

• REVIEW •

Experimental models to study cholangiocyte biology

Pamela S. Tietz, Xian-Ming Chen, Ai-Yu Gong, Robert C. Huebert, Anatoliy Masyuk, Tatyana Masyuk, Patrick L. Splinter, Nicholas F. LaRusso

Pamela S. Tietz, Xian-Ming Chen, Ai-Yu Gong, Robert C. Huebert, Anatoliy Masyuk, Tatyana Masyuk, Patrick L. Splinter, Nicholas F. LaRusso, Center for Basic Research in Digestive Diseases, Department of Internal Medicine and Biochemistry and Molecular Biology, Mayo Medical School, Clinic and Foundation, Rochester, MN 55905

Supported by grants DK24031 and DK57993 (N. F. LaRusso) from the National Institutes of Health and by the Mayo Foundation.

Correspondence to: Nicholas F. LaRusso, Center for Basic Research in Digestive Diseases, Mayo Medical School, Clinic and Foundation, 200 First Street, SW Rochester, MN 55905, United States. larusso.nicholas@mayo.edu

Telephone: +1-507284-1006 Fax: +1-507284-0762

Received 2002-01-14 Accepted 2002-01-18

Abstract

Cholangiocytes-the epithelial cells which line the bile ducts-are increasingly recognized as important transporting epithelia actively involved in the absorption and secretion of water, ions, and solutes. This recognition is due in part to the recent development of new experimental models. New biologic concepts have emerged including the identification and topography of receptors and flux proteins on the apical and/or basolateral membrane which are involved in the molecular mechanisms of ductal bile secretion. Individually isolated and/or perfused bile duct units from livers of rats and mice serve as new, physiologically relevant *in vitro* models to study cholangiocyte transport. Biliary tree dimensions and novel insights into anatomic remodeling of proliferating bile ducts have emerged from three-dimensional reconstruction using CT scanning and sophisticated software. Moreover, new pathologic concepts have arisen regarding the interaction of cholangiocytes with pathogens such as *Cryptosporidium parvum*. These concepts and associated methodologies may provide the framework to develop new therapies for the cholangiopathies, a group of important hepatobiliary diseases in which cholangiocytes are the target cell.

Tietz PS, Chen XM, Gong AY, Huebert RC, Masyuk A, Masyuk T, Splinter PL, LaRusso NF. Experimental models to study cholangiocyte biology. *World J Gastroenterol* 2002;8(1):1-4

INTRODUCTIONS

The liver contains two types of epithelia: hepatocytes, accounting for ~65% of the liver cell population; and intrahepatic bile duct cells, or cholangiocytes, the epithelial cells that line the intrahepatic biliary tree and account for ~5% of the liver cell population.

In the past decade, interest in cholangiocyte pathobiology has exploded due to: (i) the development of new experimental techniques that allow hypotheses related to cholangiocyte biology to be directly addressed (Figure 1); (ii) the recognition that cholangiocytes are critically important to normal liver function, especially solute and water transport, cell-cycle phenomena, cell signaling, and interactions with other cells, matrix components, foreign organisms and xenobiotics; and (iii) the appreciation that cholangiocytes

represent the major target of a group of serious genetic and acquired diseases termed the cholangiopathies. In a coordinated series of hypothesis-driven studies, we have explored selective aspects of cellular processing by cholangiocytes focusing on proteins (receptors, channels, exchangers, transporters, junctional proteins, molecular motors, pro/anti-apoptotic molecules) that we hypothesized were likely critically important in cholangiocyte secretion, absorption, intracellular transport, and structural modifications. Thus, we briefly review here a variety of novel *in vivo* and *in vitro* experimental models that have allowed us to expand our understanding of how cholangiocytes function and what happens when disease alters their normal physiology. Several more extensive reviews on cholangiocyte pathobiology are referenced for readers interested in more comprehensive reviews.

IN VIVO MODELS

The rat biliary tree has been shown to undergo selective proliferation in response to different experimental stimuli such as bile duct ligation (BDL)^[1], 70% hepatectomy^[2], carbon tetrachloride treatment^[3], and feeding of α -naphthylisothiocyanate (ANIT)^[4,5]. As best we know, the proliferated cholangiocytes retain a normal cholangiocyte phenotype. The bile duct ligated rat model has been useful in initiating studies on the effect of hormones on bile secretion. Infusion of secretin and somatostatin results in a choleric and cholestatic response, respectively, in the bile duct ligated but not sham-operated rat, due not only to an increased number of cells but an increased expression of the receptors for secretin and somatostatin on individual cholangiocytes^[6-8]. Much less is known about how the mouse biliary tree responds to hormones. To further explore the regulatory mechanisms of ductal bile secretion, it was necessary to develop additional novel *in vitro* experimental models.

IN VITRO MODELS

Freshly Isolated Cells

The development of *in vitro* models of biliary epithelia essentially began with the ability to isolate cholangiocytes of high purity from normal rat, mouse and human liver^[9,10]. This experimental model allowed direct studies on the effects of hormones on cholangiocytes which demonstrated among other things, that secretin stimulated exocytosis via a cyclic AMP mechanism, and that this effect was blocked by somatostatin^[11].

The technique of counter-flow elutriation has allowed refinement of cell isolation techniques from normal or BDL rats^[12,13] by allowing separation of subpopulations of cholangiocytes which differ in size. Using this model, we have provided evidence that these small, medium and large cholangiocytes originate from different portions of the intrahepatic biliary ductal system. Using molecular and physiological approaches, we have also demonstrated that these subpopulations of cholangiocytes differ in their transport and proliferative capabilities^[12,13].

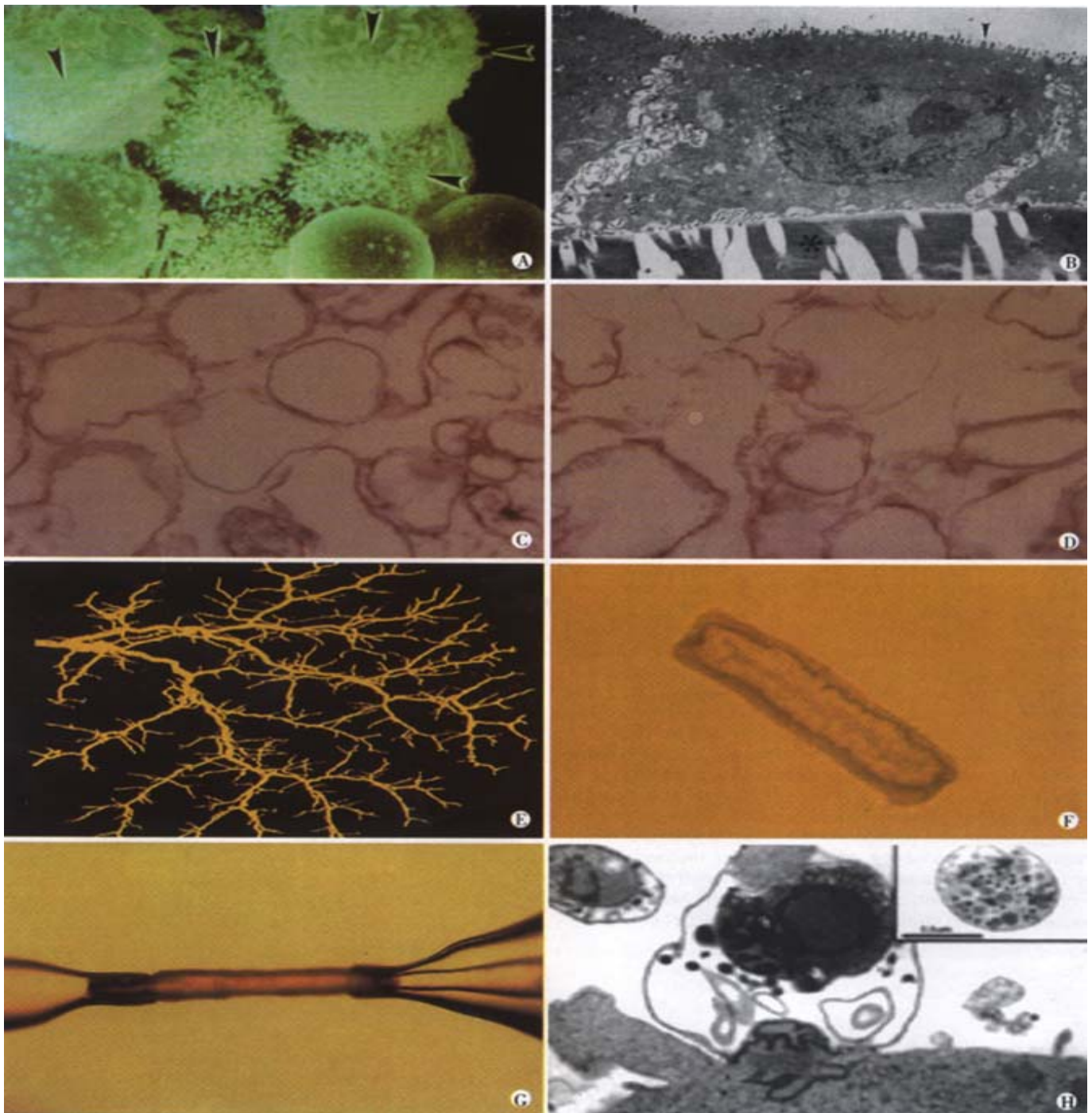


Figure 1 Experimental *in vitro* models of biliary epithelia.

(a) A scanning electron micrograph of a group of isolated cholangiocytes after separation using immunomagnetic beads. Note that the prominent microvilli (arrowheads) are limited to one side of the cells. Mag = 4,400.

(b) A transmission electron micrograph cross-section of normal rat cholangiocytes in culture demonstrates characteristics of polarized cells with apical microvilli (arrowheads) and numerous basolateral intercellular interdigitations near the collagen coated filter denoted by *, (Bar = 2 mm, Mag = 7,500).

(c) (d) A transmission electron micrograph of apical (c) and basolateral (d) plasma membrane domains revealed similar homogenous vesiculated membranes of varied shapes and sizes without apparent contamination of other organelles (Bar = 0.5 mm, Mag = 22,500).

(e) A three-dimensional reconstructed image of the intrahepatic biliary tree isolated from normal rat liver.

(f) A light micrograph of an unstained isolated bile duct unit from rat liver. After overnight culture, the two ends seal forming an enclosed unit. A single layer of epithelial cells with a thin outer layer of connective tissue surrounds the lumen.

(g) A microperfused intrahepatic bile duct unit isolated from rat liver, manually dissected and cannulated with micropipettes.

(h) Transmission electron micrograph of *C. parvum* infection of cultured human cholangiocytes. A parasitophorous vacuole contains a developing parasite stage which is intracellular but extracytoplasmic. A macrogamete is shown in the inset, demonstrating development of sexual stages of the parasite. Bar = 1 mm.

Cholangiocyte cDNA Library

A unique cDNA library has been constructed from highly purified cholangiocytes isolated from rats subjected to bile duct ligation for 2 weeks^[14]. Total cellular RNA was extracted from cholangiocytes and poly(A)+ mRNA isolated. Subsequently, the poly(A)+ mRNA was reverse transcribed and directionally cloned. The cholangiocyte cDNA library allows screening and sequencing of positive clones for numerous molecules yet to be identified.

Cultured Cells

Freshly isolated cells maintained in short-term culture provided the opportunity to perform patch-clamp studies yielding novel insights into the electrophysiology of cholangiocytes^[15]. Established long-term cultured cholangiocytes can be grown on semi-permeable cell culture filters by which they quickly reach confluence, maintain morphologic polarity and develop adequate transepithelial electrical resistance, making them a prototype for use in transport studies. This model has been utilized to characterize the uptake of glucose and bile acids and to study water transport^[16-19].

Isolated Organelles

In order to perform more rigorous transport studies and to generate accurate kinetic transport parameters (i.e., Km and Vmax), we developed techniques for isolating vesicles enriched in either the apical or the basolateral domain of cholangiocytes starting either with whole rat liver or with cholangiocytes in culture^[20,21]. An initial application of these vesicles was to generate kinetic values for sodium-dependent taurocholate uptake, a process that we demonstrated occurs in apical but not basolateral vesicles^[17]. This tool allows continued studies to localize and functionally evaluate transport processes in cholangiocytes.

Intrahepatic Bile Duct Units

Experiments using intact intrahepatic bile duct units isolated by mechanical and enzymatic techniques from normal rats to study biliary epithelial transport physiology have been previously described^[22]. An advantage of this model is that we can not only control the luminal contents (by manipulating components of the perfusate) but we can independently and simultaneously modify the basolateral milieu (by manipulating components of the bathing buffer). With this approach, we were able to detect changes in intraluminal pH and electrolyte concentrations in response to agonists. We could also demonstrate water transport across this epithelial barrier in response to osmotic gradients, the characteristics of which (kinetics, temperature independence and mercury sensitivity) all suggested the presence of water selective channel proteins (i.e., aquaporins) (AQP) on the membranes of cholangiocytes. Using quantitative computer-assisted image analysis to measure expansion and reduction of luminal area as a reflection of water movement, we have demonstrated that water movement across the bile duct units is transcellular and channel-mediated^[13].

We have subsequently expanded this model using a microperfusion technique and an epifluorescence detection system^[24]. With this modification, we have demonstrated the movement of water into (secretion) and out of (absorption) the lumen of the perfused ducts in response to inward and outward osmotic gradients. The calculation of both net water movement (Jv) and osmotic water permeability (Pf) provide evidence that the measured bi-directional fluxes reflect water movement through water channels.

In addition, we have demonstrated that isolated bile duct units actively absorb solutes such as bile acids and glucose, and transport ions such as bicarbonate. We have also shown that luminal perfusion of ATP and other nucleotides activates P2Y

ATP receptors on the apical cholangiocyte plasma membrane and induces increases in $[Ca^{2+}]_i$ and net ductular alkalization, suggesting that ductal bile secretion is regulated by these signaling molecules^[25].

This technique has now been adapted to the mouse in which we can reproducibly isolate and microperfuse intact bile duct units from normal mouse liver with the anticipated application to transgenic or knockout mouse models^[26]. Transgenic mice continue to be developed in which there is a selective knockout of one or more aquaporin water channels^[27]. The isolated and perfused bile duct unit model would allow us to test the hypothesis that knockout mice lacking AQP1 and AQP4 water channels or perhaps other naturally expressed aquaporins may have substantially reduced choleretic and cholestatic responses to hormones since the flux of water molecules through these water channels should be absent.

The isolation of intact, polarized intrahepatic bile duct units from both rat and mouse allows the direct study of secretory and absorptive activities of the bile ducts in a way which most closely approximates the normal biliary ductal system.

Three-Dimensional Modeling

Although cholangiocyte functional and morphological heterogeneity likely contributes to the selective involvement of different portions of the biliary tree in the cholangiopathies, our understanding of the nature and mechanisms for normal and abnormal anatomical remodeling of the biliary tree is limited. To better define the heterogeneous nature of the biliary tree, we utilized a computer-aided three-dimensional imaging technique, first described in a study of the normal human biliary tree^[28], to perform quantitative anatomical studies of the rat intrahepatic biliary system^[29].

Computer generated three-dimensional reconstruction of the intrahepatic biliary tree using microscopic-computed tomography scanning and sophisticated software allowed us to generate key biliary tract dimensions (length, surface area, duct diameter, volume) and branching patterns (distance from the junction of intra- and extrahepatic ducts, number of bile duct branches and branching angles).

In various forms of liver disease, including the cholangiopathies, proliferation of cholangiocytes is a common pathological response^[1, 30, 31]. The anatomical basis and remodeling process which occurs in response to various stimuli remain unclear. We have since applied the three-dimensional reconstruction of the biliary tree to rats in whom selective cholangiocyte proliferation was induced by ANIT feeding^[4,5]. The anatomical remodeling and quantitative observations after selective cholangiocyte proliferation suggest that the proliferation process involves sprouting of new side branches. Recently three-dimensional modeling has been applied to generate data for the hepatic artery and portal vein within the same liver (Masyuk, LaRusso unpublished). This descriptive study allowed key findings on the length of vascular segments, diameter of blood vessel segments and volume of the hepatic artery and portal vein, associated with experimentally-induced cholangiocyte proliferation.

Three-dimensional reconstruction will provide complementary data that, at a minimum, will yield structural information on biliary tract architecture and biliary mapping (i.e., which branches of the biliary tree are involved in absorption or secretion, the mechanisms by which ducts proliferate in response to injury, and the impact of these modifications on the peribiliary vasculature.) The significance of these studies relates not only to the intrinsic value of understanding cholangiocyte physiology but also to providing a biologic rationale for why only certain segments of the biliary tree are involved in the individual cholangiopathies. Primary biliary cirrhosis, for example, leads to destruction of interlobular bile ducts, while intrahepatic cholestasis induced by drugs affects principally the cholangiocytes that line small bile ducts^[30, 32, 33].

In Vitro Infection Model of Biliary Cryptosporidiosis

Using monolayers of human cholangiocytes derived from normal liver and immortalized by SV40 transformation, we developed an *in vitro* infection model of biliary cryptosporidiosis^[34]. Cryptosporidiosis is an infectious disease caused by *Cryptosporidium parvum* (*C. parvum*), an emerging parasite which causes self-limited diarrhea in immunocompetent subjects and potentially life-threatening syndromes in immunocompromised individuals, primarily those with acquired immunodeficiency syndrome (AIDS). Despite the magnitude and severity of cryptosporidial infection, the pathogenesis is poorly understood, and there is currently no effective therapy. Using this novel infection model, we found that *C. parvum* sporozoites (derived from oocysts excysted *in vitro*) attach to the apical surface of biliary epithelia, invade the cells, reside in a parasitophorous vacuole, and undergo both sexual and asexual development.

C. parvum attachment to cholangiocytes involves interactions between specific glycoproteins on cholangiocytes and *C. parvum* sporozoite lectins while the invasion into cholangiocytes works through actin-dependent membrane spreading mediated by cortactin and RhoGTP-binding proteins^[34-36]. While *C. parvum* is cytopathic to uninfected cells adjacent to infected cholangiocytes via Fas/FasL-dependent apoptosis, the organism prevents cell death of infected cells by inhibiting apoptosis via activation of NF- κ B^[37, 38]. This model provides a useful system for the development of novel therapeutic strategies for *C. parvum* induced enterology and AIDS-cholangiopathy.

CONCLUSION

Advances in medical knowledge most often are preceded by advancements in technology and experimental models. Results from experiments using these new models and methods have clarified which flux proteins are expressed in cholangiocytes, their intracellular topography and segmental distribution, what molecules control their cellular compartmentalization, and their physiologic relevance to ductal bile formation. In addition, the information has provided a theoretical framework for development of novel therapeutic strategies for the cholangiopathies, a group of cholestatic genetic/acquired hepatobiliary diseases in which the cholangiocyte is the principal target of diverse destructive processes.

Abbreviations

ANIT	α -naphthylisothiocyanate
AQP	aquaporin
BDL	bile duct ligation
<i>C. parvum</i>	<i>Cryptosporidium parvum</i>

Acknowledgement We greatly appreciate the secretarial assistance of Deb Hintz in preparation of this manuscript.

REFERENCES

- Alpini G, Phillips JO, LaRusso NF. The biology of biliary epithelia. Edited by Arias IM, Boyer JL, Fausto N, Jakoby WB, Schachter DA, Shafritz DA. The Liver: Biology and Pathobiology. New York: Raven Press 1994:623-653
- LeSage G, Glaser SS, Gubba S, Robertson W, Phinizz JL, Lasater J, Rodgers R, Alpini G. Regrowth of the rat biliary tree after 70% partial hepatectomy is coupled to increased secretin-induced ductal secretion. *Gastroenterology* 1996; 111:1633-1644
- LeSage G, Benedetti A, Glaser S, Marucci L, Tretjak Z, Caligiuri A, Rodgers R, Phinizz JL. Acute carbon tetrachloride feeding selectively damages large, but not small, cholangiocytes from normal rat liver. *Hepatology* 1999;29:307-319
- Desmet VJ, Krsulovic B, van Damme B. Histochemical study of rat liver in alpha-naphthylisothiocyanate (ANIT) induced cholestasis. *Am J Pathol* 1968;52:401-421
- Kossor DC, Goldstein RS, Ngo W, DeNicola DB, Leonard TB, Dulik DM, Meunier PC. Biliary epithelial cell proliferation following alpha-naphthylisothiocyanate (ANIT) treatment: relationship to bile duct obstruction. *Fundam Appl Toxicol* 1995;26:51-62
- Alpini G, Ulrich C, Pham LD, Phillips JO, Miller LJ, LaRusso NF. Upregulation of secretin receptor gene expression in rat cholangiocytes after bile duct ligation. *Am J Physiol* 1994;266:G922-G928
- Tietz P, Alpini G, Pham L, LaRusso NF. Somatostatin inhibits secretin-induced ductal hyperchloresis and exocytosis by cholangiocytes. *Am J Physiol* 1995; 269:G110-G118
- Tietz PS, Hadac E, Miller LJ, LaRusso NF. Upregulation of secretin receptors on cholangiocytes after bile duct ligation. *Regul Pept* 2001;297:1-6
- Ishii M, Vroman B, LaRusso NF. Isolation and morphologic characterization of bile duct epithelial cells from normal rat liver. *Gastroenterology* 1989;97:1236-1247
- Vroman B, LaRusso NF. Development and characterization of polarized primary cultures of rat intrahepatic bile duct epithelial cells. *Lab Invest* 1996;74:303-313
- Kato A, Gores GJ, LaRusso NF. Secretin stimulates exocytosis in isolated bile duct epithelial cells by a cyclic AMP-mediated mechanism. *J Biol Chem* 1992; 267:15523-15529
- Alpini G, Roberts S, Kuntz SM, Ueno Y, Gubba S, Podilla PV, LeSage G, LaRusso NF. Morphologic, molecular and functional heterogeneity of cholangiocytes from normal rat liver. *Gastroenterology* 1996;110:1636-1643
- Alpini G, Ulrich C, Roberts S, Phillips JC, Ueno Y, Podila PV, Colegio O, LeSage G, Miller LJ, LaRusso NF. Molecular and functional heterogeneity of cholangiocytes from rat liver after bile duct ligation. *Am J Physiol* 1997;272:G289-G297
- Pham L, Lazaridis K, LaRusso NF, deGroen PC. Development and characterization of a cDNA library prepared from isolated rat cholangiocytes. *Gastroenterology* 1997;112:A1358
- Balan V, Larkin J, Pham L, Vroman B, McNiven MA, LaRusso NF. Identification of Rab3d in intrahepatic bile duct epithelial cells: Implications for exocytosis and bile secretion. *Gastroenterology* 1994;106:A863
- Lazaridis KN, Pham L, Vroman B, DeGroen PC, LaRusso NF. Kinetic and molecular identification of sodium-dependent glucose transporter in normal rat cholangiocytes. *Am J Physiol* 1997;272:G1168-1174
- Lazaridis KN, Pham L, Marinelli RA, Tietz P, deGroen PC, Levine S, Dawson PA, LaRusso NF. Rat cholangiocytes absorb bile acids at their apical domain via the ileal sodium-dependent bile acid transporter. *J Clin Invest* 1997;100:2714-2721
- Lazaridis KN, Tietz PS, Kip S, Dawson P, LaRusso NF. Alternative splicing of the rat sodium/bile acid transporter changes its cellular localization and transport properties. *Proc Natl Acad Sci USA* 2000;97:11092-11097
- Marinelli RA, Pham LD, Tietz PS, LaRusso NF. Expression of aquaporin 4-water channels in rat cholangiocytes. *Hepatology* 2000;31:1313-1317
- Tietz PS, Holman RT, Miller LJ, LaRusso NF. Isolation and characterization of rat cholangiocyte vesicles enriched in apical or basolateral plasma membrane domains. *Biochemistry* 1995;34:15436-15443
- Tietz P, Levine S, Holman R, Fretham C, LaRusso NF. Characterization of apical and basolateral plasma membrane domains derived from cultured rat cholangiocytes. *Anal Biochem* 1997;254:192-199
- Roberts SK, Kuntz SM, Gores GJ, LaRusso NF. Regulation of bicarbonate-dependent ductular bile secretion assessed by luminal micropuncture of isolated rodent intrahepatic bile ducts. *Proc Natl Acad Sci USA* 1993;90:9080-9084
- Cova E, Gong A, Marinelli RA, LaRusso NF. Water movement across rat bile duct units is transcellular and channel-mediated. *Hepatology* 2001;34:456-463
- Masyuk AI, Gong AY, Kip S, Burke MJ, LaRusso NF. Perfused rat intrahepatic bile ducts secrete and absorb water, solute and ions. *Gastroenterology* 2000; 119:1672-1680
- Dranoff JA, Masyuk AI, Kruglov EA, LaRusso NF, Nathanson MH. Polarized expression and function of P2YATP receptors in rat bile duct epithelia. *Am J Physiol* 2001;281:G1059-G1067
- Gong AY, Masyuk AI, Splinter PL, LaRusso NF. Development and initial application of a micropfusion model of intrahepatic mouse bile duct units. *Hepatology* 2000;32(4, Pt2):433A
- Verkman AS, Yang B, Song Y, Manley GT, Ma T. Role of water channels in fluid transport studied by phenotype analysis of aquaporin knockout mice. *Exp Physiol* 2000;85:233S-241S
- Ludwig J, Ritman EL, LaRusso NF, Sheedy PF. Anatomy of the human biliary system studies by quantitative computer-aided three-dimensional imaging techniques. *Hepatology* 1998;27:893-889
- Masyuk TV, Ritman EL, LaRusso NF. Quantitative assessment of the rat intrahepatic biliary system by three-dimensional reconstruction. *Am J Pathol* 2001;158:2079-2088
- LaRusso NF. Morphology, physiology and biochemistry of biliary epithelia. *Toxicol Pathol* 1996;24:84-89
- Thung SN. The development of proliferating ductular structures in liver disease. *Arch Pathol Lab Med* 1990;114:407-411
- Roberts SK, Ludwig J, LaRusso NF. The pathology of biliary epithelia. *Gastroenterology* 1997;112:269-279
- Birnbaum A, Suchy FJ. The intrahepatic cholangiopathies. *Semin Liver Dis* 1998;18:263-269
- Chen XM, Levine SA, Tietz P, Krueger E, McNiven MA, Jefferson DM, Mahle M, LaRusso NF. Cryptosporidium parvum is cytopathic for cultured human biliary epithelia via an apoptotic mechanism. *Hepatology* 1998;28:906-913
- Chen XM, LaRusso NF. Mechanisms of attachment and internalization of Cryptosporidium parvum to biliary and intestinal epithelial cells. *Gastroenterology* 2000;118:368-379
- Chen XM, Huang BQ, Splinter PL, McNiven MA, LaRusso NF. Molecular mechanism of Cryptosporidium parvum invasion of biliary epithelia. *Gastroenterology* 2001;120:A325
- Chen XM, Gores GJ, Paya CV, LaRusso NF. Cryptosporidium parvum induces apoptosis in biliary epithelia by a Fas/Fas ligand-dependent mechanism. *Am J Physiol* 1999;277:G599-608
- Chen XM, Levine SA, Splinter PL, Tietz PS, Ganong AL, Jobin C, Gores GJ, Paya CV, LaRusso NF. Cryptosporidium parvum activates nuclear factor kappa B in biliary epithelia preventing epithelial cell apoptosis. *Gastroenterology* 2001;120:1774-1783

• BASIC RESEARCH •

Direct effect of croton oil on intestinal epithelial cells and colonic smooth muscle cells

Xin Wang, Mei Lan, Han-Ping Wu, Yong-Quan Shi, Ju Lu, Jie Ding, Kai-Cun Wu, Jian-Ping Jin, Dai Ming Fan

Xin Wang, Mei Lan, Han-Ping Wu, Yong-Quan Shi, Jie Ding, Kai-Cun Wu, Dai Ming Fan, Institute of Digestive Diseases, Xijing Hospital, Fourth Military Medical University, Xi'an 710032, Shaanxi Province, China

Ju Lu, Class EE 87, Department of Electronic Engineering, Tsinghua University, Beijing 100084, China

Jian-Ping Jin, Department of Physiology and Biophysics, Case Western Reserve University School of Medicine, Cleveland, 44106-4970, Ohio, USA

Supported by the National Natural Science Foundation of China, No. 39970901

Correspondence to: Prof. Dai-Ming Fan, Institute of Digestive Disease, Xijing Hospital, Fourth Military Medical University, Xi'an 710033, Shaanxi Province, China. Daimfan@pub.xaonline.com
Telephone: +86-29-3375221 Fax: +86-29-2539041

Received 2001-08-08 Accepted 2001-10-23

Abstract

AIM: To investigate the direct effect of croton oil (CO) on human intestinal epithelial cell (HIEC) and guinea pig colonic smooth muscle cells *in vitro*.

METHODS: Growth curves of HIEC were drawn by MTT colorimetry. The dynamics of cell proliferation was analyzed with flow cytometry, and morphological changes were observed under light and electron microscopy after long-term (6 weeks) treatment with CO. Expression of cyclooxygenase-2 (COX-2) mRNA was detected by dot blot in HIEC treated with CO. Genes related to CO were screened by DD-PCR, and the direct effect of CO on the contractility of isolated guinea pig colonic smooth muscle cells was observed.

RESULTS: High concentration (20 - 40 mg · L⁻¹) CO inhibited cell growth significantly (1, 3, 5, 7d OD sequence: (20 mg · L⁻¹) 0.040±0.003, 0.081±0.012, 0.147±0.022, 0.024±0.016; (40 mg · L⁻¹) 0.033±0.044, 0.056±0.012, 0.104±0.010, 0.189±0.006; OD control 0.031±0.008, 0.096±0.012, 0.173±0.009, 0.300±0.016, *P*<0.01), which appeared to be related directly to the dosage. Compared with the control, the fraction number of cells in G1 phase decreased from 0.60 to 0.58, while that in S phase increased from 0.30 to 0.34 and DNA index also increased after 6 weeks of treatment with CO (the dosage was increased gradually from 4 to 40 mg · L⁻¹). Light microscopic observation revealed that cells had karyomegaly, less plasma and karyoplasm lopsidedness. Electron microscopy also showed an increase in cell proliferation and in the quantity of abnormal nuclei with pathologic mitosis. Expression of COX-2 mRNA decreased significantly in HIEC treated with CO. Thirteen differential cDNA fragments were cloned from HIEC treated with CO, one of which was 100 percent homologous with human mitochondrial cytochrome C oxidase subunit II. The length of isolated guinea pig colonic smooth muscle cells was significantly shortened after treatment with CO (*P*<0.05).

CONCLUSION: At a high CO concentration (>20 mg · L⁻¹),

cell growth and proliferation are inhibited in a dosage-dependent manner. Increase in cell proliferation and in malignant conversion of the cellular phenotype is observed in cells cultured chronically with CO. COX-2 mRNA expression decreases significantly, while human mitochondrial cytochrome C oxidase subunit II mRNA expression increases markedly in HIEC treated with CO. CO also has a direct effect on the contractility of Guinea pig colonic smooth muscle cells.

Wang X, Lan M, Wu HP, Shi YQ, Lu J, Ding J, Wu KC, Jin JP, Fan DM. Direct effect of croton oil on intestinal epithelial cells and colonic smooth muscle cells. World J Gastroenterol 2002; 8(1):103-107

INTRODUCTION

Croton is the fruit of *Croton tiglium* L, which consists of 34%-57% croton oil and 18% proteins. Croton oil (CO) contains crotonoleic acid, crotonic acid, crotonyl alcohol, 16 kinds of crotonyl alcohol bisester and many kinds of crotonyl alcohol trisester. Also contained in the seed of croton are croton, cocarcinogen C-3, crotonoside, isoguanine, β-sitosterol, amino acids and many kinds of enzymes. However, the principal component of croton extract is CO, which possesses multiple drug effects. CO is a stimulant in making inflammatory models, especially in models of skin and mucosal inflammation^[1], such as animal models of hemorrhoids, pleuritis, ear edema and uveitis^[2]. Investigations have shown that allergic contact dermatitis (ACD) induced by CO is not a kind of late pleoergy response, but is mediated by the immune system in skin^[3,4]. Metalloprotease neutral endopeptidase (NEP) and neuropeptide play an important role in ACD^[5]. After CO administration to mice for 3 h^[6,7], there was no change in the mucosa of stomach and intestine under light microscope, but mucosal epithelial cell inflammation was observed under electron microscopy.

According to the recent, that dehydrocrotonin (DCTN), an extract of CO, had anti-ulcer effect^[8], especially in ulcers induced by hypothermia, alcohol and pyloric ligation. This effect was supposed to be related to the increase in the release of prostaglandin E2, the non-specific competitive binding of H2 and M receptors of stomach, the reinforcement of mucosal protective action and the weakening of mucosa-impairing factors. So DCTN has the potential to be a new anti-ulcer drug^[9,10].

It was reported that croton extract could not only suppress tumor growth but also promote tumor development. It has been confirmed that t-DCTN, which possesses neither genetic toxicity nor cytotoxicity, has anti-tumor activity and can significantly elongate the survival period of mice with S180 sarcoma and ascites neoplasia^[11,12]. Recent research showed that 2,3-dihydroxy-labda-8 (17), 12(E), 14-triene, one of the croton extracts, had non-specific cytotoxicity for various tumor cells^[13]. However, some investigations found that CO could cause skin carcinoma by lipid peroxidation and hydroperoxide production; it could directly bind protein kinase C, stimulating over-proliferation of epidermis, and repeatedly impair skin, which induces skin hyperplasia.

Croton is a strong cathartic; trace of croton can cause severe

diarrhea because of its potent in accelerating gastrointestinal motility. Now, Chinese medicine is the hot spot in the development of new drugs promoting gastrointestinal motility^[14-28]. However, its mechanism in inducing diarrhea and accelerating gastrointestinal motion is not yet clarified^[29-32].

The aim of this research is to observe the effect of CO on intestinal epithelial cells and isolated colonic smooth muscle cells; investigate the effect of CO on biological properties of intestinal epithelia, mRNA differential expression and intestinal smooth muscle cell contraction; and further clarify its molecular mechanism so as to lay the foundation of the development of new drugs promoting gastrointestinal motility.

MATERIALS AND METHODS

Cell lines and culture

Human intestinal epithelial cell line (HIEC), presented as a gift by Dr. Ren DQ from Department of Radiation Medicine, Fourth Military Medical University, was grown in RPMI 1640 medium with 100 mL·L⁻¹ fetal bovine serum. CO dissolved in dimethyl sulfoxide (DMSO) was added into the culture medium when the medium was exchanged^[32]. The end-concentration of CO was 4 mg·L⁻¹; then the concentration increased progressively to 40 mg·L⁻¹ in 6 weeks.

Effects of CO on HIEC growth (MTT)

Add HIEC into 96 well plate (200 µL/well); and add CO of different concentrations (4, 20, 40, 80 mg·L⁻¹) and control DMSO (0.2, 1, 2, 4 mL·L⁻¹) to corresponding groups, with three wells in each group. Put the culture plates into culture cassette, then take out one 96-well plate each time (1, 3, 5, 7 d), add 20 µL MTT solution (5 g·L⁻¹) into each well, and resume culturing at 37°C for 4 h. Afterwards, suck and throw away the culture medium from the 96-well plate and add 150 µL DMSO to the plate. Detect OD in each well with photometer (wave length: 490 nm) and draw the growth curve.

Flow cytometry analysis of HIEC proliferation treated with CO

Harvest HIEC in log phase growth that was treated with CO for 6 weeks. Cell proliferation cycle of HIEC was analyzed with flow cytometry after HIEC was routinely digested, washed twice with PBS and fixed with 700 mL·L⁻¹ ethanol. DNA index (DI) was calculated with the formula: DI = experimental group cells G0/1 / control cells G0/1. DNA.

Judgment standard of ploidy^[33]. DI = 0.95-1.05 (DI = 1 ± CV, CV is 0.05): diploid; DI ≠ 1.00, between 0.90-1.10: proximal diploid; DI > 1.10 or DI < 0.9: increased or decreased heteroploid DNA content.

Morphological changes of HIEC treated with CO

Changes in cell morphology were observed dynamically under inverted microscope. HIEC in log phase growth that was treated with CO for 6 weeks was harvested, and its proliferation cycle was analyzed with flow cytometry after routinely digested, washed twice with PBS, centrifuged for 5 min at 1200-1400 r·min⁻¹, fixed with glutaraldehyde for 30 min at 4°C, and prepared into ultrathin section for transmission electron microscopic observation.

Expression of COX-2 mRNA in HIEC (Dot blot)

Total RNA was extracted from control and experimental cells treated with CO for 6 wk. RNA samples were pointed onto the nitric cellulose membrane, and specific COX-2 oligonucleotide probes were end-labeled. Expression of COX-2 mRNA was detected with dot blot.

mRNA differential display of HIEC treated with CO (DD-

PCR)

Gene expressions of HIEC treated with CO for 6 weeks and of control were compared through DD-PCR. Primers were designed according to the literature: 3' end anchor primer H-T₁₁C: 5'-AAGCTTTTTTTTTTTC-3', 8 strips of 5' end random primers: H-AP₁-H-AP₈. The first chain of cDNA was synthesized by reverse transcription; then with RT products as templates, and PCR was performed with 8 strips of 5' end random primers individually. Products of RT-PCR were run on 60 g·L⁻¹ urea denaturation polyacrylamide gels until the indicator arrived at the basal part of the gel at 200-300 V for 6-8 h. The gels were stained with modified silver-stain. Differential cDNA fragments were cut, recovered and purified for secondary amplification with PCR, and amplification products were isolated by agarose gel electrophoresis and ligated with pUC-Tm vector after recovery and purification. Recombinant plasmids were transfected into DH5α Escherichia coli and the bacteria were plated and incubated at 37°C overnight. Positive clones were picked out and the plasmids were extracted, followed by restriction enzyme cleavage identification. Further identification of the positive clones included reverse Northern blot and sequencing by automatic sequencer. Homology of the sequences of the differential expression cDNA fragments was searched in Gene Bank Database.

Direct effect of CO on Guinea pig colonic smooth muscle cells

Guinea pig colonic smooth muscle cells were isolated by modified methods reported by Bitar and Makhoul^[34,35]. Activity of the smooth muscle cells was detected with trypan blue, and the number of the cells were calculated under invert microscope. The number of smooth muscle cells with vitality must exceed 90% for experiment. CO was dissolved in dimethyl sulfoxide (DMSO) to make 4, 2, and 0.25 g·L⁻¹ CO solutions. Ten µL CO solutions of different concentrations were added into 200 µL colonic smooth muscle cell suspensions, the end-concentration of CO being 0.14, 0.07, and 0.009 g·L⁻¹, respectively. The cells were incubated with CO at 30°C for 30 s and 80 µL of 25 g·L⁻¹ glutaraldehyde was added to terminate the reaction.

The length change of the smooth muscle cells was detected with micrometer under invert microscope. The average length was calculated from every 50 cells randomly. The contractile response of the smooth muscle cells was measured by the decrease of average length of cells treated with CO compared with that of the control. The formula is:

Percentage of cell contractile change = (average length of experimental cells - average length of control cells) / average length of control cells × 100%.

RESULTS

Effect of CO on the growth and cell cycle-phase of HIEC

High dosage (80 mg·L⁻¹) CO resulted in the death of all HIEC; moderate dosage (20-40 mg·L⁻¹) significantly inhibited cell growth (1, 3, 5, 7 d OD sequence: (20 mg·L⁻¹) 0.040 ± 0.003, 0.081 ± 0.012, 0.147 ± 0.022, 0.024 ± 0.016; (40 mg·L⁻¹) 0.033 ± 0.044, 0.056 ± 0.012, 0.104 ± 0.010, 0.189 ± 0.006; OD control 0.031 ± 0.008, 0.096 ± 0.012, 0.173 ± 0.009, 0.300 ± 0.016, *P* < 0.01) in a dosage-dependent manner (IC₅₀ is 52 mg·L⁻¹); and low dosage (4 mg·L⁻¹) had no effect on cell growth (*P* > 0.05). The flow cytometry showed that S phase HIEC quantity significantly increased, G₂/M phase cell quantity decreased and DI rose to 1.15 after HIEC was treated with CO for 6 weeks.

Changes of HIEC morphology treated with CO

Morphologic changes of HIEC were dynamically observed under invert microscope in cells incubated with CO. Initially many cells exhibited

sheet shedding, intercellular space increased, toxic granules accumulated in the cytoplasm, and cell growth was significantly delayed. The growth behavior of the cells improved after treatment with CO for 11d. After the dosage of CO was progressively increased to $40 \text{ mg} \cdot \text{L}^{-1}$ at the 6th week, the following phenomena occurred: fusiform cells significantly increased, cell bodies shrank, the nuclei were enlarged, the cytoplasm was reduced, karyoplasm lopsidedness was developed, and cell growth was accelerated. Under transmission electron microscope, we observed many wide apophyses in cell membrane, abundant microvilli, enlarged nuclei, multiplied nucleoli, and abnormal nuclei with pathologic mitosis (Figure 1).

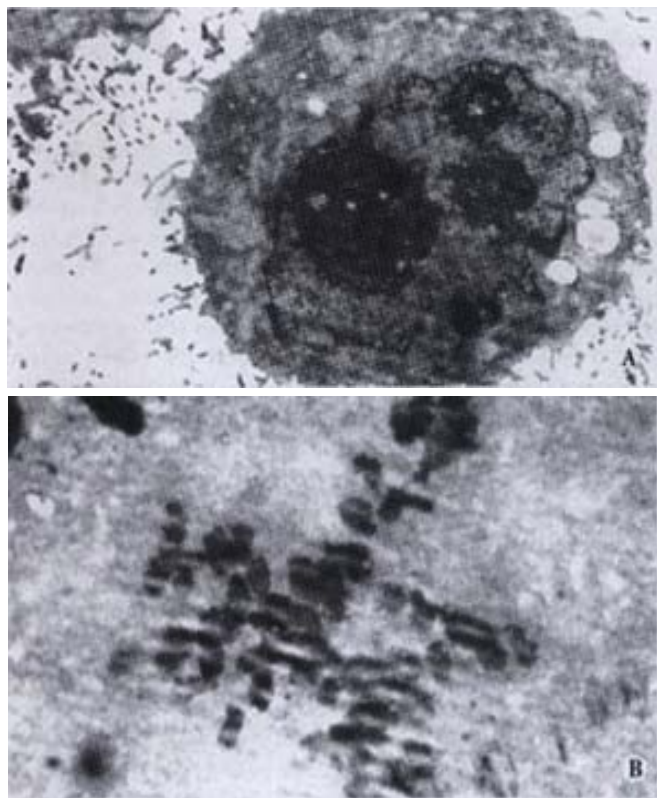


Figure 1 A: Rich microvilli, enlarged nuclei and increased nucleoli in HIEC treated with CO (left);
B: Abnormal nuclei with pathologic mitosis in HIEC treated with CO (right).

Expression of COX-2 mRNA in HIEC

Expression of COX-2 mRNA was significantly down regulated in HIEC after treated with CO for 6 week (Figure 2).

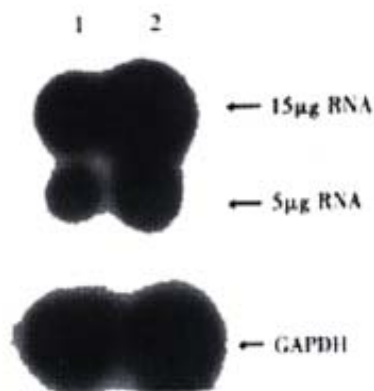


Figure 2 Expression of COX-2mRNA in HIEC 1:HIEC treated with CO for 6week; 2:Control HIEC

DD-PCR

Some cDNA fragments found in HIEC treated with CO were up-regulated, down-regulated, newly born or deleted in comparison of experimental cells with controls (Figure 3). Thirteen different cDNA fragments were successfully cloned; among the 13 positive clones, 2 fragments were significantly up-regulated and 11 down-regulated in HIEC treated with CO, which was confirmed through reverse Northern blot analysis. Sequencing and homology demonstrated that one over-expressed cDNA fragment is 100% homologous with the homeobox gene of mitochondrial cytochrome C oxidase subunit-2 gene.

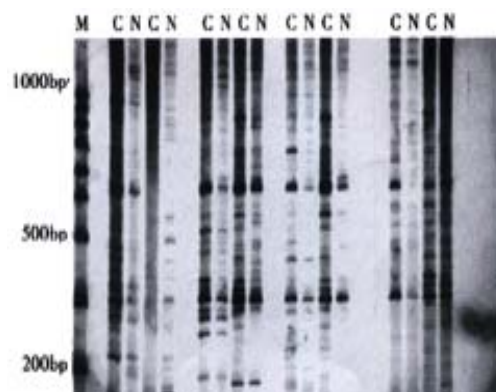


Figure 3 Differential display of mRNA in HIEC treated with COM: 100bp ladder; C: HIEC treated by CO; N: Normal HIEC

Direct effect of CO on guinea pig colonic smooth muscle cells

Free Guinea pig colonic smooth muscle cells appeared in fusiform shape with diverse length. Some of them were relaxed while others were at different phases of contraction (Figure 4). The length of normal guinea pig colonic smooth muscle cells ranged from $60 \mu\text{m}$ to $160 \mu\text{m}$, with an average length being $(102 \pm 23) \mu\text{m}$. After incubated with different concentrations of CO (0.14 , 0.07 , $0.009 \text{ g} \cdot \text{L}^{-1}$), the average length of colonic smooth muscle cells became $(72 \pm 27) \mu\text{m}$, $(74 \pm 26) \mu\text{m}$ and $(72 \pm 17) \mu\text{m}$, respectively, while that of the control cells was $(104 \pm 22) \mu\text{m}$ (Figure 5). The percentages of decrease in cell length were 29.5%, 28% and 29.6%, respectively, significantly smaller than that of the control ($P < 0.05$).

DISCUSSION

Our study showed that^[36] high dosage of CO could result in the death of HIEC; middle dosage could inhibit cell growth in a dose-dependent manner; low dosage had no effect on cell growth. Meanwhile, after long-term continuous incubation with CO, the cycle from G_1 to S of HIEC was shortened, the quantity of G_1 phase cells was reduced, the quantity of S phase cells was increased, and DI was raised. We found that the principal phenomena of HIEC treated with CO included cell degeneration, necrosis, diminished ability of cells adhesion, and delayed cell growth. As the drug action persisted, degenerated cell quantity decreased and cell proliferation was accelerated. We also observed that HIEC treated with CO proliferated faster than control cells, and abnormal nuclei with pathologic mitosis were observed under electron microscope. These phenomena indicated that the cytotoxicity of high concentration CO might be the major cause for cell growth suppression. CO had the potential effect on promoting cell over-proliferation and increasing the content of heteroploid DNA when HIEC was incubated with CO for a long time.



Figure 4 A: Relaxed colonic smooth muscle cell; B: Contracted colonic smooth muscle cell

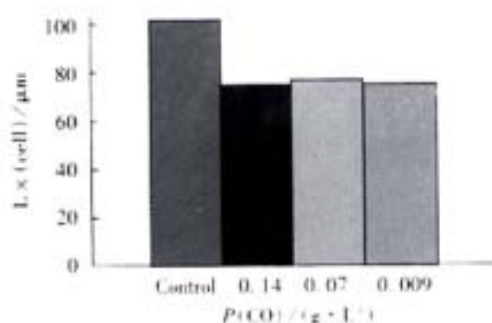


Figure 5 Direct contractile effect of CO on the colonic smooth muscle cells

COX-2 is an isoenzyme of cyclooxygenase discovered recently. Under normal conditions, COX-2 expression was low or non-existent in most tissues and cells in human body, but its expression could be promptly enhanced when cells were stimulated by a variety of factors. Recent studies showed that COX-2 is closely related to the development and progression of many kinds of human tumors, especially gastrointestinal tumors, such as colon cancer and gastric cancer. It has been confirmed that the expression of COX-2 increases more significantly in colon cancer tissues than in normal colonic tissues^[37], and its expression is higher in many kinds of gastric cancer cell lines and tissues than in their normal counterparts^[38,39]. The incidence and mortality of colon cancer were decreased with the long-term intake of non-steroidal anti-inflammatory drugs (NSAIDs), a COX-2 inhibitor, which is effective on familial adenomatous polyposis. These data indicated that COX-2 might play an important role in the pathology of these tumors. The specific mechanism of COX-2 induced tumorigenesis is yet unclear, but it is suspected to be related to the following factors: catalysis of carcinogen synthesis; catalysis of prostaglandin (PGs) synthesis, which can regulate the expression of genes and accelerate DNA synthesis and cell proliferation; inhibition of cell apoptosis; enhancement of adhesion between cells and extracellular matrix; promotion of tumor angiogenesis^[40,41]; inhibition of immunological response^[42]. The expression of COX-2 mRNA was detected in HIEC treated with CO for 6 weeks, and the results revealed its significant down-regulation. The relationship between CO-induced tumorigenesis and down-regulation of COX-2 in HIEC remains to be elucidated.

Thirteen differential expression gene fragments were detected in HIEC treated with CO for long time through mRNA differential display. Therefore, these genes may be related to the biological effects of CO on HIEC. One of the genes is human mitochondria cytochrome C oxidase subunit II gene, whose expression is high in CO treated HIEC. Human mitochondria cytochrome C oxidase consists of subunit I, II and III, which contributes substantially to the respiratory function of mitochondrion. In addition, two notably highly expressed genes were separated from Cisplatin-resistant human head and neck squamous epithelium cancer by Higuchi^[43] through DDRT-PCR, and

one of them is again the human mitochondria cytochrome C oxidase subunit II gene, which is putatively related to Cisplatin-resistance of tumor cells. We have also separated the highly expressed mitochondria cytochrome C oxidase subunit II gene from vincristine-resistant human gastric cancer cell SGC7901/VCR by DDRT-PCR (to be published separately). This suggests that mitochondria cytochrome C oxidase subunit II gene is closely correlated with drug-resistance. We found that CO-resistance of HIEC could be induced by gradually increasing the concentration of CO. However, the mechanism of CO-resistance in HIEC is unclear. As normal intestinal epithelial cells express certain multidrug resistance genes and proteins, such as P-glycoprotein (P-gp) in small intestinal epithelial cell line^[44,45], it demands further investigation about whether the CO-resistance is mediated by P-gp or mitochondria cytochrome C oxidase subunit II gene product.

Croton possesses many kinds of drug actions; however, its clinical application is largely limited to treating constipation, while its effect in promoting gastrointestinal motility is neglected. The neglect is not only due to its complexity in components and severe side effects, but also to the ignorance of its molecular mechanism in promoting gastrointestinal motility. Pol^[46] found that CO could accelerate gastrointestinal movement of mice at 3h after gastric administration. When CO was administrated to dogs^[47], it could quickly evoke a rapid complex wave similar to the interdigestive myoelectric complex (IMC) III phase, although its contractile time was shorter its velocity of conduction faster than normal IMC. However, it was not affected by vagus nerve, which showed no relationship with α and β receptors. IMC cycle shortening induced by CO was the principal cause of diarrhea. Albuquerque made a series of gastrointestinal movement experiments on animals with CO^[48]. The results showed that CO and its preparations could directly affect intestinal smooth muscles and rat diaphragm muscles and cause them to contract. Other researchers reported^[49,50,51] that senna could induce diarrhea and accelerate gastrointestinal movement by enhancing the synthesis and release of endogenous prostaglandin E₂ (PGE₂). Although we do not know whether the gastrointestinal motility enhancement of CO is related to PGE₂, the significant down-regulation of COX-2 expression in HIEC with long-term treatment of CO indicated that the mechanism of CO promoted motility is different from that induced by senna. Furthermore, our experiment confirmed that the average length of colonic smooth muscle cells was significantly shortened when they were incubated with CO of different concentrations, which showed that CO had a direct contractile effect on colonic smooth muscle cells.

To sum up, the effect of CO on the HIEC growth was in a dose-dependent manner. High dosage of CO could delay cell growth or cause cell death; and low dosage had no effect. A long-term administration with progressively increased CO dosage could promote cell proliferation, increase heteroploid DNA content, and induce malignant conversion of cells. COX-2 expression was significantly down-regulated and mitochondria cytochrome C oxidase subunit-2 gene was significantly up-regulated in HIEC after induced by CO for a long time. At the same time, the expression of many genes

was changed. CO has a direct contractile effect on the colonic smooth muscle cells of guinea pig.

REFERENCES

- Moon SH, Seo KI, Han WS, Suh DH, Cho KH, Kim JJ, Eun HC. Pathological findings in cumulative irritation induced by SLS and croton oil in hairless mice. *Contact Dermatitis* 2001; 44: 240-245
- Villena C, Vivas JM, Villar AM. Ocular inflammation models by topical application: croton oil induced uveitis. *Curr Eye Res* 1999; 18: 3-9
- Zhang L, Tinkle SS. Chemical activation of innate and specific immunity in contact dermatitis. *J Invest Dermatol* 2000; 115: 168-176
- Kaminski MJ, Mroczkowski TF, Krotoski WA. Dendritic epidermal gamma/delta T cells (DETC) activated in vivo proliferate in vitro in response to Mycobacterium leprae antigens. *Int J Dermatol* 2000; 39: 603-608
- Scholzen TE, Steinhoff M, Bonaccorsi P, Klein R, Amadesi S, Geppetti P, Lu B, Gerard NP, Olerud JE, Luger TA, Bunnett NW, Grady EF, Armstrong CA, Ansel JC. Neutral endopeptidase terminates substance P-induced inflammation in allergic contact dermatitis. *J Immunol* 2001; 166: 1285-1291
- Pol O, Ferrer I, Puig MM. Diarrhea associated with intestinal inflammation increased the potency of Mu and Delta Opioids on the inhibition of gastrointestinal transit in mice. *J Pharmacol Exp Ther* 1994; 270: 386-391
- Pol O, Planas E, Puig MM. Peripheral effects of naloxone in mice with acute diarrhea associated with intestinal inflammation. *J Pharmacol Exp Ther* 1995; 272: 1271-1276
- Hiruma-Lima CA, Spadari Bratfisch RC, Grassi Kassisse DM, Brito AR. Antiulcerogenic mechanisms of dehydrocrotonin, a diterpene lactone obtained from Croton cajucara. *Planta Med* 1999; 65: 325-330
- Hiruma-Lima CA, Gracioso JS, Rodriguez JA, Haun M, Nunes DS, Souza Brito AR. Gastroprotective effect of essential oil from Croton cajucara Benth. (Euphorbiaceae). *J Ethnopharmacol* 2000; 69: 229-234
- Brito AR, Rodriguez JA, Hiruma-Lima CA, Haun M, Nunes DS. Antiulcerogenic activity of trans-dehydrocrotonin from Croton cajucara. *Planta Med* 1998; 64: 126-129
- Grynberg NF, Echevarria A, Lima JE. Anti-tumour activity of two 19-nor-clerodane diterpenes, trans-dehydrocrotonin and trans-crotonin, from Croton cajucara. *Planta Med* 1999; 65: 687-689
- Agner AR, Maciel MA, Pinto AC. Investigation of genotoxic activity of trans-dehydrocrotonin, a clerodane diterpene from Croton cajucara. *Teratog Carcinog Mutagen* 1999; 19: 377-384
- Roengsumran S, Petsom A, Kuptiyanuwat N. Cytotoxic labdane diterpenoids from Croton oblongifolius. *Phytochemistry* 2001; 56: 103-107
- Wang ZH, Lu LS. Effect of Weichangtong on gastrointestinal motility disorders. *Xin Xiaohuabingxue Zazhi* 1997; 5: 448-449
- Zheng TZ, Li W, Qu SY, Ma YM, Ding YH, Wei YL. Effects of Dangshen on isolated gastric muscle strips in rats. *World J Gastroenterol* 1998; 4: 354-356
- Ma XS, Fan XP, Chen Z, Li CW, Xing YS. Effects of rhizoma atracylodes macrocephalae on the contraction of isolated ileum of guinea pig. *Xin Xiaohuabingxue Zazhi* 1996; 4: 603-604
- Li SZ, Tan XH. Effect of Astragalus membranaceus on intestinal blood flow and motility in dogs. *Xin Xiaohuabingxue Zazhi* 1997; 5: 659-660
- Hao Q, Li Y, Yin HT. Comparative effect of different varieties of Bupleurum and Citrus on gastrointestinal motility in mice. *Huaren Xiaohua Zazhi* 1998; 6: 205-207
- Li Y, Sun SY, Zou Z, Chen SN, Wang XY. Influences of 6 formula compositions combined of 8 kinds of Chinese medicinals on gastro intestinal motility in mice. *Huaren Xiaohua Zazhi* 1998; 6: 208-209
- Li HM, Liang H, Tang HQ, Li X. Therapeutic effects of pinaverium bromide in functional constipation and diarrhea in mice. *Huaren Xiaohua Zazhi* 1998; 6: 36-39
- Pang L, Zhou DR. Regulative action of Chinese traditional medicine in gastrointestinal motility. *Huaren Xiaohua Zazhi* 1998; 6: 535-536
- Zhu JZ, Yang GH, Leng ER, Chen DF. Gastrointestinal motility promoting action of traditional Chinese medicine. *Shijie Huaren Xiaohua Zazhi* 1999; 7: 689-690
- Wang J, Hou JY. Effect of granulae Li Wei on gastrointestinal activity. *Shijie Huaren Xiaohua Zazhi* 2000; 8: 377-381
- Shi BJ, Liu HY. Comparison between cisapride and metoclopramide in the treatment of irritable bowel syndrome. *Xin Xiaohuabingxue Zazhi* 1997; 5: 51-52
- Xiang AM, Zhou DD. Traditional Chinese medicine and gastric mucosal barrier. *Huaren Xiaohua Zazhi* 1998; 6: 537-538
- Gao F, Zhang SB, Zhang LY, Liu F, Tong WD, Li FZ. An experiment study of the small intestinal transit injured by contact laxatives. *Shijie Huaren Xiaohua Zazhi* 1999; 7: 659-660
- Lin J, Cai G, Xu JY. A comparison between Zhishi Xiaopiwan and cisapride in treatment of functional dyspepsia. *World J Gastroenterol* 1998; 4: 544-547
- Tian XL, Mourelle M, Li YL, Guarner F, Malagelada JR. The role of Chinese herbal medicines in a rat model of chronic colitis. *World J Gastroenterol* 2000; 6: 40-42
- Zhang HX, Ren P, Huang X, Li Yuan. Regulation of the traditional Chinese medicine on gastrointestinal hormone and motility. *Shijie Huaren Xiaohua Zazhi* 2000; 8
- Zhu JZ, Yang GH, Leng EF, Chen DF. Effects of the traditional Chinese medicine on gastrointestinal motility. *Shijie Huaren Xiaohua Zazhi* 1999; 7: 689-690
- Pang L, Zhou DR. Regulation of the traditional Chinese medicine on gastrointestinal motility. *Huaren Xiaohua Zazhi* 1998; 6: 535
- Wang X, Zhang ZY, Shi YQ, Lan M, Han QL, Wu HP, Jin JP, Fan DM. Preliminary study on protein differential expression of small bowel in BALB/c mice induced by croton oil. *Weichangbingxue He Ganzhangbingxue Zazhi* 2000; 9: 103-106
- Hu CJ, Yang DL, Yin GP, Song XM, Li JS, Cao YC. Quantitative studies of RNA, DNA and proliferation index in Hepatocarcinoma cells. *Xinxiaohua Bingxue Zazhi* 1997; 5: 516
- Ennes HS, McRoberts JA, Hyman PE, Snape WJ. Characterization of colonic circular smooth muscle cells in culture. *Am J Physiol* 1992; 263: G365-G370
- Murthy, Karnam S, Makhlof GM. cGMP-mediated Ca²⁺ release from IP₃-insensitive Ca²⁺ stores in smooth muscle. *Am J Physiol* 1998; 274: C1199-C1205
- Mei Lan, Xin Wang, Han Ping Wu, Dai Ming Fan. Effect of croton extract on biological characterization of human intestinal epithelial cells. *Shijie Huaren Xiaohua Zazhi* 2001; 9: 366-373
- Sano H, Kawahito Y, Wilder RL, Hashimoto A, Mukai S, Asai K, Kimura S, Kato H, Kondo M, Hla T. Expression of cyclooxygenase-1 and -2 in human colorectal cancer. *Cancer Res* 1995; 55: 3785-3789
- Li L, Wu KC, Wu HP, Wang X, Nie YZ, Fan DM. Expression and biological activity of COX-2 in human gastric cancer cells. *J Cell Mol Immunol* 2000; 16: 255-259
- Wu KC, Jackson L, Mahida YR. Cyclooxygenase (Cox)-1 and -2 in human gastric mucosa: Constitutive expression by parietal cells and induction of Cox-2 in lamina propria cells proximal to ulcers. *Gastroenterology* 1998; 114: G1365
- Gke M, Kanai M, Lynch Devaney K, Podolsky DK. Rapid mitogen activated protein kinase activation by transforming growth factor α in wounded rat intestinal epithelial cells. *World J Gastroenterol* 1998; 4: 263
- Sujii M, Kawano S, Tsuji S, Sawaono H, Hori M, DuBois RN. Cyclooxygenase regulates angiogenesis induced by colon cancer cells. *Cell* 1998; 93: 705-716
- Huang M, Stoling M, Sharma S, Mao JT, Zhu L, Miller PW, Wollman J, Herschman H, Dubinett SM. Non-small cell lung cancer cyclooxygenase-2-dependent regulation of cytokine release in lymphocytes and macrophages: up-regulation of interleukin-10 and down-regulation of interleukin-12 production. *Cancer Res* 1998; 58: 1208-1216
- Higuchi. Up-regulation of human chorionic gonadotropin α subunit gene and human mitochondrial cytochrome C oxidase subunit II gene in cis-Diamminedichloroplatinum (II)-resistant human head and neck squamous carcinoma cells. *Hokkaido Igaku Zasshi* 1999; 74: 231-238
- Li M, Hurren R, Zastawny RL, Ling V, Buick RN. Regulation and expression of multidrug resistance (MDR) transcripts in the intestinal epithelium. *Br J Cancer* 1999; 80: 1123-1131
- Edelmann H M, Duchek P, Rosenthal FE, Foger N, Glackin C, Kane SE, Kuchler K. Cmdr1, a chicken P-glycoprotein, confers multidrug resistance and interacts with estradiol. *Biol Chem* 1999; 380: 231-241
- Margarita M, Puig MM, Pol O. Peripheral effects of Opioids in a model of chronic intestinal inflammation in mice. *J Pharmacol Exp Ther* 1998; 287: 1068-1075
- Xu JD, Zhang JJ, Hu GQ. Change of small intestinal electric activity during diarrhea induced by croton oil in dog. *Chin J Appl Physiol* 1991; 7: 139-142
- Albuquerque AA, Sorenson AL, Leal JH. Effects of essential oil of Croton zehntneri, and of anethole and estragole on skeletal muscles. *J Ethnopharmacol* 1995; 49: 41-49
- Qin XM, Li HF, Wang LD. Effects of metoclopramide on gastrointestinal myoelectric activity in rats. *Chin Natl J New Gastroenterol* 1997; 3: 169-170
- Beubler E, Kollmar G. Prostaglandin-mediated action of sennosides. *Pharmacology* 1993; 36(Suppl 1): 85-91
- Nijs G, Witter P, Geboes K, Lemli J. Influence of rhein anthrone and rhein on small intestine transit rate in rats: evidence of prostaglandin mediation. *Eur J Pharmacol* 1992; 218: 199-203

• BASIC RESEARCH •

Identification of CD226 ligand on colo205 cell surface

Kai Sun, Bo-Quan Jin, Qi Feng, Yong Zhu, Kun Yang, Xue-Song Liu, Bang-Quan Dong

Kai Sun, Department of Hepatobiliary Surgery, Xijing Hospital, Xi'an 710032, Shaanxi province, China

Bo-Quan Jin, Yong Zhu, Kun Yang, Xue-Song Liu, Bang-Quan Dong, Department of Immunology, The Fourth Military Medical University, Xi'an 710032, Shaanxi province, China

Qi Feng, Department of Hematology, Xijing Hospital; Xi'an 710032, Shaanxi province, China

Supported by the National Nature Science Foundation. No 39700065

Correspondence to: Kai Sun, M.D, Department of Hepatobiliary Surgery, Xijing Hospital, Xi'an 710032, Shaanxi province, China. iamsunkai@263.net

Telephone: +86-029-3242969 Fax: +86-029-3242969

Received 2001-06-11 Accepted 2001-10-16

Abstract

AIM: To confirm the existence of CD226 ligand and its distribution, which is a novel molecule that was cloned in 1996.

METHODS: The mRNA was extracted from TPA activated Jurkat cells and used as a template for reverse-transcription. After PCR amplification, the fragment including CD226 extracellular region and the splice donor sequence "ACTTACCTGT" was obtained and cloned into fusion expression vector pIG. The recombinant vector pCD226/Ig was transfected in COS-7 cells by DEAE-Dextran method, the secreting fusion protein was identified by Sandwich ELISA, and was purified by anti-CD226 affinity chromatography. This fusion protein was used as a probe in the investigation of CD226 ligand by immunohistochemistry. Existence of CD226 ligand was further identified by adhesion experiment.

RESULTS: Expression of a secreting fusion protein was identified by sandwich ELISA, indicating that both CD226 extracellular domain and IgGFC domain could be recognized respectively by anti-CD226 and anti-IgGFC mAb. About 130µg CD226/Ig fusion protein could be obtained from 100mL COS-7 culture supernatants by anti-CD226 affinity chromatography purification. SDS-PAGE showed that this fusion protein has a molecular mass of 83 ku. It was confirmed by immunohistochemistry that CD226 ligand expressed on the Colo205 cells, but not on Jurkat cell, U937 cell and mixed lymphocyte culture cells. In adhesive assay, resting Jurkat cells did not have significant adhesion to Colo205 cells. In contrast, activated Jurkat cells could bind to colon carcinoma Colo205 cells and this adhesive reaction could be blocked by CD226/Ig fusion protein or anti-CD226 mAb. Immunochemical experiment showed that Colo205 cells could be specifically stained by CD226/Ig, indicating that CD226 ligand exists on the surface of Colo205 cells.

CONCLUSION: Existence of CD226 ligand on the surface of Colo205 cells was identified by immunohistochemistry and adhesion blocking experiment. In addition, the secreting CD226/Ig fusion protein prepared in this study will be a potential tool for further investigation of CD226 ligand.

INTRODUCTION

CD226 was initially reported by Burns in 1985 with a name TLI SA1 (T lineage specific activation antigen 1, TLI SA1)^[1], and was renamed PTA1 (platelet and T cell antigen 1, PTA1) in 1989 because of its expression on platelet as well^[2]. Since 1985, a lot of investigations have been done on CD226 expression, functions and its relationship with diseases^[2-6]. CD226 was mainly expressed on the activated T cells, NK cells, monocytes, platelets and megakaryocytes lineage^[4-8], taking part in signal transduction of T cell activation and differentiation as well as platelet activation and aggregation. CD226 mAb was found to stimulate the activation and aggregation of platelets^[2,3], inhibit differentiation of CTL^[2,9] and T and NK cell mediated cytotoxicity^[7]. In 1997, PTA1 cDNA was cloned from cDNA library of TPA activated Jurkat cells^[10]. It belongs to an immunoglobulin super family (IgSF) with a 232aa extracellular region, 25aa transmembrane region and 61aa intracellular region. Interestingly, PTA1 cDNA was almost the same as that of DNAM-1 (DNAM associated molecule-1), a novel molecule cloned by Shibuya in 1996^[7]. In 2000, PTA1 (DNAM-1) was designated as CD226 on the 7th Workshop and Conference on the Human Leucocyte Differentiation Antigen in Harrogate. CD226 is the only IgSF member whose extracellular region consists of two IgV-like domains.

Almost all the important Ig-superfamily members are highly conserved during molecular evolution^[11-13], such as CD2, CD4/CD8 and CD28. Homological analysis showed that CD226 molecules are highly conserved (93%-95%) among human, ape and monkey, suggesting that CD226 may have very important functions^[14]. It seems that CD226 takes part in the mechanism of platelet function disorders, autoimmune diseases, transplantation, virus infection diseases and tumors^[3,15-20], suggesting that CD226 plays an important role in immune system and may have a potential application to clinical diagnosis and treatment. Up to, little is known about CD226 ligand. So, the aim of this study is to make a preliminary research on CD226 ligand.

MATERIAL AND METHODS

Materials

pIG vector was a gift kindly presented by Dr. Xu. COS-7, U937, Jurkat, Colo205 cell line and CD226 hybridoma (secreting mAb Leo-A1 against the extracellular domain of CD226) were provided by Prof. Jin. Goat anti-human Ig-SABC immunohistochemistry kit was purchased from Boster Co. Vectors and restrict enzymes were purchased from Huamei Co; Trizol reagent kit was purchased from Gibco Co, and CNBr-Sepharose 4B is a product of Pharmacia Co.

Design of the primers for semi-nest RT-PCR

Primers were designed according to the sequence of CD226 cDNA: primer 1, 5'-GCAAGCTTCAGAGATGGATTATCCTACT-3' (forward, containing HindIII enzyme site at 5'); primer 2, 5'-GCGGATCCACTTACCTGTAGCCACAAAGAGGGTA TATTGG-3' (reverse, containing BamHI enzyme site and donor splice region "ACTTACCTGT" at 5'); primer 3, 5'-ACTCTAGTCTTTGGTCCTGC-3'. Primer1 and Primer 3 were used to amplify the whole length CD226 cDNA, and primer 1 and primer 2 were used to amplify cDNA encoding CD226 extracellular region (Figure 1).

				P1→	<u>gcaagcttca</u>	<u>gagatggatt</u>	
121	agagcgagca	gcactcacat	ctcaagaacc	agcctttcaa	acagtttcca	gagATGgatt	180
	<u>atcctact</u>						
181	atcctacttt	actttttggt	cttcttcatg	tatacagagc	tctatgtgaa	gaggtgcttt	240
241	ggcatacatc	agttcccttt	gccgagaaca	tgtctctaga	atgtgtgtat	ccatcaatgg	300
301	gcattctaac	acaggtggag	tggttcaaga	tccgggacca	gcaggattcc	atagccattt	360
361	tcagccctac	tcatggcatg	gtcataagga	agccctatgc	tgagagggtt	tactttttga	420
421	attcaacgat	ggcttccaat	aacatgactc	ttttcttctg	gaatgcctct	gaagatgatg	480
481	ttggctacta	ttcctgtctt	ctttacactt	acccacaggg	aacttggcag	aaggtgatac	540
541	aggtgggttca	gtcagatagt	tttgaggcag	ctgtgccatc	aaatagccac	attgtttcgg	600
601	aacctggaaa	gaatgtcaca	ctcacttgte	agcctcagat	gacgtggcct	gtgcaggcag	660
661	tgaggtggga	aaagatccag	ccccgtcaga	tgcacctctt	aacttactgc	aacttgggtc	720
721	atggcagaaa	tttcacctcc	aagttcccaa	gacaaatagt	gagcaactgc	agccacggaa	780
781	ggtggagctg	categtcate	cccgatgtca	cagtcctcaga	ctcggggctt	taccgtgct	840
841	acttgccaggc	cagcgcagga	gaaaacgaaa	ccttcgtgat	gagattgact	gtagccgagg	900
	P3←	<u>gggttata</u>	<u>tgggagaaac</u>	<u>accgatgtcc</u>	<u>attcacctag</u>	<u>gcg</u>	
901	gtaaaaccga	taaccaatat	accctctttg	tggtggagg	gacagtltta	ttgtttgtgt	960
961	ttgttatctc	aattaccacc	atcattgtca	ttttctttaa	cagaaggaga	aggagagaga	1020
1021	gaagagatct	atttacagag	tcttgggata	cacagaaggc	acccaataac	tatagaagtc	1080
1081	ccatctctac	cagtcacact	accaatcaat	ccatggatga	tacaagagag	gatattttatg	1140
		P2←	<u>cgctcctgg</u>	<u>ttctgatctc</u>	<u>a</u>		
1141	tcaactatcc	aaccttctct	cgcaggacca	aagacTAGag	tttaagctta	ttcttgacat	1200
1201	gagtgcatta	gtaatgactc	ttatgtactc	atgcattggat	c		
Primer 1 5'GCAAGCTTCAGAGATGGATTATCCTACT3'							
Primer 2 5'ACTCTAGTCTTTGGTCCTGC3'							
Primer 3 5'GCGGATCCACTTACCTGTAGCCACAAAGAGGGTATATTGG3'							

Figure 1 Sequence of CD226 cDNA and primers.

174-923bp: extracellular region of CD226; 174-227bp: signal peptide sequence; 924-998bp: transmembrane region; □labeled sequence: primers; underlined sequence was the splicing donor sequence.

Reverse transcription-polymerase chain reaction (RT-PCR)

Jurkat cells were cultured at a concentration of $1 \times 10^6 \text{ L}^{-1}$ with TPA ($50 \mu\text{g} \cdot \text{L}^{-1}$) for 18-30 h at 37°C , and the total RNA was isolated by Trizol reagent kit. RNA was primed and reverse transcribed into cDNA in a $20 \mu\text{L}$ reaction volume containing 10U reverse transcriptase, $10 \mu\text{g}$ RNA, $10 \times \text{Buffer}$ $2 \mu\text{L}$, $10 \text{mmol} \cdot \text{L}^{-1}$ dNTP complex $4 \mu\text{L}$, and primer 3. After incubation at 42°C for 1 h, the reverse transcription product was PCR amplified by Primer 1 and Primer 3, and then by Primer 1 and Primer 2. The PCR parameters were 94°C for 1 min, 60°C for 1 min, and 72°C for 80 s for 35 cycles.

Plasmid construction

Expression vector for CD226 extracellular region was prepared as previously described^[21]. The corresponding PCR fragment was cloned into pUC-19 and M13mp18/19 vector for DNA sequencing. After DNA sequencing, the 793bp fragment encoding CD226 extracellular region and the splice donor sequence "ACTTACCTGT" was subcloned into pIG, a mammalian fusion protein expression vector containing the cytomegalovirus (CMV) promoter, splice acceptor, genomic human IgG1, and SV40 polyadenylation signal. The resulting expression vector pCD226/Ig was identified by PCR and restrict enzyme digestion.

COS-7 cell Transfection

COS-7 cell transfection was performed by a modified method^[22]. Briefly, COS-7 cells at 50%-75% confluence were transfected in 7mL glucose Dulbecco's modified Eagle's medium (DMEM) containing $100 \text{mL} \cdot \text{L}^{-1}$ fetal calf serum (FCS), $400 \mu\text{g}$ DEAE-dextran/mL, $100 \mu\text{mol} \cdot \text{L}^{-1}$ chloroquine diphosphate, and $40 \mu\text{g}$ purified DNA. After 3 h at 37°C , the transfection mixture was removed and the cells were treated with $100 \text{g} \cdot \text{L}^{-1}$ dimethyl sulfoxide in PBS for 2 min. Cells were then returned to DMEM supplemented with $10 \text{mL} \cdot \text{L}^{-1}$ fetal calf serum (FCS) for 4 d to allow CD226/Ig expression.

Purification and identification of CD226/Ig fusion protein

Leo-A1 affinity chromatography column was prepared as previously described^[23]. The pCD226/Ig transfected COS-7 supernatant was spined out cell debris for 5 minutes at $10000 \text{ r} \cdot \text{min}^{-1}$, filtered through a $0.45 \mu\text{m}$ filter and then purified by Leo-A1 affinity chromatography. The expression of a secreting fusion protein was identified by sandwich ELISA (anti-CD226 mAb and HRP-conjugated anti-hIg mAb, anti-IL-8 antibody was used as control). SDS-PAGE and Western-blot (polyclonal anti-hIgG antibody) were performed by routine methods.

Immunohistochemical staining by CD226/Ig

Immunohistochemical experiment was performed by SABC methods. For light microscopy, cytospin preparations of Colo205 cells were incubated with $3 \text{g} \cdot \text{L}^{-1}$ methanol-hydrogen peroxide solution at 37°C for 30 min to inactivate endogenous peroxidases. The slides were then blocked in goat serum blocking solution at 37°C for 30 min. Without washing, the slides were incubated with CD226/Ig fusion protein ($10 \text{mg} \cdot \text{L}^{-1}$) at 4°C . After overnight incubation, the slides were washed three times with PBS, and incubated with biotin labeled goat anti human IgG for 4 h at room temperature. Finally, the slides were washed, allowed to sit for 2 min, and then reacted with SABC complex and DAB peroxidase substrate solution. Human IgG1 was used instead of CD226/Ig in the control experiment.

Adhesion assay

In 96 well plate, Colo205 cells with the density of $0.5 \times 10^5/\text{well}$ were cultured for one day to let cells confluence, and 3.7 MBq ^{51}Cr labeled resting or activated Jurkat cells were added with $1 \times 10^5/\text{well}$ and cultured for 4 h, and non-adhered cells were moved by gently washing, the adhered cells were lysed by $20 \text{g} \cdot \text{L}^{-1}$ Triton X-100, and Bq was measured. Different concentrations of CD226/Ig fusion protein and anti-CD226 mAb Leo-A1 were used in the adhesion blocking experiment.

RESULTS

Construction of pCD226/Ig fusion expression vector

A very low level of CD226 molecules was expressed on resting Jurkat cells, and the expression level could be enhanced by TPA stimulation for 24 h. The CD226 mRNA from Jurkat cells was enriched by TPA stimulating. After retro-transcription, semi-nests PCR amplification, a single band about 800bp has been obtained. This fragment was then ligated into pUC19 and subcloned into M13mp18/19 vector for sequencing. The sequencing data showed that the fragment was 793bp long in total, a HindIII enzyme site could be found at the upstream and the "ACTTACCTGT" donor splicing sequence and a BamHI site could be found at the downstream. The 793 bp fragment was ligated between HindIII and BamHI sites of pIG vector. The recombinant vector pCD226/Ig was identified by restrict enzyme digestion assay and PCR identification (Figure 2).

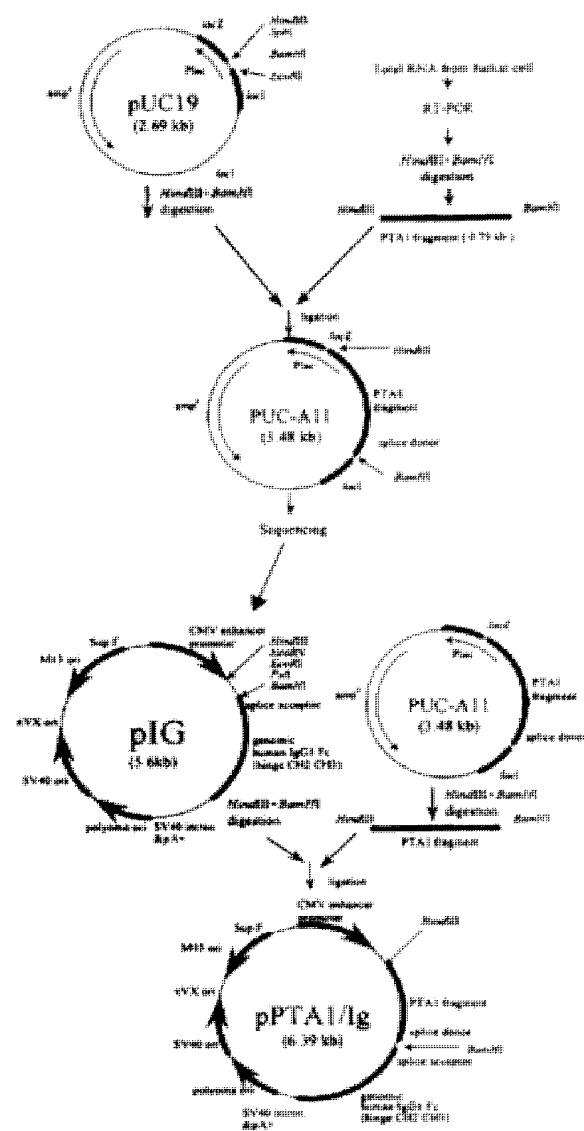


Figure 2 Construction of pCD226/Ig fusion vector.

Expression, identification and purification of CD226/Ig fusion protein

The pCD226/Ig vector was transiently transfected into COS-7 cells. The optimal conditions was checked before large-scale transfection, and it was found that transfected COS-7 cells cultured in medium with 10ml·L⁻¹ serum for 96 h could produce CD226/Ig most effectively. The secreted CD226/Ig fusion protein was purified by Leo-A1 affinity chromatography. About 130μg CD226/Ig fusion protein could be obtained from 100mL COS-7 culture supernatants by anti-CD226 affinity chromatography purification. SDS-PAGE showed CD226/Ig fusion protein has a molecular mass of 83 ku (Figure 3) and could be recognized by anti-IgG polyclonal antibody in Western-blot assay (Figure 4). In ELISA assay, CD226/Ig expression could be identified in pCD226/Ig transfected COS-7 supernatant, but a negative result was obtained in pIG vector transfected COS-7 supernatant (Table 1). Both CD226 extracellular domain and Fc domain of the CD226/Ig protein could be recognized respectively by anti-CD226 and anti-hIg Fc mAb, suggesting that CD226/Ig could mimic the nature CD226 molecule and be a potential tool in the research of CD226 ligand and its functions.

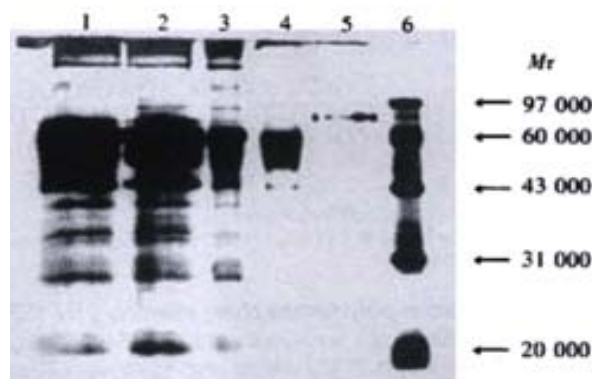


Figure 3 Identification of CD226/Ig fusion protein purified by Leo-A1 Sepharose-4B affinity column.

1. Supernatant of pIG vector transfected COS-7 cells; 2. Supernatant of pCD226/Ig transfected COS-7 cells; 3. Supernatant of pCD226/Ig transfected COS-7 cells after concentrated by ammonium sulfate; 4. Flow through solution of pCD226/Ig transfected COS-7 cells after affinity chromatography; 5. CD226/Ig fusion protein purified by Leo-A1 sepharose-4B affinity column; 6. Marker.



Figure 4 Western-blot result of CD226/Ig by anti-IgG polyclonal antibody Lane 1. Supernatant of pCD226/Ig transfected COS-7 cells; Lane 2. Supernatant of pIG transfected COS-7 cells

Table 1 Identification of CD226/Ig fusion protein expression by sandwich-ELISA

Coated antibody	Samples tested	Conjugated secondary antibody	Results
Anti-CD226	pCD226/Ig transfected COS supernatant	HRP-GohlgG	+++
Anti-CD226	pIG transfected COS supernatant	HRP-GohlgG	-
Anti-IL-8	pCD226/Ig transfected COS supernatant	HRP-GohlgG	-

Identification of CD226 ligand on Colo205 cells

Immunohistochemical experiment showed that Colo205 cells could be specifically stained by CD226/Ig but not by control protein (hIgG), indicating that CD226 ligand exists on the surface of Colo205 cells (Figure 5). Resting Jurkat cells had a low-level expression of CD226 on cell surface, whereas activated Jurkat cells expressed high level of CD226 after TPA treatment for 24h. In adhesive assay, resting Jurkat cells have a very low level adhesion to Colo205 cells. In contrast, activated Jurkat cells could bind to colon carcinoma Colo205 cells and this adhesive reaction could be blocked by CD226/Ig fusion protein or Leo-A1 mAb but not control Ig and anti-IL-1 mAb, indicating that CD226 takes part in this specific adhesion (Figure 6).

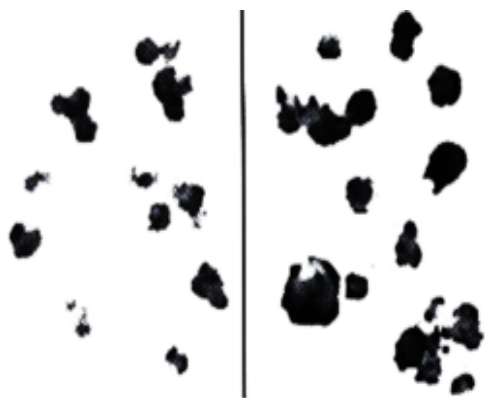


Figure 5 CD226L expression on Colo205 cells identified by CD226/Ig immunohistochemistry.

A: Colo205 negative control (stained with hIg); B: Colo205 cells were specifically stained by CD226/Ig.

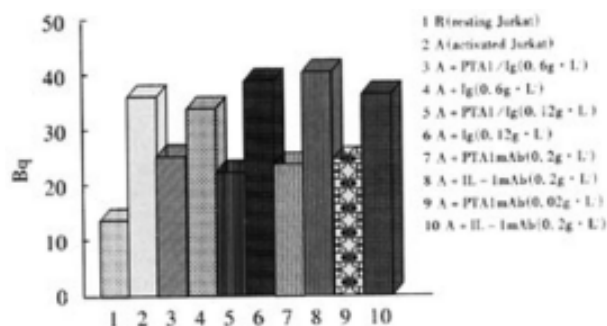


Figure 6 Adhesion experiments of activated Jurkat cells with Colo205 cells. Density of Colo205 was 0.5×10^5 per well. Density of Jurkat was 1×10^5 per well. R stand for resting Jurkat cells. A stand for activated Jurkat cells.

DISCUSSION

CD226 is a 65 ku glycoprotein expressed on the surface of activated T cells, NK cells, and platelets. It is a member of the Ig-superfamily containing 2 Ig-like domains of the V-set and is encoded by a gene on human chromosome 18q22.3^[24]. Ig-superfamily members play essential roles in many aspects of immune responses by acting as immunoglobulin Fc receptors, cytokine receptors, adhesive molecules and accessory molecules^[11,25-27]. The main function of Ig-super family concentrated in cell-to-cell recognition and interaction, such as LFA-1/CD2, CD4/MHC, CD28/B7, and many of these Ig-super family members are involved in the T cell activation^[28-32]. Cross-linking CD226 with antibodies cause the activation of T cells and aggregation of platelets. Previous studies also showed the cross-linking of LFA-1 induced tyrosine phosphorylation of CD226, in which the Fyn protein tyrosine kinase may play a role^[33,34]. The above results indicate that CD226 mediates cellular adhesion to other cells bearing an unidentified ligand and takes part in signal transduction. Interaction

between ligand and receptor is the basis of immune response. So, identification of CD226L is very important for the further investigation of CD226.

Intercellular adhesive molecules play an important role in the immune response, they provide not only intercellular binding, but also participate in signal transduction, and are closely related with allograft rejection, tolerance, cell differentiation, lymphocyte homing and tumor immunity^[35-39]. In addition to the specific antigen recognition signal provided by CD3-TCR complex, a lot of other signals are required in the T cells mediated immune response, such as signals provided by CD4/CD8, CD2, LFA-1, CD28^[40-42]. Our previous results showed that resting T cells expressed low-level of CD226 molecule. When T cells were activated, they expressed high-level CD226 molecules. This finding suggested that CD226 might be closely related to the function of activated T cells. Differentiation of T cell to CTL could be inhibited when Leo-A1 mAb or Leo-A1 F(ab')₂ were added into mixed lymphocyte culture (MLC), and production of LAK cells was also reduced, this action of Loe-A1 was not dependent on Fc of Leo-A1. The inhibiting effect of Loe-A1 only works in the differentiation phase of CTL but not in the cytotoxicity phase, suggesting that the epitope recognized by CD226 is related with the differentiation of CTL^[1,2,7]. Another mAb DX11 against CD226 (DNAM-1) was reported to significantly inhibit the cytotoxicity of CTL to several tumor cell lines, such as Colo205, PA-1, MCF7^[7]. Therefore, epitope recognized by DX11 mAb was different from that recognized by Leo-A1 mAb, and these two different epitopes may take part in the differentiation and cytotoxicity of CTL.

Since the mid 1980s, there has been a rapid increase in our knowledge about the specific cell surface molecules mediating cell-cell interaction and adhesion events. This has been largely due to the success of molecular cloning techniques, allowing the isolation of functional cDNA clones that encoding these glycoproteins. Always methods have been successfully used in the cloning of novel cDNA. One of these methods reported by Aruffo and Seed is very effective^[43,44]. This method is based on the transient expression of cDNA library in cells and specific mAb recognition (capture and panning). Several molecules, such as CD2, CD22, CD28, CD36 and CD58^[43-47], have been cloned by this method. So, once a suitable antibody, ligand or cell line has been identified to recognize a cell surface molecule, the cDNA encoding this molecule could be cloned by this method. CD226 molecule or its homologue to be used in the investigation of CD226 ligand should have the following characteristics: easy to obtain, high in purity and natural in motif. So these molecules could be obtained by purification from platelet, preparations of anti-idiotypic mAb or preparations of recombinant CD226 molecule. In this study, we prepared the CD226/Ig fusion protein containing CD226 extracellular region 232aa (including 10 glycosylation sites, 57ku) and IgG Fc region (CH2, CH3 and H region, 26ku), the putative molecule weight is consistent with that identified in SDS-PAGE and Western-blot. CD226/Ig fusion protein is expressed in secreting form that was detected by Sandwich-ELISA, its two different domains could be recognized by anti-CD226 mAb and anti-hIg Fc mAb, respectively, but could not be recognized by other mAb, suggesting CD226/Ig can mimic the nature of CD226 molecule and can be used in the research of CD226 ligand. Ig fusion proteins have many advantages such as easy to purify, easy to label and easy to detect, and thus were widely used in ligand identification^[48-53], and disease protection^[54-56]. These advantages make it more convenient to further clone CD226 ligand.

Immunohistochemical research suggested that CD226 ligand was expressed on Colo205 cells and this result was also supported by adhesion-blocking experiment. It was shown that resting Jurkat cells expressed very low level of CD226 molecules, but activated Jurkat cells expressed high-level CD226 molecules after TPA activation for 24

h, and the expression of CD226 was regulated by cytokines, such as TGF- β , TNF- α and IL-2^[57]. In the experiment about adhesion, activated Jurkat cells could bind to colon carcinoma Colo205 cells and this adhesion reaction could be blocked by CD226/Ig fusion protein or Leo-A1 mAb but not by control Ig and anti-IL-1 mAb, indicating that CD226 ligand exist in Colo205 cells and takes part in this specific adhesion.

When T cells were activated, they expressed high-level CD226 molecules. Interestingly, CD226 ligand seemed to express on the surface of tumor cells. Activated T cells not only need the specific antigen recognition by TCR, but also the engagement of accessory molecules on T cells by their respective ligands expressed on the target cells.^[38,39,58,59] More researches need to be done to reveal their relationship and what signal have CD226 transduced during immune response against tumors. The above results made a solid foundation for further cloning of CD226 ligand and is helpful for thorough investigations on CD226L structure and function.

ACKNOWLEDGMENT Dr. Xu and Dr. Lan for their valuable technical advice and assistance.

REFERENCES

- Burns GF, Triglia T, Werkmeister JA, Begley CG, Boyd AW. TLISA, a human T lineage-specific activation antigen involved in the differentiation of cytotoxic T lymphocytes and anomalous killer cells from their precursors. *J Exp Med* 1985; 161: 1063-1078
- Scott JL, Dunn SM, Jin B, Hillam AJ, Walton S, Berndt MC, Murray AW, Krissansen GW, Burns GF. Characterization of a novel membrane glycoprotein involved in platelet activation. *J Biol Chem* 1989; 264: 13475-13482
- Zuzel M, Walton S, Burns GF, Berndt MC, Cawley JC. A monoclonal antibody to a 67 kD cell membrane glycoprotein directly induces persistent platelet aggregation independently of granule secretion. *Br J Haematol* 1991;79:466-473
- Sun Chen, Jin Boquan, Liu Xuesong, Yang Kun, Zhang Tingting, Dong Bangquan, Li Jiazeng, Wu huaizhu, Peng Lin, Bao Chengxin, Wu Wenjie. PTA1 monoclonal antibody induce human platelet aggregation and intra-cytoplasmic Ca²⁺ elevation. *Zhonghua Xueye Zazhi* 1998;19:133-137
- Li Demin, Jin Boquan, Su Li, Jia Wei, Sun Kai, Liu Xuesong, Zhang Tingting. Distribution and function of murine platelets and T cell activation antigen 1. *Zhonghua Weishengwu Xuehemian Yixue Zhazhi* 1999;19:232-235
- Sun Kai, Feng Qi, Jin Boquan. Platelet and T cell antigen 1 (PTA1). *Zhonghua Wei Sheng Wu Xue He Mian Yi Xue Zha Zhi* 1999;19:261-264
- Shibuya A, Campbell D, Hannum C, Yssel H, Franz Bacon K, McClanahan T, Kitamura T, Nicholl J, Sutherland GR, Lanier LL, Phillips JH. DNAM-1, A Novel Adhesion Molecule Involved in the Cytolytic Function of T Lymphocytes. *Immunity* 1998; 4: 573-581
- Slupsky JR, Cawley JC, Kaplan C, Zuzel M. Analysis of CD9, CD32 and p67 signalling: use of degranulated platelets indicates direct involvement of CD9 and p67 in integrin activation. *Br J Haematol* 1997;96:275-286
- Chen LK, Bensussan A, Burns GF, Tourvieille B, Soulie A, Sasportes M. Allospecific proliferative human T-cell clones acquire the cytotoxic effector function after three months in culture, in IL-2 conditioned medium. *Hum Immunol* 1986;17:30-36
- Sherrington PD, Scott JL, Jin B, Simmons D, Dorahy DJ, Lloyd J, Brien JH, Aebersold RH, Adamson J, Zuzel M, Burns GF. TLISA (PTA1) activation antigen implicated in T cell differentiation and platelet activation is a member of the regulation of expression. *J Biol Chem* 1997; 272: 21735-21744
- Halaby DM, Mornon JP. The immunoglobulin superfamily: an insight on its tissular, species, and functional diversity. *J Mol Evol* 1998; 46:389-400
- Hawke NA, Yoder JA, Litman GW. Expanding our understanding of immunoglobulin, T-cell antigen receptor, and novel immune-type receptor genes: a subset of the immunoglobulin gene superfamily. *Immunogenetics* 1999;50:124-133
- Ioerger TR, Du C, Linthicum DS. Conservation of cys-cys trp structural triads and their geometry in the protein domains of immunoglobulin superfamily members. *Mol Immunol* 1999;36:373-386
- Tian Fang, Li Demin, Xia Haibin, Liu Xuesong, Jia Wei, Sun Chen, Sun Kai, Jin Boquan. Isolation of cDNAs Encoding Gibbon and Monkey Platelet and T Cell Activation Antigen 1(PTA1). *DNA Sequence* 1999; 10: 155-161
- Huang Chuanshu, Jin Boquan, Wang Meixian, Li Enshan. Study on the activated antigen expression on the lymphocytes and lymphoblasts from HFRS patients. *Shanghai Mian Yi Xue Zha Zhi* 1991;11:94-96
- Su Min, Niu Shumiao, Tian Dongping, Li Jian, Li Hengli, Guo Shangwen, Shi Bingyin. The clinical significance of aberrant HLA-DR antigen expression on thyrocytes. *Zhonghua Bing Li Xue Za Zhi* 1994;23:34-36
- Tabata H, Hara M, Kitani A, Hirose T, Norioka K, Harigai M, Suzuki K, Kawakami M, Kawagoe M, Nakamura H. Hirose-T Expression of TLISA1 on T cells from patients with rheumatoid arthritis and systemic lupus erythematosus. *Clin Immunol Immunopathol* 1989;52:366-375
- Miller FW, Love LA, Barbieri SA, Balow JE, Plotz PH. Lymphocyte activation markers in idiopathic myositis: changes with disease activity and differences among clinical and autoantibody subgroups. *Clin Exp Immunol* 1990; 81:373-379
- Huang Chuanshu, Jin Boquan, Wang Meixian, Li Enshan, Sun Chen. Hemorrhagic fever with renal syndrome: relationship between pathogenesis and cellular immunity. *J Infect Dis* 1994;169:868-870
- Loertscher R, Forbes RD, Halabi G, Lavery P, Quinn T. Expression of early and late activation markers on peripheral blood T lymphocytes does not reliably reflect immune events in transplanted hearts. *Clin Transplant* 1994;8:230-238
- Sun Kai, Jin Boquan, Sun Chen, Tian Fang, Zhu Yong, Yang Kun, Liu Xuesong. Construction and expression of a novel human platelet/T cell activation antigen 1(PTA1) fusion protein in COS-7 cells. *Xi Bao Yu Fen Zi Mian Yi Xue Zha Zhi* 1998;14:1-4
- Lena Serghides, Ian Crandall, Eric Hull, and Kevin C. Kain. The Plasmodium falciparum-CD36 Interaction Is Modified by a Single Amino Acid Substitution in CD36. *Blood* 1998;92:1814-1819
- Sun Kai, Jin Boquan, Sun Chen, Zhu Yong, Jia Wei, Yang Kun, Liu Chenggang. Purification of PTA1/Ig fusion protein by affinity chromatography for PTA1. *Xi Bao Yu Fen Zi Mian Yi Xue Zha Zhi* 1998;14: 113-116
- Callen DF, Baker E, Eyre HJ, Chernos JE, Bell JA, Sutherland GR. Reassessment of two apparent deletions of chromosome 16p to an ins (11;16) and a t(1;16) by chromosome painting. *Ann Genet* 1990;33:219-221
- Hawke NA, Yoder JA, Litman GW. Expanding our understanding of immunoglobulin, T-cell antigen receptor, and novel immune-type receptor genes: a subset of the immunoglobulin gene superfamily. *Immunogenetics* 1999;50:124-133
- Linsley PS, Peach R, Gladstone P, Bajorath J. Extending the B7 (CD80) gene family. *Protein Sci* 1994;3:1341-1343
- Taheri M, Saragovi U, Fuks A, Makkerh J, Mort J, Stanners CP. Self recognition in the Ig superfamily. Identification of precise subdomains in carcinoembryonic antigen required for intercellular adhesion. *J Biol Chem* 2000;275:26935-26943
- Bierer BE, Sleckman BP, Ratnoffsky SE, Burakoff SJ. The biologic roles of CD2, CD4, and CD8 in T-cell activation. *Annu Rev Immunol* 1989; 7:579-599
- Kupfer A, Singer SJ. Cell biology of cytotoxic and helper T cell functions: immunofluorescence microscopic studies of single cells and cell couples. *Annu Rev Immunol* 1989;7:309-337
- Springer TA, Dustin ML, Kishimoto TK, Marlin SD. The lymphocyte function-associated LFA-1, CD2, and LFA-3 molecules: cell adhesion receptors of the immune system. *Annu Rev Immunol* 1987;5:223-252
- Dustin ML, Sanders ME, Shaw S, Springer TA. Purified lymphocyte function-associated antigen 3 binds to CD2 and mediates T lymphocyte adhesion. *J Exp Med* 1987;165:677-692
- Kishimoto TK, O'Connor K, Lee A, Roberts TM, Springer TA. Cloning of the beta subunit of the leukocyte adhesion proteins: homology to an extracellular matrix receptor defines a novel supergene family. *Cell* 1987;48:681-690
- Shibuya K, Lanier LL, Phillips JH, Ochs HD, Shimizu K, Nakayama E, Nakauchi H, Shibuya A. Physical and functional association of LFA-1 with DNAM-1 adhesion molecule. *Immunity* 1999;11:615-623
- Shibuya A, Lanier LL, Phillips JH. Protein kinase C is involved in the regulation of both signaling and adhesion mediated by DNAM-1 receptor. *J Immunol* 1998;161:1671-1676
- Isobe M, Suzuki J, Yamazaki S, Yazaki Y, Horie S, Okubo Y, Maemura K, Yazaki Y, Sekiguchi M. Regulation by differential development of Th1 and Th2 cells in peripheral tolerance to cardiac allograft induced by blocking ICAM-1/LFA-1 adhesion. *Circulation* 1997;96:2247-2253
- Gunji Y, Nakamura M, Hagiwara T, Hayakawa K, Matsushita H,

- Osawa H, Nagayoshi K, Nakauchi H, Yanagisawa M, Miura Y. Expression and function of adhesion molecules on human hematopoietic stem cells: CD34+ LFA-1- cells are more primitive than CD34+ LFA-1+ cells. *Blood* 1992;80:429-436
- 37 Hogg N, Landis RC. Adhesion molecules in cell interactions. *Curr Opin Immunol* 1993;5:383-390
- 38 Springer TA. Adhesion receptors of the immune system. *Nature* 1990;346:425-434
- 39 Phillips JH, McKinney L, Azuma M, Spits H, Lanier LL. A novel beta 4, alpha 6 integrin-associated epithelial cell antigen involved in natural killer cell and antigen-specific cytotoxic T lymphocyte cytotoxicity. *J Exp Med* 1991;174:1571-1581
- 40 Adler B, Ashkar S, Cantor H, Weber GF. Costimulation by extracellular matrix proteins determines the response to TCR ligation. *Cell Immunol* 2001;210:30-40
- 41 Park WR, Park CS, Tomura M, Ahn HJ, Nakahira Y, Iwasaki M, Gao P, Abe R, Hamaoka T, Fujiwara H. CD28 costimulation is required not only to induce IL-12 receptor but also to render janus kinases/STAT4 responsive to IL-12 stimulation in TCR-triggered T cells. *Eur J Immunol* 2001;31:1456-1464
- 42 Clavreul A, Fisson S, D'hellencourt CL, Couez D. Interrelationship between CD3 and CD28 pathways in a murine T cell thymoma. *Mol Immunol* 2000;37:571-577
- 43 Aruffo A, Seed B. Molecular cloning of a CD28 cDNA by a high-efficiency COS cell expression system. *Proc Natl Acad Sci U S A* 1987;84:8573-8577
- 44 Seed B, Aruffo A. Molecular cloning of the CD2 antigen, the T-cell erythrocyte receptor, by a rapid immunoselection procedure. *Proc Natl Acad Sci U S A* 1987;84:3365-3369
- 45 Sewell WA, Brown MH, Dunne J, Owen MJ, Crumpton MJ. Molecular cloning of the human T-lymphocyte surface CD2 (T11) antigen. *Proc Natl Acad Sci U S A* 1986;83:8718-8722
- 46 Wilson GL, Fox CH, Fauci AS, Kehrl JH. cDNA cloning of the B cell membrane protein CD22: a mediator of B-B cell interactions. *J Exp Med* 1991;173:137-146
- 47 Wyler B, Daviet L, Bortkiewicz H, Bordet JC, McGregor JL. Cloning of the cDNA encoding human platelet CD36: comparison to PCR amplified fragments of monocyte, endothelial and HEL cells. *Thromb Haemost* 1993;70:500-505
- 48 Ianelli CJ, Edson CM, Thorley-Lawson DA. A ligand for human CD48 on epithelial cells. *J Immunol* 1997;159:3910-3920
- 49 Koopman G, Keehnen RM, Lindhout E, Zhou DF, de Groot C, Pals ST. Germinal center B cells rescued from apoptosis by CD40 ligation or attachment to follicular dendritic cells, but not by engagement of surface immunoglobulin or adhesion receptors, become resistant to CD95-induced apoptosis. *Eur J Immunol* 1997;27:1-7
- 50 Piepkorn M, Hovingh P, Bennett KL, Aruffo A, Linker A. Chondroitin sulphate composition and structure in alternatively spliced CD44 fusion proteins. *Biochem J* 1997;327:499-506
- 51 Lee JW, Gersuk GM, Kiener PA, Beckham C, Ledbetter JA, Deeg HJ. HLA-DR-triggered inhibition of hemopoiesis involves Fas/Fas ligand interactions and is prevented by c-kit ligand. *J Immunol* 1997;159:3211-3219
- 52 Zollner O, Lenter MC, Blanks JE, Borges E, Steegmaier M, Zerwes HG, Vestweber D. L-selectin from human, but not from mouse neutrophils binds directly to E-selectin. *J Cell Biol* 1997;136:707-716
- 53 Mannori G, Santoro D, Carter L, Corless C, Nelson RM, Bevilacqua MP. Inhibition of colon carcinoma cell lung colony formation by a soluble form of E-selectin. *Am J Pathol* 1997;151:233-243
- 54 Dmitrieva N, Shelton D, Rice AS, McMahon SB. The role of nerve growth factor in a model of visceral inflammation. *Neuroscience* 1997;78:449-459
- 55 Kirk AD, Harlan DM, Armstrong NN, Davis TA, Dong Y, Gray GS, Hong X, Thomas D, Fechner JH Jr, Knechtle SJ. CTLA4-Ig and anti-CD40 ligand prevent renal allograft rejection in primates. *Proc Natl Acad Sci U S A* 1997;94:8789-8794
- 56 Moreland LW, Baumgartner SW, Schiff MH, Tindall EA, Fleischmann RM, Weaver AL, Ettlinger RE, Cohen S, Koopman WJ, Mohler K, Widmer MB, Bloch CM. Treatment of rheumatoid arthritis with a recombinant human tumor necrosis factor receptor (p75)-Fc fusion protein. *N Engl J Med* 1997;337:141-147
- 57 Jin Boquan, Scott JL, Vadas MA, Burns GF. TGF beta down-regulates TLiSA1 expression and inhibits the differentiation of precursor lymphocytes into CTL and LAK cells. *Immunology* 1989;66:570-576
- 58 O'Rourke AM, Mescher MF. Cytotoxic T-lymphocyte activation involves a cascade of signalling and adhesion events. *Nature* 1992;358:253-255
- 59 Rodrigues M, Nussenzweig RS, Romero P, Zavala F. The *in vivo* cytotoxic activity of CD8+ T cell clones correlates with their levels of expression of adhesion molecules. *J Exp Med* 1992;175:895-905

Edited by Ma JY

• BASIC RESEARCH •

Effect of manganese on heat stress protein synthesis of new-born rats

Ben-Yan Zhang, Sheng Chen, Fang-Li Ye, Chang-Cai Zhu, He-Xi Zhang, Rui-Bo Wang, Cheng-Fen Xiao, Tang-Chun Wu, Guo-Gao Zhang

Ben-Yan Zhang, Fang-Li Ye, Chang-Cai Zhu, Department of Preventive Medicine, College of Medicine, Wuhan University of Science and Technology, Wuhan 430080. Hubei Province, China
Sheng Chen, Rui-Bo Wang, Cheng-Fen Xiao, Tang-Chun Wu, Guo-Gao Zhang, Department of Labor Hygiene, Wuhan Tongji Medical University, Wuhan 430030, Hubei Province, China
He-Xi Zhang, Department of Preventive Medicine, Xinxiang Medical College, Xinxiang 453002, Henan Province, China
Supported by Natural Science Foundation of Metallurgical Industry Ministry. No. (1996) 254-21

Correspondence to: Ben-Yan Zhang, Department of Preventive Medicine, College of Medicine, Wuhan University of Science and Technology, 205 Yejin Road Wuhan 430080. Hubei Province, P.R.China.
zhangbe7020@sina.com

Telephone: +86-27-86831703 / 86830745

Received 2001-06-02 Accepted 2001-10-26

Abstract

AIM: To study the effect of manganese (Mn) on heat stress protein 70 (HSP70) synthesis in the brain and liver of new-born rats whose mother-rats were exposed to Mn.

METHODS: 32 female rats were randomly divided into four groups. One group was administrated with physiological saline only as control group, the other three groups were administrated with 7.5, 15 and 30 mg·kg⁻¹ manganese chloride (MnCl₂) by intraperitoneal injection every two days for two weeks. After delivery, the mother-rats received MnCl₂ unceasingly for a week with the same method. Then the contents of Mn, Zn, Cu and Fe in the livers of the new-born rats were determined by atomic absorption spectroscopy; The level of HSP70 in the brains and the livers of the new-born rats as detected by Western-dot-blotting, and the SOD activities were measured simultaneously.

RESULTS: The contents of Mn in the livers of new-born rats of the experimental groups (respective 1.38±0.18, 2.73±0.65, 3.44±0.89 μg·g⁻¹) were significantly increased compared with the control group (0.88±0.18 μg·g⁻¹; *P*<0.01); The contents of Fe in the livers of new-born rats of 15 and 30 mg·kg⁻¹ experimental groups (426±125, 572±175 μg·g⁻¹, respectively) were significantly increased compared with the control group (286±42 μg·g⁻¹; *P*<0.05); the levels of Zn in the livers of the new-born rats of three experimental groups (254±49, 263±47, 213±28 μg·g⁻¹, respectively) were lower than those of the control group (335±50 μg·g⁻¹; respective *P*<0.05, *P*<0.01); and the levels of Cu showed no significant difference among the four groups (three experimental groups: 75±21, 68±241 and 78±18 μg·g⁻¹; control group: 83±9 μg·g⁻¹; *P*>0.05). There was a significant increase in the levels of HSP70 in the brains of new-born rats of the 30 mg·kg⁻¹ group (19.5×10³±1.3×10³ A; control group: 14.3×10³±1.4×10³ A; *P*<0.01), and the levels of HSP70 in the livers of new-born rats of three experimental groups (respective 19.6×10³±3.9×10³ A, 18.5×10³±3.8×10³ A, 22.4×10³±1.9×10³ A) also increased

than control group (13.3×10³±1.0×10³ A; *P*<0.01), but the SOD activities showed no significant difference among brains of the four groups (experimental groups: 5.04±0.43, 4.83±0.48, 4.60±0.84 ku·g⁻¹; control group: 4.91±0.37 ku·g⁻¹; *P*>0.05). The SOD activities in the livers of 15 mg·kg⁻¹ group (5.41±0.44 ku·g⁻¹) was lower than the control group (5.95±0.36 ku·g⁻¹; *P*<0.05).

CONCLUSION: While mother-rats were exposed to manganese, the metabolisms of Mn, Zn and Fe of new-born rats in the livers were influenced and were situated in a stress status, thus HSP70 syntheses is induced in the brains and livers of new-born rats, but the mechanism of this effect in the developmental toxicity of Mn remains to be further studied.

Zhang BY, Chen S, Ye FL, Zhu CC, Zhang HX, Wang RB, Xiao CF, Wu TC, Zhang GG. Effect of manganese on heat stress protein synthesis of new-born rats. *World J Gastroenterol* 2002;8(1):114-118

INTRODUCTION

Manganese (Mn) has bi-directional effect on the mammal^[1-3], both deficient and excess intake of Mn result in altered enzymatic reactions and brain function because of its essential element nutrition^[4] and neurotoxic effect. With exposure to higher concentrations is harmful to health^[5,6]. Excessive manganese has been associated with neurobehavioral deficits and neurological and/or neuropsychiatric illness^[7]. As a nervous toxicant, Mn damages central nervous system, and has procreant toxicity. Mn also could transplacenta to embryo and affects growth of offspring^[8,9]. Thus, excessive manganese also is an embryotoxicant and fetotoxicant in mammals^[10], but the mechanism of this effect has not been elucidated yet. It is well known that heat stress / shock proteins (Hsps) are induced by a series of occupational factors and their main biological action is to participate in thermotolerance and toxicant tolerance. Hsps participate in protein synthesis, folding, assemblage and intracellular protein transport as the molecular chaperones^[11,12]. It has not been reported whether these functions are relative with toxicity of Mn. The HSP70 levels and the SOD activities of the brains and livers and the trace-element contents of the livers were measured in the new-born rats after their mother-rats were exposed to the manganese.

MATERIALS AND METHODS

Animal Treatment

Thirty-two healthy Wistar female rats that weigh 200~240g (obtained from center of experimental animal of Tongji Medical University) were randomly divided into four groups. Except one group as control, the other three groups were treated with Manganese chloride tetrahydrate (MnCl₂·H₂O₂). By mean of single intraperitoneal injection administration every two days for two weeks, the doses were 7.5, 15 and 30 mg·kg⁻¹ respectively. The control group was similarly injected physiological saline. Then the rats (1 ♂ : 1 ♀) were housed together. The next morning gestation was defined as d 0 when sperms were founded in the vaginal smear. After

pregnancy, the mother-rats were treated with MnCl_2 at the same concentration of before, then harvested at time points up to a week with the same method as before. These female rats received MnCl_2 11 times. The newborn rats were killed by cervical dislocation in 24 h. The brain and liver of the newborn rats was reserved in -20°C immediately.

Determination of trace elements

The reserved livers were put into roaster for 2 h at 105°C and reserved into desiccator. Drying sample accurately Weighed up 0.0500–0.1000g was put into conical flask and added 2 mL nitric acid (G.R), 0.5 mL perchloric acid (G.R) and digested to dry approximately. After cooling, the digestive sample was dissolved with redistilled water that was distilled for 4 times, the sample was put into 10 mL test tube and fixed volume to 5 mL. Trace elements were measured with atomic absorption spectroscopy (Spectr AA-40 atomic absorption apparatus, VARIAN corp., USA). Mn was measured with graphite stove atomic absorption spectroscopy analysis, and adopted flame atomic absorption spectroscopy to mensurate Cu, Zn and Fe.

Brains and livers homogenate

Prepared homogenates of the brains and livers were done as described by routine technique. Mensurated contents of the protein of the brains and livers as Lowry.

Detection of SOD activities

Taking equal quality proteins of the brains and livers to determine SOD activities in the brains and livers with SOD kits supplied by Nanjing Jiancheng Bioengineering Graduate Institute.

Determination of HSP70

Equal amount proteins of the brains and livers was taken to determine the HSP70 levels in the brains and livers with Western-dot-blotting^[13]. After Western blotting, HSP70 was detected using anti-HSP70 rabbit polyclonal antibodies (provided by Lab of Cell & Developmental Genetics, University Laval, Canada) and anti-rabbit

horseradish peroxidase-conjugated secondary antibodies (Sigma), and visualized using 3-3'-diaminobenzidine (DAB). The results were quantified by a densitometry (CS-930, Japan).

Statistic analysis

The results were analyzed with SAS programs in IBM-PC.

RESULTS

Effect of Mn on female rat Reproduction

After female rats exposed to Mn, their gestation periods had no significant difference from the control group ($P>0.05$). The parturition indexes seem to reduce along with manganic dosage increment, but the difference is not significant compared with control group ($P>0.05$) yet. Average of fetiferous quality of puerperal female rats seem to reduce in 7.5 and $15\text{mg}\cdot\text{kg}^{-1}$ groups, but the differences are not significant compared with control group ($P>0.05$) yet. However, $30\text{mg}\cdot\text{kg}^{-1}$ group significantly reduced compared with control group ($P<0.01$). Average of fetiferous quality of pregnant female rats in 15 and $30\text{mg}\cdot\text{kg}^{-1}$ groups significantly reduced compared with the control group ($P<0.05$, $P<0.01$). The viability index of 1-day-old filial rats in $30\text{mg}\cdot\text{kg}^{-1}$ group significantly reduced compared with the control group ($P<0.01$). The newborn rats' weight and height showed no significant difference among four groups ($P>0.05$, Table 1).

Effect of Mn on traceelements in newborn rats

The manganese contents of the new-born rats' livers in three experimental groups significantly increased compared with control group ($P<0.01$), and there was a dose-dependent increase in these groups. The levels of zinc in the new-born rats' livers in three experimental groups were lower than those of control group too ($P<0.05$, $P<0.01$, respectively). The iron contents of the new-born rats' livers in 15 and $30\text{mg}\cdot\text{kg}^{-1}$ experimental groups were higher than control group ($P<0.05$, $P<0.01$, respectively), but the copper levels of the newborn rats' livers showed no significant difference among four rroups ($P>0.05$, Table 2).

Table 1 Effect of Mn on reproduction in female rats

Mn ($\text{mg}\cdot\text{kg}^{-1}$)	Gestation (d)	Puerpera female rats (n)	Paturition index (%)	Tatol Filial rats (n)	puerperal female rats Fetiferous quality (n)	pregnant female rats fetiferous quality (n)	Livabilit of d 1 filial rats (%)	Newborn rats' mass (g)	Newborn rats' height (cm)
control	21.3±0.8	7	87.5	68	9.7±2.1	8.5±3.9*	98.5	5.89±0.49	5.2±0.25
7.5	21.8±1.2	6	75.0	41	6.8±3.1	5.1±4.1	95.1	5.47±0.54	5.1±0.36
15	22.2±0.8	5	62.5	33	6.6±2.7	4.1±3.9*	87.9	5.38±0.53	4.98±0.35
30	22.7±1.5	3	37.5	15	5.0±2.6*	1.8±2.9*	73.3*	5.13±0.51	4.87±0.38

* $P<0.05$, $P<0.01$, vs control.

Effect of Mn on SOD activities in newborn rats

Although the SOD activities of the newborn rat' brains seem to reduce in 15, $30\text{mg}\cdot\text{kg}^{-1}$ groups and increase in $7.5\text{mg}\cdot\text{kg}^{-1}$ group, but no significant difference showed among all the four groups ($P>0.05$). The

SOD activities of the newborn rat' livers were lower in $15\text{mg}\cdot\text{kg}^{-1}$ group than control group ($P<0.05$), but showed no significant difference among 7.5, $30\text{mg}\cdot\text{kg}^{-1}$ and control groups ($P>0.05$, Table 3).

Table 2 Effect of Mn on traceelements in newborn rats' livers ($\bar{x}\pm s$, $\mu\text{g}\cdot\text{g}^{-1}$)

Mn ($\text{mg}\cdot\text{kg}^{-1}$)	Filialrats (n)	Mn	Cu	Zn	Fe
control	5	0.88±0.18	83±9	335±50	286±42
7.5	5	1.38±0.18*	75±21	254±50*	271±88
15	7	2.73±0.65*	68±24	263±47*	426±125*
30	5	3.44±0.89*	78±18	213±28*	572±175*

* $P<0.05$, $P<0.01$, vs control.

Table 3 Effect of Mn on SOD and HSP70 in brains and livers ($\bar{x} \pm s$)

Mn (mg·kg ⁻¹)	Filial Rats (n)	Brain		Liver	
		SOD / ku·g ⁻¹	HSP70/×10 ³ A	SOD / ku·g ⁻¹	HSP70/×10 ³ A
control	8	4.91±0.37	14.3±1.4	5.95±0.36	13.4± 1.0
7.5	9	5.04±0.43	16.0±1.8	5.96±0.41	19.6±3.9 ^b
15	7	4.83±0.48	14.4±1.4	5.41±0.44 ^a	18.5±3.8 ^b
30	6	4.60±0.84	19.5±1.3 ^b	5.87±0.68	22.4±1.9 ^b

^aP<0.05, ^bP<0.01, vs control**Effect of Mn on HSP70 synthesis in newborn rats**

The level of HSP70 in the brain showed no significant difference among 7.5, 15mg·kg⁻¹ and control groups ($P>0.05$), but showed significantly increased between 30mg·kg⁻¹ and control groups ($P<0.01$). The level of HSP70 in the livers significantly increased in three experimental groups to be compared with control group ($P<0.01$, Table 3).

DISCUSSION

The fetiferous quality reduces after female rats are imbued with Mn; parturition index also tended to reduce along with the manganese dosage increase, and livability of d 1 old filial rats significantly reduced along with the manganese dosage increase. The fact illustrates that manganese influences female rats' reproductive function. Manganese could transplacenta to enter filial central nervous system^[15]. Yang BN reported that the new-born rats' manganese contents of the brain were significantly higher than those of control group with inductance coupling plasmic emanant spectroscopy after mother-rats exposed to by manganese^[16]. This study determined that the new-born rats' manganese contents of the livers are significantly higher than control group with atomic absorption spectroscopy after mother-rats exposed to manganese, and have a dose-effect relationship. The results show that the manganese could be transferred to the embryo by placental barrier and accumulate in filial rat's brains and livers after mother-rats to be exposed by manganese in gestation. It has not been reported that the effect of Mn on other microelements in the newborn rats' liver of intoxicated mother-rats. This study also detected that the levels of Zn in the new-born rats' livers of three experimental groups were lower than those of control group, and the iron contents in the new-born rats' livers of and 30mg·kg⁻¹ treated groups were higher than the control group, but the copper levels showed no significant difference among four groups. It was obvious that the zinc and iron metabolism were disturbed in the livers of new-born rats after mother-rats exposed to manganese. Zn is an essential microelement and has much to do with many enzymatic bioactivities. Zn is very important to maintain normal body growth and reproductive function. While the body zinc deficiency, the hormone syntheses reduce and their activities decrease, which, therefore, result in serious obstruction of the growth, children's testicles agenesis, reducing spermic quantity, weakening spermic activity, agenesis of the immune apparatus in the thymus gland etc and immune estate. While serum zinc contents descend, it is degressive that the levels of neuropeptide somatostatin and arginine-vasopressin have much to do with capability of the learning and memory in rats' hippocampi, and make the rats' capability of learning and memory clearly decline^[17]. When filial rats lack the zinc during the lactation and weaning stage, the brain weight, the hippocampal weight, the serum and hippocampal zinc concentrations are significantly lowered, and proportion of induced long-term potentiation (LTP) is zero and proportion of active avoidance response decreased profoundly^[18]. Cognition is a field of thought processes by which an individual processes information through skills of perception, thinking, memory, learning and attention. Zinc deficiency may affect cognitive development by alterations in attention, activity, neuropsychological behavior and motor development. The exact mechanisms are not clear but it appears that zinc is essential for neurogenesis, neuronal migration, synaptogenesis^[19]. Excessive manganese arising zinc deficiency could interfere with

neurotransmission and subsequent neuropsychological behavior.

This study determined zinc decrease in newborn rats' livers after mother-rats were administrated by manganese, it tallies with the phenomenon that as we observed, filial rats' neurobehavior functions deferred and the capability of learning and memory weakened^[20]. The result enlightens that the effect of Mn on filial rats' developmental toxicity might be responsible for the manganese which leads to the zinc deficiency in the brain and liver. A new pathway is suggested in the manganese mechanism research on filial rats' neurotoxicity. Fe is also an essential microelement and has important physiologic function. The study also discovered that newborn rats' irons to heighten in the livers after mother-rats were imbued by manganese. The most actions are antagonistic between Fe and Zn. It is uncertain that whether the manganese cumulated in the liver to arise the zinc decreases and results in heightening Fe antagonistically. So, the reason needs further study.

Mn has an especial affinity with the mitochondrial and can largely cumulate in the cells that contain plentiful mitochondrial, so the manganese content is highest in the liver and the content is higher in the spleen, the kidney and brain^[21]. The manganese mainly damages extrapyramidal system on central nervous system, which is related to specifically organization and the neurons distribution in the substantia nigra and corpus striatum. Many melanin neurons and aminergic neurons are distributed in the dense area of substantia nigra. They have a speciality that collect and cumulate the amine and metal elements, such as manganese etc. Superfluous manganese on one hand activate the cytochrome oxidase P-450 to engender the free radicals to deplete the sulthydyls and impair cellular resistivity, Mn on the other hand can also produce plentiful free radicals to damage mitochondrial, and to disturb energy metabolism, then mediate the toxicity of excitability amino acids and result in increasing intracellular calcium, activating the calcium-dependent protease, nuclease, phosphatase and promoting the cellular recessive denaturalization. The increase of calcium ions again, promotes the production of free radicals as result, forms a vicious circle. Therefore, cumulative manganese may destroy the protective barrier of the melanin neurons and constantly releases to beget continual toxicity in the extrapyramidal system). The free radicals play very important role in manganese neurotoxicity. SOD is a important enzyme among enzymes system that eliminates free radicals. The manganese is able to inhibit SOD by forming free radicals. In our study only the SOD activities of livers in 15mg·kg⁻¹ group were lower than the control group. Although it inclined depression that the SOD activities of the livers in 7.5 and 30mg·kg⁻¹ groups and of the brains in the three experimental groups, the differences were not significant to be compared with control group. This causation may be that SOD have a insensitivity on free radicals by the manganese toxicity, also may have other cause to be elucidated. The body was situated in a toxicant stress status and oxidative stress after the manganese was accumulated in the filial rat's brain and liver^[22]. When body was situated in a toxicant stress / oxidative stress status, heat stress protein is markedly elevated *in vivo* on response of toxicant stress / oxidative stress.^[23-26] The stress response is a common physiological response from the prokaryotes to the human. It is the character of various stress responses that Hsps syntheses appear as increase or grow out of nothing in the cells. Hsps are a kind proteins that have protective function as quite conservation in the evolution. Hsps could respond stress responses by some injurious environmental factors, such as Pb^[27], Cd^[28], Hg^[29], As^[30,31], benzene^[32,33], CO^[34], ischemia^[35], psychological tension^[36] etc. Hsps have been proposed as

general markers of cellular aggression and their use for environmental monitoring is often suggested^[37]. Hsps endow with resumptive capability of the cells or biology from various stress responses and protect them to keep from the damages of these factors^[38-46]. The primary signification of Hsps is to keep protect the cells from suffering from ill conditions of high temperature, low oxygen, heavy metal and illness etc^[47-54]. Therefore it is obvious that thermotolerance was formed, in other words, after the cells or organisms were exposed to subthermal death point, the livability significantly increases on the thermal death point. HSP70 exerts main action in the form of stress tolerance. HSP70 has important protective function in intracellular hereditary substance DNA, the process of biologic growth, development, differentiation and regulation^[55-57]. HSP70 connects with many internal bioactive substances and take part in many biochemical processes. It is principal that HSP70 promote protein synthesis, folding, assemblage, transportation and take part in the elimination of metamorphic proteins as molecular chaperones under non-stress conditions^[58-62]. These important functions may have to do with the function of the thermotolerance and poison tolerance. When cells experience thermal or toxicant stress, Hsps take on a new role, conserved from poison to humans, of protecting cells from the detrimental effects of stress. This role takes on added significance for the embryo in which the developmental program must be read linearly, with little opportunity to cycle backward to complete a missed segment of the program. Thereby Hsps will afford protection to the human embryo/fetus exposed to thermal/toxicant stress^[63-65].

This study showed that some HSP70 were synthesized in normal newborn rats' brains and livers. The HSP70 contents of the newborn rats' brains in Low and medium dosage groups had a few increase, but the differences were not significant compared with control group. The HSP70 contents in the newborn rats' brains of high manganese dosage group significantly increased. The HSP70 contents all significantly increased in the newborn rats' livers of three experimental groups to be compared with control group. These results indicated that HSP70 had a certain degree role in normal growth and the manganese had effect on HSP70 syntheses in the newborn rats' brains and livers. However the HSP70 syntheses were low in very few newborn rats' brains and livers of experimental groups too. It remains to be elucidated that HSP70 synthesis is related to manganese toxicity in the pathology, clinic, susceptibility of manganese poisoning and other biochemical variety.

Through contrast affected degree of HSP70 syntheses in newborn rats' brain and livers, induction of HSP70 is sensitive in the liver than in the brain. The reason may have to do with manganese accumulation that is higher in the liver than in the brain in the newborn rats. Recently some researcher explore HSP70 to relate to the fetation from the point of the development and had acquired many interesting results. They considered stress response to have diploid effects. On the one hand protect embryonic growth, on the other hand disturb as well as embryonic growth. Final procreant consequence mainly depend on the intensity and duration in the stress response whether to exceed self regulative level in intracellular HSP70 synthesis and also relate to injured period in fetation. Many results all had proved that HSP70 could influence embryonic growth *in vivo* and *in vitro*. HSP70 maybe is a biomaker as screening developmental toxicant^[66], and excessive manganese may be considered a developmental toxicant.. Moreover, the stress status also leads to disorder of digestive system, for instance, gastrointestinal motility disorders^[67,68], vasoactive intestinal peptide (VIP), neuropeptide Y (NPY) of colonic mucosa was increased^[69], platelet derived growth factor (PDGF)^[70], and tissue inhibitor of metalloproteinase 1 (TIMP-1) are increased^[71], and heme oxygenase-1 (HO-1) mRNA and protein were highly induced and HO enzyme activity was higher after hemorrhagic shock and resuscitation (HR)^[72]. Besides accelerates HSP70 synthesis *in vivo*, The manganese could induce the nitric oxide synthase(NOS) yet. The NOS begets increasing the synthesis of nitric oxide(NO). Superfluous NO could mediate neurotoxicity of excitative amino acid as a cytotoxicity molecule and could damage central nervous system in budding filial generation^[73]^[28], whereas, HSP70 could diminish the liver damage

by NO. Re-induction of HSP70 expression by stress effect re-established resistance to NO toxicity^[74].

Our study demonstrates that the excessive manganese cumulated largely filial rat's brain and liver by way of placenta after mother-rats exposed to manganese, and disturbed the microelement metabolisms of the l manganese, zinc and iron *in vivo* and injured the growth on the offspring. On the other hand the body was situated in a stress status and the embryo and filial generation growth were damaged by the inducement of HSP70 synthesis in the brain and liver. The mechanism of this effect in the developmental toxicity of Mn remains to be further researched.

REFERENCES

- Greger JL. Nutrition versus toxicology of manganese in humans: evaluation of potential biomarkers. *Neurotoxicology* 1999;20:205-212
- Greger JL. Dietary standards for manganese: overlap between nutritional and toxicological studies. *J Nutr* 1998;128(2 Suppl):368-371
- Kafritsa Y, Fell J, Long S, Bynevelt M, Taylor W, Milla P. Long-term outcome of brain manganese deposition in patients on home parenteral nutrition. *Arch Dis Child* 1998;79:263-265
- Amemiya T. The eye and nutrition. *Jpn J Ophthalmol* 2000;44:320-329
- Chua AC, Morgan EH. Effects of iron deficiency and iron overload on manganese uptake and deposition in the brain and other organs of the rat. *Biol Trace Elem Res* 1996;55:39-54
- Verity MA. Manganese neurotoxicity: a mechanistic hypothesis. *Neurotoxicology* 1999;20:489-497
- Mergler D, Baldwin M, Belanger S, Larribe F, Beuter A, Bowler R, Panisset M, Edwards R, de Geoffroy A, Sassine MP, Hudnell K. Manganese neurotoxicity, a continuum of dysfunction: results from a community based study. *Neurotoxicology* 1999;20:327-342
- Zhang D, He X, Zhang W, Tan J. Effect of manganese on the growth and development of rat offspring. *Wei Sheng Yan Jiu* 1998;27:237-240
- Spencer A. Whole blood manganese levels in pregnancy and the neonate. *Nutrition* 1999; 15:731-734
- Olomina MT, Domingo JL, Llobet JM, Corbella J. Effect of day of exposure on the developmental toxicity of manganese in mice. *Vet Hum Toxicol* 1996;38:7-9
- Zhang GG, He HZ, Wu TC. Heat Stress Proteins and It Expectation of Application Study in Occupational Medicine. *Zhonghua Laodong Weisheng Zhiyebing Zazhi* 1998; 17: 67-71
- Wu TC, Yuan Y, Bi YY, He HZ, Zhang GG. Plasma free amino acid in workers working under different stress conditions. *J Occupa Health* 1998; 40: 203-206
- He XS, Pan QP, Wu TC, Yuan Y, Tang PT, He HZ. Determine Chief Heat Stress Proteins with Western Blot Doting. *Zhonghua Laodong Weisheng Zhiyebing Zazhi* 1996; 13: 376-378
- Krachler M, Rossipal E, Micetic-Turk D. Trace element transfer from the mother to the newborn—investigations on triplets of colostrum, maternal and umbilical cord sera. *Eur J Clin Nutr* 1999;53:486-494
- Brenneman KA, Cattley RC, Ali SF, Dorman DC. Manganese-induced developmental neurotoxicity in the CD rat: is oxidative damage a mechanism of action. *Neurotoxicology* 1999;20:477-487
- Yang BL, Zang DX, Tan JF, Ke MH, Wu xj, Song SH, Xet. Effect of Mn on manganese, zinc, copper and iron of filial rats' brains during pregnancy of maternal rats. *Weisheng Dulixue Zazhi* 1997; 11: 101-103
- Li JS, Xu PX, Ren HM, Hu HT, Ling FD. changes of the somatostatin and arginine vasopressin contents of the rat hippocampus in zinc deficiency. *Acta Nutrimeta Sinica* 1998; 21: 21-24
- Kong X, Ren R, Liu L. Effects of zinc deficiency in fodder on brain development, learning and memory in rats. *Zhonghua Yu Fang Yi Xue Za Zhi* 1997;31:295-298
- Bhatnagar S, Taneja S. Zinc and cognitive development. *Br J Nutr* 2001;85(Suppl 2):139-145
- Zhang BY, Zhu ZC, Ye FL, Xiao BS, Xu T. Effect of manganese on neurobehavioral function of offsprings of intoxicated rat. *Zhongguo zhiye Yixue* 1999;26:5-7
- He FS. Manganese and manganic compounds. In: He FS. Chinese occupational medicine. Beijing: People's Medical Publishing House. 1999; 241-247
- Jauniaux E, Watson AL, Hempstock J, Bao YP, Skepper JN, Burton GJ. Onset of maternal arterial blood flow and placental oxidative stress. A possible factor in human early pregnancy failure. *Am J Pathol* 2000;157:2111-2122
- Lin KC, Krieg RJ Jr, Saborio P, Chan JC. Increased heat shock protein-70 in unilateral ureteral obstruction in rats. *Mol Genet Metab* 1998;65:303-310
- Wong HR, Menendez IY, Ryan MA, Denenberg AG, Wispe JR. Increased expression of heat shock protein-70 protects A549 cells against hyperoxia. *Am J Physiol* 1998;275(4 Pt 1):L836-841

- 25 Sugaya K, Chou S, Xu SJ, McKinney M. Indicators of glial activation and brain oxidative stress after intraventricular infusion of endotoxin. *Brain Res Mol Brain Res* 1998;58:1-9
- 26 Singh AK, Lakhota SC. Tissue-specific variations in the induction of Hsp70 and Hsp64 by heat shock in insects. *Cell Stress Chaperones* 2000; 5:90-97
- 27 Ait-Aissa S, Porcher J, Arrigo A, Lambre C. Activation of the hsp70 promoter by environmental inorganic and organic chemicals: relationships with cytotoxicity and lipophilicity. *Toxicology* 2000;145:147-157
- 28 Damelin LH, Vokes S, Whitcutt JM, Damelin SB, Alexander JJ. Hormesis: a stress response in cells exposed to low levels of heavy metals. *Hum Exp Toxicol* 2000;19:420-430
- 29 Goering PL, Fisher BR, Noren BT, Papaconstantinou A, Rojko JL, Marler RJ. Mercury induces regional and cell-specific stress protein expression in rat kidney. *Toxicol Sci* 2000;53:447-457
- 30 Sok J, Calton M, Lu J, Lichtlen P, Clark SC, Ron D. Arsenite-inducible RNA -associated (AIRAP) protects cells from arsenite toxicity. *Cell Stress Chaperones* 2001; 6:6-15
- 31 Ibrahim EC, Morange M, Dausset J, Carosella ED, Paul P. Heat shock and arsenite induce expression of the nonclassical class I histocompatibility HLA-G gene in tumor cell lines. *Cell Stress Chaperones* 2000;5:207-218
- 32 Vojdani A, Lapp CW. Interferon-induced proteins are elevated in blood samples of patients with chemically or virally induced chronic fatigue syndrome. *Immunopharmacol Immunotoxicol* 1999;21:175-202
- 33 Wu TC, Yuan Y, Wu Y, He HZ, Zhang GG, Tanguay RM. Presence of antibodies to heat stress proteins and its potential significance in workers exposed to benzene and patients with benzene-poisoning. *Cell Stress Chaperones* 1998;3:161-167
- 34 Wu TC, Tanguay RM, Wu Y, He HZ, Xu DG, Feng JD, Shi WX, Zhang GG. Presence of antibodies to heat stress proteins and its possible significance in workers exposed to high temperature and carbon monoxide. *Biomedical and Environmental Science* 1996;9:370-379
- 35 Kumar Y, Tatu U. Induced hsp70 is in small, cytoplasmic complexes in a cell culture model of renal ischemia: a comparative study with heat shock. *Cell Stress Chaperones* 2000;5:314-327
- 36 Wu TC, Xiong YL, Chen S, Leng ST, Hai T, Tanguay RM. Biochemical changes of plasma in paratroops after parachuting: a preliminary investigation. *Space medicine & medical engineering* 1999; 12:235-239
- 37 Mun HS, Aosai F, Norose K, Chen M, Hata H, Tagawa YI, Iwakura Y, Byun DS, Yano A. Toxoplasma gondii Hsp70 as a danger signal in toxoplasma gondii-infected mice. *Cell Stress Chaperones* 2000;5:328-335
- 38 Wagner M, Hermanns I, Bittinger F, Kirkpatrick CJ. Induction of stress proteins in human endothelial cells by heavy metal ions and heat shock. *Am J Physiol* 1999;277(5 Pt 1):L1026-1033
- 39 Weber H, Wagner AC, Jonas L, Merkord J, Hofken T, Nizze H, Leitzmann P, Goke B, Schuff-Werner P. Heat shock response is associated with protection against acute interstitial pancreatitis in rats. *Dig Dis Sci* 2000;45:2252-2264
- 40 Matranga V, Toia G, Bonaventura R, Muller WE. Cellular and biochemical responses to environmental and experimentally induced stress in sea urchin coelomocytes. *Cell Stress Chaperones* 2000;5:113-120
- 41 Hamel L, Kenney M, Jayyosi Z, Ardati A, Clark K, Spada A, Zilberstein A, Perrone M, Kaplow J, Merkel L, Rojas C. Induction of heat shock protein 70 by herbimycin A and cyclopentenone prostaglandins in smooth muscle cells. *Cell Stress Chaperones* 2000;5:121-131
- 42 Volloch V, Gabai VL, Rits S, Force T, Sherman MY. HSP72 can protect cells from heat-induced apoptosis by accelerating the inactivation of stress kinase JNK. *Cell Stress Chaperones* 2000;5:139-147
- 43 Locke M, Atance J. The myocardial heat shock response following sodium salicylate treatment. *Cell Stress Chaperones* 2000;5:359-368
- 44 He H, Chen C, Xie Y, Asea A, Calderwood SK. HSP70 and heat shock factor 1 cooperate to repress Ras-induced transcriptional activation of the c-fos gene. *Cell Stress Chaperones* 2000;5:406-411
- 45 Hightower LE, Brown, Renfro JL, Perdrizet GA, Rewinski M, Guidon PT Jr, Mistry T, House SD. Tissue-level cytoprotection. *Cell Stress Chaperones* 2000;5:412-414
- 46 Basu S, Srivastava PK. Heat shock proteins: the fountainhead of innate and adaptive immune responses. *Cell Stress Chaperones* 2000;5:443-451
- 47 Multhoff G, Mizzen L, Winchester CC, Milner CM, Wenk S, Eissner G, Kampinga HH, Laumbacher B, Johnson J. Heat shock protein 70 (Hsp70) stimulates proliferation and cytolytic activity of natural killer cells. *Exp Hematol* 1999;27:1627-1636
- 48 Hantschel M, Pfister K, Jordan A, Scholz R, Andreesen R, Schmitz G, Schmetzer H, Hiddemann W, Multhoff G. Hsp70 plasma membrane expression on primary tumor biopsy material and bone marrow of leukemic patients. *Cell Stress Chaperones* 2000;5:438-442
- 49 van Eden W, Wendling U, Paul L, Prakken B, van Kooten P, van der Zee R. Arthritis protective regulatory potential of self-heat shock protein cross-reactive T cells. *Cell Stress Chaperones* 2000;5:452-457
- 50 Ostberg JR, Patel R, Repasky EA. Regulation of immune activity by mild (fever-range) whole body hyperthermia: effects on epidermal Langerhans cells. *Cell Stress Chaperones* 2000;5:458-461
- 51 Hasday JD, Singh IS. Fever and the heat shock response: distinct, partially overlapping processes. *Cell Stress Chaperones* 2000;5:471-480
- 52 Samali A, Robertson JD, Peterson E, Manero F, van Zeijl L, Paul C, Cotgreave IA, Arrigo AP, Orrenius S. Hsp27 protects mitochondria of thermotolerant cells against apoptotic stimuli. *Cell Stress Chaperones* 2001;6:49-58
- 53 Ip SP, Che CT, Kong YC, Ko KM. Effects of schisandrin B pretreatment on tumor necrosis factor-alpha induced apoptosis and Hsp70 expression in mouse liver. *Cell Stress Chaperones* 2001;6:44-48
- 54 Wu TC, Chen S, Xiao CF, Wang CL, Pan Q, Wang ZZ, Xie MX, Mao ZC, Wu Y, Tanguay RM. Presence of antibody against the inducible Hsp71 in patients with acute heat-induced illness. *Cell Stress Chaperones* 2001;6:113-120
- 55 Kozawa O, Matsuno H, Niwa M, Hatakeyama D, Kato K, Uematsu T. AlphaB-crystallin, a low-molecular-weight heat shock protein, acts as a regulator of platelet function. *Cell Stress Chaperones* 2001;6:21-28
- 56 Loones MT, Chang Y, Morange M. The distribution of heat shock proteins in the nervous system of the unstressed mouse embryo suggests a role in neuronal and non-neuronal differentiation. *Cell Stress Chaperones* 2000;5:291-305
- 57 Constitutive expression of heat shock proteins Hsp90, Hsc70, Hsp70 and Hsp60 in neural and non-neural tissues of the rat during postnatal development. *Cell Stress Chaperones* 1998;3:188-199
- 58 Kimmins S, MacRae TH. Maturation of steroid receptors: an example of functional cooperation among molecular chaperones and their associated proteins. *Cell Stress Chaperones* 2000;5:76-86
- 59 Fernando P, Heikkila JJ. Functional characterization of Xenopus small heat shock protein, Hsp30C: the carboxyl end is required for stability and chaperone activity. *Cell Stress Chaperones* 2000;5:148-159
- 60 Asea A, Kabingu E, Stevenson MA, Calderwood SK. HSP70 peptidomimetic and peptide-negative preparations act as chaperokines. *Cell Stress Chaperones* 2000;5:425-431
- 61 Kedzierska S, Jezierski G, Taylor A. DnaK/DnaJ chaperone system reactivates endogenous E. coli thermostable FBP aldolase *in vivo* and *in vitro*; the effect is enhanced by GroE heat shock proteins. *Cell Stress Chaperones* 2001;6:29-37
- 62 Locke M. Heat shock transcription factor activation and hsp72 accumulation in aged skeletal muscle. *Cell Stress Chaperones* 2000;5:45-51
- 63 Mirkes PE. Molecular/cellular biology of the heat stress response and its role in agent-induced teratogenesis. *Mutat Res* 1997;396:163-173
- 64 Lang L, Miskovic D, Lo M, Heikkila JJ. Stress-induced, tissue-specific enrichment of hsp70 mRNA accumulation in Xenopus laevis embryos. *Cell Stress Chaperones* 2000;5:36-44
- 65 Martin CC, Tang P, Barnardo G, Krone PH. Expression of the chaperonin 10 gene during zebrafish development. *Cell Stress Chaperones* 2001;6:38-43
- 66 Todd MD, Lin X, Stankowski LF Jr, Desai M, Wolfgang GH. Chiron Corporation, Emeryville, CA. Toxicity Screening of a Combinatorial Library: Correlation of Cytotoxicity and Gene Induction to Compound Structure. *J Biomol Screen* 1999;4:259-268
- 67 Wood JD. Enteric nervous system in pathogenesis of gastrointestinal motility disorders. *Chin Natl J New Gastroenterol* 1996;2(Suppl 1):26-31
- 68 Schmelz M, Schmid VJ, Parrish AR. Selective disruption of cadherin/catenin complexes by oxidative stress in precision-cut mouse liver slices. *Toxicol Sci* 2001;61:389-394
- 69 Chen ZY, Yan MX, Xiang BK, Zhan HW. Alterations of gut hormones of blood and colonic mucosa in rats with chronic stress. *Shijie Huaren Xiaohua Zazhi* 2001;9:59-61
- 70 Lin H, LO M, Zhang YX, Wang BY, Fu BY. Induction of a rat model of alcoholic liver diseases. *Shijie Huaren Xiaohua Zazhi* 2001;9:24-28
- 71 Lo XH, Xie YH, Fu BY, Liu CR, Wang BY. Dynamic expression of tissue inhibitor of metallo- proteinase1 in alcoholic liver disease in rats. *Shijie Huaren Xiaohua Zazhi* 2001;9:29-33
- 72 Hoetzel A, Vagts DA, Loop T, Humar M, Bauer M, Pahl HL, Geiger KK, Pannen BH. Effect of nitric oxide on shock-induced hepatic heme oxygenase-1 expression in the rat. *Hepatology* 2001;33:925-937
- 73 Zhang BY, Zhu ZC, Ye FL, Fan YH. Effect of manganese on activity of nitric oxide synthase of filial rat's brain. *Weisheng Dulixue Zazhi* 1999;13:255-257
- 74 Burkart V, Liu H, Bellmann K, Wissing D, Jaattela M, Cavallo MG, Pozzilli P, Briviba K, Kolb H. Natural resistance of human beta cells toward nitric oxide is mediated by heat shock protein 70. *J Biol Chem* 2000;275:19521-19528

• BASIC RESEARCH •

Severe biliary complications after hepatic artery embolization

Xiao-Qiang Huang, Zhi-Qiang Huang, Wei-Dong Duan, Nin-Xing Zhou, Yu-Quan Feng

Xiao-Qiang Huang, Zhi-Qiang Huang, Wei-Dong Duan, Nin-Xing Zhou, Yu-Quan Feng, Department of Hepatobiliary Surgery, General Hospital of PLA, Beijing 100853, China

Correspondence to: Xiao-Qiang Huang, The General Hospital of PLA, 28 Fuxing Road, Beijing 100853, China. huangxq@ht.rol.cn.net
Telephone: +86-10-66937343

Received 2001-07-12 Accepted 2001-10-12

Abstract

AIM: To study the mechanism and treatment of severe biliary complications arising from hepatic artery embolization (HAE).

METHODS: Of seven cases of intra- and extrahepatic biliary damage resulting from hepatic artery embolization reported since 1987, 6 patients suffered from hepatic haemangioma, the other case was due to injection of TH compound into the hepatic artery during operation. The hepatic artery was injected with ethanol so as to evaluate the liver damage in experimental rats.

RESULTS: All the cases were found to have destructive damage of intra- and extrahepatic bile duct at the hilum with biliary hepatocirrhosis. Experimental results revealed necrosis of the liver parenchyma, especially around the portal tract and obliteration of intrahepatic bile duct.

CONCLUSIONS: To prevent the severe biliary complications of HAE, the use of HAE for hepatic haemangioma which was widely practiced in China, should be re-evaluated. Hepatic arterial embolization of hepatic haemangioma may result in severe destructive biliary damages and its indiscriminate use should be prohibited.

Huang XQ, Huang ZQ, Duan WD, Zhou NX, Feng YQ. Severe biliary complications after hepatic artery embolization. *World J Gastroenterol* 2002;8(1):119-123

INTRODUCTION

Hepatic artery embolization (HAE) has been used for the treatment of malignant tumors of the liver. At present, in Chinese literatures, HAE has been widely used for liver cancer therapy^[1-6]. Recent reports showed that the method has been advocated for the treatment of liver benign tumors especially in hepatic hemangioma^[7-15]. However, the value of HAE as well as the pitfalls of this form of treatment in hepatic hemangioma have not been fully evaluated. Some basic differences of hepatic hemodynamics between hepatic hemangioma and hepatic cell carcinoma^[16], may in turn affect the result of treatment. Severe complications after HAE for hepatic hemangioma had rarely been mentioned in the literature, therefore, such kind of non-operative treatment may be taken as an "innocuous" procedure and it has been used indiscriminately. Little attention to the biliary complications of HAE has been paid and the treatment of the biliary complication is a very knotty problem^[17]. We have treated 7 consecutive cases of severe destructive damages of the bile duct resulting from HAE from February 1987 to September 1999. In addition, damage of bile duct after HAE has been testified by a series

of animal experiments. This report reviews our experience in the treatment of severe biliary complications of HAE and the results of animal experiment.

MATERIALS AND METHODS

Animal experiment

Male and female Wistar rats (220g-280g) purchased from the Laboratory Animal Unit of the General Hospital of PLA, Beijing. All animals were reared on a standard laboratory diet, and tap water. They were kept in a room where the temperature (20°C±2°C), humidity (65%-70%), and day : night cycle (12:12 light:dark) were controlled.

Hepatic artery embolization

Ethanol (100%) was selected as the embolizing agent for the study. Hepatic artery embolization was performed under inhalant anesthesia. Branches of the abdominal aorta, and the branches from coeliac artery to spleen, stomach and duodenum were temporarily ligated. Ethanol (100%) with small amount of methylene blue was injected into the abdominal aorta with syringe, 0.2 milliliter ethanol for each rat. After the injection, the ligated arteries were loosened.

The animals lost appetite and 3/20 had obstructive jaundice after the operation. The rats were randomly divided into two groups, ten rats for each group.

Ten rats were killed 3 days (group A) after the embolization, the others were killed after 7 days (group B). Blood samples of Group A, Group B and control (abdominal operation but without ethanol injection) were collected for liver function test including glutamic pyruvic transaminase (GPT), glutamic oxaloacetic transaminase (GOT), bilirubin, alkaline phosphatase (ALP) and total bile acid (TBA). At the same time, the liver was removed and fixed in 10% formalin solution and embedded in paraffin. The specimens were sectioned and stained with hematoxylin-eosin (H&E).

Statistical analysis

The results were expressed as mean ±S.E. ($\bar{x} \pm S\bar{e}$).

RESULTS

Liver function changes

Changes of liver function differed among rats with or without jaundice after the embolization. GPT, GOT, ALP and TBA were significantly increased after HAE on the 3rd day and 7th day when compared with the control group, these changes seemed to be recovered on the 7th day (Table 1).

Table 1 Liver function changes ($\bar{x} \pm S\bar{e}$)

	GPT(U/L)	GOT(U/L)	TB(μmol/L)	DB(μmol/L)	ALP(U/L)	TBA(μmol/L)
Control	30±8	63±6	10±9	5±5	146±115	6±2
Group A	245±191	443±382	129±213	61±99	104±11	161±249
Group B	55±67	233±266	5±2	3±1	243±174	48±36

GPT=glutamic pyruvic transaminase, GOT= glutamic oxaloacetic transaminase, TB= total bilirubin, DB= direct bilirubin, ALP= alkaline phosphatase, TBA= total bile acid.

Pathological changes

Small yellowish necrosis patches can be seen by naked eyes in some lobes of the liver of groups A and B. There were small local necrotic areas in the liver parenchyma of groups A and B, the control group showed no liver necrosis. Most of the necrosis was located near the portal triad, the necrotic areas showed eosinophilic staining. The damaged areas presented coagulation necrosis of hepatocytes, where the hepatocytes showed uniformly eosinophilic, the liver cell plate was still visible but the hepatic cell nuclei disappeared. There was a clear borderline around the necrotic areas after the 7th day with infiltration of inflammatory cells. Most of the portal veinules remained normal, but the wall of the surviving artery was thickened and bile duct disappeared from the portal tract. Proliferation of small bile ducts was easily seen outside the necrotic areas (Figure 1). Obliteration of the bile duct with impairment of biliary drainage was responsible for the above findings.

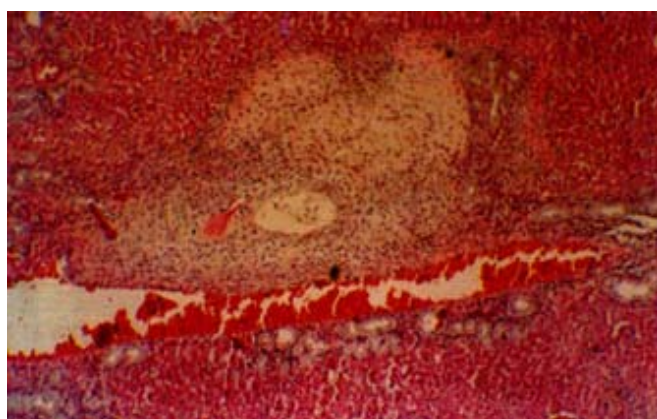


Figure 1 Liver necrosis after HAE in rats. The necrotic area is seen near the portal triad. HE×100

The above findings showed that the liver damage of HAE could be reproduced in animal experiment. Injecting ethanol through hepatic artery can certainly result in local necrosis of the liver, especially the biliary tract in the portal triads of the liver. Necrosis of portal triads or liver parenchyma will lead to biliary abscess formation and fibrosis of the liver.

CASE REPORTS

Case 1

A 55-year-old male was found to have a 4cm×4.5cm hemangioma in the right lobe of the liver during a routine physical examination in March 1989. He was advised to have his liver thrombosed. HAE with iodized oil 10ml and sodium morrhuate 4ml were injected with Seldinger technique. He felt severe abdominal pain at once after the injection. Pain was not relieved until 5 days after the embolization. Intense vomiting appeared 20 min after the embolization, and persisted for 4 days. Obstructive jaundice appeared after 20 days. Percutaneous transhepatic cholangiogram (PTC) showed changes of the right and left hepatic duct. Occlusion of extrahepatic bile duct was noted in July 1989. Ultrasound showed dilatation of the gallbladder and fluid accumulated around the gallbladder. Gallbladder necrosis with segmental bile duct necrosis were confirmed at operation on July 29, 1989. Cholecystectomy, partial hepatic bile duct excision and choledochocholedochostomy with T-tube stenting were performed. Serum icterus index descended from 90U to 20U with T-tube kept in place for two years. He was admitted to the General Hospital of PLA, Beijing, because of biliary cirrhosis, portal hypertension, enlarged spleen and ascites in 1994. Due to severe hepatocirrhosis, atrophy of the right lobe of the liver and portal hypertension, reconstructive biliary operation was deemed to be unsafe unless the portal pressure has been lowered down. So he was to under go staged

operation, the first operation consisted of splenectomy and splenicocaval shunt on June 9, 1994. Hepatocholedochojejunostomy was performed 6 months afterwards. The patient remained well without jaundice since the last operation.

Case 2

A 55-year-old female was found to have a large mass (5cm×6cm) in the right lobe of liver in June 1996, but she experienced no remarkable symptoms. Nevertheless, HAE was performed with ethanol (100%) following doctor's advice. The patient suffered from irregular fever and epigastric pain after the HAE. Ultrasound showed liver abscess formation two months later. She was still febrile and appeared toxic in spite of drainage of bile containing pus by a percutaneous catheter. Laparotomy and liver abscess drainage were performed three months later. But jaundice reappeared 4 months after the operation. Computed tomography scan showed left hepatic duct dilatation, and infective necrotic lesion of unhomogenous density in the right lobe of the liver. Fistulography through the right liver drainage tube showed abnormal communication between the drainage tract and the extrahepatic bile duct, as well as a duodenal fistula. Hepatectomy, hepatocholedocho-jejunostomy and U-tube stenting were performed 4 months later in April 1997. Jaundice disappeared after the operation. The stenting tube was maintained for one and half years. She recovered after withdrawal of the tube.

Case 3

A 62-year-old woman was found to have an asymptomatic hemangioma (10cm×9cm) in the right liver by ultrasound in December 1994. HAE was advised and performed with iodized oil and sodium morrhuate. Persisted epigastric pain followed the procedure. Ultrasound and CT showed cystic lesions (5.6cm×6.1cm) in the left lobe of the liver 2 months later (Figure 2). The patient had had repeated attacks of high fever with chills, and antibiotics administration was not effective. She was admitted with the diagnosis of biliary multi-abscesses of the liver. A transcatheter catheter was placed with drainage of about 180-200 mL bile each day. The last operation was performed in June 1996. A large amount of bile stained necrotic tissue along the portal tract on both sides of the liver was removed. During the operation, the normal intrahepatic ducts were found destroyed. The right and left liver parenchyma was atrophied while the caudate lobe became hypertrophied. A fibrous stricture band was present around the common hepatic duct. The stricture band was removed and U-tube stents were placed during the operation. Jaundice disappeared 2 years after the operation.

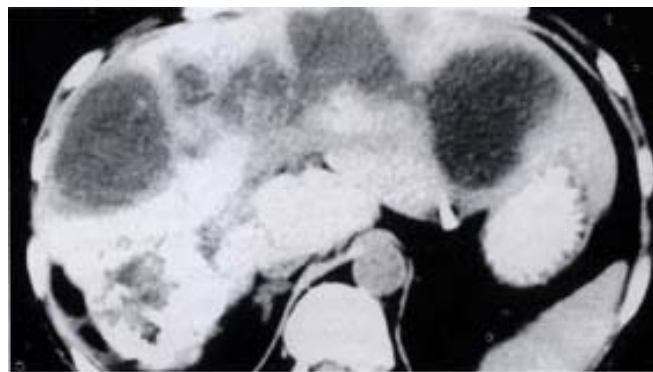


Figure 2 Biliary abscess of liver after HAE. CT shows multi-abscess along portal tract.

Case 4

A 24-year-old female was diagnosed having a space occupying lesion in the right liver. She was operated upon in 1987. Multiple nodular lesions were found in her right liver, which were supposed to be

metastatic nodules. A nodule was taken for pathological sections, and the hepatic artery was ligated and methacrylate (TH glue) was injected through distal end of the hepatic artery during operation. The postoperative course was very stormy. She developed continued abdominal pain with high fever and jaundice after the operation. The abdominal X-ray showed that the branches of the left, and right hepatic artery and gastroduodenal artery were embolized. However, the tissues from the right lobe of the liver was inflammatory in nature pathologically. Seven months later, she was admitted to the General Hospital of PLA, and PTC showed that stricture of hilar bile duct and the left hepatic duct with diffuse fibrosis in the perihilar region and necrosis of the right liver and the gallbladder. GI examination revealed an internal fistula between the first portion of duodenum and hepatic hilum. The operation undertaken was very difficult. However, the intestinal fistula was repaired, anastomosis of the dilated segment III bile duct and a long Roux-en-Y jejunal loop was created with a U-tube stent. The tube was removed 11/2 years later. The patient recovered from the operation. She delivered a child two years later, but eventually, the patient died of hepatocellular carcinoma 5 years after the operation.

Case 5

A 60-year-old male was found to have a hepatic hemangioma (5cm×5cm) in 1994. CT examination in 1998 showed an increase in the size of the tumor. HAE was advised and performed with iodized oil, steel wire ring and pingyangmycinum in July 1998. Persistent epigastric pain occurred for 3 days after the procedure, followed by jaundice and fever with gray colored stool 20 days later. This condition was aggravated 4 months later. The patient when seen was suffering from continual high fever and deep jaundice and was admitted to the hospital in January 1999. Diagnoses of hepatic abscesses and gallbladder necrosis after the embolization were made. ERCP showed extensive hepatic bile duct stricture (Figure 3), which was thought to be not amenable to surgery. The patient was treated conservatively.



Figure 3 Intrahepatic bile duct stricture after HAE. ERCP shows biliary stricture.

Case 6

A 43-year-old female was found to have a liver hemangioma in October 1998. HAE was performed which was complicated by severe abdominal pain and repeated vomiting for a week, and jaundice occurred 3 months later. Antibiotic therapy was effective. The patient was admitted with the diagnosis of obstructive jaundice in September 1999. MRI showed gallbladder necrosis perforation and with fluid collection around it (Figure 4). Intrahepatic bile ducts were dilated. A hemangioma (3cm×3.5cm) in the right lobe of the liver was still seen. The gallbladder was found to be necrotic, and the abscess cavity communicated with the common bile duct as seen at operation. Cholecystectomy, and T tube stenting were performed. Jaundice disappeared after the operation.



Figure 4 MRI showed fluid around the gallbladder.

Case 7

A 43-year-old man was found to have a hemangioma of the right liver during physical examination in June 1993. HAE was advised and was performed using iodized oil and sodium morrhuate. Serious epigastric pain occurred immediately after the embolization. Jaundice appeared in July 1995. He was then operated upon, three coagulated blood coagula were taken out during choledochostomy. The patient was reoperated in June 1996. Choledochenterostomy and drainage of the III segmental duct were performed in January 1998. An external bile fistula was formed and biliary drainage of 300 mL was given each day but jaundice did not subside. The patient was admitted for operation in September 1999, marked biliary cirrhosis and atrophy of right lobe were found at operation. Cholangioenterostomy of the dilated III segmental duct and T tube stenting were performed. Jaundice subsided very slowly after the operation.

DISCUSSION

Blood supply of the hepatic duct and mechanism of bile duct injury in HAE

Branches of intrahepatic bile duct, artery and portal vein come together in the same Glisson sheath in the portal tract. Arterioles from the hepatic artery form a dense capillary network around the bile duct, which is the so-called peribiliary plexus. Therefore, only a small portion of hepatic arterial blood directly enters the sinusoids. The blood supply of the bile duct and structure of portal tract comes completely from hepatic artery. Hence, the intrahepatic bile duct receives unique nutrient blood supply from the hepatic artery in contrast to the double blood supply of hepatic cell^[18-25]. Therefore, damages of the biliary system are more severe than the liver cell in hepatic arterial embolization. Clinically, continuous hepatic artery infusion of FUDR is expected to cause development of permanent stricture of the biliary system^[26]. The complication was thought to be the result of regional drug toxicity and biliary vascular embolism. The end result is sclerosing cholangitis and diffuse fibrosis as well as scarring of biliary tree. Stapleton *et al*^[27] in the study of the blood supply of the right and left hepatic ducts found that the peribiliary plexus of the caudate lobe has bilateral artery blood supply. This may be the reason for atrophy of right and left lobes but accompanied with hypertrophy of the caudate lobe after HAE injury which was consistently found in the cases in this report.

Hemangioma occurs more frequently in the right liver lobe and stricture of hilar hepatic duct was found in the HAE of right lobe lesions as shown in this report. This is explained by the finding that hilar bile duct blood supply chiefly derived from right hepatic and cystic arteries^[28-30].

Sodium morrhuate is commonly used as a vascular sclerosing agent^[31-33], but it is a strong irritant, it can cause local tissue necrosis and inflammation as well as complete occlusion of large blood

vessels in the injecting area. It was used for sclerosing therapy of varicosity vein and it is scarcely used for HAE. Four cases in this report used sodium morrhuate as the sclerosent, resulting in liver necrosis and abscess formation. We are of the opinion that the use of sclerosing drug as an embolizing agent in HAE is very dangerous.

Ethanol caused protein coagulation and damage of vascular endothelium which causes thrombosis and obstruction of blood vessel^[34-36]. In this report, one case received ethanol as the embolizing agent. Animal experiment demonstrated that ethanol causes intrahepatic biliary obliteration and acute liver focal necrosis in the rat model.

Surgical treatment

Cases in this report have the following characteristics of: ① 6/7 cases were hepatic hemangiomas and strong destructive embolizing agents were employed; ②clinically, all patients presented persistent abdominal pain following the procedure; ③all resulted in extensive hepatic necrosis and damage of the biliary tree, hepatic biliary abscesses developed after the embolization; ④ damage of the intra- and extra-hepatic biliary system was destructive, it was difficult to rehabilitate the patients and a prolonged hospitalization is needed.

Treatment of the complications after HAE: Liver parenchyma necrosis was distributed along the portal tract after the HAE. Because of the disruptive effect of sclerosing agent on the biliary tract and the focal necrosis liver cells, some of the liver cells near the foci of necrosis are still secreting bile, the end result is biliary abscess forming in the necrosed area. The bile duct in its entire course may be completely destroyed. The damaged hepatic lobe will eventually be atrophied. Necrosis and fibrous stricture often consequently involve the hepatic duct bifurcation as well as the left hepatic duct, which results in obstructive jaundice in the end. In late cases, when complicated with biliary cirrhosis and portal hypertension, restorative biliary surgery is very difficult. Under such conditions, it is our experience that the treatment needs to be divided into several steps. The first step is the drainage of bile collection and removal of necrotic tissue to control the infection. First step of treatment is to improve patients'ä general status as well as the local condition by maintaining biliary drainage. Treatment of the second step is hepatotomy and necrotic tissue elimination. If biliary stricture is of perihilar type, operation to relieve hilar bile duct stricture and Roux-en-Y hepatocholecho-jejuno-stomy and place U tubes for stenting are necessary^[37-41]. If patients are complicated with biliary cirrhosis and portal hypertension, preliminary operation of portal pressure decompression, for example spleno-renal shunt is often needed before the difficult biliary restoration operation is attempted^[42]. If bile ducts were badly damaged, bilateral biliary drainage with U tubes is a better alternative.

To prevent severe biliary complications of HAE, the use of HAE for hepatic hemangioma should be re-evaluated and the indiscriminate use of sclerosing agents in HAE should be prohibited.

REFERENCES

- Jia YC, Tian JM, Wang ZT, Chen D, Ye H, Liu Q, Yang JJ, Sun F, Lin L, Lu JP, Wang F, Cheng HY. A retrospective review on interventional treatment of 10000 cases of liver cancer. *Huaren Xiaohua Zazhi* 1998;6:2-3
- Ji XL, Liu YX, Wang YH, Zhao H. Histopathological study of hepatocellular carcinoma after transcatheter hepatic arterial

- embolization. *China Natl J New Gastroenterol* 1996;2:79-81
- Zheng CS, Feng GS, Zhou RM, Liang B, Liang HM, Zhen J, Yu JM, Liu H. Hepatic arterial infusion chemotherapy and embolization in the treatment of primary hepatic carcinoma. *China Natl J New Gastroenterol* 1997;3:104-107
- Fan J, Ten GJ, He SC, Guo JH, Yang DP, Weng GY. Arterial chemoembolization for hepatocellular carcinoma. *World J Gastroenterol* 1998;4:33-37
- Cheng XM, Luo PF, Shao PJ, Zhou ZJ, Ma Z. Analysis of the Cause of Death after Chemoembolization for Liver Cancer. *Jieru Yixue Zazhi* 1997;2: 11-13
- Huang FG, Li Y, Xie XD. Side effects and complications of hepatic arterial infusion and embolization of liver carcinoma in aged patients and its management. *World J Gastroenterol* 1998;4:67-68
- Li GW, Zhao ZR, Li BS, Liu XG, Wang ZL, Liu QF. Source of blood supply of liver cavernous hemangioma and sclerosis and embolization treatment. *China Natl J New Gastroenterol* 1997;3: 147-149
- Xie ZG, Wang ZD. Blood supply of hepatic cavernous haemangioma and interventional treatment. *Xinxiaohuabingxue Zazhi* 1996; 4:46-48
- Li Y, Li S. An experiment study of sodium morrhuate as an agent for arterial embolization. *Zhonghua Fangshe Zazhi* 1987;21:357-360
- Jiang XX. Hepatic artery embolization in treatment of huge cavernous hemangioma. *Zhonghua Fangshe Zazhi* 1992; 26:88-90
- Yan XF, He JG, Song HZ, Zhao CZ. Interventional therapy of hepatic cavernous hemangioma. *Zhonghua Waikexue Zazhi* 1994;32: 563-564
- Panis Y, Fagniez PL, Cherqui D, Roche A, Schaaill JC, Jaeck D. Successful arterial embolization of giant liver hemangioma. Report of a case with five-year computed tomography follow-up. *HPB-Surg* 1993; 7:141-146
- Li GW, Zhao ZR, Li BS, Liu XG, Wang ZL, Liu QF. Embolization therapy and its mechanism of cavernous hemangioma of liver. *Shanxi Yixue Zaizhi* 1993; 22:515-517
- Li IQ, Li JL, Wu S, Liang ST, Liao QH. Fifteen cases lipidol embolization treatment of hepatic cavernous haemangioma. *Zhonghua Shiyianwaikexue Zazhi* 1994; 14:1-3
- Li GW, Liu XG, Li BS, Wang ZL, Le XB, Wang Y, Liu QF, Gao H. Study of sclerosing treatment of liver haemangioma. *Zhonghua Shiyianwaikexue Zazhi* 1992;9:1-3
- Zhou Runsu, Qiao Hongqing, Deng Jinglan, Huo JP, Ma XR. Analysis of radioimage of hepatic artery perfusion in patients with hepatic space-occupying lesions. *Zhongguo Zhongliu Linchuang* 1995; 22:381-383
- Huang XQ, Huang ZQ, Duan WD, Zhou NX, Feng YQ. Destructive damage of bile duct of hepatic artery embolization in treatment of hepatic cavernous haemangioma. *Junyijingxiu xueyan Xuebao* 2000; 21:88-91
- Jing JG, Wang CL, Han MJ, Yang MW. The experimental study of local blood flow and pathologic changes after embolization of portal vein branch with two kinds of embolic materials. *Zhongguo Yikedaxue Xuebao* 1995;24:602-604
- Wang X, Zhong YX, Zhang LL, Huang YX, Wen QS, Chu YK, Zhang HX, Wang QL. Effect of IL-8 and ET-1 on secondary liver injury by hepatic arterial embolization in rabbits. *Shijie Huaren Xiaohua Zazhi* 2000;8:413-416
- Motta PM. The three-dimensional microanatomy of the liver. *Arch Histol Jap* 1984;47:1-30
- Huang XQ. Changes of liver microcirculation in cirrhosis and biliary obstruction. *Guowaiyixue Waikexue Fence* 1986;6:321-323
- Huang XQ, Yang KZ, Huang ZQ, Ying GQ, Wang BZ. An experiment study of liver microcirculation after ligation bile duct. *Zhonghua Shiyianwaikexue Zazhi* 1987; 4:151-154
- Compagno J, Grisham JW, Louis St. Scanning electron microscopy of extrahepatic biliary obstruction. *Arch Pathol* 1974;97: 348-351
- Bosch J, Enriquez R, Groszmann RJ, Storer EH. Chronic bile duct ligation in the dog: Hemodynamic characterization of a portal hypertensive model. *Hepatology* 1983;3:1002-1007
- Jones AL, Schmuker DL. Current concepts of liver structure as related to function. *Gastroenterology* 1977;73:833-851
- Margaret K M, Hector B, Blayney D W, Cecchi G, Goldberg D A, Leong L A, Margolin K A, Terz J J. Sclerosing cholangitis after continuous hepatic artery infusion of FUDR. *Ann Surg* 1985; 202: 176-181
- Stapleton GN, Hickman R, Jerblanche J. Blood supply of the right and left hepatic ducts. *Br J Surg* 1998;85:202-207
- Zheng JF, Sun FL, Yu XF, Dou YC. Transhepatic arterial

- chemoembolization using lipiodol and ischemic injury to the gallbladder. *Linchuang Waike Zazhi* 1998; 6: 270-271
- 29 Wang X, Huang YX, Wen QS, Cu YK, Li DY, Zhang HX, Zhang JZ, Wang YD. Experimental study on gastric mucosal injury by hepatic arterial embolization in rabbits. *Huaren Xiaohua Zazhi* 1998; 6:997-999
 - 30 Chen WJ, Ying DJ, Liu ZJ, Liu ZJ, He ZP. Analysis of the arterial supply of the extrahepatic bile ducts and its clinical significance. *Clinical Anatomy* 1999;12:245-249
 - 31 Zhang TL, Cheng HH, Hou KY, Yan NS. Necrosis of the gastric wall after alpha-cyanoacrylate embolization of gastric coronary vein. *Beijing Yikedaxue Xuebao* 1996; 28:452-453
 - 32 Jing YC, Yang ZD, Ding HY, Ma FC. Pathological changes of perivascular tissues after gastric and hepatic vascular embolization with medical TH tissue adhesive in rabbits. *Linchuang Yushiyang Binglixue Zazhi* 1997; 13: 51-52
 - 33 Lu MD, Chen JW, Xie XY, Liang LJ, Huang JF. Portal vein embolization by fine needle ethanol injection: experimental and clinical studies. *World J Gastroenterol* 1999;5:506-510
 - 34 Lu MD, Yin YY, Ren W. A study of portal vein embolization with absolute ethanol injection in cirrhotic rats. *World J Gastroenterol* 1998; 4:415-417
 - 35 Lu MD, Liang LJ, Peng BG, Ren W. Study of portal vein embolization with ethanol injection in cirrhotic rats. *Zhonghua Shiyian Waike Zazhi* 1998; 15: 75-76
 - 36 Lu MD, Chen JW, Xie XY, Liang LJ, Huang JF. Portal vein embolization by fine needle ethanol injection: experimental and clinical studies. *World J Gastroenterol* 1999;5:506-510
 - 37 Liu YX, Huang ZQ, Zhou YB, Chai ZJ, Qiang GX, Chi YB, Han BL, He ZP, Zhang QZ, Tu JM. Surgical treatment of injury bile duct strictures. *Puwai Linchuang* 1986;234-237
 - 38 Huang ZQ. New development of biliary surgery in China. *World J Gastroenterol* 2000;6:187-192
 - 39 Wang J, Liu YU, Huang ZQ, Feng YQ, Zhou NX, Gu WQ, Duan YP, Huang XQ, Zhang WZ. Surgical treatment of 42 cases of traumatic strictures of bile duct. *Gandanyipi Waike Zazhi* 1995; 1:81-84
 - 40 Huang ZQ. Surgical treatment of biliary obstruction in posterior segment of the right lobe. *Zhonghua Waike Zazhi* 1988;26: 593-597
 - 41 Huang XQ, He ZP, Zhou YB, Zhong JC, Guo ZY, Feng YQ. Repair biliary stricture used mucous segments with blood supply. *Zhonghua Waike Zazhi* 1986; 24:523-526
 - 42 Huang ZQ, Zai JX, Han BL, Qian GX. Surgical treatment of bile duct strictures with portal hypertension. *Zhonghua Waike Zazhi* 1979;17:351-356

Edited by Ma JY

• BASIC RESEARCH •

Lipopolysaccharide induced synthesis of CD14 proteins and its gene expression in hepatocytes during endotoxemia

Sheng-Wei Li, Jian-Ping Gong, Chuan-Xin Wu, Yu-Jun Shi, Chang-An Liu

Sheng-Wei Li, Jian-Ping Gong, Chuan-Xin Wu, Yu-Jun Shi, Chang-An Liu, Department of General Surgery, The Second College of Clinical Medicine & the Second Affiliated Hospital of Chongqing University of Medical Sciences, Chongqing 400010, China

Supported by the National Natural Science Foundation of China (No. 39970719)

Correspondence to: Sheng-Wen Li, Department of General Surgery, The Second College of Clinical Medicine & the Second Affiliated Hospital of Chongqing Medical University, 74 Linjiang Road, Central District, Chongqing 400010, China. lswgg@163.com

Telephone: +86-23-63849075-2100

Received 2001-08-23 Accepted 2001-09-05

Abstract

AIM: To observe synthesis of CD14 protein and expression of CD14 mRNA in hepatic tissue and hepatocytes of rats during endotoxemia.

METHODS: The endotoxemia model of Wistar rat was established by injection of a dose of lipopolysaccharide (LPS) ($5\text{mg}\cdot\text{kg}^{-1}$, *Escherichia coli* O111:B4) via the tail vein, and then the rats were sacrificed after 3, 6, 12 and 24 h in batches. Hepatocytes were isolated from normal and LPS-injected rats by in situ collagenase perfusion technique and were collected to measure the expression of CD14 mRNA and synthesis of CD14 protein by reverse transcript-polymerase chain reaction (RT-PCR) or Western blot analysis. The binding of fluorescein isothiocyanate (FITC)-CD14 polyclonal antibody to isolated hepatocytes was also assessed by flow cytometric analysis (FCM).

RESULTS: In the rats with endotoxemia, the expressions of CD14 mRNA in hepatic tissue and isolated hepatocytes were stronger at 3, 6, and 12 h than that in control rats (3.48 ± 0.15 , 5.89 ± 0.62 , 4.33 ± 0.18 , vs 1.35 ± 0.14 in hepatic tissue, $P<0.01$; 4.12 ± 0.17 , 6.24 ± 0.64 , 4.35 ± 0.18 , vs 1.87 ± 0.15 in hepatocytes, $P<0.01$). The synthesis of CD14 protein in hepatic tissue and isolated hepatocytes increases also obviously in 6 and 12 h when compared to that in control rats (13.27 ± 1.27 , 17.32 ± 1.35 , 11.42 ± 1.20 , vs 7.34 ± 0.72 in hepatic tissue, $P<0.01$; 14.68 ± 1.30 , 17.95 ± 1.34 , 11.65 ± 1.19 , vs 7.91 ± 0.70 in hepatocytes, $P<0.01$). FCM showed that mean fluorescence intensity (MFI) and numbers of FITC-CD14 positive cells in the rats with endotoxemia increased obviously at 3, 6, 12 and 24 h when compared with normal control group (43.4%, 70.2%, 91.4%, 32.6% vs 4.5%, $P<0.01$).

CONCLUSION: LPS can markedly promote the synthesis of CD14 protein and up-regulate the expression of CD14 mRNA in isolated hepatocytes and hepatic tissue. Liver might be a main source for soluble CD14 production during endotoxemia.

Li SW, Gong JP, Wu CX, Shi YJ, Liu CA. Lipopolysaccharide induced synthesis

of CD14 proteins and its gene expression in hepatocytes during endotoxemia. *World J Gastroenterol* 2002;8(1):124-127

INTRODUCTION

CD14 is a glycosylphosphatidylinositol-anchored lipopolysaccharide (LPS) receptor, and first reported to be a differentiation marker expressed on the surface of macrophages, neutrophils and other myeloid lineage cells^[1,2]. Recent works have shown that the CD14 antigen is expressed in many types of cell and tissues^[3-8]. But it is not yet clear whether hepatocytes can express CD14 protein and gene. Hepatocytes are the major source of most acute-phase proteins. If in fact soluble CD14 (sCD14) is an acute-phase protein, then hepatocytes might be expected to express CD14, which is upregulated during endotoxemia^[9-11]. Furthermore, hepatocytes isolated from endotoxemic animals exhibit markedly enhanced responses to LPS, raising the possibility that these cells may express CD14^[3,4,12-14]. To determine whether hepatocytes express CD14, our experiments were to observe the synthesis of CD14 protein and expression of CD14 mRNA in hepatocytes and hepatic tissue of rats during endotoxemia and to verify hepatocytes as a main source for soluble CD14 (sCD14) production.

MATERIALS AND METHODS

Reagents

LPS (*Escherichia coli* O111:B4) and type IV of collagenase were purchased from Sigma Chemical Company (St. Louis, Mo.). An anti-CD14 polyclonal antibody was purchased from Santa Cruz Biotechnology (Santa Cruz, Calif.). SP Reagent boxes and fluorescein isothiocyanate (FITC)-IgG were purchased from Zhongshan Biotechnology Company (Beijing, China).

Animals

Male Wistar rats, which were pathogen-free and weighed approximately 250 g each, were purchased from the Animal Center of Chongqing University of Medical Science. The rats were exposed each day 12 h of light and darkness. Rodent chow and water were provided ad libitum. Experimental protocols were approved by the Institutional Care and Use Committee of the Chongqing university of Medical Science.

The endotoxemia model of animals

The acute endotoxemia model of Wistar rat was established as described by Li SW, *et al*^[4]. In brief, animals were injected with a dose of LPS ($5\text{mg}\cdot\text{kg}^{-1}$, *Escherichia coli* O111:B4) via the tail vein, and then the rats were sacrificed at 3, 6, 12 and 24 h respectively. There were six rats at each time point, and other six animals were used as controls (0 h).

Hepatocyte Isolation

Hepatocytes were isolated from normal and LPS-injected rats by an in situ collagenase perfusion technique, modified as described previously^[15, 16]. In brief, livers were removed after a portal vein

perfusion with Hanks' balanced salt solution (HBSS) and the homogenate was digested in a solution of $0.5\text{g}\cdot\text{L}^{-1}$ collagenase. Hepatocytes were separated from the nonparenchymal cells by two cycles of differential centrifugation (50g for 2 min) and further purified over a 30% Percoll gradient. Hepatocyte purity exceeded 90% as assessed by light microscopy, and viability was typically greater than 95% as determined by trypan blue exclusion assay.

RNA Isolation and Complementary DNA Synthesis

Total RNA was isolated from rat liver tissue and hepatocytes by using the TRIZOL Reagent (Life Technologies, USA). The quality of RNA was controlled by the intactness of ribosomal RNA bands. A total of 0.5mg of each intact total RNA samples was reverse-transcribed to complementary DNA (cDNA) by using the reverse transcription-polymerase chain reaction (RT-PCR) kit (Roche, USA). cDNA was stored at -70°C until polymerase chain reaction (PCR) analysis.

Determination of CD14 mRNA by RT-PCR

The PCR primers used were CD14: sense ($5'$ -CTCAACCTAGAGCCGTTTCT- $3'$), anti-sense ($5'$ -CAGGATTGTCAGACAGGTCT- $3'$); β -actin: sense ($5'$ -ACCACAG-CTGAGAGGGAAATCG- $3'$), anti-sense ($5'$ -AGAGGTCTTTACGGATGTCAACG- $3'$). The sizes of the amplified PCR products were 267 bp for CD14 and 281 bp for β -actin. The conditions for amplification were as follows: denaturation at 93°C for 1 min, annealing at 57°C for 1 min, and extension at 70°C for 2 min for 30 cycles. The PCR products were electrophoresed in $20\text{g}\cdot\text{L}^{-1}$ agarose gels, and the gels were ethidium bromide stained and video photographed on an ultraviolet transilluminator, and the results were showed with the relative absorbance (Ar: relative optical density, ROD).

Western blot analysis of CD14 protein

Cultured hepatocytes were washed twice with phosphate-buffered saline (PBS), pelleted by centrifugation. Cell pellets were resuspended in 50 μl of lysis buffer containing 20 $\text{mmol}\cdot\text{L}^{-1}$ HEPES (pH 7.9), 25% glycerol, $0.42\text{ mmol}\cdot\text{L}^{-1}$ NaCl, $15\text{ mmol}\cdot\text{L}^{-1}$ MgCl_2 , $0.2\text{ mmol}\cdot\text{L}^{-1}$ EDTA, $0.5\text{ mmol}\cdot\text{L}^{-1}$ phenylmethylsulfonyl fluoride (PMSF) and $0.5\text{ mmol}\cdot\text{L}^{-1}$ dithiothreitol (DTT). After three freeze-thaw cycles, cell lysates were centrifuged at 12000g for 30 min, and the supernatant was saved. The liver tissue was homogenized with homogenizer before the freeze-thaw lysis, as described above for cultured hepatocytes. For Western blot analysis, samples (20 μg per lane) were separated on an SDS- $100\text{g}\cdot\text{L}^{-1}$ polyacrylamide gel and transferred to nitrocellulose membrane. The membrane was sequentially blocked in PBS-Tween ($1\text{g}\cdot\text{L}^{-1}$) containing $50\text{ml}\cdot\text{L}^{-1}$ milk and then incubated with 5 μg of anti-rat CD14 polyclonal antibody per mL, washed three times, and further incubated with a goat anti-rabbit immunoglobulin G horseradish peroxidase-conjugated secondary antibody. Blocking and antibody incubations each lasted 1 h at room temperature. After several washes, the membrane was developed with DAB reagent, and the results were showed with relative absorbance Ar (relative optical density, ROD).

Flow cytometric analysis (FCM)

Expression of CD14 protein in hepatocytes was examined by FCM. In brief, hepatocytes were incubated with the anti-CD14 polyclonal antibody ($0.1\text{mg}\cdot\text{L}^{-1}$) after washing, cells were incubated with goat anti-rabbit immunoglobulin G labeled with FITC, after being washed three times, and 10000 cells were analyzed by flow cytometry (Coulter, USA).

Statistical Analysis

All results were expressed as $\bar{x}\pm s$. Statistical difference between means were determined by using Student's *t* test. A *P* value of <0.01 was considered significant.

RESULTS

Expression of CD14 mRNA in liver tissue and hepatocytes

We postulated that hepatocytes and hepatic tissue could express CD14 gene which could be upregulated during endotoxemia. Rats were injected with LPS and total RNA was extracted from freshly isolated and purified hepatocytes and hepatic tissue at different time points indicated. RT-PCR analysis showed that hepatocytes and liver tissue from controls had low but detectable levels of CD14 mRNA. LPS treatment showed steady-state CD14 mRNA levels in hepatocytes, inducing a threefold elevation by as early as 3 h after LPS treatment. The levels increased with times, reaching a maximum of six-fold by 6 h after treatment, and subsequently declined to near baseline levels by 24 h. We also examined the CD14 mRNA levels in RNA isolated from hepatic tissue during endotoxemia and found that the pattern of CD14 mRNA induction by LPS was similar to that of the isolated hepatocytes, indicating that the upregulation of CD14 mRNA was not likely to be simply a consequence of the hepatocyte isolation procedure (Figure 1).

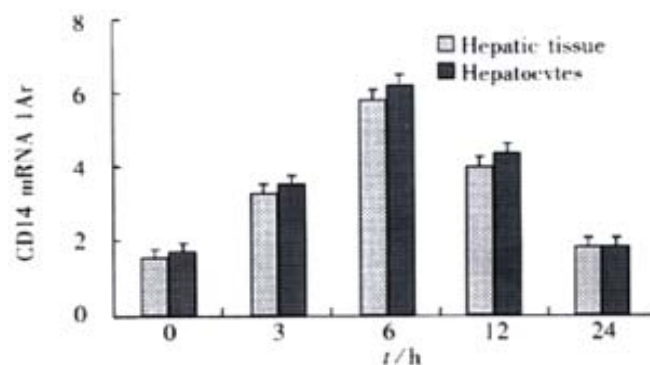


Figure 1 Expression of CD14 mRNA in hepatic tissue and hepatocytes $P<0.01$, vs 0 h.

CD14 protein expression in hepatocytes and hepatic tissue

To determine if the upregulation of CD14 expression could also be appreciated in protein levels, Western blot analysis was performed on both hepatocytes and hepatic tissue sample from LPS-treated animals or control animals. In hepatocytes extracts, increases of CD14 protein were seen 6 h after LPS treatment, peaked at 12 h, and declined thereafter. A similar increase of CD14 protein in hepatic tissue was observed. there were significantly different when compared with control animals ($P<0.01$, Figure 2).

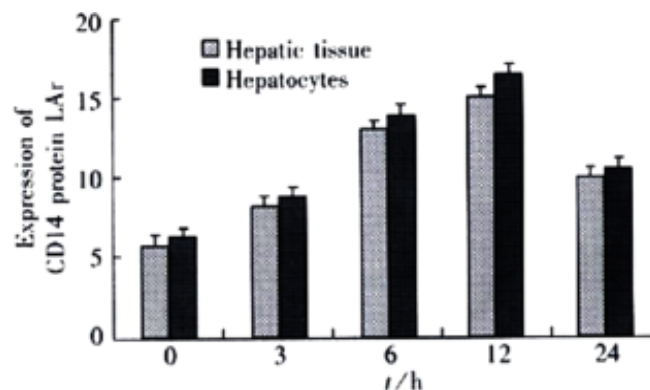


Figure 2 Expression of CD14 protein in hepatic tissue and hepatocytes $P<0.01$, vs 0 h

Binding of FITC to Hepatocytes

To confirm the expression of CD14 on hepatocytes, we also examined the binding of FITC to the cells. FITC-CD14 positive cells were 4.5% in rats of normal group. But in rats with endotoxemia, the mean fluorescence intensity (MFI) increased, the numbers of FITC-CD14 positive cells were 43.4%, 70.2%, 91.4%, and 32.6%, respectively in 3, 6, 12 and 24 h after stimulation of LPS. There was significant difference when compared to normal group animals ($P < 0.01$, Figure 3).

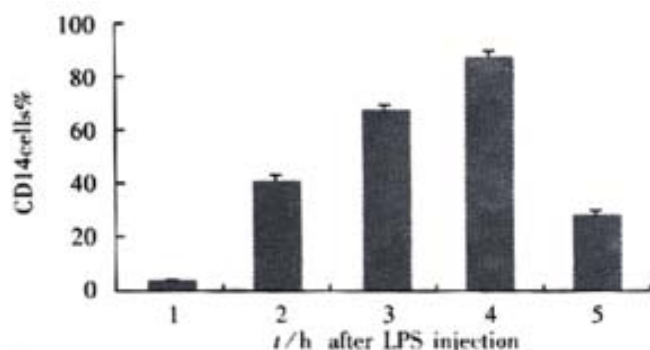


Figure 3 Percentage of CD14 positive cells $P < 0.01$, vs 0 h.

DISCUSSION

CD14 was first described as a myeloid differentiation antigen in 1980^[1]. It is a 55-kDa glycoprotein with multiple leucine-rich repeats and is encoded on chromosome (5q) together with growth factors, such as granulocyte macrophage colony stimulating factor. CD14 has been identified as a receptor for complexes of LPS and LPS-binding protein but it also binds other bacterial products^[17-22]. The LPS-binding region within the CD14 molecule is remarkably conserved across species with a high degree of gene sequence homology, and it has therefore been suggested that CD14 is a pattern recognition receptor^[17,23-25]. CD14 as a key LPS signaling molecule was reported to be expressed mainly in the monocyte-macrophages system^[1,26-29]. Recent works have shown that the CD14 antigen is expressed in many types of cells and tissues^[5-8,12]. But it is not yet clear whether hepatocytes express CD14. Although shedding from leukocytes has been proposed as the major source of sCD14 in blood, it is likely that other sources exist^[3,5,30-32]. Some reports suggested that sCD14 behaves like other acute-phase proteins^[9-11,33-36]. Hepatocytes are the major source of most acute-phase proteins. So we think if sCD14 is an acute-phase protein, then hepatocytes might be expected to express CD14 gene and synthesize CD14 protein, which is upregulated during endotoxemia^[37-40].

To determine whether hepatocytes synthesize CD14 protein and express CD14 gene, we measured steady-state CD14 protein and its mRNA both *in vivo* and *in vitro*. We found that: ① isolated hepatocytes and liver tissue could synthesize basal levels of CD14 protein and express basal levels of CD14 gene and that synthesis and expression of CD14 were markedly upregulated by LPS during endotoxemia; these results are in agreement with previous report^[41,42]; ② synthesis of CD14 protein and expression of CD14 mRNA in both Hepatocytes and liver tissue indicated that such synthesis and expression were not likely to be simple a consequence of hepatocyte isolation procedure; ③ in liver, besides hepatocytes, nonparenchymal cells such as Kupffer cells, endothelial cells, neutrophils and other cells can also express CD14 gene and synthesize CD14 protein^[4,43-47], but the fact that both isolated hepatocytes and hepatic tissue expressed CD14 protein and its mRNA indicated that the nonparenchymal cells could hardly have any effect on such expression in liver tissue.

Although we do not provide direct evidence here that sCD14 in plasma originates from hepatocytes during endotoxemia, our results showed that there was the possibility that the liver is an important source for sCD14 during endotoxemia. Pan *et al*^[5] found that the liver is one of the major organs for the production of soluble CD14. Liu *et al*^[41,42] reported also that CD14 transcription rates were significantly increased in hepatocytes from LPS-treated rat, indicating that the upregulation in CD14 mRNA levels observed in rats hepatocytes after LPS treatment was dependent, in part, on increased transcription, and their observations supported the idea that sCD14 would be an acute-phase protein and hepatocytes might be a source for circulating sCD14 production^[3,4,8,48-52]. Our data indicate that hepatocytes from LPS-stimulated rats express higher amounts of CD14 gene and CD14 protein, and may release more sCD14. Further investigation of the expression of CD14 in hepatocytes is actively ongoing in our laboratory.

In summary, our *in vitro* and *in vivo* data indicate that hepatocytes can synthesize CD14 protein and express CD14 mRNA and their synthesis and expression are upregulated effectively by LPS during endotoxemia. Liver is a main source for sCD14 production during sepsis or endotoxemia.

REFERENCES

- Lichtman SN, Wang J, Lemasters JJ. LPS receptor CD14 participates in release of TNF-alpha in RAW 264.7 and peritoneal cells but not in kupffer cells. *Am J Physiol* 1998;275:G39-46
- Fearns C, Ulevitch RJ. Effect of recombinant interleukin-1beta on murine CD14 gene expression *in vivo*. *Shock* 1998;9:157-163
- Su GL, Dorko K, Strom SC, Nussler AK, Wang SC. CD14 expression and production by human hepatocytes. *J Hepatol* 1999;31:435-442
- Li SW, Wu CX, ShiYJ, Liu CA. Lipopolysaccharide upregulates expression of CD14 gene and CD14 proteins of hepatocytes in rats. *Zhonghua Ganzangbing Zazhi* 2001;9:103-104
- Pan Z, Zhou L, Hetherington CJ, Zhang DE. Hepatocytes contribute to soluble CD14 production, and CD14 expression is differentially regulated in hepatocytes and monocytes. *J Biol Chem* 2000;275:36430-36435
- Ahmed AF, Nio M, Ohtani H, Nagura H, Ohi R. In situ CD14 expression in biliary atresia: comparison between early and late stages. *J Pediatr Surg* 2001;36:240-243
- Furusako S, Takahashi T, Mori S, Takahashi Y, Tsuda T, Namba M, Mochizuki H. Protection of mice from LPS-induced shock by CD14 antisense oligonucleotide. *Acta Med Okayama* 2001;55:105-115
- Jersmann HP, Hii CS, Hodge GL, Ferrante A. Synthesis and surface expression of CD14 by human endothelial cells. *Infect Immun* 2001;69:479-485
- Patino R, Ibarra J, Rodriguez A, Yague MR, Pintor E, Fernandez-Cruz A, Figueredo A. Circulating monocytes in patients with diabetes mellitus, arterial disease, and increased CD14 expression. *Am J Cardiol* 2000;85:1288-1291
- Choi YH, Lee WH, Lee Y, Kim JK, Lee SY, Park JE. Correlation between monocyte and T-lymphocyte activation markers in patients with acute coronary syndrome. *Jpn Heart J* 2000;41:605-615
- Gluck T, Silver J, Epstein M, Cao P, Farber B, Goyert SM. Parameters influencing membrane cd14 expression and soluble cd14 levels in sepsis. *Eur J Med Res* 2001;6:351-358
- Nanbo A, Nishimura H, Muta T, Nagasawa S. Lipopolysaccharide stimulates HepG2 human hepatoma cells in the presence of lipopolysaccharide-binding protein via CD14. *Eur J Biochem* 1999;260:183-191
- Fang WH, YaoYM, Shi ZG, YuY, WuY, Lu LR, Sheng ZY. Significance of the expressions of lipopolysaccharide binding protein mRNA and lipopolysaccharide receptor CD14mRNA in the liver of burned rat. *Zhonghua Shaoshang Zazhi* 2000;16:157-160
- Jiang JX, Xie GQ, Chen YH, Liu DW, Zhou JH, Zhu PF, Wang ZG, Zhang HJ. Expression of scavenger receptor and CD14 on Kupffer cells and its relationship with endotoxin-induced hepatic injury. *Zhonghua Chuangshang Zazhi* 2000;16:478-481
- Gong JP, Xu MQ, LiK. Expression of CD14 in Kupffer's cells induced by Lipopolysaccharide. *Di-San Junyi Daxue Xuebao* 2001;23:425-428
- Gong JP, Hun BL. Isolation, culture and identification of live cells. *Shijie Huaren Xiaohua Zazhi* 1999;7:417-419
- Bernardo J, Billingslea AM, Blumenthal RL, Seetoo KF, Simons ER, Fenton MJ. Differential responses of human mononuclear phagocytes to mycobacterial lipoarabinomannans: role of CD14 and the mannose

- receptor. *Infect Immun* 1998;66:28-35
- 18 Means TK, Lien E, Yoshimura A, Wang S, Golenbock DT, Fenton MJ. The CD14 ligands lipopolysaccharide and lipopolysaccharide differ in their requirement for Toll-like receptors. *J Immunol* 1999;163:6748-6755
 - 19 Hetherington CJ, Kingsley PD, Crocicchio F, Zhang P, Rabin MS, Palis J, Zhang DE. Characterization of human endotoxin lipopolysaccharide receptor CD14 expression in transgenic mice. *J Immunol* 1999;162:503-509
 - 20 Fang WH, Yao YM, Shi ZG, Yu Y, Wu Y, Lu LR, Chang GY, Sheng ZY. Gene expression of lipopolysaccharide receptor CD14 and tumor necrosis factor- α in rats after thermal injury. *Zhonghua Waike Zazhi* 1999;37:271-273
 - 21 Ben DF, Huan JN, Yang Y, Wang L, Chen YL, Xia ZF. Increased expression of peritoneal macrophage CD14 in severely burned mice. *Zhonghua Shaoshang Zazhi* 2000;16:96-99
 - 22 Peng Z, Zhang ZX, Xu YJ. Expressions of CD11c, CD14 and TGF- β 1 mRNA in alveolar macrophages in chronic bronchitis. *Zhonghua Weishengwuxue He Mianyixue Zazhi* 2000;20:408-410
 - 23 Gong JP, Hum BL. Role of CD14 in activation of Kupffer cell induced by lipopolysaccharide. *Shijie Huaren Xiaohua Zazhi* 1999;7:875-877
 - 24 Su GL, Rahemtulla A, Thomas P, Klein RD, Wang SC, Nanji AA. CD14 and lipopolysaccharide binding protein expression in a rat model of alcoholic liver disease. *Am J Pathol* 1998;152:841-849
 - 25 Heumann D, Adachi Y, Le Roy D, Ohno N, Yadomae T, Glauser MP, Calandra T. Role of plasma, lipopolysaccharide-binding protein, and CD14 in response of mouse peritoneal exudate macrophages to endotoxin. *Infect Immun* 2001;69:378-385
 - 26 Devitt A, Moffatt OD, Raykundalia C, Capra JD, Simmons DL, Gregory CD. Department of Immunology, University of Birmingham Medical School, UK. Human CD14 mediates recognition and phagocytosis of apoptotic cells. *Nature* 1998;392:442-443
 - 27 Peppelenbosch MP, DeSmedt M, ten Hove T, van Deventer SJ, Grooten J. Lipopolysaccharide regulates macrophage fluid phase pinocytosis via CD14-dependent and CD14-independent pathways. *Blood* 1999;93:4011-4018
 - 28 Liu S, Morris SM Jr, Nie S, Shapiro RA, Billiar TR. cAMP induces CD14 expression in murine macrophages via increased transcription. *J Leukoc Biol* 2000;67:894-901
 - 29 Stelter F, Witt S, Furl B, Jack RS, Hartung T, Schutt C. Different efficacy of soluble CD14 treatment in high- and low-dose LPS models. *Eur J Clin Invest* 1998;28:205-213
 - 30 Hiki N, Berger D, Prigl C, Boelke E, Wiedeck H, Seidelmann M, Staib L, Kaminishi M, Oohara T, Beger HG. Endotoxin binding and elimination by monocytes: secretion of soluble CD14 represents an inducible mechanism counteracting reduced expression of membrane CD14 in patients with sepsis and in a patient with paroxysmal nocturnal hemoglobinuria. *Infect Immun* 1998;66:1135-1141
 - 31 Hiki N, Berger D, Dentener MA, Mimura Y, Buurman WA, Prigl C, Seidelmann M, Tsuji E, Kaminishi M, Beger HG. Changes in endotoxin-binding proteins during major elective surgery: important role for soluble CD14 in regulation of biological activity of systemic endotoxin. *Clin Diagn Lab Immunol* 1999;6:844-850
 - 32 Bessler H, Komlos L, Punsky I, Ntambi JA, Bergman M, Straussberg R, Sirota L. CD14 receptor expression and lipopolysaccharide-induced cytokine production in preterm and term neonates. *Biol Neonate* 2001;80:186-192
 - 33 Wang SC, Klein RD, Wahl WL, Alarcon WH, Garg RJ, Remick DG, Su GL. Tissue coexpression of LBP and CD14 mRNA in a mouse model of sepsis. *J Surg Res* 1998;76:67-73
 - 34 Imai K, Takeshita A, Hanazawa S. Transforming growth factor-beta inhibits lipopolysaccharide-stimulated expression of inflammatory cytokines in mouse macrophages through downregulation of activation protein 1 and CD14 receptor expression. *Infect Immun* 2000;68:2418-2423
 - 35 Liu S, Salyapongse AN, Geller DA, Vodovotz Y, Billiar TR. Hepatocyte toll-like receptor 2 expression *in vivo* and *in vitro*: role of cytokines in induction of rat TLR2 gene expression by lipopolysaccharide. *Shock* 2000;14:361-365
 - 36 Hiki N, Berger D, Mimura Y, Frick J, Dentener MA, Buurman WA, Seidelmann M, Kaminishi M, Beger HG. Release of endotoxin-binding proteins during major elective surgery: role of soluble CD14 in phagocytic activation. *World J Surg* 2000;24:499-506
 - 37 van Oosten M, van de Bilt E, van Berkel TJ, Kuiper J. New scavenger receptor-like receptors for the binding of lipopolysaccharide to liver endothelial and Kupffer cells. *Infect Immun* 1998;66:5107-5112
 - 38 Kono H, Wheeler MD, Rusyn I, Lin M, Seabra V, Rivera CA, Bradford BU, Forman DT, Thurman RG. Gender differences in early alcohol-induced liver injury: role of CD14, NF-kappaB, and TNF-alpha. *Am J Physiol Gastrointest Liver Physiol* 2000;278:G652-661
 - 39 Jiang S, Naito M, Kaizu C, Kuwata K, Hasegawa G, Mukaida N, Shultz LD. Lipopolysaccharide-induced cytokine and receptor expression and neutrophil infiltration in the liver of osteopetrosis (op/op) mutant mice. *Liver* 2000;20:465-474
 - 40 Jiang J, Xie G, Chen Y, Liu D, Qiu J, Zhou J, Zhu P, Wang Z. Intrahepatic expression of scavenger receptor and CD14 and their relationship with local inflammatory responses in endotoxemia in mice. *Shock* 2001;16:75-80
 - 41 Liu S, Khemlani LS, Shapiro RA, Johnson ML, Liu K, Geller DA, Watkins SC, Goyert SM, Billiar TR. Protein Expression of CD14 by hepatocytes: upregulation by cytokines during endotoxemia. *Infect Immun* 1998;66:5089-5098
 - 42 Liu S, Shapiro RA, Nie S, Zhu D, Vodovotz Y, Billiar TR. Characterization of rat CD14 promoter and its regulation by transcription factors AP1 and Sp family proteins in hepatocytes. *Gene* 2000;250:137-147
 - 43 Netea MG, Kullberg BJ, van der Meer JW. Lipopolysaccharide-induced production of tumour necrosis factor and interleukin-1 is differentially regulated at the receptor level: the role of CD14-dependent and CD14-independent pathways. *Immunology* 1998;94:340-344
 - 44 Toshima K, Mochida S, Ishikawa K, Matsui A, Arai M, Ogata I, Fujiwara K. Contribution of CD14 to endotoxin-induced liver injury may depend on types of macrophage activation in rats. *Biochem Biophys Res Commun* 1998;246:731-735
 - 45 Lukkari TA, Jarvelainen HA, Oinonen T, Kettunen E, Lindros KO. Short-term ethanol exposure increases the expression of Kupffer cell CD14 receptor and lipopolysaccharide binding protein in rat liver. *Alcohol Alcohol* 1999;34:311-319
 - 46 Yin M, Ikejima K, Wheeler MD, Bradford BU, Seabra V, Forman DT, Sato N, Thurman RG. Estrogen is involved in early alcohol-induced liver injury in a rat enteral feeding model. *Hepatology* 2000;31:117-123
 - 47 Song PI, Abraham TA, Park Y, Zivony AS, Harten B, Edelhauser HF, Ward SL, Armstrong CA, Ansel JC. The Expression of Functional LPS Receptor Proteins CD14 And Toll-Like Receptor 4 in Human Corneal Cells. *Invest Ophthalmol Vis Sci* 2001;42:2867-2877
 - 48 Su GL, Rahemtulla A, Thomas P, Klein RD, Wang SC, Nanji AA. CD14 and lipopolysaccharide binding protein expression in a rat model of alcoholic liver disease. *Am J Pathol* 1998;152:841-849
 - 49 Fang W, Yao Y, Shi Z. The effect of bactericidal/permeability-increasing protein on lipopolysaccharide-binding protein and lipopolysaccharide receptor CD14 mRNA expression in rats after thermal injury. *Zhonghua Yi Xue Za Zhi* 1999;79:289-291
 - 50 Wang F, Wang LY, Wright D, Parmely MJ. Redox imbalance differentially inhibits lipopolysaccharide-induced macrophage activation in the mouse liver. *Infect Immun* 1999;67:5409-5416
 - 51 Jarvelainen HA, Orpana A, Perola M, Savolainen VT, Karhunen PJ, Lindros KO. Promoter polymorphism of the CD14 endotoxin receptor gene as a risk factor for alcoholic liver disease. *Hepatology* 2001;33:1148-1153
 - 52 Urbaschek R, McCuskey RS, Rudi V, Becker KP, Stickel F, Urbaschek B, Seitz HK. Endotoxin, endotoxin-neutralizing-capacity, sCD14, sICAM-1, and cytokines in patients with various degrees of alcoholic liver disease. *Alcohol Clin Exp Res* 2001;25:261-268

• BASIC RESEARCH •

Multivariate regression analysis on early mortality after orthotopic liver transplantation

Ye-Ben Qian, Gui-Hua Cheng, Jie-Fu Huang

Ye-Ben Qian, Department of hepatic biliary surgery, first affiliated hospital An Hui Medical University, HeFei 230022, Anhui Province, China

Gui-Hua Cheng, Jie-Fu Huang, Organ transplantation center, first affiliated hospital, Sun Yat-Sen University of Medical Sciences, GuangZhou 510089 Guangdong Province China

Supported by clinic major project foundation of minister of health, No. 97040230

Correspondence to: Dr Ye-Ben Qian, Department of hepatic biliary surgery, first affiliated hospital An Hui Medical University, HeFei 230022, Anhui Province, China. ayqianyb@163.net
Telephone: +86-551-5129029

Received 2001-05-30 Accepted 2001-10-26

Abstract

AIM: To identify the risk factors relating to early mortality after orthotopic liver transplantation.

METHODS: Clinical data of 37 adult patients undergoing liver transplantation were retrospectively collected and divided into two groups: the survived group (survival time ≥ 30 d) and the death group (survival time < 30 d). The relationship between multivariate risk factors and early mortality after orthotopic liver transplantation were analyzed by stepwise logistic regression.

RESULTS: The survival rate was 73%. Early mortality rate was 27%. APACHE III, preoperative serum creatinine level and intraoperative bleeding quantity had a significant independent association with early mortality. ($R=0.1841$, 0.2056 and 0.3738).

CONCLUSION: APACHE III, preoperative serum creatinine level and intraoperative bleeding quantity are significant risk factors relating to early mortality after orthotopic liver transplantation. To improve the recipient's preoperative critical condition and renal function and to reduce intraoperative bleeding quantity could lower the early mortality after orthotopic liver transplantation.

Qian YB, Cheng GH, Huang JF. Multivariate regression analysis on early mortality after orthotopic liver transplantation. *World J Gastroenterol* 2002;8(1):128-130

INTRODUCTION

In recent years, the success rates of orthotopic liver transplantation (OLT) have improved markedly as a result of rapid advances in immunosuppressions, surgical and preservation techniques. One-year survival rate after liver transplantation exceeds 80%. Orthotopic liver transplantation, as an accepted treatment for end-stage liver disease, has been widely performed in the world^[1-5]. In our country, the early mortality after OLT remains relatively high and current studies have focused on the improvement of survival rate after liver transplantation^[6,7]. Clinical data of 37 adult patients undergoing liver transplantation were retrospectively collected in our study. The significant risk factors relating to early mortality after OLT were analyzed and determined, which may contribute to the selection of candidate and improvement of survival in patients with liver

transplantation.

MATERIALS AND METHODS

Materials

Thirty-seven adult patients undergoing OLT procedures at our transplantation center from September 1993 to January 2000 were studied. The study population consisted of 32 men and 5 women with a mean age of 39.8 (range 17-64) years. The grafts were obtained from donors. Indications for liver transplantation were end-stage liver cirrhosis ($n=9$), fulminant hepatic failure ($n=8$), primary liver cancer ($n=14$), primary sclerosing cholangitis ($n=2$), Willson's disease ($n=1$), polycystic liver and kidney ($n=1$), hepatoma ($n=1$), and cholangiocarcinoma ($n=1$).

Multiple risk factors

Thirty-seven patients were divided into two groups: survival group (survival time ≥ 30 d) and death group (Survival time < 30 d). There were different possible risk factors relating to early mortality after liver transplantation including preoperative, intraoperative and postoperative ones. Preoperative information consisted of age, APACHE III, hepatoencephalopathy, previous abdominal surgery, serum albumin, prothrombin time (PT), serum creatinine level (Cr), serum Aspartate transaminase (AST), white blood cells counts (WBC), platelet counts (PLC) and mismatch ABO group. Intraoperative information included heat ischemic time, cold ischemic time, anhepatic time and bleeding quantity. Postoperative information included rate of acute rejection and postoperative complications rate (including biliary leakage, cytomegalovirus (CMV) infection, hepatic artery thrombosis, hydrothorax and myocardial infarction, etc).

Statistical methods

Experimental data were presented as $\bar{x} \pm s$ and frequency. For continuous data, independent 2-tailed t tests were used to determine whether there were significant differences between the two groups. Pearson's Chi-square statistics were used to test differences in all frequencies. Data with significant difference were entered into a stepwise logistic regression analysis. And all of the statistical calculations were performed using the SPSS (version: 9.0, Chicago, USA).

RESULTS

Twenty-seven of the 37 adult patients survived more than one month after liver transplantation. Early survival rate was 73% while early mortality was 27%. The other 10 patients died postoperatively within 30 d and the major cause for their death were disseminated intravascular coagulation (DIC $n=2$), myocardial infarction ($n=2$), acute renal failure ($n=2$), hepatic artery thrombosis ($n=1$), cerebral bleeding ($n=1$) and adult respiratory distress syndrome (ARDS) ($n=1$).

Comparison between the survival group and the death group showed significant differences only in terms of age, APACHE III, serum creatinine level, PT, was PLC and intraoperative bleeding quantity, ($P < 0.05$, Table 1). The stepwise logistic regression were used to create the best statistical model relating to early mortality after transplantation. The factors that had significant independent

associations with early mortality after the stepwise procedure were APACHE III, serum creatinine level and intraoperative bleeding quantity, with regression coefficients of 0.1841, 0.2056 and 0.3738, respectively (Table 2).

Table 1 Risk factors relating to early mortality after liver transplantation

Risk factors	Survival group (n=27)	Death group (n=10)	P value
Age(yrs)	38.3±2.5	47.8±2.2	0.0000
Previous abdominal surgery	11% (3/27)	30% (3/10)	0.3130
APACHE III (score)	40.5±6.7	63.4±12.9	0.0000
Hepatoencephalopathy	15% (4/27)	40% (4/10)	0.1712
Serum creatinine level (μmol·L ⁻¹)	82.2±10.8	132.8±33.2	0.0000
AST (nkat·L ⁻¹)	97.9±18.6	125.8±80.5	0.0951
Albumin (g·L ⁻¹)	36.9±1.7	32.7±2.9	0.0000
TB (imol·L ⁻¹)	298.3±67.9	314.9±87.1	0.5447
PT /s	22.5±3.2	25.5±3.7	0.0175
WBC/ (×10 ⁹ ·L ⁻¹)	7.3±1.2	6.8±1.1	0.2351
PLC / (×10 ⁹ ·L ⁻¹)	129.5±17.5	53.4±12.3	0.0000
Dismatch ABO group	7.3% (2/27)	30% (3/10)	0.1102
Heat ischemic time /min	3.8±0.1	3.9±0.3	0.1478
Cold ischemic time /s	464.9±26.9	471.2±46.3	0.6104
Anhepatic time/s	87.5±4.9	90.3±10.5	0.2704
Intraoperative bleeding quantity /ml	5615.1±1003.7	12263.6±3606.1	0.0000
Rate of acute rejection	18% (5/27)	20% (2/10)	1.0000
Rate of postoperative complications	59% (16/27)	70% (7/10)	0.709

Table 2 Stepwise logistic regression analysis

Variable	B	SE	Wald	df	Sig	R
APACHE III	0.340	0.0141	5.8481	1	0.0156	0.1841
Serum creatinine level (Cr)	3.6542	1.4013	6.8002	1	0.0091	0.2056
Intraoperative bleeding quantity	2.0194	0.7516	7.2182	1	0.0020	0.3738

DISCUSSION

Orthotopic liver transplantation is a treatment for end-stage liver disease. Early mortality was below 10%^[8,9], which remains high in our country. The serious preoperative condition of recipient and the late timing for operation may account for this result^[10,11]. A number of investigators have examined the factors associated with outcome after liver transplantation including PT, APACHE III and so on^[12-16]. In our study, 10 of 37 patients died postoperatively, with an early mortality of 27%. After analyzed with stepwise logistic regression, APACHE III, preoperative serum creatinine level (Cr) and intraoperative bleeding quantity showed significant associations with early mortality after liver transplantation.

While APACHE III score is a best predictor of mortality^[17,18,19], APACHE III that results from the addition of 3 groups of variables (acute physiology, age and chronic health) consists of multiple organ function evolution, including heart, lung, liver, kidney, brain, etc. It is more accurate than APACHE III. And now it has been widely used to evaluate the severely ill in patients' condition and to predict the mortality of patients^[20,21]. In our study, the APACHE III score was 40.5±6.7 and 63.4±12.9 in the survival group and the death group respectively. There was a statistical difference between the two groups in APACHE III score, $P < 0.001$. The stepwise logistic regression analysis showed a significant independent association with early mortality after transplantation, with a regression coefficient of 0.1841. As one of the main risk factors, it can act as a reference index of the selection of recipient and timing for operation. However because it is not specific to liver function, it needs combination with other indexes when used to predict outcome of OLT.

Renal dysfunction is a common dangerous complication in patients with end-stage liver disease. It results from acute tubular necrosis and caused by hepatorenal syndrome^[22-25]. Gunning^[26] reported a significant decrease of 43% in glomerular filtration rate (GFR) during transplantation in patients with normal renal function. Both high preoperative serum creatinine level and intraoperative venovenous bypass can lead to renal hemodynamic instability during operation^[27,28,29]. The postoperative nephrotoxic immunosuppressions can also contribute to the irreversible renal insufficiency, leading to renal failure after liver transplantation^[30,31]. In our study, 2 of 10

patients died of renal failure, who were all along with high preoperative serum creatinine level and hepatorenal syndrome before transplantation. A significant difference was found between the survival group and the death group was shown in serum creatinine level ($P < 0.001$), with a mean of 82±11 and 133±33, respectively. The stepwise logistic regression analysis, it also showed a statistical independent association with early mortality after liver transplantation, with a regression coefficient of 0.2056. It is also a main risk factor which predicts early mortality after OLT. It is very important to correct renal malfunction before transplantation. How to prevent and treat renal failure Kuse^[32] reported that Urotilatin can treat acute renal failure following OLT. Gonwa and the other investigators^[33-36] reported that renal failure need dialysis. Our principles were to avoid using nephrotoxic treatments and drugs, to maintain stable hemodynamically and monitor central venous pressure, to use small dose of Dopamine (2-5 μg·kg⁻¹·min⁻¹) and Procaine to dilate renal artery and protect renal function, to use diuretics appropriately, to perform hemodialysis properly performed if needed, and not to use Alprostadil (PGE₁)^[37].

Intraoperative bleeding quantity is the third important risk factor relating to early mortality after liver transplantation^[38]. If it exceeded 1000ml, mortality was very high. The intraoperative bleeding quantity of the death group was more than that of the survival group statistically ($P < 0.05$), with a mean of 12264±3606mL and 5615±1004mL respectively. Logistic regression analysis showed a significant relationship between intraoperative bleeding quantity and early mortality after transplantation, with a regression coefficient of 0.3738. Severe bleeding and a large amount of transfusion during operation may lead to hemodynamic instability and DIC. And long-term hypoplasia may accelerate preoperative renal insufficiency, leading to irreversible renal failure, and increasing the early mortality after operation^[39,40]. Intraoperative severe bleeding may due to previous upper abdominal surgery, abdominal extensive adhesions, portal hypertension, splenic hyperfunction, severe coagulation disorders, etc.^[41-44]. In our study, there was no significant difference between the two groups with previous surgical histories. But it should be emphasized that some of our findings might be accidental because of insufficient cases involved in the study. We should pay attention to these patients with previous surgical histories. In these patients, severe bleeding and coagulation disorders may occur during operation because of abdominal extensive adhesions and difficulties in sequestration and ligation, consequently DIC and acute renal failure may follow. In our centre, 2 patients developed DIC.

The other risk factors showed no significant associations with early mortality after liver transplantation. But some of the factors did influence the outcome of the recipients and should be considered carefully, including mismatch ABO group, heat ischemic time, cold ischemic time, rate of acute rejection, rate of postoperative complications, etc.^[45-51]. Except emergent cases, the recipients and the donors were matched in ABO group at our center. Heat ischemic time and cold ischemic time were also limited strictly within 5 min and 12 h respectively during operation. After transplantation, ultrasonography B, chest X-ray examination, CMV detection and liver biopsy were performed periodically. Acute rejection and other postoperative complications were diagnosed and treated earlier. In patients diagnosed as having acute rejection, a large dose of methylprednisolone and FK506 were administered with a treatment rate of 100%. Therefore, these risk factors showed no significant value in statistical analysis in our study.

REFERENCES

- Starzl TE, Demetris AJ. Liver transplantation: a 31-year perspective. *Curr Probl Surg* 1990; 27:55-106
- Bismuth H, Farges O, Castaing D, Samuel D, Adam R, Johann M, Azoulay D, Feray C, Astarciglu I, Saliba F. Evaluation of results of liver transplantation: Experience based on a series of 1052 transplantation. *Presse Med* 1995; 24:1106-1110

- 3 Parrilla P, Sanchez-Bueno F, Figueras J, Jaurrieta E, Mir J, Margarit C, Lazaro J, Herrera L, Gomez-Fleitas M, Varo E, Vicente E, Robles R, Ramirez P. Analysis of the complications of the piggy-back technique in 1,112 liver transplants. *Transplantation* 1999; 67: 1214-1217
- 4 Ryckman FC, Alonso MH, Bucuvalas JC, Balistreri WF. Long-term survival after liver transplantation. *J Pediatr Surg* 1999; 34: 849-850
- 5 Goss JA, Shackleton C, Farmer D, Amout W, Seu P, Markowitz J, Martin P. Orthotopic liver transplantation for primary sclerosing cholangitis-a 12 year, single-center experience. *Ann Surg* 1997; 225: 472-481
- 6 Xia SuiSheng. Current status of liver transplantation in China. *Shijie Huaren Xiaohua Zazhi* 1999;7:645-646
- 7 Huang Jiefu. Organ transplantation in china: current status and strategy. *ZhongHua Waike Zazhi* 1999; 37:535-537
- 8 Doyle HR, Marino IR, Jabbour N,Zetti G, McMichael J, Mitchell S, Fung J, Starzl TE. Early death or retransplantation in adults after orthotopic liver transplantation. *Transplantation* 1994; 57:1028-1036
- 9 Deschenes M, Belle SH, Krom RA, Zetterman RK, Lake JR. Early allograft dysfunction after liver transplantation. *Transplantation* 1998; 66: 302-310
- 10 Chung SW, Kirkpatrick AW, Kim HL, Scudamore CH, Yoshida EM. Correlation between physiological assessment and outcome after liver transplantation. *Am J Surg* 2000; 179: 396-399
- 11 Spanier TB, Klein RD, Nasraway SA, Rand WM, Rohrer RJ, Freeman RB, Schwaitzberg SD. Multiple organ failure after liver transplantation. *Crit Care Med* 1995; 23: 466-473
- 12 Baliga P, Merion RM, Turcotte JG, Ham JM, Henley KS, Lucey MR, Schork A, Yushyr R, Campbell DA Preoperative risk factor assessment in liver transplantation. *Surgery* 1992; 112:704-711
- 13 Cillo U, Tedeschi U, Carraro P, Burra P, Varagnolo M, Ambrosino G, Cionfoli M, Brolese A,Borin L, Zanus G. Early predictive markers of irreversible graft dysfunction After liver transplantation. *Transplant Proc* 1994; 26: 3599-3601
- 14 Bein T, Frhlich D, Pmsl J, Forst H, Pratschke E. The predictive value of four scoring systems in liver transplant recipients. *Intensive Care Med* 1995; 21: 32-37
- 15 Clavien PA, Camargo CA, Croxford R, Langer B, Levy GA, Greig PD. Definition and classification of negative outcomes in solid organ transplantation. Application in liver transplantation. *Ann Surg* 1994; 220: 109-120
- 16 Ricci P, Therneau TM, Malinchoc M, Benson JT, Petz JL, Klintmalm GB, Crippin JS. A prognostic Model for the outcome of liver transplantation in patients with cholestatic liver disease. *Hepatology* 1997; 25: 672-677
- 17 Angus DC, Clermont G, Kramer DJ, Linde-Zwirble WT, Pinsky MR. Short-term and long-term outcome prediction with the Acute Physiology and Chronic Health Evaluation II system after orthotopic liver transplantation. *Crit Care Med* 2000; 28:150-156
- 18 Sawyer RG, Durbin CG, Rosenlof LK, Pruett TL. Comparison of APACHE II scoring in liver and kidney transplant recipients versus trauma and general surgical patients in a single intensive-care unit. *Clin Transplant* 1995;9:401-405
- 19 Bein T, Forst H, Pratschke E. Apache-II-scoring in the liver transplant recipient. *Intensive Care Med* 1992; 18:60-61
- 20 Knaus WA, Wagner DP, Draper EA, Zimmerman JE, Bergner M, Bastos PG, Sirio CA, Murphy D, Tedlotring MS, Damiano A MS, Harrell. The APACHE c6 prognostic system risk prediction of hospital mortality for critically hospitalized adults. *Chest* 1991; 100:1619-1636
- 21 Bernal W, Wendon J, Rela M, Heaton N, Williams R. Use and outcome of liver transplantation in acetaminophen-induced acute liver failure. *Hepatology* 1998; 27:1050-1055
- 22 Fraley DS, Burr R, Bernardini J, Angus D, Kramer DJ, Johnson JP. Impact of acute renal failure on mortality in end-stage liver disease with or without transplantation. *Kidney Int* 1998; 54:518-522
- 23 Alvares-da-Silva MR, Waechter FL, Francisconi CF, Barros E, Thome F, Traiber C, Fonseca DL, Zingani JM,Sampaio JA, Pinto RD, Pereira-Lima L. Risk factors for postoperative acute renal failure at a new orthotopicliver transplantation program. *Transplant Proc* 1999; 31: 3050-3052
- 24 Palapattu GS, Barbaric Z, Rajfer J.Acute bilateral renal cortical necrosis as a cause of postoperative renal failure. *Urology* 2001; 58:281
- 25 Kes P. Hepatorenal syndrome: new perspectives in pathophysiology and management. *Acta Med Croatica* 2000; 54:165-173
- 26 Gunning TC, Brown MR, Swygert TH, et al. Perioperative renal function in patients undergoing orthotopic liver transplantation. *Transplantation* 1991; 51: 422-427
- 27 Lafayette RA, Paré G, Schmid CH, King AJ, Rohrer RJ, Nasraway SA. Pretransplant renal dysfunction predicts poorer outcome in liver transplantation. *Clin Nephrol* 1997; 48:159-164
- 28 Thomas G, Kelly D, Norris S, Crosby O, Hegarty J, Crowley K, McEntee G, Traynor O, Watson A, Keogh B Acute renal failure in orthotopic liver transplantation. *Ir J Med Sci* 1996; 165:271-273
- 29 Pascual E, Gomez-Arnau J, Pensado A, de la Quintana B, Carrera A, Arribas MJ, Garcia-Guiral M, Cuervas- Mons V. Incidence and risk factors of early acute renal failure in liver transplant patients. *Transplant Proc* 1993; 25:1837
- 30 Platz KP, Mueller AR, Blumhardt G, Bachmann S, Bechstein WO, Kahl A, Neuhaus P. Nephrotoxicity following orthotopic liver transplantation. A comparison between cyclosporine and FK506. *Transplantation* 1994; 58:170-178
- 31 Van Buren D, Payne J, Geevarghese S, MacDonell R, Chapman W, Wright JK, Helderma JH, Richie R, Pinson CW. Renal function in primary liver transplant recipients receiving neoral (cyclosporine) versus prograf (tacrolimus). *Transplant Proc* 1998; 30:1401-1402
- 32 Kuse ER, Meyer M, Constantin R, Oldhafer K, Schlitt HJ, Schulz-Knappe P, Uberbacher HJ, Pichlmayr R, Forssmann WG. Urodelatin (INN: ularitide). A new peptide in the treatment of acute kidney failure following liver transplantation. *Anaesthesist* 1996; 45:351-358
- 33 Gonwa TA, Mai ML, Melton LB, Hays SR, Goldstein RM, Levy MF, Klintmalm GB.Renal replacement therapy and orthotopic liver transplantation: the role of continuous veno-venous hemodialysis. *Transplantation* 2001; 71:1424-1428
- 34 L'htkes P, Lutz J, Loock J, Daul A, Broelsch C, Philipp T, Heemann U. Continuous venovenous hemodialysis treatment in critically ill patients after liver transplantation. *Kidney Int Suppl* 1999;72:S71-74
- 35 Richardson D. Dialysis in non-renal organ (liver) transplantation. *Nephron* 2001;88:296-306
- 36 Morales JM. Management and prevention of acute renal failure in solid organ transplantation. *Ren Fail* 1996; 18:481-488
- 37 Manasia AR, Leibowitz AB, Miller CM, Silverstein JH, Schwartz M, Delguidice R, Vallabhajosula S, Oropello JM, Benjamin E. Postoperative intravenous infusion of alprostadil (PGE1) does not improve renal function in hepatic transplant recipients. *J Am Coll Surg* 1996; 182:347-352
- 38 Nasraway SA, Klein RD, Spanier TB, Rohrer RJ, Freeman RB, Rand WM, Benotti PN. Hemodynamic correlates of outcome in patients undergoing orthotopic liver transplantation. Evidence for early post-operative myocardial depression. *Chest* 1995;107:218-224
- 39 Bilbao I, Charco R, Balsells J, Lazaro JL, Hidalgo E, Llopart L, Murio E, Margarit C. Risk factors for acute renal failure requiring dialysis after liver transplantation. *Clin Transplant* 1998; 12:123-129
- 40 Bartosh SM, Alonso EM, Whittington PF. Renal outcomes in pediatric liver transplantation. *Clin Transplant* 1997; 11:354-360
- 41 Cacciarelli TV, Esquivel CO, Moore DH, Cox KL, Berquist WE, Concepcion W, Hammer GB, So SKS.Factors affecting survival after liver transplantation in Infants. *Transplantation* 1997;64:242-248
- 42 Neuberger J, Gunson B, Komolmit P, Davies MH, Christensen E. Pretransplant prediction of prognosis after liver Transplantation in primary sclerosing cholangitis using a Cox regression model. *Hepatology* 1999;29:1375-1379
- 43 Gonzalez FX, Rimola A, Grande L, Antolin M, Garcia-Valdecasas JC, Fuster J, Lacy AM,Cugat E, Visa J, Rodes J. Predictiver factors of early postoperative graft function in human liver transplantation. *Hepatology* 1994;20:565-573
- 44 Wong T, Devlin J, Roland N, Heaton N, Williams R. Clinical characteristics affecting the outcome of liver transplantation. *Transplantation* 1997;64878-64888
- 45 Lo CM, Shaked A, Busuttil RW. Risk factors liver transplantation across the ABO barrier. *Transplantation* 1994; 58: 543-548
- 46 Figuras J, Busquets J, Grande L, Jaurrieta E, Perez-Ferreiroa J, Mir J, Margarit G, Loper P, Vazquez J, Casanova D, Bernardos A, De-Vicente E, Parrilla P, Ramon JM, Bou R. The deleterious effect of donor hight plasma sodium and extended preservation in liver transplantation. A multivariate analysis. *Transplantation* 1996;61:410-413
- 47 Chavez-Cartaya R, Rasmussa A, Tokat Y, Jamieson NV. Effect of preservation time on early graft function And outcome of orthotopic liver transplants. *Transplant Proc* 1995;27:724
- 48 Strasberg SM, Howard TK, Molmenti EP, Hretil M. Selecting the door live, risk factors for poor function after orthotopic liver transplantation. *Hepatology* 1994;20:829-838
- 49 Garcia S, Roque J, Ruza F, Gonzalez M, Madero R, Alvarado F, Herruzo R. Infection and associated risk factors in the immediate postoperative period of pediatric liver transplantation: a study of 176 transplants. *Clin Transplant* 1998; 12:190-197
- 50 Doyle HR, Morelli F, Mc Michael J. Hepatic retransplantation: an analysis of risk factor associated with outcome. *Transplantation* 1996; 61: 1499-1505
- 51 Goss JA, Shackleton CR, McDiarmid SV. Long-term results of pediatric liver transplantation. An analysis of 569 transplants. *Ann Surg* 1998; 228:411-420

• REVIEW •

The management of patients with the short bowel syndrome

Cameron F. E. Platell, Jane Coster, Rosalie D. McCauley, John C. Hall

Cameron F. E. Platell, Jane Coster, Rosalie D. McCauley, John C. Hall, Department of Surgery, The University of Western Australia, Perth, Australia

Correspondence to: Dr. Cameron Platell, University Department of Surgery, Fremantle Hospital. cplatell@cyllene.uwa.edu.au

Telephone: +8-9-431 2500 Fax: +8-9-431 2623

Received 2001-10-21 Accepted 2001-11-25

Abstract

The surgeon is invariably the primary specialist involved in managing patients with short bowel syndrome. Because of this they will play an important role in co-ordinating the management of these patients. The principal aims at the initial surgery are to preserve life, then to preserve gut length, and maintain its continuity. In the immediate postoperative period, there needs to be a balance between keeping the patient alive through the use of TPN and antisecretory agents and promoting gut adaptation with the use of oral nutrition. If the gut fails to adapt during this period, then the patient may require therapy with more specific agents to promote gut adaptation such as growth factors and glutamine. If following this, the patient still has a short gut syndrome, then the principal options remain either long term TPN, or intestinal transplantation which remains a difficult and challenging procedure with a high mortality and morbidity due to rejection.

Platell CFE, Coster J, McCauley RD, Hall JC. The management of patients with the short bowel syndrome. *World J Gastroenterol* 2002;8(1):13-20

INTRODUCTIONS

A remarkable feature of the gastrointestinal tract is how little of it we require in order to maintain a normal nutritional state. Nonetheless, there is a small group of patients who, following extensive loss of principally the small intestine, are unable to maintain their nutrition by oral intake alone. These patients are defined as having the short bowel syndrome.

The pathophysiological consequences of loss of the bowel is dependent upon two important points. Firstly, the extent and site of the intestinal resection, and secondly, the adaptability of the remaining intestine. In general, we need 50 to 70 cm (i.e. around 1 cm/kg weight) of healthy jejunum or ileum in continuity with a section of the colon in order to avoid developing the short bowel syndrome. This is remarkable considering that the normal human small intestine ranges from about 3 to 5 metres in length. Some have defined short bowel syndrome as the loss of 70% or more of the length of the small intestine^[1]. But length is not everything, and if the remaining bowel is involved with the underlying disease process (e.g. Crohn's disease or ischaemia) then its capacity to adapt will be limited. The minimum amount of small intestinal absorptive area required to sustain life varies from individual

to individual. Survival on an oral diet alone may occur in patients with as little as 15 cm of residual jejunum.

This review addresses the medical and surgical management of patients with short bowel syndrome. Particular emphasis is placed on the conduct of the initial surgical procedure and the therapies that may either constitute definitive methods of treatment or serve as useful adjuncts to other forms of surgery. The latter consisting of autologous gastrointestinal reconstruction and small bowel transplantation.

INITIAL SURGICAL PROCEDURE

The causes of short bowel syndrome differ between adults and children. In adults, it most often results after surgery for Crohn's disease or mesenteric infarction. Whilst in infants, the causes more commonly include necrotizing enterocolitis, gastroschisis, atresia, and volvulus^[2-4].

It goes without saying that it is important to preserve as much of the small and large intestine as possible at the initial surgery. However, the subsequent patient progress will depend on not only the length of gut removed, but on whether the patient has a primary anastomosis or a stoma. Nightingale^[5] has classified patients with short bowel syndrome into two groups: those with a primary jejunocolic anastomosis, and those with a jejunostomy. The latter have major problems with losses of water, sodium, and divalent cations such as magnesium; whereas, patients with a jejunocolic anastomosis rarely have problems with their fluid and electrolyte balance. Maintaining colonic continuity serves to decrease gastric emptying and decreases energy/carbohydrate losses. Nonetheless, if a surgeon is concerned regarding the risk of performing a primary anastomosis for fear of an anastomotic dehiscence, then it is safer to consider a primary stoma with reconstruction delayed for 2-3 mo. Although this can create its own problems of leaving *in situ* a segment of excluded gut. Careful consideration should be given to the siting of stomas. It may be advantageous to have an end stoma in close proximity to a mucus fistula.

Preservation of colonic length is not only important for the absorption of fluid and electrolytes, as has been discussed, but it also has nutritional advantages. Patients with the short bowel syndrome have malabsorption of carbohydrates, even after the ingestion of small amounts of otherwise easily absorbed carbohydrates, and this causes a spill-over of the ingested carbohydrates into the residual colon where it undergoes bacterial fermentation^[6].

Jeppesen and Mortensen^[7] have noted that colonic digestion can salvage up to 3-4 MJ/d⁻¹ in patients with the short bowel syndrome, which is about 50% of the daily requirements. They observed that preservation of more than one-half of colonic function is unusual in patients who require parenteral nutrition and have more than 100 cm of residual small bowel. This data reinforces the concept of the colon as an energy-salvaging organ.

Excluded gut may act as a reservoir for bacterial translocation and recurrent sepsis^[8]. Defunctioned gut is

associated with mucosal atrophy and bacterial overgrowth that predispose to bacterial translocation. Reynolds *et al*^[8], reported a case where a patient with excluded bowel suffered episodes of clinical deterioration, fever and rigors without isolation of bacteria from blood cultures. It is possible that these episodes may have been the result of migration of viable bacteria from the excluded gut lumen into the mesenteric lymph system and peritoneum. In this situation pathogenic organisms cannot be cultured from the blood but may be isolated from the peripheral lymph nodes. Schafer *et al*^[9], reviewed the progress of newborns who had stomas created during surgery for a mechanical ileus or intrauterine perforation of the small bowel. To avoid non-use of the distal bowel, they used a roller pump to pass the effluent from the end enterostomy into the distal bowel through the mucus fistula. They reported that this enabled subsequent re-anastomosis to be performed under optimum bowel conditions. Al-Harbi *et al*^[10], described a similar experience in six neonates (gestational ages of 27-38 wk, birth mass of 533-3400g). Mass gain during refeeding ranged from 5 to 25g·kg⁻¹·d⁻¹ with the refeeding lasting for 16-169 d. It was concluded that this technique lessens the need for parenteral nutrition and electrolyte supplementation prior to reanastomosis.

NATURAL HISTORY OF GUT ADAPTATION

Intestinal failure associated with the short bowel syndrome

may be either transient or permanent. Most patients require nutritional support until their gut has undergone sufficient adaptation to allow survival on an oral diet. Results from animal studies have shown that structural adaptation of the remnant bowel involves both an increase in villous height and mucosal surface area, and an increase in bowel luminal circumference and wall thickness. Functional adaptation is characterised by an increase in rate of absorption of nutrients. This is postulated to be the result of structural change, a slowing of transit rate and/or alterations in intracellular molecular events such as increased transport and/or enzyme activity.

The intestinal mucosa produces several peptides that have a trophic effect upon the intestine (Table 1). Following small bowel resection the rate of secretion of these peptides increases in an attempt to compensate for the missing tissue. Recently, Nightingale^[17] has discussed the role of one of these peptides, glucagon-like peptide-2 (GLP-2), in intestinal adaptation. L cells, located in the ileum and jejunum, secrete GLP-2. Nightingale noted that, in patients without an ileum, intake of a meal does not alter plasma GLP-2 concentration and that remnant jejunum of these patients does not adapt^[18,19]. In contrast, intake of a meal induces an increase in plasma GLP-2 concentrations in ileal resected patients with a retained colon and remnant jejunum of these patients does adapt^[20,21]. Collectively, these pieces of information suggest GLP-2 may be useful in adjunctive therapy for short bowel syndrome.

Table 1 The effect of small bowel resection on intestinal peptides that are known regulate intestinal growth

Factor	Source	Effect of Small Bowel Resection on Factor
Epidermal Growth	Salivary glands and Brunner's glands in the jejunum	EGF levels are increased in saliva and diminished in urine 3 d after resection in mice ^[11] .
Factor (EGF)		
Enteroglucagon	L cells of ileum and colon	12 d after a 75% small bowel resection there was a significant increase in concentration of enteroglucagon in the plasma of rats ^[12] .
Glucagon-like	L cells of ileum and colon	There is an increase in expression of GLP-2 mRNA in the ileum of rats after small bowel resection ^[13] .
Peptide 2 (GLP-2)		There is a decrease in expression of dipeptidyl peptidase IV mRNA, the enzyme that inactivates GLP-2, in the ileum of rats after small bowel resection ^[14] .
Insulin-like Growth factor-I (IGF-1)	Cells of the small intestine	80% small bowel resection led to a 183% and 249% increase in IGF-1 mRNA in the jejunum and ileum respectively of rats ^[15] .
Peptide tyrosine tyrosine (PYY)	L cells of ileum	After 70% resection in rats the concentration of PYY in plasma was elevated for at least 2 wk and there was a four and six-fold increase in PYY mRNA in ileum and colon at six hours after resection ^[14] .
Neurotensin	Gut mucosal endocrine cells (N cells) in the jejunum and ileum	50% resection of the distal intestine in dogs was associated with a transient increase in neurotensin ^[16] .

INITIAL SUPPORTIVE MANAGEMENT

The aim of supportive care of patients is to maintain nutritional state and promote gut adaptation.

Parenteral nutrition

An important historical use of parenteral nutrition was in keeping patients with short bowel syndrome alive both in the short and long term. The decision to commence parenteral therapy is based on a number of issues. These include, the extensive loss of gut where the clinician believes the patient will be unable to maintain their own nutrition, or where in the post operative period, the patient is unable to maintain their weight and plasma albumin concentration via oral intake alone. Once parenteral nutrition is commenced, for most patient, there follows a period of gradual transition to enteral nutrition and diet therapy.

The use of parenteral nutrition is associated with a number of side effects. Parenteral nutrition has been found to cause intestinal atrophy in humans and animals^[22-24] and long-term parenteral nutrition is associated with complications that

include recurring central venous line sepsis, high costs (Aus \$ 150·d⁻¹), high mortality (20% in children, mainly due to liver dysfunction) and poor quality of life.

In children with short-bowel syndrome receiving long-term parenteral nutrition, hepatic dysfunction is a major problem. Its aetiology is multifactorial and includes alterations in gut motility which lead to intraluminal stasis which is thought to be a major etiologic factor for bacterial overgrowth and subsequent cholestasis, especially when the ileocecal valve is absent. Sondheimer *et al*^[25], reported that 67% of neonates with short bowel syndrome which were nourished by parenteral nutrition developed cholestasis. This progressed to liver failure in 17% of the neonates. As cholestasis developed shortly after the first infection in 90 % of infants^[25] it seems sepsis may sensitize the liver to cholestatic injury. In spite of the problems associated with parenteral nutrition, Suita *et al*^[26], have commented that advances in parenteral nutrition have meant that infants with a small bowel measuring only 20 cm either with or without an ileocecal valve can survive. However, patients do best in the presence of an ileocecal valve and an intact colon^[27].

Medical Therapy

High-volume output from a jejunostomy requires restriction of oral fluids, a high-energy iso-osmolar diet with added salt, and the use of drugs that reduce motility (loperamide, codeine phosphate) and secretions (proton pump inhibitors, octreotide). Nightingale^[5] has stressed that patients who have less than 100 cm of jejunum *in situ* and a stomal output in excess of their oral intake have the most to gain from the use of antisecretory drugs. This is because they usually lose more from the jejunostomy than they take in orally ('secretors') and are more likely to require long-term parenteral therapy. Yet Octreotide reduces nutrient transport in the small intestine, reduces the number of functional nutrient carriers, and is in general detrimental to gut adaptation. Hence its use in all patients with short bowel syndrome is not indicated.

Gastric hyperacidity is a frequently observed change which occurs transiently in the postoperative period following a massive bowel resection. Unless it is controlled with either proton pump inhibitors or H2 receptor blockers, it may result in extensive gastric or duodenal ulceration.

Enteral nutrition

Enteral nutrition is a key element in promoting the intestinal

hyperplasia which is characteristic of gut adaptation. It does this by several mechanisms. Enteral nutrition provides epithelial work and stimulates the release of pancreatico-biliary secretions that are known to maintain the structure and function of the intestine. Food within the intestine also stimulates the release of various regulatory peptides from the intestine and can deliver specific nutrients to the cells of the intestinal mucosa.

There are a number of specific gut nutrients that are important in adaptation (Table 2). These nutrients promote intestinal structure and function by providing cells of the intestinal mucosa with substrates for the synthesis of essential molecules or by providing energy. For example, polyamines, small molecules that are essential for cell growth and regulation of the cell cycle, are synthesised from ornithine. Whereas, fermentable fibres and their products (i.e. short chain fatty acids) are important fuels for enterocytes. Glutamine is another important gut nutrient that promotes intestinal adaptation. This amino acid is the main fuel of enterocytes and also is a substrate for the synthesis of nucleic acids^[34]. The information presented in Table 2 indicate that supplements of glutamine only promote adaptation in parenterally-fed animals. This suggests that supplements of glutamine can only enhance intestinal adaptation in the absence of epithelial work.

Table 2 Nutrients that regulate gut adaptation

Nutrient	Effect on Intestinal Adaptation
Soluble fibre and short chain fatty acids	SCFA-supplemented parenteral nutrition led to an increase in ileal uptake of D-glucose in rats with an 80% small bowel resection ^[28] .
Triglycerides	A 2% pectin-enriched elemental diet led to a significant increase in intestinal weight, mucosal protein content, and mucosal DNA content in rats with an 80% small bowel resection ^[29] . Rats fed with an elemental diet containing 60% long chain triglycerides after a 60% resection had a greater intestinal adaptation than rats fed a diet containing 17% long chain triglycerides ^[30] .
Ornithine α -ketoglutarate	Enteral supplements of ornithine 2g·kg ⁻¹ ·d ⁻¹ significantly increased jejunal crypt depth ratio and significantly increased glutamine concentration in anterior tibialis muscle ^[31] . Enteral supplements of ornithine 1g·kg ⁻¹ ·d ⁻¹ significantly increased ileal villus height and expression of ornithine decarboxylase mRNA in the ileum ^[32] .
Glutamine	In rats with an 85% small bowel resection, feeding a 2% glutamine-enriched TPN solution, enhanced intestinal adaptation as assessed by mucosal villus height, and mucosal DNA content ^[33] . A glutamine-enriched diet enhanced ileal hyperplasia in rats with an 80% small bowel resection ^[34] . In rats with a 70% small bowel resection, feeding a 5% glutamine-enriched rats chow diet inhibited intestinal adaptation as assessed by duodenal protein content and ileal DNA content ^[35] . A 2% glutamine-enriched elemental diet did not alter markers of intestinal adaptation in rats with a massive small bowel resection ^[36] . A 4% glutamine-enriched oral diet did not significantly alter intestinal adaptation after intestinal resection in rats ^[37] .

There are a number specific gut peptides which mediate the trophic effect of gut nutrients. Glucagon-like peptide-2, which is released by the intestinal L cells, plays a role in the trophic effect of short chain fatty acids (SCFA) on intestinal adaptation. Treatment of rats with SCFA leads to an increase in expression of proglucagon mRNA, a precursor of GLP-2, in the L-cells^[28,39]. Furthermore, Vanderhoof *et al*^[30] speculated that slower absorption of long chain triglycerides allows them to stimulate release of intestinal regulatory peptides, such as GLP-2 and PYY, from L-cells in the ileum. There also may be links between glutamine and PYY as a glutamine-enriched oral diet led to an increase in concentration of PYY in the portal blood after small bowel resection in a rat model^[40].

Epithelial work is important for gut adaptation. Clarke^[41] used a rat model to examine the effect of epithelial work on the structure of the intestine. Isotonic solutions of either glucose, galactose, sodium chloride, *D*-methyl *D*-glucoside, or *D*-mannose were infused into surgically prepared sacs of upper small intestine in rats which fed normally via the gut-in-continuity. Treatment with the glucose, a nutrient and galactose and α -methyl *D*-glucoside, molecules with no nutritional value, led to an increase in villus height. In

addition, treatment with sodium chloride, a molecule that is absorbed by the intestinal mucosa, also led to an increase in villus height.

Age may influence intestinal adaptation as pediatric patients undergo better bowel adaptation than adults. Wasa *et al*^[42] reviewed 12 pediatric and 18 adult patients with short bowel syndrome from Osaka University Hospital. The length of the residual small intestine ranged from 0 to 75 cm (mean 47 cm) in pediatric patients and from 0 to 150 cm (mean 47 cm) in adult patients. Eight pediatric patients (67%) and 4 adult patients (22%) were weaned from TPN. None of the adult patients with residual small intestinal length less than 40 cm could achieve complete intestinal adaptation.

A number of specific oral nutritional regimens have been evaluated to assess their ability to promote gut adaptation. The provision of oral medium-chain triglycerides increases the absorption of energy in patients with short bowel syndrome who have a functioning colon^[43]. Short-chain fatty acids are readily absorbed across the colonic mucosa, whereas long-chain fatty acids are not absorbed by the colon. Hence, patients with a short bowel syndrome and a functioning colon are able to absorb both short-chain and medium-chain C8-C10

triglycerides. Part of their efficacy in this role relates to the fact that both of these types of fat are water-soluble. Manipulation of the dietary fat intake has little appreciable advantage in patients without a functioning colon^[44]. Sales *et al*^[45] reported on four patients, aged 40 - 65 years, with on average 54.5 cm of remaining bowel, who were managed with a progressive step diet. It involved the administration of pectin (Step 1), the use of medium-chain triacylglycerols and complex, nonfermentable sugars (Step 2); coconut oil (47% medium - chain triacylglycerols) and simple sugars (Step 3); and finally long-chain triacylglycerols and lactose (Step 4). Total parenteral nutrition was interrupted at steps 3 or 4 when the energy content of the diet reached 150% of the patient's resting energy expenditure, if serum albumin and weight were stable, or if there were no alterations in frequency, amount and consistency of the stool.

IRREVERSIBLE SMALL BOWEL FAILURE

From studies of patients on long-term parenteral nutrition, it seems that there are between two and three patients per million of population per year who develop irreversible small bowel failure^[46]. Messing *et al*^[47] assessed prognostic factors in 124 consecutive adults with non-malignant short bowel syndrome. Survival and parenteral nutrition-dependence probabilities were 86% and 49% at 2 years, and 75% and 45% at 5 years. In multivariate analysis, survival was related negatively to end-enterostomy, to small bowel length of <50 cm, and to arterial infarction as a cause of short bowel syndrome, but not to parenteral nutrition dependence. The latter was related negatively to post-duodenal small bowel lengths of <50 and 50-99 cm and to absence of terminal ileum and/or colon in continuity. Cutoff values of small bowel lengths separating transient and permanent intestinal failure were 100, 65, and 30 cm in end-enterostomy, jejunocolic, and jejunoleocolic type of anastomosis. In adult short bowel

syndrome patients, small bowel length of <100 cm is highly predictive of permanent intestinal failure. Presence of terminal ileum and/or colon in continuity enhances both weaning off parenteral nutrition and survival probabilities. After 2 years of parenteral nutrition, probability of permanent intestinal failure is 94%. These rates may lead to selection of other treatments, especially intestinal transplantation, instead of parenteral nutrition, for permanent intestinal failure caused by short bowel syndrome.

Gambarara *et al*^[48] have accumulated data that suggests that rather than depending on the length of intestine remaining or the presence of the ileocecal valve, the prognosis of patients with the extreme-short-bowel syndrome depends on recurrent sepsis and early onset liver impairment. In addition, their case review shows that the extreme-short-bowel syndrome is not necessarily an indication for bowel transplantation.

Patients with short bowel syndrome frequently develop other clinical problems which may require therapy. These include, hyperphagia, hyponatremia and hypochloremia, metabolic acidosis, including D-lactic acidosis, cholelithiasis and urolithiasis, gastro-esophageal reflux, dystrophy and symptoms caused by secondary dilatation of the lengthened bowel loops: a protruding abdomen, enteral stasis, leading to constipation or diarrhoea with bacterial overgrowth^[49].

ADAPTATION

The main long term aim of therapy of short bowel syndrome is to promote intestinal adaptation to allow transition to an oral diet. Such management has focused on the use of preferred gut nutrients such as glutamine, and the use of either specific (e.g. intestinal growth factor IGF-1) or general growth factors (e.g. growth hormone). These treatments have followed from the knowledge that both nutrient and growth factor related events drive intestinal adaptation.

Table 3 Molecules that regulate intestinal adaptation

Molecule	Effect on Intestinal Adaptation
Glucagon-Like Peptide 2	Treatment of rats with a 75% mid small bowel resection with twice daily injections of 0.1 µg per gram of bodyweight for 21 d induced led to mucosal hyperplasia in the proximal jejunum but not in the terminal ileum and a significant increase in intestinal absorptive capacity ^[50] .
Interleukin-11	Treatment of rats with a 90% small bowel resection with twice daily injections of 125 mg·g ⁻¹ IL-11 significantly increased villus height and crypt cell mitotic rates ^[51] .
Keratinocyte Growth Factor (KGF)	Treatment of rats with a 75% small bowel resection with 3 mg·kg ⁻¹ ·d ⁻¹ of KGF enhanced intestinal adaptation as assessed by mucosal cellularity, and biochemical activity in duodenal, jejunal and ileal segments ^[52] .
Transforming factor-α	Treatment of mice with a 50% small bowel resection with intraperitoneal TGF-α enhanced intestinal adaptation ^[53] .
Growth Hormone	Treatment of rats with a 75% small intestinal resection with 0.1 mg·kg ⁻¹ ·d ⁻¹ for 28 d enhanced ileal adaptation as assessed by ileal mucosal height. Treatment with growth hormone did not alter ileal mucosal DNA content or ileal mucosal IGF-1 content ^[54] . Treatment of rats with an 80% jejunoileal resection with synthetic rat GH for up to 14 d did not enhance ileal adaptation ^[55] . Treatment of an infant with only 25 cm of jejunum and 2 cm of ileum, with an ileocecal valve, with a 4-week course of 0.5 U/kg of GH allowing weaning from TPN ^[56] . Ten patients with short bowel syndrome were treated with daily subcutaneous doses of recombinant human GH (rhGH) of 0.024 mg·kg ⁻¹ ·d ⁻¹ or a placebo for 8 wk in a crossover clinical trial that included a wash-out period of at least 12 wk. Low-dose rhGH doubled serum levels of IGF-1 and increased body weight and lean body mass; but there were no significant changes in absorptive capacity of water, energy, or protein ^[57] .
Insulin-like Growth Factor-1	Treatment of rats with 70% and 80% jejuno-ileal resection with IGF-1 or analogues significantly attenuated malabsorption of fat and increased weight of stomach and proximal small bowel ^[58] . Gastrostomy-fed rats underwent 80% jejuno-ileal resection followed by infusion of 2.4 mg·kg ⁻¹ ·d ⁻¹ IGF-1 for 7 d. IGF-1 infusion led to a modest increase in ileal but not jejunal growth ^[59] . Treatment of TPN-fed rats for 7 d with IGF-1 after a 60% jejunoileal resection led to an increase in jejunal mass, enterocyte proliferation and migration rates yet had minimal effect on colonic structure ^[59] .
Epidermal Growth Factor (EGF)	Treatment of rabbits with 2/3 proximal resection with oral EGF (40 µg·kg ⁻¹ ·d ⁻¹) for 5 d led to an increase in maltase specific activity and a 3-4 fold increase in glucose transport and phlorizin binding ^[60] . Treatment of rabbits with a 50%-60% small bowel resection with 0.3 µg·kg ⁻¹ ·h ⁻¹ for 7 d led to a fourfold increase in mucosal dryweight at 3 wk post-resection ^[61] . Treatment of rats with a 75% small bowel resection with 6.25 µg·kg ⁻¹ ·h ⁻¹ of EGF increased mucosal thickness at 28 d post-resection ^[62] .
Neurotensin	Treatment of rats with a 75% small bowel resection with 600 µg·kg ⁻¹ ·d ⁻¹ led to an increase in the rate of mucosal proliferation ^[63] .

It makes sense to combine the administration of growth factors with an abundant supply of appropriate nutrients. Such approaches have worked well in animal models. Table 3 presents the results of studies that have evaluated the effect of cytokines and growth factors on intestinal adaptation. Clearly, there are a number of agents that can enhance adaptation. However, the effect of these agents is influenced by factors such as nutrition regimen and type of surgery. For example, Ziegler *et al.*^[15], found that treatment of gastrostomy-fed rats with 2.4mg·kg⁻¹·d⁻¹ IGF-1 for 7 d after 80% jejuno-ileal resection led to a modest increase in ileal but not jejunal growth. In contrast, treatment of TPN-fed rats for 7 d with IGF-1 after a 60% jejunoileal resection and cecectomy did not alter colonic structure^[59]. The effect of treatment with other combinations on intestinal adaptation has yielded less equivocal results. Ziegler *et al.*^[34], used a rat model to examine the effect of glutamine and IGF-1 on intestinal adaptation in rats. Treatment with a glutamine-enriched diet or daily injections of IGF-1 enhanced ileal hyperplasia. More importantly, treatment with glutamine and IGF-1 synergistically increased ileal weight and protein content. Fiore *et al.*^[64], examined the effect of treatment with IL-11 and EGF on intestinal adaptation in rats after 85% small bowel resection. The animals were treated with either 0.10µg·g⁻¹ EGF, 125µg·kg⁻¹

IL-11, or 0.10µg·g⁻¹ EGF and 125µg·kg⁻¹ IL-11 for 8 d. Rats which received EGF and IL-11 had the most number of proliferating cells in the mucosal crypts.

The results in humans have been less convincing. In 1995, Byrne *et al.*^[65], published the results of their investigation of the effect of GH, glutamine and a high complex carbohydrate/low fat diet on 47 patients with short bowel syndrome who had been dependent on TPN for many years. All patients were treated in hospital over a 4 week period. This treatment enabled 40% of patients to be weaned off TPN at one-year follow-up (Table 4). A number of these patients had small bowel length to weight ratios of a little as 0.5cm·kg⁻¹. Subsequent studies have been unable to reproduce these results^[66-68]. The data presented in Table 4 indicates that there was little difference in the type of patients involved in each of the three clinical studies, nor were there large differences in treatment regimens. However, the patients involved in the study by Byrne *et al.*^[65], were treated as inpatients whereas the other patients were all treated as outpatients. It is possible that this may have affected the results as outpatients may have been less compliant. Scolapio *et al.*^[67], considered this issue and believed that the patients involved in their study did comply with the treatment regimen. These conflicting data emphasise the need for further studies to evaluate the effect of trophic agents on intestinal adaptation.

Table 4 The effect of glutamine, growth hormone, and a modified diet on patients with short-bowel syndrome

Authors	Design of Study	Treatment	Number and Type of Patients	Average Length of Remnant Bowel 43	Results
Byrne <i>et al.</i> ^[65]	Uncontrolled study. Patients admitted to hospital and treated for 21d.	GH 0.11mg·kg ⁻¹ ·d ⁻¹ , glutamine 0.16g·kg ⁻¹ ·d ⁻¹ ^{1a8} by the parenteral route with up to 30g·d ⁻¹ by the enteral route, and a diet containing 60% of total calories as carbohydrate, 20% as fat and 20% from protein.	47 patients that were chronically dependent on parenteral nutrition	patients with a colonic remnant had (50±7)cm ^[4] , patients with no colon had (102±24)cm.	At the end of the study 57% of the patients no longer needed TPN, 30% had reduced TPN requirements, and 6% required approximately the same amount of TPN as they did at the start of the study. One year later 40% of the patients no longer needed TPN, 40% had reduced TPN requirements, and 20% required approximately the same amount of TPN as they did at the start of the study.
Scolapio ^[66] Scolapio <i>et al.</i> ^[67]	Double-blind, placebo controlled, randomized crossover study. Patients were treated for 21d as out-patients.	GH 0.14mg·kg ⁻¹ ·d ⁻¹ , glutamine 0.63g·kg ⁻¹ ·d ⁻¹ by oral route, and a diet containing 60% total calories as carbohydrate, 20% as fat and 20% as protein.	8 patients that were dependent on parenteral nutrition for an average of 12.9 years.	71 cm ² patients had colonic continuity.	Treatment led to a significant increase in bodyweight and lean body mass, a significant decrease in percent body fat and induced peripheral edema. All parameters returned to baseline levels within 14 d of stopping treatment. Treatment had no significant effect on intestinal villus height or crypt depth.
Szkudlarek <i>et al.</i> ^[68]	Double-blind, placebo controlled, randomized crossover study. Patients were treated for 28 d as out-patients.	GH 0.14mg·kg ⁻¹ ·d ⁻¹ , glutamine 30g·d ⁻¹ by oral route and glutamine-enriched parenteral nutrition (17% of nitrogen as glutamine).	8 patients that were dependent on parenteral nutrition for an average of 7 years.	104 cm.4 patients had colonic continuity.	No significant effect of treatment on absorption of energy, carbohydrate, nitrogen, wet weight, sodium, potassium, calcium or magnesium. Treatment induced adverse effects.

SURGICAL MANAGEMENT

Non-Transplant Procedures - Autologous Gastrointestinal Reconstruction

Only a few patients with short bowel syndrome are candidates for non-transplant procedures. Surgery in the form of autologous gastrointestinal reconstruction is designed to redistribute the patient's own residual absorptive bowel to enhance adaptation and, possibly, to increase the absorptive mucosal surface by neomucosal growth. The majority of such reconstructions have been performed on paediatric patients. Intestinal lengthening, as described by Bianchi, is the most commonly used method of gastrointestinal reconstruction for the therapy of short bowel syndrome. It divides the bowel in two longitudinal halves based on the bifurcated mesenteric blood supply, then reconnects the two halves in series with the rest of the small intestine.

Bianchi^[69] has recently reviewed his 16-year experience of longitudinal intestinal lengthening procedures for 20 neonates and infants with short-bowel syndrome that included a dysfunctional dilated jejunum. There was no operative

mortality and the long-term survival was 45%. Survivors had >40 cm residual jejunum and a greater number also retained their ileocaecal valve and a longer colonic length. Death was commonly due to end-stage liver failure. Weber^[54] reviewed the outcome of 16 infants and children who had this procedure performed, with a resultant increase in the length of their bowel by 22%-85% (mean 42%). There were marked improvements in stool counts, intestinal transit time, intestinal clearance of barium, D-xylose absorption, and fat absorption. Fourteen of the 16 patients (88%) no longer required parenteral nutrition.

Small Bowel Transplantation

Intestinal transplantation, either alone or in combination with the liver, may eventually emerge as the preferred therapy for patients with permanent intestinal failure. However, in comparison with solid organ transplantations, such as the kidney and the liver, there has been slower progression from experimentation towards routine clinical practice. The first intestinal transplant was performed in Boston in 1964. It

involved the transfer of an ileal segment from the patients mother, but the recipient died 12 hours after surgery. In New York in 1970, a 170 cm jejunoileal segment was transplanted from an identical sister and the recipient lived for 79 d and was able to eat for 6 wk. At Kiel University in 1988, an intestinal transplant from an identical sister resulted in a survival for 4 years^[70].

The high level of immune surveillance within the small intestine means that large number of 'passenger' immunocytes and dendritic cells are transplanted along with the intestinal tissue. This increases the risk of acute rejection, which leads to the use of high doses of immunosuppressive agents and a greater incidence of side effects. In addition, the immunocompromized recipient is vulnerable to infections such as cytomegalovirus enteritis. In fact, recipients can die of side effects in the presence of a functioning graft^[71]. Improved results are only expected with newer immunosuppressive agents, better antiviral prophylaxis and treatment, and improved preservation and surgical techniques^[72].

Grant^[73] has recently reviewed the world experience in which 33 intestinal transplant programs provided data on 273 transplants in 260 patients. These patients received their transplants before March 1997. Only one-thirds of the recipients were adults and the commonest indication for transplantation was the short bowel syndrome. Many of the transplants involved other organs - intestine plus liver (48%); multi-viscera (11%). The one year graft survival for isolated intestinal transplants performed after early 1995 was 55% (the patient survival was 69%). Overall, 77% of the survivors were being sustained on oral nutrition and had no requirement for parenteral nutrition. The overall three-year survival has been about 40%, which is comparable with the results of lung transplantation.

Organ retrieval from a living donor can be performed safely for small bowel transplantation. However, further study of the management of rejection as well as viral infection is necessary for both living and non-living-related small bowel transplantation^[74]. Endoscopic surveillance may be useful to detect early allograft rejection^[75]. It has been suggested that a lower severity of graft rejection in combined liver-small bowel transplantation improves functional results of intestinal transplantation in children without additional mortality or morbidity^[76].

Goulet *et al*^[77], have stressed that, because parenteral nutrition is generally well tolerated, even for long periods, each indication for transplantation must be weighed carefully in terms of risk and quality of life. In this regard, it is of interest that a T cell lymphoma has been reported in the intestinal graft of a multivisceral organ recipient^[78]. It may have special significance because the lymphoproliferative disorders that are usually observed after transplantation are invariably of B cell origin. Furthermore, Crohn's disease in the recipient can recur in the intestinal transplant^[79].

Kato *et al*^[80], have used a rodent model to demonstrate that EGF augments both the structural and functional adaptation of intestinal grafts. Recipient Lewis rats underwent resection of the distal 80% of the small bowel followed by the insertion of a 20 cm isograft. EGF (30 µg·kg⁻¹·d⁻¹), or a control, was infused intraperitoneally for 3 d immediately after surgery. After 7 d, the graft was isolated for morphologic studies and was used for analysis of glucose and water absorption and the expression of sodium glucose cotransporter 1. These were used as indicators of functional adaptation. After seven days, the EGF-treated group exhibited significantly increased mucosal villous height, crypt cell proliferation, glucose and water absorption, and expression of sodium glucose co-transporter 1 protein

compared to the control group.

Other Surgical Techniques

A variety of surgical techniques have been devised to promote oral absorption of nutrients and delay emptying. These include a reversed intestinal segments, artificial intestinal valves, and recirculating loops. None of these procedures has been associated with significant clinical success. Thompson *et al*^[81], studied 48 adults and 112 children with short-bowel syndrome. The eventual outcome was that 44% adapted and survived on enteral nutrition alone, 28% required long-term parenteral nutrition, and 28% underwent surgery. Thirteen of 15 patients with adequate intestinal length (>120 cm in adults), but dilated dysfunctional bowel, were improved by either stricturoplasty or tapering. However, the patients who received an artificial valve (*n*= 2) or a reversed segment (*n*= 1) did poorly and required further surgery for revision or reversal. In general, success is lowest for procedures designed to prolong intestinal transit time; thus, these procedures should be used only in carefully selected patients^[82].

This is in contrast with the experience of Panis *et al*^[83], who reported their experience with segmental reversal of the small bowel. Eight patients with short bowel syndrome underwent, at the time of intestinal continuity restoration, a segmental reversal of the distal (*n*= 7) or proximal (*n*= 1) small bowel. The median length of the remnant small bowel was 40 cm (range, 25-70cm), including a median length of reversed segment of 12 cm (range, 8-15 cm). Parenteral nutrition cessation was obtained in 3 of 5 patients at 1 years and in 3 of 3 patients at 4 years. Segmental reversal of the small bowel could be proposed as an alternative to intestinal transplantation in patients with short bowel syndrome before the possible occurrence of parenteral nutrition-related complications.

COORDINATED INTERDISCIPLINARY MANAGEMENT

There have been proposals to develop multidisciplinary teams to care for patients with the short bowel syndrome. The key issues are the maintenance of optimum growth and development in infants and children, the promotion of intestinal adaptation, and the safe progression towards an oral diet. Koehler *et al*^[84], evaluated the effect of co-ordinated interdisciplinary team management of children with intestinal failure on nutritional outcome measures. Using an established registry, the authors conducted a comprehensive evaluation of patient data including anthropometric measures, organ system function, and mode of nutrition support. Linear growth velocity of neither pre- nor post-pubescent patients significantly improved during the 2-year study period of interdisciplinary team management.

When innovative, not yet fully proven therapies are introduced, physicians may have neither experience nor sufficient data in the medical literature to assist in their decision. When multiple physicians caring for a single patient have reached different conclusions regarding this new therapy, the potential for disagreement exists that could give rise to ethical issues as well as cause confusion to the patient. To explore these topics, Cooper *et al*^[85], investigated the attitudes of specialists to therapies for short bowel syndrome. A forced choice questionnaire was distributed to clinicians in neonatology and pediatric gastroenterology. Significant differences were noted among specialists as to whom would be involved in discussions of therapeutic options with patients about short bowel syndrome. Differences also were noted in the willingness of specialists to discuss and recommend therapies, in the perceived survival and quality of life by various specialists after transplant and palliative surgery, and in the local availability of various options. The neonatologists

and gastroenterologists at the same institution disagreed on responses in 34% of the questions with only 1 of the 25 pairs in full agreement. There is the potential for much patient confusion when counselling physicians recommend different options. Colleagues as individuals and specialists as groups should talk to each other before individual discussions with families to ensure that there is a clear understanding of differing beliefs.

REFERENCES

- Coran AG, Spivak D, Teitelbaum DH. An analysis of the morbidity and mortality of short-bowel syndrome in the pediatric age group. *Eur J Ped Surg* 1999;9:228-230
- Vennarecci G, Kato T, Misiakos EP, Neto AB, Verzaro R, Pinna A, Nery J, Khan F, Thompson JF, Tzakis AG. Intestinal transplantation for short gut syndrome attributable to necrotizing enterocolitis. *Pediatrics* 2000; 105:E25
- Ramsden WH, Arthur RJ, Martinez D. Gastroschisis: a radiological and clinical review. *Ped Radiol* 1997;27:166-169
- Horwitz JR, Lally KP, Cheu HW, Vazquez WD, Grosfeld JL, Ziegler MM. Complications after surgical intervention for necrotizing enterocolitis: a multicenter review. *J Ped Surg* 1995;30:994-998
- Nightingale JM. Management of patients with a short bowel. *Nutrition* 1999;15:633-637
- Olesen M, Gudmand-Hoyer E, Holst JJ, Jorgensen S. Importance of colonic bacterial fermentation in short bowel patients: small intestinal malabsorption of easily digestible carbohydrate. *Dig Dis Sci* 1999;44: 1914-1923
- Jeppesen PB, Mortensen PB. Significance of a preserved colon for parenteral energy requirements in patients receiving home parenteral nutrition. *Scan J Gastroenterol* 1998;33:1175-1179
- Reynolds N, Zentler-Munro P, Cuschieri A, Pennington CR. Potential hazards of excluded bowel and use of parenteral nutrition: a case report. *Nutrition* 1997;13:971-974
- Schafer K, Zachariou Z, Loffler W, Daum R. Continuous extracorporeal stool-transport system: a new and economical procedure for transitory short-bowel syndrome in prematures and newborns. *Ped Surg Int* 1997; 12:73-75
- Al-Harbi K, Walton JM, Gardner V, Chessell L, Fitzgerald PG. Mucous fistula refeeding in neonates with short bowel syndrome. *J Ped Surg* 1999; 34:1100-1103
- Shin CE, Helmrath MA, Falcone RA, Fox JW, Duane KR, Erwin CR, Warner BW. Epidermal growth factor augments adaptation following small bowel resection: optimal dosage, route, and timing of administration. *J Surg Res* 1998;77:11-16
- Sagor GR, Al-Mukhtar MY, Ghatti MA, Wright NA, Bloom SR. The effect of altered luminal nutrition on cellular proliferation and concentrations of enteroglucagon and gastrin after small bowel resection. *Br J Surg* 1982; 69:14-18
- Fuller PJ, Beveridge DJ, Taylor RG. Ileal proglucagon gene expression in the rat: characterization in intestinal adaptation using in situ hybridisation. *Gastroenterology* 1993;104:459-466
- Dunphy JL, Justice FA, Taylor RG, Fuller PJ. mRNA levels of dipeptidyl peptidase IV decrease during intestinal adaptation. *J Surg Res* 1999;87: 130-133
- Ziegler TR, Mantell MP, Chow JC, Rombeau JL, Smith RJ. Intestinal adaptation after extensive small bowel resection: differential change in growth and insulin-like growth factor system messenger ribonucleic acids in jejunum and ileum. *Endocrinology* 1998;139:3119-3126
- Thompson JS, Quigley EM, Adrian TE. Factors affecting outcome following proximal and distal intestinal resection in the dog: an examination of the relative roles of mucosal adaptation, motility, luminal factors, and enteric peptides. *Dig Dis Sci* 1999;44:63-74
- Nightingale J. Short bowel, short answer. *Gut* 1999;45:478-479
- Jeppesen PB, Hartmann B, Hansen BS, Thulesen J, Holst JJ, Mortensen PB. Impaired meal stimulated glucagon-like peptide 2 response in ileal resected short bowel patients with intestinal failure. *Gut* 1999;45: 559-563
- De Francesco A, Malfi G, Delsedime L. Histological findings regarding jejunal mucosa in short bowel syndrome. Measurement by calcium absorption. *Dig Dis Sci* 1989;34:709-715
- Jeppesen PB, Hartmann B, Thulesen J, Hansen BS, Holst JJ, Poulsen SS, Mortensen PB. Elevated plasma glucagon-like peptide 1 and 2 concentrations in ileum resected short bowel patients with a preserved colon. *Gut* 2000;47:370-376
- Dowling RH, Booth CC. Functional compensation after small bowel resection in man: Demonstration by direct measurement. *Lancet* 1966;ii:146-147
- Platell C, McCauley R, McCulloch R, Hall J. The influence of parenteral glutamine and branched-chain amino acids on total parenteral nutrition-induced atrophy of the gut. *JPEN* 1993;17: 348-354
- Buchman AL, Moukarzel AA, Ament ME, Eckhart C, Bhuta S, Mestecky J, Hollander D. Effects of total parenteral nutrition on intestinal morphology and function in humans. *Trans Proc* 1994; 26:1457
- Pironi L, Paganelli GM, Miglioli M, Biasco G, Santucci R, Ruggeri E, Di-Febo G, Barbara L. Morphologic and cytoproliferative patterns of duodenal mucosa in two patients after long-term parenteral nutrition: changes with oral feeding and relation to intestinal resection. *JPEN* 1994;18:351-354
- Sondheimer JM, Asturias E, Cadnapaphornchai M. Infection and cholestasis in neonates with intestinal resection and long-term parenteral nutrition. *J Ped Gastroenterol Nut* 1998;27:131-137
- Suita S, Masumoto K, Yamanouchi T, Nagano M, Nakamura M. Complications in neonates with short bowel syndrome and long-term parenteral nutrition. *JPEN* 1999;23:S106-S109
- Mayr JM, Schober PH, Weissensteiner U, Hollwarth ME. Morbidity and mortality of the short-bowel syndrome. *Eur J Ped Surg* 1999;9: 231-235
- Tappenden KA, McBurney MI. Systemic short-chain fatty acids rapidly alter gastrointestinal structure, function, and expression of early response genes. *Dig Dis Sci* 1998;43:1526-1536
- Korunda MJ, Rolandelli RH, Settle RG, Saul SH, Rombeau JL. The effect of a pectin supplemented elemental diet on intestinal adaptation to massive small bowel resection. *JPEN* 1986;10:343-350
- Vanderhoof JA, Grandjean CJ, Kaufman SS, Burkley KT, Antonson DL. Effect of high percentage medium-chain triglyceride diet on mucosal adaptation following massive bowel resection in rats. *JPEN* 1984;8:685-689
- Dumas F, De Bandt JP, Colomb V, Le Boucher J, Coudray-Lucas C, Lavie S, Brousse N, Riccours C, Cynober L, Goulet O. Enteral ornithine α -ketoglutarate enhances intestinal adaptation after small bowel resection in rats. *Metabolism* 1998;47:1366-1371
- Czernichow B, Nsi-Envo E, Galluser M, Gosse F, Raul F. Enteral supplementation with ornithine α -ketoglutarate improves the early adaptive response to resection. *Gut* 1997;40:67-72
- Tamada H, Nezu R, Matsuo Y, Imamura I, Takagi Y, Okada A. Alanine glutamine-enriched total parenteral nutrition restores intestinal adaptation after either proximal or distal massive resection in rats. *JPEN* 1993;17:236-242
- Ziegler TR, Mantell MP, Chow JC, Rombeau JL, Smith RJ. Gut adaptation and the insulin-like growth factor system: regulation by glutamine and IGF-I administration. *Am J Physiol* 1996;271:G866-G875
- Vanderhoof JA, Blackwood DJ, Mommadpour H, Park JH. Effects of oral supplementation of glutamine on small intestinal mucosa following resection. *J Am Coll Nutr* 1992;11:223-227
- Michail S, Mohammadpour H, Park JH, Vanderhoof JA. Effect of glutamine-supplemented elemental diet on mucosal adaptation after small bowel resection in rats. *J Pediatr Gastroenterol Nutr* 1995; 21:394-398
- Wiren ME, Permert J, Skulman SP, Wang F, Larsson J. No differences in mucosal adaptive growth one week after intestinal resection in rats given enteral glutamine supplementation or deprived of glutamine. *Eur J Surg* 1996;162:489-498
- McCauley R, Kong SE, Hall JC. Glutamine and nucleotide metabolism within enterocytes. *JPEN* 1998;22:105-111
- Reimer RA, McBurney MI. Dietary fiber modulates intestinal proglucagon messenger ribonucleic acid and postprandial secretion of glucagon-like peptide-1 and insulin in rats. *Endocrinology* 1996; 137:3948-3956
- Wiren M, Adrian TE, Arnelo U, Permert J, Staab P, Larsson J. Early gastrointestinal regulatory peptide response to intestinal resection in rats is stimulated by enteral glutamine supplementation. *Dig Surg* 2000;16:197-203
- Clarke RM. 'Luminal nutrition' versus 'functional work-load' as controllers of mucosal morphology and epithelial replacement in the rat small intestine. *Digestion* 1977;15:411-424
- Wasa M, Takagi Y, Sando K, Harada T, Okada A. Long-term outcome of short bowel syndrome in adult and pediatric patients. *JPEN* 1999;23:S110-S112
- Jeppesen PB, Mortensen PB. Colonic digestion and absorption of energy from carbohydrates and medium-chain fat in small bowel failure. *JPEN* 1999;23:S101-S105
- Jeppesen PB, Mortensen PB. The influence of a preserved colon on the absorption of medium chain fat in patients with small bowel resection. *Gut* 1998;43:478-483

- 45 Sales TR, Torres HO, Couto CM, Carvalho EB. Intestinal adaptation in short bowel syndrome without tube feeding or home parenteral nutrition: report of four consecutive cases. *Nutrition* 1998;14:508-512
- 46 Hakim NS, Papalois VE. Small bowel transplantation. *Int Surgery* 1999;84:313-317
- 47 Messing B, Crenn P, Beau P, Boutron-Ruault MC, Rambaud JC, Matuchansky C. Long-term survival and parenteral nutrition dependence in adult patients with the short bowel syndrome. *Gastroenterology* 1999;117:1043-50
- 48 Gambarara M, Ferretti F, Bagolan P, Papadatou B, Rivosecchi M, Lucchetti MC, Nahom A, Castro M. Ultra-short-bowel syndrome is not an absolute indication to small-bowel transplantation in childhood. *Eur J Ped Surg* 1999;9:267-270
- 49 Waag KL, Hosie S, Wessel L. What do children look like after longitudinal intestinal lengthening. *Eur J Ped Surg* 1999;9:260-262
- 50 Scott RB, Kirk D, MacNaughton WK. GLP-2 augments the adaptive response to massive intestinal resection in the rat. *Am J Physiol* 1998;275:G911-G921
- 51 Liu Q, Du XX, Schindel DT, Yang ZX, Rescorla FJ, Willaims DA, Grossfeld JL. Trophic effects of interleukin-11 in rats with experimental short bowel. *J Pediatr Surg* 1996;31:1047-1050
- 52 Johnson WF, DiPalma CR, Ziegler TR, Scully S, Farrell CL. Ketatinocyte growth factor enhances early gut adaptation in a rat model of short bowel syndrome. *Vet Surg* 2000;29:17-27
- 53 Falcone RA, Stern LE, Kemp CJ, Erwin CR, Warner BW. Intestinal adaptation occurs independent of transforming growth factor alpha. *J Pediatr Surg* 2000;35:365-370
- 54 Shulman DI, Hu CS, Duckett G, Lavalee-Grey M. Effects of short-term growth hormone therapy in rats undergoing 75% small intestinal resection. *J Pediatr Gastroenterol* 1992;14:3-11
- 55 Ljungmann K, Grfte T, Kissmeyer-Nielsen P, Flyvbjerg A, Vilstrup H, Tygstrup N, Laurberg S. GH decrease hepatic amino acid degradation after small bowel resection in rats without enhancing bowel adaptation. *Am J Physiol* 2000;279:G700-G706
- 56 Velasco B, Lassaletta L, Gracia R, Tovar JA. Intestinal lengthening and growth hormone in extreme short bowel syndrome: a case report. *J Ped Surg* 1999;34:1423-1424
- 57 Ellegard L, Bosaeus I, Nordgren S, Bengtsson BA. Low-dose recombinanthuman growth hormone increases body weight and lean body mass in patients with short bowel syndrome. *Ann Surg* 1997;225:88-96
- 58 Lemmey AB, Ballard FJ, Martin AA, Tomas FM, Howarth GS, Read LC. Treatment with IGF-1 peptides improves function of the remnant gut following small bowel resection in rats. *Growth Factors* 1994;10:243-252
- 59 Gillingham MB, Dahly EM, Carey HV, Clark MD, Kritsch KR, Ney DM. Differential jejunal and colonic adaptation due to resection and IGF-I in parenterally fed rats. *Am J Physiol* 2000;278:G700-G709
- 60 O'Loughlin E, Winter M, Shun A, Hardin JA, Gall DG. Structural and functional adaptation following jejunal resection in rabbits: effect of epidermal growth factor. *Gastroenterology* 1994;107:87-93
- 61 Swaniker F, Gou W, Diamond J, Fonkalsrud EW. Delayed effects of epidermal growth factor after extensive small bowel resection. *J Pediatr Surg* 1996;31:56-59
- 62 Chaet MS, Arya G, Ziegler MM, Warner BW. Epidermal growth factor enhances intestinal adaptation after massive small bowel resection. *J Pediatr Surg* 1994;29:1035-1038
- 63 Mata A, Gomez de Segura IA, Largo C, Codesal J, De Miguel E. Neurotensin increases intestinal adaptation and reduces enteroglucagon immunoreactivity after large bowel resection in rats. *Eur J Surg* 1997;163:387-393
- 64 Fiore NF, Ledniczy G, Liu Q, Orazi A, Du X, Williams DA, Grosfeld JL. Comparison of interleukin 11 and epidermal growth factor on residual intestine after massive small bowel resection. *J Pediatr Surg* 1998;33:24-29
- 65 Byrne TA, Persinger RL, Younf LS, Ziegler TR, Wilmore DW. A new treatment for patients with short-bowel syndrome. Growth hormone, glutamine, and a modified diet. *Ann Surg* 1995;222:243-255
- 66 Scolapio JS. Effect of growth hormone, glutamine, and diet on body composition in short bowel syndrome: a randomized, controlled study. *JPEN* 1999;23:309-312
- 67 Scolapio JS, Camilleri M, Fleming CR, Oenning LV, Burton DD, Sebo TJ, Batts KP, Kelly DG. Effect of growth hormone, glutamine, and diet on adaptation in short-bowel syndrome: A randomized, controlled study. *Gastroenterology* 1997;113:1074-1081
- 68 Szkudlarek J, Jeppesen PB, Mortensen PB. Effect of high dose growth hormone with glutamine and no change of diet on intestinal absorption in short bowel patients: a randomised, double blind, crossover, placebo controlled study. *Gut* 2000;47:199-205
- 69 Bianchi A. Experience with longitudinal intestinal lengthening and tailoring. *Eur J Ped Surg* 1999;9:256-259
- 70 Margreiter R. Living-donor pancreas and small-bowel transplantation. *Lan Arch Surg* 1999;384:544-549
- 71 Novelli M, Muesan P, Mieli-Vergani G, Dhawan A, Rela M, Heaton ND. Oral absorption of tacrolimus in children with intestinal failure due to short or absent small bowel. *Transplant Int* 1999;12:463-465
- 72 Makisalo H, Ericzon BG. Intestinal transplantation. *Ann Chir Gyn* 1997;86:155-162
- 73 Grant D. Intestinal transplantation: 1997 report of the international registry. Intestinal Transplant Registry. *Transplantation* 1999;67:1061-1064
- 74 Morel P, Kadry Z, Charbonnet P, Bednarkiewicz M, Faidutti B. Paediatric living related intestinal transplantation between two monozygotic twins: a 1-year follow-up. *Lancet* 2000;355:723-724
- 75 Kato T, O'Brien CB, Nishida S, Hoppe H, Gasser M, Berho M, Rodriguez MJ, Ruiz P, Tzakis AG. The first case report of the use of a zoom videoendoscope for the evaluation of small bowel graft mucosa in a human after intestinal transplantation. *Gastrointest. Endoscopy* 1999;50:257-261
- 76 Jan D, Michel JL, Goulet O, Sarnacki S, Lacaille F, Damotte D, Cezard JP, Aigrain Y, Brousse N, Peuchmaur M, Rengeval A, Colomb V, Jouviet P, Ricour C, Revillon Y. Up-to-date evolution of small bowel transplantation in children with intestinal failure. *J Ped Surg* 1999;34:841-843
- 77 Goulet O, Jan D, Lacaille F, Colomb V, Michel JL, Damotte D, Jouviet P, Brousse N, Faure C, Cezard JP, Sarnacki S, Peuchmaur M, Hubert P, Ricour C, Revillon Y. Intestinal transplantation in children: preliminary experience in Paris. *JPEN* 1999;23:S121-S125
- 78 Berho M, Viciano A, Weppler D, Romero R, Tzakis A, Ruiz P. T cell lymphoma involving the graft of a multivisceral organ recipient. *Transplantation* 1999;68:1135-1139
- 79 Sustento-Reodica N, Ruiz P, Rogers A, Viciano AL, Conn HO, Tzakis AG. Recurrent Crohn's disease in transplanted bowel. *Lancet* 1997;349:688-691
- 80 Kato Y, Hamada Y, Ito S, Okumura T, Hioki K. Epidermal growth factor stimulates the recovery of glucose absorption after small bowel transplantation. *J Surg Res* 1998;80:315-319
- 81 Thompson JS, Langnas AN. Surgical approaches to improving intestinal function in the short-bowel syndrome. *Arch Surg* 1999;134:706-709
- 82 Thompson JS, Langnas AN, Pinch LW, Kaufman S, Quigley EM, Vanderhoof JA. Surgical approach to short-bowel syndrome. Experience in a population of 160 patients. *Ann Surg* 1995;222:600-605
- 83 Panis Y, Messing B, Rivet P, Coffin B, Hautefeuille P, Matuchansky C, Rambaud JC, Valleur P. Segmental reversal of the small bowel as an alternative to intestinal transplantation in patients with short bowel syndrome. *Ann Surg* 1997;225:401-407
- 84 Koehler AN, Yaworski JA, Gardner M, Kocoshis S, Reyes J, Barksdale EM Jr. Coordinated interdisciplinary management of pediatric intestinal failure: a 2-year review. *J Ped Surg* 2000;35:380-385
- 85 Cooper TR, Garcia-Prats JA, Brody BA. Managing disagreements in the management of short bowel and hypoplastic left heart syndrome. *Pediatrics* 1999;104:48

• BASIC RESEARCH •

Relationship between cytokine mRNA expression and organ damage following cecal ligation and puncture

Rong-Qian Wu, Ying-Xin XU, Xu-Hua Song, Li-Jun Chen, Xian-Jun Meng

Rong-Qian Wu, Ying-Xin XU, Xu-Hua Song, Li-Jun Chen, Xian-Jun Meng, Institute of Surgical Research, Chinese PLA General Hospital, Beijing 100853, China

Supported by the National Natural Science Foundation of China, No. 39870796

Correspondence to: Dr. Rong-Qian Wu, Institute of surgical Research, General Hospital of PLA, Beijing 100853, China

Received 2001-04-21 Accepted 2001-08-15

Abstract

AIM: To investigate the role of cytokine gene expression in organ damage at different tissue sites during sepsis.

METHODS: Male NIH mice were subjected to cecal ligation and puncture (CLP) or sham operation (Sham). Pro-inflammatory cytokine (TNF α , IL-1 β and IL-6) and anti-inflammatory cytokine (IL-4) gene expression in the liver and lung tissue were assessed by RT-PCR. The permeability of microvascular and water content in the lungs and liver were also examined.

RESULTS: Significant increase in TNF α , IL-1 β and IL-6 gene expression was observed at 3 and 12 h after CLP both in the liver and lungs ($P < 0.01$). The level of IL-4 gene expression was not changed after CLP in the lungs, but increased at 12 h after CLP ($P < 0.01$) in the liver tissue. Both the liver and lungs showed a significant increase in microcirculatory permeability at 12 h after CLP ($P < 0.01$), and the increase in the lungs was higher than that in the liver. The water mass fractions in the liver ($P < 0.05$) and lungs ($P < 0.01$) were increased after CLP, and the increase in the lungs happened earlier and more severely than that in the liver.

CONCLUSION: The inflammatory response in the liver and lungs was different during sepsis. At the early stage of sepsis, pro-inflammatory reaction dominates both in the liver and lungs. But at the later stage of sepsis, induction of compensatory anti-inflammatory response was seen in the liver but not in the lungs. This difference *in situ* activity may contribute to the different vulnerability of organ damage during sepsis. The strategy of systemic administration of anti-inflammatory drugs to sepsis should be reconsidered.

Wu RQ, Xu YX, Song XH, Chen LJ, Meng XJ. Relationship between cytokine mRNA expression and organ damage following cecal ligation and puncture. *World J Gastroenterol* 2002;8(1):131-134

INTRODUCTION

Despite modern techniques of resuscitation and intensive care and an ever-increasing number of powerful and effective antibiotics, sepsis remains a major cause of death in the critically ill^[1], including severe trauma, burns, hemorrhage, major operations^[2], etc. Sepsis-related mortality frequently results from multiple organ dysfunction syndrome,

which is characterized by impaired pulmonary function, hepatic failure, cardiac dysfunction, acute renal failure, and disseminated intravascular coagulation^[3,4]. The physiologic derangements of MODS are believed to result from the excessive activation of the systemic inflammatory response by infection, ischemia, injury, or immunologic activation^[5,6].

Post-sepsis MODS is now believed to be caused by an overexpression of host defenses^[7]. Mediators such as TNF α , IL- β and other cytokines are acknowledged to be pivotal early effectors. There is evidence that the development of tissue damage in sepsis is closely related to the release of an ever-increasing number of cytokines and accumulation of neutrophils at the sites of infection or injury^[8,9]. Though there were many studies on the role of cytokines in sepsis. Most studies detect only circulating mediators, not mediators bound to cells or receptors^[10,11]. Analyses of serum levels are troublesome to interpret. They may underestimate the effective amount of mediator acting at a cellular level. Bioassays, which measure the functional activity of cytokines, often lack specificity and may over-report amounts.

Polymicrobial sepsis induced by cecal ligation and puncture (CLP) is a model of sepsis which reproduces many of the inflammatory and pathological sequelae that are observed clinically^[12]. Following CLP, animals develop bacteremia, hypothermia, hypotension, and damage to multiple organ systems^[13]. The present study was designed to observe the gene expression of cytokines in hepatic and pulmonary tissues with CLP model, in order to investigate the role of cytokines in organ damage during sepsis.

MATERIALS AND METHODS

Animal model and experimental groups

NIH mice were obtained from the animal center of the general hospital of Chinese PLA. The mice were randomly divided into two groups: CLP group and sham group. Sepsis was induced by cecal ligation and puncture (CLP). The mice were anesthetized, and the cecum was ligated below the ileocecal junction; and intestinal continuity was maintained. The cecum was punctured twice with a 20-gauge needle and a small amount of cecal contents was expressed through the punctures. The incision was closed and 1 ml of normal saline was administered subcutaneously. Sham-operated mice underwent the same surgical procedure, but without CLP. The mice were sacrificed at 3 or 12 h after the procedure.

Preparation of RNA

Total RNA was extracted from liver and lung tissues according to the guanidinium isothiocyanate single-step methods. The RNA concentration of each sample was estimated by measuring the absorbance at 260 nm.

Reverse transcription and PCR

Total RNA from experimental samples was used to synthesize cDNA using AMV reverse transcriptase. β -actin and β_2 -MG were used as

internal control primers. The primers for the cytokines and control were as follows: β -actin (478bp): 5'AGG GAA ATC GTG CGT GAC ATC AAA 3', 5'ACT CAT CGT ACT CCT GCT TGC TGA 3'; β_2 -MG (300bp): 5'GGC TCG CTC GGT GAC CCT AGT CTT T 3', 5'TCT GCA GGC GTA TGT ATC AGT CTC A 3'; TNF- α (349bp): 5'TTC TGT CCC TTT CAC TCA CTG G3', 5'TTG GTG GTT TGC TAC GAC GTG G 3'; IL-1 β (441bp): 5'ATT AGA CAG CTG CAC TAC AGG CTC 3', 5'AGA TTC CAT GGT GAA GTC AAT TAT 3'; IL-6 (156bp): 5'TGG AGT CAC AGA AGG AGT GGC TAA G 3', 5'TCT GAC CAC AGT GAG GAA TGT CCA C 3'; IL-4 (181bp): 5'CGA AGA ACA CCA CAG AGA GTG AGC T 3', 5'GAC TCA TTC ATG GTG CAG CTT ATC G 3'. PCR was performed in a 25 μ L reaction volume. A hot start was applied for 5min at 95°C. The amplification cycle (denaturation step at 94°C for 30s, an annealing step at 55°C for 30s and an extension step at 72°C for 90s) was repeated 30 times and followed by a final extension for 10 min at 72°C. Amplified products were separated by electrophoresis in ethidium bromide-stained 15g·L⁻¹ agarose gel and visualized with UV illumination. The bands representing reaction product on the film were scanned by densitometry. A normalization quotient (Q) was calculated between the integrated optical density values (IOD) for the adhesion molecules and the β -actin or β_2 -MG bands ($Q = \text{IOD adhesion molecules band} / \text{internal control band}$). The level of adhesion molecules mRNA were expressed as the quotient of the integrated values for the adhesion molecules and the β -actin or β_2 -MG bands.

Microvascular permeability in the liver and lungs

Evans blue (15g·L⁻¹) was injected intravenously in concentrations of 10 μ L·g⁻¹ 0.1ml/10g. The liver and lung tissues were excised and weighed. To each sample of tissues, 4.0mL formamide was added and incubated at 56°C for 72 h. If necessary, the incubation time was prolonged, until the blue color of the samples completely disappeared. After filtration with glass filter, the absorbance of the filtrate was measured at 620nm in a Beckman spectrophotometer. The total amount of dye can be calculated by means of a standard calibration curve. The permeability of microvascular in the liver and lungs was shown as the μ g of Evans blue in every mg tissues.

Water mass fractions in the liver and lungs

Water mass fractions were used as a parameter of organ water accumulation after CLP. The liver and lung tissues were removed in a humidity chamber and the wet mass was measured immediately. The tissues were dried at 70°C to a constant mass for the determination of dry mass. Organ edema was determined by calculating tissue water content according to the following formula: Water mass fractions (%) = (1-dry mass / wet mass) × 100%.

Statistics

All data were reported as $\bar{x} \pm s$. Data were analyzed by *t* test for comparisons between two groups. $P < 0.05$ was accepted as the level of significance.

RESULTS

Cytokine mRNA expression in the liver and lungs

Significant increase in TNF α , IL-1 β and IL-6 gene expression was observed at 3 and 12 h after CLP both in the liver and lungs. But the level of IL-4 gene expression was not changed after CLP in the lungs, while it was increased at 12 h after CLP (Figure 1, 2) in the liver tissue.

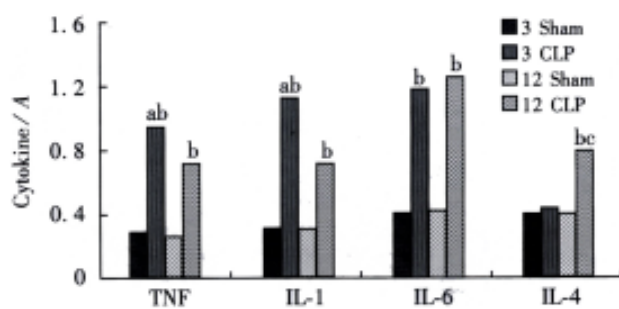


Figure 1 The cytokines gene expression in the liver ^a $P < 0.01$, vs CLP 12h group, ^b $P < 0.01$, vs sham group, ^c $P < 0.01$, vs CLP 3h group

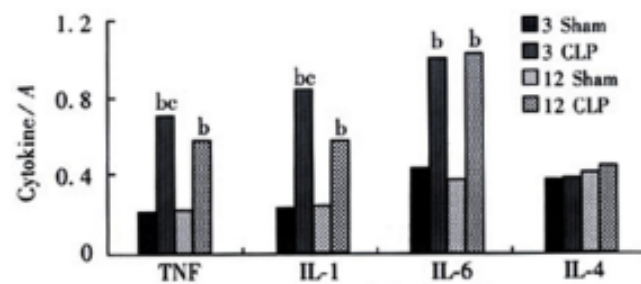


Figure 2 The cytokines gene expression in the lungs ^b $P < 0.01$, vs sham group, ^c $P < 0.05$, vs CLP 12h group

Microvascular permeability in the liver and lungs

Both the liver and lungs showed a significant increase in microcirculatory permeability at 12 h after CLP, and the increase in the lungs was higher than that in the liver (Figure 3).

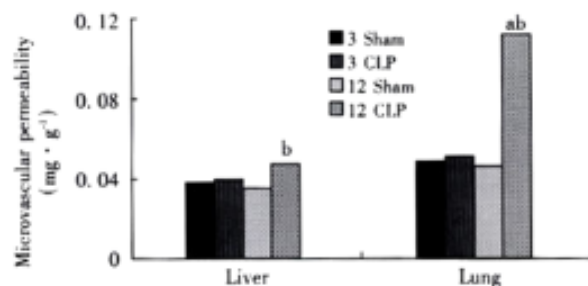


Figure 3 Microvascular permeability in the liver and lungs ^a $P < 0.01$, vs CLP 3h group, ^b $P < 0.01$, vs sham group.

Water mass fractions in the liver and lungs

The water mass fractions in the liver and lungs were increased after CLP, and the increase in the lungs happened earlier and more severely than that in the liver (Figure 4).

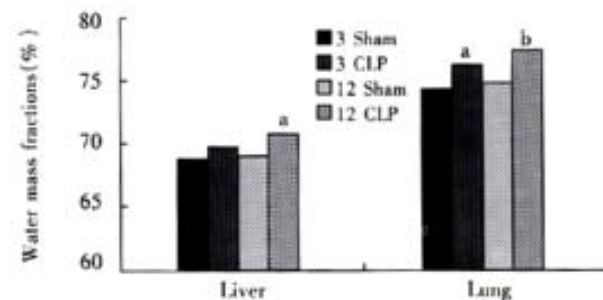


Figure 4 Water mass fractions in the liver and lungs ^a $P < 0.05$, vs sham group, ^b $P < 0.01$, vs sham group

DISCUSSION

SIRS affects all aspects of systemic homeostasis. It is arbitrary, but convenient, to consider its effects from the perspective of the dysfunction of certain key organ systems. It must be recognized, however, that there is no defining combination of systems or temporal sequence of physiologic deterioration that characterizes the syndrome^[14]. A systematic review of 30 descriptions of MODS published between 1969 and 1993 revealed that respiratory system is the most commonly cited organ system^[15,16]. The liver with its rich supply of blood and sinusoid is directly exposed to bacteria and endotoxins drained from the GI tract^[17-19]. Previous works have proclaimed that liver is the most susceptible and vulnerable organ during sepsis and multiple organ failure^[20]. So in this study, we chose the liver and lungs as the samples to study the role of local cytokine gene expression in organ damage.

Cytokines are polypeptides or glycoproteins of low molecular weight. Most cytokines are not stored as preformed molecules, hence their production requires new gene transcription and translation. Unlike mediators derived from the classical endocrine system, cytokines are produced. The production of cytokines at various tissue sites depends, in part, on the proximity of the site to the injurious stimulus. A lot of cells such as macrophage^[21] and endothelial cells^[22] can produce cytokines. Cytokines act predominantly as paracrine and autocrine messengers, not endocrine mediators. Thus, cytokines may exert their major effects locally, within organs and tissues. Assays of circulating cytokine concentrations may be misleading because they do not detect cytokines bound to soluble receptors^[23]. These assays may also fail to detect cytokines when inhibitors or receptor antagonists are present^[24]. Therefore investigations in this area require more precise determination of the temporal sequencing and tissue-specific expression of cytokines.

In this study we assessed the gene expression of pro-inflammatory and anti-inflammatory cytokines in the hepatic and pulmonary tissues. Pro-inflammatory cytokines such as TNF α , and IL-1 β are known to play predominant roles in the normal inflammatory response. But exaggerated endogenous production is likely responsible for the complications associated with sepsis as tissue injury and ultimate organ failure^[25]. These pro-inflammatory cytokines result in the production of secondary mediators (including nitric oxide, arachidonic acid metabolites, bradykinin, and histamine) which in turn activate neutrophils and endothelial cells to perpetuate tissue injury^[26, 27]. But attempts to modulate the biological activity of cytokines with monoclonal antibodies against endotoxin, TNF α , IL-1 have not been successful in improving outcome in several clinical series. Recently, evidence is accumulating that in response to the original inciting event (the inflammatory response), the body also mounts an anti-inflammatory response. Agents that have been identified so far as participating in this anti-inflammatory response include interleukins-4, -10, -11 and -13; transforming growth factor- α ; colony-stimulating factors; soluble receptors to tumor necrosis factor and receptor antagonists to IL-1^[28]. Because most of these mediators have been discovered recently, we know very little about their actions, and even less about their effects on the pro-inflammatory cascade. However, it had already been shown that some of these mediators, especially some of these interleukins, have a profound effect on monocyte function, including antigen presenting activity^[29]. They also inhibit T- and B-lymphocyte activity, including antigen-specific T-lymphocyte proliferation. The result is immune suppression, which can sometimes be profound. Of great interest is the fact that these mediators can down-regulate their own synthesis, thereby providing a mechanism through which homeostasis can be restored. Results in this study showed that the conditions of inflammatory reaction in the liver and lungs were different during

sepsis. At the early stage of sepsis, the power of pro-inflammatory reaction was stronger than that of anti-inflammatory reaction both in the liver and lungs. But at the later stage of sepsis, compensatory anti-inflammatory response was found in the liver but not in the lungs.

The consensus of the concept of systemic inflammatory responses has brought about a promising approach in the treatment of SIRS/MODS^[30] - anti-inflammatory instead of anti-infection^[31,32]. Various approaches aimed to interrupt the cascade of host inflammatory responses have been tested^[33]. These include interventions targeted at the inflammation effector cells as monoclonal antibodies or receptor antagonist to pro-inflammatory cytokines^[34,35]. However, many of these seemingly effective measures in experimental study failed when moved from the laboratory bench to clinical ward^[36,37]. As results showed in this study that the conditions of inflammatory reaction in the liver and lungs were different during sepsis, it is postulated that in the strategy of anti-inflammatory interventions such as monoclonal antibodies against endotoxin and TNF α , in addition to timing, organ targeting may also be considered.

REFERENCES

- Memmini G, Buggiani B, Ciulli L, Cavallini MR, Turini M, Pierini A, Bianchi F, Moggi C. Study on 480 hospitalized febrile children: evaluation of the septic risk and results of the antibiotic and corticosteroid combined therapy. *Pediatr Med Chir* 1999; 21:119-123
- D'Amico D, Cillo U. Impact of severe infections on the outcome of major liver surgery: a pathophysiologic and clinical analysis. *J Chemother* 1999; 11:513-517
- Jarrar D, Chaudry IH, Wang P. Organ dysfunction following hemorrhage and sepsis: mechanisms and therapeutic approaches. *Int J Mol Med* 1999; 4:575-583
- Crouser ED, Julian MW, Weinstein DM, Fahy RJ, Bauer JA. Endotoxin-induced ileal mucosal injury and nitric oxide dysregulation are temporally dissociated. *Am J Respir Crit Care Med* 2000; 161:1705-1712
- Brun-Buisson C. The epidemiology of the systemic inflammatory response. *Intensive Care Med* 2000; 26 Suppl 1(-EM-):S64-74
- Qin RY, Zou SQ, Wu ZD, Qiu FZ. Influence of splanchnic vascular infusion on the content of endotoxins in plasma and the translocation of intestinal bacteria in rats with acute hemorrhage necrosis pancreatitis. *World J Gastroenterol* 2000; 6:577-580
- Vincent JL. Update on sepsis: pathophysiology and treatment. *Acta Clin Belg* 2000; 55:79-87
- Terregino CA, Lopez BL, Karras DJ, Killian AJ, Arnold GK. Endogenous mediators in emergency department patients with presumed sepsis: are levels associated with progression to severe sepsis and death? *Ann Emerg Med* 2000; 35:26-34
- Todoroki H, Nakamura S, Higure A, Okamoto K, Takeda S, Nagata N, Itoh H, Ohsato K. Neutrophils express tissue factor in a monkey model of sepsis. *Surgery* 2000; 127:209-216
- Presneill JJ, Waring PM, Layton JE, Maher DW, Cebon J, Harley NS, Wilson JW, Cade JF. Plasma granulocyte colony-stimulating factor and granulocyte - macrophage colony - stimulating factor levels in critical illness including sepsis and septic shock: relation to disease severity, multiple organ dysfunction, and mortality. *Crit Care Med* 2000; 28:2344-2354
- Paterson RL, Webster NR. Sepsis and the systemic inflammatory response syndrome. *J R Coll Surg Edinb* 2000; 45:178-182
- Salkowski CA, Detore G, Franks A, Falk MC, Vogel S. Pulmonary and hepatic gene expression following cecal ligation and puncture: monophosphoryl lipid A prophylaxis attenuates sepsis-induced cytokine and chemokine expression and neutrophil infiltration. *Infect Immun* 1998; 66: 3569-3578
- Matsukawa A, Hogaboam CM, Lukacs NW, Lincoln PM, Evanoff HL, Kunkel SL. Pivotal role of the CC chemokine, macrophage-derived chemokine, in the innate immune response. *J Immunol* 2000; 164: 5362-5368
- Zhang WZ, Han TQ, Tang YQ, Zhang SD. Rapid detection of sepsis complicating acute necrotizing pancreatitis using polymerase chain reaction. *World J Gastroenterol* 2001; 7:289-292
- Somogyi-Zalud E, Zhong Z, Lynn J, Dawson NV, Hamel MB, Desbiens NA. Dying with acute respiratory failure or multiple organ system failure with sepsis. *J Am Geriatr Soc* 2000; 48(5 Suppl):S140-145
- Medoff BD, Harris RS, Kesselman H, Venegas J, Amato MB, Hess D. Use of recruitment maneuvers and high-positive end-expiratory pressure in a patient with acute respiratory distress syndrome. *Crit Care Med* 2000; 28:

- 1210-1216
- 17 Fu WL, Xiao GX, Yue XL, Hua C, Lei MP. Tracing method study of bacterial translocation *in vivo*. *World J Gastroenterol* 2000;6:153-155
- 18 Koo DJ, Chaudry IH, Wang P. Mechanism of hepatocellular dysfunction during sepsis: the role of gut-derived norepinephrine. *Int J Mol Med* 2000; 5:457-465
- 19 Gong JP, Han BL. Effect of CD14 in LPS mediating inactivation of Kupffer cells. *Shijie Huaren Xiaohua Zazhi* 1999;7:875-877
- 20 Wu RQ, Xu YX, Song XH, Chen LJ, Meng XJ. Adhesion molecule and proinflammatory cytokine gene expression in hepatic sinusoidal endothelial cells following cecal ligation and puncture. *World J Gastroenterol* 2001; 7: 128-130
- 21 Ebong S, Call D, Nemzek J, Bolgos G, Newcomb D, Remick D. Immunopathologic alterations in murine models of sepsis of increasing severity. *Infect Immun* 1999; 67:6603-6610
- 22 Marie C, Muret J, Fitting C, Payen D, Cavaillon JM. Interleukin-1 receptor antagonist production during infectious and noninfectious systemic inflammatory response syndrome. *Crit Care Med* 2000; 28:2277-2282
- 23 Zhang GQ, Yu H, Zhou XQ, Liao D, Xie Q, Wang B. TNF- α induced apoptosis and necrosis of mice hepatocytes. *Shijie Huaren Xiaohua Zazhi* 2000; 8: 303-306
- 24 Bulger EM; Maier RV. Lipid mediators in the pathophysiology of critical illness. *Crit Care Med* 2000; 28(4 Suppl):N27-36
- 25 Yu PW, Xiao GX, Fu WL, Yuan JC, Zhou LX, Qin XJ. Pathogenetic effects of platelet activating factor on enterogenic endotoxemia after burn. *World J Gastroenterol* 2000;6:451-453
- 26 Takahashi Y, Katayose D, Shindoh C. Interleukin-13 prevents diaphragm muscle deterioration in a septic animal model. *Tohoku J Exp Med* 1999; 189:191-202
- 27 Matsukawa A, Hogaboam CM, Lukacs NW, Lincoln PM, Evanoff HL, Strieter RM, Kunkel SL. Expression and contribution of endogenous IL-13 in an experimental model of sepsis. *J Immunol* 2000; 164:2738-2744
- 28 Bernard GR. Research in sepsis and acute respiratory distress syndrome: are we changing course? *Crit Care Med* 1999; 27: 434-436
- 29 Ishikawa K, Tanaka H, Nakamori Y, Hosotsubo H, Ogura H, Nishino M, Shimazu T, Sugimoto H. Difference in the responses after administration of granulocyte colony-stimulating factor in septic patients with relative neutropenia. *J Trauma* 2000; 48:814-824
- 30 Faist E, Kim C. Therapeutic immunomodulatory approaches for the control of systemic inflammatory response syndrome and the prevention of sepsis. *New Horiz* 1998; 6: S97-S102
- 31 Suputtamongkol Y, Intaranongpai S, Smith MD, Angus B, Chaowagul W, Permpikul C, Simpson JA, Leelarasamee A, Curtis L, White NJ. A double-blind placebo-controlled study of an infusion of lexipafant (Platelet-activating factor receptor antagonist) in patients with severe sepsis. *Antimicrob Agents Chemother* 2000; 44:693-696
- 32 Abraham E. Why immunomodulatory therapies have not worked in sepsis. *Intensive Care Med* 1999; 25: 556-566
- 33 Deitch EA, Goodman ER. Prevention of multiple organ failure. *Surg Clin North Am* 1999; 79:1471-1488
- 34 Lazon V, Barke RA. Gram-negative bacterial sepsis and the sepsis syndrome. *Urol Clin North Am* 1999; 26:687-699
- 35 Nasraway SA. Sepsis research: we must change course. *Crit Care Med* 1999; 27: 427-430

Edited by Ma JY

• BASIC RESEARCH •

Construction of HCV-core gene vector and its expression in cholangiocarcinoma

Xiao-Fang Liu, Sheng-Quan Zou, Fa-Zu Qiu

Xiao-Fang Liu, Sheng-Quan Zou, Fa-Zu Qiu, Department of General Surgery of Tongji Hospital, Wuhan 430030, Hubei Province, China
Correspondence to: Dr.Xiao-Fang Liu, Department of Genneral Surgery of Tongji Hospital, 1095 Jiefang Road, Wuhan 430030, Hubei Province, China. Liu634@263.net

Telephone: +86-27-83662134

Received 2001-04-21 Accepted 2001-08-15

Abstract

AIM: To establish an experimental model for exploring the role of hepatitis C virus (HCV) in the development of cholangiocarcinoma.

METHODS: Recombinant plasmid of HCV-core gene was constructed with molecular cloning technique and transfected into QBC939 cells with lipofection. After it was selected with G418, resistant colonies were obtained. The colonies were analysed by immunocytochemistry and Western blotting. The morphology was observed under transmission electron microscope(TEM) and microscope.

RESULTS: The recombinant plasmid was proved to carry the target gene by PCR and restriction enzymed mapping. Moreover, it could express HCV-C protein efficiently in QBC939 cells. The HCV-like particles were found in the cytoplasm by electron microscope, which were spherical with a diameter of 50nm-80nm possessing outer membrane. The transfected cells had lower differentiation and higher malignant degree under microscope.

CONCLUSION: Because HCV-core gene could express steadily in cholangiocarcinoma cells, the transfected tumor cells(QBC939-HCVC) could be used to study the effect of HCV in the development of cholangiocarcinoma.

Liu XF, Zou SQ, Qiu FZ. Construction of HCV-core gene vector and its expression in cholangiocarcinoma. *World J Gastroenterol* 2002;8(1):135-138

INTRODUCTION

Cholangiocarcinoma is the second cancer of hepatobiliary system. The incidence and mortality of cholangiocarcinoma are increasing yearly. There are 3000 new patients in America each year. Recent reports showing the expression of HCV RNA and HCV antigens in cholangiocarcinoma^[1-8], have provided new insights into the pathogenesis of cholangiocarcinoma. Hepatitis C virus(HCV) is recognized as a kind of serious infectious source to harm the health of the humans. It could lead to cancer^[9-17]. Moreover, its core protein could act as a transcriptional regulator of various viral and cellular promoters to potentially disrupt normal cellular functions^[18-21]. Thus, the function of core protein is important for carcinogenesis. We constructed the recombinant plasmid of HCV core gene with molecular cloning technique and transfected into cholangiocarcinoma cells with lipofection, and established an experimental model for exploring the role of HCV in the development of cholangiocarcinoma.

MATERIALS AND METHODS

Materials

Plasmids and bacterium strain PBK-HCV encompassing the core and envelope genomic regions of HCV, containing 330nt - 2020nt of HCV II strain, was provided as a gift by Dr.Chen (Institute of Infectious Disease, Zhejiang University), whose restriction sites were *Pst*I and *Eco*RI. The prokaryotic expressing vector of PBK-CMV containing MCS(multiple cloning site), the neomycin- and kanamycin-resistance gene, SV40 poly(A), was purchased from Stratagene Co. *E.coli* JM109 was obtained from the collection kept in our research group.

Cells The QBC939 cells(a cholangiocarcinoma cell line) were a generous gift from Dr. Wang Shuguang(Third Military Medical University, China). QBC939 cells were cultured in RPMI 1640 supplemented with 100mL·L⁻¹ FBS and incubated at 37°C in a 50mL·L⁻¹ CO₂ atmosphere.

Reagents Restriction enzymes(*Sal*I and *Bam*H I), Taq DNA polymerase, T₄ DNA ligase, were purchased from Hua Mei Co. Lipofection was provided by Boehringer Mannheim Co. Mouse anti-HCV C protein monoclonal antibody was purchased from Chemicon Co. House anti-mouse IgG(mouse)-AP, NBT/BICP were purchased from Zhong Shan Co. Biotinylated-conjugated sheep anti-mouse IgG was purchased from Boster Co.

PCR primers Two primers were designed according to the sequence of HCV core genomic regions and synthesized by the Shanghai GeneCore Bio Technologies Co. Primer 1: 5'-CTCGTCGACCATGAGCACAAATCCTAA-3'; Primer 2: 5'-CTCGGATCCTAAGCGGAAGC-TGGGATG-3'. Primer 1 was 5' primer containing *Sal*I site and Primer 2 was 5' primer containing *Bam*HI site.

Methods

PCR amplification PCR amplification was done using the PBK-HCV as a template and primers 1 and 2 as primers. The reaction was performed according to the parameters of 94°C 3min, 94°C 1min, 55°C 30s and 72°C 1min for 35 cycles. Then it was extended 10min at 72°C. The amplified fragment (approx 600bp) was analyzed by 9 g·L⁻¹ agarose-gel electrophoresis. The product was purified and used for DNA recombination.

DNA recombination DNA recombination was performed according to the methods described in reference^[22]. A 0.6kb fragment, containing HCV core gene, was obtained from the PCR product after digestion with *Sal*I and *Bam*HI. The fragment was recombined into plasmid PBK-CMV and the resulted recombinant plasmid was designated as PBK-HCVC (Figure 1).

Transfection of cells Transfection was performed with lipofection. The constructed vector and control plasmid were used to transfect QBC939 cells in culture. Seven-two h after transfection, they were selected with G418. Then the cells were harvested and used for the detections.

Immunocytochemistry for HCV core protein Detection of HCV core protein expression was performed using a mouse anti-HCV core protein monoclonal antibody(1 : 50) on cell sections of transfected QBC939 and control plasmid.

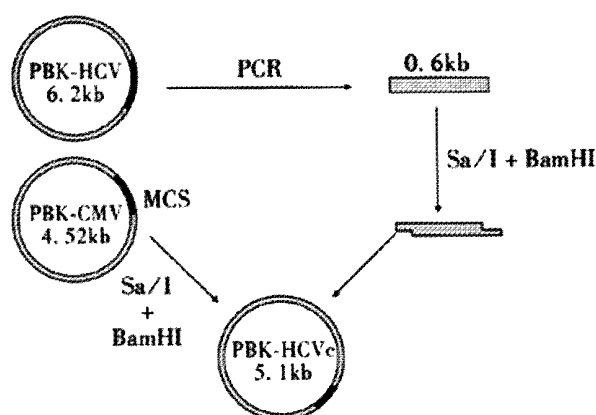


Figure 1 Construction of plasmid PBK-HCVC.

Western blotting Detection of HCV core protein by immunoblotting was performed. Briefly, cells (1×10^6) were scraped, centrifuged briefly, and lysed for 30 min on ice in $50 \text{ mmol} \cdot \text{L}^{-1}$ Tris-cl (pH 7.5), $150 \text{ mmol} \cdot \text{L}^{-1}$ NaCl, $0.2 \text{ mmol} \cdot \text{L}^{-1}$ EDTA, $1 \text{ mmol} \cdot \text{L}^{-1}$ PMSF and $10 \text{ g} \cdot \text{L}^{-1}$ NP-40. The samples were cleared by centrifugation ($14000 \text{ r} \cdot \text{min}^{-1}$, 30 min, 4°C), and assessed for protein concentration. SDS-PAGE was performed, and proteins were electroblotted onto nitrocellulose membranes. After 1 h incubation in blocking solution, the membrane was exposed to the primary antibody 2 h at 4°C . After washing in PBS, the secondary AP-labeled antibody was added for 2 h at room temperature. The proteins were visualized with NBT-BICP.

Transmission electron microscope A pellet of the transfected cells was fixed in $2.5 \text{ g} \cdot \text{L}^{-1}$ glutaraldehyde, postfixed with $10 \text{ g} \cdot \text{L}^{-1}$ osmium tetroxide, treated with $20 \text{ g} \cdot \text{L}^{-1}$ uranyl acetate, dehydrated in ethanol, infiltrated with propylene oxide, and embedded in Epon mixture. Ultrathin sections were observed under Opton EM 10C (German).

Microscope After selected with G418, the cell sections were stained with HE. The cell sections were observed under microscope.

RESULTS

Identification of reconstructed plasmid by PCR and restriction enzymes

The reconstructed plasmid was amplified by PCR, using the PBK-HCVC as a template and primers 1 and 2 as primers, the reaction was performed according to the same parameters. PCR product was approx 600 bp (Figure 2). Then it was identified by the digestion with restriction enzymes (*SmaI* and *BamHI*). Fragments of 4500 bp and 600 bp were produced from the digestion. It was proved to carry the target gene (Figure 3).

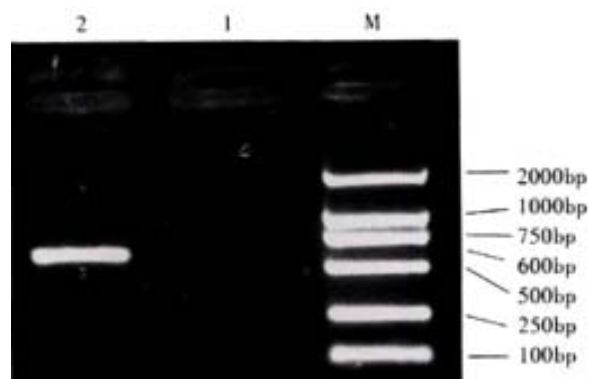


Figure 2 Electrophoretic analysis of PCR product.
M: Marker DL2000; 1: Negative control; 2: PCR product

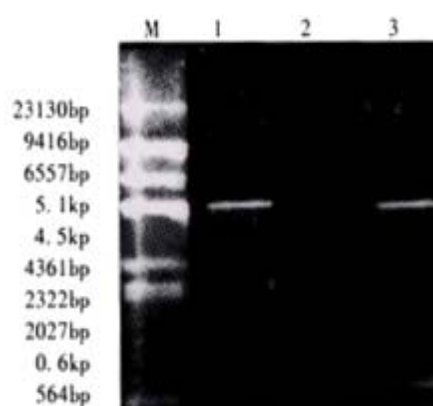


Figure 3 The restriction mapping of PBK-HCVC
M: Maker; ϕ DNA/Hindc6; 1: PBK-CMV; 2: PBK-HCVC; 3: PBK-HCVC restricted by *SmaI* and *BamHI*

Expression of the HCV core protein

Cell sections of transfected with PBK-HCVC and control plasmid (PBK-CMV) were stained for HCV core protein. Staining for HCV core protein was seen in the PBK-HCVC transfected QBC939 cells. Positive staining was located to the cytoplasm (Figure 4).

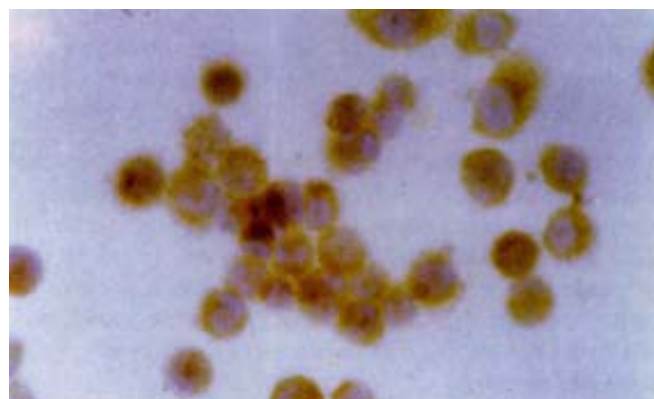


Figure 4 Detection of expressed HCV C antigen by immunocytochemistry. $\times 200$

The expressed products in the supernatant which were transfected with PBK-HCVC and control plasmid (PBK-CMV) were identified by Western blotting. A approx 21 ku band, similar to the size of HCV core protein, was observed in the supernatant of transfection with PBK-HCVC (Figure 5). These results showed that the QBC939 cells transfected with PBK-HCVC could express HCV core protein.

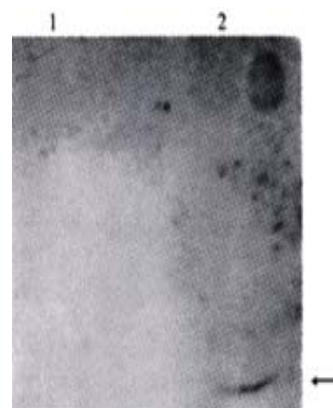


Figure 5 Western blotting detection of the expressed HCV-C protein
1: Transfected QBC939 cells with PBK-CMV; 2: Transfected QBC939 cells with PBK-HCVC

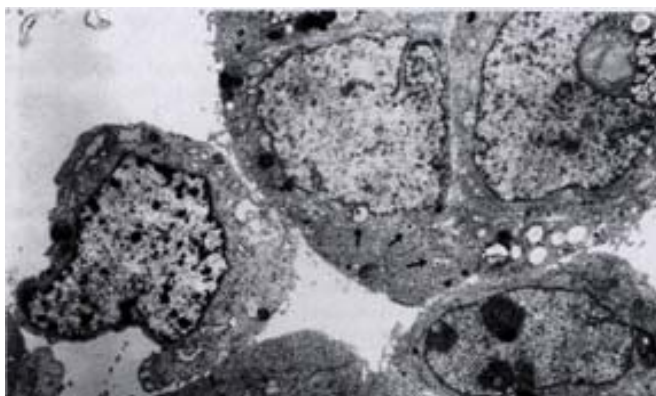


Figure 6 Morphology of QBC939-HCVC cells by TEM. $\times 6500$

The morphologic alteration of the transfected cells

On day 15 after QBC939 cells were transfected with PBK-HCVC, the HCV-like particles were found in the cytoplasm under TEM, which were spherical with a diameter of 50nm-80nm possessing outer membrane (Figures 6,7). The structures were absent in the negative control. The results suggested that the recombinant plasmid could express HCV core protein efficiently in cholangiocarcinoma cell lines. The splits of nuclei were increased significantly in transfected QBC939 cells with PBK-HCVC than PBK-CMV and QBC939 cells (Figure 8). It suggested that the extent of the differentiation was reduced and malignant degree was enhanced after QBC939 cells were transfected with PBK-HCVC.

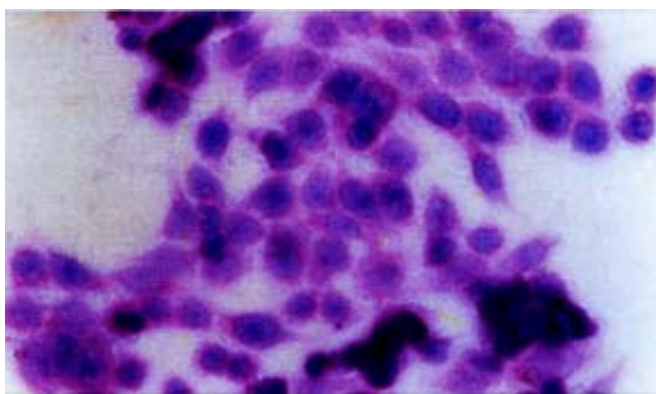


Figure 8 The morphologic alteration of the transfected cells HE. $\times 200$

DISCUSSION

The pathogenesis of cholangiocarcinoma is not clear. Cholelithiasis, cystic dilation of the biliary system, ulcerative colitis and primary sclerosing cholangitis are thought to be the risk factors for cholangiocarcinoma. Recently, laboratory and epidemiological studies found and epidemic found the infection of HCV was related to the development of cholangiocarcinoma [1-8,23-25]. But the mechanism of how they are related has not been studied deeply. HCV infection is an important cause of morbidity and mortality worldwide, causing a spectrum of liver diseases ranging from an asymptomatic carrier state to end-stage liver disease. The most important feature of persistent HCV infection is the development of chronic hepatitis in half of the infected individuals and the potential for disease progression to hepatocellular carcinoma. In our country there are 30-40 million of HCV-carriers patients [26-28].

HCV are hepatotropic viruses. Viral replication and cellular injury are largely confined to the liver. Recent studies, however, have suggested that HCV may replicate in tissues other than in hepatocyte only. Many scholars have reported the presence of HCV RNA and

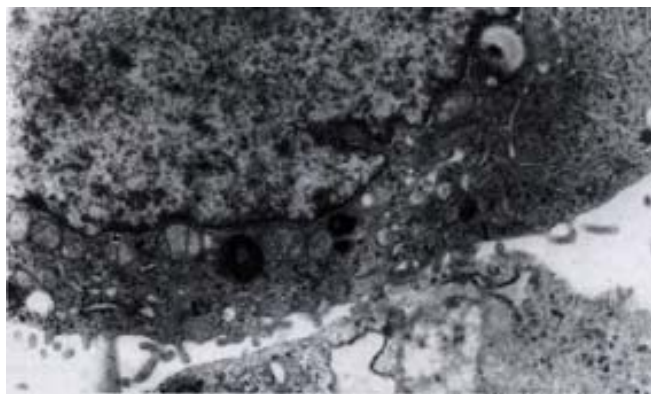


Figure 7 Morphology of QBC939-HCVC cells by TEM. $\times 60\ 000$

HCV-antigens in lymph nodes, pancreas, ovary, kidney, heart and bile duct epithelial cells [29-35]. The infection of HCV could lead to bile duct damage and loss. Moreover, bile duct injury is more commonly associated with HCV than either HBV or autoimmune hepatitis, which is the characteristic histologic feature of HCV. The bile duct damage and loss are defined as variable epithelial, steatosis, lymphocytic infiltration of bile ducts [36-38]. The more injury of HCV infection in bile duct provides new evidence that bile duct epithelial cells could be an important reservoir of HCV and might lead to the pathogenesis of cholangiocarcinoma. An HCV genome contains a linear, positive-strand RNA molecule of 9500 nucleotides encoding a single polypeptide precursor of 3000 amino acids. The polypeptide is cleaved by viral proteases to generate three putative structural proteins (C, E1 and E2) and at least six nonstructural proteins (NS2, NS3, NS4A, NS4B, NS5A and NS5B) [39,40]. The genomic region encoding the putative C protein is also called core protein. The HCV core protein could act as a transcriptional regulator of various viral and cellular promoters to potentially disrupt normal cellular functions [18-21]. The core protein may cooperate with ras oncogene and transform primary rat embryo fibroblasts to a tumorigenic phenotype [41]. It may also cause anti-apoptosis by reversion of tumor suppressor gene-p53 and activation of NF- κ B and implicate a mechanism by which HCV may evade the host immune surveillance leading to viral persistence and possibly to carcinogenesis [42-51]. Thus, the HCV core protein plays a major role in the malignant transformation of cells. It is important to explore the role of HCV in the development of cholangiocarcinoma by establishing an experimental model which expresses efficiently HCV core protein in cholangiocarcinoma cell lines.

In our study, recombinant plasmid of HCV-core gene was constructed with molecular cloning technique, it was identified by restriction enzymes. Then it was transfected into QBC939 cells with lipofection. After it was selected with G418 made by the presence of the neomycin and kanamycin resistance gene, resistant colonies were obtained. The colonies were analysed by immunocytochemistry and Western blotting. The results suggest that the recombinant plasmid was proved to carry the target gene by PCR and restricted enzyme map, and it could express HCV core protein efficiently in QBC939 cells. The morphology was observed under transmission electron microscopy (TEM), and the HCV-like particles in the cytoplasm, were found spherical with a diameter of 50nm-80nm possessing outer membranes. Moreover, we also found that the splits of nuclei were increased in transfected QBC939 cells with PBK-HCVC, and the extent of differentiation was reduced. It suggested that the malignant degree was enhanced after QBC939 cells were transfected with PBK-HCVC. Because HCV-core gene could express steadily in cholangiocarcinoma cells, the transfected tumor cells (QBC939-HCVC) could be used to study the effect of HCV in the development of cholangiocarcinoma.

REFERENCES

- Tomimatsu M, Ishiguro N, Tanai M, Okuda H, Saito A, Obata H, Yamamoto M, Takasaki K, Nakano M. Hepatitis C virus antibody in patients with primary liver cancer (hepatocellular carcinoma, cholangiocarcinoma and hepatocellular-cholangiocarcinoma) in Japan. *Cancer* 1993;72:683-688
- Zhang HZ, Tang YB, Lu XY. Detection of hepatitis B virus DNA and hepatitis C virus RNA in human hepatocellular carcinoma by polymerase chain reaction. *Zhonghua Binglixue Zazhi* 1996;25:70-726
- Yin FZ, Chen BF, Xu CS. HCV RNA sequences in cholangiocarcinoma tissues. *Zhonghua Shiyao Waikao Zazhi* 1998;15:109-110
- Chen RF, Zou SQ, Zhao XP. The expression of hepatitis C virus gene in hilar cholangiocarcinoma and implication. *Zhonghua Shiyao Waikao Zazhi* 2000;17:223-224
- Lu HY, Michele Q Ye, Swan N Thung, Dash S, Gerber MA. Detection of hepatitis C virus RNA sequences in cholangiocarcinomas in Chinese and American patients. *Chin Med J* 2000;113:1138-1141
- Chen MY, Huang ZQ, Chen LZ, Gao YB, Peng RY, Wang DW. Detection of hepatitis C virus NS5 protein and genome in Chinese carcinoma of the extrahepatic bile duct and its significance. *World J Gastroenterol* 2000;6:800-804
- Zhai SH, Liu JB, Liu YM, Zhang LL, Du ZP. Expression of HBsAg, HCV-Ag and AFP in liver cirrhosis and hepatocarcinoma. *Shijie Huaren Xiaohua Zazhi* 2000;8:524-527
- Wang WL, Wang CJ, Wang BF. Significance of HCV gene and its antigen expression in human primary intrahepatic cholangiocarcinoma. *Shijie Huaren Xiaohua Zazhi* 2001;9:542-545
- Hiramatsu N, Hayashi N, Haruna Y, Kasahara A, Fusamoto H, Mori C, Fuke I, Okayama H, Kamada T. Immunohistochemical detection of hepatitis C virus-infected hepatocytes in chronic liver disease with monoclonal antibodies to core, envelope and NS3 regions of the hepatitis C virus genome. *Hepatology* 1992;16:306-311
- Yan XB, Wu WY, Wei L. Clinical features of infection with different genotypes of hepatitis C virus. *Huaren Xiaohua Zazhi* 1998;6:653-655
- Zhang LF, Peng WW, Yao JL, Tang YH. Immunohistochemical detection of HCV infection in patients with hepatocellular carcinoma and other liver diseases. *World J Gastroenterol* 1998;4:64-65
- Sorensen HT, Friis S, Olsen JH, Thulstrup AM, Mellemkjaer L, Linet M, Trichopoulos D, Vilstrup H, Olsen J. Risk of liver and other types of cancer in patients with cirrhosis: a nationwide cohort study in Denmark. *Hepatology* 1998;28:921-925
- Yang JM, Wang RQ, Bu BG, Zhou ZC, Fang DC and Luo YH. Effect of HCV infection on expression of several cancer-associated gene products in HCC. *World J Gastroenterol* 1999;5:25-27
- Feng DY, Chen RX, Peng Y, Zheng H, Yan YH. Effect of HCV NS3 protein on p53 protein expression in hepatocarcinogenesis. *World J Gastroenterol* 1999;5:45-46
- Huang F, Zhao GZ, Li Y. HCV genotypes in hepatitis C patients and their clinical significances. *World J Gastroenterol* 1999;5:547-549
- Caselmann WH. Clinical characteristics and outcome of a cohort of 101 patients with hepatocellular carcinoma. *World J Gastroenterol* 2001;7:208-215
- Tang ZY. Hepatocellular Carcinoma Cause, Treatment and Metastasis. *World J Gastroenterol* 2001;7:445-454
- Liu QY, Tackney C, Bhat RA, Prince AM, Zhang P. Regulated processing of hepatitis C virus core protein is linked to subcellular localization. *J Virol* 1997;71:657-662
- Dai YM, Shou ZP, Ni CR, Wang NJ, Zhang SP. Localization of HCV RNA and capsid protein in human hepatocellular carcinoma. *World J Gastroenterol* 2000;6:136-137
- Liu LH, Xiao WH, Liu WW. Effect of deoxycytidine on the P16 tumor suppressor gene in hepatocellular carcinoma cell line HepG2. *World J Gastroenterol* 2001;7:131-135
- Ray RB, Meyer K, Ray R. Hepatitis C virus core protein promotes immortalization of primary human hepatocytes. *Virology* 2000;271:197-204
- Sambrook J, Fritsch EF, Maniatis T (Translated by Jin DY, Liang MF). Molecular Cloning: A Laboratory Manual (2nd Ed). Beijing: Science Press 1996:672-898
- Yamamoto M, Takasaki K, Nakanom M. Minute nodular intrahepatic cholangiocarcinoma. *Cancer* 1998;82:2145-2149
- Suriawinata A, Ivanov K, Haim MB, Schwartz ME. A 67-year-old man with hepatitis C virus infection and a liver tumor. *Semi In Liver Dis* 2000;20:227-231
- Kobayashi M, Ikeda K, Saitoh S, Suzuki F, Tsubota A, Arase Y, Murashima N, Chayama K, Kumada H. Incidence of primary cholangiocellular carcinoma of the liver in Japanese with HCV-related cirrhosis. *Cancer* 2000;88:2471-2477
- Zhang SL, Liang XS, Lin SM, Peng Chao Qiu. Relation between viremia level and liver disease in patients with chronic HCV infection. *China Natl J New Gastroenterol* 1996;2:115-117
- Assy N, Minuk GY. A comparison between previous and present histologic assessments of chronic hepatitis C viral infections in humans. *World J Gastroenterol* 1999;5:107-110
- Li LF, Zhou Y, Xia S, Zhao LL, Wang ZX, Wang CQ. The epidemiologic feature of HCV prevalence in Fujian. *World J Gastroenterol* 2000;6:80
- Shimizu YK, Iwamoto A, Hijikata M, Purcell RH, Yoshikura H. Evidence of *in vitro* replication of hepatitis C virus genome in a human T-cell line. *Proc Natl Acad Sci USA* 1993;89:5477
- Moldvay J, Deny D, Pol S, Brechot C, Lamas E. Detection of hepatitis C virus RNA in peripheral blood mononuclear cells of infected patients by *in situ* hybridization. *Blood* 1994;38:269
- Zhou P, Cai Q, Chen YC, Zhang MS, Guan J, Li XJ. Hepatitis C virus RNA detection in serum and peripheral blood mononuclear cells of patients with hepatitis C. *China Natl J New Gastroenterol* 1997;3:108-110
- Kato N, Nakazawa T, Mizutani T, Shimotohno K. Susceptibility of human T-lymphotropic virus type I infected cell line MT-2 to hepatitis C virus infection. *Biochem Bio Res Commun* 1995;26:863-869
- Fan XG, Tang FQ, Ou ZM, Zhang JX, Liu GC, Hu GL. Lymphoproliferative response to hepatitis C virus (HCV) antigens in patients with chronic HCV infection. *Shijie Huaren Xiaohua Zazhi* 1999;7:1038-1040
- Yan FM, Chen AS, Hao F, Zhao XP, Gu CH, Zhao LB, Yang DL, Hao LJ. Hepatitis C virus may infect extrahepatic tissues in patients with hepatitis C. *World J Gastroenterol* 2000;6:805-811
- Cheng JL, Tong WB, Liu BL, Zhang Y, Yan Z, Feng BF. Hepatitis C virus in human B lymphocytes transformed by Epstein-Barr virus *in vitro* by *in situ* reverse transcriptase-polymerase chain reaction. *World J Gastroenterol* 2001;7:370-375
- Bach N, Thung SN, Schaffner F. The histological features of chronic hepatitis C and autoimmune chronic hepatitis: A comparative analysis. *Hepatology* 1992;15:572-577
- Goldin RD, Patel NK, Thomas HE. Hepatitis C and bile duct loss. *J Clin pathol*, 1996;49: 836-838
- Giannini E, Ceppa P, Botta F, Fasoli A, Romagnoli P, Cresta E. Steatosis and bile duct damage in chronic hepatitis C: distribution and relationships in a group of Northern Italian patients. *Liver* 1999;19:432-437
- Zhang SZ, Liang JJ, Qi ZT, Hu YP. Cloning of the non-structural gene 3 of hepatitis C virus and its inducible expression in cultured cells. *World J Gastroenterol* 1999;5:125-127
- Jiang RL, Lu QS, Luo KX. Cloning and expression of core gene cDNA of Chinese hepatitis C virus in cosmid pTM3. *World J Gastroenterol* 2000;6:220-222
- Ray RB, Lagging LM, Meyer K, Ray R. Hepatitis C virus core protein cooperates with ras and transforms primary rat embryo fibroblasts to tumorigenic phenotype. *J Virol* 1996;70:4438-4443
- Xiao WH, Liu WW, Lu YY, Li Z. Mutation of p53 tumor suppressor gene in hepatocellular carcinoma. *Xin Xiaohuabingxue Zazhi* 1997;5:573-574
- Wei HS, Li DG, Lu HM. Hepatic cell apoptosis and fas gene. *Shijie Huaren Xiaohua Zazhi* 1999;7:531-532
- Li J, Chen YF, Wang WL, Lin SG. Translocated expression of HCV core protein inhibits apoptosis in the tissue of hepatocellular carcinoma. *Shijie Huaren Xiaohua Zazhi* 1999;7:579-582
- Si XH, Yang LJ. Extraction and purification of TGF α and its effect on the induction of apoptosis of hepatocytes. *World J Gastroenterol* 2001;7:527-531
- Ray RB, Meyer K, Ray R. Suppression of apoptotic cell death by hepatitis C virus core protein. *Virology* 1996;226:176-182
- Marusawa H, Hijikata M, Chiba J, et al. Hepatitis C virus core protein inhibits Fas- and Tumor Necrosis Factor Alpha-mediated apoptosis via NF- κ B activation. *J Virol* 1999;73:4713-4720
- Ray RB, Meyer K, Steele R, Shrivastava A, Aggarwal BB, Ray R. Inhibition of tumor necrosis factor (TNF- α)-mediated apoptosis by hepatitis C virus core protein. *J BioChem* 1998;273:2256-2259
- Tai DI, Tsai SL, Chen YM, Chuang YL, Peng CY, Sheen IS, Yeh CT, Chang KS, Huang SN, Kuo GC, Liaw YF. Activation of nuclear factor κ B in hepatitis C virus infection: Implication for pathogenesis and hepatocarcinogenesis. *Hepatology* 2000;31:656-664
- Hiramatsu N, Hayashi N, Katayama K, Mochizuki K, Kawanishi Y, Kashara A, Fusamoto H, Kamada T. Immunohistochemical detection of Fas antigen in liver tissue of patients with chronic hepatitis C. *Hepatology* 1994;19:1354-1359
- Yen TS. Nuclear factor κ B and hepatitis C-Is there a connection. *Hepatology* 2000;31:785-787

• BASIC RESEARCH •

CCK8 inhibits expression of TNF- α in the spleen of endotoxic shock rats and signal transduction mechanism of p38 MAPK

Ai-Hong Meng, Yi-Ling Ling, Xiao-Peng Zhang, Xiao-Yun Zhao, Jun-Lan Zhang

Ai-Hong Meng, Yi-Ling Ling, Xiao-Yun Zhao, Jun-Lan Zhang, Department of Pathophysiology, Hebei Medical University, Shijiazhuang 050017, Hebei Province, China

Xiao-Peng Zhang, Department of Chest Surgery of Hebei Provincial People's Hospital, Shijiazhuang, 050000, China

Supported by the Health Committee of Hebei Province (No.2k002), project supported by Science and Technology Department of Hebei Province (01276410D) and project supported by Natural Science Foundation of Hebei Province (No.302490). The paper published on *World J Gastroenterol*, 2001; 7 (5): 667-671 is key project supported by the Health Committee of Hebei Province (No.2k002), project supported by Science and Technology Department of Hebei Province (01276410D) and project supported by Natural Science Foundation of Hebei Province (No.302490)

Correspondence to: Professor Yi-Ling Ling, Department of Pathophysiology, Hebei Medical University, Shijiazhuang 050017, Hebei Province, China. LingYL20@sina.com.cn

Telephone: +86-311-6052263

Received 2001-10-21 Accepted 2001-12-08

Abstract

AIM: To study the effect of sulfated cholecystokinin-octapeptide (CCK-8) on systemic hypotension, gene and protein expression of TNF- α in spleen of lipopolysaccharide (LPS) induced endotoxic shock (ES) rats, and further investigate the signal transduction mechanism of p38 mitogen-activated protein kinase (MAPK).

METHODS: The changes of blood pressure were observed using physiological record instrument in four groups of rats: LPS (8 mg·kg⁻¹, iv), CCK-8 (40 μ g·kg⁻¹, iv) pretreatment 10 min before LPS (8 mg·kg⁻¹), CCK-8 (40 μ g·kg⁻¹, iv) or normal saline (control) group. The content of TNF- α in the spleen was assayed 2 h after LPS administration using ELISA kit and the expression of TNF- α mRNA was examined 30 min, 2 h and 6 h after LPS administration by reverse transcribed polymerase chain reaction (RT-PCR). Activation of p38 MAPK was detected with Western blot 30 min after LPS administration.

RESULTS: CCK-8 reversed LPS-induced decrease of mean arterial pressure (MAP) in rats. The content of TNF- α in the spleen was (282 \pm 30) ng·L⁻¹ in control group, while it increased to (941 \pm 149) ng·L⁻¹ in LPS group, $P < 0.01$. CCK-8 significantly inhibited the LPS-induced increase of TNF- α content in spleen. It decreased to (462 \pm 87) ng·L⁻¹ in CCK-8+LPS group, $P < 0.01$. The expression of TNF- α mRNA 30 min and 2 h after treatment was stronger in LPS group, while it was lowered after CCK-8 pretreatment. The p38 MAPK expression increased significantly in LPS group (5.84 times of control) and CCK-8 increased the activation of p38 MAPK in ES rats (10.74 times of control).

CONCLUSION: CCK-8 reverses the decrease of MAP in ES rats and has inhibitory effect on the gene and protein expression of TNF- α in spleen, and p38 MAPK may be involved in its signal transduction mechanisms.

Meng AH, Ling YL, Zhang XP, Zhao XY, Zhang JL. CCK-8 inhibits expression of TNF- α in the spleen of endotoxic shock rats and signal transduction mechanism of p38 MAPK. *World J Gastroenterol* 2002;8(1):139-143

INTRODUCTION

Lipopolysaccharide (LPS), main component of Gram-negative bacterial endotoxin^[1], is the leading cause of sepsis or endotoxic shock (ES), and when administered experimentally to animals, mimics the same inflammatory response. LPS exerts its effects through cytokines^[2]. The pathophysiological changes seen in sepsis are often not due to the infectious organism itself but instead to the uncontrolled production of pro-inflammatory cytokines, including tumor necrosis factor (TNF)- α ^[3]. TNF- α , which is produced by LPS-activated target cells, is thought to be LPS's primary mediator^[4]. TNF is known to have cytotoxic and cytostatic effects on certain tumor cells, and with a pivotal role in inflammatory reactions and regulation of immunological response^[5,6]. TNF- α was mainly produced in the early stage of endotoxemia, and decreased obviously from 6 h to 9 h after challenge^[7]. Specific intracellular signaling pathways that modulate cytokine gene expression probably exist in target cells and may represent novel targets for tomorrow's antisepsis therapies^[8]. Mitogen-activated protein kinases (MAPKs) are members of discrete signaling cascades that form focal points for diverse extracellular stimuli and function to regulate fundamental cellular processes^[9]. The p38 MAPK, one class of MAPK family, is involved in intracellular signals that regulate a variety of cellular responses during inflammation^[10].

CCK-8 possessed both excitatory and inhibitory action on contractile activity of different regions of stomach in guinea pigs^[11]. In the spleen, CCK-8 is formed in high abundance in the white pulp where it appears to surround cell clusters. CCK-8 is a chemoattractant for human monocytes and rat macrophages, enhances human eosinophil chemotaxis induced by PAF and LTB₄ in allergic patients. Our previous study demonstrated that CCK-8 could protect animals from LPS-induced ES and the protective effect of CCK-8 may be related to its modulation of cytokines^[12-14]. Spleen, one of the targets stimulated by LPS, is an important immunological organ. In this study, we examined the expression of TNF- α with reverse transcribed polymerase chain reaction (RT-PCR) and enzyme linked immunoabsorbant assay (ELISA) in spleen and further investigated the mechanism involving p38 MAPK.

MATERIAL AND METHODS

Material

CCK-8 (sulfated), LPS (*E.coli* LPS, serotype 0111:B4), leupeptin, pepstatin A and Triton X-100 were all purchased from Sigma, and aprotinin from Boehringer. The ELISA kit was purchased from Medsystem (Austria) for assay of TNF- α . Total RNA isolation system and access RT-PCR system were purchased from Promega (USA). Monoclonal anti-p38 MAPK (diphosphorylated p38) was purchased from Sigma (USA). All other reagents used were of analytic grade. Healthy male Sprague-Dawley rats ($n=52$, weighing 150 g-200 g BW) were obtained from Experimental Animal Center of Hebei Province.

Methods

The rats were randomly assigned to four groups and injected different agents via caudal vein. A bolus dose ($8 \text{ mg} \cdot \text{kg}^{-1}$, $5 \text{ g} \cdot \text{L}^{-1}$) of LPS was injected to group receiving LPS and a bolus dose ($40 \mu\text{g} \cdot \text{kg}^{-1}$, $0.05 \text{ g} \cdot \text{L}^{-1}$) of CCK-8 was given to the group of CCK-8+LPS 10 min before injection of LPS. Saline or CCK-8 ($40 \mu\text{g} \cdot \text{kg}^{-1}$) was administered separately to the control or CCK-8 group. Catheter was inserted into femoral artery and Mean arterial pressure (MAP) was detected using physiological record instrument (RM-6000, Japan). The agents were injected through caudal vein after the MAP became steady. Animals were sacrificed at 30 min, 2 h or 6 h after treatment, spleen was rapidly excised, rinsed of blood. The samples were stored at -80°C . The samples collected at different time points were for the assay of TNF- α mRNA using RT-PCR, samples collected at 2 h were for the assay of TNF- α protein by ELISA and at 30 min for the expression of p38 MAPK by Western blot.

TNF- α detection by ELISA

Frozen tissue samples were weighed and placed in homogenization buffer (4°C) at a ratio of 100 mg per milliliter of buffer. Buffer contained a protease-inhibitor cocktail including $1 \text{ mmol} \cdot \text{L}^{-1}$ phenylmethylsulfonyl fluoride (PMSF), $1 \text{ mg} \cdot \text{L}^{-1}$ pepstatin A, $1 \text{ mg} \cdot \text{L}^{-1}$ aprotinin, and $1 \text{ mg} \cdot \text{L}^{-1}$ leupeptin in phosphate-buffered saline solution, pH 7.2, containing $5 \text{ g} \cdot \text{L}^{-1}$ Triton X-100. Samples were homogenized and centrifuged at $18\,000 \text{ r} \cdot \text{min}^{-1}$, 4°C . Tissue supernatants were analyzed for TNF- α using ELISA kit.

Analysis of TNF- α mRNA by RT-PCR

Total RNA was extracted from spleen tissues. The concentration of RNA was determined from absorption at 260 nm. The primers for TNF- α and β -actin were as follows: β -actin (420bp), 5'-GAGACCTTC AACACCCAGCC-3', 5'-TCGGGGCATCGG AACCGCTCA-3'; TNF- α (468bp), 5'-GGATCATCTTCT CAAAACTCG-3', 5'-TCACAGAGCAATGACTCCAAA-3'. Polymerase chain reactions were performed in a $50 \mu\text{L}$ reaction volume. RT-PCR reaction was run in the following procedures: 48°C for 45 min, 1 circle; 94°C for 2 min, 1 circle; 94°C for 30 s, 57°C for 30 s, 68°C for 1 min, 30 circles; 68°C for 7 min, 1 circle. Six μL PCR product was placed on to $15 \text{ g} \cdot \text{L}^{-1}$ agarose gel and observed by EB staining using Gel-Pro analyzer.

Detection of p38 MAPK expression by Western blot

Spleen was rapidly excised 30 min after agents administration. Tissues were homogenized with PBS (pH 7.2) and centrifuged at 4°C , $18\,000 \text{ r} \cdot \text{min}^{-1}$ for 10 min. Protein contents were detected in supernatants by coomassie brilliant blue (CBB). Sample loading buffer was added, and each sample was boiled for 8 min prior to loading equal content of protein onto a $12 \text{ g} \cdot \text{L}^{-1}$ SDS-polyacrylamide gels, transferred to polyvinylidene fluoride (PVDF) membranes, and incubated with phospho-specific anti-p38 MAPK. Being washed three times in T-PBS, membranes were incubated in horseradish peroxidase-linked secondary antibody for 1 h at room temperature. Membranes were again washed three times with T-PBS and stained with diaminobenzidine (DAB).

Statistical analysis

Data were reported as $\bar{x} \pm s$. Statistical differences between values from different groups were determined by one way ANOVA and Newman-Keuls q test. Significance was set at $P < 0.05$. Gel-Pro Analyzer was used to analyze the PCR and Western results.

RESULTS

Changes of MAP

There was no significant difference between groups before treatment. LPS administration resulted in a significant sustained decrease in MAP during the period of 2 h, decreased to $(7.82 \pm 0.43) \text{ kPa}$ 30 min after LPS administration and restored to $(9.33 \pm 0.63) \text{ kPa}$ by pretreatment with CCK-8 (Figure 1).

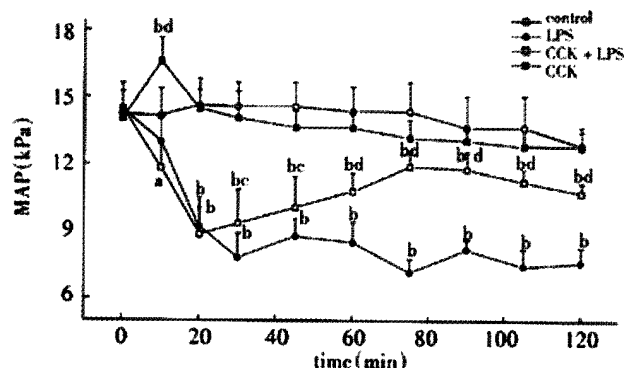


Figure 1 Mean arterial pressure (MAP) of animals injected normal saline, LPS, CCK+LPS and CCK, $n=6$. ^a $P < 0.05$, ^b $P < 0.01$, vs Control, ^c $P < 0.05$, ^d $P < 0.01$, vs LPS.

TNF- α content in spleen 2 h after LPS

Spleen TNF- α content became significantly higher 2 h after administration of LPS as compared to the control animals ($941 \pm 149 \text{ ng} \cdot \text{L}^{-1}$ vs $(282 \pm 30) \text{ ng} \cdot \text{L}^{-1}$, $P < 0.01$), while CCK-8 significantly inhibited the LPS induced increase of TNF- α ($462 \pm 87 \text{ ng} \cdot \text{L}^{-1}$, $P < 0.01$). No significant changes were noted in TNF- α content following CCK-8 administration compared with normal saline administration (Figure 2).

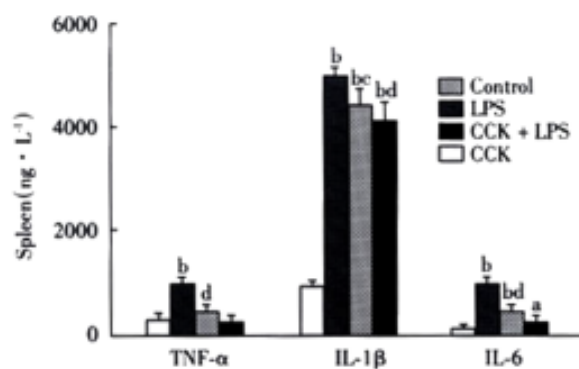


Figure 2 Effects of CCK on TNF- α , IL-1 β and IL-6 2 h (TNF- α) or 6 h (IL-1 β and IL-6) following LPS administration. $n=6$. ^a $P < 0.05$, ^b $P < 0.01$, vs Control; ^c $P < 0.05$, ^d $P < 0.01$, vs LPS.

RT-PCR detection of TNF- α

TNF- α mRNA in spleen was detected by RT-PCR analysis. The results showed that the spleen of rats 30 min and 2 h after LPS administration expressed the gene coding for TNF- α because RT-PCR generated a DNA fragment corresponding to the predicted length, 468bp, of the TNF- α amplification product. The expression of TNF- α decreased in CCK-8+LPS group compared with LPS group. The ratios of β -actin at 30 min and 2 h were $(85 \pm 8)\%$ and $(57 \pm 7)\%$ in LPS group, while it decreased to $(30 \pm 6)\%$ and $(16 \pm 2)\%$ respectively in CCK-8+LPS group. The TNF- α amplification product was not detected 6 h after agents administration. In each tissue sample, all β -actin amplification products were of 420bp length (Figure 3).

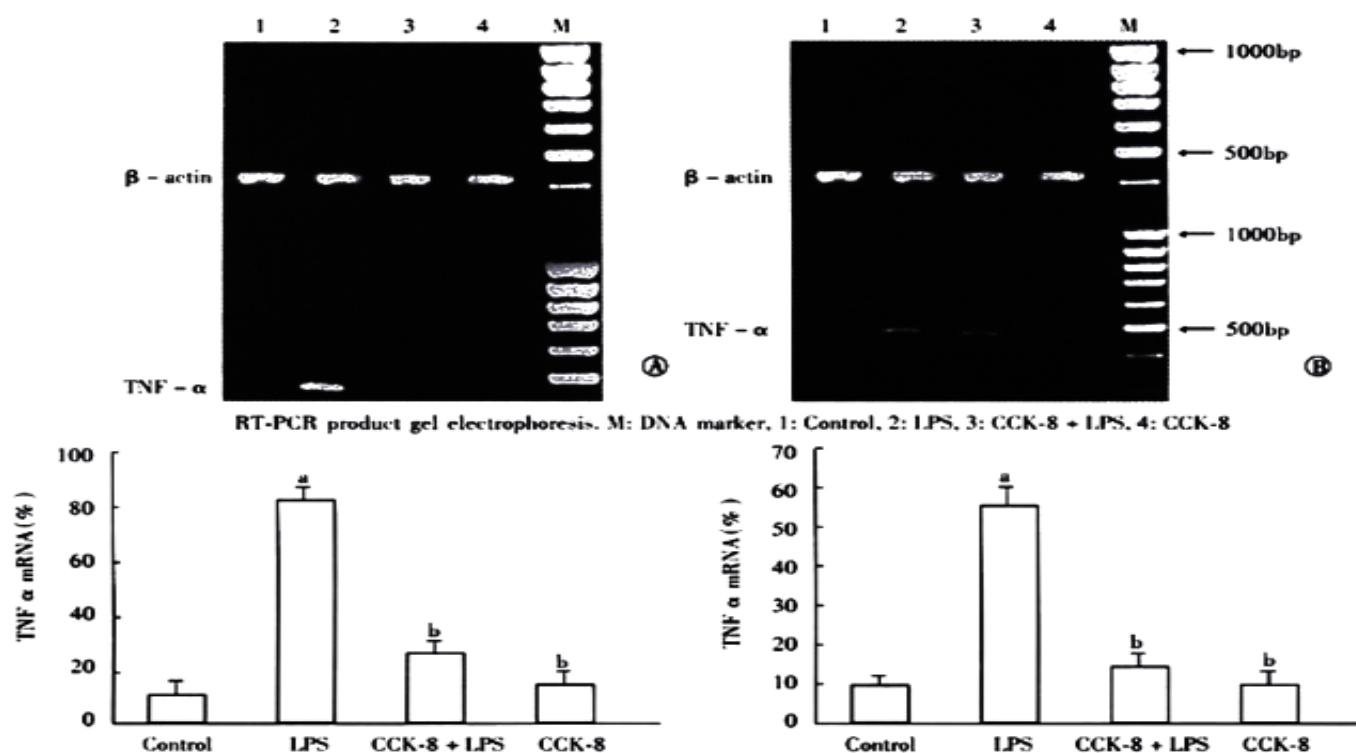


Figure 3 Effect of CCK-8 on LPS-induced TNF- α mRNA expression. Total RNA from the rat spleen was extracted at 30 min(A) or 2h(B) after LPS administration. $n=3$. ^a $P<0.01$ vs Control; ^b $P<0.01$ vs LPS.

Analysis of p38 MAPK expression by Western blot

Significant phosphorylation of p38 MAPK was observed in the spleen of rats 30 min after LPS administration, the densitometry units (DU) of LPS group is 5.84 times that of control. CCK-8 can enhance LPS-induced phosphorylation of p38 MAPK significantly, the DU of CCK-8+LPS group is 10.74 times that of control. Phosphorylation of p38 MAPK was also observed in control and CCK-8 groups (4.64 times of control)(Figure 4).

DISCUSSION

Although macrophages are the main secretors of TNF- α , other spleen cells, such as lymphocytes, may secrete low amounts of TNF- α and may influence macrophage ability to generate and secrete the cytokine^[15]. This has led to the suggestion that spleen is an important organ in the production of TNF- α following LPS administration, releasing the cytokines into the circulation, thereby contributing to the elevated serum level of the cytokine. Numerous TNF- α and IL-1 β mRNA positive cells were observed using *in situ* hybridization in the marginal zone and in the red pulp of the spleen in rats after LPS injections, whereas sections from saline-treated animals showed minimal cytokine mRNA expression^[16]. LPS resulted in a greater increase in circulating levels of TNF- α which peaked at 90 min and decreased at 150 min after LPS administration^[17]. We found that CCK-8 significantly inhibits LPS-induced increase of TNF- α in spleen, which agreed with the results we obtained before^[14]. While Cunningham *et al*^[18] reported that CCK-8 stimulated production of TNF- α , IL-1 β and IL-6 by monocytes, but was considerably less than LPS response. Later studies^[19] suggest that the increase of cytokines induced by CCK-8 may be due to the detection of endotoxin/LPS in medium.

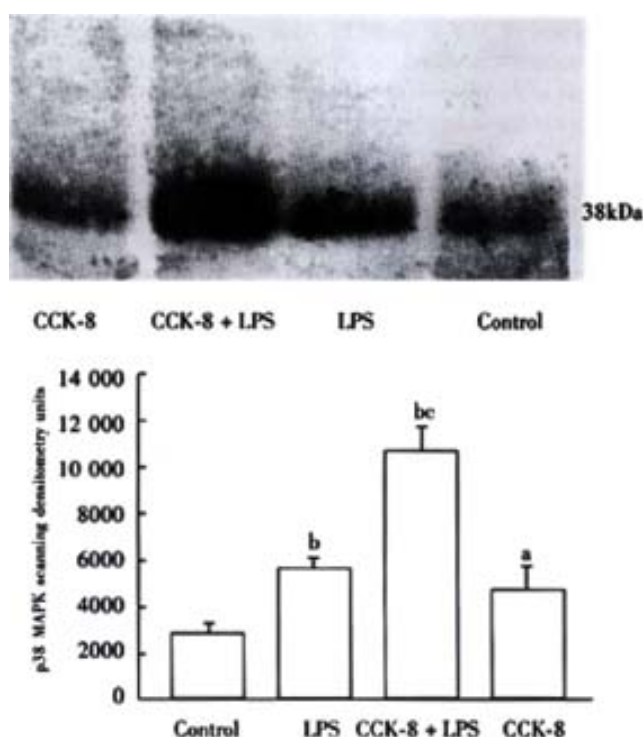


Figure 4 CCK-8 increases p38 MAPK activation induced by LPS in spleen. ^a $P<0.05$, ^b $P<0.01$ vs Control; ^c $P<0.01$ vs LPS.

Despite convincing data indicating the protective function of

CCK-8 to organism in ES, the precise mechanism remains elusive. Our previous studies showed that CCK can protect pulmonary arterial endothelium against detrimental effects by LPS or TNF- α ^[20,21]. The anti-inflammatory effect of CCK-8 shown in this study may mediate the cell protective function of CCK-8 in ES. The p38 MAPK pathway may be involved. Members of the MAPK cascade are considered to play key roles in signal transduction pathways activated by a wide range of stimuli^[22]. CCK is known to activate MAPK signaling pathways^[23]. Activated MAPK then transduces into the nucleus and phosphorylates the ternary complex factor TCF which activates the expression of immediate-early genes, such as c-fos and egr-1^[24]. The three best characterized members of this growing family of serine/threonine kinases are extracellular signal regulated kinase (ERK), c-jun N-terminal kinase (JNK) and p38. While ERK responds vigorously to growth factors and certain hormones, JNK and p38 are rather activated by stress stimuli and are widely believed to be part of the cellular stress response machinery^[22,25]. The p38 MAPK is associated with immune cell activation, because this kinase is activated by a variety of inflammatory mediators. Challenge of neutrophils with LPS leads to activation of p38 but with slower kinetics than G-protein-coupled chemoattractant receptors^[26]. CCK-A and CCK-B receptors are G-protein-coupled^[27]. p38 is expressed in the pancreas and rapidly activated by CCK receptor agonist, cerulein^[28,29]. p38 inhibition aggravated cerulein pancreatitis, indicating that p38 activation may support protection of the pancreas against damage through hyperstimulation stress. CCK activated p38 MAPK and increased the phosphorylation of HSP27^[30]. The p38-MAPK/HSP27 pathway may be important for organ protection in the pancreas. Other studies indicate that p38 activation can indeed be protective^[14]. Sodium salicylate (NaSal) significantly reduced TNF- α production in LPS-stimulated macrophages. LPS-stimulated activation of ERK and SAPK/JNK was inhibited by NaSal pretreatment. NaSal treatment of macrophages activated p38 MAPK independent of LPS stimulation^[8]. Our data have raised the question of how the increase in p38 MAPK activity, a potent intermediate signal transducer involved in the production of TNF- α after LPS administration, could be associated with decreased production of TNF- α , detected by ELISA and RT-PCR analysis in the presence of CCK-8. LPS-induced production of TNF- α is regulated mainly, but not exclusively, through the p38 MAPK pathway^[31]. TNF- α expression in T cells is regulated by several distinct MAPK pathways that functionally cooperate and are critical for transcriptional as well as for posttranscriptional processes^[32]. Carbon oxide inhibited the LPS-induced production of TNF- α in mice, which was mediated by p38 MAPK activation^[3]. Perhaps a delicate balance exists in the actions of p38, in that subtle cellular activation, as with LPS alone, is stimulatory for TNF- α synthesis, whereas hyperstimulation, as seen in spleen treated with CCK-8 and LPS, becomes inhibitory and thus results in downregulation of TNF- α . This modulation by CCK-8 of LPS-induced production of TNF- α exemplifies accumulating evidence emphasizing the complexity of the molecular regulation of TNF- α expression.

The results of the present study show that administration of CCK-8 prevents LPS-induced decrease of MAP and attenuates LPS-induced increase of TNF- α gene and protein expression in spleen. The different activation of p38 MAPK by LPS or CCK-8 may be involved in their effect on TNF- α production. CCK-8, therefore, might be used therapeutically to treat septic shock syndrome and other inflammatory disease states.

REFERENCES

- Fan K. Regulatory effects of lipopolysaccharide in murine macrophage proliferation. *World J Gastroenterol* 1998; 4:137-139
- Turrin NP, Gayle D, Ilyin SE, Flynn MC, Langhans W, Schwartz GJ, Plata-Salaman CR. Pro-inflammatory and anti-inflammatory cytokine mRNA induction in the periphery and brain following intraperitoneal administration of bacterial lipopolysaccharide. *Brain Res Bull* 2001; 54: 443-453
- Ottervein LE, Bach FH, Alam J, Soares, Lu HT, Wysk M, Davis RJ, Flavell RA, Choi AMK. Carbon monoxide has anti-inflammatory effects involving the mitogen-activated protein kinase pathway. *Nat Med* 2000; 6:422-428
- Yamakawa T, Eguchi S, Matsumoto T, Yamakawa Y, Numaguchi K, Miyata I, Reynolds CM, Motley ED, Inagami T. Intracellular signaling in rat cultured vascular smooth muscle cells: roles of nuclear factor-kappaB and p38 mitogen-activated protein kinase on tumor necrosis factor-alpha production. *Endocrinology* 1999; 140: 3562-3572
- Bai XY, Jia XH, Cheng LZ, Gu YD. Influence of IFN α -2b and BCG on the release of TNF and IL-1 by Kupffer cells in rats with hepatoma. *World J Gastroenterol* 2001; 7:419-421
- Wu RQ, Xu YX, Song XH, Chen LJ and Meng XJ. Adhesion molecule and proinflammatory cytokine gene expression in hepatic sinusoidal endothelial cells following cecal ligation and puncture. *World J Gastroenterol* 2001; 7:128-130
- Zang GQ, Zhou XQ, Yu H, Xie Q, Zhao QM, Wang B, Guo Q, Xiang YQ and Liao D. Effect of hepatocyte apoptosis induced by TNF- α on acute severe hepatitis in mouse models. *World J Gastroenterol* 2000; 6: 688-692
- Vittimberga FJ, McDade TP, Perugini RA, Callery MP. Sodium salicylate inhibits macrophage TNF- α production and alters MAPK activation. *J Surg Res* 1999; 84:143-149
- Browning DD, Windes ND, Ye RD. Activation of p38 mitogen-activated protein kinase by lipopolysaccharide in human neutrophils requires nitric oxide-dependent cGMP accumulation. *J Biol Chem* 1999; 274:537-542
- Ohashi N, Matsumori A, Furukawa Y, Ono K, Okada M, Iwasaki A, Miyamoto T, Nakano A, Sasayama S. Role of p38 mitogen-activated protein kinase in neointimal hyperplasia after vascular injury. *Arterioscler Thromb Vasc Biol* 2000; 20:2521-2526
- Li W, Zheng TZ and Qu SY. Effect of cholecystokinin and secretin on contractile activity of isolated gastric muscle strips in guinea pigs. *World J Gastroenterol* 2000; 6:93-95
- Ling YL, Huang SS, Wang LF, Zhang JL, Wan M and Hao RL. Cholecystokinin-octapeptide (CCK-8) reverses experimental endotoxin shock. *Acta Physiol Sin* 1996; 48: 390-394
- Ling YL, Huang SS, Zhang JL, Wan M, Hao RL. Effect of cholecystokinin on SOD, MDA contents and phagocyte chemiluminescence of reversing endotoxin shock rat. *Zhongguo Bingli Shengli Zazhi* 1997; 13: 483-486
- Ling YL, Meng AH, Zhao XY, Shan BE, Zhang JL and Zhang XP. Effect of cholecystokinin on cytokines during endotoxic shock in rats. *World J Gastroenterol* 2001; 7:667-671
- Lahat N, Rahat MA, Brod V, Cohen S, Weber G, Kinarty A, Bitterman H. Abdominal surgery reduces the ability of rat spleen cells to synthesize and secrete active tumor necrosis factor-alpha (TNF- α) by a multilevel regulation. *Clin Exp Immunol* 1999; 115: 19-25
- Meltzer JC, Sanders V, Grimm PC, Stern E, Rivier C, Lee S, Rennie SL, Gietz RD, Hole AK, Watson PH, Greenberg AH, Nance DM. Production of digoxigenin-labelled RNA probes and the detection of cytokine mRNA in rat spleen and brain by in situ hybridization. *Brain Res Brain Res Protoc* 1998; 2: 339-351
- Molina PE, Abumrad NN. Differential effects of hemorrhage and LPS on tissue TNF- α , IL-1 and associate neuro-hormonal and opioid alterations. *Life Sci* 2000; 66:399-408
- Cunningham ME, Shaw TA, Bernstein LH, Tinghitella TJ, Claus RE, Brogan DA, McMillen MA. Cholecystokinin-stimulated monocytes produce inflammatory cytokines and eicosanoids. *Am J Gastroenterol* 1995; 90: 621-626
- Lieb K, Fiebich BL, Grawitz MB, Hull M, Berger M. Effect of substance P and selected other neuropeptides on the synthesis of interleukin-1 beta and interleukin-6 in human monocytes: a re-examination. *J Neuroimmunol* 1996; 67: 77-81
- Gu ZY, Ling YL, Meng AH, Cong B, Huang SS. Effect of cholecystokinin octapeptide on the response of rabbit pulmonary artery induced by LPS in vitro. *Zhongguo Bingli Shengli Zazhi* 1999; 15: 484-487
- Meng AH, Ling YL, Wang DH, Gu ZY, Li SJ and Zhu TN. Cholecystokinin-octapeptide alleviates tumor necrosis factor-alpha induced changes in rabbit pulmonary arterial reactivity and injuries of endothelium in vitro. *Shengli Xuebao* 2000; 52:502-506
- Widmann C, Gibson S, Jarpe MB, Johnson GL. Mitogen-activated protein kinase: conservation of a three-kinase module from yeast to human. *Physiol*

- Rev 1999; 79:143-180
- 23 Tapia JA, Ferris HA, Jensen RT, Garcia LJ. Cholecystokinin activates PYK2/CAKbeta by a phospholipase C-dependent mechanism and its association with the mitogen-activated protein kinase signaling pathway in pancreatic acinar cells. *J Biol Chem* 1999; 274: 31261-31271
- 24 Feng DY, Zheng H, Tan Y and Cheng RX. Effect of phosphorylation of MAPK and Stat3 and expression of c-fos and c-jun proteins on hepatocarcinogenesis and their clinical significance. *World J Gastroenterol* 2001; 7: 33-36
- 25 Fleischer F, Dabew R, Ke BG and Wagner ACC. Stress kinase inhibition modulates acute experimental pancreatitis. *World J Gastroenterol* 2001; 7: 259-265
- 26 Browning DD, Windes ND and Ye RD. Activation of p38 mitogen-activated protein kinase by lipopolysaccharide in human neutrophils requires nitric oxide-dependent cGMP accumulation. *J Biol Chem* 1999; 274:537-542
- 27 Monstein HJ, Nylander AG, Salehi A, Chen D, Lundquist L and Hakanson R. Cholecystokinin-A and cholecystokinin-B/gastrin receptor mRNA expression in the gastrointestinal tract and pancreas of the rat and man. *Scand J Gastroenterol* 1996; 31:383-390
- 28 Metzler W, Hofken T, Weber H, Printz H, Goke B, Wagner AC. Hyperthermia, inducing pancreatic heat-shock protein, fails to prevent cerulein-induced stress kinase activation. *Pancreas* 1999; 19:150-157
- 29 Wagner AC, Metzler W, Hofken T, Weber H, Goke B. p38 MAP kinase is expressed in the pancreas and is immediately activated following cerulein hyperstimulation. *Digestion* 1999; 60: 41-47
- 30 Schafer C, Clapp P, Welsh MJ, Benndorf R, Williams JA. HSP27 expression regulates CCK-induced changes of the actin cytoskeleton in CHO-CCK-A cells. *Am J Physiol* 1999; 277:C1029-1031
- 31 Wysk M, Yang D, Lu HT, Flavell RA and Davis RJ. TNF-induced cytokine expression mediated by the p38 MAP kinase activator MKK3. *Proc Natl Acad Sci USA* 1999; 96: 3763-3768
- 32 Hoffmeyer A, Wilde AG, Flory E, Neufeld B, Kunz M, Rapp UR and Ludwig S. Different mitogen-activated protein kinase signaling pathways cooperate to regulate tumor necrosis factor- α gene expression in T lymphocytes. *J Biol Chem* 1999; 274:4319-4327

Edited by Ma JY

• BASIC RESEARCH •

Effect of cholesterol liposomes on calcium mobilization in muscle cells from the rabbit sphincter of Oddi

Xin-Jiang Wang, Jing-Guo Wei, Chun-Mei Wang, Yao-Cheng Wang, Qiu-Zhen Wu, Jia-Kuan Xu, Xiang-Xin Yang

Xin-Jiang Wang, Jing-Guo Wei, Yao-Cheng Wang, Qiu-Zhen Wu, Jia-Kuan Xu, Xiang-Xin Yang, Department of Radiology, Tangdu Hospital, Chun-Mei Wang, Department of Electron Microscope, Fourth Military Medical University, Xi'an 710038, Shaanxi Province, China

Correspondence to: Dr. Xin-Jiang Wang, Department of Radiology, Tangdu Hospital, the Fourth Military Medical University, Xi'an 710038, Shaanxi Province, China. tdradio@fmmu.edu.cn

Telephone: +86-29-3577163 Fax: +86-29-3577163

Received 2001-04-08 Accepted 2001-06-10

Abstract

AIM: To analyze the influence of cholesterol liposome on the Ca^{2+} mobilization of cultured muscle cells in rabbit sphincter of Oddi's.

METHODS: New Zealand rabbit was sacrificed and the sphincter of Oddi (SO) segment was obtained aseptically. The SO segment was cut into pieces and cultured in DMEM solution. Then the smooth muscle cells were subcultured, and the 4th-7th passage cells were used for further investigation. The intracellular Ca^{2+} increase was measured under confocal microscope after the addition of $20\text{mmol}\cdot\text{L}^{-1}$ KCl, $10^{-7}\text{mol}\cdot\text{L}^{-1}$ acetylcholine and $10^{-7}\text{mol}\cdot\text{L}^{-1}$ cholecystokinin, and different antagonists were added to analyze the Ca^{2+} mobilization pathway. After the cells were incubated with $1\text{g}\cdot\text{L}^{-1}$ cholesterol liposome (CL) (molar ratio was $\sim 2:1$), the intracellular Ca^{2+} increase was measured again to determine the effect of CL on cellular Ca^{2+} mobilization.

RESULTS: The resting cellular calcium concentration of cultured SO cell was $108\text{nmol}\cdot\text{L}^{-1}\pm 21\text{nmol}\cdot\text{L}^{-1}$. The intracellular Ca^{2+} increases induced by $20\text{mmol}\cdot\text{L}^{-1}$ KCl, $10^{-7}\text{mol}\cdot\text{L}^{-1}$ ACh and $10^{-7}\text{mol}\cdot\text{L}^{-1}$ CCK were $183\%\pm 56\%$, $161\%\pm 52\%$ and $130\%\pm 43\%$, respectively. When the extracellular Ca^{2+} was eliminated by $2\text{mmol}\cdot\text{L}^{-1}$ EGTA and $5\mu\text{mol}\cdot\text{L}^{-1}$ verapamil, the intracellular Ca^{2+} increases induced by KCl, ACh and CCK were $20\%\pm 14\%$, $82\%\pm 21\%$ and $104\%\pm 23\%$, respectively. After the preincubation with heparin, the Ca^{2+} increases were $62\%\pm 23\%$ and $23\%\pm 19\%$ induced by ACh and CCK, as for preincubation with procaine they were $72\%\pm 28\%$ and $85\%\pm 37\%$ induced by ACh and CCK, respectively. Pretreatment with CL for 18h, the resting cellular Ca^{2+} concentration elevated to $152\text{nmol}\cdot\text{L}^{-1}\pm 26\text{nmol}\cdot\text{L}^{-1}$, however, the cellular Ca^{2+} increase percentages in response to these agonists were $67\%\pm 32\%$, $56\%\pm 33\%$ and $34\%\pm 15\%$.

CONCLUSION: KCl elicits the SO cellular Ca^{2+} increase depends on influx of extracellular Ca^{2+} , ACh evoked the SO

cellular Ca^{2+} increase is through the mobilization of intracellular Ca^{2+} pool and influx of extracellular Ca^{2+} as well, CCK excites the SO cells mainly through mobilization of intracellular IP3-sensitive Ca^{2+} store. After the incorporation with cholesterol liposome, KCl, ACh and CCK induced cellular Ca^{2+} increase percentages decreased.

Wang XJ, Wei JG, Wang CM, Wang YC, Wu QZ, Xu JK, Yang XX. Effect of cholesterol liposomes on calcium mobilization in muscle cells from the rabbit sphincter of Oddi. *World J Gastroenterol* 2002;8(1):144-149

INTRODUCTION

Biliary tract diseases are becoming more common in recent years in China^[1-10]. Sphincter of Oddi (SO) is an important part located at the distal part of biliary tract. And it is well accepted that SO plays an important role in the regulation of biliary system hydraulic pressure and bile flow^[11-13]. SO dysfunction (SOD) is one of the causes responsible for biliary tract disorders^[14-16], pancreatitis^[17-18] and other disorders^[19-21]. The mechanism underlying the occurrence of SOD is controversial, however, several investigators have noticed the relation between hypercholesterolemia and SOD^[22-24]. Szilvassy *et al*^[23] reported that patient has an impaired SO relaxation due to high serum lipids, but normalization of serum lipids improved the sphincter of Oddi relaxation. Wei *et al*^[24] found the abnormalities in ultrastructure of SO in rabbits with hypercholesterolemia. Therefore, hypercholesterolemia might be one of causes of SOD. Meanwhile, the effect of cholesterol on gallbladder contractility has been interpreted by many authors^[25-27], who found that the cholesterol incorporated into membrane can impair the cellular signal transduction and contractility as well.

The thin optical sectioning capability of laser scanning confocal microscopy rejects light from out-of-focus planes and permits imaging of $[\text{Ca}^{2+}]_i$ in single alive cells in optical sections less than $1\mu\text{m}$ thick, which makes it possible to measure intracellular Ca^{2+} alteration instantaneously. So, this experiment was designed to analyze the effect of different agonists on Ca^{2+} mobilization of SO cells and cholesterol liposome on this process, in order to explore the mechanism that hypercholesterolemia affected the SO motility.

MATERIAL AND METHODS

Materials

The fluo 3/AM was obtained from Molecular Probes (USA), trypsin, HEPES, cholecystokinin-octapeptide (CCK) and bovine serum albumin (BSA) were from Sigma Chemicals (USA), and Dulbecco's modified Eagle's medium (DMEM) was from Gibco Laboratories (USA). The ethylene glycol-bis(β -amino ethyl ether)-N,N,N',N'-tetraacetic acid (EGTA), verapamil, procaine, egg phosphatidylcholine and cholesterol were obtained from Shanghai Chemical Co. (China), and the acetylcholine from Suzhou Chemical Co. The dimethyl sulfoxide (DMSO) was purchased from Beijing

Chemical Co. All other chemicals were commercial products of the highest available grade of purity.

Cells preparation

The New Zealand rabbits (<30d) were euthanized by intravenous injection of ketamine (20mg·kg⁻¹), and the segment of Oddi was removed quickly and washed by PBS solution containing penicillin (500×10³u·L⁻¹). The experiments were conducted in accordance with the institutional ethical guidelines. Mucosa and serosa were dissected carefully, then washed twice with culture medium. The sphincter strip was cut into 1-2 mm³ squares and placed into culture chamber, the chamber was everted and added into 3mL DMEM medium, and pH was adjusted to 7.4 by addition of 24mmol·L⁻¹ NaHCO₃ before the use. After 3 h incubation at 37°C, when the tissue squares stuck to the chamber then turn over the chamber, replaced the medium every 4-5 d.

Subculture: Cells migrated from the explants 10-15d, as the chamber was confluent with cells, then subcultured by addition with 2.5g·L⁻¹ trypsin at 37°C for 10 min. The trypsin was inactivated by bovine serum, and the cell suspension was centrifuged at 1000r·min⁻¹ for 7 min. The supernatant was removed and cell pellet resuspended in fresh medium to a concentration of 5-7×10⁵·mL⁻¹ and repassaged into several chambers.

Differentiation: Three glass cover slips (18mm×18mm) placed into a 6cm diameter chamber, then cell suspension was added and incubated for 48 h. The slips covered with cells and fixed with 950mL·L⁻¹ ethanol for 30min, washed with PBS for 5min and desiccated naturally. The β -actin staining was performed with immunohistological kits. The positive stain was localized in long, straight, noninterrupted fibrils scattered densely along the longitudinal axis. Under phase-contrast microscope, the cultured cells showed a characteristic “hill- and - valley” growth pattern, and the 4th-7th passage cells were used in this experiments.

Preparation of cholesterol liposome

Liposomes were prepared as described previously^[28,29]. Cholesterol (200mg) and phosphatidylcholine (100mg) were added into 5mL chloroform and soluted completely. After the organic solution was evaporated, the container was placed in the desiccator overnight at 4°C. Then PBS (pH 7.2) was added into the container, the final concentration of CL was 10g·L⁻¹. After the sonication, the mixture was centrifuged at 21 000×g for 30min to sediment the undispersed lipid, then the supernatant was collected. The cholesterol-to-phospholipid molar ratio (FC/ PL) of the liposome was ~2:1. Control liposome (Cholesterol 100mg and phosphatidylcholine 200mg) was prepared in the same way, FC/PL molar ratio was ~0.5:1. Both liposomes were sterilized by filtration through a 0.45 μ m filter and mixed with sterile DMEM (Dulbecco's modified Eagle's medium) at a concentration of 1g·L⁻¹, which is in accordance with the serum concentration of rabbit model with hypercholesterolemia^[57], pH was adjusted to 7.4, control and cholesterol-rich media were determined to be isomolar before experimentation.

Calcium measurement

A 10mm hole was made in a plastic chamber (Made in Denmark), then a 22mm glass coverslip was used to seal the hole tightly from the bottom. Then it was cleaned thoroughly and sterilized by ultra-violet lamp for 2h. The cell suspension was added into the chambers and incubated for 48h, they were incubated with or without CL overnight.

Preparation of fluo-3/AM: The concentration of free cytosolic Ca²⁺ in SMCs was determined using the fluorescent Ca²⁺ indicator fluo-3/ AM. Fifty μ g fluo-3 was dissolved in 50 μ L dimethyl sulfoxide (DMSO) (about 885 μ mol·L⁻¹), and mixed thoroughly. Then it was

subdivided into ten vials and stored at -20°C. Five μ L of vial of stock solution was diluted by D-Hanks with a proportion of 1:200(V/V). The final concentration of fluo-3 was about 4.5 μ mol·L⁻¹. This loading solution should be used in 3 h, to maximize loading efficiency. **Ca²⁺ measurement:** The SO cells culture media was removed and washed for 10 min with D-Hanks solution. Remove the final wash solution, add the loading solution, incubate about 50 min at 37°C. Then remove the loading solution, wash the cells with D-Hanks, measure the fluorescence soon after loading. The measurement was performed under Bio-Rad MRC 1024 laser scanning confocal microscope, select cellular Ca²⁺ indicator from the method menu, then select the button for fluo-3, numerical aperture being 1.3, and pixel 512. The data was treated at Compaq Pentium 90. The peak excitation was about 506nm and the peak emission was about 526nm.

Solution

HEPES buffered solution (in mmol·L⁻¹): 134 NaCl, 6 KCl, 2 CaCl₂, 1 MgCl₂, 10 HEPES, 10 Glucose, 0.49 EDTA; D-Hanks: 138 NaCl, 5.4 KCl, 0.37 Na₂HPO₄·H₂O, 0.44 KH₂PO₄, 4.17 NaHCO₃. PBS: 138 NaCl, 2.7 KCl, 10 Na₂HPO₄·H₂O, 1.6 KH₂PO₄; High K⁺ solution contained the following (in mmol·L⁻¹): 120 NaCl, 20 KCl, 2 CaCl₂, 1 MgCl₂, 10 HEPES, 10 Glucose. Heparin was diluted by D-Hanks with 7×10⁵U·L⁻¹, procaine concentration was 10mmol·L⁻¹.

Statistical analyses

Results were expressed as $\bar{x} \pm S\bar{x}$. Student's test or an analysis of variance (ANOVA) was performed to test the statistical significance as necessary, $P < 0.05$ was regarded as significant.

RESULTS

Cultured SO cells showed a typical smooth muscle cell characteristics which presented as “hill-and -valley” and α -SM actin positive staining, filament was demonstrated along the longitudinal axis of the cells (Figure 1). Loading with fluo-3/AM for 50min, the fluorescence distributed inhomogenously under LSCM, which may represent the Ca²⁺ pool, is inhomogenous. All experiments were conducted at room temperature (21°C-23°C). The value of Ca²⁺ concentration was calculated and based on the following equation: $[Ca^{2+}]_i = K_d \times (F - F_{min}) / (F_{max} - F)$, where K_d is the dissociation constant for Ca²⁺ (316nmol·L⁻¹), F_{max} is fluorescence maxima which was obtained by saturating intracellular signal values; F_{min} is fluorescence minima which represented zero-Ca²⁺ signal. The resting cellular Ca²⁺ concentration was 108±21nmol·L⁻¹.



Figure 1 Cultured SO cells characterized with α -SM actin positive staining, filament were demonstrated along the longitudinal axis of the cells.

Distinctive agonists induced alteration of intracellular fluorescence

At the presence of extracellular Ca^{2+} , intracellular Ca^{2+} concentration changed under the LSCM after the addition of agonists, and it showed spatially heterogeneous alteration of fluorescent intensity in SO cells (Figure 2).

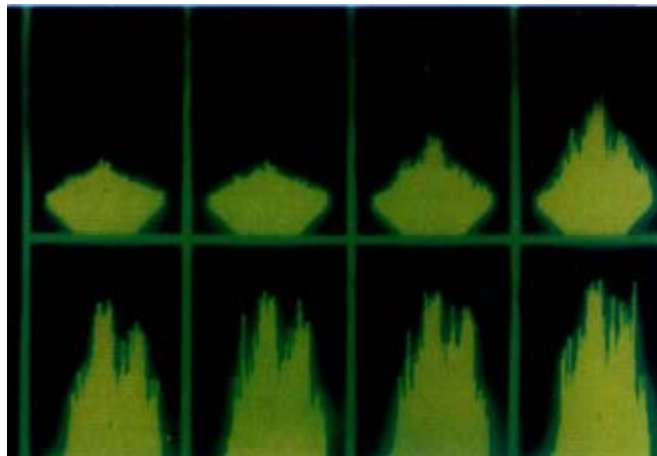


Figure 2 At the presence of extracellular Ca^{2+} , intracellular Ca^{2+} concentration changed under the LSCM (1 image·s⁻¹) after the addition of agonists, and it shows spatially heterogeneous alteration of fluorescent intensity in SO cells.

After the addition of 20mmol·L⁻¹ KCl, the increase of intracellular fluorescence was 183±56% ($n=4$), 10⁻⁷ mol·L⁻¹ ACh caused fluorescence increase was 161±52 % ($n=4$), 10⁻⁷ mol·L⁻¹ CCK agonized an increase of 130±43 % ($n=4$), the maximum Ca^{2+} concentration were 297±66nmol·L⁻¹, 275±58nmol·L⁻¹ and 251±45nmol·L⁻¹, respectively. ($n=4$, Figure 3).

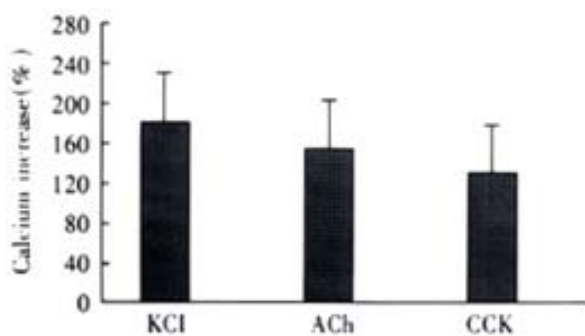


Figure 3 Intracellular fluorescence increases induced by different agonists. Ca^{2+} concentration increased from resting level of 108±21nmol·L⁻¹ to 297±66nmol·L⁻¹, 275±58nmol·L⁻¹ and 251±45nmol·L⁻¹, respectively. ANOVA was performed for the analysis, $F=0.9184$, no significant difference between three groups ($n=4$).

The elimination of extracellular Ca^{2+} was performed by incubation of 2mmol·L⁻¹ EGTA and 10μmol·L⁻¹ verapamil for 10min. The extracellular Ca^{2+} was chelated by EGTA (a highly specific chelator for free Ca^{2+} ions) and inward Ca^{2+} current was inhibited by verapamil (inhibitor of L-type Ca^{2+} channels). Compared with the presence of extracellular Ca^{2+} , under this circumstance, the cellular fluorescence decreased from the peak rapidly.

At absence of extracellular Ca^{2+} treated by EGTA and verapamil, 20mmol·L⁻¹ KCl induced an Ca^{2+} increase of 20%±14% ($P<0.01$, vs control, $t=4.882$), with maximal Ca^{2+} concentration of 131±17nmol·L⁻¹, which indicated the induction of KCl depends on the presence of extracellular Ca^{2+} . Under the same condition, ACh increased the cellular Ca^{2+} by 82%±21%, with a

maximal Ca^{2+} concentration of 192nmol·L⁻¹±22nmol·L⁻¹. After pretreatment of heparin (inhibitor of IP3-sensitive Ca^{2+} release channel) and procaine (inhibitor of IP3-insensitive Ca^{2+} release channel), the cellular fluorescence increase by 62%±23 % and 72%±28%, respectively, the maximal cellular calcium was 175nmol·L⁻¹±26nmol·L⁻¹ and 186nmol·L⁻¹±30nmol·L⁻¹, and there was no significant difference from that of untreated cells (Figure 4).

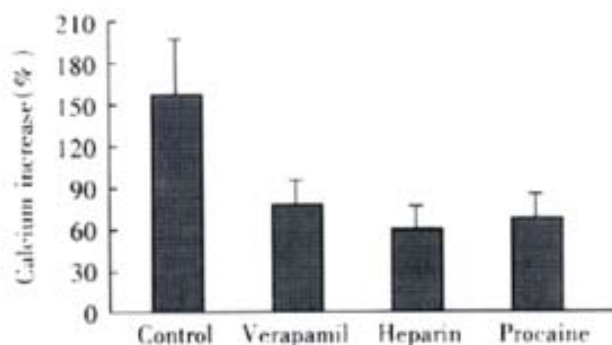


Figure 4 Effect of different antagonists on ACh induced cellular Ca^{2+} increase ($\bar{x}\pm Sx$, $n=4$). Maximal Ca^{2+} concentration increased to 192±22nmol·L⁻¹, 175nmol·L⁻¹±26nmol·L⁻¹ and 186±30nmol·L⁻¹, respectively. ANOVA was performed for the analysis, $F=1.324$, with no significant difference between the three experimental groups ($n=4$).

CCK induced an cellular Ca^{2+} increase of 104%±23% after the elimination of extracellular Ca^{2+} . After incubation of heparin and procaine, CCK induced calcium increase were 23%±19% and 85%±37%, which was different from that of acetylcholine (Figure 5).

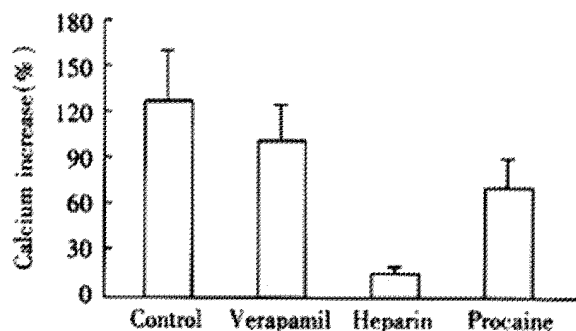


Figure 5 Effect of different antagonists on CCK induced cellular Ca^{2+} increase ($\bar{x}\pm Sx$, $n=4$). Maximal Ca^{2+} concentration increased to 220±26nmol·L⁻¹, 133±21nmol·L⁻¹ and 201±40nmol·L⁻¹, respectively. SNK-q test was performed, there was a statistical difference between heparin treated group and other two groups, $P<0.01$.

Intracellular calcium increase after the incubation of cholesterol liposome

After the incubation of 1g·L⁻¹ CL for 18h, many CL incorporated into the membrane, the cells changed slightly as mentioned by others^[45]. The intracellular calcium concentration of control liposome (FC/PL molar ratio with ~0.5:1) treated cells were 117±19nmol·L⁻¹, there was no significant difference as compared with untreated cells. However, the resting cellular Ca^{2+} concentration was elevated obviously by incubation of CL (FC/PL molar ratio with ~2:1), which was 152±26nmol·L⁻¹. But, after addition of agonists, the Ca^{2+} concentrations increased to 257±54nmol·L⁻¹, 238±57nmol·L⁻¹ and 204nmol·L⁻¹±26nmol·L⁻¹, respectively, the calcium increase percentages were significantly decreased, the cellular fluorescence increases induced by KCl, ACh and CCK were 67±32% ($t=3.597$), 56±33% ($t=3.410$) and 34±15% ($t=4.216$), respectively, ($P<0.05$, vs control) (Figure 6).

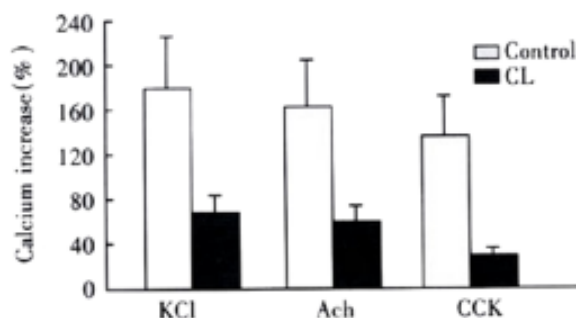


Figure 6 Effect of cholesterol liposome on cellular Ca^{2+} mobilization ($\bar{x} \pm \text{Sx}$, $n=4$). Agonists induced cellular fluorescence increase percentages were markedly less than that of control group.

DISCUSSION

The present study shows that Ca^{2+} mobilization of SO cells evoked by potassium, acetylcholine and cholecystinin were impaired after the cells incubated with cholesterol liposome (CL). And it also indicated that CL affects the different pathways of Ca^{2+} mobilization, for our results demonstrated that KCl induced intracellular Ca^{2+} increase depends on the extracellular Ca^{2+} influx, acetylcholine may agonize the Ca^{2+} increase through both intra- and extracellular pathway, while CCK elicited SO cells via mobilizing intracellular Ca^{2+} store. These observations agree with other authors' in gallbladder muscle cells^[30-34].

Based on literatures and our results, potassium excited the smooth muscle cells depend on Ca^{2+} influx through L-type voltage-dependent Ca^{2+} channel which could be inhibited by verapamil. As for acetylcholine and cholecystinin, $2\text{mmol}\cdot\text{L}^{-1}$ EGTA and $10\mu\text{m}$ verapamil could not inhibit the cellular Ca^{2+} increase completely, demonstrating that both ACh and CCK elicit SO cells do not depend on influx of extracellular calcium. However, heparin could inhibit the cellular Ca^{2+} increase induced by CCK, which indicate a CCK evoked Ca^{2+} increase of SO cells through IP₃-sensitive pathway.

The normal function of SO is the precondition of biliary tract homeostasis, and the motility was under the coordination of hormone and innervation^[35-38]. SOD is responsible for many disorders including gallbladder stasis, stone formation and unexplainable upper abdominal ache post-cholecystectomy^[13]. Additionally, it was proved that the occurrence of SOD was correlated with intestinal dysmotility^[20,39,40] and it was also correlated with recurrent and chronic pancreatitis^[41,42]. On the other hand, most researches on SO were concentrated on the SO manometry, in such a situation, the results and conclusions were always full of discrepancy due to the complex effect of hormone and nerve or differences in species^[12,13]. Therefore, isolated and cultured SO cells were used to study its characteristics in order to rule out complex influences *in vivo*^[43-46].

It was well known that motility regulation of smooth muscle cells depends on several mechanisms, including: influx of extracellular Ca^{2+} , intracellular Ca^{2+} mobilization and sensitivity modulation of intracellular Ca^{2+} . If this process was inhibited, the contractility will be impaired. In our previous experiments, high molar ratio CL (molar ratio~2:1) impaired the SO muscle cell contractility^[43], whereas, low molar ratio CL(0.5:1) had no effect on cells contractility. According to previous literatures, cholesterol enrichment of the SMC membrane occurs rapidly, and the aortic smooth muscle cells in hypercholesterolemic rabbit has impaired relaxation^[47-49], and reduced contraction as well^[50]. Cholesterol incorporation into

membrane could also result in an alteration of membrane conduction of ions^[51,63]. Because the cholesterol liposome was readily incorporated into cells membrane, that the duration, CL and cells incubation needed, was not a routine one. In another previous experiment, we used 2h for incubation^[43]. Broderick *et al* used 3h in the study of CL effect on arterial smooth muscle^[50].

Our aim was mainly to observe the Ca^{2+} mobilization alteration affected by CL. There are many evidence *in vivo* and *in vitro* showing an impaired contractility in human and animal gallbladders with cholesterol stones^[28,52]. Li *et al*^[53] measured the actin and myosin isoform in gallbladders smooth muscle following feeding in prairie dogs and found that cholesterol feeding induced a shift in actin isoforms, but whether it is really responsible for the decreased contractility is uncertain. It was proved that cholesterol could alter smooth muscle membrane and cell function by changing the physical state of the membrane phospholipid bilayer^[54], and therefore affect the function of integral membrane proteins, such as Ca^{2+} and potassium channels, as well as transmembrane receptors^[26]. Membrane fluidity decreased with excessive cholesterol incorporation and subsequently restricted optimal function of membrane proteins, such as receptor binding of ligands, receptor coupling with G proteins and activation of enzymes^[55,56]. Thus, it could explain the impaired activation of signal transduction pathways responsible for contractile responses to receptor-dependent agonists, such as CCK and ACh. It has been shown that muscle cell contraction, membrane fluidity, membrane cholesterol and phospholipid content are reversible after the membrane cholesterol was leached out by incubation of cholesterol-free liposomes for several hours^[27,28]. Whether the effects of cholesterol liposome observed in this study were due to cytotoxicity Other authors reported that high concentration of CL might have influence to cultured muscle cells^[46]. The similar procedures had been done by many researchers^[27,29,64], and the cholesterol was within the serum concentration range of hypercholesterolemia rabbit model^[57]. So, the cytotoxicity of liposomes to cells in this study, if any, might be unconsiderable.

The effect of cholesterol on SO has not been elucidated yet. SO manometry of hypercholesterolemic rabbit shows that abnormal SO motility had been observed before the formation of gallstone^[57], basal pressure rose and amplitude of phasic contraction decreased that represented an impaired relaxation and decreased contraction, too. Szilvassy *et al*^[58] observed that the SO of hypercholesterolemic rabbits restored the nitrergic transmitter mediated relaxation by farnesol treatment. The SO segments of rabbits, prairie dogs and guinea pigs belong to extraduodenal type^[59-61] and were able to pump fluid from the bile duct to duodenum. Therefore, it could be concluded that cholesterol affected the SO contractility which was responsible for a reduced peristaltic function to pump bile into duodenum. CCK receptors located in SO neurons and muscle cells were G-protein coupled receptors^[62] which could be affected by excessive cholesterol incorporation resulting in decreased release of neural mediators or an impaired contraction. Therefore, we can conclude that hypercholesterolemia could not only impair relaxation but also contraction of rabbits sphincter of Oddi, which could lead to the occurrence of SO dysfunction.

In summary, the present study shows that potassium induced rabbits SO cells Ca^{2+} increase depends on Ca^{2+} influx through L-type channel; acetylcholine induces SO cells Ca^{2+} increase from both intra- and extra-cellular Ca^{2+} release; cholecystinin evokes the SO cells by mobilizing IP₃-sensitive Ca^{2+} stores; and cholesterol liposome could affect the intracellular Ca^{2+} increase induced by

different agonists.

REFERENCES

- Fang CH, Yang JZ, Kang HG. A PCR study on Hp DNA of bile, mucosa and stone in gallstones patients and its relation to stone nuclear formation. *Shijie Huaren Xiaohua Zazhi* 1999;7: 233-235
- Gu SW, Luo KX, Zhang L, Wu AH, He HT, Weng JY. Relationship between ductule proliferation and liver fibrosis of chronic liver disease. *Shijie Huaren Xiaohua Zazhi* 1999;7:845-847
- Zhou LS, Shi JS, Wang ZR, Wang L. Tumor necrosis factor α in gallbladder and gallstone. *Shijie Huaren Xiaohua Zazhi* 2000;8: 426-428
- Fang CH, Yang J. A study on DNA of aerobic and anaerobic bacteria in bile, mucosa and stone in gallstone patients. *Shijie Huaren Xiaohua Zazhi* 2000; 8:66-68
- Li XP, Mao XZ. Effect of estrogen, cholic acid loading and bile draining on hepatobiliary functions in rats. *Shijie Huaren Xiaohua Zazhi* 2000;8:1009-1012
- He XS, Huang JF, Liang LJ, Lu MD, Cao XH. Surgical resection for hepato portal bile duct cancer. *World J Gastroenterol* 1999;5: 128-131
- Huang ZQ. New development of biliary surgery in China. *World J Gastroenterol* 2000;6:187-192
- Li LB, Cai XI, Li JD, Mu YP, Wang YD, Yuan XM, Wang XF, Bryner B, Finley RK Jr. Will intraoperative cholangiography prevent biliary duct injury in laparoscopic cholecystectomy *World J Gastroenterol* 2000;6:21
- Yang YK, Qiu KX, Zhan YZ, Zhan EY, Yang HM, Zheng P. Determination of cholesterol in human biliary calculus by TLC scanning. *World J Gastroenterol* 2000;6:62
- Chen XM, LaRusso NF. Human intestinal and biliary cryptosporidiosis. *World J Gastroenterol* 1999;5:424-429
- Coelho JC, Moody FG. Certain aspects of normal and abnormal motility of sphincter of Oddi. *Dig Dis Sci* 1987;32:86-94
- Toouli J. What is sphincter of Oddi dysfunction? *Gut* 1989;30:753-761
- Dodds WJ. Biliary tract motility and its relationship to clinical disorders. *AJR* 1990;155:247-258
- Herman F, Delforge M, Basten B, Masy V, Lilet H, Brassine A. Dysfunction of the sphincter of Oddi in cholecystectomy patients. *Rev Med Liege* 1998;53:193-198
- Toouli J. Biliary motility disorders. *Baillieres Clin Gastroenterol* 1997; 11:725-740
- Eversman D, Fogel EL, Rusche M, Sherman S, Lehman GA. Frequency of abnormal pancreatic and biliary sphincter manometry compared with clinical suspicion of sphincter of Oddi dysfunction. *Gastrointest Endosc* 1999;50:637-641
- Guelrud M, Morera C, Rodriguez M, Jaen D, Pierre R. Sphincter of Oddi dysfunction in children with recurrent pancreatitis and anomalous pancreaticobiliary union: an etiologic concept. *Gastrointest Endosc* 1999;50:194-199
- Tomas A, Vida F, Ponce J. Acute recurrent pancreatitis in a patient with Oddi's sphincter dysfunction. *Gastroenterol Hepatol* 1999;22: 279-281
- Chen SZ, Sha JP, Chen XC, Hou CC, Fu WH, Liu W. Dysrelaxation of sphincter of Oddi in patients with bile reflux gastritis: study on effect of nifedipine of gallbladder emptying. *Shijie Huaren Xiaohua Zazhi* 1999;7:1020-1023
- Chen SZ, Bu X, Hou CC, Li S, Chen XC. Mechanism of nifedipine for improving abnormal gallbladder emptying function in patients with irritable bowel syndrome. *Shijie Huaren Xiaohua Zazhi* 1998; 6: 423-426
- Chen SZ, Zhao H, Wu CY, Fu WJ, Chen XC. Gallbladder emptying function in patients with bile reflux gastritis. *Shijie Huaren Xiaohua Zazhi* 1998; 6: 427-429
- Szilvassy Z, Nagy I, Szilvassy J, Jakab I, Csati S, Lonovics J. Impaired nitrenergic relaxation of the sphincter of Oddi of hyperlipidaemic rabbits. *Eur J Pharmacol* 1996;301: R17-18
- Szilvassy Z, Nagy I, Madacsy L, Hajnal F, Velosy B, Takacs T, Lonovics J. Beneficial effect of lovastatin on sphincter of Oddi dyskinesia in hypercholesterolemia and hypertriglyceridemia. *Am J Gastroenterol* 1997; 92: 900-902
- Wei JG, Wang YC, Du F, Yu HJ. Dynamic and ultrastructural study of sphincter of Oddi in early-stage cholelithiasis in rabbits with hypercholesterolemia. *World J Gastroenterol* 2000;6: 102-106
- Chen Q, Amaral J, Oh S, Biancani P, Behar J. Gallbladder relaxation in patients with pigment and cholesterol stones. *Gastroenterology* 1997;113: 930-937
- Chen Q, De Petris G, Yu P, Amaral J, Biancani P, Behar J. Different pathways mediate cholecystokinin action in cholelithiasis. *Am J Physiol* 1997;272: G838-G844
- Chen Q, Amaral J, Biancani P, Behar J. Excess membrane cholesterol alters human gallbladder muscle contractility and membrane fluidity. *Gastroenterology* 1999;116:678-685
- Yu P, Chen Q, Biancani P, Biancani J. Membrane cholesterol alters gallbladder muscle contractility in prairie dogs. *Am J Physiol* 1996; 271:G56-G61
- Bialecki RA, Tulenko TN. Excess membrane cholesterol alters calcium channels in arterial smooth muscle. *Am J Physiol* 1989;257: C306-C314
- Xu QW, Shaffer EA. The potential site of impaired gallbladder contractility in an animal model of cholesterol gallstone disease. *Gastroenterology* 1996; 110:251-257
- Mansour A, Dawoud I, Gad-El-Hak-N. The potential site of disordered gallbladder contractility during the early stage of cholesterol gallstone formation. *Hepatogastroenterology* 1998;45: 1404-1409
- Yu P, Chen Q, Harnett KM, Amaral J, Biancani P, Behar J. Direct G protein activation reverses impaired CCK signaling in human gallbladders with cholesterol stones. *Am J Physiol* 1995; 269: G659-G665
- Behar J, Rhim BY, Thompson W, Biancani P. Inositol trisphosphate restores impaired human gallbladder motility associated with cholesterol stones. *Gastroenterology* 1993; 104:563-568
- Yu P, De Petris G, Biancani P, Amaral J, Behar J. Cholecystokinin-coupled intracellular signaling in human gallbladder muscle. *Gastroenterology* 1994;106:763-770
- Hogan WJ, Geenen JE. Biliary dyskinesia. *Endoscopy* 1988;20:179-183
- Luman W, Williams AJ, Pryde A, Smith GD, Nixon SJ, Heading RC, Palmer KR. Influence of cholecystectomy on sphincter of Oddi motility. *Gut* 1997;41:371-374
- Mawe GM, Kennedy AL. Duodenal neurons provide nicotinic fast synaptic input to sphincter of Oddi neurons in guinea pig. *Am J Physiol* 1999;277: G226-234
- Middelfart HV, Matzen P, Funch-Jensen P. Sphincter of Oddi manometry before and after laparoscopic cholecystectomy. *Endoscopy* 1999;31:146-151
- Soffer EE, Johlin FC. Intestinal dysmotility in patients with sphincter of Oddi dysfunction. A reason for failed response to sphincterotomy. *Dig Dis Sci* 1994; 39:1942-1946
- Evans PR, Dowsett JF, Bak YT, Chan YK, Kellow JE. Abnormal sphincter of Oddi response to cholecystokinin in postcholecystectomy syndrome patients with irritable bowel syndrome. The irritable sphincter. *Dig Dis Sci* 1995; 40: 1149-1156
- Tarnasky PR, Hoffman B, Aabakken L, Knappe WL, Coyle W, Pineau B, Cunningham JT, Cotton PB, Hawes RH. Sphincter of Oddi dysfunction is associated with chronic pancreatitis. *Am J Gastroenterol* 1997; 39: 1125-1129
- Di-Francesco V, Brunori MP, Rigo L, Toouli J, Angelini G, Frulloni L, Bovo P, Filippini M, Vaona B, Talamini G, Cavallini G. Comparison of ultrasound-secretin test and sphincter of Oddi manometry in patients with recurrent acute pancreatitis. *Dig Dis Sci* 1999; 44: 336-340
- Wang XJ, Wei JG, Wang YC, Xu JK, Wu QZ, Wu DC, Yang XX. Effect of cholesterol liposome on contractility of rabbit Oddi's sphincter smooth muscle cells. *Shijie Huaren Xiaohua Zazhi* 2000; 8: 633-637
- Zhang JS, Wei JG, Zhang ML, Wang D, Shi YH, Ji ZL. Effects of cholesterol liposome on cytoskeleton of rabbit sphincter of Oddi cells in culture. *J Fourth Milit Med Univ* 1997;18:528-531
- Zhang JS, Wei JG, Wu JZ, Chen JY. Culture and morphologic observation of rabbit Oddi's sphincter cells. *Shijie Huaren Xiaohua Zazhi* 1999;7:316-319
- Zhang JS, Wei JG, Wu JZ, Zhang YH, Wang H. Experimental study of the effects of cholesterol liposome on rabbit sphincter of Oddi cells proliferation in culture. *J Fourth Milit Med Univ* 1998;19:494-497
- Tulenko TN, Laury-Kleintop L, Walter MF, Mason RP. Cholesterol, calcium and atherosclerosis: is there a role for calcium channel blockers in atheroprotection? *Int J Cardiol* 1997;62: S55-66
- Weisbrod RM, Griswold MC, Du Y, Bolotina VM, Cohen RA. Reduced responsiveness of hypercholesterolemic rabbit aortic smooth muscle cells to nitric oxide. *Arterioscler Thromb Vasc Biol* 1997;17:394-402
- Kitagawa S, Yamaguchi Y, Shinozuka K, Kwon YM, Kunitomo M. Dietary cholesterol enhances impaired endothelium-dependent relaxations in aortas of salt-induced hypertensive Dahl rats. *Eur J Pharmacol* 1996;297:

- 71-76
- 50 Van Diest MJ, Herman AG, Verbeuren TJ. Influence of hypercholesterolemia on the reactivity of isolated rabbit arteries to 15-Lipoxygenase metabolites on arachidonic acid, comparison with platelet-derived agents and vasodilators. *Prostaglandins Leukot Essent Fatty Acids* 1996;54:135-145
- 51 Cox RH, Tulenko TN. Altered contractile and ion channel function in rabbit portal vein with dietary atherosclerosis. *Am J Physiol* 1995;268: H2522-2530
- 52 Behar J, Lee KY, Thompson WR, Biancani P. Gallbladder contraction in patients with pigment and cholesterol stones. *Gastroenterology* 1989; 97:1479-1484
- 53 Li YF, Bowers RL, Russell DH, Moody FG, Weisbrodt NW. Actin and myosin isoforms in gallbladder smooth muscle following cholesterol feeding in prairie dogs. *Gastroenterology* 1990;99: 1460-1466
- 54 Gleason MM, Medow MS, Tulenko TN. Excess membrane cholesterol alters calcium movements, cytosolic calcium levels, and membrane fluidity in arterial smooth muscle cells. *Circ Res* 1991;69:216-227
- 55 Squier TC, Bigelow DJ, Thomas DD. Lipid fluidity directly modulates the overall protein rotational mobility of the Ca-ATPase in sarcoplasmic reticulum. *J Biol Chem* 1988;263:9178-9186
- 56 Fong TM, McNamee MG. Stabilization of acetylcholine receptor secondary structure by cholesterol and negatively charged lipids. *Biochemistry* 1987; 26:3871-3880
- 57 Du F, Wei JG. Function of Oddi's sphincter disorders in formation of cholelithiasis (abstract). *Zhonghua Waikao Zazhi* 1999;37:383
- 58 Szilvassy Z, Sari R, Nemeth J, Nagy I, Csati S, Lonovics J. Improvement of nitroergic relaxation by farnesol of the sphincter of Oddi from hypercholesterolaemic rabbits. *Eur J Pharmacol* 1998;353:75-78
- 59 Calabuig R, Ulrich -Baker MG, Moody FG, Weems WA. Propulsion in the opossum sphincter of Oddi. *Am J Physiol* 1990;258:G138-G142
- 60 Calabuig R, Weems WA, Moody FG. Choledochoduodenal flow: effect of the sphincter of Oddi in opossums and cats. *Gastroenterology* 1990;99:1641-1646
- 61 Toouli J. Sphincter of Oddi motility. *Br J Surg* 1984;71:251-256
- 62 Wank SA. G protein-coupled receptors in gastrointestinal physiology I. CCK receptors: an exemplary family. *Am J Physiol* 1998; 274 (Gastrointest. Liver physiol.37):G607-G613
- 63 Zhou Q, Jimi S, Smith TL, Kummerow FA. The effect of cholesterol on the accumulation of intracellular calcium. *Biochim Biophys Acta* 1991; 1085:1-6
- 64 Broderick R, Bialecki R and Tulenko TN. Cholesterol-induced changes in rabbit arterial smooth muscle sensitivity to adrenergic stimulation. *Am J Physiol* 1989;257: H170-H178

Edited by Ma JY

• BASIC RESEARCH •

Early diagnosis and treatment of severe acute cholangitis

Wei-Zhong Zhang, Yi-Shao Chen, Jin-Wei Wang, Xue-Rong Chen

Wei-Zhong Zhang, Yi-Shao Chen, Jin-Wei Wang, Xue-Rong Chen, Department of Surgery, Huangyan First Hospital, Huangyan 318020, Zhejiang Province, China

Correspondence to: Dr. Wei-Zhong Zhang, Department of Surgery, Huangyan First Hospital, Huangyan 318020, Zhejiang Province, China. pgmh@mail.tzptt.zj.cn

Telephone: +86-576-4016922

Received 2001-07-05 Accepted 2001-11-15

Abstract

AIM: To investigate the diagnostic standard for early identification of severe acute cholangitis in order to lower the incidence of morbidity and mortality rate.

METHODS: A diagnostic standard was proposed in this study as follows: documented biliary duct obstruction by ultrasound or computerized tomography or other imaging tools with the manifestation of systemic inflammatory response syndrome (SIRS). The surgical procedures included emergency common bile duct exploration with T tube insertion or cholecystostomy with secondary common bile duct exploration. And incidence of postoperative multiple organ dysfunction syndrome (MODS), duration of systemic inflammatory response and hospital mortality were analyzed.

RESULTS: Forty-three patients conforming to the diagnostic standard described above were employed in this study. 1 patient was admitted in acutely ill condition and complicated with acute relapse of chronic bronchitis, cholecystostomy procedure was performed but the patient was complicated with postoperative acute lung injury which was treated by assisted mechanical ventilation for 5 d; 2 wk later, two-stage common bile duct Exploration and T tube insertion were performed. The remaining 42 patients underwent primary common bile duct exploration and T tube insertion, 1 developed acute lung injury and recovered 3 d later, 2 patients developed acute renal dysfunction, 1 of which recovered 2 d later and the other died on d 4. For all patients, the postoperative systemic inflammatory response persisted for 2 to 8 d with median of 3 d.

CONCLUSION: Early diagnosis of severe acute cholangitis can be made using this diagnostic standard, further development of systemic inflammatory response could be prevented and incidence of MODS as well as hospital mortality decreased.

Zhang WZ, Chen YS, Wang JW, Chen XR. Early diagnosis and treatment of severe acute cholangitis. *World J Gastroenterol* 2002;8(1):150-152

INTRODUCTION

Severe acute cholangitis takes a severe clinical course, systemic inflammatory response syndrome (SIRS) appears at early stage and followed by multiple organ dysfunction syndrome (MODS), which signifies poor prognosis^[1-8]. Recently, the perioperative management and technique of anesthesia have been much improved,

however, the mortality and morbidity of the patients with severe acute cholangitis remain high, especially in local hospitals. This study was performed to investigate the standard for early diagnosis of severe acute cholangitis and its surgical timing in order to decrease the complications.

MATERIALS AND METHODS

Diagnostic criteria

In this study, we proposed the diagnostic criterion for severe acute cholangitis as follows: documented obstruction of biliary duct by ultrasound, CT or other radiological imaging^[9-19] if the patient presents two or more of the following conditions: ① temperature more than 38°C or less than 36°C, ② elevated heart rate more than 90·min⁻¹, ③ respiratory rate more than 20·min⁻¹ or PaCO₂ less than 4.27KPa, and ④ white blood cell count more than 12×10⁹·L⁻¹, less than 4×10⁹·L⁻¹, or immature granulocyte more than 0.10^[20].

Clinical materials

Between January 1997 and November 2000, 43 consecutive patients conforming to proposed diagnostic criterion for severe acute cholangitis were admitted in surgical department of our hospital, of which 26 were male and 17 were female, the average age was 53±8 years and the average APACHE II score was 9. 2±2.6. 27 patients had stones only in common bile duct; the remaining 16 had both intrahepatic and extrahepatic stones.

After admission, proper preoperative preparation was carried out and all patients underwent emergency biliary duct decompression, including common bile duct exploration with T tube drainage or cholecystostomy with secondary choledochostomy.

After operation, patients were intensively monitored on multiple organ systems. Hospital mortality was taken as death during hospitalization for the severe cholangitic attack, and death attributed to the underlying biliary sepsis in the absence of other obvious contributory cause within 48 h after emergency biliary duct drainage. When postoperative serum creatinine doubled or exceeded 180μmol·L⁻¹ among patients who had a normal preoperative value or when it increased 100μmol·L⁻¹ over its deranged preoperative level, the diagnosis was renal dysfunction. Respiratory dysfunction was taken as the necessity for mechanical ventilation at any time after admission because of acute cholangitis. And duration of systemic inflammatory response was measured.

RESULTS

One patient aged 65 years was admitted in critically ill condition with APACHE II score of 15 and was complicated with acute relapse of chronic bronchitis, therefore, cholecystostomy procedure was performed but he was complicated with postoperative acute lung injury which was treated by assisted mechanical ventilation for 5 d; 2 wk later, common bile duct was explored and T tube inserted. After 20 d, he was discharged. The remaining 42 patients underwent first-stage common bile duct exploration and T tube placement, however, 1 developed acute lung injury and was managed by mechanical ventilation for 3 d; 2 patients developed acute renal dysfunction, one of which recovered 2 d later and the other died on d4. For all

patients, the postoperative systemic inflammatory response persisted for 2 to 8 d with median of 3 d.

DISCUSSION

Acute cholangitis caused by obstruction of common bile duct can easily induce systemic inflammatory response and later MODS or MOF, the clinical mortality is high. In China, a symposium on hepatic and biliary duct stones was held by Chinese Association of Surgery at Chongqing city in 1983, and the diagnostic standards for severe acute cholangitis was recommended. The diagnosis was met when patient presents shock or two of following six parameters: nervous symptoms; pulse more than $120 \cdot \text{min}^{-1}$; white blood cell counts more than $20 \times 10^9 \cdot \text{L}^{-1}$; temperature more than 39°C or less than 35°C ; biliary duct filled with pus and highly pressured; positive blood culture. In western country, diagnosis of severe acute cholangitis was established when septic shock or mental obtundation was confirmed in patients with acute cholangitis^[21]. However, many patients with severe acute cholangitis were not manifested with nervous dysfunction and hypotension; the incidence of Reynolds' pentad was low; recent study showed that culture is far less sensitive than PCR method in detecting microbes present in blood^[22-23]; and with progress in technique of modern imaging, obstruction of biliary duct can be identified early and accurately and proper management can be achieved timely; last but not least, patients with the diagnosis of severe acute cholangitis by this standard usually presented severe systemic inflammatory response, suggestive of the presence of multiple organ dysfunction, so if the patients were operated on at this time, second hit would ensue and course leading to MOF was accelerated^[24], mortality increased accordingly. At that time, when diagnosis was established, biliary drainage was of immediate concern, the surgical procedures included common bile duct exploration and T tube insertion, or cholecystostomy when patient's condition was unstable, but mortality rate carried between 10 per cent and 40 per cent.^[1-3, 25]

In the era of minimally-invasive surgery, when the diagnosis of severe acute cholangitis is confirmed, the principle of management has much changed^[26-32]. Non-operative biliary decompression is attempted before any definitive surgical procedure is undertaken. A nasobiliary catheter by endoscopy can be left in place to provide short-term biliary decompression until the patient's cholangitis resolves. The goal of such treatment is to convert an urgent or emergent problem into one that can be managed in an elective setting. Emergent surgical decompression of the common bile duct is reserved for patients in whom endoscopic procedure is either unsuccessful or unavailable. Should a surgical procedure be necessary, the goal is to establish biliary decompression only by means of a choledochotomy, and placement of a large diameter T-tube. Overall, non-operative drainage can be accomplished with morbidity rates of less than 40 per cent and overall mortality of less than 10 per cent.

Lai *et al* in early 1990s conducted a randomized prospective study on the role of endoscopic biliary drainage for severe acute cholangitis, the diagnosis of severe acute cholangitis was based on the presence of either septicemic shock or evidence of progressive biliary sepsis including mental confusion and persistent or relapsing fever despite appropriate antibiotic treatment, however, the mortality rate remained up to 10 percent. Recently, they conducted a retrospective study to evaluate the combined endoscopic and laparoscopic approach in managing gallstone cholangitis, in their series, 60 patients had severe acute cholangitis defined by the presence of septic shock, mental confusion, or persistent high fever despite antibiotic treatment and the mortality rate among patients with severe acute cholangitis decreased to 5.0 per cent (3/60)^[21]. They concluded that combined approach is safe and effective for managing gallstone cholangitis. Other authors had reported similar advantages of nonoperative

decompression^[27-30].

The advent of endoscopic retrograde cholangiopancreatography, endoscopic sphincterotomy and newer laparoscopic procedures including common bile duct exploration has remarkably decreased the mortality of severe acute cholangitis^[33-37]. However, the performance of these procedures is dependent on training, technical skills and experience of the surgeon. In the hands of an experienced surgeon, a laparoscopic approach is reasonable for the treatment of acute cholangitis in the tertiary hospitals^[33]. But in the primary or local hospitals which don't have the experienced endoscopic surgeon or equipment, the management of patients with severe acute cholangitis has to be turned to traditional procedures. Furthermore, a recent multicenter randomized trial comparing surgical treatment with endoscopic management in patients with common bile duct stones showed that surgical treatment was associated with lower major complications like MODS (4% vs 13%) and less retained stones (6% vs 16%) than endoscopic management^[38]. And other complications of nonoperative management were also noted.^[39-40]

As we know, in the situation of severe acute cholangitis, the intraductal pressure rises secondary to obstruction, bacteria and endotoxins can leak into the systemic circulation and induce systemic inflammatory response^[4-7] and a frequent complication of this inflammatory response is the development of organ system dysfunction or failure^[20, 41-42]. Therefore, the management of severe acute cholangitis should be based on the early awareness of the disease by clinicians, the objective of this study was to establish the early diagnosis of severe acute cholangitis.

An American College of Chest Physicians/Society of Critical Care Medicine Consensus Conference (ACCP/SCCM) was held in August 1991 to produce a series of universal definitions for SIRS (systemic inflammatory response syndrome), sepsis and other clinical conditions related to sepsis, the aim of the consensus conference was to improve our ability to make early detection of the disease possible, and thus allow early therapeutic intervention to decrease morbidity and mortality^[20, 42]. Based on this background, we recommended a new diagnostic standard since January 1997, that was, SIRS manifestation with documented obstruction of biliary duct by imaging, and surgical procedure for decompression mainly was common bile duct exploration and T tube drainage. 43 consecutive patients conforming to proposed diagnostic criterion for severe acute cholangitis were employed in this study. 1 patient aged 65 years was admitted in acutely ill condition and complicated with acute relapse of chronic bronchitis, cholecystostomy procedure was performed but he was complicated with postoperative acute lung injury which was treated by assisted mechanical ventilation for 5 d; 2 wk later, two-stage common bile duct Exploration and T tube insertion were performed. The remaining 42 patients underwent primary common bile duct exploration and T tube insertion, however, 1 developed acute lung injury and recovered later; 2 patients developed acute renal dysfunction, one of which recovered 2 d later and the other died on d4. Therefore, all patients in this cohort were diagnosed and managed timely, preventing SIRS from further progressing, thus the incidence of MOD was low (9.3%, 4/43) and mortality rate decreased (2.3%, 1/43).

In conclusion, the preliminary results of this prospective study showed that if the systemic inflammatory response is identified early in the disease process of severe acute cholangitis, MODS can be effectively prevented and mortality decreased, the proposed definition for severe acute cholangitis is practical and should be clinically accepted. Furthermore, a randomized controlled prospective study should be done to confirm this conclusion.

REFERENCES

- 1 Xi XM. Treatment of severe acute cholangitis in 106 elderly patients with integrated traditional and western medicine. *Xin Xiaohuabingxue Zazhi*

- 1993; 1: 182-183
- 2 Liu YG, Xu FH. 57 cases of severe acute cholangitis with multiple organ system failure. *Xin Xiaohuabingxue Zazhi* 1996; 4: 124
- 3 Fulcher AS. Case 1: Recurrent pyogenic cholangitis. *Radiology* 1998; 208: 341-344
- 4 Dong JH, Huang ZQ, Han BL, Duan HC, Li K, Peng ZM, Wang AC. Clinical and pathophysiological characteristics of the new experimental model of biliary sepsis in rabbits. *Xin Xiaohuabingxue Zazhi* 1994; 2: 140-143
- 5 Lei ZM, Li J, Yang WJ, Li DY. Change of nitric oxide and endothelin and its significance in the course of biliary obstruction by stones. *Shijie Huaren Xiaohua Zazhi* 2000; 8(suppl 8): 16
- 6 Kimmings AN, van Deventer SJH, Rauws EAJ, Huibregtse K, Gouma DJ. Systemic inflammatory response in acute cholangitis and after subsequent treatment. *Eur J Surg* 2000; 166: 700-705
- 7 Shi TF, Yang WL. Study on bacterial translocation of intestine and endotoxin concentration of plasma in obstructive jaundice. *World J Gastroenterol* 1998; 4 (Suppl 2): 92
- 8 Shang D, Guan FL, Jin PY, Chen HL, Cui JH. Effect of combined therapy of Yinchenhao Chengqi decoction and endoscopic sphincterotomy for endotoxemia in acute cholangitis. *World J Gastroenterol* 1998; 4: 443-445
- 9 Guo GH, Xu JH, Sun SM, Ma T, Wu LB, Yang YH, Zhuang QW, Jing XB. Experimental study of cholangiogram for refractory jaundice. *World J Gastroenterol* 1999; 5: 75-76
- 10 Li T, Li HP, Huang QR. Imaging features of primary extrahepatic bile duct carcinoma. *Xin Xiaohuabingxue Zazhi* 1996; 4: 266-267
- 11 Gong B, Zhou DY, Zhang FM, Hu B, Cheng HY. Endoscopic treatment of 207 patients with bile duct diseases. *Xin Xiaohuabingxue Zazhi* 1996; 4:270-272
- 12 Li ZS. Current situation in ERCP studies in China. *Shijie Huaren Xiaohua Zazhi* 2000; 8:446-448
- 13 Li ZS. Progress in endoscopic management of pancreas disease. *World J Gastroenterol* 1998; 4: 178-180
- 14 Lu WF. ERCP and CT diagnosis of pancreas divisum and its relation to etiology of chronic pancreatitis. *World J Gastroenterol* 1998; 4: 150-152
- 15 Li LB, Cai XJ, Li JD, Mu YP, Wang YD, Yuan XM, Wang XF, Bryner B, Finley RK Jr. Will intraoperative cholangiography prevent biliary duct injury in laparoscopic cholecystectomy *World J Gastroenterol* 2000; 6(Suppl 3): 21
- 16 Assy N, Jacob G, Spira G, Edoute Y. Diagnostic approach to patients with cholestatic jaundice. *World J Gastroenterol* 1999; 5: 252-262
- 17 Lu B, Sun J, Zhou K, Chai ZB, Zhou J. Percutaneous transhepatic gallbladder cholangiography in the diagnosis of obstructive jaundice. *Shijie Huaren Xiaohua Zazhi* 2000; 8(Suppl 8): 7
- 18 Long ST, Long F, Xu QR, Tang XY, Gao ZW. Percutaneous transhepatic cholangiography with gastrointestinal imaging in the diagnosis of obstructive hepatobiliary disease. *Huaren Xiaohua Zazhi* 1998; 6(Suppl 7): 456
- 19 Ma BY, Yuan CX, Peng YL, Hu YK. Ultrasonographic diagnosis of 584 patients with obstructive jaundice. *Shijie Huaren Xiaohua Zazhi* 2001; 9: 116-117b
- 20 Fry DE. Sepsis syndrome. *Am Surg* 2000; 66: 126-132
- 21 Poon RTP, Liu CL, Lo CM, Lam CM, Yuen WK, Yeung C, Fan ST, Wong J. Management of gallstone cholangitis in the era of laparoscopic cholecystectomy. *Arch Surg* 2001; 136: 11-16
- 22 Kane TD, Alexander JW, Johannigman JA. The detection of microbial DNA in the blood: a sensitive method for diagnosing bacteremia and /or bacterial translocation in surgical patients. *Ann Surg* 1998; 227: 1-9
- 23 Zhang WZ, Han TQ, Tang YQ, Zhang SD. Rapid detection of sepsis complicating acute necrotizing pancreatitis using polymerase chain reaction. *World J Gastroenterol* 2001; 7: 289-292
- 24 Schwartz JD, Shamamian P, Schwartz DS, Grossi EA, Jacobs CE, Steiner F, Minneci PC, Baumann FG, Colvin SB, Galloway AC. Cardiopulmonary bypass primes polymorphonuclear leukocytes. *J Surg Res* 1998; 75: 177-182
- 25 Li ZH, Luo YT, Zhong ZM. Surgical procedures in 21 patients with acute obstructive suppurative cholangitis. *Xin Xiaohuabingxue Zazhi* 1995; 3: 45
- 26 Feng ZT, Song QY, Liu JD, Pan YM, Li SM, Dong CJ, Liu WG. Endoscopic therapy of acute suppurative cholangitis. *Shijie Huaren Xiaohua Zazhi* 2000; 8(Suppl 8): 86
- 27 Gong JP, Zhou YB, Han BL, Li ZH. Endoscopic sphincterotomy in treatment of secondary common bile duct stones. *Shijie Huaren Xiaohua Zazhi* 1999; 7: 320-322
- 28 Liu HY, Tong WH, Hu WM, Li HR, Wen ZS, Wang JK, Huang WX, Liu X. Percutaneous expandable metallic stent biliary endoprotheses used in malignant and benign obstructive jaundice. *World J Gastroenterol* 2000; 6(Suppl 3): 51
- 29 Kozarek RA. Metallic biliary stents for malignant obstructive jaundice: a review. *World J Gastroenterol* 2000; 6: 643-646
- 30 Hong DF, Gao M, Bryner U, Cai XJ, Mou YP. Intraoperative endoscopic sphincterotomy for common bile duct stones during laparoscopic cholecystectomy. *World J Gastroenterol* 2000; 6: 448-450
- 31 Ren X, Kong QY, Xu XH, Zhang GL. Management of acute obstructive suppurative cholangitis by nonoperative biliary decompression procedure. *Xin Xiaohuabingxue Zazhi* 1996; 4: 507-508
- 32 Hu B, Zhou DY, Gong B, Zhang FM, Wang SZ, Cheng HY, Wu MC. Metal stent implantation for palliation of malignant biliary obstruction- a report of 57 cases. *China Natl J New Gastroenterol* 1996; 2: 149-151
- 33 Lillemo KD. Surgical treatment of biliary tract infections. *Am Surg* 2000; 66:138-144
- 34 Schwesinger WH, Sirinek KR, Strodel III WE. Laparoscopic cholecystectomy for biliary tract emergencies: state of the art. *World J Surg* 1999; 23: 334-342
- 35 Crawford DL, Phillips EH. Laparoscopic common bile duct exploration. *World J Surg* 1999; 23: 343-349
- 36 Hammarstrom LE, Andersson R, Stridbeck H, Ihse I. Influence of bile duct stones on patient features and effect of endoscopic sphincterotomy on early outcome of edematous gallstone pancreatitis. *World J Surg* 1999; 23: 12-17
- 37 Geenen DJ, Geenen JE, Jafri FM, Hogan WJ, Catalano MF, Johnson GK, Schmalz MJ. The role of surveillance endoscopic retrograde cholangiopancreatography in preventing episodic cholangitis in patients with recurrent common bile duct stones. *Endoscopy* 1998; 30: 18-20
- 38 Suc B, Escat J, Cherqui D, Fourtanier G, Hay JM, Fingerhut A, Millat B. Surgery vs endoscopy as primary treatment in symptomatic patients with suspected common bile duct stones. *Arch Surg* 1998; 133: 702-708
- 39 Wojtun S, Gil M, Gil J. Recognition of ERC-induced pancreatitis in patients with choledocholithiasis by an analysis of laboratory findings. *Hepatogastroenterology* 2000; 47: 550-553
- 40 Tiscornia OM, Hamamura S, de Lehmann ES, Otero G, Waisman H, Tiscornia WP, Bank S. Biliary acute pancreatitis: a review. *World J Gastroenterol* 2000; 6: 157-168
- 41 Barkun AN, Barkun JS, Baillie J. A Taiwanese woman with acute cholangitis. *Endoscopy* 2000; 32: 890-894
- 42 Dellinger RP, Bone RC. To SIRS with love. *Crit Care Med* 1998; 26: 178-179

Edited by Wang JH and Xu XQ

• BASIC RESEARCH •

Upregulation of vascular endothelial growth factor by hydrogen peroxide in human colon cancer

Jian-Wei Zhu, Bao-Ming Yu, Yu-Bao Ji, Ming-Hua Zheng, Dong-Hua Li

Jian-Wei Zhu, Bao-Ming Yu, Yu-Bao Ji, Ming-Hua Zheng, Dong-Hua Li, Shanghai Institute of Digestive Surgery, Ruijin Hospital, Shanghai Second Medical University, Shanghai 200025, China

Correspondence to: Dr. Jian-Wei Zhu, Shanghai Institute of Digestive Surgery, Ruijin Hospital, Shanghai Second Medical University, Shanghai 200025, China. tozhujw@263.net

Telephone: +86-21-64370045-662211

Received 2001-07-19 Accepted 2001-09-27

Abstract

AIM: To evaluate the effect of reactive oxygen species such as hydrogen peroxide on the progression of human colon cancer.

METHODS: Human colon carcinoma cell lines, LS174T and HCT8, were treated respectively with 10^{-5} , 10^{-7} or 10^{-9} mol·L⁻¹ hydrogen peroxide for 24h, and co-cultured with human endothelial cell line ECV-304. The migration of ECV-304 induced by cancer cells was calculated and the expression level of vascular endothelial growth factor in cancer cells was determined by RT-PCR analysis and ELISA. Dactinomycin of 1.5mg·L⁻¹ which could block transcription of cancer cells was applied to observing the effects of H₂O₂ on transcriptional activity and the relative half-life of VEGF mRNA. Finally, to evaluate the effect of H₂O₂ on NF-κB activity in colon cancer cells, NF-κB in cytoplasm and nucleus of the cells were detected with FITC-tagged antibody and its presence in the nucleus(Fn) vs cytoplasm(Fc) was monitored by measuring the green fluorescence integrated over the nucleus by laser scanning cytometry(LSC).

RESULTS: Exogenous hydrogen peroxide of low concentration increased the migration of endothelial cell induced by colon cancer cells. When cancer cells were treated with 10^{-5} mol·L⁻¹ H₂O₂, the migration number of endothelial cells induced by LS174T cells was 203±70, and the number induced by HCT8 cells was 145±65. The two values were significantly higher than those treated with other concentrations of H₂O₂ ($P<0.01$). The expression of vascular endothelial growth factor in cancer cells, which could be blocked by dactinomycin, were increased to a certain degree, while the relative half-life of VEGF mRNA was not prolonged after treatment with hydrogen peroxide. The activity of NF-κB in colon cells rose after the cells were exposed to hydrogen peroxide for 24h. The Fn values in HCT8 cells were 91±13 (0 mol·L⁻¹ H₂O₂) and 149±40 (10^{-5} mol·L⁻¹ H₂O₂) ($P<0.05$), in LS174T cells were 127±35 (0 mol·L⁻¹ H₂O₂) and 192±11 (10^{-5} mol·L⁻¹ H₂O₂) ($P<0.05$). It is similar to the case of VEGF expression in cancer cells.

CONCLUSION: Hydrogen peroxide increases vascular endothelial growth factor expression in colon cancer cells, and it is likely that reactive oxygen species such as hydrogen peroxide facilitates the development of colon cancer.

Zhu JW, Yu BM, Ji YB, Zheng MH, Li DH. Upregulation of vascular

endothelial growth factor by hydrogen peroxide in human colon cancer. *World J Gastroenterol* 2002;8(1):153-157

INTRODUCTION

Reactive oxygen species (ROS) can be easily produced in intracolonic cavity, due to large amounts of bacteria and dietary metabolites in it. Several reports on the relationship between ROS and cancer suggested that ROS such as oxygen radicals, hydroxyl radicals and hydrogen peroxide (H₂O₂), were involved in the pathogenesis of colon tumors^[1-14]. H₂O₂, a special intermediate in redox reaction, is able to cross cell membranes in a free manner and modify protein and nucleic acid after being changed into radicals, and now it is thought to be a kind of signal molecular which plays an important role in the growth of tumor cells. Evidences have been given in some reports that H₂O₂ could promote cell growth and related gene expression in human tumors such as prostate cancer and breast cancer. Considering the special environment in colon and rectum we think it is necessary to evaluate the effects of ROS, especially H₂O₂, on the progression of colorectal cancer^[15-27]. As angiogenesis, which induced by several factors such as vascular endothelial growth factor(VEGF), is often demonstrated in solid tumors, and thought to be an essential requirement for the development of malignant tumors^[28-33], we investigated the effects of H₂O₂ on VEGF expression in colon cancers in this study to find evidences that ROS such as H₂O₂ plays a role in the progression of the tumor.

MATERIALS AND METHODS

Cell culture and culture conditions

Human colon cancer cell lines, LS174T and HCT8, and human umbilical vein endothelial cell line ECV-304 were purchased from American Type Culture Collection. These cell lines were cultured and maintained in RPMI1640 supplemented with 100 ml·L⁻¹ fetal bovine serum at 37°C in 50 ml·L⁻¹ carbon dioxide and 950 ml·L⁻¹ air.

H₂O₂ treatment of cancer cells and MTT assay

To determinate the effects of H₂O₂ on the growth of cancer cells, LS174T and HCT8 cells were grown (10^3 per well) on 96-well plates and treated with the culture media containing H₂O₂ (ten concentrations from 10^{-10} mol·L⁻¹ to 10^{-1} mol·L⁻¹) (300 ml·L⁻¹ H₂O₂ solution was purchased from Sigma). After 48h, MTT assay showed that H₂O₂ inhibited the growth of cancer cells when its concentration was $>10^{-5}$ mol·L⁻¹, while had no effect on cell growth when its concentration was $\leq 10^{-5}$ mol·L⁻¹. Therefore, those concentrations of H₂O₂, 10^{-5} , 10^{-7} and 10^{-9} mol·L⁻¹, were used in subsequent studies.

Endothelial cell migration induced by cancer cells

To clarify the effects of H₂O₂ on the migration of vascular endothelial cells, which could be promoted by VEGF, colon cancer cells were co-cultured with endothelial cells. LS174T and HCT8 cells were plated on 12-well plates (Falcon) at a density of 4×10^5 per well. Four hours later, the cells were washed with serum-free medium, and

exposed to 10^{-5} , 10^{-7} or 10^{-9} mol·L⁻¹ H₂O₂ with the H₂O₂-containing complete media for 24h. Cell culture inserts with polyethylene terephthalate membranes (PET) and 8 μm pore size (Becton Dickinson, USA) were then placed into the 12-well plates, and endothelial cells ECV-304 were seeded into the inserts with a density of 1×10^4 . Six hours later, the cells on the upper surface of the PET membranes were wiped off completely, and the inserts were fixed and stained. The migration capacity of endothelial cells was estimated by counting the number of the cells beneath the PET membranes. The controls were the groups without cancer cells in the wells or without treating cancer cells with H₂O₂.

Expression of VEGF in colon cancer cell

To determine the effects of H₂O₂ on expression of VEGF, LS174T and HCT8 were grown to 90% confluence to avoid the effects of cell density and incubated in complete media in the presence of H₂O₂ (10^{-5} , 10^{-7} and 10^{-9} mol·L⁻¹) for 24h. Total RNA was extracted and resuspended in sterile RNase-free water for storage at -70°C. Access RT-PCR system (Promega) with the sensitive feature was used to determine the relative VEGF mRNA expression. All primers were synthesized by Life Technology, Hongkong.

VEGF sense: 5'-AAGCCATCCTGTGTGCCCTG ATG-3'
antisense: 5'-GCGAATTCCTCTGCCGCGCTGAC-3'
β-actin sense: 5'-AACACCCAGCCATGTACGTTG-3'
antisense: 5'-CGGATGTCCACGTCACACTTCAT-3'

The 50 μL mixture for reverse transcription and PCR amplification were added in one-tube including AMV reverse transcriptase 5U, Tfl DNA polymerase 5U, MgSO₄, 20 μL dNTP mixture, reaction buffer and 20 pmol of each primer and 0.1 μg total RNA sample. The condition for RT-PCR included a 48°C reverse transcription, a 94°C AMV inactivation and denaturation, a 60°C annealing and a 72°C extension. PCR amplification was subjected to 40 cycles. A volume of 10 μL RT-PCR products was added in 20 g·L⁻¹ agarose gel containing 0.5 mg·L⁻¹ EB. After electrophoresis, the density and area of each band were measured using Fluro-sTM image software (Bio-Rad, USA). The relative RNA level of VEGF in tumor cells was calculated using the house-keeping gene β-actin as an internal control. The experiments were repeated at least four times.

Analysis VEGF transcriptional activity and VEGF mRNA half-life

To confirm that the effect of H₂O₂ on expression of VEGF in colon cancer cells was due to an increase in transcription, transcription activity of cancer cells was blocked by Dactinomycin (ActD, purchased from Sigma). LS174T cells were incubated in the presence of ActD ($1.5 \text{ mg} \cdot \text{L}^{-1}$) for 4h before their exposure to 10^{-5} mol/L H₂O₂ in serum-free medium. Total RNA was extracted from cells after 24h, and RT-PCR analysis was made. Control cells were treated with ActD without H₂O₂.

To determine the effect of H₂O₂ on VEGF mRNA stability, LS174T cells were incubated in the presence or absence of 10^{-5} mol·L⁻¹ H₂O₂ for 24h. Further transcription in cells was then blocked by addition of $1.5 \text{ mg} \cdot \text{L}^{-1}$ ActD. Total RNA was extracted from cells at 0, 0.25, 0.5, 1, 2 and 4h. RT-PCR analysis was made and the relative level of VEGF mRNA expression at each point was compared with the control value (total RNA extracted from cells before ActD treatment was defined as 100%). The relative half-life of VEGF mRNA was determined by plotting relative VEGF mRNA expression levels on a semilogarithmic axis versus time.

Determination of VEGF protein levels

The VEGF protein levels in the supernatant were

determined with an enzyme-linked immunosorbent assay (ELISA) kit. Examinations were repeated three times.

Activity of transcriptional factor NF-κB in colon cancer cells

To evaluate the effects H₂O₂ on NF-κB activity in colon cancer cells, NF-κB in cytoplasm and nucleus of the cells was detected with FITC-tagged antibody and its presence in the nucleus vs cytoplasm was monitored by measuring the green fluorescence integrated over the nucleus by laser scanning cytometry (LSC) according to the Deptala's report. Briefly, the cells were first attached to the microscope slides, and exposed to 10^{-5} mol·L⁻¹ H₂O₂ for 0.5, 1, 3, 6, 12 and 24h. The cells on slides were fixed and incubated with NF-κB P65 antibody (Santa Cruz) and FITC-tagged goat-antirabbit Ig (Santa Cruz) at room temperature. Cellular DNA was then counterstained by addition of a solution containing propidium iodide and RNase (Sigma). The cells were placed on microscope slides mounted under coverslips and analyzed by LSC. At least 10^3 cells were analyzed by LSC per slide. Fluorescence intensity in nucleus (Fn) and in cytoplasm (Fc) were detected and the activity of NF-κB was detected by estimating the value of Fn or Fn/Fc.

Statistics

When appropriate, data were expressed as $\bar{x} \pm s$. Analysis of variance and *t* test were applied to assess the significance of differences. Statistical significance was accepted at $P < 0.05$.

RESULTS

H₂O₂ promotes the migration of endothelial cells induced by colon cancer cells

The migration of endothelial cells induced by cancer cells was promoted to a certain degree when LS174T and HCT8 cells were exposed to 10^{-5} , 10^{-7} or 10^{-9} mol·L⁻¹ H₂O₂ for 24h. When cancer cells were treated with 10^{-5} mol·L⁻¹ H₂O₂, the migration number of endothelial cells induced by LS174T cells was 203 ± 70 , and the number induced by HCT8 cells was 145 ± 65 . The two values were significantly higher than those treated with other concentrations of H₂O₂ (Table 1, Figure 1). When there was no cancer cell in the co-culture system, the number of random motility of endothelial cells was about ten cells.

Upregulation of VEGF expression by H₂O₂

Electrophoresis of RT-PCR products showed the three positive bands, 243, 375 and 509 bp, representing VEGF121, VEGF165 and β-actin respectively. The internal control demonstrated a stable expression in colon cells treated with each dose of H₂O₂. The analysis of electrophoresis showed that expression levels of VEGF were elevated in LS174T and HCT8 cells with H₂O₂ exposure, especially with 10^{-5} mol·L⁻¹ H₂O₂ (Figure 2). After inhibition of transcriptional activity by ActD before addition of H₂O₂, induction of VEGF mRNA expression was completely inhibited in LS174T cells (Figure 3), indicating that H₂O₂-induced VEGF expression possibly occurred at the transcriptional level. The relative half-life of VEGF mRNA in LS174T cells treated with H₂O₂ was similar to that of the cells without H₂O₂ exposure, demonstrating that the stability of VEGF mRNA was not affected by the treatment with H₂O₂ (Figure 4). To determine whether secretion of VEGF is increased by H₂O₂ in colon cancer cells, the supernatant was assayed and the results showed that H₂O₂ also promoted the VEGF protein expression. The levels of VEGF protein peaked when LS174T and HCT8 cells were incubated in the media containing 10^{-5} mol·L⁻¹ H₂O₂. This situation is similar to the increase of VEGF expression.

Table 1 The migration of endothelial cells induced by colon cancer cells ($\bar{x} \pm s$)

Cell line	H ₂ O ₂ in media(mol·L ⁻¹)			
	0	10 ⁻⁹	10 ⁻⁷	10 ⁻⁵
LS174T	155±38	162±38	174±40	202±70 ^a
HCT8	113±73	114±71	122±68	145±65 ^b

^a*P*<0.01, *t*=3.4751, vs LS174T, without H₂O₂ treatment ^b*P*<0.01, *t*=3.4183, vs HCT8, without H₂O₂ treatment

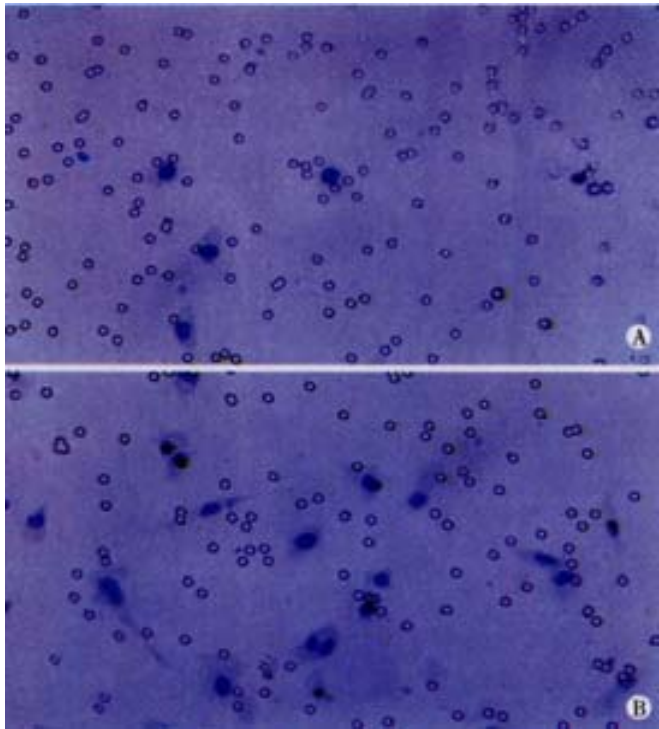


Figure 1 The migration of endothelial cells induced by LS174T cells was increased after the cancer cells were exposed to 10⁻⁵mol·L⁻¹ H₂O₂. The regular circles is the 8μm pores located in PET membrane. A: induced by cancer cells without H₂O₂ treatment. B: induced by cancer cells with H₂O₂ treatment. ×200

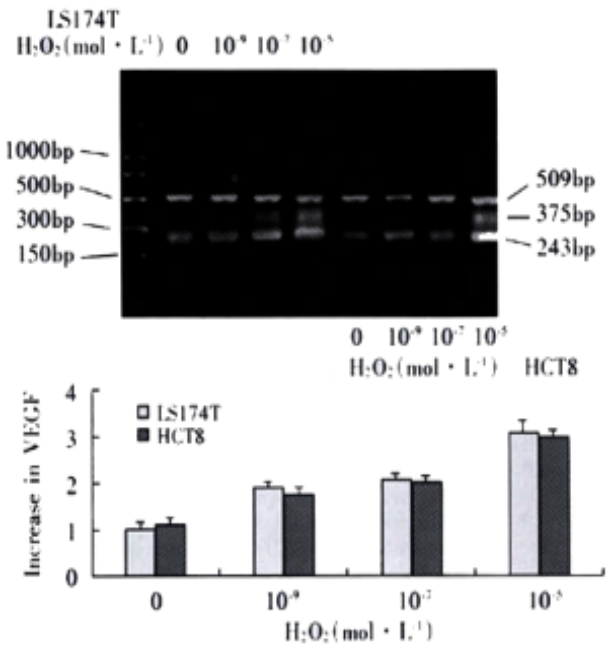


Figure 2 Expression levels of VEGF were increased in LS174T and HCT8 after exposure to 10⁻⁹,10⁻⁷and 10⁻⁵mol·L⁻¹ H₂O₂, demonstrating a dose-dependent feature.

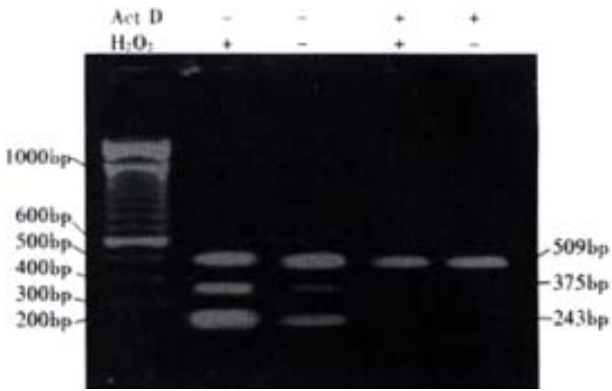


Figure 3 LS174T cells were treated with 1.5mg·L⁻¹ Act D for 4h, followed by exposure to 10⁻⁵ mol·L⁻¹ H₂O₂ for 24h. RT-PCR was done. The control was those without Act D treatment.

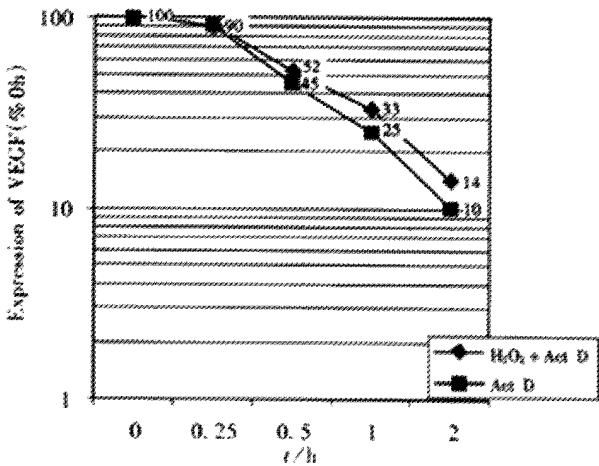


Figure 4 Effect of H₂O₂ on the half-life of VEGF mRNA in LS174T cells with or without H₂O₂ exposure following Act D treatment. No difference in half-life was showed between the two groups.

H₂O₂ increases the activity of NF-κB

LS174T and HCT8 cells were incubated in the presence of H₂O₂ (10⁻⁵mol·L⁻¹) for 0.5,1,3,6,12 and 24h in complete medium. NF-κB activity peaked after exposure to H₂O₂ for 24h. We investigated the changes of NF-κB activity in LS174T and HCT8 cells treated with 10⁻⁵, 10⁻⁷and 10⁻⁹ mol·L⁻¹H₂O₂ in media. Compared with the cells without H₂O₂ treatment, administration of 10⁻⁵ mol·L⁻¹ H₂O₂ for 24h led to a more remarkable increase in green fluorescence intensity measured over nuclear area (Fn) (Table 2,Figure 5), indicating the increase of NF-κB activity in LS174T and HCT8 cells.

Table 2 Change of NF-κB activity in colon cancel cells ($\bar{x} \pm s$)

Cell line	H ₂ O ₂ (mol·L ⁻¹)	
	0	10 ⁻⁵
HCT8 Fn	91±13	149±40 ^a
Fn/Fc	0.75±0.14	2.18±0.54
LS174T Fn	127±35	192±11 ^b
Fn/Fc	2.18±1.17	3.99±1.38

^a*P*<0.05, *t*=3.4179, vs HCT8, no H₂O₂ treatment

^b*P*<0.05, *t*=3.0981, vs LS174T, no H₂O₂ treatment

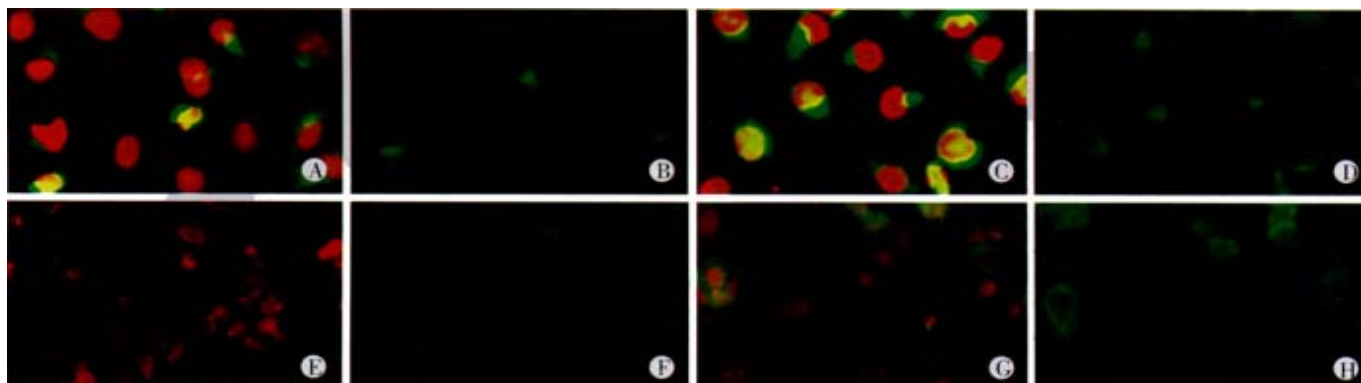


Figure 5 Measurement of nuclear and cytoplasmic NF- κ B associated fluorescence by LSC. The red fluorescence represents the nuclear area, and the intensity of green fluorescence over nucleus(Fn) reflects NF- κ B activity. A, B: LS174T cells without H_2O_2 treatment. C, D: Increase in NF- κ B activity of LS174T cells with H_2O_2 exposure. E, F: HCT8 cells without H_2O_2 treatment. G, H: Increase in NF- κ B activity of LS174T cells with H_2O_2 exposure.

DISCUSSION

The reactive oxygen species(ROS), which are ubiquitous and occur naturally in all aerobic species, may be divided into two categories :free oxygen radicals ($\cdot OH$, $\cdot NO$ and $O_2^{\cdot -}$) and nonradical ROS such as H_2O_2 . For decades, H_2O_2 has been one of the ROS that has been well investigated in inflammatory response and oxidant-induced stress. Recently, numerous evidence has been presented to show that H_2O_2 can act as a signaling molecule involved in many cellular function such as apoptosis and proliferation^[1-10]. And the regulation of series of genes involved in carcinogenesis and progression is associated with the function of H_2O_2 ^[3,5,6,9,11-14]. Several reports have suggested that ROS such as H_2O_2 plays a role in the pathogenesis of tumor in colon, where there are a great deal of bacteria and dietary metabolites^[15-27]. Diet rich in fat increased the formation of ROS in feces, which then possibly damaged the stem cells in the colon^[20,22,26]. However, up to date, little information has been available about the role of H_2O_2 the special reactive oxygen intermediate, in the biological behaviors of colon cancer cells.

VEGF is a potent and unique angiogenic protein that stimulates capillary formation and has specific mitogenic and chemotactic activity for vascular endothelial cells^[28]. In colon cancer, VEGF levels are elevated and correlated with a poor clinical outcome^[29-33]. VEGF expression is regulated by some pathological processes such as hypoxia^[34-36] and by numerous cytokines and growth factors including interleukin1 β , interleukin 6, platelet-derived growth factor, transforming growth factor β , epidermal growth factor, hepatocyte growth factor, insulin-like growth factor, angiotensin II, hypoxia -inducible factor I and EIF4E etc.^[37-52]. Recently, oncogene p53 is also found to be a regulator of VEGF gene in colon cancer cells^[53,54]. In the present study, we found, to our knowledge, for the first time, that exogenous H_2O_2 could up-regulate the expression of VEGF in human colon cancer cells and the migration of endothelial cells induced by the cancer cells after we reviewed those results from RT-PCR assay, ELISA and migration experiment of endothelial cells. Considering the important role of VEGF in neovascularization in solid tumors, we believe that hydrogen peroxide may have the promoting effects on the progression of colon cancer. Related studies also found that hydrogen peroxide could not only increase the expression of VEGF in cultured human vascular smooth muscle cell, human retinal pigment epithelial, melanoma cells and glioblastoma cells, but also promote the growth of prostate and breast cancer cells^[55-58].

NF- κ B activation, as expressed by its translocation from the cytoplasm to nucleus, can be conveniently assayed by LSC by measuring the intensity of NF- κ B-associated immunofluorescence over the area of cell nucleus and comparing it with the intensity over cytoplasm^[59]. NF- κ B, as a transcriptional factor controlling a variety

of target genes such as adhesion molecular and apoptosis, is closely related to the pathogenesis and progression of tumors. NF- κ B activity in cells like leukocyte, could be increased by hydrogen peroxide and NF- κ B activation was an essential step before VEGF expression level was increased by hydrogen peroxide in murine osteoblastic cells^[60,61]. It is noteworthy in the present experiment that the increase of NF- κ B activity was accompanied by the promotion of expression of VEGF in colon cancer cells exposed to hydrogen peroxide. Thereby, we estimate that the NF- κ B activation may be the prerequisite of the effect of hydrogen peroxide on VEGF expression in colon cancer cells.

In view that such reactive oxygen species as hydrogen peroxide are likely to promote the development of colon cancer, it would be helpful in releasing oxidative stress by antioxidants in the colon cancer therapy.

REFERENCES

- 1 Rhee SG. Redox signaling:hydrogen peroxide as intracellular messenger. *Exper Mol Med* 1999;35:53-59
- 2 Gata L,Paul J,Ba GN, Tew KD, Tapiero H. Oxidative stress induced in pathologies:the role of antioxidants. *Biomed Pharmac Ther* 1999;53:169-180
- 3 Schwieger A, Bauer L, Hanusch J, Sers C, Schafer R, Bauer G.Ras oncogene expression determines sensitivity for intercellular induction of apoptosis. *Carcinogenesis* 2001;22:1385-1392
- 4 Chen Y, Kramer DL, Diegelman P, Vujcic S, Porter CW. Apoptotic signaling in polyamine analogue-treated SK-MEL-28 human melanoma cells. *Cancer Res* 2001;61:6437-6444
- 5 Del Bello B, Valentini MA, Zunino F, Comporti M, Maellaro E. Cleavage of Bcl-2 in oxidant- and cisplatin-induced apoptosis of human melanoma cells. *Oncogene* 2001;20:4591-4595
- 6 Chung YM, Yoo YD, Park JK, Kim YT, Kim HJ.Increased expression of peroxiredoxin II confers resistance to cisplatin. *Anticancer Res* 2001; 21:1129-1133
- 7 Dare E, Li W, Zhivotovsky B, Yuan X, Ceccatelli S.Methylmercury and H(2)O(2) provoke lysosomal damage in human astrocytoma D384 cells followed by apoptosis. *Free Radic Biol Med* 2001;30:1347-1356
- 8 Moriya K, Nakagawa K, Santa T, Shintani Y, Fujie H, Miyoshi H, Tsutsumi T, Miyazawa T, Ishibashi K, Horie T, Imai K, Todoroki T, Kimura S, Koike K. Oxidative stress in the absence of inflammation in a mouse model for hepatitis C virus-associated hepatocarcinogenesis. *Cancer Res* 2001; 61:4365-4370
- 9 Joseph P, Muchnok TK, Klishis ML, Roberts JR, Antonini JM, Whong WZ, Ong T. Cadmium-induced cell transformation and tumorigenesis are associated withtranscriptional activation of c-fos, c-jun, and c-myc proto-oncogenes: role of cellular calcium and reactive oxygen species. *Toxicol Sci* 2001;61:295-303
- 10 Huang RP, Peng A, Golarad A, Hossain MZ, Huang R, Liu YG, Boynton AL. Hydrogen peroxide promotes transformation of rat liver non-neoplastic epithelial cells through activation of epidermal growth factor receptor. *Mol Carcinog* 2001;30:209-217
- 11 Chen YR, Shrivastava A, Tan TH.Down-regulation of the c-Jun N-terminal kinase (JNK) phosphatase M3/6 and activation of JNK by hydrogen peroxide and pyrrolidine dithiocarbamate. *Oncogene* 2001; 20:367-374
- 12 Zmijewski JW, Song L, Harkins L, Cobbs CS, Jope RS. Oxidative stress

- and heat shock stimulate RGS2 expression in 1321N1 astrocytoma cells. *Arch Biochem Biophys* 2001;392:192-196
- 13 Mendoza L, Carrascal T, De Luca M, Fuentes AM, Salado C, Blanco J, Vidal-Vanaclocha F. Hydrogen peroxide mediates vascular cell adhesion molecule-1 expression from interleukin-18-activated hepatic sinusoidal endothelium: implications for circulating cancer cell arrest in the murine liver. *Hepatology* 2001;34:298-310
 - 14 Hardman RA, Afshari CA, Barrett JC. Involvement of mammalian MLH1 in the apoptotic response to peroxide-induced oxidative stress. *Cancer Res* 2001;61:1392-1397
 - 15 Risau W. Development and differentiation of endothelium. *Kidney Int Suppl* 1998; 67:s3-6
 - 16 Landriscina M, Cassano A, Ratto C, Longo R, Ippoliti M, Palazzotti B, Crucitti F, Barone C. Quantitative analysis of basic fibroblast growth factor and vascular endothelial growth factor in human colorectal cancer. *Br J Cancer* 1998;78:765-770
 - 17 Ishigami SI, Arai S, Furutani M, Niwano M, Harada T, Mizumoto M, Mori A, Onodera H, Imamura M. Predictive value of vascular endothelial growth factor in metastasis and prognosis of human colorectal cancer. *Br J Cancer* 1998;78:1379-1384
 - 18 Nanashima A, Ito M, Sekine I, Naito S, Yamaguchi H, Nakagoe T, Ayabe H. Significance of angiogenic factor in liver metastatic tumors originating from colorectal cancers. *Dig Dis Sci* 1998;43:2634-2640
 - 19 Wang MP, Cheung N, Yuen ST, Leung SY, Chung LP. Vascular endothelial growth factor is up-regulated in the early pre-malignant stage of colorectal tumor progression. *Int J Cancer* 1999;81:845-850
 - 20 Zebrowski BK, Liu W, Ramirez K, Akagi Y, Mills GB, Ellis LM. Markedly elevated level of vascular endothelial growth factor in malignant ascites. *Ann Surg Oncol* 1999;6:373-378
 - 21 Dachs GU, Chaplin DJ. Microenvironmental control of gene expressions: implications for tumor angiogenesis, progression and metastasis. *Semi Radiat Oncol* 1998; 8:208-216
 - 22 Ortega N, L'Fagih FE, Plouet J. Control of vascular endothelial growth factor angiogenic activity by the extracellular matrix. *Biol Cell* 1998; 90:381-390
 - 23 Neufeld G, Cohen T, Gengrinovitch S, Poltorak Z. Vascular endothelial growth factor and its receptors. *FASEB J* 1998;90:381-390
 - 24 Lufc FC, Mervaa E, Muller DN, Gross V, Schmidt F, Park JK, Schmitz C, Lippoldt A, Breu V, Dechend R, Dragun D, Schneider W, Ganten D, Haller H. Hypertension-induced end organ damage: A new transgenic approach to an old problem. *Hypertension* 1999;33:212-218
 - 25 Semenza GL, Agani F, Iyer N, Kotch L, Laughner E, Leung S, Yu A. Regulation of cardiovascular development and physiology by hypoxia-inducible factor 1. *Ann N Y Acad Sci* 1999;874:262-268
 - 26 Nanthan CA, Franklin S, Abreo KW, Nassar R, Debenedatti A, Williams J, Stucker FJ. Expression of eIF4E during head and neck tumorigenesis: possible role in angiogenesis. *Laryngoscope* 1999;109:1253-1258
 - 27 Arri S, Mori A, Uchida S, Fujimoto K, Shimada Y, Imamura M. Implication of vascular endothelial growth factor in the development and metastasis of human cancers. *Hum Cell* 1999;12:25-30
 - 28 Holash J, Wiegand SJ, Yancopoulos GD. New model of tumor angiogenesis: dynamic balance between vessel regression and growth mediated by angiopoietins and VEGF. *Oncogene* 1999;18:5356-5362
 - 29 Lamszus K, Lateral J, Westphal m, rosen EM. Scatter factor/hepatocyte growth factor content and function in human gliomas. *Int J Dev Neurosci* 1999;17:517-530
 - 30 Saari A, Karpanen T, Alitalo K. Mechanism of angiogenesis and their use in the inhibition of tumor growth and metastasis. *Oncogene* 2000;19:6122-6129
 - 31 Akagi Y, Liu W, Zebrowski B, Xie K and Ellis LM. Regulation of vascular endothelial growth factor expression in human colon cancer by insulin-like growth factor 1. *Cancer Res* 1998;58:4008-4014
 - 32 Akagi Y, Liu W, Xie K, Zebrowski B, Shaheen RM and Ellis LM. Regulation of vascular endothelial growth factor expression in human colon cancer by Interleukin-1 α . *Br J Cancer* 1999;80:1506-1511
 - 33 Bouvet M, Ellis LM, Nishizaki M, Fujiwara T, Liu W, Bucana CD, Fang B, Lee JJ and Roth JA. Adenovirus-mediated wild-type p53 gene transfer down-regulates vascular endothelial growth factor expression and inhibits angiogenesis in human colon cancer. *Cancer Res* 1998;58:2288-2292
 - 34 Kondo Y, Arai S, Furutani M, Ishigami S, Mori A, Onodera H, Chiba T, Imamura M. Implication of vascular endothelial growth factor and p53 status for angiogenesis in noninvasive colorectal carcinoma. *Cancer* 2000;88:1820-1827
 - 35 Pool-Zobel BL, Abrahamse SL, Collins AR, Kark W, Gugler R, Oberreuther D, Siegel Treptow-van Lishaut S, Rechkemmer G. Analysis of DNA strand breaks, oxidized bases, and glutathione S-transferases in human colon cells from biopsies. *Cancer Epidemiol biomarkers prev* 1999;8:609-614
 - 36 Kondo S, Toyokuni S, Iwasa Y, Tanaka T, Onodera H, Imamura M. Persistent oxidative stress in human colorectal carcinoma, but not in adenoma. *Free Radic Biol Med* 1999;27:401-410
 - 37 Bras A, Sanches R, Cristovao L, Fidalgo P, Mexia J, Leitao N, Rueff J. Oxidative stress in familial adenomatous polyposis. *Eur J Cancer* 1999;8:305-310
 - 38 Wen RW, Giacosa A, Hull WE, Haubner R, Spiegelhalter B, Bartsch H. The antioxidant/anticancer potential of phenolic compounds isolated from olive oil. *Eur J Cancer* 2000;36:1235-1247
 - 39 Van Rossen ME, Sluiter W, Bonthuis F, Jeekel H, Marquet RL, Van Eijck CH. Scavenging of reactive oxygen species leads to diminished peritoneal tumor recurrence. *Cancer Res* 2000;60:5625-5629
 - 40 Owen RW, Spiegelhalter B, Bartsch H. Generation of reactive oxygen species by the faecal matrix. *Gut* 2000;46:225-232
 - 41 Edmiston KH, Shoji Y, Mizoi T, Ford R, Nachman A, Jessup JM. Role of nitric oxide and superoxide anion in elimination of low metastatic colorectal carcinomas by unstimulated hepatic sinusoidal endothelial cell. *Cancer Res* 1998;58:1524-1531
 - 42 Giardina C, Inan MS. Nonsteroidal anti-inflammatory drugs, short-chain fatty acids, and reactive oxygen metabolism in human colorectal cancer cells. *Biochim Biophys Acta* 1998;1401:277-288
 - 43 Polyak K, Li Y, Zhu H, Lengauer C, Willson JK, Markowitz SD, Trush MA, Kinzler KW, Vogelstein B. Somatic mutations of the mitochondrial genome in human colorectal tumor. *Nat Genet* 1998;20:291-293
 - 44 Jessup JM, Battle P, Waller H, Edmiston KH, Stolz DB, Watkins SC, Locker J, Skena. Reactive nitrogen and oxygen radicals formed during hepatic ischemia-reperfusion kill weakly metastatic colorectal cancer cells. *Cancer Res* 1999;59:1825-1829
 - 45 Liegibel UM, Abrahamse SL, Pool-Zobel BL, Rechkemmer G. Application of confocal laser scanning microscopy to detect oxidative stress in human colon cells. *Free Radic Res* 2000;32:535-547
 - 46 Zheng ZH, Zhang H, Pan YX, Gao Y, Yang JZ. Prevention of postoperative abdominal adhesions by an antibody to VEGF in mice. *Shijie Huaren Xiaohua Zazhi* 1999;7:227-229
 - 47 Pan X, Ke CW, Pan WF, He X, Cao GW, Qi ZT. Killing effect of DT/VEGF system on gastric carcinoma cell. *Shijie Huaren Xiaohua Zazhi* 2000;8:393-396
 - 48 Mao H, Yuan AL, Zhao MF, Lai ZS, Zhang YL, Zhou DY. Effect of p38MAPK signal pathway on ultrastructural change of liver cancer cells induced by VEGF. *Shijie Huaren Xiaohua Zazhi* 2000;8:536-538
 - 49 Pan X, Pan W, Ni CR, Ke CW, Cao GW, Qi ZT. Killing effect of tetracycline controlled expression of DT/VEGF system on liver cell cancer. *Shijie Huaren Xiaohua Zazhi* 2000;8:867-873
 - 50 Pan X, Pan W, Ke CW, Zhang B, Cao GW, Qi ZT. Tetracycline controlled DT/VEGF system gene therapy mediated by adenovirus vector. *Shijie Huaren Xiaohua Zazhi* 2000;8:1121-1126
 - 51 Assy N, Paizi M, Gaitini D, Baruch Y, Spira G. Clinical implication of VEGF serum levels in cirrhotic patients with or without portal hypertension. *World J Gastroenterol* 1999;5:296-300
 - 52 Tian XJ, Wu J, Meng L, Dong ZW, Shou CC. Expression of VEGF121 in gastric carcinoma MGC803 cell line. *World J Gastroenterol* 2000;6: 281-283
 - 53 Bruce WR, Giacca A, Medline A. Possible mechanisms relating diet and risk of colon cancer. *Cancer Epidemiol Biomarkers Prev* 2000;9:1271-1279
 - 54 Bianchi NO, Bianchi MS, Richard SM. Mitochondrial genome instability in human cancers. *Mutat Res* 2001;488:9-23
 - 55 Ellis EA, Guberski DL, Somogyi-Mann M, Grant MB. Increased H₂O₂, vascular endothelial growth factor and receptors in the retina of the BBZ/Wor diabetic rat. *Free Radic Biol Med* 2000;28:91-101
 - 56 Castilla MA, Carmelo C, Gazapo RM, Martin O, Gonzalez-Pacheco FR, Tejedor A, Bragado R, Arroyo MV. Role of vascular endothelial growth factor (VEGF) in endothelial cell protection against cytotoxic agents. *Life Sci* 2000; 67:1003-1013
 - 57 Haklar G, Sayin-Ozveri E, Yuksel M, Aktan AO, Yalcin AS. Different kinds of reactive oxygen and nitrogen species were detected in colon and breast tumors. *Cancer Lett* 2001;165:219-224
 - 58 Wartenberg M, Dierschagen H, Hescheler J, Sauer H. Growth stimulation versus induction of cell quiescence by hydrogen peroxide in prostate tumor spheroids is encoded by the duration of the Ca²⁺ response. *J Biol Chem* 1999; 274:27759-27767
 - 59 Deptala A, Bedner E, Gorczyca W, Darzynkiewicz Z. Activation of nuclear factor KappaB (NF- κ B) assayed by laser scanning cytometry. *Cytometry* 1998; 33: 376-382
 - 60 Kaul N, Choi J, Forman HJ. Transmembrane redox signaling activates NF-KappaB in macrophages. *Free Radical Biol Med* 1998; 24: 202-207
 - 61 Chua CC, Hamdy RC, Chua BH. Mechanism of transforming growth factor- β 1 induced expression of vascular endothelial growth factor in murine osteoblastic MC3T3-E1 cells. *Biochim Biophys Acta* 2000; 1497: 69-76

• BASIC RESEARCH •

An analysis of 10218 ulcerative colitis cases in China

Xue-Liang Jiang, Hui-Fei Cui

Xue-Liang Jiang, Department of Gastroenterology, Chinese PLA General Hospital of Jinan Command, Jinan 250031, China
Hui-Fei Cui, Department of Biochemical Pharmaceutics, Shandong University, Jinan 250012, Shandong Province, China
Supported by the Key Research Fund of Jinan Command, No.9801
Correspondence to: Dr. Xue Liang Jiang, Department of Gastroenterology, Chinese PLA General Hospital of Jinan Command, 25 Shifanlu, Jinan 250031, Shandong Province, China. chfjxl@jn-public.sd.cninfo.net
Telephone: +86-531-2600132 Fax: +86-531-2600132
Received 2001-07-19 Accepted 2001-08-01

Abstract

AIM: To analyze the characteristics of ulcerative colitis (UC) in China.

METHODS: From 1981 to 2000, a total of 10218 patients of UC reported in Chinese medical literature and including our cases diagnosed were analyzed according to the diagnostic criteria of Lennard-Jones.

RESULTS: The number of cases increased by 3.08 times over the past 10 years (2506 patients were diagnosed from 1981 to 1990 while 7512 patients were diagnosed from 1991 to 2000). Lesion range were described in 7966 patients, 5592 (70.20%) were proctosigmoiditis or proctitis, 1792 (22.50%) left-sided colitis, 582 (7.30%) pancolitis. Among the 8122 patients, 2826 (34.8%) had first episode, 4272 (52.6%) had chronic relapse, 869 (10.7%) were of chronic persist type, 154 (1.9%) were of acute fulminant type. The course of the illness were described in 5867 patients, 4427 (75.5%) were less than 5 years, 910 (15.5%) between 5 and 10 years, 530 (9.1%) more than 10 years. Six hundred and sixteen patients (6.1%) had extraintestinal manifestations. The mean age at the diagnosis was 40.7 years (range 6-80 years, and the peak ages 30-49 years). The male to female ratio was 1.09. Among 270 patients diagnosed in our hospital, 36 had histories of smoking, there was no negative association between the severity of UC and smoking ($P > 0.05$), 21 smokers were followed up for one year, 15 of them had given up smoking when the disease were diagnosed, and one year later, 7 patients relapsed, another 6 patients continued smoking, and one year later, 2 patients relapsed. Among 270 UC patients diagnosed in our hospital, 4 patients (1.48%) from 2 families had familial history of UC. Treatment was mentioned in 6859 patients, only 5-ASA and/or corticosteroid only in 1276 patients (18.6%), only Chinese herbs in 1377 patients (20.1%), combined Chinese and western medicine in 4056 patients (59.1%), surgery was performed in 87 patients (1.3%), other treatments in 63 patients (0.9%).

CONCLUSIONS: In China, number of UC patients increased significantly in the past 10 years. Lesions are commonly located to left side colon. The course is short with rare extraintestinal manifestations. The age of onset is relatively high. Males and females are nearly equally affected. No negative relation was found between smoking and severity of the disease. Familial relatives are rarely involved

Traditional Chinese medicine (TCM) is widely used in the treatment of UC.

Jiang XL, Cui HF. An analysis of 10218 ulcerative colitis cases in China. *World J Gastroenterol* 2002;8(1):158-161

INTRODUCTION

Ulcerative colitis (UC) was first described by Wilks in 1859. In China, the first case of UC was reported in 1956^[1]. The diagnostic criteria of UC was published firstly in 1978 and was revised in 1993 on the National Conference of Chronic non-infective Diarrhea Disease in Taiyuan city, China^[2-4]. The criteria are similar to Lennard-Jones, on the three major aspects: mainly by exclusion. A multi-center study was set up in Chinese PLA General Hospital of Jinan Command (Shandong province, China) in 1999, with eight comprehensive hospitals from different areas using unique diagnostic criteria and method treatment^[1].

UC was thought to be infrequent in China in the past, however, it was increasing over the last 20 years^[1,2,5]. Figure 1.

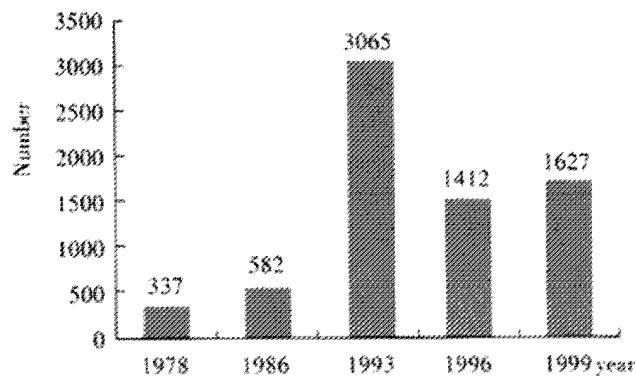


Figure 1 Cases reported on the conferences in China.

No precise statistics are available in China, in our hospital, 57 cases were admitted from 1981 to 1990, whereas 213 cases were hospitalized from 1991 to 2000^[1]. According to the statistics of World Digestology Network (<http://www.wd.org.cn>) data base, more than 1560 Chinese papers on this subject were published in the past 20 years, of which, 102 articles were published on World Chinese Journal of Digestology (founded in 1993) and World Journal of Gastroenterology (founded in 1995), regarding the animal model^[6-16], etiology and pathogenesis^[17-36], diagnostic criteria^[1-4] and results of treatment, etc^[37-102]. Of these 1560 papers, a total of 10218 patients of UC were reported in Chinese medical literature including those diagnosed in our hospital.

MATERIALS AND METHODS

The diagnosis of UC was based on endoscopic or radiological findings and mucosal biopsies or surgical pathology using Lennard-Jones criteria. Only those verified were included in the study. A total of 10218 patients of UC reported in Chinese medical literature including ours according to the diagnostic criteria of Lennard-Jones were

analyzed. Redit test was used, a value of $P < 0.05$ was regarded as statistically significant.

RESULTS

Case number

From 1981 to 2000, a total of 10218 cases of UC were reported, of these, 2506 were diagnosed from 1981 to 1990 whereas 7512 were diagnosed from 1991 to 2000, an increasing to 3.08 times in the past 10 years.

Extent of lesions range

As described in 7966 patients, 5592 (70.20%) were proctosigmoiditis/proctitis, 1792 (22.50%) left-sided colitis, 582 (7.30%) pancolitis.

Clinical types

Of those described in 8122 cases, 34.8% (2826 patients) were first presentation, 52.6% (4272 patients) were chronic relapsing, 10.7% (869 patients) were chronic persistent, 1.9% (154 patients) were acute fulminant.

Course

Of those described in 5867 cases, 4427 (75.5%) patients were less than 5 years, 910 patients (15.5%) between 5 and 10 years, 530 patients (9.1%) more than 10 years.

Extraintestinal manifestations

618 patients (6.1%) had extraintestinal manifestations.

Age

The mean age at the diagnosis was 40.7 years (range 6-80 years, peak age range 30-49 years).

Sex

The male to female ratio was 1.09.

Smoking

In our 270 patients, 36 patients (30 male, 6 female) had histories of smoking (more than 20 cigarette one day), there was no negative association between the severity of UC and smoking ($P > 0.05$, Table 1), 21 smokers were followed up for one year, 15 of them had given up smoking when the disease were diagnosed, and one year later, 7 patients relapsed, another 6 patients continued smoking, and one year later, 2 patients relapsed.

Table 1 The association between the severity of UC and smoking

Group/severity	mild	moderate	severe
Smokers	20	11	5
Non-smokers	130	72	32

Ridit test, $P > 0.05$

Family study

In our 270 UC patients, 4 patients (1.48%) from 2 families had familial history of UC. In one family, the patients were mother and son, in the other family, the patient were two sisters, and their mother had a history of bloody stool more than 9 years without seeking medical advise.

Treatment

Of the 10218 patients, treatment was mentioned in 6859 cases, only 5-ASA and/or corticosteroid only in 1276 patients (18.6%), only

Chinese herbs in 1377 patients (20.1%), combined Chinese and western medicine in 4056 patients (59.1%), surgery was performed in 87 patients (1.3%), other treatments in 63 patients (0.9%). Figure 2.

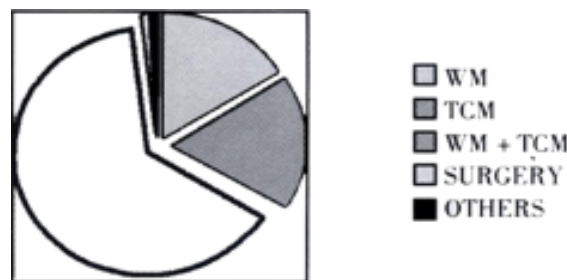


Figure 2 Treatment of UC in China. WM:western medicine TCM:traditional Chinese medicine.

DISCUSSION

The characteristic features of UC in China are as follows:

UC increased significantly in the past 10 years

The incidence of UC varies greatly in different geographical areas of the world^[90-92,95,101-102]. A high incidence is seen in Northern Europe and North America. In the western world, a sharp rise in the incidence of UC has been observed since early 1950s^[95], and now the incidence is stable. UC has been thought uncommon in China, however, an analysis of 1560 papers and 10218 cases indicate that the incidence is rising in recent years. From 1981 to 1990, 2506 patients were diagnosed while 7512 patients were diagnosed from 1991 to 2000. The number of cases increase by 3.08 times in the past 10 years. This is due to increasing awareness, better health care and improved study diagnostics. However, it may also be a real increase, reflecting changes in life style and dietary composition. These may shed some light on the role of environmental factors in the etiology of UC^[1].

Lesions mostly affect left sided colon

In China, UC is usually restricted to the rectum, sigmoid and descending colon, proctocolitis are common. Our data showed 92.7% were restrict to left colon (70.20% proctosigmoiditis/proctitis, 22.50% left-sided colitis), 7.30% pancolitis, the later was commonly seen in the Western countries^[101].

The course of illness is shorter with less extraintestinal manifestations

Occasionally, the disease may present as a single mild episode of diarrhea, but may at anytime relapse. In China, 34.8% were first presentation, 52.6% chronic relapsing, 10.7% chronic persistent, only 1.9% acute fulminant. Usually, the history revealed months or years of general ill health with continuous or intermittent diarrhea. In China, among that, the course of UC is commonly less than 5 years (75.5%), only 9.1% more than 10 years. Symptoms may be mild, systemic complications are rare, only 6.1% has extraintestinal manifestations, much less than that in the Western countries^[99].

The onset of illness is relatively higher

In china, the onset of UC is relatively higher in the middle and old-age group (30-49 years old), mean age at the diagnosis was 40.7 years, but may occur at any age (range 6-80 years), while in the western countries the peak age is 30 years old^[91].

Male and female are nearly equally affected

The reports on sex difference are variable, but there seem to be a

tendency to a male preponderance especially in high incidence areas. Our data suggest that the male to female ratio was 1.09, with nearly equal frequencies.

No relation between smoking and severity of illness

Smoking is the only consistent risk factor in case-control studies of UC, and there is no apparent relation seen between ulcerative colitis and cigarette smoking in our cases.

Familial relatives are rarely involved

Genetic study of UC are rarely performed in China. In our 270 UC patients, 4 patients (1.48%) from 2 families had family history of UC, which is much rarer than expected. The familial tendency may be much lower than that seen in western countries^[91,102].

Traditional Chinese medicine are widely used for the treatment of UC

SASP, is still the major drug used for the treatment of UC in China, which is effective in inducing remission and maintenance in mild-to-moderate cases. 5-ASA is too costly, corticosteroids are more commonly used, whereas 6-MP is only used by some authors. Heparin or oral low molecular weight heparin has been found to paradoxically induce remission in occasional patients with corticosteroid-resistant UC in China^[48,57,60]. In China, herb medicine as heartleaf houttuynia^[12,13], has been widely used in patients with mild-to-moderate disease, as well as an adjunct to patient with moderate-to-severe disease. Combined Chinese and western medicine is the predominance treatment in China.

REFERENCES

- Jiang XL, Wang ZK, Qin CY. Current research status and strategy on ulcerative colitis in China. *Shijie Huaren Xiaohua Zazhi* 2000;8:610-613
- Jiang XL. Diagnosis and treatment of ulcerative colitis. *Shijie Huaren Xiaohua Zazhi* 2000;8:332
- Jiang XL, Quan QZ, Wang ZK. Diagnosis, clinical types and criteria of effectiveness of ulcerative colitis. *Shijie Huaren Xiaohua Zazhi* 2000;8:332-334
- An ZY. Diagnostic criteria of ulcerative colitis. *Xin Xiaohuabingxue Zazhi* 1994;2:57
- Jiang XL, Pan BR, Ma JY, Ji ZH, Ma LS. Review for the 20th century and prospect for the 21st century of digestology. *Shijie Huaren Xiaohua Zazhi* 2000;8:1161-1176
- Cui SY, Zhang HB, Wu CZ, Sun GC, Zhao WP, Xu T, Li M. The clinical and experimental treatment of ulcerative colitis using Bupisan. *Xin Xiaohuabingxue Zazhi* 1997;5:219-220
- Yi JY, Xia B, Huang MF, Fu N, Deng CS. Observation of experimental model of ulcerative colitis in rats. *Xin Xiaohuabingxue Zazhi* 1997;5:721-722
- Zhu BX, Lu YM, Ye SM. Effects of sulfphasalazine on oxygen free radicals in experimental colitis. *Xin Xiaohuabingxue Zazhi* 1997;5:769-770
- He QW, Chen YM, Jia YL, Li XY, Jiang HY. The pathogenetic effects of immunocomplex on ulcerative colitis. *Huaren Xiaohua Zazhi* 1998;6:87
- Zou YH, Zhang YB, Chen WQ, Zhong TJ, Liu XQ, Zhao H, Lian ZC, Su Q, Su XR, Huang HD. Effects of Chinese medicine compound Weichangkang on rat ulcerative colitis and its NO abnormality. *Huaren Xiaohua Zazhi* 1998;6:288-290
- Jiang XL, Quan QZ, Wang D, Sun ZQ, Wang YJ. A new ulcerative colitis model induced by compound method and the change of immunity and ultrastructures. *Shijie Huaren Xiaohua Zazhi* 1999;7:381
- Jiang XL, Quan QZ, Wang D, Sun ZQ, Wang YJ, Qi F. Effect of heartleaf houttuynia herb on colonic pressure in rats with ulcerative colitis. *Shijie Huaren Xiaohua Zazhi* 1999;7:639
- Jiang XL, Quan QZ, Wang D, Sun ZQ, Wang YJ, Qi F. Experimental and clinical study of heartleaf houttuynia herb on ulcerative colitis. *Shijie Huaren Xiaohua Zazhi* 1999;7:786
- Zheng L, Gao ZQ, Wang SX. A chronic ulcerative colitis model in rats. *World J Gastroenterol* 2000;6:150-152
- Li L, Wang ZL, Ke JT, Zhang M, Shao JF, Zhong CN. Animal model selection for experimental ulcerative colitis. *Shijie Huaren Xiaohua Zazhi* 2001;9:584-585
- Jiang XL, Cui HF. A new chronic ulcerative colitis model produced by combination methods in rats. *World J Gastroenterol* 2000;6:742-746
- Wu XN. New advance on pathogenesis of ulcerative colitis. *Xin Xiaohuabingxue Zazhi* 1995;129-131
- Xu CT, Wang RL, Ma LS. Alterations of serum motilin, peptide YY, IgG and ferritin in patients with ulcerative colitis. *Xin Xiaohuabingxue Zazhi* 1997;5:247-248
- Zhang L, Wang AM, Guo RF, Zhang WN. Serum soluble interleukin-2 receptor level in patients with ulcerative colitis. *Xin Xiaohuabingxue Zazhi* 1997;5:251-252
- Chen X, Zhang ZY, Xu ED, Na JH, Yang NH. Bone mineral density and serum Ca, P and Mg in ulcerative colitis patients. *Xin Xiaohuabingxue Zazhi* 1997;5:385-386
- Jiang XL, Quan QZ, Liu TT, Wang YJ, Sun ZQ, Qi F, Ren HB, Zhang WL, Zhang L. Detection of blood platelet activation in patients with ulcerative colitis. *Xin Xiaohuabingxue Zazhi* 1997;5:736
- Jiang XL, Quan QZ, Sun ZQ, Wang YJ, Qi F. Expression of adhesion molecules in tissues and peripheral lymphocyte of patients with ulcerative colitis. *Huaren Xiaohua Zazhi* 1998;6:54-55
- Li HM. The characteristic of pathogenesis and the rule of treatment in spleen-weak patients with chronic colitis and ulcerative colitis. *Huaren Xiaohua Zazhi* 1998;6:726
- Jin W, Wu SH, Zhang ZJ, Lin PG, Ren XQ, Sui WL. Effect of Chinese herb Changyannin on T lymphocyte subgroup in patients with ulcerative colitis. *Shijie Huaren Xiaohua Zazhi* 1999;7:616-617
- Jiang XL, Quan QZ, Sun ZQ, Wang YJ, Qi F, Wang D, Zhang XL. Expression of lymphocyte apoptosis in patients with ulcerative colitis. *Shijie Huaren Xiaohua Zazhi* 1999;7:903-904
- Jiang XL, Quan QZ, Wang D, Sun ZQ, Wang YJ, Qi F. One case report of ulcerative colitis accompanied with acute myocardial infarction. *Shijie Huaren Xiaohua Zazhi* 1999;7:963
- Jiang XL, Quan QZ, Sun ZQ, Wang YJ, Qi F, Wang D, Zhang XL. Detection of soluble CD44v6 in patients with inflammatory bowel disease. *Shijie Huaren Xiaohua Zazhi* 1999;7:1028
- Tai WP, Luo HS. The role of short chain fatty acid on the etiology and treatment of ulcerative colitis. *Shijie Huaren Xiaohua Zazhi* 2000;8:96-97
- Jiang XL, Quan QZ, Cheng GR, Sun ZQ, Wang YJ, Wang YP. Expression of apoptosis on biopsy tissue in patients with ulcerative colitis. *Shijie Huaren Xiaohua Zazhi* 2000;8:107-108
- Jiang XL, Quan QZ, Liu T, Dong XC. Recent advances in research of ulcerative colitis. *Shijie Huaren Xiaohua Zazhi* 2000;8:216-218
- Wen B, Ma GF. Determination of plasma nitric oxide, motilin and their significances in ulcerative colitis. *World J Gastroenterol* 1998;4:69s
- Xia B, Guo HJ, JBA Crusius 2, Deng CS, SGM Meuwissen, AS Pena. In vitro production of TNF α , IL-6 and sIL-2R in Chinese patients with ulcerative colitis. *World J Gastroenterol* 1998;4:256
- Wang JN, Li ZF, Fu Y, Ke Y, Xu RC, Lin GB. The change of serum TNF α and IL-6 in patients with ulcerative colitis. *Shijie Huaren Xiaohua Zazhi* 1999;7:727-728
- Luo YJ, Yu JP. Molecular marker of IBD activity. *Shijie Huaren Xiaohua Zazhi* 2001;9:698-701
- Feng BS, Niu ZX, Zhang LF. LPO Change in experimental ulcerative colitis in rats. *Xin Xiaohuabingxue Zazhi* 1995;3(Suppl 4):7
- Cui SL, Tang B, Wang WM, Chen K, Liang J, Wang SC. Clinical investigation of serum TNF- α and IL-8 levels in patients with ulcerative colitis. *Xin Xiaohuabingxue Zazhi* 1997;5:719-720
- Li GQ, Feng YK. Clinical presentation and differential diagnosis of ulcerative colitis. *Shijie Huaren Xiaohua Zazhi* 2000;8:334-335
- Chen ZH, Shao XY. Examination of X ray and colonoscopy in ulcerative colitis. *Shijie Huaren Xiaohua Zazhi* 2000;8:335-336
- Wang Q, Xu L. Laboratory test and activity evaluation of ulcerative colitis. *Shijie Huaren Xiaohua Zazhi* 2000;8:336-337
- Han Y, Li SR. Current medical therapy for ulcerative colitis. *Shijie Huaren Xiaohua Zazhi* 2000;8:1273-1275
- Xu CT, Pan BR. Current medical therapy for ulcerative colitis. *World J Gastroenterol* 1999;5:64-72
- Du YC, Wang JM, Du XL. Effectiveness evaluation of different pathway of administration in ulcerative colitis. *Xin Xiaohuabingxue Zazhi* 1993;1:187-188
- Zhou ZY. Treatment of 97 ulcerative colitis patients. *Xin Xiaohuabingxue Zazhi* 1995;3:167
- Wang JD. Drug treatment of ulcerative colitis. *Xin Xiaohuabingxue Zazhi* 1996;4:338
- Li Q, Shen J. Treatment and follow up of 58 patient with ulcerative colitis. *Xin Xiaohuabingxue Zazhi* 1996;4:535
- Zhu XL, Li SX. Curative effect of drug injection via intra arterial catheter in ulcerative colitis. *Huaren Xiaohua Zazhi* 1998;6:705-706
- Chen QP. Surgical treatment of ulcerative colitis. *Shijie Huaren Xiaohua Zazhi* 2000;8:339-340
- Jiang XL, Qin CY, Li GQ. Other treatments for ulcerative colitis. *Shijie Huaren Xiaohua Zazhi* 2000;8:341-342

- 49 Rampton DS, Phil D. New treatments for inflammatory bowel disease. *World J Gastroenterol* 1998;4:369
- 50 Qing GL, Zhang AG, Niu YH, Yu DS, Guo YR. Treatment of ulcerative colitis with SASP suppository. *Xin Xiaohuabingxue Zazhi* 1994;2:120
- 51 Cui GT, Bu XZ, Chen ZX, Chen JS, Zhang PY. Treatment of ulcerative colitis with cimitidine and microwave. *Xin Xiaohuabingxue Zazhi* 1996;4:345
- 52 Sun QJ. Treatment of ulcerative colitis with metronidazole and anisodamine. *Xin Xiaohuabingxue Zazhi* 1996;4:510
- 53 Liu JY, Li YF, Fan MM. Treatment of ulcerative colitis with 4-ASA. *Xin Xiaohuabingxue Zazhi* 1997;5:183
- 54 Li SQ, Zhang JB. Treatment of ulcerative colitis with sucralfate paste. *Xin Xiaohuabingxue Zazhi* 1997;5:330
- 55 Zhou BX, Lv YM. Influence of sulphasalazine on propane dialdehyde of ulcerative colitis intestinal mucosa. *Xin Xiaohuabingxue Zazhi* 1997;5:619
- 56 Cui GT, Lv ZF. Treatment of ulcerative colitis with ranitidine enema. *Xin Xiaohuabingxue Zazhi* 1997;5:86s
- 57 Jiang XL, Liu T. Treatment of refractory ulcerative colitis with heparin. *Shijie Huaren Xiaohua Zazhi* 1999;7:694
- 58 Qin QY, Han GQ. Treatment of ulcerative colitis with aminosaliclate and corticosteroids. *Shijie Huaren Xiaohua Zazhi* 2000;8:338-339
- 59 Li RP, Wang YB. Treatment of inflammatory bowel disease with immunosuppressive agent. *Huaren Xiaohua Zazhi* 1998;6:718
- 60 Cui HF, Jiang XL. Treatment of corticosteroid-resistant ulcerative colitis with oral low molecular weight heparin. *World J Gastroenterol* 1999;5:448-450
- 61 Qiu BX, Qiu SS. Treatment of ulcerative colitis with traditional Chinese medicine. *Xin Xiaohuabingxue Zazhi* 1997;5:58s-59s
- 62 Jiang B, Wu XW, Wang Y, Si YL, Hu WJ. Treatment of ulcerative colitis with traditional Chinese herb Ziqintang. *Xin Xiaohuabingxue Zazhi* 1994;2:174
- 63 Wu ZQ, Wang HL. Treatment of ulcerative colitis with traditional Chinese herb. *Xin Xiaohuabingxue Zazhi* 1996;4:356-357
- 64 Cao GL. Treatment of ulcerative colitis with traditional Chinese herb Changanye. *Xin Xiaohuabingxue Zazhi* 1997;5:100s
- 65 Li L, Wei JQ, Zhang CQ. Treatment of ulcerative colitis with traditional Chinese herb Sanhuangtang and Binpengsan. *Xin Xiaohuabingxue Zazhi* 1997;5:125s
- 66 Li SL, Meng FS, Wang SL, Wang SQ. Treatment of ulcerative colitis with traditional Chinese herb. *Xin Xiaohuabingxue Zazhi* 1997;5:132
- 67 Wu B, Liu CL, Li WH. Treatment of ulcerative colitis with traditional Chinese herb. *Xin Xiaohuabingxue Zazhi* 1997;5:185s
- 68 Zhao XX, Long ZX, Han CB. Treatment of nonspecific ulcerative colitis with Chinese medicine. *Huaren Xiaohua Zazhi* 1998;6:78-79
- 69 Chen ZS, Nie ZW, Shun QL, Yan H. Clinical and pharmacological effect of Jianpiling on chronic ulcerative colitis. *Shijie Huaren Xiaohua Zazhi* 1999;7:960-963
- 70 Wang ZK, Xin ZP, Fan SD. Treatment of ulcerative colitis with traditional Chinese medicine. *Shijie Huaren Xiaohua Zazhi* 2000;8:340-341
- 71 Chen ZS, Zhou CM, Lu Y, Nie ZW, Sun QL, Wang YX, Chi Y. Study on TCM syndrome-typing of chronic ulcerative colitis. *China Natl J New Gastroenterol* 1996;2:141-143
- 72 Zhao LM, Guan DA, Pei HW. Treatment of ulcerative colitis with traditional Chinese medicine and western medicine. *Xin Xiaohua bingxue Zazhi* 1993;1:105
- 73 Zhu YJ, Chen WS, Wang XL. Treatment of ulcerative colitis with traditional Chinese medicine and western medicine. *Xin Xiaohua bingxue Zazhi* 1994;2:103
- 74 Guo SH, Guo JS. Treatment of ulcerative colitis with traditional Chinese medicine and western medicine. *Xin Xiaohua bingxue Zazhi* 1994;2:122
- 75 Liu QM, Bi F, Zhou SJ. Treatment of ulcerative colitis with traditional Chinese and western medicine. *Xin Xiaohua bingxue Zazhi* 1995;3:115-116
- 76 Chen ZS, Yan H, Lu Y. Advance of treatment on ulcerative colitis with traditional Chinese and western medicine. *Xin Xiaohua bingxue Zazhi* 1996;4:301-303
- 77 Sheng YZ, Ru PY, Wang SY. Treatment of ulcerative colitis with combined therapy. *Xin Xiaohua bingxue Zazhi* 1996;4:346
- 78 Ding ZQ, Wang YF, Lv CL. Treatment of ulcerative colitis with traditional Chinese medicine and western medicine. *Xin Xiaohua bingxue Zazhi* 1996;4:355-356
- 79 Sun SR, Liang LJ, Guo JQ, Song DL. Treatment of ulcerative colitis with traditional Chinese medicine and western medicine. *Xin Xiaohua bingxue Zazhi* 1997;5:400
- 80 Chen HW, Miao ZD. Treatment of ulcerative colitis with cimitidine and Yunzhigantai. *Huaren Xiaohua Zazhi* 1999;6:1009
- 81 Wang BH. Advances in treatment of ulcerative colitis. *Shijie Huaren Xiaohua Zazhi* 1999;7:177-179
- 82 Wu HG, Zhou LB, Huang C, Pan YY, Chen HP, Shi Z, Hua XG. Gene expression of cytokines in acupuncture and moxibustion treatment for ulcerative colitis in rats. *Huaren Xiaohua Zazhi* 1998;6:853-855
- 83 Wu HG, Lu HB, Zhao C, Shi Z, Liu HR, Chen HP. The mechanism of iNOS gene modulation on acupuncture and moxibustion treatment for ulcerative colitis in rats. *World J Gastroenterol* 2000;6(Suppl 3):64
- 84 Wu HG, Zhou LB, Shi DR, Liu SM, Liu HR, Zhang BM, Chen HP, Zhang LS. Morphological study on colonic ulcerative colitis treated by moxibustion. *World J Gastroenterol* 2000;6:861-865
- 85 Hu QY, Hu XY, Jiang Y. Clinical investigation of ulcerative colitis patients treated by integrated traditional Chinese and Western medicine. *World J Gastroenterol* 1998;4:93
- 86 Jiao JL, Wang SM, Li YC, Yao LY, Li SJ, Meng YX, Liu QG, Liu GQ. Treatment of ulcerative colitis with Kuijiekang. *Shijie Huaren Xiaohua Zazhi* 2000;8:572 *World J Gastroenterol* 1998;4:93s
- 87 Hu FF, Ni DQ. Treatment of ulcerative colitis with folic acid and TCM. *Shijie Huaren Xiaohua Zazhi* 2000;8:1144
- 88 Zhou QH, Gu SL, Yu J. Clinical and experimental study on treatment of retention enema for chronic nonspecific ulcerative colitis with quick-acting kuijie powder. *World J Gastroenterol* 2000;6(Suppl 3):76
- 89 Wu HG, Zhou LB, Pan YY, Huang C, Chen HP, Shi Z, Hua XG. Study of the mechanisms of acupuncture and moxibustion treatment for ulcerative colitis rats in view of the gene expression of cytokines. *World J Gastroenterol* 1999;5:515-517
- 90 Xia B, S. ShivanandaI, Zhang GS, Yi JY, JBA CRUSIUS, AS PE A. Inflammatory bowel disease in Hubei Province of China. *China Natl J New Gastroenterol* 1997;3:119-120
- 91 Xia B, JBA Crusius, SGM Meuwissen, AS Pena. Inflammatory bowel disease definition, epidemiology, etiologic aspects, and immunogenetic studies. *World J Gastroenterol* 1998;4:446-458
- 92 Shivananda S. Epidemiology and disease outcome in inflammatory bowel disease: observations from the European Collaborative Study. *World J Gastroenterol* 1998;4:25s
- 93 Geng X, Taniguchi M, Dai HH, Lin JJC, Lin J, Das KM. Autoimmunity in ulcerative colitis: humoral and cellular immune response by tropomyosin in ulcerative colitis. *World J Gastroenterol* 2000;6:9
- 94 Rask-Madsen J. Current concepts of the pathogenesis of IBD. *World J Gastroenterol* 1998;4:20-22
- 95 Russel M. The epidemiology of IBD worldwide. *World J Gastroenterol* 2000;6:6
- 96 Das KM, Farag SA. Current medical therapy of inflammatory bowel disease. *World J Gastroenterol* 2000;6:6
- 97 Rampton DS. Management of difficult inflammatory bowel disease: where are we now *World J Gastroenterol* 2000;6:8
- 98 Rampton DS. Management of difficult inflammatory bowel disease: where are we now *World J Gastroenterol* 2000;6:315-323
- 99 Das KM, Farag SA. Current medical therapy of inflammatory bowel disease. *World J Gastroenterol* 2000;6:483-489
- 100 Das KM, Farag SA. Current medical therapy of inflammatory bowel disease. *World J Gastroenterol* 2000;6:6
- 101 Salupere R. Inflammatory bowel disease in Estonia: a prospective epidemiologic study 1993-1998. *World J Gastroenterol* 2001;7:387-388
- 102 Kirsner JB. Historical origins of current IBD concepts. *World J Gastroenterol* 2001;7:175-184

• BASIC RESEARCH •

Screening and identification of proteins mediating senna induced gastrointestinal motility enhancement in mouse colon

Xin Wang, Yue-Xia Zhong, Mei Lan, Zong-You Zhang, Yong-Quan Shi, Ju Lu, Jie Ding, Kai-Cun Wu, Jian-Ping Jin, Bo-Rong Pan, Dai Min Fan

Xin Wang, Mei Lan, Zong-You Zhang, Yong-Quan Shi, Jie Ding, Kai-Cun Wu, Dai Min Fan, Institute of Digestive Disease, Xijing Hospital, Fourth Military Medical University, Xi'an 710032, Shaanxi Province, China

Yue-Xia Zhong, Department of Emergency, Tangdu Hospital, Fourth Military Medical University, Xi'an 710032, Shaanxi Province, China
Ju Lu, Class EE 87, Department of Electronic Engineering, Tsinghua University, Beijing 100084, China

Jian-Ping Jin, Department of Physiology and Biophysics, Case Western Reserve University School of Medicine, Cleveland, 44106-4970, Ohio, USA

Bo-Rong Pan, Oncology Center of Xijing Hospital, Fourth Military Medical University, Xi'an 710032, Shaanxi Province, China

Supported by the National Natural Science Foundation of China, No. 39970901

Correspondence to: Prof. Dai-Ming Fan, Institute of Digestive Diseases, Xijing Hospital, Fourth Military Medical University, Xi'an 710033, Shaanxi Province, China. Daimfan@pub.xaonline.com

Telephone: +86-29-3375221 Fax: +86-29-2539041

Received 2001-08-24 Accepted 2001-11-05

Abstract

AIM: To isolate the proteins involved in pharmacologic action of senna extract (SE) from mouse gastrointestinal tract and to explore the molecular mechanism of gastrointestinal motility change induced by SE.

METHODS: SE was administrated to mice by different routes. Gastrointestinal motility of mice was observed using cathartic, gastrointestinal propellant movement experiments and X-ray analysis. Mouse model for gastrointestinal motility enhancement was established through continuous gastric administration of SE at progressively increased dose. At 3 h and week 3, 4, 6 and 10, morphological changes of gastrointestinal tissues were found under light microscope. Ultrastructural changes of intestinal and colonic tissues at week 6 were observed under transmission electron microscope. The colonic proteomic changes in model mice were examined by two-dimension polyacrylamide gel electrophoresis with immobilized pH gradient isoelectric focusing to screen the differentially expressed proteins, and their molecular masses and isoelectric points were determined. Two N-terminal sequences of the samples were also determined by mass spectrometry.

RESULTS: SE (0.3g) caused diarrhea after gastric administration in 1-6h and enhanced gastrointestinal propellant ($65.1 \pm 7.5\%$; $45.8 \pm 14.6\%$, $P < 0.01$) in mice, but intramuscular and hypodermic injection had no cathartic effect. X-ray analysis of gastrointestinal motility demonstrated that gastric administration of SE enhanced gastric evacuation and gastrointestinal transferring function. At 3 h and week 3 and 4 after gastric administration of SE, light microscopic examination revealed no apparent change in gastrointestinal mucosal tissues, but transmission

electron microscopic examination revealed inflammatory changes in whole layer of intestinal and colonic wall. Twenty differential proteins were detected in the colonic tissues of the model mice by two-dimensional electrophoresis, and the N-terminal amino acid sequences of two proteins were determined.

CONCLUSION: SE causes diarrhea and enhances gastrointestinal motility through digestive tract administration. Long-term gastric administration of SE induces inflammatory changes and cell damage in the whole gastrointestinal tract. The differential proteins screened from the colonic tissues of the model mice might mediate the enhancing effect of SE on gastrointestinal motility.

Wang X, Zhong YX, Lan M, Zhang ZY, Shi YQ, Lu J, Ding J, Wu KC, Jin JP, Pan BR, Fan DM. Screening and identification of proteins mediating senna induced gastrointestinal motility enhancement in mouse colon. *World J Gastroenterol* 2002;8(1):162-167

INTRODUCTION

Senna, a traditional Chinese medicine, has potent cathartic effect^[1-4]. Its extract(SE), composed of a few dozens of chemical substances, possesses multiple pharmacological activities. Especially, it can promote the motility and secretion of gastrointestinal tract. However, its application is greatly restricted due to its toxicity^[5-17]. Much attention is being paid to the effect of traditional Chinese medicine on the regulation of gastrointestinal motility^[18-37]. We analyzed the role of senna in gastrointestinal motility and in diarrhea of mice and observed its action pattern, the ultrastructural changes in the active sites, and the changes in protein expression. In doing so we intended to screen from the gastrointestinal tissues the biological molecules mediating diarrhea and the enhancement of gastrointestinal movement, to elucidate the mechanism of catharsis induced by senna at the molecular level, and to lay a foundation for the development of pharmaceutical agents enhancing gastrointestinal motility.

MATERIALS AND METHODS

Materials

Imported senna (Shaanxi Medicine Corporation) was used, and its quality was confirmed by the Institute of Pharmaceutics, Fourth Military Medical University. The extract was obtained through solvent recovery and stored at -20°C. Acrylamide, bisacrylamide, SDS, Tris base, PMSF (all from Sino-America Biotechnology Co); ultrapure urea (Shanghai Biotechnology Co); ampholyte pH 3-10L, IPG dry strips pH 3-10L, IPGphorTM Isoelectric Focusing System (Pharmacia Co); ultradispersor GF-1 (Jiangsu Qilin Medical Equipment Factory); two-dimensional electrophoresis bath DYY-III 26, gradient mixer (Beijing 61 Factory); electrophoresis apparatus (Bio-Rad Co) were used.

Induction of diarrhea by SE in different Administration routes

Thirty Balb/c mice (both sexes, 8 week, 18g-23g) were used. Before experimental manipulation, the mice was fasted without water deprivation for 24h, and each was kept in a single cage re-based with filter paper. After being divided into different groups, the mice were administered 0.3g SE in different routes, and the diarrhea status was examined.

Effect of SE on gastrointestinal motility in mice

Effect of SE on gastrointestinal motility for carbon Thirty Balb/c mice (both sexes, 6-8weeks, 18-23 g) were divided randomly into 3 groups: Group I, II, and Control Group. SE of 0.3g was delivered to each mouse in Group I through gastric administration; 0.3g SE was im injected into each mouse in Group II; and the same volume of 9g·L⁻¹ NaCl was delivered through gastric administration to the mice in control group. After 20 min, 0.1 mL of 100 g·L⁻¹ mixture of Arabic gum and charcoal powder was administrated to all mice. Then, all mice were killed after 20 min. Whole gastrointestinal tract was taken out and pulled straight. The length of gastrointestinal tract from pylorus to anus and that from pylorus to the anterior extremity of carbon powder were measured. Percentage of migration distance of carbon powder out of whole length was calculated.

Effect of SE on gastrointestinal motility for barium Eight Balb/c mice (both sexes, 8weeks, 18~20 g), fasting without water deprivation within 24 h prior to the experimental manipulation, were divided randomly into 2 groups. SE of 0.3g was given through gastric administration to each mouse in Group I, and the same volume of 9 g·L⁻¹ NaCl to each mouse in the control group. After 20 min, 0.8 mL of 1.6kg·L⁻¹ barium sulfate suspension was given to each mouse. The mice were put into cloth bags that could restrict their movement, and the bags were placed on the flat of the X-ray digital machine. The migration of barium in the gastrointestinal tract was visualized and X-ray photos were taken at 5 and 40 min, 1, 1.5, 2, and 3h after barium administration^[38].

Effect of SE on morphology of gastrointestinal tissue

Thirty Balb/c mice (both sexes, 8weeks, 18-23 g) were fed separately according to their sexes. Ten were classified into the control group, and 20 into the experimental group. SE was given through gastric administration to the mice in the experimental group once a day. The frequency of drug delivery increased progressively from 1·d⁻¹ to 4·d⁻¹ and the dosage increased progressively from 0.1g·d⁻¹ to 0.8g·d⁻¹ in 6 weeks. The same volume of 9 g·L⁻¹ NaCl was given to the control group. Four mice in the experimental group and 2 in the control group were killed at 3 h, 3, 4 and 6week after reagent administration. Gastric, intestinal and colonic tissues were obtained and fixed in 40 g·L⁻¹ paraformaldehyde and embedded routinely with paraffin. Sections were made. Morphological changes were examined under light microscope after HE staining. Intestinal and colonic tissues at week 6 were collected and fixed with 30 g·L⁻¹ glutaraldehyde for 6h at 4°C. Ultrathin sections were routinely made. Cellular ultrastructural changes in the whole layer of the intestinal wall were examined under transmission electron microscope.

Two-dimensional polyacrylamide gel electrophoresis of proteins^[39]

Establishment of animal model for chronic gastrointestinal motility enhancement Forty Balb/c mice (both sexes, 8 weeks, 18-20 g) were selected. Twenty five mice in the experimental group received SE through gastric administration once a day, with the frequency and dosage increasing progressively from 0.1g, 1·d⁻¹ to 0.8g, 4·d⁻¹.

Fifteen mice in the control group received the same volume of 9 g·L⁻¹ NaCl.

Preparation of protein sample from intestinal tissue of mice

Twenty mice were killed at 6 weeks after receiving gastric administration of SE (10 mice) and 9g·L⁻¹ NaCl (10 mice). The colons were collected and put immediately into ice-cold 9g·L⁻¹ NaCl containing 0.1mmol·L⁻¹PMSF. The colonic tracts were dissected and colonic contents were washed out. The moisture on the tissues was absorbed with filter paper, and the tissues were put into liquid nitrogen immediately. The whole procedure must be finished in 5 min. Then, the tissues were either stored at -70°C until used again, or taken for immediate use. In the latter case, the tissues were weighed on electric scale, and lysed by adding tissue lytic solution (9.5mol·L⁻¹ urea, 20g·L⁻¹ NP, 402g·L⁻¹ ampholyte pH 3-10, 20g·L⁻¹ 2-ME, 1.5 mmol·L⁻¹ EDTA, 40 mmol·L⁻¹Tris and ion-free water) by a mass volume ratio of 1 : 5. Tissue homogenate was prepared with high-speed disperser in ice-bath (3500 r·min⁻¹×5s×5), and DNase and RNase (both 0.4 g·L⁻¹) were added into the homogenate. After the incubation for 20 min in ice-bath and addition of PMSF (0.1 mmol·L⁻¹), the homogenate was centrifuged at 10,000×g for 10 min. The supernatant was harvested and stored in designated volume at -70°C until used again. The total protein concentration in the supernatant was measured by Bradford method^[40-42].

Solid-phase pH gradient isoelectric focusing For each group, 100 µg protein sample was solved in 250µL mixture of deuterioxide solution and IPG buffer, placed at room temperature for 1h, and then applied to sample tank which was placed with IPG dry gel strip (13 cm in length), and covered with mineral oil. The isoelectric focusing program was: deuterioxidation for 12 h; isoelectric focusing 0-300 V, 1 h; 300-500 V, 1 h; 500-1000 V, 1 h; 1000-2000 V, 1 h; 2000-4000 V, 1 h; 4000-8000 V, 4 h. All operations above were performed at 20°C.

Equilibration and transfer of IPG slab gels The slab gels were collected and equilibrated with SDS-balanced buffer (50mmol·L⁻¹ Tris, 6 mol·L⁻¹ urea, 300 g·L⁻¹ glycerol, 10 g·L⁻¹ DTT, ion-free water) for 15 min followed by a second equilibration with balanced buffer (50 mmol·L⁻¹ Tris, 6 mol·L⁻¹ urea, 300 g·L⁻¹glycerol, 25 g·L⁻¹ idocetamide, ion-free water) for another 15 min. Two pieces of 125 g·L⁻¹ separation gel (17cm×17cm×0.15cm) was prepared in absence of sticking gels. IPG slab gels were fixed on the top of the separation gel using 5 g·L⁻¹ agarose. Protein marker was applied at the other terminus.

Second dimension SDS-PAGE Two pieces of 125 g·L⁻¹ SDS-PAGE (17cm×17cm×0.15cm) were prepared and underwent polymerization for 2 h in absence of sticking gels; IPG slab gels were fixed onto the top of SDS-PAGE gels; electrophoresis was performed for 11 h at room temperature (15°C -20°C) with constant electric current (20 mA/gel, 40mA in total) and terminated when the marker arrived at the bottom.

Silver staining of gels The gels were collected and stained with silvery salt based on a modified protocol. The gels were fixed with the fixing solution (300 g·L⁻¹ ethanol, 0.5 mol·L⁻¹ sodium acetate, 5 g·L⁻¹ glutaraldehyde, 2 g·L⁻¹ sodium thiosulfate), rinsed with ion-free water for 15 min×3, stained with 1 g·L⁻¹ AgNO₃ and 0.1 g·L⁻¹ formaldehyde for 20 min, washed with ion-free water for 30sec, and colored with 25 g·L⁻¹ sodium carbonate, 0.5 g·L⁻¹ sodium thiosulfate and 0.1 g·L⁻¹ formaldehyde. The color development was terminated with 10 g·L⁻¹ acetic acid.

Analysis of protein map on two-dimensional gels After silvery salt staining, the gels were scanned with transmission laser scanner at 500 bpi resolution and analyzed with image pattern analyzer under identical conditions. The position, shape and density information for each

detected spot was compared to screen obviously differentially expressed proteins and to determine their molecular masses and isoelectric points.

Identification of the screened proteins by sequencing^[43] One mg colonic proteins from the animal model was sampled and underwent solid-phase pH gradient isoelectric focusing and second dimension SDS-PAGE and transferred from gel slabs to polyvinylidene difluoride (PVDF) membranes (transferring buffer: CAPS, DTT, methanol and ion-free water, pH 11.0; transferring condition: 350 mA, 4.5 h, 10°C). The proteins on the PVDF membranes were stained with 1 g·L⁻¹ Coomassie brilliant blue. PDVF membrane was air-dried at room temperature. The protein spots stained with Coomassie brilliant blue were excised from the membrane, and their amino acid sequences at the N-termini were determined by mass spectrometry.

Statistical analysis

Student's *t* test and χ^2 test were used for data measurement and enumeration, respectively.

RESULTS

Cathartic Effect of SE in different Administration routes

One to 1.5 h after gastric administration of SE, mice started to suffer from diarrhea, defecating water-thin feces, which lasted 4-5h. When the mice received im and sc injection of extract of doubled dosage, they did not develop diarrhea within 6 h (Table 1).

Table 1 Carthartic effect of SE in different administration routes

	Groups	Dose/g	n	Administration routes	Diarrhea (in 6h)
I	Normal saline	0.3	6	ig	-
II	SE	0.3	6	ig	+(6) ^b
III	Normal saline	0.3	6	im	-
IV	SE	0.3	6	im	-
VC	SE	0.3	6	sc	-

^b*P*<0.01, vs all other groups.

Effect of SE on gastrointestinal motility in mice

Effect of SE on gastrointestinal propellant movement While ig administration of SE could enhance gastric motility, im delivery did not show such effect (Table 2).

Table 2 Effect of SE on gastrointestinal propellant rate in mice ($\bar{x}\pm s$)

	Group	Dose/g	Administration routes	n	Propellant rate/%
I	Normal saline	0.3	ig	10	45.8±14.6
II	SE	0.3	ig	10	65.1± 7.5 ^b
III	SE	0.3	im	10	48.3±12.4

^b*P*<0.01, vs I, III groups.

X-ray analysis of SE effect on gastrointestinal motility In mice with gastric administration of SE (0.3 g), barium sulfate was excreted at 40 min, and more at 2 h. The migration speed was significantly higher than that shown in the control group (Figure 1).

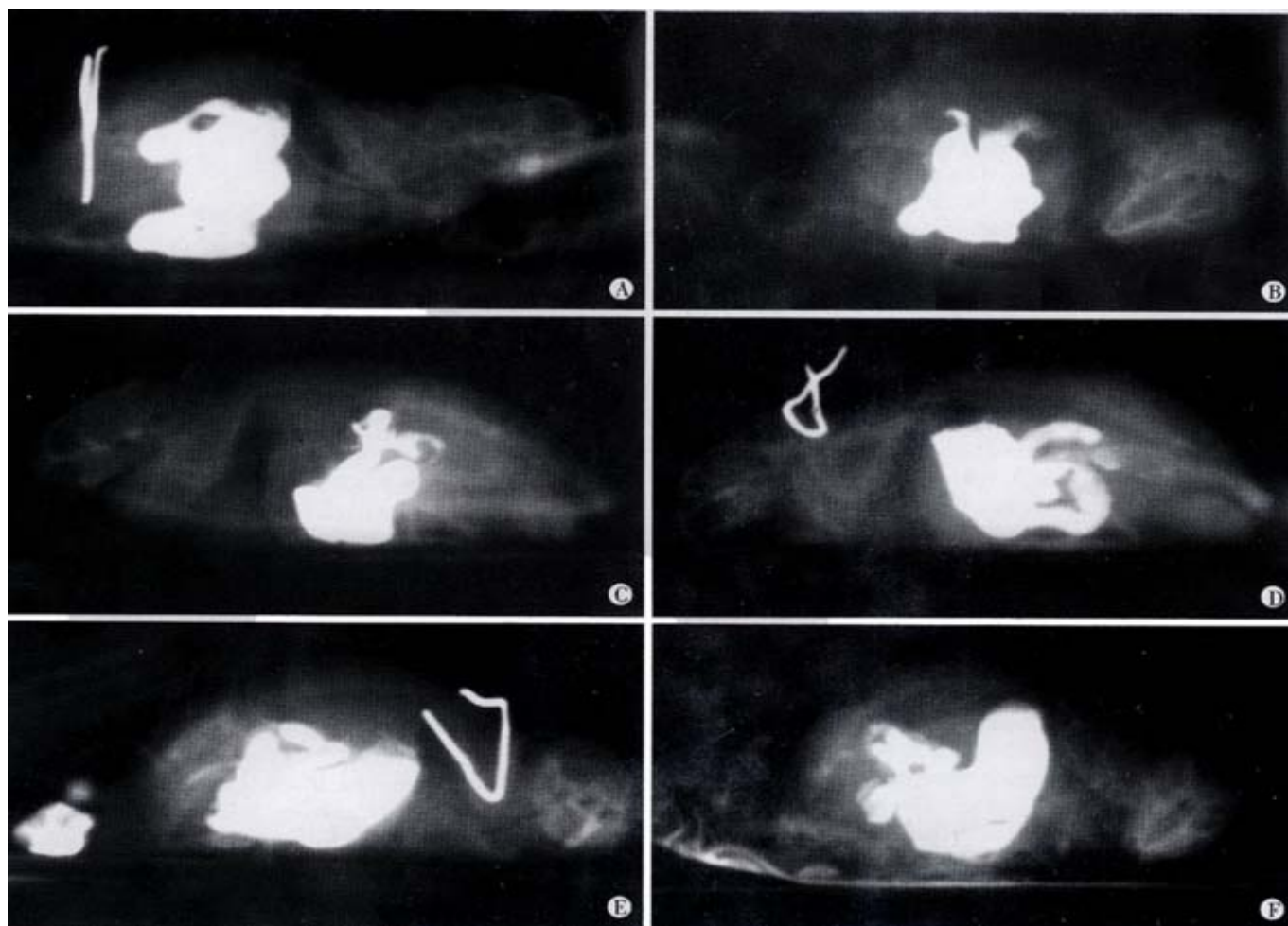


Figure 1 X- rays of gastrointestinal peristalsis in mice administered with SE
A, B, C: 5min, 2h, 3h after 9 g·L⁻¹ NaCl gastric administration, respectively D, E, F: 5 min, 2h, 3h after 0.3 g SE gastric administration, respectively

Morphological effects of SE on gastrointestinal tissue No pathological changes were observed in gastrointestinal tissues under light microscopy examination at 3 h, 3, 4 and 6 weeks after gastric administration of SE. However, at week 6, it was observed under transmission electron microscope that some small intestine epithelial cells underwent degeneration and necrosis. Although the microvilli were normal, the mitochondria in the cells were slightly swollen, with

part of the cristae broken. In the mucosa, macrophages containing phagocytic particles were found to increase, and so were plasmacytes. Cell degeneration and necrosis occurred more frequently in the mucosal epithelial cells in colon than those in the small intestine (Figure 2). The mitochondrial abnormalities mentioned above were observed in both small intestine and colon smooth muscle cells, along with the occurrence of vacuolation.

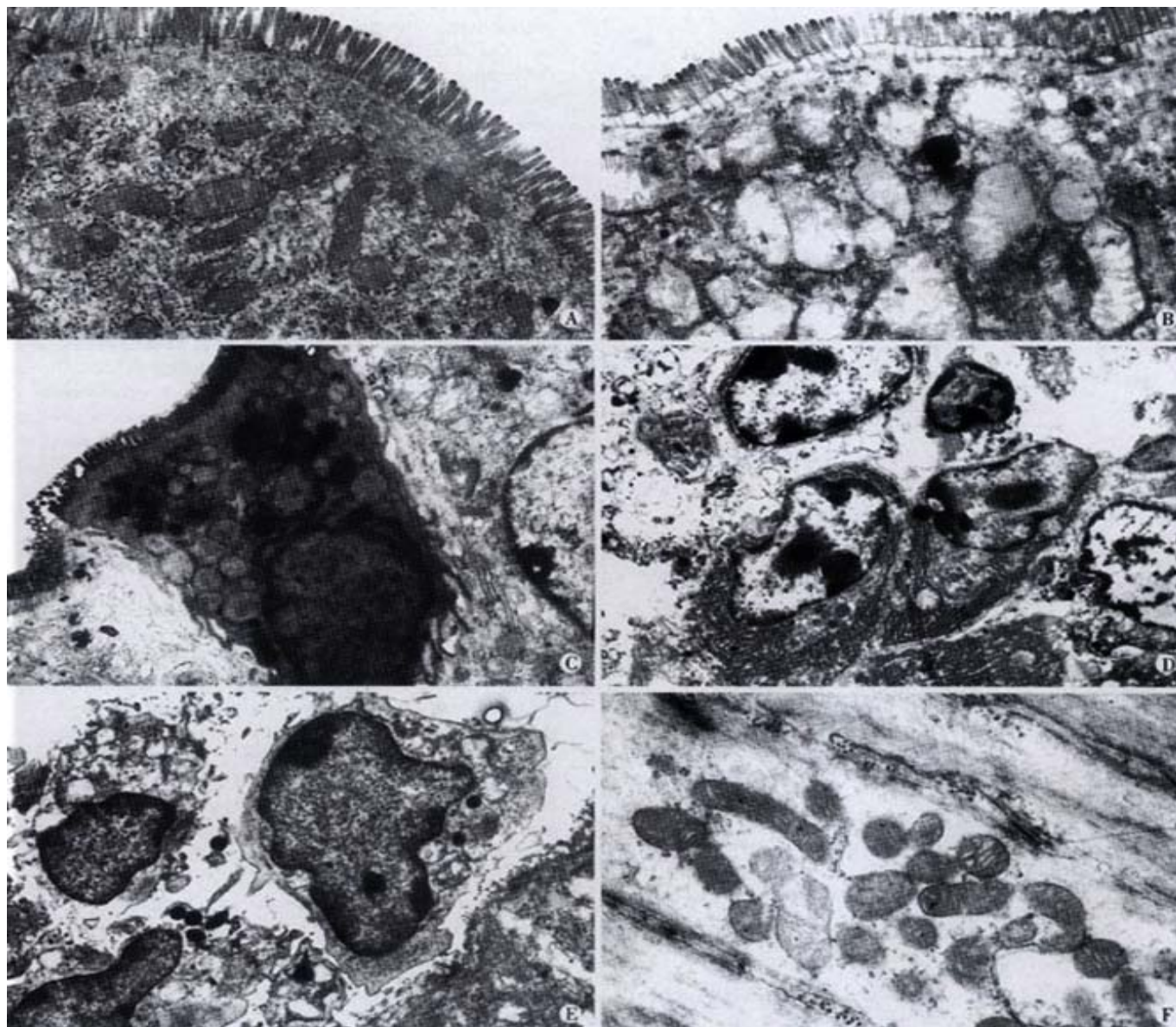


Figure 2 Ultrastructure of intestine and colon cells in mice receiving SE at week 10.

A: Normal epithelial cell; B: Intestinal cell after treatment with SE; C: Colon cell after treatment with SE; D: Increase in submucosal plasmacytes; E: Increase in submucosal macrophages; F: Minor degeneration of smooth muscle cells in intestine

Gastrointestinal proteins in mice

Establishment of mice model for chronic gastrointestinal movement enhancement Gastrointestinal propellant movement experiment and X-ray analysis of gastrointestinal motility demonstrated that gastric administration of SE could significantly enhance the gastrointestinal motility in Balb/c mice. Therefore, continuous gastric administration of SE might keep the gastrointestinal tract in constant enhanced motility. At week 6, the weight of the mice in the model group was significantly lower than that in the control group.

Differential expression of gastrointestinal tissue proteins in mice In the first dimension IPG isoelectric focusing, pH gradient was pH 3-10 L, 100 μ g protein sample was added. In the second dimension IPG -PAGE 125 $\text{g}\cdot\text{L}^{-1}$ uniform gel was used, the gels were stained with silver salt (Figure 3).

Identification of differentially expressed proteins The colonic proteins of one control mouse and one model mouse were screened and compared, and the process repeated for 5 such pairs. Twenty proteins were found different in abundance (Table 3).

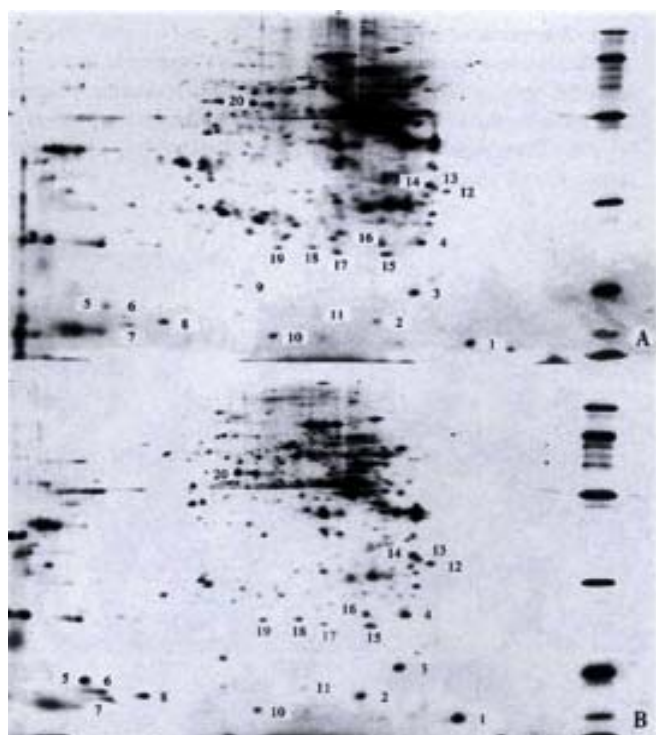


Figure 3 Proteins on two-dimension electrophoresis maps
A: Normal mice; B: Model mice

Table 3 Identification of the differential proteins

No.	Molecular mass/ku	Isoelectric point/pI	No.	Molecular mass/ku	Isoelectric Point/pI
1	15.0	3.9	11	18.0	5.9
2	17.5	5.2	12	33.0	4.3
3	19.0	4.7	13	34.0	4.5
4	26.0	4.6	14	35.0	4.6
5	18.0	8.8	15	24.0	5.1
6	17.5	8.6	16	26.0	5.2
7	16.5	8.5	17	24.5	5.7
8	17.0	8.0	18	25.0	6.1
9	20.0	7.0	19	25.0	6.5
10	16.0	6.6	20	52.0	7.0

Identification of differential proteins by sequencing The N-terminal amino acid sequences of protein No. 4 and No 12 were determined by sequencing (No. 4: N-MIX/IYR-C; No 12: N-GFXDX/L-C). Protein database search showed that these two proteins were unknown proteins.

DISCUSSION

Senna is a traditional Chinese medicine containing various chemicals, the effective components of which are sennoside A, B, C and D. It has been shown that sennosides are decomposed into Rhein anthrone by bacteria in colon, and then take effects on the colonic smooth muscle, significantly promoting colonic motility in animals and humans. The mechanism is that sennoside and its active forms affect on the intestinal mucosal epithelium and submucosal nerve bundles, stimulating prostaglandin (PG) synthesis and endogenous acetylcholine release, and subsequently enhancing colonic smooth muscle contraction.^[44-46] Meanwhile, sennosides may affect directly the colonic smooth muscle, evoking its spontaneous spike potential and promoting its contraction^[47]. In addition, sennosides can stimulate the colonic mucosa to release PG, NO and 5-HT, efficiently inducing the excretion of water and electrolytes by epithelial cells^[48-50]. Our study showed that 1-1.5 h after gastric administration of SE, mice started

to suffer from diarrhea, defecating water-thin feces, which lasted 4-5h. When the mice received im injection of extract of doubled dosage, they did not develop diarrhea within 6 h, but after 6 h, 3 mice had light diarrhea. It suggested that the possible pathway might be that the drug delivered through im injection entered blood circulation and was excreted into the intestinal tract with bile. With hypodermic injection of larger dosage of extract, no mice developed diarrhea. However, no enhanced gastrointestinal motility was observed after im injection of SE. These results indicate that the cathartic effect of SE can only be exerted through the digestive tract rather than other pathways.

Our study also indicated that SE could promote the propellant movement in mice, a result in agreement with the reports of other researchers. Although most researchers believe that the active components of senna mainly work on colon and promote colonic motility. We think that it may also affect small intestine, as our gastrointestinal propellant movement experiment has revealed that it promoted the motility of mice small intestine in mice. In order to locate the effective site of the drug, we continuously observed the movement of marked liquid (BaSO₄) in the gastrointestinal tract after administration of SE, and discovered that it inhibited rather than promoted gastric empty; however, it promoted small intestinal motility, and especially colonic motility.

We made histological examinations of mouse gastrointestinal tracts at different stages after gastric administration of SE. No apparent change was found under light microscope, but transmission electron microscopy showed lesions and degenerative changes of small intestinal mucosal epithelial cells, increase in submucosal macrophages and plasmacytes, minor degeneration of smooth muscle cells, and severe extensive degeneration and necrosis of colonic epithelial cells. Mengs *et al*^[10] observed the changes in guinea pig colonic epithelial cells after continuous gastric administration of sennoside for 2 weeks, and discovered epithelial cell degeneration. These results show that SE can injure the intestinal cells.

Using improved two-dimensional electrophoresis of proteomic analysis^[42,51,52], we compared the protein expression in the colon tissues of promoted gastrointestinal motility model mice and that of normal controls. The conditions in the whole process were identical for the two groups, and the location, shape, size and density of many protein spots were similar on the two-dimensional electrophoresis maps. Hence, the two groups were comparable. Image analysis showed differential proteins in the colon tissues of the model animals; the differences were primarily the increase or decrease in the amount of protein expression. Most of the differential proteins had moderate or low molecular mass, as shown in Table 3, which are probably regulatory proteins induced or affected by SE. Two of the proteins were sequenced with mass spectrometry and were confirmed to be novel ones through protein database search. However, the pharmacological functions they mediate remain to be discovered.

SE administered through the gastrointestinal tract promotes diarrhea and gastrointestinal motility, especially that of the small intestine and the colon; it also injures the digestive tract mucosa and smooth muscles, and promotes differential protein expression in the colon tissues of model animals. We have isolated and identified some of the molecules that may be involved in mediating the motility promotion and secretion effect of senna, and will continue to investigate the molecular mechanism of the aforementioned effects so as to lay the foundation for further research.

REFERENCES

- 1 Arezzo A. Prospective randomized trial comparing bowel cleaning preparations for colonoscopy. *Surg Laparosc Endosc Percutan Tech* 2000; 10:215-217
- 2 Chilton AP, O'Sullivan M, Cox MA, Loft DE, Nwokolo CU. A blinded, randomized comparison of a novel, low-dose, triple regimen with fleet phospho-soda: a study of colon cleanliness, speed and success of

- colonoscopy. *Endoscopy* 2000;32:37-41
- 3 Krumbiegel G, Schulz HU. Rhein and aloe-emodin kinetics from senna laxatives in man. *Pharmacology* 1993;47:120-124
 - 4 Valverde A, Hay JM, Fingerhut A, Boudet MJ, Petroni R, Pouliquen X, Msika S, Flamant Y. Senna vs polyethylene glycol for mechanical preparation the evening before elective colonic or rectal resection: a multicenter controlled trial. *Arch Surg* 1999;134:514-519
 - 5 Lan M, Wang X, Wu HP, Fan DM. Biological effects of senna extract on human intestinal epithelial cells. *Shijie Huaren Xiaohua Zazhi* 2001; 9:555-559
 - 6 Stickel F, Seitz HK, Hahn EG, Schuppan D. Liver toxicity of drugs of plant origin. *Z Gastroenterol* 2001;39:225-232, 234-237
 - 7 Adam SE, Al-Yahya MA, Al-Farhan AH. Combined toxicity of Cassia senna and Citrullus colocynthis in rats. *Vet Hum Toxicol* 2001;43:70-72
 - 8 Tasaka AC, Weg R, Calore EE, Sinhorini IL, Dagli ML, Haraguchi M, Gorniak SL. Toxicity testing of Senna occidentalis seed in rabbits. *Vet Res Commun* 2000;24:573-582
 - 9 Calore EE, Weg R, Haraguchi M, Calore NM, Cavaliere MJ, Sesso A. Mitochondrial metabolism impairment in muscle fibres of rats. chronically intoxicated with Senna occidentalis seeds. *Exp Toxicol Pathol* 2000;52:357-363
 - 10 Mascolo N, Mereto E, Borrelli F, Orsi P, Sini D, Izzo AA, Massa B, Boggio M, Capasso F. Does senna extract promote growth of aberrant crypt foci and malignant tumors in rat colon? *Dig Dis Sci* 1999;44: 2226-2230
 - 11 Mengs U, Grimminger W, Krumbiegel G, Schuler D, Silber W, Volkner W. No clastogenic activity of a senna extract in the mouse micronucleus assay. *Mutat Res* 1999;444:421-426
 - 12 Mukhopadhyay MJ, Saha A, Dutta A, De B, Mukherjee A. Genotoxicity of sennosides on the bone marrow cells of mice. *Food Chem Toxicol* 1998;36:937-940
 - 13 Haraguchi M, Calore EE, Dagli ML, Cavaliere MJ, Calore NM, Weg R, Raspantini PC, Gorniak SL. Muscle atrophy induced in broiler chicks by parts of Senna occidentalis seeds. *Vet Res Commun* 1998;22: 265-271
 - 14 Calore EE, Cavaliere MJ, Haraguchi M, Gorniak SL, Dagli ML, Raspantini PC, Calore NM, Weg R. Toxic peripheral neuropathy of chicks fed Senna occidentalis seeds. *Ecotoxicol Environ Saf* 1998;39:27-30
 - 15 Cavaliere MJ, Calore EE, Haraguchi M, Gorniak SL, Dagli ML, Raspantini PC, Calore NM, Weg R. Mitochondrial myopathy in Senna occidentalis-seed-fed chicken. *Ecotoxicol Environ Saf* 1997;37:181-185
 - 16 Calore EE, Cavaliere MJ, Haraguchi M, Gorniak SL, Dagli ML, Raspantini PC, Perez Calore NM. Experimental mitochondrial myopathy induced by chronic intoxication by Senna occidentalis seeds. *J Neurol Sci* 1997;146:1-6
 - 17 Brusick D, Mengs U. Assessment of the genotoxic risk from laxative senna products. *Environ Mol Mutagen* 1997;29:1-9
 - 18 Zhang HX, Ren P, Huang X, Li Yuan. Regulation of the traditional Chinese medicine on gastrointestinal hormone and motility. *Shijie Huaren Xiaohua Zazhi* 2000; 8:
 - 19 Zhu JZ, Yang GH, Leng EF, Chen DF. Effects of the traditional Chinese medicine on gastrointestinal motility. *Shijie Huaren Xiaohua Zazhi* 1999;7:689-690
 - 20 Pang L, Zhou DR. Regulation of the traditional Chinese medicine on gastrointestinal motility. *Huaren Xiaohua Zazhi* 1998; 6: 535
 - 21 Qin XM, Li HF, Wang LD. Effects of metoclopramide on gastrointestinal myoelectric activity in rats. *Chin Natl J New Gastroenterol* 1997;5:169
 - 22 Zheng TZ, Li W, Qu SY, Ma YM, Ding YH, Wei YL. Effects of Dangshen on isolated gastric muscle strips in rats. *World J Gastroenterol* 1998;4:354-356
 - 23 Lin J, Cai G, Xu JY. A comparison between Zhishi Xiaopiwan and cisapride in treatment of functional dyspepsia. *World J Gastroenterol* 1998;4:544-547
 - 24 Zhang ZQ, Zhang HP, Ha CL, Li XZ, Lu GQ, Chen GL, Zhang GH. Clinical analysis of therapeutic effect of traditional Chinese medicine on peptic ulcer. *World J Gastroenterol* 1998; 4: 88-89
 - 25 Li W, Zheng TZ, Qu SY. Effect of cholecystokinin and secretin on contractile activity of isolated gastric muscle strips in guinea pigs. *World J Gastroenterol* 2000; 6: 93-95
 - 26 Lin XZ, Ma DL, Cui ZQ, Kang Y. Effects of rhubarb and the active ingredients of rhubarb on the cytoplasmic free calcium in INT-MNC of rabbits. *World J Gastroenterol* 2000;6:301-303
 - 27 Tian XL, Mourelle M, Li YL, Guarner F, Malagelada JR. The role of Chinese herbal medicines in a rat model of chronic colitis. *World J Gastroenterol* 2000; 6(Suppl 3): 40
 - 28 Ma XS, Fan XP, Chen Z, Li CW, Xing YS. Effects of rhizoma atracylodes macrocephalae on the contraction of isolated ileum of guinea pig. *Xin Xiaohuabingxue Zazhi* 1996;4: 603-604
 - 29 Wang ZH, Lu LS. Effect of Weichangtong on gastrointestinal motility disorders. *Xin Xiaohuabingxue Zazhi* 1997;5:448-449
 - 30 Li Y, Sun SY, Zou Z, Chen SN, Wang XY. Influences of 6 formula compositions combined of 8 kinds of Chinese medicinals on gastro intestinal motility in mice. *Huaren Xiaohua Zazhi* 1998;6:208-209
 - 31 Pang L, Zhou DR. Regulative action of Chinese traditional medicine in gastrointestinal motility. *Huaren Xiaohua Zazhi* 1998;6:535-536
 - 32 Gao F, Zhang SB, Zhang LY, Liu F, Tong WD, Li FZ. An experiment study of the smallintestinal transit injured by contact laxatives. *Shijie Huaren Xiaohua Zazhi* 1999;7:659-660
 - 33 Zhu JZ, Yang GH, Leng ER, Chen DF. Gastrointestinal motility promoting action of traditional Chinese medicine. *Shijie Huaren Xiaohua Zazhi* 1999;7:689-690
 - 34 Wang J, Hou JY. Effect of granulae Li Wei on gastrointestinal activity. *Shijie Huaren Xiaohua Zazhi* 2000;8:377-381
 - 35 Hao Q, Li Y, Yin HT. Comparative effect of different varieties of Bupleurum and Citrus on gastrointestinal motility in mice. *Huaren Xiaohua Zazhi* 1998;6:205-207
 - 36 Li SZ, Tan XH. Effect of Astragalus membranaceus on intestinal blood flow and motility in dogs. *Xin Xiaohuabingxue Zazhi* 1997;5:659-660
 - 37 Wang X, Zhang ZY, Shi YQ, Lan M, Wang QL, Wu HP, Jin JP, Fan DM. Preliminary study on protein differential expression of small bowel in BALB/c mice induced by croton oil. *Chin J Gastroenterol Hepatol* 2000;9:103-106
 - 38 Pfeifer A, Klatt P, Massberg S, Ny L, Sausbier M, Hirneiss C, Wang GX, Korth M, Aszodi A, Andersson KE, Krombach F, Mayerhofer A, Ruth P, Fassler R, Hofmann F. Defective smooth muscle regulation in cGMP kinase I-deficient mice. *EMBO J* 1998;17:3045-3051
 - 39 Wang X, Wang BL, Zhang ZY, Lan M, Wang JC, Yao LB, Chen NC, Jin JP, Fan DM. Improvement and application of two-dimensional gel electrophoresis in proteome analysis. *J Cell Mol Immunol* 2001;17:191-192
 - 40 Radloff M, Delling M, Marti T, Gercken G. Hsp27 phosphorylation is induced in alveolar macrophages exposed to Cdo-coated silica particles. *Biochem Biophys Res Commun* 1998;248:219-222
 - 41 Staudenmann W, Hatt PD, Hoving S, Lehmann A, Kertesz M, James P. Sample handling for proteome analysis. *Electrophoresis* 1998;19:901-908
 - 42 Arnott D, O'Connell KL, King KL, Stults JT. An integrated approach to proteome analysis: Identification of proteins associated with cardiac hypertrophy. *Anal Biochem* 1998;258:1-18
 - 43 Qiu YC, Benet LZ, Burlingame AL. Identification of the hepatic protein targets of reactive metabolites of acetaminophen *in vivo* in mice using two-dimensional gel electrophoresis and mass spectrometry [J]. *J Biol Chem* 1998;273:17940-17953
 - 44 Yagi T, Miyawaki Y, Nishikawa A, Yamauchi K, Kuwano S. Suppression of the purgative action of rhein anthrone, the active metabolite of sennosides A and B, by indomethacin in rats. *J Pharm Pharmacol* 1991; 43:307-310
 - 45 Yagi T, Yamauchi K, Kuwano S. The synergistic Purgative action of aloe-emodin anthrone and rhein anthrone in mice: Synergism in large intestinal propulsion and water secretion. *J Pharm Pharmacol* 1997;49: 21-25
 - 46 Nijs G, de-witte P, Geboesk J. Influence of rhein anthrone and rhein on small intestine transit rate in rats: evidence of prostaglandin mediation. *Eur J Pharmacol* 1992;218:199-203
 - 47 Lan M, Wang X, Liu Na, Fan DM. Effect of senna extract on contraction of colonic smooth muscle cells in guinea pig. *Di-si Junyi Daxue Xuebao* 2001;(in press)
 - 48 van Gorkom BA, Karrenbeld A, van Der Sluis T, Koudstaal J, de Vries EG, Kleibeuker JH. Influence of a highly purified senna extract on colonic epithelium. *Digestion* 2000;61:113-120
 - 49 Izzo AA, Mascolo N, Capasso F. Nitric oxide as a modulator of intestinal water and electrolyte transport. *Dig Dis Sci* 1998;43:1605-1620
 - 50 Izzo AA, Sautebin L, Rombola L, Capasso F. The role of constitutive and inducible nitric oxide synthase in senna- and cascara-induced diarrhoea in the rat. *Eur J Pharmacol* 1997;323:93-97
 - 51 Wang X, Zhang ZY, Shi YQ, Lan M, Ma Z, Jin JP, Fan DM. Differential expression of colonic proteins induced by extract of senna in mice. *Di-si Junyi Daxue Xuebao* 2001;22:16-19
 - 52 Wang X, Shi YQ, Zhao YQ, Wang JC, Yao LB, Zhang ZY, Lan M, Jin JP, Fan DM. Differential display of Vincristine-resistance-related proteins in gastric cancer SGC7901 cell line. *Zhonghua Zhongliu Zazhi* 2001;23: 281-284

• BASIC RESEARCH •

Preventive effect of glutamine on intestinal barrier dysfunction induced by severe trauma

Jun-You Li, Yi Lu, Sen Hu, Dan Sun, Yong-Ming Yao

Jun-You Li, Yi Lu, Sen Hu, Dan Sun, Yong-Ming Yao, Burn Institute, Chinese PLA 304 Hospital, Beijing 100037, China
Supported by the Key Project of the "Tenth Five-Year Plan" of the Chinese PLA (01L081)

Correspondence to: Jun-You LI, Burn Institute, Chinese PLA 304 Hospital, 51 Fu Cheng Road, Beijing 100037, China. WuZG@A-1.net.cn
Telephon: +86-10-66867395 Fax: +86-10-68429998

Received 2001-06-03 Accepted 2001-11-15

Abstract

AIM: To investigate the mechanism underlying intestinal barrier function damage after severe trauma and the therapeutic effect of glutamine.

METHODS: Burned patients, and animal models of severe trauma replicated by hemorrhagic shock combined with endotoxin infusion and burn injury, were included in a serial experiment. Effects of oral glutamine on intestinal barrier function were observed in scalded rats. Parameters measured in these experiments were as follows: plasma levels of diamine oxidase (DAO), tumor necrosis factor (TNF α), endotoxin (LPS), and lactate as well as D-lactate by biochemical methods, lactose/mannitol (L/M) ratio in urine by SP-3400, and pathological examination of intestinal mucosa under light microscopy.

RESULTS: Plasma DAO activity was significantly increased after injury. There was a negative correlation between plasma DAO and intestinal mucosal DAO or pH_i ($r=-0.93$, plasma 0.80 ± 0.93 , 2.83 ± 1.71 , 1.14 ± 0.64 , 2.36 ± 2.06 and 2.49 ± 1.67 vs intestinal 0.52 ± 0.12 , 0.34 ± 0.03 , 0.45 ± 0.18 , 0.37 ± 0.26 and 0.41 ± 0.07 ; $r=-0.533$, plasma 0.87 ± 0.75 , 1.89 ± 1.13 , 1.21 ± 0.23 , 3.03 ± 2.61 and 4.70 ± 1.22 vs pH_i 7.03 ± 0.05 , 7.05 ± 0.06 , 7.14 ± 0.096 , 7.20 ± 0.08 and 7.05 ± 0.07 ; $P<0.01-0.05$). Positive correlations were found between DAO activity and plasma TNF α , LPS, lactate, L/M and D-lactate ($r=0.817$, 0.842 , 0.872 , and 0.951 ; plasma DAO 0.87 ± 0.75 , 1.89 ± 1.13 , 1.21 ± 0.23 , 3.03 ± 2.61 and 4.70 ± 1.22 vs TNF α 0.08 ± 0.02 , 0.03 ± 0.25 , 0.17 ± 0.09 , 0.34 ± 0.15 and 0.33 ± 0.18 ; vs LPS 0.14 ± 0.03 , 0.16 ± 0.04 , 0.21 ± 0.02 , 0.18 ± 0.16 and 0.37 ± 0.10 ; vs lactate 9.03 ± 2.19 , 18.30 ± 2.56 , 9.81 ± 2.83 , 12.01 ± 6.83 , 12.01 ± 6.84 and 43.61 ± 11.27 ; vs L/M 0.03 ± 0.01 , 0.41 ± 0.27 , 0.62 ± 0.20 , 1.70 ± 0.60 ; $r=0.774$, plasma DAO 1.25 ± 0.41 , 2.17 ± 0.71 , 2.29 ± 0.87 , 1.23 ± 0.55 and 1.11 ± 0.47 vs D-lactate 8.37 ± 2.48 , 18.25 ± 6.18 , 13.96 ± 4.94 , 8.93 ± 3.00 and 12.39 ± 4.94 ; all $P<0.01$), respectively. Damage of intestinal mucosa was found by pathological examination. Intestinal barrier function was improved to a certain extent by oral glutamine in scalded rats.

CONCLUSION: Intestinal barrier function was damaged in the early stage after trauma. Plasma DAO activity, D-lactate content, intestinal pH_i and urine L/M may be sensitive markers of intestinal mechanical injury, and glutamine may protect against intestinal barrier dysfunction after severe trauma.

Li JY, Lu Y, Hu S, Sun D, Yao YM. Preventive effect of glutamine on intestinal barrier dysfunction induced by severe trauma. *World J Gastroenterol* 2002;8(1):168-171

INTRODUCTION

It is generally accepted that the intestine may serve as an important organ in the development of severe complications under critically ill conditions, including trauma, burns, shock, etc.^[1-3] Hemorrhagic shock and/or gut ischemia-reperfusion injury commonly occur in the early stage after acute insults, leading to gut-derived sepsis as a result of gut barrier dysfunction^[4-10]. In order to investigate the mechanism underlying intestinal barrier function damage and its potential interventional measures, burned patients and animal models of severe trauma were employed in our current experiments^[6,11-15].

MATERIALS AND METHODS

Animal models

Animal models of severe trauma were replicated by hemorrhagic shock combined with endotoxin infusion. Male Wistar rats, weighing 190g-230g, were anaesthetized with intraperitoneal injection of 30g·L⁻¹ barbitone sodium (35mg·kg⁻¹), and the femoral artery and jugular vein were cannulated under aseptic conditions. The rats were then bled via the jugular vein catheter until a mean arterial pressure of 30-35 mmHg (4.6 kPa) was reached. At the end of shock, endotoxin (*E.coli*O55 B5, Sigma) was infused through tail vein at a dose of 2mg·kg⁻¹. A goat model of hemorrhagic shock combined with endotoxin challenge was established according to the previous report ($n=20$)^[5]. Animals received *E.coli*O26 B6 endotoxin via portal vein 24h after the recovery from shock, and the dosage was 30 ng·kg⁻¹·min⁻¹, which was given in a continuous infusion lasting for 5d. Wistar rats were divided randomly into three groups: normal controls, early feeding with standard feed phase Gln 0.5g after scalding, and animals (except control group) sustained a 30% TBSA full-thickness scald covering the back and flanks^[6]. Determination of plasma diamine oxidase in 21 burned patients (17 male and 4 female) at the age of 33±10 years, with burn area (64±21)%, and (35±20)% III°. Plasma DAO activity was determined on day 1, 3, 7, 14 and 21 postburn. Blood and intestinal DAO levels were tested according to our previous report^[17]. Plasma lactate and D-lactate concentrations were determined by biochemical methods as described by Brandt *et al*^[18]. Microassay for quantitation of endotoxin in blood was made with new PCA treatment using chromogenic limulus amebocyte lysate^[19].

Tumor necrosis factor (TNF α) assay. Plasma TNF content was measured by radioimmunoassay. Lactulose/mannitol (L/M) ratio tests in urine were made by SP-3400^[20].

Pathological examination. Tissue samples were examined under light microscopy.

Statistical Analyses

Data were expressed as the mean±standard error, and were statistically evaluated by Students *t* test and correlation analysis. Differences were considered to be significant with $P<0.05$.

RESULTS

Plasma DAO levels were elevated in double-peak patterns, one at early stage after trauma and another during invading infection in animal models. Similar results were also obtained in burned patients. Meanwhile, intestinal DAO levels were decreased to certain extent after trauma in animal model. There was a significantly negative correlation between plasma and intestinal DAO activity (Table 1; Figures 1 and 2).

Table 1 Changes in plasma DAO in trauma animal model ($\bar{x} \pm s \times 10^3 \text{U} \cdot \text{L}^{-1}$)

Animal model	Before injury	T (after injury)/h				
		2	6	24	48	72
Goat	0.9±0.8	1.9±1.1 ^a		1.2±0.2	3.0±2.6	4.7±1.2 ^b
Rats	1.3±0.4	2.2±0.7 ^b	2.3±0.87 ^b	1.2±0.6	1.1±0.5	
Scalded rats	0.8±0.9	0.8±1.8 ^b		1.1±0.6	2.4±2.1 ^a	
Burned pigs	4.1±1.4	4.7±1.5		4.7±1.4	4.8±1.1	5.8±1.4 ^a
Gun shooting	1.5±0.6	1.2±0.5	2.0±0.6 ^b	1.9±0.2 ^b		

Dog in hypothermia

^a $P < 0.05$; ^b $P < 0.01$, vs before injury.

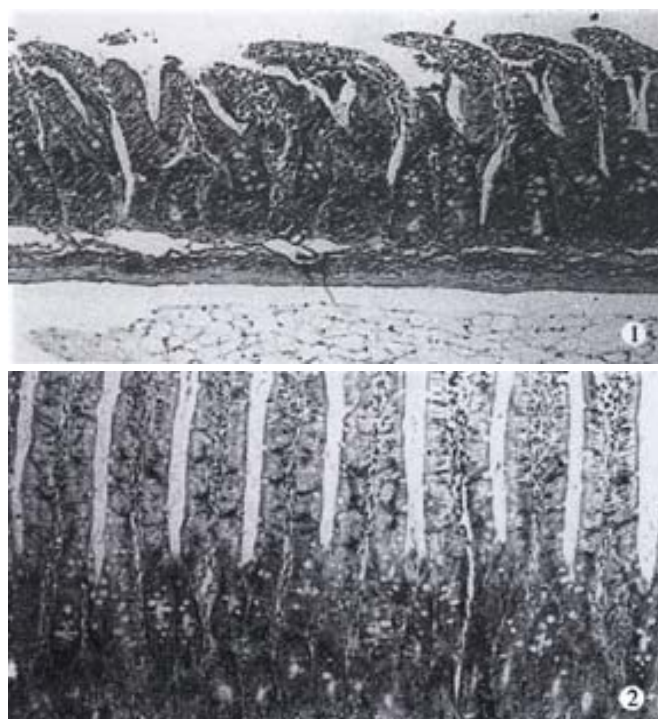


Figure 1 Pathological changes of intestinal mucosa after 8d in scalded rats. HE×100

Figure 2 Pathological changes of intestinal mucosa after 8d oral GLN in scalded rats. HE×100

Plasma DAO concentrations and the level of the related index, and plasma $\text{TNF}\alpha$ significantly increased at various intervals after trauma in goats. Plasma endotoxin levels notably increased at 24h and 72h after injury. Blood lactic acid significantly increased from 2h to 72h after trauma. The plasma DAO activity was obviously correlated with plasma $\text{TNF}\alpha$, LPS and lactate ($P < 0.01$; Table 2 and 3). Changes in DAO activity were significantly related with plasma $\text{TNF}\alpha$ and LPS levels in scalded rats. Plasma DAO activity and plasma D-lactate were significantly correlated in rats secondary to hemorrhage followed by endotoxin challenge ($r = 0.774$; $P < 0.01$).

Glutamine could protect against intestinal barrier function damage. The results indicated that plasma DAO activity was decreased in animals with early glutamine supplementation compared with those without glutamine treatment (10h after trauma $P < 0.05$).

Results of intestinal pathological examination. The pathologic examination of the intestine showed that the damage of epithelial cells of intestinal mucosa, hemorrhage and necrosis, accompanied by the inflammatory cell infiltration in intestinal wall in goats suffering from hemorrhagic shock combined with endotoxin infusion. It was revealed that there was disruption of intestinal mucosa after scald and gut ischemia-reperfusion combined with endotoxin challenge in rats, whereas oral glutamine supplementation could markedly improve intestinal mucosa following acute insults (Figure 2).

Table 2 Changes in parameters in goats after hemorrhagic shock combined with endotoxin infusion

	Before injury	T (after injury)/h			
		2	24	48	72
$\text{TNF}/\mu\text{g} \cdot \text{L}^{-1}$	0.08±0.02	0.03±0.25 ^a	0.17±0.09 ^a	0.34±0.15 ^a	0.33±0.18 ^a
$\text{LPS}/\times 10^3 \text{Eu} \cdot \text{L}^{-1}$	0.14±0.03	0.16±0.04	0.21±0.02 ^a	0.18±0.16	0.37±0.10 ^b
$\text{Lactate}/\text{nmol} \cdot \text{L}^{-1}$	9.03±2.19	18.30±2.56 ^a	9.81±2.83	12.01±6.84	43.61±11.27 ^b
L/M rat	0.03±0.01	0.41±0.27	0.62±0.20		1.70±0.60 ^b
Intestinal pHi	7.03±0.05	7.05±0.06 ^b	7.14±0.09 ^b	7.20±0.08 ^a	7.05±0.07 ^b

^a $P < 0.05$; ^b $P < 0.01$, vs before injury.

Table 3 Correlation analysis in goats subjected to hemorrhagic shock combined with endotoxin infusion

X	Y	r	P
DAO	$\text{TNF}\alpha$	0.817	<0.01
DAO	LPS	0.842	<0.01
DAO	Lactate	0.872	<0.01
DAO	L/m	0.951	<0.01
DAO	Intestinal pHi	-0.553	<0.05

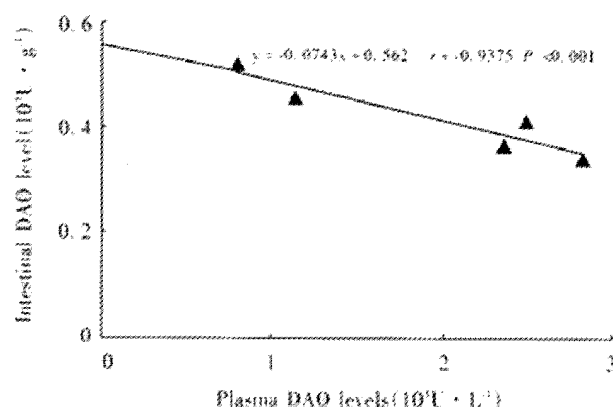


Figure 3 Relationship between intestinal and plasma DAO level.

DISCUSSION

DAO is located in the upper part of intestinal mucosa in human as well as in mammals, and is a highly active intracellular enzyme. Under certain circumstances, intestinal mucosa cells became necrosed and dropped into the intestinal cavity, leading to decrease in intestinal mucosal DAO, and increase in DAO activity inside the intestinal cavity. DAO can also enter into the mucosal space between cells, lymphatic vessel^[21-27] and blood flow, making plasma DAO markedly elevated. Gut as an important organ, may play an important role in the pathogenesis of serious complications. Intestinal mucosal surface layer with tight epithelial cells is an important component for intestinal barrier function, thus it can be seen that intestinal epithelial tissue integrated property is a key part to preserve intestinal barrier function. The changes in DAO activity is an ideal index to investigate intestinal barrier function damage after trauma, specially the changes in plasma DAO activity^[2,6,10,11]. Therefore, intestinal barrier function injury after severe trauma could result in bacterial/toxin translocation, in turn evoke systemic inflammatory response syndrome

and multiple organ dysfunction syndrome^[3,28-29].

The intestinal blood flow might keep relatively low despite of systemic circulation recovery during trauma, which was evident by significant decrease in intestinal mucosal pH_i^[30-33]. This may be the pathological basis for intestinal origin sepsis and multiple organ dysfunction syndrome. The changes in intestinal permeability were reflected by blood D-lactate and L/M rate in urine. Secretory IgA is an important component part for regulation intestinal immune function, it can prevent the bacteria from adhering to intestinal epithelial cells, and prevent gut-derived bacteria from invading through the intestinal barrier, which might reduce the toxicity of bacterial products to epithelial cells. Therefore, IgA may possess the beneficial effect on the preservation of intestinal mechanical barrier^[34-37]. From our data that changes in several indexes of intestinal barrier function in various animal models after trauma, it was shown that DAO was released to increase in blood, and decreased in intestinal tissues. Thus, determination of DAO activity might reflect the condition of intestinal injury and repaired process.

The change in plasma D-lactate, lactulose, mannitol and ratio of L/M could reflect the increased intestinal permeability. The intestinal IgA levels appear to be associated with the local immunological dysfunction^[38-41]. The change in intestinal pH_i showed that intestinal hemorrhagic injury may result in the release of intestinal mucosal enzyme, subsequently leading to significant elevation of plasma DAO activity. This study showed that there is a close relationship between plasma DAO and TNF α , LPS, D-lactate, lactate, L/M, and the change of intestinal pathology and intestinal barrier function index was similar, indicating that intestinal barrier function was damaged after trauma.

We also observed that the plasma DAO activity was increased 2h and 72h after trauma, especially at 72h, and change of plasma TNF α and LPS was similar to the former. These results suggest that stress injury can cause changes of intestine barrier function index following intestinal ischemia-reperfusion injury, repair or endo/inextra protection, but the trends and degrees of changes were varied. Therefore, it is important to reduce development of SIRS to MODS by protection of intestinal barrier function in early trauma, and prevention of translation of intestinal origin bacteria and toxins^[6,10,14,42-45].

Recent studies have shown that GLN may provide protection against intestinal barrier function injury after trauma^[46-52]. Blood DAO activity was reduced to different extents at 10h, 5d and 8d after early stage of oral GLN in scalded rats. Intestinal pathological examination showed that the damage of epithelial cells of intestinal mucosa could be markedly improved, and the close correlation between plasma DAO and LPS and TNF α could also be changed after scalding^[6]. The results indicate that GLN can protect against the intestinal barrier function damage after trauma.

REFERENCES

- Li JY, Hu S, Sun XQ, Yan M, Jin H, Jiang XG, Zhou BT, Sheng ZY. Study on pathophysiological changes during early stage of sepsis after trauma. *Zhong guo wei zhong bing ji jiu yi xue* 2001;13:291-294
- Li JY, Sun SR, Xue LB, Lu Y, Jing H, Gu ZR. Sequential changes in diamine oxidase activity after burns. *Zhong hua zheng xing shao shang za zhi* 1997;13:40-42
- Swank GM, Deitch EA. Role of the gut in multiple organ failure: bacterial translocation and permeability changes. *World J Surg* 1996;20:411-417
- Chen HL, Wu JZ, Pei DK, Guan FL. Damage of gut barrier in the pathogenesis of multiple organ dysfunction syndrome. *Zhong hua pu tong wai ke za zhi* 1998;13:50-53
- Hu S, Sheng ZY, Xue XB, Zhou BT, Lu JY, Jin H, Yu Y, Sun XQ, Li JY, Zheng YQ, Xiong DX. A serilized studies of animal models of posttraumatic multiple organ dysfunction syndrome. *Jie fang jun yi xue za zhi* 1996;21:5-9
- Li JY, Lu Y, Xue LB, Wan SY, Sun SR, Yu Y, Xu HJ, Sheng ZY. The effect of oral glutamine gut mucosa Function and structure in scalded rat. *Jie fang jun yi xue za zhi* 1996;21:91-93
- Yao YM, Sheng ZY, Wu Y, Yu Y, Lu LR. Relationship between plasma D-lactate levels and acute intestinal injury in rats following ischemia-reperfusion. *Zhong hua zheng xing shao shang za zhi* 1998;14:266-269
- Lu Y, Sheng ZY, Li JY, Sun XQ, Jin H, Jiang XG. The relationship between the ICAM-1 expression of hemangioendothelial cell and the dysfunction of murine small bowel in an intestinal ischemia-reperfusion model. *Zhong guo pu tong wai ke za zhi* 2000;15:145-147
- Cui XL, Sheng ZY, Guo ZR, He LX, Zao J, Ren XW, Sun SR, Jiang LX. Mechanisms of early gastro-intestinal ischemia after burn: hemodynamic and hemorrhologic features. *Zhong hua zheng xing shao shang za zhi* 1998;14:262-265
- Li JY, Lu Y, Fu XB, Jin H, Hu S, Sun XQ, Sheng ZY. The significance of changes in diamine oxidase activity in intestinal injury after trauma. *Zhong guo wei zhong bing ji jiu yi xue* 2000;12:482-484
- Li JY, Lu Y, Hu S, Jin H. An experimental study on monitoring of barrier function of small intestine. *Chuang shang wai ke za zhi* 2001;3:109-112
- Li JY, Lu Y, Jin H, Hu S, Sun XQ, Jiang XG, Sheng ZY. Sequential changes of diamine oxidase activity after trauma. *An ji suan he sheng wu zi yuan* 1999;21:17-19
- Fang WH, Yao YM, Shu HG, Yu Y, Wu Y, Zheng YQ. The time course and tissue distribution of endotoxin in rats after thermal injury. *Zhong hua zheng xing shao shang za zhi* 1999;15:298-300
- Fu XB, Yang YH, Sun XQ, Gu XM, Sheng ZY. Protective effects of endogenous basic fibroblast growth factor activated by 2.3 butanedion monoxide on functional changes of ischemic intestine, liver and kidney in rats. *Zhong guo wei zhong bing ji jiu yi xue* 2000;12:69-72
- Fu XB, Sheng ZY, Wang YP, Ye YX, Xu MH, Sun TZ, Zhou BT. Basic fibroblast growth factor reduces the gut and liver morphologic and functional injuries after ischemia and reperfusion. *J Trauma* 1997;42:1080-1087
- Wu CT, Li ZL. Effect of DAO on intestinal damage in acute necrotizing pancreatitis in dogs. *Shi jie hua ren xiao hua za zhi* 1999;7:64-65
- Li JY, Yu Y, Hao J, Jin H, Xu HJ. Determination of diamine oxidase activity in intestinal tissue and blood using spectrophotometry. *An ji suan he sheng wu zi yuan* 1996;18:28-30
- Sun XQ, Fu XB, Zhang R, Lu Y, Deng Q, Zhang C, Jiang XG, Sheng ZY. Plasma D-lactate levels as a useful marker of increased intestinal permeability after severe injuries. *Zhong guo wei zhong bing ji jiu yi xue* 2000;12:476-478
- Yao YM, Tian HM, Wang YP, Yu Y, Shi ZG, Sheng ZY. Microassay for quantitation of endotoxin in blood with new PCA treatment using chromogenic limulus amoebocyte lysate. *Shang hai yi xue jian yan za zhi* 1993;8:31-33
- Zhu XF, Xiong DX, Sheng ZY. Establish measuring Method of alterations in intestinal permeability. *Zhong guo wei sheng tai za zhi* 1994;6:36-38
- Hosoda N, Nishi M, Nakagawa M, Hiramatsu Y, Hioki K, Yamamoto D M. Structural and functional alterations in the gut of parenterally or enterally fed rats. *J Surg Res* 1989;47:129-133
- Yan BG, Yang ZC, Huang YS, Liu ZY, Li A. Effect of delayed rapid fluid resuscitation on plasma diamine oxidase in early postburn dogs. *Shi jie hua ren xiao hua za zhi* 2000;8:178-180
- Lu Y, Li JY, Sun SR, Jin H, Jiang XG, Sun XQ, Sheng ZY. Relationship between change of plasma diamine oxidase activity and gut injury in rats during gut ischemia-reperfusion. *An ji suan he sheng wu zi yuan* 2000;22:50-53
- Liu MH, Gao LX. The effect of oral glutamine supplementation on small intestinal function in burned rats. *Ying yang xue bao* 1995;17:17-21
- Dong HL, Cai JW, Si ZX. Effects of radiation on intestinal and plasma DAO activity in rats. *Shi jie xiao hua za zhi* 1998;6:698
- Bragg LE, Thompson JS, West WW. Intestinal diamine oxidase levels reflect ischemic injury. *J Surg Res* 1991;50:228-233
- Ci XL, Wang BS, Zhang SW, Zhang NN. Experimental treatment with herbal medicines for impaired intestinal mucosal barrier induced by endotoxin plus tumor necrosis factor- α . *Zhong guo wei zhong bing ji jiu yi xue* 1999;11:262-265
- Rush BF, Sori AJ, Murphy TF, Smith S, Flanagan JJ, Machiedo GW. Endotoxemia and bacteremia during hemorrhagic shock: The link between and sepsis? *Ann Surg* 1988;207:549-552
- Yao YM, Sheng ZY, Tian HM, Wang YP, Yu Y, Fu XB, Lu LY, Wang DW, Ma YY. Gut-derived endotoxemia and multiple system organ failure following gunshot wounds combined with hemorrhagic shock an experimental study in the dog. *J Trauma* 1995;38:742-746
- Hu S, Jin H, Lu Y, Li JY, Zhou BT. The changes of PH on gastroduodenal mucosa after hemorrhage shock and resuscitation in goats. *Zhong guo wei zhong bing ji jiu yi xue* 1997;9:708-710
- Murray MJ, Gonze MD, Nowak LR, Cobb CF. Serum D(-)-Lactate levels as an aid to diagnosing acute intestinal ischemia. *The American Journal of Surgery* 1994;167:575-578
- Sun XQ, Lu Y, Jin H, Li JY, Jiang XG, Hu S, Fu XB. Change of intestine mucosal barrier induced by intestine ischemia-reperfusion injury.

- Chuang shang wai ke za zhi* 1999;1:208-210
- 33 Murray MJ, Barbose JJ, Cobb CF. Serum D-lactate levels, as a predictor of acute intestinal ischemia in a rat model. *J Surg Res* 1993;54:507-509
 - 34 Doe WF. The intestinal immune system. *Gut* 1989;30:1679-1685
 - 35 Yu Y, Shi ZG, Chai JK, Guo ZY, Yao YM, Li G, Ho XX, Jiang W, Wang HB, Sheng ZY. The clinical significance of changes in IgA levels in intestinal tract after major burns. *Zhong guo wei zhong bing ji jiu yi xue* 1998;10:725-727
 - 36 Yu Y, Sheng ZY, Tian HM, Wang YP, Yu Y, Lu LR, Chang GY, Ma RS. An experimental study on injury of intestinal immuno-barrier in rat after scald. *Zhong hua zheng xing shao shang wai ke za zhi* 1996;12:86-89
 - 37 Biesbrock AR, Reddy MS, Levine MJ. Interaction of a salivary mucin-secretory immunoglobulin a complex with mucosal pathogens. *Infection and Immunity* 1991;59:3492-3497
 - 38 Harmatz PR, Cater EA, Sullivan D, Hatz RA, Baker R, Breazlale E, Grant K, Bloch KJ. Effect of thermal injury in the rat on transfer of IgA protein into bile. *Ann Surg* 1989;210:203-207
 - 39 Cappeler WA, Bloch KJ, Hatz RA, Carter EA, Fagundes J, Sullivan DA, Harmatz PR. Reduction in biliary IgA after burn injury. *Ann Surg* 1992;215:338-341
 - 40 Alverdy JC, Aoys E. The Effect of dexamethasone and endotoxin administration on biliary IgA and bacterial adherence. *J Surg Res* 1992;53:450-454
 - 41 Yu Y, Chai JK, Li JY, Jin H, Dong N. A preliminary study on the relationship between level of IgA in intestinal content and urine after burns. *An ji suan he sheng wu zi yuan* 2001;23:49-51
 - 42 Diebel LN, Liberati DM, Brown WJ, Dulchavsky SA, painter TM, Diglio CA, Montgomery PC. Secretory immunoglobulin A blocks hypoxia-augmented bacterial passage across madin-darby canine kidney cell monolayers. *J Trauma* 1997;43:759-763
 - 43 Noguchi Y, James JH, Fischer JE, Hasselgren PO. Increased glutamine consumption in small intestine epithelial cell during sepsis in rats. *Am J Surg* 1997;173:199-205
 - 44 Yu B, Wang SL, You ZY, Li A, Zhao Y. Effects of L-Glutamine on ghe tut nutrient metabolism in severe burned miniswines. *Chang nei yu chang wai ying yang* 1995;2:7-10
 - 45 Li N, Liu FN, Li YS, Kang J, Li FJ, Li JS. The Changes of plasma glutamine and its influence on intestinal permeability after abdominal Surgery. *Chang nei chang wai ying yang* 1998;5:3-6
 - 46 Rhoads JM, Keku EO, Quinn J, Woosely J, Lecce JG. L-Glutamine stimulates jejunal sodium and chloride absorption in pig rotavirus enteritis. *Gastroenterology* 1991;100:683-691
 - 47 Yu B, Wang SL, You ZY, Zhao Y, Li A. Enhancement of gut absorptive function by early enteral feeding enriched with L-Glutamine in severe burned miniswines. *Zhong hua wai ke za zhi* 1995;33:742-744
 - 48 Wu F, Jin XQ, Wu SX, Li J, Xu JL. The experimental study of cholestasis due to parenteral nutrition. *Chang nei chang wai ying yang* 1998;5:96-98
 - 49 Yang JT, Wang ZG, Zhu PF. The Effects of glutamine supplementation on the cellular immunity in traumatized rats. *Ying yang xue bao* 1999;21:8-12
 - 50 Dai DW, Wu SM, Li M, Chen HJ, Cai W. Protective effect of Glutamine in the anoxia/reoxygenation induced injury of human intestinal epithelial cells *in vitro*. *An ji suan he sheng wu zi yuan* 1997;19:1-3
 - 51 Tu WF, Li JS, Zhu WM, Li ZD, Liu FN, Chen YM, XU JG, Shao HF, Xiao GX, LI A. Influence of glutamine on gut bacteria/endotoxin translocation in acute severe pancreatitis. *Chang wai yu chang nei ying yang* 1999;6:29-32
 - 52 Yu B, Wang SL, You ZY, Zhao Y, Li A. Protection against intestinal injury with oral feeding L-glutamine in severe burned mini-swines. *Zhong hua wai ke za zhi* 1998;14:19-21

Edited by Ma JY

• BASIC RESEARCH •

Localization of neurokinin B receptor in mouse gastrointestinal tract

Hong Wang, Yuan-Qiang Zhang, Yu-Qiang Ding, Jin-Shan Zhang

Hong Wang, Yuan-Qiang Zhang, Jin-Shan Zhang, Department of Histology and Embryology, Yu-Qiang Ding, Institute of Neurosciences, the Fourth Military Medical University, Xi'an, 710032, China

Supported by the Grants of the National Natural Science Foundation of China, No.39600045, No.39870109

Correspondence to: Professor Yuan Qiang Zhang, Changle Road 17, Xi'an 710032, China. Zhangyuanqiang@fmmu.edu.cn

Telephone: +86-29-3374508 Fax: +86-29-3374508

Received 2001-07-19 Accepted 2001-10-20

Abstract

AIM: To observe the location of neurokinin receptor (NK3r) in the mouse gastrointestinal tract.

METHODS: The abdomens of 8 male Kunming mice were opened under anaesthesia with sodium pentobarbital. The exposed gut organs were kept moisture and temperature at the same time. Then the esophagus, jejunum, ileum, colon, etc were respectively cut and the segments from the stomach to the distal colon were opened along the mesenteric border. A circular 4mm~6mm enteric part(pieces of 1 cm² were to be prepared) and mucosa and submucosa were removed, then the longitudinal muscle layer was pulled off from the circular muscle layer under microphotograph. They were rinsed in 50n mol·L⁻¹ potassium phosphate-buffered saline(PBS). Immunohistochemistry and immunoreactive fluorescence were used in the staining procedures.

RESULTS: There was not NK3r-Like(-Li) positive material on the smooth muscle cells of the esophagus, stomach, and intestines and other regions. The nerve cell bodies with immunoreactivity for NK3r were mainly distributed in the submucosal nerve plexus or myenteric nerve plexus of the gastrointestinal tract except for the esophagus, stomach and rectum. The reaction product was located on the surface of the nerve cell plasma. It was occasionally observed in the cell plasma endosomes, but was very weakly stained. Among the NK3-like positive neurons in the plexus, the morphological type in many neurons appeared like Dogiel II type cells. Some neuron cell bodies were big, having many profiles, some were long ones or having grading structure. Cell body diameter was about 10μm-46μm and 8μm-42μm in myenteric plexus and submucous plexus.

CONCLUSION: This study not only described the distribution of neurokinin B receptor in the mouse gut in detail, but also provided a morphological basis for deducing the functional identity of the NK3r-LI immunoreactivity neurons, suggesting the possibility that these neurons were closely related to gastrointestinal tract contraction and relaxing activity.

Wang H, Zhang YQ, Ding YQ, Zhang JS. Localization of neurokinin B receptor in mouse gastrointestinal tract. *World J Gastroenterol* 2002;8(1):172-175

INTRODUCTION

The tachykinin family of neuropeptides mainly includes neurokinin A(NKA) neurokinin B(NKB), and the neurotransmitters in the peripheral and central nerve systems^[1]. Tachykinin and their receptors (NK1/NK2/NK3) play an important role in the nerve system. Various studies have been undertaken in NK3 receptor's distribution in rat CNS^[2,3]. Our previous experiments suggest that NK3 receptor in the paraventricular and supraoptic nuclei of the rat hypothalamus may be involved in the modulation of the release of vasopressin from the hypothalamus when the internal environment was disturbed^[3]. Some research results^[4] implicated that tachykinin located in the intestine intrawall neurons is attributable to the activation of gut and its modification. Pharmacological research work has proved that NK3r was located in neurons rather than in muscle cells^[5,6]. Having characterized the antisera, researchers localized the neurokinin receptor in the rat/guinea gut^[6,7]. NK2r was also detected in the muscularis mucosa of the small intestine and the colon. NK2r was localized in the plasma membrane of smooth muscle cells and was present on numerous nerve terminals in both the submucosal and the myenteric plexus of the small intestine^[4,7,8], but NK1r-Li reactive product existed only in the neurons that resemble the interstitial cells of Cajal^[9-11]. Mann *et al*^[12] and Grady *et al*^[7] reported that in rat myenteric plexus there were neurons that could express NK1r. These neurons had colocalization with NK3r-Li positive neurons. Although all these results implicated that tachykinin receptors existed in the mouse gastrointestinal tract, and that they might be related to intestinal muscle contractile activity^[13] in addition to its influence in blood pressure and increase of vascular penetration. Up to now, we have not seen reports about this receptor's distribution in mouse gastrointestinal tract. Our aim was to further investigate this receptor distribution in mouse gut.

MATERIALS AND METHODS

Animals and material preparation

Ten male Kunming mice weighing 20g-30g were chosen and the abdomens of 8 mice were opened under anaesthesia with sodium pentobarbital. To keep moisture and temperature we cleaned the exposed gut organs with 0.01 mol·L⁻¹ PBS (phosphate-buffered saline, pH 7.0) continuously. Then the esophagus, jejunum, ileum, colon, etc were respectively cut and the segments from the stomach to the distal colon were opened and cleaned by 0.01 mol·L⁻¹ PBS containing smooth muscle relaxing medicine. And they were filled with 40g·L⁻¹ polyformaldehyde and the two ends were closed tightly and fixed for 6-8 h. The stomachs were fixed for 8 h following Peng Xi's suggestion(1999)^[14] and incubated in 300g·L⁻¹ sucrose for 24 h (overnight) together with other organs after cut and cleaned with 0.01 mol·L⁻¹ PBS. Gastrointestinal tract was processed from stomach to the distal colon and was opened along the mesenteric border. A circular 4-6mm enteric part(pieces of 1 cm² were to be prepared)

was obtained, the longitudinal muscle layer was pulled off from the circular muscle layer with fine forceps and processed for immunohistochemical examination along the mesenteric border rinsed in phosphate-buffered saline and prepared for layer separation. Gastrointestinal tracts were cut into small pieces of 1 cm² and mucosa and submucosa were removed with forceps. Then they were rinsed in 50 nmol·L⁻¹ potassium phosphate-buffered saline(PBS) and prepared for layer separation. These procedures can be done under anatomy microphotography.

Staining procedures

Staining procedures: whole-mount free-floating tissues and slide-mounted sections were washed in 50 mmol·L⁻¹ KPBS, incubated with 0.3% H₂O₂ (30min), rinsed again in 50 mmol·L⁻¹ KPBS, and incubated in diluent containing of 50mM KPBS, 4g·L⁻¹ Triton X-100, 10 g·L⁻¹ bovine serum albumin, and 10 ml·L⁻¹ normal goat serum for 30min at 22°C, then transferred to NK3r affinity-purified antibodies diluted to 1:50 in the same diluent for 48-96 h at 4°C. Tissues were washed in 50 mmol·L⁻¹ KPBS with 0.2g·L⁻¹ TritonX-100 and incubated with biotinylated goat anti-rabbit IgG(Vector) diluted to 1:200 for 3 h at 22°C(Vector), followed by avidin-biotin complex coupled with horseradish peroxidase 1:200 for 2 h at 22°C(Vector). The horseradish peroxidase reaction product was visualized with 0.4 g·L⁻¹ diaminobenzidine tetrahydrochloride and 0.1 mL·L⁻¹ H₂O₂ dissolved in 0.1 mol·L⁻¹ sodium acetate. The reaction was terminated by two consecutive 9 g·L⁻¹ NaCl washes.

The gastrointestinal tracts of the remaining mice were pulled off and cut on a cryostat at -20°C, rinsed by 0.01 mol·L⁻¹ PBS and incubated in 40 g·L⁻¹ formaldehyde fixative overnight at 4°C. They were incubated again in 300 g·L⁻¹ sucrose and embedded by OCT on the next day. Their cryostat sections were 10µm in thickness, and immunohistochemically stained after the slides were cooled according to the earlier procedure.

RESULTS

Immunohistochemical results showed that NK3-Li neurons and fibers existed in enteric plexus(submucous plexus and myenteric plexus) in the duodenum, jejunum, ileum and colon (Figures 1-8). Staining intensity in myenteric plexus was a little stronger. And the esophagus and the stomach were immunoreactively negative. No positive immunoreactive product was found in esophagus smooth muscle cells.

NK3-Li positive substance existed mostly in the membrane, some or a little in the plasma, but none in the nuclei. The surface of the positive neurons was well stained and was more apparent than those in the cell body(Figures 1,2,4,8). The neurons stained in

myenteric plexus had high intensity, the NK3-Li neurons and fibers were web-like(Figure 3). And the fibers between the positive neurons were often of a beaded or granular appearance(Figure 7). Between fibers just like necklace among longitudinal muscle-myenteric plexus neuronal fibers there were striated fibers, that connect with them. From the cryostat sections, NK3r-Li immunoreactive product was found in intestinal myenteric plexus.

Among the NK3-like positive neurons in the plexus, the morphological type of many neurons were like Dogiel II type cells: round or ellipse shape or presenting several dividing beaded profiles. Some neuron cell bodies were bigger, having many profiles, some of which were long or having grading structures. Results by microscopic counting are shown in Figures 1 and 2.

Table 1 The number of NK3r immunoreactivity neuron cell bodies in mouse gastrointestinal Tract*

Region	Neuronal density / (cells·cm ⁻²) ($\bar{x} \pm s$)	
	Myenteric plexus	Submucous plexus
Esophagus	Almost no	Almost no.
Stomach	Almost no.	Almost no.
Duodenum	82±14	95±12
Jejunum	249±37	237±31
Ileum	143±24	140±19
Colon	118±17	107±15

*neurons in areas of 0.05 cm² were counted.

Table 2 Morphological characteristics of NK3r stained neurons in the mouse gastrointestinal tract

plexus	Region	Shape		d (cell soma)/µm	
		Unipolar or bipolar	Multipolar	Major	Minor
Myenteric	Oesophagus	(+/-)	(+)		
	Stomach	(+/-)	(+)		
	Duodenum	++	+++	17-38	10-26
	Jejunum	++	+++	25-46	13-20
	Ileum	++	+++	21-37	12-18
	Colon	+	++	15-36	14-16
Submucous	Rectum	+/-	+	13-34	8-19
	Stomach	(+/-)	(+)		
	Duodenum	++	+++	16-35	8-11
	Jejunum	++	+++	19-42	10-13
	Ileum	++	+++	14-35	9-17
	Colon	+	++	13-27	8-15

(+/-) almost no; (+) very rare; + infrequent; ++ common; +++ abundant



Figure 1 NK3r-like(Li) neurons in myenteric nerve plexus of duodenum, mainly located on cell membrane. Arrow: positive neuron; Duo: duodenum, mp: myenteric plexus.

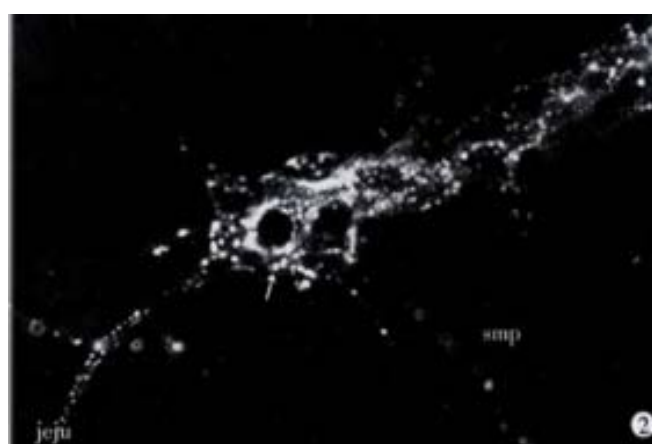


Figure 2 NK3r-Li neurons in submucosa neural plexus of jejunum. Arrow: positive neuron cell bodies; Smp: submucosa nerve plexus; Jeju: jejunum.

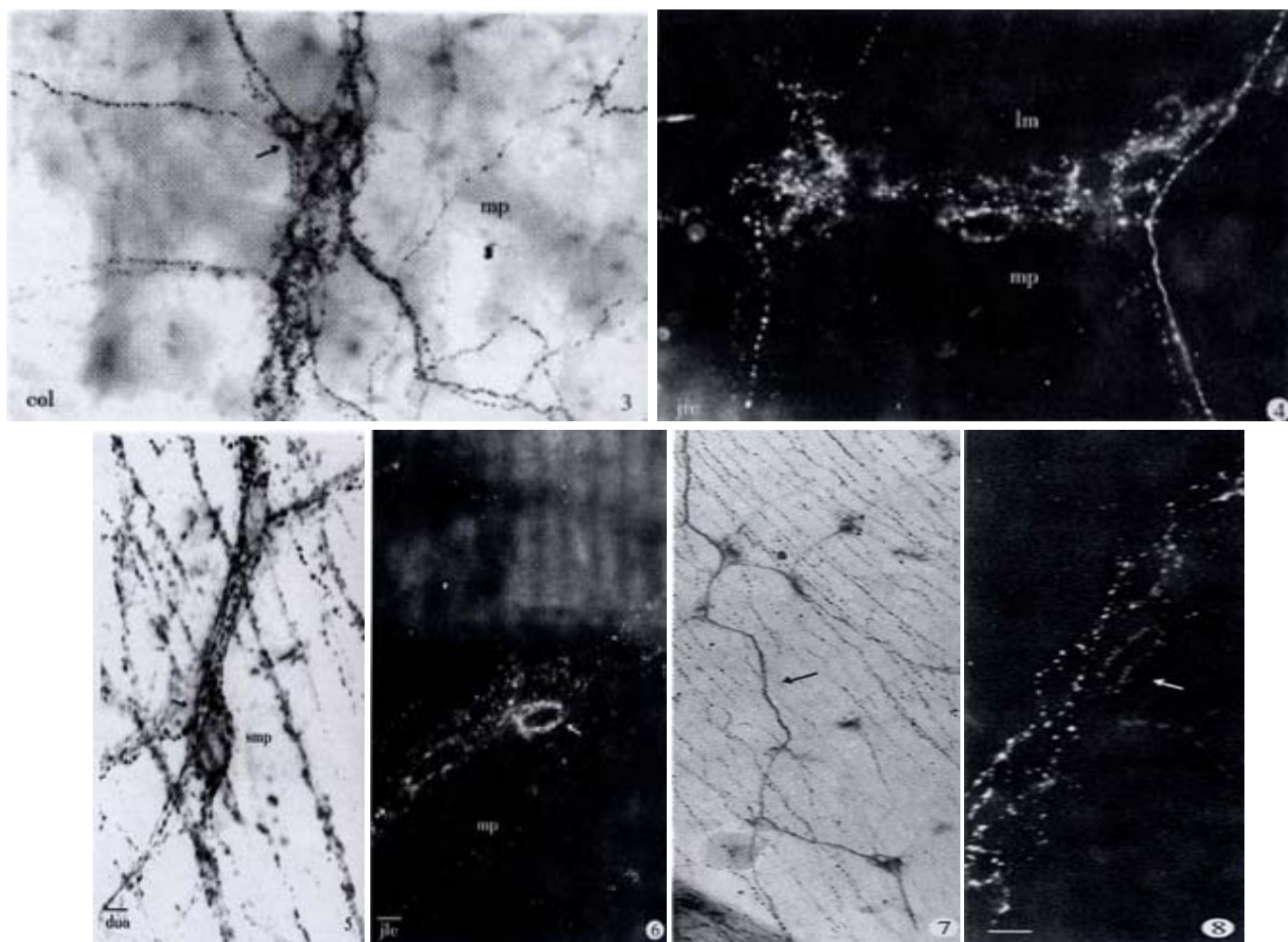


Figure 3 NK3r-Li product mainly found on the cell membrane in the colon's myenteric plexus. Dark arrow: positive neuron; Col: colon; mp: myenteric plexus.

Figure 4 The NK3r-Li neurons in the myenteric nerve plexus of the ileum. Mp: myenteric plexus; Ile: ileum; Lm: longitudinal muscles; Cm: circular muscles.

Figure 5 The NK3r-Li neurons in the submucosa nerve plexus of the duodenum. Dark arrow: positive neuron; Smp: submucosa nerve plexus. Bar=20µm in Figures 1-5

Figure 6 NK3r-Li neurons in the neuron ganglion of the ileum myenteric nerve plexus; mp: myenteric plexus. Bar=40µm

Figure 7 The NK3r-Li nerve fibers like a necklace.

Figure 8 The higher magnification of Dogiel II type NK3r-Li neurons. Arrow: positive products on the cell membrane. Bar=6µm in Figures 7,8

DISCUSSION

There were some reports about tachykinin B receptor(NK3r) distribution in mammal gastrointestinal tract^[7,12]. It was proved that NK3r-Li neurons were localized in enteric nervous system of rats and guinea pig^[15]. We observed the NK3r distribution in mouse gastrointestinal tract. Our results were consistent with the previous results, and support the research work of Mann *et al*^[12], and Grady *et al*^[7], but we must claim several valuable differences: ① In our experiments we found that immunoreactivity was mainly located in the enteric nervous system neurons, rather than in mouse esophagus or other parts of the gut smooth muscles, which was different from the results of Maggi *et al*^[5] and Guard *et al*^[16]. ② We also found that there were different morphological type of NK3r-Li neurons in mouse jejunum and ileum nervous plexus: the first part gut plexus had more neurons than the second part gut plexus. In ileum plexus NK3r-Li neurons were mostly of Dogiel II type neurons^[17], which was different from the results by other authors that NK3r-Li neurons were only located in the ileum. ③ Although the immunoreactive products existed mainly in the enteric system neurons membrane, they were also detected in some positive neurons plasma. On the whole, cell

morphology(size and shape) was similar to the cells that were observed and described by Mann *et al.* and Furness^[18]. We also found that there were some small cell body neurons, which did not have clear characteristic positive shapes, so we might deduce that they had possibly different functions or belonged to dividing disparity. The location of the NK3r-Li immunoreactivity observed through the subnuclei of the NTS (solitary tract nucleus) suggested that NK3r-Li immunoreactive neurons might be involved in the medullar integration of the information conveyed by the afferent vagus nerve from the lower digestive tract^[19]. The distribution of the NK3r-containing neurons coincided with the afferent fibers arising from the lower digestive tract. Vagal afferent fibers from the stomach and intestine terminated preferentially in the subnuclei medialis and commissuralis and in the substantia gelatinosa of the NTS (solitary tract nucleus)^[20] as well. In the NTS, the subnucleus centralis represented the preferential termination sites for afferent fibers arising from the esophagus(vagus nerve). No or very few NK3r-Li neurons have been found in this subnucleus. We also found the supporting example for these references of NK3 receptor in the central nervous system and added proof to NK3 receptor in the peripheral nervous system. In the rat

brain, by situ hybridization method for NK3r mRNA, the results agreed well with the immunohistochemical results, however low levels of NK3r mRNA were found in rat stomach and intestines^[21] which suggests that our detection of a large population of enteric neurons with NK3r immunoreactivity contradicts with Tsuchida *et al.*'s results^[22]. Binding studies also failed to detect NK3r in the gastrointestinal tract^[22]. Our experiments showed that morphology of NK3r-Like neurons was in agreement with Dogiel II type neurons in size, shape and localization. The number of neurons was not very large and was less than the proportion of NK1r-Li neurons in the enteric nervous system. Considering NK3r-Li neurons' size in diameter, and the morphologic and pharmacological results, we speculate that NK3r-Li neurons are possibly a part of afferent internal neurons related to the enteric construction, relaxing the activity of mouse enteric nervous system, which was closely related to with some vice sympathetic nerve fiber functions. This is determined according to Furness *et al.*'s^[23] dividing method in guinea enteric nervous system neurons that is regarded as right, but at the same time it needs further verifications by functional test. Functional experiments supported the neuronal localization of the NK3r: the NK3 agonists NKB senktide stimulated contraction of rat duodenum and guinea pig ileum^[24,25]. The response of the guinea pig ileum were abolished by tetrodotoxin and reduced by atropine which indicated the presence of NK3r in the cholinergic neurons of the myenteric plexus^[26]. Indeed, senktide stimulated acetyl choline to release from the myenteric neurons^[16]. Barthó *et al.* (1999)^[24,25] proved that NK3r existed in rodent gastrointestinal (interwall) neurons and regulated tachykinin inducing the excitement of the enteric nervous system thus influencing construction^[27]. Our findings that neurons in the myenteric plexus could express NK3r is of particular interest and NK3r reacting production existed mainly on the plasma membrane of gastrointestinal tract intrawall neurons, implicating that tachykinin B transmitter possibly influence membrane receptor thus influencing the contraction and relaxing smooth muscle and even regulating the exocrine of gastrointestinal tract as well as the contents that some articles have described^[28-33].

In summary, our research not only observed the distribution of NK3r-like neurons and fibers in mouse gastrointestinal tract, but also provided new insight into the cellular colocalization of receptor proteins in the mouse gut tract and a base for investigating NK3r-like neuron functions in the gut tract. These results might also give implications about muscle activity of contracting or relaxing action related to the neurokinin receptor.

REFERENCES

- Blanchet F, Gauchy C, Perez S, Soubrie P, Glowinski J, Kemel ML. Distinct modifications by neurokinin1 (SR140333) and neurokinin2 (SR48968) tachykinin receptor antagonists of the N-methyl-D-aspartate-evoked release of acetylcholine in striosomes and matrix of the rat striatum. *Neuroscience* 1998; 85:1025-1036
- Chen LW, Guan ZL, Ding YQ. Mesencephalic dopaminergic neurons expressing neuromedin K receptor (NK3): a double immunocytochemical study in the rat. *Brain Res* 1998; 780:148-152
- Ding YQ, Shigemoto R, Takada M, Ohishi H, Nakanishi S, Mizuno N. Localization of the neuromedin K receptor (NK3) in the central nervous system of the rat. *J Comp Neurol* 1996; 364:290-310
- Portbury AL, Furness JB, Southwell BR, Wong H, Walsh JH, Bunnett NW. Distribution of neurokinin-2 receptors in the guinea-pig gastrointestinal tract. *Cell Tissue Res* 1996; 286:281-292
- Maggi CA, Patacchini R, Rovero P, Giachetti A. Tachykinin receptors and tachykinin receptor antagonists. *J Auton Pharmacol* 1993; 13:23-93
- Bertrand PP, Galligan JJ. Tachykinin- and synaptically-activated chloride current in myenteric neurons of guinea-pig ileum. *J Physiol (Lond)* 1994; 481:47-60
- Grady EF, Baluk P, Böhm S, Gamp PD, Wong H, Payan DG, Ansel J, Portbury AL, Furness JB, McDonald DM, Bunnett NW. Characterisation of antisera specific to NK1, NK2, NK3 neurokinin receptors and their utilization to localize receptors in the rat gastrointestinal tract. *J Neurosci* 1996; 16:6975-6986
- Alex G, Kunze WA, Furness JB, Clerc N. Comparison of the effects of neurokinin 3 receptor blockade on two forms of slow synaptic events in myenteric AH neurons. *Neuroscience* 2001; 104:263-269
- Portbury AL, Furness JB, Young HM, Southwell BR, Vigna SR. Localization of NK1 receptor immunoreactivity to neurons and interstitial cells of the guinea-pig gastrointestinal tract. *J Comp Neurol* 1996; 367:342-351
- Vigna SR, Bowden JJ, McDonald DM, Fisher J, Okamoto A, McVey DC, Payan DG, Bunnett NW. Characterisation of antibodies to the rat substance P(NK1) receptor and to a chimeric substance P receptor expressed in mammalian cells. *J Neurosci* 1994; 14:834-845
- Sternini C, Su D, Gamp PD, Bunnett NW. Cellular sites of expression of the neurokinin-1 receptor in the rat gastrointestinal tract. *J Comp Neurol* 1995; 358:531-540
- Mann PT, Southwell BR, Ding YQ, Shigemoto R, Mizuno N, Furness JB. Localisation of neurokinin 3(NK3) receptor immunoreactivity in the rat gastrointestinal tract. *Cell Tissue Res* 1997; 289:1-9
- Furness JB, Clerc N. Responses of afferent neurons to the contents of the digestive tract, and their relation to endocrine and immune responses. *Progr. Brain Res* 2000; 122:157-170
- Peng X, Feng JB, Wang SHL. Methods of showing rats stomach myenteric neural plexus. *Jiepouxue Zazhi* 1999; 22:368-369
- Li JC, Busch LC, Kuhnle W. Immunohistochemical study on the gastroenteric nervous system in trisomy 16 mice-an animal model of Down syndrome. *World J Gastroenterol* 2000;6:793-799
- Guard S, Watson SP. Tachykinin receptor types: classification and membrane signaling mechanisms. *Neurochem Int* 1991; 18:149-165
- Furness JB, Clerc N, Gola M, Kunze WA, Fletcher EL. Identification of component neurons and organisation of enteric nerve circuits. In : *Neurogastroenterology - From the Basics to the Clinics. Kluwer Academic Publishers, Dordrecht, The Netherlands* 2000:134-147
- Furness JB, Clerc N, Lomax AEG, Bornstein JC, Kunze WA. Shapes and projections of tertiary plexus neurons of the guinea-pig small intestine. *Cell and Tissue Res* 2000;300:383-387
- Carpentier C, Baude A. Immunocytochemical localization of NK3 receptors in the dorsal vagal complex of rat. *Brain Research* 1996; 734:327-331
- Furness JB, Clerc N, Kunze WA. Memory in the enteric nervous system. *Gut* 2000; 47:60-62
- Tsuchida K, Shigemoto R, Yokota Y, Nakanishi S. Tissue distribution and quantitation of the mRNAs for three rat tachykinin receptors. *Eur J Biochem* 1990; 193:751-757
- Mantyh PW, Gates T, Mantyh CR, Maggio JE. Autoradiographic localization and characterization of tachykinin receptor binding sites in the rat brain and peripheral tissues. *J Neurosci* 1989; 9:258-279
- Furness JB, Bornstein JC, Pompolo S, Young HM, Kunze WA, Yuan SY, Kelly H. The nerve circuits for motility control in the gastrointestinal tract. *J Smooth Muscle Res* 1993; 29:143-144
- Bartho L, Lenard JRL, Patacchini R, Halmi V, Wilhelm M, Holzer P, Maggi CA. Tachykinin receptors are involved in the "local efferent" motor response to capsaicin in the guinea-pig small intestine and esophagus. *Neuroscience* 1999; 90:221-228
- Kunze WA, Clerc N, Furness JB, Gola M. The soma and neurites of primary afferent neurons in the guinea-pig intestine respond differentially to deformation. *J Physiol* 2000;526:375-385
- Guard S, Watson SP. Evidence for NK3 receptor-mediated tachykinin release in the guinea-pig ileum. *Eur J Pharmacol* 1987; 144:409-412
- Clerc N, Furness JB, Kunze WA, Thomas EA, Bertrand PP. Long term effects of synaptic activation at low frequency on excitability of enteric AH neurons. *Neuroscience* 1999;90: 279-289
- Furness JB, Bornstein JC, Kunze WA, Clerc N. The enteric nervous system and its extrinsic connections. In : Yamada, T., Alpers, D.H., Laine, L., Owyang, C., Powel, D.W. eds. *Textbook of gastroenterology*, Vol. 1, 3rd ed., Lippincott, Williams & Wilkins, Philadelphia. 1999: 11-35
- Furness JB, Kunze WA, Clerc N. Nutrient tasting and signaling mechanisms in the gut. II. The intestine as a sensory organ: neural, endocrine, and immune responses. *Am J Physiol* 1999; 277:G922-G928
- Jiang ZW, Li JS, Li N, Li YS, Liu FL, Sheng XQ, Cheng YM. Recovery of the allografted small intestine functions. *China Natl J New Gastroenterol* 1997;3:67-68
- Liu CY, Liu JZ, Zhou JH, Wang HR, Li ZY, Li AJ, Liu KJ. TRH microinjection into DVC enhances motility of rabbits gallbladder via vagus nerve. *World J Gastroenterol* 1998;4:162-164
- Huang XQ. Helicobacter pylori infection and gastrointestinal hormones: a review. *World J Gastroenterol* 2000;6:783-788
- Pan QS, Fang ZP, Huang FJ. Identification, localization and morphology of APUD cells in gastroenteropancreatic system of stomach containing teleosts. *World J Gastroenterol* 2000;6:842-847

• BASIC RESEARCH •

Study on of bioadhesive property of carbomer934 by a gamma camera *in vivo*

Jie Fu, Xun Sun, Zhi-Rong Zhang

Jie FuXun Sun, Zhi-Rong Zhang, West China School of Pharmacy, Sichuan University, Chengdu 610041, China

Supported by the Nation Distinguished Youth Scientific Fund (No. 39925039)

Correspondence to: Zhi-Rong Zhang, Ph.D., West China School of Pharmacy, Sichuan University, Chengdu, 610041, China. zrzzl@mail.sc.cninfo.net

Telephone: +86-28-5501566 Fax: +86-28-5456898

Received 2001-07-19 Accepted 2001-10-27

Abstract

AIM: To study the bioadhesive property of carbomer934 in dog alimentary tract.

METHODS: Carbomer934 and ethylcellulose were radiolabelled with technetium-99m; and Gastrointestinal emptying rate of materials was measured using the technique of gamma scintigraphy.

RESULTS: After oral administration, the maximum intestinal radioactivity of non-bioadhesive granules and bioadhesive granules were observed in the second hour and the sixth hour respectively. Constants of stomach emptying rate of nonadhesive granules, bioadhesive granulesI and bioadhesive granulesII were $0.774h^{-1}$, $0.265h^{-1}$ and $0.321h^{-1}$ respectively on the base of gastric residual amount. Compared to nonadhesive material (ethylcellulose), the migration rate of adhesive material (carbomer934) was remarkably slower in dog alimentary canal.

CONCLUSION: It is concluded that, in the dog, interactions between gastrointestinal mucus layer and adhesive material or nonadhesive material were significantly different. Carbomer934 had stronger *in vivo* bioadhesive property than ethylcellulose.

Fu J, Sun X, Zhang ZR. Study on of bioadhesive property of carbomer934 by a gamma camera *in vivo*. *World J Gastroenterol* 2002;8(1):176-179

INTRODUCTION

A problem frequently encountered with controlled release dosage forms is the inability to increase residence time of the dosage form in the stomach and proximal portion of the small intestine. Under fast condition, gastric residence of a dosage form is typically short, which is not more than an hour and it is also common for dosage forms to transit rapidly through the small intestine for not more than 3h^[1]. Rapid GI transit phenomena may consequently diminish the extent of absorption of many drugs. Since many drug compounds are absorbed exclusively in the small intestine or in a limited segment of the intestine, it would therefore be beneficial to develop sustained release dosage forms, which remain in the stomach for an extended period of time. Several approaches have been tried to prolong gastric residence, one of which is the use of oral bioadhesive formulation^[2,3]. A number of charged and neutral polymers have been classified as bio-

mucoadhesives, since they are known to bind very strongly to mucus via non-covalent bonds.^[4,5] Carbomer is a polyacrylic acid polymer, crosslinked with allyl sucrose. As a mucoadhesive polymer, carbomer has been investigated extensively by the pharmaceutical researchers because of its high viscosity at low concentration and low toxicity.^[6-15] *In vitro* experiment has proved that carbomer934 have good bioadhesion with the gastrointestinal mucus^[16-19]. Our research strategy is to investigate the *in vivo* bioadhesion of carbomer934 through measuring the migration rate of radioactive carbomer934 granules in dog alimentary tract by a gamma camera. Gamma scintigraphy is an elegant imaging technique which allows the intestinal performance of pharmaceutical formulations to be visualized.^[20] Over the past 20 years the approach has become the technique of choice for probing the complex interaction of drug preparation/formulations with the heterogeneous environment of the gut.^[21-29]

MATERIALS AND METHODS

Materials and apparatus

Ethylcellulose200cps (EC, imported from Roth Co. Ltd., obtained from Shanghai Chemical Agents Distributing Factory); Stearic acid(AP, supplied by Shanghai Stock and Accommodate Station of Chemical Agents); Carbomer934 (Cb934, purchased from Shanghai Shenxing Pharmacy Co. Ltd); ^{99m}TcO₄(China Institute for A-energy and Isotope); γ-ray camera(Orbiter, Semens Co. Ltd, Germany); and Dog (provided by Laboratory Animal Center, Sicuan University).

Methods

Radiolabeling of Cb934 and ethylcellulose Procedures of Cb934 and ethylcellulose radiolabelled were described in brief as follows: In vacuum bottle, 1ml of 0.1mol·L⁻¹ hydrochloric acid containing 1mg SnCl₂ and 1mg vitamin C was added to 2mL of 15g·L⁻¹Cb934(or 30g·L⁻¹EC) of ethanol solution, then with incorporation of Tc ^{99m}O₄. The mixture was warmed at 90°C for 10 minutes. Radioactivity chemical purity of radiolabelled materials measured by TLC was beyond 95%.

Preparation of radioactive granules According to the materials proportion of granules listed in Table 1, the mixed materials were solved in ethanol and dried in a rotated vaporizing apparatus. The product was crushed, then manually sieved. The collecting fraction have a size range of 20-40 mesh. An amount of the final blend was filled into hard gelatin capsules (size No.0). Each capsule has an activity of about 111MBq technetium99m at the time of administration.

Table 1 Component proportion of radioactive granules

granules	Percentage/%		
	EC	Cb934	Stearic acid
Non-bioadhesive	100	0	0
Bioadhesive I	0	100	0
Bioadhesive II	0	50	50

Measurement of migration rate of granules in dog alimentary tract

The study was an open-labeled, three-period, three treatment crossover study in three dogs (15-20kg). Each subject received the

following treatment in a randomized order: Treatment A: control nonbioadhesive granules, $2 \times 111\text{MBq}$ radioactivity following 24 h fast. Treatment B: bioadhesive granulesI, $2 \times 111\text{MBq}$ radioactivity following 24 h fast. Treatment C: bioadhesive granulesII $2 \times 111\text{MBq}$ radioactivity following 24 h fast. Percentage of granules in different segments of dog alimentary canal could be determined according to radioactivity by a γ -ray camera.

RESULTS

Migration rate of three kinds of granules

The dog alimentary tract was divided into three segments of stomach, intestine and colon(including colon,rectum and anus). Radioactivity was measured respectively in different segments (Tables). The gastric emptying rate of granules containing Cb934 (bioadhesive granules I and bioadhesive granulesII) was significantly slower than the control non-bioadhesive granules. After 4h, percentage of non-bioadhesive granules in stomach was only 7.63%, while bioadhesive granulesI 45.92% and bioadhesive granulesII 37.52%. In the sixth hour, percentage of non-bioadhesive granules, bioadhesive granulesI and bioadhesive granulesII in dog stomach was 0, 23.2% and 15% respectively.

Table 2 Non-bioadhesive granules in alimentary tract of dog ($n=3$)

Sites	Granules in different segment of alimentary tract(%)					
	1h	2h	4h	6h	8h	12h
Stomach	83.7	26.9	7.6	0	0	0
Intestine	16.3	73.2	59.7	0	0	0
Colon	0	0	32.6	43.2	10.6	0

Table 3 Bioadhesive granulesI in alimentary tract of dog ($n=3$)

Sites	Granules in different segment of alimentary tract(%)					
	1h	2h	4h	6h	8h	12h
Stomach	100	79.6	45.4	23.3	7.5	0
Intestine	20.4	54.7	59.7	55.1	30.9	0
Colon	0	0	0	21.8	61.6	54.3

Table 4 Bioadhesive granules II in alimentary tract of dog ($n=3$)

Sites	Granules in different segment of alimentary tract(%)					
	1h	2h	4h	6h	8h	12h
Stomach	100	67.1	37.5	15	0	0
Intestine	0	32.8	51.6	57.9	29.6	0
Colon	0	0	10.9	29.7	70.4	64.8

Non-bioadhesive granules were emptied to intestine in the first hour and the maximum intestinal radioactivity was observed in the

second hour, then intestinal radioactivity was completely eliminated in the sixth hour, bioadhesive granulesI and bioadhesive granulesII began to intestine migrated to in the second hour, and the maximum intestinal radioactivity was observed in the sixth hour. Furthermore considerable intestinal radioactivity could be inspected in the eighth hour. Compared with the non-bioadhesive granules, the bioadhesive granules had delayed onset of emptying to intestine and the maximum radioactivity in intestine. This result indicated that bioadhesion of Cb934 granules on the intestinal mucus was stronger than nonbioadhesive granules. In the fourth hour, a considerable non-bioadhesive pellets have entered the colon and were completely discharged out of anus in the eighth hour. Meanwhile, only very small parts of bioadhesive granules migrated into colon, and as long as the twelfth hour a great deal of granules were still in the dog alimentary tract.

Emptying half life of three kinds of granules in dog stomach

Emptying rate of stomach is fit to the first order kinetics^[30]. $\text{Log}V_t = \text{Log}V_0 - \text{Kemt}/2.303$ V_t :Gastric residual amount at the time of t V_0 :Gastric residual amount at the time of 0 in stomach Kemt : Constant of stomach emptying rate.

Constants of stomach emptying rate of nonadhesive granules, bioadhesive granulesI and bioadhesive granulesII can be calculated as 0.774h^{-1} , 0.265h^{-1} , 0.321h^{-1} respectively on the base of gastric residual amount. According to gastric residual amount of the first three points of time, constant of gastric emptying rate of bioadhesiveI granules can be calculated as 0.265h^{-1} , while according to the latter three points of time, constant can be calculated as 0.449h^{-1} .

Pictures of γ -ray camera

A majority of nonadhesive granules have been emptied into intestine in the second hour (Figure 1B), then reached colon in the fourth hour (Figure 1C) and a great deal collected at anus in the seventh hour (Figure 1D). In the fourth hour, most bioadhesiveI granules still mustered in the stomach(Figure 2C) and reached colon in the twelfth hour(Figure 2D). In the fifth hour, most bioadhesiveII granules were still in the intestine (Figure 3C) and reached colon in the seventh hour.

DISCUSSION

According to radioactivity measured by a gamma camera, migration rate of granules containing Cb934 was significantly slower than nonbioadhesive granules. It can be concluded that Cb934 has good bioadhesive properties *in vivo* and is a possible candidate material for oral bioadhesive preparation.

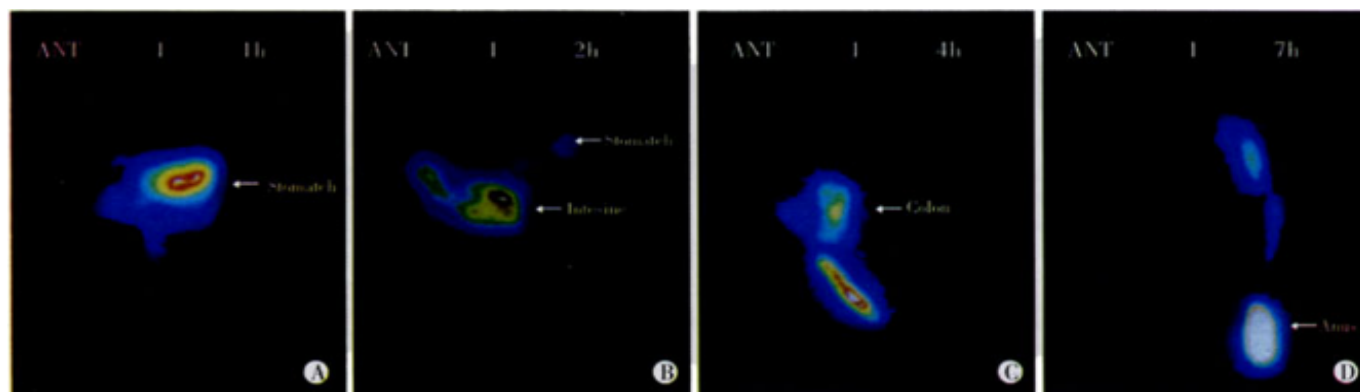


Figure 1 Radioactivity in alimentary tract of dog swallowing nonadhesive granules.

A, B, C, D: radioactivity at 1, 2, 4 and 7h.

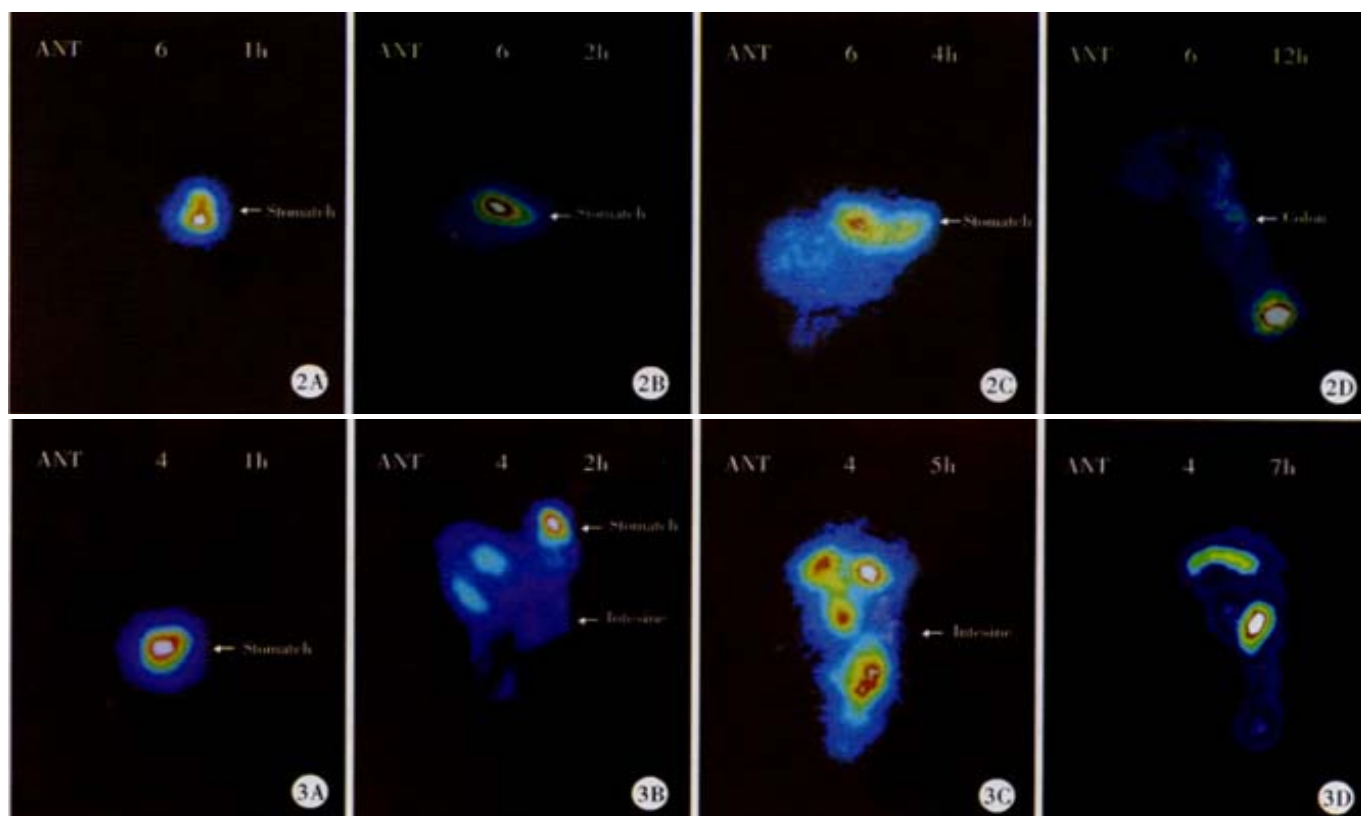


Figure 2 Radioactivity in alimentary tract of dog swallowing bioadhesive granules.

A, B, C, D: radioactivity at 1, 2, 4 and 12h.

Figure 3 Radioactivity in alimentary tract of dog swallowing bioadhesive granules.

A, B, C, D: radioactivity at 1, 2, 4 and 7h.

Compared with the rate constant (0.265h^{-1}) at gastric prophase emptying, gastric anaphase emptying rate constant (0.449h^{-1}) of bioadhesive granules became larger. This result showed that gastric emptying rate of Cb934 granules became faster as time went along. It can be inferred that Cb934 was excessively hydrated and caused a lubricative effect, which quickened the gastric emptying of granules. This implied that materials, which not only have good bioadhesive properties and but also can maintain gel status to avoid excessive hydrating, should be preferably considered in oral bioadhesive preparation design.

REFERENCES

- Barara Naisbett, John Woodley. The potential use of tomato lectin for oral drug delivery: 3. Bioadhesion *in vivo*. *Int J Pharm* 1995; 114: 227-236
- Schnurch A.B, Humenberger C, Vlaenta C. Basic studied on bioadhesive delivery systems for peptide and protein drugs. *Int J Pharm* 1998; 165: 217-225
- Arango M.A, Ponchel G, Orecchioni A.M, Renedo M.J, Duchene D, Irache J.M. Bioadhesive potential of gliadin nanoparticulate systems. *Eur J Pharm Sci* 2000; 11:333-341
- Madsen F, Eberth K, Smart JD. A rheological examination of the mucoadhesive/mucus interaction: the effect of mucoadhesive type and concentration. *J Control Release* 1998; 50:167-178
- Eouani C, Piccerelle Ph, Prinderre P, Bourret E, Joachim J. In-vitro comparative study of buccal mucoadhesive performance of different polymeric films. *Eur J Pharm Biopharm Sci* 2001; 52:45-55
- Nakanishi T, Kaiho F, Hayashi M. Improvement of drug release rate from Carbopol 934P formulation. *Chem Pharm Bull* 1998; 46:171-173
- Tan Y.T.F, Peh KK, Al-Hanbali O. Investigation of interpolymer complexation between carbopol and various grades polyvinylpyrrolidone and effects on adhesion strength and swelling properties. *J Pharm Pharmaceut Sci* 2001; 4:7-14
- Nakanishi T, Kaiho F, Hayashi M. Use of sodium salt of Carbopol 934P in oral peptide delivery. *Int J Pharm* 1998; 171: 177-183
- Callens C, Adriaens E, Dierckens K, Remon JP. Toxicological evaluation of a bioadhesive nasal powder containing a starch and Carbopol 974P on rabbit nasal mucosa and slug mucosa. *J Control Release* 2001; 76:81-91
- Repka MA, McGinity JW. Bioadhesive properties of hydroxypropylcellulose topical films produced by hot-melt extrusion. *J Control Release* 2001; 70:341-351
- Khan GM, Zhu JB. Studies on drug release kinetics from ibuprofen-carbomer hydrophilic matrix tablets: influence of co-excipients on release rate of the drug. *J Control Release* 1999; 57:197-203
- Ozeki T, Yuasa H, Kanaya Y. Controlled release from solid dispersion composed of poly(ethylene oxide)-Carbopol interpolymer complex with various cross-linking degrees of Carbopol. *J Control Release* 2000; 63:287-295
- Khan GM, Zhu JB. Formulation and *in vitro* evaluation of ibuprofen-carbopol 974P-NF controlled release matrix tablets: influence of co-excipients on release rate of the drug. *J Control Release* 1998; 54:185-190
- Muramatsu M, Kanada K, Nishida A, Ouchi K, Saito N. Application of Carbopol to controlled release preparations. Carbopol as a novel coating material. *Int J Pharm* 2000; 199: 77-83
- Senel S, Capan Y, Sargon MF, Giray CB, Hincal AA. Histological and bioadhesion studies on buccal bioadhesive tablets containing a penetration enhancer sodium glycodeoxycholate. *Int J Pharm* 1998; 170: 239-245
- Bogataj M, Mrhar A, Korosec L. Influence of physicochemical and biological parameter on drug release from microspheres adhered on vesical and intestinal mucosa. *Int J Pharm* 1999; 177: 211-220
- Riley RG, Smart JD, Tsibouklis J, Dettmar PW, Hampson F, Davis JA, Kelly G, Wilber WR. An investigation of mucus/polymer rheological synergism using synthesised and characterised poly(acrylic acid)s. *Int J Pharm* 2001; 217: 87-100
- Hagerstrom H, Paulsson M, Edsman K. Evaluation of mucoadhesion for two polyelectrolyte gels in simulated physiological conditions using a rheological method. *Eur J Pharm Sci* 2001; 9:301-309
- Dash AK, Gong Z., Miller DW, Han HY, Laforet JP. Development of a rectal nicotine delivery system for the treatment of ulcerative colitis. *Int J Pharm* 1999; 190: 21-34
- Connor AL, Wray H, Cottrell J, Wilding IR. A scintigraphic study to

- investigate the potential for altered gut distribution of loperamide from a loperamide-simethicone formulation in man. *Eur J Pharm Sci* 2001; 13: 369-374
- 21 Sangalli ME, Maroni A, Zema L, Busetti C, Giordano F, Gazzaniga A. *in vitro* and *in vivo* evaluation of an oral system for time and/or site-specific drug delivery. *J Control Release* 2001; 73:103-110
- 22 Digenis GA, Sandefer EP, Page RC, Doll WJ, Gold TB, Darwazeh NB. Bioequivalence study of stressed and nonstressed hard gelatin capsules using amoxicillin as a drug marker and gamma scintigraphy to confirm time and GI location of *in vivo* capsule rupture. *Pharm Res* 2000; 17: 572-580
- 23 Krishnaiah YSR, Satyanrayana S, Rama Prasad YV, Rao SN. Gamma scintigraphic studies on guar gum matrix tablets for colonic drug delivery in healthy human volunteers. *J Control Release* 1998; 55: 245-252
- 24 Ishibashi T, Pitcairn GR, Yoshino H, Mizobe M, Wilding IR. Scintigraphic Evaluation of a new capsule-type colon specific drug delivery system in healthy volunteers. *J Pharma Sci* 1998; 87: 531-535
- 25 Billa N, Yuen KH, Khader MAA, Omar A. Gamma-scintigraphic study of the gastrointestinal transit and *in vivo* dissolution of a controlled release diclofenac sodium formulation in xanthan gum matrices. *Int J Pharm* 2000; 201: 109-120
- 26 Haruta S, Kawai K, Jinnouchi S, Ogawara KI, Higaki, Tamura S, Arimori K, Kimura T. Evaluation of absorption kinetics of orally administered theophylline in rats based on gastrointestinal transit monitoring by gamma scintigraphy. *J Pharma Sci* 2001; 90: 464-473
- 27 Tang GH, Tang XL. Application of nuclear medicine techniques in drug development. *Acta Pharmaceutica Sinica* 2001; 36: 390-395
- 28 Wilson CG. *In vivo* monitoring of dosage forms. *J Pharm Pharmacol* 1998; 50: 383-386
- 29 Wilding IR, Coupe AJ, Davis SS. The role of scintigraphy in oral drug delivery. *Adv Drug Deliv Rev* 2001; 46: 103-124
- 30 Liang WQ. Biopharmaceutics and pharmacokinetics. Beijing: Renming Health Press. 2000:134-136

Edited by Ma JY

• BASIC RESEARCH •

Gastric myoelectrical activity and gastric emptying in diabetic patients with dyspeptic symptoms

Hui-Bin Qi, Jin-Yan Luo, You-Ling Zhu, Xue-Qin Wang

Hui-Bin Qi, Jin-Yan Luo, You-Ling Zhu, Xue-Qin Wang, Department of Gastroenterology, The Second Hospital of Xi'an Jiaotong University, Xi'an 710004, Shannxi, China

Correspondence to: Hui-bin Qi, Xiwu Road 36, Xi'an 710004, Shannxi, China. qihuibin123@163.net

Telephone: +86-29-7262029 Fax: +86-29-7231758

Received 2001-04-05 Accepted 2001-07-10

Qi HB, Luo JY, Zhu YL, Wang XQ. Gastric myoelectrical activity and gastric emptying in diabetic patients with dyspeptic symptoms. *World J Gastroenterol* 2002;8(1):180-182

INTRODUCTION

Recently, electrogastrography (EGG) has received more and more attention. Although gastroenterologists are interested in its clinical application, concerns remain to the reliability and analysis of the EGG and the correlation between the EGG and gastric motility^[1-13]. This study was to investigate gastric myoelectrical activity and gastric emptying (GE) and their relationship in diabetic patients with dyspeptic symptoms using electrogastrography and isotopic method.

MATERIALS AND METHODS

Subjects

The study was performed on 22 healthy asymptomatic subjects (11 women, 11 men, mean age 50 yr) and 32 non-insulin dependent diabetes mellitus (NIDDM) patients with dyspeptic symptoms (15 women, 17 men, mean age 51 yr) based on clinical and laboratory diagnoses. NIDDM was diagnosed by the WHO criteria (1980). All patients had a minimum 3-month history of chronic, persistent, or recurrent epigastric pain and fullness, early satiety, nausea and/or vomiting. The result of esophagogastroduodenoscopic examination were negative for any focal lesions, including esophagitis, gastric, or duodenal ulcers or erosions, or esophageal or gastric malignancy. Exclusion criteria were: ① history of abdominal surgery; ② history of gastroesophageal reflux disease or irritable bowel syndrome; ③ evidence of cardiovascular, pulmonary, hepatic, or renal disease. All subjects fasted an overnight before the study and took no medications known to affect gastrointestinal motility during 3 d before the study.

Gastric emptying test

Gastric emptying test was taken by using SPECT technique. The standard meal for gastric emptying test consisted of 100g scrambled eggs labeled with ^{99m}Tc-DTPA (11.1 MBq) and 200mL of water. After eating, the anterior/posterior images of the stomach were taken by the same operator using a technetium scanner for 2 h. Retention and half-emptying time ($T_{1/2}$) were calculated by a specialist at the Department of Nuclear Medicine. Delayed gastric emptying was defined as the half-emptying time $\geq x+2s$ as controls.

Recording of gastric myoelectrical activity

Gastric myoelectrical activity was measured with surface EGG. The EGG recording including a 30-min fasting study using an EGG recording unit (Digitrapper, Syneetics Medical, Sweden), after which the patient ate a standard test meal

(1883J). This was immediately followed by another 30-min recording. The EGG data was analyzed by the "multigram" Syneetics software package running on a personal computer. The EGG parameters including dominant frequency (DF), dominant power (DP), postprandial / preprandial DF, postprandial / preprandial DP.

Statistical analysis

Data were expressed as $\bar{x} \pm s$. Statistical analyses used are *t* test and χ^2 test. Statistical significance is taken as $P < 0.05$.

RESULTS

Gastric emptying test

The mean percentage of gastric retention and half-emptying time in diabetic patients with dyspeptic symptoms were substantially higher than in the healthy subjects (Table 1). Of 32 patients, 15 (47%) had delayed gastric emptying. Of 22 controls, 1 (5%) had delayed gastric emptying. The incidence of gastric emptying delay was higher in patients than in controls ($P < 0.01$).

Table 1 Gastric Emptying In NIDDM ($\bar{x} \pm s$)

Groups	n	Percentage of gastric retention %				$T_{1/2}$ min
		30min	60min	90min	120min	
NIDDM	32	75 \pm 7 ^a	61 \pm 8 ^b	54 \pm 10 ^b	43 \pm 10 ^b	92 \pm 10 ^b
Controls	22	61 \pm 7	45 \pm 6	33 \pm 4	24 \pm 10	49 \pm 9

^a $P < 0.05$ vs controls; ^b $P < 0.01$ vs controls

Electrogastrographic findings

EGG dominant frequency corresponds to gastric slow wave. DF ranging from 2.4 to 3.7 cycle per min (cpm) was considered as normogastria, DF < 2.4 cpm was defined as bradygastria, DF > 3.7 cpm was defined as tachygastria. DF < 2.4 cpm and/or DF > 3.7 cpm was defined as dysrhythmia or abnormal EGG. The patients had a lower incidence of normogastria than did controls both in the fed state (34% vs 86%, $P < 0.01$) and in the fasting state (38% vs 96%, $P < 0.01$). However, the patients had a higher incidence of dysrhythmia (tachygastria and bradygastria) than did controls both in the fed state (66% vs 14%, $P < 0.01$) and in the fasting state (63% vs 5%, $P < 0.01$). The mean postprandial dominant frequency and postprandial/preprandial dominant frequency ratio were lower in patients than in controls (2.61 \pm 0.29 cpm vs 3.76 \pm 0.14 cpm, $P < 0.05$; 1.01 \pm 0.10 vs 1.28 \pm 0.11, $P < 0.05$). The mean postprandial dominant power increase and the mean postprandial/preprandial dominant power ratio was significantly less in the patients than in the controls (121.50 \pm 67.02 V².cpm vs 688.61 \pm 72.73 V².cpm, $P < 0.01$; 0.71 \pm 0.60 vs 2.40 \pm 0.61, $P < 0.01$). No differences were found in the mean preprandial dominant frequency and the mean preprandial dominant power (2.57 \pm 0.24 cpm vs 2.91 \pm 0.22 cpm, $P > 0.05$; 144.10 \pm 27.40 V².cpm vs 288.40 \pm 56.72 V².cpm, $P > 0.05$).

Comparison of EGG and gastric emptying

Of 32 diabetic patients with dyspeptic symptoms, 15 (47%) had

delayed gastric emptying and 21 (66%) patients with dysrhythmia. 12 patients with dysrhythmia had slow gastric emptying. There was no significant correlation between gastric electrical rhythm and gastric emptying ($P>0.05$).

DISCUSSION

Gastric emptying and EGG were measured in diabetic patients with dyspeptic symptoms in this study. The results showed that fifteen of 32 (47%) diabetic patients with dyspeptic symptoms had delayed gastric emptying, and 21 of 32 (66%) patients had abnormal gastric myoelectrical activity. 12 patients with dysrhythmia had slow gastric emptying. The major abnormalities in gastric myoelectrical activity observed in diabetic patients with dyspeptic symptoms were the abnormal rhythmicity of the gastric slow wave and the reduced postprandial increase in the dominant power.

Our findings in this study are similar to those in previous studies in patients with various gastric motor disorders^[14-19]. In studies using cutaneous electrodes, abnormal EGG were found in 50% of patients with functional dyspepsia^[14]. In an electrogastrographic study using cutaneous electrodes, a high proportion of adult patients (60%) with functional dyspepsia had abnormally slow gastric emptying and abnormalities in gastric myoelectrical activity^[15]. We found that 66% of the patients had abnormal rhythmicity of the gastric slow wave (bradygastria and tachygastria) and some patients had a reduced postprandial increase in the dominant power. EGG findings similar to those in this study have been also reported in studies in patients with gastroparesis^[20,21]. However, Pfaffenbach *et al.* reported that the EGG values obtained in diabetics did not differ significantly from those in healthy subjects and did not correlate with radioscinigraphy, the EGG values in diabetics with delayed gastric emptying (about 40%) did not differ from data in diabetics without gastroparesis^[22]. Jebbink *et al.* also reported that no differences between patients with functional dyspepsia and healthy volunteers were found in the incidence of dysrhythmias^[23]. These discrepancies probably result from differences in patient selection, differences in definition of dyspepsia and EGG analysis method^[24]. Prior studies have demonstrated that gastric emptying in dyspeptic patients was found to be delayed in 30~80% of the patients^[15,20, 25-28]. In agreement with prior studies, this study demonstrated 47% delayed gastric emptying in diabetic patients with dyspeptic symptoms. The present study shows that 12 patients with dysrhythmia had delayed gastric emptying, but there was no correlation between gastric rhythmicity and gastric emptying. An other interesting finding was the reduced increment of amplitude (power), expressed as absolute or relative changes (fed/fasting power ratio). A possible cause for a decrease in the power ratio was the reduced gastric distention or/and contractility of the stomach. An increase in amplitude were reported in numerous studies in normal adults and in normal children^[29-32]. Some authors believed that it was related to the increased contractility of the stomach after the meal^[30,33-35], whereas others reported a major effect of gastric distention. Faure *et al.* suggested that both gastric distention and motor activity contributed to the increase in EGG amplitude, the greater contribution being attributable to gastric distention^[36]. Gastric emptying and EGG findings were agreement with our finding in previous study^[37] and other authors' findings^[38]. A study by Barbar *et al.* showed that EGG did not correlate with nuclear scintigraphic gastric emptying studies in children with suggestive symptoms of gastric motility disorders^[38]. Zhang *et al.* reported that they can't predict a delayed GET by an abnormal EGG^[39]. However, controversial findings were reported. Pfaffenbach *et al.* reported that in 25 adult patients with functional dyspepsia, patients with delayed gastric emptying showed significantly more pre- and post prandial tachygastrias than patients with normal gastric emptying^[40]. Gastric emptying is a complex procedure. EGG reflects gastric myoelectrical

activity and gastric emptying reflects gastric motility, so EGG and gastric emptying should complement each other in studying gastric motor disorders^[14,41].

In conclusion, diabetic patients with dyspeptic symptoms have delayed gastric emptying and abnormalities in gastric myoelectrical activity including dysrhythmia and the reduced postprandial increase in the dominant power. However, the abnormal EGG isn't able to predict delayed gastric emptying.

REFERENCES

- Mathur R, Pimentel M, Sam CL, Chen JD, Bonorris GG, Barnett PS, Lin HC. Postprandial improvement of gastric dysrhythmias in patients with type II diabetes: identification of responders and nonresponders. *Digestive Diseases and Sciences* 2001;46:705-712
- Sanmiquel CP, Mintchev MP, Bowes KL. Electrogastrography: An noninvasive technique to evaluate gastric activity. *Can J Gastroenterol* 1998;12:423-430
- Ma GR, Guo SC, Sun J. Study on the relations between some common gastrointestinal disorders and testing results of electrogastrogram. *Chin Natl J Gastroenterol* 1996;2:81
- Zhang J, Chen D, Gao HY. Function of electrogastrogram in the diagnosis of GI diseases in children. *Chin Natl J Gastroenterol* 1996;2 (Suppl. 1):81-82
- Ouyang S. The new investigation on wave form of electrogastrography. *Chin Natl J Gastroenterol* 1996;2(Suppl. 1):79
- Wang DS, Zhang LD, Chai JY, Zhang Y, Lu YY. Specific EGG wave figure in gastric and duodenal ulcer. *Chin Natl J Gastroenterol* 1996;2 (Suppl. 1):88
- Li JS. Experience in clinical application of electrogastrogram. *Chin Natl J Gastroenterol* 1996;2(Suppl. 1):83
- Ravelli AM. Electrogastrography in childhood. *Chin Natl J Gastroenterol* 1996;2(Suppl. 1):18-21
- Koch KL. Clinical applications of electrogastrography. *Chin Natl J Gastroenterol* 1996;2(Suppl. 1):15-17
- Chen JD. Spectral analysis of electrogastrogram and its clinical significance. *Chin Natl J Gastroenterol* 1996;2(Suppl. 1):11-13
- Chung OY. The clinical significance of gastric dysrhythmias. *Chin Natl J Gastroenterol* 1996;2(Suppl. 1):5-8
- Chen YM, Zhao S, Wan P, Wang J, Fan H, Luo HM, Long YL, Ma BD. Electrogastrography in patients with uremia. *Huaren Xiaohua Zazhi* 1998;6:979-981
- Wang SY. The clinical significance of electrogastrogram application. *Xin Xiaohuabingxue Zazhi* 1994;2(Suppl. 2):157-158
- Parkman HP, Miller MA, Trate D, Knight LC, Urbain JL, Maurer AH, Fisher RS. Electrogastrography and gastric emptying scintigraphy are complementary for assessment of dyspepsia. *J Clin Gastroenterol* 1997;24:214-219
- Lin Z, Eaker EY, Sarosiek I, McCallum RW. Gastric myoelectrical activity and gastric emptying in patients with functional dyspepsia. *Am J Gastroenterol* 1999;94:2384-2389
- Reizzo G, Chiloiro M, Guerra V, Borrelli O, Salvia G, Cucchiara S. Comparison of gastric electrical activity and emptying in healthy and dyspeptic children. *Digestive Diseases and Sciences* 2000;45: 517-524
- Feng YY, Xu RP, Wang Y. The influence of fasting electrogastrograph in patients with functional dyspepsia using cisapride treatment. *Chin Natl J Gastroenterol* 1996;2(Suppl. 1):88
- Li YS, Zhu RM. Mechanisms of functional dyspepsia. *Huaren Xiaohua Zazhi* 1998;6:439-440
- Fu M, Xu GM. Stomach motility in 30 patients with gastric dysrhythmia. *Xin Xiaohuabingxue Zazhi* 1995;3:81-83
- Qi HB, Luo JY, Dai XG, Wang XQ. A study on motility in patients with diabetic gastroparesis. *Xin Xiaohuabingxue Zazhi* 1997; 5:661-662
- Huang YQ, Wang X, Liu L, Li C. Serum NO and the changes of cutaneous electrogastrogram in patients with NIDDM. *Shijie Huaren Xiaohua Zazhi* 2000;8:1177-1178
- Pfaffenbach B, Wegener M, Adamek RJ, Schaffstein J, Lee YH, Ricken D. Antral myoelectric activity, gastric emptying, and dyspeptic symptoms in diabetics. *Scand J Gastroenterol* 1995;30:1166-1171
- Jebbink HJA, Van Berge-Henegouwen GP, Bruijs PPM, *et al.* Gastric myoelectrical activity and gastrointestinal motility in patients with functional dyspepsia. *Eur J Clin Invest* 1995;25:492-437
- Levanon D, Zhang M, Chen JD. Efficiency and efficacy of the electrogastrogram. *Digestive Diseases and Sciences* 1998;43:1023-1030
- Soykan I, Lin Z, Sarosiek I, McCallum RW. Gastric myoelectrical activity, gastric emptying, and correlations with symptoms and fasting blood glucose levels in diabetic patients. *Am J Med Sci* 1999;317:226-231

- 26 Lin X, Chen JZ. Abnormal gastric slow waves in patients with functional dyspepsia assessed by multichannel electrogastrography. *Am J Physiol Gastrointest Liver Physiol* 2001;280:G1370-1375
- 27 Lu CL, Chen CY, Chang FY, Kang LJ, Lee SD, Wu HC, Kuo TS. Impaired postprandial gastric myoelectrical activity in Chinese patients with nonulcer dyspepsia. *Digestive Diseases and Sciences* 2001; 46:242-249
- 28 Chen JD, Ke MY, Lin XM, Wang Z, Zhang M. Cisapride provides symptomatic relief in functional dyspepsia associated with gastric myoelectrical abnormality. *Aliment Pharmacol Ther* 2000;14:1041-1047
- 29 Chen JD, Co E, Liang P, Sutphen J, Torres-Pinedo RB, Orr WC. Patterns of gastric myoelectrical activity in human subjects of different ages. *Am J Physiol* 1997;272:G1022-G1027
- 30 Riezzo G, Chilioro M, Guerra V. Electrogastrography in healthy children: evaluation of normal values, influence of age, gender and obesity. *Digestive Diseases and Sciences* 1998;43:1646-1651
- 31 Cucchiara S, Franzese A, Salvia G, Alfonsi L, Iula VD, Montisci A, Moreira FL. Gastric emptying delay and gastric derangement in IDDM. *Diabetes Care* 1998;21:438-443
- 32 Lin Z, Chen JD, Schirmer BD, McCallum RW. Postprandial response of gastric slow waves: correlation of serosal recordings with the electrogastrograms. *Digestive Diseases and Sciences* 2000;45:645-651
- 33 Zhang KG, Hu YB, Shi XH, Xiao SD. Response of the electrogastrogram in normal subjects to water, milk and solid meal. *Xin Xiaohuabingxue Zazhi* 1996;4:194-195
- 34 Zhou SC, He QN, He P, Feng ZT, Wang YJ. The effect erythromycin on cutaneous electrogastrogram in patients with non-ulcer dyspepsia. *Xin Xiaohuabingxue Zazhi* 1996;4:59-60
- 35 Huang LX, Zhao JX. The effect erythromycin on gastric electrical rhythm in patients with diabetes mellitus. *Xin Xiaohuabingxue Zazhi* 1996;4:612
- 36 Faure C, Wolff P, Navarro J. Effect of meal and intravenous erythromycin on manometric and electrogastrographic measures of gastric motor and electrical activity. *Dig Dis Sci* 2000;45:525-528
- 37 Luo JY, Zhu YL, Wang XQ, Qi HB. Assessment of clinical values of electrogastrography and gastric emptying test. *Weichangbing Xue* 2000; 5:223-225
- 38 Barbar M, Steffen R, Wyllie R, Goske M. Electrogastrography versus gastric emptying scintigraphy in children with suggestive symptoms of gastric motility disorders. *J Pediatr Gastroenterol Nutr* 2000;30:193-197
- 39 Zhang KG, Hu YB, Wang CD, Mo JZ, Wang SX, Xiao SD. Studies in patients with NIDDM by gastric emptying time and electrogastrogram. *Chin Natl J Gastroenterol* 1996;2:81
- 40 Pfaffenbach B, Adamek RJ, Bartholomaeus C, Wegener M. Gastric dysrhythmias and delayed gastric emptying in patients with functional dyspepsia. *Digestive Diseases and Sciences* 1997;42:2094-2099
- 41 Quigley EMM. The evaluation of gastrointestinal function in diabetic patients. *World Journal of Gastroenterology* 1999;5:277-282

Edited by Wang QY

• BASIC RESEARCH •

Proliferation of intestinal crypt cells by gastrin-induced ornithine decarboxylase

Zi-Li Zhang, Wei-Wen Chen

Zi-Li Zhang, Wei-Wen Chen, Guangzhou University of Traditional Chinese Medicine (TCM), Guangzhou 510405, China
Supported by National Natural Science Foundation of China, No. 39970906

Correspondence to: Dr. Chen Weiwen, Piwei Institute, Guangzhou University of TCM, Guangzhou 510405, China. pwxh@gzhtcm.edu.cn
Telephone: +86-20-86591233 ext 2444

Received 2001-07-03 Accepted 2001-10-16

Abstract

AIM: To determine whether the gastrin stimulated intestinal crypt cell (IEC-6) proliferation by induction of ornithine decarboxylase (ODC).

METHODS: IEC-6 cells were grown in DMEM containing 50 mL·L⁻¹ dialyzed fetal bovine serum for 24h and then were treated with gastrin. The proliferative capability of the cells was monitored subsequently on d 1, 2, 3, and 4 after treatment with MTT assay at absorbance 570nm. The cellular ODC mRNA expression, ODC activity, and putrescine content were examined by RT-PCR method, radiometric technique and high-performance liquid chromatography (HPLC) analysis respectively after 12h of treatment.

RESULTS: On d1 after exposure of IEC-6 cells to pentagastrin, the proliferation increased initially and reached a peak on d3 at 250 μg·L⁻¹ concentration. Pentagastrin 500 μg·L⁻¹ increased cell proliferation on day 1 and day 2, and then decreased. Compared with control group, pentagastrin 250 μg·L⁻¹ increased ODC mRNA level by 1.09-fold ($P < 0.05$), ODC activity by 1.71-fold ($P < 0.01$), and putrescine content 5.30-fold ($P < 0.01$), respectively. Similarly, pentagastrin of 500 μg·L⁻¹ also increased ODC mRNA level by 1.16-fold ($P < 0.05$), ODC activity 1.63-fold ($P < 0.05$), and putrescine content 4.41-fold ($P < 0.01$), respectively. But there was not significant difference between them.

CONCLUSION: Gastrin is an agent which promotes IEC-6 cell proliferation involved in regulating ODC activity mechanism.

Zhang JL, Chen WW. Proliferation of intestinal crypt cells by gastrin-induced ornithine decarboxylase. *World J Gastroenterol* 2002;8(1):183-187

INTRODUCTION

Increasing evidence has demonstrated that cell proliferation, differentiation and migration in the intestinal mucosa is dependent on the supply of polyamines to the dividing cells^[1-8]. Intracellular polyamine levels are highly regulated^[9-15] and completely depend on the activation or inhibition of ornithine decarboxylase (ODC), which is the first rate-limiting step in polyamine biosynthesis^[16-22]. In addition to the general effect of metabolic hormones, the amount of ODC in the gastrointestinal mucosa is also regulated by growth-related gut peptides present in the diet or secreted from digestive glands^[23-29]. Gastrin is an important gut peptide which stimulates cell proliferation in the mucosa under physiological condition^[30]. Administration of gastrin significantly increases ODC activity and intracellular polyamine levels in intestinal epithelial cells^[30]. Intestinal epithelial restitution is a complex process. Because of the limitation to

study such issues in natural mucosae, cultured rat small intestinal epithelial cell lines (IEC-6) were commonly employed to characterize the physiological events such as growth, differentiation, metabolism and so on during restitution in detail. In the present study, we investigated the influence of gut peptide gastrin on the proliferation, expression of the ODC gene, ODC activity and polyamine biosynthesis in cultured normal rat intestinal crypt cells (IEC-6 cell line).

MATERIALS AND METHODS

Chemicals and supplies

IEC-6 cell line (CRL-1592) was purchased from American Type Culture Collection (ATCC, Rockville, MD) at passage 13. Disposable culture was purchased from Corning Glass Works (Corning, NY). Dulbecco's modified Eagle's medium containing 4500 mg·L⁻¹ D-glucose, L-glutamine, 25 mmol·L⁻¹ HEPES buffer and pyridoxine hydrochloride (DMEM), dialyzed fetal bovine serum (dFBS), trypsin-EDTA solution, gentamicin sulfate and insulin, Dulbecco's PBS (D-PBS), and biochemicals such as pentagastrin, putrescine, sodium dodecyl sulfate (SDS) and 3-(4,5-dimethylthiazol-2-yl)-2,5-diphenyl-tetrazolium bromide (MTT) were from Sigma (St. Louis, MO). L-[1-¹⁴C]ornithine (sp act 1.93 TBq·mol⁻¹) was purchased from NEN (Boston, MA).

General experimental protocol

To insure the highest level of viability, the culture was started as soon as possible upon receipt of the vial. Thaw the vial by gentle agitation in 37°C water bath and decontaminate by dipping in 700 mL·L⁻¹ ethanol, transfer the vial contents to 25 cm² tissue culture flasks containing 10 mL DMEM supplemented with 50 g·L⁻¹ dFBS, 10 mg·L⁻¹ insulin, and 50 mg·L⁻¹ gentamicin sulfate (cDMEM) then place into the incubator for 15 min prior to addition of the vial contents to allow the medium to reach its normal pH (7.2). Incubate the cells at 37°C in a humidified atmosphere of 900 mL·L⁻¹ air-100 mL·L⁻¹ CO₂. Stock cells were subcultured once a week; and the medium was changed three times weekly. The cells were restarted from frozen stock every five to six passages. Tests for mycoplasma were routinely negative. For cell counting and subculturing, the cells were dispersed with 0.5 g·L⁻¹ trypsin and 0.2 g·L⁻¹ EDTA. Remove the solution and add 1 - 2 mL of trypsin-EDTA solution. Allow the flask to sit at room temperature until the cells detach. Add fresh culture medium, aspirate and dispense into new culture flasks.

Treatment of pentagastrin on IEC-6 cells

IEC-6 cell numbers were directly measured with the help of a cell counter, and plated in 96-wells with 200 μL cDMEM, or 6-wells with 2000 μL cDMEM. The cells were incubated in a humidified atmosphere at 37°C in 900 mL·L⁻¹ air-100 mL·L⁻¹ CO₂, which was followed by a period of different experimental treatments. Pentagastrin was dissolved in two or three drops of 300 g·L⁻¹ ammonium hydroxide (sterile), adjusted to pH 7.5, and then diluted with medium to the desired concentrations before use. Media pentagastrin were prepared immediately before the experiments.

In the first series of studies, we examined the effect of pentagastrin on cell proliferation in IEC-6 cells. Cells were plated in

96-well microplates at a density of 1×10^4 cells per well with 200 μ L cDMEM and grown in incubator under the condition described above. After 24h, 10 μ L media pentagastrin were added at final concentrations of 500 and 250 μ g \cdot L $^{-1}$. Control cells were fed with fresh medium without gastrin as well. To determine the time course of cell proliferation, cell numbers were measured at different time points after exposure of the cells to pentagastrin with MTT assay.

In the second series of studies, we examined the effect of pentagastrin on cellular ODC mRNA levels, ODC enzyme activity and putrescine content in IEC-6 cells. Cells were plated in 6-well microplates at a density of 2×10^6 cells per well with 2000 μ L cDMEM and grown under incubator at the condition described above. After 24h, 100 μ L media pentagastrin were added at final concentrations of 250 and 500 μ g \cdot L $^{-1}$, respectively. Control cells were fed with fresh medium without gastrin as well. Cultures were harvested at 12h after exposure of the cells to pentagastrin. The dishes were placed on ice, the monolayers were washed three times with ice-cold D-PBS, and different solutions were then added according to the assays to be conducted.

Measurement of ODC mRNA level

Total RNA was isolated from IEC-6 cells using RNA TRIzol reagent from Gibco(Gaithersburg, MD). Isolation and extraction were performed according to the manufacturer's protocol. Briefly, the cells were washed with Dulbecco's PBS and were lysed with 1.0mL Trizol/well.

RNA was extracted with 0.2mL chloroform and precipitated with 0.5 mL isopropanol. The precipitated RNA was washed with 1mL 700mL \cdot L $^{-1}$ ethanol and redissolved in RNase-free water. The concentration of the extracted RNA was calculated by measuring the absorbance at 260nm. The ratio of the absorbance at 260nm to that at 280nm was always >1.9 .

Aliquots of RNA (5 μ g) were reverse-transcribed using an RT-PCR kit from Gibco(Gaithersburg, MD). Briefly, 5 μ g RNA in 10 μ L of diethyl pyrocarbonate-treated water(DEPC-water) was mixed with 1 μ L of 50 μ mol \cdot L $^{-1}$ oligo(dT) $_{20}$, heated at 65 $^{\circ}$ C for 5min, and then placed on ice. The following reagents were added to the tubes: 4 μ L of 5 \times concentrated cDNA synthesis buffer, 1 μ L of 0.1mol \cdot L $^{-1}$ DTT, 1 μ L of RNaseOUT(40MU \cdot L $^{-1}$), 1 μ L of DEPC-water, 2 μ L of 10mmol \cdot L $^{-1}$ dNTP Mix, and 1 μ L of Thermoscript RT(15MU \cdot L $^{-1}$). The reaction mixture was incubated for 50min at 50 $^{\circ}$ C before the reaction was terminated by incubating the tube at 85 $^{\circ}$ C for 5min. The mixture was added with 1 μ L RNase H and incubated at 37 $^{\circ}$ C for 20min. The tube was stored at -80 $^{\circ}$ C until PCR was performed using the Platinum Taq DNA polymerase with rat-specific primers prepared on a DNA synthesizer (Seagon, Shanghai, China). The primers were designed according to sequences of rat ornithine decarboxylase gene (EC 4.1.1.17). as follows: upstream primer: 5' $>$ TGG CTG GCG CTG GTC TGT AGT $<$ 3'; downstream primer: 5' $>$ AGC TCC TGC CTG GGT.CTT.ATG A $<$ 3'.

The cDNA amplification products were predicted to be 300bp in length for ODC. To initiate the PCR, 2 μ L RT products were added to the PCR master mix, including 5 μ L 10 \times PCR reaction buffer, 2 μ L 50mmol \cdot L $^{-1}$ MgCl $_2$, 0.2 μ L Platinum Taq DNA polymerase(5MU \cdot L $^{-1}$), 1 μ L 10 μ mol \cdot L $^{-1}$ each of the primers, 10mmol \cdot L $^{-1}$ dNTP Mix and 37.8 μ L DEPC-water. Tubes were placed in a programmed tempcontrol system (PE) as follows: 1) incubation at 94 $^{\circ}$ C for 2min (initial denaturation); 2) 40 cycles of the following sequential steps: 94 $^{\circ}$ C for 30s (denaturation), 60 $^{\circ}$ C for 30s (annealing), and 72 $^{\circ}$ C for 1min (extension); and 3) incubation at 72 $^{\circ}$ C for 7min (final extension). The PCR products were size-fractionated by agarose gel electrophoresis. After electrophoresis and ethidium bromide staining, DNA bands were visualized and the relative levels of mRNA for ODC were corrected for cDNA loading as measured with an ultraviolet transilluminator.

Assay for ODC activity

ODC activity was determined with radiometric technique in which the amount of 14 CO $_2$ liberated from DL-[L- 14 C]ornithine was estimated. Samples were collected as described above and placed in 0.5mL of 20mmol \cdot L $^{-1}$ Tris buffer (pH7.4) containing 0.05mmol \cdot L $^{-1}$ EDTA, 0.05mmol \cdot L $^{-1}$ pyridoxal phosphate, and 5mmol \cdot L $^{-1}$ dithiothreitol. The cells were frozen and thawed three times, scraped, and transferred to Eppendorf tubes. Cells were centrifuged at 12000g at 4 $^{\circ}$ C for 15min. The ODC activity of an aliquot of the supernatant was determined during incubation in stoppered vials in the presence of 7.6nmol of [14 C] ornithine (sp act 1.93TBq \cdot mol $^{-1}$) for 15min at 37 $^{\circ}$ C. The 14 CO $_2$ liberated by the decarboxylation of ornithine was trapped on a piece of filter paper impregnated with 20 μ L of 2mol \cdot L $^{-1}$ NaOH, which was suspended in a center well above the reaction mixture. The reaction was stopped by the addition of trichloroacetic acid to a final concentration of 100g \cdot L $^{-1}$. The 14 CO $_2$ trapped in the filter paper was measured by liquid scintillation spectroscopy at a counting efficiency of 95%. Aliquots of the 12000g supernatant were assayed for total protein, by Lowry method. Enzymatic activity was expressed as picomoles of CO $_2$ per milligram of protein per hour.

Analysis of cellular putrescine

The cellular putrescine content was analyzed by HPLC as described previously^[5]. In brief, after monolayers were washed three times with ice-cold D-PBS, 0.5mol \cdot L $^{-1}$ perchloric acid were added and the monolayers were frozen at -80 $^{\circ}$ C until ready for extraction, dansylation, and HPLC cells were harvested, and centrifuged at 1600g for 10min. This supernatant was collected, neutralized to pH 7.0 with 3mol \cdot L $^{-1}$ KOH, and centrifuged to remove the precipitate. A 0.5mL aliquot of solution was delivered to clean Eppendorf tubes. After addition of 0.25mL saturated Na $_2$ CO $_3$ and 0.5mL dansyl chloride solution(10g \cdot L $^{-1}$ acetone), reaction was allowed to proceed by heating at 70 $^{\circ}$ C for 30min and then added to 1.5mL toluene. After mixing and centrifugation, the organic protein portion was collected and dried by vacuum centrifugation. To the residue, 300 μ L methanol was added and filtered, and an aliquot of 200 μ L was used for HPLC analysis. Solvent A and B were composed of acetonitrile, water, glacial acetic acid, and triethylamine in the volume proportions of 80:20:0.02:0.001 and 95:5:0.02:0.005, respectively. The mobile phases used in this separation consisted of 60% solvent A and 40% solvent B. Each sample was run for 20min, and the equilibration delay between injections was 2min. Sufficient mobile phases (A and B) were prepared fresh before starting the automatic injector. The polyamine putrescine was measured by comparing ratios of polyamines to 1,10-diaminodecane peak areas with a standard curve. Protein was dissolved in 1mol \cdot L $^{-1}$ NaOH and determined by the Lowry method. The results were expressed as nanomoles of polyamines per milligram of protein.

Statistics

All data are expressed as $\bar{x} \pm s$ from three-four dishes. The significance of the difference between means was determined by independent *t* test using SPSS statistical software.

RESULTS

Effect of gastrin on the proliferation Of IEC-6 cells

IEC-6 cells were grown in cDMEM in the presence or absence of pentagastrin. Exposure of IEC-6 cells to pentagastrin, the proliferation increased initially on d1 and reached a peak on d3 in 250 μ g \cdot L $^{-1}$ concentration. Pentagastrin 500 μ g \cdot L $^{-1}$ increased cell proliferation on d1 and d2 and then decreased as shown in Figure 1.

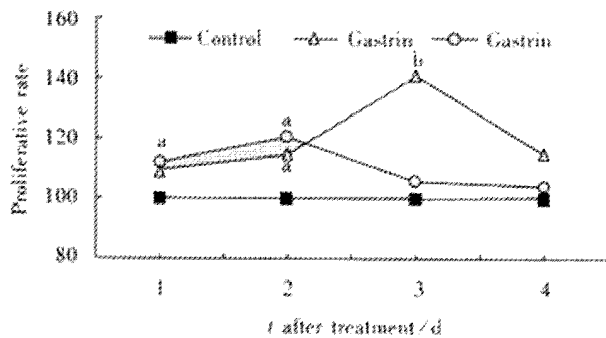


Figure 1 Gastrin effect on IEC-6 proliferation by the MTT assay. ^a $P < 0.05$, ^b $P < 0.01$ vs control.

ODC mRNA amount in IEC-6 cells treated with gastrin

Administration of pentagastrin 250 and 500 $\mu\text{g}\cdot\text{L}^{-1}$ significantly raised the ODC mRNA levels by 1.16-fold and 1.09-fold, respectively as compared with control group (Figure 2). But there was no significant difference between the two doses of gastrin.

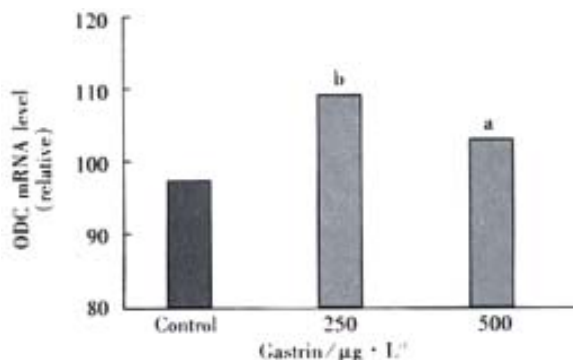


Figure 2 ODC mRNA levels in IEC-6 cells.

^a $P < 0.05$, ^b $P < 0.01$ vs control.

Gastrin induction of ODC activity

In these studies, IEC-6 cells were grown in cDMEM in the presence or absence of pentagastrin. This exposure of IEC-6 cells to pentagastrin 250 and 500 $\mu\text{g}\cdot\text{L}^{-1}$ caused ODC activity to increase significantly by 1.71-fold and 1.63-fold, respectively at 12h after treatment as compared with control group. But there was no significant difference between them (Figure 3).

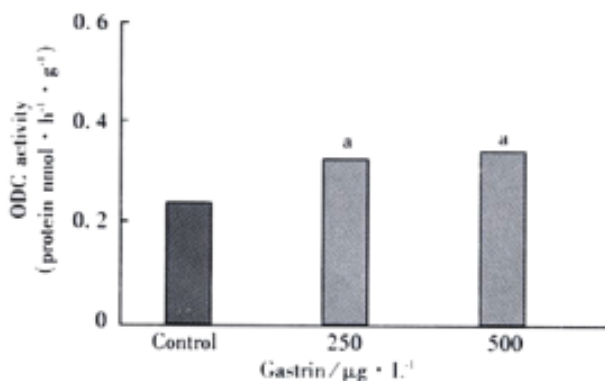


Figure 3 ODC activity in IEC-6 cells exposed to pentagastrin.

^a $P < 0.05$ vs control.

Effect of pentagastrin on putrescine content in IEC-6 cells

Increases in ODC activity in cells exposed to pentagastrin were paralleled with increases in cellular putrescine levels. Compared with a value of $0.46 \pm 0.02 \mu\text{mol}\cdot\text{g}^{-1}$ from 4 cultures in the control group, the cellular putrescine levels treated with pentagastrin 250 and 500 $\mu\text{g}\cdot\text{L}^{-1}$ significantly increased ($P < 0.01$), the values were $2.44 \pm 0.05 \mu\text{mol}\cdot\text{g}^{-1}$ and $2.03 \pm 0.03 \mu\text{mol}\cdot\text{g}^{-1}$ from 4 cultures, which were 5.30-fold and 4.41-fold of control group, respectively.

DISCUSSION

Numerous studies have demonstrated that polyamine biosynthesis plays a critical role in the control of normal mucosal growth and repair^[1-12] and that ODC in small intestinal mucosa has a high basal activity compared with most tissues and significantly increases in response to a variety of chronic and acute mitogenic stimuli^[16-29]. The rapid and striking increases in ODC and polyamine levels are absolutely required for the stimulation of intestinal mucosal growth^[16-21].

IEC-6 cells which were established by Quaroni *et al* are derived from neonatal normal rat small intestine and have characteristics of crypt-type epithelial cells as judged by morphological and immunologic criteria which do not exhibit differentiated morphology or specific gene expression. They are nontumorigenic and retain the undifferentiated character of epithelial stem cells. These cells exhibit a number of features of normal cells in culture: i.e. a normal rat diploid karyotype, strong density inhibition of growth, lack of growth in soft agar, and a low plating efficiency when seeded at low density. The establishment of IEC-6 cell lines play an important role in functional researches of small intestine epithelial cells such as growth, differentiation, metabolism, the pharmacological effects, and the pathophysiological changes and the mechanism of intestinal mucosa resulted from various pathogenic factors. This cell line also provided an appropriate *in vitro* model for the study on cell proliferation and mucosal healing. This cell line was broadly used in the studies on cellular, molecular and genetic mechanism of small intestinal mucosal repair since the establishment^[31-40].

The gastrointestinal mucosa must maintain a barrier against the harsh luminal contents of acid, enzymes, bacteria, and toxins. Disruption of this barrier is the salient feature of a variety of common and important gastrointestinal disorders, including inflammatory bowel disease and peptic ulcers. The mucosal epithelium of the small intestine has the capacity for rapid renewal and adaptation after injury or resection. Crypt cell proliferation leading to intestinal growth and promoting re-establishment of mucosal integrity after injury are essential processes for the differentiation, maintenance, and repair of the intestinal epithelium and are regulated via a complex interplay of nutrients, pancreatic and biliary secretions, and both locally derived and circulating growth factors^[41-51].

It is of interest and important to investigate the effect of growth-related gut peptides on the regulation of ODC activity in intestinal epithelial cells. The current study clearly shows that, in small intestinal crypt cells maintained in cDMEM, gastrin stimulates cell proliferation, increases ODC mRNA levels, ODC activity and polyamine content, in which the effects of pentagastrin 250 $\mu\text{g}\cdot\text{L}^{-1}$ seems to be better than those of 500 $\mu\text{g}\cdot\text{L}^{-1}$. Consistent with the results reported by other authors^[30] higher dosage of pentagastrin ($>1000 \mu\text{g}\cdot\text{L}^{-1}$) inhibited IEC-6 cell proliferation (data not shown).

In summary, our results indicate that the increased ODC activity in IEC-6 cells treated with gastrin is associated with a rise in ODC mRNA levels and an increase of intracellular putrescine resulting in cell proliferation. It suggests that the induction of ODC activity by gastrin plays an important role in the regulation of cell proliferation in the intestinal mucosa under physiological condition.

ACKNOWLEDGEMENTS We would like to thank Prof. Wang

Zhou, Drs Han and Yu, and Mr Pan for their technical advice and excellent assistance.

REFERENCES

- 1 Loser C, Eisel A, Harms D, and Folsch UR. Dietary polyamines are essential luminal growth factors for small intestinal and colonic mucosal growth and development. *Gut* 1999 Jan; 44: 12-16
- 2 Bardocz S, Grant G, Brown DS, and Pusztai A. Putrescine as a source of instant energy in the small intestine of the rat. *Gut* 1998; 42: 24-28
- 3 Greco S, Huguency I, George P, Perrin P, Louisot P, and Biol MC. Influence of spermine on intestinal maturation of the glycoprotein glycosylation process in neonatal rats. *Biochem J* 2000; 345(Pt 1): 69-75
- 4 Banan A, McCormack SA, and Johnson LR. Polyamines are required for microtubule formation during gastric mucosal healing. *Am J Physiol* 1998;274: G879-885
- 5 Patel AR, Li J, Bass BL, and Wang JY. Expression of the transforming growth factor beta gene during growth inhibition following polyamine depletion. *Am J Physiol* 1998; 275: C590-598
- 6 McCormack SA, Blanner PM, Zimmerman BJ, Ray R, Poppleton HM, and Patel TB. Polyamine deficiency alters EGF receptor distribution and signaling effectiveness in IEC-6 cells. *Am J Physiol* 1998; 274: C192-205
- 7 Wang JY, Wang J, Golovina VA, Li L, Platoshy O, and Yuan JX. Role of K(+) channel expression in polyamine-dependent intestinal epithelial cell migration. *Am J Physiol Cell Physiol* 2000; 278: C303-314
- 8 Wang JY, Viar MJ, Shi HJ, Patel AR, and Johnson LR. Differences in transglutaminase mRNA after polyamine depletion in two cell lines. *Am J Physiol* 274 (Cell Physiol. 43): C522-C530
- 9 Wang W and Higuchi CM. Dietary soy protein is associated with reduced intestinal mucosal polyamine concentration in male Wistar rats. *J Nutr* 2000; 130: 1815-1820
- 10 Noack J, Kleessen B, Proll J, Dongowski G, and Blaut M. Dietary guar gum and pectin stimulate intestinal microbial polyamine synthesis in rats. *J Nutr* 1998; 128: 1385-1391
- 11 Patel AR, and Wang JY. Polyamine depletion is associated with an increase in JunD/AP-1 activity in small intestinal crypt cells. *Am J Physiol* 1999;276:G441-450
- 12 Ray RM, Viar MJ, Yuan Q, and Johnson LR. Polyamine depletion delays apoptosis of rat intestinal epithelial cells. *Am J Physiol Cell Physiol* 2000; 278: C480-489
- 13 Ray RM, Zimmerman BJ, McCormack SA, Patel TB, and Johnson LR. Polyamine depletion arrests cell cycle and induces inhibitors p21(Waf1/Cip1), p27(Kip1), and p53 in IEC-6 cells. *Am J Physiol* 1999; 276: C684-691
- 14 McCormack SA, Ray RM, Blanner PM, and Johnson LR. Polyamine depletion alters the relationship of F-actin, G-actin, and thymosin beta4 in migrating IEC-6 cells. *Am J Physiol* 1999; 276: C459-468
- 15 Li L, Li J, Rao JN, Li M, Bass BL, and Wang JY. Inhibition of polyamine synthesis induces p53 gene expression but not apoptosis. *Am J Physiol* 1999; 276: C946-954
- 16 Guo Y, Harris RB, Rosson D, Boorman D, and O'Brien TG. Functional Analysis of Human Ornithine Decarboxylase Alleles. *Cancer Res* 2000;60: 6314-6317
- 17 Noda J, Iwakiri R, Fujimoto K, Matsuo S, and Aw TY. Programmed cell death induced by ischemia-reperfusion in rat intestinal mucosa. *Am J Physiol* 1998 Aug; 274 (Gastrointest.Liver Physiol. 37):G270-276
- 18 Ray RM, Viar MJ, Patel TB, and Johnson LR. Interaction of asparagine and EGF in the regulation of ornithine decarboxylase in IEC-6 cells. *Am J Physiol* 1999; 276: G773-780
- 19 Wang JY, Li J, Patel AR, Summers S, Li L, and Bass BL. Synergistic induction of ornithine decarboxylase by asparagine and gut peptides in intestinal crypt cells. *Am J Physiol* 1998; 274: C1476-1484
- 20 Jacoby RF, Cole CE, Tutsch K, Newton MA, Kelloff G, Hawk ET, and Lubet RA. Chemopreventive efficacy of combined piroxicam and difluoromethylornithine treatment of Apc mutant Min mouse adenomas, and selective toxicity against Apc mutant embryos. *Cancer Res* 2000; 60: 1864-1870
- 21 Meyskens FL, and Gerner EW. Development of difluoromethylornithine (DFMO) as a chemoprevention agent. *Clin. Cancer Res* 1999;5:945-951
- 22 Hori T, Wanibuchi H, Yano Y, Otani S, Nishikawa A, Osugi H, Kinoshita H, and Fukushima S. Epithelial cell proliferation in the digestive tract induced by space restriction and water-immersion stress. *Cancer Lett* 1998; 125: 141-148
- 23 Gke M, Kanai M, and Daniel KP. Intestinal fibroblasts regulate intestinal epithelial cell proliferation via hepatocyte growth factor. *Am J Physiol* 1998;274 (Gastrointest-Liver Physiol.5): G809-G818
- 24 DeMarco V, Dyess K, Strauss D, West CM, and Neu J. Inhibition of glutamine synthetase decreases proliferation of cultured rat intestinal epithelial cells. *J Nutr* 1999; 129: 57-62
- 25 Jehle PM, Fussgaenger RD, Angelus NK, Jungwirth RJ, Saile B, and Lutz MP. Proinsulin stimulates growth of small intestinal crypt-like cells acting via specific receptors. *Am J Physiol* 1999; 276: E262-268
- 26 Taupin DR, Kinoshita K, and Podolsky DK. Intestinal trefoil factor confers colonic epithelial resistance to apoptosis. *Proc Natl Acad Sci U S A* 2000; 97: 799-804
- 27 Rao JN, Li J, Li L, Bass BL, and Wang JY. Differentiated intestinal epithelial cells exhibit increased migration through polyamines and myosin II. *Am J Physiol* 1999; 277: G1149-1158
- 28 Qing Y, Viar MJ, Ray RM, and Johnson LR. Putrescine does not support the migration and growth of IEC 6 cells. *Am J Physiol* 2000; 278 (Gastrointest-Liver Physiol.1): G49-G56
- 29 Pfeffer LM, Yang CH, Pfeffer SR, Murti A, McCormack SA, and Johnson LR. Inhibition of ornithine decarboxylase induces STAT3 tyrosine phosphorylation and DNA binding in IEC-6 cells. *Am J Physiol Cell Physiol* 2000; 278: C331-335
- 30 Jonson L, Bundgaard JR, Johnsen AH, and Rourke JJ. Identification and expression of gastrin and cholecystokinin mRNAs from the turtle, *Pseudemys scripta*: evidence of tissue-specific tyrosyl sulfation (1). *Biochim Biophys Acta* 1999; 1435: 84-93
- 31 Chen XM, and Larusso NF. Mechanisms of attachment and internalization of *Cryptosporidium parvum* to biliary and intestinal epithelial cells. *Gastroenterology* 2000;118:368-378
- 32 Miyazaki Y, Shinomura Y, Tsutsui S, Kitamura S, Hiraoka S, and Matsuzawa Y. Calphostin C induces expression of amphiregulin mRNA via reactive oxygen species in IEC-6 cells. *Life Sci* 1998; 63: PL361-365
- 33 Sonoyama K, Rutatip S, and Kasai T. Gene expression of activin, activin receptors, and follistatin in intestinal epithelial cells. *Am J Physiol* 2000; 278 (Gastrointest.Liver Physiol.37):G89-97
- 34 Fabbri A, Falzano L, Frank C, Donelli G, Matarrese P, Raimondi F, Fasano A, Fiorentini C. *Vibrio parahaemolyticus* thermostable direct hemolysin modulates cytoskeletal organization and calcium homeostasis in intestinal cultured cells. *Infect Immun* 1999; 67: 1139-1148
- 35 Kumar CK, Nguyen TT, Gonzales FB, and Said HM. Comparison of intestinal folate carrier clone expressed in IEC-6 cells and in *Xenopus* oocytes. *Am J Physiol* 1998; 274: C289-294
- 36 Shinohara H, Killion JJ, Bucana CD, Yano S, and Fidler IJ. Oral administration of the immunomodulator JBT-3002 induces endogenous interleukin 15 in intestinal macrophages for protection against irinotecan-mediated destruction of intestinal epithelium. *Clin Cancer Res* 1999; 5: 2148-2156
- 37 Jobin C, Holt L, Bradham CA, Streetz K, Brenner DA, and Sartor RB. TNF receptor-associated factor-2 is involved in both IL-1 beta and TNF-alpha signaling cascades leading to NF-kappa B activation and IL-8 expression in human intestinal epithelial cells. *J Immunol* 1999; 162: 4447-4454
- 38 Rivard N, Boucher MJ, Asselin C, and L'Allemain G. MAP kinase cascade is required for p27 downregulation and S phase entry in fibroblasts and epithelial cells. *Am J Physiol* 1999; 277: C652-664
- 39 Erwin CR, Helmrath MA, Shin CE, Falcone RA Jr, Stern LE, and Warner BW. Intestinal overexpression of EGF in transgenic mice enhances adaptation after small bowel resection. *Am J Physiol* 1999; 277 (Gastrointest-Liver Physiol. 3): G533-G540
- 40 Sturm A, Sudermann T, Schulte KM, Goebell H, and Dignass AU. Modulation of intestinal epithelial wound healing *in vitro* and *in vivo* by lysophosphatidic acid. *Gastroenterology* 1999; 117: 368-377

- 41 Quaroni A, Tian JQ, Goke M, and Podolsky DK. Glucocorticoids have pleiotropic effects on small intestinal crypt cells. *Am J Physiol* 1999; 277: G1027-1040
- 42 Nishimura S, Takahashi M, Ota S, Hirano M, and Hiraishi H. Hepatocyte growth factor accelerates restitution of intestinal epithelial cells. *J Gastroenterol* 1998; 33: 172-178
- 43 Varedi M, Greeley GH Jr, Herndon DN, and Englander EW. A thermal injury-induced circulating factor(s) compromises intestinal cell morphology, proliferation, and migration. *Am J Physiol* 1999; 277: G175-182
- 44 Ruthig DJ, and Meckling Gill KA. Both (n-3) and (n-6) fatty acids stimulate wound healing in the rat intestinal epithelial cell line, IEC-6. *J Nutr* 1999; 129: 1791-1798
- 45 Bocker U, Damiao A, Holt L, Han DS, Jobin C, Panja A, Mayer L, and Sartor RB. Differential expression of interleukin 1 receptor antagonist isoforms in human intestinal epithelial cells. *Gastroenterology* 1998; 115: 1426-1438
- 46 Vreugdenhil AC, Dentener MA, Snoek AM, Greve JW, and Buurman WA. Lipopolysaccharide binding protein and serum amyloid A secretion by human intestinal epithelial cells during the acute phase response. *J Immunol* 1999; 163: 2792-2798
- 47 Awane M, Andres PG, Li DJ, and Reinecker HC. NF-kappa-B-inducing kinase is a common mediator of IL-17-, TNF-alpha-, and IL-1 beta-induced chemokine promoter activation in intestinal epithelial cells. *J Immunol* 1999; 162: 5337-5344
- 48 Nikawa T, Rokutan K, Nanba K, Tokuoka K, Teshima S, Engle MJ, Alpers DH, and Kishi K. Vitamin A up-regulates expression of bone-type alkaline phosphatase in rat small intestinal crypt cell line and fetal rat small intestine. *J Nutr* 1998; 128: 1869-1877
- 49 Cario E, Rosenberg IM, Brandwein SL, Beck PL, Reinecker HC, and Podolsky DK. Lipopolysaccharide activates distinct signaling pathways in intestinal epithelial cell lines expressing Toll-like receptors. *J Immunol* 2000; 164: 966-972
- 50 Shigematsu T, Miura S, Hirokawa M, Hokari R, Higuchi H, Watanabe N, Tsuzuki Y, Kimura H, Tada S, Nakatsumi RC, Saito H1, and Ishii H. Induction of endothelin-1 synthesis by IL-2 and its modulation of rat intestinal epithelial cell growth. *Am J Physiol* 1998; 275 (Gastrointest.Liver Physiol.3): G556-G563
- 51 Rhoads JM, Argenzio RA, Chen W, Graves LM, Licato LL, Blikslager AT, Smith J, Gatzky J, and Brenner DA. Glutamine metabolism stimulates intestinal cell MAPKs by a cAMP-inhibitable, Raf-independent mechanism. *Gastroenterology* 2000; 118: 90-100

• BASIC RESEARCH •

Study on the mechanism of regulation on peritoneal lymphatic stomata with Chinese herbal medicine

Shi-Ping Ding, Ji-Cheng Li, Jian Xu, Lian-Gen Mao

Shi-Ping Ding, Ji-Cheng Li, Lian-Gen Mao, Department of Lymphology, Department of Histology and Embryology, Medical College of Zhejiang University, School of Medicine, Hangzhou 310031, China

Jian Xu, Hangzhou First People's Hospital, Hangzhou 310001, China

Supported by the National Natural Science Foundation of China, No. 39970934, Scientific Research Fund by the Science Technology Committee of Hangzhou, State Administration of Traditional Chinese Medicine, No. 927031, Zhejiang Provincial Administration of Traditional Chinese Medicine, fund for outstanding talents by the Chinese Ministry of Health and Analysis and Testing Fund of Zhejiang Province, No. 00159

Correspondence to: Dr. Ji-Cheng Li, Department of Lymphology, Department of Histology and Embryology, Zhejiang University, School of Medicine, Hangzhou 310031, China. lijc@mail.hz.zj.cn

Telephone: +86-571-87217139 Fax: +86-571-87217139

Received 2001-08-23 Accepted 2001-11-05

Abstract

AIM: To study the mechanism of Chinese herbal medicine (CHM, the prescription consists of *Radix Salviae Miltiorrhizae*, *Radix Codonopsis*, *Pilosulae*, *Rhizoma Atractylodis Alba* and *Rhizoma Alismatis*, *Leonurus Heterophyllus* Sweet, etc) on the regulation of the peritoneal lymphatic stomata and the ascites drainage.

METHODS: The mouse model of live fibrosis was established with the application of intragastric installations of carbon tetrachloride once every three days; scanning electron microscope and computer image processing were used to detect the area and the distributive density of the peritoneal lymphatic stomata; and the concentrations of urinary ion and NO in the serum were analyzed in the experiment.

RESULTS: Two different doses of CHM could significantly increase the area of the peritoneal lymphatic stomata, promote its distributive density and enhance the drainage of urinary ion such as sodium, potassium and chlorine. Meanwhile, the NO concentration of two different doses of CHM groups was $133.52 \pm 23.57 \mu\text{mol/L}$, and $137.2 \pm 26.79 \mu\text{mol/L}$ respectively. In comparison with the control group and model groups ($48.36 \pm 6.83 \mu\text{mol/L}$, and $35.22 \pm 8.94 \mu\text{mol/L}$, $P < 0.01$), there existed significantly marked difference, this made it clear that Chinese herbal medicine could induce high endogenous NO concentration. The effect of Chinese herbal medicine on the peritoneal lymphatic stomata and the drainage of urinary ion was altered by adding NO donor (sodium nitroprusside, SNP) or NO synthase (NOS) inhibitor (N(G)-monomethyl-L-arginine, L-NMMA) to the peritoneal cavity.

CONCLUSION: There existed correlations between high NO concentration and enlargement of the peritoneal lymphatic stomata, which result in enhanced drainage of ascites. These data supported the hypothesis that Chinese herbal medicine could regulate the peritoneal lymphatic stomata by accelerating the synthesis and release of endogenous NO.

Ding SP, Li JC, Xu J, Mao LG. Study on the mechanism of regulation on

peritoneal lymphatic stomata with Chinese herbal medicine. *World J Gastroenterol* 2002;8(1):188-192

INTRODUCTION

Numerous investigations have demonstrated that the peritoneal lymphatic stomata are small openings of the subperitoneal lymphatic vessels both in animals and in humans^[1-18]. It has also been observed that particles, cells and solutions containing vital dyes are absorbed rapidly by the peritoneal lymphatic stomata^[19-22]. Subsequent researches suggested that the peritoneal cavity is an integral part of the lymphatic system with enormous absorption powers, functioning primarily by means of the subperitoneal lymphatics via the peritoneal lymphatic stomata^[23-29]. Thus, it has important clinical implications, especially in ascites drainage^[30-32]. In recent years, therapeutic effect of Chinese herbal medicine (CHM) on the ascites has also drawn world wide attention among the scholars. It is further confirmed that Chinese herbal medicine can regulate the lymphatic stomata and promote the excretion of substance from the peritoneal cavity, which showed a good future in the treatment of the hepatocirrhosis with ascites^[33-44]. However, it is still unclear how the lymphatic stomata is regulated by the Chinese herbal medicine. This article aimed at the regulation of CHM on the lymphatic stomata in the mouse liver fibrosis model induced by CCl_4 , which provided theoretical evidence on ascites. Furthermore, by the application of NO donor (SNP) and NOS inhibitor (L-NMMA), the effect of NO was studied on the peritoneal lymphatic stomata in order to clarify the mechanism of CHM on the regulation of the peritoneal lymphatic stomata.

MATERIAL AND METHODS

Experimental CHM

By examining a computerized media index, the conventional remedies of CHM was selected for the treatment of hepatocirrhosis with ascites. The Chinese composite prescription was supplied by Zhejiang Academy of Traditional Chinese Medicine. The prescription consisted of *Radix Salviae Miltiorrhizae*, *Radix Codonopsis*, *Pilosulae*, *Rhizoma Atractylodis Alba* and *Rhizoma Alismatis*, *Leonurus Heterophyllus* Sweet. The medicament was immersed in the $750 \text{ mL} \cdot \text{L}^{-1}$ alcohol for 24 hrs, then purified with rotatory evaporator (ZFQ85A type, produced by Shanghai 11th Factory of Electron Tube). The crude drug content was $15.2 \text{ g} \cdot \text{mL}^{-1}$.

Animal and grouping

Ninety healthy mature NIH male mice, weighing 25g-30g, provided by the Experimental Animal Center of Zhejiang Academy of Medical Sciences, were selected and divided at random into six groups (each of 15 mice): the control group (NS group), model group, low dose of CHM group (CHM I), high dose of CHM group (CHM II), the donor group (DR group) and the inhibitor group (IR group).

Mouse liver fibrosis model

Except the NS group, the other experimental mice were fed freely with $50 \text{ mL} \cdot \text{L}^{-1}$ alcohol solution instead of water for 1 week, then the

mice were given 100ml·L⁻¹ CCl₄ rape-seed oil solution 0.1ml/10g by gastrogavage every 3 days for 6 weeks to induce liver fibrosis. After liver fibrosis was confirmed by pathological examination, low dose of the Chinese herbal medicine (0.1ml/10g/day) was given to CHM I group, high dose of the Chinese herbal medicine (0.2ml/10g/day) was give to CHMII group, normal saline (0.2ml/10g/day) was given to DR group, for 3 weeks respectively. After the 10th week, DR and IR group was additionally injected intraperitoneally with 50μg/10g/day NO donor (SNP) or 80μg/10g/day NOS inhibitor (L-NMMA) for two days respectively. Model group was untreated and NS group was given 0.2ml/10g of normal saline per day.

Preparation of samples for scanning electron microscopic examination and computer image processing

The diaphragmatic peritoneum on the right side was cut into 5.0×5.0 mm² pieces and put into 25ml·L⁻¹ glutaraldehyde solution for 1 h, then postfixed for 1h in 10ml·L⁻¹ OsO₄, dehydrated in a graded series of alcohol, CO₂ critical-point dried, mounted on aluminum tubs and sputter-coated with gold. Specimens were examined with a Stereoscan 260 SEM operated at 25kV. The result was treated with the computer image processing system attached to SEM. The system consists of video, A/D, IBM386. Software was designed for processing and quantitatively analyzing the area and the distributive density of the lymphatic stomata.

Urinary volume and ionic concentration analysis

Mouse urine was collected in 2 hrs and ionic concentration of Na⁺, K⁺ and Cl⁻ was measured using auto-biochemical analyzer (Beckman CX Δ7 type).

Measurement of serum NO

Five hundred microliters of the serum was de-proteinized with 200mL of 75mM zinc sulfate and 250mL of 55mM sodium hydroxid and subsequently were centrifuged at 3000rpm for 10min. One hundred microliters of the deproteinized solution was mixed with 0.3ml ddH₂O and 0.25g newly-activated Cadmium sufficiently for 1h. The nitrite concentration was determined by mixing 0.1ml of the supernatants from the mixed solution with an equal volume of Griess reagent (1 part of 0.2% N-(1-naphthyl) ethylenediamine dihydrochloride to 1 part of 1% sulfanilamide in 2% phosphoric acid) for 15min. The absorbance at 545 nm was measured, and the nitrite concentration was determined from a standard curve calibrated with NaNO₂ solution^[45].

Statistic analysis

The experimental results were described by $\bar{x} \pm s$ and the difference among the groups was analyzed by *t* test.

RESULTS

Changes of peritoneal lymphatic stomata

In SEM, there were cuboidal and flattened cells in the mesothelium. The lymphatic stomata which was round or ellipse were located only among the cuboidal cells and most of them were distributed in cluster. In NS group and model groups, there were few and small lymphatic stomata (Figures 1,2). In contrast, there were many and large lymphatic stomata in CHMI and CHMII groups (Figure3, 4). In DR group, there were fewer and larger lymphatic stomata than in the model group (Figure 5), while in the IR group fewer and smaller than that of the CHMII group (Figure 6).

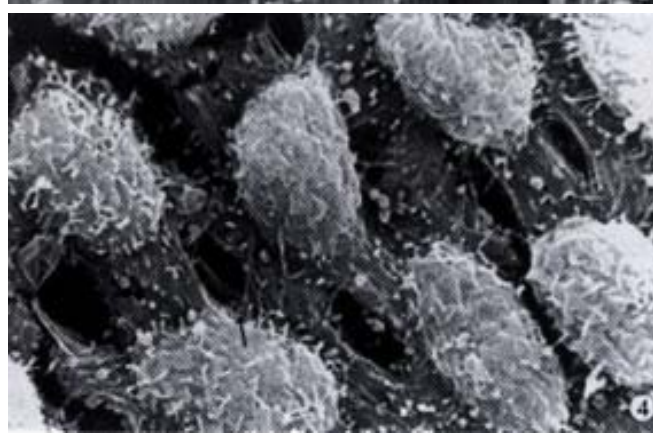
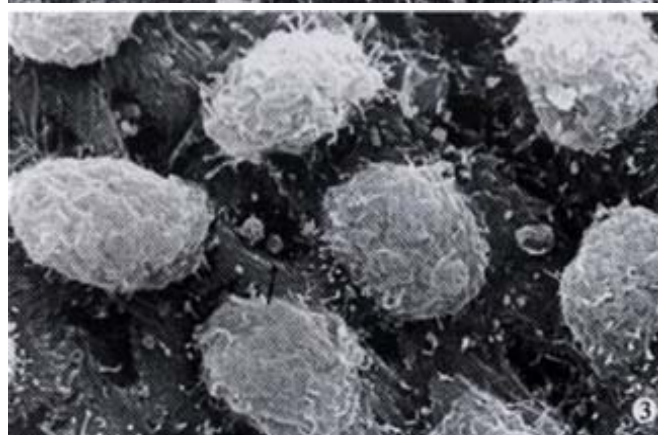
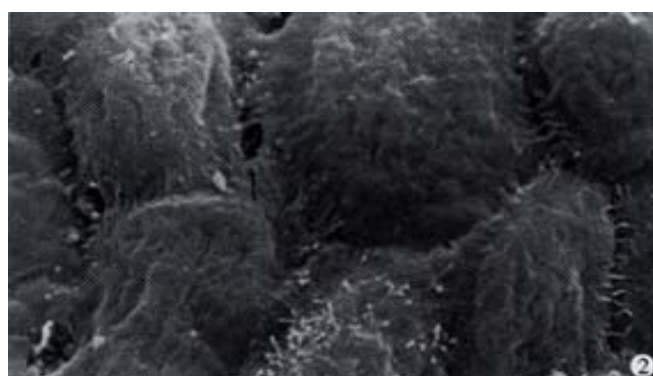
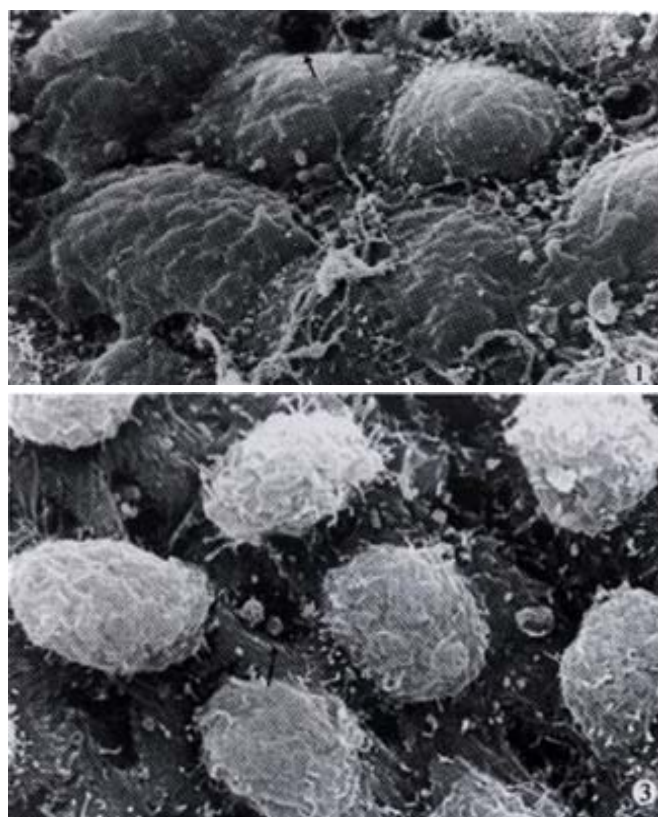


Figure 1 SEM observation of mouse diaphragmatic peritoneum in the control group. Both the area and distribution density of the peritoneal lymphatic stomata (arrow) are small. ×3500

Figure 2 SEM observation of mouse diaphragmatic peritoneum in model group showing the peritoneal stomata (arrow).×3500

Figure 3 SEM observation of mouse diaphragmatic peritoneum in CHMI group. The area and distribution density of the peritoneal lymphatic stomata (arrow) are significantly increased. ×3500

Figure 4 SEM observation of mouse diaphragmatic peritoneum in CHMII group. The area and distribution density of the peritoneal lymphatic stomata (arrow) are significantly increased. ×3500

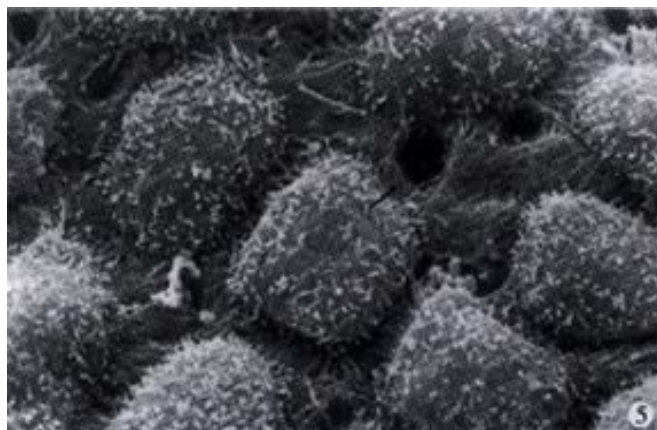


Figure 5 SEM observation of mouse diaphragmatic peritoneum in DR group. Compared with model group, the area and distribution density of the peritoneal lymphatic stomata (arrow) are relatively increased. $\times 3500$

Figure 6 SEM observation of mouse diaphragmatic peritoneum in IR group. Compared with CHMII group, the area and distribution density of the peritoneal lymphatic stomata (arrow) are relatively decreased. $\times 3500$

With image processing, the average area of the stomata was $3.59 \pm 1.29 \mu\text{m}^2$ in NS group and $3.02 \pm 1.11 \mu\text{m}^2$ in model group, whereas in CHMI group and CHMII group, the average area of the stomata was $5.89 \pm 0.33 \mu\text{m}^2$, and $5.93 \pm 1.87 \mu\text{m}^2$ respectively. There were significant differences in the enlargement of the stomata between CHMI and CHMII groups, based on the analysis of variance ($P < 0.01$). By comparing the area at the 99% confidence interval of population means, we found that the stomata area of CHMI and CHMII groups were much larger than those of NS and model groups (Table 1).

When the mouse was injected intraperitoneally by SNP, the average area of the stomata was $4.37 \pm 0.10 \mu\text{m}^2$, which was larger than that of the corresponding model group. When the mouse was injected intraperitoneally by L-NMMA, the average area of the stomata was $2.70 \pm 1.30 \mu\text{m}^2$, which was smaller than that of the corresponding CHMII group. These showed that the area of the stomata could be altered by SNP or L-NMMA significantly ($P < 0.05$ or $P < 0.01$).

Table 1 The influence of CHM, NO donor and NOS inhibitor ($n=15$) on the area of the lymphatic stomata

Groups	Mean (μm^2)	SD	Min. (μm^2)	Max. (μm^2)
NS	3.59	1.29	0.91	8.93
model group	3.02	1.11	1.83	7.53
CHMI ^{bd}	5.89	0.33	2.00	9.82
CHMII ^{bd}	5.93	1.87	2.08	10.15
DR ^c	4.37	0.10	1.92	8.70
IR ^f	2.70	1.30	1.75	9.19

^a $P < 0.05$, ^b $P < 0.01$, vs NS group; ^c $P < 0.05$, ^d $P < 0.01$, vs model group; ^e $P < 0.05$, ^f $P < 0.01$, vs CHMII group

The average distribution density of the stomata of NS group, and model group were $66.99 \pm 5.43/0.01\text{mm}^2$, $42.80 \pm 13.35/0.01\text{mm}^2$, whereas those of CHMI and CHMII group were $92.08 \pm 4.44/0.01\text{mm}^2$, and $96.24 \pm 4.62/0.01\text{mm}^2$ respectively. The results showed that CHM can promote the distribution density of the stomata significantly (Figure 7) ($P < 0.01$).

When the mouse was injected intraperitoneally by SNP, the average distribution density of the stomata was $79.06 \pm 5.37\text{mm}^2/0.01\text{mm}^2$, which was much higher than that of the corresponding model group. When the mouse was injected intraperitoneally by L-NMMA, the average distribution density of the stomata was $60.82 \pm 30.79\text{mm}^2/0.01\text{mm}^2$, which was much lower than that of the corresponding CHM group. The above statistics show that the distribution density of the stomata could be altered by SNP or L-

NMMA significantly ($P < 0.01$).

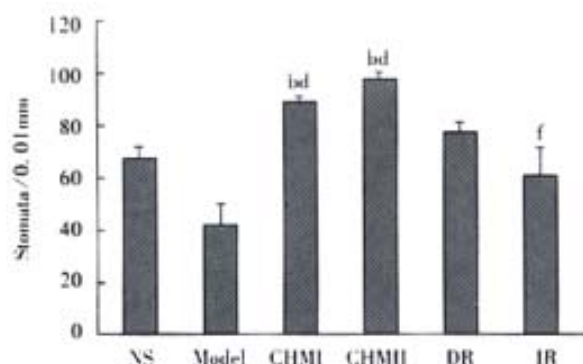


Figure 7 The influence of CHM, NO donor and NOS inhibitor on the distribution density of the lymphatic stomata.

Comparison of urinary ionic concentration

Subsequent experiment showed that the excretion of Na^+ , K^+ and Cl^- in CHMI and CHMII group was significantly higher than those in NS group and model groups respectively ($P < 0.01$) (Table 2).

When NO donor was injected intraperitoneally, the excretion of Na^+ , K^+ and Cl^- in DR group was significantly higher than those in the model group ($P < 0.05$ or $P < 0.01$). When NO inhibitor was injected intraperitoneally, the excretion of Na^+ , K^+ and Cl^- in IR group decreased significantly in comparison with the corresponding CHMII group ($P < 0.05$ or $P < 0.01$).

Table 2 The effect of CHM, NO donor, NOS inhibitor on the urinary ion of the mice (mmol/L, $n=15$)

Groups	Na^+	K^+	Cl^-
NS	91.55 ± 23.42	106.15 ± 34.16	111.18 ± 30.05
model group	97.48 ± 42.12	129.65 ± 46.91	121.90 ± 41.65
CHMI	$202.09 \pm 35.30^{\text{bd}}$	$217.30 \pm 57.78^{\text{bd}}$	$176.00 \pm 0.00^{\text{bc}}$
CHMII	$170.78 \pm 17.05^{\text{bd}}$	$210.11 \pm 51.49^{\text{bd}}$	$184.72 \pm 13.81^{\text{bd}}$
DR	$126.74 \pm 51.27^{\text{d}}$	$142.16 \pm 6.33^{\text{c}}$	$134.18 \pm 30.36^{\text{c}}$
IR	$139.28 \pm 26.02^{\text{f}}$	$88.29 \pm 22.59^{\text{f}}$	$154.98 \pm 14.88^{\text{e}}$

^a $P < 0.05$, ^b $P < 0.01$, vs NS group; ^c $P < 0.05$, ^d $P < 0.01$, vs model group; ^e $P < 0.05$, ^f $P < 0.01$, vs CHMII group

Comparison of NO concentration

There were significant difference in the concentration of NO between groups. The NO concentration of NS, model groups was $48.36 \pm$

6.83 $\mu\text{mol/L}$ and $35.22 \pm 8.94 \mu\text{mol/L}$ respectively, however that of CHMI and CHMII group was $133.52 \pm 23.57 \mu\text{mol/L}$ and $137.2 \pm 26.79 \mu\text{mol/L}$. The results showed that the concentration of NO in CHMI and CHMII groups was higher than that in NS and model groups ($P < 0.01$) (Figure 8). The results indicated that Chinese herbal medicine could induce higher endogenous NO. When NO donor was injected intraperitoneally, NO concentration in DR group was $62.56 \pm 18.91 \mu\text{mol/L}$, which was significantly higher than that in the model group ($P < 0.05$). When NO inhibitor was injected intraperitoneally, NO concentration in IR group was $99.88 \pm 21.03 \mu\text{mol/L}$, which decreased significantly as compared with that of CHMII group ($P < 0.01$).

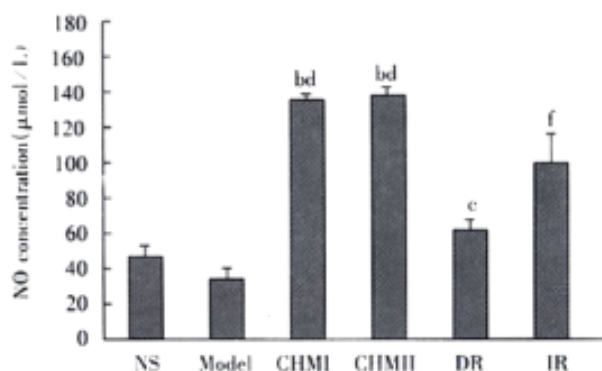


Figure 8 The change of NO concentration by using CHM, NO donor and NOS inhibitor in the mice.

DISCUSSION

In the mesothelial cells constituting the lymphatic stomata, there exists bundles of actin microfilaments, the contraction and relaxation of the microfilaments could result in the change of the diameter of the lymphatic stomata. Because the lymphatic stomata is the main pathway of the drainage of the material from the peritoneal cavity^[23-29], further investigation on regulating mechanism of the lymphatic stomata could promote the treatment of ascites and other associated illness.

With regard to the regulation of patency of the stomata, some authors have proposed that the peritoneal lymphatic stomata open passively when the diaphragm stretches during expiration, and close passively when it contracts during inspiration. Tsilibary and Wissig observed the regulation of the stomata by means of intravenously injecting carbacholine and succinylcholine, which cause the contraction and relaxation of the mouse diaphragm^[3]. Their experimental results showed that stomata opened and closed with drug-induced relaxation and contraction of the diaphragm. Changes of the intra-abdominal pressure also play an important role on the regulation of the peritoneal lymphatic stomata. When the intra-abdominal pressure is increased experimentally by injecting normal saline intraperitoneally, the amount of the peritoneal lymphatic stomata is much larger than that of the normal group. On the contrary, when the intra-abdominal pressure is decreased experimentally, the patent number of the peritoneal lymphatic stomata is much less than that of the normal group^[3].

Li *et al* and Lv *et al* further confirmed the effect of some Chinese herbal medicine such as Radix Salviae Miltiorrhizae, Radix Codonopsis Pilosulae, Rhizoma Atractylodis Alba and Rhizoma Alismatis in the regulation of the peritoneal lymphatic stomata significantly by increasing the average diameter and the average distribution densities respectively, which can enhance fluid drainage into the vascular system^[37-44]. This is of important clinical significance in treating ascites caused by liver cirrhosis. In the present study, the prescription is made up according to the traditional Chinese medicinal therapeutic principle in treating “hypocondriac pain”, “lump” and “tympanites”. The drug has the effects of activating blood

circulation to remove stasis, strengthening Spleen, supplementing Qi, and smoothening Qi to eliminate fullness. Our study showed that the CHM in the experiment could regulate the peritoneal lymphatic stomata significantly by increasing the average area and the average distribution densities respectively. Meanwhile, the medicines could enhance the drainage of urinary ion such as sodium, potassium and chlorine. The finding has further confirmed Li *et al*'s results^[37-39] and Lv *et al*'s results^[40-44].

It can also be seen that both dosage of CHM could induce higher concentration of NO, that is, the high endogenous NO production is associated with the enlargement of the peritoneal lymphatic stomata and the increase of the drainage of urinary ion. Further results indicated that great changes could occur in the area and the distribution density of the lymphatic stomata when the NO donor or NOS inhibitor was injected intraperitoneally. When NO donor was injected intraperitoneally, i.e., the concentration of the endogenous NO increased, the area and the distribution density of the lymphatic stomata in the NO donor group were much larger than those of the model group ($P < 0.05$ or $P < 0.01$). Moreover, when NO inhibitor was given, the concentration of the endogenous NO decreased, these indexes of the lymphatic stomata in NO inhibitor group were much less than those of the corresponding large dose of CHM ($P < 0.01$). Thus, it could be seen that the effect of CHM on the peritoneal lymphatic stomata was altered by adding NO donor or NOS inhibitor to the peritoneal cavity.

It has confirmed that the endothelium-derived relaxing factor (EDRF) is nitric oxide^[46-49], which has an effect in relaxing the blood vessel. Li *et al* reported that, with the proceeding of the peritoneal dialysis. Clinically, numerous macrophages were found to enter the peritoneal cavity to form milky spots. Damages of mesothelial cells, increased density of their distribution and enlargement of the peritoneal lymphatic stomata were found to be associated with the increase of macrophage NO quantity. Furthermore, increased NO production was related to the enlargement of the peritoneal lymphatic stomata in the long-term peritoneal dialysis. Therefore, Li *et al* proposed that NO could relax the lymphatic stomata which lead to the enhanced lymph absorption or ultrafiltration failure^[50]. On these grounds, we suggested that the regulation of CHM on the lymphatic stomata may be related to endogenous NO. Chinese herbal medicine may regulate the lymphatic stomata by accelerating the synthesis and release of endogenous NO. Nitric oxide as an endothelium-derived relaxing factor, mediates its biological effects by activating soluble guanylyl cyclase and increasing cyclic GMP synthesis from GTP and decreasing the concentration of Ca^{2+} . These reactions result in the strong relaxation of the lymphatic stomata, with the area and the distribution densities of the lymphatic stomata enlarged, which would lead to the drainage of ascites from the peritoneal cavity.

REFERENCES

- 1 Leak LV, Rahil K. Permeability of the diaphragmatic mesothelium: the ultrastructural basis for stomata. *Am J Anat* 1978;151:557-593
- 2 Tsilibary EC, Wissig SL. Absorption from the peritoneal cavity: SEM study of the mesothelium covering the peritoneal surface of the muscular portion of the diaphragm. *Am J Anat* 1977;149:127-133
- 3 Tsilibary EC, Wissig SL. Lymphatic absorption from the peritoneal cavity: regulation of patency of mesothelial stomata. *Microvasc Res* 1983;25:22-39
- 4 Tsilibary EC, Wissig SL. Light and electron microscope observation of the lymphatic drainage units of the peritoneal cavity of rodents. *Am J Anat* 1987;180:195-207
- 5 Li JC, Yu SM. Ultrastructural study on the peritoneal stomata in human fetuses. *Jiepo Xuebao* 1990;21:359-361
- 6 Li JC, Yu SM. Study on the ultrastructure of the peritoneal stomata in humans. *Acta Anat* 1991;141:26-30
- 7 Li JC. Electron microscopic study of mesothelial cells in the diaphragm peritoneum of human fetus using the freeze-fracture replica method. *Zhongguo Yixue Kexueyuan Xuebao* 1991;13:189-194
- 8 Li JC. A scanning electron microscopic study on capillary configuration of

- human diaphragmatic peritoneum. *Keji Tongbao* 1992;8:57-61
- 9 Li JC, Chen XB. Study of the human peritoneal stomata and its clinical significance. *Zhonghua Shiyian Waikexue* 1992;9:38-39
 - 10 Li JC, Gao YS, Yong TW. Study on the pelvic stomata and computer image processing. *Zhongguo Yixue Kexueyuan Xuebao* 1994;16:264-269
 - 11 Li JC, Gao YS. The study of quantitative image processing on the ultrastructure of the pelvic stomata in humans. XVIIIth meeting of the European group of lymphology, Belgium, Brussels, 1994: Abstracts
 - 12 Li JC, Zhao ZR, Gao YS, Zhou JL. Study on human pelvic stomata by using the self-made SEM image processing system. *Zhonghua Wuli Yixue Zazhi* 1995;17:104-106
 - 13 Li JC, Zhou JL, Gao YS. The ultrastructure and computer imaging of the lymphatic stomata in the human pelvic peritoneum. *Ann Anat* 1997;179:215-220
 - 14 Li JC, Lv ZL, Shi YH, Shen Y, Yu SM. Experimental study on the peritoneal stomata. *Zhongguo Zhongyi Jichu Yixue Zazhi* 1998;4:20
 - 15 Gao YS, Li JC, Xu LS, Qian BQ. A SEM image processing system and its application in peritoneal stomata study. *Shengwu Yixue Gongchengxue Zazhi* 1993;10:239-243
 - 16 Azzali G. The lymphatic vessels and the so-called "lymphatic stomata" of the diaphragm: A morphologic ultrastructural and three-dimensional study. *Microvasc Res* 1999;57:30-40
 - 17 Fukuo Y, Shinohara H, Matsuda T. The distribution of lymphatic stomata in the diaphragm of the golden hamster. *Anat Rec* 1990;169:13-21
 - 18 Negrini D, Mukenge S, Del Fabbro M, Gonano C, Miserocchi G. Distribution of diaphragmatic stomata. *J Appl Physiol* 1991;70:1544-1549
 - 19 Bettendorf U. Lymph flow mechanism of the subperitoneal diaphragmatic lymphatics. *Lymphology* 1978;11:111-116
 - 20 Mahedero G, Moran JM, Salas J. Absorption of intralipid and interferences from nutrients infused into the peritoneal cavity of the rat. *Am J Surg* 1992;164:45-50
 - 21 Marco AJ, Domingo M, Ruberte J, Carretero A, Briones V, Dominguez L. Lymphatic drainage of listeria monocytogenes and Indian ink inoculated in the peritoneal cavity of the mouse. *Lab Animals* 1992;26:200-205
 - 22 Negrini D, Mukenge S, Del Fabbro M, Gonano C. Distribution of diaphragmatic lymphatic lacunae. *J Appl Physiol* 1992;72:1166-1172
 - 23 Li JC, Shi YH, Chen XB, Yu SM. Study on the peritoneal stomata and absorptive mechanism of ascites. *Zhongguo Yixue Kexueyuan Xuebao* 1992;14:328-333
 - 24 Li JC, Jiang BY. A scanning electron microscopic study on three-dimensional organization of human diaphragmatic lymphatics. *Functional and Developmental Morphology* 1993;3:129-131
 - 25 Li JC, Jiang BY. Studies on three-dimensional configuration of diaphragmatic lymphatics and absorptive mechanism of lymph from the peritoneal cavity. *Zhongguo Yixue Kexueyuan Xuebao* 1994;16:183-187
 - 26 Li JC, Chen XB, Zhang CW, Zhou LJ, Yu SM. Ultrastructural study on human lymphatic drainage units in peritoneal stomata of human. *Jiepo Xuebao* 1995;26:101-104
 - 27 Li JC, Shen Y, Gao YS, Yong TW. Quantitative study of a SEM image processing system on the absorptive mesothelium of the diaphragmatic peritoneum. *Zhongguo Yixue Kexueyuan Xuebao* 1995;17:264-268
 - 28 Li JC, Zhao ZR, Zhou JL, Yu SM. A study of three-dimensional organization of the human diaphragmatic lymphatic lacunae and lymphatic drainage units. *Ann Anat* 1996;178:537-544
 - 29 Li JC, Chen XB, Yu SM. The ultrastructure of vesicle-containing cells and ER-cells of human peritoneum. *Ann Anat* 1996;178:365-367
 - 30 Khoroshaev VA, Vorozheikin VM, Baibekov IM. Routes of resorption of peritoneal fluid in the diaphragm in liver cirrhosis (morphologic study). *Arkh Patol* 1991;53:40-44
 - 31 Hasbargen JA, Hasbargen BJ, Fortenberry EJ. Effect of intraperitoneal neostigmine on peritoneal transport characteristics in CAPD. *Kidney Int* 1992;42:1398-1400
 - 32 Li JC, Yu SM. Study on the relation between the peritoneal stomata and net ultrafiltration in CAPD. *Zhonghua Shenjangbing Zazhi* 1994;10:49-52
 - 33 Zhang B, Wang LT. The cytological mechanism of Chinese herbal medicines in antagonizing liver fibrosis. *Zhongxiyi Jiehe Ganbing Zazhi* 1997;7:249-252
 - 34 Li J, Li YH, Xue LC, Wu CZ. Protective effect of Tanshinone on experimental damage of hepatocytes. *Zhongxiyi Jiehe Ganbing Zazhi* 1996;6:29-30
 - 35 Aiza I, Perez GO, Schiff ER. Management of ascites in patients with chronic liver disease. *Am J Gastroenterol* 1994;89:1994-1996
 - 36 Zhao JP, Yuan SH, Li JC, Liu JD. Advances in the treatment of cirrhosis. *Yixue Zongshu* 1999;5:477-479
 - 37 Li JC, Lv ZL, Wu NP, Zhou JL, Shi YH. A scanning electron microscopy and computer image processing morphometric study of the pharmacological regulation of patency of the peritoneal stomata. *Ann Anat* 1996;178:443-447
 - 38 Li JC, Lv ZL, Shi YH, Shen Y, Chen YF. Study on pharmacological regulation of the peritoneal stomata and its computer image processing. *Zhongguo Yixue Kexueyuan Xuebao* 1996;18:219-223
 - 39 Li JC, Ding WY, Shen Y, Shi YH, Zhong HL, Yu SM, Lv ZL. The influence of Chinese herbal medicines on the peritoneal lymphatic stomata in the mice. *Zhongguo Bingli Shengli Zazhi* 1999;15:414
 - 40 Lv ZL, Li JC. The influence of Chinese herbal medicines for diuresis on the peritoneal stomata in mice. *Zhongxiyi Jiehe Ganbing Zazhi* 1996;6:31-32
 - 41 Lv ZL, Li JC, Shi YH, Chen HM. The mechanism of Jianpi-yiqi Chinese herbal medicine treating the cirrhosis. *Zhongyao Yaoli Yu Linchuang* 1996;11-12
 - 42 Lv ZL, Li JC. The mechanism of Chinese herbal medicine for blood circulation to eliminate turbid in curing ascites: observation on the regulation of red sage root on the peritoneal lymphatic stomata. *Shiyong Zhongxiyi Jiehe Zazhi* 1996;9:1147-1148
 - 43 Lv ZL, Li JC, Shi YH, Chen HM. Experimental observation on the regulation of Chinese herbal medicine on the peritoneal lymphatic stomata. *Zhongyi Zazhi* 1996;37:560-561
 - 44 Lv ZL, Li JC. Experimental study on the regulation of Chinese herbal medicine for diuresis to dispel tympanites on the peritoneal lymphatic stomata of the mouse. *Zhongguo Zhongxiyi Jiehe Zazhi* 1997;17:199-200
 - 45 Mao HM. Determination of nitrate in serum by a copper-coated cadmium reduction method. *Linchuang Jianyan Zazhi* 1995;13:6-8
 - 46 Murad F. Discovery of some of the biological effects of nitric oxide and its role in cell signaling (Nobel Lecture). *Angew Chem Int Ed* 1999;38:1856-1868
 - 47 Yu J, Guo F, Ebert MPA, Malfertheiner P. Expression of inducible nitric oxide synthase in human gastric cancer. *World J Gastroenterol* 1999;5:430-431
 - 48 Huang YQ, Xiao SD, Zhang DZ, Mo JZ. Nitric oxide synthase distribution in esophageal mucosa and hemodynamic changes in rats with cirrhosis. *World J Gastroenterol* 1999;5:213-216
 - 49 Peng X, Feng JB, Wang SL. Distribution of nitric oxide synthase in stomach wall in rats. *World J Gastroenterol* 1999;5:92
 - 50 Li JC, Zhang K, Yang ZR. Effects of peritoneal dialysis on macrophage nitric oxide production and its relation with peritoneal lymphatic stomata. *Shenzangbing Yu Touxishen Yizhi Zazhi* 2000;9:13-17

• REVIEW •

Early diagnosis for colorectal cancer in China

Ya-Li Zhang, Zhen-Su Zhang, Ba-Ping Wu, Dian-Yuan Zhou

Ya-Li Zhang, Zhen-Su Zhang, Ba-Ping Wu, Dian-Yuan Zhou, PLA Institute for Digestive Diseases, Nanfang Hospital, The First Medical University of PLA, Guangzhou 510515, Guangdong Province, China
Supported by Key University Teacher Funds by the Ministry of Education
Correspondence to: Dr. Ya-Li Zhang, PLA Institute for Digestive Diseases, Nanfang Hospital, Guangzhou 510515, China. zhangyl@fimmu.edu.cn

Telephone: +86-20-85141544

Received 2001-03-05 Accepted 2001-06-25

Abstract

AIM: To review the present studies on early diagnosis of colorectal cancer.

METHODS: The detective rate for early cancer is 1.7%-26.1% based on various statistical data, with much higher detective rate in endoscopy. Since early cancer means invasion involved in the mucosa or submucosa, the diagnosis can only be made when the invasive depth is identified. Pathological tissue materials from both surgical operation or endoscopic resection are suitable for early cancer evaluation.

RESULTS: Incidence of polyp malignancy is 1.4%~20.4%. The various constitutive proportion of polyps may explain the different rates. Malignant incidence is higher in adenomatous polyps, that for villous polyps can reach 21.3%-58.3%. Type II early stage of colorectal carcinoma is rarely reported in China. It is showed that majority of them were not malignant, most of type IIa being adenoma or hyperplasia, and IIb being inflammatory and IIc might be the isolated ulcers. The occurrence of malignancy of type II is far lower than that of polypoid lesion. In China, the qualitative diagnosis and classification of neoplasm generally adopted the WHO standard, including surgical excision or biopsies. There is impersonal evaluation between colorectal pre-malignancy and cancer. The former emphasizes the dysplasia of nuclei and gland, while the latter is marked with cancer invasion. Diagnosis of early stage colorectal cancer in endoscopy is made with too much caution which made the detective rate much lower. Mass screening for asymptomatic subjects and follow-up for high risk population are mainly used to find the early stage colorectal cancer in China. Fecal occult blood test is also widely made as primary screening test, galactose oxygenase test of rectal mucus (T antigen), fecal occult albumin test are also used. The detective rate of colorectal cancer is 24-36.5 per 105 mass population.

CONCLUSION: Although carcinoma associated antigen in blood or stool, microsatellite DNA instability for high risk familial history, molecular biology technology for stool oncogene or antioncogene, telomerase activity and exfoliative cytological examination for tumor marker, are utilized, none of them is used in mass screening by now.

Zhang YL, Zhang ZS, Wu BP, Zhou DY. Early diagnosis for colorectal cancer in China. World J Gastroenterol 2002;8(1):21-25

INTRODUCTION

The colorectal cancer is one of the most common malignant tumors which threatens the people's health^[1-3]. The occurrence of colorectal cancer has been rising over the past 3 decades. At present, the colorectal cancer is the second cause of death in western countries, and the forth in China^[4,5]. It is clear that the prognosis of colorectal cancer is related to early diagnosis^[6-8]. For instance, the five-year survival after operation of colorectal cancer, diagnosed in early stage, is over 80%, but in the advanced stage it is lower than 40%. So, it is very important to improve the colorectal cancer's prognosis by means of early diagnosis^[9-13]. Recently, much attention has been paid to early detection for colorectal cancer in China. The popularity of the colonoscopy and the mass screening for colorectal cancer in the population who have no symptoms has raised the rate of the early diagnosis of colorectal cancer greatly. However, the study and progress vary among regions in the country, and there are also misdiagnoses. This paper reviews the present study of early diagnosis of colorectal cancer in China.

THE DETECTIVE RATE OF EARLY STAGE COLORECTAL CANCER IN CHINA

At present, the data of detective rate for early stage colorectal cancer are not perfect, and the detective rate is 1.7%-26.1%, based on various reports (Table 1)^[14-20]. The major reason for the different rate is the various statistical data. In virtue of the endoscopy popularity, the early stage of cancers are detected increasingly. Most of them can be treated by non-surgically. So, there are great differences between the endoscopic and the surgical data. For example, 997 cases of colorectal cancer were treated surgically during 1990-1999 in Nan Fang Hospital, 21 cases are in early stage (2.1%), while 1087 cases of colorectal cancer were found from 20 353 colonoscoped cases during the corresponding period, in which, 146 early stage of cancers were identified (13.4%). Because most of early cancers are polyps-like and easy to be resected under endoscopy, the percentage of early stage cancer in surgical samples is low.

Table 1 The detective rate for early stage of colorectal cancer in China

Authors	Colorectal cancer		
	Total n	Early stage n (%)	Year
Lu <i>et al</i> ^[14]	569	85(15.1)	1997
Ni <i>et al</i> ^[15]	132	15(11.4)	1997
Yang <i>et al</i> ^[16]	721	65(22.9)	1997
NI <i>et al</i> ^[17]	296	32(10.8)	1997
Cai <i>et al</i> ^[18]	1058	59(5.6)	1999
Zeng <i>et al</i> ^[19]	300	5(1.7)	1996
Sun <i>et al</i> ^[20]	180	47(26.1)	1998

MORPHOLOGY OF EARLY STAGE COLORECTAL CANCER UNDER ENDOSCOPY

There are two types of early colorectal cancer based on the morphological classification under endoscopy. Type I also called protruded or polyps type, can be further grouped as pedunculated (Ip), subpedunculated (Isp) and sessile (Is) superficial type. Type II can be classified as elevated (IIa), flat (IIb) and depressed (with or without protruded)^[6,19]. Since early cancer means invasion involving the mucosa or submucosa, which is not related to the tumor size or special morphology, the diagnosis only can be

made when the invasive depth is identified. Pathological tissues from both surgical operation and endoscopic resection are suitable for early cancer evaluation. It is important that early cancer diagnosis can not be made based on the endoscopic biopsy since invasion is not observed.

Histopathological examination of polyps under endoscopy is a crucial method to detect early cancer in China, and most of them are polyp malignancy^[9,14,21,22]. Generally, polyp formation is mostly involved in the proliferation of mucosa and submucosal tissues. As long as cancerous tissues do not touch upon pedicle, they can attribute to early-stage carcinoma. If pedicle of polyp invasion in colorectal cancer can not be observed for incomplete resection or embedded in the wrong direction, diagnosis of early-stage carcinoma can not be made rashly. Incidence of polyp malignant transformation is 1.4%-20.4% (Table 2). Different result may be from various constitutive proportion of polyps. Malignant incidence is high in adenomatous polyps. In villous polyps, it can reach 21.3%-58.3% according to the documents in China^[23-31]. Moreover, as some adenomatous ingredient are observed by biopsy, some advanced colorectal cancers are diagnosed as polyp malignancy by pathologists. This kind of lesions can not be included in the early-stage carcinoma. In our previous study, 87/127 (68.6%) advanced colorectal carcinoma had residual of adenoma.

Table 2 The malignant transformation rate of polyps in China

Authors	Area	n	Incidence (%)
Zhou <i>et al</i> ^[22]	Guangzhou	539	3.4
Cai <i>et al</i> ^[23]	Guangzhou	216	9.7
Zhang <i>et al</i> ^[24]	Changchun	2000	5.1
Shen <i>et al</i> ^[25]	Kunming	533	6.4
Zhu <i>et al</i> ^[26]	Beijing	219	1.4
Zhu <i>et al</i> ^[27]	Nanjing	644	5.8
Wang <i>et al</i> ^[28]	Xi'an	548	9.7
Zhang <i>et al</i> ^[29]	Zhejiang	321	14.6
Zhang <i>et al</i> ^[30]	Ha-erbing	494	20.4
Gao <i>et al</i> ^[31]	Shanghai	334	6.6

Type II early stage of colorectal carcinoma is rarely reported in China. Huang *et al* first summarized 6304 patients detected by colonoscopy from 1974 to 1996 in a hospital of Beijing^[32], only 36 Type II lesions were discovered, including 31 (86.1%) type IIa, 4 (11.1%) type IIb and 1 (7%) type IIc. Thirty-two tubular adenomas, 3 villous adenoma and 1 carcinoid were confirmed by histopathological examination. Only one case was identified as malignancy by follow-up.

In 137 cases of early stage colorectal cancer detected in Nanfang Hospital from 1990 to 1999, 95.6% were polypoid type, only 6 cases were considered as type II (4.4%) (Table 3). We also analyzed the histopathological features of 186 cases of type II lesions, only 3.2% were diagnosed as early stage carcinoma (Table 4). It indicated that the majority of so-called type II cancer under endoscopy were not real malignancy. Most of type IIa were adenoma or hyperplasia polyps, and most of type IIb were inflammatory changes of mucosa. A large number of type IIc cases might be the isolated ulcers. The occurrence of malignancy of type II is far lower than that of polypoid lesion.

Table 3 Morphology of 137 cases of early stage colorectal cancer under endoscopy

Morphology	Type	n	Ratio
Polypoid	I	131	95.6
Elevated	IIa	2	1.4
Flat	IIb	1	0.7
Depressed	IIc or IIc+IIa	3	2.3

Table 4 Histopathology of 186 cases of type II lesion

Morphology	Type	n (%)	Histopathologic diagnosis		
			Early cancer	Adenoma	Other
Elevated	IIa	155 (83.3)	2 (1.3)	86 (55.4)	67 (43.3)
Flat	IIb	22 (11.8)	1 (4.5)	2 (9.00)	19 (86.4)
Depressed	IIc or IIc+IIa	9 (4.8)	3 (33.3)	4 (44.4)	2 (22.2)

THE DIAGNOSTIC STANDARD FOR EARLY STAGE OF COLORECTAL CANCER

In China, the qualitative diagnosis and classification of neoplasm generally adopted the WHO standard for both surgical excision and biopsies^[17,33]. The evaluation is objective between colorectal pre-malignancy and cancer. The former emphasizes the dysplasia of nuclei and gland, while the latter is marked with cancer invasion^[34-37]. Although pathologists hold different opinions about the classification of dysplasia, it could be classified generally into 3 grades. The simplest classification depends on the ratio of dysplasia karyon in epithelium. Mild dysplasia indicates the crowding nuclei limited within 1/2 depth of epithelium in basement, moderate dysplasia means that atypical nuclei occupied more than 1/2 epithelium, and severe dysplasia refers to the atypical nuclei occupying the whole epithelium with integrated basement. The essential difference between dysplasia and malignancy is invasion. The malignancy is manifested by the destroyed basement, and sporadic dysplasia glands. It is called intra-mucosal cancer if the cancer cell invasion limited within the mucosa. If the cancer destroyed mucosal muscle into submucosa, it is called sub-mucosal cancer. These two types are generally designated as early stage cancer. From the literature reviews, we found that the diagnosis of early stage colorectal cancer in China is made with much cautions under endoscopy. On the one hand, pathologic diagnosis generally adopted the WHO standard, which depends on the invasion, and sometimes it is difficult to observe the invasion on biopsy sections. On the other hand, patients always feel panic to cancer, once the colorectal cancer is diagnosed, they would rather choose surgical operation than endoscopic resection. Besides, they often require consultation of the pathological sections, if diagnostic standard is different, this may cause the psychological pressure to the pathologic doctors in different regions.

In European countries, colorectal cancer is the most common malignant tumor of digestive tract. But the diagnostic rate of early cancer is usually reported less than 9%. In Japan, the diagnostic rate of early stage of cancer detected by endoscopy is 17%-53%. The cases of early stage cancer reported in China is the same as in European countries but far lower than in Japan^[14-20]. Schlemper RJ *et al* compared the differences in pathological diagnosis of early carcinoma from stripping or surgically resected specimens of colonic mucosa between Japan and Europe-America^[34]. It was found that 4 cancer cases were diagnosed by Japanese pathologists in 11 adenoma with mild dysplasia based on European-American standard. This is because Japanese pathologists emphasize the nuclei dysplasia and gland structural change evaluating malignancy^[37], but pathologists in China usually take above changes as markers of pre-malignancy.

DETECTION FOR EARLY STAGE OF COLORECTAL CANCER

Mass screening for asymptomatic subjects and follow-up for high risk population are the major ways to find the early stage of colorectal cancer in China^[38-42]. High risk factors are old age, histories of colorectal polyps, familial history of cancer and some colorectal related positive tests^[43-51]. Since mass screening for asymptomatic population need a large amount of work, and exact diagnosis must depend on endoscopic and histopathological examination, screening test has been paid much attention. So far, fecal occult blood test is widely used as primary screening test in China^[52-55]. Other screening tests include galactose oxygenase

test of rectal mucus(T antigen)^[56-60], and fecal occult albumin test^[61,62]. If the screening tests appear positive, colonoscopy is then taken. Although carcinoma associated antigen in blood or stool^[63-81], microsatellite DNA instability for high risk familial history^[82-86], molecular biology technology for stool oncogene or antioncogene^[87-99], telomerase activity^[100-104] and exfoliative cytological examination^[105,107] have been used for tumor marker, none of them is used in mass screening.

There are some excellent work reported in China on mass screening for colorectal cancer. Most of them are based on immune fecal occult blood test(Table 5)^[54,55,62]. In mass screening (age above 35 years), the occurrence of colorectal cancer is 24-36 per 10⁵ population.

Table 5 Mass screening for colorectal cancer in asymptomatic population

Authors	Region	Age(yrs)	Population	Cancer	Dukers(%) A/B	Detection rate
Li <i>et al</i>	North	>35	102 800	25	52.0	24/10 ⁵
Zhen <i>et al</i>	East	>35	62 667	16	57.2	25.5/10 ⁵
Zhou <i>et al</i>	Mid-south	>45	24 677	9	55.6	36.5/10 ⁵

Tantigen detection in rectal mucus is also used in some mass screenings^[57-60,108,109]. In 3820 asymptomatic population, the positive rate of T antigen is 9.1%, among them, 2 cases of early cancer and 28 cases of adenoma were identified. The detective rate of pathologic change is 12.7%. It is shown that T antigen test is not specific for colorectal examination. In 103 cases of T antigen positive subjects, 85 cases were found without any lesion under colonoscopy. The sensitivity is not better than that of feces occult blood examination^[110-114].

Since screening tests used so far are not specific for colorectal detection, there are some misdiagnoses either by feces occult blood examination or rectal mucous T antigen test. To improve the detective rate of the early stage cancer, it is suggested that combined complementary screening should be taken. Zhejiang University School of Medicine optimized the screening protocol for colorectal cancer among a high-incidence population^[113]. Through increasing the cases for colonoscopy follow-up, the detective rate of early cancer was increased. Beijing General Hospital reported that by combined test of sequential fecal occult blood and albumin in the screening of colorectal neoplasma, 3 cases of carcinoma were found from 883 positive asymptomatic subjects^[114]. The Nanfang Hospital recommended the complementary schemes by combining occult blood and T antigen detection. In 5 cases of colorectal cancer, which were found by colonoscopy in 2832 asymptomatic subjects, 3 were positive in feces occult blood examination and 2 in T antigen test. The missed cases will be reduced if complementary screening was taken^[13]. Our study showed that the mass screening can reduce the colorectal occurrence(Table 6)^[113].

FUTURE STUDY IN EARLY DIAGNOSIS FOR COLORECTAL CANCER

It is definite that asymptomatic mass screening is the important way to identify the early cancer. Because of the poor specificity of screening test, and the high cost, it is difficult to popularize. Target screening will be highlighted. In 1992, Sidransky *et al* first extracted DNA successfully from feces and reported ras gene variation with Southern-Blot^[116]. It is considered an effective screening for colorectal cancer in the 21st century. PCR-SSCP technology has a high sensitivity, good specificity and easy manipulation. Gene mutation such as P53, ras, c-erbB-2, APC and MCC was identified in feces

(Table 7)^[94-96,117,118]. Since no specific gene mutation is found in colorectal cases, the detective rate by molecular technique is low. Though combined genes detection can enhance the screening rate, it is too complex and expensive.

Table 6 The follow-up results in 3,641 cases of asymptomatic population

	Cancer (n)	Adenoma	
		n	>1.0 cm Dysplasia(>II grade)
First screen	4	48	17(35.4%) 12(25.0%)
Two years later	0	18	4(22.2%) 2(11.1%)

Table 7 Gene mutation analysis in colorectal cancer stool (Nanfang Hospital)

Gene	n	Tissue DNA		Fecal DNA	
		Positive	%	Positive	%
APC	41	20	48.8	14	34.1
MCC	45	13	28.9	11	24.4
P53	32	32	37.5	10	31.3

Analysis of gene offers possibility and practical significance for detecting high risk population. For example, HNPCC generally represents the microsatellite DNA instability and characteristic DNA mismatch repair gene. Therefore, detecting MIN and DNA mismatch repair gene may identify some high risk population with cancer familial predisposition^[119-122]. We analyzed 46 cases of colorectal carcinoma for MIN, and found 14 cases of MIN positive patients, 12 of them with familial predisposition (85.7%). It is suggested that MIN might reflect colorectal carcinoma with familial predisposition in some extent.

REFERENCES

- Zhang YL, Nie J, Zhou J, Guo W, Guan CP, Zhou DY. Incidence and geographical features of colorectal cancer in patients under 30 years of age in china. *Zhonghua Xiaohua Neijing Zazhi* 1997;14:11-14
- Zhang ZS, Zhang YL. Progress in research of colorectal cancer in China. *Shijie Huaren Xiaohua Zazhi* 2001;9:489-494
- Wang SH, Zheng YQ. A clinicopathologic analysis of 354 cases of large intestinal cancer in western Hunan. *Xin Xiaohuabingxue Zazhi* 1996;4:325-326
- Jing F, Zhou SZ, Tao YF, Fang RY, Xiang YB, Shun L, Gao YT. Cancer incidence trend in Shanghai 1972-1994. *Zhongliu* 1999;19:255-258
- Yu JP, Dong WG. Current situation about early diagnosis of cancer of large intestine. *Shijie Huaren Xiaohua Zazhi* 1999;7:553-554
- Li GY, Lu YM, Chen FL, Gong JZ. Current situation about diagnosis and treatment of early colorectal cancer. *Huaren Xiaohua Zazhi* 1998; 6: 377-382
- Zhang Y. Guwai Yixue. Advances of diagnosis and treatment of early colorectal cancer. *Zhongliuxue Fengzhe* 1999; 26: 114-118
- Xiao XW. The value of selective chemoembolization in the treatment of hepatometastases in colorectal carcinoma. *World J Gastroenterol* 1998;4(Suppl 2):38-41
- Jia XD, Han C. Chemoprevention of tea on colorectal cancer induced by dimethylhydrazine in Wistar rats. *World J Gastroenterol* 2000;6: 699-703
- Feng FC, Zhang YL. Canceration and endoscope treament of large intestine polys. *Zhongguo Shiyong Neike Zazhi* 1996;16: 390-392
- Sheng J, Zhang ZZ, Mo SJ, Liu SY, Wang YL. Endoscopic diagnosis and therapy for early colorectal cancer. *Zhonghua Xiaohua Neijing Zazhi* 1998; 15: 297-298
- Cheng FQ, Du H, Zhu C, Jiang H, Wang HZ, Liu SY. Endoscopic diagnosis and therapy for early colorectal cancer: report of 63 cases. *Zhonghua Xiaohua Neijing Zazhi* 1998; 15: 94-96
- Zhou DY, Feng FC, Zhang YL, Lai ZS. Study on combination mass screening protocol for colorectal cancer. *Zhonghua Neijing Zazhi* 1994; 33:367-369
- Lu YM, Gu F, Lin SR, Zhu ZM. Significance of clinical screening colonoscopy and colonoscopic polypectomy with pathology in diagnosis of early colon cancer. *Zhonghua Xiaohua Neijing Zazhi* 1997; 14: 222-224
- Ni PY, Qu HT. Summary of five years follow up colonoscopy on patients with colorectal polyps and cancer. *Zhongguo Neijing Zazhi* 1997; 3: 1-2
- Yang YX, Li HB, Liu FS, Zhu XD, Zhang YR, Li XL, Xu QX. Preliminary approach of the relationship between colorectal polyps and

- carcinoma:analysis to 2,237 cases. *Zhongguo Neijing Zazhi* 1997; 3: 17-18
- 17 Zhang YL. The diagnosis standard of endoscopic biopsy for colorectal cancer. *Zhonghua Xiaohua Neijing Zazhi* 2001; 18: 135-138
 - 18 Cai BY, Yu DY, Wang Y, Gong BQ, Ma B. The clinical pathological analysis of 1058 cases of colon carcinoma. *Qiqihaer Yixueyuan Xuebao* 1999; 20: 5-6
 - 19 Zeng XJ, Guo RD, Guo PC. A Clinical Analuses of 300 Cases of Carcinoma of the Large Intestine. *Fujian Yiyao Zazhi* 1996;18:13-15
 - 20 Shun CJ, Yao Q, Xu JZ, Yu BM. Detection of early large intestine cancer during clinical symptomatic inspection: clinical and pathological characteristics. *Zhongliu* 1998; 18: 49-51
 - 21 Zhang YL. Canceration and endoscope biopsy diagnosis of large intestine polys. *Zhonghua Xiaohua Neijing Zazhi* 1999;16:188-200
 - 22 Zhou DY, Zhang YC, Zhang YL, Feng HC, Hu Q, Xiao GS. Study on anaplasia potentiality of colorectal adenoma. An analysis of 611 adenomas by endoscope biopsy. *Zhongguo Guangdian Yixue Zazhi* 1992; 1:166-169
 - 23 Cai KY, Huang SZ, Yu XB, Yu JP. An analysis of follow up colonoscopy on 216 aged patients with colorectal polyps. *Fubu Waikes* 2000; 13: 105-106
 - 24 Zhang B, Zhen YG, Zhang DH. The clinical pathological features of colorectal polyps by colonoscope management in 2000 cases. *Zhongguo Shiyong Waikes Zazhi* 1999; 19: 661-662
 - 25 Sheng LJ, Feng SZ, Zhang L, Pu P. Pathological analysis of 533 cases of large bowel polyps. *Yunnan Yiyao* 1995; 16: 267-268
 - 26 Zu C, Zhang JP, Zhang ZQ, Zhao DH. Treatment of large bowel polyps in elderly people with over five years;a follow-up. *Zhonghua Xiaohua Zazhi* 1995; 15: 198-199
 - 27 Zu MQ. Endoscopic Excision of Colonic Polyps. A report of 456 cases. *Zhongguo Zhongliu Linchuang*1995; 22: 334-337
 - 28 Wang ZX, Xu DP, Zhou HZ, Lei PS, Cheng SZ. An analysis of canceration of 53 large intestine polys. *Zhongliu Fangzhi Yanjiu* 1994; 21: 236-238
 - 29 Zhang HZ, Tian HY, Xu JH. Clinical analysis of 321 cases of colorectal polyps. *Shiyong Zhongliu Zazhi* 1994; 9: 30-31
 - 30 Zhang ZY, Pan LN, Wu HX, Li SY. Relation of colorectal polyps and colorectal cancer.A report of 494 cases. *Neijing* 1994; 11: 1-2
 - 31 Gao WD, Yao LQ, Zhou PH, Gu SH. Treatment on canceration colorectal adenomas by colonscope. *Zhonghua Neijing Zazhi* 1996; 2: 42-43
 - 32 Han Y, Li SY. Diagnosis and treatment on early colorectal neoplasmas of type flat and concave by endoscopy. *Zhonghua Neijing Zazhi* 1997; 3: 39-41
 - 33 Zhang YL. The dysplasia of colorectal adenoma. In: Zhang YL eds. Colorectal cancer: Basic and clinical research. *Shanghai Sci Press* 1999: 13-15
 - 34 Schlemper RJ,Itabashi M, Kato Y, Lewin KJ, Riddell RH, Shimoda T, Sipponen P, Stolte M, Watanabe H. Differences in the diagnostic criteria used by Japanese and Western pathologists to diagnose colorectal carcinoma. *Cancer* 1998; 82: 60-69
 - 35 Schlemper RJ, Borchard F, Dixon MF, Koike M, Mueller J, Stolte M, Watanabe H. International comparability of the pathological diagnosis for early cancer of the digestive tract: Munich meeting. *J Gastroenterol* 2000; 35(Suppl 12):102-110
 - 36 Riddell RH. East meets West: what is early cancer? *Can J Gastroenterol* 1999;13:495-497
 - 37 Lauwers GY, Shimizu M, Correa P, Riddell RH, Kato Y, Lewin KJ, Yamabe H, Sheahan DG, Lewin D, Sipponen P, Kubilis PS, Watanabe H. Evaluation of gastric biopsies for neoplasia: differences between Japanese and Western pathologists. *Am J Surg Pathol* 1999; 23: 511-518
 - 38 Chen K, Jiao DA, Zheng S, Zhou L, Yu H, Yuan YC, Yao KY, Ma XY, Zhang Y. Diagnostic value of fecal occult blood testing for screening colorectal cancer. *China Natl J New Gastroenterol* 1997;3:166-168
 - 39 Zhou DY, Feng FC, Zhang YL. Route of early diagnosis on colorectal cancer. *Zhonghua Xiaohua Zazhi* 1992;12:319-321
 - 40 Zhou DY, Zhang YL. Progress on biologic characteristics and early diagnosis of colorectal cancer. *Guowai Yixue: Xiaohua Jibing Fengce* 1992;1:17-18
 - 41 Zhang YL, Zhou DY, Zhang WD, Lai ZS. Speculation on early diagnosis of colorectal cancer. *Yixue Yu Zhexue* 1993;43-44
 - 42 Zhang YL, Zhou DY. Prophylactic and therapeutic strategy of colorectal cancer. *Weichangbingxue He Ganchangbingxue Zazhi* 1994;3:241-243
 - 43 Xu SB, Zhang WX, Wang LL. Expression of antigen a new tumor marker Sc6 byimmunohistochemical method. *Xin Xiaohuabingxue Zazhi* 1994;2(Suppl 2):49-50
 - 44 Feng FC, Huang W, Zhou DY, Zhang YL, Lai ZS. Study on detection of cancer associated antigen in serum and feces by monoclonal antibodies against human colorectal cancer. *Xin Xiaohuabingxue Zazhi* 1995;3:36-38
 - 45 Chen B, Zhou SJ, Fan DM. Establishment of a quick ConA-mAb-LISA for detection of serum MC3-Ag, a novel colorectal cancer-associated antigen. *Xin Xiaohuabingxue Zazhi* 1995;3(Suppl 4):12-13
 - 46 Luo YH, Fang DC, Lu R, Liu FX, Liang ZY, Liu WW, Men RP, Zhou ZC. Heterozygosity loss at the APC/MCC locus in colorectal cancer. *Xin Xiaohuabingxue Zazhi* 1996;4:309-311
 - 47 Zhuang XQ, Yuan SZ, Wang XH, Lai RQ, Luo ZQ. Expression and prognostic significance of EGF receptor and proliferating cell nuclear antigen in colorectal cancer. *Xin Xiaohuabingxue Zazhi* 1996;4:483-484
 - 48 Liu Y, Li QM, Lu MZ. Expressions of nm23-H1, p53 and PCNA in human colorectal carcinoma tissues. *Xin Xiaohuabingxue Zazhi* 1997;5: 431-432
 - 49 Zhao J, Pan X, Yin GP, Shan LC, Wang CL. Peripheral blood CD44 contents in 26 patients with colorectal cancer. *Xin Xiaohuabingxue Zazhi* 1997;5:510-511
 - 50 Feng FC, Huang W, Zhang YL, Wang JD, Zhou DY. Clinical significance of serum sIL-2R and TNF in patients with colorectal carcinoma. *Xin Xiaohuabingxue Zazhi* 1997;5:567-568
 - 51 Qiu SL, Huang JQ. Significance of CD44 gene products for colorectal carcinoma diagnosis and prognosis evaluation. *Xin Xiaohuabingxue Zazhi* 1997;5(Suppl 6):32-33
 - 52 Zhang YL, Zhou DY, Lai ZS. Evaluation of immunological fecal occult blood test for colorectal tumor by specific antibody coated staphylococcal protein A coagglutination. *J Med Coll PLA* 1992; 7:382-358
 - 53 Yu SP, Zheng SJ, Zhou HY. Evaluation of colorectal carcinoma screening with fecal monoclonal antibody. *World J Gastroenterol* 1998;4(Suppl 2):9-11
 - 54 Chen K, Jiao DA, Zheng S, Zhou L, Yu H, Yuan YC, Yao KY, Ma XY, Zhang Y. Diagnostic value of fecal occult blood testing for screening colorectal cancer. *China Natl J New Gastroenterol* 1997;3:166-168
 - 55 Zhu WX. Comparative fecal occult blood test with the kit of RPHA-Z and RPHA-T. *Zhonghua Yixue Zazhi* 1987: 673-674
 - 56 Zhou DY, Zhang YL, Nai ZS. A study on the screening of large intestinal carcinoma by reactum mucus T-antigen method. *Zhonghua Xiaohua Zazhi* 1991;11:261-262
 - 57 Xu SY, Lin GJ, Lu Y. Clinical significance of T-antigen in the premalignant condition of colorectal cancer. *Zhonghua Xiaohua Neijing Zazhi* 1998; 15: 285-288
 - 58 Li DB, Wang HB. Application of T-antigen detective kit in screening colorectal cancer. *Zhongguo Gangchangbing Zazhi* 1998; 18: 27-28
 - 59 Lu Y, Xu SY, Wang QY, Li ZM. Determination of T-antigen in large intestinal mucus by galactose oxidase method. *Zhonghua Yixue Jianyan Zazhi* 1995; 18: 133-135
 - 60 Tan J, Zhang Q, Fang XZ, Kan AP, Cai XL, Zhang SM, Zhang L, Zhang SH. Clinical significance of galactose oxidase-schiff reaction in the detection of carcinoma and precancerous lesions of large intestine. *Zhonghua Zhongliu Zazhi* 1997; 19: 157-159
 - 61 Wang ZH. Mass screening for colorectal cancer by semi-quantum testing fecal occult albumin. *Zhongguo Lingchuang Mianyixue Zazhi* 1993: 39-42
 - 62 Wang ZH, Li SY, Cheng ZM. Preparation of rabbit anti-human immuno-carboxylate and its application in screening of colorectal tumor. *Zhongguo Zhongliu Lingchuang* 1999; 26: 450-452
 - 63 Feng FC, Huang W, Zhong DY, Zhang YL. Study on detection of cancer associated antigen in serum and feces by monoclonal antibodies against human colorectal cancer. *Xingxiaohuabing Zazhi* 1995;3:36-38
 - 64 Hu JY, Su JZ, Pi ZM, Zhu JG, Zhou GH, Sun QB. Radioimmunoimaging of colorectal cancer using 99mTc labeled monoclonal antibody. *World J Gastroenterol* 1998;4:303-306
 - 65 Fang DC, Luo YH, Lu R, Liu WW, Lui FX, Liang ZY. Loss of heterozygosity at APC, MCC and DCC genetic loci in colorectal cancers. *China Natl J New Gastroenterol* 1995;1:21-24
 - 66 Zhao CH, Jiang CY, Zhang YY, Liu XX, Luo DC, Zhang XT, Lin YQ. Analysis of LDH activities and its isoenzyme patterns in colorectal cancer tissues. *China Natl J New Gastroenterol* 1997;3:41-42
 - 67 Wu GJ, Shan XN, Li MF, Shi SL, Zheng QP, Yu L, Zhao SY. A preliminary study on the loss of heterozygosity at 17p13 in gastric and colorectal cancers. *China Natl J New Gastroenterol* 1997;3:160-162
 - 68 Zhang J, Lai MD, Chen J. Methylation status of p16 gene in colorectal carcinoma and normal colonic mucosa. *World J Gastroenterol* 1999;5: 451-454
 - 69 Xu QW, Li YS, Zhu HG. Relationship between expression P53 protein, PCNA and CEA in colorectal cancer and lymph node metastasis. *World J Gastroenterol* 1998;4:218-219
 - 70 Cai Q, Lu HF, Sun MH, Du X, Fan YZ, Shi DR. Expression of two CD44 variant proteins (v3 and v6) in human colorectal carcinoma and its relevance for prognosis. *World J Gastroenterol* 2000;6(Suppl 3):75
 - 71 He SW, Shen KQ, He YJ, Xie B, Zhao YM. Regulatory effect and mechanism of gastrin and its antagonists on colorectal carcinoma. *World J Gastroenterol* 1999;5:408-416

- 72 He Y, Zhou J, Wu JS, Dou KF. Inhibitory effects of EGFR antisense oligodeoxynucleotide in human colorectal cancer cell line. *World J Gastroenterol* 2000;6:747-749
- 73 Jiang CP, Chen YQ, Zhu JW, Shen HX, Yu X. Immunohistochemical study of gastrin in colorectal carcinoma tissues and its adjacent mucosa. *China Natl J New Gastroenterol* 1997;3:84-86
- 74 Chen DW, Wang YH, Chen XY, Wang Q, Gao H. Clinical significance of immunohistochemical study of P53 protein in colorectal carcinoma. *China Natl J New Gastroenterol* 1996;2:25-26
- 75 Hu JY, Wang S, Zhu JG, Zhou GH, Sun QB. Expression of B7 costimulation molecules by colorectal cancer cells reduces tumorigenicity and induces antitumor immunity. *World J Gastroenterol* 1999;5: 147-151
- 76 Feng S, Song JD. Determination of α -glucuronidase in human colorectal carcinoma cell lines. *China Natl J New Gastroenterol* 1997;3:251-252
- 77 Hu JY, Su JZ, Pi ZM, Zhu JG, Zhou GH, Sun QB. Radioimmunoinaging of colorectal cancer using ^{99m}Tc labeled monoclonal antibody. *World J Gastroenterol* 1998;4:303-306
- 78 Zhou ZF, Yuan SZ. Prognostic value of silver stained nucleolar organizer regions in colorectal carcinoma. *China Natl J New Gastroenterol* 1995;1:43-47
- 79 Xu YH, Song JD. Expression of tumor associated antigen-LEA in pre-malignant and malignant lesions of colorectal mucosa. *Shijie Huaren Xiaohua Zazhi* 1999;7:992
- 80 Xu SP, Zheng SJ, Zhou HY, Guo XL. Colorectal cancer mass screening by cancer associated monoclonal antibody in feces. *Zhonghua Xiaohua Zazhi* 1998; 18: 216-217
- 81 Wu BP, Zhang YL, Zhang ZS, Zhang LL, Guo W, Zhou DY. Microsatellite instability, MMR gene expression in colorectal cancer with familial predisposition. *Zhonghua Liuxingbingxue Zazhi* 1998;19:331
- 82 Wang YP, Waltraut F, Peter P. Analysis of hMLH1 and hMSH2 gene mutation in hereditary non-polyposis colorectal cancer. *Zhonghuayixue Yichuanxue Zazhi* 1998;15: 333-336
- 83 Wu BP, Zhang YL, Zhou DY, Gao CF, Lai ZS. Microsatellite instability, MMR gene expression and proliferation kinetics in colorectal cancer with familial predisposition. *World J Gastroenterol* 2000;6:902-905
- 84 Zhang LL, Zhang ZS, Zhang YL, Wu BP, Guo W, Liu XX, Zhou DY. Microsatellite instability in multiple primary colorectal cancers. *Shijie Huaren Xiaohua Zazhi* 1999;7:397-399
- 85 Capozzi E, Della Puppa L, Fornasari M, Pedroni M, Boiocchi M, Viel A. Evaluation of the replication error phenotype in relation to molecular and clinicopathological features in hereditary and early onset colorectal cancer. *Eur J Cancer* 1999; 35:289-295
- 86 Lin H, Lin JY, Zhang YL, Zhang ZS, Zhou MY, Zhou DY. The detection of the mutation of APC gene in the stool of the patients with sporadic colorectal carcinoma. *Zhonghua Xiaohua Zazhi* 2000;20:60-61
- 87 Ji DJ, Cao Y, Zhang YL, Jiang P, Yu N, Feng FC, Zhou DY. Synchronous studies on variations of p53 gene transcriptions and expressions in colorectal carcinomas HT-29 and Lovo cell lines. *Shijie Huaren Xiaohua Zazhi* 2000;8:77-79
- 88 Zhen S, Cai YH, Chao J, Zhen L, Mo YQ, Zhang YM, Geng LY, Shi ZZ, Gu JR. Colorectal cancer associated gene analysis by SSH technique. *Zhonghua Yixue Zazhi* 1997; 77: 256-259
- 89 Mo YQ, Zhen L, Cai XH, Chao J, Zhu LJ, Zhen S. Expression of new cancer associated gene - HSU 17714 in colorectal cancer and other malignant tumors. *Zhongguo Zhongliu Linchuang* 1997; 24: 504-508
- 90 Li M, Wang B, Yu BM, Zhen MH. Relationship between p53 gene mutation and prognosis in colorectal cancer. *Shijie Huaren Xiaohua Zazhi* 1999;7:425-426
- 91 Zhuan XQ, Lai RQ, Sun GH, Wang XH, Yuan SZ. The expression of p53 protein and PCNA in colorectal tumors. *Shijie Huaren Xiaohua Zazhi* 1999;7:616
- 92 Shen XB, Zhang XC, Mei LX, Zhao XM, Hu JG. The signification of the expression of nm23/NDPK and p53 in colorectal cancer. *Shijie Huaren Xiaohua Zazhi* 1999;7:809-810
- 93 Lin H, Lin JY, Zhang YL, Zhang ZS, Zhou MY, Zhou DY. The detection of the mutation of APC gene in the stool of the patients with sporadic colorectal carcinoma. *Zhonghua Xiaohua Zazhi* 2000; 20: 60-61
- 94 Gan YB, Cai XH, Zheng S. Detection of Ki-ras gene mutations in tumor tissues and stools of patients with colorectal carcinoma. *Zhejiang Yike Daoxue Xuebao* 1995; 24: 241-247
- 95 Luo CY, Li SY, Zhu XG. The detection of the rearrangements of bcl-2 gene in the cancer tissues and the stool of the patients with colorectal carcinoma by semi-nest PCR. *Zhonghua Shiyang Waikexue Zazhi* 1999;16: 197-198
- 96 Cao GW, Qi ZT, Pan X, Zhang XQ, Miao XH, Feng Y, Lu XH, Kuriyama S, Du P. Gene therapy for human colorectal carcinoma using human CEA promoter controlled bacterial ADP-ribosylating toxin genes human CEA: PEA & DTA gene transfer. *World J Gastroenterol* 1998;4: 388-391
- 97 Xu CT, Pan BR. The study of gene change in colorectal tumors. *Huaren Xiaohua Zazhi* 1998;6:58-60
- 98 Yu BM, Zhao R. The recent study on molecular biology in colorectal cancer. *Shijie Huaren Xiaohua Zazhi* 1999;7:173-175
- 99 Liu BY, Sun ZL, Pan SW, Chui DX, Yuan XJ, Li D, Lei YF, Wang S. Gene expression and early diagnosis in colorectal cancer. *Shijie Huaren Xiaohua Zazhi* 2000;8:43-44
- 100 Sun ZJ, Zhang YL, Zhang ZS, Guo W, Zhou DY. Study on activity of telomerase in colorectal cancer screening. *Zhonghua Liuxingbingxue Zazhi* 1998;19:327
- 101 Jiang CY, Ding K, Liu XX, Zhao CH, Zhu S. Study on histoenzymes markers in colorectal cancer. *Zhongguo Zhongxiyi Jiehe Waikexue Zazhi* 1998; 4: 336-339
- 102 Wang W, Luo HS, Yu BP. Telomerase and colorectal cancer. *Shijie Huaren Xiaohua Zazhi* 2000;8:800-802
- 103 Cuo SL, Huang JQ, Wang YF, Peng ZH. Telomerase analysis in pre-malignant and malignant tumors in colon. *Huaren Xiaohua Zazhi* 1998; 6: 992-993
- 104 Wu XW, Li SY, Wang ZH, Wu X, Cheng ZM, Wu ZT. The evaluation of colonic exfoliative cell for the screening of colorectal cancer. *Aizheng* 1997; 16: 386-387
- 105 Fan RY, Li SR, Wu X, Wu ZT, Cheng ZM, Deng YJ, Chao JB, Zhang HG. The expression of telomerase in exfoliate cells of colorectal cancer. *Shijie Huaren Xiaohua Zazhi* 2000;8:814-815
- 106 Li J, Li SR, Cao JB, Gao G. Laser-induced fluorescence spectrum of colon cancer *in vivo*. *Shijie Huaren Xiaohua Zazhi* 1999;7:164-165
- 107 Luo DC, Dai HJ, Ni YZ, Ci W. A study on the screening of large intestinal carcinoma by t-antigen monoclonal antibody method. *Zhongguo Aizheng Zazhi* 1998; 8: 256-257
- 108 Liu SC, Bai X, Wei YG, Wang ZL. Reresearch of galactose oxidase in screening carcinoma of the large intestine. *Huaren Xiaohua Zazhi* 1998; 6: 990-991
- 109 Zhou DY, Feng FC, Zhang YL, Lai ZS. Comparative analysis of detecting rectum mucus T-antigen and Immuno-fecal occult blood test in screening colorectal cancer. *Chinese Med J* 1993;106:739-742
- 110 Zhou DY, Feng FC, Pan DS, Lai ZS, Zhang WD, Zhang YL, Wan TM, Li LB, Xu GL, Zhou D. Evaluation of optimized screening protocol for colorectal cancer among a high-incidence population. *Zhonghua Xiaohua Zazhi* 1993;13:315-317
- 111 Liu XY, Zheng S, Yang G, Yu H, Zhou L, Zhang X, Shun QY, Shen GF, Shen YZ, Ding XF. Evaluation of combined test of sequential fecal occult blood and albumin in the screening of colorectal neoplasia. *Zhonghua Fangzhi Yanjiu* 1997; 24: 197-200
- 112 Li SY, Zhang CL, Xu ED, Yang TZ, Cheng NP, Liu YH, He YN. Evaluation of combined test of sequential fecal occult blood and albumin in the screening of colorectal neoplasia. *Zhonghua Zhongliu Zazhi* 1995; 17: 381-383
- 113 Zhou DY, Zhang YL, Feng FC, Lai ZS, Pan DS. Combined test of spa fecal occult blood and rectum mucus t-antigen in the screening and follow-up of colorectal cancer. *Weichangbingxue* 1997;2:67-69
- 114 Sidransky D, Tokino T, Hamilton SR, Kinzler KW, Levin B, Frost P, Vogelstein B. Identification of ras oncogene mutations in the stool of patients with curable colorectal tumors. *Science* 1992; 256:102-105
- 115 Eguchi S, Kohara N, Komuta K, Kanematsu T. Mutations of the p53 gene in the stool of patients with resectable colorectal cancer. *Cancer* 1996; 77(Suppl): 1707-1710
- 116 Sidransky D. Molecular screening: how long can we afford to wait? *J Natl Cancer Inst* 1994; 86: 955-956
- 117 Luo CY, Li SY. The detection and their clinical significance of C-erbB-2 amplification and p53 mutation in the stools of patients with colorectal carcinomas. *Zhonghua Putong Waikexue Zazhi* 1999; 14: 371-373
- 118 Lin JY, Lin H, Zhou DY, Jiang P, Zhang YL. Detection of suppress oncogene mutations in tumor tissues and stools of patients with colorectal carcinoma. *Zhonghua Liuxingbingxue Zazhi* 1998; 19: 326
- 119 Yu N, Qiu HM, Ding YQ, Xu L, Zhang SJ. The relation between DNA replication error and clinicopathological features of colorectal carcinoma. *Zhonghua Binglixue Zazhi* 1998; 27: 359-361
- 120 Yu N, Qiu HM, Ding YQ, Xu L. MSI-a useful molecular indicator of hereditary nonpolyposis colorectal cancer: a report of 4 cases. *Diyi Junyi Daoxue Xuebao* 1999;19: 160-162
- 121 Guo QX, Wei N, Guo CH, Lin LM, Chen BJ. Analysis on microsatellite DNA instability in sporadic nonpolyposis colorectal cancer. *Shandong Yike Daxue Xuebao* 1999; 37: 114-116
- 122 Wu BP, Zhang YL, Zhou DY, Gao CF, Lai ZS. Microsatellite instability, MMR gene expression and proliferation kinetics in colorectal cancer with familial predisposition. *World J Gastroenterol* 2000;6:902-905

• ESOPHAGEAL CANCER •

RRR- α -tocopheryl succinate inhibits human gastric cancer SGC-7901 cell growth by inducing apoptosis and DNA synthesis arrest?

Kun Wu, Yan Zhao, Bai-He Liu, Yao Li, Fang Liu, Jian Guo, Wei-Ping Yu

Kun Wu, Yan Zhao, Bai-He Liu, Yao Li, Fang Liu, Jian Guo, Department of Nutrition and Food Hygiene, Public Health School, Harbin Medical University, Harbin 150001, Heilongjiang Province, China
Wei-Ping Yu, Genetics Institute, Texas University of USA, Austin, USA
Supported by National Natural Science Foundation of China, No.39870662
Correspondence to: Prof. Kun Wu, Department of Nutrition and Food Hygiene, Public Health School, Harbin Medical University, Harbin 150001, Heilongjiang Province, China. wukun@public.hr.hl.cn
Telephone: +86-451-3648665

Received 2001-04-25 Accepted 2001-10-15

Abstract

AIM: To investigate the effects of growth inhibition of human gastric cancer SGC-7901 cell with RRR- α -tocopheryl succinate (VES), a derivative of natural Vitamin E, via inducing apoptosis and DNA synthesis arrest.

METHODS: Human gastric cancer SGC-7901 cells were regularly incubated in the presence of VES at 5, 10 and 20 mg·L⁻¹ (VES was dissolved in absolute ethanol and diluted in RPMI 1640 complete condition media correspondingly to a final concentration of VES and 1 mL·L⁻¹ ethanol), succinic acid and ethanol equivalents as vehicle (VEH) control and condition media only as untreated (UT) control. Trypan blue dye exclusion analysis and MTT assay were applied to detect the cell proliferation. 37 kBq of tritiated thymidine was added to cells and [³H] TdR uptake was measured to observe DNA synthesis. Apoptotic morphology was observed by electron microscopy and DAPI staining. Flow cytometry and terminal deoxynucleotidyl transferase-mediated dUTP nick end labeling (TUNEL) assay were performed to detect VES-triggered apoptosis.

RESULTS: VES inhibited SGC-7901 cell growth in a dose-dependent manner. The growth curve showed suppression by 24.7%, 49.2% and 68.7% following 24h of VES treatment at 5, 10 and 20 mg·L⁻¹, respectively, similar to the findings from MTT assay. DNA synthesis was evidently reduced by 35%, 45% and 98% after 24h VES treatment at 20 mg·L⁻¹ and 48h at 10 and 20 mg·L⁻¹, respectively. VES induced SGC-7901 cells to undergo apoptosis with typically apoptotic characteristics, including morphological changes of chromatin condensation, chromatin crescent formation/margination, nucleus fragmentation and apoptotic body formation, typical apoptotic sub-G1 peak by flow cytometry and increase of apoptotic cells by TUNEL assay in which 90% of cells underwent apoptosis after 48h of VES treatment at 20 mg·L⁻¹.

CONCLUSION: VES can inhibit human gastric cancer SGC-7901 cell growth by inducing apoptosis and DNA synthesis arrest. Inhibition of SGC-7901 cell growth by VES is dose- and time-dependent. Therefore VES can function as a potent chemotherapeutic agent against human gastric

carcinogenesis.

Wu K, Zhao Y, Liu BH, Li Y, Liu F, Guo J, Yu WP. RRR- α -tocopheryl succinate inhibits human gastric cancer SGC-7901 cell growth by inducing apoptosis and DNA synthesis arrest. *World J Gastroenterol* 2002;8(1):26-30

INTRODUCTION

Vitamin E is characterized as a fat-soluble membrane antioxidant^[1,2]. Vitamin E succinate (RRR- α -tocopheryl succinate; VES), a derivative of natural vitamin E, however, does not possess antioxidant properties unless the succinate group is removed by a nonspecific esterase. VES has been demonstrated to be a potent growth inhibitor of various cancer cell types *in vitro* and *in vivo*^[3,4]. For example, VES has been shown to inhibit the growth of human monoblastic leukemia cells *in vitro*^[5], murine B-16 melanoma cells *in vitro*^[6], hamster buccal pouch tumor cells *in vivo*^[7], avian lymphoid cells *in vitro*^[8,9], murine EL4 T lymphoma cells *in vitro*^[4,10], human gastric cancer cells *in vitro* and *in vivo*^[11-13], and human breast cancer cells *in vitro* and *in vivo*^[14,15].

The exact mechanisms are not clearly known, but the inhibitory effect of VES on the proliferation of rapidly dividing cells can be attributed to the induction of cell cycle blockage^[16], increased secretion and activation of transforming growth factor- β , (TGF- β) and TGF- β receptor II^[9,14,17], and the induction of apoptosis^[18-20]. In many instances, growth inhibition following terminal differentiation^[21-23] or anticancer drug treatment^[24-26] results in apoptosis. Apoptosis, namely, programmed cell death, is an active and physiological process characterized by a series of morphological and biological alterations including condensation of cytoplasm, loss of plasma membrane microvilli, segmentation of nucleus and extensive degradation of chromosomal DNA into oligomers of 180bp^[27-30]. The exact mechanisms of apoptosis are still unclear, but our earlier studies indicated that VES can secrete and activate biologically active TGF- β and then TGF- β increases the kinase activity of c-Jun N-terminal kinase (JNK) followed by phosphorylation of c-Jun, and finally activated c-Jun triggers apoptosis in human gastric cancer SGC-7901 cells^[31].

Gastric cancer is common in China^[32-41]. Since VES is a potential tumor chemopreventive and chemotherapeutic agent, it is worthwhile to investigate the manner in which VES inhibits the cell growth and thereafter gain a better understanding of the molecular events involved. In this study, we demonstrate the ability of VES to inhibit cell proliferation, arrest DNA synthesis and induce human gastric cancer SGC-7901 cells to undergo apoptosis, address the involvement of certain apoptosis-related events in this process and prove that VES-triggered apoptosis is different from VES-induced DNA synthesis arrest.

MATERIALS AND METHODS

Materials

VES, DAPI (4',6-diamidino-2'-phenylindole dihydrochloride,

succinic acid, MTT [3-(4,5-dimethylthiazole-2-yl)-2,5-diphenyltetrazolium bromide] and propidium iodide were purchased from Sigma Co. Ltd. RPMI 1640 media was obtained from Gibco, BRL. *In situ* cell death detection kit was purchased from Boehringer Mannheim, Indianapolis, Inc. ^3H -TdR was supplied by Chinese Academy of Sciences.

Methods

Cell culture Human gastric cancer cell lines SGC-7901 were maintained in RPMI 1640 medium supplemented with 100mL·L⁻¹ fetal calf serum (FCS), 100kU·L⁻¹ penicillin, 100mg·L⁻¹ streptomycin and 2mmol·L⁻¹ L-glutamine under 50mL·L⁻¹ CO₂ in a humidified incubator at 37°C. SGC-7901 cells were incubated for different time periods in the presence of VES at 5, 10 and 20mg·L⁻¹ (VES was dissolved in absolute ethanol and diluted in RPMI 1640 complete condition media correspondingly to a final concentration of VES and 1mL·L⁻¹ ethanol), succinic acid and ethanol equivalents as vehicle (VEH) control and condition media only as untreated (UT) control.

Growth curve Exponentially growing SGC-7901 cells were trypsinized and aliquoted into 24-well flat-bottomed tissue culture plates at 5×10^4 ·well⁻¹. The cells were allowed to attach overnight and then incubated for seven days in the presence or absence of VES. Cell number and viability were determined by trypan blue dye exclusion analysis.

MTT assay The cells were inoculated in a 96-well plate (5×10^3 ·well⁻¹) as described previously^[42]. In brief, cells after 24h of incubation were treated with VES and controls and then cultured for six days. The cells in eight wells at every dose were supplemented with 0.2mL of 5g·L⁻¹ MTT every day. After 4h, culture media were discarded followed by addition of 0.2ml of DMSO and vibration for 10min. The absorbance (A) was measured at 570nm using a microplate reader. The percentage of viable cells was calculated as follow: (A of experimental group / A of control group) × 100%. [^3H] Thymidine incorporation. The cells were treated with VES for 24 or 48h as described previously^[43]. 37kBq of tritiated thymidine were added to cells during the last 6h of culture and harvested onto glass fiber filters. [^3H] TdR uptake was measured in a Beckman LS5000 TD liquid scintillation counter.

Electron microscopy The cells treated with VES or VEH were trypsinized and harvested after 24h and 48h, respectively. Subsequently the cells were immersed with Epon 821, imbedded in capsules and converged for 72h at 60°C, the cells were prepared into ultrathin section (60nm) and stained with uranyl acetate and lead citrate. Cell morphology was examined by transmission electron microscopy.

DAPI staining Treated cells were pelleted and washed three times with distilled water, and then stained with 2mg·L⁻¹ DAPI in 100% methanol for 15min at 37°C. Cells were viewed using a fluorescence microscope with ultraviolet (UV) excitation at 300~500nm. Cells with nuclei that contained clear condensed chromatin or cells with fragmented nuclei were scored as apoptosis.

TUNEL assay Apoptosis of SGC-7901 cells was analyzed by using *in situ* cell death detection kit. The method is essentially based on the terminal deoxynucleotidyl transferase-mediated dUTP nick end labeling (TUNEL) technique, and it can detect apoptosis at very early stages. In brief, cells were treated in the presence or absence of VES and fixed overnight in 100g·L⁻¹ formaldehyde, treated with proteinase K and then H₂O₂, labeled with fluorescein dUTP in a humid box for

1h at 37°C. The cells were then combined with POD-Horseradish peroxidase, colorized with DAB (3,3-diaminobenzidine) and counterstained with methyl green. Cells were visualized with light microscope.

Flow cytometry Cells were incubated with various doses of VES, harvested, washed with phosphate-buffered saline (PBS) twice and fixed with 700mL·L⁻¹ ethanol at 4°C overnight. Fixed cells were washed twice with PBS and stained with 800μL propidium iodide and 200μL deoxyribonulcease-free ribonuclease A in PBS. The fluorescence intensity of propidium iodide-stained nuclei was determined by a FACscan.

Statistical analysis Student's *t* test was used to assess statistical significance of differences. If *P* < 0.05, the difference was considered significant.

RESULTS

Inhibition of Human Gastric Cancer SGC-7901 Cell Proliferation by VES

Growth curve VES has been previously shown to function as a growth inhibitory agent. In this study, VES inhibited SGC-7901 cell growth in a dose-dependent manner. The growth curve showed that cell growth was suppressed by 24.7%, 49.2% and 68.7% following 24h of VES treatment at 5, 10 and 20mg·L⁻¹, respectively. The percentage of inhibition was 100% on day 4 with the treatment of VES at 20mg·L⁻¹ (Figure 1).

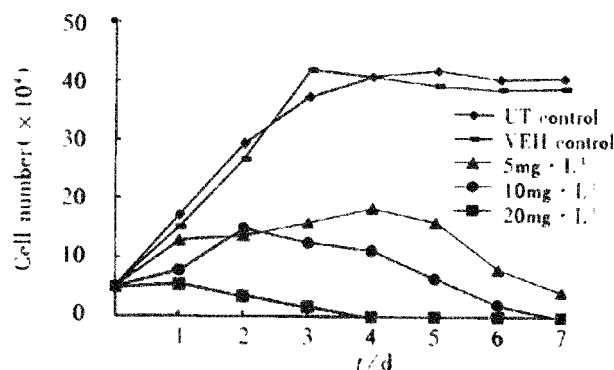


Figure 1 Growth curve of SGC-7901 cell treated with VES.

MTT assay SGC-7901 cells were treated in the presence or absence of VES for six days and cell viability was daily measured by MTT proliferation analysis. VES significantly inhibited cell growth and VES at 10 and 20 mg·L⁻¹ had an obviously inhibitory effect by 100% on the 5th and 4th days, respectively (Table1), similar to the findings from growth curve.

Table 1 Effect of VES on the viability of SGC-7901 cells

Group	Rate of viable cells/%					
	1	2	3	4	5	6
UT control	100	100	100	100	100	100
VEH control	105.5	102.4	92.1	95.3	105.7	97.5
5 mg·L ⁻¹ VES	94.8	101.2	91.4	144.3	91.4	74.6
10 mg·L ⁻¹ VES	91.4	64.6	20.8	4.2	0	0
20 mg·L ⁻¹ VES	53.4	32.9	4.3	0	0	0

DNA synthesis arrest by VES

VES treatment of SGC-7901 cells inhibited [^3H] thymidine

uptake with a dose-response relationship. DNA synthesis was evidently reduced by 35%, 45% and 98% after 24h VES treatment at 20 mg·L⁻¹ and 48h at 10 and 20 mg·L⁻¹, respectively, compared with UT control ($P<0.01$). On the other hand, VEH control did not affect SGC-7901 cell proliferation (Table 2).

Table 2 Inhibitory effect of VES on DNA synthesis incorporated with ³H-TdR ($\bar{x}\pm s$, $n=6$)

Group	Radioactive intensity/Bq·10 ⁴ cell ⁻¹	
	24h(% of inhibition ratio)	48h(% of inhibition ratio)
UT control	64.1±10.2(0)	143.2±13.7(0)
VEH control	63.8±10.3(1)	141.9±14.7(0)
5 mg·L ⁻¹ VES	61.8±10.4(4)	137.1±16.3(4)
10 mg·L ⁻¹ VES	57.2±10.7(11)	79.3±10.0(45) ^b
20 mg·L ⁻¹ VES	41.4± 8.0(35) ^b	2.2±0.3(98) ^b

^b $P<0.01$, vs UT control.

VES induction of apoptosis

Morphological changes Apoptotic characteristics including chromatin condensation, chromatin crescent formation/margination, DNA fragmentation and apoptotic body formation were seen by electron microscopy (Figure 2) and by fluorescence microscopy of DAPI-labelled cells (Figure 3). The cells undergoing apoptosis evidently increased when the concentration of VES was elevated and reaction time was prolonged.

Flow cytometry VES-induced apoptosis was studied further in SGC-7901 cells using flow cytometry. Cell cycle analysis after VES treatment revealed the presence of a sub-G1 apoptotic peak (Figure 4).

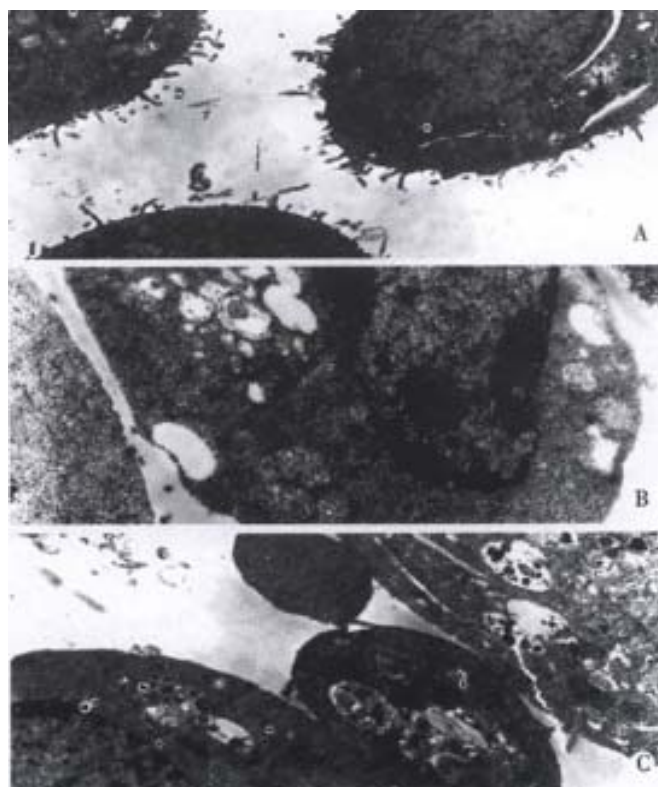


Figure 2 VES-induced apoptosis in SGC-7901 cells with transmission electron microscope

A: Normal cell; B: Apoptotic cell with chromatin condensation, chromatin crescent formation/margination; C: Cell with apoptotic body.

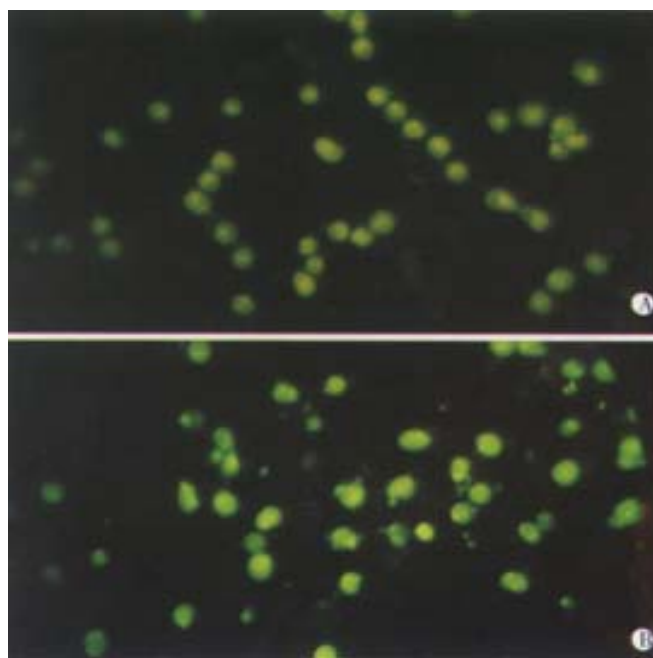


Figure 3 VES-induced apoptosis in SGC-7901 cells with DAPI staining UT control; VES at 20 mg·L⁻¹

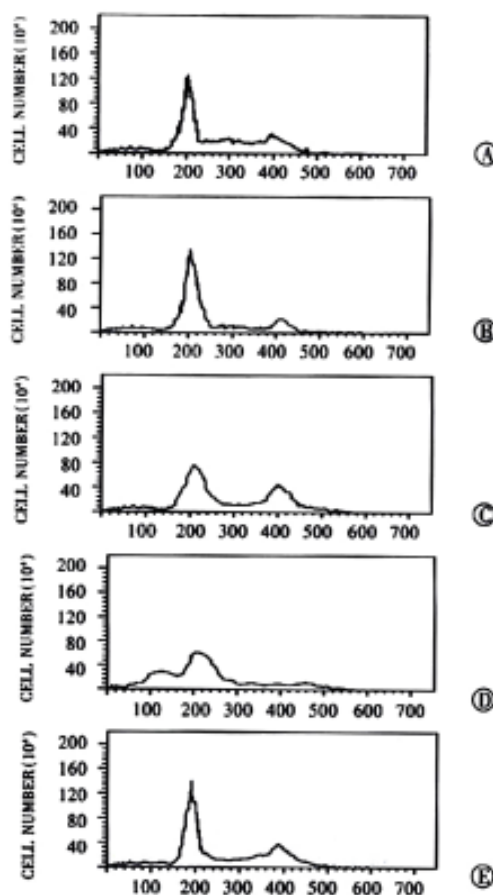


Figure 4 VES-induced apoptosis in SGC-7901 cells with flow cytometry A: UT control; B: VEH control; C: VES at 5 mg·L⁻¹; D: VES at 10 mg·L⁻¹; E: VES at 20 mg·L⁻¹.

TUNEL assay Apoptotic cell death was determined by TUNEL assay according to the manufacturer's instructions. The results showed that apoptotic cells increased with the increase of the concentration of VES in an obviously dose-dependent manner. The percentage of apoptosis was 90% after VES treatment at 20 mg·L⁻¹ (Figure 5 and Table 3).

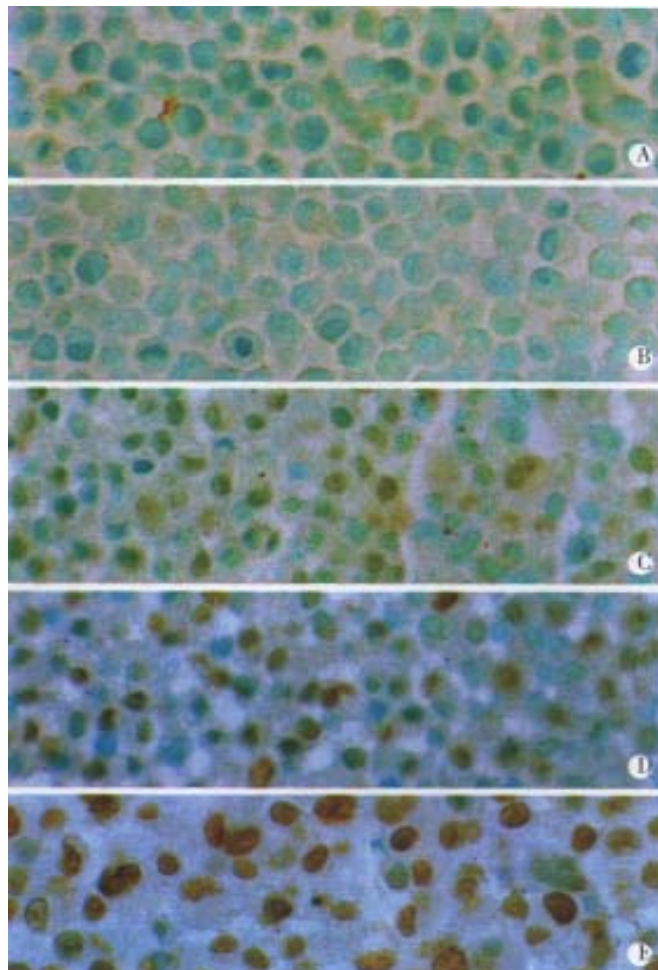


Figure 5 VES-induced apoptosis by TUNEL assay.

A: UT control; B: VEH control; C: VES at 5 mg·L⁻¹; D: VES at 10 mg·L⁻¹; E: VES at 20 mg·L⁻¹.

Table 3 Induction of apoptosis after 48h of VES treatment in SGC-7901 cells

Group	Apoptotic cells/10 ⁴ cells	Rate of apoptosis/%
UT control	6	0.06
VEH control	28	0.28
5 mg·L ⁻¹ VES	1248 ^b	12.48
10 mg·L ⁻¹ VES	5736 ^b	57.63
20 mg·L ⁻¹ VES	8996 ^b	89.96

^bP<0.01, vs UT control.

DISCUSSION

Cell growth is regulated by the interaction of cell proliferation and cell death. When cell growth is inhibited, the decrease of cell proliferation and increase of cell death will occur. Cell proliferation is performed by continuously proceeding into cell cycle and will be suppressed if cell cycle is disturbed^[44-46]. The disorder of DNA synthesis, however, is a common reason for the disturbance of cell cycles^[47,48]. Cell death is another principal reason for cell growth inhibition and is relevant to cell proliferation. Apoptotic cell death is a naturally occurring process of cell suicide which plays a crucial role in the development and homeostasis of metazons by eliminating superfluous or unwanted cells (reviewed by^[49-53]).

Previous studies showed that VES can block DNA synthesis in tumor cells^[43,54]. The percent of DNA synthesis arrest is more than 90% when human breast cancer cells are treated with VES at 10 mg·L⁻¹, similar to the rate of breast cancer cell growth inhibition which exceeds 80%^[15]. A recent study shows that VES can function as an apoptosis inducer in tumor cells. In this study, VES was found to inhibit cell proliferation in human gastric cancer SGC-7901 cells by trypan blue exclusion analysis and MTT assay. Cell growth was inhibited by 100% with treatment of VES at 10 mg·L⁻¹ on day 7 and at 20 mg·L⁻¹ on day 4 in the former experiment, while on the 6th and 4th days in the latter one. Meanwhile, VES significantly suppressed cell growth by DNA synthesis arrest via preventing SGC-7901 cells from progressing into S-phase, ultimately blocking the cell proliferation. In order to further elucidate the mechanisms of inhibitory effects of VES on cell growth, we determined the incidence of VES-mediated apoptosis in SGC-7901 cells by electron microscopy, DAPI staining, flow cytometry and TUNEL assay on the basis of morphological and molecular level. The results demonstrated that VES-treated SGC-7901 cells were characteristic by typical apoptotic alterations, including morphological changes by electron microscopy and DAPI staining, typical apoptotic sub-G₁ peak observed by flow cytometry; increase of apoptotic cells with the elevation of the concentration of VES in a clearly dose-dependent manner by TUNEL assay. The data above implicated that VES inhibits human gastric cancer SGC-7901 cell growth by inducing apoptosis and DNA synthesis arrest.

Apoptosis is a complex and programmed process which is regulated by a variety of factors^[55-60]. The antiproliferative actions of VES may be due, in part, to the ability of VES to induce autocrine acting biologically active TGF-βs^[9,14,17]. In addition, VES-mediated apoptosis is inhibited when c-Jun mutant is transfected into breast cancer cells^[61]. JNK, mitogen-activated protein kinase (MAPK) family member, plays an important role in the course of VES-triggered apoptosis^[31,61]. Although the exact mechanisms involved in VES-induced apoptosis have not been well known up to now, the ability of a compound to induce 90% apoptosis in a tumor cell population within 48h is noticeable. It is also noteworthy that VES can selectively inhibit the growth of tumor cells but not normal cells^[8,62-64]. The research in our laboratory demonstrated that VES inhibited benzo (a)pyrene (B(a)P)-induced forestomach carcinogenesis in female mice^[11], while the inhibition and inhibitory mechanisms of VES *in vivo* are worth further investigating.

REFERENCES

- Wang YF, Li QF, Wang H, Mao Q, Wu CQ. Effects of vitamin E on experimental hepatic fibrosis in rats. *Huaren Xiaohua Zazhi* 1998; 6: 207-209
- Jiang ZS, Gao Y. Biological feature of matrix metalloproteinase and its action in metastasis of liver cancer. *Shijie Huaren Xiaohua Zazhi* 2000;8:1403-1404
- Kline K, Yu W, Zhao B, Israel K, Charpentier A, Simmons-Menchaca M, Sanders BG. Vitamin E Succinate: Mechanisms of action as tumor cell growth inhibitor. In: Prasad KN, Santamaria L, Williams RM, eds. *Nutrients in Cancer Prevention and Treatment*. Totowa, NY: Humana, 1995:39-56
- Yu W, Sanders BG, Kline K. RRR-α-tocopheryl succinate inhibits EL4 thymic lymphoma cell growth by inducing apoptosis and DNA synthesis arrest. *Nutr Cancer* 1997;27:92-101
- Fariss MW, Fortuna MB, Everett CE, Smith JD, Trent DF, Djuric Z. The selective antiproliferation effects of α-tocopheryl hemisuccinate and cholesteryl hemisuccinate on murine leukemia cells result from the action of the intact compounds. *Cancer Res* 1994;54:3346-3351
- Ottino P, Duncan JR. Effect of α-tocopheryl succinate on free radical and lipid peroxidation levels in BL6 melanoma cells. *Free Radical Biol Med* 1997;22:1145-1151
- Schwartz J and Shklar G. The selective cytotoxic effect of carotenoids and α-tocopherol on human cancer cell lines *in vitro*. *J Oral Maxillofac Surg* 1992;50:367-373
- Kline K, Yu W, Sanders BG, Vitamin E. Mechanisms of action as tumor cell growth inhibitors. In: Prasad KN, Cole WC, eds. *Cancer and Nutrition*. Amsterdam: IOS, 1998:37-53

- 9 Simmons-Menchaca M, Qian M, Yu W, Sanders BG, Kline K. RRR- α -Tocopheryl succinate inhibits DNA synthesis and enhances the production and secretion of biologically active transforming growth factor- α by avian retrovirus-transformed lymphoid cells. *Nutr Cancer* 1995; 24:171-185
- 10 Yu W, Sanders BG, Kline K. Modulation of murine EL-4 thymic lymphoma cell proliferation and cytokine production by Vitamin E succinate. *Nutr Cancer* 1996;25:137-149
- 11 Wu K, Shan YJ, Zhao Y, Yu JW, Liu BH. Inhibitory effects of RRR- α -tocopheryl succinate on bezo(a)pyrene (B(a)P)-induced forestomach carcinogenesis in female mice. *World J Gastroenterol* 2001;17:60-65
- 12 Wu K, Guo J, Shan YJ, Liu BH. The effects of vitamin E succinate on apoptosis in human gastric cancer. *Weisheng Dulixue Zazhi* 1999;13:84-90
- 13 Wu K, Ren Y, Guo J. The effects of vitamin E succinate on the cyclic regulation protein of human gastric cancer cells. *Weisheng Dulixue Zazhi* 1998;12:203-207
- 14 Turley JM, Ruscetti FW, Kim SJ, Fu T, Gao FV, Birchenall-Roberts MC. Vitamin E succinate inhibits proliferation of BT-20 human breast cancer cells: increased binding of cyclin A negatively regulates E2F transactivation activity. *Cancer Res* 1997;57:2668-2675
- 15 Malafa MP, Neitzel LT. Vitamin E succinate promotes breast cancer tumor dormancy. *J Surg Res* 2000;93:163-170
- 16 Kim SJ, Bang OS, Lee YS, Kang SS. Production of inducible nitric oxide is required for monocytic differentiation of U937 cells induced by vitamin E-succinate. *J Cell Sci* 1998;111 (Pt 4):435-441
- 17 Ariazi EA, Satomi Y, Ellis MJ, Haag JD, Shi W, Sattler CA, Gould MN. Activation of the transforming growth factor beta signaling pathway and induction of cytoskeleton and apoptosis in mammary carcinomas treated with the anticancer agent perillyl alcohol. *Cancer Res* 1999;59:1917-1928
- 18 Neuzil J, Weber T, Schroder A, Lu M, Ostermann G, Gellert N, Mayne GC, Olejnicka B, Negre-Salvayre A, Sticha M, Coffey RJ, Weber C. Induction of cancer cell apoptosis by alpha-tocopheryl succinate: molecular pathways and structural requirements. *FASEB J* 2001;15:403-415
- 19 Turley JM, Fu T, Ruscetti FW, Mikovits JA, Bertolette DC, Birchenall-Roberts MC. Vitamin E succinate induces Fas-mediated apoptosis in estrogen receptor-negative human breast cancer cells. *Cancer Res* 1997;57:881-890
- 20 Yu W, Israel K, Liao QY, Aldaz CM, Sanders BG, Kline K. Vitamin E succinate (VES) induces Fas sensitivity in human breast cancer cells: role for Mr 43,000 Fas in VES-triggered apoptosis. *Cancer Res* 1999;59:953-961
- 21 Foehr ED, Bohuslav J, Chen LF, DeNoronha C, Geleziunas R, Lin X, O'Mahony A, Greene WC. The NF-kappa B-inducing kinase induces PC12 cell differentiation and prevents apoptosis. *J Biol Chem* 2000; 275:34021-34024
- 22 Sementchenko VI, Watson DK. Ets target genes: past, present and future. *Oncogene* 2000;19:6533-6548
- 23 Steff AM, Trop S, Maira M, Drouin J, Hugo P. Opposite Ability of Pre-TCR and alphabetaTCR to induce apoptosis. *J Immunol* 2001;166:5044-5050
- 24 Liu HF, Liu WW, Fang DC, Men RP. Relationship between Fas antigen expression and apoptosis in human gastric carcinoma and adjacent noncancerous tissues. *Huaren Xiaohua Zazhi* 1998;6:321-322
- 25 Xu HY, Yang YL, Guan XL, Song G, Jiang AM, Shi LJ. Expression of regulating apoptosis gene and apoptosis index in primary liver cancer. *World J Gastroenterol* 2000;6:721-724
- 26 Lacour S, Hammann A, Wotawa A, Corcos L, Solary E, Dimanche-Boitrel MT. Anticancer agents sensitize tumor cells to tumor necrosis factor-related apoptosis-inducing ligand-mediated caspase-8 activation and apoptosis. *Cancer Res* 2001;61:1645-1651
- 27 Liang WJ, Huang ZY, Ding YQ. Time effect of TNF α on apoptosis of Lovo cells of human colorectal carcinoma. *Huaren Xiaohua Zazhi* 1998;6:27-29
- 28 Nagata S. Symposium on apoptosis and medical diseases-Fas-induced apoptosis. *Internal Med* 1998;37:179-181
- 29 Leblanc V, Delumeau I, Tocqué B. Ras-GTPase activating protein inhibition specifically induces apoptosis of tumour cells. *Oncogene* 1999;18:4884-4889
- 30 Lu SY, Pan XZ, Peng XW, Shi ZL, Lin L, Chen MH. Effect of Hp infection on gastric epithelial cell kinetics in stomach diseases. *Shijie Huaren Xiaohua Zazhi* 2000;8:386-388
- 31 Wu K, Liu BH, Zhao DY, Zhao Y. The effect of vitamin E succinate on the expression of TGF- β 1, c-Jun and JNK1 in human gastric cancer SGC-7901 cells. *World J Gastroenterol* 2001;17:83-87
- 32 Mao ZB, Meng XY, Ge ZJ, Li RZ, Shi GS. Expression of arylamidase isoenzyme in gastric carcinoma and precancerous lesions. *Huaren Xiaohua Zazhi* 1998;6:323-325
- 33 Wang LP, Yu JY, Deng YJ, Tian YW, Wu X, Liu G, Ding HY. Relationship between the expression of somatostatin and epidermal growth factor receptor in gastric carcinoma. *Huaren Xiaohua Zazhi* 1998;6:606-609
- 34 Zhang QX, Dou YL, Shi XY, Ding Yi. Expression of somatostatin mRNA in various differentiated types of gastric carcinoma. *World J Gastroenterol* 1998;4:48-51
- 35 Liu ZM, Shou NH. Expression significance of mdrl gene in gastric carcinoma tissue. *Shijie Huaren Xiaohua Zazhi* 1999;7:145-146
- 36 Yu WL, Huang ZH. Progress in studies on gene therapy for gastric cancer. *Shijie Huaren Xiaohua Zazhi* 1999;7:887-889
- 37 Chen GY, Wang DR. The expression and clinical significance of CD44v in human gastric cancers. *World J Gastroenterol* 2000;6:125-127
- 38 Wang RQ, Fang DC, Liu WW. MUC2 gene expression in gastric cancer and preneoplastic lesion tissues. *Shijie Huaren Xiaohua Zazhi* 2000;8:285-288
- 39 Guo YQ, Zhu ZH, Li JF. Flow cytometric analysis of apoptosis and proliferation in gastric cancer and precancerous lesion. *Shijie Huaren Xiaohua Zazhi* 2000;8:983-987
- 40 Chen SY, Wang JY, Ji Y, Zhang XD, Zhu CW. Effects of *Helicobacter pylori* and protein kinase C on gene mutation in gastric cancer and precancerous lesions. *Shijie Huaren Xiaohua Zazhi* 2001;9:302-307
- 41 Xu AG, Li SG, Liu JH, Gan AH. Function of apoptosis and expression of the proteins Bcl-2, p53 and C-myc in the development of gastric cancer. *World J Gastroenterol* 2001;7:403-406
- 42 Liu BH, Wu K, Zhao DY. Inhibition of human gastric cancer SGC-7901 cell growth by vitamin E succinate. *Weisheng Yanjiu* 2000;29:172-174
- 43 Liu BH, Wu K. Study on the growth inhibition of Vitamin E Succinate in human gastric cancer cell. *Aibian Jibian Tubian* 2000;12:79-81
- 44 Sturla LM, Westwood G, Selby PJ, Lewis JJ, Burchill SA. Induction of cell death by basic fibroblast growth factor in Ewing's sarcoma. *Cancer Res* 2000;60:6160-6170
- 45 Wang H, Chow DA. Natural antibody-induced intracellular signaling and growth control in C3H 10T1/2 fibroblast variants. *Immunology* 2000;101:458-467
- 46 Shen MR, Droogmans G, Eggermont J, Voets T, Ellory JC, Nilius B. Differential expression of volume-regulated anion channels during cell cycle progression of human cervical cancer cells. *J Physiol* 2000;529:385-394
- 47 Keller C, Krude T. Requirement of Cyclin/Cdk2 and protein phosphatase 1 activity for chromatin assembly factor 1-dependent chromatin assembly during DNA synthesis. *J Biol Chem* 2000;275:35512-35521
- 48 Khan SH, Moritsugu J, Wahl GM. Differential requirement for p19ARF in the p53-dependent arrest induced by DNA damage, microtubule disruption, and ribonucleotide depletion. *Proc Natl Acad Sci U S A* 2000;97:3266-3271
- 49 Green DR, Reed JC. Mitochondria and apoptosis. *Science* 1998;281: 1309-1312
- 50 Xue XC, Fang GE, Hua JD. Gastric cancer and apoptosis. *Shijie Huaren Xiaohua Zazhi* 1999;7:359-361
- 51 Ashkenazi A, Dixit VM. Apoptosis control by death and decoy receptors. *Curr Opin Cell Biol* 1999;11:255-260
- 52 Wu K, Zhao Y, Yu W. Study on apoptosis. *Guowai Yixue Yichuanxue Fence* 2001;24:134-138
- 53 Li Y, Wu K. Effectors of apoptosis. *Guowai Yixue Weishengxue Fence* 2001;28:50-54
- 54 Wu K, Guo J, Shan YJ. Inhibitory effects of VES on the growth of human squamous gastric carcinoma cells. In: Johnson IT and Fenwick GR, eds. Dietary anticarcinogens and antimutagens-Chemical and biological aspects. RS-C, UK: *Athenaum Press* 2000:304-307
- 55 Yang WC, Wang LD. The mechanisms of cell proliferation control by tumor inhibitory genes and oncogenes. *Xin Xiaohuabingxue Zazhi* 1997;5:262-263
- 56 Aravind L, Dixit VM, Koonin EV. The domains of death: evolution of the apoptosis machinery. *TIBS* 1999;24:47-53
- 57 Gu XH, Li QF, Wang YM. Expression of hepatocyte apoptosis and Fas/FasL in liver tissues of patients with hepatitis D. *Shijie Huaren Xiaohua Zazhi* 2000;8:35-38
- 58 Sun BH, Zhao XP, Wang BJ, Yang DL, Hao LJ. FADD and TRADD expression and apoptosis in primary human hepatocellular carcinoma. *World J Gastroenterol* 2000;6:223-227
- 59 Zhao Y, Wu K. Cell death molecule Fas/CD95 and apoptosis. *Aibian Jibian Tubian* 2001;13:55-58
- 60 Yang JQ, Yang LY, Zhu HC. Mitomycin C induced apoptosis of human hepatoma cell. *Shijie Huaren Xiaohua Zazhi* 2001;9:268-272
- 61 Yu W, Simmons-Menchaca M, You H. RRR- α -Tocopheryl Succinate induction of prolonged activation of c-Jun amino-terminal kinase and c-Jun during induction of apoptosis in human MDA-MB-435 breast cancer cells. *Mol Carcinogenesis* 1998;22:247-267
- 62 Simmons-Menchaca M, Qian M, Yu W, Sanders BG, Kline K. RRR- α -tocopheryl succinate inhibits DNA synthesis and enhances the production and secretion of biologically active transforming growth factor- β by avian retrovirus-transformed lymphoid cells. *Nutr Cancer* 1995;24:171-185
- 63 Kline K, Sanders BG. RRR- α -tocopheryl succinate inhibition of lectin-induced T cell proliferation. *Nutr Cancer* 1993;19:241-252
- 64 Neuzil J, Weber T, Gellert N, Weber C. Selective cancer cell killing by alpha-tocopheryl succinate. *Br J Cancer* 2000;84:87-89

• ESOPHAGEAL CANCER •

Morphological and functional changes of mitochondria in apoptotic esophageal carcinoma cells induced by arsenic trioxide

Zhong-Ying Shen, Jian Shen, Qiao-Shan Li, Cai-Yun Chen, Jiong-Yu Chen, Yi Zeng

Zhong-Ying Shen, Jian Shen, Qiao-Shan Li, Department of Pathology, Medical College of Shantou University, Shantou 515031, Guangdong Province, China

Cai-Yun Chen, Central Lab. Medical College of Shantou University
Jiong-Yu Chen, Central Lab. of Tumor Hospital, Medical College of Shantou University

Yi Zeng, Institute of Virology, Chinese Academy of Preventive Medicine, Beijing 100052, China

Supported by the National Natural Science Foundation of China No. 39830380

Correspondence to: Dr. Zhong-Ying Shen, Department of Pathology, Medical College of Shantou University, 22 Xinglin Road, Shantou 515031, Guangdong Province, China. zhongyingshen@yahoo.com
Telephone: +86-754-8538621 Fax: +86-754-8537516

Received 2001-06-02 Accepted 2001-11-20

Abstract

AIM: To demonstrate that mitochondrial morphological and functional changes are an important intermediate link in the course of apoptosis in esophageal carcinoma cells induced by As_2O_3 .

METHODS: The esophageal carcinoma cell line SHEEC1, established in our laboratory, was cultured in 199 growth medium, supplemented with $100\text{mL}\cdot\text{L}^{-1}$ calf serum and $3\mu\text{mol}\cdot\text{L}^{-1}\text{As}_2\text{O}_3$ (the same below). After 2, 4, 6, 12, 24 h of drug adding, the SHEEC1 cells were collected for light-and electron-microscopic examination. The mitochondria were labeled by Rhodamine fluorescence probe and the fluorescence intensity of the mitochondria was measured by flow cytometer and cytofluorimetric analysis. Further, the mitochondrial transmembrane potential (MTP, $\Delta\Psi\text{m}$) change was also calculated.

RESULTS: The mitochondrial morphological change after adding As_2O_3 could be divided into three stages. In the early-stage (2-6 h) after adding As_2O_3 , an adaptive proliferation of mitochondria appeared; in the mid-stage (6-12 h) a degenerative change was observed; and in the late-stage (12-24 h) the mitochondria swelled with outer membrane broken down and then cells death with apoptotic changes of nucleus. The functional change of the mitochondria indicated by fluorescent intensity, which reflected the MTP status of mitochondria, was in accordance with morphological change of the mitochondria. The fluorescent intensity increased at early-stage, declined in mid-stage and decreased to the lowest in the late-stage. 24 h after As_2O_3 adding, the cell nucleus showed typical apoptotic changes.

CONCLUSION: Under the inducement of As_2O_3 , the early apoptotic changes of SHEEC1 cells were the apparent morphological and functional changes of mitochondria, afterwards the nucleus changes followed. It is considered that changes of mitochondria are an important intermediate link in the course of apoptosis of esophageal carcinoma

cells induced by As_2O_3 .

Shen ZY, Shen J, Li QS, Chen CY, Chen JY, Zeng Y. Morphological and functional changes of mitochondria in apoptotic esophageal carcinoma cells induced by arsenic trioxide. *World J Gastroenterol* 2002;8(1):31-35

INTRODUCTION

Esophagus cancer is common in China^[1-11]. The treatment is still a focus of research^[12-17]. Induction of cell apoptosis is a novel therapeutic strategies for cancer^[18-25]. In our previous work, we used As_2O_3 to induce apoptosis of esophageal carcinoma cells^[26]. The pathomorphological changes evinced that cells became smaller, the cells shrank, the nuclei rounded up, chromatin agglutinated and marginated, nuclear membrane broke down and then followed by the degenerative changes of the cells. All these changes indicated typical morphological changes of apoptosis^[27]. The necrotic changes were also found with a large dosage of As_2O_3 ^[28]. We discovered that in the early-stage of cell apoptosis, prior to the obvious change of cell nuclei, the mitochondria showed proliferation. The detailed morphological changes of mitochondria of esophageal carcinoma cells induced by As_2O_3 were firstly described in our paper^[29]. We also found that nitric oxide (NO) was released from the cultured esophageal carcinoma cell line after administration of As_2O_3 with increasing amounts at the early apoptotic stage^[30]. Furthermore, down regulated expression of bcl-2 and over expression of bax were always found in apoptotic cells induced by As_2O_3 ^[31].

Some authors hold that apoptosis is a programmed cell death (PCD); the death signal originates from the inside of cells; the change chiefly involves the cell nucleus with no apparent changes seen in the cytoplasm and cell organelle^[32-33]; making it different from cell necrosis^[34]. In our studies, the morphological changes of apoptotic cells induced by As_2O_3 were different from the programmed cell death in which the latter showed the nuclear changes at first and then cytoplasm, and the former were vice versa^[35]. In recent years, it has been explained that apoptosis is related to certain factors, such as Bcl-2/Bax,^[36-39] Ca^{2+} ^[40] and cytochrome c^[41-42], which are all located on mitochondria^[43]. When they are released from mitochondria, they can inhibit or promote cell apoptosis. Therefore, mitochondria are thought to be the apoptosis regulation center^[44]. Mitochondria are also an important organelle. They are concerned with cell breathing, oxygen metabolism, enzyme activity and energy supply. All of those functions relate to the permeability of the mitochondria and mitochondrial transmembrane potential (MTP, $\Delta\Psi\text{m}$). When MTP decreases, the mitochondria generate morphological and functional changes^[45-47].

Rhodamine 123 (Rho123), a kind of fluorescent dye, is traditionally used as a mitochondria probe^[48]. Rho 123 can quickly gather on living cell mitochondria. The fluorescence intensity of Rho123 represents MTP which reflects the cell in a quiescent or active condition, and in a proliferative or differentiative manner^[49]. Flow cytometer and fluorescent microphotometry are the satisfactory

instruments to measure Rho123 fluorescent intensity. The purpose of this paper is to study the mitochondrial morphological and functional changes during the cell apoptosis of esophageal carcinoma cell line induced by As_2O_3 , thus demonstrating that mitochondrial changes play an important role in the course of cell apoptosis.

MATERIALS AND METHODS

Cell line and As_2O_3 adding

The esophageal carcinoma cell line SHEEC1 is the human embryonic esophageal epithelial cells malignantly transformed by HPV18 E6 E7 in synergy with TPA^[50]. It is cultured in 199 growth medium, supplemented with $100\text{mL}\cdot\text{L}^{-1}$ calfserum and antibiotics. In experiments, SHEEC1 cells were cultured separately in culture flasks and on 24-well culture plates (Corning Co.) with the cover slide inside the well, in every well 10^4 SHEEC1 cells were inoculated. As_2O_3 (Sigma, St. Louis, Mo; Lot A 1010) was prepared in concentration of $3\mu\text{mol}\cdot\text{L}^{-1}$ with 199 growth medium. The experimental group and the control group without As_2O_3 administered were examined at definite times. The experiments were repeated once.

Examination under light-and electron-microscope

At 2,4,6,12,24 h after As_2O_3 adding, one culture flask of SHEEC1 cultured cells was taken for examination. The floating cells in the flasks were collected by centrifugation (CytospinIII, Shandon Co.), Giemsa stained and examined by light-microscope. Cells attached to flask were digested with $2.5\text{g}\cdot\text{L}^{-1}$ trypsin, centrifuged, the cell pallet was fixed with $25\text{g}\cdot\text{L}^{-1}$ glutaraldehyde, and were routinely prepared for electron-microscopic examination.

Rhodamine fluorescent probe labeling and cytofluorimetric analysis (CFA)^[51,52]

SHEEC1 cells were placed on the slide after reacting with As_2O_3 at various times, stained by Rhodamine 123 (Rho123, MW381, Molecular Probe Inc. Eugene) at the concentration of $10\text{mg}\cdot\text{L}^{-1}$, and the cells were incubated in 37°C , $50\text{mL}\cdot\text{L}^{-1}$ CO_2 incubator for 15 min. It was examined by fluorescent microscopy and cytofluorimetry. Using the Nikon fluorescent microscope (Fluophot, Nikon) with Low-cost cooled digital CCD camera system and software STARI (Photometrics LTD. USA), the fluorescent image of mitochondria of SHEEC1 cells labeled by Rho123 were displayed on the screen of monitor, the fluorescent intensity of cells was measured by scanning method, and the average amount of cellular fluorescence was calculated by software.

Flow cytometer (FCM) examination^[53]

Following As_2O_3 treatment, SHEEC1 cell cultured in flasks were harvested with trypsinization, washed once with PBS, resuspended in PBS, and incubated with Rho123 ($10\text{mg}\cdot\text{L}^{-1}$) at 37°C for 15 min, stained cells were wash twice with PBS, dispersed, filtered through a 360 mesh nylon net to make single cell suspension. 10^9 cell $\cdot\text{L}^{-1}$ were detected by flow cytometer (FACSort, B-D Co. USA) using exciting light 488nm and emission light 515nm to detect Rho123 fluorescent intensity. The histogram managed by the computer was drawn according to the fluorescent intensity value of one cell. Partial of SHEEC1 cells were fixed with $700\text{mL}\cdot\text{L}^{-1}$ alcohol, stained with propidium iodide (Sigma) and analyzed with flow cytometer. The cell cycle and apoptotic cell rate were calculated.

Calculation of mitochondrial transmembrane potential (MTP. $\Delta\Psi\text{m}$)^[46]

Examining 10^4 cells by FCM, the average fluorescent intensity of the

cells labeled by Rho 123 before and after As_2O_3 adding were drawn as histograms for comparing. By cytofluorimetric analysis the average fluorescent intensity value ($\bar{x}\pm s$) was calculated from one cell.

RESULTS

Cell apoptosis

Twenty-four hours after As_2O_3 acting on SHEEC1 cells, the apoptotic peak (28% of the cells) before G_1G_0 in DNA histogram of FCM examination appeared (Figure 1). Collecting the floating cells by cytospin and Giesma staining, the cell nuclei showed typical cell apoptotic changes with chromatin agglutinated and margined (Figure 2).

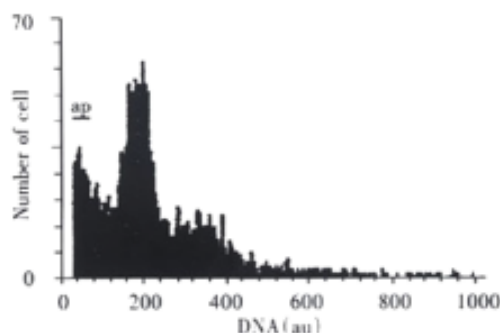


Figure 1 DNA histogram of SHEEC1 cells 24 h after Figure 2 Apoptotic changes 24 h after As_2O_3 .

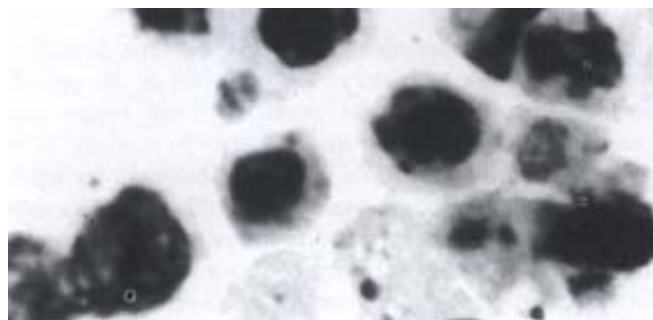


Figure 2 As_2O_3 adding. ap, apoptotic peak. adding, HE $\times 400$.

Morphological changes of mitochondria under transmission electron-microscope

Before adding As_2O_3 the mitochondria were located around the nucleus in one or two arrays (Figure 3A). There were fixed intervals between mitochondria, in which other organelles were present. When adding As_2O_3 2-4 h, the mitochondria increased, which showed either concentration in certain areas or in one pole of the cytoplasm or distributed in inner, middle or outer layer of the cytoplasm (Figure 3B). Mitochondria were oval in shape and different in size. The newly proliferated mitochondria were smaller with dense matrix. Some mitochondria were condensed with indistinct ridges and some mitochondria were crowded closely together. After 6 h, the high electron dense and irregular shaped substances precipitated in the mitochondrial matrix, even filled up the whole mitochondria (Figure 3C). The autophagosomes resulting from wrapping of condensed mitochondria by the lysosomes were frequently seen. After 12 h, the mitochondria swelled, its outer membrane broke down, left a single layer of membrane, which were seen like a balloon or a vacuole. After 24 h, the cell nucleus shrank and chromatin agglutinated locating near the nuclear membrane with mitochondria swelling, or becoming vacuole-like or broken down (Figure 3D).

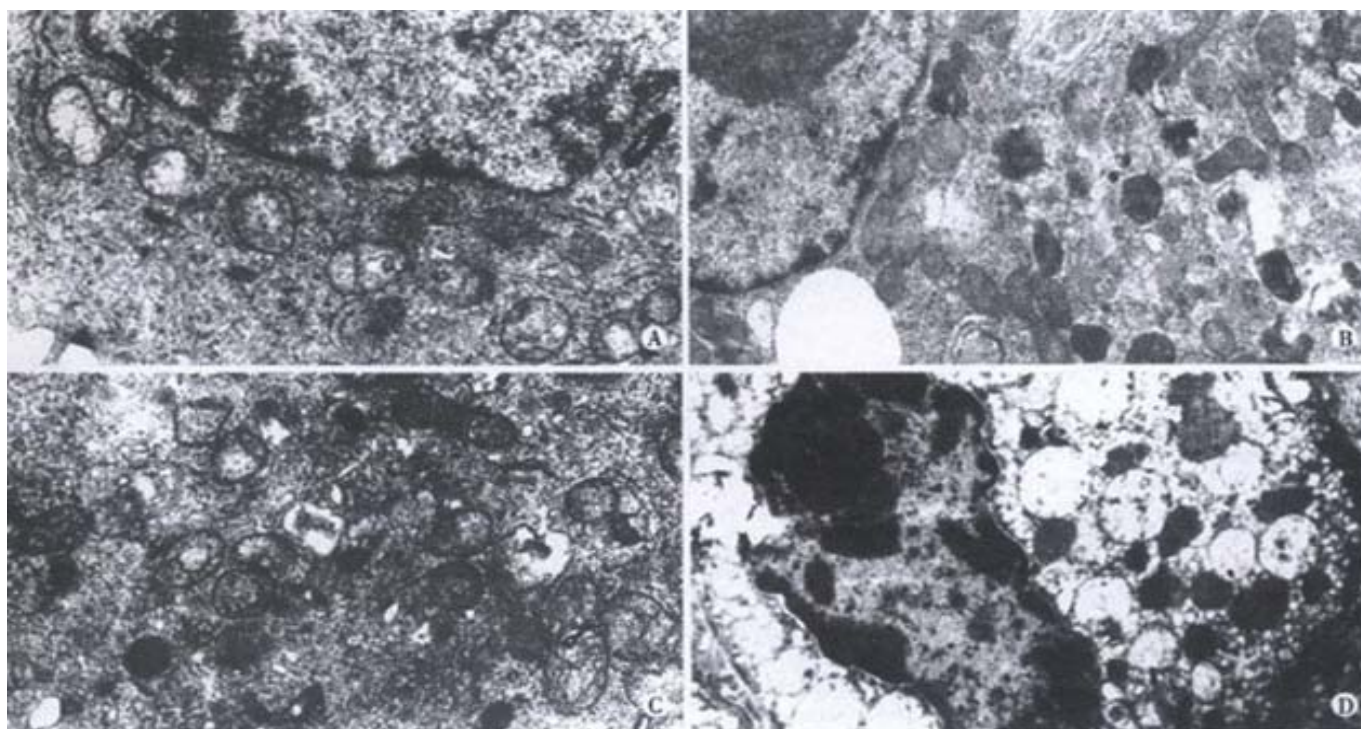


Figure 3 Apoptotic cells (EM x 15000). Mitochondria in 1-2 arrays located around the cell nucleus, not adding As₂O₃; Increment of mitochondria 2-4 h after As₂O₃ adding; Dense substances deposition in mitochondria 4-6h after As₂O₃ adding; Apoptotic cell showed cell nucleus shrank, chromatin agglutinated, mitochondria increased and swelled as balloon-like 24h after As₂O₃ adding.

Functional changes of mitochondria in cell apoptosis: the dynamic changes of MTP ($\Delta\Psi_m$)

Mitochondrial fluorescence intensity detected by FCM After As₂O₃ was added to SHEEC1 cells, the changes of mitochondria fluorescence intensity from different reacting times were seen in histogram (Figure 4 A,B,C,D). A slight increase of mitochondrial fluorescence intensity was observed at 2h after added As₂O₃. With treatment of As₂O₃ for 4-6h, fluorescent intensity of mitochondria was decreased sharply. After 12-24h fluorescent intensity was the lowest.

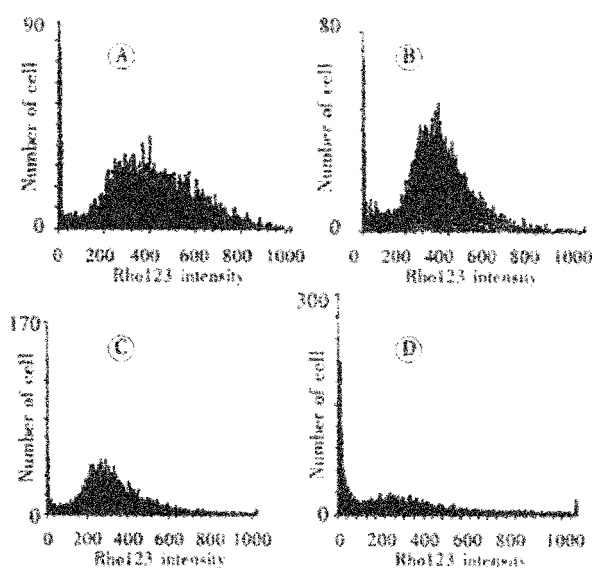


Figure 4 The histogram of mitochondrial fluorescent intensity by FCM after As₂O₃ adding.

A: Control; B: 2-4 h; C: 4-6 h; D: 12-24 h.

Fluorescent intensity by cytofluorimetric analysis Under fluorescent microscope, the number of mitochondria of cells was increased at first (Figure 5) and then decreased. The fluorescent intensity increased in 2h after As₂O₃ added, declined in 4-6h and decreased to the lowest in the 12-24h (Table 1). An increment of fluorescence intensity in partial early-stage apoptotic cells after 2 h of As₂O₃ adding and the intensity decreased hereafter. Following fluorescence associated with the uptake of dye Rho123 allows to evaluate $\Delta\Psi_m$ modifications, the results showed the dynamic MTP changes in the apoptotic process induced by As₂O₃.

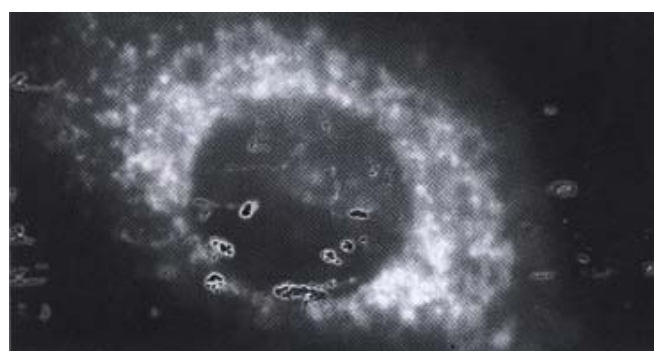


Figure 5 Increment of mitochondria with Rho123 labeled in cytoplasm of SHEEC1 after 2-4 h As₂O₃ adding. $\times 1000$

The Rho123 fluorescence intensity of the labeled mitochondria differed from different reacting times after adding As₂O₃. At first fluorescent intensity increased and then the rapidly declining value of fluorescence intensity was in accordance with both results of FCM and CFA. It taking cell morphology into account, the fluorescence intensity changes may reflect the consequence of As₂O₃ stimulation to mitochondria for different times. 2 h after As₂O₃ was added, the mitochondria proliferated and the fluorescent intensity increased, soon after the

intensity swiftly declined and went to the lowest at 24 h, which indicated that morphological and functional changes of mitochondria induced by As_2O_3 represented the process cell apoptosis.

Table 1 Average fluorescence intensity value of SHEEC1 after As_2O_3 adding (arbitrary unit $\times 10^{-4}/\text{cell}$)

T (after As_2O_3) h	Fluorescence intensity ($\bar{x} \pm s$)
Control	180.3 \pm 75.7
2	206.4 \pm 93.2
4	170.2 \pm 80.3
6	168.2 \pm 72.2
12	114.4 \pm 70.3
24	90.7 \pm 85.6

DISCUSSION

Reports about As_2O_3 inducement of apoptosis of cancer cells have been seen frequently in hemopoietic stem cells and leukemia cells^[54-60], but rarely in epithelial tumor cells^[61-64]. We have tried to explore the possibility of curing esophageal carcinoma by using As_2O_3 treatment *in vitro*. The experimental results have shown that As_2O_3 can induce cancer cell apoptosis, large doses of As_2O_3 can even induce cell necrosis. Our previous works indicated that at the early-stage of cell apoptosis, morphological changes of the mitochondria might be an important phenomenon in the course of esophageal carcinoma cell apoptosis induced by As_2O_3 ^[29, 31]. Our results showed that morphological and functional changes of mitochondria of SHEEC1 cells were induced by As_2O_3 . It could divide into three stages. Two to four h after As_2O_3 administration, the mitochondria proliferated with a lot of new small mitochondria, distributing from the inner layer to the outer layer of cytoplasm. This was the early reaction of mitochondria of SHEEC1 cells to the effect of As_2O_3 . 6 h after As_2O_3 inducement, many ridges on mitochondria were seen. The dense substances began to precipitate in the matrix of mitochondria and the condensed or damaged mitochondria were engulfed by lysosomes to form autophagosomes as seen in lymphocytes^[65]. Twelve hours after As_2O_3 inducement, the mitochondria were swelling, or vacuolation with mitochondria ridges decreased or disappeared. Twenty-four h after As_2O_3 inducement, apoptotic cells appeared with coagulating chromatin in nucleus and shrinking in the whole cell. The mitochondria swelled like a balloon. During the whole course of cell apoptosis, changes of mitochondria preceded the changes in nuclei.

The fluorescent intensity value detected by CFA and FCM reflects the function of mitochondria^[66]. The change of Rho123 fluorescent intensity under As_2O_3 treatment may be divided into 3 time phases: 2-4h after As_2O_3 inducement, mitochondria increased fluorescent intensity, but began to decline after 4-6 h and decreased to the lowest after 12-24 h. These functional changes of mitochondria were in accordance with mitochondrial morphological changes.

The functional changes of mitochondria may be accompanied with decreasing the formation of ATP, reducing the activity of dehydrogenase^[67], thus influencing cell respiration, cell metabolism, energy supply and even the cell death. If the mitochondrial release cytochrome c or apoptotic inducement factors (AIF), they may activate the caspases enzyme system, which further act upon cell nucleus and cell keratinoprotein to induce irreversible apoptotic changes^[68]. If the mitochondrial changes resulted in lowering of $\Delta\Psi_m$, increase of oxygen free radical and blocking up the formation of ATP, the cells will be finally undergo necrosis, because they lose the ability of electron bond transmission. Therefore, the mitochondrial changes may induce cell apoptosis and also cell necrosis^[69]. When the inducement factor is strong or highly concentrated it induces cell necrosis. If less in amount and strength, it may give times to activate the caspases enzyme system^[70], the cell apoptosis will develop. Mitochondrial fluorescent probe Rho123 is a very useful tool, which may specifically conjugate with mitochondria to indicate cells living

state or metabolic state^[25]. Detecting Rho123 fluorescence intensity of mitochondria may reveal mitochondrial quantity and function under different kinds of stimuli. The Rho123 fluorescence intensity is stronger in proliferative cells than in quiescent cells, and the intensity decreases in damaged mitochondria caused by harmful stimuli^[48]. The amount of Rho123 conjugated with mitochondria differs in different types of cells and in different cell functional status^[66]. The mitochondrial changes of SHEEC1 cells induced by As_2O_3 occurred 2-4 h after drug adding. Under the same cultured conditions, mitochondria were supposed to be the firstly targeting site in the course of cell apoptosis. Therefore, under As_2O_3 inducement, the morphological and functional in mitochondria of SHEEC1 cells, which happened prior to cell nuclear DNA change, may be regarded as the important link in cell apoptosis.

REFERENCES

- He LJ, Wu M. The distribution of esophageal and cardiac carcinoma and precancerous of 2238. *World J Gastroenterol* 1998; 4(Suppl 2):100
- Yu GQ, Zhou Q, DING Ivan, Gao SS, Zheng ZY, Zou JX, Li YX, Wang LD. Changes of p53 protein blood level in esophageal cancer patients and normal subjects from a high incidence area in Henan, China. *World J Gastroenterol* 1998; 4:365-366
- Gao SS, Zhou Q, Li YX, Bai YM, Zheng ZY, Zou JX, Liu G, Fan ZM, Qi YJ, Zhao X, Wang LD. Comparative studies on epithelial lesions at gastric cardia and pyloric antrum in subjects from a high incidence area for esophageal cancer in Henan, China. *World J Gastroenterol* 1998; 4:332-333
- Wang LD, Zhou Q, Wei JP, Yang WC, Zhao X, Wang LX, Zou JX, Gao SS, Li YX, Yang CS. Apoptosis and its relationship with cell proliferation, p53, Waf1p21, bcl-2 and c-myc in esophageal carcinogenesis studied with a high risk population in northern China. *World J Gastroenterol* 1998; 4:287-293
- Qiao GB, Han CL, Jiang RC, Sun CS, Wang Y, Wang YJ. Overexpression of P53 and its risk factors in esophageal cancer in urban areas of Xi'an. *World J Gastroenterol* 1998; 4:57-60
- Jiao LH, Wang LD, Xing EP, Yang GY, Yang CS. Frequent inactivation of p16 and p15 expression in human esophageal squamous cell carcinoma detected by RT-PCR. *World J Gastroenterol* 1998; 4(Suppl 2):105-
- Bai YM, Wang LD, Seril DN, Liao J, Yang GY, Yang CS. Expression of hMSH2 in human esophageal cancer from patients in a high incidence area in Henan, China. *World J Gastroenterol* 1998; 4(Suppl 2):107
- Qi YJ, Wang LD, Nie Y, Cai C, Yang GY, Xing EP, Yang CS. Alteration of p19 mRNA expression in esophageal cancer tissue from patients at high incidence area in northern China. *World J Gastroenterol* 1998; 4(Suppl 2):108
- Zhang X, Geng M, Wang YJ, Cao YC. Expression of epidermal growth factor receptor and proliferating cell nuclear antigen in esophageal carcinoma and pre-cancerous lesions. *Huaren Xiaohua Zazhi* 1998; 6:229-230
- Wang D, Su CQ, Wang Y, Ye YK. Deletion of p16 gene at a high frequency in esophageal carcinoma. *Huaren Xiaohua Zazhi* 1998; 6:1052-1053
- Zou JX, Wang LD, SHI Stephanie T, Yang GY, Xue ZH, Gao SS, Li YX, YANG Chung S. p53 gene mutations in multifocal esophageal precancerous and cancerous lesions in patients with esophageal cancer in high risk northern China. *Shijie Huaren Xiaohua Zazhi* 1999; 7:280-284
- Deng LY, Zhang YH, Xu P, Yang SM, Yuan XB. Expression of interleukin 1 β converting enzyme in 5-FU induced apoptosis in esophageal carcinoma cells. *World J Gastroenterol* 1999; 5:50-52
- Xiao ZF, Zhang Z, Wang Z, Zhang HZ, Wang M, Shi ML, Yin WB. Value of CT Scan on radiotherapy of esophageal carcinoma. *Huaren Xiaohua Zazhi* 1998; 6(Suppl 7): 181-184
- Fu JH, Rong TH, Huang ZF, Yang MT, Wu YL. Comparative assessment of three prostesis types of palliative intubation for late stage esophageal carcinoma. *Huaren Xiaohua Zazhi* 1998; 6:984-986
- Chen KN, Xu GW. Diagnosis and treatment of esophageal cancer. *Shijie Huaren Xiaohua Zazhi* 2000; 8:196-202
- Wu XY, Zhang XF, Yin FS, Lu HS, Guan GX. Clinical study on surgical treatment of esophageal carcinoma in patients after subtotal gastrectomy. *World J Gastroenterol* 1998; 4(Suppl 2):68-69
- Gao ZD, Xu XY, Mao AW, Zhou XF, Jiang H. Combination of arterial infusion chemotherapy and radio therapy in the treatment of 36 cases of middle and late stage esophageal cancer. *World J Gastroenterol* 1998; 4(Suppl 2):72
- Guo WJ, Yu EX, Zheng SG, Shen ZZ, Luo JM, Wu GH, Xia SA. Study on the apoptosis and cell cycle arrest in human liver cancer SMMC7721 cells induced by Jianpili qi herbs. *Shijie Huaren Xiaohua Zazhi* 2000; 8:52-55
- Tu SP, Jiang SH, Qiao MM, Cheng SD, Wang LF, Wu YL, Yuan YZ,

- Wu YX. Effect of trichosanthin on cytotoxicity and induction of apoptosis of multiple drugs resistance cells in gastric cancer. *Shijie Huaren Xiaohua Zazhi* 2000; 8:150-152
- 20 Liang WJ, Huang ZY, Ding YQ, Zhang WD. Lovo cell line apoptosis induced by cyclo heximide combined with TNF α . *Shijie huaren Xiaohua Zazhi* 1999; 7:326-328
 - 21 Lu XP, Li BJ, Chen SL, Lu B, Jiang NY. Effect of chemotherapy or targeting chemotherapy on apoptosis of colorectal carcinoma. *Shijie Huaren Xiaohua Zazhi* 1999; 7:332-334
 - 22 Shen YF, Zhuang H, Shen JW, Chen SB. Cell apoptosis and neoplasms. *Shijie Huaren Xiaohua Zazhi* 1999; 7:267-268
 - 23 Sun ZX, Ma QW, Zhao TD, Wei YL, Wang GS, Li JS. Apoptosis induced by norcantharidin in human tumor cells. *World J Gastroenterol* 2000; 6:263-265
 - 24 Zhu HZ, Ruan YB, Wu ZB, Zhang CM. Kupffer cell and apoptosis in experimental HCC. *World J Gastroenterol* 2000; 6:405-407
 - 25 Evan G and Littlewood T. A matter of life and cell Death. *Science* 1998; 281: 1317-1320
 - 26 Shen ZY, Tan LJ, Cai WJ, Shen J, Chen C, Tang XM, Zheng MH. Arsenic trioxide induces apoptosis of oesophageal carcinoma *in vitro*. *Intern J Mol Med* 1999;4:33-37
 - 27 Shen ZY, Tan LJ, Cai WJ, Shen J, Chen CY, Tang XM. Morphologic study on apoptosis of esophageal carcinoma cell line induced by arsenic trioxide. *Shijie Huaren Xiaohua Zazhi* 1998; 6:(Suppl 7)226-229
 - 28 Shen J, Wu MH, Cai WJ, Shen ZY. The effects of arsenite trioxide in various concentration on the esophageal carcinoma cell line. *Zhongguo Zhongliu Shengwu Zhiliao Zazhi* 2001; 8:106-109
 - 29 Shen ZY, Shen J, Cai WJ, Hong C, Zheng MH. The alteration of mitochondria is an early event of arsenic trioxide induced apoptosis in esophageal carcinoma cells. *Intern J Mol Med* 2000;5: 155-158
 - 30 Shen ZY, Shen WY, Chen MH, Hong CG, Shen J. Alterations of nitric oxide in apoptosis of esophageal carcinoma cells induced by arsenite. *Shijie Huaren Xiaohua Zazhi* 2000; 8: 1101-1104
 - 31 Shen ZY, Shen J, Chen MH, Li QS, Hong CQ. Morphological changes of mitochondria in apoptosis of esophageal carcinoma cells induced by As₂O₃. *Zhonghua Binglixue Zazhi* 2000; 29: 200-203
 - 32 Deng LY, Zhang YH, Zhang HX, Ma CL, Chen ZG. Observation of morphological changes and cytoplasmic movement in apoptosis process. *World J Gastroenterol* 1998; 4: 66-67
 - 33 Floryk D, Ucker DS. Molecular mapping of the physiological cell death process. Mitochondrial events may be disordered. *Ann N Y Acad Sci* 2000; 926: 142-148
 - 34 Shen ZY, Chen CY, Shen J, Cai WJ. Ultrastructural study of apoptosis and necrosis in the esophageal carcinoma cell line induced by arsenic trioxide. *Zhongguo Yixue Wulixue Zazhi* 1999; 16: 91-94
 - 35 Shen ZY, Chen MH, Li QS, Shen J. An ultrastructural study on the programmed cell death of human amniotic epithelium. *Dianzi Xianwei Xuebao* 2000; 19: 259-260
 - 36 Zhang CS, Wang WL, Peng WD, Hu PZ, Chai YB, Ma FC. Promotion of apoptosis of SMMC7721 cells by bcl-2 ribozyme. *Shijie Huaren Xiaohua Zazhi* 2000; 8: 417-441
 - 37 Yuan RW, Ding Q, Jiang HY, Qin XF, Zou SQ, Xia SS. Bcl-2, p53 protein expression and apoptosis in pancreatic cancer. *Shijie Huaren Xiaohua Zazhi* 1999; 7: 851-854
 - 38 Wang LD, Zhou Q, Wei JP, Wang WC, Zhao X, Wang LX, Zou X, Gao SS, Li YX, Yang CS. Apoptosis and its relationship with cell proliferation, p53, waf/p21, bcl-2 and c-myc in esophageal carcinogenesis studied with a high risk population in northern China. *World J Gastroenterol* 1998; 4: 287-293
 - 39 Pastorino JG, Chen ST, Tafani M, Snyder JW and Farber JL. The overexpression of Bax produces cell death upon induction of the mitochondrial permeability transition. *J Biol Chem* 1998; 273: 7770-7775
 - 40 Fang M, Zhang HQ, Xue SB, Li N, Wang L. Intracellular calcium distribution in apoptosis of HL-60 cells induced by harringtonine: intranuclear accumulation and regionalization. *Cancer Letters* 1998; 127: 113-121
 - 41 Mootha VK, Wei MC, Buttle KF, Scorrano L, Panoutsakopoulou V, Mannella CA, Korsmeyer SJ. A reversible component of mitochondrial respiratory dysfunction in apoptosis can be rescued by exogenous cytochrome c. *EMBO J* 2001; 20: 661-671
 - 42 Zimmermann KC, Waterhouse NJ, Goldstein JC, Schuler M, Green DR. Aspirin induces apoptosis through release of cytochrome c from mitochondria. *Neoplasia* 2000;2:505-513
 - 43 Li H, Kolluri SK, Gu J, Dawson MI, Cao XH, Hobbs PD, Lin BZ, Chen GQ, Lu JS, Lin F, Xie ZH, Fontana JA, Reed JC, Zhang XK. Cytochrome c release and apoptosis induced by mitochondrial targeting of nuclear orphan receptor TR3. *Science* 2000; 289: 1159-1164
 - 44 Brenner C and Kroemer G. Apoptosis Mitochondria—the death signal intergrators. *Science* 2000; 289: 1150-1151
 - 45 Heerdt BG, Houston MA, Anthony GM, Augenlicht LH. Mitochondrial membrane potential ($\Delta \psi_{mt}$) in the coordination of p53-independent proliferation and apoptosis pathways in human colonic carcinoma cells. *Cancer Res* 1998; 58: 2869-2875
 - 46 Wakabayashi T, Karbowski M. Structural changes of mitochondria related to apoptosis. *Biol Signals Recept* 2001; 10: 26-56
 - 47 Hail NJ, Lotan R. Mitochondrial permeability transition is a central coordinating event in N-(4-hydroxyphenyl) retinamide-induced apoptosis. *Cancer Epidemiol Biomarkers Prev* 2000; 9: 1293-1301
 - 48 Shapiro HM. Membrane potential estimation by flow cytometer. *Methods* 2000; 21: 271-279
 - 49 Buckman JF, Reynolds IJ. Spontaneous changes in mitochondrial membrane potential in cultured neurons. *J Neurosci* 2001; 21: 5054-5065
 - 50 Shen ZY, Cen S, Shen J, Cai WJ, Xu JJ, Ten ZP, Hu Z, Zeng Y. Study of immortalization and malignant transformation of human embryonic esophageal epithelial cells induced by HPV18E6E7. *J Cancer Res Clin Oncol* 2000; 126: 589-594
 - 51 Canete M, Juaranz A, Lopez-Nieva P, Alonso-Torcal C, Villanueva A, Stockert JC. Fixation and permanent mounting of fluorescent probes after vital labeling of cultured cells. *Acta Histochem* 2001; 103: 117-126
 - 52 Follstad BD, Wang DI, Stephanopoulos G. Mitochondrial membrane potential differentiates cells resistant to apoptosis in hybridoma cultures. *Eur J Biochem* 2000; 267: 6534-6540
 - 53 Bedner E, Li X, Gorczyca W, Melamed MR, Darzynkiewicz Z. Analysis of apoptosis by laser scanning cytometry. *Cytometry* 1999; 35: 181-195
 - 54 Li YM, Broome JD. Arsenic targets tubulins to induce apoptosis in myeloid leukemia cells. *Cancer Res* 1999; 59: 776-780
 - 55 Bazarbachi A, El-Sabban ME, Nasr R, Quignon F, Awaraji C, Kersual J, Dianoux L, Zermati Y, Haidar JH, Hermine O, de-The H. Arsenic trioxide and interferon-alpha synergize to induce cell cycle arrest and apoptosis in human T-cell lymphotropic virus type I-transformed cells. *Blood* 1999; 93: 278-283
 - 56 Jing Y, Dai J, Chalmers-Redman RM, Tatton WG, Waxman S. Arsenic trioxide selectively induces acute promyelocytic leukemia cell apoptosis via a hydrogen peroxide-dependent pathway. *Blood* 1999; 94: 2102-2111
 - 57 Lallemand-Breitenbach V, Guillemin MC, Janin A, Daniel MT, Degos L, Kogan SC, Bishop JM, de-The H. Retinoic acid and arsenic synergize to eradicate leukemic cells in a mouse model of acute promyelocytic leukemia. *J Exp Med* 1999; 189: 1043-1052
 - 58 Rousselot P, Labaume S, Marolleau JP, Larghero J, Noguera MH, Brouet JC, Fermand JP. Arsenic trioxide and melarsoprol induce apoptosis in plasma cell lines and in plasma cells from myeloma patients. *Cancer Res* 1999; 59:1041-1048
 - 59 Huang XJ, Wiernik PH, Klein RS, Gallagher RE. Arsenic trioxide induces apoptosis of myeloid leukemia cells by activation of caspases. *Med Oncol* 1999; 16: 58-64
 - 60 Zhu XH, Shen YL, Jing YK, Cai X, Jia PM, Huang Y, Tang W, Shi GY, Sun YP, Dai J, Wang ZY, Chen SJ, Zhang TD, Waxman S, Chen Z, Chen GQ. Apoptosis and growth inhibition in malignant lymphocytes after treatment with arsenic trioxide at clinically achievable concentrations. *J Nat Cancer Inst* 1999; 91: 772-778
 - 61 Chen HY, Liu WH, Qin SK. Induction of arsenic trioxide on apoptosis of hepatocarcinoma cell lines. *Shijie Huaren Xiaohua Zazhi* 2000; 8: 532-535
 - 62 Gu QL, Li NL, Zhu ZG, Yin HR, Lin YZ. A study on arsenic trioxide inducing *in vitro* apoptosis of gastric cancer cell lines. *World J Gastroenterol* 2000; 6: 435-437
 - 63 Tu SP, Jiang SH, Tan JH, Jiang XH, Qiao MM, Zhang YP, Wu YL, Wu YX. Proliferation inhibition and apoptosis induction by arsenic trioxide on gastric cancer cell SGC 7901. *Shijie Huaren Xiaohua Zazhi* 1999; 7: 18-21
 - 64 Tan L, Chen X, Shen ZY. Study on the proliferative inhibition of human esophageal cancer cells with treatment DMSO and As₂O₃. *Shanghai Di-er Yike Daxue Xuebao* 1999; 19: 5-8
 - 65 Huo X, Piao YJ, Huang XX, Quao DF. Ultrastructural observation of mitochondria in apoptotic lymphocytes induced with cycloheximide. *Dianzi Xianwei Xuebao* 1998; 17: 702-705
 - 66 Hu Y, Moraes CT, Savaraj N, Priebe W, Lampidis TJ. Rho (0) tumor cells: a model for studying whether mitochondria are targets for rhodamine 123, doxorubicin, and other drugs. *Biochem Pharmacol* 2000; 60: 1897-1905
 - 67 Green DR, Reed JC. Mitochondria and apoptosis. *Science* 1998;281: 1309-1312
 - 68 Sugrue MM, Tatton WG. Mitochondrial membrane potential in aging cells. *Biol Signals Recept* 2001; 10: 176-188
 - 69 Lee HC, Yin PH, Lu CY, Chi CW, Wei YH. Increase of mitochondria and mitochondrial DNA in response to oxidative stress in human cells. *Biochem J* 2000; 348: 425-432
 - 70 Seol JG, Park WH, Kim ES, Jung CW, Hyun JM, Lee YY, Kim BK. Potential role of caspase-3 and -9 in arsenic trioxide-mediated apoptosis in PCI-1 head and neck cancer cells. *Int J Oncol* 2001; 18: 249-255

• ESOPHAGEAL CANCER •

The sensitivity of digestive tract tumor cells to As₂O₃ is associated with the inherent cellular level of reactive oxygen species

Fei Gao, Jing Yi, Gui-Ying Shi, Hui Li, Xue-Geng Shi, Xue-Ming Tang

Fei Gao, Jing Yi, Gui-Ying Shi, Hui Li, Xue-Geng Shi, Xue-Ming Tang, Department of Cell Biology, Shanghai Second Medical University, Shanghai 200025, China

Supported by the grants from National Natural Science Foundation of China, No. 39730270 and Shanghai Science and Technology Development fund of Education Committee, No.2000B101

Correspondence to: Prof. YI Jing, Department of Cell Biology, Shanghai Second Medical University, Shanghai 200025, China. yijing@shsmu.edu.cn Telephone: +86-21-63846590 Ext.421 Fax: +86-21-53065329

Received 2001-04-25 Accepted 2001-10-18

Abstract

AIM: To explore the correlation of the inherent cellular ROS level with the susceptibility of the digestive tract tumor cells to apoptosis induced by As₂O₃.

METHODS: Two gastric carcinoma cell lines, SGC7901 and MKN45, and two esophageal carcinoma cell lines, EC/CUHK1 (alternatively named EC1.71) and EC1867 with low concentration (2 μmol·L⁻¹) of As₂O₃ were cultured respectively, which confirmed the difference in apoptosis susceptibility between SGC7901 and MKN45, and between EC/CUHK1 and EC1867. The cells were incubated with dihydrogenrhodamine123 (DHR123), used as a ROS capture in absence of As₂O₃. The fluorescent intensity of rhodamine123, which was the product of cellular oxidation of DHR123, was detected by flow cytometry, and ROS was measured.

RESULTS: Apoptosis induced by a low concentration of As₂O₃ was more readily to occur in SGC7901 (22.4%±2.4%) and EC/CUHK1 (27.0%±2.9%) than in MKN45 (2.1%±0.5%) and EC1867 (0.8%±0.5%). In other words, SGC7901 was more sensitive than MKN45 to As₂O₃, meanwhile EC/CUHK1 was more sensitive than EC1867 to As₂O₃. The level of inherent cellular ROS in SGC7901 (650±37) was higher than that in MKN45 (507±22) (*P*<0.01), and the level of inherent cellular ROS in EC/CUHK1 (462±17) was higher than that in EC1867 (187±12) (*P*<0.01).

CONCLUSIONS: The cellular sensitivity to apoptosis induced by As₂O₃ is associated with the difference in cellular ROS level. The inherent ROS level might determinate the apoptotic sensitivity of tumor cells to As₂O₃.

Gao F, Yi J, Shi GY, Li H, Shi XG, Tang XM. The sensitivity of digestive tract tumor cells to As₂O₃ is associated with the inherent cellular level of reactive oxygen species. *World J Gastroenterol* 2002;8(1):36-39

INTRODUCTION

Arsenic trioxide (As₂O₃) has proved to be effective in the treatment of acute promyelocytic leukemia (APL)^[1-7]. While many researchers aimed at the effectiveness of As₂O₃-induced apoptosis on the other leukemic cells and some solid tumor cells, a lot of evidence showed that some types of tumor cells were sensitive while others

were insensitive to apoptosis-inducing effect of As₂O₃^[2,8-20]. Unraveling the causes of such sensitivity difference in the tumor cells will benefit not only the clinical selection of patients, to which As₂O₃ can be given, but also understanding the mechanisms underlying the apoptosis induced by As₂O₃.

Previously we investigated the sensitivity of a series of digestive tumor cell lines to As₂O₃. We identified that there were difference of sensitivity to apoptosis induced by low concentration (2 μmol/L) of As₂O₃ between the gastric carcinoma cell line SGC7901 and MKN45, and between the esophageal carcinoma cell line EC/CUHK1 (alternatively named EC1.71) and EC1867; SGC7901 was more sensitive than MKN45, and EC/CUHK1 was more sensitive than EC1867 to As₂O₃^[15-16]. We found that As₂O₃ induced cell apoptosis via directly influencing mitochondrion, consequently causing decrease of transmembrane potential and increase of reactive oxygen species (ROS) level^[17]. Recently it was evidenced that ROS participate the apoptosis induction of acute promyelocytic leukemia^[18,19,21,22]. But whether the difference of sensitivity of digestive tumor cells to apoptosis-inducing effect of As₂O₃ is associated with the inherent cellular ROS level is not clearly understood. In this study, we demonstrated the difference between SGC7901 versus MKN45, and EC/CUHK1 versus EC1867, thereby explored the relation between the sensitivity of cell to apoptosis induction of As₂O₃ and the inherent cellular ROS level.

MATERIALS AND METHODS

Cell Lines and Culture Conditions

Gastric carcinoma cell line SGC7901 vs MKN45, and esophageal carcinoma cell line EC/CUHK1 vs EC1867 (kindly provided by professor Shen, Shantou University) were cultured in DMEM medium supplemented with 100kU·L⁻¹ penicillin, 100mg·L⁻¹ streptomycin, and 100mL·L⁻¹ fetal bovine serum (Gibco) in a fully humidified atmosphere with 50mL·L⁻¹ CO₂ at 37°C. Cells were split when reached to 80% confluency.

Inducing Cell Apoptosis by As₂O₃

About 5×10⁵ tumor cells in logarithmic stage were treated with 2 μmol·L⁻¹ concentration of As₂O₃ (Sigma) for 72h and analyzed by flow cytometry and electron microscopy for apoptosis^[15-17]. As₂O₃ powder was dissolved in small amounts of 1.0 mol·L⁻¹ NaOH, then diluted to 10.0 mmol·L⁻¹ with phosphate-buffered saline (PBS) as stock solutions.

Detection Inherent ROS Level

The cells were incubated with 1 μmol·L⁻¹ dihydrorhodamine123 (DHR123, Sigma), as a ROS capture^[23-25], for 1 or 24h. Blank and positive controls were set, in which DHR123 was either omitted or plus 50 μmol·L⁻¹ of hydrogen peroxide (H₂O₂). DHR123 could be oxidized intracellularly to form the fluorescent compound rhodamine123 (Rh123) by ROS, and be pumped into mitochondria and remained there. After incubated with DHR123, cells were trypsinized and harvested before an immediate detection of

fluorescence intensity of Rh123 by flow cytometry FACScan (Becton Dickinson), and the cellular ROS level was thus measured.

RUSULTS

Cell Apoptosis Induced by As₂O₃

A significant apoptosis was observed in EC/CUHK1 and SGC7901 cells with 2μmol/L of As₂O₃ for 3 days while no remarkable apoptosis could be seen in EC1867 and MKN45 cells with the equivalent As₂O₃. The characteristic morphological changes were displayed in the apoptotic cells, including the shrinkage of the nuclear membrane, condensation and margination of the chromatin, and nuclear breakage (Figure1). DNA flow cytometry showed that the some cells with fractional DNA, as typical display of apoptosis, appeared, (27.0±2.9)% and (22.4±2.4)% ($\bar{x} \pm s, n=5$) respectively in EC/CUHK1 and SGC7901 cells, but hardly visible in EC1867 (0.8±0.5)% and MKN45 (2.1±0.5)%. (Figure 2).

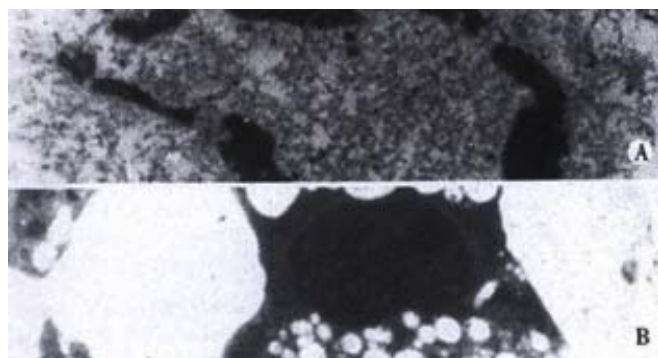


Figure 1 Apoptotic cells in EC/CUHK1 and SGC7901 with the condensation and margination of chromatin, and nuclear breakage EM×6000

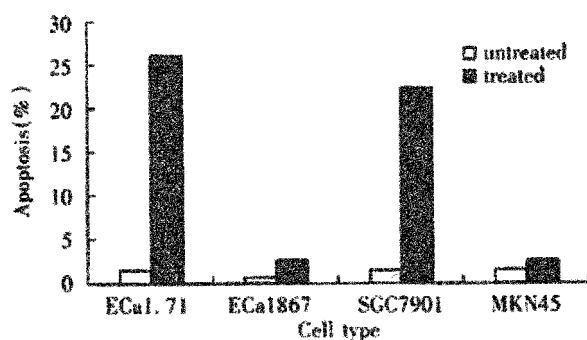


Figure 2 Flow cytometry with PI staining: apoptosis proportions in EC/CUHK1, EC1867, SGC7901 and MKN45

Inherent Cellular ROS Level

After incubation with DHR123 for 1 or 24h in absence of As₂O₃, the values ($\bar{x} \pm s, n=3$) of fluorescent intensity for Rh123 were 29±4.1 and 650±37 in SGC7901 cells; 21±1.4 and 507±22 in MKN45 cells; 50±3.9 and 462±17 in EC/CUHK1; 46±6.4 and 187±12 in EC1867 cells. The fluorescent intensity in blank control was less than 3. The values for the positive controls (DHR123 plus hydrogen peroxide incubation for 1h) were 80±4.9 in SGC7901; 27±3.0 in MKN45; 72±5.8 in EC/CUHK1; and 19±2.1 in EC1867. Figure 3 displayed the fluorescence histograms for four types of cells after incubation with DHR123 for 24h. The data showed that, in absence of As₂O₃, the cellular ROS level was higher in SGC7901 than in MKN45, and higher in EC/CUHK1 than in EC1867. Such differences were augmented in 24h incubation as shown above, where the value in SGC7901 was as 1.3 times as in MKN45, and in EC/CUHK1 was 2.5 times as in EC1867.

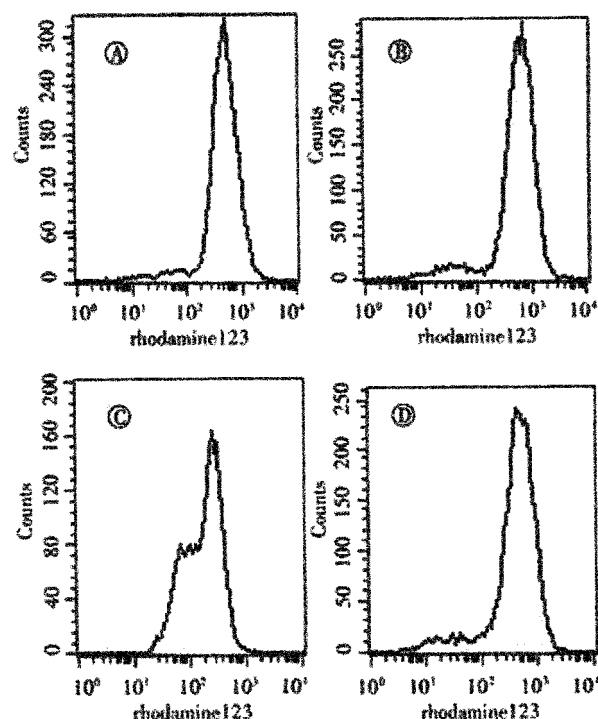


Figure 3 Flow cytometry displaying the inherent ROS level of cells A:MKN45; B:SGC7901; C:EC1867; D:EC/CUHK1

DISCUSSION

ROS, including superoxide anion (O₂⁻), hydrogen peroxide (H₂O₂), hydroxyl free radical (OH) and singlet oxygen (¹O₂), continuously generated from mitochondrial respiratory chain, have powerfully oxidative potential. ROS is capable of attacking lipids, nuclear acids and proteins, resulting in certain degree of oxidative damages^[26-35]. It has been thought recently to involve in apoptosis triggering and signaling^[36-43]. Cell possesses an efficient antioxidant defense system, mainly composed of the enzymes such as superoxide dismutase, glutathione peroxidase, and catalase, which can scavenge the ROS excessive to cellular metabolism, and make ROS level relatively stable under physiological conditions^[26-35]. Though it has been noticed that ROS were involved in As₂O₃-induced apoptosis^[18,19,21,22], evaluation of ROS level differences directly by a flow cytometric detection of ROS, to our knowledge, has not been frequently reported. Instead, H₂O₂, a kind of ROS, was adopted to represent the total ROS level, usually judged from a decrease in activity of glutathione peroxidase or catalase, or a decrease in ratio of reductive/oxidative glutathione^[18,19]. The total ROS level in the resting cells, however, was directly measured in the present study, by flow cytometric detection of Rh123. The comparative investigation on the inherent ROS levels in the cells showed that there were different apoptosis susceptibility to As₂O₃. In this study, inherent ROS level signified the basal cellular level of ROS in absence of any drug or exogenous ROS.

Detecting ROS level by flow cytometry has been a novel approach with characteristic of rapidness, convenience and reproducibility. DHR123, one of common ROS captures, is membrane permeable. It is oxidized by ROS intracellularly to become fluorescent Rh123, and is pumped into mitochondria and remain there, then is detectable by flow cytometry after a period of accumulation^[23-25]. 6-carboxy-2',7'-dichlorodihydrofluorescein diacetate (DCFH-DA) is another agent used to capture ROS. It is

cleaved by nonspecific esterases to form DCFH, which was further oxidized to form the fluorescent compound DCF and kept inside cells^[19,44,45]. It proved important, as we realized in this study, to prolong the incubation time with the ROS capture in order to visualize the nuance in ROS, since the absolute quantity of ROS is scarce. We selected two time intervals to visualize the accumulation of Rh123 fluorescence, finding that difference began to display at 1 h and became much pronounced by 24 h. These parameters definitely represented the difference of ROS level inherently existed in the respective types of cells. A similar result was obtained by using DCFH-DA in our study. Recently it was evidenced that NB4 leukemia cell line, which is sensitive to low concentration of As_2O_3 (1-2 μ mol/L), had higher H_2O_2 level than the U937 leukemia cell line which is insensitive to As_2O_3 , and exposure of cells to low concentration of As_2O_3 elevated the level of H_2O_2 in NB4 but not in U937^[19]. Though these studies indicated that a higher H_2O_2 level in NB4 might link to its higher sensitivity to As_2O_3 -induced apoptosis^[19], whether there existed a difference in total ROS level between cell lines which possessed different susceptibility to As_2O_3 -induced apoptosis, prior to As_2O_3 treatment, has not been documented.

Based on our previous work, we selected two pairs of digestive tract cell lines EC/CUHK1 versus EC1867, SGC7901 versus MKN45 in which one type of cell was susceptible and the other type was unsusceptible to As_2O_3 -induced apoptosis in this study, and measured the inherent levels of total ROS in these cells. The data on both pairs showed that the inherent ROS level was higher in sensitive cells. These results indicated that difference in apoptosis susceptibility of tumor cells to low concentration of As_2O_3 , was associated with the difference in the inherent cellular level of ROS, and what's more, the inherent ROS level might be pivotal in determination of the cellular susceptibility to As_2O_3 -induced apoptosis. The difference of inherent ROS level between cells probably resulted from the differential expression of enzymes involved in ROS generation and elimination^[46-51]. An interference to the expression of relevant enzymes or simply ROS is likely an approach by which an improved effect and expanded usage of arsenic trioxide can be achieved clinically.

REFERENCES

- Cai X, Shen YL, Zhu Q, Jia PM, Yu Y, Zhou L, Huang Y, Zhang JW, Xiong S.M., Chen SJ, Wang ZY, Chen Z and Chen GQ. Arsenic trioxide-induced apoptosis and differentiation are associated respectively with mitochondrial transmembrane potential collapse and retinoid acid signaling pathways in acute promyelocytic leukemia. *Leukemia* 2000;14:262-270
- Murgo AJ. Clinical trials of arsenic trioxide in hematologic and solid tumors: overview of the National Cancer Institute Cooperative Research and Development Studies. *Oncologist* 2001; 6(Suppl 2):22-28
- Kinjo K, Kizaki M, Muto A, Fukuchi Y, Umezawa A, Yamato K, Nishihara T, Hata J, Ito M, Ueyama Y, Ikeda Y. Arsenic trioxide (As_2O_3)-induced apoptosis and differentiation in retinoic acid-resistant acute promyelocytic leukemia model in hGM-CSF-producing transgenic SCID mice. *Leukemia* 2000; 14:431-438
- Ma DC, Sun YH, Chang KZ, Ma XF, Huang SL, Bai YH, Kang J, Liu YG, Chu JJ. Selective induction of apoptosis of NB4 cells from G2+M phase by sodium arsenite at lower doses. *Eur J Haematology* 1998; 61:27-35
- Munshi NC. Arsenic trioxide: an emerging therapy for multiple myeloma. *Oncologist* 2001; 6(Suppl 2):17-21
- Soignet SL, Maslak P, Wang ZG, Jhanwar S, Calleja E, Dardashti LJ, Corso D, DeBlasio A, Gabrilove J, Scheinberg DA, Pandolfi PP, Warrell RP Jr. Complete remission after treatment of acute promyelocytic leukemia with arsenic trioxide. *N Engl J Med* 1998;339:1341-1348
- Zhu XH, Shen YL, Jing YK, Cai X, Jia PM, Huang Y, Tang W, Shi GY, Sun YP, Dai J, Wang ZY, Chen SJ, Zhang TD, Waxman S, Chen Z, Chen GQ. Apoptosis and growth inhibition in malignant lymphocytes after treatment with arsenic trioxide at clinically achievable concentrations. *J Natl Cancer Inst* 1999;91:743-745
- Tu SP, Zhong J, Tan JH, Jiang XH, Qiao MM, Wu YX, Jiang SH. Induction of apoptosis by arsenic trioxide and hydroxy camptothecin in gastric cancer cells *in vitro*. *World J Gastroenterol* 2000;6:532-539
- Shen ZY, Tan LJ, Cai WJ, Shen J, Chen CY, Tang XM. Morphologic study on apoptosis of esophageal carcinoma cell line induced by arsenic trioxide. *Huaren Xiaohua Zazhi* 1998;6(Suppl 7):226-229
- Tu SP, Jiang SH, Tan JH, Jiang XH, Qiao MM, Zhang YP, Wu YL, Wu YX. Proliferation inhibition and apoptosis induction by arsenic trioxide on gastric cancer cell SGC-7901. *Shijie Huaren Xiaohua Zazhi* 1999; 7:18-21
- Chen HY, Liu WH, Qin SK. Induction of arsenic trioxide on apoptosis of hepatocarcinoma cell lines. *Shijie Huaren Xiaohua Zazhi* 2000;8:532-535
- Maeda H, Hori S, Nishitoh H, Ichijo H, Ogawa O, Kakehi Y, Kakizuka A. Tumor growth inhibition by arsenic trioxide (As_2O_3) in the orthotopic metastasis model of androgen-independent prostate cancer. *Cancer Res* 2001;61:5432-5440
- Xu HY, Yang YL, Gao YY, Wu QL, Gao GQ. Effect of arsenic trioxide on human hepatoma cell line BEL-7402 cultured *in vitro*. *World J Gastroenterol* 2000;6:681-687
- Gu QL, Li NL, Zhu ZG, Yin HR, Lin YZ. A study on arsenic trioxide inducing *in vitro* apoptosis of gastric cancer cell lines. *World J Gastroenterol* 2000;6:435-437
- Shi YH, Tan LJ, Li H, Shi GY, Shi XG, Tang XM. Study on arsenic trioxide induced apoptosis in tumor cell lines of digestive tract. *Shanghai Di-er Yike Daxue Xuebao* 1999;19:242-245
- Tan LJ, Shi GY, Shi XG, Tang XM. Induction of apoptosis of human esophageal cancer cell lines treated with arsenic trioxide. *Zhongguo Aizheng Zazhi* 1999;9:85-87
- Tan LJ, Shi YH, Shi GY, Li H., Shi XG, Tang XM. Study on the mechanism of As_2O_3 -induced apoptosis of human esophageal carcinoma cell lines. *Shanghai Di-er Yike Daxue Xuebao* 2000;20:12-17
- Dai J, Weinberg RS, Waxman S, Jing Y. Malignant cells can be sensitized to undergo growth inhibition and apoptosis by arsenic trioxide through modulation of the glutathione redox system. *Blood* 1999;93:268-277
- Jing Y, Dai J, Chalmers-Redman RME, Tatton WG, Waxman S. Arsenic trioxide selectively induces acute promyelocytic leukemia cell apoptosis via a hydrogen peroxide-dependent pathway. *Blood* 1999; 94:2102-2111
- Shen ZY, Tan LJ, Cai WJ, Shen J, Chen C, Tang XM, Zheng MH. Arsenic trioxide induces apoptosis of oesophageal carcinoma *in vitro*. *Int J Mol Med* 1999;4:33-37
- Gao F, Yi J, Shi GY, Li H, Jin HF, Shi XG, Tang XM. The susceptibility of leukemia cells to arsenic trioxide-induced apoptosis is determined by cellular reactive oxygen species level. *Shengwu Huaxue Yu Shengwu Wuli Xuebao* 2001;33:109-113
- Gao F, Yi J, Shi GY, Jin HF, Shi XG, Tang XM. Cell cycle-related induction of apoptosis of NB4 cells by arsenic trioxide is associated with difference in reactive oxygen species level in cell cycle. *Shanghai Di-er Yike Daxue Xuebao* 2001;21:296-299
- Shi GY, Gao F, Shi XG, Tang XM. Detection of cellular reactive oxygen species by flow cytometry. *Shanghai Di-er Yike Daxue Xuebao* 2001; 21:122-124
- Navarro-Antolin J, Hernandez-Perera O, Lopez-Ongil S, Rodriguez-Puyol M, Rodriguez-Puyol D, Lamas S. CsA and FK506 up-regulate eNOS expression: role of reactive oxygen species and AP-1. *Kidney Int* 1998;68(Suppl):S20-S24
- Lopez-Ongil S, Hernandez-Perera O, Navarro-Antolin J, Perez de Lema G, Rodriguez-Puyol M, Lamas S, Rodriguez-Puyol D. Role of reactive oxygen species in the signalling cascade of cyclosporine A-mediated up-regulation of eNOS in vascular endothelial cells. *Br J Pharmacol* 1998;124:447-454
- Allen RG and Tresini M. Oxidative Stress and Gene Regulation. *Free Radic Biol* 2000;28:463-499
- Yeldandi AV, Rao MS, Reddy JK. Hydrogen peroxide generation in peroxisome proliferator-induced oncogenesis. *Mutation Res* 2000;448: 159-177
- Sun GY, Liu WW. Free radicals and digestive system neoplasms. *Huaren Xiaohua Zazhi* 1998;6:272-273
- Greene EL, Velarde V, Jaffa AA. Role of reactive oxygen species in bradykinin-induced mitogen-activated protein kinase and c-fos induction in vascular cells. *Hypertension* 2000;35:942-947
- Sun GY, Liu WW, Zhou ZQ, Fang DC, Men RP, Luo YH. Free radicals in development of experimental gastric carcinoma and precancerous lesions induced by N-methyl-N'-nitro N-nitrosoguanidine in rats. *Huaren Xiaohua Zazhi* 1998;6:219-221
- Sun GY, Liu WW, Zhou ZQ, Fang DC, Men RP, Luo YH. Free radicals in development of experimental gastric carcinoma and precancerous lesions induced by N-methyl-N'-nitro N-nitrosoguanidine in rats. *World J Gastroenterol* 1998;4:124
- Mates JM, Sanchez-Jimenez FM. Role of reactive oxygen species in apoptosis: implications for cancer therapy. *Int J Biochem Cell Biol* 2000; 32:157-170

- 33 Chen DZ, Wei MX, Gu YC, Guan XZ. Oxygen free radical harm in Piyinxu and Shenyinxu patients. *Huaren Xiaohua Zazhi* 1998;6:660-662
- 34 Nath KA, Norby SM. Reactive oxygen species and acute renal failure. *Am J Med* 2000;109:665-678
- 35 Thannickal VJ, Fanburg BL. Reactive oxygen species in cell signaling. *Am J Physiol Lung Cell Mol Physiol* 2000;279:L1005-1028
- 36 Perkins C, Kim CN, Fang G, Bhalla KN. Arsenic induces apoptosis of multidrug-resistant human myeloid leukemia cells that express Bcr-Abl or overexpress MDR, MRP, Bcl-2, or Bcl-xL. *Blood* 2000;95:101-022
- 37 Carmody RJ, Cotter TG. Signalling apoptosis: a radical approach. *Redox Rep* 2001;6:77-90
- 38 Fadeel B, Cihlin A, Henter J-I, Orrenius S, Hampton MB. Involvement of caspases in neutrophil apoptosis: regulation by reactive oxygen species. *Blood* 1998; 92:4808-4818
- 39 Zhang C, Gong Y, Ma H, An C, Chen D. Reactive oxygen species involved in trichosanthin-induced apoptosis of human choriocarcinoma cells. *Biochem J* 2001;355:653-661
- 40 Arai T, Endo N, Yamashita K, Sasada M, Mori H, Ishii H, Hirota K, Makino K, Fukuda K. 6-formylpterin, a xanthine oxidase inhibitor, intracellularly generates reactive oxygen species involved in apoptosis and cell proliferation. *Free Radic Biol Med* 2001;30:248-259
- 41 Jones DC, Gunasekar PG, Borowitz JL, Isom GE. Dopamine-induced apoptosis is mediated by oxidative stress and is enhanced by cyanide in differentiated PC12 cells. *J Neurochem* 2000;74:2296-2304
- 42 Moreno-Manzano V, Ishikawa Y, Lucio- Cazana J, Kitamura M. Selective involvement of superoxide anion, but not downstream compounds hydrogen peroxide and peroxynitrite, in tumor necrosis factor- α -induced apoptosis of rat mesangial cells. *J Biol Chem* 2000; 275:12684-12691
- 43 Hildeman DA, Mitchell T, Teague TK, Henson P, Day BJ, Kappler J, Marrack PC. Reactive oxygen species regulate activation-induced T cell apoptosis. *Immunity* 1999;10:735-744
- 44 Sawada M, Nakashima S, Kiyono T, Nakagawa M, Yamada J, Yamakawa H, Banno Y, Shinoda J, Nishimura Y, Nozawa Y, Sakai N. p53 regulates ceramide formation by neutral sphingomyelinase through reactive oxygen species in human glioma cells. *Oncogene* 2001;20:1368-1378
- 45 Sureda FX, Gabriel C, Comas J, Pallas M, Escubedo E, Camarasa J, Camins A. Evaluation of free radical production, mitochondrial membrane potential and cytoplasmic calcium in mammalian neurons by flow cytometry. *Brain Res Brain Res Protoc* 1999;4:280-287
- 46 Atlante A, Calissano P, Bobba A, Giannattasio S, Marra E, Passarella S. Glutamate neurotoxicity, oxidative stress and mitochondria. *FEBS Lett* 2001;497:1-5
- 47 Faist V, Konig J, Hoger H, Elmadfa I. Decreased mitochondrial oxygen consumption and antioxidant enzyme activities in skeletal muscle of dystrophic mice after low-intensity exercise. *Ann Nutr Metab* 2001; 45:58-66
- 48 Caillaud C, Py G, Eydoux N, Legros P, Prefaut C, Mercier J. Antioxidants and mitochondrial respiration in lung, diaphragm, and locomotor muscles: effect of exercise. *Free Radic Biol Med* 1999;26:1292-1299
- 49 Zini R, Morin C, Bertelli A, Bertelli AA, Tillement JP. Effects of resveratrol on the rat brain respiratory chain. *Drugs Exp Clin Res* 1999;25:87-97
- 50 Esposito LA, Melov S, Panov A, Cottrell BA, Wallace DC. Mitochondrial disease in mouse results in increased oxidative stress. *Proc Natl Acad Sci USA* 1999;96:4820-4825
- 51 Paradies G, Petrosillo G, Pistolesi M, Ruggiero FM. The effect of reactive oxygen species generated from the mitochondrial electron transport chain on the cytochrome oxidase activity and on cardiolipin content in bovine heart submitochondrial particles. *FEBS letter* 2000; 466:323-326

Edited by Wang JH and Xu XQ

• ESOPHAGEAL CANCER •

Nitric oxide and calcium ions in apoptotic esophageal carcinoma cells induced by arsenite

Zhong-Ying Shen, Wen-Ying Shen, Ming-Hua Chen, Jian Shen, Wei-Jie Cai, Zeng Yi

Zhong-Ying Shen, Ming-Hua Chen, Jian Shen, Wei-Jie Cai,
Department of Pathology

Wen-Ying Shen, Department of Chemistry Medical College of Shantou
University, Shantou, 515031, Guangdong, China

Zeng Yi, Institute of Virology, Chinese Academy of Preventive Medicine,
Beijing, 100052, China

Supported by the National Natural Science Foundation of China.
No. 39830380

Correspondence to: Dr. Zhong-Ying Shen, Department of Pathology,
Medical College of Shantou University, 22 Xinling Road. Shantou 515031,
Guandong Province, China. Zhongyingshen@yahoo.com

Telephone: +86-754-8538621 Fax: +86-754-8537516

Received 2001-08-09 Accepted 2001-11-12

Abstract

AIM: To quantitatively analyze the nitric oxide (NO) and Ca^{2+} in apoptosis of esophageal carcinoma cells induced by arsenic trioxide (As_2O_3).

METHODS: The cell line SHEEC1, a malignant esophageal epithelial cell induced by HPV in synergy with TPA in our laboratory, was cultured in a serum-free medium and treated with As_2O_3 . Before and after administration of As_2O_3 , NO production in cultured medium was detected quantitatively using the Griess Colorimetric method. Intracellular Ca^{2+} was labeled by using the fluorescent dye Fluo3-AM and detected under confocal laser scanning microscope (CLSM), which was able to acquire data in real-time enabling Ca^{2+} dynamics of individual cells *in vitro*. The apoptotic cells were examined under electron microscopy.

RESULTS: Intracellular concentration of Ca^{2+} increased from 1.00 units to 1.09-1.38 units of fluorescent intensity at As_2O_3 treatment and NO products subsequently released from As_2O_3 -treated cells increased from $0.98-1.00 \times 10^{-2} \mu\text{mol} \cdot \text{L}^{-1}$ up to $1.48-1.52 \times 10^{-2} \mu\text{mol} \cdot \text{L}^{-1}$ and maintained in a high level continuously. Finally apoptosis of cells occurred, chromatin being agglutinated, cells shrunk, nuclei became round and mitochondria swelled.

CONCLUSION: Ca^{2+} and NO increased with cell damage and apoptosis in cells treated by As_2O_3 . The Ca^{2+} is an initial messenger to the apoptotic pathway. To investigate Ca^{2+} and NO will be a new direction for studying the apoptotic signaling messenger of the esophageal carcinoma cells induced by As_2O_3 .

Shen ZY, Shen WY, Chen MH, Shen J, Cai WJ, Yi Z. Nitric oxide and calcium ions in apoptotic esophageal carcinoma cells induced by arsenite. World J Gastroenterol 2002;8(1): 40-43

INTRODUCTION

Arsenic trioxide (As_2O_3) has been proved to be a genotoxic and a carcinogenic agent^[1-6]. Previous studies also showed that As_2O_3 induced cellular apoptosis in leukemia^[7-15], in cancer cells of head and neck^[16] and other cancer cells^[17-22]. So As_2O_3 has antitumoral

effect. We found that As_2O_3 induced apoptosis in esophageal squamous carcinoma cells^[23]. The pathomorphological changes induced by As_2O_3 revealed that cells became smaller and shrank, nucleus rounded up, chromatin agglutinated and marginated, the nuclear membrane broke down followed by degenerative changes and cell mortality. All these changes indicated typical morphological changes of apoptosis^[24, 25]. Mitochondria, an important cellular apparatus, is related to cell breathing, oxygen metabolism, enzyme activity and energy supply. Our data demonstrated that the primary target of As_2O_3 inducing apoptosis of esophageal carcinoma cells might be the mitochondria^[26]. It is likely that As_2O_3 is a mitochondriotoxic agent^[27, 28]. At the early stage of cellular apoptosis induced by As_2O_3 , the mitochondria generated morphological and functional changes^[29, 30].

NO exerts a wide range of its biological properties via its interaction with mitochondria and NO mediated mitochondria damage^[31]. In our previous data, an increase level of nitrite, a stable product of NO, was detected in the culture medium of esophageal carcinoma cells in arsenite-treated apoptosis^[32]. Calcium ions (Ca^{2+}) act as a universal second messenger in a variety of cells. Numerous functions of all types of cells are regulated by Ca^{2+} to a greater or lesser degree. Because of the importance of Ca^{2+} in biology, numerous methods of analyzing cellular Ca^{2+} activity have been established. Confocal laser scanning microscopy (CLSM) allows the precise spatial and temporal analysis of intracellular Ca^{2+} activity at the subcellular level. This optical technique has enabled scientists to document the dynamic changes of intracellular Ca^{2+} *in vitro*^[33].

Arsenic may generate reactive oxygen species to exert its toxicity, which is implicated in DNA damage, signal transduction and apoptosis. What we are interested in is to see if NO and Ca^{2+} are involved in arsenic-induced apoptosis and to observe the changes of its target organelle—mitochondria. This study is to investigate which are the original messengers that initiate apoptosis and to detect quantitatively Ca^{2+} and NO in the apoptotic process of esophageal carcinoma cell line induced by As_2O_3 .

MATERIALS AND METHODS

Cell line generation and cell culture

The esophageal carcinoma cell line (SHEEC1) was a malignant transformed cell line of human embryonic esophageal epithelium induced by HPV18 E₆E₇ in synergy with TPA (12-O-tetradecanoyl-phorbol-13-acetate)^[34]. Cells were cultured in 50ml flasks and 24-well plate (Corning) with serum-free medium. The culture medium contained of the basal medium (MCDB151) with trace elements (M-6645 Sigma) and added transferrin, hydrocortisone, epidermal growth factor (EGF), insulin (Sigma Chemical Co.) and extracts of bovine hypophysis (Gibco, BRL), but without calf serum, nitrite and nitrate, while containing streptomycin and penicilline ($50\text{mg} \cdot \text{L}^{-1}$ for each).

The administration of arsenic

Arsenic trioxide (As_2O_3) obtained from Sigma Chemical Co. (St. Louis MO, Lot A 1010) at concentrations of 0, 1, 3 and $5 \mu\text{mol} \cdot \text{L}^{-1}$ was added into the culture flasks and 24-well plates, respectively, for

0, 2, 4, 8, 12 and 24 h. The experiment was repeated once.

Transmission electron-microscopy (EM) examination

At the endpoints of As_2O_3 (24h), cells of each group were digested with 0.25% trypsin, centrifuged, fixed with 2.5% glutaraldehyde, and routinely prepared for electron microscopic examination. The samples were observed under transmission electron microscope (Hitachi 300).

Cell cycle and apoptotic rate analyzed by flow cytometry (FCM)

Cells of repeated experiment were harvested to measure the ratio of apoptotic cells to survived cells. The cells were washed twice with PBS, dispersed, and filtered through 360 mesh nylon net to make a single cell suspension. It was fixed with 700mL·L⁻¹ precooled alcohol in ice. Before analysis cells were suspended in PBS and stained with propidium iodide. 1×10^9 cells·L⁻¹ were detected by flow cytometry (FACSort, B-D Co, USA). The DNA histogram was drawn according to the fluorescent intensity value of 10^4 cells.

Procedure of NO detection^[35]

The nitrite/nitrate colorimetric method, using the kit purchased from Boehringer Mannheim Co, was used to detect NO in culture medium. The culture medium of 0.2 mL from flask was regularly deactivated at 80°C for 5 min and deproteinated by centrifugation in 12000 r·min⁻¹ for 30min, and the supernatant was determined. The procedure for NO determination was as follows: sample solution of 100μL, 50μL of nicotinamide adenine dinucleotide phosphate (NADPH) and 4μL of the enzyme nitrate reductase (NR) were placed in a 3mL test tube, mixed, incubated for 30 min at room temperature, and added 50μL color reagent I & II, respectively, mixed, and allowed to stand in the dark at room temperature for 10 to 15min. The NO content of the samples and the blank was estimated with Shimadzu UV/120 spectrophotometry by 450nm and was calculated by calibration curve of standard addition method. The standards were prepared from known amounts of stock NO_3 and NO_2 and run in parallel with test samples in each assay.

Determination of intracellular calcium level using CLSM^[33, 36]

The cells were cultured on the coverslips within the glass bottom of a small cultured dish (No. 0, uncoated, and irradiated. MatTek Co., USA). At the exponential growth period, the cells were stained with $10\mu\text{mol}\cdot\text{L}^{-1}$ fluo-3/AM (Molecular Probe) for 30min at 37°C, and washed with $135\text{ mol}\cdot\text{L}^{-1}$ NaCl, $10\text{ mol}\cdot\text{L}^{-1}$ HEPES, $0.4\text{ mol}\cdot\text{L}^{-1}$ MgCl_2 , $1\text{ mol}\cdot\text{L}^{-1}$ CaCl_2 , $1\text{ g}\cdot\text{L}^{-1}$ D-glucose, $1\text{ g}\cdot\text{L}^{-1}$ bovine serum albumin, pH 7.3 at least 3 times. Then the cells were placed in the culture medium 199 to maintain them in living state. Before and after administration of As_2O_3 the fluorescence intensity was determined by CLSM in dynamic changes for up to 900 s. Using scan-time series menu, time series was used to scan some definite cells repeatedly to monitor the dynamic changes in fluorescent intensity of intracellular Ca^{2+} content over time. The parameters of the CLSM (Ultima 312, Meridian Instruments Inc., USA) were as follows: the excited light 488nm, the emission light 530 nm and pinhole 10-40nm. The fluorescent intensity of pixel was collected and managed with the software of the instrument.

RESULTS

Cell apoptosis

Ultrastructural morphological changes of mitochondria in As_2O_3 treated cells were described in the previous reports^[25,26]. Cells treated with

As_2O_3 at different concentrations for 24 h displayed an apoptotic appearance. Under electron microscope, condensed and margined chromatin in most of the nuclei appeared accompanying swelling mitochondria (Figure 1). By flow cytometry, time course study on As_2O_3 induced apoptosis revealed that apoptotic peak can be observed as early as 12 h after the incubation of arsenic trioxide in $3\mu\text{mol}\cdot\text{L}^{-1}$. The apoptotic cells accounted for 5.0% of total cell population at 12 h and 28.3% at 24 h (Figure 2).

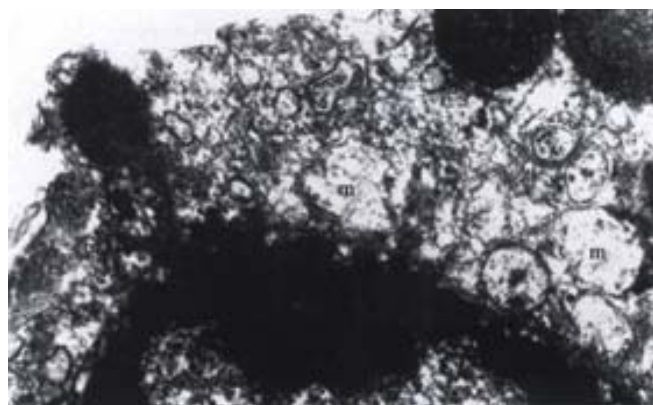


Figure 1 Ultrastructure of SHEEC1 cell treated with $3\mu\text{mol}\cdot\text{L}^{-1}$ As_2O_3 . Apoptotic appearance displayed with swelling of mitochondria and nuclear chromatin coagulating and merging. m, mitochondria. n, nucleus. EM, $\times 7000$

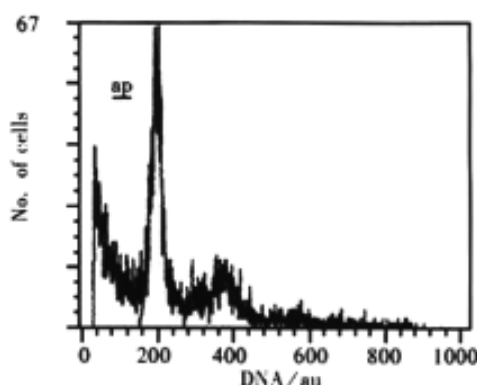


Figure 2 DNA histogram of SHEEC1 cell in 24 h after $3\mu\text{mol}\cdot\text{L}^{-1}$ of As_2O_3 adding. ap, apoptotic peak.

NO determination

When As_2O_3 acted on the SHEEC1 for 2-24h, in 0, 1, 3 and $5\mu\text{mol}\cdot\text{L}^{-1}$ As_2O_3 , NO in cultured medium was increased at the time points. The amount of NO released from SHEEC1 was increased from the basal condition ($0.98\text{--}1.00 \times 10^{-2}\mu\text{mol}\cdot\text{L}^{-1}$) up to the high level ($1.48\text{--}1.52 \times 10^{-2}\mu\text{mol}\cdot\text{L}^{-1}$) (8h) and maintained for 24h (Figure 3). The concentration of NO in different groups varied, high concentration of NO in $5\mu\text{mol}\cdot\text{L}^{-1}$ of As_2O_3 and low concentration of NO in $1\mu\text{mol}\cdot\text{L}^{-1}$ of As_2O_3 .

Dynamic change calcium of intracellular calcium

To show the time course of changes in Ca^{2+} in individual cells, the changes in fluorescence intensity (arbitrary unit, au) at different representative cells were measured. Upon the initiation of stimulation by As_2O_3 , all the cells responded with a rapid rise in $[\text{Ca}^{2+}]$ from 1.00 au. to 1.09-1.38 au of fluorescent intensity. The peak levels of Ca^{2+} in all cells were consistently reached at about 900s after stimulation (Figure 4A). In the control group, without being treated with As_2O_3 , the fluorescent intensity of cell, were remained on the basal line (Figure 4B).

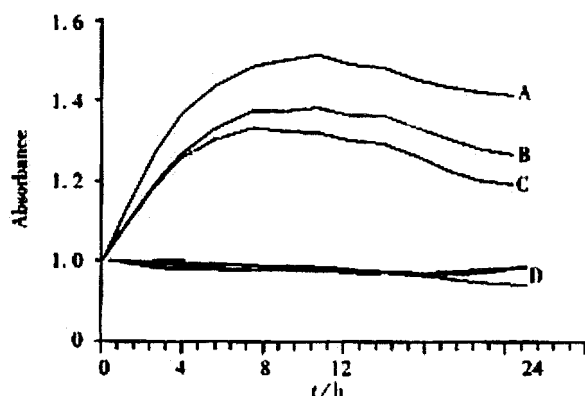


Figure 3 NO determination of SHEEC1 treated with different concentration of As_2O_3 . NO increased markedly in $5\mu\text{mol}\cdot\text{L}^{-1}$ of As_2O_3 group (A), intermediately in $3\mu\text{mol}\cdot\text{L}^{-1}$ of As_2O_3 group (B) and lowly in $1\mu\text{mol}\cdot\text{L}^{-1}$ of As_2O_3 group (C). The control group, $0\mu\text{mol}\cdot\text{L}^{-1}$ of As_2O_3 , were remained on the basal lines (D).

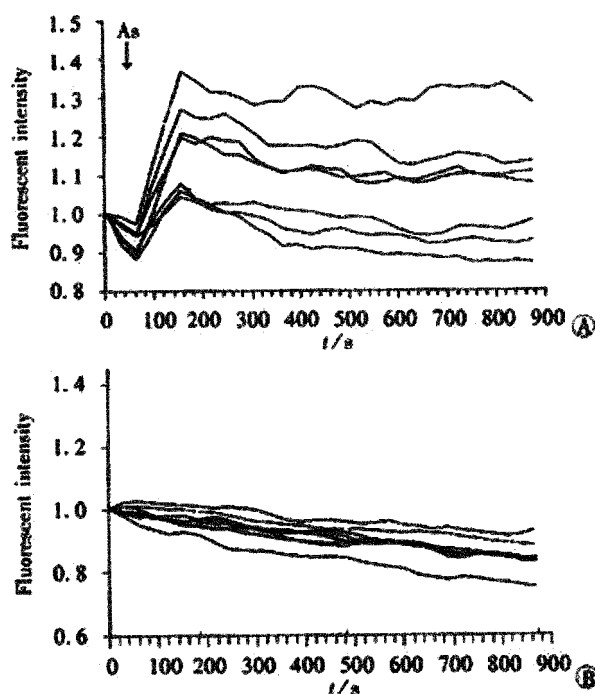


Figure 4 Dynamic changes of intracellular calcium in 7 cells of SHEEC1 treated with As_2O_3 . A, SHEEC1 cells treated with As_2O_3 in $3\mu\text{mol}\cdot\text{L}^{-1}$. B, Control group without adding As_2O_3 .

DISCUSSION

In general, the process of cell apoptosis involved three phases: the initiation phase, the effector phase and the degradation phase^[37]. The initiation (or signal transduction) phase is the stage in which specific or non-specific pro-apoptotic signal transduction pathways are activated. The effector (or central control) phase mainly occurs in the mitochondria^[38] where mitochondria membranes are unstable as a result of the action of the permeability alternation. Some genes such as p53 and bcl-2, activate in this phase^[39-41]. The degradation (or morphological and biochemical changes) phase manifest the postmitochondrial features of apoptosis, in which soluble intermembrane proteins released from mitochondria played an active role in the activation of proteolytic destruction. In our previous reports, we investigated the early changes of the apoptotic cells

induced by As_2O_3 and defined the phase in which As_2O_3 was involved^[26, 27]. Our results demonstrated that As_2O_3 acted directly on mitochondria for the early stage of apoptosis. The alteration of mitochondria in arsenic trioxide treated tumor cells could be observed as early as 2 h after the treatment^[27, 30]. In this study we investigated signal messengers of apoptosis, by first selecting both messengers of NO and Ca^{2+} in the apoptotic pathway.

Experiments on the effects of various modulators (dose and time lag) of arsenic in the level of Ca^{2+} and NO were carried out. Nitric oxide (NO) is a free radical generated in cells by nitric oxide synthases (NOS)^[42]. It is a gaseous inter- and intra-cellular messenger that plays as a signaling molecular in many physiological and pathological processes and it is also a cytotoxic agent involved in many diseases, which has been elaborated extensively during the last decade. Various intra- or extra-cellular factors act on mitochondria to produce NO. NO binds to cytochrome oxidase^[43], blocks respiratory chain and induces apoptosis^[44, 45].

Cells themselves control intracellular Ca^{2+} concentration ($[\text{Ca}^{2+}]_i$) strictly with several Ca^{2+} regulatory mechanisms, such as Ca^{2+} channels, Ca^{2+} pumps, and Ca^{2+} exchangers. The role of calcium is as the important intracellular signal element in regulating cell death^[46]. As revealed by previous reports, it seems that calcium changes in apoptosis vary with stimuli and cell lines^[47]. This data suggested that an early, gradual and sustained increase in intracellular Ca^{2+} is necessary for the appearance of apoptotic characteristics. In the examination of CLSM with Fuo-3 AM as a calcium indicator, we found that a rise in intracellular calcium was elicited at once after application of As_2O_3 . The mechanism of how arsenic increases intracellular calcium levels was not clear at this moment. Arsenic has been shown to disrupt mitochondria and may elevate intracellular calcium via a signal transduction pathway. Arsenite has also been reported to activate protein kinase C and mitogen-activated protein kinase^[48]. These kinases are known to be involved in the calcium signal transduction pathway.

According to the previous reports, the relationship between NO, Ca^{2+} and mitochondria in apoptosis is as follows: various extracellular factors can induce the increase of intracellular Ca^{2+} levels ($[\text{Ca}^{2+}]_i$), modulating cellular signaling and gene expression, and the increased ($[\text{Ca}^{2+}]_i$) effect on NO production through the iNOS pathway^[49, 50]; mitochondria are a source of NO^[51], the production of which may affect energy metabolism, O_2 consumption and O_2 free radical formation^[52]; mitochondrial Ca^{2+} uptake in combination with NO production triggers the collapse of mitochondrial membrane potential, affecting mitochondrial respiration and culminating in delayed cell death^[53].

In conclusion, our data proved that increased calcium ions and nitric oxide triggered by As_2O_3 may play an important role in arsenite-induced apoptosis in esophageal carcinoma cells. The demonstration of the involvement of Ca^{2+} and NO in arsenite-induced apoptosis suggests a new direction for studying the apoptotic pathway.

REFERENCES

- Matsui M, Nishigori C, Toyokuni S, Takada J, Akaboshi M, Ishikawa M, Imamura S, Miyachi Y. The role of oxidative DNA damage in human arsenic carcinogenesis: detection of 8-hydroxy-2'-deoxyguanosine in arsenic-related Bowen's disease. *J Invest Dermatol* 1999; 113:26-31
- Goering PL, Aposhian HV, Mass MJ, Cebrian M, Beck BD, Waalkes MP. The enigma of arsenic carcinogenesis: role of metabolism. *Toxicol Sci* 1999; 49:5-14
- Schaumloffel N, Gebel T. Heterogeneity of the DNA damage provoked by antimony and arsenic. *Mutagenesis* 1998; 13: 281-286
- Ho IC, Yih LH, Kao CY, Lee TC. Tin-protoporphyrin potentiates arsenite-induced DNA strand breaks, chromatid breaks and kinetochore-negative micronuclei in human fibroblasts. *Mutat Res* 2000; 452:41-50
- Gebel T. Suppression of arsenic-induced chromosome mutagenicity by antimony. *Mutat Res* 1998; 412:213-218

- 6 Gebel T, Birkenkamp P, Luthin S, Dunkelberg H. Arsenic (III), but not antimony (III), induced DNA-protein crosslinks. *Anticancer Res* 1998; 18: 4253-4257
- 7 Zhu XH, Shen YL, Jing YK, Cai X, Jia PM, Huang Y, Tang W, Shi GY, Sun YP, Dai J, Wang ZY, Chen SJ, Zhang TD, Waxman S, Chen Z, Chen GQ. Apoptosis and growth inhibition in malignant lymphocytes after treatment with arsenic trioxide at clinically achievable concentrations. *J Natl Cancer Inst* 1999; 91:772-778
- 8 Look AT. Arsenic and apoptosis in the treatment of acute promyelocytic leukemia. *J Natl Cancer Inst* 1998; 90: 86-88
- 9 Shao W, Fanelli M, Ferrara FF, Riccioni R, Rosenauer A, Davison K, Lamph WW, Waxman S, Pelicci PG, Lo-Coco F, Avvisati G, Testa U, Peschle C, Gambacorti-Passerini C, Nervi C, Miller WH. Arsenic trioxide as an inducer of apoptosis and loss of PML/RAR alpha protein in acute promyelocytic leukemia cells. *J Natl Cancer Inst* 1998; 90: 124-133
- 10 Soignet SL, Maslak P, Wang ZG, Jhanwar S, Calleja E, Dardashti LJ, Corso D, DeBlasio A, Gabrilove J, Scheinberg DA, Pandolfi PP, Warrell RP. Complete remission after treatment of acute promyelocytic leukemia with arsenic trioxide. *N Engl J Med* 1998; 339: 1341-1348
- 11 Tamm I, Paternostro G and Zapata JM. Treatment of acute promyelocytic leukemia with arsenic trioxide. *N Engl J Med* 1999; 340: 1043-1045
- 12 Jing Y, Dai J, Chalmers-Redman RM, Tatton WG, Waxman S. Arsenic trioxide selectively induces acute promyelocytic leukemia cell apoptosis via a hydrogen peroxide-dependent pathway. *Blood* 1999; 94:2102-2111
- 13 Huang XJ, Wiernik PH, Klein RS, Gallagher RE. Arsenic trioxide induces apoptosis of myeloid leukemia cells by activation of caspases. *Med Oncol* 1999; 16:58-64
- 14 Lallemand-Breitenbach V, Guillemin MC, Janin A, Daniel MT, Degos L, Kogan SC, Bishop JM, de The H. Retinoic acid and arsenic synergize to eradicate leukemic cells in a mouse model of acute promyelocytic leukemia. *J Exp Med* 1999; 189:1043-1052
- 15 Li YM, Broome JD. Arsenic targets tubulins to induce apoptosis in myeloid leukemia cells. *Cancer Res* 1999; 59:776-780
- 16 Seol JG, Park WH, Kim ES, Jang CW, Hyun JM, Lee YY, Kim BK. Potential role of caspase-3 and -9 in arsenic trioxide-mediated apoptosis in PCI-1 head and neck cancer cells. *Int J Oncol* 2001; 18: 249-255
- 17 Chen HY, Liu WH, Qin SK. Induction of arsenic trioxide on apoptosis of hepatocarcinoma cell lines. *Shijie Huaren Xiaohua Zazhi* 2000; 8: 532-535
- 18 Gu QL, Li NL, Zhu ZG, Yin HR, Lin YZ. A study on arsenic trioxide inducing *in vitro* apoptosis of gastric cancer cell lines. *World J Gastroenterol* 2000; 6: 435-437
- 19 Tu SP, Jiang SH, Tan JH, Jiang XH, Qiao MM, Zhang YP, Wu YL, Wu YX. Proliferation inhibition and apoptosis induction by arsenic trioxide on gastric cancer cell SGC 7901. *Shijie Huaren Xiaohua Zazhi* 1999; 7: 18-21
- 20 Xu HY, Yang YL, Gao YY, Wu QL, Gao GQ. Effect of arsenic trioxide on human hepatoma cell line BEL-7402 cultured *in vitro*. *World J Gastroenterol* 2000; 6:681-687
- 21 Wang W, Qin SK, Chen BA, Chen HY. Experimental study on antitumor effect of arsenic trioxide in combination with cisplatin or doxorubicin on hepatocellular carcinoma. *World J Gastroenterol* 2001; 7:702-705
- 22 Xu HY, Gao YY, Wu QL, Gao GQ, Yang YL, Chen SX, Liu TF. Proliferation inhibition and apoptosis induction by arsenic trioxide on human hepatoma cell line *in vitro*. *Shijie Huaren Xiaohua Zazhi* 2000; 8:1233-1237
- 23 Shen ZY, Tan LJ, Cai WJ, Shen J, Chen C, Tang XM, Zheng MH. Arsenic trioxide induces apoptosis of oesophageal carcinoma *in vitro*. *Int J Mol Med* 1999;4:33-37
- 24 Shen ZY, Tan LJ, Cai WJ, Shen J, Chen CY, Tang XM. Morphologic study on apoptosis of esophageal carcinoma cell line induced by arsenic trioxide. *Shijie Huaren Xiaohua Zhazhi* 1998;6:226-229
- 25 Shen ZY, Chen CY, Shen J, Cai WJ. Ultrastructural study of apoptosis and necrosis in the esophageal carcinoma cell line induced by arsenic trioxide. *Zhongguo Yixue Wulixue Zazhi* 1999; 16: 91-94
- 26 Shen ZY, Shen J, Chen MH, Li QS, Hong CQ. Morphological changes of mitochondria in apoptosis of esophageal carcinoma cells induced by As₂O₃. *Zhonghua Binluxe Zazhi* 2000; 29: 200-203
- 27 Shen ZY, Shen J, Cai WJ, Hong CQ, Zheng MH. The alteration of mitochondria is an early event of arsenic trioxide induced apoptosis in esophageal carcinoma cells. *Int J Mol Med* 2000; 5: 155-158
- 28 Kroemer G and de The H. Arsenic trioxide, a novel mitochondriotoxic anticancer agent? *J Natl Cancer Inst* 1999; 91:743-74
- 29 Shen ZY, Chen MH, Li QS, Shen J. An ultrastructural study on the programmed cell death of human amniotic epithelium. *Dianzi Xianwei Xuebao* 2000; 19: 259-260
- 30 Shen ZY, Shen J, Li QS, Chen CY, Chen JY, Zeng Y. The morphological and functional changes of mitochondria in apoptotic esophageal carcinoma cells induced by arsenic trioxide. *World J Gastroenterol* 2001 (in press)
- 31 Rachmilewitz D. Role of nitric oxide in gastrointestinal tract. *World J Gastroenterol* 1998; 4:28-29
- 32 Shen ZY, Shen WY, Chen MH, Hong CQ, Shen J. Alterations of nitric oxide in apoptosis of esophageal carcinoma cells induced by arsenite. *Shijie Huaren Xiaohua Zhazhi* 2000; 8: 1101-1104
- 33 Takahashi A, Camacho P, Lechleiter JD, Herman B. Measurement of intracellular calcium. *Physiol Rev* 1999; 79: 1089-1125
- 34 Shen ZY, Cen S, Shen J, Cai WJ, Xu JJ, Teng ZP, Hu Z, Zeng Y. Study of immortalization and malignant transformation of human embryonic esophageal epithelial cells induced by HPV18E6E7. *J Cancer Res Clin Oncol* 2000; 126:589-594
- 35 Shen WY, Chen MH, Shen ZY, Zhang LM. Microspectrophotometric determination of nitric oxide. *J Shantou Univ Med College* 2000; 13:10-11
- 36 Satoh Y, Nishimura T, Kimura K, Mori S, Saino T. Application of real-time confocal microscopy for observation of living cells in tissue specimens. *Hum Cell* 1998; 11: 191-198
- 37 Kroemer G, Dallaporta B and Resch-Rigon M. The mitochondrial death/life regulator in apoptosis and necrosis. *Annu Rev Physiol* 1998; 60: 619-642
- 38 Brenner C and Kroemer G. Apoptosis Mitochondria—the death signal integrators. *Science* 2000; 289: 1150-1151
- 39 Zhang CS, Wang WL, Peng WD, Hu PZ, Chai YB, Ma FC. Promotion of apoptosis of SMMC7721 cells by bcl-2 ribozyme. *Shijie Huaren Xiaohua Zazhi* 2000; 8: 417-419
- 40 Yuan RW, Ding Q, Jiang HY, Qin XF, Zou SQ, Xia SS. Bcl-2, p53 protein expression and apoptosis in pancreatic cancer. *Shijie Huaren Xiaohua Zazhi* 1999; 7: 851-854
- 41 Wang LD, Zhou Q, Wei JP, Wang WC, Zhao X, Wang LX, Zou X, Gao SS, Li YX, Yang CS. Apoptosis and its relationship with cell proliferation, p53, waf/p21, bcl-2 and c-myc in esophageal carcinogenesis studied with a high risk population in northern China. *World J Gastroenterol* 1998; 4: 287-293
- 42 Kuai XL, Ge ZJ, Meng XY, Ni RZ. Expression of nitric oxide synthase in human gastric carcinoma. *Shijie Huaren Xiaohua Zazhi* 2000; 8:22-24
- 43 Li H, Kolluri SK, Gu J, Dawson MI, Cao X, Hobbs PD, Lin B, Chen G, Lu J, Lin F, Xie Z, Fontana JA, Reed JC, Zhang X. Cytochrome c release and apoptosis induced by mitochondrial targeting of nuclear orphan receptor TR3. *Science* 2000; 289: 1159-1164
- 44 Brown GC. Nitric oxide and mitochondrial respiration. *Biochim Biophys acta* 1999; 1411: 351-369
- 45 Brown GC. Regulation of mitochondrial respiration by nitric oxide inhibition of cytochrome c oxidase. *Biochim Biophys Acta* 2001; 1504: 46-57
- 46 Duchon MR. Mitochondria and calcium: from cell signaling to cell death. *J Physiol* 2000; 529: 57-68
- 47 Fang M, Zhang H, Xue S. Role of calcium in apoptosis of HL-60 cells induced by harringtonine. *Sci China* 1998; 41: 600-607
- 48 Jun CD, Oh CD, Kwak HJ, Pae HO, Yoo JC, Choi BM, Chun JS, Park RK, Chung HT. Overexpression of protein kinase C isoforms protects RAW 264.7 macrophages from nitric oxide-induced apoptosis: involvement of c-Jun N-terminal kinase stress-activated protein kinase, p38 kinase, and CPP-32 protease pathways. *J Immunol* 1999; 162: 3395-3401
- 49 Korhonen R, Kankaanranta H, Lahti A, Lahde M, Knowles RG, Moilanen E. Bi-directional effects of the elevation of intracellular calcium on the expression of inducible nitric oxide synthase in J774 macrophages exposed to low and to high concentration of endotoxin. *Biochem J* 2001; 354: 351-358
- 50 Gurr JR, Liu F, Lynn S, Jan KY. Calcium-dependent nitric oxide production is involved in arsenite-induced micronuclei. *Mutat Res* 1998; 416: 137-148
- 51 Giulivi C, Poderoso JJ, Boveris A. Production of nitric oxide by mitochondria. *J Biol Chem* 1998; 273: 11038-11043
- 52 Nishikawa M, Takeda K, Sato EF, Kuroki T, Inoue M. Nitric oxide regulates energy metabolism and Bcl-2 expression in intestinal epithelial cells. *Am J Physiol* 1998; 274: G797-801
- 53 Umansky V, Ushmorov A, Ratter F, Chlichlia K, Bucur M, Lichtenauer A, Rocha M. Nitric oxide-mediated apoptosis in human breast cancer cells requires changes in mitochondrial functions and is independent of CD95 (APO-1/Fas). *Int J Oncol* 2000; 16:109-117

• ESOPHAGEAL CANCER •

VEGF₁₆₅ antisense RNA suppresses oncogenic properties of human esophageal squamous cell carcinoma

Zhong-Ping Gu, Yun-Jie Wang, Jin-Ge Li, Yong-An Zhou

Zhong-Ping Gu, Yun-Jie Wang, Yong-An Zhou, Department of Thoracic Surgery, Jin-Ge Li, Department of Infectious Disease, Fourth Military Medical University, Xi'an 710038, Shaanxi Province, China
Correspondence to: Zhong Ping Gu, Department of Thoracic Surgery, Fourth Military Medical University, Xi'an 710038, Shaanxi Province, China. Zhongpg@pub.xaonline.com
Telephone: +86-29-3577737

Received 2001-08-09 Accepted 2001-10-23

Abstract

AIM: To investigate the effect of antisense RNA to vascular endothelial growth factor₁₆₅ (VEGF₁₆₅) on human esophageal squamous cell carcinoma cell line EC109 and the feasibility of gene therapy for esophageal carcinoma.

METHODS: By using subclone technique, the full length of VEGF₁₆₅ amino acid cDNA, which was cut from pGEM-3Zf (+), was cloned inversely into the eukaryotic expression vector pCEP4. The recombinant plasmid pCEP-AVEGF₁₆₅ was transfected into EC109 cell with lipofectamine. After a stable transfection, dot blot, enzyme-linked immunosorbent assay (ELISA), laser confocal imaging system analysis, transmission electron microscopy and flow cytometry were performed to determine the biological characteristics of EC109 cell line before and after transfection *in vitro* and whether there was a reversion in the tumorigenic properties of the EC109 cell *in vivo*.

RESULTS: The eukaryotic expression vector pCEP-AVEGF₁₆₅ was successfully constructed and transfected into EC109 cells. The expression of VEGF₁₆₅ was significantly decreased in the transfected cells while the biological characteristics of the cells were not influenced by the expression of antisense gene. The tumorigenic and angiogenic capabilities were greatly reduced in nude mice, as demonstrated by reduced tumor end volume (820 ± 112.5) mm³ vs (7930 ± 1035) mm³ and (7850 ± 950) mm³, $P = 0.01$ and microvessel density (8.5 ± 1.2) mm⁻² vs (44.3 ± 9.4) mm⁻² and (46.4 ± 12.6) mm⁻², $P < 0.01$ in comparison between experimental groups empty vector transfected group and control group.

CONCLUSION: The angiogenesis and tumorigenicity of human esophageal squamous cell carcinoma were effectively inhibited by VEGF₁₆₅ antisense RNA. Antisense RNA to VEGF₁₆₅ can potentially be used as an adjuvant therapy for solid tumors.

Gu ZP, Wang YJ, Li JG, Zhou YA. VEGF₁₆₅ antisense RNA suppresses oncogenic properties of human esophageal squamous cell carcinoma. *World J Gastroenterol* 2002;8(1):44-48

INTRODUCTION

Angiogenesis, which is defined as the formation of new blood vessel from the pre-existing vascular bed, is essential for solid tumor

growth, for the entrance of tumor cell into the circulation, and for the subsequent establishment and growth of metastasis. Many studies demonstrated that tumor angiogenesis is associated with patient outcome and is an independent prognostic marker in almost all solid tumors, including esophageal carcinoma^[1-10]. Tumor angiogenesis is a complex process, involving growth factors and extracellular matrix enzymes. Among the many known triggers of tumor angiogenesis, vascular endothelial growth factor (VEGF), also known as vascular permeability factor, is an endothelial cell-specific mitogen and an angiogenesis inducer released by a variety of tumor cells and expressed in human tumors *in situ*. VEGF₁₆₅ is the most effective angiogenic factor in the VEGF family. Tumor cells engineered to express VEGF constitutively exhibit enhanced tumor growth and angiogenic phenotypes^[11-13]. Conversely, inhibition of the expression of VEGF₁₆₅ was considered as a therapeutic strategy for the treatment of solid tumors^[14-24].

In this report, we constructed antisense RNA to VEGF₁₆₅ eukaryotic expression vector and applied gene transfer technology to modulate the expression in stably transfected human esophageal squamous cell carcinoma cells. We assessed the effects of down-regulation of VEGF expression on the biological characteristics *in vitro*, microvessel density and tumorigenic capability in nude mice.

MATERIALS AND METHODS

Cell line and vector

The EC109 human esophageal squamous cell carcinoma cell line was generously provided by Dr. Sun (Department of Thoracic Surgery, Tangdu Hospital, Fourth Military Medical University). Cells were maintained in Dulbecco's modified Eagle's medium (DMEM), high glucose media (Life Technologies) and supplemented with 100 mL·L⁻¹ fetal calf serum (HyClone Laboratories), penicillin, streptomycin, and nonessential amino acids (Life Technologies). The vector pGEM-3Zf (+) (carrying the full length aminoacids cDNA of VEGF₁₆₅) was kindly provided by Dr. Abraham (Columbia University, USA) and vector pCEP4 was a gift from Dr. Li (Department of Infectious Disease, Tangdu Hospital, Fourth Military Medical University, China).

Plasmid construction

The expression vector for VEGF₁₆₅ antisense RNA was constructed by subcloning cDNA fragment that code for VEGF₁₆₅ into the eukaryotic expression vector pCEP4. pGEM-3Zf (+) was digested by *Kpn*I and *Hind* III. The fragment was purified by gel. The VEGF₁₆₅ amino acids cDNA was cloned inversely in the *Hind* III/*Kpn*I site of pCEP4 to generate plasmid pCEP-AVEGF₁₆₅ (Figure 1).

Transfection and selection

The transfection and selection of the EC109 cells were carried out in a 6-well plate. When the cells reached 70% confluence, the transfection process began. Briefly, solution A was prepared by diluting 10 µg of pCEP-AVEGF₁₆₅ into 200 µL serum-free medium, and solution B was prepared by diluting 20 µL Lipofectamine 2000 (Life

Technologies) into 200 μ L serum-free medium. The two solutions were combined for 20 min at room temperature, and then 0.6mL serum-free medium was added to the tube containing the complex, and subsequently added to the rinsed cells. The medium was replaced with fresh and complete medium 18 h after the start of transfection. Seventy-two hours after transfection, it was replaced again with the selective medium containing 200g \cdot L⁻¹ hygromycin B (Boehringer Mannheim). Once stable transfections were obtained, the cells were maintained in 100g \cdot L⁻¹ of hygromycin B. The EC109 cells were transfected with either the empty pCEP4 vector or pCEP-AVEGF₁₆₅.

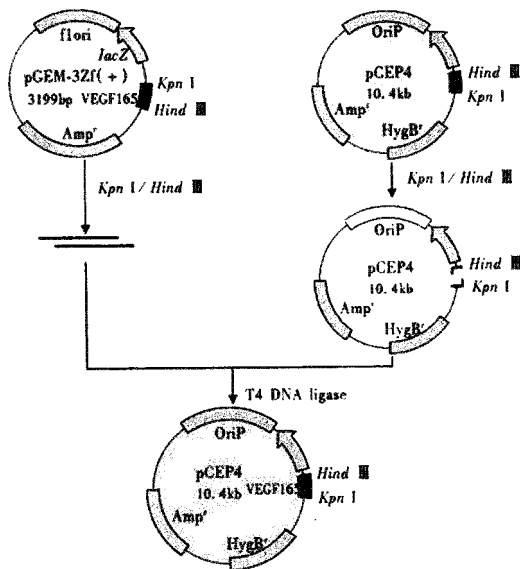


Figure 1 Diagram of the construction of the vector pCEP-AVEGF₁₆₅.

Dot blot analysis

Total cellular RNA was extracted from the cultured cells using the Trizol isolation kit (Life Technologies) according to the manufacturer's instruction. The recovered total RNA was redissolved in diethyl pyrocarbonate-treated water and 20 μ g was immobilized onto a gene screen plus membrane (DuPont) by gentle suction with a blotting manifold (Bethesda Research Laboratories). The membrane was then probed with a 5'-end-radiolabeled synthetic oligodeoxyribonucleotide complementary.

Flow cytometry analysis

Approximately 5×10^6 centrifugal sedimentation cells were immediately fixed in 700mL \cdot L⁻¹ ethanol and stored at 4 $^{\circ}$ C in PBS in preparation for fluorescent-activated cell sorting. Flow cytometry analysis was performed on a FACStar flow cytometer (Becton Dickinson). Histograms of cell number logarithmic fluorescence intensity were recorded for 10 000 cells per sample.

Transmission electron microscope examination

The centrifugalized cells were placed in 40g \cdot L⁻¹ glutaraldehyde and then post-fixed in osmium tetroxide and embedded in Epon. Routine thin sections were stained with uranyl acetate and lead citrate. Thin sections were mounted on grids and examined under a transmission electron microscope (JEM-2000EX) at 60kV.

Laser confocal microscope analysis

Indirect immunofluorescence techniques were applied in the transfected EC109 cells and the parental cells. VEGF₁₆₅ protein was detected with mouse anti-human VEGF₁₆₅ antibody and sheep anti-mouse IgG-FITC (Dako A/S Denmark). FITC was activated by light with a wavelength of 488nm. The data of laser scanning were 3%. The

expression of VEGF₁₆₅ was analyzed by confocal microscope system controlled by software obtained by Bio-Rad.

Tumorigenicity assay

Athymic Balb/c nude mice were obtained from the Animal Center of Fourth Military Medical University. The mice were maintained in a laminar airflow cabinet under specific pathogen-free conditions and used at 8-12 weeks of age. Cells used for injection were grown to subconfluence, trypsinized, washed once, and resuspended in serum-free DMEM. The cell suspensions were examined microscopically to ensure that they were composed of single-cell suspensions. Mice were injected s.c. on the hind leg with 5×10^6 single cells in 0.1mL. The mice were then separated into three groups, depending on whether they were injected with pCEP-AVEGF₁₆₅ transfected cells, pCEP4 empty vector transfected cells, or control cells. Each group contained five mice. Calipers was used for the calculation of tumor size. Microvessel density was determined under light microscopy after immunostaining of sections with anti-CD34 monoclonal antibody according to the strepto ABC kit (Dako A/S Denmark) instruction.

Statistical analysis

The data were analyzed for significance by ANOVA.

RESULTS

VEGF₁₆₅ antisense vector construction

After ligation, transformation and selection, three clones were found likely to contain the desired recombinant. These clones were digested by restriction enzymes *KpnI/HindIII* or *KpnI/SfiI*. The 640bp or the 660bp fragment was found by using polyacrylamide gel electrophoresis. These recombinant plasmids were the eukaryotic expression vectors of antisense RNA to VEGF₁₆₅ (Figure 2).

Expression of VEGF₁₆₅ antisense RNA

Two weeks after being transfected and selected by hygromycin B, the EC109 cells transfected by pCEP-AVEGF₁₆₅ expressed antisense RNA to VEGF₁₆₅ which was confirmed by dot blot analysis, whereas the cells transfected by pCEP4 empty vector and control group cells were negative (Figure 3).

Expression of VEGF₁₆₅ in vitro

ELISA showed that a great number of VEGF₁₆₅ accumulated in the pCEP4 empty vector transfected group and control group cells, whereas in the pCEP-AVEGF₁₆₅ transfected group cells, the level of VEGF₁₆₅ was very low. The level of VEGF₁₆₅ expression was significantly lower in EC109 cells transfected by pCEP-AVEGF₁₆₅ than that in the pCEP4 empty vector transfected group and control group cells ($P < 0.01$) determined under confocal microscope, as indicated in Figure 4.

The change of ultrastructure and cell cycle

There was no substantial change neither in the ultrastructure examined under transmission electron microscope nor in the cell cycle determined by flow cytometer.

The change of tumorigenic capacity in vivo

The nude mice were sacrificed at week 5. Tumor volume was measured and morphological characteristics were assessed in HE stained sections. pCEP-AVEGF₁₆₅ transfected xenografts grew very slowly, pCEP4 empty vector transfected group and nontransfected control xenografts were significantly larger than pCEP-AVEGF₁₆₅ transfected xenografts ($P < 0.01$), and the mean tumor volumes were $(820 \pm 112.5)\text{mm}^3$, $(7930 \pm 1035)\text{mm}^3$ and $(7850 \pm 950)\text{mm}^3$,

respectively. pCEP-AVEGF₁₆₅ transfected xenografts had a relatively large area of central necrosis. Immunohistochemical staining for CD34 was performed to evaluate tumor microvessel density. The microvessel density was expressed as the average number of the five highest areas



Figure 2 Identification of recombinant clone by restriction enzyme.

- 1: Fragment of 640bp digested with *KpnI/Hind III*
- 2: DL2000 markers (2000,1000,750,500,250,100bp)
- 3: Fragment of 660bp digested with *KpnI/SfiI*

identified within a single×200 field, for the pCEP-AVEGF₁₆₅ transfected mice, pCEP4 empty vector group and nontransfected controls were (8.5±1.2)mm⁻², (44.3±9.4) mm⁻² and (46.4±12.6) mm⁻², respectively ($P<0.01$).

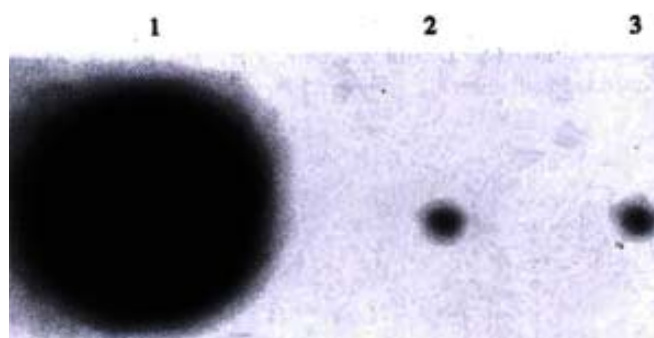


Figure 3 Expression of antisense RNA to VEGF₁₆₅ in EC109 cell

- 1: Transfected by pCEP-AVEGF₁₆₅
- 2: Transfected by empty vector
- 3: Control group

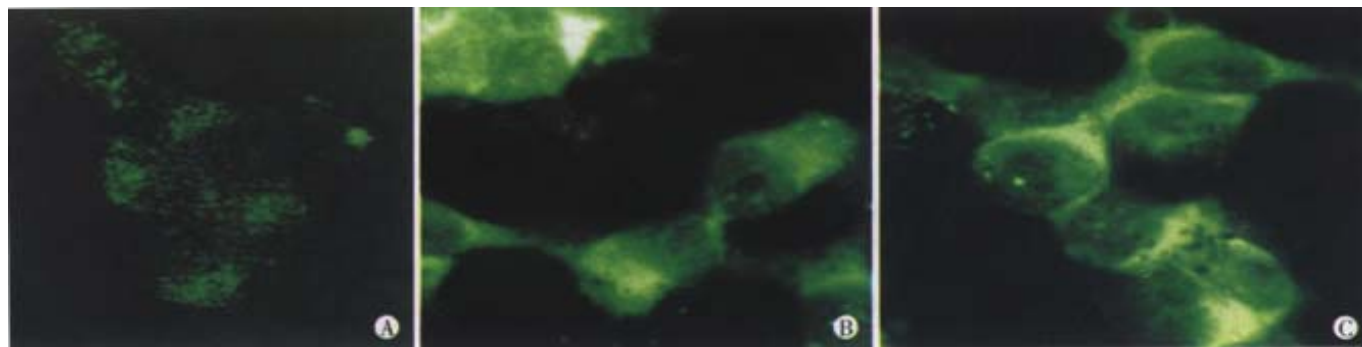


Figure 4 Expression of VEGF₁₆₅ in EC109 cell (×40): transfected by pCEP-AVEGF₁₆₅ (A), transfected by empty vector (B), and control group (C).

DISCUSSION

Mammalian cells require oxygen and nutrients for their survival and are therefore located within 100μm-200μm blood vessels-the diffusion limit for oxygen. For multicellular organisms which grow beyond this size, they must recruit new blood vessels by angiogenesis and vasculogenesis. This process is regulated by a balance between pro- and anti-angiogenic molecules, and is derailed in various diseases, especially cancer. Without blood vessels, tumor can not grow beyond a critical size or metastasize to another organ^[25-29]. In 1971, Folkman^[30] proposed that solid tumor growth and metastasis are critically dependent on angiogenesis, the formation of new blood vessels from pre-existing vasculature, and hence, blocking angiogenesis could be a strategy to arrest tumor growth. The induction of angiogenesis is mediated by several factors released by both tumor and host cells. One of the key mediators of angiogenesis is VEGF, a multifunctional growth factor that is overexpressed and secreted by a majority of human and animal tumors. VEGF was purified by Ferrara *et al*^[31] from the conditioned medium of bovine pituitary folliculo stellate cells. VEGF is a homodimeric 46ku heparin-binding glycoprotein with potent angiogenic, mitogenic, and vascular permeability-enhancing activities specific for endothelial cells. By alternative splicing of messenger RNA, VEGF may exist in at least four different homodimeric molecular species each monomer having 121, 165, 189 or 206 amino acids, respectively (VEGF₁₂₁, VEGF₁₆₅, VEGF₁₈₉, VEGF₂₀₆). Among this family, VEGF₁₆₅ is the most important effector. Antiangiogenic therapy targeting VEGF has been

proposed as a means of inhibiting VEGF-dependent tumor growth and metastasis^[32-40].

It has been suggested that antisense RNA could block the translation progress of aim protein effectively and inhibit expression^[41-45]. DeFatta *et al*^[46] found that reducing eIF4E express on *via* antisense RNA suppressed both the tumorigenic and angiogenic properties of the head and neck squamous cell cancers, cell line FaDu, as demonstrated by lowered capacity to grow in soft agar, reduced expression of angiogenic factors, and loss of tumorigenicity in nude mice. Oku and associates^[47] transfected human SK-MEL-2 melanoma cells with antisense VEGF which resulted in substantial inhibition of intracerebral tumor growth in nude mice, and a decrease in tumor vascularity, blood flow, and permeability.

The prognosis of human esophageal squamous cell carcinoma after curative resection is dismal. Radiotherapy and several conventional chemotherapeutic agents have been tried to improve the prognosis, but the results are generally disappointing. In this regard, antiangiogenic therapy could be a promising and hopeful strategy for esophageal cancer^[48-51]. In this study, an antisense RNA to VEGF₁₆₅ eukaryotic expression vector pCEP-AVEGF₁₆₅ was constructed successfully. We transfected it into human esophageal squamous cell carcinoma cell line EC109. Under immunohistochemistry and confocal microscopy, it was found that the expression of VEGF₁₆₅ decreased significantly in the cells transfected with VEGF₁₆₅ antisense RNA compared with the empty vector transfected and control group. Under transmission electron microscopy and flow cytometry, we observed that the ultrastructure

and cell cycle had no change among transfected and control groups. In the nude mice tumor model, the tumorigenicity, the rate of tumor growth, and microvessel density were significantly decreased for the tumors derived from antisense RNA transfected cells as compared with the empty vector transfected and parental cells. pCEP-AVEGF₁₆₅ transfected tumors had a very low initial growth rate with central necrosis. These results suggested that inhibition of tumor growth might be achieved by VEGF₁₆₅ antisense RNA's down-regulation of endogenous VEGF expression in tumor tissues. In the meantime, we found that the VEGF₁₆₅ antisense RNA therapy could slow the rate of tumor growth and not inhibit completely the tumorigenicity. This demonstrated that the process of angiogenesis and tumorigenicity is complex and involves multifactors. To the best of our knowledge, this is the first experimental report which shows that VEGF₁₆₅ antisense RNA suppresses the growth of human esophageal squamous cell carcinoma *in vivo* in association with decreased vessel number in the treated tumors.

Esophageal carcinoma is still common in China^[52-58], and the treatment remains a big problem up to date^[59-65]. Our present study suggests that antisense RNA to VEGF₁₆₅ can potentially be used as an adjuvant therapy for human esophageal squamous cell carcinoma. Further studies are needed to understand the details of the mechanisms for appropriate clinical application.

ACKNOWLEDGMENTS We especially thank Dr. Xiao Yan Sun for providing us the EC109 cell line, Dr. Abraham for providing the pGEM-3Zf (+) vector, we also thank Dr. Zhi Pei Zhang for his assistance with the animal experiments, and Prof. Bo Rong Pan for improving the paper.

REFERENCES

- Carmeliet P, Jain RK. Angiogenesis in cancer and other diseases. *Nature* 2000; 407:249-257
- Park JS, Qiao L, Su ZZ, Hinman D, Willoughby K, McKinstry R, Yacoub A, Duigou GJ, Young CS, Grant S, Hagan MP, Ellis E, Fisher PB, Dent P. Ionizing radiation modulates vascular endothelial growth factor (VEGF) expression through multiple mitogen activated protein kinase dependent pathways. *Oncogene* 2001;20:3266-3280
- Millikan KW, Mall JW, Myers JA, Hollinger EF, Doolas A, Saclarides TJ. Do angiogenesis and growth factor expression predict prognosis of esophageal cancer? *Am Surg* 2000;66:401-5; discussion 405-406
- Kollermann J, Hulpap B. Expression of vascular endothelial growth factor (VEGF) and VEGF receptor Flk-1 in benign, premalignant, and malignant prostate tissue. *Am J Clin Pathol* 2001;116:115-121
- Volm M, Koomagi R, Mattern J. PD-ECGF, bFGF, and VEGF expression in non-small cell lung carcinomas and their association with lymph node metastasis. *Anticancer Res* 1999; 19:651-655
- Assy N, Paizi M, Gaitini D, Baruch Y, Spira G. Clinical implication of VEGF serum levels in cirrhotic patients with or without portal hypertension. *World J Gastroenterol* 1999;5:296-300
- Tian XJ, Wu J, Meng L, Dong ZW, Shou CC. Expression of VEGF 121 in gastric carcinoma MGC803 cell line. *World J Gastroenterol* 2000;6: 281-283
- Volm M, Mattern J, Koomagi R. Inverse correlation between apoptotic (Fas ligand, caspase-3) and angiogenic factors (VEGF, microvessel density) in squamous cell lung carcinomas. *Anticancer Res* 1999;19: 1669-1671
- Borre M, Nerstrom B, Overgaard J. Association between immunohistochemical expression of vascular endothelial growth factor (VEGF), VEGF-expressing neuroendocrine-differentiated tumor cells, and outcome in prostate cancer patients subjected to watchful waiting. *Clin Cancer Res* 2000;6:1882-1890
- Korshunov A, Golanov A. The prognostic significance of vascular endothelial growth factor (VEGF C-1) immunorexpression in oligodendroglioma. An analysis of 91 cases. *J Neurooncol* 2000;48:13-19
- Carmeliet P. Mechanisms of angiogenesis and arteriogenesis. *Nature Med* 2000; 6:389-395
- Ferrara N, Alitalo K. Clinical applications of angiogenic growth factors and their inhibitors. *Nat Med* 1999;5:1359-1364
- Ferrara N. Vascular endothelial growth factor: molecular and biological aspects. *Curr Top Microbiol Immunol* 1999;237:1-30
- Nishizaki M, Fujiwara T, Tanida T, Hizuta A, Nishimori H, Tokino T, Nakamura Y, Bouvet M, Roth JA, Tanaka N. Recombinant adenovirus expressing wild-type p53 is antiangiogenic: a proposed mechanism for bystander effect. *Clin Cancer Res* 1999;5:1015-1023
- Kido Y. Vascular endothelial growth factor (VEGF) serum concentration changes during chemotherapy in patients with lung cancer. *Kurume Med J* 2001;48:43-47
- Takayama K, Ueno H, Nakanishi Y, Sakamoto T, Inoue K, Shimizu K, Ohashi H, Hara N. Suppression of tumor angiogenesis and growth by gene transfer of a soluble form of vascular endothelial growth factor receptor into a remote organ. *Cancer Res* 2000; 60:2169-2177
- Morino F, Tokunaga T, Tsuchida T, Handa A, Nagata J, Tomii Y, Kijima H, Yamazaki H, Watanabe N, Matsuzaki S, Ueyama Y, Nakamura M. Hammerhead ribozyme specifically inhibits vascular endothelial growth factor gene expression in a human hepatocellular carcinoma cell line. *Int J Oncol* 2000;17:495-499
- Sandberg JA, Sproul CD, Blanchard KS, Bellon L, Sweedler D, Powell JA, Caputo FA, Kornbrust DJ, Parker VP, Parry TJ, Blatt LM. Acute toxicology and pharmacokinetic assessment of a ribozyme (angiozyme) targeting vascular endothelial growth factor receptor mRNA in the cynomolgus monkey. *Antisense Nucleic Acid Drug Dev* 2000;10:153-162
- Oshika Y, Nakamura M, Tokunaga T, Ohnishi Y, Abe Y, Tsuchida T, Tomii Y, Kijima H, Yamazaki H, Ozeki Y, Tamaoki N, Ueyama Y. Ribozyme approach to downregulate vascular endothelial growth factor (VEGF) 189 expression in non-small cell lung cancer (NSCLC). *Eur J Cancer* 2000;36:2390-2396
- Nguyen JT, Wu P, Clouse ME, Hlatky L, Terwilliger EF. Adeno-associated virus-mediated delivery of antiangiogenic factors as an antitumor strategy. *Cancer Res* 1998;58:5673-5677
- Brekken RA, Overholser JP, Stastny VA, Waltenberger J, Minna JD, Thorpe PE. Selective inhibition of vascular endothelial growth factor (VEGF) receptor 2 (KDR/Flk-1) activity by a monoclonal anti-VEGF antibody blocks tumor growth in mice. *Cancer Res* 2000; 60:5117-5124
- Kotoh T, Dhar DK, Masunaga R, Tabara H, Tachibana M, Kubota H, Kohno H, Nagasue N. Antiangiogenic therapy of human esophageal cancers with thalidomide in nude mice. *Surgery* 1999;125:536-544
- Gaddipati JP, Mani H, Shefali, Raj K, Mathad VT, Bhaduri AP, Maheshwari RK. Inhibition of growth and regulation of IGFs and VEGF in human prostate cancer cell lines by shikonin analogue 93/637 (SA). *Anticancer Res* 2000;20:2547-2552
- Zimmermann RC, Hartman T, Bohlen P, Sauer MV, Kitajewski J. Preovulatory treatment of mice with anti-vegf receptor 2 antibody inhibits angiogenesis in corpora lutea. *Microvasc Res* 2001;62:15-25
- Risau W. Mechanisms of angiogenesis. *Nature* 1997;386:671-674
- Shibuya M. Structure and function of VEGF/VEGF-receptor system involved in angiogenesis. *Cell Struct Funct* 2001;26:25-35
- Rohan RM, Fernandez A, Udagawa T, Yuan J, D'Amato RJ. Genetic heterogeneity of angiogenesis in mice. *FASEB J* 2000;14:871-876
- Ramanujan S, Koenig GC, Padera TP, Stoll BR, Jain RK. Local imbalance of proangiogenic and antiangiogenic factors: a potential mechanism of focal necrosis and dormancy in tumors. *Cancer Res* 2000;60:1442-1448
- Isner JM, Asahara T. Angiogenesis and vasculogenesis as therapeutic strategies for postnatal neovascularization. *J Clin Invest* 1999;103: 1231-1236
- Folkman J. Tumor angiogenesis: therapeutic implications. *N Engl J Med* 1971;285:1182-1186
- Ferrara N, Henzel WJ. Pituitary follicular cells secrete a novel heparin-binding growth factor specific for vascular endothelial cells. *Biochem Biophys Res Commun* 1989; 161: 851-858
- Hyder SM, Murthy L, Stancel GM. Progesterone regulation of vascular endothelial growth factor in human breast cancer cells. *Cancer Res* 1998; 58: 392-395
- Ferrara N. Role of vascular endothelial growth factor in regulation of physiological angiogenesis. *Am J Physiol Cell Physiol* 2001;280: C1358-366
- Neufeld G, Cohen T, Gengrinovitch S, Poltorak Z. Vascular endothelial growth factor (VEGF) and its receptors. *FASEB J* 1999; 13: 9-22
- Salven P, Lymboussaki A, Heikkila P, Jaaskela-Saari H, Enholm B, Aase K, von Euler G, Eriksson U, Alitalo K, Joensuu H. Vascular endothelial growth factors VEGF-B and VEGF-C are expressed in human tumors. *Am J Pathol* 1998; 153:103-108
- Gerber HP, McMurtrey A, Kowalski J, Yan M, Keyt BA, Dixit V, Ferrara N. Vascular endothelial growth factor regulates endothelial cell survival through the phosphatidylinositol 3'-kinase/Akt signal transduction pathway. Requirement for Flk-1/KDR activation. *J Biol Chem* 1998; 273: 30336-30343
- Bates DO, Heald RI, Curry FE, Williams B. Vascular endothelial growth factor increases Rana vascular permeability and compliance by different signalling pathways. *J Physiol* 2001;533:263-272
- Rousseau S, Houle F, Huot J. Integrating the VEGF signals leading to

- actin-based motility in vascular endothelial cells. *Trends Cardiovasc Med* 2000;10:321-327
- 39 Pepper MS, Wasi S, Ferrara N, Orci L, Montesano R. In vitro angiogenic and proteolytic properties of bovine lymphatic endothelial cells. *Exp Cell Res* 1994; 210: 298-305
- 40 Laughner E, Taghavi P, Chiles K, Mahon PC, Semenza GL. Her2 (neu) signaling increases the rate of hypoxia-inducible factor 1 alpha (hif-1alpha) synthesis: novel mechanism for hif-1-mediated vascular endothelial growth factor expression. *Mol Cell Biol* 2001;21:3995-4004
- 41 Fu L, Mei Y, Li H. Effect of PAI-1 antisense RNA on vascular endothelial growth factor expression in aorta smooth muscle cells cultured in vitro. *Zhonghua Yixue Yi Chuanxue Zazhi* 2001;18:110-113
- 42 Nguyen JT. Vascular endothelial growth factor as a target for cancer gene therapy. *Adv Exp Med Biol* 2000;465:447-456
- 43 Belletti B, Ferraro P, Arra C, Baldassarre G, Bruni P, Staibano S, De Rosa G, Salvatore G, Fusco A, Persico MG, Viglietto G. Modulation of in vivo growth of thyroid tumor-derived cell lines by sense and antisense vascular endothelial growth factor gene. *Oncogene* 1999;18: 4860-4869
- 44 Cheng SY, Huang HJ, Nagane M, Ji XD, Wang D, Shih CC, Arap W, Huang CM, Cavenee WK. Suppression of glioblastoma angiogenicity and tumorigenicity by inhibition of endogenous expression of vascular endothelial growth factor. *Proc Natl Acad Sci U S A* 1996;93:8502-8507
- 45 Inoue K, Slaton JW, Kim SJ, Perrotte P, Eve BY, Bar-Eli M, Radinsky R, Dinney CP. Interleukin 8 expression regulates tumorigenicity and metastasis in human bladder cancer. *Cancer Res* 2000;60:2290-2299
- 46 DeFatta RJ, Nathan CA, De Benedetti A. Antisense RNA to eIF4E suppresses oncogenic properties of a head and neck squamous cell carcinoma cell line. *Laryngoscope* 2000;110:928-933
- 47 Oku T, Tjuvajev JG, Miyagawa T, Sasajima T, Joshi A, Joshi R, Finn R, Claffey K P, Blasberg RG. Tumor growth modulation by sense and antisense vascular endothelial growth factor gene expression: effects on angiogenesis, vascular permeability, blood volume, blood flow, fluorodeoxyglucose uptake, and proliferation of human melanoma intracerebral xenografts. *Cancer Res* 1998; 58:4185-4192
- 48 Wu XY, Zhang XF, Yin FS, Lu HS, Guan GX. Clinical study on surgical treatment of esophageal carcinoma in patients after subtotal gastrectomy. *World J Gastroenterol* 1998;4:68-69
- 49 Chen DF, Yang ZY, Yin WB. Radiotherapy of 180 cases of operable esophageal carcinoma. *China Natl J New Gastroenterol* 1997;3:123-126
- 50 Xiao ZF, Yang ZY, Zhou ZM, Yin WB, Gu XZ. Radiotherapy of double primary esophageal carcinoma. *World J Gastroenterol* 2000;6:145-146
- 51 Zhang YH, Xu P, Yang SM, Yuan XB. Expression of interleukin 1 and LY converting enzyme in 5-FU induced apoptosis in esophageal carcinoma cells. *World J Gastroenterol* 1999;5:50-52
- 52 Zhang HX, Li XL, Zhao WX, Gao XP, Fu HM, Shang YQ. The study of trace elements in the hair of patients with esophageal carcinoma in high risk area. *World J Gastroenterol* 2000;6:20
- 53 Shen ZY, Shen WY, Chen MH, Hong CQ, Shen J. Quantitative detection of nitric oxide (NO) in apoptosis of esophageal carcinoma cell induced by arsenite. *World J Gastroenterol* 2000;6:65
- 54 Wu QM, Li SB, Wang Q, Wang DH, Li XB, Liu CZ. The expression of COX-2 in esophageal carcinoma and its relation to clinicopathologic characteristic. *Shijie Huaren Xiaohua Zazhi* 2001;9:11-14
- 55 Zhang J, Yan XJ, Yan QJ, Duan J, Hou Y, Su CZ. Cloning and expression of HPV16 L-2 DNA from esophageal carcinoma in *E. coli*. *Shijie Huaren Xiaohua Zazhi* 2001;9:273-278
- 56 Zhang X, Geng M, Wang YJ, Cao YC. Expression of epidermal growth factor receptor and proliferating cell nuclear antigen in esophageal carcinoma and pre cancerous lesions. *Huaren Xiaohua Zazhi* 1998;6:229-230
- 57 Wang D, Su CQ, Wang Y, Ye YK. Deletion of p16 gene at a high frequency in esophageal carcinoma. *Huaren Xiaohua Zazhi* 1998;6: 1052-1053
- 58 Gu HP, Shang PZ, Su H, Li ZG. Association of CD15 antigen expression with cathepsin D in esophageal carcinoma tissues. *Shijie Huaren Xiaohua Zazhi* 2000;8:259-261
- 59 Liu J, Chen SL, Zhang W, Su Q. P21WAF1 gene expression with P53 mutation in esophageal carcinoma. *Shijie Huaren Xiaohua Zazhi* 2000; 8:1350-1353
- 60 Wang D, Su CQ, Wang Y, Ye YK. Deletion of p16 gene at a high frequency in esophageal carcinoma. *Huaren Xiaohua Zazhi* 1998;6: 1052-1053
- 61 Shen ZY, Shen WY, Chen MH, Hong CQ, Shen J. Alterations of nitric oxide in apoptosis of esophageal carcinoma cells induced by arsenite. *Shijie Huaren Xiaohua Zazhi* 2000;8:1101-1104
- 62 Shen ZY, Tan LJ, Cai WJ, Shen J, Chen CY, Tang XM. Morphologic study on apoptosis of esophageal carcinoma cell line induced by arsenic trioxide. *Huaren Xiaohua Zazhi* 1998;6:226-229
- 63 Chen J, Zhang ZY, Zhu JQ, Wang CW, Xie Y, Huang DQ. Expression of CD44v6 in esophageal carcinoma and its clinical significance. *Huaren Xiaohua Zazhi* 1998;6:534
- 64 He FX, Fan SH, Ge LZ, Shen YF, Lu XK. Radioprotection of radiated auto blood transfusion on patients with esophageal carcinoma. *Huaren Xiaohua Zazhi* 1998;6:867-868
- 65 Fu JH, Rong TH, Huang ZF, Yang MT, Wu YL. Comparative assessment of three prosthesis types of palliative intubation for late stage esophageal carcinoma. *Huaren Xiaohua Zazhi* 1998;6:984-986

• ESOPHAGEAL CANCER •

Relationship of tobacco smoking, CYP1A1, GSTM1 gene polymorphism and esophageal? cancer in Xi'an

An-Hui Wang, Chang-Sheng Sun, Liang-Shou Li, Jiu-Yi Huang, Qing-Shu Chen

An-Hui Wang, Chang-Sheng Sun, Liang-Shou Li, Jiu-Yi Huang, Department of Epidemiology, Faculty of Preventive Medicine, Fourth Military Medical University Xi'an 710033, Shaanxi Province, China
Qing-Shu Chen, Department of Thoracic Surgery, Tangdu Hospital, Fourth Military Medical University, Xi'an 710038, Shaanxi Province, China
Supported by National Natural Science Foundation of China, No.39670651
Correspondence to: An-Hui Wang, Department of Epidemiology, Faculty of Preventive Medicine, Fourth Military Medical University Xi'an 710032, Shaanxi Province, China. wanganhui@hotmail.com
Telephone: +86-29-3374871

Received 2001-06-13 Accepted 2001-11-15

Abstract

AIM: To analyze the association of tobacco smoking, polymorphism of CYP1A1 (7th exon) and GSTM1 genotype and esophageal cancer(EC) in Xi'an.

METHODS: A hospital based case-control study, with molecular epidemiological method, was carried out. Polymorphism of CYP1A1 and GSTM1 of samples from 127 EC cases and 101 controls were detected by PCR method.

RESULTS: There were no significant difference of age and gender between cases and controls. Tobacco smoking was the main risk factor(OR=1.97, 95% CI=1.12-3.48) for EC in Xi'an. The proportions of CYP1A1 *Ile/Ile*, *Ile/Val* and *Val/Val* gene types in cases and controls was 19.7%, 45.7%, 34.6% and 30.7%, 47.5%, 21.8% respectively ($P=0.049$). Individuals with CYP1A1 *Val/Val* genotype compared to those with CYP1A1 *Ile/Ile* genotype had higher risk for EC increased (OR=2.48, 95%CI=1.12-5.54). The proportions of GSTM1 deletion genotype in cases and controls were 58.3% and 43.6% (OR=1.81, 95%CI=1.03-3.18, $P=0.028$). Analysis of gene-environment interaction showed that tobacco smoking and CYP1A1 *Val/Val* genotype; tobacco smoking and GSTM1 deletion genotype had synergism interaction respectively. Analysis of gene-gene interaction did not find synergistic interaction between these two genes. But in GSTM1 deletion group, there was significant difference of distribution of CYP1A1 genotype between cases and controls ($P=0.011$).

CONCLUSION: CYP1A1 *Val/Val* and GSTM1 deletion genotypes are genetic susceptibility biomarkers for EC. The risk increases, when person with CYP1A1 *Val/Val* and/or GSTM1 deletion genotype. And these two-metabolic enzymes seem to have interactions with tobacco smoking, in which the mechanism still needs further study.

Wang AH, Sun CS, Li LS, Huang JY, Chen QS. Relationship of tobacco smoking, CYP1A1, GSTM1 gene polymorphism and esophageal cancer in Xi'an. *World J Gastroenterol* 2002;8(1):49-53

INTRODUCTION

Esophageal cancer (EC) is one of the most common malignant tumors of human being. The incidence of EC varies in different countries. China is the country with highest incidence and

mortality rate of EC. Research showed that risks for EC in different countries or different places were different^[1-6]. In western countries alcohol intake and tobacco smoking were studied deeply^[7-12]. It was thought that besides tobacco smoking and alcohol drinking, nutrition factors, life style, viruses infection, heredity or exposure to nitrosamines, fungi or AFB1 maybe involved in the process of EC^[1,3,13-19]. In China, researches showed risks for EC were different in areas with different incidence^[1-5,16,18,20,21]. The mortality rate of EC of Xi'an city in Shaanxi province is about 24 per 100,000, which ranks first in all cancer mortalities. Previous studies showed that both of tobacco smoking and family history of EC were main risk factors for EC in Xi'an city^[2,22,23].

EC is a multi-etiology disease; environmental risks exposures and genetic susceptibility may take the role part^[2,22-24]. Almost all of the environmental carcinogens (procarcinogens) are activated to be ultimate carcinogens before initiate the process of carcinogenesis. Some metabolic enzymes are closely related to the activation and detoxification of procarcinogens. Alterations of the key oncogene or tumor suppress gene can disturb the cycle of cell proliferation, which can also initiate the process of carcinogenesis^[23,25,26]. Susceptibility of cancer is associated with the genetics polymorphism of related metabolic enzymes. Both certain susceptibility related biomarkers and certain environmental carcinogens perhaps are indispensable factors for EC^[20,23,27,28]. To explore the bio-basis of genetic susceptibility of EC in Xi'an, we carried out a hospital based case-control study to analyze the associations of tobacco smoking, CYP1A1, GSTM1 gene polymorphism and EC.

MATERIALS AND METNODS

Selecion of patients and controls

All cases with esophageal cancer (confirmed by pathological diagnosis) came from inpatients of Tandu Hospital during half a year period (December, 1999 to April, 2000). All controls were stratified randomly selected from non-cancer inpatients from different department of the same hospital during the same period. Both cases and controls were confined to residents with long-term living in Xi'an (with similar proportion of gender and age).

Collected data

Trained interviewers using a structured questionnaire interviewed cases and controls in the hospital. The questionnaire obtained detailed information on residence, occupation, tobacco smoking habit and so on. Here tobacco smoking was defined as smoking at least one cigarette per day and persisting for more than one year. 127 cases (male 97, female 30) and 101 (male 78, female 23) controls were included. Blood samples were also collected for extraction of DNA genome. All blood samples had been stored at -70°C before started DNA extraction.

PCR methods to detect polymorphism of CYP1A1 and GSTM1

Digested by Proteinase K, DNA genomes were extracted from blood

clot of cases and controls with hydroxybenzene, chloroform method in a uninterrupted period. CYP1A1 and GSTM1 polymorphisms were identified by polymerase chain reaction (PCR) before which DNA samples were stored at 4°C. Primers for GSTM1(P1:5'-GTA CCC TAC TTG ATT GAT GGG-3'; P2:5'-CTG GAT TGT AGC AGA TCA TGC-3') and for CYP1A1 (P3: 5'-CGG AAG TGT ATC GGT GAG ACC A -3' P4: 5'-CGG AAG TGT ATC GGT GAG ACC G -3'; P5:5'-GTA GAC AGA GTC TAG GCC TCA-3') were synthesized by Shenggong bio-technical company of Shanghai. PCR condition for GSTM1 as follows, 50μL solution including 10×buffer 5μL, Mg²⁺ 2μL, P1,P2 1μL respectively, template DNA1.5μL, dNTPs 1μL and Taq DNA polymerase 3^U. After denaturation at 94°C for 10 min, Taq DNA polymerase was added,followed by 30 cycles with 94°C 1min, 60°C 1min, and 72°C 1min.20g·L⁻¹ agar was used to electrophoresis PCR production, then observed under the violate light. GSTM1 exist genotype was characterized as had a 273bp fragment; while GSTM1 deletion genotype had no fragment (Figure 1).

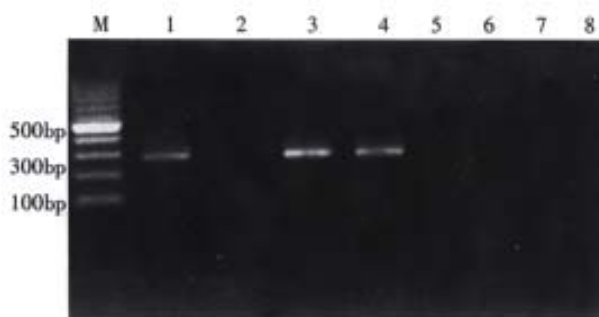


Figure 1 Identify the GSTM1 genotype
M:100bp DNA ladder, 3,4 were GSTM1 exist 2,5 were GSTM1 deletion; 1 positive control,6 negative control,7 was blank control (without DNA template)

We used two pairs of primers to detect the polymorphism of CYP1A1 (7th exon). For each DNA sample two sets of PCR were carried out using P3, P5 (marked as tube A) and P4, P5 (marked as tube B) respectively. PCR conditions were the same:50μL solution including 10×buffer 5μL,Mg²⁺ 2μL, P3,P5 (or P4,P5) 1μL, template DNA 1.5μL, dNTPs 1μL and Taq DNA polymerase 3^U, then 94°C 10min followed by 94°C 1min,55°C 1min, 72°C 1min, 35 cycles,72°C extending 10 min. PCR products were observed. The PCR was conducted to detect the mutation of A-G in CYP1A1 7th exon, the mutation can leads to change of one amino acid (Ile to Val). If there was only tube A had the specifically fragment (200bp), the DNA was regarded as CYP1A1 *Ile/Ile* genotype (pure wild genotype); if only tube B had the positive fragment, CYP1A1 *Val/Val* genotype (pure mutation) was considered; and CYP1A1 *Ile/Val* genotype was identified with both tube A and tube B had the fragment (Figure 2).

Quality control

DNA extraction and PCR were conducted in different period and places. The genotypes of DNA samples were identified blindly. Every PCR had were set controls as blanket control (without DNA template), positive control and negative control, and when any one of these controls was failure, PCR wasre-conducted.

Statistical analysis

Data were input into computer, then the values of χ^2 , odds ratio (OR) and OR95% CI (confidence intermediate) were

calculated. And ORs of gene-environment and gene-gene interaction were also estimated.



Figure 2 Identified the genotypes of CYP1A1
M: 100bp DNA ladder; 1(A),2(B) represent *Ile/Ile* genotype; 3(A),4(B) represent *Ile/Val* genotype; 5(A),6(B) represent *Val/Val* genotype; 7(A),8 (B) as blank control(without DNA template).

RESULTS

Comparability between cases and controls

The age and gender in cases and controls were comparable(Table 1).

Table 1 Comparability of age and gender in cases and controls

Factor	Case	Control	χ^2	P
Age(year)				
<50	28	16		
50-	38	44		
≥60	61	41	4.73	0.094
Gender				
Male	97	78		
Female	30	23	0.02	0.80

Risk factors for EC

The proportions of tobacco smoking, *GSTM1* deletion genotype and *CYP1A1* genotype (*Val/Val*) in cases and controls were significantly different ($P<0.05$) (Table 2).

Table 2 Distributions of smoking, *GSTM1* deletion and *CYP1A1* genotypes

Factors	Case	Control	OR	OR95%CI	χ^2	P
Smoking						
Yes	69	38	1.97	1.12-3.48	6.28	0.012
No	58	63				
<i>GSTM1</i>						
Deletion	74	44	1.81	1.03-3.18	4.85	0.028
Exist	53	57				
<i>CYP1A1</i>						
<i>Ile/Ile</i>	25	31	1.00		1.00	
<i>Ile/Val</i>	58	48	1.50	0.74-3.03	1.48	0.22
<i>Val/Val</i>	44	22	2.48	1.12-5.54	5.93	0.015

Interaction of tobacco smoking and *GSTM1* deletion genotype or *CYP1A1 Val/Val* genotypes

Analysis showed that there was synergistic interaction between tobacco smoking and *GSTM1* deletion genotype (Table 3).

Table 3 Interaction of smoking and *GSTM1* deletion genotype.

Smoking	<i>GSTM1</i> deletion	Case	Control	OR	OR95%CI	χ^2	P
No	No	25	37	1.00			
Yes	No	28	20	2.07	0.90-4.80	3.48	0.062
No	Yes	33	26	1.88	0.86-4.13	2.93	0.087
Yes	Yes	41	18	3.37	1.49-7.69	10.29	0.0013

$$SIA=3.37/(1.88+2.07-1.00)=1.14$$

Tobacco smoking and CYP1A1 *Val/Val* genotype also appeared synergistic interaction (Table 4).

Table 4 Interaction of tobacco smoking and CYP1A1 *Val/Val* genotype

Smoking	CYP1A1(<i>Val/Val</i>)	Case	Control	OR	OR95%CI	χ^2	P
No	No	36	47	1.00			
Yes	No	47	32	1.92	0.98-3.76	4.18	0.04
No	Yes	22	16	1.80	0.77-4.20	2.18	0.14
Yes	Yes	22	6	4.79	1.62-14.83	10.30	0.0013

SIM=4.79/(1.92×1.80)=1.39

But CYP1A1 mutation genotypes(*Val/Val*, *Ile/Val*) and GSTM1deletion genotype did not show significant interaction (Table 5).

Table 5 Interaction of CYP1A1mutation genotypes(*Val/Val*, *Ile/Val*) and GSTM1deletion genotype

GSTM1 deletion	CYP1A1 mutation	Case	Control	OR	OR95%CI	χ^2	P
No	No	10	20	1.00			
No	Yes	43	37	2.32	0.89-6.14	3.61	0.057
Yes	No	15	11	2.73	0.81-9.42	3.28	0.070
Yes	Yes	59	33	3.58	1.39-9.38	8.66	0.0033

OR of individuals with CYP1A1 mutation genotype and GSTM1deletion genotype was greater than those with of any other forms of the two genotypes. But there did not show any synergistic interaction between CYP1A1 mutation genotypes and GSTM1deletion genotype.

Stratified with GSTM1 deletion genotype to analyze the distributions of CYP1A1 genotypes in cases and controls. Results showed that there were significant different in cases and controls ($P=0.011$) in GSTM1 exist genotype CYP1A1 genotypes, whereas there were no significant difference ($P=0.83$) between cases and controls in GSTM1 deletion genotype (Table 6).

Table 6 Analysis of CYP1A1 genotypes in cases and controls with Stratified GSTM1deletion

CYP1A1 genotype	GSTM1 deletion		existing GSTM1	
	Case	Control	Case	Control
<i>Ile/Ile</i>	15	11	10	20
<i>Ile/Val</i>	35	19	23	29
<i>Val/Val</i>	24	14	20	8
χ^2	0.39		9.04	
P	0.83		0.011	

DISCUSSION

Under similar environmental carcinogens exposure only a few of individuals get neoplasm, for there were individual difference to environmental exposure. The different liability to cancer was called genetic susceptibility of cancer. Genetic susceptibility can affect on every step of carcinogenesis, including modify the effect of environmental carcinogens^[24,29-35]. Oncogenes and tumor suppressor genes can also affect individual's susceptibility to cancer. Cancer susceptibility genes includes typeI, typeII metabolism enzyme gene, DNA repair gene and those affect cell proliferation rate gene. In recent years evidence has accumulated to support the hypothesis that cancer susceptibility gene may be of importance in determining individual susceptibility to cancer^[34,36-46].

EC is a multi-factor determined disease; including environmental risk factors and genetic factors. In recent years, more and more researches considered environmental and genetic susceptibility factors and their interactions in evaluating the risks of cancer^[2,17,43,47-50]. Investigations showed the mortality rate of EC in Shaanxi province did not

decreased during the late 20 years, and risks factors for EC in Xi'an city were discussed in several researches^[2,22,23]. In this hospital based case- control study, the results showed that tobacco smoking was a risk factor; and tobacco smoking had interactions with GSTM1deletion genotype and CYP1A1 *Val/Val* genotype.

Most chemical carcinogens in environment are pro-carcinogens. And aromatic hydrocarbons (AHs) in tobacco smoking are pro-carcinogens, they need to be activated to reactive electrophilic forms by type I metabolic enzymes (CYP450s), then initiate the carcinogenesis. On the other hand the reactive electrophilic forms of carcinogen can be detoxified and excreted by type I metabolic enzymes such as GSTM1. Although theoretically the increase of activity of type II metabolic enzymes and/or decrease of activity of type I metabolic enzymes can increase the risk for cancer, there were different results in different researches, some supported this hypothesis and others did not^[27,34,35,37,40-42,51-56]. Our results showed that individuals with the GSTM1 deletion genotype or/and CYP1A1 *Val/Val* genotype had increased risks for EC.

P450 CYP1A1 gene located in chromosome 15q22 mainly metabolizes pro-carcinogens. There are three kinds of polymorphism of CYP1A1: *MspI* site, 7th exon (*Ile-Val*) and AA polymorphism. *MspI* polymorphism include three genotypes: without *MspI* enzyme cleavage site allele gene *m1(m1/m1)* as A genotype; having *MspI* cleavage site allele (*m2/m2*) as C genotype and *m1/m2* as B genotype. In different populations the distribution of these three genotypes were different. CYP1A1 *Ile-Val* polymorphism caused by 7th exon 4889th base difference (A or G), transition of A to G results in 462th amino turned from isoleucine to valine^[13], then form three kinds of genotypes: homozygote wild genotype (*Ile/Ile*), mutation genotype (*Val/Val*) and heterozygote *Ile/Val* genotype. Polymorphism of 7th exon correlated with polymorphism of *MspI* in Asia and Caucasian populations, and in Americans from Africa these two kind of CYP1A1 polymorphism were independent, CYP1A1 7th exon polymorphism and *MspI* site were incomplete linkage. Research showed CYP1A1 *Val/Val* genotype have higher ability to activate pro-carcinogen than CYP1A1 *Ile/Ile* genotype. PAH-DNA adducts in leukocyte were higher in heavy smoking population with CYP1A1 *Val/Val* genotype than those with CYP1A1 *Ile/Val* or *Ile/Ile* genotype. AA polymorphism was new special *MspI* polymorphism, which still under discussion.

Although evidence showed that CYP1A1 mutation genotype (*Val/Val*) had the strongest ability to activate pro-carcinogens, the associations between CYP1A1 genotype and susceptibility to cancers were varied^[30-33,37,57,58]. Data from Guangdong province in China showed that *MspI* C correlated with no-smoking population's lung cancer susceptibility^[52]. Study in Shanghai and Haerbin no significant relation was discovered between CYP1A1 (*Ile-Val*) polymorphism and lung cancer susceptibility in non-smoking female patients^[51]. CYP1A1 *Val/Val* genotype only appear about 3.2%~5% in white population, while in Japanese it was about 19.8%, in Chinese it was 22.3%. Our study showed that distributions of CYP1A1 genotypes in cases and controls were different ($P=0.049$), CYP1A1 *Val/Val* genotype was associated with EC (OR= 2.48, 95%CI=1.12-5.54) and there was interaction of tobacco smoking and CYP1A1 *Val/Val* genotype.

GSTM1 can detoxify a number of reactive electrophilic compound substances, including the carcinogens PAHs. If

individuals with GSTM1 deletion genotype, the ability of detoxify the carcinogens decreased. Individuals with GSTM1 deletion can have the increased risk of cancers^[24,43,46]. In China there were similar research on GSTM1 deletion genotype and the risks of lung cancer(OR=2.56)^[53], and stomach cancer(OR=1.90, 95%CI=1.01-3.56)^[54]. Researches showed that in Henan province, high incidence of EC in China, GSTM1 deletion gene polymorphisms had not significant relation with EC susceptibility^[20]. Results of our study indicated GSTM1 deletion genotype was significant different in cases and controls ($P=0.028$) and the OR was 1.81(OR95%CI=1.03-3.18). GSTM1 deletion genotype had synergistic interaction with tobacco smoking.

In summary, we found tobacco smoking, CYP1A1 Val/Val genotype; GSTM1 deletion genotype had associations with EC in Xi'an area. Gene-environment interaction analysis showed that tobacco smoking had synergistic interactions with CYP1A1 Val/Val genotype, and with GSTM1 deletion genotype. Gene-gene interaction analysis did not find synergistic interaction between CYP1A1 mutation genotypes and GSTM1 deletion genotype, though individuals with these two genotypes had increased risk for EC. The synergistic interactions and their mechanisms of tobacco smoking with these two metabolic enzymes gene polymorphisms still need further study with large (population-based) samples and modified designs.

Acknowledgment We would like to thank Bing-Quan Gu for their help in collecting blood sample.

REFERENCES

- Zhang W, Bailey-Wilson JE, Li W, Wang X, Zhang C, Mao X, Liu Z, Zhou C, Wu M. Segregation analysis of esophageal cancer in a moderately high-incidence area of northern China. *Am J Hum Genet* 2000; 67: 110-119
- Li LS, Sun CS, Zhang XL, Qiao GB, Xu DZ, Han CL, Yang WX, Chang GS, Yan MX, Wang Y, Zhang HY. A comparative molecular epidemiological study on esophageal cancer between Xi'an and Linzhou. *Jiefangjun Yufangyixue Zazhi* 1999; 17: 255-259
- Zhou XG, Watanabe S. Factor analysis of digestive cancer mortality and food consumption in 65 Chinese countries. *J Epidemiol* 1999; 9: 275-284
- Wang LD, Zou JX, Hong JY, Zhou Q, Deng CJ, Xie DW, Holly C. Identification of a novel genetic polymorphism of human O-6-alkylguanine-DNA alkyltransferase in patients with esophagus cancer. *Huren Xiaohua Zazhi* 1998; 6: 560-463
- Lu JB, Lian SY, Sun XB, Zhang ZX, Dai DX, Li BW, Cheng LP, Wei JR, Duan WJ. A case-control study on the risk factors of esophageal cancer in Linzhou. *Zhonghua Liuxingbingxue Zazhi* 2000; 21: 434-436
- Li WD, Wang XQ, Zhang CL, Han XY, Chen DQ, Zhang T, Pan XF, Jia YT, Mao XZ, Zhang R. Esophageal carcinoma in part of population of yangquan city. *Zhonghua Yixue Zazhi* 1998; 78: 203-206
- Castellsague X, Munoz N, De Stefani E, Vitoria CG, Quintana MJ, Castelletto R, Rolon PA. Smoking and drinking cessation and risk of esophageal cancer (Spain). *Cancer Causes Control* 2000; 11: 813-818
- Lagregren J, Bergstrom R, Lindgren A, Nyren O. The role of tobacco, snuff and alcohol use in the aetiology of cancer of the oesophagus and gastric cardia. *Int J cancer* 2000; 85: 340-346
- Launoy G, Milan C, Faivre J, Pienkowski P, Gignoux M. Tobacco type and risk of squamous cell cancer of the oesophagus in males: a French multicentre case-control study. *Int J Epidemiol* 2000; 29: 36-42
- Talamini G, Capelli P, Zamboni G, Mastromauro M, Pasetto M, Castagnini A, Angelini G, Bassi C, Scarpa A. Alcohol, smoking and papillomavirus infection as risk for esophageal squamous-cell papilloma and esophageal squamous-cell carcinoma in Italy. *Int J cancer* 2000; 86: 874-878
- Castellsague X, Munoz N, De Stefani E, Vitoria CG, Castelletto R, Rolon PA, Quintana MJ. Independent and joint effects of tobacco smoking and alcohol drinking on the risk of esophageal cancer in men and women. *Int J Cancer* 1999; 82: 657-664
- Castellsague X, Munoz N, De Stefani E, Vitoria CG, Castelletto R, Rolon PA. Influence of mate drinking, hot beverages and diet on esophageal cancer risk in South America. *Int J Cancer* 2000; 88: 658-664
- Dhillon PK, Farrow DC, Vaughan TL, Chow WH, Risch HA, Gammon MD, Mayne ST, Stanford JL, Schoenberg JB, Ahsan H, Dubrow R, West AB, Rotterdam H, Blot WJ, Fraumeni JF Jr. Family history of cancer and risk of esophageal and gastric cancers in the United States. *Int J Cancer* 2001; 93: 148-152
- Nayar D, Kapil U, Joshi YK, Sundara KR, Sriastava SP, Shukla NK, Tandon RK. Nutritional risk factors in esophageal cancer. *J Assoc Physicians India* 2000; 48: 781-787
- Chang F, Syrjanen S, Shen Q, Cintorino M, Santopietro R, Tosi P, Syrjanen K. Evaluation of HPV, CMV, HSV and EBV in esophageal squamous cell carcinomas from a high-incidence area of China. *Anticancer Res* 2000; 20: 3935-3940
- Li T, Lu ZM, Chen KN, Guo M, Xing HP, Mei Q, Yang HH, Lechner JF, Ke Y. Human papillomavirus type 16 is an important infectious factor in the high incidence of esophageal cancer in Anyang area of China. *Carcinogenesis* 2001; 22: 929-934
- Shi QL, Xu DZ, Sun CS, Li LS. Study on family aggregation of esophageal cancer in Linzhou city. *Zhonghua Yufang Yixue Zazhi* 2000; 34: 269-270
- Shen YP, Gao YT, Dai Q, Hu X, Xu TL, Xiang YB, Tang ZL, Li WL. A case-control study on esophageal cancer in Huaian city, Jiangsu province (I): role of the cigarette smoking and alcohol drinking. *Zhongliu* 1999; 19: 363-367
- Lagergren J, Ye W, Lindgren A, Nyren O. Heredity and risk of cancer of the esophagus and GASTRIC cardia. *Cancer Epidemiol Biomarkers Prev* 2000; 9: 757-760
- Lin DX, Tang YM, Lu SX, Kadlubar FF. Glutathione S-transferase M1, T1 genotypes and risks of esophageal cancer: a case-control study. *Zhonghua Liuxingbing Zazhi* 1998; 19: 195-199
- Gao YT, Den J, Xiang YB, Ruan ZX, Wang ZX, Hu BY, Guo MR, Ten WK, Han JJ, Zhang YS. Smoking, related cancers, and other diseases in Shanghai: A 10-year prospective study. *Zhonghua Yufang Yixue Zazhi* 1999; 33: 5-8
- Zhang HY, Sun CS, Li LS, Yan MX. Cytochrome P4501A1 and the genetic susceptibility to esophageal carcinoma. *Zhonghua Yufang Yixue Zazhi* 2000; 34: 69-71
- Wang AH, Zhang HY, Wang Y, Yan MX, Sun CS, Li LS, Huang JY, Cheng QS, Zhu YF. Molecular epidemiological study on esophageal cancer in Xi'an. *Disi Junyi Daxue Xuebao* 2001; 22: 61-63
- Tan W, Song N, Wang GQ, Liu Q, Tang HJ, Kadlubar FF, Lin DX. Impact of genetic polymorphisms in cytochrome P450 2E1 and glutathione S-transferases M1, T1, and P1 on susceptibility to esophageal cancer among high-risk individuals in China. *Cancer Epidemiol Biomarkers Prev* 2000; 9: 551-556
- Hu N, Huang J, Emmert-buck MR, Tang ZZ, Roth MJ, Wang C, Dawsey SM, Li WJ, Wang QH, Han XY, Ding T, Giffen C, Goldstein AM, Taylor PR. Frequent inactivation of the TP53 gene in esophageal squamous cell carcinoma from a high-risk population in China. *Clin Cancer Res* 2001; 7: 883-891
- Taniere P, Martel-Planche G, Puttawibul P, Casson A, Montesano R, Chanvitan A, Hainaut P. TP53 mutations and MDM2 gene amplification in squamous-cell carcinomas of the esophagus in south Thailand. *Int J Cancer* 2000; 88: 223-227
- Shao GZ, Hu Z, Li EM, Li J, Wen BG. Relationship between the GSTM1 genetic polymorphism and susceptibility to squamous cell carcinoma of esophagus. *Shantou Daxue Yixueyuan Xuebao* 1999; 12: 1-3
- Mizobuchi S, Furihata M, Sonobe H, Ohtsuki Y, Ishikawa T, Murakami H, Kurabayashi A, Ogoshi S, Sasaguri S. Association between p53 immunostaining and cigarette smoking in squamous cell carcinoma of the esophagus. *Jpn J Clin Oncol* 2000; 30: 423-428
- van Lieshout EM, Roelofs HM, Dekker S, Mulder CJ, Wobbes T, Jansen JB, Peters WH. Polymorphic expression of the glutathione S-transferase P1 gene and its susceptibility to Barrett's esophagus and esophageal carcinoma. *Cancer Res* 1999; 59: 586-589
- Roth MJ, Dawsey SM, Wang G, Tangrea JA, Zhou B, Ratnasinghe D, Woodson KG, Olivero OA, Poirier MC, Frye

- BL, Taylor PR, Weston A. Association between GSTM1*0 and squamous dysplasia of the esophagus in the high risk region of Linxian, China. *Cancer Lett* 2000; 156: 73-81
- 31 Morita S, Yano M, Tsujinaka T, Akiyama Y, Taniguchi M, Kaneko K, Miki H, Fujii T, Yoshino K, Kusuoka H, Monden M. Genetic polymorphisms of drug-metabolizing enzymes and susceptibility to head-and-neck squamous-cell carcinoma. *Int J Cancer* 1999; 80: 685-688
 - 32 Butler WJ, Ryan P, Roberts-Thomson IC. Metabolic genotypes and risk for colorectal cancer. *J Gastroenterol Hepatol* 2001;16:631-635
 - 33 Rojas M, Cascorbi I, Alexandrov K, Kriek E, Auburtin G, Mayer L, Kopp-Schneider A, Roots I, Bartsch H. Modulation of benzo^[a]pyrene diolepoxide-DNA adduct levels in human white blood cells by CYP1A1, GSTM1 and GSTT1 polymorphism. *Carcinogenesis* 2000; 21: 35-41
 - 34 Tanimoto K, Hayashi S, Yoshiga K, Ichikawa T. Polymorphisms of the CYP1A1 and GSTM1 gene involved in oral squamous cell carcinoma in association with a cigarette dose. *Oral Oncol* 1999; 35: 191-196
 - 35 Sato M, Sato T, Izumo T, Amagasa T. Genetic polymorphism of drug-metabolizing enzymes and susceptibility to oral cancer. *Carcinogenesis* 1999; 20: 1927-1931
 - 36 Xing DY, Tan W, Song N, Lin DX. Genetic polymorphism in hOGG1 and susceptibility to esophageal cancer in Chinese. *ZhonghuaYiue Yichuanxue Zazhi* 2000; 17: 377-380
 - 37 Chen S, Xue K, Xu L, Ma G, Wu J. Polymorphisms of the CYP1A1 and GSTM1 genes in relation to individual susceptibility to lung carcinoma in Chinese population. *Mutat Res* 2001;458:41-47
 - 38 Song C, Xing D, Tan W, Wei Q, Lin D. Methylenetetrahydrofolate reductase polymorphisms increase risk of esophageal squamous cell carcinoma in a Chinese population. *Cancer Res* 2001;61:3272-3275
 - 39 Lee JM, Lee YC, Yang SY, Yang PW, Luh SP, Lee CJ, Chen CJ, Wu MT. Genetic polymorphisms of XRCC1 and risk of the esophageal cancer. *Int J Cancer* 2001;95:240-246
 - 40 Chao YC, Wang LS, Hsieh TY, Chu CW, Chang FY, Chu HC. Chinese alcoholic patients with esophageal cancer are genetically different from alcoholics with acute pancreatitis and liver cirrhosis. *Am J Gastroenterol* 2000;95:2958-2964
 - 41 Sato M, Sato T, Izumo T, Amagasa T. Genetically high susceptibility to oral squamous cell carcinoma in terms of combined genotyping of CYP1A1 and GSTM1 genes. *Oral Oncol* 2000;36: 267-671
 - 42 Gsur A, Haidinger G, Hollaus P, Herbacek I, Madersbacher S, Trieb K, Pridun N, Mohn-Staudner A, Vetter N, Vutuc C, Micksche M. Genetic polymorphisms of CYP1A1 and GSTM1 and lung cancer risk. *Anticancer Res* 2001;21:2237-2242
 - 43 Dong CH, Yu SZ, Chen GC, Zhao DM, Hu Y. Association of polymorphisms of glutathione S transferase M1 and T1 genotypes with elevated aflatoxin and increased risk of primary liver cancer. *Huaren Xiaohua Zazhi* 1998; 6: 463-466
 - 44 Bian JC, Shen FM, Shen L, Wang TR, Wang XH, Chen GC, Wang JB. Susceptibility to hepatocellular carcinoma associated with genotypes of GSTM1 AND gstm1. *World J Gastroenterol* 2000; 6:228-230
 - 45 Cai L, Yu SZ, Zhang ZF. Glutathione S-transferase M1, T1 genotypes and the risk of gastric cancer: a case-control study. *World J Gastroenterol* 2001;7:506-509
 - 46 Cai L, Yu SZ. A molecular epidemiologic study on gastric cancer in Changde, Fujian province. *Shijie Huaren Xiaohua Zazhi* 1999; 7: 652-655
 - 47 Lee JM, Lee YC, Yang SY, Shi WL, Lee CJ, Luh SP, Chen CJ, Hsieh CY, Wu MT. Genetic polymorphisms of p53 and GSTP1, but not NAT2, are associated with susceptibility to squamous-cell carcinoma of the esophagus. *Int J Cancer* 2000; 89: 458-464
 - 48 Bartsch H, Nair U, Risch A, Rojas M, Wikman H, Alexandrov K. Genetic polymorphism of CYP genes, alone or in combination, as a risk modifier of tobacco-related cancers. *Cancer Epidemiol Biomarkers Prev* 2000;9:3-28
 - 49 Butkiewicz D, Cole KJ, Phillips DH, Harris CC, Chorazy M. GSTM1, GSTP1, CYP1A1 and CYP2D6 polymorphisms in lung cancer patients from an environmentally polluted region of Poland: correlation with lung DNA adduct levels. *Eur J Cancer Prev* 1999;8: 315-323
 - 50 Liu G, Zhou Q, Wang LD, Hong JY, Deng CJ, Wang YY, Zou JX. Blood clot as a DNA source for studying genetic polymorphism of human carcinogen-metabolizing enzymes. *World J Gastroenterol* 1998; 4(Suppl 2): 108-109
 - 51 Qu YH, Shi YB, Peter S, Zhong LJ, Sun L, Sun XW, Cheng JR, Lin YJ, Xian YB, Dai XD, Gao YT. The genotypes of cytochrome P4501A1 and GST M1 in non-smoking female lung cancer. *Zhongliu* 1998; 18: 80-82
 - 52 Hu YL, Zhang Q. Genetic Polymorphisms of CYP1A1 and susceptibility of lung cancer. *Zhonghua Yixue Yichuanxue ZaZhi* 1999; 16: 26-28
 - 53 Gao JR, Ren CL, Zhang Q. CYP2D6 and GSTM1 genetic polymorphism and lung cancer susceptibility. *Zhonghua Zhongliu Zazhi* 1998; 20: 185-186
 - 54 Cai L, Yu SZ. Preliminary studies on cytochrome P4502E1 and glutathione transferase M1 polymorphisms and susceptibility to gastric cancer. *Zhongguo Gonggong Weisheng* 1999; 15: 895-897
 - 55 Olshan AF, Mark CW, Watson MA, Bell DA. GSTM1, GSTT1, GSTP1, CYP1A1 and NAT1 Polymorphisms, Tobacco use, and the risk of head and neck cancer. *Cancer Epidemiol Biomarkers Prev* 2000; 9:185-191
 - 56 London SJ, Yuan JM, Coetzee GA, Gao YT, Ross RK, Yu MC. CYP1A1 I462V genetic polymorphism and lung cancer risk in a cohort of men in Shanghai, China. *Cancer Epidemiol Biomarkers Prev* 2000;9:987-991
 - 57 Murata M, Watanabe M, Yamanaka M, Kubota Y, Ito H, Nagao M, Katoh T, Kamataki T, Kawamura J, Yatani R, Shiraishi T. Genetic polymorphisms in cytochrome P450 (CYP) 1A1, CYP1A2, CYP2E1, glutathione S-transferase (GST) M1 and GSTT1 and susceptibility to prostate cancer in the Japanese population. *Cancer Lett* 2001; 165: 171-177
 - 58 Shen J, Wang RT, Xing HX, Wang LW, Wang ZX, Wang BY, Li MS, Wang JM, Hua ZL, Guo CH, Wang XR, Xu XP. Research on the interaction models of cytochrome P450 1A1 polymorphism(s) in the agents of stomach cancer. *Zhonghua Yufang Yixue Zazhi* 2001;35:167-170

• REVIEW •

Changing patterns of traumatic bile duct injuries: a review of forty years experience

Zhi-Qiang Huang, Xiao-Qiang Huang

Zhi-Qiang Huang, Xiao-Qiang Huang, Research Institute of General Surgery, The General Hospital of Chinese PLA, Beijing 100853, China
Correspondence to: Zhi-Qiang Huang, 28 Fuxin Road, Beijing 100853, China. zhiqianghuang2000@yahoo.com

Telephone: +86-10-66939871 Fax: +86-10-68181689

Received 2001-08-23 Accepted 2001-12-20

Abstract

AIM: To summarize the experiences of treating bile duct injuries in 40 years of clinical practice.

METHODS: Based on the experience of more than 40 years of clinical work, 122 cases including a series of 61 bile duct injuries of the Southwest Hospital, Chongqing, and 42 cases (1989-1997) and 19 cases (1998-2001) of the General Hospital of PLA, Beijing, were reviewed with special reference to the pattern of injury. A series of cases of the liver and the biliary tract injuries following interventional therapy for hepatic tumors, most often hemangioma of the liver, were collected. Chinese medical literature from 1995 to 1999 dealing with 2742 traumatic bile duct strictures were reviewed.

RESULTS: There was a changing pattern of the bile duct injury. Although most of the cases of bile duct injuries resulted from open cholecystectomy. Other types of trauma such as laparoscopic cholecystectomy (LC) and hepatic surgery were increased in recent years. Moreover, serious hepato-biliary injuries following HAE using sclerotic agents such as sodium morrhuate and absolute ethanol for the treatment of hepatic hemangiomas were encountered in recent years. Experiences in how to avoid bile duct injury and to treat traumatic biliary strictures were presented.

CONCLUSION: Traumatic bile duct stricture is one of the serious complications of hepato-biliary surgery, its prevalence seemed to be increased in recent years. The pattern of bile duct injury was also changed and has become more complicated. Interventional therapy with sclerosing agents may cause serious hepatobiliary complications and should be avoided.

Huang ZQ, Huang XQ. Changing patterns of traumatic bile duct injuries: a review of forty years experience. *World J Gastroenterol* 2002;8(1):5-12

INTRODUCTION

Since the first total cholecystectomy performed by Carl Langenbuch in 1882, there has been the likelihood of bile duct injury. But it was not mentioned until 1905 that Mayo reported the first two cases of bile duct stricture following cholecystectomy treated by choledochoduodenostomy^[1]. This might be due to the small number of operations performed by that time. However, the number of cases of bile duct injuries has been rapidly increased since then^[2]. In China, the prevalence of cholelithiasis is increasing, and cholecystectomy has become one of the most frequent operations in daily surgical

practice^[3-5]. The victims of bile duct injuries often suffered from great misery and the fatality rate can be as high as 30%^[6]. Efforts have been made in the training and standardization of conventional biliary operations such as cholecystectomy, the result being encouraging. Roslyn^[7] (1993) revealed 42,474 cases of open cholecystectomy from 1988 to 1989 (8% of cholecystectomies performed in America at the same period of time), and the bile duct injury rate has been lowered to 0.2%. In China, however, the bile duct injury during conventional open cholecystectomy has been claimed to be low, in spite of the lack of statistical data. In recent years, the number of reports on bile duct injuries due to cholecystectomies has been rapidly increased in the Chinese medical literature. The seriousness of the problem caused great concern from the medical professionals^[8]. Furthermore, the pattern of bile duct injuries at present also differed in some way from the traditional ones which imposed different methods of treatment. These may be complicated and unfamiliar to the practicing physicians and surgeons. In this report, we present our clinical experiences in the treatment of bile duct injuries over the past 40 years and specially the importance in laparoscopic, and bile duct injuries during liver resection and interventional therapy of hepatic lesions.

CLINICAL MATERIALS

Case records of traumatic bile duct injuries were reviewed. All patients in Group A and Group B series were the cases attended by the senior author either as the director or as senior surgeon of the department. Group A consisted of 61 cases of bile duct injury admitted to the South-west Hospital, Chongqing from 1963 to 1986;^[9] and Group B were 61 cases admitted to the General Hospital of PLA in Beijing from 1989 to 1997^[10] and from 1998 to 2001 (Tables 1,2).

Before 1990, the cases of traumatic bile duct stricture were mostly due to open celiotomy by conventional technique. Cases of bile duct stricture following laparoscopic cholecystectomy have been encountered since the turn of 1990 and cases of bile duct injuries resulting from the so-called 'mini-cholecystectomy' have been found in recent years. Up till now, bile duct injuries chiefly result from conventional surgery but not laparoscopic operations. Traumatic injuries and operations of the upper abdominal organs may cause bile duct injury, but biliary tract operations was the most common cause.

Table 1 Types of primary operations in 61 cases of traumatic biliary strictures (Group A, 1963/1986, South-West Hospital Series)

Types of operation	Cases
Cholecystectomy	39
Cholecystectomy + choledochostomy	10
Gastrectomy (B-II)	7
Hepatic injury - Rt lobectomy	1
Suture + gauze packing	2
Suture + choledochostomy	1
Suture + repair of duodenum	1
Total cases	61
**29 of the 61 cases were recognized by the operator during the primary operation	

Table 2 Changing trend of primary operations in cases of traumatic biliary strictures (Group B: The General Hospital of PLA Series)

Types of operations	Cases	
	(1989-1997)	(1998-2001)
Cholecystectomy	27	8
Mini-cholecystectomy	2	
Laparoscopic cholecystectomy(LC)	4	5
Cholecystectomy + choledochostomy	9	
Hepatic resection	3	
Hepatic resection + HAE	1	
HAE		1
Gastrectomy(B-I)	1	
Total cases	42	19

In these 122 cases of traumatic bile duct injuries, cholecystectomy, especially simple cholecystectomies, was responsible for the majority of cases. As to the patterns of injuries, laparoscopic surgery, hepatic resection and interventional therapy for hepato-biliary diseases made a significant contribution in the Group B series.

Gastric resection The next common cause of extra-hepatic bile duct injury is gastric resection, which has been frequently employed for the treatment of chronic duodenal ulcer disease before the advent of the present anti-ulcer drugs. In series A, there were 2 cases of bile duct injury due to gastric resection probably through a not well-known mechanism which was differed from the ordinary direct operative injury. The first one was a male patient aged 42 years with a history of repeated hemorrhage from chronic duodenal ulcer for 7 years. On operation, a mass involving the posterior duodenal wall and the head of the pancreas was found and a Bancroft's type of gastric resection was performed. Four years following the operation, the patient still suffered from episodes of massive G-I bleeding accompanied with low blood pressure. Therefore, another operation was undertaken. The operation consisted of vagotomy and resection of the remanding portion of the gastric antrum together with the duodenal "ulcer" so as to control bleeding. However, the patient experienced a very stormy postoperative course. Jaundice appeared on the 4th postoperative day associated with daily chills and fever, while the gastric aspiration showed no bile. The patient's general condition was thus rapidly deteriorated. Re-operation was performed on the 6th postoperative day. A large amount of blood and bile tinged fluid was found inside the peritoneal cavity, and fatty necrosis was found around the head of the pancreas. A cholecystostomy was performed to relieve jaundice and drainage of the abdominal cavity. After the operation, a large amount of bile mixed with pancreatic juice (amylase activity was 1280 Winslow's unit) was drained outdaily through the cholecystostomy tube. Subsequently, further additional operations were performed for intra-abdominal residual abscesses. Eventually, the patient died of sepsis and wide spread intra-cranial hemorrhage. At autopsy, left-sided residual suphrenic abscess and empyema of left thorax was found, the ruptured duodenal stump was healed, and obstruction of the common bile duct at the ampulla below the confluence of the bile and pancreatic ducts was found so that pancreatic fluid was drained through the cholecystostomy tube by retrograde flow. There was no evidence of direct surgical injury or suturing of the lower end of the bile duct as the cause of biliary obstruction, however.

Another case was a middle-aged patient who also suffered from chronic duodenal ulcer complicated with repeated G-I hemorrhage. He was also treated at first by Bancroft's gastric resection and followed by resection of the gastric remnant and the ulcer because episodes of G-I hemorrhage recurred. The patient developed disruption of the duodenal stump and obstructive jaundice. PTC showed bile duct obstruction at the ampulla of Vater. This patient was firstly treated by abdominal drainage and cholecystostomy followed by Roux-en-Y

choledocho-jejunostomy and pancreatico-jejunostomy with an uneventful convalescence. This patient showed no excessive pancreatic drainage through the cholecystostomy tube because of the common bile and the pancreatic ducts were both obstructed at the ampullary level. In these two cases, the obstruction of the ampulla may be the result of operative interruption of blood supply to this particular region. However, the mechanism of such kind of bilio-pancreatic duct injury has not been well understood.

Interventional therapy and bile duct injury In recent years, a particular type of bile duct injury was noted^[11], i.e., bile duct injuries following interventional treatment for hepatic tumors, most frequently for hepatic hemangiomas^[12] (Table 3). But such kind of bile duct injuries was usually not categorized under the heading of traumatic bile duct injury in hospital files.

Table 3 Hepato-biliary complications following HAE for cavernous hemangioma of liver

Case	Embolizing No. agents	Complications	Operations	Results
1	Sod.mo.+Lip.	Rt.Lt.CHD,GB Necrosis Biliary cirrhosis Liver abscess	S-R shunt B-jejunostomy	Jaundice ↓
2	Ethanol	Biliary fistula	Rt. Lobectomy B-jejunostomy	Jaundice ↓
3	Sod.mo.+Lip.	Rt-Lt-HD necrosis Liver abscess	PTBD Necrosectomy, U-tube	Jaundice ↓ Jaundice ↑
4	Lip.wire Phnyanmycin	GB necrosis HD stricture Liver abscess	No	Jaundice ↓
5	Sod. Mo+Lip.	GB,CBD necrosis Liver abscess	Cholecystectomy T-tube stent	Jaundice ↓
6*	Sod. Mo+Lip.	Bile fistula Rt lobe atrophy Biliary cirrhosis	B-jejunostomy T-tube stent	Jaundice ↓
7*	Ethanol	Rt liver, GB,duodenum necrosis	Cholecystectomy Gastro-jejunostomy	Died
8	Sod.mo+Lip.	Rt liver abscess GB necrosis	Cholecystectomy Rt lobectomy Repair HD	Jaundice ↓
9*	Sod. Mo+Lip	Rt liver necrosis HD stricture Portal hypertension	No	Jaundice ↑ Repeated hematemesis

(Such type of bile duct injury was not included under the category of traumatic biliary injuries in the hospital records)

* Treated by consultation; Sod mo.=sodium morrhuate; Lip.=iodized oil; B=biliary; GB=gallbladder; CBD=common bile duct; HD=hepatic duct; S-R=spleno-renal; PTBD=percutaneous transhepatic biliary drainage

Since interventional therapy was advocated for hepatocellular carcinoma in recent years with encouraging results, the method of percutaneous transarterial embolism (HAE) has also been advocated and used for the treatment of hepatic hemangioma^[13,14]. The embolizing agent used was usually sodium morrhuate which is a strong sclerosing agent commonly employed for injection of varicose vein of the lower extremities. But in hepatic hemangioma, after HAE with sodium morrhuate, the patient usually experienced a chronic course of progressive sclerosis of the intrahepatic and extrahepatic hepatic bile duct, persistent jaundice, progression of hepatic fibrosis and portal hypertension^[15].

A male patient aged 43 years, he was diagnosed having a hemangioma of the right liver after a routine physical examination with ultrasound scanning. He was advised to have a "catheter treatment" (HAE) for the tumor. According to the doctor's advice, he received a HAE treatment with injection of 10mL iodized oil and 4mL sodium morrhuate. He developed severe right upper abdominal pain, nausea and vomiting immediately after the injection. He was then admitted and treated in the hospital for one week, but he had constant upper abdominal discomfort after discharged from the hospital. Two years later, jaundice appeared which had been diagnosed as "viral hepatitis" and treated accordingly for 3 months. Exploratory celiotomy was

followed. A cholecystectomy was performed, exploring the common bile duct, in which a red-colored mucoid plug was found and removed. Three years later, a percutaneous transhepatic drainage of left intrahepatic bile duct was made because of persistent jaundice. A second operation of choledcho-jejunostomy was then performed. Despite of the operations, jaundice still persisted. He was at last admitted to the General Hospital of PLA in 1999, 6 years after interventional therapy for the liver hemangioma. Preoperative evaluation revealed fibrosis and atrophy of the right liver with the hemangioma still in situ, extensive fibrosis and stricture of the right hepatic duct involving the hepatic duct confluence and the left hepatic duct, and, hypertrophy of the left lateral segment of the liver with dilated intrahepatic bile ducts (Figures 1,2). A third operation was then performed. The left lateral intrahepatic bile duct was chosen for biliary-intestinal anastomosis. Because of the sclerotic changes of the hepatic duct confluence, a trans-round ligament approach for left hepatic duct-jejunostomy of Roux-en-Y type with stent was adopted. Jaundice decreased following the last operation. The other cases of HAE biliary injuries showed more or less similar clinical courses (Table 3). The clinical course and type of subsequent surgical treatment depended on the extensiveness of hepatic and biliary damages and the progression of hepatic fibrosis. Portal hypertension secondary to hepatic fibrosis may be developed and complicated with G-I hemorrhage. In all the cases under this category, the caudate lobe of the liver was found to be much enlarged and in a state of functional compensation.

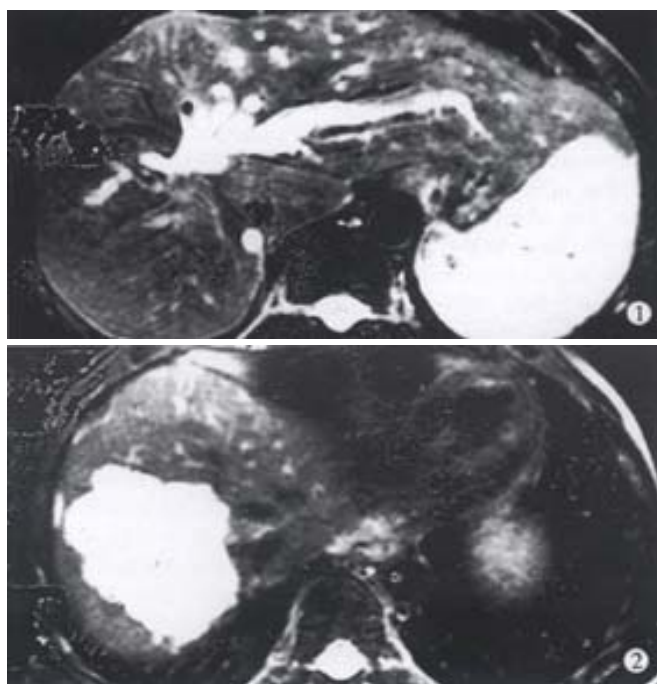


Figure 1 Hepatobiliary damages 6 years after HAE with sod. morrhuate: MRI showed atrophy of right liver, hypertrophy of the left lateral segment and obstruction of hepatic duct at the hila hepatis.

Figure 2 Hemangioma of right liver years after HAE. The same patient. MRI showed hemangioma still in place.

Hepatic trauma and bile duct injury Traumatic injury of the liver may be the cause of bile duct injury. Hepatic resections in daily surgical practice as one of the causes of bile duct injury is of increasing importance due to the rapid development of hepatic surgery in recent 20 years. In Group A series, we met a middle-aged male patient who sustained from severe laceration of the right lobe of the liver in a road accident. Resuscitation including emergency right hepatic lobectomy was undertaken in another hospital. However, injury to the left hepatic duct was inflicted and was recognized at

completion of the operation. Hence, repeated operations to treat the bile duct stricture and its complications were necessary subsequently, such as spleno-renal shunt for the treatment of portal hypertension and G-I bleeding, and attempts to recreate a patent biliary-intestinal passage. But operative attempts failed repeatedly because of marked enlargement of the left hepatic lobe and the extreme right posterior rotating displacement of the hilum which became inaccessible to the operation through the conventional surgical approach. The thirteenth operation was performed for the patient to complete a mucosa-to-mucosa anastomosis between the left hepatic duct and a Roux-en-Y jejunal loop through a low thoraco-abdominal incision. The patient recovered from the operation uneventfully and reported to have a satisfactory outcome. There was a young male patient in Group A. He had a severe crushing injury of the liver in a road accident. An external biliary fistula developed following incision and drainage treatment of a subphrenic abscess in right side after the primary operation, and 200-300ml bile was drained from the wound every day. Reoperation revealed traumatic rupture and occlusion of the right hepatic duct. He was treated, during the operation, using the gallbladder to form a conduit bridging between the right hepatic duct and the common bile duct. The biliary fistula healed after the operation.

Bile duct injury and hepatic resection In the past 10 years, more and more cases of bile duct injury due to elective liver tumor resections were admitted to the General Hospital of PLA for further treatment. In the Group B series, 1 case of bile duct injuries as a result of hepatic resection was recorded from 1989-1997. From 1998-2001, 3 additional cases were admitted to the General Hospital of PLA. According to our knowledge, besides the above mentioned cases, more than 6 cases were actually caused by hepatic tumor excision in our hospital. Five of these 6 cases had injuries to the left hepatic duct during the resection of tumors involving the left medial segment of the liver (Figure 3). The history of a case of left hepatic duct injury as a result of extended right hepatic resection for neurilemmoma and gauze packing to check bleeding was very illustrative to show the complexity of bile duct injury following hepatic surgery.

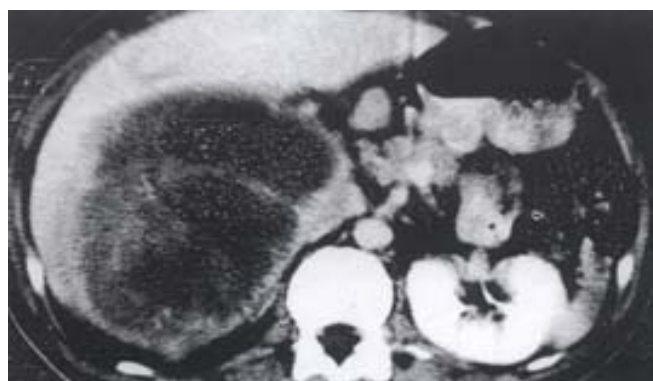


Figure 3 Neurilemmoma of the right liver: Resection of the tumor with right-sided tri-segmentectomy resulted into injury of the left hepatic duct.

A male patient aged 32 years was admitted to the General Hospital of PLA on 4 January, 2000. He had operative bile duct injury during resection of a neurilemmoma on 27 August, 1998. The tumor, weighting 5.0kg, situated in the right liver, was resected with difficulty and complicated with profuse bleeding. The estimated blood loss was about 27 000 mL. Gauze packing was used to stop the hemorrhage from the liver hilum upon completion of the operation. There was clinical jaundice on the second post-operative day. The gauze packing was removed on the 5th postoperative day through the celiotomy wound. On October 21, 1998, PTCD of the left intrahepatic bile duct was performed because of persistent jaundice.

As the indwelling catheter was withdrawn accidentally later on, another PTCD of the left intrahepatic duct was performed on December 23, 1999 when the serum bilirubin level was $543\mu\text{mol/L}$. The catheter was kept on draining of bile in the amount of $500\text{--}700\text{mL}\cdot\text{d}^{-1}$. Retrograde cholangiography showed complete obstruction of the left segmental bile duct (Figure 4). After admission to the General Hospital of PLA, the patient was reexamined and prepared for reoperation. During the operation, there was so dense fibrous adhesions and rich vascular communications in the hilar region that dissection of the extrahepatic bile duct was very difficult. Therefore, the left segmental bile duct was approached along the surface plane of the left external hepatic segment under the guidance of intraoperative ultrasound scanner. The site of the obstructed left intrahepatic duct was found posterior to the left portal vein. The operation was completed with a cholangio-jejunostomy over a U-typed silicone rubber tube. This case illustrated the changing scope of traumatic bile duct strictures at the present that restorative treatment in many cases may be very complicated, and this might be the reason why this patient carried on his PTCD tube for as long as 2 years before referral to our hospital without further surgical intervention. The use of intraoperative BU-scan was important for the success of the operation in this case. Since bile duct injuries inflicted from hepatic surgery may have a very complicated clinical feature, therefore, for one or another reason, such patients may be withheld from appropriate and timely surgical intervention. This was reflected from what happened to a male patient at 40 years of age in Group B. He was diagnosed as having a cavernous hemangioma of quadrate lobe of the liver by ultrasound. The tumor was resected in another hospital. Following the operation, the patient developed obstructive jaundice, biliary peritonitis, and a big "biloma" in the upper abdomen. Re-exploration of the abdomen was carried out, bile-like fluid of about 2500mL was evacuated, however, the extrahepatic bile duct could not be found. The patient suffered from obstructive jaundice and subphrenic abscess without further treatment for 7 months. At last, when the patient was admitted to the General Hospital of PLA, his general condition was very poor and cachectic, the serum bilirubin level was $600\mu\text{mol/L}$. MRI examination showed a large subphrenic collection of fluid and markedly dilated intrahepatic bile ducts (Figure 5). Aspiration of the subphrenic abscesses showed infected bile collection. He was further treated by PTCD of the intrahepatic duct instead of reconstructive operation. In spite of the minimally invasive procedure, the patient developed hepatic coma and recovered only after a period of intensive medical treatment. He was waiting for further surgery when his condition was indicated for the operation. This was a typical case of negligence of medical profession. The difficult situations facing to the surgeon are the lack of knowledge and experience in handling bile duct injury following hepatic operations.



Figure 4 The same case as Fig 3. Retrograde cholangiography of the intraphepatic duct through a PTBD catheter showing obstruction of left intrahepatic ducts and hypertrophy of the left hepatic segment.

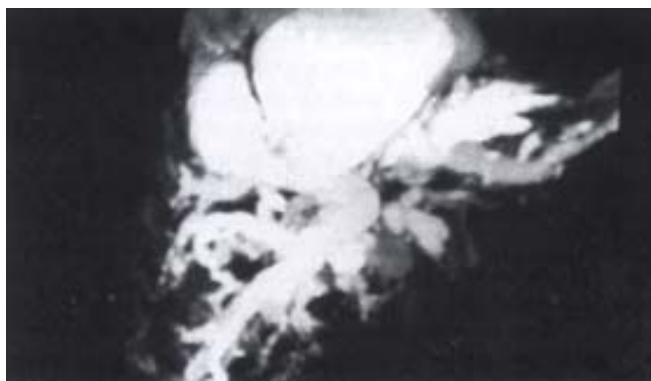


Figure 5 Bile duct injury in resection of quadrate lobe hemangioma: MRCP showing marked dilatation of the intrahepatic duct system with suphrenic collection of fluid. Extrahepatic bile duct not visualized.

DISCUSSION

Safety of cholecystectomy The current cholecystectomy should be a safe and effective operation. For example, in a review reported on the safety of laparoscopic cholecystectomy for cholelithiasis^[16], 4655 consecutive cases of cholecystectomies for gallstones one year before laparoscopic cholecystectomy (LC) was initiated were collected from 34 well equipped hospitals in China. Among these cases, postoperative complications which needed reoperative intervention occurred in 17 cases (0.36%), complications with lasting sequelae in 2 cases (0.05%), and death in 8 cases with a mortality rate of 0.18%. Most of the deaths were related to emergency operation in high risk patients^[16]. More or less similar result was obtained by Roslyn^[7] who revealed 42,474 open cholecystectomies performed in the year 1989 in America with a mortality rate of 0.17%. Injury to the bile duct is still a serious complication during cholecystectomy. Presently, incidence of bile duct injuries in open cholecystectomy has been decreased to a rather low level. Clavien *et al*^[17] reviewed the result of open cholecystectomy in the hospitals in North America and in Europe, injuries to the extrahepatic bile duct was found in 0.2% of the 1, 252 operations. But, bile duct injuries occurred more frequently in laparoscopic cholecystectomy than in conventional open cholecystectomy^[18-21]. The latest data about laparoscopic cholecystectomy collected by Huang *et al* showed that bile duct injuries occurred in 0.30% and biliary complications (including postoperative bile fistula which might be the result of minor bile duct injuries) occurred in 0.60% of the cases in China^[22]. The reported incidence of operative injury of the bile duct may be much lower than actually existed, however. This is true in China and as well as in the other parts of the world. Therefore, the reported incidence of traumatic bile duct injury in laparoscopic cholecystectomy was around 0.15% (9/5680)^[23] from a single hospital to 0.19% in a review series, but the result of about 0.5% in some western countries^[24,25]. A review of recent Chinese medical literature (1995.1-1999.12) on trauma to the extra-hepatic bile duct^[26] revealed that the spectrum of bile duct injuries occurring most frequently was the operations related to cholecystectomy, which accounted for 94% in 2,566 cases (Table 4).

Table 4 Bile duct injury and the type of operations in 2742 cases (Chinese literature review 1995-1999)

Type of operation	No. of cases	%
Cholecystectomy	1 933	70
Laparoscopic cholecystectomy	310	11
Cholecystectomy + choledochostomy	165	6
Gastrectomy	66	2
HAE*	16	0.6
Hepatic resection	10	0.4
Other operations	66	2
Unspecified	176	6

*HAE = Hepatic arterial embolization

There were cases of bile duct injuries from HAE and hepatic resections (0.6% and 0.4% respectively), and bile duct injuries due to laparoscopic cholecystectomy accounting for 11% of the total series. This variations in the disease pattern of benign biliary stricture were in accordance with the current changing practice of hepato-biliary surgery.

Surgical treatment of traumatic biliary stricture Since bile duct injury cannot be eradicated by biliary surgery as human beings are not exempt from errors. Therefore, prevention as well as treatment of bile duct injuries is still most important in biliary surgery [27-29]. In our experience, the long-term good results of reparative operation of traumatic bile duct stricture may be as high as 90% and 95% [9,10]. In average, especially when reconstructive surgery was performed in those hospitals lack of expertise in biliary surgery, the result may be far from satisfactory, the postoperative morbidity rate and reoperation rate was high, and the mortality rate may be as high as 30%. Many of the patients carried on a miserable life (so-called biliary cripple) and eventually died of hepatic failure. Option of methods of surgical treatment for traumatic biliary strictures is varied according to different authors. In our experience, the best result was obtained after bilio-enterostomy of Roux-en-Y type with application of plastic reconstructions of hilar bile duct remnant. Therefore, in the two series of cases in this report, satisfactory result was obtained in more than 90% of the treated cases. In our series, all of the patients were referred from elsewhere in our country, and most of them have had multiple unsuccessful operations and came to our hospital as the last resort. One patient with traumatic bile duct injury had been operated upon as many as 12 times. Secondary surgical repair of biliary stricture is more difficult than the primary reparation because of the much distorted local anatomy and, in many of the cases, the level of bile duct stricture may be extended above the hepatic confluence to involving both hepatic ducts (Bismuth classification type IV), which is the most difficult situation to be treated.

In the treatment of traumatic bile duct stricture, the type of surgery seems to have important influence on the outcome of the disease. We preferred cholangio-jejunostomy of the Roux-en-Y type for reconstruction, especially for those late cases and those high strictures in which one or both hepatic ducts may be involved. Therefore, we used such type of operative repair in 47 of the 61 cases (77%) of Group A. Besides, in 4 cases with a functioning distal common bile duct, we adopted the principle of preservation of the sphincter of Oddi's function by using a pedicled gastric or jejunal patch for the repair. With an interposed jejunal loop with artificial nipple formation, hepatico-duodenostomy was employed in 2 cases. By such methods of management, we obtained good long-term result of 95.6% (including 2 reoperations 2 and 30 years after the first repair respectively). Two patients (4.4%) in Group A died of suppurative cholangitis 4 and 12 years respectively after the repair. Based on our experience in bile duct surgery, we have set up some guidelines for the surgery of biliary stricture which were proved to be important in clinical practice. They are: ① Strategy of traumatic biliary stricture repair: primary repair is critical, but early repair is more frequent, thus being, more important; though reoperations are difficult, they should be performed with confidence; operation should be staged in the presence of marked portal hypertension; operations should be a wait ted till marked biliary cirrhosis with liver dysfunction; ②. Technical essentials in reparative operation: side-to-side bilio-enterostomy is the first choice to minimize late stricture formation; single-layered anastomosis is essential; absorbable or single strand suturing materials should be provided; stent placement of 9 months or 1 year, if possible; good quality stenting tube should be selected to prevent accidental breakage; It should be kept in mind that there were '3 hepatic ducts' at the hilum of liver instead of only 2 as generally believed; ③ Alternatives: T-tube, Y-tube, and U-tube all

have merits for stenting; straight-tube, and shape-memory tube may be used at special occasions; Trans-hepatic tube may also be used for prolonged stenting and instrumentation; Finally, bile duct surgery is more or less alike to cannal engineering.

LC bile duct stricture Treatment of traumatic injury of extrahepatic bile duct due to laparoscopic cholecystectomy is a special problem of current biliary surgery. Though the number of laparoscopic injuries was relatively low in comparison with the open technique, for example, 310 of 2742 cases of bile duct injuries (12%) in a literature survey [26] and 4 of 42 cases (9.5%) of bile duct injuries in the General Hospital of PLA from 1989-1997 [10]. In a review of 182 cases of bile duct injuries from 4 medical centers (1999), 30 cases (17%) were due to LC [30]. Reports of LC bile duct injury have appeared since 1991 when the technique of laparoscopic cholecystectomy was first introduced to China mainland, but the number of patients rapidly increased as time went on. Therefore, LC bile duct injuries were found in 5 of the 19 cases treated in the General Hospital of PLA between the years 1998 and 2000, accounting for 26.3%. With accumulated experience of treatment of LC bile duct injuries, certain characteristic features were apparent. Most of the severe bile duct injuries of LC belonged to the so-called "classical injury" classified by Davidoff [31]. Usually there was loss of a segment of the upper bile duct and involvement of one or both hepatic ducts. Sometimes, one of the injured hepatic ducts in the hepatic hilum may be hidden from the operator's sight (the right posterior duct being the most often and also occasionally the left hepatic duct) (Figures 6,7). Retained foreign materials (usually a broken piece of plastic tube which was used for internal stenting) were found more often. Spontaneous biliary duodenal fistula may be found in cases with no clinical jaundice. On the other hand, in many cases, when secondary repair was undertaken, the degree of intra-abdominal inflammatory changes and extent of adhesions was less than in the operation after conventional open surgery, therefore, a repair operation for the injury or anastomosis with the gut can be considered. These characteristic features of LC bile duct injuries demanded a change of surgical policy in the management of bile duct injuries for a better result [32-34].

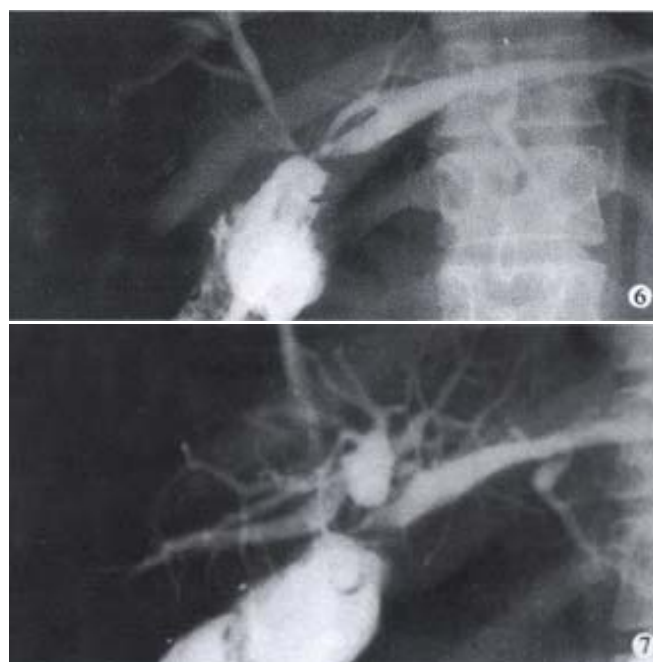


Figure 6 LC bile duct injury: Bile duct repair by hepatico-jejunostomy of Roux-en-Y type. Postoperative retrograde cholangiography only the right anterior segmental duct and the left hepatic duct visualized.

Figure 7 The same case. PTC showing the dilated blind end of the right posterior segmental duct which was "missed" during the operation.

Gastric resection and bile duct injury Gastric resection is the next most common cause of operative bile duct injury. In a review of 2742 cases of bile duct injuries reported in Chinese literature by Huang *et al*^[35], 66 cases occurred during gastric resection operation, accounting for 2.4% of the total. The most severe type of such kind injury was trans-section of the common bile duct together with the hepatic artery and the portal vein. Such type of injury gave a high fatality rate (11/11). Among the patients in series A, two incidences showed a similar clinical manifestations following gastric operation for bleeding chronic penetrating duodenal ulcer. The mechanism of such type of damages may be related to the disruption of blood supply to the duodeno-ampullary region. Disturbance of local blood supply resulted in the coexistence of disruption of the duodenal stump and fibrotic obstruction at the ampulla. Blood supply of the extrahepatic bile duct is segmental. The supra-duodenal portion of the common bile duct received arterial blood supply chiefly from branches sent by the hepatic artery proper, while the lower portion of the common bile duct including the ampullary region received blood supply chiefly from the posterior pancreatico-duodenal artery that was derived from the gastroduodenal artery^[36,37]. Operation of excising the bleeding duodenal ulcer would inevitably result in the disruption of local blood supply and lead to the dishesion of the duodenal stump and fibrotic occlusion change of the ampulla.

Interventional therapy and bile duct injury Since bile duct injuries and its consequences are the ever existing problem of hepato-biliary surgery including interventional therapies of many hepato-biliary affections^[38,39]. A kind of severe extensive damage of the intraand extra-hepatic bile duct as a result of inadvertent use of sclerosing agents in the treatment of liver tumors (most often hemangioma of the liver) was noted^[11,13,14,40]. Six cases were admitted to our hospital on account of complications such as liver necrosis and abscesses, biliary intestinal fistula, extensive hepatic fibrosis complicated with portal hypertension, G-I bleeding, extensive destruction of the intra- and hilar bile duct with obstructive jaundice, etc. The sclerosing agents that most commonly employed were sodium morrhuate and absolute ethanol^[13,14,41]. Furthermore, we have also attended 3 cases through consultation. One case of asymptomatic haemangioma of the right liver was treated in another hospital by injecting 19ml absolute alcohol through the hepatic arterial catheter. The patient suffered from severe abdominal pain soon after the injection and was operated upon because of signs of acute peritonitis on the third day after the procedure. During operation, necrosis of the right liver, the biliary tract and the duodenum was found. The patient developed biliary fistula, and eventually died of multiple organs failure on the 10th day after the therapy. The other 2 patients suffered from repeated G-I bleeding because of portal hypertension due to hepatic fibrosis. Trans-hepatic arterial embolization (HAE) is a kind of interventional therapy which was widely employed as the current non-surgical treatment for advanced hepatocellular carcinoma(HCC)^[42-47]. In general, the embolizing agents consisted of lipoidal oil and small particles of gelform sponge. Particles of 1-2 mm in size would block the small intrahepatic arteriols about 50 μ m in diameter, and caused necrosis of the tumor mass. The gelform sponge particles will be dissolved in a course of about 2 weeks. While, on the other hand, if liquid materials are used as embolizing agent, such as absolute ethanol and sodium morrhuate, the drug may reach the end of the hepatic arterioles, causing damages to the liver parenchyma wherever the drug reached. Therefore, liquid embolizing agents will cause more extensive liver necrosis and damages to the intrahepatic bile duct by way of the peribiliary plexus. The resulting complications will be necrosis of the gallbladder, destruction of the intrahepatic bile duct system, liver abscesses formation, sclerosis of intra- and extra-hepatic duct, necrosis of the gall bladder with biliary duodenal fistula formation, and hepatic fibrosis (Figures 8, 9). If a more caustic agent (such as absolute ethanol) is used, immediate coagulation necrosis of the bile duct and liver parenchyma will occur. If the drug

was used in excessive amount or being injected too rapidly (as often the case when mechanical automatic injector is used), there will be retrograde flow of the drug causing extensive damage of extrahepatic intra-abdominal organs.

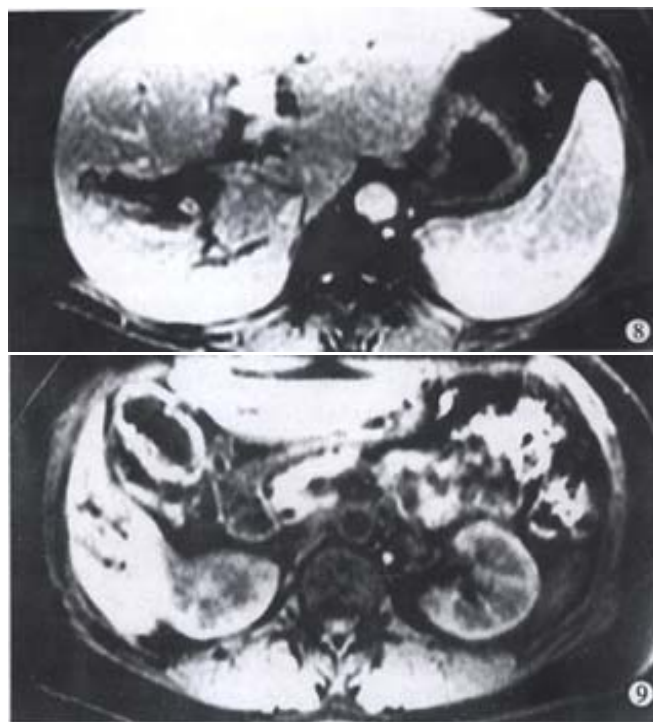


Figure 8 Fibrosis and obstruction of hepatic duct following HAE with injection of sodium morrhuate: 2 years after the procedure.

Figure 9 The same case. Necrosis of the gallbladder and the hepatic duct.

Liver receives double-sourced blood supply, arterial blood composed of 25%-30% of the hepatic blood inflow and supply 50% of the total oxygen expenditure of the liver. The hepatic artery, after entering into the liver parenchyma, sends branches to the hepatic duct, forming a complicated peribiliary plexus which by way of the portal vessels reaches hepatic sinusoids^[48]. The intrahepatic bile duct system, differing from the hepatic cells, received blood supply exclusively from hepatic artery. Blood supply of the common hepatic duct and the right and left hepatic duct is derived directly from the right and left hepatic artery, forming a peribiliary vascular plexus in direct connection with the intrahepatic peribiliary vascular plexus^[49]. Therefore, inadvertent intra-arterial injection of sclerosing agents into the hepatic artery will result in destruction of the intrahepatic bile duct, as well as sclerosis and obstruction of the right and left hepatic duct at the hilum hepatis. However, the common bile duct under such conditions was often found to be exempt except when retrograde flow of a large amount of the drug occurred. This is explained on the ground of vascular pattern of the common bile duct that the vascular plexus of the common bile duct is derived chiefly from the branches of gastroduodenal artery that connect with the vascular plexus of the intrahepatic bile duct indirectly. Furthermore, as we found in the reported cases of intrahepatic bile duct damage resulting from HAE that in spite of atrophy of the right and left hepatic lobes, the caudate lobe was usually markedly hypertrophied so as to take over the functional role of the liver. This phenomenon is also explained on the basis of blood supply of the caudate lobe. The caudate lobe of liver received bilateral hepatic arterial and portal venous blood supply, therefore, may be exempt from the injurious effect of HAE.

In recent years, HAE has been widely used as a therapeutic modality in the treatment of advanced HCC and was claimed to be safe and effective. However, serious biliary damage was found when

HAE was applied to treat cases of hepatic haemangiomas with sclerosing agents as shown in this report. There may be fundamentally different hemodynamic patterns between malignant and benign lesions of the liver. It was well known that arterial blood supply to HCC is much increased with dilatation and increased number of arterial branches to the tumor. Under such conditions, intra-arterial injection of sclerosing agents may be diverted from the accompanying intrahepatic bile ducts. While, in case of liver hemangioma, configuration of vascularity of the liver remained almost the same as found in the normal liver, therefore, more injected toxic agents will be directed to the intrahepatic biliary plexus and caused damages. A large volume of injected material (such as absolute ethanol) by high speed under pressure injection, and displacement of the intra-arterial catheter may render the situation worst as wide spread retrograde flow may occur as result of arterial spasm. Many cases of bile duct damage resulting from HAE employing sclerosing agents (generally not categorized under traumatic bile duct injury) may not be amendable to surgical treatment because of the extensiveness of the lesion. The authors have treated 11 such cases during the last 10 years (including 3 cases by consultation). Among these cases, 2 were not treated surgically because of extensive sclerotic cholangitis of the intrahepatic bile duct. One case of intrahepatic sclerosing cholangitis resulting from injection of absolute ethanol into a hydatid cyst of the right liver which happened to have a fistula communicating with the hepatic duct. One case of hemangioma of the liver died of multiple organs failure after the injection of absolute ethanol. The other 6 patients were treated by drainage of liver abscess, resection of damaged liver lobe, reconstruction of cholangio-enterostomy with an indwelling U-tube for stenting, and, in one case, a preliminary spleno-renal shunt was required before definite bile duct operation was attempted because of portal hypertension and G-I bleeding. One patient died of liver carcinoma 5 years after surgery. Because of the serious complications in HAE for benign hepatic lesions, re-evaluation of the rationale of such kind of treatment should be undertaken.

Hepatic resection and bile duct injury Injury to the extrahepatic bile duct during hepatic surgery occurred most frequently in operations for those lesions located in the perihilar region. Operations involving resection of tumors of quadrate lobe of the liver are most vulnerable because of the close proximity of these structures. Bile duct injury and stricture formation following hepatic resection should deserve more scrutiny because of its detrimental effect on the outcome of the surgery and the difficulty of repairing operation under such situation^[50-52]. In our experience, bile duct stricture resulting from hepatic surgery has become more common over the past 10 years, the increase of number of patients kept pace with the development and propagation of hepatic surgery in our country. In this report, bile duct injury in hepatic surgery accounted for 0.82%-15.7% of the total bile duct strictures. Furthermore, bile duct injuries occurred only in cases of hepatic trauma in Group A. In Group B, the incidence of bile duct injuries rose to 15.7 % as a result of resection of hepatic tumors. In fact, to our knowledge, numbers of bile duct injury in hepatic surgery were much larger than what was reported. The apparent reason is that many cases were recorded and filed as 'operative complications' or 'bile fistulae' instead of the diagnosis of traumatic bile duct injuries^[53-55]. Injury to the hilar bile duct is most vulnerable during resection of tumors, either benign or malignant, of the quadrate lobe of the liver. The transverse portion of the left hepatic duct courses along the underneath border of the quadrate lobe and with its peribiliary connective tissue fibers interwoven with that from the hilar plate. Identification and isolation of the left hepatic duct may be difficult especially when the normal anatomical relationship was distorted by local tumor growth. Furthermore, branches of bile duct to the left middle segment of the liver were difficult to be identified and individually divided, laceration injury of the left hepatic duct may occur when the hepatic tumor mass was mobilized. Therefore, we emphasized that technique of mobilizing the left hepatic duct with the hilar

plate for the prevention of bile duct injury should be a safeguard measure in liver resection and should be followed in case of perihilar tumor resection.

In recent years, a kind of small incision (3cm-5cm) cholecystectomy (minilaparotomy) has been introduced^[56-58]. The result of such type of operation is not different from that of conventional surgery so far as the probability of bile duct injury is concerned.

REFERENCES

- 1 Braasch JW. Historical perspectives of biliary tract injuries. *Surg Clin North Am* 1994; 74:731-740
- 2 Chapman WC, Halevy A, Blumgart LH, Benjamin IS. Postcholecystectomy bile duct strictures: Management and outcome in 130 patients. *Arch Surg* 1995; 130:597-604
- 3 Guo ZY, Huang ZQ. Characteristics of gallstones in China. *Zhonghua Waike Zazhi* 1987;25:321-329
- 4 Huang ZQ. Development of Hepatobiliary and pancreatic surgery in the last fifty years in China. *Zhonghua Waike Zazhi* 2001; 39:9-16
- 5 Huang ZQ. New development of biliary surgery in China. *World J Gastroenterol* 2000; 6:187-192
- 6 Huang ZQ. Laparoscopic surgery and the evolution of surgical treatment of cholelithiasis. *Zhonghua Waike Zazhi* 1993; 31:387-389
- 7 Roslyn JJ, Binns GS, Hughes EFX, Saunders-Kirkwood K, Zinner MJ, Cates JA. Open cholecystectomy. A contemporary analysis of 42 474 patients. *Ann Surg* 1993;218:129-137
- 8 Huang ZQ. The safety of laparoscopic cholecystectomy should be guarded. *Zhonghua Waike Zazhi* 1995; 33:645-646
- 9 Liu YX, Huang ZQ, Zhou YB, Cai ZJ, Qian GX, Chi YB, Han BL, He ZP, Zhang CZ, Tao JM. Surgical treatment of traumatic bile duct stricture. *Puwai Linchuang* 1986; 1:234-245
- 10 Wang J, Liu YX, Feng YQ, Zhou NX, Gu WQ, Huang XQ, Zhang WZ, Huang ZQ. Surgical treatment of traumatic stricture of bile duct. *Zhonghua Gandan Waike Zazhi* 1998; 4: 73-75
- 11 Huang XQ, Huang ZQ, Duan WD, Zhou NX, Feng YQ. Damage to intra- and extrahepatic bile duct after hepatic artery embolization. *Zhonghua Waike Zazhi* 2000;38:169-172
- 12 Huang XQ, Huang ZQ, Duan WD, Zhou NX, Feng YQ. Hepato-biliary complications following hepatic artery embolism for hepatic hemangioma (Report of 9 cases). *Zhongguo Shiyong Waike Zazhi* 2001;21:319-320
- 13 Li YH, Li SX. An experimental study of sod morrhuate as an agent for arterial embolization. *Zhonghua Fangshexue Zazhi* 1987;21:357-359
- 14 Yan XF, He JG, Song HZ, Zhao CZ. Interventional therapy of hepatic cavernous hemangioma. *Zhonghua Waike Zazhi* 1994; 32:563-565
- 15 Huang XQ, Huang ZQ, Duan WD, Zhou NX, Feng YQ. Destructive damage of bile duct of hepatic artery embolization in treatment of hepatic cavernous haemangioma. *Acad J PLA Postgrad Med Sch* 2000; 21:88-91
- 16 Huang ZQ, Wang YS, Jia SY. On safety of laparoscopic cholecystectomy (Analysis of 4655 cases from 34 hospitals). *Gandan Yipi Zazhi* 1995; 1:73-76
- 17 Clavien PA, Sanabria JR, Mentha G, Borst F, Buhler L, Roche B, Cywes R, Tibshirani R, Rohner A, Strasberg SM. Recent results of elective open cholecystectomy in a North American and a European Center. *Ann Surg* 1992; 216:613-626
- 18 Dunn D, Fowler S, Nair R, McCloy R. Laparoscopic cholecystectomy in England and Wales: results of an audit by The Royal College of Surgeons of England. *Ann R Coll Surg Engl* 1994; 76:269-275
- 19 Kerin MJ, Gorey TF. Biliary injuries in the laparoscopic era. Clinical review. *Eur J Surg* 1994;160:195-201
- 20 Wherry DC, Marohn MR, Malanoski MP, Hetz SP, Rich NM. An external audit of laparoscopic cholecystectomy in the steady state performed in medical treatment facilities of the department of defense. *Ann Surg* 1996; 224:145-154
- 21 Gouma DJ, Go MNYH. Bile duct injury during laparoscopic and conventional cholecystectomy. *J Am Coll Surg* 1994;178:229-233
- 22 Huang XQ, Feng XQ, Huang ZQ. Complications of laparoscopic cholecystectomy in China.:An analysis of 39 238 cases. *Chin Med J* 1997; 110: 704-706
- 23 Zhou ZD, Chen XR, Mao JS, Yu SM. Prevention and treatment of extrahepatic bile duct injuries in laparoscopic cholecystectomy. *Gandan Waike Zazhi* 1999; 7:261-262
- 24 Huang ZQ. Iatrogenic bile duct injuries: Old problem with new meaning. *Zhongguo Shiyong Waile Zazhi* 1999;19: 451-452
- 25 Martin RF, Rossi RL. Bile duct injuries: Spectrum, mechanism of injury, and their prevention. *Surg Clin North Am* 1994; 74:781-803
- 26 Huang XQ, Huang ZQ. Treatment of iatrogenic bile duct injury. *Zhongguo Shiyong Waike Zazhi* 2001; 21:413-414
- 27 Huang ZQ. Bile duct injury in the era of laparoscopic surgery. *Gandan Waike*

- Zazhi 1998; 6:65-66
- 28 Rutledge R, Fakhry SM, Baker CC, Meyer AA. The impact of laparoscopic cholecystectomy on the management and outcome of biliary tract disease in North Carolina: A statewide, population-based, time-series analysis. *J Am Coll Surg* 1996; 183:31-45
 - 29 Strasberg SM, Hertl M, Soper NJ. An analysis of the problem of biliary injury during laparoscopic cholecystectomy. *J Am Coll Surg* 1995; 180:101-124
 - 30 Dai XW, Chen YJ, Gao ZQ, Shi JS, Yang FQ, Ma K, et al. Iatrogenic extrahepatic bile duct injury and treatment (a report of 182 cases). *Zhongguo Shiyong Waike Zazhi* 1999; 19:485-487
 - 31 Davidoff AM, Pappas TN, Murray EA, Hilleren DJ, Johson RD, Baker ME, Newman GE, Cotton PB, Meyers WC. Mechanism of major biliary injury during laparoscopic cholecystectomy. *Ann Surg* 1992; 215:196-199
 - 32 Madariaga JR, Dodson SF, Selby R, Todo S, Iwatsuki S. Corrective treatment and anatomic considerations for laparoscopic cholecystectomy injuries. *J Am Coll Surg* 1994; 179:321-325
 - 33 Woods MS, Traverso LW, Kozarek RA, Tsao J, Rossi RL, Gough D, Donohue JH. Characteristics of biliary tract complications during laparoscopic cholecystectomy: A multi-institutional study. *Am J Surg* 1994; 167:27-34
 - 34 Kwon AH, Inui H, Kamiyama Y. Laparoscopic management of bile duct and bowel injury laparoscopic cholecystectomy. *World J Surg* 2001; 25:856-861
 - 35 Huang XQ, Huang ZQ. Present status of bile duct injuries in China. Proceedings of The 9th National Conference on Biliary and The 2nd Chinese General Surgeon Association, 2000, Nov. Wuhan 49-52
 - 36 Xu ND. Anatomy and anatomical variations of extrahepatic biliary passage. In Huang ZQ: Modern Biliary Surgery (Dangdai Dandao Waikexue), Shanghai: Archives of Science and Technology Publisher 1998:26-27
 - 37 Chen WJ, Ying DJ, Liu ZJ, He ZP. Analysis of the arterial supply of the extrahepatic bile ducts and its clinical significance. *Clinical Anatomy* 1999; 12: 245-249
 - 38 Huang ZQ. Bile duct injury-The ever-lasting theme in hepato-biliary surgery. *Zhonghua Putongwaik Zazhi* 2001; 16:371-373
 - 39 Huang FG, Li Y, Xie XD. Side effects and complications of hepatic arterial infusion and embolization of liver carcinoma in aged patients and its management. *World J Gastroenterol* 1998; 4:67-68
 - 40 Huang XQ, Yang KZ, Huang ZQ, Yi GQ, Wang BZ. Changes of hepatic micro-circulation after obstruction of bile duct: An experimental study. *Zhonghua Shiyong Waik Zazhi* 1987; 4:151-154
 - 41 Cao XC, He NS, Sun JZ, Wang S, Ji XM, Wang JS, Zhang CL, Yang JG, Lu TW, Li JH, Zhang GH. Interventional treatment of huge hepatic cavernous hemangioma. *Chin Med J* 2000; 113:927-929
 - 42 Wang JH, Lin G, Yan ZP, Wang XL, Cheng JM, Li MQ. Stage II surgical resection of hepatocellular carcinoma after TAE of 38 cases. *World J Gastroenterol* 1998; 4:133-136
 - 43 Li L, Wu PH, Li JQ, Zhang WZ, Lin HG, Zhang YQ. Segmental transcatheter arterial embolization for primary hepatocellular carcinoma. *World J Gastroenterol* 1998; 4:511-512
 - 44 Huang FG, Yuan J, Xie XD. Long-term follow-up of patients with carcinoma after hepatic arterial infusion and embolization. *World J Gastroenterol* 1998; 4:66
 - 45 Lu MD, Chen JW, Xie XY, Liang LJ, Huang JF. Portal vein embolization by fine needle ethanol injection: experimental and clinical studies. *World J Gastroenterol* 1999; 5:506-510
 - 46 Tang ZY. Hepatocellular carcinoma-cause, treatment and metastasis. *World J Gastroenterol* 2001; 7:445-454
 - 47 Fan J, Ten GJ, He SC, Guo JH, Yang DP, Weng GY. Arterial chemembolization for hepatocellular carcinoma. *World J Gastroenterol* 1998; 4:33-37
 - 48 Stapleton GN, Hickman R, Terblanche J. Blood supply of the right and left hepatic ducts. *Brit J Surg* 1998; 85:202-207
 - 49 Lillemoe KD, Melton GB, Cameron JL, Pitt HA, Campbell KA, Talamini MA, Sauter PA, Coleman J, Yeo CJ. Postoperative bile duct strictures: management and outcome in the 1990s. *Ann Surg* 2000; 232:430-441
 - 50 Matthews JB, Gertsch P, Baer HU, Schweizer WP, Blumgart LH. Biliary stricture following hepatic resection. *HPB Surgery* 1991; 3:181-189
 - 51 Yamashita YI, Hamatsu T, Rikimaru T, Tanaka S, Shirabe K, Shimada M, Sugimachi K. Bile leakage after hepatic resection. *Ann Surg* 2001; 233:45-50
 - 52 Torzilli G, Makuuchi M, Midorikawa Y, Sano K, Inoue K, Takayama T, Kubota K. Liver resection without total vascular exclusion: hazardous or beneficial. *Ann Surg* 2001; 233:167-175
 - 53 Schweizer WP, Matthews JB, Baer HU, Nudelman LI, Triller J, Halter F, Gertsch P, Blumgart LH. Combined surgical and interventional radiological approach for complex benign biliary tract obstruction. *Br J Surg* 1991; 78:559-563
 - 54 Tocchi A, Costa G, Lepre L, Liotta G, Mazzoni G, Sita A. The long-term outcome of hepaticojunostomy in the treatment of benign bile duct stricture. *Ann Surg* 1996; 224:162-167
 - 55 Keulemans YC, Bergman JJ, de Wit LT, Rauws EA, Huibregtse K, Tytgat GN, Gouma DJ. Improvement in the management of bile duct injuries. *J Am Coll Surg* 1998; 187:246-254
 - 56 Luo KY, Lin SJ, Yang Y, Wang MZ, Liu WZ, Wo HZ, Chen QS. The comparison of conventional open cholecystectomy, laparoscopic cholecystectomy and minor incision cholecystectomy. *Zhonghua Waik Zazhi* 1997; 35:660-662
 - 57 O'Dwyer PJ, Murphy JJ, O'Higgins NJ. Cholecystectomy through a 5 cm sub-costal incision. *Br J Surg* 1990; 77:1189-1190
 - 58 Nagakawa T. Biliary surgery via minilaparotomy-A limited procedure for biliary lithiasis. *HPB Surgery* 1993; 6:245-254

Edited by Zhu LH

• GASTRIC CANCER •

Differential display of vincristine-resistance-related genes in gastric cancer? SGC7901 cell

Xin Wang, Mei Lan, Yong-Quan Shi, Ju Lu, Yue -Xia Zhong, Han-Ping Wu, Hui-Hong Zai, Jie Ding, Kai-Cun Wu, Bo-Rong Pan, Jian-Ping Jin, Dai-Ming Fan

Dai-Ming Fan-Xin Wang, Mei Lan, Yong-Quan Shi, Han-Ping Wu, Hui-Hong Zai, Jie Ding, Kai-Cun Wu, Dai-Ming Fan, Institute of Digestive disease, Xijing Hospital, Fourth Military Medical University, Xi'an 710032, Shaanxi Province, China

Ju Lu, Department of Electronic Engineering, Tsinghua University, Beijing 100084, China

Yue-Xia Zhong, Emergency Department, Tangdu Hospital, Fourth Military Medical University, Xi'an 710038, Shaanxi Province, China

Bo-Rong Pan, Oncology Center of Xijing Hospital, Fourth Military Medical University, Xi'an 710032, Shaanxi Province, China

Jian-Ping Jin, Department of Physiology and Biophysics, Case Western Reserve University School of Medicine, Cleveland, 44106-4970, Ohio, USA

Supported by the National Natural Science Foundation of China, No. 30030140, 39970901

Correspondence to: Prof. Dai-Ming Fan, Institute of Digestive disease, Xijing Hospital, Fourth Military Medical University, Xi'an 710033, Shaanxi Province, China. Daimfan@pub.xao

Telephone: +86-29-3375221 Fax: +86-29-2539041

Received 2001-04-21 Accepted 2001-08-15

Abstract

AIM: To isolate and clone the vincristine-resistance-related genes in gastric cancer SGC7901 cell line and to clarify the multidrug-resistant molecular mechanism of gastric cancer cells.

METHODS: The modified differential-display polymerase chain reaction (DD-PCR) was used to examine the differences in the mRNA composition of Vincristine-resistant gastric cancer SGC 7901 cells (SGC7901/VCR), induced by vincristine sulfate versus SGC7901 cells. The differentially expressed cDNA fragments were confirmed by reverse Northern analysis, sequencing, BLAST analysis and Northern blot analysis.

RESULTS: DD-PCR identified that 54 cDNA fragments were preferentially expressed in SGC 7901/VCR cells. When these cDNA fragments were analyzed by reverse Northern blot, 20 were reproducibly expressed at a high level in SGC7901/VCR. Sequencing and BLAST analysis revealed that seven of the genes were known genes: ADP-ribosylation factor 4, Cytochrome oxidase subunit II, Ss-A/Ro ribonucleoprotein autoantigen 60kd subunit, ribosomal protein S13, galectin-8 gene, oligophrenin 1 mRNA, ribosomal protein L23 mRNA; thirteen of the genes were unknown genes. The length and abundance of the four unknown genes mRNA were further confirmed by Northern blot analysis.

CONCLUSION: The twenty differential known and unknown genes may be related to the vincristine-resistant mechanism in human gastric cancer SGC7901 cell line.

Wang X, Lan M, Shi YQ, Lu J, Zhong YX, Wu HP, Zai HH, Ding J, Wu KC, Pan BR, Jin JP, Fan DM. Differential display of vincristine-resistance-related genes in gastric cancer SGC7901 cell. *World J Gastroenterol* 2002;8(1):54-59

INTRODUCTION

The primary factor affecting the chemotherapy for gastric cancer is the resistance of cancer cells to anti-tumor drugs. This phenomenon is called multidrug-resistance (MDR). Previous studies have shown that the mechanisms of MDR involved P-glycoprotein (P-gp), multidrug-resistance related protein (MRP 1-5), lung drug-resistance related protein (LRP), and recently discovered breast cancer drug-resistance related protein (BCRP), GSH/GST, PKC, Topo DNA plerosis^[1-3], genes related to apoptosis and changes of cellular environment (such as pH, hypoxia and temperature). However, over-expression of the genes encoding these proteins cannot completely account for MDR, nor can the treatment aiming at these mechanisms significantly revert MDR. Thus, it is most likely that MDR involves multi-genes. Little has been known about MDR of gastric carcinoma cells. Preliminary studies have shown specific features in MDR of gastric carcinoma cells^[4-19], which cannot be completely explained by any known mechanisms of gastric carcinoma MDR^[20-32]. We therefore used mRNA differential display to investigate the differential expression of the genes in MDR gastric cells in order to elucidate the molecular mechanism of gastric cancer MDR and to discover the related genes so as to lay the foundation for the eventual solution of the problem.

MATERIALS AND METHODS

Induction of vincristine-resistant gastric cancer SGC 7901 cells

Gastric cancer SGC7901 cell (preserved by the Institute), grown in RPMI1640 medium containing 100g·L⁻¹ fetal bovine serum and cultured in incubator filled with 950mL·L⁻¹ O₂, 50 mL·L⁻¹ CO₂ at 37°C. The procedure of SGC7901/VCR cell induction was as follows^[33]: SGC7901 cells were harvested at the mid log-growth phase, and then cultured in the medium containing 0.2 mg·L⁻¹ vincristine; the medium exchanged every two or three days, and then the vincristine concentration was increased by 0.1 mg·L⁻¹ every other week, until it reached 0.8-1.0mg·L⁻¹. SGC7901/VCR cells with stable phenotype were obtained after three months of continuous culture.

DD-PCR^[34-38]

Total RNA of gastric cancer SGC7901 and SGC7901/VCR cells was extracted and underwent RNA formaldehyde denatured agarose gel electrophoresis. The purity and RNA content of the samples were measured by OD260/280. Five µg of total RNA were taken from SGC7901 and SGC7901/VCR respectively, and combined with anchoring primers 5'-AAGCTTTTTTTTTTTTA-3', 5'-AAGCTTTTTTTTTTTTG-3', and 5'-AAGCTTTTTTTTTTTC to undergo RT-PCR. The procedure is as follows: to each 20µL reaction system, 5µg total RNA and 1.6µL anchoring primer were added, and the system was put at 70°C for 5 min and then into ice bathing. Buffer of 5×RT 4µL, 10mmol·L⁻¹ dNTP (each)2µL, RNase inhibitor 20U, M-MuLV retrotranscriptase (MBI) 2µL (40U) were added into the reaction system sequentially, and put in H₂O to get a total volume of 20µL. The reaction went at 37°C for 1h, and for

10min at 70°C to terminate.

Eight random primers AP1-8 were employed in PCR. Three kinds of cDNA products of retrotranscription were each combined with the eight random primers to form 24 PCR reaction systems. There were 48 PCR reactions for two kinds of cells. In each 20μL PCR reaction system, there were 2μL RT product cDNA, 1μL anchoring primer (4μmol·L⁻¹), 1μL random primer (4μL), 10×PCR buffer 2μL, MgCl₂ (25μmol·L⁻¹) 1.6μL, dNTP (5μmol·L⁻¹) 1.6μL, Taq plus I DNA polymerase (MBI) 0.15μL (0.4U), α-³²P-dNTP 0.5μL (185kBq), and ion-free water. The conditions of PCR: 95°C 3min; 94°C 30s→40°C 2min→72°C 40s for 40 cycles; and then 70°C 10min for termination. PCR product was 95°C heat denatured for 3min, and underwent ice-bathing, and 60 g·L⁻¹ urea denatured polyacrylamide gel (sequencing gel) electrophoresis. The gel was preserved with membrane after electrophoresis and underwent X-ray film autoradiography at -70°C in black box for 48h.

Cloning and restriction enzymatic cleavage identification of differential DNA bands

Differential bands were cut from the gel and the DNA was recovered and amplified with secondary PCR. The primers and conditions were identical to that of DD-PCR. The amplified product was separated with agarose gel electrophoresis, purified and retrieved, cloned into PUCm-T vector (Shanghai Shenggong Co.), and underwent restriction enzymatic cleavage identification.

Reverse Northern analysis

The plasmids were extracted from the bacteria with positive clones of the 46 differential DNA bands; the quantities were determined through 10 g·L⁻¹ agarose gel electrophoresis. One μg plasmid was used to solve in 6(SSC buffer, boiled at 100°C for 10min to denature, put into ice-water, and pointed onto two NC membranes, each NC membrane having 46 points, and 1μg plasmid. The location of the points on the two membranes were identical. The NC membranes were dried at room temperature. The samples were alkaline-denatured on the membranes; and the membranes were heated at 80°C for 2h to fix the plasmid DNA and preserved at room temperature.

Preparation of radioactive cDNA probe: Total RNA was extracted from SGC7901 and SGC7901/VCR cells by the same method as in DD-PCR. Ten μg total RNA was taken; 2μL Olig dT₁₈ (0.5mg·L⁻¹) were added, and put at 70°C for 5min, and ice-water bathed for 5min. Buffer of 5×RT 10μL, dNTP (10mmol·L⁻¹/each) 2.5μL, RNase inhibitor 2.5μL (50U), α-³²P-dATP 5μL (1850kBq), α-³²P-dCTP 5μL (1850kBq), M-MuLV 4μL (80U), and water 50μL were added. The reaction was processed at 37°C for 1h, and 70°C for 5min to terminate. EDTA of 0.5 mol·L⁻¹ (pH 8.0) 2μL, 100 g·L⁻¹ SDS 2μL and 10 mol·L⁻¹ NaOH 1.8μL were put into the retrotranscription product, and incubated at 68°C for 30min. Ten μL 1mol·L⁻¹ Tris.Cl (pH 7.4) and 3μL 2 mol·L⁻¹ HCl were added to neutralize at room temperature. Pre-hybridization was made at 42°C for 6h, and different cDNA probes were added onto the two membranes to hybridize at 42°C for 20h. The membranes were washed, dried and underwent X-ray film autoradiography at -70°C for 72h.

Sequencing and homologous analysis of cDNA clones

The cDNA fragments were sequenced and confirmed through reverse Northern blot to be highly expressed in SGC7901/VCR. BLAST program was used for homologous comparison in genetic library and FASTA was used to analyze the results.

Northern Blot analysis

The total RNA of the two kinds of cells was extracted by the method

identical to that mentioned above. Sixteen μg total RNA of each sample was denatured; 10 g·L⁻¹ formaldehyde denature agarose gel electrophoresis (16μg RNA/lane) was performed; the mRNA was transferred onto the NC membranes by capillary blot, and heated at 80°C for 2h to fix the mRNA. Plasmids were extracted from positive clone bacteria; restriction endonuclease cleavage and electrophoresis were performed; the target cDNA fragments were recovered and purified; the cDNA probes were labeled by random primer method, and pre-hybridized on the NC membrane for 3h at 42°C. The probes were added and hybridized at 42°C for 20h. The membranes were washed, dried and undergone for X-ray film autoradiography at -70°C in black box for 48h.

RESULTS

DD-PCR separation of differential cDNA of SGC7901/VCR cell

The mRNA of SGC7901 and SGC7901/VCR cells was amplified by RT-PCR, each was divided into 24 groups, and each group was further separated into 150-200 cDNA fragments of diverted length (100-1500bp) after 60 g·L⁻¹ polyacrylamide gel electrophoresis. The comparison showed that the abundance of certain DNA bands in SGC7901/VCR cells was up-regulated, down-regulated, newly generated or lost. A total of 196 differential cDNA fragments were obtained (Figure 1).

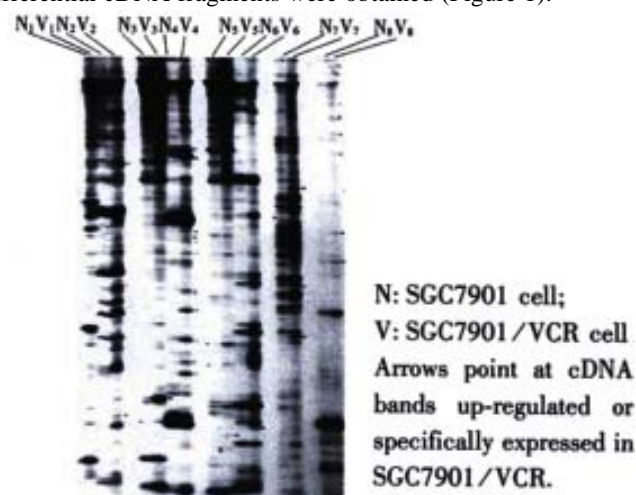


Figure 1 Differential display of mRNA of SGC7901/VCR.

Cloning and restriction enzymatic cleavage identification of differential cDNA fragments in SGC7901/VCR

Fifty-four of the 196 differential cDNA fragments were specifically or significantly highly expressed in SGC7901/VCR cells. Restriction enzymatic cleavage identification showed that 46 cDNA fragments were successfully cloned (Figure 2).



Figure 2 Restriction endonuclease cleavage identification of differential cDNA clones in SGC7901/VCR.

Reverse northern analysis of differential cDNA fragments

In order to confirm the abundance changes of the differential genes and exclude false positive, reverse Northern blot was performed and the high expression of the 20 cDNA fragments in SGC7901/VCR was further validated (Figure 3).

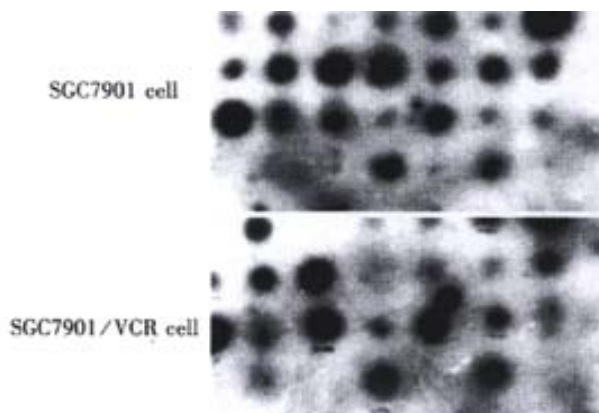


Figure 3 Reverse Northern analysis of genes significantly highly expressed in SGC7901/VCR.

cDNA sequencing and homologous analysis

Sequencing and homologous analysis of the 20 highly expressed genes in SGC7901/VCR cells, confirmed by reverse Northern blot, showed that 7 of the 20 positive clones were highly homologous with known gene sequences (Table 1), and 13 were unknown sequences: GRP-2, GRP-8, GRP-12, GRP-15, GRP-18, GRP-19, GRP-24, GRP-28, GRP-31, GRP-36, GRP-37, GRP-38, GRP-41.

Table 1 Up-regulated cDNA sequence in SGC7901/VCR homologous with known genes

Serial number	Homologous genes
GRP-44(168bp)	ADP-ribosylation factor4 (ARF4) mRNA (1610bp)
GRP-39(181bp)	Cytochrome oxidase subunit II mRNA
GRP-33(199bp)	Ss-A/Ro ribonucleoprotein autoantigen 60kd subunit mRNA
GRP-42(498bp)	Ribosomal protein S13 (RPS13) mRNA (530bp)
GRP-6 (390bp)	Galaectin-8 (LGALS 8) gene, exons4, mRNA
GRP-16(197bp)	Oligophrenin 1 (OPHN1) mRNA (7350bp)
GRP-1 (442bp)	Ribosomal protein L23 (RPL23) mRNA (490bp)

GRP:Gastric cancer drug-resistance related protein; serial numbers are numbering of positive cDNA clones.

GRP-2

CAGTGACTTTATTTAATGGGTTTTTCAGACATACAGAAAGGGATTCTTTAGATGGGGCTGTGTCAGTCACTAGTCAACCATCTTCACTGTGGAGTCTAGTCACTAT
GATTTTGTGTTTGTAGATCATGAGGATTCATTCAAATGTCTCCTCTTCCACTCCTTCGTAATAGGTTACATGATCTGAAAGTACATCCCTCTTATGACATTG
TATTCAAACAGGTTGCTGCTACTTCTCTACTGTCATTAATCTTTTCATCATCTTCTTATTCCTCTTAGC—

GRP-8

GTTTGAGAGGATACTCATCTTTTGAATCCTGACCTTAGGTTCCGGCATGTAGACCAAGTGATGAGAAGTGAATACATGGAAGAGTTTTTAAGTGTGACTTGA
AAAATATGC—

GRP-12

GGAACCTGGATTCTTTAATAGTTGTTGAAGCCTCCAGGGGGCCAGGCGGATCACTTGAGGCCAGCCTGGCCAACATAGCGAAACCCTGCCTCTACTAAAA
CCACAAAAATCAGCCGGGATGTTGGCACACGCTTATAATCCAGCTACTTGGGACGCTGAGGTGGGATATAGCTTGAACCCGGGAAGGAGACTGCAGTCAG
GGAAGCTAGGGAAGCCTCAGACCAAGGATGATTGAATAACAAAGAAAAGGTGTAAGTAAAGATCTCCAACCTCTAGGGAGTACTAATTAGGAAAGTTAAGG
GTAGAAAAAGATAAATTAAGGAAAATAC—

GRP-15

GAAAGACAGAAAACAAGGGCAAAACAGGAGATGAGGAAATGTTAAAGGATAAAGGAAAGCCAGAGAGTGAGGGAGAGGCAAAAGAAGGAAAGTCAGAGA
GGGAGGGAGAGTCAGAGATGGAGGGAGGATCAGAGAGAGAGGAAAACCAGAGATAGAGGGAAGCCAGAGAGTGAAGGAGAGCCAGGGAGTGAACAA
GGGCTGCAGGAAAGCGCCAGCTGAGGATGATGTACCCAGGAAAGC—

GRP-18

GGAACCTGGATTCTTTAATAGTTGTTGAAGCCTCCAGGGGGCCAGGCGGATCACTTGAGGCCAGCCTGGCCAACATAGCGAAACCCTGCCTCTACTAAAA
CCACAAAAATCAGCCGGGATGTTGGCACACGCTTATAATCCAGCTACTTGGGACGCTGAGGTGGGATATAGCTTGAACCCGGGAAGGAGACTGCAGTCA
GGGAAGCCTAGGGAAGCCTCAGACCAAGGATGATTGAATAACAAAGAAAAGGTGTAAGTAAAGATCTCCAACCTCTAGGGAGTACTAATTAGGAAAGTTAA
GGGTAGAAAAAGATAAATTAAGGAAAATACCGTTGAGAAGCTTAAGACTGGAGATCTGGATCCCTCGAGTCTAGAGTCGACCTGCA—

GRP-19

AAAAGAAGAAAATAAACACCAAAAAACAAGGAGAATAAATGGCAGCAGACTTGATGCAAAAAATTAATAAATTAAGAGAAATTACAGATGCACCTTTTATT
GATTGCAAAAAAGCTTTAGAGCAACAGGTGCTGATTAGATAAAGCAGTTGCTTGATTACAAGAAAACGGAAAACTAAAGCACTTAAAAAGCTGATAGA
ATTGCTGCTGAAGGTTTAGTTTTTGCTACTAAAAATGAAACACATGGTGTATAGTAGAATTAAACTCAGAAACAGACTTTGTTG—

GRP-24

GGAACCTGGATTCTTTAATAGTTGTTGAAGCCTCCAGGGGGCCAGGCGGATCACTTGAGGCCAGCCTGGCCAACATAGCGAAACCCTGCCTCTACTAAAA
CCACAAAAATCAGCCGGGATGTTGGCACACGCTTATAATCCAGCTACTTGGGACGCTGAGGTGGGATATAGCTTGAACCCGGGAAGGAGACTGCAGTCAG
GGAAGCCTAGGGAAGCCTCAGACCAAGGATGATTGAATAACAAAGAAAAGGTGTAAGTAAAGATCTCCAACCTCTAGGGAGTACTAATTAGGAAAG
TTAAGGGTAGAAAAAGATAAATTAAGGAAAATAC—

GRP-28

CTGTGGCAATATTGTGTTCCAAATAAAGACTTGGTTTCCTCAGATCTACGCCATTTTCAATCTTCCCTAACAATACGTGCATTTTTAACAAAGCTGGTATT
TGAATACTTACCTGAGGTAACATGCCTTGGTATAGTTTCTTCTAAAGTTCACTGCAGGCTGGGTGCTGTGGCTCGTGCCTGTAATCCTAGCACTTTGGGAGGC
CGAGTCGGGAGAATTGCTTGAGCCCGGGAGTTCAAGACCAGCCTGCGGGACAAAATGAGACCCCATCCATA—

GRP-31

CTGTGATTTTTTTAAGGTCTTAATATTGAAGGAAGTCAACAGTCATTTATCCGAATTAAGTTGAGGTTAATAAAGTTTCAATTCGTAATTTTCCAAACC
AACCAATGTAAAAACCCAGATTTTCTGAATTGAGTCATGTAAGGATTTTTGTAAAGTG—

GRP-36

ACGGCAACTGATAGCTTTAAGGAGGAAGAGAGAATAGAGAGAGTGTGTGTTGGGGGGTGTGTGTGCGTTTAGTCCTATAAAATGTTTACTATTGATTTTT
TCTGTTTACTACCTCTTTCTCAAATAGGTTGGTTGTGAAGATGGATCTGTGAAACTATTTCAAATTACCCAGACAAAATTCAGTTTGAAAGAAATTTTGATC
GGCAGAAAAGTAAGCGTCATTTTTCATGGG-

GRP-37

TCATTTTACAAAAGGAACATTAATATTAATATAAGAAAAGAATTTCTTATACGTACCAATATGGTATCACATTTTCAGCTCAACATCAGACATGCAATAAATG
TATACAAGTACTTCAATTTGCATTAGAACATTTTAAAGAAATACACAATTATTTCTAAATTATTTTATATATACTAAGGCGGTAAAAGCTTAAGACTGG
AGATCTGGATCCCTCGAGTCTAGAGTCGACCTGCAGGCATGCAAGCTTGGCGTAATCATGGTCATAGCTGTTCTCTGTGTGAAATTGTTATCCGCTCACAAT
TCCACACAACATACGAGCCGGAAGCATA—

GRP-38

TAGAACCTGAGTGGGAACAGAAATCTCAAAATAAATAAATGGAAATGAGATCATGGCTGTAAATGGTAATTATATTATGTCAAAAACACCTTTAGAGTTACT
TTAGAGCTCCCTAAAAATAACAATTAAGTAGCTGTAGAGGATATTTCCTCTCTCTTACATTTATGTGGTGTTCAGGTGGACAAAGTACTTTTG

GRP-41

TCAGAAATGAGAATGCACTGGAGGCTGGTGATTCTCTGGACCCCTCTTCCCATCCATCGTTTCGGCTAAAAGTCATCATAAATTGGGAGTCCTTCCCTT
TACTGGTCTAGAAGTTCCCTCAGGAAGCAGCGTCACCTCTCTCCCTGCTCTTCACTGAGGAGGGAGGAAGAGGAGCAAGAGAAGACTTTCCGGTTTCCAA
ATGGCAGATTTGGTTTCGGGCATGTGAGGAGCCACATA—

Northern blot analysis of unknown differential genes in SGC7901/VCR cell

The cDNA fragments of four genes randomly selected from the 13 unknown genes mentioned above were used to produce probes for Northern blot, and the result was in agreement with that of DD-PCR and reverse Northern analysis. All the four genes were specifically (GRP-2) or highly expressed in SGC7901/VCR.

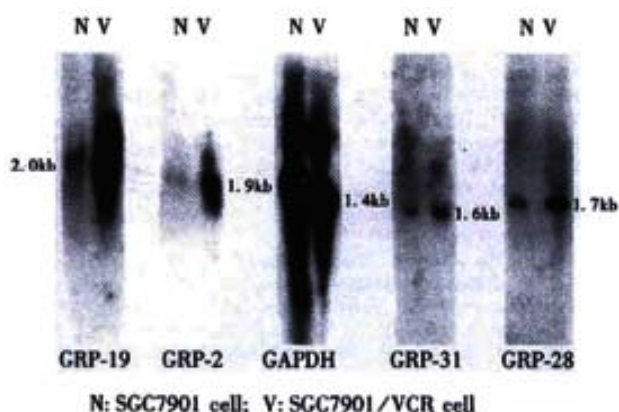


Figure 4 Northern analysis of unknown genes up-regulated in SGC7901/VCR cells.

DISCUSSION

MDR is a major obstacle to tumor chemotherapy. In recent years, progress has been made concerning the mechanism of MDR at the molecular level, which includes the separation and identification of some proteins encoded by MDR-related genes, including P-gp, MRP, LRP and BCRP. All of them are membrane proteins, which engender MDR by reducing the accumulation of chemotherapeutic drugs in the target cells or redistributing the drugs, which consequently reduce the drug concentration in the target organelles. Their expressions differ in different tumors. Certain anti-MDR drugs with some specific MDR mechanisms have been applied clinically. The first generation anti-MDR drugs require that the drug concentration to be high enough to revert MDR, so their side-effects often exceed the tolerance of patients. The second and third generation drugs (PSC833, GF 120918, VX-710, LY335979 etc) cannot revert MDR effectively, either. This phenomenon suggests that tumor cells may tolerate anti-tumor drugs through various mechanisms. The changes at the genetic level are usually more sensitive and prompt than those at the protein level, so screening MDR-related genes at the genetic level has great advantages. One method for screening differential expression genes is

mRNA differential display, which contributes substantially in many researches. We employed this technique to screen 20 gene fragments that were highly expressed in gastric cancer MDR cells. This result indicates that MDR involves multi-genes, each playing its own role in the process. Among these genes, seven were separated and identified as known genes.

Human mitochondrial cytochrome C oxidase subunit II

Human mitochondrial cytochrome C oxidase consists of three subunits. It has essential functions in mitochondrial respiration. Higuchi^[39] obtained two highly expressed genes in human head and neck squamous epithelium cancer cells that were cisplatin-resistant, using differential display, and one of the two encodes human mitochondrial cytochrome C oxidase subunit II. It is regarded as a sign of cisplatin-resistance. Denis-Gay *et al.*^[40] discovered that the concentration and activity of mitochondrial cytochrome C oxidase did not change in K562 leukemia cells that were adriamycin-resistant, while the concentrations of most other cytochrome oxidases declined significantly. A noteworthy phenomenon recently reported is that methamphetamine or 3,4-methylenedioxymethamphetamine (MDMA) could suppress the activity of mitochondrial cytochrome C oxidase, which implied that they could probably revert MDR^[41].

Galectin-8 cDNA is closely related to PCTA-1^[42]

If transferred into tumor 11299 cells, galectin-8 could suppress the formation of the clones by 75%. Galectin-8 is a binding protein of integrin, and has effects against tumor cell adhesion after binding. It can also induce apoptosis, too^[43-45].

Human ribosomal protein L23(RPL23)

It is homologous with *E. coli* ribosomal protein L11. As the drug-resistant mutant strain of *E. coli* lacks L11, it is postulated that L23 may be related to drug-resistance^[46].

Ss-A/Ro ribonucleoprotein autoantigen subunit

Its mRNA (1890 bp) has an open reading frame (ORF), encoding a polypeptide of 417 amino acid residues whose apparent molecular mass is 60ku. It is the antigen of several autoimmune diseases. In ultraviolet radiation resistant bacteria, an RNA-binding protein was recently discovered to mediate the resistance and to be highly homologous with Ss-A/Ro 60ku protein. Therefore, Ss-A/Ro ribonucleoprotein autoantigen 60ku subunit presumably has the similar function in the recovery of cells after UV radiation in higher eukaryotes^[47].

Oligophrenin-1 (OPHN1)

Its gene covers 500 kb genomic DNA and is composed of 25 exons. It is highly expressed primarily in fetal brain, encoding a protein whose

molecular mass is 91ku. It has a typical Rho GTPase activation protein (rhoGAP) domain, the activation of which induces GAP to inactivate Rho and Ras. Therefore, the inactivation of rhoGAP can activate its target molecules and subsequently influence cell differentiation and migration. Its mutation can result in non-specific X-chromosome linked mental retardation, as its loss of function probably interferes with or affects cell signal transduction pathways, impeding cell migration and axonal growth in the development of cells in the neural system^[48,49].

ADP-ribosylation factor 4 (ARF4)

It is a member of the G-protein family, with a molecular mass of about 20ku. It was first identified to activate cholera toxin ribosyltransferase, and was recently discovered to effect essentially in vesicular transport in cell, and to be an activator of phospholipase D^[50]. Human ribosomal protein S13 (RPS13) is a translation initiation factor and is related to cell growth and differentiation^[51]. Some of these seven genes are apparently related to MDR, and the relationship of others to MDR remains to be further studied.

Two cDNAs (GRP-24, GRP-41) which are highly expressed in SGC7901/VCR cells, are 100% homologous with human genomic clone fragments. The two genomic clones contain the genes of dynamin, neuroendocrine secretory protein 55 (NESP55), and GANS1. Dynamin is a membrane protein with GTPase activity; its alternative splicing produces six subtypes engaging in endocytosis, exocytosis, pinocytotic vesicle cycle, intracellular and Golgi complex vesicular transport, and cell membrane transport. NESP55 and GANS1 are both G-proteins, involved in cell signal transduction. Further confirmation of homologous genes of the two cDNA fragments is necessary.

We randomly selected 4 cDNA fragments (GRP-2, GRP-19, GRP-28, GRP-31) from the rest 11 unknown genes to do Northern analysis. The result was in agreement with that of reverse Northern analysis; and gave the lengths of the four genes and also confirmed the reliability of reverse Northern blot. The result is conducive to the cloning of the entire length of the genes.

To sum up, we managed to separate and clone 20 significantly highly or specifically expressed genes from drug-resistant gastric cancer SGC7901/VCR cells using DD-PCR. Some known genes are related to drug-resistance and others may enhance drug-resistance. It is necessary to conduct further research on the unknown genes.

REFERENCES

- Fan K, Fan D, Cheng LF, Li C. Expression of multidrug resistance-related markers in gastric cancer. *Anticancer Res* 2000;20:4809-4814
- Jonker JW, Smit JW, Brinkhuis RF, Maliepaard M, Beijnen JH, Schellens JH, Schinkel AH. Role of breast cancer resistance protein in the bioavailability and fetal penetration of topotecan. *J Natl Cancer Inst* 2000; 92: 1651-1656
- Tan B, Pinwnica WD, Ratner L. Multidrug resistance transporters and modulation. *Curr Opin Oncol* 2000;12: 450-458
- Liu ZM, Shou NH, Jiang XH. Expression of lung resistance protein in patients with gastric carcinoma and its clinical significance. *World J Gastroenterol* 2000; 6:433-434
- Zhang LJ, Chen KN, Xu GW, Xing HP, Shi XT. Congenital expression of Mdr-1 gene in tissues of carcinoma and its relation with pathomorphology and prognosis. *World J Gastroenterol* 1999;5:53-56
- Fan DM, Xiao B, Shi YQ, Ming-Feng, Qiao TD, Chen BJ, Chen Z. A novel cDNA fragment associated with gastric cancer drug resistance was screened out from a library by monoclonal antibody MGr1. *World J Gastroenterol* 1998; 4:110-111
- Liu Y, Lu MZ, Li QM, Wang YL. Expression of p53 C-myc and P-gp in gastric cancer. *Xin Xiaohuabingxue Zazhi* 1997; 5:585-586
- You HN, Chen Q, Jiang HP, Li DG, Zhang WZ. The influence of P-glycoprotein expression on the prognosis of gastric carcinoma. *Xin Xiaohuabingxue Zazhi* 1997; 5(Suppl 6):23-24
- Zhou WJ, Pan FQ. Significance of P-gp and P53 in patients with gastric cancer. *Huaren Xiaohua Zazhi* 1998; 6:318-319
- Xiao B, Shi YQ, Zhao YQ, You H, Liu XL, Fan DM. Expression of Fas gene in gastric cancer cells transduced with Fas gene. *Huaren Xiaohua Zazhi* 1998;6:400-403
- Cheng SD, Wu YL, Zhang YP, Qiao MM, Guo QS. Abnormal drug accumulation in multidrug resistant gastric carcinoma cells. *Shijie Huaren Xiaohua Zazhi* 2001; 9:131-134
- Lage H, Jordan A, Scholz R, Dietel M. Thermosensitivity of multidrug-resistant human gastric and pancreatic carcinoma cells. *Int J Hyperthermia* 2000;16:291-303
- Yin L, Chen K, Li D. Inherent mdr-1 gene expression in fresh tumor tissue specimens from several high-incidence malignancies. *Zhonghua Zhongliu Zazhi* 1997;19:420-422
- Gurel S, Yerci O, Filiz G, Dolar E, Yilmazlar T, Nak SG, Gulten M, Zorluoglu A, Memik F. High expression of multidrug resistance-1 (MDR-1) and its relationship with multiple prognostic factors in gastric carcinomas in patients in Turkey. *J Int Med Res* 1999;27:79-84
- Anzai H, Kitadai Y, Bucana CD, Sanchez R, Omoto R, Fidler IJ. Expression of metastasis-related genes in surgical specimens of human gastric cancer can predict disease recurrence. *Eur J Cancer* 1998; 34:558-565
- Motoo Y, Su SB, Nakatani MT, Sawabu N. Expression of multidrug resistance gene (mdr-1) mRNA in gastric and colorectal cancers. *Anticancer Res* 1998;18:1903-1906
- Yeh KH, Chen CL, Shun CT, Lin JT, Lee WJ, Lee PH, Chen YC, Cheng AL. Relatively low expression of multidrug resistance-1 (MDR-1) and its possible clinical implication in gastric cancers. *J Clin Gastroenterol* 1998;26:274-278
- Son YS, Suh JM, Ahn SH, Kim JC, Yi JY, Hur KC, Hong WS, Muller MT, Chung IK. Reduced activity of topoisomerase II in an Adriamycin-resistant human stomach-adenocarcinoma cell line. *Cancer Chemother Pharmacol* 1998;41:353-360
- Endo K, Maehara Y, Kusumoto T, Ichiyoshi Y, Kuwano M, Sugimachi K. Expression of multidrug-resistance-associated protein (MRP) and chemosensitivity in human gastric cancer. *Int J Cancer* 1996;68:372-377
- Liu XL, Xiao B, Yu ZC, Guo JC, Zhao QC, Xu L, Shi YQ, Fan DM. Downregulation of Hsp90 could change cell cycle distribution and increase drug sensitivity of tumor cells. *World J Gastroenterol* 1999; 5:199-208
- Darimont BD. The Hsp90 chaperone complex-A potential target for cancer therapy? *World J Gastroenterol* 1999; 5:195-198
- Xiao B, Shi YQ, Zhao YQ, You H, Wang ZY, Liu XL, Yin F, Qiao TD, Fan DM. Transduction of Fas gene or Bcl-2 antisense RNA sensitizes cultured drug resistant gastric cancer cells to chemotherapeutic drugs. *World J Gastroenterol* 1998; 4:421-425
- Yin F, Shi YQ, Zhao WP, Xiao B, Miao JY, Fan DM. Suppression of P-gp induced multidrug resistance in a drug resistant gastric cancer cell line by overexpression of Fas. *World J Gastroenterol* 2000;6:664-670
- Shi YQ, Xiao B, Miao JY, Li MF, Qiao TD, Chen BJ, Chen Z, Han JL, Zhou SJ, Fan DM. A novel cDNA fragment associated with gastric cancer drug resistance screened from a library by mAb MGr1. *Huaren Xiaohua Zazhi* 1998; 6:656-659
- Xiao B, Shi YQ, Zhao YQ, You H, Wang ZY, Liu XL, Yin F, Qiao TD, Fan DM. Transduction of fas gene or bcl-2 antisense RNA sensitizes cultured drug resistant gastric cancer cells to chemotherapeutic drugs. *Huaren Xiaohua Zazhi* 1998;6:675-679
- Liu B, Staren E, Iwamura T, Appert H, Howard J. Effects of Taxotere on invasive potential and multidrug resistance phenotype in pancreatic carcinoma cell line SUIT-2. *World J Gastroenterol* 2001; 7:143-141
- Wang X, Shi YQ, Zhao YQ, Wang JC, Yao LB, Zhang ZY, Lan M, Jin JP, Fan DM. Differential display of Vincristine-resistance-related proteins in gastric cancer SGC7901 cell line. *Zhonghua Zhongliu Zazhi* 2001;23:281-284
- Lin HL, Liu TY, Wu CW, Chi CW. Berberine modulates expression of mdr1 gene product and the responses of digestive track cancer cells to Paclitaxel. *Br J Cancer* 1999;81:416-226
- Zheng GQ, Han FS, Liu XY, Xu GW. Drug resistance mechanism of doxorubicin-resistant human gastric cancer cells BGC-823/DOX. *Zhonghua Waikexue Zazhi* 1997;35:325-328
- Varga A, Sokolowska-Kohler W, Presber W, Von Baehr V, Von Baehr R, Lucius R, Volk D, Nacsas J, Hever A. Toxoplasma infection and cell free extract of the parasites are able to reverse multidrug resistance of mouse lymphoma and human gastric cancer cells *in vitro*. *Anticancer Res* 1999;19:1317-1324
- Nakamura T, Oka M, Aizawa K, Soda H, Fukuda M, Terashi K, Ikeda K, Mizuta Y, Noguchi Y, Kimura Y, Tsuruo T, Kohno S. Direct interaction between a quinoline derivative, MS-209, and multidrug resistance protein (MRP) in human gastric cancer cells. *Biochem Biophys Res Commun* 1999; 255:618-624
- Kellner U, Hutchinson L, Seidel A, Lage H, Danks MK, Dietel M, Kaufmann SH. Decreased drug accumulation in a mitoxantrone-resistant gastric carcinoma cell line in the absence of P-glycoprotein. *Int J Cancer* 1997;71:817-824

- 33 Nitta A, Chung YS, Nakata B, Yashiro M, Onoda N, Maeda K, Sawada T, Sowa M Establishment of a cisplatin-resistant gastric carcinoma cell line OCUM-2M/DDP. *Cancer Chemother Pharmacol* 1997;40:94-97
- 34 Wang X, Huang YX, Wen QS, Wang QL. Silver-staining mRNA differential display method and cloning of tumor related genes in HepG2 cell line. *Di-si Junyi Daxue Xuebao* 2001;22:843-845
- 35 Wang L, Lu W, Chen YG, Zhou XM, Gu JR. Comparison of gene expression between normal colon mucosa and colon carcinoma by means of messenger RNA differential display. *World J Gastroenterol* 1999; 5:533-534
- 36 Ji F, Peng QB, Zhan JB, Li YM. Study of differential polymerase chain reaction of C-erbB 2 oncogene amplification in gastric cancer. *World J Gastroenterol* 1999; 5:152-155
- 37 You H, Xiao B, Cui DX, Shi YQ, Fan DM. Two novel gastric cancer associated genes identified by differential display. *World J Gastroenterol* 1998;4:334-336
- 38 Cui DX, Yan XJ, Su CZ. Differentially expressed genes were isolated in gastric carcinoma by optimised differential display PCR. *Shijie Huaren Xiaohua Zazhi* 1999; 7:139-144
- 39 Higuchi E. Up-regulation of human chorionic gonadotropin alpha subunit gene and human mitochondrial cytochrome oxidase subunit II gene in cis-Diamminedichloroplatinum(II) -resistant human head and neck squamous carcinoma cells. *Hokkaido Igaku Zasshi* 1999;74:231-238
- 40 Denis-Gay M, Petit JM, Mazat JP, Ratinaud MH. Modifications of oxido-reductase activities in adriamycin-resistant leukaemia K562 cells. *Biochem Pharmacol* 1998;56: 451-457
- 41 Burrows KB, Gudelsky G, Yamamoto BK. Rapid and transient inhibition of mitochondrial function following methamphetamine or 3,4-methylenedioxymethamphetamine administration. *Eur J Pharmacol* 2000;398:11-18
- 42 Gopalkrishnan RV, Roberts T, Tuli S, Kang D, Christiansen KA, Fisher PB. Molecular characterization of prostate carcinoma tumor antigen-1, PCTA-1, a human galectin-8 related gene. *Oncogene* 2000;19:4405-4416
- 43 Hadari YR, Arbel-Goren R, Levy Y, Amsterdam A, Alon R, Zaick Y. Galectin-8 binding to integrins inhibits cell adhesion and induces apoptosis. *J Cell Sci* 2000;113:2385-2397
- 44 Bassen R, Brichory F, Caulet-Maugendre S, Bidon N, Delaval P, Desrues B, Dazord L. Expression of Po66-CBP, a type-8 galectin, in different healthy, tumoral and peritumoral tissues. *Anticancer Res* 1999 ;19:5429-5433
- 45 Camby I, Belot N, Rorive S, Lefranc F, Maurage CA, Lahm H, Kaltner H, Hadari Y, Ruchoux MM, Brotchi J, Zick Y, Salmon I, Gabius HJ, Kiss R. Galectins are differentially expressed in supratentorial pilocytic astrocytomas, astrocytomas, anaplastic astrocytomas and glioblastomas, and significantly modulate tumor astrocyte migration. *Brain Pathol* 2001 ;11:12-26
- 46 Mcelwain KB, Boynton JE, Gillham NW. A nuclear mutation conferring thiostrepton resistance in chlamydomonas reinhardtii affects a chloroplast ribosomal protein related to Escherichia coli ribosomal protein L11. *Mol Gen Genet* 1993; 241: 564-572
- 47 Chen X, Quinn AM, Wolin SL. Ro ribonucleoproteins contribute to the resistance of Deinococcus radiodurans to ultraviolet irradiation. *Genes Dev* 2000;14:777-782
- 48 Billuart P, Bienvenu T, Ronce N, des Portes V, Vinet MC, Zemni R, Roest Crollius H, Carrie A, Fauchereau F, Cherry M, Briault S, Hamel B, Fryns JP, Beldjord C, Kahn A, Moraine C, Chelly J. Oligophernin-1 encodes a rho GAP protein involved in X-linked mental retardation. *Nature* 1998;392: 923-926
- 49 Ljubimova JY, Khazenzon NM, Chen Z, Neyman YI, Turner L, Riedinger MS, Black KL. Gene expression abnormalities in human glial tumors identified by gene array. *Int J Oncol* 2001;18:287-295
- 50 Lebeda RA, Haun RS. Cloning and characterization of the human ADP-ribosylation factor 4 gene. *Gene* 1999;237: 209-214
- 51 Ito T, Kim GT, Shinozaki K. Disruption of an Arabidopsis cytoplasmic ribosomal protein S13-homologous gene by transposon-mediated mutagenesis causes aberrant growth and development. *Plant J* 2000;22:257-264

• GASTRIC CANCER •

Overexpression of cyclin E in Mongolian gerbil with *Helicobacter pylori*- induced gastric precancerosis

Yong-Li Yao, Bo Xu, Yu-Gang Song, Wan-Dai Zhang

Yong-Li Yao, Yu-Gang Song, Wan-Dai Zhang, Institute of Gastrointestinal Diseases, Nanfang Hospital, First Military Medical University, Guangzhou 510515, Guangdong Province, China

Bo Xu, Department of Orthopedics, Nanfang Hospital, First Military Medical University, Guangzhou 510515, Guangdong Province, China

Correspondence to: Yong-Li Yao, Institute of Gastrointestinal Diseases, Nanfang Hospital, First Military Medical University, Guangzhou 510515, Guangdong Province, China. xbyyl@fimmu.edu.cn

Telephone: +86-20-85141544

Received 2001-03-12 Accepted 2001-08-15

Abstract

AIM: To explore dysregulation of cyclin E in malignancies, and to further investigate the role of cyclin E in *Helicobacter pylori* (*H. pylori*)-induced gastric precancerosis.

METHODS: Four-week-old specific pathogen-free male Mongolian gerbils were employed in the study. 0.5 mL 1×10^8 cfu \cdot L⁻¹ suspension of *H. pylori* NTCC11637 in Brucella broth was inoculated orally into each of 20 Mongolian gerbils, and a further 20 gerbils were inoculated with Brucella broth as controls. 10 of the infected gerbils and 10 of the non-infected control gerbils were sacrificed at 25, 45 wk after infection. The expression of cyclin E was analyzed by RT-PCR and immunohistochemical studies with monoclonal antibody to cyclin E in Mongolian gerbil of *H. pylori*-induced gastric precancerosis.

RESULTS: *H. pylori* was constantly detected in all infected animals throughout the study. At 25 wk after infection of *H. pylori*, ulcers were observed in the antral and body of stomach ($n=6$). Histological examination showed that all animals developed severe inflammation and multifocal lymphoid follicles appeared in the lamina propria and submucosa of gastric antrum. At 45 wk after infection of *H. pylori*, severe atrophic gastritis ($n=10$), intestinal metaplasia ($n=8$) and dysplasia ($n=6$) could be observed. Cyclin E mRNA levels were significantly more at 25 wk after infection of *H. pylori* (1.27 ± 0.26), and at 45 wk after infection of *H. pylori* (1.82 ± 0.39) than control-animals (0.59 ± 0.20 , $P < 0.01$); cyclin E mRNA levels were evaluated by 2.2-fold at 25 wk ($P < 0.01$) and 3.1-fold at 45 wk ($P < 0.01$) precancerosis induced by *H. pylori*, when compared with control gastric epithelium of Mongolian gerbil. Immunohistochemical staining revealed exclusive nuclear staining of cyclin E. Furthermore, there was a sequential increase in cyclin E positive cells from normal epithelium to precancerosis.

CONCLUSION: Overexpression of cyclin E occurs relatively early in gastric tumorigenesis in this model.

Yao YL, Xu B, Song YG, Zhang WD. Overexpression of cyclin E in Mongolian gerbil with *Helicobacter pylori*- induced gastric precancerosis. World J Gastroenterol 2002;8(1):60-63

INTRODUCTION

Gastric cancer is a major health problem^[1-3] and remains the second

most common cancer in the world^[4-6]. Although epidemiological studies have indicated that *H. pylori* infection plays a crucial role in gastric carcinogenesis in humans^[7-22], there is no direct proof that *H. pylori* is actually associated with gastric carcinogenesis^[23-26]. The purpose of this study was to elucidate the relationship between *H. pylori* infection and gastric carcinogenesis by using an animal model of long-term *H. pylori* infection, and explore the role played by cyclin E in gastric tumorigenesis^[27-29].

Cyclins are positive regulators of cell cycle progression. They function by forming a complex with and activating a class of protein kinases which are essential for cell cycle transitions. As the major regulatory events leading to cell proliferation occur in the G1 phase of the cell cycle, altered expression of cyclins involved in the G1 phase may be an important step in oncogenesis^[30-33]. Among G₁ cyclins, an accumulating body of evidence suggests that over expression and rearrangement of cyclin E is associated with malignancy. Over expression of cyclin E has also been found in mouse mammary tumors and is associated with tumor development; altered expression of cyclin E can accelerate occurrence and early progression of colorectal cancer, and plays an important role in occurrence of breast cancer^[34-37]. But cyclin D₁, over expression in esophageal cancer and breast cancer, has no over expression in gastric cancer, which suggests expression of cyclins has specificity of organs. To gain a further understanding of the role played by cyclin E in gastric tumorigenesis, the study investigates the role of cyclin E in *H. pylori*-induced gastric precancerosis^[38-39].

MATERIALS AND METHODS

Animals and preparation

Four-week-old specific pathogen-free male Mongolian gerbils, weighing (20 \pm 5)g, were employed in the study. They were housed in individual metabolic cages in a temperature conditioned room (23 \pm 2) $^{\circ}$ C with a 12 h light-dark cycle, allowed access to standard rat chow (provided by Experimental Animal Center, First Military Medical University) and water ad libitum, and acclimatized to the surrounding for 7 d prior to the experiments. *H. pylori* (NTCC11637) was obtained from American Type Culture Collection and cultured on Brucella agar plates containing 70 mL \cdot L⁻¹ goat blood in a microaerobic condition (volume fraction; N₂:85%, O₂:5%, CO₂:10%, in aerobic globe box) at 37 $^{\circ}$ C for 3 d. The strain was identified by morphology, Gram's stain, urease production and so on.

Experimental protocol

Suspension 0.5 mL 1×10^8 cfu \cdot L⁻¹ of *H. pylori* NTCC11637 in Brucella broth was inoculated orally into each of 20 Mongolian gerbils which had been fasted overnight, for 14 d continuously. A further 20 gerbils were inoculated with Brucella broth as controls. 10 of the infected gerbils and 10 of the non-infected control gerbils were sacrificed at 25, 45 wk after infection. The stomach of each animal was removed and opened for macroscopic observation. For half of each gastric antrum mucosa was dissected for RNA isolation. The remainders of the stomach samples were used for histological examination, which were fixed with neutral-buffered 100 mL \cdot L⁻¹

formalin and processed by standard methods that embedded in paraffin, sectioned and stained with haematoxylin for analyzing histological changes, Giemsa stain for detecting for *H. pylori* and Alcian blue (AB)/PAS stain for examining intestinal metaplasia.

RNA isolation and RT-PCR analysis

Using Tripure isolation reagent (Boehringer Mannheim, Germany), total cellular RNA was isolated from previously frozen tissues according to the manufacturer's instruction. All RNA samples were analyzed for integrity of 18s and 28s rRNA by ethidium bromide staining of 0.5µg RNA resolved by electrophoresis on 12g·L⁻¹ agarose-formaldehyde gels. RT-PCR analysis was performed as follows. RNA was incubated at 60°C for 10 min and chilled to 4°C immediately before being reverse transcribed. Reverse transcription of 1µg total RNA using antisense primers was performed in a volume of 20µL for 40 min at 50°C, containing 200 U MMLV reverse transcriptase, 1×buffer RT, 1 MU·L⁻¹ Rnasin, 0.5mmol·L⁻¹ dATP, dGTP, dCTP and dTTP respectively and 0.2µmol·L⁻¹ antisense primers including cyclin E and β-actin respectively. The samples were heated to 99°C for 5 min to terminate the reverse transcription reaction. By using a Perkin-Elmer DNA Thermocycler 4800 (Perkin-Elmer, Norwalk, CT), 5µL cDNA mixture obtained from the reverse transcription reaction was then amplified for cyclin E and β-actin. β-actin was used as the housekeeping gene and amplified with cyclin E as contrast. The amplification reaction mixture consisted of 10×buffer 5µL, 0.2 mmol·L⁻¹ dATP, dGTP, dCTP and dTTP respectively, 2.5 U Taq DNA polymerase, and 0.2µmol·L⁻¹ each of sense and antisense primers in a final volume of 50µL. The reaction mixture was first heated at 94°C for 2 min and amplification was carried out for 29 cycles at 94°C for 0.5 min, 53°C for 1 min, 70°C for 1.5 min, followed by an incubation for 7 min at 70°C. The number of amplification cycles was previously determined to keep amplification in the linear range to avoid the "plateau effect" associated with increased numbers of PCR cycles. The PCR primers used were: cyclin E, sense 5'-TAT GGC GAC ACA AGA AAA TG-3' and antisense 5'-GCA AGA GAA GAC AGA CAA CG-3'; β-actin, sense 5'-CCA AGG CCA ACC GCG AGA AGA TGA C-3' and antisense 5'-AGG GTA CAT GGT GGT GCC GCC AGA C-3'. The length of PCR products for cyclin E and β-actin was 770 bp and 587 bp. PCR products were run on a 15g·L⁻¹ agarose gel in 0.5×TBE buffer and then analyzed by gel image analysis system. The level of cyclin E was reflected with the ratio of cyclin E/β-actin.

Immunohistochemical staining

Four micrometers paraffin-embedded tissue sections were deparaffinized and rehydrated. Endogenous peroxidase activity was ablated with 10 mL·L⁻¹ hydrogenperoxide in methanol. The immunostaining for cyclin E was conducted using the StreptAvidin-Biotin-enzyme Complex kit (Boster, Wuhan). Immunostaining by replacing primary antibody with PBS was also conducted as a negative control. The staining was evaluated semiquantitatively on the basis of the percentage of positive cells, and classified as follows^[40]: diffusely positive (+++) when positive cells accounted for more than 70% of the total cells, partially positive (++) when positive cells were 35%-70%, partially positive (+) when positive cells accounted for 5%-35%, and negative (-) when positive cells accounted for less than 5%.

Statistical Analysis

Experimental results were analyzed with Chi-square Tests and K Related Samples Test by SPSS software. Statistical significance was determined at $P < 0.05$.

RESULTS

Histopathological findings

H. pylori was detected in gastric antrum and gastric body of all infected animals throughout the study, and more in gastric antrum than gastric body. By the 25th wk after infection of *H. pylori*, ulcers were observed in the antral and body of stomach ($n=6$). Histological examination showed that all animals developed severe inflammation in the area close to ulcers; multifocal lymphoid follicles appeared in the lamina propria and submucosa; and there were mild atrophic gastritis in all infected animals. By the 45th wk after infection of *H. pylori*, severe atrophic gastritis ($n=10$), intestinal metaplasia ($n=8$) and dysplasia ($n=6$) could be observed. Those metaplastic glands appeared more atypical than the surrounding nonmetaplastic and hyperplastic glands. Severe atrophic gastritis, intestinal metaplasia and dysplasia were gastric precancerosis. In the uninfected animals, there were no significant changes throughout the study.

RT-PCR analysis of cyclin E mRNA expression

There were cyclin E mRNA expression in gastric antrum mucosa of control-animals. cyclin E mRNA levels were significantly more at 25 wk after infection of *H. pylori* (1.27 ± 0.26), and at 45 wk after infection of *H. pylori* (1.82 ± 0.39) than control-animals (0.59 ± 0.20 , $P < 0.01$); Cyclin E mRNA levels were evaluated by 2.2-fold at 25 wk ($P < 0.01$) and 3.1-fold at 45 wk ($P < 0.01$) precancerosis induced by *H. pylori*, when compared with control gastric epithelium of Mongolian gerbil (Figure 1-3).

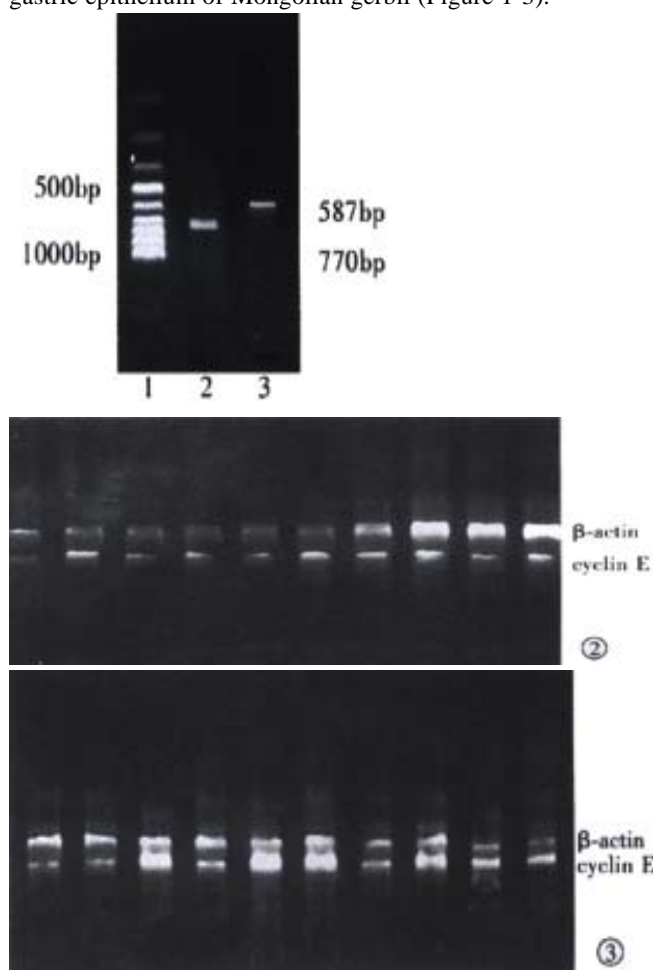


Figure 1 1:cyclin E; 2:PCR marker; 3:β-actin

Figure 2 RT-PCR analysis of cyclin E mRNA levels using β-actin as internal control. Total RNA was first reverse transcribed into cDNA and then amplified by PCR in control.

Figure 3 In 25 wk after infection of *H. pylori*.

Immunohistochemical analysis of cyclin E protein expression

To examine whether increased cyclin E mRNA expression were accompanied by increased expression of cyclin E protein, immunohistochemical analysis was performed. cyclin E protein expression lied in nuclei and cytoplasm. Cyclin E protein expressions were evaluated significantly at 25 wk ($P<0.01$) and at 45 wk ($P<0.01$) precancerosis induced by *H. pylori*, when compared with control gastric epithelium of Mongolian gerbil (Figure 4 and Table 1).

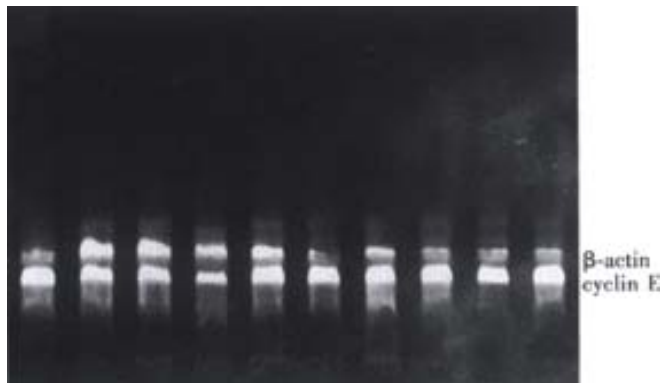


Figure 4 In 45 wk after infection of *H. pylori*.

Table 1 Expression of cyclin E by immunohistochemical staining (n=10)

Groups	Cyclin E				Positive %
	-	+	++	+++	
Control	8	2			20 ^a
25 wk after <i>H. pylori</i> inf	2	7	1		80 ^b
45 wk after <i>H. pylori</i> inf	1	6	2	1	90 ^c

K related samples test: $P=0.002$ Chi-square test: $\chi^2=12.344$, $P=0.002^b$ vs $^aP=0.007$, c vs $^aP=0.002$

DISCUSSION

H. pylori infection is now know as a major cause of acute and chronic active gastritis, peptic ulcer disease and atrophic gastritis and is also suspected to be involved in the genesis of gastric adenocarcinoma and mucosa-associated lymphoid tissue lymphoma^[41-49]. In 1994, the International Agency for Research on Cancer (IRAC), a branch of the World Health Organization (WHO), convened experts from 11 countries to examine the evidence linking a number of infectious agents with human cancer. Although there is no direct proof that *H. pylori* is actually associated with gastric carcinogenesis, epidemiological studies have indicated that *H. pylori* infection plays an important role in gastric carcinogenesis in humans; *H. pylori* was designated as a definite carcinogen (group I) to the human stomach based on prospective case-control studies reported in 1991. Several experiments were conducted in Japan that demonstrated that chronic *H. pylori*-infection models of Mongolian gerbils developed gastric carcinoma. These results will be extremely significant to elucidate the mechanism of gastric carcinogenesis due to *H. pylori* infection^[5,50]. Apoptosis, a programmed cell death, was ignored, just like *H. pylori*, only to reappear recently. However, the number of current publications dealing with apoptosis of *H. pylori* has increased exponentially. Although gastric epithelial apoptosis is a programmed physiological event in the superficial aspect of the mucosa and is important for healthy cell turnover, *H. pylori* infection reportedly promotes such a cell death sequence^[51-52]. Because apoptosis regulates the cycle of cell turnover in balance with proliferation, dysregulation of apoptosis or proliferation evoked by *H. pylori* colonization would be linked to the gastric

carcinogenesis^[53-56].

Cyclins are positive regulators of cell cycle progression, initially identified in early cleavage embryos of marine invertebrates as proteins that accumulated during interphase and were degraded at mitosis. Cyclins are now known to be positive regulatory subunits of a class of protein kinase termed cyclin-dependent kinases. These protein kinases have been shown in a number of diverse eukaryotic systems to be the master regulators of major cell cycle transitions^[57-59]. Cyclin E is essential for the G1/S phase transition in the cell cycle. Cyclin E gene amplification and altered expression has been reported in a variety of human cancers^[60-61]. Now Cyclin E gene has been detected as oncogene^[38]. Cyclin E was synthesized in the mid-term of the cell cycle, expressed the highest level when entering S phase, and degraded through S phase. The level of cyclin-dependent kinase2 kept constant during the cell cycle. Cyclin E, cyclin-dependent kinase2 and cyclin-dependent kinase inhibitor regulated G1/S phase transition by two-way at late stage of G1 phase, Cyclin E accelerated G1/S phase transition by composing and activating cyclin-dependent kinase2.

In the present study, to explore dysregulation of cyclin E in malignancies, and to further investigate the role of cyclin E in *H. pylori*-induced gastric precancerosis, cyclin E mRNA level was measured by quantitative RT-PCR analysis in Mongolian gerbil gastric antrum mucosa. In addition, the expression and localization of protein product was analyzed by immunohistochemistry. Sample size requirement for obtaining sufficient amounts of RNA for RT-PCR analysis did not allow detection of either cyclin E mRNA level in any specific type of preneoplastic lesions. However, using immunohistochemical technique, cyclin E protein expression in preneoplastic lesions was observed from paraffin-embedded tissue sections. Cyclin E mRNA levels were increased 2.2-fold at 25 wk and 3.1-fold at 45 wk precancerosis induced by *H. pylori*, when compared with normal gastric epithelium of Mongolian gerbil. Immunohistochemical staining revealed exclusive nuclear staining of cyclin E. Furthermore, there was a sequential increase in cyclin E positive cells from normal epithelium to precancerosis. The present study indicated that expression of cyclin E increased from normal epithelium to precancerosis, dysregulation of cyclin E expression occurred relatively early in gastric tumorigenesis in this model and might participate in tumor progression. These findings suggested that *H. pylori*-induced gastric precancerosis was associated with dysregulation of gastric epithelial cell cycle. Further studies were needed to delineate the mechanism of these alterations.

REFERENCES

- Deng DJ. Progress of gastric cancer etiology: N-nitrosamides in the 1990s. *World J Gastroenterol* 2000;6:613-618
- Chen GY, Wang DR. The expression and clinical significance of CD44v in human gastric cancers. *World J gastroenterol* 2000;6:125-127
- Ma JL, Liu WD, Zhang ZZ, Zhang L, You WC, Chang YS. Relationship between gastric cancer and precancerous lesions. *Shijie Huaren Xiaohua Zazhi* 1998;6:223-224
- Pan ZR. Study on chronic gastritis and gastric cancer. *Xin Xiaohua Bingxue Zazhi* 1996;4:95-96
- Watanabe T, Tada M, Nagai H, Sasaki S, Nakao M. *Helicobacter pylori* infection induces gastric cancer in Mongolian gerbils. *Gastroenterology* 1998;115:642-648
- Zhuang XQ, Lin SR. Study on the relationship between *Helicobacter pylori* and gastric cancer. *Shijie Huaren Xiaohua Zazhi* 2000;8:206-207
- Vandenplas Y. *Helicobacter pylori* infection. *World J Gastroenterol* 2000; 6:20-31
- Takahashi S, Keto Y, Fujita H, Muramatsu H, Nishino T, Okabe S. Pathological changes in the formation of *Helicobacter pylori*-induced gastric lesions in Mongolian gerbils. *Dig Dis Sci* 1998;43:754-765
- Pan KF, Liu WD, Ma JL, Zhou T, Zhang L, Chang YS, You WC. Infection of *Helicobacter pylori* in children and mode of transmission in a high-risk area of gastric cancer. *Shijie Huaren Xiaohua Zazhi* 1998;6:42-44
- Zhang L, Jiang J, Pan KF, Liu WD, Ma JL, Zhou T, Perez-Perez GT,

- Blaser MJ, Chang YS, You WC. Infection of *H. pylori* with cagA+ strain in a high risk area of gastric cancer. *Shijie Huaren Xiaohua Zazhi* 1998;6:40-41
- 11 Zhuang XQ, Lin SR. Study on *Helicobacter pylori* infection in gastric cancer and precancerosis. *Shijie Huaren Xiaohua Zazhi* 2000;8:710-711
- 12 Hu PJ. *Helicobacter pylori* and gastric cancer. *Shijie Huaren Xiaohua Zazhi* 1999;7:1-2
- 13 Huang XQ. *Helicobacter pylori* infection and gastrointestinal hormones: a review. *World J Gastroenterol* 2000;6:783-788
- 14 Shang SH, Zheng JW. Treatment on *Helicobacter pylori* induced diseases. *Shijie Huaren Xiaohua Zazhi* 2000;8:556-557
- 15 Wang XH, Zahgn WD, Zahgn YL, Zeng JZ, Sun Y. Relationship between *Hp* infection and oncogene and tumor suppressor gene expressions in gastric cancer and precancerosis. *Shijie Huaren Xiaohua Zazhi* 1998;6:516-518
- 16 Ye GA, Zhang WD, Liu LM, Shi L, Xu ZM, Chen Y, Zhou DY. *Hp vac A* gene and chronic gastritis. *Shijie Huaren Xiaohua Zazhi* 2001;9:593-594
- 17 Quan J, Fan XG. Experimental studies on *Helicobacter pylori* and gastric cancer. *Shijie Huaren Xiaohua Zazhi* 1999;7:1068-1069
- 18 Lu SY, Pan XZ, Peng XW, Shi ZL, Lin L, Chen MH. Effect of *Hp* infection on gastric epithelial cell kinetics in stomach diseases. *Shijie Huaren Xiaohua Zazhi* 2000;8:386-388
- 19 Xiao SD. *Helicobacter pylori* and gastric cancer. *Shijie Huaren Xiaohua Zazhi* 1998;6:4
- 20 Xia HH. Association between *Helicobacter pylori* and gastric cancer: current knowledge and future research. *World J Gastroenterol* 1998;4:93-96
- 21 Gao XH, Pan BR. *Helicobacter pylori* infection and gastric cancer. *Xin Xiaohua Bingxue Zazhi* 1995;3:223-224
- 22 Zu Y, Shu J, Yang CM, Zhong ZF, Dai HY, Wang X, Qin GM. Study on *Helicobacter pylori* infection and risk of gastric cancer. *Shijie Huaren Xiaohua Zazhi* 1998;6:367-368
- 23 Wu MS, Shun CT, Lee WC, Chen CJ, Wang HP, Lee WJ, Lin JT. Gastric cancer risk in relation to *Helicobacter pylori* infection and subtypes of intestinal metaplasia. *Br J Cancer* 1998;78:125-128
- 24 Forman D. Review article: Is there significant variation in the risk of gastric cancer associated with *Helicobacter pylori* infection? *Aliment Pharmacol Ther* 1998;12:3-7
- 25 Alexander CGA, Amg MC. Association of *Helicobacter pylori* infection with gastric cancer. *Military Med* 2000;165:21-27
- 26 Cai L, Yu SZ, Zhang ZF. *Helicobacter pylori* infection and risk of gastric cancer in Changle County, Fujian Province, China. *World J Gastroenterol* 2000;6:374-376
- 27 Chi J, Fu BY, Nakajima, Hattori and Kushima. Establishment of Mongolian gerbil animal model infected with *Hp* infection and change of inflammation and proliferation before and after *Hp* eradication. *Shijie Huaren Xiaohua Zazhi* 1999;7:557-560
- 28 Zhang WD. Animal model on diseases induced by *H. pylori*: it was difficult for study of *H. pylori*. *Shijie Huaren Xiaohua Zazhi* 1999;7:555-556
- 29 Yasui W, Naka K, Suzuki T, Fujimoto J, Hayashi K, Matsutani N, Yokozaki H, Tahara E. Expression of p27Kip1, cyclin E and E2F-1 in primary and metastatic tumors of gastric carcinoma. *Oncol Rep* 1999;6:983-987
- 30 Matsumoto M, Furihata M, Ishikawa T, Ohtsuki Y, Ogoshi S. Comparison of deregulated expression of cyclin D1 and cyclin E with that of cyclin dependent kinase 4 (CDK4) and CDK2 in human oesophageal squamous cell carcinoma. *Br J Cancer* 1999;80:256-261
- 31 Loden M, Nielsen NH, Roos G, Emdin So, Landberg G. Cyclin E dependent kinase activity in human breast cancer in relation to cyclin E, p27 and p21 expression and retinoblastoma protein phosphorylation. *Oncogene* 1999;18:2557-2566
- 32 Le Cam L, Polanowska J, Fabbriozio E, Olivier M, Philips A Ng Eaton E, Classon M, Geng Y, Sardet C. Timing of cyclin E gene expression depends on the regulated association of a bipartite repressor element with a novel E2F complex. *EMBO J* 1999;18:1878-1890
- 33 Jang SJ, Park YW, Park MH, Lee JD, Lee YY, Jung TJ, Kim IS, Choi IY, Ki M, Choi BY, Ahn MJ. Expression of cell cycle regulators, cyclin E and p21 WAF1/CIP1, potential prognostic markers for gastric cancer. *Eur J Surg Oncol* 1999;25:157-163
- 34 Nielsen NH, Arnerlov C, Cajander S, Landberg G. Cyclin E expression and proliferation in breast cancer. *Anal Cell Pathol* 1998; 17:177-188
- 35 Mishina T, Dosaka Akita H, Hommura F, Nishi M, Kojima T, Ogura S, Shimizu M, Katoh H, Kawakami Y. Cyclin E expression, a potential prognostic marker for non small cell lung cancers. *Clin Cancer Res* 2000;6:11-16
- 36 Quade BJ, Park JJ, Crum CP, Sun D, Dutta A. *In vivo* cyclin E expression as a marker for early cervical neoplasia. *Mod Pathol* 1998;11:1238-1246
- 37 Ohashi R, Gao C, Miyazaki M, Hamazaki K, Tsuji T, Inoue Y, Uemura T, Hirai R, Shimizu N, Namba M. Enhanced expression of cyclin E and cyclin A in human hepatocellular carcinomas. *Anticancer Res* 2001;21:657-662
- 38 Sakaguchi T, Watanabe A, Sawada H, Yamada Y, Yamashita J, Matsuda M, Nakajima M, Miwa T, Hirao T, Nakano H. Prognostic value of cyclin E and p53 expression in gastric carcinoma. *Cancer* 1998;82:1238-1243
- 39 Ling WJ, Ma YJ, Zhang WD, Chen YP. Relationship between classification of spleen syndrome of patients with chronic gastric diseases and gastric carcinoma and cyclin E expression. *Shijie Huaren Xiaohua Zazhi* 2000;8:513-515
- 40 Shimizu M, Nikaido T, Toki T, Shiozawa T, Fujii S. Clear cell carcinoma has an expression pattern of cell cycle regulatory molecules that is unique among ovarian adenocarcinomas. *Cancer* 1999;85:669-677
- 41 Li ZM, Gao CM, Ding JH, Wang JD, Wang YP, Hu X, Liu TK, Takezaki T, Tajima K. Study on seroprevalence of *Helicobacter pylori* infection among upper digestive tract cancer patients and their kindreds. *Chin J Epidemiol* 1999;20:88-90
- 42 Tabata H, Fuchigami T, Kobayashi H, Sakai Y, Nakanishi M, Tomioka K, Nakamura S, Fujishima M. *Helicobacter pylori* and mucosal atrophy in patients with gastric cancer: a special study regarding the methods for detecting *Helicobacter pylori*. *Dig Dis Sci* 1999;44:2027-2034
- 43 Meining AG, Bayerdorffer E, Stolte M. *Helicobacter pylori* gastritis of the gastric cancer phenotype in relatives of gastric carcinoma patients. *Eur J Gastroenterol Hepatol* 1999;11:717-720
- 44 Yamaoka Y, Kodama T, Kashima K, Graham DY. Antibody against *Helicobacter pylori* CagA and VacA and the risk for gastric cancer. *J Clin Pathol* 1999;52:215-218
- 45 Danesh J. *Helicobacter pylori* infection and gastric cancer: systematic review of the epidemiological studies. *Aliment Pharmacol Ther* 1999; 13:851-856
- 46 Harris RA, Owens Dk. Witherell H, Parsonnet J. *Helicobacter pylori* and gastric cancer: what are the benefits of screening only for the CagA phenotype of *H. pylori*? *Helicobacter* 1999;4:69-76
- 47 Hansen S, Melby KK, Aase S, Jellum E, Vollset Se. *Helicobacter pylori* infection and risk of cardia cancer and non cardia gastric cancer. A nested case-control study. *Scand J Gastroenterol* 1999;34:353-360
- 48 Scheiman JM, Cutler AF. *Helicobacter pylori* and gastric cancer. *Am J Med* 1999;106:222-226
- 49 Kuipers EJ. Review article: exploring the link between *Helicobacter pylori* and gastric cancer. *Aliment Pharmacol Ther* 1999;13:3-11
- 50 Honda S, Fujioka T, Tokieda M, Satoh R, Nishizono A, Nasu M. Development of *Helicobacter pylori* induced gastric carcinoma in Mongolian gerbils. *Cancer Res* 1998;58:4255-4259
- 51 Shirin H, Sordillo EM, Oh SH, Yamamoto H, Delohery T, Weinstein B, Moss SF. *Helicobacter pylori* inhibits the G1 to S transition in AGS gastric epithelial cell. *Cancer Res* 1999;59:2277-2281
- 52 Gao H, Wang JY, Shen XZ, Liu JJ. Effect of *Helicobacter pylori* infection on gastric epithelial cell proliferation. *World J Gastroenterol* 2000;6:442-444
- 53 Suzuki H, Ishii H. Role of apoptosis in *Helicobacter pylori* associated gastric mucosal injury. *J Gastroenterol Hepatol* 2000;15:D46-D54
- 54 Rudi J, Kuck D, Strand S, Herbay AV, Mariani SM, Krammer PH, Galle PR, Stremmel W. Involvement of the CD95 (APO1/Fas) receptor and ligand system in *Helicobacter pylori* induced gastric epithelial apoptosis. *J Clin Invest* 1998;102:1506-1514
- 55 Zhuang XQ, Lin SR. Research of *Helicobacter pylori* infection in precancerous gastric lesions. *World J Gastroenterol* 2000;6:428-429
- 56 Gu JZ, Hou TW, Wang XX. Study on precancerous gastric lesions induced by *Helicobacter pylori*. *Shijie Huaren Xiaohua Zazhi* 2001;9:111
- 57 Shin JY, Kim HS, Park J, Park JB, Lee JY. Mechanism for inactivation of the KIP family cyclin dependent kinase inhibitor genes in gastric cancer cells. *Cancer Res* 2000;60:262-265
- 58 Carroll JS, Prall OW, Musgrove EA, Sutherland RL. A pure estrogen antagonist inhibits cyclin E-Cdk2 activity in MCF-7 breast cancer cells and induces accumulation of p130-E2F4 complexes characteristic of quiescence. *J Biol Chem* 2000;275:38221-38229
- 59 Fischer PM, Lane DP. Inhibitors of cyclin-dependent kinases as anti cancer therapeutics. *Curr Med Chem* 2000;7:1213-1245
- 60 Tu JF, Jiang FZ, Chen BC. The relationship between cyclin E expression in primary gallbladder carcinoma and the activity of cell proliferation. *Chin J Exp Surg* 2000;17:20-21
- 61 Huang M, Yang SM, Liao SL, Zhang B, You JF. The effects of cyclin E on the growth and other cell cycle related genes of breast carcinoma cells MCF-7. *Chin J Pathol* 2000;29:192-195

• LIVER CANCER •

Expression of gap junction genes connexin 32 and connexin 43 mRNAs and proteins, and their role in hepatocarcinogenesis

Xiang-Dong Ma, Xing Ma, Yan-Fang Sui, Wen-Liang Wang

Xiang-Dong Ma, Department of Obstetrics & Gynecology, Xijing Hospital, Fourth Military Medical University, 17 Changle Xilu, Xi'an 710033, Shaanxi Province, China

Xing Ma, Department of Orthopedics, Xinan Hospital, Third Military Medical University, Chongqing, 400038, China

Yan-Fang Sui, Wen-Liang Wang, Department of Pathology, Fourth Military Medical University, Xi'an 710033, Shaanxi Province, China

Correspondence to: Dr. Xiang-Dong Ma, Department of Obstetrics & Gynecology, Xijing Hospital, the Fourth Military Medical University, Xi'an 710033, Shaanxi Province, China. mapping@fmmu.edu.cn

Telephone: +86-27-3373569

Received 2001-02-08 Accepted 2001-03-12

Abstract

AIM: To investigate the relationship between hepatocarcinogenesis and the expression of connexin32 (cx32), connexin43 (cx43) mRNAs and proteins *in vitro*.

METHODS: Gap junction genes cx32 and cx43 mRNA in hepatocellular carcinoma cell lines HHCC, SMMC-7721 and normal liver cell line QZG were detected by *in situ* hybridization (ISH) with digoxin-labeled cx32, and cx43 cDNA probes. Expression of Cx32 and Cx43 proteins in the cell lines was revealed by indirect immunofluorescence and flow cytometry (FCM).

RESULTS: Blue positive hybridization signals of cx32 and cx43 mRNAs detected by ISH with cx32 and cx43 cDNA probes respectively were located in cytoplasm of cells of HHCC, SMMC-7721 and QZG. No significant difference of either cx32 mRNA or cx43 mRNA was tested among HHCC, SMMC-7721 and QZG ($P=2.673$, HHCC vs QZG; $P=1.375$, SMMC-7721 vs QZG). FCM assay showed that the positive rates of Cx32 protein in HHCC, SMMC-7721 and QZG were 0.7%, 1.7% and 99.0%, and the positive rates of Cx43 protein in HHCC, SMMC-7721 and QZG were 7.3%, 26.5% and 99.1% respectively. Significant differences of both Cx32 and Cx43 protein expression existed between hepatocellular carcinoma cell lines and normal liver cell line ($P=0.0069$, HHCC vs QZG; $P=0.0087$, SMMC-7721 vs QZG). Moreover, the fluorescent intensities of Cx32 and Cx43 proteins in HHCC, SMMC-7721 were lower than that in QZG.

CONCLUSION: Hepatocellular carcinoma cell lines HHCC and SMMC-7721 exhibited lower positive rates and fluorescent intensities of Cx32, Cx43 proteins compared with that of normal liver cell line QZG. It is suggested that lower expression of both Cx32 and Cx43 proteins in hepatocellular carcinoma cells could play pivotal roles in the hepatocarcinogenesis. Besides, genetic defects of cx32 and cx43 in post-translational processing should be considered.

Ma XD, Ma X, Sui YF, Wang WL. Expression of gap junction genes connexin 32 and connexin 43 mRNAs and proteins, and their role in hepatocarcinogenesis. *World J Gastroenterol* 2002;8(1):64-68

INTRODUCTION

Carcinoma of the liver is one of the most common malignant tumors which seriously threatens to human life^[1-14]. About 90% of carcinoma of the liver are hepatocellular carcinoma (HCC)^[15-19]. In each year, more than 250 thousands of new cases of HCC were reported around the world, among which 110 000 cases (44.7%) occurred in China^[20-24]. Due to the difficulty in early diagnosis and treatment, the tumor molecular mechanisms, early diagnosis and effective methods of clinical treatment for HCC have been a major research project all over the world.

Gap junctions are intercellular channels formed by the interaction of two hemichannels—connexons, one of which is composed of six protein subunits^[25,26]. Connexins (Cx) are subunits of gap junctional channels^[27,28], by which neighboring cells can exchange low molecular weight ions and molecules, i.e., gap junctional intercellular communication (GJIC)^[29,30]. GJIC mediated via gap junctions plays important roles in embryogenesis, cell proliferation, tissue homeostasis and in carcinogenesis^[31,32]. Connexins are encoded by a gene family of at least 16 members, which have been divided into two groups based on primary amino acid sequence homology. Connexin32 (Cx32) and connexin43 (Cx43) are the major gap junction forming proteins in liver tissues. Decreased expression of Cx genes and disordered signal transduction pathway of Cx genes contribute to abnormal gap junctional intercellular communication between contacting cells^[33]. Uncontrolled tumor cell growth because of the loss of gap junctional intercellular communication due to the down-regulated expression of Cx genes appears to be an important event in cell transformation^[34-37]. In this study, the hepatocellular carcinoma cell lines HHCC, SMMC-7721 and normal liver cell line QZG were employed to investigate the relationship between hepatocarcinogenesis and cx32, cx43 mRNA and their protein expression.

MATERIALS AND METHODS

Cell culture

Hepatocellular carcinoma cell lines HHCC, SMMC-7721 and normal liver cell line QZG, were kindly provided by Professor Chen in the 863 Research Group. The cells were cultured on slides in RPMI 1640 medium (Gibco BRL, USA), supplemented with 100 mL·L⁻¹ fetal bovine serum (Gibco BRL, USA), incubated in a humidified atmosphere of 950 mL·L⁻¹ air and 50 mL·L⁻¹ CO₂ at 37°C. The cells were passaged by trypsinization twice a week.

Probe labeling

pGEM-cx32 plasmid containing cx32 cDNA 1.5kb, pSG5-cx43 plasmid containing cx43 cDNA 1.1kb were gifts from Professor Li in Hunan Medical University. After amplification, isolation and purification, pGEM3-cx32 plasmid was digested by EcoR I (Gibco BRL, USA) and pSG5-cx43 by BamH I (Gibco BRL, USA). The digested plasmids were electrophorated on 7 g·L⁻¹ agarose gel with DNA/Hind III + EcoR I Marker (Gibco BRL, USA). cx32, cx43 cDNAs from gel were extracted and purified as the protocol of PCR-pure kit (Clontech, USA), and labeled using Dig

DNA labeling and detection kit (Boehringer Mannheim, Germany).

In situ hybridization

Slides of varied cells were incubated in $0.2\text{mL}\cdot\text{L}^{-1}$ DEPC at RT for 10 min, then in $0.2\text{mL}\cdot\text{L}^{-1}$ HCl for 10 min, $5\text{mg}\cdot\text{L}^{-1}$ PK at 37°C for 10 min. The digestion reaction was stopped in $0.1\text{mol}\cdot\text{L}^{-1}$ glycine and the slides were fixed in $40\text{g}\cdot\text{L}^{-1}$ PFA for 10 min, dehydrated in ethanol and air dried in sequence. Prehybridization was performed at 42°C for 30 min. The labeled cDNA probes were denatured in hybridization buffer at 100°C for 10 min, then at -20°C for 3 min, then added on tissues and coverslipped at 42°C overnight. Washing of sections was done with $2\times\text{SSC}$, $1\times\text{SSC}$, $0.5\times\text{SSC}$ and Buffer I. The slides were incubated in NSS at 37°C for 30 min, and then Dig-Ap (Boehringer Mannheim, Germany, 1:500) for 2h, finally detected with NBT / BCIP of Dig DNA labeling and detection kit (Boehringer Mannheim, Germany). Positive signals were visualized as intensive blue granules in the cytoplasm. Control sections were used. All results were verified by χ^2 test.

Flow cytometry (FCM) analysis

Total $10^6\cdot\text{L}^{-1}$ cells of HHCC, SMMC-7721 and QZG were

collected, and blocked with normal serum (Vector, USA) for 30 min at 4°C , then added mouse-anti Cx32 McAb (Zymed, USA, 1:1000) and mouse-anti Cx43 McAb (Zymed, USA, 1:1000) respectively for 30 min at 4°C , whereas IgG was added for control. FITC-IgG (Jackson, 1:100) was added in the cells for 30 min at 4°C , precipitated and washed by $0.01\text{mol}\cdot\text{L}^{-1}$ pH7.5 PBS. Detective rates and the fluorescent intensity of Cx32, Cx43 proteins in the cells were measured by ELITE ESP flow cytometer (Coulter, USA) and phoenix software (Coulter, USA).

RESULTS

Detect of cx32, cx43 mRNA in cell lines by ISH

The cx32, cx43 mRNA in hepatocellular carcinoma cell lines HHCC, SMMC-7721 and normal liver cell line QZG were detected by Dig-labeled cx32, cx43 cDNA probes. After in situ hybridization, blue positive hybridization signals of mRNA were located in cytoplasm of the cells. The results showed that bright blue specific hybridization signals of cx32 mRNA and cx43 mRNA were detected in hepatocellular carcinoma cell lines HHCC, SMMC-7721 and normal liver line QZG. χ^2 tests did not show any significant difference ($P > 0.05$) between them. The results were showed in Figure 1-3.

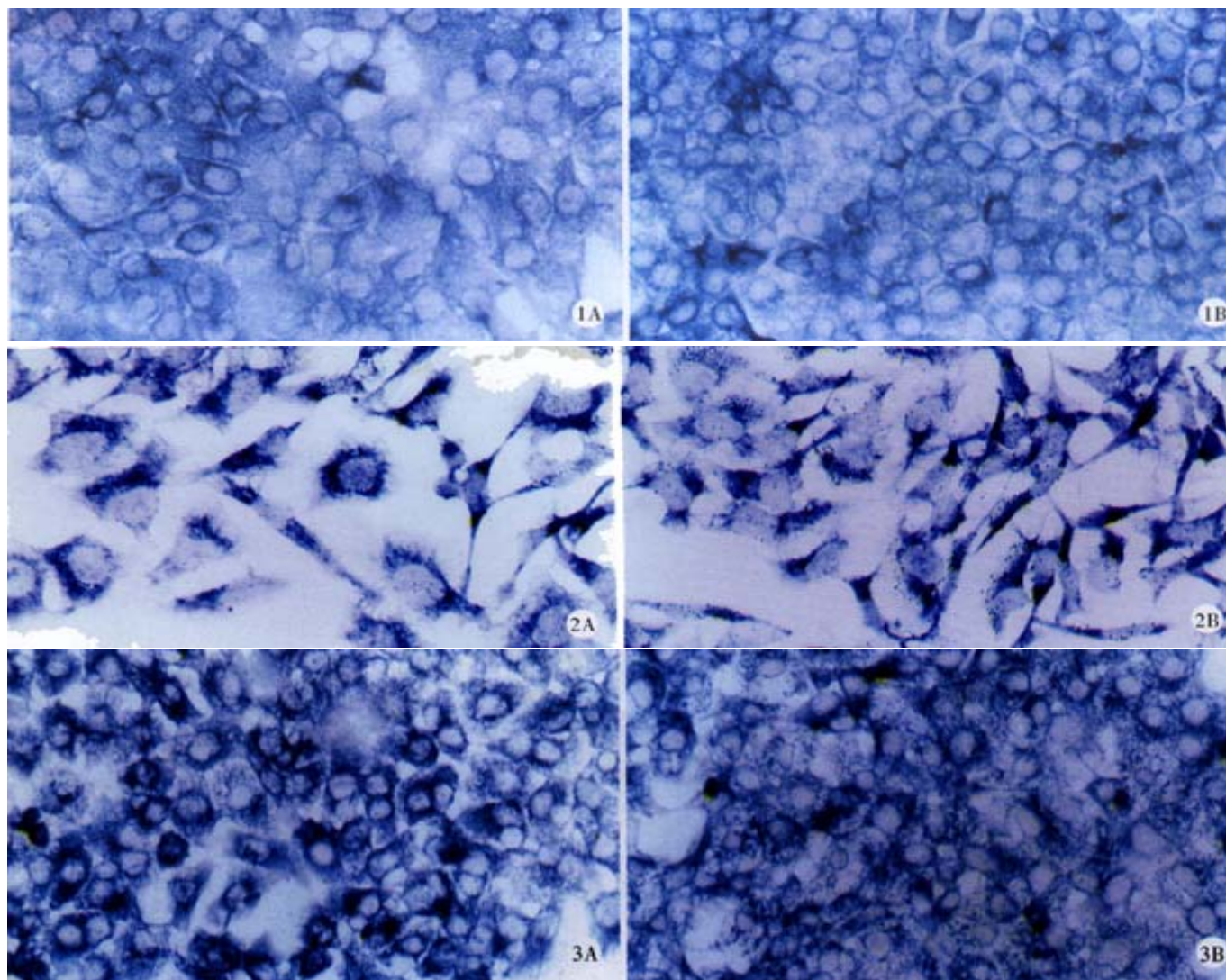


Figure 1A Positive signal of cx32 mRNA in HHCC, ISH $\times 400$
Figure 2A Positive signal of cx32 mRNA in SMMC-7721, ISH $\times 400$
Figure 3A Positive signal of cx32 mRNA in QZG, ISH $\times 400$

Figure 1B Positive signal of cx43 mRNA in HHCC, ISH $\times 400$
Figure 2B Positive signal of cx43 mRNA in SMMC-7721, ISH $\times 400$
Figure 3B Positive signal of cx43 mRNA in QZG, ISH $\times 400$

Expressions of Cx32, Cx43 proteins in hepatocellular carcinoma cell lines by FCM

Expression of Cx32, Cx43 proteins in cultured hepatocellular carcinoma cell lines HHCC, SMMC-7721 and normal liver cell line QZG were detected by FCM after immunoreaction with mouse-anti Cx32 McAb, mouse-anti Cx43 McAb. FCM examined both positive rates of Cx proteins expression and their quantities in each cell line.

FCM assay showed that positive rates of Cx32 protein expression in HHCC, SMMC-7721 and QZG were 0.7%, 1.7% and 99.0%, and those of Cx43 protein were 7.3%, 26.5% and 99.1% respectively. The fluorescent intensity of Cx32 protein and Cx43 protein in HHCC, SMMC-7721 were lower than those in QZG. QZG

cells showed both higher positive rates for Cx32, Cx43 proteins and strong fluorescent intensity. The detection rates of Cx32, Cx43 proteins were showed in Figure 4-6 and Table 1.

Table 1 Positive expression rates of Cx32 and Cx43 proteins in various cell lines

Cell line	Positive rates %	
	Cx32	Cx43
HHCC	0.7 ^b	7.3 ^b
SMMC-7721	1.7 ^b	26.5 ^b
QZG	99.0	99.1

^bP<0.01, vs QZG.

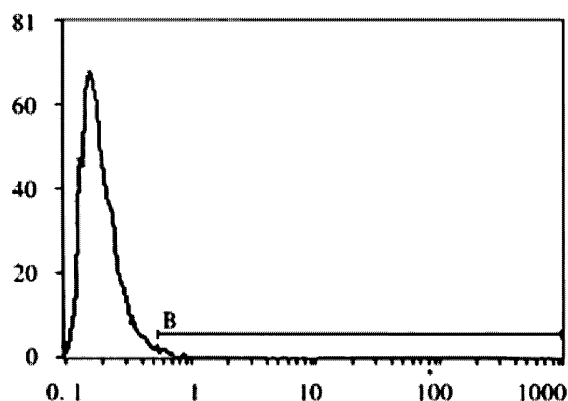


Figure 4A Positive expression rate of Cx32 protein in HHCC, FCM
(X: FL1; Y: cell count)

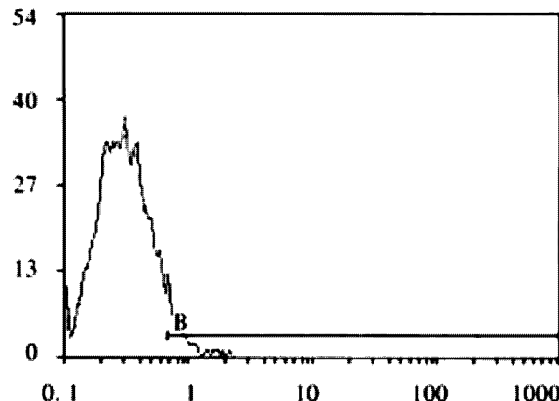


Figure 4B Positive expression rate of Cx43 protein in SMMC-7721, FCM
(X: FL1; Y: cell count)

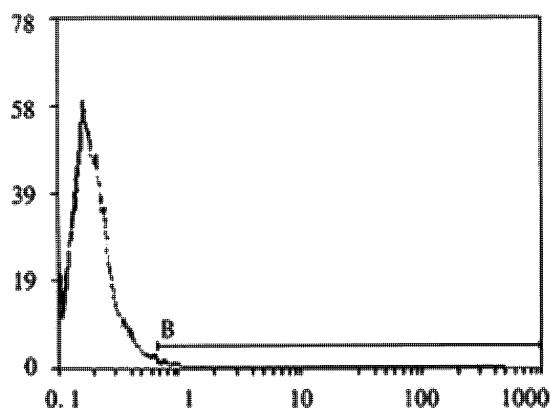


Figure 5A Positive expression rate of Cx43 protein in HHCC, FCM
(X: FL1; Y: cell count)

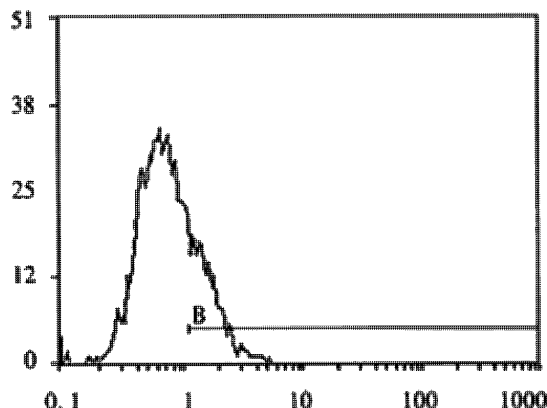


Figure 5B Positive expression rate of Cx32 protein in QZG, FCM
(X: FL1; Y: cell count)

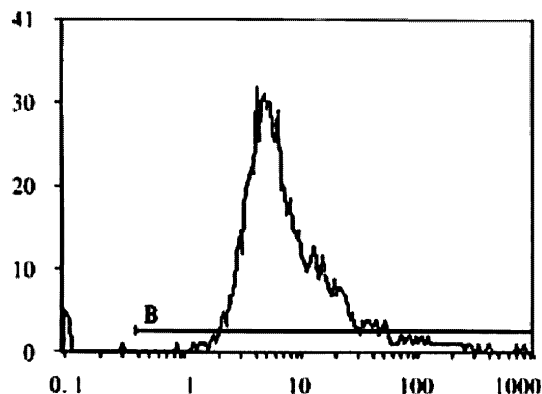


Figure 6A Positive expression rate of Cx32 protein in SMMC-7721, FCM
(X: FL1; Y: cell count)

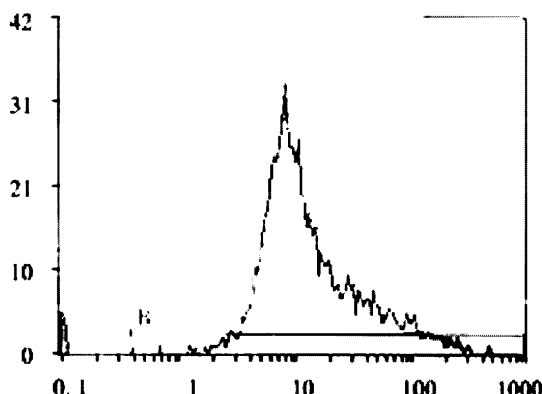


Figure 6B Positive expression rate of Cx43 protein in QZG, FCM
(X: FL1; Y: cell count)

DISCUSSION

Gap junction intercellular communication (GJIC) mediated by gap junction channels^[38,39] has been postulated to be an important tool for the maintenance of tissues homeostasis, metabolism, control growth and differentiation^[40,41]. Carcinogenesis is one of the pathological processes in which disorders of GJIC may play an important role. The inhibited GJIC in many kinds of tumor cells has been found, which could make important contributions to neoplastic progression by allowing tumor cells to escape by either systemic or local control mechanisms^[42-44].

Cx32, Cx43 are widely expressed in many tissues, especially in normal liver. This study revealed that Cx32 and Cx43 proteins expressed at a high level in normal liver cell line but at low level in hepatocellular carcinoma cell lines^[45-47].

Hepatocarcinogenesis is dramatically enhanced in liver neoplasm tissues lacking of Cx32 and Cx43 proteins, as we shown previously^[48]. The results showed that cx32 and cx43 mRNAs and their proteins were highly expressed in normal liver tissues and cell lines, and had significantly decreased in hepatocellular carcinoma tissues and cell lines except expression of Cx43 protein in hepatoma cell line SMMC-7721. cx32 is the specific expression gene in human normal liver tissues and cell line whereas cx43 is a kind of variable expressing gene in either normal liver or hepatoma cell lines. Decrease of Cx proteins related with abnormal function of GJIC between hepatocellular carcinoma cells and surrounding normal cells finally results in hepatocarcinogenesis. Aberrant localization of Cx32 and Cx43 may be not only essential for the reduced GJIC in HCC^[49], but also disturb the mechanism of a bystander effect^[50]. Expression of the gap junctional proteins is often decreased in tumor tissues, but recruited expression could suppress malignant phenotypes of the tumor cells. The mechanism is that enhanced GJIC on basis of normal gap junctional protein expression regulates homologous and heterologous communication between tumor cells, surrounding normal hepatocytes and other cells^[51].

Many observations demonstrate that the lower expression of Cx32 and Cx43 may be involved in the development of hepatocellular carcinoma^[52]. It is interesting, moreover, that our results have showed even lower expression of Cx32, Cx43 proteins in hepatocellular carcinoma cell lines HHCC, SMMC-7721 than that in normal liver cell line QZG, but ISH results have shown no decreases of cx32 and cx43 mRNA in hepatocellular carcinoma compared with normal liver cell line. Therefore, it appears that cx32 and cx43 genes transcription is not responsible for aberrant expression of Cx32 and Cx43 proteins during human liver tumorigenesis. Besides, the results have indicated that cx32 and cx43 genes, the specific genes expressing in normal liver tissues, are expected to be the potential unmutated tumor suppressor genes.

Some abnormal regulatory events promote carcinogenesis^[55,56], through multiple mechanisms, including post translation process and other potential mechanisms^[53-56]. The carcinogenesis and development of hepatocellular carcinoma are related with the abnormal expression of cx genes, signal transduction disorders^[57, 58], such as reduce of $[Ca^{2+}]$ ^[59,60] and post-translational phosphorylation on tyrosine of Cx proteins, which are associated with dramatic changes in gap junctional intercellular communication and carcinogenesis^[61]. The possibility is that defects in post-translational processing of Cx32 and Cx43 proteins may be obstacle for their transportation to cell membranes^[62]. Furthermore, phosphorylation on tyrosine of Cx protein can affect the structure of Cx proteins, which is related to channel properties^[63]. Post-translational phosphorylation on tyrosine of Cx32 and Cx43 may be important factors controlling the GJIC in hepatocellular carcinoma and substantially responsible for the assembly and function of these proteins as well. Further investigation is expected to understand the mechanism in detail.

REFERENCES

- 1 Ma XD, Sui YF, Wang WL. Expression of gap junction genes connexin32 and connexin43 and their proteins in hepatocellular carcinoma and normal liver tissues. *World J Gastroenterol* 2000;6:66-69
- 2 Wang Y, Liu H, Zhao Q, Li X. Analysis of point mutation in site 1896 of HBV procore and its detection in the tissues and serum of HCC patients. *World J Gastroenterol* 2000;6:395-397
- 3 Mei MH, Xu J, Shi QF, Yang JH, Chen Q, Qin LL. Clinical significance of serum intercellular adhesion molecule detection on patients with hepatocellular carcinoma. *World J Gastroenterol* 2000;6:408-410
- 4 Qin Y, Li B, Tan YS, Sun ZL, Zuo FQ, Sun ZF. Polymorphism of p16INK4a gene and rare mutation of p15INK4b gene exon2 in primary hepatocellular carcinoma. *World J Gastroenterol* 2000;6:411-414
- 5 Wang XZ, Chen XC, Yang YH, Chen ZX, Huang YH, Tao QM. Relationship between HBxAg and Fas/FasL in patients with hepatocellular carcinoma. *World J Gastroenterol* 2000;6(Suppl 3):17-20
- 6 Zhao CY, Li YL, Liu SX, Feng ZJ. Changes of IL6 and relevant cytokines in patients with hepatocellular carcinoma and their clinical significance. *World J Gastroenterol* 2000;6(Suppl 3):33-36
- 7 Su ZJ, Zhang YF, Shi MY, Zeng QX, Chen ML. A prospective study of nosocomial infection in 848 cases of liver diseases. *World J Gastroenterol* 2000;6(Suppl 3):38-40
- 8 Li JY, Huang Y, Lin MF. Clinical evaluation of several tumor markers in the diagnosis of primary hepatic cancer. *World J Gastroenterol* 2000;6(Suppl 3):39-41
- 9 Yin ZZ, Jin HL, Yin XZ, Li TZ, Quan JS, Jin ZN. Effect of boschniakia rossica on expression of GSTP, p53 and p21ras proteins in early stage chemical hepatocarcinogenesis and its anti inflammatory activities in rats. *World J Gastroenterol* 2000;6(Suppl 3):49-51
- 10 Lin GY, Chen ZL, Lu CM, Li Y, Wang J, Ping XJ, Huang R. Immunohistochemical study on p53, Hrasp21, cerbB2 protein and PCNA expression in tumor tissues of Han and minority ethnic patients with primary hepatic carcinoma in Xinjiang. *World J Gastroenterol* 2000;6(Suppl 3):53-56
- 11 Jiang Z, Liu L, Fang W, Shou WZ, Zhang DS, Dai MM. Local radioactive treatment of hepatocellular cancer with phosphorus32 glass microspheres to enhance the efficacy of hepatic artery chemoembolism and possibly related with MDR expressed glycoprotein. *World J Gastroenterol* 2000;6(Suppl 3):59-62
- 12 Liu LX, Jiang HC, Zhu AL, Zhou J, Wang XQ, Wu M. Gene expression profiles in liver cancer and normal liver tissues. *World J Gastroenterol* 2000;6(Suppl 3):85-88
- 13 Wang CF, Shao YF, Zhang HZ. Surgical treatment for patients with stage IVa hepatic carcinoma and related studies. *World J Gastroenterol* 2000;6(Suppl 3):86-89
- 14 Lin NF, Tang J, Mohamed-Ishmael HS. Study on environmental etiology of high incidence areas of liver cancer in China. *World J Gastroenterol* 2000;6:572-576
- 15 Tian DY, Yang DF, Xia NS, Zhang ZG, Lei HB, Huang YC. The serological prevalence and risk factor analysis of hepatitis G virus infection in Hubei Province of China. *World J Gastroenterol* 2000;6:585-587
- 16 Zhong DR, Ji XL. Hepatic angiomyolipoma misdiagnosis as hepatocellular carcinoma: A report of 14 cases. *World J Gastroenterol* 2000;6:608-612
- 17 Riordan SM, Williams R. Transplantation of primary and reversibly immortalized human liver cells and other gene therapies in acute liver failure and decompensated chronic liver disease. *World J Gastroenterol* 2000;6:636-642
- 18 Li Y, Su JJ, Qin LL, Yang C, Luo D, Ban KC, Kensler TW, Roebuck BD. Chemopreventive effect of oltipraz on AFB1 induced hepatocarcinogenesis in tree shrew model. *World J Gastroenterol* 2000;6:647-650
- 19 Xu HY, Yang YL, Gao YY, Wu QL, Gao GQ. Effect of ars enic trioxide on human hepatoma cell line BEL7402 cultured in vitro. *World J Gastroenterol* 2000;6:681-687
- 20 Zang GQ, Zhou XQ, Yu H, Xie Q, Zhao GM, Wang B, Guo Q, Xiang YQ, Liao D. Effect of hepatocytic apoptosis induced by TNF α on acute severe hepatitis in mouse models. *World J Gastroenterol* 2000;6:688-692
- 21 Huang XF, Wang CM, Dai XW, Li ZJ, Pan BR, Yu LB, Qian B, Fang L. Expression of chromogranin A and cathepsin D in human primary hepatocellular carcinoma. *World J Gastroenterol* 2000;6:693-698
- 22 Xu HY, Yang YL, Guan XL, Song G, Jiang AM, Shi LJ. Expression of regulating apoptosis gene and apoptosis index in primary liver cancer. *World J Gastroenterol* 2000;6:721-724
- 23 Chen YP, Liang WF, Zhang L, He HT, Luo KX. Transfusion transmitted virus infection in general populations and patients with various liver diseases in south China. *World J Gastroenterol* 2000;6:738-741
- 24 Ma XD, Sui YF, Wang WL. The expression of gap junction protein connexin32 in human hepatocellular carcinoma, cirrhotic and viral hepatitis liver tissues. *Aizheng* 1999; 18:133-135

- 25 Kumar NM, Gilula NB. The gap junction communication channel. *Cell* 1996; 84: 381-388
- 26 Windoffer R, Beile B, Leibold A, Thomas S, Wilhelm U, Leube RE. Visualization of gap junction mobility in living cells. *Cell Tissue Res* 2000; 299:347-362
- 27 Durnick PE, Benjamin DC, Verselis VK, Bargiello TA, Dowd TL. Structure of the amino terminus of a gap junction protein. *Arch Biochem Biophys* 2000; 381:181-190
- 28 Hopperstad MG, Srinivas M, Spray DC. Properties of gap junction channels formed by Cx46 alone and in combination with Cx50. *Biophys J* 2000; 79:1954-1966
- 29 Falk MM. Biosynthesis and structural composition of gap junction intercellular membrane channels. *Eur J Cell Biol* 2000; 79:564-574
- 30 Ruch RJ, Trosko JE. The role of oval cells and gap junctional intercellular communication in hepatocarcinogenesis. *Anticancer Res* 1999; 19: 4831-4838
- 31 Yamasaki H, Naus CC. Role of connexin genes in growth control. *Carcinogenesis* 1996;17:1199-1213
- 32 Krutovskikh V, Yamasaki H. The role of gap junctional intercellular communication (GJIC) disorders in experimental and human carcinogenesis. *Histol Histopathol* 1997;12:761-768
- 33 Hahn AF, Ainsworth PJ, Naus CC, Mao J, Bolton CF. Clinical and pathological observations in men lacking the gap junction protein connexin32. *Muscle Nerve* 2000; 999:S39-49
- 34 Moennikes O, Buchmann A, Rommaldi A, Ott T, Werringloer J, Willecke K, Schwarz M. Lack of phenobarbital-mediated promotion of hepatocarcinogenesis in connexin 32-null mice. *Cancer Res* 2000; 60:5087-5091
- 35 Moennikes O, Buchmann A, Willecke K, Tranb O, Schwarz M. Hepatocarcinogenesis in female mice with mosaic expression of connexin 32. *Hepatology* 2000; 32: 501-506
- 36 Piechocki MP, Toti RM, Fernstrom MJ, Burk RD, Ruch RJ. Liver cell-specific transcriptional regulation of connexin32. *Biochim Biophys Acta* 2000; 1491: 107-122
- 37 Ma XD, Sui YF, Wang WL. Expression of gap junction genes connexin32, connexin43 and their proteins in human hepatocellular carcinoma cell lines and normal liver cell line. *Shiyong Aizheng Zazhi* 1999;14:161-163
- 38 Ma XD, Sui YF, Wang WL, Xu QL. A flow cytometric study of gap junction cx32,cx43 in human hepatocellular carcinoma cell lines. *Xibao Yu Fenzi Mianyixue Zazhi* 1999;15:51-54
- 39 Ma XD, Sui YF, Wang WL, Wang CM. Expression of gap junction proteins Cx32, Cx43 in human hepatocellular carcinoma cell lines and normal liver cell line: Study with laser scanning confocal microscope. *Zhongguo Zhongliu Zazhi* 2000;10:1-2
- 40 Juul MH, Rivedal E, Stokke T, Sanner T. Quantitative determination of gap junction intercellular communication using flow cytometric measurement of fluorescent dye transfer. *Cell Adhes Commun* 2000; 7: 501-512
- 41 Nielsen M, Ruch RJ, Vang O. Resveratrol reverses tumor-promoter-induced inhibition of gap junctional intercellular communication. *Biochem Biophys Res Commun* 2000;275:804-809
- 42 Krutovskikh VA, Troyanovsky S M, Piccoli C, Tsuda H, Asamoto M, Yanaski H. Differential effect of subcellular localization of communication impairing gap junction protein connexin43 on tumor cell growth. *Oncogene* 2000; 19: 505-513
- 43 Christ GJ. Gap junctions and ion channels: relevance to erectile dysfunction. *Int J Impot Res* 2000;12(Suppl 4):S15-25
- 44 Piechocki MP, Burk RD, Ruch RJ. Regulation of connexin 32 and connexin43 by DNA methylation in rat liver cells. *Carcinogenesis* 1999; 20: 401-406
- 45 Ma XD, Sui YF, Wang WL. Expression of gap junction protein connexin32 in human hepatocellular carcinoma, pericancerous liver and normal liver tissues. *Disi Junyi Da xue Xuebao* 1999;20:48-50
- 46 Temme A, Buchmann A, Gabriel HD, Nelles E, Schwarz M, Willecke K. High incidence of spontaneous and chemically induced liver tumors in mice deficient for connexin32. *Curr Biol* 1997; 7: 713-716
- 47 Wang Y, Rose B. An inhibition of gap-junctional communication by cadherins. *J Cell Sci* 1997; 110(pt3): 301-309
- 48 Krutovskikh V, Yamasaki H. Connexin gene mutations in human genetic diseases. *Mutat Res* 2000;462:197-207
- 49 Krutovskikh V, Mazzoleni G, Mironov N, Omori Y, Aguelon AM, Mesnil M, Berger F, Partensky C, Yamasaki H. Altered homologous and heterologous gap-junction intercellular communication in primary human liver tumors associated with aberrant protein localization but not gene mutation of connexin 32. *Int J Cancer* 1994; 54: 87-93
- 50 Kawamura K, Bahar R, Namba H, Seimiya M, Takenaga K, Hamada H, Sakiyama S, Tagawa M. Bystander effect in uracil phosphoribosyltransferase/5-fluoracil-mediated suicide gene therapy is correlated with the level of intercellular communication. *Int J Oncol* 2001; 18:117-120
- 51 Ren P, Ruch RJ. Inhibition of gap junctional intercellular communication by barbiturates in long-term primary cultured rat hepatocytes is correlated with liver tumor promoting activity. *Carcinogenesis* 1996; 17:2119-2124
- 52 Omori Y, Krutovskikh V, Mironov N, Tsuda H, Yamasaki H. Cx32 gene mutation in a chemically induced rat liver tumor. *Carcinogenesis* 1996; 17: 2077-2880
- 53 Neveu MJ, Hully JR, Babcock KL, Hertzberg EL, Nicholson BJ, Paul DL, Pitot HC. Multiple mechanisms are responsible for altered expression of gap junction genes during oncogenesis in rat liver. *J Cell Sci* 1994; 107(pt1): 83-95
- 54 DeoCampo ND, Wilson MR, Trosko JE. Cooperation of bcl-2 and myc in the neoplastic transformation of normal rat liver epithelial cells is related to the down-regulation of gap junction-mediated intercellular communication. *Carcinogenesis* 2000;21:1501-1506
- 55 Kolaja KL, Engelken DT, Klaassen CD. Inhibition of gap-junctional-intercellular communication in intact rat liver by nongenotoxic hepatocarcinogens. *Toxicology* 2000;146:15-22
- 56 Yamasaki H, Krutovskikh V, Mesnil M, Tanaka T, Zaidan-Dagli ML, Omori Y. Role of connexin (gap junction) genes in cell growth control and carcinogenesis. *C R Acad Sci* 1999;322:151-159
- 57 Niessen H, Harz H, Bedner P, Kramer K, Willecke K. Selective permeability of different connexin channels to the second messenger inositol 1,4,5-trisphosphate. *J Cell Sci* 2000;113(pt8):1365-1372
- 58 Niessen H, Willecke K. Strongly decreased gap junctional permeability to inositol 1,4,5,-trisphosphate in connexin32 deficient hepatocytes. *FEBS Lett* 2000;466:112-114
- 59 Suadicani SO, Vink MJ, Spray DC. Slow intercellular Ca(2+) signaling in wild-type and cx43-null neonatal mouse cardiac myocytes. *Am J Physiol Heart Circ Physiol* 2000; 279:H3076-3088
- 60 Rottingen J, Iversen JG. Ruled by waves Intracellular and intercellular calcium signaling. *Acta Physiol Scand* 2000;169:203-219
- 61 Chen BL, Ma XD, Xin XY, Wang DT, Wang CM. The regulation on signal transduction pathway of gap junction gene connexin43 in HeLa cell line by all-trans-retinoic acid. *Shiyong Aizheng Zazhi* 2000; 15:337-340
- 62 Ma XD, Chen BL, Wang DT, Xin XY. Expression of antioncogene connexin43 mRNA and its protein in human cervical carcinoma cell line HeLa. *Xiandai Fuchanke Jinzhan* 1999;8:317-319
- 63 Guan XJ, Ruch RJ. Gap junction endocytosis and lysosomal degradation of connexin43-P2 in WB-F344 rat liver epithelial cells treated with DDT and lindane. *Carcinogenesis* 1996;17:1791-1798

• LIVER CANCER •

Pharmacokinetics of radioimmunotherapeutic agent of direct labeling mAb ^{188}Re -HAb18

Chao Lou, Zhi-Nan Chen, Hui-Jie Bian, Jie Li, Shou-Bo Zhou

Chao Lou, Zhi-Nan Chen, Hui-Jie Bian, Department of Cell Engineering Research Centre, Jie Li, Department of Oral Cell Biology, Qingdu Hospital, Fourth Military Medical University, Xi'an 710033, Shaanxi Province, China

Shou-Bo Zhou, School of Biological Science, University of Manchester, Oxford Road, United Kingdom

Supported by National Natural Science Foundation of China, No. 39700175 (Dr. Hui-Jie Bian)

Correspondence to: Chao Lou, Cell Engineering Research Centre, Fourth Military Medical University, Xi'an 710033, Shaanxi Province, China. wall1970@sina.com

Telephone: +86-29-3374057

Received 2001-07-19 Accepted 2001-10-24

Abstract

AIM: To label anti-hepatoma monoclonal antibody (mAb) fragment HAb18 F(ab')₂ was labeled with ^{188}Re for the pharmacokinetic model of ^{188}Re -HAb18 F(ab')₂ and to evaluate its pharmacokinetic parameters in hepatoma-bearing nude mice.

METHODS: HAb18 F(ab')₂ was directly labeled with ^{188}Re using 2-mercaptoethanol (2-ME) as reducing agents. Labeling efficiency and immunoreactivity of ^{188}Re -HAb18 F(ab')₂ were evaluated by Whatman 3MM paper chromatography and live cell assay, respectively. Biodistribution analysis was also conducted in nude mice bearing human hepatoma in which animals were sacrificed at different time points (1, 4, 18, 24 and 24h) after ^{188}Re -HAb18 F(ab')₂ was injected through tail-vein into hepatoma-bearing nude mice. The blood and radioactivity of organs and mass were measured. The concentrations of ^{188}Re -HAb18 F(ab')₂ were evaluated with a pharmacokinetic 3P97 software.

RESULTS: The optimum labeling efficiency and immunoreactive fraction were 91.7% and 0.78% respectively. The parameters of ^{188}Re -HAb18 F(ab')₂ were: $T_{1/2}$, 2.29h; V_d , $1.49 \times 10^{-9} \text{ L} \cdot \text{Bq}^{-1}$; AUC, $20.49 \times 10^9 \text{ Bq} \cdot \text{h} \cdot \text{L}^{-1}$; CL, $0.45 \times 10^{-3} \text{ L} \cdot \text{h}^{-1}$. ^{188}Re -HAb18 F(ab')₂ could locate specially in hepatoma with high selective reactivity of HAb18 F(ab')₂. ^{188}Re -HAb18 F(ab')₂ was mainly eliminated by kidney. The maximal tumor to blood ratio was at 48h, and maximal tumor to liver ratio was at 18h.

CONCLUSION: The pharmacokinetics of ^{188}Re -HAb18 F(ab')₂ fit a 1-compartment model. ^{188}Re -HAb18 F(ab')₂ can be uptaken selectively at the hepatoma site.

Lou C, Chen ZN, Bian HJ, Li J, Zhou SB. Pharmacokinetics of radioimmunotherapeutic agent of direct labeling mAb ^{188}Re -HAb18. *World J Gastroenterol* 2002;8(1):69-73

INTRODUCTION

^{188}Re is a new radioisotope^[1-16]. In the past,¹³¹I was used as the main radioisotope for radioimmunotherapy (RAIT).¹³¹I has its favour such

as simple labeling, appropriate partial energy and path length, but the high energy of γ -ray produced harmness to the whole body, and β -energy ($E_{\text{max}}=0.6\text{MeV}$) was low^[17-22]. So scientists have searched for more effective radioisotope. Rhenium-188 is of particular interest to this study as the ^{188}Re may be obtained from the $^{188}\text{W}/^{188}\text{Re}$ generator, and ^{188}Re decays by β - emission with energies ($E_{\text{max}}=2.12\text{MeV}$) similar to ^{90}Y and γ photons ($E_{\gamma}=155\text{keV}$; abundance=15%) that are useful for dosimetry calculations and radioimmunoinaging, with a half-time of 17h. Furthermore, ^{188}Re has chemical properties similar to ^{99}Tc m, thus it can be conjugated to antibodies modeling on ^{99}Tc m labeling methods using direct or indirect method^[23-29]. Direct methods require attaching the reduced form of Re to the endogenous thiols of antibodies, whereas indirect methods require the reduced Re to be complexed by a bifunctional chelator that is conjugated to the antibody^[30-32]. There has been considerable interest in the direct labeling of mAb, which would result in the formation of an instant kit formulation for imaging or therapy.

^{188}Re can be provided at reasonable costs for routine preparation of radiopharmaceuticals for cancer treatment. ^{188}Re is an important therapeutic radioisotope which is obtained on demand as carrier-free sodium perrhenate by saline elution of the tungsten-188/rhenium-188 generator system. Because of its prominent physical characters, ^{188}Re will become a new therapeutic isotope. ^{188}Re is a radioisotope currently under evaluation for a variety of therapeutic application, including that for metastatic bone pain and therapy in oncology.

The HAb18 antibody is a murine IgG₁ anti-hepatoma monoclonal antibody under investigation in our laboratory. It does not cross react with normal liver cells, and only rarely with other malignant tissues. Due to the smaller size, easier penetration into tumor tissues, rapid clearance from circulation, and less human anti-mouse antibody (HAMA) reaction, F(ab')₂ fragments showed that tumor localization is faster and better than the intact antibody. Previous studies of ^{99}Tcm labeled with HAb18 F(ab')₂ indicated that the conjugate is effective to detect hepatoma in the nude mice model^[33]. The results encourage us to continue the radioimmunotherapy for hepatoma using ^{188}Re labeled with HAb18 F(ab')₂. we have studied the pharmacokinetics of ^{188}Re -HAb18 F(ab')₂ in hepatoma-bearing nude mice in order to prove if ^{188}Re -HAb18 F(ab')₂ was located specially in hepatoma, to establish the pharmacokinetic model and get the parameters of pharmacokinetics.

MATERIALS AND METHODS

Animals

Five-week Balb/c nude mice (derived from Experimental Animals Center of our university) were implanted with 1×10^7 (0.2mL) human hepatocellular carcinoma (HCC) cells in the right thigh. When the diameter of the tumors reached 1cm, the tumor bearing mice would be investigated further.

Monoclonal antibody fragment

HAb18 F(ab')₂ fragment was generated by pepsin digestion and phenyl-sepharose HP column purification with a relative molecular mass of 110,000. The solution containing the antibody fragment was concentrated by lypholization and reconstituted with distilled water.

Isotope

A 7.4GBq $^{188}\text{W}/^{188}\text{Re}$ generator was eluted with normal saline.

Radiolabeling

The antibody concentrated at $5\text{g}\cdot\text{L}^{-1}$ was reduced by reaction with a molar excess of 2-ME at 4°C for 20-30 min. The reduced antibody was isolated from reductant through a PD-10 column (Pharmacia) equilibrated with $0.05\text{mol}\cdot\text{L}^{-1}$ acetate-buffered saline.

For labeling, the reduced HAb18 F(ab')₂ was mixed with glucoheptonate (GH) solution, SnCl_2 solution, and $50\text{-}100\mu\text{L}$ perhenium solution for 2-3 h at 37°C before it was analyzed by Whatman 3MM paper chromatography which was then developed in $100\text{g}\cdot\text{L}^{-1}$ trichloroacetic acid (TCA). R^a-f (distance of some composition moved/distance of extended reagent moved) values for $100\text{g}\cdot\text{L}^{-1}$ TCA are: mAb 0.0, ^{188}Re -GH 0.7, and $^{188}\text{ReO}_4$ 0.7. Labeled mAb was differentiated from ^{188}Re colloid by the method of Thrall *et al* [33]. The same strips impregnated with $10\text{-}20\text{g}\cdot\text{L}^{-1}$ human serum albumin before development with 5V:2V:1V; water: ethanol: $5\text{mol}\cdot\text{L}^{-1}$ NH_4OH (volum ratio). Colloid remained on the bottom of the strip while mAb-bound isotope migrated with the solvent front.

Immunoreactivity assessment

The *in vitro* immunoreactivity of the radiolabeled HAb18 F(ab')₂ was evaluated by a live cell assay [9]. Briefly, $5\times 10^9\cdot\text{L}^{-1}$ HCC cells were centrifuged at $1000\text{r}\cdot\text{min}^{-1}$ for 5 min and washed twice with $1\text{g}\cdot\text{L}^{-1}$ bovine serum albumin (BSA) in PBS, then 5 serial 1:2 dilutions were made up in $10\text{g}\cdot\text{L}^{-1}$ BSA in Eppendorf tubes precoated with BSA. Radiolabeled HAb18 F(ab')₂ at a mass concentration of $40\mu\text{g}\cdot\text{L}^{-1}$ in $10\text{g}\cdot\text{L}^{-1}$ BSA was added using a volume equal to half the volume of cell suspension. The total volume of cell-binding assay solution was 0.3 mL. After incubation for 2 h at 37°C , the total as well as the cell-bound radioactivity were counted in a gamma counter.

Study of biodistribution in nude mice

Fifteen hepatoma-bearing nude mice were divided into 5 groups randomly, the mice were tail-vein injected via tail vein with $1.85\text{MBq }^{188}\text{Re}$ -HAb18 F(ab')₂ in a volume of 0.1 mL and then they were sacrificed at 1, 4, 18, 24 and 48h (3 mice at each time). Samples of tumor, heart, liver, spleen, lung, kidney, large intestine, small intestine, muscle, bone were taken and weighed carefully. In addition, the blood sample was drawn from the heart. The radioactive concentrations in tissues were calculated and expressed as percent injected dose per gram (%ID·g⁻¹). The radioactivity of tumor/no tumor (T/NT) was also calculated.

Pharmacokinetics

The concentrations of blood and other organs were mounted by 3P97 software to get the parameters of pharmacokinetics and established the mode of pharmacokinetics was established.

RESULTS

Table 1 shows the biodistribution of ^{188}Re -HAb18 F(ab')₂. The blood concentration was measured by 3P97 software, which fits the 1-compartment model (Table 3). Figure 1 shows the curve of concentration-time in nude mice, and Table 2 shows the parameters of pharmacokinetics. The half-time (h) of each tissue was: tumor (32.99), blood (2.99), lung (5.67), bone (11.76), muscle (9.22), small intestine (7.47), large intestine (15.08), heart (2.29), liver (5.67), spleen (19.76), and kidney (11.53). Table 4 illustrates the influence of various concentrations of SnCl_2 and GH on the free $^{188}\text{ReO}_4$ amounts, colloid amounts and labeling efficiency.

Optimal complexation with labeling efficiency of 91.7% was achieved in $0.8\text{mol}\cdot\text{L}^{-1}$ GH and $2\text{g}\cdot\text{L}^{-1}$ SnCl_2 solution. As shown in Figure 2, the immunoreactive fraction, 0.78 was determined by plotting the inverse of the bound fraction as compared with the inverse of the cell concentration, which is based on the assumption that the total antigen concentration (i.e., cell density) is a good approximation for the free antigen concentration.

Table 1 Biodistribution of ^{188}Re -HAb18 F(ab')₂ in hepatoma-bearing nude mice

Tissue	T(post-inj)/h	^{188}Re -HAb18 F(ab') ₂	
		%ID·g ⁻¹ ($\bar{x}\pm s$)	T/NT ratio
Tumor	1	3.01 ± 0.89	ND
	4	3.94 ± 0.82	ND
	18	3.43 ± 0.28	ND
	24	1.96 ± 0.43	ND
	48	0.99 ± 0.32	ND
Blood	1	4.58 ± 0.63	0.66
	4	1.83 ± 0.10	2.15
	18	0.21 ± 0.04	16.30
	24	0.18 ± 0.03	10.90
	48	0.05 ± 0.01	19.80
Heart	1	1.60 ± 0.38	1.88
	4	0.80 ± 0.10	4.92
	18	0.36 ± 0.03	9.53
	24	0.30 ± 0.02	6.53
	48	0.21 ± 0.03	4.71
Liver	1	2.07 ± 0.40	1.45
	4	1.57 ± 0.31	2.51
	18	0.77 ± 0.12	4.45
	24	0.66 ± 0.10	2.97
	48	0.47 ± 0.13	2.11
Spleen	1	1.22 ± 0.25	2.47
	4	0.91 ± 0.22	4.33
	18	0.47 ± 0.07	7.30
	24	0.45 ± 0.08	4.36
	48	0.41 ± 0.10	2.40
Lung	1	1.45 ± 0.23	2.08
	4	0.86 ± 0.29	4.58
	18	0.19 ± 0.04	18.10
	24	0.18 ± 0.04	10.90
	48	0.14 ± 0.05	7.07
Kidney	1	59.81 ± 14.52	0.05
	4	47.83 ± 12.87	0.08
	18	18.72 ± 4.94	0.18
	24	15.80 ± 0.99	0.12
	48	7.31 ± 2.10	0.13
Large intestine	1	1.36 ± 0.38	2.21
	4	0.93 ± 0.24	4.24
	18	0.57 ± 0.06	6.02
	24	0.45 ± 0.00	4.36
	48	0.18 ± 0.03	5.50
Small intestine	1	1.61 ± 0.43	1.87
	4	0.88 ± 0.29	4.24
	18	0.33 ± 0.05	10.40
	24	0.29 ± 0.05	6.76
	48	0.13 ± 0.05	7.62
Muscle	1	0.74 ± 0.29	4.07
	4	0.44 ± 0.12	8.95
	18	0.19 ± 0.08	18.10
	24	0.16 ± 0.06	12.25
	48	0.05 ± 0.02	19.80
Bone	1	1.03 ± 0.31	2.92
	4	0.68 ± 0.12	5.79
	18	0.31 ± 0.09	11.06
	24	0.27 ± 0.02	7.26
	48	0.16 ± 0.02	6.19

ND: not done

Table 2 Pharmacokinetic parameters of ¹⁸⁸Re-HAb18 F(ab')₂ in hepatoma-bearing nude mice

Parameter	Unit	Value	Standard error
C0	1×10 ⁹ Bq·L ⁻¹	6.18	3.14E-01
Ke	h ⁻¹	0.30	2.88E-02
Vd	1×10 ⁻⁹ L·Bq ⁻¹	1.49	
T _{1/2} (Ke)	h	2.29	
AUC	1×10 ⁹ Bq·h·L ⁻¹	20.49	
CL	1×10 ⁻³ L·h ⁻¹	0.45	

CO: Concentration at zero time Ke: Elimination rate constant

Vd: Apparent volume of distribution T_{1/2}: Half-life time

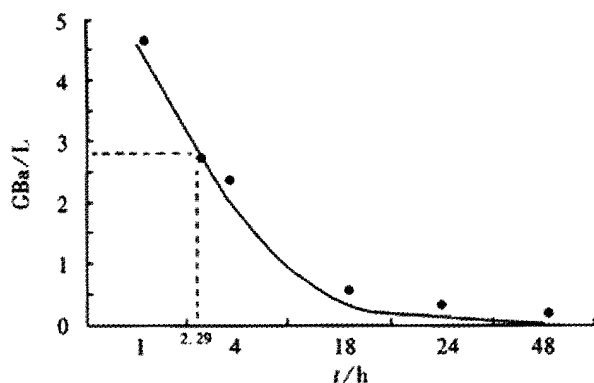
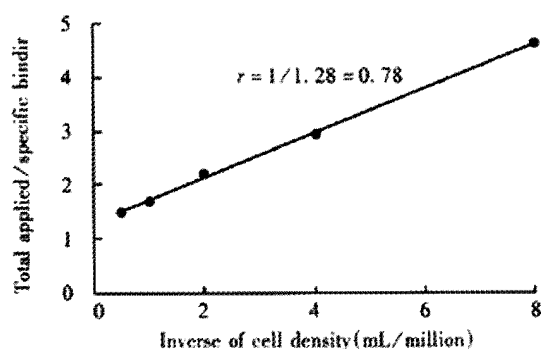
AUC: Area under the curve CL: Clearance

Table 3 Criteria for goodness of fitting for mean

REC No.	Mean No	WT	No. of camp	Weighted sum of squarers	R	R Squares	Goodness of fit	Max error C-CI	Max error %	AIC
1	1	1	1	0.672E-01	0.9993	0.9955	0.150	0.18	100.00	-9.499
2	1	1/c	1	0.329E+00	0.9856	0.9781	0.331	0.52	99.1	-1.560
3	1	1/cc	1	0.119E+01	0.9200	0.9207	0.630	3.58	78.2	4.877

Table 4 Effect of various concentration of SnCl₂ and GH on free ¹⁸⁸ReO₄ amounts, colloid amounts and labeling efficiency

Concentration		¹⁸⁸ ReO ₄	Colloid	Labeling efficiency(%)
aSnCl ₂ (g·L ⁻¹)	8	0.3	3.6	90.9
	4	0.4	2.8	90.1
	2	9.7	2.1	82.7
	1	21.8	1.2	71.2
bGH (mol·L ⁻¹)	0.8	1.1	1.1	91.7
	0.4	12.5	2.5	78.8
	0.2	16.6	2.8	72.7
	0.1	20.6	4.1	71.3

^aMolar ratio of 2-ME: F(ab')₂ = 400:1, Concentration of GH=0.5 mol·L⁻¹^bMolar ratio of 2-ME: F(ab')₂ = 400:1, Concentration of SnCl₂=2 g·L⁻¹**Figure 1** Concentration-time curve of ¹⁸⁸Re-HAb18 F(ab')₂ in nude mice**Figure 2** Binding assay for determination of immunoreactive fraction of ¹⁸⁸Re-labeled HAb18 F(ab')₂

DISCUSSION

The occurrence of hepatoma is high in Southeast Asia, East Africa and Middle Africa. In China, hepatoma is one of the most three common cancers related death, but there is no effective treatment^[34-45]. The therapy of hepatoma includes surgical operation, chemotherapy and radiotherapy. Targeting diagnosis and therapy of hepatoma with anti-hepatoma Mab have been developed quickly, giving a hopeful prospect to hepatoma treatment. Our research focuses on the targeting therapy of hepatoma.^[46-48] ¹⁸⁸Re is a generator-produced radioisotope which can be obtained. There were some studies on the biodistribution and pharmacokinetics of ¹⁸⁸Re-mAb. Safavy *et al*^[49] have reported biodistribution of ¹⁸⁸Re-labeled trisuccin-HuCC49 and trisuccin-C49deltaCh2 conjugates in athymic nude mice bearing intraperitoneal colon cancer xenografts. ¹⁸⁸Re-labeled mAb was injected, and the mice were sacrificed 24h postinjection. Biodistribution of the radiolabeled mAb at 24h after injection showed median tumor uptake values of 23.5% ID·g⁻¹ and 17.6% ID·g⁻¹ for the ¹⁸⁸Re-C49deltaCh2 and ¹⁸⁸Re-HuCC49, respectively. Yang *et al*^[50] have prepared the conjugate of staphylococcal enterotoxin A (SEA) protein which is a bacterial Sag and the F(ab')₂ fragment of HAb18. The F(ab')₂ fragment of mAb HAb18 was prepared by papainic digestion method. The conjugate of mAb HAb18 F(ab')₂ fragment and SEA was prepared with chemical conjugating reagent N-succinimidyl-1-(3-(2-pyridyldithio) propionate (SPDP) and purified through chromatography column Superose 12 with FPLC system. The molecular mass was identified with SDS-PAGE assay, the antibody activity of in the conjugate was determined by indirect immunocytochemical ABC method. SEA is a protein, the method of labeling is indirect, SEA and antibody are conjugated by SPDP. ¹⁸⁸Re's labeling method is direct, it is more convenient and quicker than indirect method. In the animal experiment, ¹⁸⁸Re-HAb18F(ab')₂ can inhibit the growth of tumor, but the pharmacokinetics of ¹⁸⁸Re-HAb18F(ab')₂ in animal is seldom reported.

¹⁸⁸Re-HAb18F(ab')₂ can last a long time at a high level (Table 1). The maximal ratio of tumor: blood was at 48h, and maximal ratio of tumor: liver was at 18h. From Table 1, we can also find that after 1, 4, and 24 h (iv) injection, the radio percent of tumor is 3.83%, 6.48%, and 9.74%, the liver is 1.64%, 2.59% and 3.19%, the kidney is 76.24%, 78.8% and 76.3% respectively, showing that the antibody and its fragments were eliminated from kidney^[51-52]. The half-time of ¹⁸⁸Re-HAb18 F(ab')₂ in the tumor was 32.99h, it was longer in tumor than that in other organs, this indicated that ¹⁸⁸Re-HAb18 F(ab')₂ was located in tumor, the rate of decay was low. It also showed that the mAb was specifically combined with tumor tissues and its harmness to normal tissues was low. Pharmacokinetic parameters (AUC, blood clearance, half-life, etc) were generated using the 3P97 software.

From 3P97 software, we can see the pharmacokinetics of conform to a 1-compartment model. Table 3 shows the criteria for goodness of fitting. we can judge the compartments from R squares, goodness of fit and AIC. 1, 1/C, 1/C/C represented three weights. To the same weight, when the F test has marked significance ($P < 0.05$ or $P < 0.01$), we should choose the compartment of small AIC, and when the F test has not prominent significance ($P > 0.05$), we should choose the small compartment.^[53] From Table 3, it can be seen that the 1-compartment model is the best. ¹⁸⁸Re-HAb18 F(ab')₂ can distribute to the whole body instantly. The elimination rate was corresponded to the concentration of the drug. The higher the concentration was, the higher the speed of elimination was.

The half-time was 32.99h in tumor, being much longer than that in any other organs. It showed that ¹⁸⁸Re-HAb18 F(ab')₂ was located specifically in hepatoma and the elimination was low. It also showed the higher selective reactivity of HAb18 F(ab')₂ with hepatoma, the

harmness to other organs was small. The half-time was 2.29h in blood, and was 32.99h in tumor, the radioation of blood can decrease more rapidly than that of the tumor. The half-time of ^{188}Re was 17h, which was also lower than that in blood, so the ^{188}Re can be eliminated through the blood. It has excellent value in the clinical therapy.^[54-62]

Carrier-free ^{188}Re is one of β emitting radionuclides recommended for RAIT because of suitable decay characteristics and availability from $^{188}\text{W}/^{188}\text{Re}$ generator. Some methods are reported in the literature for labeling mAb with ^{188}Re which imitate the labeling method of ^{99}Tcm . ^{188}Re eluted from generator will not bind to organic ligands without reduction to a lower oxidation state. We selected SnCl_2 as reductant and GH as transfer ligand and stablizer to avoid Sn- or Re-collide formation. Table 1 shows that the concentration of SnCl_2 and GH solutions is an important parameter to obtain good labeling results. The low percentage of free $^{188}\text{ReO}_4$ and radiocolloid shows that $0.8 \text{ mol} \cdot \text{L}^{-1}$ GH and $2 \text{ g} \cdot \text{L}^{-1}$ SnCl_2 are the optimal values. Under these conditions, the labeled HAb18 F(ab')₂ keeps its immunoreactivity (Figure 2).

We believe that a variety of factors make ^{188}Re a potential alternative to other β -emitting radionuclides for RAIT. They include an efficient generator system and the direct labeling of IgG at high specific activity. The enhanced clearance of ^{188}Re -IgG from the circulation and the retention of immunoreactivity and tumortargeting of the Re-mAb conjugate are also important factors. In addition, the low-energy (155keV, 15%) γ emission for imaging and the lack of accretion of metabolic products in nontarget tissues are important characteristics for further evaluation of ^{188}Re -labeled antibodies for tumor therapy.

REFERENCES

- Guhlke S, Beets AL, Oetjen K, Mirzadeh S, Biersack HJ, Knapp FF Jr. Simple new method for effective concentration of ^{188}Re solutions from alumina-based $^{188}\text{W}/^{188}\text{Re}$ generator. *J Nucl Med* 2000; 41: 1271-1278
- Jeong JM, Lee YJ, Kim YJ, Chang YS, Lee DS, Chung JK, Song YW, Lee MC. Preparation of rhenium-188-tin colloid as a radiation synovectomy agent and comparison with rhenium-188-sulfur colloid. *Appl Radiat Isot* 2000; 52: 851-855
- Kotzerke J, Glatting G, Seitz U, Rentschler M, Neumaier B, Bunjes D, Duncker C, Dohr D, Bergmann L, Reske-SN. Radioimmunotherapy for the intensification of conditioning before stem cell transplantation: differences in dosimetry and biokinetics of ^{188}Re - and $^{99\text{m}}\text{Tc}$ -labeled anti-NCA-95 mAbs. *J Nucl Med* 2000; 41: 531-537
- Sykes TR, Somayaji VV, Bier S, Woo TK, Kwok CS, Snieckus V, Noujaim AA. Radiolabeling of monoclonal antibody B43.13 with rhenium-188 for immunoradiotherapy. *Appl Radiat Isot* 1997; 48: 899-906
- Sharkey RM, Blumenthal RD, Behr TM, Wong GY, Haywood L, Forman D, Griffiths GL, Goldenberg DM. Selection of radioimmunoconjugates for the therapy of well-established or micrometastatic colon carcinoma. *Int J Cancer* 1997; 72: 477-485
- Roka R, Sera T, Pajor L, Thurzo L, Lang J, Csernay L, Pavics L. Clinical experience with rhenium-188 HEDP therapy for metastatic bone pain. *Orv Hetil* 2000; 141: 1019-1023
- Wunderlich G, Pinkert J, Andreeff M, Stintz M, Knapp FF Jr, Kropp J, Franke WG. Preparation and biodistribution of rhenium-188 labeled albumin microspheres B 20: a promising new agent for radiotherapy. *Appl Radiat Isot* 2000; 52: 63-68
- Zimmerman BE, Cessna JT, Unterweger MP, Li AN, Whiting JS, Knapp FF Jr. A new experimental determination of the dose calibrator setting for ^{188}Re . *J Nucl Med* 1999; 40: 1508-1516
- Knapp FF Jr. Rhenium-188-a generator-derived radioisotope for cancer therapy. *Cancer Biother Radiopharm* 1998; 13: 337-349
- Hafeli UO, Roberts WK, Meier DS, Ciezki JP, Pauer GJ, Lee EJ, Weinhaus MS. Dosimetry of a W-188/Re-188 beta line source for endovascular brachytherapy. *Med Phys* 2000; 27: 668-675
- Juwied M, Sharkey RM, Swayne LC, Griffiths GL, Dunn R, Goldenberg DM. Pharmacokinetics, dosimetry and toxicity of rhenium -188-labeled anti-carcinoembryonic antigen monoclonal antibody, MN-14, in gastrointestinal cancer [see comments]. *J Nucl Med* 1998; 39: 34-42
- Junfeng Y, Duanzhi Y, Xiaofeng M, Zili G, Jiong Z, Yongxian W, Knapp FF Jr. ^{188}Re Rhenium sulfide suspension: a potential radiopharmaceutical for tumor treatment following intra-tumor injection. *Nucl Med Biol* 1999; 26: 573-579
- Chen J, Gliblin MF, Wang N, Jurisson SS, Quinn TP. In vivo evaluation of $^{99\text{m}}\text{Tc}/^{188}\text{Re}$ -labeled linear alpha-melanocyte stimulating hormone analogs for specific melanoma targeting. *Nucl Med Biol* 1999; 26: 687-693
- Iznaga-Escobar N. ^{188}Re -direct labeling of monoclonal antibodies for radioimmunotherapy of solid tumors: biodistribution, normal organ dosimetry, and toxicology. *Nucl Med Biol* 1998; 25: 441-447
- Palmedo H, Guhlke S, Bender H, Sartor J, Schoeneich G, Risse J, Grunwald F, Knapp FF Jr, Biersack HJ. Dose escalation study with rhenium-188 hydroxyethylidene diphosphonate in prostate cancer patients with osseous metastases. *Eur J Nucl Med* 2000; 27: 123-130
- Melendez Alafort L, Ferro Flores G, Arteaga Murphy C, Pedraza Lopez M, Gonzalez Zavala MA, Tendilla JJ, Garcia Salinas L. Labeling peptides with rhenium-188. *Int J Pharm* 1999; 182: 165-172
- van Zanten Przybysz I, Molthoff CF, Ross JC, Plaizier MA, Visser GW, Pijpers R, Kenemans P, Verheijen RH. Radioimmunotherapy with intravenously administered ^{131}I -labeled chimerical monoclonal antibody Mov18 in patients with ovarian cancer. *J Nucl Med* 2000; 41: 1168-1176
- Behr TM, Behe M, Lohr M, Sgouros G, Angerstein C, Wehrmann E, Nebendahl K, Becker W. Therapeutic advantages of Auger electron-over beta-emitting radiometals radioiodine when conjugated to internalizing antibodies. *Eur J Nucl Med* 2000; 27: 753-756
- Clarke K, Lee FT, Brechbiel MW, Smyth FE, Old LJ, Scott AM. Therapy efficacy of anti-Lewis(y) humanized 3S193 radioimmunotherapy a breast cancer model: enhanced activity when combined with taxol chemotherapy. *Clin Cancer Res* 2000; 6: 3621-3628
- Barendswaard EC, O'Donoghue JA, Larson SM, Tschmelitsch J, Welt S, Finn RD, Humm JL. ^{131}I radioimmunotherapy and fractionated external beam radiotherapy: comparative effectiveness in a human tumor xenograft. *J Nucl Med* 1999; 40: 1764-1768
- Smith Jones PM, Vallabhaiah S, Goldsmith SJ, Navarro V, Hunter CJ, Bastidas D, Bander NH. In vitro characterization of radiolabeled monoclonal antibodies specific for the extracellular domain of prostate-specific membrane antigen. *Cancer Res* 2000; 60: 5237-5243
- Juwied ME, Zhang CH, Blumenthal RD, Hajjar G, Sharkey RM, Goldenberg DM. Prediction of hematologic toxicity after radioimmunotherapy with ^{131}I -labeled anticarcinoembryonic antigen monoclonal antibodies. *J Nucl Med* 1999; 40: 1609-1616
- Natowich DJ, Mardirossian G, Ruscowski M, Fogarasi M, Virzi F, Winnard Jr P. Directly and indirectly technetium-99m-labeled antibodies-a comparison of *in vitro* and animal *in vivo* properties. *J Nucl Med* 1993; 34: 109-119
- Colnot DR, Quak JJ, Roos JC, van Lingen A, Wilhelm AJ. Phase I therapy study of ^{186}Re -labeled chimeric monoclonal antibody U36 in patients with squamous cell carcinoma of the head and neck. *J Nucl Med* 2000; 41: 1999-2010
- Lechner P, Lind P, Snyder M, Haushofer H. Probe-guided surgery for colorectal cancer. *Recent Results Cancer Res* 2000; 157: 273-280
- Willkomm P, Bender H, Bangard M, Decker P, Grunwald F, Biersack HJ. FDG PET and immunoscintigraphy with $^{99\text{m}}\text{Tc}$ -labeled antibody fragments for detection of the recurrence of colorectal carcinoma. *J Nucl Med* 2000; 41: 1657-1663
- Line BR, Weber PB, Lukasiewicz R, Dansereau RN. Reduction of background activity through radiolabeling of antifibrin Fab' with $^{99\text{m}}\text{Tc}$ -dextran. *J Nucl Med* 2000; 41: 1264-1270
- Amato R, Kim EE, Prow D, Andreopoulos D, Kasi LP. Radioimmunodetection of residual, recurrent or metastatic germ cell tumors using technetium-99 anti-(alpha-fetoprotein) Fab' fragment. *J Cancer Res Clin Oncol* 2000; 126: 161-167
- Bian HJ, Chen ZN and Deng JL. Direct technetium-99m labeling of anti-hepatoma monoclonal antibody fragment: a radioimmunoconjugate for hepatocellular carcinoma imaging. *World J Gastroenterol* 2000; 6: 348-352
- Dadachova E, Chapman J. ^{188}Re (V)-DMSA revisited: preparation and biodistribution of a potential radiotherapeutic agent with low kidney uptake. *Nucl Med Commun* 1998; 19: 173-181
- Schmidt PF, Smith SV and Bundesen PG. ^{188}Re DD-3B6/22 Fab' for use in therapy of ovarian cancer: labeling and animal studies. *Nucl Med Biol* 1998; 25: 639-649
- Ferro-Flores G, Pimentel-Gonzalez G, Gonzalez-Zavala MA, Arteaga de Murphy C, Melendez Alafort L, Tendilla JJ, Croft BY. Preparation, biodistribution, and dosimetry of ^{188}Re -labeled McAb ior ceal and its F(ab')₂ fragments by avidin-biotin strategy. *Nucl Med Biol* 1999; 26: 57-62
- Thrall JH, Freitas JE, Swanson D, Rogers WL, Clare JM, Brown M, Pitt B. Clinical comparison of cardiac blood pool visualization with technetium-99m red blood cells labeled *in vivo* and with technetium-99m human serum albumin. *J Nucl Med* 1978; 19: 796-803
- Qian S B, Li Y, Qian GX, Chen SS. Efficient tumor regression induced by genetically engineered tumor cells secreting interleukin-2 and membrane-

- expressing allogeneic MHC class I antigen. *J Cancer Res Clin Oncol* 2001; 127: 27-33
- 35 Dai WJ, Jiang HC. Advances in gene therapy of liver cirrhosis: a review. *World J Gastroenterol* 2001;7:1-8
 - 36 Cheng ML, Wu YY, Huang KF, Luo TY, Ding YS, Lu YY, Liu RC, Wu J. Clinical study on the treatment of liver fibrosis due to hepatitis B by IFN- α 1 and traditional medicine preparation. *World J Gastroenterol* 1999;5:267-269
 - 37 Kessel D, Caruso JA, Reiners JJ Jr. Potentiation of photodynamic therapy by ursodeoxycholic acid. *Cancer Res* 2000; 60: 6985-6988
 - 38 Yang SS, Wu CH, Chen TH, Huang YY, Huang CS. TT viral infection through blood transfusion: retrospective investigation on patients in a prospective study of post transfusion hepatitis. *World J Gastroenterol* 2000;6:70-73
 - 39 Kang MA, Kim KY, Seol JY, Kim KC, Nam MJ. The growth inhibition of hepatoma by gene transfer of antisense vascular endothelial growth factor. *J Gene Med* 2000; 2: 289-296
 - 40 Ma XD, Sui YF, Wang WL. Expression of gap junction genes connexin 32, connexin 43 and their proteins in hepatocellular carcinoma and normal liver tissues. *World J Gastroenterol* 2000;6:66-69
 - 41 Huang ZH, Zhuang H, Lu S, Guo RH, Xu GM, Cai J, Zhu WF. Humoral and cellular immunogenicity of DNA vaccine based on hepatitis B core gene in rhesus monkeys. *World J Gastroenterol* 2001;7:102-106
 - 42 Fang JN, Jin CJ, Cui LH, Quan ZY, Choi BY, Ki MR, Park HB. A comparative study on serologic profiles of virus hepatitis B. *World J Gastroenterol* 2001;7:107-110
 - 43 Tietze MK, Wuestefeld T, Paul Y, Zender L, Trautwein C, Manns MP, Kubicka S. IkappaBalpha gene therapy in tumor necrosis factor-alpha- and chemotherapy-mediated apoptosis of hepatocellular carcinomas. *Cancer Gene Ther* 2000; 7: 1315-1323
 - 44 Xu J, Mei MH, Zeng SE, Shi QF, Liu YM, Qin LL. Expressions of ICAM21 and its mRNA in sera and tissues of patients with hepatocellular carcinoma. *World J Gastroenterol* 2001;7:120-125
 - 45 Hu YP, Hu WJ, Zheng WC, Li JX, Dai DS, Wang XM, Zhang SZ, Yu HY, Sun W, Hao GR. Establishment of transgenic mouse harboring hepatitis B virus (adr subtype) genomes. *World J Gastroenterol* 2001;7: 111-114
 - 46 Qiu K, Wang BF, Chen ZN, Fang P, Liu CG, Wan WX, Liu YF. ^{99m}Tc-labeled HAb18 McAb Fab fragment for radioimmunodiagnosis in nude mice bearing human hepatocellular carcinoma. *World J Gastroenterol* 1998;4:117-120
 - 47 Chen ZN, Bian HJ, Jiang JL. Recent progress in anti-hepatoma monoclonal antibody and its application. *Huaren Xiaohua Zazhi* 1998;6:461-462
 - 48 Ickman S. Antibodies stage a comeback in cancer treatment. *Science* 1998;280:1196-1197
 - 49 Safavy A, Khazaeli MB, Safavy K, Mayo MS, Buchsbaum DJ. Biodistribution study of ¹⁸⁸Re-labeled trisuccin-HuCC49 and trisuccin-HuCC49deltaCh2 conjugates in athymic nude mice bearing intraperitoneal colon cancer xenografts. *Clin Cancer Res* 1999; 5: 2994-3000
 - 50 Yang LJ, Sui YF, Chen ZN. Preparation and activity of conjugate of monoclonal antibody HAb18 against hepatoma F(ab')₂ fragment and staphylococcal enterotoxin A. *World J Gastroenterol* 2001;7:216-221
 - 51 Duan XD, Chen ZN, Bian HJ, Wen AD, Feng Q. Pharmacokinetics of technetium-99m labeled anti-hepatoma monoclonal antibody HAb18 and its F(ab')₂ fragment in mice. *Zhongguo Yaowu Xue Zazhi* 2000;35:465-467
 - 52 Chen H, Gu SF, Xiao Zh, Zeng FD, Wu WZ, Zhang QH. Pharmacokinetics and bioavailability of sustained release capsules of nicardipine hydrochloride in healthy volunteers. *Zhongguo Yaolixue Tongbao* 2000; 16:107-110
 - 53 Lan Q, Huang Q, Zhuang DL, Wu YF, Sun ZF. Study on the pharmacokinetics of immunoradiotherapeutic agent S-MAb SZ39 in glioma-bearing nude mice. *Zhongguo Yaowu Xue Zazhi* 1999;34:683-686
 - 54 Hosono MN, Hosono M, Zamora PO. Localization of colorectal carcinoma by rhenium-188-labeled B72.3 antibody in xenograft mice. *Ann Nucl Med* 1998; 12:83-88
 - 55 Gustin JF, Loussouarn A, Bardies M, Gautherot E, Gruaz Guyon A, Sai Maurel C, Barbet J, Curtet C, Chatal JF, Faivre Chauvet A. Two-step targeting of xenografted colon carcinoma using a bispecific antibody and ¹⁸⁸Re-labeled bivalent hapten: biodistribution and dosimetry studies. *J Nucl Med* 2001; 42: 146-153
 - 56 Hosono MN, Hosono M, Mishra AK, Faivre Chauvet A, Gautherot E, Barbet J, Knapp F F, Chatal JF. Rhenium-188-labeled anti-neural cell adhesion molecule antibodies with 2-iminothiolane modification for targeting small-cell lung cancer. *Ann Nucl Med* 2000; 14: 173-179
 - 57 Bian HJ, Chen ZN, Lou C, Mi L, Wang J, Yue XL. ¹⁸⁸Re-labeled HAb18 F(ab')₂ of hepatoma radioimmunodiagnosis. *Zhongliu* 2000; 20:181-183
 - 58 Qingnuan L, Xiaodong Z, Rong S, Wenxin L. Preparation of (¹⁸⁸Re) Re-AEDP and its biodistribution studies. *Appl Radiat Isot* 2000; 53: 993-997
 - 59 Kostarelos K, Emfietzoglou D. Tissue dosimetry of liposome-radionuclide complexes for internal radiotherapy: toward liposome-targeted therapeutic radiopharmaceuticals. *Anticancer Res* 2000; 20: 3339-3345
 - 60 Iznaga Escobar N, Torres LA, Morales A, Ramos M, Alvarez I, Perez N, Fraxedas R, Rodriguez O, Rodriguez N, Perez R, Lage A, Stabin MG. Technetium-99m-labeled anti-EGF-receptor antibody in patients with tumor of epithelial origin: I. Biodistribution and dosimetry for radioimmunotherapy. *J Nucl Med* 1998; 39: 15-23
 - 61 Blower PJ, Kettle AG, O'Doherty MJ, Coakley AJ, Knapp FF. ^{99m}Tc (V)DMSA quantitatively predicts ¹⁸⁸Re(V)DMSA distribution in patients with prostate cancer metastatic to bone. *Eur J Nucl Med* 2000; 27: 1405-1409
 - 62 Heppeler A, Froidevaux S, Eberle AN, Maecke HR. Receptor targeting for tumor localisation and therapy with radiopeptides. *Curr Med Chem* 2000; 7: 971-994

Edited by Ma JY

• GASTRIC CANCER •

High-dose Iodized Oil Transcatheter Arterial Chemoembolization For Patients with Large Hepatocellular Carcinoma

Min-Shan Chen, Jin-Qing Li, Ya-Qi Zhang, Li-Xia Lu, Wei-Zhang Zhang, Yun-Fei Yuan, Yong-Ping Guo, Xiao-Jun Lin, Guo-Hui Li

Min-Shan Chen, Jin-Qing Li, Ya-Qi Zhang, Yun-Fei Yuan, Yong-Ping Guo, Xiao-Jun Lin, Guo-Hui Li, Department of Hepatobiliary Cancer Center of Sun Yet-sen University of Medical Sciences, Guangzhou 510060, China

Li-Xia Lu, Wei-Zhang Zhang, Department of Radiology Cancer Center of Sun Yet-sen University of Medical Sciences, Guangzhou 510060, China

Supported by the "9-5" National Major Project of National Committee of Sciences and Technology, No.96-907-03-02

Correspondence to: Dr. Min-Shan Chen, Department of Hepatobiliary Cancer Center of Sun Yet-sen University of Medical Sciences, 651 Dongfeng Road East, Guangzhou 510060, China. Minshan@8848.net
Telephone: +86-13902241061 Fax: +86-20-87754506

Received 2001-08-23 Accepted 2001-09-08

Abstract

AIM: To conduct a randomized trial to evaluate the role of using high-dose iodized oil transcatheter arterial chemoembolization (TACE) in the treatment of large hepatocellular carcinoma (HCC).

METHODS: From January 1993 to June 1998, 473 patients with unresectable hepatocellular carcinoma were divided into two groups: 216 patients in group A received more than 20mL iodized oil during the first TACE treatment; 257 patients in group B received 5-15mL iodized oil in the same way. The Child's classification and ICG-R15 for evaluating the liver function of the patients were done before the treatment. During the TACE procedure the catheters was inserted into the target artery selectively and the tumor vessels were demonstrated with contrast medium in the hepatic angiography. The anticancer drug mixed with iodized oil (Lipiodol) were Epirubicin and Mitomycin. In group A, 112 cases received 20-29mL Lipiodol in the first procedure, 85 cases 30-39mL, 19 cases more than 40mL. The largest dose was 53 mL and the average dose was 28.3mL. In group B, 119 cases received 5-10mL Lipiodol, 138 cases received 11-15mL, and the average dose was 11.8mL.

RESULTS: High-dose Lipiodol chemoembolization caused tolerable side effects and a little hurt to the liver function in the patients with Child grade A or ICG-R15 <20. But the patients with child grade B or ICG-R15 >20 had higher risk of liver failure after high-dose TACE. More type I and type II lipiodol accumulations in CT scan after 4 weeks of TACE were seen in the group A patients than those in the group B patients ($P < 0.01$). The resection rate and complete tumor necrosis rate in group A were higher than those of group B ($P < 0.05$). The 1-, 2-, 3-year survival rates of group A patients with Child grade A were 79.2%, 51.8% and 34.9%, respectively, better than those of group B ($P < 0.001$).

CONCLUSION: High-dose Lipiodol can result in more complete tumor necrosis by blocking both arteries and small

portal vein of the tumor. High-dose TACE for treatment of large and hypervascular hepatocellular carcinoma is practically acceptable with the better effect than the routine dose. For the patients with large and hypervascular tumor of Child grade A liver function or ICG-R15 less than 20%, oily chemoembolization with 20-40mL Lipiodol is recommended.

Chen MS, Li JQ, Zhang YQ, Lu LX, Zhang WZ, Yu YF, Guo YP, Lin XJ, Li GH. High-dose Iodized Oil Transcatheter Arterial Chemoembolization For Patients with Large Hepatocellular Carcinoma. *World J Gastroenterol* 2002;8(1):74-78

INTRODUCTION

Hepatocellular carcinoma (HCC) is one of the most common malignant tumors in human beings. It was estimated that in 1985, about 315, 000 new cases of primary liver cancer occurred worldwide, accounting for 4.1% of all human cancer cases^[1]. In the same year, 312,000 patients died as a consequence of the disease. In China, HCC is responsible for 130,000 deaths every year and is the second cause of the cancer deaths^[2]. The crude mortality of HCC was 20.4 per 100,000 population, accounting for 18.8% of the total cancer deaths in 1990-1992^[3].

About 80% of HCC are associated with cirrhosis that makes treatment more difficult^[4]. Surgical resection is the best options for the treatment of HCC and the 5-year survival rate after hepatectomy was about 20%-40%^[5]. But in only 20% of HCC patients the surgical resection is feasible. About 60%-70% HCC were in late stages at the time of diagnosis and had lost the chance of operation^[6-8]. Transcatheter arterial chemoembolization (TACE) is one of the most common method for the treatment of the unresectable HCC^[9,10]. The results achieved by using TACE were much better than those of systemic or regional chemotherapy^[11, 12]. TACE with anticancer agent suspended in an oily substance has become one of the standard forms of treatment for advanced HCC. In the treatment, iodized oil is used as an embolic agent and carrier of anticancer drugs^[13,14]. After entering into the small arteries and peritumoral sinusoid of HCC through a catheter, the iodized oil can be retain there to block the terminal blood flow. The more iodized oil entering into the small arteries and peritumoral sinusoid of HCC, the more complete blocking of the terminal blood supply to the cancer will occur^[15,16]. But in such case more iodized oil may flow into the portal vein causing infarction or necrosis in the noncancerous hepatic tissue, and thus lead to the more liver dysfunction. Generally the amount of iodized oil recommended is about 5-15 mL at each procedure for fear that more iodized oil could lead to liver dysfunction^[17,18]. In clinical practice, most patients who received TACE were those with large HCC. For the large and hypervascular liver tumor, using 5-15 mL iodized oil is not enough to attain complete filling of tumor vessel bed. To get a full blocking of the tumor vessels, a larger volume of iodized oil is necessary. Basing on the experience of our clinical practice and the good evaluation of liver function, we conducted a high-dose (more

than 20mL) iodized oil TACE for the large HCC.

MATERIALS AND METHODS

Eligibility of patients

From January 1993 to June 1998, 473 patients with large HCC who were eligible for this study were treated at the Tumor Hospital of Sun Yat-sen University of Medical Sciences. The eligibility criteria for entering this study were as follows: ① a diagnosis of HCC was established on the basis of the patient's high serum alpha-fetoprotein (AFP) value, findings obtained at computed tomography(CT) scan and clinical manifestations; ② the largest diameter of the tumor exceeded 5 cm; ③ there was no evidence of portal trunk occlusion by thrombosis, extrahepatic metastasis, jaundice or ascites; ④ during the TACE procedure the catheter was successfully inserted into the target artery selectively as proved by angiography. We excluded patients who had Child's C grade liver function or ICG-R15 (indocyanine green retention rate in 15 min)>30%. All patients were randomly divided into two treatment groups. In Group A, 216 patients received more than 20mL of iodized oil in the first TACE, and in Group B, 257 patients received 5-15mL.

Clinical Characteristics of the patients

The clinical characteristics of the patients including age, sex, size of tumor, thrombosis in portal branch, AFP, serum alanine aminotransferase(ALT), Child's grading, ICG-R15 were collected before the treatment. The patients in the two groups did not differ significantly with respect to these clinical characteristics (Table 1).

Table 1 Pretreatment clinical characteristics of 473 patients

Characteristics	Group A (N=216)	Group B (N=257)	Probability value
Age			
Mean	44.6	45.1	0.348
Range	22-67	24-71	
Sex			
Male	213	246	0.065
Female	3	11	
Diameter of tumor			
6-9.9cm	32	9	0.133
10-14.9cm	105	135	
≥15cm	79	73	
Thrombosis			
Yes	54	81	0.118
No	162	176	
AFP (μg/L)			
≥400	91	114	0.626
<400	125	143	
ALT			
<40	117	109	0.023
40-79	78	103	
80-119	17	39	
≥120	4	7	
Child's class			
A	203	238	0.553
B	13	19	
ICG-R15*			
<10	71	89	0.314
10-19	127	137	
20-29	18	31	

*ICG-R15 refers to the indocyanine green retention rate at 15 minutes

Methods of chemoembolization

During the hepatic angiography that demonstrated the tumor vessels and tumor contour, the catheter was inserted selectively into the target artery. The catheter tip was placed as close as possible to the tumor for attaining the high-selective embolization^[19]. The first 5-10 mL iodized oil (Lipiodol, Laboratoire Guerbet, Aulnay-sous-Bois, France) were mixed with anticancer drugs, Epirubicin(50 mg·m⁻²) and Mitomycin(8mg·m⁻²), to form an emulsion. The emulsion was slowly injected under fluoroscopic control. The remainder Lipiodol was added according to the state of accumulation of the emulsion within the tumor at the first injection, speed of blood flowing to the tumor, and appearance of portal vein around the tumor (Figure 1). Gelatin sponge impregnated with contrast medium was injected into the tumor, if the blood flow to the tumor wasn't slowed down enough after the Lipiodol injection^[20]. Any embolization was terminated when the blood flow to the tumor had slowed down.



Figure 1 Portal vein branches around the tumor as visualized by high-dose iodized oil

In group A, 112 cases received 20-29mL Lipiodol in the first procedure, 85 cases 30-39mL, 19 cases more than 40mL; the largest dose was 53 mL and the average dose was 28.3mL. In group B, 119 cases received 5-10mL Lipiodol and 138 cases received 11-15mL; the average dose was 11.8mL.

Follow-up

Four weeks after TACE, the therapeutic effect was assessed by double phase CT scan and AFP test. The CT was performed after a bolus administration of 50-100mL of contrast material^[21]. The pattern of Lipiodol accumulation on CT were classified into following four kinds according to Nishimine^[22]: type I, homogeneous; type II, defective; type III, inhomogeneous; and type IV, only slight accumulation, if any (Table 2). Type I was further subgrouped into type I a (with accumulation around the tumor) and type I b (without accumulation around the tumor). AFP was tested at 4 wk intervals after first TACE.

Type	I	II	III	IV
L-CT				
L-CT				
	Homogeneous	Defective	Uneven	No/slight Accumulation

A repeat TACE and other therapies were performed depending on the conditions of the patient after the first TACE. 11 patients underwent totally 5 times TACE; 32 underwent 4; 139 underwent 3; 207 underwent 2; 84 underwent 1. 59 patients underwent percutaneous ethanol injection(PEI) after TACE and 46 patients received surgical

resection. Survival was measured from date of the first treatment until death. The causes of death were determined for 347 patients during the follow-up period. When a patient died from advanced carcinoma, hepatic failure or a deterioration of his or her general condition shortly after the procedure, the patients death was considered to be due to treatment failure.

Statistical analysis

The changes of liver dysfunction and CT type was analyzed by chi-square test. Cumulative survival rates were estimated by the Kaplan-Meier method. The relationship between each of the variable and survival was assessed by log rank test. "Significant" indicated a calculated two-tailed value of <0.05 .

RESULTS

Side Effects

The most frequent side effects of TACE were fever and abdominal pain. In Group A abdominal pain occurred in 53.7% of the patients, fever in 71.3%, vomiting in 20.8%, appetite loss in 41.7% and upper digestive tract bleeding in 0.93%. In group B, abdominal pain occurred in 49.8% patients, fever in 47.5%, vomiting in 14.8%, appetite loss in 42.8% and upper digestive bleeding in 1.17%. The toxic effect of the drugs on the hemopoietic system reflected in slight decreases in the white blood cell counts, platelet counts, and hemoglobin levels of peripheral blood in both groups. Elevations in the serum alanine aminotransferase, alkaline phosphatase, or total bilirubin levels were seen in the patients of both groups, but the changes were not severe and no significant differences were found between the two groups. Liver dysfunction occurred in 24 patients of group A and in 28 patients of group B. The patients with child's grade B or ICG-R15 >20 had higher risk of liver failure after high-dose TACE (Table 2).

Table 2 The comparison of liver dysfunction** in two group

Group	Child-Pugh Classification		ICG-R15		
	A	B	$<10\%$	10-19%	$\geq 20\%$
Group A	5.9%(12/203)	92.3%(12/13)	1.4%(1/71)	7.9%(10/127)	72.2%(13/18)
Group B	5.5%(13/238)	84.2%(15/19)	2.2%(2/89)	5.8%(8/137)	58.1%(18/31)

**Liver dysfunction is referred to ascites, jaundice(Tbil $>34.2\mu\text{mol/L}$), or hepatic encephalopathy

CT and AFP

CT scan was done four weeks after TACE: In group A there were 77 cases of type I, 130 cases of type II, 9 cases of type III; whereas in group B there were 27 cases of type I, 108 cases of type II, 90 cases of type III and 32 cases of type IV (group A vs group B $P<0.001$, Figure 2). In group A, the AFP level in 78 of 91 AFP-positive patients ($\geq 400\mu\text{g}\cdot\text{L}^{-2}$) had decreased and in 12 of them down to normal; in group B, 81 of 114 AFP-positive patients had their AFP decrease and in 9 down to normal ($P<0.01$).

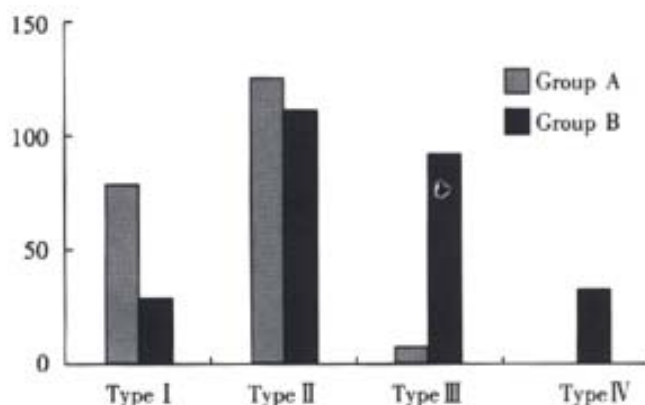


Figure 2 Comparison of CT type between the two groups.

Resection

After TACE, 47 cases achieved surgical resection in group A, and 19 of them were found to have complete tumor necrosis pathologically. In group B, 25 patients received surgical resection and only 4 cases were found to have complete tumor necrosis. The resection rate and complete tumor necrosis rate of group A were higher than those of group B ($P<0.05$).

Survival Rates

The 1-, 2-, 3-year cumulative survival rates of the patients with Child's grade A in group A were 79.2%, 51.8%, 34.9% and in group B was 59.1%, 26.7%, 14.9%, respectively (Figure 3). The cumulative survival rates were significantly better in group A than in group B ($P<0.001$). The 1-, 2-, 3-year cumulative survival rates of the patients with Child's grade B in group A were 42.1%, 21.1%, 7.7% and in group B was 46.8%, 23.7%, 0%, respectively (no significantly difference in between the two groups).

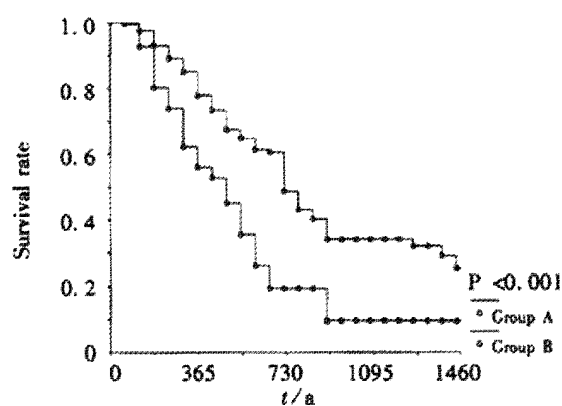


Figure 3 Cumulative survival rates of patients with Child's A in two groups.

DISCUSSION

For use in TACE, Iodized oil (mostly lipiodol) mixed with anticancer drugs has been reported to be one of the most effective agents^[23,24]. Iodized oil plays an important role as an embolic agent. It not only occludes the small arteries supplying the tumor but also acts as the carrier bringing the drug to the tumor. The lipiodol can enter into the microcirculation of the tumor and stay there to stop the blood flow^[25]. The experimental investigations in animal and human resected specimens revealed that the lipiodol could stay in the small artery, sinusoid, and small portal vein within the tumor. In general, the recommended amount of lipiodol is 5-15mL. The use of large volume of iodized oil is more prone to invade the normal liver parenchyma, causing more liver injury^[26]. Matsuo^[27] reported the relationship between the lipiodol dose and the tumor necrosis rates in 198 HCC cases. He found that the prognosis was better in the group of patients with big tumors in which the doses of lipiodol were correspondingly larger tumor diameter, but the total dose must not be more than 10mL in small HCC. Other authors^[28,29] confirmed that the dose of iodized oil played an important role in TACE. A sufficiently high dose of Lp-TACE would be a factor of good tumor response, if the tumor was large. Therefore the volume of lipiodol is an important factor influencing the antitumor effect of TACE. The large and hypervascular liver tumors have vast vessel bed. So it is necessary to inject high-dose lipiodol to attain complete filling of tumor vessel bed. While the tumor 5cm in diameter needs 5mL lipiodol to fill the vessel bed, the 10cm tumor would need at least 8 times of lipiodol to do the same work. In this situation a high-dose of iodized oil must be used for complete filling of the large tumor^[30,31]. Some portal branches around the tumors are displayed after the high-

dose lipiodol pooled into the tumor; this is considered to be the sign of complete arterial block. After a certain amount of lipiodol is pooled into the hepatic microcirculation and sinusoid, any additional volume of lipiodol enter into the branches of portal vein via the sinus between hepatic artery and portal vein. And then some lipiodol is seen in the small branches of portal vein around the tumor. As the amount of lipiodol delivered into artery increase, the portal vein branches become more prominent^[32]. Prominent portal vein appearances were seen in 29% patients given 10 mL or less of lipiodol, in 67% with 10-20 mL, and in 86% with more than 20 mL. It was known that infiltrating portion and nonencapsulated daughter nodules of the tumor are nourished by both the portal vein and the hepatic artery. So even if the tumor arteries are successfully embolized, some tumor cells can survive because the portal vein blood supply still exists. This may be the reason for incomplete tumor necrosis with subsequent tumor recurrence^[28,15]. High-dose lipiodol fully fills the sinus and stops the portal vein supply to tumor cells after the arteries are embolized. Embolization of both hepatic artery and small portal veins may cause complete necrosis of the tumor infiltrating portion and nonencapsulated daughter nodules^[13,14]. The visualization of some portal vein tributaries around the tumor may be a sign of complete embolization.

After Lp-TACE it is important to estimate the amount and state of iodized oil accumulating within the tumor, because this has much bearing on the prognosis of the patients^[33]. Matsuo^[27] found that the volume of lipiodol infusion correlated with the CT type. If the lipiodol volume is greater than the tumor mass in the small HCC, more type I lipiodol accumulation will be seen in the CT scan after Lp-TACE. He suggested that the lipiodol volume should be greater than the tumor mass, but the maximum dose should be less than 10 mL for fear of liver dysfunction even in the large HCC. Nishimine^[22] reported that tumors of CT type I have the highest cumulative survival rates and those of the type I have higher cumulative survival rates than type III and type IV. The iodized oil retention was again evaluated by using CT scan one month after TACE. It was found that the patients with iodized oil retention in the tumor greater than 50 per cent of tumor size survived longer than patients with retention of less than 50 per cent^[34-36]. Our study showed that high-dose lipiodol could bring about more type I and type II lipiodol accumulation than a routine dose. Pathological study of resected specimen after TACE showed that the area of lipiodol retention in CT was the necrotic area of the tumor. The high-dose lipiodol would lead to more lipiodol retention in the necrotic tumor^[37,38].

For preventing severe side effects, attention must be paid. The liver reserve function must be evaluated by Child's grading and ICG-R15^[39,40,41,42]. Our data showed that the liver dysfunction most frequently occurred in the patients with child's B or ICG-R15>20. The patients with Child's A or ICG-R15<20 were usually tolerant of 20-40mL lipiodol. Nonetheless, a high-dose lipiodol is contraindicated for the patients with child's B or ICG-R15>20. Second, to avoid normal liver parenchyma damage a high-selective placement of the catheter is crucial for injecting high-dose lipiodol. We mainly used the 5F Yasilo catheter or 5F RH catheter to perform the high selective catheterization. Subsegmental or segmental embolization is necessary for the high-dose lipiodol infusion^[43,44]. If the tip of catheter can't pass over all the arteries that flow to normal tissue and organ, high-dose lipiodol injection should be done with caution. Finally, slow injection under fluorescent guidance is also important to let all the lipiodol flow clearly into the tumor vessels. Whenever the lipiodol flows to the outside of tumor, injection should be stopped immediately. In the condition that all the lipiodol selectively enters into the tumor and doesn't flow to the normal liver tissue, the hepatic function will not be deteriorated^[45,46]. We safely injected 53mL into a large HCC with a diameter >20cm. If the blood flow is still fast toward the tumor after lipiodol infusion, Gelatin

sponge should be prescribed^[47]. High-dose lipiodol TACE can bring about more tumor necrosis. So high-dose lipiodol TACE results in higher survival rate.

It is concluded that high-dose lipiodol can bring about more completely tumor necrosis by blocking both the arteries and small portal veins of the tumor. High-dose TACE for treatment of large and hypervascular hepatocellular carcinoma is practically acceptable and gives a better effect than those using a routine dose. For the patients with large and hypervascular tumors and with Child A or ICG-R15 less than 20%, chemoembolization with 20-40mL lipiodol is recommended.

REFERENCES

- 1 Wu MC, Shen F. Progress in research of liver surgery in China. *World J Gastroenterol* 2000;6:773-776
- 2 Tang ZY, Yu YQ, Zhou XD, Ma ZC, Wu ZQ Progress and prospects in hepatocellular carcinoma surgery. *Ann Chir* 1998;52:558-563
- 3 Zhang SW, Li LD, Lu FZ, Mo R, Sun XT, Huanfu XM, Sun J, Zhou YC, Dai XD. Mortality of primary liver cancer from 1990 through 1992. *Zhonghua Zhongliu Zazhi* 1999;21:245-249
- 4 Rabe C, Pilz T, Klostermann C, Berna M, Schild HH, Sauerbruch T, Caselmann WH. Clinical characteristics and outcome of a cohort of 101 patients with hepatocellular carcinoma. *World J Gastroenterol* 2001; 7:208-215
- 5 Wu MC. Progresses in surgical treatment of primary hepatocellular carcinoma. *Huaren Xiaohua Zazhi* 1998;6:921-923
- 6 Sithinamsuwan P, Piratvisuth T, Tanomkiat W, Apakupakul N, Tongyoo S. Review of 336 patients with hepatocellular carcinoma at Songklanagarind Hospital. *World J Gastroenterol* 2000;6:339-343
- 7 Tang ZY. Hepatocellular carcinoma cause, treatment and metastasis. *World J Gastroenterol* 2001;7:445-454
- 8 Yip D, Findlay M, Boyer M, Tattersall MH. Hepatocellular carcinoma in central Sydney: a 10 year review of patients seen in a medical oncology department. *World J Gastroenterol* 1999;5:483-487
- 9 Tu SP, Wu DM, Yuan YZ, Wu YL, Jiang SH, Wu YX. Treatment of hepatocellular carcinoma by transcatheter arterial chemoembolization with hydroxycamptothecin. *Shijie Huaren Xiaohua Zazhi* 1999;7:158-160
- 10 Zhang XQ, Yang XM, Sun HL, Li ZR. Effects of hepatic artery chemoembolization on hepatic carcinoma. *Xin Xiaohuabingxue Zazhi* 1997;5:112-113
- 11 Fan J, Ten GJ, He SC, Guo JH, Yang DP, Weng GY. Arterial chemoembolization for hepatocellular carcinoma. *World J Gastroenterol* 1998;4:33-37
- 12 Okusaka T, Okada S, Ueno H, Ikeda M, Yoshimori M, Shimada K, Yamamoto J, Kosuge T, Yamasaki S, Iwata R, Furukawa H, Moriama N, Sakamoto M, Hirohashi S. Evaluation of the therapeutic effect of transcatheter arterial embolization for hepatocellular carcinoma. *Oncology* 2000; 58: 2093-2099
- 13 Ono Y, Yoshimasu T, Ashikaga R, Inoue M, Shindou H, Fuji K, Araki Y, Nishimura Y. Long-term results of lipiodol-transcatheter arterial embolization with cisplatin or doxorubicin for unresectable hepatocellular carcinoma. *Am J Clin Oncol* 2000; 23: 564-568
- 14 Ueno K, Miyazono N, Inoue H, Nishida H, Kanetsuki I, Nakajo M. Transcatheter arterial chemoembolization therapy using iodized oil for patients with unresectable hepatocellular carcinoma: evaluation of three kinds of regimens and analysis of prognostic factors. *Cancer* 2000; 88: 1574-1581
- 15 Takayasu K, Muramatsu Y, Maeda T, Iwata R, Furukawa H, Muramatsu Y, Moriama N, Okusaka T, Okada S, Ueno H. Targeted transarterial oily chemoembolization for small foci of hepatocellular carcinoma using a unified helical CT and angiography system: analysis of factors affecting local recurrence and survival rates. *Am J Roentgenol* 2001; 176: 681-688
- 16 Mizoe A, Yamaguchi J, Azuma T, Fujioka H, Furui J, Kanematsu T. Transcatheter arterial embolization for advanced hepatocellular carcinoma resulting in a curative resection: report of two cases. *Hepatogastroenterology* 2000; 47: 1706-1710
- 17 Vogl TJ, Trapp M, Schroeder H, Mack M, Schuster A, Schmitt J, Neuhaus P, Felix R. Transarterial chemoembolization for hepatocellular carcinoma: volumetric and morphologic CT criteria for assessment of prognosis and therapeutic success-results from a liver transplantation center. *Radiology* 2000; 214: 349-357
- 18 Ernst O, Sergeant G, Mizrahi D, Delemazure O, Paris JC, L'Hermine C. Treatment of hepatocellular carcinoma by transcatheter arterial chemoembolization: comparison of planned periodic chemoembolization and chemoembolization based on tumor response. *Am J Roentgenol* 1999; 172: 59-64

- 19 Inoue H, Ito T, Siraki K, Sugimoto K, Sakai T, Oomori S, Takase K, Nakano T. Effect of segmental transcatheter arterial chemoembolization on branched chain amino acids and tyrosine ratio in patients with hepatocellular carcinoma. *Int J Oncol* 2000; 17: 977-980
- 20 Kwok PC, Lam TW, Chan SC, Chung CP, Wong WK, Chan MK, Lo HY, Lam WM. A randomized clinical trial comparing autologous blood clot and gelfoam in transarterial chemoembolization for inoperable hepatocellular carcinoma. *J Hepatol* 2000; 32: 955-964
- 21 Katyal S, Oliver JH, Peterson MS, Chang PJ, Baron RL, Carr BI. Prognostic significance of arterial phase CT for prediction of response to transcatheter arterial chemoembolization in unresectable hepatocellular carcinoma: a retrospective analysis. *Am J Roentgenol* 2000; 175: 1665-1672
- 22 Nishimine K, Uchida H, Matsuo N. Segmental transarterial chemoembolization with Lipiodol mixed with anticancer drugs for nonresectable hepatocellular carcinoma: Follow-up CT and therapeutic results. *Cancer Chemother Pharmacol* 1994; (Suppl 33):S60-S68
- 23 Llado L, Virgili J, Figueras J, Valls C, Dominguez J, Rafecas A, Torras J, Fabregat J, Guardiola J, Jaurrieta E. A prognostic index of the survival of patients with unresectable hepatocellular carcinoma after transcatheter arterial chemoembolization. *Cancer* 2000; 88: 50-57
- 24 Pelletier G, Ducreux M, Gay F, Lubinski M, Hagege H, Dao T, Van Steenberghe W, Buffet C, Rougier P, Adler M, Pignon JP, Roche A. Treatment of unresectable hepatocellular carcinoma with lipiodol chemoembolization: a multicenter randomized trial. Groupe CHC. *J Hepatol* 1998; 29: 129-134
- 25 Savastano S, Miotto D, Casarrubea G, Teso S, Chiesura Corona M, Feltrin GP. Transcatheter arterial chemoembolization for hepatocellular carcinoma in patients with Child's grade A or B cirrhosis: a multivariate analysis of prognostic factors. *J Clin Gastroenterol* 1999; 28: 334-340
- 26 Kamada K, Nakanishi T, Kitamoto M, Aikata H, Kawakami Y, Ito K, Asahara T, Kajiyama G. Long-term prognosis of patients undergoing transcatheter arterial chemoembolization for unresectable hepatocellular carcinoma: comparison of cisplatin lipiodol suspension and doxorubicin hydrochloride emulsion. *J Vasc Interv Radiol* 2001; 12: 847-854
- 27 Matsuo N, Uchida H, Sakaguchi H, Nishimine K, Nishimura Y, Hirohashi S, Ohishi H. Optimal lipiodol volume in transcatheter arterial chemoembolotherapy for hepatocellular carcinoma: Study based on lipiodol accumulation patterns and histopathologic findings. *Seminars in Oncology* 1997;24:61-70
- 28 Takayasu K, Arai S, Matsuo N, Yoshikawa M, Ryu M, Takasaki K, Sato M, Yamanaka N, Shimamura Y, Ohto M. Comparison of CT findings with resected specimens after chemoembolization with iodized oil for hepatocellular carcinoma. *Am J Roentgenol* 2000;175: 699-704
- 29 Bizollon T, Rode A, Bancel B, Gueripel V, Ducerf C, Baulieux J, Trepo C. Diagnostic value and tolerance of Lipiodol-computed tomography for the detection of small hepatocellular carcinoma: correlation with pathologic examination of explanted livers. *J Hepatol* 1998;28: 491-496
- 30 Oi H, Kim T, Kishimoto H, Matsushita M, Tateishi H, Okamura J. Effective cases of transcatheter arterioportal chemoembolization with high-dose iodized oil for hepatocellular carcinoma. *Cancer Chemother Pharmacol* 1994;33 Suppl: S69-73
- 31 Oi H, Kishimoto H, Matsushita M, Katsushima S, Tateishi H, Okamura J. Antitumor effect of transcatheter oily chemoembolization for hepatocellular carcinoma assessed by computed tomography: role of iodized oil. *Semin Oncol* 1997;24(Suppl 6): 56-60
- 32 Nakayama A, Imamura H, Matsuyama Y, Kitamura H, Miwa S, Kobayashi A, Miyagawa S, Kawasaki S. Value of lipiodol computed tomography and digital subtraction angiography in the era of helical biphasic computed tomography as preoperative assessment of hepatocellular carcinoma. *Ann Surg* 2001;234: 56-62
- 33 Caturelli E, Siena DA, Fusilli S, Villani MR, Schiavone G, Nardella M, Balzano S, Florio F. Transcatheter arterial chemoembolization for hepatocellular carcinoma in patients with cirrhosis: evaluation of damage to nontumorous liver tissue-long-term prospective study. *Radiology* 2000; 215: 123-128
- 34 Colagrande S, Fargnoli R, Dal Pozzo F, Bindi A, Rega L, Villari N. Value of hepatic arterial phase CT versus lipiodol ultrafluid CT in the detection of hepatocellular carcinoma. *J Comput Assist Tomogr* 2000; 24: 878-883
- 35 Higashi S, Tabata N, Kondo KH, Maeda Y, Shimizu M, Nakashima T, Setoguchi T. Size of lipid microdroplets effects results of hepatic arterial chemotherapy with an anticancer agent in water-in-oil-in-water emulsion to hepatocellular carcinoma. *J Pharmacol Exp Ther* 1999; 289: 816-819
- 36 Vogl TJ, Schroeder H, Trapp M, Straub R, Schuster A, Schuster M, Mack M, Souchon F, Neuhaus P. Multi-sequential arterial chemoembolization of advanced hepatocellular carcinomas: computerized tomography follow-up parameters for evaluating effectiveness of therapy. *Rofo Fortschr Geb Rontgenstr Neuen Bildgeb Verfahren* 2000;172:43-50
- 37 Kamada K, Nakanishi T, Kitamoto M, Aikata H, Kawakami Y, Ito K, Asahara T, Kajiyama G. Long-term prognosis of patients undergoing transcatheter arterial chemoembolization for unresectable hepatocellular carcinoma: comparison of cisplatin lipiodol suspension and doxorubicin hydrochloride emulsion. *J Vasc Interv Radiol* 2001;12: 847-854
- 38 Okusaka T, Okada S, Ueno H, Ikeda M, Yoshimori M, Shimada K, Yamamoto J, Kosuge T, Yamasaki S, Iwata R, Furukawa H, Moriyama N, Sakamoto M, Hirohashi S. Evaluation of the therapeutic effect of transcatheter arterial embolization for hepatocellular carcinoma. *Oncology* 2000;58: 293-299
- 39 Jiao LR, El Desoky AA, Seifalian AM, Habib N, Davidson BR. Effect of liver blood flow and function on hepatic indocyanine green clearance measured directly in a cirrhotic animal model. *Br J Surg* 2000; 87: 568-574
- 40 Hashimoto M, Watanabe G. Hepatic parenchymal cell volume and the indocyanine green tolerance test. *J Surg Res* 2000; 92: 222-227
- 41 Tang ZY. Advances in clinical research of hepatocellular carcinoma in China. *Huaren Xiaohua Zazhi* 1998;6:1013-1016
- 42 Zhou HG, Gu GW. New trend in clinicopathology of primary liver cancer. *Huaren Xiaohua Zazhi* 1998;6:714-715
- 43 Wu ZQ, Fan J, Qiu SJ, Zhou J, Tang ZY. The value of postoperative hepatic regional chemotherapy in prevention of recurrence after radical resection of primary liver cancer. *World J Gastroenterol* 2000; 6:131-133
- 44 Li L, Wu PH, Li JQ, Zhang WZ, Lin HG, Zhang YQ. Segmental transcatheter arterial embolization for primary hepatocellular carcinoma. *World J Gastroenterol* 1998;4:511-512
- 45 Tarazov PG, Polysalov VN, Prozorovskij KV, Grishchenkova IV, Rozengauz EV. Ischemic complications of transcatheter arterial chemoembolization in liver malignancies. *Acta Radiol* 2000; 41: 156-160
- 46 Caturelli E, Siena DA, Fusilli S, Villani MR, Schiavone G, Nardella M, Balzano S, Florio F. Transcatheter arterial chemoembolization for hepatocellular carcinoma in patients with cirrhosis: evaluation of damage to nontumorous liver tissue-long-term prospective study. *Radiology* 2000;215:123-128
- 47 Ono Y, Yoshimasu T, Ashikaga R, Inoue M, Shindou H, Fuji K, Araki Y, Nishimura Y. Long-term results of lipiodol-transcatheter arterial embolization with cisplatin or doxorubicin for unresectable hepatocellular carcinoma. *Am J Clin Oncol* 2000;23:564-568

• LIVER CANCER •

Anti-hepatoma activity of resveratrol in vitro

Zhong-Jie Sun, Cheng-En Pan, Hong-Shan Liu, Guo-Jun Wang

Zhong-Jie Sun, Cheng-En Pan, Hong-Shan Liu, Guo-Jun Wang,
Department of Hepatobiliary Surgery, First Hospital of Xi'an Jiaotong
University, Xi'an 710061, Shaanxi Province, China

Correspondence to: Dr. Zhong-Jie SUN, Department of Hepatobiliary
Surgery, First Hospital of Xi'an Jiaotong University Xi'an 710061,
Shaanxi Province, China. szhjje@21cn.com

Telephone: +86-029-5260273 Fax: +86-029-5260273

Received 2001-08-09 Accepted 2001-08-23

Abstract

AIM: To study the anti-tumor effect of resveratrol alone and the synergistic effects of resveratrol with 5-FU on the growth of H22 cells line *in vitro*.

METHODS: The number of cells was measured by MTT method, the morphological changes of H₂₂ cells were investigated under microscopy and electron microscopy.

RESULTS: Resveratrol inhibited the growth of hepatoma cells line H₂₂ in a dose- and time-dependent manner. IC₅₀ of the resveratrol on H₂₂ cells was 6.57 mg·L⁻¹. The synergistic anti-tumor effects of resveratrol with 5-FU increased to a greater extent than for H22 cells treated with 5-FU alone (70.2% vs 28.4%) ($P < 0.05$). Under microscope and electron microscope, characteristics of apoptosis such as typical apoptotic bodies were commonly found in tumor cells in the drug-treated groups.

CONCLUSION: Resveratrol can suppresses the growth of H₂₂ cells *in vitro*, its anti-tumor activity may occur through the induction of apoptosis.

Sun ZJ, Pan CE, Liu HS, Wang GJ. Anti-hepatoma activity of resveratrol *in vitro*. *World J Gastroenterol* 2002;8(1):79-81

INTRODUCTION

Hepatoma is common in China^[1-20], but only a few chemotherapeutic drugs hold a high place in the treatment of human primary hepatocellular carcinoma (PHC). Resveratrol, a phytoalexin found in grapes, fruits, and root extracts of the weed *Polygonum cuspidatum*, has been an important constituent of Japanese and Chinese folk medicine. Indirect evidence suggests that the presence of resveratrol in white and rose wine may explain for the reduced risk of coronary heart disease associated with moderate wine consumption. This effect has been attributed to the inhibition of platelet aggregation and coagulation, in addition to the antioxidant and anti-inflammatory activity of resveratrol^[21-28]. Moreover, a recent report shows that resveratrol is a potent cancer chemopreventive agent in assays representing three major stages of carcinogenesis^[29-35]. The ability to inhibit cellular events associated with tumor initiation, promotion, and progression has been attributed to the anticyclooxygenase activity (COX-1) of resveratrol^[36]. We report here the results of our findings showing that resveratrol inhibited the growth of hepatoma cells line H₂₂.

MATERIALS AND METHODS

Reagents

Resveratrol was kindly provided by Prof Li (Environment and

Chemical Engineering School, Xi'an Jiaotong University) and dissolved in dimethylsulfoxide (DMSO); MTT was obtained from Sigma. RPMI 1640 containing 100 mL·L⁻¹ fetal bovine serum (FBS) was bought from Gibco. All other chemicals were standard commercial products of analytical grade.

Cell culture

H₂₂ cells were obtained from Center of Molecular Biology of First Hospital, Xi'an Jiaotong University and routinely cultured in RPMI 1640 containing 100 mL·L⁻¹ FBS at 37°C in an atmosphere with 50 mL·L⁻¹ CO₂.

Assay of cell proliferation

H₂₂ cells were plated in 96-well plates (2×10⁴/well) for 24 h before the addition of resveratrol. Medium was then aspirated and replaced with fresh RPMI 1640 + 100 mL·L⁻¹ FBS containing resveratrol for 48 h. Different compositions to be tested were added according to designed groups: group A (cell control group) with nothing added, group B (DMSO control group) with DMSO 5 mL·L⁻¹, group C1-5 with Resveratrol (1.25, 2.50, 5.0, 10.0 and 20.0 mg·L⁻¹), group D 1-25-FU (2400 and 1200 mg·L⁻¹), group E with Resveratrol 5.0 mg·L⁻¹+5-FU 1200 mg·L⁻¹. Each group had 4 wells and was cultured for 48 h. The number of cells was determined by MTT (3-[4,5-dimethylthiazol-2-yl]-2,5-diphenyl tetrazolium bromide) method as described in Sigma Technical Bulletin (Sigma, MO). Absorbance at 570 nm (A) was assayed at different time points. The A value was adjusted with the living cell number. Each sample was assayed three times. Inhibition rate (%) = (1 - experimental A/control A) × 100%.

Morphologic observation

After the cellular culture for 48 h, cells in groups A, C and E were observed and photographed with an Olympus BH-I microscope and a Hitachi-600 electron microscope.

RESULTS

Growth inhibition of H₂₂ cells

H₂₂ cells at 2×10⁴/well were incubated with different concentrations of resveratrol for 8 - 48 h and the effect of resveratrol on the cells growth was examined by MTT assay. The growth of H₂₂ cells was markedly inhibited by resveratrol with the IC₅₀ value of 6.57 mg·L⁻¹. Moreover, the cytotoxicity of resveratrol was in concentration-dependent and time-dependent manners (Table 1). The inhibition ability of 5-FU was 49.2% (2400 mg·L⁻¹), 28.4% (1200 mg·L⁻¹) respectively; The inhibiting ability of resveratrol (5.0 mg·L⁻¹) combined with 5-FU (1200 mg·L⁻¹) was higher than that of 5-FU alone (70.2% vs 28.4%, $P < 0.05$).

Morphology observation

Apoptotic cells were found in cells incubated with resveratrol. Light microscopic observation showed that apoptotic cells were characterized with cytoplasmic condensation, vacuolated bubbles, and condensed nuclei (Figure 1). Under electron microscope, H₂₂ cells exhibited the characteristics of apoptosis including cytoplasmic condensate, pyknotic nuclei, condensed chromatin and apoptotic bodies (Figures 2,

3). Compared with control groups, group C and E had much more cells with the apoptotic characteristics.

Table 1 Effect of various concentrations of resveratrol on the growth of hepatoma cells H₂₂

c(resveratrol)/mg · L ⁻¹	8h	12h	24h	48h
0.00	-	-	-	-
1.25	11.4	12.6	13.4	16.8
2.50	23.4	29.3	30.2 ^a	32.6 ^a
5.00	30.5 ^a	31.2 ^a	36.4 ^a	43.5 ^a
10.0	32.2 ^a	38.3 ^a	45.1 ^a	62.2
20.0	38.2 ^a	45.9 ^a	65.2 ^b	74.9 ^b

^aP<0.05; ^bP<0.01 vs control

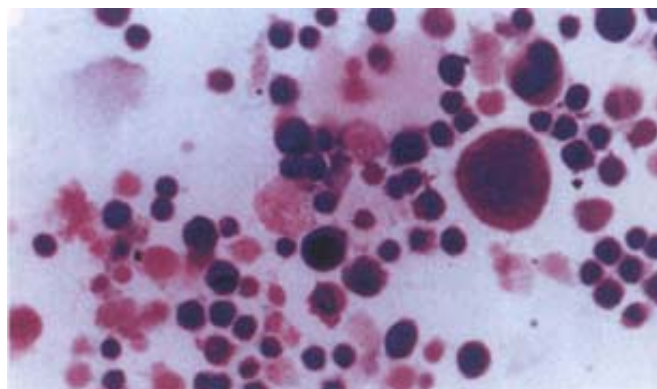


Figure 1 Treatment with resveratrol for 48 hours: apoptotic cell with condensed nuclei and cytoplasmic condensation (×200).

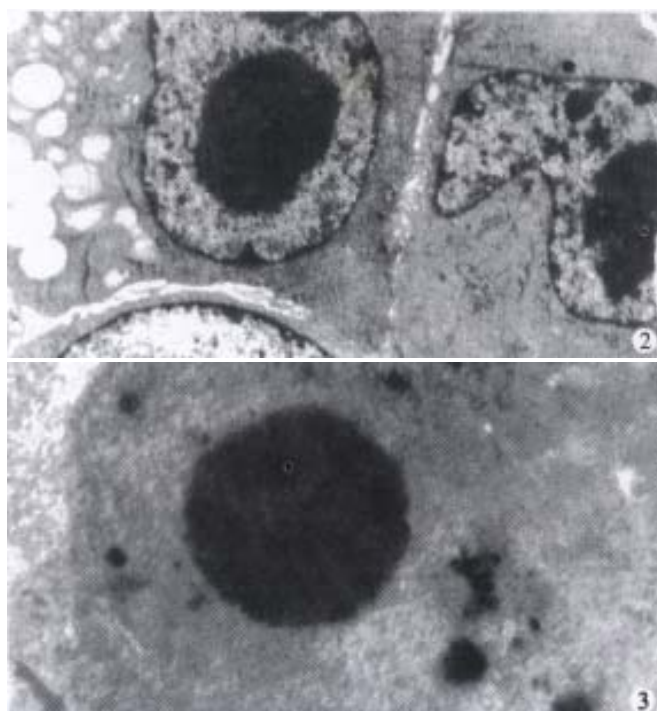


Figure 2 Cytoplasmic condensation with vacuoles, pyknotic nuclei, some with condensed chromatin inside (×5000).

Figure 3 Apoptotic body (×10 000).

DISCUSSION

To date, only a few chemotherapeutic drugs hold a high place in the treatment of human primary hepatocellular carcinoma (PHC) and there is clearly a need for evaluation of new anti-hepatoma drugs. Resveratrol (3,5,4'-trihydroxystibene), a natural compound present in grapes and other food, has been shown to provide cancer

chemopreventive effects in different systems based on its striking inhibition of diverse cellular events associated with tumor initiation, promotion, and progression^[29-35,37]. At the molecular level, these effects were related to the inhibition of free radical formation and cyclooxygenase activity^[36], as well as induction of differentiation. In addition, resveratrol was shown to be a remarkable inhibitor of ribonucleotide reductase and DNA synthesis with cellular arrest in the S phase or the S-G₂ phase transition^[38-40]. In the present study, MTT assay was used to observe the effect of resveratrol on the growth of H₂₂ mouse hepatoma cells *in vitro*, indicating that the drug could inhibit the growth of hepatoma cells. Its concentration- and time-effect relationships were also significant. Compared with control groups, group C had much more cells with apoptotic characteristics. The plausible mechanisms that could account for the anti-tumor activity of resveratrol might be related to induce apoptosis of tumor cells^[41-48].

Resveratrol combined with 5-FU inhibited the cell growth much more strongly than each agent used alone. At a certain concentration, resveratrol inhibits H₂₂ cell growth with the same effect as using 5-FU alone. Combination of resveratrol and 5-FU could have a cooperative effect. Both drugs inhibit cell growth at different phases of the cell cycle, i.e., resveratrol mainly causes G₂/M arrest^[39-40] and 5-FU mainly inhibits DNA synthesis(S phase) which naturally decreases the cellular growth more significantly. Our study indicates that combined use of resveratrol and 5-FU at low concentration that is used to treat hepatoma may be more efficient than using a single drug at higher concentration. The side-effects produced by 5-FU at the high doses can be avoided by its combination at low doses. These results suggest that resveratrol, may be potentially useful as a biochemical modulator to enhance the therapeutic effects of 5-FU in cancer chemotherapy.

REFERENCES

- Tang ZY. Hepatocellular Carcinoma Cause, Treatment and Metastasis. *World J Gastroenterol* 2001;7:445-454
- Lin NF, Tang J, Mohamed Ismael HS. Study on environmental etiology of high incidence areas of liver cancer in China. *World J Gastroenterol* 2000;6:572-576
- Yang CS. Chinese diet in the causation and prevention of cancer. *World J Gastroenterol* 1998;4:36-37
- Liu E, Zhang QN, Li WG. Effect of various drinking water on human micronucleus frequency in high-risk population of PHC. *World J Gastroenterol* 1998;4:183-184
- Wu MC. Clinical research advances in primary liver cancer. *World J Gastroenterol* 1998;4:471-474
- Tang ZY. Advances in clinical research of hepatocellular carcinoma in China. *World J Gastroenterol* 1998;4:4-7
- Wu MC, Shen F. Progress in research of liver surgery in China. *World J Gastroenterol* 2000;6:773-776
- Jiang YF, Yang ZH, Hu JQ. Recurrence or metastasis of HCC: predictors, early detection and experimental antiangiogenic therapy. *World J Gastroenterol* 2000;6:61-65
- Li JY, Huang Y, Lin MF. Clinical evaluation of several tumor markers in the diagnosis of primary hepatic cancer. *World J Gastroenterol* 2000;6:39
- Wang CF, Shao YF, Zhang HZ. Surgical treatment for patients with stage IVa hepatic carcinoma and related studies. *World J Gastroenterol* 2000;6:86
- Gu GW, Zhou HG. Traditional Chinese Medicine in prevention of liver cancer. *Shijie Huaren Xiaohua Zazhi* 1999;7:80-81
- Liu WW. Etiological studies of hepatocellular carcinoma. *Shijie Huaren Xiaohua Zazhi* 1999;7:93-95
- Zhou XD. Prevention and treatment of recurrences and metastases of hepatocellular carcinoma. *Shijie Huaren Xiaohua Zazhi* 1999;7:260-261
- Lu B, Dai YM. Abnormal cycle regulation of cells in the HCC. *Shijie Huaren Xiaohua Zazhi* 2001;9:205-208
- Li L, Wu PH, Li JQ, Zhang WZ, Lin HG, Zhang YQ. Segmental transcatheter arterial embolization for primary hepatocellular carcinoma. *World J Gastroenterol* 1998;4:511-512
- Huang FG, Li Y, Xie XD. Side effects and complications of hepatic arterial infusion and embolization of liver carcinoma in aged patients and its management. *World J Gastroenterol* 1998;4:67-68
- Wang JH, Lin G, Yan ZP, Wang XL, Cheng JM, Li MQ. Stage II surgical resection of hepatocellular carcinoma after TAE: a report of 38

- cases. *World J Gastroenterol* 1998;4:133-136
- 18 Cai WX, Zheng H, Sheng J, Ye QL. Combined measurement of serum tumor markers in patients with hepatocellular carcinoma. *World J Gastroenterol* 1998;4:181-182
 - 19 Deng ZL, Ma Y, Yuan L, Teng PK. The importance of hepatitis C as a risk factor for hepatocellular carcinoma in Guangxi. *World J Gastroenterol* 2000;6:75
 - 20 Fan J, Wu ZQ, Tang ZY, Zhou J, Qiu SJ, Ma ZC, Zhou XD, Ye SL. Multimodality treatment in hepatocellular carcinoma patients with tumor thrombi in portal vein. *World J Gastroenterol* 2001;7:28-32
 - 21 Huang K, Lin M, Cheng G. Anti-inflammatory tetramers of resveratrol from the roots of *Vitis amurensis* and the conformations of the seven-membered ring in some oligostilbenes. *Phytochemistry* 2001;58:357-362
 - 22 Surh Y, Chun K, Cha H, Han SS, Keum Y, Park K, Lee SS. Molecular mechanisms underlying chemopreventive activities of anti-inflammatory phytochemicals: down-regulation of COX-2 and iNOS through suppression of NF-kappaB activation. *Mutat Res* 2001;480-481:243-268
 - 23 Olas B, Wachowicz B, Saluk-Juszczak J, Zielinski T, Kaca W, Buczynski A. Antioxidant activity of resveratrol in endotoxin-stimulated blood platelets. *Cell Biol Toxicol* 2001;17:117-125
 - 24 Stojanovic S, Sprinz H, Brede O. Efficiency and mechanism of the antioxidant action of trans-resveratrol and its analogues in the radical liposome oxidation. *Arch Biochem Biophys* 2001;391:79-89
 - 25 Wu JM, Wang ZR, Hsieh TC, Bruder JL, Zou JG, Huang YZ. Mechanism of cardioprotection by resveratrol, a phenolic antioxidant present in red wine (Review). *Int J Mol Med* 2001;8:3-17
 - 26 Russo P, Tedesco I, Russo M, Russo GL, Venezia A, Cicala C. Effects of de-alcoholated red wine and its phenolic fractions on platelet aggregation. *Nutr Metab Cardiovasc Dis* 2001;11:25-29
 - 27 Murcia MA, Martinez-Tome M. Antioxidant activity of resveratrol compared with common food additives. *J Food Prot* 2001;64:379-384
 - 28 Olas B, Zbikowska HM, Wachowicz B, Krajewski T, Buczynski A, Magnuszewska A. Inhibitory effect of resveratrol on free radical generation in blood platelets. *Acta Biochim Pol* 1999;46:961-966
 - 29 Igura K, Ohta T, Kuroda Y, Kaji K. Resveratrol and quercetin inhibit angiogenesis *in vitro*. *Cancer Lett* 2001;171:11-16
 - 30 Gusman J, Malonne H, Atassi G. A reappraisal of the potential chemopreventive and chemotherapeutic properties of resveratrol. *Carcinogenesis* 2001;22:1111-1117
 - 31 Kimura Y, Okuda H. Resveratrol isolated from *Polygonum cuspidatum* root prevents tumor growth and metastasis to lung and tumor-induced neovascularization in Lewis lung carcinoma-bearing mice. *J Nutr* 2001;131:1844-1849
 - 32 Yang CS, Landau JM, Huang MT, Newmark HL. Inhibition of carcinogenesis by dietary polyphenolic compounds. *Annu Rev Nutr* 2001;21:381-406
 - 33 Kozuki Y, Miura Y, Yagasaki K. Resveratrol suppresses hepatoma cell invasion independently of its anti-proliferative action. *Cancer Lett* 2001;167:151-156
 - 34 Nakagawa H, Kiyozuka Y, Uemura Y, Senzaki H, Shikata N, Hioki K, Tsubura A. Resveratrol inhibits human breast cancer cell growth and may mitigate the effect of linoleic acid, a potent breast cancer cell stimulator. *J Cancer Res Clin Oncol* 2001;127:258-264
 - 35 Mollerup S, Ovrebø S, Haugen A. Lung carcinogenesis: resveratrol modulates the expression of genes involved in the metabolism of PAH in human bronchial epithelial cells. *Int J Cancer* 2001;92:18-25
 - 36 MacCarrone M, Lorenzon T, Guerrieri P, Agro AF. Resveratrol prevents apoptosis in K562 cells by inhibiting lipoxygenase and cyclooxygenase activity. *Eur J Biochem* 1999;265:27-34
 - 37 Jang M, Cai L, Udeani G, O, Slowing KV, Thomas CF, Beecher CW, Fong HH, Farnsworth NR, Kinghorn AD, Mehta RC, Moon RC, Pezzuto JM. Cancer chemopreventive activity of resveratrol, a natural product derived from grapes. *Science (Washington DC)* 1997;275: 218-220
 - 38 Fontecave M, Lepoivre M, Elleingand E, Gerez C., Guittet O. Resveratrol, a remarkable inhibitor of ribonucleotide reductase. *FEBS Lett* 1998;421: 277-279
 - 39 Park JW, Choi YJ, Jang MA, Lee YS, Jun DY, Suh SI, Baek WK, Suh MH, Jin IN, Kwon TK. Chemopreventive agent resveratrol, a natural product derived from grapes, reversibly inhibits progression through S and G2 phases of the cell cycle in U937 cells. *Cancer Lett* 2001;163:43-49
 - 40 Ragione FD, Cucciolla V, Borriello A, Pietra V. D., Racioppi L., Soldati G., Manna C., Galletti P., Zappia V. Resveratrol arrests the cell division cycle at S/G2 phase transition. *Biochem Biophys Res Commun* 1998;250: 53-58
 - 41 Pervaiz S. Resveratrol-from the bottle to the bedside? *Leuk Lymphoma* 2001;40:491-498
 - 42 Huang C, Ma WY, Goranson A, Dong ZG. Resveratrol suppresses cell transformation and induces apoptosis through a p53-dependent pathway. *Carcinogenesis (Lond)* 1999;20: 237-242
 - 43 Dorrie J, Gerauer H, Wachter Y, Zunino SJ. Resveratrol induces extensive apoptosis by depolarizing mitochondrial membranes and activating caspase-9 in acute lymphoblastic leukemia cells. *Cancer Res* 2001;61:4731-4739
 - 44 She QB, Bode AM, Ma WY, Chen NY, Dong Z. Resveratrol-induced activation of p53 and apoptosis is mediated by extracellular-signal-regulated protein kinases and p38 kinase. *Cancer Res* 2001;61:1604-1610
 - 45 Tsan MF, White JE, Maheshwari JG, Bremner TA, Sacco J. Resveratrol induces Fas signalling-independent apoptosis in THP-1 human monocytic leukaemia cells. *Br J Haematol* 2000;109:405-412
 - 46 Szende B, Tyihak E, Kiraly-Veghely Z. Dose-dependent effect of resveratrol on proliferation and apoptosis in endothelial and tumor cell cultures. *Exp Mol Med* 2000;32:88-92
 - 47 Bernhard D, Tinhofer I, Tonko M, Hubl H, Ausserlechner MJ, Greil R, Kofler R, Csordas A. Resveratrol causes arrest in the S-phase prior to Fas-independent apoptosis in CEM-C7H2 acute leukemia cells. *Cell Death Differ* 2000;7:834-842
 - 48 Tian XM, Zhang ZX. The anticancer activity of resveratrol on implanted tumor of HepG2 in nude mice. *Shijie Huaren Xiaohua Zazhi* 2001;9:161-164

• LIVER CANCER •

Characterization of focal hepatic lesions with SPIO-enhanced MRI

Wei-Wei Zheng, Kang-Rong Zhou, Zu-Wang Chen, Ji-Zhang Shen, Cai-Zhong Chen, Shu-Jie Zhang

Wei-Wei Zheng, Kang-Rong Zhou, Zu-Wang Chen, Ji-Zhang Shen, Cai-Zhong Chen, Shu-Jie Zhang, Department of Radiology, Affiliated Zhongshan Hospital, Medical College of Fudan University, Shanghai 200032, P.R.China

Supported by the Health Ministry Programme No.97030220

Correspondence to: Dr. Wei Wei Zheng, Department of Radiology, Zhongshan Hospital, Medical Center of Fudan University, 180 Fenglin Road, Shanghai 200032, China. Viviannc@online.sh.cn

Telephone: +86-21-64041990 Ext.2416

Received 2001-08-08 Accepted 2001-08-23

Abstract

AIM: To evaluate the value of superparamagnetic iron oxide (SPIO) enhanced MRI in characterizing focal hepatic lesions.

METHODS: Forty-three patients (32 men, 11 women, mean age 51 years, age range 25-74 years) with previously identified focal hepatic lesions were enrolled into this study. All the patients underwent plain, Gd-DTPA enhanced MRI and the SPIO enhanced MRI 1-7 d later. The surgicopathologic diagnosis was established in 31 cases and the diagnosis in other 12 cases was made on the basis of clinical findings and biochemical tests. The signal changes of lesions were analyzed and the CNRs of lesion-to-liver were measured before and after SPIO enhancement. The data were analyzed by paired *t* test.

RESULTS: Focal hepatic lesions included primary hepatocellular carcinoma (HCC, *n*=22), hemangioma (*n*=5), cyst (*n*=4), metastases (*n*=5), cirrhotic nodule (*n*=4), focal nodular hyperplasia (FNH, *n*=5) and other miscellaneous lesions (*n*=6). After SPIO enhancement HCC demonstrated iso- or slight hyperintensity on T1WI and moderate hyperintensity on T2WI, hemangioma showed moderate hyperintensity on T1WI and obvious hyperintensity on T2WI, the SI of cyst had no change either on T1WI or on T2WI, cirrhotic nodules revealed iso-intensity on T2WI, and the SI of FNH decreased significantly on T2WI. No specific manifestations were found in the other 6 miscellaneous lesions after SPIO enhancement.

CONCLUSION: SPIO enhanced-MRI can improve the characterization confidence for diagnosis of focal hepatic lesions.

Zheng WW, Zhou KR, Chen ZW, Shen JZ, Chen CZ, Zhang SJ. Characterization of focal hepatic lesions with SPIO-enhanced MRI. *World J Gastroenterol* 2002;8(1):82-86

INTRODUCTION

Superparamagnetic iron oxide (SPIO) is a newly developed tissue-specific contrast material. Intravenously administered SPIO particles can be specifically taken up by reticulo-endothelial system, and the signal intensities of normal hepatic and splenic parenchyma are significantly decreased on MR images. Therefore, it has been widely applied for lesion detection in the liver^[1-6]. After SPIO-enhancement the detectability of focal hepatic lesions smaller than

1cm could be increased from 65.9% to 97.5%. However, to our knowledge, the previously reported studies were mainly concerned about the detection of hepatic metastatic lesions and only a few studies focused on the characterization of focal hepatic lesions^[4-13]. Thus, the purpose of this study is to evaluate the diagnostic value of superparamagnetic iron oxide in demonstrating benign and malignant focal hepatic lesions.

MATERIAL AND METHODS

Patients

Forty-three patients (32 men, 11 women, mean age 51 years, age range 25-74 years) with previously identified focal hepatic lesions were enrolled into this study. The pathologically proven diagnosis was achieved in 31 cases and the other 12 cases were diagnosed on the basis of clinical findings and biochemical tests. Most lesions were smaller than 3cm. Three cases previously suspected of having focal hepatic lesion were finally confirmed as cirrhotic nodules after SPIO-enhancement. In the remaining 40 patients showed multiple hepatic lesions were found in 22 and solitary in 18, including malignant lesions in 29 cases and benign lesions in 11 cases. The malignant lesions included: primary hepatocellular carcinoma (HCC, *n*=22) associated with hemangioma or cyst in 4, cholangiocarcinoma with cysts (*n*=1), and cholangiohepatocarcinoma (*n*=1), metastases (*n*=5). The benign lesions included: multiple hemangiomas (*n*=2), focal nodular hyperplasia (FNH, *n*=5), angiolipoleiomyoma (*n*=1), inflammatory pseudotumor with hemangioma and cysts (*n*=1), multiple abscess (*n*=1) and focal inflammation with hemangioma (*n*=1).

Contrast agent

Gadopentetate dimeglumine (Magnevist; Schering, Berlin, Germany) was manually administered through antecubital intravenous bolus of 0.1mmol/kg. Feridex (Advanced Magnetix, USA) is an iron oxide preparation coated with low-molecular-weight dextran available in 5mL vial containing 11.2mg iron and 61.3mg mannitol/mL. Feridex at a dose of 0.05mL·kg⁻¹ (0.56mg Fe·kg⁻¹) was diluted with 100mL of 5g·L⁻¹ glucose and infused intravenously at a rate of 3mL·min⁻¹.

Imaging procedure

The GE Signa 1.5T MR imaging system was used. The whole procedure including: ① non-enhanced images: SE T1-weighted (TR/TE=540ms/15ms), FSE T2-weighted with fat suppression (TR/TE=3000-4000ms/98ms); ② Gd-DTPA enhanced images: FMPSGR with dynamic enhancement; and ③ SPIO-enhanced images: 1-7 d later, SE T1-weighted, FSE T2-weighted, FSE T2-weighted with fat suppressed sequences, were performed after SPIO administration. Transverse images were obtained with a slice thickness of 8mm, a section gap of 1-2mm, a field of view of 360mm and matrix size of 256×160.

Imaging analysis

The images were reviewed by 3 experienced radiologists. The signal intensities (SI) of normal hepatic parenchyma, hepatic lesions and

signal change of lesion-to-liver were measured before and after administration of SPIO. Regions of interest (ROI) with at least 50 pixels on homogeneous background free of artifacts. ROI were chosen to be representative of the tissue being evaluated. Measurements were made at the same anatomic level for unenhanced and enhanced images in each patient. If patient had multiple lesions with the homogeneous character, the typical one was selected, otherwise the lesions were analyzed individually.

RESULTS

Totally 12 kinds of benign and malignant diseases were observed in 43 patients. The CNR of lesion-to-liver was evaluated on each sequence (Tables 1 and 2). After SPIO-enhancement the ratios of lesion-to-liver were significantly raised on T₁-weighed images except that of cyst, while on T₂-weighed images the hepatic cirrhotic nodules and FNH's ratios of lesion-to-liver showed no significant difference before and after SPIO-enhancement.

Table 1 The CNR of lesion-to-liver on T₁WI

Lesion (cases)	T ₁ WI	SPIO-enhanced T ₁ WI	P
HCC (22)	-10.2±8.3	19.9±23.8	<0.001
Hemangioma (5)	-16.4±8.6	71±33	<0.05
Cyst (4)	-457±12.1	-33.7±17.9	>0.05
Metastases (5)	-15.4±9.3	6.8±28.1	<0.05
Cirrhosis nodules (4)	2.3±9.3	21.3±17	<0.05
FNH (5)	-4.3±14.1	18.8±18.6	<0.05
Cholangiocarcinoma (1)	-32	0	-
inflammatory pseudotumor (1)	-15	47	-
Hepatic abscess (1)	-19	1	-
Focal inflammatory lesion (1)	-17	12	-
Angiolipoleiomyoma (1)	16	85	-
Cholangiohepatocarcinoma (1)	-5	34	-

Table 2 The CNR of lesion-to-liver on T₂WI

Lesion (cases)	T ₂ WI	SPIO-enhanced T ₂ WI	P
HCC (22)	98.39±58.59	465.77±272.73	<0.001
Hemangioma (5)	354.57±119.78	1452.63±205.68	<0.001
Cyst (4)	509.48±145.02	1256.33±333.39	<0.001
Metastases (5)	104.36±52.02	416.11±324.94	<0.05
Cirrhosis nodules (4)	16.34±15.76	13.77±12.54	>0.05
FNH (5)	65.78±68.4	77.5±104.7	>0.05
Cholangiocarcinoma (1)	63.33	766.95	-
inflammatory pseudotumor (1)	45.58	618.01	-
Hepatic abscess (1)	114.97	587.55	-
Focal inflammatory lesion (1)	89.33	575.53	-
Angiolipoleiomyoma (1)	145.26	523.91	-
Cholangiohepatocarcinoma (1)	106.09	1390.6	-

HCC was found in 22 patients. The lesions were iso- or hypointense on T₁-weighed images and slightly hyperintense on T₂-weighed images before enhancement. After SPIO administration, 11 cases of the lesions became slightly hyperintense, 10 were isointense and 1 was hypointense on T₁WI, while on T₂WI all lesions appeared hyperintense. The mean CNRs of lesion-to-liver on T₁WI and T₂WI were greatly improved from -10.2±8.3, 98.4±58.6 to 19.9±23.8, 465.8±272.7 respectively after SPIO administration. The difference had statistical significance ($P<0.001$). After Gd-DTPA administration, 17 cases showed obvious enhancement while the other 5 cases enhanced mildly in early phase. Characteristically, the signal

intensity or enhancement of the lesions decreased significantly in portal and delayed phases (Figure 1A-C).

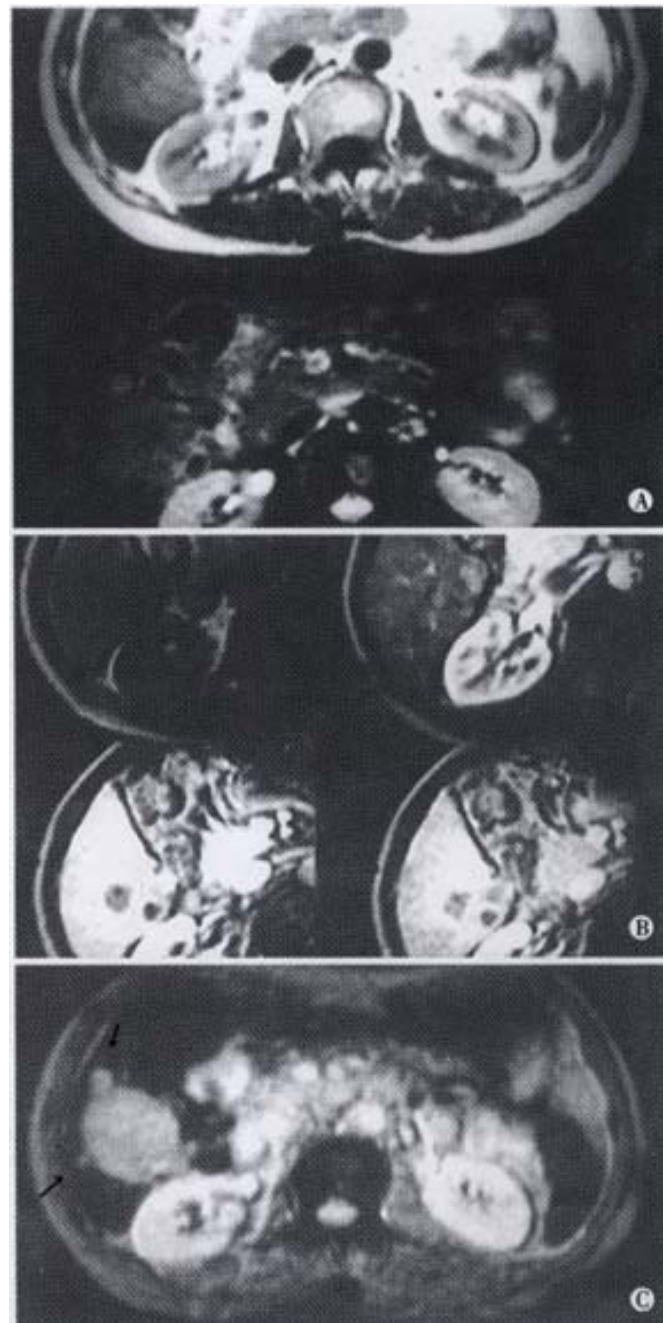


Figure 1 Primary hepatocellular carcinoma in posterior right lobe. The lesions appear hypointensity on T₁WI and mildly hyperintensity on T₂WI (A). On Gd-DTPA enhanced images, early enhancement can be seen in arterial phase and appear relatively hypointensity in portal phase. (B) On SPIO-enhanced image, the conspicuity is clearer than pre-contrast and Gd-DTPA enhanced images. Two micro-lesions (arrow) are obviously showed (C).

Hepatic hemangioma was revealed in 5 cases. The lesions were iso- or hypointense on T₁WI and markedly hyperintense on T₂WI in pre-contrast images. After SPIO-enhancement distinct SI increase was noted and the CNR of lesion-to-liver increased from -16.4±8.6 to 71±33 ($P<0.05$) on T₁WI. The signal intensity showed no perceivable change on T₂WI, but the CNR of lesion-to-liver was greatly increased because of the signal loss of the background after SPIO administration (Figure 2A, B). After Gd-DTPA enhancement, the lesions were gradually filled by the contrast from peripheral to central area and were kept hyperintense in portal and delayed phases.

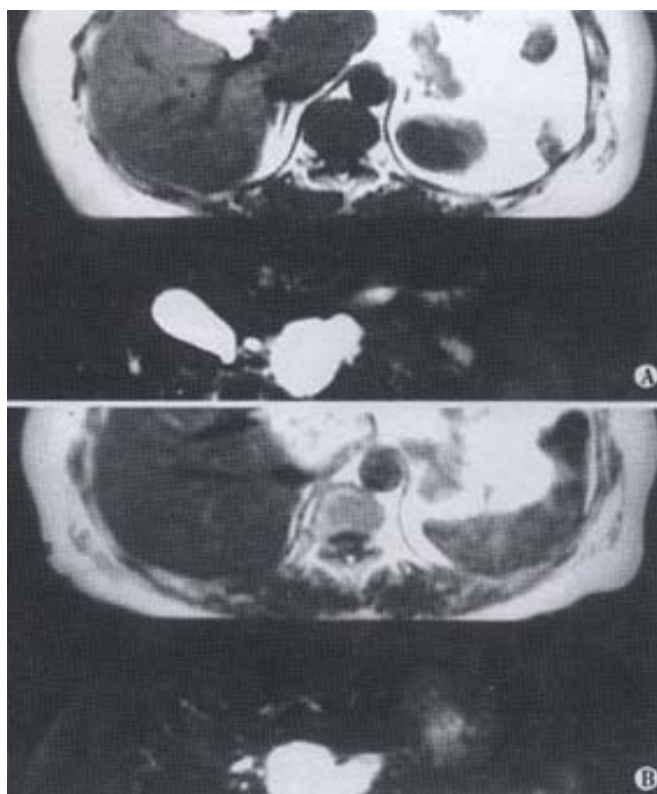


Figure 2 Hepatic hemangioma. (A) The lesion shows hypointensity on T₁WI and hyperintensity on T₂WI on pre-contrast images. (B) After SPIO administration, the lesion become hyperintense on both T₁WI and T₂WI (arrow).

Hepatic cyst was found in 4 patients. The SI of the cyst had no change after SPIO-enhancement. The hypointensity of cystic lesions on T₁WI after SPIO-enhancement was characteristic, thus it could be distinguished from other focal hepatic lesions. The hepatic cyst showed no enhancement after Gd-DTPA administration.

Metastasis was observed in 5 cases. The lesions were hypointense on T₁WI pre-enhancement and iso- or hypointense during post-enhancement. On T₂WI they were mildly hyperintense before enhancement and relatively hyperintense after enhancement because of obvious signal decrease of adjacent normal liver parenchyma. Such change of SI had no diagnostic value because many other focal hepatic lesions could have the similar appearance after SPIO enhancement. The appearance of lesions varied after Gd-DTPA administration, most of them showed peripheral enhancement, or with “bull eyes” sign, or only slightly enhanced.

Cirrhotic nodule was found in 4 patients, which was associated with HCC in one patient. On pre-contrast T₁WI cirrhotic nodules appeared slightly hyperintense differing from other focal hepatic lesions. That the cirrhotic nodule contained Kupffer cells which could take up SPIO particles made it have the same SI as that of the surrounding liver parenchyma after SPIO administration. The cirrhotic nodules showed no early enhancement after Gd-DTPA administration and pertained iso- or hypo-intense in portal and delayed phases.

Focal nodular hyperplasia (FNH) was observed in 5 cases. The lesions were slightly hypointense on unenhanced T₁WI. The appearances of FNH on T₂WI were variable and could be hyperintense ($n=2$), heterogeneously intense ($n=2$) and iso-intense ($n=1$) which was unable to be detected. After SPIO-enhancement, SI of the lesion decreased markedly and appeared iso- or slightly hyper-intense on T₂WI, which was characteristic for FNH. On Gd-DTPA enhanced image, the manifestation was also characteristic: it was obviously enhanced in early phase and continuously kept hyperintense in portal and delayed phases (Figure 3A-C).

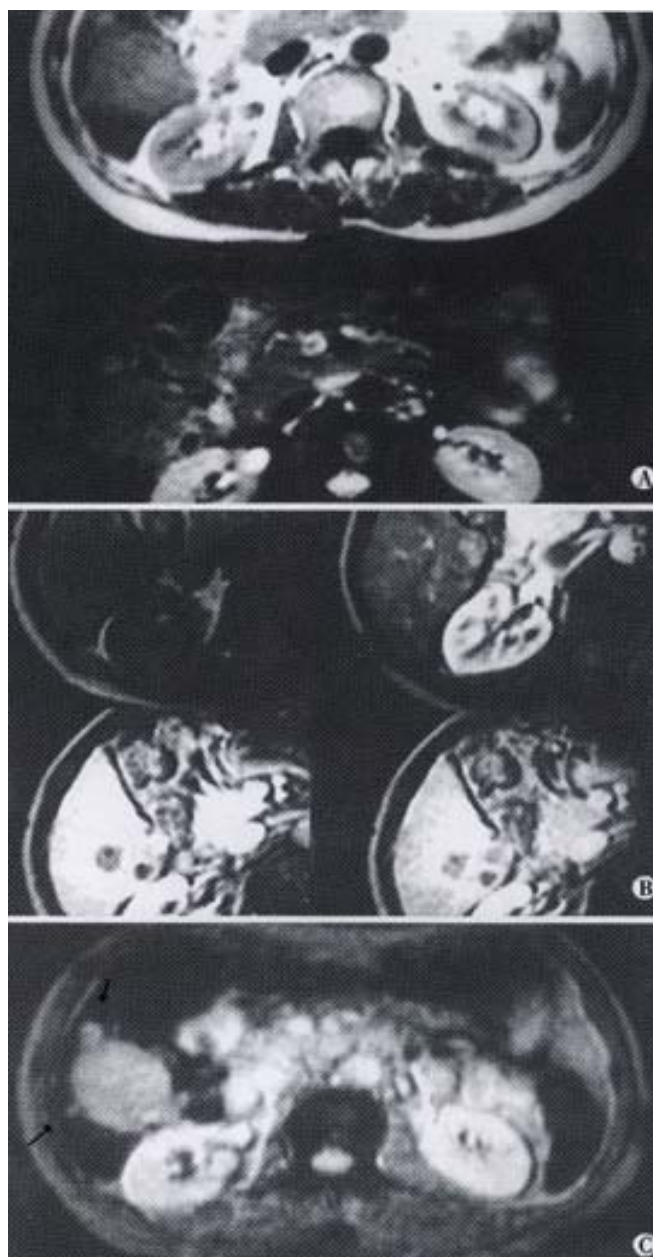


Figure 3 Focal nodular hyperplasia (FNH). Before enhancement, the lesion (arrow) presents hypointensity on T₁WI and heterogeneous hyperintensity on T₂WI (A). After Gd-DTPA administration, the lesion is obviously enhanced in arterial phase and remains hyperintense in portal and delayed phase (B). On T₂WI after SPIO enhancement, the lesion (arrow) has focal signal loss compared with the un-enhanced image (C).

Other focal hepatic lesions were found in 6 cases including cholangiocarcinoma ($n=1$), inflammatory pseudotumor ($n=1$), hepatic abscess ($n=1$), focal inflammatory lesion ($n=1$), angiolipoleiomyoma ($n=1$), and cholangiohepatocarcinoma ($n=1$). These lesions were hypointense on T₁WI and slightly or moderately hyperintense on T₂WI before enhancement. The appearances were non-specific after SPIO-enhancement although the contour of lesions was clear and the CNR of lesion-to-liver increased, which was helpful in improving the detectability or conspicuity. The appearances of these lesions on Gd-DTPA enhanced images were also diversified.

DISCUSSION

As a non-specific extracellular contrast material, Gd-DTPA has been widely used in MR imaging of the liver. Dynamic Gd-DTPA-

enhanced MR images can provide much useful information of the blood supply of lesions and thus highly improving the accuracy of diagnose of focal hepatic lesions. However, Gd-DTPA has several disadvantages such as non-specific distribution, quickly reaching equilibrium throughout extracellular compartment and having slightly nephrotic toxicity. As a negative contrast material, namely reticulo-endothelial system specific contrast agent, the particles of SPIO can be taken up primarily by the hepato-splenic Kupffer cells. The collection of SPIO particles can produce a focal heterogeneous magnetic field which shortens T2 relaxation time predominantly, leading to a significant decrease of SI of normal hepatic parenchyma and remarkable improvement for the focal lesion detection. The prolonged half-life time and widened scanning time-window are also helpful in making examination more convenient^[1,4,5,13-15,17].

The signal intensity of normal hepatic parenchyma decreased both on T₁WI and T₂WI after SPIO-enhancement, especially on T₂WI. The SI of HCC changed a little due to lack of Kupffer cells, but the signal loss of background inversely makes the HCC appear hyperintense. As a result, the CNR of lesion-to-liver increased and the detection of HCC after SPIO-enhancement being improved. There are a few of reports dealing with the appearance of HCC on SPIO-enhanced MR images^[9,14,17-22]. Grangier described HCC's feature in 10 cases after SPIO enhancement and concluded that the HCC presenting iso-intensity on T1WI was the key point for differentiating HCC from hemangioma and cyst^[11]. However, we believe that it might be inappropriate because the appearances of HCC in our 22 cases on enhanced-T₁WI were slightly hyperintense, isointense and hypointense which were 50% (11/22), 45.5% (10/22) and 4.5% (1/22) respectively. This might be attributed to more examples in our study or the difference of HCC's differentiation between the two studies. The non-characteristic appearances of HCC on pre- and post-SPIO-enhanced T₂WI made it difficult to distinguish from other malignant lesions. Moreover, the signal changes on pre- and post-enhanced T₁WI can exclude the possibility of hemangioma and cyst. Accordingly, the accurate diagnosis of HCC must not merely rely on the appearance of lesion on SPIO-enhanced MRI but on the combination with the clinical findings and biochemical tests. After Gd-DTPA administration, the precise diagnosis in most cases can be made according to the enhancement pattern of the lesion. Typically, HCC is enhanced rapidly in arterial phase and the contrast agent is soon washed out in portal phase. So we believe that, only for those the diagnoses are indefinite or the appearances of lesion are untypical on Gd-DTPA-enhanced images, SPIO-enhanced MRI could be a method of choice to make further diagnosis^[17-21].

The hemangioma had high SI on unenhanced T₂WI and showed no change on SPIO-enhanced T₂WI. The hemangioma presenting moderate hyper-intensity on T₁WI after SPIO-enhancement is a key point to distinguish it from cyst and other focal hepatic lesions. However, such typical appearance did not present, owing to the partial volume effect in tiny hemangioma in our study, manifesting iso- or slight hyper-intensity on post-enhanced T₁WI which might make the diagnosis confused. Grangier and Hahn *et al* reported that on SPIO-enhanced T₂WI, the SI of hemangioma could decrease significantly and its enhancement pattern was as the same as that on Gd-DTPA enhanced T1WI (the lesion was filled with contrast agent gradually)^[10,11]. Although the signal of lesion decreased a little, 11 lesions of 5 patients in our study had no such appearance and remained hyper-intensitive namely "Bright Bulb" on SPIO-enhanced T₂WI. Whether such difference is attributed to the different dosage of contrast agent used in studies (10(mol Fe·kg⁻¹ in our group vs 15(mol Fe·kg⁻¹ in others) needs further investigations.

SPIO has unique advantages in diagnosing liver cirrhotic nodules and FNH. Both contain Kupffer cells which can take up the SPIO particles. Accordingly, on post-contrast T₂WI, the former showed identical intensity to that of adjacent normal hepatic parenchyma and the latter had signal loss of different degree. Hepatic cirrhotic nodule

and FNH were the only two diseases that had signal loss in our study. As hepatic cirrhotic nodules usually have a cirrhosis background, the lesion presented the SI similar to that of surrounding liver parenchyma after SPIO-administration and no early enhancement after Gd-DTPA administration is the key factor to make the accurate diagnosis. In our study there were 3 liver cirrhotic nodules, which had difficulty in characterization on pre- and Gd-DTPA enhanced MR images, accurate diagnoses were made after SPIO-administration. Thus, SPIO-enhanced MRI is supposed to be the first choice when the cirrhotic nodule is suspected to be associated with early stage of canceration and has no obvious early enhancement after Gd-DTPA administration^[15]. FNH has no cirrhotic background with abnormally arrayed lobuli hepatis. The various appearances on pre-contrast T₂WI might be corresponding to its different cellular components. Most lesions were iso- or slightly hyperintense on T₂WI and had signal loss on SPIO-enhanced image. The CNR of lesion-to-liver had no statistical significance between pre- and post-contrast images in our study. This can exactly demonstrate that Kupffer cell in FNH uptake the contrast media and decrease the SI while the background has signal loss at the same time (the mean SI of lesion and liver decreased from 138.6 to 43 and 85.3 to 23.6 respectively on pre- and post-contrast images). The change of SI was different from other diseases and had statistical significance ($P < 0.05$). The central scar was reported to present as mildly hyperintense and 2 cases in our study had this appearance. The characterized appearance of FNH on Gd-DTPA enhanced MR image demonstrated markedly early enhancement as homogeneous hyperintense and iso- to slightly hyperintense in portal or delayed phase. Central scar in 3 lesions enhanced in delayed phase. The results in our study were consistent with other report^[24-29].

Cyst had no signal change on both pre- and post-contrast T₁W, and T₂W images. There were 4 inflammatory cases and 1 case of abscess in our study which had no visible difference on pre- and post- SPIO enhanced images. Diagnoses were made only by Gd-DTPA enhanced images and confirmed after clinical antibiotics treatment and follow-up. One case of inflammatory pseudotumor was pathologically proven^[30]. One case of cholangiocarcinoma was diagnosed mainly on Gd-DTPA enhanced images which provided more information of the blood supply of lesions. Another case of angiolipoleiomyoma was misdiagnosed as HCC before surgery on both Gd-DTPA and SPIO-enhanced images because it had early enhancement and no SPIO uptake. When retrospectively reviewed, the patchy hyperintensity on T₁W and T₂W images corresponding to fatty component might suggest the diagnosis. Since there was no obvious difference of SI, SPIO-contrasted image had little specificity in diagnosing such hepatic inflammation, cholangiocarcinoma and angiolipoleiomyoma^[30-33]. To characterize these lesions, SPIO-enhanced image was inferior to Gd-DTPA image although the lesions showed better circumscription.

As a specific MR contrast media, there is no doubt that SPIO has superiority in detection of hepatic micro-lesions. It is also useful in characterization of some lesions and is superior to unenhanced MR with Gd-DTPA enhanced image when differential diagnosis of HCC, FNH and cirrhotic nodule is needed. As most hepatic lesions could be precisely diagnosed by conventional MR combined with Gd-DTPA dynamic contrast enhancement, SPIO-enhanced image would be a supplementary modality to those which are difficult to be defined.

REFERENCES

- 1 Peter F, Sanjay S. Liver-specific MR imaging contrast agents. *Radiol Clin North Am* 1998;36:287-296
- 2 Anthony B, Janice W, Daniel W, *et al.* Hepatic lesion detection at MR imaging: A comparative study with four sequences. *Radiology* 1997; 203:759-765
- 3 Fretz CJ, Elizondo G, Weissleder R, Hahn PF, Stark DD, Ferrucci JT. Superparamagnetic iron oxide-enhanced MR imaging: Pulse sequence optimization for detection of liver cancer. *Radiology* 1989;172:393-397
- 4 Masayuke M, Kanematsu M, Itoh K, Maetani Y, Kondo H, Matsunaga N, Hoshi H, Shiraishi J. Detection of malignant hepatic tumors:

- comparison of Gadolinium- and Ferumoxide-enhanced MR imaging. *AJR* 2001;177:637-643
- 5 Taylor PM, Hawnaur JM, Hutchinson CE. Superparamagnetic iron oxide imaging of focal liver Disease. *Clinical Radiology* 1995;50:215-219
- 6 Lwakatare F, Yamashita Y, Nakayama M, Takahashi M. SPIO-enhanced MR imaging of focal fatty liver lesions. *Abdom Imaging* 2001;26:157-160
- 7 Ros PR, Freeny PC, Harms SE, Seltzer SE, Davis PL, Chan TW, Stillman AE, Muroff LR, Runge VM, Nissenbaum MA. Hepatic MR imaging with ferumoxides: a multicenter clinical trial of the safety and efficacy in the detection of focal hepatic lesions. *Radiology* 1995;196:481-488
- 8 Winter TC, Freeny PC, Nghiem HV, Mack LA, Patten RM, Thomas CR, Elliott S. MR Imaging with IV superparamagnetic ironoxide: efficacy in the detection of focal hepatic lesions. *AJR* 1993;161:1191-1198
- 9 Bluemke DA, Paulson EK, Choti MA, DeSena S, Clavien PA. Detection of hepatic lesions in candidates for surgery: comparison of Ferumoxides-enhanced MR imaging and dual-phase helical CT. *AJR* 2000;175:1653-1658
- 10 Bellin NB, Zaim S, Auberton E, Sarfati G, Duron VJ, Khayat D, Grellet J. Liver metastases: Safety and efficacy of detection with superparamagnetic iron oxide in MR imaging. *Radiology* 1994;193:657-663
- 11 Grangier C, Tourniaire J, Mentha G, Schiau R, Howarth N, Chachuat A, Grossholz M, Terrier F. Enhancement of liver hemangiomas on T1-weighted MR SE images by superparamagnetic iron oxide particles. *J Comput Assist Tomogr* 1994;18:888-896
- 12 Hahn RF, Stark DD, Weissleder R, Elizondo G, Saini S Ferrucci JT. Superparamagnetic iron oxide: Clinical application to imaging tissue perfusion in vascular liver tumors. *Radiology* 1990;174:361-366
- 13 Grandin C, Van Beers BE, Robert A, Gigot JF, Geubel A, Pringot J. Benign hepatocellular tumors: MRI after superparamagnetic iron oxide administration. *J Comput Assist Tomogr* 1995;19:412-418
- 14 Parley MR, Mergo PJ, Torres GM, Ros PR. Characterization of focal hepatic lesions with Ferumoxides-enhanced T2-weighted MR imaging. *AJR* 2000;175:159-163
- 15 Clement O, Frija G, Chambon C, Schouman-Clayes E, Mosnier JF, Poupon MF, Balkau B. Liver tumors in cirrhosis: experimental study with SPIO-enhanced MR imaging. *Radiology* 1991;180:31-36
- 16 Krinsky GA, Lee VS, Theise ND, Weinreb JC, Rofsky NM, Diflo T, Teperman LW. Hepatocellular carcinoma and dysplastic nodules in patients with cirrhosis: prospective diagnosis with MR imaging and explantation correlation. *Radiology* 2001;219:445-454
- 17 Fernandez MDP, Redvanly R. Primary hepatic malignant neoplasms. *Radiol Clin North Am* 1998;36:333-348
- 18 Reimer P, Jahnke N, Fiebich M, Schima W, Deckers F, Marx C, Holzknecht N, Saini S. Hepatic lesion detection and characterization value of nonenhanced MR imaging, superparamagnetic iron oxide-enhanced MR imaging, and spiral CT -ROC analysis. *Radiology* 2000;217:152-158
- 19 Arbab AS, Ichikawa T, Araki T, Toyama K, Nambu A, Ohsawa S, Kumagai H, Aikawa Y. Detection of hepatocellular carcinoma and its metastases with various pulse sequences using superparamagnetic iron oxide (SHU-555-A). *Abdom Imaging* 2000;25:151-158
- 20 Kondo H, Kanematsu M, Hoshi H, Murakami T, Kim T, Hori M, Matsuo M, Nakamura H. Preoperative detection of malignant hepatic tumors: comparison of combined methods of MR imaging with combined methods of CT. *AJR* 2000;174:947-954
- 21 Mori K, Yoshioka H, Itai Y, Okamoto Y, Takahashi N, Saida Y. Arteriportal shunts in cirrhotic patients: Evaluation of the difference between tumorous and nontumorous arteriportal shunts on MR imaging with superparamagnetic iron oxide. *AJR* 2000;175:1659-1664
- 22 Hahn PF, Stark DD, Weissleder R, Elizondo G, Saini S, Ferrucci JT. Clinical Application of superparamagnetic iron oxide of MR imaging of tissue perfusion in vascular liver tumors. *Radiology* 1991;174:361-366
- 23 Paley MR, Ros PR. Hepatic metastases. *Radiol Clin North Am* 1998;36:349-368
- 24 Mergo PJ, Ros PR. Benign lesions of the liver. *Radiol Clin North Am* 1998;36:319-332
- 25 Mortelet KJ, Praet M, Van Vlierberghe H, et al. CT and MR imaging findings in focal nodular hyperplasia of the liver: radiologic-pathologic correlation. *AJR* 2000;175:687-692
- 26 Carlson SK, Daniel JC, Bender CE, Welth TJ. CT of focal nodular hyperplasia of the liver. *AJR* 2000;174:705-712
- 27 Ji Y, Zhu XZ, Tan YS, Zeng HY, Ye QH, Tang ZY. A clinicopathological study of hepatic focal nodular hyperplasia. *Zhonghua Binglixue Zazhi* 2000;29:334-336
- 28 Yi Y, Zhu XZ, Sun HC, Tan YS, Ma ZC, Ye QH, Sujie A, Tang ZY. Hepatocellular adenoma and focal nodular hyperplasia: a series of 24 patients with clinicopathological and radiological correlation. *Chinese Medical Journal* 2000;113:852-857
- 29 Ruppert-Kohlmayr AJ, Uggowitz MM, Kugler C, Zebedin D, Schaffler G, Ruppert GS. Focal nodular hyperplasia and hepatocellular adenoma of the liver: differentiation with multiphasic helical CT. *AJR* 2001;176:1493-1498
- 30 Yan FH, Zhou KR, Jiang YP, Shi WB. Inflammatory pseudotumor of the liver: 13 cases of MRI findings. *World J Gastroenterol* 2001;7:422-424
- 31 Ye HY, Xie ZF, Gao YG, Liang Y, Ji XL, Yu G. Hepatic angiomyolipoma: correlation of MRI and pathologic findings. *Zhonghua Fangshexue Zazhi* 2001;35:679-681
- 32 Braga HJ, Imam K, Bluemke DA. MR imaging of intrahepatic cholangiocarcinoma: use of Ferumoxides for lesion localization and extension. *AJR* 2001;177:111-114
- 33 Ahmadi T, Itai Y, Takahashi M, Onaya H, Kobayashi T, Tanaka YO, Matsuzake Y, Tanaka N, Okada Y. Angiomyolipoma of the liver: significance of CT and MR dynamic study. *Abdom Imaging* 1998;23:520-526

• LIVER CANCER •

Antitumor activities of human dendritic cells derived from peripheral and cord blood

Jin-Kun Zhang, Jun Li, Hai-Bin Chen, Jin-Lun Sun, Yao-Juan Qu, Juan-Juan Lu

Jin-Kun Zhang, Jun Li, Hai-Bin Chen, Jin-Lun Sun, Yao-Juan Qu, Juan-Juan Lu, Cancer Pathology Laboratory, Shantou University Medical College, Shantou 515031, Guangdong Province, China
Supported by Natural Science Foundation of the Higher Education Office of Guangdong Province, No. 9501 and No.9816

Correspondence to: Prof. Jin Kun Zhang, Cancer Pathology Laboratory, Shantou University Medical College, 22 Xinlinglu, Shantou 515031, Guangdong Province, China. Jkzhang@stu.edu.cn

Telephone: +86-754-8900443 Fax: +86-754-8557562

Received 2001-07-19 Accepted 2001-12-29

Abstract

AIM: To observe the biological specialization of human peripheral blood dendritic cells (DC) and cord blood derived DC and its effects on effector cells killing human hepatocarcinoma cell line BEL-7402 *in vitro*.

METHODS: The DC biological characteristics were detected with immunohistochemical and MTT assay. Two antitumor experimental groups are: peripheral blood DC and cord blood DC groups. Peripheral blood DC groups used LAK cells as the effector cells and BEL-7402 as target cells, while cord blood DC groups used CTL induced by tumor antigen twice pulsed DC as effector cells and BEL-7402 as target cells, additional peripheral blood DC and cord blood DC are added to observe its stimulating activities to effector cells. The effector's cytotoxicity to tumor cells were detected with neutral red colorimetric assay at two effector/target ratios of 5:1 and 10:1.

RESULTS: Peripheral blood DC and cord blood DC highly expressed HLA-ABC, HLA-DR, HLA-DQ, CD54 and S-100 protein. The stimulating activities to lymphocyte proliferation were compared between experimental groups (DC added) and control group (no DC added), in six experiment subgroups, the DC/lymphocyte ratio was sequentially 0.25:100, 0.5:100, 1:100, 2:100, 4:100 and 8:100, A values ($\bar{x} \pm s$) were 0.75396 \pm 0.009, 0.84916 \pm 0.010, 0.90894 \pm 0.012, 0.98371 \pm 0.007, 1.01299 \pm 0.006 and 1.20384 \pm 0.006 in peripheral blood DC groups and 0.77650 \pm 0.005, 0.83008 \pm 0.007, 0.92725 \pm 0.007, 1.05990 \pm 0.010, 1.15583 \pm 0.011, 1.22983 \pm 0.011 in cord blood DC groups. A value was 0.59517 \pm 0.005 in control group. The stimulating activities were higher in experimental groups than in control group ($P < 0.01$), which were increased when the DC concentration was enlarged ($P < 0.01$). Two differently derived DCs had the same phenotypes and similar stimulating activities ($P > 0.05$). In peripheral blood DC groups, the cytotoxicity ($\bar{x} \pm s$) of the LD groups (experimental groups) and L groups (control group) was 58.16% \pm 2.03% (5:1), 46.18% \pm 2.25% (10:1) and 38.13% \pm 1.29% (5:1) and 65.40% \pm 1.56% (10:1) respectively; in cord blood DC groups, TD groups (experimental groups) and T groups (control groups) were 69.71% \pm 2.33% (5:1), 77.64% \pm 1.94% (10:1) and 56.89% \pm 1.82% (5:1) and 60.99% \pm 1.42% (10:1) respectively. The cytotoxicity activities were enhanced with increased effector/target ratio ($P < 0.01$). At the same

effector/target ratio, the cytotoxicity of experimental groups were bigger than that of control groups ($P < 0.01$). The cytotoxicity activities of cord blood DC groups were higher than that of peripheral blood DC groups ($P < 0.01$).

CONCLUSION: Peripheral blood DC and cord blood DC are mature DC in morphology and function, both can enhance the effector cell killing activities to hepatocarcinoma cells. DC pulsed with tumor antigen can induce higher specific CTL activity than unpulsed DC.

Zhang JK, Li J, Chen HB, Sun JL, Qu YJ, Lu JJ. Antitumor activities of human dendritic cells derived from peripheral and cord blood. *World J Gastroenterol* 2002;8(1):87-90

INTRODUCTION

Dendritic cells (DC) is a potent professional antigen presenting cell, the only one that can stimulate the naive T cell^[1-4]. DC can present exogenous antigen to CD4⁺ cell by MHC-II antigen presenting pathways as well as to CD8⁺ cell by MHC-I pathways. It also provides plenty of costimulating signals, so that it plays a key role in antitumor immunity^[5-9]. Although the peripheral blood DC is easily separated, DC was able to enhance the killing activity of Lymphokine and PHA activated killer (LAK) cells *in vitro*^[10-12], but in some patients with tumors, especially some patients with advanced tumors, autogenous DC may be defective. In this article, two differently derived DCs are studied on their induction of anti-hepatocarcinoma cell activity. It provides experimental evidence for clinical application of DC directed tumor immunotherapy.

MATERIAL AND METHODS

Blood

Human peripheral blood provided by young volunteers, and cord blood provided by Shantou University Medical College First Affiliated Hospital.

Tumor cell line

BEL-7402 tumor cell line was bought from Experimental Animal Center, Sun Yat-Sen University of Medical Sciences.

Main reagents

Percoll was purchased from Pharmacia. Mini-MACS (magnetic activated cell sorter) and CD34 cell separation kit were purchased from Miltenyi GmbH Biotec, a kit including the following reagents: A1-human Ig (FcR), A2-haptin coupled CD34 monoclonal antibody, B-colloid anti-haptin antibody and microbead. rhSCF, rhGM-CSF and rhTNF- α were obtained from Pepro Tech Ltd or Institute of Basic Medicine Sciences, Chinese Military Medical Academy. Mouse anti-human antibody CD54, HLA-ABC, HLA-DR, HLA-DQ, S-100 protein and SABC immunohistochemical kit were obtained from Biotec, Boehringer Mannheim and Boster, respectively. MTT was from Amresco.

Isolation of human blood DC

Isolation of Human Peripheral blood DC^[9] Four step method of our laboratory was used. Peripheral blood mononuclear cells from

healthy volunteers were prepared using Ficoll-Hypaque ($\rho=1077 \text{ g}\cdot\text{L}^{-1}$) centrifugation method. Interface cells were collected and washed three times to remove platelets. Discontinuous Percoll density gradient centrifugation was employed, and interface cells between 35% and 50% called preliminary enrichment of DC were collected, cultured in PRMI 1640 with $100\text{mL}\cdot\text{L}^{-1}$ inactivated fetal calf serum ($100 \text{ mL}\cdot\text{L}^{-1}$ FCS PRMI 1640) at 37°C , in a saturation humidity, atmosphere of $50\text{mL}\cdot\text{L}^{-1} \text{ CO}_2$ for 36 hours, then panned on Ig coated petri dish for further purification, nonadhesive cells were collected as the mature DC.

Isolation of human cord blood DC The $\text{CD}34^+$ stem cells, were separated using $\text{CD}34^+$ stem cell separation kit and microbead, Mini-MACS cell sorter, cultured with rhGM-CSF, rhTNF- α and rhSCF for 14 d, mature DC was acquired.

Immunohistochemistry method for DC phenotypes

Peripheral blood DC smear and cord blood DC smear were prepared and incubated with mouse anti human HLA-ABC, CD54, HLA-DQ, HLA-DR and S-100 protein primary antibody. ABC staining and DAB were used to display the result.

DC stimulating activity to homogenous lymphocyte

DC stimulating activity to homogenous lymphocyte proliferation Human peripheral blood lymphocytes were obtained by Ficoll separation method. Two groups of peripheral blood DC and cord blood DC were divided. In each group, six subgroups were divided according to the DC/lymphocyte ratio of 0.25:100, 0.5:100, 1:100, 2:100, 4:100 and 8:100 respectively. Lymphocyte concentration was $8\times 10^8\cdot\text{L}^{-1}$, PHA was $50\text{mg}\cdot\text{L}^{-1}$. Control group as DC+PHA served as control in each subgroup. Additional lymphocyte+PHA and PHA also served as control groups. Each subgroup set three wells on 96 multiwell culture plates. Each experiment repeated 4 times.

MTT colorimetric method detecting the lymphocyte proliferation Add $20 \mu\text{L}$ MTT ($5\text{g}\cdot\text{L}^{-1}$) to each well of multiwell culture plate, incubate for 4 hours, then add $150\mu\text{L}$ DMSO, mixed about 10 min until the crystal completely dissolved. The absorption value (A value) of each well was immediately read by Bio-Rad 3550-UV type automatic enzyme linked detector at 490nm wavelength. The minus of A value in experimental group and A in DC+PHA shows the proliferative response. The minus of A value in lymphocyte + PHA group and A in PHA shows the lymphocyte proliferation of control group. SPSS software was applied for analysis of variation.

Effector cells induced

LAK cell induced The human peripheral blood mononuclear cells were prepared by the same procedure above, cultured at $2\times 10^9\cdot\text{L}^{-1}$ population with the final concentration of rhIL-2 $1000\text{kU}\cdot\text{L}^{-1}$ and PHA $20\text{mg}\cdot\text{L}^{-1}$ in $100\text{mL}\cdot\text{L}^{-1}$ FCS PRMI-1640 at 37°C in a full humidified $50\text{mL}\cdot\text{L}^{-1} \text{ CO}_2$ atmosphere for 7 d. Half volume of solution was replaced by fresh culture medium at d4.

CTL induced twice by antigen pulsed DC The whole culture system included human peripheral mononuclear cells $1\times 10^8\cdot\text{L}^{-1}$, cord blood DC $5\times 10^6\cdot\text{L}^{-1}$, ultrasonic disrupted BEL-7402 cells $1\times 10^9\cdot\text{L}^{-1}$, IL-2 $80 \text{ kU}\cdot\text{L}^{-1}$. They were cultured for 5 d and pulsed again at d3. Control culture system (no DC added) was set.

Antitumor experiment

DC induced CTL killing activity to hepatocarcinoma cells The experiment was conducted two groups: peripheral blood DC group and cord blood DC group, each group being divided into two subgroups. Peripheral blood DC groups: BEL-7402+LAK (L group) as control

group, BEL-7402 +LAK +DC (LD group) as experiment group. BEL-7402 cell concentration was $8\times 10^8\cdot\text{L}^{-1}$, DC was $8\times 10^6\cdot\text{L}^{-1}$, two LAK /BEL-7402 ratio of 5:1 and 10:1 were applied. Cord blood DC groups: BEL7402+CTL (T group) as control group, BEL7402+DC-CTL (TD group) as experimental group. Cell concentration and ratio were the same as above. Additional BEL-7402 culture media was set as control group. Each group set three paralleled wells, cultured in 96 multiwell culture plate for 48 hours, the effector cell killing activities were detected. The procedure above was repeated for 4 times.

Neutral red uptake method Neutral red uptake method was applied to detect the cytotoxicity activities of effector cells. 0.1 mL neutral red solution $0.3\text{g}\cdot\text{L}^{-1}$ was added to each well, incubated at 37°C for 1 h, rinsed with PBS, solution of hydrochloride ethanol 0.1 mL was added, and absorbance was detected at 570 nm by Bio-Rad automatic enzyme linked detector. Formula for cytotoxicity calculation is below:

$$(1 - \frac{\text{A value of experiment group} - \text{A value of medium control group}}{\text{A value of control group} - \text{A value of medium control group}}) \times 100\%$$

SPSS for windows statistic software are used for data variation analysis.

RESULTS

DC phenotypes analysis

Immunohistochemical ABC method showed that human peripheral blood DC and human cord blood DC had high expression of HLA-ABC, HLA-DR, HLA-DQ and CD54. S-100 protein was also positive. Positive cells were big and irregular in shaped and filled with diffuse brown-yellow particles in cytoplasm, the neucleus was also big and irregular. However, the phenotype difference between peripheral blood DC and cord blood DC was not distinct.

DC stimulating activity to lymphocyte

In human peripheral blood DC and human cord blood DC groups, lymphocyte proliferation activities were significantly higher than control groups ($P<0.01$), which was increased when DC concentration was enlarged ($P<0.01$). Human peripheral blood DC and human cord blood derived DC had no significant difference in lymphocyte stimulation ($P>0.05$, Figure 1).

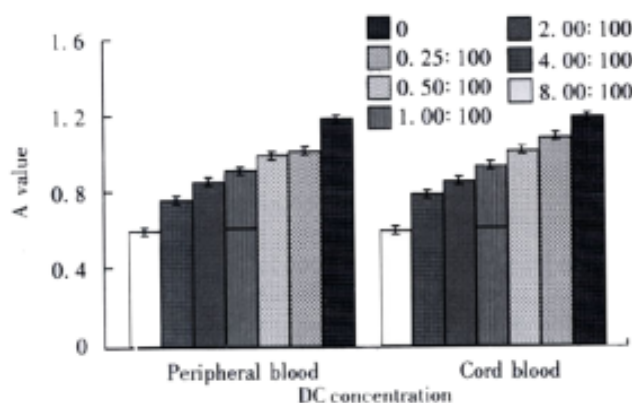


Figure 1 Lymphocyte proliferation response by different DC concentrations.

DC induced effector's cytotoxicity activities

In groups of human peripheral blood DC and human cord blood DC, cytotoxicity activities enhanced with the increased effector/target ratio ($P<0.01$). Within the same ratio, cytotoxicity activities of experimental groups were higher than control groups ($P<0.01$). Cytotoxicity activities of human cord blood DC groups were bigger

than human peripheral blood DC groups ($P < 0.01$, Figure 2)

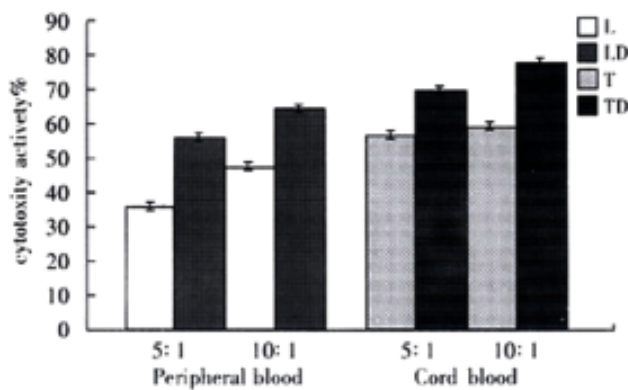


Figure 2 DC's effect to cytotoxicity activity of effector against BEL7402.

DISCUSSION

DC is a potent antigen presenting cells, mainly takes part in cell immunity and T cell dependent humoral immunity, and plays a key role in antitumor immunity^[13-21]. Recently, with the construction of DC isolation method and expanding culture *in vitro*, research has transfer red from the relationship between tumor infiltrating DC and the prognosis to DC application in tumor immunotherapy, especially how to improve the tumor cell immunogenicity and enhance the DC antigen presenting efficacy and stimulating activity to CTL^[22-30]. In this experiment, DC of human peripheral blood and cord blood were studied on its potential in clinical application.

Human peripheral blood DC isolation was made according to four step method modified in this laboratory. This method is easy to operate, low in cost and reliable, and has been used in this laboratory for many years, and high purity of DC can be obtained by this method^[31,32]. Another method is used in cord blood DC isolation: CD34⁺ cell isolation kit combined with cell factor expanding culture for preparation of cord blood derived DC. This is an advancing method. The principle of CD34⁺ cell isolation kit is as follows: CD34⁺ monoclonal antibody recognizes the specific antigen of stem cell membrane, by which the antibody coupled magnetic microbead binds to cells, when the cells pass through column in the magnetic field, the CD34⁺ can be acquired by positive selection. Three reagents comprises in CD34⁺ isolation kit: A1, human Ig, used as blocking reagent to FcR for preventive non specific binding of CD34⁺ monoclonal antibody to CD34⁺ cells. A2, hapten coupled CD34 monoclonal antibody, can specifically bind with CD34 molecule. B, anti-hapten antibody linked with microbead, can link the microbead with CD34⁺ cells. When the cells pass through MACS (magnetic cell sorter) column in magnetic field, negative cells can pass through the column, while positive cells were absorbed to column. When the column was taken away from magnetic field, the elution from column included the positive cells. MACS cell isolation has been verified by immunofluorescent PCR, FISH and FACS method. It has the characteristics of high purity (93%-99.9%)^[14], large number of cells processing ability in a single time, and easy operating, simple procedure. When cell factors such as rhGM-CSF, rhTNF- α and SCF are added to stem cell culture media, most of CD34⁺ cells differentiate to DC^[33]. Though the GM-CSF can stimulate cell growth of both the DC progenitor and monocyte or macrophage, for high purity of CD34⁺ cell in initiate culture system, clearance most of monocyte and macrophage by its adherence to flask by replacing media and culture plate. Cell factor secreted by monocyte and macrophage also benefits DC development.

In this article, a series of antibodies were used for immunohistochemical staining of DC, results showed that human peripheral blood DC had and CD34⁺ derived cord blood DC high

expression of CD54, HLA-ABC, HLA-DR, HLA-DQ, and S-100 protein. The positive cells accounted for above 95% and 90% respectively, demonstrating that DC here is mature^[34,35].

For DC functional analysis, MTT assay was used to detect the DC activity of stimulating the allogeneous lymphocyte. The principle of MTT assay is that the living proliferating cells can deoxidize the MTT (thiazoyl blue tetrazolium bromide) to purple crystal formazan and deposit in cytoplasm, so we can use the colorimetric method to detect the cell proliferation. With continuous modification, it has become a very consummate method with characteristics of sensitivity, simple procedure, safety and no radioactivity. In this experiment, DC can clearly stimulate the lymphocyte response to PHA. It shows that the DC has potent MLR stimulating activity which contributes to DC expression of adherence and MHC- II molecule. Phenotype and functionally mature DC of high purity provided primitive condition for DC application in antitumor.

Tumor cells expressed low level antigen and has antigen modulation, so tumor antigen can not be efficiently presented and the T cell mediated immune response can not be activated, by which tumor can escape the surveillance of immune system. As a nonprofessional APC, tumor cells with no expression of costimulator often leads to T cell anergy. Special attention has been paid to DC for its present exogenous antigen to CD8⁺ cell by MHC- I antigen presenting pathway as well as its expression of costimulating signal^[36-40]. In this article, peripheral and human cord blood DC can significantly improve effector's cytotoxicity, due to a large quantity of dendrites, and many kinds of surface molecules and receptors and cytokine secreted^[41,42]. LAK cells induced for 7 days chiefly demonstrated CTL's characteristic of CD16⁺, CD8⁺ and CD3⁺, which can efficiently kill the target cells^[43-46]. It has been found recently that DC secretion of exosome can present antigen and induce immune response. This is another path for effector activation^[47]. In general, from patients in well condition, autogenous peripheral blood DC and LAK cells can be acquired, for it is low in cost; while in patient in bad condition, cord blood DC can be used as an alternative.

Cord blood DC can more efficiently induce effector's cytotoxicity than peripheral blood DC, due to the following factors: ① Cord blood DC comprises some immature DC, the coexistence of mature and immature DC can be synergetic, immature DC can ingest and process antigen, while mature DC can present antigen and activate T cells, therefore, coexistence of mature and immature DC is better than single mature DC^[48]. ② Both cord DC and CTL were pulse twice with tumor antigen, and specific antitumor activity improved. LAK cells induced 7 days can secrete perforin and granular particles nonspecific to ally kill target cells while human cord blood DC pulsed *in vitro* by tumor antigen can efficiently present tumor antigen to effector which occupy the TCR of CTL, and activate the specific CTL, with the help of costimulator such as CD80, CD86 and CD40. Furthermore, DC can secrete nave T specific chemotactic factor DC-CKK. Some other cell factors such as MCP-1, RANTES and IL-8 also can also play a chemotactic role in DC emigrant. DC can form a cluster of cells and secrete a large number of IL-12 which bind with IL-12R of CTL and enhance CTL proliferating response and cytotoxicity. IL-12 mediates T_H1 immune response and inclines to tumor killing activity^[42,49-51]. If permitted, twice antigen pulsed DC should be used.

Summary, human blood DC and cord blood DC have a potential application in the clinical therapy of hepatocarcinoma, especially late hepatocarcinoma.

REFERENCES

- 1 Rissoan MC, Soumelis V, Kadowaki N, Grouard G, Briere F, Malefyt MDW, Liu YJ. Reciprocal control of T helper cell and

- dendritic cell differentiation. *Science* 1999;283:1183-1186
- 2 Steinman RM, Inaba K. Myeloid dendritic cells. *J Leukocyte Bio* 1999; 66:205-208
 - 3 Bottomly K. T cells and dendritic cells get intimate. *Science* 1999;283: 1124-1125
 - 4 Cao X, Zhang W, Wang J, Zhang M, Huang X, Hamada H, Chen W. Therapy of established tumor with a hybrid cellular vaccine generated by using granulocyte-macrophage colony-stimulating factor genetically modified dendritic cells. *Immunology* 1999;97:616-625
 - 5 Hu JY, Wang S, Zhu JG, Zhou GH, Sun QB. Expression of B7 costimulation molecules by colorectal cancer cells reduces tumorigenicity and induces anti tumor immunity. *World J Gastroenterol* 1999;5: 147-151
 - 6 De VM, Heirman C, Van MS, Devos S, Corthals J, Moser M, Thielemans K. Retrovirally transduced bone marrow-derived dendritic cells require CD4⁺ T cell help to elicit protective and therapeutic antitumor immunity. *J Immunology* 1999;162:144-151
 - 7 Albert ML, Sauter B, Bhardwaj N. Dendritic cells acquire antigen from apoptotic cells and induce class I-restricted CTLs. *Nature* 1998; 392: 86-89
 - 8 Banchereau J, Steinman RM. Dendritic cells and the control of immunity. *Nature* 1998; 392:245-252
 - 9 Luft T, Pang KC, Thomas E, Hertzog P, Hart DN, Trapani J, Cebon J. Type I IFNs enhance the terminal differentiation of dendritic cells. *J Immunol* 1998;161:1947-1953
 - 10 Zhang JK, Chen HB, Sun JL, Zhou YQ. Effect of dendritic cells on LPAK cells induced at different time in killing hepatoma cells. *Shijie Huaren Xiaohua Zazhi* 1999;7:673-675
 - 11 Sun JL, Zhang JK, Chen HB, Cheng JD, Qiu YQ. Promoting effects of dendritic cells on LPAK cells killing human hepatoma cells. *Zhongguo Zhongliu Linchuang yu Kangfu* 1998;5:16-18
 - 12 Chen HB, Zhang JK, Huang ZL, Sun JL, Zhou YQ. Effects of cytokines on dendritic cells against human hepatoma cell line. *Shijie Huaren Xiaohua Zazhi* 1999;7:191-193
 - 13 Shimizu Y, Guidotti LG, Fowler P, Chisari FV. Dendritic cell immunization breaks cytotoxic T lymphocyte tolerance in hepatitis B virus transgenic mice. *J Immunol* 1998;161:4520-4529
 - 14 Mackensen A, Krause T, Blum U, Uhrmeister P, Mertelsmann R, Lindemann A. Homing of intravenously and intralymphatically injected human dendritic cells generated *in vitro* from CD34⁺ hematopoietic progenitor cells. *Cancer Immunol Immunother* 1999; 48: 118-122
 - 15 Salgaller ML, Tjoa BA, Lodge PA, Ragde H, Kenny G, Boynton A, Murphy GP. Dendritic cell-based immunotherapy of prostate cancer. *Crit Rev Immunol* 1998;18:109-119
 - 16 Lim SH, Bailey Wood R. Idiotypic protein-plused dendritic cell vaccination in multiple myeloma. *Int J Cancer* 1999;83:215-222
 - 17 Greten TF, Jaffee EM. Cancer vaccines. *J Clin Oncol* 1999; 17: 1047-1060
 - 18 Chen CH, Wu TC. Experimental vaccine strategies for cancer immunotherapy. *J Biomed Sci* 1998; 5: 231-252
 - 19 Wang RF. Human tumor antigens: implications for cancer vaccine development. *J Mol Med* 1999; 77: 640-655
 - 20 Li MS, Yuan AL, Zhang WD, Liu SD, Lu AM, Zhou DY. Dendritic cells *in vitro* induce efficient and special anti tumor immune response. *Shijie Huaren Xiaohua Zazhi* 1999;7:161-163
 - 21 Li MS, Yuan AL, Zhang WD, Chen XQ, Tian XH, Piao YJ. Immune response induced by dendritic cells induce apoptosis and inhibit proliferation of tumor cells. *Shijie Huaren Xiaohua Zazhi* 2000;8:56-58
 - 22 Xiao LF, Luo LQ, Zhou Y, Huang SL. Study of the phenotype of PBLs activated by CD28/CD80 and CD2/CD58 and acting with hepatoma cells and the restricted usage of TCR V α gene subfamily. *Shijie Huaren Xiaohua Zazhi* 1999;7:1044-1046
 - 23 Gilboa E, Nair SK, Lysterly HK. Immunotherapy of cancer with dendritic cell based vaccines. *Cancer Immunol* 1998;46:82-87
 - 24 Morse MA, Coleman RE, Akabani G, Niehaus N, Coleman D, Lysterly HK. Migration of human dendritic cells after injection in patients with metastatic malignancies. *Cancer Res* 1999;59:56-58
 - 25 Marriott I, Bost KL, Inscho EW. Extracellular uridine nucleotides initiate cytokine production by murine dendritic cells. *Cellular Immunology* 1999;195:147-156
 - 26 Sun JL, Zhang JK, Chen HB, Zhou YQ. Morphology of cultured human peripheral blood dendritic cells and their antitumor activity. *Zhongguo Zuzhihuaxue yu Xibaoxue Zazhi* 1999; 8: 28-31
 - 27 Nunez R, Grob P, Baumann S, Zuniga A, Ackermann M, Suter M. Immortalized cell lines derived from mice lacking both type I and type II IFN receptors unify some functions of immature and mature dendritic cells. *Immunology and Cell Bio* 1999;77:153-163
 - 28 Wu MC. Progress in surgical treatment of primary hepatocellular carcinoma. *Huaren Xiaohua Zazhi* 1998;6:921-923
 - 29 Zou QY, Li RB, Zheng PL, Yang LP, Chen YZ, Kong XP. Effect of embryohepatic extracts on proliferation and differentiation of hepatoma BEL-7402 cells. *Shijie Huaren Xiaohua Zazhi* 1999;7:243-245
 - 30 Kanto T, Hayashi N, Takehara T, Tatsumi T, Kuzushita N, Ito A, Sasaki Kasahara A, Hori M. Impaired allostimulatory capacity of peripheral blood dendritic cells recovered from hepatitis C virus infected individuals. *J Immunol* 1999;162: 5584-5591
 - 31 Zhang JK, Sun JL, Chen HB, Zang Y, Qu YJ. Influence of granulocyte-macrophage colony-stimulating factor and tumor necrosis factor upon the anti-hepatoma activities of human dendritic cells. *World J Gastroenterol* 2000; 6:718-720
 - 32 Sun JL, Zhang JK, Chen JD, Chen HB, Chew YQ, Chen JX. *in vitro* study on the morphology of human blood dendritic cells and LPAK cells inducing apoptosis of the hepatoma cell line. *Chinese medical journal* 2001; 114: 600-605
 - 33 Herlyn D, Birebent B. Advances in cancer vaccine development. *Ann Med* 1999; 31: 66-78
 - 34 Austyn JM. Dendritic cells. *Curr Opin Hematol* 1998;5:3-15
 - 35 Zhai SH, Liu JB, Zhu P, Wang YH. CD54, CD80, CD86 and HLA-ABC expressions in liver cirrhosis and hepatocarcinoma. *Shijie Huaren Xiaohua Zazhi* 2000;8:292-295
 - 36 Reid SD, Penna G, Adorini L. The control of T cell responses by dendritic cell subsets. *Curr Opin Immunol* 2000; 12:114-121
 - 37 Macpherson G, Kushnir N, Wykes M. Dendritic cells, B cells and the regulation of antibody synthesis. *Immun Rev* 1999;172:325-334
 - 38 Lanzavecchia A, Sallusto F. From synapses to immunological memory: the role of sustained T cell stimulation. *Curr Opin Immunol* 2000; 12: 92-98
 - 39 Dubois B, Bridon JM, Fayette J, Barthelemy C, Banchereau J, Caux C, Briere F. Dendritic cells directly modulate B cell growth and differentiation. *J Leuk Biol* 1999; 66: 224-229
 - 40 Mailliard RB, Dallal RM, Son YI, Lotze MT. Dendritic cells promote T-cell survival or death depending upon their maturation state and presentation of antigen. *Immunol Invest* 2000; 29: 177-185
 - 41 Stockwin LH, McGonagle D, Martin IG, Blair GE. Dendritic cells: immunological sentinels with a central role in health and disease. *Immunol and Cell Biol* 2000; 78: 91-102
 - 42 Macpherson G, Wykes M. Dendritic cell-B cell interaction: dendritic cells provide B cells with CD40-independent proliferation signals and CD40-dependent survival signals. *Immunology* 2000; 100:1-3
 - 43 Huang SL, Xiao LF, Luo LQ, Chen HQ. Phenotype analysis and restricted usage of TCR V α genes subfamily in mAb-costimulated T cells after incubated with hepatocellular carcinoma cell line. *Shijie Huaren Xiaohua Zazhi* 1998;6:1033-1035
 - 44 Tang ZY. Advances in clinical research of hepatocellular carcinoma in China. *Shijie Huaren Xiaohua Zazhi* 1998; 6:1013-1016
 - 45 Chen Q, Ye YB, Chen Z. Activation of killer cells with soluble gastric cancer antigen combined with anti CD3 McAb. *World J Gastroenterol* 1999;5:179-180
 - 46 Zhang JK, Sun JL, Chen HB, Zhou YQ. Ultrastructural comparison of apoptosis of human hepatoma cells and LAK cells. *Shijie Huaren Xiaohua Zazhi* 1998;6:877-879
 - 47 Zitvogel L, Regnault A, Lozier J, Wolfers J, Flament C, Tenza D, Ricciardi Castagnoli P, Paposo G, Amigorena S. Eradication of established murine tumors using a novel cell-free vaccine: dendritic cell-derived exosomes. *Nat Med* 1998;4: 594-600
 - 48 Fujii S, Fujimoto K, Shimizu K, Ezaki T, Kawano F, Takatsuki K, Kawakita M, Matsuno K. Presentation of tumor antigens by phagocytic dendritic cell clusters generated from human CD34⁺ hematopoietic progenitor cells: induction of autologous cytotoxic T lymphocytes against leukemic cells in acute myelogenous leukemia patient. *Cancer Res* 1999;59:2150-2158
 - 49 Chiodoni C, Paglia P, Stoppacciaro A, Rodolfo M, Parenza M, Colombo MP. Dendritic cells infiltrating tumors cotransduced with granulocyte/macrophage colony-stimulating factor (GM-CSF) and CD40 ligand genes take up and present endogenous tumor-associated antigens, and prime naive mice for a cytotoxic T lymphocyte response. *J Exp Med* 1999;190:125-133
 - 50 Rosenzweig M, Camus S, Guigon M, Gluckman JC. The influence of interleukin (IL)-4, IL-13, and Flt3 ligand on human dendritic cell differentiation from cord blood CD34⁺ progenitor cells. *EXP Hematol* 1998;26:63-72
 - 51 Holtl L, Rieser C, Papesh C, Ramoner R, Herold M, Klocker H, Radmayr C, Stenzl A, Bartsch G, Thurnher M. Cellular and humoral immune responses in patients with metastatic renal cell carcinoma after vaccination with antigen pulsed dendritic cells. *J Urol* 1999; 161: 777-782

• VIRAL LIVER DISEASES •

Anti-HBV hairpin ribozyme-mediated cleavage of target RNA in vitro

Yu-Hu Song, Ju-Sheng Lin, Nan-Zhi Liu, Xin-Juan Kong, Na Xie, Nan-Xia Wang, You-Xin Jin, Kuo-Huan Liang

Ju-Sheng Lin, Nan-Zhi Liu, Xin-Juan Kong, Na Xie, Nan-Xia Wang, Kuo-Huan Liang, Institute of Liver Diseases, Tongji Hospital, Tongji Medical College, Huazhong University of Science and Technology, Wuhan 430030, Hubei Province, China

Yu-Hu Song, You-Xin Jin, State Key Laboratory of Molecular Biology, Shanghai Institute of Biochemistry, Chinese Academy of Science, Shanghai 200031, China

Supported by Ministry of Health (No 98-1-140) and Chinese Academy of Sciences (No KJ951-B1-610)

Correspondence to: Dr. JIN You-Xin, State Key Laboratory of Molecular Biology, Shanghai Institute of Biochemistry, Chinese Academy of Science, Shanghai 200031, China. yxjin@sunm.shnc.ac.cn
Telephone: +86-21-64374430-221

Received 2001-07-19 Accepted 2001-10-28

Abstract

AIM: To study the preparation and cleavage activity of HpRz directed against the transcript of HBV core gene *in vitro*.

METHODS: HpRz gene designed by computer targeting the transcript of HBV core gene was cloned into the vector p1.5 between 5'-cis-Rz and 3'-cis-Rz. ³²P-labeled HpRz transcript proved whether the vector fit for the preparation of hairpin ribozyme *in vitro*. ³²P-labeled pKC transcript containing HBV core region as target-RNA was transcribed using T₇ RNA polymerase and purified by denaturing PAGE. Cold HpRz transcript was incubated with ³²P-labeled target-RNAs under different conditions and radio autographed after denaturing polyacrylamide gel electrophoresis.

RESULTS: HpRz has the specific ability of cleavage of target RNA at 37°C and 12 mM MgCl₂. K_m=26.31nmol/L, K_{cat}=0.18/min. These results revealed that the design of HpRz was correct.

CONCLUSION: HpRz prepared in this study possesses specific catalytic activity from the identification of cleavage activity. These results indicate that hairpin ribozyme may intracellularly inhibit the replication of HBV, therefore it may become a novel potent weapon for the treatment of hepatitis B.

Song YH, Lin JS, Liu NZ, Kong XJ, Xie N, Wang NX, Jin YX, Liang KH. Anti-HBV hairpin ribozyme-mediated cleavage of target RNA *in vitro*. *World J Gastroenterol* 2002;8(1):91-94

INTRODUCTION

Hepatitis B is a major worldwide health problem^[1-5]. Hepatitis B virus is a small hepatotropic DNA virus, causing acute and chronic B-type hepatitis in man. Chronic infection is associated with a high risk of liver cirrhosis and primary liver carcinoma^[6-14]. Currently available therapies are of limited efficacy^[15-33]. Ribozyme is a kind of catalytic RNA which can catalyze the cleavage of sequence-specific RNA. Compared with antisense RNA, ribozyme may be a more effective experimental tool to suppress the gene expression. Possessing both antisense and RNA cleavage activity, the enzymatic nature of

ribozyme may facilitate effectiveness even at low level of expression^[34]. Hepatitis B virus is a DNA virus that replicates through reverse transcription of a RNA intermediate (pregenic RNA). So engineered anti-HBV ribozyme can potentially be multifunctional, targeting pregenomic RNA and viral mRNA to suppress the replication of hepatitis B virus. Since previous attempt to use hammerhead ribozyme for the intracellular inhibition of HBV replication have been largely unsuccessful in intact cell^[35,36], however engineered hairpin ribozymes have been shown to inhibit replication of human immunodeficiency virus, hepatitis C virus and human papilloma virus *in vivo*^[37-44]. So we designed hairpin ribozyme to inhibit HBV replication. It is well known that HBV C region is associated with viral replication. In this report we have designed hairpin ribozyme targeting core gene of HBV by computer, prepared hairpin ribozyme by transcription of recombinant plasmid *in vitro*, and proved its ability to cleave HBV *in vitro* from identification of activity of anti-HBV hairpin ribozyme.

MATERIALS AND METHODS

Materials

E. coli DH5α has been maintained in our laboratory. The ribozyme vector p1.5 (kind gift of Qi GR, Shanghai Institute of Biochemistry), Plasmid pKC^[45] for target-RNAs (constructed by Dr Lian JQ, the Forth Military Medical University) has been maintained in our laboratory. DNA sequence Kit, *in vitro* transcription kit, restriction endonucleases, T4 DNA ligase, RNase A free DNase I were purchased from Promega Company; and RNase inhibitor, T4 DNA polymerase from Takara Company, α³²P dATP and α³² UTP from Beijing Yahui Company, Materials were used all of analytical purification.

Oligonucleotides of HpRz: R1 5'-CTA GAT CCG GAA GAA CTA AAC CAG AGA AAC AGA TCT CTT CGG AGA TCG TAC ATT ACC TGG TAG GTA C-3'; R2 5'-CTA CCA GGT AAT GTA CGA TCT CCG AAG AGA TCT GTT TCT CTG GTT TAG TTC TTC CGG AT-3'. They were chemically synthesized in Beckman Oligo-1000 DNA synthesizer.

Methods

***In vitro* transcription and purification of target RNA** The template pKC was linearized with BstXI, the 3'-overhangs of linearized pKC was blunted with T4 DNA polymerase. *in vitro* transcription was carried out at 37°C for 90 min in a 20 μL final volume containing 40 mmol·L⁻¹ Tris·HCl (pH 7.5), 50 mmol·L⁻¹ DTT, 2 mmol·L⁻¹ spermidine, 8 mmol·L⁻¹ MgCl₂, 0.25 mmol·L⁻¹ ATP, GTP, CTP, 0.05 mmol·L⁻¹ UTP, 370 KBq alpha ³²P-UTP, 80 U T₇ RNA polymerase and 4 μg linearized template. Target RNA was purified by 60g·L⁻¹ denaturing gel electrophoresis by cutting off the autoradiograph bands. Labeled target RNA was dissolved in DEPC H₂O and reserved under -20°C.

Construction of recombinant plasmid for ribozyme and preparation of ribozyme *in vitro* The hairpin ribozyme HpRz for HBV was designed according to the computer software pcFOLD compiled by Professor Zuker (Canadian Academy of Science). The

homologous possibility with the gene of human being was excluded by consulting with RNA sequence of human cell from NCBI Genbank. Synthesized ribozyme fragments were cloned into XbaI/KpnI sites of p1.5 as pHpRz. Recombinant plasmid was identified by being digested with EcoRI and HindIII, then the DNA sequence of recombinant plasmid was analyzed through the dideoxy method developed by Sanger (Figure 1). The template pHpRz was linearized with EcoRI and *in vitro* transcription and purification of ribozyme were the same as those of target RNA. To get a large amount of transcribed HpRz without isotope, the transcription of HpRz was set up according to manufacture's instruction, then template was digested with RNase A free DNase I, the RNA was dissolved in DEPC H₂O and measured by spectrophotometer containing 3'-cis-Rz and 5'-cis-Rz.

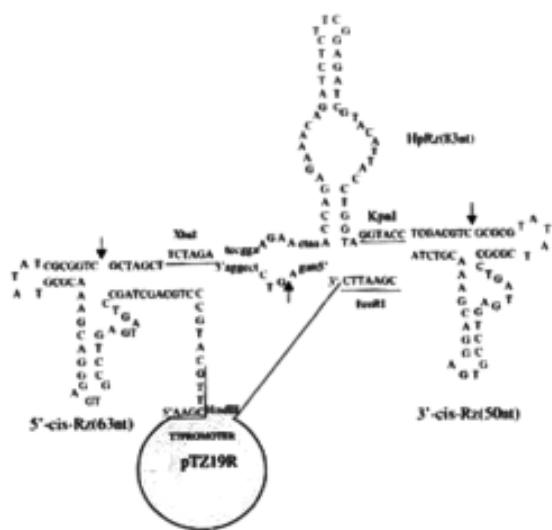


Figure 1 Structure of HpRz plus 5'-cis-Rz and 3'-cis-Rz.

***In vitro* cleavage reaction of HpRz** The cold hairpin ribozyme and target RNA labeled by alpha-³²P UTP were quantified. The cleavage reaction of ribozyme was performed in ribozyme buffer (40 mmol·L⁻¹ Tris·HCl pH7.5/ 12 mmol·L⁻¹ MgCl₂) at 37°C with 10 nmol·L⁻¹ ³²P-labeled substrate and 10 n mol·L⁻¹ cold ribozyme. In this condition the cleavage mixture was incubated at different time points. The volume of the reaction is 5 μL. One μL loading buffer (2.5g·L⁻¹ Bromophenol Blue, 2.5g·L⁻¹ Xylene cyanol FF, 20 mmol·L⁻¹ EDTA and saturated Urea) was added to stop the reaction. The result could be analyzed after running a 60g·L⁻¹ denaturing polyacrylamide gel electrophoresis. The cleavage efficiency was calculated from Bq values of the bands of substrate (S) and products (P) $CE = [P/(P+S)] \cdot 100\%$.

Kinetics of the cleavage reaction The procedure was described by Uhlenbeck^[46]. The cleavage reactions were done and the results were analyzed as above. K_m and K_{cat} were calculated by Lineweaver-Burk method (double- reciprocal plot).

RESULTS

Identification of recombinant plasmid pHpRz

The result of digested recombinant plasmid by EcoRI and HindIII was analyzed by running 20g·L⁻¹ agarose gel electrophoresis (Figure 2). This result and the DNA sequence analysis showed that the clone was correct.

Identification of transcription of ribozyme

The transcription of ribozyme from EcoRI-linearized template should include three bands: 50nt, 63nt and 83nt. The result showed our design was correct (Figure 3).

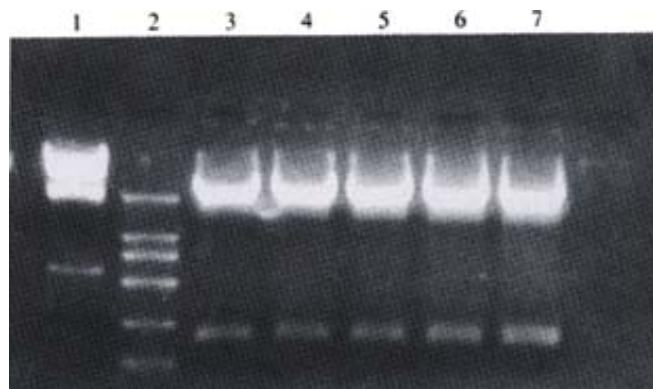


Figure 2 The analysis of HpRz digested by EcoRI and HindIII (20g·L⁻¹ agarose gel). lane 1: λ DNA/HindIII marker; lane 2: DL2000 DNA marker; lane 3-7: HpRz digested by EcoRI and HindIII.

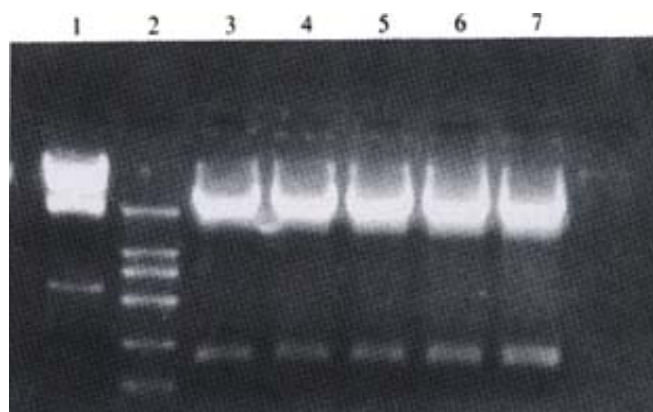


Figure 3 *in vitro* transcript of pHpRz. HpRz is 83nt. 5'-cis-Rz is 63nt, 3'-cis-Rz is 50nt.

In vitro cleavage reaction of ribozyme and kinetics of the cleavage reaction

Time course The cleavage mixture (Rz : substrate = 1:1 mol·L⁻¹) were incubated at 37°C for different time points, it was shown that the reaction product increased with the increase in incubation time and within 60 min it was linear, $CE = 32.67\%$ (Figures 4 and 5).

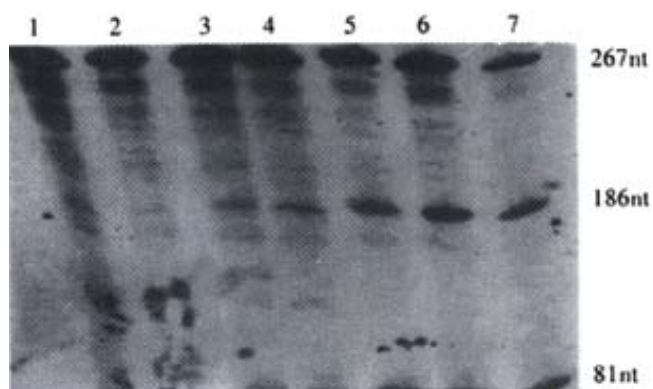


Figure 4 Time course. Specific cleavage of HBV RNA target molecules by HpRz *in vitro*. Lane 1: substrate control; lane 2: incubated for 6 min; lane 3: 10 min; lane 4: 20 min; lane 5: 40 min; lane 6: 60 min; lane 7: 90 min.

The kinetics of cleavage reaction Under the condition of 37°C and 40-minute reaction time, the cleavage efficiency was calculated at Rz:S = 1:1, 1:2, 1:4, 1:8 and 1:16 (mol/L) ratio. K_m and K_{cat} were obtained by the Lineweaver-Burke method (Figure 6) $K_m = 26.31 \text{ nmol} \cdot \text{L}^{-1}$, $K_{cat} = 0.18 \cdot \text{min}^{-1}$.

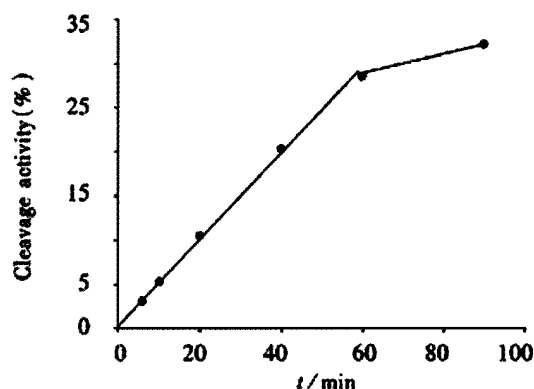


Figure 5 Time curves of cleavage reactions of HpRz prepared *in vitro*.

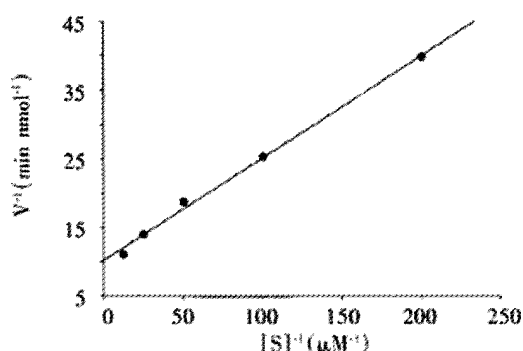


Figure 6 Lineweaver-burk kinetic plots of the specific cleavage of HBV RNA target molecules by HpRz prepared *in vitro*. HpRz concentration is 5 nmol·L⁻¹, substrate concentration is 80,40,20,10 5nmol·L⁻¹. Reaction is at 37°C for 40 min.

DISCUSSION

Ribozyme is classified into six kinds. Hammerhead ribozyme and hairpin ribozyme have been studied extensively as experimental tools for trans suppression of gene expression and possible therapeutic application. Hammerhead ribozyme is small and easy to design and there is less restriction of selection of target site, so its application is extensive. Although hammerhead ribozyme was used to suppress HBV replication, and hammerhead ribozyme-mediated cleavage of target RNA could be achieved *in vitro* and in cell extract, they showed poor effect in intact cells^[35, 36]. Cellular protein and low Mg²⁺ concentration limited intracellular ribozyme activity. It will be difficult to raise the intracellular Mg²⁺ level. Protein can influence the ribozyme intracellular performance. However, cellular protein may also have positive effect on ribozyme-mediated catalysis. Because of limited knowledge on mechanisms of protein modulation of catalytic RNA activity and the complex formed by ribozyme and ribonucleoprotein are frequently large, poorly defined and difficult to study, it is hard for us to use protein to enhance ribozyme activity. Compared with hammerhead ribozyme, hairpin ribozyme has complex structure, hard to design and there is too much restriction of target site and its application is limited. It possesses the better cleavage activity under physiological condition from *in vitro* assays done under standard condition at 37°C and low Mg²⁺ concentration. PJ Welch^[47] designed three hairpin ribozymes against the pgRNA (pregenic RNA) encoding HBV surface antigen, the polymerase and the X protein and demonstrated that two of them can cleave target RNA *in vitro* and reduced the level of HBV expression and suppressed HBV replication *in vivo*. Zu *et al.*^[48] used hairpin ribozyme library to identify accessible target sites within HBV pregenomic RNA, four hairpin ribozyme targeting conserved region in subtypes of HBV can inhibit HBV replication in intact cell. Until now no report on hairpin

ribozyme directed against core gene of HBV has available. In this report we have designed and constructed hairpin ribozyme to cleave transcripts of HBV core gene *in vitro*. Our experiment was the study of preparation and cleavage activity of hairpin ribozyme-HpRz by means of the computer design, cloning the ribozyme gene into the vector that possessed cis-cleavage ribozymes and labeled it with isotope. The *in vitro* transcription effect of ribozyme was satisfactory, 5'-cis-Rz and 3'-cis-Rz cut themselves and released the purposed ribozyme. The ribozyme flanking sequences could be shortened and ribozyme structure induced by the secondary structure of long flanking sequences would be eliminated. That would affect ribozyme turnover ratio/binding activity in the result of an accurate hybridization and better cleavage for ribozyme. Moreover isolation of ribozyme is very convenient by cutting off autoradiograph bands. Ribozyme is quantified more accurately. In this paper the number of nucleotide of hairpin ribozyme was similar to that of the cleavage product, so we can not use transcribed HpRz labeled by isotope. The ribozyme vector was proved to fit for preparation of hammerhead ribozyme^[49-51]. In our study we also used the preparation of hairpin ribozyme and its efficacy is similar to that of hammerhead ribozyme. So the vector possesses wide applicability in the study of preparation of ribozyme *in vitro*, not only hammerhead ribozyme, but also hairpin ribozyme.

HBV is a double-stranded DNA virus replicates through pregenomic RNA intermediate, which provides a therapeutic opportunity for a novel antiviral gene therapy based on ribozyme RNA cleavage. In our experiment, we have designed and constructed hairpin ribozyme directed against HBV core region. The kinetics of hairpin ribozyme showed that HpRz possessed specific ability of cleaving the HBV transcripts *in vitro*. These results indicated that HpRz is worthy of being further studied in intact cells and developed as a nucleic acid drug in the future. However the *in vitro* result can not completely reflect *in vivo* performance. The total HBV mRNA transcript in cell forms the secondary and tertiary structure which affect ribozyme combination with the substrate and cleavage activity. The subcellular compartment where the ribozyme is located, degradation of ribozyme, the complexes which are formed by ribozyme and ribonucleoprotein within cell and gene delivery system, affect the combination with substrate and cleavage of ribozyme. So *in vivo* effect of the ribozyme should be investigated as soon as possible. The ribozyme fragments would be cloned into eucaryotic vectors and transfected into HepG2 cell or Huh7 cell. Experimental analysis of the anti-HBV ribozyme activity *in vivo* is in progress and should help determine its potential use as antiviral agents against HBV.

REFERENCES

- Shi H, Wang FS. Host factors in chronicity of hepatitis B virus infection and their significances in clinic. *Shijie Huaren Xiaohua Zaizhi* 2001;9:66-69
- Befeler AS, Di Bisceglie AM. Hepatitis B. *Infect Dis Clin North Am* 2000; 14:617-632
- Maddrey WC. Hepatitis B: an important public health issue. *J Med Virol* 2000; 61:362-366
- Lau GK. Hepatitis B infection in China. *Clin Liver Dis* 2001;5:361-379
- Merican I, Guan R, Amarapuka D, Alexander MJ, Chutaputti A, Chien RN, Hasnain SS, Leung N, Lesmana L, Phiet PH, Sjalfoellah Noer HM, Sollano J, Sun HS, Xu DZ. Chronic hepatitis B virus infection in Asian countries. *J Gastroenterol Hepatol* 2000;15:1356-1361
- Guo SP, Wang WL, Zhai YQ, Zhao YL. Expression of nuclear factor-κB in hepatocellular carcinoma and its relation with the X protein of hepatitis B virus. *World J Gastroenterol* 2001;7:340-344
- Shi DR, Lu L, Wang JH, Dong CL, Cong WT. HBV DNA distribution of hepatitis B virus in pancreas and liver of patients with cirrhosis. *Shijie Huaren Xiaohua Zazhi* 2000;8:751-754
- Wu C, Cheng ML, Ding YS, Liu RC, Li J, Wang WL, Hu L. A five-year follow up survey of risk factor of viral hepatic cirrhosis. *Shijie Huaren Xiaohua Zazhi* 2000; 8:1365-1367
- Wang HY, Yan RQ, Long JB, Wu QL. Cyclin D1 amplification is associated with HBV DNA intergration and pathology in human hepatocellular carcinoma. *Shijie Huaren Xiaohua Zazhi* 1999;7:98-100
- Fang ZR, Yang DH, Qin HR, Hua CZ, Xu Z, Qiu HL. Expression of

- IGF-I, IGF-I receptor mRNA in hepatocellular carcinomas and adjacent nontumor tissue. *Shijie Huaren Xiaohua Zazhi* 1999;7:848-850
- 11 Yan JC, Ma Y, Chen WB, Shun XH. Pathological significance of expression intrahepatic smooth muscle fiber in hepatitis B. *Shijie Huaren Xiaohua Zazhi* 2000;8:1242-1246
 - 12 Zhai SH, Liu JB, Liu YM, Zhang LL, Du ZH. Expression of HBsAg, HCV-Ag and AFP in liver cirrhosis and hepatocarcinoma. *Shijie Huaren Xiaohua Zazhi* 2000;8:524-527
 - 13 Feitelson MA. Hepatitis B virus in hepatocarcinogenesis. *J Cell Physiol* 1999;181:188-202
 - 14 Arbuthnot P, Kew M. Hepatitis B virus and hepatocellular carcinoma. *Int J Exp Pathol* 2001;82:77-100
 - 15 Zhuang L, You J, Tang BZ, Ding SY, Yan KH, Peng D, Zhang YM, Zhang L. Preliminary results of Thymosin- α 1 versus interferon- α treatment in patient with HBeAg negative and serum HBV DNA positive chronic hepatitis B. *World J Gastroenterol* 2001;7:407-410
 - 16 Xie Q, Guo Q, Zhou XQ, Gu RY. Effect of adenine arabinoside monophosphate coupled to lactosaminated human serum albumin on duck hepatitis B virus. *Shijie Huaren Xiaohua Zazhi* 1999;7:125-126
 - 17 Li J, Tang B. Effect on replication of hepatitis B virus by Chinese traditional medicine. *Shijie Huaren Xiaohua Zazhi* 2000; 8:945-946
 - 18 Zhu Y, Wang YL, Shi L. Clinical analysis of the efficacy of interferon alpha treatment of hepatitis. *World J Gastroenterol* 1998; 4:85-86
 - 19 Xu KC, Wei BH, Yao XX, Zhang WD. Recently therapy for chronic hepatitis B virus by combined traditional Chinese and Western medicine. *Shijie Huaren Xiaohua Zazhi* 1999; 7:970-974
 - 20 Zoulim F, Trepo C. New antiviral agents for the therapy of chronic hepatitis B virus infection. *Intervirology* 1999; 42:125-144
 - 21 Lau GK. Use of immunomodulatory therapy (other than interferon) for the treatment of chronic hepatitis B virus infection. *J Gastroenterol Hepatol* 2000;15 Suppl:E46-52
 - 22 Guan R. Interferon monotherapy in chronic hepatitis B. *J Gastroenterol Hepatol* 2000;15 Suppl:E34-40
 - 23 Torresi J, Locarnini S. Antiviral chemotherapy for the treatment of hepatitis B virus infections. *Gastroenterology* 2000;118:S83-103
 - 24 Schiff ER. Lamivudine for hepatitis B in clinical practice. *J Med Virol* 2000;61:386-391
 - 25 Farrell G. Hepatitis B e antigen seroconversion: effects of lamivudine alone or in combination with interferon alpha. *J Med Virol* 2000;61: 374-379
 - 26 Lai CL, Yuen MF. Profound suppression of hepatitis B virus replication with lamivudine. *J Med Virol* 2000;61:367-373
 - 27 Jarvis B, Faulds D. Lamivudine. A review of its therapeutic potential in chronic hepatitis B. *Drugs* 1999;58:101-141
 - 28 Malik AH, Lee WM. Chronic hepatitis B virus infection: treatment strategies for the next millennium. *Ann Intern Med* 2000;132:723-731
 - 29 Lok AS. Hepatitis B infection: pathogenesis and management. *J Hepatol* 2000;32(1 Suppl):89-97
 - 30 Liu J, McIntosh H, Lin H. Chinese medicinal herbs for chronic hepatitis B: a systematic review. *Liver* 2001;21:280-286
 - 31 Doo E, Liang TJ. Molecular anatomy and pathophysiologic implications of drug resistance in hepatitis B virus infection. *Gastroenterology* 2001;120:1000-1008
 - 32 Farrell GC. Clinical potential of emerging new agents in hepatitis B. *Drugs* 2000;60:701-710
 - 33 Shaw T, Locarnini S. Combination chemotherapy for hepatitis B virus: the path forward? *Drugs* 2000;60:517-531
 - 34 Muotri AR, da Veiga Pereira L, dos Reis Vasques L, Menck CF. Ribozymes and the anti-gene therapy: how a catalytic RNA can be used to inhibit gene function. *Gene* 1999;237:303-310
 - 35 von Weizsacker F, Blum HE, Wands JR. Cleavage of hepatitis B virus RNA by three ribozymes transcribed from a single DNA template. *Biochem Biophys Res Commun* 1992; 189:743-748
 - 36 Beck J, Nassal M. Efficient hammerhead ribozyme-mediated cleavage of the structured hepatitis B virus encapsidation signal *in vitro* and in cell extracts, but not in intact cells. *Nucleic Acids Res* 1995; 23:4954-4962
 - 37 Feng Y, Leavitt M, Tritz R, Duarte E, Kang D, Mamounas M, Gilles P, Wong-Staal F, Kennedy S, Merson J, Yu M, Barber JR. Inhibition of CCR5-dependent HIV-1 infection by hairpin ribozyme gene therapy against CC-chemokine receptor 5. *Virology* 2000;276:271-278
 - 38 Klebba C, Ottmann OG, Scherr M, Pape M, Engels JW, Grez M, Hoelzer D, Klein SA. Retrovirally expressed anti-HIV ribozymes confer a selective survival advantage on CD4⁺ T cells *in vitro*. *Gene Ther* 2000; 7:408-416
 - 39 Andang M, Hinkula J, Hotchkiss G, Larsson S, Britton S, Wong-Staal F, Wahren B, Ahrlund-Richter L. Dose-response resistance to HIV-1/MuLV pseudotype virus *ex vivo* in a hairpin ribozyme transgenic mouse model. *Proc Natl Acad Sci* 1999;96:12749-12753
 - 40 Perez-Ruiz M, Sievers D, Garcia-Lopez PA, Berzal-Herranz A. The antisense sequence of the HIV-1 TAR stem-loop structure covalently linked to the hairpin ribozyme enhances its catalytic activity against two artificial substrates. *Antisense Nucleic Acid Drug Dev* 1999; 9:33-42
 - 41 Koizumi M, Ozawa Y, Yagi R, Nishigaki T, Kaneko M, Oka S, Kimura S, Iwamoto A, Komatsu Y, Ohtsuka E. Design and anti-HIV-1 activity of hammerhead and hairpin ribozymes containing a stable loop. *Nucleosides Nucleotides* 1998;17:207-218
 - 42 Li X, Gervais A, Kang D, Law P, Spector SA, Ho AD, Wong-Staal F. Gene therapy targeting cord blood-derived CD34⁺ cells from HIV-exposed infants: preclinical studies. *Gene Ther* 1998; 5:233-239
 - 43 Welch PJ, Tritz R, Yei S, Leavitt M, Yu M, Barber J. A potential therapeutic application of hairpin ribozymes: *in vitro* and *in vivo* studies of gene therapy for hepatitis C virus infection. *Gene Ther* 1996;3:994-1001
 - 44 Alvarez-Salas LM, Cullinan AE, Siwkowski A, Hampel A, DiPaolo JA. Inhibition of HPV-16 E6/E7 immortalization of normal keratinocytes by hairpin ribozymes. *Proc Natl Acad Sci* 1998; 95:1189-1194
 - 45 Lian JQ, Zhou YX and Jin YX. Effect of specific connected ribozyme-mediated cleave on anti-HBV *in vitro*. *Disi Junyi Daxue Xuebao* 1999; 20: 97-101
 - 46 Uhlenbeck OC. A small catalytic oligoribonucleotide. *Nature* 1987; 328:596-600
 - 47 Welch PJ, Tritz R, Yei S, Barber J, Yu M. Intracellular application of hairpin ribozyme genes against hepatitis B virus. *Gene Ther* 1997;4:736-743
 - 48 zu Putlitz J, Yu Q, Burke JM, Wands JR. Combinatorial screening and intracellular antiviral activity of hairpin ribozymes directed against hepatitis B virus. *J Virol* 1999;73:5381-5387
 - 49 Liu DZ, Jin YX, Hou H, Huang YZ, Yang GC, Xu Q. Preparation and identification of activity of anti-HPV-6b/11E1 universal ribozyme-Rz1198 *in vitro*. *Asian J Androl* 1999;1:195-201
 - 50 Xu R, Zhou X, Xie Q, Jin Y, Liao D. Preparation and identification of hammerhead ribozyme *in vitro* against rat caspase-3 mRNA fragment *Zhonghua Gan Zang Bing Za Zhi* 2000;8:361-363
 - 51 Xu RH, Liu J, Zhou XQ, Xie Q, Jin YX, Yu H, Liao D. Activity identification of anti-caspase-3 mRNA hammerhead ribozyme in both cell-free condition and BRL-3A cells. *Chinese Medical Journal* 2001;114:606-611

• VIRAL LIVER DISEASES •

Seek protein which can interact with hepatitis B virus X protein from human liver cDNA library by yeast two-hybrid system

Xiao-Zhong Wang, Xiang-Rong Jiang, Xiao-Chun Chen, Zhi-Xing Chen, Dan Li, Jian-Yin Lin, Qi-Min Tao

Xiao-Zhong Wang, Xiang-Rong Jiang, Xiao-Chun Chen, Zhi-Xing Chen, Dan Li, Department of Gastroenterology, Union Hospital of Fujian Medical University, Fuzhou 350001, Fujian Province, China
Jian-Yin Lin, Laboratory of molecular biology, Fujian Medical University, Fuzhou 350004, Fujian Province, China
Qi-Min Tao, Liver Disease Institute, Beijing University, Beijing 100044, China

Correspondence to: Dr. Xiao-Zhong Wang, Department of Gastroenterology, Union Hospital of Fujian Medical University, Fuzhou 350001, Fujian Province, China. drwangxz@pub6.fz.fj.cn
Telephone: +86-591-3357896 ext 8482

Received 2001-05-31 Accepted 2001-07-15

Abstract

AIM: To seek the X associated protein (XAP) with the constructed bait vector pAS2-1X from normal human liver cDNA library.

METHODS: The X region of the HBV gene was amplified by PCR and cloned into the eukaryotic expression vector pAS2-1. The reconstituted plasmid pAS2-1X was transformed into the yeast cells and the expression of X protein (pX) was confirmed by Western blot analysis. Yeast cells were cotransformed with pAS2-1X and the normal human liver cDNA library and were grown in selective SC/-trp-leu-his-ade medium, the second screen was performed with the LacZ report gene. Furthermore, segregation analysis and mating experiment were performed to eliminate the false positive and the true positive clones were selected for PCR and sequencing.

RESULTS: Reconstituted plasmid pAS2-1X including the anticipated fragment of X gene was proved by auto-sequencing assay. Western blot analysis showed that reconstituted plasmid pAS2-1X expressed BD:X fusion protein in yeast cells. Of 5×10^6 transformed colonies screened, 65 grew in the selective SC/-trp-leu-his-ade medium, 5 scored positive for β -gal activity, and only 2 remaining clones passed through the segregation analysis and mating experiment. Sequence analysis identified that two clones contained similar cDNA fragment: GAAGTTGCG.

CONCLUSION: The short peptide (glutacid-leucine-alanine) is a possible required site for XAP binding to pX. Normal human liver cDNA library has difficulties in expressing the integrated XAP on yeast cells.

Wang XZ, Jiang XR, Chen XC, Chen ZX, Li D, Lin JY, Tao QM. Seek protein which can interact with hepatitis B virus X protein from human liver cDNA library by yeast two-hybrid system. *World J Gastroenterol* 2002;8(1):95-98

INTRODUCTION

Modern biological investigations indicate many proteins have relationship with the development of hepatocellular carcinoma^[1-8]. More and more evidences have demonstrated hepatitis B virus (HBV)

X protein which encoded by the smallest open reading frame (ORF) of the HBV genome plays an important role in the carcinogenesis^[9-13]. At a molecular level, several endogenous genes critical for cell proliferation or apoptosis and the inflammatory response seemed interacted with HBx, such as c-Fos, c-Jun, CREB, CD44, TNF- α , p21 and p53^[14-21]. In addition, DNA transfection approaches have clearly demonstrated that pX is a transactivator of a wide variety of viral and cellular promoters^[22-24], but the underlying mechanism of transactivation is currently obscure. Since HBx has no ability to bind DNA, protein-protein interaction seems to be crucial for HBx transactivation^[25-28]. One most direct way to identify the mechanism of HBx transactivation is to find out host proteins that interact specifically with HBx. We use the yeast two-hybrid system, a genetic approach to search the clone genes that interact with a protein of interest by *in vivo* complementation in yeast cells, to seek XAP from normal human liver cDNA library.

MATERIALS AND METHODS

Plasmid Construction

To make the bait plasmid, the X region of the HBV gene was amplified by PCR using as forward and reverse primers XF and XR, which contain an EcoRI and Pst I site respectively for ease of cloning. The sequence of the primers, with the restriction enzyme site underlined are: XF: ACGGAATTCATGGCTGCTAGGCTGTG, XR: ATCCTGCAGAGGTGAAAAAGTTGCAT. These bind to nucleotide positions 1374 and 1838 on HBV genome. The templates for this reaction were sera of HBV DNA positive patients. The 464bp product was cloned into the respective restriction enzyme sites of plasmid pAS2-1 (Clontech) and this plasmid was subsequently named pAS2-1X.

Western Blot analysis

Saccharomyces cerevisiae AH109 (Clontech) was grown in YPD medium (10g·L⁻¹ yeast extract, 20 g·L⁻¹ peptone, 20 g·L⁻¹ dextrose). This yeast strain carries LacZ, HIS3 and ADE2 reporter genes under the control of Gal4-binding sites was used to screen the liver cDNA library. Yeast cells were transformed with pAS2-1X using lithium acetate method previously published by Gietz *et al*^[29] and were grown in selective SC/-trp medium. Cells were collected by centrifugation and lysates were prepared according to Urea/SDS method. A part of protein extract were resolved on a 120g·L⁻¹ SDS-polyacrylamide gel and transferred onto polyvinylidene difluoride membrane. After blocking with nonfat dried milk, the membrane was treated with 1:3000 diluted Gal4 DNA-BD monoclonal antibody (Clontech) followed by 1:1000 diluted alkaline phosphatase-conjugated goat anti-mouse IgG. Subsequently the blot was developed by 5-bromo-4-chloro-3-indolyl phosphate and nitro blue tetrazolium. The untransformed yeast cells were used for negative control.

Screening of the liver cell cDNA library by the yeast two-hybrid system

The screening procedure used was a modification of the method

described by Gietz *et al*^[29]. Yeast cells AH109 were transformed with pAS2-1X and pACT2-cDNA library (Clontech) by Liac-mediated transformation and were grown in selective SC/-trp-leu-his-ade medium for 7 days. After about 3 days at 30°C, the growing colonies were assayed for α -gal activity by replica plating the yeast transformants onto Whatman filter papers, the filters were snap frozen in liquid nitrogen for 10s twice and incubated for 1-8h at 30°C in a buffer containing 5-bromo-4-chloro-3-indolyl- α -D-galactopyranoside(X-gal) solution. Positive interactions were detected by the appearance of blue colonies. Segregation analysis and mating experiment were done to exclude the type I,II, III false positive and true positive colonies were obtained.

Sequence analysis of pACT2-cDNA

The pACT2-cDNA plasmid genome was isolated following the standard protocol. Briefly, the true positive clones were grown in SC/-leu medium, cells were collected by centrifugation and resuspended in lysis buffer (20g·L⁻¹ Triton 100, 10g·L⁻¹ SDS, 10mmol L⁻¹ NaCl, 10mmol·L⁻¹ Tris-HCl pH8.0, 1mmol·L⁻¹ Na₂EDTA) and phenol, chloroform and isoamyl alcohol(volume fraction 25:24:1). After addition of acid-washed glass beads (Sigma), samples were centrifugated and plamid DNA recovered. The pACT2-cDNA plasmid DNA was purified by CsCl gradient centrifugation to permit PCR using the Matchmaker AD LD-Insert Screening Amplimers (Clontech) which anneals to GAL4-AD. Auto-sequencing assay was performed in Shanghai Shengong Biological Corporation.

RESULTS

Plasmid construction

The HBV X fragment was successfully generated by PCR(figure 1) and cloned into plasmid pAS2-1. Reconstituted plasmid pAS2-1X including the anticipated fragment of X gene was proved by digesting with restricted endonuclease and auto-sequencing assay as follows: GACTGTATCGCCGGTATTGCAATACCCAGCTTTGACTCATATGGCCATGGAGGCCGAATTCATGGCTGCTAGGCTGTGCTGCCAACTGGATCCTGCGCGGGACGTCCTTTGTGTACGTCCCGTCACGCGTG AATCCCGCGGACGACCCCTCCCGGGGCCGCTTGGGGCTCTACCGCCCCTTCTCCGCTGTGTGATCCGACCGACACGGGGCGCACCTCTCTTTACGCGGACTCCCCGTCTGTGCCTTCTCATCTGCCGGACCGTGTGCACTTCGCTTCACCTCTGCACGTCGCATGGAAACCACCGTGAACGCCACCGGAACCTGCCCAAGGCCTTGCAAGAGGACTCTTGACTTGACAGCAATGTCAACGACCGACCTTGAGGCATACTCAAAGACTGTGTGTTAACGAGTGGGAGGAGTTGGGGAGGAGATTAGGTTAAAGGTCTTTGTACTAGGAGGCTGTAGGCATAAATGGTGTGTTACACAGCACCATGCAATTTTACCTCTGCAGCCAAGCTAATCCGGGCGAATTTCTTATGATTTATGATTTTATTATTAATAAGTTATAAAAAAATAAGTGTATACAAATTTTAAAGGTGACTTTTANGTTTTAAACGAAAATNTTATNTTGAGTAACTNTTTCCTGGAGGTCAAGGTTGCTT (underlined fractions are restriction enzyme site).

Western Blot analysis

Western Blot Analysis proved that yeast cells transformed with pAS2-1X have positive signal which can not be seen in the control, pAS2-1X can express BD:X fusion protein yeast cells(figure 2). Besides, The colony-lift assay showed that the reconstruted plasmid could not active LacZ reporter gene in yeast. pAS2-1X can be used as bait vector in yeast two-hybrid system.

Screening of the liver cell cDNA library

Of 5×10⁶ transformed colonies screened, 65 grew in the selective SC/-trp-leu-his-ade medium. Out of these HIS⁺ ADE⁺

prototrophs, 5 scored positive for β -gal activity, only 2 remaining clones passed through the segregation analysis and mating experiment.

Sequence analysis

PCR (Figure 3) and sequence analysis identified that two clones contained the same cDNA sequence: GAACTTGCG, which encodes glutacid-leucine -alanine.

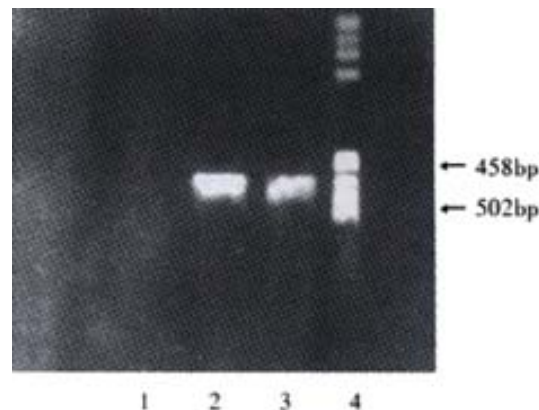


Figure 1 Electrophoresis of X gene PCR products
1: Negative control; 2:Positive control; 3:Sample; 4: Marker

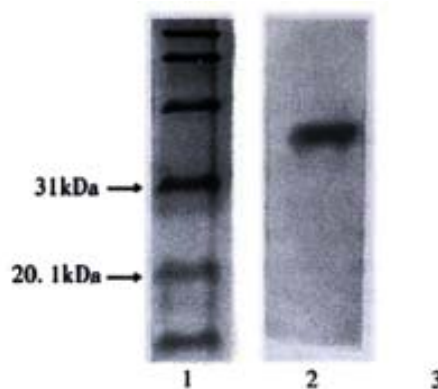


Figure 2 Western blot of yeast after being transformed with pAS2-1X
1:Marker; 2: pX; 3: Negative control

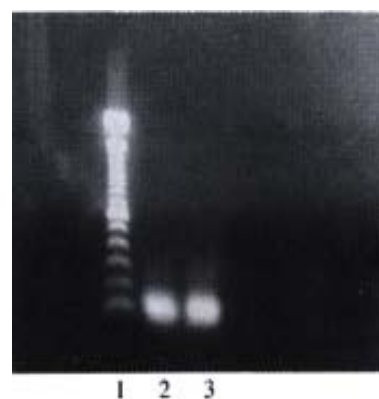


Figure 3 Library cDNA amplified from positive yeast clones
1:100bp DNA ladder; 2: positive cloned

DISCUSSION

Persistent Hepatitis B virus infection is strongly associated with the development of hepatocellular carcinoma(HCC). The viral X gene encodes a 17-kd protein, termed pX, fuctions a transcriptional activator of a variety of viral and cellular genes, it is capable of interacting with a wide variety of cellular protein, including cell-cycle control and apoptosis protein. There are well documented that pX acts through apoptosis pathway involving Fas and caspase 3^[30-33], it also

interacts with p53, a wellknown tumor suppressor gene^[34-36] and inhibits nucleotide excision repair^[37-39]. However, ample evidences showed that pX may function by additional profound mechanisms in HCC^[40-43].

Identification and characterization of proteins in a cell with which a given protein interacts is often helpful for understanding the function and mechanisms of action of that protein. The yeast two-hybrid system is a molecular genetic test for protein interaction, which is firstly established by Fileds *et al* in 1989^[44]. It's a powerful and sensitive technique for the identification of genes that code for proteins which interact in a biologically significant fashion with a protein of interest. The assay is performed in the yeast cells so as to reflect the real situations *in vivo* and has the potential to identify the weak and transient interaction between two protein. In addition, since the cDNA library can be constructed according to various type of tissues, organs and cells, many proteins interact with transcription factors, protein kinases, phosphatases, receptors, cytoskeletal proteins as well as proteins involved in cell cycle regulation and apoptosis can be study by this elegant approach. Although the yeast two-hybrid system has become a standard procedure for molecular biologists, it remains some deficiency. The most important problem is different types of false positives, fortunately, they can be eliminated by other method such as segregation analysis and mating experiment^[29,45].

Our study successfully constructed the bait vector pAS2-1X, HIS and ADE independent growth and blue -colony formation in the α -gal assay by yeast cells harboring both pAS2-1X and pACT2-cDNA recombinant plasmids and the behaviors of cells in false-positive elimination tests suggested the isolated clones can specifically interact with pX and the results were reliable.

It should be greatly concerned that XAPs studied by the yeast two-hybrid system in the past were different in size, structure and biological functions^[46]. Lee *et al*^[47] indentified an XAP1 that is a human homolog of the monkey UV-damaged DNA-binding protein in 1995; Kuzhandaivelu *et al*^[48] discovered an XAP2 which is known as the p38 subunit of the aryl hydrocarbon receptor complex (ARA9) in 1996; Huang *et al*^[49] reported an XAPC7 contained a polypeptide with high sequence homology to the PROS-28.1 subunit of proteasome of *Drosophila melanogaster* and the α proteasome subunit of *Arabidopsis thaliana* in 1996; Cong *et al*^[50] isolated an XAP3 which is a human homolog of the rat protein kinase C-binding protein in 1997; Melegari *et al*^[51] proved an XIP including two consensus phosphorylation sites for protein kinase C and Casein kinase II in 1998; Sun *et al*^[52] demonstrated a p55sen appeared to be related to the family of EGF-like protein in gengeral in 1998; Rahmani *et al*^[53,54] identified an HVDVC3 which is a third member of the family of human genes that encode the voltage-dependent anion channel. The reasonable explantation for these distinct results has not been obtained yet. Whether there exists different kinds of XAP or funtional fragment interacting with pX or the repetitive results depend on the high transformation efficiency remains obscure. One of the possible mechanism may be a specific fragment can interact with pX specially and the proteins containing this fragment thus can bind to pX. Sequence analysis shown that both two true positive clones we isolated contained the sequence encodes glutacid-leucine -alanine, therefore, it's rational to deduce this short peptide is a required site for XAP binding to pX.

The interaction of proteins shall locate at nucleus in yeast two-hybrid system. However, some proteins require modification such as glycosylation outside the necleus after the expression, and others are only correctly folded and actived in the cooperation of some particular proteins which don't exist in yeast cells, so not all proteins can obtain normal structure and biological function in yeast cells. The cDNA library used for seeking XAP in the past research including Epstein-Barr virus transformed human peripheral lymphocyte cDNA library,

Hela λ gt11 cDNA library or senescent human liver cDNA library, were all library consititued from abnormal cells. Our study had not isolated integrated cDNA sequence of XAP partly owing to the difference between normal human liver cDNA library and abnormal cells cDNA library in protein's expression, modification and activation.

In conclusion, the short peptide (glutacid-leucine-alanine) is a possibly required site for XAP binding to pX. Normal human liver cDNA library has difficulties in expressing the integrated XAP on yeast cells.

REFERENCES

- Kong XB, Yang ZK, Liang LJ, Huang JF, Lin HL. Overexpression of P-glycoprotein in hepatocellular carcinoma and its clinical implication. *World J Gastroenterol* 2000;6:134-135
- Sun JJ, Zhou XD, Liu YK, Zhou G. Phase tissue intercellular adhesion molecule-1 expression in nude mice human liver cancer metastasis model. *World J Gastroenterol* 1998;4:314-316
- Xiao CZ, Dai YM, Yu HY, Wang JJ, Ni CR. Relationship between expression of CD44v6 and nm23-H1 and tumor invasion and metastasis in hepatocellular carcinoma. *World J Gastroenterol* 1998;4:412-414
- Feng T, Zeng ZC, Zhou L, Chen WY, Zuo YP. Detection of human liver-specific F antigen in serum and its preliminary application. *World J Gastroenterol* 1999;5:175-176
- Lin GY, Chen ZL, Lu CM, Li Y, Ping XJ, Huang R. Immunohistochemical study on p53, H-rasp21, c-erbB-2 protein and PCNA expression in HCC tissues of Han and minority ethnic patients. *World J Gastroenterol* 2000;6:234-238
- Huang XF, Wang CM, Dai XW, Li ZJ, Pan BR, Y LB, Qian B, Fan L. Expressions of chromograninA and cathepsinD in human primary hepatocellular carcinoma. *World J Gastroenterol* 2000;6:693-698
- Mei MH, Xu J, Shi QF, Yang JH, Chen Q, Qin LL. Clinical significance of serum intercellular adhesion molecule-1 detection in patients with hepatocellular carcinoma. *World J Gastroenterol* 2000;6:408-410
- Zhao CY, Li YL, Liu SX, Feng ZJ. Changes of IL-6 and relevant cytokines in patients with hepatocellular carcinoma and their clinical significance. *World J Gastroenterol* 2000;6(Suppl 3):33
- Yu DY, Moon HB, Son JK. Incidence of hepatocellular carcinoma in transgenic mice expressing the hepatitis B virus X-protein. *J Hepatol* 1999;31:123-132
- Zhu HZ, Cheng GX, Chen JQ, Kuang SY, Cheng Y, Zhang XL, Li HD, Xu SF, Shi JQ, Qian GS, Gu JR. Preliminary study on the production of transgenic mice harboring hepatitis B virus X gene. *World J Gastroenterol* 1998;4:536-539
- Wang XZ, Tao QM. The relationship between HBV x gene and hepatocellular carcinoma. *Shijie Huaren Xiaohua Zazhi* 1999;7:1063-1064
- Yu DY, Moon HB, Son JK, Jeong S, Yu SL, Yoon H, Han YM, Lee CS, Park JS, Lee CH, Hyun BH, Murakami S, Lee KK. Incidence of hepatocellular carcinoma in transgenic mice expressing the hepatitis B virus X-protein. *J Hepatol* 1999; 31: 123-132
- Gao FG, Sun WS, Cao YL, Zhang LN, Song J, Li HF, Yan SK. HBx-DNA probe preparation and its application in study of hepatocarcinogenesis. *World J Gastroenterol* 1998;4:320-322
- Feitelson MA. Hepatitis B X antigen and P53 in the development of hepatocellular carcinoma. *J Hepatobiliary Pancreat Surg* 1998; 5:367-374
- Qin LL, Su JJ, Li Y, Yang C, Ban KC, Yian RQ. Expression of IGF-c α , p53, p21 and HBxAg in precancerous events of hepatocarcinogenesis induced by AFB1 and /or HBV in tree shrews. *World J Gastroenterol* 2000;6:138-139
- Lara-Pezzi E, Serrador JM, Montoya MC, Zamora D, Yanez-Mo M, Carretero M, Furthmayr H, Sanchez-Madrid R, Lopez-Cabrera M. The hepatitis B virus x protein induces a migratory phenotype in a CD44-dependent manner: possible role of HBx in invasion and metastasis. *Hepatology* 2001;33:1271-1281
- Lin GY, Chen ZL, Lu CM, Li Y, Ping XJ, Huang R. Immunohistochemical study on p53, H-rasp21, c-erbB-2 protein and PCNA expression in HCC tissues of Han and minority ethnic patients. *World J Gastroenterol* 2000;6:234-238
- Sun BH, Zhang J, Wang BJ, Zhao XP, Wang YK, Yu ZQ, Yang DL, Hao LJ. Analysis of *in vivo* patterns of caspase 3 gene expression in primary hepatocellular carcinoma and its relationship to p21^{WAF1} expression and hepatic apoptosis. *World J Gastroenterol* 2000;6:356-360
- Feng DY, Zheng H, Tan Y, Cheng RX. Effect of phosphorylation of MAPK and Stat3 and expression of ca2fos and ca2jun proteins on

- hepatocarcinogenesis and their clinical significance. *World J Gastroenterol* 2001;7:33-36
- 20 Natoli G, Avantaggiati ML, Chirillo P, Puri PL, Ianni A, Balsano C, Levrero M. Ras- and raf-dependent activation of c-jun transactivational activity by the hepatitis B virus transactivator pX. *Oncogene* 1994; 9: 2837-2843
- 21 Lara PE, Majano PL, Gomez GM, Garcia MC, Moreno OR, Levrero M, Lopez CM. The hepatitis B virus X protein up-regulates tumor necrosis factor alpha gene expression in hepatocytes. *Hepatology* 1998; 28: 1013-1021
- 22 Caselmann WH. Trans-activation of cellular genes by hepatitis B virus proteins: a possible mechanism of hepatocarcinogenesis. *Adv Virus Res* 1996; 47:253-302
- 23 Hildt E, Hofschneider PH, Urban S. The role of hepatitis B virus (HBV) in the development of hepatocellular carcinoma. *Semin Virol* 1999; 7:333-3347
- 24 Nomura T; Lin Y,Dorjsuren D,Ohno S, Yamashita T, Murakami S. Human hepatitis B virus X protein is detectable in nuclei of transfected cells, and is active for transactivation. *Biochem Biophys Acta* 1999; 1453: 330-340
- 25 Hu Z, Zhang Z,Doo E, Coux O,Goldberg AL, Liang TJ. Hepatitis B virus X protein is both a substrate and a potential inhibitor of the proteasome complex. *J Virol* 1999; 73: 7231-7240
- 26 Shintani Y, Yotsuyanagi H, Moriya K, Fujie H, Tsutsumi T, Kanegae Y, Kimura S, Saito I, Koike K. Induction of apoptosis after switch-on of the hepatitis B virus X gene mediated by the Cre/loxP recombination system. *J Gen Viro* 1999; 80(Pt 12): 3257-3265
- 27 Maguire H F, J P Hoeffler, A Siddiqui. HBV X protein alter the DNA binding specificity of CREB and ATF-2 by protein-protein interaction. *Science* 1991;252:842-844
- 28 Lara PE, Armesilla AL, Majano PL, Redondo JM, Lopez CM. The hepatitis B virus X protein activates nuclear factor of activated T cells (NF-AT) by a cyclosporin A-sensitive pathway. *EMBO J* 1998; 17: 7066-7077
- 29 Gietz RD, Raine BT, Robbins A,Graham KC, Woods RA. Identification of proteins that interact with a protein of interest: applications of the yeast two-hybrid system. *Molecular Cellular Biochemistry* 1997; 172:67-69
- 30 Sun BH, Zhao XP, Wang BJ, Yang DL, Hao LJ. FADD and TRADD Expression and apoptosis in primary hepatocellular carcinoma. *World J Gastroenterol* 2000;6:223-227
- 31 Wang XZ, Chen XC, Yang YH, Chen ZX, Huang YH, Tao QM. Relationship between HBxAg and Fas/FasL in patients with hepatocellular carcinoma. *World J Gastroenterol* 2000;6(suppl 3):17
- 32 Shin EC, Shin JS, Park JH, Kim H,Kim SJ. Expression of fas ligand in human hepatoma cell lines: role of hepatitis-B virus X (HBX) in induction of Fas ligand. *Int J Cancer* 1999; 82: 587-591
- 33 Gottlob K, Fulco M, Levrero M, Graessmann A. The hepatitis B virus HBx protein inhibits caspase 3 activity. *J Biol Chem* 1998; 273: 33347-33353
- 34 Lee SG, Rho HM. Transcriptional repression of the human p53 gene by hepatitis B viral X protein. *Oncogene* 2000; 19: 468-471
- 35 Lee H, Kim HT, Yun Y. Liver-specific enhancer II is the target for the p53-mediated inhibition of hepatitis B viral gene expression. *J Biol Chem* 1998; 273: 19786-19791
- 36 Prost S, Ford JM, Taylor C, Doig J, Harrison DJ. Hepatitis B x protein inhibits p53-dependent DNA repair in primary mouse hepatocytes. *J Biol Chem* 1998; 273: 33327-33332
- 37 Groisman IJ, Koshy R, Henkler F, Groopman JD, Alaoui-Jamali MA. Downregulation of DNA excision repair by the hepatitis B virus-x protein occurs in p53-proficient and p53-deficient cells. *Carcinogenesis* 1999; 20: 479-483
- 38 Jia L, Wang XW, Harris CC. Hepatitis B virus X protein inhibits nucleotide excision repair. *Int J Cancer* 1999; 80: 875-879
- 39 Becker SA, Lee TH, Butel JS, Slagle BL Hepatitis B virus X protein interferes with cellular DNA repair. *J Virol* 1998; 72: 266-272
- 40 Lin GY, Chen ZL, Lu CM, Li Y, Wang J, Ping XJ, Huang R. Immunohistochemical study on p53, H-rasp21, c-erbB-2 protein and PCNA expression in tumor tissues of Han and minority ethnic patients with primary hepatic carcinoma in Xinjiang. *World J Gastroenterol* 2000;6 (suppl):53
- 41 Lee SW, Lee YM, Bae SK, Murakami S, Yun Y, Kim KW. Human hepatitis B virus X protein is a possible mediator of hypoxia-induced angiogenesis in hepatocarcinogenesis. *Biochem Biophys Res Commun* 2000; 268: 456-461
- 42 Lian Z, Liu J, Pan J, Satioglu Tufan NL, Zhu M, Arbuthnot P, Kew M, Clayton MM, Feitelson MA. A cellular gene up-regulated by hepatitis B virus-encoded X antigen promotes hepatocellular growth and survival. *Hepatology* 2001;34:146-157
- 43 Qin LL, Su JJ, Li Y, Yang C, Ban KC, Yian RQ. Expression of IGF- α , p53, p21 and HBxAg in precancerous events of hepatocarcinogenesis induced by AFB1 and/or HBV in tree shrews. *World J Gastroenterol* 2000;6:138-139
- 44 Fields S, Song OK. A novel genetic system to detect protein-protein interactions. *Nature* 1989; 340:245-246
- 45 Bartel P, Chien CT, Sternglanz R. Elimination of false positives that arise in using the two hybrid system. *Biotechniques* 1993;14: 920-924
- 46 Wang XZ, Tao QM. Advances on research of hepatitis B virus pX associated Protein. *GanZang* 2000;5:55-56
- 47 Lee TH, Elledge SJ, Butel JS. Hepatitis B virus X protein interacts with a probable cellular DNA repair protein. *J Virol* 1995; 69:1107-1114
- 48 Kuzhandaivelu N, Cong YS, Inouye C, Yang W M, Seto E. XAP2, a novel hepatitis B virus X-associated protein that inhibits X transactivation. *Nucleic Acids Res* 1996; 24:4741-4750
- 49 Huang J, Kwong J, Sun ECY, Liang TJ. Proteasome complex as a potential cellular target of hepatitis B virus X protein. *J Virol* 1996; 70:5582-5591
- 50 Cong YS, Yao YL, Yang WM, Kuzhandaivelu N, Seto. The hepatitis B virus X-associated protein, XAP3, is a protein kinase C-binding protein. *J Biological Chemistry* 1997;272:16482-16489
- 51 Melegari M, Scaglioni PP, Wands JR. Cloning and characterization of a novel hepatitis B virus X binding protein that inhibit viral replication. *J Virol* 1998; 72:1737-1743
- 52 Sun BS, Zhu X, Clayton MM, Pan J, Feitekson MA. Identification of a protein isolated from senescent human cells that binds to hepatitis B virus X antigen. *Hepatol* 1998; 27:228-239
- 53 Rahmani Z, C.Maunoury, A.Siddiqui. Isolation of a novel human voltage-dependent anion channel gene. *Eur J Hum Genet* 1998; 6:337-340
- 54 Rahmani Z, K Huh, R Lasher. Hepatitis virus x protein colocalizes to mitochondria with a human voltage-dependent anion channel HVDAC3 and alter it transmembrane potential. *J Virol* 2000; 74:2840-2846

Edited by Wang JH and Xu XQ

• BASIC RESEARCH •

Expression and bioactivity identification of soluble MG7 scFv

Zhao-Cai Yu, Jie Ding, Bo-Rong Pan, Dai-Ming Fanm, Xue-Yong Zhang

Zhao-Cai Yu, Jie Ding, Dai-Ming Fan, Xue-Yong Zhang, Department of Gastroenterology, Xijing Hospital, Fourth Military Medical University, Xi'an 710032, Shaanxi Province, China
Bo-Rong Pan, Oncological Center, Xijing Hospital, Fourth Military Medical University, Xi'an 710032, Shaanxi Province, China
Supported by the Foundation for Medical Science Research of PLA (No. 962047)

Correspondence to: Prof. Xue-Yong Zhang, Department of Gastroenterology, Xijing Hospital, Fourth Military Medical University, Xi'an 710033, Shaanxi Province, China. xyzhang@fmmu.edu.cn.
Telephone: +86-029-3374576

Received 2001-09-25 Accepted 2001-10-29

Abstract

AIM: To examine the molecular mass and identify the bioactivity of MG₇ scFv for its application as a targeting mediator in gene therapy of gastric cancer.

METHODS: Two strongly positive recombinant phage clones screened from MG₇ recombinant phage antibody library were separately transfected into *E.coli* TG1. Plasmid was isolated from the transfected *E.coli* TG1 and digested by EcoR I and Hind III to examine the length of exogenous scFv gene. Then, the positive recombinant phage clones were individually transfected into *E.coli* HB2151. The transfectant was cultured and induced by IPTG. Perplasmic extracts was prepared from the induced transfectant by osmotic shock. ELISA was used to examine the antigen-binding affinity of the soluble MG₇ scFv. Immunodotting assay was adopted to evaluate the yield of soluble MG₇ scFv produced by transfected *E.coli* HB2151. Western blot was used to examine the molecular mass of MG₇ scFv. Finally, the nucleotide sequence of MG₇ scFv was examined by DNA sequencing.

RESULTS: two positive recombinant phage clones were found to contain the exogenous scFv gene. ELISA showed that MG₇ scFv had strong antigen-binding affinity. Immunodotting assay showed that transfected *E.coli* HB2151 could successfully produce the soluble MG₇ scFv with high yield via induction by IPTG. The molecular mass of MG₇ scFv was 30 kDa by western blot. DNA sequencing demonstrated that the V_H and V_L genes of MG₇ scFv were 363bp and 321bp, respectively.

CONCLUSION: We have successfully developed the soluble MG₇ scFv which possessed strong antigen-binding affinity.

Yu ZC, Ding J, Pan BR, Fan DM, Zhang XY. Expression and bioactivity identification of soluble MG₇ scFv. *World J Gastroenterol* 2002;8(1):99-102

INTRODUCTION

Gastric cancer takes the leading place in the incidence of various tumors in china^[1]. Many conventional approaches, including surgical, chemical and physical treatments, appear palliative in most advanced cases. Because these conventional approaches cannot selectively target at the tumor cells and completely eradicate them,

and recurrence and metastasis of tumor may develop due to the existence of residual tumor cells. Therefore, targeting therapy for tumor is badly needed to achieve a greater curative effect and overcome the obstacle existing in the conventional approaches^[2-13]. Recent studies showed that the targeting therapy had a promise in the treatment of gastric cancer^[14-29]. In the present study, we produced the soluble MG₇ scFv and evidenced that MG₇ scFv is a favorable mediator for targeting therapy of gastric cancer.

MATERIALS AND METHODS

Restriction analysis of the strong recombinant phage clones

The strong positive recombinant phage clones (3 μ L containing 2×10^9 pfu) were separately added into 5mL log-phase *E.coli* TG1 and incubated for 1 h at 37°C with shaking at 250 r·min⁻¹. Plasmid was isolated from the culture product and digested by EcoR I and Hind III. Electrophoresis was performed to check the digested product.

Production and antigen-binding affinity test of the soluble MG₇ scFv

The strongly positive recombinant phage clones (3 μ L containing 2×10^9 pfu) were separately added into 5mL log-phase *E.coli* HB2151 and incubated for 1 h at 37°C with shaking at 250 r·min⁻¹. 10 μ L IPTG (isopropyl β -D-thiogalactopyranoside) were added and incubated overnight at 37°C with shaking at 250 r·min⁻¹. Cells were precipitated by centrifugation and supernatant was also collected. The precipitated cells were subjected to osmotic shock for preparation of soluble MG₇ scFvs. KATOIII cells in log phase were transferred into a 96 wells-plate and immobilized on the wall by centrifugation at 1000g for 10min, and finally fixed in 0.25mL·L⁻¹ glutaraldehyde. 0.2 mL perplasmic extracts and supernatant were applied to each well and incubated at 4°C overnight. 0.2 mL anti-E tag antibody were applied to each well and incubated at 37°C for 2 h. 0.1 ml HRP-labeled goat anti-mouse (HRP-GAM) Ig solution was added into each well. The absorbance value (A) at 450nm of reactant in each well was measured after incubation for 1 h at 37°C and staining with TMB.

Immunodotting test of the yield of soluble MG₇ scFv

40 μ L of perplasmic extracts and supernatant were separately dotted on the Hybond-C super membrane and dried at 60°C for 30 min. After being blocked by 50 mL·L⁻¹ nonfat milk for 2 h, the Hybond-C super membrane was incubated in 5mL diluted anti-E tag antibody solution at 37°C for 2 h. 5 mL HRP- labeled goat anti-mouse (HRP-GAM) Ig solution were added for another incubation at 37°C for 1 h and eventually stained by DAB.

Western blot test of the molecular mass of soluble MG₇ scFv

40 μ L of perplasmic extracts and supernatant were firstly analyzed by SDS-PAGE and then transferred onto the Hybond-C super membrane. After being blocked by 50 mL·L⁻¹ nonfat milk, the Hybond-C super membrane was incubated in 5mL diluted anti-E tag antibody solution at 37°C for 2 h. 5 mL of HRP- labeled goat anti-mouse (HRP-GAM) Ig solution were added for another incubation at 37°C for 1 h and

eventually stained by DAB.

DNA sequencing of MG₇ scFv

DNA sequencing was performed by ABI PRISM™ 377 DNA sequencer.

RESULTS

Restriction analysis of the strong positive recombinant phage clones

Two strongly positive clones were found to be recombinant clones which contained the exogenous gene. One of the two strongly positive clones contained a 450bp fragment of exogenous gene (Lane 1) and the other one contained a 750bp fragment of exogenous gene (Lane 2, Figure 1).

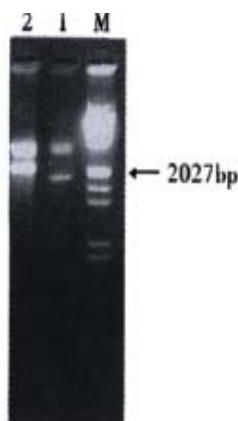


Figure 1 Restriction analysis of the strong positive recombinant phage clones. M: λ /EcoR I and Hind II; 1,2: Recombinant clones

Antigen-binding affinity of the soluble MG₇ scFv by ELISA

One of the strong positive clones was shown to produce soluble form of MG₇ scFv with Antigen-binding activity (Table 1). This clone was confirmed to contain a 750bp fragment of exogenous gene by restriction analysis above and chosen for later use.

Table 1 ELISA of the soluble MG₇ ScFv for binding with KATOIII cells (A value)

ELISA	Number of strong positive clones		Neg. ctrl
	1	2	
First round	0.287	0.776	0.201
Second round	0.346	0.802	0.223

The yield of soluble MG₇ scFv

The positive signal displayed on the dotting site with perplasmic

extracts from induced *E.coli* HB2151 was significantly stronger than that from non-induced *E.coli* HB2151 (Figure 2). It implied that *E.coli* HB2151 had successfully produced the soluble MG₇ scFv via induction by IPTG.



Figure 2 Immunodotting of soluble MG₇ scFv. 1: Periplasmic extracts from induced *E.coli* HB2151; 2: Supernatant from induced *E.coli* HB2151; 3: Periplasmic extracts from non-induced *E.coli* HB2151

The molecular mass of MG₇ scFv

A protein band with positive signal was found at Mr 30 indicating that the soluble MG₇ scFv was a protein of Mr 30 (Figure 3).

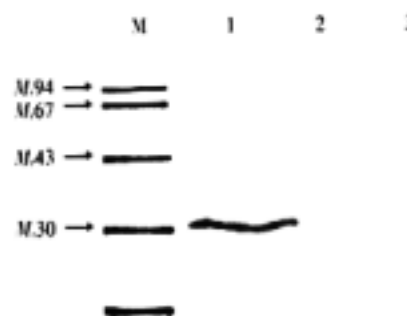


Figure 3 Western blot of the molecular mass of soluble MG₇ scFv. M: Protein marker; 1: Periplasmic extracts from induced *E.coli* HB2151; 2: Supernatant from induced *E.coli* HB2151; 3: Periplasmic extracts from non-induced *E.coli* HB2151

DNA sequence of MG₇ scFv

The V_H and V_L genes of MG₇ scFv were respectively 363 bp and 321 bp in length. The V_H gene has two conserved codon for cysteine at 67-69bp and 289-291bp. The V_L gene has two conserved codon for cysteine at 472-474bp and 664-666bp. Both of the V_H and V_L genes are highly homologous with the variable fragment of some known antibodies (Figure 4).

ATG GCC CAG GTG AAG CTG CAG CAG TCT GGG CCT GAA GTG GTA AAG CCT GGG GCT TCA GTG AAG TTG TCC TGC
AAG GCT TCT GGC TAC ATC TTC ACA AGT TAT GAT ATA GAC TGG GTG AGG CAG ACG CCT GAA CAG GGA CTT GAG
TGG ATT GGA TGG ATT TTT CCT GGA GAG GGG AGT ACT GAA TAC AAT GAG AAG TTC AAG GGC AGG GCC ACA CTG

VH

AGT GTA GAC AAG TCC TCC AGC ACA GCC TAT ATG GAG CTC ACT AGG CTG ACA TCT GAG GAC TCT GCT GTC TAT
TTC TGT GCT AGA GGG GAC TAC TAT AGG CGC TAC TTT GAC TTG TGG GGC CAA GGG ACC ACG GTC ACC GTC TCC
TCA GGT GGA GGC GGT TCA GGC GGA GGT GGC TCT GGC GGT GGC GGA TCG GAC ATC GAG CTC ACT CAG

Linker

TCT CCA GCA ATC ATG TCT GCA TCT CCA GGG GAG AGG GTC ACC ATG ACC TGC AGT GCC AGC TCA AGT ATA CGT
TAC ATA TAT TGG TAC CAA CAG AAG CCT GGA TCC TCC CCC AGA CTC CTG ATT TAT GAC ACA TCC AAC GTG GCT

VL

CCT GGA GTC CCT TTT CGC TTC AGT GGC AGT GGG TCT GGG ACC TCT TAT TCT CTC ACA ATC AAC CGA ATG GAG
GCT GAG GAT GCT GCC ACT TAT TAC TGC CAG GAG TGG AGT GGT TAT CCG TAC ACG TTC GGA GGG GCA CCA AGC
TGG GAA ATC AAA CGG

Figure 4 Nucleotide sequence of MG₇ scFv

DISCUSSION

MG₇, a monoclonal antibody against human gastric cancer, was proved to possess quite high specificity and sensitivity to gastric cancer associated antigen. It was successfully used in experimental targeting therapy in nude mice bearing transplanted human gastric cancer^[30]. But owing to its murine origin, like many other similar antibodies, MG₇ antibody can elicit anti-mouse immunoreaction in man and thus its use in clinical practice is restricted^[31,32]. One of the efficient strategies to this problem is to remove the constant region of antibody which makes main contribution to the immunogenicity of the murine antibody to human being^[33-38]. On the other hand, antibody without constant region, termed scFv, is less antigenic and induces weaker repulsive reaction. In addition, it is a smaller molecule and comprises 1/6 of its original antibody in molecular mass which ensure that scFv can more readily penetrate into the tumor tissue *in vivo* and be easily cleared up from the normal tissue^[39,40]. Besides, the scFv is more available than its original antibody by gene engineering technology which can provide an economical means for diagnosis of gastric cancer^[41-47].

As mentioned above, the scFv is advantageous to its original antibody in clinical practice. Therefore, developing the MG₇ scFv is of great significance in both early diagnosis and therapy of gastric cancer. For example, MG₇ scFv fused with avidin can be used as a reagent in immuno-PCR for early diagnosis of gastric cancer. Additionally, a new immunotoxin for treatment of gastric cancer can be developed by fusing the MG₇ ScFv and A subunit of ricin together. MG₇ ScFv can direct the A subunit of ricin to MG₇ positive gastric cancer cells^[48-50]. In our previous study, the MG₇ recombinant phage antibody derived from MG₇ hybridoma was constructed and subsequently two strong positive phage antibody clones were screened out from this library^[51].

Targeting therapy for tumors in the last decade has become a highlight in the field of tumor therapy^[52-57]. In past, the discoveries of many tumor specific antigen (TSA) and tumor associated antigen (TAA) assured the practicability of antibody as a tool in tumor targeting therapy^[58-69]. Ascribed to its high specificity and sensitivity in recognizing associated antigen, antibody is the optimal candidate for targeting mediator. Therefore, targeting therapy mediated by antibody still remains as a promising curative modality among the ways of tumor therapy and attracts worldwide attention^[70].

This study was conducted with the purpose to produce the soluble MG₇ scFv, identify its antigen-binding affinity, determine its molecular mass and get an understanding of its nucleotide sequence. We first examined the length of exogenous MG₇ scFv gene harbored in the two strong positive phage antibody clones by restriction analysis and found that one of the phage antibody clones contained a 750bp fragment of exogenous gene which was identical to many discovered scFvs in length. Secondly, we prepared the periplasmic extracts (containing majority of the soluble scFv) from IPTG-induced *E.coli* HB2151 and detected the antigen-binding affinity of MG₇ scFv by ELISA. One of the soluble MG₇ scFvs was shown to possess apparent antigen-binding activity. Subsequently, immunodotting test exhibited that *E.coli* HB2151 had successfully produced the soluble MG₇ scFv with high yields via induction by IPTG. Meanwhile, western blot suggested that the molecular mass of soluble MG₇ scFv was Mr 30. Finally, DNA sequencing unraveled that the MG₇ scFv had the common characteristics shared by other known scFvs in nucleotide sequence. Collectively, we have successfully developed the soluble MG₇ scFv and created an opportunity to study its application in targeting therapy of gastric cancer.

REFERENCE

- Niu WX, Qin XY, Liu H, Wang CP. Clinicopathological analysis of patients with gastric cancer in 1200 cases. *World J Gastroenterol* 2001; 7: 281-284
- Wang SH, Wang HT, Jiang SC. Selection of human anti-HAV McAb from a phage antibody library. *Zhongguo shengwu jishu Zazi* 1998; 14: 173-178
- Lu XP, Li BJ, Chen SL, Lu B and Jiang NY. Effect of chemotherapy or targeting chemotherapy on apoptosis of colorectal carcinoma. *Shijie Huaren Xiaohua Zazhi* 1999; 7:3332-334
- Liu HF, Liu WW, Fang DC. Induction of apoptosis in human gastric carcinoma cell line SGC7901 by anti-Fas monoclonal antibody. *Shijie Huaren Xiaohua Zazhi* 1999; 7: 476-487
- Ning XY, Yang DH. Research and progress is *in vivo* gene therapy for primary liver cancer. *Shijie Huaren Xiaohua Zazhi* 2000; 8:89-90
- Chen JP, Lin C, Xu CP, Zhang XY, Fu M, Deng YP, Wei Y and Wu M. Transduction efficiency, biologic effect and mechanism of recombinant RA538, antisense C-myc adenovirus on different cell lines. *Shijie Huaren Xiaohua Zazhi* 2000;8:266-270
- Guo SY, Gu QL, Liu BY, Zhu ZG, Yin HR and Lin YZ. Experimental study on the treatment of gastric cancer by TK gene combined with mL-2 gene. *Shijie Huaren Xiaohua Zazhi* 2000;8:974-978
- Pan X, Pan W, Ni CR, Ke CW, Cao GW and Qi ZT. Killing effect of tetracycline-controlled expression of DT/VEGF system on liver cell cancer. *Shijie Huaren Xiaohua Zazhi* 2000; 8:867-873
- Leng JJ, Chen YQ, Leng XS. Genetic therapy for pancreatic neoplasms. *Shijie Huaren Xiaohua Zazhi* 2000; 8: 916-918
- Pan X, Pan W, Ke CW, Zhang B, Cao GW, Qi ZT. Tetracycline controlled DT/VEGF system gene therapy mediated by adenovirus vector. *Shijie Huaren Xiaohua Zazhi* 2000;8:1121-1126
- Wang FS, Wu ZZ. Current situation in studies of gene therapy for liver cirrhosis and liver fibrosis. *Shijie Huaren Xiaohua Zazhi* 2000;8:371-396
- Pan X, Ke CW, Pan W, He X, Cao GW, Qi ZT. Killing effect of DT/VEGF system on gastric carcinoma cell. *Shijie Huaren Xiaohua Zazhi* 2000; 8: 393-396
- Cao GW, Qi ZT, Pan X, Pan W, He X, Ke CW. Gene therapy for human colorectal carcinoma using promoter controlled bacterial ADP-ribosylating toxin genes human CEA, PEA and DTA gene transfer. *World J Gastroenterol* 1998;4:388-391
- Lu XP, Li BJ, Chen SL, Lu B, Jiang NY. Anti-CEA monoclonal antibody targeting therapy for colorectal carcinoma. *Shijie Huaren Xiaohua Zazhi* 1999;7:329-331
- Engelstadter M, Bobkova M, Baier M, Stitz J, Holtkamp N, Chu TH, Kurth R, Dornburg R, Buchholz CJ, Cichutek K. Targeting human T cells by retroviral vectors displaying antibody domains selected from a phage display library. *Hum Gene Ther* 2000;11:293-303
- Wu YD, Song XQ, Zhou DN, Hu XH, Gan YQ, Li ZG, Liao P. Experimental and clinical study on targeting treatment of liver cancer using radionuclide- anti-AFP antibody -MMC doublet. *Shijie Huaren Xiaohua Zazhi* 1999; 7: 387-390
- Zhang J, Liu YF, Yang SJ, Sun ZW, Qiao Q and Zhang SZ. Construction and expression of mouse/humanized ScFv and their fusion to humanized mutant TNF- α against hepatocellular carcinoma. *Shijie Huaren Xiaohua Zazhi* 2000; 8: 616-620
- Chen ZN, Bian HJ, Jiang JL. Recent progress in anti-hepatoma monoclonal antibody and its application. *Shijie Huaren Xiaohua Zazhi* 1998; 6: 461-462
- Romanczuk H, Galer CE, Zabner J, Barsomian G, Wadsworth SC, O'Riordan CR. Modification of an adenoviral vector with biologically selected peptides: a novel strategy for gene delivery to cells of choice. *Hum Gene Ther* 1999; 10: 2615-2626
- Wang W, Zhou J, Xu L and Zhen Y. Antineoplastic effect of intracellular expression of a single-chain antibody directed against type IV collagenase. *J Environ Pathol Toxicol Oncol* 2000; 19: 61-68
- Li J, Wang Y, Li Q. Construction and expression of ScFv from anti-human gastric cancer McAb 3H11. *Zhonghua Zhongliu Zazhi* 1998; 20: 85-87
- Wei XC, Wang XJ, Chen K, Zhang L, Liang Y, Lin XL. Killing effect of TNF-related apoptosis inducing ligand regulated by tetracycline on gastric cancer cell line NCI-N87. *World J Gastroenterol* 2001; 7: 559-562
- Liu DH, Zhang W, Su YP, Zhang XY, Huang YX. Construction of eukaryotic expression vector of sense and antisense VEGF165 and its expression regulation. *Shijie Huaren Xiaohua Zazhi* 2001; 9: 886-891
- Liu WC, Mu HX, Ren J, Zhang XY, Pan BR. Anti-tumor activity of defensin on gastric cancer cell line *in vitro*. *Shijie Huaren Xiaohua Zazhi* 2001; 9: 622-626
- Yang JT, Fang DC, Yang SM, Luo YH, Lu R, Luo KL, Liu WW. Construction of sense and antisense hTR eukaryotic expression vector. *Shijie Huaren Xiaohua Zazhi* 2000; 8: 491-493
- Huang ZH, Qian WF, Chi DB, Jiang ZS. Apoptosis in human colorectal cancer Lovo cells induced by HSVtk/GCV system *in vitro*. *Shijie Huaren Xiaohua Zazhi* 2001;9:194-197
- Qian WF, Huang ZH, Chi DB. Herpes simplex virus thymidine kinase/ganciclovir system combined with 5-FU for the treatment of experimental colorectal cancer. *Shijie Huaren Xiaohua Zazhi* 2001;9: 190-193
- Xu DX, Chen WS, Ye ZJ. The antisense gene of growth factor receptor

- reversing the malignant phenotype of human hepatoma cells. *Shijie Huaren Xiaohua Zazhi* 2001; 9: 175-179
- 29 Tang YC, Li Y, Qian GX. Reduction of tumorigenicity of SMMC-7721 hepatoma cells by vascular endothelial growth factor antisense gene therapy. *World J Gastroenterol* 2001; 7: 22-27
- 30 Fan DM, Zhang XY, Chen XT, Qiao TD, Chen BJ. Preparation and immunohistologic identification of mAbs against a poor differentiated gastric cancer line MKN-46-9. *Jiefangjun Yixue Zhazhi* 1988; 13: 12-15
- 31 Klimka A, Matthey B, Roovers RC, Barth S, Arends JW, Engert A, Hoogenboom HR. Human anti-CD30 recombinant antibodies by guided phage antibody selection using cell panning. *Br J Cancer* 2000; 83: 252-260
- 32 Watkins NA, Ouwehand WH. Introduction to antibody engineering and phage display. *Vox Sang* 2000; 78: 72-79
- 33 Zhai W, Davies J, Shang DZ, Chan SW, Allain JP. Human recombinant single-chain antibody fragments, specific for the hypervariable region 1 of hepatitis C virus, from immune phage-display libraries. *J Viral Hepat* 1999; 6: 115-124
- 34 De Greeff A, van Alphen L, Smith HE. Selection of recombinant antibodies specific for pathogenic *Streptococcus suis* by subtractive phage display. *Infect Immun* 2000; 68: 3949-3955
- 35 Long MC, Jager S, Mah DC, Jebailey L, Mah MA, Masri SA, Nagata LP. Construction and characterization of a novel recombinant single-chain variable fragment antibody against Western equine encephalitis virus. *Hybridoma* 2000; 19: 1-13
- 36 Johns M, George AJ, Ritter MA. In vivo selection of ScFv from phage display libraries. *J Immunol Methods* 2000; 239: 137-151
- 37 Mao S, Gao C, Lo CH, Wirsching P, Wong CH, Janda KD. Phage-display library selection of high-affinity human single-chain antibodies to tumor-associated carbohydrate antigens sialyl Lewisx and Lewisx. *Proc Natl Acad Sci U S A* 1999; 96: 6953-6958
- 38 Kupsch JM, Tidman NH, Kang NV, Truman H, Hamilton S, Patel N, Newton Bishop JA, Leigh IM, Crowe JS. Isolation of human tumor-specific antibodies by selection of an antibody phage library on melanoma cells. *Clin Cancer Res* 1999; 5: 925-931
- 39 Franconi R, Roggero P, Pirazzi P, Arias FJ, Desiderio A, Bitti O, Pashkoulou D, Mattei B, Bracci L, Masenga V, Milne RG, Benvenuto E. Functional expression in bacteria and plants of an ScFv antibody fragment against tospoviruses. *Immunotechnology* 1999; 4: 189-201
- 40 Yi K, Chung J, Kim H, Kim I, Jung H, Kim J, Choi I, Suh P, Chung H. Expression and characterization of anti-NCA-95 ScFv (CEA 79 ScFv) in a prokaryotic expression vector modified to contain a Sfi I and Not I site. *Hybridoma* 1999; 18: 243-249
- 41 McCall AM, Adams GP, Amoroso AR, Nielsen UB, Zhang L, Horak E, Simmons H, Schier R, Marks JD, Weiner LM. Isolation and characterization of an anti-CD16 single-chain Fv fragment and construction of an anti-HER2/neu/anti-CD16 bispecific scFv that triggers CD16-dependent tumor cytotoxicity. *Mol Immunol* 1999; 36: 433-445
- 42 Winthrop MD, DeNardo SJ, DeNardo GL. Development of a hyperimmune anti-MUC-1 single chain antibody fragments phage display library for targeting breast cancer. *Clin Cancer Res* 1999; 5(10 Suppl): 3088s-3094s
- 43 Stadler BM. Antibody production without animals. *Dev Biol Stand* 1999; 101: 45-48
- 44 Topping KP, Hough VC, Monson JR, Greenman J. Isolation of human colorectal tumour reactive antibodies using phage display technology. *Int J Oncol* 2000; 16: 187-195
- 45 Adams GP, Schier R. Generating improved single-chain Fv molecules for tumor targeting. *J Immunol Methods* 1999; 231: 249-260
- 46 Lekkerkerker A, Logtenberg T. Phage antibodies against human dendritic cell subpopulations obtained by flow cytometry-based selection on freshly isolated cells. *J Immunol Methods* 1999; 231: 53-63
- 47 van Kuppevelt TH, Dennissen MA, van Venrooij WJ, Hoet RM, Veerkamp JH. Generation and application of type-specific anti-heparan sulfate antibodies using phage display technology. Further evidence for heparan sulfate heterogeneity in the kidney. *J Biol Chem* 1998; 273: 12960-12966
- 48 Yang LJ, Sui YF, Chen ZN. Preparation and activity of conjugate of monoclonal antibody HAB18 against hepatoma F(ab')₂ fragment and staphylococcal enterotoxin A. *World J Gastroenterol* 2001; 7: 216-221
- 49 Cheng H, Liu YF, Zhang HZ, Shen WA, Zhang SZ. Construction and expression of anti-HCC immunotoxin of sFv-TNF- α and GFP fusion proteins. *Shijie Huaren Xiaohua Zazhi* 2001; 9: 640-644
- 50 Rodenburg CM, Mernaugh R, Bilbao G, Khazaeli MB. Production of a single chain anti-CEA antibody from the hybridoma cell line T84.66 using a modified colony-lift selection procedure to detect antigen-positive ScFv bacterial clones. *Hybridoma* 1998; 17: 1-8
- 51 Yu ZC, Ding J, Nie YZ, Fan DM and Zhang XY. Preparation of single chain variable fragment of MG₇ mAb by phage display technology. *World J Gastroenterol* 2001; 7: 510-514
- 52 Darimont BD. The Hsp90 chaperone complex-A potential target for cancer therapy *World J Gastroenterol* 1999; 5: 195-198
- 53 Bi WX, Xu SD, Zhang PH, Kong F. Antitumoral activity of low density lipoprotein acalacinomycin complex in mice bearing H22 tumor. *World J Gastroenterol* 2000; 6: 140-142
- 54 Yang CQ, Wang JY, Fang JT, Liu JJ, Guo JS. A comparison between intravenous and peritoneal route on liver targeted uptake and expression of plasmid delivered by Glyco poly L-lysine. *World J Gastroenterol* 2000; 6: 508-512
- 55 Chen YP, Zhang L, Lu QS, Feng XR, Luo KX. Lactosamination of liposomes and hepatotropic targeting research. *World J Gastroenterol* 2000; 6: 593-596
- 56 He Y, Zhou J, Wu JS, Dou KF. Inhibitory effects of EGFR antisense oligodeoxynucleotide in human colorectal cancer cell line. *World J Gastroenterol* 2000; 6: 747-749
- 57 Wang XW, Yuan JH, Zhang RG, Guo LX, Xie Y, Xie H. Antihepatoma effect of alpha fetoprotein antisense phosphorothioate oligodeoxyribonucleotides *in vitro* and in mice. *World J Gastroenterol* 2001; 7: 345-351
- 58 Wang L, Lu W, Chen YG, Zhou XM, Gu JR. Comparison of gene expression between normal colon mucosa and colon carcinoma by means of messenger RNA differential display. *World J Gastroenterol* 1999; 5: 533-534
- 59 Kong XB, Yang ZK, Liang LJ, Huang JF, Lin HL. Overexpression of P-glycoprotein in hepatocellular carcinoma and its clinical implication. *World J Gastroenterol* 2000; 6: 134-135
- 60 Qin LL, Su JJ, Li Y, Yang C, Ban KC, Yian RQ. Expression of IGF-c α , p53, p21 and HBxAg in precancerous events of hepatocarcinogenesis induced by AFB1 and/or HBV in tree shrews. *World J Gastroenterol* 2000; 6: 138-139
- 61 Li J, Feng CW, Zhao ZG, Zhou Q, Wang LD. A preliminary study on ras protein expression in human esophageal cancer and precancerous lesions. *World J Gastroenterol* 2000; 6: 278-280
- 62 Tian XJ, Wu J, Meng L, Dong ZW, Shou CC. Expression of VEGF121 in gastric carcinoma MGC803 cell line. *World J Gastroenterol* 2000; 6: 281-283
- 63 Xu AG, Li SG, Liu JH, Gan AH. The function of apoptosis and protein expression of bcl2, p53 and C-myc in the development of gastric cancer. *World J Gastroenterol* 2000; 6(Suppl 3): 27-33
- 64 Li JY, Huang Y, Lin MF. Clinical evaluation of several tumor markers in the diagnosis of primary hepatic cancer. *World J Gastroenterol* 2000; 6(Suppl 3): 39-41
- 65 Lin GY, Chen ZL, Lu CM, Li Y, Wang J, Ping XJ, Huang R. Immunohistochemical study on p53, Hrasp21, cerbB2 protein and PCNA expression in tumor tissues of Han and minority ethnic patients with primary hepatic carcinoma in Xinjiang. *World J Gastroenterol* 2000; 6(Suppl 3): 53-58
- 66 Fan ZR, Yang DH, Cui J, Qin HR, Huang CC. Expression of insulin like growth factor and its receptor in hepatocellular carcinogenesis. *World J Gastroenterol* 2001; 7: 285-288
- 67 Zheng CX, Zhan WH, Zhao JZ, Zheng D, Wang DP, He YL, Zheng ZQ. The prognostic value of preoperative serum levels of CEA, CA19-9 and CA72-4 in patients with colorectal cancer. *World J Gastroenterol* 2001; 7: 431-434
- 68 Xu AG, Li SG, Liu JH, Gan AH. Function of apoptosis and expression of the proteins Bcl-2, p53 and C-myc in the development of gastric cancer. *World J Gastroenterol* 2001; 7: 403-406
- 69 Li XG, Song JD, Wang YQ. Differential expression of a novel colorectal cancer differentiation-related gene in colorectal cancer. *World J Gastroenterol* 2001; 7: 551-554
- 70 Chen QK, Yuan SZ, Zeng ZY, Huang ZQ. Tumoricidal activation of murine resident peritoneal macrophages on pancreatic carcinoma by interleukin2 and monoclonal antibodies. *World J Gastroenterol* 2000; 6: 287-289

• REVIEW •

The prognostic significance of clinical and pathological features in hepatocellular carcinoma

Lun-Xiu Qin, Zhao-You Tang

Lun-Xiu Qin, Zhao-You Tang, Liver Cancer Institute and Zhongshan Hospital, Fudan University, Shanghai, China

Correspondence to: Zhao-You Tang, M.D. Professor of Surgery Chairman, Liver Cancer Institute & Zhongshan Hospital, 136 Yi Xue Yuan Road, Shanghai 200032, China. zytang@srcap.stc.sh.cn

Telephone: +86-21-64037181 Fax: +86-21-64037181

Received 2001-12-20 Accepted 2002-01-24

Abstract

The prognosis of patients with HCC still remains dismal. The life expectancy of HCC patients is hard to predict because of the high possibility of postoperative recurrence. Many factors, such as patient's general conditions, macroscopic tumor morphology, as well as tumor histopathology features, have been proven of prognostic significance. Female HCC patient often has a better prognosis than male patient, which might be due to the receptor of sex hormones. Younger patients often have tumors with higher invasiveness and metastatic potentials, and their survival and prognosis are worse than the older ones. Co-existing hepatitis status and hepatic functional reserve have been confirmed as risk factors for recurrence. Serum alpha-fetoprotein (AFP) is useful not only for diagnosis, but also as a prognostic indicator for HCC patients. AFP mRNA has been proposed as a predictive marker of HCC cells disseminated into the circulation and for metastatic recurrence. Many pathologic features, such as tumor size, number, capsule state, cell differentiation, venous invasion, intrahepatic spreading, and advanced pTNM stage, are the best-established risk factors for recurrence and important aspects affecting the prognosis of patients with HCC. Marked inflammatory cell infiltration in the tumor could predict a better prognosis. Clinical stage is still the most important factor influencing on the prognosis. Extratumor spreading and lymph nodal metastasis are independent predictors for poor outcome. Some new predictive systems have recently been proposed. Different strategies of treatment might have significant different effects on the patients' prognosis. To date, surgical resection is still the only potentially curative treatment for HCC, including localized postoperative recurrences. Extent of resection, blood transfusion, occlusion

of porta hepatis, and blood loss affect the survival and prognosis of HCC patients. Regional therapies provide alternative ways to improve the prognosis of HCC patients who have no opportunity to receive surgical treatment or postoperative recurrence. The combination of these treatment modalities is hopeful to further improve the prognosis. The efficacies of neoadjuvant (preoperative) or adjuvant (postoperative) chemotherapy or chemoembolization in preventing recurrence and on the HCC prognosis still remain great controversy, and deserves further evaluation. Biotherapy, including IFN-alpha therapy, will play more important role in preventing recurrence and metastasis of HCC after operation.

Qin LX, Tang ZY. The prognostic significance of clinical and pathological features in hepatocellular carcinoma. *World J Gastroenterol* 2002;8(2):193-199

INTRODUCTION

The outcome for patients with hepatocellular carcinoma (HCC) still remains dismal, although it has been proven much in the past few decades, a definitive subset is cured by surgery only, and encouraging long-term survival of patients have been obtained in some clinical centers. The high possibility of intrahepatic and/or extrahepatic recurrence postoperatively remains one major obstacle for further improving the survival and prognosis of HCC patients. The life expectancy of HCC patients is hard to predict, making it difficult to decide the patient's prognosis. Many factors, such as the patient's general conditions (age, sex, co-existing hepatitis, liver function, AFP level), macroscopic tumor morphology (tumor size, number, capsule status, intra- or extrahepatic spreading, vessel invasion), tumor pathohistology features, as well as effective treatment and adjuvant therapies, have been proven of prognostic significance. In recent years, as the understanding of tumor biology and the development of molecular biology techniques, many molecular factors (biomarkers) have been shown related to prognosis^[1-11]. In this review, we will focus on the prognostic significance of clinical and pathological features of HCC.

PATIENTS' SEX AND AGE

Sex and sex hormone related factors

Many reports indicate that female HCC patient more frequently has a well-encapsulated, less invasive tumor, and longer survival, lower recurrent rate, and better prognosis than male patient. These might be due to the receptor of sex hormones^[5,12]. Both androgen receptor (AR) and estrogen receptor (ER) are found closely related to the prognosis of HCC patients. The 5-year survival rates of AR negative, ER negative, ER positive, or AR positive HCC patients were 55%,

24%, 10%, and 0%, respectively. ER positive HCC has less malignant biologic behavior and a better prognosis than ER negative ones, with higher percentages of single nodule, complete encapsulation, and lower PCNA labeled index. And the ER positive rate of small HCC (62.5%) is higher than that of large HCC (30.4%). The presence of variant liver ER transcripts in the tumor is the strongest negative predictor of survival in inoperable HCC, with spontaneous survival significantly worse than that of patients with wild-type ER. HBsAg-positive patients with variant receptors have a even worse survival^[112]. But there is still controversy with the relationship between the better prognosis of female HCC patients and the sex hormone receptors.

Age

Younger HCC patients often have tumors with higher invasiveness and metastatic potentials, higher recurrence possibility, and their survival and prognosis are worse than the older ones. However, Chedid found male, older patients often had poorly differentiated tumors, and poorer survivals, and age younger than 45 years was a good prognostic factor^[113]. In authors' institute, no significant difference between the younger and older patients was found^[14].

CO-EXISTING HEPATITIS STATUS AND LIVER CIRRHOSIS

Co-existing hepatitis status and liver cirrhosis are other important factors influencing the prognosis of HCC patients. The inflammatory activity and hepatic reserve have been confirmed as risk factors for recurrence. Longer disease-free survival (DFS) is found in patients without active hepatitis, and suppression of co-existing hepatitis is necessary to achieve better DFS^[115]. The postoperative overall and disease-free survival rates of patients without hepatitis viral infection (N-HCC) are better than those hepatitis B virus-related HCC (B-HCC) and HBV-HCV double infection HCC(D-HCC)patients. The postoperative long-term survival rate of patients seronegative for HBsAg is greater than that of patients seropositive for HBsAg^[116]. This is due to N-HCC cases have a good liver function reservation, and have no synchronous and metachronous multicentric occurrence^[117]. D-HCC often has a higher surgical complication rate and hospital mortality, and recurred earlier after hepatectomy^[118].

A high viral load is an independent risk factor for recurrence. The HBeAg, wild-type HBV are more likely to be found in patients with a high viral load, while precore mutant-type HBV is useful for estimating a patient's prognosis after resection of B-HCC^[119]. Patients infected with genotype 1b of HCV may have a relatively high risk of ongoing hepatocarcinogenesis and more aggressive progression of associated liver dysfunction, resulting in a poorer outcome than with other genotypes^[120, 211].

Functional reserve of the remnant cirrhotic liver is another independent prognostic factor. Hepatic functional damage immediately after hepatectomy is a significant risk factor for early intrahepatic recurrence^[122]. Some liver functional markers, such as alanine transaminase (ALT), gamma-glutamyl transpeptidase (GGT), serum albumin level, the preoperative indocyanine green (ICG) retention value at 15 minutes after injection, particularly the Child-Pugh classification, are important predictive markers for DFS of HCC patients^[123-25]. According to the scoring of hepatitis activity index (HAI), the histologic activity of hepatitis was closely related to the HCC recurrence, the HCC patients with middle hepatitis activity (HAI score of 6-9) in the non-tumor liver tissue had a higher 2-year intrahepatic recurrent rate^[126]. Recurrence hardly could be avoided in the patients with liver dysfunction^[127, 28]. The serum albumin level of patients was also an independent risk factor of early recurrence, while liver cirrhosis and serum bilirubin were independent prognostic factors

for late recurrence after HCC resection^[29]. Patients with Karnofsky index <80%, serum bilirubin >50micromol/l, serum alkaline phosphatase at least twice the upper limit of normal range, and prothrombin time <70% of normal level have been found to have a poor prognosis^[14, 30].

TUMOR MAKERS

Serum alpha-fetoprotein (AFP) is useful not only for diagnosis, but also as a prognostic indicator for HCC patients. Patients with high AFP levels at diagnosis tended to have greater tumor size, bilobar involvement, massive or diffuse types, and portal vein thrombosis. The median survival rates with normal AFP (<20IU/mL), or with moderately elevated AFP (20-399IU/mL) (6-7 months) were significantly longer than that with markedly elevated AFP (> or =400IU/mL) (3months)^[31]. Nonetheless, a correlation could not be established between increased AFP and Okuda's stages, degree of tumor differentiation, or extrahepatic metastasis.

AFP mRNA has been proposed as a predictive marker of HCC cells disseminated into the circulation and for metastatic recurrence in many reports^[32-37], but its clinical significance remains controversial^[38-40]. The patients with positive AFP mRNA in peripheral blood were found to have a higher possibility of extrahepatic metastasis than those negative. Some of them could change to negative after adjacent treatment, whose overall and disease-free survival rates are much better than those with permanent positive AFP mRNA. So, AFP mRNA in peripheral blood of HCC patients in perioperative period might be a predictive marker for the early intrahepatic recurrence and distant metastasis after HCC resection^[32, 33]. In a recent report, circulating AFP mRNA was transiently detected in cirrhosis with no predictive value for HCC development.

Lens culinaris agglutinin A-reactive fraction of alpha-fetoprotein (AFP-L3) is found to be a useful indicator of distant metastasis and a poor prognosis for HCC. Patients with AFP-L3-positive had worse liver function and larger tumors compared to the negative group. They also had more advanced cancer with poor tumor histology compared to the negative group. Distant metastasis was diagnosed significantly more often in the positive group than that in the negative group^[41].

Although DCP was not an independent prognostic factor, its measurement was effective in predicting HCC recurrence and had the advantage that it can be assessed before operation^[42]. However, albumin mRNA in peripheral blood has no confirmed value for predicting circulating spread of HCC cells.

PATHOLOGICAL FEATURES OF TUMOR

Many pathologic factors of tumor itself, such as tumor size, number, capsule state, cell differentiation, venous invasion, presence of satellite nodules, and advanced pTNM stage, are the best-established risk factors for recurrence and important aspects affecting the prognosis of patients with HCC^[43-46]. Assal *et al.* proposed an invasiveness scoring system to predict recurrence and survival after curative HCC resection, which consists of six variables including portal venous invasion, intrahepatic spreading, hepatic venous invasion, membrane invaded, and no tumor capsule, or capsule invaded. According to this system, HCC could be divided into three groups: low invasiveness HCC (A): 0-1 score, middle invasiveness (B): 2-4, and high invasiveness HCC (C): 5-11 scores. The recurrent rate increased as the score became higher. The prognosis of Group B and C patients were much worse than Group A^[47].

Tumor size

Many studies have confirmed that tumor size is one independent

prognostic factor^[46,50]. Both of the 5-year overall survival (OS) and disease-free survival (DFS) rates of small HCC (tumor largest diameter ≤ 5 cm) are better than that of large HCC (tumor diameter > 5 cm)^[3,4-8,14,48].

Tumor number and capsule status

The prognosis of patient with single tumor nodule is much better than those with multiple nodules. However, there was still a different result, no significant difference between their overall and DFS rates could be found^[49].

The patients with well-encapsulated HCC have a better prognosis than those with poor encapsulated. However, well-encapsulated and nonnecrotic HCCs have a significantly higher tumor pressure (TP) and great pressure gradient (TP-PVP), both of them are found to associate with venous invasion or intrahepatic metastasis^[50].

Venous invasion and intra-or extrahepatic spreading

Venous invasion and intrahepatic metastasis (IM) might strongly reflect the invasiveness of HCC. They are also important independent factors for poor prognosis^[45, 49, 51,52]. In Authors' institute, the 5-year survival rate of the HCC patients without portal vein thrombi (PVT) (63.9%) after operation is much higher than that of patients with PVT (40.8%). Ouchi K, *et al.* defined portal vein invasion (Vp) and IM as the extratumor spread, and found it was the only significant variable influencing recurrence in multivariate analysis. As a predictive factor for recurrence after resection of HCC, the extratumor spreads was found to be more accurate than is any single invasiveness parameter such as Vp or IM^[53]. The patients with macroscopic portal vein invasion, microscopic vascular invasion, intrahepatic metastasis, poor differentiation, pleomorphism, sarcomatous change, vascular lake, and angiographic condensed pooling were more frequently found to have extremely poor prognosis^[54]. The prognosis of patients with lymph nodal metastasis from HCC is generally poor, even if hepatic resection with regional LN dissection is performed^[52,55].

Inflammatory cell infiltration

Marked inflammatory cell infiltration in the tumor could predict a better prognosis, which could attribute to the anti-tumor effect induced by cellular immunity of CD8+ and CD4+ T lymphocytes. Wada found the patients with HCCs less than 3 cm in diameter with marked inflammatory cell infiltration had a much lower recurrence rate after resection (9.1%) (compared with 47.7% in the controls), and a higher 5-year survival rate (100%) (compared with 65.1% in the controls). The tumor invasion into the portal vein in the vicinity of the tumor was much lower. Varying degrees of piecemeal necrosis of cancer nests produced by infiltrating lymphocytes were observed in all patients with marked inflammatory cell infiltration in the tumor^[56].

CLINICAL STAGING

It is well known that clinical stage is the most important factor influencing on the prognosis of HCC patients. The most common used staging system is UICC's TNM (tumor, nodes, metastases). Okuda system is also used in some regions. Based on the current TNM staging system for human HCC, a new T staging system has been proposed to correlate the staging group with patient outcome after curative liver resection. In this new system, T1 is defined as no vascular invasion, small size ($< \text{or} = 5$ cm), and solitary tumor; T2 as the presence of one of the following factors: size greater than 5 cm, vascular invasion, or multiple tumors; T3 as the presence of two of the above three factors; and T4, the presence of all three factors. The new T staging system shows good correlation between the staging group and patient outcome. But this modified TNM system is not

superior to the UICCpTNM system in predicting survival of HCC patients^[43]. Portal vein invasion (Vp) and intrahepatic metastasis (IM) strongly reflect the invasiveness of HCC, and are predictive factors for recurrence and prognosis after resection of HCC^[53]. Lymph nodal metastasis is one independent predictor for poor outcome^[55].

A new score system, the Cancer of the Liver Italian Program (CLIP) score, recently is proposed, which includes the parameters involved in the Child-Pugh stage, plus macroscopic tumor morphology, AFP levels, and the presence or absence of portal thrombosis. The CLIP score is able to predict survival better than the Okuda or TNM staging system, accurately identify patients with different prognoses, particularly in the early phases of HCC^[57]. Besides, Schoniger-Hekele developed a multivariate Cox proportional hazard model (Vienna survival model for HCC=VISUM-HCC) predicting survival, and found patients with serum bilirubin > 2 mg/dl, portal vein thrombosis, prothrombin time $< 70\%$, AFP > 180 mg/l, tumour mass $> 50\%$, and enlarged lymph nodes were independent predictors of survival. Applying the VISUM-HCC survival model to patients in Okuda stage 2 identified subgroups with an excellent and very poor prognosis for which different treatment modalities should be offered^[52].

TREATMENT STRATEGIES RELATED

Effective treatment is important for prolonging the survival and improving the prognosis of HCC patients. Different strategies of treatment might have significant different effects on the patients' prognosis.

At present, surgery is still the only potentially curative treatment for HCC, including either partial hepatectomy or total hepatectomy with orthotopic liver transplantation (OLT). Although the survival rates of selected patients for transplantation and partial hepatectomy are comparable, the use of OLT is limited by the difficulty of obtaining donor livers, the expensive cost (particularly in developing countries)^[58]. So, surgical resection is still the most important way to obtain long-term survivals. In recent years, regional cancer therapies, such as transcatheter arterial chemoembolization (TACE), and vary kinds of liver tumor ablation therapies (including percutaneous ethanol injection-PEI, percutaneous microwave coagulation therapy-PMCT, radiofrequency ablation-RF, etc.) have been developed. These regional therapies are hopeful in further improving the prognosis of HCC patients who have no opportunity to receive surgical treatment or postoperative recurrence. The combination of these treatment modalities is hopeful to further improve the prognosis of HCC patients^[59,60].

OPERATION RELATED

Many operation-related factors, such as extent of resection, blood transfusion, occlusion time of porta hepatis, blood loss, affect the survival and prognosis of HCC patients.

Surgical margin

The significance of the extent of surgical resection remains controversial. Some reports indicated it had no significant influence on the OS and DFS rates. No significant difference between the major hepatectomy (2 segments or more) and a minor hepatectomy group (one segment or less) could be observed in patient OS and DFS. So, a major hepatectomy is therefore not recommended for patients with solitary small HCC^[61,62]. However, many other reports emphasized the importance of surgical margin in the prognosis of HCC patients. Anatomical resection appeared to have a beneficial effect on recurrence-free survival after hepatectomy for HCC. If the liver

functional reserve is good, the extent of surgical resection should be big enough to increase the DFS^[63,64]. Some reports indicated that surgical margin might have some effect on the survival rate of patients with small HCC, while no obvious influence on the overall survival of HCC patients^[65]. However, in China, co-existing liver cirrhosis is found in most of the HCC patients, which limits the extent of surgical resection. If major liver resection is performed in the patients with severe liver cirrhosis, the patients could be died of the poor remnant liver function. And more, when tumor locates in the porta hepatis or is closed to the important vessels (blood vessels and bile duct), it is impossible to have the surgical margin >1cm. In authors' institute, no significant difference in the survival rates between the HCC patients received different extensions of liver resection was found. So, it is not necessary to try to have an extended surgical margin for the patients with obvious liver cirrhosis.

Blood transfusion

Many reports indicate perioperative blood transfusion enhances the risk of intrahepatic recurrence of HCC, and is a significant independent factor that influence cumulative survival rate of patients^[48,66]. Cox regression analysis for recurrence revealed that blood transfusion was the most significant prognostic indicator for recurrence in stage I-II patients but not in stage III-IV patients^[67].

ADJUVANT THERAPIES

Adjuvant therapies are hoped to decrease or elimination of intrahepatic recurrence of HCC after liver resection and satisfactory OS. However, in 2000, Chen *et al.* reviewed all of the eight truly randomized and quasi-randomised clinical trials (totaling 548 patients) (RLT) that compared HCC patients who were given and not given neoadjuvant/adjuvant therapy as a supplement to curative liver resection. Both pre- (neoadjuvant) and post-operative (adjuvant), systemic and locoregional (+/- embolization), chemo- and immunotherapy interventions were tested. Seven of the eight trials reported no survival benefit from adjuvant therapy. Only one trial reported a statistically significant difference for survival and DFS for the treatment arm, but the results of both its arms were very poor when compared to other studies. So, there is no evidence for efficacy of any of the adjuvant protocols reviewed on the survival and prognosis of HCC patients^[68]. Little and Fong also thought as yet there were no evidence demonstrated benefit from the various neoadjuvant and adjuvant therapies investigated^[58].

Preoperative adjuvant therapy (neoadjuvant therapy)

The value of preoperative TACE on the prognosis still remains great controversy. Many reports indicated that it could increase the possibility of recurrence and lung metastasis, showed no contribution to prognosis, should be avoided for the resectable HCC, particularly in patients with advanced cirrhosis of the liver^[69,70]. Partial tumor necrosis caused by preoperative TACE might facilitate postoperative disease recurrence. The possible reason is that the remaining tumor cells might become more aggressive, and less firmly attached, more likely to be dislodged into the bloodstream during hepatic resection^[71]. And more, preoperative TACE for resectable HCC results in delayed surgery and operational difficulty, without any benefit. It might also increase the possibility of liver failure in those with severe liver cirrhosis^[32]. Preoperative TACE should only be performed to reduce tumor bulk in patients with HCC with borderline resectability, and increased the resectability. Peng *et al.* found preoperative TACE might only benefit patients with tumors >8cm but not those with tumors 2 to 8cm^[72]. Yoshida found preoperative TACE could not improve DFS after liver resection, but preoperative

transarterial immunoembolization (TIE), a newly developed arterial embolization technique using OK-432 and fibrinogen, seemed to be more effective than conventional TAE against extracapsular invasion and intrahepatic metastasis, could improve the disease-free survival^[73]. However, Wu *et al.* found effective preoperative TACE might be one of the best methods for resectable HCCs including small HCCs for improving disease-free survival after hepatectomy^[74].

Preoperative portal vein embolization could improve prognosis after right hepatectomy for HCC in patients with impaired hepatic function, but cannot prevent tumor recurrence after HCC resection^[75]. Main portal branch transection combined with major liver resection and neoadjuvant and adjuvant locoregional immunochemotherapy could increase the resectability rate and the overall survival and DFS^[76]. Preoperative administration of 5-FU and interferon LFN-beta may prevent recurrence of co-existing hepatitis B and C virus infections^[77].

Postoperative adjuvant therapy

Effective postoperative adjuvant treatment might also be helpful in further improving the prognosis of HCC patients^[78].

The effectiveness of postoperative chemotherapy and chemoembolization on the prognosis of HCC patients still remains controversial. Some reports indicated TACE or hepatic arterial infusion chemotherapy (HAIC) was an effective in preventing recurrence after radical hepatectomy for HCC, it could suppress residual liver recurrence from intrahepatic micrometastases rather than multicentric carcinogenesis^[79-82]. This was confirmed by one RCT^[83]. However, another RCT indicated that TACE after radical resection for HCC could increase the possibility of extrahepatic metastasis, and the prognosis would be even worse^[84]. And more recently, Ono *et al.* summarized three RCTs of postoperative chemotherapy, and found postoperative chemotherapy was associated with significantly worse disease-free and overall survival rates, enhanced the cancer recurrence in the remnant liver is enhanced and deteriorated the long-term outcome in patients with cirrhosis^[85].

According to authors' institute data, postoperative adjuvant TACE or HACE or combined IFN-alpha therapy, or autologous lymphocytes activated vitro with recombinant interleukin-2 (LAK) therapies could decrease significantly the 3-year recurrent rate of patients received radical liver resection for HCC^[3,86,87]. Postoperative TACE is useful for prevention and treatment of HCC recurrence, particularly in treating the postoperative residual tumor^[88,89].

Biotherapy plays more and more important role in the prevention of recurrence and metastasis of HCC after operation^[33]. Adoptive immunotherapy can lower recurrence and improve recurrence-free outcomes of HCC^[78].

Postoperative IFN-alpha therapy can decrease recurrence after resection of hepatitis C virus-related HCC^[90]. This result was further confirmed by two pilot RCTs^[91,92]. A similar effect was obtained by preoperative IFN-alpha therapy, it might due to IFN can prevent the recurrence of hepatitis B and C virus, and decrease the incidence of HCC in patients with HCV^[48,93]. We found high-dose and long-term therapy with IFN-alpha dose-dependently inhibited tumor growth and recurrence after resection of HCC. The result of RCT carried in authors' institute also showed that IFN-alpha therapy could decrease the postoperative recurrence rate of HCC and prolong the DFS after HCC resection. This might be attributed to antiangiogenesis effect of IFN-alpha^[94].

Recently, one RCT indicated that a single 1850 MBq dose of intra-arterial ¹³¹I-lipiodol given after curative resection significantly decreased the rate of recurrence and increased the 3-year overall survival rate from 46.3% to 86.4%^[95].

TIME OF RECURRENCE

Recent studies have shown that the prognosis of recurrent HCC after resection was dependent on the time of recurrence. Based on the time of recurrence, Poon *et al.* classified the intrahepatic recurrences into early (≤ 1 year) and late (> 1 year) recurrences, and found that early and late intrahepatic recurrences were associated with different risk factors and prognostic factors. By multivariate analysis, preoperative tumor rupture and venous invasion were independent risk factors for early recurrence, whereas cirrhosis was the only significant risk factor for late recurrence. The prognosis for patients with early recurrence was worse than that of patients with late recurrence. Independent prognostic factors for early recurrence were serum albumin level and initial tumor pTNM classification, whereas only serum bilirubin level was found to be an independent prognostic factor for late recurrence. Early recurrences appear to arise mainly from intrahepatic metastases, whereas late recurrences are more likely to be multicentric in origin^[29]. Prognosis was determined by the interval to recurrence, number of recurrent tumors, any concurrent extrahepatic recurrence, and type of treatment^[24, 30, 45].

SUMMARY AND PERSPECTIVE

In summary, the prognosis of patients with HCC is still dismal. In addition to clinical stage, age, sex, hepatitis activity in the nontumorous liver, treatment strategies, and perioperative transfusion also appear to have some prognostic significance. Pathologic factors indicative of tumor invasiveness such as venous invasion, presence of satellite nodules, large tumor size, and advanced pTNM stage, are the best-established risk factors for recurrence.

Effective treatment is important for prolonging the survival and improving the prognosis of HCC patients. Different strategies of treatment might have significant different effects on the patients' prognosis. To date, surgical resection is still the only potentially curative treatment for HCC, including localized postoperative recurrences. There is a lack of convincing evidence for the efficacy of neoadjuvant or adjuvant chemotherapy in preventing recurrence, which deserves further evaluation. Regional therapies, such as TACE, PEI, RF, etc, are alternative modalities for the nonresectable HCC and nonresectable recurrences. Combination of regional therapy modalities, may offer additional benefit. Biotherapy, particularly IFN- α therapy, will play more important role in the preventing recurrence.

REFERENCES

- Pisani P, Parkin M, Bray F, Ferlay J. Estimates of the worldwide mortality from 25 cancers in 25 cancers in 1990. *Int J Cancer* 1999;83:18-29
- Greenlee RT, Hill-Harmon MB, Murray T, Thun M. Cancer Statistics, 2001. *CA Cancer J Clin* 2001;51:15-36
- Tang ZY. Hepatocellular carcinoma-Cause, treatment and metastasis. *World J Gastroenterol* 2001;7:445-454
- Zhou XD, Tang ZY, Yang BH, Lin ZY, Ma ZC, Ye SL, Wu ZQ, Fan J, Qin LX, Zhang BH. Experience of 1000 patients who underwent hepatectomy for small hepatocellular carcinoma. *Cancer* 2001;91:1479-1486
- Wu MC, Shen F. Progress in research of liver surgery in China. *World J Gastroenterol* 2000;6:773-776
- Rabe C, Pilz T, Klostermann C, Berna M, Schild HH, Sauerbruch T, Caselmann WH. Clinical characteristics and outcome of a cohort of 101 patients with hepatocellular carcinoma. *World J Gastroenterol* 2001;7:208-215
- Yip D, Findlay M, Boyer M, Tattersall MH. Hepatocellular carcinoma in central Sydney: a 10 year review of patients seen in a medical oncology department. *World J Gastroenterol* 1999;5:483-487
- Sithinamsuwan P, Piratvisuth T, Tanomkiat W, Apakupakul N, Tongyoo S. Review of 336 patients with hepatocellular carcinoma at Songklanagarind Hospital. *World J Gastroenterol* 2000;6:339-343
- Niu Q, Tang ZY, Ma ZC, Qin LX, Zhang LH. Serum vascular endothelial growth factor is a potential biomarker of metastatic recurrence after curative resection of hepatocellular carcinoma. *World J Gastroenterol* 2000;6:565-568
- Tang ZY. Hepatocellular carcinoma. *J Gastroenterol Hepatol* 2000;15 Suppl:G1
- Cance WG, Stewart AK, Menck HR. The National Cancer Data Base Report on treatment patterns for hepatocellular carcinomas: improved survival of surgically resected patients, 1985-1996. *Cancer* 2000;88:912-920
- Villa E, Moles A, Ferretti I, Buttafoco P, Grottola A, Del Buono M, De Santis M, Manenti F. Natural history of inoperable hepatocellular carcinoma: estrogen receptors' status in the tumor is the strongest prognostic factor for survival. *Hepatology* 2000;32:233-238
- Chedid A, Ryan LM, Dayal Y, Wolf BC, Falkson G. Morphology and other prognostic factors of hepatocellular carcinoma. *Arch Pathol Lab Med* 1999;123:524-528
- Sun HC, Tang ZY, Ma ZC. The factors affecting the recurrent rate after radical resection of liver cancer. *Zhonghua Gandanwaike Zazhi* 2000;6:7-9(in Chinese)
- Takata M, Yamanaka N, Tanaka T, Yamanaka J, Maeda S, Okamoto E, Yasojima H, Uematsu K, Watanabe H, Urugari Y. What patients can survive disease free after complete resection for hepatocellular carcinoma: A multivariate analysis. *Jpn J Clin Oncol* 2000;30:75-81
- Wu CC, Ho WL, Chen JT, Tang JS, Yeh DC, P'eng FK. Hepatitis viral status in patients undergoing liver resection for hepatocellular carcinoma. *Br J Surg* 1999;86:1391-1396
- Noguchi K, Nakashima O, Nakashima Y, Shiota K, Nawata H, Kojiro M. Clinicopathologic study on hepatocellular carcinoma negative for hepatitis B surface antigen and antibody to hepatitis C virus. *Int J Mol Med* 2000;6:661-665
- Chen JH, Chau GY, Lui WY, Tsay SH, King KL, Loong CC, Hsia CY, Wu CW. Surgical results in patients with hepatitis B-related hepatocellular carcinoma and positive hepatitis B early antigen. *World J Surg* 2000;24:383-387
- Kubo S, Hirohashi K, Tanaka H, Tsukamoto T, Shuto T, Yamamoto T, Ikebe T, Wakasa K, Nishiguchi S, Kinoshita H. Effect of viral status on recurrence after liver resection for patients with hepatitis B virus-related hepatocellular carcinoma. *Cancer* 2000;88:1016-1024
- Murase J, Kubo S, Nishiguchi S, Hirohashi K, Shuto T, Ikebe T, Kinoshita H. Correlation of clinicopathologic features of resected hepatocellular carcinoma with hepatitis C virus genotype. *Jpn J Cancer Res* 1999;90:1293-1300
- Hanazaki K, Wakabayashi M, Sodeyama H, Mochizuki Y, Machida T, Yokoyama S, Sode Y, Kawamura N, Miyazaki T. Surgical outcome in cirrhotic patients with hepatitis C-related hepatocellular carcinoma. *Hepatogastroenterology* 2000;47:204-210
- Hanazaki K, Wakabayashi M, Sodeyama H, Kajikawa S, Amano J. Hepatic function immediately after hepatectomy as a significant risk factor for early recurrence in hepatocellular carcinoma. *Hepatogastroenterology* 1999;46:3201-3207
- Hanazaki K, Kajikawa S, Shimozaawa N, Mihara M, Shimada K, Hiraguri M, Koide N, Adachi W, Amano J. Survival and recurrence after hepatic resection of 386 consecutive patients with hepatocellular carcinoma. *J Am Coll Surg* 2000;191:381-388
- Poon RT, Fan ST, Lo CM, Liu CL, Wong J. Intrahepatic recurrence after curative resection of hepatocellular carcinoma: long-term results of treatment and prognostic factors. *Ann Surg* 1999;229:216-222
- Poon RT, Fan ST, Lo CM, Liu CL, Ng IO, Wong J. Long-term prognosis after resection of hepatocellular carcinoma associated with hepatitis B-related cirrhosis. *J Clin Oncol* 2000;18:1094-1101
- Ueno S, Tanabe G, Yoshida A, Yoshidome S, Takao S, Aikou T. Postoperative prediction of and strategy for metastatic recurrent hepatocellular carcinoma according to histologic activity of hepatitis. *Cancer* 1999;86:248-254
- Lise M, Bacchetti S, Da Pian P, Nitti D, Pilati PL, Pigato P. Prognostic factors affecting long term outcome after liver resection for hepatocellular carcinoma: results in a series of 100 Italian patients. *Cancer* 1998;82:1028-1036
- Taketomi A, Shimada M, Shirabe K, Kajiyama K, Gion T, Sugimachi K. Natural killer cell activity in patients with hepatocellular carcinoma: a new prognostic indicator after hepatectomy. *Cancer* 1998;83:58-63
- Poon RT, Fan ST, Ng IO, Lo CM, Liu CL, Wong J. Different risk factors and prognosis for early and late intrahepatic recurrence after resection of hepatocellular carcinoma. *Cancer* 2000;89:500-507
- Chevret S, Trinchet JC, Mathieu D, Rached AA, Beaugrand M, Chastang C. A new prognostic classification for predicting survival in patients with hepatocellular carcinoma. Groupe d'Etude et de Traitement du Carcinome Hepatocellulaire. *J Hepatol* 1999;31:133-141
- Tangkijvanich P, Anukulkarnkusol N, Suwangool P, Lertmaharit S, Hanvivatvong O, Kullavanijaya P, Poovorawan Y. Clinical characteristics and prognosis of hepatocellular carcinoma: analysis based on serum alpha-fetoprotein levels. *J Clin Gastroenterol* 2000;31:302-308

- 32 Matsumura M, Shiratori Y, Niwa Y, Tanaka T, Ogura K, Okudaira T, Imamura M, Okano K, Shiina S, Omata M. Presence of alpha-fetoprotein mRNA in blood correlates with outcome in patients with hepatocellular carcinoma. *J Hepatol* 1999;31:332-339
- 33 Okuda N, Nakao A, Takeda S, Oshima K, Kanazumi N, Nonami T, Kurokawa T, Takagi H. Clinical significance of alpha-fetoprotein mRNA during perioperative period in HCC. *Hepatogastroenterology* 1999;46:381-386
- 34 Minata M, Nishida N, Komeda T, Azechi H, Katsuma H, Nishimura T, Kuno M, Ito T, Yamamoto Y, Ikai I, Yamaoka Y, Fukuda Y, Nakao K. Postoperative detection of alpha-fetoprotein mRNA in blood as a predictor for metastatic recurrence of hepatocellular carcinoma. *J Gastroenterol Hepatol* 2001;16:445-451
- 35 Wong IH, Lau WY, Leung T, Yeo W, Johnson PJ. Hematogenous dissemination of hepatocytes and tumor cells after surgical resection of hepatocellular carcinoma: a quantitative analysis. *Clin Cancer Res* 1999;5:4021-4027
- 36 Wong IH, Yeo W, Leung T, Lau WY, Johnson PJ. Circulating tumor cell mRNAs in peripheral blood from hepatocellular carcinoma patients under radiotherapy, surgical resection or chemotherapy: a quantitative evaluation. *Cancer Lett* 2001;167:183-191
- 37 Jiang YF, Yang ZH, Hu JQ. Recurrence or metastasis of HCC: predictors, early detection and experimental antiangiogenic therapy. *World J Gastroenterol* 2000;6:61-65
- 38 Lemoine A, Le Bricon T, Salvucci M, Azoulay D, Pham P, Raccuia J, Bismuth H, Debuire B. Prospective evaluation of circulating hepatocytes by alpha-fetoprotein mRNA in humans during liver surgery. *Ann Surg* 1997;226:43-50
- 39 Kienle P, Weitz J, Klaes R, Koch M, Benner A, Lehnert T, Herfarth C, von Knebel Doeberitz M. Detection of isolated disseminated tumor cells in bone marrow and blood samples of patients with hepatocellular carcinoma. *Arch Surg* 2000;135:213-218
- 40 He P, Tang ZY, Ye SL, Liu BB. Relationship between expression of α -fetoprotein messenger RNA and some clinical parameters of human hepatocellular carcinoma. *World J Gastroenterol* 1999;5:111-115
- 41 Yamashiki N, Seki T, Wakabayashi M, Nakagawa T, Imamura M, Tamai T, Nishimura A, Inoue K, Okamura A, Arita S, Harada K. Usefulness of Lens culinaris agglutinin A-reactive fraction of alpha-fetoprotein (AFP-L3) as a marker of distant metastasis from hepatocellular carcinoma. *Oncol Rep* 1999;6:1229-1232
- 42 Imamura H, Matsuyama Y, Miyagawa Y, Ishida K, Shimada R, Miyagawa S, Makuuchi M, Kawasaki S. Prognostic significance of anatomical resection and des-gamma-carboxy prothrombin in patients with hepatocellular carcinoma. *Br J Surg* 1999;86:1032-1038
- 43 Farinati F, Rinaldi M, Gianni S, Naccarato R. How should patients with hepatocellular carcinoma be staged Validation of a new prognostic system. *Cancer* 2000;89:2266-2273
- 44 Llado L, Virgili J, Figueras J, Valls C, Dominguez J, Rafecas A, Torras J, Fabregat J, Guardiola J, Jaurrieta E. A prognostic index of the survival of patients with unresectable hepatocellular carcinoma after transcatheter arterial chemoembolization. *Cancer* 2000;88:50-57
- 45 Poon RT, Fan ST, Wong J. Risk factors, prevention, and management of postoperative recurrence after resection of hepatocellular carcinoma. *Ann Surg* 2000;232:10-24
- 46 Ohkubo T, Yamamoto J, Sugawara Y, Shimada K, Yamasaki S, Makuuchi M, Kosuge T. Surgical results for hepatocellular carcinoma with macroscopic portal vein tumor thrombosis. *J Am Coll Surg* 2000;191:657-660
- 47 el-Assal ON, Yamanai A, Soda Y, Yamaguchi M, Yu L, Nagasue N. Proposal of invasiveness score to predict recurrence and survival after curative hepatic resection for hepatocellular carcinoma. *Surgery* 1997;122:571-577
- 48 Makino Y, Yamanai A, Kimoto T, El-Assal ON, Kohno H, Nagasue N. The influence of perioperative blood transfusion on intrahepatic recurrence after curative resection of hepatocellular carcinoma. *Am J Gastroenterol* 2000;95:1294-300
- 49 Utsunomiya T, Shimada M, Taguchi KI, Hasegawa H, Yamashita Y, Hamatsu T, Aishima SI, Sugimachi K. Clinicopathologic features and postoperative prognosis of multicentric small hepatocellular carcinoma. *J Am Coll Surg* 2000;190:331-335
- 50 Tanaka T, Yamanaka N, Oriyama T, Furukawa K, Okamoto E. Factors regulating tumor pressure in hepatocellular carcinoma and implications for tumor spread. *Hepatology* 1997; 26:283-287
- 51 Paquet KJ, Gad HA, Lazar A, Koussouris P, Mercado MA, Heine WD, Jachman-Jahn V, Ruppert W. Analysis of factors affecting outcome after hepatectomy of patients with liver cirrhosis and small hepatocellular carcinoma. *Eur J Surg* 1998;164:513-519
- 52 Schoniger-Hekele M, Muller C, Kutilek M, Oesterreicher C, Ferenci P, Gangl A. Hepatocellular carcinoma in Central Europe: prognostic features and survival. *Gut* 2001;48:103-109
- 53 Ouchi K, Sugawara T, Fujiya T, Kamiyama Y, Kakugawa Y, Mikuni J, Yamanami H, Nakagawa K. Prediction of recurrence and extratumor spread of hepatocellular carcinoma following resection. *J Surg Oncol* 2000;75:241-245
- 54 Yamanaka J, Yamanaka N, Nakasho K, Tanaka T, Ando T, Yasui C, Kuroda N, Takata M, Maeda S, Matsushita K, Uematsu K, Okamoto E. Clinicopathologic analysis of stage II-III hepatocellular carcinoma showing early massive recurrence after liver resection. *J Gastroenterol Hepatol* 2000;15:1192-1198
- 55 Uenishi T, Hirohashi K, Shuto T, Kubo S, Tanaka H, Sakata C, Ikebe T, Kinoshita H. The clinical significance of lymph node metastases in patients undergoing surgery for hepatocellular carcinoma. *Surg Today* 2000;30:892-895
- 56 Wada Y, Nakashima O, Kutami R, Yamamoto O, Kojiro M. Clinicopathological study on hepatocellular carcinoma with lymphocytic infiltration. *Hepatology* 1998;27:407-414
- 57 Lui WY, Chiu ST, Chiu JH, Loong CC, Chau GY, King KL, Hsia CY, Wu CW, P'eng FK. Evaluation of a simplified staging system for prognosis of hepatocellular carcinoma. *J Formos Med Assoc* 1999;98:248-253
- 58 Little SA, Fong Y. Hepatocellular carcinoma: current surgical management. *Semin Oncol* 2001;28:474-486
- 59 Seki T, Tamai T, Nakagawa T, Imamura M, Nishimura A, Yamashiki N, Ikeda K, Inoue K. Combination therapy with transcatheter arterial chemoembolization and percutaneous microwave coagulation therapy for hepatocellular carcinoma. *Cancer* 2000;89:1245-1251
- 60 Parks RW, Garden OJ. Liver resection for cancer. *World J Gastroenterol* 2001;7:766-771
- 61 Takano S, Oishi H, Kono S, Kawakami S, Nakamura M, Kubota N, Iwai S. Retrospective analysis of type of hepatic resection for hepatocellular carcinoma. *Br J Surg* 2000;87:65-70
- 62 Shimada M, Gion T, Hamatsu T, Yamashita Y, Hasegawa H, Utsunomiya T, Takenaka K, Sugimachi K. Evaluation of major hepatic resection for small hepatocellular carcinoma. *Hepatogastroenterology* 1999;46:401-406
- 63 Nonami T, Harada A, Kurokawa T, Nakao A, Takagi H. Hepatic resection for hepatocellular carcinoma. *Am J Surg* 1997;173:288-291
- 64 Shuto T, Hirohashi K, Kubo S, Tanaka H, Yamamoto T, Ikebe T, Kinoshita H. Efficacy of major hepatic resection for large hepatocellular carcinoma. *Hepatogastroenterology* 1999;46:413-416
- 65 Torii A, Nonami T, Harada A, Yasui M, Nakao A, Takagi H. Extent of hepatic resection as a prognostic factor for small, solitary hepatocellular carcinomas. *J Surg Oncol* 1993;54:13-17
- 66 Fan ST, Ng IO, Poon RT, Lo CM, Liu CL, Wong J. Hepatectomy for hepatocellular carcinoma: the surgeon's role in long-term survival. *Arch Surg* 1999;134:1124-1130
- 67 Asahara T, Katayama K, Itamoto T, Yano M, Hino H, Okamoto Y, Nakahara H, Dohi K, Moriwaki K, Yuge O. Perioperative blood transfusion as a prognostic indicator in patients with hepatocellular carcinoma. *World J Surg* 1999;23:676-680
- 68 Chan ES, Chow PK, Tai B, Machin D, Soo K. Neoadjuvant and adjuvant therapy for operable hepatocellular carcinoma. *Cochrane Database Syst Rev* 2000;CD001199
- 69 Nagasue N, Kohno H, Tachibana M, Yamanai A, Ohmori H, El-Assal ON. Prognostic factors after hepatic resection for hepatocellular carcinoma associated with Child-Turcotte class B and C cirrhosis. *Ann Surg* 1999;229:84-90
- 70 Hanazaki K, Kajikawa S, Shimozaawa N, Mihara M, Shimada K, Hiraguri M, Koide N, Adachi W, Amano J. Survival and recurrence after hepatic resection of 386 consecutive patients with hepatocellular carcinoma. *J Am Coll Surg* 2000;191:381-388
- 71 Huang J, He X, Lin X, Zhang C, Li J. Effect of preoperative transcatheter arterial chemoembolization on tumor cell activity in hepatocellular carcinoma. *Chin Med J* 2000;113:446-448
- 72 Lu CD, Peng SY, Jiang XC, Chiba Y, Tanigawa N. Preoperative transcatheter arterial chemoembolization and prognosis of patients with hepatocellular carcinomas: retrospective analysis of 120 cases. *World J Surg* 1999;23:293-300
- 73 Yoshida T, Sakon M, Umeshita K, Kanai T, Miyamoto A, Takeda T, Gotoh M, Nakamura H, Wakasa K, Monden M. Appraisal of transarterial immunoembolization for hepatocellular carcinoma: a clinicopathologic study. *J Clin Gastroenterol* 2001;32:59-65
- 74 Zhang Z, Liu Q, He J, Yang J, Yang G, Wu M. The effect of preoperative transcatheter hepatic arterial chemoembolization on disease-free survival after hepatectomy for hepatocellular carcinoma. *Cancer* 2000; 89:2606-2612
- 75 Tanaka H, Hirohashi K, Kubo S, Shuto T, Higaki I, Kinoshita H. Preoperative portal vein embolization improves prognosis after right hepatectomy for hepatocellular carcinoma in patients with impaired hepatic function. *Br J Surg* 2000;87:879-882
- 76 Lygidakis NJ, Sgourakis G, Dedemadi G, Spentzouris N, Kontis A, Nestoridis J. Preoperative main portal branch transection combined with

- liver locoregional transarterial neo and adjuvant immunochemotherapy for patients with hepatocellular carcinoma. *Hepatogastroenterology* 2000;47:1546-1554
- 77 Sato Y, Ichida T, Ito S, Hatakeyama K. Preoperative administration of 5-FU and interferon beta may prevent recurrence of hepatitis B and C virus. *Am J Gastroenterol* 2002;97:215-216
 - 78 Takayama T, Sekine T, Makuuchi M, Yamasaki S, Kosuge T, Yamamoto J, Shimada K, Sakamoto M, Hirohashi S, Ohashi Y, Kakizoe T. Adoptive immunotherapy to lower postsurgical recurrence rates of hepatocellular carcinoma: a randomised trial. *Lancet* 2000;356:802-807
 - 79 Tanaka K, Shimada H, Togo S, Takahashi T, Endo I, Sekido H, Yoshida T. Use of transcatheter arterial infusion of anticancer agents with lipiodol to prevent recurrence of hepatocellular carcinoma after hepatic resection. *Hepatogastroenterology* 1999;46:1083-1088
 - 80 Asahara T, Itamoto T, Katayama K, Ono E, Dohi K, Nakanishi T, Kitamoto M, Azuma K, Ito K. Adjuvant hepatic arterial infusion chemotherapy after radical hepatectomy for hepatocellular carcinoma—results of long-term follow-up. *Hepatogastroenterology* 1999;46:1042-1048
 - 81 Franco D, Usatoff V. Resection of hepatocellular carcinoma. *Hepatogastroenterology* 2001;48:33-36
 - 82 Shimoda M, Bando T, Nagata T, Shirosaki I, Sakamoto T, Tsukada K. Prophylactic chemolipiodolization for postoperative hepatoma patients. *Hepatogastroenterology* 2001;48:493-497
 - 83 Huang YH, Wu JC, Lui WY, Chau GY, Tsay SH, Chiang JH, King KL, Huo TI, Chang FY, Lee SD. Prospective case-controlled trial of adjuvant chemotherapy after resection of hepatocellular carcinoma. *World J Surg* 2000;24:551-555
 - 84 Lai EC, Lo CM, Fan ST, Liu CL, Wong J. Postoperative adjuvant chemotherapy after curative resection of hepatocellular carcinoma: a randomized controlled trial. *Arch Surg* 1998;133:183-188
 - 85 Ono T, Yamanoi A, Nazmy El Assal O, Kohno H, Nagasue N. Adjuvant chemotherapy after resection of hepatocellular carcinoma causes deterioration of long-term prognosis in cirrhotic patients: metaanalysis of three randomized controlled trials. *Cancer* 2001;91:2378-2385
 - 86 Wu ZQ, Fan J, Qiu SJ, Zhou J, Tang ZY. The value of postoperative hepatic regional chemotherapy in prevention of recurrence after radical resection of primary liver cancer. *World J Gastroenterol* 2000;6:131-133
 - 87 Tang ZY, Qin LX, Sun HC, Zhou J, Wang L, Ling ZY, Ma ZC, Ye SL, Wu ZQ. The studies on the recurrence and metastasis of hepatocellular carcinoma. *Zhong Hua Pu Tong Wai Ke Za Zhi* 2000;15:517-520
 - 88 Ren Z, Lin Z, Ye S. Transcatheter arterial chemoembolization for postoperative residual tumor of hepatocellular carcinoma. *Zhonghua Zhong Liu Za Zhi* 2001;23:332-334 (in Chinese)
 - 89 Lin Z, Ren Z, Xia J. Appraisal of postoperative transcatheter arterial chemoembolization (TACE) for prevention and treatment of hepatocellular carcinoma recurrence. *Zhonghua Zhong Liu Za Zhi* 2000;22:315-317 (in Chinese)
 - 90 Kubo S, Nishiguchi S, Hirohashi K, Tanaka H, Shuto T, Yamazaki O, Shiomi S, Tamori A, Oka H, Igawa S, Kuroki T, Kinoshita H. Effects of long-term postoperative interferon-alpha therapy on intrahepatic recurrence after resection of hepatitis C virus-related hepatocellular carcinoma. A randomized, controlled trial. *Ann Intern Med* 2001;134:963-967
 - 91 Suou T, Mitsuda A, Koda M, Matsuda H, Maruyama S, Tanaka H, Kishimoto Y, Kohno M, Hirooka Y, Kawasaki H. Interferon alpha inhibits intrahepatic recurrence in hepatocellular carcinoma with chronic hepatitis C: a pilot study. *Hepatol Res* 2001;20:301-311
 - 92 Ikeda K, Arase Y, Saitoh S, Kobayashi M, Suzuki Y, Suzuki F, Tsubota A, Chayama K, Murashima N, Kumada H. Interferon beta prevents recurrence of hepatocellular carcinoma after complete resection or ablation of the primary tumor—A prospective randomized study of hepatitis C virus-related liver cancer. *Hepatology* 2000;32:228-232
 - 93 Kubo S, Nishiguchi S, Hirohashi K, Tanaka H, Tsukamoto T, Shuto T, Takemura S, Yamamoto T, Ikebe T, Wakasa K, Shiomi S, Kinoshita H. Influence of previous interferon therapy on recurrence after resection of hepatitis C virus-related hepatocellular carcinoma. *Jpn J Cancer Res* 2001;92:59-66
 - 94 Wang L, Tang ZY, Qin LX, Wu XF, Sun HC, Xue Q, Ye SL. High-dose and long-term therapy with interferon-alfa inhibits tumor growth and recurrence in nude mice bearing human hepatocellular carcinoma xenografts with high metastatic potential. *Hepatology* 2000;32:43-48
 - 95 Lau WY, Leung TW, Ho SK, Chan M, Machin D, Lau J, Chan AT, Yeo W, Mok TS, Yu SC, Leung NW, Johnson PJ. Adjuvant intra-arterial iodine-131-labelled lipiodol for resectable hepatocellular carcinoma: a prospective randomised trial. *Lancet* 1999;353:797-801

Edited by Pagliarini R

• ESOPHAGEAL CANCER •

The abnormal expression of retinoic acid receptor- β , p53 and Ki67 protein in normal, premalignant and malignant esophageal tissues

Min Xu, Yu-Lan Jin, Jun Fu, Hong Huang, Sheng-Zu Chen, Ping Qu, Hai-Mei Tian, Zhao-Yang Liu, Wei Zhang

Min Xu, Sheng-Zu Chen, Department of Nuclear Medicine, Cancer Hospital (Institute), Peking Union Medical College and Chinese Academy of Medical Sciences, Beijing 100021, China
Yu-Lan Jin, Jun Fu, Hong Huang, Ping Qu, Hai-Mei Tian, Zhao-Yang Liu, Wei Zhang, Central Laboratory for Tumor Biology, Cancer Hospital (Institute), Peking Union Medical College and Chinese Academy of Medical Sciences, Beijing 100021, China

Correspondence to: Professor Wei Zhang, Central Laboratory for Tumor Biology, Cancer Hospital (Institute), Peking Union Medical College and Chinese Academy of Medical Sciences, Beijing 100021, China. zhangwe@public.bta.net.cn

Telephone: +86-10-67141838 Fax: +86-10-67141838

Received 2002-01-28 Accepted 2002-02-20

Abstract

AIM: Esophageal cancer remains a significant health problem worldwide. It is important to investigate alterations in expression of retinoic acid receptor- β , p53 and Ki67 proteins in esophageal carcinogenesis.

METHODS: To find biomarkers for early identification of esophageal cancer, we analyzed the retinoic acid receptor- β , p53 protein and the proliferation marker Ki67 in surgical specimens of normal, mildly, and severely dysplastic and malignant esophageal tissues by *in situ* hybridization of RNA and immunohistochemistry.

RESULTS: RAR- β was expressed in 94.3% (33/35) of normal mucosae, 67.8% (19/28) of the mild, 58.1% (18/31) of the severe lesions and 53.2% (116/218) of tumor samples. RAR- β mRNA was expressed in 62.7% (42/67), 55.1% (43/78) and 29.2% (7/24) of well, moderated and poorly differentiated SSCs. The p53 and Ki67 proteins were 5.9% (2/34) of the normal mucosa. P53 and Ki67 stained positively in 10.7% (3/28) and 21.4% (6/28) of mild dysplasia, and 51.6% (16/31) and 58.1% (18/31) of severely dysplasia respectively. Samples from esophageal cancer showed no higher levels of p53 and Ki67 expression than seen in severely dysplastic lesions. There was significant difference of RAR- β , p53 and Ki67 expression between normal mucosa and dysplastic tissue or esophageal cancer.

CONCLUSION: Loss of RAR- β expression and accumulation of p53 and Ki67 proteins may serve as biomarkers for early identification of esophageal cancer in the high-risk populations.

Xu M, Jin YL, Fu J, Huang H, Chen SZ, Qu P, Tian HM, Liu ZY, Zhang W. The abnormal expression of retinoic acid receptor- β , p53 and Ki67 protein in normal, premalignant and malignant esophageal tissues. *World J Gastroenterol* 2002;8(2):200-202

INTRODUCTION

Esophageal cancer remains a significant health problem in the world because the 5-year survival rate is low^[1]. Chemoprevention is very important for the esophageal cancer. But it remains a problem to

identify the premalignant esophageal tissues in the people with high risk. In this study, we investigate the expression of retinoic acid receptor- β (RAR- β), Ki67 and p53 protein in normal, premalignant, and malignant esophageal tissues to find biomarkers for early identification of the disease.

Retinoids, a group of nature and synthetic analogues of vitamin A, can modulate cell growth and differentiation^[2]. Retinoids are known to exert their biological effects by binding to specific nuclear retinoid receptors, which belong to a steroid/thyroid hormone-receptor superfamily. The nuclear retinoid receptors are divided into retinoic acid receptors (RARs) and retinoid X receptors (RXRs), both with three subtypes (α , β , γ)^[3]. Retinoids can suppress or reverse epithelial carcinogenesis and to prevent the development of invasive cancer in many animal models^[4-6]. In a Chinese clinical trial using the synthetic retinoid N-4-(ethoxycarbonylphenyl) retinamide, the incidence of cancer in the treatment group with severe esophageal dysplasia was 43.2%, that was lower than of the group treated with placebo^[7]. Our previous study demonstrated that all-trans RA can induce esophageal cancer cell lines to undergo apoptosis, which was associated with the expression and upregulation of RAR- β ^[8]. In this study, we tried to explore the earliest loss of RAR- β expression.

Deletion or mutation of tumor suppressor genes may be a key event in carcinogenesis. The human p53 gene encodes a nuclear protein that may be vital in the regulatory control of cell proliferation^[9,10]. Loss of wild-type p53 function is considered to be a key event in the induction of malignant transformation in many cancers, including esophageal cancers^[11-14].

Ki67 is a nuclear antigen expressed during G1, S, M and G2 periods of cell cycle. The expression level of Ki67 indicated the status of cell proliferation. Some studies have showed that Ki67 protein could be a biomarker to identify the high-risk precancerous tissue^[15,16]. The present study was undertaken to determine the accumulation of p53 and Ki67 protein in normal, premalignant, and malignant esophageal tissues to gain insight into the possible involvement of them in the early stage of esophageal carcinogenesis.

MATERIALS AND METHODS

Tissue specimens

Three hundred and twelve tissue specimens were obtained from the Ci County, Hebei Province and the Cancer Hospital, China, respectively. The esophageal specimens of normal mucosae ($n=35$) used in this study were obtained from a clinical chemopreventive trial in Ci County with a high prevalence of esophageal cancer. These samples were reviewed by pathologists and considered to be morphologically normal epithelium. There were 59 specimens of dysplastic lesions and 218 specimens of esophageal cancer from the Cancer Hospital, China. Of these dysplastic lesions, there were 28 cases of mild dysplastic lesions and 31 cases of severe dysplastic lesions. Of these esophageal cancers, there were 169 cases of squamous cell carcinoma (SCC), 29 cases of adenocarcinoma (AC) and 20 cases of adenosquamous cell carcinoma (AC-SSC). There were 67 well differentiated SSCs, 78 moderately differentiated and 24 poorly differentiated SSCs among the SSCs. All samples were

routinely fixed in 10% buffered formalin, embedded in paraffin, and cut into 4 μ m sections. One of each of these sections was stained with hematoxylin and eosin for classification.

In Situ Hybridization of RNA

Levels of RAR- β expression were measured by using a previously described method of nonradioactive *in situ* hybridization. The quality and specificity of the digoxigenin-labeled anti-sense and sense riboprobes were determined using Northern blotting, and the specificity of the binding of antisense riboprobes was verified using negative control sections. Briefly, the tissue sections were treated with 0.2 N HCl and proteinase K, respectively, after deparaffinization and rehydration. The slides were then postfixed with 4% paraformaldehyde and acetylated in freshly prepared 0.25% acetic anhydride in a 42°C for 1h with a hybridization solution containing 50% deionized formamide, 2X standard saline citrate, 2X Denhardt's solution, 10% dextran sulfate, 400 μ g/ml yeast tRNA, 250 μ g/ml salmon-sperm DNA, and 20mm dithiothreitol in diethylpyrocarbinat-treated water. Next the slides were incubated in 50 μ l per slide hybridization solution containing 20ng of a freshly denatures dig-cRNA probe at 42°C for 4h. After that, the slides were washed for 2h in 2XSSC containing 2% normal sheep serum (NSS) and 0.05% Triton X-100 and then for 20minutes at 42°C in 0.1XSSC. For color reaction, the slides were incubated for 30min at 23°C in 0.1mol/L maleic acid and 0.15mol/L NaCl (PH 7.5, buffer 1) containing 2% NSS and 0.3% Triton X-100 and then incubated overnight at 4°C with a sheep anti-digoxigenin antibody. After being washed in buffer 1 twice, the color was developed in a chromogen solution (45 μ l of nitroblue tetrazolium and 35 μ l of an X-phosphate solution in 10ml of buffer 2, which consisted of 0.1M Tris, 0.1M NaCl, and 0.05M MgCl₂ (PH9.5)) for 6h with occasional observation for color development. The slides were then mounted with cover glass in Aqua mounting medium.

Immunohistochemistry

The immunohistochemical detection of p53 protein and the proliferation marker Ki67 was performed using a modified ABC technique. Briefly, tissue sections were deparaffinized in xylene and rehydrated in a series of ethanol solutions (100-50%). The sections were then microwaved for 15min to retrieve antigens in 0.02M citric acid solution. The endogenous peroxidase activity was blocked by incubation in a 1% methanolic hydrogen peroxide solution for 30min. This was followed by preincubation with 20% normal horse serum to minimize nonspecific binding of the second antibody. The sections were then incubated at 23°C for 4h with monoclonal mouse anti-p53 or Ki 67 antibody from Vector Laboratories (Burlingame, Calif., USA) both diluted at 1 : 50 in PBS. After being washed three times in PBS, the sections were incubated with biotinylated horse anti-mouse IgG (H+L) (Vector) for 30min at 23°C and then incubated with the ABC kit (Vector) for 30min in the dark. This was followed by incubation with 3-amino-9-ethylcarbazole (Sigma Chemical, St. Louis, Mo., USA) solution were finally mounted with Aqua mount medium under coverslips. Control sections were incubated with normal mouse IgG instead of primary antibodies or with the second antibody only.

Review and scoring of the sections

The stained sections were reviewed and scored independently by two investigators using an Olympus microscope. The sections stained for nuclear retinoid receptors were assigned to positive or negative staining categories only. Positively staining means that 10% or more epithelial cells stained positively. Sections stained for p53 protein and Ki67 were assigned scores of 0-3, with 0 meaning no staining; 1, weak positive, the mounts of positive cells are less than 10%; 2, positive, the mounts of positive cells are more than 10% but less than 50%;

and 3, strong positive, the mounts of positive cells are more than 50%. Scores 0 and 1 were counted as negative and scores 2 and 3 as positive cases. Statistical analysis was performed using fisher's exact test to determine the association between normal or dysplastic tissues and tumors. P values were generated using Statistica version 3.0a for a Macintosh computer (StatSoft, Tulsa, Okla., USA).

RESULTS

RAR- β expression

Our preliminary study showed that RAR- α , RAR- γ and RXR- α were expressed in all of the esophageal samples without significant difference, so we excluded RAR- α , RAR- γ and RXR- α from this study and only investigate the expression of RAR- β . In 33 of 35 samples of normal mucosae, RAR- β was expressed, whereas RAR- β were detected in only 67.8% (19/28) and 58.1% (18/31) of the mild and severe lesions, respectively. In 116 of 218 tumor samples, RAR- β was expressed (Table 1). The expression of RAR- β decreased significantly between normal mucosae and dysplastic tissues or esophageal cancers (Table 2). But it was similar among the three subtypes of esophageal cancer (Table 1). However RAR- β expression was associated with the degree of squamous cell differentiation: RAR- β mRNA was expressed in 62.7% (42/67) of well differentiated SSCs, but in only 55.1% (43/78) of moderated differentiated SSCs, and in 29.2% (7/24) of poorly differentiated SSCs (Table 3).

Table 1 Expression of the biomarkers in all kinds of esophageal tissues

Biomarker	% (positive/total)					
	Normal	Mild Dysplasia	Severe dysplasia	SSC	AC	AC-SSC
RAR- β	94.3 (33/35)	67.9 (19/28)	58.1 (18/31) ^a	54.4 (92/169)	51.7 (15/29)	45.0 (9/20)
P53	5.7 (2/35)	10.7 (3/28)	51.6 (16/31) ^b	56.8 (96/169)	62.1 (18/29)	60.0 (12/20)
Ki67	5.9 (2/34)	21.4 (6/28)	58.1 (18/31) ^c	62.1 (105/169)	58.6 (17/29)	65.0 (13/20)

^aP<0.01 vs χ^2 test between normal tissues and severe dysplastic tissues.

^bP<0.0001 vs χ^2 test between normal tissues and severe dysplastic tissues.

^cP<0.00002 vs χ^2 test between normal tissues and severe dysplastic tissues.

Table 2 Expression of the biomarkers in normal, dysplastic, and malignant esophageal tissues

Biomarker	% (positive/total)	
	Normal	dysplasia tumor
RAR- β	94.3(33/35)	62.7(37/59) ^a
P53	5.7(2/35)	32.2(19/59) ^c
Ki67	5.9(2/34)	40.7(24/59) ^d

^aP=0.016 vs χ^2 test between normal tissues and dysplastic tissues. ^bP<0.0003 vs χ^2 test between normal tissues and tumor tissues. ^cP=0.006 vs χ^2 test between normal tissues and dysplastic tissues. ^{ad}P<0.0008 vs χ^2 test between normal tissues and dysplastic tissues.

Table 3 Expression of RAR- β in the three subtypes of esophageal squamous cell carcinomas

Tumor differentiation	% (positive/total)
Well differentiated SCC	62.7(42/67)
Moderately differentiated	55.1(43/78)
Poorly differentiated	29.2(7/24) ^a

^aP<0.005 vs χ^2 test between well differentiated and poorly differentiated SSCs.

P53 and Ki67 expression

In contrast to RAR- β expression, the p53 tumor-suppressor gene and the proliferation marker Ki67 were only detected immunohistochemically in two cases each in the normal mucosa. P53 and Ki67 stained positively in 10.7% (3/28) and 21.4% (6/28) of mild dysplasia, respectively. A dramatic increase in their expression, however, was seen in 51.6% (16/31) and 58.1% (18/31) of

severely dysplastic esophageal lesions. Samples from esophageal cancers showed no higher levels of *p53* and Ki67 expression than seen in severely dysplastic lesions. And there was no significant alteration found in the three subtypes of esophageal cancers (Table 1). However, there was significant accumulation between normal mucosae and dysplastic tissues or esophageal cancers. (Table 2).

DISCUSSION

In this study, we first analyzed the expression of RAR- β by using *in situ* hybridization, and then the *p53* tumor-suppressor gene product and proliferation marker Ki67 protein using immunohistochemistry in normal, mild dysplastic, severely dysplastic, and cancerous mucosae. We found that RAR- β expression was progressively lost as early as in the mildly dysplastic stage of esophageal mucosae. And RAR- β expression was significantly lost with esophageal squamous differentiation. *p53* and Ki67 were also accumulated in the later precancerous stage of the esophagus. These results suggest that the detection of RAR- β expression and of *p53* and Ki67 protein may be biomarkers for early identification of esophageal cancer in the high-risk populations.

It is well established that retinoids can modulate epithelial cell growth, differentiation, and apoptosis *in vitro* and *in vivo*. Retinoids can prevent abnormal squamous differentiation of epithelial cells in nonkeratinizing tissues physiologically. Retinoids can also reverse squamous metaplasia, which develops during vitamin A deficiency^[2]. The abrogation in the retinoid signal pathway may be due to the loss of expression of RAR- β ^[17]. Indeed, in our recent study, we demonstrated that the sensitivity of esophageal cancer cells to RA was correlated not only with the constitutive expression but also with RA-induced upregulation of RAR- β ^[17]. Cell lines that failed to express RAR- β were resistant to RA and could form colonies in soft agar^[17]. Thus, loss of RAR- β expression could contribute to the resistance to treatment with 13-cis RA in esophageal cancer. In addition, a more recent study demonstrated that RAR- β 2 knockout in F9 cells resulted in the loss of RA-associated growth arrest^[18]. Various studies have clearly demonstrated that altered expression of retinoid receptors is associated with malignant transformation in human cells. Alter expression of RAR- β is a common event in different types of tumors, including head and neck, lung, and breast tumors^[8,17,19,20]. In our previous study, RAR- β was expressed in all of the distant normal epithelia from esophageal cancer patients^[21]. In this study, RAR- β expression is just a little low in the histologically normal mucosa. Taken together, it could be inferred that RAR- β serves as a biomarker for the early identification of esophageal cancer for chemoprevention strategy.

Previous studies demonstrated that lots of genetic alterations existed in specimens from esophageal cancer patients. For instance, *p53* and *p16* mutations were revealed to be early events during esophageal carcinogenesis^[22, 23]. Loss of *p53* activity could lead to malignant transformation of normal human cells^[24,25]. The studies by Dr. Yang's group demonstrated that accumulation of *p53* protein was due to *p53* gene mutation, which occurred at very early stages of esophageal carcinogenesis^[26]. Some studies have also showed that Ki67 protein could be a biomarker to identify the high-risk precancerous tissue^[15,16]. In our study, both Ki67 and *p53* proteins accumulated at early stages of esophageal carcinogenesis.

Since the RAR- β , *p53*, Ki67 expression shows significant changes at the early stage of esophageal carcinogenesis, then they could be biomarkers to identify the high-risk precancerous tissue. The combination of them may improve the accuracy of identification greatly. But the underlying mechanism of the change is largely unknown, therefore more additional work is needed to investigate the mechanism and the correlation of lost expression of RAR- β , *p53* gene protein mutation and Ki67 protein expression in esophageal cancers.

REFERENCES

- McCann J. Esophageal cancers: changing character, increasing incidence. *J Natl Cancer Inst* 1999; 91: 497-498
- De Luca LM. Retinoids and their receptors in differentiation, embryogenesis, and neoplasia. *FASEB J* 1991; 5: 2924-2933
- Chambon P. A decade of molecular biology of retinoid acid receptors. *FASEB J* 1996; 10: 940-954
- Moon RC, Mehta RG, Rao KVN. Retinoids and cancer in experimental animals. In: Sporn MB, Roberts AB, Goodman DS (eds). *The retinoids: Biology, Chemistry and Medicine* (2nd ed). New York: Raven Press 1994:573-595
- Kelloff GJ, Boone CW, Steele VK, Perloff M, Crowell J and Doody LA. Development of chemopreventive agents for lung and upper aerodigestive tract cancers. *J Cell Biochem Suppl* 1993; 17:2-17
- Inayama Y, Kitamura H, Shibagaki T, Usuda Y, Ito T, Nakatani Y, Kanisawa M. In vivo growth and differentiation potential of tracheal basal cells of rabbits in vitamin A deficiency. *Int J Exp Pathol* 1996; 77: 89-97
- Han J. Highlights of the cancer chemoprevention studies in China. *Prev Med* 1993; 22: 712-722
- Xu XC, Liu X, Tahara E, Lippman SM, Lotan R. Expression and up-regulation of retinoic acid receptor-beta is associated with retinoid sensitivity and colony formation in esophageal cancer cell lines. *Cancer Res* 1999; 59: 2477-2483
- Levine AJ, Momand J, Finlay CA. The *p53* tumor suppressor gene. *Nature (Lond.)* 1991; 351: 453-456
- Ullrich SJ, Anderson CW, Mercer WE, Appella E. The *P53* tumor suppressor protein, a modulator of cell proliferation. *J Biol Chem* 1992; 267: 15259-15262
- Oren M. *P53*: the ultimate tumor suppressor gene. *FASEB J* 1992; 6: 3169-3176
- Hollstein MC, Peri L, Mandard AM, Welsh JA, Montesano R, Metcalf RA, Bak M, Harris CC. Genetic analysis of human esophageal tumors from two high incidence geographic areas: frequent *P53* base substitutions and absence of ras mutations. *Cancer Res* 1991; 51:4102-4106
- Qiao GB, Han CL, Jiang RC, Sun CS, Wang Y, Wang YJ. Overexpression of *P53* and its risk factors in esophageal cancer in urban areas of Xi'an. *World J Gastroenterol* 1998; 4: 57-60
- Yu GQ, Zhou Q, Ivan D, Gao SS, Zheng ZY, Zou JX, Li YX, Wang LD. Changes of *P53* protein blood level in esophageal cancer patients and normal subjects from a high incidence area in Henan, China. *World J Gastroenterol* 1998; 4:365-366
- Polkowski W, van Lanschot JJ, Ten Kate FJ, Baak JP, Tytgat GN, Obertop H, Voorn WJ, Offerhaus GJ. The value of *P53* and Ki67 as markers for tumor progression in the Barrett's dysplasia carcinoma sequence. *Surg Oncol* 1995; 4:163-171
- Liu SC, Sauter ER, Clapper ML, Feldman RS, Levin L, Chen SY, Yen TJ, Ross E, Engstrom PF, Klein-Szanto AJ. Markers of cell proliferation in normal epithelia and dysplastic leukoplakias of the oral cavity. *Cancer Epidemiol Biomarkers Prev* 1998; 7:597-603
- Enzinger PC, Ilson DH, Saltz LB, Martin LK, Kelsen DP. Phase II clinical trial of 13-cis-retinoic acid and interferon-alpha-2a in patients with advanced esophageal carcinoma. *Cancer* 1999; 85: 1213-1217
- Slabber CF, Falkson G, Burger W, Schoeman L. 13-Cis-retinoic acid and interferon-alpha-2a in patients with advanced esophageal cancer: a phase II trial. *Invest New Drugs* 1996; 14: 391-394
- Xu XC, Ro JY, Lee JS, Shin DM, Hong WK, Lotan R. Differential expression of nuclear retinoic receptors in normal, premalignant, and malignant head and neck tissues. *Cancer Res* 1994; 54: 3580-3587
- Lotan R, Xu XC, Lippman SM, Ro JY, Lee JS, Lee JJ, Hong WK. Suppression of retinoic acid receptor-beta in premalignant oral lesions and its upregulation by isotretinoin. *N Engl J Med* 1995; 332:1405-1410
- Qiu H, Zhang W, El-Naggar AK, Lippman SM, Lin P, Lotan R, Xu XC. Loss of retinoic acid receptor-beta expression is an early event during esophageal carcinogenesis. *Am J Pathol* 1999;155:1519-1523
- Bennett WP, von Brevern MC, Zhu SM, Bartsch H, Muehlbauer KR, Hollstein MC. *P53* mutations in esophageal tumors from a high incidence area of China in relation to patient diet and smoking history. *Cancer Epidemiol Biomarkers Prev* 1997; 6: 963-966
- Barrett MT, Galipeau PC, Sanchez CA, Emond MJ, Reid BJ. Determination of the frequency of loss of heterozygosity in esophageal adenocarcinoma by cell sorting, whole genome amplification and microsatellite polymorphisms. *Oncogene* 1996; 12: 1873-1878
- Lane DP. The regulation of *P53* function: Steiner Award Lecture. *Int J Cancer* 1994; 57: 623-627
- Vogelstein B, Kinzler KW. *P53* function and dysfunction. *Cell* 1992; 70: 523-526
- Gao H, Wang LD, Zhou Q, Hong JY, Huang TY, Yang CS. *P53* tumor suppressor gene mutation in early esophageal precancerous lesions and carcinoma among high-risk populations in Henan, China. *Cancer Res* 1994;54:4342-4346

• ESOPHAGEAL CANCER •

Transcription factor EGR-1 inhibits growth of hepatocellular carcinoma and esophageal carcinoma cell lines

Miao-Wang Hao, Ying-Rui Liang, Yan-Fang Liu, Li Liu, Ming-Yao Wu, Huan-Xing Yang

Miao-Wang Hao, Li Liu, Department of Internal Medicine, Tangdu Hospital, Xi'an 710038, Shaanxi Province, China
Ying-Rui Liang, Ming-Yao Wu, Huan-Xing Yang, Department of Pathology, Medical College of Shantou University, Shantou 515031, Guangdong Province, China

Yan-Fang Liu, Department of Pathology, Fourth Military Medical University, Xi'an 710032, Shaanxi Province, China

Supported by the National Natural Scientific Foundation of China, No. 39670298

Correspondence to: Dr. Miao-Wang Hao, Department of Internal Medicine, Tangdu Hospital, Fourth Military Medical University, Xi'an 710038, Shaanxi Province, China. haomwg@fmmu.edu.cn

Telephone: +86-29-3377726

Received 2001-09-14 Accepted 2001-10-11

Abstract

AIM: The transcription factor EGR-1 (early growth response gene-1) plays an important role in cell growth, differentiation and development. It has identified that EGR-1 has significant transformation suppression activity in some neoplasms, such as fibrosarcoma, breast carcinoma. This experiment was designed to investigate the role of *egr-1* in the cancerous process of hepatocellular carcinoma (HCC) and esophageal carcinoma (EC), and then to appraise the effects of EGR-1 on the growth of these tumor cells.

METHODS: Firstly, the transcription and expression of *egr-1* in HCC and EC, paracancerous tissues and their normal counterpart parts were detected by *in situ* hybridization and immunohistochemistry, with normal human breast and mouse brain tissues as positive controls. *egr-1* gene was then transfected into HCC (HHCC, SMMC7721) and EC (ECa109) cell lines in which no *egr-1* transcription and expression were present. The cell growth speed, FCM cell cycle, plate clone formation and tumorigenicity in nude mice were observed and the controls were the cell lines transfected with vector only.

RESULTS: Little or no *egr-1* transcription and expression were detected in HCC, EC and normal liver tissues. The expression of *egr-1* were found higher in hepatocellular paracancerous tissue (transcription level $P=0.000$; expression level $P=0.143$, probably because fewer in number of cases) and dysplastic tissue of esophageal cancer (transcription level $P=0.000$; expression level $P=0.001$). The growth rate of *egr-1*-transfected HHCC (HCC cell line) cells and ECa109 (EC cell line) cells was much slower than that of the controls. The proportion of S phase cell, clone formation and tumorigenicity were significantly lower than these of the controls' (decreased 45.5% in HHCC cells and 34.1% in ECa109 cells; 46.6% and 41.8%; 80.4% and 72.6% respectively). There were no obvious differences between SMMC7721 (HCC) *egr-1*-transfected cells and the controls with regard to the above items.

CONCLUSION: The decreased expression of *egr-1* might play a role in the dysregulation of normal growth in the cancerous process of HCC and EC. *egr-1* gene of

transfected HHCC and ECa109 cells showed obvious suppression of the cell growth and malignant phenotypes, but no suppression in SMMC7721 (HCC cell line) cells.

Hao MW, Liang YR, Liu YF, Liu L, Wu MY, Yang HX. Transcription factor EGR-1 inhibits growth of hepatocellular carcinoma and esophageal carcinoma cells lines. *World J Gastroenterol* 2002;8(2):203-207

INTRODUCTION

The tumor suppressorgene therapy research has become increasingly interested. Tumor suppressor genes have two categories: Type 1, they undergo mutation or deletion, such as p53, Rb, WT1 and BRCA1 etc. Type 2, they express little or nil and with rare mutation or deletion, such as cx34, maspin and integrin $\alpha 6$ etc^[1]. In designing the tumor gene therapy, the type II tumor suppressor genes are evidently more advantageous. We only need to induce or to promote more expression of the genes to get rid of many technical difficulties such as replacing the deleted gene or knocking out the mutated gene.

The early growth response gene, *egr-1* (Zfp-6 in standardized genetic Nomenclature for mice^[2], also known as NGFI-A, Krox-24, Zif-268, or TIS-8) is one of the important members of the immediate early gene family. It encodes a protein EGR-1 with 3 adjacent zinc-finger motifs, and structures that are present in many DNA-binding transcription factors. Its special zinc-finger structure can bind with "GC-rich" DNA regulatory elements and can control that particular gene to transcribe^[3]. The expression of *egr-1* is closely related to cell growth^[4] and differentiation^[5]. Some researching results have revealed that EGR-1 can reverse the malignant phenotype of HT-1080 fibrosarcoma and ZR-75-1 mammary carcinoma cell lines, and can also EGR-1 inhibit the tumorigenicity and transforming growth of these cells^[6-8]. *egr-1* may act as a type II tumor suppressor gene.

Both hepatocellular carcinoma (HCC) and esophageal carcinoma (EC) are common malignant tumors in China. Many research works on HCC and EC^[9-24], especially on the effects of the tumor suppressor genes such as p53, p16 and p21 etc^[25-38] had been reported, but the reports about *egr-1* for these two cancers are still lacking. In this paper, the transcription and expression of *egr-1* in HCC, EC tissues and their normal counterparts were detected by *in situ* hybridization and immunohistochemistry in order to investigate the role of *egr-1* in the cancerous process of HCC and EC. The constructed *egr-1* eukaryo-expressing vector was transfected into HCC and EC lines, where there was absence of expression of *egr-1*, with a view to observe how the high level of exogenous expression of EGR-1 in the cancer cell influenced their growth, clone formation and tumorigenicity. The inhibitory action of *egr-1* on HCC and EC is to be probed so as to provide an experimental evidence for the study of gene therapy of the two cancers.

MATERIALS AND METHODS

Materials

The plasmids, pAC-h-*egr-1* (fragment of single and double enzyme digestion by BamH I and/or SalI was determined by 10g·L⁻¹ agarose gel electrophoresis. The size of the fragments was identical to that of

plasmid map), containing the whole cDNA fragment of human wild-type *egr-1* gene and pAC- Φ eukaryo-expressing vectors, were kindly granted by Dr. JG Monore, Pennsylvania University School of Medicine^[39].

Human hepatocellular, esophageal carcinomas and breast tissue specimens were collected from the Pathology Department of Fourth Military Medical University and Medical College of Shantou University. All patients providing the specimens were not treated by radiotherapy or chemotherapy before operation. The specimens were fixed with 40g·L⁻¹ formaldehyde solution (for *in situ* hybridization) and Carnoy solution (for immuno-histochemistry). Mouse brain tissues were from Balb/c mice.

The cell lines HHCC and SMMC7721 of HCC were purchased from Shanghai Cytology Institute, China. The EC cell line ECa109 was from Cytology Institute of Chinese Medical Academy. All the cell lines were cultured in RPMI 1640 medium supplemented with 100mL·L⁻¹ new born bovine serum and grown in the circumstance of 37°C, 50mL·L⁻¹ CO₂ and saturated humidity. Cell numbers were determined by Coulter counting method.

The Lipofectamine™, G418 and TRIzol™ total RNA extraction kit were purchased from Gibco/BRL Co. The Wizard™ plus Minipreps DNA purification kit was the product of Promega Co. The polyclonal rabbit anti-human EGR-1 (C[#]-19) antibody was from Santa Cruz Co. *in situ* hybridization (POD) detection kit and SABC immunohistochemistry kit were from Boster Co, Wuhan, China. The Advantage™ PCR purification kit was from Clontech Co, and γ -³²P-dATP was provided by Yuhui Biomedical Engineering Co, Beijing.

Methods

Probe preparation and labeling

The plasmid pAC-h-*egr-1* was digested by both *Sal* I and *Bam* H I, and the products were determined by agarose gel electrophoresis; the 400 bp DNA fragments were recovered by promega DNA purification kit. The recovered DNA was dissolved in 20ul sterile three-distilled water and ultraviolet spectrophotometry was taken for quantitation analysis. γ -³²P-dATP 5' end Label method was used for probe labeling. After alcohol precipitation, the probe was dissolved in TE; the specific radiation activity was determined by TAC method, and stored at -20°C.

In situ hybridization and Immunohistochemistry

In situ hybridization was performed according to the kit instructions on the formaldehyde-fixed and paraffin-embedded sections. Human normal breast and mouse brain tissue sections were used as positive controls. According to the SABC stain instructions, immunohistochemistry was done on the Carnoy-fixed or frozen section. Positive control was frozen section of human normal mammary adenosis, and negative control was primary antibody-blank.

Gene transfection and identification after transfection

Transfection was performed according to the legend of Lipofectamine™ kit, and 48h later selective culture was added with 600mg·L⁻¹ G418. 2 weeks later, the cells and clones appeared all (the cells of blank control died). The concentration of G418 was changed to 400mg·L⁻¹ G418 for maintenance. The clones were digested *in situ*, and transferred to a 6-well plate for amplification, which were used for detection of every item.

mRNA dot hybridization: 2×10⁶ cells were collected and total RNA was extracted according to TRIzol™ total RNA extraction kit. The extracted RNA was dissolved in the RNase-free water. A absorbance value was determined, RNA quantity was calculated and purified was identified; stored at -80°C; procedures of RNA dot blot was according to the directions.

Western blot hybridization and immunohistochemistry: Western blot hybridization was performed according to the directions. The "cell crawling slide" in logarithm stage was collected, rinsed with PBS×2, fixed in 700mL·L⁻¹ alcohol and stained by SABC kit. The positive control was frozen section of mammary adenosis, and the negative control was primary antibody-blank.

Assay of cell phenotype

FCM cell cycle examination: The transfected cells were digested by 2.5g·L⁻¹ trypsin to a single cell suspension when they were 80% confluent, counted, 1×10⁶ cells were fixed in 700mL·L⁻¹ alcohol and FCM was performed.

Cell growth curve: cells of transfected and blank vector groups were digested by trypsin and counted in 1×10³ cells. Each group was inoculated in 24-well plate, and 1ml RPMI 1640 medium containing 100mL·L⁻¹ FCS was added. In the culture period, cells of 3 wells were digested and counted every day, and the mean values were also calculated. Of the remainder, the medium was changed every 3-4d and counted every 6-7d according to the cell growth conditions, growth curves were then made.

Examination of plate cloning: HCC and EC lines, which had been transfected with *egr-1* gene, G418 selected and amplified were digested to a single cell suspension. Cells counted were inoculated into 6-well tissue culture plates; each well contained 100 cells. The control cells were transfected with blank vector. Changing the medium 1~2 times per wk; by about 2 wk plates were taken out to observe the clone formation; fixed in methyl alcohol, Giemsa stained, clones over 50 cells were counted, and the mean value was adopted and clone formation rates were made.

Nude mice tumorigenicity: After trypsin digestion, the cells of the experimental and control groups were inoculated into nude mice subcutaneously with 1×10⁷ cell (about 0.1-0.2mL) for each mouse. About 3wk later the mice were killed according to the tumor growth, and then pictures were taken. The tumor mass was separated carefully and weighed, and the daily growing mass was calculated then. Tumor tissues were fixed, paraffin embedded, HE stained and observed microscopically.

Statistical analysis

Results were expressed as mean±SE. To compare the mean values, Stata statistical software was used. *P*<0.05 was considered significant.

RESULTS

Egr-1 mRNA and protein expression in HCC and EC

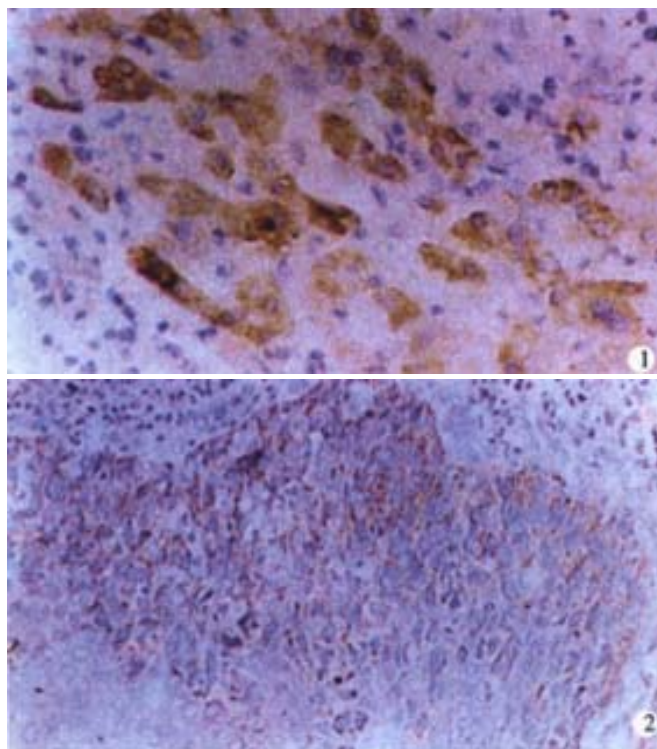
In situ hybridization and SABC immunohistochemistry staining for *egr-1* mRNA and protein in human HCC, EC tissues and their normal counterparts were performed. Little or no *egr-1* transcription was detected in HCC and normal liver tissues. Higher transcription of *egr-1* was detected in hepatocellular paracancerous tissues such as large cell hyperplasia (LCD) and "atrophic-like liver plate (reluctant LCD)". *egr-1* mRNA signal was present in the cytoplasm. EGR-1 expression in HCC, normal liver and hepatocellular paracancerous tissues was consistent with the transcription (When EGR-1 expression in HCC compared with the expression in the paracancerous tissue, *P*=0.143. Table 1, Figure 1). EGR-1 protein signal was in the nucleus. Little or no *egr-1* transcription was detected in the aggressive EC and normal esophageal epithelial tissues (not including basal layer cells). Higher transcription of *egr-1* was detected in dysplastic esophageal epithelium. EGR-1 expression in aggressive EC, normal esophageal epithelium and dysplastic tissues was also consistent with the transcription (Table 2, Figure 2).

Table 1 *egr-1* transcription and expression in HCC tissue and its normal counterparts

Tissue	n	mRNA (%)	n	Protein (%)
Normal liver	8	0(0.0)	2	0(0.0)
Hepatic paracancerous tissue	22	21(95.5)	5	4(80.0)
Liver carcinoma	24	6(25.0) ^a	3	0(0.0) ^b

^aP=0.000, ^bP=0.143, vs hepatic paracancerous tissue**Table 2** *egr-1* transcription and expression in EC tissue and its normal counterparts

Tissue	n	mRNA(%)	Protein (%)
Agressive carcinoma	47	8(17.0) ^a	6(12.8) ^b
Dysplasia	29	18 (62.1)	14 (48.3)
Normal epithelium	28	9(32.1)	2(7.1)

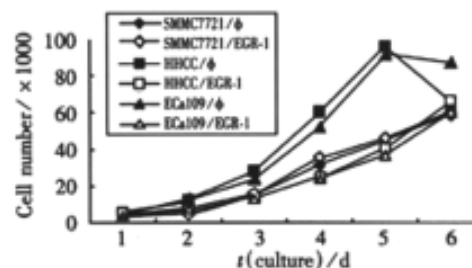
^aP=0.000, ^bP=0.001, vs dysplasia**Figure 1** Positive signal of *egr-1* mRNA in the cytoplasm paracancerous "atrophic-like liver plate" tissue of HCC. SP×400**Figure 2** Positive signal of EGR-1 mRNA in the cytoplasm of moderately dysplastic esophageal epithelium. SP×400**Egr-1 mRNA and protein detection in transfected tumor cells**

mRNA level (mRNA dot blot): The total RNA of *egr-1* and vector transfected HCC and EC cells were dot hybridized by ³²P labeled *egr-1* probe. The result revealed that *egr-1* group had stronger signals than that of the control.

Western blot and immunohistochemistry: The proteins of *egr-1* and vector transfected HCC and EC cells were extracted and quantitatively analyzed. Then both groups with identical quantitative proteins were determined by SDS-PAGE; electrical transfer onto the nitro-cellulose membrane was made, and Western blot hybridization was performed. The results revealed that in *egr-1* transfected groups of both HCC and EC cells, there were strongly stained bands just at the molecular mass of 59ku, which was identical to that of EGR-1, whereas in all the controls there were no such bands present. This suggested that the tumor cells transfected by *egr-1* could strongly express EGR-1 protein. The results of immunohistochemistry by primary antibody EGR-1 and SABC method showed 50-70% positive staining of *egr-1* transfected cells were, while in the controls the results were all negative; which was consistent with that of the Western blot.

Malignant phenotype examination**Curves of cell growth**

The growth rates of the *egr-1* transfected HHCC liver carcinoma cells and EC109 esophageal carcinoma cells were obviously slower than that of the controls. But the difference was not significant in the SMMC7721 liver carcinoma cell line (Figure 3).

**Figure 3** Cell growth curve of liver and esophageal carcinoma cells transfected *egr-1* and vector**FCM cell cycle assay**

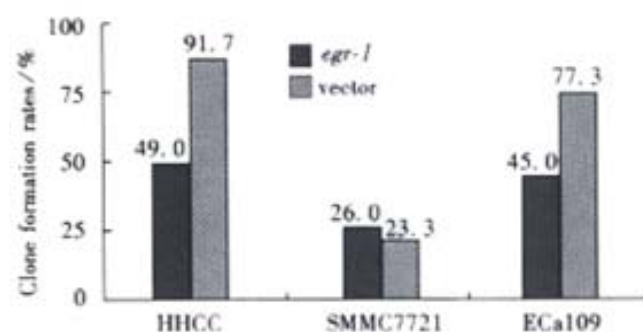
In *egr-1* transfected HHCC, the number of fraction of S phase accounted for 0.15, lower than that of the controls (0.28, $P=0.038$); i. e., the proportion of S phase was 0.46 lower than that of the control (Table 3). In ECa109, the number of fraction of S phase accounted for 0.18 (control 0.27, $P=0.048$), and was 0.34 lower than that of the control. In SMMC7721 (HCC), there was no marked difference between the experimental and the control groups (0.21 to 0.22, $P=1.000$). As for the G₁ and G₂/M phases, there were neither significant differences between experiment groups and control groups.

Table 3 Cell cycle of HCC and EC cells expressing EGR-1 with FCM (number of fraction)

Cell clone	G ₁	G ₂ /M	S
HHCC/EGR-1	0.77	0.08	0.15 ^a
HHCC/φ	0.64	0.08	0.28
SMMC7721/EGR-1	0.70	0.09	0.21 ^b
SMMC7721/φ	0.70	0.09	0.22
ECa109/EGR-1	0.73	0.11	0.18 ^c
ECa109/φ	0.64	0.10	0.27

^aP=0.038, ^bP=1.000, ^cP=0.048, vs their controls**Plate cloning formation**

In HHCC cell line, the clone forming rate of transfected cells was 49.0±10.6%, 42.7% lower than that of control 91.7±6.1%. In ECa109 line, the clone forming rate of transfected cells was 45.0±5.3%, 32.3% lower than that of control 77.3±3.1%. In SMMC7721, There were no statistical difference between the experimental group 26.0±2.6% and the control group 23.3±2.1% (Figure 4).

**Figure 4** Clone formation rates of exogenous high EGR-1 expression HCC and EC

Nude mice tumorigenicity

All the inoculated nude mice had tumor mass growth except in one case (one of the three SMMC7721/ ϕ inoculated mice). In HHCC cell line, the tumor growth rate of transfected group was 80.7%, lower than that of the control ($P=0.001$). In ECa109 cell, the growth rate of transfected group was 72.6%, also lower than that of the control ($P=0.001$). In SMMC7721, there was no growth rate difference between the experimental and the control group ($P=0.681$)(Table 4).

Table 4 Nude mice tumorigenicity of gene transfected groups in HCC and EC cells

Cell clone	n	Tumorigenicity rate	Tumor growth rate (x \pm s, mg·d ⁻¹)
HHCC/EGR-1	3	3/3	13.9 \pm 5.2 ^a
HHCC/ ϕ	3	3/3	70.9 \pm 7.8
SMMC7721/EGR-1	3	3/3	18.7 \pm 4.3 ^b
SMMC7721/ ϕ	3	2/3	15.2 \pm 13.0
ECa109/EGR-1	4	4/4	12.9 \pm 2.1 ^c
ECa109/ ϕ	4	4/4	47.1 \pm 11.3

^a $P=0.001$, ^b $P=0.681$, ^c $P=0.001$, vs their controls

DISCUSSION

Although *egr-1* is a member of immediate early genes, its expression is also elevated during the process of growth^[4] and differentiation^[5]. Observations suggest that EGR-1 have pleiotropic roles such as growth, development, differentiation etc. This is Supported by the finding that the GC-rich DNA-binding element for *egr-1* (GCE) is present in a large number of gene regulating regions, including growth factors, signal transduction genes, other transcription factors and oncogenes. In this report, we showed that *egr-1* transcription and expression decreased obviously in HCC and EC tissues compared with their paracancerous tissues. Another (large) study also indicated that human small cell lung tumors express little or no *egr-1* mRNA compared with adjacent normal tissues^[40], further supporting our findings. Except that the *egr-1* gene was deleted only in all 5q syndrome cases^[41], *egr-1* expression was profoundly decreased in a number of other human tumor cell lines such fibroblastoma, glioblastoma, osteosarcoma and lung cancer^[6]. Therefore it seems likely that the inactivation of *egr-1* expression is a generalized phenomenon in the developmental process of a number of tumors.

Egr-1 is ubiquitously expressed at low levels but accumulates to relatively high levels in only a few adult organs as brain, heart, lung, kidney^[42] and breast^[11]. We showed here that normal liver and esophageal epithelial tissues expressed undetectable level of *egr-1*, but the *egr-1* gene was activated in the tissues of hepatic paracancerous tissue such as LCD and "atrophic liver plate" (reluctant LCD) and dysplastic tissue of esophageal carcinoma. During regeneration of normal liver tissue, increased *egr-1* expression is induced^[43]. In mouse fibroblast NIH3T3 cells, *egr-1* expression increases two-fold 10min after UV irradiation, which rises to a maximum (eightfold induction) after 2h^[6]. Human HT1080 fibrosarcoma subclone, cells H4, express little or no *egr-1*. Phorbol ester treatment only can elicit a small increase in *egr-1* expression in H4, in contrast to the normally rapid, high transient expression of *egr-1* observed after the addition of a wide range of stimulating agents to normal or immortalized cell lines^[7]. Therefore, the meaning of little or no *egr-1* expression in liver and esophageal carcinomas is different to their counterparts. *egr-1* gene in the hepatic paracancerous tissue such as LCD and dysplasia of esophageal carcinoma can be activated when they are stimulated, but the stimulations is invalidated in carcinomas. The decreased expression of *egr-1* may play a role in the dysregulation of normal growth in the cancerous process of HCC and EC.

To confirm the development of liver and esophageal carcinomas involves the inactivation of *egr-1*. It would deserve further investigation of the effects of exogenous EGR-1 on the growth and malignant phenotypes of the cancer. Like tumor suppressor gene WT1, EGR-1 can also bind with GCE elements^[44], this suggests that EGR-1 might have inhibitory activity on cancer growth. In the

experimental report^[8], EGR-1 could reverse the malignant phenotype of *v-sis* transformed NIH3T3 cells. The results of this paper also showed that stably expressed EGR-1 could inhibit the cancer's growth rate, reduce the number of fraction of S phase, decrease the plate clone formation rate and reduce the tumorigenicity of HHCC and ECa109 cell lines. In recent years, studies have revealed that in human tumors, EGR-1 expression suppressing tumor cell growth is a common phenomenon. In human HT-1080 fibrosarcoma cells, the growth rates in 6 groups of expressing different EGR-1 level are inhibited proportionately and are dose-dependent. The total inhibition rate of these cells' tumorigenicity is over 50%. The growth of human ZR-75-1 breast carcinoma, U251 glioblastoma and SAOS-2 osteosarcoma cells has also been demonstrated to be suppressed by EGR-1 in different degree^[6]. However, in this experiment EGR-1 did not suppress the malignant phenotypes of SMMC7721, HCC cell line, this might be due to different transformation mechanism in this cell line, which needs investigation further.

The mechanism of EGR-1 inhibition on cancer growth is complicated, which interacts with TGF- β 1, PDGF and WT1. TGF- β 1 specifically inhibits PDGF β -dependent cells' growth^[4], while EGR-1 inhibits the malignant phenotype and growth of the PDGF β /*v-sis* that were transformed from NIH3T3 cells. This suggests that EGR-1 is closely related with TGF- β 1 and PDGF. Meanwhile, EGR-1 can also activate the transcription of TGF- β 1 in a dose-dependent manner, this activation might be one of the potential mechanisms of EGR-1 of inhibiting tumor growth^[45]. Interestingly, WT1 can bind with the GC element of TGF- β 1 promoter, and then inhibit the activity of that promoter (but this reaction is weaker than that of inhibition on PDGF β). One recent study has shown that the inhibitory reaction of EGR-1 on cancer growth is also by inducing the expression of TGF- β 1, fibronectin, p21 and focal adhesion kinase (FAK) in human fibrosarcoma cell line^[46]. EGR-1 may also regulate cell interaction with the extracellular matrix by synergistic induction of TGF- β 1, FN, and PAI-1 in human HT-1080 glioblastoma cells^[47] and directly transactivates the fibronectin gene and enhances attachment of human glioblastoma cell line U251^[48]. Other reports show that the suppression by *egr-1* also involves down-regulation of bcl-2^[49] and stimulates apoptosis by transactivation of the p53 gene^[50].

Recent studies^[6, 8, 50] as well as this experiment suggest that EGR-1 can act as a tumor suppressor factor. EGR-1 has been identified to be little or no expression in several human malignant tumors such as fibroblastoma, glioblastoma, osteosarcoma, lung cancer, breast carcinoma (including cancer cells and tumor tissues)^[1, 6], as well as hepatocellular carcinoma and esophageal carcinoma in this experiment. Another (larger) study also indicates that human small cell lung tumors express little or no *egr-1* mRNA compared with adjacent normal tissues^[40]. Furthermore, 5q-syndrome is the exclusive tumor with *egr-1* gene deletion^[41]. Hence we suspect that *egr-1* might be belonged to typeII tumor suppressor genes as mentioned above. The reintroduction of *egr-1* gene products by drugs might be a promising approach to normalize growth regulation, which can avoid the difficult problem of replacing defective gene DNA.

ACKNOWLEDGEMENT

Thanks to Prof. Bo-Rong Pan in the Oncology Center of Xijing Hospital for his help in the preparation of this article.

REFERENCES

- Huang RP, Fan Y, de-Belle I, Niemeyer C, Gottardis MM, Mercola D, Adamson ED. Decreased *egr-1* expression in human, mouse and rat mammary cells and tissues correlates with tumor formation. *Int J Cancer* 1997;72:102-109
- Darland T, Samuels M, Edwards SA, Sukhatme VP, Adamson ED. Regulation of Egr-1 (Zfp-6) and c-fos expression in differentiating embryonal carcinoma cells. *Oncogene* 1991;6:1367-1376
- Gashler AL, Swaminathan S, Sukhatme VP. A novel repression module, an extensive activation domain, and a bipartite nuclear localization signal defined in the immediate-early transcription factor *egr-1*. *Mol Cell Biol*

- 1993;13:4556-4571
- 4 Liu C, Calogero A, Ragona G, Adamson E, Mercola D. EGR-1, the reluctant suppression factor: EGR-1 is known to function in the regulation of growth, differentiation, and also has significant tumor suppressor activity and a mechanism involving the induction of TGF-beta1 is postulated to account for this suppressor activity. *Crit Rev Oncog* 1996;7:101-125
- 5 Nguyen HQ, Hoffman Liebermann B, Liebermann DA. The zinc finger transcription factor *egr-1* is essential for and restricts differentiation along the macrophage lineage. *Cell* 1993;7:197-209
- 6 Huang RP, Liu C, Fan Y, Mercola D, Adamson ED. *egr-1* negatively regulates human tumor cell growth via the DNA-binding domain. *Cancer Res* 1995;55:5054-5062
- 7 Liu C, Adamson E, Mercola D. Transcription factor EGR-1 suppresses the growth and transformation of human HT-1080 fibrosarcoma cells by induction of transforming growth factor beta1. *Proc Natl Acad Sci USA* 1996;93:11831-11836
- 8 Huang RP, Darland T, Okamura D, Mercola D, Adamson ED. Suppression of v-sis-dependent transformation by the transcription factor, *egr-1*. *Oncogene* 1994;9:1367-1377
- 9 Tang ZY, Schmid. Advances in clinical research of hepatocellular carcinoma in China. *World J Gastroenterol* 1998;4(Suppl 2):4-7
- 10 Wu XY, Zhang XF, Yin FS, Lu HS, Guan GX. Clinical study on surgical treatment of esophageal carcinoma in patients after subtotal gastrectomy. *World J Gastroenterol* 1998;4(Suppl 2):68-69
- 11 Bai YM, Wang LD, Seril DN, Liao J, Yang GY, Yang CS. Expression of hMSH2 in human esophageal cancer from patients in a high incidence area in Henan, China. *World J Gastroenterol* 1998; 4(Suppl 2): 107
- 12 Qi YJ, Wang LD, Nie Y, Cai C, Yang GY, Xing EP, Yang CS. Alteration of p19 mRNA expression in esophageal cancer tissue from patients at high incidence area in northern China. *World J Gastroenterol* 1998; 4(Suppl 2): 108-109
- 13 Qian QJ, Xue HB, Qu ZQ, Fang SG, Cao HF, Wu MC. *in situ* detection of tumor infiltrating lymphocytes expressing perforin and fas ligand genes in human HCC. *World J Gastroenterol* 1999; 5: 12-14
- 14 Gao SS, Zhou Q, Li YX, Bai YM, Zheng ZY, Zou JX, Liu G, Fan ZM, Qi YJ, Zhao X, Wang LD. Comparative studies on epithelial lesions at gastric cardia and pyloric antrum in subjects from a high incidence area for esophageal cancer in Henan, China. *World J Gastroenterol* 1998;4:332-333
- 15 Liang YR, Zheng SY, Shen YQ, Wu XY, Huang ZZ. Relationship between expression of apoptosis related antigens in hepatocellular carcinoma and *in situ* end labeling. *World J Gastroenterol* 1998; 4: 99
- 16 Xiao L, Zhou HY, Luo ZC, Liu J. Telomeric associations of chromosomes in patients with esophageal squamous cell carcinomas. *World J Gastroenterol* 1998; 4: 231-233
- 17 Huang B, Wu ZB, Ruan YB. Expression of nm23 gene in hepatocellular carcinoma tissue and its relation with metastasis. *World J Gastroenterol* 1998; 4: 266-267
- 18 Sun HC, Li XM, Xue Q, Chen J, Gao DM, Tang ZY. Study of angiogenesis induced by metastatic and non metastatic liver cancer by corneal micropocket model in nude mice. *World J Gastroenterol* 1999; 5: 116-118
- 19 Luo YQ, Wu MC, Cong WM. Gene expression of hepatocyte growth factor and its receptor in HCC and nontumorous liver tissues. *World J Gastroenterol* 1999; 5: 119-121
- 20 Liu CG, Zhu MC, Chen ZN. Preparation and purification of F(ab')₂ fragment from anti hepatoma mouse IgG1 mAb. *World J Gastroenterol* 1999; 5: 522-524
- 21 Ma XD, Sui YF, Wang WL. Expression of gap junction genes connexin 32, connexin 43 and their proteins in hepatocellular carcinoma and normal liver tissues. *World J Gastroenterol* 2000; 6: 66-69
- 22 Tang YC, Li Y, Qian GX. Reduction of tumorigenicity of SMMC-7721 hepatoma cells by vascular endothelial growth factor antisense gene therapy. *World J Gastroenterol* 2001; 7: 22-27
- 23 Feng DY, Zheng H, Tan Y, Cheng RX. Effects of phosphorylation of MARK and Stat3 and expression of c-fos and c-jun proteins on hepatocarcinogenesis and their clinical significance. *World J Gastroenterol* 2001; 7: 33-36
- 24 Fan ZR, Yang DH, Cui J, Qin HR, Huang CC. Expression of insulin-like growth factor II receptor in hepatocellular carcinogenesis. *World J Gastroenterol* 2001; 7: 285-288
- 25 Yang SM, Zhou H, Chen RC, Wang YF, Chen F, Zhang CG, Zhen Y, Yan JH, Su JH. Sequencing of P53 mutation in established human hepatocellular carcinoma cell line of HHC4 and HHC15 in nude mice. *World J Gastroenterol* 1998; 4: 506-510
- 26 Luo F, Kan B, Lei S, Yan LN, Mao YQ, Zou LQ, Yang YX, Wei YQ. Study on P53 protein and C erbB2 protein expression in primary hepatic cancer and colorectal cancer by flow cytometry. *World J Gastroenterol* 1998; 4(Suppl 2): 87
- 27 Zhou Q, Wang LD, Gao SS, Li YX, Zhao X, Wang LX. P53 immunostaining positive cells correlated positively with S phase cells as measured by BrdU in the esophageal precancerous lesions from the subjects at high incidence area for esophageal cancer in northern China. *World J Gastroenterol* 1998; 4 (Suppl 2): 106
- 28 Feng DY, Chen RX, Peng Y, Zheng H, Yan YH. Effect of HCV NS3 protein on P53 protein expression in hepatocarcinogenesis. *World J Gastroenterol* 1999; 5: 45-46
- 29 Casson AG. Molecular biology of Barrett's esophagus and esophageal cancer: role of P53. *World J Gastroenterol* 1998;4:277-279
- 30 Wang LD, Zhou Q, Wei JP, Yang WC, Zhao X, Wang LX, Zou JX, Gao SS, Li YX, Yang CS. Apoptosis and its relationship with cell proliferation, P53, Waf1p21, bcl-2 and c-myc in esophageal carcinogenesis studied with a high risk population in northern China. *World J Gastroenterol* 1998;4:287-293
- 31 Yu GQ, Zhou Q, Ding I, Gao SS, Zheng ZY, Zou JX, Li YX, Wang LD. Changes of P53 protein blood level in esophageal cancer patients and normal subjects from a high incidence area in Henan, China. *World J Gastroenterol* 1998; 4: 365-366
- 32 Deng ZL, Ma Y. Aflatoxin sufferer and P53 gene mutation in hepatocellular carcinoma. *World J Gastroenterol* 1998; 4: 28-29
- 33 Qiao GB, Han CL, Jiang RC, Sun CS, Wang Y, Wang YJ. Overexpression of P53 and its risk factors in esophageal cancer in urban areas of Xi'an. *World J Gastroenterol* 1998; 4: 57-60
- 34 Luo D, Liu QF, Gove C, Naomov NV, Su JJ, Williams R. Analysis of N ras gene mutation and P53 gene expression in human hepatocellular carcinomas. *World J Gastroenterol* 1998; 4: 97-98
- 35 Peng XM, Peng WW, Yao JL. Codon 249 mutations of P53 gene in development of hepatocellular carcinoma. *World J Gastroenterol* 1998; 4:125-127
- 36 Jiao LH, Wang LD, Xing EP, Yang G, Yu Y, Yang CS. Frequent inactivation of P16 and P15 expression in human esophageal squamous cell carcinoma detected by RT-PCR. *World J Gastroenterol* 1998;4(Suppl 2):105
- 37 Liu LH, Xiao WH, Liu WW. Effects of 5-Aza-2'-deoxycytidine on the P16 tumor suppressor gene in hepatocellular carcinoma cell line HepG2. *World J Gastroenterol* 2001; 7: 131-135
- 38 Qin LL, Su JJ, Li Y, Yang C, Ban KC, Yian RQ. Expression of IGFII, p53, P21 and HBxAg in precancerous events of hepatocarcinogenesis induced by AFB1 and/or HBV in tree shrews. *World J Gastroenterol* 2000; 6: 138-139
- 39 Maltzman JS, Carman JA, Monroe JG. Role of EGR1 in regulation of stimulus-dependent CD44 transcription in B lymphocytes. *Mol Cell Biol* 1996; 16: 2283-2294
- 40 Levin WJ, Press MF, Gaynor RB, Sukhatme VP, Boone TC, Reissmann PT, Figlin RA, Holmes EC, Souza LM, Slamon DJ. Expression patterns of immediate early transcription factors in human non-small cell lung cancer. The Lung Cancer Study Group. *Oncogene* 1995; 11: 1261-1269
- 41 Le Beau MM, Espinosa R, Neuman WL, Stock W, Roulston D, Larson RA, Keinonen M, Westbrook CA. Cytogenetic and molecular delineation of the smallest commonly deleted region of chromosome 5 in malignant myeloid diseases. *Proc Natl Acad Sci USA* 1993; 90: 5484-5488
- 42 Herms J, Zurmohle U, Schlingensiepen R, Brysch W, Schlingensiepen KH. Developmental expression of the transcription factor zif268 in rat brain. *Neurosci Lett* 1994; 165: 171-174
- 43 Columbano A, Shinozuka H. Liver regeneration versus direct hyperplasia. *FASEB J* 1996; 10: 1118-1128
- 44 Rauscher FJ 3d, Morris JF, Tournay OE, Cook DM, Curran T. Binding of the Wilms' tumor locus zinc finger protein to the EGR-1 consensus sequence. *Science* 1990; 250: 1259-1262
- 45 Dey BR, Sukhatme VP, Roberts AB, Sporn MB, Rauscher FJ 3rd, Kim SJ. Repression of the transforming growth factor-beta 1 gene by the Wilms' tumor suppressor WT1 gene product. *Mol Endocrinol* 1994;8:595-602
- 46 Belle I, Huang RP, Fan Y, Liu C, Mercola D, Adamson ED. P53 and *egr-1* additively suppress transformed growth in HT1080 cells but *egr-1* counteracts P53-dependent apoptosis. *Oncogene* 1999; 18: 3633-3642
- 47 Liu C, Yao J, de Belle I, Huang RP, Adamson E, Mercola D. The transcription factor EGR-1 suppresses transformation of human fibrosarcoma HT1080 cells by coordinated induction of transforming growth factor-beta1, fibronectin, and plasminogen activator inhibitor-1. *J Biol Chem* 1999; 274: 4400-4411
- 48 Liu C, Yao J, Mercola D, Adamson E. The transcription factor EGR-1 directly transactivates the fibronectin gene and enhances attachment of human glioblastoma cell line U251. *J Biol Chem* 2000; 275: 20315-20323
- 49 Huang RP, Fan Y, Peng A, Zeng ZL, Reed JC, Adamson ED, Boynton AL. Suppression of human fibrosarcoma cell growth by transcription factor, *egr-1*, involves down-regulation of Bcl-2. *Int J Cancer* 1998;77:880-886
- 50 Liu C, Rangnekar VM, Adamson E, Mercola D. Suppression of growth and transformation and induction of apoptosis by EGR-1. *Cancer Gene Ther* 1998; 5: 3-28

• GASTRIC CANCER •

Construction of cDNA representational difference analysis based on two cDNA libraries and identification of garlic inducible expression genes in human gastric cancer cells

Yong Li, Lin Yang, Jian-Tao Cui, Wen-Mei Li, Rui-Fang Guo, You-Yong Lu

Yong Li, Jian-Tao Cui, Wen-Mei Li, You-Yong Lu, Beijing Institute for Cancer Research, Beijing Laboratory of Molecular Oncology, School of Oncology, Peking University, Beijing 100034, China
Lin Yang, Department of Gastroenterology, PLA Institute for Digestive Diseases, First Affiliated Hospital of First Military Medical University, Chinese, Guangzhou, 510000, Guangdong Province, China
Rui-Fang Guo, Department of Physiology, Neimenggu Medical College, Huhehaote, 010000, Neimengguzhizhi, China
Supported by the Natural Scientific Foundation of China (NSFC3962526) and National High-Technology Project-863 (102-10-01-04).
Correspondence to: Dr. You-Yong Lu, Beijing Institute for Cancer Research, Beijing Laboratory of Molecular Oncology, School of Oncology, Peking University, 1 Da-Hong-Luo-Chang Street, Western District, Beijing 100034, China. yongylu@public.bta.net.cn
Telephone: +86-10-66163061 Fax: +86-10-66175832
Received 2001-08-09 Accepted 2001-11-14

Abstract

AIM: To elucidate molecular mechanism of chemopreventive efficacies of garlic against human gastric cancer (HGC).

METHODS: HGC cell line BGC823 was treated with Allitridi (a kind of garlic extract) and Allitridi-treated and parental BGC823 cDNA libraries were constructed respectively by using λ ZAP II vector. cDNA Representational Difference Analysis (cDNA RDA) was performed using *Bam*H I cutting-site and abundant cDNA messages provided by the libraries. Northern blot analysis was applied to identify the obtained difference products.

RESULTS: Two specific cDNA fragments were obtained and characterized to be derived from homo sapiens folate receptor α (FR α) gene and calcyclin gene respectively. Northern blot results showed a 4-fold increase in FR α gene expression level and 9-fold increase in calcyclin mRNA level in BGC823 cells after Allitridi treatment for 72h.

CONCLUSION: The method of cDNA RDA based on cDNA libraries combines the high specificity of cDNA RDA with abundant cDNA messages in cDNA library; this expands the application of cDNA library and increases the specificity of cDNA RDA. Up-regulation of FR α gene and calcyclin gene expressions induced by Allitridi provide valuable molecular evidence for the efficacy garlic in treating HGC as well as other diseases.

Li Y, Yang L, Cui JT, Li WM, Guo RF, Lu YY. Construction of cDNA representational difference analysis based on two cDNA libraries and identification of garlic inducible expression genes in human gastric cancer cells. *World J Gastroenterol* 2002;8(2):208-212

INTRODUCTION

Gastric cancer is common in China^[1-38]. Garlic has been used for over three thousand years in traditional Chinese medicine and is widely used in preventing manifold diseases all over the world. Epidemiological

studies indicated that garlic in diet had remarkable antithrombotic, hypolipidemic, hypocholesterolemic and antineoplastic effects^[39-41]. Both Chinese and Italian scholars reported protective efficacies of garlic in cases of human gastric cancer (HGC)^[40]. Allitridi is an important constituent of garlic oil mainly containing diallyl trisulfide (DATS) and diallyl disulfide (DADS), which are widely used in cancer chemoprevention and anti-cardiovascular disease research^[42]. Our data also indicated that Allitridi could arrest HGC cell line BGC823 in G1 phase and induce morphological changes of such cells (data not shown). Recent studies suggested that garlic may exert its chemopreventive effects by modulating lipid peroxidation, enhancing the levels of glutathione (GSH), glutathione peroxidase (GPx), glutathione S-transferase (GST) and NAD(P)H:quinone oxidoreductase (NQO)^[43,44]. However, a definitive molecular mechanism of anticarcinogenic activities of garlic has not been established.

The cDNA Representational Difference Analysis (cDNA RDA) method with high specificity is widely used in identifying differentially expressed genes in different developmental stages and cell cycle phases or in following the progression of expression in proceeding with a particular event, for example, stimulation of cells with a growth factor^[45-47]. Enough double stranded cDNA will be available in cDNA libraries for subtractive cloning. In order to detect the feasibility of cDNA RDA based on cDNA libraries and to identify Allitridi inducible expression genes at the same time, Allitridi-treated and parental BGC823 cell cDNA libraries were constructed respectively by using λ ZAP II vector. We further took advantage of restriction site harbored in the vector and replaced four-cutting restriction endonuclease *Dpn* II used in classical cDNA RDA with six-cutting enzyme *Bam*H I to select representations and to perform cDNA RDA following the classical procedure.

MATERIALS AND METHODS

Cell culture and cDNA library construction

The HGC cell line BGC823 was grown at 50mL·L⁻¹ CO₂ in DMEM medium supplemented with 50mL·L⁻¹ fetal calf serum. Allitridi used in our experiments contained 97.98% DATS and 0.85% DADS. BGC823 cells were incubated in medium containing 25mg·L⁻¹ Allitridi for 72h. Total RNA isolated from parental and Allitridi-treated BGC823 cells was separated by using guanidinium thiocyanate acid-phenol-chloroform method, followed by purification of poly(A)+ mRNA with the Poly(A)+ Quik mRNA Isolation Kit (Stratagene). 5 μ g mRNA were collected and λ ZAP-cDNA Gigapack III Gold Cloning Kit (Stratagene) was used to construct two cDNA libraries which were Allitridi-treated and parental cell cDNA libraries respectively.

Establishment of cDNA RDA based on cDNA libraries

By using Allitridi-treated BGC823 (Alli823) library DNA as tester and parental cell (BGC823) library DNA as driver, we performed cDNA RDA following the protocol supplied by classical cDNA RDA. Library DNAs (40 μ g) of the two cDNA libraries were prepared respectively and digested with *Bam*H I, phenol extracted, ethanol

precipitated and resuspended in 20 μ L 1 \times TE. 12 μ L (about 24 μ g) digested DNAs were then conjugated to 18 μ L R-Bam-24 (10 μ mol \cdot L⁻¹) and R-Bam-12 (10 μ mol \cdot L⁻¹) adapters. PCRs were set up to generate the initial representations by using R-Bam-24 as a primer. Afterward the R-adapters were removed from the representation of BGC823 with *Bam*H I to form the driver. Representation of Alli823 was also digested with *Bam*H I and the product was purified using Qiaex resin (Qiagen). This formed the tester, of which 2 μ g was conjugated to the J-Bam-12/24 adapters. For the first subtractive hybridization, 0.4 μ g J-conjugated tester was mixed with 24 μ g driver, and the mixture was allowed to anneal 20 h at 67°C. The annealing products were used as templates and 25 cycles of PCR were performed to generate the first difference product (DP1). J-adapters on DP1

were changed for N-Bam-12/24 adapters. The ratio for subtractive hybridization was changed for 50 ng : 40 μ g and the processes were repeated to generate the second difference product (DP2). To generate the third difference product (DP3), 400 pg J-conjugated DP2 was mixed with 40 μ g driver and the process repeated. Sequences of oligonucleotides used in cDNA RDA were as follows: R-Bam-24 5'-AGCACTCTCCAGCCTCTC ACCGAG-3'; R-Bam-12 5'-GATCCTCGGTGA-3'; J-Bam-24 5'-ACCGACGT CGACTATCCATGAACG-3'; J-Bam-12 5'-GATC CGTTCATG-3'; N-Bam-24 5'-AGGCAACTGTGCTATCCGA GGGAG-3'; N-Bam-12 5'-GATCCTCCCTCG-3'. The 5' end of 12-mer adapters was dephosphorylated. cDNA RDA based on cDNA libraries is showed schematically in Figure 1.

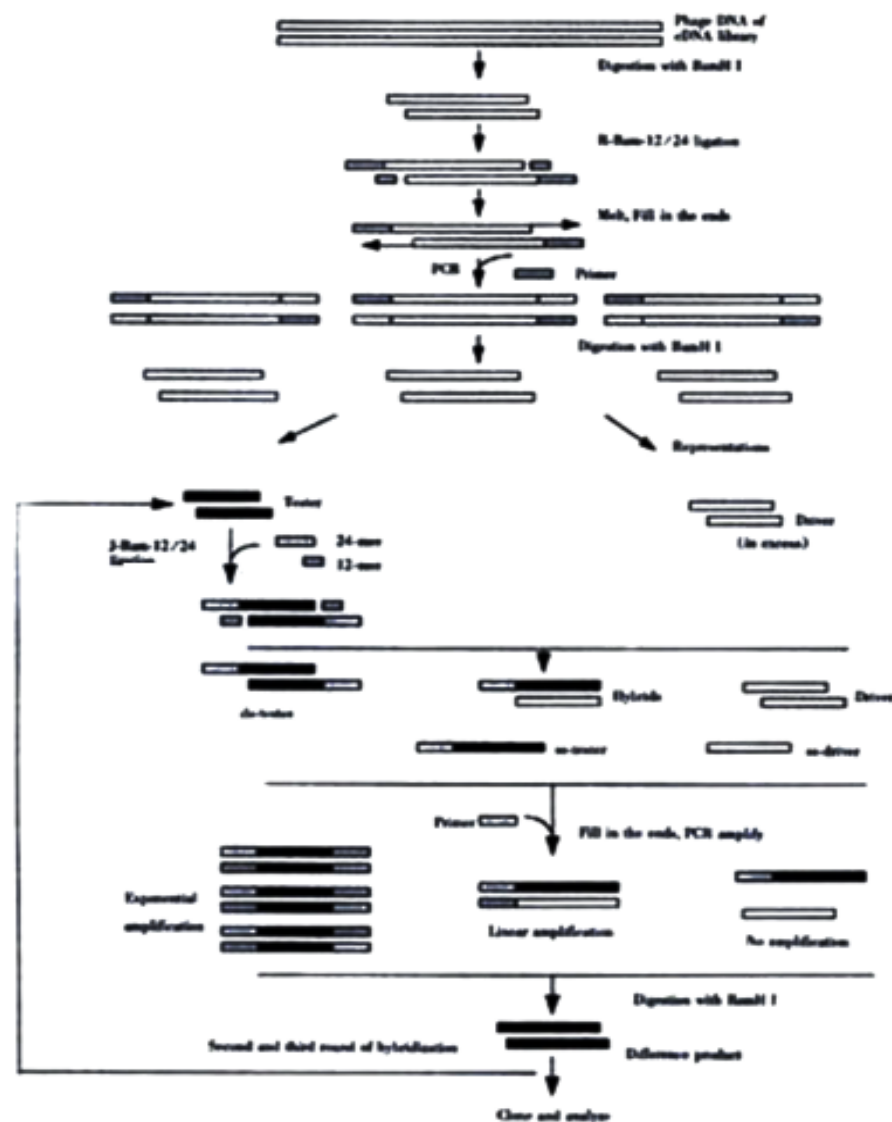


Figure 1 Schematic diagram of cDNA RDA based on cDNA libraries, illustrating the subtractive hybridization and amplification steps following the representation stage and preparation of amplicons. Gray boxes (24-mer, 12-mer) represent R (or J, N)-Bam adapters

Northern blot hybridization

Total RNA extracted from parental and Allitridi-treated BGC823 cells for 72h (10µg for each sample) were fractionated on formaldehyde agarose gel and transferred onto Nitrocellulose filters (S&S Company), then cross-linked by using a UV Stratalinker. Probes (DP3s) were labeled by random primer extension and hybridization carried out in 1mmol·L⁻¹ EDTA, 0.25mmol·L⁻¹ Na₂HPO₄ and 70g·L⁻¹ SDS solution for 16h at 60°C. Following hybridization, the filters were washed twice in 1mmol·L⁻¹ EDTA, 40mmol·L⁻¹ Na₂HPO₄ and 50g·L⁻¹ SDS for 25min at 60°C and twice in 1mmol·L⁻¹ EDTA, 40mmol·L⁻¹ Na₂HPO₄ and 10g·L⁻¹ SDS for 25min at 60°C again. Filters were exposed to a phosphor screen for 48h and analyzed.

Sequencing and Database Searching

Final difference products were amplified and cloned into pGEM-T Easy Vector (Promega). Double stranded plasmid DNA was prepared using miniprep columns (Promega) and sequenced with Ultra VGI 1280 (applying User Manual version 3.0). Resulting sequences were compared to the GenBank database by using the BLAST program.

RESULTS

Parental and Allitridi-treated BGC823 cell cDNA libraries

Morphological changes were observed in BGC823 cells after exposure to 25mg·L⁻¹ Allitridi for 96h. The cells after treatment dramatically changed to an elongated shape with filamentous protrusions. Neurite-like structures outgrew from the cell bodies and formed interconnections (Figure 2). Titer for Allitridi-treated BGC823 (Alli823) cDNA library was 1.1×10¹³ clones·L⁻¹, and titer for parental cell (BGC823) cDNA library 2.0×10¹³ clones·L⁻¹. The size of insert sequences for those two cDNA libraries ranged from several hundred base pairs to several kilobase pairs (kb), and the average length was about 2 kb (Figure 3).

cDNA RDA based on two cDNA libraries

cDNA RDA based on cDNA libraries is an extension of classical cDNA RDA in application and follows the protocol of the latter. λZAP II vector used to construct cDNA libraries has three *Bam*H I restriction sites with one site located very near the 5'-end of insert sequence. Thus *Bam*H I adapters can be introduced into the 5'-end of insert sequence. The shortest fragment cleaved from library vector DNA is 6.4kb in size, unable to compete with insert sequence during subsequent PCR amplification. Therefore, we could replace four-cutting restriction endonuclease *Dpn* II used in classical cDNA RDA with six-cutting enzyme *Bam*H I to select representations and perform cDNA RDA. With same copies three distinct fragments appeared in the digestion products of library DNA (about 22.1, 11.3 and 6.4kb in size respectively). We saw a stepwise reduction of complexity of the products in each successive difference product, until two clear bands with little background were visible by ethidium staining in the third difference products (DP3). The larger band named as DP3-1 is about 340 bp and the shorter one DP3-2 about 180bp in size. The amplicons and difference products obtained after the first, second and third round hybridization-amplification steps are showed in Figure 4.

Identification of differentially expressed genes in parental and Allitridi treated BGC823 cells

The third difference products, DP3-1 and DP3-2 were cloned into pGEM-T Easy Vector and resulting sequences were compared to the GenBank database using the BLAST program. Results showed that: DP3-1 had remarkable homology with FRα mRNA as high as 98%; DP3-2 sequence showed a remarkable homology of 97% with human calcylin mRNA. Northern blot results using DP3-1 and DP3-2 as probes showed a 4-fold increase in FRα gene expression level and 9-fold increase in calcylin mRNA level in BGC823 cells after Allitridi treatment for 72h (Figure 5).

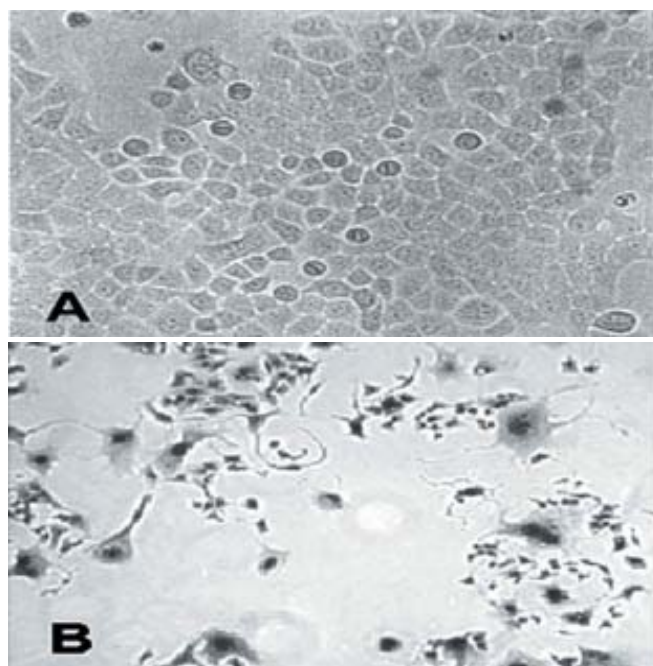


Figure 2 Morphological changes of human gastric cancer cell line BGC823 after Allitridi treatment. A: The parental cells (used as control); B: Neurite-like structures outgrew from the cell bodies and formed interconnections after exposure to 25mg·L⁻¹ Allitridi for 96h (5×40).

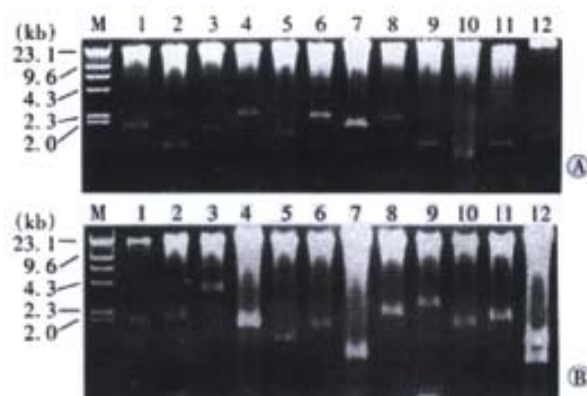


Figure 3 Insert sequences released from randomly selected clones (Lanes 1-12) of parental cell (BGC823) cDNA library (A) and Allitridi-treated cell (Alli823) cDNA library (B) by digestion with *Eco*I and *Xho*I. λPhage/*Hind* III size marker was indicated in Lane M.

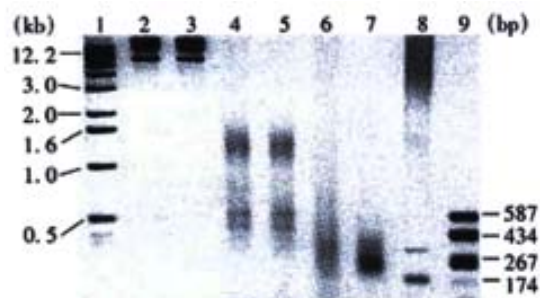


Figure 4 Agarose gel electrophoresis of difference products obtained after the first, second and third round hybridizations. *Bam*H I-digested library DNA extracted from Alli823 and BGC823 cDNA libraries respectively (Lanes 2,3); Amplicons of cDNA population prepared from Allitridi-treated and parental groups (used as tester and driver respectively) (Lane 4,5); First, second and third difference products respectively (Lanes 6,7,8); 1 kb size marker (Lane 1) and PUC18/*Hae* III DNA size marker (Lane 9).

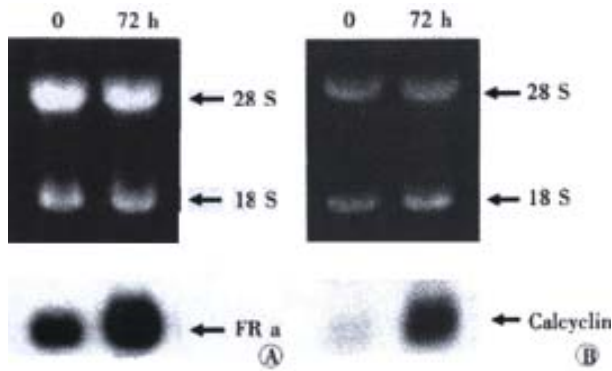


Figure 5 Northern blot analysis of FR α gene and calcyclin gene expression in BGC823 cells. FR α mRNA (A) and calcyclin mRNA (B) level was elevated after exposure to 25mg·L⁻¹ Allitridi for 72h.

DISCUSSION

cDNA RDA based on cDNA libraries shares the chief merits of classical cDNA RDA, and has in addition several distinct advantages: Firstly, enough double stranded cDNAs needed for subtractive hybridization can be obtained from cDNA libraries and thus expand the application of cDNA libraries. Next, with same copies, three distinct fragments (about 22.1, 11.3 and 6.4kb in size respectively) appear in the products of library DNA digestion with *Bam*H I and act as good marks indicating the appropriate digestion degree for library DNA and thus increasing the specificity and reproducibility of cDNA RDA. Thirdly, by replacing four-cutting enzyme *Dpn* II with six-cutting enzyme *Bam*H I to digest library DNA, longer difference products can be obtained; this will increase the specificity of subsequent Northern blot analysis, Database homology searching and library screening. Finally, through replacing or combining *Bam*H I cutting site with other restriction sites (for example, *Eco*I or *Xho*I) harbored in library vector, more difference products including low abundant messages can be obtained.

FR α functions as a membrane receptor to mediate the high-affinity internalization and delivery of folate and 5-methyltetrahydrofolate to the cytoplasm of the cell^[48]. Deficiency of folate has already been linked with increased incidence of neural tube defects and of cardiovascular disease through elevated plasma homocysteine levels^[49]. Recent studies showed that folate deficiency may cause an imbalance in DNA precursors, uracil misincorporation into DNA, and chromosome breakage. By reducing intracellular S-adenosylmethionine (SAM), it can also cause global DNA hypomethylation, leading to inappropriate activation of proto-oncogenes and induction of malignant transformation^[50-52]. Folate deficiency is reported to be associated with increased risk of colorectal carcinoma and breast cancer^[53-55]. Our findings suggested that up-regulation of FR α gene expression by Allitridi may compensate for folate deficiency and correspond with the preventive efficacy of garlic against HGC as well as other human diseases. Calcyclin gene, as a member of the S100 family for generating small calcium-binding proteins, was reported to be a cell cycle-dependent gene and to be associated with cell differentiation^[56-59]. Our results showed that calcyclin gene expression in BGC823 cells was up-regulated by Allitridi treatment before the neurite-like structures generated in the cells, and this would suggest the impact of garlic on regulating calcium metabolism and the involvement of calcyclin gene in HGC cell differentiation.

In conclusion, cDNA RDA based on cDNA libraries combines the high specificity of cDNA RDA with the abundant cDNA messages in cDNA library, and thus expands the application of cDNA library and increases specificity of cDNA RDA. Our findings suggest that up-regulation of FR α gene and calcyclin gene expression induced by Allitridi may play an important role in HGC cell differentiation and

may provide valuable molecular evidence for demonstrating the important preventive efficacy of garlic against HGC.

REFERENCES

- Xue FB, Xu YY, Wan Y, Pan BR, Ren J, Fan DM. Association of *H. pylori* infection with gastric carcinoma: a Meta analysis. *World J Gastroenterol* 2001;7:801-804
- Wu YL, Sun B, Zhang XJ, Wang SN, He HY, Qiao MM, Zhaong J, Xu JY. Growth inhibition and apoptosis induction of Sulindac on Human gastric cancer cells. *World J Gastroenterol* 2001;7:796-800
- Cai L, Yu SZ, Zhan ZF. Cytochrome P450 2E1 genetic polymorphism and gastric cancer in Changle, Fujian Province. *World J Gastroenterol* 2001;7:792-795
- Xu CT, Huang LT, Pan BR. Current gene therapy for stomach carcinoma. *World J Gastroenterol* 2001;7:752-759
- Cai L, Yu SZ, Zhang ZF. Glutathione S-transferases M1, T1 genotypes and the risk of gastric cancer: A case control study. *World J Gastroenterol* 2001;7:506-509
- Niu WX, Qin XY, Liu H, Wang CP. Clinicopathological analysis of patients with gastric cancer in 1200 cases. *World J Gastroenterol* 2001;7:281-284
- Miehlke S, Kirsch C, Dragosics B, Gschwantler M, Oberhuber G, Antos D, Dite P, Luter J, Labenz J, Leodolter A, Malfertheiner P, Neubauer A, Ehninger G, Stolte M, Bayerdrffer E. *Helicobacter pylori* and gastric cancer: current status of the Austrian Czech German gastric cancer prevention trial (PRISMA Study). *World J Gastroenterol* 2001;7:243-247
- Li XY, Wei PK. Diagnosis of stomach cancer by serum tumor markers. *Shijie Huaren Xiaohua Zazhi* 2001;9:568-570
- Gao HJ, Yu LZ, Bai JF, Peng YS, Sun G, Zhao HL, Miu K, Lu XZ, Zhang XY, Zhao ZQ. Multiple genetic alterations and behavior of cellular biology in gastric cancer and other gastric mucosal lesions: *H. pylori* infection, histological types and staging. *World J Gastroenterol* 2000;6:848-854
- Cai L, Yu SZ, Ye WM, Yi YN. Fish sauce and gastric cancer: an ecological study in Fujian Province, China. *World J Gastroenterol* 2000;6:671-675
- Cai L, Yu SZ, Zhang ZF. *Helicobacter pylori* infection and risk of gastric cancer in Changle County, Fujian Province, China. *World J Gastroenterol* 2000;6:374-376
- Zhang WD, Wang XH, Zeng JZ, Zhang YL, Sun Y. The relationship of traditional Chinese medicine and *Helicobacter pylori* infection, expression of oncogene and tumor suppressor genes in patients with gastric cancer and precancerous lesions. *World J Gastroenterol* 2000;6:71
- Yuan Y, Gong W, Xu RT, Wang XJ, Gao H. Gastric cancer screening in 16 villages of Zhuanghe region: a mass screening report from a high risk area of stomach cancer in China. *World J Gastroenterol* 2000;6:54
- Li M, Chen XZ, Lin ZX, Chen L. A preliminary clinical report of 2LC reagent for early gastric cancer diagnosis. *World J Gastroenterol* 2000;6:18
- Guan J, Zhang JP, Zhou TH. Relationship between telomerase *Helicobacter pylori* and stomach cancer. *Shijie Huaren Xiaohua Zazhi* 2000;8:910-911
- Wang DX, Fang DC, Liu WW. Study on alteration of multiple genes in intestinal metaplasia, atypical hyperplasia and gastric cancer. *Shijie Huaren Xiaohua Zazhi* 2000;8:855-859
- Shen J, Wang RT, Xu XP. Progress in studies of relationship between NO, iNOS and gastric cancer. *Shijie Huaren Xiaohua Zazhi* 2000;8:320-322
- Wang Q, Jin PH, Lin GW, Xu SR. Cost effectiveness of population based *Helicobacter pylori* screening to prevent gastric cancer. *Shijie Huaren Xiaohua Zazhi* 2000;8:262-265
- Deng DJ, EZ. Overview on recent studies of gastric carcinogenesis: human exposure of N nitrosamides. *Shijie Huaren Xiaohua Zazhi* 2000;8:250-252
- Zhuang XQ, Lin SR. Progress in research on the relationship between Hp and stomach cancer. *Shijie Huaren Xiaohua Zazhi* 2000;8:206-207
- Mi JQ, Zhang ZH, Shen MC. Significance of CD44v6 protein expression in gastric carcinoma and precancerous lesions. *Shijie Huaren Xiaohua Zazhi* 2000;8:156-158
- Ji F, Wang WL, Yang ZL, Li YM, Huang HD, Chen WD. Study on the expression of matrix metallo proteinase 2 mRNA in human gastric cancer. *World J Gastroenterol* 1999;5:455-457
- Cai L, Yu SZ. A molecular epidemiologic study on gastric cancer in Changle, Fujian Province. *Shijie Huaren Xiaohua Zazhi* 1999;7:652-655
- Zhou XW. Current status and prospect of clinical studies on TCM treatment of precancerous lesions of stomach. *Shijie Huaren Xiaohua Zazhi* 1999;7:277-279
- Shen J, Chen XR. Significance of cathepsin B activity in gastric cancer tissue. *Shijie Huaren Xiaohua Zazhi* 1999;7:147-149
- Liu ZM, Shou NH. Expression significance of mdrl gene in gastric carcinoma tissue. *Shijie Huaren Xiaohua Zazhi* 1999;7:145-146
- Yan XJ. Establishing early diagnosis and warning system of gastric carcinoma. *Shijie Huaren Xiaohua Zazhi* 1999;7:96-97

- 28 Hu PJ. *Hp* and gastric cancer: challenge in the research. *Shijie Huaren Xiaohua Zazhi* 1999;7:1-2
- 29 Ye WM, Yi YN, Luo RX, Zhou TS, Lin RT, Chen GD. Diet and gastric cancer: a casecontrol study in Fujian Province, China. *World J Gastroenterol* 1998;4:516-518
- 30 Yuan Y, Cong W, Xu RT, Wang XJ, Gao H. Gastric cancer screening in 16 villages of Zhuanghe region: a high risk area of stomach cancer in China. *World J Gastroenterol* 1998;4:111
- 31 Yu XE, Zhao AX, Wei DL, Du JZ. Relationship between *Helicobacter pylori* infection and gastric cancer. *World J Gastroenterol* 1998;4:96
- 32 Xia HX. Association between *Helicobacter pylori* and gastric cancer: current knowledge and future research. *World J Gastroenterol* 1998;4:93-96
- 33 Cao GH, Yan SM, Yuan ZK, Wu L, Liu YF. A study of the relationship between trace element Mo and gastric cancer. *World J Gastroenterol* 1998;4:55-56
- 34 Wang ZQ, He J, Chen W, Chen Y, Zhou TS, Lin YC. Relationship between different sources of drinking water, water quality improvement and gastric cancer mortality in Changle County-A retrospective-cohort study in high incidence area. *World J Gastroenterol* 1998;4:45-47
- 35 Li ZS, Zhu ZG, Yin HR, Chen SS, Lin YZ. Modified TRAP-PCR in detection of telomerase activity in early diagnosis of stomach tumors. *Huaren Xiaohua Zazhi* 1998;6:939-941
- 36 Sheng HG, Sun LZ, Zhang M, Wu TH, Liu GS, Guo CL. Preliminary studies on serum MGAg in patients with gastric cancer. *Huaren Xiaohua Zazhi* 1998;6:884-886
- 37 Pan KF, Liu WD, Ma JL, Zhou T, Zhang L, Chang YS, You WC. Infection of *Helicobacter pylori* in children and mode of transmission in a high risk area of gastric cancer. *Huaren Xiaohua Zazhi* 1998;6:42-44
- 38 Zhang L, Jiang J, Pan KF, Liu WD, Ma JL, Zhou T, Perez GI, Blaser MJ, Chang YS, You WC. Infection of *H.pylori* with *cagA*+ strain in a high risk area of gastric cancer. *Huaren Xiaohua Zazhi* 1998;6:40-41
- 39 Fleischauer AT, Poole C, Arab L. Garlic consumption and cancer prevention: meta-analyses of colorectal and stomach cancers. *Am J Clin Nutr* 2000;72:1047-1052
- 40 You WC, Zhang L, Gail MH, Ma JL, Li JY, Chang YS, Blot WJ, Zhao CL, Liu WD, Li HQ, Ma JL, Hu YR, Bravo JC, Correa P, Xu GW, Fraumeni JF. Comparisons of precancerous lesions in two countries of Shandong Province, China with contrasting risk of gastric cancer. *Int J Epidemiol* 1998;27:945-948
- 41 Su Q, Luo ZY, Teng H, Yun WD, Li YQ, He XE. Effect of garlic and garlic green tea mixture on serum lipids in MNNG-induced experimental gastric carcinoma and precancerous lesion. *Huaren Xiaohua Zazhi* 1998;6:112-113
- 42 Singh SV, Pan SS, Srivastava SK, Xia H, Hu X, Zaren HA, Orchard JL. Differential induction of NAD(P)H:quinone oxidoreductase by anti-carcinogenic organosulfides from garlic. *Biochem Biophys Res Commun* 1998;244:917-920
- 43 Balasenthil S, Nagini S. Inhibition of 7,12-dimethylbenz[a]anthracene-induced hamster buccal pouch carcinogenesis by S-allylcysteine. *Oral Oncol* 2000;36:382-386
- 44 Balasenthil S, Arivazhagan S, Ramachandran CR, Nagini S. Effects of garlic on 7,12-Dimethylbenz[a]anthracene-induced hamster buccal pouch carcinogenesis. *Cancer Detect Prev* 1999;23:534-538
- 45 Seidita G, Polizzi D, Costanzo G, Costa S, Di Leonardo A. Differential gene expression in P53-mediated G arrest of human fibroblasts after gamma-irradiation or N-phosphoacetyl-L-aspartate treatment. *Carcinogenesis* 2000;21:2203-2210
- 46 Yamashita Y, Yokoyama M, Kobayashi E, Takai S, Hino O. Mapping and determination of the cDNA sequence of the *Erc* gene preferentially expressed in renal cell carcinoma in the Tsc2 gene mutant (Eker) rat model. *Biochem Biophys Res Commun* 2000;275:134-140
- 47 Liu X, Rapp N, Deans R, Cheng L. Molecular cloning and chromosomal mapping of a candidate cytokine gene selectively expressed in human CD34+ cells. *Genomics* 2000;65:283-292
- 48 Sierra EE, Goldman ID. Recent advances in the understanding of the mechanism of membrane transport of folates and antifolates. *Semin Oncol* 1999;26:11-23
- 49 Al-Gazali LI, Padmanabhan R, Melnyk S, Yi P, Pogribny IP, Pogribna M, Bakir M, Hamid ZA, Abdulrazzaq Y, Dawodu A, James SJ. Abnormal folate metabolism and genetic polymorphism of the folate pathway in a child with Down syndrome and neural tube defect. *Am J Med Genet* 2001;103:128-132
- 50 Chern CL, Huang RF, Chen YH, Cheng JT, Liu TZ. Folate deficiency-induced oxidative stress and apoptosis are mediated via homocysteine-dependent overproduction of hydrogen peroxide and enhanced activation of NF-kappaB in human Hep G2 cells. *Biomed Pharmacother* 2001;55:434-442
- 51 Zhu SS, Xiao SD, Chen ZP, Shi Y, Fang JY, Li RR, Mason JB. DNA methylation and folate metabolism in gastric cancer. *World J Gastroenterol* 2000;6:18
- 52 Duthie SJ, Narayanan S, Blum S, Pirie L, Brand GM. Folate deficiency *in vitro* induces uracil misincorporation and DNA hypomethylation and inhibits DNA excision repair in immortalized normal human colon epithelial cells. *Nutr Cancer* 2000;37:245-251
- 53 Ryan BM, Weir DG. Relevance of folate metabolism in the pathogenesis of colorectal cancer. *J Lab Clin Med* 2001;138:164-176
- 54 Sellers TA, Kushi LH, Cerhan JR, Vierkant RA, Gapstur SM, Vachon CM, Olson JE, Therneau TM, Folsom AR. Dietary folate intake, alcohol, and risk of breast cancer in a prospective study of postmenopausal women. *Epidemiology* 2001;12:420-428
- 55 Ames BN. DNA damage from micronutrient deficiencies is likely to be a major cause of cancer. *Mutat Res* 2001;475:7-20
- 56 Fullen DR, Reed JA, Finnerty B, McNutt NS. S100A6 preferentially labels type C nevus cells and nevic corpuscles: additional support for Schwannian differentiation of intradermal nevi. *J Cutan Pathol* 2001;28:393-399
- 57 Konrad L, Aumuller G. Calcyclin is differentially expressed in rat testicular cells. *Biochim Biophys Acta* 1999;1489:440-444
- 58 Yang Q, O'Hanlon D, Heizmann CW, Marks A. Demonstration of heterodimer formation between S100B and S100A6 in the yeast two-hybrid system and human melanoma. *Exp Cell Res* 1999;246:501-509
- 59 Smith SP, Shaw GS. A novel calcium-sensitive switch revealed by the structure of human S100B in the calcium-bound form. *Structure* 1998;6:211-222

Edited by Lu HM

• GASTRIC CANCER •

Applying a highly specific and reproducible cDNA RDA method to clone garlic up-regulated genes in human gastric cancer cells

Yong Li, You-Yong Lu

Yong Li, You-Yong Lu, Beijing Institute for Cancer Research, Beijing Laboratory of Molecular Oncology, School of Oncology, Peking University, Beijing 100034, China

Supported by the Natural Scientific Foundation of China (NSFC3962526) and National High-Technology Project-863 (102-10-01-04)

Correspondence to: Dr. You-Yong Lu, Beijing Institute for Cancer Research, Beijing Laboratory of Molecular Oncology, School of Oncology, Peking University, 1 Da-Hong-Luo-Chang Street, Western District, Beijing 100034, China. yongylu@public.bta.net.cn
Telephone: +86-10-66163061 Fax: +86-10-66175832

Received 2001-09-14 Accepted 2001-10-21

Abstract

AIM: To develop and optimize cDNA representational difference analysis (cDNA RDA) method and to identify and clone garlic up-regulated genes in human gastric cancer (HGC) cells.

METHODS: We performed cDNA RDA method by using abundant double-stranded cDNA messages provided by two self-constructed cDNA libraries (Allitridi-treated and paternal HGC cell line BGC823 cells cDNA libraries respectively). *Bam*H I and *Xho* I restriction sites harbored in the library vector were used to select representations. Northern and Slot blots analyses were employed to identify the obtained difference products.

RESULTS: Fragments released from the cDNA library vector after restriction endonuclease digestion acted as good marker indicating the appropriate digestion degree for library DNA. Two novel expressed sequence tags (ESTs) and a recombinant gene were obtained. Slot blots result showed a 8-fold increase of glia-derived nexin/protease nexin 1 (GDN/PN1) gene expression level and 4-fold increase of hepatitis B virus x-interacting protein (XIP) mRNA level in BGC823 cells after Allitridi treatment for 72h.

CONCLUSION: Elevated levels of GDN/PN1 and XIP mRNAs induced by Allitridi provide valuable molecular evidence for elucidating the garlic's efficacies against neurodegenerative and inflammatory diseases. Isolation of a recombinant gene and two novel ESTs further show cDNA RDA based on cDNA libraries to be a powerful method with high specificity and reproducibility in cloning differentially expressed genes.

Li Y, Lu YY. Applying a highly specific and reproducible cDNA RDA method to clone garlic up-regulated genes in human gastric cancer cells. *World J Gastroenterol* 2002;8(2):213-216

INTRODUCTION

cDNA representational difference analysis (cDNA RDA), with high specificity by eliminating those fragments present in two compared populations and leaving only the differences, has been employed with some degree of success^[1-6]. While cDNA RDA, like other PCR-

based difference screening methods, is prone to produce false positive results^[7,8]. In our study, we used cDNA RDA method to isolate garlic inducible differentially expressed genes in human gastric cancer (HGC) cells. Allitridi is a critical constituent of garlic oil, mainly containing diallyl trisulfide (DATS) and diallyl disulfide (DADS), which is widely used in cancer chemoprevention and anti-cardiovascular disease research^[9-16]. Differences between two double-stranded cDNAs populations derived from Allitridi-treated and paternal HGC cell line BGC823 cells cDNA libraries were identified by using cDNA RDA. *Bam*H I and *Xho* I restriction sites harbored in the library vector were employed to select representations. We found another major source of false positives in cDNA RDA, which was inappropriate enzyme digestion of sample DNAs, and introduced improvements to minimize their production.

MATERIALS AND METHODS

Allitridi-treated and paternal HGC cell line BGC823 cells cDNA libraries

Allitridi is a critical constituent of garlic oil, containing 97.98% diallyl trisulfide (DATS) and 0.85% diallyl disulfide (DADS) in concentration. BGC823 cells were incubated in medium containing 25mg·L⁻¹ Allitridi for 72h. Total RNA isolated from paternal and Allitridi-treated BGC823 cells were extracted, followed by synthesis of double stranded cDNAs using λZAP-cDNA Gigapack III Gold Cloning Kit (Stratagene). cDNAs derived from Allitridi-treated and paternal BGC823 cells, with *Eco* I cutting site at 5'-end and *Xho* I site at 3'-end, were unidirectionally cloned into λZAP II vector for cDNA library construction.

cDNA RDA based on cDNA libraries: generation of representations

Difference between Allitridi-treated BGC823 (Alli823) cDNA library DNA (used as tester) and paternal cell (BGC823) library DNA (used as driver) was identified by using cDNA RDA to isolate Allitridi up-regulated genes. Library DNAs of the two cDNA libraries were prepared and digested with *Bam*H I respectively in a mixture containing 40μg library DNAs, 8μL *Bam*H I (10kU·L⁻¹, Promega), and 10μL 10×Buffer H in a final volume of 100μL. The digestions were carried out at 37°C for 2, 4, and 12h respectively to obtain the most appropriately digested fragments. After phenol extraction and ethanol precipitation, digested DNAs (about 24μg) were then ligated to 18μL R-Bam-24 (10μmol·L⁻¹) and 18μL R-Bam-12 (10μmol·L⁻¹) adapters. PCR reactions were set up to generate the initial representations by using R-Bam-24 as primer.

In order to expand the content of messages in the representations, we further employed *Bam*H I and *Xho* I together to digest the library DNAs. Library DNAs (about 40μg) of Alli823 and BGC823 cDNA libraries were digested with *Xho* I respectively. Digested DNAs were then ligated to *Xho* I Linker-15 (5'-TCGAGGATCCATTCA-3') and *Xho* I Linker-13 (5'-ACTGAATGGATCC-3'). Resulting ligations were digested with *Bam*H I and then ligated to R-Bam-12/24 adapters (10μmol·L⁻¹),

followed by PCR amplification to generate amplicons.

Using *Bam*H I alone or *Bam*H I and *Xho* I together to digest library DNAs and to prepare representations is showed schematically in Figure 1.

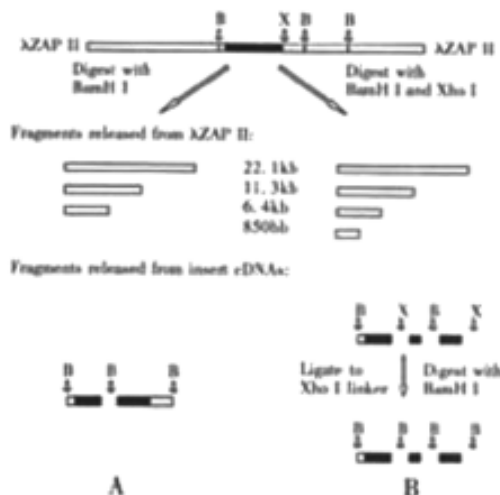


Figure 1 Schematic diagram of preparing representations for cDNA RDA based on cDNA libraries. Using *Bam*H I alone (A) or *Bam*H I and *Xho* I together (B) to digest library DNAs. Black boxes represent insert cDNAs of cDNA libraries. White boxes represent two arms of cDNA library vector (λ ZAP II vector). "B" represents *Bam*H I and "X" *Xho* I.

The followed three rounds of hybridizations and selective amplifications were performed according to the protocol supplied by typical cDNA RDA. Sequences of adapters used here are as follows: R-Bam-24 5'-AGCACTCTCCAGCCTCTCACCGAG-3'; R-Bam-12 5'-GATCCTCGGTGA-3'; J-Bam-24 5'-ACCGACGTCGACTATCC ATGAACG-3'; J-Bam-12 5'-GATCCGTTTCATG-3'; N-Bam-24 5'-AGGCAACTGTGCTATCCGAGGGAG-3'; N-Bam-12 5'-GATCCTCCCTCG-3'.

Slot and Northern blots analyses

Reamplified difference products (100ng each) were mixed with 2.5 μ L 3mmol·L⁻¹ NaOH respectively and incubated for 1h at 65°C, and then transferred onto Nitrocellulose filters (S&S Com) by using Slot Minifold® II (Schleicher&Schull). Two same filters were prepared and then cross-linked using a UV Stratalinker. Reverse transcription products (the first stranded cDNAs) of 5 μ g total RNA of Allitridi-treated and paternal BGC823 cells were used as probes respectively. Probes were labeled with ³²P using a Random-Primer labeling kit (Promega) and hybridization carried out in 1mmol·L⁻¹ EDTA, 0.25mmol·L⁻¹ Na₂HPO₄ and 70g·L⁻¹ SDS solution for 16h at 60°C. Following hybridization, the filters were washed twice in 1mmol·L⁻¹ EDTA, 40mmol·L⁻¹ Na₂HPO₄ and 50g·L⁻¹ SDS for 25min at 60°C and twice in 1mmol·L⁻¹ EDTA, 40mmol·L⁻¹ Na₂HPO₄ and 10g·L⁻¹ SDS for 25min at 60°C again. Filters were exposed to a phosphor screen for 48h and analyzed.

Total RNA (10 μ g each) isolated from HGC cell lines BGC823, MGC803, PAMC82, SGC7901 and MKN45 were transferred onto Nitrocellulose filters. Probe (the third difference product, DP3) was labeled by random primer extension and Northern blots hybridization carried out in the same manner described above.

Sequencing and Database Searching

Difference products were amplified and cloned into pGEM-T Easy Vector (Promega). Double stranded plasmid DNAs were prepared using miniprep columns (Promega) and sequenced with Ultra VGI 1280 (applying User Manual version 3.0). Resulting sequences were compared to the GenBank database by using the BLAST program.

RESULTS

Generation of representations for cDNA RDA based on cDNA libraries

Double stranded cDNAs, with *Eco* I cutting site at 5'-end and *Xho* I site at 3'-end, were unidirectionally cloned into λ ZAP II vector for cDNA library construction. Library vector (λ ZAP II vector) has three *Bam*H I restriction sites with one site located very near to 5'-end of insert cDNAs. Thus *Bam*H I adapters can be introduced into the 5'-end of insert cDNAs. With the same copies three distinct fragments appeared in the products of library DNA digested with *Bam*H I at 37°C for 4h (about 22.1, 11.3 and 6.4kb in size respectively), which indicated appropriate digestion degree. However, library DNAs were not fully digested at 37°C for 2h, and the smears of library DNAs after digestion for 12h showed excessive reactions. When *Bam*H I and *Xho* I were used together to digest library DNAs (1 cut/2 kb insert cDNAs in average), another vector-derived fragment (850 bp in size) was released from 3'-end of insert cDNAs. We further designed *Xho* I Linker-15/13 to convert *Xho* I cutting site to *Bam*H I site. Thus the content of cDNA messages available for difference analysis was expanded. The results for library DNAs after digestion with different enzymes or different conditions are showed in Figure 2. Subsequently, PCR reactions were set up to generate the initial representations (amplicons) (Figure 3).

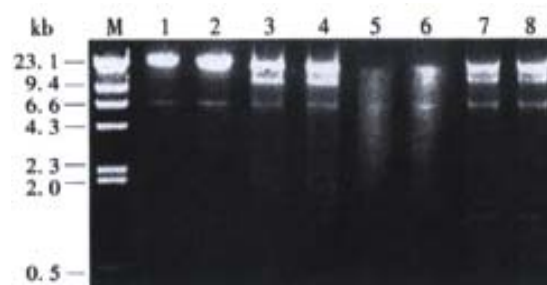


Figure 2 Agarose gel electrophoresis of digestion products of Alli823 (lanes 1,3,5) and BGC823 (lanes 2,4,6) cDNA library DNAs digested with *Bam*H I at 37°C for 2 (lanes 1,2), 4 (lanes 3,4), and 12h (lanes 5,6) respectively. The digestion products of Alli823 (lane 7) and BGC823 (lane 8) library DNAs digested with *Bam*H I and *Xho* I together (A fragment, 850 bp in size, appeared in the digestion products). ϕ Phage/*Hind* III size marker (lane M).

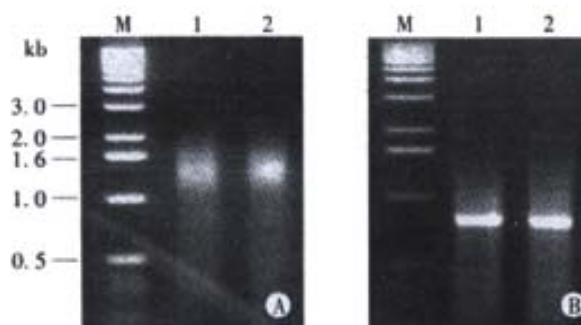


Figure 3 Agarose gel electrophoresis of amplicons derived from different enzyme digestions. A: The amplicons obtained by using *Bam*H I to digest Alli823 (lane 1) and BGC823 (lane 2) cDNA library DNAs respectively; B: The amplicons obtained by using *Bam*H I and *Xho* I together to digest Alli823 (lane 1) and BGC823 (lane 2) library DNAs respectively. 1kb size marker (lane M).

Identification of differentially expressed genes in Allitridi-treated BGC823 cells

Results of Slot blots analysis showed that expression of 4 cDNAs was up-regulated by Allitridi treatment and the degree to which each cDNA was up-regulated ranged from 3- to 8-fold (Figure 4). Sequencing and GenBank database searching results showed that two isolated

difference fragments (SH2 and SH3) had remarkable homology over 97% with glia-derived nexin/protease nexin 1 (GDN/PN1) mRNA and hepatitis B virus x-interacting protein (XIP) mRNA respectively. No homology was found in fragment SH1, which indicated SH1 to

be a novel EST. SH4 showed remarkable homology as high as 98% with a piece of human DNA sequence on chromosome 20 and was also showed to be a novel EST. The sequences of SH1 and SH4 were showed in Figure 5.

SH1 (434bp)

```
TAGGCAACTGTGCTATCCGAGGGAGCAACGCCCTTCGTGCGCCACATGACGCATACTACCTGCCACATCTCAC
GCTCGTCCACCGTCGGCGCGCACACACTTGACAGCCCTTGCGGTACATCGCCGTACGACGAGCGGCATCATG
TTTTCCAGCACACCGCGCGCTGACCCGCCCTACCGCCGTGTCGATACCGGCAAGGTGGAGCCATCGCCCTT
GCCCCAGATCAAACGTTTCGGTGCCAGTGGGCATCAGCTTGCGGTGCTTGACCACCAGGCCGCCAGACGGTTTCG
AAATACAGCACGGTGCAATACAGGGTGCTGCCACTGCGCTCGATCACACCCAGGACCAGGCTCGCGCCGGTTTCG
GGCCGACAACCCCGCCAGCGCCTCGGTCTTGGTGCCCGCCTTCCTTGGATAGCACAGTTGCCTA
```

SH4 (400bp)

```
TAGGCAACTGTGCTATCCGAGGGAGATCCTTTTGCCTTAATCTCAGTGCTCGTTACTTTCATGGTCCCAAGATGGCT
GCTGTATCCCAAGAATCATGTCTGCGTTCAAGGAAGGAGGGGTGGAGGAAGAGGAAGGGCCAAACTAGCTGG
ACCCGTACCTTCTATCAGAAAGTAGAACCTCGTCAGAAAGTCTGTTTCTGCTCTCTCCCTCTGCATATCTTCACT
TAGATGCCCTTGGCCCCAGCCAGCTACCATTCACCTCTAGCTGCAAACAAAGCTAAGACAGCAGGGAACAGGA
TTGTCATGGCTGAATAGACCAATCGTGTTCATCTACTGAGACTGGCACACTGCCTCTGCAATAAACTGGGAT
CTCCCTCGGATAGCACAGTTGCCTA
```

Figure 5 Sequences of two novel ESTs (SH1 and SH4) isolated by cDNA RDA based on cDNA libraries.

Northern blots analysis was employed to detect the expression level of another obtained difference product (derived from calyculin mRNA) and a novel transcript about 2 kb in size appeared only in the hybridization result of BGC823 total RNA (Figure 6). Further cDNA library screening and database searching showed this novel transcript to be a recombinant gene merged from calyculin gene and homo sapiens heterogeneous nuclear ribonucleoprotein A0 (HNRPA0) gene.

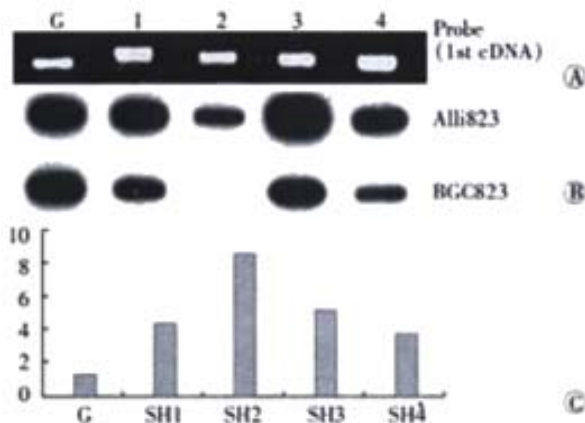


Figure 4 A: Agarose gel electrophoresis of reamplified difference products SH1-4 (lanes 1-4 respectively). PCR product of GAPDH (400bp in size) used as quantity control (lane G). B: Slot blots analysis showing differentially expressed cDNAs. Reverse transcription products (first stranded cDNA) of total RNA of BGC823 and Alli823 cells used as probe respectively. C: The degree to which each cDNA was up-regulated.

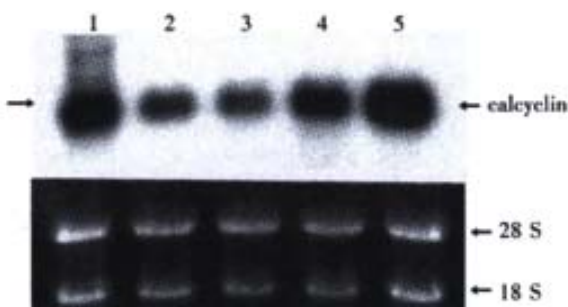


Figure 6 Northern blotting result showing the expression level of calyculin gene in human gastric cancer cell lines BGC823, MGC803, PAMC82, SGC7901 and MKN45 (lanes 1-5) respectively. The arrow showing the novel transcript derived from the recombinant gene merged from calyculin gene and HNRPA0 gene.

DISCUSSION

When cDNA RDA^[1-6] or RDA^[17-19] is performed, sample cDNAs or genome DNAs are digested into fragmented populations to prepare representations, and the digestion products showed as smears by agarose gel electrophoresis. Therefore, it is difficult to determine the most appropriate digestion degree. However, deficient or excessive enzyme digestion of sample DNAs can undoubtedly result in false positive results. In our study, cDNA RDA was performed based on cDNA libraries. Our data showed that time for enzyme digestion affected the digestion degree obviously. With the same copies, three or four fragments released from library vector after enzyme digestion acted as good marks indicating appropriate digestion, which increased the specificity and reproducibility of cDNA RDA. Moreover, when *Bam*H I and *Xho* I were used together to digest library DNAs, the content of cDNA messages available for difference analysis was expanded and more specific products were obtained.

Thrombin, as the principal component of the blood coagulation cascade, also prevents neurite outgrowth and modulates morphologic changes in both neurons and astrocytes^[20-22]. Recent studies have showed that thrombin mediates polynuclear synapse elimination, both *in vivo* and *in vitro*^[23]. Glia-derived nexin/protease nexin 1 (GDN/PN1) is the most potent vertebrate inhibitor for thrombin, which, acting as neurite-promoting factor, plays an important role in neurotrophic and neuroprotective properties^[24-29]. Garlic extract contains antioxidant phytochemicals that prevent the oxidant-mediated brain cell damage and produce neurotrophic effects^[30-33]. Our results showed the potential effect of garlic on reducing the risk of neurodegenerative disease through up-regulation of GDN/PN1 expression.

The hepatitis B virus (HBV) has been reported to be a risk factor in the development of hepatocellular carcinoma^[34-42]. The HBV X protein (HBx) is a small transcriptional activator and has been showed capable of transactivating many different viral and cellular promoters. It is essential for virus infection and is implicated in the development of hepatocellular carcinoma^[43-49]. An HBx-interacting protein that specifically binds to the carboxy terminus of wild-type HBx was identified in 1998 and designated as HBx interacting-protein (XIP), which could inhibit HBx activity and thus decrease HBV replication^[50]. Elevated level of XIP mRNA induced by garlic extract provided valuable molecular evidence for elucidating the garlic's efficacies against inflammatory diseases.

Identification of recombinant gene in our study showed the feasibility of employing cDNA RDA method to the discovery of probes for anonymous loci that suffered genetic rearrangements. Cloning of two novel ESTs further showed cDNA RDA based on cDNA libraries to be a powerful method in isolating novel genes.

REFERENCES

- 1 Yoon DY, Buchler P, Saarikoski ST, Hines OJ, Reber HA, Hankinson O. Identification of genes differentially induced by hypoxia in pancreatic cancer cells. *Biochem Biophys Res Commun* 2001;288:882-886
- 2 Graveel CR, Jatko E, Madore SJ, Holt AL, Farnham PJ. Expression profiling and identification of novel genes in hepatocellular carcinomas. *Oncogene* 2001;20:2704-2712
- 3 Seidita G, Polizzi D, Costanzo G, Costa S, Di Leonardo A. Differential gene expression in P53-mediated G(1) arrest of human fibroblasts after gamma-irradiation or N-phosphoacetyl-L-aspartate treatment. *Carcinogenesis* 2000;21:2203-2210
- 4 Xu W, Wang S, Wang G, Wei H, He F, Yang X. Identification and characterization of differentially expressed genes in the early response phase during liver regeneration. *Biochem Biophys Res Commun* 2000;278:318-325
- 5 Davenport J, Neale GA, Goorha R. Identification of genes potentially involved in LMO2-induced leukemogenesis. *Leukemia* 2000;14:1986-1996
- 6 Yamashita Y, Yokoyama M, Kobayashi E, Takai S, Hino O. Mapping and determination of the cDNA sequence of the Erc gene preferentially expressed in renal cell carcinoma in the Tsc2 gene mutant (Eker) rat model. *Biochem Biophys Res Commun* 2000;275:134-140
- 7 Kim S, Zeller K, Dang CV, Sandgren EP, Lee LA. A strategy to identify differentially expressed genes using representational difference analysis and cDNA arrays. *Anal Biochem* 2001;288:141-148
- 8 Bole-Feysot C, Perret E, Roustan P, Bouchard B, Kelly PA. Analysis of prolactin-modulated gene expression profiles during the Nb2 cell cycle using differential screening techniques. *Genome Biol* 2000;1:RESEARCH0008
- 9 Nakagawa H, Tsuta K, Kiuchi K, Senzaki H, Tanaka K, Hioki K, Tsubura A. Growth inhibitory effects of diallyl disulfide on human breast cancer cell lines. *Carcinogenesis* 2001;22:891-897
- 10 Wu CC, Sheen LY, Chen HW, Tsai SJ, Lii CK. Effects of organosulfur compounds from garlic oil on the antioxidant system in rat liver and red blood cells. *Food Chem Toxicol* 2001;39:563-569
- 11 Gupta N, Porter TD. Garlic and garlic-derived compounds inhibit human squalene monooxygenase. *J Nutr* 2001;131:1662-1667
- 12 Hong YS, Ham YA, Choi JH, Kim J. Effects of allyl sulfur compounds and garlic extract on the expression of Bcl-2, Bax, and P53 in non small cell lung cancer cell lines. *Exp Mol Med* 2000;32:127-134
- 13 Cho BH, Xu S. Effects of allyl mercaptan and various allium-derived compounds on cholesterol synthesis and secretion in Hep-G2 cells. *Comp Biochem Physiol C Toxicol Pharmacol* 2000;126:195-201
- 14 Munday R, Munday CM. Low doses of diallyl disulfide, a compound derived from garlic, increase tissue activities of quinone reductase and glutathione transferase in the gastrointestinal tract of the rat. *Nutr Cancer* 1999;34:42-48
- 15 Li XG, Xie JY, Lu YY. Suppressive action of garlic oil on growth and differentiation of human gastric cancer cell line BGC-823. *Huaren Xiaohua Zazhi* 1998;6:10-12
- 16 Singh SV, Pan SS, Srivastava SK, Xia H, Hu X, Zaren HA, Orchard JL. Differential induction of NAD(P)H:quinone oxidoreductase by anti-carcinogenic organosulfides from garlic. *Biochem Biophys Res Commun* 1998;244:917-920
- 17 Toder R, Grutzner F, Haaf T, Bausch E. Species-specific evolution of repeated DNA sequences in great apes. *Chromosome Res* 2001;9:431-435
- 18 Cummings M, Brown KW. Low frequency of genetic lesions in Wilms tumors by representational difference analysis. *Cancer Genet Cytogenet* 2001;127:155-160
- 19 Endoh D, Cho KO, Tsukamoto K, Morimura T, Kon Y, Hayashi M. Application of representational difference analysis to genomic fragments of Marek's disease virus. *J Clin Microbiol* 2000;38:4310-4314
- 20 Smirnova IV, Citron BA, Arnold PM, Festoff BW. Neuroprotective signal transduction in model motor neurons exposed to thrombin: G-protein modulation effects on neurite outgrowth, Ca(2+) mobilization, and apoptosis. *J Neurobiol* 2001;48:87-100
- 21 Fritsche J, Reber BF, Schindelholz B, Bandtlow CE. Differential cytoskeletal changes during growth cone collapse in response to hSema III and thrombin. *Mol Cell Neurosci* 1999;14:398-418
- 22 Turgeon VL, Houenou LJ. Prevention of thrombin-induced motoneuron degeneration with different neurotrophic factors in highly enriched cultures. *J Neurobiol* 1999;38:571-580
- 23 Kim S, Nelson PG. Transcriptional regulation of the prothrombin gene in muscle. *J Biol Chem* 1998;273:11923-11929
- 24 Hengst U, Albrecht H, Hess D, Monard D. The phosphatidylethanolamine-binding protein is the prototype of a novel family of serine protease inhibitors. *J Biol Chem* 2001;276:535-540
- 25 Docagne F, Nicole O, Marti HH, MacKenzie ET, Buisson A, Vivien D. Transforming growth factor-beta1 as a regulator of the serpins/t-PA axis in cerebral ischemia. *FASEB J* 1999;13:1315-1324
- 26 Mbebi C, Hantai D, Jandrot-Perrus M, Doyennette MA, Verdier-Sahuque M. Protease nexin I expression is up-regulated in human skeletal muscle by injury-related factors. *J Cell Physiol* 1999;179:305-314
- 27 Kariko K, Harris VA, Rangel Y, Duvall ME, Welsh FA. Effect of cortical spreading depression on the levels of mRNA coding for putative neuroprotective proteins in rat brain. *J Cereb Blood Flow Metab* 1998;18:1308-1315
- 28 Kim S, Buonanno A, Nelson PG. Regulation of prothrombin, thrombin receptor, and protease nexin-1 expression during development and after denervation in muscle. *J Neurosci Res* 1998;53:304-311
- 29 Lee P, Spector JG, Derby A, Roufa DG. Effects of thrombin and protease nexin-1 on peripheral nerve regeneration. *Ann Otol Rhinol Laryngol* 1998;107:61-69
- 30 Youdim KA, Joseph JA. A possible emerging role of phytochemicals in improving age-related neurological dysfunctions: a multiplicity of effects. *Free Radic Biol Med* 2001;30:583-594
- 31 Sumi S, Tsuneyoshi T, Matsuo H, Yoshimatsu T. Isolation and characterization of the genes up-regulated in isolated neurons by aged garlic extract (AGE). *J Nutr* 2001;131:1096S-1099S
- 32 Borek K. Antioxidant health effects of aged garlic extract. *J Nutr* 2001;131:1010S-1015S
- 33 Iqbal M, Athar M. Attenuation of iron-nitritotriacetate (Fe-NTA)-mediated renal oxidative stress, toxicity and hyperproliferative response by the prophylactic treatment of rats with garlic oil. *Food Chem Toxicol* 1998;36:485-495
- 34 Wang ZX, Hu GF, Wang HY, Wu MC. Expression of liver cancer associated gene HCCA3. *World J Gastroenterol* 2001;7:821-825
- 35 Tang ZY. Hepatocellular Carcinoma Cause, Treatment and Metastasis. *World J Gastroenterol* 2001;7:445-454
- 36 Rabe C, Pilz T, Klostermann C, Berna M, Schild HH, Sauerbruch T, Caselmann WH. Clinical characteristics and outcome of a cohort of 101 patients with hepatocellular carcinoma. *World J Gastroenterol* 2001;7:208-215
- 37 Arbutnot P, Kew M. Hepatitis B virus and hepatocellular carcinoma. *Int J Exp Pathol* 2001;82:77-100
- 38 Wang Y, Liu H, Zhou Q, Li X. Analysis of point mutation in site 1896 of HBV precore and its detection in the tissues and serum of HCC patients. *World J Gastroenterol* 2000;6:395-397
- 39 Yu MC, Gu CH. Mutation of hepatitis B virus and its association with liver diseases. *Shijie Huaren Xiaohua Zazhi* 1999;7:978-979
- 40 Wang HY, Yan RQ, Long JB, Wu QL. Cyclin D1 amplification is associated with HBV DNA integration and pathology in human hepatocellular carcinoma. *Shijie Huaren Xiaohua Zazhi* 1999;7:98-100
- 41 Tang RX, Gao FG, Zeng LY, Wang YW, Wang YL. Detection of HBV DNA and its existence status in liver tissues and peripheral blood lymphocytes from chronic hepatitis B patients. *World J Gastroenterol* 1999;5:359-361
- 42 Wu GY, Wu CH. Gene therapy and liver diseases. *World J Gastroenterol* 1998;4:18-19
- 43 Kim YC, Song KS, Yoon G, Nam MJ, Ryu WS. Activated ras oncogene collaborates with HBx gene of hepatitis B virus to transform cells by suppressing HBx-mediated apoptosis. *Oncogene* 2001;20:16-23
- 44 Diao J, Khine AA, Sarangi F, Hsu E, Iorio C, Tibbles LA, Woodgett JR, Penninger J, Richardson CD. X protein of hepatitis B virus inhibits Fas-mediated apoptosis and is associated with up-regulation of the SAPK/JNK pathway. *J Biol Chem* 2001;276:8328-8340
- 45 Guo SP, Wang WL, Zhai YQ, Zhao YL. Expression of nuclear factor-κB in hepatocellular carcinoma and its relation with the X protein of hepatitis B virus. *World J Gastroenterol* 2001;7:340-344
- 46 Chen WN, Oon CJ, Leong AL, Koh S, Teng SW. Expression of integrated hepatitis B virus X variants in human hepatocellular carcinomas and its significance. *Biochem Biophys Res Commun* 2000;276:885-892
- 47 Klein NP, Bouchard MJ, Wang LH, Kobarg C, Schneider RJ. Src kinases involved in hepatitis B virus replication. *EMBO J* 1999;18:5019-5027
- 48 Yu DY, Moon HB, Son JK, Jeong S, Yu SL, Yoon H, Han YM, Lee CS, Park JS, Lee CH, Hyun BH, Murakami S, Lee KK. Incidence of hepatocellular carcinoma in transgenic mice expressing the hepatitis B virus X protein. *J Hepatol* 1999;31:123-132
- 49 Lee YH, Yun Y. HBx protein of hepatitis B virus activates Jak1-STAT signaling. *J Biol Chem* 1998;273:25510-25515
- 50 Melegari M, Scaglioni PP, Wands JR. Cloning and characterization of a novel hepatitis B virus x binding protein that inhibits viral replication. *J Virol* 1998;72:1737-1743

Edited by Hu DK

• GASTRIC CANCER •

JTE-522-induced apoptosis in human gastric adenocarcinoma cell line AGS cells by caspase activation accompanying cytochrome C release, membrane translocation of Bax and loss of mitochondrial membrane potential

Hong-Liang Li, Dan-Dan Chen, Xiao-Hong Li, Hai-Wei Zhang, Jun-Hua Lü, Xian-Da Ren, Cun-Chuan Wang

Hong-Liang Li, Xiao-Hong Li, Jun-Hua Lü, Xian-Da Ren, Department of Pharmacology, Jinan University Pharmacy College, Guangzhou 510632, Guangdong Province, China

Dan-Dan Chen, Department of Cardiology, First Affiliated Hospital, Zhongshan University, Guangzhou 510089, Guangdong Province, China
Hai-Wei Zhang, Department of Pathology, Jinan University Medical College, Guangzhou 510632, Guangdong Province, China

Cun-Chuan Wang, Department of laparoscopic surgery, First Affiliated Hospital, Jinan University Medical College, Guangzhou 510632, Guangdong Province, China

Supported by National Natural Science Foundation of China, No. 39770300, 30070873, and the Overseas Chinese Affairs Office of the State Council Foundation, No. 98-33

Correspondence to: Prof. Xian-Da Ren, Department of Pharmacology, Jinan University Pharmacy College, Guangzhou 510632, Guangdong Province, China. tsam@jnu.edu.cn

Telephone: +86-20-8522-0261

Received 2001-11-15 Accepted 2001-12-08

Abstract

AIM: To investigate the role of the mitochondrial pathway in JTE-522-induced apoptosis and to investigate the relationship between cytochrome C release, caspase activity and loss of mitochondrial membrane potential ($\Delta\Psi_m$).

METHODS: Cell culture, cell counting, ELISA assay, TUNEL, flow cytometry, Western blot and fluorometric assay were employed to investigate the effect of JTE-522 on cell proliferation and apoptosis in AGS cells and related molecular mechanism.

RESULTS: JTE-522 inhibited the growth of AGS cells and induced the apoptosis. Caspases 8 and 9 were activated during apoptosis as judged by the appearance of cleavage products from procaspase and the caspase activities to cleave specific fluorogenic substrates. To elucidate whether the activation of caspases 8 and 9 was required for the apoptosis induction, we examined the effect of caspase-specific inhibitors on apoptosis. The results showed that caspase inhibitors significantly inhibited the apoptosis induced by JTE-522. In addition, the membrane translocation of Bax and cytosolic release of cytochrome C accompanying with the decrease of the uptake of Rhodamin 123, were detected at an early stage of apoptosis. Furthermore, Bax translocation, cytochrome C release, and caspase 9 activation were blocked by Z-VAD.fmk and Z-IETD-CHO.

CONCLUSION: The present data indicate a crucial association between activation of caspases 8, 9, cytochrome C release, membrane translocation of Bax, loss of $\Delta\Psi_m$ and JTE-522-induced apoptosis in AGS cells.

Li HL, Chen DD, Li XH, Zhang HW, Lü JH, Ren XD, Wang CC. JTE-522-induced apoptosis in human gastric adenocarcinoma cell line AGS cells by caspase activation accompanying cytochrome C release, membrane translocation of Bax and loss of mitochondrial membrane potential. *World J Gastroenterol* 2002;8(2):217-223

INTRODUCTION

Previous studies have showed that non-steroidal anti-inflammatory drugs (NSAIDs) can induce apoptosis in several cell type, including human colorectal tumor cell lines^[1,2], human breast cancer cells^[3], human lung cancer cells^[4], B cell chronic lymphocytic leukemia cells^[5] and myeloid leukemia cell line^[6]. JTE-522 is a novel NSAIDs, which is a specific inhibitor of cyclooxygenase-2 with significant anti-inflammatory and analgesic properties^[7]. In a previous study, we have demonstrated that JTE-522 induced apoptosis in human gastric adenocarcinoma AGS cells, but the detail mechanism is not clear.

Caspase, a family of cysteine protease, is the common executor of apoptosis induced by various stimuli^[8,9]. Caspase 8 and caspase 9 are recognized as upstream apoptosis initiators, which activate downstream caspases 3, 6 and 7^[10]. The apoptotic action of NSAIDs was inhibited by the caspase inhibitor Z-VAD.fmk, demonstrating the involvement of caspases^[5]. However, the pathway leading to caspase activation remains unknown. Caspases play a central role in the execution of apoptosis. The two most well-studied pathways of caspase activation include the surface death receptor pathway and the mitochondrion-initiated pathway. In the mitochondrion pathway, cytochrome C and other apoptogenic proteins (e.g apoptosis-inducing factor) are released from the intermembrane space to the cytosol^[12]. Once released, cytochrome C binds to apoptotic protease-activating factor-1 (Apaf-1) and induces activation of caspase 9^[12]. Recently, it was shown that bax, a proapoptotic member of bcl-2 family, promoted apoptosis by triggering the release of cytochrome C from mitochondria^[13-18]. In the present study, our aims are to investigate the role of the mitochondrial pathway in JTE-522-induced apoptosis and to investigate the relationship between cytochrome C release, caspase activity and loss of mitochondrial membrane potential ($\Delta\Psi_m$).

MATERIALS AND METHODS

Cell line and reagents

AGS, a gastric adenocarcinoma cell line, was provided by Cancer Institute, Sun-Yet Sen University of Medical Sciences (China). The cells were grown in RPMI-1640 medium and supplemented with 10% fetal calf serum, penicillin G (100kU/L) and kanamycin (0.1g·L⁻¹) at 37°C in a 5% CO₂. Antibodies used in this study were obtained from Santa Cruz. All other chemicals were purchased from Sigma Chemical Co (St. Louis, MO, USA).

Determination of cell proliferation rate

AGS cells (1×10^5) were seeded in 12-well plates and cultured for 24h. The cultures were divided into two groups: the first group (control) was cultured in the RPMI1640 medium, and the second was cultured in the continuous presence of 1mmol/L JTE-522. The cells were then harvested every 24h by trypsinization and cell numbers counted with a hemocytometer. Three cultures were used for experiments at each time point.

Detection of apoptotic DNA fragmentation

AGS cells were grown in 96-well culture plates. The cells were incubated with various doses of JTE-522 for 6h. Apoptotic DNA fragmentation was determined using a commercially obtained enzyme-linked immunosorbent assay (ELISA) kit from Sigma. This assay was based on a quantitative sandwich enzyme-immunoassay directed against cytoplasmic histone-associated DNA fragments. Briefly, the cells were incubated in 200 μ L of lysis buffer provided in the kit, the lysates were centrifuged, and 20 μ L of the supernatant containing cytoplasmic histone-associated DNA fragments were reacted overnight at 4 $^{\circ}$ C in streptavidin-coated microtiter wells with 80 μ L of the immunoreagent mixture containing biotinylated anti-histone antibody and peroxidase-conjugated anti-DNA antibody. After washing, the immunocomplex-bound peroxidase was probed with 2,2'-azino-di[3-ethylbenzthiazoline sulfonate] for spectrophotometric detection at 405nm.

TUNEL

TUNEL assay was performed using the apoptosis detection system. Cells were fixed by 4% paraformaldehyde in PBS overnight at 4 $^{\circ}$ C. The samples were washed three times with PBS and were permeabilized by 0.2% Triton X-100 in PBS for 15min on ice. After washing twice, cells were equilibrated at room temperature for 15 to 30min in equilibration buffer (200mmol/L potassium cacodylate, 0.2mmol/L dithiothreitol, 0.25g \cdot L $^{-1}$ bovine serum albumin, and 2.5mmol/L cobalt chloride in 25mmol/L Tris-HCL, PH 6.6) and then incubated in the presence of 5 μ mol/L fluorescein-12-dUTP, 10 μ mol/L dATP, 100 μ mol/L ethylenediaminetetraacetic acid (EDTA), and terminal deoxynucleotidyl transferase at 37 $^{\circ}$ C for 1.5h in dark. The tailing reaction was terminated by 2 \times standard saline citrate (SSC). The samples were washed three times with PBS and were analyzed by fluorescence microscopy. At least 1000 cells were counted, and the percentage of TUNEL-positive cells was determined.

Ladder detection assay

After induction of apoptosis, cells (5×10^6 /sample, both attached and detached cells) were lysed with 150 μ L hypotonic lysis buffer (10mmol/L EDTA, 0.5% Triton X-100 in 1mmol/L Tris-HCL, Ph7.4) for 15min on ice and were precipitated with 2.5% polyethylene glycol and 1mol/L NaCl for 15min at 4 $^{\circ}$ C. After centrifugation at 16000g for 10min at room temperature, the supernatant was incubated in the presence of proteinase K (0.3g \cdot L $^{-1}$) at 37 $^{\circ}$ C for one hour and precipitated with isopropanol at -20 $^{\circ}$ C. After centrifugation, each pellet was dissolved in 10 μ L of Tris-EDTA (pH 7.6) and electrophoresed on a 1.5% agarose gel containing ethidium bromide. Ladder formation of oligonucleosomal DNA was detected under ultraviolet light.

Cytosolic release of cytochrome C and membrane translocation of Bax

The analysis was performed according to the method of Euguchi *et al* [19], with minor modifications. Briefly, cells were collected and suspended in mitochondria isolation buffer [20mmol/L Hepes-KOH, PH 7.5; 210mmol/L sucrose; 70mmol/L mannitol; 1mmol/L

EDTA; 1mmol/L dithiothreitol (DTT); 1.5mmol/L MgCl $_2$, 10 mmol/L KCl; and protease inhibitor cocktail supplemented with 10 μ mol/L digitonin]. The suspensions were incubated at 37 $^{\circ}$ C for 5min and centrifuged at 15000g for 15min. The supernatants and pellets were collected for Western blotting according to the method described by Tsuchida *et al* [20].

Caspase activity assay

Activities of caspase 8 and caspase 9 were determined by using a fluorometric assay kit according to the method described by Gao *et al* [20]. Briefly, 5×10^5 cells were collected and lysed in 50 μ L lysis buffer and incubated with fluorochromic caspase substrate, Ile-Glu-Thr-Asp-7-amino-4-trifluoromethylcoumarin (IETD-AFC) and Leu-Glu-His-Asp-7-amino-4-trifluoromethylcoumarin (LEHD-AFC) for caspase 8 and caspase 9, respectively. After incubation at 37.5 $^{\circ}$ C for 1h, the fluorescence was measured by a spectrofluorophotometer with excitation at 400nm and emission at 550nm.

Mitochondrial membrane potential analysis

Rhodamine 123, a cationic fluorescent dye whose mitochondria fluorescence intensity decreased quantitatively in response to dissipation of $\Delta\Psi_m$, was used to evaluate perturbations in $\Delta\Psi_m$. Cells were incubated with 5 μ mol/L rhodamine 123 for 30min, and then were collected, washed, and stained with 10 μ mol/L PI. The uptake of rhodamine 123 was measured by flow cytometry.

Statistics analysis

The data shown were mean value of at least three different experiments and expressed as mean \pm SD. Student's test was used to compare data. A *P* value of less than 0.05 was considered as statistically significant.

RESULTS

Effect of JTE-522 on cell proliferation and apoptosis in AGS cells

In order to understand the potential role of JTE-522 in the induction of apoptosis and its possible contribution to AGS cell loss in human gastric adenocarcinoma, the inhibitory effect of JTE-522 on cell proliferation was studied in AGS cells. As shown in Figure 1.

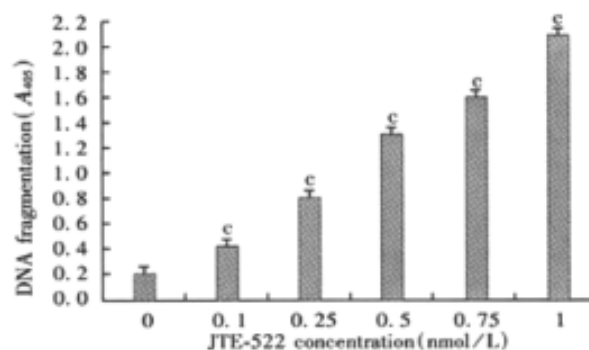


Figure 1 Effect of JTE-522 on AGS cell proliferation. Cells were incubated in the absence or presence of 1mmol/L JTE-522 and cell numbers determined at the time replicates at each time point (**P*<0.01).

The cells were cultured in the presence or absence of JTE-522 and cell numbers determined over three days. AGS cell proliferation was markedly inhibited by 1 mmol/L JTE-522. In the absence of JTE-522, the number of control cells doubled approximately every 24h in RPMI1640 medium supplemented with 10% fetal calf serum. The effect of JTE-522 at concentrations from 0.1mmol/L to 1mmol/L on DNA fragmentation in AGS cells was shown in Figure 2.

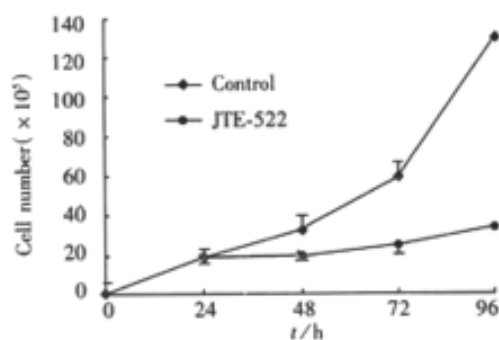


Figure 2 Effect of JTE-522 on DNA fragmentation in AGS cells. Cytoplasmic histone-associated DNA fragments were determined using a commercial ELISA kit. Results were representative of four independent determinations.

JTE-522 was found to significantly induce DNA fragmentation after the onset of incubation and this effect was in a dose-dependent manner. The same results were obtained by TUNEL assay. The number of TUNEL-positive cells was dramatically increased after treatment with JTE-522 for 48h, that is, the percentage of TUNEL-positive cells increased from $19.3 \pm 1.7\%$ to $59.8 \pm 2.6\%$ (Figure 3).

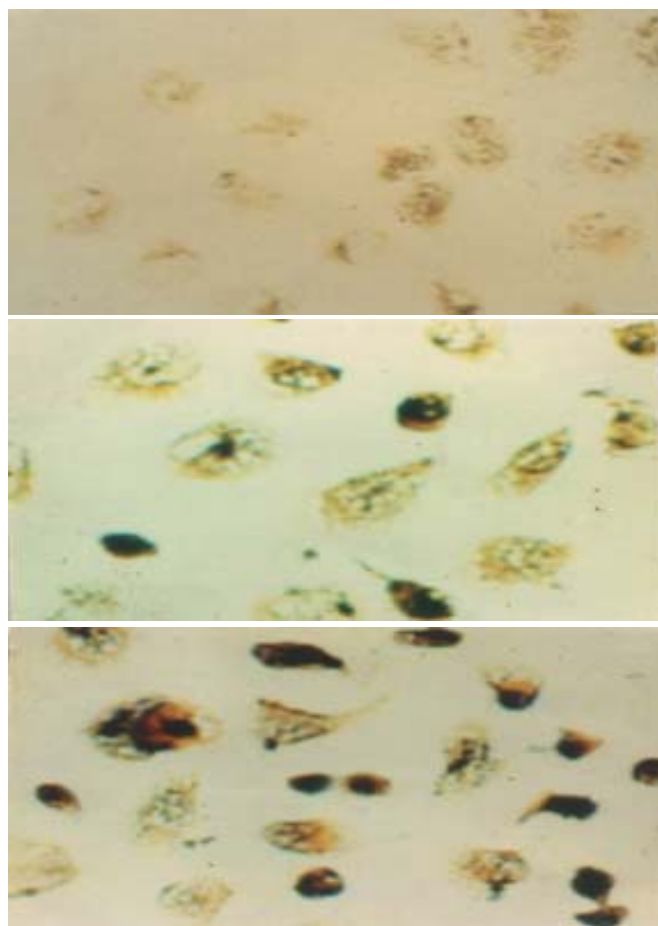


Figure 3 TUNEL assay demonstrating marked morphological changes in AGS cells after treatment with different concentrations of JTE-522. A: control; B: 0.1mmol/L JTE-522; C: 1mmol/L JTE-522

Effect of JTE-522 on caspases 8, 9 in AGS cells

In order to demonstrate the role of caspase 8 and caspase 9 in JTE-522-induced apoptosis, we examined the activities of caspase 8 and caspase 9 after treatment with JTE-522 for indicated time. The results showed that caspase 8 activity increased at 9h after JTE-522 treatment in AGS cells (Figure 4A), and the activity of caspase 9 also increased. To further confirm the activation of these two caspases, we

conducted Western blot analysis (Figure 4B). The results showed that both caspases were activated, as judged by the decrease of the procaspases and the increase of their cleavage products. These experiments clearly showed that caspase 8 and caspase 9 played an important role during apoptosis induced by JTE-522. To investigate whether the activation of caspases 8 and 9 was required for the apoptosis induction, we examined the effect of caspase-specific inhibitors on apoptosis. The results showed extensive DNA fragmentation after treatment with JTE-522, while the treatment of Z-VAD.fmk, Ac-IETD-CHO or Ac-LEHD-CHO significantly blocked it (Figure 4C). These results suggested that both caspase 8 and caspase 9-like activity was required for JTE-522 apoptosis during the apoptotic process.

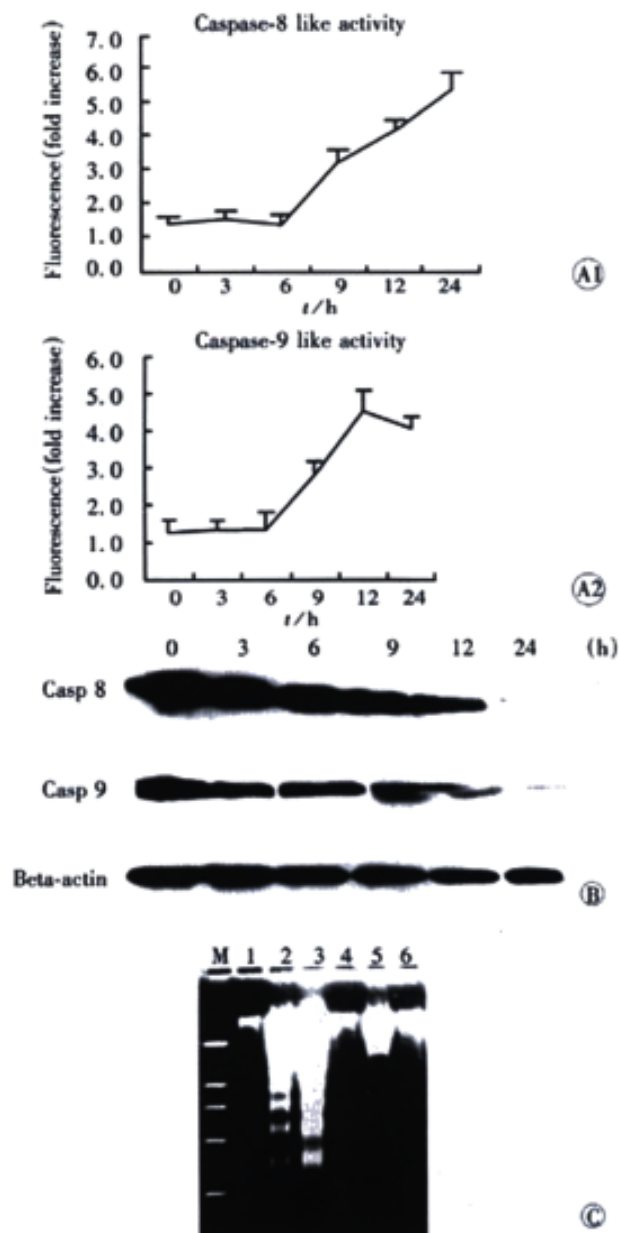


Figure 4 The role of procaspase 8 and procaspase 9 in JTE-522 induced apoptosis for indicated time. 4A: Effect of JTE-522 on caspase activities for indicated time. Data presented are the mean value of three separate experiments. 4B: Western blot shows the cleavage of procaspase 8 (Casp 8) and procaspase 9 (Casp 9). AGS cells were treated with JTE-522 for the indicated times. 4C: Effect of caspase inhibitor on JTE-522 induced DNA fragmentation. AGS cells were treated with: 1: control; 2: 1mmol/L JTE-522; 3: 0.5mmol/L JTE-522; 4: 50μmol/L Z-VAD.fmk+1mmol/L JTE-522; 5: 50μmol/L Ac-IETD-CHO +1mmol/L JTE-522; 6: 50μmol/L Ac-LEHD-CHO+1mmol/L JTE-522 for 24h.

Effect of JTE-522 on cytosolic release of cytochrome C and membrane translocation of bax

Cytochrome C, which is released from mitochondria, has recently been identified as a key factor that could activate caspase in a cell-free system^[19]. In fact, it has been reported that levels of cytosolic cytochrome C were increased in response to various apoptotic stimuli such as staurosporine, P53, etoposide, and ultraviolet-B irradiation^[20-22]. We therefore performed Western blotting to examine the distribution of cytochrome C in cytosol and membrane fractions before and after apoptosis induction. AGS cells were treated with JTE-522 for 24h, and the cells treated with 0.1 μ mol/L staurosporine for 24h were used as a positive control. After treatment, the cells were collected and suspended in the mitochondrial isolation buffer containing digitonin. Treatment with digitonin made small pores on cell membranes that allow the releases of cytosolic cytochrome C to the buffer fraction^[19]. The supernatant and the pellet that represented cytosol and membrane fractions, respectively, were collected separately and subjected to Western blot analysis (Figure 5A). The result showed that cytochrome C in membrane fractions decreased significantly in both staurosporine and JTE-522 treated cells, while in cytosol fractions, high levels of cytochrome C were detected in both treated cells but not in control cells. On the contrary, bax protein increased in membrane fractions and decreased in cytosol fractions after treatment with staurosporine or JTE-522. Bcl-2 protein, as well as cytochrome C oxidase subunit IV (cyto oxi, as a control for mitochondrial protein loading), which were located in mitochondria and not released to cytosol. This result indicated that the cytosolic release of cytochrome C was specially triggered by apoptotic stimuli, but not due to the experimental manipulation.

There was a growing evidence for two pathways of cytochrome C release from mitochondria during apoptosis: rupture of the outer membrane following swelling, or through a specific pore in the outer membrane^[23]. In liposomes and yeast Bax and Bak interacted with voltage-dependent anion channel (VDAC) to cause selective cytochrome C release^[21]. Addition of recombinant Bax to isolated mitochondria induced cytochrome C loss without swelling. However, others had shown that Bax did induce the permeability transition in isolated mitochondria and within cells^[24]. Therefore, we questioned whether the cytosolic release of cytochrome C and membrane translocation of Bax in JTE-522-induced apoptosis were caspase-dependent or not. The cells were pretreated with Z-VAD.fmk at 50 μ mol/L for 1h before treatment with staurosporine or JTE-522. Levels of cytochrome C and Bax in cytosol were examined by Western blotting (Figure 5C). The results showed that the increase of cytochrome C and the decrease of Bax in cytosol induced by staurosporine or JTE-522 were blocked by Z-VAD.fmk. The cleavage of procaspase 3 and 8 was also blocked. These results indicated that the Bax translocation and cytochrome C release were dependent on the activation of caspases.

Since it has been well documented that caspase-8 was the first caspase activated in Fas-, P53-, TRAIL- and TNF-induced apoptosis^[20, 25, 26], we sought to determine whether caspase-8 activation occurs prior to, as in Fas-, P53- and TNF-induced apoptosis or after caspase-9, caspase 3 activation and cytochrome C release, and examined the effects of Ac-IETD-CHO on cytochrome C release and caspase 9 activation. The results showed that Ac-IETD-CHO effectively blocked cytochrome C release and the processing of caspase 8. The caspase 9-like activity was also blocked by both Z-VAD.fmk and Ac-IETD-CHO (Figure 5D). This result suggested that caspase 8-like caspase might work as an initiation caspase that triggered the release of cytochrome C and caspase 9 activation in this system.

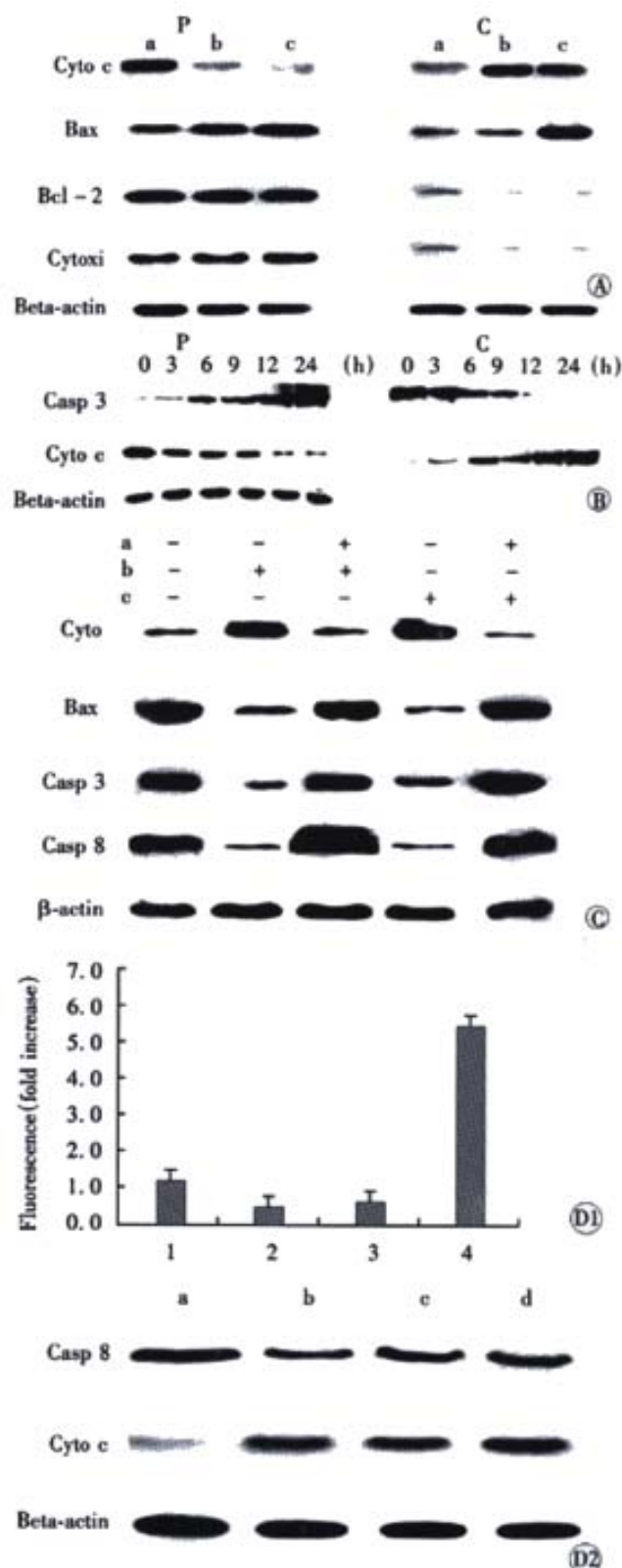


Figure 5 Effect of JTE522 on the activation of caspase, cytochrome C release and membrane translocation of Bax. Figure 5A: AGS cells were treated with: RPMI 1640 medium for control (a) or 0.1 μ mol/L staurosporine (b) or 1mmol/L JTE-522(c). After 24h, the cells were collected and suspended in mitochondria isolation buffer. Cytosol (C) and pellet (P) fractions were separated and subjected to Western blotting as described in Materials and Methods. Cytochrome C (cyto c), cytochrome C oxidase subunit IV (Cyt oxi); Figure 5B: Effect of JTE522 on the changes of cytosolic cytochrome C release and procaspase 3 (casp-3); Figure 5C: Effect of caspase inhibitors on cytochrome C release and translocation of Bax. AGS cells were treated with 50

$\mu\text{mol/L}$ Z-VAD.fmk (a) for 1h or $0.1\mu\text{mol/L}$ staurosporine(b) or 1mmol/L JTE-522(c) or without any treatment. The cytosol was prepared as in (A) and analyzed by Western blotting with indicated antibodies, Casp 3 (procaspase 3), Casp 8 (procaspase 8); Figure 5D: AGS cells were cultured at RPMI 1640 medium or treated with caspase inhibitors: Figure 5D1: Effect of caspase inhibitor on the activity of caspase 9: 1: control; 2: Z-VAD.fmk+ 1mmol/L JTE-522; 3: Ac-IETD-CHO+ 1mmol/L JTE-522; 4: 1mmol/L JTE-522 for 24h; Figure 5D2: Effect of caspase inhibitor on caspase 8 cleavage, cytochrome c release: 1: control(a); 2: Z-VAD.fmk+ 1mmol/L JTE-522 (b); 3: Ac-IETD-CHO+ 1mmol/L JTE-522(c); 4: Ac-LEHD-CHO + 1mmol/L JTE-522(d). Cells were collected and analyzed for caspase 8 cleavage, cytochrome C release, or caspase-like activity as described in Materials and Methods.

Effect of JTE-522 and Z-VAD.fmk on mitochondrial membrane potential

It had been described that cytochrome C release could be induced by mitochondrial permeability transition (PT) characterized by loss of $\Delta\Psi\text{m}$ ^[27]. As salicylates induced mitochondrial PT and loss of $\Delta\Psi\text{m}$ in isolated mitochondria and hepatocytes, we analyzed the effect of JTE-522 on $\Delta\Psi\text{m}$ in AGS cells using rhodamin 123 dye. As shown in Figure 6, JTE-522 had no significant effect on $\Delta\Psi\text{m}$ at 3h and decrease the uptake of rhodamin 123 at 6h, 9h and 12h, earlier than mitochondrial cytochrome C release and caspases 8 and 9 processing. In addition, Z-VAD.fmk blocked loss of $\Delta\Psi\text{m}$ induced by JTE-522 at 9h and had a marked inhibitory effect at 12h, indicating that loss of $\Delta\Psi\text{m}$ was caspase-dependent and this loss was in a time-dependent manner.

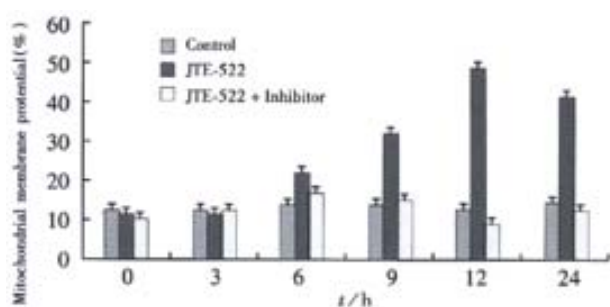


Figure 6 Time-lapsed changes of mitochondrial $\Delta\Psi\text{m}$ in AGS cells under the treatment of JTE-522. The data were the means of three experiment \pm SD

DISCUSSION

NSAIDs have another interesting effect which is seemingly unrelated to their anti-inflammatory action. Administration of some NSAIDs to patients and animals suffering from colonic polyps and colon cancer causes regression of the aberrant growth, while epidemiological studies have shown that long-term consumption of NSAIDs, greatly reduces the risk of developing colon cancer and gastric adenocarcinoma^[28-33]. However, the mechanism remains unclear. Many studies showed that apoptosis was likely to play an extremely important part in the pathogenesis of NSAIDs-induced ulcerogenesis, and also likely to be involved in regression of colon cancer and other neoplasms^[34]. The mechanism underlying the inducing of apoptosis by JTE-522 and other NSAIDs is unknown and currently under research. So far, several pathways have been implicated inducing cyclooxygenase inhibition^[32-35], arrest of cell cycle^[36] and nuclear factor- κB inhibition^[37,38]. Although several groups have demonstrated the involvement of caspases^[5], the pathways leading to caspase activation remain unknown. In this study, we observed for the first time the caspase-dependent membrane translocation of Bax and cytosolic release of cytochrome C and the loss of $\Delta\Psi\text{m}$ in JTE-522-induced apoptosis. These results indicate that mitochondria play an important role in JTE-522-induced apoptosis.

A number of pro- and anti-apoptotic members of the Bcl-2 protein family regulate the release of cytochrome C and apoptosis inducing factor (AIF) from the mitochondrial intermembrane space into the cytosol^[39-43]. Cytochrome C then interacts with pro-caspase 9 and Apaf-1 to activate caspase 9 and thus switch on caspase 3, 6 and 7, leading to apoptosis. The cytosolic release of cytochrome C has been reported in apoptosis induced by various stimuli, including NSAIDs^[43]. In this study, we observed the cytosolic release of cytochrome C, as well as the activation of caspase 9. In contrast to the caspase-independent release of cytochrome C in Raji cells induced by aspirin^[44] the release of cytochrome C was almost completely blocked by caspase inhibitor in our system, suggesting that different mechanisms are involved in cytochrome C release in these two systems.

Disruption of mitochondrial function is a critical event in the apoptotic process leading to the elimination of cells treated with chemotherapeutic agents. Opening of the mitochondrial megachannel has been implicated as a key event in the disruption of mitochondrial membrane integrity during apoptosis. Many intrinsic factors can induce opening if the megachannel including members of the Bcl-2/Bax family, cellular redox status, and cytosolic Ca^{2+} levels^[45]. Disruption of mitochondrial membrane integrity involves the loss of metabolic functions and release of proteins from the mitochondrial intermembrane space into the cytosol. Cytochrome C and AIF represent two such proteins, which are released into the cytosol, and promote caspase and/or nuclease activation. However, there are considerable uncertainties about how cytochrome C and AIF are released from mitochondria and about the events leading up to their appearance in the cytosol. One of them is that the pro-apoptotic proteins Bax and Bak that accelerate opening of the voltage-dependent anion channel (VDAC) in the outer membrane and thereby specifically release cytochrome C^[46,47]. Bax is a proapoptotic member of Bcl-2 family proteins, which can form channels in synthetic membrane^[48-50] and induce cytochrome C release from isolated mitochondria^[51]. However, the mechanism by which Bax stimulates cytochrome C release is unclear. Bax contains the hydrophobic membrane-anchoring domain at its C-terminus, but the membrane-anchoring potential is repressed by its N-terminal domain, allowing Bax to distribute typically in cytosol^[52]. Upon apoptotic stimulation, Bax inserts into mitochondria membrane, where it exerts its function^[53,54]. The overexpression^[55], enforced dimerization^[56], and Bid-induced conformation change^[57] trigger the redistribution of Bax. In this study, we observed JTE-522-induced membrane translocation of Bax and this translocation was not associated with the increase of Bax protein level, but dependent on caspase activity. Caspase 8 has been shown to cleave Bid and the cleaved Bid is reported to be more efficient for triggering the oligomerization and insertion of Bax into mitochondria membrane. In agreement with these observations, we detected caspase 8 activation by cleavage activity of a caspase 8-specific fluorogenic substrate, as well as cleavage of caspase 8 in our system. In addition, the caspase 8-preferential inhibitor effectively blocked cytochrome C release and caspase 9 activation, suggesting caspase 8 to be an upstream caspase.

The most informative measure of the changes associated with cytochrome C release is the mitochondrial membrane potential. However, such measurement in apoptotic cells has produced conflicting results, with reports of no decrease in potential until after cytochrome C release, a decrease in membrane potential associated with cytochrome C release^[50], and an initial increase in potential followed by cytochrome C release without loss of membrane potential^[58]. These measurements rely on the uptake of fluorescent dyes, which gives a qualitative indication of the membrane potential. In this study, our results indicate that JTE-522-induced decrease in $\Delta\Psi\text{m}$ precedes the release cytochrome C at an early phase of apoptosis. This result is different from the report that aspirin induced cytochrome c release precedes the decrease of $\Delta\Psi\text{m}$ in Raji cells. This

discrepancy might reflect that multiple pathways mediated NSAIDs-induced apoptosis depending on experimental systems.

In summary, The present data indicate a crucial association between activation of caspases 8 and 9, cytochrome C release, membrane translocation of Bax, loss of mitochondrial membrane potential and JTE-522-induced apoptosis in AGS cells.

ACKNOWLEDGEMENTS

We gratefully acknowledge Prof Geng-Tao Lui, Institute of Material Medica, Chinese Academy of Medical Sciences for the many helpful discussion and suggestions relating to this work; Special thanks to Chris Simmet and Pasricha Jerriment for proofreading the manuscript and for useful suggestions; Dr Cheng Wei He for technical advice and helpful discussion; Dr Gang Fei Peng for FCM; Dr Wang Tao for Western blot; Dr Guo Qing Xie and Mr Hai Nan Wang for photo processing.

REFERENCES

- Qiao L, Shiff SJ, Rigas B. Sulindac sulfide alters the expression of cyclin proteins in HT-29 colon adenocarcinoma cells. *Int J Cancer* 1998;76:99-104
- Shiff SJ, Koutsos MI, Qiao L. NSAIDs inhibits the proliferation of colon adenocarcinoma cells: effects on cell cycle and apoptosis. *Exp Cell Res* 1996; 222: 179-188
- Robertson FM, Parrett ML, Joarder FS, Ross M, Harris RE. Ibuprofen-induced inhibition of cyclooxygenase isoform gene expression and regression of rat mammary carcinomas. *Cancer Lett* 1998; 122: 165-175
- Duffy CP, Elliott RA, Heenan MM, Coyle S, Cleary IM, Clynes M. Enhancement of chemotherapeutic drug toxicity to human tumor cells *in vitro* by a subset of non-steroidal anti-inflammatory drugs. *Eur J Cancer* 1998; 34: 1250-1259
- Bellosillo B, Colomer D, Montserrat E, Pons G, Gil J. Aspirin and salicylate induce apoptosis and activation of caspases. *Blood* 1998; 92: 1406-1414
- Zhang GS, Tu CQ, Zhang GY, Zhou GB, Zheng WL. Indomethacin induces apoptosis and inhibits proliferation in chronic myeloid leukemia cells. *Leukemia Res* 2000; 24: 385-392
- Tomozawa S, Nagawa H, Tsuno N. Inhibition of haematogenous metastasis of colon cancer in mice by a selective COX-2 inhibitor, JTE-522. *Br J Cancer* 1999; 81: 1274-1279
- Cohen GM. Caspases: the executioners of apoptosis. *Biochem J* 1997; 326: 1-6
- Kumar S, Lavin MF. The ICE family of cysteine proteases as effectors of cell death. *Cell Death Differ* 1996; 3: 255-267
- Salvesen GS, Dixit VM. Caspases: intracellular signaling by proteolysis. *Cell* 1997; 91: 443-446
- Luo X, Budihardjo L, Zou H, Slaughter C, Wang X. Bid, a Bcl-2 interacting protein, mediates cytochrome C release from mitochondria in response to activation of cell surface death receptors. *Cell* 1998; 94: 481-490
- Li P, Nijhawan D, Budihardjo I, Srinivasula SM, Ahmad M, Alnemri ES, Wang X. Cytochrome C and dATP-dependent formation of Apaf-1/caspase-9 complex initiates an apoptotic protease cascade. *Cell* 1999; 91: 479-489
- Shimizu S, Narita M, Tsujimoto Y. Bcl-2 family proteins regulate the release of apoptogenic cytochrome C by the mitochondrial channel VDAC. *Nature* 1999; 399: 483-485
- Antonsson B, Montessuit S, Lauper S. Bax oligomerization is required for channel-forming activity in liposomes and to trigger cytochrome C release from mitochondria. *Biochem J* 2000;345: 271-278
- Goping IS, Gross A, Lavoie JN, Nguyen M, Shore GC. Regulated targeting of bax to mitochondria. *J Cell Biol* 1998; 143: 207-215
- Hsu YT, Wolter KG, Youle RJ. Cytosol-to-membrane redistribution of Bax and Bcl-XL during apoptosis. *Proc Natl Acad Sci USA* 1997; 94: 3668-3672
- Li HL, Zhang HW, Ren XD. Synergism between heparin and adriamycin on cell proliferation and apoptosis in human nasopharyngeal carcinoma CNE2 cells. *Acta Pharmacol sin* 2002;23:167-172
- Li HL, Ye KH, Ren XD. Heparin induced apoptosis in human nasopharyngeal carcinoma CNE2 cells. *Cell Research* 2001;11:311-315
- Eguchi Y, Srinivasan A, Tomaselli KJ, Shimizu S, Tsujimoto Y. ATP-dependent steps in apoptosis signal transduction. *Cancer Res* 1997; 59: 2174-2181
- Gao CF, Ren S, Zhang LL, Ichinose S, Tsuchida N. Caspase-dependent cytosolic release of cytochrome C and membrane translocation of Bax in P53-induced apoptosis. *Exp Cell Res* 2001; 265: 145-151
- Akihiro I, Uehara T, Tokumitsu A, Okuma Y, Nomura Y. Possible involvement of cytochrome C release and sequential activation of caspases in ceramide-induced apoptosis in SK-N-MC cells. *Biochim Biophys Acta* 1999; 1452: 263-274
- Ferrer I, Lopez E. Staurosporine- and H-7-induced cell death in SH-SY5Y neuroblastoma cells is associated with caspase-2 and caspase-3 activation, but not with activation of the FAS/FAS-caspase-8 signaling pathway. *Mol Brain Res* 2000; 85: 61-67
- Scarlett JL, Sheard PW, Hughes G, Ledgerwood EC, Ku HH, Murphy MP. Changes in mitochondrial membrane potential during staurosporine-induced apoptosis in Jurkat cells. *FEBS Lett* 2000; 475: 267-272
- Zamzani N, Susin SA, Marchetti P. Mitochondrial control of nuclear apoptosis. *J Exp Med* 1996; 183: 1533-1544
- Zhang JG, Cohen GM. Release of mitochondrial cytochrome C is upstream of caspase activation in chemical-induced apoptosis in human monocytic tumor cells. *Toxicol Lett* 1998; 102-103: 121-129
- Murphy KM, Streips UN, Lock RB. Bax membrane insertion during Fas (CD95)-induced apoptosis precedes cytochrome C release and is inhibited by Bcl-2. *Oncogene* 1999; 18: 5991-5999
- Petit PX, Susin SA, Zamzani N. Mitochondrial and programmed cell death: back to the future. *FEBS Lett* 1996; 396: 7-9
- Thun MJ. Aspirin and gastrointestinal cancer. *Adv Exp Med Bio* 1997; 400A: 395-402
- Waston AJM. Review article: manipulation of cell death-the development of novel strategies for the treatment of gastrointestinal disease. *Aliment Pharmacol* 1995; 9: 215-226
- Smith ML, Havvcraft G, Hull MA. The effect of non-steroidal anti-inflammatory drugs on human colorectal cancer cells: evidence of different mechanisms of action. *Eur J Cancer* 2000; 36: 664-674
- Zhu GH, Ching CK, Lai KC, Lam SK. Differential apoptosis by indomethacin in gastric epithelial cell through the constitutive expression of wild-type P53 and/or up-regulation of c-myc. *Biochem Pharmacol* 1999; 58: 193-200
- Sheng M, Dinchuk JE, Kargman SL. Suppression of intestinal polyposis in Apc716 knockout mice by inhibition of COX-2. *Cell* 1996; 87: 803-809
- Wu YL, Sun B, Zhang XJ, Wang SN, He HY, Qiao MM, Zhong J, Xu JY. Growth inhibition and apoptosis induction of Sulindac on human gastric cancer cells. *World J Gastroenterol* 2001;7:796-800
- Huang S, Li JY, Wu J, Meng L, Shou CC. Mycoplasma infections and different human carcinomas. *World J Gastroenterol* 2001;7:266-269
- Sheng GG, Shao J, Sheng H. A selective COX-2 inhibitor suppresses cells. *Gastroenterology* 1997; 113: 1883-1897
- Antonsson B, Conti F, Ciavatta A, Montessuit SL, Sano H, Kawahito Y, Wilder R. Expression of COX-1 and COX-2 in human colorectal cancer. *Cancer Res* 1995; 55: 3785-3789
- Qiao L, Shiff SJ, Rigas B. Sulindac sulfide inhibits the proliferation of colon cancer cells: diminished expression of the proliferation markers PCNA and ki-67. *Cancer Lett* 1997; 115: 229-234
- Kipp E, Ghosh S. Inhibition of NF-kB by sodium salicylate and aspirin. *Science* 1994; 265: 956-959
- Giardina C, Boulares H, Inan MS. NSAIDs and butyrate sensitize a human colorectal cancer cell line to TNF and Fas ligation: the role of reactive oxygen species. *Biochim Biophys Acta* 1999; 1448: 425-438
- Scarlett JL, Sheard PW, Hughes G, Murphy MP. Changes in mitochondrial membrane potential during staurosporine-induced apoptosis in Jurkat cells. *FEBS Lett* 2000; 475: 267-272
- Xu CT, Huang LT, Pan BK. Current gene therapy for stomach carcinoma. *World J Gastroenterol* 2001;7:752-759
- Kroemer G, Reed JC. Mitochondrial control of cell death. *Nature Med* 2000; 6: 513-519
- Shen ZY, Shen J, Li QS, Chen CY, Chen JY, Zeng Y. Morphological and functional changes of mitochondria in apoptosis esophageal carcinoma cells induced by arsenic trioxide. *World J Gastroenterol* 2002;8:31-35
- Du C, Fang M, Li Y, Wang X, Smac A. Mitochondrial protein that promotes cytochrome C dependent caspase activation by eliminating IAP inhibition. *Cell* 2000; 102: 43-53
- Pique M, Pons G, Gil J. Aspirin induce apoptosis through mitochondrial cytochrome C release. *FEBS Lett* 2000; 480: 193-196
- Zhivotovsky B, Orrenius S, Brustugun OT. Injected cytochrome C release in apoptosis. *Nature* 1998; 391: 449-457
- Bossy-Wetzel E, Newmeyer DD, Green DR. Mitochondrial cytochrome C release in apoptosis occurs upstream of the DEVD-specific caspase activation and independently of mitochondrial transmembrane depolarization. *EMBO J* 1998; 17: 37-45
- Yang J, Liu X, Bhalla K, Kim CN, Ibrado AM, Cai J, Peng T, Jones DP, Wang X. Prevention of apoptosis by Bcl-2: release of cytochrome C from mitochondria blocked. *Nature* 1997; 275: 1129-1132
- Adachi S, Cross AR, Babior BM, Gottlieb RA. Bcl-2 and the outer mitochondrial membrane in the inactivation of cytochrome C during Fas-mediated apoptosis. *J Biol Chem* 1997; 272: 21878-21882
- Ewis S, Martinou I, Bernasconi L, Bernard A, Mermod J, Maazzei G,

- Maundrell K, Gambale F, Sadoul R, Martinou J. Inhibition of Bax channel-forming activity by Bcl-2. *Science* 1997; 272: 370-372
- 51 Jurgensmier JM, Xie Z, Deveraux Q, Ellerby L, Bredesen D, Reed JC. Bax directly induces release of cytochrome C from isolated mitochondria. *Proc Natl Acad Sci USA* 1997; 95: 4997-5002
- 52 Goping I, Gross A, Lavoie JN, Nguyen M, Jemmeeerson R, Roth K, Korsmeyer SJ, Hore GC. Regulated targeting of BAX to mitochondria. *J Biol Chem* 1998; 143: 207-215
- 53 Wolter KG, Hsue YT, Smith CL, Nechushtan AX. Movement of Bax from the cytosol to mitochondria during apoptosis. *J Cell Biol* 1997; 139: 1281-1292
- 54 Bruel A, Karenty E, Schmid M, McDonnell TJ, Lanotte M. Altered sensitivity to retinoid-induced apoptosis associated with changes in the subcellular distribution of Bcl-2. *Exp Cell Res* 1997; 223: 281-287
- 55 Rosse T, Oliver R, Monney L, Rager M, Conus S, Fellay I, Jansen B, Broner C. Bcl-2 prolongs cell survival after Bax-induced release of cytochrome C. *Nature* 1998; 391: 496-499
- 56 Gross A, Jockel J, Wei MC, Korsmeyer SJ. Enforced dimerization of BAX results in its translocation, mitochondria dysfunction and apoptosis. *EMBO J* 1998; 17: 3878-3885
- 57 Desagher S, OsenSand A, Nichols A, Eskes R, Montessuit S, Lauper S, Maundrell K, Antonsson B, Martinou JC. Bid-induced conformational cytochrome C release during apoptosis. *J Cell Biol* 1999; 144: 891-901
- 58 Eskes R, Desaggher S, Antonsson B, Martinou JC. Bid induced the oligomerization and insertion of Bax into the outer mitochondrial membrane. *Mol Cell Biol* 2000; 20: 929-935
- 59 Green DR, Reed JC. Mitochondria and apoptosis. *Science* 1998; 281: 1309-1312

Edited by Zhang JZ

• GASTRIC CANCER •

Effect of *cis*-9,*trans*-11-conjugated linoleic acid on cell cycle of gastric adenocarcinoma cell line (SGC-7901)

Jia-Ren Liu, Bai-Xiang Li, Bing-Qing Chen, Xiao-Hui Han, Ying-Ben Xue, Yan-Mei Yang, Yu-Mei Zheng, Rui-Hai Liu

Jia-Ren Liu, Bai-Xiang Li, Bing-Qing Chen, Ying-ben Xue, Yan-Mei Yang, Yu-Mei Zheng, Department of Toxicological Health, Public Health College, Harbin Medical University, Harbin 150001, Heilongjiang Province, China

Xiao-Hui Han, ICU of Cardiological Surgery, The Second Hospital, Harbin Medical University, Harbin 150001, Heilongjiang Province, China

Rui-Hai Liu, Food Science and Toxicology, Department of Food Science, Cornell University, Ithaca, NY 14853-7201, USA

Supported by the National Natural Science Foundation of China, No. 39870661

Correspondence to: Dr. Jia-ren Liu, 199 Dongdazhi Street, Nangang District, Harbin 150001, Heilongjiang Province, China. jiaarenliu@yahoo.com

Telephone: +86-451-3639459 Fax: +86-451-3641253

Received 2001-08-23 Accepted 2001-09-05

Abstract

AIM: To determine the effect of *cis*-9,*trans*-11-conjugated linoleic acid (*c9,t11*-CLA) on the cell cycle of gastric cancer cells (SGC-7901) and its possible mechanism in inhibition cancer growth.

METHODS: Using cell culture and immunocytochemical techniques, we examined the cell growth, DNA synthesis, expression of PCNA, cyclin A, B₁, D₁, p16^{ink4a} and p21^{cip/waf1} of SGC-7901 cells which were treated with various *c9,t11*-CLA concentrations (25, 50, 100 and 200 μmol·L⁻¹) of *c9,t11*-CLA for 24 and 48h, with a negative control (0.1% ethane).

RESULTS: The cell growth and DNA synthesis of SGC-7901 cells were inhibited by *c9,t11*-CLA. SGC-7901 cells. Eight day after treatment with various concentrations of *c9,t11*-CLA mentioned above, the inhibition rates were 5.92%, 20.15%, 75.61% and 82.44%, respectively and inhibitory effect of *c9,t11*-CLA on DNA synthesis (except for 25 μmol/L, 24h) showed significantly less ³H-TdR incorporation than that in the negative controls (*P* < 0.05 and *P* < 0.01). Immunocytochemical staining demonstrated that SGC-7901 cells preincubated in media supplemented with different *c9,t11*-CLA concentrations at various times significantly decreased the expressions of PCNA (the expression rates were 7.2-3.0%, 24h and 9.1-0.9% at 48h, respectively), Cyclin A (11.0-2.3%, 24h and 8.5-0.5%, 48h), B₁ (4.8-1.8% at 24h and 5.5-0.6% at 48h) and D₁ (3.6-1.4% at 24h and 3.7%-0 at 48h) as compared with those in the negative controls (the expressions of PCNA, Cyclin A, B₁ and D₁ were 6.5% at 24h and 9.0% at 48h, 4.2% at 24h and 5.1% at 48h, 9.5% at 24h and 6.0% at 48h, respectively) (*P* < 0.01), whereas the expressions of p16^{ink4a} and p21^{cip/waf1}, cyclin-dependent kinases inhibitors (CDKI), were increased.

CONCLUSION: The cell growth and proliferation of SGC-7901 cell is inhibited by *c9,t11*-CLA via blocking the cell cycle, with reduced expressions of cyclin A, B₁ and D₁ and enhanced expressions of CDKI (p16^{ink4a} and p21^{cip/waf1}).

Liu JR, Li BX, Chen BQ, Han XH, Xue YB, Yang YM, Zheng YM, Liu RH. Effect of *cis*-9,*trans*-11-conjugated linoleic acid on cell cycle of gastric adenocarcinoma cell line (SGC-7901). *World J Gastroenterol* 2002;8(2):224-229

INTRODUCTION

Gastric cancer is common in China^[1-12], and it is currently thought to be caused by environmental factors, with diet being an important modifying agent^[13-17]. Its mechanism of prevention and treatment still makes it become a hot spot in this area^[18-39]. Its anticancerous potential Dietary fat has been implicated as an enhancing agent in carcinogenesis by both epidemiological and animal studies. Consumption of meat, specifically animal fat, has been implicated in a number of disease processes^[40-42]. However, several epidemiological studies have suggested an association between increased consumption of meat and fat and decreased risk of stomach, mammary and esophageal cancers^[43,44]. Among the fatty acids, only the essential fatty acid, linoleic acid (LA), has been clearly shown to enhance mammary tumorigenesis^[43]. However, isomeric derivatives of *cis*-9,*cis*-12-octadecadienoic acid (linoleic acid, LA) containing a conjugated double-bond system (conjugated linoleic acid, CLA) showed inhibitory effect on carcinogenesis in animal studies^[45,46]. CLA has a mixture of positional (9/11 or 10/12 double bonds) and geometric (various *cis/trans* combinations) isomers of LA formed by rumen and colon bacteria. The ability of CLA to prevent mammary and other tumors in rodents has been identified and has been the subject of several reviews^[43]. There are eight potential isomers of CLA, but the *cis*-9,*trans*-11 and *trans*-9,*cis*-11 isomers are thought to be active as potential antioxidant and anticarcinogenic agents. Therefore, it is of interest to investigate more extensively the anticancer activities of CLA.

In the present study, we investigated the effect of *cis*-9,*trans*-11-CLA (*c9,t11*-CLA) on the cell cycle of human gastric adenocarcinoma cells (SGC-7901).

MATERIALS AND METHODS

Materials

c9,t11-CLA, a monoisomer of *c-9,t11*-octadecadienoic acid with 98% purity, was obtained from Dr. Rui-Hai Liu (Food Science and Toxicology, Department of Food Science, Cornell University, Ithaca, NY, USA). The *c9,t11*-CLA was dissolved in 96 ml·L⁻¹ ethanol, and was then diluted to the following concentrations: 0, 25, 50, 100 and 200 μmol·L⁻¹.

Methods

Cell culture Human gastric adenocarcinoma cells (SGC-7901), purchased from Cancer Research Institute of Beijing (China), were cultured in RPMI 1640 (Gibco) medium, supplemented with calf serum 100 ml·L⁻¹, penicillin (100×103 u·L⁻¹) and streptomycin (100 mg·L⁻¹). The pH was maintained at 7.2-7.4, by equilibration with 5% CO₂. The temperature was maintained at 37 °C. The cells were sub-cultured with a mixture Ethylenedinitrile tetraacetic acid (EDTA) and trypsin.

Cell growth curve The SGC-7901 cells were seeded in six 24 well plates (Nuc.Co.); each well contained 2×10⁴ cells. After 24h, the medium of different plates was replaced with media supplemented with *c9,t11*-CLA at different concentrations. On the next day, the numbers of cells of 3 wells from each plate were determined daily by using the trypan blue staining. The means were obtained on each of

eight days and were used to draw a cellular growth curve. The inhibitory rates(IR) on the 8th day was calculated, as follows:

$$\text{IR}(\%) = \frac{\text{Total Number of cells in negative control (8d)} - \text{Number of cells in test groups(8d)}}{\text{Total number of cells in negative control(8d)}} \times 100\%$$

[³H]-Labeled precursor incorporation SGC-7901 cells (5×10^4 /well in 24 well plate) were cultured in appropriate medium for 24h prior to beginning the experiment. The medium was, then, replaced with different concentrations *c9*, *t11*-CLA. After 18 and 42h, the cells were incubated with [³H] thymidine (China Nucleus Institute, 0.5μCi/mL, 1.0μCi/well). After 6h the cells were harvested with trypsin/EDTA. Cells were collected in an acetic fiber filter with cellular collector and washed three times with PBS. The filter was dried overnight at 37°C. The filter was transferred into liquid of scintillation(containing 1% po and 2% pop in xylene) and cpm value determined by liquid Scintillation Counter (LS6500, Beckmen Co.).

Cell samples

SGC-7901 cells were treated for 24 and 48h with various concentrations of *c9*, *t11*-CLA and collected by centrifugation. Specimens were fixed immediately in 40g·L⁻¹ formaldehydum polymerisatum and embedded in paraffin. Gastric cancer tissue from a patient served as a reference.

Primary antibodies

To examine the proliferating cell nuclear antigen(PCNA) in cell proliferation and to determine cyclins (A, B₁ and D₁) and cyclin-dependent kinases inhibitors (*p16^{ink4a}* and *p21^{waf1}*) in cell cycle of SGC-7901, we used six primary antibodies: corresponding mouse monoclonal antibodies for cyclin B₁ and D₁, PCNA and *p21^{waf1}* and corresponding rabbit polyclonal antibodies for cyclin A and *p16^{ink4a}*. PCNA, *p16^{ink4a}*, and cyclin D₁ were purchased from Calbiochem Co. USA; others from Zhongshan Co. China.

Immunocytochemistry

Immunocytochemical staining was performed on serial sections at room temperature, using the horseradish peroxidase method. The sections were deparaffinized in xylene and rehydrated through graded alcohol. The sections were incubated for 10min at 95°C in 10mmol·L⁻¹ sodium citrate(pH 6.0) buffer for PCNA staining. Endogenous peroxidases were inactivated by immersing the sections in hydrogen peroxide for 10min, and then were incubated for 10min with 100ml·L⁻¹ normal goat serum in PBS to block non-specific binding. The sections were subsequently incubated overnight at 4°C with relevant antibodies (1 : 50 dilution) respectively. The next day, the sections were incubated with biotinylated anti-mouse or anti-rabbit IgG(Zhongshan Co. China) for 30min, followed by peroxidase-conjugated streptavidin(Zhongshan Co.China) for 30min. The chromogenic reaction was developed with DAB (diaminobenzidine) for 10min, and all sections were counterstained with hematoxylin. Controls consisted of omission of the primary antibody. The Positive Rate(PR) was calculated as follows:

$$\text{PR}(\%) = \frac{\text{Number of positive cells}}{\text{Total number}(2 \times 10^4)} \times 100$$

Statistical analysis

Analysis of data was performed using the student's *t* test or χ^2 test. A value of $P < 0.05$ is considered to be statistically significant.

RESULTS

Effect of *c9*, *t11*-CLA on SGC-7901 cell growth

As shown in Figure 1, Growth of the cells in various concentrations of

c9, *t11*-CLA did not differ from the negative control within 3d. After 3d, SGC-7901 cells incubated in 25 and 50μmol·L⁻¹ of *c9*, *t11*-CLA grew at a lower rate than the negative control. While in 100 and 200μmol·L⁻¹ concentrations of *c9*, *t11*-CLA, cell proliferation was significantly inhibited. The inhibitory rate of various *c9*, *t11*-CLA concentrations were 5.9%, 20.2%, 75.6% and 82.4%, respectively.

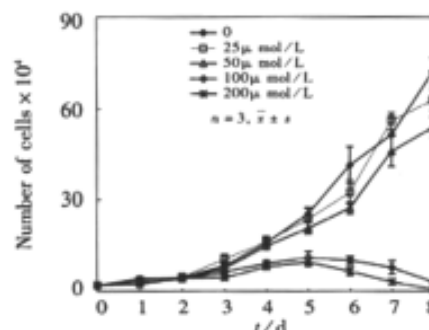


Figure 1 Growth curve of SGC-7901 cells cultured in various concentration of *c9*, *t11*-CLA

Effect on DNA synthesis

The effect of CLA on isotope incorporation into SGC-7901 cells are presented in Table 1. SGC-7901 cells preincubated in media supplemented with various *c9*, *t11*-CLA concentration (except for 25μmol/L, 24h) incorporated significantly less ³H-TdR than did the negative control ($P < 0.05$ and $P < 0.01$, Table 1). The inhibitory rate (IR) displayed a dose-response relationship as the concentration of *c9*, *t11*-CLA increased.

Table 1 Inhibitory effect of *c9*, *t11*-CLA on DNA synthesis in SGC-7901 cells ($n=6$)

<i>c9</i> , <i>t11</i> -CLA (μmol/L)	³ H-TdR incorporation (cpm, $\bar{x} \pm s$)		Inhibitory Rate (%)	
	24h	48h	24h	48h
0	2165±172	3598±603	-	-
25	1810±505	3093±323	16.4	14.0
50	2208±291	2640±607 ^a	-2.0	26.6
100	2065±261	2063±495 ^b	4.6	42.7
200	472±260 ^b	88±15 ^b	78.2	97.5

^a $P < 0.05$, ^b $P < 0.01$ vs negative control

Cell proliferation

As shown in Figure 2, expression rates of PCNA (Figure 3.1) on SGC-7901 cells gradually decreased after SGC-7901 cells were incubated with different concentrations of *c9*, *t11*-CLA at various times. Moreover, SGC-7901s cell expressed significantly less PCNA than did the negative control ($P < 0.01$). The expression rate displayed a dose-response relationship as the concentrations of CLA increased.

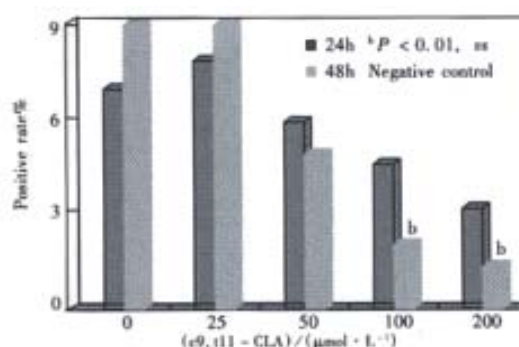


Figure 2 Expression of PCNA on SGC-7901 cells treated with *c9*, *t11*-CLA

Expressions of cyclin A,B₁ and D₁ and p16^{ink4a}, p21^{waf1}

The the expression of rates cyclin A, B₁, and D₁ (Figure 3.2-4)on SGC-7901 cells was decreased (Table 2) after SGC-7901 cell were

incubated with different concentrations of c9, t11-CLA for 24h and 48h while cyclin-dependent kinases inhibitors (P16^{ink4a}, and P21^{waf1}) increased (Table 3; Figure 3.5-6).

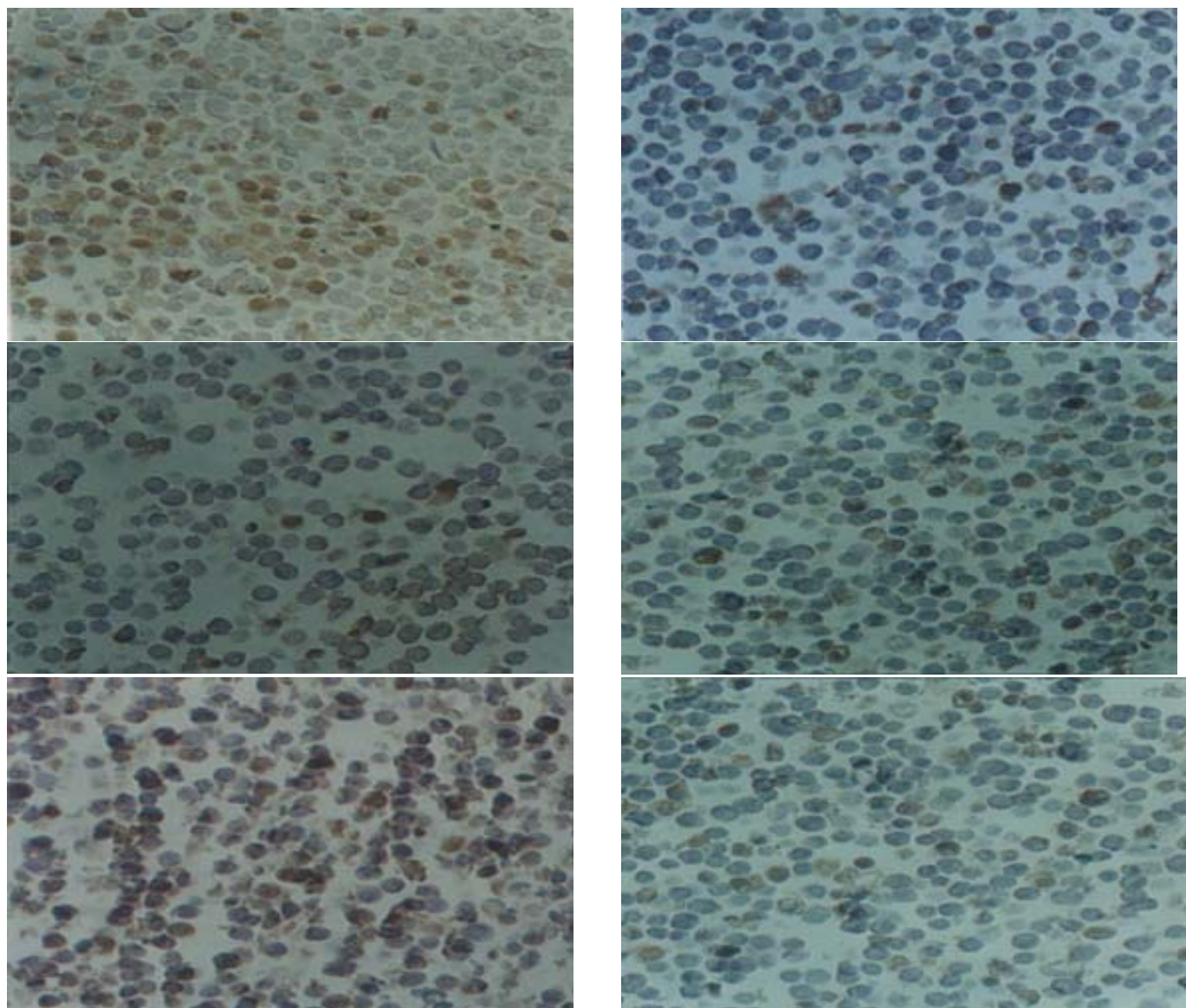


Figure 3 A: The expression of PCNA on SGC-7901 cells of the negative controls (immunocytochemistry staining SP method, original magnification ×400); B: The expression of cyclin A on SGC-7901 cells of the negative controls (immunocytochemistry staining SP method, original magnification ×400); C: The expression of cyclin B₁ on SGC-7901 cells of the negative controls (immunocytochemistry staining SP method, original magnification ×400); D: The expression of cyclin D₁ on SGC-7901 cells of the negative controls (immunocytochemistry staining SP method, original magnification ×400); E:The expression of p16^{ink4a} on SGC-7901 cells of c9,t11-CLA group (100μmol·L⁻¹) (immunocytochemistry staining SP method, original magnification ×400); F:The expression of p21^{clp/waf1} on SGC-7901 cells of c9,t11-CLA group (100μmol·L⁻¹) (immunocytochemistry staining SP method, original magnification ×400)

Table 2 Positive rates of cyclin A, B₁, and D₁ on SGC-7901 cells treated with c9,t11-CLA(%)

c9,t11-CLA (μmol/L)	24h			48h		
	Cylin A	Cylin B ₁	Cylin D ₁	Cylin A	Cylin B ₁	Cylin D ₁
0	10.7	4.2	9.5	5.9	5.1	6.0
25	11.0	4.8	3.6 ^b	8.5	5.5	3.7 ^b
50	7.9	2.5	3.5 ^b	5.0	3.1 ^b	3.7 ^b
100	4.4 ^b	2.6 ^b	2.1 ^b	1.3 ^b	0.7 ^b	0.6 ^b
200	2.3 ^b	1.8 ^b	0.4 ^b	0.5 ^b	0.6 ^b	0

^bP<0.01 vs negative control

Table 3 Positive rates of p16^{ink4a} and p21^{waf1} on SGC-7901 cells treated with c9,t11-CLA(%)

c9,t11-CLA (μmol/L)	24h		48h	
	p16 ^{ink4a}	p21 ^{waf1}	p16 ^{ink4a}	p21 ^{waf1}
0	1.0	0.2	0.8	0.6
25	0.7	1.4 ^b	0.2	0.8
50	1.4	1.0 ^b	3.0 ^b	2.5 ^b
100	2.8 ^b	4.1 ^b	4.6 ^b	3.8 ^b
200	3.6 ^b	5.2 ^b	5.0 ^b	6.3 ^b

^bP<0.01 vs negative control

DISCUSSION

CLA is a naturally occurring fatty acid in animal's food. Dietary sources of CLA include grilled beef, cheese, and related foods^[47]. Another source of CLA is its endogenous generation via the carbon centered free radical oxidation of linoleic acid^[45]. Over the past ten years, a number of research works of animal experiments have supported the observation that CLA is an effective chemopreventive agent of cancer, and that it can inhibit carcinogenesis of different tissues at different stages of induction by chemical agents^[44,45]. Several investigators in our group have reported that *c9, t11*-CLA is an effective agent to prevent carcinogenesis^[48,49] and cancer^[50-52]. Zhu's study^[48] demonstrated that *c9, t11*-CLA could significantly inhibit the mice forestomach neoplasia induced by B(a)P(50mg·kg⁻¹) in post-initiation in short term(23weeks). The incidences of tumors of mice in the B(a)P group, B(a)P with high dose CLA(5μL·g⁻¹) group and B(a)P with low dose CLA(2.5μL·g⁻¹) group were 100%, 60% and 69% respectively ($P < 0.05$). Xue's research^[49] also indicated that the incidence of neoplasm in mouse forestomach in the B(a)P group, 75% pure *c9, t11*-CLA group, 98% pure *c9, t11*-CLA group and 98% pure *t10, c12*-CLA group were 100.0%, 75.0%, 69.2%, and 53.8%, respectively. This may be due to an inhibition mitogen of activated protein kinase(MAPK)-a way to reduce carcinogenesis. The data from our research group suggested that *c9, t11*-CLA could inhibit proliferation of cancer cells, i.e. SGC-7901 cells^[50] and MCF-7 cells^[51,52], and induced cancer cell (SGC-7901) apoptosis^[53]. Moreover, the inhibiting effect of *c9, t11*-CLA on SGC-7901 cell proliferation may be related to cell cycle.

As shown in Figure 1, *c9, t11*-CLA at various concentrations in 8 days reduced the proliferative activity of SGC-7901 cells and its inhibitory rates were from 5.92% to 82.44%, but the mechanism of such inhibition of *c9, t11*-CLA has not been clarified. However, we discovered that SGC-7901 cells supplemented with *c9, t11*-CLA incorporated significantly less [³H] thymidine than negative controls (shown in Table I). The inhibitory rates of, from 16.4% to 78.2% after incubating with *c9, t11*-CLA for 24h and from 14.0% to 97.5% after 48h displayed a dose-response relationship. In the meantime, we investigated further the expressions of PCNA and protein from cell cycle such as cyclins and cyclin-dependent kinase inhibitors (CDKI) on SGC-7901 cells treated with various concentrations of *c9, t11*-CLA. PCNA (proliferating cell nuclear antigen) plays an essential role in both the replication and repair of DNA, and is an essential component of the DNA replication machinery, acting as the processing factor for polymerases and DNA. In addition to its role in replication, PCNA is not only required for base excision-repair of nucleotides, but also binds to cell cycle regulatory proteins such as *p21* and Gadd45^[54]. In this study, we discovered that the expression of PCNA on SGC-7901 cells gradually decreased with increasing concentrations of *c9, t11*-CLA in comparison with negative controls (shown in Figure 2). In other words, DNA replication lessens, thereby resulting in slower on SGC-7901 cell proliferation.

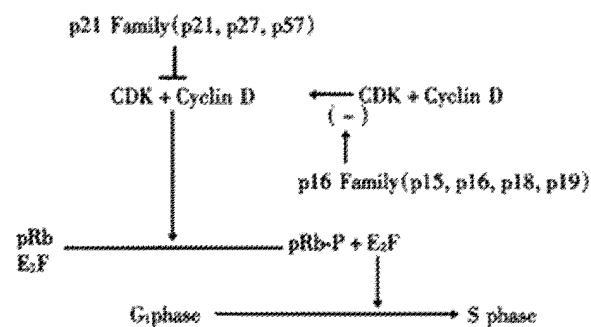


Figure 4 The relationship between CDKI(*p16* and *p21*) and cyclins in G₁/S transition

The fundamental task of the cell cycle is to ensure that DNA is faithfully replicated once during S phase and that identical chromosomal copies are distributed equally to two daughter cells during M phase. The cell cycle is a complex process, regulated by many factors, which can be divided into three groups: cyclins(A,B,D,E...H); cyclin-dependent kinases (CDK, including CDK₁-CDK₇); CDK inhibitors (CDKI, including *p16* family and *p21* family). They are balanced through mutual interactions. Uncontrolled cell proliferation is the hallmark of cancers which are the result of damage to genes that directly regulate their cell cycles. Using immunocytochemical technique to detect expressions of cyclins and CDKI, we demonstrated that the expressions of cyclin A,B₁ and D₁ on SGC-7901 cells treated with various concentrations *c9, t11*-CLA were reduced, whereas expressions of CDKI(*p16*^{ink4a} and *p21*^{waf1}) increased, as compared with those of negative controls. Successive actions of CDKs promote cell-cycle progression in mammalian cells. Various cyclins bind and activate CDKs at specific times during the cell cycle.

Mammalian cyclin A activates CDK₂^[55] in S-phase and CDK₁ (Cdc₂) in G₂- and M-phases. One important mechanism that enables sequential activation of cyclin-CDK complexes is the periodic synthesis and destruction of cyclins. Cyclin A expression starts late in G₁-phase and is increasing through S- and G₂-phase before the protein is degraded in M-phase. The cell cycle-dependent expression of cyclin B₁ is critical for the proper timing of a cell's entry into mitosis which is dependent both upon the binding of CDK₁ to cyclin B₁, as well as a series of phosphorylation and dephosphorylation events. The cyclin B₁ protein accumulates during interphase and peaks at the G₂-M phase transition^[56]. One of the crucial substrates of G₁ phase CDK, including CDK₄ in the complex with D-type cyclins(cyclin D₁, D₂ and D₃), is Rb protein (pRb), which is the product of the retinoblastoma susceptibility gene. Rb protein plays an important role in the regulation of the G₁ to S phase progression in normal cells and the function of pRb is regulated by phosphorylation. Thus, during the G₀ and G₁ phase, Rb protein is in an un- or underphosphorylated stage and binds to E₂F family transcription factors. Cyclin Ds/CDK₄ becomes activated around the mid G₁ phase, resulting in the accumulation of increasingly phosphorylated, inactive forms pRb. This causes the release of E₂F family transcription factors which induce the expression of S-phase genes by positive regulation through E₂F-binding sites(see Figure 4)^[57]. It is also known that abrogation of the functions of Cyclin A prevents entry into the S phase. From the beginning of the S phase Rb protein remains in the hyperphosphorylated inactive state until the end of M phase; such condition is thought to be due to both cyclin A/CDK₂ and Cyclin A,B₁/Cdc₂ in catalyzing the phosphorylation reaction^[58]. *p16*^{ink4a} is the founder member of a family of proteins with the ability to inhibit CDK₄ and the CDK₄-related kinase CDK₆.

The INK4 family is composed of four members in mammalian organisms: *p16*^{ink4a}, *p15*^{ink4b}, *p18*^{ink4c}, and *p19*^{ink4d}. The four mammalian INK4 proteins have similar biochemical properties: all of them bind to CDK₄ and CDK₆ and inhibit the kinase activity of the CDK₄₋₆/Cyclin D complexes(Figure 4)^[59]. The INK4 inhibitor causes G₁ arrest indicating that the phosphorylation of pRb on residues specific for CDK₄(and possibly CDK₆) is critical for G₁/S progression. While *p21*^{CIP1/waf1} family, comprising *p21*^{CIP1/waf1}, *p27*^{CIP1} and *p57*^{CIP2}, bind to a variety of CDKs and cyclins, preferentially to cyclin/CDK complexes rather than monomeric forms and also inhibit performed active cyclin/CDK complexes(see Figure 4)^[59]. In addition to its role as a CDKI, *p21*^{CIP1/waf1} has been shown to block DNA replication by direct interaction with PCNA mentioned above. However, *p21*^{CIP1/waf1} does not inhibit the PCNA-dependent nucleotide excision-repair of DNA. In deed, DNA damage leads to an increase in the level of *p53*, and result in *p21*-mediated cell cycle arrest in the G₁ phase, which persists

until DNA repair is completed^[60]. Thus, it is proposed that $p21^{Cip/waf1}$ plays an important role under such conditions as terminal differentiation and cell senescence.

In conclusion, $c9,t11$ -CLA may inhibit cell growth and proliferation by a decrease in the expressions of cyclin A, B₁ and D₁ and an increase in that of CDKI($p16^{ink4a}$ and $p21^{Cip/waf1}$) on SGC-7901 cells in comparison with the negative controls. This result suggested that the inhibition effect of $c9,t11$ -CLA on SGC-7901 cell proliferation is related to the cell cycle. The whole mechanism of the action of $c9,t11$ -CLA on SGC-7901 cell cycle further research.

REFERENCES

- Gao HJ, Yu LZ, Bai JF, Peng YS, Sun G, Zhao HL, Miu K, Lu XZ, Zhang XY, Zhao ZQ. Multiple genetic alterations and behavior of cellular biology in gastric cancer and other gastric mucosal lesions: *H. pylori* infection, histological types and staging. *World J Gastroenterol* 2000;6:848-854
- Deng DJ, E Z. Overview on recent studies of gastric carcinogenesis: human exposure of N nitrosamides. *Shijie Huaren Xiaohua Zazhi* 2000; 8:250-252
- Deng DJ. progress of gastric cancer etiology: N-nitrosamides 1999s. *World J Gastroenterol* 2000;6:613-618
- Li DG, Wang ZR, Lu HM. Pharmacology of tetrandrine and its therapeutic use in digestive diseases. *World J Gastroenterol* 2001;7:627-629
- Niu WX, Qin XY, Liu H, Wang CP. Clinicopathological analysis of patients with gastric cancer in 1200 cases. *World J Gastroenterol* 2001;7: 281-284
- Kimura K. Gastritis and gastric cancer. Asia. *Gastroenterol Clin North Am* 2000;29:609-621
- Hua JS. Effect of Hp: cell proliferation and apoptosis on stomach cancer. *Shijie Huaren Xiaohua Zazhi* 1999;7:647-648
- Xia HX, Zhang GS. Apoptosis and proliferation in gastric cancer caused by Hp infection. *Shijie Huaren Xiaohua Zazhi* 1999;7:740-742
- Cai L, Yu SZ, Ye WM, Yi YN. Fish sauce and gastric cancer: an ecological study in Fujian Province, China. *World J Gastroenterol* 2000;6: 671-675
- Cai L, Yu SZ, Zhang ZF. *Helicobacter pylori* infection and risk of gastric cancer in Changle County, Fujian Province, China. *World J Gastroenterol* 2000;6:374-376
- Cai L, Yu SZ. A molecular epidemiologic study on gastric cancer in Changle, Fujian Province. *Shijie Huaren Xiaohua Zazhi* 1999;7:652-655
- Cai L, Yu SZ, Zhang ZF. Glutathione S-transferases M1, T1 genotypes and the risk of gastric cancer: A case-control study. *World J Gastroenterol* 2001;7:506-509
- Sugie S, Okamoto K, Watanabe T, Tanaka T, Mori H. Suppressive effect of irsogladine maleate on N-methyl-N-nitro-N-nitrosoguanidine (MNNG)-initiated and glyoxal-promoted gastric carcinogenesis in rats. *Toxicology* 2001;166:53-61
- Palli D, Russo A, Saieva C, Salvini S, Amorosi A, Decarli A. Dietary and familial determinants of 10-year survival among patients with gastric carcinoma. *Cancer* 2000;89:1205-1213
- Mathew A, Gangadharan P, Varghese C, Nair MK. Diet and stomach cancer: a case-control study in South India. *Eur J Cancer Prev* 2000;9:89-97
- Palli D. Epidemiology of gastric cancer: an evaluation of available evidence. *J Gastroenterol* 2000;35:84-89
- Palli D, Russo A, Ottini L, Masala G, Saieva C, Amorosi A, Cama A, D'Amico C, Falchetti M, Palmirotta R, Decarli A, Costantini RM, Fraumeni JF Jr. Red meat, family history, and increased risk of gastric cancer with microsatellite instability. *Cancer Res* 2001;61:5415-5419
- Tu SP, Jiang SH, Tan JH, Jiang XH, Qiao MM, Zhang YP, Wu YL, Wu YX. Proliferation inhibition and apoptosis induction by arsenic trioxide on gastric cancer cell SGC-7901. *Shijie Huaren Xiaohua Zazhi* 1999;7:18-21
- Chen YQ, Shen HX, Zhou SJ, Chen L, Yu X, Lu LP. Experimental study of the inhibitory effect of fufang shenqitang on gastric adenocarcinoma of rats. *Shijie Huaren Xiaohua Zazhi* 1999;7:117-119
- Gao GL, Yang Y, Ren CW, Yang SF. Effect of vitamin D3 on forestomach carcinogenesis induced by N methyl N'nitro N nitroso-guanidine and tween 20 in rats. *Shijie Huaren Xiaohua Zazhi* 1999;7:763-765
- Xiao B, Xiao LC, Lai ZS, Zhang YL, Zhang ZS, Zhang WD. Experimental study of the inhibition affect of Zhen'ailing on the growth of gastric cancer in vitro. *Shijie Huaren Xiaohua Zazhi* 1999;7:951-954
- Xin Y, Zhao FK, Zhang SM, Wu DY, Wang YP, Xu L. Relationship between CD44v6 expression and prognosis in gastric carcinoma patients. *Shijie Huaren Xiaohua Zazhi* 1999; 7:210-214
- Li XS, Zhang XJ, Sun YR, Wang XF, Liu HW, Li W, Sa HJ, Liu HY, Zhang XM, Yang JC. Studies on cytokine activity in sera and ascites of patients with digestive tumor. *Shijie Huaren Xiaohua Zazhi* 1999;7:13-14
- Wang SW, Xie YH, Li YR, Lin HS, Zhu LZ. Antineoplastic effect and short-term effect on advanced malignant tumor of digestive tract of Chinese herbs antike. *Shijie Huaren Xiaohua Zazhi* 1999;7:236-239
- Liu HF, Liu WW, Fang DC, Men RF, Wang ZH. Apoptosis and its relationship with Fas ligand expression in gastric carcinoma and its precancerous lesion. *Shijie Huaren Xiaohua Zazhi* 1999;7: 561-563
- Zhou HP, Wang X, Zhang NZ. Early apoptosis in intestinal and diffuse gastric carcinomas. *World J Gastroenterol* 2000;6:898-901
- Liu XB, Li L, Zhuang BZ, Jiang YD, Wang JH. Cyclin E expression in gastric carcinoma and its clinicopathological significance. *Shijie Huaren Xiaohua Zazhi* 1999;7:656-658
- Wang XS, Wang RB, Zhang ZL, Cao TJ, Jin WD. Effect of short time heating with MMC and 5-FU on cancer cells. *Shijie Huaren Xiaohua Zazhi* 1999;7:576-578
- Zhang FX, Zhang XY, Fan DM, Deng ZY, Yan Y, Wu HP, Fan JJ. Antisense telomerase RNA induced human gastric cancer cell apoptosis. *World J Gastroenterol* 2000;6:430-432
- Zhao AG, Yang JK, Zhao HL. Chinese Jianpi herbs induce apoptosis of human gastric cancer grafted onto nude mice. *Shijie Huaren Xiaohua Zazhi* 2000;8:737-740
- Zhu ZH, Xia ZS, He SG. The effects of ATRA and 5Fu on telomerase activity and cell growth of gastric cancer cells in vitro. *Shijie Huaren Xiaohua Zazhi* 2000;8:669-673
- Xia ZS, Zhu ZH, He SG. Effects of ATRA and 5-Fu on growth and telomerase activity of xenografts of gastric cancer in nude mice. *Shijie Huaren Xiaohua Zazhi* 2000;8:674-677
- Guo YQ, Zhu ZH, Li JF. Flow cytometric analysis of apoptosis and proliferation in gastric cancer and precancerous lesion. *Shijie Huaren Xiaohua Zazhi* 2000;8:983-987
- Gu QL, Li NL, Zhu ZG, Yin HR, Lin YZ. A study on arsenic trioxide inducing in vitro apoptosis of gastric cancer cell lines. *World J Gastroenterol* 2000;6:435-437
- Wu K, Shan YJ, Zhao Y, Yu JW, Liu BH. Inhibitory effects of RRRa2tocopheryl succinate on benzo(a)pyrene (B(a)P) a 2induced forestomach carcinogenesis in female mice. *World J Gastroenterol* 2001;7: 60-65
- Wu K, Liu BH, Zhao DY, Zhao Y. Effect of vitamin E succinate on expression of TGF- β -1, c-jun and JNK1 in human gastric cancer SGC-7901 cells. *World J Gastroenterol* 2001;7:83-87
- Cui RT, Cai G, Yin ZB, Cheng Y, Yang QH, Tian T. Transretinoic acid inhibits rats gastric epithelial dysplasia induced by N-methyl-N-nitro-N-nitrosoguanidine: influences on cell apoptosis and expression of its regulatory genes. *World J Gastroenterol* 2001;7:394-398
- He XS, Su Q, Chen ZC, He XT, Long ZF, Ling H, Zhang LR. Expression, deletion and mutation of p16 gene in human gastric cancer. *World J Gastroenterol* 2001;7:515-521
- Liu S, Wu Q, Chen ZM, Su WJ. The effect pathway of retinoic acid through regulation of retinoic acid receptor in gastric cancer cells. *World J Gastroenterol* 2001;7:662-666
- Zhang B, Zhang LH, Li N, Wang YJ, Li JS. Effects of n-3 fatty acids on glucose metabolism of septic rats and its mechanism. *Shijie Huaren Xiaohua Zazhi* 1999;7:335-337
- Lewis CJ, Yetley EA. Health claim and observational human data: relation between dietary fat and cancer. *Am J Clin Nutr* 1999;69: 1357-1364
- Mantzioris E, Cleland LG, Gibson RA, Neumann MA, Demasi M, James MJ. Biochemical effects of a diet containing foods enriched with n-3 fatty acid. *Am J Clin Nutr* 2000; 72:42-48
- MacDonald HB. Conjugated linoleic acid and disease prevention: a review of current knowledge. *J Am Coll Nutr* 2000;19:111-118
- Kimoto N, Hirose M, Futakuchi M, Iwata T, Kasai M, Shirai T. Site-dependent modulating effects of conjugated fatty acids from safflower oil in a rat two-stage carcinogenesis model in female Sprague-Dawley rats. *Cancer Lett* 2001; 168: 15-21
- Ip C, Banni S, Angioni E, Carta G, McGinley J, Thompson HJ, Barbano D, Bauman D. Conjugated linoleic acid-enriched butter fat alters mammary gland morphogenesis and reduces cancer risk in rats. *J Nutr* 1999;129:2135-2142
- Brodie AE, Manning VA, Ferguson KR, Jewell DE, Hu CY. Conjugated linoleic acid inhibits differentiation of pre- and post-confluent 3T3-L1 preadipocytes but inhibits cell proliferation only in pre-confluent cells. *J Nutr* 1999; 129: 602-606
- Parodi PW. Conjugated linoleic acid and other anticarcinogenic agents of bovine milk fat. *J Dairy Sci* 1999;82:1339-1349
- Zhu Y, Qiu J, Chen BQ, Liu RH. The inhibitory effect of conjugated linoleic acid on mice forestomach neoplasia induced by benzo(a) pyrene. *Zhonghua Yufang Yixue* 2001;35:19-22
- Xue YB, Chen BQ, Liu JR, Zheng YM, Liu RH. The inhibition of mouse forestomach neoplasm induced by B(a)p through MAPKs pathway by conjugated Linoleic acid. *Zhonghua Yufang Yixue* 2001;35:1-4

- 50 Liu JR, Chen BQ, Liu RH, Lu GF, Zhu Y, Han XH. The Inhibited effect on gastric carcinoma cell induced by conjugated linoleic acid (CLA). *Weisheng Yanjiu* 1999;28:353-357
- 51 Liu JR, Chen BQ, Xue YB, Han XH, Yang YM, Liu RH. Inhibitory effect of conjugated linoleic acid on the *in vitro* growth of human mammary cancer cells (MCF-7). *Zhonghua Yufang Yixue* 2001;35:244-247
- 52 O'Shea M, Devery R, Lawless F, Murphy J, Stanton C. Milk fat conjugated linoleic acid (CLA) inhibits growth of human mammary MCF-7 cancer cells. *Anticancer Res* 2000;20:3591-3601
- 53 Liu JR, Chen BQ, Deng H, Han XH, Liu RH. Cellular apoptosis induced by conjugated linoleic acid in human gastric cancer (SGC-7901) cells. *Gongye Weisheng Yu Zhiyebing* 2001;27:129-133
- 54 Tsurimoto T. PCNA binding proteins. *Front Biosci* 1999; 4: D849-858
- 55 Mani S, Wang C, Wu K, Francis R, Pestell R. Cyclin-dependent kinase inhibitors: novel anticancer agents. *Expert Opin Investig Drugs* 2000;9: 1849-1870
- 56 Ito M. Factors controlling cyclin B expression. *Plant Mol Biol* 2000;43: 677-690
- 57 Pyronnet S, Sonenberg N. Cell-cycle-dependent translational control. *Curr Opin Genet Dev* 2001;11:13-18
- 58 Viallard JF, Lacombe F, Belloc F, Pellegrin JL, Reiffers J. Molecular mechanisms controlling the cell cycle: fundamental aspects and implications for oncology. *Cancer Radiother* 2001;5: 109-129
- 59 Israels ED, Israels LG. The cell cycle. *Stem cells* 2001;19:88-91
- 60 Sowa Y, Sakai T. Butyrate as a model for "gene-regulating chemoprevention and chemotherapy". *Biofactors* 2000;12:283-287

Edited by Lu HM

• GASTRIC CANCER •

Methionine-dependence and combination chemotherapy on human gastric cancer cells *in vitro*

Wei-Xin Cao, Jing-Min Ou, Xu-Feng Fei, Zheng-Gang Zhu, Hao-Ran Yin, Min Yan, Yan-Zhen Lin

Wei-Xin Cao, Jing-Min Ou, Xu-Feng Fei, Department of Clinical Nutrition, Shanghai Institute of Digestive Surgery, Ruijin Hospital, Shanghai Second Medical University, Shanghai 200025, China
Zheng-Gang Zhu, Hao-Ran Yin, Min Yan, Yan-Zhen Lin, Department of Surgery, Shanghai Institute of Digestive Surgery, Ruijin Hospital, Shanghai Second Medical University, Shanghai 200025, China

Supported by the Science Foundation of Ministry of Health of China, No.96-2-296

Correspondence to: Dr. Wei-Xin Cao, Department of Clinical Nutrition, Ruijin Hospital, Shanghai Second Medical University, 197 Ruijiner Road, Shanghai 200025, China. fische@citiz.net

Telephone: +86-21-64370045 Ext.661688 Fax: +86-21-64333548

Received 2001-08-24 Accepted 2001-09-05

Abstract

AIM: To elucidate whether human primary gastric cancer and gastric mucosa epithelial cells *in vitro* can grow normally in a methionine (Met) depleted environment, i.e. Met-dependence, and whether Met-depleting status can enhance the killing effect of chemotherapy on gastric cancer cells.

METHODS: Fresh human gastric cancer and mucosal tissues were managed to form monocellular suspensions, which were then cultured in the Met-free but homocysteine-containing (Met⁻Hcy⁺) medium, with different chemotherapeutic drugs. The proliferation of the cells was examined by cell counter, flow cytometry (FCM) and microcytotoxicity assay (MTT).

RESULTS: The growth of human primary gastric cancer cells in Met⁻Hcy⁺ was suppressed, manifested by the decrease of total cell counts [$1.46 \pm 0.42 (\times 10^5 \cdot L^{-1})$ in Met⁻Hcy⁺ vs $1.64 \pm 0.44 (\times 10^5 \cdot L^{-1})$ in Met⁺Hcy⁻, $P < 0.01$], the decline in the percentage of G₀G₁ phase cells (0.69 ± 0.24 in Met⁻Hcy⁺ vs 0.80 ± 0.18 in Met⁺Hcy⁻, $P < 0.01$) and the increase of S cells (0.24 ± 0.20 in Met⁻Hcy⁺ vs 0.17 ± 0.16 in Met⁺Hcy⁻, $P < 0.01$); however, gastric mucosal cells grew normally. If Met⁻Hcy⁺ medium was used in combination with chemotherapeutic drugs, the number of surviving gastric cancer cells dropped significantly.

CONCLUSION: Human primary gastric cancer cells *in vitro* are Met-dependent; however, gastric mucosal cells have not shown the same characteristics. Met⁻Hcy⁺ environment may strengthen the killing effect of chemotherapy on human primary gastric cancer cells.

Cao WX, Ou JM, Fei XF, Zhu ZG, Yin HR, Yan M, Lin YZ. Methionine-dependence and combination chemotherapy on human gastric cancer cells *in vitro*. *World J Gastroenterol* 2002;8(2):230-232

INTRODUCTION

Gastric cancer is common in China and abroad^[1-20], and chemotherapy is still a main method for advanced cancer so far^[21-30]. Up to now, quite a few studies have elucidated the property of methionine (Met) dependence of cancer cells^[31-34]. If that property was utilized in

combination with specific chemotherapeutic drugs, the proliferation of tumor cells would be suppressed. This study intended to culture the human primary gastric cancer cells in diverse environments to judge whether the gastric cancer cells were Met-dependent and whether Met⁻Hcy⁺ could enhance the effect of chemotherapy.

MATERIALS AND METHODS

Study on Met-dependence

Human primary gastric cancer cells were collected from gastric cancer tissues of 37 advanced gastric cancer patients in our hospital, and human gastric mucosal epithelial cells were simultaneously obtained in 31 patients. Based on the Met-free RPMI-1640 medium, dialyzed bovine serum, and other ingredients necessary for cell growth, Met-free but homocysteine-containing (Met⁻Hcy⁺) medium and Met-containing but Hcy-depleting (Met⁺Hcy⁻) medium were prepared^[31]. Fresh gastric cancer and mucosa tissues were obtained during operations. After being clipped into pieces and digested, the samples were made into monocellular suspensions, which were then shared out equally in the Met⁻Hcy⁺ medium (test group) and Met⁺Hcy⁻ medium (control group) separately. The cell concentration was adjusted to $5 \times 10^5 \cdot L^{-1}$. Seeded in the bottles the inside of which was covered with mouse tail collagen, the cells were incubated at 37°C in an atmosphere containing 50 mL·L⁻¹ CO₂. After being cultured continuously for 96h, the cells were digested by protease to monocellular suspensions, which were then examined by cell counter and phase-contrast microscope and submitted to FCM study for cell kinetics.

Study on Met⁻Hcy⁺ environment in combination with chemotherapeutic drugs

Human primary gastric cancer cells were sampled from gastric cancer tissues of 40 advanced gastric cancer patients. The methods and conditions of gastric cancer sampling, treatment, and culture were the same as mentioned above. Human primary gastric cancer cells were inoculated in 96-well plates, in which any one of adriamycin (ADM), cisplatin (DDP), 5-fluorouracil (5-FU), mitomycin C (MMC) and methotrexate (MTX) was then added. The concentrations of those drugs were 0.4, 3.0, 10.0, 3.0 and 4.0 mg·L⁻¹ respectively. Each drug group was designed to be repeated for 3 times, and the concentration of 0 was the empty control. Tetrazolium salt was added after the cells were incubated at 37°C in a 50 mL·L⁻¹ CO₂ atmosphere for 48h. The cell suspensions were centrifuged, added with dimethyl sulfoxide (DMSO), shaken and aspirated until crystals dissolved completely. Microcytotoxicity assay (MTT) was applied, and the cells were colorimetrically analyzed by Bio-tek Instruments at 490nm to obtain the A (absorbance) value, which reflected the amount of surviving cells.

Statistical analysis

Paired *t* test was used.

RESULTS

Human primary gastric cancer cell cycle and amount

After a 96-h culture, the proliferation of human primary gastric cancer cells in the test group was affected, showing bad adherence and cytotoxicity; however, the cancer cells in the control group did not show

the similar phenomenon. The percentage of cells in G₀G₁ phases in the test group was significantly lower than that in the control group while the percentage of S phase cells in test group was obviously higher than that in the control group. There was no statistical significance between the percentage of G₂M cells in the test group and that in the control group. The result of cell counting was that human primary gastric cancer cells in the test group were apparently less than those in the control group (Table 1).

Table 1 The distribution of human primary gastric cancer cell cycle and the amount of cells ($\bar{x} \pm s$, $n = 37$)

Groups	Fractions in different phases			Amount of cells ($\times 10^6 \cdot L^{-1}$)
	G ₀ G ₁	S	G ₂ M	
Met ⁺ Hcy ⁻	0.80±0.18	0.17±0.16	0.04±0.06	1.64±0.44
Met ⁺ Hcy ⁺	0.69±0.24 ^b	0.24±0.20 ^b	0.07±0.13	1.46±0.42 ^b

^bP<0.01, vs Met⁺Hcy⁻ group.

Human gastric mucosa cell cycle and amount

Gastric mucosa epithelial cells grew well both in the test group and in the control group. There was no obvious difference in the percentages in various phases in cell cycle between the two groups. The amount of cells in the test group was slightly higher than that in the control group but without statistical significance (Table 2).

Table 2 The distribution of human gastric mucosa epithelial cell cycle and the amount of cells ($\bar{x} \pm s$, $n = 31$)

Groups	Fractions in different phases			Amount of cells ($\times 10^6 \cdot L^{-1}$)
	G ₀ G ₁	S	G ₂ M	
Met ⁺ Hcy ⁻	0.90±0.13	0.07±0.11	0.02±0.02	1.70±0.44
Met ⁺ Hcy ⁺	0.90±0.14	0.08±0.11	0.03±0.04	1.75±0.45

Different media in combination with chemotherapeutic drugs

The surviving gastric cancer cells in the test group without chemotherapeutic drugs were fewer than those in the corresponding control group, with lower A value. The proliferation of gastric cancer cells in the Met⁺Hcy⁺ group was suppressed much more strongly than that in the Met⁺Hcy⁻ group, no matter which drug was added. The former group had the manifestation of the decrease in surviving gastric cancer cells to various extents, with lower A value (Table 3).

Table 3 The influence of Met⁺Hcy⁻ or Met⁺Hcy⁺ in combination with chemotherapeutic drugs to gastric cancer cells ($\bar{x} \pm s$, A)

Drug	Met ⁺ Hcy ⁻	Met ⁺ Hcy ⁺
ADM	0.3807±0.3114	0.3175±0.2003 ^a
DDP	0.3878±0.3050	0.3189±0.1848 ^b
5-FU	0.3657±0.2597	0.3182±0.2049 ^a
MMC	0.3861±0.2734	0.3105±0.2103 ^b
MTX	0.3649±0.2811	0.3120±0.2003 ^b
Control	0.4834±0.4337	0.3981±0.3056 ^b

^aP<0.05, ^bP<0.01, vs Met⁺Hcy⁻.

DISCUSSION

Met-dependence and Met starvation

Methionine is an essential amino acid containing an S-methyl, which is used to synthesize through methylation quite a few important physiological active substances. Homocysteine is the direct precursor of Met. Hcy and Met may be converted into each other *in vitro*, but it is not as such *in vivo*. Hcy is continuously consumed with the need of metabolism, and hence is transformed and supplied by Met. Met depletion *in vivo* is easily produced once Met supply is stopped, as there is no pathway *in vivo* of Hcy transforming to Met, which is an essential amino acid. Normal cells can grow well in the environment

containing Hcy instead of Met. The proliferation of tumor cells, however, may be suppressed under such condition. This phenomenon is called Met-dependence. It is one of research focuses in the past decades that Met starvation is made artificially in tumor-bearing body to inhibit the tumor growth based on the therapy of Met-dependence. There are several methods to produce Met starvation^[32-34]: (1) degradation of Met by methioninase; (2) fast plus Met-depleting total parenteral nutrition (Met-TPN). Due to its unsatisfactory specificity methioninase can degrade Met irreversibly, but it can also degrade Hcy, homocystine, cysteine and cystine during a short period of time so that the normal cells are hard to survive. Only through fast and Met-TPN may Met starvation be produced and have little impact on normal tissue cells.

Met-dependence of tumor cells

Studies *in vivo* and *in vitro* can be used to judge whether tumor cells have the property of Met-dependence and to explore the impact of Met starvation on the proliferation of tumor cells. The research *in vivo* is not easy to conduct because of many inevitable factors. The prominent characteristic of the research *in vitro* is that the cells cultured are not influenced by complex internal environment and the rule of cell life activity can be studied. The change of cell physiological functions under the influence of single or multi-factors may be further observed when culture conditions such as physical, chemical and biological factors are altered artificially. Goseki *et al* explored the relationship of tumor growth and Met-dependence by animal experiment. We have also done such work in the past years^[35,36]. The studies suggested that Met starvation in tumor-bearing animals could inhibit the proliferation of tumor cells. In the experiment *in vitro* of gastric cell line SGC-7901, we found that the percentages of SGC-7901 cells in S and G₂M phases in the Met⁺Hcy⁺ medium were both obviously elevated and the percentage of G₀G₁ cells significantly declined in comparison with those in the Met⁺Hcy⁻ medium. The results meant that the cell cycle of SGC-7901 was inhibited in the G₂M phase. The present study showed again that *in vitro* the proliferation of human primary gastric cancer cells in the environment of Met⁺Hcy⁺ had the similar results to that of human gastric cancer cell line SGC-7901. The cell cycle of tumor cells was disturbed and the amount of cancer cells decreased significantly; however, no same phenomenon was observed in the gastric mucosa epithelial cells. The results suggested that human gastric cancer cells were Met-dependent. The cause of Met-dependence of tumor cells remains unclear. As far as we know now, the causes include: (1) decreased amount and activity of Met synthetase; (2) deficiency of 5-methyltetrahydrofolate reductase; (3) inability to make use of endogenous Met; (4) rise in the rate of basal transmethylation; (5) activated EJ/T24HRAS1 oncogene leading to the expression of Met-dependence.

Significance of Met starvation in combination with chemotherapeutic drugs

Chemotherapy can not be replaced by surgery and radiotherapy in the treatment of malignancies. At present most chemotherapeutic drugs are phase-specific, despite some without phase-specificity, all of which are hard to kill tumor cells completely. So the aim of tumor therapy is to take measures to improve the effect of chemotherapy. It is a new trial to drive the G₀ cells to enter into the proliferating phase. Our previous clinical study and tumor-bearing rat experiment^[37-39] showed that after the treatment of parenteral nutrition, the percentages of S and S+G₂+M gastric cancer cells increased obviously while that of G₀G₁ cells decreased dramatically. Met deprivation can produce Met starvation in Met-dependent tumor cells, then metabolism of cancer cells is suppressed and more cells remain in the phases of S and G₂. As a result, the effect of phase-specific chemotherapeutic drugs is enhanced significantly. This provides a new way to improve the therapeutical effect on tumors by using Met-TPN combined with chemotherapeutic drugs. Many authors^[40-44] have made the researches, both experimentally and clinically, on Met-TPN in

combination with chemotherapeutic drugs to improve the effect of chemotherapy. They confirmed that Met-TPN in combination with 5-FU, DDP and ADM respectively can enhance the sensitivity of chemotherapy of gastric cancer, breast cancer and Yashida sarcoma. Our present study supported the above results. It is hypothesized that Met starvation could make primary gastric cancer cells blocked in the phases of S/G₂M. Theoretically, the more numerous are the cells in the proliferating phase, the stronger effect of phase-specific chemotherapeutic drugs have been produced.

REFERENCES

- Cai L, Yu SZ. A molecular epidemiologic study on gastric cancer in Changle, Fujian Province. *Shijie Huaren Xiaohua Zazhi* 1999; 7: 652-655
- Wang Q, Jin PH, Lin GW, Xu SR. Cost effectiveness of population based *Helicobacter pylori* screening to prevent gastric cancer. *Shijie Huaren Xiaohua Zazhi* 2000; 8:262-265
- Wong BC, Lam SK, Ching CK, Hu WH, Kwok E, Ho J, Yuen ST, Gao Z, Chen JS, Lai KC, Ong LY, Chen BW, Wang WH, Jiang XW, Hou XH, Lu JY. The China gastric cancer study group. Differential *Helicobacter pylori* infection rates in two contrasting gastric cancer risk regions of South China. *J Gastroenterol Hepatol* 1999; 14:120-125
- Gao GL, Yang Y, Yang S, Ren CW. Relationship between proliferation of vascular endothelial cells and gastric cancer. *Shijie Huaren Xiaohua Zazhi* 2000; 8:282-284
- Zou SC, Qiu HS, Zhang CW, Tao HQ. A clinical and long term follow up study of peri operative sequential triple therapy for gastric cancer. *World J Gastroenterol* 2000; 6:284-286
- Zhang XQ, Lin SR. The study advance of *Helicobacter pylori* and gastric cancer. *Shijie Huaren Xiaohua Zazhi* 2000; 8:206-207
- Ma JL, Liu WD, Zhang ZZ, Zhang L, You WC, Chang YS. Relationship between gastric cancer and precancerous lesions. *World J Gastroenterol* 1998; 4: 180-182
- Xue XC, Fang GE, Hua JD. Gastric cancer and apoptosis. *Shijie Huaren Xiaohua Zazhi* 1999; 7: 359-361
- Xia HX. Association between *Helicobacter pylori* and gastric cancer: current knowledge and future research. *World J Gastroenterol* 1998; 4:93-96
- Wang WX, Yuan Y, Gao H, Wang L, Wu YQ, Dong M. Screening of *Helicobacter pylori* infection in 16 villages of high risk population of gastric cancer. *World J Gastroenterol* 1998; 4: 112
- Cai L, Yu SZ, Zhang ZF. *Helicobacter pylori* infection and risk of gastric cancer in Changle Country, Fujian Province, China. *World J Gastroenterol* 2000; 6: 374-376
- Yuan Y, Cong W, Xu RT, Wang XJ, Gao H. Gastric cancer screening in 16 villages of Zhuanghe region: a high risk area of stomach cancer in China. *World J Gastroenterol* 1998; 4: 111
- Wu YA, Lu B, Liu J, Li J, Chen JR, Hu SX. Consequence alimentary reconstruction in nutritional status after total gastrectomy for gastric cancer. *World J Gastroenterol* 1999; 5: 34-37
- Hu PJ. *Hp* and gastric cancer: challenge in the research. *Shijie Huaren Xiaohua Zazhi* 1999; 7: 1-2
- Liu XB, Li L, Zhuang BZ, Jiang YD, Wang JH. Cyclin E expression in gastric carcinoma and its clinicopathological significance. *Shijie Huaren Xiaohua Zazhi* 1999; 7:656-658
- Folli S, Morgagni P, Roviello F, De Manzoni G, Marrelli D, Saragoni L, Di Leo A, Gaudio M, Nanni O, Carli A, Cordiano C, Dell'Amore D, Vio A. Risk factors for lymph node metastases and their prognostic significance in early gastric cancer (EGC) for the Italian Research Group for Gastric Cancer (IRGGC). *Jpn J Clin Oncol* 2001; 31: 495-499
- Yokota T, Kunii Y, Teshima S, Yamada Y, Saito T, Takahashi M, Kikuchi S, Yamauchi H. Significant prognostic factors in patients with early gastric cancer. *Int Surg* 2000; 85:286-290
- Kocher HM, Linklater K, Patel S, Ellul JP. Epidemiological study of oesophageal and gastric cancer in south-east England. *Br J Surg* 2001; 88: 1249-1257
- Barchielli A, Amorosi A, Balzi D, Crocetti E, Nesi G. Long-term prognosis of gastric cancer in a European Country: a population-based study in Florence (Italy). 10-year survival of cases diagnosed in 1985-1987. *Eur J Cancer* 2001; 37: 1674-1680
- Stein HJ, Feith M, Siewert JR. Cancer of the esophagogastric junction. *Surg Oncol* 2001; 9: 35-41
- Wang XS, Wang RB, Zhang ZL, Cao TJ, Jin WD. Effect of short time heating with MMC and 5-FU on cancer cells. *Shijie Huaren Xiaohua Zazhi* 1999; 7: 576-578
- Tu SP, Jiang SH, Qiao MM, Cheng SD, Wang LF, Wu YL, Yuan YZ, Wu YX. Effect of trichosanthin on cytotoxicity and induction of apoptosis of multiple drugs resistance cells in gastric cancer. *Shijie Huaren Xiaohua Zazhi* 2000; 8: 150-152
- Zhang XY. Some recent works on diagnosis and treatment of gastric cancer. *World J Gastroenterol* 1999; 5: 1-3
- Li GF, Xie SB, Sun H, Yang XH, Liu WJ, Zhai Q, Zhou YX, Li ZH, Zhang GM. An investigation of intra arterial chemotherapy infusion and embolization combined with abdominal chemotherapy for advanced gastric cancer. *World J Gastroenterol* 1998; 4: 71
- Yu WL, Huang ZH. Progress in studies on gene therapy for gastric cancer. *Shijie Huaren Xiaohua Zazhi* 1999; 7:887-889
- Murashima N, Gochi A, Kenmotsu M, Hamazaki K, Funaki M, Ohtsuka S, Tanaka N. Schedule-dependent combined sensitivity testing of anti-cancer agents in human gastric carcinoma cell lines. *J Int Med Res* 2001; 29: 189-197
- Itoh Y, Fuwa N, Shinoda M. A case of esophageal carcinoma surgically treated after discontinuance of the simultaneous application of radiotherapy and chemotherapy with low doses of CDDP and 5-FU. *J Radiat Med* 2000; 18:55-58
- Takahashi M, Yanoma S, Yamamoto Y, Rino Y, Amano T, Imada T. Combined effect of CDDP and caffeine against human gastric cancer cell line *in vivo*. *Anticancer Res* 1998; 18: 4399-4401
- Harstrick A, Gonzales A, Schleucher N, Vanhoef U, Lu K, Formento JL, Milano G, Wilke H, Seeber S, Rustum Y. Comparison between short or long exposure to 5-fluorouracil in human gastric and colon cancer cell lines: biochemical mechanism of resistance. *Anticancer Drugs* 1998; 9:625-634
- Raida M, Kath R, Arnrich M, Kahler G, Scheele J, Hoffken K. A phase II study of weekly high-dose 5-fluorouracil and leucovorin plus bi-weekly alternating doxorubicin and cisplatin for advanced gastric carcinoma. *Cancer Res Clin Oncol* 1998; 124: 335-340
- Guo HY, Herrera H, Groce A, Hoffman RM. Expression of the biochemical defect of methionine dependence in fresh patient tumors in primary histoculture. *Cancer Res* 1993; 53: 2479-2483
- Kreis W, Baker A, Ryan A, Bertasso A. Effect of nutritional and enzymatic methionine deprivation upon human normal and malignant cells in tissue culture. *Cancer Res* 1980; 40: 634-641
- Yoshida S, Yomasaki K, Kaibara A, Takagi K, Noake T, Ishibashi N, Kakegawa T. Effect of methionine-deprived total parenteral nutrition on tumor protein turnover in rats. *Cancer* 1995; 76:1275-1282
- Poirson-Bichat F, Gonfalone G, Bras-Goncalves RA, Dutrillaux B, Poupon MF. Growth of methionine dependent human prostate cancer (PC-3) is inhibited by ethionine combined with methionine starvation. *Br J Cancer* 1997; 75: 1605-1612
- Xiao HB, Cao WX, Yin HR, Lin YZ. The study of methionine-deprived total parenteral nutrition on gastric carcinoma bearing rat. *Changwai Yu Changnei Yingyang* 1997; 4: 16-18
- Cao WX, Xu N, Yin HR, Chen XH. The implication of tumor cells' methionine dependence in chemotherapy. *Zhonghua Shiyian Waikexue* 1999; 16: 319-320
- Cao WX, Yan M, Lin YZ, Yin HR, Zhu ZG, Li SF, Lu YP. The influence of intravenous nutrition on gastric cancer cell kinetics. *Zhonghua Zhongliu Zazhi* 1992; 14:418-420
- Cao WX, Xiao HB, Yin HR, Yan M, Zhu SZ, Lin YZ. The influence of intravenous nutrition on the effect of chemotherapy in gastric cancer. *Zhonghua Zhongliu Zazhi* 1994; 16:137-140
- Yan M, Cao WX, Zhu ZG, Yin HR, Zhu SZ, Lin YZ. The study of the parenteral nutrition on the gastric cancer cell kinetics in Wistar rats. *Zhongguo Linchuang Yingyang Zazhi* 1993; 1: 31-34
- Hoshiya Y, Kubota T, Matsuzaki SW, Kitajima M, Hoffman RM. Methionine starvation modulates the efficacy of cisplatin on human breast cancer in nude mice. *Anticancer Res* 1996; 16: 3515-3517
- Goseki N, Maruyama M, Nagai K, Kando F, Endo M, Shimoju K, Wada Y. Clinical evaluation of anticancer effect of methionine-depleting total parenteral nutrition with 5-fluorouracil and/or mitomycin C. *Gan To Kagaku Ryoho* 1995; 22: 1028-1035
- Kitamura S, Ohtani T, Kurihara M, Kosaki G, Akazawa S, Sasaki T, Takahashi H, Nakano S, Tokunaga K. A controlled study of AO-90, a methionine-free intravenous amino acid solution, in combination with 5-fluorouracil and mitomycin C in advanced gastric cancer patients (internal medicine group evaluation). *Gan To Kagaku Ryoho* 1995; 22: 765-775
- Taguchi T, Kosaki G, Onodera T, Endo M, Nakagawara G, Sano K, Kaibara N, Kakegawa T, Nakano S, Kurihara M. A controlled study of AO-90, a methionine-free intravenous amino acid solution, in combination with 5-fluorouracil and mitomycin C in advanced gastric cancer patients (surgical group evaluation). *Gan To Kagaku Ryoho* 1995; 22: 753-764
- Cao WX, Cheng QM, Fei XF, Li SF, Yin HR, Lin YZ. A study of preoperative methionine-depleting parenteral nutrition plus chemotherapy in gastric cancer patients. *World J Gastroenterol* 2000; 6: 255-258

• LIVER CANCER •

Effects of cryopreservation and phenylacetate on biological characters of adherent LAK cells from patients with hepatocellular carcinoma

Ning Zheng, Sheng-Long Ye, Rui-Xia Sun, Yan Zhao, Zhao-You Tang

Ning Zheng, Sheng-Long Ye, Rui-Xia Sun, Yan Zhao, Zhao-You Tang, Liver Cancer Institute and Zhongshan Hospital, Fudan University, Shanghai 200032, China

Supported by the National 9th Five-Year Program of China, No. 96-906-01-20
Correspondence to: Prof. Sheng-Long Ye, Liver Cancer Institute, Zhongshan Hospital, Fudan University, Shanghai 200032, China. slye@shmu.edu.cn

Telephone: +86-21-64041990-2137

Received 2001-11-15 Accepted 2001-12-10

Abstract

AIM: To improve the preparation of adherent lymphokine-activated killer (A-LAK) cells and to study the effects of cryopreservation and phenylacetate (PA) on biological characters of A-LAK cells.

METHODS: A-LAK cells were obtained from peripheral blood mononuclear cells (PBMCs) of the patients with hepatocellular carcinoma (HCC) by using L-phenylalanine methyl ester (PME) to deplete immunosuppressive monocytes. Proliferative activity of SMMC7721 cell line after treatment with phenylacetate (PA) was observed. A-LAK cells were treated with the supernatant of SMMC7721 cells that had been pretreated with PA. The changes of proliferation, cytotoxicity and phenotype of A-LAK cells were investigated after cryopreservation.

RESULTS: The expansion of A-LAK cells (96.79 ± 69.10 folds on Day 14) was significantly higher than that of non-adherent LAK (NA-LAK) cells (22.77 ± 13.20) as well as conventional LAK cells (4.64 ± 0.91). PA significantly suppressed the growth of SMMC7721 cells, and the inhibitor ratio was 46%. The supernatant of cultured tumor cells intensively suppressed the proliferation and cytotoxicity of A-LAK cells, but the suppressive effect of the supernatant was previously decreased after treatment with PA. Impairments in proliferation and cytotoxicity of A-LAK cells immediately after thawing of cryopreservation and recovery after reincubation with IL-2 were observed. The cytotoxicity of thawed A-LAK cells on Day 5 was significantly higher than that of fresh A-LAK before freezing ($54.8 \pm 10.2\%$ vs $40.5 \pm 6.4\%$). No significant change in the percentage of lymphocyte subsets was identified in frozen A-LAK cells as compared with that in the fresh control cells.

CONCLUSION: A-LAK cells can be simply prepared by using PME, and showed a synergistic anti-tumor effect with the combination of PA. Cryopreservation can increase the immunoactivities of A-LAK cells from the patients with hepatocellular carcinoma.

Zheng N, Ye SL, Sun RX, Zhao Y, Tang ZY. Effects of cryopreservation and phenylacetate on biological characters of adherent LAK cells from patients with hepatocellular carcinoma. *World J Gastroenterol* 2002;8(2):233-236

INTRODUCTION

Biotherapy of cancer, as the forth modality of tumor treatment, has been accepted^[1-4]. Adoptive transfer of LAK cells together with IL-2 has been found to be an effective immunotherapeutic modality for eradication of several tumors^[5-8]. However, some reports indicated that clinical responses have been infrequent and transient, and that severe toxicity was associated with the administration of high doses of rIL-2^[6,9,10]. Adherent-lymphokine activated killer (A-LAK) cells have significantly higher cytolytic activity on a per cell basis and greater proliferative capacity than LAK cells^[9-14]. But the usage of A-LAK cells was limited by the complex traditional preparation by using nylon wool columns^[15-17]. To harvest a large number of actively immunocompetent cells at the right time now becomes an important point of adoptive immunotherapy. The freezing of peripheral blood mononuclear cells (PBMCs) is a common practice, and does not significantly alter the functional activities of immunocompetent cells^[18]. The recent reports showed that frozen PBMCs produced significantly larger quantities of IL-1, IL-2, IL-6, and IFN- γ than the fresh cells^[19]. These results indicated that cryopreservation could increase the immunoactivities of immunocytes. We improved the preparation of A-LAK cells and studied the effects of cryopreservation and phenylacetate (PA) on biological characters of A-LAK cells from the patients with hepatocellular carcinoma.

MATERIALS AND METHODS

Cell lines and Reagents

A human hepatocellular carcinoma cell line, SMMC7721, was maintained in RPMI1640 medium supplemented with 10% heat-inactivated fetal calf serum (FCS, Gibco) at 37°C in a 5% CO₂ humidified atmosphere. Phenylacetate (PA, Sigma) and L-phenylalanine methyl ester (PME, Sigma) were dissolved in RPMI1640 medium, brought to pH7.0 and 7.4, respectively and stored in aliquots at 4°C.

Preparation of A-LAK cells

PBMCs were isolated from the patients with hepatocellular carcinoma (HCC) by using a cell separator (CS-3000 plus, Baxter), and then by centrifugation on Ficoll-Hypaque gradients. Cells collected from the gradient interface were washed twice in RPMI 1640 medium (GIBCO) and incubated in medium containing PME (5mmol/L) for 40min at room temperature to remove monocytes. After two washes with complete tissue culture medium (TCM) containing RPMI 1640 medium supplemented with 10%(v/v) heat-inactivated pooled AB human serum. The monocyte-depleted PBMCs were adjusted to the concentration of 2×10^6 /ml and incubated in TCM containing rIL-2 (1000U/ml) in a plastic culture flasks positioned on its flat side for 24hr at 37°C in humidified atmosphere of 5% CO₂. Following 24hr of activation in rIL-2, supernatants containing cells that did not adhere to plastic were decanted from the flasks, collected, and centrifuged. The recovered non-adherent cells (NA-LAK cells) were resuspended in fresh TCM plus rIL-2 (1000U/L) and cultured for 8-12 days. The cell-free supernatant of the non-adherent cell population was collected

and used as autologous conditioned medium (AuCM). The cells adherent to plastic (A-LAK cells) were washed twice with prewarmed TCM to remove cells that were not firmly attached to plastic, and then were supplemented with TCM containing 50% (v/v) of AuCM and rIL-2 (1000U/ml). These A-LAK cells were also cultured for 8-12 days and maintained at a concentration of 2×10^6 cells/ml by supplying fresh TCM containing rIL-2 (1000U/ml) as needed. PBMCs were also established in cultures with rIL-2 (1000U/L) and cultured for 4 days as standard, regular LAK cells.

Procedures of freezing and thawing

After 10 days of incubation with rIL-2, A-LAK cells were washed and counted. Then the cells were diluted in the cold freezing medium in an ice bath to give a final concentration of 5×10^6 cells/ml. The freezing medium consisted of 10% (v/v) heat-inactivated pooled AB human serum, 10% dimethyl sulfoxide (DMSO), and 80% RPMI-1640 containing rIL-2 (1000U/ml). The cells were distributed in precooled plastic vials. The vials were frozen according to the routine procedure: at 4°C for 30min → at 0°C for 30min → at -20°C for 30min → at -80°C for 60min → transferred to liquid nitrogen for storage.

The frozen cells were thawed in a 37°C water bath, and washed at 1000rpm in phosphate-buffered saline twice to remove DMSO. Cell recovery and viability were calculated by trypan blue exclusion. After thawing, the cells were cultured in complete media as described above with 1000U of rIL-2/ml at the concentration of 2×10^6 cells/ml for 7~10 days.

Tumor cell culture and PA treatment

The SMMC7721 cells growing in logarithmic phase were seeded into flasks at a concentration of 2×10^5 cells/flask. The following day, the medium was changed, and PA was added to the medium at 0 and 5mmol/L for 7 days. After cell counts, the mediums were changed. Twenty-four hours later, the cell-free supernatants of SMMC7721 cells with PA pre-treatment and non-treatment were collected.

Proliferative activity of A-LAK cells

Fold expansions of fresh A-LAK cells, NA-LAK cells, regular LAK and frozen A-LAK cells were determined by cell counts performed in the presence of trypan blue on day 1, 4, 7, 10, and 14, respectively.

On the other hand, A-LAK cells were incubated by supplying fresh TCM containing 10% (v/v) cell-free supernatant derived from SMMC7721 cells with and without PA administration previously for 14 days. Cell numbers were calculated by hemocytometer cell counts in trypan blue.

Cytotoxicity Assays^[20]

The fresh A-LAK cells, frozen A-LAK cells and A-LAK cells treated with SMMC7721 cell supernatant administered with or without PA were tested as effector cells for cytotoxicity against cultured SMMC7721 cells in MTT assays. SMMC7721 cells as target cells were seeded 2×10^4 cells/well in wells of U-bottomed 96-well plates and incubated for 24hr. Effector cells were added to target cells in effector-to-target ratio of 10 : 1. After 48-hour incubation at 37°C, stock MTT solution (50μl/well) was added to all wells of an assay, and plates were incubated at 37°C for 6hr. Acid-isopropanol was added to all wells and mixed thoroughly to dissolve the dark blue crystals. After a few minutes at room temperature to ensure that all crystals were dissolved, the plates were read on a Microplate Reader (3550-UV, Bio-Rad), using a test wavelength of 570nm, a reference wavelength of 630nm.

Analyses of phenotype

The surface phenotype of cells was analyzed before freezing, after

thawing and after 3 days of restimulation with rIL-2 using monoclonal antibodies CD3, CD4, CD8, CD16, and CD25. Analyses were performed on a flow cytometer (EPI CV-V, Culter Corp.).

Statistics

Statistics analysis of the data was performed using the Student's *t*-test; *P* < 0.05 was considered statistically significant.

RESULTS

Proliferation of A-LAK cells

A-LAK cells expanded better and faster than autologous non-adherent cells or regular LAK cells under the same growth conditions (Table 1). For HCC patients, the expansions of A-LAK cells varied from 23- to 243- fold by 14 days in culture, which were much higher than those of NA-LAK cells and regular LAK cells.

Table 1 Proliferative capacity of A-LAK cells

Culture Days	Cells expansion folds		
	A-LAK	NA-LAK	Regular LAK
1	1.35±0.39	0.87±0.21 ^a	0.83±0.09 ^a
4	2.22±0.85	1.09±0.33 ^a	0.99±0.03 ^a
7	4.42±2.05	2.13±0.83 ^a	1.55±0.14 ^b
10	22.52±10.47	8.49±3.91 ^a	3.25±0.64 ^b
14	96.79±69.10	22.77±13.20 ^a	4.64±0.91 ^a

^a*P* < 0.05, vs compared with A-LAK cells of the same day; ^b*P* < 0.01, vs compared with A-LAK cells of the same day

The recovery rate after thawing of the cryopreserved A-LAK cells was 84.3±4.2%. The viability of frozen cells was 96.4±3.8%. The length of storage in liquid nitrogen (ranged from 1 day to 6 months) did not have any detectable effect. The frozen A-LAK cells after thawing maintained a high ability of proliferation. After 3 days of reculture with rIL-2, the expansion folds of thawed A-LAK cells was in the same range as A-LAK cells before freezing (Figure 1).

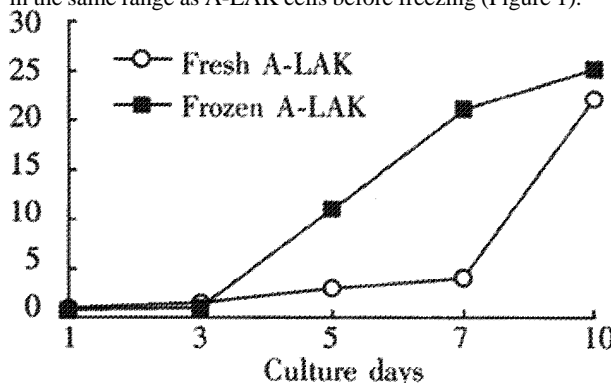


Figure 1 Proliferative capacity of A-LAK cells

Effect of PA on SMMC7721 cell proliferation

Having treated with PA at 5mmol/L for 7 days, the SMMC7721 cells propagated from 2.0×10^5 cells/flask to 1.54×10^6 cells/flask. At the same time, the tumor cells without PA treatment proliferated to 2.86×10^6 cells/flask. The inhibitory ratio of PA affecting SMMC7721 proliferation was 46%.

Effect of PA and supernatant of Tumor cells on A-LAK propagation

On day 14 of cell culture, the expansion folds of A-LAK cells treated with the supernatant of SMMC7721 cells were only 55.22±42.37, which were significantly lower than those of normal cultured A-LAK cells (96.79±69.10, *P* < 0.01). However, the expansion folds of A-LAK cells treated with the supernatant of SMMC7721 cells with PA administration previously recovered to 84.72±58.98, which had no

significant statistical difference from those normal cultured A-LAK cells ($P>0.05$).

Effect of PA and supernatant of tumor cells on A-LAK cell cytotoxicity

The cytotoxicity of A-LAK cells treated with the supernatant of SMMC7721 cells $31.2\pm9.01\%$ was significantly lower than that of normal cultured A-LAK cells $68.4\pm8.82\%$ ($P<0.001$). However, the cytotoxicity of A-LAK cells treated with the supernatant of SMMC7721 cells with PA administration previously approached the normal level $57.1\pm10.1\%$ ($P>0.05$).

Effect of cryopreservation on A-LAK cell cytotoxicity

Immediately after thawing, there was a significant decrease in cytotoxic activities. This impairment in activity was temporary, and the complete cytotoxicity could be restored by reincubation of the thawed A-LAK cells with rIL-2 for 1 day (Figure 2). After 5 days of postthaw culture with rIL-2, the cytotoxicity of the thawed A-LAK cells ($54.8\pm10.2\%$) was significantly higher than that of fresh A-

LAK cells before freezing ($40.5\pm6.4\%$, $P<0.05$).

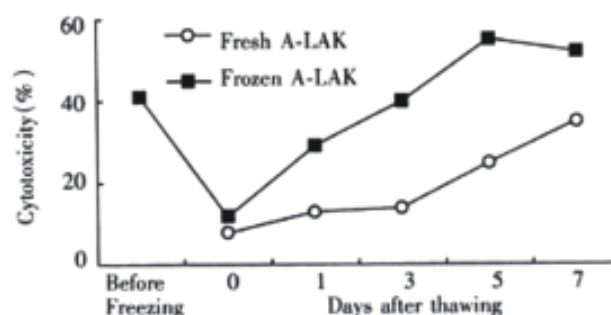


Figure 2 Effect of cryopreservation on A-LAK cells cytotoxicity

Change of phenotype of frozen A-LAK cells

As shown in Table 2, no significant change in the percentage of lymphocyte subpopulations of A-LAK cells before freezing, immediately after thawing, and 3 days after thawing was identified ($P>0.05$).

Table 2 Changes of phenotype of cryopreserved A-LAK cells

	Case No.	CD3	CD4	CD8	CD4/CD8	CD16	CD25
Before freezing	6	76.5±10.3	41.4±7.5	40.3±5.3	1.03±0.31	10.4±3.1	52.3±5.9
Day 0 after thawing	6	80.5±11.4	35.9±6.4	36.5±4.9	1.07±0.38	14.1±4.3	49.7±3.1
Day 3 after thawing	6	86.3±8.9	33.1±7.5	42.6±6.0	0.78±0.19	15.4±2.7	46.5±4.7

DISCUSSION

The application of LAK cells in immunotherapeutic treatment of cancer began in the past decade. The biotherapy may be the most effective method in delayed treatment of residual neoplastic diseases after classic reductive therapy (i.e. chemotherapy and bone marrow transplantation). A large number of immunocompetent cells are required for each adoptive immunotherapy. In some patients, because of the complexity of the preparation of immunocytes, such as LAK cells and A-LAK cells, the immunosuppressive status of the tumor host, and the procedures of the treatment of malignant tumor (i.e. the side effects of chemotherapy on the immune system of the host), it is difficult to obtain sufficient effector cells when they are needed. Therefore, we have carried out experiments to improve the preparation of A-LAK cells, and to determine the effects of cryopreservation and PA on the immunologic function of A-LAK cells obtained from the patients with HCC.

A major contributor to host immunity and immune surveillance against infection, tissue or cell damage and malignancy is the monocyte/macrophage system. The monocytes/macrophages play both positive and negative regulator roles in immune responses^[21-23]. They can secrete some kinds of cytokines (i.e. IL-1, IL-6), which may lead to an enhancement effect on both humoral and cellular immunity of human bodies^[24,25]. Meanwhile, they can also produce some chemotactic factors (such as prostaglandin E2, lipocortin) to intensively suppress the immune responses^[26,27]. In addition, some reports indicated that monocytes/macrophages could inhibit the proliferation and cytotoxicity of LAK cells^[28]. Thus, the therapeutic effects of LAK cells would be improved by removing monocytes/macrophages from PBMC. The monocyte-depleted PBMC cells could be incubated with rIL-2 in a plastic flask and the plastic-adherent cells could be harvested as adherent LAK cells. There are several methods that can be used to get rid of monocytes/macrophages from peripheral blood. The routine one is to load PBMC onto prewarmed nylon wool column to remove monocytes/macrophages by adherence to nylon wool. But the complexity of this procedure limited the usage of A-LAK cells. Some reports demonstrated that PME could remove the monocytes/macrophages efficiently without changing the phenotype and cytotoxicity of lymphocytes. Triozzi and colleagues used this procedure

to harvest A-LAK cells with efficient anti-tumor activities from the patients with renal cancer^[15]. Our results using the same method to prepare A-LAK cells from patients with HCC are similar to those reports.

There are evidences that the immune system of tumor hosts has been destroyed, and that the immune function of hosts is suppressed^[29-32]. Thus, LAK cells and A-LAK cells prepared from peripheral blood of tumor hosts were different from those of normal individuals. Melden *et al* reported that for normal individuals, the expansion of A-LAK cells varied from 190- to 800- folds by 14 days in culture^[9], whereas the numbers of A-LAK cells harvested from HCC patients in our study were only increased by 23- to 243- folds. We also indicated that the human HCC cell line (SMMC7721) intensively suppressed the proliferation and cytotoxic activity of A-LAK cells by secreting some immunosuppressive factors. The suppression of immune system of tumor host caused by secretion of immunosuppressive factors from tumor cells has become one reason for the limitation of the usage of the adoptive immunotherapy such as LAK/rIL-2.

The cryopreservation of human mononuclear cells is a common practice, but the effect of the cryopreservation of the effector cells on the functional activities is not well documented. Some reports indicated that high concentration of DMSO, rapid cooling rate, and rapid diluting after thawing could injure the hemopoietic stem cells and lymphocytes^[33]. Recent results showed that freezing not only did not significantly affect the functional activities of immunocompetent cells, but also increased the secreting abilities of some cytokines of these cells^[19]. In our tests, optimal proliferation and cytotoxicity of A-LAK cells from the patients with HCC were generated after 10 days of culture with rIL-2. Cryopreservation was performed on cells after 10 days of culture. Our results demonstrated that impairments in proliferation and cytotoxicity of A-LAK cells immediately after thawing of cryopreservation and recovery after reincubation with IL-2 were observed. The cytotoxicity of thawed A-LAK cells on Day 5 was significantly higher than that of fresh A-LAK before freezing. The results indicated that cryopreservation could increase the immunoactivities of A-LAK cells from the patients with hepatocellular carcinoma. The difference of the immunologic activities of A-LAK cells during the distinct periods after thawing may explain the

divergence of views from different investigators.

Phenylacetate (PA) is a member of a class of aromatic fatty acids and common metabolite of phenylalanine that is present in human plasma and cerebrospinal fluid in micromolar concentrations^[34]. Experimental data indicated that PA was able to promote differentiation, growth inhibition, tumor maturation, and apoptosis *in vitro* and *in vivo* of various human leukemia cells, prostate carcinoma cells, breast cancer cells, brain tumor cells and renal cancer cells^[35-38]. The phase I clinical trials at the National Cancer Institute with phenylacetate as a novel, nontoxic differentiation inducers have been finished^[39]. Currently in clinical trials, PA was examined for its ability to modify tumor immunogenicity and revealed that it was able to reduce biosynthesis and secretion of TGF- β 2, the tumor-derived T-cell suppressor factor, and reverse the tumor associated inhibition of IL-2 secretion by PHA-treated peripheral blood lymphocytes^[40]. In our study, PA could significantly inhibit the growth of tumor cells, and the suppressive effect of the supernatant of tumor cells with pre-treatment of PA on the proliferation and cytotoxicity of A-LAK cells was decreased. Our data indicated that PA could decrease the immunosuppressive factors derived from tumor cells, antagonize the inhibition of tumor in biotherapy, and coordinate to attack tumor cells.

REFERENCES

- Ye SL. Biotherapy of tumor. In: Tang ZY. Contemporary oncology. 2nd ed. Shanghai: Shanghai Med University Press 2000:513-522
- Bremers AJ, Parmiani G. Immunology and immunotherapy of human cancer: present concepts and clinical developments. *Crit Rev Oncol Hematol* 2000;34:1-25
- Cheng JD, Rieger PT, von-Mehren M, Adams GP, Weiner LM. Recent advances in immunotherapy and monoclonal antibody treatment of cancer. *Semin Oncol Nurs* 2000;16(Suppl 1): 2-12
- Kobari M, Egawa S, Shibuya K, Sunamura M, Saitoh K, Matsuno S. Effect of intraportal adoptive immunotherapy on liver metastases after resection of pancreatic cancer. *Br J Surg* 2000;87:43-48
- Ye SL. Biotherapy of hepatocellular carcinoma. In: Tang ZY, Yu YQ. Primary liver cancer, 2nd ed. Shanghai: Shanghai Sci Technical Press 1999:382-296
- Hoffman DM, Gitlitz BJ, Belldgrun A, Figlin RA. Adoptive cellular therapy. *Semin Oncol* 2000;27:221-233
- Pawelec G, Rees RC, Kiessling R, Madrigal A, Dodi A, Baxevas C, Gambacorti-Passerini C, Masucci G, Zeuthen J. Cells and cytokines in immunotherapy and gene therapy of cancer. *Crit Rev Oncog* 1999;10:83-127
- Semino C, Martini L, Queirolo P, Cangemi G, Costa R, Aloisio A, Ferlazzo G, Sertoli MR, Reali UM, Ratto GB, Melioli G. Adoptive immunotherapy of advanced solid tumors: an eight year clinical experience. *Anticancer Res* 1999;19:5645-5649
- Melder RJ, Whiteside TL, Vujanovic NL, Hiscrodt JC, Herberman RB. A new approach to generating antitumor effectors for adoptive immunotherapy using human adherent lymphokine-activated killer cells. *Cancer Res* 1988;48:3461-3469
- Schwarz RE, Vujanovic N L, Hiscrodt JC. Enhanced antimetastatic activity of lymphokine-activated killer cells purified and expanded by their adherence to plastic. *Cancer Res* 1989;49:1441-1446
- Kiremidjian-Schumacher L, Roy M, Wishe HI, Cohen MW, Stotzky G. Supplementation with selenium augments the functions of natural killer and lymphokine-activated killer cells. *Biol Trace Elem Res* 1996;52:227-239
- Koberda J, Przepiorka D, Moser RP, Grimm EE. Sequential TNF and TGF-beta regulation of expansion and induction of cytotoxicity in long-term cultures of lymphokine-activated killer cells. *Lymphokine Cytokine Res* 1994;13:139-145
- Boiardi A, Silvani A, Ruffini PA, Rivoltini L, Parmiani G, Broggi G, Salmaggi A. Loco-regional immunotherapy with recombinant interleukin-2 and adherent lymphokine-activated killer cells (A-LAK) in recurrent glioblastoma patients. *Cancer Immunol Immunother* 1994;39:193-197
- Basse PH, Herberman RB, Hokland ME, Goldfarb RH. Tissue distribution of adoptively transferred adherent LAK cells: role of the route of administration. *Nat Immun* 1992;11:193-202
- Trionzi PL, Aldrich W, Kim J, Kinney P, Sagone A, Rinehart J. Biologic effects of the adoptive transfer of cells depleted of monocytes with L-phenylalanine methyl ester. *Immunopharmacology* 1994;28:39-45
- Koyama S, Fukao K. Phenotypic analysis of nylon-wool-adherent suppressor cells that inhibit the effector process of tumour cell lysis by lymphokine-activated killer cells in patients with advanced gastric carcinoma. *J Cancer Res Clin Oncol* 1994;120:240-247
- Jaso-Friedmann L, Leary JH 3rd, Evans DL. Role of function-associated molecules in target cell lysis: analysis of rat adherent lymphokine-activated killer cells. *Nat Immun* 1993;12:316-325
- Marti F, Miralles A, Peiro M, Amill B, de Dalmases C, Pinol G, Rueda F, Garcia J. Differential effect of cryopreservation on natural killer cell and lymphokine-activated killer cell activities. *Transfusion* 1993;33:651-655
- Venkataraman M. Effects of cryopreservation on immune responses. VIII. Enhanced secretion of interferon- α by frozen human peripheral blood mononuclear cells. *Cryobiology* 1995;32:528-534
- Riberiro-Dias F, Marzagao-Barbuto JA, Tsujita M, Jancar S. Discrimination between NK and LAK cytotoxic activity of murine spleen cells by MTT assay: differential inhibition by PGE2 and EDTA. *J Immuno Methods* 2000;241:121-129
- Hsieh CL, Chen DS, Hwang LH. Tumor-induced immunosuppression: a barrier to immunotherapy of large tumors by cytokine-secreting tumor vaccine. *Hum Gene Ther* 2000;11:681-692
- Williams MA, Newland AC, Kelsey SM. The potential for monocyte-mediated immunotherapy during infection and malignancy. Part I: apoptosis induction and cytotoxic mechanisms. *Leuk Lymphoma* 1999; 34:1-23
- Rhoades CJ, Williams MA, Kelsey SM, Newland AC. Monocyte-macrophage system as targets for immunomodulation by intravenous immunoglobulin. *Blood Rev* 2000;14:14-30
- Schwacha MG, Schneider CP, Bland KI, Chaudry IH. Resistance of macrophages to the suppressive effect of interleukin-10 following thermal injury. *Am J Physiol Cell Physiol* 2001;281:C1180-C1187
- Marselli L, Marchetti P, Tellini C, Giannarelli R, Lenciono C, Del-Guerra S, Lupi R, Carmellini M, Mosca F, Navalesi R. Lymphokine release from human lymphomononuclear cells after co-culture with isolated pancreatic islets: effects of islet species, long-term culture, and monocyte-macrophage cell removal. *Cytokine* 2000;12:503-505
- Luo JS, Kammere R, von-Kleist S. Comparison of the effects of immunosuppressive factors from newly established colon carcinoma cell cultures on human lymphocyte proliferation and cytokine secretion. *Tumor Biol* 2000;21:11-20
- Sakata T, Iwagami S, Tsaroka Y, Teraoka H, Hojo K, Suzukis S, Sato K, Suzuki R. The role of lipocortin I in macrophage-mediated immunosuppression in tumor-bearing mice. *J Immunol* 1990;145:387-396
- Bergmann L, Schui DK, Brieger J, Weidmann E, Mitron PS, Hoelzer D. The inhibition of lymphokine-activated killer cells in acute myeloblastic leukemia is mediated by TGF- β 1. *Exp Hematol* 1995;23:1574-1580
- Pardoll D. T cells and tumors. *Nature* 2001; 411:1010-1012
- Dagleish AG. Current problems in the development of specific immunotherapeutic approaches to cancer. *J Clin Pathol* 2001;54:675-676
- Biggs MW, Eiselein JE. Suppression of immune surveillance in melanoma. *Med Hypotheses* 2001;56:648-652
- Karimine N, Arinaga S, Inoue H, Nanbara S, Ueo H, Akiyoshi T. Lymphokine-activated killer cell function of peripheral blood mononuclear cells, spleen cells and regional lymph node cells in gastric cancer patients. *Clin Exp Immunol* 1994;96:484-490
- Cai JM, Ding ZH, Mai GZ, Li XC. Different susceptibility of murine hemopoietic cells and lymphocytes to freezing-thawing process. *Dier Junyi Daxue Xuebao* 1994;15:110-114
- Samid D, Hudgins WR, Shack S, Liu L, Prasanna P, Myers CE. Phenylacetate and phenylbutyrate as novel, nontoxic differentiation inducers. *Adv Exp Med Biol* 1997;400A:501-505
- Han S, Wada RK, Sidell N. Differentiation of human neuroblastoma by phenylacetate is mediated by peroxisome proliferator-activated receptor gamma. *Cancer Res* 2001;61:3998-4002
- Vasse M, Thibout D, Paysant J, Legrand E, Soria C, Crepin M. Decrease of breast cancer cell invasiveness by sodium phenylacetate (NaPa) is associated with an increased expression of adhesive molecules. *Br J Cancer* 2001;84:802-807
- Watanabe M, Sugano S, Imai J, Yoshida K, Onodera R, Amin MR, Uchida K, Yamaguchi R, Tateyama S. Suppression of tumourigenicity, and induction of differentiation of the canine mammary tumor cell line MCM-B2 by sodium phenylacetate. *Res Vet Sci* 2001;70:27-32
- Thibout D, DiBenedetto M, Kraemer M, Sainte CO, Derbin C, Crepin M. Sodium phenylacetate modulates the synthesis of autocrine and perigrine growth factors secreted by breast cancer cell lines. *Anticancer Res* 1998;18:2657-2661
- Thibault A, Samid D, Cooper MR, Figg WD, Tompkins AC, Patronas N. Phase I study of phenylacetate administered twice daily to patients with cancer. *Cancer* 1995;75:2932-2938
- Liu L, Bar-ner M, Weber J, Danielpour D, Qian SW, Shearer GM, Bernutt RM. Enhancement of tumor immunogenicity by phenylacetate and derivatives: Changes in surface antigens and tumor-derived immunosuppressive factors. *Proc Am Assoc Cancer Res* 1994;35:481

• LIVER CANCER •

Prediction of recurrence and prognosis in patients with hepatocellular carcinoma after resection by use of CLIP score

Wen-He Zhao, Zhi-Min Ma, Xing-Ren Zhou, Yi-Zheng Feng, Bao-Shan Fang

Wen-He Zhao, Zhi-Min Ma, Xing-Ren Zhou, Yi-Zheng Feng, Bao-Shan Fang, Department of Oncosurgery, the First Affiliated Hospital, Zhejiang University, Medical College, Hangzhou 310003, Zhejiang Province, China

Correspondence to: Dr. Wen-He Zhao, Department of Oncosurgery, the First Affiliated Hospital, Zhejiang University, Medical College, 79 Qingchun, Hangzhou 310003, Zhejiang Province, China. zhaowh@mail.hz.zj.cn
Telephone: +86-571-87236880

Received 2001-10-12 Accepted 2001-10-29

Abstract

AIM: The survival time of patients with hepatocellular carcinoma (HCC) after resection is hard to predict. Both residual liver function and tumor extension factors should be considered. A new scoring system has recently been proposed by the Cancer of the Liver Italian Program (CLIP). CLIP score was confirmed to be one of the best ways to stage patients with HCC. To our knowledge, however, the literature concerning the correlation between CLIP score and prognosis for patients with HCC after resection was not published. The aim of this study is to evaluate the recurrence and prognostic value of CLIP score for the patients with HCC after resection.

METHODS: A retrospective survey was carried out in 174 patients undergoing resection of HCC from January 1986 to June 1998. Six patients who died in the hospital after operation and 11 patients with the recurrence of the disease were excluded at 1 month after hepatectomy. By the end of June 2001, 4 patients were lost and 153 patients with curative resection have been followed up for at least three years. Among 153 patients, 115 developed intrahepatic recurrence and 10 developed extrahepatic recurrence, whereas the other 28 remained free of recurrence. Recurrences were classified into early (≤ 3 year) and late (> 3 year) recurrence. The CLIP score included the parameters involved in the Child-Pugh stage (0-2), plus macroscopic tumor morphology (0-2), AFP levels (0-1), and the presence or absence of portal thrombosis (0-1). By contrast, portal vein thrombosis was defined as the presence of tumor emboli within vascular channel analyzed by microscopic examination in this study. Risk factors for recurrence and prognostic factors for survival in each group were analyzed by the chi-square test, the Kaplan-Meier estimation and the COX proportional hazards model respectively.

RESULTS: The 1-, 3-, 5-, 7-, and 10-year disease-free survival rates after curative resection of HCC were 57.2%, 28.3%, 23.5%, 18.8% and 17.8%, respectively. Median survival time was 28, 16, 10, 4, and 5 mo for CLIP score 0, 1, 2, 3, and 4 to 5, respectively. Early and late recurrence developed in 109 patients and 16 patients respectively. By the chi-square test, tumor size, microsatellite, venous invasion, tumor type (uninodular, multinodular, massive), tumor extension (\leq or $> 50\%$ of liver parenchyma replaced by tumor),

TNM stage, CLIP score, and resection margin were the risk factors for early recurrence, whereas CLIP score and Child-Pugh stage were significant risk factors for late recurrence. In univariate survival analysis, Child-Pugh stages, resection margin, tumor size, microsatellite, venous invasion, tumor type, tumor extension, TNM stages, and CLIP score were associated with prognosis. The multivariate analysis by COX proportional hazards model showed that the independent predictive factors of survival were resection margins and TNM stages.

CONCLUSION: CLIP score has displayed a unique superiority in predicting the tumor early and late recurrence and prognosis in the patients with HCC after resection.

Zhao WH, Ma ZM, Zhou XR, Feng YZ, Fang BS. Prediction of recurrence and prognosis in patients with hepatocellular carcinoma after resection by use of CLIP score. *World J Gastroenterol* 2002;8(2):237-242

INTRODUCTION

Hepatocellular carcinoma (HCC) is one of the major causes of death in the world^[1-4]. In China, HCC ranked second of cancer mortality since 1990s^[5]. Within the past decade, as a result of advances in the diagnosis and disease management of HCC, significant improvement of overall and disease-free survival rates after resection of HCC have been achieved^[6-9]. However, even when curative resection is performed, a considerable number of patients develop intrahepatic and/or extrahepatic recurrence postoperatively^[10-16]. The recurrence and prognostic assessment of patients with HCC after resection is an important clinical issue^[13,14,17-21].

After Okuda made a suggestion of clinical stage system^[22], UICC introduced the tumor node metastasis (TNM) stage that was widely used in China for predicting the prognosis of HCC^[17,18,23]. TNM stage took into account of the tumor extension alone and it did not deal with liver function. HCC mainly arose in patients already affected with chronic hepatitis or cirrhosis^[12,24]. The prevalence of hepatitis B surface antigen (HbsAg) and antibody to HCV in HCC patients were reported to be 63.2% and 11.2% respectively in China^[25], and coexisting cirrhosis occurred in 88.8% (888/1000 patients) for patients with small HCC^[14]. The liver damage in patients with HCC after resection is also a risk factor for recurrence and prognosis^[26-32]. Hence, a new stage accounting for both liver function and tumor extension is necessary to predict HCC prognosis.

In 1998, by a retrospective evaluation of 435 Italian patients, the Cancer of the Liver Italian Program (CLIP) had proposed a new prognostic system that included four parameters involved in the Child-Pugh stage, plus macroscopic tumor morphology, alpha-fetoprotein (AFP) levels, and the presence or absent portal thrombosis and confirmed that the CLIP score, compared with the Okuda staging system, gave more accurate prognostic information, was statistically more efficient, and had a greater survival predictive power^[33,34]. After that, Farinati *et al*^[35] pointed that the CLIP score was able to

predict survival better than TNM staging system, especially in the subgroup of patients undergoing chemoembolization. However, the number of patients with HCC after resection in these two studies was small and limited. Correlation between CLIP score and prognosis of patients with HCC after resection was not reported. The aim of this study is to validate the prognostic value of CLIP score in the patients with HCC by means of disease-free survival rate and time to recurrence for patients enrolled between 1986 and 1998 in our department.

MATERIALS AND METHODS

Patients

From January 1986 to June 1998, 174 patients underwent resection of HCC at our department. The mean age was 49.8 (range, 9-75) years old and the ratio of male to female was 156 to 18. Six patients who died in the hospital after operation and 11 patients were excluded because of the disease detected in the remnant liver by a routine ultrasound or CT scan or arteriography performed at 1 month after hepatectomy, which was considered residual disease. By the end of June 2001, 4 patients were lost and 153 patients with curative resection have been followed up for at least three years. Among 153 patients, 115 developed intrahepatic recurrence and 10 developed extrahepatic recurrence, whereas the other 28 remained recurrence free after a mean follow up period of 60 months. Figure 1 showed the patients distribution of the time to recurrences or death after operation. There were two peaks at 6 months and 15 months among those with early recurrence. Our data indicated that 3-year' survival after hepatectomy was a distinctive point of early from late recurrence when compared with other time intervals such as 1 and 2 years.

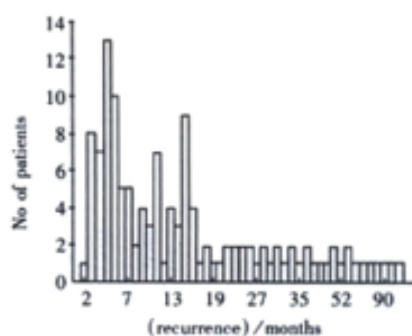


Figure 1 The recurrent time distribution of patients with HCC after complete resection

Methods

The CLIP score system included Child-Pugh stage^[36], tumor morphology and extension, AFP levels, and the presence or absence of portal thrombosis (Table1).

Table 1 CLIP score system

Variable	Scores		
	0	1	2
Child-Pugh stage	A	B	C
Tumor morphology	Uninodular and extension ≤50%	Multinodular and extension ≤50%	Massive or extension >50%
AFP(ng/Dl)	<400	≥400	
Portal vein thrombosis	No	Yes	

The scores was calculated by addition of each individual value of the four items^[34]. What was the difference from the CLIP data, that portal vein thrombosis was defined as the presence of tumor emboli within vascular channel analyzed by microscopic examination in this study.

Disease-free survival rate was defined as the time relapsed from the date of image diagnosis and either the date of death or the date of the latest follow-up visit, with final evaluation at June 30, 2000. Recurrences were classified into early (<=3 year) and late recurrence (>3 year) after the date of hepatectomy. Patients with early or late recurrences were compared respectively with patients who did not develop any recurrent disease during the follow-up periods to identify risk factors.

Statistical Analysis

Comparisons between groups were performed by the chi-square test (Pearson's methods or Fisher's exact test). Univariate survival curves were evaluated using the Kaplan-Meier method and compared by using the Long-rang test. The COX proportional hazards model was used to determine the significance of each significant univariate variable in multivariate analysis of prognostic factors. All analyses were performed using SPSS 8.0 for windows software. All *P* values of less than 0.05 in two-tailed were considered statistically significant.

RESULTS

The 1-, 3-, 5-, 7-, and 10-year cumulative disease-free survival rates were 57.2%, 28.3%, 23.5%, 18.8% and 17.8% respectively after hepatectomy. Among the 125 patients with recurrence, 109 had early recurrences and 16 had late recurrences. 28 patients were recurrence free within follow-up period.

Risk factors for early and late recurrence

The characteristics of the host-and treatment-related factors were showed in Table 2. Among of six host-related factors, age, gender, hepatitis B surface antigen status, tumor family history and cirrhosis were associated with neither early nor late recurrence.

Table 2 Characteristics of host-and treatment-related factors in patients with HCC after resection

Characteristics	Early recurrence (n=109)	Late recurrence (n=16)	No recurrence (n=28)
Age	50.7±9.8	49.2±8.5	48.3±10.2
Gender(M/F)	100/9	13/3	24/4
HbsAg			
positive	78	12	18
negative	31	4	10
Tumor family history			
Yes	16	5	4
No	91	11	24
Unknown	2	0	0
Cirrhosis			
Yes	82	12	18
No	27	4	10
Child-Pugh			
A	91	10	26
B	31	6	2
C	1	0	0
Preoperative TAE			
Yes	18	0	4
No	97	16	24
splenectomy			
Yes	11	1	4
No	98	15	24
Resection margin (cm)			
<1	67	4	4
≥1	42	12	24
Postoperative chemotherapy			
Yes	58	9	13
No	51	7	15

Child-Pugh stage had not correlation with early recurrence, whereas it had significant correlation with late recurrence [Child stage B: 37.5% (6/16) in late recurrence versus 7.1% (2/28) in no-recurrence, $P=0.019$]. The four treatment-related factors, preoperative transcatheter arterial embolization (TAE), postoperative chemotherapy, with or without splenectomy, were associated with neither early nor late recurrence. The proportion of resection margin less than one centimeter in early recurrence was significant higher than that in no-recurrence ($P=0.000$), but had not correlated with late recurrence. Eight tumor-related factors except serum AFP levels were associated with early recurrence, namely tumor size $>5\text{cm}$ ($P=0.001$), presence of microsatellite ($P=0.000$), venous invasion ($P=0.001$), tumor type ($P=0.024$), tumor extension ($P=0.013$), advanced TNM stages ($P=0.000$), and CLIP scores ($P=0.005$). In contrast, only CLIP score has significant correlation with late recurrence [CLIP score 0-1: 92.9% (26/28) in no-recurrence versus 56.2% (9/16) in late recurrence, $P=0.006$] (Table 3).

Table 3 Characteristics of tumor-related factors in patients with HCC after resection

Characteristics	Early recurrence ($n=109$)	Late recurrence ($n=16$)	No recurrence ($n=28$)
Serum AFP ($\mu\text{g}\cdot\text{L}^{-1}$)			
<400	66	8	14
≥ 400	43	8	14
Tumor size/cm			
≤ 5	43*	7	21
>5	66	9	7
Microsatellite			
Absent	69	14	28
present	40	2	0
Venous invasion			
Absent	78	15	28
present	31	1	0
Tumor type			
Uninodular	78	14	27
Multinodular	17	2	1
Massive	14	0	0
Tumor extension			
$\leq 50\%$	90	15	28
$>50\%$	19	1	0
UICC TNM stage			
I	1	1	9
II	36	11	18
III	51	12	1
IV	21	2	0
CLIP scores			
0	21	6	11
1	38	3	15
2	25	6	1
3	4	0	1
4-5	11	1	0

Survival curve analysis

Univariate survival curve analysis showed that Child stage ($P=0.0358$), resection margin ($P=0.0000$), tumor size ($P=0.0000$), presence of microsatellite ($P=0.0000$), venous invasion ($P=0.0000$), tumor type ($P=0.0000$), tumor extension ($P=0.0000$), TNM stage ($P=0.0000$), and CLIP score ($P=0.0000$) were associated with prognosis. The multivariate analysis by COX proportional hazards model revealed that the independent prognostic factors for survival were resection margin ($P=0.0000$) and TNM stage ($P=0.0035$). Figure 2 and 3 demonstrated cumulative disease free

survival curves of TNM stage and CLIP score respectively. Table 3 showed 1-, 3-, and 5-year disease free survival rates and median survival time of TNM stage and CLIP score.

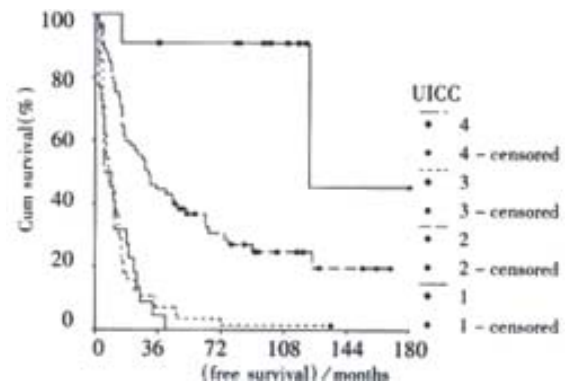


Figure 2 TNM stages and disease-free survival rate in patients with HCC after resection

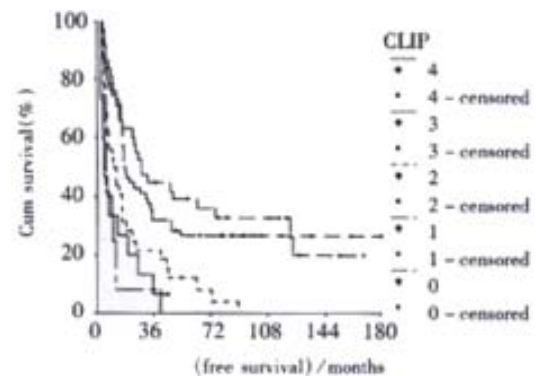


Figure 3 CLIP stages and disease-free survival rate in patients with HCC after resection

Table 4 Patients survival by TNM stages and CLIP scores in HCC

	<i>n</i>	Survival rate/%			Median survival /Months	95%CI
		1-	3-	5-year		
CLIP						
0	38	71.0	44.7	39.1	28	17-39
1	56	73.2	32.1	26.7	16	11-21
2	32	43.8	21.9	12.5	10	4-16
3	15	33.3	6.7	6.7	4	0-8
4-5	12	8.3	8.0	0	5	2-8
UICC						
1	11	100	90.9	90.9	122	95-182
2	65	75.4	44.6	35.1	30	18-42
3	55	38.2	7.3	3.6	7	3-11
4	22	31.8	4.5	0	5	0-10

DISCUSSION

Recurrences of HCC in the remnant after surgical resection could originate from either intrahepatic metastasis from the primary tumor or multicentric occurrence^[19,32,37,38]. Some authors have been found that recurrence was mainly associated with adverse tumor factors such as tumor size, vascular invasion, and microsatellite^[10-14,17,18]. Others demonstrated a liver function status^[26-32,38]. Poon *et al* showed that

tumor factors were linked to early recurrence, whereas the nontumorous liver status was linked to late recurrence^[19]. Thus, a good stage system should include both tumor-related factors and host-related factor. In 1998, a retrospective analysis of 435 cases of HCC diagnosed at 16 Italian institutions was performed by CLIP^[33]. Four independent predictive factors of survival were Child-Pugh stage, tumor morphology, AFP, and portal vein thrombosis by multivariate analysis. Adding each individual value for the four items, the CLIP score was produced. The median survival time for CLIP score 0, 1, 2, 3, 4, and 5 to 6 were 42.5, 32.0, 16.5, 4.5, 2.5, and 1.0 months respectively. Compared with Okuda stage I (32.5 months), II (12.0 months), and III (1.5 months), the CLIP score has a higher number of categories and a greater discriminating ability, and gives more precise information^[33,34]. After that, 154 patients with histologically ascertained HCC and cirrhosis were recruited by Farinati *et al*^[35] and found that the median survival rate in patients with CLIP stages 0, 1, 2, 3, 4, and 5 to 6 were 31, 27, 13, 8, 2, and 2 months respectively. The TNM staging was much less effective in distinguishing patients with respect to median survival (TNM stage I, 34 months; stage II, 25 months; stage III, 20 months; and stage IV, 14 months) and TNM was not significantly correlated with survival rate in patients undergoing a single treatment (TACE). In conclusion, Farinati *et al* confirmed that the CLIP score was currently the best way to stage patients with HCC, it could accurately identify patients with different prognosis, particularly in the early phases (CLIP0-3) of HCC^[35]. However, in those data, the major treatment of the HCC were not surgical resection, 12 of 435 patients in the CLIP group^[33] and 17 of 154 patients in Farinati group^[35] were surgical treatment. The CLIP score was based on prognostic parameters of unresectable patients. This study introduced the CLIP score into the patients with HCC after resection and studied its prognostic value. The results suggested that CLIP score were significantly associated with early and late recurrence, but TNM stage was only associated with early recurrence. It meant that the risk of early recurrence was dependent on the primary tumor factors, but the late recurrence was dependent on the underlying liver status. The CLIP score has a unique superiority for predicting recurrence, because of that accounting for both liver function and tumor extension. The survival analysis showed that the CLIP score was associated with prognosis in the univariate survival and did not associated with that in the multivariate survival. Otherwise, the TNM stage was associated with prognosis in the both univariate and multivariate survival analysis. We had reported before^[18] that the TNM stage was inefficient for multicentric origin and Long-term survival patients because the TNM stage depended only on tumor characteristics, but not on patient factors^[32]. In addition, CLIP score also solved out a problem of TNM stage, that is HCC with two nodes located in both lobes of the liver may be a multicentric origin and the patient after complete resection will have a good prognosis, which was identified stage IV in TNM stage. Recently, Ueno *et al*^[39] investigated the value of CLIP score in 662 Japanese patients with HCC at 4 Japanese institutions from 1990 and 1998. Compared with the Okuda and AJCC staging systems, the CLIP score revealed a class of patients with an impressively more favorable prognosis and another class with a relatively shorter life expectancy. Moreover, the likelihood ratio test showed that the CLIP score had additional homogeneity of survival within each score above that of the Okuda stage or the AJCC stage. This was true for 3 subgroups of patients who received surgery, TAE, and percutaneous ethanol injections.

The patients with portal vein tumor thrombosis (PVTT), which was one of the most important predictive factor identified with the multivariate analysis^[10-12,14,17,18,40-42] showed higher recurrence rate and a poor prognosis, as has been found previously. However, unlike the resectable cases, the PVTT had been a relatively rare condition prevalently in unresectable patients^[43]. With the development of image technology, the CT and Doppler ultrasound characteristics of

benign and malignant PVTT have been described^[43,44]. But the PVTT detected by image examination were either located in the main and/or the first portal branch or large thrombosis^[43,44]. For the resectable HCC, macroscopic tumor thrombus rate was 4.9%^[14]. Cong *et al*^[45] reported the rate of microscopic vascular embolus was 28% in 93 hepatectomies of <3cm small HCC. In the 336 patients with HCC reported by Sithinamsuwan *et al*^[40], the PVTT was 50%. Liver Cancer Study Group of Japan^[11] reported that image TVPP positive rate was 23%, whereas microscopic PVTT rate was 72.8%. Thus, whether the portal thrombosis was benign or malignant, and PVTT was defined by image or pathology, those all would affect patient's prognosis, and result in the difference of scores of CLIP stage. Under similar circumstances, it will effect predictive capacity of CLIP score.

AFP level is the most effective marker for HCC diagnosis and recurrent surveillance^[11,46-48]. The prognostic significance of AFP level is still a controversial issue^[11,12,14,17,18,33,40,46,48]. The large series data (Liver Cancer Study Group of Japan in 1995, 9099 patients^[11], Zhang in 2000, 1725 patients^[17]) showed that AFP level was associated with prognosis, and the higher AFP was, the poorer patient's prognosis was. To our knowledge, no study has been reported that AFP level has correlated with prognosis in multivariate analysis in China^[17,18,49,50], and the literature also did not show any relationship between AFP level and prognosis. Rabe *et al*^[12] reported that while AFP positivity itself was not associated with lower survival, AFP-level greater than 100ug·L⁻¹ was associated with a median survival of 3 months, and lower AFP-level was associated with a survival of 12.5 months ($P < 0.01$). Hanazaki *et al*^[51] reported that AFP $> \text{or} = 1000\text{ug}\cdot\text{L}^{-1}$ and the presence of vascular invasion were independent unfavorable prognostic factors affecting overall survival and that AFP $> \text{or} = 1000\text{ug}\cdot\text{L}^{-1}$ was an independently significant factor of poor disease-free survival. Thus, the both all were inefficient and need to be considered that the critical value of AFP was more than 400ug·L⁻¹ and the prognostic weight of preoperative variable AFP level was defined zero or one score in CLIP, which was the same as present or absent portal vein thrombosis.

Tumor morphology, including the microsatellite, tumor size, uni- or multinodular and tumor extension, can be regarded as indices of tumor burden and was defined as prognostic factors previously for patients with HCC^[9,18,33-35,41,49]. Recently, the literature regarding the correlation of remnant liver function status and prognosis after operation, increased gradually. 246 patients with curative resection of HCC were observed. Intrahepatic recurrences were classified into early (≤ 1 year) and late (> 1 year) recurrences. By multivariate analysis, preoperative tumor rupture and venous invasion were independent risk factors for early recurrence, whereas cirrhosis was the only significant risk factor for late recurrence. By comparing histological features of resected recurrent and primary tumors, 8 of 9 resected early recurrent tumors (89%) were classified as intrahepatic metastases, whereas all 6 resected late recurrent tumors (100%) were multicentric occurrences^[19]. For resectable cases of HCC, the most patients have a good liver function in preoperation, whereas the late recurrence or death only associated with Child stage in this study, which suggest that liver function damage is the one of reasons which result in late death (no-tumor factors) beside early operative mortality or easy to recurrence. Ariizumi *et al*^[52] showed that multicentric HCC tended to grow in more damaged segments of the liver. Thus, influence of tumor-related factors to patients who survived more than three years with no recurrence decreased gradually, meanwhile the influence of host-related factors, including liver functional status and multicentric in origin increased gradually^[18,32]. Consequently, a question occurs: why HCC only found some patients but not all. The answer only is that the liver background with or without HCC is different from each other. In other word, some livers have a predisposition to cancer. Donato *et al*^[53] have studied risk factors and clinical significance of high liver cell proliferative activity in 208 well-compensated cirrhotic patients with immunostaining for proliferating

cell nuclear antigen (PCNA). The overall PCNA labeling index (LI) ranged from 0.1% to 12.5% (mean, 2.1%), being significantly higher in the 50 patients who developed HCC during 88 \pm 42 months of follow-up than in the 158 patients who remained cancer-free (3.6% \pm 2.4% vs 1.6% \pm 1.5%; $P<0.0001$). In conclusion, development of HCC in patients with compensated cirrhosis seems to be reliably predicted by liver cell proliferation status. Sangiovanni *et al*^[54] assessed whether hepatocyte proliferation is an independent risk factor for HCC when considered together with clinical and demographic characteristics. Total 97 consecutive patients with a histological diagnosis of cirrhosis and preserved liver tissue function were retrospectively evaluated. Hepatocyte proliferation was evaluated by flow-cytometric analysis in liver samples collected at the time of histological diagnosis of cirrhosis. The results showed that S-phase fraction of 1.8% or higher significantly correlated with the development of HCC. To study the liver status of patients with HCC have important role in clarification of histogenesis of HCC.

In summary, CLIP score, because of giving consideration to both tumor and patients, has displayed a unique superiority in predicting the tumor recurrence and prognosis in patients with HCC.

REFERENCES

- Tang ZY. Advances in clinical research of hepatocellular carcinoma in China. *World J Gastroenterol* 1998; 4(Suppl 2):4-7
- Yip D, Findlay M, Boyer M, Tattersall MH. Hepatocellular carcinoma in central Sydney: a 10-year review of patients seen in a medical oncology department. *World J Gastroenterol* 1999; 5:483-487
- Schmid R. Prospect of gastroenterology and hepatology in the next century. *World J Gastroenterol* 1999; 5:185-190
- Roberts LR, LaRusso NF. Potential roles of tumor suppressor genes and microsatellite instability in hepatocellular carcinogenesis in southern African blacks. *World J Gastroenterol* 2000; 6:37-41
- Zhang SW, Li LD, Lu FZ, Mu R, Sun XD, Huangpu XM, Sun J, Zhou SY, Dai XD. Mortality of primary liver cancer in China from 1990 through 1992. *Zhonghua Zhongliu Zazhi* 1999; 21:245-249
- Poon RT, Fan ST, Lo CM, Ng IO, Liu CL, Lam CM, Wong J. Improving survival results after resection of hepatocellular carcinoma: a prospective study of 377 patients over 10 years. *Ann Surg* 2001; 234: 63-70
- Parks RW, Garden OJ. Liver resection for cancer. *World J Gastroenterol* 2001; 7:766-771
- Wu MC, Shen F. Progress in research of liver surgery in China. *World J Gastroenterol* 2000; 7:773-776
- Tang ZY. Advances in clinical research of hepatocellular carcinoma in China. *World J Gastroenterol* 1998; 4(Suppl 2): 4-7
- Paquet KJ, Lazar A, Heine WP, Jachmann-Jahn V. Small unilobar hepatocellular carcinoma ($<5\text{cm}$) in patients with liver cirrhosis. Early diagnosis, surgical indications, resection and prognosis. *Zentralbl Chir* 2000; 125:629-636
- Liver cancer study group of Japan. Survey and follow-up study of primary liver cancer in Japan-Report 11. *Liver* 1995; 36:208-217
- Rabe C, Pilz T, Klostermann C, Berna M, Schild HH, Sauerbruch T, Caselmann WH. Clinical characteristics and outcome of a cohort of 101 patients with hepatocellular carcinoma. *World J Gastroenterol* 2001; 7:208-215
- Ono T, Yamanoi A, Assal ONE, Kohno H, Nagasue N. Adjuvant chemotherapy after resection of hepatocellular carcinoma causes deterioration of long-term prognosis in cirrhosis patients-metaanalysis of three randomized controlled trials. *Cancer* 2001; 91:2378-2385
- Zhou XD, Tang ZY, Yang BH, Lin ZY, Ma ZC, Ye SL, Wu ZQ, Fan J, Qin LX, Zheng BH. Experience of 1000 patients who underwent hepatectomy for small hepatocellular carcinoma. *Cancer* 2001; 91: 1479-1486
- Wu MC. Clinical research advances in primary liver cancer. *World J Gastroenterol* 1998; 4:471-474
- Jiang YF, Yang ZH, Hu JQ. Recurrence or metastasis of HCC: predictors, early detection and experimental antiangiogenic therapy. *World J Gastroenterol* 2000; 6:61-65
- Zhang ZJ, Wu MC, Shen F, He J, Chen H, Yang GS, Cong WM, Zong M. Significance of TNM classification in prognostic evaluation of hepatocellular carcinoma following surgical resection. *Zhonghua Zhongliu Zazhi* 1999; 21:293-295
- Zhao WH, Feng YZ, Ma ZM, Zhou XR. Study on prognostic factors for hepatocellular carcinoma after resection by Cox proportional hazard. *Zhonghua Putong Waikes Zazhi* 2001; 16:472-474
- Poon RT, Fan ST, Ng IO, Lo CM, Liu CL, Wong J. Different risk factors and prognosis for early and late intrahepatic recurrence after resection of hepatocellular carcinoma. *Cancer* 2000; 89:500-507
- Kwon AH, Matsui Y, Kamiyama Y. Perioperative blood transfusion in hepatocellular carcinomas-influence of immunologic profile and free survival. *Cancer* 2001; 91:771-778
- Toyada H, Kumada T, Nakano S, Takeda I, Sugiyama K, Kiriya S, Tanikawa M, Sone Y, Hisanaga Y. Impact of diabetes mellitus on the prognosis of patients with hepatocellular carcinoma. *Cancer* 2001; 91: 957-963
- Okuda K, Ohtsuki T, Obata H, Tomimatsu M, Okazaki N, Hasegawa H, Nakajima Y, Ohnishi K. Natural history of hepatocellular carcinoma and prognosis in relation to treatment. *Cancer* 1985; 56:918-928
- Yan LN, Zeng Y, Wen TF, Zhou JC, Lu SC, Li P, Chen XL. The feasibility of a new clinical staging for primary liver cancer. *Zhonghua Putong Waikes Zazhi* 2001; 16:455-456
- Tang ZY. Hepatocellular carcinoma-cause, treatment and metastasis. *World J Gastroenterol* 2001; 7:445-454
- Zhang JY, Dai M, Wang X, Lu WQ, Li DS, Zhang H. A case-control study of hepatitis B and C virus infection as risks for hepatocellular carcinoma in Henan, China. *Int J Epidemiol* 1998; 27:574-578
- Takata M, Yamanaka N, Tanaka T, Yamanaka J, Maeda S, Okamoto E, Yasojima H, Uematsu K, Watanabe H, Uragari Y. What patients can survive disease free after complete resection for hepatocellular carcinoma A multivariate analysis. *Jpn J Clin Oncol* 2000; 30:75-81
- Tarao K, Rino Y, Ohkawa S, Shimizu A, Tamai S, Miyakawa K, Aoki H, Imada T, Shindo K, Okamoto N, Totsuka S. Association between high serum alanine aminotransferase levels and more rapid development and higher rate of incidence of hepatocellular carcinoma in patients with hepatitis C virus-associated cirrhosis. *Cancer* 1999; 86:589-595
- Hanazaki K, Wakabayashi M, Sodeyama H, Kajikawa S, Amano J. Hepatic function immediately after hepatectomy as a significant risk factor for early recurrence in hepatocellular carcinoma. *Hepatogastroenterology* 1999; 46:3201-3207
- Poon RT, Ng IO, Fan ST, Lai EC, Lo CM, Liu CL, Wong J. Clinicopathologic features of long-term survivors and disease-free survivors after resection of hepatocellular carcinoma: a study of a prospective cohort. *J Clin Oncol* 2001; 19:3037-3044
- Poon RT, Fan ST, Lo CM, Liu CL, Ng IO, Wong J. Long-term prognosis after resection of hepatocellular carcinoma associated with hepatitis B-related cirrhosis. *J Clin Oncol* 2000; 18:1094-1101
- Ko S, Nakajima Y, Kanehiro H, Hisanaga M, Aomatsu Y, Kin T, Yagura K, Ohya T, Nishio K, Ohashi K, Sho M, Yamada T, Nakano H. Significant influence of accompanying chronic hepatitis status on recurrence of hepatocellular carcinoma after hepatectomy, results of multivariate analysis. *Ann Surg* 1996; 224:591-595
- Yamasaki S, Kosuge T, Yamamoto J, Shimada K. Long-term results after hepatectomy for hepatocellular carcinoma according to cancer stage. *Nippon Geka Gakkai Zasshi* 1998; 99: 219-222
- The cancer of the liver Italian program (CLIP) investigators. A new prognostic system for hepatocellular carcinoma: A retrospective study of 435 patients. *Hepatology* 1998; 28:751-755
- The cancer of the liver Italian program (CLIP) investigators. Prospective validation of the CLIP score: a new prognostic system for patients with cirrhosis and hepatocellular carcinoma. *Hepatology* 2000; 31:840-845
- Farinati F, Rinaldi M, Gianni S, Naccarato R. How should patients with hepatocellular carcinoma be staged validation of a new prognostic system. *Cancer* 2000; 89:2266-2273
- Pugh RNH, Murray-Lyon IM, Dawson JL, Pietroni MC, Williams R. Transection of the oesophagus for bleeding oesophageal varices. *Br J Surg* 1973; 60:646-649
- Matsumoto Y, Fujii H, Matsuda M, Kono H. Multicentric occurrence of hepatocellular carcinoma: diagnosis and clinical significance. *J Hepatobiliary Pancreat Surg* 2001; 8:435-440
- Ueno S, Tanabe G, Yoshida A, Yoshidome S, Takao S, Aikou T. Postoperative prediction of and strategy for metastatic recurrent hepatocellular carcinoma according to histologic activity of hepatitis. *Cancer* 1999; 86:248-254
- Ueno S, Tanabe G, Sako K, Hiwaki T, Hokotate H, Fukukura Y, Baba Y, Imamura Y, Aikou T. Discrimination value of the new western prognostic system (CLIP score) for hepatocellular carcinoma in 662 Japanese patients. Cancer of the Liver Italian Program. *Hepatology* 2001; 34:529-534
- Sithinamsuwan P, Piratvisuth T, Tanomkiat W, Apakupakul N, Tongyoo S. Review of 336 patients with hepatocellular carcinoma at Songklanagarind Hospital. *World J Gastroenterol* 2000; 6:339-343
- Tung-Ping Poon R, Fan ST, Wong J. Risk factors, prevention, and management of postoperative recurrence after resection of hepatocellular carcinoma. *Ann Surg* 2000; 232:10-24
- Llado L, Virgili J, Figueras J, Valls C, Dominguez J, Rafecas A, Torras

- J, Fabregat J, Guardiola J, Jaurrieta E. A prognostic index of the survival of patients with unresectable hepatocellular carcinoma after transcatheter arterial chemoembolization. *Cancer* 2000; 88:50-57
- 43 Tublin ME, Dodd III GD, Baron RL. Benign and malignant portal vein thrombosis: differentiation by CT characteristics. *Am J Roentgenol* 1997; 168:719-723
- 44 Dodd III GD, Memel DS, Baron R, Eichner L, Santiguida LA. Portal vein thrombosis in patients with cirrhosis: does sonographic detection of intrathrombus flow allow differentiation of benign and malignant thrombus. *Am J Roentgenol* 1995; 165:573-577
- 45 Cong WM, Wu MC, Chen H, Wang Y, Zhang XZ. Clinicopathologic features of small hepatocellular carcinoma-an analysis of ninety-three cases. *Zhonghua ZhongL. Zazhi* 1993; 15:372-374
- 46 Tangkijvanich P, Anukulkarnkusol N, Suwangool P, Lertmaharit S, Hanvivatvong O, Kullavanijaya P, Poovorawan Y. Clinical characteristics and prognosis of hepatocellular carcinoma: analysis based on serum alpha-fetoprotein levels. *J Clin Gastroenterol* 2000; 31:302-308
- 47 Johnson PJ. The role of serum alpha-fetoprotein estimation in the diagnosis and management of hepatocellular carcinoma. *Clin Liver Dis* 2001; 5:145-159
- 48 Yamanaka J, Yamanaka N, Nakasho K, Tanaka T, Ando T, Yasui C, Kuroda N, Takata M, Maeda S, Matsushita K, Uematsu K, Okamoto E. Clinicopathologic analysis of stage II-III hepatocellular carcinoma showing early massive recurrence after liver resection. *J Gastroenterol Hepatol* 2000; 15:1192-1198
- 49 Zhang ZJ, Wu MC, He J, Chen H, Yang JM, Yang GS, Cong WM, Zhang BH, Sheng F, Zong M. Influencing factors of disease free survival in hepatocellular carcinoma after hepatectomy. *Zhonghua Yixue Zazhi* 2000; 80:42-43
- 50 Chen MS, Li JQ, Li GH. Clinical factors affecting prognosis of small hepatocellular carcinoma after hepatectomy. *Zhonghua Zhongliu Zazhi* 1994; 16:225-227
- 51 Hanazaki K, Kajikawa S, Koide N, Adachi W, Amano J. Prognostic factors after hepatic resection for hepatocellular carcinoma with hepatitis C viral infection: univariate and multivariate analysis. *Am J Gastroenterol* 2001; 96:1243-1250
- 52 Ariizumi S, Takasaki K, Yamamoto M, Ohtsubo T, Saito A, Nakano M. Multicentric hepatocellular carcinomas tend to grow in more damaged segments of the liver. *J Gastroenterol* 2000; 35: 441-444
- 53 Donato MF, Arosio E, Del Ninno E, Ronchi G, Lampertico P, Morabito A, Balestrieri MR, Colombo M. High rates of hepatocellular carcinoma in cirrhotic patients with high liver cell proliferative activity. *Hepatology* 2001; 34:523-528
- 54 Sangiovanni A, Colombo E, Radaelli F, Bortoli A, Bovo G, Casiraghi MA, Ceriani R, Roffi L, Redaelli A, Rossini A, Spinzi G, Minoli G. Hepatocyte proliferation and risk of hepatocellular carcinoma in cirrhotic patients. *Am J Gastroenterol* 2001; 96:1575-1580

Edited by Zhang JZ

• LIVER CANCER •

Mechanical properties of hepatocellular carcinoma cells

Gang Zhang, Mian Long, Zhe-Zhi Wu, Wei-Qun Yu

Gang Zhang, Department of Pathophysiology, The Third Military Medical University, Chongqing 400038, China
Mian Long, Zhe-Zhi Wu, Wei-Qun Yu, College of Bioengineer, Chongqing university, Chongqing 400044, China
Supported by the National Science Foundation of China, No.39370198
Correspondence to: Gang Zhang, Department of Pathophysiology, The Third Military Medical University, Chongqing 400038, China. a65412423@public.cta.cq.cn
Telephone: +86-23-68752339 Fax: +86-23-68752340
Received 2001-08-24 Accepted 2001-09-05

Abstract

AIM: To study the viscoelastic properties of human hepatocytes and hepatocellular carcinoma (HCC) cells under cytoskeletal perturbation, and to further to study the viscoelastic properties and the adhesive properties of mouse hepatoma cells (HTC) in different cell cycle.

METHODS: Micropipette aspiration technique was adopted to measure viscoelastic coefficients and adhesion force to collagen coated surface of the cells. Three kinds of cytoskeleton perturbing agents, colchicines (Col), cytochalasin D (CD) and vinblastine (VBL), were used to treat HCC cells and hepatocytes and the effects of these treatment on cell viscoelastic coefficients were investigated. The experimental results were analyzed with a three-element standard linear solid. Further, the viscoelastic properties of HTC cells and the adhesion force of different cycle HTC cells were also investigated. The synchronous G₁ and S phase cells were achieved through thymine-2-desoxyriboside and colchicines sequential blockage method and thymine-2-desoxyriboside blockage method respectively.

RESULTS: The elastic coefficients, but not viscous coefficient of HCC cells ($K_1=103.6\pm12.6\text{N}\cdot\text{m}^{-2}$, $K_2=42.5\pm10.4\text{N}\cdot\text{m}^{-2}$, $\mu=4.5\pm1.9\text{Pa}\cdot\text{s}$), were significantly higher than the corresponding value for hepatocytes ($K_1=87.5\pm12.1\text{N}\cdot\text{m}^{-2}$, $K_2=33.3\pm10.3\text{N}\cdot\text{m}^{-2}$, $\mu=5.9\pm3.0\text{Pa}\cdot\text{s}$, $P<0.01$). Upon treatment with CD, the viscoelastic coefficients of both hepatocytes and HCC cells decreased consistently, with magnitudes for the decrease in elastic coefficients of HCC cells (K_1 : $68.7\text{N}\cdot\text{m}^{-2}$ to $81.7\text{N}\cdot\text{m}^{-2}$, 66.3% to 78.9% ; K_2 : $34.5\text{N}\cdot\text{m}^{-2}$ to $37.1\text{N}\cdot\text{m}^{-2}$, 81.2% to 87.3% , $P<0.001$) larger than those for normal hepatocytes (K_1 : $42.6\text{N}\cdot\text{m}^{-2}$ to $49.8\text{N}\cdot\text{m}^{-2}$, 48.7% to 56.9% ; K_2 : $17.2\text{N}\cdot\text{m}^{-2}$ to $20.4\text{N}\cdot\text{m}^{-2}$, 51.7% to 61.3% , $P<0.001$). There was a little decrease in the viscous coefficient of HCC cells (2.0 to $3.4\text{Pa}\cdot\text{s}$, 44.4 to 75.6% , $P<0.001$) than that for hepatocytes (3.0 to $3.9\text{Pa}\cdot\text{s}$, 50.8 to 66.1% , $P<0.001$). Upon treatment with Col and VBL, the elastic coefficients of hepatocytes generally increased or tended to increase while those of HCC cells decreased. HTC cells with 72.1% of G₁ phase and 98.9% of S phase were achieved and high K_1 , K_2 value and low μ value were the general characteristics of HTC cells. G₁ phase cells had higher K_1 value and lower μ value than S phase cells had, and G₁ phase HTC cells had stronger adhesive forces [$(275.9\pm232.8)\times10^{-10}\text{N}$] than S phase cells [$(161.2\pm120.4)\times10^{-10}\text{N}$, $P<0.001$].

CONCLUSION: The difference in both the pattern and the magnitude of the effect of cytoskeletal perturbing agent on the viscoelastic properties between HCC cells and hepatocytes may reflect differences in the state of the cytoskeleton structure and function and in the sensitivity to perturbing agent treatment between these two types of cells. Change in the viscoelastic properties of cancer cells may affect significantly tumor cell invasion and metastasis as well as interactions between tumor cells and their micro-mechanical environments.

Zhang G, Long M, Wu ZZ, Yu WQ. Mechanical properties of hepatocellular carcinoma cells. *World J Gastroenterol* 2002;8(2):243-246

INTRODUCTION

Current advances in oncology have shown that the continuous growth of malignancy, invasion and metastasis are a multi-step pathophysiological process, which consists of successive steps of tumor cell deformation and locomotion^[1-3]. For an understanding of the mechanisms involved, advanced methodologies of cellular and molecular biology have been extensively used in the study of the related oncogenes and anti-oncogenes, as exemplified in hepatocellular carcinoma (HCC)^[4-8], and in the elucidation of the interaction between tumor cells and vascular endothelial cells^[9,10]. These studies have already led to considerable knowledge in the event involved in tumor metastasis.

The mechanical properties are very important for biologic behaviors of tumor cells in following reasons. Firstly, tumor cells are destined to experience shear-induced deformation in blood flow if they metastasize through the blood vasculature. The mechanical properties determine whether tumor cells can pass through the microvasculature to form metastases, and probably whether they can survive in the blood shear environment. Secondly, the mechanical properties are related to active pseudopod formation and motility, in which they probably have a similar structural basis and are the main cellular events of tumor cell invasion, and a relationship between active pseudopod formation and cytoskeletal structures has already been demonstrated^[11-13]. To the aim of this study was to try to understand how the viscoelastic properties of HCC cells are altered compared to those of normal hepatocytes, how the viscoelastic properties of these two types of cells respond to treatment with cytoskeleton perturbing agents [cytochalasin D (CD), colchicines (Col) and vinblastine (VBL)] and what changes occur in viscoelastic properties and the adhesive properties of hepatoma cells in different phases.

MATERIALS AND METHODS

Cell sample preparation

HCC cells (SMMC 7721) were obtained from the 2nd Military Medical University (Shanghai, China); HTC cells were kindly given by department of clinical biochemistry of Chongqing Medical University. Normal hepatocytes were prepared from human fetal liver tissue by a combination of $0.5\text{g}\cdot\text{L}^{-1}$ collagenases IV (Sigma) digestion and density gradient centrifugation^[14-17]. Cells were maintained in an incubator at 37°C in an atmosphere of $950\text{mL}\cdot\text{L}^{-1}$ humidified air and $50\text{mL}\cdot\text{L}^{-1}$ carbon dioxide. The final concentration of the cells for micropipette experiment was of the order of $10^6\text{cells}\cdot\text{L}^{-1}$.

Preparation of synchronous G₁ and S phase HTC cells

The synchronous G₁ phase cells were achieved through thymine-2-desoxyriboside and colchicines sequential blockage method^[18].

Micropipette system and analysis of the viscoelastic properties of cells

The structure of micropipette system and experimental procedures were described in literatures^[19-21]. Micropipettes were pulled from capillary glass tubes in a micropipette puller (P87, Sutler Instrument Co, USA). The weighted average values of the internal radius of the pipette used in the present investigation were $2.47 \pm 0.91 \mu\text{m}$.

Experimental results were analyzed with a three-element standard linear solid model^[22], in which an elastic element, K_1 , was in parallel with a Maxwell element composed of another elastic element, K_2 , in series with a viscous element, μ . Viscoelastic coefficients were expressed as $\bar{x} \pm s$. Student's *t*-test was used for statistical analysis.

Analysis of the adhesive properties of HTC cells in different cycle

The adhesive model used was schematically shown in Figure 1, F_a was adhesive force of cell, R_p was the inner radius of micropipette, ΔP was negative pressure pulled the adhesive cell away from basement membrane coated by collagen IV, and θ was the angle of micropipette between basement membrane, F_a can be calculated from the following equation: $F_a = R_p^2 \times \Delta P \times \cos \theta$

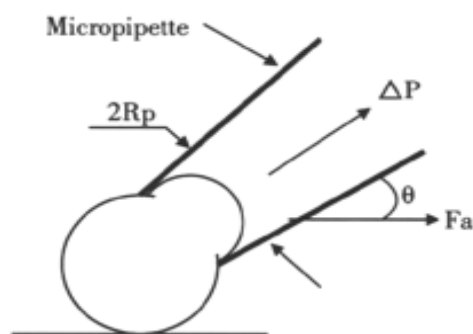


Figure 1 Geometry of adhesive model

RESULTS

Viscoelastic properties of HCC cells and hepatocytes and effects of cytoskeleton inhibitions

The values of the viscoelastic coefficients of hepatocytes and HCC and the effects of treatment with CD, Col and VBL were shown in Tables 1-3, respectively. The results were summarized as follows: (1) Compared to those of normal hepatocytes, the values of the elastic coefficients K_1 and K_2 of HCC cells were significantly higher ($P < 0.01$). However, the viscous coefficient, μ , of the HCC cells was not significantly different from that of hepatocytes. (2) Treatment with $1-60 \text{ mg} \cdot \text{L}^{-1}$ of Col resulted in a little but significant

increase in K_1 for hepatocytes with independent of [Col], whereas in the case of K_2 there appeared to be no significant change. In the case of the viscous coefficient, there was a significant decrease with independent of [Col]. In contrast to hepatocytes, the HCC cells resulted in a significant decrease in all 3 coefficients with dependence on [Col] (Table 1). (3) Treatment of the hepatocytes with VBL in the concentration range of $0.05-2.00 \text{ mg} \cdot \text{L}^{-1}$ resulted in a marked increase in the elastic coefficients at all concentrations, whereas the viscous coefficient only increased significantly at $0.25 \text{ mg} \cdot \text{L}^{-1}$ and $0.75 \text{ mg} \cdot \text{L}^{-1}$ of VBL. In the case of the HCC cells, K_1 exhibited a little but significant increase at $0.05 \text{ mg} \cdot \text{L}^{-1}$ of VBL, but then decreased continuously with increasing [VBL], whereas the values of K_2 and μ decreased monotonously with increasing [VBL] (Table 2). (4) Upon treatment with 0.25 to $5.00 \text{ mg} \cdot \text{L}^{-1}$ of CD, the coefficients K_1 , K_2 and μ decreased significantly from the control values, but the decrease exhibited no significant dependence on the perturbing agent concentration. In the case of the K_1 and K_2 , the magnitude of the above decrease was significantly greater for the HCC cells. For μ , the magnitude of the decrease for HCC cells was less than that of the hepatocytes (Table 3).

Viscoelastic and adhesive properties of HTC in different cycle

The synchronization results detected with flow cytometer showed that it could meet the requirements of the experiments nicely. HTC with 72.1% of G₁ phase and 98.9% of S phase were achieved. The values of the adhesive force of HTC on different concentration of artificial basement membrane (collagen IV coated) were shown in Table 4. The adhesive force of G₁ phase HTC on basement membrane coated by collagen IV $5 \text{ mg} \cdot \text{L}^{-1}$ was $(275.9 \pm 232.8) \times 10^{-10} \text{ N}$, and the corresponding value of S phase HTC was $(161.2 \pm 120.4) \times 10^{-10} \text{ N}$. Difference between them was considered significant ($P < 0.001$). The viscoelastic coefficients of HTC cells in different cycle were shown in (Table 5).

Table 4 Adhesive forces of HTC on artificial basement membrane ($\bar{x} \pm s$)

Concentration of collagen IV ($\text{mg} \cdot \text{L}^{-1}$)	F_a (10^{-10} N)
1	107.8 ± 65.4
2	182.6 ± 107.9^b
5	298.9 ± 144.1^d

^b $P < 0.001$ vs collagen IV $1 \text{ mg} \cdot \text{L}^{-1}$; ^d $P < 0.001$ vs collagen IV $2 \text{ mg} \cdot \text{L}^{-1}$

Table 5 Viscoelastic coefficients of HTC in different cycle ($\bar{x} \pm s$)

Viscoelastic coefficients	General	G ₁ phase	S phase
K_1 ($\text{N} \cdot \text{m}^{-2}$)	186.5 ± 35.6	215.3 ± 50.2	179.7 ± 33.0^b
K_2 ($\text{N} \cdot \text{m}^{-2}$)	224.4 ± 114.5	181.9 ± 102.9	188.6 ± 87.1
μ ($\text{Pa} \cdot \text{s}$)	3.1 ± 2.3	2.9 ± 1.3	4.7 ± 2.4^b

^b $P < 0.001$ vs G₁ phase.

Table 1 Viscoelastic properties of hepatocytes and HCC cells under the action of colchicines ($\bar{x} \pm s$)

[colchicine] ($\text{mg} \cdot \text{L}^{-1}$)	Hepatocytes			HCC cells		
	K_1 ($\text{N} \cdot \text{m}^{-2}$)	K_2 ($\text{N} \cdot \text{m}^{-2}$)	μ ($\text{Pa} \cdot \text{s}$)	K_1 ($\text{N} \cdot \text{m}^{-2}$)	K_2 ($\text{N} \cdot \text{m}^{-2}$)	μ ($\text{Pa} \cdot \text{s}$)
0.0	87.5 ± 12.1	33.3 ± 10.3	5.9 ± 3.0	103.6 ± 12.6	42.5 ± 10.4	4.5 ± 1.9
1.0	95.4 ± 14.1^a	33.2 ± 7.7	3.9 ± 1.7^b	86.7 ± 10.0^b	20.6 ± 2.9^b	4.5 ± 1.5
15.0	107.1 ± 23.0^b	39.6 ± 12.2^a	5.3 ± 1.9	31.4 ± 8.0^b	7.0 ± 1.9^b	1.3 ± 0.6^b
30.0	99.5 ± 11.1^b	28.0 ± 7.3^a	4.0 ± 1.8^b	53.5 ± 12.9^b	12.3 ± 4.8^b	2.1 ± 1.0^b
60.0	104.4 ± 13.0^b	30.6 ± 6.5	3.5 ± 1.1^b	61.6 ± 16.0^b	16.5 ± 6.5^b	2.3 ± 1.2^b

^a $P < 0.05$, ^b $P < 0.01$ vs normal control

Table 2 Viscoelastic properties of hepatocytes and HCC cells under the action of vinblastine ($\bar{x} \pm s$)

[vinblastine] (mg.L ⁻¹)	Hepatocytes			HCC cells		
	K ₁ (N.m ⁻²)	K ₂ (N.m ⁻²)	μ (Pa.s)	K ₁ (N.m ⁻²)	K ₂ (N.m ⁻²)	μ (Pa.s)
0.00	87.5±12.1	33.3±10.3	5.9±3.0	103.6±12.6	42.5±10.4	4.5±1.9
0.05	115.9±15.9 ^b	42.4±8.8 ^b	6.1±2.3	118.4±19.7 ^b	23.1±6.0 ^b	5.6±2.3
0.25	128.7±2.4 ^b	54.0±6.3 ^b	9.8±1.6 ^b	93.2±11.3 ^b	17.0±3.2 ^b	2.9±1.0 ^b
0.75	138.3±23.2 ^b	51.4±13.4 ^b	8.2±3.3 ^a	84.5±6.2 ^b	15.2±3.1 ^b	2.6±0.8 ^b
2.00	117.0±9.1 ^b	43.9±7.7 ^b	6.2±2.3	53.4±12.0 ^b	8.7±2.8 ^b	1.0±0.5 ^b

^aP<0.05, ^bP<0.01 vs normal control**Table 3** Viscoelastic properties of hepatocytes and HCC cells under the action of cytochalasin D ($\bar{x} \pm s$)

[cytochalasin D] (mg.L ⁻¹)	Hepatocytes			HCC cells		
	K ₁ (N.m ⁻²)	K ₂ (N.m ⁻²)	μ (Pa.s)	K ₁ (N.m ⁻²)	K ₂ (N.m ⁻²)	μ (Pa.s)
0.00	87.5±12.1	33.3±10.3	5.9±3.0	103.6±12.6	42.5±10.4	4.5±1.9
0.25	37.7±7.1 ^b	12.9±3.3 ^b	2.0±0.8 ^b	29.5±11.4 ^b	6.5±2.6 ^b	1.6±0.8 ^b
0.50	39.5±6.4 ^b	13.8±3.4 ^b	2.6±1.1 ^b	21.9±5.2 ^b	5.4±1.7 ^b	1.1±0.5 ^b
2.50	42.4±5.9 ^b	16.1±3.3 ^b	2.9±1.4 ^b	31.7±3.8 ^b	7.1±1.8 ^b	2.5±1.0 ^b
5.00	44.9±7.5 ^b	16.1±3.0 ^b	2.6±1.3 ^b	34.9±9.4 ^b	8.0±2.7 ^b	1.9±0.7 ^b

^aP<0.05, ^bP<0.01 vs normal control

DISCUSSION

Viscoelasticity is an important mechanical property of a cell that is related to its motility and deformability^[23-25]. For HCC cells, the viscoelasticity has probably significant bearing on tumor cell invasion and metastasis, in which it determines the flowing behavior of tumor cells in the circulation and whether such cells can be arrested to form metastasis. In addition, mechanical stiffness is closely related to cell adhesion behavior^[26,27], which is the first step in tumor cell invasion. With the three-element standard linear solid viscoelastic model, we clearly showed that HCC cells have higher values for the elastic coefficients but not the viscous coefficient than hepatocytes. This result indicated that HCC cells were more rigid than normal hepatocytes under the experimental conditions. One possible explanation of this result is that, in HCC cells, interconnections between microfilaments and microtubules might have changed as compared to those in normal hepatocytes, and thus microfilaments are affected upon disorganization of microtubules.

As the primary force-bearing structure of a cell, the cytoskeleton may be very important in determining cell mechanical behavior^[28-30]. We used three microfilament- or microtubule- targeting perturbing agents (Col, VBL and CD) to treat hepatocytes and HCC cells and found the effects of agents on viscoelastic properties of HCC cells were different obviously in both pattern and extents from those on hepatocytes. Such differences might reflect differences in the state of the cytoskeleton structure and organization, and in the cell's sensitivity to agents. These results also suggested that cytoskeleton play a role in the maintenance of cell viscoelasticities.

Our results of the viscoelastic properties of HTC in different cycle indicated that high K₁, K₂ and low μ were the general characteristics of HTC, and these were coincided with the result of HCC cells. G₁ phase cells had higher K₁ value and lower μ value than S phase cells had, but there was no obviously difference in K₂ between two phase cells, which reflected the discrepancies of cytoskeletal protein assemble and synthesis in different cell cycle. Those resultson relevance of cytoskeletal structure to viscoelastic coefficient of HCC cells suggested that microfilaments could play a major rule in the maintenance of cell viscoelasticity, especially in G₁ phase cells. In contrary to these, synthesis of microtubules in S phase cells increased, and more microtubules took part in determination the cells viscoelasticity, which could endow G₁ phase cells with higher elasticity and lower viscosity than S phase of cells. These characteristics evidently contributed to G₁

phase cells survival from the blood shear environment and arrest to form metastases.

The adhesive properties of HTC in different cycle

Current study has shown that action of tumor cells on basement membrane is a multi-step pathophysiological process^[31]. Our results showed the adhesive force of HTC cells on basement membrane coated by collagen VI had the obvious correlation with the concentration of collagen. Wang *et al*^[32] reported that the content of collagen IV and laminin in basement membrane increased along with the growth of tumor, but basement membrane became to decrease, even damaged when tumor transferred. So, the different thickness of basement membrane could reflected the different interaction between tumor cells and the membrane. Increased thickness of basement membrane might play the important rule in tumor cell invasion, which was conducive to the chemotactic motion of tumor cell, active orientation movement, and supplied strong adhesive force and adhesive site for tumor cell. The adhesive force of G₁ phase of HTC was obviously greater than that of S phase cells. In general, expression of fibronectin receptor in transferred tumor cell would decrease and laminin receptor would increase. Fibronectin play a more important rule in improving tumor cell spreading and increasing the synthesis and proliferation of DNA in S/G₂ phase. Laminin has many functions on the tumor cell adhesion and movement^[33]. So, the difference of adhesive force between G₁ phase cell and S phase cell could reflect the difference of expression of adhesive molecule receptor on the cell surface, especially the difference of periodic distribution of fibronectin receptor and laminin receptor. In addition, a strong affinity existed between laminin and thrombolysin, and both of them binded together to form thrombolysin by activating profibrinolysin and hydrolyzing laminin and fibronectin, and finally activation of procollagen and degradation of basement membrane occurred. The phenomenon of high adhesive force value in G₁ phase cell may be also relevant to these changes, which made G₁ phase cells in active condition in adhesion and movement. In the course of tumor invasion and metastasis, G₁ phase cell were more capable of adhering to and getting through basement membranes than S phase cells.

REFERENCES

- Okuda K. Hepatocellular carcinoma. *J Hepatol* 2000; 32:225-237
- Wu MC. Clinical research advances in primary liver cancer. *World J Gastroenterol* 1998; 4: 471-475

- 3 Jiang YF, Yang ZH, Hu JQ. Recurrence or metastasis of HCC: predictors, early detection and experimental antiangiogenic therapy. *World J Gastroenterol* 2000; 6: 61-66
- 4 Tang ZY. Hepatocellular Carcinoma - Cause, Treatment and Metastasis. *World J Gastroenterol* 2001; 7: 445-455
- 5 Liu WW. Etiological studies of hepatocellular carcinoma. *Shijie Huaren Xiaohua Zazhi* 1999; 7: 93-95
- 6 Ji Y, Ling MY, Li Y, Xie H. Effect of cell fusion on metastatic ability of mouse hepatocarcinoma cell lines. *World J Gastroenterol* 1999; 5: 22-25
- 7 Cao XY, Lin J, Lian ZR, Clayton M, Hu JL, Zhu MH, Fan DM, Feitilson M. Cloning of differentially expressed genes in human hepatocellular carcinoma and nontumor liver. *World J Gastroenterol* 2001; 7: 579-583
- 8 Zhou XP, Wang HY, Yang GS, Chen ZJ, Li BA, Wu MC. Cloning and expression of MXR7 gene in human HCC tissue. *World J Gastroenterol* 2000; 6: 57-61
- 9 Sun JJ, Zhou XD, Zhou G, Liu YK. Expression of intercellular adhesive molecule-1 in liver cancer tissues and liver cancer metastasis. *World J Gastroenterol* 1998; 4: 202-206
- 10 Sun JJ, Zhou XD, Lin YK, Zhou G. Phase tissue intercellular adhesion molecule-1 expression in nude mice human liver cancer metastasis model. *World J Gastroenterol* 1998; 4: 314-317
- 11 Dong C, Aznavoorian S, Liotta LA. Two phases of pseudopod protrusion in tumor cells revealed by a micropipette. *Microvasc Res* 1994; 47: 55-67
- 12 You J, Mastro AM, Dong C. Application of the dual-micropipette technique to the measure of tumor cell locomotion. *Exp Cell Res* 1999; 248:160-171
- 13 Sun WB, Han BL, Peng ZM, Li K, Ji Q, Chen J, Wang HZ, Ma RL. Effect of aging on cytoskeleton system of Kupffer cell and its phagocytic capacity. *World J Gastroenterol* 1998; 4: 77-80
- 14 Wang YJ, Li MD, Wang YM, Nie QH, Chen GZ. Experimental study of bioartificial liver with cultured human liver cells. *World J Gastroenterol* 1999; 5: 135-138
- 15 Chen K, Gao Y, Pan YX, Yang JZ. Separation and cultivation of porcine hepatocytes. *Shijie Huaren Xiaohua Zazhi* 1999; 7: 200-202
- 16 Gong JP, Han BL. Technique of isolation, culture and identification of liver cells. *Shijie Huaren Xiaohua Zazhi* 1999; 7: 375-378
- 17 Wang YJ, Lin GD, Lin J, Li MD. Large-scale isolation of sucking pig hepatocytes. *Shijie Huaren Xiaohua Zazhi* 1999; 7: 661-662
- 18 Yu QU, Song GB, Wu ZZ, Long M, Cai SX. Investigation of the viscoelasticity of synchronous HTC cells. *Shengwu Wuli Xuebao* 1999; 15: 431-435
- 19 Zhang G, Long M, Wu ZZ. Experiment study on viscoelastic properties of hepatocellular carcinoma cells. *Jiefangjun Yixue Zazhi* 2001; 26: 204-207
- 20 Zhang G, Wu ZZ, Wang HB, Long M, Song GB, Cai SX. Effect of vinblastine and cytochalasin D on viscoelastic properties of hepatocellular carcinoma cells. *Zhongguo Shengwu Yixue Gongcheng Xuebao* 2000; 19: 213-217
- 21 Zhang G, Long M, Wu ZZ. Comparative study on the viscoelastic properties of hepatocytes and hepatocellular carcinoma cells. *Disan Junyi Daxue Xuebao* 2001; 23: 751
- 22 Chien S, Sung KL. Effects of colchicines on viscoelastic properties of neutrophils. *Biophys* 1984; 46: 383-386
- 23 Riquelme BD, Foresto PG, Valverde JR, Rasia JR. Alterations to complex viscoelasticity of erythrocytes during storage. *Clin Hemorheol Microcirc* 2000; 22: 181-188
- 24 Chung TW, Ho CP. Changes in viscosity of low shear rates and viscoelastic properties of oxidative erythrocyte suspensions. *Clin Hemorheol Microcirc* 1999; 21: 99-103
- 25 Undar A, Henderson N, Thurston GB, Masai T, Beyer EA, Frazier OH, Fraser CD Jr. The effects of pulsatile versus nonpulsatile perfusion on blood viscoelasticity before and after deep hypothermic circulatory arrest in a neonatal piglet model. *Artif Organs* 1999; 23: 717-721
- 26 Chang KC, Hammer DA. Adhesive dynamics simulations of sialyl-Lewis (x)/E-selectin-mediated rolling in a cell-free system. *Biophys J* 2000; 79: 1891-1902
- 27 Heymann B, Grubmuller H. Dynamic force spectroscopy of molecular adhesion bonds. *Phys Rev Lett* 2000 26; 84: 6126-6129
- 28 Svetina S, Bozic B, Derganc J, Zeks B. Mechanical and functional aspects of membrane skeletons. *Cell Mol Biol Lett* 2001; 6: 677-690
- 29 Wang N, Stamenovic D. Contribution of intermediate filaments to cell stiffness, stiffening, and growth. *Am J Physiol Cell Physiol* 2000; 279: C188-194
- 30 Stamenovic D, Coughlin MF. The role of prestress and architecture of the cytoskeleton and deformability of cytoskeletal filaments in mechanics of adherent cells: a quantitative analysis. *J Theor Biol* 1999; 201: 63-74
- 31 Okada Y. Tumor cell-matrix interaction: pericellular matrix degradation and metastasis. *Verh Dtsch Ges Pathol* 2000; 84: 33-42
- 32 Wang F, Gao J. Relationship between extracellular matrix and progressive growth of malignant tumor. *Zhonghua Zhongliu Zazhi* 1998; 2: 112-115
- 33 Kitayama J, Nagawa H, Tsuno N, Osada T, Hatano K, Sunami E, Saito H, Muto T. Laminin mediates tethering and spreading of colon cancer cells in physiological shear flow. *Br J Cancer* 1999; 80: 1927-1934

Edited by Zhang JZ

Study of apoptosis in human liver cancers

Chang-Min Shan, Juan Li

Chang-Min Shan, Department of Biology, Binzhou Medical College, Binzhou 256603, China

Juan Li, Department of Pharmacy, Affiliated Hospital Binzhou Medical College, Binzhou 256603, China

Correspondence to: Chang-Min Shan, Department of Biology, Binzhou Medical College, Binzhou 256603, China. shancm@bzmc.edu.cn
Telephone: +86-543-3256143

Received 2002-01-28 Accepted 2002-02-23

Abstract

AIM: To investigate the action of apoptosis in occurrence of liver carcinomas *in vivo* and the biological effect of Solanum lyratum Thumb on BEL-7404 cell line inducing apoptosis *in vitro*.

METHODS: The apoptosis in the liver carcinoma was detected with terminal deoxynucleotidyl transferase mediated dUTP nick end labelling (TUNEL); the cancer cells cultured in DMED medium were treated with extract of Solanum lyratum Thumb and observed under microscope, and their DNA was assayed by gel electrophoresis.

RESULTS: *In vivo* apoptotic cells in the cancer adjacent tissues increased; *in vitro* treatment of liver cancers with extract of Solanum lyratum Thumb could induce the cells to manifest a typical apoptotic morphology. Their DNA was fractured and a characteristic ladder pattern could be found using electrophoresis.

CONCLUSION: *In vivo* the apoptosis of carcinomas was lower; maybe the cells divided quickly and then the cancers occurred. In the cancer adjacent tissues, the apoptosis picked up, and *in vitro* Solanum lyratum Thumb could induce the apoptosis of BEL-7404 cells.

Shan CM, Li J. Study of apoptosis in human liver cancers. *World J Gastroenterol* 2002;8(2):247-252

INTRODUCTION

The balance between cell proliferation and apoptosis is essential for the development and maintenance of normal organs. The occurrence of cancers is purportedly due to the smother of normal apoptosis process, which caused the imbalance between cell proliferation and apoptosis^[1,2]. To investigate the action of apoptosis in the occurrence of liver carcinomas *in vivo*, the apoptosis in the cancers was detected with terminal deoxynucleotidyltransferase mediated dUTP nick end labelling (TUNEL). Solanum lyratum Thumb is usually used as an anticancer drug to treat liver cancers, lung cancers, esophagus cancers and so on. Modern scientific research revealed that Solanum lyratum Thumb can promote the formation of cycle adenocine monophosphate (cAMP) and the activity of protein kinase A(PKA) in the gastric cancer cells^[3]. Yet, there has been no report as to whether Solanum lyratum Thumb could induce the apoptosis of cancer cells. This paper studied the apoptosis-inducing action of the extracts of Solanum lyratum Thumb on human hepatoma cell line BEL-7404.

MATERIALS AND METHODS

Selection of samples

20 liver tissue samples were collected from the patients of liver cancer hospitalized in Department of Pathology of Affiliated Hospital to Binzhou Medical College as the liver cancer group(12 from males, 8 from females). Their tissues adjacent to the cancer were used as the cancer adjacent tissue group. The preparation of tissue block and slices: the samples obtained surgically were fixed with 10% formalin, dehydrated by conventionality, embedded by paraffin, cut into slices 5μm thick. One slice for each sample was stained by HE; it was used for pathological identification.

In vivo detection of apoptosis

TUNEL staining was used to detect DNA degradation *in situ* in the relatively late stage of apoptosis. Apoptotic cells were labelled by the TUNEL reaction using *in situ* Cell Apoptosis Detection Kit. *In situ* Cell Apoptosis Detection Kits were purchased from WUHAN BOSTER Biological Technology Co, Ltd. The detailed manipulation were conducted according to introductions for users. Negative controls consists of the process except that the labelling buffer was substituted for TdT and DIG-dUTP. positive controls were hypothyroid cancer samples. Result identification: After DAB staining the cells whose nuclei were orange counted as positive. Photomicrographs were taken with an Olympus microphoto-microscope (see Figure 1).

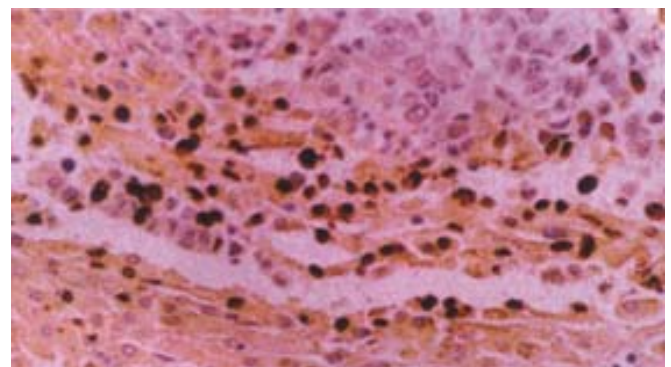


Figure 1 shows apoptotic cells in liver carcinomas and in cancer adjacent tissues(positive).TUNEL ×200

Data processing

The positive rates for each group were calculated. Four visual fields were randomly selected from each tissue section and analyzed under 10×20 fold statistics microscope with the imaging analysis system of CMIAS. The integrated optical density (IOD) was measured, and data were expressed as means±s.e.m, and analyzed with t-test by software Microsoft Excel 97. *P* value less than 0.05 was regarded as representing significant difference.

Drug preparation

Solanum lyratum Thumb is the whole plant of Solanum lyratum Thumb deadly nightshade. After extraction using ethanol, and there after using acetidine, the fat-soluble extracts of Solanum lyratum Thumb were distilled in DMSO and then diluted in RPMI 1640 medium to different concentrations for later use.

Cell culture and drug application

Human hepatoplastoma cell line BEL-7404 was purchased from Institute of Materia Medica, Chinese Academy of Medical Science, Beijing. BEL-7404 cells were seeded at 37°C in a humidified incubator under 5% CO₂/95% air in RPMI1640 supplemented with 200IU/ml penicillin, 200µg/ml streptomycin, and cultured for 24h. This medium was replaced by another medium containing extracts of *Solanum lyratum* Thumb 10µg·ml⁻¹, 5µg·ml⁻¹, 2.5µg·ml⁻¹ respectively. The cells went on to be cultured for 24, 48, 72h.

In vitro detection of apoptosis

Cellular morphological observation: First the cell shapes were observed and apoptosis was detected and photomicrographs were taken with an Olympus microphoto-microscope. **DNA isolation and electrophoresis:** After the cells were cultured in deferent concentrations of the drug for deferent time lengths, DNA isolation was done as follows: After they were washed twice with RPMI1640 medium and resuspended, the cells (5×10⁵ or 2×10⁶ cells) were collected by centrifugation (200×g, 10min), and then 50µl of cell cracking liquid was added to resuspend the cells. They were incubated at 37°C until the lysates containing liquid became clear, and then centrifuged at 12000r·min⁻¹ 5min at 4°C. DNA fragments were extracted from the supernatant with phenol-chloroform(1:1) phenol-chloroform-isoamyl alcohol(25:14:1), precipitated by addition of 2 volumes of absolute ethanol and 0.1 volume of 3mol·L⁻¹ sodium acetate at -20°C for 24h, centrifuged at 12000r·min⁻¹ -10°C, for 10min. The precipitate was dissolved in 20µl TE with 1µl RNase and kept at 37°C for 1h. The pattern of DNA fragmentation was visualized by electrophoresis (at room temperature, 75mA, 1-2h) in 1% agarose gel containing ethidium bromide and photographed under UV light.

RESULTS

In vivo detection of apoptosis

It was found with TUNEL technique that the partial tissues in the liver cancer group were positive; its positive rate was lower than in the tissues adjacent to cancers. The IOD in the cancer group was lower than in the cancer adjacent tissue group. There was significant deference between the two groups (see Table 1).

Table 1 Cell apoptosis in liver carcinoma

Group	Number of cases	Positive rate	IOD number ($\bar{x} \pm s$)
Cancer	20	2/20	2.9±10.85
Cancer adjacent tissue	20	20/20	266.8±536.7

t=2.2011, P<0.05

In vitro morphological observation of cells and production of apoptotic body

The morphological changes took place in BEL-7404 cells exposed to extracts of *Solanum lyratum* Thumb (2.5µg·ml⁻¹, 5µg·ml⁻¹, 10µg·ml⁻¹) for 24h. As is shown in Figure 2, a lot of cells became round; their cytoplasm and chromatin became condensed; their membranes became crooked, and vesicles shaped. The nuclei cracked and typical apoptotic bodies formed. BEL-7404 cells exposed to extracts of *Solanum lyratum* Thumb (2.5µg·ml⁻¹, 5µg·ml⁻¹, 10µg·ml⁻¹) for 48h showed an increase in the number of apoptotic cells, and a decrease in the number of normal cells. The cells came off and suspended in the medium. In BEL-7404 cells exposed to extracts of *Solanum lyratum* Thumb (2.5µg·ml⁻¹, 5µg·ml⁻¹, 10µg·ml⁻¹) for 72h, most cells suspended, the apoptotic bodies of a few cells enlarged. Their membrane bursted, exhibiting the death state of these cells.

DNA ladder production

In BEL-7404 cells exposed to extracts of *Solanum lyratum* Thumb (2.5µg·ml⁻¹, 5µg·ml⁻¹, 10µg·ml⁻¹) for 24h, 48h and 72h, the DNA

changed obviously. Just as shown in Figure 3, they showed ladder bands after electrophoresis. It proved that cellular apoptosis happened, which was significantly different from the controls.

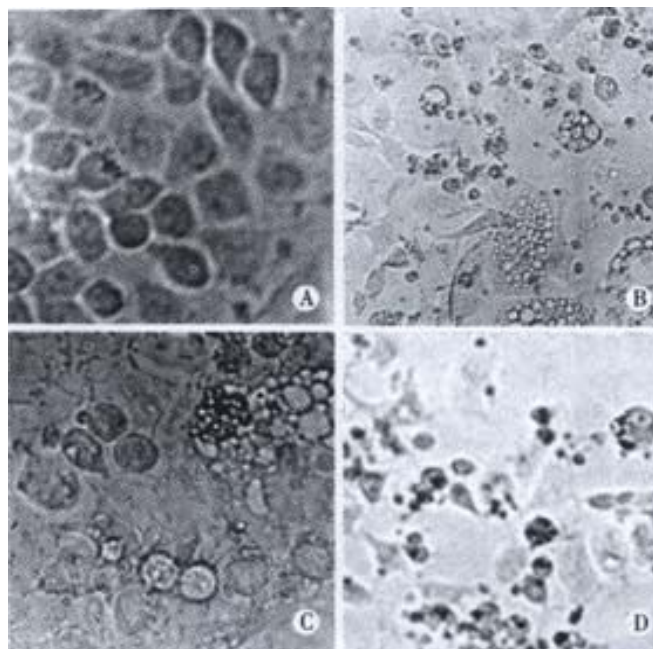


Figure 2 Morphological change in BEL-7404 cells exposed to the extract of *Solanum lyratum* Thumb. 5µg·ml⁻¹ for untreated (2A), 24h (2B), 48h (2C), 72h (2D). ×100

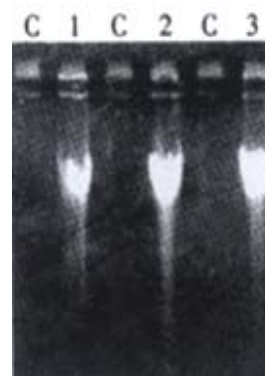


Figure 3 DNA ladder in agarose gel after BEL-7404 cells treated with extract of *Solanum lyratum* Thumb 5µg·ml⁻¹ for 24, 48, 72h. Column C: control; 1, 2, 3, column: the cells treated with extract of *Solanum lyratum* Thumb for 24h, 48h, 72h respectively.

DISCUSSION

The term 'apoptosis' was introduced into modern science by Kerr *et al.* in 1972 to describe the special morphology of physiological cell death. The word itself is an ancient Greek word meaning the 'falling off' of leaves from a tree or petals from a flower and was originally used in the medical and philosophical writings of classical Greek and Roman times. Apoptosis or 'programmed cell death' represents the regulated activation of a pre-existing death program encoded in the genome. It is a highly orchestrated form of cell death and plays a central role in the control of tissue cell numbers in organs' development, homeostasis and normal functioning, such as cell proliferation and differentiation. Dysregulation of apoptosis may be involved in the pathogenesis of human diseases^[4,5].

There are two central pathways that lead to apoptosis: (1) positive induction by ligand binding to a plasma membrane receptor and (2) negative induction by loss of a suppressor activity. Each leads to activation of cysteine proteases with homology to IL-1β converting enzyme (ICE) (i.e., caspases). Positive-induction

involves ligands related to TNF. The ligands are typically trimeric and bind to cell surface receptors causing aggregation (trimerization) of cell surface receptors. The intracellular portion of these receptors contains an 80 amino acid death domain (DD) that through homophilic interactions recruits adaptor proteins to form a signaling complex on the cytosolic surface of the receptor. The bringing together of the three receptors, thereby orienting the intracellular DDs, appears to be the critical feature for signaling by these receptors. The adaptor complex then recruits caspase-8; caspase-8 is activated, and the cascade of caspase-mediated disassembly proceeds^[6,7]. Cytosolic Aspartate-Specific Proteases, called CASPases, are responsible for the deliberate disassembly of a cell into apoptotic bodies. Caspases are present as inactive proenzymes, most of which are activated by proteolytic cleavage. Caspase-8, caspase-9, and caspase-3 are situated at pivotal junctions in apoptotic pathways. Caspase-8 initiates disassembly in response to extracellular apoptosis-inducing ligands and is activated in a complex associated with the receptors' cytoplasmic death domains. Caspase-9 activates disassembly in response to agents that trigger release of cytochrome c from the mitochondria and is activated when complexed with dATP, APAF-1, and extramitochondrial cytochrome c. Caspase-3 appears to amplify caspase-8 and caspase-9 signals into full-fledged commitment to disassembly. Both caspase-8 and caspase-9 can activate caspase-3 by proteolytic cleavage and caspase-3 may then cleave vital cellular proteins or activate additional caspases by proteolytic cleavage^[8-10].

Negative induction of apoptosis by loss of a suppressor activity involves the mitochondria. Release of cytochrome c from the mitochondria into the cytosol serves as a trigger to activate caspases^[11]. Permeability of the outer mitochondrial membrane is essential to initiation of apoptosis through this pathway. Proteins belonging to the Bcl-2 family appear to regulate the membrane permeability to ions and possibly to cytochrome c as well. Although these proteins can themselves form channels in the membrane, the actual molecular mechanisms underlying the regulation of mitochondrial permeability and the release of solutes remain to be elucidated. The Bcl-2 family is composed of a large group of anti-apoptosis members that when overexpressed prevent apoptosis and a large group of pro-apoptosis members that when overexpressed induce apoptosis. The balance between the anti-apoptotic and pro-apoptotic Bcl-2 family members may be critical to determining whether a cell undergoes apoptosis. Thus, the suppressor activity of the anti-apoptotic Bcl-2 family appears to be negated by the pro-apoptotic members^[12]. Many members of the pro-apoptotic Bcl-2 family are present in cells at levels sufficient to induce apoptosis. However, these members do not induce apoptosis because their activity is maintained in a latent form. Bax is present in the cytosol of living cells. After an appropriate signal, Bax undergoes a conformational change and moves to the mitochondrial membrane where it causes release of mitochondrial cytochrome c into the cytosol. BID is also present in the cytosol of living cells. After cleavage by caspase-8, it moves to the mitochondria where it causes release of cytochrome C possibly by altering the conformation of Bax. Similarly, BAK appears to undergo a conformational change that converts it from an inactive to an active state. Thus, understanding the molecular mechanisms responsible for regulating the Bcl-2 family activities creates the potential for pharmaceutical intervention to control apoptosis^[13-16].

Liver carcinoma is one of the most common cancers. Further progress has been made in its diagnoses, treatments and the mechanism of its occurrence. The study of its apoptosis is very important^[17,18]. It has been proved that occurrence of cancers is due to the loss of control of normal apoptosis and the disturbance of balance between cell apoptosis and cell proliferation^[1,2]. The apoptosis related genes (bcl-2 family) is divided into two categories: apoptotic repressor and apoptotic promoter. Bcl-2 is an important apoptotic repressor, while Bax is one of the most important apoptotic promoters. The protein it encodes can combine with Bcl-2 to form

compounds which resist the action of repressing apoptosis. But it has a positive regulatory action^[19-21]. Recent studies indicate that the regulation of apoptosis by bcl-2 and bax is not only based on the level of either of the two regulatory proteins but also based on the ratio of them. If the ratio is high, the cells go to apoptosis^[22-24]. In our experiment the *in vivo* apoptosis in liver cancers was detected by TUNEL technique. The result showed that IOD in the liver cancer group was lower than in the cancer adjacent tissue group, which was a significant difference ($t=2.2011$, $P<0.05$). Our results were consistent with that of Peng *et al*^[25]. We found that apoptotic cells in the cancer adjacent tissue were more and there were less in the cancer. This showed that apoptosis in the cancer adjacent tissue is more active. The apoptosis may be caused by a negative induction of apoptosis. First the level of BAX can increase. Its conformations can change, and then move to the outer membrane of mitochondria thus making cytochrome c to release from mitochondria. There after CASPASE is activated, and then the cascade of CASPASE-mediated disassembly proceeds. Thus apoptosis emerges. The pathway may be blocked in liver cancers, and apoptosis slow down, so proliferation of the cells cannot be balanced, and the cancers occur.

Some drugs (e.g. adriamycin, doxorubicin, propolis) can induce apoptosis, repress the division of liver cancer cells and thus treat cancers^[26-28]. Tamoxifen can induce apoptosis of HepG2 hepatoblastoma cells, because Tamoxifen activates Ca^{2+} influx pathways. After the human hepatocellular SK-HEP-1 carcinoma cells were treated with methylglyoxal bis (cyclopentylamidino)hydrazone (MGBCP), their cell morphology changed, and the cell growth rate decreased. It may induce cell apoptosis^[29,30]. Human hepatoma cell line (HepG2) were treated with Sodium selenite. Selenite-induced DNA alterations in apoptosis were studied, and characteristic apoptotic morphological alterations were observed. The results clearly show that Se-induced cell death occurs predominantly in the form of apoptosis^[31]. Apoptosis in human hepatoma BEL-7402 cells can be induced by Octreotide, which may be related to the mechanism of antineoplastic action of Octreotide in hepatoma^[32]. It has been proved that baicalein, chlorinated fatty acids, troglitazone (an antidiabetic agent) and cisplatin could respectively induce apoptosis in hepatoma cells HepG2^[33-36]. Their results were similar to ours. The apoptotic characteristics, DNA fragment, cellular morphological changes emerged in the hepatoma cells treated with different agents.

Solanum Lyratum is one of Chinese anticancer herbs. The damage effect of Solanum Lyratum on different phases of PC chromosomes in CHO cells was studied by cell fusion technique. The result showed that obvious damage were observed in G2-PCC in cells treated with the drug at 0.5-1.0g·ml⁻¹ for 45min at 37°C. The obvious damage of PC chromosomes indicated that Solanum Lyratum may markedly block the G2 phase of cell cycle. But treatment with different doses of the drug showed no effect on the progression of cells in M phase. A study found that Chinese Herbal Mixture containing Solanum Lyratum has a stronger killing action on Human Tumor Cells BGC-823 and MCF-7 *In Vitro*. Flowcytometric analysis showed that the drug can stop the cell cycle of BGC-823 at G1 phase and cause a significant decrease in the number of S phase cells. It was found that the drug can inhibit DNA synthesis, expressions of antioncogenes Rb, p21 and enhance the expression of oncogene c-myc in BGC-823 cells^[37]. Apoptosis of cancers is induced with the Chinese herbal medicine^[38-40]. Solanum Lyratum can suppress the proliferation of hepatoma cells via G0/G1 arrest and inhibition of DNA synthesis followed by apoptosis. Arsenic trioxide has significant selective apoptosis-inducing effect on human hepatocarcinoma cells, which is regulated by several genes. Bcl-2 gene expression down-regulated, Bax and Fas gene expressions up-regulated^[41]. A Chinese herb-magnolol can also inhibit the proliferation of tumor cells and activate apoptosis *in vitro* and *in vivo*^[42].

In our experiment, after BEL-7404 human hepatoblastoma cell line was cultured in the medium containing Solanum Lyratum extract

(concentration: $2.5\mu\text{g}\cdot\text{mL}^{-1}$, $5\mu\text{g}\cdot\text{mL}^{-1}$, $10\mu\text{g}\cdot\text{mL}^{-1}$) for 24h, the morphologic change took place in these cells, and the apoptotic bodies and DNA ladders appeared. After 48h, 72h they changed acutely. This indicated that *Solanum Lyratum* may exert an anticancer action through promoting apoptosis and resulting in the death of the liver cancer cells. It may stimulate the cells to bring out a positive gene directed apoptosis. It probably induce overexpression of gene bax and inhibit expression of gene bcl-2, making the ratio of proteins of bax/bcl-2 increase and then promoting the cell apoptosis. This may be a positive induction of apoptosis. First *Solanum Lyratum* as a ligand binds to cell surface receptor. It causes aggregation of cell surface receptors. The signaling complex on the cytosolic surface of the receptor forms. CASPASE is activated, and then the cascade of CASPASE-mediated disassembly proceeds.

Several genes, factors and TNF receptor family are involved in the apoptosis of liver cancer cells. In the human hepatocellular carcinoma cell line, Hep3B, an increased level of bax expression mediates apoptosis^[43]. It was found that bcl-2-positive cells did not show apoptosis, and p53 protein (stimulative) may regulate apoptosis in some cases of human liver tumors, the mutant p53 protein may inhibit the cancer cells going to the apoptosis, whereas c-myc, Fas and Lewisy are not relevant to apoptosis^[25,44,45]. Bcl-2 was focally expressed in hepatic tumor epithelium^[21]. Using immuno-histochemical methods, the expression of Bcl-2, an anti-apoptotic protein was studied in hepatocellular tumors of B6C3F1 mice. Normal mouse hepatocytes did not express detectable amounts of Bcl-2, whereas most diethylnitrosamine-induced tumors were positive for this protein. This explained that expression of bcl-2 might inhibit the normal proliferation of cells, and result in the occurrence of tumors^[46]. In the BEL-7404 cells where apoptosis was mediated by AFP, Fas apoptosis signals and Bcl-2 survival signals from apoptosis were expressed^[47]. the proapoptotic protein Bax is translocated from the cytosol to mitochondria, where a potent proapoptotic 18-kDa fragment (Bax/p18) at its N-terminus of Bax was cleaved. It promotes release of cytochrome c, a caspase-activating protein, activation of caspase-3, cleavage of poly(ADP-ribose) polymerase, and fragmentation of DNA and apoptosis. On the contrary Bcl-2 overexpression inhibited etoposide-induced calpain activation, Bax cleavage, cytochrome c release, and apoptosis^[48]. In human hepatoma cells, Bcl-2 may protect cells from TGF-beta-F-induced apoptosis by interfering TGF-beta generated signals leading to the production of reactive oxygen species^[49]. Ethanol could induce apoptosis in liver cells, which was initiated by the intracellular Ca^{2+} elevation in the cytoplasm. N-p-tosyl-L-lysine chloromethyl ketone (TLCK)-sensitive serine proteases was activated^[50].

Combination of drugs can increase the pharmacotherapeutic effect on liver cancers. Co-administration of the chemosensitizer verapamil increased the antitumor efficacy of paclitaxel by up to five-fold. cyclin A and cdc2 kinase accumulated in paclitaxel-treated cells. Exposure to paclitaxel decreased [^3H]thymidine incorporation into DNA in cells at 24h but this significantly increased at 72h, that was most likely due to DNA repair mechanisms related to cell cycle restriction^[51]. Glutathione-doxorubicin (GSH-DXR) effectively induced apoptosis in rat hepatoma cells (AH66) at a lower concentration than DXR. DXR and GSH-DXR induce apoptotic DNA fragmentation via caspase-3 activation, but not via caspase-1 activation, and GSH-DXR enhances the activation of caspase-3 approximately 100-fold more effectively than DXR used alone. An upstream apoptotic signal that can activate caspase-3 is activated within 6 h by treating AH66 cells with the drug^[52]. Internucleosomal DNA fragmentation, a biological hallmark of apoptosis, was detected in hepatoma cells after continuous incubation with a combination of sodium butyrate and interferon-alpha (IFN-alpha) for 72h. Sodium butyrate potently enhances the anti-tumour effect of IFN-alpha *in vitro* and a rational combination of these two drugs may be useful for the treatment of liver cancer^[53]. After 96h in HepG2, Hep1B, Hepa1-6

and MH1C1 hepatoma cells, combination therapy of an acyclic retinoid and tamoxifen (TAM) on proliferation and apoptosis of hepatoma cell enhanced apoptosis from a maximum of 60% after monotherapy to more than 90%. Apoptosis increased p27, bax, caspase 3 expression was accompanied by upregulation of caspase 3 and 8 activity, while the levels of p21cip/waf and bcl-2 were unchanged or decreased^[54]. The combination of human peripheral blood dendritic cells (DCs) and lymphokine and phytohaemagglutinin (PHA) activated killer (LPAK) cells could induce apoptosis of BEL-7402 cells effectively, with some LPAK cells manifesting the characteristics of autophagic apoptosis^[55].

Clinical resistance to chemotherapeutic drugs is a major problem in the treatment of cancers. Increased bcl-2 expression in epithelium adjacent to tumors represents a genetically variation in the morphologically normal epithelium because it occurs without the corresponding high proliferative state seen in the normal crypt-regenerative compartment. Heterogeneity may provide a mechanistic explanation for chemotherapeutic resistance in tumors with cells having high bcl-2^[22]. Treatment with taxol can induce apoptosis of HepG2 thus killing liver cancer cells. DNA ladder of 200bp emerged. In the meantime bcl-xl, or bad and bax were expressed in HepG2 cells; and the expression levels of bcl-xl and bak remained unchanged, whereas the level of bad was down-regulated. It was thought that the change of bcl-2 family proteins caused by anticancer drugs in liver cancer cells may be involved in chemoresistance^[56]. A new somatostatin analogue, TT-232 has a pronounced antiproliferative effect on differentiated and dedifferentiated, drug-sensitive and multidrug-resistant hepatocellular carcinoma cell lines. TT-232 induces apoptosis at comparable levels in all these hepatoma variants, which demonstrates that the multidrug resistance of hepatomas does not correlate with a reduced susceptibility to apoptosis induction. The mechanism involved in apoptosis is functional in both drug-sensitive and resistant hepatoma variants and can be activated by the somatostatin analogue TT-232^[57].

The gene therapeutics to liver cancer is a new technique. Human genes p53, B7-1, GM-CSF, IL-2 were transduced into liver cancer cells by adenovirus. The ad-multigenes can induce apoptosis and elevate sensitivity of liver cancer cells to chemotherapy drug-cisplatin^[58]. After gene therapy with HSV thymidine kinase, inhibition of enhanced glucose transport in ganciclovir-treated Morris hepatoma cells increased apoptosis^[59]. For gene therapy of hepatocellular carcinoma (HCC), the *Escherichia coli* purine nucleoside phosphorylase (PNP)/fludarabine suicide gene system may be more useful than the herpes simplex virus thymidine kinase/ganciclovir (HSV-tk/GCV) system. Human HCC cells of the cell lines, HepG2 and Hep3B were transduced with PNP or HSV-tk using adenoviral vectors, followed by prodrug incubation. Both systems predominantly induced apoptosis in HepG2 and Hep3B cells. The results showed that cell line-specific differences in response to treatment with PNP/fludarabine and HSV-tk/GCV, respectively. PNP/fludarabine may be superior to HSV-tk/GCV for the treatment of human HCC because of its independence from p53 and the Fas/FasL system^[60].

ACKNOWLEDGEMENTS

The authors thank professor Guan-Hua Du Ph.D., Teacher of doctors and Director of National Center for Pharmaceutical Screening, Institute of Materia Medica, Chinese Academy of Medical Science, Beijing, 100050, China for his support and help to this work, checking and approving to this paper.

REFERENCES

- 1 Kanzler S, Galle PR. Apoptosis and the liver. *Semin Cancer Biol* 2000; 10: 173-184
- 2 Park YN, Chae KJ, Kim YB, Park C, Theise N. Apoptosis and proliferation in hepatocarcinogenesis related to cirrhosis. *Cancer* 2001; 92: 2733-2738

- 3 Gu SQ, Liang YY, Fang LR, Li BY, Wang DS. Co-regulative effects of the cAMP/PKA and DAG/PKC signal pathways on human gastric cells during differentiation induced by tradition Chinede medicines. *China Natl J New Gastroenterol* 1997; 3: 50-53
- 4 Andrikoula M, Tsatsoulis A. The role of Fas-mediated apoptosis in thyroid disease. *Eur J Endocrinol* 2001; 144: 561-568
- 5 Wang LD, Zhou Q, Wei JP, Yang WC, Zhou X, Wang LX, Zou JX, Gao SS, Li YX, Yang CS. Apoptosis and its relationship with cell proliferation, P53, Waf1p21, bcl-2 and c-myc in esophageal carcinogenesis studied with a high-risk population in northern China. *World J Gastroenterol* 1998; 4: 287-293
- 6 Thornberry NA, Lazebnik Y. Caspsase: Enemies Within. *Science* 1998; 281: 1312-1315
- 7 Ashkenazi A, Dixit VM. Death Receptor: Signaling and Modulation. *Science* 1998; 281: 1305-1309
- 8 Slee EA, Harte MT, Kluck RM, Wolf BB, Casiano CA, Newmeyer DD, Wang HG, Reed JC, Nicholson DW, Alnemri ES, Green DR, Martin SJ. Ordering the cytochrome c-initiated caspase cascade: hierarchical activation of caspases-2, -3, -6, -7, -8, and -10 in a caspase-9-dependent manner. *J Cell Biol* 1999; 144: 281-292
- 9 You KR, Shin MN, Park RK, Lee SO, Kim DG. Activation of caspase-8 during N-(4-hydroxyphenyl) retinamide-induced apoptosis in Fas-defective hepatoma cells. *Hepatology* 2001; 34: 1119-1127
- 10 Lin SY, Chang YT, Liu JD, Yu CH, Ho YS, Lee YH, Lee WS. Molecular mechanisms of apoptosis induced by magnolol in colon and liver cancer cells. *Mol Carcin* 2001; 32: 73-83
- 11 Madesh M, Hajnoczky G. VDAC-dependent permeabilization of the outer mitochondrial membrane by superoxide induces rapid and massive cytochrome c release. *J Cell Biol* 2001; 155: 1003-1015
- 12 Green DR, Reed JC. Mitochondria and Apoptosis. *Science* 1998; 281: 1309-1315
- 13 Wolter KG, Hsu YT, Smith CL, Nechushtan A, Xi XG, Youle RJ. Movement of Bax from the cytosol to mitochondria during apoptosis. *J Cell Biol* 1997; 139: 1281-1292
- 14 Goping IS, Gross A, Lavoie JN, Nguyen M, Jemmerson R, Roth K, Korsmeyer SJ, Shore GC. Regulated targeting of BAX to mitochondria. *J Cell Biol* 1998; 143: 207-215
- 15 Desagher S, Sand AO, Nichols A, Eskes R, Montessuit S, Lauper S, Maundrell K, Antonsson B, Martinou JC. Bid-induced conformational change of Bax is responsible for mitochondrial cytochrome c release during apoptosis. *J Cell Biol* 1999; 144: 891-901
- 16 Griffiths GJ, Dubrez L, Morgan CP, Jones NA, Whitehouse J, Corfe BM, Dive C, Hickman JA. Cell damage-induced conformational changes of the pro-apoptotic protein Bak in vivo precede the onset of apoptosis. *J Cell Biol* 1999; 144: 903-914
- 17 Zhang RG, Wang XW, Guo LX, Xie H. Growth inhibition of BEL-7404 human hepatoma cells by expression of mutant telomerase reverse transcriptase. *International J Cancer* 2002; 97: 173-179
- 18 Wu MC. Clinical research advances in primary liver cancer. *World J Gastroenterol* 1998; 4: 471-474
- 19 Bold RJ, Virudachalam S, McConkey DJ. BCL2 expression correlates with metastatic potential in pancreatic cancer cell lines. *Cancer* 2001; 92: 1122-1129
- 20 Lowe SL, Rubinchik S, Honda T, McDonnell TJ, Dong JY, Norris JS. Prostate-specific expression of Bax delivered by an adenoviral vector induces apoptosis in LNCaP prostate cancer cells. *Gene Ther* 2001; 8: 1363-1371
- 21 Weihsing RR, Shintaku IP, Geller SA, Petrovic LM. Hepatocellular and pancreatic mucinous cystadenocarcinomas with mesenchymal stroma: analysis of estrogen receptors/progesterone receptors and expression of tumor-associated antigens. *Mold Pathol* 1997; 10: 372-379
- 22 Bell K, Bronner MP, Pasha T, Furth EE. Expression of proliferating cell nuclear antigen in gastrointestinal therapeutic lesions and its relationship to bcl-2 expression. *Pathobiology* 1996; 64: 91-98
- 23 Sejima T, Miyagawa I. Expression of bcl-2, P53 oncoprotein, and proliferating cell nuclear antigen in renal cell carcinoma. *Eur Urol* 1999; 35: 242-248
- 24 Ho YS, Liu HL, Duh JS, Chen RJ, Ho WL, Jeng JH, Wang, Lin JK. Induction of apoptosis by S-Nitrosoglutathione and Cu²⁺ or Ni²⁺ ion through modulation of bax, bad, and bcl-2 proteins in human colon adenocarcinoma cells. *Mol Carcin* 1999; 26: 201-211
- 25 Peng XM, Peng WW, Chen Q, Yao JL. Apoptosis, Bcl-2 and p53 protein expressions in tissues from hepatocellular carcinom. *Shijie Huaren Xiaohua Zazhi* 1998; 6: 834-836
- 26 Zhang XD, Wang WL. Establishment of an apoptotic model induced by adriamycin in human hepatocellular carcinoma. *Zhonghua Zhongliu Zazhi* 1997; 19: 260-263
- 27 Li J, Wang WL, Yang XK, Yu XX, Hou YD, Zhang J. Inducible overexpression of Bak sensitizes HCC-9204 cells to apoptosis induced by doxorubicin. *Acta Pharmacol Sin* 2000; 21: 769-776
- 28 Choi YH, Lee WY, Nam SY, Choi KC, Park YE. Apoptosis induced by propolis in human hepatocellular carcinoma cell line. *Int J Mol Med* 1999; 4: 29-32
- 29 Kim JA, Kang YS, Jung MW, Lee SH, Lee YS. Involvement of Ca²⁺ influx in the mechanism of tamoxifen-induced apoptosis in HepG2 human hepatoblastoma cell. *Cancer Lett* 1999; 147: 115-123
- 30 Hashimoto Y, Hibasami H, Tamaki S, Kamei A, Ikoma J, Kaito M, Imoto I, Watanabe S, Nakashima K, Adachi Y. Induction Of Apoptotic Cell Death In Human Hepatocellular Carcinoma SK-HEP-1 Cells By A Polyamine Synthesis Inhibitor, Methylglyoxal Bis(Cyclopentylamido)hydrazine. *Anticancer Drugs* 1999; 10: 323-327
- 31 Shen HM, Yang CF, Ong CN. Sodium selenite-induced oxidative stress and apoptosis in human hepatoma HepG2 cells. *Int J Cancer* 1999; 81: 820-828
- 32 Chen X, Liu Z, Ai Z. Antineoplastic mechanism of Octreotide action in human hepatoma. *Chin Med J* 2001; 114: 1167-1170
- 33 Chen CH, Huang LL, Huang CC, Lin CC, Lee Y, Lu FJ. Baicalein, a novel apoptotic agent for hepatoma cell lines: a potential medicine for hepatoma. *Nutr Cancer* 2000; 38: 287-295
- 34 Lystad E, Hostmark AT, Jebens E. Apoptotic effects of dichloro stearic and dichloro myristic acid in human hepatoma cells (HepG2). *Pharmacol Toxicol* 2001; 89: 85-91
- 35 Yamamoto Y, Nakajima M, Yamazaki H, Yokoi T. Cytotoxicity and apoptosis produced by troglitazone in human hepatoma cells. *Life Sci* 2001; 70: 471-482
- 36 Qin LF, Ng IO. Induction of apoptosis by cisplatin and its effect on cell cycle-related proteins and cell cycle changes in hepatoma cells. *Cancer Lett* 2002; 175: 27-38
- 37 Liu J, Liu HT, Liang YY, Wang DS. Effect of compound Chinese drug Bailong on the expression of tumor suppressor genes and relationship with prekallikrein activator signal pathway in human gastric carcinoma BGC82-3 cell line. *Zhongguo Zhongxiyi Jiehe Zazhi* 1999; 19: 613-615
- 38 Deng YP, Lin C, Zhang XY, Chen DQ, Xiao PG, Wu M. Arsenic Trioxide Induced Human Esophageal Cancer Ec109 Cell Apoptosis With Downregulation of c-myc Gene Expression. *Zhongguo Yixue Kexue Xuebao* 2000; 22: 67-70
- 39 Kao ST, Yeh CC, Hsieh CC, Yang MD, Lee MR, Liu HS, Lin JG. The Medicine BU-ZHONG -YI -QI-TANG Inhibited Proliferation of Hepato Chines Cell Lines by Inducing Apoptosis via G0/G1 Arrest. *Life Sci* 2001; 69: 1485-1496
- 40 Li ZQ. Traditional Chinese medicine for primary liver cancer. *World J Gastroenterol* 1998; 4: 360-364
- 41 Liu L, Qin SK, Chen HY, Wang JH, Chen H, Ma J, Liu WH. An experimental study on arsenic trioxide- selectively induced human hepatocarcinoma cell lines apoptosis and its related genes. *Zhonghua Ganzhangbing Zazhi* 2000; 8: 367-379
- 42 Lin SY, Liu JD, Chang HC, Yeh SD, Lin CH, Lee WS. Magnolol suppresses proliferation of cultured human colon and liver cancer cells by inhibiting DNA synthesis and activating apoptosis. *J Cell Biochemistry* 2002; 84: 532-544
- 43 Mitry RR, Sarraf CE, Wu CG, Pignatelli M, Habib NA. WILD-type P53 induces in Hep3B through up-regulation of bax expression. *Lab Invest* 1997; 77: 369-378
- 44 Terada T, Nakanuma Y. Expression of apoptosis, proliferating cell nuclear antigen, and apoptosis-related antigen (bcl-2, c-myc, Fas, Lewis (y) and P53) in human cholangiocarcinomas and hepatocellular carcinomas. *Pathol Int* 1996; 46: 764-770
- 45 Haitel A, Wiener HG, Blaschitz U, Marberger M, Susani M. Biologic behavior of and P53 overexpression in multifocal renal cell carcinoma of clear cell type: an immunohistochemical study correlating grading, staging, and proliferation markers. *Cancer* 1999; 85: 1593-1598
- 46 Lee GH. Correlation between bcl-2 expression and histopathology in diethylnitrosamine-induced mouse hepatocellular tumors. *Am J Pathol* 1997; 151: 957-961
- 47 Wang XW, Xie H. Presence of Fas and Bcl-2 proteins in BEL-7404 human hepatoma cells. *World J Gastroenterol* 1998; 4: 540-543
- 48 Gao G, Dou QP. N-terminal cleavage of Bax by calpain generates a potent proapoptotic 18-kDa fragment that promotes Bcl-2-independent cytochrome C release and apoptotic cell death. *J Cell Biochem* 2001; 80: 53-72
- 49 Huang YL, Chou CK. Bcl-2 blocks apoptotic signal of transforming growth factor-beta in human hepatoma cells. *J Biomed Sci* 1998; 5: 185-191
- 50 Nakayama N, Eichhorst ST, Muller M, Krammer PH. Ethanol-induced apoptosis in hepatoma cells proceeds via intracellular Ca²⁺ elevation, activation of TLCK-sensitive proteases, and cytochrome c release. *Exp Cell Res* 2001; 269: 202-213
- 51 Gagandeep S, Novikoff PM, Ott M, Gupta S. Paclitaxel shows cytotoxic activity in human hepatocellular carcinoma cell line. *Cancer Lett* 1999; 136: 109-118
- 52 Asakura T, Sawai T, Hashidume Y, Ohkawa S, Yokoyama S, Ohkawa K.

- Caspase-3 activation during apoptosis caused by glutathione-doxorubicin conjugate. *Br J Cancer* 1999; 80: 711-715
- 53 Hung WC, Chuang LY. Sodium butyrate enhances STAT 1 expression in PLC/PRF/5 hepatoma cells and augments their responsiveness to interferon-alpha. *Br J Cancer* 1999; 80: 705-710
- 54 Herold C, Ganslmayer M, Ocker M, Hermann M, Hahn EG, Schuppan D. Combined *in vitro* anti-tumoral action of tamoxifen and retinoic acid derivatives in hepatoma cells. *Int J Oncol* 2002; 20: 89-96
- 55 Sun J, Zhang J, Chen J, Chen H, Chew Y, Chen J. *in vitro* study on the morphology of human blood dendritic cells and LPAK cells inducing apoptosis of the hepatoma cell line. *Chin Med J (Engl)* 2001; 114: 600-605
- 56 Luo D, Cheng SCS, Xie Yong. Expression of bcl-2 family proteins during chemotherapeutic agents-induced apoptosis in the hepatoblastoma HepG2 cell line. *Br J Biomed Sci* 1999; 56: 114-118
- 57 Diaconu CC, Szathmari M, Keri G, Venetianer A. Apoptosis is induced in both drug-sensitive and multidrug-resistant hepatoma cells by somatostatin analogue TT-232. *Br J Cancer* 1999; 80: 1197-1203
- 58 Wang ZX, He ZP, Wu ZZ, Zhang WW. Induction of apoptosis in human hepatocellular carcinoma cells by adenoviral-mediated transfer human multigenes. *Zhongguo Ganzangbing Zazhi* 2000; 8: 224-226
- 59 Haberkorn U, Altmann A, Kamencic H, Morr I, Traut U, Henze M, Jiang S, Metz J, Kinscherf R. Glucose transport and apoptosis after gene therapy with HSV thymidine kinase. *Eur J Nucl Med* 2001; 28: 1690-1696
- 60 Krohne TU, Shankara S, Geissler M, Roberts BL, Wands JR, Blum HE, Mohr L. Mechanisms of cell death induced by suicide genes encoding purine nucleoside phosphorylase and thymidine kinase in human hepatocellular carcinoma cells *in vitro*. *Hepatology* 2001; 34: 511-518

Edited by Wu XN

• LIVER CANCER •

Inhibitory effect of endostatin expressed by human liver carcinoma SMMC7721 on endothelial cell proliferation *in vitro*

Xuan Wang, Fu-Kun Liu, Xi Li, Jai-Sou Li, Gen-Xin Xu

Xuan Wang, Fu-Kun Liu, Xi Li, Jai-Sou Li, Research Institute of General Surgery, Clinical School of Medicine, Nanjing University, Nanjing 210002, Jiangsu Province, China
Gen-Xin Xu, Department of Molecular Biology, Nanjing Military Medical School, Nanjing 210002, Jiangsu Province, China
Correspondence to: Dr.Xuan Wang, Research Institute of General Surgery, Clinical School of Medicine, Nanjing University, No.305, Eastern Road of Zhongshan, Nanjing 210002, Jiangsu Province, China. wx58cn@yahoo.com.cn
Telephone: +86-25-4513749 Fax: +86-25-4364753
Received 2001-09-14 Accepted 2001-10-11

Abstract

AIM: To construct a stable transfectant of human liver carcinoma cell line SMMC7721 that could secrete human endostatin and to explore the effect of human endostatin expressed by the transfectant on endothelial cell proliferation.

METHODS: Recombinant retroviral plasmid pLncx-Endo containing the cDNA for human endostatin gene together with rat albumin signal peptide was engineered and transferred into SMMC7721 cell by lipofectamine. After selection with G418, endostatin-transfected SMMC7721 cells were chosen and expanded. Immunohistochemical staining and Western blot were used to detect the expression of human endostatin in transfected SMMC7721 cells and its medium. The conditioned medium of endostatin-transfected and control SMMC7721 cells were collected to cultivate with human umbilical vein endothelial cells for 72 hours. The inhibitory effect of endostatin, expressed by transfected SMMC7721 cells, on endothelial proliferation *in vitro* was observed by using MTT assay.

RESULTS: A 550 bp specific fragment of endostatin gene was detected from the PCR product of endostatin-transfected SMMC7721 cells. Immunohistochemistry and Western blot analysis confirmed the expression and secretion of foreign human endostatin protein by endostatin-transfected SMMC7721 cells. *in vitro* endothelial proliferation assay showed that 72 hours after cultivation with human umbilical vein endothelial cells, the optical density (OD) in group using the medium from endostatin-transfected SMMC7721 cells was 0.51 ± 0.06 , lower than that from RPMI 1640 group (0.98 ± 0.09) or that from control plasmid pLncx-transfected SMMC7721 cells (0.88 ± 0.11). The inhibitory rate for medium from endostatin-transfected SMMC7721 cells was 48%, significantly higher than that from empty plasmid pLncx-transfected SMMC7721 cells (10.2%, $P < 0.01$).

CONCLUSION: Human endostatin can be stably expressed by SMMC7721 cell transferred with human endostatin gene and its product can significantly inhibit the proliferation of human umbilical vein endothelial cell *in vitro*.

Wang X, Liu FK, Li X, Li JS, Xu GX. Inhibitory effect of endostatin expressed by human liver carcinoma SMMC7721 on endothelial cell proliferation *in vitro*. *World J Gastroenterol* 2002;8(2):253-257

INTRODUCTION

Recent studies have shown that angiogenesis is essential for tumor growth and metastases^[1-9]. Hanahan *et al*^[10,11] noted that angiogenesis is regulated by a balance between factors of proangiogenesis and antiangiogenesis. The pathological formation of new blood vessel could be generated if the balance was undermined^[12]. This provides the rationale for antiangiogenic therapy for cancer. Endostatin, a specific inhibitor of endothelial cell proliferation, first isolated as a M_r22000 protein from the conditioned medium of a murine hemangioendothelioma cell line (EOMA), is a C-terminal fragment of collagen 18a consisting of 184 amino acids. Its potent antiangiogenic effect can specifically inhibit the proliferation and migration of endothelial cell and subsequently promote the development of apoptosis and atrophy of tumor without direct influence on tumor cell or nonneoplastic cell growth^[13-21]. To explore the inhibitory effect of human endostatin expressed by SMMC7721 on endothelial cell proliferation, retroviral pLncx carrying human endostatin gene was used to transfect human liver carcinoma cell line SMMC7721, and the supernatant of transfected SMMC7721 was collected to incubate with human umbilical vein endothelial cell (HUVEC) *in vitro*.

MATERIALS AND METHODS

Plasmids

The plasmid pUC19-Endo containing the cDNA for human endostatin was generously provided by Professor Genxin Xu (Nanjing Military Medical College, Nanjing, China). In this plasmid, human endostatin cDNA was put downstream from rat serum albumin signal peptide and influenza virus HA tag. Plasmid pUC19-Endo and retroviral pLncx were digested with HindIII and Cla I respectively, and resulting products were ligated. The recombinant plasmid was designated as pLncx-Endo. Correct in-frame insertion of human endostatin cDNA was confirmed by electrophoresis showing the pattern of pLncx-Endo digested with restriction enzyme.

Cell lines

Virus packaging cell PA317 and NIH3T3 cell lines were provided by Dr. Qian (Second Military Medical University, Shanghai, China). PA317 and NIH3T3 cells were maintained in DMEM supplemented with 100mL L⁻¹ fetal bovine serum, 100units/ml penicillin and 100ug/ml streptomycin. HUVEC was purchased from Shanghai Cellular Research Institute. SMMC7721 and HUVEC were maintained in 1640 medium.

Transfection of PA317 cells and determination of viral titre

Plasmids of pLncx-Endo and pLncx were transferred into PA317 cells respectively by lipofectamine (Gibco) following the manufacturer's instructions. G418 selection at 500mg·L⁻¹ was added at the same time. Two weeks after transfection, G418-resistant colonies emerged and were expanded. The supernatant of G418-resistant PA317 colony was collected and diluted to infect NIH3T3 cells with a final

concentration of polybrene at $2\text{mg}\cdot\text{L}^{-1}$. After transfection, NIH3T3 cells were also placed under G418 selection. Two weeks later, G418-resistant NIH3T3 colonies were counted for determination of viral titre.

Generation of stable transfectant

Total of 5×10^5 SMMC7721 cells were plated on 6-well plate and incubated for 24h. The cells were rinsed with serum-free 1640 medium twice, and $100\mu\text{L}$ supernatant of endostatin-transfected PA317 colony was added and incubated for 3h. Another 3mL 1640 medium was added with the final concentration of polybrene at $2\text{mg}\cdot\text{L}^{-1}$ and G418 at $500\text{mg}\cdot\text{L}^{-1}$. Four weeks after transfection, G418-resistant cells were expanded for preservation and detected for endostatin-HA fusion protein by immunohistochemistry and Western blot analysis. The G418-resistant colony was designated as SMMC-Endo. Control transfectant (SMMC-pLncx) was generated in a similar way except that the parent plasmid pLncx-Endo was replaced by pLncx.

PCR amplification of endostatin gene

SMMC-Endo and SMMC-pLncx cells were harvested and DNA was extracted. The primers used were: 5'CCG GAA TTC ATG CAC AGC CAC CGC GAC TTC CAG CCG and 5'GCC GGA TCC CTA CTT GGA GGC AGT CAT GAA GCT based on human endostatin sequence. PCR was performed in $50\mu\text{L}$ reactive volume containing $2\mu\text{L}$ cDNA, $2\mu\text{L}$ $10\times\text{PCR}$ buffer, $2\mu\text{L}$ $4\times\text{dNTP}$ ($2\text{mmol}\cdot\text{L}^{-1}$), $50\text{pmol}\cdot\text{L}^{-1}$ primer, and $1\mu\text{L}$ Tag DNA polymerase. The samples were subjected to 30 thermal cycles, consisting of 5min at 94°C for predenaturation, 1min at 94°C for denaturing, 1min at 60°C for annealing, 1min at 72°C for extension, and 10min at 72°C for final extension after the last cycle. PCR products were run on $10\text{g}\cdot\text{L}^{-1}$ agarose gels (containing $0.5\text{mg}\cdot\text{L}^{-1}$ ethidium bromide) and visualized under UV light.

Immunohistochemical staining

Immunohistochemical staining was accomplished utilizing an avidin-biotin technique. Anti-HA monoclonal antibody was purchased from Jing Mei Biotechnology Co. Ltd. SMMC-Endo and SMMC-pLncx cells were grown on six-well glass slides and fixed in acetone. After washing in PBS, the cells were incubated with a $10\text{mL}\cdot\text{L}^{-1}$ H_2O_2 solution at room temperature for ten minutes to quench endogenous peroxidases. Nonspecific binding was blocked with $50\text{mL}\cdot\text{L}^{-1}$ normal horse serum at room temperature for five minutes. The cells then were incubated with anti-HA at a 1:300 dilution at 4°C overnight. Following washing in PBS, the secondary antibody, biotinylated anti-rat Ig G, was added and the cells were incubated at room temperature for an hour. After washes in PBS, Vectastain reagent (a solution containing streptavidin-horseradish peroxidase) was added and then incubated at room temperature for ten minutes. 3,3-diaminobenzidine was used as the chromagen. After ten minutes, the brown color signifying the presence of antigen bound to antibodies was detected by light microscopy and photographed at $\times 400$.

Western blot analysis

SMMC-Endo and SMMC-pLncx cells were plated in six-well plates at 2.5×10^5 cells/well respectively and incubated for 24h. The medium was replaced with 1mL serum-free RPMI 1640 and collected after 48h. One mL of conditioned medium was concentrated in a microconcentrator (Amicon, Beverly, MA) to $20\mu\text{L}$ and subjected to a $120\text{g}\cdot\text{L}^{-1}$ reducing SDS/PAGE gel. Protein were transferred to a nitrocellulose membrane and incubated overnight in $50\text{mL}\cdot\text{L}^{-1}$ nonfat milk in PBS at 4°C . After briefly washing in $10\text{mL}\cdot\text{L}^{-1}$ nonfat milk,

the membrane was incubated with anti-HA mouse monoantibody diluted 1:500. After three 10min washes in $10\text{mL}\cdot\text{L}^{-1}$ nonfat milk, the membrane was incubated in horseradish peroxidase-conjugated antimouse immunoglobulin diluted 1:1000. After three 10min washes in TBS, the proteins were detected using the Amersham ECL kit.

Endothelial cell proliferation assay

SMMC7721, SMMC-Endo and SMMC-pLncx cells were plated onto six-well culture plates at a density of 2.5×10^5 cells/well and incubated for 24h. The cells were washed with PBS, and 1.5mL of serum-free 1640 were added and incubated for another 48h. The total of 9mL serum-free RPMI 1640 were collected and concentrated to 1.8mL using Centrifuplus 10 concentrator (Amicon), and stored at -80°C for usage. HUVEC cells were plated at a density of 4000 cells/well onto gelatinized 40-well culture plates and incubated (37°C , $50\text{mL}\cdot\text{L}^{-1}\text{CO}_2$) for 24h in $100\mu\text{L}$ RPMI 1640 medium. The medium was replaced with $20\mu\text{L}$ of above concentrated conditioned medium and incubated for 30min. $80\mu\text{L}$ of 1640 supplemented with $10\text{mL}\cdot\text{L}^{-1}$ fetal bovine serum and $1\mu\text{g}\cdot\text{L}^{-1}$ bFGF (Sigma) was then added for 72h. The numbers of cells were quantified using a colorimetric MTT assay. Tests were conducted in quadruplicate.

RESULTS

Identification of a recombinant retroviral pLncx-Endo and determination of the recombinant virus titre

The plasmid pLncx and the recombinant retroviral pLncx-Endo were digested by Hind III and Cla I respectively. Only in recombinant retroviral pLncx-Endo contained a 640-bp endostatin gene fragment separated by electrophoresis in $10\text{g}\cdot\text{L}^{-1}$ agarose gel (Figure 1). It proved that the foreign endostatin gene together with signal peptide and HA-tag was correctly inserted in retroviral pLncx. After transfection of NIH3T3 cells with supernatant of endostatin-transfected PA317, NIH3T3 cells were maintained in DMEM supplemented with G418 $500\text{mg}\cdot\text{L}^{-1}$. Two weeks later, total 34 colonies were detected under microscopy and the titre of the recombinant virus (pLncx-Endo) was $1.36\times 10^8\text{cfu}\cdot\text{L}^{-1}$.

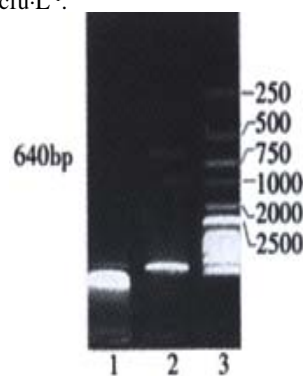


Figure 1 Identification of recombinant plasmids digested with restriction enzymes (Hind III and Cla I)
1: pLncx plasmid digested with Hind III and Cla I; 2: pLncx-Endo plasmid digested with Hind III and Cla I; 3: DNA Marker.

Generation of stable transfectants

The PCR products amplified from DNA of SMMC-Endo and SMMC-pLncx cells were analyzed under ultraviolet light after $10\text{g}\cdot\text{L}^{-1}$ agarose gel electrophoresis. A 550-bp fragment was seen in the PCR product from DNA of SMMC-Endo cells, but not from the control (Figure 2). It indicated that endostatin was successfully transferred into SMMC7721 cells by way of retroviral pLncx-Endo. The expression of endostatin in the transfected SMMC-Endo cells was also detected by immunohistochemical staining. A lot of brown granules were seen in endostatin-transfected SMMC-Endo cell cytoplasm while control SMMC-pLncx cells showing negative. Thus, it proved that endostatin

gene can be expressed stably in SMMC7721 cells (Figure 3). Transgene expression was also tested by Western blot for the expressed protein. On a reducing 120g·L⁻¹ SDS/PAGE gel, a distinct band at around *M*_r22000, corresponding to the size of endostatin, was visualized in the supernatant of SMMC-Endo cells but not in the supernatant of SMMC-pLncx cells. Monoclonal mouse anti-HA antibody reacted positively in a Western blot with the *M*_r22000 protein only. It was confirmed that endostatin could be efficiently secreted into the supernatant of cells transduced by retroviral pLncx-Endo (Figure 4).

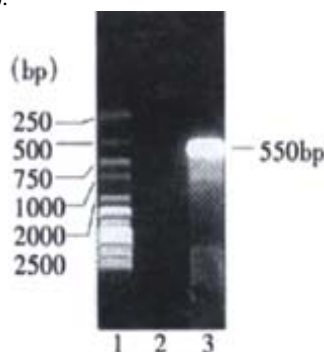


Figure 2 Analysis of PCR product of SMMC7721 transferred with pLncx-endo by 1% agarose gel electrophoresis. 1: DNA Marker; 2: PCR product of SMMC7721 cell DNA transfected with pLncx; 3: PCR product of SMMC7721 cell DNA transfected with pLncx-endo

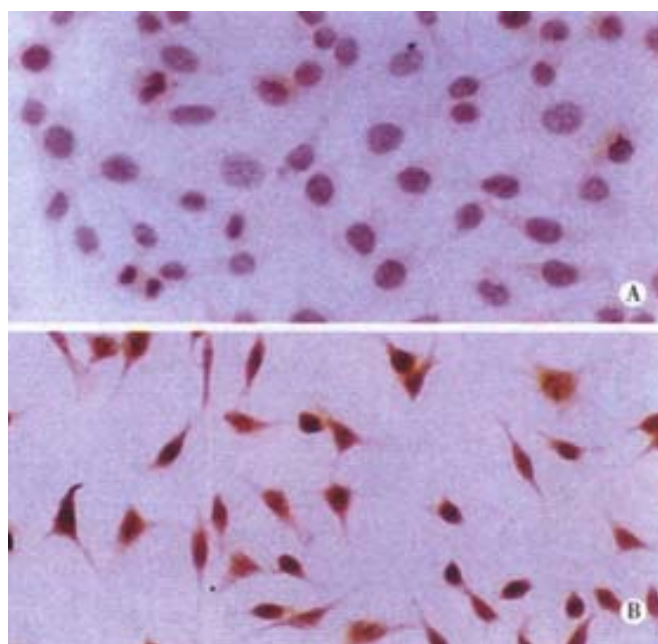


Figure 3 Expression of human endostatin-HA fusion protein in endostatin-transfected cells. Anti-HA monoclonal antibody was applied to SMMC7721 transfected with pLncx (A) and SMMC7721 transfected with pLncx-endo (B), followed by a HRP-conjugated secondary antibody. Hematoxylin counterstain. $\times 400$.

Human endostatin inhibits endothelial cell proliferation

Three days after incubation with conditioned medium, cell number, as measured by absorbance (OD), was quantified by using a colorimetric MTT assay. The results showed that the optical density in groups using concentrated conditioned medium from SMMC7721 cells, RPMI1640 and SMMC-pLncx cells were 1.01 ± 0.09 , 0.98 ± 0.09 and 0.88 ± 0.1 respectively. It revealed that conditioned medium both from SMMC7721 cells and empty plasmid pLncx-transfected SMMC7721 cells did not have inhibitory effect on the growth of HUVEC, compared with 1640 medium ($P > 0.01$). While the optical density in group using conditioned medium from endostatin-

transfected SMMC-Endo cells was 0.51 ± 0.06 , significantly lower than that from SMMC-pLncx group (0.88 ± 0.1). It meant that inhibitory rate on endothelial proliferation for conditioned medium from endostatin-transfected SMMC7721 group was 48%, significantly higher than that from control pLncx-transfected SMMC7721 group (10.2%, $P < 0.01$), (Figure 5).

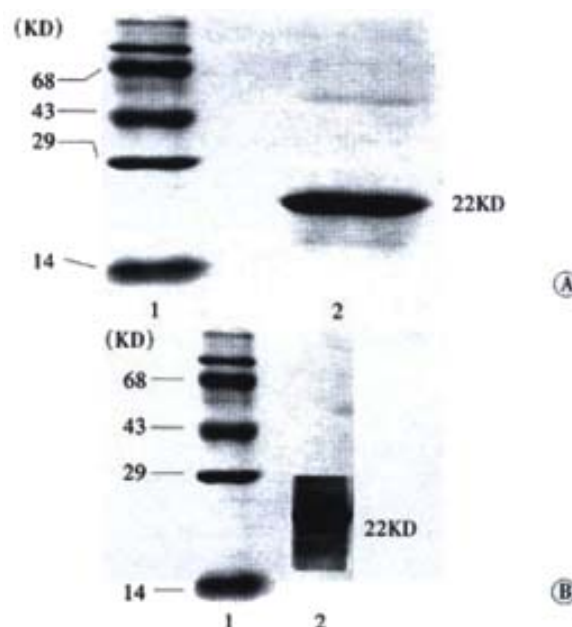


Figure 4 SDS-PAGE analysis and Western blot of endostatin expressed in supernatant of viral transduced SMMC7721 cells (A) SDS-PAGE analysis; 1, protein marker; 2, supernatant of SMMC7721 cells transfected with pLNCX-Endo; (B) Western blot analysis; 1, protein marker; 2, supernatant of SMMC7721 cells transfected with pLNCX-Endo

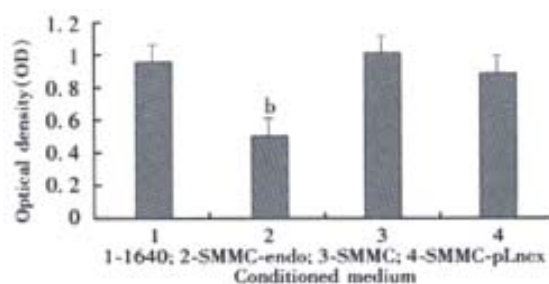


Figure 5 Inhibition of endothelial cell proliferation by conditioned medium from transfected and untransfected cells. Conditioned medium from endostatin-transfected SMMC-Endo cells (2), conditioned medium from SMMC7721 cells (3), and conditioned medium from SMMC-pLncx cells (4) were concentrated and applied to cultivate with HUVEC cells grown in 40-well plate. Three days later, cell number, as measured by absorbance (OD), was then quantified by using a colorimetric MTT assay. Bars, SD. $^b P < 0.01$, compared with conditioned medium from control SMMC-pLncx cells.

DISCUSSION

It is well known that the growth and metastases of tumor is dependent on the formation of new blood vessel. The new blood vessel provides not only nutrient for tumor, but also the ways for excretion and metastases. Numerous studies have proven that tumor cells will stop growing or die when it exceeds 2mm to 3mm in diameter if new blood vessel for tumor is not formed^[5,6]. So, anti-angiogenesis is one of the effective ways to inhibit and control the development of tumor by inducing tumor dormancy or apoptosis.

Endostatin is a new kind of potent antiangiogenic factor

consisting of 184 amino acids in C- terminal fragment of endogenous collagen 18a. It was isolated as a M_r 22000 protein from conditioned medium of the EOMA murine hemangioendothelioma cell line by Professor O'Reilly in 1997^[22-27]. *In vivo* and *in vitro* experiments have demonstrated that endostatin have specific inhibitory effect on tumor metastases and primary tumor with no observed sign of toxicity^[16,28-33]. Furthermore, the genome of endothelial cell, targeted by endostatin, has a stable inherent property and rare mutation. So, there is no acquired resistance to endostatin during endostatin therapy. But the production of functional polypeptide has proven difficult because of its unstable physical property. In addition, antiangiogenic therapy with endostatin in cancer requires prolonged administration and high doses of the recombinant protein. It will result in heavy economic burden and inconvenience to recipients by repeated administrations. Therefore, transfer of foreign endostatin gene into host cells represents an alternative method to treat tumor by generating high efficient endostatin in areas around tumor^[34-36]. The aims of generating a high efficient protein with no toxin and keeping a long time and relatively high expression of endostatin can be achieved by single administration^[37]. A few groups have demonstrated that antiangiogenic gene therapy with viral vectors is a potentially useful approach for inhibiting tumor growth in mouse model^[35,38-44]. By the way, gene transfer mediated by retroviral vectors is most commonly used among the various ways of transducing methods^[45]. As retroviral vectors can be integrated into chromosome of host cells, gene transferred by retrovirus can be inherited to next generation and stably expressed in host cells. In this experiment, in order to explore the effect of endostatin on endothelial cell proliferation expressed by SMMC7721, endostatin gene was inserted into retroviral vector pLncx by recombinant technology and subsequently used to infect human liver carcinoma cell line SMMC7721. After transfection, PCR products and immunohistochemical staining showed that endostatin gene had been successfully transferred into and expressed in endostatin-transfected SMMC7721 cells. For the purpose of the protein expressed by SMMC7721 cells being excreted outside the cell, rat albumin signal peptide, which can lead to the expressed protein being secreted outside cell while without any effect on the activity of the protein, was put into the upstream of endostatin gene during the construction of recombinant plasmid^[16,28,46]. The effect of signal peptide was also demonstrated by Western blot analysis, which revealed that endostatin protein did exist in the concentrated supernatant of endostatin-transfected SMMC7721 cells. The endothelial cell proliferation assay indicated that conditioned medium from endostatin-transfected SMMC7721 cells significantly inhibited the proliferation of endothelial cell by 48%, compared to conditioned medium from control SMMC7721 cells transferred with empty plasmid pLncx. In another word, endostatin expressed by SMMC7721 cells can remarkably inhibit the proliferation of endothelial cell. In conclusion, gene therapy with endostatin mediated by retrovirus is effective *in vitro*, and perhaps it might also have a significant inhibitory effect on tumor growth *in vivo*, but that remains to be confirmed by further experiments.

REFERENCES

- Folkman J, Watson K, Ingber D, Hanahan D. Induction of angiogenesis during the transition from hyperplasia to neoplasia. *Nature* 1989;339:58-62
- Hahnfeldt P, Panigrahy D, Folkman J, Hlatky L. Tumor development under angiogenic signaling: a dynamical theory of tumor growth, treatment response and postvascular dormancy. *Cancer Res* 1999;59:4770-4775
- Liu DH, Zhang XY, Fan DM, Huang YX, Zhang JS, Huang WQ, Zhang YQ, Huang QS, Ma WY, Chai YB, Jin M. Expression of vascular endothelial growth factor and its role in oncogenesis of human gastric carcinoma. *World J Gastroenterol* 2001;7:500-507
- Dhanabal M, Ramchandra R, Waterma MJF, Lu H, Knebelmann B, Segal M, Sukhatme VP. Endostatin induce endothelial cell apoptosis. *J Biol Chem* 1999;274:1721-1726
- Folkman J. Clinical applications of research on angiogenesis. *N Engl J Med* 1995;333:1757-1763
- Perletti G, Concar P, Giardini R, Marras E, Piccinini F, Folkman J, Chen L. Antitumor activity of endostatin against carcinogen-induced rat primary mammary tumors. *Cancer Res* 2000;60:1793-1796
- Jiang YF, Yang ZH, Hu JQ. Recurrence or metastasis of HCC: predictors, early detection and experimental antiangiogenic therapy. *World J Gastroenterol* 2000;6:61-65
- Liu H, Wu JS, Li LH, Yao X. The expression of platelet-derived growth factor and angiogenesis in human colorectal carcinoma. *Shijie Huaren Xiaohua Zazhi* 2000;8:661-664
- Fan ZR, Yang DH, Cui J, Qin HR, Huang CC. Expression of insulin like growth factor II and its receptor in hepatocellular carcinogenesis. *World J Gastroenterol* 2001;7:285-288
- Hanahan D, Folkman J. Patterns and emerging mechanisms of the angiogenic during tumorigenesis. *Cell* 1996;86:353-364
- Bohem T, Folkman J, Browder T, O'Reilly MS. Antiangiogenic therapy of experimental cancer does not induce acquired drug resistance. *Nature* 1997;390:404-407
- Liu XP, Song SB, Li G, Wang DJ, Zhao HL, Wei LX. Correlations of microvessel quantification in colorectal tumors and clinicopathology. *Shijie Huaren Xiaohua Zazhi* 1999;7:37-39
- O'Reilly MS, Bohem T, Shing Y, Fukai N, Vasios G, Lane WS, Flynn E, Folkman J. Endostatin: an endogenous inhibitor of angiogenesis and tumor growth. *Cell* 1997;88:277-285
- Berger AC, Feldman AL, Gnani MF, Kruger EA, Sim Bk, Hewitt S, Figg WD, Alexander HR, Libutti SK. The angiogenesis inhibitor, endostatin, does not affect murine cutaneous wound healing. *J Surg Res* 2000;91:26-31
- Dhanabal M, Volk R, Ramchandran R, Simons M, Sukhatme V. Cloning, expression, and *in vitro* activity of human endostatin. *Biochem and Biophys Res Commun* 1999;258:345-352
- Yokoyama Y, Dhanabal M, Griffioen AW. Synergy between angiostatin and endostatin: inhibition of ovarian cancer growth. *Cancer Res* 2000;60:2190-2196
- Feldman AL, Restifo NP, Alexander HR, Bartlett DL, Hwu P, Seth P, Libutti K. Antiangiogenic gene therapy of cancer utilizing a recombinant adenovirus to elevate systemic endostatin levels in mice. *Cancer Res* 2000;60:1503-1506
- Sasaki T, Fukai N, Mann K, Gohring W, Olsen BR, Timpl R. Structure, function and tissue forms of the C-terminal globular domain of collagen containing the angiogenesis inhibitor endostatin. *Embo J* 1998;17:4249-4256
- Wen W, Moses MA, Wiederschain D, Arbiser JL, Folkman J. The generation of endostatin is mediated by elastase. *Cancer Res* 1999;59:6052-6056
- Felbor U, Dreier L, Bryant RA, Ploegh HL, Olsen BR, Mothes W. Secreted cathepsin L generates endostatin from collagen XVIII. *Embo J* 2000;19:1187-1194
- Kim YM, Jang JW, Lee OH, Yeon J, Choi EY, Kim EW, Lee ST, Kwon YG. Endostatin inhibits endothelial and tumor cellular invasion by blocking the activation and catalytic activity of matrix metalloproteinase. *Cancer Res* 2000;60:5410-5413
- Taddei L, Chiarugi P, Brogelli L. Inhibitory effect of full-length human endostatin on *in vitro* angiogenesis. *Biochem and Biophys Res Commun* 1999;263:340-345
- Ding I, Sun JZ, Fenton B, Liu WM, Kinsely P, Okunieff P, Min W. Intratumoral administration of endostatin plasmid inhibits vascular growth and perfusion in Mca-4 murine mammary carcinomas. *Cancer Res* 2001;61:526-531
- Kuger EA, Durat PH, Tsokos MG, Venzon DJ, Libutti SK, Dixon SC, Rudek MA, Pluda J, Allegra C, Figg WD. Endostatin inhibits microvessel formation in the ex vivo rat aortic ring angiogenesis assay. *Biochem and Biophys Res Commun* 2000;268:183-191
- Musso O, Theret N, Heljasvaara R, Rehn M, Turlin B, Campion JP, Pihlajaniemi T, Clement B. Tumor hepatocytes and basement membrane-producing cells specifically express two different forms of the endostatin precursor, collagen XVIII, in human liver cancers. *Hepatology* 2001;33:868-876
- Musso O, Rehn M, Theret N, Turlin B, Paulette BS, Lotrian D, Campion JP, Pihlajaniemi T, Clement B. Tumor progression is associated with a significant decrease in the expression of the endostatin precursor collagen XVIII in human hepatocellular carcinomas. *Cancer Res* 2001;61:45-49
- Lietard J, Theret N, Rehn M, Musso O, Dargere D, Pihlajaniemi T, Clement B. The promoter of the long variant of collagen XVIII, the precursor of endostatin, contains liver-specific regulatory elements. *Hepatology* 2000;1377-1385
- Yoon SS, Eto H, Lin CM, Nakamura H, Pawlik TM, Song SU, Tanabe KK. Mouse endostatin inhibits the formation of lung and liver metastases. *Cancer Res* 1999;59:6251-6256
- Oehler MK, Blicknell R. The promise of anti-angiogenic cancer therapy.

- Br J Cancer* 2000;82:749-752
- 30 Sauter BV, Martinet O, Zhang WJ, Mandeli J, Woo SLC. Adenovirus-mediated gene transfer of endostatin *in vivo* results in high level of transgene expression and inhibition of tumor growth and metastases. *Proc Natl Acad Sci USA* 2000;97:4802-4807
 - 31 Blezinger P, Wang J, Gondo M, Quezada A, Mehrens D, French M, Singhai A, Sullivan S, Rolland A, Ralston R, Min W. Systemic inhibition of tumor growth and tumor metastases by intramuscular administration of the endostatin gene. *Nat Biotechnol* 1999;17:343-348
 - 32 Huang X, Wong MKK, Zhao Q, Zhu Z, Wang KZQ, Huang N, Ye C, Gorelik E, Li M. Soluble recombinant endostatin purified from *Escherichia coli*: antiangiogenic activity and antitumor effect. *Cancer Res* 2001;61:478-481
 - 33 Strik H, Schluesener HJ, Seid K, Meyermann R, Deininger M. Localization of endostatin in rat and human gliomas. *Cancer* 2001;91:1013-1019
 - 34 Wu J, Fan DM. Angiogenesis and antiangiogenesis therapy. *Shijie Huaren Xiaohua Zazhi* 2001;9:316-321
 - 35 Tang YC, Li Y, Qian GX. Reduction of tumorigenicity of SMMC7721 hepatoma cells by vascular endothelial growth factor antisense gene therapy. *World J Gastroenterol* 2001;7:22-27
 - 36 Feldman AL, Pak H, Yang JC, Alexander HR, Libutti SK. Serum endostatin levels are elevated in patients with soft tissue sarcoma. *Cancer* 2001;91:1525-1529
 - 37 Naguen JT, Wu P, Clouse ME, Hlatky L, Terwillinger EF. Adeno-associated virus-mediated delivery of anti-angiogenic factors as an anti-tumor strategy. *Cancer Res* 1998;58:5673-5677
 - 38 Yoon SS, Carroll NM, Chiocca EA, Tanabe KK. Cancer gene therapy using a replication -competent herpes simplex virus type I vector. *Ann Surg* 1998;228:366-374
 - 39 Folkman J. Antiangiogenic gene therapy. *Proc Natl Acad Sci USA* 1998;95:9064-9066
 - 40 Dhanabal M, Ramchandran R, Volk R, Stillman IE, Lombardo M, Iruela-Arispe ML, Simons M, Sukhatme VP. Endostatin: Yeast production, mutants and antitumor effect in renal cell carcinoma. *Cancer Res* 1999;59:189-197
 - 41 Yokoyama Y, Green JE, Sukhatme VP, Ramakrishnan S. Effect of endostatin on spontaneous tumorigenesis of mammary adenocarcinomas in a transgenic mouse model. *Cancer Res* 2000;60:4362-4365
 - 42 Qin LX, Sun HC, Wang L, Zhou J, Li Y, Ma ZC, Zhou XD, Wu ZQ, Lin ZY, Yang BH. Metastatic human hepatocellular carcinoma models in nude mice and cell line with metastatic potential. *World J Gastroenterol* 2001;7:597-601
 - 43 Xiao B, Jing B, Zhang YL, Zhou DY, Zhang WD. Tumor growth inhibition effect of hIL-6 on colon cancer cells transfected with the target gene by retroviral vector. *World J Gastroenterol* 2000;6:89-92
 - 44 Wang XW, Yuan JH, Zhang RG, Guo LX, Xie Y, Xie H. Antihepatoma effect of alpha-fetoprotein antisense phosphorothioate oligodeoxyribonucleotides in vitro and in mice. *World J Gastroenterol* 2001;7: 345-351
 - 45 Lohr F, Lo DY, Zaharoff DA, Hu K, Zhang XW, Li YP, Zhao YL, Dewhirst MW, Yuan F, Li CY. Effective tumor therapy with plasmid-encoded cytokines combined with *in vivo* electroporation. *Cancer Res* 2001;61:3281-3284
 - 46 Cao MM, Pan W, Chen QL, Ma ZC, Ni ZJ, Wu WB, Pan X, Cao GW, Qi ZT. Construction of the eukaryotic expression vector expressing the fusion protein of human endostatin protein and IL-3 signal peptide. *Shijie Huaren Xiaohua Zazhi* 2001;9:43-46

Edited by Zhang JZ

• LARGE INTESTINAL CANCER •

Expression and identification of recombinant soluble single-chain variable fragment of monoclonal antibody MC3

Feng-Tian He, Yong-Zhan Nie, Bao-Jun Chen, Tai-Dong Qiao, Dai-Ming Fan, Rong-Fen Li, Yun-Sheng Kang, Yan Zhang

Feng-Tian He, Rong-Fen Li, Yun-Sheng Kang, Yan Zhang, Department of Biochemistry & Molecular Biology, Third Military Medical University, Chongqing 400038, China
Yong-Zhan Nie, Bao-Jun Chen, Tai-Dong Qiao, Dai-Ming Fan, Institute of Digestive Disease, Xijing Hospital, Fourth Military Medical University, Xi'an 710032, Shaanxi Province, China
Correspondence to: Dr. Feng-Tian He, Department of Biochemistry & Molecular Biology, Third Military Medical University, Chongqing 400038, China. hefengtian@163.net
Telephone: +86-23-68752262 Fax: +86-23-68753462
Received 2001-09-25 Accepted 2001-12-05

Abstract

AIM: To generate soluble single chain variable fragments (ScFv) of monoclonal antibody MC3 recognizing colorectal and gastric carcinomas.

METHODS: mRNA was isolated from the hybridoma cell line producing MC3 and the DNAs encoding variable domains of heavy and light chains (VH and VL) of the antibody were amplified separately by RT-PCR and assembled into ScFv DNA with a linker DNA. The ScFv DNA was ligated into the phagemid vector pCANTAB5E and the ligated sample was transformed into *E. coli* TG1. The transformed cells were infected with M13K07 helper phage to yield recombinant phages. After two rounds of panning with gastric carcinoma cell line AGS highly expressing MC3-binding antigen, the phage clones displaying ScFv fragments of the antibody were selected by ELISA. 4 phage clones showing strong signal in ELISA were used to infect *E. coli* HB2151 to express soluble ScFvs. The soluble ScFvs were identified by Dot blot and Western blot, and their antigen-binding activity was assayed by ELISA. The VH and VL DNAs of the ScFv DNA derived from phage clone 19 were sequenced.

RESULTS: The VH, VL and ScFv DNAs were about 340 bp, 320 bp and 750 bp respectively. After two rounds of panning to the recombinant phages, 18 antigen-positive phage clones were selected from 30 preselected phage clones by ELISA. All the soluble ScFvs derived from the 4 out of the 18 antigen-positive phage clones were about M_r 32000 and concentrated in periplasmic space under the given culture condition. The soluble ScFvs could bind the antigen, and they shared the same binding site with MC3. The sequences of the VH and VL DNAs of the MC3 ScFv showed that the variable antibody genes belonged to the IgG1 subgroup, κ -type.

CONCLUSION: The soluble ScFv of MC3 is successfully produced, which not only provides a possible novel targeting vehicle for *in vivo* and *in vitro* study on associated cancers, but also offers the antibody a stable genetic source.

He FT, Nie YZ, Chen BJ, Qiao TD, Fan DM, Li RF, Kang YS, Zhang Y. Expression and identification of recombinant soluble single-chain variable fragment of monoclonal antibody MC3. *World J Gastroenterol* 2002;8(2):258-262

INTRODUCTION

Progress in the use of murine monoclonal antibodies (McAbs) for the *in vivo* study on diagnosis and treatment of human tumors is limited by a number of factors, including poor penetration of the intact antibody molecule into the tumors, their inability to reach the tumor in sufficient quantities without significant toxicity to normal tissue, and the development of a human anti-mouse antibody response to the injected McAb^[1-5]. One possible way to alter the pharmacology of antibody is via the use of smaller molecular weight antibody fragment called ScFv. ScFv molecules offer several advantages as carriers for the selective delivery of radionuclides and toxins to tumors, including rapid blood clearance, low kidney uptake, small size suitable for rapid penetration through tumor tissue and less possibility of developing antimouse antibody response^[6-18]. Colorectal and gastric carcinomas are frequent causes of death of the cancers of digestive system. MC3 is a specific monoclonal antibody directed against colorectal and gastric carcinomas^[19], which has a potential use for *in vivo* diagnosis and therapy of the corresponding carcinomas. In order to overcome the disadvantages of the intact McAb applied *in vivo* and to offer the antibody a stable genetic source, soluble ScFv of MC3 was generated by advanced recombinant phage antibody technique, which may provide a novel tumor-targeting vehicle for *in vivo* study on the diagnosis and treatment of colorectal and gastric carcinomas.

MATERIALS AND METHODS

Materials

The hybridoma cell line producing McAb MC3 (isotype IgG1, κ) was generated by the Institute of Digestive Disease, Xijing Hospital, Fourth Military Medical University, Xi'an, China^[19]. Mouse ScFv DNA construction kit, phage-displayed ScFv expression and detection kits, anti-E tag antibody and pCANTAB5 Sequencing Primer Set were purchased from Pharmacia, Sweden. mRNA isolation kit, Taq DNA polymerase, T4 DNA ligase, SfiI and NotI restriction enzymes were bought from Promega, USA. The gastric carcinoma cell line AGS highly expressing MC3-binding antigen was from ATCC, USA. Horseradish peroxidase (HRP)-labeled goat anti-mouse IgG was from Sino-American Biotechnology Company, China.

Preparation of the phage-displayed ScFv

Total RNA was extracted from guanidine thiocyanate homogenates from 5×10^6 MC3-producing hybridoma cells^[20], and the mRNA was isolated from the total RNA using mRNA isolation system according to the protocol supplied by the manufacturer. Subsequently the phage-displayed ScFvs were generated using the Mouse ScFv DNA construction kit and ScFv expression kit^[21-27]. The purified mRNA was transcribed into cDNA using random primers, and the VH and VL DNAs were separately amplified through PCR program 1 (30 cycles: 94°C×1min, 55°C×2min, 72°C×2min). Gel-purified VH and VL DNAs were mixed with linker primers at an equimolar ratio and assembled into ScFv DNA in fill-in reaction, designed

program 2 (7 cycles: 94°C×1min, 63°C×4min). In a second PCR reaction (same as program 1), the ScFv DNA was amplified and provided with a SfiI site at the 5' end and a NotI site at the 3' end. After digestion with restriction enzymes SfiI and NotI, the ScFv DNA was ligated into the phagemid vector pCANTAB5E, and the ligated sample was transformed into competent *E. coli* TG1 cells to express phage-displayed ScFv. The transformants were grown in 2×YT medium containing ampicillin and glucose (2×YT-AG medium) up to an OD₆₀₀=0.5. Bacteria were infected with M13KO7 helper phage for 1 h at 37°C with shaking. The cells were sedimented by centrifugation, and the supernatant was carefully removed and discarded. The pellet was gently resuspended in 2×YT medium containing ampicillin and kanamycin (2×YT-AK medium) and incubated overnight at 37°C with shaking. The supernatant containing the recombinant phages was harvested by centrifugation and the phages were precipitated with PEG8000 and NaCl and resuspended in 2×YT medium, filtered through a 0.45µm filter and stored at 4°C.

Panning to select for antigen-positive phage-displayed ScFvs

Recombinant phage expressing the MC3 ScFv were selected by panning^[25-27]. The AGS cells highly expressing MC3-binding antigen were grown as an attached monolayer in 25-cm² flasks until almost confluent, washed with PBS, and fixed with 0.25% glutaraldehyde for 8min at room temperature (RT). The fixed cells were washed with PBS and blocked with 50g/L nonfat dry milk in PBS for 2h at RT. The cells were washed 3 times with PBS and the PEG-precipitated recombinant phages diluted 8:7 with 100g/L nonfat dry milk in PBS containing 0.1g/L sodium azide were added to the fixed cells. The culture flask was shaken gently for 2h at 37°C and the cells were washed 20 times with PBS and 20 times with PBS containing 0.1% Tween20 (PBST). Log phase *E. coli* TG1 cells were incubated with bound phages for 1h at 37°C with shaking. Ampicillin, glucose and M13KO7 were added to the bacterial suspension, and the culture was incubated for 1h at 37°C with shaking. Subsequently, preparation of PEG-precipitated recombinant phage was completed as above, and the second round of panning was performed as described for the first panning step. After the second round of panning, the reinfecting TG1 bacteria were plated on SOBAG plates and grown overnight at 30°C, and single colonies were grown in 2×YT-AG medium overnight at 30°C with shaking. 40µL of the saturated culture of single clone was infected with 400µL of M13KO7 helper phage in 2×YT-AG medium for 2h at 37°C with shaking. Cells were pelleted by centrifugation, resuspended in 400µL of 2×YT-AK medium and grown overnight at 37°C with shaking. After centrifugation, phage supernatants were harvested and screened by ELISA.

Detection of phage-displayed MC3 ScFv by ELISA

Phage supernatants obtained from single recombinant cell clones were screened for binding to the AGS cells by ELISA^[25,26,28-33]. The AGS cells were grown in 96-well plates, fixed and blocked as described in the panning step. Phage supernatants obtained from single recombinant cell clones were diluted 4:1 with 20g/L nonfat dry milk in PBS and incubated for 10min at RT, then added to the cell-grown wells (100µL/well) and shaken gently for 1.5h at RT. The cells were washed 6 times with PBST, and the bound phages were detected by incubation for 1 hr at RT with 1:5000 diluted HRP-labeled mouse McAb directed against major coat protein (gene 8 protein) of M13 (100µL/well). Plates were washed 6 times, ABTS substrate was added and incubated for 40min in the dark at RT with shaking, and the A value was measured at 405 nm (A₄₀₅). M13KO7 helper phage served as a negative control, and the phage antibodies were regarded as antigen-positive when A₄₀₅ was at least 2× higher compared to the negative control.

Expression of soluble MC3 ScFv

Log-phase *E. coli* HB2151 cells were infected separately with phage clones 12, 19, 23 and 30 (which previously showed strong signal in phage ELISA, clone 19 showed the strongest signal) for 30min at 37°C with shaking and the infected cells were plated on SOBAG plates containing 100mg/L of nalidixic acid. Single colonies were grown in 5mL of SB-AG medium overnight at 30°C with shaking and diluted with 50mL of fresh SB-AG medium for further incubation for 1h at 30°C with shaking. After centrifugation, the sedimented cells were resuspended in 50mL freshly prepared SB-AI (1: IPTG, 1mmol/L) and incubated for 5h at 30°C with shaking to induce the expression of soluble ScFv. Bacterial culture was divided into two separate centrifuge tubes and centrifuged and supernatants (extracellular fraction) were stored at -20°C until use. One of the two cell pellets was resuspended in 0.5mL of ice-cold 1×TES (0.2mol/L Tris-HCl, pH8.0, 0.5mmol/L EDTA, 0.5mol/L sucrose) followed by adding 0.75mL of 1/5×TES. After incubation for 30min on ice, the supernatant containing the periplasmic fraction was centrifuged and stored at -20°C. Whole-cell extract was prepared by resuspending the second pellet in 0.5mL PBS and boiling for 5 min following centrifugation.

Detection of soluble ScFv by Dot blot

Extracellular fraction and its concentrate precipitated by ice-cold 200g/L trichloroacetic acid (TCA) (to 1/5 of the original volume), periplasmic extract diluted 1:4 with PBS, and whole-cell extracts were spotted onto the nitrocellulose membrane separately (2µL/spot). The membrane was blocked for 2h at RT with PBS containing 100g/L nonfat dry milk (blocking buffer, BB) followed by incubation for 1h at RT with anti-E tag antibody (directed against the E tag-peptide fused to the VL region of the ScFv) diluted to a final concentration of 8mg/L with an equal volume mixture of PBS and BB containing 0.05% Tween20 (PBS/BBT). After being washed once with PBS containing 0.05% Tween20 and 4 times with PBS and followed by a 5min soak in PBS, the membrane was incubated for 1h at RT with HRP-labeled goat anti-mouse IgG diluted 1:150 with PBS/BBT, and washed as above and developed using diaminobenzidine (DAB) substrate.

Detection of soluble ScFv by Western blot

Routine method was applied^[34,35]. Periplasmic extract diluted 1:4 with PBS and TCA-concentrated extracellular fraction were loaded into the wells (10µL/well) of 120g/L SDS polyacrylamide gels and followed by electrophoresis, and the fractionated proteins were then transferred onto a nitrocellulose membrane. The membrane was blocked and developed as described in Dot blot.

ELISA for assay of the reactivity with antigen of soluble ScFv

The AGS cells were grown in 96-well plates, fixed and blocked as described in phage ELISA followed by incubation with 50µL of periplasmic and extracellular fraction for 1 h at RT. After washed 6 times with PBST, anti-E tag antibody diluted 1:1000 with PBS/BBT was added (50µL/well) and incubated as above. The plate was washed and 50µL of HRP-labeled goat anti-mouse IgG diluted 1:1000 with PBS/BBT was added and incubated as above. After being washed, ABTS substrate was added and A₄₀₅ was measured. PBS was as a negative control, and the ScFv was considered as a binder when the ELISA response was at least 2× higher compared to the negative control.

ELISA for assay of the competition of soluble ScFv with MC3 in antigen-binding

It was done as described in references^[36-38]. The AGS cells were

grown in 96-well plates, fixed and blocked as described in phage ELISA followed by incubation with 50 μ L of periplasmic fraction for 1 h at RT, with PBS as a negative control. After washed 6 times with PBST, MC3 was added to the plate (50 μ L/well) at a final concentration of 20 mg/L, and incubated for 1 h at RT. After washed as above, HRP-labeled goat anti-mouse IgG diluted 1:1000 was added (50 μ L/well) and incubated and washed as above. Then TMB substrate was added and A_{450} was measured. Binding of MC3 with the cells was inhibited by the soluble ScFv, which was described as the inhibition rate: Inhibition rate (%) = $1 - (A_{450} \text{ of the tested sample} / A_{450} \text{ of the control}) \times 100\%$.

DNA Sequencing

The phagemid derived from phage antibody clone 19 was used for DNA sequencing of VH and VL DNAs of the ScFv DNA, based on the dideoxy method, with the primers taken from the pCANTAB5 Sequencing Primer Set.

RESULTS

Cloning of MC3 ScFv DNA and Screening of phage-displayed ScFv

The amplified VH, VL and ScFv DNAs were about 340 bp, 320 bp and 750 bp respectively. After two rounds of panning to the recombinant phages, 18 antigen-positive phage clones were selected from 30 preselected phage clones by ELISA. 4 out of the 18 clones (clones 12, 19, 23 and 30), which showed strong signal (clone 19 showed the strongest signal), were selected for expression of soluble MC3 ScFv in *E. coli* HB2151.

Identification of soluble MC3 ScFv

After expression of soluble ScFv in *E. coli* HB2151, extracellular, periplasmic, and whole-cell fractions were checked for the presence and reactivity of ScFv by Dot blot, Western blot and ELISA. In a Dot blot, no visible signal was achieved for the whole-cell extracts, and only weak signal was shown for the extracellular extracts, while a strong signal for periplasmic and TCA-precipitated extracellular extracts. Based on the results in the Dot blot, Western blot analysis was performed only with periplasmic and TCA-precipitated extracellular extracts, and ELISA for reactivity of soluble ScFv with antigen was performed only with periplasmic and extracellular fractions. Western blot showed that in both periplasmic and TCA-precipitated extracellular extracts, a distinct band of M_r 32000, lying within the expected molecular weight range of soluble ScFv, was visualized, and the periplasmic fractions showed stronger reactivity in comparison to the TCA-precipitated extracellular extracts (Figure 1 and Figure 2). The results displayed in Dot blot and Western blot indicated that most of soluble ScFv was secreted into the periplasm under the given culture condition.

ELISA showed that MC3 ScFv secreted into the periplasm could

react with AGS cells expressing MC3-binding antigen at a high level, whereas no significant binding signal was obtained in extracellular extracts. The periplasmic fraction containing soluble ScFv derived from the phage clone 19 showed the strongest signal in ELISA.

Based on the above result in ELISA, the competition ELISA was performed only with periplasmic fraction, and the result showed that all the soluble ScFv-containing periplasmic extracts derived from the clones 12, 19, 23 and 30 could inhibit the binding of MC3 with its corresponding antigen, and the inhibition rates were 36.9%, 41.2%, 31.9% and 33.8% respectively, which indicated that the soluble ScFvs shared the same antigen binding site with McAb MC3.

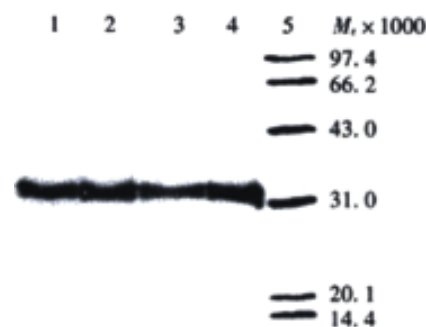


Figure 1 Detection of soluble MC3 ScFv in periplasmic extract by Western blot. Lanes 1-4: periplasmic extracts derived from phage clones 12, 19, 23 and 30 respectively, diluted 1:4 with PBS; Lane 5: low molecular weight protein marker.

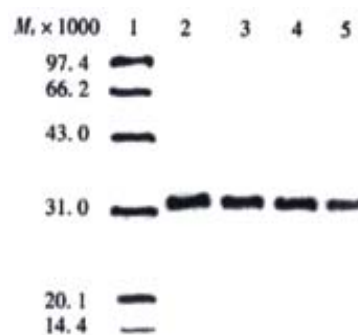


Figure 2 Detection of soluble MC3 ScFv in TCA-precipitated extracellular fraction by Western blot. Lane 1: low molecular weight protein marker; Lane 2-5: TCA-precipitated extracellular fractions (to 1/5 of the original volume) derived from the phage clones 12, 19, 23 and 30 respectively.

DNA Sequence analysis

The phagemid derived from clone 19 was used for DNA sequencing, and the result showed that the VH and VL DNAs of MC3 ScFv DNA were 336 bp and 312 bp respectively, and they were identified as variable antibody genes belonging to the IgG1 subgroup, κ -type. The detail sequence of the VH and VL DNAs were listed as follows.

VH DNA of MC3 ScFv (336 bp)

5'-ATGGCCCAGG TGAAGCTGCA GCAGTCAGGA CCTGAACTGA AGAAGCCTGG AGAGACAGTC AGGATCTCCT
GCAAGGCTTC TGGATATACC TTCACAACTG CTGGAATGCA GTGGGTGCAA AAGATGCCAG GAAAGGGTTT
GAAGTGGATT GGCTGGATAA ACACCCACTC TGGAGTGCCA AAGTATGCAG AAGAGTTCAA GGGACGCTTT
GCCTTCTCTT TGGAAACCTC TGCCAGCACT GCATATTTAC AGATAAGCAA CCTCAAAAAT GAGGACACGG
CTACGTATTT CTGTATGAGA TGGGATTACG ACGGGGGGTT TGCTTACTGG GGCCAA-3'

VL DNA of MC3 ScFv (312 bp)

5'-GCTTCTTTGG CTGTGTCTCT AGGGCAGAGG GCCACCATCT CCTGCAGAGC CAGCGAAAGT GTTGATAATA
TTGGCATTAG TTTTATGAAC TGGTTCCAGC AGAAACCAGG ACAGCCACCC AAACCTCTCA TCTATGCTGC
ATCCAAGCAA GGATCCGGGG TCCCTGCCAG GTTACTGGC AGTGGGTCTG GGACAGATTT CAGCCTCAAC
ATATATCCTA TGGAGGAGGA TGATCCTGCA GTGTATTTCT GTCACCAAAG TAAGGAGGTT CCTTACACGT
TCGGAGGGGG GACCAAGCTG GAAATAAAAC GG-3'

DISCUSSION

Recent progress in antibody engineering have been directed toward the expression of antibody fragments in bacterial and phage display systems, leading to increase of various applications in biology, clinical diagnosis and therapy. The power of the phage display system to express antibody fragments offers several advantages over hybridoma technology, allowing quick, economical production and generation of antibodies with increasing affinity and specificity by mimicking affinity maturation in the normal immune system, and offering the antibody a stable genetic source which can be easily manipulated^[39-51]. Antibody fragments showed less possibility of developing anti-antibody response in comparison to the intact antibodies when applied *in vivo*. In this study, the ScFv of murine McAb MC3 directed against colorectal and gastric carcinomas was successfully produced by advanced phage antibody technology, which offered it the above advantages of the engineering antibody. MC3 ScFv was displayed on the surface of M13 phage as a fusion protein with gene III protein (g3p) and additionally expressed in a soluble form secreted in the bacterial periplasm. Both expression forms retained their reactivity to the antigen. Because of the advantage of MC3 ScFv compared to the intact MC3 for *in vivo* diagnosis and therapy of the associated carcinomas, we have focused on the production of soluble ScFv.

A critical step in cloning of the ScFv DNA was the assembly of VH and VL DNAs with linker DNA. The linker primers consist of two 93-base oligonucleotides which are complementary to each other and have homology with the 3' end of the VH gene and the 5' end of the VL gene. 24 bases on either end of the linkers are complementary to the ends of the VH and the VL. The central 45 bases of the linkers encode the flexible (Gly⁴-4Ser)³ linker which joins the VH and the VL to form a ScFv fragment. In the assembly and fill-in reactions, an exact quantification of purified VH and VL products and linker DNA was very essential. Even slight deviations of the equimolar ratio VH:VL:linker lead to either no visible ScFv product or to the formation of VH-linker or VL-linker dimers, apparently 450bp in size.

McAb MC3 was prepared by immunizing mice with human colorectal carcinoma cells, but immunohistochemical detection indicated that the MC3-binding antigen was highly expressed in both colorectal and gastric carcinomas^[19]. Because no purified antigen was available so far, the recombinant phages were selected in a panning reaction with AGS cells highly expressing MC3-binding antigen. After two rounds of panning, 18 antigen-positive phage clones were selected by ELISA, and 4 clones showing strong signal were used to express soluble ScFv. Clone 19, which showed the strongest signal in ELISA, was used for DNA sequencing and identified as variable antibody genes belonging to the IgG1 subgroup, κ -type.

The *E. coli* strain HB2151 was used to express soluble MC3 ScFv because in this strain the amber stop codon interposed between the E-tag sequence and g3p gene prevented the expression of a ScFv-g3p fusion protein. The soluble ScFv is secreted into the periplasm via the g3p leader sequence, where it is folded in its native form. Dot blot, Western blot, and ELISA verified that soluble ScFv was concentrated in periplasmatic fraction under the given culture condition. Location of functional ScFv in the periplasm is preferred for large-scale preparation because of smaller volume in comparison to the extracellular fraction. The soluble ScFv-containing extracts (such as periplasmatic fraction) may be used directly for some immunoassays. Alternatively, the soluble ScFv may be purified from *E. coli* proteins if the components of the bacterial extract interfere with the immunoassay or/and when the ScFv is for *in vivo* use. In conclusion, the preparation of soluble ScFv of MC3 may provide a promising targeting vehicle for *in vitro* and potential *in vivo* imaging and therapeutic applications to colorectal and gastric carcinomas, and also offer the antibody a stable genetic source.

REFERENCES

- DeNardo SJ, Kramer EL, O'Donnell RT, Richman CM, Salako QA, Shen S, Noz M, Glenn SD, Ceriani RL, DeNardo GL. Radioimmunotherapy for breast cancer using indium-111/yttrium-90 BrE-3: results of a phase I clinical trial. *J Nucl Med* 1997;38:1180-1185
- Alvarez RD, Partridge EE, Khazaeli MB, Plott G, Austin M, Kilgore L, Russell CD, Liu T, Grizzle WE, Schlom J, LoBuglio AF, Meredith RF. Intraperitoneal radioimmunotherapy of ovarian cancer with 177Lu-CC49: a phase I/II study. *Gynecol Oncol* 1997;65:94-101
- Tempero M, Lechner P, Dalrymple G, Harrison K, Augustine S, Schlam J, Anderson J, Wisecarver J, Colcher D. High dose therapy with iodine-131-labeled monoclonal antibody CC49 in patients with gastrointestinal cancers: a phase I trial. *J Clin Oncol* 1997;15:1518-1528
- Buchsbaum D, Khazaeli MB, Liu T, Bright S, Richardson K, Jones M, Meredith R. Fractionated radioimmunotherapy of human colon carcinoma xenografts with ¹³¹I-labeled monoclonal antibody CC49. *Cancer Res* 1995;55(Suppl):5881s-5887s
- Liu HF, Liu WW, Fang DC, Men RP. Expression and significant of proapoptotic gene Bax in gastric carcinoma. *World J Gastroenterol* 1999; 5:15-17
- Goel A, Augustine S, Baranowska-Kortylewicz J, Colcher D, Booth BJ, Pavlinkova G, Tempero M, Batra SK. Single-Dose versus fractionated radioimmunotherapy of human colon carcinoma xenografts using 131I-labeled multivalent CC49 single-chain fvs. *Clin Cancer Res* 2001;7:175-184
- Goel A, Baranowska-Kortylewicz J, Hinrichs SH, Wisecarver J, Pavlinkova G, Augustine S, Colcher D, Booth BJ, Batra SK. ^{99m}Tc-labeled divalent and tetravalent cc49 single-chain fvs: novel imaging agents for rapid *in vivo* localization of human colon carcinoma. *J Nucl Med* 2001;42:1519-1527
- Khare PD, Shao XL, Kuroki M, Hirose Y, Arakawa F, Nakamura K, Tomita Y, Kuroki M. Specifically targeted killing of carcinoembryonic antigen (CEA)-expressing cells by a retroviral vector displaying single-chain variable fragmented antibody to CEA and carrying the gene for inducible nitric oxide synthase. *Cancer Res* 2001;61:370-375
- Schmidt M, McWatters A, White RA, Groner B, Wels W, Fan Z, Bast RC Jr. Synergistic interaction between an anti-p185 HER-2 pseudomonas exotoxin fusion protein [scFv(FRP5)-ETA] and ionizing radiation for inhibiting growth of ovarian cancer cells that overexpress HER-2. *Gynecol Oncol* 2001;80:145-155
- Mayer A, Tsiompanou E, O'Malley D, Boxer GM, Bhatia J, Flynn AA, Chester KA, Davidson BR, Lewis AA, Winslet MC, Dhillon AP, Hilson AJ, Begent RH. Radioimmunoguided surgery in colorectal cancer using a genetically engineered anti-CEA single-chain Fv antibody. *Clin Cancer Res* 2000;6:1711-1719
- Barth S, Huhn M, Matthey B, Tawadros S, Schnell R, Schinkothe T, Diehl V, Engert A. Ki-4(scFv)-ETA', a new recombinant anti-CD30 immunotoxin with highly specific cytotoxic activity against disseminated Hodgkin tumors in SCID mice. *Blood* 2000;95:3909-3914
- Barth S, Huhn M, Matthey B, Schnell R, Tawadros S, Schinkothe T, Lorenzen J, Diehl V, Engert A. Recombinant anti-CD25 immunotoxin RFT5(SCFV)-ETA' demonstrates successful elimination of disseminated human Hodgkin lymphoma in SCID mice. *Int J Cancer* 2000;86:718-724
- Onda M, Olafsen T, Tsutsumi Y, Bruland OS, Pastan I. Cytotoxicity of antiosteosarcoma recombinant immunotoxins composed of TP-3 Fv fragments and a truncated Pseudomonas exotoxin A. *J Immunother* 2001; 24:144-150
- Hoffmann P, Mueller N, Shively JE, Fleischer B, Neumaier M. Fusion proteins of B7.1 and a carcinoembryonic antigen (CEA)-specific antibody fragment opsonize CEA-expressing tumor cells and coactivate T-cell immunity. *Int J Cancer* 2001; 92:725-732
- Roovers RC, van der Linden E, de Bruine AP, Arends JW, Hoogenboom HR. *in vitro* characterisation of a monovalent and bivalent form of a fully human anti Ep-CAM phage antibody. *Cancer Immunol Immunother* 2001;50:51-59
- Mersmann M, Schmidt A, Rippmann JF, Wuest T, Brocks B, Rettig WJ, Garin-Chesa P, Pfizenmaier K, Moosmayer D. Human antibody derivatives against the fibroblast activation protein for tumor stroma targeting of carcinomas. *Int J Cancer* 2001;92:240-248
- Kashentseva EA, Seki T, Curiel DT, Dmitriev IP. Adenovirus targeting to c-erbB-2 oncoprotein by single-chain antibody fused to trimeric form of adenovirus receptor ectodomain. *Cancer Res* 2002;62:609-616
- Tur MK, Sasse S, Stocker M, Djabelkhir K, Huhn M, Matthey B, Gottstein C, Pfizner T, Engert A, Barth S. An anti-GD2 single chain Fv selected by phage display and fused to Pseudomonas exotoxin A develops specific cytotoxic activity against neuroblastoma derived cell lines. *Int J Mol Med* 2001;8:579-584
- Fan DM, Zhang XY, Chen XT, Mou ZX, Chen BJ, Qiao TD, Yang HB, Yang ZD. Establishment of four monoclonal antibodies to colonic cancer cells and immunohistochemical study on their corresponding antigens. *Disi*

- Junyi Daxue Xuebao 1988;9:74-77
- 20 Chomczynski P, Sacchi N. Single-step method of RNA isolation by acid guanidinium thiocyanate-phenol-chloroform extraction. *Anal Biochem* 1987;162:156-159
- 21 McCafferty J, Griffiths AD, Winter G, Chiswell DJ. Phage antibodies: filamentous phage: displaying antibody variable domains. *Nature* 1990;348:552-554
- 22 Marks JD, Hoogenboom HR, Bonnert TP, McCafferty J, Griffiths AD, Winter G. By-passing immunization: Human antibodies from V-gene libraries displayed on phage. *J Mol Biol* 1991;222:581-597
- 23 Winter G, Milstein C. Man-made antibodies. *Nature* 1991;349:293-299
- 24 Hoogenboom HR, Griffiths AD, Johnson KS, Chiswell DJ, Hudson P, Winter G. Multi-subunit proteins on the surface of filamentous phage: methodologies for displaying antibody (Fab) heavy and light chains. *Nucl Acid Res* 1991;19:4133-4137
- 25 He FT, Chen BJ, Nie YZ, Han ZY, Qiao TD, Fan DM. Production of phage-displayed single chain variable fragments of monoclonal antibody MGb1. *Zhonghua Neike Zazhi* 2000;39:585-587
- 26 He FT, Nie YZ, Han ZY, Chen BJ, Qiao TD, Fan DM. Production of phage-displayed anti-idiotypic antibody single chain variable fragments to MG7 monoclonal antibody directed against gastric carcinoma. *Zhonghua Yixue Zazhi* 2001;81:33-36
- 27 Schlebusch H, Reinartz S, Kaiser R, Grunn U, Wagner U. Production of a single-chain fragment of the murine anti-idiotypic antibody ACA125 as phage-displayed and soluble antibody by recombinant phage antibody technique. *Hybridoma* 1997;16:47-52
- 28 George J, Meroni PL, Gilburd B, Raschi E, Harats D, Shoenfeld Y. Anti-endothelial cell antibodies in patients with coronary atherosclerosis. *Immunol Lett* 2000;73:23-27
- 29 Liu Z, Gurlo T, von Grafenstein H. Cell-ELISA using beta-galactosidase conjugated antibodies. *J Immunol Methods* 2000;234:153-167
- 30 Devereux G, Hall AM, Barker RN. Measurement of T-helper cytokines secreted by cord blood mononuclear cells in response to allergens. *J Immunol Methods* 2000;234:13-22
- 31 Salih AM, Nixon NB, Dawes PT, Matthey DL. Antibodies to neuroblastoma cells in rheumatoid arthritis: a potential marker for neuropathy. *Clin Exp Rheumatol* 2000;18:23-30
- 32 Pereira S, Maruyama H, Siegel D, Van Belle P, Elder D, Curtis P, Herlyn D. A model system for detection and isolation of a tumor cell surface antigen using antibody phage display. *J Immunol Methods* 1997;203:11-24
- 33 Heitner T, Moor A, Garrison JL, Marks C, Hasan T, Marks JD. Selection of cell binding and internalizing epidermal growth factor receptor antibodies from a phage display library. *J Immunol Methods* 2001;248:17-30
- 34 Kupsch JM, Tidman NH, Kang NV, Truman H, Hamilton S, Patel N, Newton Bishop JA, Leigh IM, Crowe JS. Isolation of human-specific antibodies by selection of an antibody phage library on melanoma cells. *Clin Cancer Res* 1999;5: 925-931
- 35 Tordsson JM, Ohlsson LG, Abrahmsen LB, Karlstrom PJ, Lando PA, Brodin TN. Phage-selected primate antibodies fused to superantigens for immunotherapy of malignant melanoma. *Cancer Immunol Immunother* 2000;48:691-702
- 36 Wang CD, Chen YL, Wu T, Liu YR. Association between low expression of somatostatin receptor II gene and lymphoid metastasis in patients with gastric cancer. *Shijie Huaren Xiaohua Zazhi* 1999;7:864-866
- 37 Han FC, Yan XJ, Hou Yu, Xiao LY, Guo YH, Su CZ. Gold immunochromatographic assay for anti-Helicobacter pylori antibody. *Shijie Huaren Xiaohua Zazhi* 1999;7:743-746
- 38 Cui DX, Yan XJ, Zhang L, Zhao JR, Jiang M, Guo YH. Screening and its clinical significance of 6 fragments of highly expressing genes in gastric cancer and precancerous mucosa. *Shijie Huaren Xiaohua Zazhi* 1999;7:770-773
- 39 Winter G, Griffiths AD, Hawkins RE, Hoogenboom HR. Making antibodies by phage display technology. *Annu Rev Immunol* 1994;12:433-435
- 40 Chowdhury PS, Pastan I. Improving antibody affinity by mimicking somatic hypermutation *in vitro*. *Nat Biotechnol* 1999;17:568-572
- 41 Chowdhury PS, Viner JL, Beers R, Pastan I. Isolation of a high-affinity stable single-chain Fv specific for mesothelin from DNA-immunized mice by phage display and construction of a recombinant immunotoxin with anti-tumor activity. *Proc Natl Acad Sci USA* 1998;95:669-674
- 42 Mao S, Gao C, Lo CH, Wirsching P, Wong CH, Janda KD. Phage-display library selection of high-affinity human single-chain antibodies to tumor-associated carbohydrate antigens sialyl Lewisx and Lewisx. *Proc Natl Acad Sci USA* 1999;96:6953-6958
- 43 Roovers RC, van der Linden E, de Bruine AP, Arends JW, Hoogenboom HR. Identification of colon tumour-associated antigens by phage antibody selections on primary colorectal carcinoma. *Eur J Cancer* 2001;37:542-549
- 44 Palmer DB, Crompton T, Marandi MB, George AJ, Ritter MA. Intrathymic function of the human cortical epithelial cell surface antigen gp200-MR6: single-chain antibodies to evolutionarily conserved determinants disrupt mouse thymus development. *Immunology* 1999;96:236-245
- 45 He J, Zhou G, Liu KD, Qin XY. Construction and preliminary screening of a human phage single-chain antibody library associated with gastric cancer. *J Surg Res* 2002;102:150-155
- 46 Graus YF, Verschuuren JJ, Degenhardt A, van Breda Vriesman PJ, De Baets MH, Posner JB, Burton DR, Dalmau J. Selection of recombinant anti-HuD Fab fragments from a phage display antibody library of a lung cancer patient with paraneoplastic encephalomyelitis. *J Neuroimmunol* 1998;82:200-209
- 47 Figini M, Obici L, Mezzanzanica D, Griffiths A, Colnaghi MI, Winter G, Canevari S. Panning phage antibody libraries on cells: isolation of human Fab fragments against ovarian carcinoma using guided selection. *Cancer Res* 1998;58:991-996
- 48 Watkins JD, Beuerlein G, Pecht G, McFadden PR, Glaser SM, Huse WD. Determination of the relative affinities of antibody fragments expressed in *Escherichia coli* by enzyme-linked immunosorbent assay. *Anal Biochem* 1997;253:37-45
- 49 Tordsson J, Abrahmsen L, Kalland T, Ljung C, Ingvar C, Brodin T. Efficient selection of scFv antibody phage by adsorption to *in situ* expressed antigens in tissue sections. *J Immunol Methods* 1997;210:11-23
- 50 Govorko D, Cohen G, Solomon B. Single-chain antibody against the common epitope of mutant p53: isolation and intracytosolic expression in mammalian cells. *J Immunol Methods* 2001;258:169-181
- 51 Shadidi M, Sioud M. An anti-leukemic single chain Fv antibody selected from a synthetic human phage antibody library. *Biochem Biophys Res Commun* 2001;280:548-552

Edited by Wu XN

• LARGE INTESTINAL CANCER •

Report of 16 kindreds and one kindred with hMLH1 germline mutation

Bo Zhao, Zhen-Jun Wang, Yu-Feng Xu, Yuan-Lian Wan, Peng Li, Yan-Ting Huang

Bo Zhao, Zhen-Jun Wang, Yuan-Lian Wan, Peng Li, Yan-Ting Huang, Department of Surgery, Peking University First Hospital, Beijing 100034, China

Yu-Feng Xu, Experimental Center, Peking University First Hospital, Beijing 100034, China

Supported by National Natural Science Foundation of China, No. 39970817, and by a Fund from National Education Committee (1999)
Correspondence to: Zhen-Jun Wang, Department of Surgery, Peking University First Hospital, No.8 Xishiku Street, Western District, Beijing, 100034, China. wang3zj@sohu.com

Received 2001-09-25 Accepted 2001-10-29

Abstract

AIM: To analyze the diagnosis and treatment of 16 hereditary nonpolyposis colorectal cancer (HNPCC) kindreds, and to report the first kindred with hMLH1 germline mutation in Mainland China.

METHODS: The diagnosis, treatment and follow-up study of 16 HNPCC kindreds were retrospectively reviewed. Data concerning site of the malignant tumor, age at the diagnosis, history of synchronous and/or metachronous cancer, and histopathology of tumors were recorded. All treatments had won formal consent. PCR and SSCP were used to screen the coding region of hMLH1 and hMSH2 genes. Variant bands were sequenced by a 377 DNA sequencer.

RESULTS: Among sixteen kindreds, sixty-eight patients had a mean age of 50.8 years, including twenty-one multiple cancer patients and forty-six colorectal cancer patients (metachronous colorectal cancers in sixteen). A total of one hundred and one malignant neoplasms were found in these sixty-eight patients, including 50 colonic, 17 rectal, 11 gastric, 7 endometrial, and 4 esophageal cancers. 39.5% colorectal patients had metachronous cancers within ten years who needed reoperations. A germline G265T nonsense mutation was found in the third exon of hMLH1, resulting in a stop codon and truncated protein. Three phenotypically normal family members were also found to carry the mutated gene.

CONCLUSION: HNPCC is a typical auto-dominant hereditary disease, the main characteristics include early onset and frequency of cancers; predominance of colorectal, especially right-sided colon cancers; frequency of multiple primary cancers (especially colorectal cancers). Segmental resection for colorectal cancers is not eligible for colorectal cancer patient in HNPCC kindreds. Intensive follow-up is essential for all patients and possible gene carriers. The first HNPCC kindred with hMLH1 gene germline mutation was identified in Mainland China, and three phenotypically normal family members were found to be carriers of the mutated gene. The G265T germline (nonsense) mutation in the third exon of hMLH1 found here had not been reported previously in the literature.

Zhao B, Wang ZJ, Xu YF, Wan YL, Li P, Huang YT. Report of 16 kindreds and one kindred with hMLH1 germline mutation. *World J Gastroenterol* 2002; 8(2):263-266

INTRODUCTION

Hereditary nonpolyposis colorectal cancer, or Lynch syndrome, is an autosomal, dominantly inherited disease characterized by an excess of early age onset colorectal cancers. It is estimated that hereditary nonpolyposis colorectal cancer may account for 5 to 10 percent of the total colorectal cancers worldwide^[2]. There are two main variants of the disorder^[1,3], Lynch syndrome I, which is susceptible to colorectal carcinoma only, and the more common Lynch syndrome II, which is characterized by excessive colorectal carcinoma and malignancies of extracolonic tissue, especially the endometrium in the western world. Other tumors belong to the spectrum of this syndrome include those of the stomach, esophagus, ovaries, pancreas, and urinary tract^[3,4]. HNPCC has no premonitory symptoms, and the cancer is usually found at an advanced stage at around 50 years of age.

Five causative mismatch repair genes for HNPCC (hMSH2, hMLH1, hPMS1, hPSM2, and hMSH6/GTBP) have been identified, and a germline mutation in one of them predisposes carriers to early onset cancers^[5-10]. hMSH2 and hMLH1 genes contribute at least 40 and 35 percent of all HNPCC germline mutations, respectively. Mutational analysis of the two main genes not only permit diagnosis of most cancer families or patients, but also earlier detection of cancer through targeted surveillance and chemoprevention of the gene carriers.

Despite the fact that China might have the biggest HNPCC population, the disease is rare reported. And also the mismatch repair gene mutation of HNPCC families from Mainland China has not been reported. We retrospectively reviewed the clinical characteristics and treatments of 16 HNPCC kindreds registered in our hospital, and report the first hMLH1 gene mutation family in Mainland China.

MATERIALS AND METHODS

Diagnostic criteria of HNPCC family

Kindreds of independent Chinese families that included multiple patients with colorectal cancer were clinically reviewed. The strict criteria for HNPCC were the Amsterdam criteria^[11]. The criteria are (1) three or more relatives with histologically verified colorectal cancer, with one of them being a first-degree relative to the other two relatives; (2) at least two successive generations were affected; (3) one or more colorectal cancer cases diagnosed under 50 years of age; and (4) familial polyposis of colon is excluded. Japanese clinical diagnostic criteria for HNPCC^[12] was used for highly suspected families that did not fully met the Amsterdam criteria. Families that met either A or B were clinically diagnosed as HNPCC. The criteria include A: a case with three or more colorectal cancers within the first-degree relatives; B: a case with two or more colorectal cancers within the first-degree relatives meeting the following criteria (1) age onset of colorectal cancers being earlier than 50 years old; (2) with right colon involvement; (3) with synchronous or metachronous multiple colorectal cancers; (4) associated with synchronous or metachronous extracolonic malignancies.

Family investigation

The diagnosis is made upon the compilation of a detailed family history. The family history of cancer was thoroughly reviewed when a

patient was admitted with the diagnosis of colorectal cancer. Suspected families were further reviewed by a specific surgeon (Wang ZJ). The history covered at least all first-degree relatives and selected second-degree relatives. Families fulfilling the Amsterdam criteria or Japanese clinical diagnostic criteria were registered and family members were reviewed by telephone or outpatients visits. Before this review, all patients were reinvestigated by follow-up records or telephone interviews. Data concerning the site of cancer, age of diagnosis, history of synchronous and/or metachronous cancers, and histopathology of cancers were documented. The Clinical characteristics, diagnosis, treatments and follow-up study of sixteen HNPCC pedigrees were retrospectively analyzed in this report.

Germline hMLH1 gene mutation analysis

Peripheral blood was obtained from the affected and unaffected normal family members, all of whom signed the formal consent. Genomic DNA was extracted by standard organic methods. The coding regions of hMLH1 and hMSH2 gene were PCR amplified according to Weber methods^[13] with minor modifications. SSCP was used to screen the coding regions and variant bands were then sequenced by a 377DNA sequencer. After a mutation was found, specific regions of DNA from their offspring were PCR amplified and sequenced.

RESULTS

HNPCC families

A total sixteen kindreds were diagnosed, among there, eleven met Amsterdam criteria and five met the Japanese clinical diagnosis criteria. There were three Lynch syndrome I families, and thirteen Lynch syndrome II families respectively. HNPCC constituted about 5.2% of colorectal cancer patients within the same period in our hospital.

Tumor spectrum

One hundred and one malignant neoplasms were found in sixty-eight patients (multiple cancer in twenty-one) with a mean age of 50.8 years in sixteen kindreds, including fifty colonic, seventeen rectal, eleven gastric, seven endometrial, and four esophageal, two each skin, pancreatic, lung and cervical, one each breast, ovarian cancer, gastric leiomyosarcoma and brain glioblastoma, respectively. There were forty-six colorectal cancer patients (including sixteen metachronous colorectal cancers). In the present group, 67.6% patients and 66.3% cancers are of colorectal ones. Right-side colon cancers constitute 47.8% of total cancers and 74.6% of colorectal cancers. 34.8% of colorectal cancers were metachronous ones.

Patient treatment and follow-up

81.6% patients received radical operations; other patients received chemotherapy, irradiation and traditional Chinese medicine treatment. 39.5% colorectal cancer patients had metachronous colorectal cancers within 10 years and required re-operations. A multiple primary cancer patient, after rectal cancer was resected, developed subsequently ascending colon cancer 12 years later, stomach cancer 18 years later, transverse colon cancer 19 years later, and descending colon cancer 28 years after the first operation.

hMLH1 mutation RESULTS

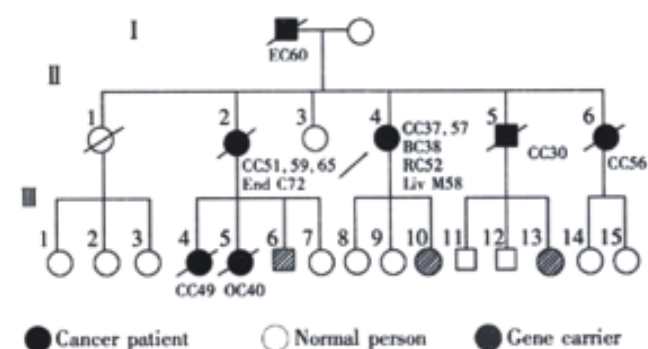
In one large HNPCC family, a germline G265T nonsense mutation was found in the third exon of hMLH1 gene. The mutation turned GAG in codon 89 to a stop codon TAG, resulting in a truncated protein. The normal family member over 50 years old did not have the same germline mutation. Three phenotypically normal family members were also found to carry the mutated gene. Two of them subsequently

received colonoscopy examinations. One was found to have an adenoma of 2cm and was resected endoscopically. We searched the Human Gene Mutation Database (HGMD) (uwcm.web.cf.ac.uk/uwcm/mg/hgmdo.html), and found this mutation had not been reported previously in the literature.

DISCUSSION

Hereditary nonpolyposis colorectal cancer is a typical auto-dominant hereditary disease^[14], constituting about 5.2% of colorectal cancer patients within the same period in our hospital, which is consistent with the published reports^[14,15]. Early onset of the colorectal cancer is an important feature of HNPCC patients^[16]. The average age onset of colon cancer in the general population in China is around 60 years of age. Patients with HNPCC in our group developed colorectal cancer at an average of 49 years, 10 years earlier than the general population. Colorectal cancers occur most frequently in HNPCC kindred. In the present group, 67.6% patients and 66.3% cancers are colorectal ones, consistent with previously published reports^[17,18]. Colon cancers are more often right-sided, constituting 47.8% of total cancer and 74.6% of colorectal cancers, whereas in sporadic colon cancer, the opposite is true^[17,18]. The next most frequently seen cancer is gastric cancer, about 10.8% in this group, well above the reported frequency in the literature^[19,20]. It is interesting that gastric cancer occurred at a higher frequency and ovarian cancer at a lower frequency in our group^[21,22]. More research study should be done to clarify if this is just a reflection of case selection bias or the difference is related to ethnic or geographical groups^[23,24]. Endometrium is the third predisposing organ, and about 6.9% cancer is in the endometrium^[21]. A small number of other cancers included pancreatic, esophageal, skin, lung, cervical, and breast cancers. There was one gastric leiomyosarcoma and glioblastoma, respectively.

Two breast and two lung cancers in our small group of patients are worthy of particular comment. Controversy exists whether these two kinds of cancers belong to the spectrum of HNPCC^[25,26]. In China, breast and lung cancers are much less prevalent than those in the western world, and it is interesting that the incidence of these two cancers among those families is far above the average level in China. One breast cancer occurred in the index patients of a Lynch syndrome II kindred (Figure 1) that received sequence analysis in this study. The patient developed ascending colon cancer at 37 years of age, breast cancer at 38, rectum cancer at 52, descending colon cancer at 57. The possibility of a sporadic breast cancer in this patient is small. The two lung cancers occurred in two patients of classical Lynch syndrome II kindred, but they developed rather late. More cases and studies are needed to clarify if these two cancers are integral to cancer spectrum of this syndrome^[27].



CC: colon cancer; RC: rectal cancer; BC: breast cancer; OC: ovarian cancer; EC: esophageal cancer; End C: endometrial cancer; Liv M: liver metastasis.
Figure 1 A Lynch syndrome II pedigree with hMLH1 gene germline mutation

Another cardinal features of the HNPCC in this group and in the medical literature is the occurrence of metachronous colorectal cancer^[28,29]. In our group, 39.5% colorectal cancer patients developed metachronous colorectal cancer within ten years after their initial colorectal cancer resection. But in contrast to the literature, none of the patients were found to have synchronous colorectal cancers. Although it is quite possible that small benign adenomas were not recorded or missed during the colonoscopic or barium examination, but the possibility of missing a cancer is quite small. The reason for the lack of synchronous cancer remains unclear.

81.6% our patients received routine radical resection. Among colorectal patients who received routine segmental resections, 39.5% developed metachronous colorectal cancer, and needed re-operations. After segmental resection, a multiple primary cancer patient developed ascending colon cancer twelve years later, gastric cancer eighteen years later, transverse colon cancer nineteen years later, and descending colon cancer twenty eight years later after the first operation. Therefore, the most eligible choice is subtotal or total colectomy with ileorectal anastomosis or with ileopouch anal anastomosis^[30,31], which removes the colonic segment as much as possible, and avoids permanent ileostomy. Two patients, one had primary cancer, the other had metachronous colon cancer, both received total colectomy with ileopouch anal anastomosis. A short term follow-up of the patients showed good life quality. In literature^[30-33], different views exist regarding prophylactic colectomy for gene carriers of HNPCC. Firstly, not all carriers of the germline hMSH2 and hMLH1 gene mutations develop colorectal cancer; Vasen *et al* reported that up to 60 years of age, 92% of the carriers developed colorectal cancers in affected families^[32]. Secondly, complications even mortality occurred around 8% and 1% respectively in these operations^[30]. The timing of prophylactic operation in an HNPCC gene carrier is unknown. The median age at diagnosis of colorectal cancer is around 45 years, but Rodriguez-Bigas showed that 27% of their patients were diagnosed before 39 years and 88% by 69 years of age^[33]. Other uncertainties include: the optimal procedure has yet to be considered, the psychologic impact of the invasive procedure on body image and sexuality in young adult carriers.

Colonoscopy remains the most important surveillant measure in revealing synchronous and metachronous cancers or polyps in the follow-up of patients and in symptomatic gene-carriers. polypectomy should performed if present^[34]. J vinen *et al*^[35] reported a 62 percent decrease of colorectal cancer in HNPCC patients who underwent colonoscopic screening vs. those who did not.

The first family with hMLH1 gene mutation from Mainland China was identified in our study. In the large HNPCC kindred, a germline G265T nonsense mutation was found in the third exon of hMLH1, resulting in a stop codon and truncated protein. The mutation segregated with the disease in the family. We made a search in the Human Gene Mutation Database (HGMD) (uwcm.web.cf.ac.uk/uwcm/mg/hgmdo.html), and found this to be a new mutation previously unreported in the medical literature. In three phenotypical normal family members, the same mutated gene was found in the germline. Two of them subsequently received colonoscopy examinations, and one was found to have an adenoma of 2cm which was resected endoscopically. These carriers are now needed an intensive follow-up regime.

ACKNOWLEDGMENT

We appreciate the invaluable technical assistance and great help of Dr. Ding-fang Bu from Experimental Center of our hospital.

REFERENCES

- Lynch HT, Smyrk T, Lynch J. An update of HNPCC (Lynch syndrome). *Cancer Genet Cytogenet* 1997;93:84-99
- Stephenson BM, Finan PJ, Gascoyne J, Garbett F, Murday VA, Bishop DT. Frequency of familial colorectal cancer. *Br J Surg* 1991;78:1162-1166
- Vasen HF, Offerhaus GJ, den Hartog Jager FC, Menko FH, Nagengast FM, Griffioen G, van Hogezaand RB, Heintz AP. The tumor spectrum in hereditary non-polyposis colorectal cancer: a study of 24 kindreds in the Netherlands. *Int J Cancer* 1990;46:31-34
- Watson P, Lynch HT. OMIM. Extracolonic cancer in hereditary nonpolyposis colorectal cancer. *Cancer* 1993;71:677-685
- Fishel R, Lescoe MK, Rao MR, Copeland NG, Jenkins NA, Garber J, Kane M, Kolodner R. The human mutator gene homolog MSH2 and its association with hereditary nonpolyposis colon cancer. *Cell* 1994;77:167
- Leach FS, Nicolaides NC, Papadopoulos N, Liu B, Jen J, Parsons R, Peltomaki P, Sistonen P, Aaltonen L, Nystrom-Lahti M. Mutations of a mutS homolog in hereditary nonpolyposis colorectal cancer. *Cell* 1993;75:1215-1225
- Bronner CE, Baker SM, Morrison PT, Warren G, Smith LG, Lescoe MK, Kane M, Earabino C, Lipford J, Lindblom A. Mutation in the DNA mismatch repair gene homologue hMLH1 is associated with hereditary non-polyposis colon cancer. *Nature* 1994;36:258-261
- Papadopoulos N, Nicolaides NC, Wei YF, Ruben SM, Carter KC, Rosen CA, Haseltine WA, Fleischmann RD, Fraser CM, Adams MD. Mutation of a mutL homolog in hereditary colon cancer. *Science* 1994;263:1625-1629
- Nicolaides NC, Papadopoulos N, Liu B, Wei YF, Carter KC, Ruben SM, Rosen CA, Haseltine WA, Fleischmann RD, Fraser CM. Mutations of two PMS homologues in hereditary nonpolyposis colon cancer. *Nature* 1994;371:75-80
- Akiyama Y, Sato H, Yamada T, Nagasaki H, Tsuchiya A, Abe R, Yuasa Y. Germ-line mutation of the hMSH6/MTBP gene in an atypical hereditary nonpolyposis colorectal cancer kindred. *Cancer Res* 1997;57:3920-3923
- Vasen HF, Mecklin JP, Khan PM, Lynch HT. The International Collaborative Group on Hereditary Non-Polyposis Colorectal Cancer (ICG-HNPCC). *Dis Colon Rectum* 1991;34:424-425
- Baba S. Hereditary nonpolyposis colorectal cancer: an update. *Dis Colon Rectum* 1997;40:S86-95
- Weber TK, Conlon W, Petrelli NJ, Rodriguez-Bigas M, Keitz B, Pazik J, Farrell C, O'Malley L, Oshali M, Abdo M, Anderson G, Stoler D, Yandell D. Genomic DNA-based hMSH2 and hMLH1 mutation screening in 32 Eastern United States hereditary nonpolyposis colorectal cancer pedigrees. *Cancer Res* 1997;57:3798-3803
- Ponz de Leon M. Prevalence of hereditary nonpolyposis colorectal carcinoma (HNPCC). *Ann Med* 1994;26:209-214
- Marra G, Boland CR. Hereditary nonpolyposis colorectal cancer: the syndrome, the genes, and historical perspectives. *J Natl Cancer Inst* 1995;87:1114-1125
- Lynch HT, Richardson JD, Amin M, Lynch JF, Cavaliere RJ, Bronson E, Fusaro RM. Variable gastrointestinal and urologic cancers in a Lynch syndrome II kindred. *Dis Colon Rectum* 1991;34:891-895
- Mecklin JP, Jarvinen HJ. Clinical features of colorectal carcinoma in cancer family syndrome. *Dis Colon Rectum* 1986;29:160-164
- Fitzgibbons RJ Jr, Lynch HT, Stanislav GV, Watson PA, Lanspa SJ, Marcus JN, Smyrk T, Krieger MD, Lynch JF. Recognition and treatment of patients with hereditary nonpolyposis colon cancer (Lynch syndromes I and II). *Ann Surg* 1987;206:289-295
- Green SE, Bradburn DM, Varma JS, Burn J. Hereditary non-polyposis colorectal cancer. *Int J Colorectal Dis* 1998;13:3-12
- Lin KM, Shashidharan M, Ternent CA, Thorson AG, Blatchford GJ, Christensen MA, Lanspa SJ, Lemon SJ, Watson P, Lynch HT. Colorectal and extracolonic cancer variations in MLH1/MSH2 hereditary nonpolyposis colorectal cancer kindreds and the general population. *Dis Colon Rectum* 1998;41:428-433
- D'Emilia JC, Rodriguez-Bigas MA, Petrelli NJ. The clinical and genetic manifestations of hereditary nonpolyposis colorectal carcinoma. *Am J Surg* 1995;169:368-372
- Watson P, Lynch HT. OMIM. Related Articles. Extracolonic cancer in hereditary nonpolyposis colorectal cancer. *Cancer* 1993;71:677-685
- Froggatt NJ, Joyce JA, Davies R, Gareth D, Evans R, Ponder BA, Barton DE, Maher ER. A frequent hMSH2 mutation in hereditary non-polyposis colon cancer syndrome. *Lancet* 1995;345:727
- Peltomaki P, Vasen HF. Mutations predisposing to hereditary nonpolyposis colorectal cancer: database and results of a collaborative study. The International Collaborative Group on Hereditary Nonpolyposis Colorectal Cancer. *Gastroenterology* 1997;113:1146-1158
- Itoh H, Houlston RS, Harocopos C, Slack J. Risk of cancer death in first-degree relatives of patients with hereditary non-polyposis cancer syndrome (Lynch type II): a study of 130 kindreds in the United Kingdom. *Br J Surg* 1990;77:1367-1370
- Nelson CL, Sellers TA, Rich SS, Potter JD, McGovern PG, Kushi LH. Familial clustering of colon, breast, uterine, and ovarian cancers as assessed by family history. *Genet Epidemiol* 1993;10:235-244
- Risinger JJ, Barrett JC, Watson P, Lynch HT, Boyd J. Molecular genetic evidence of the occurrence of breast cancer as an integral tumor in patients with the hereditary nonpolyposis colorectal carcinoma syndrome. *Cancer*

- 1996;77:1836-1843
- 28 Lynch HT, Lanspa SJ, Boman BM, Smyrk T, Watson P, Lynch JF, Lynch PM, Cristofaro G, Bufo P, Tauro AV. Hereditary nonpolyposis colorectal cancer-Lynch syndromes I and II. *Gastroenterol Clin North Am* 1988;17:679-712
- 29 Svendsen LB, Bulow S, Mellemaard A. Metachronous colorectal cancer in young patients: expression of the hereditary nonpolyposis colorectal cancer syndrome? *Dis Colon Rectum* 1991;34:790-793
- 30 Rodriguez-Bigas MA. Prophylactic colectomy for gene carriers in hereditary nonpolyposis colorectal cancer. Has the time come? *Cancer* 1996;78:199-201
- 31 Lynch HT. Is there a role for prophylactic subtotal colectomy among hereditary nonpolyposis colorectal cancer germline mutation carriers? *Dis Colon Rectum* 1996;39:109-110
- 32 Vasen HF, Taal BG, Griffioen G, Nagengast FM, Cats A, Menko FH, Oskam W, Kleibeuker JH, Offerhaus GJ, Khan PM. Clinical heterogeneity of familial colorectal cancer and its influence on screening protocols. *Gut* 1994;35:1262-1266
- 33 Rodriguez-Bigas MA, Lee PH, O'Malley L, Weber TK, Suh O, Anderson GR, Petrelli NJ. Establishment of a hereditary nonpolyposis colorectal cancer registry. *Dis Colon Rectum* 1996;39:649-653
- 34 Gaglia P, Atkin WS, Whitelaw S, Talbot IC, Williams CB, Northover JM, Hodgson SV. Variables associated with the risk of colorectal adenomas in asymptomatic patients with a family history of colorectal cancer. *Gut* 1995;36:385-390
- 35 Jarvinen HJ, Mecklin JP, Sistonen P. Screening reduces colorectal cancer rate in families with hereditary nonpolyposis colorectal cancer. *Gastroenterology* 1995;108:1405-1411

Edited by Wu XN

• LARGE INTESTINAL CANCER •

Colonoscopic screening and follow-up for colorectal cancer in the elderly

Jun Wan, Zi-Qi Zhang, Cheng Zhu, Meng-Wei Wang, Dong-Hai Zhao, Yong-He Fu, Jian-Ping Zhang, Ya-Hong Wang, Ben-Yan Wu

Jun Wan, Zi-Qi Zhang, Cheng Zhu, Meng-Wei Wang, Dong-Hai Zhao, Yong-He Fu, Jian-Ping Zhang, Ya-Hong Wang, Ben-Yan Wu, Department of Gastroenterology, General Hospital of the Chinese PLA, Beijing 100853, China

Correspondence to: Jun Wan, Department of Gastroenterology, General Hospital of the Chinese PLA, Beijing 100853, China. jfjzyy301@163.com
Telephone: +86-10-66937622 Fax: +86-10-66937622

Received 2001-09-25 Accepted 2001-11-14

Abstract

AIM: To improve the prevention and treatment of senile patients with colorectal cancer by evaluating the importance of colonoscopy in clinical screening and follow-up.

METHODS: Clinical screening of colonoscopy was performed for 2196 patients aged 60-90 years old according to the protocol, and 1740 of them (79.2%) were followed-up.

RESULTS: Colorectal cancer was found in 52 patients, and the detectable rate was 2.4%. Among them, 19 were diagnosed as early colorectal cancer, accounting for 36.5% of the detected colorectal cancer. Among the followed-up patients, early colorectal cancer was found in 9, accounting for 45.0% of the detected colorectal cancer. The resectable rate and 5 years survival rate of colorectal cancer were 97.7% and 80.9% respectively. The incidence of complication was 0.05%, and the successful rate of cecum intubation was 98.9%.

CONCLUSION: Colonoscopic screening and follow-up of the elderly for colorectal cancer and pre-cancerous lesion (adenomatoid polyp) can increase the detectable rate of early colorectal cancer and improve its prevention and treatment.

Wan J, Zhang ZQ, Zhu C, Wang MW, Zhao DH, Fu YH, Zhang JP, Wang YH, Wu BY. Colonoscopic screening and follow-up for colorectal cancer in the elderly. *World J Gastroenterol* 2002;8(2):267-269

INTRODUCTION

Sequential method is usually used in clinical screening of colorectal cancer^[1-3], but some experts hold that direct sigmoidoscopy should be performed for the screening of large intestinal cancer^[4-6]. Colonoscopy screening of large intestinal cancer is advocated abroad due to the significant incidence of proximal cancer of colon in the past 10 years^[7-14]. Colonoscopy screening and follow-up were conducted for 2196 old patients who had not received barium enema contrast radiography from September 1985 to July 1998 in this study.

MATERIALS AND METHODS

All the 2196 patients to be screened were retired or veteran officers in active service. Age ranged from 60 to 90 (averaged 70.5) years old, 2067 male and 129 female. Enteroscopy was performed for 8298 with

times, and 1740 of the 2196 patients (79.2%) were followed-up for 1-12 years. The number of follow-up per patient was 4.5 times and the time of follow-up per patient was 5.9 years. Among the screened patients, 1618 (73.7%) were asymptomatic. The main symptoms of the remainder were anorexia, abdominal uncomfortableness, constipation, irregular feces and loss of body weight. Among the 2196 patients, heart disease, encephalopathy, lung disease and nephrosis were found in 1911 (87.0%), in which more than 3 vital organ diseases were found in 534 (24.3%). 639 patients (29.1%) were found to have a history of abdominal operation such as subtotal gastrectomy, cholecystectomy, appendectomy, abdominal exploratory operation and colon cancer operation.

Colonoscopy screening was performed by using Olympus CF-MB3W, CF-IBM, PCF-10, CF-1T20I, CF-V10L, CF-200L colonoscopes made in Japan, and colonoscopic follow-up was conducted according to the patients' physical conditions every years.

RESULTS

The detectable rate of colorectal polypus

Among the 2196 patients, 9893 polypi were found in 1364 (62.1%), in which 8587 polyps were detected in 1618 asymptomatic patients (86.8%). 3435 and 6458 polypi were found in the first diagnosis and follow-up respectively, which accounted for 65.3% of the total detected polypi. Among the 8537 polypi confirmed by pathologic examination, 1841 (21.6%) were inflammatory polypi, and 5801 (67.9%) were adenomatoid polypi, and 895 (10.5%) were hyperplastic and hamartoma. 21 were adenomatoid polypi with malignant transformation, accounting for 0.2% of the detected colorectal polypi.

The detectable rate and follow-up of colorectal cancer

Among the 2196 patients, colorectal cancer was found in 52 patients, and the detectable rate was 2.4%. Among the 52 patients with colorectal cancer, early colorectal cancer and early multiple colorectal cancer were found in 19 (36.5%) and in 3 (5.8%) respectively, and 22 early cancerous foci were found as well. Among the asymptomatic patients, colorectal cancer was found in 24, which accounted for 46.2% of the total detected colorectal cancer, and early colorectal cancer was found in 13 asymptomatic patients, which accounted for 54.2% of the total asymptomatic colorectal cancer. Colorectal cancer was found in 20, and early colorectal cancer in 9 of them (45.0%) during the follow-up, which was higher than that (31.3%) by colonoscopic screening. Surgical treatment was performed for 24 of the 32 patients with colorectal cancer found in the screening. The Duck's pathologic staging was as follows: 7 patients (29.2%) were in stage A, 15 (62.5%) in stage B, and 2 (8.3%) in stage C.

Treatment and prognosis of the patients with colorectal cancer

Treatment of the 52 patients with colorectal cancer was shown in Table 1. Surgical operation and or electric coagulation resection under colonoscope was performed according to the patient's condition. Among the 44 patients who received surgical treatment,

colorectostomy was performed for 43 (97.7%) with all the early colorectal cancer removed (100.0%). 22 survived for more than 5 years, and 5 years survival rate was 80.9% (Figure 1).

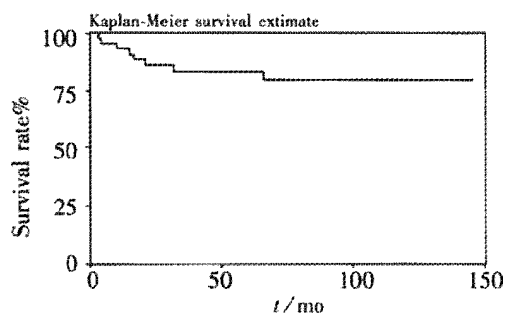


Figure 1 The survival curve of 44 operated patients with colorectal cancer

Table 1 Treatment of 52 patients with colorectal cancer

Type of cancer	n	Treated by endoscope	Operation		Not operated	Not followed up
			Removed	Not removed		
Early	19	6	12	0	1	0
Progressive	33	0	31	1	0	1

Complication and successful rate of intubation

8298 times of colonoscopy were performed, in which the incidence rate of complication was 0.05%, complication was found in 4 patients (bleeding in 2 and collapse in 2), and the successful rate of intubation was 98.9%. Colonoscopy was not performed in the ileocecum of 91 patients due to their poor tolerance, history of abdominal operation, long and tortuous intestinal canal, obstruction by tumors, and poor preparation of intestinal tract.

DISCUSSION

Colonoscopic clinical screening and follow-up is an ideal method for the detection of early colorectal cancer and pre-cancerous lesion (adenoma). In this study, clinical screening and follow-up by colonoscopy were performed for patients over 60 years old, and the detectable rate of colorectal cancer was 2.4%, and the detectable rate of early colorectal cancer was 36.5%, which was higher than that (21.0%) reported by using screening method^[15,16]. The detectable rate of early colorectal cancer was 15.2-16.8% in this country^[17,18], and 45.0% in our follow-up by colonoscopy. It indicates that persistent follow-up by colonoscopy is of great importance for the detection of early colorectal cancer. Among the 2196 screened patients, colorectal polypi was found in 1364 (62.1%), and 67.9% of them were adenomatoid polyps confirmed by pathologic examination. The detected polypi by colonoscopy in the follow-up accounted for 65.2% of the total detected polypi. Therefore, we hold that colonoscopic screening should be performed for the patients over 60 years old including those with no symptoms, and those with their adenomas removed. The latter should be followed up every year. Experts^[14,19] also advocated that colonoscopic screening should be performed for the ordinary population every year, because they believed that it was more economic and effective for the patients over 60 years old.

Clinical screening and follow-up by colonoscopy lead to the prompt treatment of colorectal cancer and improve the excision rate and 5 years survival rate of the patients with colorectal cancer, which are higher than those (71-92.8% and 62-74%)^[20-24] reported in other countries and are significantly higher than those (84.8% and 53.0%) reported in China^[25]. The treatment of pre-cancerous lesion (adenomatoid polyp) under colonoscopy reduced the incidence of colorectal cancer and improved its prevention and treatment. 9566 of

the 9893 (96.7%) colorectal polypi were treated under colonoscopy. Among the 21 cancerous polypi, surgical operation and excision under colonoscopy were performed for 20 patients respectively, except one case due to the patient's condition. Researchers found that the incidence of colorectal cancer can be decreased by 76-90% by removing adenomatoid polypus under colonoscopy with the recurrent and regenerated adenomas resected in the follow-up by colonoscopy^[26-28]. The colorectal polypi were treated when clinical screening and follow-up by colonoscopy were performed in this study. It would greatly decrease the expected incidence of colorectal cancer.

In this study 87% of the patients suffered from multiple organ diseases such as heart disease, encephalopathy, and nephrosis, and 24.3% of them had diseases in more than 3 vital organs, but the incidence of complication was significantly lower than that (0.4-1.4%)^[29-31] with no occurrence of death and perforation^[31] as a result of the improvement of intestinal canal preparation, simplification of colonoscopy intubation, and the appropriate measures taken for them according to the changes of their blood pressure and ECG when colonoscopy was performed. 29.2% of the patients in this study had a history of abdominal operation, but the successful rate of intubation was 98.9%. Therefore, we hold that clinical screening and follow-up by colonoscopy for old patients can lead to early diagnosis and treatment of patients with colorectal cancer and pre-cancerous lesion (adenomatoid polypus), and it is a safe and effective method to detect early colorectal cancer and decrease the death rate of colorectal cancer.

REFERENCES

- 1 Yu JP, Dong WG. Current situation about early diagnosis of cancer of large intestine. *Shijie Huaren Xiaohua Zazhi* 2001;7:553-554
- 2 Li SR. Diagnosis and treatment of colorectal cancer. *Shijie Huaren Xiaohua Zazhi* 2001;9:780-782
- 3 Wang YB, Yang ZX. Routine diagnosis of colorectal cancer. *Shijie Huaren Xiaohua Zazhi* 2001;9:792-793
- 4 Komuta K, Furui J, Haraguchi M, Kanematsu T. The detection of colorectal cancer at an asymptomatic stage by screening is useful. *Hepatogastroenterology* 2000; 47: 1011-1014
- 5 Kavanagh AM, Giovannucci EL, Fuchs CS, Colditz GA. Screening endoscopy and risk of colorectal cancer in United States men. *Cancer Causes Control* 1998; 9: 455-462
- 6 Khullar SK, Disario JA. Colon cancer screening. Sigmoidoscopy or colonoscopy. *Gastrointest Endosc Clin N Am* 1997; 7:365-386
- 7 Inciardi JF, Lee JG, Stijnen T. Incidence trends for colorectal cancer in California: implications for current screening practices. *Am J Med* 2000; 109: 277-281
- 8 Zhang B, Fattah A, Nakama H. Characteristics and survival rate of elderly patients with colorectal cancer detected by immunochemical occult blood screening. *Hepatogastroenterology* 2000; 47: 414-418
- 9 Han Y. Early endoscopic diagnosis of colorectal cancer. *Shijie Huaren Xiaohua Zazhi* 2001;9(Suppl 7):789-790
- 10 Imperiale TF, Wagner DR, Lin CY, Larkin GN, Rogge JD, Ransohoff DF. Risk of advanced proximal neoplasms in asymptomatic adults according to the distal colorectal findings. *N Engl J Med* 2000; 343: 169-174
- 11 Lieberman D. Colonoscopy as a mass screening tool. *Eur J Gastroenterol Hepatol* 1998; 10: 225-228
- 12 Borum ML. Colorectal cancer screening. *Prim Care* 2001; 28: 661-674
- 13 Scintu F, Canalis C, Capra F, D'Alia G, Giordano M, Mocci P, Pisano M, Casula G. Colonoscopic screening in first-degree relatives of patients with sporadic colorectal cancer. *Ann Ital Chir* 2000; 71: 693-699
- 14 Mandel JS. Colorectal cancer screening. *Cancer Metastasis Rev* 1997; 16:263-279
- 15 Nakama H, Zhang B, Fukazawa K, Zhang X. Comparisons of cancer detection rate and costs of one cancer detected among different age-cohorts in immunochemical occult blood screening. *J Cancer Res Clin Oncol* 2001; 127: 439-443
- 16 Iishi H, Kitamura S, Nakaizumi A, Tatsuta M, Otani T, Okuda S, Ishiguro S. Clinicopathological features and endoscopic diagnosis of superficial early adenocarcinomas of the large intestine. *Dig Dis Sci* 1993; 38:1333-1337
- 17 Li CQ, Wang LY. An analysis of 283 patients with colon cancer detected by colonoscopy. *Huaren Xiaohua Zazhi* 1998; 6:239-239
- 18 Lu Y, Gu F, Lin SR, Chu ZM. Significance of endoscopy screening and pathologic examination of removed polypus in the diagnosis of early colon cancer. *Zhonghua Xiaohua Neijing Zazhi* 1997; 14:222-224

- 19 Anderson J. Clinical practice guidelines. Review of the recommendations for colorectal screening. *Geriatrics* 2000; 55: 67-73
- 20 Staudacher C, Chiappa A, Zbar AP, Bertani E, Biella F. Curative resection for colorectal cancer in the elderly. Prognostic factors and five-year follow-up. *Ann Ital Chir* 2000; 71: 491-496
- 21 Park YJ, Park KJ, Park JG, Lee KU, Choe KJ, Kim JP. Prognostic factors in 2230 Korean colorectal cancer patients: analysis of consecutively operated cases. *World J Surg* 1999; 23: 721-726
- 22 Semmens JB, Platell C, Threlfall TJ, Holman CD. A population-based study of the incidence, mortality and outcomes in patients following surgery for colorectal cancer in Western Australia. *Aust N Z J Surg* 2000; 70: 11-18
- 23 Han-Shiang C. Curative resection of colorectal adenocarcinoma: multivariate analysis of 5-year follow-up. *World J Surg* 1999; 23: 1301-1306
- 24 Barillari P, Ramacciato G, Manetti G, Bovino A, Sammartino P, Stipa V. Surveillance of colorectal cancer: effectiveness of early detection of intraluminal recurrences on prognosis and survival patients treated for cure. *Dis Colon Rectum* 1996; 39: 388-393
- 25 Zhang PD, Guan JA, Feng GQ. An analysis of 113 venerable patients with colon cancer. *Zhongguo Zhongliu Linchuang* 1994; 21: 120-122
- 26 Burchert A, Schmassmann A. Evaluation of various screening and surveillance methods in colorectal carcinoma. *Schweiz Med Wochenschr* 1998; 128: 999-1011
- 27 Donovan JM, Syngal S. Colorectal cancer in women: an underappreciated but preventable risk. *J Womens Health* 1998; 7: 45-48
- 28 Citarda F, Tomaselli G, Capocaccia R, Barcherini S, Crespi M. Efficacy in standard clinical practice of colonoscopic polypectomy in reducing colorectal cancer incidence. *Gut* 2001; 48: 812-815
- 29 Robinson MH, Hardcastle JD, Moss SM, Amar SS, Chamberlain JO, Armitage NC, Scholefield JH, Mangham CM. The risks of screening: data from the Nottingham randomised controlled trial of faecal occult blood screening for colorectal cancer. *Gut* 1999; 45: 588-592
- 30 Jentschura D, Raute M, Winter J, Henkel T, Kraus M, Manegold BC. Complications in endoscopy of the lower gastrointestinal tract. Therapy and prognosis. *Surg Endosc* 1994; 8: 672-676
- 31 Waye JD. Management of complications of colonoscopic polypectomy. *Gastroenterologist* 1993; 1: 158-164

Edited by Zhang JZ

• LARGE INTESTINAL CANCER •

Specific CEA-producing colorectal carcinoma cell killing with recombinant adenoviral vector containing cytosine deaminase gene

Li-Zong Shen, Wen-Xi Wu, De-Hua Xu, Zhong-Cheng Zheng, Xin-Yuan Liu, Qiang Ding, Yi-Bing Hua, Kun Yao

Li-Zong Shen, Wen-Xi Wu, Qiang Ding, Yi-Bing Hua, Department of General Surgery, The First Affiliated Hospital of Nanjing Medical University, Nanjing, 210029, Jiangsu Province, China
De-Hua Xu, Zhong-Cheng Zheng, Xin-Yuan Liu, Shanghai Institute of Biochemistry and Cell Biology, The Chinese Academy of Sciences, Shanghai, 200031, China
Kun Yao, Department of Microbiology and Immunology, Nanjing Medical University, Nanjing, 210029, Jiangsu Province, China
Supported by the Creation Foundation of Nanjing Medical University, No.Cx9905

Correspondence to: Prof. Wen-Xi Wu, Department of General Surgery, The First Affiliated Hospital of Nanjing Medical University, 300 Guangzhou Road, Nanjing, 210029, Jiangsu Province, China. wuwenxi@yahoo.com
Telephone: +86-25-3718836 Ext.6863

Received 2001-09-14 Accepted 2001-10-12

Abstract

AIM: To kill CEA positive colorectal carcinoma cells specifically using the *E coli* cytosine deaminase (CD) suicide gene, a new replication-deficient recombinant adenoviral vector was constructed in which CD gene was controlled under CEA promoter and its *in vitro* cytotoxic effects were evaluated.

METHODS: Shuttle plasmid containing CD gene and regulatory sequence of the CEA gene was constructed and recombined with the right arm of adenovirus genome DNA in 293 cell strain. Dot blotting and PCR were used to identify positive plaques. The purification of adenovirus was performed with ultra-concentration in CsCl step gradients and the titration was measured with plaque formation assay. Cytotoxic effects were assayed with MTT method. The fifty percent inhibition concentration (IC_{50}) of 5-FC was calculated using a curve-fitting parameter. The human colorectal carcinoma cell line, which was CEA-producing, and the CEA-nonproducing Hela cell line were applied in cytological tests. An established recombinant adenovirus vector AdCMVCD, in which the CD gene was controlled under CMV promoter, was used as virus control. Quantitative results were expressed as the mean \pm SD of the mean. Statistical analysis was performed using ANOVA test.

RESULTS: The desired recombinant adenovirus vector was named AdCEACD. The results of dot blotting and PCR showed that the recombinant adenovirus contained CEA promoter and CD gene. Virus titer was about 5.0×10^{14} pfu/L⁻¹ after purification. The CEA-producing Lovo cells were sensitive to 5-FC and had the same cytotoxic effect after infection with AdCEACD and AdCMVCD (The IC_{50} values of 5-FC in parent Lovo cells, Lovo cells infected with 100 M.O.I AdCEACD and Lovo cells infected with 10 M.O.I AdCMVCD were >15000 , 216.5 ± 38.1 and $128.8 \pm 25.4 \mu\text{mol} \cdot \text{L}^{-1}$, $P < 0.001$, respectively), and the cytotoxicity of 5-FC increased accordingly when the m.o.i of adenoviruses were enhanced (The value of IC_{50} of 5-FC was reduced to $27.9 \pm 4.2 \mu\text{mol} \cdot \text{L}^{-1}$ in 1000 M.O.I AdCEACD infected Lovo cells and $24.8 \pm 7.1 \mu\text{mol} \cdot \text{L}^{-1}$ in 100 M.O.I AdCMVCD infected Lovo cells, $P < 0.05$, $P < 0.01$, respectively).

The CEA-nonproducing Hela cells had no effect after infection with AdCEACD, but Hela cells had the cytotoxic sensitivity to 5-FC after infection with AdCMVCD (The IC_{50} of 5-FC in parent Hela cells and Hela cells infected with AdCMVCD at 10 M.O.I was >15000 and $214.5 \pm 31.3 \mu\text{mol} \cdot \text{L}^{-1}$, $P < 0.001$). AdCEACD/5-FC system also had bystander effect, and the viability was about 30 percent when the proportion of transfected cells was only 10 percent.

CONCLUSION: The recombinant adenovirus vector AdCEACD has the character of cell type-specific gene delivery. The AdCEACD/5-FC system may become a new, potent and specific approach for the gene therapy of CEA-positive neoplasms, especially colon carcinoma.

Shen LZ, Wu WX, Xu DH, Zheng ZC, Liu XY, Ding Q, Hua YB, Yao K. Specific CEA-producing colorectal carcinoma cell killing with recombinant adenoviral vector containing cytosine deaminase gene. *World J Gastroenterol* 2002;8(2):270-275

INTRODUCTION

Gene therapy is a novel approach that might lead to improved treatments of some types of cancer^[1-9]. A suicide gene is a gene encoding a protein, which under appropriate conditions (i.e., exposure to prodrugs) is toxic to the genetically modified cell (i.e., tumor cell). Apart from the direct killing effects, further investigation led to the fundamental discovery, termed the "bystander effect", which allowed a therapeutic application of suicide gene therapy. The bystander effect demonstrated that a tumor population could be killed if only a fraction of the tumor expressed the suicide gene, and thus was a seminal finding that overcame the limitations of gene therapy technology, i.e., the inability to genetically modify an entire tumor mass^[10,11]. The gene for herpes simple virus-thymidine kinase (HSV-1 TK) has been the subject of many investigations *in vitro* and *in vivo*^[12-19]. The *Escherichia coli* gene coding for the cytosine deaminase (CD) enzyme is another suicide gene. CD transforms nontoxic prodrug 5-fluorocytosine (5-FC) into an antitumor chemotherapeutic agent 5-fluorouracil (5-FU). This gene has already been tested *in vitro* as well as in several animal models; most of them being based on colorectal carcinoma cells^[20-24].

If suicide gene were delivered into cells, these cells, either target cells or normal cells, might be killed. The ability to direct suicide gene to transfer to particular cell will be important not only to achieve a therapeutic effect but also to limit potential adverse effects. But gene targeting continues to be a major obstacle to the overall success of gene therapy. For such strategies to have clinical applications the therapeutic gene should be expressed in the cells of interest, while avoiding expression in non-target cell population. In the case of cancer therapy, one such method would be the use of tumor cell-specific or tissue-specific promoters capable of directing expression of a heterologous gene in the cells^[25-27]. Systemic delivery

of a vector, which contains a tumor- or tissue-specific expression cassette, would then be feasible since expression of the transgene would be limited to these cells exclusively^[28,29].

Previously we constructed a replication-deficient recombinant adenovirus vector containing CD gene controlled under cytomegalovirus (CMV) promoter, termed AdCMVCD, and confirmed that AdCMVCD/5-FC system presented direct killing and bystander effect for many kinds of neoplasms *in vitro* and *in vivo*^[30]. In the present study we constructed a new replication-deficient recombinant adenovirus vector, termed AdCEACD, containing CD gene under control of the carcino-embryonic antigen (CEA) promoter, and investigated its *in vitro* effects.

MATERIALS AND METHODS

Cells and cell culture

Ad5-transformed human embryonic kidney (293) cell line, human colorectal carcinoma (Lovo) cell line and human cervix carcinoma (Hela) cell line were grown in Dulbecco's modified Eagle's medium (DMEM) (Gibco) supplemented with 100mL·L⁻¹ fetal bovine serum (FBS) (Gibco) in a 50mL·L⁻¹ CO₂ atmosphere at 37°C.

Plasmid and virus

Expression plasmid pCEACD contained whole length CD gene sequence and CEA promoter sequence. Shuttle plasmid pAdE1CMV contained the E1A enhancer linked to the cytomegalovirus (CMV) promoter. The recombinant adenoviral vector AdCMVlacZ carried the *E. coli* lacZ gene for β -galactosidase under control of the CMV enhancer/promoter. We constructed a recombinant adenoviral vector, termed AdCMVCD, containing CD gene under CMV promoter.

Shuttle plasmid containing CEA promoter and CD gene

A fragment of CEA promoter (about 0.4kb) and CD gene (about 1.3kb) was obtained from pCEACD by digestion with HindIII and BamHI (Promega), then the terminal of BamHI was treated with Klenow fragment of *E. coli* DNA polymerase (Promega), finally the fragment was subcloned into pAdE1CMV with XbaI and HindIII (Promega). The resulting plasmid was named pAdCEACD.

Preparation of the "right arm" of adenovirus genome and recombination of adenovirus vector AdCEACD

Preparation of the "right arm" of adenovirus genome DNA and construction of recombinant adenovirus by homologous recombination AdCEACD were conducted according to methods we had reported^[31].

Identification of AdCEACD

Adenovirus supernatant of each clone were degraded by boiling, ten minutes later the supernatant was laid on ice. CEA fragment, 0.3kb, obtained from pCEACD by digestion with HindIII and EcoI, was used to prepare [α -³²P]-labeled probe according to product instruction (Amersham Pharmacia Biotech). The probe was used to dot blotting with DNA of all clones on nylon membrane (Amersham Life Science) in Rapid-hyb buffer (Amersham Pharmacia Biotech).

For positive clones with dot blotting, polymerase chain reaction (PCR) assay was applied to determine CD gene. The sense sequence of CD primer was 5'-TATGGATCCTCAACGTTTGTAAATCGA TGGCTT-3', while the antisense sequence was 5'-ATAGAATTAAGGCTAACAATGTCGAATAACGCTT-3'. Each 50 μ L PCR system contained 3 μ L DMSO, 1.5 μ L dNTP (10mmol·L⁻¹), upstream primer 20pmol, downstream primer 20pmol, adenovirus supernatant 2 μ L, 4u pfu DNA polymerase (Sangon, Shanghai), 5 μ L 10 \times pfu DNA polymerase buffer. PCR was performed for 30 cycles (94°C 1min, 60°C 1.5min, 72°C 1.5min) in an automated DNA Thermal Cycler (Perkin-Elmer Cetus).

Propagation, purification and titration of AdCEACD

AdCEACD was propagated in 293 monolayer cells. The purification of adenovirus was performed with ultra-concentration in CsCl step gradients for 2h at 20°C and 22000r·min⁻¹. The titration of AdCEACD was measured with plaque formation assay.

CEA secretions of Lovo and Hela cells

Lovo cells or Hela cells were subcultured in 60-mm cell culture dishes respectively. After determining the number of cells on a dish that was about over 90% confluent, we removed the medium, and added 3ml fresh complete media and continue to incubate for 24h, then collected the supernatant to test the concentration of CEA with radioimmunoassay.

The sensitivity of cells infected by adenovirus to 5-FC

Lovo or Hela cells were seeded at a concentration of 2000 cells/well on 96-well, flat-bottom microplates in medium supplemented with 100mL·L⁻¹ FBS. After 12h, cells were infected by adenoviruses in different multiplicity of infection (M.O.I). After 12h, cells were cultivated in fresh medium containing various concentrations of 5-FC (0, 0.15, 1.5, 15, 150, 1500 and 15000 μ mol·L⁻¹; Sigma). After 48h of incubation with the drug, cell viability was measured using MTT (Huamei Corporation) assay. The fifty percent inhibition concentration (IC₅₀) of 5-FC was calculated using a curve-fitting parameter, and the results were represented as the means \pm SD from three independent experiments.

The bystander effect of AdCEACD/5-FC

After tumor cells had been infected by adenovirus for 12h in 1000 M.O.I, the bystander effect was measured by co-culturing different proportions of transfected cells and untransfected cells at a concentration of 2 \times 10⁵ cells/well on 6-well, flat-bottom plates in 5-FC-containing medium that was replaced every day. After 5d of incubation with the drug, cell viability was measured by counting live cells with trypan blue staining.

Statistical Analysis

Quantitative results were expressed as the mean \pm SD of the mean. Statistical analysis was performed using ANOVA test. *P*<0.05 was considered statistically significant.

RESULTS

Construction of shuttle plasmid pAdCEACD

The structure of pAdCEACD is depicted in Figure 1. The map of pAdCEACD after treatment with restriction endonuclease is showed in Figure 2.

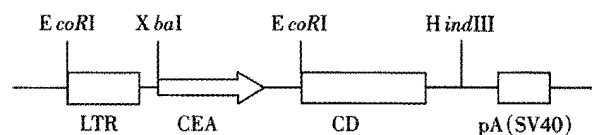


Figure 1 Schematic representation of the adenovirus shuttle plasmid, LTR, left inverted terminal repeats; pA, polyadenylation signal.



Figure 2 Map of pAdCEACD. There was a fragment of 1.8kb containing CEA and CD after being digested with XbaI and HindIII; As there were two coI restriction sites, there were three fragments after treatment with EcoI and HindIII, 0.9kb for LTR and CEA, 1.3 kb for CD, 2.2kb for LTR and CEA and CD.

Identification of AdCEACD

The result of dot blotting: There were 36 clones after recombination, 11 of which were hybridized. The result is showed in Figure 3.

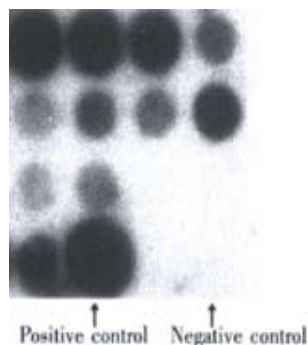


Figure 3 The identification of the recombinant adenovirus AdCEACD by dot blotting

During dot blotting the expression plasmid CEACD was used as positive control while virus AdCMVLacZ was used as negative control. The three well around negative controls were vacancy. The result showed that 6 of 11 clones were positive (over 50 percent). The left upper clone was to be further identified. The result of PCR Figure 4.

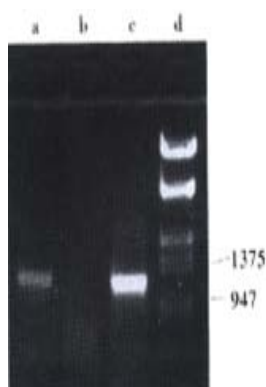


Figure 4 The identification of the recombinant adenovirus AdCEACD by PCR. a, PCR product using AdCEACD as template; b, PCR product using pAdE1CMV as template; c, PCR product using pAdCMVCD as template; d, λ DNA Marker.

During identification by PCR, pAdCMVCD was used as positive control while pAdE1CMV as negative control. The result showed that the recombinant adenovirus (left upper clone) contained CD gene in its genome.

The titration of AdCEACD

After purification the titration of the recombinant adenovirus AdCEACD was 5.0×10^{14} pfu/L⁻¹.

CEA secretions of Lovo or Hela

The concentration of CEA in the supernatant of Lovo cells was estimated to be $100 \mu\text{g} \cdot \text{L}^{-1}$, while lower $0.5 \mu\text{g} \cdot \text{L}^{-1}$ (beyond test) in the supernatant of Hela cells. So we consider that Lovo cell is CEA-producing and Hela cell CEA-nonproducing.

Sensitivity of the cells infected with AdCMVCD to 5-FC (Figure 5)

CMV promoter is ubiquitously strong, and effective in a variety of cells and tissues. As showed in Figure 5, after infected with AdCMVCD, the sensitivity of both Lovo cells (CEA-positive) and Hela cells (CEA-negative) to 5-FC had been enhanced, the IC₅₀ values of 5-FC for Lovo cells and Hela cells infected with AdCMVCD at 10 M.O.I were 128.8 ± 25.4 and $214.5 \pm 31.3 \mu\text{mol} \cdot \text{L}^{-1}$,

respectively, while the value of IC₅₀ for parent cells of these two cell lines was more than $15000 \mu\text{mol} \cdot \text{L}^{-1}$ ($P < 0.001$, respectively). The cytotoxicity of 5-FC increased accordingly when the m.o.i of adenovirus was enhanced, the value of IC₅₀ was reduced to 24.8 ± 7.1 and $23.9 \pm 5.2 \mu\text{mol} \cdot \text{L}^{-1}$, respectively, when the adenovirus concentration was 100 M.O.I ($P < 0.01$, respectively).

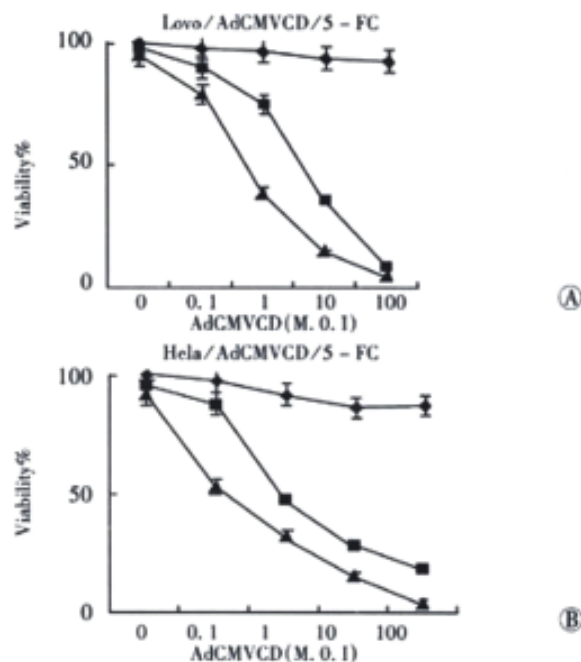


Figure 5 Sensitivity of cells infected with AdCMVCD to 5-FC. ◆: 5-FC 0; ■: 5-FC, $15 \mu\text{mol} \cdot \text{L}^{-1}$; ▲: 5-FC, $150 \mu\text{mol} \cdot \text{L}^{-1}$.

Sensitivity of the cells infected with AdCEACD to 5-FC (Figure 6)

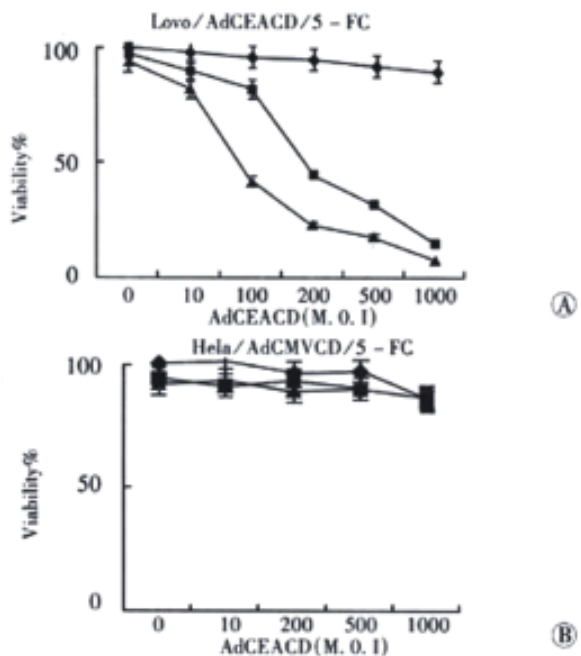


Figure 6 Sensitivity of cells infected with AdCEACD to 5-FC. ◆: 5-FC 0; ■: 5-FC, $15 \mu\text{mol} \cdot \text{L}^{-1}$; ▲: 5-FC, $150 \mu\text{mol} \cdot \text{L}^{-1}$.

CEA promoter is cell- or tissue- specific, so it makes CD gene express only in CEA-producing cells. Figure 6 shows that, human colorectal carcinoma cell strain Lovo cells (CEA-positive) became sensitive to 5-FC significantly when they were infected with AdCEACD, the IC₅₀ of 5-FC for Lovo cells infected with AdCEACD

at 100 M.O.I was $216.5 \pm 38.1 \mu\text{mol} \cdot \text{L}^{-1}$ ($P < 0.001$, compared with the IC_{50} of 5-FC in parent Lovo cells). The cytotoxicity of 5-FC increased accordingly when the m.o.i of adenovirus was enhanced, the value of IC_{50} of 5-FC was reduced to $27.9 \pm 4.2 \mu\text{mol} \cdot \text{L}^{-1}$ in Lovo cells infected with 1000 M.O.I AdCEACD ($P < 0.05$). However, the sensitivity of Hela cells (CEA-negative) infected with AdCEACD to 5-FC was not enhanced (the IC_{50} of 5-FC in 100 M.O.I AdCEACD infected Hela cells and 1000 M.O.I AdCEACD infected Hela cells was more than $15000 \mu\text{mol} \cdot \text{L}^{-1}$ too, $P > 0.05$, compared with the IC_{50} of 5-FC in parent Hela cells, respectively), indicating that AdCEACD/5-FC system can result in specific killing of CEA-producing cells.

The bystander effect of AdCEACD/5-FC system (Figure 7)

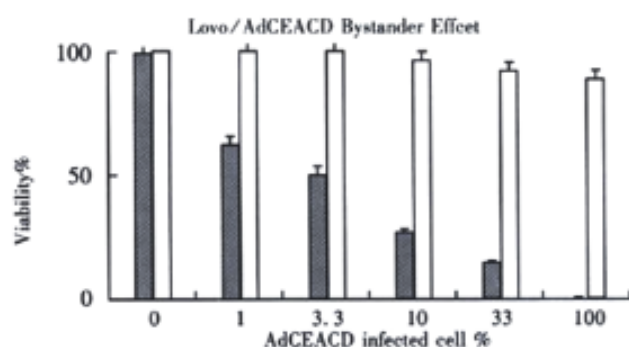


Figure 7 The bystander effect of AdCEACD/5-FC system. □: without 5-FC; ■: 5-FC $150 \mu\text{mol} \cdot \text{L}^{-1}$

After tumor cells had been infected by AdCEACD for 12h in 1000 M.O.I, the bystander effect was measured by co-culturing different proportions of transfected cells and untransfected cells at a concentration of 2×10^5 cells/well on 6-well, flat-bottom plates in 5-FC-containing medium that was replaced every day. After 5d of incubation with the drug, cell viability decreased significantly. The viability was $24.7 \pm 3.4\%$ when the proportion of transfected cells was only 10 percent, while the value of according control was $98.7 \pm 8.9\%$ ($P < 0.05$), indicating that the AdCEACD/5-FC system had excellent bystander effect.

DISCUSSION

Gene therapy has made rapid progress during the past few years and appears to be approaching clinical application in medical practice^[32-35]. Cancer is one of the most common causes of death in many countries and conventional treatments have not been able to cope with cancer adequately. Advances in our knowledge of molecular biology of cancer have brought a better understanding of the pathomechanism, as well as the development of molecular diagnostics and the basics of gene therapy. Cancer protocols (both marker and therapy) constitute about 70 percent of all current gene therapy protocols. Suicide gene therapy is one of these protocols and has a promising perspective. The purpose of this study is to apply CD gene, one of suicide genes, to treat colorectal carcinoma. One of the most important techniques of gene therapy is the choice of certain vector for gene transfer. Vectors are carriers or delivery vehicles for therapeutic genetic materials. There are two kinds of vectors available, non-viral vectors and viral vectors, the former contains liposomes, ligand-polylysine-DNA-complexes, dendrimers, cochleates, synthetic peptide complexes, electroporation and microinjection, etc, while the latter is composed of retroviral vectors, adenoviral vectors and adeno-associated virus vector.

Adenovirus vector system has many advantages. Adenovirus vectors can be prepared at much higher titres than retroviral vectors

and have a high efficiency gene transfer regardless of the proliferative state of the tissues whereas retroviral vectors insert their genes only into dividing cells. Adenovirus genomes usually do not integrate into the host cell chromosome^[36-42]. Although the duration of *in vivo* gene expression with adenovirus vector is short, the level of therapeutic gene expression is much higher. The purpose of suicide gene therapy is to kill transfected cells, so we choose adenoviral vector for suicide gene transfer. Suicide gene with efficient expression disappears rapidly after transfected tumor cells are killed, resulting in minimizing the underlying side effects of suicide gene. The adenovirus can infect a wide range of different cells, making it impossible to deliver genes to special target cells by intravenous administration. CD gene encodes cytosine deaminase which can transform 5-FC to cytotoxic 5-FU. 5-FU is often used for the treatment of colorectal carcinoma in combination with another chemotherapeutic agent. It causes cell death by inhibiting both RNA and DNA syntheses. If CD gene is delivered into normal cells, it may kill them when 5-FC is administrated.

The ability to target gene transfer to a particular class of cells is an important aspect of improving efficacy of gene therapy and limiting undesirable side effects. Ideal gene therapy vectors would be delivered intravenously to transfect only specific cells. Existing vectors only transfect cells *in vivo* in a manner determined by blood flow and the site of introduction. Various strategies for targeted gene therapy have been designed, one of which is transcriptional targeting^[43-46]. For certain procedures it may be necessary to deliver genes under the control of appropriate tissue- or cell-specific promoters, perhaps for the lifetime of the individual^[47-50]. Transcriptional targeting of vectors is important for gene therapy of cancer because of the requirement to limit toxic therapies to the malignant target cells. It may be possible to identify and use transcriptional control elements that drive expression of proteins unique to, or overexpressed in malignant cells. These genes would reduce collateral expression of the transgene, and hence toxicity to healthy cells. For colorectal carcinoma, carcino-embryonic antigen (CEA) is one of such elements. CEA is a tumor-associated marker for human colorectal carcinoma and CEA is transcriptionally silent in adult normal tissues but over-expressed in approximate 60 to 80 percent human colorectal carcinomas^[51-54]. Therefore we have used CEA as a transcriptional element to construct a new replication-deficient recombinant adenoviral vector containing CD gene controlled under CEA promoter in this study, and we have constructed the desired adenovirus vector, AdCEACD, successfully. We have applied dot blotting and PCR to identify CEA gene and CD gene in the vector respectively. *in vitro* experiments have showed the vector delivers CD gene only to CEA-producing cells, and only CEA-producing cells can be killed by 5-FC.

Currently available *in vivo* gene transfer vectors are not capable of transferring a gene to all tumor cells; however, successful application of suicide gene therapy *in vivo* relies on the bystander effect, where the active chemotherapeutic agent diffuses in the tumor cells and neighboring malignant cells in sufficient concentrations to suppress growth. In this study we also demonstrated that the AdCEACD/5-FC system presented bystander effect, as did AdCMVCD. The correlation between CEA secretion and induction of CD activity and 5-FC/5-FU sensitivity is not straightforward. It is presumed that transcriptional targeting is due to transcriptional activation. There are transcriptional activators in CEA-producing cells, which can activate CEA promoter, hence can drive the expression of CD gene, whereas CEA-nonproducing cells lack certain activators and CD gene can not express. The current results suggest that the recombinant adenovirus transfer of the CD gene under control of CEA promoter could theoretically be a useful vector for the CEA-producing tumors, such as colorectal carcinoma. It is not perfect that

Hela cells had been used as CEA-nonproducing cell control, but we lack cell lines of normal intestinal mucosa or normal bone marrow. We will continue this research in vivo to further investigate the specificity of the recombinant adenoviral vector AdCEACD.

REFERENCES

- Tang YC, Li Y, Qian GX. Reduction of tumorigenicity of SMMC-7721 hepatoma cells by vascular endothelial growth factor antisense gene therapy. *World J Gastroenterol* 2001;7:22-27
- He Y, Zhou J, Wu JS, Dou KF. Inhibitory effects of EGFR antisense oligodeoxynucleotide in human colorectal cancer cell line. *World J Gastroenterol* 2000;6:747-749
- Lou GL, Cao XT, Min BH, Zhang WP, Meng PL. Effect of TNF gene transfected LAK cells on the ascitic liver carcinoma bearing mice. *World J Gastroenterol* 2000;6(Suppl 3):12
- Yang DH, Zhang MQ, Du J, Xu C, Liang QM, Mao JF, Qin HR, Fan ZR. Inhibitory effect of IGFII antisense RNA on malignant phenotype of hepatocellular carcinoma. *World J Gastroenterol* 2000;6:266-267
- Fan YF, Huang ZH. Progress in the studies of gene therapy for colorectal cancer. *Shijie Huaren Xiaohua Zazhi* 2001;9:427-430
- Leng JJ, Chen YQ, Leng XS. Genetic therapy for pancreatic neoplasms. *Shijie Huaren Xiaohua Zazhi* 2000;8:916-918
- Xu DX, Chen WS, Ye ZJ. The antisense gene of growth factor receptor reversing the malignant phenotype of human hepatoma cells. *Shijie Huaren Xiaohua Zazhi* 2001;9:175-179
- Wang SM, Wu JS, Yao X, He ZS, Pan BR. Effect of TGF- α , EGFR antisense oligodeoxynucleotides on colon cancer cell line. *Shijie Huaren Xiaohua Zazhi* 1999;7:522-524
- Li ZS, Zhu ZG, Yin HR, Chen SS, Lin YZ. Diversity of telomerase activity in human and murine tumor cells transfected with cytokine genes. *Shijie Huaren Xiaohua Zazhi* 1999;7:194-196
- Dai YM. Targeting chemotherapy: a new focus in gene therapy research. *Shijie Huaren Xiaohua Zazhi* 1999;7:469-472
- Mesnil M, Yamasaki H. Bystander effect in herpes simplex virus-thymidine kinase/ganciclovir cancer gene therapy: role of gap-junctional intercellular communication. *Cancer Res* 2000;60:3989-3999
- Howard BD, Boenicke L, Schniewind B, Henne-Bruns D, Kalthoff H. Transduction of human pancreatic tumor cells with vesicular stomatitis virus G-pseudotyped retroviral vectors containing a herpes simplex virus thymidine kinase mutant gene enhances bystander effects and sensitivity to ganciclovir. *Cancer Gene Ther* 2000;7:927-938
- Beltinger C, Fulda S, Kammertoens T, Uckert W, Debatin KM. Mitochondrial amplification of death signals determines thymidine kinase/ganciclovir-triggered activation of apoptosis. *Cancer Res* 2000;60:3212-3217
- Guo SY, Gu QL, Liu BY, Zhu ZG, Yin HR, Lin YZ. Experimental study on the treatment of gastric cancer by TK gene combined with mIL-2 gene. *Shijie Huaren Xiaohua Zazhi* 2000;8:974-978
- Du KH, Guo SY, Gong DQ, Gu QL, Zhu ZG, Yin HR, Lin YZ. Experimental study on the treatment of gastric cancer by TK gene and GCV. *Shijie Huaren Xiaohua Zazhi* 2000;8:1293-1295
- Zhao YG, Zhang XY, Hui HX, Wang CJ. Effect of HSV-tk/GCV suicide gene system on human esophageal carcinoma cells. *Shijie Huaren Xiaohua Zazhi* 2001;9:961-962
- Huang ZH, Qian WF, Chi DB, Jiang ZS. Apoptosis in human colorectal cancer Lovo cells induced by HSVtk/GCV system *in vitro*. *Shijie Huaren Xiaohua Zazhi* 2001;9:194-197
- Qian WF, Huang ZH, Chi DB. Herpes simplex virus thymidine kinase/ganciclovir system combined with 5-FU for the treatment of experimental colorectal cancer. *Shijie Huaren Xiaohua Zazhi* 2001;9:190-193
- Huang ZH, Yu WL, Yang L, Song HJ, Yang JZ. Effect of retrovirus-mediated HSVtk suicide gene on colon cancer *in vitro*. *Shijie Huaren Xiaohua Zazhi* 2001;9:84-86
- Bentires-Alj M, Hellin AC, Lechanteur C, Princen F, Lopez M, Fillet G, Gielen J, Merville MP, Bours V. Cytosine deaminase suicide gene therapy for peritoneal carcinomatosis. *Cancer Gene Ther* 2000;7:20-26
- Block A, Freund CTF, Chen SH, Nguyen KP, Finegold M, Windler E, Woo SLC. Gene therapy of metastatic colon carcinoma: regression of multiple hepatic metastases by adenoviral expression of bacterial cytosine deaminase. *Cancer Gene Ther* 2000;7:438-445
- Chen MJ, Chung-Faye GA, Searle PF, Young LS, Kerr DJ. Gene therapy for colorectal cancer: therapeutic potential. *Bio Drugs* 2001;15:357-367
- Cui L, Lin YZ, Zhu ZG, Chen XH, Gu QL, Liu BY, Yu BM. Killing effect of 5-FC/CD system on nude mice bearing human colorectal carcinoma. *Shijie Huaren Xiaohua Zazhi* 1999;7:473-475
- Chung-Faye GA, Chen MJ, Green NK, Burton A, Anderson D, Mautner V, Searle PF, Kerr DJ. *in vivo* gene therapy for colon cancer using adenovirus-mediated, transfer of the fusion gene cytosine deaminase and uracil phosphoribosyltransferase. *Gene Ther* 2001;8:1547-1554
- Chen Z, Du Y. Application of specific receptor of vascular endothelial cells in the tumor vascular target treatment. *Shijie Huaren Xiaohua Zazhi* 2001;9:702-705
- Humphreys MJ, Ghaneh P, Greenhalf W, Campbell F, Clayton TM, Everett P, Huber BE, Richards CA, Ford MJ, Neoptolemos JP. Hepatic intra-arterial delivery of a retroviral vector expressing the cytosine deaminase gene controlled by the CEA promoter and intraperitoneal treatment with 5-fluorocytosine suppresses growth of colorectal liver metastases. *Gene Ther* 2001;8:1241-1247
- Uchida A, O'Keefe DS, Bacich DJ, Molloy PL, Heston WD. *in vivo* suicide gene therapy model using a newly discovered prostate-specific membrane antigen promoter/enhancer: a potential alternative approach to androgen deprivation therapy. *Urology* 2001;58:132-139
- Koyama F, Sawada H, Fujii H, Hirao T, Ueno M, Hamada H, Nakano H. Enzyme/prodrug gene therapy for human colon cancer cells using adenovirus-mediated transfer of the Escherichia coli cytosine deaminase gene driven by a CAG promoter associated with 5-fluorocytosine administration. *J Exp Clin Cancer Res* 2000;19:75-80
- Cao GW, Qi ZT, Pan X, Zhang XQ, Miao XH, Feng Y, Lu XH, Kuriyama S, Du P. Gene therapy for human colorectal carcinoma using human CEA promoter controlled bacterial ADP-ribosylating toxin genes: PEA and DTA gene transfer. *World J Gastroenterol* 1998;4:388-391
- Xu DH, Ge K, Jiang Q, Zheng ZC, Liu XY. The construction of an adenovirus vector containing cytosine deaminase gene and its application. *Shengwu Huaxue Yu Shengwu Wuli Xuebao* 1998;30:164-168
- Wu WX, Shen LZ, Ding Q, Xu DH, Zheng ZC, Liu XY, Yao K. Construction and initial identification of an adenoviral vector containing cytosine deaminase gene controlled under carcino-embryonic antigen promoter. *Nanjing Yike Daxue Xuebao* 2001;21:356-357
- Shen LZ, Wu WX, Ding Q, Xu DH, Zheng ZC, Liu XY, Hua YB. Establishment of human colorectal carcinoma cell strain modified by human interferon- γ gene. *Shijie Huaren Xiaohua Zazhi* 2001;9:1310-1312
- Ning XX, Wu KC, Shi YQ, Wang X, Zhao YQ, Fan DM. Construction and expression of gastric cancer MG7 mimic epitope fused to heat shock protein 70. *Shijie Huaren Xiaohua Zazhi* 2001;9:892-896
- Zhang J, Yan XJ, Yan QJ, Duan J, Hou Y, Su CZ. Cloning and expression of HPV16 L2 DNA from esophageal carcinoma in *E. coli*. *Shijie Huaren Xiaohua Zazhi* 2001;9:273-278
- Zheng SX, Li XG, Zhou LJ, Zhu XZ. Construction of pcDNA3/p16 plasmid and its inhibitory role in the proliferation of hepatoma cell line. *Shijie Huaren Xiaohua Zazhi* 2000;8:49-51
- Wickham TJ. Targeting adenovirus. *Gene Therapy* 2000;7:110-114
- Pan X, Pan W, Ke CW, Zhang B, Cao GW, Qi ZT. Tetracycline controlled DT/VEGF system gene therapy mediated by adenovirus vector. *Shijie Huaren Xiaohua Zazhi* 2000;8:1121-1126
- Hao CQ, Zhou YX, Feng ZH, Li JG, Jia ZS, Wang PZ. Construction, identification and expression of framework plasmid pAd.HCV-C of adenovirus expression vector of HCV C. *Shijie Huaren Xiaohua Zazhi* 2001;9:635-639
- Lu JG, Lin C, Huang ZQ, Wu JS, Fu M, Zhang XY, Liang X, Yao X, Wu M. Inhibitory effects of human cholangiocarcinoma cell line by recombinant adenoviruses p16 with CDDP. *Shijie Huaren Xiaohua Zazhi* 2000;8:641-645
- Chen JP, Lin C, Xu CP, Zhang XY, Fu M, Deng YP, Wei Y, Wu M. Transduction efficiency, biologic effects and mechanism of recombinant RA538, antisense C-myc adenovirus on different cell lines. *Shijie Huaren Xiaohua Zazhi* 2000;8:266-270
- Chen JP, Lin C, Xu CP, Zhang XY, Fu M, Deng YP, Kui Y, Wu M. *in vitro* and *in vivo* molecular therapy with Asc-myc adenovirus for human gastric carcinoma cell line. *Shijie Huaren Xiaohua Zazhi* 1999;7:482-486
- Chen JP, Lin C, Xu CP, Zhang XY, Wu M. The therapeutic effects of recombinant adenovirus RA538 on human gastric carcinoma cells *in vitro* and *in vivo*. *World J Gastroenterol* 2000;6:855-860
- Russell SJ, Cosset FL. Modifying the host range properties of retroviral vectors. *J Gene Med* 1999;1:300-311
- Nishikawa M, Yamauchi M, Morimoto K, Ishida E, Takakura Y, Hashida M. Hepatocyte-targeted *in vivo* gene expression by intravenous injection of plasmid DNA complexed with synthetic multi-functional gene delivery system. *Gene Ther* 2000;7:548-555
- Haisma HJ, Pinedo HM, van Rijswijk A, van der Meulen-Muileman I, Sosnowski BA, Ying W, van Beusechem VW, Tillman BW, Gerristen WR, Curiel DT. Tumor-specific gene transfer via an adenoviral vector targeted to the pan-carcinoma antigen EpCAM. *Gene Ther* 1999;6:1469-1474

- 46 Jenkins RG, Herrick SE, Meng QH, Kinnon C, Laurent GJ, McAnulty RJ, Hart SL. An integrin-targeted non-viral vector for pulmonary gene therapy. *Gene Ther* 2000;7:393-400
- 47 Nagayama Y, Nishihara E, Iitaka M, Namba H, Yamashita S, Niwa M. Enhanced efficacy of transcriptionally targeted suicide gene/prodrug therapy for thyroid carcinoma with the Cre-lox-P system. *Cancer Res* 1999;59:3049-3052
- 48 Ueno M, Koyama F, Yamada Y, Fujimoto H, Takayama T, Kamada K, Naito A, Hirao S, Mukogawa T, Hamada H, Nakajima Y. Tumor-specific chemo-radio-gene therapy for colorectal cancer cells using adenovirus vector expressing the cytosine deaminase gene. *Anticancer Res* 2001;21:2601-2608
- 49 Morimoto E, Inase N, Miyake S, Yoshizawa Y. Adenovirus-mediated suicide gene transfer to small cell lung carcinoma using a tumor-specific promoter. *Anticancer Res* 2001;21:329-331
- 50 Ueda K, Iwahashi M, Nakamori M, Nakamura M, Matsuura I, Yamaue H, Tanimura H. Carcinoembryonic antigen-specific suicide gene therapy of cytosine deaminase/5-fluorocytosine enhanced by the Cre/loxP system in the orthotopic gastric carcinoma model. *Cancer Res* 2001;61:6158-6162
- 51 Zheng CX, Zhan WH, Zhao JZ, Zheng D, Wang DP, He YL, Zheng ZQ. The prognostic value of preoperative serum levels of CEA, CA19-9 and CA72-4 in patients with colorectal cancer. *World J Gastroenterol* 2001;7:431-434
- 52 Li JY, Huang Y, Lin MF. Clinical evaluation of several tumor markers in the diagnosis of primary hepatic cancer. *World J Gastroenterol* 2000;6(Suppl 3):39
- 53 Reiter W, Stieber P, Reuter C, Nagel D, Lau-Werner U, Lamerz R. Multivariate analysis of the prognostic value of CEA and CA19-9 serum levels in colorectal cancer. *Anticancer Res* 2000;20:5195-5198
- 54 Yamamoto H, Miyake Y, Noura S, Ogawa M, Yasui M, Ikenaga M, Sekimoto M, Monden M. Tumor markers for colorectal cancer. *Gan To Kagaku Ryoho* 2001;28:1299-1305

Edited by Hu DK

• VIRAL LIVER DISEASES •

Detection of anti-preS1 antibodies for recovery of hepatitis B patients by immunoassay

Jun Wei, Yu-Qin Wang, Zhi-Meng Lu, Guang-Di Li, Yuan Wang, Zu-Chuan Zhang

Jun Wei, Guang-Di Li, Yuan Wang, Zu-Chuan Zhang, Institute of Biochemistry and Cell Biology, Shanghai Institutes for Biological Sciences, Chinese Academy of Sciences, Shanghai 200031, China

Yu-Qin Wang, Zhi-Meng Lu, Department of Clinical virology, Rui-Jin Hospital, Shanghai Second Medical University 200025, Shanghai, China

Supported by the grants No. KY951-A1-301 and No. KY95T-06-03 from the 9th Five Years Plan Key Research Programs of the Chinese Academy of Sciences.

Correspondence to: Zu-Chuan Zhang, Institute of Biochemistry and Cell Biology, Shanghai Institutes for Biological Sciences, Chinese Academy of Sciences, Shanghai 200031, China. zhangzc@sunm.shenc.ac.cn

Telephone: +86-21-64374430 Fax: +86-21-64338357

Received 2001-06-02 Accepted 2001-10-29

Abstract

AIM: To establish a convenient immunoassay method based on recombinant antigen preS1(21-119aa) to detect anti-preS1 antibodies and evaluate the clinical significance of antibodies in hepatitis B.

METHODS: The expression plasmid pET-28a-preS1 was constructed, and a large quantity of preS1(21-119aa) fragment of the large HBsAg protein was obtained. The preS1 fragment purified by Ni²⁺-IDA affinity chromatography was used as coated antigen to establish the indirect ELISA based on streptavidin-biotin system for detection of the anti-preS1 antibodies in sera from HBV-infected patients. For follow-up study, serial sera were collected during the clinical course of 21 HBV-infected patients and anti-preS1 antibodies, preS1 antigen, HBV-DNA and other serological HBV markers were analyzed.

RESULTS: preS1(21-119aa) fragment was highly expressed from the plasmid pET-28a-preS1 in a soluble form in *E. Coli* (30mg·L⁻¹), and easily purified to high purity over 90% by one step of Ni²⁺-IDA-sepharose 6B affinity chromatography. The purity and antigenicity of the purified preS1(21-119aa) protein was determined by 150g·L⁻¹ SDS-PAGE, Western blot and a direct ELISA. Recombinant preS1(21-119aa) protein was successfully applied in the immunoassay which could sensitively detect the anti-preS1 antibodies in serum specimens of acute or chronic hepatitis B patients. Results showed that more than half of 19 acute hepatitis B patients produced anti-preS1 antibodies during recovery of the disease, however, the response was only found in a few of chronic patients. In the clinical follow-up study of 11 patients with anti-preS1 positive serological profile, HBsAg and HBV-DNA clearance occurred in 6 of 10 acute hepatitis B patients in 5-6 months, and seroconversion of HBeAg and disappearance of HBV-DNA occurred in 1 chronic patients treated with lamivudine, a antiviral agent.

CONCLUSION: The high-purity preS1(21-119aa) coated antigen was successfully prepared by gene expression and affinity chromatography. Using this antigen, a conveniently detective system of anti-preS1 antibodies in sera was established. Preliminary clinical trial the occurrence of anti-

preS1 antibodies in acute hepatitis B patients suggests the clearance of HBV from serum in a short-term time, and anti-preS1 positive in chronic patients means health improvement or recovery from the disease.

Wei J, Wang YQ, Lu ZM, Li GD, Wang Y, Zhang ZC. Detection of anti-preS1 antibodies for recovery of hepatitis B patients by immunoassay. *World J Gastroenterol* 2002;8(2):276-281

INTRODUCTION

Human hepatitis B virus (HBV) is a small enveloped DNA virus which causes acute and chronic hepatitis in humans^[1]. Worldwide, the number of infected persons is predicted to reach 400 million during 2000. Areas with high prevalence of HBV include China^[2,3], Southeast Asia and Africa, where approximately 10% of the population are chronic carriers^[4]. The envelope of HBV contains three related proteins, encoded by the S open reading frame (ORF) of the viral genome, composed of three regions: preS1, preS2 and S. The major protein, termed small HBs protein (SHBs), is encoded by the S gene, whereas the two minor envelop proteins, termed the middle protein (MHBs) and the large protein (LHBs), are encoded by the preS2+S and preS1+preS2+S region, respectively^[5]. The preS1 region contains epitopes that elicit immune responses at the B-cell and T-cell level over a broader range of MHC haplotypes than those on the preS2 and S protein^[6-8]. The preS1 domain also contains potential viral attachment sites to hepatocytes^[9] and elicit antibodies capable of neutralizing HBV in the chimpanzee^[10].

The preS1 epitopes have been extensively analyzed using synthetic peptides, anti-peptide sera and anti-preS1 monoclonal antibodies. B cell epitopes have been mapped to residues 27-35aa, 72-78aa, 32-47aa, 41-53aa, 94-105aa and 106-117aa in the preS1 region^[11-13]; and T cell epitopes mainly located in residues 12-21aa, 21-30aa, 29-48aa and 94-117aa of the preS1 region^[13,14]. These findings explain why the preS1 region has good immunogenicity and can easily elicit the anti-preS1 responses^[15]. Additionally, nearly all preS1 epitopes concentrate on residues 21-119aa in the preS1 region (ad subtypes of HBV LHBs carry a 119aa-residue preS1, and HBV in most Chinese belong to adr subtype; 8 residues on N-terminus of preS1 are absent in ay subtype). Because the preS1 region locates on the outside of the mature virion and has many overlapping epitopes, anti-preS1 immune response occurred early in the course of the disease and is involved in the clearance and neutralization of HBV. As anti-preS1 antibodies have been mainly detected early during acute hepatitis B^[16,17], the anti-preS1 antibodies could represent an early serological marker for HBV clearance^[18]. About 1/2 of subjects in the convalescence phase of acute hepatitis B were serological positive for anti-preS1 antibodies, whereas persistence of preS1 antigen and lack of corresponding antibodies have been the predict of the evolution of a chronic course of disease^[19]. In this study, preS1(21-119aa) peptide was chosen and highly expressed in a soluble form. Using this protein as the antigen, an effective enzyme-linked immunosorbent assay was established. The sensitive test can provide a basis for monitoring anti-preS1 in sera of patients with hepatitis B and offers a prognostic implication for patients.

MATERIALS AND METHODS

Materials

Plasmids, *E. Coli* strain The plasmid pADR-1 containing HBV genome (adr subtype) was constructed by Wu *et al*^[20]. Expression vector pET-28a(+) was purchased from Novagen. *E. Coli* strain BL21 (DE3)plyS was used for the production of the preS1(21-119aa) peptide.

Enzymes and Reagents Restriction enzymes and T₄ DNA ligase were purchased from New England Biolabs, Boehringer Mannheim and GIBCO BRL. DNA sequence kit was from USB. Agrose and LMP agarose were from GIBCO BRL. Acrylamide, bisacrylamide, isopropylthio-β-D-galactoside (IPTG), imidazole and iminodiacetic acid (IDA)-Sephacrose 6B, biotinamidocaproate-N-hydroxy-succinimide ester (BNSE) and 3,3',5,5'-tetramethylbenzidine (TMB) were from Sigma. Protein A was from Pharmacia. Diaminobenzidine (DAB) and streptavidin-horseradish peroxidase (HRP) conjugate were from Sino-American Biotech. Anti-preS1(21-47aa) monoclonal antibody (mAb) 125E11 and 125E11 conjugated with HRP were made in our lab^[21]. Tetrabutyl ammoniumborohydride (TBABH) was from Fluka.

Serum specimens and kits for HBV markers Serum specimens were collected from patients admitted to the Rui-Jin Hospital with clinical and biochemical evidence of hepatitis B. As a control, sera of healthy persons with normal liver function and without any markers of HBV infection were used. HBsAg and anti-HBs, HBeAg and anti-HBe, anti-HBc were determined by commercially available ELISA kits from Abbott laboratories. PreS1 protein were detected by a double mAb sandwich ELISA^[22]. HBV-DNA level in serum samples was assayed by HBV PCR fluorogence diagnostic kit from PJ (Shenzhen,China).

Methods

Construction of expression plasmid containing preS1(21-119aa) DNA sequence.

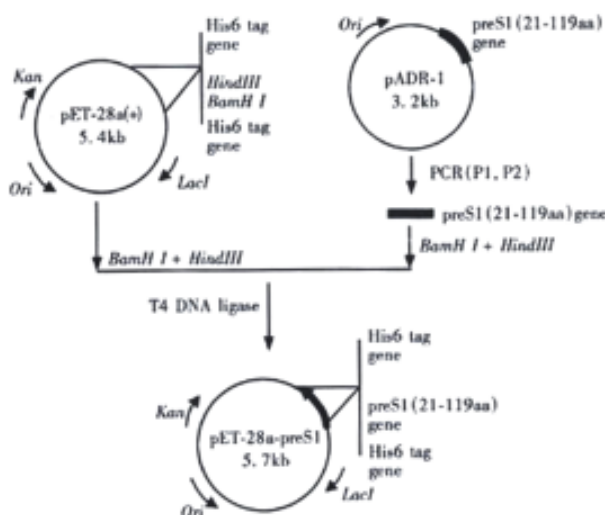


Figure 1 Construction of expression plasmid pET-28a-preS1

Figure 1 depicts the steps leading to the final construction of the expression plasmid pET-28a-preS1 which expresses a fusion protein containing preS1(21-119aa) peptide with His₆ tags. PCR primers were designed as follows:

Forward primer P₁: 5'-CATAGGATCCCTCTGGGATTCTTT-3'

BamHI

Reverse primer P₂: 5'-ATCG AAGCTTGAATTC GGCCTGAGGATGACT-3'

HindIII EcoRI

Preparation of plasmid DNA, PCR, digestion of DNA with restriction enzymes, agarose gel electrophoresis, recovery and purification of DNA fragment, ligation of terminus created by restriction enzymes and transformation of competent *E. Coli* were performed according to Sambrook^[23].

Cell culturing and harvesting *E. Coli* strain BL21(DE3)plyS cells harboring the expression plasmid pET-28a-preS1 were inoculated into LB medium containing kanamycin (50mg·L⁻¹). The seed culture was inoculated into 100-fold volume of fresh LB medium (kanamycin, 50mg·L⁻¹) and cultured at 37°C up to 0.4-0.6 of A₆₀₀. To this culture IPTG was added to give a final concentration of 0.2mmol·L⁻¹, and incubation was continued at 37°C for 6h or 22°C for 24h. The induced cells, as well as the uninduced cells, were harvested by centrifugation, and cell lysates were analyzed by 150g·L⁻¹ SDS-PAGE.

Western analysis of the preS1(21-119aa) fusion protein After SDS-PAGE, proteins were transferred to nitrocellulose membrane (Schleicher & Schuell), and the membrane was incubated with a murine monoclonal antibody 125E11 (1:1000, volume ratio), which recognizes preS1(21-47aa) fragment within the preS1 region, followed by goat anti-mouse IgG peroxidase conjugate (1:1000, volume ratio). After washing, substrate solution containing DAB (0.5g·L⁻¹) and H₂O₂ (0.02mL·L⁻¹) was added to have 125E11 specific binding protein bands visualized.

Purification of the preS1(21-119aa) fusion protein In order to characterize whether the expressed fusion protein is soluble or insoluble, the cell pellet from 100ml culture was resuspended in 4ml buffer A (20mmol·L⁻¹ Tris-HCl pH7.9, 0.5mol·L⁻¹ NaCl, 100g·L⁻¹ glycerol, 1mmol·L⁻¹ PMSF, 25mmol·L⁻¹ imidazole), and sonicated in ice bath. Then the sonicate was centrifuged at 18000r·min for 15min, and the resulting supernatant was concentrated to 2mL and the pellet was resuspended in 2mL buffer A as the insoluble protein sample. The soluble and insoluble samples were subjected to 150g·L⁻¹ SDS-PAGE and Western blot analysis.

2mL supernatant was applied to 2mL Ni²⁺-IDA sepharose 6B column (2mL) preequilibrated with buffer A at 4°C. The column was washed with 30ml buffer B (20mmol·L⁻¹ Tri-HCl pH7.9, 0.5mol·L⁻¹ NaCl, 100g·L⁻¹ glycerol, 1mmol·L⁻¹ PMSF, 45mmol·L⁻¹ imidazole), and the bound protein was eluted with 4mL buffer C (20mmol·L⁻¹ Tri-HCl pH7.9, 0.5mol·L⁻¹ NaCl, 100g·L⁻¹ glycerol, 1mmol·L⁻¹ PMSF, 100mmol·L⁻¹ imidazole) and the elution samples were collected^[24, 25]. The fractions enriched for preS1(21-119aa)-His₆ tag fusion protein was identified by 150g·L⁻¹ SDS-PAGE and Western blot analysis.

Biotin labeling of protein A The procedure is essentially the same as that described by Kittigul *et al*^[26]. Protein A (2.0g·L⁻¹) is dialyzed against 0.01mol·L⁻¹ NaHCO₃ at 4°C. After dialysis, 1mL of the protein A solution was mixed with 120μL of BNSE (1.0g·L⁻¹ in dimethyl sulfoxide). The mixture was incubated at 4°C overnight and dialyzed overnight against PBS at 4°C with several changes of PBS.

Antigenicity analysis of preS1(21-119aa) domain of the fusion protein The antigenicity of preS1(21-119aa) fusion protein was analyzed by a direct ELISA. The microtiter plate was coated with preS1(21-119aa) fusion protein from 10 to 2500ng/well, and mAb 125E11 labeled with HRP was added to each well and incubated at 37°C for 1h. The plate was washed, and substrate solution containing TMB (7.5g·L⁻¹) and H₂O₂ (0.3mL·L⁻¹) was added to each well to develop a color change, then the reaction was stopped with 1.0mol·L⁻¹ H₂SO₄ and A (absorbance) value was measured at 450nm in an ELISA reader (Labsystem Multiscan, Finland).

Establishment of indirect ELISA for detecting anti-preS1 antibodies in serum The optimal dilutions of the reagents are

determined by checkerboard titration. Microtiter plates (Nunc, Denmark) were coated by incubation overnight at 4°C with 2mg·L⁻¹ preS1(21-119aa) protein in 100μL volume of per well in carbonate buffer (15mmol·L⁻¹ Na₂CO₃, 35mmol·L⁻¹ NaHCO₃, pH9.6). The microplates were then washed three times with a washing solution (20mmol·L⁻¹ Tris-HCl pH7.4, 0.5mL·L⁻¹ Tween-20), and postcoated with 5g·L⁻¹ bovine serum albumin (BSA) in PB (2.7mmol·L⁻¹ KCl, 0.5mmol·L⁻¹ KH₂PO₄, 6.5mmol·L⁻¹ Na₂HPO₄, pH7.5) for 1h at 37°C. After washing, 100μL diluted serum samples [1:30 in PBFST (100mL·L⁻¹ fetal calf serum(FCS), 0.5mol·L⁻¹ NaCl and 0.5g·L⁻¹ Tween-20 in PB)] were added and incubated for 2h at 37°C. After washing, 100μL biotin labeled protein A solution (2mg·L⁻¹ in PBFST) diluted in PBFST was dispensed into wells, and the plates were incubated for 1h at 37°C. After washing 4 times, streptavidin-HRP conjugate diluted in PBFST was added into each well of the plates, and the plates were incubated for 1h at 37°C. Finally, after washing, 100μL of the substrate mixture (1.0mmol·L⁻¹ TMB, 0.2mmol·L⁻¹ TBABH, 0.2mol·L⁻¹ potassium citrate and 0.5mL·L⁻¹ H₂O₂)^[27] was added and incubated for 20min at 37°C. The reaction was stopped by the addition of 50μL of 1.0mol·L⁻¹ H₂SO₄. The optical density was measured at 450nm (A₄₅₀) with the ELISA reader. To determine cut-off value for the established ELISA, A₄₅₀ value of negative control for anti-preS1 antibodies was evaluated by testing a serum mixture from 100 normal individuals. The cut-off value was defined as 2.1 folds of mean of negative control. Specimens were considered to be positive when the obsorbance value exceeded the cut-off value.

Specificity of established ELISA for detection of anti-preS1 antibodies Twenty-five μL anti-preS1 antibodies positive serum with the same volume of 0.15g·L⁻¹ preS1(21-119aa) protein or PBS was incubated at 37°C, and mixture was stepwise diluted and added to wells coated by preS1(21-119aa), and then indirect ELISA was performed. A parallel test with normal human serum was also performed in the same experiment.

Follow-up study The serum specimens from 11 anti-preS1 positive patients and 10 anti-preS1 negative patients with hepatitis B were collected at monthly intervals and their HBV markers^[28], including HBV-DNA^[29-31], HBsAg, anti-HBs, HBeAg, anti-HBe, anti-HBc, preS1^[32] and anti-preS1 were analyzed.

RESULTS

Construction of expression plasmid pET-28a-preS1

PreS1(21-119aa) gene fragment was synthesized by PCR using the primers P₁, P₂ and the plasmid pADR-1 containing HBV genome (adr subtype) as the template. The PCR product was digested with *Bam*HI and *Hind*III and then subcloned into the *Bam*HI-*Hind*III sites of pET-28a(+) to yield expression plasmid pET-28a-preS1 (Figure 1). Two His tag fragments which coded a stretch of six histamine residues located in both terminus of inserted fragment, respectively. This made it easy to purify preS1(21-119aa) fusion protein by Ni²⁺-IDA-sepharose 6B affinity chromatography. DNA sequence analysis confirmed that the expression plasmid coded the correct nucleotide sequence. The nucleotide sequence and deduced amino acid sequence of the preS1(21-119aa) region gene fragment inserted in the pET-28a-preS1 is shown in Figure 2.

Expression of preS1(21-119aa) fusion protein

In order to express the preS1(21-119aa) fusion protein, the expression plasmid pET-28a-preS1 was transformed into *E. Coli* BL21(DE3) plysS, and the cells were cultured and induced by IPTG. The expressive levels were determined by SDS-PAGE and Western blot analysis of the cell lysates. As show in lane 2 of Figure 3, more than

30% of total stainable proteins was about 17000 fusion protein. The analysis of solubility showed that about 80% of the fusion protein was soluble (lane 3 of Figure 3). Thus, the soluble form was convenient for the followed purification and clinical application.

1	OCT	CTC	CGA	TTC	TTT	CCC	GAT	CAC	CAG	TTC	GAC	CGT	CCC	TTC	CGA	45
	P	L	G	F	F	P	D	H	Q	L	D	P	A	F	G	
46	GCG	AAC	TEA	AAC	AAT	CGA	GAT	TGG	GAC	TTC	AAC	CCC	AAC	AAG	GAT	90
	A	N	S	N	N	P	D	W	D	F	N	P	N	K	D	
91	CAC	TGG	CGA	GAG	CGA	AAT	CAG	GTA	CGA	CGC	CGA	CGA	TTC	GGG	CGA	135
	H	W	P	E	A	N	Q	V	G	A	G	A	F	G	P	
136	GGG	TTC	ACC	CGA	CAC	CGC	CGT	CTT	TTC	GGG	TGG	AGC	CGT	CAG		180
	G	F	T	P	P	H	G	G	L	L	G	W	S	P	Q	
181	OCT	CAG	CGC	ATT	TTC	ACA	ACA	GTC	CGA	GTA	CGA	CGT	CGT	CGT	CGC	225
	A	Q	C	I	L	T	T	V	P	V	A	P	P	P	A	
226	TCC	ACC	AAT	CGG	CAG	TEA	CGA	AGC	CAG	CGT	ACT	CGC	ATC	TCT	CGA	270
	S	T	N	R	Q	S	G	R	Q	P	T	P	I	S	P	
271	OCT	CGA	ACA	GAC	AGT	CGT	CGT	CAG	CGC							297
	P	L	R	D	S	H	P	Q	A							

Figure 2 Nucleotide and derived amino acid sequence of PreS1(21-119aa) region gene fragment inserted into the expression vector pET-28a-preS1.

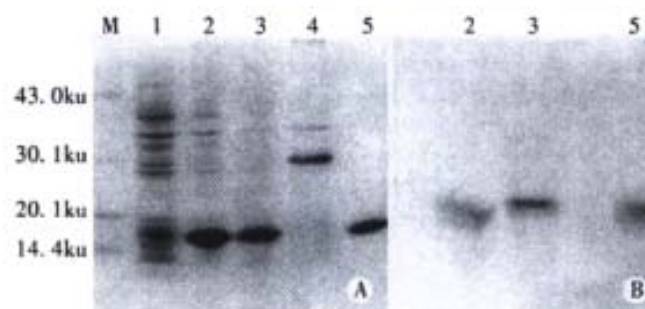


Figure 3 Expression and intracellular location of preS1(21-119aa) in *E. Coli*. BL21(DE3)plysS cells. Protein samples were subjected to 15% SDS-PAGE and stained with Commassia brilliant blue (A), and the duplicate gel was electrobotted onto a nitrocellulose membrane for western analysis (B). Lane M: molecular mass standards. Lane 1-2 are culture lysates of uninduced BL21 cells (lane 1) and induced BL21 cells (lane 2). Lane 3,4: Supernatant (soluble) and precipitate (insoluble) fractions, respectively; Lane5: purified fusion protein by Ni²⁺-IDA-sepharose 6B.

Purification and antigenicity analysis of the preS1(21-119aa) fusion protein

The fusion protein was purified by affinity chromatography on Ni²⁺-IDA sepharose 6B column as described in Materials and Methods. The purity of purified fusion proteins was evaluated to be over 90% (Lane 5, Figure 3). In order to analyze antigenicity of the fusion proteins, microtiter plates were coated with stepwise diluted solutions (from 2500ng to 10ng per well) of purified preS1(21-119aa) protein, GST-preS1(21-47aa) or artificially synthesized preS1(21-47aa) peptide. Direct ELISA showed that they all reacted well with the preS1-specific mAb 125E11 in a dose-dependent manner, meanwhile the antigenicity of preS1(21-119aa) protein was better than GST-preS1(21-47aa) and much better than synthesized preS1(21-47aa) peptide (Figure 4).

Detection of anti- preS1(21-119aa) antibodies in sera from hepatitis B patients

In order to observe specificity of established indirect ELISA, anti-preS1 antibodies positive serum (confirmed by Western Blotting) was preincubated with preS1(21-119aa) fusion protein and used to test. The result showed in a drop of the extinction to a value close to the negative control, thus demonstrating specificity of the method (Figure 5).

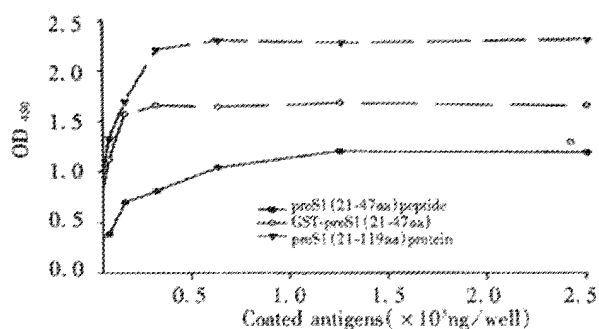


Figure 4 Immunoreactivity of preS1(21-119aa), GST-preS1(21-47aa) peptide. Microtiter plate was coated with different amount (10-2500ng) of the purified preS1 proteins or peptide. Then direct ELISA was performed.

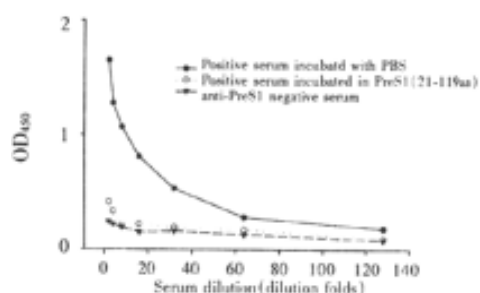


Figure 5 Specificity test of indirect ELISA for detection of anti-preS1 antibodies

In order to inspect established indirect ELISA, 192 serum specimens were collected from patients admitted to the Rui-Jin Hospital, Shanghai Second Medical University. Among them, there were 92 serum specimens with clinical and biochemical evidence of hepatitis B; and 100 sera of individuals without any markers of HBV infection and with normal liver function were assigned as negative controls. Additionally, 3 sera known to contain antibodies against preS1(21-

119aa) with different level tested by Western analysis were used as positive controls. Through the indirect ELISA based on recombinant preS1(21-119aa) fusion protein, anti-preS1 antibodies were detected in none of 100 HBV negative controls. In HBsAg positive individuals (Table 1), anti-preS1 antibodies were noted in more than half of patients with acute hepatitis before or after recovery, but only found in a few of patients with chronic hepatitis, and the level of anti-preS1 antibodies had significant difference between acute hepatitis patients and chronic hepatitis patients (*t* test, $P < 0.01$).

Table 1 Anti-preS1 antibodies in HBV-infected patients detected by indirect biotin-labeled protein A ELISA

Subjects	n	anti-preS1 Ab(+)	positive/%
Acute hepatitis			
Before recovery(HBsAg+)	16	10	62.5
After recovery (HBsAg-)	17	9	52.9
Chronic carriers			
Healthy chronic carriers	30	1	3.3
Chronic hepatitis	29	2	6.9
Total	92	22	23.9
Control (negative for all HBV markers)	100	0	0.0

Follow-up study

Diagnosed by clinical symptoms and serological profile, the inpatients for follow-up study were assigned to 10 acute hepatitis patients and 11 chronic hepatitis patients. Sera from 21 hepatitis B inpatients were collected at monthly intervals in half a year and anti-preS1 antibodies were detected by indirect ELISA. In Figure 6A, a typical profile of an acute episode of hepatitis B followed by seroconversion to anti-preS1 are presented. HBV-DNA and preS1 antigen were detectable simultaneously in the acute phase of the disease. Anti-preS1 developed early in infection, still in the presence of low level of preS1 antigen, and climbed the highest with disappearance of HBV-DNA and preS1 antigen. The results of detection of the other serological markers showed that anti-HBe and antiBs in sera of patients was followed by appearance of anti-preS1 antibodies.

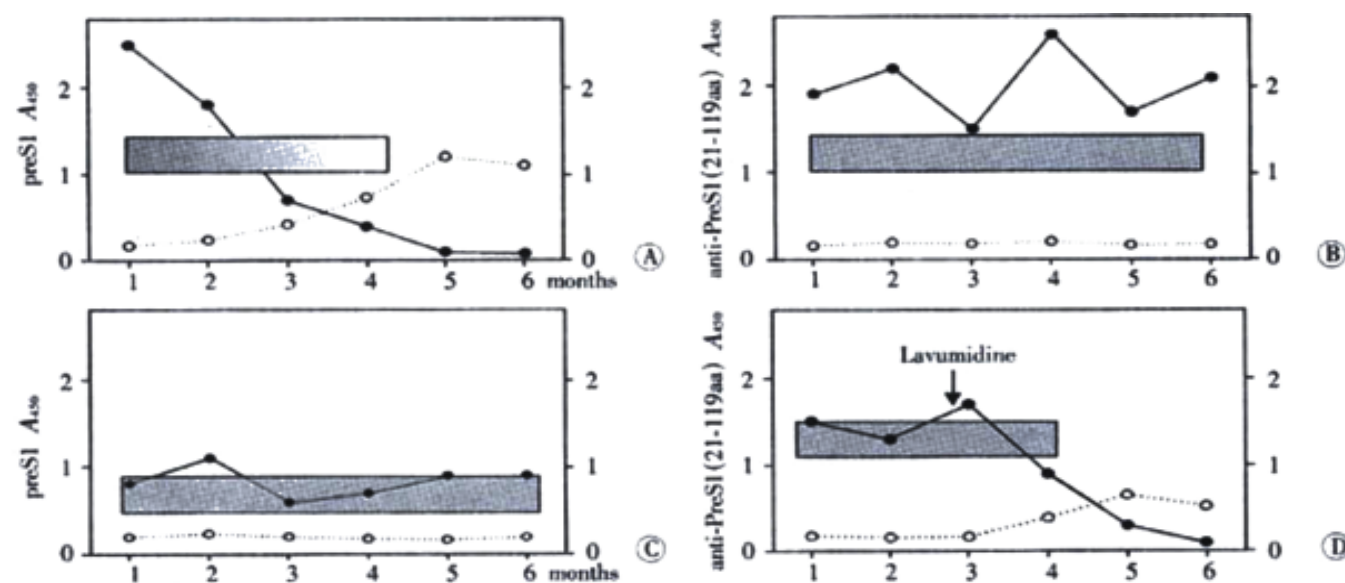


Figure 6 The profiles of serologic markers during acute chronic HBV infection with immuno-diagnosis for preS1 antigen and anti-preS1 (21-119aa) antibodies. A: Typical serologic profile of HBV markers during acute infection, with disappearance of preS1 antigen and seroconversion to anti-preS1(21-119aa) antibodies; elimination of HBV-DNA in 2-4 months from the appearance of antibodies. B: Chronic patients with HBeAg+ serologic profile; high level of preS1 antigen and HBV-DNA but absence of anti-preS1(21-119aa) antibodies. C: Chronic patients with anti-HBe+ serologic profile; low level of preS1 domain and HBV-DNA and absence of anti-preS1(21-119aa) antibodies. D: One patient persisting of HBsAg, HBeAg and preS1 for almost 3 years until treated with Lamivudine. Appearance of anti-preS1(21-119aa) antibodies with simultaneous health improvement; disappearance of HBV-DNA and declining level of preS1 antigen in serum. OD₄₅₀ value of Y axis (‘•’ preS1 antigen and ‘•’ anti-preS1 antibody) was mean value of inpatients in every group; different shade (■) in the rectangle (A) represented different level of HBV-DNA in patients.

Ten chronic hepatitis B inpatients were divided into two groups: one group was healthy chronic carriers (Figure 6B) who were seropositive HBeAg and high level of HBV-DNA and preS1 antigen; the other group was chronic hepatitis B patients (Figure 6C) who had seropositive anti-HBe and low level of HBV-DNA and preS1 antigen during the course of the disease. During follow-up period, anti-preS1 antibodies were not found and there were no apparent improvement in both groups. Interestingly, a patient (Figure 6.D) treated with lavumidine, a anti-HBV-DNA replication agent, was different from the other chronic patients. Seroconversion of preS1 antigen to anti-preS1 antibodies was observed after lavumidine treatment. Although no elimination of HBsAg was observed in this patient, the development of anti-preS1 response correlated well with improvement in health.

DISCUSSION

The PreS1 domain is found exclusively in LHBs, which is a major component of the envelope of mature virions, but it is significantly less represented in subviral particles of HBV^[5]. These findings suggest that PreS1 domain is located on the out surface of the virion and thought to be involved in virus-host cell interaction^[33-35]. Moreover, a sequence between amino acid residues 21 and 47 of the PreS1 domain was found to be the dominant binding site for hepatocytes^[9, 36-38]. PreS1 domain induces an immune responses in patients recovering from HBV infection and are considered to be essential in initiating the clearance of the infectious virus for recovery from HBV infection^[19, 39]. Above materials indicate that the anti-preS1 antibodies in the serum of hepatitis B patients may well be a new serological marker for clinical diagnosis of hepatitis B. Previous experimental data showed that none of important epitopes were found in preS1(1-20aa) fragment. Therefore, in present study preS1(21-119aa) sequence of HBV (adr subtype) envelope protein was chosen for recombinant expression and application for detection of anti-preS1 antibodies.

Under the control of inducible T₇ promoter, preS1(21-119aa) fusion protein was highly expressed in soluble form by the expression plasmid pET-28a-preS1 transfected BL21(DE3)plysS cells, and was easily purified by single step of affinity chromatography, owing to His6 tags on both terminus of preS1(21-119aa) sequence. The antigenic properties of the recombinant preS1(21-119aa) protein were determined by the reactivity with anti-preS1 monoclonal antibody 125E11, which recognizes a linear preS1 sequence between 21aa and 47aa^[21], and it is suitable for identification of preS1 proteins containing preS1(21-47aa) fragment.

Recently, Wei *et al*^[40] reported that they have expressed preS1(21-47aa) fusion proteins, which were successfully used in preliminary trial to detect anti-preS1(21-47aa) antibody. Because there are more epitopes in preS1(21-119aa) sequence, ELISA established in this study was much better in sensitivity compared with the assay based on preS1(21-47aa) fusion proteins as coated antigen. In this study, streptavidin-biotin system was introduced into ELISA, and this system has been used widely to detect immunoglobulin^[41, 42]. Protein A is known to bind IgG in human and several species of animals via the Fc portion of the IgG molecule^[43]. In our experimental condition, the sensitivity and specificity of ELISA based on biotin labeled protein A were much improved than ELISA based on anti-human IgG.

Clinical follow-up results showed that appearance of anti-preS1 antibody in the course of most acute hepatitis patients could predict the clearance of HBeAg and disappearance of preS1 dominants and HBV-DNA^[44, 45] followed by elimination of HBsAg and seroconversion to anti-HBs. The antibodies directly against preS1 region are distinct from anti-HBs, and anti-preS1 response developed after onset of the symptom in-patients and early than other HBV-related immune-responses^[46, 47]. The role of anti-preS1 antibodies might be neutralization of HBsAg with preS1-coded epitopes (particularly infective HBV virions), as the antibodies were found in most cases of

acute hepatitis followed by recovery^[48]. Anti-preS1 antibodies were hardly observed in patients with acute hepatitis progressing to chronic disease and in chronic hepatitis patients with continuing presence of preS1 domain and seropositive of HBeAg or anti-HBe^[49, 50]. But anti-preS1 antibodies was detected in a few patients with chronic aggressive hepatitis undergoing treatment with antiviral agents, and the appearance of the antibodies correlated well with healthy improvement^[51, 52]. The apparent prognostic implications of anti-preS1 antibodies are of interest in screening for this marker in hepatitis B patients.

In conclusion, the study suggested that presence of antibodies against preS1(21-119aa) region in serum during acute infection may indicate subsequent recovery. Through detection of anti-preS1(21-119aa) antibodies based on biotin-labeled protein A indirect ELISA and follow-up study, it afforded some information about the state and future prognosis of hepatitis B patients. The detection system has potential to be developed to a new kit for diagnosis and prognosis of hepatitis B patients.

REFERENCES

- 1 Worman HJ, Lin F, Mamiya N, Mustacchia PJ. Molecular biology and the diagnosis and treatment of liver diseases. *World J Gastroenterol* 1998; 4: 185-191
- 2 Xu KC, Wei BH, Yao XX, Zhang WD. Recent therapy for chronic hepatitis B by combined traditional Chinese and western medicine. *Shijie Huaren Xiaohua Zazhi* 1999; 7:970-974
- 3 Wu XN. Update therapy of chronic hepatitis B in China: recent progress. *China Natl J New Gastroenterol* 1996; 2:65-68
- 4 Yu LC, Gu CH. Mutation of hepatitis B virus and its association with liver disease. *Shijie Huaren Xiaohua Zazhi* 1999; 7:978-979
- 5 Cho EW, Park JH, Yoo OJ, Kim KJ. Translocation and accumulation of exogenous hepatitis B virus PreS surface antigen in the cell nucleus. *J Cell Sci* 2001; 114:1115-1123
- 6 Pride MW, Bailey CR, Muchmore E, Thanavala Y. Evaluation of B and T-cell response in chimpanzees immunized with Hepagene, a hepatitis B vaccine containing pre-S1, pre-S2 gene products. *Vaccine* 1998; 16:543-550
- 7 Milich DR, McLachlan A, Moriarty A, Thornton GB. A single 10 residue pre-S(1) peptide can prime T-cell help for antibody production to multiple epitopes within the pre-S-(1), pre-S-(2) and S regions of HBsAg. *J Immunol* 1987; 138:4457-4465
- 8 Yang JY, Hui JY, Li GD, Wang Y, Yuan HY, Li YY. Expression of the recombinant hepatitis B virus surface antigen carrying PreS epitopes in *Pichia pastoris*. *Shengwu Huaxue Yu Shengwu Wuli Xuebao* 2000; 32:139-144
- 9 Bock CT, Tillmann HL, Manns MP, Trautwein C. The Pre-S region determines the intracellular localization and appearance of hepatitis B virus. *Hepatology* 1999; 30:517-525
- 10 Neurath AR, Seto B, Strick N. Antibodies to synthetic peptides from the preS1 region of the hepatitis B virus (HBV) envelop (env) protein are virus-neutralizing and protective. *Vaccine* 1989; 7:234-236
- 11 Park JH, Cho EW, Lee YJ, Shin SY, Kim KL. Determination of the protective effects of neutralizing anti-hepatitis B virus (HBV) immunoglobulins by epitope mapping with recombinant HBV surface antigen protein. *Microbiol Immunol* 2000; 44:703-710
- 12 Kuroki K, Floerani M, Mimms LT, Ganem D. Epitope mapping of the preS1 domain of the hepatitis B virus large surface protein. *Virology* 1990; 176:620-624
- 13 Maeng CY, Ryu CJ, Gripon P, Guguen-Guillouzo C, Hong HJ. Fine mapping of virus-neutralizing epitopes on hepatitis B virus preS1. *Virology* 2000; 270:9-16
- 14 Ferrari C, Cavalli A, Penna A, Valli A, Bertoletti A, Pedretti G, Pilli M, Vitali P, Neri TM, Giuberti T. Fine specificity of the human T-cell response to the hepatitis B virus preS1 antigen. *Gastroenterology* 1992; 103:255-263
- 15 Le Seyec J, Chouteau P, Cannie I, Guguen-Guillouzo C, Gripon P. Infection process of the hepatitis B virus depends on the presence of a defined sequence in the pre-S1 domain. *J virol* 1999; 73:2052-2057
- 16 Borisova G, Borschukova O, Skrastina D, Dislers A, Ose V, Pumpens P, Grens E. Behavior of a short preS1 epitope on the surface of hepatitis B core particles. *Biol Chem* 1999; 380:315-324
- 17 Coursaget P, Buisson Y, Bourdil C, Yvonnet B, Molinie C, Diop MT, Chiron JP, Bao O, Diop-Mar I. Antibody response to preS1 in hepatitis B virus-induced liver disease and after immunization. *Res Virol* 1990; 141:563-570
- 18 Ryu CJ, Kim YK, Hur H, Kim HS, Oh JM, Kang YJ, Hong HJ. Mouse monoclonal antibodies to hepatitis B virus preS1 produced after immunization with recombinant preS1 peptide. *Hybridoma* 2000; 19:185-189

- 19 Prange R, Werr M. DNA-mediated immunization to hepatitis B virus envelope proteins: preS antigen secretion enhances the humoral responses. *Vaccine* 1999; 17:617-623
- 20 Wu XF, Zhou YZ, Feng ZM, Li ZP, Xia SY. Cloning and restriction mapping of human HBV genome seratype adr. *Zhongguo kexue (B)* 1983; 26:954-960
- 21 Yang HL, Jin Y, Cao HT, Xu X, Li GD, Wang Y, Zhang ZC. Affinity purification of HBV surface antigen carrying preS1 region. *Shengwu Huaxue Yu Shengwu Wuli XueBao* 1996; 28: 412-417
- 22 Yang HL, Cao HT, Li MY, Ping BF, Li GD, Wang Y, Zhang ZC. Development of the diagnostic kit to detect preS1 protein-marker of the intact Hepatitis B Virus Dane particle. *Shanghai Yixue Jianyan Zazhi* 1995; 10:204-206
- 23 Sambrook J, Fritsch EF, Manniatis T. Molecular cloning: a laboratory manual. (2nd ed). *Cold Spring Laboratory Press* 1989:25-98
- 24 Park JH, Na SY, Lee HH, Lee YJ, Kim KL. Detection of pET-vector encoded, recombinant S-tagged proteins using the monoclonal antibody ATOM-2. *Hybridoma* 2001; 20:17-23
- 25 Nunez E, Wei X, Delgado C, Rodriguez-Crespo I, Yelamos B, Gomez-Gutierrez J, Peterson DL, Gavilanes F. Cloning, expression, and purification of histidine-tagged preS domains of hepatitis B virus. *Protein Expr Purif* 2001; 21:183-191
- 26 Kittigul L, Temprom W, Sujirarat D, Kittigul C. Determination of tumor necrosis factor-alpha levels in dengue virus infected patients by sensitive biotin-streptavidin enzyme-linked immunosorbent assay. *J Virol Methods* 2000; 90:51-57
- 27 Frey A, Meckelein B, Externest D, Schmidt MA. A stable and highly sensitive 3', 3', 5', 5'-tetramethylbenzidine-based substrate reagent for enzyme-linked immunosorbent assays. *J Immunol Methods* 2000; 233: 47-56
- 28 Fang JN, Jin CJ, Cui LH, Quan ZY, Choi BY, Ki MR, Park HB. A comparative study on serologic profiles of virus hepatitis B. *World J Gastroenterol* 2001; 7:107-110
- 29 Zhou P, Zhang MS, Cai Q, Chen YC, Li XJ, Yu JG, Guan J, Liu CL. Detection of HBV DNA in serum of patients with HBV infection by polymerase chain reaction. *Shijie Huaren Xiaohua Zazhi* 1998; 6:263-264
- 30 Wang PZ, Zhang ZW, Zhou YX, Bai XF. Quantitative PCR detection of HBV-DNA in patients with chronic hepatitis B and its significance. *Shijie Huaren Xiaohua Zazhi* 2000; 8:755-758
- 31 Zheng Z, Yang SW, Xiao W, Sun P, Li XJ, Hu YQ. Evaluation of the HBV in HbsAg negative inpatients by HBV DNA measured with PCR. *World J Gastroenterol* 1998; 4(suppl 2):77
- 32 Le Guillou DB, Duclos-Vallee JC, Eberle F, Capel F, Petit MA. Evaluation of an enzyme-linked immunosorbent assay for detection and quantification of hepatitis B virus PreS1 envelope antigen in serum samples: comparison with two commercial assays for monitoring hepatitis B virus DNA. *J viral Hepat* 2000; 7:387-392
- 33 Kuijpers L, Koens M, Murray-Lyon I, Coleman JC, Karayiannis P, Thomas HC, Zanetti A, Cargnel A, Harrison TJ, Zukerman AJ. Pre-S proteins in hepatitis B. *J Med Virol* 1989; 28: 47-51
- 34 Chen K, Han BG, Ma XK, Zhang HQ, Meng L, Wang GH, Xia F, Song XG, Ling SG. Establishment and preliminary use of hepatitis B virus preS1/2 antigen assay. *World J Gastroenterol* 1999; 5:550-552
- 35 Choi IH, Park SG, Chung JH, Kim JJ, Hong HJ. Generation of human Fab monoclonal antibodies against preS1 of hepatitis B virus using repertoire cloning. *Hybridoma* 1998; 17:535-540
- 36 Neurath AR, Kent SB, Strick N, Parker K. Identification and chemical synthesis of a host cell receptor binding site on hepatitis B virus. *Cell* 1986; 46:429-436
- 37 Hui J, Mancini M, Li G, Wang Y, Tiollais P, Michel ML. Immunization with a plasmid encoding a modified hepatitis B surface antigen carrying the receptors binding site of hepatocytes. *Vaccine* 1999; 17: 1711-1718
- 38 Ono M, Morisawa K, Nie J, Ota K, Taniguchi T, Saibara T, Onishi S. Transactivation of transforming growth factor alpha gene by hepatitis B virus preS1. *Cancer Res* 1998; 58:1813-1816
- 39 Hu YP, Yao YC, Li JX, Wang XM, Li H, Wang ZH, Lei ZH. The cloning of 3' truncated preS/S gene from HBV genomic DNA and its expression in transgenic mice. *World J Gastroenterol* 2000; 6:734-737
- 40 Wei J, Liu XJ, Li GD, Wang Y, Wang YQ, Lu ZM, Zhang ZC. Expression, Purification and Preliminary Clinical Use of Recombinant HBsAg GST-PreS1(21-47aa) Fusion Proteins. *Shengwu Huaxue Yu Shengwu Wuli XueBao* 2001; 33:379-385
- 41 Bolton J, Sanders J, Oda Y, Chapman C, Konno R, Furmaniak J, Rees Smith B. Measurement of thyroid-stimulating hormone receptor autoantibodies by ELISA. *Clin Chem* 1999; 45:2285-2287
- 42 Santora KE, Nelson SA, Lewis KA, LaRochelle WJ. Avidin- or streptavidin-biotin as a highly sensitive method to stain total protein on membranes. *Mol Biotechnol* 2000; 15:161-165
- 43 Prual CA, Brubaker KD, Leach RM, Gay CV. Detection of endogenous biotin-containing proteins in bone and cartilage cells with streptavidin systems. *Biochem Biophys Res Commun* 1998; 247:312-314
- 44 Tang RX, Gao FG, Zeng LY, Wang YW, Wang YL. Detection of HBV DNA and its existence status in liver tissues and peripheral blood lymphocytes from chronic hepatitis B patients. *World J Gastroenterol* 1999; 5:359-361
- 45 Reshetnyak VI, Sharafanova TI, Ilchenko LU, Golovanova EV, Poroshenko GG. Peripheral blood lymphocytes DNA in patients with chronic liver diseases. *World J Gastroenterol* 2001; 7:235-237
- 46 Heermann KH, Goldmann U, Schwartz W, Seyffarth T, Baumgarten H, Gerlich WH. Large surface proteins of hepatitis B virus containing the pre-S sequence. *J Virol* 1984; 52:396-402
- 47 Yang JY, Jin J, Kong YY, Wei J, Zhang ZC, Li GD, Wang Y, Yuang HY, Li YY. Purification and characterization of recombinant hepatitis B surface antigen SS1 expressed in *Pichia pastoris*. *Shengwu Huaxue Yu Shengwu Wuli XueBao* 2000; 32:503-508
- 48 Milich DR, Thornton GB, Neurath AR, Kent SB, Michel ML, Tiollais P, Chisari FV. Enhanced immunogenicity of pre-S region of hepatitis B surface antigen. *Science* 1985; 228:1195-1199
- 49 Mimms LT, Floreani M, Tyner J, Whitters E, Rosenlof R, Wray L, Goetze A, Sarin V, Eble K. Discrimination of hepatitis B virus (HBV) subtypes using monoclonal antibodies to the preS1 and preS2 domains of the viral envelop. *Virology* 1990; 176:604-619
- 50 Pontisso P, Ruvoletto MG, Gerlich WH, Heermann KH, Bandini R, Alberti A. Identification of a attachment site for human liver plasma membranes in hepatitis B virus particles. *Virology* 1989; 173:522-530
- 51 Klinkert MQ, Theilmann L, Pfaff E, Schaller H. Pre-S1 antigens and antibodies early in the course of acute hepatitis B virus infection. *J Virol* 1986; 58:522-525
- 52 Milich DR. Genetic and molecular basis for T- and B- cell recognition of hepatitis B viral antigen. *Immune Rev* 1987; 99:71-103

Edited by Wang JH and Xu XQ

• VIRAL LIVER DISEASES •

Methodologic research on TIMP-1, TIMP-2 detection as a new diagnostic index for hepatic fibrosis and its significance

Qing-He Nie, Yong-Qian Cheng, Yu-Mei Xie, Yong-Xing Zhou, Xian-Guang Bai, Yi-Zhan Cao

Qing-He Nie, Yong-Qian Cheng, Yu-Mei Xie, Yong-Xing Zhou, Bai-Xian Guang, Yi-Zhan Cao, The Centre of Diagnosis and Treatment for Infectious Disease of Chinese PLA, Tangdu Hospital, Fourth Military Medical University, Xi'an 710038, Shanxi Province, China

Supported by the Postdoctoral Science Foundation of China, No. 1999-10 State Postdoctoral Foundation Commission

Correspondence to: Dr. Qing-He Nie, The Centre of Infectious Disease Diagnosis and Treatment of Chinese PLA, Tangdu Hospital, Fourth Military Medical University, Xi'an 710038, Shaanxi Province, China. nieqinghe@hotmail.com

Telephone: +86-29-3377595

Received 2001-11-02 Accepted 2002-01-15

Abstract

AIM: To set up a new method to detect tissue inhibitors of metalloproteinase-1 and -2 (TIMP-1 and TIMP-2) in sera of patients with hepatic cirrhosis, and to investigate the expression and location of TIMP-1 and TIMP-2 in liver tissue of patients with hepatic cirrhosis, and the correlation between TIMPs in liver and those in sera so as to discuss whether TIMPs can be used as a diagnosis index of hepatic fibrosis.

METHODS: The monoclonal antibodies (McAbs) of TIMP-1 and TIMP-2 were used to sensitize erythrocytes, and solid-phase absorption to sensitized erythrocytes (SPASE) was used to detect TIMP-1 and TIMP-2 in the sera of patients with hepatic cirrhosis. Meanwhile, with the method of *in situ* hybridization and immunohistochemistry, we studied the mRNA expression and antigen location of TIMP-1 and TIMP-2 in the livers of 40 hepatic cirrhosis patients with pathologic diagnosis.

RESULTS: With SPASE, they were 16.4% higher in the acute hepatitis group, 33.3% higher in the chronic hepatitis group, and the positive rates were 73.6% and 61.2% respectively in sera of hepatic cirrhosis patients, which were remarkably higher than those in chronic hepatitis and acute hepatitis group ($P < 0.001$). In 40 samples of hepatic cirrhosis tissues, all of them showed positive expression of TIMP-1 and TIMP-2 mRNA detected with immunohistochemistry or *in situ* hybridization (positive rate was 100%). Expression of TIMPs in different degrees could be found in liver tissue with cirrhosis. TIMPs were located in cytoplasm of liver cells of patients with hepatic cirrhosis. There was a significant correlation between serum TIMPs level and liver TIMPs level.

CONCLUSION: SPASE is a useful method to detect the TIMP-1 and TIMP-2 in sera of patients with hepatic cirrhosis, and TIMP-1 and TIMP-2 can be considered as a useful diagnostic index of hepatic fibrosis, especially TIMP-1.

Nie QH, Cheng YQ, Xie YM, Zhou YX, Bai XG, Cao YZ. Methodologic research on TIMP-1, TIMP-2 detection as a new diagnostic index for hepatic fibrosis and its significance. *World J Gastroenterol* 2002;8(2):282-287

INTRODUCTION

SPASE (solid-phase absorption to sensitized erythrocytes) is an immunological detecting method possessing the similar principle with ELISA (enzyme-linked immunosorbent assay) and SPRIA (solid-phase radioimmunoassay)^[1]. Erythrocytes sensitized by antibodies are used as the indicator, taking the place of enzyme or isotope labeled antibody. The result is judged by the hemagglutination phenomena. SPASE has the same sensitivity and specificity as ELISA and SPRIA, and is so simple and rapid as RPHA (reverse passive hemagglutination)^[2,3]. The monoclonal antibodies (McAbs) of TIMP-1 and TIMP-2 were used to sensitize erythrocytes. SPASE was used to detect TIMP-1 and TIMP-2 in the sera of patients with hepatic cirrhosis, and proved pretty well. At the same time, with the method of *in situ* hybridization and immunohistochemistry, the mRNA expression and antigen location of TIMP-1 and TIMP-2 in the livers of 40 hepatic cirrhosis patients diagnosed by pathology were studied.

MATERIALS AND METHODS

Materials

The U shape 96 well plexiglass microhemagglutination plate was used as the solid phase support. The solid-phase antibody (McAbs of TIMP-1 and TIMP-2) was purchased from Maxim Biologic Technology Corp, America, (No: MAB-0282, MAB-0283). Formaldehyde-chicken or sheep erythrocytes were sensitized by TIMP-1 and TIMP-2 McAb, according to the method introduced by Han^[4] to prepare for sensitized erythrocytes. The concentration of McAbs was 50-100 mg·L⁻¹. The positive samples that simulated positive sample were obtained from the sera of hepatic cirrhotic patients pathologically diagnosed, and normal human sera were used as the negative control, and PBS as the blank control. To test the thermal stability, McAb was bathed at 60°C water with different time, and its activity was detected by RIA.

We collected 408 serum samples from Tangdu Hospital and Xijing Hospital affiliated to the Fourth Military Medical University, and Southwest Hospital affiliated to the Third Military Medical University, The First and Fourth Hospitals of Chinese PLA. The diagnosis of viral hepatitis accorded with the diagnosis standard revised by the Fifth National Academic Conference^[5] for Infectious and Parasitic Diseases. According to the standard, there were 128 serum samples of acute hepatitis, 174 of chronic hepatitis, and 106 of hepatic cirrhosis. 40 liver samples were collected from the pathologic departments of Tangdu and Xijing Hospitals affiliated to the Fourth Military Medical University. All the 40 samples were proved pathologically with nodular hepatic cirrhosis. Male, 40; female, 8; the mean age, 50 years.

Methods

Procedure of SPASE 50 mg·L⁻¹ McAb were added into U shape 96 well plexiglass micro hemagglutination plate (100 μL·well), to make one layer and the unnecessary solution should be removed, the sparing solution could be reused, and then dried under room

temperature, fixed at 56°C, washed with PBS 3-4 times, to get rid of the unfixed McAb molecule. 100μL per well of the prepared serum sample (diluted at the ratio volume of 1:10) was added, reacted at 37°C for 1h, washed with PBS 3-4 times, and then 50μL per well of McAb sensitized erythrocytes were added. After shaking mixed, they were standing for 1h at 37°C or 2h at room temperature. The results were determined according to the absorbed condition of erythrocytes (like RPHA). The erythrocytes depositing on the bottom of the well was considered as negative result, showing a spot or a little circle in the center of the well without scattered erythrocytes around. The positive result was determined when the erythrocytes were absorbed and a layer spread on the bottom of the well.

Immunohistochemical staining The laboratory procedure referred to references 6-12.SP immunostaining was performed as described by streptomycin avidin-peroxidase immunochemistry kit (purchased from Maxim Biological Technology Company). Briefly, the liver samples were embedded with paraffin, and serial sections at 4μm thickness were prepared. Paraffin was removed from the sections with xylene and rehydrated with graded ethanol. After the antigens were repaired, unspecific immunoglobulin-binding sites were blocked by a 20min preincubation with 100mL·L⁻¹ normal human sera. The sections were then incubated with monoclonal antibody against TIMP-1 or TIMP-2 at 4°C overnight, and then secondary antibody was added at 37°C for 30-40min, avidin-peroxidase at 37°C for 20min, and finally DAB was added to be stained. After the sections were washed several times, they were counterstained with hematoxylin, dehydrated with ethanol, rinsed in xylene, and the sections were mounted with gum for microscopic examination and photography. To make sure of the reliability and specificity of the result of immunohistochemical staining, rabbit sera and PBS were used to replace the first antibody in our control test. 10 normal liver tissues were also used as the normal control samples.

Liver tissue *in situ* hybridization The investigation procedure referred to related references^[13-17]. The *in situ* hybridization kit was purchased from Boshide Biological Technology Limited Company (Wuhan, China, No. MK1549). *In situ* hybridization was performed according to the manufacturer's direction. Briefly, the paraffin embedded serial sections(thickness 4μm), were dried at 80°C, and their paraffin was removed by xylene and rehydrated with graded ethanol. The sections were acidified in HCl for 30min, and blocked in 3mL 300mL·L⁻¹H₂O₂ for 10min before digestion in proteinase K for 30min, and then dehydrated with graded ethanol. After prehybridization at 37-40°C for 2h, the labeled cDNA probes of TIMP-1 and TIMP-2 were denatured in hybridization buffer at 95°C for 10min, then -20°C for 10min, added on tissues which had been prehybridized at 37°C overnight. Sections were washed in turn with 2×SSC, 1×SSC, 0.2×SSC, and Buffer I, blocking water was added at room temperature for 20min, and then rabbit anti-digoxin serum at 37°C for 60min, biotinylated goat anti-rabbit serum at 37°C for 30min, SABC at 37°C for 30min, finally DAB was added to be stained. After several times of washing, the sections were counterstained with hematoxylin, dehydrated with ethanol, rinsed in xylene, and mounted with gum for microscopic examination and photography. (1) Blank control: prehybridization solution was replaced by the cDNA probes of TIMP-1 and TIMP-2 to be hybridized with the positive liver sections; (2) Negative control: the *in situ* hybridization was performed with 10 normal liver sections.

Semi-quantitative index was used to determine the results of immunohistochemistry and *in situ* hybridization: no positive cells (-); positive cells occupied hepatocytes of hepatic lobule less than 1/3(+); 1/3~2/3(++); more than 2/3(+++).

RESULTS

Methodologic Optimization

The best laboratory condition and influence factors To study the related factor of sensitivity and specificity of this technique, the simulated positive samples were used, and we concluded that there were two main factors might directly influence the experiment condition. One was the concentration of coated antibodies and the other the density of sensitized erythrocytes. Much higher or less concentration of coated antibodies would decrease the sensitivity, while 50-100mg·L⁻¹ might be the best (Table 1). There was a close relation between the density of sensitized erythrocytes, which is the indicator, and at 2.5·L⁻¹ the sensitivity appeared to be the best (Table 2).

Degree of accuracy and repetitive test The coefficient of variation (CV) in one lot of samples in the same plate was 6.06%. The coefficient of variation (CV) in different lot of samples in different plate was 7.65%. Both of them were less than 10% (Table 3), which showed that this technique was provided with good degree of accuracy and repetition.

Table 1 Relationship between coated McAb and the sensitivity of SPASE

Coated McAb (mg·L ⁻¹)	Serum titer							Negative control
	1:1	1:10	1:20	1:50	1:100	1:200	1:500	
12.5	+++	++	+	-	-	-	-	-
25	++++	+++	++	+	-	-	-	-
50	++++	++++	++++	++++	++	+	-	-
100	++++	++++	++++	+++	++	+	-	-
200	++++	+++	+++	++	+	-	-	-
400	+++	++	++	++	+	-	-	-

Table 2 Relation between the density of sensitized erythrocytes and the sensitivity of SPASE

Density of sensitized erythrocytes	Serum titer							Negative control
	1:1	1:10	1:20	1:50	1:100	1:200	1:500	
1.5·L ⁻¹	+++	++	+	-	-	-	-	-
2.5·L ⁻¹	++++	++++	++++	+++	++	+	-	-
3.0·L ⁻¹	++++	++++	+++	++	+	+	-	-
6.0·L ⁻¹	+++	+++	++	+	-	-	-	-
10.0·L ⁻¹	++	+++	++	-	-	-	-	-

Table 3 Repetitive experiment of samples

	Well numbers	($\bar{x} \pm s$)	CV(%)
In the same lot	15	0.642±0.0389	6.06
In different lot	5	0.575±0.044	7.65

Table 4 Results of detecting TIMP-1 and TIMP-2 in different sera

Clinical type	n	TIMP-1		TIMP-2	
		Positive number	%	Positive number	%
Acute hepatitis	128	21	16.4	16	12.6
Chronic hepatitis	174	59	33.9	48	27.6
Hepatic cirrhosis	106	78	73.6	65	61.3

Clinical Application

Serum samples The 408 serum samples of patients with liver disease were used to detect TIMP-1 and TIMP-2 with SPASE. The

positive rates were 73.6% and 61.2% respectively, which were remarkably higher than those in chronic hepatitis and acute hepatitis group. There was a significant statistical difference ($P < 0.001$, Table 4).

Immunohistochemistry By immunohistochemistry detection, the positive signal as brown particles were scattered or diffused only in cytoplasm other than nuclei in liver cells. Table 5 represented the result of detecting TIMP-1 and TIMP-2 of 40 liver samples of hepatic cirrhosis, in which, for TIMP-1, 28 samples were (+++), 70.0% of cytoplasm; 4 were (++), 10.0%; 8 were (+), accounted for 20.0%. For TIMP-2, 22 samples were (+++), 55.0% of cytoplasm; 10 were (++), 25.0%; 8 were (+), 20.0%. 10 normal liver tissues were negative. There was no positive signal after abridging the first antibody or the second one, and there was no positive signal when the first antibody replaced by rabbit serum or PBS, which proved that the results of immunohistochemistry detecting were specific.

In situ hybridization The positive signal of *in situ* hybridization showed brown particles, and distributed in the cytoplasm, scattered or diffused. There was no positive signal in nuclei. All the 40 samples of hepatic cirrhosis tissues showed positive expression of TIMP-1 and TIMP-2 mRNA, and the positive rate was 100%. Table 6 showed the intensity of TIMP-1 and TIMP-2 mRNA expression in the liver samples. For TIMP-1 mRNA, 32 samples were (+++), 80.0% of cytoplasm; 6 were (++), 15.0%; 2 were (+), 5.0%. Of TIMP-2 mRNA, 22 samples were (+++), in which 55.0% of cytoplasm; 16 were (++), accounted for 40.0%; 2 were (+), 5.0%. The expression intensity of TIMP-1 mRNA was stronger than that of TIMP-2 mRNA. There was no positive signal when TIMP-1 cDNA probes or TIMP-2 cDNA probes were replaced by the prehybridization solution, and when the 10 normal liver tissues were hybridized with TIMP-1 cDNA probes or TIMP-2 cDNA probes, all were negative. These proved that the results of *in situ* hybridization were specific.

Table 5 Expressing of TIMP-1 and TIMP-2 in liver

Group	n	TIMP-1				TIMP-2			
		-	+	++	+++	-	+	++	+++
Normal group	10	10	0	0	0	10	0	0	0
Hepatic cirrhosis	40	0	8	4	28	0	8	10	22

Table 6 Expressing of TIMP-1 mRNA and TIMP-2 mRNA in liver of hepatic cirrhosis

Group	n	TIMP-1				TIMP-2			
		+++	++	+	-	+++	++	+	-
Hepatic cirrhosis	40	32	6	2	0	22	16	2	0
Normal liver	10	0	0	0	10	0	0	0	10

DISCUSSION

SPASE is a new method used to detect the TIMP-1 and TIMP-2 in sera of patient with hepatic cirrhosis. During the setting up of this technique, we preliminarily tried to find out how to treat the influence factors and choose the condition. We consider that this method can not only possess both the advantages of SPA and IHT (indirect hemagglutination test), but also avoid the radiation pollution of RIA or cancer-causing danger of ELISA. Meanwhile, this method possesses many other advantages, such as wider range of usage, less influence factors, saving McAb, being easy to operate and judge detecting results. In a word, this is a specific, sensitive, rapid and economic method. There are two main factors that may influence the

laboratory condition. Firstly, lower concentration of coated antibodies may result in fewer antibodies combined on the surface of support, which won't be able to catch antigens, while higher density may result in overlap of antibodies on the surface of support, which will have effect on the space position of conjunction of antigens and antibodies, and then antigens can't be effectively caught. Secondly, acting as the indicator system, a reverse correlation exists between the density of sensitized erythrocyte and sensitivity of detection. When the density of sensitized erythrocyte is higher than $3 \cdot L^{-1}$, the detection sensitivity will be significantly decreased, while clarity of the result would be impaired if the density is lower than $1 \cdot L^{-1}$. Because the erythrocytes can only react with one layer of the agent on the surface of solid support, excessive erythrocytes didn't combine with agents and would deposit at the bottom of wells, then the judgment of the results would be affected. For this reason, a layer of the sensitized erythrocytes with adequate density is better. The density we used in practice is about $2.5 \cdot L^{-1}$, which is lower than that used in RPHA. In present study, the way of coating the antibodies was improved, and proved that the method of heating-fixed antibodies was feasible. Sheep erythrocytes and chicken erythrocytes sensitized by formaldehyde were detected with sensitization test, and no specific difference was observed except a little faster sedimentation rate of the former. This insured the source of erythrocytes.

The occurrence and progress of hepatic cirrhosis were the result of the interaction between hepatocytes and extracellular matrixes (ECM)^[18-25]. The increase of ECM synthesis and decrease of ECM degradation will result in excess deposition of ECM in liver. More important reason of the excess deposition of ECM is the decrease of ECM degradation in the late stage. The metrical metalloproteinases played a leading role during the degradation of ECM^[26-35]. MMPs were a group of zinc-ion dependent enzymes, which created conditions for further degradation of other proteinases though reducing the stability of helical structure of collagen and changing the secondary structure of substrates. TIMPs were a group of polypeptides with the ability of inhibiting the function of MMPs. TIMPs would inhibit the degradation of ECM through two main ways, which is non-covalent modification or conjugated with proenzyme. Research work showed that TIMP could be divided into four classes: TIMP-1, TIMP-2, TIMP-3, and TIMP-4. However, only TIMP-1 and TIMP-2 could be detected in liver^[37-44]. All the 40 samples of hepatic cirrhosis tissues, showed positive expression of TIMP-1 and TIMP-2, and the positive rate was 100%. TIMP-1 and TIMP-2 were expressed at the same time, and were located in the liver cytoplasm, not in the nuclei. The expression of TIMP-1 was more obvious than that of TIMP-2. No expression of related antigens of TIMP-1 and TIMP-2 were detected. All these indicated that TIMP-1 did play an important role in the development of liver fibrosis and liver cirrhosis. The inhibitory effect of MMPs was enhanced with the high level expressing of TIMP-1 and TIMP-2 which resulted in the decrease of degradation of ECM, the deposit of ECM and the development of liver fibrosis and liver cirrhosis. The cause of the higher expression of TIMP-1 probably lay in two main reasons. First, the different classes of MMP resulted in the different inhibition activity of TIMP to MMP. TIMP-1 to procollagenase (MMP1) and TIMP-2 to gelatinase -A (MMP2), and gelatinase -B (MMP9) had assumed stronger inhibition activity. During the degradation of ECM, the main one was MMP1, and collagens I,III were the main object of MMP1. Second, the promotion of TIMP-1 was 10 times more than TIMP-2 to the proliferation of cells (including fibroblast, epithelial cells, endothelial cells, and smooth muscle cells). Furthermore, this action had no relation with the inhibition action of TIMP to MMP^[45-59].

In situ hybridization was mainly used to observe the characteristics and accurate location of gene expression. The high sensitivity and strong specificity of this technique will be preferable to

study the pathogenesis of hepatic fibrosis and to demonstrate the diagnosis. Recently, digoxin has become a widely used non-isotope labeled compound characterized by its perfect specific and stability. Its sensitivity is almost the same as isotope, but without pollution. So, it is easily accepted and used to label TIMP-1 and TIMP-2 cDNA probe to detect the paraffin sections of liver. The results showed that this technique was high sensitive and specific. The rates of positive expressions of TIMP-1 and TIMP-2 were 80.0% and 55.0% respectively. The location of TIMPs expression was in cytoplasm of hepatocyte, except nuclei, and the mRNA expression of TIMP-1 was stronger than that of TIMP-2, which was in accordance with the results of immunohistochemistry, and further proved that the TIMPs played a key role in the development of hepatic fibrosis and hepatic cirrhosis.

It is now known that there is a noticeable increase of TIMP-1 in the injured liver, which takes place earlier and increases faster, therefore, more and more researchers has regarded it as the diagnostic index of hepatic fibrosis. Detecting TIMP-1 and TIMP-2 with SPASE was used as a quick laboratory diagnosis of hepatic fibrosis. The sera from hepatic cirrhosis patients pathologically confirmed and normal people served as positive and negative control respectively. The results of detecting TIMP-1 and TIMP-2 in the sera of 408 patients with hepatic disease showed that positive rate of TIMPs was higher in sera of hepatic cirrhosis patients than that of acute or chronic hepatitis ($P < 0.001$). TIMPs in sera of chronic hepatitis patients were apparently higher than those of acute hepatitis patients. This conclusion enumerated above was Supported by the detecting results of TIMP-1 and TIMP-2 by using immunohistochemistry and in situ hybridization.

Recently, Murawaki *et al*^[60-62] has detected TIMP-1 and TIMP-2 in sera of patients with chronic liver disease by means of ELISA, and found a good relation between TIMP-1 and TIMP-2 in sera and in liver. The sensitivity and specificity of TIMP-1 were higher than those of TIMP-2. In injured liver, especially in fibrotic liver, TIMP-1 predominated, and the degree of TIMP-1 was remarkably related to the severity of hepatic fibrosis. Compared with TIMP-1, the specificity and sensitivity of TIMP-2 were inadvisable for diagnosis of hepatic fibrosis. So, TIMP-1 was more important than TIMP-2 in the determination of histological change of hepatic fibrosis^[63-70]. This was proved by our study of the expression of related antigens and the location of mRNA of TIMP-1 and TIMP-2. The expression of related antigens in liver could be reflected through detecting TIMPs in sera. So, TIMP-1 and TIMP-2 could be considered as useful diagnostic index of hepatic fibrosis, especially TIMP-1. Because viral hepatitis is common in China^[71-99], liver fibrosis is the focus of research^[18-24,100,101]. So serum TIMP-1 and TIMP-2 will find wide use in practice in the future.

ACKNOWLEDGEMENT

I acknowledge the advice and help of Prof. Bo-Rong Pan!

REFERENCES

- Nie QH, Huang C, Zhang KR, Peng BM. SPASE for rapid detection of *Shigella flexneri* from fecal samples with monoclonal antibody. *Zhonghua Chuanranbing Zazhi* 1995;13:145-148
- Nie QH, Huang C, Zhang KR, Peng BM. Preparation of prevalent monoclonal antibodies of *Shigella flexneri* and their application in rapid diagnosis of shigellosis. Seventh International Congress on Rapid Methods and Automation in Microbiology and Immunology (LONDON). *Programme Abstracts* 1993:41
- Li CW. The modern immunochemistic technique. First ban. Shanghai: Shanghai Sci. & Tech. Publishing House 1992:235-239
- Han CY. Indirect hemagglutinative Technique. *Beijing: Sci Publi House* 1979:94-111
- The prevention and treatment program of viral hepatitis. *Zhonghua Neike Zazhi* 1995;34:788-791
- Nie QH, Xie Q, Hu DR, Li MD, Li L. The expression of hepatitis G virus-related antigens in the liver tissue of patients with HGV/GBV-C infection. *Di-san Junyi Daxue Xuebao* 1997;19:394-396
- Nie QH, Hu DR, Li MD, Xie Q. The expression of HGV/GBV-C or HCV related antigens in the liver tissue of patients coinfectd with hepatitis C and G viruses. *Shijie Huaren Xiaohua Zazhi* 2000;8:114-115
- Nie QH, Li MD, Hu DR, Li L. The expression of hepatitis G virus-related antigens in the liver tissues of with hepatitis patients. *Zhonghua Chuanranbing Zazhi* 2000;18:173-175
- Wang D, Shi JQ, Liu FX. Immunohistochemical detection of proliferating cell nuclear antigen in hepatocellular carcinoma. *China Natl J New Gastroenterol* 1997;3:101-103
- Zhang LF, Peng WW, Yao JL, Tang YH. Immunohistochemical detection of HCV infection in patients with hepatocellular carcinoma and other liver diseases. *World J Gastroenterol* 1998;4:64-65
- Yan JP, Liu JC, Ma XH, Jia JB, Zhao YC, Xu RL, Li CM, Han DW. Immunohistochemical study on basic fibroblast growth factor in experimental liver fibrosis. *Xin Xiaohuabingxue Zazhi* 1997;5:642-644
- Nie QH, Li L, Li MD, Hu DR. Clinical and immunopathological study on GB virus B (GBV-B) infection. *Shijie Huaren Xiaohua Zazhi* 2000;8: 775-781
- Nie QH, Li MD, Hu DR. Detection of hepatitis G virus RNA in liver tissue using digoxigenin labelled probe by in situ hybridization. *J Gastroenterol Hepatol* 1999;14:A365
- Liu YJ, Cong WM, Xie TP, Wang H, Shen F, Guo YJ, Chen H, Wu MC. Detecting the localization of hepatitis B and C virus in hepatocellular carcinoma by double in situ hybridization. *China Natl J New Gastroenterol* 1996;2:187-189
- Zhao GQ, Xue L, Xu HY, Tang XM, Hu RD, Dong J. In situ hybridization assay of androgen receptor gene in hepatocarcinogenesis. *World J Gastroenterol* 1998;4:503-505
- Qian QJ, Xue HB, Qu ZQ, Fang SG, Cao HF, Wu MC. In situ detection of tumor infiltrating lymphocytes expressing perforin and fas-ligand genes in human HCC. *World J Gastroenterol* 1999;5:12-14
- Nie QH, Hu DR, Li MD, Li L, Zhu YH. Detection of hepatitis G virus RNA in liver tissue using digoxigenin labelled probe by in situ hybridization. *Shijie Huaren Xiaohua Zazhi* 2000;8:771-774
- Friedman SL. The cellular basis of hepatic fibrosis: mechanism and treatment strategies. *N Engl J Med* 1993;328:1828-1835
- George DK, Ramm GA, Walker NI, Powell LW, Crawford DH. Elevated serum type IV collagen: a sensitive indicator of the presence of cirrhosis in haemochromatosis. *J Hepatol* 1999; 31: 47-52
- Kossakowska AE, Edwards DR, Lee SS, Urbanski LS, Stabblar AL, Zhang CL, Phillips BW, Zhang Y, Urbanski SJ. Altered balance between matrix metalloproteinases and their inhibitors in experimental biliary fibrosis. *Am J Pathol* 1998; 153: 1895-1902
- Arthur MJ, Mann DA, Iredale JP. Tissue inhibitors of metalloproteinases, hepatic stellate cells and liver fibrosis. *J Gastroenterol Hepatol* 1998; 13: S33-38
- Arthur MJ. Role of Ito cells in the degradation of matrix in liver. *J Gastroenterol Hepatol* 1995; 10: S57-62
- Arthur MJ. Collagenases and liver fibrosis. *J Hepatol* 1995; 22: S43-48
- Arthur MJ. Degradation of matrix proteins in liver fibrosis. *Pathol Res Pract* 1994; 190: 825-833
- Liu XS, Li DG, Lu HM, Xu QF. Effects of tetrandrine and verapamil on fibroblastic growth and proliferation. *China Natl J New Gastroenterol* 1997;3:70
- Wang YF, Li QF, Wang H, Mao Q, Wu CQ. Effects of vitamin E on experimental hepatic fibrosis in rats. *World J Gastroenterol* 1998;4:157
- Huang ZG, Zhai WR, Zhang YE, Zhang XR. Study of heterosera induced rat liver fibrosis model and its mechanism. *World J Gastroenterol* 1998;4:206-209
- Jia JB, Han DW, Xu RL, Gao F, Zhao LF, Zhao YC, Yan JP, Ma XH. Effect of endotoxin on fibronectin synthesis of rat primary cultured hepatocytes. *World J Gastroenterol* 1998;4:329-331
- Cheng ML, Wu YY, Huang KF, Luo TY, Ding YS, Lu YY, Liu RC, Wu J. Clinical study on the treatment of liver fibrosis due to hepatitis B by IFN α -1 and traditional medicine preparation. *World J Gastroenterol* 1999;5:267-269
- Du WD, Zhang YE, Zhai WR, Zhou XM. Dynamic changes of type I, III and IV collagen synthesis and distribution of collagen producing cells in carbontetrachloride induced rat liver fibrosis. *World J Gastroenterol* 1999;5:397-403
- Zhu YH, Hu DR, Nie QH, Liu GD, Tan ZX. Study on activation and cfos, cjun expression of in vitro cultured human hepatic stellate cells. *Shijie Huaren Xiaohua Zazhi* 2000;8:299-302
- Sun ZQ, Wang YJ, Quan QZ, Liu XF, Pan X, Jiang XL. Prevention and treatment action of tetrandrine on experimental liver fibrosis in rats. *Xin Xiaohuabingxue Zazhi* 1994;2:19-20
- Sun ZQ, Wang YJ, Quan QZ, Han GY, Jin XH. Change of serum phosphonate esterase in hepatic fibrosis in rats. *Xin Xiaohuabingxue Zazhi* 1994;2:206-207

- 34 Wang YJ, Sun ZQ, Quan QZ, Zhang ZJ. Controlled study of Cordyceps sinensis and colchicine on the antifibrosis effect of liver. *Xin Xiaohuabingxue Zazhi* 1994;2:208-209
- 35 Quan QZ, Sun ZQ, Li DG, Wang YJ, Che JT, Qi F, Fan P. Experimental and clinical study of calcium channel blockers on antifibrosis in chronic liver diseases. *Xin Xiaohuabingxue Zazhi* 1994;2:214-216
- 36 Olaso E, Friedman SL. Molecular regulation of hepatic fibrogenesis. *J Hepatol* 1998;29:836-842
- 37 Pinzari M, Marra F, Carloni V. Signal transduction in hepatic stellate cells. *Liver* 1998;18:2-13
- 38 Alcolado R, Arthur MJ, Iredale JP. Pathogenesis of liver fibrosis. *Clin Sci* 1997;92:103-112
- 39 Iredale JP. Tissue inhibitors of metalloproteinases in liver fibrosis. *Int J Biochem Cell Biol* 1997;29:43-54
- 40 Yang SM, Fang DC, Feng HF, Chen GM, Gao LQ. Diagnostic value of serum prolydase, procollagen type III and hyaluronic acid levels for liver fibrosis. *Xin Xiaohuabingxue Zazhi* 1995;3:27-28
- 41 Torres L, Garcia-Trevijano ER, Rodriguez JA, Carretero MV, Bustos M, Fernandez E, Eguinoa E, Mato JM, Avila MA. Induction of TIMP-1 expression in rat hepatic stellate cells and hepatocytes: a new role for homocysteine in liver fibrosis. *Biochim Biophys Acta* 1999;1455:12-22
- 42 George DK, Ramm GA, Walker NI, Powell LW, Crawford DH. Elevated serum type IV collagen: a sensitive indicator of the presence of cirrhosis in haemochromatosis. *J Hepatol* 1999;31:47-52
- 43 Arthur MJ, Iredale JP, Mann DA. Tissue inhibitors of metalloproteinases: role in liver fibrosis and alcoholic liver disease. *Alcohol Clin Exp Res* 1999;23:940-943
- 44 Li DG, Lu HM, Chen YW. Studies on anti liver fibrosis of tetrandrine. *Shijie Huaren Xiaohua Zazhi* 1999;7:171-172
- 45 Sakaida I, Uchida K, Hironaka K, Okita K. Prolyl 4-hydroxylase inhibitor (HOE 077) prevents TIMP-1 gene expression in rat liver fibrosis. *J Gastroenterol* 1999;34:376-377
- 46 Wang FS, Wu ZZ. Current situation in studies of gene therapy for liver cirrhosis and liver fibrosis. *Shijie Huaren Xiaohua Zazhi* 2000;8:371-373
- 47 Han GY, Jin XH, Wu CQ, Wang HF, Liu WJ. Alteration of serum phosphatase esterase in liver fibrosis in rats. *Xin Xiaohuabingxue Zazhi* 1996;4:369-370
- 48 Chen F, Chai WM. The progress of diagnosis and therapy for liver fibrosis during the latest three years. *Xin Xiaohuabingxue Zazhi* 1997;5:69-71
- 49 Yang YX, Kang JY. Mechanism and serum diagnosis of liver fibrosis. *Xin Xiaohuabingxue Zazhi* 1997;5:119-120
- 50 Hou ZJ, Li HZ, Liu XW. Enzymology in diagnosis of liver fibrosis. *Xin Xiaohuabingxue Zazhi* 1997;5:325-326
- 51 Qiu DK, Li H, Zeng MD, Li JQ. Effect of cordyceps polysaccharides-liposome on the expression of interstitial mRNA in rats with hepatic fibrosis. *Xin Xiaohuabingxue Zazhi* 1997;5:417-418
- 52 Yan JP, Liu JC, Ma XH, Jia JB, Zhao YC, Xu RL, Li CM, Han DW. Immunohistochemical study on basic fibroblast growth factor in experimental liver fibrosis. *Xin Xiaohuabingxue Zazhi* 1997;5:642-644
- 53 Wang X, Chen YX, Xu CF, Zhao GN, Huang YX, Wang QL. Relationship between tumor necrosis factor- α and liver fibrosis. *Huaren Xiaohua Zazhi* 1998;6:106-108
- 54 Xu LX, Xie XC, Jin R, Ji ZH, Wu ZZ, Wang ZS. Effect of selenium in rat experimental liver fibrosis. *Huaren Xiaohua Zazhi* 1998;6:133-135
- 55 Wu YA, Kong XT. Anti-hepatic fibrosis effect of pentoxifylling. *Shijie Huaren Xiaohua Zazhi* 1999;7:265-266
- 56 Wang GQ, Kong XT. Action of cell factor and Decorin in tissue fibrosis. *Shijie Huaren Xiaohua Zazhi* 2000;8:458-460
- 57 Liu F, Wang XM, Liu JX, Wei MX. Relationship between serum TGF β 1 of chronic hepatitis B and hepatic tissue pathology and hepatic fibrosis quantity. *Shijie Huaren Xiaohua Zazhi* 2000;8:528-531
- 58 Liu F, Liu JX, Cao ZC, Li BS, Zhao CY, Kong L, Zhen Z. Relationship between TGF β 1, serum indexes of liver fibrosis and hepatic tissue pathology in patients with chronic liver diseases. *Shijie Huaren Xiaohua Zazhi* 1999;7:519-521
- 59 Gu SW, Luo KX, Zhang L, Wu AH, He HT, Weng JY. Relationship between ductule proliferation and liver fibrosis of chronic liver disease. *Shijie Huaren Xiaohua Zazhi* 1999;7:845-847
- 60 Murawaki Y, Ikuta Y, Idobe Y, Kawasaki H. Serum matrix metalloproteinase-1 in patients with chronic viral hepatitis. *J Gastroenterol Hepatol* 1999;14:138-145
- 61 Murawaki Y, Ikuta Y, Kawasaki H. Clinical usefulness of serum tissue inhibitor of metalloproteinases (TIMP)-2 assay in patients with chronic liver disease in comparison with serum TIMP-1. *Clin Chim Acta* 1999;281:109-120
- 62 Murawaki Y, Ikuta Y, Idobe Y, Kitamura Y, Kawasaki H. Tissue inhibitor of metalloproteinase-1 in the liver of patients with chronic liver disease. *J Hepatol* 1997;26:1213-1219
- 63 Li BS, Wang J, Zhen YJ, Liu JX, Wei MX, Sun SQ, Wang SQ. Experimental study on serum fibrosis markers and liver tissue pathology and hepatic fibrosis in immunodamaged rats. *Shijie Huaren Xiaohua Zazhi* 1999;7:1031-1034
- 64 Wang Y, Gao Y, Huang YQ, Yu JL, Fang SG. Gelatinase A proenzyme expression in the process of experimental liver fibrosis. *Shijie Huaren Xiaohua Zazhi* 2000;8:165-167
- 65 Yao XX. Diagnosis and treatment of liver fibrosis. *Shijie Huaren Xiaohua Zazhi* 2000;8:681-689
- 66 Iredale JP, Murphy G, Hembry RM, Friedman SL, Arthur MJ. Human hepatic lipocytes synthesize tissue inhibitor of metalloproteinases-1. Implications for regulation of matrix degradation in liver. *J Clin Invest* 1992;90:282-287
- 67 Roeb E, Purucker E, Breuer B, Nguyen H, Heinrich PC, Rose-John S, Matern S. TIMP expression in toxic and cholestatic liver injury in rat. *J Hepatol* 1997;27:535-544
- 68 Herbst H, Wege T, Milani S, Pellegrini G, Orzechowski HD, Bechstein WO, Neuhaus P, Gressner AM, Schuppan D. Tissue inhibitor of metalloproteinase-1 and -2 RNA expression in rat and human liver fibrosis. *Am J Pathol* 1997;150:1647-1659
- 69 Kasahara A, Hayashi N, Mochizuki K, Oshita M, Katayama K, Kato M, Masuzawa M, Yoshihara H, Naito M, Miyamoto T, Inoue A, Asai A, Hijioka T, Fusamoto H, Kamada T. Circulating matrix metalloproteinase-2 and tissue inhibitor of metalloproteinase-1 as serum markers of fibrosis in patients with chronic hepatitis C. Relationship to interferon response. *J Hepatol* 1997;26:574-583
- 70 Kossakowska AE, Edwards DR, Lee SS, Urbanski LS, Stabblar AL, Zhang CL, Phillips BW, Zhang Y, Urbanski SJ. Altered balance between matrix metalloproteinases and their inhibitors in experimental biliary fibrosis. *Am J Pathol* 1998;153:1895-1902
- 71 Song CH, Wu MY, Wang XL, Dong Q, Tang RH, Fan XL. Correlation between HDV infection and HBV serum markers. *China Natl J New Gastroenterol* 1996;2:230-231
- 72 Gao JE, Tao QM, Guo JP, Ji HP, Lang ZW, Ji Y, Feng BF. Preparation and application of monoclonal antibodies against hepatitis C virus nonstructural proteins. *China Natl J New Gastroenterol* 1997;3:114-116
- 73 Yang DH, Xiu C, Yang B, Gu JR, Qian LF, Qu SM. Expression of insulin-like growth factor II and its receptor in liver cells of chronic liver diseases. *China Natl J New Gastroenterol* 1997;3:117-118
- 74 Yu SJ. A comparative study on proliferating activity between HBV related and HCV related small HCC. *China Natl J New Gastroenterol* 1997;3:236-237
- 75 Zhang SL, Han XB, Yue YF. Relationship between HBV viremia level of pregnant women and intrauterine infection: nested PCR for detection of HBV DNA. *World J Gastroenterol* 1998;4:61-63
- 76 Gao FG, Sun WS, Cao YL, Zhang LN, Song J, Li HF, Yan SK. HBx DNA probe preparation and its application in study of hepatocarcinogenesis. *World J Gastroenterol* 1998;4:320-322
- 77 Wang WL, Gu GY, Hu M. Expression and significance of HBV genes and their antigens in human primary intrahepatic cholangiocarcinoma. *World J Gastroenterol* 1998;4:392-396
- 78 Zhong S, Wen SM, Zhang DF, Wang QL, Wang SQ, Ren H. Sequencing of PCR amplified HBV DNA pre c and c regions in the 2,2,15 cells and antiviral action by targeted antisense oligonucleotide directed against sequence. *World J Gastroenterol* 1998;4:434-436
- 79 Zhong S, Wen SM, Zhang DF, Wang QL, Wang SQ, Ren H. Sequencing of PCR amplified HBV DNA pre c and c regions in the 2215 cells and antiviral action by targeted antisense oligonucleotide directed against sequence. *World J Gastroenterol* 1998;4:434-436
- 80 Zheng Z, Yang SW, Xiao W, Sun P, Li XJ, Hu YQ. Evaluation of the HBV in HBsAg by HBV DNA measured with PCR. *World J Gastroenterol* 1998;4:577
- 81 Lee JH, Ku JL, Park YJ, Lee KU, Kim WH, Park JG. Establishment and characterization of four human hepatocellular carcinoma cell lines containing hepatitis B virus DNA. *World J Gastroenterol* 1999;5:289-295
- 82 Guo SP, Ma ZS, Wang WL. Construction of eukaryotic expression vector of HBV x gene. *World J Gastroenterol* 1999;5:351-352
- 83 Tang RX, Gao FG, Zeng LY, Wang YW, Wang YL. Detection of HBV DNA and its existence status in liver tissues and peripheral blood lymphocytes from chronic hepatitis B patients. *World J Gastroenterol* 1999;5:359-361
- 84 Wen SJ, Xiang KJ, Huang ZH, Zhou R, Qi XZ. Construction of HBV specific ribozyme and its recombinant with HDV and their cleavage activity *in vitro*. *World J Gastroenterol* 2000;6:377-380
- 85 Wang Y, Liu H, Zhou Q, Li X. Analysis of point mutation in site 1896 of HBV precore and its detection in the tissues and serum of HCC patients. *World J Gastroenterol* 2000;6:395-397
- 86 Hu YP, Yao YC, Li JX, Wang XM, Li H, Wang ZH, Lei ZH. The cloning of 3'truncated preS/S gene from HBV genomic DNA and its expression in transgenic mice. *World J Gastroenterol* 2000;6:734-737
- 87 Wei L, Wang Y, Chen HS, Tao QM. Sequencing of hepatitis C virus

- cDNA with polymerase chain reaction directed sequencing. *China Natl J New Gastroenterol* 1997;3:12-15
- 88 Zhou P, Cai Q, Chen YC, Zhang MS, Guan J, Li XJ. Hepatitis C virus RNA detection in serum and peripheral blood mononuclear cells of patients with hepatitis C. *China Natl J New Gastroenterol* 1997;3:108-110
- 89 Sun DG, Liu CY, Meng ZD, Sun YD, Wang SC, Yang YQ, Liang ZL, Zhuang H. A prospective study of vertical transmission of hepatitis C virus. *China Natl J New Gastroenterol* 1997;3:111-113
- 90 Gao JE, Tao QM, Guo JP, Ji HP, Lang ZW, Ji Y, Feng BF. Preparation and application of monoclonal antibodies against hepatitis C virus nonstructural proteins. *China Natl J New Gastroenterol* 1997;3:114-116
- 91 Zhang LF, Peng WW, Yao JL, Tang YH. Immunohistochemical detection of HCV infection in patients with hepatocellular carcinoma and other liver diseases. *World J Gastroenterol* 1998;4:64-65
- 92 Zhu FL, Lu HY, Li Z, Qi ZT. Cloning and expression of NS3 cDNA fragment of HCV genome of Hebei isolate in *E. coli*. *World J Gastroenterol* 1998;4:165-168
- 93 Soresi M, Carroccio A, Bonfissuto G, Agate V, Magliarisi C, Aragona F, Levrero M, Notarbartolo A, Montalto M. Ultrasound detection of abdominal lymphadenomegaly in subjects with hepatitis C virus infection and persistently normal transaminases: a predictive index of liver histology severity. *World J Gastroenterol* 1998;4:270
- 94 Yang JM, Wang RQ, Bu BG, Zhou ZC, Fang DC, Luo YH. Effect of HCV infection on expression of several cancer associated gene products in HCC. *World J Gastroenterol* 1999;5:25-27
- 95 Feng DY, Chen RX, Peng Y, Zheng H, Yan YH. Effect of HCV NS3 protein on p53 protein expression in hepatocarcinogenesis. *World J Gastroenterol* 1999;5:45-46
- 96 Huang F, Zhao GZ, Li Y. HCV genotypes in hepatitis C patients and their clinical significances. *World J Gastroenterol* 1999;5:547-549
- 97 Dai YM, Shou ZP, Ni CR, Wang NJ, Zhang SP. Localization of HCV RNA and capsid protein in human hepatocellular carcinoma. *World J Gastroenterol* 2000;6:136-137
- 98 Dai YM, Shou ZP, Ni CR, Wang NJ, Zhang SP. Localization of HCV RNA and capsid protein in human hepatocellular carcinoma. *World J Gastroenterol* 2000;6:136-137
- 99 Cheng JL, Tong WB, Liu BL, Zhang Y, Yan Z, Feng BF. Hepatitis C virus in human B lymphocytes transformed by Epstein-Barr virus *in vitro* by in situ reverse transcriptase chain reaction. *World J Gastroenterol* 2001;7:370-375
- 100 Nie QH, Li MD, Hu DR, Chen GZ. Study on the cause of human protective immunodeficiency after HCV infection. *Shijie Huaren Xiaohua Zazhi* 2000;8:28-30
- 101 Nie QH, Cheng YQ, Xie YM, Zhou YX, Cao YZ. Inhibiting effect of antisense oligonucleotides phosphorothioate on gene expression of TIMP-1 in rat liver fibrosis. *World J Gastroenterol* 2001;7: 363-369

Edited by Hu DK

• VIRAL LIVER DISEASES •

Clinicopathological study on TTV infection in hepatitis of unknown etiology

Zhong-Jie Hu, Zhen-Wei Lang, Yu-Sen Zhou, Hui-Ping Yan, De-Zhuang Huang, Wan-Rong Chen, Zhao-Xia Luo

Zhong-Jie Hu, Zhen-Wei Lang, Yu-Sen Zhou, Hui-Ping Yan, De-Zhuang Huang, Wan-Rong Chen, Zhao-Xia Luo, Department of Pathology, Beijing You'an Hospital, Beijing 100054, China
Supported by the National Natural Science Foundation of China, No. 39900133 and Beijing Natural Science Foundation, No. 7992023
Correspondence to: Zhong-Jie Hu, Department of Pathology, Beijing You'an Hospital, 8 You'an Men Wai, Beijing 100054, China. huzhong-jie@263.net
Telephone: +86-10-63292211-2402 Fax: +86-10-63055834
Received 2001-08-23 Accepted 2001-09-05

Abstract

AIM: To investigate the state of infection, replication site, pathogenicity and clinical significance of transfusion transmitted virus (TTV) in patients with hepatitis, especially in patients of unknown etiology.

METHODS: Liver tissues taken from 136 cases of non-A non-G hepatitis were tested for TT virus antigen and nucleic acid by *in situ* hybridization (ISH) and nested-polymerase chain reaction (PCR). Among them, TT virus genome and its complemental strand were also detected in 24 cases of autopsy liver and extrahepatic tissues with ISH. Meanwhile, TTV DNA was detected in the sera of 187 hepatitis patients by nested-PCR. The pathological and clinical data of the cases infected with TTV only were analyzed.

RESULTS: In liver, the total positive rate of TTV DNA was 32.4% and the positive signals were located in the nuclei of hepatocytes. In serum, TTV DNA was detected in 21.4% cases of hepatitis A-G, 34.4% of non-A non-G hepatitis and 15% of healthy donors. The correspondence rate of TTV DNA detection between liver tissue with ISH and sera with PCR was 63.2% and 89.3% in the same liver tissues by ISH and by PCR, respectively. Using double-strand probes and single-strand probes designed to detect TTV genome, the correspondence rate of TTV DNA detected in liver and extrahepatic tissues was 85.7%. Using single-strand probes, TTV genome could be detected in liver and extrahepatic tissues by PCR, but its complemental strands (replication strands) could be observed only in livers. The liver function of most cases infected with TTV alone was abnormal and the liver tissues had different pathological damage such as ballooning, acidophilia degeneration, formation of apoptosis bodies and focus of necrosis, but the inflammation in the lobule and portal area was mild.

CONCLUSION: The positive rate of TTV DNA among cases of hepatitis was higher than that of donors, especially in patients with non-A non-G hepatitis, but most of them were coinfecting with other hepatitis viruses. TTV can infect not only hepatocytes, but also extrahepatic tissues. However, the chief replication place may be liver. The infection of TTV may have some pathogenicity. Although the pathogenicity is comparatively weak, it can still damage the liver tissues.

The lesions in acute hepatitis (AH) and chronic hepatitis (CH) are mild, but in severe hepatitis (SH), it can be very serious and cause liver function failure, therefore, we should pay more attention to TTV when studying the possible pathogens of so-called "liver hepatitis of unknown etiology".

Hu ZJ, Lang ZW, Zhou YS, Yan HP, Huang DZ, Chen WR, Luo ZX. Clinicopathological study on TTV infection in hepatitis of unknown etiology. *World J Gastroenterol* 2002;8(2):288-293

INTRODUCTION

In 1997, Nishizawa first found and reported a virus which was associated with post-transfusion hepatitis and named it transfusion transmitted virus. TTV is an unenveloped, single-stranded and circular DNA virus, which consists of 3852 nucleotides and most closely resembles the members of the Circoviridae family^[1-3]. Meanwhile, different studies suggested that TTV genotypes were so much and could vary frequently^[4-8]. It is believed that TTV belongs to hepadnavirus and replicates chiefly in the liver^[9-11], however, some researchers think that the replication site is in the bone marrow rather than in the livers^[12]. At present, epidemiological studies suggest that TTV is mainly transmitted by blood^[13-15]; blood products^[16] and body fluid routes^[13,17], it can also be transmitted by mother-to-child vertical^[18] and horizontal^[19,20] route, fecal-oral route^[9,15,21] and sexual route^[22]. The infection rate of TTV DNA varies largely in healthy population and patients with liver diseases, but generally, it is higher in patients than in healthy donors^[7,23-26]. The discovery of TTV once put a light on the etiological diagnoses of hepatitis cases of unknown etiology, unfortunately, the pathogenicity and clinical significance of TTV remain doubtful at this time^[25,27-29]. To clarify the infection status, replication place, pathogenicity and clinical significance of TTV among hepatitis cases, especially in patients of unknown etiology, we conducted the research to test TTV DNA comprehensively among large-sample cases of hepatitis.

MATERIALS AND METHODS

Patients

We studied 136 hepatitis cases of unknown etiology, including 45 females and 91 males, aged 16-77 years. By serological screening, all the cases were proved to have not been infected by hepatitis A virus (HAV), hepatitis B virus (HBV), hepatitis C virus (HCV), hepatitis E virus (HEV), hepatitis G virus (HGV), cytomegalovirus (CMV) or Epstein-Barr virus (EBV). Meanwhile, alcohol hepatopathy, hepatopathy caused by drugs, autoimmunity hepatopathy and liver damage caused by other systemic diseases were eliminated on the basis of the history and other clinical indexes. According to the pathological diagnostic criteria set up at the 10th National Meeting of Infection Diseases in September 2000, Xi'an, China, there were 51 cases of acute hepatitis (AH), 41 chronic hepatitis (CH), 9 acute severe hepatitis (ASH), 11 subacute severe hepatitis (SSH), 5 chronic severe hepatitis (CSH), 11 liver cirrhosis (LC) and 8

hepatocarcinoma (HCC). The liver biopsies were performed in all patients except 28 who died of liver failure and autopsies were performed. Among the 28 cases, extrahepatic tissue samples (including pancreases, kidneys, spleens and hearts) were obtained from 24 cases. The control group consists of 31 patients who had undergone abdominal operations for other diseases except liver diseases. Paired sera were also obtained from 19 of 136 cases. Sera were collected from 42 cases of non-A non-G hepatitis and from 126 cases of hepatitis A-G. Sera of 20 donors from blood bank in Beijing You'an Hospital served as controls. All the specimens of the liver tissues and the extrahepatic tissues were fixed immediately in 100mL·L⁻¹ neutral formalin and embedded in paraffin, and then sliced continuously to make 5μm thick sections and stained with hematoxylin-eosin (HE). After that, the common pathological damages of virus hepatitis were observed under microscopy and the inflammation and fibrosis of the hepatic lobules were assessed according to the Histology Activation Index (HAI, Knodell Grade) and the pathological diagnoses were made.

Methods

Design and synthesis of primers The primers of PCR were contrived using the molecular biology software "Goldkey" (by the Chinese Academy of Military Medical Sciences, Beijing, China) and OLIGO 5.0 (USA), the sequence was based on the full-length TTV genome published in the Gen Bank (registry code: AF079173). The sequences were as follows: outer primers: P₁: 5'-ACAGACAGAGGAGAGAGGCAAC-3'; P₂: 5'-AACAGGCACATTACTACTACC-3', inner primers: P₃: 5'-CCAGGAGCATATACAGAC-3', P₄: 5'-TGTTACTTCTTGCTGGTGAAAT-3'.

Label of double-strand TTV DNA probes Using the plasmid pGEM-ORF1 that contains the sequences of TTV genome as template (plasmid pGEM-ORF1 was provided by the Chinese Academy of Military Medical Sciences), the double-strand probes of TTV DNA were labeled with digoxigenin by PCR following the manual of Boehringer Mannheim digoxigenin kit. In the presence of template (3μL), 10×PCR buffer (6μL), labeling mixture with Dig-11-dUTP (2μL), primer P1 and P2 (1μL separately) and Taq DNA polymerase (1μL), PCR was performed for 30 cycles (94°C for 40s with an additional 3min in the first cycle, 55°C for 40s, and 72°C for 50s) in a reaction volume of 60μL. The products were separated by electrophoresis to purify the probes. The labeled probes were homologous with the 1900-2208bp region of the TTV DNA that was a part of the TTV DNA ORF1. The total length of the probe was 309bp and the titer was 1mg·L⁻¹.

Label of single-strand TTV DNA probes The single-strand TTV DNA probes were labeled by asymmetric PCR, which was performed under the same conditions as the double-strand probes, except that the primer P1 and P2 were added in a rate of 1:100. The two primers were used to label the two single-strand probes. One could be used to detect the genome strand of TTV DNA (probe P37), the other could be used to detect its complementary strand (probe P38).

In situ hybridization Paraffin embedded sections were first parched at 60°C for 3-5h, deparaffined in xylene, digested by protease K, fixed in 40g·L⁻¹ polyformaldehyde, dehydrated through graded alcohol, and prehybridized for 10min. Then hybridization liquid was added (5-10 drops/section). After denatured for 10min (95°C in wet bin), the sections were subsequently incubated for 16-20h at 68°C in water bath bin, washed by 2×SSC, blocked by goat serum/BSA, incubated with anti-Dig-Ap. At last, chromogenic reaction was developed with NBT, BCIP lucifugously.

The confirmation assays included: (1) blank controls: the positive sections were hybridized with prehybridization solution instead of Dig-TTV DNA probes; (2) replacement assays by other probes: the positive sections were hybridized with Dig-HBV DNA probes but not TTV DNA probes; and (3) the negative sections of normal liver tissues were rehybridized, using probes with higher titer.

Nested-PCR After the paraffin-embedded sections had been deparaffined and treated with alcohol, the liver tissues were homogenized and incubated in proteinase K-sodium dodecyl sulfate at 52°C for 3h. And then, nucleic acids were extracted from them with phenol-chloroform and precipitated with ethanol. DNA species of chromosomal origin, which emerged as a cloudy precipitate immediately after addition of ethanol, were removed. The remaining nucleic acids were collected by centrifugation and dissolved in 200μL Tris-HCl buffer (10mmol·L⁻¹, pH 8.0) containing 1m·L⁻¹ EDTA (TE buffer). Sera (1mL) was diluted twofold with Tris-HCl buffer (50mmol·L⁻¹, pH 8.0) containing 150mmol·L⁻¹ NaCl and 1mmol·L⁻¹ EDTA and centrifuged in a TLA 100.3 rotor (Beckman Instruments, Inc., Palo Alto, Calif.) at 190583G for 1h. The pellet was suspended in Tris-HCl buffer (10mmol·L⁻¹, pH 8.0) containing 5mmol·L⁻¹ EDTA and supplemented with 0.5mg proteinase K per mL as well as 5g·L⁻¹ sodium dodecyl sulfate and incubated at 65°C for 2h as the direction of the STG Kit (Biotronics Tech. Corp., USA). Then, nucleic acids were extracted with phenol-chloroform, precipitated with ethanol and dissolved in 100μL of TE buffer.

Using DNA (0.1ng) extracted from the sera or livers as a template, the first-round PCR was performed with P1 and P2 (100μmol·L⁻¹ respectively) for 35 cycles (94°C for 40s with an additional 3min in the first cycle, 55°C for 40s, and 72°C for 40s with an additional 7min in the last cycle) in the presence of 10×PCR buffer (3μL), dNTPs (100μmol·L⁻¹) and Taq DNA polymerase (1U) in 30μL of reaction volume (the reverse transcriptase, Taq DNA polymerase, dNTPs and T4 DNA Ligase were provided by Sino-American Biotech. Inc. Beijing). On the products of the first-round PCR (2μL), the second round was performed for 30 cycles under the same conditions as in the first round.

Detection of other pathogens The markers of hepatitis A-G viruses, CMV and EBV in sera were screened by ELISA, the steps were according to the directions of the Kits (anti-HAV IgM Kit, HBV-M Kit, anti-HCV IgM IgG Kit, HDV-M Kit and anti-HEV IgM Kit were purchased from Sino-American Biotech. Inc. Beijing, and anti-CMV IgM, anti-EBV IgM were the products of Delyea Inc., Italy). The antigens of HBV, HCV, HGV, EBV and CMV expressed in liver tissues were assayed by immunohistochemical staining using the streptavidin-peroxidase (S-P) method. The monoclonal antibody Kit against HBsAg and polyclonal antibody Kit against HBcAg were purchased from Maxim Biotech. Inc. Fuzhou, China. Purified rabbit monoclonal antibodies against HCV NS5-Ag, HGV NS5-Ag and EBV-Ag were provided by the Institute of virology of Chinese Academy of Preventive Medicine and Institute of Bacteriology & Epidemiology of Chinese Academy of Military Medical Sciences. Serum alanine aminotransferase (ALT) and total serum bilirubin (TSB) were assayed by automatic analyzer (COMBAS).

Statistical analysis

Aided by statistical software SPSS 10.0, statistical analysis was performed. χ^2 test was used for unpaired enumeration data and McNemar test for paired enumeration data. If they were measurement data and normal distribution, we expressed them as $\bar{x} \pm s$ (standard deviation) and the comparison among groups were performed by unpaired Student's *t* test. *P* values less than 0.05 was considered significant.

RESULTS

TTV DNA in liver tissues

In all the 136 samples of liver tissues, the total positive rate of TTV DNA was 32.4% (44/136). It was 27.5% (14/51) in acute mild hepatitis group, 36.6% (15/41) in chronic hepatitis, 45.5% (5/11) in subacute severe hepatitis, 40.0% (2/5) in chronic severe hepatitis, 36.4% (4/11) in active liver cirrhosis and 50% (4/8) in primary hepatocarcinoma. No TTV DNA could be detected in the cases of acute severe hepatitis. The positive rate in chronic liver diseases (39.5%) was significantly higher than that in acute liver diseases (23.3%, $P=0.046$). However, there was no significant difference as compared with control group. After detection of other pathogen by immunohistochemical staining and *in situ* hybridization, 13 cases were confirmed to be infected by TTV alone, including 5 cases of acute hepatitis, 6 cases of chronic hepatitis and 2 cases subacute severe hepatitis (Table 1).

Table 1 TTV DNA in liver tissues of hepatitis

Type	n	TTV(+) n(%)	TTV(-) n(%)	TTV alone n(%)
AH	51	14(27.5)	37(72.5)	5(9.8)
CH	41	15(36.6)	26(63.4)	6(14.6)
ASH	9	0(0.0)	9(100.0)	2(18.2)
SSH	11	5(45.5)	6(54.5)	0(0.0)
CSH	5	2(40.0)	3(60.0)	0(0.0)
LC	11	4(36.4)	7(63.6)	0(0.0)
HCC	8	4(50.0)	4(50.0)	0(0.0)
Total	136	44(32.4)	92(67.6)	13(9.6)
Normal	31	8(25.8)	23(74.2)	

The positive signal of TTV DNA predominantly located in the nucleoli of the hepatocytes with an appearance of blue grain. It also could be found in the cytoplasm of the hepatocytes but much weaker than that in the nucleoli. In acute hepatitis, the positive cells were distributed diffusely in the interlobular areas, and in chronic hepatitis they were aggregated in the periportal areas and in active liver cirrhosis they clustered in the pseudolobules. The positive signals could also be found in the hepatocarcinoma cells.

TTV DNA in sera

TTV DNA could be detected in 21.4% (27/126) cases of hepatitis A-G, 34.3% (21/61) cases of non A non G hepatitis and 15% (3/20) healthy donors. There was no significant difference between the donors and the patients of hepatitis. Classified by the clinical diagnosis in AH, CH, SH and LC groups, the positive rates were 29.0% (18/

62), 23.5 % (19/81), 52.9 % (9/17) and 7.4 % (2/27), respectively. The positive rate in SH group was significantly higher than in control group ($P=0.014$, Table 2).

Table 2 TTV DNA in sera of patients

Type	n	TTV(+) n(%)	TTV(-) n(%)
NA-NG	61	21(34.4)	40(65.6)
A-G	126	27(21.4)	99(78.6)
AH	62	18(29.0)	44(71.0)
CH	81	19(23.5)	62(76.5)
SH	17	9(52.9)	8(47.1) ^a
LC	27	2(7.4)	25(92.6)
Total	187	48(25.7)	139(74.3)
Control	20	3(15.0)	17(85.0)

^a $P<0.05$, vs Control

In liver tissues and sera of patients of non-A non-G hepatitis, the positive rate of TTV DNA (33.0%) was significantly higher than that of hepatitis A-G (21.4%) ($P=0.025$).

Among the 19 paired samples of sera and liver tissues, 12 cases had the same results when testing liver tissues by ISH and testing sera by PCR, although 5 liver tissues were positive while the paired sera were negative and 2 sera were positive but the paired liver tissues were negative. However, there was no significant difference between them ($P=0.453$).

Fifty-six liver tissue specimens were assayed by PCR and at the same time by ISH. The coincidence rate of the results was 89.3% (50/56). Five cases were positive by PCR while negative by ISH and only 1 case was negative by PCR but positive by ISH. The difference was not statically significant either ($P=0.219$). Fifty-six specimens of liver, pancreas, kidney, spleen and heart tissues were tested by PCR using the two probes respectively. The results suggested that the total coincidence rate was 85.7% (48/56). The rest showed positive outcomes using one probe but negative outcomes using another probe in equal proportion. The difference using the two probes was not significant ($P=1.000$).

Paired specimens of liver, pancreas, kidney, spleen and heart tissues from 8 patients in whom TTV DNA had been found in the liver tissues by PCR using double-strand probes, were assayed again using P37 probes and P38 probes, respectively. The results showed that using P37 probes, 7, 7, 3, 5, 1 cases were positive in liver, pancreas, kidney, spleen and heart tissues, respectively. However, using P38 probes, only 5 specimens of liver tissues were positive and all the extrahepatic tissues were negative (Table 3).

Table 3 TTV DNA genome and its complement chain in liver and extrahepatic tissues by PCR using single-strand probes

No.	Diagn.	Liver			Pancreas			Kidney			Spleen			Heart		
		DP	P37	P38	DP	P37	P38	DP	P37	P38	DP	P37	P38	DP	P37	P38
1	CSH	+	+	+	-	+	-	+	+	-	+	+	-	-	/	/
2	CSH	+	-	+	-	-	-	+	-	-	+	-	-	/	/	/
3	HCC	+	+	-	+	+	-	-	-	-	+	+	-	/	/	/
4	HCC	+	+	-	-	+	-	-	-	-	-	-	-	/	/	/
5	LC	+	+	+	+	+	-	+	+	-	+	+	-	+	/	/
6	LC	+	+	+	+	+	-	-	-	-	+	+	-	/	/	/
7	LC	+	+	+	+	+	-	+	+	-	-	+	-	/	/	/
8	SSH	+	+	-	+	+	-	+	-	-	-	-	-	/	/	/

DP: double-strand probe

Liver damage of cases infected with TTV alone

In AH group, serum ALT and TSB in patients infected with TTV alone ($325 \pm 222 \text{ nkat} \cdot \text{L}^{-1}$, $91 \pm 115 \mu\text{mol} \cdot \text{L}^{-1}$, respectively) were lower than that in patients infected with HBV only ($931 \pm 630 \text{ nkat} \cdot \text{L}^{-1}$, $134 \pm 118 \mu\text{mol} \cdot \text{L}^{-1}$, respectively), the difference of ALT being statistically significant ($P=0.005$). However, in SH group, there was no significant difference of ALT and TSB between cases infected with TTV alone ($509 \pm 361 \text{ nkat} \cdot \text{L}^{-1}$, $304 \pm 125 \mu\text{mol} \cdot \text{L}^{-1}$, respectively) and cases infected with HBV alone ($435 \pm 239 \text{ nkat} \cdot \text{L}^{-1}$, $226 \pm 96 \mu\text{mol} \cdot \text{L}^{-1}$, respectively) ($P>0.05$, Table 4).

Table 4 Liver function of cases infected by TTV alone and by HBV alone

	Pathogen	ALT(nkat·L ⁻¹)	TSB(μmol·L ⁻¹)
AH	TTV alone	325±222 ^b	91±115
	HBV alone	931±630	134±118
SH	TTV alone	509±361	304±125
	HBV alone	435±239	226±96
CH	TTV alone	187±150	98±199

^b $P<0.01$, vs HBV

In the liver tissues of patients with chronic hepatitis caused by TTV alone, some histological lesions could be found in hepatic lobule, including ballooning degeneration, acidophile degeneration, formation of apoptotic bodies, focus of necrosis, amplification of portal areas and infiltration of mononuclear cells, but the inflammation and fibrosis were mild. The histological activity index (3.23 ± 1.86) was lower than that in cases infected by HBV only (5.69 ± 1.34), the difference being statistically significant ($P=0.001$).

In cases without detectable pathogens in sera at present, after histological assay, 25.7% (35/136) were still of unknown etiology and 50.0% (68/130) could be explained to be the infection of HBV and/or HCV. Infection with TTV alone and with HGV only accounted for 9.6% (13/136) respectively, and the rate of coinfection with TTV and HGV was 5.1% (7/136) and the others were mixed infected with TTV/HGV and HBV/HCV.

DISCUSSION

Up to now, the epidemiological survey of TTV suggested that the infection of TTV globally distributed in all kinds of species. It was reported that the positive rate of TTV in healthy donors differed largely, ranging from 1% to 93%^[30-34]. Nevertheless, in patients with hepatopathy it ranged from 20% to 80%^[23-25,35]. These data show that the positive rate of TTV in population varies remarkably, it may be the result of the difference of the primers used in test or the imbalance of the different regions. However, it was higher in cases of liver diseases than that in healthy donors. These conclusions were chiefly drawn on the basis of serological studies, as the investigation of the liver tissues was scarce. In our study, we detected TTV DNA directly in liver tissue specimens by ISH. The results suggested that the total positive rate of TTV DNA was 32.4% in liver tissues of cases of unknown etiology, which was coincident with that in sera (34.4%). It could be conjectured that the results from serological screening can mirror the situation of TTV DNA in liver. Moreover, the positive rate of TTV DNA in AH group (27.5%) was similar to that in the normal controls (25.8%), but it was significantly higher in chronic hepatopathy (39.5%), especially in SSH, CSH and HCC groups, than in acute hepatopathy (23.5%) and control group. It indicated that TTV was common in population, and its infection could cause acute hepatitis and fulminant hepatitis and could develop to chronic hepatitis too. It may be one of the promoters of chronicity and deterioration of acute hepatitis and can affect the development of liver

cirrhosis and hepatocarcinoma. It is worthy notice that no TTV DNA could be found in acute severe hepatitis group. We think that it might be due to the large portion of the necrosis areas.

In sera, the positive rate of TTV DNA in cases of unknown etiology was much higher than that of hepatitis A-G and the lowest in healthy donors, but the difference was not significant. We thought that it was because the samples were not enough, thus we merged the samples of liver tissues and sera to enlarge the samples and perform the statistical analysis again. The results showed the positive rate of TTV DNA in cases of non-A non-G hepatitis (33.0%) was significantly higher than that of hepatitis A-G. Therefore, when we search the pathogens of "hepatopathy with unknown etiology", we must pay more attention to the infection of TTV.

In our study, we used different methods to confirm the results. The data suggested that the positive rate in liver tissues by ISH was similar to that in sera by PCR, there were 5 cases in which TTV was positive in the liver by ISH but negative in sera by PCR, and only 2 cases were reversed. The reason might be the small number of cases or that the copies in liver tissues were higher than that in sera, and in some cases the replication of TTV DNA was so inactive that the corresponding viremia was absent. In the liver, the results of test by ISH were not significantly different from that by PCR and there was no significant difference between the results of test by PCR using the double-strand probes and single-strand probes which were complemented with the genome of TTV DNA. These methods could be used to supplement and verify each other.

TTV was once regarded as a particular hepadnavirus^[36], but some studies suggested that TTV DNA could be detected in the bone marrows and the peripheral blood mononuclear cells (PBMC), and the hepatocytes were not the only site where TTV infected and existed^[11,12]. In our study, we screened the paired tissues of liver, pancreas, kidney, spleen and heart by PCR using double-strand probes and P37 probes. The results showed that TTV DNA could be detected in livers as well as in extrahepatic tissues, but in extrahepatic tissues, the positive rate was lower, and the density and intensity of positive signals were much weaker than that in liver tissues. In general, only in cases with positive TTV in liver, were there positive signals in extrahepatic tissues and there was only one case was reversed. Furthermore, there was no obvious pathological damage in the extrahepatic tissues. In conclusion, TTV can infect not only the liver, but also extrahepatic tissues. Yet, the liver is still the mainly infected site and the infection in extrahepatic tissues is an accompanying status that may act as a refuge to escape the attack of the immunity system of the host. As a result, these places can reinfect the liver as a source of infection and might be responsible for the chronicity of TTV infection and the high prevalence in all populations.

Concerning the replication site of TTV, there are much disputations at present. Okamoto *et al*^[11] discovered that separated by gel electrophoresis and characterized biophysically, TTV DNA in sera migrated in sizes ranging from 2.0 to 2.5kb. However, TTV DNA in liver tissues migrated at 2.0 to 2.5kb as well as at 3.5 to 6.1kb. Both faster and slower migrating forms of TTV DNA in the liver were found to be circular and the full genomic length being 3.8kb. The further study suggested that TTV DNA migrated at 3.5 to 6.1kb represents a circular, double-strand replication intermediates of TTV. The author concluded that TTV replicated in the liver via a circular double-strand DNA. However, Kikuchi *et al*^[12] found that in hepatocytes there was only TTV DNA but no mRNA by PCR and Southern hybridization, while in bone marrow tissues, especially specimens coming from biopsy, there were high titers of TTV DNA. The author suggested that TTV replicates chiefly in bone marrows but not in liver, and Okamoto *et al*^[37] found replication intermediates in marrows too. Furthermore,

Maggi *et al*^[38] found that TTV can replicate in activated mononuclear cells, and recent studies^[39,40] suggest that viral replication takes place in multiple tissues at distinct levels in infected individuals. In order to clarify the problem, we contrived and labeled 2 single-strand probes by asymmetric PCR. Because TTV is a single-strand DNA virus, in the process of replication the replication intermediates will appear. Detection of the genomes and its complementary chains using single-strand probes could explain the existence and replication of TTV DNA in different tissues. The results suggested that in positive cases using double-strand probes, positive signals could be detected in parts of the specimens of liver, pancreas, kidney, spleen and heart tissues using single-strand probes designed to detect the TTV genome. However, using single-strand probes designed to detect the replication chain of TTV DNA, positive signals could be seen in part of liver tissues but all the extrahepatic tissues were negative. These results showed again that TTV can infect extrahepatic tissues, but the infection belongs to an accompanying state and liver is still one of the main replication places. Although we have studied the bone marrow tissues and had not compared it to the liver, it is clear at least that TTV can replicate in liver and it is the prerequisite to investigate the pathogenicity of TTV.

Discovery of TTV once triggered the expectations to explain the cases of non-A non-G hepatitis, unfortunately, the pathogenicity and clinical significance of TTV remain doubtful at this time. Most studies suggest that TTV is not responsible for hepatitis and is not one of the chief pathogens of hepatitis^[23,25,30,41-43], and in hepatitis B/C, TTV does not seem to cooperate with HBV/HCV and coinfection with TTV does not modify the clinical feature and exacerbate liver damage^[44,45]. And TTV plays an insignificant role in acute fulminant and non-fulminant hepatitis^[46]. But some researchers did not think so. They think that TTV may cause epidemic outbreak of hepatitis of unknown etiology by fecal-to-mouth route^[28], and be responsible for some cases of non-A non-G hepatitis^[47,48]. Some studies suggest that TTV can make other systems abnormal^[49,50] and may be responsible for the development of hepatocellular carcinoma in patients with type C liver disease^[51]. We selected the patients of non-A non-G hepatitis who had been screened by serological and histological assays by ISH and confirmed to be infected by TTV alone, and then we observed the pathological damages, assessed the damage degree of the liver tissues by the criterion of global “Knodell Grade” and analyzed the liver function. The results show that TTV DNA is mainly located in the nuclei or cytoplasm of the hepatocytes. In the liver tissues of cases infected with TTV only the common pathological damages and inflammation would be found in the interlobular and periportal areas. The positive cells scattered diffusely in the interlobular areas in acute hepatitis and aggregated in periportal areas in chronic hepatitis or in the form of cluster in pseudolobules in the liver cirrhosis. The grade of HAI of acute or chronic hepatitis caused by TTV only was much lower than that caused by HBV. Clinically, the patients might have a raised ALT and TSB in AH group, but the elevation was mostly moderate and ALT was significantly lower than that caused by HBV. However, in SH group, the liver function change caused by TTV was similar to that caused by HBV. In CH group, the grades of inflammation activity of all the cases with TTV alone were G1-2. Therefore, TTV may have some pathogenicity, but the pathogenicity is comparatively weak and the liver damage is not serious in AH or CH. The result is identical with that of the study performed by Ge *et al*^[52]. However, when it caused fulminant hepatitis, the pathogenicity is not weaker than that of HBV and Yusufu’s study^[53] demonstrated that TTV may contribute to fulminant hepatic failure as a solitary infectious agent or a co-infectious agent with HCV. In addition, among these 136 cases of unknown etiology, the pathogen of 25.7% (35/136) patients was still unknown after the histological tests, 50% were caused by HBV and/or HCV,

9.6% were infected by TTV alone while 24.3% were contaminated by TTV and/or HGV, the others were coinfecting with TTV/HGV and HBV/HCV. These results suggest that we ought to pay more attention to TTV when we study the possible pathogen of so-called “liver diseases of unknown etiology”, although the conclusion should be verified by more data and more thorough studies.

On the whole, TTV is widespread in population. The positive rate of TTV DNA among hepatitis cases is higher than that of donors, especially in patients of non-A non-G hepatitis, but most of them are coinfecting with other hepatitis viruses. TTV can infect not only hepatocytes, but also extrahepatic tissues. However, the chief replication place may be the liver. The infection of TTV may have some pathogenicity. Although the pathogenicity is comparatively weak, it can still damage the liver tissues. The lesions in acute hepatitis (AH) and chronic hepatitis (CH) groups are mild, but in severe hepatitis (SH) group, it can be very serious and cause failure of liver function, therefore, we should pay more attention to TTV when studying the possible pathogens of so-called “liver hepatitis of unknown etiology”.

REFERENCES

- 1 Mushahwar IK, Erker JC, Muerhoff AS, Leary TP, Simons JN, Birkenmeyer LG, Chalmers ML, Pilot-Matias TJ, Dexai SM. Molecular and biophysical characterization of TT virus: evidence for a new virus family infecting humans. *Proc Natl Acad Sci USA* 1999; 96: 3177-3182
- 2 Miyata H, Tsunoda H, Kazi A, Yamada A, Khan MA, Murakami J, Kamahora T, Shiraki K, Hino S. Identification of a novel GC-rich 113-nucleotide region to complete the circular, single-stranded DNA genome of TT virus, the first human circovirus. *J Virol* 1999; 73: 3582-3586
- 3 Takahashi K, Iwasa Y, Hijikata M, Mishihiro S. Identification of a new human DNA virus (TTV-like mini virus, TLMV) intermediately related to TT virus and chicken anemia virus. *Arch Virol* 2000; 145: 979-993
- 4 Mulyanto, Hijikata M, Matsushita M, Ingkokusmo G, Widjaya A, Sumarsidi D, Kanai K, Ohta Y, Mishihiro S. TT virus (TTV) genotypes in native and non-native prostitutes of Irian Jaya, Indonesia: implication for non-occupational transmission. *Arch Virol* 2000; 145: 63-72
- 5 Khudyakov YE, Cong ME, Nichols B, Reed D, Dou XG, Viazov SO, Chang J, Fried MW, Williams I, Bower W, Lambert S, Purdy M, Roggendorf M, Fields HA. Sequence heterogeneity of TT virus and closely related viruses. *J Virol* 2000; 74: 2990-3000
- 6 Romeo R, Hegerich P, Emerson SU, Colombo M, Purcell RH, Bukh J. High prevalence of TT virus (TTV) in naive chimpanzees and in hepatitis C virus-infected humans: frequent mixed infections and identification of new TTV genotypes in chimpanzees. *J Gen Virol* 2000; 81 (Pt 4): 1001-1007
- 7 Okamoto H, Fukuda M, Tawara A, Nishizawa T, Itoh Y, Hayasaka I, Tsuda F, Tanaka T, Miyakawa Y, Mayumi M. Species-specific TT viruses and cross-species infection in nonhuman primates. *J Virol* 2000; 74: 1132-1139
- 8 Toyoda H, Fukuda Y, Nakano I, Katano Y, Yokozaki S, Hayashi K, Ito Y, Suzuki K, Nakano H, Saito H, Takamatsu J. TT virus genotype changes frequently in multiply transfused patients with hemophilia but rarely in patients with chronic hepatitis C and in healthy subjects. *Transfusion* 2001; 41: 1130-1135
- 9 Ukita M, Okamoto H, Kato N, Miyakawa Y, Mayumi M. Excretion into bile of a novel unenveloped DNA virus (TT virus) associated with acute and chronic non-A-G hepatitis. *J Infect Dis* 1999; 179: 1245-1248
- 10 Rodriguez Inigo E, Casqueiro M, Bartolome J, Ortiz Movilla N, Lopez Alcorocho JM, Herrero M, Manzarbeitia F, Oliva H, Carreno V. Detection of TT virus DNA in liver biopsies by in situ hybridization. *Am J Pathol* 2000; 156: 1227-1234
- 11 Okamoto H, Ukita M, Nishizawa T, Kishimoto J, Hoshi Y, Mizuo H, Tanaka T, Miyakawa Y, Mayumi M. Circular double-stranded forms of TT virus DNA in the liver. *J Virol* 2000; 74: 5161-5167
- 12 Kikuchi K, Miyakawa H, Abe K, Kako M, Katayama K, Fukushima S, Mishihiro S. Indirect evidence of TTV replication in bone marrow cells, but not in hepatocytes, of a subacute hepatitis/aplastic anemia patient. *J Med Virol* 2000; 61: 165-170
- 13 Matsubara H, Michitaka K, Horiike N, Yano M, Akbar SM, Torisu M, Onji M. Existence of TT virus DNA in extracellular body fluids from normal healthy Japanese subjects. *Intervirology* 2000; 43: 16-19
- 14 Chan YJ, Hsu YH, Chen MC, Wong WW, Wu JC, Yang WC, Liu CY. TT virus infection among hemodialysis patients at a medical center in Taiwan. *Chung Hua Min Kuo Wei Sheng Wu Chi Mien I Hsueh Tsa Chih* 2000; 33: 14-18
- 15 Luo K, Liang W, He H, Yang S, Wang Y, Xiao H, Liu D, Zhang L.

- Experimental infection of nonenveloped DNA virus (TTV) in rhesus monkey. *J Med Virol* 2000; 61: 159-164
- 16 Bjoro K, Petrova EP, Thomas MG, Froland SS, Williams R, Naoumov NV. TT virus infection in patients with primary hypogammaglobulinaemia: natural history and relationship to liver disease in the immunocompromised host. *Scand J Gastroenterol* 2001; 36: 987-993
 - 17 Inami T, Konomi N, Arakawa Y, Abe K. High prevalence of TT virus DNA in human saliva and semen. *J Clin Microbiol* 2000; 38: 2407-2408
 - 18 Schroter M, Polywka S, Zollner B, Schafer P, Laufs R, Feucht HH. Detection of TT virus DNA and GB virus type C/Hepatitis G virus RNA in serum and breast milk: determination of mother-to-child transmission. *J Clin Microbiol* 2000; 38: 745-747
 - 19 Kazi A, Miyata H, Kurokawa K, Khan MA, Kamahora T, Katamine S, Hino S. High frequency of postnatal transmission of TT virus in infancy. *Arch Virol* 2000; 145: 535-540
 - 20 Iriyama M, Kimura H, Nishikawa K, Yoshioka K, Wakita T, Nishimura N, Shibata M, Ozaki T, Morishima T. The prevalence of TT virus (TTV) infection and its relationship to hepatitis in children. *Med Microbiol Immunol Berl* 1999; 188: 83-89
 - 21 Itoh M, Shimomura H, Fujioka S, Miyake M, Tsuji H, Ikeda F, Tsuji T. High prevalence of TT virus in human bile juice samples: importance of secretion through bile into feces. *Dig Dis Sci* 2001; 46: 457-62
 - 22 Krekulova L, Rehak V, Killoran P, Madrigal N, Riley LW. Genotypic distribution of TT virus (TTV) in a Czech population: evidence for sexual transmission of the virus. *J Clin Virol* 2001; 23: 31-41
 - 23 Gerner P. TT virus infection in healthy children and in children with chronic hepatitis B or C. *J Pediatr* 2000; 136: 606-610
 - 24 Colombatto P, Brunetto MR, Kansopon J, Oliveri F, Maina A, Aragon U, Bortoli ML, Scatena F, Baicchi U, Houghton M, Bonino F, Weiner AJ. High prevalence of G1 and G2 TT-virus infection in subjects with high and low blood exposure risk: identification of G4 isolates in Italy. *J Hepatol* 1999; 31: 990-996
 - 25 Kim SR, Hayashi Y, Kudo M, Imoto S, Song KB, Ando K, Shintani S, Koterazawa T, Kim KI, Taniguchi M. TTV positivity and transfusion history in non-B, non-C hepatocellular carcinoma compared with HBV- and HCV-positive cases. *Intervirology* 2000; 43: 13-15
 - 26 Abe K, Inami T, Ishikawa K, Nakamura S, Goto S. TT virus infection in nonhuman primates and characterization of the viral genome: identification of simian TT virus isolates. *J Virol* 2000; 74: 1549-1553
 - 27 Hijikata M, Iwata K, Ohta Y, Nakao K, Matsumoto M, Matsumoto H, Kanai K, Baba K, Samokhvalov EI, Mishiro S. Genotypes of TT virus (TTV) compared between liver disease patients and healthy individuals using a new PCR system capable of differentiating 1a and 1b types from others. *Arch Virol* 1999; 144: 2345-2354
 - 28 Luo KX, Zhang L, Wang SS, Nie J, Yang SC, Liu DX, Liang WF, He HT, Lu Q. An outbreak of enterically transmitted non-A, non-E viral hepatitis. *J Viral Hepat* 1999; 6: 59-64
 - 29 Christensen JK, Eugen Olsen J, Srensen M, Ullum H, Gjedde SB, Pedersen BK, Nielsen JO, Krogsgaard K. Prevalence and prognostic significance of infection with TT virus in patients infected with human immunodeficiency virus. *J Infect Dis* 2000; 181: 1796-1799
 - 30 Love A, Stanzeit B, Li L, Olafsdottir E, Gudmundsson S, Briem H, Widell A. TT virus infections among blood donors in Iceland: prevalence, genotypes, and lack of relationship to serum ALT levels. *Transfusion* 2000; 40:306-309
 - 31 Niel C, Saback FL, Lampe E. Coinfection with multiple TT virus strains belonging to different genotypes is a common event in healthy Brazilian adults. *J Clin Microbiol* 2000; 38: 1926-1930
 - 32 Biagini P, Gallian P, Touinssi M, Cantaloube JF, Zapitelli JP, de Lamballerie X, de Micco P. High prevalence of TT virus infection in French blood donors revealed by the use of three PCR systems. *Transfusion* 2000; 40: 590-595
 - 33 Okamoto H, Takahashi M, Nishizawa T, Ukita M, Fukuda M, Tsuda F, Miyakawa Y, Mayumi M. Marked genomic heterogeneity and frequent mixed infection of TT virus demonstrated by PCR with primers from coding and noncoding regions. *Virology* 1999; 259: 428-436
 - 34 Chen XJ, Peng XM, Gao ZL, Lu JX, Yao JL. The significance of TTV infection in normal population and patients liver diseases. *Shijie Huaren Xiaohua Zazhi* 1999; 7: 5-7
 - 35 Fu EQ, Bai XF, Pan L, Li GY, Yang WS, Tang YM, Wang PZ, Sun JF. Investigation of TT virus infection in groups of defferent people in Xi'an. *Shijie Huaren Xiaohua Zazhi* 1999; 7: 967-969
 - 36 Ohbayashi H, Tanaka Y, Ohoka S, Chinzei R, Kakinuma S, Goto M, Watanabe M, Marumo F, Sato C. TT virus is shown in the liver by in situ hybridization with a PCR-generated probe from the serum TTV-DNA. *J Gastroenterol Hepatol* 2001; 16: 424-428
 - 37 Okamoto H, Takahashi M, Nishizawa T, Tawara A, Sugai Y, Sai T, Tanaka T, Tsuda F. Replicative forms of TT virus DNA in bone marrow cells. *Biochem Biophys Res Commun* 2000; 270: 657-662
 - 38 Maggi F, Fornai C, Zaccaro L, Morrica A, Vatteroni ML, Isola P, Marchi S, Ricchiuti A, Pistello M, Bendinelli M. TT virus (TTV) loads associated with different peripheral blood cell types and evidence for TTV replication in activated mononuclear cells. *J Med Virol* 2001; 64: 190-194
 - 39 Okamoto H, Nishizawa T, Takahashi M, Asabe S, Tsuda F, Yoshikawa A. Heterogeneous distribution of tt virus of distinct genotypes in multiple tissues from infected humans. *Virology* 2001; 288: 358-368
 - 40 Chan PK, Chik KW, Li CK, Tang NL, Ming MS, Cheung JL, Ng KC, Yuen PM, Cheng AF. Prevalence and genotype distribution of TT virus in various specimen types from thalassaemic patients. *J Viral Hepat* 2001;8: 304-309
 - 41 Wang JT, Lee CZ, Kao JH, Sheu JC, Wang TH, Chen DS. Incidence and clinical presentation of posttransfusion TT virus infection in prospectively followed transfusion recipients: emphasis on its relevance to hepatitis. *Transfusion* 2000; 40: 596-601
 - 42 Kadayifci A, Guney C, Uygun A, Kubar A, Bagci S, Dagalp K. Similar frequency of TT virus infection in patients with liver enzyme elevations and healthy subjects. *Int J Clin Pract* 2001; 55: 434-436
 - 43 Ikeuchi T, Yokosuka O, Kanda T, Imazeki F, Seta T, Saisho H. Roles of TT virus infection in various types of chronic hepatitis. *Intervirology* 2001; 44: 219-223
 - 44 Zhao Y, Wang JB. Epidemiological survey on TTV infection and the association with other viral liver diseases in Changchun area. *Shijie Huaren Xiaohua Zazhi* 2001; 9: 747-750
 - 45 Hagiwara H, Hayashi N, Mita E, Oshita M, Kobayashi I, Iio S, Hiramatsu N, Sasaki Y, Kasahara A, Kakinuma K, Yamauchi T, Fusamoto H. Influence of transfusion-transmitted virus infection on the clinical features and response to interferon therapy in Japanese patients with chronic hepatitis C. *J Viral Hepat* 1999; 6: 463-469
 - 46 Huang YH, Wu JC, Chiang TY, Chan YJ, Huo TI, Huang YS, Hwang SJ, Chang FY, Lee SD. Detection and viral nucleotide sequence analysis of transfusion-transmitted virus infection in acute fulminant and non-fulminant hepatitis. *J Viral Hepat* 2000; 7: 56-63
 - 47 Huang CH, Zhou YS, Chen RG, Xie CY, Wang HT. The prevalence of transfusion transmitted virus infection in blood donors. *World J Gastroenterol* 2000; 6: 268-270
 - 48 Sioda A, Moriyama M, Matsumura H, Kaneko M, Tanaka N, Arakawa Y. Clinicopathological features of serum TTV DNA-positive non-A-G liver diseases in Japan. *Hepatol Res* 2001; 21: 169-180
 - 49 Tokita H, Murai S, Kamitsukasa H, Yagura M, Harada H, Takahashi M, Okamoto H. Influence of TT virus infection on the thrombocytopenia of patients with chronic liver disease. *Hepatol Res* 2001; 20: 288-300
 - 50 Shibayama T, Masuda G, Ajisawa A, Takahashi M, Nishizawa T, Tsuda F, Okamoto H. Inverse relationship between the titre of TT virus DNA and the CD4 cell count in patients infected with HIV. *AIDS* 2001; 15: 563-570
 - 51 Moriyama M, Matsumura H, Shimizu T, Shioda A, Kaneko M, Miyazawa K, Miyata H, Tanaka N, Uchida T, Arakawa Y. Histopathologic impact of TT virus infection on the liver of type C chronic hepatitis and liver cirrhosis in Japan. *J Med Virol* 2001; 64: 74-81
 - 52 Ge Y, Ren XF, Li DZ, Hu TH, Yang Q. Liver histologic characteristics of patients with TTV infection during an epidemic of TTV infection in Wuhan. *Shijie Huaren Xiaohua Zazhi* 1999; 7: 1029-1030
 - 53 Yusufu Y, Mochida S, Matsui A, Okamoto H, Fujiwara K. TT virus infection in cases of fulminant hepatic failure-evaluation by clonality based on amino acid sequence of hypervariable regions. *Hepatol Res* 2001;21:85-96

Edited by Ma JY

• VIRAL LIVER DISEASES •

Construction and characterization of an experimental ISCOMS-based hepatitis B polypeptide vaccine

Xiao-Ju Guan, Xiao-Jun Guan, Yu-Zhang Wu, Zheng-Cai Jia, Tong-Dong Shi, Yan Tang

Xiao-Ju Guan, Shanghai Institute of Materia Medica, Chinese Academy of Sciences, Shanghai 200031, China, previously worked as a postdoc in Institute of Immunology, Third Military Medical University, Chongqing 400038, China

Xiao-Jun Guan, Department of Science & Research, Second Military Medical University, Shanghai 200433, China

Yu-Zhang Wu, Zheng-Cai Jia, Tong-Dong Shi, Yan Tan, Institute of Immunology, Third Military Medical University, Chongqing 400038, China

Supported by the National Natural Science Foundation of China, No. 39789010

Correspondence to: Yu-Zhang Wu, Institute of Immunology, Third Military Medical University, Chongqing 400038, China. wuyuzhang@yahoo.com

Received 2001-04-05 Accepted 2001-07-10

Abstract

AIM: To characterize the biochemical and immunological properties of an experimental ISCOMS vaccine prepared from a novel therapeutic polypeptide based on T cell epitopes of HBsAg, and a hepatitis B-ISCOMS was prepared and investigated.

METHODS: An immunostimulating complexes (ISCOMS)-based vaccine containing a novel therapeutic hepatitis B polypeptide was prepared by dialysis method, and its formation was visualized by electron microscopy and biochemically verified by SDS-polyacrylamide gel electrophoresis. Amount of the peptide within ISCOMS was determined by Bradford assay, and specific CTL response was detected by ELISPOT assay.

RESULTS: Typical cage-like structures of submicroparticle with a diameter of about 40nm were observed by electron microscopy. Results from Bradford assay showed that the level of peptide incorporation was about $0.33\text{g}\cdot\text{L}^{-1}$. At the paralleled position close to the sixth band of the molecular weight marker (3480kDa) a clear band was shown in SDS-PAGE analysis, indicating successful incorporation of polypeptide into ISCOMS. It is suggested that ISCOMS delivery system could efficiently improve the immunogenicity of polypeptide and elicit specific immune responses *in vivo* by the results of ELISPOT assay, which showed that IFN- γ producing cells (specific CTL responses) were increased (spots of ISCOMS-treated group: 47 ± 5 , $n=3$; control group: 5 ± 2 , $n=3$).

CONCLUSION: ISCOMS-based hepatitis B polypeptide vaccine is successfully constructed and it induces a higher CTL response compared with short polypeptides vaccine *in vivo*.

Guan XJ, Guan XJ, Wu YZ, Jia ZC, Shi TD, Tang Y. Construction and characterization of an experimental ISCOMS-based hepatitis B polypeptide vaccine. *World J Gastroenterol* 2002;8(2):294-297

INTRODUCTION

Infection of hepatitis B virus (HBV) is very common in China^[1-25], and nearly 100 million people have a persistent infection with HBV who are at risk of developing chronic hepatitis leading to liver cirrhosis and

hepatocellular carcinoma. Up to now, vaccination is a main way in prevention^[26-36]. Based on our knowledge and work on epitopes of HBV natural nucleocapsids, using SGI O2 workstation and Insight II software modeling the configuration of natural HBV PreS2, HBsAg and HbcAg, we have screened out several novel HBV therapeutic polypeptides containing immunodominant B-, T helper (Th) and cytotoxic T lymphocyte responses (CTL) epitopes of HBV PreS2, HBsAg and HbcAg. It is well known that natural antigens and their dominant epitope peptides can not induce sufficient antigen-specific CTL responses *in vivo*, although they could pulse antigen-specific CTLs *in vitro*. Therefore efforts should be made to potentially promote or enhance their antigenicity so as to induce efficient immune responses including CTLs *in vivo*, among which utilization of appropriate adjuvants or delivery systems is a promising and useful strategy.

Elaborate work has demonstrated that ISCOMS, or immunostimulating complexes, first described by Sweden scientist Bror Morein and his colleagues in 1984, is a good vehicle for antigen presentation. Previously antigens used in earlier works in this complexes were isolated from crude molecular components of microbes while is prepared from phosphatidylcholine (or phosphatidylethanolamine), cholesterol and glucoside Quil A (also called Spikoside) and antigen molecule now, which are approximately 40nm submicroscopic cage-like particles (the size is similar to virus particle). ISCOMS formed in the absence of antigen molecules is termed ISCOMS matrix or empty ISCOMS compared to ISCOMS formed in the presence of antigen(s). Elaborate work has demonstrated that ISCOMS is a good vehicle for antigen presentation. Incorporation into ISCOMS not only allows protein antigens to induce strong antibody, major histocompatibility complex (MHC) class II-restricted T cell responses and mucosal immunity, but also allow antigens to enter the endogenous pathway of antigen processing to induce MHC class I-restricted CTL *in vivo*^[37-39]. Immunization with antigens in ISCOMS induces protective immunity against a number of experimental infections, including influenza, toxoplasmosis, measles, feline leukemia, EBV infection, and herpes simplex^[40-42]. An ISCOMS-based vaccine against equine influenza was produced and sold by Iscotec AB in Sweden in 1988. Compared with liposomes, ISCOMS structure is much more rigid, three-dimensional with marked symmetry, which is extremely stable under many conditions, including in the intestine, and may be present for long periods of time intra- and extracellularly in lymphoid tissues. On the basis of our previous work on the design and synthesis of HBV epitope-based vaccines, choosing a polypeptide containing both Th and CTL epitopes of HBV as a model antigen, an experimental ISCOMS-based vaccine was constructed and prepared, and its biochemical and immunological properties were then investigated and discussed in this study.

MATERIALS AND METHODS

Reagents and preparation

Phosphatidylcholine, cholesterol, and decanoyl-N-methyl-glucamide (Mega-10) were all from Sigma. Quil A was kindly provided by Dr. Erik B Lindblad. SDS molecular mass marker (2500-17000u) was from Sigma (MWM-100). Hepatitis B polypeptide, glycopeptide and lipopeptide were synthesized by the solid-phase method with an automated peptide synthesizer (431A, Applied Biosystems, Foster City, CA).

Lipid mixture stock solution

Phosphatidylcholine and cholesterol($10\text{g}\cdot\text{L}^{-1}$ each) were fully dissolved in $200\text{g}\cdot\text{L}^{-1}$ (in distilled water) Mega10, aliquot and store at low temperature until required.

Bradford solution

Dissolve 100mg Coomassie blue G and 30mg SDS in 50mL $950\text{mL}\cdot\text{L}^{-1}$ ethanol. Add 100mL of $850\text{g}\cdot\text{L}^{-1}$ orthophosphoric acid and make up to 1L with water. Filter before use.

Preparation of an experimental ISCOMS-based vaccine from a therapeutic hepatitis B short polypeptide

To a solution of hepatitis B polypeptide($1\text{g}\cdot\text{L}^{-1}$) and Quil A($1\text{g}\cdot\text{L}^{-1}$), add $100\mu\text{L}$ of lipid mixture stock solution and mix thoroughly. After reaction at room temperature for 2h, the mixture was transferred to a dialysis bag, dialyzed 24h at room temperature, then at 4°C for another 48h. To confirm the presence of typical structure of ISCOMS, a small aliquot($\sim 80\mu\text{L}$) was negatively stained and examined by electron microscopy analysis. Sterilize by filtration through a $0.22\mu\text{m}$ filter.

Amount of polypeptide incorporated into ISCOMS determined by Bradford method

To each $50\mu\text{L}$ sample of ISCOMS and to each $50\mu\text{L}$ dilution of BSA add 1mL Bradfords solution. Incubate 5min at room temperature. Measure the A_{595} of each sample and BSA standard. Plot a standard curve from the BSA values and determine the protein concentration of the ISCOMS by interpolation from this curve.

Incorporation of short peptide into ISCOMS examined by peptide SDS-PAGE analysis

Table 1 Formulation of gels

Components	Stacking gel (mL)	Spacer gel (mL)	Separating gel (mL)
Acrylamide solution	5.00	3.05	1.00
Gel buffer	5.00	5.00	3.10
Glycerol	1.60	—	—
Water	3.40	6.95	8.40
Total	15.00	15.00	12.50

Prepare gels as indicated in Table1. After the gel has set, allow to equilibrate by leaving overnight at 4°C . Remove the comb and rinse wells with water, then with Cathode Buffer. Load the samples and molecular weight marker. Electrophoresis condition: constant current at 20mA for 1h and 30mA for 4-6h (the marker dye is within 1cm of the anodic end of the gel). Immerse in the fixative solution for 30min. Transfer to staining solution for 1h and destaining solution for 2h, renewing the solution every 30 minutes. The gel now is ready for visualization, analysis or qhotography.

ELISPOT assay

Female Balb/c mice, obtained from the Animal Research Center of Academy of Military Medical Sciences(Beijing, China) were sc injected to the hind footpad with hepatitis B polypeptide-ISCOMS and hepatitis polypeptide(5nmol each) alone. After 7d of the first priming, the animals were boosted and lymph nodes were removed 7d later to prepare single cell suspension for the ELISPOT assay, which was performed according to the instruction of the murine IFN- γ ELISPOT kit(Diaclone, France).

RESULTS

Typical structure of ISCOMS prepared from hepatitis B polypeptide by electron microscopy

Hepatitis B-ISCOMS unique structure was examined by electron microscopy, which showed uniform honeycomb-like open structure composed of several subunits and confirmed the formation of ISCOMS (Figure 1).

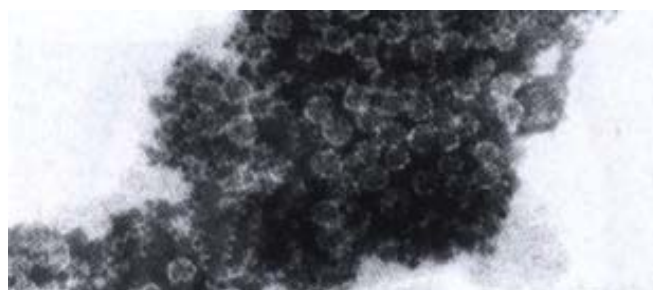


Figure 1 Visualization of hepatitis B-ISCOMS by electron microscopy.

Amount of hepatitis B polypeptide incorporated into ISCOMS

Standard curve was shown as Figure 2($r=0.9968$). The mean A_{595} value of ISCOMS was 0.0835. According to the standard curve, the corresponding peptide concentration was about $0.33\text{g}\cdot\text{L}^{-1}$.

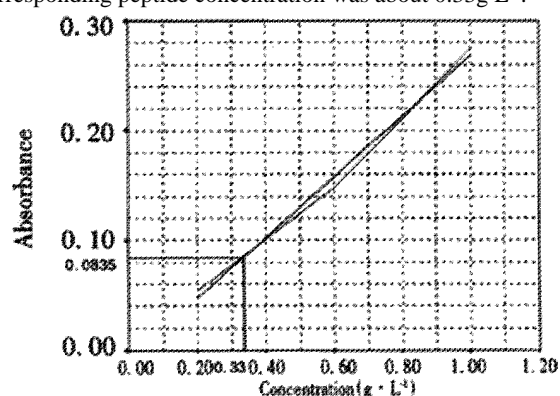


Figure 2 Standard curve of Bradford assay

SDS-PAGE analysis of ISCOMS

In the SDS-PAGE separation of ISCOMS prepared from different hepatitis B polypeptides we observed that at the paralleled position close to the sixth band of the molecular weight marker there was a clear band indicating the peptide incorporated into ISCOMS(Figure 3). Compared to the polypeptide sample, it was at the similar position but somewhat with a slight tailer, which might be affected by other components in the ISCOMS.

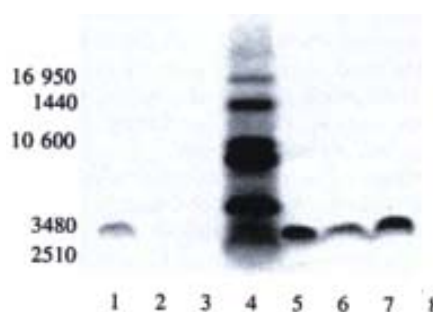


Figure 3 SDS-polyacrylamide gel separation of hepatitis B polypeptide-ISCOMS. 1.Hepatitis B peptide(30)-ISCOMS; 2.ISCOMS matrix; 3.Hepatitis B lipopeptide-ISCOMS; 4.Molecular weight marker; 5.Hepatitis B peptide(30)(as control); 6,7.Hepatitis B peptide(30)-ISCOMS; 8.Hepatitis B glycopeptide -ISCOMS.

IFN- γ linked-CTL activity of Hepatitis B polypeptide-ISCOMS determined by ELISPOT assay

Swelling of lymph nodes were obvious in ISCOMS treated group. In ELISPOT assay, significantly improved IFN- γ linked cytotoxic T lymphocyte(CTL) proliferation response to hepatitis B polypeptide was observed in HBP-ISCOMS group compared to the polypeptide control group(spots of B: 47 ± 5 , $n=3$; A: 5 ± 2 , $n=3$, respectively)(Figure 4).

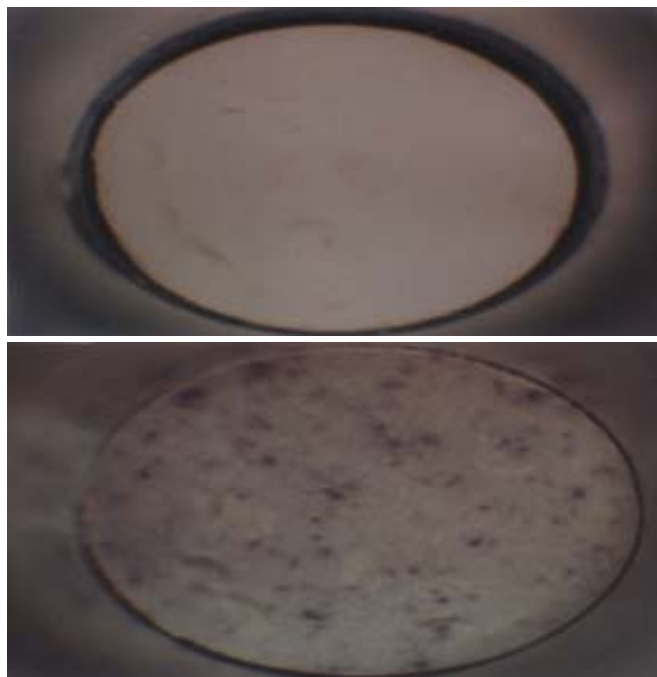


Figure 4 ELISPOT results showing improved specific CTL responses induced by hepatitis B polypeptide incorporated into ISCOMS (B) compared with the polypeptide (A)

DISCUSSION

Studies in immunological mechanisms and T cell function have demonstrated that class I major histocompatibility complex(MHC)-restricted cytotoxic T lymphocytes(CTL) play a critical role in the control of intracellular pathogens and tumor cells growth, but the problems of CTL responses induced *in vivo* and cell-mediated immunity have not been solved yet. Exogenous soluble antigens are not allowed to enter the endogenous pathway necessary for MHC class I-restricted presentation, therefore are not capable of stimulating MHC class I-restricted CD8⁺ CTL responses. Obviously, intracellular expression and synthesis of antigens by infection or through pathological/physiological genes could lead to MHC class I restricted-representation pathway, but vaccination of infectants or transfected cells might lead to certain diseases, thus development of adequate novel vaccine adjuvants, especially those themselves are not immunogenic and could present non-replicable soluble antigens to the endogenous pathway and are capable of inducing MHC class I restricted-CTL responses, are badly in demand.

ISCOMS technique is just one of the novel adjuvanted-vaccine systems to meet this demand. Since the first description of ISCOMS appeared more than a decade ago, ISCOMS has been widely used to generate antigen-adjuvant complex in vaccine development, especially in viral antigen studies to promote immune responses. ISCOMS has a unique ability to provoke a full range of immune response to protein antigens, which is efficient after both parenteral and oral immunization. It has a unique ability to allow the antigen molecules to enter the endogenous pathway for antigen processing, which in turn to provoke MHC class I-restricted CTL. It is safe and stable, prepared

in mild conditions. Furthermore, as ISCOMS is a non-viable adjuvant vesicle and is not immunogenic and antigenic itself, it could enhance antigen specific immune responses, but not unwanted immunity. Different antigen molecules are able to produce vaccine-adjuvant complex with ISCOMS matrix after proper modification, so are useful and promising in various vaccine design.

Preparations of experimental ISCOMS-based vaccines, have been done with large number of whole microbe or isolated from microbe, especially viruses such as HIV^[43-46], influenza virus^[38,47-49], EBV^[41], HSV^[42,50] and Measles^[40,51]. The work with the major S gene products (HBsAg) of the hepatitis B virus genome has been reported, but not with epitope-based hepatitis B polypeptide. In our study, on the basis of the molecular design and synthesis of therapeutic hepatitis B peptides previously, different hepatitis B polypeptides were investigated for their abilities to incorporating into ISCOMS.

Formation of typical structure of ISCOMS was verified by electron microscopy. Adequate proportion of the components, extensive dialysis and purification by density gradient ultracentrifugation when necessary, are important factors involved in the preparation of ISCOMS. The presence of typical cage-like microparticles visualized by electron microscopy is a simple and direct method to examine the formation of ISCOMS, but ISCOMS matrix also shows similar structure as ISCOMS containing antigen molecules, so other methods are required to verify the presence of antigen component. Results from Bradford assay suggested that ISCOMS was successfully formed with polypeptide(30) and other components. In our study, polypeptide incorporated into ISCOMS was about 0.33g·L⁻¹(incorporation rate 33%). In addition, we observed that the short polypeptide which was easily degraded in a couple of days even at 4°C, was stable while stored at 4°C for months without notable degradation, indicating markedly improved stability of antigen peptide after the formation of hepatitis B short polypeptide-ISCOMS.

SDS-PAGE separation of short polypeptide showed an apparent band close to 3480Da which confirmed the successful incorporation of hepatitis B polypeptide into ISCOMS(peptide failed to incorporate into ISCOMS was removed during dialysis). The peptide control showed a straight and regular band, while those for peptide-ISCOMS were broad which indicated effects of other components on SDS-PAGE separation. Specific CTL responses were markedly enhanced by ISCOMS-adjuvanted hepatitis B vaccine compared to antigen peptide control in mice visualized by ELISPOT assay. More work will be done to investigate the immunological properties and mechanisms underlying of this experimental ISCOMS-based vaccine from hepatitis B polypeptide *in vivo*.

ACKNOWLEDGMENTS

We are grateful to Dr. Soren Kamstrup and Dr. Erik B Lindblad from Denmark, Dr. Anna Lunden from Sweden and Dr. John Simms from United Kingdom for their kind help in this study.

REFERENCES

- 1 Wang PZ, Zhang ZW, Zhou YX, Bai XF. Quantitative PCR detection of HBV-DNA in patients with chronic hepatitis B and its significance. *Shijie Huaren Xiaohua Zazhi* 2000; 8: 755-758
- 2 Shi H, Wang FS. Host factors in chronicity of hepatitis B virus infection and their significances clinic alh. *Shijie Huaren Xiaohua Zazhi* 2001; 9: 66-69
- 3 Fang DX, Li FQ, Tan WG, Chen HB, Jin HY, Li SQ, Lin HJ, Zhou ZX. Transient expression and antigenic characterization of HBsAg of HBV nt551 A to G mutant. *World J Gastroenterol* 1999; 5: 73-74
- 4 Guo SP, Ma ZS, Wang WL. Construction of eukaryotic expression vector of HBV x gene. *World J Gastroenterol* 1999; 5: 351-352
- 5 Tang RX, Gao FG, Zeng LY, Wang YW, Wang YL. Detection of HBV DNA and its status of existence in liver tissues and peripheral blood lymphocytes from chronic hepatitis B patients. *World J Gastroenterol* 1999; 5: 359-361
- 6 Chen K, Han BG, Ma XK, Zhang HQ, Meng L, Wang GH, Xia F, Song XG, Ling SG. Establishment and preliminary use of hepatitis B virus preS1/2 antigen assay. *World J Gastroenterol* 1999; 5: 550-552
- 7 Qin LL, Su JJ, Li Y, Yang C, Ban KC, Yian RQ. Expression of IGF- II, p53, P21 and HBxAg in precancerous events of hepatocarcinogenesis induced by AFB1 and/or HBV in tree shrews. *World J Gastroenterol* 2000; 6: 138-139

- 8 He XS, Huang JF, Chen GH, Fu Q, Zhu XF, Lu MQ, Wang GD, Guan XD. Orthotopic liver transplantation for fulminant hepatitis B. *World J Gastroenterol* 2000;6: 398-399
- 9 Hu YP, Yao YC, Li JX, Wang XM, Li H, Wang ZH, Lei ZH. The cloning of 3'truncated preS/.S gene from HBV genomic DNA and its expression in transgenic mice. *World J Gastroenterol* 2000; 6: 734-737
- 10 Wang XZ, Chen XC, Yang YH, Chen ZX, Huang YH, Tao QM. Relationship between HBxAg and Fas/FasL in patients with hepatocellular carcinoma. *World J Gastroenterol* 2000; 6: 17
- 11 Wang SP, Xu DZ, Yan YP, Shi MY, Li RL, Zhang JX, Bai GZ, Ma JX. Hepatitis B virus infection status in the PBMC of newborns of HBsAg positive mothers. *World J Gastroenterol* 2000; 6: 58
- 12 Ma CH, Sun WS, Zhang LN, Ding PF. Inhibitory effect of antisense oligodeoxynucleotides complementary to HBV on HepG2.2.15 cell line. *World J Gastroenterol* 2000; 6: 72
- 13 Gao XW, Jia SY, Liu XM. BCG vaccine combined with dipyrindamole in the treatment of HBV infection. *World J Gastroenterol* 2000; 6: 76
- 14 You J, Zhuang L, Tang BZ, Yang H, Yang WB, Li W, Zhang HL, Zhang YM, Zhang L, Yan SM. Interferon alpha with Thymopeptide in the treatment of chronic hepatitis B. *Shijie Huaren Xiaohua Zazhi* 2001; 9: 388-391
- 15 Chen XS, Wang GJ, Cai X, Yu HY, Hu YP. Inhibition of hepatitis B virus by oxymatrine *in vivo*. *World J Gastroenterol* 2001; 7: 49-52
- 16 Huang ZH, Zhuang H, Lu S, Guo RH, Xu GM, Cai J, Zhu WF. Humoral and cellular immunogenicity of DNA vaccine based on hepatitis B core gene in rhesus monkeys. *World J Gastroenterol* 2001; 7: 102-106
- 17 Fang JN, Jin CJ, Cui LH, Quan ZY, Choi BY, Ki MR, Park HB. A comparative study on serologic profiles of virus hepatitis B. *World J Gastroenterol* 2001; 7: 107-110
- 18 Guo SP, Wang WL, Zhai YQ, Zhao YL. Expression of nuclear factor- κ B in hepatocellular carcinoma and its relation with the X protein of hepatitis B virus. *World J Gastroenterol* 2001; 7: 340-344
- 19 Zhuang L, You J, Tang BZ, Ding SY, Yan KH, Peng D, Zhang YM, Zhang L. Preliminary results of Thymosin- α 1 versus interferon- α treatment in patients with HBeAg negative and serum HBV DNA positive chronic hepatitis B. *World J Gastroenterol* 2001; 7: 407-410
- 20 Wang JP, Li XH, Zhu Y, Wang AL, Lian JQ, Jia ZS, Xie YM. Detection of serum sIL-2R, IL-6, IL-8, TNF- α and lymphocytes subsets, mL-2R in patients with chronic hepatitis B. *Shijie Huaren Xiaohua Zazhi* 2000;8:763-766
- 21 Zhao LS, Qin S, Zhou TY, Tang H, Liu L, Lei BJ. DNA-based vaccination induces humoral and cellular immune responses against hepatitis B virus surface antigen in mice without activation of C-myc. *World J Gastroenterol* 2000; 6: 239-243
- 22 Wang Y, Liu H, Zhou Q, Li X. Analysis of point mutation in site 1896 of HBV precore and its detection in the tissues and serum of HCC patients. *World J Gastroenterol* 2000; 6: 395-397
- 23 Li Y, Su JJ, Qin LL, Yang C, Luo D, Ban KC, Kensler TW, Roebuck BD. Chemopreventive effect of oltipraz on AFB1-induced hepatocarcinogenesis in tree shrew model. *World J Gastroenterol* 2000;6:647-650
- 24 Cheng ML, Lu YY, Wu J, Luo TY, Huang KF, Ding YS, Liu RC, Li J, Li Z. Three-year follow-up study on hepatic fibrosis due to chronic hepatitis B treated by interferon- α 1b and traditional medicine preparation. *World J Gastroenterol* 2000; 6: 81
- 25 Zheng W, Tan H, Song SB, Lu HY, Wang Y, Yu YX, Yin R. The construction and expression of a fusion protein consisting of anti-HBsAg antibody fragment Fab and interferon- α in *E.coli*. *World J Gastroenterol* 2000; 6: 83
- 26 Li WB, Yao ZQ, Zhou YX, Feng ZH. Studies on immunization with HBV gene vaccine plus HBsAg protein in mice. *Shijie Huaren Xiaohua Zazhi* 1999; 7: 188-190
- 27 Du DW, Zhou YX, Feng ZH, Li GY, Yao ZQ. Study on immunization of anti-subcutaneous transplanting tumor induced by gene vaccine. *Shijie Huaren Xiaohua Zazhi* 1999; 7: 955-957
- 28 Du DW, Zhou YX, Feng ZH, Yao ZQ, Li GY. Immune responses to interleukin 12 and hepatitis B gene vaccine in H2 d mice. *Shijie Huaren Xiaohua Zazhi* 2000; 8: 128-130
- 29 Wang QC, Zhou YX, Yao ZQ, Feng ZH. Effects of DNA vector constructs and different genes on the induction of immune responses by HBV DNA based vaccine. *Shijie Huaren Xiaohua Zazhi* 2000; 8: 289-291
- 30 Huang ZH, Zhuang H, Lu S, Guo RH, Xu GM, Cai J, Zhu WF. Humoral and cellular immunogenicity of DNA vaccine based on hepatitis B core gene in rhesus monkeys. *World J Gastroenterol* 2001; 7: 102-106
- 31 Liu HB, Meng ZD, Ma JC, Han CQ, Zhang YL, Xing ZC, Zhang YW, Liu YZ, Cao HL. A 12-year cohort study on the efficacy of plasma-derived hepatitis B vaccine in rural newborns. *World J Gastroenterol* 2000;6:381-383
- 32 Li H, Wang L, Wang SS, Gong J, Zeng XJ, Li RC, Nong Y, Huang YK, Chen XR, Huang ZN. Research on optimal immunization strategies for hepatitis B in different endemic areas in China. *World J Gastroenterol* 2000; 6: 392-394
- 33 Zeng XJ, Yang GH, Liao SS, Chen AP, Tan J, Huang ZJ, Li H. Survey of coverage, strategy and cost of hepatitis B vaccination in rural and urban areas of China. *World J Gastroenterol* 1999; 5: 320-323
- 34 Li H, Li RC, Liao SS, Yang JY, Zeng XJ, Wang SS. Persistence of hepatitis B vaccine immune protection and response to hepatitis B booster immunization. *World J Gastroenterol* 1998; 4: 493-496
- 35 Liao SS, Li RC, Li H, Yang JY, Zeng XJ, Gong J, Wang SS, Li YP, Zhang KL. Long-term efficacy of plasma derived hepatitis B vaccine among Chinese children: a 12-year follow-up study. *World J Gastroenterol* 1999; 5: 165-166
- 36 Kong LB, Gao DS, Mi XQ, Wang FL. The relationship between non-and-hyporesponders to hepatitis B vaccine and their serum interleukine-2 or interleukine 6 levels. *World J Gastroenterol* 2000; 6: 31
- 37 Polakos NK, Drane D, Cox J, Ng P, Selby MJ, Chien D, O'Hagan DT, Houghton M, Paliard X. Characterization of hepatitis C virus core-specific immune responses primed in rhesus macaques by a nonclassical ISCOM vaccine. *J Immunol* 2001; 166: 3589-3598
- 38 Rimmelzwaan GF, Nieuwkoop N, Brandenburg A, Sutter G, Beyer WE, Maher D, Bates J, Osterhaus AD. A randomized, double blind study in young healthy adults comparing cell mediated and humoral immune responses induced by influenza ISCOM vaccines and conventional vaccines. *Vaccine* 2000; 19: 1180-1187
- 39 Voeten JT, Rimmelzwaan GF, Nieuwkoop NJ, Lovgren-Bengtsson K, Osterhaus AD. Introduction of the haemagglutinin transmembrane region in the influenza virus matrix protein facilitates its incorporation into ISCOM and activation of specific CD8(+) cytotoxic T lymphocytes. *Vaccine* 2000; 19: 514-522
- 40 Wyde PR, Stittelaar KJ, Osterhaus AD, Guzman E, Gilbert BE. Use of cotton rats for preclinical evaluation of measles vaccines. *Vaccine* 2000; 19: 42-53
- 41 Wilson AD, Lovgren-Bengtsson K, Villacres-Ericsson M, Morein B, Morgan AJ. The major Epstein-Barr virus (EBV) envelope glycoprotein gp340 when incorporated into ISCOMS primes cytotoxic T-cell responses directed against EBV lymphoblastoid cell lines. *Vaccine* 1999;17:1282-1290
- 42 Mohamedi SA, Brewer JM, Alexander J, Heath AW, Jennings R. Antibody responses, cytokine levels and protection of mice immunized with HSV-2 antigens formulated into NISV or ISCOM delivery systems. *Vaccine* 2000; 18: 2083-2094
- 43 Heeney J, Akerblom L, Barnett S, Bogers W, Davis D, Fuller D, Koopman G, Lehner T, Mooij P, Morein B, de-Giuli-Morghen C, Rosenwirth B, Verschoor E, Wagner R, Wolf H. HIV-1 vaccine-induced immune responses which correlate with protection from SHIV infection: compiled preclinical efficacy data from trials with ten different HIV-1 vaccine candidates. *Immunol Lett* 1999; 66: 189-195
- 44 Verschoor EJ, Mooij P, Oostermeijer H, van der Kolk M, ten-Haaf P, Verstrepen B, Sun Y, Morein B, Akerblom L, Fuller DH, Barnett SW, Heeney JL. Comparison of immunity generated by nucleic acid-MF59, and ISCOM-formulated human immunodeficiency virus type 1 vaccines in Rhesus macaques: evidence for viral clearance. *J Virol* 1999;73:3292-3300
- 45 Rytting AS, Akerblom L, Albert J, Unger T, Bjorling E, Al-Khalili L, Gronowitz JS, Kallander CF. Monoclonal antibodies to native HIV type 1 reverse transcriptase and their interaction with enzymes from different subtypes. *AIDS Res Hum Retroviruses* 2000; 16: 1281-1294
- 46 Oscherwitz J, Zeigler ME, Gribbin TE, Cease KB. A V3 loop haptenic peptide sequence, when tandemly repeated, enhances immunogenicity by facilitating helper T-cell responses to a covalently linked carrier protein. *Vaccine* 1999; 17: 2392-2399
- 47 Rimmelzwaan GF, Baars M, van-Beek R, de-Lijster P, de-Jong JC, Claas EC, Osterhaus AD. Influenza virus subtype cross-reactivities of haemagglutination inhibiting and virus neutralising serum antibodies induced by infection or vaccination with an ISCOM-based vaccine. *Vaccine* 1999; 17: 2512-2516
- 48 Ennis FA, Cruz J, Jameson J, Klein M, Burt D, Thippawong J. Augmentation of human influenza A virus-specific cytotoxic T lymphocyte memory by influenza vaccine and adjuvant carriers (ISCOMS). *Virology* 1999; 259: 256-261
- 49 Rimmelzwaan GF, Claas EC, van-Amerongen G, de-Jong JC, Osterhaus AD. ISCOM vaccine induced protection against a lethal challenge with a human H5N1 influenza virus. *Vaccine* 1999; 17: 1355-1358
- 50 Simms JR, Heath AW, Jennings R. Use of herpes simplex virus (HSV) type 1 ISCOMS 703 vaccine for prophylactic and therapeutic treatment of primary and recurrent HSV-2 infection in guinea pigs. *J Infect Dis* 2000; 181: 1240-1248
- 51 Stittelaar KJ, Boes J, Kersten GF, Spiekstra A, Mulder PG, de-Vries P, Roholl PJ, Dalsgaard K, van-den-Dobbelsteen G, van-Alphen L, Osterhaus AD. In vivo antibody response and *in vitro* CTL activation induced by selected measles vaccine candidates, prepared with purified Quil A components. *Vaccine* 2000; 18: 2482-249

mIL-2R, T cell subsets & hepatitis C

Chao-Pin Li, Ke-Xia Wang, Jian Wang, Bo-Rong Pan

Chao-Pin Li, Ke-Xia Wang, Jian Wang, Department of Aetiology and Immunology, School of Medicine, Huainan University of Technology, Huainan 232001, Anhui Province, China
Bo-Rong Pan, the Fourth Military Medical University
Supported by the Youth Scientific Foundation of the Ministry of Coal Industry of China, No. 96-072

Correspondence to: Dr. Chao-Pin Li, School of Medicine, Huainan Institute of Technology, Huainan 232001, Anhui Province, China. yxfy@hnt.edu.cn
Telephone: +86-554-6658770 Fax: +86-554-6662469

Received 2001-09-14 Accepted 2001-10-11

Abstract

AIM: To study the levels of membrane interleukin-2 receptor (mIL-2R) and T cell subsets in peripheral blood mononuclear cells (PBMC) from patients with hepatitis C and their role in the pathogenesis of hepatitis C.

METHODS: The levels of mIL-2R and T cells subsets in PBMC were detected by biotin-streptavidin (BSA) technique before and after stimulation with PHA in 203 patients with hepatitis C with HCV-RNA(+), anti-HCV(+), anti-HCV(-).

RESULTS: The total expressive levels of mIL-2R before and after stimulation with PHA (0.03 ± 0.01 , 0.03 ± 0.02 , 0.04 ± 0.02 , 0.36 ± 0.03), and T cell subsets in PBMC (0.62 ± 0.06 , 0.37 ± 0.05 , 0.35 ± 0.07) were all lower in patients with hepatitis C than those in normal controls (0.66 ± 0.07 , 0.41 ± 0.06 , 0.31 ± 0.05 , $P < 0.01$). Among the patients, the levels of mIL-2R were lower in silence than those in situation of PHA inducing ($P < 0.01$). However, the levels of mIL-2R were similar in acute hepatitis C to that in chronic hepatitis C ($P > 0.05$). The levels of CD_3^+ , CD_4^+ , CD_4^+/CD_8^+ were lower and CD_8^+ was higher in patients with acute and chronic hepatitis C with anti-HCV(+) than those in normal controls (0.62 ± 0.06 , 0.37 ± 0.05 , 0.35 ± 0.07 , 1.18 ± 0.30 , 0.61 ± 0.07 , 0.37 ± 0.05 , 1.39 ± 0.33 , 0.31 ± 0.05 , $P < 0.05$ - $P < 0.01$).

CONCLUSION: The cellular immunity is obviously changed in patients with hepatitis C. The levels of mIL-2R and activation of T cells are closely associated with chronicity of hepatitis C.

Li CP, Wang KX, Wang J, Pan BR. mIL-2R, T cell subsets & hepatitis C. *World J Gastroenterol* 2002;8(2):298-300

INTRODUCTION

In acute and chronic hepatitis C virus (HCV) infection liver damage is thought to be the results of T-lymphocyte-mediated destruction of virus infected liver cells^[1-51]. The factors that affected the immune response to viral antigens, particularly those that regulate the function of virus-specific cytotoxic T-lymphocyte-mediated lymphocytes, most likely play an important role in determining the states of liver injury. Interleukin-2 (IL-2) has a crucial role in several immunologic functions and its effect is dependent on the interaction with IL-2 receptors (IL-2R) expressed on surface of activated T lymphocytes and other immunocompetent cells^[52-54]. Decreased IL-2 activity in supernatants of mitogen-activated peripheral blood mononuclear cells (PBMC) has been measured in patients with chronic HCV infection who had active liver disease, while normal levels have been detected in chronic HCV carriers with milder or no liver damage. The impaired

IL-2 activity of PBMC, which has been claimed to be associated with high levels of virus duplication, has been interpreted as the reflection of an immune regulatory disorder of chronic active hepatitis C, which may be responsible for reduced differentiation of cytotoxic, virus-specific T cells and could explain the failure to eliminate all infected cells. Recently, methods for detecting membrane interleukin-2 receptor (mIL-2R), which exists on surface of T cells and can be released from activated lymphocytes, have been available, and high levels of these serum factors have been detected in a variety of pathologic conditions. To analyze IL-2R dependent immunoregulatory function in viral hepatitis, the levels of mIL-2R in the course of acute and chronic HCV infection in relation to the activity of liver disease and of virus replication have been investigated. The results suggest that in chronic active hepatitis C there is a state of activation rather than of depression of the IL-2 system, and the pathogenesis is related to the cellular immune function of the patients. PBMC are aggregation of immune cells, which have a lot of T lymphocytes, and play an important role in the anti-HCV infection. The cellular immune function of the patients may be the reflection of the level of T cell subsets and mIL-2R. The method of biotin-streptavidin (BSA) has higher specificity and sensitivity. In order to study the influence on the cellular immune function after being infected by HCV in PBMC and the effect on the mechanism of hepatitis C, the T cell subsets and mIL-2R of 203 patients with acute and chronic hepatitis C were detected by the above methods.

MATERIALS AND METHODS

Subjects

The 203 patients with confirmed diagnosis of hepatitis C (male 116 and female 87), aged 19-52 (average: 36.4 years), from our affiliated and teaching hospitals were chosen whose HCV-RNA in serum and PBMC were detected. Among them, the positive number of HCV-RNA in acute and chronic patients was 58 and 145 respectively. All diagnoses were made according to the diagnosis criterion of Chinese Hepatitis Conference 1995 (Beijing). The controls ($n=20$) were normal blood donors from the local Central Blood Bank.

Reagents and instruments

The antibodies against T cell subsets, Ficoll-Hypaque sedimentation gradient were produced by Shanghai Jingan Medical Institute, the Second Reagent Factory of Shanghai, and Huamei Bioengineering Company of Shanghai (No. 981010, 980215, 980422). Carbon dioxide gas incubator (MDF-135) was made in Japan.

Samples

The peripheral vein blood 5mL from each of the patients with hepatitis C was collected at 08:00, which was distributed 2.5mL in a sterile test tube and an anticoagulant test tube with heparin respectively.

Separation of PBMC and detection of T cell subsets, mIL-2R

After the anticoagulant heparinized blood was mixed with equal volume of Hanks' liquid without Ca^{2+} and Mg^{2+} , the PBMC were harvested from heparinized whole blood by centrifugation on Ficoll-Hypaque sedimentation gradient and diluted to $(1-3) \times 10^9 \cdot L^{-1}$ cells suspension with RPMI 1640 culture liquid. The $10 \mu L$ suspension of

PBMC was smeared on sheet glass pores so that the cells with CD_3^+ , CD_4^+ , CD_8^+ could be detected. Of the PBMC suspension, 0.5mL was mixed with RPMI 1640 culture liquid, which had PHA 200mg·L⁻¹. The cells were grown in continuous culture (37°C, 50mL·L⁻¹ CO₂ in atmosphere) for 72h and its mL-2R induced by PHA could be measured by the antibodies against membrane of T cells.

Immunocytochemical method of Biotin-streptavidin system (BSA)

The different mAb against CD_3 , CD_4 , CD_8 and Tac with biotin and SA-HRP were smeared on different sheet glasses. These smears were left dry naturally and fixed with acetone for 15-20min. The cells were incubated in continuous culture (37°C, 50mL·L⁻¹ CO₂ in atmosphere) for 30min. The immune sheet glass pores were measured after being stained with the color-developing agent and several washings with Tris Buffer Solution (TBS). The total number

of 200 PBMC was counted and its positive cells were statistically analyzed with the help of high power lens. The positive criterion was that the color of endoplasm or cell membrane was brown, if not being negative.

Statistical analysis was made by using Student's *t* test.

RESULTS

The results showed that the absolute positive rates of CD_3^+ , CD_4^+ and CD_4^+/CD_8^+ were lower and CD_8^+ was higher in patients with anti-HCV(+) than those in normal controls ($P<0.01$, Table 1). However, there was no significant difference between the patients with acute hepatitis C and normal controls ($P>0.05$). But there was a higher significant difference between the patients with chronic hepatitis C and normal controls ($P<0.05$). The reactivity of T cells in peripheral blood before and after being induced by PHA was all lower in acute, chronic hepatitis C than those in normal controls ($P<0.01$).

Table 1 The detective results of T cell subsets and mL-2R in peripheral blood of patients with hepatitis C ($\bar{x}\pm s$)

Group	n	CD_3^+	CD_4^+	CD_8^+	CD_4^+/CD_8^+	mIL-2R	
						Silent	Induced
Anti-HCV(+)AH	58	0.62±0.05 ^a	0.37±0.05 ^b	0.35±0.07 ^a	1.18±0.30	0.03±0.01 ^b	0.34±0.02 ^b
Anti-HCV(-)CH	145	0.61±0.07 ^b	0.37±0.05 ^b	0.36±0.06 ^b	1.04±0.42 ^b	0.03±0.01 ^b	0.35±0.02 ^b
Normal controls	20	0.66±0.07	0.41±0.06	0.31±0.05	1.39±0.33	0.04±0.02	0.36±0.03
F	-	5.32	6.45	5.96	7.08	8.33	9.05
P		<0.01	<0.01	<0.01	<0.01	<0.01	<0.01
MS within group		40.347	26.186	32.022	0.150	1.39	5.354

^a $P<0.05$, ^b $P<0.01$, vs normal control. AH: acute hepatitis; CH: chronic hepatitis

DISCUSSION

The chronicity of hepatitis is easier in patients with hepatitis C than that with hepatitis B^[6,12,20,26,36]. The T cell subsets of the 203 patients with hepatitis C were detected by the method of BSA, and the results showed that the positive rate of T cell subsets and their mutual proportion were significantly different ($P<0.01$), and there were significant disorders of cellular immune function and obvious pathologic injury.

It seems probable that mL-2R is an important symbol of active T cells and plays a key role in biologic effect and its expression level can reflect the course of T cells activity and immune situation. The expressive level of T cells in silence was lower in hepatitis C patients than in normal controls ($P<0.01$), which showed that the T cell activity was interfered. The possible reasons seemed to be as follows: (1)The mL-2R on surface of T cells of the patients was inhibited by HCV; (2)The infection, duplication, proliferation of HCV in PBMC promoted the soluble interleukin-2 receptor to (sIL-2R) produced and released from T cells and inhibited the expression of mL-2R^[55-59]. This manifestation was caused by the low inducing cellular immune ability. Some active Tc cells could be combined tightly with the complex of HCV antigen-MHC-I molecule on the surface of liver cells by T cells receptor (TCR) and released perforin. This irrevocable and progressive injury was one of the important reasons for chronicity of hepatitis C; (3)sIL-2R and mL-2R could competitively combine with IL-2, and sIL-2R, being an immunosuppressive factor (similar to blocking factor), which could activate the IL-2 around the T cells so that the self-secretion effect of T cells decreased and the disorder of cellular immune function was enforced and the infection of HCV would be persisted^[60-62]. These conclusions were in agreement with the concept that both acute and chronic active hepatitis C liver cell damages were caused mainly by cytotoxic T lymphocytes directed against viral antigens expressed on the surface of infected cells and that CD_8^+ lymphocytes were abundant in the infiltrates of the liver.

The present study demonstrates that the receptor of PHA exists on the surface of T cells. The level of mL-2R obviously increased after stimulation with PHA, which showed that mL-2R could be induced by PHA and was significantly different between acute hepatitis C patients and chronic hepatitis C patients ($P<0.05$). The more serious the patient's condition, the longer the course of disease, and the lower the level of mL-2R. The low level of mL-2R was not beneficial for clearing away HCV and easy to reduce chronicity of hepatitis C.

CD_3^+ , CD_4^+ and CD_8^+ are major function subsets of T cells and play a key role in response to HCV. Its counts and mutual relationship could be used to identify the cellular immune level and immunoregulation and is one of the valuable immunologic targets to forecast the change of patients' condition. The results showed that the lower positive rate of CD_3^+ in chronic hepatitis C and the immunity to HCV were partly deficient. The lower positive rate and poor activation of CD_4^+ are important reasons for the disorder of the immune function and can not clean HCV in time. Another key reason is the high level of CD_8^+ in chronic active hepatitis C, which can cause injury of liver cells and increase of ALT persistently. The proportion of CD_4^+/CD_8^+ could play an important role in the network of immunoregulation. The high level of CD_8^+ identified the injury of liver cells caused by CTL. These findings indicated that the immune response of the body to HCV was limited, and the infection of HCV existed persistently so that the patient's condition would change from acute to chronic.

REFERENCES

- Chen YD, Tao QM, Zhang CY. The treatment of oral interferon for thirty patients with hepatitis C. *Xin Xiaohuabingxue Zazhi* 1996; 4:12-14
- Liu YJ, Cong WM, Xie TP, Wang H, Shen F, Guo YJ, Chen H, Wu MC. Detecting the localization of hepatitis B and C virus in hepatocellular carcinoma by double in situ hybridization. *China Natl J New Gastroenterol* 1996; 2:187-189
- Wei L, Wang Y, Chen HS, Tao QM. Sequencing of hepatitis C virus cDNA with polymerase chain reaction directed sequencing. *China Natl J New Gastroenterol* 1997; 3:12-15

- 4 Gao JE, Tao QM, Guo JP, Ji HP, Lang ZW, Ji Y, Feng BF. Preparation and application of monoclonal antibodies against hepatitis C virus nonstructural proteins. *China Natl J New Gastroenterol* 1997; 3:114-116
- 5 Yu SJ. A comparative study on proliferating activity between HBV related and HCV related small HCC. *China Natl J New Gastroenterol* 1997; 3:236-237
- 6 Zhang LF, Peng WW, Yao JL, Tang YH. Immunohistochemical detection of HCV infection in patients with hepatocellular carcinoma and other liver diseases. *World J Gastroenterol* 1998; 4:64-65
- 7 Tong WB, Zhang CY, Feng BF, Tao QM. Establishment of a nonradioactive assay for 2' 5' oligoadenylate synthetase and its application in chronic hepatitis C patients receiving interferon α . *World J Gastroenterol* 1998; 4:70-73
- 8 Liu YH, Zhou RL, Rui JA. Detection of hepatoma cells in peripheral blood of HCC patients by nested RT-PCR. *World J Gastroenterol* 1998; 4:106-108
- 9 Zhu FL, Lu HY, Li Z, Qi ZT. Cloning and expression of NS3 cDNA fragment of HCV genome of Hebei isolate in *E. coli*. *World J Gastroenterol* 1998; 4:165-168
- 10 Yang JM, Wang RQ, Bu BG, Zhou ZC, Fang DC, Luo YH. Effect of HCV immunization on expression of several cancer associated gene products in HCC. *World J Gastroenterol* 1999; 5: 25-27
- 11 Chen SB. The infection of HCV and primary hepatocellular carcinoma. *Xin Xiaohuabingxue Zazhi* 1994; 2:239-240
- 12 Sun ZQ, Wang YJ. The positive and negative growth factors for modulate on replication of hepatocellular. *Xin Xiaohuabingxue Zazhi* 1994; 2: 247-248
- 13 Deng C, Su XS. The studied advance on growth factors of hepatocellular. *Xin Xiaohuabingxue Zazhi* 1994; 2:61
- 14 Chen SB. The relationship between hepatic disease and heredity. *Xin Xiaohuabingxue Zazhi* 1995; 3:1-2
- 15 Li JX, Sun DY, Li H, Zhu XZ, Liou QK, Su SL, Zhang D, Shen XY. Detection the marker of hepatitis virus and cytonmegalovirus for blood donors with ELISA. *Xin Xiaohuabingxue Zazhi* 1995; 3:181
- 16 Li XY, Yin FQ, Hou YF. The treatment of Ligalong dilution for 68 patients with hepatitis C. *Xin Xiaohuabingxue Zazhi* 1995; 3:116
- 17 Tian SB, Li DG, Lu HM. Transformation growth factor α and hepatic disease. *Xin Xiaohuabingxue Zazhi* 1995; 3:55
- 18 Jia KL, Zhang XF. Analysis on the detection of anti-HCV and ALT for 1050 blood donors. *Xin Xiaohuabingxue Zazhi* 1995; 3:154
- 19 An P, Yuan F, Han CF. Risk factos of hepatitis C virus infevion in hemodialysis patients. *Xin Xiaohuabingxue Zazhi* 1996; 4:12-14
- 20 Li JQ, Si PR, Yang LG, Liu BY, Min JR, Sun ZH, Cheng SM. Superinfection and mutual relation of hepatitis B and C virus. *Xin Xiaohuabingxue Zazhi* 1996; 4:15-17
- 21 Dong SX, Chen SB. Tumor necrosis factor and chronic hepatic disease. *Xin Xiaohuabingxue Zazhi* 1996; 4:44-45
- 22 Li JX, Zhu XZ, Li H. The detective rate of HBV, HCV, HDV in fresh serum of HBsAg (+) and ALT(-). *Xin Xiaohuabingxue Zazhi* 1996; 4:52
- 23 Li C, Zhan SL, Wang BN. The significance of detection of anti-HCV and hematometachysis. *Xin Xiaohuabingxue Zazhi* 1996; 4:55-56
- 24 Ren ZX, Pei WX, Wang LS, Liou JX. The change of viral marker in serum for overlapping infection of HBV and HCV. *Xin Xiaohuabingxue Zazhi* 1996; 4:379-380
- 25 Li JQ, Si PR, Yang LG, Liou BY, Min JR. Study on the viral marker in serum of 311 patients with hepatitis. *Xin Xiaohuabingxue Zazhi* 1996; 4:387-388
- 26 Zhang SL, Lan SM, Li YF. The diagnosis and treatment of chronic hepatitis C. *Xin Xiaohuabingxue Zazhi* 1996; 4:397-398
- 27 Cheng SQ. The advance of hepatic manifestat- tion of viral disease. *Xin Xiaohuabingxue Zazhi* 1996; 4: 401-402
- 28 Tang ZN, Hao LJ. The treatment of interferon on hepatitis C. *Xin Xiaohuabingxue Zazhi* 1996; 4: 403-404
- 29 Zhan SL, Li C, Wang BN. The manifestation of auto-antibody in serum of patients with positive of anti-HCV. *Xin Xiaohuabingxue Zazhi* 1996; 4:382
- 30 Ji JM, Li JX. The detective rate of anti-HCV in serum of patients in hospital. *Xin Xiaohuabingxue Zazhi* 1996; 4:411
- 31 Wang M, Li JX. Detection of viral marker of patients with hematometachysis and hemodialysis. *Xin Xiaohuabingxue Zazhi* 1996; 4:413-414
- 32 Zhang YR, Ding SZ, Li HB, Fan XM, Yang YX. The influence of HBV, HCV on liver function. *Xin Xiaohuabingxue Zazhi* 1996; 4: 417-418
- 33 Wang YJ, Wang XH, Wang YM, Li MD. Ultrastructural changes of neutrophils in patients with chronic severe viral hepatitis. *Xin Xiaohuabingxue Zazhi* 1996; 4:452-453
- 34 Lin SM, Zhang SL, Di PC, Liang XS. The significance of recombinant immunoblot assay in acute hepatitis C. *Xin Xiaohuabingxue Zazhi* 1996; 4:511-512
- 35 Zhao YY, Yang HY, Liu GX, Li ZQ, Liu L, He LL, Deng WJ. Hepatitis C virus infection in patients with primary liver cancer. *Xin Xiaohuabingxue Zazhi* 1996; 4:43-44
- 36 Jiang ZK, Zhang XF, Zhang C, Li LH, Yan MH. Study on the aetiology of posthepatic cirrhosis. *Xin Xiaohuabingxue Zazhi* 1997; 5:136
- 37 Shen J, Xu YC, Gao Z, Niu JY, Shen HB, Ye FF. Epidemiological statocellauldy on the etiologic synergistic interaction of HCV and HBV in the development of hepar carcinoma. *Xin Xiaohuabingxue Zazhi* 1997; 5:72-74
- 38 Li SL, Ma XX, Jing XJ. Investigation on HCV contamination of blood products in hospitals. *Xin Xiaohuabingxue Zazhi* 1997; 5:94-95
- 39 Tang ZY, Qi JY, Shen HX, Yang DL, Hao LJ. Short and long term effect of interferon therapy of patients with chronic hepatitis C. *Xin Xiaohuabingxue Zazhi* 1997; 5:104-105
- 40 Luo YQ, Wu MC. Hepatocyte growth factor. *Xin Xiaohuabingxue Zazhi* 1997; 5:198-199
- 41 Liang XS, Zhang SL, Di PC, Lin SM. Serum hepatitis C virus RNA in patients with chronic hepatitis C virus infection treated with interferon α . *Xiaohuabingxue Zazhi* 1997; 5:311-312
- 42 Lin SM, Zhang SL. Diagnostic value of RIBA and RIA-2 in detection of anti HCV in chronic hepatitis C. *Xin Xiaohuabingxue Zazhi* 1997; 5: 444-445
- 43 Tang W, Du SC, Tao QM, Zhu L. A study on anticontamination of RT-PCR in detection of HCV-RNA. *Xin Xiaohuabingxue Zazhi* 1997; 5:638-639
- 44 Yan XB, Wei L, Wu WT. Clinical analysis on gene-type and different type of HCV overlapping infection of HBV. *Xin Xiaohuabingxue Zazhi* 1997; 5:805-806
- 45 Li SL, Su K, Fang JT. Epidemiologic analysis of HBV, HCV and HDV infection in natural population in Fushun. *Xin Xiaohuabingxue Zazhi* 1997; 5:42-43
- 46 Li LF, Zhou Y, Xia S, Zhao LL, Wang ZX, Wang CQ. The epidemiologic feature of HCV prevalence in Fujian. *World J Gastroenterol* 2000; 6:80
- 47 Du JH, Cha WZ. Interrelation between hepatitis C and primary hepatocellular carcinoma. *Shijie Huaren Xiaohua Zazhi* 1999; 7:176
- 48 Worman HJ, Lin F. Molecular biology of liver disorders: the hepatitis C virus and molecular targets for drug development. *World J Gastroenterol* 2000; 6:465-469
- 49 Jiang RL, Lu QS, Luo KX. Cloning and expression of core gene cDNA of Chinese hepatitis C virus in cosmid pTM3. *World J Gastroenterol* 2000; 6:220-222
- 50 Zhou YX, Feng ZH, Jia ZS, Lian JQ, Li JG, Li WB. A study of gene immunization with recombinant expression plasmid of hepatitis C virus core antigen. *Huaren Xiaohua Zazhi* 1998; 6:966-968
- 51 Guo YH, Yan XJ, Hou Y, Ren FL, Zhao JR, Cui DX, Han FC, Duan J, Li XQ, Su CZ. Quantitative detection HCV-RNA in serum of Chinese people with RT-PCR. *Huaren Xiaohua Zazhi* 1999; 7: 810-811
- 52 Zhao XM, Duan DL, Zhang AL, Wang ZG, Zhu M, Hu R. Effect of antineoplastic agent huisheng oral liquid on human IL-2 level and activity of LAK cells. *Huaren Xiaohua Zazhi* 1998; 6:409-411
- 53 Jing DD, Qiu DK. Relationship between IL-2 activity, IL-2R expression and liver function in patients with post hepatitis B cirrhosis. *Huaren Xiaohua Zazhi* 1998; 6: 900-901
- 54 Zhao CY, Liu JX, Tang HH, Feng ZJ, Zhen Z, Zhang SH. Significance of IL-2 and related indexes in patients with hepatitis and hepatocellular carcinoma. *Huaren Xiaohua Zazhi* 1998; 6:479-481
- 55 Liu YH, Zhou RL, Rui JA. Detection of hepatoma cells in peripheral blood of HCC patients by nested RT-PCR. *World J Gastroenterol* 1998; 4: 106-108
- 56 Wu HB, Li ZW, Li Y. Clinical significance of detection of positive and negative strands of HCV RNA in peripheral blood mononuclear cells. *Shijie Huaren Xiaohua Zazhi* 1999; 7:220-221
- 57 Zhao XP, Shen HX, Tian DY, Zhang DS, Peng ZH, Yang DL, Hao LJ. Expression and significance of HCV RNA and HCV NS5 antigen in liver tissues of patients with hepatitis C. *Shijie Huaren Xiaohua Zazhi* 1999; 7: 516-518
- 58 Fan XG, Tang FQ, Ou ZM, Zhang JX, Liu GC, Hu GL. Lymphoproliferative response to hepatitis C virus (HCV) antigens in patients with chronic HCV infection. *Shijie Huaren Xiaohua Zazhi* 1999; 7:1038-1040
- 59 Liou WN, Tan DM, Fan XG, Zhang Z, Ou YK. The significance of detection of HCV in peripheral blood mononuclear cells of patients. *Shijie Huaren Xiaohua Zazhi* 2001; 9:235
- 60 Wang JP, Li XH, Zhu Y, Wang AL, Lian JQ, Jia ZS, Xie YM. Detection of serum sIL-2R, IL-6, IL-8, TNF- α and lymphocytes subsets, mIL-2R in patients with chronic hepatitis B. *Shijie Huaren Xiaohua Zazhi* 2000; 8: 763-766
- 61 Huang PC. Clinical manifestation of detection of sIL-2R in serum and ascites for the patients with cirrhosis and hepatocellular carcinoma. *Huaren Xiaohua Zazhi* 1998; 6:455-456
- 62 Zhang SL, Liang XS, Lin SM, Qiu PC. Relation between viremia level and liver disease in patients with chronic HCV infection. *China Natl J New Gastroenterol* 1996; 2:115-117

• *H. pylori* •

Modalities of testing *Helicobacter pylori* in patients with nonmalignant bile duct diseases

Milutin Bulajic, Bojan Stimec, Miroslav Milicevic, Matthias Loehr, Petra Mueller, Ivan Boricic, Nada Kovacevic, Mirko Bulajic

Milutin Bulajic, Department of Internal Medicine, Clinical Center "Dr Dragisa Misovic"-Dedinje, Belgrade, Yugoslavia
Bojan Stimec, Institute for Anatomy, School of Medicine, Belgrade, Yugoslavia
Miroslav Milicevic, First Surgical Clinic, Institute for digestive Diseases, University Clinical Center, Belgrade, Yugoslavia
Matthias Loehr, Department of Medicine II, Medical Faculty Mannheim, University of Heidelberg, Germany
Petra Mueller, Department of Medicine, University of Rostock, Germany
Ivan Boricic, Institute for Pathology, School of Medicine, Belgrade, Yugoslavia

Nada Kovacevic and Mirko Bulajic, Clinic for Gastroenterology and Hepatology, Institute for Digestive Diseases, University Clinical Center, Belgrade, Yugoslavia

Supported by Gastrointestinal Research Laboratory, Department of Medicine, University of Rostock, Germany

Correspondence to: Dr. Milutin Bulajic, Department of Internal Medicine, Clinical Center "Dr Dragisa Misovic"-Dedinje, Heroja Milana Tepica 1, 11000 Belgrade, Yugoslavia. mbulajic@EUnet.yu

Telephone: +381-11-667122 Fax: +381-11-4442452

Received 2001-12-21 Accepted 2002-01-25

Abstract

AIM: This paper describes the procedure of detection of *Helicobacter pylori* (*H. pylori*) in bile specimens in patients suffering from benign diseases of biliary ducts (lithiasis with/without nonspecific cholangitis).

METHODS: The group of 72 patients entering the study consisted of 32 male and 40 female (45% and 55%, respectively). Bile was obtained during ERCP in 68 patients, and during cholecystectomy in 4 patients. A fast urease test (FUT) to determine the existence of *H. pylori* in gastric mucosa was carried out for all the patients during the endoscopic examination. The existence of genetic material of *H. pylori* was determined by detection of ureA gene by the method of nested PCR. The results of this reaction were shown by electrophoresis on 10g·L⁻¹ agarose gel in a band of 256bp.

RESULTS: The majority of the patients included in our study had biliary lithiasis without signs of cholangitis (48 patients, 67%), whereas other patients were complicated by cholangitis (17 patients, 24%). Seven patients (9%) had normal ERCP, forming thus the control group. In the group of patients with lithiasis 26 patients (54.2%) had positive PCR of *H. pylori* in bile and among the patients with associated cholangitis positive PCR was detected in 9 patients (52.9%). Among the seven patients with normal ERCP only one (14%) had positive PCR of *H. pylori*. A high percentage of *H. pylori* infection of gastric mucosa was observed (57 patients, 79%). It was also observed that its slightly higher positivity was in the patients with distinct bile pathology: 81% FUT positive patients in the group with choledocholithiasis alone and 76% in the group with choledocholithiasis associated with cholangitis. Seventy-one percent of the patients with regular findings had positive FUT.

CONCLUSION: The prevalence of *H. pylori* infection both in bile and in gastric mucosa in patients with benign diseases of biliary ducts does not show a statistically significant difference in relation to the prevalence of the same with the patients with normal ERCP. The existence of *H. pylori* infection possibly does not play a role in pathogenesis of benign biliary diseases.

Bulajic M, Stimec B, Milicevic M, Loehr M, Mueller P, Boricic I, Kovacevic N, Bulajic M. Modalities of testing *Helicobacter pylori* in patients with nonmalignant bile duct diseases. *World J Gastroenterol* 2002;8(2):301-304

INTRODUCTION

Helicobacter pylori (*H. pylori*) is a microaerophilic and Gram-negative microorganism which could represent the main causative agent in the development of chronic antral gastritis, duodenal ulcer, or even gastric cancer^[1-3]. In the last few years, the interests of scientists in the correlation between *H. pylori* infection and various extradigestive diseases^[4] have been significantly increasing. Due to the complexity of pathophysiologic mechanisms of the infection with this microorganism, diagnostic procedures for the detection of *H. pylori* infection in extragastric specimens did not meet high standards. Fast urease test for the detection of *H. pylori* infection in stomach often had false negative or false positive results^[5]. Microscopic analysis of the specimens by means of various staining also proved to be nonspecific without sufficient sensitivity to detect this organism. The incubation process takes even from 3 to 7 days in order to obtain cultures of *H. pylori*. This was the reason to undertake cloning of urease gene of *H. pylori*, which was specific for this species, thus obtaining high sensitivity and specificity^[6]. Urease genes (EMBL acc. No. X17079)^[7] were sequestered and specific *H. pylori* oligonucleotide primers were synthesized. Having used fumes of these oligonucleotide primers for detection and identification of *H. pylori*, the method of PCR (polymerase chain reaction) permits the recognition of *H. pylori* even in a trace, by multiplying the aimed genetic sequence of a specific ureA gene^[8].

This paper describes the procedure of *H. pylori* microorganism detection in specimens of bile with the patients subject to the test suffering from benign diseases of biliary ducts (lithiasis with/without nonspecific cholangitis).

MATERIALS AND METHODS

The study was carried out on 72 patients, admitted at the Institute for Digestive Diseases (the Clinic for Gastroenterology and Hepatology and First Surgical Clinic) of the University Clinical Centre of Serbia in Belgrade. Laboratory workup was accomplished at the Gastrointestinal Research Laboratory, University of Rostock. The group of 72 patients who were tested consisted of 32 male and 40 female (45% and 55%, respectively). The age range was from 11-90 yrs. The average age of all the patients was 56.7 years with SD±16.45. Thirty two patients (44%) had undergone previous cholecystectomy.

The patients were examined at the University Clinical Centre of

Serbia from September 20, 1998 to October 5, 1999. Prior to this, the patients did not undergo any endoscopic biliary therapeutical procedures. In 68 patients, the specimens of bile were obtained during endoscopic retrograde cholangio-pancreatography (ERCP) and in 4 patients during cholecystectomy. In all the patients which underwent ERCP, endoscopic papillotomy (EPT) was carried out with a variety of subsequent extraction procedures (basket, mechanical lithotripsy, balloon). Sampling of bile in those cases was performed prior to EPT. The existence of *H. pylori* in gastric mucosa was checked by fast urease test in all the patients at the Clinic of Gastroenterology and Hepatology of the Clinical Centre of Serbia during endoscopic examination.

DNA was isolated from bile specimens by a sequence of procedures including respectively: centrifugation, followed by a 2-hour incubation in lysis buffer, extraction via phenol chloroform, precipitation with acid ethanol, and dissolution in Tris-EDTA buffer. The final DNA sample was tested in respect of the existence of ure A gene by means of PCR method. In order to detect *H. pylori* infection of bile ducts nested (two-step) PCR was used, with two pairs of primers: outer primer with its own sense and antisense as follows: 5'-GCCAATGGTAAATTAGTTCC-3' (s) 5'-TTACTCCTTAATTGTTTTTAC-3' (as) and the other pair is so-called inner primer with its own sense and antisense: 5'-TTCTTTGAAGTGAATAGATGC-3' (s) 5'-ATAGTTGTCATCGCTTTTAGC-3' (as)^[9]. Taq polymerase, 5MU·L⁻¹ (Perkin Elmer Biosystems) was used during the reaction. The master mix for the first reaction (outer primers) consisted of 5μL of DNA template, 3μL of MgCl₂, 5μL Taq reaction buffer II, 4μL dNTPs, 0.2μL Taq polymerase, 1.3μL of outer sense primer, 1.2μL of outer antisense primer, and H₂O up to the final volume of 50μL. The master mix for the second reaction (inner primers) differed from the first one in the amount of primers: 1.7μL of outer sense primer, 1.0μL of outer antisense primer. Both PCR reactions were performed in a DNA thermal cycler in three steps, 1min. at 94 °C, 1min. at 50 °C, and 1min. at 72 °C, for 25 cycles each. The *H. pylori* gene was presented by electrophoresis on 10g·L⁻¹ agarose gel at the level of 258 base pairs.

RESULTS

Based on the clinical tests, we diagnosed biliary lithiasis in the patients included in our study. Forty-eight of them (67%) had no signs of cholangitis (Figure 1), and 17 cases were complicated by cholangitis (24%, Figure 2). Seven patients (9%) had normal ERCP findings and constituted the control group.

In the group of patients with lithiasis 54.2% patients had a positive PCR *H. pylori* in bile and in the group of patients with inflammation a positive PCR was detected in 52.9% of the patients (Table 1). Among the seven patients with regular findings only one patient (14%) was PCR positive. There was a statistically significant difference in the positivity of PCR *H. pylori* in the joint group of patients who had non-malignant diseases of bile ducts (gallstones and inflammation) in relation to the controls (Chi-square test, $P=0.0467$). After the tested group was divided into two basic pathologies and the statistical analysis repeated, it was clear that only the patients with lithiasis alone had a significantly higher frequency of positive *H. pylori* in bile ($P=0.0486$), contrary to the ones with associated cholangitis (Fischer's precision test, $P=0.0967$).

Fast urease test revealed a high percentage of *H. pylori* of gastric mucosa (57 patients - 79%). There was a slightly higher positivity in patients with distinct biliary pathology - 81% FUT positive patients in the group with cholelithiasis and 76% in the group with associated cholangitis, compared to the controls, where FUT was positive in 71%. There was no statistical difference between the groups (Chi-square test, $P=0.5957$).

Finally, if we compare findings of *H. pylori* in bile (by PCR method) with the same in gastric mucosa (by FUT method), we come to the conclusion that there is no statistically significant difference between them. However, if we extract only the subgroup of patients with lithiasis then the difference becomes highly significant (Chi square, $P=0.0045$).

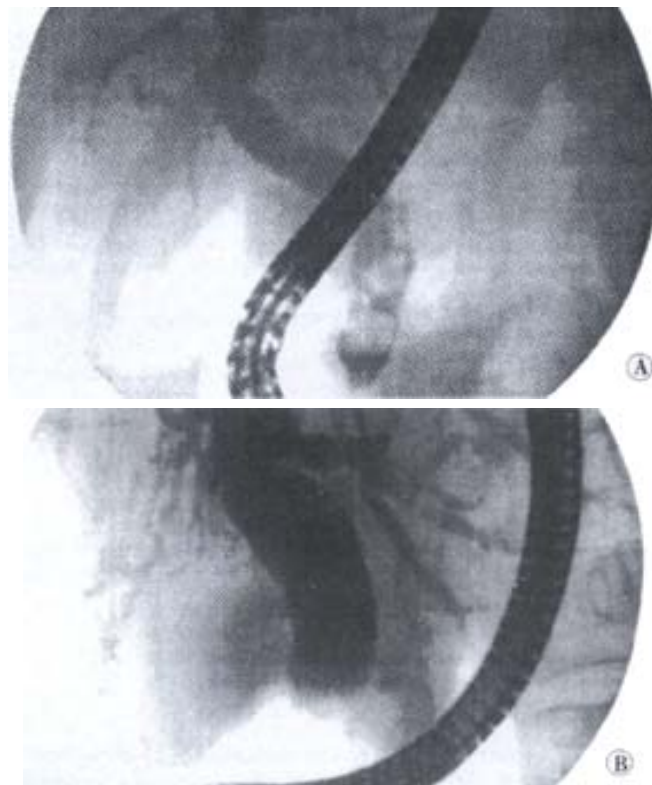


Figure 1 ERCP: Biliary calculosis

Figure 2 ERCP: Cholangitis

Table 1 *H. pylori* positivity in bile (PCR) and in gastric mucosa (FUT)

Test	Biliary lithiasis		controls
	without cholangitis	with cholangitis	
PCR +	26	9	1
PCR -	22	8	6
FUT +	39	13	5
FUT -	9	4	2

PCR: for ureA gene; FUT: Fast urease test

DISCUSSION

Bile acids in physiological concentrations inhibit the growth of various sorts of intestinal bacteria^[10], including lactobacilli and clostridia, which are sensitive to unconjugated bile acids, such as cholic, deoxycholic and lithocholic acids. Since *H. pylori* is a Gram negative bacteria, it also shows sensitivity *in vitro* to deoxycholic and chenodeoxycholic acids^[11]. They are the main free bile acids in human bile. However, under different pathological conditions, this inhibition factor of *H. pylori* growth can be changed: for example, the concentration of various matter in bile can be influenced by biliary obstruction^[12]. Further, the *in vivo* inhibitory effect of bile acids to *H. pylori* has been proven by various studies through testing the role of *H. pylori* in biliary reflux gastritis, which, however, has given contradictory results^[13], as some studies suggested that biliary reflux from the duodenum into the antrum did not affect the growth of *H. pylori* in antrum.

In our study, out of the total of 72 patients *H. pylori* was identified in bile of 36 patients (50%). This study demonstrates that there is a possibility to identify this microorganism by means of PCR method in the environment which is known to inhibit its growth under *in vitro* conditions. Since *H. pylori* infection was more frequent in the patients with the diseases of biliary ducts than in the controls (53.8% vs 14.3%), it is possible to suppose that under the pathological conditions there was a change of the conditions for the growth of this bacteria *in vivo* and this would be the subject of further research. Although it seems unlikely that *H. pylori* could grow in the environment which contains bile, it has been proven for some of *Helicobacter* species to be living in the gallbladder (*H. hepaticus*, *H. bilis*, *H. pullorum* and others)^[14]. Fox *et al* detected *H. bilis*, *H. pullorum* and *H. rappini* by means of PCR method in 23 patients with the diagnosis of chronic cholecystitis although there were no cases where microorganisms had grown from bile cultures. Based on these data, it is possible that *H. pylori* caused certain idiopathic hepatobiliary diseases. *H. pullorum* is known to cause infection in people and chicken manifested with diarrhoea or increased hepatic enzymes and liver enlargement^[15]. *H. rappini*, which causes abortion in sheep and acute insufficiency of liver of the sheep fetus, was isolated in people complaining of diarrhoea. Finally, *H. bilis* was proved to be a cause of hepatitis in mice^[16].

Offner *et al*^[17] announced in 1994 that the presence of M_r130 proteins caused crystalization of cholesterol. It was also found that CagA protein of *H. pylori* had this identical molecular weight, and also that both of these proteins had crossed reactions with human leucine-aminopeptidase^[18]. Figura *et al*^[19] found anti-CagA antibodies in 15 of 16 bile specimens in patients undergoing cholecystectomy for stones and were proven to have CagA *H. pylori* within the stomach. All these findings support the role of these microorganisms in the initiation of crystalization of cholesterol which induces cholelithiasis. Recent researches devoted to the studies of *Helicobacter* sp. in different diseases of biliary ducts and liver show that *Helicobacter* can survive not only in stomach but also in human bile, and, additionally, that it can be the cause of various hepatobiliary diseases. For this reason, Roe *et al*^[20] tested the survival of *Helicobacter* sp. in bile of the patients having various diseases of biliary system which contained changed bile acids or bile acids to which *H. pylori* was resistant. The study included 20 patients with intrahepatic lithiasis, three patients had pancreas cancer and two patients had common bile duct cancer. Bile was obtained by means of PTBD method and tested in respect of the presence of 16s rRNA specific gene of *H. pylori* by PCR method. The result of the PCR were the product of 375 bp. After the sequencing and analysis of sequences, 20 (80%) of PCR product were suited to *H. pylori* genome while the rest of 5 (20%) were suited to *H. bilis* genome. Based on the obtained results the authors concluded that *H. pylori* was the most important and the most frequent cause of infection among all sorts of *Helicobacter* sp. in diseases of biliary ducts. However, the authors did not give any explanation how the infection of biliary ducts with this bacteria happens but suggested further research in future.

In order to analyse the path and source of infection of biliary ducts utilizing the most sensitive methodology, we tested the positivity of *H. pylori* by PCR method (in bile) and FUT (in gastric mucosa) the result of which was a statistically very significant difference. This surprising finding could imply that the pathogenesis of biliary system and gastric mucosa are independent. In this difference the main portion belongs to lithiasis, since in the case of the subgroup with associated cholangitis no statistically significant difference was found. Taking into account that in the subgroup of lithiasis there were some deviations in the positivity of *H. pylori* towards the controls, it is clear that biliary pathogenesis is not uniform in all its forms. It has been pointed out earlier that *H. sp.* exist in the biliary system and

gallbladder of the patients belonging to the Chilean population^[13], being one of the main causes of chronic inflammation which can stimulate forming of biliary stones. Ponzetto *et al*^[21] tested the presence of *H. sp.* in bile and mucosa of bile bladder of the patients having cholelithiasis and prevalence of *H. pylori* antibodies in serum of the patients. Sixty four patients were subjected to cholecystectomy and from whom bile was collected at operation as well as the mucosa of gallbladder. The specimens of serum were compared to the specimens of 610 blood donors. Serum was tested in respect of the presence of specific IgG antibodies in relation to *H. pylori* (ELISA). Bile and mucosa of bile bladder were tested by means of PCR method with respect to the presence of genetic sequence 16s rRNA *H. sp.* In 22 out of 64 tested specimens of bile PCR for *H. sp.* was positive. *H. pylori* infection was significantly more frequent in the patients with cholelithiasis than in the controls, and *H. pylori* DNA was also present in the bile of the patients.

Our clinical and molecular biological tests for *H. pylori* in patients with biliary diseases were undertaken in a larger population than that previously reported.

It is possible to conclude that PCR method can detect *H. pylori* infection of biliary ducts. Prevalence of *H. pylori* infection in the patients with benign diseases of bile ducts does not show a statistically significant difference in relation to the prevalence with the patients presentign with normal ERCP. However, in the patients with biliary lithiasis there is a certain difference which is on the borderline of statistical significance. The analysis of *H. pylori* in gastric mucosa by means of FUT method did not have a statistically significant difference either among the patients with benign biliary pathology and controls. Based on all the data stated above it can be said that the presence of *H. pylori* infection, either in bile or in gastric mucosa, does play a role in pathogenesis of benign biliary diseases although more explicit conclusions require a larger control group.

ACKNOWLEDGEMENT

Warmest gratitude to the Department of Medicine, University of Rostock, and particularly to the Head and staff of the Gastrointestinal Research Laboratory for their kind help, support and contribution in this article.

REFERENCES

- 1 Hobsley M, Tovey F. *Helicobacter pylori*: the primary cause of duodenal ulceration or a secondary infection? *World J Gastroenterol* 2001; 7:149-151
- 2 Miehke S, Kirsch C, Dragosics B, Gschwandler M, Oberhuber G, Antos D, Dite P, Lauter J, Labenz J, Leodolter A, Malfertheiner P, Neubauer A, Ehninger G, Stolte M, Bayerdorffer E. *Helicobacter pylori* and gastric cancer: current status of the Austrian-Czech-German gastric cancer prevention trial (PRISMA) study. *World J Gastroenterol* 2001; 7:243-247
- 3 Veldhuyzen van Zanten SJ, Sherman PM. *Helicobacter pylori* infection as a cause of gastritis, duodenal ulcer, gastric cancer and nonulcer dyspepsia: a systematic over-view. *Can Med Assoc J* 1994; 150:177-185
- 4 Gasbarrini A, Franceschi F, Gasbarrini G, Pola P. Extradigestive diseases and *Helicobacter pylori* infection. *Eur J Gastroenterol Hepatol* 1997; 9:231-233
- 5 Hazell SL, Borody TJ, Gal A. *Campylobacter pyloridis*. I. Detection of urease as a marker of bacterial colonisation and gastritis. *Am J Gastroenterol* 1987; 82:292-296
- 6 Clayton CL, Wren BW, Mullanu P, Topping A, Tabaqchali S. Molecular cloning and expression of *Campylobacter pylori* species-specific antigens in *Escherichia coli* K-12. *Infect Immun* 1989; 57:623-629
- 7 Clayton CL, Pallen MJ, Kleanthous H, Wren BW, Tabaqchali S. Nucleotide sequence of two genes from *Helicobacter pylori* encoding for urease subunits. *Nucleic Acids Res* 1990; 18:362
- 8 Clayton CL, Kleanthous H, Coates PJ, Morgan DD, Tabaqchali S. Sensitive detection of *Helicobacter pylori* by using polymerase chain reaction. *J Clin Microbiol* 1992; 30:192-200
- 9 Lin T, Yeh CT, Wu CS, Liaw IF. Detection and partial sequence analysis of *Helicobacter pylori* DNA in the bile samples. *Dig Dis Sci* 1995; 40:2214-2219
- 10 Floch MH, Gerhengoren W, Elliott S, Spiro HM. Bile acid inhibition of intestinal microflora. A function of simple bile acid *Gastroenterology*

- 1971; 61:228-233
- 11 Hanninen ML. Sensitivity of *Helicobacter pylori* to different bile salts. *Eur J Clin Microb Infect Dis* 1991; 10:515-518
- 12 Xu G, Kirk CTC, Goode AW. Changes in biliary lipid concentrations in bile duct obstruction: An experimental study. *J R Soc Med* 1986; 79:522-527
- 13 Kelloso J, Alavaikko M, Laitinen S. Effects of biliary tract produce on duodenogastric reflux and the gastric mucosa. *Scand J Gastroenterol* 1991; 26:1272-1278
- 14 Fox JG, Dewhirst FE, Shen Z, Feng Y, Taylor NS, Paster BJ, Ericson RL, Lau CN, Correa P, Araya JC, Roa I. Hepatic *Helicobacter* species identified in bile and gallbladder tissue from Chileans with chronic cholecystitis. *Gastroenterology* 1998; 114:755-763
- 15 Stanley J, Linton D, Burens AP, Dewhirst FE, On SL, Porter A, Owen RJ, Costas M. *Helicobacter pullorum* sp. Novel genotype and phenotype of a new species isolated from poultry and from human patients with gastroenteritis. *Microbiology* 1994; 140:3441-3449
- 16 Franklin C, Riley L, Hunziker R. Enteropathic lesions in scid mice infected with *Helicobacter bilis*. *Lab Anim Sci* 1997; 47:438-439
- 17 Offner GD, Gong D, Afdhal NH. Identification of a 130-kDa human biliary concavalin A binding protein as aminopeptidase N. *Gastroenterology* 1994; 106:755-762
- 18 Covacci A, Censini S, Bugnoli M, Petraccia R, Burrone D, Macchia G, Massone A, Papini E, Xiang Z, Figura N, Rappuoli R. Molecular characterization of the 128-kDa immunodominant antigen of *Helicobacter pylori* associated with cytotoxicity and duodenal ulcer. *Proc Natl Acad Sci USA* 1993; 90:5791-5795
- 19 Figura N, Cetta F, Angelico M, Montalto G, Cetta D, Pacenti L, Vindigni C, Vaira D, Festuccia F, De Santis A, Rattan G, Giannace R, Campagna S, Gennari C. Most *Helicobacter pylori*-infected patients have specific antibodies, and some also have *H. pylori* antigens and genomic material in bile. Is it a risk factor for gallstone formation? *Dig Dis Sci* 1998; 43:854-866
- 20 Roe IH, Kim JT, Lee HS, Lee JH. Detection of *Helicobacter* DNA in bile from bile duct diseases. *J Korean Med Sci* 1999; 14:182-186
- 21 Ponzetto A, Vergnano G, Soldati T, Cutufo MA, Giustetto A, Angelino R, Pellicano R, Leone N, Arena V, Rizzetto M, Fronda GR. Detection of *Helicobacter pylori* in the bile of patients with cholelithiasis. *Gut* 1999; 45:A162

Edited by Pan BR and Zhang JZ

• *H. pylori* •

Detection of *H.pylori* DNA in gastric epithelial cells by *in situ* hybridization

Xin-Liang Lu, Ke-Da Qian, Xun-Qiu Tang, Yong-Liang Zhu, Qin Du

Xin-Liang Lu, Ke-Da Qian, Xun-Qiu Tang, Yong-Liang Zhu, Qin Du, Department of Digestive Diseases, Second Affiliated Hospital, Zhejiang University Medical College, Hangzhou 310009, Zhejiang Province, China

Correspondence to: Xin-Liang Lu, Department of Digestive Diseases, Second Affiliated Hospital, Zhejiang University Medical College, Hangzhou 310009, Zhejiang Province, China. luxl@haoyisheng.com.cn

Received 2001-10-12 Accepted 2001-11-01

Abstract

AIM: To investigate the presence of *H.pylori* DNA within gastric epithelial cells in patients with *H.pylori* infection and its possible carcinogenic mechanism.

METHODS: Total 112 patients, with pathologically confirmed chronic superficial gastritis, chronic atrophic gastritis, intestinal metaplasia, atypical hyperplasia or gastric cancer were studied. Among them, 28 were *H.pylori* negative and 84 *H.pylori* positive. *H.pylori* DNA in gastric epithelial cells was detected by GenPoint catalyzed signal amplification system for *in situ* hybridization.

RESULTS: In the *H.pylori* positive group, zero out of 24 chronic superficial gastritis (0.0%), four out of 25 precancerous changes (16.0%) and thirteen out of 35 gastric cancers (37.1%) showed *H.pylori* DNA in the nucleus of gastric epithelial cells, the positive rates of *H.pylori* DNA in the nucleus of gastric epithelial cells were progressively increased in chronic superficial gastritis, precancerous changes and gastric cancer groups ($\chi^2=12.56$, $P=0.002$); One out of 24 chronic superficial gastritis (4.2%), eleven out of 25 precancerous changes (44.0%) and thirteen out of 35 gastric cancers (37.1%) showed *H.pylori* DNA in the cytoplasm of gastric epithelial cells ($\chi^2=10.86$, $P=0.004$). In the *H.pylori* negative group, only one patient with gastric cancer was found *H.pylori* DNA in the nucleus of gastric epithelial cells; Only two patients, one patient with precancerous changes and another with gastric cancer, showed *H.pylori* DNA in the cytoplasm of gastric epithelial cells. Furthermore, *H.pylori* DNA must have been in the cytoplasm as long as it existed in the nucleus of gastric epithelial cells.

CONCLUSION: *H.pylori* DNA exists both in the nucleus and the cytoplasm of gastric epithelial cells in patients with *H.pylori* infections. The pathological progression from chronic superficial gastritis, precancerous changes to gastric cancer is associated with higher positive rates of *H.pylori* DNA presence in the nucleus of gastric epithelial cells.

Lu XL, Qian KD, Tang XQ, Zhu YL, Du Q. Detection of *H.pylori* DNA in gastric epithelial cells by *in situ* hybridization. *World J Gastroenterol* 2002; 8(2): 305-307

INTRODUCTION

Gastric cancer is the second most common fatal malignancy in the

world and is the cause of more than 750000 deaths annually^[1-3]. Many studies have showed that *H.pylori* infection is closely related with gastritis, peptic ulcer and gastric cancer, and may play a causative role at the early phases of this chain^[3-16]. *H.pylori* was classified as a class I carcinogen by the International Agency for Research on Cancer in 1994. So far the mechanism of *H.pylori* carcinogenesis has not been illuminated^[3-7]. The *H.pylori* DNA must invade gastric epithelial cells first, and then exists chronically in gastric epithelial cell in an unknown manner before integration. The *in situ* hybridization technique has become an essential tool for detecting the localization of DNA transcripts on tissue sections^[17-19]. The aims of our study are to investigate whether there is *H.pylori* DNA within gastric epithelial cells and the possible carcinogenic mechanism by GenPoint catalyzed signal amplification system for *in situ* hybridization in patients with *H.pylori* infections.

MATERIALS AND METHODS

Clinical data

By *H.pylori* diagnostic criteria, 112 patients, including 28 *H.pylori* that were negative and 84 *H.pylori* that were positive, were studied. There were 24 cases with chronic superficial gastritis, 25 cases with precancerous changes and 35 cases with gastric cancer among the *H.pylori* positive group, and 10, 16 and 2 cases, respectively among the *H.pylori* negative group. Histological examination was by routine haematoxylin and eosin stain, and by the *H.pylori* methylene blue staining kit as suggested by the manufacturer (Fujian Sanqiang, China). Rapid urease tests (Digestech, China), ¹³C-urea breath tests (Isodiagnostak, Canada) or ¹⁴C-urea breath tests (Shenzhen Headway, China), and serological *H.pylori*-IgG tests (Orion Diagnostica, Finland) were carried out as suggested by each manufacturer. The positive criteria were randomly for two positive items among the following three items: (1) histology (routine haematoxylin and eosin stain, methylene blue stain), (2) urease dependent tests (rapid urease tests, ¹³C- or ¹⁴C- urea breath tests), and (3) serological *H.pylori*-IgG tests. Negative criteria were met if three items were negative.

In situ hybridization

The size of biotinylated Long DNA Probe for *H.pylori* M₂6000 Protein Gene (Maxim Biotech, USA.) is 303 base pair. 5μm sections were coated on single well slides and hot plated for 12h before deparaffination and rehydration with ethanol. The sections were treated sequentially with 2g·L⁻¹ Triton-X100 for 15min, 1mM HCl for 10min and digested with 10g·L⁻¹ pepsin (Sigma, USA) for 15min, and 20mg·L⁻¹ proteinase K (Meack, Germany) for 30min. The enzyme was inactivated by treatment with 2g·L⁻¹ glycine in pH7.4 phosphate-buffered saline (PBS) for 5min. Then the sections were incubated sequentially with 10g·L⁻¹ RNase at 37°C for 30min, 3ml·L⁻¹ H₂O₂ in methanol for 30min and prehybridized with hybridization buffer solution at 37°C for 60min. To denature the probe and cellular DNA, the sections were heated with hybridization buffer solution containing 1mg·L⁻¹ of *H.pylori* probe at 95°C for 15min. The sections were hybridized at 42°C in a humidified chamber for 60min, then treated with Dako GenPoint catalyzed signal amplification system

for *in situ* hybridization as suggested by the manufacturer. The sections were counterstained with hematoxylin and examined under a light microscope.

Catalyzed signal amplification system for *in situ* hybridization

The Dako GenPoint system created an additional level of amplification for biotin detection. After an initial binding of streptavidin-peroxidase to the biotinylated probe, the peroxidase catalyzed the oxidation of biotinyl-tyramide, which immediately formed covalent bonds with aromatic groups in the specimen. This reaction deposited large amounts of biotin at the site of hybridization. The additional biotin was then used to capture more streptavidin-peroxidase. The signal was finally developed by adding the chromogenic indicator dye diaminobenzidine (DAB), which was oxidized by the precipitate at the site of hybridization.

RESULTS

In the *H. pylori* positive group, zero out of 24 chronic superficial gastritis (0.0%), four out of 25 precancerous changes (16.0%) and thirteen out of 35 gastric cancers (37.1%) showed *H. pylori* DNA in the nucleus of gastric epithelial cells, the positive rates of *H. pylori* DNA in the nucleus of gastric epithelial cells were progressively increased in chronic superficial gastritis, precancerous changes and gastric cancer groups ($\chi^2=12.56$, $P=0.002$); One out of 24 chronic superficial gastritis (4.2%), eleven out of 25 precancerous changes (44.0%) and thirteen out of 35 gastric cancers (37.1%) showed *H. pylori* DNA in the cytoplasm of gastric epithelial cells ($\chi^2=10.86$, $P=0.004$). In the *H. pylori* negative group, only one patient with gastric cancer was found *H. pylori* DNA in the nucleus of gastric epithelial cells; Just two patients, one patient with precancerous changes and another with gastric cancer, showed *H. pylori* DNA in the cytoplasm of gastric epithelial cells. Furthermore, *H. pylori* DNA must have been in the cytoplasm as long as it existed in the nucleus of gastric epithelial cells.

DISCUSSION

H. pylori has been acknowledged as a possible carcinogen^[3-16]. Genome integration is the most important carcinogenic mechanism in some microorganisms^[19-21]. However, there is no reliable evidence of integration of the *H. pylori* DNA in the human genome at this time^[22-24]. Parsonnet proposed that *H. pylori* has a similar mechanism as virus carcinogenesis^[4], viz, *H. pylori* DNA integrated into the gastric epithelial cells genome, which may induce transformation or malignancy of the normal cell. The *H. pylori* DNA must invade the gastric epithelial cells first, and then exists chronically in gastric epithelial cell in an unknown manner before integration. We found that the *H. pylori* DNA can exist both in the nucleus and cytoplasm of gastric epithelial cells in patients with *H. pylori* infections, predominately in cases with precancerous changes and gastric cancer by *in situ* hybridization technique that has been proved a powerful tool for *in situ* gene localization in individual cell^[17-19]. *H. pylori* DNA can invade into host cells, even into the nucleus, and exist chronically within cells, which is indicated *H. pylori* DNA and genome of host cell would affect each other, even *H. pylori* DNA integrated into genome of host cell. Chiou and his colleagues^[25] demonstrated that *H. pylori* infection caused an alteration of gene expression in AGS cells and identified 21 overexpressed genes and 17 suppressed genes from the cDNA expression arrays. Some other studies have also showed the alteration of gene expression, cell proliferation and apoptosis^[14-16,26-38] in patients with gastric cancer or *H. pylori* infection.

We collected 84 *H. pylori* positive cases, including 25 precancerous changes and 35 gastric cancers, and significantly

increased sensitivity by Dako GenPoint catalyzed signal amplification system. The rates of *H. pylori* DNA in the nucleus of gastric epithelial cells was progressively increased in chronic superficial gastritis, precancerous changes and gastric cancer, at 0.0%, 16.0% and 37.1%, respectively in the *H. pylori* positive group. So the progression from chronic superficial gastritis to precancerous changes and to gastric cancer was associated with the presence of *H. pylori* DNA in the nucleus of gastric epithelial cells. This may indicate that *H. pylori* DNA and the genome of the host cell may affect each other, as *H. pylori* DNA is integrated into genome of the host cell. As a result this may change the structure and function of the host cell genome, and thus destroy the stability of the genome. We also found there was *H. pylori* DNA in the *H. pylori* negative group. High sensitivity of *in situ* hybridization^[17-19] and previous *H. pylori* infection may explain the result. *H. pylori* DNA was also located in the cytoplasm of gastric epithelial cells. *H. pylori* can be seen to invade gastric mucosa by electron or immunoelectron microscopy^[39-42]. *H. pylori* was able to destroy the junction of cells, and even invade into the cytoplasm of stromal cells in the lamina propria. Yang and his colleagues^[41] found that *H. pylori* could be engulfed and degraded by the human gastric cancer cell line SGC-7901 using transmission electron microscopy. Once the *H. pylori* DNA invaded the gastric epithelial cells, it could enter the nucleus when the karyotheca disappears during the metaphase of mitosis. If the *H. pylori* DNA was found in nucleus, it was also found in the cytoplasm in our study. In the *H. pylori* positive group, the positive rates of finding *H. pylori* DNA in cytoplasm in precancerous changes and gastric cancer were higher than that in chronic superficial gastritis, while there was no statistic significance in the rate between precancerous changes and gastric cancer.

ACKNOWLEDGEMENT

We thank Dr EB Holm for suggesting improvements to the manuscript.

REFERENCES

- 1 Niu WX, Qin XY, Liu H, Wang CP. Clinicopathological analysis of patients with gastric cancer in 1200 cases. *World J Gastroenterol* 2001; 7: 281-284
- 2 Cai L, Yu SZ. A molecular epidemiologic study on gastric cancer in Changle, Fujian Province. *Shijie Huaren Xiaohua Zazhi* 1999; 7: 652-655
- 3 Forman D. *Helicobacter pylori*: the gastric cancer problem. *Gut* 1998; 43: S33-S34
- 4 Parsonnet J. *Helicobacter pylori* and gastric cancer. *Gastroenterol Clin North Am* 1993; 22: 89-104
- 5 Xia HX. Association between *Helicobacter pylori* and gastric cancer: current knowledge and future research. *World J Gastroenterol* 1998; 4: 93-96
- 6 Hu PJ. *Hp* and gastric cancer: challenge in the nesearch. *Shijie Huaren Xiaohua Zazhi* 1999; 7: 1-2
- 7 Zhuang XQ, Lin SR. Progress in research on the relationsh between *Hp* and stomach cancer. *Shijie Huaren Xiaohua Zazhi* 2000; 8: 206-207
- 8 Li H, Kalies I, Helander HF. Infection of *Helicobacter pylori* in rats and mice-a one year study. *World J Gastroenterol* 1998; 4: S57
- 9 Axon A. *Helicobacter pylori* is not a commensal. *Curr Opin Gastroenterol* 1999; 15: S1-S4
- 10 Quan J, Fan XG. Progress in experimental research of *Helicobacter pylori* infection and gastric carcinoma. *Shijie Huaren Xiaohua Zazhi* 1999; 7: 1068-1069
- 11 Zhuang XQ, Lin SR. Research of *Helicobacter pylori* infection in precancerous gastric lesions. *World J Gastroenterol* 2000; 6: 428-429
- 12 Maeda S, Yoshida H, Ogura K, Yamaji T, Ikenoue T, Mitsushima T, Tagawa H, Kawaguchi R, Mori K, Mafune KI, Kawabe T, Shiratori Y, Omata M. Assessment of gastric carcinoma risk associated with *Helicobacter pylori* may vary depending on the antigen used. *Cancer* 2000; 88:1530-1535
- 13 Cai L, Yu SZ, Zhang ZF. *Helicobacter pylori* infection and risk of gastric cancer in Changle County, Fujian Province, China. *World J Gastroenterol* 2000; 6: 374-376
- 14 Yang Y, Deng CS, Yao XJ, Liu HY, Chen M. Effect of *Helicobacter pylori* on morphology and growth of gastric epithelial cells. *Shijie Huaren*

- Xiaohua Zazhi 2000;8: 500-504
- 15 Rokkas T, Wotherspoon A. Carcinogenesis. *Curr Opin Gastroenterol* 1999; 15: S23-S28
 - 16 Xia HX, Zhang GS. Apoptosis and proliferation in gastric cancer caused by *Hp* infection. *Shijie Huaren Xiaohua Zazhi* 1999; 7: 740-742
 - 17 Su CQ, Qiu H, Zhang Y. Localization of keratin mRNA and collagen I mRNA in gastric cancer by *in situ* hybridization and hybridization electron microscopy. *World J Gastroenterol* 1999; 5: 527-530
 - 18 Xie YM, Nie QH, Zhou YX, Cheng YQ, Kang WZ. Detection of TIMP-1 and TIMP-2 RNA expressions in cirrhotic liver tissue using digoxigenin labelled probe by *in situ* hybridization. *Shijie Huaren Xiaohua Zazhi* 2001; 9: 251-254
 - 19 Huang PL, Lu LG, Shi ZY, Yin KZ, Zhang XM. Detection of human papillomavirus DNA in colorectal neoplasms by *in situ* hybridization with digoxin labelled DNA probes. *Huaren Xiaohua Zazhi* 1998; 6: 771-773
 - 20 Gao FG, Sun WS, Cao YL, Zhang LN, Song J, Li HF, Yan SK. HBx-DNA probe preparation and its application in study of hepatocarcinogenesis. *World J Gastroenterol* 1998; 4: 320-322
 - 21 Wang Y, Liu H, Zhou Q, Li X. Analysis of point mutation in site 1896 of HBV precore and its detection in the tissues and serum of HCC patients. *World J Gastroenterol* 2000; 6: 395-397
 - 22 Makino S, Suzuki M. Bacterial genomic reorganization upon DNA replication. *Science* 2001; 292: 803
 - 23 Bart A, Smeets LC, Kusters JG. DNA uptake sequences in *Helicobacter pylori*. *Microbiology* 2000; 146: 1255-1256
 - 24 Smeets LC, Bijlsma JJ, Boomkens SY, Vandenbroucke Grauls CM, Kusters JG. comH, a novel gene essential for natural transformation of *Helicobacter pylori*. *J Bacteriol* 2000; 182: 3948-3954
 - 25 Chiou CC, Chan CC, Sheu DL, Chen KT, Li YS, Chan EC. *Helicobacter pylori* infection induced alteration of gene expression in human gastric cells. *Gut* 2001; 48: 598-604
 - 26 Liu HF, Liu WW, Fang DC, Yang SM, Zhao L. Gastric epithelial apoptosis induced by *Helicobacter pylori* and its relationship with Bax protein expression. *Shijie Huaren Xiaohua Zazhi* 2000; 8: 860-862
 - 27 Satoh K, Kihira K, Kawata H, Tokumaru K, Kumakura Y, Ishino Y, Kawakami S, Inoue K, Kojima T, Satoh Y, Mutoh H, Sugano K. P53 Expression in the Gastric Mucosa Before and After Eradication of *Helicobacter pylori*. *Helicobacter* 2001; 6: 31-36
 - 28 Gao HJ, Yu LZ, Bai JF, Peng YS, Sun G, Zhao HL, Miu K, Li XZ, Zhang XY, Zhao ZQ. Multiple genetic alterations and behavior of cellular biology in gastric cancer and other gastric mucosal lesions: *H. pylori* infection, histological types and staging. *World J Gastroenterol* 2000; 6: 848-854
 - 29 Wang DX, Fang DC, Liu WW. Study on alteration of multiple genes in intestinal metaplasia, atypical hyperplasia and gastric cancer. *Shijie Huaren Xiaohua Zazhi* 2000; 8: 855-859
 - 30 Zhu YH, Wang YR, Sun JJ, Zhu CL, Wu X, Lu B. Study on the relationship between *Helicobacter pylori* infection and proliferative kinetics of gastric mucosa. *World J Gastroenterol* 1998; 4: S96
 - 31 Gao H, Wang JY, Shen XZ, Liu JJ. Effect of *Helicobacter pylori* infection on gastric epithelial cell proliferation. *World J Gastroenterol* 2000; 6: 442-444
 - 32 Chen SY, Wang JY, Ji Y, Zhang XD, Zhu CW. Effects of *Helicobacter pylori* and protein kinase C on gene mutation in gastric cancer and precancerous lesions. *Shijie Huaren Xiaohua Zazhi* 2001; 9: 302-307
 - 33 Wang DX, Fang DC, Li W, Du QX, Liu WW. A study on relationship between infection of *Helicobacter pylori* and inactivation of antioncogenes in cancer and pre-cancerous lesion. *Shijie Huaren Xiaohua Zazhi* 2001; 9: 984-987
 - 34 Hamanaka Y, Nakashima M, Wada A, Ito M, Kurazono H, Hojo H, Nakahara Y, Kohno S, Hirayama T, Sekine I. Expression of human beta-defensin 2 (hBD-2) in *Helicobacter pylori* induced gastritis: antibacterial effect of hBD-2 against *Helicobacter pylori*. *Gut* 2001; 49: 481-487
 - 35 Leung WK, Yu J, To KF, Go MY, Ma PK, Chan FK, Sung JJ. Apoptosis and proliferation in *Helicobacter pylori*-associated gastric intestinal metaplasia. *Aliment Pharmacol Ther* 2001; 15: 1467-1472
 - 36 Mori N, Ueda A, Geleziunas R, Wada A, Hirayama T, Yoshimura T, Yamamoto N. Induction of monocyte chemoattractant protein 1 by *Helicobacter pylori* involves NF-kappaB. *Infect Immun* 2001; 69: 1280-1286
 - 37 Xia HH, Talley NJ. Apoptosis in gastric epithelium induced by *Helicobacter pylori* infection: implications in gastric carcinogenesis. *Am J Gastroenterol* 2001; 96: 16-26
 - 38 Anti M, Armuzzi A, Gasbarrini A, Gasbarrini G. Importance of changes in epithelial cell turnover during *Helicobacter pylori* infection in gastric carcinogenesis. *Gut* 1998; 43: S27-S32
 - 39 Zhou LY, Chen CY, Liang P, Chen LY, Zhong XR, Chen LY. *Helicobacter pylori* infection induced changes of anionic sites on surface of mucous cells and their basement membrane. *Huaren Xiaohua Zazhi* 1998; 6: 570-573
 - 40 Ko GH, Kang SM, Kim YK, Lee JH, Park CK, Youn HS, Baik SC, Cho MJ, Lee WK, Rhee KH. Invasiveness of *Helicobacter pylori* into human gastric mucosa. *Helicobacter* 1999; 4: 77-81
 - 41 Yang Y, Deng CS, Yao XJ, Liu HY, Chen M. Electron microscopic observation after interaction between *Helicobacter pylori* and gastric epithelial cells. *Zhonghua Neike Zazhi* 2000; 39: 454-456
 - 42 Blom J, Gernow A, Holck S, Wewer V, Norgaard A, Graff LB, Krasilnikoff PA, Andersen LP, Larsen SO. Different patterns of *Helicobacter pylori* adherence to gastric mucosa cells in children and adults. An ultrastructural study. *Scand J Gastroenterol* 2000; 35: 1033-1040

Edited by Zhang JZ

• *H. pylori* •

A study of recombinant protective *H. pylori* antigens

Zheng Jiang, Xiao-Hong Tao, Ai-Long Huang, Pi-Long Wang

Zheng Jiang, Xiao-Hong Tao, Pi-Long Wang, Department of Gastroenterology, the First Affiliated Hospital, Chongqing University of Medical Sciences, Chongqing 400016, China

Ai-Long Huang, Institute of Viral Hepatitis, Chongqing University of Medical Sciences, Chongqing 400010, China

Correspondence to: Dr. Zheng Jiang, Department of Gastroenterology, the First Affiliated Hospital, Chongqing University of Medical Sciences, Chongqing 400016, China. jzh053@mail.china.com
Telephone: +86-23-68891218

Received 2001-09-26 Accepted 2001-11-08

Abstract

AIM: To construct a recombinant vector which can express *M*₂₆₀₀₀ outer membrane protein (OMP) from *Helicobacter pylori* (*Hp*), and to obtain the vaccine protecting against *Hp* infection and a diagnostic reagent kit quickly detecting *Hp* infection.

METHODS: The gene encoding the structural *M*₂₆₀₀₀ outer membrane protein of *Hp* was amplified from *Hp* chromosomal DNA by PCR, and inserted in the prokaryotic expression vector pET32a (+), which was transformed into the Top10 *E. coli* strain. Recombinant vector was selected, identified and transformed into BL-21(DE3) *E. coli* strain. The recombinant fusion proteins were expressed. The antigenicity of recombinant protein was studied by ELISA or immunoblotting and immunized Balb/c mice.

RESULTS: The gene of *M*₂₆₀₀₀ OMP was amplified to be 594 base pairs, 1.1% of the cloned genes was mutated and 1.51% of amino acid residues was changed, but there was homogeneity between them. The recombinant fusion protein encoded objective polypeptides of 198 amino acid residues, corresponding to calculated molecular masses of *M*₂₆₀₀₀. The level of soluble expression products was about 38.96% of the total cell protein. After purification by Ni-NTA agarose resin columniation, the purity of objective protein became about 90%. The ELISA results showed that recombinant fusion protein could be recognized by patient serum infected with *Hp* and rabbit serum immunized with the recombinant protein. Furthermore, Balb/c mice immunized with the recombinant protein were protected against *H. pylori* infection.

CONCLUSION: *M*₂₆₀₀₀ OMP may be a candidate vaccine preventing *Hp* infection.

Jiang Z, Tao XH, Huang AL, Wang PL. A study of recombinant protective *H. pylori* antigens. *World J Gastroenterol* 2002;8(2):308-311

INTRODUCTION

Helicobacter pylori (*Hp*) is a microaerophilic, spiral and gram-negative bacillus first isolated from human gastric antral epithelium in 1982. It is recognized as a human-specific gastric pathogen that colonizes the stomachs of at least half of the world's population^[1]. Most infected individuals are asymptomatic. However, in some subjects, the infection is associated with the development of peptic ulcer, gastric adenocarcinoma, mucosa-associated lymphoid tissue

(MALT) lymphoma and primary gastric non-Hodgkin's lymphoma^[2-11]. Furthermore, this organism was recently categorized as a class I carcinoma by the World Health Organization^[12], and direct evidence of carcinogenesis was recently demonstrated in an animal model^[13,14]. Immunization against the bacterium represents a cost-effective strategy to reduce the incidence of global gastric cancer and would also have a major impact on *H. pylori*-peptic ulcer disease^[15]. The selection of antigenic targets is critical in the design of an *Hp* vaccine. To date, this area is scarcely touched upon. The majority of studies focused on the urease enzyme, heat shock protein, VacA, and so on^[1,16-19], but not *M*₂₆₀₀₀ outer membrane proteins. So, in this study, the recombinant plasmid of *H. pylori* *M*₂₆₀₀₀ outer membrane protein genes was constructed, and expressed for development of *Hp* vaccine.

MATERIALS AND METHODS

Materials

A well-characterized strain, *H. pylori* (*Hp*), was afforded by the Department of Microbiology, Chongqing University of Medical Sciences. Top10, BL21 *E. coli* strains and pET32a(+) plasmid were presented by the Institute of Viral Hepatitis of Chongqing University of Medical Sciences. Restriction enzymes (HindIII, BamHI) and T₄ DNA ligase were purchased from Promega, TagDNA polymerase was produced by Immunology Department of the former Beijing Medical University. Isopropyl-β-D-thiogalactopyranoside (IPTG), dNTP and oligonucleotide primers were obtained from Sigma Chemical Co. and so on.

Cloning of *Hp* *M*₂₆₀₀₀ OMP gene

Oligonucleotide primers were designed to amplify *H. pylori* open reading frame (ORFs) of *M*₂₆₀₀₀ outer membrane protein based on the published genome sequence^[20]. The primers were designed with a BamHI site incorporated into the 5' end and a Hind III site at the 3' end as follows (5'-3'): GCGGATCCATGTTAGTTACAAA CTTGCC (forward) and AAGCTTAATGGAATTTCTTT (reverse). Genomic DNA prepared from Chongqing *H. pylori* strains was used as the template in the PCR. The PCR cycle consisted of 30 cycles of denaturation at 94°C for 60s, annealing at 58°C for 45s, with an extension step at 72°C for 90s. Products were visualized on 10g·L⁻¹ agarose gel and purified using a PCR purification kit. After digestion with the restriction enzymes BamHI and Hind III simultaneously, the purified products were cloned into the compatible sites of the expression vectors pET32a(+) using T₄ DNA ligase at a molar ratio of 4:1 at 4°C overnight.

Fifty μL Top10 incubated at 37°C overnight was added into 2mL Luria-Bertani broths and routinely grew at 37°C, and shaken at 300r·min⁻¹ for 4h. When optical density at 600nm was 0.5, it was ultracentrifuged at 10000r·min⁻¹ at room temperature (RT) for 2min. The resulting deposits were suspended with 100mmol·L⁻¹ CaCl₂ 150μL and incubated at 0°C for 2h. Ten μL connected products (aboved) was resuspended and incubated at 0°C for 30min, at 42°C for 2min and at 0°C for 2min respectively. At last, it was incubated at 37°C at 180r·min⁻¹ for 30min after the addition of 1mL LB broth, 200μL was collected and spread onto an LB plate containing 100mg·L⁻¹ ampicillin as the selectable marker and incubated at 37°C overnight.

Extraction and expression of recombinant plasmid

The next day, the single cloned bacterial drop was selected, and cultured in 2mL LB broth containing 100mg·L⁻¹ ampicillin at 37°C overnight at 300r·min⁻¹, then recombinant plasmids were extracted and screened with plasmid extraction kit according to the manufacturer's instruction, in the meantime, identified by PCR and restriction enzyme digestion. The recombinant plasmids were selected and transformed into competent BL21(DE3) *E. coli* strains using standard procedures. BL21 *E. coli* strains containing recombinant plasmid were grown until mid-log phase (optical density at 600nm= 0.5 to 1.0), and expression of the fusion proteins was induced by addition of 0.5-4.0mmol·L⁻¹ IPTG for 4h. Following induction, the bacteria were harvested by ultracentrifugation at 12000r·min⁻¹, resuspended in protein-buffer and seethed for 5min. Total protein was electrophoresed on SDS-PAGE gel and stained with coomassie.

Immunoblotting analysis

Briefly, the *M*_r26000 OMP was purified using Ni-NTA agarose resin after bacteria were cultured and broken down by microwave with the energy of 600W×35% for 40min, ultracentrifuged (10000g, 15min, 4°C), and then quantified. *H. pylori* *M*_r26000 outer membrane protein-specific antibody was produced following subcutaneous immunization of the New Zealand rabbits, while age-matched control rabbits were immunized with PBS as described previously^[17]. Serum antibody specificity was determined by ELISA or immunoblotting following electrophoretic transfer of SDS-PAGE-separated (150g·L⁻¹ acrylamide) *H. pylori* *M*_r26000 outer membrane protein to 0.45μm pore size PVDF membrane. After a 30min wash in Tris-saline blotting buffer, antigen-impregnated PVDF strips were incubated with the rabbit sera for 2h at RT. After washing, bound rabbit antibodies were detected by incubation of the strips in alkaline phosphatase-conjugated goat anti-rabbit IgG antibody for 1h at RT.

Prophylactic immunization

Six- to eight-week-old mice were immunized three times by subcutaneous immunization using emulsified *M*_r26000 OMP with Freund's adjuvant at intervals of 1, 14 and 21 days respectively, to produce antibody responded to *M*_r26000 outer membrane protein. The dose consisted of 1mL (100mg·L⁻¹) of purified *M*_r26000 OMP and 1mL complete Freund's adjuvant. Thereafter, the dose consisted of 0.5mL OMP and 0.5mL incomplete Freund's adjuvant. Age-matched control mice were immunized with PBS. The antibody titers in immunized mice were monitored by ELISA with purified fusion protein. Mice were challenged with a single dose of 10⁸ *H. pylori* organisms 7 days after the last immunization. Twenty-eight days after challenge, the mice were killed by cervical dislocation. The stomach of each animal was removed, bisected longitudinally, and pinned out. Full-thickness tissue was taken from the antrum-body area of one-half of each stomach and placed into 0.2mL of urease test medium. Urease activity in the sample, identified by a distinctive color change in the medium, was assessed after 24h incubation at RT. The remainder of the stomach was fixed in 100mL·L⁻¹ buffered formalin and embedded in paraffin. Longitudinal sections, stained with a modified May-Grunwald Giemsa stain, were scanned by full length under light microscopy. Mice were considered protected or not according to the previously report^[17].

Statistical analysis

The Student test was used to evaluate the presence or absence of experimental infection in test and control animals as well as the anti-*M*_r26000 outer membrane protein response to immunization. *P* values <0.05 were considered as statistically significant.

RESULTS

PCR amplification of *H. pylori* *M*_r26000 OMP gene

According to the literature, the gene encoding the *M*_r26000 outer membrane protein, was amplified by PCR with Chongqing *H. pylori* strain's chromosomal DNA as the templates. The cloning products were electrophoresed and visualized on 10g·L⁻¹ agarose gel (Figure 1). It revealed that *M*_r26000 OMP DNA fragment amplified by PCR contained a gene of approximately 594 nucleotides, which was compatible with the previous reports^[21].

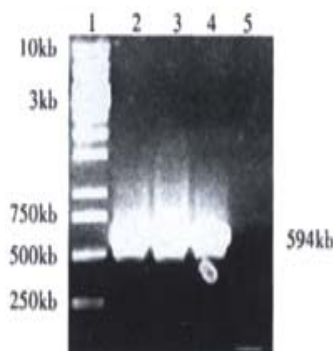


Figure 1 Ten g·L⁻¹ agarose gel electrophoreses of *M*_r26000 OMP DNA fragment amplified by PCR from *Helicobacter pylori*. Lane1: Nucleotide marker; Lane2-4: PCR products; Lane 5: Negative control.

Identification of recombinant plasmid by restriction enzyme digestion

The recombinant plasmids pET32a(+) were all digested by *Hind*III or *Bam*HI, and by *Hind*III and *Bam*HI simultaneously, then digestive products were visualized on 10g·L⁻¹ agarose gel electrophoreses (Figure 2). It demonstrated that recombinant plasmid contained the objective gene.

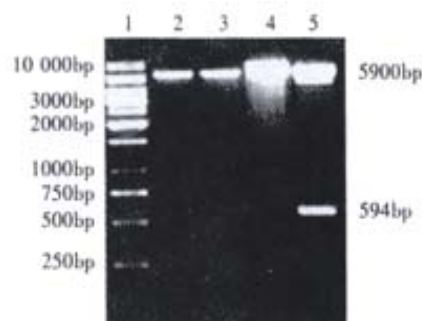


Figure 2 The identification of recombinant plasmid by restriction enzyme digestion. Lane1:Nucleotide marker; Lane2: pET32a(+)/*Hind*III; Lane3: pET32a(+)/*Hind*III, *Bam*HI; Lane4: Recombinant plasmid/*Hind*III; Lane5: Recombinant plasmid/*Hind*III, *Bam*HI.

Sequence analysis of cloned *M*_r26000 OMP nucleotide

The nucleotide sequence of the cloned genes inserted in pET32a(+) was analyzed by automated sequencing across the cloning junction, using the universal primer T₇. The results were: the cloned genes contained 594 nucleotides with a promoter and a start codon coding a putative protein of 198 amino acid residues with a calculated molecular mass of *M*_r26000. As compared with previously reports, 1.1% of the cloned genes were mutated, and 1.51% amino acid residues were changed. The homogeneity was about 98% between them. The cloned gene and mutative protein sequences were published in GenBank (AY 033499).

Analysis of the recombinant fusion protein

Following recombinant vector transformed into BL21 *E. coli* strains,

the fusion protein was amply expressed. Its molecular mass was M_r 46000 by $150\text{g}\cdot\text{L}^{-1}$ SDS-PAGE gel analysis (the expression of the pET32a(+) vector, M_r 20000). After the recombinant bacteria broken down by microwave and ultracentrifuged ($10000\text{r}\cdot\text{min}^{-1}$, 15min, 4°C), the level of soluble fusion protein in the supernatant was about 38.96% of total cell protein. After purification by Ni-NTA agarose resin columniation, the purity of objective protein was about 90% (Figure 3).

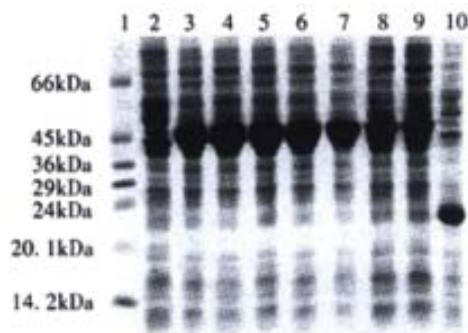


Figure 3 $150\text{g}\cdot\text{L}^{-1}$ SDS-PAGE analysis of the fusion protein expressed in BL21(DE3). Lane1: Molecular weight marker; 2Lane: BL21 after 4h induction with IPTG; Lane3-9: BL21/recombinant vector expression after 4h induction with 0.5, 1, 1.5, 2, 2.5, 3, 4mmol·L⁻¹ IPTG respectively; Lane10: BL21/pET32a(+) vector expression after 4h induction with IPTG.

Antigenicity study of recombinant fusion protein

Sera were obtained from persons infected and not infected with *H. pylori* respectively. The recombinant fusion protein was recognized by the *H. pylori* positive sera, not recognized by the *H. pylori* negative sera, while the expressed protein of BL21/pET32a(+) not recognized by the *H. pylori* positive sera; the recombinant fusion protein was also recognized by the rabbit sera immunized with M_r 26000 OMP, however the expressed protein of BL21/pET32a(+) not recognized by the rabbit sera immunized with M_r 26000 OMP.

Prophylactic efficacy with *H. pylori* M_r 26000 OMP

Subcutaneous immunization with *H. pylori* OMP and FA(Freund's adjuvant) conferred immune protection against *H. pylori* challenge in 19 (95%) of 20 mice. In contrast, 15 (100%) of 15 naive control animals were infected with *H. pylori*. These differences were statistically significant ($P<0.05$). The protection from infectious challenge was correlated with serum antibody reactivity to M_r 26000 OMP by immunoblotting. Similar reactivity was absent in the sera collected from same animals prior to immunization, while sera from mice sham immunized with PBS and FA failed to display similar immune responsiveness.

DISCUSSION

The outer membrane is a continuous structure on the surface of gram-negative bacteria and an asymmetric bilayer with phospholipids in the inner monolayer and the bulky glycolipid lipopolysaccharide (LPS) in the outer monolayer, in bacterial pathogens, has bilateral particular significance as a potential target for protective immunity and avoiding the host's immune system. Outer membrane vaccines have been used with considerable success to induce protection against a number of organisms, including *H. pylori* the heat shock protein, urease A, B and so on. M_r 26000 OMP is a low molecular mass Hsp protein belonging to family I of *H. pylori*^[20]. An earlier study showed that it was commonly expressed in all *H. pylori* strains examined so far. Furthermore, no cross-reaction is shown when antibodies (polyclonal and monoclonal) to *H. pylori* low-molecular outer membrane protein

are used to immunoscreen closely related species of helicobacter, campylobacter, or a diverse range of other bacteria. *Hp* low molecular outer membrane protein is unique.

In our study, 1.1% of the cloned genes was mutated, 1.51% of amino acid residues was changed as compared with other reports^[20]. The reasons of difference might be summarized as follows: (1)*H. pylori* chromosomal DNA as templates were different; (2) there is heterogeneity among strains; and (3) *H. pylori* was provided with the ability of transformation, which could lead to *H. pylori* varied and genome reseted^[22]. But there was homogeneity between them. The purified recombinant M_r 26000 OMP antigen could be recognized by the sera of patients infected with *H. pylori* and rabbit sera immunized with the recombinant protein. Moreover, in animal model, Balb/c mice immunized with the recombinant fusion protein were protected against *H. pylori* infection. These were consistent with previous reports^[23-26]. While being an immunogenic marker, M_r 26000 OMP showed a high sensitivity and specificity^[27]. Moreover, a significant association was found between the serologic response to M_r 26000 antigen and malignant outcome of *H. pylori* infection^[28-31]. So the serum test for detecting antibody with low molecular weight proteins of *H. pylori* could be useful for identifying *H. pylori*-infected patients at risk of peptic ulcer or malignancy. The results showed that M_r 26000 OMP is not only an immunogenic marker for detecting *Helicobacter pylori* infection and gastric carcinoma, but also a true vaccine candidate.

In addition to constructing the recombinant vector, we also tried to seek live carriers, because antigen delivery systems can influence the immune response qualitatively as well as quantitatively. Immunization via the mucosal route offers the advantage that it has the potential to stimulate both mucosal immunity and systemic immunity. It is simple, safe and can be used for the immunization of large population groups. Another advantage is the existence of the common mucosal immune system which induced protective immune responses at one mucosal site to be expressed at another^[32]. So live carriers on oral route are ideal vaccine delivery systems and are being increasingly used to express large amounts of protective recombinant antigens. We are investigating live carriers to provide a mucosal vaccine vector to deliver M_r 26000 OMP to antigen-presenting cells on the mucosal surface.

REFERENCES

- 1 Michetti P, Kreiss C, Kotloff K, Porta N, Blanco JL, Bachmann D, Herranz M, Saldinger P, Cortes-Thoulaz I, Losonsky G, Nichols R, Simon J, Stolte M, Ackerman S, Monath TP, Blum AL. Oral immunization with urease and *Escherichia coli* heat-labile enterotoxin is safe and immunogenic in *Helicobacter pylori*-infected adults. *Gastroenterology* 1999; 116: 804-812
- 2 Suganuma M, Kurusu M, Okabe S, Sueoka N, Yoshida M, Wakatsuki Y, Fujiki H. *Helicobacter pylori* membrane protein 1: a new carcinogenic factor of *Helicobacter pylori*. *Cancer Res* 2001; 61: 6356-6359
- 3 Nakamura S, Matsumoto T, Suekane H, Takeshita M, Hizawa K, Kawasaki M, Yao T, Tsuneyoshi M, Iida M, Fujishima M. Predictive value of endoscopic ultrasonography for regression of gastric low grade and high grade MALT lymphomas after eradication of *Helicobacter pylori*. *Gut* 2001; 48:454-60
- 4 Uemura N, Okamoto S, Yamamoto S, Matsumura N, Yamaguchi S, Yamakido M, Taniyama K, Sasaki N, Schlemper RJ. *Helicobacter pylori* infection and the development of gastric cancer. *N Engl J Med* 2001; 345: 829-32
- 5 Casella G, Buda CA, Maisano R, Schiavo M, Perego D, Baldini V. Complete regression of primary gastric MALT-lymphoma after double eradication *Helicobacter pylori* therapy: role and importance of endoscopic ultrasonography. *Anticancer Res* 2001;21(2B): 1499-1502
- 6 Morgner A, Miehke S, Fischbach W, Schmitt W, Muller-Hermelink H, Greiner A, Thiede C, Schetelig J, Neubauer A, Stolte M, Ehninger G, Bayerdorffer E. Complete remission of primary high-grade B-cell gastric lymphoma after cure of *Helicobacter pylori* infection. *J Clin Oncol* 2001; 19:2041-2048
- 7 Kate V, Ananthakrishnan N, Badrinath S. Effect of *Helicobacter pylori* eradication on the ulcer recurrence rate after simple closure of perforated

- duodenal ulcer: retrospective and prospective randomized controlled studies. *Br J Surg* 2001; 88: 1054-1058
- 8 Zhuang XQ, Lin SR. Progress in research on the relationship between *Hp* and stomach cancer. *Shijie Huaren Xiaohua Zazhi* 2000; 8:206-207
 - 9 Yu XE, Zhao AX, Wei DL, Du JZ. Relationship between *Helicobacter pylori* infection and gastric cancer. *World J Gastroenterol* 1998; 4(Suppl 2): 96
 - 10 Gao HJ, Yu LZ, Bai JF, Peng YS, Sun G, Zhao HL, Miu K, Li XZ, Zhang XY, Zhao ZQ. Multiple genetic alterations and behavior of cellular biology in gastric cancer and other gastric mucosal lesions: *H. pylori* infection, histological types and staging. *World J Gastroenterol* 2000; 6:848-854
 - 11 Yao YL, Zhang WD. Relation between *Helicobacter* and gastric cancer. *Shijie Huaren Xiaohua Zazhi* 2001; 9:1045-1049
 - 12 Goto T, Nishizono A, Fujioka T, Ikewaki J, Mifune K, Nasu M. Local secretory immunoglobulin A and postimmunization gastritis correlated with protection against *Helicobacter pylori* infection after oral vaccination of mice. *Infect Immun* 1999; 67:2531-2539
 - 13 Watanabe T, Tada M, Nagai H, Sasaki S, Nakao M. *Helicobacter pylori* infection induces gastric cancer in Mongolian Gerbils. *Gastroenterology* 1998; 115:642-648
 - 14 Honda S, Fujioka T, Tokieda M, Satoh R, Nishizono A, Nasu M. Development of *Helicobacter pylori*-induced gastric carcinoma in Mongolian Gerbils. *Cancer Res* 1998; 58:4255-4259
 - 15 Hatzifoti C, Wren BW, Morrow JW. *Helicobacter pylori* vaccine strategies-triggering a gut reaction. *Immuno Today* 2000; 21: 615-619
 - 16 Kotloff KL, Sztein MB, Wasserman SS, Losonsky GA, DiLorenzo SC, Walker RI. Safety and immunogenicity of oral inactivated whole-cell *Helicobacter pylori* vaccine with adjuvant among volunteers with or without subclinical infection. *Infect Immun* 2001; 69: 3581-3590
 - 17 Keenan J, Oliaro J, Domigan N, Potter H, Aitken G, Allardyce R, Roake J. Immune response to an 18-kilodalton outer membrane antigen identifies lipoprotein 20 as a *Helicobacter pylori* vaccine candidate. *Infect Immun* 2000; 68: 3337-3343
 - 18 Dubois A, Lee CK, Fiala N, Kleanthous H, Mehlman PT, Monath T. Immunization against natural *Helicobacter pylori* infection in nonhuman primates. *Infect Immune* 1998; 66: 4340-4346
 - 19 Ikewaki J, Nishizono A, Goto T, Fujioka T, Mifune K. Therapeutic oral vaccination induces mucosal immune response sufficient to eliminate long-term *Helicobacter pylori* infection. *Microbiol Immunol* 2000; 44:29-39
 - 20 Alm RA, Bina J, Andrews BM, Dolg P, Hancock REW, Trust TJ. Comparative genomics of *Helicobacter pylori*: analysis of the outer membrane protein families. *Infect Immun* 2000; 68: 4155-4168
 - 21 Toomb JF, White O, Kerlavage AR, Clayton RA, Sutton GG, Fleischmann RD, Ketchum KA, Klenk HP, Gill S, Dougherty BA, Nelson K, Quackenbush J, Zhou L, Kirkness EF, Peterson S, Loftus B, Richardson D, Dodson R, Khalak HG, Glodek A, McKenney K, Fitzgerald LM, Lee N, Adams MD, Hickey EK, Berg DE, Gocayne JD, Utterback TR, Peterson JD, Kelley JM, Cotton MD, Weldman JM, Fujii C, Bowman C, Wathley L, Wallin E, Hayess WS, Borodovskys M, Karp PD, Smiths HO, Fraser CM, Venter JC. The complete genome sequence of the gastric pathogen *Helicobacter pylori*. *Nature* 1997; 388:739-747
 - 22 Zhong P, Wu KX, Xu FH, Xu CD, Xu JY. Cloning and characterization of *Hp* *cagA* gene sequences derived from Chinese strains. *Shijie Huaren Xiaohua Zazhi* 1999; 7: 669-672
 - 23 Li MF, Ling Z, Ma AY, Zhao JH, Sun JX, Yu SZ, Wu XF. Cloning, expression and immunogenicity of *Hp* *UreB* gene. *Shijie Huaren Xiaohua Zazhi* 1999; 7:596-600
 - 24 Saldinger PF, Porta N, Launois P, Louis JA, Waanders GA, Bouzourene H, Michetti P, Blum AL, Corthesy-theulaz IE. Immunization of Balb/c mice with *Helicobacter* *Urease B* induces a Thelper 2 response absent in *Helicobacter* infection. *Gastroenterology* 1998; 115: 891-897
 - 25 Ghiara P, Ross M, Marchetti M, Tommaso AD, Vindingni C, Ciampolini F, Covacci A, Telford J, Magistris MTD, Pizza M, Rappuoli R, Giudice GD. Therapeutic intragastric vaccination against *Helicobacter pylori* in mice eradicates an otherwise chronic infection and confers protection against reinfection. *Infect Immun* 1997; 65:4996-5002
 - 26 Kleanthous H, Myers GA, Georgakopoulos KM, Tibbitts TJ, Ingrassia JW, Gray HL, Ding R, Zhang ZZ, Lei W, Nichols R, Lee CK, Ermak TH, Monath TP. Rectal and intranasal immunizations with recombinant *Urease* induce distinct local and serum immune responses in mice and protect against *Helicobacter pylori* infection. *Infect Immun* 1998; 66:2879-2886
 - 27 Yang WH, Lin SR, Wang LX, Ding SG, Jin Z. The relation between the pathogenetic factors of *Helicobacter pylori* and gastric diseases. *J Beijing Med Univ* 2000; 32:34-38
 - 28 Shieh SJ, Sheu BY, Yang SB, Tsao HJ, Lin XZ. Serologic response to lower-molecular-weight proteins of *Helicobacter pylori* is related clinical outcome of *Helicobacter pylori* infection in Taiwan. *Dig Dis Sci* 2000; 45:781-788
 - 29 Mitchell HM, Hazell SL, Li YY, Hu PJ. Serological response to specific *Helicobacter pylori* antigen: antibody against *cagA* antigen is not predictive of gastric cancer in a developing country. *Am J Gastroenterol* 1996; 91:1785-1789
 - 30 Raymond J, Sauvestre C, Kalach N, Bergeret M, Dupont C. Immunoblotting and serology for diagnosis of *Helicobacter pylori* infection in children. *Pediatr Infect Dis J* 2000; 19:118-121
 - 31 Lu JJ, Perng CL, Shyu RY, Chen CH, Lou Q, Chong SKF, Lee CH. Comparison of five PCR methods for detection of *Helicobacter pylori* DNA in gastric tissues. *J Clin Microbiol* 1999; 37:772-774
 - 32 Hasan UA, Abai AM, Harper DR, Wren BW, Morrow WJW. Nucleic acid immunization: concepts and techniques associated with third generation vaccines. *J Immunol Methods* 1999; 229:1-22

Edited by Ma JY

• BASIC RESEARCH •

Morphological properties and residual strain along the small intestine in rats

Jing-Bo Zhao, Hong Sha, Feng-Yuan Zhuang, Hans Gregersen

Jing-Bo Zhao, Hans Gregersen, Biomechanics Lab, Centre for Sensory-Motor Interaction, Aalborg University and Department of surgery A, Aalborg Hospital, Denmark

Hong Sha, Clinical Institute, China-Japan Friendship Hospital, Beijing, 100029 China

Feng-Yuan Zhuang, Institute of Bio-Science and Bio-Engineering, Beijing University of Aeronautics and Astronautics, Beijing 100084, China

Supported by Karen Elise Jensens Foundation and the Danish Technical Research Council

Correspondence to: Hans Gregersen, M.D., Dr.M.Sci., Centre for Sensory-motor Interaction, Aalborg University, Fredrik Bajersvej 7D-3, DK-9220 Aalborg, Denmark. hag@smi.auc.dk

Telephone: +45-99322064 Fax: +45-98154008

Received 2001-11-02 Accepted 2002-01-25

Abstract

AIM: Residual stress and strain are important for gastrointestinal function and relate to the geometric configuration, the loading conditions and the zero-stress state of the gastrointestinal tract. The purpose of this project is to provide morphometric data and residual strains for the rat small intestine ($n=11$).

METHODS: To approach the no-load state, the intestine was surgically excised, transferred to an organ bath and cut transversely into short ring-shaped segments. Each ring was cut radially for obtaining the zero-stress state. The residual stress can be characterised by an opening angle. The strain difference between the zero-stress state and the no-load state is called residual strain.

RESULTS: Large morphometric variations were found along the small intestine. The wall thickness was highest in the proximal duodenum and decreased in distal direction along the axis of the small intestine ($P<0.001$). The circumferential length of the inner and outer surfaces decreased rapidly along the length of duodenum by 30-50% ($P<0.001$). The wall area and lumen area showed a similar pattern ($P<0.001$). In zero-stress state the rings always opened up after making the cut. The experiments resulted in larger inner circumferential length and smaller outer circumferential length when compared to the no-load state. The wall thickness and wall area did not differ between the no-load and zero-stress state. The opening angle and tangent rotation angle increased along the length of the duodenum and had its highest value 30% down the intestine. Further down the intestine it decreased again ($P<0.001$). The serosal residual strain was tensile with the highest value close to the ligament of Treitz ($P<0.001$). The mucosal residual strain was compressive in all segments of the small intestine with average values between -0.25 and -0.4 and with the lowest values close to the ligament of Treitz ($P<0.001$).

CONCLUSION: Axial variation in morphometric properties and residual strains were found in the small intestine. Existence of large residual strains indicates that the zero-stress state must be considered in future biomechanical studies in the gastrointestinal tract.

Zhao JB, Sha H, Zhuang FY, Gregersen H. Morphological properties and residual strain along the small intestine in rats. *World J Gastroenterol* 2002;8(2):312-317

INTRODUCTION

The gastrointestinal (GI) tract is a hollow muscular tube serving as a digestive organ. The small intestine transports, digests and absorbs nutrients. It extends from the pylorus to the caecum and comprises the duodenum, jejunum and ileum which merges into the large intestine at the ileocaecal valve. Our knowledge of GI motility has increased considerably during the last decades. Most data dealt with motility patterns, flow rates, peristaltic reflexes, and tone in sphincter regions^[1-5]. The GI tract, like other hollow organs such as the heart, blood vessels, urinary bladder and the urethra, is functionally subjected to dimensional changes. Hence, biomechanical properties are of particularly functional importance. Data in the literature pertaining to the passive mechanical properties of small intestine were concerned with the length-tension relationship in circular and longitudinal tissue strips^[6-8], the compliance^[9], and the stress-strain relationship of the intact wall^[10, 11]. However, a complete biomechanical analysis of GI physiology requires a full set of data describing the geometric properties and a valid reference state.

The zero-stress state of an organ is the state at which the organ is stress-free, meaning that all external and internal forces are removed. Thus, the morphometric properties are best described at the zero-stress state where no internal or external forces deform the tissue. Furthermore, knowing the zero-stress configuration is essential in any mechanical analysis since it serves as the reference state for computing stress and strain under physiological or pathophysiological conditions. Until 1983, it was believed that biological organs were free of stress when all external loads were removed (now known as the no-load state). Vaishnav and Vossoughi^[12] and Fung^[13] independently reported in 1983 that the no-load state of a blood vessel was not the zero-stress state. This was shown by an experiment where tissue rings that were cut radially opened up into sectors. The difference in stress and strain between the no-load and zero-stress state was called residual stress and strain, respectively, and it was found that the opening angle of the sector was a convenient way to quantitate the residual stress (Figure 1). Since then, a large number of studies have been published on the zero-stress state of different organ systems. The majority of these studies focused on the zero-stress state of systemic and pulmonary arteries, the heart and veins in normal animals and in various disease models such as experimental hypertension and diabetes and in venous grafts. Studies were also presented on the airway^[14] and ureter^[15].

The first data on residual strains and stresses in the gastrointestinal tract appeared in 1996^[16]. Now we realize that the zero-stress configuration of the gastrointestinal tract is very different from that of the no-load condition and that the zero-stress state is sensitive to growth and remodeling by surgical resection (Dou *et al*, unpublished data). Gregersen *et al*^[17] made an attempt to describe the geometry of the duodenum at the zero-stress state, and studied the strain distribution with reference to the zero-stress state in guinea pig duodenum using an elastomer casting method. It was found that the duodenum had very large opening angles and circumferential residual strains with axial variation. These studies opened up a whole new field of investigation in relation to gastrointestinal physiology and pathophysiology. The aims of the current study were to provide morphometric data at the no-load and zero-stress states of the entire

small intestine in rats and the axial distribution of residual circumferential strains.

MATERIALS AND METHODS

Eleven three-month-old male SD rats weighing 293 ± 18 g were included in this study. The rats were anaesthetised with pentobarbital sodium ($100 \text{ mg} \cdot \text{kg}^{-1}$, ip). Following laparotomy, the calcium antagonist, papaverine ($60 \text{ mg} \cdot \text{kg}^{-1}$) was injected into the lower thoracic aorta through a cannula (22G/25mm) in order to abolish contractile activity in the GI tract. After obtaining smooth muscle relaxation, the whole small intestine was harvested and 12 segments from various parts of the intestine were isolated. The most proximal segment was close to the pylorus whereas the most distal segment was close to the ileo-caecal valve. Within a short time, the residual contents in the lumen were gently cleared using saline. Then the segments were placed immediately into cold aerated Krebs solution containing $60 \text{ g} \cdot \text{L}^{-1}$ dextran. Three rings, 1-2mm in length, were cut from each segment for no-load and zero-stress state tests. The rings were photographed in the no-load state using a video camera (SONY CCD Camera, Japan) and then cut radially on the anti-mesenteric side to obtain their zero-stress state (Figure 1). A 60-min-period was allowed for equilibration and the specimens were photographed again. The selection of this time period was based on pilot experiments.

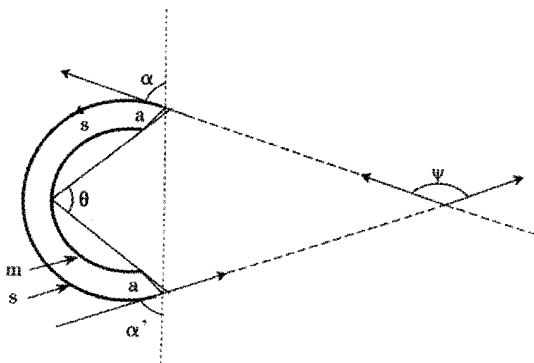


Figure 1 Definition of the zero-stress state. Traditionally, the zero-stress state is characterized by an opening angle defined as the angle subtended by two radii drawn from the mid-point of the inner wall to the inner tips of two ends of the sector in the zero-stress state. The opening angle is denoted by θ . The labels m and s denote the mucosal and serosal surfaces and a is the line cutting. The angle between the tip tangents, which is described in the text, is denoted by ψ . The angles between the tangents at the tip of the sector and the line joining the tips are designated as α and α' , respectively. The mean value $(\alpha + \alpha')/2$ is referred to as the mean tangential angle.

Data Analysis

The morphometric data were obtained from the digitised images of the photographs of segments in the zero-stress and no-load states (Figure 2). Measurements were done using SigmaScan software (Jandel Scientific, Germany). The following data were measured from each specimen: the circumferential length (C), the wall thickness (h), the wall and lumen area, and the opening angle (α) at the zero-stress state. The subscripts i, o, n and z referred to the inner (mucosal) surface, outer (serosal) surface, no-load state and zero-stress state condition. The data from triplet of rings were averaged before further analysis.

Figure 2 shows a schematic of a tissue sector in the zero-stress state. The subtended angle is called the opening angle, θ , and is defined as the subtended angle between the two radii from the midpoint of the arc of the inner wall of the specimen to the inner tips of the sector.

The opening angle was a convenient measure but might not always be useful in practice. First, it required that both the no-load

and the zero-stress state to be circular. However, neither configuration might be exactly circular. The opening angle is a measure of the angle between the two radii and does not account for the shape of the curve. It provides no information on the curvature of the wall. The angles between the tangents at the tip of the sector and the line joining the tips are designated as α and α' , respectively (Figure 1). The mean value $(\alpha + \alpha')/2$ was referred to as the mean tangential angle. If the sector is exactly circular, then $\theta = (\alpha + \alpha')/2$. The second difficulty with the opening angle is when its value exceeds 360° (i.e., the sector inverts inside out). Some organs such as the guinea-pig duodenum often have θ greater than 360° ^[17]. The geometry of the duodenum at the zero-stress state can also be characterized by the angle between the two tangents of the tip, ψ , as shown in Figure 1. ψ refers to the angle between the tip tangents. The value of ψ is relatively independent on where the cuts are made in the ring and does not require the no-load or zero-stress shape to be circular (see reference 18).

The measured data was used for computation of residual strains defined as:

Residual Green's strain at the mucosal surface: $\epsilon_i = (C_{i-n}/C_{i-z}) - 1/2$

Residual Green's strain at the serosal surface: $\epsilon_o = (C_{o-n}/C_{o-z}) - 1/2$

Thus, from the circumferential lengths at the no-load and zero-stress state, we can compute the circumferential residual strain, at the mucosal and serosal surfaces in the sense of green. Green strain is used when large deformations are encountered as in this study. Negative strain implies that the tissue is in compression whereas positive strain implies extension.

Statistical Analysis

The data were representative of a normal distribution and accordingly the results were expressed as mean \pm SD unless otherwise stated. Analysis of variance was used to detect possible variations in axial direction of the small intestine and between no-load and zero-stress state (Sigmastat 2.0™). In case of significance, data were evaluated in pairs by a multiple comparison procedure Student-Newman-Keuls method. If the normality test or the equal variance test failed, Kruskal-Wallis one-way analysis of variance on ranks was used. The results were regarded as significant when $P < 0.05$.

RESULTS

Representative images of rings in the no-load state and after cutting into the zero-stress state are illustrated in Figure 2. Figure 3 presented the morphometric data measured from the photographs of the segments in the no-load state and zero-stress state. In the no-load state (Figure 3A), the wall thickness was highest in the proximal duodenum (average value approximately 1.2mm) and decreased in distal direction along the axis of the small intestine to a value close to 0.6mm ($f=66.48$, $P < 0.001$). The circumferential length and the inner and outer surfaces decreased rapidly along the length of duodenum by 30-50% in both no-load state and zero-stress state (Figure 3B, inner, $f=22.46$ and $P < 0.001$; outer, $f=37.68$ and $P < 0.001$). The wall area and lumen area showed a similar pattern (Figure 3C, wall area, $f=43.43$ and $P < 0.001$; Lumen area, $f=12.50$ and $P < 0.001$). The wall thickness-to-inner circumferential length ratio increased along the length of duodenum after it decreased continuously towards the distal ileum (Figure 3D, $f=38.52$ and $P < 0.001$). The highest average value was found close to the ligament of Treitz (0.21) and the lowest value of 0.08 was found close to the ileo-caecal valve.

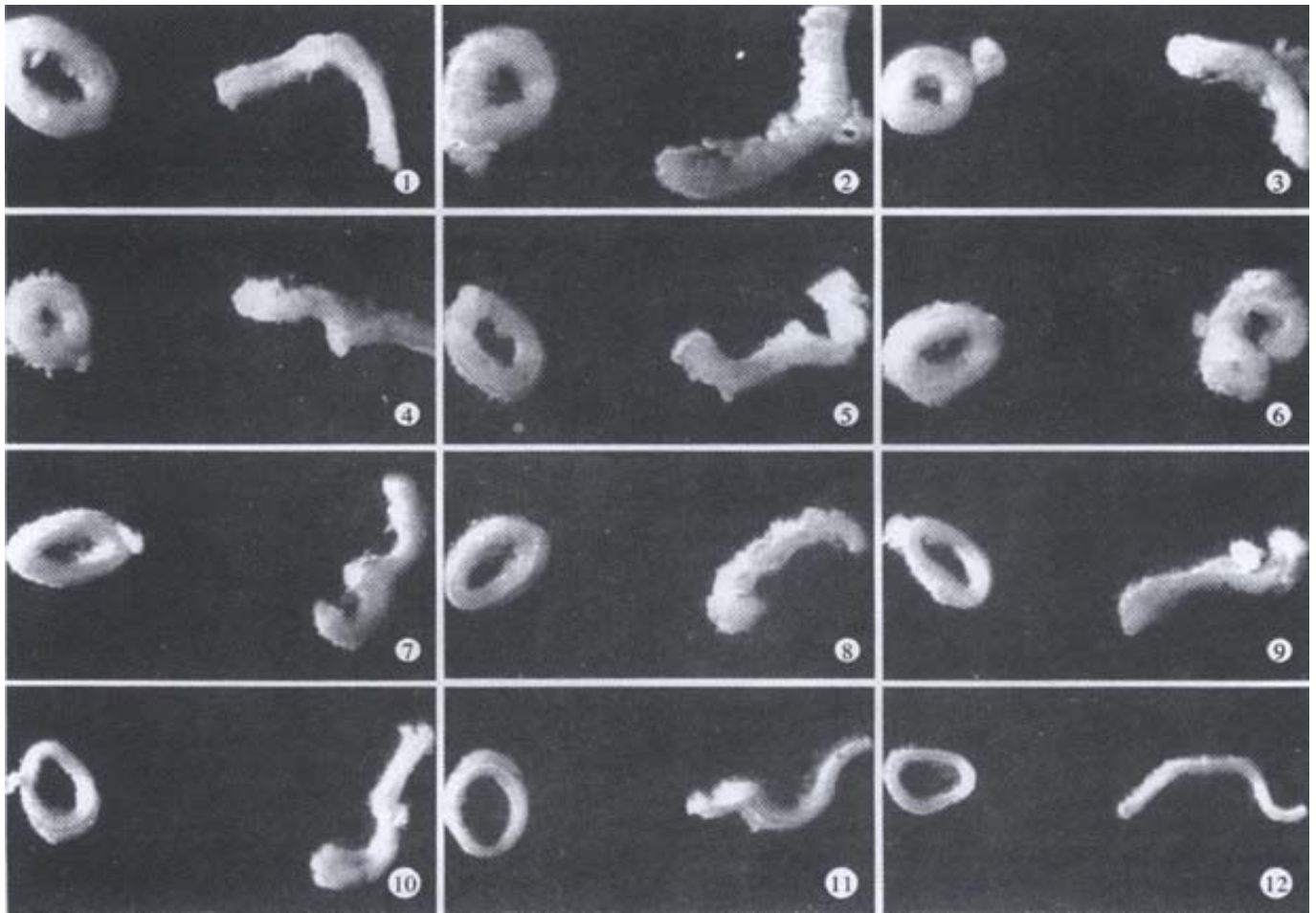


Figure 2 Photographs showing specimens obtained from different locations in the intestine in the no-load state (left, closed rings) and the zero-stress state (right, open sectors). The rings of jejunum (site 5 to site 8) turned inside out when cut open.

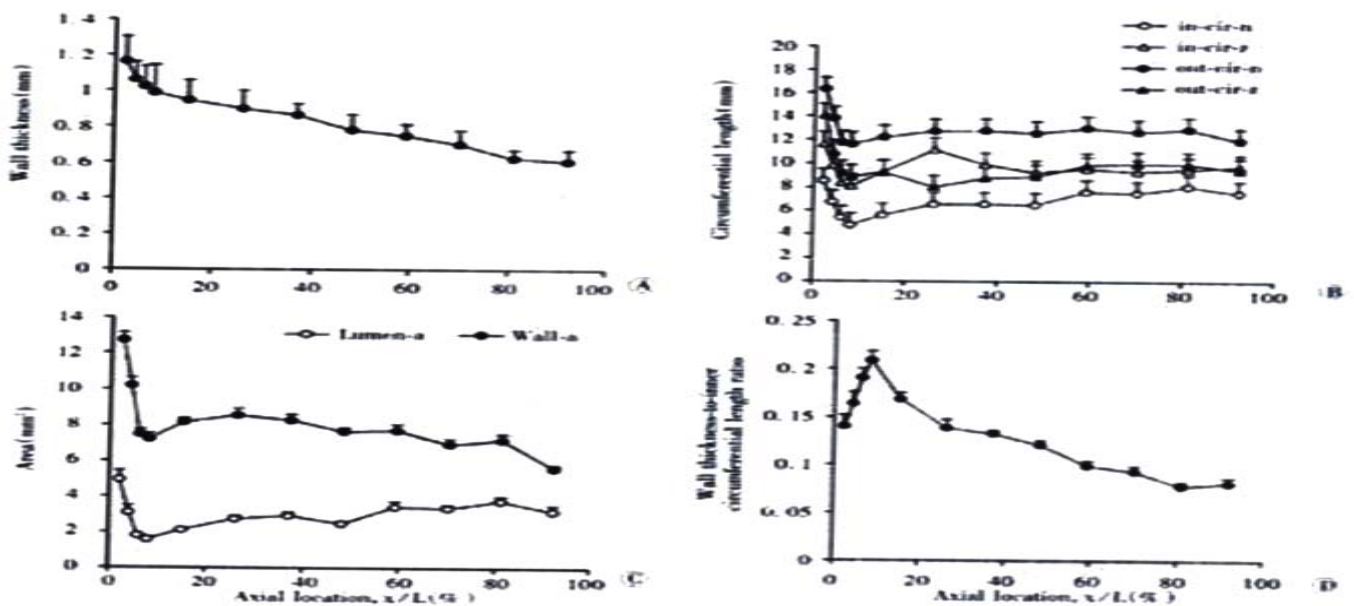


Figure 3 Photographs showing morphometry of rat small intestine including wall thickness in the no-load state (A), inner and outer circumferential length in the no-load state and zero-stress state (B), the wall and lumen area in the no-load state (C) and wall thickness-to-inner circumferential length ratio (D). Values are (S). Variation of all morphometric parameters related to location along the axis of the small intestine was found ($P < 0.001$).

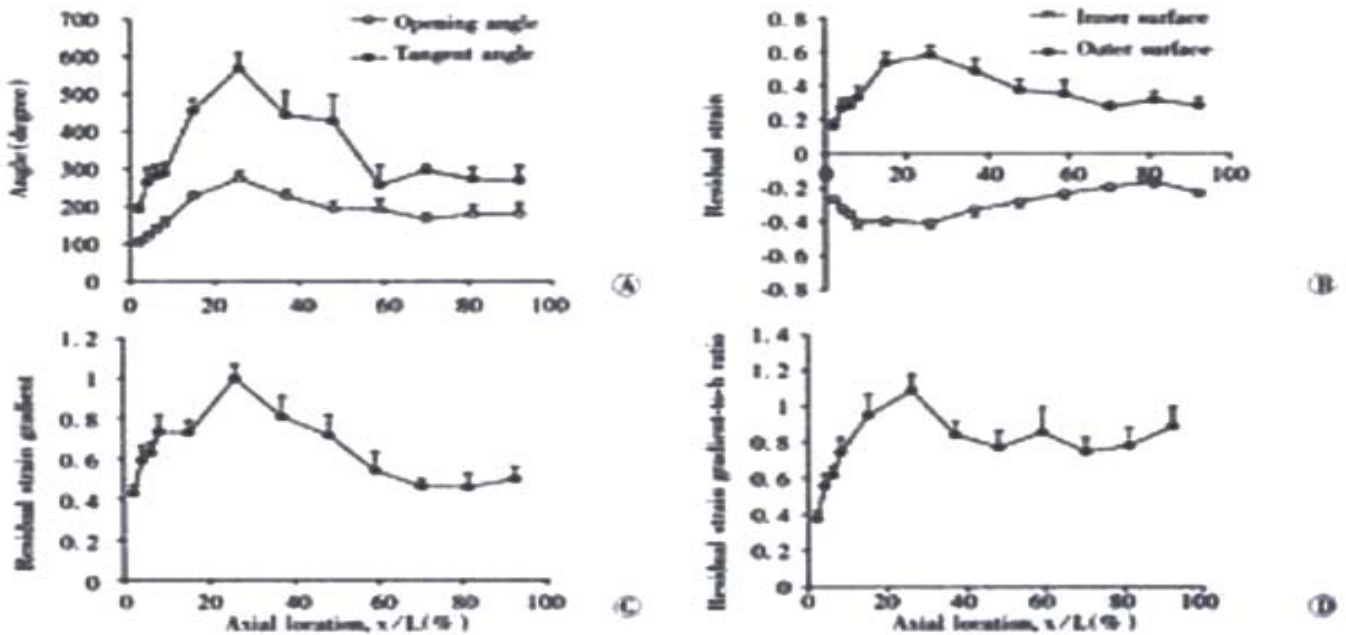


Figure 4 Photographs showing (A) the distributions of the opening angle and tangent rotation angle, (B) residual strains at the mucosal and serosal surfaces, (C) the residual strain gradient and (D) residual strain gradient normalised with respect to the wall thickness (h). Values are $\bar{x} \pm s$. A significant variation was found along the small intestine for all variables ($P < 0.001$).

In the zero-stress state, the rings always opened up after making the cut. This resulted in larger inner circumferential length and smaller outer circumferential length when compared to the no-load state. Otherwise, the wall thickness and wall area did not differ between the no-load and zero-stress state ($P > 0.5$). The distributions of the opening angle and residual strains at the mucosal and serosal surfaces are shown in Figure 4. The opening angle and tangent rotation angle increased along the length of the duodenum and had its highest value 30% down the intestine. They decreased again further down the intestine (opening angle, $f=5.07$ and $P < 0.001$; tangent rotation angle, $f=11.95$ and $P < 0.001$). The opening angle attained values higher than 180 degrees in the jejunum and ileum, meaning that the rings turned themselves inside-out (Figure 4A). The serosal residual strain was tensile with the highest value close to the ligament of Treitz (approximately 0.6) and decreased to approximately 0.3 in the distal ileum (Figure 4B, $f=5.20$ and $P < 0.001$). The mucosal residual strain was compressive in all segments of the small intestine with average values between -0.25 and -0.4. A significant variation was found along the small intestine with the lowest values close to the ligament of Treitz ($f=8.17$ and $P < 0.001$). The curve for the residual strain gradient (i.e. the difference between mucosal and serosal residual strains) showed a pattern similar to that for the tangent rotation angle (Figure 4C, $f=7.11$ and $P < 0.001$). Furthermore, the residual strain gradient normalised as the wall thickness increased rapidly along the length of the duodenum from average values of 0.4 to 1.1 and dropped to a constant level of approximately 0.8 in more distal parts of the small intestine (Figure 4D, $f=4.43$ and $P < 0.001$).

DISCUSSION

Mechanical properties are important for cardiovascular^[18,19] and urogenital function^[15,20]. The GI tract is similar to these organs in which it is functionally subjected to changes in wall stresses and strains. Therefore, during the last decade, acquiring biomechanical information in the digestive tract has increasingly called attention.

Some studies have provided data on the small intestine^[9-11,17]. However, many aspects are still left largely unexplored. With respect to biomechanics of the small intestine, we still lack a database on its geometry to fulfil a detailed biomechanical analysis of small intestinal physiology. Moreover, our knowledge about the small intestine at the zero-stress state is very limited. Gregersen H *et al.*^[17] provided the first data on the zero-stress state of the guinea pig duodenum. The current study aimed to describe the morphometry at the no-load and zero-stress states of the small intestine and to analyse the residual strain in the small intestine. The duodenal residual strains obtained in pigs^[21] and rats in this study are less than that in the guinea-pig. In general, the opening angle in pigs and rats is not larger than 360 degrees.

Our results demonstrated large axial variations of all the morphometric parameters. The outer circumferential length and the luminal area increased whereas the wall thickness decreased in distal direction. A decrease in wall thickness is in line with findings in prior studies^[22,23]. When radial cuts were made, the rings from the proximal small intestine were more likely to turn inside out resulting in a larger opening angle and larger residual strains than those in the jejunal and ileal rings. In accordance with observations in other hollow organs, the circumferential residual strain in the small intestine was compressive at the inner wall and tensile at the outer wall. From the mechanical point of view, a large residual strain may be nature's way to resist luminal pressures. The present study showed that the small intestinal mucosa at the no-load state was under compression and with axial variation from duodenum to ileum. This variation seems to correlate to morphometric variation along the small intestine^[22]. In this sense we hypothesise that the compressed duodenal mucosa might be better protected against injury from frequent pressure changes produced by frequent contractions and the rush of luminal contents ejected at intervals from the stomach. By contrast, the less compressed ileal mucosa fulfils the protection in a region under relatively lower and stable pressure. From our studies, it is evident that a gradient in residual stress and strain exists and that the mucosal and submucosal layers are in compression. It still remains to be investigated whether mucosal growth is determined by the compression induced by residual

stresses or whether the residual stress largely is a result of mucosal growth. It is of interest to notice that Rodriguez *et al*^[24] predicted how volumetric tissue growth altered residual stress. Particularly, it was predicted that concentric hypertrophy (increase in wall thickness-to-radius ratio) increased residual stress and strain. The prediction is in accordance with the data in this study (comparison of Figure 3D with Figure 4).

Our previous data showed that the duodenal wall was stiffer than the jejunal and the ileal wall in circumferential direction. That is, the elastic properties differed among the small intestinal segments. The differences in stiffness may be associated with the specialised functions of the proximal and distal segments of the small intestine. The duodenum has a large influence on gastric emptying and has been proposed to act as a capacitative resistor^[25], whereas the distal ileum acts as a reservoir^[4]. The transit time is slower distally^[1], which may be partly explained by the difference in the viscosity of the chyme. However, the passive elastic properties may also contribute to differences in intestinal flow patterns: a passing bolus will be slowed to a lesser degree in the duodenum where the wall stiffness is high whereas the compliant ileal walls bulges lead to pooling of luminal contents and decreased flow. Though we find the highest residual strains in the proximal small intestine, the association between the stiffness^[9] and the residual strains found in this study does not seem that the mechanism is clear cut and further investigation is needed.

There are several important implications of the zero-stress state, some of which are, as yet, hypothetical. It is clear from the above discussion that using any state other than the zero-stress state will lead to error in the computed stresses and strains. Analysis of strain must refer to the zero-stress state in order to compare the specimens obtained from different locations of the GI tract in different species, and in remodeling induced by diseases, growth or degeneration. Furthermore, since the zero-stress state is not influenced by external or internal forces, it provides a standard state for describing tissue morphology.

All GI studies done thus far show that the rings open into sectors when cut radially. This implies that the mucosa is under compression in the no-load state (and at physiological conditions in the low pressure range) whereas the muscle layers are in tension. The residual tension in the muscle may provide a more optimum length for muscle contraction. It has been demonstrated that residual stress reduces the stress concentration at the inner wall of the GI tract at no-load and homeostatic states^[17, 21, 26, 27]. Thus, the compressed mucosa may be better protected against injury from the flow of luminal contents than uncompressed mucosa. These protection mechanisms could be important when unphysiologically high pressures are reached, such as in mechanical obstruction. Since peristaltic bolus transport bulges out the intestinal wall in the vicinity of the bolus^[28,29], the residual strain would likely influence the resistance to bolus flow under normal conditions. Since residual strains exist, the mucosa will inevitably be under compressive stress and strain in the no-load condition, for instance, where the transmural pressure is zero. The GI muscles are usually passive since phasic contractions occur infrequently^[30]. We may also ask if there are any other functions of the mucosa compression than those mentioned above. It is well known that the mucosa is one of the tissues with the fastest turnover rate. The fast growth of the mucosal surface could easily cause mucosal compression and hence explain the presence of large residual strains. Likewise the large compressive stresses may affect mucosal growth. Studies on the intestine and other organs have shown that mechanical stresses are important factors in regulating gene expression and growth^[31] (Gregersen *et al.*, unpublished data). Well-known examples are cardiac hypertrophy caused by hypertension and muscle atrophy in space flight. Theoretically, absorption of luminal contents may also be affected by the residual compression. It is well known that a gradient in the height of the mucosal villi exists along the small intestine, with the highest villi found in the proximal duodenum^[23], and that small

intestinal absorption depends on the luminal pressure^[32]. Thus, there may exist a correlation between the residual strain gradient and the gradient in the height of villi. These interesting aspects of small intestinal function should be the focus of future studies.

Other important issues pertain to the function of the mechanoreceptors (endings of the sensory afferent nerves) in the gastrointestinal wall. Such receptors include noci-sensitive receptors and receptors in the peristaltic reflex pathway. It is well known that the receptors are located both in the submucosa and in the muscle layers. We have shown that a strain gradient exists from the mucosa to the serosa of the wall under physiological conditions. This suggests that the population of receptors from different locations in the wall may have different zero-settings and respond differently to the same stimuli. A difference in the responses of mucosal and muscle receptors to stimuli has in fact been observed^[33]. The present results emphasize the importance of studying the receptor kinematics by using experimental models on the intact organ approximating the *in vivo* conditions. Data on receptor kinematics obtained from tissue strips or otherwise cut-open segments would likely give erroneous results.

Differences in morphometric properties and residual strains were found between rat duodenum, jejunum and ileum. Existence of a large residual circumferential strain indicates that the zero-stress state must be considered in future biomechanical studies. Residual stress may affect the tissue remodeling in response to disease and interventions by varying the stress distribution in the organ. The data on residual strains in the GI tract and the non-uniform remodeling may be used to improve surgery (for example, the procedures may be designed to prestress the tissue to make it more resistant to injury).

REFERENCES

- Huang X, Zhu HM, Deng CZ, Porro GB, Sangaletti O, Pace F. Gastroesophageal reflux: the features in elderly patients. *World J Gastroenterol* 1999;5: 421-423
- Kellow JE, Borody TJ, Phillips SF, Tucker RL, Haddad AC. Human interdigestive motility: variations in patterns from oesophagus to colon. *Gastroenterology* 1986; 91: 386-395
- Li W, Zheng TZ, Qu SY. Effect of cholecystokinin and secretin on contractile activity of isolated gastric muscle strips in guinea pigs. *World J Gastroenterol* 2000;6: 93-95
- Schulze-Delrieu K. Intrinsic differences in the filling response of the guinea pig duodenum and ileum. *J Lab Clin Med* 1991; 117: 44-50
- Zheng TZ, Li W, Qu SY, Ma YM, Ding YH, Wei YL. Effects of Dangshen on isolated gastric muscle strips in rats. *World J Gastroenterol* 1998; 4: 354-356
- Meiss RA. Some mechanical properties of cat intestinal muscle. *Am J Physiol* 1971; 220: 2000-2007
- Price JM, Patitucci PJ, Fung YC. Mechanical properties of resting taenia coli smooth muscle. *Am J Physiol* 1979; 236: C211-C220
- Elbrond H, Tottrup A, Forman A. Mechanical properties of isolated smooth muscle from rabbit sphincter of Oddi and duodenum. *Scand J Gastroenterol* 1991; 26: 289-294
- Storkholm JH, Jrgensen CS, Dall FH, Jensen SL, Gregersen H. Differences exist in Passive elastic wall properties between segments of isolated guinea-pig distal ileum and duodenum *in vitro*. *Neurogastroenterol Mot* 1994; 6: 21-27
- Duch BU, Petersen JA, Vinter-Jensen L, Gregersen H. Elastic properties in the circumferential direction in isolated rat small intestine. *Acta Physiol Scand* 1996; 157: 157-163
- Storkholm JH, Villadsen GE, Jensen SL, Gregersen H. Passive elastic wall properties in isolated guinea pig small intestine. *Dig Dis Sci* 1995; 40: 976-982
- Vaishnav RN, Vossoughi J. Estimation of residual strains in aortic segments. In: Hall CW, eds. Biomedical engineering II. Recent Developments. New York: Pergamon Press 1983: 330-333
- Fung YC. What principle governs the stress distribution in living organs In: Fung YC, Fukada E, Junjian W, eds. Biomechanics in China, Japan and USA. Beijing, China: Science, 1983: 1-13
- Han HC, Fung YC. Residual strains in porcine and canine trachea. *J Biomech* 1991; 24: 307-315
- Hansen I, Gregersen H. Morphometry and residual strain in porcine ureter. *Scand J Urol Nephrol* 1999; 33: 10-16
- Gregersen H, Kassab GS. Biomechanics of the gastrointestinal tract. *Neurogastroenterol Motility* 1996; 8: 277-297

- 17 Gregersen H, Kassab GS, Pallencaoe E, Lee C, Chien S, Skalak R, Fung YC. Morphometry and strain distribution in guinea pig duodenum with reference to the zero-stress state. *Am J Physiol* 1997; 273: G865-G874
- 18 Dobrin PB. Mechanical properties of arteries. *Physiol Rev* 1978; 58: 397-460
- 19 Mulvany MJ. Determinants of vascular hemodynamic characteristics. *Hypertension* 1984; 6: III13-III18
- 20 Van Duyl WA. A model for both the passive and active properties of urinary tissue related to bladder function. *Neurourol Urodyn* 1985; 4: 275-283
- 21 Gao C, Zhao J, Gregersen H. Histomorphometry and strain distribution in pig duodenum with reference to the zero-stress state. *Dig Dis Sci* 2000; 45: 1500-1508
- 22 Gabella G. On the musculature of the gastrointestinal tract of the guinea pig. *Anat Embryol* 1981; 163: 135-156
- 23 Gabella G. Structure of muscles and nerves in the gastrointestinal tract. In: Johnson LR, eds. *Physiology of the Gastrointestinal tract*. New York: Raven 1987: 335-382
- 24 Rodriguez EK, Hoger A, McCulloch AD. Stress-dependent finite growth in soft elastic tissues. *J Biomech* 1994; 27: 455-467
- 25 Shirazi S, Schulze-Delrieu K, Brown CK. Duodenal resistance to the emptying of various solutions from the isolated cat stomach. *J Lab Clin Med* 1988; 111: 654-660
- 26 Gregersen H, Lee TC, Chien S, Skalak R, Fung YC. Strain Distribution in the Layered Wall of the Esophagus. *J Biomech Eng* 1999; 121: 442-448
- 27 Lu X, Gregersen H. Regional distribution of axial strain and circumferential residual strain in the layered rabbit esophagus. *J Biomech* 2001; 34: 225-233
- 28 Bayliss VM, Starling EH. The movements and innervation of the small intestine. *J Physiol* 1991; 26: 125-138
- 29 Siegle ML, Ehrlein HJ. Effects of various agents on ileal postprandial motor patterns and transit of chyme in dogs. *Am J Physiol* 1989; 257: G698-G703
- 30 Kellow JE, Borody TJ, Phillips SF, Tucker RL, Haddad RC. Human interdigestive motility: variations in patterns from esophagus to colon. *Gastroenterology* 1986; 91: 386-395
- 31 Fung YC, Liu SQ. Changes of the zero-stress state of rat pulmonary arteries in hypoxic hypertension. *J Applied Physiol* 1994; 70: 2455-2470
- 32 Murakami H, Takeda T, Kawaga K, Morita H, Tanaka S, Hosomi H. The role of extrinsic nervous system in jejunal absorption during elevation of intraluminal pressure in anesthetized dogs. *J Auton Nerv System* 1995; 51: 237-244
- 33 Grundy D. Mechanoreceptors in the gastrointestinal tract. *J Smooth Muscle Res* 1993; 29: 37-46

Edited by Pan BR and Zhang JZ

• BASIC RESEARCH •

Cloning of cytochrome P-450 2C9 cDNA from human liver and its expression in CHL cells

Ge-Jian Zhu, Ying-Nian Yu, Xin Li, Yu-Li Qian

Ge-Jian Zhu, Ying-Nian Yu, Department of Pathophysiology and Laboratory of Medical Molecular Biology, Zhejiang University School of Medicine, Hangzhou 310031, Zhejiang Province, China

Xin Li, Department of pharmaceutical analysis & drug metabolism, College of Pharmacology Science, Zhejiang University, Hangzhou 310031, Zhejiang Province, China

Yu-Li Qian, Present address: Center of laboratory, Women's hospital, School of Medicine, Zhejiang University, Hangzhou 310031, Zhejiang Province, China

Supported by National Natural Science Foundation of China, No.39770868 and Natural Science Foundation of Zhejiang Province, No.397490

Correspondence to: Prof. Ying-Nian Yu, Department of Pathophysiology and Laboratory of Medical Molecular Biology, Zhejiang University School of Medicine, Hangzhou 310031, Zhejiang Province, China. ynyu@mail.hz.zj.cn
Telephone: +86-571-87217149 Fax: +86-571-87217149

Received 2001-11-15 Accepted 2001-12-12

Abstract

AIM: Using bacterial, yeast, or mammalian cell expressing a human drug metabolism enzyme would seem good way to study drug metabolism-related problems. Human cytochrome P-450 2C9 (*CYP2C9*) is a polymorphic enzyme responsible for the metabolism of a large number of clinically important drugs. It ranks among the most important drug metabolizing enzymes in humans. In order to provide a sufficient amount of the enzyme for drug metabolic research, the *CYP2C9* cDNA was cloned and expressed stably in CHL cells.

METHODS: After extraction of total RNA from human liver tissue, the human *CYP2C9* cDNA was amplified with reverse transcription-polymerase chain reaction (RT-PCR), and cloned into cloning vector pGEM-T. The cDNA fragment was identified by DNA sequencing and subcloned into a mammalian expression vector pREP9. A transgenic cell line was established by transfecting the recombinant vector of pREP9-*CYP2C9* into CHL cells. The enzyme activity of *CYP2C9* catalyzing oxidation of tolbutamide to hydroxy tolbutamide in S9 fraction of the cell was determined by high performance liquid chromatography (HPLC).

RESULTS: The amino acid sequence predicted from the cDNA segment was identical to that of *CYP2C9*1*, the wild type *CYP2C9*. However, there were two base differences, i.e. 21T>C, 1146C>T, but the encoding amino acid sequence was the same, L7, P382. The S9 fraction of the established cell line metabolizes tolbutamide to hydroxy tolbutamide; tolbutamide hydroxylase activity was found to be $0.465 \pm 0.109 \mu\text{mol} \cdot \text{min}^{-1} \cdot \text{g}^{-1}$ S9 protein or $8.62 \pm 2.02 \text{mol} \cdot \text{min}^{-1} \cdot \text{mol}^{-1}$ CYP, but was undetectable in parental CHL cell.

CONCLUSION: The cDNA of human *CYP2C9* was successfully cloned and a cell line of CHL-*CYP2C9*, efficiently expressing the protein of *CYP2C9*, was established.

Zhu GJ, Yu YN, Li X, Qian YL. Cloning of cytochrome P-450 2C9 cDNA from human liver and its expression in CHL cells. *World J Gastroenterol* 2002; 8(2):318-322

INTRODUCTION

Cytochrome P-450 (CYP) is a heme-containing enzyme widely distributed from bacteria to mammals, which catalyzes oxidative or reductive metabolism of a wide variety of substances including endogenous as well as exogenous compounds. Mammalian CYP present in liver microsomes is one of the key enzymatic mechanisms for the metabolism of drugs, pesticides, environmental pollutants, and carcinogens^[1]. Mammals possess at least 17 distinct CYP gene families that together code for an estimated 50-60 individual CYP genes in any given species^[2]. The human CYP2C subfamily comprises four members, *CYP2C8*, *CYP2C9*, *CYP2C18* and *CYP2C19*^[3], accounting for 20% of the total CYP in human liver. *CYP2C9* is a polymorphic enzyme responsible for the metabolism of a large number of clinically important drugs such as S-warfarin, phenytoin, tolbutamide, torsemide, losartan, fluoxetine, dapsone^[4], cyclooxygenase-2 inhibitor: celecoxib^[5,6], nonpeptide angiotensin II receptor antagonist: irbesartan^[7] and numerous nonsteroidal anti-inflammatory drugs. It ranks among the most important drug metabolizing enzymes in humans^[8].

The combination of gene technology and cell culture technology has provided new opportunities for studying proteins because any gene from any species encoding an protein may be cloned and expressed in bacterial, yeast, or mammalian cells in a defined way^[9-18]. This approach to drug metabolism is of particular importance because some of the enzymes are difficult to purify and prepare in sufficient quantities, or expression levels are low, expression is organ-specificity, or the enzyme-product organs are very scarce. These restrictions apply especially for human enzymes. The heterologous expression of the cDNA allows to bypass these restrictions^[19]. Human *CYP2C9* previously has been expressed in *E. coli*^[20], *Salmonella typhimurium*^[21], yeast^[22] COS-1^[3], human liver epithelial cell THLE^[23], and human hepatic cell line HepG2^[24]. Several cell lines stably expressing human CYP1A1^[25], CYP2B6^[25], CYP2A6^[26], CYP3A4^[27], *CYP2C18* (in press) and a phase II metabolism enzyme UDP-glucuronosyltransferase, UGT1A9^[28] have been established in our laboratory. In this study human *CYP2C9* cDNA was amplified with reverse transcription-polymerase chain reaction (RT-PCR), and a transgenic cell line stably expressing *CYP2C9* was established.

MATERIALS AND METHODS

Materials

Restriction endonucleases, Moloney murine leukemia virus (M-MuLV) reverse transcriptase were purchased from MBI Fermentas AB, Lithuania. Taq plus I DNA polymerase, dNTPs, PCR primers, DNA sequence primers and random hexamer primer were supplied or synthesized by Shanghai Sangon Biotechnology Corp. DNA sequencing kit was supplied by Perkin-Elmer Corp. The TRIzol reagent, G418, minimum essential media (MEM) and newborn bovine calf sera from Gibco. NADPH from Roche Molecular Biochemicals. Diethyl pyrocarbonate (DEPC), tolbutamide and hydroxytolbutamide were obtained from Sigma Chemical Company. T4 DNA ligase and pGEM-T vector system were supplied by

Promega. Other chemical reagents used were all of analytical purity from commercial sources.

Methods

Cloning of human *CYP2C9* cDNA from a Chinese human liver

The total RNA was extracted from a surgical specimen of human liver with TRIzol reagent according to the manufacture's instructions, and then the first strand of cDNA was reverse transcribed from mRNA. Procedure: 5 µg of the total RNA and 2 µg of random hexamer primer in deionized DEPC-treated water were denatured at 65°C for 15min, then 4 µL 5×reverse transcription buffer, 3 µL 10mmol·L⁻¹ dNTP, 1 µL M-MuLV reverse transcriptase (200u) and essential deionized DEPC treated water was added to a total volume of 20 µL. The reaction was performed at 25°C for 10min, then at 42°C for 1h, and finally at 70°C for 10min to inactivate reverse transcriptase. The reactant then was stored at 4°C. To amplify the human *CYP2C9* cDNA by PCR, 2 µL of the reactant were mixed with 2 µL of 10mmol·L⁻¹ each of dNTPs, 20pmol of PCR primers and 4u of Taq plus I DNA polymerase in 1×PCR buffer containing 1.5mmol·L⁻¹ MgCl₂. A total volume of 100 µL was reached by adding deionized water. Two specific 32 mer and 28 mer oligonucleotide PCR primers were designed according to the cDNA sequence of *CYP2C9* clone 25 reported by Romkes *et al*^[3] (GenBank accession no. M61855, J05326). The sense primer corresponding to base position 1 to 32 was 5'-GAGAAGGTACCAATGGATTCTCTTGTGGTCT-3', with a restriction site of *Kpn* I, and the anti-sense one, corresponding to the base position from 1513 to 1540, was 5'-AGAGGAAAGAGAGCTCGAGGGACTGCAC-3' with a restriction site of *Xho* I. The PCR was performed at 94°C 2min, then 35 cycles of 94°C 60s, 60°C 60s, 72°C 2min, and lastly 72°C 10min. The product was stored at 4°C. An aliquot of 10 µL from the PCR was subjected to electrophoresis in a 10g·L⁻¹ agarose gel stained with ethidium bromide.

Construction of recombinant pGEM-*CYP2C9* and sequencing of *CYP2C9* cDNA^[29]

The PCR product of about 1.5 kb in length, recovered and purified by electroelution into dialysis bag was ligated with a clone vector, pGEM-T (Promega), by T4 DNA ligase. *E.coli* DH5α was transformed with the resulted recombinant pGEM-*CYP2C9* and the replicated plasmid was harvested from the bacteria screened by ampicillin resistant and blue-white selection with X-gal and IPTG. The cDNA of *YP2C9* cloned in pGEM-T was sequenced on both strands by dideoxy chain-termination method marked with BigDye with primers of T7 and SP6 promoters and two specific primers of 5'-TGCCTTGTGGAGTTG-AGA-3' (463-483), and 5'-ACAGAGACGACAAGCACAAC -3' (907-926). The termination products were resolved and detected using an automated DNA sequencer (Perkin-Elmer-ABI Prism 310).

Construction of the pREP9 based expression plasmid for *CYP2C9*

The *Kpn* I/ *Xho* I fragment of the human *CYP2C9* cDNA cleaved from the recombinant pGEM-*CYP2C9* recovered and purified by electroelution into dialysis bag was cloned directly into a unique site *Kpn* I/ *Xho* I within the multiple cloning sites of the mammalian expression vector pREP9 (Invitrogen) with T4 DNA ligase. The recombinant was transformed to *E. coli* Top 10, and screened by ampicillin resistant. The recombinant was identified by restriction mapping.

Transfection and selection^[29]

Chinese hamster lung (CHL) cells were transfected with the resultant

recombinant, pREP9-*CYP2C9*, using a modified calcium phosphate method. After 24h incubation in MEM containing 10% newborn bovine calf sera at 37°C, the culture was rinsed and re-fed with fresh growth medium. After 72h post-transfection, the culture were split and then selected in the culture medium containing the neomycin analogue G418 (400mg·L⁻¹). The selective medium was changed every 3-4d to remove dead cells and to allow the growth of resistant colonies. After 1mo, surviving colonies (termed CHL-*CYP2C9*) were harvested as a pool and propagated in medium containing G418.

Preparation of S9 of CHL-*CYP2C9*

CHL-*CYP2C9* cells grown in the culture medium containing G418 (400mg·L⁻¹) were rinsed with phosphate balanced solution (PBS), scraped and collected from the bottle with 11.5g·L⁻¹ KCl aqua solution and then sonicated in 200W, 5 s for 10 times with 10s of interval break. The resulted homogenate was centrifuged at 9000g at 4°C for 20min and the postmitochondrial supernatant (S9) was transferred carefully to a clean tube for assay or storage under -70°C. The protein in S9 was determined by the method described by Lowry *et al*, with bovine serum albumin as standard. CYP was measured spectrally using the method of Johannesen *et al*^[30].

Tolbutamide hydroxylase assay^[22,31]

The *CYP2C9* tolbutamide hydroxylase activity of S9 fraction was determined by high performance liquid chromatography (HPLC). The assay was performed in a total volume of 500 µL containing final concentrations of 5mmol·L⁻¹ HEPES (pH 7.4), 1.5mmol·L⁻¹ MgCl₂, 0.1mmol·L⁻¹ EDTA, 0.25mg S9 and 1mmol·L⁻¹ sodium tolbutamide. The reaction was initiated with 0.5mmol·L⁻¹ NADPH and terminated after 60min at 37°C by the addition of 50 µL of 4mmol·L⁻¹ HCl. Reaction product was extracted by vortex-mixing of 3mL of water-saturated ethyl acetate with the mixture for 2min. The organic layer was collected after centrifugation in a table top centrifuge at 1000g for 5min. After most of the ethyl acetate extract had air-dried, the rest was removed in a heating block at 75°C. The residue was resolubilized in 200 µL of methanol, and reaction product, hydroxytolbutamide was then assayed using HPLC by injecting 20 µL of the solubilized extract on to a reversed phase column (Shim-pack CLC-ODS 15cm×0.6cm id, 10 µm particle size), using 0.5g·L⁻¹ phosphoric acid, pH 2.6, acetonitrile (6:4/V:V) as the mobile phase with a flow rate of 1mL·min⁻¹. The column elution was monitored at 230nm, and rates of product formation were determined from standard curves prepared by adding varying amounts of hydroxytolbutamide to incubations conducted without NADPH.

RESULTS

Construction of recombinants

The recombinant of pGEM-*CYP2C9* (Figure 1) was constructed with the human *CYP2C9* cDNA inserted into the cloning site of vector pGEM-T between the promoters of T7 and SP6. Selection and identification of the recombinant was carried out by *Kpn* I/*Xho* I endonuclease digestion and agarose gel electrophoresis (Figure 1). The cloned cDNA segment was sequenced. In comparison with the *CYP2C9* clone 65 cDNA sequence reported by Romkes *et al*^[3] (GenBank accession no. M61857, J05326), our preparation showed two base differences, i.e. 21T>C, 1146C>T, but the encoding amino acid sequence was the same, i.e. L7, P382 respectively.

The *Kpn* I/*Xho* I fragment (1.5 kb) containing the complete *CYP2C9* cDNA was subcloned into the *Kpn* I/*Xho* I site of mammalian expression vector pREP9 (Figure 2). Selection and identification of the recombinants were carried out by *Kpn* I/*Xho* I endonuclease digestion and agarose gel electrophoresis (Figure 2). The resulting plasmid was designated as pREP9-*CYP2C9* and

contained the entire coding region, along with 2 bp of the 5'-end and 41 bp of the 3'-end untranslated region of the *CYP2C9* cDNA, respectively.

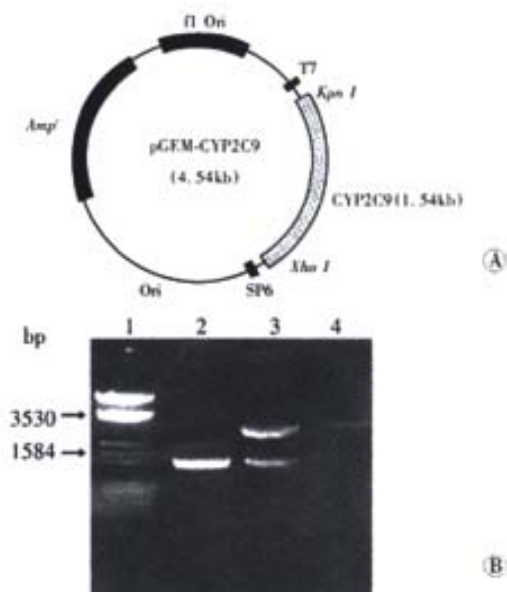


Figure 1 Scheme and electrophoresis identification of recombinant pGEM-*CYP2C9*. A: Scheme of recombinant pGEM-*CYP2C9*; B: Electrophoresis identification of recombinant pGEM-*CYP2C9*; 1: Marker (λ /EcoRI and Hind III); 2: PCR product of *CYP2C9* (1.54 kb); 3: Recombinant of pGEM-*CYP2C9* digested by *Kpn* I and *Xho* I; 4: pGEM-T vector

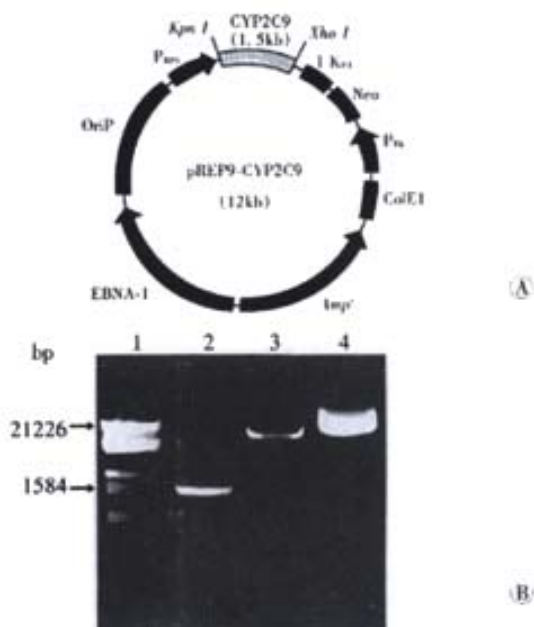


Figure 2 Scheme and electrophoresis identification of recombinant pREP9-*CYP2C9*. A: Scheme of pREP9-*CYP2C9*; B: Electrophoresis identification of recombinant pREP9-*CYP2C9*; 1: Marker (λ /EcoRI and Hind III); 2: PCR product of *CYP2C9* (1.54 kb); 3: Recombinant of pREP9-*CYP2C9* digested by *Kpn* I and *Xho* I; 4: pREP9 vector

Establishment of transgenic cell lines with *CYP2C9* enzyme activity

CHL cells were transfected with pREP9-*CYP2C9*, and selected with G418 (400 mg·L⁻¹). The surviving colonies were propagated and a cell line termed CHL-*CYP2C9* was established. The tolbutamide

hydroxylase activity of *CYP2C9* in S9 fraction of CHL-*CYP2C9* cells was assayed by HPLC. A typical elution profile of hydroxytolbutamide in extracts is shown (Figure 3). *CYP2C9* enzyme activity with tolbutamide was found to be $0.465 \pm 0.109 \mu\text{mol} \cdot \text{min}^{-1} \cdot \text{g}^{-1}$ S9 protein or $8.62 \pm 2.02 \text{ mol} \cdot \text{min}^{-1} \cdot \text{mol}^{-1}$ CYP ($n=3$), but none was detectable in parental CHL cells. The CYP content was $57.7 \text{ nmol} \cdot \text{g}^{-1}$ S9 protein from CHL-*CYP2C9* but no detectable CYP was present in CHL cell.

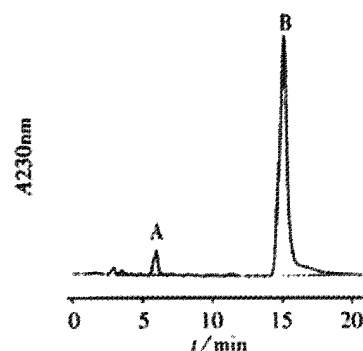


Figure 3 Representative chromatogram of extracts. A Shim-pack CLC-ODS column (15 cm × 0.6 cm i.d.) was used. The mobile phase was constituted with phosphoric acid (pH 2.6), acetonitrile (6:4/V/V) with the flow rate at $1 \text{ mL} \cdot \text{min}^{-1}$. Hydroxytolbutamide was monitored at 230 nm. A: hydroxytolbutamide; B: tolbutamide

DISCUSSION

Direct cloning of human *CYP* cDNAs from cDNA libraries generally has been successful using anti-rodent or anti-human *CYP* antibodies and rodent *CYP* cDNA probes. But these cloning procedures are applicable only for the most abundantly expressed *CYP* mRNAs. Using the RT-PCR to clone low abundance *CYP* cDNA is a simple and direct method. *CYP2C9* mRNA was present in human liver^[32], HepG2 cells^[33], kidney, testes, adrenal gland, prostate, ovary, duodenum^[34], and brain tumors^[35]. The pGEM-T vector system possessing single 3'-T overhangs at the insertion site greatly improves the efficiency of ligation of a PCR product into the plasmid by preventing recircularization of the vector and providing a compatible overhang for PCR products generated by Taq Plus I DNA polymerases.

The human *CYP2C9* gene is located on chromosome 10q24. Up to date, 12 *CYP2C9* alleles have been identified (see: Table 1 and *CYP2C9* alleles nomenclature <http://www.imm.ki.se/CYPalleles/cyp2c9.htm>). *CYP2C9**1 is the wild type of human *CYP2C9*. *CYP2C9**2 exhibit a base substitute 430C>T, resulting in a R144C substitution which has been suggested to affect the interaction between the CYP enzyme molecule and the cytochrome P450 reductase^[36]; this may explain the slower metabolism of some *CYP2C9* substrates such as S-warfarin and tolbutamide^[8, 37]. *CYP2C9**3 has a base substitute 1075A>C, which leads to an I359L substitute. Takanashi *et al*^[38] expressed the *CYP2C9**1 and *CYP2C9**3 cDNA in yeast and examined the kinetics of seven individual metabolic reactions by wild-type *CYP2C9**1 and its *CYP2C9**3 variant. Their results indicated that the I359L exchange significantly reduces the catalytic activity with all *CYP2C9*-mediated substrates studied, although the extent of the reduction in activity and kinetic parameters varied between different substrates. Interestingly Kidd *et al*^[39] reported a male Caucasian, homozygous for *CYP2C9**3, who poorly metabolized phenytoin and glipizide/tolbutamide. This study establishes that the I359L mutation is responsible for the poor metabolizer phenotype. The *CYP2C9**2 and *CYP2C9**3 are responsible for the poor metabolizing celecoxib^[5], losartan^[40], torsemide^[41]. *CYP2C9**4^[42] has a base substitute of 1076T>C,

leading to a I359T substitution. Ieiri *et al*^[43] evaluated the catalytic activity of three variants (I, L, and T) at codon 359 of *CYP2C9* enzymes expressed in a yeast cDNA expression system. The specific catalytic activities were assessed by diclofenac-4'-hydroxylation. The *in vitro* study revealed that recombinant I359, L359, and T359 (2 batches) exhibited a mean K_m of 2.0, 16.5 and (3.8 and 2.9) μmol and V_{max} of 12.4, 17.9 and (4.4 and 5.1) $\text{nmol}\cdot\text{min}^{-1}\cdot\text{nmol}^{-1}\text{CYP}$, respectively. The *CYP2C9**5 variant is derived from a 1080C>G transversion in exon 7 of *CYP2C9* that leads to a D360E substitution in the encoded protein^[44]. The *CYP2C9**5 variant was found to be expressed in African-Americans with a frequency of approximately 3% in this population group. This variant was expressed in, and purified from, insect cells infected with a recombinant baculovirus. The *in vitro* data suggest that carriers of the *CYP2C9**5 allele would eliminate *CYP2C9* substrates at slower rates compared to individuals expressing the wild-type protein^[44]. Kidd *et al*^[45] reported a new *CYP2C9* allele (*CYP2C9**6) with the deletion of an adenine at base pair 818 of the cDNA. The clearance of phenytoin in this individual is estimated to be approximately 17% of that observed in normal patients. The frequency of this allele was 0.6% in 79 African-Americans and 0% in 172 Caucasians. Shintani *et al*^[46] reported that mutations in the 5'-flanking region of the human *CYP2C9* gene appear to contribute to the large interindividual variability in drug metabolism activity. Compared with *CYP2C9**1 cDNA, there are two base differences in the *CYP2C9* cDNA cloned by us, but the encoded amino acid sequence remains unchanged. This obviously is the molecular basis for full enzymatic activity.

Table 1 Nomenclature and characteristics of *CYP2C9* alleles

Allele	Protein	Nucleotide changes	Effect	Enzyme activity		References
				<i>In Vivo</i>	<i>In vitro</i>	
<i>CYP2C9</i> *1	<i>CYP2C9.1</i>	None		Normal	Normal	3
<i>CYP2C9</i> *2	<i>CYP2C9.2</i>	430C>T	R144C		Decr	36
<i>CYP2C9</i> *3	<i>CYP2C9.3</i>	1075A>C	I359L	Decr	Decr	37,38,39,43
<i>CYP2C9</i> *4	<i>CYP2C9.4</i>	1076T>C	I359T			42,43
<i>CYP2C9</i> *5	<i>CYP2C9.5</i>	1080C>G	D360E	Decr		44
<i>CYP2C9</i> *6		818delA	frame shift	Decr		45
<i>CYP2C9</i> *7-12						<i>In press</i>

To express the functional activity of a CYP, a cell evidently must have adequate heme supply, either by intracellular biosynthesis or extracellular provision^[47]. CYPs also require other enzymatic components for full activity, including the flavoprotein NADPH-P450 oxidoreductase (OR) and, in some cases, cytochrome b₅. The OR must interact directly with the CYP to transfer the required two electrons from NADPH. Cytochrome b₅ is necessary for increasing electron transfer for certain CYP forms and specific substrates. The CHL is the cell line originally derived from the lung of a newborn female Chinese hamster and has no or very limited activities of CYP enzymes, but has adequate OR and cytochrome b₅ levels to support CYP activities.

To achieve high expression levels of *CYP2C9*, the *CYP2C9* cDNA was cloned into the eukaryotic expression vector pREP9, which had previously been used in this laboratory for the expression of human CYP1A1, CYP2B6, CYP2A6, CYP3A4 and UGT1A9 in CHL cells^[25-28]. The salient feature of this vector has an Epstein Barr Virus origin of replication and nuclear antigen (EBNA-1) to allow high-copy episomal replication in mammal cell lines. The Rous sarcoma virus long terminal repeat (RSV LTR) early promoter controls the expression of the *CYP2C9* cDNA.

Tolbutamide (1-butyl-3-p-tolylsulfonylurea) is an oral hypoglycemic agent which is being used in the treatment of diabetes. In humans it undergoes CYP-catalyzed hydroxylation of the tolyl methyl group which is the initial and rate-limiting reaction followed by

further oxidation by cytosolic dehydrogenases yielding carboxytolbutamide. Overall this pathway accounts for up to 85% of tolbutamide clearance in humans. Evidence that *CYP2C9* is solely responsible for tolbutamide hydroxylation is convincing and tolbutamide is widely accepted as a prototypic substrate for the assessment of hepatic *CYP2C9* activity, both *in vitro* and *in vivo*^[8].

We used tolbutamide as a substrate for evaluating the expressing of human *CYP2C9* activity in CHL-*CYP2C9* cell. The tolbutamide hydroxylase activity was $0.465\pm 0.109\mu\text{mol}\cdot\text{min}^{-1}\cdot\text{g}^{-1}$ S9 protein or $8.62\pm 2.02\text{mol}\cdot\text{min}^{-1}\cdot\text{mol}^{-1}$ CYP. These value, were somewhat higher than these obtained with recombinant *CYP2C9* purified from *E. coli*: $4.67\text{--}4.96\text{nmol}\cdot\text{min}^{-1}\cdot\text{nmol}^{-1}$ CYP^[48] or human liver microsomes: $0.189\pm 0.0083\text{nmol}\cdot\text{min}^{-1}\cdot\text{mg}^{-1}$ microsome^[49] and $2.29\text{--}4.33\text{nmol}\cdot\text{min}^{-1}\cdot\text{nmol}^{-1}$ CYP^[48]. This clearly stated that CHL-*CYP2C9* expressed the *CYP2C9* efficiently and this may be a useful tool for further studies of its enzymatic function and mechanism.

REFERENCES

- Anzenbacher P, Anzenbacherova E. Cytochromes P450 and metabolism of xenobiotics. *Cell Mol Life Sci* 2001;58:737-747
- Nelson DR. Cytochrome P450 and the individuality of species. *Arch Biochem Biophys* 1999; 369: 1-10
- Romkes M, Falletto MB, Blaisdell JA, Raucy JL, Goldstein JA. Cloning and expression of complementary DNAs for multiple members of the human cytochrome P450IIC subfamily. *Biochemistry* 1991; 30: 3247-3255
- Winter HR, Wang Y, Unadkat JD. *CYP2C8/9* mediate dapsone N-hydroxylation at clinical concentrations of dapsone. *Drug Metab Dispos* 2000; 28: 865-868
- Tang C, Shou M, Rushmore TH, Mei Q, Sandhu P, Woolf EJ, Rose MJ, Gelmann A, Greenberg HE, De-Lepeleire I, Van-Hecken A, De-Schepper PJ, Ebel DL, Schwartz JL, Rodrigues AD. In-vitro metabolism of celecoxib, a cyclooxygenase-2 inhibitor, by allelic variant forms of human liver microsomal cytochrome P450 2C9: correlation with *CYP2C9* genotype and in-vivo pharmacokinetics. *Pharmacogenetics* 2001;11:223-235
- Tang C, Shou M, Mei Q, Rushmore TH, Rodrigues AD. Major role of human liver microsomal cytochrome P450 2C9 (*CYP2C9*) in the oxidative metabolism of celecoxib, a novel cyclooxygenase-II inhibitor. *J Pharmacol Exp Ther* 2000; 293: 453-459
- Bourrie M, Meunier V, Berger Y, Fabre G. Role of cytochrome P-4502C9 in irbesartan oxidation by human liver microsomes. *Drug Metab Dispos* 1999; 27: 288-296
- Miners JO, Birkett DJ. Cytochrome P450 2C9: an enzyme of major importance in human drug metabolism. *Br J Clin Pharmacol* 1998; 45: 525-538
- Liu XF, Zou SQ, Qiu FZ. Construction of HCV-core gene vector and its expression in cholangiocarcinoma. *World J Gastroenterol* 2002; 8:135-138
- Wu C, Zou QM, Guo H, Yuan XP, Zhang WJ, Lu DS, Mao XH. Expression, purification and immuno-characteristics of recombinant UreB protein of *H. pylori*. *World J Gastroenterol* 2001; 7:389-393
- Li XJ, Wu JG, Si JL, Guo DW, Xu JP. High-level expression of human calmodulin in *E.coli* and its effects on cell proliferation. *World J Gastroenterol* 2000; 6:588-592
- Cheng J, Zhong YW, Liu Y, Dong J, Yang JZ, Chen JM. Cloning and sequence analysis of human genomic DNA of augmenter of liver regeneration. *World J Gastroenterol* 2000; 6:275-277
- Guo SP, Ma ZS, Wang WL. Construction of eukaryotic expression vector of HBV x gene. *World J Gastroenterol* 1999; 5:351-352
- Qu S, Li QF, Deng YZ, Zhang JM, Zhang J. Cloning and expression of HLA-B7 gene. *World J Gastroenterol* 1999; 5:345-348
- Liu ZG, Yang JH, An HZ, Wang HY, He FT, Han ZY, Han Y, Wu HP, Xiao B, Fan DM. Cloning and identification of an angiostatic molecule IP10/crg-2. *World J Gastroenterol* 1999; 5:241-244
- He Y, Zhou J, Dou KF. Construction of hepatocyte growth factor expression vector and detection of expression in human hepatocytes. *Shijie Huaren Xiaohua Zazhi* 2001; 9:1143-1146
- Pan X, Pan W, Ke CW, Zhang B, Cao GW, Qi ZT. Tetracycline controlled DT/VEGF system gene therapy mediated by adenovirus vector. *Shijie Huaren Xiaohua Zazhi* 2000; 8:1121-1126
- Lu JG, Lin C, Huang ZQ, Wu JS, Fu M, Zhang XY, Liang X, Yao X, Wu M. Inhibitory effects of human cholangiocarcinoma cell line by recombinant adenoviruses P16 with CDDP. *Shijie Huaren Xiaohua Zazhi* 2000; 8: 641-645
- Crespi CL, Miller VP. The use of heterologously expressed drug metabolizing enzymes-state of the art and prospects for the future. *Pharmacol Therapeutics* 1999;84:121-131
- McGinnity DF, Griffin SJ, Moody GC, Voice M, Hanlon S, Friedberg T, Riley RJ. Rapid characterization of the major drug-metabolizing human

- hepatic cytochrome P-450 enzymes expressed in *Escherichia coli*. *Drug Metab Dispos* 1999; 27: 1017-1023
- 21 Fujita K, Kamataki T. Role of human cytochrome P450(CYP) in the metabolic activation of N-alkylnitrosamines: application of genetically engineered *Salmonella typhimurium* YG7108 expression each form of CYP together with human NADPH-cytochrome P450 reductase. *Mutat Res* 2001; 483: 35-41
- 22 Goldstein JA, Faletto MB, Romkes-Sparks M, Sullivan T, Kitareewan S, Raucy JL, Lasker JM, Ghanayem BI. Evidence that *CYP2C19* is the major (S)-mephenytoin 4'-hydroxylase in humans. *Biochemistry* 1994; 33: 1743-1752
- 23 Bort R, Castell JV, Pfeifer A, Gomezlechón MJ, Mace K. High expression of human CYP2C in immortalized human liver epithelial cells. *Toxicol in Vitro* 1999; 13: 633-638
- 24 Yoshitomi S, Ikemoto K, Takahashi J, Miki H, Namba M, Asahi S. Establishment of the transformants expressing human cytochrome P450 subtypes in HepG2, and their applications on drug metabolism and toxicology. *Toxicol in Vitro* 2001; 15: 245-256
- 25 Wu JM, Dong HT, Cai ZN, Yu YN. Stable expression of human cytochrome CYP2B6 and CYP1A1 in chinese hamster CHL cells: their use in micronucleus assays. *Chin Med Sci J* 1997; 12:148-155
- 26 Yan LQ, Yu YN, Zhuge J, Xie HY. Cloning of human cytochrome P450 2A6 cDNA and its expression in mammalian cells. *Zhongguo Yaolixue Yu Dulixue Zazhi* 2000; 14:31-35
- 27 Chen Q, Wu J, Yu Y. Establishment of transgenic cell line CHL-3A4 and its metabolic activation. *Zhonghua Yufang Yixue Zazhi* 1998; 32: 281-284
- 28 Li X, Yu YN, Zhuge J, Qian YL. Cloning of UGT1A9 cDNA from liver tissues and its expression in CHL cells. *World J Gastroenterol* 2001; 7:841-845
- 29 Sambrook J, Fritsch EF, Maniatis T. Molecular cloning, a laboratory manual. 2nd ed. New York: Cold Spring Harbor Laboratory Press, 1989;6:28-29, 1:63-86, 16:39-40
- 30 Johannesen KA, DePierre JW. Measurement of cytochrome P-450 in the presence of large amounts of contaminating hemoglobin and methemoglobin. *Anal Biochem* 1978; 86: 725-732
- 31 Ho JW, Moody DE. Determination of tolbutamide hydroxylation in rat liver microsomes by high-performance liquid chromatography: effect of psychoactive drugs on *in vitro* activity. *Life Sci* 1993; 52: 21-28
- 32 Rodriguez-Antona C, Donato MT, Pareja E, Gomez-Lechon MJ, Castell JV. Cytochrome P-450 mRNA expression in human liver and its relationship with enzyme activity. *Arch Biochem Biophys* 2001; 393: 308-315
- 33 Sumida A, Fukuen S, Yamamoto I, Matsuda H, Naohara M, Azuma J. Quantitative analysis of constitutive and inducible CYPs mRNA expression in the HepG2 cell line using reverse transcription-competitive PCR. *Biochem Biophys Res Commun* 2000; 267: 756-760
- 34 Klose TS, Blaisdell JA, Goldstein JA. Gene structure of *CYP2C8* and extrahepatic distribution of the human CYP2Cs. *J Biochem Mol Toxicol* 1999; 13: 289-295
- 35 Knapfer H, Knapfer MM, Hotfilder M, Preiss R. P450-expression in brain tumors. *Oncol Res* 1999; 11: 523-528
- 36 Crespi CL, Miller VP. The R144C change in the CYP2C9*2 allele alters interaction of the cytochrome P450 with NADPH:cytochrome P450 oxidoreductase. *Pharmacogenetics* 1997; 7:203-210
- 37 Aithal GP, Day CP, Kesteven PJ, Daly AK. Association of polymorphisms in the cytochrome P450 *CYP2C9* with warfarin dose requirement and risk of bleeding complications. *Lancet* 1999; 353:717-719
- 38 Takanashi K, Tainaka H, Kobayashi K, Yasumori T, Hosakawa M, Chiba K. *CYP2C9* Ile359 and Leu359 variants: enzyme kinetic study with seven substrates. *Pharmacogenetics* 2000; 10: 95-104
- 39 Kidd RS, Straughn AB, Meyer MC, Blaisdell J, Goldstein JA, Dalton JT. Pharmacokinetics of chlorpheniramine, phenytoin, glipizide and nifedipine in an individual homozygous for the *CYP2C9**3 allele. *Pharmacogenetics* 1999; 9: 71-80
- 40 Yasar U, Tybring G, Hidestrand M, Oscarson M, Ingelman-Sundberg M, Dahl ML, Eliasson E. Role of *CYP2C9* polymorphism in losartan oxidation. *Drug Metab Dispos* 2001; 29: 1051-1056
- 41 Miners JO, Coulter S, Birkett DJ, Goldstein JA. Torsemide metabolism by *CYP2C9* variants and other human CYP2C subfamily enzymes. *Pharmacogenetics* 2000; 10: 267-270
- 42 Imai J, Ieiri I, Mamiya K, Miyahara S, Furuumi H, Nanba E, Yamane M, Fukumaki Y, Ninomiya H, Tashiro N, Otsubo K, Higuchi S. Polymorphism of the cytochrome P450 (CYP) 2C9 gene in Japanese epileptic patients: genetic analysis of the *CYP2C9* locus. *Pharmacogenetics* 2000;10:85-89
- 43 Ieiri I, Tainaka H, Morita T, Hadama A, Mamiya K, Hayashibara M, Ninomiya H, Ohmori S, Kitada M, Tashiro N, Higuchi S, Otsubo K. Catalytic activity of three variants (Ile, Leu, and Thr) at amino acid residue 359 in human CYP2C9 gene and simultaneous detection using single-strand conformation polymorphism analysis. *Ther Drug Monit* 2000; 22: 237-244
- 44 Dickmann LJ, Rettie AE, Kneller MB, Kim RB, Wood AJ, Stein CM, Wilkinson GR, Schwarz UI. Identification and functional characterization of a new CYP2C9 variant (*CYP2C9**5) expressed among African Americans. *Mol Pharmacol* 2001; 60:382-387
- 45 Kidd RS, Curry TB, Gallagher S, Edeki T, Blaisdell J, Goldstein JA. Identification of a null allele of *CYP2C9* in an African-American exhibiting toxicity to phenytoin. *Pharmacogenetics* 2001; 11: 803-808
- 46 Shintani M, Ieiri I, Inoue K, Mamiya K, Ninomiya H, Tashiro N, Higuchi S, Otsubo K. Genetic polymorphisms and functional characterization of the 5'-flanking region of the human *CYP2C9* gene: *in vitro* and *in vivo* studies. *Clin Pharmacol Ther* 2001;70:175-182
- 47 Correia MA, Farrell GC, Schmid R, Ortiz-de-Montellano PR, Yost GS, Mico BA. Incorporation of exogenous heme into hepatic cytochrome P-450 *in vivo*. *J Biol Chem* 1979; 254: 15-17
- 48 Lasker JM, Wester MR, Aramsombatdee E, Raucy J. Characterization of CYP2C19 and CYP2C9 from human liver: respective roles in microsomal tolbutamide, S-mephenytoin, and omeprazole hydroxylations. *Arch Biochem Biophys* 1998;353:16-28
- 49 Easterbrook J, Fackett D Li AP. A comparison of aroclor 1254-induced and uninduced rat liver microsomes in phenytoin O-deethylation, coumarin 7-hydroxylation, tolbutamide 4-hydroxylation, S-mephenytoin 4'-hydroxylation, chloroxazone 6-hydroxylation and testosterone 6β-hydroxylation. *Chem Biol Interact* 2001; 134: 243-249

Edited by Schmid R

• BASIC RESEARCH •

Infrared thermoimages display of body surface temperature reaction in experimental cholecystitis

Dong Zhang, Yuan-Gen Zhu, Shu-You Wang, Hui-Min Ma, Yan-Yan Ye, Wei-Xing Fu, Wei-Guo Hu

Dong Zhang, Yuan-Gen Zhu, Shu-You Wang, Hui-Min Ma, Yan-Yan Ye, Wei-Xing Fu, Wei-Guo Hu, Institute of Acupuncture, China Academy of Traditional Chinese Medicine, Beijing 100700, China
Supported by China National Key Projects for Fundamental Research (No. 95-Yu-19-313) and National Natural Science Foundation of China, No.30171176

Correspondence to: Prof. Dong Zhang, Institute of Acupuncture, China Academy of Traditional Chinese Medicine, Beijing 100700, China. zhang-d@btamail.net.cn

Telephone: +86-10-64014411 Ext.2776 Fax: +86-10-64513164

Received 2001-07-19 Accepted 2001-08-23

Abstract

AIM: To display the thermoimages of the body surface in experimental cholecystitis, to observe the body surface temperature reaction in visceral disorders, and to study if the theory of body surface-viscera correlation is true and the mechanism of temperature changes along the meridians.

METHODS: By injecting bacteria suspension into the stricture bile duct and gallbladder, 21 rabbits were prepared as acute pyogenic cholangiocholecystitis models, with another 8 rabbits prepared by the same process except without injection of bacteria suspension as control. The body surface infrared thermoimages were continuously observed on the hair shaven rabbit skin with AGA-782 thermovision 24h before, 1-11d after and (2,3wk) 4wk after the operation with a total of over 10 records of thermoimages.

RESULTS: Twelve cases out of 21 rabbits with cholecystitis revealed bi-lateral longitudinal high temperature lines in its trunk; with negative findings in the control group. The high-temperature line appeared on d1-d2, first in the right trunk, after the preparation of the model, about 7d after the model preparation, the lines appeared at the left side too, persisting for 4wk. The hyper-temperature line revealed 1.1-2.7°C higher than before the model preparation, 0.7-2.5°C higher than the surrounding skin. The length of the high temperature line might reach a half length of the body trunk, or as long as the whole body itself.

CONCLUSION: The appearance of the longitudinal high temperature lines at the lateral aspects of the trunk in the experimental group is directly bound up with the experimental animals pyogenic cholecystitis, with its running course quite similar to that of the Gallbladder Channel of Foot Shaoyang, but different to the zones of hyperalgesia and site of referred pain in cholecystitis.

Zhang D, Zhu YG, Wang SY, Ma HM, Ye YY, Fu WX, Hu WG. Infrared thermoimages display of body surface temperature reaction in experimental cholecystitis. *World J Gastroenterol* 2002;8(2):323-327

INTRODUCTION

The reactions on body surface due to visceral lesion have long aroused the interest of investigators. As early as 1889, the Head's zone was observed and the referred pain was interpreted by the two concepts of pre-spinal and intra-spinal viscerosomatic association neurons several decades later. The above-mentioned zones of hyperalgesia were

mainly based on the complaint of the patients themselves, and the accompanying reaction of nerve-blood vessel-muscle-sclerotic zone-dermatome is again a kind of pathological changes with indefinite boundary, still short of objective examination. Formerly, some scholars have explored the relation between the visceral lesion and temperature of the body surface, which was limited only to the region around the lesion, like observation, for instance, around cholecystitis. The theory of meridian in Traditional Chinese Medicine (TCM) maintains that, the meridians connect the viscera internally and the body surface externally. Physiologically, it serves for the flowing of blood-qi, and pathologically, reflects disease changes. Acupuncture is a therapy of entrails by stimulating acupoints along channels on the body surface^[1-6]. However, exactly how the temperature changes induced by visceral disorders, whether it occurs at the meridians and acupoints through TCM theory or appears at the special regions of Head's zone or referred pain on the basis of Western medicine, or even only appears around the lesions, is still a question attracting investigators' interests. Infrared thermography, a modern measuring temperature method, could be used for diagnosing some diseases and medical basic researches, such as the displaying of temperature imaging of cerebral cortex^[7,8], effect of acupuncture on brain^[9,10] and study of principle of acupuncture^[11,12], etc. Based on past work^[13], we have studied this topic by the above-mentioned animal models for continuous follow-up examinations so as to investigate whether cholecystitis can lead to body surface temperature reactions and their locations in this paper.

MATERIALS AND METHODS

Experimental animal

Adult healthy rabbits, 21 in the experimental group, and 8 in the control group in both sexes, weighing 3.0±0.35kg, supplied by Department of Experimental Animals from our Academy.

Animal model

The models were made based on the method reported by Xu *et al*^[14]. The animals were anesthetized with sodium phenobarbital through auricular marginal vessel (45mg·kg⁻¹) with abdominal hairs shaved. After routine anesthesia, an incision was made at the mid-abdominal line from the xyphoid process to the umbilicus and the abdomen was opened. We isolated a small segment of the common bile duct 1cm from the duodenum, inserted a hard plastic tube 0.5cm long opened longitudinally with a caliber just a little more slender than the common bile duct, and then put outside the bile duct. The lower end of the tube was penetrated with a thread and ligated to close its open end. Thus, the duct was strictured in an incomplete blocked manner. 1mL suspension prepared by mixing a piece of rabbit dung with 10mL was injected with saline into the gallbladder to create a pyogenic cholecystitis. We sutured the wound and applied some antibiotics locally and continued to feed the animal. After the animals resumed its consciousness, there were manifestations including loss of appetite, icteric jaundice in the sclera, auricles, and skin to different degrees, with deep-colored urine. By anatomy, when the experiment was over, the gallbladder could be seen enlarged, dilated, with thickened wall and fibrosis, indicating a chronic inflammation. By the same process, the common bile ducts of the animals in the control group were isolated but with no bacterial suspension administered. After we sutured the wounds the feeding was continued.

Observation process

Before every thermoinage was taken and the model operations were performed in the two groups, the hairs at the back and both sides of the trunk were cut. The infrared thermoinages were taken 24h before the operation and 1-11d, and (2, 3wk) 4wk after the operations at the hairless areas to investigate the temperature changes and its evolution before and after the models were formed.

Experimental instrument and surroundings

Swedish AGA-782 Infrared thermovision was applied for observation of thermoinages with the thermosensitivity being 0.1 (0.025°C available after computerized processing). The images of temperature distribution of the observed parts were taken with the infrared camera of the instrument, and continuous images were taken by the black-white demonstrator and color monitor. The infrared thermoinage was processed, reserved and analyzed by equipment system TC-800 computer and DISCO3.1 thermoinage program, while the absolute values of temperature were checked by the DH-1 Model Thermal Calibration Source (Figure 1). The room temperatures were 25.5-29.6°C, and relative humidities 33-60%.

Method for observation and recording of thermoinages of body surface

The camera of the thermovision was placed 1 meter above the observed parts, while the Thermal Calibration Source within the visual field of the camera so as to indicate the absolute temperature. The thermoinages were recorded at the hairless areas (for fixation of the animal, Figure 2), more than 10 follow-up continuous observations were made 1d before and 4 wk after the operation.



Figure 1 AGA-782 infrared thermovision system

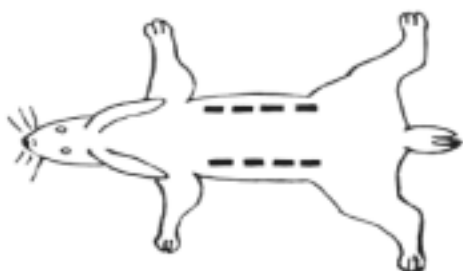


Figure 2 The method for recording the thermoinage of the rabbit's trunk

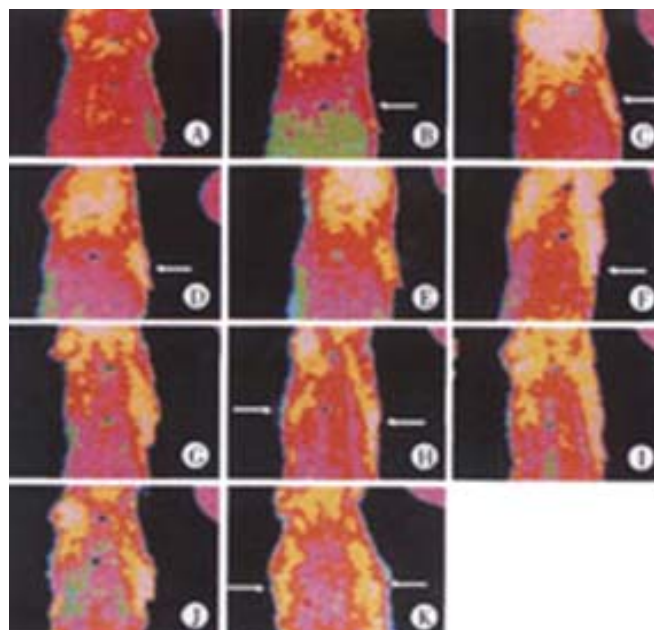
RESULTS

Symptoms of the animal models

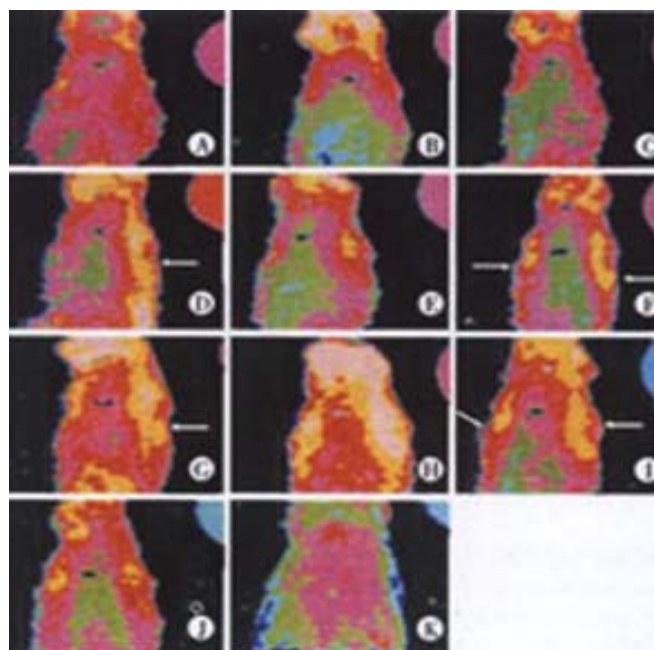
The operation process went smoothly, with the animals resuming its consciousness 4-5h after the operation. All conditions but food taking remained normal, without any inflammatory reactions in the wound. In three cases, the sclera and auricle became icteric 1d after operation, another 16 cases showed such jaundice 2-5d after operation. Generally, general jaundice of the skin appeared 3-5d after operation. All 21 animals had deep-colored urine and fever to certain

degree. One week later, the animal returned to normal temperature without jaundice, but the appetite was still abnormal, with emaciation, indicating chronic inflammation. In our series, 5 cases died 7d later, 1 died 9d later, and another 1 died 18d later. The remaining animals survived, and 12 revealed longitudinal high temperature lines along the lateral aspects of the trunk, which was similar to the running course of Gallbladder Channel of Foot Shaoyang. The lines elongated as time went on (Figure 3).

Figure 3 Continuous display of the infrared thermoinages of rabbit trunk with cholecystitis in 2 rabbits.



I. The distribution and evolution of high temperature line on the infrared thermoinage of No.11 rabbit's trunk (back and axillary aspect) A: before cholecystitis model; B:1d after cholecystitis, high temperature line appeared in the lateral aspect; C: on d2; D: on d3; E: on d4; F: on d7, high temperature line began to appear at the left side; G: on d8; H: on d9, marked bilateral high temperature lines; I: on d10; J: on d11; K: on d30, high temperature line remained.



II. The distribution and evolution of high temperature line on the infrared thermoinage of No.8 rabbit's trunk (back and axillary aspect) A: before

cholecystitis model; B: 1d after cholecystitis; C: on d2, right high temperature line; D: on d3, marked right high temperature line appeared; E: on d4; F: on d7, left high temperature line appeared; G: on d8; H: on d9, marked bilateral high temperature lines; I: on d10; J: on d11; K: on d30, bilateral high temperature lines disappeared.

The distribution is shown by the dotted line in Figure 1. The other 9 rabbits didn't show such lines. Only some spotted high temperature areas could be seen. There might even be lower temperature of the body surface.

Features of high temperature lines in the trunk in acute cholecystitis

The features included: (1) 9 out of the 12 animals with longitudinal high temperature line in the trunk were bilateral, and the other 3 unilateral; (2) Most of the high temperature lines first appeared in the right side, among them, 3 cases appeared 1d after operation; 5 cases after d2. The lines in the left side appeared rather late. All left high temperature lines appeared 7d after operation except 1 case appeared only 2d after; (3) The lines were thread (band) shaped, first rather short and elongated as time elapsed, the longest being as long as the trunk itself; (4) The duration of the existing lines lasted, with over 30d as the longest; (5) The temperature of the lines was about 0.7-2.5°C higher than that of the surrounding region, about 1.1-2.7°C higher than that before the lesion appeared in the same region.

The thermoimages of body surface and symptoms of the control animals after operation

All 8 cases resumed consciousness 4-5h after the operation, with normal activities, without swelling or infection in the wound, without icteric sclera, auricles or deep-colored urine. Body temperatures rose in different degree, with normal appetite and better survival condition. No longitudinal high temperature lines appeared in the trunk 1mo after the operation except that 1 case had some high temperature areas that appeared remittently (Figure 4).

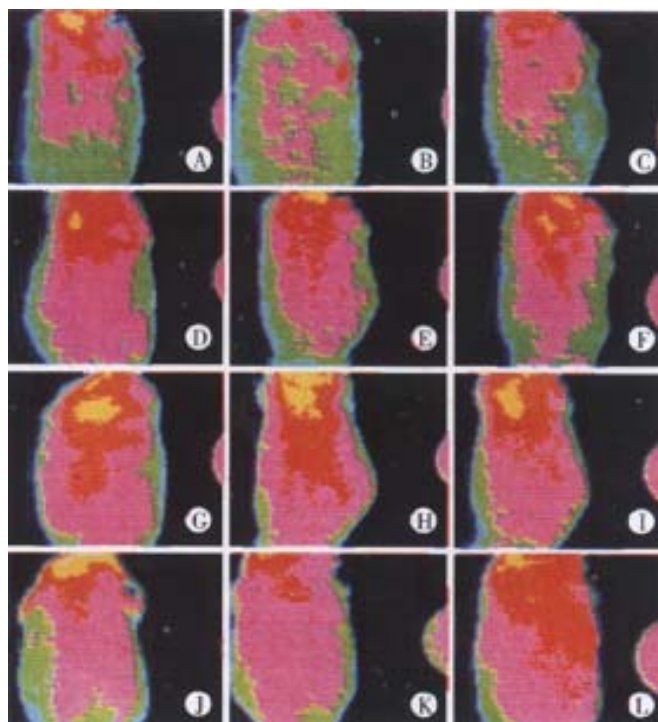


Figure 4 The distribution and evolution on infrared thermoimage of control rabbit's trunk (back and axillary aspect) A: before operation; B: 1d after operation; C: on d2; D: on d3; E: on d4; F: on d7; G: on d8; H: on d9; I: on d10; J: on d11; K: on d22; L: on d30. It can be seen here that there was no longitudinal high temperature line 1 month after the operation.

DISCUSSION

Reaction on the body surface due to visceral disorders, a phenomenon recognized in both traditional Chinese medicine and western medicine, is called "correlation of body surface and viscera" in modern medicine and "correlation of meridian and viscera" in TCM theory. Though not exactly identical in the description of both systems, yet, they bear the common idea that viscera lesions might be reflected on the body surface. As the largest organ of the body, skin receives all stimulations from outside, preserves body fluid and maintains body heat balance, with a comprehensive function of sensation, secretion, excretion, temperature regulation, and metabolism. There is a close relationship between the body surface and internal viscera. The former always reflects the disorders of the latter. Visible changes can be seen on the skin in diseases such as scleroderma, lupus erythematosus, and iatrogenic dermatitis, therefore, visceral diseases can sometimes be diagnosed by changes in the skin, and conversely, abnormal cutaneous sensation also reflects visceral ailments. The left shoulder pain, for instance, can be seen in myocardial ischemia; inter-scapular pain, in stomach and pancreas diseases; referred pain in the right shoulder, and scapular pain in liver and gallbladder disorders (Figure 5A), as well as the Head's zone with clear distribution (pain hypersensitivity) (Figure 5B), and so on.

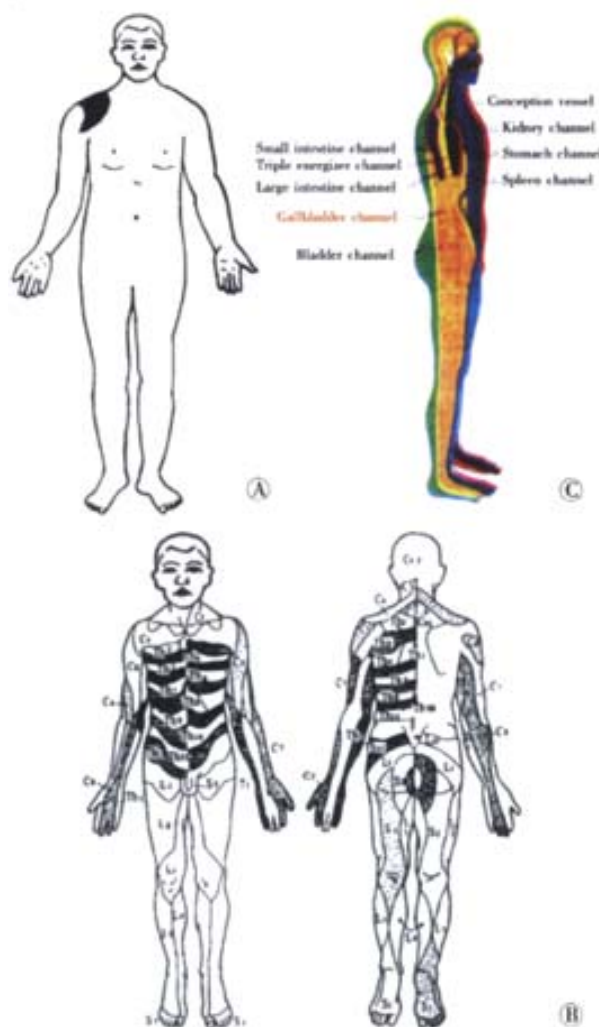


Figure 5 Diagram showing referred pain in cholecystitis, Head's zone and "cutaneous portion" of gallbladder channel.

A: Referred pain in cholecystitis; B: Head's zone; C: "Cutaneous portion" of gallbladder channel on the lateral aspect of the body

For the Head's zone, it is interpreted that the nerve impulse comes from the stimulus in the internal organ which, through the posterior root of the spinal cord, arrives at a specific spinal segment and forms an excitation focus in the cord and then reaches the efferent nerve fibers of the same segment via the intermediary association neurons, resulting in the sensory hypersensitivity of the correlative body surface part. This is a visceral-sensory reflection related to a kind of pain sensitive phenomenon that appeared on a certain part of the body surface due to disorders of the internal organs whereas referred pain may be due to the fact that the afferent nerve of the body surface and affected organ share the same spinal posterior nerve root entering the spinal cord, whose never endings project to the sane visceros-somatic association neuron. Abundant clinical facts and basic research reveal that there are minute description and summary for the specificities and law of distribution of Head's zone and referred pain. Though the mechanism of body surface reaction for visceral disorders is still unclear, yet, it is of clinical significance to judge the disorders of the organs by these reaction areas on the body surface. However, the subjective complaints of sensation are not to be used as objective basis for diagnosis. This is why someone observed the relations between the temperature and pain sensation, attempting to apply temperature in the place of subjective complaints. Unfortunately, the correlative relations are still indefinite^[5]. Objective phenomena and records for the external manifestations of disorders of internal organ are still rare. The goal of our study is to record the longitudinal zone of high temperature on the lateral trunk by infrared thermography. We noticed that there are significant differences between the recorded longitudinal and the distribution of the 2 pain hypersensitive areas on the body surface.

The past studies show that there are high temperature lines running longitudinally on the human surface whose course is related to the meridians, hence, the title "high temperature lines along meridian" (HTLM). The study of these phenomena with infrared thermography is a great advance on the basis of biophysical studies on acupoints. Acupuncture-moxibustion can raise the skin temperature^[15,16]. Although observation on HTLM reveals that the rate of their appearance is rather low under natural condition, it can be raised by acupuncturing-moxibusting^[17], indicating that the appearance of HTLM might need certain inducing factors, inside or outside the body. For the outside inducing factor, such as acu-moxibusting stimuli, there have been a lot of reports; but there are no reports concerning inside stimuli (such as visceral disorders) so far. In the theory of traditional Chinese medicine, it is the meridian system that connects the interior with the exterior, provides the passage for the flowing of blood and Qi, communicates the superficies with the interior, and regulates Yin and Yang. All internal viscerae connect them through corresponding meridian and collaterals. Once a viscera is ill, it can be manifested on the body surface through their corresponding meridian. The above description in traditional Chinese medicine is rather identical with the observation and study of Head's zone and referred pain in modern medicine. In the modern studies of meridian phenomena, the dematosis, capillary dilatation in the skin, cutaneous and subcutaneous nodules, depressions, elevation, tenderness, acupoints electric measurement and acupoints temperature examination, etc. along the meridian were all focused on the search for the correlation between the viscera and its corresponding meridian, so as to prove the scientific theory of meridian. Unfortunately, the conclusion is still unclear. Compared with the above theories between traditional Chinese medicine and western medicine, there are both similarities and dissimilarities. The idea that body surface can reflect the diseases of the viscera is the same between the two medical systems, while their locations reflecting the affected viscera are different. Head's zone is distributed on the basis of neural segments, viz. being transversely distributed in the trunk, while referred pain is distributed in regions or in patches; whereas meridians are distributed longitudinally and in bands. The satisfactory results of Chinese herbal medicine^[18-20] and acupunctura-moxibustion^[21-28] on digestive diseases

demonstrate that it is feasible to apply traditional Chinese medical therapies for diseases in western medicine, acupuncture plays also an impotent role on the research of pathogeny and treatment^[29-32], and the difference in the theories of the two medical systems can be unified and verified with objective indices. The acute pyogenic cholecystitis falls under the category of gallbladder disorders in traditional Chinese medicine. In the thermoimage of body surface recorded by infra-red thermography, we observed, for the first time, the longitudinal distribution of high temperature lines on the body trunk, which is different to the zones of hyperalgesia and referred pain area on the body surface in gallbladder disease, but similar to the distribution of "cutaneous portion" of Gallbladder Channel of Foot Shaoyang (Figure 5C), indicating that there is a tendency of temperature reaction on the body surface along the meridian in visceral diseases.

Gallbladder diseases could be diagnosed by modern instrument^[33]. The rise of body temperature is an index of infection^[34,35]. Due to the inflammatory reaction in experimental pyogenic cholecystitis, body temperature is raised, which is a systematic phenomenon. However, in our experiment, the temperature of the longitudinal high temperature lines on the lateral trunk was higher than the surrounding skin, indicating that the existence of the lines was not due to the rise of temperature, or rather, a specific mechanism. Physiologically, high body temperature indicates the degree of energy metabolism and the flowing blood volume in the local part^[36-39]. In addition to the interpretation that the distribution of high temperature lines on body surface in cholecystitis can be made by the running course of Gallbladder channel and theory of traditional Chinese medicine, it can also be preliminarily interpreted by blood circulation, metabolism and nervous function. After the gallbladder is affected, the nervous reflex on the body surface reactive area is increased, leading to the increase of metabolism of the skin tissue and blood circulation to meet the needs of recovery of the viscera, hence, the high temperature lines. Formerly, we observed many phenomena of high temperature lines along the meridians, their depths^[40,41] and the relationship between autonomic nervous system and the lines^[42]. We now further understand, through our present experiment, the mechanism of its appearance, viz. visceral disease being one of the factors responsible for the appearance of the high temperature lines, and the lines along the meridians being a kind of manifestation reflecting visceral pathology. Here, we offer a pictorial basis for the objective verification of meridian-visceral correlation in traditional Chinese medicine, and a supplement to the theory of zones of hyperalgesia and referred pain in modern medicine.

REFERENCES

- 1 Akimova LG. Laser puncture in the combined treatment of stenocardia with concomitant chronic cholecystitis. *Lik Sprava* 1998;3:135-137
- 2 Zhang J, Huang YX, Gao W, Pan BR, Wang JJ, Li YM, Wang QL. Effects of acu-poin electro acupuncture on gastrointestinal mucosa immunologic function in rats. *Shijie Huaren Xiaohua Zazhi* 2001;9:1116-1119
- 3 Chang XR, Yan J, Yi SX, Lin YP, Yang RD, Huang BQ. Effect of needling points of lower extremities of foot Yangming meridian on area of gastric antrum with ultrasonography B observation. *World J Gastroenterol* 1998;4:99
- 4 Liu YC, Liang QS, Zhang YC, Ling XW, Xue DN. Blockade with Innovar and Atropine to prevent internal organ pull response. *World J Gastroenterol* 2000;6:43
- 5 Liang QS, Liu YC, Zhang YC. Drug injection of Lanwei acupoint to prevent pull response during appendectomy. *World J Gastroenterol* 2000;6:45
- 6 Qin M, Huang YX. Progress in studies on protective effect of acupuncture in gastric mucosa and its mechanism. *Shijie Huaren Xiaohua Zazhi* 2000;8:456-457
- 7 Zhang D, Fu WX, Wang SY. Cortical infrared thermography. *Zhongguo Yixue Yingxiangxue Zazhi* 1998;6:224-226
- 8 Zhang D, Li L, Ma HM, Ye CF, Wang SY, Fu WX, Chen DS. Comparison of cortical microcirculation flow on regions of different temperature in cerebral hemisphere. *Zhongguo Yixue Wulixue Zazhi* 2000;

- 17:179-181
- 9 Zhang D, Fu WX, Wang SY. Study on Effects of electro-acupuncture (EA) on cortical temperature by Cortical Infrared Thermomaging (CIT). *Zhenci Yanjiu* 1999;24:146-152
- 10 Zhang D, Ma HM, Fu WX, Wang SY, Li L, Ye CF, Chen DS. Effect of electric acupuncture on micro circulation flow on cerebral cortical regions of different temperature. *Zhongguo Zhongyi Jichu Yixue Zazhi* 2000; 6:49-52
- 11 Ovechkin A, Lee SM, Kim KS. Thermovisual evaluation of acupuncture points. *Acupunct Electrother Res* 2001;26:11-23
- 12 Zhang D, Wang SY, Fu WX, Ye YY, Wang SY, Ma HM, Zhu YG. A preliminary study on evaluation of electro-acupuncture effect by Cortical Infrared Thermography. *Chin J Intera Tradit West Med* 1998;4: 286-289
- 13 Zhang D, Fu WX, Ye YY, Wang SY, Ma HM, Zhu YG. Display of high-thermal line along meridian on body surface of experimental cholecystitis rabbits. *Shanghai Zhenjiu Zazhi* 2001;4:77-79
- 14 Xu YL, Ye YY, Zhu YG. Effect of electroacupuncture at acuriculo- and body-acupoints on gallbladder motility of the experimental cholecystitis in rabbits. *Zhenci Yanjiu* 2000;25:27-30
- 15 Zhang D, Wei ZX, Fu WX, Wang SY, Wang FL. Thermography observation on effect of moxibustion on Jing-point for eye temperature. *Zhongyi Yanjiu* 1998;11:46-47
- 16 Cramp AF, Noble JG, Lowe AS, Walsh DM. Transcutaneous electrical nerve stimulation (TENS): the effect of electrode placement upon cutaneous blood flow and skin temperature. *Acupunct Electrother Res* 2001;26:25-37
- 17 Zhang D, Fu WX, Wang SY, Ma HM, Wang YC. Comparison of phenomenon of high thermal lines along channels induced by different acupuncture-moxibustion methods. *Zhongguo Zhenjiu* 2000;20: 349-353
- 18 Li ZQ. Traditional Chinese medicine for primary liver cancer. *World J Gastroenterol* 1998;4:360-364
- 19 Zhang P, Yang WM, Shui WX, Du YG, Jin GY. Effect of Chinese herb Mixture, shock decoction on bacterial translocation from the gut. *World J Gastroenterol* 2000;6:74
- 20 Huang ZM. Modern research in traditional herbal medicine *Oenanthe Javanica*. *Shijie Huaren Xiaohua Zazhi* 2001; 9:1-5
- 21 Wan Q. Auricular-plaster therapy plus acupuncture at zusanli for postoperative recovery of intestinal function. *J Tradit Chin Med* 2000; 20:134-135
- 22 Yi SX, Lin YP, Yan J, Chang XR, Yang Y. Effect of electro-acupuncture on gastric motility, substance P (SP) and motilin (MTL) in rats. *Shijie Huaren Xiaohua Zazhi* 2001;9:284-287
- 23 Li YM, Huang YX, Zhang J, Wang QL. Effect of electro-acupuncture on gastric emptying of rats treated with lipopolysaccharide and its relation with serum cytokines. *Shijie Huaren Xiaohua Zazhi* 2001;9:1110-1115
- 24 Wu HG, Zhou LB, Pan YY, Huang C, Chen HP, Shi Z, Hua XG. Study of the mechanisms of acupuncture and moxibustion treatment for ulcerative colitis rats in view of the gene expression of cytokines. *World J Gastroenterol* 1999;5:515-517
- 25 Pei WF, Xu GS, Sun Y, Zhu SL, Zhang DQ. Protective effect of electroacupuncture and moxibustion on gastric mucosal damage and its relation with nitric oxide in rats. *World J Gastroenterol* 2000;6:424-427
- 26 Ma ZY, Fan QS, Zhang DF. The effect of acupuncture on the IL2-IFN-NKC immunoregulatory system of mice with HAC grafting hepatocarcinoma. *World J Gastroenterol* 2000;6:32
- 27 Sun DY, Huang YX, Cu ZH, Gao W, Wang QL, Liu GS. Effects of electroacupuncture on gastric mucosal blood flow and plasma gut hormone level in dogs. *Huaren Xiaohua Zazhi* 1998;6:936-938
- 28 Wang JJ, Huang YX. Effect of CGRP in regulating gastrointestinal function by electroacupuncture. *Shijie Huaren Xiaohua Zazhi* 2000;8: 913-915
- 29 Gao W, Huang YX, Chen H, Zhao NX, Sun DY, Zhang HX, Wang QL. Regulatory mechanism of electroacupuncture on the stomach channel brain gut peptide immune network. *Shijie Huaren Xiaohua Zazhi* 2001;9:279-283
- 30 Wu HG, Zhou LB, Shi DR, Liu SM, Liu HR, Zhang BM, Chen HP, Zhang LS. Morphological study on colonic ulcerative colitis treated by moxibustion. *World J Gastroenterol* 2000;6:861-865
- 31 Xu GS, Sun Y, Wang ZJ, Zhang DQ, Gu XJ. Effects of electroacupuncture on gastric mucosal blood flow and transmucosal potential difference in stress rats. *Huaren Xiaohua Zazhi* 1998;6:4-6
- 32 Zhao BM, Huang YX. Mechanism and action of acupuncture in regulation of gastric acid secretion. *Shijie Huaren Xiaohua Zazhi* 2000;8:318-319
- 33 Cheng YS, Xiao KZ. Gastrointestinal imageology in china: a 50 year evolution. *Shijie Huaren Xiaohua Zazhi* 2000;118:1225-1232
- 34 Halachmi S, DiCastro N, Matter I, Cohen A, Sabo E, Mogilner JG, Abrahamson J, Eldar S. Laparoscopic cholecystectomy for acute cholecystitis: how do fever and leucocytosis relate to conversion and complications? *Eur J Surg* 2000; 166:136-140
- 35 Eldar S, Sabo E, Nash E, Abrahamson J, Matter I. Laparoscopic cholecystectomy for the various types of gallbladder inflammation: a prospective trial. *Surg Laparosc Endosc* 1998; 8:200-207
- 36 Zhang D, Xue LG, Wei ZX, Gao HH, Tang JR, Zhang ZP, Wen BZ. Analysis of the relationship between the facial skin temperature and blood flow. *J Biomed Eng* 1999;16:81-85
- 37 Zhang D, Mai HM, Wang SY, Wang YC, Fu WX. Effect of blood circulation in skin temperature. *Zhongguo Yixue Yingxiangxue Zazhi* 2001; 9:140-142
- 38 Sandner-Kieslin A, Litscher G, Voit-Augusti H, James RL, Schwarz G. Laser doppler flowmetry in combined needle acupuncture and moxibustion: a pilot study in healthy adults. *Lasers Med Sci* 2001;16: 184-191
- 39 Cramp AF, Noble JG, Lowe AS, Walsh DM. Transcutaneous electrical nerve stimulation (TENS): the effect of electrode placement upon cutaneous blood flow and skin temperature. *Acupunct Electrother Res* 2001;26:25-37
- 40 Zhang D, Wang SY, Wang YC, Fu WX, Ma HM. Temperature measurement on the body surface of the different temperature points and thermal lines along meridian and in its depths. *Beijing Shengwu Yixue Gongcheng* 2001;20:296-299
- 41 Zhang D, Wang SY, Wang YC, Fu WX, Ma HM. Measurement of depth's temperature under thermal lines along meridian. *Zhongguo Zhongyi Jichu Yixue Zazhi* 2001;7:62-64
- 42 Zhang D, Wang SY, Ma HM, Wang YC, Fu WX. Effect of autonomic nervous in skin temperature. *Zhongguo Yixue Yingxiangxue Zazhi* 2001; 9: 142-144

Edited by Hu DK

• BASIC RESEARCH •

Effect of L-NAME on nitric oxide and gastrointestinal motility alterations in cirrhotic rats

Xin Wang, Yue-Xia Zhong, Zong-You Zhang, Ju Lu, Mei Lan, Ji-Yan Miao, Xue-Gang Guo, Yong-Quan Shi, Yan-Qiu Zhao, Jie Ding, Kai-Cun Wu, Bo-Rong Pan, Dai-Ming Fan

Xin Wang, Zong-You Zhang, Mei Lan, Ji-Yan Miao, Xue-Gang Guo, Yong-Quan Shi, Yan-Qiu Zhao, Jie Ding, Kai-Cun Wu, Dai-Ming Fan, Institute of Digestive disease, Xijing Hospital, Fourth Military Medical University, Xi'an 710032, Shaanxi Province, China

Yue-Xia Zhong, Emergency Department, Tangdu Hospital, Fourth Military Medical University, Xi'an 710038, Shaanxi Province, China
Ju Lu, Class EE 87, Department of Electronic Engineering, Tsinghua University, Beijing 100084, China

Bo-Rong Pan, Oncology Center, Xijing Hospital, Fourth Military Medical University, Xi'an 710032, Shaanxi Province, China

Supported by National Natural Science Foundation of China, No.39970901
Correspondence to: Prof. Dai-Ming Fan, Institute of Digestive Diseases, Xijing Hospital, Fourth Military Medical University, Xi'an 710033, Shaanxi Province, China. daimfan@pub.xaonline.com

Telephone: +86-29-3375221 Fax: +86-29-2539041

Received 2001-08-23 Accepted 2001-09-05

Abstract

AIM: To investigate the effect of L-NAME on nitric oxide and gastrointestinal motility alterations in cirrhotic rats.

METHODS: Rats with cirrhosis induced by carbon tetrachloride were randomly divided into two groups, one ($n=13$) receiving $0.5\text{mg}\cdot\text{kg}^{-1}$ per day of N-G-nitro-L-arginine methyl ester (L-NAME), a nitric oxide synthase inhibitor, for 10 days, whereas the other group ($n=13$) and control ($n=10$) rats were administered the same volume of $9\text{g}\cdot\text{L}^{-1}$ saline. Half gastric emptying time and 2h residual rate were measured by SPECT, using $^{99\text{m}}\text{Tc}$ -DTPA-labeled barium sulfate as test meal. Gastrointestinal transition time was recorded simultaneously. Serum concentration of nitric oxide (NO) was determined by the kinetic cadmium reduction and colorimetric methods. Immunohistochemical SABC method was used to observe the expression and distribution of three types of nitric oxide synthase (NOS) isoforms in the rat gastrointestinal tract. Western blot was used to detect expression of gastrointestinal NOS isoforms.

RESULTS: Half gastric emptying time and trans-gastrointestinal time were significantly prolonged ($124.0\pm 26.4\text{min}$; $33.7\pm 8.9\text{min}$; $72.1\pm 15.3\text{min}$; $P<0.01$), ($12.4\pm 0.5\text{h}$; $9.5\pm 0.3\text{h}$; $8.2\pm 0.8\text{h}$; $P<0.01$), 2h residual rate was raised in cirrhotic rats than in controls and cirrhotic rats treated with L-NAME ($54.9\pm 7.6\%$, $13.7\pm 3.2\%$, $34.9\pm 10.3\%$, $P<0.01$). Serum concentration of NO was significantly increased in cirrhotic rats than in the other groups ($8.20\pm 2.48\mu\text{mol}\cdot\text{L}^{-1}$, $5.94\pm 1.07\mu\text{mol}\cdot\text{L}^{-1}$, and control $5.66\pm 1.60\mu\text{mol}\cdot\text{L}^{-1}$, $P<0.01$). NOS staining intensities which were mainly located in the gastrointestinal tissues were markedly lower in cirrhotic rats than in the controls and cirrhotic rats after treated with L-NAME.

CONCLUSION: Gastrointestinal motility was remarkably inhibited in cirrhotic rats, which could be alleviated by L-NAME. Nitric oxide may play an important role in the inhibition of gastrointestinal motility in cirrhotic rats.

Wang X, Zhong YX, Zhang ZY, Lu J, Lan M, Miao JY, Guo XG, Shi YQ, Zhao YQ, Ding J, Wu KC, Pan BR, Fan DM. Effect of L-NAME on nitric oxide and gastrointestinal motility alterations in cirrhotic rats. *World J Gastroenterol* 2002;8(2):328-332

INTRODUCTION

Investigation in gastrointestinal motility has promoted the interest of researchers in the functional changes in gastrointestinal motility of cirrhotic patients^[1-8]. It is validated that nitric oxide (NO) plays a pivotal role in neural transduction and gastrointestinal motility regulation as a neurotransmitter and messenger molecule with various physiological functions^[9-19]. However, the relationship between NO and functional changes in cirrhotic gastrointestinal motility is not yet clear^[20-27]. We used nitric oxide synthase (NOS) -specific inhibitor to treat cirrhosis model rats and observe changes in their gastrointestinal motility so as to disclose the role of NO in such changes and to provide experimental basis for diagnosis of cirrhotic gastrointestinal motility abnormalities.

MATERIALS AND METHODS

Preparation of animal model

Male SD rats were provided by the Experimental Animal Center, the Fourth Military Medical University, weighting (250 ± 50)g, fed with standard granule food, and randomly divided into model group (26 rats) and normal control group (10 rats). CCl_4 toxic cirrhosis model preparation: rats in the model group received subcutaneous injection of CCl_4 ($3\text{mL}\cdot\text{kg}^{-1}$) twice a week for 12 weeks; and rats in the control group received olive oil ($3\text{mL}\cdot\text{kg}^{-1}$) twice a week for 12 weeks. At the end of 12 weeks, cirrhosis model group was randomly subdivided into treated group and untreated group. Normal SD rats were served as controls, each group having 10 rats. Rats in the treated group were given $0.5\text{mg}\cdot\text{kg}^{-1}\cdot\text{d}^{-1}$ N-G-nitro-L-arginine methyl ester (L-NAME, Sigma product, USA), a NOS inhibitor, through intragastric administration for 10 days, and the untreated group and control group received gastric delivery of $9\text{g}\cdot\text{L}^{-1}$ NaCl once a day for 10 days. Hepatic tissue samples were normally fixed with $40\text{g}\cdot\text{L}^{-1}$ polyformaldehyde, prepared into paraffin wrapped sections, stained with HE and observed under light microscope.

Analysis of gastrointestinal motility

Examination of gastric emptying Experimental animals were fast for over 12h without receiving drugs or food that might influence gastric motility during the previous 2 weeks. Each rat received 2mL BaSO_4 mixed with $3.7\text{GBq}\cdot\text{L}^{-1}$ $^{99\text{m}}\text{Tc}$ -DTPA through the esophagus into the stomach in 2min, and was placed lying on the back. SPECT (Type CT, Sophy camera Co, France) detector was focused on the abdomen of the animals with the whole stomach as the Region of Interest (ROI); radioactivity was recorded and images were displayed for 60s as the total radioactivity. Gastric images were then taken at 15, 30, 45, 60, 90 and 120min, delineating the ROI; the curve of time-half gastric emptying was drawn and gastric residual radioactivity rates at different time points were calculated by computer.

Total gastrointestinal transition time (TGIT) After isotopic scanning, the time of BaSO₄ excretion through anus was recorded.

Alterations of NO and NOS

Assay of serum NO₂/NO₃-content Rats were decapitated and the blood was collected and quietly placed for 60min. After 4000r·min⁻¹ centrifugation for 15min, the supernatant was used for NO₂/NO₃-measurement. Operation was performed following the instructions of the reagent kit (purchased from Institute of Nuclear Medicine, General Hospital of Chinese PLA).

Expression of NOS in gastrointestinal tract Immunohistochemical method was used with immunohistochemical reagents from Wuhan Boshide Biotech Co Ltd. Five rats were randomly selected from each of the three groups. Each rat was anesthetized with 10g·L⁻¹ sodium pentobarbital (50mL·kg⁻¹) through abdominal cavity injection and perfused with 40g·L⁻¹ polyformaldehyde for 1.5h. Gastric, small intestinal and colonic tissues were immediately taken out and immersed in 200g·L⁻¹ sucrose solution at 4°C for 24h until the tissues sank to the bottom. Then the tissues were cryotomized at -20°C into slices 14-16μm thick. The tissues were rinsed three times with 0.01mmol·L⁻¹ PBS for 5min; treated with peroxide and methanol for 15min; vibrated and washed with PBS for 5min three times; and blocked with normal bovine serum for 30min. Rabbit anti-NOS₁ (1:100 rabbit polyclonal antibody), anti-NOS₂ (1:50 rabbit polyclonal antibody), anti-NOS₃ (100 rabbit polyclonal antibody) were added and the solution was incubated at 4°C overnight. Then it was vibrated and washed with PBS three times for 5min. Biotinized sheep-anti-rabbit IgG was added and the solution was let react at 37°C for 30min. The system was washed again with 0.01mmol·L⁻¹ PBS for 5min×3; SABC was added and let react at 37°C for 30min; and washed with 0.01mmol·L⁻¹ PBS for 5min×4. The stain was developed with DAB and stained with lignin. The sample was normally dehydratized till transparent and sealed with neutral resin. Microscopic observation was done and photo taken under microscope.

Determination of NOS in gastrointestinal tract with Western blot Animals fasted 12h before experiment without water deprivation. Three rats each from treated group, untreated group and control group were randomly chosen, decapitated, and eviscerated immediately to obtain the stomach, small intestine and colon, which were rinsed in ice-water containing 0.1mmol·L⁻¹ PMSF, frozen in liquid nitrogen and moved into -70°C refrigerator for preservation. The whole process should be finished within 5min. Tissue lysis liquid was prepared with ion-free water containing 0.1mmol·L⁻¹ PMSF. The gastrointestinal tissues were weighed and homogenized (3500r·min⁻¹, 5s×5) in ice-bathing, the mass/volume ratio of tissue to tissue lysis liquid being 1:5. Centrifugation was then performed at 12500r·min⁻¹ for 10min; the supernatant was separated and preserved at -70°C; the protein concentration in the extract was measured by the Bradford method.

Eighty g·L⁻¹ PAGE gel was prepared and 2×SDS loading buffer was added to the protein samples, followed by heating at 100°C for 3min. Centrifugation was performed again and protein samples of the same amount were added. Electrophoresis was done with 20mA current; and the gel was stained with Coomassie brilliant blue. Separation of protein extracts of the stomach, small intestines and colons of the rats was accomplished with 80g·L⁻¹ SDS-PAGE. After electrophoresis, electric transfer of the proteins onto NC membrane was done with a constant current of 0.8mA·cm⁻² for 1h using semi-dry electric transfer device (Beijing 61 Factory). Transfer buffer ingredients (25mmol·L⁻¹ Tris-HCl, 192mmol·L⁻¹ glycine, 10g·L⁻¹ SDS, 200g·L⁻¹ methanol, pH8.3. TBS pH7.5+50g·L⁻¹ non-fat milk+0.5g·L⁻¹ NP-40) were used for blocking the sample for 2h at

RT. Primary antibody NOS₁, NOS₂ and NOS³-3 (1:100 rabbit multiclonal antibody) was diluted with TBS buffer containing 1g·L⁻¹ BSA and added. The sample was incubated at 4°C for 16-18h and rinsed in TBS three times for 10min. HRP linked sheep-anti-rabbit secondary antibody (1:400, Boshide Co.) was diluted with TBS, added to the sample and let react for 2h at RT. The sample was then rinsed in TBS+1 g·L⁻¹ NP-40 10min×5 and developed with DAB.

Statistical analysis

Analysis of variance was conducted using NOSA statistics program (Fourth Military Medical University), and the results were presented in form of $\bar{x} \pm s$.

RESULTS

Establishment of rat model with cirrhosis

Model rats had hepatomegaly and splenomegaly, the liver became hard, the edge turned blunt, and the surface was not smooth, with nodules of varied sizes. Light microscopy showed hepatocyte regeneration, fat degeneration, proliferation of collagen fibers, and pseudo-lobulation.

Gastrointestinal motility

Gastrointestinal motility for barium Gastric semi-solid emptying: after intragastric administration of BaSO₄ containing ^{99m}Tc-DTPA, abdominal radioactivity images were taken in 8 rats in normal group (Figure 1A), untreated group (Figure 1B) and treated group (Figure 1C) each at 5, 30, 90 and 120min. The images showed that gastric emptying of cirrhotic rats was slowed down, and after treatment it was accelerated. The residual rate of gastric semi-solid substance of rats was observed dynamically.

Gastric emptying of cirrhotic rats was slowed down, the 2h residual rate being increased significantly. After L-NAME treatment, the gastric emptying was accelerated, the 2h residual rate decreased significantly (Figure 2 and Table 1).

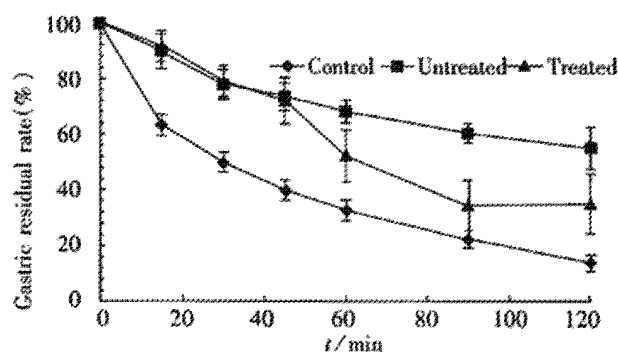


Figure 2 Residual rate curves of gastric semi-solid substance of rats

Table 1 Half-emptying time and 2h residual rate (n=8)

Groups	GET _{1/2} (min)	RR2h(%)
Control	33.7	13.7
Untreated	124.0	54.9 ^b
Treated	72.1	34.9

^bP<0.01, vs control and treated. GET_{1/2}: half-emptying time; RR2h: 2h residual rate

Gastrointestinal transition time TGIT of rats in untreated group (12.4±0.5)h was significantly longer (P<0.01) than that in the control group (9.5±0.3)h, whereas TGIT of rats in treated group (8.2±0.8)h was significantly shorter (P<0.01). Figure 3 shows that gastrointestinal transition of barium sulfate apparently slowed down in cirrhotic rats, and was significantly accelerated after L-NAME treatment; and barium sulfate was excreted in 6h after delivery.

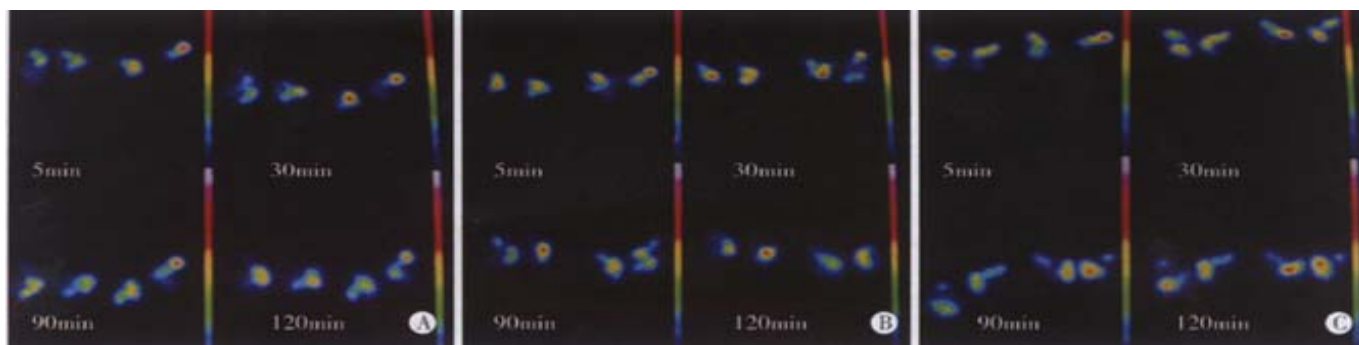


Figure 1 Gastric emptying for barium in rats. A: Normal; B: Cirrhotic; C: Cirrhotic treated with L-NAME

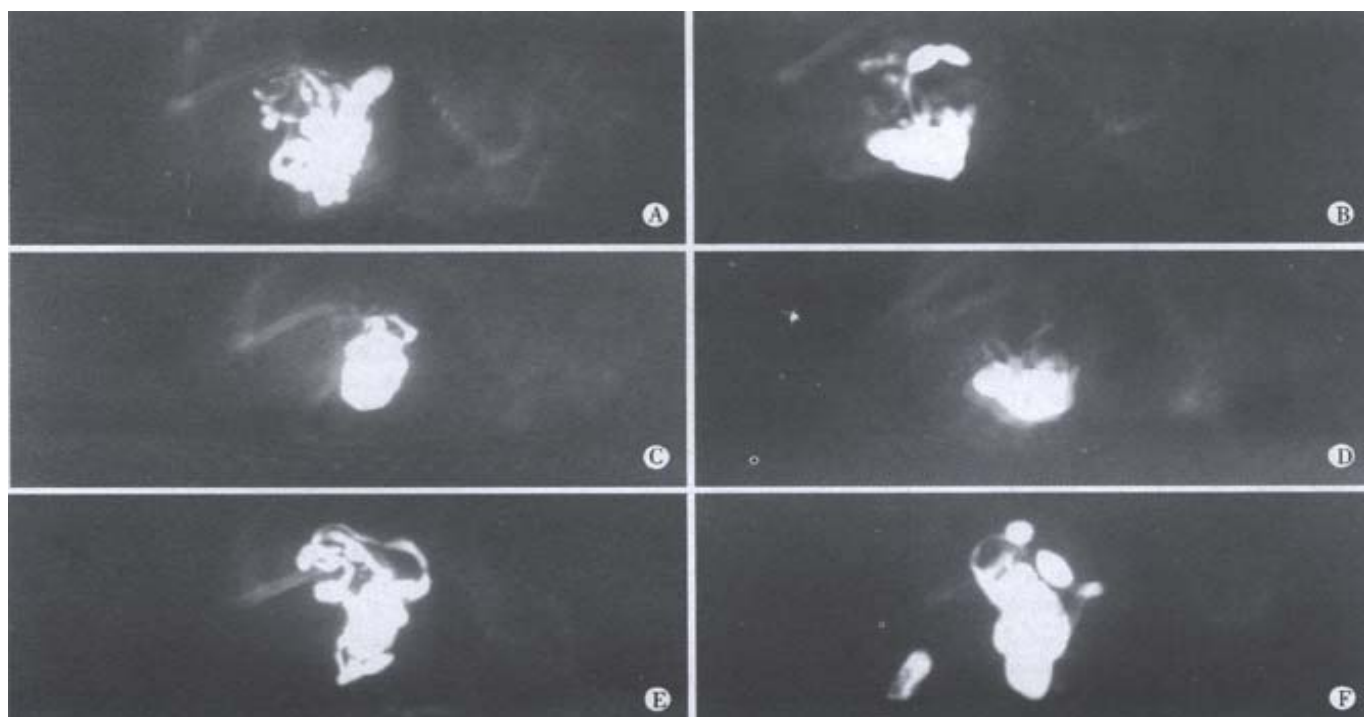


Figure 3 X-ray analysis of rat gastrointestinal motility.

A, B: Control rats at 5min and 6h; C, D: Untreated rats at 5min and 6h; E, F: Treated rats 5min and 6h

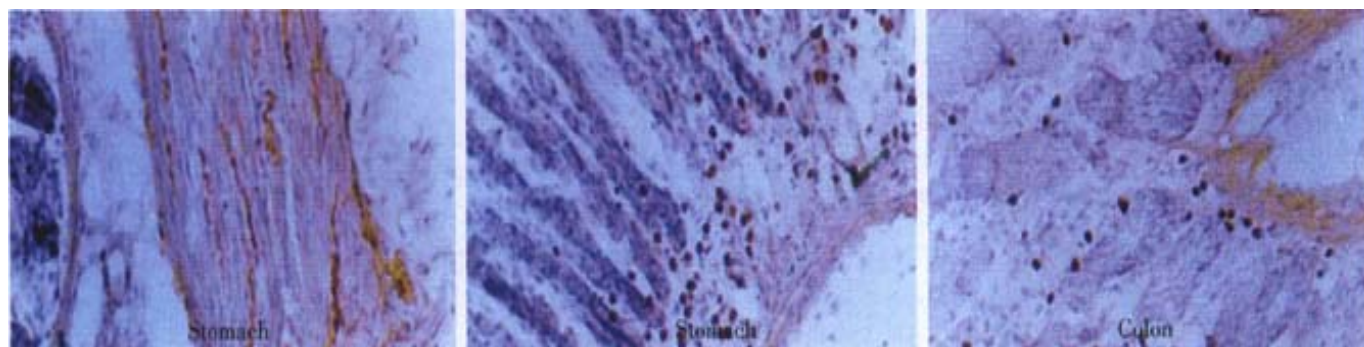


Figure 4 Expression and distribution of NOS in rat gastrointestinal tract with cirrhosis.

Alterations of NO and NOS

Serum concentration of NO The serum $\text{NO}_2^-/\text{NO}_3^-$ concentrations were $(8.20 \pm 2.48) \mu\text{mol} \cdot \text{L}^{-1}$, $(5.94 \pm 1.07) \mu\text{mol} \cdot \text{L}^{-1}$, and $(5.66 \pm 1.60) \mu\text{mol} \cdot \text{L}^{-1}$ in the rats of untreated group, normal control group, and treated group, respectively. It was apparent that NO concentration in the untreated group was significantly higher than

in other groups ($P < 0.01$).

Expression of NOS in rat gastrointestinal tract NOS immunohistochemical staining showed that NOS_1 , NOS_2 and NOS_3 had similar distribution in gastrointestinal mucosal lamina propria layer, principally in neutrophils, monocytes, macrophages and some lymphocytes of gastrointestinal mucosal lamina propria layer

interstitial. NOS₁ existed mainly in intermuscular nerve bundles in the gastrointestinal wall, endocrine cells in the mucosal layer, macrophages in gastrointestinal mucosal lamina propria layer interstitial, and some lymphocytes. In normal rats, NOS positive cells were mainly located in the lower third part of the gastric mucosal layer, in the intermuscular nerve bundles and villus interstitial of small intestine, and pervasively in colonic mucosal villus interstitial (Figure 4). In cirrhotic rats, NOS positive cells decreased significantly in the whole gastrointestinal tract and intermuscular nerve bundle. These two indexes in cirrhotic rats treated with L-NAME were significantly higher than those in untreated rats.

Western blot analysis Protein electrophoresis showed that the sampling amounts of gastric, small intestinal and colonic proteins of rats in the three groups were the same, and that the protein composition in the small intestine was quite different from that in the stomach and the colon. Western blot showed that NOS expression decreased significantly in the gastric and colonic tissues of cirrhotic rats, and it returned to normal after treated with L-NAME. NOS was not detected in the small intestine in either groups.

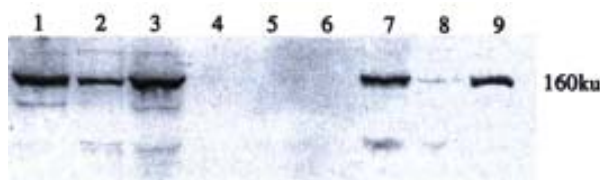


Figure 5 Expression of NOS₁ in stomach(1,2,3), intestine(4,5,6) and colon(7, 8,9) of rats 1,4,7: Control; 2,5,8: Cirrhotic; 3,7,9: Treated

DISCUSSION

NO plays an important role in gastrointestinal physiological activities as well as in the pathogenesis and progress of many severe diseases^[27-31]. It is involved in the regulation of gastrointestinal smooth muscle contraction and secretion of water and salt of intestinal epithelial cells^[32,33]. It mediates endotoxin-induced inhibition of gastric acid secretion, protects gastrointestinal mucosa, sustains mucosal blood flow, inhibits neutrophil adhesion to vascular endothelium and blocks platelet adhesion; prevents macrophage activation. NOS is the rate-limiting enzyme of NO synthesis, which exists pervasively in gastrointestinal tissues, including epithelia, fibroblasts, macrophages, inherent and infiltrating lymphocytes, neutrophils, monocytes, smooth muscle cells, endocrine cells, and intramuscular ganglia. The kinds and densities of NOS positive cells diverse at different regions^[34-40]. NOS can be classified into 3 types according to biological characters and encoding genes: neuronal type nNOS (NOS₁), endothelial type eNOS (NOS₃) and induced type iNOS (NOS₂). There are 50% homology between them. NOS₁ primarily exists in neural and epithelial cells. NOS₂ was firstly separated from macrophages and later discovered to exist in other kinds of cells such as vascular smooth muscle cells. NOS₃ mainly exists in vascular endothelial cells. According to the activity dependence on Ca²⁺/CaM, NOS has two subtypes: constitutive NOS (cNOS), including NOS₁ and NOS₃ whose activity is regulated by Ca²⁺/CaM, and induced NOS, including NOS₂ whose enzymatic activity is not dependent on Ca²⁺/CaM but needs inducing factors. The cNOS primarily exists in normal vascular endothelial cells, and is also found in adrenal gland cells, platelets, fibroblasts, PMNs, brain cells and certain non-cholinergic, non-adrenergic synapses^[41,42].

NOS expression in gastrointestinal tissues differs in certain pathological situations. In abdominal inflammation, positive cells on the small intestinal wall mainly exist in the mucosal lamina propria layer, over 80% of the positive cells are CD45 positive inflammatory

cells, about 15% are CD3 positive T lymphocytes, and epithelial cells are all negative. In ulcerative colitis, iNOS positive cells are mainly intestinal epithelial cells, while mucosal inherent cells are all negative. The status in cirrhosis is not known yet^[43-45]. NO is the major inhibitory neurotransmitter released by non-adrenaline, non-cholinergic neurons, which is closely related to gastrointestinal motility and pathology. Gastric physiological expansion and intestinal peristalsis are regulated by NO, which can directly inhibit gastrointestinal smooth muscle contraction and retard gastrointestinal motility. NOS inhibitor can promote ascites re-absorption and urinary sodium excretion of cirrhotic rats, and the rats' colonic motility recovery after abdominal operations. We prepared a toxic cirrhotic rat model, used radioactive isotopic method to determine gastric emptying functions of the rats, and recorded the total gastrointestinal transition time (TGIT). The results showed that TGIT of the rats in untreated group was significantly longer than that of the rats in the control group and the treated group, while gastric emptying was significantly slower in the former. It suggested the dysfunction of gastrointestinal motility in cirrhosis.

Cirrhotic patients are prone to develop endotoxemia due to floratranslocation, enhanced absorption of endotoxins and reduced hepatic detoxification. Endotoxins stimulate vascular endothelial cells, activate NOS, and consequently increasing NO synthesis. The serum NO concentration in cirrhotic patients rose significantly^[46-48], and the same findings were observed in cirrhotic rat's model in our experiment. However, immunohistochemical staining revealed the different distribution of NOS₁, NOS₂ and NOS₃ as described above. The quantity of NOS positive cells in cirrhotic rat gastrointestinal tissues was significantly lower than that in rats treated with L-NAME and normal control, so was NOS staining intensity in nerve bundles. Western blot was used to examine the expression of the three types of NOS in gastric, small intestinal and colonic tissues of rats and the same results were obtained as we did through NOS immunohistochemistry. These results indicate that local synthesis of NO is regulated by many factors in cirrhotic rat gastrointestinal tissues^[49].

NOS-specific competitive inhibitor L-NAME was used to treat cirrhotic rats and the results were as follows: TGIT of untreated cirrhotic rats was significantly longer than that of normal or treated cirrhotic rats, and gastric emptying in the former group was significantly slower. L-NAME treatment significantly accelerated gastric emptying and reduced TGIT. The serum NO concentration in cirrhotic rats was elevated, and L-NAME treatment reduced the serum NO concentration and gastrointestinal NO synthesis as well. These results indicate that NO contributes greatly to cirrhotic gastrointestinal motility dysfunction. NOS inhibitor L-NMMA can reduce the duration of small intestinal digestive interval MMC I phase as well as the total duration of MMC, whereas the occurrence frequency of MMC was raised and small intestinal motility was enhanced. This might be one of the mechanisms of L-NAME enhancing cirrhotic rat gastrointestinal motility^[50].

Disorder of cirrhotic gastrointestinal motility is a multi-factor disease. Our research showed that the gastrointestinal motility of cirrhotic rats was significantly inhibited, which was demonstrated by slowed gastric emptying and prolonged gastrointestinal transition time. As NO activity in the serum and tissues of cirrhotic rats was comparatively high, we used NOS-specific inhibitor to treat the rats and removed such inhibition, and found that NO played an important role in cirrhotic gastrointestinal motility dysfunction. Thus, we conclude that drugs inhibiting NO synthesis would be clinically conducive to alleviate the gastrointestinal motility dysfunction of cirrhotic patients and could consequently reduce the occurrence of cirrhosis-related complications.

REFERENCES

- Madrid AM, Hurtado C, Venegas M, Cumsille F, Defilippi C. Long-term treatment with cisapride and antibiotics in liver cirrhosis: effect on small intestinal motility, bacterial overgrowth, and liver function. *Am J Gastroenterol* 2001;96:1251-1255

- 2 Chen CY, Lu CL, Chang FY, Huang YS, Lee FY, Lu RH, Lih-Jiun K, Lee SD. The impact of chronic hepatitis B viral infection on gastrointestinal motility. *Eur J Gastroenterol Hepatol* 2000;12:995-1000
- 3 Madrid AM, Brahm J, Antezana C, Gonzalez-Koch A, Defilippi C, Pimentel C, Oksenberg D, Defilippi C. Small bowel motility in primary biliary cirrhosis. *Am J Gastroenterol* 1998;93:2436-2440
- 4 Madrid AM, Cumsille F, Defilippi C. Altered small bowel motility in patients with liver cirrhosis depends on severity of liver disease. *Dig Dis Sci* 1997;42:738-742
- 5 Chang CS, Chen GH, Lien HC, Yeh HZ. Small intestine dysmotility and bacterial overgrowth in cirrhotic patients with spontaneous bacterial peritonitis. *Hepatology* 1998;28:1187-1190
- 6 Zhang ZY, Wang X, Miao JY, Guo XG. Investigational progress of gastrointestinal motility changes induced by cirrhosis. *Di-si Junyi Daxue Xuebao* 1999;20:47-55
- 7 Zhang ZY, Wang X, Miao JY, Guo XG, Fan DM. Change of the gastrointestinal motility in cirrhotic rats. *Di-si Junyi Daxue Xuebao* 2001;22:16-19
- 8 Russo A, Fraser R, Adachi K, Horowitz M, Boeckxstaens G. Evidence that nitric oxide mechanisms regulate small intestinal motility in humans. *Gut* 1999; 44: 72-76
- 9 Zhang H, Jiang SL, Yao XX. Study of T lymphocyte subsets, nitric oxide, hexosamine and Helicobacter pylori infection in patients with chronic gastric diseases. *World J Gastroenterol* 2000;6:601-604
- 10 Zhou JF, Cai D, Zhu YG, Yang JL, Peng CH, Yu YH. A study on relationship of nitric oxide, oxidation, peroxidation, lipoperoxidation with chronic cholecystitis. *World J Gastroenterol* 2000;6:501-507
- 11 Zhao WM, Ma XH, Li ZJ, Yang CF. The effect of nitric oxide on gastric carcinoma metastasis. *World J Gastroenterol* 1998;4:78-79
- 12 Wu HG, Lu HB, Zhao C, Shi Z, Liu HR, Chen HP. The mechanism of iNOS gene modulation on acupuncture and moxibustion treatment for ulcerative colitis in rats. *World J Gastroenterol* 2000;6:64
- 13 Shao RX, Wang JB, Guo JH. The plasma level of nitric oxide and the expression of inducible nitric oxide synthase in human hepatocellular carcinoma. *World J Gastroenterol* 2000;6:61
- 14 Wang QG, He LY, Chen YW, Hu SL. Enzymohistochemical study on burn effect on rat intestinal NOS. *World J Gastroenterol* 2000;6: 421-423
- 15 Pei WF, Xu GS, Sun Y, Zhu SL, Zhang DQ. Protective effect of electroacupuncture and moxibustion on gastric mucosal damage and its relation with nitric oxide in rats. *World J Gastroenterol* 2000;6: 424-427
- 16 Yu J, Guo F, Ebert MPA, Malfertheiner P. Expression of inducible nitric oxide synthase in human gastric cancer. *World J Gastroenterol* 1999;5:430-431
- 17 Peng X, Feng JB, Wang SL. Distribution of nitric oxide synthase in stomach wall in rats. *World J Gastroenterol* 1999;5:92
- 18 Peng X, Wang SL. Nitric oxide and gastroenteric movement. *Huaren Xiaohua Zazhi* 1998;6:445-446
- 19 Xu CT, Yin QF, Li L, Pan BR. Serum levels of gastrin, motilin and leu-enkephalin in patients with liver cirrhosis. *Xin Xiaohuabingxue Zazhi* 1996;4:25-27
- 20 Li XR, He ZS, Wu JS, Ma QJ, Gao DM. Serum levels of NO in portal and peripheral vein of portal hypertensive rats. *Xin Xiaohuabingxue Zazhi* 1997;5:351-352
- 21 Zhang ZY, Ren XL, Yao XX. Alterations and relationship of plasma endotoxin and nitric oxide in patients with cirrhosis. *Xin Xiaohuabingxue Zazhi* 1997;5: 369-370
- 22 Huang YQ, Zhang DZ, Mo JZ, Li RR, Xiao SD. Nitric oxide concentration of esophageal tissues and hemodynamics in cirrhotic rats. *Xin Xiaohuabingxue Zazhi* 1997;5:558-559
- 23 Xu DH, Li DG, Lu HM. Nitric oxide and cirrhosis. *Xin Xiaohuabingxue Zazhi* 1997;5:69-70
- 24 Huang YQ, Wang X, Li C, Liu L. Clinical significance of nitric oxide level, esophageal pH and esophageal dynamic changes in diabetic patients. *Shijie Huaren Xiaohua Zazhi* 2000;8:374-376
- 25 Xu KD, Liu TF, Cing X. Significance of detection of plasma nitric oxide, endothelin, endotoxin in patients with liver cirrhosis. *World J Gastroenterol* 1998;4:64
- 26 Rachmilewitz D. Role of nitric oxide in gastrointestinal tract. *World J Gastroenterol* 1998;4:28-29
- 27 Quigley EMM. Is there a pathologic basis for gastrointestinal dysmotility? *World J Gastroenterol* 1998;4:10-17
- 28 Li XR, He ZS, Wu JS, Ma QJ, Gao DM. Nitric oxide and hyperdynamic circulation in portal hypertension. *Xin Xiaohuabingxue Zazhi* 1997;5:71-72
- 29 Yang CJ, Zhen CE, Yao XX. Study on relationship between plasma NO and sex hormones in patients with hepatic cirrhosis. *Huaren Xiaohua Zazhi* 1998;6:976-978
- 30 Huang YQ, Wang X, Li C, Liu L. Effect of nitric oxide on pathogenesis in patients with gastroesophageal reflux disease. *Shijie Huaren Xiaohua Zazhi* 2000;8:253-255
- 31 Li XR, Wu JS, He ZS, Ma QJ, Gao DM. Overproduction of nitric oxide inhibits vascular reactivity in portal hypertensive rats. *China Natl J New Gastroenterol* 1997;3:221-224
- 32 Jin NG, Li Y, Li ZL, Jin YW. Exogenous nitric oxide directly inhibits antral circular muscle motility of rat stomach *in vitro*. *Huaren Xiaohua Zazhi* 1998;6:188-191
- 33 Martin PY, Ohara M, Gines P. Nitric oxide synthase (NOS) inhibition for one week improves renal sodium and water excretion in cirrhotic rats with ascites. *J Clin Invest* 1998; 101: 235-242
- 34 Peng X, Feng JB, Wang SL, You ZY, Li A. Alterations of nitric oxide synthase and nitric oxide in gastric tissues of burned rats. *Xin Xiaohuabingxue Zazhi* 1997;5:765-766
- 35 Peng X, Feng JB, Wang SL. Nitric oxide synthase distribution in myenteric plexus of rat digestive tract. *Huaren Xiaohua Zazhi* 1998;6:250-252
- 36 Tong WD, Zhang SB, Zhang LY, Gao F, Du WH, Mou JH. Significance of nitric oxide synthase and substance P distribution in enteric nervous system of slow transit constipation. *Huaren Xiaohua Zazhi* 1998;6:380-382
- 37 Huang YQ, Xiao SD, Zhang DZ, Mo JZ. Nitric oxide synthase distribution in esophageal mucosa and hemodynamic changes in rats with cirrhosis. *World J Gastroenterol* 1999;5:213-216
- 38 Feng ZJ, Feng LY, Sun ZM, Song M, Yao XX. Expression of nitric oxide synthase protein and gene in the splanchnic organs of liver cirrhosis and portal hypertensive rats. *World J Gastroenterol* 2000;6:33
- 39 Teng B, Murthy KS, Kuemmerle JF, Grider JR, Sase K, Michel T, Akhlouf GM. Expression of endothelial nitric oxide synthase in human and rabbit gastrointestinal smooth muscle cells. *Am J Physiol* 1998;275:G342-351
- 40 Jarvinen MK, Wollmann WJ, Powrozek TA, Schultz JA, Powley TL. Nitric oxide synthase-containing neurons in the myenteric plexus of the rat gastrointestinal tract: distribution and regional density. *Anat Embryol Berl* 1999; 199: 99-112
- 41 Barbiers M, Timmermans JP, Scheuermann DW, Adriaensen D, Mayer B. Nitric oxide synthase-containing neurons in the pig large intestine: topography, morphology, and viscerofugal projections. *Microsc Res Tech* 1994; 29: 72-78
- 42 Nichols K, Staines W, Krantis A. Nitric oxide synthase distribution in the rat intestine: a histochemical analysis. *Gastroenterology* 1993; 105: 1651-1661
- 43 Alican I, Kubes P. A critical role for nitric oxide in intestinal barrier function and dysfunction. *Am J Physiol* 1996;270:G225-237
- 44 Beckett CG, Dell'Olio D, Ellis HJ, Rosen Bronson S, Ciclitira PJ. The detection and localization of inducible nitric oxide synthase production in the small intestine of patients with coeliac disease. *Eur J Gastroenterol Hepatol* 1998; 10: 641-647
- 45 Kolios G, Rooney N, Murphy CT, Robertson DA, Westwick J. Expression of inducible nitric oxide synthase activity in human colon epithelial cells: modulation by T lymphocyte derived cytokines. *Gut* 1998; 43: 56-63
- 46 Sarela AI, Mihaimeed FM, Batten JJ, Davidson BR, Mathie RT. Hepatic and splanchnic nitric oxide activity in patients with cirrhosis. *Gut* 1999; 44: 749-753
- 47 Genesca J, Gonzalez A, Segura R. Interleukin-6, nitric oxide, and the clinical and hemodynamic alteration of patients with liver cirrhosis. *Am J Gastroenterol* 1999; 94:169-177
- 48 Huang YQ, Xiao SD, Mo JZ, Zhang DZ. Effects of nitric oxide synthesis inhibitor in long term treatment on hyperdynamic circulatory state in cirrhotic rats. *World J Gastroenterol* 2000;6:31
- 49 Wang X, Wen QS, Huang YX. Effect of L-NAME on expression of NOS isoforms in cirrhotic rat intestines. *Di-Si Junyi Daxue Xuebao* 2001;22:817-820
- 50 Russo A, Fraser R, Adachi K, Horowitz M, Boeckxstaens G. Evidence that nitric oxide mechanisms regulate small intestinal motility in humans. *Gut* 1999; 44: 72-76

• BASIC RESEARCH •

Regulating effect of Chinese herbal medicine on the peritoneal lymphatic stomata in enhancing ascites absorption of experimental hepatofibrotic mice

Ji-Cheng Li, Shi-Ping Ding, Jian Xu

Ji-Cheng Li, Shi-Ping Ding, Department of Lymphology, Department of Histology and Embryology, Medical College of Zhejiang University, Hangzhou 310031, Zhejiang Province, China
Jian Xu, Hangzhou First People's Hospital, Hangzhou 310006, Zhejiang Province, China

Supported by the National Natural Science Foundation of China, No. 39970934; Scientific Researches by Science Committee of Hangzhou; State Administration of Traditional Chinese Medicine, No.97Z031; Zhejiang Provincial Administration of Traditional Chinese Medicine; excellent young talented person by Chinese Ministry of Health and Analysis and Testing fundation of Zhejiang Province.

Correspondence to: Dr. Ji-Cheng Li, Department of Lymphology, Department of Histology and Embryology, Medical College of Zhejiang University, Hangzhou 310031, Zhejiang Province, China. lijc@mail.hz.zj.cn
Telephone: +86-571-87217139 Fax: +86-571-87217139

Received 2001-08-24 Accepted 2001-08-28

Abstract

AIM: To observe the regulatory effect of Chinese herbal medicine on peritoneal lymphatic stomata and its significance in treating ascites in liver fibrosis model mice.

METHODS: Two Chinese herbal composite prescriptions were used separately to treat the carbon tetrachloride-induced mouse model of liver fibrosis. The histo-pathologic changes of the liver sections (HE and VG stainings) were observed. The peritoneal lymphatic stomata was detected by scanning electron microscopy and computer image processing. The changes of urinary volume and sodium ion concentration were measured.

RESULTS: In the model group, lots of fibrous tissue formed in liver and extended into the hepatic lobules to separate them incompletely. In the treated and prevention groups, the histo-pathologic changes of liver was rather milder, only showed much less fibrous tissue proliferation in the hepatic lobules. The peritoneal lymphatic stomata enlarged with increased density in the experimental groups (diameter: PA, $3.07 \pm 0.69 \mu\text{m}$; PB, $2.82 \pm 0.37 \mu\text{m}$; TA, $3.25 \pm 0.82 \mu\text{m}$ and TB, $2.82 \pm 0.56 \mu\text{m}$; density: PA, $7.11 \pm 1.90 \text{ stomata} \cdot 1000 \mu\text{m}^{-2}$; PB, $8.76 \pm 1.45 \text{ stomata} \cdot 1000 \mu\text{m}^{-2}$; TA, $6.55 \pm 1.44 \text{ stomata} \cdot 1000 \mu\text{m}^{-2}$ and TB, $8.76 \pm 1.79 \text{ stomata} \cdot 1000 \mu\text{m}^{-2}$), as compared with the model group (diameter: $2.00 \pm 0.52 \mu\text{m}$; density: $4.45 \pm 1.05 \text{ stomata} \cdot 1000 \mu\text{m}^{-2}$). After treatment, the urinary volume and sodium ion excretion increased in the experimental groups (PA, $231.28 \pm 41.09 \text{ mmol} \cdot \text{L}^{-1}$; PB, $171.69 \pm 27.48 \text{ mmol} \cdot \text{L}^{-1}$ and TA, $231.44 \pm 34.12 \text{ mmol} \cdot \text{L}^{-1}$), which were significantly different with those in the model group ($129.33 \pm 36.75 \text{ mmol} \cdot \text{L}^{-1}$).

CONCLUSION: Chinese herbal medicine has marked effects in alleviating liver fibrosis, regulating peritoneal lymphatic stomata, improving the drainage of ascites from peritoneal cavity and causing increase of urinary volume and sodium ion excretion to reduce the water and sodium retention, and thus have favorable therapeutic effect in treating ascites.

Li JC, Ding SP, Xu J. Regulating effect of Chinese herbal medicine on the peritoneal lymphatic stomata in enhancing ascites absorption of experimental hepatofibrotic mice. *World J Gastroenterol* 2002;8(2):333-337

INTRODUCTION

Since von Recklinghausen first reported the peritoneal lymphatic stomata, numerous investigators demonstrated that these are small openings of the subperitoneal lymphatic vessels in animals and in humans^[1]. It has also been observed that particles, cells and solutions containing vital dyes are absorbed rapidly by the peritoneal lymphatic stomata. Subsequent researchers suggested that the peritoneal cavity is an integral part of the lymphatic system with enormous absorption powers, functioning primarily by means of the subperitoneal lymphatics via the peritoneal stomata^[2-4]. Thus it has played an extremely important role in pathological conditions such as ascites absorption^[2-4], peritoneal dialysis^[3], intrauterine fetal hemolytic hemorrhage, and neoplastic metastasis of the peritoneal cavity^[5].

Liver cirrhosis is a common progressive pathological lesion of chronic liver diseases in response to various liver-damaging factors^[6-38]. Among liver cirrhosis of various causes, one common feature is the increased hepatic deposition of extracellular matrix, which consists mainly of collagen, leading to portal hypertension, esophageal varices and ascites. In the treatment of the ascites, the methods such as catharsis, diuresis, diaphoresis were used, but these methods would have side-effects which limit their clinical use^[32-35]. In recent years, attention has been paid to the therapeutic effect of Chinese medicine on the ascites^[36-41]. With the discovery of the human lymphatic stomata and the study of the lymphatic drainage system in the peritoneal cavity, Li *et al* confirmed that Chinese medicine can regulate the lymphatic stomata and promote the excretion of substance from the peritoneal cavity, and provided a new approach to the management of liver cirrhosis with ascites^[4].

In the present case, based on the previous study of peritoneal lymphatic stomata (PLS) regulation, mouse liver fibrosis model induced by carbon tetrachloride gastrogavage was used for studying the effect of two kinds of Chinese herbal medicine in anti-fibrosis, regulating PLS and promoting urine output and urinary ion excretion, so as to provide an experimental basis for clinical trial in cirrhosis with ascites.

MATERIALS AND METHODS

Animal and grouping

One hundred and two male ICR mice, weighing 18.2-25.4g, provided by Experimental Animal Center of Zhejiang Academy of Medical Sciences, were randomly divided into six groups: 17 in the prevention A group (PA group), 17 in the prevention B group (PB group), 20 in the treatment A group (TA group), 20 in the treatment B group (TB group), 20 in the model group and 8 in the control group.

Drugs

Chinese composite prescription I and II (CP I and II) were supplied by Zhejiang Academy of Traditional Chinese Medicine. The former consisted of radix *Salviae Miltiorrhizae*, *Radix Codonopsisitis*

Pilosulae, Rhizoma Atractylodis Alba and Rhizoma Alismatis, and the latter consisted of rhizoma Ligustici Wallichii, Semen Persicae and radix Salviae Miltiorrhizae. The herbal drugs were steeped in 75% alcohol for 24h, then purified with rotatory evaporator (ZFQ85A type, produced by Shanghai 11th Factory of Electron Tube). The crude drug content in CP I was $9\text{Kg}\cdot\text{L}^{-1}$ and in CP II $6\text{Kg}\cdot\text{L}^{-1}$.

Establishment of mouse liver fibrosis model

All the experimental animals were fed freely with $380\text{mg}\cdot\text{L}^{-1}$ pentobarbital solution instead of water for 10d. Excepting the control group, the mice were given 10% CCl_4 in rape-seed oil solution ($100\text{ml}/900\text{ml}$) $0.2\text{ml}/\text{mouse}$ by gastro-gavage every 4 days for 10 weeks to induce liver fibrosis. CP I or CP II ($0.2\text{ml}/\text{mouse}$) was given to the PA and PB groups respectively at the same time of CCl_4 administration. For the TA and TB groups, equal volumes of CP I and CP II were given respectively beginning from wk 7 of the experiment, after liver fibrosis formation was confirmed by pathological examination. The model group was untreated and the control group was given $0.2\text{ml}/\text{mouse}$ of normal saline per day. The experiment was lasted to wk10.

Preparation of pathological samples

The livers were taken out after the mice were killed, fixed with Bouin liquid, embedded in paraffin, sectioned, and stained with HE and VG methods for observation under light microscopy.

Preparation of sample for transmission electron microscopic examination

The tissue blocks of about 1-2mm in diameter were fixed with $25\text{mL}\cdot\text{L}^{-1}$ glutaraldehyde solution in 0.1 M phosphate buffer. Then they were postfixed in $10\text{g}\cdot\text{L}^{-1}$ OsO_4 in $0.1\text{mol}\cdot\text{L}^{-1}$ phosphate buffer for 1h at 4°C . After dehydration in a graded series of ethanol and steeping in propylene oxide, they were embedded in Epon 812. Semi-thin serial sections were made for orientation and identification of the mesothelium, and then fine sections of the mesothelium were cut with Leica Ultracut UCT ultramicrotome and stained with uranyl acetate and lead citrate. The sections were examined with a Philips EM 410 TEM operated at 60 kV.

Preparation of sample for scanning electron microscopic examination

The diaphragmatic peritoneum of mice was cut into pieces $3\times 3\text{mm}$ in size, double fixed with $25\text{mL}\cdot\text{L}^{-1}$ glutaraldehyde solution and $10\text{g}\cdot\text{L}^{-1}$ OsO_4 , gradiently dehydrated with ethanol, managed by $20\text{g}\cdot\text{L}^{-1}$ tannic acid electric conduction, CO_2 dried under critical point by HCP-2 type apparatus, Hitachi, and examined with Hitachi S-570 scanning electron microscope after metallizing with 20kV of accelerating voltage.

Computer image processing

Computerized digital processor of electronic microscopic image was used. The whole set of instruments consisted of camera, A/D, IBMP II computer, high resolution color display monitor of 64 grey level / 256 false color (including VGA adapter) and application software.

Urinary volume and ionic concentration determination

Urine in 2 hrs was collected with a filter and ionic concentration of Na^+ , K^+ and Cl^- were determined using auto-biochemical analyzer (Beckman CX Δ 7 type).

Statistic analysis

Student's *t*-test was adopted.

RESULTS

Body weight and death of CCl_4 -treated mice

After intake of CCl_4 , the mice generally manifested sluggish motion,

loose skin with lusterless hairs, obvious lowering of body weight 24h afterward but recovered gradually in the later 3d until the next CCl_4 medication, and these formed a cyclic change. The lowest number of deaths due to CCl_4 intake occurred in the PA group (3 mice), and then the TA group (7 mice), PB group (11 mice), TB group (13 mice) and the model group (13 mice) in the order. The mortalities in PA and TA group were significantly lower than that in the model group ($P<0.05$).

Pathological changes of liver

In the model group, the margin of liver was uneven; lots of fibrous tissue formed in pental areas and extended into the hepatic lobules to separate them incompletely; a large amount of inflammatory cells infiltrated in the intralobular and the interlobular regions; the liver structure was disordered with some displacement of central veins, and there were more necrotic and degenerated liver cells compared with the control (Figure 1, 2). Under transmission electron microscopy, there were numerous collagenous fibers around the liver cells (Figure 3). In the two preventive and two treated groups, the pathological changes of liver was rather milder, showing less fibrous tissue proliferation and inflammatory cell infiltration in the interlobular space; the hepatic cell cords arranged radially with less displacement of central veins and less degenerated or necrosis hepatic cells (Figure 4). The pathologic changes in the PA and TA groups were milder than those in the PB and TB groups.

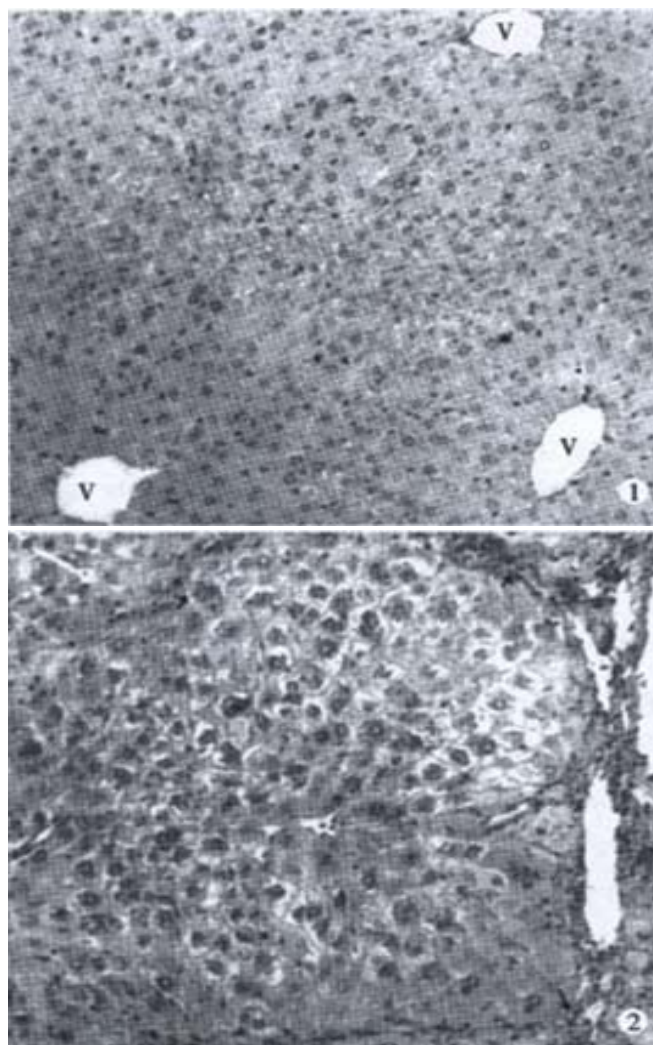


Figure 1 Light microscope observation of normal liver tissue in the control group. V: central vein. $\times 100$

Figure 2 Light microscope observation of liver fibrosis tissue in model group. Lots of fibrous tissue (arrows) formed in liver. A large amount of inflammatory cells soaked into the intralobular and the interlobular (tsiangle). $\times 200$

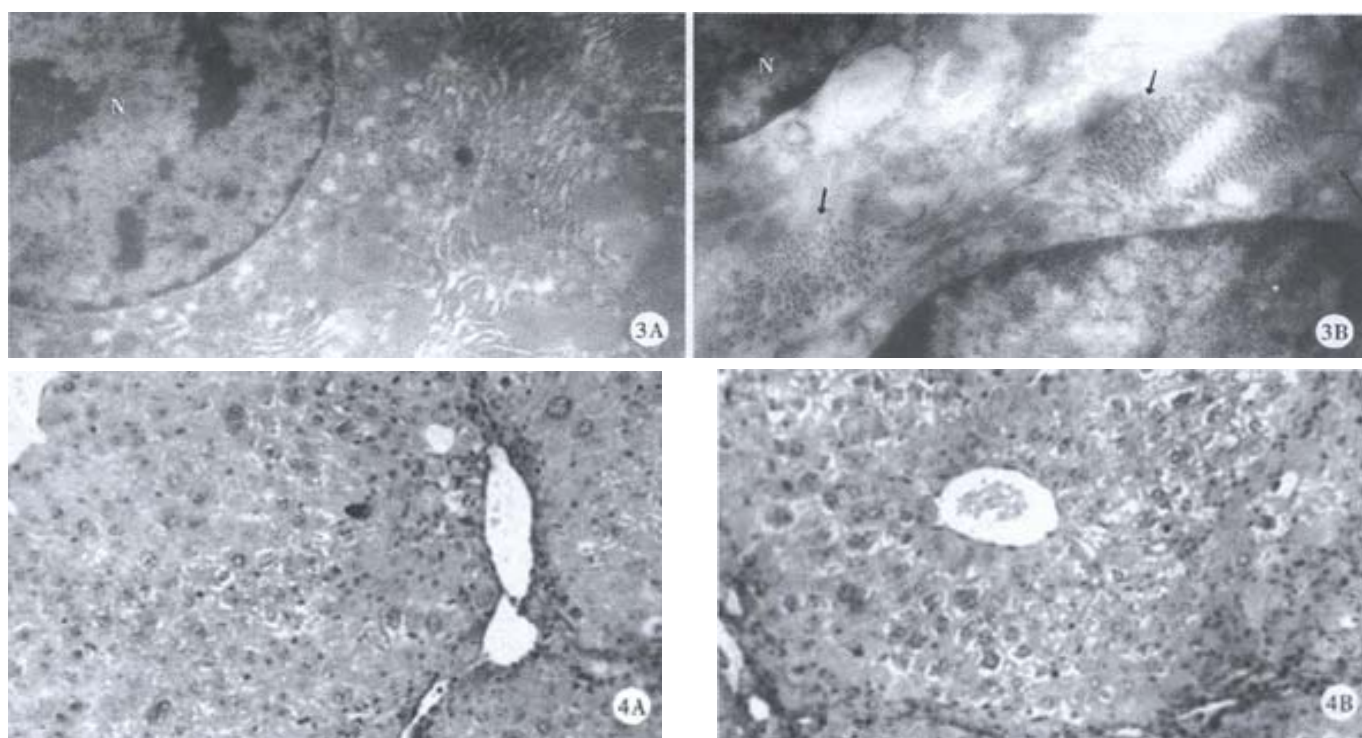


Figure 3 TEM observation of liver in the control (A) and model group (B).

Lot of collagenous fiber (arrows) formed in model group. N: nucleus. A $\times 12000$, B $\times 13500$

Figure 4 Light microscope observation of liver fibrosis tissue in PA group (A) and TA group (B).

The pathological changes of liver was rather lighter compared with the model. $\times 200$

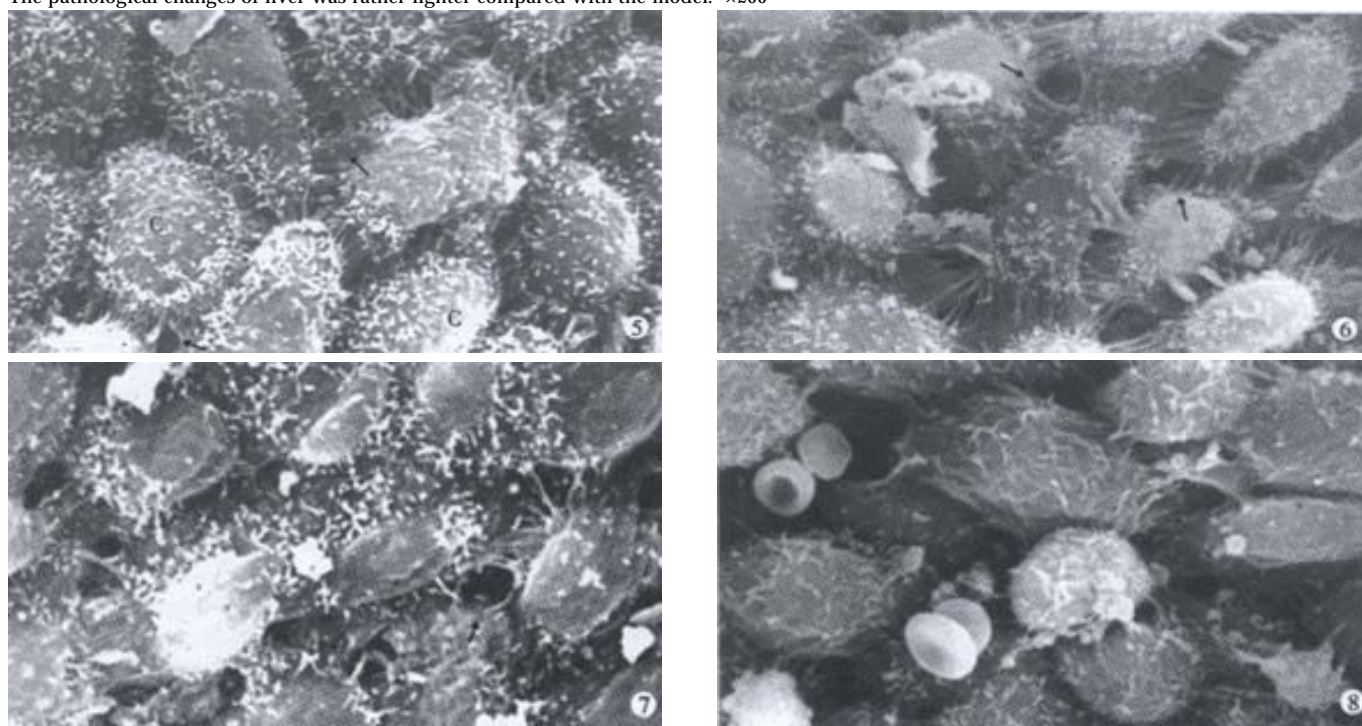


Figure 5 SEM observation of the peritoneal stomata (arrow) in the control group.

The mesothelial cells (C) and locked stomata (triangle) of the diaphragmatic peritoneum in the mice. $\times 2000$

Figure 6 SEM observation of mice diaphragmatic peritoneum in the prevention A group.

Both diameter and distributive density of the peritoneal stomata (arrows) are significantly increased. $\times 2000$

Figure 7 SEM observation of mice diaphragmatic peritoneum in the treatment A group.

Both diameter and distributive density of the peritoneal stomata (arrow) are significantly increased. $\times 2000$

Figure 8 SEM observation of mice diaphragmatic peritoneum in the treatment A group.

Some erythrocytes (arrow) could be seen to pass through the lymphatic stomata. $\times 3000$

Changes of peritoneal lymphatic stomata

Many microvilli on the mesothelial surface of diaphragmatic peritoneum of mice could be seen with electron microscopy. The microvilli seemed to be less at the place where the mesothelial cell with its nucleus protruding to peritoneal cavity and to be more at the junctions neighboring mesothelial cells. Such uneven distribution of the villi drew out the rhomboid or polygonal outlines of mesothelial cells, which were ordinarily of the flat form and the cubical form. Peritoneal lymphatic stomata (PLS) could be found only between the neighboring cubical mesothelial cells, distributed in cluster distribution and were round or elliptical shaped. In physiological condition, only a part of PLS are opened, most are in the locked manner (Figure 5).

Observations in this study showed that the diameters of PLS in the PA and PB groups increased significantly with more stomata opened, and thus resulted in an increase in their density (Table 1, Figure 6). Similar changes also occurred in the TA and TB groups (Table 1, Figure 7). Through PLS, one could see the lymphatic drainage units (LDU) formed by endothelial cytoplasmic protrusions and connective tissue fibers at the bottom of PLS (Figure 8). Intraperitoneal substances could enter through PLS into the subperitoneal lymphatic vessels so as to accelerate the absorption of ascites from the peritoneal cavity.

Table 1 Comparison of Diameter and Density of PLS between Groups ($\bar{x}\pm s$)

Group	n	Diameter/ μm	Density/(stomata $\cdot 1000\mu\text{m}^{-2}$)
Control	8	2.11 \pm 0.78	5.70 \pm 1.25
Model	20	2.00 \pm 0.52	4.45 \pm 1.05
PA	17	3.07 \pm 0.69 ^{bd}	7.11 \pm 1.90 ^{ad}
TA	20	3.25 \pm 0.82 ^{bd}	6.55 \pm 1.44 ^{ad}
PB	17	2.82 \pm 0.37 ^{bd}	8.76 \pm 1.45 ^{bd}
TB	20	2.82 \pm 0.56 ^{bd}	8.76 \pm 1.79 ^{bd}

^a $P<0.05$, ^b $P<0.01$, vs control group; ^c $P<0.01$, vs model group.

Comparison of urinary ionic concentration

The excretions of Na^+ , K^+ and Cl^- in the PA and PB group were significantly increased than those in the control group and the model group respectively ($P<0.05$ or $P<0.01$) (Table 2). The excretion of these ions in the TA group was also increased, but in the TB group, increase in ionic excretion was only limited to K^+ and Cl^- , whereas the Na^+ excretion was not significantly different from that in the model or the control group (Table 2).

Table 2 Comparison of urinary ionic concentration between groups (mmol $\cdot\text{L}^{-1}$, $\bar{x}\pm s$)

Group	n	Na^+	K^+	Cl^-
Control	8	117.98 \pm 42.29	100.16 \pm 31.32 ^c	93.43 \pm 36.20
Model	20	129.33 \pm 36.75	162.21 \pm 39.42 ^a	120.49 \pm 42.34
PA	17	231.28 \pm 41.09 ^{ac}	241.63 \pm 59.43 ^{ac}	212.17 \pm 44.01 ^{ac}
TA	20	231.44 \pm 34.12 ^{ac}	306.45 \pm 79.53 ^{ac}	240.66 \pm 31.37 ^{ac}
PB	17	171.69 \pm 27.48 ^{ac}	185.97 \pm 54.92 ^{ac}	158.10 \pm 32.79 ^{ac}
TB	20	135.33 \pm 34.59	188.17 \pm 73.91 ^{ac}	149.50 \pm 45.79 ^a

^a $P<0.05$, vs control group; ^c $P<0.05$, vs model group

Comparison of urine volume between groups

The urine volumes 2h after CP I and CP II gastrogavage in the prevention or treatment groups (average 1250 μL) were more than that in the control group (average 550 μL), and that in the model group was the least one (average 150 μL).

DISCUSSION

It is considered currently that liver fibrosis is the basic pathologic change of chronic liver diseases. No matter what the pathogenic mechanism of different liver diseases is, the ultimate consequence of progressive pathologic processes is the development of cirrhosis, portal hypertension and ascites^[42-46]. CCl_4 is a super-hepatotoxin, with which the CCl_3 free radical is produced during metabolic processes and acts

on liver cells to covalently conjugate with the cyto-membranous unsaturated lipid to cause lipid peroxidation and necrosis of hepatocytes^[16,47,48].

CP I and CP II are made up according to the traditional Chinese medicinal therapeutic principle in treating "hypochondriac pain", "lump" and "tympanites". The former has the effects of activating blood circulation to relieve stasis, strengthening "Spleen", supplementing Qi, and smoothening Qi to eliminate fullness. The latter is mainly used to activate blood circulation and remove stasis. *Salviae miltiorrhizae* in the prescriptions could preserve the integrity of hepatocytes, eliminate toxic free radicals, inhibit lipid peroxidation of cytomembrane and relieve necrosis of hepatocytes^[49]. The two composite Chinese herbal prescriptions contain equal dosage of *Salviae miltiorrhizae*, aiming at antagonizing the CCl_3 free radical, preserving the integrity of hepatocytes and decreasing the toxic action of CCl_4 on hepatocytes. However, view from the mortality of hepato-fibrosis mice, the mortality in the PA group was the lowest, and that in the PB and TB groups was not significantly different from that in the model group, the results suggested that the effect of CP I in protecting against acute damage of hepatocytes was superior to that of CP II. Wang held that the main mechanisms of Chinese herbal medicine in antagonizing liver fibrosis were: (1) To protect liver cells from degeneration, necrosis and immunological damage so as to eliminate the inducing factors of liver fibrosis; (2) to inhibit the activation and proliferation of hepatic stellate cells; (3) to decrease the expression of the genes responsible for ECM secretion; (4) to promote the activity and production of collagenase^[14,50].

According to traditional Chinese medical theory, cirrhotic ascites, one of the serious complications of liver cirrhosis, is caused by insufficiency of Yuan-Qi (vigour) and ferociousness of evil Water in the late decompensatory stage. *Radix Codonopsis Pilosulae* used in the prescriptions may strengthen "Spleen" and promote its function, activate Yuan-Qi of Middle-Jiao; *Rhizoma Atractylodis Alba* may strengthen "Spleen" and promote urination, and supplement "Spleen" to remove ascites; and *Rhizoma Alismatis* has special function in inducing diuresis. The collocation of the four drugs has effects not only in strengthening Spleen, supplementing Qi, activating blood circulation to relieve stasis, and inducing diuresis to relieve abdominal distension, but also in antagonizing liver fibrosis and protecting liver.

In the previous study, it was shown that PLS are opening of subperitoneal lymphatic capillary vessels on the surface of peritoneum, possessing an active absorptive function for liquid and granular substances in the peritoneal cavity, and the drugs for treating ascites can accelerate the absorption of peritoneal lymph by PLS. This experiment touched preliminarily upon the function of PLS regulation and changes of urinary volume and ions excretion during prevention and treatment of liver fibrosis with traditional Chinese drugs. It was shown in the experiment that the diameter and density of PLS in the CP I or CP II prevention or treatment groups were all higher than those in the control or the model groups respectively. Our previous study also revealed that when the diameter and density of PLS were increased by drugs, the quantity of absorption through PLS was increased significantly^[4]. It was further proved that the urinary volume and ionic excretion in the CP I and CP II prevention groups were increased significantly and also increased in the two treatment groups except Na^+ in CP II group. These results coincide with the regulatory effects of PLS, and indicate that both the two composite prescriptions have the effects in promoting the absorption through PLS on intraperitoneal substances of PLS, so as to accelerate liquid and ion excretion in cirrhotic patients with ascites.

REFERENCES

- 1 Azzali G. The lymphatic vessels and the so-called "lymphatic stomata" of the diaphragm: A morphologic ultrastructural and three-dimensional study. *Microvasc Res* 1999;57:30-43
- 2 Wu Y, Li JC, Mao LG, Dong XQ. Study of Chinese herbal medicine in

- treating ascites and their mechanism in regulating lymphatic stomata. *Zhongguo Zhongxiyi Jiehe Zazhi* 2001;21:677-679
- 3 Li JC, Zhang K, Yang ZR. Effects of peritoneal dialysis on macrophage nitric oxide production and its relation with peritoneal lymphatic stomata. *Shenzangbing Yu Touxu Shenyizhi Zazhi* 2000;9:13-17
 - 4 Li JC, Ding WY, Shen Y, Shi YH, Zhong HL, Yu SM. The influence of Chinese herbal medicines on the peritoneal lymphatic stomata in the mice. *Zhongguo Bingli Shenglixue Zazhi* 1999;15:414
 - 5 Funatsu K, Nishihara H, Nozaki Y. A case of a solitary metastatic diaphragmatic tumor-relation to the peritoneal stomata of the diaphragm. *Adiat Med* 1998;16:363-365
 - 6 Ma X, Qiu DK, Peng YS. Immunohistochemical study of hepatic oval cells in human chronic viral hepatitis. *World J Gastroenterol* 2001;7:238-242
 - 7 Reshetnyak VI, Sharafanova TI, Ilchenko LU, Golovanova EV, Poroshenko GG. Peripheral blood lymphocytes DNA in patients with chronic liver diseases. *World J Gastroenterol* 2001;7:235-237
 - 8 vom Dahl S, Kircheis G, Hussinger D. Hepatic encephalopathy as a complication of liver disease. *World J Gastroenterol* 2001;7:152-156
 - 9 Wang JY, Zhang QS, Guo JS, Hu MY. Effects of glycyrrhetic acid on collagen metabolism of hepatic stellate cells at different stages of liver fibrosis in rats. *World J Gastroenterol* 2001;7:115-119
 - 10 Weng HL, Cai WM, Liu RH. Animal experiment and clinical study of effect of gamma-interferon on hepatic fibrosis. *World J Gastroenterol* 2001;7:42-48
 - 11 Huang X, Li DG, Wang ZR, Wei HS, Cheng JL, Zhan YT, Zhou X, Xu QF, Li X, Lu HM. Expression changes of activin A in the development of hepatic fibrosis. *World J Gastroenterol* 2001;7:37-41
 - 12 Dai WJ, Jiang HC. Advances in gene therapy of liver cirrhosis: a review. *World J Gastroenterol* 2001;7:1-8
 - 13 Li X, Meng Y, Yang XS, Wu PS, Li SM, Lai WY. CYP11B2 expression in HSCs and its effect on hepatic fibrogenesis. *World J Gastroenterol* 2000;6:885-887
 - 14 Wang LT, Zhang B, Chen JJ. Effect of anti fibrosis compound on collagen expression of hepatic cells in experimental liver fibrosis of rats. *World J Gastroenterol* 2000;6:877-880
 - 15 Liu HL, Li XH, Wang DY, Yang SP. Matrix metalloproteinase 2 and tissue inhibitor of metalloproteinase 1 expression in fibrotic rat liver. *World J Gastroenterol* 2000;6:881-884
 - 16 Wei HS, Lu HM, Li DG, Zhan YT, Wang ZR, Huang X, Cheng JL, Xu QF. The regulatory role of AT 1 receptor on activated HSCs in hepatic fibrogenesis: effects of RAS inhibitors on hepatic fibrosis induced by CCl₄. *World J Gastroenterol* 2000;6:824-828
 - 17 Huang GC, Zhang JS, Zhang YE. Effects of retinoic acid on proliferation, phenotype and expression of cyclin dependent kinase inhibitors in TGF β 1 stimulated rat hepatic stellate cells. *World J Gastroenterol* 2000;6:819-823
 - 18 Chen YP, Liang WF, Zhang L, He HT, Luo KX. Transfusion transmitted virus infection in general populations and patients with various liver diseases in south China. *World J Gastroenterol* 2000;6:738-741
 - 19 Zang GQ, Zhou XQ, Yu H, Xie Q, Zhao GM, Wang B, Guo Q, Xiang YQ, Liao D. Effect of hepatocyte apoptosis induced by TNF α on acute severe hepatitis in mouse models. *World J Gastroenterol* 2000;6:688-692
 - 20 Riordan SM, Williams R. Transplantation of primary and reversibly immortalized human liver cells and other gene therapies in acute liver failure and decompensated chronic liver disease. *World J Gastroenterol* 2000;6:636-642
 - 21 Nie QH, Cheng YQ, Xie YM, Zhou YX, Cao YZ. Inhibiting effect of antisense oligonucleotides phosphorothioate on gene expression of TIMP-1 in rat liver fibrosis. *World J Gastroenterol* 2001;7:363-369
 - 22 Ma XD, Sui YF, Wang WL. Expression of gap junction genes connexin 32, connexin 43 and their proteins in hepatocellular carcinoma and normal liver tissues. *World J Gastroenterol* 2000;6:66-69
 - 23 Braet F, Zanger RD, Spector I, Wisse E. Structure and dynamics of hepatic endothelial fenestrae. *World J Gastroenterol* 2000;6:1
 - 24 Zhang SC, Dai Q, Wang JY, He BM, Zhou K. Gut derived endotoxemia: one of the factors leading to production of cytokines in liver diseases. *World J Gastroenterol* 2000;6:16
 - 25 Feng ZJ, Feng LY, Sun ZM, Song M, Yao XX. Expression of nitric oxide synthase protein and gene in the splanchnic organs of liver cirrhosis and portal hypertensive rats. *World J Gastroenterol* 2000;6:33
 - 26 Liu XJ, Liu F, Xiao WJ, Huang MH, Huang SM, Wang YP. Effects of sinusoidal endothelial cell conditioned medium on the expression of connective tissue growth factor in rat hepatic stellate cells. *World J Gastroenterol* 2000;6:42
 - 27 Wei HS, Li DG, Lu HM, Zhan YT, Wang ZR, Huang X, Zhang J, Cheng JL, Xu QF. Effects of AT1 receptor antagonist, losartan, on rat hepatic fibrosis induced by CCl₄. *World J Gastroenterol* 2000;6:540-545
 - 28 Du WD, Zhang YE, Zhai WR, Zhou XM. Dynamic changes of type I, III and α 1(I) collagen synthesis and distribution of collagen producing cells in carbon tetrachloride induced rat liver fibrosis. *World J Gastroenterol* 1999;5:397-403
 - 29 Li D, Zhang LJ, Chen ZX, Huang YH, Wang XZ. Effects of TNF α , IL-6 and IL-10 on the development of experimental rat liver fibrosis. *Shijie Huaren Xiaohua Zazhi* 2001;9:1242-1245
 - 30 Jian HQ, Zhang XL. Pathogenesis of hepatic fibrosis. *Shijie Huaren Xiaohua Zazhi* 2000;8:687-689
 - 31 Bai WY, Yao XX, Feng LY. Research of hepatic fibrosis. *Shijie Huaren Xiaohua Zazhi* 2000;8:1267-1268
 - 32 Xiang DD, Wei YL, Li QF. Molecular mechanism of transforming growth factor β 1 on Ito cell. *Shijie Huaren Xiaohua Zazhi* 1999;7:980-981
 - 33 Zhang LJ, Wang XZ. Transmitter and Portal hypertension. *Shijie Huaren Xiaohua Zazhi* 2000;8:1280-1281
 - 34 Li D, Wang XZ. Relationship among liver fibrosis and TNF- α , IL-6 and IL-10. *Shijie Huaren Xiaohua Zazhi* 2001;9:808-810
 - 35 Yao XX. Diagnosis and treatment of liver fibrosis. *Shijie Huaren Xiaohua Zazhi* 2000;8:681-683
 - 36 Xu KC, Wei BH, Yao XX, Zhang WD. Recent therapy for chronic hepatitis B by combined traditional Chinese and Western medicine. *Shijie Huaren Xiaohua Zazhi* 1999;7:970-974
 - 37 Wang QC, Shen DL, Zhang CD, Xu LZ, Nie QH, Xie YM, Zhou YX. Effects of Ruangansuopiwan on expression of tissue inhibitor of metalloproteinase-1/2 in rat liver fibrosis. *Shijie Huaren Xiaohua Zazhi* 2001;9:379-382
 - 38 Yang Q, Yan YC, Gao YX. Inhibitory effect of Quxianruangan Capsulae on liver fibrosis in rats and chronic hepatitis patients. *Shijie Huaren Xiaohua Zazhi* 2001;9:1246-1249
 - 39 Wang XL, Liu P, Liu CH, Liu C. Effects of coordination of FZHY decoction on functions of hepatocytes and hepatic stellate cells. *Shijie Huaren Xiaohua Zazhi* 1999;7:663-665
 - 40 Sun YH, Yao XX, Jiang SL. The liver fibrosis treated with chinese traditional drugs. *Shijie Huaren Xiaohua Zazhi* 2000;8:686-687
 - 41 Huang ZM. Modern research in traditional herbal medicine-Oenanthe Javanica. *Shijie Huaren Xiaohua Zazhi* 2001;9:1-5
 - 42 Sun DL, Sun SQ, Li TZ, Lu XL. Serologic study on extracellular matrix metabolism in patients with viral liver cirrhosis. *Shijie Huaren Xiaohua Zazhi* 1999;7:55-56
 - 43 Gao ZL, Li DG, Lu HM, Gu XH. The effect of retinoic acid on Ito cell proliferation and content of DNA and RNA. *World J Gastroenterol* 1999;5:443-444
 - 44 Lu P, Luo HS, Yu BP. Hepatocellular apoptosis and its apoptosis-regulating gene in rat liver fibrosis model. *Shijie Huaren Xiaohua Zazhi* 2001;9:165-169
 - 45 Lu LG, Zeng MT, Li JQ, Fan JG, Hua J, Fan ZP, Tai N, Qiu TK. Effect of arachidonic acid and linoleic acid on proliferation of rat hepatic stellate cells. *Shijie Huaren Xiaohua Zazhi* 1999;7:10-12
 - 46 Yao XX, Tang YW, Yao DM, Xiu HM. Effect of Yigan Decoction on the expression of type I,III collagen proteins in experimental hepatic fibrosis in rats. *Shijie Huaren Xiaohua Zazhi* 2001;9:263-267
 - 47 Yan JC, Ma Y, Chen WB, Xu CJ. Dynamic observation on vascular diseases of liver tissues of rats induced by CCl₄. *Shijie Huaren Xiaohua Zazhi* 2000;8:42-45
 - 48 Yan JC, Chen WB, Ma Y, Xu CJ. Immunohistochemical study on hepatic vascular forming factors in liver fibrosis induced by CCl₄ in rats. *Shijie Huaren Xiaohua Zazhi* 2000;8:1238-1241
 - 49 Shen M, Chen Y, Qiu DK, Xiong WJ. Effects of recombinant augmentin of liver regeneration protein, danshen and oxymatrine on rat fibroblasts. *Shijie Huaren Xiaohua Zazhi* 2001;9:1129-1133
 - 50 Wang Y, Gao Y, Huang YQ, Yu JL, Fang SG. Gelatinase A proenzyme expression in the process of experimental liver fibrosis. *Shijie Huaren Xiaohua Zazhi* 2000;8:165-167

Edited by Lu HM

• BASIC RESEARCH •

Effects of progesterone on gastric emptying and intestinal transit in male rats

Chuan-Yong Liu, Lian-Bi Chen, Pei-Yi Liu, Dong-Ping Xie, Paulus S. Wang

Chuan-Yong Liu, Lian-Bi Chen, Dong-Ping Xie, Department of Physiology, School of Medicine, Shandong University, Jinan, 250012, Shandong Province, China

Pei-Yi Liu, Paulus S. Wang, Department of Physiology, School of Medicine, National Yang-Ming University, Taipei 11221, China

Supported by Chinese Developing Funds (provided by Taiwan) and Scientific Initiating Grants of Shandong University

Correspondence to: Associate Prof. Dr. Chuan-Yong Liu, Department of Physiology, School of Medicine, Shandong University, Jinan 250012, Shandong Province, China. liucy@sdu.edu.cn

Telephone: +86-531-2942037 Fax: +86-531-2942156

Received 2001-11-15 Accepted 2002-01-04

Abstract

AIM: To study the dose-dependent of progesterone (P) effect and the interaction between the oxytocin (OT) and P on gastrointestinal motility.

METHODS: In order to monitor the gastric emptying and intestinal transit, the SD male rats were intubated via a catheter with normal saline (3ml/kg) containing $\text{Na}_2^{51}\text{CrO}_4$ (0.5 $\mu\text{Ci}/\text{ml}$) and 10% charcoal. OT was dissolved into normal saline and P was dissolved into 75% alcohol.

RESULTS: Low doses of P (1mg/kg, i.p.) enhanced the gastric emptying (75 \pm 3%, $P<0.05$) and high dose of P (5mg/kg, i.p.) inhibit it (42 \pm 11.2%, $P<0.01$). P (1mg/kg) increased the intestinal transit (4.2 \pm 0.3, $P<0.05$) while the higher dose (10-20mg/kg) had no effect. OT (0.8mg/kg, i.p.) inhibited the gastric emptying (23.5 \pm 9.8%, $P<0.01$). The inhibitory effects of P (20mg/kg) (32 \pm 9.7%, $P<0.05$) and OT (0.8mg/kg) on gastric emptying enhanced each other when the two chemicals were administrated simultaneously (17 \pm 9.4%, $P<0.01$).

CONCLUSION: Low dose of P increased GI motility while high dose of P decreased it. During the later period of pregnancy, elevated plasma level of OT may also participate in the gastrointestinal inhibition.

Liu CY, Chen LB, Liu PY, Xie DP, Wang PS. Effects of progesterone on gastric emptying and intestinal transit in male rats. *World J Gastroenterol* 2002;8(2):338-341

INTRODUCTION

Gastrointestinal motility is disturbed in pregnant women because of the changes of some hormone levels in the plasma, such as estrogen (E), progesterone (P), and other gastrointestinal hormones^[1,2]. Steroids, especially P and E, participate the regulation of gastrointestinal motility^[3-5] and are involved in the pathogenesis of some functional disorders in the gut^[6]. We reported that administration of estrogen inhibited the rat gastric emptying and intestinal transit while P enhanced the gut motility^[7]. The effects of E were testified by other scholars while the inhibitory effect of P was observed^[8]. Oxytocin (OT) is also a hormone related to pregnancy, and its plasma concentration is higher during the late phase^[9,10]. It is reported that OT inhibited gastric motility and secretion^[11-13]. We recently found

that administration of OT inhibited the rat gastrointestinal motility through inducing the release of cholecystokinin (CCK) (unpublished data). Progesterone affects the OT effect on uterine smooth muscle^[14], but it is unknown if P and OT interact with each other on the effect of gut motility. In this study, three experiments were conducted to investigate the dose-dependent effect of P and the interaction between P and OT on gastric emptying and intestinal transit in male rats.

MATERIALS AND METHODS

Animals

Male Sprague-Dawley rats weighing 250-350g were housed at 22°C and light-controlled environment (6a.m.-8p. m.) and fed with rat chow. Tap water was given *ad libitum*.

Experiment protocol

Experiment 1. The male rats were randomly divided into four groups ($n=6$ each). They were fasted but with access to water for 24h before use. On the day of experiment, the four groups of animals were injected intraperitoneally (i. p.) with 0, 0.3, 1.0 and 3.0mg/kg of P, respectively 15min before gastric intubation of a non-nutrient liquid meal. Fifteen min after the administration of the liquid meal, the rats were decapitated and the gastric emptying and intestinal transit were measured.

Experiment 2. The procedure was identical to that in experiment 1, except the dose of P was 0, 5, 10 and 20mg/kg, respectively in the four groups of animals ($n=7$).

Experiment 3. Male rats were divided into four groups with 7 animals each and fasted for 24h before use. Fifteen min before gastric intubation of a non-nutrient liquid meal, the animals were injected i.p. with the normal saline and 75% alcohol (1ml/kg) in group 1, OT (0.8mg/kg) and 75% alcohol (1ml/kg) in group 2, normal saline (1ml/kg) and P (20mg/kg) in group 3, and OT (0.8mg/kg) and P (20mg/kg) in group 4. OT was dissolved in the normal saline and P was dissolved in the alcohol (75%).

Measurement of gastric emptying and GI transit

Gastric emptying and GI transit were measured as described by Doong *et al*^[15]. Rats were intubated via a catheter (PE-205, ID 1.67mm, OD 2.42mm, Clay-Adam, Parsippany, NJ, USA) with normal saline (3mL/kg) containing $\text{Na}_2^{51}\text{CrO}_4$ (0.5 $\mu\text{Ci}/\text{mL}$) and 10% charcoal. The test meal was continuously stirred before intubation. Air (0.5mL) was used to flush the residual charcoal suspension in the catheter into the rats. Fifteen min later, the rats were decapitated and the stomach and attached small intestine immediately exposed by laparotomy. After ligation of the esophagogastric, gastroduodenal, and ileocecal junctions, the whole stomach and small intestine were carefully removed and placed on a wooden board to observe the leading edge of the charcoal in the intestine. The small intestine was then divided into 10 equal segments and the radioactivity in the stomach and each segment of small intestine was measured in an automatic gamma counter (1470 Vizard, Pharmacia, Turku, Finland). Gastric emptying was measured by determining the amount of labeled chromium contained in the small intestine 15min after

intubation, expressed as a percentage of the amount given. Intestinal transit was assessed by calculating the geometric center of distribution of the radioactivity with the 10 segments by summation of the radioactivity in each segment multiplied by the segment number.

Statistical analysis

The data were expressed as the mean value \pm S. E. M. The treatment means were tested for homogeneity using one-way analysis of variance, and the significance of any difference between means was tested using Duncan's multiple range test. A difference between two means was considered to be statistically significant when P was less than 0.05.

RESULTS

Low dose of P on gastric emptying and intestinal transit

Gastric emptying was enhanced slightly after P (0.3mg/kg) was injected i. p., and was elevated significantly by administration of P (1mg/kg) in the same way ($P < 0.05$, $n=6$). P (3mg/kg) inhibited the gastric emptying, although the difference was not significant (Figure 1-1). Administration of P, 1mg/kg or 3mg/kg, increased the intestinal transit significantly ($P < 0.05$, $n=6$), but the dose of 0.3mg/kg did not influence it (Figure 1-2).

High dose of P on gastric emptying and intestinal transit

Administration of P (5-20mg/kg, i.p.) dose dependently decreased the gastric emptying (Figure 2-1). In this experiment, only the lowest dose of P (5mg/kg, i.p.) significantly increased the intestinal transit, P with much higher dose (10 and 20mg/kg) did not influence the intestinal transit (Figure 2-2).

Interaction of OT and P on gastric emptying and intestinal transit

Compared with control, both OT (0.8mg/kg, i.p.) and P (20mg/kg i.p.) significantly inhibited the gastric emptying. When both OT and P were administrated, the gastric emptying was further inhibited (Figure 3). Administration of OT (0.8mg/kg) and/or P (20mg/kg) did not influence the intestinal transit.

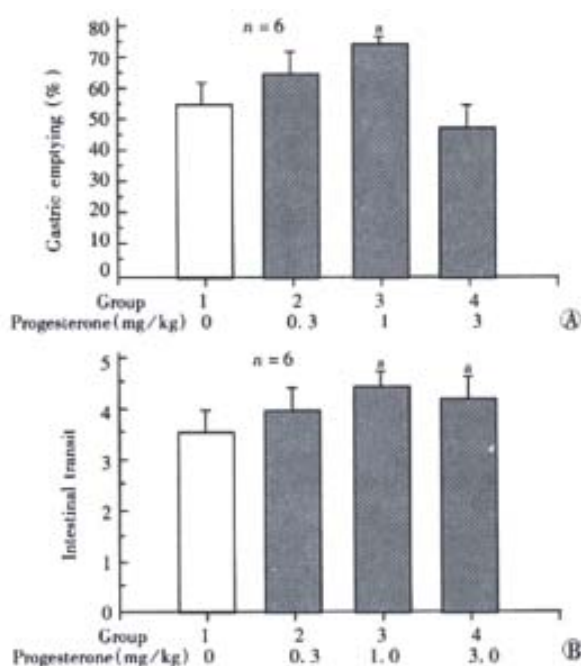


Figure 1 A: Effect of low dose of progesterone (i.p.) on gastric emptying in male rats. ^a $P < 0.05$ vs group 1; B: Effect of low dose of progesterone (i.p.) on intestinal transit in male rats. ^a $P < 0.05$ vs group 1

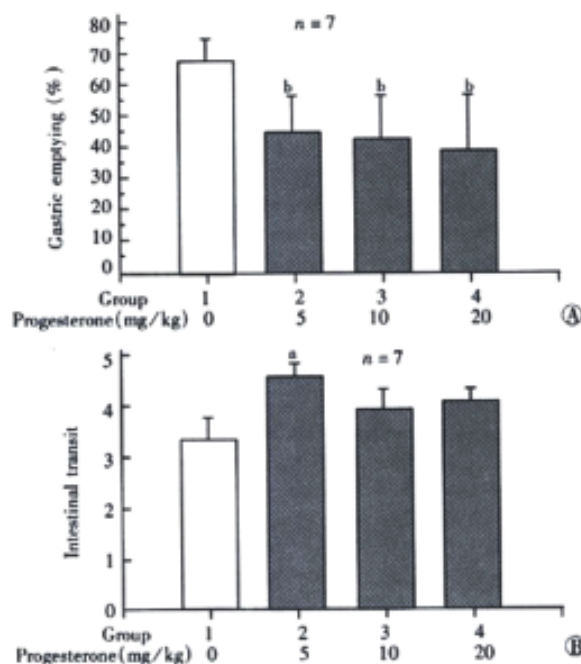


Figure 2 A: Effect of high dose of progesterone (i.p.) on gastric emptying in male rats. ^b $P < 0.01$ vs group 1; B: Effect of high dose of progesterone (i.p.) on intestinal transit in male rats. ^a $P < 0.05$ vs group 1

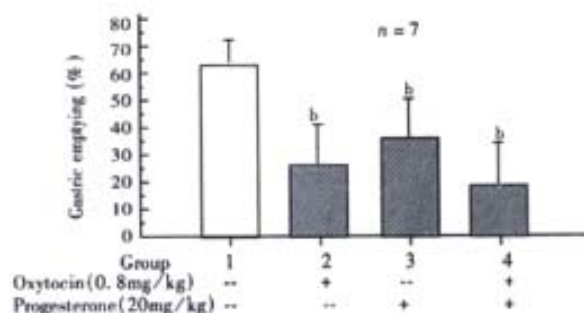


Figure 3 Interaction of progesterone and oxytocin (i.p.) on gastric emptying in male rats. ^b $P < 0.01$ vs group 1

DISCUSSION

It is known that the liquid emptying slows as the calorie content increases. For nutrient liquid that stimulates intestinal feedback inhibition, there is an initial rapid emptying phase followed by a linear phase. In this study, we used non-nutrient liquid meal, and therefore the emptying rate was rapid, representing the initial rapid emptying of nutrient liquid. Because the volume in the initial rapid emptying contributes greatly to the nutrient liquid being half emptied, it is reasonable to assume that the changes of liquid emptying caused by the hormones from our study could influence the half-emptying time of nutrient liquid.

The result in this study indicated that the lower dose of P enhanced the gastrointestinal motility while the higher dose inhibited it. This data could explain why different effects of P on gastric emptying and intestinal transit were observed. Different routes of administration could make the chemicals absorbed at different velocity, thus making the plasma level of this hormone different. Besides the central nervous system, other organs such as the uterus also secrete OT into blood^[16, 17]. In the pregnant women with or without pain, the OT concentration in plasma is much higher than that in the cerebrospinal fluid, so the higher level of OT during the late period of pregnancy may mainly come from the peripheral organs^[18].

Although there is no direct evidence that there exists OT receptor in the gut, our data indicated that OT could inhibit the gastric emptying.

Disturbed gastrointestinal motility was observed in the pregnant women. In the early period, the high level of estrogen and progesterone may contribute to this pathophysiological phenomenon. During the late period, the OT level in plasma was elevated^[9, 10]. In the present study, when administrated simultaneously, the inhibitory effects of P and OT on gastrointestinal were strengthened each other. Thus, OT may also participate in the inhibition of gastrointestinal motility during the late period of pregnancy.

In the uterus, The OT receptor is upregulated in the secretory phase during the oestrous cycle and downregulated during the early pregnancy^[19-21]. Two levels of interaction between OT and steroid hormones were reported, the genomic and non - genomic mechanisms^[22]. Estrogen induces the OT receptor (OTR) mRNA expression, and then increases the OTR density on the membrane of the uterus smooth muscle^[22-35]. This effect of estrogen was also observed in the central nervous system^[36]. The effect of P on OTR expression is controversial. It has been suggested that, through the nuclear receptors, P inhibits the OTR mRNA expression, and makes the target cell less sensitive to OT stimulation^[25, 26, 37-43]. Giacalone also reported that, RU-486, a P receptor antagonist, increases the incidences of tachysystole, hypertonia and fetal heart rat abnormality^[44]. However, Al-Matubsi reported that pretreatment with P enhanced the OTR mRNA expression in the ovine corpus luteum^[45]. OT excites the uterus smooth muscle mainly through two mechanisms: binding the membrane receptor directly and increasing the secretion of prostaglandin (PG)^[46-48]. P enhanced uterine PGF 2 α secretion in response to OT in ovariectomized sows^[49].

Direct interaction, but not through the regulation of RNA expression, between P and OT was also reported. Grazzini *et al* found that P specially binded to the OTR and inhibited its ligand binding and signal functions^[14, 50]. Burger also reported that P inhibited the calcium signaling evoked by ligand stimulation of G protein-coupled receptor. This kind of P effect was fast, reversible and was not prevented by cycloheximide, indicating a non-genomic nature^[51].

In this experiment, administration of P (20mg/kg) and OT (0.8mg/kg) in combination inhibited the gastric emptying, and the gastric motility was further attenuated. Because this effect was found within 30min after the chemical treatment, it is clear that the nature of the potentiation between P and OT is non - genomic.

In conclusion, the data indicated that high dose of P inhibited the GI motility while low dose of P enhanced it. During pregnancy, especially during the later period, high levels of P and OT enhance each other to disturb the gastrointestinal motility.

REFERENCES

- Chiloiro M, Darconza G, Piccioli E, De Carne M, Clemente C, Riezzo G. Gastric emptying and orocecal transit time in pregnancy. *J Gastroenterol* 2001; 36: 538-543
- Chang FY, Lee SD, Yeh GH, Lu CC, Wang PS, Wang SW. Disturbed small intestinal motility in the late rat pregnancy. *Gynecol Obstet Invest* 1998; 45:221-224
- Bradesi S, Eutamene H, Fioramonti J, Bueno L. Acute restraint stress activates functional NK1 receptor in the colon of female rats: involvement of steroids. *Gut* 2002; 50:349-354
- Sheen-Chen SM, Ho HT, Chen WJ, Sheen CW, Eng HL, Chou FF. Progesterone receptor in patients with hepatolithiasis. *Dig Dis Sci* 2001; 46:2374-2377
- Tierney S, Nakeeb A, Wong O, Lipsett PA, Sostre S, Pitt HA, Lillemoe KD. Progesterone alters biliary flow dynamics. *Ann Surg* 1999; 229: 205-209
- Mathias JR, Clench MH. Relationship of reproductive hormones and neuromuscular disease of the gastrointestinal tract. *Dig Dis* 1998;16: 3-13
- Chen TS, Doong ML, Chang FY, Lee SD, Wang PS. Effects of sex steroid hormones on gastric emptying and gastrointestinal transit in rats. *Am J Physiol* 1995; 268: G171-G176
- Coskun T, Sevinc A, Tevetoglu I, Alican I, Kurtel H, Yegen BC. Delayed gastric emptying in conscious male rats following chronic estrogen and progesterone treatment. *Exp Med (Berl)* 1995; 195: 49-54
- Mizutani S, Hayakawa H, Akiyama H, Sakura H, Yoshino M, Oya M, Kawashima Y. Simultaneous determinations of plasma oxytocin and serum placental leucine aminopeptidase (P-LAP) during late pregnancy. *Clin Biochem* 1982; 15:141-145
- Kumaresan P, Subramanian M, Anandarangam PB, Kumaresan M. Radioimmunoassay of plasma and pituitary oxytocin in pregnant rats during various stages of pregnancy and parturition. *J Endocrinol Invest* 1979; 2:65-70
- Wang F, Luo JQ, Zheng TZ, Qu SY, Li W, He DY. Effect of oxytocin on the contractile activity of isolated gastric strips in rats. *Zhongguo Yaolixue Yu Dulixue Zazhi* 1999; 13: 285-287
- Duridanova DB, Nedelcheva DM, Gagov HS. Oxytocin induced changes in single cell K⁺ currents and smooth muscle contraction of guinea-pig gastric antrum. *Eur J Endocrinol* 1997; 136: 531-538
- Asad M, Shewade DG, Koumaravelou K, Abraham BK, Vasu S, Ramaswamy S. Gastric antisecretory and antiulcer activity of oxytocin in rats and guinea pigs. *Life Sci* 2001; 70:17-24
- Grazzini E, Guillon G, Mouillac B, Zingg HH. Inhibition of oxytocin receptor function by direct binding of progesterone. *Nature* 1998; 392: 509-512
- Doong ML, Lu CC, Kau MM, Tsai SC, Chiao YC, Chen JJ, Yeh JY, Lin H, Huang SW, Chen TS, Chang FY, Wang PS. Inhibition of gastric emptying and intestinal transit by amphetamine through a mechanism involving an increased secretion of CCK in male rats. *Br J Pharmacol* 1998; 124: 1123-1130
- Mitchell BF, Chibbar R. Synthesis and metabolism of oxytocin in late gestation in human decidua. *Adv Exp Med Biol* 1995;395:365-380
- Shojo H, Kaneko Y. Characterization and expression of oxytocin and the oxytocin receptor. *Mol Genet Metab* 2000;71:552-558
- Takagi T, Tanizawa O, Osuki Y, Sugita N, Haruta M, Yamaji K. Oxytocin in the cerebrospinal and plasma of pregnant and nonpregnant subjects. *Horm Metab Res* 1985; 17: 308-310
- Fuchs AR, Behrens O, Maschek H, Kupsch E, Einspanier A. Oxytocin and vasopressin receptors in human and uterine myomas during menstrual cycle and early pregnancy. *Hum Reprod Update* 1998; 4: 594-604
- Robinson RS, Mann GE, Lamming GE, Wathes DC. Expression of oxytocin, oestrogen and progesterone receptors in uterine biopsy samples throughout the oestrous cycle and early pregnancy in cows. *Eproduction* 2001;122: 965-979
- Einspanier A, Bielefeld A, Kopp JH. Expression of the oxytocin receptor in relation to steroid receptors in the uterus of a primate model, the marmoset monkey. *Hum Reprod Update* 1998; 4:634-646
- Aingg HH, Grazzini E, Breton C, Larcher A, Rozen F, Russo C, Guillon G, Mouillac B. Genomic and non-genomic mechanisms of oxytocin receptor regulation. *Adv Exp Med Biol* 1998; 449: 287 - 295
- Engstrom T, Bratholm P, Christensen NJ, Vilhardt H. Up-regulation of oxytocin receptors in non-pregnant rat myometrium by isoproterenol: effects of steroids. *J Endocrinol* 1999;161:403-411
- Zingg HH, Grazzini E, Breton C, Larcher A, Rozen F, Russo C, Guillon G, Mouillac B. Genomic and non-genomic mechanisms of oxytocin receptor regulation. *Adv Exp Med Biol* 1998; 449: 287-295
- Behrendt-Adam CY, Adams MH, Simpson KS, McDowell KJ. Oxytocin-neurophysin I mRNA abundance in equine uterine endometrium. *Domes Anim Endocrinol* 1999; 16: 183-192
- Leung ST, Wathes DC. Regulatory effect of steroid hormones and fetal tissues on expression of oxytocin receptor in the endometrium of late pregnant ewes. *J Reprod Fertil* 1999; 115: 243-250
- Vasudevan N, Davidkova G, Zhu YS, Koibuchi N, Chin WW, Pfaff D. Differential interaction of estrogen receptor and thyroid hormone receptor isoforms on the rat oxytocin receptor promoter leads to differences in transcriptional regulation. *Neuroendocrinology* 2001; 74:309-324
- Leung ST, Wathes DC. Oestradiol regulation of oxytocin receptor expression in cyclic bovine endometrium. *J Reprod Fertil* 2000; 119: 287-292
- Ivell R, Walther N. The role of sex steroids in the oxytocin hormone system. *Mol Cell Endocrinol* 1999;151:95-101
- Mittaud P, Labourdette G, Zingg H, Guenot-Di Scala D. Neurons modulate oxytocin receptor expression in rat cultured astrocytes: Involvement of TGF-beta and membrane components. *Glia* 2002;37:169-177
- Terenzi MG, Jiang QB, Cree SJ, Wakerley JB, Ingram CD. Effect of gonadal steroids on the oxytocin-induced excitation of neurons in the bed nuclei of the stria terminalis at parturition in the rat. *Neuroscience* 1999; 91:1117-1127
- Amico JA, Davis AM, McCarthy MM. An ovarian steroid hormone regimen that increases hypothalamic oxytocin expression alters [³H] muscimol binding in the hypothalamic supraoptic nucleus of the female rat. *Brain Res* 2000; 857:279-282

- 33 Brussaard AB, Devay P, Leyting-Vermeulen JL, Kits KS. Changes in properties and neurosteroid regulation of GABAergic synapses in the supraoptic nucleus during the mammalian female reproductive cycle. *J Physiol* 1999; 516: 513-524
- 34 Israel JM, Poulain DA. 17-Oestradiol modulates *in vitro* electrical properties and responses to kainate of oxytocin neurones in lactating rats. *J Physiol* 2000; 524: 457-470
- 35 Leng G. Steroidal influences on oxytocin neurones. *J Physiol* 2000; 524:315
- 36 Ivell R, Kimura T, Muller D, Augustin K, Abend N, Bathgate R, Telgmann R, Balvers M, Tillmann G, Fuchs AR. The structure and regulation of the oxytocin receptor. *Exp Physiol* 2001;86:289-296
- 37 Murata T, Murata E, Liu CX, Narita K, Honda K, Higuchi T. Oxytocin receptor gene expression in rat uterus: regulation by ovarian steroids. *J Endocrinol* 2000; 166:45-52
- 38 Mann GE. Hormone control of prostaglandin F(2 alpha) production and oxytocin receptor concentrations in bovine endometrium in explant culture. *Domest Anim Endocrinol* 2001; 20: 217-226
- 39 Bouchard P. Progesterone and the progesterone receptor. *J Reprod Med* 1999;44: 153-157
- 40 Sladek CD, Swenson KL, Kapoor R, Sidorowicz HE. The role of steroid hormones in the regulation of vasopressin and oxytocin release and mRNA expression in hypothalamo-neurohypophysial explants from the rat. *Exp Physiol* 2000; 85:171S-177S
- 41 Mann GE, Payne JH, Lamming GE. Hormonal regulation of oxytocin-induced prostaglandin F(2alpha) secretion by the bovine and ovine uterus *in vivo*. *Domest Anim Endocrinol* 2001; 21:127-141
- 42 Breton C, Di Scala-Guenot D, Zingg HH. Oxytocin receptor gene expression in rat mammary gland: structural characterization and regulation. *J Mol Endocrinol* 2001;27:175-189
- 43 Leung ST, Reynolds TS, Wathes DC. Regulation of oxytocin receptor in the placental capsule throughout pregnancy in the ewe: the possible role of oestradiol receptor, progesterone receptor and aromatase. *J Endocrinol* 1998; 158: 173-181
- 44 Giacalone PL, Daures JP, Faure JM, Boulot P, Hedon B, Laffargue F. The effects of mifepristone on uterine sensitivity to oxytocin and on fetal heart rate patterns. *Eur J Obstet Gynecol Reprod Biol* 2001; 97: 30-34
- 45 Al-Matubsi HY, Frazer S, Fairclough RJ, Jenkin G. Effects of progesterone on expression of messenger RNA encoding oxytocin-neurophysin, oxytocin receptor and prostaglandin G/H synthase-1 and -2 during the early oestrous cycle in the ovine corpus luteum. *Eprod Fertil Dev* 1999;11:435-442
- 46 Gimpl G, Fahrenholz F. The oxytocin receptor system: structure, function, and regulation. *Physiol Rev* 2001; 81: 629-683
- 47 Engstrom T, Bratholm P, Christensen NJ, Vilhardt H. Effect of oxytocin receptor blockade on rat myometrial responsiveness to prostaglandin f(2) (alpha). *Biol Reprod* 2000; 63: 1443-1449
- 48 Wu WX, Verbalis JG, Hoffman GE, Derks JB, Nathaniwlsz PW. Characterization of oxytocin receptor expression and distribution in the pregnant sheep uterus. *Endocrinology* 1996; 137: 722-728
- 49 Edgerton LA, Kaminski MA, Silvia WJ. Effects of progesterone and estradiol on uterine secretion of prostaglandin f (2 alpha) in response to oxytocin in ovariectomized sows. *Biol Reprod* 2000; 62:365-369
- 50 Gimpl G, Burger K, Politowska E, Ciarkowski J, Fahrenholz F. Oxytocin receptors and cholesterol: interaction and regulation. *Exp Physiol* 2000; 85:41S-49S
- 51 Burger K, Fahrenholz F, Gimpl G. Non-genomic effects of progesterone on the signaling functions of G-protein-coupled receptors. *FEBS Lett* 1999; 464: 25-29

Edited by Ma JY

• BASIC RESEARCH •

Liver sinusoidal endothelial cell injury by neutrophils in rats with acute obstructive cholangitis

Jian-Ping Gong, Chuan-Xin Wu, Chang-An Liu, Sheng-Wei Li, Yu-Jun Shi, Xu-Hong Li, Yong Peng

Jian-Ping Gong, Chuan-Xin Wu, Chang-An Liu, Sheng-Wei Li, Yu-Jun Shi, Xu-Hong Li, Yong Peng, Department of General Surgery, The Second College of Clinical Medicine & the Second Affiliated Hospital of Chongqing University of Medical Science, 74 Linjiang Road, Chongqing 400010, China

Supported by the National Natural Science Foundation of China, No. 39970719, 30170919

Correspondence to: Dr. Jian-Ping Gong, Department of General Surgery, The Second College of Clinical Medicine & the Second Affiliated Hospital of Chongqing University of Medical Science, 74 Linjiang Road, Chongqing 400010, China. gongjianping11@hotmail.com
Telephone: +86-28-5541610

Received 2001-09-26 Accepted 2001-11-08

Abstract

AIM: The objective of this study is to elucidate the potential role of poly-morphonuclear neutrophils (PMN) in the development of such a sinusoidal endothelial cell (SEC) injury during early acute obstructive cholangitis (AOC) in rats.

METHODS: Twenty one Wistar rats were divided into three groups: the AOC group, the bile duct ligated group (BDL group), and the sham operation group (SO group). The common bile duct (CBD) of rats in AOC group was dually ligated and 0.2ml of the *E. coli* O₁₁₁ B₄ (5×10^9 cfu/ml) suspension was injected into the upper segment, in BDL group, only the CBD was ligated and in SO group, neither injection of *E. coli* suspension nor CBD ligation was done, but the same operative procedure. Such group consisted of seven rats, all animals were killed 6h after the operation. Morphological changes of the liver were observed under light and electron microscope. Expression of intercellular adhesion molecule-1 (ICAM-1) mRNA in hepatic tissue was determined with reverse transcription polymerase chain reaction (RT-PCR). The serum levels of alanine aminotransferase (ALT) were determined with autoanalyser and cytokine-induced neutrophil chemoattractant (CINC) was determined by enzyme-linked immunosorbent assay (ELISA).

RESULTS: Neutrophils was accumulated in the hepatic sinusoids and sinusoidal endothelial cell injury existed in AOC group. In contrast, in rats of BDL group, all the features of SEC damage were greatly reduced. Expression of ICAM-1 mRNA in hepatic tissue in three groups were 7.54 ± 0.82 , 2.87 ± 0.34 , and 1.01 ± 0.12 , respectively. There were significant differences among three groups ($P < 0.05$). The serum CINC levels in the three groups were 188 ± 21 ng·L⁻¹, 94 ± 11 ng·L⁻¹, and 57 ± 8 ng·L⁻¹, respectively. There were also significant differences among the three groups ($P < 0.05$). Activity of the serum ALT was 917 ± 167 kat·L⁻¹, 901 ± 171 kat·L⁻¹, and 908 ± 164 kat·L⁻¹, respectively, ($P > 0.05$).

CONCLUSION: Hepatic SEC injury occurs earlier than hepatic parenchymal cells during AOC. Recruitments of circulating

neutrophils in the hepatic sinusoidal space might mediate the SEC injury, and ICAM-1 in the liver may modulate the PMN of accumulation.

Gong JP, Wu CX, Liu CA, Li SW, Shi YJ, Li XH, Peng Y. Liver sinusoidal endothelial cell injury by neutrophils in rats with acute obstructive cholangitis. *World J Gastroenterol* 2002;8(2):342-345

INTRODUCTION

Biliary tract infection, especially acute obstructive cholangitis (AOC) is common^[1,2]. Despite a multitude of advances in treatment of surgical infection, this remains a significant cause of morbidity and mortality^[3,4], where sepsis and endotoxemia from AOC are important causes of multiple organ failure (MOF) and deaths^[5-9]. Ohtsuka *et al*^[10] reported that polymorphonuclear neutrophils (PMN) accumulated in the hepatic sinusoidal space increased obviously in rats with obstructive jaundice and there were interaction between PMN and sinusoidal endothelial cells (SEC) causing injury during AOC. This study was study the potential role of PMN in the development of SEC injury and the mechanism of accumulation of PMN during early period of AOC.

MATERIALS AND METHODS

Animal Experiment

Male Wistar rats weighing 200-230g were purchased from Laboratory Animal Center of Chongqing University of Medical Science. These animals were divided into three groups: the AOC group, bile duct ligated group of (BDL group), and sham operation group (SO group). All the animals were killed 6 hour after operation, the surgical procedures were carried out under light diethyl ether anesthesia. The animal models were performed as follows. In AOC group, a 1.5cm medium incision was made over the upper abdomen, the common bile duct (CBD) was mobilized and dually ligated, and 0.2mL of the *E. coli* O₁₁₁ B₄ (5×10^{12} cfu·L⁻¹) (Sigma, USA) suspension was injected into the upper segment. In BDL group, the CBD was doubly ligated but without injection of *E. coli* O₁₁₁ B₄ suspension. In SO group, neither *E. coli* injection of suspension nor CBD ligation was done, but only routine operative procedure was performed. Seven rats constituted each group.

Serum ALT & CINC

Hepatic injury was assessed by measuring the serum alanine aminotransferase (ALT) which was performed with autoanalyser. The serum cytokine-induced neutrophil chemoattractant (CINC) concentration was measured by enzyme-linked immunosorbent assay (ELISA) according to the manufacturer's direction with a lower limit of 10ng·L⁻¹. For CINC, microtitre plates were coated with anti CINC mAb overnight at room temperature on a plate shaker, after the blockage, samples were then added. The detected antibody was biotinylated anti-CINC. Standard curves were made with a natural CINC calibrated against the WHO interim International Standard.

Expression of ICAM-1 mRNA in Hepatic Tissue

Total RNA was isolated from rat liver tissue by using the Trizol Reagent (Life Technologies, USA). The quality of RNA was controlled by the intactness of ribosomal RNA bands. A total of 0.5mg of each intact total RNA sample was reverse-transcribed to complementary DNA (cDNA) by using reverse transcription polymerase chain reaction (RT-PCR) kit (Roche, USA). cDNA was stored at -70°C until PCR analysis. The PCR primers used were ICAM-1: sense (5'-CTTCTCCTGCTCTGCAACCC-3'), antisense (5'-GGGAGAGCACATTCAGGTC-3'); β -actin: sense (5'-ACCACAGCTGAGAGGGAAATCG-3'), antisense (5'-AGAGGTCTTTACGGATGTCAACG-3'). The sizes of the amplified PCR products were 326 bp for ICAM-1 and 281 bp for β -actin. The procedure was as follows: denaturation at 95°C for 30sec, annealing at 55°C for 1min, and extension at 71°C for 1min for 28 cycles. The PCR products were electrophoresed in $20\text{g}\cdot\text{L}^{-1}$ agarose gels, and the gels were ethidium bromide stained and video photographed on an ultraviolet transilluminator. The bands representing reactive product were scanned by densitometer of a Bio-Image Analysis System (Doc Gel 2000). The relative optical density (ROD) values were expressed as the level of ICAM-1 mRNA in hepatic tissue.

Morphologic Observations of Hepatic Tissue

Liver samples from different liver lobes were fixed with $100\text{mL}\cdot\text{L}^{-1}$ buffered formalin or $25\text{g}\cdot\text{L}^{-1}$ glutaraldehyde immediately. For light microscopy, the tissue blocks were embedded in paraffin, and the sections were stained with hematoxylin and eosin (H&E). For transmission electron microscopy (TEM), the tissue blocks were embedded in Epon 618 resin and ultrathin sections were stained with uranyl acetate and lead citrate. A H-2000 transmission electron microscope was used.

Statistical Analysis

Results were presented as $\bar{x}\pm s$. Statistical difference was analysed by means of the analysis of Variance (ANOVA). $P<0.05$ is considered significant.

RESULTS

Accumulation of PMN in hepatic sinusoidal space

Accumulation of PMN in the hepatic sinusoidal space was found, under light microscopy, PMN counts in hepatic sinusoidal space increased significantly after 6h in AOC group in comparison with BDL group or SO group. Under electron microscopy, PMN were seen easily in hepatic sinusoidal space in AOC group (Figure 1A).

Sinusoidal endothelial cell injury

Under light microscopy, no distinct change in SEC could be shown in any of the above groups. Electron microscopically, however, focal detachment, decreased electron density of cytoplasm, and swollen or even vacuolated mitochondria in SEC could often be observed in the AOC group (Figure 1B). In this group, the Kupffer cells were enlarged, but normal surface structures were retained and no degenerative changes of the nucleus or cytoplasm were shown (Figure 1-C). In contrast such changes could be occasionally seen in the SEC of BDL group. No evident morphological changes of SEC could be observed in SO group.

Expression of ICAM-1 mRNA in hepatic tissue

Expression of ICAM-1 mRNA in hepatic tissues was distinctly enhanced after 6h in AOC group when compared to other two groups ($P<0.05$). There was less expression of ICAM-1 gene in BDL group and no expression of ICAM-1 gene in SO group (Figure 2).

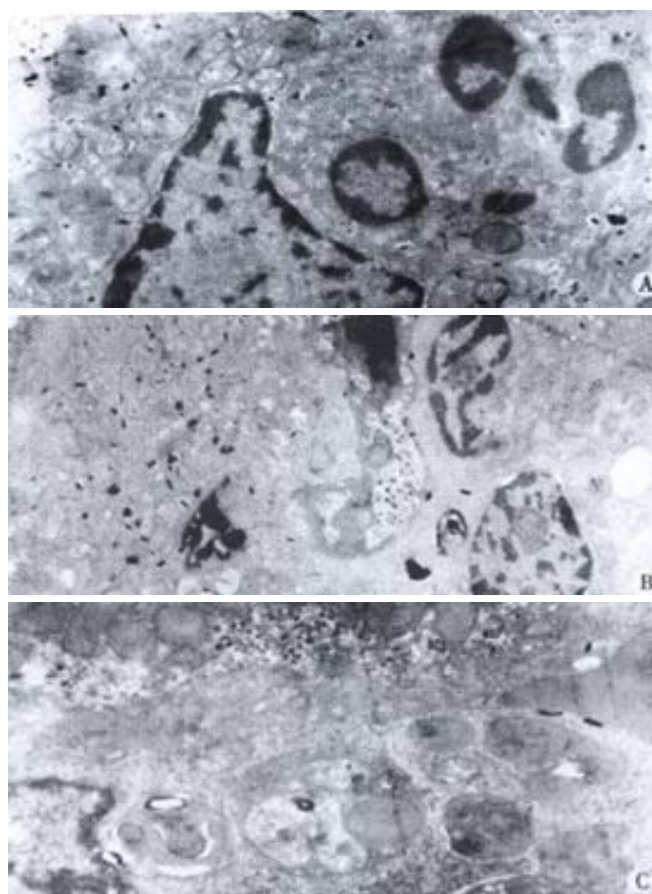


Figure 1 A: In AOC group, PMN was seen easily in hepatic sinusoidal. TEM $\times 4000$; B: In AOC group, two PMNs were seen in hepatic sinusoid with decreased electronic density of cytoplasm, and swollen or even vacuolated mitochondria in SEC. TEM $\times 3000$; C: In AOC group, KC was also seen easily in hepatic sinusoid with active phagocytosis. TEM $\times 4000$

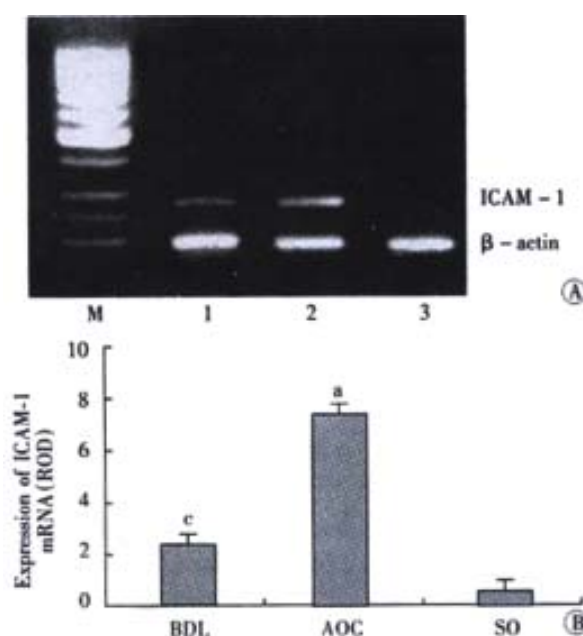


Figure 2 A: Expression of ICAM-1 mRNA. M, Marker. Lane 1: BDL; Lane 2: AOC; Lane 3: SO; B: Expression of ICAM-1 mRNA. $^aP<0.05$, vs other two groups, $^cP<0.05$, vs control group

The serum ALT level and CINC concentration

The serum ALT level and CINC concentration were shown in Table 1. The serum ALT activity in the three groups was evidently unchanged in the same period ($P>0.05$). but, the serum CINC concentration in the AOC group was significantly higher than that in the BDL group or the SO group ($P<0.05$).

Table 1 The changes of serum ALT level and CINC concentration in the three groups ($\bar{x}\pm s$, $n=7$)

Serum parameters	AOC	BDL	SO
ALT (nkat·L ⁻¹)	917±167	901±171	908±164
CINC (ng·L ⁻¹)	188±21 ^a	94±11 ^c	57±8

^a $P<0.05$, vs other two groups. ^c $P<0.05$, vs SO group.

DISCUSSION

Neutrophils and macrophages play a central role in the host defence against microbial infections. However, they also produce damage to normal tissue by releasing oxygen free radicals, elastase, and various cytokines^[11,12]. The hepatic sinusoidal endothelia are fenestrated allowing exchange of substance between the circulating blood and hepatocytes^[13]. The Kupffer cells are located at the luminal side of the SEC and is able to phagocytize pathogens and release cytokines, such as tumor necrosis factor- α (TNF- α), interleukin (IL)-1, IL-6, IL-8, and adhesion molecules ICAM-1 (CD54), etc^[14-16], these inflammatory cytokines and chemokines can be upregulated in inflammatory processes within the liver^[17-20]. Recent reports have revealed the interaction between neutrophils and SEC in sepsis, and neutrophils have the potential to cause endothelial cell injury by producing protease and superoxides^[13,16,21]. Overreaction of neutrophils may be responsible for organ failure in cholestatic rats^[10,12,22]. We found that accumulation of PMNs in the hepatic sinusoidal space was accompanied by SEC injury with decreased electron density of cytoplasm, and swollen or even vacuolated mitochondria in the early period of AOC. Our results indicated that damage of SEC occurred earlier than that of hepatic parenchymal cells and the vascular endothelium which was a critical and initial event in AOC and organ failure processes. SEC injury might develop microcirculatory disturbance in the liver, resulted in hepatocytic damage and hepatic dysfunction.

Although obvious parenchymal cell necrosis was not observed in our study, it is likely that the microcirculatory disturbance could provoke liver dysfunction during AOC. CINC, a member of IL-8 family and a major neutrophil chemotactic factor in rats, increased in the liver during sepsis^[23]. Substantial neutrophil accumulation in the liver and the role of these cells in the pathophysiology of liver injury was found in models of endotoxin shock and hepatic ischemia-reperfusion injury^[24-32]. But, the relationship between PMN accumulation, ICAM-1 expression and SEC injury during AOC is unclear. The injury to SECs was induced by the interaction of the activated PMNs and SECs via ICAM-1 and CD18^[33-37]. Ohtsuka *et al* reported ICAM-1 expression on SEC started to rise 6-12h after partial hepatectomy, reaching a peak after 24-48h. ICAM-1 is particularly expressed on Kupffer cells, endothelial cells, and leukocytes and it promotes accumulation of PMN in the hepatic sinusoids and is linked to endothelial cell injury^[38-52]. The mechanisms of upregulated ICAM-1 gene expression during AOC may included (1) inflammatory cytokines upregulate ICAM-1 expression in endotoxemia^[28]; (2) synthesis of ICAM-1 is increased and /or its elimination is decreased through the bile in bile duct ligated animals.

In conclusion, hepatic SEC injury occurs earlier than hepatic parenchymal cells damage during AOC. Recruitment of circulating neutrophils in the hepatic sinusoidal space enhance the SEC injury, and ICAM-1 in the liver can modulate the accumulation of PMN.

REFERENCES

- Huang ZQ. New development of biliary surgery in China. *World J Gastroenterol* 2000; 6:187-192
- Kimmings AN, van Deventer SJH, Rauws EAJ, Huibregtse K, Gouma DJ. Systemic inflammatory response in acute cholangitis and after subsequent treatment. *Eur J Surg* 2000; 166: 700-705
- Lillemoe KD. Surgical treatment of biliary tract infections. *Am Surg* 2000; 66: 138-144
- Gong JP, Liu CA, Wu CX, Li SW, Shi YJ, Li XH. Nuclear factor κ B activity in patients with acute severe cholangitis. *World J Gastroenterol* 2002; 8:346-349
- Ling YL, Meng AH, Zhao XY, Shan BE, Zhang JL, Zhang XP. Effect of cholecystokinin on cytokines during endotoxic shock in rats. *World J Gastroenterol* 2001; 7: 667-671
- Tomioaka M, Iinuma H, Okinaga K. Impaired Kupffer cell function and effect of immunotherapy in obstructive jaundice. *J Surg Res* 2000; 92:276-282
- Kordzaya DJ, Goderdzishvili VT. Bacterial translocation in obstructive jaundice in rats: role of mucosal lacteals. *Eur J Surg* 2000; 166: 367-374
- Kimmings AN, van Deventer SJH, Obertop H, Rauws EAJ, Huibregtse K, Gouma DJ. Endotoxin, cytokines, and endotoxin binding protein in obstructive jaundice and after preoperative biliary drainage. *Gut* 2000; 46: 725-731
- Gil LT, Rosello AM, Torres AC, Moreno RL, Orihuela JAF. Modulation of soluble phases of endothelial/leukocyte adhesion molecule 1, intercellular adhesion molecule 1, and vascular cell adhesion molecule 1 with interleukin-1 β after experimental endotoxin challenge. *Crit Care Med* 2001; 29: 776-781
- Ohtsuka M, Miyazaki M, Kubosawa H, Kondo Y, Ito H, Shimizu H, Shimizu Y, Nozawa S, Furuya S, Nakajima N. Role of neutrophils in sinusoidal endothelial cell injury after extensive hepatectomy in cholestatic rats. *J Gastroenterol Hepatol* 2000; 15: 880-886
- Xu MQ, Gong JP, Xue L, Han BL, Xu F. Effects of Kupffer cell NF- κ B activation on liver regeneration after partial hepatectomy in biliary obstructive rats. *Di-San Junyi Daxue Xuebao* 2001; 23: 1143-1145
- Ito Y, Machen NW, Urbaschek R, McCuskey RS. Biliary obstruction exacerbates the hepatic microvascular inflammatory response to endotoxin. *Shock* 2000; 14: 599-604
- Braet F, Zanger RD, Spector I, Wisse E. Structure and dynamics of hepatic endothelial fenestrae. *World J Gastroenterol* 2000; 6(Suppl): 1
- Bone-Larson CL, Simpson KJ, Colletti LM, Lukacs NW, Chen SC, Lira S, Kunkel SL, Hogaboam CM. The role chemokines in the immunopathology of the liver. *Immunol Rev* 2000; 177:8-20
- Han DW. The clinical sine of subsequent liver injury induced by gut derived endotoxemia. *Shijie Huaren Xiaohua Zazhi* 1999; 7: 1055-1058
- Liu BH, Chen HS, Zhou JH, Xiao N. Effects of endotoxin on endothelin receptor in hepatic and intestinal tissues after endotoxemia in rats. *World J Gastroenterol* 2000; 6:298-300
- Zhang SC, Dai Q, Wang JY, He BM, Zhou K. Gut-derived endotoxemia: one of the factors leading to production of cytokines in liver diseases. *World J Gastroenterol* 2000; 6(Suppl): 16
- Lin E, Calvano SE, Lowry SF. Inflammatory cytokines and cell response in surgery. *Surgery* 2000; 127:117-126
- Gong JP, Xu MQ, Zhu J, Han BL, Li K. Expression of CD14 in Kupffer cells induced by lipopolysaccharide. *Di-San Junyi Daxue Xuebao* 2001; 23: 425-428
- Koo DJ, Chaudry IH, Wang P. Kupffer cells are responsible for producing inflammatory cytokines and hepatocellular dysfunction during early sepsis. *J Surg Res* 1999; 83: 151-157
- Hardaway RM. A review of septic shock. *Am Surg* 2000; 66: 22-27
- Roggin KK, Papa EF, Kurkchubasche AG, Tracy TF. Kupffer cell inactivation delays repair in a rat model of reversible biliary obstruction. *J Surg Res* 2000; 90: 166-173
- Bautista AP. Impact of alcohol on the ability of Kupffer cells to produce chemokines and its role in alcoholic liver disease. *J Gastroenterol Hepatol* 2000; 15: 349-356
- Deaciuc IV, D'Souza NB, Sarphie TG, Schmidt J, Hill DB, McClain CJ. Effects of exogenous superoxide anion and nitric oxide on the scavenging function and electron microscopic appearance of the sinusoidal endothelium in the isolated, perfused rat liver. *J Hepatol* 1999; 30:213-221
- Fan K. Regulatory effects of lipopolysaccharide in murine macrophage proliferation. *World J Gastroenterol* 1998; 4:137-139
- Angus DC, Linde-Zwirble WT, Lidicker J, Clermont G, Carcillo J, Pinsky MR. Epidemiology of severe sepsis in the United States: Analysis of incidence, outcome, and associated costs of care. *Crit Care Med* 2001; 29: 1303-1310
- Roy DL, Padova FD, Adachi Y, Glauser MP, Calandra T, Heumann D. Critical role of lipopolysaccharide-binding protein and CD14 in immune responses against gram-negative bacteria. *J Immunol* 2001; 167: 2759-2765
- Wu RQ, Xu YX, Song XH, Chen LJ, Meng XJ. Adhesion molecule and proinflammatory cytokine gene expression in hepatic sinusoidal endothelial cells following cecal ligation and puncture. *World J Gastroenterol* 2001;

- 7: 128-130
- 29 Jackson GDF, Dai Y, Sewell WA. Bile mediates intestinal pathology in exdotoxemia in rats. *Infect Immun* 2000; 68: 4714-4719
 - 30 Knolle PA, Gerken G. Local control of the immune response in the liver. *Immunol Rev* 2000; 174:21-34
 - 31 Gong JP, Han BL. Effects of CD14 in LPS mediating activation of Kupffer cells. *Shijie Huaren Xiaohua Zazhi* 1999;7:875-877
 - 32 Bai XY, Jia XH, Cheng LZ, Gu YD. Influence of IFN α -2b and BCG on the release of TNF and IL-1 by Kupffer cells in rats with hepatoma. *World J Gastroenterol* 2001; 7: 419-421
 - 33 Guo XW, Dudman NP. Homocysteine induces expressions of adhesive molecules on leukocytes in whole blood. *Chin Med J* 2001;114:1235-1239
 - 34 Mack C, Jungermann K, Gotze O, Schieferdecker HL. Anaphylatoxin C5a actions in rat liver: synergistic enhancement by C5a of lipopolysaccharide-dependent $\alpha 2$ -macroglobulin gene expression in hepatocytes via IL-6 release from Kupffer cells. *J Immunol* 2001; 167: 3972-3979
 - 35 Hedin KE, Kaczynski JA, Gibson MR, Urrutia R. Transcription factors in cell biology, surgery, and transplantation. *Surgery* 2000; 128: 1-5
 - 36 Lehmann C, Konig JP, Dettmann J, Birnbaum J, Kox WJ. Effects of iloprost, a stable prostacyclin analog, on intestinal leukocyte adherence and microvascular blood flow in rat experimental endotoxemia. *Crit Care Med* 2001; 29:1412-1416
 - 37 Soler-Rodriguez AM, Zhang H, Lichenstein HS, Qureshi N, Niesel DW, Crowe SE, Peterson JW, Klimpel GR. Neutrophil activation by bacterial lipoprotein versus lipopolysaccharide: differential requirements for serum and CD14. *J Immunol* 2000; 164: 2674-2683
 - 38 Neubauer K, Ritzel A, Saile B, Ramadori G. Decrease of platelet-endothelial cell adhesion molecule-1 gene-expression in inflammatory cells and in endothelial cells in the rat liver following CCl₄-administration and in vitro after treatment with TNF α . *Immunol Lett* 2000; 74: 153-64
 - 39 Madorin WS, Cepinskas G, Kvietys PR. Peritonitis induces rat cardiac myocytes to promote polymorphonuclear leukocyte emigration and activate endothelial cells: Effect of lipopolysaccharide pretreatment. *Crit Care Med* 2001; 29: 1774-1779
 - 40 Emmanuils K, Weighardt H, Maier S, Gerauer K, Fleischmann T, Zheng XX, Hancock WW, Holzmann B, Heidecke CD. Critical role of Kupffer cell-derived IL-10 for host defense in septic peritonitis. *J Immunol* 2001; 167: 3919-3927
 - 41 Funda DP, Tuckova L, Farre MA, Iwase T, Moroi I, Tlaskalova-Hogenova H. CD14 is expressed and released as soluble CD14 by human intestinal epithelial cells *in vitro*: lipopolysaccharide activation of epithelial cells revisited. *Infect Immun* 2001; 69: 3772-3781
 - 42 Assy N, Jacob G, Spira G, Edoute Y. Diagnostic approach to patients with cholestatic jaundice. *World J Gastroenterol* 1999; 5: 252-262
 - 43 Zuo GQ, Gong JP, Liu CA, Li SW, Wu XC, Yang K, Li Y. Expression of lipopolysaccharide binding protein and its receptor CD14 in experimental alcoholic disease. *World J Gastroenterol* 2001; 7: 836-840
 - 44 Seki S, Habu Y, Kawamura T, Takeda K, Dobashi H, Ohkawa T, Hiraide H. The liver as a crucial organ in the first line of host defence: the role of Kupffer cells, natural killer (NK) cells and NK1.1 Ag+ T cells in T helper 1 immune responses. *Immunol Rev* 2000; 174: 35-46
 - 45 Arai M, Peng XX, Currin RT, Thurman RG, Lemasters JJ. Protection of sinusoidal endothelial cells against storage/reperfusion injury by prostaglandin E₂ derived from Kupffer cells. *Transplantation* 1999;68: 440-445
 - 46 Watanabe M, Chijiwa K, Kameoka N, Yamaguchi K, Kuroki S, Tanaka M. Gadolinium pretreatment decreases survival and impairs liver regeneration after partial hepatectomy under ischemia/reperfusion in rats. *Surgery* 2000; 127: 456-463
 - 47 Enomoto N, Ikejima K, Yamashina S. Kupffer cell-derived prostaglandin E₂ is involved in alcohol-induced fat accumulation in rat liver. *Am J Physiol Gastrointest Liver Physiol* 2000; 279: G100-G106
 - 48 Wang LS, Zhu HM, Zhou DY, Wang YL, Zhang WD. Influence of whole peptidoglycan of bifidobacterium on cytotoxic effectors produced by mouse peritoneal macrophages. *World J Gastroenterol* 2001; 7: 440-443
 - 49 Islam AFMW, Moss ND, Dai Y, Smith MSR, Collins A, Jackson GDF. lipopolysaccharide-induced biliary factors enhance invasion of *Salmonella enteritidis* in a rat model. *Infect Immun* 2000; 68: 1-5
 - 50 Gong JP, Wu CX, Liu CA, Li SW, Shi YJ, Yang K, Li Y, Li XH. Intestinal damage mediated by Kupffer cells in rats with endotoxemia. *World J Gastroenterol* 2002; 8: press
 - 51 Sindram D, Porte RJ, Hoffman MR, Bentley RC, Clavien PA. Synergism between platelets and leukocytes in inducing endothelial cell apoptosis in the cold ischemic rat liver: a Kupffer cell mediated injury. *FASEB J* 2001; 15: 1230-1232
 - 52 Li SW, Gong JP, Wu CX, Shi YJ, Liu CA. Lipopolysaccharide induced synthesis of CD14 proteins and its gene expression in hepatocytes during endotoxemia. *World J Gastroenterol* 2002; 8: 124-127

Edited by Wu XN

• BASIC RESEARCH •

Nuclear factor κ B activity in patients with acute severe cholangitis

Jian-Ping Gong, Chong-An Liu, Chuan-Xin Wu, Sheng-Wei Li, Yu-Jun Shi, Xu-Hong Li

Jian-Ping Gong, Chong-An Liu, Chuan-Xin Wu, Sheng-Wei Li, Yu-Jun Shi, Xu-Hong Li, Department of General Surgery, The Second College of Clinical Medicine & the Second Affiliated Hospital of Chongqing University of Medical Science, 74 Linjiang Road, Central District, Chongqing 400010, China

Supported by the National Natural Science Foundation of China, No. 39970719, 30170919

Correspondence to: Dr. Jian-Ping Gong, Department of General Surgery, The Second College of Clinical Medicine & the Second Affiliated Hospital of Chongqing University of Medical Science, 74 Linjiang Road, Central District, Chongqing 400010, China. gongjianping11@hotmail.com
Telephone: +86-23-63766701 Fax: +86-23-63822815

Received 2001-09-14 Accepted 2001-10-22

Abstract

AIM: To determine the NF- κ B activity in peripheral blood mononuclear cells (PBMC) in patients with acute cholangitis of severe type (ACST) and correlate the degree of NF- κ B activation with severity of biliary tract infection and clinical outcome.

METHODS: Twenty patients with ACST were divided into survivor group (13 cases) and nonsurvivor group (7 cases). Other ten patients undergoing elective gastrectomy or inguinal hernia repair were selected as control group. Peripheral blood samples were taken 24 hours postoperatively. PBMC were separated by density gradient centrifugation, then nuclear proteins were isolated from PBMC, and Electrophoretic Mobility Shift Assay (EMSA) used determined. The results were quantified by scanning densitometer of a Bio-Image Analysis System and expressed as relative optical density (ROD). The levels of TNF- α , IL-6, and IL-10 in the plasma of patients with ACST and healthy control subjects were determined by using an enzyme-linked immunoassay (ELISA).

RESULTS: The NF- κ B activity was 5.02 ± 1.03 in nonsurvivor group, 2.98 ± 0.51 in survivor group and 1.06 ± 0.34 in control group. There were statistical differences in three groups ($P < 0.05$). The levels of TNF- α and IL-6 in plasma were $(498 \pm 53) \text{ ng} \cdot \text{L}^{-1}$ and $(587 \pm 64) \text{ ng} \cdot \text{L}^{-1}$ in nonsurvivor group, $(284 \pm 32) \text{ ng} \cdot \text{L}^{-1}$ and $(318 \pm 49) \text{ ng} \cdot \text{L}^{-1}$ in survivor group and $(89 \pm 11) \text{ ng} \cdot \text{L}^{-1}$ and $(102 \pm 13) \text{ ng} \cdot \text{L}^{-1}$ in control group. All patients with ACST had increased levels of TNF- α and IL-6, which were many-fold greater than those of control group, and there was an evidence of significantly higher levels in those of nonsurvivor group than that in survivor group ($P < 0.05$). The levels of IL-10 in plasma were $(378 \pm 32) \text{ ng} \cdot \text{L}^{-1}$, $(384 \pm 37) \text{ ng} \cdot \text{L}^{-1}$ and $(68 \pm 11) \text{ ng} \cdot \text{L}^{-1}$ in three groups, respectively. All patients had also increased levels of IL-10 when compared with control group ($P < 0.05$), but the IL-10 levels were not significantly higher in nonsurvivors than in survivors ($P > 0.05$).

CONCLUSION: NF- κ B activity in PBMC in patients with ACST

increases markedly and the degree of NF- κ B activation is correlated with severity of biliary tract infection and clinical outcome.

Gong JP, Liu CA, Wu CX, Li SW, Shi YJ, Li XH. Nuclear factor κ B activity in patients with acute severe cholangitis. *World J Gastroenterol* 2002; 8(2):346-349

INTRODUCTION

Acute cholangitis of severe type (ACST) is a common problem facing today's surgeons^[1-3]. Despite a multitude of advances in the area of surgical infection and surgical or nonsurgical interventions to treat biliary tract diseases, ACST and biliary sepsis remain a significant cause of morbidity and mortality^[4-9]. Many reports have focused on aspects of the proinflammatory cytokines which are believed to be central to the pathophysiology of the sepsis syndrome^[10-11]. Recent investigations have shown that expression of many cytokines is closely linked to the activation of transcriptional factors^[12-13]. Among several transcriptional regulatory factors involved in immuno-regulatory genes expression, nuclear factor kappa B (NF- κ B) acts as a critical step for directing the transcription of many proinflammatory cytokine genes in animal models of sepsis or endotoxemia^[14-16]. Investigations regarding the role of NF- κ B in human inflammatory diseases are scarce^[17-20]. So far, no study has aimed to examine in patients with ACST the relationship among NF- κ B activity in peripheral blood mononuclear cells (PBMC), the concentrations of the pro-inflammatory cytokines in plasma, and clinical outcome. The purpose of this study was to determine the NF- κ B DNA binding activity in circulating blood cells and the cytokines tumor necrosis factor alpha (TNF- α), interleukin (IL)-6, and IL-10 profile in patients with ACST. Attempts were made also to correlate degree of NF- κ B activation with severity of biliary tract infection and clinical outcome.

MATERIALS AND METHODS

Patients

The study population was recruited from a series of 20 patients with a clinical diagnosis of ACST. Among them, 13 were male, and 7 female, ranging in age from 27 to 78 yr. All patients had manifestations of fever, chill, jaundice, and right upper quadrant pain. Other manifestations included two or more of the following clinical conditions: Blood cultures were positive; Core body temperature $>39^{\circ}\text{C}$ or $<36^{\circ}\text{C}$; Heart rate >120 beats/min; Hypotension: A systolic blood pressure of <12.0 kPa or a reduction of >5.33 kPa from baseline in the absence of other causes of hypotension; White blood cell count $>1.5 \times 10^9 \text{ L}^{-1}$. These patients were divided into nonsurvivor group (7 cases) and survivor group (13 cases). Ten patients undergoing elective gastrectomy or inguinal hernia repair were selected as control group. Peripheral blood samples were taken 24h postoperatively.

Isolation of PBMC

PBMC were separated by density gradient centrifugation, as previously described^[18]. In brief, PBMC were isolated from blood

freshly collected on sodium citrate by centrifugation on Ficoll-Hypaque. Before Ficoll, a fraction of the blood was centrifuged 5min at $1500r \cdot \text{min}^{-1}$ and 1mL of plasma was collected and put immediately at -20°C for further cytokine measurements.

Isolation of nuclear proteins

Nuclear proteins were isolated from PBMC extract by placing the sample in 0.8mL of ice-cold hypotonic buffer [$10\text{mmol} \cdot \text{L}^{-1}$ HEPES (pH7.9), 10mL KCL, $0.1\text{mmol} \cdot \text{L}^{-1}$ EDTA, $0.1\text{mmol} \cdot \text{L}^{-1}$ ethylene glycol tetraacetic acid, $1\text{mmol} \cdot \text{L}^{-1}$ DTT; Protease inhibitors (aprotinin, pepstatin, and leupeptin, $10\text{mg} \cdot \text{L}^{-1}$ each)]. The homogenates were incubated on ice for 20min, vortexed for 20s after adding $50\mu\text{L}$ of 10 per cent Nonidet P-40, and then centrifuged for 1 minute at 4°C in an Eppendorf centrifuge. Supernatants were decanted, the nuclear pellets after a single wash with hypotonic buffer without Nonidet P-40 were suspended in an ice-cold hypertonic buffer [$20\text{mmol} \cdot \text{L}^{-1}$ HEPES (pH7.9), $0.4\text{mol} \cdot \text{L}^{-1}$ NaCL, $1\text{mmol} \cdot \text{L}^{-1}$ EDTA, $1\text{mmol} \cdot \text{L}^{-1}$ DTT; Protease inhibitors], incubated on ice for 30min at 4°C , mixed frequently, and centrifuged for 15min at 4°C . The supernatants were collected as nuclear extracts and stored at -70°C . Concentrations of total proteins in the samples were determined according to the method of Bradford.

Electrophoretic Mobility Shift Assay (EMSA)

NF- κ B binding activity was performed in a 10- μL binding reaction mixture containing $1 \times$ binding buffer [$50\text{mg} \cdot \text{L}^{-1}$ of double-stranded poly(dI-dC), $10\text{mmol} \cdot \text{L}^{-1}$ Tris-HCl (pH 7.5), $50\text{mmol} \cdot \text{L}^{-1}$ NaCl, $0.5\text{mmol} \cdot \text{L}^{-1}$ EDTA, $0.5\text{mmol} \cdot \text{L}^{-1}$ DTT, $1\text{mmol} \cdot \text{L}^{-1}$ MgCl_2 , and $100\text{mL} \cdot \text{L}^{-1}$ glycerol], $5\mu\text{g}$ of nuclear protein, and 35 fmol of double-stranded NF- κ B consensus oligonucleotide ($5'$ -AGT TGA GGG GAC TTT CCC AGG- $3'$) that was endly labeled with γ - ^{32}P (111TBq mmol^{-1} at 370GBq L^{-1}) using T4 polynucleotide kinase. The binding reaction mixture was incubated at room temperature for 20min and analyzed by electrophoresis on 7 per cent nondenaturing polyacrylamide gels. After electrophoresis the gels were dried by Gel-Drier (Bio-Rad Laboratories, Hercules, CA) and exposed to Kodak X-ray films at -70°C .

Quantifying with the Phosphor Imager

The binding bands were quantified by scanning densitometer of a Bio-Image Analysis System. The results were expressed as relative optical density (ROD).

Measurement of cytokines in plasma

TNF- α , IL-6, and IL-10 levels in the plasma of patients with ACST and healthy control subjects were determined with using an enzyme-linked immunoassay (ELISA). The detection limits of the assays were $50\text{ng} \cdot \text{L}^{-1}$ (TNF- α), $49\text{ng} \cdot \text{L}^{-1}$ (IL-6), and $49\text{ng} \cdot \text{L}^{-1}$ (IL-10). All cytokines assays were performed in duplicate and had intra- and interassay variations lower than 8% and 11%, respectively.

Statistical Analysis

Data were analyzed with using Microsoft Excel with Astute statistical add-in and were expressed as median \pm standard error. A value of $P \leq 0.05$ was considered statistically significant.

RESULTS

Methods

The patients of nonsurvivor group died within 35d, all from complications of SIRS, sepsis or MOF. The patients of survivor group were well discharged from hospital postoperatively in 28 days. The median age in nonsurvivor group was 54 yr, which was not significantly different from that of survivor group (53yr) ($P > 0.05$).

An admission APACHE II score in nonsurvivor group was 25, which was also not different from that of survivor group (24) ($P > 0.05$).

The NF- κ B activity was 5.02 ± 1.03 in nonsurvivor group, 2.98 ± 0.51 in survivor group and 1.06 ± 0.34 in control group. There were statistical differences in three groups ($P < 0.05$). The NF- κ B activity increased in all patients with ACST, versus the control group ($P < 0.05$), and the patients of nonsurvivor group had higher levels of NF- κ B activation than those of survivor group ($P < 0.05$, Figure 1).

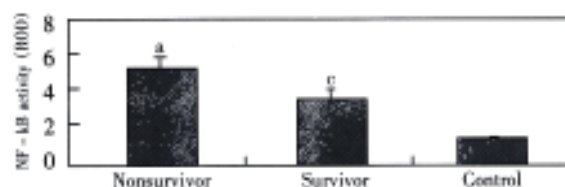


Figure 1 The activity of NF- κ B in three groups. ^a $P < 0.05$, vs other groups, ^c $P < 0.05$, vs control.

The levels of TNF- α and IL-6 in plasma were $(498 \pm 53)\text{ng} \cdot \text{L}^{-1}$ and $(587 \pm 64)\text{ng} \cdot \text{L}^{-1}$ in nonsurvivor group, $(284 \pm 32)\text{ng} \cdot \text{L}^{-1}$ and $(318 \pm 49)\text{ng} \cdot \text{L}^{-1}$ in survivor group and $(89 \pm 11)\text{ng} \cdot \text{L}^{-1}$ and $(102 \pm 13)\text{ng} \cdot \text{L}^{-1}$ in control group. All patients with ACST had increased levels of TNF- α and IL-6, which were many-fold greater than those of control group, and there was an evidence of significantly higher levels in those of nonsurvivor group than that in survivor group ($P < 0.05$). The levels of IL-10 in plasma were $(378 \pm 32)\text{ng} \cdot \text{L}^{-1}$, $(384 \pm 37)\text{ng} \cdot \text{L}^{-1}$ and $(68 \pm 11)\text{ng} \cdot \text{L}^{-1}$ in three groups, respectively. All patients had also increased levels of IL-10 when compared with control group ($P < 0.05$), but the IL-10 levels were not significantly higher in nonsurvivors than in survivors ($P > 0.05$). (Figure 2).

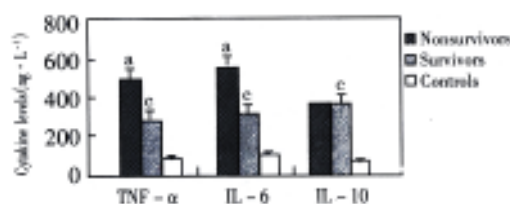


Figure 2 Changes of cytokines in plasma. ^a $P < 0.05$, vs other groups, ^c $P < 0.05$, vs control

DISCUSSION

The overwhelming inflammatory response in patients with ACST is a major cause which induces systemic inflammatory response syndrome (SIRS) and MOF^[1-4]. Mortality in patients with ACST reflects a multifactorial pathology, and neither cytokine concentrations in plasma nor even the APACHE II score can be expected to accurately predict patients' outcomes^[5-9]. NF- κ B is a protein found in inflammatory cells such as lymphocytes, monocytes, and macrophages. NF- κ B activation is stimulated by LPS, TNF- α , and IL-1, the very early mediators or factors in the inflammatory cascade^[21,22]. Once stimulated NF- κ B activates various parts of the inflammatory responses: TNF- α , IL-6 and IL-10, and adhesion molecules such as selectins and integrin^[23-25]. These mediators and factors then promote further activity of the inflammatory cascade and "off" goes the SIRS and MOF^[2,8,9,24]. Therefore, we chose to focus on NF- κ B as an important regulatory factor to regulate the expression of multiple cytokine genes. NF- κ B is a ubiquitous transcription factor involved in the signal transduction pathway of many inducers of the inflammatory response and is therefore a potentially attractive target for

immunomodulation to reduce sepsis and organ dysfunction^[26], but we are not yet clear about changes of NF- κ B and relation between NF- κ B and cytokines in patients with ACST. Foulds *et al*^[20] reported that levels of nuclear-bound NF- κ B (activated NF- κ B) were greater in patients who developed organ dysfunction after surgery, and patients with lower levels of nuclear NF- κ B who recovered from surgery without organ dysfunction. Bohrer *et al* investigated activity of NF- κ B in nuclear extracts from PBMC of 15 patients with sepsis, of whom 10 survived. NF- κ B activity was measured on days 1, 2, 3, 4, 5, 6, 8, 10, and 14 after admission where available. All patients with NF- κ B binding activity exceeding 200% of day 1 died. This small study concluded that NF- κ B activation might be an important event in clinical sepsis. But, Adib-Conquy *et al*^[27] found the expression of NF- κ B was significantly reduced for all patients with sepsis and trauma as compared with control subjects. In our study, by comparing the predictive value of measuring NF- κ B activity in PBMC and the concentrations of some pro- and anti-inflammatory mediators in plasma in patients with ACST, we found that the NF- κ B activity measured in the PBMC was a better overall predictor of mortality than the balance and time course of pro- and anti-inflammatory cytokines released in plasma. On the basis of these results NF- κ B would seem to be a more sensitive molecular marker assay when compared with cytokines used as an indicator of sepsis. The expressions of many genes involved in the inflammatory and immune processes are regulated by NF- κ B, TNF- α , IL-6, and IL-10, and they possess NF- κ B binding sites in the promoter region, enabling messenger ribonucleic acid to express in response to extracellular stimuli^[28-31]. TNF- α , IL-6, and IL-10 have all been implicated in the pathogenesis of SIRS and MOF that results from trauma, injury, infection, and sepsis^[32-43]. In the present study, we found that TNF- α and IL-6 were elevated in the patients with ACST and there were higher levels of TNF- α and IL-6 in patients who survived than in patients who died, which is in agreement with previous reports. These previous studies also showed that levels were higher in patients with sepsis when compared with trauma patients. We found significant relationship between NF- κ B activation and circulating concentrations of TNF- α and IL-6. IL-10, as an anti-inflammatory mediator, was elevated in the patients with ACST but reduced in patients who died. There might be other transcription factor as AP-1 involved in the signal transduction pathway of the inflammatory response^[16,21,23,44-48] and its mechanism is going on.

In conclusion, we have shown NF- κ B activation in PBMCs in patients with ACST increased markedly before death and was related to plasma TNF- α and IL-6 concentrations. These findings have important implications for the development of future therapeutic interventions in the critically ill and support the need for further study of the role of NF- κ B activation in mortality from ACST and MOF.

REFERENCES

- Huang ZQ. New development of biliary surgery in china. *World J Gastroenterol* 2000; 6: 187-192
- Kimmings AN, Deventer SJH, Rauws EAJ, Huibregtse K, Gouma DJ. Systemic inflammatory in acute cholangitis and after subsequent treatment. *Eur J Surg* 2000; 166: 700-705
- Lillemoe KD. Surgical treatment of biliary tract infections. *Am Surg* 2000; 66: 138-144
- Fry DE. Sepsis syndrome. *Am Surg* 2000; 66: 126-132
- Parker SJ, Watkins PE. Experimental models of gram-negative sepsis. *Br J Surg* 2001; 88:22-30
- Tabrizi AR, Zehnbauser BA, Freeman BD, Buchman TG. Genetic markers in sepsis. *J Am Coll Surg* 2001; 192: 106-117
- Jackson GDF, Dai Y, Sewell WA. Bile mediates intestinal pathology in endotoxemia in rats. *Infect Immun* 2000; 68: 4714-4719
- Islan AFMW, Moss NM, Dai Y, Smith MSR, Collins AM, Jackson GDF. Lipopolysaccharide-induced biliary factors enhance invasion of salmonella enteritidis in a rat model. *Infect Immun* 2000; 68: 1-5
- Erwin PJ, Lewis H, Dolan S, Tobias PS, Schumann RR, Lamping N, Wisdom GB, Rowlands BJ, Halliday MI. Lipopolysaccharide binding protein in acute pancreatitis. *Crit Care Med* 2000; 28: 104-109
- Kordzaya DJ, Goderdzishvili VT. Bacterial translocation in obstructive jaundice in rats: role of mucosal lacteals. *Eur J Surg* 2000; 166: 367-374
- Kimmings AN, van Deventer SJH, Obertop H, Rauws EAJ, Huibregtse K, Gouma DJ. Endotoxin, cytokines, and endotoxin binding protein in obstructive jaundice and after preoperative biliary drainage. *Gut* 2000; 46: 725-731
- Ohtsuka M, Miyazaki M, Kubosawa H, Kondo Y, Ito H, Shimizu H, Shimizu Y, Nozawa S, Furuya S, Nakajima N. Role of neutrophils in sinusoidal endothelial cell injury after extensive hepatectomy in cholestatic rats. *J Gastroenterol Hepatol* 2000; 15: 880-886
- Ito Y, Machen NW, Urbaschek R, McCuskey RS. Biliary obstruction exacerbates the hepatic microvascular inflammatory response to endotoxin. *Shock* 2000; 14: 599-604
- Han SJ, Choi JH, Ko HM, Yang HW, Choi II W, Lee HK, Lee OH, Im SY. Glucocorticoids prevent NF- κ B activation by inhibiting the early release of platelet-activating factor in response to lipopolysaccharide. *Eur J Immunol* 1999; 29: 1334-1341
- West MA, Clair L, Kraatz J, Rodriguez JL. Endotoxin tolerance from lipopolysaccharide pretreatment induces nuclear factor- κ B alterations not present in C3H/HeJ mice. *J Trauma* 2000; 49: 298-305
- Reddy SAG, Huang JH, Liao WSL. Phosphatidylinositol 3-kinase as a mediator of TNF-induced NF- κ B activation. *J Immunol* 2000; 164: 1355-1363
- Paterson RL, Galley HF, Dhillon JK, Webster NR. Increased nuclear factor κ B activation in critically ill patients who die. *Crit Care Med* 2000; 28: 1047-1051
- Arnalich F, Garcia-Palomero E, Lopez J, Jimenez M, Madero R, Renart J, Vazquez JJ, Montiel C. Predictive value of nuclear factor κ B activity and plasma cytokine levels in patients with sepsis. *Infect Immun* 2000; 68: 1942-1945
- Pennington C, Dunn J, Li C, Ha T, Browder W. Nuclear factor κ B activation in acute appendicitis: a molecular marker for extent of disease? *Am Surg* 2000; 66: 914-919
- Foulds S, Galustian C, Mansfield AO, Schachter M. Transcription factor NF- κ B expression and postsurgical organ dysfunction. *Ann Surg* 2001; 233: 70-78
- Kono H, Wheeler MD, Rusyn I, Lin M, Seabra V, Rivera CA, Bradford BU, Forman DT, Thurman RG. Gender differences in early alcohol-induced liver injury: role of CD14, NF- κ B, and TNF- α . *Am J Gastrointest Liver Physiol* 2000; 278:G652-661
- Ninomiya-Tsuji J, Kishimoto K, Hiyama A, Inoue J, Cao Z, Matsumoto K. The kinase TAK1 can activate the NIK-I κ B as well as the MAP kinase cascade in the IL-1 signalling pathway. *Nature* 1999; 398: 252-256
- Hedin KE, Kaczynski JA, Gibson MR, Urrutia R. Transcription factors in cell biology, surgery, and transplantation. *Surgery* 2000; 128: 1-5
- Starkel P, Horsmans Y, Sempoux C, Saeger CD, Wary J, Lause P, Maier D, Lambotte L. After portal branch ligation in rat, nuclear factor κ B, interleukin-6, signal transducers and activators of transcription 3, c-fos, c-myc, and c-jun are similarly induced in the ligated and nonligated lobes. *Hepatology* 1999; 29:1463-1470
- Matsukawa A, Hogaboam CM, Lukacs NW, Lincoln PM, Evanoff HL, Strieter RM, Kunkel S. Expression and contribution of endogenous IL-13 in an experimental model of sepsis. *J Immunol* 2000; 164: 2738-2744
- Jiang Q, Akashi S, Miyake K, Petty HR. Cutting Edge: lipopolysaccharide induces physical proximity between CD14 and Toll-like receptor 4 (TLR4) prior to nuclear translocation of NF- κ B. *J Immunol* 2000; 165: 3541-3544
- Adib-Conquy M, Adrie C, Moine P, Asehnoune K, Fitting C, Pinsky MR, Dhainaut JF, Cavaillon JM. NF- κ B expression in mononuclear cells of patients with sepsis resembles that observed in lipopolysaccharide tolerance. *Am J Respir Crit Care Med* 2000; 162: 1877-1883
- Heumann D, Adachi Y, Roy DL, Ohno N, Yadoma T, Glauser MP, Calandra T. Role of plasma, lipopolysaccharide-binding protein, and CD14 in response of mouse peritoneal exudate macrophage to endotoxin. *Infect and Immun* 2001; 69: 378-385
- Belich MP, Salmeron A, Johnston LH, Ley SC. TPL-2 kinase regulates the proteolysis of the NF- κ B-inhibitory protein NF- κ B1 p105. *Nature* 1999; 397: 363-368
- Bone-Larson CL, Simpson KJ, Colletti LM, Lukacs NW, Chen SC, Lira S, Kunkel S, Hogaboam CM. The role chemokines in the immunopathology of the liver. *Immunol Rev* 2000; 177:8-20
- Han DW. The clinical sine of subsequent liver injury induced by gut derived endotoxemia. *Shijie Huaren Xiaohua Zazhi* 1999; 7: 1055-1058
- Zhang SC, Dai Q, Wang JY, He BM, Zhou K. Gut-derived endotoxemia: one of the factors leading to production of cytokines in liver diseases. *World J Gastroenterol* 2000; 6(Suppl): 16
- Lin E, Calvano SE, Lowry SE. Inflammatory cytokines and cell response in surgery. *Surgery* 2000; 127:117-126
- Gong JP, Xu MQ, Li K, Zhu J, Han BL. Expression of CD14 in Kupffer cells induced by lipopolysaccharide. *Acta Acad Med Mil Tert* 2001; 23:

- 425-428
- 35 Koo DJ, Chaudry IH, Wang P. Kupffer cells are responsible for producing inflammatory cytokines and hepatocellular dysfunction during early sepsis. *J Surg Res* 1999; 83: 151-157
- 36 Hardaway RM. A review of septic shock. *Am Surg* 2000; 66: 22-27
- 37 Sindram D, Porte RJ, Hoffman MR, Bentley RC, Clavien PA. Synergism between platelets and leukocytes in inducing endothelial cell apoptosis in the cold ischemic rat liver: a Kupffer cell mediated injury. *FASEB J* 2001;15: 1230-1232
- 38 Deaciuc IV, D'Souza NB, Sarphie TG, Schmidt J, Hill DB, McClain CJ. Effects of exogenous superoxide anion and nitric oxide on the scavenging function and electron microscopic appearance of the sinusoidal endothelium in the isolated, perfused rat liver. *J Hepatol* 1999; 30: 213-221
- 39 Wu RQ, Xu YX, Song XH, Chen LJ, Meng XJ. Adhesion molecule and proinflammatory cytokine gene expression in hepatic sinusoidal endothelial cells following cecal ligation and puncture. *World J Gastroenterol* 2001; 7: 128-130
- 40 Neubauer K, Ritzel A, Saile B, Ramadori G. Decrease of platelet-endothelial cell adhesion molecule 1-gene-expression in inflammatory cells and in endothelial cells in the rat liver following CCl₄-administration and *in vitro* after treatment with TNF α . *Immunol Lett* 2000; 74: 153-164
- 41 Assy N, Jacob G, Spira G, Edoute Y. Diagnostic approach to patients with cholestatic jaundice. *World J Gastroenterol* 1999; 5: 252-262
- 42 Blunck R, Scheel O, Muller M, Brandenburg K, Seitzer U, Seydel U. New insights into endotoxin-induced activation of macrophages: involvement of a K⁺ channel in transmembrane signaling. *J Immunol* 2001; 166: 1009-1015
- 43 Scott MG, Vreugdenhil ACE, Buurman WA, Hancock REW, Gold MR. Cutting edge: cationic antimicrobial peptides block the binding of lipopolysaccharide (LPS) to LPS binding protein. *J Immunol* 2000; 164: 549-553
- 44 Ling YL, Meng AH, Zhao XY, Shan BE, Zhang JL, Zhang XP. Effect of cholecystokinin on cytokines during endotoxic shock in rats. *World J Gastroenterol* 2001; 7: 667-671
- 45 Gordon H. Detection of alcoholic liver disease. *World J Gastroenterol* 2001; 7: 297-302
- 46 Bai XY, Jia XH, Cheng LZ, Gu YD. Influence of IFN α -2b and BCG on the release of TNF and IL-1 by Kupffer cells in rats with hepatoma. *World J Gastroenterol* 2001; 7: 419-421
- 47 Wang LS, Zhu HM, Zhou DY, Wang YL, Zhang WD. Influence of whole peptidoglycan of bifidobacterium on cytotoxic effectors produced by mouse peritoneal macrophages. *World J Gastroenterol* 2001; 7: 440-443
- 48 Zuo GQ, Gong JP, Liu CH, Li SW, Wu XC, Yang K, Li Y. Expression of lipopolysaccharide binding protein and its receptor CD14 in experimental alcoholic liver disease. *World J Gastroenterol* 2001; 7: 836-840

Edited by Hu DK

• BASIC RESEARCH •

Effect of areca on contraction of colonic muscle strips in rats

Dong-Ping Xie, Wei Li, Song-Yi Qu, Tian-Zhen Zheng, Ying-Li Yang,
Yong-Hui Ding, Yu-Ling Wei, Lian-Bi Chen

Dong-Ping Xie, Lian-Bi Chen, Department of Physiology, Medical College, Shandong University, Jinan 250012, Shandong Province, China
Wei Li, Song-Yi Qu, Tian-Zhen Zheng, Department of Physiology, Lanzhou Medical College, Lanzhou 730000, Gansu Province, China
Ying-Li Yang, Northwest Normal University, Lanzhou 730070, Gansu Province, China

Yong-Hui Ding, Yu-Ling Wei, Drug Control Institute of Gansu Province, Lanzhou 730000, Gansu Province, China

Supported by the Natural Scientific Foundation of Shandong Province, No. Y2001C06

Correspondence to: Dong-Ping Xie, Department of Physiology, Medical College, Shandong University, Jinan 250012, Shandong Province, China. xiedping@sdu.edu.cn

Telephone: +86-531-2942037 Fax: +86-531-2942156

Received 2001-07-19 Accepted 2002-01-20

Abstract

AIM: To investigate the effects of areca on the contractile activity of isolated colonic muscle strips in rats and mechanism involved.

METHODS: Each strip (LMPC, longitudinal muscle of proximal colon; CMPC, circular muscle of proximal colon; LMDC, longitudinal muscle of distal colon; CMDC, circular muscle of distal colon.) was suspended in a tissue chamber containing 5 mL Krebs solution (37°C), bubbled continuously with 950 mL·L⁻¹ O₂ and 50 mL·L⁻¹ CO₂. The mean contractile amplitude (A), the resting tension (T), and the contractile frequency (F) were simultaneously recorded on recorders.

RESULTS: Areca dose dependently increased the mean contractile amplitude, the resting tension of proximal and distal colonic smooth muscle strips in rats ($P < 0.05$). It also partly increased the contractile frequency of colonic smooth muscle strips in rats ($P < 0.05$). The effects were partly inhibited by atropine (the resting tension of LMPC decreased from 0.44 ± 0.12 to 0.17 ± 0.03 ; the resting tension of LMDC decreased from 0.71 ± 0.14 to 0.03 ± 0.01 ; the mean contractile amplitude of LMPC increased from -45.8 ± 7.2 to -30.5 ± 2.9 ; the motility index of CMDC decreased from 86.6 ± 17.3 to 32.8 ± 9.3 ; $P < 0.05$ vs areca), but the effects were not inhibited by hexamethonium ($P > 0.05$).

CONCLUSION: Areca stimulated the motility of isolated colonic smooth muscle strips in rats. The stimulation of areca might be relevant with M receptor partly.

Xie DP, Li W, Qu SY, Zheng TZ, Yang YL, Ding YH, Wei YL, Chen LB. Effect of areca on contraction of colonic muscle strips in rats. *World J Gastroenterol* 2002;8(2):350-352

INTRODUCTION

Areca (*Areca catechu* L.) had already been shown to relieve indigestion, unblocked stagnation of the circulation of vital energy. It had been used to treat abdominal distention and constipation, which

were caused by stagnation of the circulation of vital energy in taste. But the actions and mechanisms of areca on the colonic smooth muscle motility are not reported. In this study, we observed the effect of areca on the different colonic smooth muscle strips in rats and investigated the mechanism involved.

MATERIALS AND METHODS

Animal preparation

Wistar rats of either sex (grade I, purchased from Animal Center of Lanzhou Medical College), weighing 200-250 g, were sacrificed, and the proximal colon and distal colon were removed^[1]. The segments of the colon were opened along the mesentery. Muscle strips (8×3 mm) were cut, parallel to either the circular or the longitudinal fibers, and named circular muscle of proximal colon (CMPC), longitudinal muscle of proximal colon (LMPC), circular muscle of distal colon (CMDC), and longitudinal muscle of distal colon (LMDC). The mucosa on each strip was carefully removed.

Experiments

The muscle strip was suspended in a tissue chamber containing 5 mL Krebs solution (37°C) and bubbled continuously with 950 mL·L⁻¹ O₂ and 50 mL·L⁻¹ CO₂^[2]. One end of the strip was fixed to a hook on the bottom of the chamber. The other end was connected to an external isometric force transducer (JZ-BK, BK). Motility of colonic strips (under an initial tension of 1 g) in 4 tissue chambers were simultaneously recorded on ink-writing recorders (LMS-ZB, Cheng-Du). After 1 h equilibration, areca (10, 100, 1000 g·L⁻¹) was added in the tissue chamber to observe their effects on colon; atropine (0.01 μmol·L⁻¹) or hexamethonium (10 μmol·L⁻¹), given 3 min before the administration of areca (100 g·L⁻¹), was added separately to investigate whether the actions of areca were relevant with M receptor or N receptor. The resting tension, the frequency, and the mean contractile amplitude of LMPC, CMPC and LMDC, as well as the motility index of CMDC were measured. Motility index = $\sum (\text{amplitude} \times \text{duration})$.

Drugs preparation

Areca was broken into pieces, boiled, filtrated, and diluted to 1000 g·L⁻¹ (the drug was appraised and prepared by Drug Control Institute of Gansu Province). The following agents were used: atropine (Pharmaceutical Factory in Yancheng, Jiangsu Province), hexamethonium (Sigma Chemical Company).

Data analysis

The results were presented as $\bar{x} \pm s$, and statistically analyzed by paired *t* test, $P < 0.05$ was considered to be significant.

RESULTS

Effect of areca on the spontaneous contraction of colonic smooth muscle strips

Areca (10, 100, 1000 g·L⁻¹) dose dependently increased the mean contractile amplitude of CMPC and LMDC, the motility index of CMDC, and the resting tension of LMPC, LMDC and CMDC; but it

decreased the mean contractile amplitude of LMPC (Figure 1). It increased the contractile frequency of CMPC and LMDC (Table 1). It had no significant effects on the resting tension of CMPC and the contractile frequency of LMPC and CMDC.

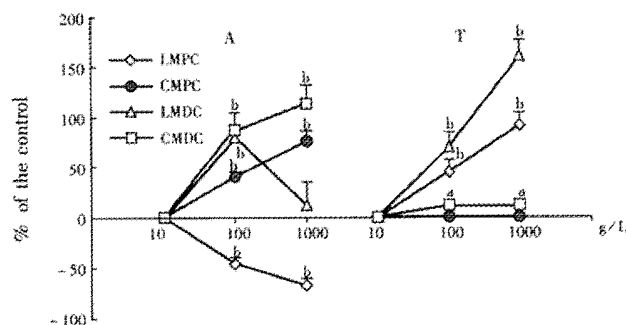


Figure 1 Effect of areca on the mean contractile (the motility index of CMDC) and the resting tension ($\bar{x} \pm s$, $n=12$)
LMPC: longitudinal muscle of proximal colon; CMPC: circular muscle of proximal colon; LMDC: longitudinal muscle of distal colon; CMDC: circular muscle of distal colon. A, the mean contractile amplitude; T, the resting tension. ^a $P<0.05$, ^b $P<0.01$ vs control.

Table 1 Effect of areca on the contractile frequency of colonic contractile in rats ($\bar{x} \pm s$, waves·min⁻¹, $n=12$)

	Areca (g·L ⁻¹)					
	0	10	0	100	0	1000
LMPC	1.8±0.2	1.9±0.2	2.2±0.2	2.5±0.3	1.8±0.2	1.8±0.4
CMPC	1.5±0.1	1.5±0.1	1.6±0.1	2.1±0.2 ^a	1.6±0.1	2.3±0.1 ^b
LMDC	1.3±0.1	1.3±0.1	1.5±0.1	2.3±0.2 ^a	1.5±0.2	2.7±0.5 ^b
CMDC	0.7±0.1	0.7±0.1	0.6±0.1	0.6±0.1	0.6±0.1	0.6±0.1

LMPC: longitudinal muscle of proximal colon; CMPC: circular muscle of proximal colon; LMDC: longitudinal muscle of distal colon; CMDC: circular muscle of distal colon. ^a $P<0.05$, ^b $P<0.01$ vs control (0).

Effect of atropine on the responses caused by areca

Atropine (0.01 μmol·L⁻¹) itself had no significant effects on rat colon. But when given 3min before the administration of areca (100g·L⁻¹), it reduced the increasing action of areca on the resting tension of LMPC and LMDC, the motility index of CMDC, and the mean contractile amplitude of LMPC. It had no significant effects on the other action of areca (Table 2).

Table 2 Effect of areca on the mean contractile amplitude and the resting tension of colon, and the motility index of distal colon after atropine pretreatment in rats ($\bar{x} \pm s$, $n=12$)

	LMPC		CMPC		LMDC		CMDC	
	T/g	A/mm	T/g	A/mm	T/g	A/mm	T/g	MI/mm·s ⁻¹
Areca	0.44±0.12 ^b	-45.8±7.2 ^b	0	40.0±3.5 ^b	0.71±0.14 ^b	79.7±12.8 ^b	0.11±0.05 ^a	86.6±17.3 ^b
Atropine 0	0.1±0.1	0	0.6±1.4	0	1.3±3.0	0	0.9±1.3	
Atropine 0.17±	-30.5±	0	36.9±	0.03±	70.9±	0.03±	32.±	
+Areca	0.03 ^{bc}	2.9	2.5 ^b	0.01 ^{ab}	13.6 ^b	0.02	98.3 ^{bc}	

T, the resting tension; A, the mean contractile amplitude; MI, the motility index. ^a $P<0.05$, ^b $P<0.001$ vs control. ^c $P<0.05$, ^d $P<0.001$ vs areca.

Effect of hexamethonium on the responses caused by areca

Hexamethonium (10 μmol·L⁻¹) had no significant effect on the contractile activity of each colonic smooth muscle strip. Hexamethonium given 3 minute before administration of areca (100g·L⁻¹) had no significant effects on the action of areca.

DISCUSSION

There are many diseases which are caused by colonic motility disorder or accompany with colonic motility abnormality, such as constipation, diarrhea, irritable bowel syndrome and so on^[3-11]. There are some reports on the study of normal colonic motility and intestinal diseases that are connected with colonic motility^[12-25]. The studies on how to treat the diseases that are caused by colonic motility disorder have also been reported^[26-35]. But it still needs a long time for us to recognize the colonic motility completely.

Recently, the effects of Chinese herbals on the gastrointestinal motility have been reported^[36-46]. Areca had been used to treat abdominal distention, constipation, abdominal pain and non-ulcer dyspepsia, which were considered to be connected with intestinal motility disorder^[47-49]. Whether the clinical use is connected with its effects on colonic motility. The present study revealed that areca dose dependently stimulated the contractions of proximal and distal colonic smooth muscle strips of rats. The exciting actions suggested that areca might caused the colonic contents to be mixed, stirred, promoted, and even excreted. These results can partly explained why areca was used to treat intestinal motility disorder.

Areca has been showed to stimulate both cholinergic M and N receptors. Our results showed that the stimulating effects of areca were partly blocked by atropine but not by hexamethonium. Our results suggested that the stimulating effects of areca on rat colonic smooth muscle strips were relevant with M receptor but irrelevant with N receptor. When M receptor was stimulated, the potential sensitive Ca²⁺ channel was opened, which will cause the influx of extracellular Ca²⁺ and then cause the contraction of smooth muscle^[50]. Areca might stimulate M receptor and then cause the concentration of intracellular Ca²⁺ increased, areca might also act on the Ca²⁺ channel receptor directly, which still need to be further studied. In conclusion, areca stimulates the contractile activity of colonic smooth muscle of rats *in vitro*. The effect of areca is partly relevant with M receptor, but irrelevant with N receptor.

REFERENCES

- Xie DP, Li W, Qu SY, Zheng TZ, Yang YL, Ding YH, Wei YL. Effects of ranitidine and cimetidine on the contractile activity of colonic smooth muscle strips in rats. *Zhongguo Yaolixue Yu Dulixue Zazhi* 2001;15:12-16
- Qu SY, Zheng TZ, Li W. Comparative study of ranitidine and cimetidine on contractile activity of isolated gastric muscle strips in rats. *Xin Xiaohuabingxue Zazhi* 1997;5:75-76
- Rajapakse R, Warman J, Korelitz BI. Colchicine for persistent constipation after total abdominal colectomy with ileorectostomy for colonic inertia. *J Clin Gastroenterol* 2001;33:81-84
- O'Sullivan MA, O'Morain CA. Bacterial supplementation in the irritable bowel syndrome. A randomised double-blind placebo-controlled crossover study. *Dig Liver Dis* 2000;32:294-301
- Chey WY, Jin HO, Lee MH, Sun SW, Lee KY. Colonic motility abnormality in patients with irritable bowel syndrome exhibiting abdominal pain and diarrhea. *Am J Gastroenterol* 2001;96:1499-1506
- Coulie B, Camilleri M, Bharucha AE, Sandborn WJ, Burton D. Colonic motility in chronic ulcerative proctosigmoiditis and the effects of nicotine on colonic motility in patients and healthy subjects. *Aliment Pharmacol Ther* 2001;15:653-663
- Bonapace ES, Maurer AH, Davidoff S, Krevsky B, Fisher RS, Parkman HP. Whole gut transit scintigraphy in the clinical evaluation of patients with upper and lower gastrointestinal symptoms. *Am J Gastroenterol* 2000;95:2838-2847
- Borum ML. Irritable bowel syndrome. *Prim Care* 2001;28:523-538
- Knowles CH, Scott SM, Lunniss PJ. Slow transit constipation: a disorder of pelvic autonomic nerves. *Dig Dis Sci* 2001;46:389-401
- Knowles CH, Nickols CD, Scott SM, Bennett NI, de Oliveira RB, Chimelli L, Feakins R, Williams NS, Martin JE. Smooth muscle inclusion bodies in slow transit constipation. *J Pathol* 2001;193:390-397
- Ringel Y, Sperber AD, Drossman DA. Irritable bowel syndrome. *Annu Rev Med* 2001;52:319-338
- Eglen RM. Muscarinic receptors and gastrointestinal tract smooth muscle function. *Life Sci* 2001;68:2573-2578
- Plattner V, Leray V, Leclair MD, Aube AC, Cherbut C, Galmiche JP. Interleukin-8 increases acetylcholine response of rat intestinal segments. *Aliment Pharmacol Ther* 2001;15:1227-1232

- 14 Percy WH, Brunz JT, Burgers RE, Fromm TH, Merkwand CL, van Dis J. Interrelationship between colonic muscularis mucosae activity and changes in transmucosal potential difference. *Am J Physiol Gastrointest Liver Physiol* 2001;281:G479-G489
- 15 Lin VW, Hsiao I, Goodwin D, Perikash I. Functional magnetic stimulation facilitates colonic transit in rats. *Arch Phys Med Rehabil* 2001;82:969-972
- 16 Shafik A, El-Sibai O, Ahmed A. Study of the mechanism underlying the difference in motility between the large and small intestine: the "single" and "multiple" pacemaker theory. *Front Biosci* 2001; 6:B1-B5
- 17 Onori L, Aggio A, Taddei G, Ciccocioppo R, Severi C, Carnicelli V, Tonini M. Contribution of NK3 tachykinin receptors to propulsion in the rabbit isolated distal colon. *Neurogastroenterol Motil* 2001;13:211-219
- 18 Herve S, Leroi AM, Mathieix-Fortunet H, Garnier P, Karoui S, Menard JF, Ducrotte P, Denis P. Effects of polyethylene glycol 4000 on 24-h manometric recordings of left colonic motor activity. *Eur J Gastroenterol Hepatol* 2001;13:647-654
- 19 Al-Saffar A, Hellstrom PM. Contractile responses to natural tachykinins and selective tachykinin analogs in normal and inflamed ileal and colonic muscle. *Scand J Gastroenterol* 2001;36:485-493
- 20 Sun WM, Hasler WL, Lien HC, Montague J, Owyang C. Nizatidine enhances the gastrocolonic response and the colonic peristaltic reflex in humans. *J Pharmacol Exp Ther* 2001;299:159-163
- 21 Portincasa P, Moschetta A, Giampaolo M, Palasciano G. Diffuse gastrointestinal dysmotility by ultrasonography, manometry and breath tests in colonic inertia. *Eur Rev Med Pharmacol Sci* 2000;4:81-87
- 22 Carini F, Lecci A, Tramontana M, Giuliani S, Maggi CA. Tachykinin NK(2) receptors and enhancement of cholinergic transmission in the inflamed rat colon: an *in vivo* motility study. *Br J Pharmacol* 2001;133:1107-1113
- 23 Ye JH, Ponnudurai R, Schaefer R. Ondansetron: a selective 5-HT(3) receptor antagonist and its applications in CNS-related disorders. *CNS Drug Rev* 2001;7:199-213
- 24 Lecci A, Carini F, Tramontana M, D'Aranno V, Marinoni E, Crea A, Bueno L, Fioramonti J, Crisculi M, Giuliani S, Maggi CA. Nepadutant pharmacokinetics and dose-effect relationships as tachykinin nk(2) receptor antagonist are altered by intestinal inflammation in rodent models. *J Pharmacol Exp Ther* 2001;299:247-254
- 25 Bassotti G, Fratini M. Of tubes and men: studying manometrically the effects of laxatives on colonic motility. *Eur J Gastroenterol Hepatol* 2001;13:631-633
- 26 Crowell MD. The role of serotonin in the pathophysiology of irritable bowel syndrome. *Am J Manag Care* 2001;7:S252-S260
- 27 Menzies JR, McKee R, Corbett AD. Differential alterations in tachykinin NK(2) receptors in isolated colonic circular smooth muscle in inflammatory bowel disease and idiopathic chronic constipation. *Egul Pept* 2001;99:151-156
- 28 Schwartz D, Stollman N. University of Miami Division of Clinical Pharmacology therapeutic rounds: irritable bowel syndrome-pathophysiology, diagnosis, and treatment. *Am J Ther* 2000;7:265-272
- 29 Talley NJ. Drug therapy options for patients with irritable bowel syndrome. *Am J Manag Care* 2001;7:S261-S267
- 30 Niedzielin K, Kordecki H, Birkenfeld B. A controlled, double-blind, randomized study on the efficacy of *Lactobacillus plantarum* 299V in patients with irritable bowel syndrome. *Eur J Gastroenterol Hepatol* 2001;13:1143-1147
- 31 Villanueva A, Dominguez-Munoz JE, Mearin F. Update in the therapeutic management of irritable bowel syndrome. *Dig Dis* 2001;19:244-250
- 32 Beglinger C. Tegaserod a novel, selective 5-HT4 receptor partial agonist for irritable bowel syndrome. *Int J Clin Pract* 2002;56:47-51
- 33 De Ponti F, Tonini M. Irritable bowel syndrome: new agents targeting serotonin receptor subtypes. *Drugs* 2001;61:317-332
- 34 De Schryver AM, Samsom M. New developments in the treatment of irritable bowel syndrome. *Scand J Gastroenterol* 2000; 232:38-42
- 35 Bouras EP, Camilleri M, Burton DD, Thomforde G, McKinzie S, Zinsmeister AR. Prucalopride accelerates gastrointestinal and colonic transit in patients with constipation without a rectal evacuation disorder. *Gastroenterology* 2001;120:354-360
- 36 Tian XL, Mourelle M, Li YL, Guarner F, Malagelada JR. The role of Chinese herbal medicines in a rat model of chronic colitis. *World J Gastroenterol* 2000;6:40
- 37 Zheng BJ. Understanding of gastrointestinal prokinetic Chinese drugs. *Zhongyi Zazhi* 1996; 37:697-698
- 38 Yang YL, Zheng TZ, Qu SY, Li W, Xie DP. Action of Binglang on contractile activity of isolated small intestinal strips in rats. *Lanzhou Daxue Xuebao* 2000;36:43-46
- 39 Yang YL, Zheng TZ, Qu SY, Li W, Xie DP, Ding YH, Wei YL. Action of Zhishi on the smooth muscle of isolated small intestine in rats. *Xibei Shifan Daxue Xuebao* 1998;34:69-72
- 40 Xie DP, Li W, Qu SY, Zheng TZ, Yang YL, Ding YH, Wei YL, Zhang MY. Effect of *Fructus Aurantii Immaturus* on contractile activity of colonic muscle strips in rats. *Shandong Yike Daxue Xuebao* 2001;39:437-438
- 41 Xie DP, Li W, Qu SY, Zheng TZ, Yang YL, Ding YH, Wei YL. Effect of Qing Pi on contractile of colonic muscle strips in rats. *Lanzhou Yixueyuan Xuebao* 1998;24:1-3
- 42 Song YI. Treatment of chronic colitis by integration of traditional and western medicine method in 92 cases. *Huaren Xiaohua Zazhi* 1998;6:454
- 43 Li Y, Sun SY, Zhou Z. Effect of Chinese herbal medicines Xiaoshixingqi on gastrointestinal motility in mice. *Xin Xiaohuabingxue Zazhi* 1997;5:153
- 44 Chen RS, Zhang YF, Deng LM, Guo DQ. The Influences of Jiechang-Kangtai on the Movement Function of Intestine. *Zhongguo Zhongxiyi Jiehe Piwei Zazhi* 1998;6:157-159
- 45 Zhang HX, Ren P, Huang X, Li Y. Regulation of Chinese herbal on gastrointestinal hormones and gastrointestinal motility. *Shijie Huaren Xiaohua Zazhi* 2000;8:1141-1144
- 46 Dou DP, Cai G. Regulation of gastric motility. *Shijie Huaren Xiaohua Zazhi* 1999;7:353-354
- 47 Zhao XP, Zhang BL. Therapy of qingfutongchangchongji for 46 patients with intestinal disorder after abdomen operated. *Shanxi Zhongyi* 1999;20: 57-58
- 48 Qin ZD. Abstracts about therapy of muxiangbinglangwan for patients with rectostenosis in 23 cases. *Guangxi Zhongyiyao* 1999;22:33
- 49 Xiao ChQ, Huo GQ. Therapy of simowubeitang for 60 patients with non-ulcer dyspepsia. *Shijie Huaren Xiaohua Zazhi* 2000;8:98
- 50 Zhou L, Ke MY. Textbook of Gastrointestinal Motility-Basic and Clinical Aspects. Beijing: Science Press 1999:202

Edited by Wang YQ

• BASIC RESEARCH •

Identification and characterization of a novel isoform of hepatopoietin

Jun Lu, Wang-Xiang Xu, Yi-Qun Zhan, Xiao-Lin Cui, Wei-Min Cai, Fu-Chu He, Xiao-Ming Yang

Jun Lu, Wei-Min Cai, Institute of Infectious Disease, First Affiliated Hospital, Medical School, Zhejiang University, Hangzhou 310003 China
Wang-Xiang Xu, Yi-Qun Zhan, Xiao-Lin Cui, Fu-Chu He, Xiao-Ming Yang, Institute of Radiation Medicine, Academy of Military Medical Sciences, Beijing 100850, China

Supported by the National Natural Science Foundation of China, No. 39830440

Correspondence to: Dr. Xiao-Ming Yang, Institute of Radiation Medicine, Academy of Military Medical Sciences, Beijing 100850, China. xiaomingyang@sina.com.cn

Telephone: +86-10-66931424 Fax: +86-10-68214653

Received 2001-09-14 Accepted 2001-11-14

Abstract

AIM: To isolate a novel isoform of human HPO (HPO-205) from human fetal liver Marathon-ready cDNA and characterize its primary biological function.

METHODS: 5'-RACE (rapid amplification of cDNA 5' ends) was used to isolate a novel isoform of hHPO in this paper. The constructed pcDNA^{HPO-205}, pcDNA^{HPO} and pcDNA eukaryotic expression vectors were respectively transfected by lipofectamine method and the stimulation of DNA synthesis was observed by ³H-TdR incorporation assay. Proteins extracted from different cells were analyzed by Western blot.

RESULTS: A novel isoform of hHPO (HPO-205) encoding a 205 amino acid ORF corresponding to a translated production of 23 kDa was isolated and distinguished from the previous HPO that lacked the N-terminal 80 amino acids. The dose-dependent stimulation of DNA synthesis of HepG2 hepatoma cells by HPO-205 demonstrated its similar biological activity with HPO *in vitro*. The level of MAPK (Mitogen-activated protein kinase) phosphorylation by Western blot analysis revealed that HPO-205 might have the stronger activity of stimulating hepatic cell proliferation than that of HPO.

CONCLUSION: A novel isoform of hHPO (HPO-205) was isolated from hepatic-derived cells. The comparison of HPO-205 and HPO will lead to a new insight into the structure and function of hHPO, and provide the new way of thinking to deeply elucidate the biological roles of HPO/ALR.

Lu J, Xu WX, Zhan YQ, Cui XL, Cai WM, He FC, Yang XM. Identification and characterization of a novel isoform of hepatopoietin. *World J Gastroenterol* 2002;8(2):353-356

INTRODUCTION

Hepatic stimulatory activity was identified from human fetal liver lysate, which was named as hepatopoietin (HPO)^[1]. Later we proved that HPO was encoded by mRNA of human fetal liver^[2]. Recombinant human hepatopoietin (rhHPO) showed its activity of specifically stimulating DNA synthesis of hepatic cells and promoting healing after liver injury *in vitro* and *in vivo*^[3-6]. Recently, HPO/ALR/EVR1 homologous cDNAs (including EST sequences) have been isolated in many laboratories^[7,8]. Sequence analysis of these homologous cDNAs revealed that the same 3' sequence was presented

in all reported sequences, however, the 5' sequence varied in these cDNAs^[9]. Furthermore, The analysis of genomic sequences of HPO/ALR also suggested there might exist different transcripts in nature. In this paper, we reported the identification and characterization of a novel isoform of human HPO in hepatic-derived cells. This cDNA with a 205 amino acid ORF was named HPO-205 to distinguish it from the previous HPO that lacked the N-terminal 80 amino acids.

MATERIALS AND METHODS

Sequence analysis and RNA extraction

HPO sequences and their proteins were analyzed by using DNA tools, Biosoft software and GenBank blast program. The primer for 5'RACE was: 5'-GGT CTT CAG GTT CAG ACA CAT GTT GGC-3'. The human fetal liver Marathon-ready cDNA (Clontech) served as template to amplify 5' end of HPO by using a kit (Clontech). The PCR products were ligated to pGEM-T vector and sequenced using T7 and SP6 primers by PE (ABI PRISM) DNA Sequencer. Cos7 (African green monkey kidney cell line), HepG2 and HLE (human hepatoma cell line) were purchased from the American Type Culture Collection. BEL-7402 (epithelial hepatoma cell lines, derived from male, 75 years) and SMMC-7721 (epithelial hepatoma cell lines, derived from male, 50 years) were purchased from the Cell Institute of Chinese Academy of Science. All cell lines were cultured in Dulbecco's Modified Eagle Media (DMEM) (GiBco BRL, Life Technologies.) supplemented with antibiotics and 100mL·L⁻¹ heat-inactivated fetal bovine serum in a humidified atmosphere of 50mL·L⁻¹ CO₂. Total RNA was isolated from the cells using TRIzolTM reagent (GiBco).

RT-PCR

Forward and reverse primers for human HPO-250 and G3PDH genes were designed and applied to amplify transcripts. Briefly, Total RNAs were extracted with Trizol (GiBco) reagent. Reverse-transcribed and amplified for 30 cycles, using RT and PCR kit (TaKaRa LA Taq with GC buffer, TaKaRa Biotech, Dalian, China), according to the manufacturer's instructions. The expression of G3PDH mRNA was detected as an internal control. Primer pairs for RT-PCR were: HPO-250 sense: 5'-ATG GCG GCG CCC GGC GAG CGG GGC CGC TT-3'; antisense: 5'-CTA GTC ACA GGA GCC ATC CTT CCA-3'; G3PDH sense: 5'-ACC ACA GTC CAT GCC ATC AC-3'; antisense: 5'-TCC ACC ACC CTG TTG CTG TA-3'. The expected size of the amplified DNA fragments for HPO-250 and G3PDH were 618 and 1000 bp respectively. The PCR products were separated on 10g·L⁻¹ agarose gel with ethidium bromide staining and photographed under UV. The photographs of the gels were analysed using Bio-Print (M&S Instruments Trading Inc, Tokyo). The values of these DNA fragments were calculated as relative intensity against G3PDH mRNA.

Construction of HPO expression vectors and Transfection

Both *Eco*R I and *Bam*H I sites were introduced by PCR *in vitro* mutagenesis, and the full length cDNA encoding human HPO and HPO-250 were inserted into pcDNA 3.1(+) vector downstream of CMV promoter. The recombinant pcDNA 3.1 plasmids were isolated and used for transfection. Cos-7 or Bel-7402 cells were subsequently harvested and reseeded at a density of 1×10⁶ cells/100-mm plate.

The cells were transfected the next day with different plasmids (2 μ g) using lipofectamine reagent (Gibco). For transient expression, the conditional medium of Cos-7 cells transfected with pcDNA^{HPO-250} or pcDNA plasmid was harvested 48h after transfection. For stable expression, the Bel-7402 cells after being transfected with pcDNA^{HPO-250} or pcDNA^{HPO} or pcDNA plasmid by 72h were selected in DMEM medium containing 400mg·L⁻¹ G418 for 14d. G418-resistant clones were isolated and grown in DMEM medium containing G418 to maintain the phenotype.

Western blot analysis

Protein was extracted from different cells, and the protein concentration was determined by Coomassie Brilliant Blue G-250 staining. Samples containing equivalent amounts (50 μ g) were separated on a 10% SDS polyacrylamide gel under reducing conditions and transferred to a Hybond-N nitrocellulose membrane (Amersham, Arlington Heights, Illinois). The membrane was incubated respectively with rabbit polyclonal anti-human HPO antibody or rabbit polyclonal anti-perk or ERK antibody (Santa Cruz) and developed with an ECL western blotting detection system (Santa Cruz) using horseradish peroxidase-conjugated second antibody (Santa Cruz).

³H-TdR incorporation assay

HepG2 hepatoma cells were counted and adjusted to 1 \times 10⁸ cells·L⁻¹, then 100 μ L of cell suspension was inoculated into 96-well plates and incubated at 37°C, 50mL·L⁻¹ CO₂ for 12h. Then the fresh medium containing prepared samples was added. After 48h of culture in presence of various medium supplements, 37kBq/well ³H-TdR was added and incubated for 3h. The cells were collected to filters, and radioactivity was determined in an LKB liquid scintillation counter, and results were expressed as median counts per minute from triplicate cultures.

RESULTS

Sequence analysis of HPO

Searching against GenBank with human HPO sequence, this sequence showed homology with 11 human cDNAs encoding HPO-like proteins. Protein sequence alignment showed that all of these encoding proteins were highly conserved in the 125 amino acid of C terminal but varied in the N terminal. Further analysis of their nucleotide sequences demonstrated no stop codon was found before the same open reading frame (ORF). This result indicated that deposited 125 amino acid HPO might be incomplete.

Isolation of HPO-205 cDNA and sequence analysis

To investigate whether a novel isoform of HPO exists in nature, a Marathon-ready cDNA from human fetal liver served as the template to amplify 5' ends of hHPO. The PCR products containing different sizes of 375, 500, 750 and 1200 bp bands were cloned into pMD18-T vectors and transformed *E. coli* DH5 α . Then the clones were screened by hybridization with ³²P-HPO cDNA as a probe, and more than 50 positive clones were obtained. After we sequenced 10 positive clones, we obtained the novel isoform HPO cDNA that encoded a 205 amino acid ORF. This cDNA with a 205 amino acid ORF was named HPO-205 (GenBank CI 11559825) to distinguish it from the previous HPO that lacked the N-terminal 80 amino acids (Figure 1).

```

1  MAAPGERGRF HGGNLFPLG GARSEMMDDL ATDARGRGAG RRDAASAST
51  PAQAPTSDSP VAEDASRRRP CRACVDFKTW MRTQQKRDTK FREDCPPDRE
      MRTQQKRDTK FREDCPPDRE
101 ELGRHSWAVL HTLAAYYDDL PTPEQQRDMA QFIHLFSKFY PCECAEDLR
      ELGRHSWAVL HTLAAYYDDL PTPEQQRDMA QFIHLFSKFY PCECAEDLR
151 KRLCRNHPDT RTRACFTQWL CHLHNEVNRE LGKPDFDCSK VDERWRDQWK
      KRLCRNHPDT RTRACFTQWL CHLHNEVNRE LGKPDFDCSK VDERWRDQWK
201 DGSCD*
      DGSCD*

```

Figure 1 Amino acid sequence alignment of HPO-205 and HPO(GenBank CI 11559825)

Expression of HPO-205 in hepatoma cell lines

The expression of HPO-205 was determined by semi-quantitative RT-PCR and Western blotting. As shown in Figure 2 and Figure 3, the cell lines showed interesting and revealing differences in the levels of HPO-205. The levels of hHPO-205 mRNA in HepG2 and HLE cell lines were significantly higher (4-5 folds) than in BEL-7402 and 7721 cell lines (Figure 2). Similarly, we also observed HPO-205 protein in HepG2 and HLE cell lines were significantly higher (4-5 folds) than in BEL-7402 and 7721 cell lines (Figure 3) by Western blot analysis. The M_r of HPO-205 in these four hepatoma cell lines is 23000 identical to the predicted molecular weight (Figure 3).

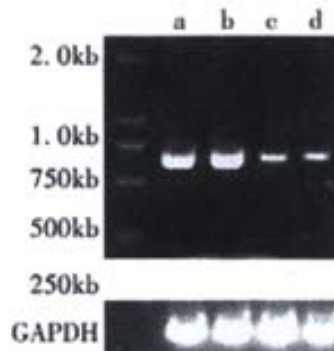


Figure 2 The mRNA expression of HPO-205 was determined by RT-PCR in hepatoma cell lines. a: HepG2 cell line; b: HLE cell line; c: SMMC-7721 cell line; d: Bel-7402 cell line; GAPDH as a control.



Figure 3 HPO-205 protein was detected by Western blot in hepatoma cell lines. a: HepG2 cell line; b: Bel-7402 cell line; c: SMMC-7721 cell line; d: HLE cell line

HPO-205 stimulated HepG2 cells proliferation in vitro

We demonstrated that biological activity of HPO-205 could be expressed from its cDNA in transient expression experiment in Cos7 cells. As shown in Figures 4A and 4B, the conditional medium from transfected cells with the pcDNA^{HPO-205} revealed the dose-dependent stimulation of DNA synthesis of HepG2 hepatoma cells. However, as a negative control, the conditional medium from mock-transfected did not show any activity.

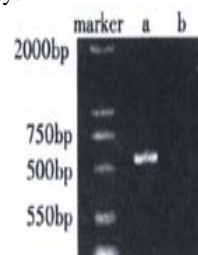


Figure 4A The HPO-205 mRNA expression in transfected Cos7 cells was detected by RT-PCR method. a: DNA marker; b: pcDNAHPO-205 vector; c: pcDNA vector.

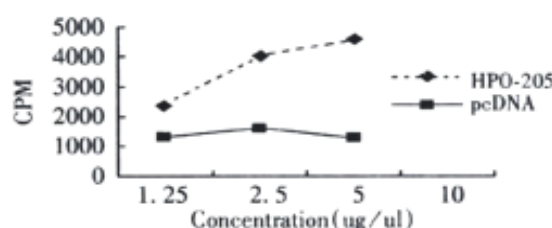


Figure 4B The effect of DNA synthesis of HepG2 cells stimulated by the different expressed protein.

Activation of Mitogen-activated protein kinase (MAPK) by expression of HPO-205 in Bel-7402 hepatoma cells

MAPK could be activated by a number of growth factors and cytokines. To assess whether HPO-205 activated the MAPK pathway, the pcDNA^{HPO-205}, pcDNA^{HPO} and pcDNA plasmids were transfected into Bel-7402 cells with low level expression of HPO. Expression of HPO-205 and HPO protein were analyzed by western blotting using antibody against HPO protein. As shown in Figure 5A, a protein band with an apparent M_r of 23000 only was detected in the HPO-205 transfected Bel-7402 cells, and a protein band with an apparent M_r of 15000 only was detected in the HPO transfected Bel-7402 cells. As shown in Figure 5B, the level of MAPK phosphorylation in BEL-7402 cells could be elevated by HPO and HPO-205 ($P<0.01$), and the level of MAPK phosphorylation activated by HPO-205 was higher than that by HPO ($P<0.01$).

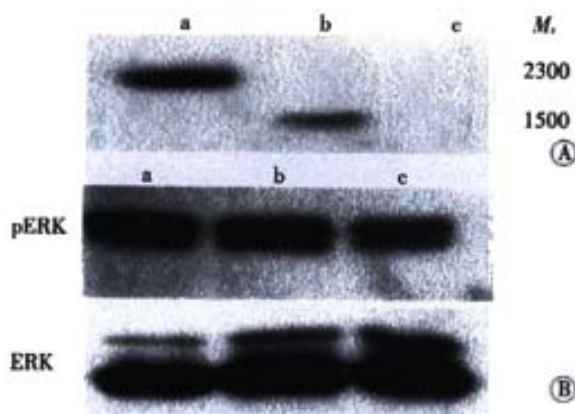


Figure 5 The stably transfected cell lines were confirmed and MAPK activation was examined by Western Blot.

A. HPO and HPO-205 protein in transfected Bel-7402 cells;
B. MAPK levels in different transfected cell lines.

DISCUSSION

We isolated and characterized a novel isoform of HPO (HPO-205) cDNA that encoded a 205 amino acid ORF. This cDNA with a 205 amino acid ORF was named HPO-205 (GenBank CI 11559825) to distinguish it from the previous HPO that lacked the N-terminal 80 amino acids. The molecular weight of HPO-205 was 23 kDa identified in four human hepatoma cell lines by Western blot, and the HPO-205 mRNA expressions were detectable in human hepatoma cell lines including HepG2, HLE, 7402 and 7721 by RT-PCR method. Our sequence analysis of HPO-205 shows presence of very rich GC bases in 5' end of HPO mRNA (more than 75%). Such high amount of GC bases will affect the efficiency of mRNA transcription. Therefore, it will lead to obtaining different kinds of incomplete HPO mRNA under different conditions in many laboratories^[10].

As we know, human HPO is a specific growth factor and plays an important role in liver regeneration *in vivo*^[11-14]. Many experiments demonstrated that HPO could stimulate the proliferation of hepatic cells *in vitro* and *in vivo*^[1,2,15]. Therefore, identification and characterization of the biological function of HPO-205 and the relationship between HPO-205 and HPO are very important. Some data have shown they are different in intracellular location, tissue distribution and mRNA expression under different pathological conditions, which have suggested their different biological functions^[16]. In this paper, we find, as human HPO, HPO-205 also stimulated the DNA synthesis of HepG2 cells. However, whether HPO-205 can specifically stimulate DNA synthesis of hepatic cells and promote healing after liver injury *in vitro* and *in vivo*, just like HPO,

remain to be under investigation.

Our previous study demonstrated that HPO stimulated the hepatic cell proliferation through its specific receptor^[4]. Recently, another report indicates that HPO/ALR assigns a FAD-linked sulphydryl oxidase activity, which plays a role in modifying some molecules *in vivo*^[17], and regulates the expression of some mitochondrial genes^[18-21]. These data suggest that there are many different mechanisms of HPO/ALR involved in stimulating cell proliferation and improving hepatic repair. Recently, Li *et al*^[22] have reported that HPO promotes the proliferation of hepatic cells through activating MAPK signal pathway. Here we have also found that both of HPO-205 and HPO could increase the activation of MAPK phosphorylation compared with the control. Moreover, the result also showed that the level of MAPK phosphorylation in HPO-205 transfected cells was significantly higher than that in HPO transfected cells by Western blot. These data indicate that HPO-205 might have the stronger activity of stimulating hepatic cell proliferation than that of HPO.

REFERENCES

- 1 Yang XM, Xie L, Oiu ZH, Wu ZZ, He FC. Human Augmenter of liver regeneration: Molecular cloning, biological activity and roles in liver regeneration. *Sci China C* 1997;40:642-647
- 2 Yang XM, Wang AM, Zhou P, Xie L, Wang QM, Wu ZZ, He FC. Human hepatopoietin—A hepatotrophic factor or liver regeneration, and its potential antihepatitis effect *in vivo*. *Chin Sci Bull* 1998;43: 1026-1031
- 3 Yang XM, Hu ZY, Xie L, Wu ZZ, He FC. *in vitro* stimulation of HTC hepatoma cell growth by recombinant human augmenter of liver regeneration (ALR). *Shengli Xuebao* 1997;49:557-561
- 4 Wang G, Yang XM, Zhang Y, Wang QM, Chen HP, Wei HD, Xing GC, Xie L, Hu ZY, Zhang CG, Fang DC, Wu CT, He FC. Identification and characterization of receptor for mammalian hepatopoietin that is homologous to yeast ERV1. *J Biol Chem* 1999;274:11469-11472
- 5 Yang XM, Wang AM, Zhou P, Wang QM, Wei HD, Wu ZZ, He FC. Protective effect of recombinant human augmenter of liver regeneration on CCl₄-induced hepatitis in mice. *Chin Med J* 1998;111:625-629
- 6 Tanigawa K, Sakaida I, Masuhara M, Hagiya M, Okita K. Augmenter of liver regeneration (ALR) may promote liver regeneration by reducing natural killer (NK) cell activity in human liver diseases. *J Gastroenterol* 2000;35:112-119
- 7 Cheng J, Zhong YW, Liu Y, Dong J, Yang JZ, Chen JM. Cloning and sequence analysis of human genomic DNA of augmenter of liver regeneration hepatitis. *Zhonghua Ganzangbing Zazhi* 2000;8:12-14
- 8 Dong J, Cheng J, Liu YS, Wang QH, Wang G, Shi SS, Si CW. Cloning and sequence analysis of a pseudogene of liver regeneration augmentin in rats. *Zhonghua Ganzangbing Zazhi* 2001;9:105-107
- 9 Hofhaus G, Stein G, Polimeno L, Francavilla A, Lisowsky T. Highly divergent amino termini of the homologous human ALR and yeast scERV1 gene products define species specific differences in cellular localization. *Eur J Cell Biol* 1999;78:349-356
- 10 Yi XR, Kong XP, Tong MH, Yang LP, Li RB, Zhang YJ. Cloning and sequencing of rat and human augmentin of liver regeneration gene. *Shijie Huaren Xiaohua Zazhi* 1998;6:392-393
- 11 Gandhi CR, Kuddus R, Subbotin VM, Prelich J, Murase N, Rao AS, Nalesnik MA, Watkins SC, DeLeo A, Trucco M, Starzl TE. A fresh look at augmentin of liver regeneration in rats. *Hepatology* 1999;29:1435-45
- 12 Francavilla A, Vujanovic NL, Polimeno L, Azzarone A, Iacobellis A, Deleo A, Hagiya M, Whiteside TL, Starzl TE. The *in vivo* effect of hepatotrophic factors augmentin of liver regeneration, hepatocyte growth factor, and insulin-like growth factor-II on liver natural killer cell functions. *Hepatology* 1997;25:411-415
- 13 Shen M, Qiu DH, Chen Y, Xiong WJ. Effects of recombinant augmentin of liver regeneration protein, danshen and oxymatrine on rat fibroblasts. *Shijie Huaren Xiaohua Zazhi* 2001;9:1129-1133
- 14 Zhou P, Yang XM, Li QF, He H, He FC, Zhang MS. Detection of augmentin of liver regeneration in sera of patients with various liver disease. *Shijie Huaren Xiaohua Zazhi* 1998;6:768-770
- 15 Yang XM, Xie L, Xing GC, Wu ZZ, He FC. Partial isolation and identification of hepatic stimulator substance mRNA extracted from human fetal liver. *World J Gastroenterol* 1998;4:2
- 16 Lu CR, Li Y, Zhao YL, Xing GC, Tang F, Wang QM, Sun YH, Wei HD, Yang XM, Wu ZZ, Chen JG, Guan KL, Zhang CG, Chen HP, He FC. Intracrine hepatopoietin potentiates AP-1 activity through JAB1 independent of MAPK pathway. *FASEB J* 2001;14

- 17 Lisowsky T, Lee JE, Polimeno L, Francavilla A, Hofhaus G. Mammalian augmenter of liver regeneration protein is a sulfhydryl oxidase. *Dig Liver Dis* 2001;33:173-180
- 18 Lee J, Hofhaus G, Lisowsky T. ERV1p from *saccharomyces cerevisiae* is a FAD-linked sulfhydryl oxidase. *FEBS Lett* 2000;477:62-66
- 19 Polimeno L, Capuano F, Marangi LC, Margiotta M, Lisowsky T, Lerardi E, Francavilla R, Francavilla A. The augmenter of liver regeneration induces mitochondrial gene expression in rat liver and enhances oxidative phosphorylation capacity of liver mitochondria. *Dig Liver Dis* 2000;32:510-517
- 20 Lange H, Lisowsky T, Gerber J, Muhlenhoff U, Kispal G, Lill R. An essential function of the mitochondrial sulfhydryl oxidase Erv1p/ALR in the maturation of cytosolic Fe/S proteins. *EMBO Rep* 2001;2:715-720
- 21 Polimeno L, Margiotta M, Marangi L, Lisowsky T, Azzarone A, Lerardi E, Francavilla R, Frassanito MA, Francavilla A. Molecular mechanisms of augmenter of liver regeneration as immunoregulator: its effect on interferon-gamma expression in rat liver. *Dig Liver Dis* 2000;32:217-225
- 22 Li Y, Li M, Xing GC, Hu ZY, Wang QM, Dong CN, Wei HD, Fan GC, Chen JZ, Yang XM, Zhao SF, Chen HP, Guan KL, Wu ZZ, Zhang CG, He FC. Stimulation of the mitogen-activated protein kinase cascade and tyrosine phosphorylation of the epidermal growth factor receptor by hepatopoietin. *J Biol Chem* 2000;275:37443-37447

Edited by Hu DK

• BASIC RESEARCH •

Telomere and telomerase in the initial stage of immortalization of esophageal epithelial cell

Zhong-Ying Shen, Li-Yan Xu, En-Min Li, Wei-Jia Cai, Min-Hua Chen, Jian Shen, Yi Zeng

Zhong-Ying Shen, Li-Yan Xu, Wei-Jia Cai, Min-Hua Chen, Jian Shen, Department of Tumor Pathology, Medical College of Shantou University, Shantou 515031, Guangdong Province, China
En-Min Li, Department of Biochemistry and Molecular Biology, Medical College of Shantou University, Shantou 515031, Guangdong Province, China

Yi Zeng, Institute of Virology, Chinese Academy of Preventive Medicine, Beijing 100052, China

Supported by the National Natural Science Foundation of China, No. 39830380

Correspondence to: Dr. Zhong-Ying Shen, Department of Tumor Pathology, Medical College of Shantou University, 22 Xinling Road, Shantou 515031, Guangdong Province, China. zhongyingshen@yahoo.com
Telephone: +86-75-8538621 Fax: +86-754-8537516

Received 2001-09-26 Accepted 2001-11-01

Abstract

AIM: To search for the biomarker of cellular immortalization, the telomere length, telomerase activity and its subunits in cultured epithelial cells of human fetal esophagus in the process of immortalization.

METHODS: The transgenic cell line of human fetal esophageal epithelium (SHEE) was established with E₆E₇ genes of human papillomavirus (HPV) type 18 in our laboratory. Morphological phenotype of cultured SHEE cells from the 6th to 30th passages, was examined by phase contrast microscopy, the telomere length was assayed by Southern blot method, and the activity of telomerase was analyzed by telomeric repeat amplification protocol (TRAP). Expressions of subunits of telomerase, hTR and hTERT, were assessed by RT-PCR. DNA content in cell cycle was detected by flow cytometry. The cell apoptosis was examined by electron microscopy (EM) and TUNEL label.

RESULTS: SHEE cells from the 6th to 10th passages showed cellular proliferation with a good differentiation. From the 12th to the 16th passages, many senescent and apoptotic cells appeared, and the telomere length sharply shortened from 23kb to 17kb without expression of hTERT and telomerase activity. At the 20th passage, SHEE cells overcame the senescence and apoptosis and restored their proliferative activity with expression of telomerase and hTERT at low levels, but the telomere length shortened continuously to the lowest of 3kb. After the 30th passage cells proliferation was restored by increment of cells at S and G2M phase in the cell cycle and telomerase activity expressed at high levels and with maintenance of telomere length.

CONCLUSION: At the early stage of SHEE cells, telomeres are shortened without expression of telomerase and hTERT causing cellular senescence and cell death. From the 20th to the 30th passages, the activation of telomerase and maintenance of telomere length show a progressive process for immortalization of esophageal epithelial cells. The expression of telomerase may constitute a biomarker for detection of immortalization of cells.

Shen ZY, Xu LY, Li EM, Cai WJ, Chen MH, Shen J, Zeng Y. Telomere and telomerase in the initial stage of immortalization of esophageal epithelial cell. *World J Gastroenterol* 2002;8(2):357-362

INTRODUCTION

Telomerase activity was demonstrated in cancer of digestive tract^[1-3], such as gastric^[4-7], hepatic^[8-10] colorectal^[11-13] and esophageal cancers^[14-19]. Inhibition of telomerase activity will be a new therapeutic for cancer^[20-26]. Telomerase activity can be used as a diagnostic marker for cancer^[27-30]. Normal mammalian cells grow in cultural medium with a limited number of passages before entering senescence and death^[31], which are associated with shortening of telomere. Telomeres are specialized structures at chromosomal ends that are composed of TTAGGG DNA repeats^[32]. Telomerase is a ribonuclear protein complex, which contains human telomerase reverse transcriptase (hTERT) as a catalytic domain, and human telomerase RNA component (hTR)^[33]. Telemetries cap chromosomal ends perform the function of preventing abnormal chromosomal fusions and rearrangement^[34]. However, each time a cell divides, the most distal part of the chromosome is incompletely duplicated and the telomere becomes shorter. Critically short telomeres enable the formation of aberrant chromosomal structures resulting in growth arrest or senescence^[35]. With expression of telomerase or hTR and hTERT, the length of telomere extends to maintain the life span of the cells. There are other roles of telomerase in immortal and malignant lesion, such as proliferative potential^[36], delaying senescence^[37, 38], promoting cell cycle, cell immortalization and carcinogenesis^[39].

Recently, many papers have indicated that human papillomavirus (HPV) are the important etiologic factor in esophageal carcinoma^[40-42]. Induced by HPV 18 E₆E₇ genes, we established an immortalized cell line (SHEE) from the esophageal epithelium which underwent^[43-46] malignant transformation^[47, 48]. Changes of telomere length and telomerase activity in the cell line are not clear at this early stage, nor is which criteria to use to detect immortalization of cells and what the relationship between telomerase and cell phenotype in SHEE cells is. The goal of this study is to explore when telomerase activity appears in the immortalized progressive process and study the relationship between telomerase and cellular phenotype.

MATERIALS AND METHODS

Cell culture and EM examination

The SHEE cell line was a kind of immortal embryonic esophageal epithelium induced by E₆E₇ genes of human papillomavirus (HPV) type 18 in our laboratory^[43]. The continual growth cells from the 6th to 30th passages were routinely cultivated in flasks and the 24-well plates (Corning Co.) with culture medium 199 (Gibco), 100mL·L⁻¹ bovine serum, 100u penicillin and streptomycin in a humidified atmosphere of 50mL·L⁻¹ CO₂ and 950mL·L⁻¹ air. The cell shape and size, anchorage-dependent growth and contact-inhibited growth were examined by phase contrast microscopy. For electron microscopic assessment, cells were spun to form a pellet and fixed with 25g·L⁻¹ glutaraldehyde. They were dehydrated in graded ethanol and

embedded in Araldite. Ultra-thin sections were cut with glass knives and mounted on copper grids. They were contrasted for 15 min with uranyl acetate and for 3 min with lead citrate. The sections were examined by electron microscope (Hitachi, H-300).

Cell proliferative Cycle and apoptosis

Cells cultured in the flask were digested, washed twice with PBS, fixed by 70% alcohol, prepared as single-cell suspension and stored at 4°C. Cells were stained with propidium iodide (Sigma) and analyzed with flow cytometry (FACSsort, B-D Co.). The percentage of cells in various stages of the cell cycle, the apoptotic cell rate (AI) and proliferation index ($PI = S + G_2M / G_0G_1 + S + G_2M$) were calculated. These cells on the glass coverslips within the 24-well plate were incubated with $10\text{mg}\cdot\text{L}^{-1}$ proteinase K for 15 min at room temperature. After the quenching of endogenous peroxidase, labeled nuclei with TUNEL (*In-Situ* Death Detection kit, Boehringer Mannheim Co.) were detected according to the instructions of the manufacturer. The brownish nucleus was considered positive apoptotic nucleus.

Telomere length analysis^[49]

The genomic DNA of 10^6 - 10^8 cells was extracted. The telomeric restriction fragment (TRF) was measured by Southern blot. Briefly, $20\mu\text{g}$ of genomic DNA was digested with *Hinf*I and run on $7\text{g}\cdot\text{L}^{-1}$ agarose gel with marker DNA/*Hind*III. After electrophoresis the gel was blotted to nylon membrane (HybondTM N⁺, Amersham, Life Science) and hybridized to the Dig-labeled probes (CCCTAA)³ at 50°C in $5\times\text{SSC}$, $1\text{g}\cdot\text{L}^{-1}$ Sod. n-Lauroylsarcosine (SLS), $0.2\text{g}\cdot\text{L}^{-1}$ SDS for 12-16h and washed twice at room temperature in $2\times\text{SSC}$, $1\text{g}\cdot\text{L}^{-1}$ SDS for 5min, once at 50°C in $1\times\text{SSC}$, $1\text{g}\cdot\text{L}^{-1}$ SDS for 10min, twice at 50°C in $1\times\text{SSC}$, $1\text{g}\cdot\text{L}^{-1}$ SDS for 10min, twice at 50°C in $0.1\times\text{SSC}$, $1\text{g}\cdot\text{L}^{-1}$ SDS for 5min, stained with NBT/BCIP and the median points were measured to obtain the mean telomere length^[50].

Telomerase activity assay

Telomerase activity was measured using the telomeric repeat amplification protocol (TRAP). Frozen samples were homogenized in $10\sim 50\mu\text{L}$ of ice-cold lyses buffer ($10\text{mmol}\cdot\text{L}^{-1}$ Tris-HCl, pH7.5, $1\text{mmol}\cdot\text{L}^{-1}$ EGTA, $0.1\text{mmol}\cdot\text{L}^{-1}$ Benzamidine, $5\text{mmol}\cdot\text{L}^{-1}$ β -mercaptoethanol, $5\text{g}\cdot\text{L}^{-1}$ CHAPS, $100\text{mL}\cdot\text{L}^{-1}$ glycerol). After 30min of incubation on ice, the lysate was centrifuged at 12000g for 20min at 4°C. TRAP-eze Telomerase Detection Kit (Oncor Inc.) reaction was performed using $1\mu\text{L}$ lysate or 1/10 diluted lysate, $2.5\mu\text{L}$ $10\times\text{TRAP}$ buffer ($200\text{mmol}\cdot\text{L}^{-1}$ Tris-HCl, pH8.3, $15\text{mmol}\cdot\text{L}^{-1}$ MgCl_2 , $630\text{mmol}\cdot\text{L}^{-1}$ KCl, 0.5% Tween 20, $10\text{mmol}\cdot\text{L}^{-1}$ EGTA, $1\text{g}\cdot\text{L}^{-1}$ BSA), $0.5\mu\text{L}$ $2.5\text{mmol}\cdot\text{L}^{-1}$ dNTP, $0.5\mu\text{L}$ Ts primer, $0.5\mu\text{L}$ TRAP primer mix, $19.5\mu\text{L}$ water, $0.5\mu\text{L}$ taq ($2\times 10^6\text{u}\cdot\text{L}^{-1}$). After incubation at 30°C for 30min, the reaction mix was immediately transferred to 94°C and performed PCR (GeneAmp PCR System 2400, PE, USA) at 94°C for 30s, 55°C for 30s, for 30 cycles. PCR products were separated in a non-denaturing $120\text{g}\cdot\text{L}^{-1}$ PAGE in $1\times\text{TBE}$ at $5\text{V}\cdot\text{cm}^{-1}$. The gel was stained using AgNO_3 and was photographed.

Subunits of telomerase analysis

The activities of telomerase were performed by hTERT and hTR analysis. Analysis of expression of hTR and hTERT was determined by reverse transcription-PCR (RT-PCR) amplification in contrast with house-keeping gene GAPDH. Total RNA was isolated from the cell using GstracTM RNA Isolation Kit (Maxim Biotech, Inc.). cDNA was synthesized from $10\mu\text{g}$ of total RNA using Ready-to-use First Strand cDNA Synthesis Kit (Maxim Biotech, Inc.). PCR reaction was performed using $2\mu\text{L}$ aliquots of the reverse-transcribed cDNA,

$2.5\mu\text{L}$ $10\times\text{PCR}$ buffer, $1.5\mu\text{L}$ $25\text{mmol}\cdot\text{L}^{-1}$ MgCl_2 , $2.5\mu\text{L}$ $1.0\text{mmol}\cdot\text{L}^{-1}$ dNTP, $2.0\mu\text{L}$ specific primers, $14\mu\text{L}$ water, $0.5\mu\text{L}$ taq ($2\times 10^6\text{u}\cdot\text{L}^{-1}$). hTERT mRNA was amplified using the primer pair: 5'-CGGAAGAGTGCTCTG-GAGCAA-3' and 5'-GGATGAAGCGAGTCTGGA-3' for 31 cycles (94°C for 45s, 55°C for 45s, 72°C for 90s). hTR was amplified using the primer pair: 5'-TCTAACCCTAACTGAGAAGGGCGTAG-3' and 5'-GTTTGCTCTAGAATGAACGGTGGGAAG-3'. GAPDH was amplified using the primer pair: 5'-GAAGGTGAAGGTCCGAGTC-3' and 5'-GAAGATGGTGATGGGATTTC-3' for 33 cycles (94°C for 60s, 55°C for 60s, 72°C for 60s). PCR products of each sample were subjected to electrophoresis in a $15\text{g}\cdot\text{L}^{-1}$ agarose gel containing $0.5\text{mg}\cdot\text{L}^{-1}$ ethidium bromide.

RESULTS

In the initiated passages, the cells in the 6th to the 10th passages were uniform in size and shape (Figure 1A), and grew as an even monolayer with characteristics of anchorage-dependent and attachment-inhibited growth. Cells continuously cultured in the 12th to the 16th passages exhibited morphologic changes in which cells were enlarged and flattened and exhibited differentiation and senescence. When many cells had shrunk, were round and floated freely, the majority underwent apoptosis and cell death with a few cells surviving (Figure 1B). Over coming senescence and apoptosis, the cells of the 20th passage restored their proliferation capacity (Figure 1C). After 30 passage the cells proliferated again and exhibited diphasic differentiation, a portion of cells displayed the undifferentiated basal epithelium and the other portion displayed differentiated squamous epithelium (Figure 1D).

Proliferative index (PI) and apoptosis

The PI of cell in 10, 16, 20, 30 the passage were 25.5%, 17.3%, 43.3%, and 43.0% respectively (Figure 2, A, B, C, D). Apoptotic cells index (AI) was in 10th passage, 7.3%; 16th, 57.5%; 20th, 5.7% and 30th, 7.5%. The cells in the 16th passage were at the stage of senescence and death, and the 10th, 20th and 30th were at their proliferated stages at various levels. Cells in G_0G_1 phase were identified as the differentiated cells containing some senescent cells.

The TUNEL assay was also used to characterize the biological features of cells apoptosis. Many TUNEL-positive nuclei were observed in cells of passage 16th (Figure 3), and in a few cells in other passages. By EM examination, many apoptotic cells revealed rounded and shrunken nuclei with condensed chromatin stuck closely to the nuclear membrane (Figure 4).

Telomere length

Following continuous growth of the cells, the telomere length of the cells in the 6th to 10th passages exhibited shortening from a mean size of 23kb in the normal esophageal mucosa to 17kb at passage 10. At 20th passage telomere length was shortened continually to the shortest 3kb, but maintained till the 30th passage (Figure 5).

Telomerase activity, expression of hTR and hTERT

Expression of hTR and hTERT in SHEE cells was determined by RT-PCR. The hTERT expression was positive in the 20th and 30th passages, but negative in the 10th passage (Figure 6A). Cells of the 10th, 20th and 30th passage showed positive expression of hTR (Figure 6B). House-keeping protein GAPDH was used as a control (Figure 6C). Comparing the variation of telomerase activity in SHEE from the 10th to the 30th passage, cells of the 10th passage were negative, while the 20th was weak and the 30th was apparent. The positive control of human esophageal squamous cell carcinoma expressed the highest telomerase activity (Figure 7).

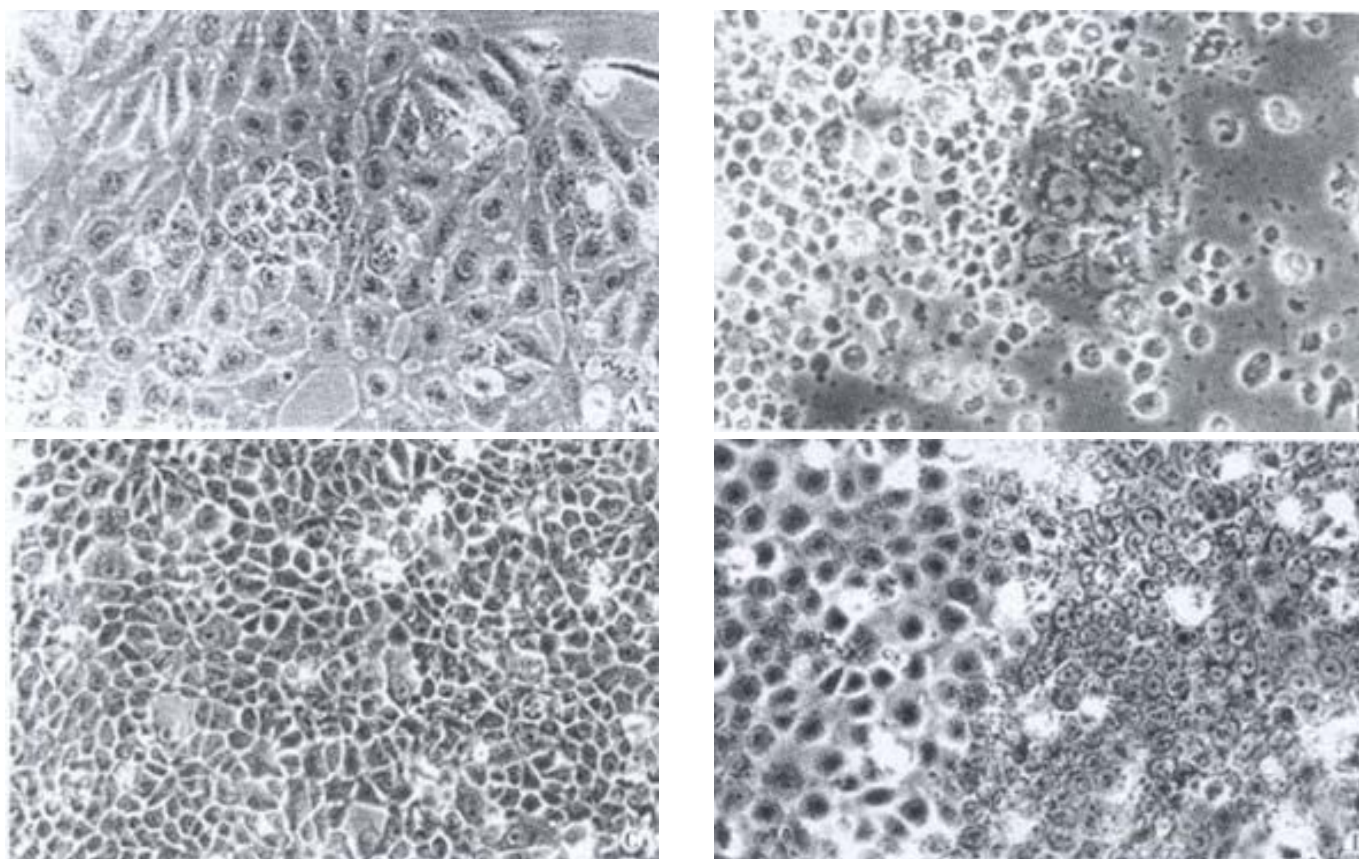


Figure 1 Morphologic changes in living cells of SHEE.

A: Cell in 6-10th passages showed differential phenotype (phase-contrast microscopy, Ph $\times 400$);

B: Cells of 16th passage displayed apoptosis with a few of cells survived (Ph $\times 400$);

C: Cells of 20th passage displayed hyperplasia (Ph $\times 200$);

D: Cells of 30th passage displayed proliferative activity with diphasic differentiation (Ph $\times 400$).

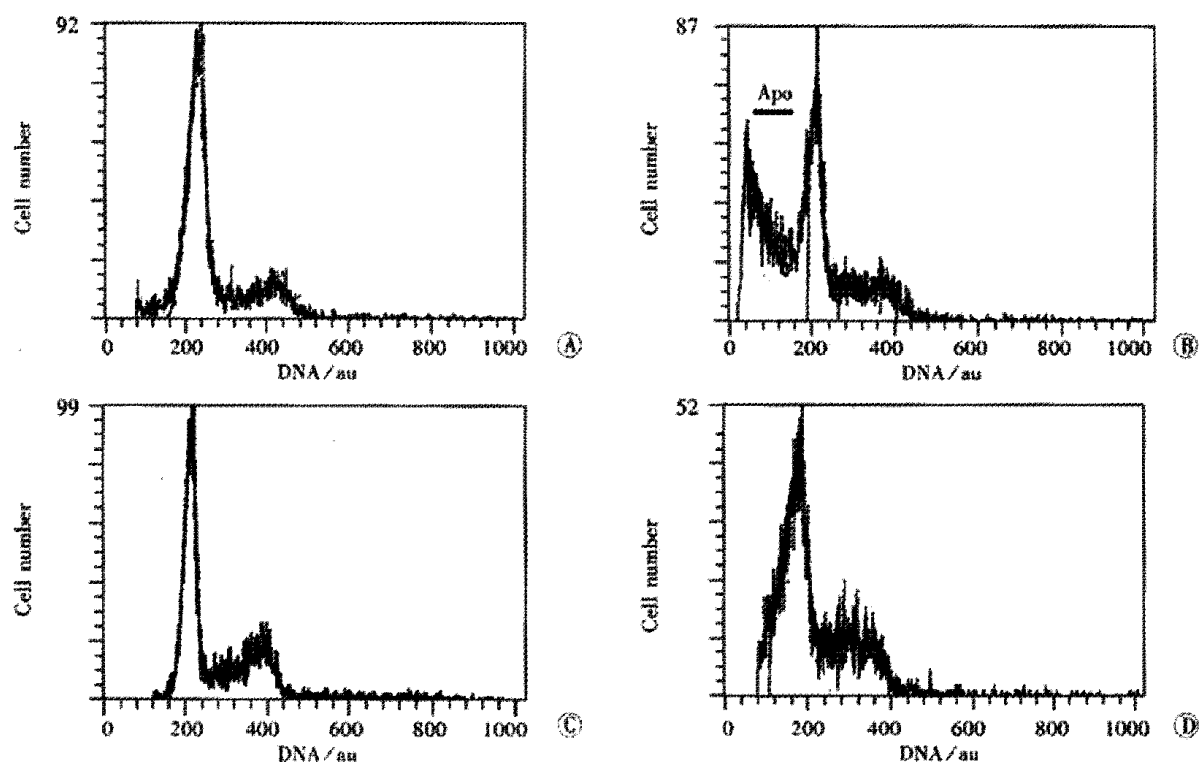


Figure 2 DNA histogram of SHEE cells.

A: 10th passage; B: 16th passage; C: 20th passage; D: 30th passage.

Apo: Apoptotic peak; AU: Arbitrary unite.



Figure 3 TUNEL positive apoptotic nuclei in 16th passage of SHEE. (x400)

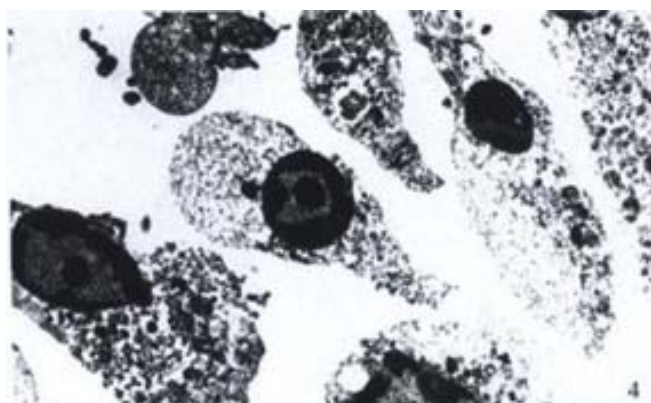


Figure 4 Electron-photomicrograph of apoptotic cells in 16th passage. Shrunken cells and rounded nuclei with margined condensed chromatin. (EM x3000)

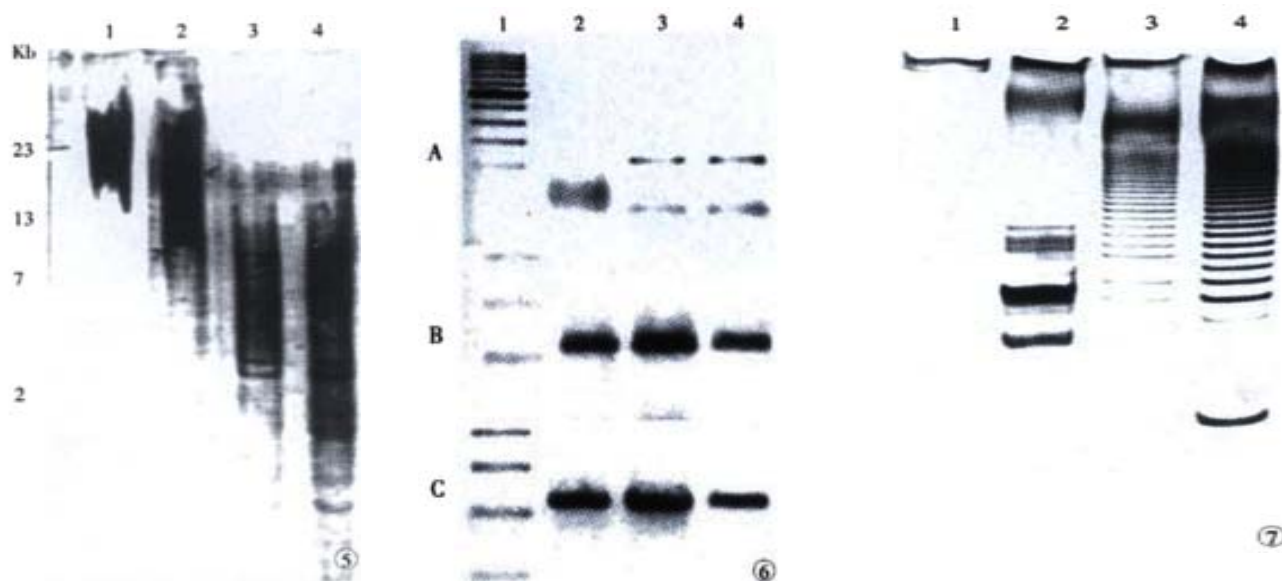


Figure 5 Telomere length of SHEE series using Southern blot.

1: Normal esophagus; 2: Cells of 10th passage; 3: Cells of 20th passage; 4: Cells of 30th passage.

Figure 6 Gel electrophoretogram of hTERT(A), hTR (B) and GAPDH (C).

Lane 1: marker; Lane 2: 10th passage; Lane 3: 20th passage; Lane 4: 30th passage.

Figure 7 Measurements of telomerase activity using TRAP assay.

Lane 1: 10th passage, negative; Lane 2: 20th passage, weak; Lane 3: 30th passage, positive; Lane 4: human esophageal squamous cell carcinoma, strong positive.

The relationship between telomerase activity and cellular proliferation

At an early stage in the immortalization process, SHEE cells could be divided into three stages. At the primary stage, telomerase activity and expression of hTERT was absent and the telomere length shortened. The cells of SHEE were proliferated and differentiated and then they were senescent and apoptotic cells in the culture. At the early immortal stage, cells exhibited telomerase activity and its subunits hTERT at low levels with telomere length being continually shortened and proliferation restored. At the immortal stage, telomerase and hTERT were expressed in high level and telomere length maintained, accompanied by cell proliferation. From 6th to 30th passages the cells expressed hTR.

DISCUSSION

After transferring the HPV18E₆E₇ genes to the fetal esophageal

epithelial cells, we established an immortal cell line designated SHEE. In order to focus on the process of immortalization, we monitored the dynamic changes of telomere length and telomerase activity of SHEE cells for extended periods of time (from the 6th passage to the 30th passage). At the primary stage the cells of passages 6-10 appeared as differentiated squamous epithelial cells with telomere length shortened without telomerase expression, after which the cells of passages 12-16 became senescent and underwent cell death. After overcoming the senescence and cell death, cells of the 20th passage expressed telomerase activity at low levels, where the length of shortened telomere was not maintained, but the proliferation of cells was restored. At the 30th passage, the cells exhibited a higher level of telomerase activity, hTR and hTERT, with maintained telomere length and continual proliferation of cells (immortalization). Therefore, one can suggest that telomerase activity and maintenance of telomere length might be necessary for immortalization of human esophageal epithelium *in vitro*.

To investigate the immortalization process, we used the SHEE cell model to define steps in aging of cells. After transduction of E₆E₇ genes from HPV type 18 normal cultured cells proliferate until they reach a discrete point (passage 12 times) in which the population growth ceases and develops to senescence. This period is termed the M1 stage of aging^[51]. After M1, a large amount of cells dead to reach a “crisis” point with a few cells survival. This period is termed the M2 stage of aging^[52]. Both M1 and M2 are therefore potential suppression pathways for tumorigenesis. The telomerase activity is sufficient to allow the cultured cells to escape from crisis^[53]. In our experiment cells transfected with HPV, cell proliferated for an extended period of time, after that cells encountered senescence (M1) and apoptosis (M2). Overcome the M1 and M2, cells exhibited accelerant hyperplasia with telomerase activity.

Recent evidence suggests that viral oncogenes might directly up-regulate telomerase activity^[54], such as HCV core protein, EBV-, HPV- and SV40 T antigen-expressing cell clones^[55-58]. In our data the increase of hTR in the primary cells of SHEE might be directly or indirectly affected by the HPV viral oncogenes. Previous reports also have shown that telomerase activity can be achieved by the E₆ and E₇ protein of HPV^[59]. HPV 16 E6 oncoprotein was capable of inducing telomerase activity in monolayer cultures of proliferating keratinocyte^[60]. It was more likely that HPV E6/E7 transcription or other additional alterations, as chromosome instability^[61,62] was prerequisite for induction of telomerase activity in proliferating cells. This hypothesis fits very well with our data on HPV-mediated immortalization of cells *in vitro*.

In summary, immortal cell line of the SHEE, up to 30th passage, may be divided into three stages. At the primary stage, telomerase activity and hTERT of cells were absent but hTR is positive with telomere length shortening and the cells became senescent and apoptotic. At the early-immortalized stage, the telomerase activity and hTERT expressed at low level and telomere length shortened continuously, but underwent cell hyperplasia occurred. At the immortalized stage, the telomerase activity and its two subunits expressed at a high level, telomere length was maintained and cell proliferation continued, in which the cells reached the stage of immortalization. The shortened telomere length and the activated telomerase activity display in a dynamic process. Our results prove that shortening of telomeres and absence of telomerase activity contribute to cellular senescence and cell death, and the activation of telomerase to maintain telomere length is necessary for immortalization. Therefore, the telomerase activity is the biomarker of immortalization of cell.

REFERENCES

- Yakoob J, Hu GL, Fan XG, Zhang Z. Telomere, telomerase and digestive cancer. *World J Gastroenterol* 1999; 5: 334-337
- He XX, Wang JL. Activity of telomerase and oncogenesis. *Huaren Xiaohua Zazhi* 1998; 6:1100-1101
- Yang SM, Fang DC, Luo YH, Lu R, Liu WW. Telomerase activity in gastrointestind submucosal tumors and its clinical significance. *Huaren Xiaohua Zazhi* 1998; 6: 765-767
- Zhan WH, Ma JP, Peng JS, Gao JS, Cai SR, Wang JP, Zheng ZQ, Wang L. Telomerase activity in gastric cancer and its clinical implications. *World J Gastroenterol* 1999; 5: 316-319
- He XX, Wang JL, Wu JL, Yuan SY, Ai L. Telomerase expression, Hp infection and gastric mucosal carcinogenesis. *Shijie Huaren Xiaohua Zazhi* 2000; 8: 505-508
- He XX, Wang JL, Wu JL, Yuan SY, Ai L. Telomere, cellular DNA content and gastric mucosal carcinogenesis. *Shijie Huaren Xiaohua Zazhi* 2000; 8: 509-512
- Yao XX, Yin L, Zhang SY, Bai WY, Li YM, Sun ZC. hTERT expression and cellular immunity in gastric cancer and precancerosis. *Shijie Huaren Xiaohua Zazhi* 2001; 9: 508-512
- Meng ZQ, Yu EX, Song MZ. Inhibition of telomerase activity of human liver cancer cell SMMC 7721 by chemotherapeutic drugs. *Shijie Huaren Xiaohua Zazhi* 1999; 7: 252-254
- Fu JM, Yu XF, Shao YF. Telomerase and primary liver cancer. *Shijie Huaren Xiaohua Zazhi* 2000; 8: 461-463
- Qu B, Li BJ, Lu ZW, Pan HL. Clinical significance of telomerase activity detected in fine-needle aspiration specimens to liver cancer diagnosis. *Shijie Huaren Xiaohua Zazhi* 2001; 9: 538-541
- Qiu SL, Huang JQ, Wang YF, Peng ZH. Analysis of telomerase activity in colorectal cancer, precancerous lesions and cancer washings. *Shijie Huaren Xiaohua Zazhi* 1998; 6: 992-993
- Sobti RC, Kochar J, Singh K, Bhasin D, Capalash N. Telomerase activation and incidence of HPV in human gastrointestinal tumors in North Indian population. *Mol Cell Biochem* 2001; 217: 51-56
- Jia L, Li YY. Telomerase activity of exfoliated cancer cells in colonic luminal washings. *Huaren Xiaohua Zazhi* 1998; 6: 955-957
- Koyanagi K, Ozawa S, Ando N, Takeuchi H, Ueda M. Clinical significance fo telomerase activity in the cancerous epithelial region of oesophageal squaous carcinoma. *Br J Surg* 1999; 86:674-679
- Hiyama T, Yokozaki H, Kitadai Y, Haruma K, Yasui W, Takara F. Overexpression of human telomerase RNA is an early oesophageal carcinogenesis. *Virchows Arch* 1999; 434: 483-487
- Kiyozuka Y, Asai A, Yamamoto D, Senzaki H, Yoshioka S, Hioki K, Tsubura A. Establishment of novel human esophageal cancer cell relation to telomere dynamics and telomerase activity. *Dig Dis Sci* 2000; 45: 870-879
- Koyanagi K, Ozawa S, Ando N, Mukai M, Kitagawa Y, Ueda MM. Telomerase activity as an indicator of malignant in iodine-nonreactive lesions of the esophagus. *Cancer* 2000; 88: 1524-1529
- Xu LY, Shen ZY, Li EM, Cai WJ, Shen J, Li C, Chen JY, Zeng Y. Telomere length and telomerase activity in immortalized and malignant transformed human embryonic esophageal epithelial cell lines by E6 and E7 genes of HPV 18 type. *Aibian Qibian Tubian* 2001; 13: 137-140
- Morales CP, Lee EL, Shay JW. *in situ* hybridization for the detection of telomerase in the progression from Barrett's esophagus to esophageal adenocarcinoma. *Cancer* 1998; 83: 652-659
- Xia ZS, Zhu ZH, He SG. Effects of ATRA and 5 Fu on growth and telomerase activity of xenografts of gastric cancer in nude mice. *Shijie Huaren Xiaohua Zazhi* 2000; 8: 674-677
- Li ZS, Zhu ZG, Yin HR, Chen SS, Lin YZ. Diversity of telomerase activity in human and murine tumor cells transfected with cytokine genes. *Shijie Huaren Xiaohua Zazhi* 1999; 7: 194-196
- Zhu ZH, Xia ZS, He SG. The effects of ATRA and 5 Fu on telomerase activity and cell growth of gastric cancer cells *in vitro*. *Shijie Huaren Xiaohua Zazhi* 2000; 8: 669-673
- Sarvesvaran J, Going J, Milroy R, Kaye SB, Nicol Keith W. Is small cell lung cancer the perfect target for anti-telomerase treatment? *Carcinogenesis* 1999; 20: 1649-1651
- Zhang FX, Zhang XY, Fan DM, Deng ZY, Yan Y, Wu HP, Fan JJ. Antisense telomerase RNA induced human gastric cancer cell apoptosis. *World J Gastroenterol* 2000; 6: 430-432
- Bednarek A, Shilkaitis A, Green A, Lubet R, Kelloff G, Christov K, Aldaz CM. Suppression of cell proliferation and telomerase activity in 4-(hydroxyphenyl) retinamide-treated mammary tumors. *Carcinogenesis* 1999; 20: 879-883
- Herbert BS, Wright AC, Passons CM, Wright WE, Ali IU, Kopelovici Shay JW. Effects of chemopreventive and antitelomerase agents on the spontaneous immortalization of breast epithelial cells. *J Natl Cancer Inst* 2001; 93:39-45
- Yeh TS, Cheng AJ, Chen TC, Jan YY, Hwang TL, Jeng LB, Chen MF, Wang TC. Telomerase activity is a useful marker to distinguish malignant pancreatic cystic tumors from benign neoplasms and pseudocysts. *J Surg Res* 1999; 87: 171-177
- Shroyer KR, Thompson LC, Enomoto T, Eskens JL, Shroyer AL, McGregor JA. Telomerase expression in normal epithelium, reactive atypia, squamous dysplasia, and squamous cell carcinoma of the uterine cervix. *Am J Clin Pathol* 1998; 109: 153-162
- Wisman GBA, Hollema H, de-Jong S, ter-Schegget J, Tjong-A-Hung SP, Ruiters MHJ, Krans M, de-Vries EGE, van-der-Zee AGJ. Telomerase activity as a biomarker for (Pre) neoplastic cervical disease in scrapings and frozen sections from patients with abnormal cervical smear. *J Clin Oncol* 1998; 16: 2238-2245
- Rudolph P, Schubert C, Tamm S, Heidorn K, Hauschild A, Michalska I, Majewski S, Krupp G, Jablonska S, Parwaresch R. Telomerase activity in melanocytic lesions: A potential marker of tumor biology. *Am J Path* 2000; 156: 1425-1432
- Jones CJ, Kipling D, Morris M, Hepburn P, Skinner J, Bounacer A, Wyllie FS, Ivan M, Bartek J, Wynford-Thomas D, Bond JA. Evidence for a telomere-independent “clock” limiting RAS oncogene-driven proliferation of human thyroid epithelial cells. *Mol Cell Biol* 2000; 20: 5690-5699
- Griffith JD, Comeau L, Rosenfield S, Stansel RM, Bianchi A, Moss H, de Lange T. Mammalian telomeres end in a large duplex loop. *Cell* 1999; 97:503-514

- 33 Nakano K, Watney E, McDougall JK. Telomerase activity and expression of telomerase RNA component and telomerase catalytic subunit gene in cervical cancer. *Am J Pathol* 1998; 153: 857-864
- 34 Schwartz JL, Jordan R, Liber H, Murnane JP, Evans HH. TP53-dependent chromosome instability is associated with transient reductions in telomere length in immortal telomerase-positive cell lines. *Genes Chromosomes Cancer* 2001; 30: 236-244
- 35 Chin L, Artandi SE, Shen Q, Tam A, Lee SL, Gottlieb GJ, Greider CW, DePinho RA. P53 deficiency rescues the adverse effects of telomere loss and cooperates with telomere dysfunction to accelerate carcinogenesis. *Cell* 1999; 97:527-538
- 36 Yang XY, Kimura M, Jeanclos E, Aviv A. Cellular proliferation and telomerase activity in CHRF-288-11 cells. *Life Sci* 2000; 66: 1545-1555
- 37 Nickoloff BJ, Chaturvedi V, Bacon P, Qin JZ, Denning MF, Diaz MO. Id-1 delays senescence but does not immortalize keratinocytes. *J Biol Chem* 2000; 275: 27501-27504
- 38 MacKenzie KL, Franco S, May C, Sadelain M, Moore MA. Mass cultured human fibroblasts overexpressing hTERT encounter a growth crisis following and extended period of proliferation. *Exp Cell Res* 2000; 259: 336-350
- 39 Sugihara M, Ohshima K, Nakamura H, Suzumiya J, Nakayama Y, Kanda M, Haraoka S, Kikuchi M. Decreased expression of telomerase-associated RNAs in the proliferation of stem cells in comparison with continuous expression in malignant tumors. *Int J Oncol* 1999; 15: 1075-1080
- 40 Wang DX, Li W. Advances in esophageal neoplasms etiology. *Shijie Huaren Xiaohua Zazhi* 2000; 8:1029-1031
- 41 Ma QF, Jiang H, Feng YQ, Wang XP, Zhou YA, Liu K, Jia ZL. Detection of human papillomavirus DNA in squamous cell carcinoma of the esophagus. *Shijie Huaren Xiaohua Zazhi* 2000; 8:1218-1224
- 42 Zou SY, Liu XM, Tang XP, Wang P. Immunohistochemical and electron microscopic observation on positive HPV 16-E6 protein in esophageal cancer. *Shijie Huaren Xiaohua Zazhi* 1998; 6:47-48
- 43 Shen ZY, Cen S, Cai WJ, Xu JJ, Ten ZP, Shen J, Hu Z, Zeng Y. Immortalization fetal esophageal epithelial cells induced by E6 and E7 genes of human papilloma virus to. *Zhonghua Shiyen He Linchuang Bingduxue Zazhi* 1999; 13: 121-123
- 44 Shen ZY, Shen J, Cai WJ, Cen S, Zeng Y. Biological characteristics of human fetal esophageal epithelial cell line immortalized by the E6 and E7 gene of HPV type 18. *Zhonghua Shiyen He Linchuang Bingduxue Zazhi* 1999; 13: 209-212
- 45 Shen ZY, Xu LY, Chen MH, Cai WJ, Shen J, Chen JY, Hon CQ, Zeng Y. Biphasic differentiation of immortalized esophageal epitheliums induced by HPW18E6E7. *Bingdu Xuebao* 2001;17:210-214
- 46 Shen ZY, Xu LY, Chen XH, Cai WJ, Shen J, Chen JY, Huang TH, Zeng Y. The genetic events of HPV-immortalized esophageal epithelium cells. *Int J Mol Med* 2001; 8:537-542
- 47 Shen ZY, Cen S, Shen J, Cai WJ, Xu JJ, Teng ZP, Hu Z, Zeng Y. Study of immortalization and malignant transformation of human embryonic esophageal epithelial cells induced by HPV18E6E7. *J Cancer Res Clin Oncol* 2000; 126: 589-594
- 48 Shen ZY, Chen XH, Shen J, Cai WH, Chen JY, Huang TFH, Zeng Y. Malignant transformation of immortalized human embryonic esophageal epithelial cells induced by human papillomavirus. *Bingdu Xuebao* 2000; 16: 97-101
- 49 Xu LY, Li EM, Shen ZY, Cai WJ, Shen J. A nonradio-labelled method assays to measure the telomere length of human chromosome. *Aibian Qibian Tubian* 2001; 13: 1-4
- 50 Hou M, Xu D, Bjorkholm M, Gruber A. Real-time quantitative telomeric repeat amplification protocol assay for the detection of telomerase activity. *Clin Chem* 2001;47:519-524
- 51 Ouellette MM, Liao M, Herbert BS, Johnson M, Holt SE, Liss HS, Shay JW, Wright WE. Subsenescent telomere lengths in fibroblasts immortalized by limiting amounts of telomerase. *J Biol Chem* 2000; 275: 10072-10076
- 52 Lustig AJ. Crisis intervention: The role of telomerase. *Proc Natl Acad Sci USA* 1999; 96: 3339-3341
- 53 Halvorsen TL, Leibowitz G, Levine F. Telomerase activity is sufficient to allow transformed cells to escape from crisis. *Mol Cell Biol* 1999; 19: 1864-1870
- 54 Zhu J, Wang H, Bishop JM, Blackburn EH. Telomerase extends the lifespan of virus-transformed human cells without net telomere lengthening. *Proc Natl Acad Sci USA* 1999; 96:3723-3728
- 55 Nowak JA. Telomerase, cervical cancer, and human papillomavirus. *Clin Lab Med* 2000; 20: 369-382
- 56 Ray RB, Meyer K, Rayt R. Hepatitis C virus core protein promotes immortalization of primary human hepatocytes. *Virology* 2000; 271: 197-204
- 57 Guo W, Kang MK, Kim HJ, Park NH. Immortalization of human oral keratinocytes is associated with elevation of telomerase activity and shortening of telomere length. *Oncol Rep* 1998; 5: 779-804
- 58 Mutirangura A, Sriuranpong V, Termrungruanglert W, Tresukosol D, Lertsaguansinchai P, Voravud N, Niruthisard S. Telomerase activity and human papillomavirus in malignant, premalignant and benign cervical lesions. *Br J Cancer* 1998; 78: 933-939
- 59 Nair P, Jayaprakash PG, Nair MK, Pillai MR. Telomerase, P53 and human papillomavirus infection in the uterine cervix. *Acta Oncol* 2000; 39: 65-70
- 60 Snijders PJ, van-Duin M, Walboomers JM, Steenbergen RD, Risse, EK, Helmerhorst TJ, Verheijen RH, Meijer PJ. Telomerase activity exclusively in cervical carcinomas and a subset of cervical intraepithelial neoplasia grade III lesions: strong association with elevated messenger RNA levels of its catalytic subunit and high-risk human papillomavirus DNA. *Cancer Res* 1998; 58: 3812-3818
- 61 Golubovskaya VM, Filatov LV, Behe CI, Presnell SC, Hooth MJ, Smith GJ, Kaufmann WK. Telomere shortening telomerase expression, and chromosome instability in rat hepatic epithelial stem-like cells. *Mol Carcinog* 1999; 24: 209-217
- 62 Filatov L, Golubovskaya V, Hurt JC, Byrd LL, Phillips JM, Kaufmann WK. Chromosomal instability is correlated with telomere erosion and inactivation of G2 checkpoint function in human fibroblasts expressing human papillomavirus type 16 E6 oncoprotein. *Oncogene* 1998; 16: 1825-1838

Edited by Wu XN

• BASIC RESEARCH •

Protective effect of estradiol on hepatocytic oxidative damage

Yan Liu, Ichiro Shimizu, Toshihiro Omoya, Susumu Ito, Xiao-Song Gu, Ji Zuo

Yan Liu, Ji Zuo Department of Biology, Medical school of Fudan University, Fudan University, Shanghai, 210032, China
Ichiro Shimizu, Toshihiro Omoya, Susumu Ito, Second Department of Internal Medicine, School of Medicine, University of Tokushima, Tokushima, 770-8503, Japan

Yan Liu, Xiao-Song Gu, Department of Biology, Nantong Medical College, Nantong, 226001, Jiangsu Province, China

Correspondence to: Yan Liu, Department of Biology, Medical School of Fudan University, 130 Dongan Road, Shanghai, 210032, China. liya9899@yahoo.com

Telephone: +86-21-64041900-2311

Received 2001-08-09 Accepted 2001-08-23

Abstract

AIM: To examine the protective effect of estradiol on the cultured hepatocytes under oxidative stress.

METHODS: Hepatocytes of rat were isolated by using perfusion method, and oxidative stress was induced by a serum-free medium and FeNTA. MDA level was determined with TBA method. Cell damage was assessed by LDH assay. Apoptosis of hepatocytes was assessed with cytoflowmetric analysis. Expression of Bcl-xl in cultured hepatocytes was detected by Western blot. The radical-scavenging activity of estradiol was valued by its ability to scavenge the stable free radical of DDPH.

RESULTS: Oxidative stress increased LDH (from $168 \pm 25 \times 10^{-6} \text{IU} \cdot \text{cell}^{-1}$ to $780 \pm 62 \times 10^{-6} \text{IU} \cdot \text{cell}^{-1}$) and MDA (from $0.28 \pm 0.07 \times 10^{-6} \text{nmol} \cdot \text{cell}^{-1}$ to $1.35 \pm 0.12 \times 10^{-6} \text{nmol} \cdot \text{cell}^{-1}$) levels in cultured hepatocyte, and estradiol inhibited both LDH and MDA production in a dose dependent manner. In the presence of estradiol $10^{-6} \text{mol} \cdot \text{L}^{-1}$, $10^{-7} \text{mol} \cdot \text{L}^{-1}$ and $10^{-8} \text{mol} \cdot \text{L}^{-1}$, the LDH levels are $410 \pm 53 \times 10^{-6} \text{IU} \cdot \text{cell}^{-1}$ ($P < 0.01$ vs oxidative group), $530 \pm 37 \times 10^{-6} \text{IU} \cdot \text{cell}^{-1}$ ($P < 0.01$ vs oxidative group), $687 \pm 42 \times 10^{-6} \text{IU} \cdot \text{cell}^{-1}$ ($P < 0.05$ vs oxidative group) respectively, and the MDA level are $0.71 \pm 0.12 \times 10^{-6} \text{nmol} \cdot \text{cell}^{-1}$ ($P < 0.01$ vs oxidative group), $0.97 \pm 0.11 \times 10^{-6} \text{nmol} \cdot \text{cell}^{-1}$ ($P < 0.01$ vs oxidative group) and $1.27 \pm 0.19 \times 10^{-6} \text{nmol} \cdot \text{cell}^{-1}$ respectively. Estradiol suppressed apoptosis of hepatocytes induced by oxidative stress, administration of estradiol ($10^{-6} \text{mol} \cdot \text{L}^{-1}$) decreased the apoptotic rate of hepatocytes under oxidative stress from $18.6 \pm 1.2\%$ to $6.5 \pm 2.5\%$, $P < 0.01$. Bcl-xl expression was related to the degree of liver cell damage due to oxidative stress, and estradiol showed a protective action.

CONCLUSION: Estradiol protects hepatocytes from oxidative damage by means of its antioxidant activity.

Liu Y, Shimizu I, Omoya T, Ito S, Gu XS, Zuo J. Protective effect of estradiol on hepatocytic oxidative damage. *World J Gastroenterol* 2002;8(2):363-366

INTRODUCTION

Hepatic fibrosis is a common consequence of chronic liver injury from many causes^[1-7], and the critical event in hepatic fibrosis is the

activation of lipocyte (also known as the stellate, fat-storing or Ito cell) which is the main source of extracellular matrix in fibrosis formation^[8-20]. The putative impetus to lipocyte activation came from cytokines released from Kupffer cells or leukocytes in liver injury^[21]. An alternative way is that parenchymal-cell necrosis itself may activate lipocyte; such activation could be mediated by the lipid peroxides formed after the membrane of parenchymal cells is injured^[22-28]. Therefore, preventing hepatocyte from injury is a matter of primary importance in blocking the fibrogenic pathway. We have reported the inhibitory effect of estradiol on activation of rat lipocytes^[29,30] and the suppressive effect on fibrogenesis in rat model^[31]. The present study is initiated to investigate the role of estradiol on the hepatocyte under oxidative stress, and to elucidate the mechanism of its inhibitory effect on hepatic fibrogenesis.

MATERIALS AND METHODS

Hepatocyte isolation and induction of lipid peroxidation

Hepatocytes were isolated from the liver of male Wistar rats (500-600g) with *in situ* perfusion method as previously described. Inocula of 2×10^5 cells per well were introduced into 12-well plate, (Nunc). The cells were cultured in 1ml Williams medium E supplemented with $50 \text{ml} \cdot \text{L}^{-1}$ FBS, $105 \text{U} \cdot \text{L}^{-1}$ penicillin, $100 \text{mg} \cdot \text{L}^{-1}$ streptomycin, and $10 \text{g} \cdot \text{L}^{-1}$ L-glutamine at 37°C in $50 \text{ml} \cdot \text{L}^{-1}$ CO_2 atmosphere and 100% humidity. After 4h, the cell medium was removed and lipid peroxidation was induced by incubating hepatocytes in serum-free Williams medium E with $100 \mu\text{mol} \cdot \text{L}^{-1}$ FeNTA (ferric nitrilotriacetate). Three groups of hepatocyte were analysed in parallel in each experiment including the hepatocytes cultured under normal condition and the hepatocyte cultured under oxidative stress in the presence or absence of $17\text{-}\beta$ -estradiol (Sigma).

Detection of (MDA) and lactate dehydrogenase (LDH) level in culture medium

Lipid peroxidation in cultured hepatocyte was determined by detecting the level of malondialdehyde (MDA), end product of lipid peroxidation in culture medium. The cell medium was collected, centrifuged at 450g to remove cell debris, and the MDA contents was determined by using a colorimetric reaction with thiobarbituric acid. A calibration curve was constructed from the conversion of tetraethoxypropane to MDA. The degree of cell damage was assessed by detecting the lactate dehydrogenase (LDH) activity released from the cytosol of damaged cells into the supernatant. The LDH activity was determined by using LDH detection Kit (Sigma). The time course of the MDA and LDH levels in culture medium was constructed to examine the lipid peroxidation and cell damage of hepatocyte during cultivation.

Flowcytometric analysis for apoptosis in hepatocytes

Rat hepatocytes were isolated and inoculated in 24-well plate as described. After oxidative stress was induced for 24h, apoptotic hepatocytes were detected by flowcytometry. Apoptotic cells expose their phosphatidylserine (PS) in the outer leaflet of cell membrane.

The exposed PS can be revealed by FITC-conjugated annexin V. Annexin V Kits(BD pharmingen) was used ,and the samples were treated according to the instruction enclosed in the kit as mannul described and analysed on the flowcytometer(Coulter Epics).

Western blot analysis of Bcl-xl

Rat hepatocytes were cultured in 35mm diameter dishes(Nunc) which were divided into 3 groups: the normal group, the oxygen stress and the oxygen stress plus estradiol group. In the presence or absence of $10^{-6}\text{mol}\cdot\text{L}^{-1}$ estradiol for the indicated time period,the dishes were then washed twice with ice cold PBS and lysed directly in 1ml SDS loading buffer($50\text{mmol}\cdot\text{L}^{-1}$ Tris, pH6.7, $20\text{g}\cdot\text{L}^{-1}$ SDS, $100\text{g}\cdot\text{L}^{-1}$ glycerol, $0.6\text{g}\cdot\text{L}^{-1}$ bromophenol blue, $100\text{mmol}\cdot\text{L}^{-1}$ dithiothreitol). The samples were boiled for 5 min and applied to a standard $120\text{g}\cdot\text{L}^{-1}$ SDS polyacrylamide protein gel. After electrophoresis, protein transfer was performed onto Hybond-ECL(Amersham Pharmacia Biotech) using a semi-dry blotting apparatus. The membrane was treated first with $100\text{ml}\cdot\text{L}^{-1}$ non-fat milk in PBS at room temperature for 2h and next with the Bcl-xl or Bcl-2 monoclonal antibody (Tanslab; diluted 1:500)for two hours at room temperature. After washing, the membrane was then incubated with HRP conjugated goat antimouse IgG(Amersham Pharmacia Biotech; diluted 1:1000)for one hour at room temperature. Immunoreactive bands were visualized using the ECL western blotting detection system kit (Amersham Pharmacia Biotech) according to the manufacturer's recommended protocol. The membranes used for Bcl-xl or Bcl-2 detection were reprobed with actin polyanitbody and the corresponding secondary antibody to normalize the signal strength of Bcl-xl and Bcl-2.

Radical-scavenging activity of estradiol

The radical-scavenging activity of estradiol was determined from its ability to scavenge the stable free radical of 1,1-diphenyl-2-picrylhydrazyl (DPPH,Wako) and was compared with that of the well-known antioxidant, α -tocopherol. $5\mu\text{l}$ of estradiol or α -tocopherol ($2,4,6,8,10\mu\text{mol}\cdot\text{L}^{-1}$) was added to 2.5ml $100\mu\text{mol}\cdot\text{L}^{-1}$ DPPH, in $20\text{mmol}\cdot\text{L}^{-1}$ 2-(N-morpholino) ethanesulfonic acid (MES) (pH 5.5) and the change in optical absorbance at 517nm was measured 30min thereafter.

Statistical analysis

Experimental results were analyzed by Student's *t* test for multiple comparisons. *P* values less than 0.05 were considered to be statistically significant.

RESULTS

Effect of estradiol on MDA and LDH level in hepatocytes under oxidative stress

The MDA and LDH levels in the medium of hepatocytes cultured under normal condition and oxidative stress were shown respectively in Figure 1 and Figure 2. The MDA level increased rapidly 5h after the oxidative stress and was maintained at a considerably high concentration during the period of continued cultivation. In normal control, MDA was kept at a low concentration in the incubating time, indicating a low level of lipid peroxidation in the normal condition. LDH level increased steadily after oxidative stress, whereas the LDH level in normal control increased slightly during culture. These data revealed that oxidative stress initiate lipid peroxidation and cause cell membrane damage in hepatocytes under stress. Twenty-four' oxidative stress was selected as the time point to examine the effect of estradiol administration on the MDA and LDH level in hepatocytes under oxidative stress. As the data showed in Table 1,estradiol decreased the MDA and LDH level in the culture medium in a dose

dependent manner.That means estradiol could inhibit the lipid peroxidation and subsequent hepatocytic membrane damage under oxidative stress.

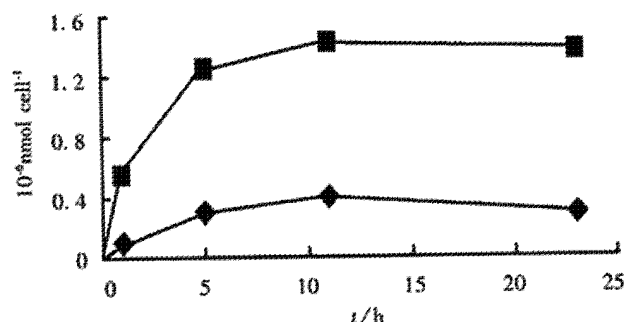


Figure 1 Effect of estradiol on MDA level in hepatocytes cultured under normal condition (◆) and oxidative stress (■)

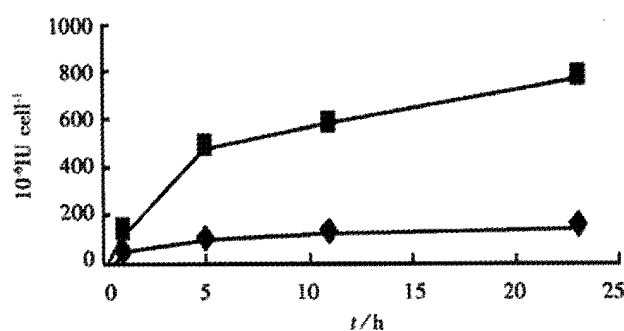


Figure 2 Effect of estradiol on LDH level in hepatocytes cultured under normal contion (◆) and oxidative stress (■)

Table 1 Effect of estradiol on MDA and LDH level in culture medium of hepatocytes under oxidative stress

Stress	MDA($10^{-6}\text{nmol}\cdot\text{cell}^{-1}$)	LDH ($10^3\text{IU}\cdot\text{cell}^{-1}$)
780±62		1.35±0.12
$10^{-8}\text{mol}\cdot\text{L}^{-1}$ estradiol	1.27±0.19	687±42 ^a
$10^{-7}\text{mol}\cdot\text{L}^{-1}$ estradiol	0.97±0.11 ^b	530±37 ^b
$10^{-6}\text{mol}\cdot\text{L}^{-1}$ estradiol	0.71±0.12 ^b	410±53 ^b
Normal control	0.28±0.07 ^b	168±25 ^b

^a*P*<0.05, ^b*P*<0.01 vs stress group.

Flowcyto-metric analysis for apoptotic hepatocytes

The aim of this investigation was to ascertain whether oxidative stress could induce apoptosis of hepatocytes, and whether estradiol could protect hepatocytes from such damage. The apoptotic rate of hepatocyte under normal culture condition was $5.9\pm1.7\%$, but in hepatocytes under oxidative stress it was $18.6\pm1.2\%$. With the administration of $10^{-6}\text{mol}\cdot\text{L}^{-1}$ estradiol,the apoptotic rate of hepatocytes under oxidative stress decreased to $6.5\pm2.5\%$. These data suggest that estradiol inhibit hepatocytic apoptosis induced by oxidative stress (results obtained from three distinct experiments).

Western blot analysis of Bcl-xl

Bcl-2 family has been investigated extensively for its proapoptotic or antiapoptotic property; Bcl-xl and Bcl-2 are well-known negative regulator of apoptosis^[32-36]. Western blot was used to examine the relationship between Bcl-xl and Bcl-2 level and estradiol administration. Estradiol applied in this experiment was $10^{-6}\text{mol}\cdot\text{L}^{-1}$. The result was depicted in Figure 3 (showing one representative result

from three independent experiments). Bcl-xl level was upregulated in hepatocytes under oxidative stress for 24h as compared with the normal control, while estradiol administration attenuated the increased expression of Bcl-xl induced by oxidative stress. After culturing for 48h, Bcl-xl expression was increased in hepatocytes both in the absence or presence of estradiol under oxidative stress. Bcl-xl level in hepatocytes was increased under oxidative stress. Bcl-2 expression was not detectable even though two antibodies from two different companies were used, indicating its low level in hepatocyte.

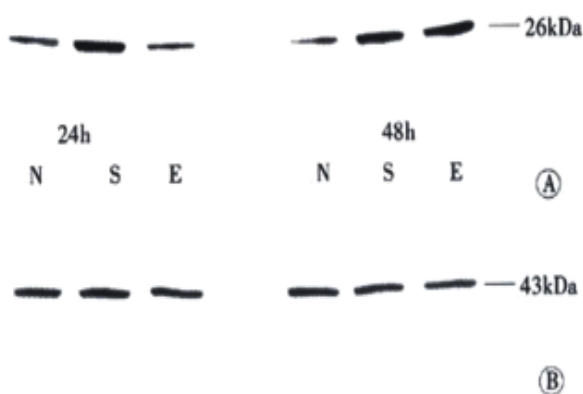


Figure 3 (A) Effect of estradiol on Bcl-xl expression in cultured hepatocytes for 24h and 48h. (B) Actin expression in cultured hepatocytes for 24h and 48h. N: Normal condition. S: Oxidative stress. E: Oxidative stress supplemented with 10^{-6} mol \cdot L $^{-1}$ estradiol.

Radical-scavenging activity of estradiol

Radical-scavenging activity of estradiol was determined by monitoring the decrease in absorbance at 517nm. Estradiol caused an immediate decrease in DPPH absorbance in a dose dependent manner (Figure 4). Its radical scavenging activity potency was approximately half that of α -tocopherol.

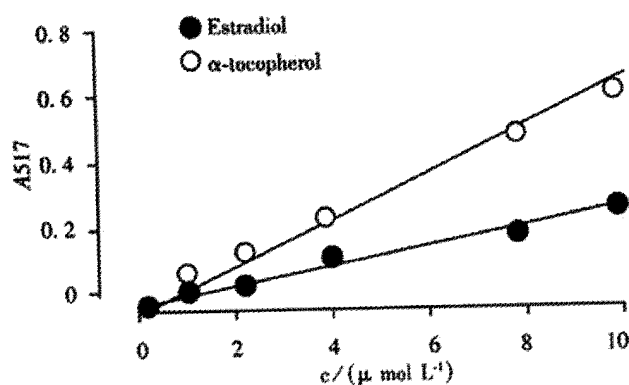


Figure 4 DPPH radical-scavenging activity of estradiol

DISCUSSION

Hepatic fibrosis and cirrhosis occur more frequently in men than in women. The ratio of male:female has been reported to range from 2.3:1 to 2.6:1 which indicates that sex hormones may play a role in the development of hepatic fibrosis and subsequent cirrhosis. We have found that estradiol treatment resulted in reduced hepatic fibrosis in male rat in which hepatic fibrosis had been induced by dimethylnitrosamine (DMN), and this phenomenon had been proven to be associated with the inhibitory effect of estradiol on the activation of lipocyte which is essential for hepatic fibrogenesis. Lipocyte can be activated by inflammatory factors released from Kupffer cells or free radicals and lipid peroxides formed in injured liver. Therefore, we examined the effect of estradiol on the cultured hepatocytes to evaluate its protective activity against oxidative damage of the liver. Estradiol is a steroidal compound that binds to specific intracellular receptors which act as transcription factors. Although the liver is not the classical sex hormone target, but livers in both men and women contain high affinity, low capacity estradiol receptors, and they are believed to respond to estradiol regulation. Another transcription independent activity of the molecule estradiol is its intrinsic antioxidant activity which makes it a potential chemical shield for cells^[37,38]. The neuroprotective effect of estradiol from oxidative damage has been extensively investigated in recent years^[39,40]. It is also noteworthy that oxygen-derived free radicals and lipid peroxidation have been implicated in hepatic injury^[41]. Our data also demonstrated that estradiol could inhibit the lipid peroxidation in hepatocyte and the free radicals induced-hepatocytic injury, and thus exerted its suppressive effect on liver fibrosis.

Hepatocytic damages induced by oxidative stress include two forms: cell necrosis and apoptosis. We also found that estradiol could inhibit the apoptosis of hepatocytes in the face of oxidative challenges. To elucidate the mechanism of its antiapoptotic effect, we examined the relationship between estradiol administration and the Bcl-2 and Bcl-x expression level by Western blotting. Figure 3 showed that Bcl-xl level in hepatocytes was increased under oxidative stress, while administration of estradiol attenuated the increased expression of Bcl-x induced by oxidative stress. These data suggested that Bcl-x expression responded directly to oxidative stress as a protective reaction, and estradiol could counteract the oxidative stress and stabilized the Bcl-xl expression before its antioxidant activity was depleted. In this study, Bcl-2 expression was not detectable even though two antibodies from different companies were used because of its low level in hepatocytes. But in another investigation we found that estradiol administration dramatically increased the Bcl-2 level in fibrotic liver tissue of rat induced by DMN injection (data not presented). Therefore, the mechanism of the antiapoptotic effect of estradiol is still elusive. The regulators, which participate in this pathway need further investigation. In conclusion, our findings suggested that estradiol could protect hepatocytes from oxidative stress, and the transcription-independent antioxidant activity of estradiol molecule may play a major role in this pathway.

REFERENCES

- 1 Wu CH. Fibrodynamics-elucidation of the mechanisms and sites of liver fibrogenesis. *World J Gastroenterol* 1999;5:388-390
- 2 Bissell DM. Hepatic fibrosis in wound repair: a progress report. *J Gastroenterol* 1998;33:295-302
- 3 Friedman SL. Molecular regulation of hepatic fibrosis, an integrated cellular response to tissue injury. *J Biol Chem* 2000;275:2247-2250
- 4 Brenner DA, Waterboer T, Choi SK, Lindquist JN, Stefanovic B, Burchardt E, Yamauchi M, Gillan A, Rippe RA. New aspects of hepatic fibrosis. *J Hepatol* 2000;32(Suppl 1):32-38
- 5 Albanis E, Friedman SL. Hepatic fibrosis. Pathogenesis and principles of therapy. *Clin Liver Dis* 2001;5:315-334
- 6 Santra A, Maiti A, Das S, Lahiri S, Chakaborty SK, Mazumder DN. Hepatic damage caused by chronic arsenic toxicity in experimental animals.

- J Toxicol Clin Toxicol* 2000;38:395-405
- 7 Maddrey WC. Alcohol-induced liver disease. *Clin Liver Dis* 2000;4: 115-131
- 8 Neubauer K, Saile B, Ramadori G. Liver fibrosis and altered matrix synthesis. *Can. J Gastroenterol* 2001;15:187-193
- 9 Shiba M, Shimizu I, Yasuda M, Ii K, Ito S. Expression of type I and type III collagens during the course of dimethylnitrosamine-induced hepatic fibrosis in rats. *Liver* 1998;18:196-204
- 10 Benyon RC, Arthur MJ. Extracellular matrix degradation and the role of hepatic stellate cells. *Semin Liver Dis* 2001;21:373-384
- 11 Ide M, Yamate J, Kuwamura M, Kotani T, Sakuma S, Takeya M. Immunohistochemical analysis of macrophages and myofibroblasts appearing in hepatic and renal fibrosis of dogs. *J Comp Pathol* 2001;124:60-69
- 12 Eng FJ, Friedman SL. Fibrogenesis I. New insights into hepatic stellate cell activation: the simple becomes complex. *Am J Physiol Gastrointest Liver Physiol* 2000;279:G7-G11
- 13 Eng FJ, Friedman SL. Transcriptional regulation in hepatic stellate cells. *Semin Liver Dis* 2001;21:385-395
- 14 Wei HS, Lu HM, Li DG, Zhan YT, Wang ZR, Huang X, Cheng JL, Xu QF. The regulatory role of AT 1 receptor on activated HSCs in hepatic fibrogenesis: effects of RAS inhibitors on hepatic fibrosis induced by CCl₄. *World J Gastroenterol* 2000;6:824-828
- 15 Iredale JP. Hepatic stellate cell behavior during resolution of liver injury. *Semin Liver Dis* 2001;21:427-436
- 16 Bataller R, Brenner DA. Hepatic stellate cells as a target for the treatment of liver fibrosis. *Semin Liver Dis* 2001;21:437-451
- 17 Pinzani M, Marra F, Carloni V. Signal transduction in hepatic stellate cells. *Liver* 1998;18:2-13
- 18 Du WD, Zhang YE, Zhai WR, Zhou XM. Dynamic changes of type I, III and IV collagen synthesis and distribution of collagen-producing cells in carbon tetrachloride induced rat liver fibrosis. *World J Gastroenterol* 1999;5:397-403
- 19 Wang LT, Zhang B, Chen JJ. Effect of anti-fibrosis compound on collagen expression of hepatic cells in experimental liver fibrosis of rats. *World J Gastroenterol* 2000;6:877-880
- 20 Liu HL, Li XH, Wang DY, Yang SP. Matrix metalloproteinase-2 and tissue inhibitor of metalloproteinase-1 expression in fibrotic rat liver. *World J Gastroenterol* 2000;6:881-884
- 21 Ramadori G, Armbrust T. Cytokines in the liver. *Eur J Gastroenterol Hepatol* 2001;13:777-784
- 22 Poli G. Pathogenesis of liver fibrosis: role of oxidative stress. *Mol Aspects Med* 2000;21:49-98
- 23 Lu LG, Zeng MD, Li JQ, Hua J, Fan JG, Fan ZP, Qiu DK. Effect of lipid on proliferation and activation of rat hepatic stellate cells (I). *World J Gastroenterol* 1998;4:497-499
- 24 Kim KY, Choi I, Kim SS. Progression of hepatic stellate cell activation is associated with the level of oxidative stress rather than cytokines during CCl₄-induced fibrogenesis. *Mol Cells* 2000;10:289-300
- 25 Hu YY, Liu CH, Wang RP, Liu C, Liu P, Zhu DY. Protective actions of salvianolic acid A on hepatocyte injured by peroxidation *in vitro*. *World J Gastroenterol* 2000;6:402-404
- 26 Chen PS, Zhai WR, Zhou XM, Zhang JS, Zhang YE, Ling YQ, Gu YH. Effects of hypoxia, hyperoxia on the regulation of expression and activity of matrix metalloproteinase-2 in hepatic stellate cells. *World J Gastroenterol* 2001;7:647-651
- 27 Greenwel P, Dominguez-Rosales JA, Mavi G, Rivas-Estilla AM, Rojkind M. Hydrogen peroxide: a link between acetaldehyde-elicited alpha1(I) collagen gene up-regulation and oxidative stress in mouse hepatic stellate cells. *Hepatology* 2000;31:109-116
- 28 Nalini G, Hariprasad C, Narayanan VA. Oxidative stress in alcoholic liver disease. *Indian J Med Res* 1999;110:200-203
- 29 Shimizu I, Mizobuchi Y, Yasuda M, Shiba M, Ma YR, Horie T, Liu F, Ito S. Inhibitory effect of oestradiol on activation of rat hepatic stellate cells *in vivo* and *in vitro*. *Gut* 1999;44:127-136
- 30 Shimizu I, Yasuda M, Mizobuchi Y, Ma YR, Liu F, Shiba M, Horie T, Ito S. Suppressive effect of oestradiol on chemical hepatocarcinogenesis in rats. *Gut* 1998;42:112-119
- 31 Yasuda M, Shimizu I, Shiba M, Ito S. Suppressive effects of estradiol on dimethylnitrosamine-induced fibrosis of the liver in rats. *Hepatology* 1999;29:719-727
- 32 Adams JM, Cory S. Life-or-death decisions by the Bcl-2 protein family. *Trends Biochem Sci* 2001;26:61-66
- 33 Zornig M, Hueber A, Baum W, Evan G. Apoptosis regulators and their role in tumorigenesis. *Biochim Biophys Acta* 2001;1551:F1-37
- 34 Budd RC. Activation-induced cell death. *Curr Opin Immunol* 2001;13: 356-362
- 35 Liu HF, Liu WW, Fang DC, Men RP. Expression of bcl-2 protein in gastric carcinoma and its significance. *World J Gastroenterol* 1998;4: 228-230
- 36 Grad JM, Zeng XR, Boise LH. Regulation of Bcl-xL: a little bit of this and a little bit of STAT. *Curr Opin Oncol* 2000;12:543-549
- 37 Huh K, Shin US, Choi JW, Lee SI. Effect of sex hormones on lipid peroxidation in rat liver. *Arch Pharm Res* 1994;17:109-114
- 38 Leal AM, Begona Ruiz-Larrea M, Martinez R, Lacort M. Cytoprotective actions of estrogens against tert-butyl hydroperoxide-induced toxicity in hepatocytes. *Biochem Pharmacol* 1998;56:1463-1469
- 39 Sawada H, Shimohama S. Neuroprotective effects of estradiol in mesencephalic dopaminergic neurons. *Neurosci Biobehav Rev* 2000;24: 143-147
- 40 Dare E, Gotz ME, Zhivotovsky B, Manzo L, Ceccatelli S. Antioxidants J811 and 17beta-estradiol protect cerebellar granule cells from methylmercury-induced apoptotic cell death. *J Neurosci Res* 2000; 62:557-565
- 41 Bruck R, Shirin H, Aeed H, Matas Z, Hochman A, Pines M, Avni Y. Prevention of hepatic cirrhosis in rats by hydroxyl radical scavengers. *J Hepatol* 2001;35:457-464

Edited by Lu HM

• BASIC RESEARCH •

Establishment of an artificial β -cell line expressing insulin under the control of doxycycline

Xin-Yu Qin, Kun-Tang Shen, Xin Zhang, Zhi-Hong Cheng, Xiang-Ru Xu, Ze-Guang Han

Xin-Yu Qin, Kun-Tang Shen, Department of General Surgery, Zhongshan Hospital, Fudan University, Shanghai 200032, China
Xin Zhang, Zhi-Hong Cheng, Xiang-Ru Xu, Ze-Guang Han, Functional Genomics Division, Chinese National Human Genome Center At Shanghai, Shanghai 201203, China

Supported by the "Hundred Talents" Program of Shanghai Municipal Government, No.98BR018

Correspondence to: Prof. Xin-Yu Qin, Department of General Surgery, Zhongshan Hospital, Fudan University, Shanghai 200032, China. xyqin@zshospital.com

Telephone: +86-21-64041900 Ext 2663 Fax: +86-21-64038472

Received 2001-09-14 Accepted 2001-12-08

Abstract

AIM: Artificial β -cell lines may offer an abundant source of cells for the treatment of type I diabetes, but insulin secretion in β -cells is tightly regulated in physiological conditions. The Tet-On system is a "gene switch" system, which can induce gene expression by administration of tetracycline (Tet) derivatives such as doxycycline (Dox). Using this system, we established 293 cells to an artificial cell line secreting insulin in response to stimulation by Dox.

METHODS: The mutated proinsulin cDNA was obtained from plasmid pcDNA3.1/C-mINS by the polymerase chain reaction (PCR), and was inserted downstream from the promoter on the expression vector pTRE2, to construct a recombinant expression vector pTRE2mINS. The promoter on pTRE2 consists of the tetracycline-response element and the CMV minimal promoter and is thus activated by the reverse tetracycline-controlled transactivator (rtTA) when Dox is administered. pTRE2mINS and plasmid pTK-Hyg encoding hygromycin were co-transfected in the tet293 cells, which express rtTA stably. Following hygromycin screening, the survived cells expressing insulin were selected and enriched. Dox was used to control the expression of insulin in these cells. At the levels of mRNA and protein, the regulating effect of Dox in culture medium on the expression of proinsulin gene was estimated respectively with Northern blot, RT-PCR, and radioimmunoassay.

RESULTS: From the 28 hygromycin-resistant cell strains, we selected one cell strain (tet293/Ins6) secreting insulin not only automatically, but in response to stimulation by Dox. The amount on insulin secretion was dependent on the Dox dose (0,10,100,200,400,800 and 1000 $\mu\text{g}\cdot\text{L}^{-1}$), the level of insulin secreted by the cells treated with Dox (1000 $\mu\text{g}\cdot\text{L}^{-1}$) was 241.0 pU $\cdot\text{d}^{-1}\cdot\text{cell}^{-1}$, which was 25-fold that of 9.7 pU $\cdot\text{d}^{-1}\cdot\text{cell}^{-1}$ without Dox treatment. Northern blot analyses and RT-PCR further confirmed that the transcription of insulin gene had already been up-regulated after exposing tet293/Ins6 cells to Dox for 15 minutes, and was also induced in a dose-dependent manner. However, the concentration of insulin in the media did not increase significantly until 5 hours following the addition of Dox.

CONCLUSION: Human proinsulin gene was transfected successfully and expressed efficiently in 293 cells, and the

expression was modulated by tetracycline and its derivatives, improving the accuracy, safety, and reliability of gene therapy, suggesting that conditional establishment of artificial β -cells may be a useful approach to develop cellular therapy for diabetes mellitus.

Qin XY, Shen KT, Zhang X, Cheng ZH, Xu XR, Han ZG. Establishment of an artificial β -cell line expressing insulin under the control of doxycycline. *World J Gastroenterol* 2002;8(2):367-370

INTRODUCTION

Owing to the steady improvement in methodology for islet and whole pancreas transplantation over the past three decades, this approach remains as the only means which is likely to substitute completely the function of the impaired β -cells in type I diabetes patients^[1]. However, the limited availability of human donors, the immunological rejection, the low survival percentage of grafts, and the high expense limit the broad-scale applicability of islet transplantation^[2-4]. As a result, in recent years much effort is being made to improve insulin secretion in the patient's non-beta cells to avoid the immune destruction^[5-9]. To successfully mimic beta cell function, it is necessary to overcome three major obstacles: proinsulin synthesis, proinsulin processing, and mature insulin storage and regulated secretion. Our previous study (unpublished) and studies by other authors had demonstrated that correct proinsulin processing and insulin storage can be obtained in somatic cells transduced with the mutated proinsulin gene^[10-13], so the major problem to ectopic insulin expression is the difficulty of reconstructing in non-beta cells the highly regulated insulin secretion of the normal beta cells^[14-19]. In 1992, Gossen and Bujard^[20] developed the tetracycline (or doxycycline)-induced gene expression (Tet-on) system, which is useful for controlling the expression of targeted genes in quantitative manner and for determining the roles of the gene products in cellular functions^[21-26]. In the present study, using this system, we generated the first non-beta cell line with doxycycline-regulated insulin secretion. The strategy described here will contribute to the development of the use of insulin gene therapy for patients with type I diabetes.

MATERIALS AND METHODS

Tet-on system

pTet-on regulator plasmid (pTet-on), pTRE2 response plasmid (pTRE2) and pTK-Hyg plasmid, which contain hygromycin-resistance gene, were purchased from Clontech. Using the polymerase chain reaction, the proinsulin cDNA was amplified from expression vector pcDNA3.1/C-mINS, which had been reconstructed from plasmids pcDNA3.1/C and pN-PEPCK-INS (the genomic sequence of human proinsulin, kindly provided by Professor LI Changchen, Dalian Medical University) in our lab. The primers used in the amplification created restriction sites *Bam*HI and *Hind*III which allowed to clone the human proinsulin cDNA into the expression vector pTRE2. The sequences of the forward and reverse promoters were: 5'-catggatcctgccatgccctgtggatg-3 and 5'-cagaagcttcgagctgcgtctagttgc-3' respectively. After verification by

restriction and sequencing, the vector, pTRE2.mINS, for expressing human insulin was generated.

Cell culture and gene transfection

To simplify the transfection procedure, the tet-293 cell line (human embryonal cell), which had been transfected with the plasmid pTet-on and stably expressed reverse tetracycline-controlled transactivator (rtTA), was purchased from Clontech. So the first step of transfection and clone selection was left out. The culture medium was DMEM supplemented with 100mL·L⁻¹ fetal bovine serum and G418 (100mg·L⁻¹). The tet-293 cells were maintained at 37°C under a 50mL·L⁻¹ CO₂ atmosphere until the cells were 80% confluent, then pTRE2.mINS was cotransfected with pTK-Hyg in a ratio of 20:1, using Lipofectin reagent (Gibco-Brl). After selection in the culture medium containing 30mg·L⁻¹ hygromycin (Sigma) for more than eight weeks, one clone (tet-293/Ins6) expressing insulin under the control of Dox was selected by screening from 28 clones.

Radioimmunoassay

Tet293/Ins6 cells (1.0×10⁶) were seeded in 35-mm-diameter dishes, and treated with Dox at 0, 10, 100, 200, 400, 800 and 1000μg·L⁻¹ for 24h, or at 1000μg·L⁻¹ for 0, 15 and 30min, 1, 2.5, 5, 12 and 24h. The amounts of insulin secreted in the medium were measured with specific radioimmunoassay kit (Haikerei Co. Peking).

RT-PCR

Total RNA was extracted from cells with TRIzol (Gibco), and the first chain of cDNA was prepared by RT with Superscript II reverse transcriptase (Gibco) using a oligo(dT)11 primer. The proinsulin gene was amplified with Taq polymerase (Progema). The PCR primers for proinsulin gene were: sense 5'-tgccatggccctgtggatg-3', and anti-sense 5'-gcaggctcgtctagtgc-3'.

Northern blot analysis

For each Northern blot, 10μg total RNA was loaded per lane and separated, transferred onto nylon membrane (Schleicher and Schuell, Germany) and cross-linked by UV irradiation. The hybridization probe specific for proinsulin, was labeled with (³²P)dCTP using a DNA labeling kit (Takera). Following hybridization at 68°C for 2h, blots were washed twice for 30min at room temperature with solution 1 (2×SSC, 0.5g·L⁻¹ SDS) and solution 2 (0.1×SSC, 1g·L⁻¹ SDS), respectively, and exposed to a phosphorimaging screen overnight. The blots were then washed with 5g·L⁻¹ SDS at 95°C until complete removal of the probe and rehybridized with human β-actin cDNA (Clontech).

RESULTS

Establishment of a stable cell line excreting insulin controlled by Dox

After screening in the culture medium containing hygromycin for more than eight weeks, a total of 28 independent Hyg-resistant cell lines were created from the tet-293 cells which had been cotransfected with pTR2.mINS and pTK-Hyg. Of the 28 clones, one (tet-293/Ins6) was obviously regulated to secrete insulin by Dox. The amount of insulin in the medium secreted by the cells treated with Dox (1mg·L⁻¹) was 241.0pU·d⁻¹·cell⁻¹, which was 25-fold that of 9.7pU·d⁻¹·cell⁻¹ released by the cells without Dox treatment.

Verify the regulation of Dox on insulin secretion in tet-293/Ins6 cells at the protein level

Tet-293/Ins6 cells were amplified and passaged (1.0×10⁶ cells) into 16 35-mm dishes, and the concentrations of insulin in the culture media were measured with RIA. As shown in Figure 1, the level of

insulin secretion increased from 18.2 to 241.0pU·d⁻¹·cell⁻¹ over a range of Dox concentrations from 10μg·L⁻¹ to 1000μg·L⁻¹. Only a slightly increasing tendency of insulin concentration was observed at 2.5h following the addition of 1 mg·L⁻¹ Dox to the culture medium. However, the amount of insulin increased significantly after exposing the cells to Dox for more than 5h (Figure 2).

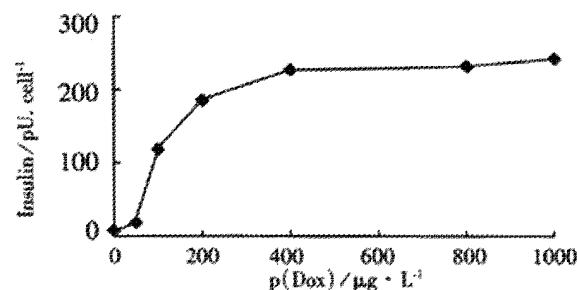


Figure 1 Insulin secretion from tet-293/Ins6 cells after treatment with Dox at different concentrations for 24h.

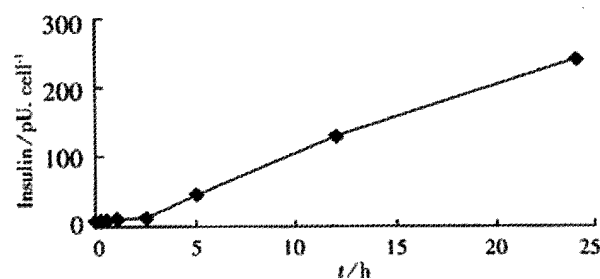


Figure 2 Time course of insulin secretion from tet-293/Ins6 cells after activation with Dox at 1000μg·L⁻¹ in 24h.

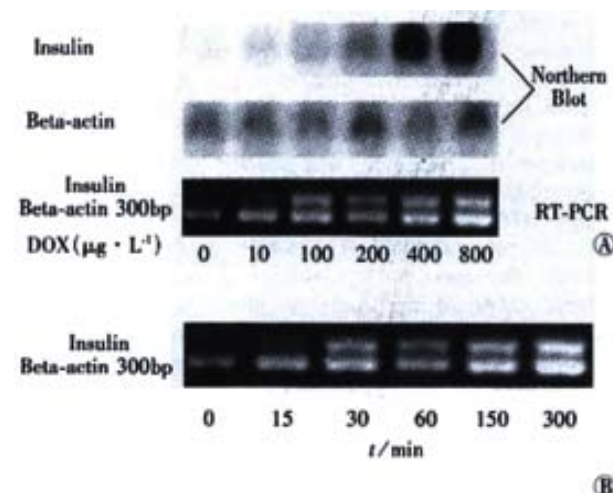


Figure 3 The conditional transcription of insulin gene by Dox in the tet-293/Ins6 cells using β-actin as loading control.

Verify the regulation of Dox on insulin expression in tet-293/Ins6 cells at the transcriptional level

Theoretically, the Tet-on system exerts its regulatory effect on target genes at the transcriptional level. So RT-PCR and Northern blot methods were used to further demonstrate the inducibility of insulin by Dox. After tet-293/Ins6 cells were cultured in the media containing different concentrations of Dox for 24h, it was found that 10μg·L⁻¹ Dox could induce insulin expression obviously, and that the insulin mRNA level was up-regulated dramatically by Dox in a dose-dependent manner (Figure 3A). As shown in Figure 3B, the result of

RT-PCR indicated that the transcription of insulin gene had already been up-regulated significantly after exposing tet-293/Ins6 cells to $1\text{mg}\cdot\text{L}^{-1}$ of Dox for 15 minutes.

DISCUSSION

Insulin-dependent diabetes mellitus (IDDM) results from the autoimmune destruction of the insulin-producing beta cells of the pancreas. As a consequence, diabetic patients experience profound metabolic derangements (hyperglycemia, ketosis and hyperlipemia) and develop vascular and neurologic chronic complications^[27-29]. These alterations can be only partially controlled by the exogenous administration of insulin, which brings patients suffering and inconvenience^[30]. In recent years, engineering insulin-secreting cell lines has received a great deal of interest and some exciting advances have been made. But the application of gene therapy to diabetes presents formidable challenges, one of which is how the level of insulin is restricted within a very narrow limit. Otherwise, if the engineered artificial β -cells were transplanted into the body, the excessive insulin for metabolism would cause hypoglycaemia^[8], and even death. Several inducible promoters originating from eukaryotic genes have been used to deliver gene in a regulated manner. The substances inducing the promoters include steroid hormones, oxygen, heavy metals, or physical stimulus (such as radiation)^[31, 32]. However, most of these promoters are not suitable for clinical application for various reasons: first, because these promoters are of mammalian origin, the exogenous regulation of transgene through such a promoter could at the same time affect the transcription of the host endogenous genes; and second, the inducers of these promoters are generally endogenous molecules (hormones, oxygen, etc.), the levels of which cannot be modulated significantly and safely. Other limitations include the potential toxicity or side effects of the inducer. Therefore, an inducer/promoter system, which regulates the transcription only of the transgene, without affecting endogenous genes, is acceptable for gene therapy in humans.

The Tet-on system, which utilizes an *E. coli* gene regulatory system^[20], appears to fulfil the criteria for clinical application for several advantages^[33-40]: (1) gene expression is easily regulated by administration of Dox; (2) Dox is minimally toxic; and (3) Dox acts specifically on the target gene, and does not activate other cellular genes. This expression system has two critical components, the regulatory plasmid and the response plasmid. The rtTA (reverse tetracycline-controlled transactivator) expressed by the regulated plasmid binds the TRE (tet-response element) in the response plasmid and activates the transcription of the target gene in the presence of Dox. Efrat *et al.*^[41] used the Tet-operon regulatory system to generate a β -cell line in transgenic mice, but there has been no report on the study of engineering non- β -cells for the treatment of diabetes in this regard. Efrat constructed a fusion protein, TETR-VP16 containing the tet repressor and the activating domain of the herpes simplex virus protein VP16, which converts the repressor into a transcriptional activator under the control of the insulin promoter. Then, the transgenic mice of the fusion protein were generated, whose β -cells could express the TETR-VP16 protein conditionally. In a separate lineage of transgenic mice, the simian virus 40 (SV40) large tumor (T) antigen (Tag) gene was introduced under the control of the tet operator sequences and a minimal promoter, which by itself is not sufficient for the expression of Tag gene. Mice from the two lineages were then crossed to generate double-transgenic mice. Expression of the TETR-VP16 protein in β -cells activated Tag transcription, resulting in the development of β -cells tumors. A stable β -cell line deriving from the tumor had the following characteristics: cell incubated in the absence of Tet proliferated normally; and cell incubation in the presence of Tet led to inhibition of proliferation. Thus, it is feasible that the expression of insulin gene can be regulated

under the control of the proliferation of these β -cells. In the present study, utilizing the Tet-on system, we have established a cell line tet-293/Ins6 in which insulin gene can be expressed conditionally by Dox treatment. Ten $\mu\text{g}\cdot\text{L}^{-1}$ Dox can activate the tet-response element and significantly enhance the expression of insulin gene in the cells in a dose-dependent manner. Additionally, the RT-PCR results showed that it is at 15min that $1\text{mg}\cdot\text{L}^{-1}$ Dox could activate the transcription of insulin gene in the tet-293/Ins6 cells following the addition of Dox, and that the amount of insulin in the media did not increase until 5 hours after the treatment of Dox, suggesting that there is a periodic interval of time from the process of gene transcription, translation, and protein synthesis, processing to the final step, secreting the protein from the cells. The strategy used here, by which a stable cell line with low background and high Dox-induced expression of insulin was generated, is more efficient and rapid for regulating insulin gene expression as compared with Efrats' method^[41], and will contribute not only to the development of artificial β -cells for the treatment of diabetes but to the generation of other condition-secreting cell lines for gene therapy of human diseases.

However, responding to the variation of blood glucose concentration, the expression level of insulin gene should be regulated strictly for gene therapy of diabetes^[42-44]. The tet-293/Ins6 cells still have their imperfections for replacing islet transplantation in humans for the treatment of diabetes. Under normal conditions, increasing glucose concentration in blood stimulates β -cells to secrete insulin immediately; but the tet-293/Ins6 cells release insulin by control of Dox at the transcriptional level, the kinetics of feedback loops on transcriptional changes is much slower than that of the secretory response in β -cells. Therefore, based on the experiments we have carried out, we are making efforts to establish an artificial β -cell line in response to glucose stimulation with gene engineering.

REFERENCES

- Newgard CB, Clark S, BeltrandelRio H, Hohmeier HE, Quade C, Normington K. Engineered cell lines for insulin replacement in diabetes: current status and future prospects. *Diabetologia* 1997;40:S42-S47
- Yuan Z, Wu GY, He YS, Shao CM, Zhan Y. Islet separation and islet cell culture *in vitro* from human embryo pancreas. *World J Gastroenterol* 1999;5:458-460
- Chen CQ, Lan P, Zhan WH. Studay on Fas-FasL system in langerhans islets transplantation. *Shijie Huaren Xiaohua Zazhi* 1999;7:422-423
- Xu JT, Yan M, Yao YW, Wu R. Effect of pentagastrin on IL-1 β induced inhibition of insulin secretion in neonatal rat islets Langerhans. *World J Gastroenterol* 2000;6(suppl 3):15
- Regazzi R, Verchere CB, Halban PA, Polonsky KS. Insulin production: from gene to granule. *Diabetologia* 1997;40:B33-B38
- Ferber S, Heimberg H, Brownlee M, Colton C. Surrogate beta cells. *Diabetologia* 1997;40:B39-B43
- Motoyoshi S, Shirotani T, Araki, E, Sakai K, Kaneko K, Motoshima H, Yoshizato K, Shirakami A, Kishikawa H, Shichiri M. Cellular characterization of pituitary adenoma cell line (AtT20 cell) transfected with insulin, glucose transporter type 2 (GLUT2) and glucokinase genes: Insulin secretion in response to physiological concentrations of glucose. *Diabetologia* 1998;41:1492-1501
- Falqui L, Martinenghi S, Berra C, Monti L, Leone BE, Pozza G, Bordignon C. Human proinsulin production in primary rat hepatocytes after retroviral vector gene transfer. *J Mol Med* 1999;77:250-253
- Cheung AT, Dayanandan B, Lewis JT, Korbutt GS, Rajotte RV, Bryer-Ash M, Boylan MO, Michael Wolfe M, Kieffer TJ. Glucose-dependent insulin release from genetically engineered K cells. *Science* 2000;290:1959-1962
- Groskreutz DJ, Sliwkowski MX, Gorman CM. Genetically engineered proinsulin constitutively processed and secreted as mature, Active insulin. *J Biol Chem* 1994;269:6241-6245
- Gros L, Montoliu L, Riu E, Lebrigand L, Bosch F. Regulation production of mature insulin by non- β -cells. *Human Gene Ther* 1997;8:2249-2259
- Falqui L, Martinenghi S, Severini GM, Corbella P, Taglietti MV, Arcelloni C, Saruger E, Monti LD, Paroni R, Dozio N, Pozza G, Bordignon C. Reversal of diabetes in mice by implantation of human fibroblasts genetically engineered to release mature human insulin. *Human Gene Ther* 1999;10:1753-1762
- Yamasaki K, Sakashi T, Nemoto M, Eto Y, Tajima N. Differentiation-

- induced insulin secretion from nonendocrine cells with engineered human proinsulin cDNA. *Biochem Bioph Res Co* 1999;265:361-365
- 14 Dochert K. Gene therapy for diabetes mellitus. *Clin Sci* 1997;92:321-330
- 15 Efrat S. Prospects for gene therapy of insulin-dependent diabetes mellitus. *Diabetologia* 1998;41:1401-1409
- 16 Rivera VM, Wang X, Wardwell S, Courage NL, Volchuk A, Keenan T, Holt DA, Gilman M, Orci L, Cerasoli Jr F, Rothman JE, Clackson T. Regulation of protein secretion through controlled aggregation in the endoplasmic reticulum. *Science* 2000;287:826-830
- 17 Ye X, Rovera VM, Zoltick P, Cerasoli Jr F, Schnell MA, Gao GP, Hughes JV, Gilman M, Wilson JM. Regulated delivery of therapeutic protein after in vivo somatic cell gene transfer. *Science* 1999;283:88-91
- 18 Lee HC, Kim SJ, Kim KS, Shin NC, Yoon JW. Remission in models of type 1 diabetes by gene therapy using a single-chain insulin analogue. *Nature* 2000;408:483-488
- 19 Grossen M, Butard H. Tight control of gene expression in mammalian cells by tetracycline-responsive promoters. *Proc Natl Acad Sci USA* 1992;89:5547-5551
- 20 Song KC, Haller GW, Giauffret D, Germana S, Reeves SA, Levy J, Sachs D, Leguern C. Regulated expression of an MHC class II gene from a promoter-inducible retrovirus. *Human Gene Ther* 2000;11:1961-1969
- 21 Dressel R, Lubbers M, Walter L, Herr W, Gunther E. Enhanced susceptibility to cytotoxic T lymphocytes without increase of MHC class I antigen expression after conditional overexpression of heat shock protein 70 in target cells. *Eur J Immunol* 1999;29:3925-3935
- 22 Hagihara Y, Saitoh Y, Arita N, Eguchi Y, Tsujimoto Y, Yoshimine T, Hayakawa T. Long-term functional assessment of encapsulated cells transfected with tet-on system. *Cell Transplant* 1999;8:431-434
- 23 Krauthauser CM, Hall LM, Wexler RS, Slee AM, Mitra J, Enders GH, Kerr JS. Regulation of gene expression and cell growth *in vivo* by tetracycline using the hollow fiber assay. *Anticancer Res* 2001;21:869-872
- 24 Lottmann H, Vanselow J, Hessabi B, Walther R. The tet-on system in transgenic mice: inhibition of the mouse pdx-1 gene activity by antisense RNA expression in pancreatic -cells. *J Mol Med* 2001;79:321-328
- 25 Milo-Landesman D, Surana M, Berkovich I, Compagni A, Christofori G, Fleischer N, Efrat S. Correction of hyperglycemia in diabetic mice transplanted with reversibly immortalized pancreatic cells controlled by the tet-on regulatory system. *Cell Transplant* 2001;10:645-650
- 26 Lin L, Lu XZ, Zhao ZQ. Electrogastrography in patients with disordered gastric motility in diabetes and effect of cisapride. *China Natl J New Gastroenterol* 1996;2(suppl 1):71-72
- 27 Wang WM, Lu GX. Research on the treatment of diabetic gastroparesis by erythromycin. *China Natl J New Gastroenterol* 1996;2(suppl 1):130
- 28 Quigley EMM. The evaluation of gastrointestinal function in diabetic patients. *World J Gastroenterol* 1999;5:277-282
- 29 Gu YP, Gu JY, Li JS. Pancreaticoduodenal transplantation with portal venous and enteric drainage in rats. *World J Gastroenterol* 2000;6:914-916
- 30 Sartoh Y, Eguchi Y, Hagihara Y, Arita N, Watahiki M, Tsujimoto Y, Hayakawa T. Dose-dependent doxycycline-mediated adrenocorticotrophic hormone secretion from encapsulated Tet-on proopiomelanocortin Neuro2A cells in the subarachnoid space. *Human Gene Ther* 1998; 9:997-1002
- 31 Paillard F. "Tet-on": a gene switch for the exogenous regulation of transgene expression. *Human Gene Ther* 1998; 9:983-985
- 32 Bachl J, Carlson C, Gray-Schopfer V, Dessing M, Olsson C. Increased transcription levels induce higher mutation rates in a hypermutating cell line. *J Immunol* 2001;166:5051-5057
- 33 Molin M, Shoshan MC, Ohman-Forslund K, Linder S, Akusjarvi G. Two novel adenovirus vector systems permitting regulated protein expression in gene transfer experiments. *J Virol* 1998;72:8358-8361
- 34 Kashima Y, Miki T, Minami K, Seino S. Establishment of a tet-on gene expression system in glucose-responsive and -unresponsive MIN6 cells. *Diabetes* 2001;50:S133
- 35 Levy LM, Warr O, Attwell D. Stoichiometry of the glial glutamate transporter GLT-1 expressed inducibly in a Chinese Hamster ovary cell line selected for low endogenous Na⁺-dependent glutamate uptake. *J Neurosci* 1998;18:9620-9628
- 36 Zhu HJ, Iaria J, Sizeland AM. Smad7 differentially regulates transforming growth factor α -mediated signaling pathway. *J Biol Chem* 1999;274:32258-32264
- 37 Wang DY, Grammer R, Cobbs CS, Stewart JE Jr, Liu ZY, Rhoden R, Hecker TP, Ding Q, Gladson CL. P125 focal adhesion kinase promotes malignant astrocytoma cell proliferation *in vivo*. *J Cell Sci* 2000; 113:4221-4230
- 38 Kobayashi T, Sawa H, Morikawa J, Zhang W, Shiku H. Bax induction activates apoptotic cascade via mitochondrial cytochrome crelease and bax overexpression enhances apoptosis induced by chemotherapeutic agents in DLD-1 colon cancer cells. *Jpn J Cancer Res* 2000;91:1264-1268
- 39 Serguera C, Bohl D, Rolland E, Provost P, Heard JM. Control of erythropoietin secretion by doxycycline or mifepristone in mice bearing polymer-encapsulated engineered cells. *Human Gene Ther* 1999; 10:375-383
- 40 Serguera C, Bohl D, Rolland E, Provost P, Heard JM. Control of erythropoietin secretion by doxycycline or mifepristone in mice bearing polymer-encapsulated engineered cells. *Human Gene Ther* 1999; 10:375-383
- 41 Efrat S, Fusco-DeMane D, Lemberg H, Emran OA, Wang XR. Conditional transformation of a pancreatic β -cell line derived from transgenic mice expressing a tetracycline-regulated oncogene. *Proc Natl Acad Sci USA* 1995;92:3576-3580
- 42 Mitancher D, Doiron B, Chen R, Kahn A. Glucose-stimulated genes and prospects of gene therapy for type I diabetes. *Endocr Rev* 1997;18:520-540
- 43 Tiedge M, Elsner M, McClenaghan NH, Hedrich HJ, Grube D, Klempnauer J, Lenzen S. Engineering of a glucose-responsive surrogate cell for insulin replacement therapy of experimental insulin-dependent diabetes. *Human Gene Ther* 2000;11:403-414
- 44 Barry S, Ramesh N, Lejnieks DV, Simonson W, Kemper L, Lernmark A, Osborne WRA. Glucose-regulated insulin expression in diabetic rats. *Human Gene Ther* 2001;12:131-139

Edited by Ma JY

• BASIC RESEARCH •

Epidemiological survey of cryptosporidiosis in Anhui Province China

Ke-Xia Wang, Chao-Pin Li, Jian Wang, Bo-Rong Pan

Ke-Xia Wang, Chao-Pin Li, Jian Wang, Department of Aetiology and Immunology, School of Medicine, Huainan University of Technology, Huainan 232001, Anhui Province, China

Bo-Rong Pan, Department of Oncology, Xijing Hospital, the Fourth Military Medical University, Xian, Shanxi Province, China

Correspondence to: Dr. Ke-Xia Wang, Department of Aetiology and Immunology, School of Medicine, Huainan Institute of Technology, Huainan 232001, Anhui Province, China. yxfy@hntu.edu.cn

Telephone: +86-554-6658770 Fax: +86-554-6662469

Received 2001-09-25 Accepted 2001-11-05

Abstract

AIM: To provide scientific evidence for prevention and controlling of cryptosporidiosis, the infection of *Cryptosporidium parvum* and its epidemiological characteristics were studied in some areas of Anhui Province.

METHODS: The oocyst of *Cryptosporidium parvum* in 5421 fresh stool samples from eleven areas of Anhui Province was tested by auramine-phenol stain and improved anti-acid stain respectively. The specific antibody of IgG, IgM and T subsets of 41 patients with positive *Cryptosporidium parvum* in stools were detected by ELISA and biotin-streptavidin (BSA) respectively.

RESULTS: The total infective rate of *Cryptosporidium parvum* was 1.33% (74/5421). Among them, the positive rates of oocyst in the areas of Huaibei (1.82%) and Fuyang (1.80%) were higher. The positive rates of oocyst in stools of infants, pupils, middle school students, college students, adults, patients with diarrhea, and those with immunodeficiency were 3.15% (28/889), 0.82% (9/1098), 0.82% (9/1092), 0.83% (8/969), 0.85% (9/1095), 2.88% (8/278) and 8.33% (3/36) respectively. The positive rates of oocyst in infants and the patients with diarrhea and immunodeficiency were significantly higher than those in controls ($P < 0.01$). The positive rate of oocyst in males was similar to that in females ($P > 0.05$). The positive rate of oocyst in urban areas (1.13%) was significantly lower than those in rural areas (1.72%, $P < 0.01$). The positive rates of specific IgG, IgM and IgG+IgM in sera of the patients with positive oocyst in stool were 63.4% (26/41), 17.1% (7/41), 19.5% (8/41) respectively. The number fractions of T subsets of CD_3^+ , CD_4^+ , CD_8^+ and CD_4^+/CD_8^+ of the patients were 0.66 ± 0.07 , 0.44 ± 0.06 , 0.28 ± 0.04 and 1.58 ± 0.32 respectively. The difference between the patients and the controls was significant ($P < 0.05$). The main manifestations of the patients were subclinical infection, in forms of slight abdominal pain, mild diarrhea, and loose stool.

CONCLUSION: There are two infection peaks in infection of *Cryptosporidium parvum* and its infection can be found more often in infants, patients with diarrhea or immunodeficiency, and in rural areas. Subclinical infection is the main manifestation and might be easily misdiagnosed. When the therapeutic

effectiveness is low for diarrhea, the infection of *Cryptosporidium parvum* should be considered, concerning their age and immune function.

Wang KX, Li CP, Wang J, Pan BR. Epidemiological survey of cryptosporidiosis in Anhui Province China. *World J Gastroenterol* 2002;8(2): 371-374

INTRODUCTION

Cryptosporidiosis is a kind of zoonoses whose clinical manifestation is diarrhea caused by *Cryptosporidium parvum*^[1-13]. Since the first report of the disease covered by Nime *et al*^[14] in 1976, more and more studies have been reported. After the first report of the disease in 1978 covered by Hanfan *et al.* in Nanjing, many reports of the disease have been published from more than ten provinces^[15-24]. In order to explore the infection, epidemiological characteristics and clinical manifestations, the investigation of the disease was taken cosmically in eleven areas of Anhui Province.

MATERIALS AND METHODS

Materials

A total of 5421 samples of stools were collected from eleven areas of Anhui Province. Among them, the number of infants, pupils, middle school students, college students, adults patients with diarrhea and immunodeficiency were 889, 1098, 1092, 969, 1373, 278 and 36 respectively. The patients with obstinate diarrhea, and immunodeficiency were the major target. The number of males and females was 3474 and 1947 respectively. The median age was 24.5 years (ranging from 4 to 63 years).

Methods

The different histories of present illness, anamnesis, health habit and healthy state of environment were taken.

Feces examination After fresh stools were collected by disposable boxes. The oocyst of *Cryptosporidium parvum* was tested by auramine-phenol stain and improved anti-acid stain respectively. The smears of stool were made on the surface of sheet glass (2cm²). After these smears were left dry naturally and fixed with methanol, the auramine-phenol stain and improved anti-acid stain were made, and the examination under microscope was taken respectively. The oocyst of *Cryptosporidium parvum* with rose bengal was positive, and the other nonspecific granules were blue-black.

Biopsy examination The examination of colon biopsy was tested by sigmoidoscope for six patients with obstinate diarrhea, or immunodeficiency.

Serological examination The antigen of oocyst coming from guinea pigs was coated on the surface of polystyrene wells, and the specific antibodies of IgG, IgM were detected by ELISA.

Examination of T subsets The T subsets (CD_3 , CD_4 , CD_8) were detected by biotin-streptavidin (BSA) in 36 patients with immunodeficiency.

Statistical analysis was made by using Student's *t* test.

RESULTS

The results of oocyst of *Cryptosporidium parvum* in stools collected from eleven areas of Anhui Province are shown in Tables 1-4. The results of specific antibodies and T subsets are shown in Tables 5-6. The common clinical symptoms of the disease are shown in Table 7.

Table 1 The distribution of infection of *Cryptosporidium parvum* in Anhui Province (n, %)

Area	n	Stain of auramine-phenol		Stain of auramine-phenol and modified acid-fast	
		Positive number	Positive rate	Positive number	Positive rate
Hefei	500	4	0.80	6	1.20
Bengbu	349	2	0.57	4	1.15
Huainan	939	10	1.06	13	1.38
Lu'an	447	4	0.89	6	1.34
Wuhu	464	4	0.86	6	1.29
Huaipei	440	5	1.14	8	1.82
Huangshan	500	5	1.00	7	1.40
Fuyang	500	6	1.20	9	1.80
Chuzhou	423	4	0.95	6	1.42
Anqing	413	3	0.73	5	1.21
Suzhou	446	5	1.12	7	1.57
Total number	5421	53	0.98	74	1.33 ^a

^a $P < 0.05$, $\chi^2 = 3.8864$.

Table 2 The distribution of infection of *Cryptosporidium parvum* in different groups (n, %)

Group	n	Stain of auramine-phenol		Stain of auramine-phenol and modified acid-fast	
		Positive number	Positive rate	Positive number	Positive rate
Infant	889	21	2.36 ^b	28	3.15 ^d
Pupil	1098	7	0.64	9	0.82
Middle school student	1092	7	0.64	9	0.82
College student	969	5	0.52	8	0.83
Adult	1059	6	0.57	9	0.85
Patients with diarrhea	278	5	1.80 ^a	8	2.88 ^d
Patients with immunodeficiency	36	2	5.56 ^b	3	8.33 ^d
Total number	5421	53	0.98	74	1.33

^a $P < 0.05$, ^b $P < 0.01$, ^d $P < 0.01$, vs college students.

Table 3 The distribution of infection of *Cryptosporidium parvum* in different sexes (n, %)

Group	n	Stain of auramine-phenol		Stain of auramine-phenol and modified acid-fast	
		Positive number	Positive rate	Positive number	Positive rate
Males	3474	37	1.07 ^d	59	1.70 ^d
Females	1947	17	0.87	30	1.54
Total number	5421	54	0.99	89	1.64

^d $P > 0.05$, vs female.

Table 4 The distribution of infection of *Cryptosporidium parvum* in urban and rural areas (n, %)

Group	n	Stain of auramine-phenol		Stain of auramine-phenol and modified acid-fast	
		Positive number	Positive rate	Positive number	Positive rate
Urban areas	3276	26	0.79 ^a	36	1.13 ^a
Rural areas	2145	27	1.26	38	1.72
Total number	5421	53	0.98	74	1.33

^a $P < 0.05$, vs Rural.

Table 5 The detective results of specific antibody against *Cryptosporidium parvum* (n, %)

Oocyst	n	IgG		IgM		IgG+IgM	
		Positive number	Positive rate	Positive number	Positive rate	Positive number	Positive rate
Positive ^b	41	26	63.41	7	17.07	8	19.51
Negative	20	0	0.00	0	0.00	0	0.00

^b $P < 0.01$, vs Negative, $\chi^2 = 25.0945$.

Table 6 The results of T subsets of patients with positive of *Cryptosporidium parvum* in stool (n, $\bar{x} \pm s$, %)

<i>cryptosporidium parvum</i>	n	CD3 ⁺	CD4 ⁺	CD8 ⁺	CD4 ⁺ /CD8 ⁺
Positive	41	65.83 \pm 6.55 ^a	43.55 \pm 6.10 ^a	28.43 \pm 4.32	1.58 \pm 0.32 ^b
Negative	20	55.87 \pm 7.23	39.26 \pm 6.43	30.04 \pm 5.67	1.36 \pm 0.41

^a $P < 0.05$, ^b $P < 0.05$, vs Negative.

Table 7 Clinical symptoms after being infected by *Cryptosporidium parvum* (n, %)

Group	n	percentage
Without symptom	62	83.78
Symptom	12	16.22
General symptom	2	2.70
Upper digestive tract symptom	1	1.35
Lower digestive tract symptom	2	2.70
Upper and lower digestive tract symptom	3	4.05
General and upper digestive tract symptom	1	1.35
General and lower digestive tract symptom	2	2.70
General and upper, lower digestive tract symptom	1	1.35
Total number	74	100.00

General symptom:acratia, fever;upper digestive tract symptom:anorexia, nausea, vomiting;Lower digestive tract symptom:abdominal distension, abdominal pain, loose stool, watery stool

Examination of living tissue The examination of biopsy was tested by sigmoidoscope in six adults and old patients with obstinate diarrhea, or immunodeficiency. The results showed that there were many oocysts on the surface of intestinal mucosa, which had villus degeneration and mononuclear leukocyte infiltrations.

DISCUSSION

Cryptosporidium parvum is recognized as an important protozoon, whose life cycle is simple with nonspecific host. Large-scale surveys of selected animals suggest that *Cryptosporidium parvum* is more often found in farm cattle, sheep, dogs and cats. The disease can be transmitted in animals and people mutually. Water polluted with *Cryptosporidium parvum* is regarded as a source of infection by some experts^[24-35]. Patients with immunodeficiency (AIDS) can easily be infected through respiratory tract. During the gastroenteritis of fulminant epidemic, the positive rate of *Cryptosporidium parvum* was 39% in 13000 patients with gastroenteritis^[14].

The pathogenicity of *Cryptosporidium parvum* hasn't been, for a long time, taken into serious consideration. Since the report of severe diarrhea caused by *Cryptosporidium parvum* breaking out in Turkey in 1955 (Stavin), and in 1976 (Nime)^[14], the infection of the disease has been reported in many countries. The different positive rates of *Cryptosporidium parvum* are 1-2% in Europe, 0.6-4.3% in North America, and 3-4% or even 10.2% in Asia, Australia, Africa, and Central and South America.

The pathogenic mechanism of *Cryptosporidiosis* hasn't been clarified. The report of Hanfan (1990)^[15,16] showed that after the infective oocyst invaded the intestine, its sporozoites intruded epithelium mucosae villus and its larva could reproduce in vacuole. With the development of the disease, the epithelium mucosae villus would collapse, light or medium inflammatory reaction with mononuclear leukocytes and watery stool could appear. Decreasing the

activity of lactase caused by infection of *Cryptosporidium parvum* was an important reason for losing lactose and diarrhea^[36-46].

Since the first patient with the disease was diagnosed in 1987 in our country, many cases of the disease have been reported, especially in Jiangsu, Fujian, Hunan, Shandong Provinces and Inner Mongolia. The total detective rate of the disease was 1.36-13.3%. It was more often found in infants and children^[47-55]. Our data of investigation suggest that the infection of *Cryptosporidium parvum* has existed in Anhui Province, and its detective rate was low (1.33%, 74/5421)^[15,16]. The infective rate of *Cryptosporidium parvum* in males and females was 1.41% and 1.28% respectively. There was no significant difference between two sexes ($P>0.05$). Although stain of auramine-phenol is one of the good methods for the detection of oocyst, the specificity of stain can be interfered by impurity in stool. The stain of auramine-phenol and modified acid-fast can overcome false positive reaction and false negative reaction of oocyst so that the detective rate of oocyst can be increased ($P<0.05$). The infectious rates of *Cryptosporidium parvum* were higher in infants and patients with obstinate diarrhea or immunodeficiency than those in middle school students and college students ($P<0.01$). The possible reason was immunodeficiency, lower positive rate of CD_3^+ , CD_4^+ and CD_4^+/CD_8^+ , so that the patients had not enough immune reaction to *Cryptosporidium parvum*. The similar results of the isolation rate had been observed in our investigation, which was more often found in infants and children with diarrhea. The possible reason was the immune organs of infants and children hadn't matured. After *Cryptosporidium parvum* invaded the intestine, the structure of pithelium mucosae villus was demolished and few antibodies were produced. The extent of the disease for adults was not only associated with the level of infection of *Cryptosporidium parvum* but also associated with the immunity. It was more often found in parasite states and self-limited diarrhea for normal population. It was more often found in severe infection and continuous diarrhea for immunodeficiency. Scavenger worm was associated with the level of Th and ADCC of the patients. The production of restrain factor and the decrease of T cells and T subsets were caused by the common antigen of different enteric bacilli and infected epithelial cells of colon. For the patients with low or no treatment effect of antibiotic, taking into consideration their living environment and individual living habits, the possible infection of *Cryptosporidium parvum* should be considered. In the study of Pan *et al*^[56-62], for thirteen patients with ulcerative colitis and ten patients with clone disease, the function of T cells and restrain index number were all deficient in the patients with inflammation intestinal tract. The infective rate of *Cryptosporidium parvum* was higher in rural areas than that in urban areas ($P<0.05$). The possible reasons were poor living conditions, lack of necessary general health knowledge and health habits in the rural areas. Food and drinking water polluted by oocyst was the possible cause of the infection.

The main antigen of *Cryptosporidium parvum* was cyst wall antigen and sporozoite antigen. Most scholars considered that cellular immunity was important and the immune mechanism of cryptosporidiosis hadn't been clarified. Moon's study showed that IgG, IgM against *Cryptosporidium parvum* couldn't repress the infection, so that the immunity of cryptosporidiosis was dependent on cellular immunity. However, other scholars, for example Chrisp and Riggs, thought that the specific antibody could easily be made after adult and young mice were vaccinated by oocyst. The detective results of specific IgA, IgM, IgG in serum, stool and duodenal juice and cellular immune function prompted that the immunity of cryptosporidiosis was dependent on ADCC. The results of our study showed that type of antibody most frequently found was IgG, with IgM, and IgG+IgM following it. For IgM as target of early infection was not necessarily a verified index, if IgG or IgM in serum was positive, possible infection of *Cryptosporidium parvum* should be considered. The positive effects of circle antibody haven't been completely clarified according to the previous results that the circle

antibody hadn't protective function^[15-17]. It is possible that the effect of antibody in serum against *Cryptosporidium parvum* in intestinal pithelium mucosae villus is ineffective.

The expressive levels of CD_3^+ , CD_4^+ and CD_4^+/CD_8^+ were lower in positive rates of oocyst in stool than those in negative rates of oocyst in stool ($P<0.05$). The result showed that the cellular immunity played a key role against the infection of *Cryptosporidium parvum*. When the levels of CD_3^+ , CD_4^+ were low, the activity of T cells and its cellular factor were inadequate, and the infection of *Cryptosporidium parvum* would persist. However, the result of general level of CD_8^+ in the patients with positive rates of oocyst indicated that the activity and number of CTL hadn't significantly increased, and severe tissue injuries, generally speaking, wouldn't take place in the patients.

Most patients neglected diagnosis and treatment when they had no or light symptoms. Most people with normal immune functions suffering from self-limited diarrhea often had symptoms of acute watery stool (5-10times/d), nausea, vomiting, headache etc, and their course of disease was less than one month. The results of our study showed that about 83.78% infected persons had no obvious symptoms, the possible reason for it was associated with the infective level and the ability of immune response. The symptoms of the patients were easily confused with general gastroenteritis. If the treatment of antibiotic failed, the infection of this disease should be considered, eliminating some associated diseases.

As a conclusion, there were two infection peaks in the infection of cryptosporidium parvum, and the infection of *Cryptosporidium parvum* has existed in Anhui Province, and was more often found in infants, children and some patients with diarrhea or immunodeficiency. The effect of specific IgM, IgG in sera of the patients against *Cryptosporidium parvum* in intestine was much inferior. If the treatment of antibiotic failed, the infection of this disease should be considered, considering age and immune function of the patients, if some associated diseases are eliminated. In order to avoid the persistent and chronic state of the illness, antiscolic treatment must be taken earlier for the subclinical infective patients with confirmed diagnosis.

REFERENCES

- 1 Cai LM, Zhang C, Chen H, Jiang WP, Mao WX. Clinicopathogenic studies of acute diarrhea in children. *China Natl J New Gastroenterol* 1997;3:162
- 2 Ma LS, Pa BR. Strengthen international academic exchange and promote development of gastroenterology. *World J Gastroenterol* 1998;4:1
- 3 Vandenplas Y. Diagnosis and treatment of gastroesophageal reflux disease in infants and children. *World J Gastroenterol* 1999;5:375-382
- 4 Komatsu S, Nimura Y, Granger DN. Intestinal stasis-associated bowel inflammation. *World J Gastroenterol* 1999;5:518-521
- 5 Guo TG, Liou XH. The report of four cases with abdominal pain caused by unusual account. *Xin Xiaohuabingxue Zazhi* 1993;1:243-244
- 6 Li ZR, He J, Shi XX, Ou LY, Meng YL, Gao HL, Ye H. The clinical analysis of 180 infants with diarrhea. *Xin Xiaohuabingxue Zazhi* 1996;4:538-539
- 7 Li SQ, Song HF. Eight cases with unusual disease in digestive tract. *Xin Xiaohuabingxue Zazhi* 1996;4:600
- 8 Ke MY. The study pulse of functional dyspepsia. *Xin Xiaohuabingxue Zazhi* 1996;4:601-602
- 9 Wang XZ. The clinical advance of functional dyspepsia. *Xin Xiaohuabingxue Zazhi* 1996;4:648
- 10 Zhao DH. The etiological diagnosis and treatment of diarrhea. *Xin Xiaohuabingxue Zazhi* 1996;4:661-662
- 11 Zeng ZH. The fifty cases with infection of parasite in upper digestive tract. *Xin Xiaohuabingxue Zazhi* 1996;4: 233
- 12 Binder HJ. The pathophysiology of diarrhea. *Xin Xiaohuabingxue Zazhi* 1997;5:62
- 13 Han Y, Li SR. The new advance of inflammatory intestinal disease. *Xin Xiaohuabingxue Zazhi* 1994;2:68
- 14 Nime FA, Burek JD, Page DL, Holscher MA, Yardley JH. Acute enterocolitis in a human being infected with the protozoan *Cryptosporidium*. *Weichangbingxue Zazhi* 1976;70:592-598
- 15 Han F, Zhu FC. Human cryptosporidiosis. *Zhongguo Jishengchongbing Fangzhi Zazhi* 1990;3:252-254
- 16 Luo MY, Wang QN, Zheng XP. The infection of cryptosporidium parvum

- and enteritis caused by cryptosporidium parvum. *Zhonghua Neikexue Zazhi* 1998; 27:686-689
- 17 Shi CS, Yao FB. The treatment advance of cryptosporidiosis. *Zhongguo Renshou Gonghuanbing Zazhi* 1998;14:57-60
- 18 Hou YS, Li JQ. First discovery of cryptosporidium parvum and its infectious status in Shanxi Province. *Xin Xiaohuabingxue Zazhi* 1997;5: 785-786
- 19 Cai LM, Zhang C, Chen H, Jiang WP, Mao WX. Clinicopathogenic studies of acute diarrhea in children. *Xin Xiaohuabingxue Zazhi* 1997;5:383-384
- 20 Gao LP. The epidemic investigation of acute diarrhea in hospital. *Xin Xiaohuabingxue Zazhi* 1996;5:103
- 21 Zhao RL. Progress in treatment of functional dyspepsia. *Huaren Xiaohua Zazhi* 1998;6:340-341
- 22 Li RS, Zhu RM. Study of pathogenesis of functional dyspepsia. *Huaren Xiaohua Zazhi* 1998;6:439-440
- 23 Zhou JL, Xu CH. The method of treatment on protozoon diarrhea. *Huaren Xiaohua Zazhi* 2000;8:93-95
- 24 Zhou X, Li N, Li JS. Growth hormone stimulates remnant small bowel epithelial cell proliferation. *World J Gastroenterol* 2000;6:909-913
- 25 Luo JZ, Zhang JC. Imbalance of intestinal flora in elderly patients with infection disease using antibiotics. *Xin Xiaohuabingxue Zazhi* 1996;4:607-608
- 26 Chang XM, Wang SY. The analysis of clinical manifestation of lower digestive tract and its results of colonoscopy. *Xin Xiaohuabingxue Zazhi* 1996;4:347-348
- 27 Yu ZL, Jin RL, Shi JH. The clinical analysis for sixty old patients with acute abdomen. *Xin Xiaohuabingxue Zazhi* 1995;3:191
- 28 Liou PL, Chen FS, Liou QL. The analysis of intoxication enteroparalysis for fifty-eight infants. *Xin Xiaohuabingxue Zazhi* 1995;3:116-117
- 29 Chen ZB, Wang KJ, Li Y. Preliminary analysis of functional dyspepsia. *Xin Xiaohuabingxue Zazhi* 1996;5:133-134
- 30 Zhang TF, Ni TM. The treatment of combing Chinese tradition medicine and Western medicine on the patients with chronic diarrhea. *Huaren Xiaohua Zazhi* 1998;6:375
- 31 Huang J. Preliminary comments on the treatment of fifteen patients with persistent diarrhea with Mahuang Jia Zhu Tang. *Huaren Xiaohua Zazhi* 1998;6:400
- 32 Zhu XP. The treatment of combing Chinese tradition medicine and Western medicine on fifty infants with chronic diarrhea. *Huaren Xiaohua Zazhi* 1998;6:415
- 33 Liou JJ. The treatment on dyspepsia for the children. *Shijie Huaren Xiaohua Zazhi* 2000;8:78
- 34 Dong YH. The evaluation of therapy measure for the infants with diarrhea. *Shijie Huaren Xiaohua Zazhi* 2000;8:111
- 35 Wang FY, Liang ZH. The study advance of oocyst of cryptosporidium parvum in water. *Zhongguo Gonggong Weisheng Zazhi* 1997;13:25-26
- 36 Kang JZ, Luo SS, Xiao BF, Chen JH. The diagnostic value of lactose test in stool for the infants with diarrhea. *Xin Xiaohuabingxue Zazhi* 1993;1:240
- 37 Cai JL, Zhao DC. The study advance of exfoliative cytologic examination in large intestine. *Xin Xiaohuabingxue Zazhi* 1994;2:102-103
- 38 Wang MR, Zhu Q, Sun JH, Cao Y, Wang CY. The treatment of Chinese tradition medicine and enema on forty-seven patients with chronic diarrhea. *Xin Xiaohuabingxue Zazhi* 1994;2:178
- 39 Hu GL, Suo AP. The treatment of combing Chinese tradition medicine and Western medicine on forty-six infants with chronic diarrhea. *Huaren Xiaohua Zazhi* 1994;2:149
- 40 Yang HB. The experience of massage therapy for 160 infants with diarrhea. *Xin Xiaohuabingxue Zazhi* 1994; 2:159
- 41 Wu ZQ, Lu JY. The report of infrequent disease in digestive tract. *Xin Xiaohuabingxue Zazhi* 1995;3:44
- 42 Lian JJ, Yan L, Lian YH. The treatment of combing Chinese tradition medicine and Western medicine on fifty infants with anorexia. *Xin Xiaohuabingxue Zazhi* 1995;3:159
- 43 Guo CL, Liou YY, Zhang ST. The treatment of Si Ni San on the patients with nonulcer dyspepsia. *Xin Xiaohuabingxue Zazhi* 1995;3:160
- 44 Zhang ZY, Zhang YQ, Xie P. Two cases of ischemic enteropathy. *Xin Xiaohuabingxue Zazhi* 1995;3:2
- 45 Liou RJ, Nie Q, Kong LF. The treatment of compound red sage root injection on digestive diseases. *Xin Xiaohuabingxue Zazhi* 1995;3:74
- 46 Liao CQ, Zhang Z. Nonulcer dyspepsia and reflux esophagitis. *Xin Xiaohuabingxue Zazhi* 1995;3:150
- 47 Cui GT, Chen ZX, Bu XZ, Song BM, Du JX. The clinical epidemiology analysis of stomach and duodenum. *Xin Xiaohuabingxue Zazhi* 1996;4:127
- 48 Wu D, He PX, Xu YE. Age distribution of 2704 patients with colon diseases detected by sigmoidoscopy. *Xin Xiaohuabingxue Zazhi* 1996; 4:319-320
- 49 Cao T, Zhu MZ, Zhang TC, Geng XC, Zhang HY. Seventeen cases of ischemic colitis. *Xin Xiaohuabingxue Zazhi* 1996;4:348
- 50 Hu JA, Zhou GY, Guo JK, Zhou J. The clinical analysis of therapy of microecosystem for 327 infants with enteritis. *Xin Xiaohuabingxue Zazhi* 1996;4:356-357
- 51 Li CQ. Nine cases of adelmorphous hemorrhage of digestive tract. *Xin Xiaohuabingxue Zazhi* 1996;4:719-720
- 52 Hong B. Thirty-two cases of chronic diarrhea treated with Ximitidin. *Xin Xiaohuabingxue Zazhi* 1996;4:175
- 53 Chen SH, Zhao SG. Eight-three cases with digestive infection treated with fluorine quinotong. *Xin Xiaohuabingxue Zazhi* 1996;4:184-185
- 54 Han QJ, Yan L, Shen ZF. One case of segmental enteritis. *Xin Xiaohuabingxue Zazhi* 1996;4:213-214
- 55 Wang GZ. 152 patients with Nonulcer dyspepsia. *Xin Xiaohuabingxue Zazhi* 1996;4:223
- 56 Pan BR, Wu XH, Xue FF. Preliminary study on T suppressor cell function in patients with inflammatory bowel diseases. *Xin Xiaohuabingxue Zazhi* 1995;3:11-12
- 57 Cai JL, Zhao DC, Li BQ. Study on the ultrastructure of rectal exfoliative cells. *Xin Xiaohuabingxue Zazhi* 1995;3:142-144
- 58 Ji XL, Gong GH, Wang MW. Histopathological study of colon mucosa in the elderly. *Xin Xiaohuabingxue Zazhi* 1995;3:154-155
- 59 Wu XT, Li JS. The therapy of nutritional support in the patients with intestinal dysfunction. *Xin Xiaohuabingxue Zazhi* 1997;5:795-796
- 60 Huang YF, Wu WK, Luo HC, Tang Y, Lin YW. Xiexieling in treatment of autonomic nervous functions in patients with chronic diarrhea with deficiency/excessiveness syndrome. *Huaren Xiaohua Zazhi* 1998;6:862-863
- 61 Chen SZ. Progress in studies of pathogenesis of IBS. *Huaren Xiaohua Zazhi* 1998;6:1094-1096
- 62 Wu CT, Huang XC, Li ZL. Increased intestinal permeability and intestinal bacterial transposition. *Shijie Huaren Xiaohua Zazhi* 1999;7:605-606

Edited by Hu DK

• BASIC RESEARCH •

Gastrin, somatostatin, G and D cells of gastric ulcer in rats

Feng-Peng Sun, Yu-Gang Song, Wei Cheng, Tong Zhao, Yong-Li Yao

Feng-Peng Sun, Yu-Gang Song, Wei Cheng, Tong Zhao, Yong-Li Yao, Department of Gastroenterology, Zhujiang Hospital, First Military Medical University, Guangzhou 510282, Guangdong Province, China. Supported by Natural Science Foundation of Guangdong Province, China, No.010578, and Important Technological Issue of Guangdong Province, No.99-13

Correspondence to: Feng-Peng Sun, Department of Gastroenterology, Zhujiang Hospital, First Military Medical University, Guangzhou 510282, Guangdong Province, China. sci@china.com

Telephone: +86-20-85140114-87101

Received 2001-05-30 Accepted 2001-11-10

Abstract

AIM: To investigate the relationship among gastrin, somatostatin, G and D cells in gastric ulcer and in its healing process in rats.

METHODS: Forty-nine Wistar rats were divided into 7 groups. The gastric ulcer model was induced by acetic acid successfully. The gastrin and the somatostatin in rat plasma, gastric fluid and antral tissue were measured by radioimmunoassay(RIA). G and D cells in antral mucosa were analyzed with polyclonal antibody of gastrin and somatostatin by immunohistochemical method and Quantimet 500 image analysis system.

RESULTS: In gastric ulcer, the level of gastrin in plasma, gastric fluid, and antral tissue increased, that of somatostatin declined, and the disorder gradually recovered to the normal level in the healing process. Immunohistochemical technique of G and D cells in antral mucosa demonstrated that the number of G cells increased and that of D cells decreased, both areas of G and D cells declined, the ratio of number and area of G/D increased in gastric ulcer, and the disorder gradually recovered in the healing process.

CONCLUSION: In gastric ulcer, the increased gastrin secreted by G cells, the declined somatostatin secreted by D cells, and the disordered G/D cell ratio can lead to gastrointestinal dysfunction.

Sun FP, Song YG, Cheng W, Zhao T, Yao YL. Gastrin, somatostatin, G and D cells of gastric ulcer in rats. *World J Gastroenterol* 2002;8(2):375-378

INTRODUCTION

Gastrin is secreted in G cells, while somatostatin is secreted in D cells. Gastrin, somatostatin and other gastrointestinal hormones regulate the function of gastrointestinal tract such as secretion, movement, absorption, circulation and nutrition of cells^[1-12]. The nerve system and the endocrine system participate in the healing process of gastric ulcer and regulate the absorption of inflammatory filtration, hyperplasia of granulation tissues, and regeneration of epithelial tissues. Obvious regular change takes place in many endocrine tissues^[13-24]. In order to investigate the relationship between gastrin, somatostatin, G and D cells in the period of gastric ulcer and its healing process in rats, the gastrin and somatostatin in plasma,

gastric juice and antral tissue were tested in rats. At the same time, the number of G and D cells was measured in the antral mucosa.

MATERIALS AND METHODS

Animal

Forty-nine healthy male Wistar rats weighing from 200g to 260g were obtained from the Experimental Animal Center of Sun Yat-Sen University of Medical Sciences. The rats were divided into seven experiment groups: 4, 7, 10, 14, 21, 28d groups, and a control group. The rats of six experimental groups were anesthetized with 30g·L⁻¹ sodium pentobarbital intraperitoneally at a dose of 30mg·kg⁻¹. The abdomen was opened and its stomach was found, 0.05mL acetic acid was injected into rat's antral tissues. Omentum majus and antral tissue of the injection site were stitched. The peritoneum, parietal abdomen and ventral muscle, and skin were stitched continually. After operation, the rats were raised separately, and fasted overnight with free access to water one day before sacrifice. No treatment was given to normal control group.

Plasma sampling

The rats' abdomen and chest chambers were opened and 4mL blood was directly withdrawn from the heart ventricle. Forty μ L(500u) aprotinin (Livzon Libao Biochemical & Pharmaceutical Co. Ltd) and 60 μ L of 100g·L⁻¹ EDTA was added to each blood sample. The samples were centrifuged at 3500r·min⁻¹ for 15min to obtain plasma. The plasma samples were then stored at -70°C until assay.

Gastric juice

After the rats' abdomen was opened, a plastic catheter was inserted into the stomach through pylorus and another catheter was inserted through oral cavity and esophagus into stomach. Two mL saline(pH7.0, 35°C) was infused into the stomach at a flow velocity of 12mL/h. The gastric fluid was collected and 40 μ L(500u) aprotinin was added. The samples were centrifuged at 3500r·min⁻¹ for 15 minutes to obtain gastric fluid. The gastric fluid samples were then stored at -70°C until assay.

Antral mucosa

The rats' stomach was separated and was split from the greater curvature of stomach. The antral tissues in the ulcer area and non-ulcer area were separately taken with ophthalmic scissors. The tissue was quickly weighed by an electric analytical balance and was boiled in a microwave stove. The boiled tissue was homogenized into homogenate in a homogenizer with 1mL of 1mol·L⁻¹ acetic acid. Then 1mL of 1mol·L⁻¹ NaOH was added to neutralize it. The homogenate was centrifuged at 3500r·min⁻¹ for 15 minutes and the supernatant was collected. The samples were then stored at -70°C until assay. The stomach was separated and was split from the greater curvature of stomach. About 1.0×0.5cm antral tissues in the ulcer area and non-ulcer area were separately taken with ophthalmic scissors. The specimen was fixed in 100mL·L⁻¹ neutrally buffered formalin. It was embedded with paraffin 24h later and was serially sectioned at 4 μ m. The sections were mounted onto histostick-coated slides. Adjacent ribbons were collected for immunohistochemical staining.

Measurement of gastrin and somatostatin

Gastrin and somatostatin were detected by using RIA method. The gastrin kits were purchased from Tianjin Qianye Biotech Co. Ltd, and the somatostatin kits were bought from the Department of Neurobiology of the Second Military Medical University. Measurement procedures were performed according to the instruction attached to the kits. The unit of result of plasma and gastric fluid was transformed to ng·L⁻¹, while the unit of result of antral mucosa tissue to ng·g⁻¹.

Immunohistochemical staining for G and D cells

The anti-gastrin antibody(Sigma Co. USA) and anti-somatostatin antibody(GYMED Co. USA) were used and immunohistochemical staining for G and D cells was performed with the strept-avidin-biotin-peroxidase complex(SABC)(Wuhan Boster Biological Technology Co. Ltd), negative control sections were normal serum blocking and PBS instead of the primary antibody. Images of 5 views randomly selected under microscope(10×40) from each anti-gastrin immunohistochemical staining section were input into the Quantimet 500 image analysis system(Leica Co, Germany). The number and area of G cells were calculated by the computer. The mean number and

area of G cells in 5 views of the section served as the number and area of G cells of a section. That of D cells was calculated in the same way as the G cells. The ratio of G/D number and G/D area was acquired by separately dividing the number of G cells and the area of G cells by the number of D cells and the area of D cells in adjacent sections.

Statistical analysis

The result of quantitative data was expressed as mean±SE. Data was analyzed using the variance analysis(ANOVA). Post hoc analysis between factors was performed using least significant difference test. Unpaired data was compared using the Wilcoxon ranksum test and correlated using Pearson's correlation.

RESULTS

The concentration of gastrin and somatostatin in the plasma, gastric juice, antral mucosa is shown in Tables 1 and 2. The number and area of G and D cells in the rat antral mucosa, and the ratio of G/D number and G/D area is shown in Table 3. The relationship between rat G and D cells, and the relationship between G or D cells with gastrin or somatostatin are shown in Table 4.

Table 1 Gastrin concentration in rat plasma, gastric juice, and antral mucosa ($\bar{x}\pm s$, $n=7$)

Group	Plasma(ng·L ⁻¹)	Gastric juice(ng·L ⁻¹)	Ulcer mucosa(ng·g ⁻¹)	Non-ulcer mucosa(ng·g ⁻¹)
Control	147±41	44±15	-	3.7±1.1
4d	397±130 ^a	56±16	2.0±0.7	6.7±2.3 ^a
7d	364±91 ^a	114±34 ^a	1.3±0.4 ^b	6.1±1.8 ^a
10d	255±87 ^a	60±20	2.3±0.8	1.9±0.7 ^a
14d	238±88	45±21	1.9±0.7	1.1±0.4 ^a
21d	211±65	44±17	1.3±0.4 ^b	1.1±0.7 ^a
28d	216±95	60±18	1.5±0.5	1.5±0.3 ^a

^a $P<0.05$, vs control group. ^b $P<0.05$, vs 4d group.

Table 2 Somatostatin concentration in rat plasma, gastric juice, and antral mucosa ($\bar{x}\pm s$, $n=7$)

Group	Plasma(ng·L ⁻¹)	Gastric juice(ng·L ⁻¹)	Ulcer mucosa(ng·g ⁻¹)	Non-ulcer mucosa(ng·g ⁻¹)
Control	45±12	64±16	-	1.4±0.4
4d	13±5 ^a	46±15 ^a	0.3±0.1	0.4±0.1 ^a
7d	22±8 ^a	42±15 ^a	0.3±0.1	0.4±0.2 ^a
10d	41±9	54±17	0.2±0.1	0.8±0.2 ^a
14d	33±8 ^a	54±12	0.9±0.4 ^b	1.3±0.4
21d	32±9 ^a	49±12	1.1±0.2 ^b	1.1±0.4
28d	35±10 ^a	51±20	1.1±0.3 ^b	1.1±0.3

^a $P<0.05$, vs control group. ^b $P<0.05$, vs 4d group.

Table 3 Number and area of G and D cells, and the ratio of G/D number and G/D area ($\bar{x}\pm s$, $n=7$)

Group	No.(G cells)	Area of G cells (×10 ⁻⁶ m ²)	No.(D cells)	Area of G cells (×10 ⁻⁶ m ²)	Number ratio of G/D	Area ratio of G/D
Control	33±6	99±7	15±2	70±11	2.3±0.1	1.4±0.1
4d	50±7 ^a	87±7 ^a	10±2 ^a	56±8 ^a	4.9±0.3 ^a	1.6±0.1 ^a
7d	69±8 ^a	91±7 ^a	9±2 ^a	60±9 ^a	7.6±0.5 ^a	1.5±0.2
10d	73±13 ^a	94±7	10±1 ^a	63±7	7.4±0.4 ^a	1.5±0.1
14d	62±11 ^a	95±9	11±2 ^a	66±11	5.8±0.5 ^a	1.5±0.1
21d	46±8 ^a	95±8	14±2	68±11	3.4±0.2 ^a	1.4±0.1
28d	43±6 ^a	95±7	14±2	66±8	3.1±0.1 ^a	1.4±0.1

^a $P<0.05$, vs control group.

Table 4 Relationship between rat G and D cells, and between G or D cells and gastrin or somatostatin

Group	No. of G cells vs No. of D cells	Area of G cells vs area of D cells	No. of G cells vs gastrin in non-ulcer mucosa	No. of D cells vs somatostatin in non-ulcer mucosa	Area of G cells vs gastrin in non-ulcer mucosa	Area of D cells vs somatostatin in non-ulcer mucosa
Control	0.97 ^b	0.95 ^b	0.95 ^b	0.93 ^b	0.94 ^b	0.93 ^b
4d	0.92 ^b	0.93 ^b	0.87 ^a	0.90 ^b	0.98 ^b	0.86 ^a
7d	0.97 ^b	0.93 ^b	0.98 ^b	0.98 ^b	0.93 ^b	0.94 ^b
10d	0.97 ^b	0.96 ^b	0.93 ^a	0.88 ^b	0.93 ^b	0.95 ^b
14d	0.91 ^b	0.99 ^b	0.87 ^a	0.89 ^b	0.78 ^a	0.99 ^b
21d	0.97 ^b	0.88 ^b	0.90 ^b	0.68	0.98 ^b	0.99 ^b
28d	0.99 ^b	0.94 ^b	0.95 ^b	0.89 ^b	0.92 ^b	0.96 ^b

^a $P<0.05$, ^b $P<0.01$, vs control group.

DISCUSSION

Both gastrin and somatostatin are gastrointestinal hormones closely related to the function of gastrointestinal system. Gastrin is mainly secreted in G cells in antral and upper small intestines. It has several kinds of molecules and distributes in plasma, tissues, gastric juice, and intestinal juice. Somatostatin is a 14 amino peptide. It also has several kinds of molecules and distributes vastly in the body. The somatostatin in gastrointestinal system is secreted in D cells. It is mainly in intestinal nerve plexus, stomach and pancreas, and it is also in gastric and intestinal fluid. In the antrum there are many G and D cells, most of which belong to the open type endocrine cells that can directly secrete gastrin or somatostatin into gastric fluid. Elevated gastrin level can increase the secretion of basal and peak gastric acid, pepsin and inner factor, increase the amount of circulating blood in the mucosa of upper gastrointestinal tract, improve the nutrition of gastric mucosa cells. Somatostatin can obstruct the secretion of basal gastric acid and pepsin and inhibit the invoking function of gastrin to the secretion of gastric acid^[25-38]. Our experiment is to reveal the change of gastrin and somatostatin in gastric ulcer rats. The result shows that when the rat had gastric ulcer, the gastrin in plasma, gastric juice and antral mucosa tissue increased, and the somatostatin declined. With the healing of ulcer, gastrin and somatostatin gradually recovered to the normal level.

G and D cells have interactive relation in the function^[39-49]. In order to study their morphology we used the immunohistochemical method to identify the G and D cells and to measure the number and area of G and D cells by the medical image analysis system. We found that with ulcer the number of G cells increased as compared with the normal control group, the D cells decreased, and both areas of G and D cells declined. And with the healing of the ulcer, the number and area of G and D cells gradually recovered to the normal level. This suggests that in the ulcer stage, the function of synthesis and secretion of G cells increased, while that of D cells declined. This inclined us that the increased secretion of gastrin in ulcer rat might be related to the increased number of G cells. The declined area of G cells may be related to the increased secretion of gastrin. The decline of somatostatin secretion in gastric ulcer is likely related to both the decreased number of D cells and the reduced area of D cells. It is known that somatostatin can inhibit G cells to secrete gastrin. Because in the gastric ulcer, the somatostatin secretion of D cells in rats lowered its inhibitory effect to G cells, gastrin secretion of G cells increased.

G and D cells are interrelated in morphology. In normal gastrointestinal mucosa, the ratio of G/D number and G/D area is stable. This is useful for keeping the normal gastrointestinal function. The ratio of G/D cells can be an important index for knowing the change of the two kinds of cells and its effect on focal endocrine function^[50-58]. Our result showed that in gastric ulcer, the ratio of G/D number and the ratio of G/D area increased than that in normal control group. In the healing process, the disorder recovered gradually to the normal level. This proves that the number of G cells increased and the number of D cells declined in gastric ulcer. It also shows that in gastric ulcer rat, the decrease of the D cell area is more obvious than that of G cells. The statistical analysis indicates that there is a relationship between the number of G and D cells, and between the area of G and D cells. There is also a relationship between the number and area of G cells and gastrin in antral mucosa, and between the number and area of D cells and somatostatin in antral mucosa. In summary, our result further proves histologically that in gastric ulcer rat, the G cell secreted gastrin increased, and the D cell secreted somatostatin reduced, the ratio and function of G/D cells were imbalanced.

REFERENCES

- Schmitz F, Schrader H, Otte J, Schmitz H, Stuber E, Herzig K, Schmidt WE. Identification of CCK-B/gastrin receptor splice variants in human peripheral blood mononuclear cells. *Egul Pept* 2001; 101:25-33
- Caplin M, Khan K, Grimes S, Michaeli D, Savage K, Pounder R, Dhillon A. Effect of gastrin and anti-gastrin antibodies on proliferation of hepatocyte cell lines. *Dig Dis Sci* 2001; 46:1356-1366
- Janecka A, Zubrzycka M, Janecki T. Somatostatin analogs. *J Pept Res* 2001; 58:91-107
- Klisovic DD, O'Dorisio MS, Katz SE, Sall JW, Balster D, O'Dorisio TM, Craig E, Lubow M. Somatostatin Receptor Gene Expression in Human Ocular Tissues: RT-PCR and Immunohistochemical Study. *Invest Ophthalmol Vis Sci* 2001; 42:2193-2201
- Hocker M, Cramer T, O'Connor DT, Rosewicz S, Wiedenmann B, Wang TC. Neuroendocrine-specific and gastrin-dependent expression of a chromogranin A-luciferase fusion gene in transgenic mice. *Gastroenterology* 2001; 121:43-55
- Monstein HJ, Ohlsson B, Axelsson J. Differential expression of gastrin, cholecystokinin-A and cholecystokinin-B receptor mRNA in human pancreatic cancer cell lines. *Scand J Gastroenterol* 2001; 36:738-743
- McWilliams DF, Grimes S, Watson SA. Antibodies raised against the extracellular tail of the CCKB/gastrin receptor inhibit gastrin-stimulated signalling. *Regul Pept* 2001; 99:157-161
- Yamamoto S, Kaneko H, Konagaya T, Mori S, Kotera H, Hayakawa T, Yamaguchi C, Uruma M, Kusugami K, Mitsuma T. Interactions among gastric somatostatin, interleukin-8 and mucosal inflammation in *Helicobacter pylori*-positive peptic ulcer patients. *Helicobacter* 2001; 6:136-145
- Morisset J, Wong H, Walsh JH, Laine J, Bourassa J. Pancreatic CCK(B) receptors: their potential roles in somatostatin release and delta-cell proliferation. *Am J Physiol Gastrointest Liver Physiol* 2000; 279:G148-G156
- Cui RT, Cai G, Yin ZB, Cheng Y, Yang QH, Tian T. Transretinoic acid inhibits rats gastric epithelial dysplasia induced by N-methyl-N-nitro-N-nitrosoguanidine: influences on cell apoptosis and expression of its regulatory genes. *World J Gastroenterol* 2001; 7:394-398
- Takeuchi K, Kawauchi S, Araki H, Ueki S, Furukawa O. Stimulation by nizatidine, a histamine H₂-receptor antagonist, of duodenal HCO₃⁻ secretion in rats: relation to anti cholinesterase activity. *World J Gastroenterol* 2000; 6:651-658
- Li W, Zheng TZ, Qu SY. Effect of cholecystokinin and secretin on contractile activity of isolated gastric muscle strips in guinea pigs. *World J Gastroenterol* 2000; 6:93-95
- Kermorgant S, Lehy T. Glycine-extended gastrin promotes the invasiveness of human colon cancer cells. *Biochem Biophys Res Commun* 2001; 285:136-141
- Berger AC, Gibril F, Venzon DJ, Doppman JL, Norton JA, Bartlett DL, Libutti SK, Jensen RT, Alexander HR. Prognostic value of initial fasting serum gastrin levels in patients with Zollinger-Ellison syndrome. *J Clin Oncol* 2001; 19:3051-3057
- Waldum HL, Aase S, Kvetoj I, Brenna E, Sandvik AK, Syversen U, Johnsen G, Vatten L, Polak JM. Neuroendocrine differentiation in human gastric carcinoma. *Cancer* 1998; 83:435-444
- Sun FP, Song YG, Zhu XS, Tang SN, Du J, Qiu QL, Zhao T. The establishment of acetic-acid-induced rat's gastric ulcer model and the observation of ulcer antral mucosa through microscope and electromicroscope. *Shijie Huaren Xiaohua Zazhi* 2001; 9:135-138
- Annibale B, Aprile MR, Ferraro G, Marignani M, Angeletti S, D'Ambra G, Caruana P, Bordini C, Delle Fave G. Relationship between fundic endocrine cells and gastric acid secretion in hypersecretory duodenal ulcer diseases. *Aliment Pharmacol Ther* 1998; 12:779-788
- Wright NA. Aspects of the biology of regeneration and repair in the human gastrointestinal tract. *Philos Trans R Soc Lond B Biol Sci* 1998; 353:925-933
- Solcia E, Rindi G, Buffa R, Fiocca R, Capella C. Gastric endocrine cells: types, function and growth. *Egul Pept* 2000; 93:31-35
- Ling YL, Meng AH, Zhao XY, Shan BE, Zhang JL, Zhang XP. Effect of cholecystokinin on cytokines during endotoxic shock in rats. *World J Gastroenterol* 2001; 7:667-671
- Zhang LH, Yao CB, Li HQ. Effects of extract F of red-rooted *Salvia* on mucosal lesions of gastric corpus and antrum induced by hemorrhagic shock-reperfusion in rats. *World J Gastroenterol* 2001; 7:672-677
- Zhang H, Jiang SL, Yao XX. Study of T-lymphocyte subsets, nitric oxide, hexosamine and *Helicobacter pylori* infection in patients with chronic gastric diseases. *World J Gastroenterol* 2000; 6:601-604
- Zhu L, Yang ZC, Li A, Cheng DC. Reduced gastric acid production in burn shock period and its significance in the prevention and treatment of acute gastric mucosal lesions. *World J Gastroenterol* 2000; 6:84-88
- Huang Y, Lu SJ, Dong JX, Li F. The new proof of neuro-endocrine-immune network-expression of islet amyloid polypeptide in plasma cells in gastric mucosa of peptic ulcer patients. *World J Gastroenterol* 2000; 6:417-418
- Zavros Y, Fleming WR, Hardy KJ, Shulkes A. Regulation of fundic and antral somatostatin secretion by CCK and gastrin. *Am J Physiol* 1998; 274:G742-G750
- Ray JM, Squires PE, Meloche RM, Nelson DW, Snutch TP, Buchan AM. L-type calcium channels regulate gastrin release from human antral G cells. *Am J Physiol* 1997; 273:G281-G288
- Kamada T, Haruma K, Kawaguchi H, Yoshihara M, Sumii K, Kajiyama G. The association between antral G and D cells and mucosal inflammation,

- atrophy, and *Helicobacter pylori* infection in subjects with normal mucosa, chronic gastritis, and duodenal ulcer. *Am J Gastroenterol* 1998; 93:748-752
- 28 Nagano T, Itoh H, Takeyama M. Effect of Dai-kenchu-to on levels of 3 brain-gut peptides (motilin, gastrin and somatostatin) in human plasma. *Biol Pharm Bull* 1999; 22:1131-1133
- 29 Naito T, Itoh H, Yasunaga F, Takeyama M. Rikkunshi-to raises levels of somatostatin and gastrin in human plasma. *Biol Pharm Bull* 2001; 24:841-843
- 30 Johansson B, Uvnas-Moberg K, Knight CH, Svennersten-Sjaunja K. Effect of feeding before, during and after milking on milk production and the hormones oxytocin, prolactin, gastrin and somatostatin. *J Dairy Res* 1999; 66:151-163
- 31 Park SM, Lee HR, Kim JG, Park JW, Jung G, Han SH, Cho JH, Kim MK. Effect of *Helicobacter pylori* infection on antral gastrin and somatostatin cells and on serum gastrin concentrations. *Korean J Intern Med* 1999; 14:15-20
- 32 Fung LC, Greenberg GR. Somatostatin-14 modulates acid-dependent inhibition of meal-stimulated gastrin via muscarinic pathways in dogs. *Regul Pept* 1998; 74:159-166
- 33 Hiraoka S, Miyazaki Y, Kitamura S, Toyota M, Kiyohara T, Shinomura Y, Mukaida N, Matsuzawa Y. Gastrin induces CXC chemokine expression in gastric epithelial cells through activation of NF-kappaB. *Am J Physiol Gastrointest Liver Physiol* 2001; 281:G735-G742
- 34 Vantus T, Keri G, Krivickiene Z, Valius M, Stetak A, Keppens S, Csermely P, Bauer PI, Bokonyi G, Declercq W, Vandenabeele P, Merlevede W, Vandenheede JR. The somatostatin analogue TT-232 induces apoptosis in A431 cells. Sustained activation of stress-activated kinases and inhibition of signalling to extracellular signal-regulated kinases. *Cell Signal* 2001; 13:717-725
- 35 Zavros Y, Paterson A, Lambert J, Shulkes A. Expression of progastrin-derived peptides and somatostatin in fundus and antrum of nonulcer dyspepsia subjects with and without *Helicobacter pylori* infection. *Dig Dis Sci* 2000; 45:2058-2064
- 36 Gromada J, Hoy M, Buschard K, Salehi A, Rorsman P. Somatostatin inhibits exocytosis in rat pancreatic alpha-cells by G(i2)-dependent activation of calcineurin and depriming of secretory granules. *J Physiol* 2001; 535:519-532
- 37 Peng X, Feng JB, Yan H, Zhao Y, Wang SL. Distribution of nitric oxide synthase in stomach myenteric plexus of rats. *World J Gastroenterol* 2001; 7:852-854
- 38 Tuo BG, Yan YH, Ge ZL, Ou GW, Zhao K. Ascorbic acid secretion in the human stomach and the effect of gastrin. *World J Gastroenterol* 2000; 6:704-708
- 39 Pesce C, Rossi R, Lenti E, Tanzi R. G-cell density in the antral mucosa: a feasibility study. *Histopathology* 1997; 30:315-318
- 40 Sun FP, Song YG, Zhu XS, Tang SN, Du J, Qiu QL, Liang QM, Zhao T. Establishment of acetic-acid-induced rat's gastric ulcer model and the histological observation of ulcer antral mucosa in healing stage. *Di Yi Jun Yi Daxue Xuebao* 2001; 21:578-581
- 41 Larsson LI. Developmental biology of gastrin and somatostatin cells in the antropyloric mucosa of the stomach. *Microsc Res Tech* 2000; 48:272-281
- 42 Mihaljevic S, Katicic M, Karner I, Vuksic-Mihaljevic Z, Dmitrovic B, Ivandic A. The influence of *Helicobacter pylori* infection on gastrin and somatostatin values present in serum. *Hepatogastroenterology* 2000; 47:1482-1484
- 43 Zavros Y, Fleming WR, Shulkes A. Concurrent elevation of fundic somatostatin prevents gastrin stimulation by GRP. *Am J Physiol* 1999; 276:G21-G27
- 44 Westbrook SL, McDowell GH, Hardy KJ, Shulkes A. Active immunization against somatostatin alters regulation of gastrin in response to gastric acid secretagogues. *Am J Physiol* 1998; 274:G751-G756
- 45 Ren J, Dunn ST, Tang Y, Wang Y, Gao J, Brewer K, Hartly RF. Effects of calcitonin gene-related peptide on somatostatin and gastrin gene expression in rat antrum. *Egul Pept* 1998; 73:75-82
- 46 Weigert N, Schepp W, Haller A, Schusdziaara V. Regulation of gastrin, somatostatin and bombesin release from the isolated rat stomach by exogenous and endogenous gamma-aminobutyric acid. *Digestion* 1998; 59:16-25
- 47 Squires PE, Meloche RM, Buchan AM. Bombesin-evoked gastrin release and calcium signaling in human antral G cells in culture. *Am J Physiol* 1999; 276:G227-G237
- 48 Cappelli E, Degan P, Thompson LH, Frosina G. Efficient repair of 8-oxo-7,8-dihydrodeoxyguanosine in human and hamster xeroderma pigmentosum D cells. *Biochemistry* 2000; 39:10408-10412
- 49 Chen YQ, Guo WH, Chen ZM, Shi L, Chen YX. Effect of gastrectomy on G-cell density and functional activity in dogs. *World J Gastroenterol* 2000; 6:419-420
- 50 Chamouard P, Walter P, Wittersheim C, Demuyne P, Meunier O, Baumann R. Antral and fundic D-cell numbers in *Helicobacter pylori* infection. *Eur J Gastroenterol Hepatol* 1997; 9:361-365
- 51 Iyo T, Kaneko H, Konagaya T, Mori S, Kotera H, Uruma M, Rhue N, Shimizu T, Imada A, Kusugami K, Mitsuma T. Effect of intragastric ammonia on gastrin-, somatostatin- and somatostatin receptor subtype 2 positive-cells in rat antral mucosa. *Life Sci* 1999; 64:2497-2504
- 52 Lloyd KC, Amirmoazzami S, Friedrik F, Chew P, Walsh JH. Somatostatin inhibits gastrin release and acid secretion by activating sst2 in dogs. *Am J Physiol* 1997; 272:G1481-G1488
- 53 Kamada T, Haruma K, Kawaguchi H, Yoshihara M, Sumii K, Kajiyama G. The association between antral G and D cells and mucosal inflammation, atrophy, and *Helicobacter pylori* infection in subjects with normal mucosa, chronic gastritis, and duodenal ulcer. *Am J Gastroenterol* 1998; 93:748-752
- 54 Tzaneva M. Light and electron microscopic immunohistochemical investigation on G and D cells in antral mucosa in *Helicobacter pylori*-related gastritis. *Exp Toxicol Pathol* 2001; 52:523-528
- 55 Magert HJ, Reinecke M, David I, Raab HR, Adermann K, Zucht HD, Hill O, Hess R, Forssmann WG. Uroguanylin: gene structure, expression, processing as a peptide hormone, and co-storage with somatostatin in gastrointestinal D-cells. *Regul Pept* 1998; 73:165-176
- 56 Beales IL. Effect of platelet-activating factor on gastrin release from cultured rabbit G-cells. *Dig Dis Sci* 2001; 46:301-306
- 57 Ford MG, Valle JD, Soroka CJ, Merchant JL. EGF receptor activation stimulates endogenous gastrin gene expression in canine G cells and human gastric cell cultures. *J Clin Invest* 1997; 99:2762-2771
- 58 Yao YL, Xu B, Zhang WD, Song YG. Gastrin, somatostatin, and experimental disturbance of the gastrointestinal tract in rats. *World J Gastroenterol* 2001; 7:399-402

Edited by Ma JY

• CLINICAL RESEARCH •

Quantitative analysis of transforming growth factor beta 1 mRNA in patients with alcoholic liver disease

Wei-Xing Chen, You-Ming Li, Chao-Hui Yu, Wei-Min Cai, Min Zheng, Feng Chen

Wei-Xing Chen, You-Ming Li, Chao-Hui Yu, Wei-Min Cai, Min-Zheng, Feng-Chen, Department of Gastroenterology, The First Affiliated Hospital, Medical College of Zhejiang University, Hangzhou 310003, Zhejiang Province, China

Correspondence to: Dr. Wei-Xing Chen, Department of Gastroenterology, The First Affiliated Hospital, Medical College, Zhejiang University, Hangzhou 310003, Zhejiang Province, China. weixng121@sina.com
Telephone: +86-571-7236568 Fax: +86-571-87236611

Received 2001-03-28 Accepted 2001-10-12

Abstract

AIM: To investigate the expression of the transforming growth factor beta 1 (TGF- β 1) mRNA in different stages of alcoholic liver disease (ALD) and its clinical value.

METHODS: One hundred and seven male alcoholics were grouped by clinical findings into four groups: alcohol abusers without liver impairment ($n=22$), alcoholic steatosis ($n=30$), alcoholic hepatitis ($n=31$), and alcoholic cirrhosis ($n=24$). Using peripheral blood mononuclear cells (PBMC) as samples the gene expression of TGF- β 1 was examined quantitatively by reverse transcription polymerase chain reaction (RT-PCR) and dot blot. There are 34 healthy subjects served as control.

RESULTS: The expression of TGF- β 1 from all ALD patients was significantly greater than that in controls (1.320 ± 1.162 vs 0.808 ± 0.276 , $P < 0.001$). The differences of the expressions were significant between the patients from each groups (alcoholic steatosis, alcoholic hepatitis and alcoholic cirrhosis) and the controls (1.168 ± 0.852 , 1.462 ± 1.657 , 1.329 ± 0.610 vs 0.808 ± 0.276 , $P < 0.050$). No significant differences of TGF- β 1 mRNA expression were observed between alcohol abusers without liver impairment and controls. The expressions in patients with alcoholic hepatitis and alcoholic cirrhosis were significantly greater than that in alcohol abusers respectively (1.462 ± 1.657 , 1.329 ± 0.610 vs 0.841 ± 0.706 , $P < 0.050$). No significant differences of TGF- β 1 mRNA expression were observed between alcoholic fatty liver men and alcohol abusers.

CONCLUSION: TGF- β 1 expression level can be a risk factor for alcoholic liver disease and might be related to the inflammatory activity and fibrosis of the liver in patients.

Chen WX, Li YM, Yu CH, Cai WM, Zheng M, Chen F. Quantitatively analysis of transforming growth factor beta 1 mRNA in patients with alcoholic liver disease. *World J Gastroenterol* 2002;8(2):379-381

INTRODUCTION

Alcoholic liver disease (ALD) is the most common cause of liver disease in late stage in the developed world^[1], and ranked as the second cause of hepatic cirrhosis in China now. The increased deposition of extracellular matrix in the liver is a key factor in the developing of the disease.

In recent years, the role of TGF- β 1 in ALD has been much emphasized^[2,3], but the study of expression of TGF- β 1 in peripheral blood mononuclear cells (PBMC) from ALD patients has

scarcely been performed. This study was aimed at quantitative analysis of the expression of TGF- β 1 mRNA in PBMC of ALD patients through reverse transcription-polymerase chain reaction (RT-PCR) technique and dot blot.

MATERIALS AND METHODS

Subjects

The subjects were from the epidemiologic survey of ALD in Zhejiang province including 107 male alcoholics, aged 25~70 years ($\chi = 43.32 \pm 10.39$), who had ingested more than 40g of alcohol a day for more than 5 years. According to the diagnostic criteria of Nanjing conference, there were 22 alcohol abusers without hepatic impairment, 30 alcoholic steatosis, 31 alcoholic hepatitis and 31 alcoholic cirrhosis. Percutaneous liver biopsy was performed in all cases, C and B hepatitis were ruled out by appropriate serological tests. 34 healthy subjects served as control, with age range from 26 to 68 years ($\chi = 45.60 \pm 10.08$). There were no significant differences in their ages among the alcoholics and healthy controls.

Design and synthesis of primers

TGF- β 1 primers and probe were synthesized by Gibco BRL Co. The forward primer, reverse primer and probe were 5'-GGA CAC CAA CTA TTG CTT CAG 3', 5'-TCC AGG CTC CAA ATG TAGG 3' and 5'-CAG CTG TAC ATT GAC TTC CGC AAG GAC CT 3' respectively. β -actin primers were synthesized by the Academy of Microorganism Science of Lubeck University, and kindly provided by Prof. Chen Zhi. The sequence of the primers were 5'-TTC CAG CCT TCC TTC CTGG 3' (forward primer) and 5'-TTG CGC TCA GGA GGA GCA AT 3' (reverse primer). The Primers were designed according to the previously reported sequence as shown in Roulot's report^[4].

Samples preparation and RNA extraction

Blood samples 3ml were mixed with Ficoll fluid to isolate the PBMC and then 150 μ l Trizol Reagent (Gibco BRL Co.) was added. Total cellular RNA was extracted by the guanidinium thiocyanate/phenol chloroform single-step method. RNA was washed in ethanol and dissolved in diethyl pyrocarbonate (DEPC)-treated water.

RT-PCR

The RT-PCR mixture consisted of RNA of each sample 5 μ l, 2mM dNTP 5 μ l, 5 \times first stand buffer 5 μ l, 100mM TT 2.5 μ l, 100pmol/ μ l oligo(dT) 15 μ l, MMLV-RT 100 unit, Rnase 1 μ l (Pharmacia Biotech) to a total volume of 20 μ l. The reaction was allowed to proceed at 41 $^{\circ}$ C for 1 hour.

The PCR mixture consisted of RT-PCR products 5 μ l, 10 \times PCR buffer 5 μ l, 20 pmol of each primer, 2mM dNTP 5 μ l and Taq polymerase 1.25 unit (Gibco BRL Co.) to a total volume of 40 μ l. This reaction mixture was overlaid with 1 drop of mineral oil.

PCR was carried out in a DNA thermal cycler (Perkin-Elmer Cetus) for 30 cycles; after initial denaturation by heating to 95 $^{\circ}$ C for 2 minutes, each cycle consisted of denaturation at 94 $^{\circ}$ C for 60 seconds, annealing at 56 $^{\circ}$ C for 60 seconds and extension at 72 $^{\circ}$ C for 45 seconds. An extra extension at 72 $^{\circ}$ C for 10 minutes was performed after the final cycle.

Dot blot

The probe was labelled using a DIG oligonucleotide 3'-end labeling kit (Boehringer Mannheim). The efficiency of the labeling reaction was checked by comparing with the labelled control-oligonucleotide by direct detection. 5 µl PCR products was dropped to on a nylon membrane. The membranes were hybridized at 60°C for 6h after being denatured, fixed, prehybridized and then washed and stained.

Quantitative analysis

Quantification of TGF-β1 mRNA was carried out using β-actin mRNA as an internal standard because the transcription levels of β-actin were very stable in all types of tissues. The dots on the membranes were quantitatively analyzed and pictures were taken using IS-1000 multifunction agarose imaging analysis system (Alpha Innotech Co.). The relative index (RI) of mRNA was calculated using a formula as RI = scan value of TGF-β1 mRNA dot / scan value of β-actin mRNA dot^[5]. Here RI might represent the relative levels of TGF-β1 mRNA in PBMC.

Statistics

The data were presented as means ± s, all the statistics were done with the software Statistical Package for the Social Sciences (SPSS) and the P value was considered significant when it was less than 0.05.

RESULTS

The expression of TGF-β1 from all ALD patients was significantly greater than that in the controls (1.320 ± 1.162 vs 0.808 ± 0.276, $t=3.811$, $P=0.0001$, Figure 1).

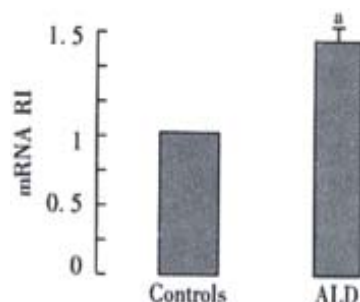


Figure 1 TGF-β1 mRNA RI values in ALD and Controls' * $P<0.05$ vs controls

The expressions in patients with the alcoholic steatosis, alcoholic hepatitis and alcoholic cirrhosis were significantly greater than the expression in the controls respectively (1.168 ± 0.852, 1.462 ± 1.657, 1.329 ± 0.610 vs 0.808 ± 0.276, $t=2.213$, $P=0.017$, $t=2.171$, $P=0.019$, $t=3.915$, $P=0.0002$). No significant differences of TGF-β1 mRNA expression were observed between alcohol abusers and the controls (Figure 2).

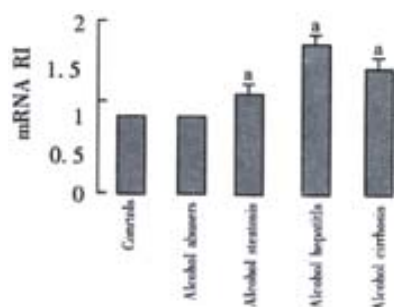


Figure 2 The TGF-β1 mRNA in alcohol abusers, alcohol steatosis, alcohol hepatitis, alcohol cirrhosis and controls. * $P<0.05$ vs controls

The expression in patients with alcoholic hepatitis and alcoholic hepatic cirrhosis was significantly greater than that in alcohol abusers respectively (1.462 ± 1.657, 1.329 ± 0.610 vs 0.841 ± 0.706, $t=1.859$, $P=0.035$, $t=2.495$, $P=0.008$). No significant differences of TGF-β1 mRNA expression were observed between alcoholic fatty liver males and alcohol abusers (Figure 3).

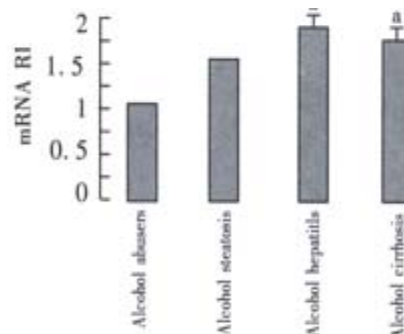


Figure 3 The TGF-β1 mRNA in alcohol abusers, alcohol steatosis, alcohol hepatitis, alcohol cirrhosis and alcohol abusers. * $P<0.05$ vs alcohol abusers

DISCUSSION

In Western societies roughly 50% of all cases of liver cirrhosis are related with alcohol abuse. The increased deposition of extracellular matrix in the liver is a key factor in the morbidity and mortality of alcoholic liver disease^[6]. This increased fibrosis may be due to a superabundance of profibrogenic factors such as transforming growth factor-beta 1 and/or relative decrease of the factors that inhibit fibrogenesis such as collagenase or interferon^[7-10]. Transforming growth factor-beta 1 (TGF-β1) is believed to play a key role in enhancing fibrogenesis and inhibiting extracellular matrix degradation^[11]. Acetaldehyde, the oxidative metabolite of ethanol damages cell membranes, initiates lipid peroxidation and forms noxious protein adducts, which result in the activation of Kupffer cells and perisinusoidal lipocytes/portal fibroblasts^[12-18]. The activation of lipocytes and fibroblasts to a proliferative and collagen-producing myofibroblast-like phenotype is triggered by the release of TGF-β1 from the activated Kupffer cells. In the liver, TGF-β1 is primarily responsible for activation of lipocytes, which are the main source of extracellular matrix proteins. Their deposition play a key role in the development of alcoholic liver cirrhosis^[19-21].

A number of investigators have shown increase of TGF-β1 mRNA and protein levels in animal models of hepatic fibrosis^[22-27]. A few studies also demonstrated increased levels of TGF-β1 mRNA and protein in animal models of ALD. Matsuoka *et al*^[28] examined Kupffer cells and hepatic lipocytes isolated from a rat model of alcoholic liver fibrosis. The collagen formation was increased significantly in alcohol-fed group more than the control, which was completely inhibited by anti-transforming growth factor beta IgG. The major peak of the molecular weight was about 25000 which was revealed by high-performance liquid chromatography and demonstrated with Northern blotting and hybridization. Kamimura *et al*^[29] examined Kupffer cell gene expression of TGF-β1 in the rat model of ALD. Kupffer cells were isolated from the model after 10 and 17 weeks of intragastric ethanol infusion, the protein and mRNA levels of TGF-β1 were significantly increased by 143% and 204% at 10 weeks and 238% and 295% at 17 weeks respectively in the ethanol-fed rats.

A number of studies have suggested a role for TGF-β1 in human liver disease^[30]. In our study, the expression of TGF-β1 was significantly greater in all the ALD patients than in the controls and the expression in the patients with the alcoholic steatosis, alcoholic hepatitis and alcoholic cirrhosis was significantly greater than

their expressions in the controls respectively. No significant differences of TGF- β 1 mRNA expression were observed between alcohol abusers and the controls. The results demonstrated that the expression of TGF- β 1 was related with ALD. Our study also showed that the expression of patients with alcoholic hepatitis and alcoholic cirrhosis was significantly greater than their expression in alcohol abusers respectively, and no significant differences of TGF- β 1 mRNA expression were observed between alcoholic steatosis men and alcohol abusers. These results indicated that the expression of TGF- β 1 was higher in more active and advanced ALD patients. Santos *et al.*^[31] also demonstrated similar results in liver specimens. The presence of TGF- β 1 expression could be recognized as a risk factor for active and advanced alcoholic liver disease.

REFERENCES

- Kumar S, Stauber RE, Gavalier JS, Basista MH, Dindzans VJ, Schade RR, Rabinovitz M, Tarter RE, Gordon R, Starzl TE, ValThiel DH. Orthotopic liver transplantation for alcoholic liver disease. *Hepatology* 1990;11:159-164
- Malizia G, Brunt EM, Peters MG, Rizzo A, Broekelmann TJ, McDonald JA. Growth factor and procollagen type I gene expression in human liver disease. *Gastroenterology* 1995;108:145-156
- Czaja MJ, Weiner FR, Flanders KC, Giambrone MA, Wind R, Biempica L, Zern MA. *in vitro* and *in vivo* association of transforming growth factor-beta 1 with hepatic fibrosis. *J Cell Biol* 1989;108:2477-2482
- Roulot D, Durand H, Coste T, Rautureau J, Strosberg AD, Benarous R, Marullo S. Quantitative analysis of transforming growth factor- α messenger RNA in the liver of patients with chronic hepatitis C: absence of correlation between high levels and severity of disease. *Hepatology* 1995;21:298-304
- Yang BB, Li FJ. Quantitative analysis of TGF- α and EGFR mRNA in laryngeal carcinoma tissues. *Chin Med J* 1999;112:1088-1092
- Breitkopf K, Lahme B, Tag CG, Gressner AM. Expression and matrix deposition of latent transforming growth factor beta binding proteins in normal and fibrotic rat liver and transdifferentiating hepatic stellate cells in culture. *Hepatology* 2001;33:387-396
- Bai WY, Yao XX, Feng LY. Current situation in studies of hepatic fibrosis. *Shijie Huaren Xiaohua Zazhi* 2000;8:1267-1268
- Blazejewski S, Preaux AM, Mallat A, Brocheriou I, Mavrier P, Dhumeaux D, Hartmann D, Schuppan D, Rosenbaum J. Human myofibroblastlike cells obtained by outgrowth are representative of the fibrogenic cells in the liver. *Hepatology* 1995;22:788-797
- Milani S, Herbst H, Schuppan D, Grappone C, Pellegrini G, Pinzani M, Casini A, Calabro A, Ciancio G, Stefanini F, Burroughs AK, Surrenti C. Differential expression of matrix-metalloproteinase-1 and -2 genes in normal and fibrotic human liver. *Am J Pathol* 1994;144:528-537
- Graham MF, Bryson GR, Diegelmann RF. Transforming growth factor beta 1 selectively augments collagen synthesis by human intestinal smooth muscle cells. *Gastroenterology* 1990;99:447-453
- Liou F, Liou JX. The role of transforming growth factor-beta 1 in hepatic fibrosis. *Shijie Huaren Xiaohua Zazhi* 2000;8:86-88
- Chen J, Robinson NC, Schenker S, Frosto TA, Henderson GI. Formation of 4-hydroxynonenal adducts with cytochrome c oxidase in rats following short-term ethanol intake. *Hepatology* 1999;29:1792-1798
- Xu D, Thiele GM, Beckenhauer JL, Klassen LW, Sorrell MF, Tuma DJ. Detection of circulating antibodies to malondialdehyde-acetaldehyde adducts in ethanol-fed rats. *Gastroenterology* 1998;115:686-692
- Li CJ, Nanji AA, Siakotos AN, Lin RC. Acetaldehyde-modified and 4-hydroxynonenal-modified proteins in the livers of rats with alcoholic liver disease. *Hepatology* 1997;26:650-657
- Israel Y. Antibodies against ethanol-derived protein adducts: pathogenic implications. *Gastroenterology* 1997;113:353-355
- Clot P, Parola M, Bellomo G, Dianzani U, Carini R, Tabone M, Arico S, Ingelman-Sundberg M, Albano E. Plasma membrane hydroxyethyl radical adducts cause antibody-dependent cytotoxicity in rat hepatocytes exposed to alcohol. *Gastroenterology* 1997;113:265-276
- Tuma DJ, Thiele GM, Xu D, Klassen LW, Sorrell MF. Acetaldehyde and malondialdehyde react together to generate distinct protein adducts in the liver during long-term ethanol administration. *Hepatology* 1996;23:872-880
- Yokoyama H, Nagata S, Moriya S, Kato S, Ito T, Kamegaya K, Ishii H. Hepatic fibrosis produced in guinea pigs by chronic ethanol administration and immunization with acetaldehyde adducts. *Hepatology* 1995;21:1438-1442
- Fan K. Regulatory effects of lipopolysaccharide in murine macrophage proliferation. *World J Gastroenterol* 1998;4:137-139
- Huang GC, Zhang JS, Zhang YE. Effects of retinoic acid on proliferation, phenotype and expression of cyclin-dependent kinase inhibitors in TGF- β 1-stimulated rat hepatic stellate cells. *World J Gastroenterol* 2000;6:819-823
- Gressner AM, Bachem MG. Molecular mechanisms of liver fibrogenesis—a homage to the role of activated fat-storing cells. *Digestion* 1995;56:335-346
- Raghow R, Irish P, Kang AH. Coordinate regulation of transforming growth factor beta gene expression and cell proliferation in hamster lungs undergoing bleomycin-induced pulmonary fibrosis. *J Clin Invest* 1989;84:1836-1842
- Kresina TF, He Q, Degli Esposti S, Zern MA. Gene expression of transforming growth factor beta 1 and extracellular matrix proteins in murine *Schistosoma mansoni* infection. *Gastroenterology* 1994;107:773-780
- Milani S, Herbst H, Schuppan D, Stein H, Surrenti C. Transforming growth factors beta 1 and beta 2 are differentially expressed in fibrotic liver disease. *Am J Pathol* 1991;139:1221-1229
- Krull NB, Zimmermann T, Gressner AM. Spatial and temporal patterns of gene expression for the proteoglycans biglycan and decorin and for transforming growth factor-beta 1 revealed by *in situ* hybridization during experimentally induced liver fibrosis in the rat. *Hepatology* 1993;18:581-589
- Xiang DD, Wei YL, Li QF. Molecular mechanism of transforming growth factor β 1 on Ito cell. *Shijie Huaren Xiaohua Zazhi* 1999;7:980-981
- Fang C, Lindros KO, Badger TM, Ronis MJ, Ingelman-Sundberg M. Zonated expression of cytokines in rat liver: effect of chronic ethanol and the cytochrome P450 2E1 inhibitor, chlormethiazole. *Hepatology* 1998;27:1304-1310
- Matsuoka M, Tsukamoto H. Stimulation of hepatic lipocyte collagen production by Kupffer cell-derived transforming growth factor beta: implication for a pathogenetic role in alcoholic liver fibrogenesis. *Hepatology* 1990;11:599-605
- Kamimura S, Tsukamoto H. Cytokine gene expression by Kupffer cells in experimental alcoholic liver disease. *Hepatology* 1995;22:1304-1309
- Bedossa P, Peltier E, Terris B, Franco D, Poynard T. Transforming growth factor-beta 1 (TGF-beta 1) and TGF-beta 1 receptors in normal, cirrhotic, and neoplastic human livers. *Hepatology* 1995;21:760-766
- Santos RM, Norton P, Esposti SD, Zern MA. TGF-beta isoforms in alcoholic liver disease. *J Gastroenterol* 1998;33:383-389

Edited by Wu XN and Ma JY

• CLINICAL RESEARCH •

Assessment of duodenogastric reflux by combined continuous intragastric pH and bilirubin monitoring

Fei Dai, Jun Gong, Ru Zhang, Jin-Yan Luo, You-Ling Zhu, Xue-Qin Wang

Fei Dai, Jun Gong, Ru Zhang, Jin-Yan Luo, You-Ling Zhu, Xue-Qin Wang, Department of Gastroenterology, Second Hospital of Xi'an Jiaotong University, Xi'an 710004, Shaanxi Province, China
Supported by the Public Health Ministry Foundation of China, No.06-9602-13
Correspondence to: Dr. Fei Dai, Department of Gastroenterology, Second Hospital of Xi'an Jiaotong University, 157 Xiwu LU, Xi'an 710004, Shaanxi Province, China. jiangdf@pub.xaonline.com
Telephone: +86-29-7231758 Fax: +86-29-7231758
Received 2001-07-19 Accepted 2001-11-15

Abstract

AIM: To assess the diagnostic value of a combination of continuous intragastric pH and bilirubin monitoring in the detection of duodenogastric reflux (DGR), and the effects of diet on the bilirubin absorbance.

METHODS: 30 healthy volunteers were divided into two groups: standard diet group (Group 1) 18 cases, free diet group (Group 2) 12 cases. Each subjects were subjected to simultaneous 24-hour intragastric pH and spectrophotometric bilirubin concentration monitoring (Bilitec 2000).

RESULTS: There was no difference of preprandial phase bilirubin absorbance between two groups. The absorbance of postprandial phase was significantly increased in group 2 than group 1. There was no difference between preprandial phase and postprandial phase absorbance in group 1. Postprandial phase absorbance was significantly higher in group 2. In a comparison of bile reflux with intragastric pH during night time, there were 4 types of reflux: Simultaneous increase in absorbance and pH in only 19.6%, increase in bilirubin with unchanged pH 33.3%, pH increase with unchanged absorbance 36.3%, and both unchanged in 10.8%. Linear regression analysis showed no correlation between percentage total time of pH<4 and percentage total time of absorbance>0.14, $r=0.068$, $P<0.05$.

CONCLUSION: Because of the dietary effect, high absorbance fluids or foods should be avoided in detection. Intragastric pH and bilirubin monitoring separately predict the presence of duodenal (and/or pancreatic) reflux and bile reflux. They can not substitute for each other. The detection of DGR is improved if the two parameters are combined simultaneously.

Dai F, Gong J, Zhang R, Luo JY, Zhu YL, Wang XQ. Assessment of duodenogastric reflux by combined continuous intragastric pH and bilirubin monitoring. *World J Gastroenterol* 2002;8(2):382-384

INTRODUCTION

Duodenogastric reflux (DGR) is a natural physiologic phenomenon often occurring during the early hours of the morning and postprandial period^[1]. When excessive, it may be pathological. Accurate detection of DGR has been a major problem for many years. Most methods used to detect DGR were of short periods, indirect and not in a physiological condition and with other shortcomings^[2,3]. Ambulatory intragastric pH monitoring allows a physiological method of measuring rises in intragastric pH with an extended sampling

period, but it can't reliably distinguish between DGR and other causes of increased pH levels and it is an indirect technique. At present an ambulatory fiberoptic spectrophotometer that detects the presence of bilirubin (Bilitec 2000) is universally recognized as a reliable method^[4-11]. This has made it feasible to qualitatively detect DGR for prolonged sampling periods in physiological setting. Up to date, there has been no report about the diagnostic value of a combined continuous intragastric pH and bilirubin monitoring in the assessment of DGR in China. We used Bilitec 2000 along with simultaneous ambulatory intragastric pH monitoring to evaluate its diagnostic value in DGR.

MATERIALS AND METHODS

Subjects

Thirty healthy control subjects, 16 male, 14 female, mean age 45 ± 11 , (range 20-70) years, were enrolled in this study. They were randomly divided into two groups: group 1 (standard diet group), 8 male, 10 female, mean age 45 ± 11 years and group 2 (free diet group), 7 male, 5 female, mean age 46 ± 10 years.

Methods

pH measurements were performed with an antimony electrode and bile measurement with a fiberoptic probe. Both catheter were connected to separate portable digital data recorders (Digitrapper Mark III and Bilitec 2000 recorder, Synectics). The pH electrodes were calibrated in buffer solution of pH 1 and pH 7 before and after the measurement. The calibration of the Bilitec 2000 was done in a small nontransparent tube before each test. The tip of pH catheter was tied with silk thread to the fiberoptic Bilitec probe, in a way the tip of the pH catheter slightly above the gap of the Bilitec probe, so that both measurements were registered almost at the same position.

Both probes were then passed transnasally after 12-h fasting and positioned in the gastric corpus 5cm below the lower border of the lower esophageal sphincter (LES)^[3,12]. The localization of the LES was determined by esophageal perfusion manometry. After 24h the probes were removed, and the data were downloaded to a PC for analysis with Esophogram software. 24-hour gastric pH record was divided in four periods: the upright period, the supine period, the prandial pH plateau period and the postprandial pH decline period^[13]. The preprandial period pH and the postprandial period (include the prandial pH plateau period and the postprandial pH decline period) pH were compared in this study. The absorbance ≥ 0.14 was used as Bilitec threshold values.

Group 1 were asked to take allowed food with bilirubin absorbance never exceeding 0.14 (range 0.02-0.11) *in vitro*, such as milk, bread, rice, noodles, fish soup, chicken soup, boiled potatoes, lotus roots, pears and so on, the total calorie of three meals being about 8.4×10^6 J. The foods were detected in another unpublicized study. Group 2 were allowed to take free food except coffee and orange juice. The foods should be finely minced to avoid solid food pollution of the tip of the probe. All subjects were advised to eat three times a day and not to drink between meals. Smoking and alcohol were not allowed.

Statistical analysis

All results were expressed as $\bar{x}\pm s$. Data were analyzed by Student's *t* test and linear regression. $P<0.05$ was considered statistically significant.

RESULTS

Intragastric pH of preprandial and postprandial period in two groups

Intragastric pH was significantly higher in postprandial period in two groups. In Group 1 and in group 2, intragastric pH of postprandial period compared with preprandial period were 3.6 ± 1.1 vs 2.0 ± 0.6 , $P < 0.05$, and 3.8 ± 1.2 vs 2.1 ± 0.8 , $P < 0.05$, respectively.

Intragastric bilirubin absorbance of preprandial and postprandial period in two groups

There was no difference of preprandial phase absorbance between two groups. The absorbance of postprandial phase was significantly increased in group 2 than group 1, 0.20 ± 0.04 vs 0.10 ± 0.08 , $P < 0.05$. There was no difference between preprandial phase and postprandial phase absorbance in group 1. Postprandial phase absorbance was significantly higher in group 2, 0.20 ± 0.04 vs 0.10 ± 0.03 , $P < 0.05$.

Intragastric pH and bile reflux changes in overnight fasting

In a comparison of bile reflux with pH monitoring during night time in group 1, there were 4 types of reflux: Simultaneous increase in absorbance and pH in only 19.6%, increase in bilirubin with unchanged pH 33.3% or pH increase with unchanged absorbance 36.3%, increase in either one of the two parameters 69.6%, and both unchanged 10.8%. Moreover, Linear regression analysis showed no correlation between percentage total time of $\text{pH} > 4$ and percentage total time of absorbance > 0.14 , $r = 0.068$, $P < 0.05$ (Figure 1-4).

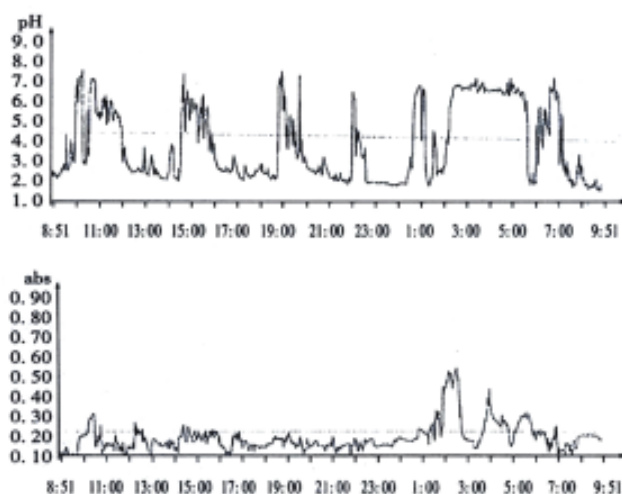


Figure 1 Simultaneous increase of intragastric pH and bilirubin absorbance

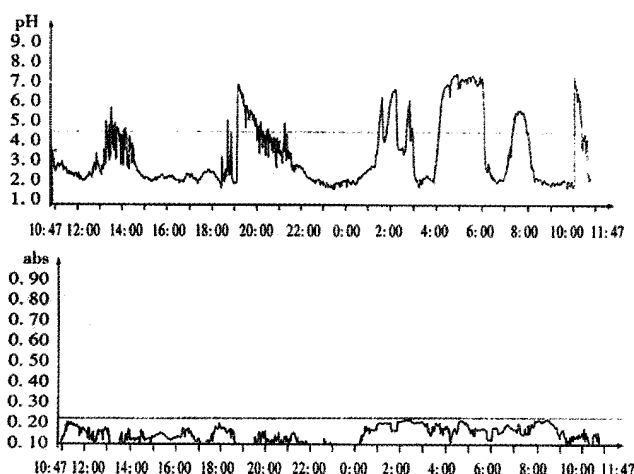


Figure 2 Intragastric pH increase with constant bilirubin absorbance

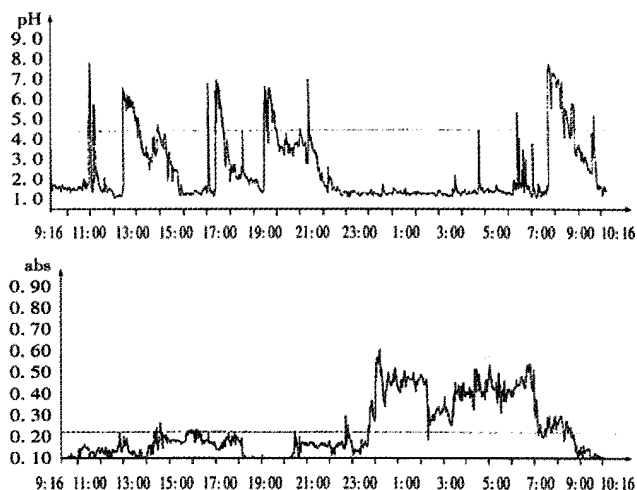


Figure 3 Bilirubin absorbance increase with constant intragastric pH

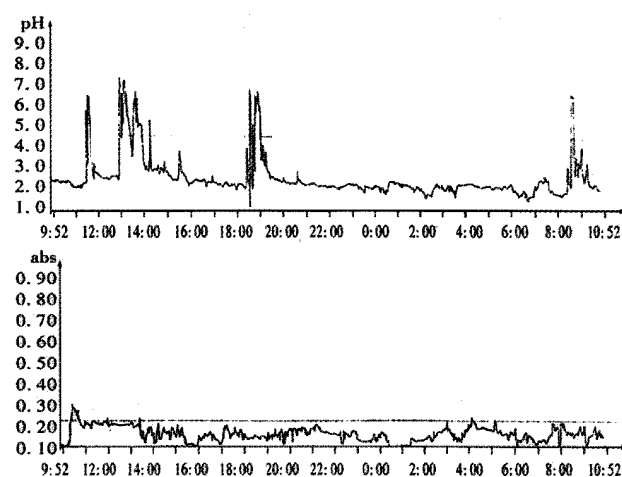


Figure 4 Intragastric pH and bilirubin absorbance both constant

DISCUSSION

Based on the experience in the esophagus in patients with gastroesophageal reflux disease, Litter *et al.*^[14] first applied intragastric 24 hour monitoring for evaluation of the alkaline reflux. Since then 24 hour intragastric pH monitoring has been used in many studies of DGR^[15-20]. It is an indirect technique and is not capable of such detection in hypochlorhydric stomachs and in the prandial period. So there exist limitations in the diagnosis of DGR^[21,22]. Bilitec 2000 is a new fiberoptic spectrophotometer that relies on the optical properties of bile to detect duodenogastric bile reflux (DGBR) in ambulatory setting independent of pH^[23]. Bilirubin is the most common pigment in bile, with a characteristic absorption peak of 470 nm^[24]. The basic working principle of the Bilitec 2000 is that an absorption at 470 nm automatically implies the presence of bilirubin, and therefore, bile in the sample under consideration. In the presence of bile alone, the degree of absorbance is proportional to the bilirubin concentration^[25]. Bilitec may be an important advancement in the field of detecting DGR, permitting more accurate studies of patients with syndromes associated with DGR.

With Bilitec 2000 a threshold value is 0.14 absorbance^[3,23,26], beyond which bile reflux is considered to be present. This threshold value takes into account scattering effects due to the gastric content such as suspended particles and mucus, which can give rise to a Bilitec readout ranging from 0 to 0.13 absorbance units, which, however, is not to be ascribed to bilirubin absorbance^[23].

In this study the results showed that the intragastric pH in the postprandial period was higher than that in preprandial in both groups because of neutralization by food. In group 1 the bilirubin absorbance was lower than 0.14 in both period. In group 2 postprandial absorbance of (0.20 ± 0.04) was significantly increased than preprandial (0.10 ± 0.03) . So measurement could be affected by the diet^[27]. Some foods with an absorbance at between 400-450 nm are capable of resulting in false positive results. In order to accurately access DGBR, the foods with high absorbance should be avoided (e.g. coffee, coke, carrot, tomato, etc). Fein *et al*^[28] reported if a threshold of absorbance of 0.25 was used, a free diet except coffee could be allowed for measurements.

In our study Bilitec 2000 along with simultaneous ambulatory intragastric pH monitoring showed a poor correlation between intragastric pH and DGBR. These results was consistent with other reports^[29,30]. How to explain the discrepancy Duodenal juice consists of intestinal secretion, pancreatic secretion and bile. A previous study^[1] using gastric aspiration and antroduodenal manometry showed a relationship among secretory activity, migrating motor complex (MMC) and DGR. DGR was highest during the late phase II of MMC and lowest after phase III. The duodenal bicarbonate output was highest after the onset of phase III while bile acid output was highest prior to the onset of phase III. Perhaps the reason for the poor correlation between intragastric pH and DGBR was related to variations of the amount of and different components in the regurgitated duodenal juice. If duodenogastric reflux fluid contains more bile and sufficient bicarbonate contents, both intragastric pH and absorbance are increased. If the reflux fluid consists mainly of duodenal bicarbonate and/or pancreatic secretion with less bile contents, rise of intragastric pH is observed owing to the buffering capacity of the fluid, and the absorbance remains unchanged. Conversely, if bile reflux occurs with less duodenal bicarbonate and pancreatic secretion, or in the absence of duodenal bicarbonate and pancreatic secretion, absorbance is increased with unchanged pH, because the low bicarbonate buffering capacity can not change the pH. Fuchs *et al*^[31] studied the variability in the composition of physiologic duodenogastric reflux and found pancreatic enzyme aspirate was significantly more often associated with a rise in pH in comparison to bile reflux ($P < 0.01$).

In conclusion, because of the dietary effect, high absorbance fluids or foods should be avoided in the detection. Intragastric pH and bilirubin monitoring separately predict the presence of duodenal (and /or pancreatic) reflux and bile reflux. They can not substitute for each other. The detection of DGR is improved if the two parameters are combined simultaneously.

REFERENCES

- Keane FB, Dimagno EP, Malagelada JR. Duodenogastric reflux in humans: Its relationship to fasting antroduodenal motility and gastric, pancreatic, and biliary secretion. *Gastroenterology* 1981;81:726-731
- Wu BY, Wang MW, Wang J. Approach to quantitation of duodenogastric reflux by ultrasonography. *Chin Natl J New Gastroenterol* 1996;2(Suppl 1):129
- Bechi P, Clanchi F. Technical aspects and clinical indications of 24-hour intragastric bile monitoring. *Hepatogastroenterology* 1999;46:54-59
- Gong J, Zhang R, Luo JY, Zhu YL, Wang XQ. The effect of bile reflux on the intragastric pH. *Xi'an Yike Daxue Xuebao* 2001;22:25-27
- Byrne JP, Romagnoli R, Bechi P, Attwood SE, Fuchs KH, Collard JM. Duodenogastric reflux of bile in health: the normal range. *Physiol Meas* 1999;20:149-158
- Vaezi MF, Richter JE. Importance of duodeno-gastro-esophageal reflux in the medical outpatient practice. *Hepatogastroenterology* 1999;46:40-47
- Gong J, Zhang R, Luo JY, Zhu YL, Wang XQ. A study on the etiology of the spontaneous nocturnal gastric alkalization. *Xi'an Yike Daxue Xuebao* 2001;22:230-232
- Okholm M, Sorensen H, Wallin L, Boesby S. Bile reflux into the esophagus. Bilitec 2000 measurements in normal subjects and in patients after Nissen fundoplication. *Scand J Gastroenterol* 1999;34:653-657
- Vaezi MF, Shay SS. New techniques in measuring nonacidic esophageal reflux. *Semin Thorac Cardiovasc Surg* 2001;13:255-264
- Kawiorski W, Herman RM, Legutko J. Current diagnosis of gastroduodenal reflux and biliary gastritis. *Przeg Lek* 2001;58:90-94
- Osugi H, Kaseno S, Takada N, Takemura M, Kisida S, Okuda E, Ueno M, Tanaka Y, Fukuhara K, Kinoshita H. Clinical significance of ambulatory intraesophageal bilirubin monitoring in diagnosis of gastroesophageal reflux. *Nippon Rinsho* 2000;58:1823-1826
- Barlow AP, Hinder RA, DeMeester TR, Fuchs K. Twenty-four-hour gastric luminal pH in normal subjects: influence of probe position, food, posture, and duodenogastric reflux. *Am J Gastroenterol* 1994;89:2006-2010
- Fuchs KH, DeMeester T, Hinder RA, Stein HJ, Barlow AP, Gupta NC. Computerized identification of pathologic duodenogastric reflux using 24-hour gastric pH monitoring. *Ann Surg* 1991;213:13-20
- Little AG, Martinez EI, DeMeester TR, Blough RM, Skinner DB. Duodenogastric reflux and reflux esophagitis. *Surgery* 1984;96:447-454
- Zhang J, Tan XL, Luo JY, Gong J. Study of 24 hour gastric pH monitoring in the diagnosis of duodenal gastric reflux. *Chin Natl J New Gastroenterol* 1996;2(Suppl 1):112-113
- Koek GH, Tack J, Sifrim D, Lerut T, Janssens J. The role of acid and duodenal gastroesophageal reflux in symptomatic GERD. *Am J Gastroenterol* 2001;96: 2033-2040
- Cuomo R, Koek G, Sifrim D, Janssens J, Tack J. Analysis of ambulatory duodenogastric reflux monitoring. *Dig Dis Sci* 2000;45:2463-2469
- Marshall RE, Anggiansah A, Owen WA, Manifold DK, Owen WJ. The extent of duodenogastric reflux in gastro-oesophageal reflux disease. *Eur J Gastroenterol Hepatol* 2001;13:5-10
- Tan XL, Luo JY, Gong J. Clinical application of 24 hour gastric pH monitoring. *Chin Natl J New Gastroenterol* 1997;5:535-536
- Gong J, Zhang Q, Zhang Y, Zhu YL, Wang XQ, Luo JY. The study on rhythm of 24h gastric pH. *Xi'an Yike Daxue Xuebao* 1999;20:326-328
- van Herwaarden MA, Samsom M, Smout AJ. 24-h recording of intragastric pH: technical aspects and clinical relevance. *Scand J Gastroenterol* 1999;230(Suppl):9-16
- Mela GS, Savarino V, Vigneri S, Zentilin P, Mansi C, DeMartini D. Limitations of continuous 24-h intragastric pH monitoring in the diagnosis of duodenogastric reflux. *Am J Gastroenterol* 1995;90:933-937
- Bechi P, Pucciani F, Baldini F, Cosi F, Falciai R, Mazzanti R, Castagnoli A, Passeri A, Boscherini S. Long-term ambulatory enterogastric reflux monitoring-validation of a new fiberoptic technique. *Dig Dis Sci* 1993;38: 1297-1306
- Baldini F, Bechi P, Cianchi F, Falai A, Fiorillo C, Nassi P. Analysis of the optical properties of bile. *J Biomed Opt* 2000;5:321-329
- Stein HJ, Kauer WKH, Feussner H, Siewert JR. Bile acids as components of the duodenogastric refluxate: Detection, relationship to bilirubin, mechanism of injury, and clinical relevance. *Hepatogastroenterology* 1999;46:66-73
- Barrett MW, Myers JC, Watson DI, Jamieson GG. Detection of bile reflux: *in vivo* validation of the Bilitec fibreoptic system. *Dis Esophagus* 2000;13:44-50
- Barrett MW, Myers JC, Watson DI, Jamieson GG. Dietary interference with the use of Bilitec to assess bile reflux. *Dis Esophagus* 1999;2:60-64
- Fein M, Fuchs KH, Bohrer T, Freys SM, Thiede A. Fiberoptic technique for 24-hour bile reflux monitoring. Standards and normal values for gastric monitoring. *Dig Dis Sci* 1996;41:216-225
- Just RJ, Leite LP, Castell DO. Changes in overnight fasting intragastric pH show poor correlation with duodenogastric bile reflux in normal subjects. *Am J Gastroenterol* 1996;91:1567-1570
- Fuchs KH, Fein M, Maroske J, Heimbucher J, Freys SM. The role of 24-hr gastric pH-monitoring in the interpretation of 24-hr gastric bile monitoring for duodenogastric reflux. *Hepatogastroenterology* 1999;46: 60-65
- Fuchs KH, Maroske J, Fein M, Tigges H, Ritter MP, Heimbucher J, Thiede A. Variability in the composition of physiologic duodenogastric reflux. *J Gastrointest Surg* 1999;3:389-395

Edited by Lu HM

• REVIEW •

The prognostic molecular markers in hepatocellular carcinoma

Lun-Xiu Qin, Zhao-You Tang

Lun-Xiu Qin, Zhao-You Tang, Liver Cancer Institute and Zhongshan Hospital, Fudan University, Shanghai, China

Correspondence to: Zhao-You Tang, M.D., Professor of Surgery & Chairman, Liver Cancer Institute & Zhongshan Hospital, Fudan University, 136 Yi Xue Yuan Road, Shanghai 200032, China. zytang@srcap.stc.sh.cn
Telephone: +86-21-64037181 Fax: +86-21-64037181

Received 2002-03-19 Accepted 2002-05-08

Abstract

The prognosis of hepatocellular carcinoma (HCC) still remains dismal, although many advances in its clinical study have been made. It is important for tumor control to identify the factors that predispose patients to death. With new discoveries in cancer biology, the pathological and biological prognostic factors of HCC have been studied quite extensively. Analyzing molecular markers (biomarkers) with prognostic significance is a complementary method. A large number of molecular factors have been shown to associate with the invasiveness of HCC, and have potential prognostic significance. One important aspect is the analysis of molecular markers for the cellular malignancy phenotype. These include alterations in DNA ploidy, cellular proliferation markers (PCNA, Ki-67, MCM2, MIB1, MIA, and CSE1L/CAS protein), nuclear morphology, the p53 gene and its related molecule MDM2, other cell cycle regulators (cyclin A, cyclin D, cyclin E, cdc2, p27, p73), oncogenes and their receptors (such as ras, c-myc, c-fms, HGF, c-met, and erb-B receptor family members), apoptosis related factors (Fas and FasL), as well as telomerase activity. Another important aspect is the analysis of molecular markers involved in the process of cancer invasion and metastasis. Adhesion molecules (E-cadherin, catenins, serum intercellular adhesion molecule-1, CD44 variants), proteinases involved in the degradation of extracellular matrix (MMP-2, MMP-9, uPA, uPAR, PAI), as well as other molecules have been regarded as biomarkers for the malignant phenotype of HCC, and are related to prognosis and therapeutic outcomes. Tumor angiogenesis is critical to both the growth and metastasis of cancers including HCC, and has drawn much attention in recent years. Many angiogenesis-related markers, such as vascular endothelial growth factor (VEGF), basic fibroblast growth factor (bFGF), platelet-derived endothelial cell growth factor (PD-ECGF), thrombospondin (TSP), angiogenin, pleiotrophin, and endostatin (ES) levels, as well as intratumor microvessel density (MVD) have been evaluated and found to be of prognostic significance. Body fluid (particularly blood and urinary) testing for biomarkers is easily accessible and useful in clinical patients. The prognostic significance of circulating DNA in plasma or serum, and its genetic alterations in HCC are other important trends. More attention should be paid to these two areas in future. As the progress of the human genome project advances, so does a clearer understanding of tumor biology, and more and more new prognostic markers with high sensitivity and specificity will be found and used in

clinical assays. However, the combination of some items, i.e., the pathological features and some biomarkers mentioned above, seems to be more practical for now.

Qin LX, Tang ZY. The prognostic molecular markers in hepatocellular carcinoma. *World J Gastroenterol* 2002;8(3):385-392

INTRODUCTION

Liver cancer is one of the common malignancies worldwide, and has been ranked the 2nd cancer killer in China since the 1990s. Although many advances in the clinical study of hepatocellular carcinoma (HCC) have been made, and long-term survival of patients has been obtained in some clinical centers, only a definitive subset of cases is cured by surgery, and the overall dismal outcome of patients with HCC has not been completely changed. Lack of control of metastatic foci and recurrence are the most prevalent causes of death in patients with HCC, and it is important for tumor control to identify the factors that predispose patients to death. Much effort has been made to predict HCC behavior, but specific prognostic indicators are still lacking^[1].

Prognostic factors in HCC conventionally consist of staging with the tumor node metastasis system (TNM) and grading by tumor cellular differentiation. There are also other factors useful in prognostic predication but most of them are clinical. With new discoveries in cancer biology, pathological and biological factors of HCC in relation to prognosis have been studied quite extensively. Morphological features of the tumor, both gross and histological, have been found to significantly associate with tumor recurrence and patient survival^[2-4]. A complementary way is to analyze molecular markers for their prognostic significance with reference to tumor recurrence and survival term in HCC. A large number of molecular biological factors have been shown to associate with the invasiveness of HCC, and have potential prognostic significance. However, routine biomarkers for the prediction of HCC prognosis are not yet available. In this review, we will focus on the recent advances in this aspect.

Cellular malignancy is a very important aspect for patient prognosis. In recent years, with the development of cellular and molecular biological techniques, many molecular markers related to invasion, metastasis, recurrence and survival have been explored. In HCC, DNA ploidy, the proliferating activity of tumor cells, tumor suppressor and promoter genes, cell cycle controllers, proteinases that degrade extracellular matrix, adhesion molecules, angiogenic factors, and metabolic genes, have been regarded as biomarkers for the malignant phenotype of HCC, and are related to prognosis and therapeutic outcomes^[5].

CELLULAR MALIGNANCY-RELATED MARKERS

DNA-ploidy

Controversy still exists regarding the prognostic significance of DNA ploidy in HCC patients. Many reports indicate that DNA ploidy could be a predictive marker for HCC prognosis^[6,7]. The overall survival rate of patients with aneuploid cells is much lower than that of patients with diploid ones, and those with multiple G0/G1 peaks have the

worst prognosis. Patients with higher cell proportions in proliferating stages have a higher early recurrence rate^[7]. However, other studies could not find a relationship between DNA ploidy and prognosis.

Proliferating activity of HCC cells

Many antigens, such as proliferating cell nuclear antigen (PCNA), Ki-67, MCM2, MIB1, MIA, and CSE1L/CAS protein (CAS), have been used as proliferation markers for cancer cells. The detection of PCNA with immunohistochemical methods is a common way to study the proliferating activity of cancer cells^[8]. Combined with histopathological characteristics, the PCNA labeling index (PCNA-LI) is one useful marker for evaluating malignant grade, and for predicting recurrence time and the patients' prognosis of HCC^[9].

The expression of the human Ki-67 protein is strictly associated with cell proliferation. The fact that the Ki-67 protein is present during all active phases of the cell cycle, but is absent from resting cells, makes it an excellent marker for determining the so-called growth fraction of a given cell population. Ki-67 protein expression is an absolute requirement for progression through the cell-division cycle. The fraction of Ki-67-positive tumor cells (the Ki-67 labeling index) is often correlated with the clinical course of the disease^[10,11]. Higher Ki-67 labeling index (Ki-67-LI) has a very similar clinical significance to PCNA-LI, reflecting the existence of biologically aggressive phenotypes and poor overall and disease-free survival rates in HCC. This could be a useful factor for predicting the long-term survival of patients with HCC following hepatic resection^[12,13].

The CSE1L/CAS protein (CAS) is a Ran-binding protein with a function as a nuclear transport (export) factor. This protein plays a role in the mitotic spindle checkpoint, which assures genomic stability during cell division. This checkpoint is frequently disturbed in neoplasias of various origins, including hepatic tumors. The degree of CAS expression correlates with the grade of tumor dedifferentiation, and could be a prognostic marker for HCC^[14].

Nuclear morphology

Nuclear profiles have been reported as useful prognostic predictors in various cancers, including HCC. The nuclear area of HCC correlates with cell differentiation and cell proliferating activity, and HCC with a large nuclear area has high potential for blood vessel invasion and intrahepatic metastasis. Computerized nuclear morphometry is more objective and quicker than conventional microscopic analysis^[15]. Recently, quantitative nuclear morphometry of cancer cells followed by computer-assisted image analysis (termed Quantitative nuclear grade, QNG) has proven to have potential use in cancer detection and predicting outcomes such as tumor stage, recurrence, and progression^[16].

p53 gene and its related molecule MDM2

p53 protein plays a central role in cellular responses, including cell-cycle arrest and cell death in response to DNA damage. p53 dysfunction can induce abnormal cell growth, increased cell survival, genetic instability, and drug resistance. Mutations in the p53 gene are the most frequently reported somatic gene alteration in human cancer. Associations of p53 mutation or positive immunohistochemistry staining with higher grade and more advanced stage has been noted for cancers of various origins. In addition, p53 mutation is considered as a strong marker predicting an increased risk of local relapse, treatment failure, and overall and disease-free survival in many kinds of human carcinomas, such as breast^[17-19], colorectal^[20], esophageal^[21], head and neck^[22], lung^[23,24], and ovarian^[25], as well as sarcoma^[26]. An increased intracellular concentration of the P53 protein, although not identical to, is sometimes seen in tumors with p53 mutation, and has been correlated with poor prognosis in some tumor types. Several studies have shown a relationship between the nuclear accumulation of p53 protein and poor disease-free and overall survival of cancer

patients^[27,28]. The presence of serum anti-p53 antibody has also been shown to associate with survival of patients with breast, ovarian, and colorectal cancer^[29,30]. p53 mutations in plasma DNA could also be detected in cancer patients, and may be used as a prognostic factor and an early marker to indicate recurrence or distant metastasis^[31]. However, there is still a great controversy as to whether alteration of the p53 gene adversely affects survival of cancer patients. Many reports failed to show the independent prognostic value of p53 in the carcinomas of tongue^[32], breast^[33,34], stomach^[35], lung^[36], ovarian^[37], bladder^[38], colorectal^[39], and non-Hodgkin's lymphoma^[40].

In a similar situation, there are many very controversial results with the prognostic value of p53 overexpression or p53 gene mutation in HCC patients. Many studies showed that p53 mutation was involved in determining the dedifferentiation, the proliferating activity, and tumor progression^[41], was strongly related to the invasiveness of HCC, and may also influence the postoperative course (particularly the recurrence within 1 year)^[42,43]. Mutations in the p53 gene or positive immunostaining for mutant P53 protein expression could be used as a significant indicator of poor prognosis. HCCs with p53 mutations have a high malignant potential, and p53 mutation in the primary lesion is useful as an indicator for the biological behavior of recurrent HCCs. It is also a useful independent prognostic factor affecting survival after recurrence^[9,44,45].

In a recent prospective study, we found the 3-year and 5-year overall survival rates of HCC patients with positive P53 nuclear accumulation were much lower than those of the HCC patients with negative P53 expression. In univariate and multivariate Cox analysis, p53 overexpression was the most significant factor that associated with the overall survival rates of HCC patients after resection. Its significance was even greater than that of factors such as tumor size, vascular invasion, and tumor capsule, though they were also related to the overall survival. p53 mutation or nuclear accumulation of p53 expression could be a valuable marker for predicting the prognosis of HCC patients after resection^[46].

Serum anti-p53 antibody also could be a useful prognostic factor for HCC patients^[47]. However, many different results showed that neither the immunohistochemical detection of p53 expression, nor the serum anti-p53 antibodies had a significant prognostic value for outcome of patients with HCC^[48,49].

The transcription of the mdm2 gene is activated by p53 and this limits the growth-suppressing activity of p53 by direct binding. It has been reported that MDM2 protein is overexpressed in several types of cancers. Endo found MDM2 overexpression correlated positively with p53 mutation, and is a useful predictor of poor prognosis in patients with HCC following hepatic resection^[50].

Cell cycle regulators

Disruption of the G1/S and G2/M checkpoints leads to uncontrolled cell growth, resulting in the development and progression of cancers. Overexpression of cyclin A, cyclin D, and cyclin E have been found to correlate with the tumor relapse of human HCC, and are independent predictive markers for their recurrence and prognosis^[51,52]. The enhanced expression of cyclin E correlates with hyperphosphorylation of pRb and a high frequency of Ki-67-positive cells. HCCs with enhanced cyclin E expression probably contain a relatively large number of proliferating cancer cells^[52]. cdc2 overexpression seems to play the most crucial role of the modulators in cell cycle progression and cell proliferation of HCC, and significantly predicts recurrence^[53].

The p27 protein binds and inhibits cyclin/cyclin-dependent kinase complexes, is a negative regulator of cell-cycle progression. The central role of p27 makes it important in a variety of disease processes, particularly in neoplasia, that involve aberrations in cellular proliferation and other cell fates. Loss of p27 cooperates with mutations in several oncogenes and tumor suppressor genes to facilitate

tumor growth, indicating that p27 may be a “nodal point” for tumor suppression. In most tumor types, reduced p27 expression correlates with poor prognosis, making p27 a novel and powerful prognostic marker^[54]. High p27 expression, correlated with prolonged survival, is a favorable independent prognostic parameter for HCC^[55,56].

The protein p73, the first identified homologue of p53 gene, has been shown to induce apoptosis. P73 expression status is significantly related to prognosis of HCC patients, and could serve as a useful indicator of prognosis in HCC patients^[57]. There is still controversy with the prognostic value of the p16INK4a and p15INK4B genes^[58].

Tumor promoter genes and their receptors

Aberrations of many tumor promoter genes, such as ras, c-myc, c-fms have been indicated as indicators of malignant potential and poor prognosis in HCC^[9,59-61]. c-myc amplification and p53 alteration may be participating events in the progression of HCC. Disease-free survival in patients showing c-myc amplification is significantly shorter than in those without amplification. Hepatocyte growth factor/scatter factor (HGF/SF) is one of the most important humoral mediators of liver regeneration. It is potentially related to molecular mechanisms of hepatocarcinogenesis via a paracrine system involving its cellular receptor, c-met. Up-regulation of c-met plays an important role in the development and progression of HCC, and may be a prognostic marker. Its expression level is inversely correlated with survival coordinated with uPA expression^[62,63]. However, there is no significant correlation between the HGF level in tumor and the survival rate of HCC patients^[5].

Among of the erb-B receptor family members, c-erbB-2 (Her-2/neu) represents a well-established prognostic marker and therapeutic target in several human tumor types, especially breast cancer. However, c-erbB-2 is neither a prognostic marker nor a relevant therapeutic target in human HCCs^[9,64]. EGF-R and c-erbB-3 play important roles in the progression of HCC, affecting disease-free survival of HCC patients^[5,65].

ets-1 has also been shown to link to cancer invasion and metastasis. ets-1 expression was observed with high incidence. However, the average labeling index (LI) in HCC is lower than in noncancerous lesions. Even lower expression levels were found in HCCs of high TNM stage, poor differentiation, portal invasion, intrahepatic metastasis, large tumor size, and high Ki-67-LI. HCC patients with high ets-1 expression showed better outcomes for disease-free survival than those with low ets-1 expression^[66].

Apoptosis related

The expression of Fas and Fas ligand (Fas L) play a role in apoptosis of cancer cells including HCCs, and associates with the prognosis of cancer patients. Fas expression level is significantly decreased in poorly differentiated HCC and of large size, while Fas L expression in carcinoma cells is observed exclusively in moderately or poorly differentiated cases. Each of them has prognostic significance for disease-free survival (DFS)^[5,67,68].

Telomerase activity

The ribonucleoprotein telomerase extends telomeres in cancer cells and has been proposed as a prognostic marker for cancer. Telomerase activity can be identified as an independent predictor for recurrence after resection of HCC^[69]. The peripheral blood telomerase activity can also be used as a molecular marker for the detection of circulating hepatoma cells in blood of HCC patients, which reflect haematogenous micrometastasis. This is potentially a practical diagnostic/predictive marker of HCC^[70]. Quantitative analysis of telomerase activity shows that the patients with positive telomerase activity in noncancerous liver tissue have a higher recurrence rate after HCC resection. The relative telomerase activity (RTA) of early recurrent patients is significantly higher than those without recurrence.

So, RTA could be a predictive marker for early recurrence after HCC resection^[71].

CELL ADHESION AND EXTRACELLULAR MATRIX RELATED

Adhesion molecules

The expression level of E-cadherin inversely correlates with HCC histological grade and prognosis. E-cadherin underexpression might have some contribution to the early recurrence of HCC^[72,73]. In contrast, alpha-, beta-, and gamma-catenin expression significantly correlated positively with HCC grade, being the highest in poorly differentiated HCC. Significant positive associations were found between gamma-catenin high expression and capsular invasion or presence of satellite nodules, and between beta-catenin high expression and vascular invasion. HCC patients with underexpression of E-cadherin, alpha-catenin, and gamma-catenin, and patients with overexpression of beta-catenin, had poorer survival rates^[73]. HCCs with a nonnuclear type of beta-catenin overexpression were frequently larger than 5cm in diameter and had poorer cellular differentiation, more invasiveness, and the patients had significantly shorter disease-free survival lengths^[74,75]. beta-catenin mutation associates with nuclear expression of the protein, and is a favorable prognostic factor related to low stage^[76].

Serum concentration of intercellular adhesion molecule-1 (sICAM-1) in patients with HCC is a marker for disease progression and prognosis. Higher sICAM-1 levels are more frequently observed in those patients with multiple lesions and intrahepatic metastasis, and their prognosis is also very poor. Detecting sICAM-1 is of important value in predicting tumor recurrence after surgery^[77-79]. The CD44 proteins form a ubiquitously expressed family of cell surface adhesion molecules involved in cell-cell and cell-matrix interactions. The major physiological role of CD44 is to maintain organ and tissue structure via cell-cell and cell-matrix adhesion, but certain variant isoforms can also mediate lymphocyte activation and homing, and the presentation of chemical factors and hormones. The expression of multiple CD44 isoforms is greatly upregulated in neoplasia. CD44, particularly its variants, may be useful as a diagnostic or prognostic marker of malignancy in at least some human cancers^[80]. Up-regulation of CD44 isoforms such as CD44s, CD44v5, CD44v6, CD44v7-8, and CD44v10, correlates with high histological grade, being the highest in poorly differentiated HCC. CD44 positivity was an independent factor. Positivity for one or more CD44 isoforms was the most useful independent factor for overall survival^[81].

Degradation of extracellular matrix

The matrix metalloproteinases (MMP) and the plasminogen activation system (PA) play crucial roles in the process of cancer invasion and metastasis. Their expression levels were found correlated to recurrence and survival after HCC resection^[82,83].

MMP-2, MMP-9, and tissue inhibitors of metalloproteinases -1, -2 (TIMP-1, TIMP-2) have been found to be of prognostic significance in HCC. The content of MMP-2, MMP-9 in HCC being higher than that in surrounding liver parenchyma could be used as an important index to judge the invasion and metastasis of HCC^[84,85]. Plasma MMP-9 levels can also be a candidate for a novel marker for HCC. The levels appear to reflect the potential and ongoing activity of vascular invasion^[5].

In several tumor types, elevated levels of urokinase plasminogen activator (uPA), its receptor (uPAR) or its inhibitor plasminogen activator inhibitor-1 (PAI-1) is associated with a poorer prognosis^[85]. uPA activity may be the most sensitive factor affecting HCC invasion in the plasminogen activation system and is a strong predictor for the recurrence and prognosis of HCC^[86,87]. The PAI-1 protein is a multifaceted proteolytic factor. It not only functions as an inhibitor of the protease uPA, but also plays an important role in signal

transduction, cell adherence, and cell migration. Thus, an apparent paradox considering its name—although it inhibits uPA during blood coagulation, it actually promotes invasion and metastasis. In many malignancies including HCC, elevated PAI-1 is associated with tumor aggressiveness and poor patient outcome^[86].

ANGIOGENESIS RELATED

Tumor angiogenesis is critical to both the growth and metastasis of cancer, and is regulated by angiogenic factors. Circulating angiogenesis regulators have been evaluated not only as diagnostic and/or prognostic factors but also as predictive factors in cancer patients. They could be used to determine the risk of developing cancer, to screen for early detection, to distinguish benign from malignant disease, and to distinguish between different types of malignancies. In established malignancies, they can be used to determine prognosis, to predict the response to therapy, and to monitor the clinical course^[5,83,88]. HCC is typically a hypervascular tumor with a rich blood supply. In recent years, many angiogenesis-related markers, such as vascular endothelial growth factor (VEGF), basic fibroblast growth factor (bFGF), platelet-derived endothelial cell growth factor (PD-ECGF), thrombospondin (TSP), angiogenin, pleiotrophin and endostatin (ES) levels, as well as intratumor microvessel density (MVD) have been evaluated and found to relate to HCC prognosis.

Intratumor microvessel density (MVD)

The intratumor MVD is a direct reflection of tumor angiogenesis. It can be visualized by immunohistochemical staining with antibodies to anti-CD34, Factor VIII, and alpha smooth muscle actin^[89]. MVD levels have a close relationship with the tumor capsule status, tumor size (HCC with 2-5cm in diameter has the highest MVD level), intrahepatic recurrence and disease-free survival, and can be a predictive marker for disease-free survival^[90]. In the authors' institute, three types of intratumor microvessels, including capillary-like, sinusoid-like, and mixed-type, were found in HCC. The MVD level was not related to tumor size, capsule status, Edmondson's grade, or alpha-fetoprotein level; was an independent factor of disease-free survival in small HCC patients; and was a predictive marker for early recurrence^[91].

Vascular endothelial growth factor (VEGF)

A substantial number of studies have demonstrated a strong association between elevated tumor expression of VEGF and advanced disease or poor prognosis in various cancers. Circulating VEGF seems to be a reliable surrogate marker of angiogenic activity and tumor progression in cancer patients. It may be predictive of tumor status and prognosis in patients with different types of cancer, and may be useful in predicting and monitoring tumor response to anticancer therapies and in follow-up surveillance for tumor relapse. It may provide new prognostic information that is not afforded by conventional clinicopathologic prognostic indicators^[92]. In HCC, a high serum VEGF level significantly correlates with absence of tumor capsule, presence of intrahepatic metastasis, presence of microscopic venous invasion, and advanced stage, and it may be useful as a biologic marker of tumor invasiveness and a prognostic factor in HCC^[93]. The data of the authors' institute also shows serum VEGF is a predictor of invasion and metastasis of HCC and a potential biomarker of metastatic recurrence after curative resection^[94,95].

Platelet-derived endothelial cell growth factor (PD-ECGF)

PD-ECGF may not be a major regulator of angiogenesis of HCC, but may play an important role in hepatocarcinogenesis, cooperating with hepatitis C virus. PD-ECGF expression associates with the venous invasion of HCC^[96].

GENOMICS AND PROTEOMICS RELATED

Molecular genetic analyses have clarified that accumulation of genomic changes provides important steps in carcinogenesis and have identified a number of valuable genetic markers for certain cancers. The association of these genomic aberrations with the progression and prognosis of cancer has drawn more and more attention. To date, allelic loss of 1p, 1q21-23, 2p21-16.3, 3p24-p25, 8p22, 8p23, 9p21, 9q, 10, 13q12, 17p13.3, and 22q13 have been proposed to be related to the survival and prognosis of cancer patients^[97-101].

Many chromosomal aberrations, including gain of 1q, 8q, and 20q, and loss of 16q, 4q, 17p, 1p, and 8p have been identified in HCC^[102]. However, the relationship between these recurrent alterations and the clinical phenotypes and prognosis is still unknown. Towards the end of 1999, we compared the differences of chromosomal aberrations between the primary HCC tumors and their matched metastatic lesions using a comparative genomic hybridization (CGH) technique, and found chromosome 8p deletions might contribute to HCC metastasis^[103]. This result was further confirmed by comparison between nude mice models of HCC with different metastatic potentials^[104]. In addition, a more accurate location was identified on 8p23.3, 8p11.2^[105]. These findings provide new targets for exploring new predictive markers for the recurrence and prognosis of HCC. Recently, Itano *et al.* used restriction landmark genomic scanning (RLGS), a new high-speed screening method for multiple genomic changes, to detect unknown genetic alterations in HCC. They found the disease-free survival rate for patients with > or = 16 changed RLGS spots was significantly lower than that for patients with fewer changed RLGS spots (< or = 15 spots). In multivariate analysis, the number of changed spots was proven to retain an independent prognostic value. These results suggest that the number of changed RLGS spots may be a useful biological marker for recurrence of HCC^[106].

One important trend in this area that should be paid attention to is the prognostic value of circulating DNA in plasma or serum, and its genetic alterations in cancer patients. Small amounts of DNA circulate in both healthy and diseased human plasma/serum, and increased concentrations of DNA are present in the plasma of cancer patients. Characteristics of tumor DNA have been found in genetic material extracted from the plasma of cancer patients. These features include decreased strand stability, the presence of specific oncogene or tumor suppressor gene mutations, microsatellite alterations, Ig rearrangements and hypermethylation of several genes. The results obtained in many different cancers have opened a new research area indicating that plasma DNA might eventually be a suitable target for the development of noninvasive diagnostic, prognostic and follow-up tests for cancer^[107]. Blood testing for circulating tumor genetic markers may provide valuable prognostic information and guide future therapy^[108].

However, there is still controversy over the prognostic significance^[109]. We found loss of heterozygosity (LOH) on chromosome 14q (D14S62 and D14S51) could be detected in plasma DNA, and could be of prognostic significance in HCC patients^[11].

Proteomics, regarded as a sister technology to genomics, is one of the technologies rapidly changing our approach to understanding tumor biology. By comparing the proteins present in diseased samples with those present in normal samples, it is possible to identify changes in expression of proteins that potentially may be related to tumor progression, invasion and metastasis, and prognosis. This technique has now made it possible to analyze proteins using high throughput, automated techniques. Proteomic profiling can be applied to tissue samples as well as body fluids (e.g. serum, urine, etc.), and it can provide surrogate markers of disease processes, potential response to treatment, possibility of recurrence and metastasis for cancers including HCC^[110].

OTHERS

In addition, higher levels of urinary TGF-beta 1^[111], heat shock protein-27 (HSP-27)^[112] and Glutamine synthetase (GS) expression

in the tumor^[113], increased levels of cyclooxygenase-2 (COX-2) in nontumor liver tissue^[114], preoperative serum IL-10^[115], and HFE mutation s^[116] or down-regulation of DRH1^[117] are also powerful prognostic indicators for shorter disease-free survival and poor prognosis, related to tumor progression of HCC.

The RECK (reversion-inducing-cysteine-rich protein with Kazal motifs) gene suppresses the invasive and metastatic activities of cancers, has negative effects on the invasiveness of HCC, and can be regarded as a promising prognostic molecular marker for HCC^[118].

EXPERIENCES OF THE AUTHORS' INSTITUTE

At the authors' institute, many molecular factors have been investigated and found to be related to HCC invasiveness in recent years. They could be divided into two groups: one is positive invasiveness-related factors, including p16 and p53 mutations, H-ras, c-erbB2, mdm2, TGF- α , epidermal growth factor receptor (EGFR), MMP-2, uPA, uPA-R and PAI-1, ICAM-1, VEGF, PD-ECGF, bFGF, and osteopontin (OPN), etc. The other group is negative invasiveness-related factors, including nm23-H1, Kai-1, TIMP-2, integrin $\alpha 5$, E-cadherin, etc. These factors could be potential predictive markers for the prognosis of HCC. Serum ICAM-1 and PAI-1 levels were higher in patients with metastasis than those without metastasis, while serum Thrombomodulin concentration negatively associated with the intrahepatic spreading and portal vein thrombosis of HCC. Deletions of chromosome 8p and 17p, overexpression of MMP-2, TGF- α , and EGFR in HCC tissues, and LOH on chromosome 14q (D14S62 and D14S51) in plasma DNA were also related to metastatic recurrence and prognosis of HCC patients. p53 mutation or nuclear accumulation of p53 expression could be a valuable marker for predicting the prognosis of HCC patients after resection. E-cadherin, nm23, TIMP-2 are promising prognostic markers^[1, 43, 46, 77, 84, 86, 91, 94-96, 104-106].

To search for metastasis-associated genes on a global genomic scale, we recently used cDNA microarrays containing approximately 9984 human transcripts to investigate the gene expression profiles of primary tumors and their corresponding metastatic lesions (intrahepatic metastasis or tumor thrombosis of portal vein). A total of 79 significantly upregulated and 69 downregulated genes were identified. Some of them have proven to promote HCC metastasis^[119]. These will provide new prognostic markers for predicting the possibility of metastatic recurrence and survival after operation.

QUESTIONS AND PROSPECTS

In summary, pathologic factors indicative of tumor invasiveness such as tumor size, number, capsule state, venous invasion, presence of satellite nodules, and advanced pTNM stage, are the best-established risk factors for recurrence and important aspects affecting the prognosis of patients with HCC. Recent molecular research has identified many tumor biological factors as potential prognostic markers (biomarkers). However, to date, none of them has been proved to be specific enough, and most of the studies for specific molecular parameters were correlative and retrospective. Methodologies, sample sizes, and definitions differ. Consideration should be given to the design of prospective clinical trials in evaluating the prognostic significance of these markers.

These biomarkers could be detected both in tissue and body fluids (serum, urine, bile, etc.). Body fluid (particularly blood and urinary) testing is easily accessible and useful in clinical patients, and is more important in "predicting" the possibility or "early diagnosis" of recurrence and metastasis. So, future work should be focused on serum or urinary markers.

The prognostic significance of circulating DNA in plasma or serum, and its genetic alterations in HCC, are important trends that deserve attention. Proteomics and cDNA array provide other ways to explore new prognostic markers. So, we can believe, with the

continuing progress of human genome project, the development of new molecular and cytogenetic techniques, and a more complete understanding of tumor biology, more and more new prognostic markers with high sensitivity and specificity will soon be found and used in clinical assays. However, the combination of some items, i.e., pathological features and some biomarkers mentioned above, seems to be more practical now.

REFERENCES

- 1 Tang ZY. Hepatocellular carcinoma-Cause, treatment and metastasis. *World J Gastroenterol* 2001;7:445-454
- 2 Qin LX, Tang ZY. The prognostic significance of clinical and pathological features in hepatocellular carcinoma. *World J Gastroenterol* 2002;8:193-199
- 3 Zhao WH, Ma ZM, Zhou XR, Feng YZ, Fang BS. Prediction of recurrence and prognosis in patients with hepatocellular carcinoma after resection by use of CLIP score. *World J Gastroenterol* 2002;8:237-242
- 4 Zheng N, Ye SL, Sun RX, Zhao Y, Tang ZY. Effects of cryopreservation and phenylacetate on biological characters of adherent LAK cells from patients with hepatocellular carcinoma. *World J Gastroenterol* 2002;8:233-236
- 5 Korn WM. Moving toward an understanding of the metastatic process in hepatocellular carcinoma. *World J Gastroenterol* 2001;7:777-778
- 6 Mise K, Tashiro S, Yogita S, Wada D, Harada M, Fukuda Y, Miyake H, Isikawa M, Izumi K, Sano N. Assessment of the biological malignancy of hepatocellular carcinoma: relationship to clinicopathological factors and prognosis. *Clin Cancer Res* 1998;4:1475-1482
- 7 Nolte M, Werner M, Nasarek A, Bektas H, von Wasielewski R, Klempnauer J, Georgii A. Expression of proliferation associated antigens and detection of numerical chromosome aberrations in primary human liver tumours: relevance to tumor characteristics and prognosis. *J Clin Pathol* 1998;51:47-51
- 8 Weber JC, Nakano H, Bachellier P, Oussoultzoglou E, Inoue K, Shimura H, Wolf P, Chenard-Neu MP, Jaeck D. Is a proliferation index of cancer cells a reliable prognostic factor after hepatectomy in patients with colorectal liver metastases? *Am J Surg* 2001;182:81-88
- 9 Lin GY, Chen ZL, Lu CM, Li Y, Ping XJ, Huang R. Immunohistochemical study on p53, H-rasp21, c-erbB-2 protein and PCNA expression in HCC tissues of Han and minority ethnic patients. *World J Gastroenterol* 2000;6:234-238
- 10 Scholzen T, Gerdes J. The Ki-67 protein: from the known and the unknown. *J Cell Physiol* 2000;182:311-322
- 11 Hernandez-Rodriguez NA, Correa E, Sotelo R, Contreras-Paredes A, Gomez-Ruiz C, Green L, Mohar A. Ki-67: a proliferative marker that may predict pulmonary metastases and mortality of primary osteosarcoma. *Cancer Detect Prev* 2001;25:210-215
- 12 Ito Y, Matsuura N, Sakon M, Takeda T, Umeshita K, Nagano H, Nakamori S, Dono K, Tsujimoto M, Nakahara M, Nakao K, Monden M. Both cell proliferation and apoptosis significantly predict shortened disease-free survival in hepatocellular carcinoma. *Br J Cancer* 1999;81:747-751
- 13 Ouchi K, Sugawara T, Ono H, Fujiya T, Kamiyama Y, Kakugawa Y, Mikuni J, Yamanami H, Komatsu S, Horikoshi A. Mitotic index is the best predictive factor for survival of patients with resected hepatocellular carcinoma. *Dig Surg* 2000;17:42-48
- 14 Wellmann A, Flemming P, Behrens P, Wuppermann K, Lang H, Oldhafer K, Pastan I, Brinkmann U. High expression of the proliferation and apoptosis associated CSE1L/CAS gene in hepatitis and liver neoplasms: correlation with tumor progression. *Int J Mol Med* 2001;7:489-494
- 15 Ikeguchi M, Sato N, Hirooka Y, Kaibara N. Computerized nuclear morphology of hepatocellular carcinoma and its relation to proliferative activity. *J Surg Oncol* 1998;68:225-230
- 16 Veltri RW, Partin AW, Miller MC. Quantitative nuclear grade

- (QNG): a new image analysis-based biomarker of clinically relevant nuclear structure alterations. *J Cell Biochem* 2000;Suppl 35:151-157
- 17 Overgaard J, Yilmaz M, Guldberg P, Hansen LL, Alsner J. TP53 mutation is an independent prognostic marker for poor outcome in both node-negative and node-positive breast cancer. *Acta Oncol* 2000;39:327-333
- 18 Takahashi M, Tonoki H, Tada M, Kashiwazaki H, Furuuchi K, Hamada J, Fujioka Y, Sato Y, Takahashi H, Todo S, Sakuragi N, Moriuchi T. Distinct prognostic values of p53 mutations and loss of estrogen receptor and their cumulative effect in primary breast cancers. *Int J Cancer* 2000;89:92-99
- 19 Blaszyk H, Hartmann A, Cunningham JM, Schaid D, Wold LE, Kovach JS, Sommer SS. A prospective trial of midwest breast cancer patients: a p53 gene mutation is the most important predictor of adverse outcome. *Int J Cancer* 2000;89:32-38
- 20 Kahlenberg MS, Stoler DL, Rodriguez-Bigas MA, Weber TK, Driscoll DL, Anderson GR, Petrelli NJ. p53 tumor suppressor gene mutations predict decreased survival of patients with sporadic colorectal carcinoma. *Cancer* 2000;88:1814-1819
- 21 Ireland AP, Shibata DK, Chandrasoma P, Lord RV, Peters JH, DeMeester TR. Clinical significance of p53 mutations in adenocarcinoma of the esophagus and cardia. *Ann Surg* 2000;231:179-187
- 22 Tamas L, Kraxner H, Mechtler L, Repassy G, Ribari O, Hirschberg A, Szentkuti G, Jaray B, Szentirmay Z. Prognostic significance of P53 histochemistry and DNA histogram parameters in head and neck malignancies. *Anticancer Res* 2000;20:4031-4037
- 23 Murakami I, Hiyama K, Ishioka S, Yamakido M, Kasagi F, Yokosaki Y. p53 gene mutations are associated with shortened survival in patients with advanced non-small cell lung cancer: an analysis of medically managed patients. *Clin Cancer Res* 2000;6:526-530
- 24 Mitsudomi T, Hamajima N, Ogawa M, Takahashi T. Prognostic significance of p53 alterations in patients with non-small cell lung cancer: a meta-analysis. *Clin Cancer Res* 2000;6:4055-4063
- 25 Shahin MS, Hughes JH, Sood AK, Buller RE. The prognostic significance of p53 tumor suppressor gene alterations in ovarian carcinoma. *Cancer* 2000;89:2006-2017
- 26 de Alava E, Antonescu CR, Panizo A, Leung D, Meyers PA, Huvos AG, Pardo-Mindan FJ, Healey JH, Ladanyi M. Prognostic impact of P53 status in Ewing sarcoma. *Cancer* 2000;89:783-792
- 27 Leibovich BC, Cheng L, Weaver AL, Myers RP, Bostwick DG. Outcome prediction with p53 immunostaining after radical prostatectomy in patients with locally advanced prostate cancer. *J Urol* 2000;163:1756-1760
- 28 Osaki T, Kimura T, Tatamoto Y, Dapeng L, Yoneda K, Yamamoto T. Diffuse mode of tumor cell invasion and expression of mutant p53 protein but not of p21 protein are correlated with treatment failure in oral carcinomas and their metastatic foci. *Oncology* 2000;59:36-43
- 29 Suzuki M, Ohwada M, Saga Y, Kohno T, Takei Y, Sato I. Micrometastatic p53-positive cells in the lymph nodes of early stage epithelial ovarian cancer: prognostic significance. *Oncology* 2001;60:170-175
- 30 Shiota G, Ishida M, Noguchi N, Oyama K, Takano Y, Okubo M, Katayama S, Tomie Y, Harada K, Hori K, Ashida K, Kishimoto Y, Hosoda A, Suou T, Kanbe T, Tanaka K, Nosaka K, Tanida O, Kojo H, Miura K, Ito H, Kaibara N, Kawasaki H. Circulating p53 antibody in patients with colorectal cancer: relation to clinicopathologic features and survival. *Dig Dis Sci* 2000;45:122-128
- 31 Shao ZM, Wu J, Shen ZZ, Nguyen M. p53 mutation in plasma DNA and its prognostic value in breast cancer patients. *Clin Cancer Res* 2001;7:2222-2227
- 32 Kantola S, Parikka M, Jokinen K, Hyrynkangas K, Soini Y, Alho OP, Salo T. Prognostic factors in tongue cancer - relative importance of demographic, clinical and histopathological factors. *Br J Cancer* 2000;83:614-619
- 33 Ferrero JM, Ramaoli A, Formento JL, Francoual M, Etienne MC, Peyrotte S, Ettore F, Leblanc-Talent P, Namer M, Milano G. P53 determination alongside classical prognostic factors in node-negative breast cancer: an evaluation at more than 10-year follow-up. *Ann Oncol* 2000;11:393-397
- 34 Reed W, Hannisdal E, Boehler PJ, Gundersen S, Host H, Marthin J. The prognostic value of p53 and c-erb B-2 immunostaining is overrated for patients with lymph node negative breast carcinoma: a multivariate analysis of prognostic factors in 613 patients with a follow-up of 14-30 years. *Cancer* 2000;88:804-813
- 35 Kaye PV, Radebold K, Isaacs S, Dent DM. Expression of p53 and p21waf1/cip1 in gastric carcinoma: lack of inter-relationship or correlation with prognosis. *Eur J Surg Oncol* 2000;26:39-43
- 36 Schiller JH, Adak S, Feins RH, Keller SM, Fry WA, Livingston RB, Hammond ME, Wolf B, Sabatini L, Jett J, Kohman L, Johnson DH. Lack of prognostic significance of p53 and K-ras mutations in primary resected non-small-cell lung cancer on E4592: a Laboratory Ancillary Study on an Eastern Cooperative Oncology Group Prospective Randomized Trial of Postoperative Adjuvant Therapy. *J Clin Oncol* 2001;19:448-457
- 37 Gadducci A, Cianci C, Cosio S, Carnino F, Fanucchi A, Buttitta F, Conte PF, Genazzani AR. p53 status is neither a predictive nor a prognostic variable in patients with advanced ovarian cancer treated with a paclitaxel-based regimen. *Anticancer Res* 2000;20:4793-4799
- 38 Fleshner N, Kapusta L, Ezer D, Herschorn S, Klotz L. p53 nuclear accumulation is not associated with decreased disease-free survival in patients with node positive transitional cell carcinoma of the bladder. *J Urol* 2000;164:1177-1182
- 39 Gallego MG, Acenero MJ, Ortega S, Delgado AA, Cantero JL. Prognostic influence of p53 nuclear overexpression in colorectal carcinoma. *Colon Rectum* 2000;43:971-975
- 40 Nieder C, Petersen S, Petersen C, Thames HD. The challenge of p53 as a prognostic and predictive factor in Hodgkin's or non-Hodgkin's lymphoma. *Ann Hematol* 2001;80:2-8
- 41 Itoh T, Shiro T, Seki T, Nakagawa T, Wakabayashi M, Inoue K, Okamura A. Relationship between p53 overexpression and the proliferative activity in hepatocellular carcinoma. *Int J Mol Med* 2000;6:137-142
- 42 Jeng KS, Sheen IS, Chen BF, Wu JY. Is the p53 gene mutation of prognostic value in hepatocellular carcinoma after resection? *Arch Surg* 2000;135:1329-1333
- 43 Tang ZY, Qin LX, Wang XM, Zhou G, Liao Y, Weng Y, Jiang XP, Lin ZY, Liu KD, Ye SL. Alterations of oncogenes, tumor suppressor genes and growth factors in hepatocellular carcinoma: with relation to tumor size and invasiveness. *Chin Med J* 1998;111:313-318
- 44 Sugo H, Takamori S, Kojima K, Beppu T, Futagawa S. The significance of p53 mutations as an indicator of the biological behavior of recurrent hepatocellular carcinomas. *Surg Today* 1999;29:849-855
- 45 Heinze T, Jonas S, Karsten A, Neuhaus P. Determination of the oncogenes p53 and C-erb B2 in the tumour cytosols of advanced hepatocellular carcinoma (HCC) and correlation to survival time. *Anticancer Res* 1999;19:2501-2503
- 46 Qin LX, Tang ZY, Ma ZC, Wu ZQ, Zhou XD, Ye QH, Ji Y, Huang LW, Jia HL, Sun HC, Wang L. P53 immunohistochemistry scoring is an independent prognostic marker of patient with hepatocellular carcinoma resection: A prospective study of 256 formalin-fixed paraffin-embedded tumor samples. *World J Gastroenterol* 2002(in press)
- 47 Shiota G, Kishimoto Y, Suyama A, Okubo M, Katayama S, Harada K, Ishida M, Hori K, Suou T, Kawasaki H. Prognostic significance of serum anti-p53 antibody in patients with hepatocellular carcinoma. *J Hepatol* 1997;27:661-668
- 48 Tangkijvanich P, Janchai A, Charuruks N, Kullavanijaya P, Theamboonlers A, Hirsch P, Poovorawan Y. Clinical associations and prognostic significance of serum anti-p53 antibodies in Thai patients with hepatocellular carcinoma. *Asian Pac J Allergy Immunol* 2000;18:237-243
- 49 Saffroy R, Lelong JC, Azoulay D, Salvucci M, Reynes M, Bismuth H, Debuire B, Lemoine A. Clinical significance of circulating anti-p53 antibodies in European patients with

- hepatocellular carcinoma. *Br J Cancer* 1999;79:604-610
- 50 Endo K, Ueda T, Ohta T, Terada T. Protein expression of MDM2 and its clinicopathological relationships in human hepatocellular carcinoma. *Liver* 2000;20:209-215
 - 51 Chao Y, Shih YL, Chiu JH, Chau GY, Lui WY, Yang WK, Lee SD, Huang TS. Overexpression of cyclin A but not Skp 2 correlates with the tumor relapse of human hepatocellular carcinoma. *Cancer Res* 1998;58:985-990
 - 52 Ohashi R, Gao C, Miyazaki M, Hamazaki K, Tsuji T, Inoue Y, Uemura T, Hirai R, Shimizu N, Namba M. Enhanced expression of cyclin E and cyclin A in human hepatocellular carcinomas. *Anticancer Res* 2001;21:657-662
 - 53 Ito Y, Takeda T, Sakon M, Monden M, Tsujimoto M, Matsuura N. Expression and prognostic role of cyclin-dependent kinase 1 (cdc2) in hepatocellular carcinoma. *Oncology* 2000;59:68-74
 - 54 Philipp-Staheli J, Payne SR, Kemp CJ. p27(Kip1): regulation and function of a haploinsufficient tumor suppressor and its misregulation in cancer. *Exp Cell Res* 2001;264:148-168
 - 55 Fiorentino M, Altamirani A, D'Errico A, Cukor B, Barozzi C, Loda M, Grigioni WF. Acquired expression of p27 is a favorable prognostic indicator in patients with hepatocellular carcinoma. *Clin Cancer Res* 2000;6:3966-3972
 - 56 Ito Y, Matsuura N, Sakon M, Miyoshi E, Noda K, Takeda T, Umeshita K, Nagano H, Nakamori S, Dono K, Tsujimoto M, Nakahara M, Nakao K, Taniguchi N, Monden M. Expression and prognostic roles of the G1-S modulators in hepatocellular carcinoma: p27 independently predicts the recurrence. *Hepatology* 1999;30:90-99
 - 57 Tannapfel A, Wasner M, Krause K, Geissler F, Katalinic A, Hauss J, Mossner J, Engeland K, Wittekind C. Expression of p73 and its relation to histopathology and prognosis in hepatocellular carcinoma. *J Natl Cancer Inst* 1999;91:1154-1158
 - 58 Qin Y, Li B, Tan YS, Sun ZL, Zuo FQ, Sun ZF. Polymorphism of p16INK4a gene and rare mutation of p15INK4b gene exon2 in primary hepatocarcinoma. *World J Gastroenterol* 2000;6:411-414
 - 59 Wang Q, Lin ZY, Feng XL. Alterations in metastatic properties of hepatocellular carcinoma cell following H-ras oncogene transfection. *World J Gastroenterol* 2001;7:335-339
 - 60 Cui J, Yang DH, Bi XJ, Fan ZR. Methylation status of c-fms oncogene in HCC and its relationship with clinical pathology. *World J Gastroenterol* 2001;7:136-139
 - 61 Kawate S, Fukusato T, Ohwada S, Watanuki A, Morishita Y. Amplification of c-myc in hepatocellular carcinoma: correlation with clinicopathologic features, proliferative activity and p53 overexpression. *Oncology* 1999;57:157-163
 - 62 Taviani D, De Petro G, Benetti A, Portolani N, Giulini SM, Barlati S. u-PA and c-MET mRNA expression is co-ordinately enhanced while hepatocyte growth factor mRNA is down-regulated in human hepatocellular carcinoma. *Int J Cancer* 2000;87:644-649
 - 63 Luo YQ, Wu MC, Cong WM. Gene expression of hepatocyte growth factor and its receptor in HCC and nontumorous liver tissues. *World J Gastroenterol* 1999;5:119-121
 - 64 Prange W, Schirmacher P. Absence of therapeutically relevant c-erbB-2 expression in human hepatocellular carcinomas. *Oncol Rep* 2001;8:727-730
 - 65 Ito Y, Takeda T, Sakon M, Tsujimoto M, Higashiyama S, Noda K, Miyoshi E, Monden M, Matsuura N. Expression and clinical significance of erb-B receptor family in hepatocellular carcinoma. *Br J Cancer* 2001;84:1377-1383
 - 66 Ito Y, Miyoshi E, Takeda T, Sakon M, Noda K, Tsujimoto M, Monden M, Taniguchi N, Matsuura N. Expression and possible role of ets-1 in hepatocellular carcinoma. *Am J Clin Pathol* 2000;114:719-725
 - 67 Ito Y, Monden M, Takeda T, Eguchi H, Umeshita K, Nagano H, Nakamori S, Dono K, Sakon M, Nakamura M, Tsujimoto M, Nakahara M, Nakao K, Yokosaki Y, Matsuura N. The status of Fas and Fas ligand expression can predict recurrence of hepatocellular carcinoma. *Br J Cancer* 2000;82:1211-1217
 - 68 Wang XZ, Chen XC, Yang YH, Chen ZX, Huang YH, Tao QM. Relationship between HBxAg and Fas/FasL in patients with hepatocellular carcinoma. *World J Gastroenterol* 2000;6:S17
 - 69 Kobayashi T, Kubota K, Takayama T, Makuuchi M. Telomerase activity as a predictive marker for recurrence of hepatocellular carcinoma after hepatectomy. *Am J Surg* 2001;181:284-288
 - 70 Tatsuma T, Goto S, Kitano S, Lin YC, Lee CM, Chen CL. Telomerase activity in peripheral blood for diagnosis of hepatoma. *J Gastroenterol Hepatol* 2000;15:1064-1070
 - 71 Suda T, Isokawa O, Aoyagi Y, Nomoto M, Tsukada K, Shimizu T, Suzuki Y, Naito A, Igarashi H, Yanagi M, Takahashi T, Asakura H. Quantitation of telomerase activity in hepatocellular carcinoma: a possible aid for a prediction of recurrent diseases in the remnant liver. *Hepatology* 1998;27:402-406
 - 72 Huang GT, Lee HS, Chen CH, Sheu JC, Chiou LL, Chen DS. Correlation of E-cadherin expression and recurrence of hepatocellular carcinoma. *Hepatogastroenterology* 1999;46:1923-1927
 - 73 Endo K, Ueda T, Ueyama J, Ohta T, Terada T. Immunoreactive E-cadherin, alpha-catenin, beta-catenin, and gamma-catenin proteins in hepatocellular carcinoma: relationships with tumor grade, clinicopathologic parameters, and patients' survival. *Hum Pathol* 2000;31:558-565
 - 74 Wong CM, Fan ST, Ng IO. beta-Catenin mutation and overexpression in hepatocellular carcinoma: clinicopathologic and prognostic significance. *Cancer* 2001;92:136-145
 - 75 Cui J, Zhou XD, Liu YK, Tang ZY, Zile MH. Abnormal Catenin gene expression with invasiveness of primary hepatocellular carcinoma in China. *World J Gastroenterol* 2001;7:542-546
 - 76 Hsu HC, Jeng YM, Mao TL, Chu JS, Lai PL, Peng SY. Beta-catenin mutations are associated with a subset of low-stage hepatocellular carcinoma negative for hepatitis B virus and with favorable prognosis. *Am J Pathol* 2000;157:763-770
 - 77 Sun JJ, Zhou XD, Liu YK, Tang ZY, Feng JX, Zhou G, Xue Q, Chen J. Invasion and metastasis of liver cancer: expression of intercellular adhesion molecule-1. *J Cancer Res Clin Oncol* 1999;125:28-34
 - 78 Mei MH, Xu J, Shi QF, Yang JH, Chen Q, Qin LL. Clinical significance of serum intercellular adhesion molecule-1 detection in patients with hepatocellular carcinoma. *World J Gastroenterol* 2000;6:408-410
 - 79 Xu J, Mei MH, Zeng SE, Shi QF, Liu YM, Qin LL. Expressions of ICAMa21 and its mRNA in sera and tissues of patients with hepatocellular carcinoma. *World J Gastroenterol* 2001;7:120-125
 - 80 Goodison S, Urquidí V, Tarin D. CD44 cell adhesion molecules. *Mol Pathol* 1999;52:189-196
 - 81 Endo K, Terada T. Protein expression of CD44 (standard and variant isoforms) in hepatocellular carcinoma: relationships with tumor grade, clinicopathologic parameters, p53 expression, and patient survival. *J Hepatol* 2000;32:78-84
 - 82 Sakamoto Y, Mafune K, Mori M, Shiraishi T, Imamura H, Mori M, Takayama T, Makuuchi M. Overexpression of MMP-9 correlates with growth of small hepatocellular carcinoma. *Int J Oncol* 2000;17:237-243
 - 83 Jiang YF, Yang ZH, Hu JQ. Recurrence or metastasis of HCC: predictors, early detection and experimental antiangiogenic therapy. *World J Gastroenterol* 2000;6:61-65
 - 84 Bu W, Tang ZY, Ye SL, Liu KD, Huang XW, Gao DM. The association of type IV collagenase with invasion and metastasis of hepatocellular carcinoma. *Zhonghua Xiaohua Zazhi* 1999;19:13-15
 - 85 Fox SB, Taylor M, Grondahl-Hansen J, Kakolyris S, Gatter KC, Harris AL. Plasminogen activator inhibitor-1 as a measure of vascular remodeling in breast cancer. *J Pathol* 2001;195:236-243
 - 86 Zheng Q, Tang ZY, Xue Q, Shi DR, Song HY, Tang HB. Invasion and metastasis of hepatocellular carcinoma in relation to urokinase-type plasminogen activator, its receptor and inhibitor. *J Cancer Res Clin Oncol* 2000;126:641-646
 - 87 Itoh T, Hayashi Y, Kanamaru T, Morita Y, Suzuki S, Wang W,

- Zhou L, Rui JA, Yamamoto M, Kuroda Y, Itoh H. Clinical significance of urokinase-type plasminogen activator activity in hepatocellular carcinoma. *J Gastroenterol Hepatol* 2000;15: 422-430
- 88 Kuroi K, Toi M. Circulating angiogenesis regulators in cancer patients. *Int J Biol Markers* 2001;16:5-26
- 89 Morinaga S, Imada T, Shimizu A, Akaike M, Sugimasa Y, Takemiya S, Takanashi Y. Angiogenesis in hepatocellular carcinoma as evaluated by alpha smooth muscle actin immunohistochemistry. *Hepatogastroenterology* 2001;48:224-228
- 90 El-Assal ON, Yamanoi A, Soda Y, Yamaguchi M, Igarashi M, Yamamoto A, Nabika T, Nagasue N. Clinical significance of microvessel density and vascular endothelial growth factor expression in hepatocellular carcinoma and surrounding liver: possible involvement of vascular endothelial growth factor in the angiogenesis of cirrhotic liver. *Hepatology* 1998;27:1554-1562
- 91 Sun HC, Tang ZY, Li XM, Zhou YN, Sun BR, Ma ZC. Microvessel density of hepatocellular carcinoma: its relationship with prognosis. *J Cancer Res Clin Oncol* 1999;125:419-26
- 92 Poon RT, Fan ST, Wong J. Clinical implications of circulating angiogenic factors in cancer patients. *J Clin Oncol* 2001;19: 1207-1225
- 93 Poon RT, Ng IO, Lau C, Zhu LX, Yu WC, Lo CM, Fan ST, Wong J. Serum vascular endothelial growth factor predicts venous invasion in hepatocellular carcinoma: a prospective study. *Ann Surg* 2001;233:227-235
- 94 Li XM, Tang ZY, Qin LX, Zhou J, Sun HC. Serum vascular endothelial growth factor is a predictor of invasion and metastasis in hepatocellular carcinoma. *J Exp Clin Cancer Res* 1999;18:511-517
- 95 Niu Q, Tang ZY, Ma ZC, Qin LX, Zhang LH. Serum vascular endothelial growth factor is a potential biomarker of metastatic recurrence after curative resection of hepatocellular carcinoma. *World J Gastroenterol* 2000;6: 565-568
- 96 Zhou J, Tang ZY, Fan J, Wu ZQ, Li XM, Liu YK, Liu F, Sun HC, Ye SL. Expression of platelet-derived endothelial cell growth factor and vascular endothelial growth factor in hepatocellular carcinoma and portal vein tumor thrombus. *J Cancer Res Clin Oncol* 2000; 126:57-61
- 97 Tada K, Shiraishi S, Kamiryo T, Nakamura H, Hirano H, Kuratsu J, Kochi M, Saya H, Ushio Y. Analysis of loss of heterozygosity on chromosome 10 in patients with malignant astrocytic tumors: correlation with patient age and survival. *J Neurosurg* 2001;95:651-659
- 98 Bisgaard ML, Jager AC, Dalgaard P, Sondergaard JO, Rehfeld JF, Nielsen FC. Allelic loss of chromosome 2p21-16.3 is associated with reduced survival in sporadic colorectal cancer. *Scand J Gastroenterol* 2001;36:405-409
- 99 Hirano A, Emi M, Tsuneizumi M, Utada Y, Yoshimoto M, Kasumi F, Akiyama F, Sakamoto G, Haga S, Kajiwaru T, Nakamura Y. Allelic losses of loci at 3p25.1, 8p22, 13q12, 17p13.3, and 22q13 correlate with postoperative recurrence in breast cancer. *Clin Cancer Res* 2001;7:876-882
- 100 Simoneau M, LaRue H, Aboukassim TO, Meyer F, Moore L, Fradet Y. Chromosome 9 deletions and recurrence of superficial bladder cancer: identification of four regions of prognostic interest. *Oncogene* 2000;19:6317-6323
- 101 Washburn JG, Wojno KJ, Dey J, Powell JJ, Macoska JA. 8pter-p23 deletion is associated with racial differences in prostate cancer outcome. *Clin Cancer Res* 2000;6:4647-4652
- 102 Wong N, Lai P, Lee SW, Fan S, Pang E, Liew CT, Sheng Z, Lau JW, Johnson PJ. Assessment of genetic changes in hepatocellular carcinoma by comparative genomic hybridization analysis: relationship to disease stage, tumor size, and cirrhosis. *Am J Pathol* 1999;154: 37-43
- 103 Itano O, Ueda M, Kikuchi K, Shimazu M, Kitagawa Y, Aiura K, Kitajima M. A new predictive factor for hepatocellular carcinoma based on two-dimensional electrophoresis of genomic DNA. *Oncogene* 2000;19:1676-1683
- 104 Qin LX, Tang ZY, Sham JST, Ma ZC, Ye SL, Zhou XD. The association of chromosome 8p deletion and tumor metastasis in human hepatocellular carcinoma. *Cancer Res* 1999;59:5662-5665
- 105 Qin LX, Tang ZY, Ye SL, Liu YK, Ma ZC, Zhou XD, Wu ZQ, Lin ZY, Sun FX, Tian J, Guan XY, Pack SD, Zhuang ZP. Chromosome 8p deletion is associated with metastasis of human hepatocellular carcinoma when high and low metastatic models are compared. *J Cancer Res Clin Oncol* 2001;127:482-488
- 106 Zhang LH, Qin LX, Ma ZC, Ye SL, Liu YK, Ye QH, Wu X, Huang W, Tang ZY. Identification of allelic imbalances regions related to metastasis of hepatocellular carcinoma: Comparison between matched primary and metastatic lesions in 22 patients by genome-wide microsatellite Analysis. *Int J Cancer* 2002 (submitted)
- 107 Anker P, Stroun M. Circulating DNA in plasma or serum. *Medicina (B Aires)* 2000;60:699-702
- 108 Taback B, Fujiwara Y, Wang HJ, Foshag LJ, Morton DL, Hoon DS. Prognostic significance of circulating microsatellite markers in the plasma of melanoma patients. *Cancer Res* 2001;61: 5723-5726
- 109 Nunes DN, Kowalski LP, Simpson AJ. Circulating tumor-derived DNA may permit the early diagnosis of head and neck squamous cell carcinomas. *Int J Cancer* 2001;92:214-219
- 110 Kennedy S. Proteomic profiling from human samples: the body fluid alternative. *Toxicol Lett* 2001;120:379-384
- 111 Tsai JF, Chuang LY, Jeng JE, Yang ML, Chang WY, Hsieh MY, Lin ZY, Tsai JH. Clinical relevance of transforming growth factor-beta 1 in the urine of patients with hepatocellular carcinoma. *Medicine (Baltimore)* 1997;76:213-226
- 112 King KL, Li AF, Chau GY, Chi CW, Wu CW, Huang CL, Lui WY. Prognostic significance of heat shock protein-27 expression in hepatocellular carcinoma and its relation to histologic grading and survival. *Cancer* 2000;88:2464-2470
- 113 Osada T, Nagashima I, Tsuno NH, Kitayama J, Nagawa H. Prognostic significance of glutamine synthetase expression in unifocal advanced hepatocellular carcinoma. *J Hepatol* 2000; 33:247-253
- 114 Kondo M, Yamamoto H, Nagano H, Okami J, Ito Y, Shimizu J, Eguchi H, Miyamoto A, Dono K, Umeshita K, Matsuura N, Wakasa K, Nakamori S, Sakon M, Monden M. Increased expression of COX-2 in nontumor liver tissue is associated with shorter disease-free survival in patients with hepatocellular carcinoma. *Clin Cancer Res* 1999;5:4005-4012
- 115 Chau GY, Wu CW, Lui WY, Chang TJ, Kao HL, Wu LH, King KL, Loong CC, Hsia CY, Chi CW. Serum interleukin-10 but not interleukin-6 is related to clinical outcome in patients with resectable hepatocellular carcinoma. *Ann Surg* 2000;231:552-558
- 116 Pirisi M, Toniutto P, Uzzau A, Fabris C, Avellini C, Scott C, Apollonio L, Beltrami CA, Bresadola F. Carriage of HFE mutations and outcome of surgical resection for hepatocellular carcinoma in cirrhotic patients. *Cancer* 2000; 89:297-302
- 117 Yamamoto Y, Sakamoto M, Fujii G, Kanetaka K, Asaka M, Hirohashi S. Cloning and characterization of a novel gene, DRH1, down-regulated in advanced human hepatocellular carcinoma. *Clin Cancer Res* 2001;7:297-303
- 118 Furumoto K, Arii S, Mori A, Furuyama H, Gorris Rivas MJ, Nakao T, Isono N, Murata T, Takahashi C, Noda M, Imamura M. RECK gene expression in hepatocellular carcinoma: correlation with invasion-related clinicopathological factors and its clinical significance. Reverse-inducing-cysteine-rich protein with Kazal motifs. *Hepatology* 2001;33:189-195
- 119 Ye QH, Qin LX, Forgues M, He P, Kim JW, Peng AC, Simon R, Robles A, Chen YD, Ma ZC, Wu ZQ, Ye SL, Liu YK, Tang ZY, Wang XW. Gene expression profiling and supervised machine learning to define metastasis-related genes in human hepatocellular carcinoma. *Nature Med* 2002 (submitted)

Edited by Pagliarini R

Radiofrequency ablation of liver cancers

Lian-Xin Liu, Hong-Chi Jiang, Da-Xun Piao

Lian-Xin Liu, Hong-Chi Jiang, Da-Xun Piao, Department of Surgery, the First Clinical College, Harbin Medical University, Harbin 150001, Heilongjiang Province, China

Supported by Youth Natural Scientific Foundation of Heilongjiang Province; Natural Scientific Foundation of Harbin

Correspondence to: Dr. Lian-Xin Liu, Department of Surgery, the First Clinical College, Harbin Medical University, 23 Youzheng Street, Nangang District, Harbin 150001, Heilongjiang Province, China. scott-lxliu@hotmail.com

Received 2002-05-10 Accepted 2002-05-18

Abstract

Primary and secondary malignant liver cancers are some of most common malignant tumors in the world. Chemotherapy and radiotherapy are not very effective against them. Surgical resection has been considered the only potentially curative option, but the majority of patients are not candidates for resection because of tumor size, location near major intrahepatic blood vessels and bile ducts, precluding a margin-negative resection, cirrhotic, hepatitis virus infection or multifocal. Radiofrequency ablation (RFA), which is a new evolving effective and minimally invasive technique, can produce coagulative necrosis of malignant tumors. RFA should be used percutaneously, laparoscopically, or during the open laparotomy under the guidance of ultrasound, CT scan and MRI. RFA has lots of advantages superior to other local therapies including lower complications, reduced costs and hospital stays, and the possibility of repeated treatment. In general, RFA is a safe, effective treatment for unresectable malignant liver tumors less than 7.0 cm in diameter. We review the principle, mechanism, procedures and experience with RFA for treating malignant liver tumors.

Liu LX, Jiang HC, Piao DX. Radiofrequency ablation of liver cancers. *World J Gastroenterol* 2002;8(3):393-399

INTRODUCTION

Hepatocellular carcinoma (HCC) is one of the most common solid cancers in the world, with an annual incidence estimated to be at least one million new patients^[1]. The mortality was secondary to lung cancer in urban and gastric carcinoma in countryside in China^[2,3]. Furthermore, the liver is second only to lymph nodes as a common site of metastasis from other solid cancers, especially abdominal cancer^[4]. It is not uncommon, particularly in patients with colorectal adenocarcinoma, for the liver to be the only site of metastatic disease^[5]. Patients with liver metastases from colorectal carcinoma or other cancers seldom survive more than 1 year if untreated^[6,7]. Surgical resection of HCC, hepatic metastases of colorectal cancer, and patients with liver-only metastases from other types of primary tumors can result in significant long-term survival benefit in at least 20-40% of patients^[8-12]. Besides these, surgical palliation through tumor cytoreduction in patients with symptomatic neuroendocrine tumor (carcinoid, functioning islet cell) with liver metastases can ameliorate the symptoms related to excess hormone production and release.

Surgical resection has been considered the only potential curative option, but only 5-20% of newly diagnosed HCC or colorectal cancer

liver metastasis patients undergo a potentially curative resection^[13,14]. Patients with disease confined to the liver may not be candidates for resection because of multifocal disease, proximity of tumor to key vascular or biliary structures that precludes a margin-negative resection, potentially unfavorable biology with the presence of multiple liver metastases, or inadequate functional hepatic reserve related to coexistent cirrhosis. Thus, for so few patients with primary or metastatic hepatic malignancies confined to the liver who are not candidates for surgical resection, Surgeons and oncologists have turned to explore novel treatment approaches to control and potentially cure the liver disease. Systemic chemotherapy for HCC and liver metastases results in less than 25% of patients; Complete responses are rare and significant improvements in survival are not sure. Although hepatic artery infusion of chemotherapeutic agents for unresectable disease has led to 40% to 55% response rates in the liver, a survival advantage has been difficult to demonstrate^[15-18].

Localized treatment was used to HCC and colorectal cancer liver metastasis and based on the principle that decreasing the volume of viable tumor or preventing new growth can lead to longer survival and potential cure in selected patients, provided that diffuse micrometastatic disease is not present. These ablative techniques include percutaneous ethanol injection^[19-21], focused ultrasound^[22-24], cryoablation^[25-28], hyperthermia (ie, microwave tumor coagulation^[29-31]), laser photocoagulation^[32-34], and radiofrequency ablation^[35-37] (RFA). Thermal energy produces destruction of tumor cells. When tumor cells are heated above 45-50°C, intracellular proteins are denatured and cell membranes are destroyed through dissolution and melting of lipid bilayers^[38-40]. RFA is a newly developed localized thermal treatment technique which was very useful in HCC and liver metastasis.

THE BACKGROUND AND MECHANISM OF RFA

The early usage of heat to treat tumors was back to early Egyptian and Greek when they used heat to cauterize ulcer and superficial neoplasm. The first experiment in RF ablation of living tissues is credited to d'Arsonval, who demonstrated that an alternating electric current greater than 10kHz could pass through living tissue without causing neuromuscular excitation. Beer and Clark used RF coagulation in human cancers in early 20th century^[41]. Coley suggested that tumors were more sensitive to the effects of hyperthermia than normal cells and that tumors could not dissipate heat by augmenting blood flow as could adjacent normal tissues. RF techniques have gained acceptance as standard method for making well-controlled thermal lesions in the fields of neurology and cardiology since then^[42-44]. It has been used in a variety of neurosurgical procedures aimed at ablating foci of spontaneous neuronal activity, in endoscopic techniques employed in gastroenterology, and in the ablation of aberrant conduction pathways in the heart for the treatment of dysrhythmias. Until the early 1990s, it is the technological modification of RF machine has made in to be used in focal thermal injuries deeper inside the body. More recently, Rossi and McGahan separately pioneered the application of RFA to primary and metastatic lesions in the liver^[45,46].

The so-called RF thermal ablation works by converting RF waves into heat. A high-frequency alternating current (100 to 500kHz), mostly 460kHz, passes from an uninsulated electrode tip into the

surrounding tissues and causes ionic vibration as the ions attempt to follow the change in the direction of the rapidly alternating current. This ionic vibration causes frictional heating of the tissues surrounding the electrode, rather than the heat being generated from the probe itself. The goal of RFA is to achieve local temperatures such that tissue destruction occurs. In general, thermal damage to cells begins at 42°C, with exposure times required for cell death at this temperature ranging from 3 to 50 hours depending on the nature of the tissue. As the temperature is increased, there is an exponential decrease in the exposure time needed for cellular destruction. At temperatures above 60°C, intracellular proteins including collagen denature, the lipid bilayer melts and cell death becomes inevitable. Thermal coagulation begins at 70°C and tissue desiccation at 100°C, producing coagulation necrosis of tumor tissue and surrounding hepatic parenchyma^[46-50]. Tissue heating also drives extracellular and intracellular water out of the tissue and results in further destruction of the tissue due to coagulative necrosis. Besides these, different studies have shown that hyperthermia can cause accelerated emigration and migration of peripheral blood mononuclear cells, activation of effect or cells, induction and secretion of cytokines, expression of heat shock proteins, and increased induction of apoptosis^[51,52].

RFA EQUIPMENT

Three primary RF devices, which worked on the same principles, are available in the world. The differences among the devices are the variations in probes and generator designs.

The device made by RITA Medical Systems consists of a 50W alternating electric current generator and a 15-gauge needle electrode. The needle electrode has a movable hub and 8 retracting curved electrodes from the tip of the needle. Each tip of the needle contains a thermocouple that can register the temperature of the heated tissues.

The device made by Radionics consists of a straight-tip internally cooled needle electrode. The tip of the needle is cooled by perfusing its inner chamber with chilled saline which can prevent scorching of the adjacent tissues and to increase the size of the thermal injury. The device can be operated with not only a single electrode but also with 3 electrodes which are placed in a triangular configuration. The device made by Radiotherapeutic is similar to the RITA device, consists of a needle with a movable hub that can deploy 10 curved needle tips. The multiple prongs are reported to produce a more uniform spherical injury than the devices with fewer prongs. But, this device does not have the temperature surveillance in the tips of the needles.

RFA PROBE

The first RFA probes were single, monopolar needles in the world. Because the RF energy delivered via the monopolar electrode decreases in proportion to the square of the distance from the electrode, coagulative necrosis was restricted to a maximum diameter of 1.6cm in which temperatures reached 80°C. Besides this, the surface temperature of the proximal and distal ends of the probe was higher than that in other parts. Thus, using a monopolar electrode results in an ellipsoid, rather than spherical, zone of necrosis, making evaluation difficult since most tumors are spherical in shape. High temperatures at the surface of the electrode cause a further limitation in size. Once the adjacent tissue reaches a high temperature and desiccates, the resulting tissue coagulum markedly reduces the propagation of RF current and heat through the tissue, yielding a smaller zone of coagulative necrosis^[52].

One method to increase the zone of ablation is to use standard 0.9% saline or hypertonic 5% saline through the needle electrode during RFA. The infused saline solution acts as a liquid electrode to increase the area of RF current conduction around the needle tip^[53]. Miao used 5% saline infusion into swine liver before and during

RFA. Both the electrode tip temperature and tissue impedance decreased and coagulation diameter increased from less than 1.0cm to greater than 5.0cm^[54].

Another technique to improve the volume of ablation involves the use of chilled perfusate into the lumen of electrodes. Lorentzen infused cool (room temperature) water into a specially designed electrode and noted a significant increase in delivered energy and ablation size in the *ex vivo* calf liver^[55]. Goldberg noted that both energy deposition and coagulation necrosis were significantly greater with electrode cooling. This was also the case with *ex vivo* and *in vivo* muscle models. Studies in animals have also suggested that the combination of internally cooled electrodes and interstitial hypertonic saline infusion may result in a larger area of ablation than either technique alone^[51, 56].

We can also use a second electrode within a few centimeters of the active electrode to increase the diameter of necrosis. In *ex vivo* experiments, this bipolar arrangement demonstrated that heat was generated not only at the active electrode, but also adjacent to the ground electrode and between the two electrodes. The resulting focus (5cm) was therefore larger than that produced by traditional single monopolar probes. The necrosis area produced by bipolar electrodes is still elliptical rather than spheroid, however, again making evaluation of its effectiveness difficult^[45,57].

Multiple active single probes can be clustered in an attempt to increase the coagulation volume as well. Goldberg *et al*^[60] investigated the effects of RFA via three electrodes placed 0.5cm apart from each other. This resulted in significant increases in the diameter of coagulation necrosis (2.9 to 7.0cm and 1.8 to 3.1cm, respectively) versus standard monopolar techniques. The use of clustered electrodes requires multiple passes and positioning and it is often laborious and difficult to ensure proper configuration. Although at times still used, this method has largely been supplanted by the development of multiprobe array electrodes^[58].

The most promising and currently the most widely used technique for RFA is the multiprobe array system. This system can be placed into the target tissue with the array retracted. Using ultrasound guidance, the array is then deployed and checked for proper positioning of all needles. These deployed multiple array needles create a series of electrodes with an overall diameter ranging up to 3.5 to 7 cm across which RFA current can be passed. Using this multiprobe needle with a standard RFA protocol, a 4-6cm tumor can be completely ablated with the array fully deployed. In general, for lesions less than 2.5cm in diameter, the needle electrode is placed parallel to the plane of the ultrasound probe. For larger tumors, either a larger multiprobe array or multiple deployments of the needle electrode are required. The treatment is planned such that the zones of necrosis overlap, keeping in mind that the entire volume of the tumor plus a margin of uninvolved tissue needs to be ablated.

RFA TECHNIQUES AND PROCEDURES

RFA of liver tumors can be performed percutaneously, using laparoscopic guidance, or as part of an open surgical procedure. The choice of treatment approach is individualized in any given patient. RFA is performed primarily by the liver surgeon and radiologist. The percutaneous approach differs from the laparoscopic and open surgical techniques only by the degree of hepatic exposure.

Patients with one to three small (<3.0cm diameter) cancers located in the periphery of the liver are considered for ultrasound-guided or CT-guided percutaneous RFA. Lesions located high in the dome of the liver near the diaphragm are not always accessible by a percutaneous approach. Furthermore, local anesthesia or monitored sedation is required for most patients treated percutaneously because of pain associated with the heating of tissue near the liver capsule. Patients treated percutaneously are usually discharged within 24h of

their RFA. Sonography is used to localize the lesion to be treated. A percutaneous approach has been used in patients with small, early-stage hepatocellular cancers with coexistent cirrhosis, and in patients with a limited number of small metastases from other organ sites^[59,60].

A laparoscopic approach offers the advantages of laparoscopic ultrasonography, which provides better resolution of the number and location of liver tumors, and a survey of the peritoneal cavity to exclude the presence of extrahepatic disease. Using laparoscopic ultrasound guidance, the RFA needle electrode is advanced percutaneously into the target tumors for treatment. The laparoscopic ultrasound permits more precise positioning of the RF needle multiple array near major blood vessels. Laparoscopic approach was used for patients with no prior history of extensive abdominal operations, and one or two liver tumors <4.0 cm in diameter located centrally in the liver near major intrahepatic blood vessels^[61,62].

The majority of patients underwent RFA of hepatic tumors during an open surgical procedure. This approach is preferred in patients with large tumors (>4.0-5.0 cm diameter), multiple tumors, if tumor locates next to a major intrahepatic blood vessel, or if a laparoscopic approach is impractical because of dense post-surgical adhesions. In contrast to percutaneous RFA treatments, it is possible to perform temporary occlusion of hepatic inflow during the intraoperative RFA procedure. Hepatic inflow occlusion facilitates RFA of large or hypervascular tumors and tumors near blood vessels. The amount of blood flow to a tumor is known to be a critical determinant of temperature response to a given increment of heat. Because heat loss or cooling effect is principally dependent on blood circulation in a given area, temperature response and blood flow are inversely related. By temporarily occluding hepatic inflow during RFA, the cooling effect of blood flow on perivascular tumor cells is minimized^[63]. The inflow occlusion increases the size of the zone of coagulative necrosis and enhances the likelihood of complete tumor cell kill, even if the tumor abuts a major intrahepatic blood vessel^[64].

The RFA needle can be placed under computed tomography (CT) or ultrasound guidance (percutaneous RFA) or ultrasound guidance (percutaneous, laparoscopic, or open RFA). Ultrasound can be used with all techniques of RFA, and offers several other advantages as well, including real-time capabilities, vascular visualization, availability, speed, and low cost. The probes are usually placed at the deep margin of the tumor and subsequently repositioned anteriorly at intervals appropriate to the size of the needle array. Once the needle is localized in the general vicinity of the tumor, the needle tip is placed into the desired portion of the tumor using a freehand technique. The ablation is started with the power setting at 25W, and the setting is automatically advanced to 50W over about 30 seconds. As the temperature at the tips of the deployed prongs exceeds 95°C, the times start to calculate. The temperature should be kept between 95-110°C at least 10 min to get full destroy^[51,65].

IMAGING TECHNIQUES IN RFA

Accurate imaging is essential for successful in situ tumor ablation. Tumors that are not seen can not be targeted, and residual foci of untreated tumor will continue to grow. With respect to tumor detection, and despite remarkable progress in US, CT and MR imaging over the past several years, no currently available imaging technique is perfectly sensitive for the detection of liver tumors, which means that some lesions will undoubtedly be overlooked with all imaging techniques. Generally, these overlooked lesions are small and will grow to a size that allows them to be detected, targeted and treated. Because currently available imaging techniques also may not precisely depict tumor margins, however, small foci of untreated tumor may not be identified. These will continue to grow in size and

result in "local recurrence" after treatments that initially appeared to be successful. Improved imaging techniques should result in not only improved detection of additional lesions but also more accurate determination of tumor margins. Recent and ongoing developments in contrast agents for US and MR imaging coupled with technical innovations in US, CT, and MR imaging may provide the much needed improvements. Additional research will be needed to determine their effect on the efficacy of in situ tumor ablation with RF.

In situ tumor ablation is virtually always performed with imaging guidance. Currently, US is most commonly used for guidance in probe placement, owing to its flexibility, widespread availability, relatively low cost, and real-time imaging capabilities. RF ablation can also be performed with CT or MR imaging guidance; however, until recently, the static nature of CT and the complexity of the MR imaging environment have limited their use. The recent development of CT fluoroscopic systems may result in a larger role for CT in the future. Similarly, the developments of open-architecture MR imaging systems and MR-compatible interventional equipment have resulted in increased interest in the use of this modality to help guide interventional procedures. Preliminary experience now suggests that MR imaging may be useful for in situ ablation procedures with RF^[66-68].

Imaging is used not only to help detect potentially treatable tumors and guide probe placement but also to monitor the effects of therapy. When procedures are performed with US guidance, hyperechogenicity is generally seen surrounding the probe tip during the application of RF energy. This has proved to be only marginally useful for monitoring the effects of therapy because the hyperechoic zones correspond only roughly to the regions of eventual tissue necrosis. Furthermore, these changes evolve rapidly over time and can disappear within minutes of ablation^[69-71]. Acoustic shadowing from more superficial treated areas can also preclude visualization of deeper portions of the tumor if one is not careful to treat deeper areas first. The use of US contrast agents may improve the accuracy of US with respect to monitoring the acute effects of therapy^[72,73]. Contrast-enhanced CT, which is probably the most widely used technique for the follow-up of treated lesions, is less useful for the immediate assessment of treatment results. CT is not particularly helpful for confirming successful treatment or identifying a small focus of untreated tumor. MR imaging appears to be more accurate than US or CT for monitoring the acute effects of^[66-68].

Follow-up imaging is very useful to assess the result of RF and the recurrence of new tumors, although sometimes it is very difficult. CT and MRI were showed more effective than ultrasound for monitoring the RFA ablation in animal studies. If the follow up imaging is performed soon after the procedure, a peripheral hyperemic halo surrounding an area of hypoattenuation devoid of parenchymal enhancement is usually seen with spiral CT or MRI. Occasionally a hyperdense central area corresponding to the needle tract is also seen. The interpretation of the follow-up CT scans required radiologists experience to prevent both diagnosis and underdiagnosis of the residual or recurrent tumor. The ablation process cause a hyperemic response in the liver parenchyma surrounding the ablation. The hyperemic prevents an accurate assessment of the completeness of the ablation in the early post-ablation period. The hyperemia usually resolved within 1 month after the procedure. After this time, persistent or new peritumoral hyperemia is considered an indication of recurrent tumor. Recurrent hypovascular tumors are detected as an enlargement of ablation area, or a subtle double-density halo developing around the margins of the treated area. All areas suspicious for tumor recurrence should be assessed by percutaneous biopsy.

RFA OF PRIMARY LIVER TUMORS

Primary liver cancer is a highly vascular cancer. A vascular sink phenomenon may contribute to the extended ablation times. Most of the

early reports on the use of RFA for HCC came from Rossi *et al*^[74] in Italy in 1995. They reported their results with percutaneous RFA in twenty-four patients (16 men and 8 women; age range, 53 to 79 years) with 36 hepatocellular carcinoma nodules of not more than 3.0cm in diameter underwent radiofrequency interstitial thermal ablation treatment with the intent to achieve a cure. In each patient, the thermal necrosis volume achieved was about double the tumor volume. During the mean follow-up interval of 24.8 months, 13 of 24 patients had recurrences, 9 of whom underwent further radiofrequency thermal ablation treatment. Radiofrequency thermal ablation was again repeated in two patients who showed a second recurrence.

Marone *et al*^[75] reported percutaneous RF results using cooling saline in the tube of 13 cirrhotic patients with 19 hepatocellular carcinoma in 1998. None of the patients had portal thrombosis or extrahepatic spread. They used a radiofrequency generator (100W power) connected to an 18G perfusion electrode needle with an exposed tip of 2-3cm. The circuit is closed through a dispersive electrode positioned under the patient's thighs. A peristaltic pump infuses a chilled (2-5°C) saline solution to guarantee the continuous cooling of the needle tip. The needle was placed into target lesions under US guidance. Complete necrosis as assessed at dynamic CT (no enhancement during the arteriographic phase) was achieved in 16 of 19 nodules (84%). No side-effects occurred. During the follow-up (median: 11 months) no death occurred and five patients had recurrent hepatocellular carcinoma appearing either as single nodule or as multi nodular liver involvement? In a large series from Curley *et al*^[76], 149 discrete HCC tumor nodules in 110 patients had been followed for a minimum of 12 months (median follow-up 19 months) after RF. Percutaneous, laparoscopic or intraoperative RFA was performed in 76 (69%) and 34 (31%) patients, respectively. Median diameter of tumors treated percutaneously (2.8cm) was smaller than lesions treated during laparotomy (4.6cm, $P<0.01$). Local tumor recurrence at the RFA site developed in four patients (3.6%); all four subsequently developed recurrent HCC in other areas of the liver. New liver tumors or extrahepatic metastases developed in 50 patients (45.5%), but 56 patients (50.9%) have no evidence of recurrence. There were no treatment-related deaths, but complications developed in 14 patients (12.7%) after RFA.

RFA OF COLORECTAL CANCER LIVER METASTASES

The liver is the most common site of distant metastasis from colorectal cancer. Colorectal cancer is the fourth most commonly diagnosed cancer and second leading cause of cancer death in the world. Nearly half of patients will develop liver metastases during the course of their disease, with 15-25% having liver metastases at the time of primary diagnosis and another 20% of patients developing metachronous liver metastases^[10,11]. About one-fourth of patients with liver metastases from colorectal cancer have no other sites of metastases and can be treated with regional therapies directed toward their liver tumors. But only a minority of the patients are candidates for surgical resection. RFA, one of the regional therapies, may be offered to patients with unresectable liver metastases.

Most of the early reports on the use of RFA for colorectal cancer liver metastases also came from Rossi *et al*^[74] in Italy. In 1996, they reported their results with percutaneous RFA in 50 patients, in which 11 patients had 13 metastases ranging from 1 to 9cm in diameter. Monopolar and bipolar needles were utilized and multiple probe insertions and treatment sessions were performed. There were no associated complications or deaths. Of the 11 patients with metastases, two underwent subsequent surgical resection, of which one had complete tumor necrosis by histopathologic examination. At a median follow-up of 22.6 months, 10 of 11 patients (90%) were

alive, but two (18%) had a local recurrence and seven (64%) had persistent or distant disease. Only one patient (9%), therefore, was alive without disease. These studies suggested that although RFA was effective in preventing local recurrence of metastases, it may not affect the progressive course of the cancer.

Solbiati *et al*^[77] reported on 117 patients with 179 metastatic lesions undergoing RFA with a mean follow-up of 3 years (range, 6 to 52 months). Computed tomographic follow-up was performed every 4-6 months. Recurrent tumors were retreated when feasible. Estimated median survival was 36 months. Estimated 1, 2, and 3-year survival rates were 93%, 69%, and 46%, respectively. Survival was not significantly related to number of metastases treated. In 77 (66%) of 117 patients, new metastases were observed at follow-up. Estimated median time until new metastases was 12 months. Percentages of patients with no new metastases after initial treatment at 1 and 2 years were 49% and 35%, respectively. Time to new metastases was not significantly related to number of metastases. Seventy (39%) of 179 lesions developed local recurrence after treatment. Of these, 54 were observed by 6 months and 67 by 1 year. This study suggests that at long-term local control can be achieved in a majority of patients, but that the development of new metastases limits improvement in overall survival.

Wood *et al*^[78] reported 231 tumors in 84 patients treated with 91 RFA procedures. The majority of patients had metastatic lesions (213 lesions in 73 patients) and 51 of the 91 treatments consisted of RFA alone. The other 40 included RFA combined with surgical resection, cryoablation, and hepatic artery infusion of chemotherapy. Of the 91 RF treatments, 39 were ablated at laparotomy, 27 by laparoscopy and 25 percutaneously; tumors ranged in size from 0.3 to 9.0cm. There were seven major complications including three deaths, one (1%) of which was directly related to the RFA procedure. Ten patients underwent a second RFA procedure (sequential ablations) and, in one case, a third RFA procedure for large (one patient), progressive (seven patients), and recurrent (three patients) lesions. At a median follow-up of 9 months (range, 1-27 months), 15 patients (18%) had developed a local recurrence. Of the remaining 69 patients, 34 were alive without disease, 14 were alive with disease, and 21 died of their disease; new hepatic tumors or extrahepatic disease therefore had developed in 35 patients. The average hospital stay was 3.6 days overall.

RFA OF OTHER LIVER METASTASES

Most of the papers discussed so far consisted of both primary liver tumors and colorectal cancer liver metastases. RFA for liver tumors has also been evaluated for specific tumor types.

Livraghi *et al*^[79] reported on 24 patients with 64 metastatic breast lesions ranging in size from 1 to 6.6cm. The liver was the only site of disease in 16 patients, while the other eight patients had stable metastatic disease elsewhere. The patients were treated with the percutaneous approach utilizing monopolar or clustered electrodes. Minor complications were noted in two patients and no deaths were reported. Complete necrosis was achieved in 59 (92%) of 64 lesions. Among the 59 lesions, complete necrosis required a single treatment session in 58 lesions (92%) and two treatment sessions in one lesion (2%). In 14 (58%) of 24 patients, new metastases developed during follow-up. Ten (71%) of these 14 patients developed new liver metastases. Currently, 10 (63%) of 16 patients whose lesions were initially confined to the liver are free of disease. One patient died of progressive brain metastases. Although a preliminary study, these results do suggest that RFA for selected patients with metastatic breast carcinoma confined to the liver can be as effective as RFA for colorectal and other metastatic tumors to the liver.

Neuroendocrine tumors metastatic to the liver often produce symptoms secondary to hormone production. Although only a minority are curable by surgical techniques, significant symptomatic relief can be obtained by surgical procedures. For those patients who are not surgical candidates, RFA may provide a viable therapeutic alternative. Siperstein *et al*^[80] reported 18 patients with 115 neuroendocrine tumors were ablated with RFA. The mean lesion size was 3.2cm (range, 1.3 to 10cm) and the average number of lesions ablated per patient was six (range, one to 14). There were two complications consisting of arterial fibrillation in one patient and an upper gastrointestinal bleed in another. Fifteen patients (83%) with 100 lesions were followed for a mean of 12.1 months (range, 3 to 35months). Local recurrence was detected in three patients (20%) and six (6%) lesions and three patients died during follow-up. However, data regarding potential symptom improvement were not reported.

FOLLOW UP OF RFA

Initial imaging serves as an indicator of complete treatment, and provides a basis for subsequent studies. However, the resolution and accuracy of current imaging techniques preclude identification of residual microscopic foci of malignancy at the periphery of a treated lesion. Hence, these viable tumor foci, if present, will grow and result in "local recurrence".

Multiphasic helical CT and contrast-enhanced MR imaging play a central role in the long-term assessment of therapeutic response, allowing confident discrimination between ablated and residual viable tumor. CT and MR studies are obtained at 3-4 months intervals and are combined with tumor marker (serum CEA, AFP, CA19-9) levels to detect local or distant recurrences. In general, sampling error and the histopathologic findings of thermally ablated tissue are too variable to render fine needle aspiration or core biopsy reliable indicators of the presence or absence of residual disease. US has proved valuable for immediate assessment of ablative results during the RF session, still in patients under general anesthesia, allowing for an immediate refinement of the ablation, if needed. US is also valuable for long-term follow-up and detection or confirmation of recurrences; in many patients contrast-guided retreatment has been performed in order to precisely direct RF energy on recurrence areas^[81-83].

ADVANTAGE AND DISADVANTAGE OF RFA

RF thermal ablation has several advantages over other therapies for primary liver cancer and metastasis liver cancer. It can be used as a percutaneous procedure, under the guiding of ultrasound, CT scan and MRI, done in local anesthesia, in out-patient department. The complications and morbidity are lower than hepatic resection and cryosurgery. RFA can be retreated in the patients whose tumors recur at the margin of treatment or have new tumors develop elsewhere in the liver. It has similar results as hepatic resection because it destroyed the tumors completely as taking it out in liver surgery, which is superior to ethanol injection. RF requires less sessions than other ablation procedures such as ethanol injection.

Although RF has a lot of advantages in the treatment of primary and metastasis liver tumors, it still has a few disadvantages and complications. These complications included symptomatic pleural effusion, fever, pain, subcutaneous hematoma, subcapsular liver hematoma, and ventricular fibrillation. The severe complication is treatment-related death. As with all methods related to tumors, the outcome of RF thermal ablation will be related to the skill of physician performing the procedure. Exact placement of the ablation needles require considerable skill and some degree of guesswork by the radiologist and surgeon, which may be the most experienced in interventional procedures. Recurrence at the treatment margin may

result from an inability to adequately kill the tumor the hepatic parenchyma adjacent to the treated tumors. The abundant portal venous blood flow present in normal hepatic parenchyma act as a heat pump, which makes the creation of the thermal injury in normal liver more difficult than that it is in liver tumors. RFA also caused skin burn in percutaneous procedures, hemorrhage, diaphragmatic necrosis, hepatic abscess, hepatic artery injuries, bile ducts injuries, renal failure, coagulopathy and liver failure, which were severe and eventually fatal.

CONCLUSION

Despite the considerable progress that has been made to date, a number of challenges remain for the future. These include the development of techniques that can increase the volume of tissue destroyed at a single treatment session, the development of more suitable and accurate imaging tests, and a better understanding of how to integrate in situ ablation techniques into the overall care of patients with different specific neoplasms.

Although long-term observations are still not available, RFA will definitely give the surgeon a helpful hand and offer the patients a better prognosis. But, RFA is unlikely to be curative for most patients, it can relieve the symptom of patients and improve the quality of life of patients. RFA has been shown to be safer and better tolerated compared to other ablative techniques, such as cryotherapy, laser ablation and microwave ablation, has been associated with fewer local recurrence. However, surgical resection remains the gold standard for treating metastatic and primary liver tumors. RFA of unresectable liver tumors provides a relatively safe, highly effective method to achieve local disease control in some liver cancer patients who are not candidates for liver resection. RFA also shown some better respect in combination with surgical resection, hepatic artery catheter and regional chemotherapy. With the development of RFA equipments and techniques, the treatment of a large primary and secondary liver cancer and malignant tumors at other body sites will be feasible and effective. The most interesting feature of RFA is the minimal-invasiveness with zero mortality rate, significantly lower complications, reduced costs and hospital days compared to surgery and other local therapies. Furthermore, with combination of other procedures, RFA will improve the survival of patients with cancer.

REFERENCES

- Schafer DF, Sorrell MF. Hepatocellular carcinoma. *Lancet* 1999;353: 1253-1257
- Tang ZY. Hepatocellular carcinoma-Cause, treatment and metastasis. *World J Gastroenterol* 2001; 7: 445-454
- Qin LX, Tang ZY. The prognostic significance of clinical and pathological features in hepatocellular carcinoma. *World J Gastroenterol* 2002; 8: 193-199
- Weiss L, Grundmann E, Torhorst J, Hartveit F, Moberg I, Eder M, Fenoglio-Preiser CM, Napier J, Horne CH, Lopez MJ. Haematogenous metastatic patterns in colonic carcinoma: an analysis of 1541 necropsies. *J Pathol* 1986;150:195-203
- Hughes KS, Simon R, Songhorabodi S, Adson MA, Ilstrup DM, Fortner JG, Maclean BJ, Foster JH, Daly JM, Fitzherbert D. Resection of the liver for colorectal carcinoma metastases: a multi-institutional study of patterns of recurrence. *Surgery* 1986; 100: 278-284
- Bengtsson G, Carlsson G, Hafstrom L, Jonsson PE. Natural history of patients with untreated liver metastases from colorectal cancer. *Am J Surg* 1981; 141: 586-589
- Wagner JS, Adson MA, Van Heerden JA, Adson MH, Ilstrup DM. The natural history of hepatic metastases from colorectal cancer. A comparison with resective treatment. *Ann Surg* 1984;199:502-508
- Fong Y, Cohen AM, Fortner JG, Enker WE, Turnbull AD, Coit DG, Marrero AM, Praesad M, Blumgart LH, Brennan MF. Liver resection for colorectal metastases. *J Clin Oncol* 1997; 15: 938-946
- Gayowski TJ, Iwatsuki S, Madariaga JR, Selby R, Todo S, Irish W, Starzl TE. Experience in hepatic resection for metastatic colorectal cancer: analysis of clinical and pathologic risk factors. *Surgery* 1994; 116: 703-710

- 10 Palmer M, Petrelli NJ, Herrera L. No treatment option for liver metastases from colorectal adenocarcinoma. *Dis Colon Rectum* 1989; 32: 698-701
- 11 Wu MC, Shen F. Progress in research of liver surgery in China. *World J Gastroenterol* 2000; 6:773-776
- 12 Nagorney DM, van Heerden JA, Ilstrup DM, Adson MA. Primary hepatic malignancy: surgical management and determinants of survival. *Surgery* 1989; 106: 740-748
- 13 Wanebo HJ, Semoglou C, Attiyeh F, Stearns MJ Jr. Surgical management of patients with primary operable colorectal cancer and synchronous liver metastases. *Am J Surg* 1978; 135:81-85
- 14 Bruinvels DJ, Stiggelbout AM, Kievit J, van Houwelingen HC, Habbema JD, van de Velde CJ. Follow-up of patients with colorectal cancer. A meta-analysis. *Ann Surg* 1994; 219:174-182
- 15 Kemeny N, Huang Y, Cohen AM, Shi W, Conti JA, Brennan MF, Bertino JR, Turnbull AD, Sullivan D, Stockman J, Blumgart LH, Fong Y. Hepatic arterial infusion of chemotherapy after resection of hepatic metastases from colorectal cancer. *N Engl J Med* 1999; 341: 2039-2048
- 16 Fowler WC, Eisenberg BL, Hoffman JP. Hepatic resection following systemic chemotherapy for metastatic colorectal carcinoma. *J Surg Oncol* 1992; 51: 122-125
- 17 Elias D, Lasser P, Rougier P, Ducreux M, Bognel C, Roche A. Frequency, technical aspects, results, and indications of major hepatectomy after prolonged intra-arterial hepatic chemotherapy for initially unresectable hepatic tumors. *J Am Coll Surg* 1995; 180:213-219
- 18 Venook AP. Update on hepatic intra-arterial chemotherapy. *Oncology* 1997; 11: 947-957
- 19 Giovannini M. Percutaneous alcohol ablation for liver metastasis. *Semin Oncol* 2002; 29: 192-195
- 20 Bartolozzi C, Lencioni R. Ethanol injection for the treatment of hepatic tumors. *Eur Radiol* 1996; 6: 682-696
- 21 Lee MJ, Mueller PR, Dawson SL, Gazelle SG, Hahn PF, Goldberg MA, Boland GW. Percutaneous ethanol injection for the treatment of hepatic tumors: indications, mechanism of action, technique, and efficacy. *AJR Am J Roentgenol* 1995; 164: 215-220
- 22 ter Haar GR. High intensity focused ultrasound for the treatment of tumors. *Echocardiography* 2001; 18: 317-322
- 23 Sibille A, Prat F, Chapelon JY, Abou el Fadil F, Henry L, Theillere Y, Ponchon T, Cathignol D. Extracorporeal ablation of liver tissue by high-intensity focused ultrasound. *Oncology* 1993; 50: 375-379
- 24 Yang R, Sanghvi NT, Rescorla FJ, Kopecky KK, Grosfeld JL. Liver cancer ablation with extracorporeal high-intensity focused ultrasound. *Eur Urol* 1993; 23 Suppl 1: 17-22
- 25 Sotsky TK, Ravikumar TS. Cryotherapy in the treatment of liver metastases from colorectal cancer. *Semin Oncol* 2002; 29: 183-191
- 26 Poston G. Cryosurgery for colorectal liver metastases. *Hepatogastroenterology* 2001; 48: 323-324
- 27 Ross WB, Horton M, Bertolino P, Morris DL. Cryotherapy of liver tumors—a practical guide. *HPB Surg* 1995; 8: 167-173
- 28 Seifert JK, Morris DL. Prognostic factors after cryotherapy for hepatic metastases from colorectal cancer. *Ann Surg* 1998; 228: 201-208
- 29 Moroz P, Jones SK, Gray BN. Status of hyperthermia in the treatment of advanced liver cancer. *J Surg Oncol* 2001; 77: 259-269
- 30 Dodd GD 3rd, Soulen MC, Kane RA, Livraghi T, Lees WR, Yamashita Y, Gil lams AR, Karahan OI, Rhim H. Minimally invasive treatment of malignant hepatic tumors: at the threshold of a major breakthrough. *Radiographics* 2000; 20: 9-27
- 31 Greve JW. Alternative techniques for the treatment of colon carcinoma metastases in the liver: current status in The Netherlands. *Scand J Gastroenterol* 2001; 234 (Suppl): 77-81
- 32 Usatoff V, Habib NA. Update of laser-induced thermotherapy for liver tumors. *Hepatogastroenterology* 2001; 48: 330-332
- 33 Heisterkamp J, van Hillegersberg R, Ijzermans JN. Interstitial laser coagulation for hepatic tumors. *Br J Surg* 1999; 86: 293-304
- 34 Schneider PD. Liver resection and laser hyperthermia. *Surg Clin North Am* 1992; 72: 623-639
- 35 Slakey DP. Radiofrequency ablation of recurrent cholangiocarcinoma. *Am Surg* 2002; 68: 395-397
- 36 Yoon SS, Tanabe KK. Surgical treatment and other regional treatments for colorectal cancer liver metastases. *Oncologist* 1999; 4:197-208
- 37 Curley SA. Radiofrequency ablation of malignant liver tumors. *Oncologist* 2001; 6: 14-23
- 38 McGahan JP, Browning PD, Brock JM, Tesluk H. Hepatic ablation using radiofrequency electrocautery. *Invest Radiol* 1990; 25: 267-270
- 39 Buscarini L, Rossi S, Fornari F, Di Stasi M, Buscarini E. Laparoscopic ablation of liver adenoma by radiofrequency electrocautery. *Gastrointest Endosc* 1995; 41: 68-70
- 40 Dickson JA, Calderwood SK. Temperature range and selective sensitivity of tumors to hyperthermia: a critical review. *Ann N Y Acad Sci* 1980; 335:180-205
- 41 Siperstein A, Garland A, Engle K, Rogers S, Berber E, String A, Foroutani A, Ryan T. Laparoscopic radiofrequency ablation of primary and metastatic liver tumors. Technical considerations. *Surg Endosc* 2000; 14:400-405
- 42 Zervas NT, Hamlin H. Stereotactic radiofrequency hypophysectomy. *Appl Neurophysiol* 1978; 41: 219-222
- 43 Cosman ER, Nashold BS, Bedenbaugh P. Stereotactic radiofrequency lesion making. *Appl Neurophysiol* 1983; 46: 160-166
- 44 Rossi S, Fornari F, Pathies C, Buscarini L. Thermal lesions induced by 480 KHz localized current field in guinea pig and pig liver. *Tumori* 1990; 76: 54-57
- 45 McGahan JP, Griffey SM, Budenz RW, Brock JM. Percutaneous ultrasound-guided radiofrequency electrocautery ablation of prostate tissue in dogs. *Acad Radiol* 1995; 2: 61-65
- 46 Wood BJ, Ramkaransingh JR, Fojo T, Walther MM, Libutti SK. Percutaneous tumor ablation with radiofrequency. *Cancer* 2002; 94: 443-451
- 47 Parikh AA, Curley SA, Fornage BD, Ellis LM. Radiofrequency ablation of hepatic metastases. *Semin Oncol* 2002; 29: 168-182
- 48 Choi H, Loyer EM, DuBrow RA, Kaur H, David CL, Huang S, Curley S, Char nsangavej C. Radio-frequency ablation of liver tumors: assessment of therapeutic response and complications. *Radiographics* 2001; 21 Spec No: S41-54
- 49 Goldberg SN. Radiofrequency tumor ablation: Principles and techniques. *Eur J Ultrasound* 2001; 13:129-147
- 50 Liu CL, Fan ST. Nonresectional therapies for hepatocellular carcinoma. *Am J Surg* 1997; 173:358-365
- 51 Buscarini L, Buscarini E, Di Stasi M, Vallisa D, Quaretti P, Rocca A. Percutaneous radiofrequency ablation of small hepatocellular carcinoma: long-term results. *Eur Radiol* 2001; 11:914-921
- 52 Hager ED, Dziambor H, Hohmann D, Gallenbeck D, Stephan M, Popa C. Deep hyperthermia with radiofrequencies in patients with liver metastases from colorectal cancer. *Anticancer Res* 1999; 19: 3403-3408
- 53 Livraghi T, Goldberg SN, Monti F, Bizzini A, Lazzaroni S, Meloni F, Pellicano S, Solbiati L, Gazelle GS. Saline-enhanced radio-frequency tissue ablation in the treatment of liver metastases. *Radiology* 1997; 202:205-210
- 54 Miao Y, Ni Y, Yu J, Marchal G. A comparative study on validation of a novel cooled-wet electrode for radiofrequency liver ablation. *Invest Radiol* 2000; 35: 438-444
- 55 Lorentzen T. A cooled needle electrode for radiofrequency tissue ablation: Thermodynamic aspects of improved performance compared with conventional needle design. *Acad Radiol* 1996; 3: 556-563
- 56 Goldberg SN, Gazelle GS, Solbiati L, Rittman WJ, Mueller PR. Radiofrequency tissue ablation: Increased lesion diameter with a perfusion electrode. *Acad Radiol* 1996; 3: 636-644
- 57 McGahan JP, Gu WZ, Brock JM, Tesluk H, Jones CD. Hepatic ablation using bipolar radiofrequency electrocautery. *Acad Radiol* 1996; 3: 418-422
- 58 Bilchik AJ, Wood TF, Allegra D, Tsioulis GJ, Chung M, Rose DM, Ramming KP, Morton DL. Cryosurgical ablation and radiofrequency ablation for unresectable hepatic malignant neoplasms: A proposed algorithm. *Arch Surg* 2000; 135: 657-662
- 59 Rhim H, Dodd GD 3rd. Radiofrequency thermal ablation of liver tumors. *J Clin Ultrasound* 1999; 27: 221-229
- 60 Goldberg SN, Gazelle GS, Compton CC, Mueller PR, Tanabe KK. Treatment of intrahepatic malignancy with radiofrequency ablation: Radiologic-pathologic correlation. *Cancer* 2000; 88: 2452-2463
- 61 Siperstein AE, Rogers SJ, Hansen PD, Gitomirsky A. Laparoscopic thermal ablation of hepatic neuroendocrine tumor metastases. *Surgery* 1997; 122:1147-1155
- 62 Curley SA, Davidson BS, Fleming RY, Izzo F, Stephens LC, Tinkey P, Croome D. Laparoscopically guided bipolar radiofrequency ablation of areas of porcine liver. *Surg Endosc* 1997; 11: 729-733
- 63 Solbiati L, Ierace T, Goldberg SN, Sironi S, Livraghi T, Fiocca R, Ser vadio G, Rizzatto G, Mueller PR, Del Maschio A, Gazelle GS. Percutaneous US-guided radio-frequency tissue ablation of liver metastases: treatment and follow-up in 16 patients. *Radiology* 1997; 202: 195-203
- 64 Stureson C, Liu DL, Stenram U, Andersson-Engels S. Hepatic inflow occlusion increases the efficacy of interstitial laser-induced thermotherapy in rats. *J Surg Res* 1997; 71: 67-72
- 65 Gazelle GS, Goldberg SN, Solbiati L, Livraghi T. Tumor ablation with radio-frequency energy. *Radiology* 2000; 217: 633-646
- 66 Lewin JS, Connell CF, Duerk JL, Chung YC, Clappitt ME, Spisak J, Gazelle GS, Haaga JR. Interactive MR-guided radiofrequency interstitial thermal ablation of abdominal tumors: clinical trial for evaluation of safety and feasibility. *J Magn Reson Imaging* 1998; 8: 40-47

- 67 Steiner P, Botnar R, Dubno B, Zimmermann GG, Gazelle GS, Debatin JF. Radio-frequency-induced thermoablation: monitoring with T1-weighted and proton-frequency-shift MR imaging in an interventional 0.5-T environment. *Radiology* 1998; 206: 803-810
- 68 Goldberg SN, Kruskal JB, Oliver BS, Clouse ME, Gazelle GS. Percutaneous tumor ablation: increased coagulation by combining radio-frequency and ethanol instillation in a rat breast tumor model. *Radiology* 2000; 217:827-831
- 69 Rossi S, Buscarini E, Garbagnati F, Di Stasi M, Quaretti P, Rago M, Zangrandi A, Andreola S, Silverman D, Buscarini L. Percutaneous treatment of small hepatic tumors by an expandable RF needle electrode. *Am J Roentgenol* 1998; 170: 1015-1022
- 70 Solbiati L, Goldberg SN, Ierace T, Livraghi T, Meloni F, Dellanoce M, Sironi S, Gazelle GS. Hepatic metastases: percutaneous radio-frequency ablation with cooled-tip electrodes. *Radiology* 1997; 205:367-373
- 71 Livraghi T, Goldberg SN, Lazzaroni S, Meloni F, Solbiati L, Gazelle GS. Small hepatocellular carcinoma: treatment with radio-frequency ablation versus ethanol injection. *Radiology* 1998; 210:655-661
- 72 Solbiati L, Goldberg SN, Ierace T, Dellanoce M, Livraghi T, Gazelle GS. Radio-frequency ablation of hepatic metastases: postprocedural assessment with a US microbubble contrast agent-early experience. *Radiology* 1999; 211:643-649
- 73 Goldberg SN, Walovitch RC, Straub JA, Shore MT, Gazelle GS. Radio-frequency-induced coagulation in rabbits: immediate detection at US using a synthetic microsphere contrast agent. *Radiology* 1999; 213:438-444
- 74 Rossi S, Di Stasi M, Buscarini E, Quaretti P, Garbagnati F, Squassante L, Paties CT, Silverman DE, Buscarini L. Percutaneous RF interstitial thermal ablation in the treatment of hepatic cancer. *Am J Roentgenol* 1996; 167: 759-768
- 75 Marone G, Francica G, D'Angelo V, Iodice G, Pastore P, Altamura G, Cusati B, Siani A. Echo-guided radiofrequency percutaneous ablation of hepatocellular carcinoma in cirrhosis using a cooled needle. *Radiol Med* 1998; 95: 624-629
- 76 Curley SA, Izzo F, Ellis LM, Nicolas Vauthey J, Vallone P. Radiofrequency ablation of hepatocellular cancer in 110 patients with cirrhosis. *Ann Surg* 2000; 232: 381-391
- 77 Solbiati L, Ierace T, Tonolini M, Osti V, Cova L. Radiofrequency thermal ablation of hepatic metastases. *Eur J Ultrasound* 2001; 13: 149-158
- 78 Wood TF, Rose DM, Chung M, Allegra DP, Foshag LJ, Bilchik AJ. Radiofrequency ablation of 231 unresectable hepatic tumors: Indications, limitations, and complications. *Ann Surg Oncol* 2000; 7: 593-600
- 79 Livraghi T. Guidelines for treatment of liver cancer. *Eur J Ultrasound* 2001; 13:167-176
- 80 Siperstein AE, Berber E. Cryoablation, percutaneous alcohol injection, and radiofrequency ablation for treatment of neuroendocrine liver metastases. *World J Surg* 2001; 25: 693-696
- 81 Fong Y, Blumgart LH, Cohen A, Fortner J, Brennan MF. Repeat hepatic resections for metastatic colorectal cancer. *Ann Surg* 1994;220: 657-662
- 82 Goya T, Miyazawa N, Kondo H, Tsuchiya R, Naruke T, Suemasu K. Surgical resection of pulmonary metastases from colorectal cancer: 10-year follow-up. *Cancer* 1989; 64:1418-1421
- 83 Gough DB, Donohue JH, Trastek VA, Nagorney DM. Resection of hepatic and pulmonary metastases in patients with colorectal cancer. *Br J Surg* 1994; 81: 94-96

Edited by Morris DL

• REVIEW •

Effects of histone acetylation and DNA methylation on p21^{WAF1} regulation

Jing-Yuan Fang, You-Yong Lu

Jing-Yuan Fang, Renji Hospital, Shanghai Institute of Digestive Disease, Shanghai Second Medical University, Shanghai, China
You-Yong Lu, Beijing Cancer Institute, Beijing University, Beijing 100000, China

Correspondence to: Jing-Yuan Fang, M.D., Ph.D., Shanghai Institute of Digestive Disease, Renji Hospital, 145 Shandong Zhong Road, Shanghai 200001, China. jingyuanfang@yahoo.com

Received 2001-12-04 Accepted 2002-02-07

Abstract

Cell cycle progression is regulated by interactions between cyclins and cyclin-dependent kinases (CDKs). p21^{WAF1} is one of the CIP/KIP family which inhibits its CDKs activity. Increased expression of p21^{WAF1} may play an important role in the growth arrest induced in transformed cells. Although the stability of the p21^{WAF1} mRNA could be altered by different signals, cell differentiation and numerous influencing factors. However, recent studies suggest that two known mechanisms of epigenesis, i.e. gene inactivation by methylation in promoter region and changes to an inactive chromatin by histone deacetylation, seem to be the best candidate mechanisms for inactivation of p21^{WAF1}. To date, almost no coding region p21^{WAF1} mutations have been found in tumor cells, despite extensive screening of hundreds of various tumors. Hypermethylation of the p21^{WAF1} promoter region may represent an alternative mechanism by which the p21^{WAF1/CIP1} gene can be inactivated. The reduction of cellular DNMT protein levels also induces a corresponding rapid increase in the cell cycle regulator p21^{WAF1} protein demonstrating a regulatory link between DNMT and p21^{WAF1} which is independent of methylation of DNA. Both histone hyperacetylation and hypoacetylation appear to be important in the carcinoma process, and induction of the p21^{WAF1} gene by histone hyperacetylation may be a mechanism by which dietary fiber prevents carcinogenesis. Here, we review the influence of histone acetylation and DNA methylation on p21^{WAF1} transcription, and effect on pathways or factors associated such as p53, E2A, Sp1 as well as several histone deacetylation inhibitors.

Fang JY, Lu YY. Effects of histone acetylation and DNA methylation on p21^{WAF1} regulation. *World J Gastroenterol* 2002;8(3):400-405

INTRODUCTION

Cell cycle progression is regulated by interactions between cyclins and CDKs^[1,2]. Especially, the transition of G₁ to S phase is known to be regulated by a family of negative cell cycle regulators, CDKIs. The latter includes two families, the CIP/KIP family and the INK4 family^[3-6]. p21^{WAF1} is one of the CIP/KIP family^[7,8]. Increased expression of p21^{WAF1} may play a crucial role in the growth arrest induced in transformed cells^[9].

p21^{WAF1} was first cloned and characterized as an important effector that acted to inhibit cyclin-dependent kinase activity in p53 mediated cell cycle arrest induced by DNA damage^[10,11]. It has been

shown that this is a G C-rich region in the human p21^{WAF1} promoter^[12]. Although the stability of the p21^{WAF1} mRNA could be altered by different signals cell differentiation^[13] and oxidative stress^[14] as well as numerous influencing factors including decorin^[15], Ras/Raf protein^[16], TGF- β ^[17] and Tax of human T cell leukemia virus type 1 (HTLV-1)^[18,19]. However, two known mechanisms of epigenetic modification, gene inactivation by methylation in promoter region and changes to an inactive chromatin by histone deacetylation, seem to be the best candidate mechanisms for the inactivation of CIP/KIP family^[20]. In this review, we focused on the methylation, histone acetylation and some transcription factor, co-transcription factor associated with acetylation.

DNA METHYLATION AND HISTONE ACETYLATION

The post-translational modifications include acetylation, phosphorylation, methylation, ubiquitination and ADP-ribosylation^[21]. In mammals, methylation of the 5' position of cytosine in the CpG dinucleotide sequence is the only naturally occurring covalent modification of the genome. The enzyme DNA 5-cytosine methyltransferase (DNMT) catalyzes the transfer of a methyl group from S-adenosylmethionine to the 5 position of cytosines residing in the dinucleotide sequence CpG^[22]. DNA methylation patterns correlate inversely with gene expression^[23] and, therefore, DNA methylation has been suggested to be an epigenetic determinant of gene expression.

DNA methylation is believed to be an on-off switch in gene expression, CpG islands present in the promoter regions have been shown to be susceptible to hypermethylation in many cancer cells^[24]. CpG islands near promoters and 5' regulatory region are usually unmethylated in normal somatic cells. In contrast, widespread methylation of CpG islands occurs in autosomal genes and leads to the silencing of the genes during oncogenic transformation.

DNA in eukaryotes is packaged with histone and non-histone proteins into chromatin. In general, regions of chromatin that are hyperacetylated are transcriptionally active, whereas regions that are hypoacetylated are silenced. Indeed, a global increase in core histone acetylation does not necessarily induce widespread transcription^[25]. Histone acetylation results in charge neutralization and separation of DNA from the histones allowing nucleosomal DNA to become more accessible to transcription factors. Histone acetylation is believed to stabilize local nucleosomal structure, thereby allowing transcription factors and the basal transcriptional machinery access to DNA. Hyperacetylation of histones has been shown to mark open chromatin and to be required for transcriptional activation^[26].

Histone acetylation is a reversible process: histone acetyltransferases (HATs) transfer the acetyl moiety from acetyl coenzyme A to the lysine neutralizes the positive charge, and histone deacetylases (HDACs) remove the acetyl groups re-establishing the positive charge in the histones. At least six human HDAC enzymes exist, and for higher eukaryotes, HDAC1 was first purified using an affinity matrix based on the deacetylase inhibitor trapoxin^[27]. HDAC inhibitor include trichostatin A (TSA)^[28,29], trapoxin (TPX)^[30], Butyrate^[31,32], MS-27-275 (a synthetic benzamide derivative)^[33] and Apicidin^[9,34]. Due to the inhibitory effects of the compounds of

endogenous genes that plays significant roles in G1-S progression of the cell cycle, HDAC inhibitors have been considered to be a novel class of cancer treatment agent^[34].

Methylation is not genomically uniform, as unmethylated CpG are found preferentially in transcriptionally active chromatin. The highest density of nonmethylated CpG islands, which usually contain promoter or other regulatory DNA that is required for active transcription of a gene. CpG island chromatin is enriched in hyperacetylated histones and deficient in linker histones^[35]. Recent studies have suggested a strong link between histone acetylation, chromatin remodeling, and gene regulation^[26,36,37]. The results from many papers established a link between DNA methylation, histone acetylation and sequence-specific DNA binding activity. In general, CpG island chromatin was found to contain highly acetylated histone H3 and H4. Deacetylation of histone H3 and H4 by the HDACs presumably leads to the formation of a chromatin environment that inhibits transcription^[38]. Hypoacetylated, transcriptionally silenced regions are often methylated^[39]. Furthermore, methylated DNA is

transcriptionally repressed, but only under conditions in which the methylated template is assembled into nucleosomal structures^[40], methylation density defines the level of histone acetylation^[41]. There are the roles of MeCP2, MBD1, MBD2, and MBD3^[35], NuRD (nucleosome-remodeling histone deacetylase)^[42,43] and DNMT1^[44], as well as DNMT1^[44,45] in the linkage of methylation with acetylation.

METHYLATION AND TRANSCRIPTION EXPRESSION OF p21^{WAF1} GENE

Usually, one could propose the negative regulation of p21^{WAF1} on the binding of DNMT1 with PCNA in normal cells^[46], however the loss of p21^{WAF1} from PCNA complexes could cause abnormal gains of methylation during repair of DNA damage^[47]. Moreover, the p21^{WAF1} gene transcription level is regulated by methylation, due to that p21^{WAF1} promoter contains high density of potentially methylatable CpG dinucleotides clustered around the initiation site of transcription (Figure 1).

CpG island
-243

```
CGAGGGACTGGGGAGGAGGGAAGTGCCTCTGCAGCACGCGAGGTTCCGGGACCCGGCTGGCCTGCTGGA
ACTCGGCCAGGCTCAGCTGCTCCGCGCTGGGCAGCCAGGAGCCTGGGC CCCGGGGAGGGCGGTC CCGGG
CGGCGCGGTGGGCCGAGCGCGGGTCCCTCTCTTGAGGCGGGCCCGGGCGGGGCGGTTGTATATCAGGGCCG
CGCTGAGCTGCGCCAGCTGAGGTGTGACAGCT G
-1 | +1
```

Figure 1 There are more CpG island at the domain near by the transcription start site in the promoter of p21^{WAF1} gene.

Dr. Nass *et al.*^[48] transfected three antisense DNMT1 (pCMV TMH) into human breast cancer MDA231 cell line, and found that the reduced DNMT1 protein and up-regulation of p21^{WAF1} suggesting that DNMT protein levels were inversely correlated with the level of p21^{WAF1} in breast cancer cells.

To date, almost no coding region p21^{WAF1} mutations have been found in tumor cells, despite extensive screening of hundreds of various tumors^[49-51]. Hypermethylation of the p21^{WAF1} promoter region may represent an alternative mechanism by which the p21^{WAF1/CIP1} gene can be inactivated. DNMT and p21^{WAF1} compete for the same binding site on PCNA, an increase in DNMT expression might promote dissociation of p21^{WAF1} from PCNA, perhaps making p21^{WAF1} more susceptible to ubiquitination and proteasome degradation^[52]. A decrease in DNMT expression would then be expected to have an opposite effect on p21^{WAF1} stability^[48]. 5-Azacytidine (5-Aza-C, a demethylating agent) mediated Sp1 expression also up-regulated activities p21^{WAF1}^[53].

Rat-1 is a cell line containing wild-type p53^[54]. Allan and co-workers found which p21^{WAF1} 5'UTR contains a putative CpG island which is methylated in Rat-1 cells that used frequently to assess transformation and for apoptosis studies, the lack of p21^{WAF1} expression appears to be the result of hypermethylation of the p21^{WAF1} promoter region, as p21^{WAF1} protein expression could be induced by growth of Rat-1 cells in the presence of 5-aza-2-deoxycytidine (5-Aza-dC). Furthermore, sequencing analysis of bisulfite-treated DNA demonstrated extensive methylation of cytosine residues in CpG dinucleotides in a CpG-rich island in the promoter region of the p21^{WAF1} gene^[55]. A report showed that altered DNA methylation was present in RMS tumors and that the DNA methyltransferase expression is increased in both embryonal and alveolar subtypes of this cancer^[56,57]. They think that hypermethylation of the p21^{WAF1} gene at the proximal STAT-binding site, correlates with decreased p21^{WAF1} expression. The p21^{WAF1} gene is subjected to methylation regulation at the transcription level and is a target of aberrant methylation in RMS cells.

However, several studies indicated that the hypermethylation of

p21^{WAF1} was not the main machineries of p21^{WAF1} expression regulation. Although Young *et al.*^[58] reported that cells arrested and p21^{WAF1} expressed by DNMT inhibition in normal human fibroblasts. Milutinovic demonstrated that inhibition of DNMT resulted in the rapid induction of the known tumor suppressor and cell cycle regulator p21^{WAF1} by a mechanism that did not involve DNA methylation of the p21^{WAF1} promoter, in human non-small cell lung cancer cell line, A549 cells^[59]. The reduction of cellular DNMT protein levels also induced a corresponding rapid increase in the cell cycle regulator p21^{WAF1} protein demonstrating a regulatory link between DNMT and p21^{WAF1} which was independent of methylation of DNA^[60]. Shin's result showed that the promoter of the p21^{WAF1} gene was not been methylated in gastric cancer cells. This confirmed that methylation was not the mechanism for inactivation of p21^{WAF1} in gastric cancer cells^[20]. In adenomatoid polyps, although DNMT1 expression coincided with the expression of other cell proliferation markers, many DNMT1-expressing cells also expressed p21^{WAF1}. The fidelity of DNMT1 expression was further undetermined in colorectal carcinomas, in which a striking heterogeneity in DNMT1 expression, with some carcinoma cells containing very high DNMT1 levels and others containing very low DNMT1. These results indicate that human colorectal carcinogenesis is accompanied by a progressive dysregulation of DNMT1 expression and suggest that abnormalities in DNMT1 expression may contribute to the abnormal CpG dinucleotide methylation which changes the characteristic of human colorectal carcinoma cell DNA^[61].

HYPERACETYLATION, HDAC INHIBITORS AND OVEREXPRESSION OF p21^{WAF1} GENE

Histone deacetylation is a general mechanism for inactivation of the p21^{WAF1} in gastric cancer cell lines^[20]. Both histone hyperacetylation and hypoacetylation appear to be important in the carcinoma process, and induction of the p21^{WAF1} gene by histone hyperacetylation may be a mechanism by which dietary fiber prevents carcinogenesis^[31].

Regarding the correlation of histone acetylation and p21^{WAF1} gene

expression, that HDAC inhibitor TSA, trapoxin, butyrate and apicidin induce p21^{WAF1} transcriptional activity involved in most studies.

TSA is originally reported to be a fungistatic antibiotic, and it appears to be a promising tool for analyzing the many functions of histone hyperacetylation in cell proliferation and differentiation. TSA can stimulate p21^{WAF1} expression in HT29 cells^[32].

TPX is the microbially derived cyclotetrapeptide^[62], Sambucetti found that it increased the level of chromatin acetylation associated with histone H3 in the trapoxin-responsive region of the p21^{WAF1} promoter, and it activated p21^{WAF1} transcription that led to elevated p21^{WAF1} protein levels in three kinds of human tumor cells. Since the domain of the promoter that is necessary for TPX-mediated activation does not contain p53 binding sites, hence p21^{WAF1} expression upregulation by TPX is independent of p53^[30].

Sodium butyrate is a short chain fatty acid produced in the human colon by bacterial fermentation of carbohydrates^[32], causes hyperacetylation of histone through the inhibition of HDAC. Three years ago, Archer and his coworkers showed firstly the critical importance of p21^{WAF1} in butyrate-mediated growth arrest was able to cause growth arrest in the human colon cancer cell line HT-29^[31]. Siavoshian^[32] suggested that butyrate and TSA stimulated, the p21^{WAF1} expression both at the mRNA and protein levels, whereas they induced histone H4 hyperacetylation. Butyrate sensitivity requires Sp1-3 site in conjunction with the Sp1-5 site and Sp1-6^[29]. Shin *et al*^[20] indicated that the overexpression of p21^{WAF1} gene occurred in human gastric cancer cell lines after butyrate treatment. Butyrate increased histone H4-acetylation in human melanoma cell lines A375 and S91 and up-regulated p21^{WAF1} gene transcription level^[63].

Apicidin is a fungal metabolite shown to exhibit antiparasitic activity by inhibition of HDAC. Han *et al*^[64] indicated that inhibition of HDAC activity by apicidin was closely associated with morphological change and induction of p21^{WAF1}, although the protein levels of cyclin D1, CDK2, HDAC1 and p53 were not affected by the addition of apicidin for 24 hrs, whereas the induction of p21^{WAF1} by apicidin was reversible.

Suberoylanilide hydroxamic acid (SAHA) is a hydroxamic acid-based hybrid polar compound, and it is an inhibitor of HDAC^[65,66]. SAHA causes an accumulation of acetylated histones H3 and H4 in total cellular chromatin by 2h, which is maintained throughout 24h of culture with increased p21^{WAF1} expression, but no change in chromatin associated with the actin and p27 genes, and SAHA also induces up to a 9-fold increase in p21^{WAF1} mRNA and protein in T24 bladder carcinoma cells. p21^{WAF1} by SAHA is regulated, at least in part, by the degree of acetylation of the gene-associated histones and that this induced increase in acetylation is gene selective^[66]. These studies also suggest that p21^{WAF1} is HDAC inhibitor and that the p21^{WAF1} promoter is a useful model for study in histone acetylation regulated transcription.

In addition, MS-27-275 inhibits HDAC and causes hyperacetylation of histones, as well as induces the expression of p21^{WAF1} various tumor cell lines^[33].

The data above indicated that the induction of histone hyperacetylation by HDAC inhibitor is responsible for the antiproliferative activity through the crucial role of p21^{WAF1} in the regulation of cell cycle.

PATHWAY OR FACTORS ASSOCIATED TO ACETYLATION OF p21^{WAF1}

Several genes or transcriptional regulatory proteins including p300/CBP associate to p21^{WAF1} gene regulation.

p53

The p21^{WAF1} expression may be dependent^[11,67] or independent of p53 regulation^[68-70]. Also, the mechanisms of p21^{WAF1} transcription

regulation fall into two general categories: dependent or independent of the p53 gene^[31]. The p21^{WAF1} promoter contains five natural p53 binding sites, at positions 4001, 3764, 2311, 2276, and 1391, respectively (GenBank accession number U24170)^[19].

p53 gene regulates the expression of p21^{WAF1}, and HDAC1,2, and 3 are all capable of downregulating p53 function, i.e., interactions of p53 and HDAC2 likely result in p53 deacetylation, thereby reducing its transcriptional activity^[71]. Clark and co-workers found that loss of the G1/S checkpoint in HIV-1-infected cells may in part be due to Tat's ability to bind p53 and sequester its transactivation activity, as seen in both in vivo and in vitro transcription assays^[72].

p21^{WAF1} overexpression has been seen to inhibit two critical checkpoints in the cell cycle, G1 and G2, through both p53-dependent and -independent^[74].

p300/CBP

Up to now, four families of nuclear proteins including p300/CBP and p300/CBP-associated cofactors contain an intrinsic HAT activity have been confirmed that possess HAT activity^[74-78]. Accumulating evidences suggest that p300 and CBP are adaptors for various DNA-binding transcription factors^[79]. Although the precise mechanism by which p300/CBP stimulates transcription remains unclear, the discovery that p300/CBP and an associated factor P/CAF have histone acetylase activities suggests that these cofactors may regulate transcription through acetylation^[80]. These activities have been proposed to modify the amino-terminal tails of the core histone proteins in a manner that may allow for some as yet uncharacterized modification of nucleosome structure.

p300 has been found to be required for induction of p21^{WAF1} expression in keratinocyte differentiation^[70]. Xiao and coworkers indicated the evidences that p300 is required for TSA-induced, Sp1-mediated p21^{WAF1} transcription: cotransfection of p300 elevated p21^{WAF1} promoter activity, and this elevation was dependent on TSA-responsive GC-box; TSA-induced promoter activation was blocked by the introduction of p300 dominant-negative mutant into cells; Sp1- or Sp3-mediated activation was also suppressed by this p300 dominant-negative mutant^[28]. Owen *et al*^[81] demonstrated the progesterone regulated transcription of the p21^{WAF1} gene through Sp1 and CBP/p300. A report^[82] showed that p21^{WAF1} stimulated trans-activation by p300/CBP, p21^{WAF1} induction of p300 results from the activity of a discrete domain in the amino-terminal half of the protein which functioned to repress transcription. they proposed a model in which p300/CBP activity might switched between promoters following p21^{WAF1} induced cell cycle arrest.

P/CAF and GCN5

Two human homologs of GCN5 have been cloned and shown to have HAT activity^[83,84]. One homolog is human p300/CBP associated factor (hP/CAF), which is a transcriptional co-activator with intrinsic histone acetylase activity, which contributes to transcriptional activation by modifying chromatin and transcriptional factors^[84,95]. The second family member is hGCN5^[85,86]. The ability of hGCN5 to acetylate nucleosomal histones is significantly reduced relative to its activity on free histones, where it predominantly modifies histone H3 at lysine 14.

The co-activator/adaptor protein GCN5 is a conserved histone acetyltransferase, which functions as the catalytic subunit in multiple yeast transcriptional regulatory complexes.

E2A

E2A gene encodes two alternatively spliced products, E12 and E47^[87,88]. The p21^{WAF1} promoter contains eight putative E-box consensus sequences, two of which lie between the TATA box and the transcription starting site, E2 and E1 (as Figure 2). E1 binds E47 hetero- and homodimers and E2 has much less affinity for E47^[89], and

TATA box E Boxes

TATATCAGGGCCG

CGCTGAGCTGCGCCCAGCTGAGGTGTGAGCAGCTGCCGAAGTCAGT

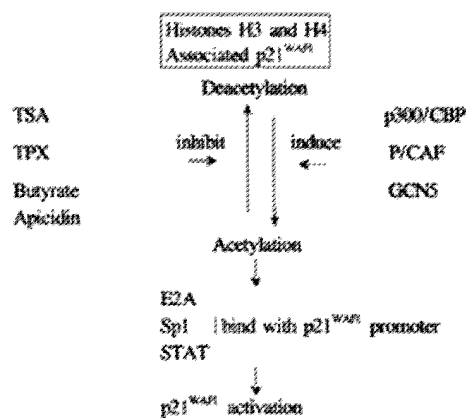
E2 E1 | →+1

The E3 box located 130 bp upstream from the TATA box also contributes to the activation of p21^{WAF1} expression, but the E4 to E8 boxes have no effect on p21^{WAF1} expression^[89]. E2A is shown to be upregulated in HTLV-1 in infected T cells.

The GC-rich region in the six consecutive Sp1 binding sites of the p21^{WAF1} promoter was digested either with methylation-sensitive HpaII or with methylation-insensitive MspI. The resulting DNA was subjected to a PCR reaction. Sp1 binding sites are the common elements that exist in the promoters of both genes^[20]. Using transient reporter gene assays, Pagliuca et al^[94] determined that Sp1 was a strong activator of p21^{WAF1} promoter, whereas Sp3 functioned as a weak transactivator.

In addition to its role in cell cycle regulation, p21^{WAF1} is also believed to inhibit DNA replication through its ability to bind proliferating cell nuclear antigen (PCNA), which is required for both replicative DNA synthesis and DNA repair. However, p21^{WAF1} has no inhibitory effect on the DNA repair function of PCNA^[100,101]. Thus, p21^{WAF1} may play a central role in preventing the replication of mutations incurred after exposure of cells to DNA damage.

Histone acetylation is the major mechanism for regulation of the p21^{WAF1} gene in most cell lines (shown as Figure 3). Both histone hyperacetylation and hypoacetylation appear to be important in the carcinoma process. The influence of methylation on p21^{WAF1} gene expression is dependent on differentiation of cells and tissue. It is our anticipation that induction of the p21^{WAF1} gene by histone hyperacetylation may become a mechanism of dietary prevention of carcinogenesis.



- 1 Norbury C, Nurse P. Animal cell cycles and their control. *Ann Rev Biochem* 1992; 61: 441-470
- 2 Marx J. How cells cycle toward cancer. *Science* 1994; 263: 319-321
- 3 Elledge SJ, Winston J, Harper JW. A question of balance: the role of cyclin-kinase inhibitors in development and tumorigenesis. *Trends Cell Biol* 1996; 6: 388-392
- 4 Sherr CJ, Roberts JM. Inhibitors of mammalian G1 cyclin-dependent kinase. *Genes Dev* 1995; 9: 1149-1163
- 5 Hall M, Bates S, Peters G. Evidence for different mode of action of cyclin-dependent kinase inhibitors: p15 and p16 bind to kinase, p21 and p27 bind to cyclins. *Oncogene* 1995; 11: 1581-1588
- 6 Chen J, Saha P, Kornbluth S, Dynlacht BD, Dutta A. Cyclin-binding motifs are essential for the function of p21CIP1. *Mol Cell Biol* 1996; 16:

- 4673-4682
- 7 Matsuoka S, Edwards MC, Bai C, Parker S, Zhang P, Baldini A, Harper JW, Elledge SJ. p57KIP2, a structurally distinct member of the p21CIP1 Cdk inhibitor family, is a candidate tumor suppressor gene. *Genes Dev* 1995; 9: 650-662
 - 8 Polyak K, Lee MH, Erdjument-Bromage H, Koff A, Roberts JM, Tempst P, Massague J. Cloning of p27Kip1, a cyclin-dependent kinase inhibitor and potential mediator of extracellular antimitogenic signals. *Cell* 1994; 78: 59-66
 - 9 Kim JS, Lee S, Lee T, Lee YW, Trepel JB. Transcriptional activation of p21^{WAF1/CIP1} by apicidin, a novel histone deacetylase inhibitor. *Biochem Biophys Res Comm* 2001; 281: 866-871
 - 10 Gu Y, Turck CW, Morgan DO. Inhibition of CDK2 activity *in vivo* by an associated 20 Kregulatory subunit. *Nature* 1993; 366: 707-710
 - 11 el-Deiry WS, Tokino T, Velculescu VE, Levy DB, Parson R, Trent JM, Li n D, Mercer WE, Kinzler KW, Vogelstein B. WAF1, a potential mediator of p53 tumor suppression. *Cell* 1993; 75: 817-825
 - 12 Prowse DM, Bolgan L, Molnar A, Dotto GP. Involvement of the Sp3 transcription factor in induction of p21Cip1/WAF1 in keratinocyte differentiation. *J Biol Chem* 1997; 272: 1308-1314
 - 13 Schwaller J, Koeffler HP, Niklaus G, Loetscher P, Nagel S, Fey MF, Tobler A. Posttranscriptional stabilization underlies p53-independent induction of p21^{WAF1/CIP1/SDI1} in differentiating human leukemic cells. *J Clin Invest* 1995; 95: 973-979
 - 14 Esposito F, Cuccovillo F, Vanoni M, Cimino F, Anderson CW, Appella E, Russo T. Redox-mediated regulation of p21(waf1/cip1) expression involves a post-transcriptional mechanism and activation of the mitogen-activated protein kinase pathway. *Eur J Biochem* 1997; 245: 730-737
 - 15 Stander M, Naumann U, Wick W, Weller M. Transforming growth factor-(and p21: multiple molecular targets of decorin-mediated suppression of neoplastic growth. *Cell Tissue Res* 1999; 296: 221-227
 - 16 Wang LG, Liu XM, Kreis W, Budman DR. The effect of antimicrotubule agents on signal transduction pathways of apoptosis: a review. *Cancer Chemother Pharmacol* 1999; 44: 355-361
 - 17 Datto MB, Yu Y, Wang XF. Functional analysis of the transforming growth factor beta responsive elements in the WAF1/Cip1/p21 promoter. *J Biol Chem* 1995; 270: 28623-28628
 - 18 Parker SF, Perkins ND, Gitlin SD, Nabel GJ. A cooperative interaction of human T-cell leukemia virus type 1 Tax with the p21 cyclin-dependent kinase inhibitor activates the human immunodeficiency virus type 1 enhancer. *J Virol* 1996; 70: 5731-5734
 - 19 de la Fuente C, Santiago F, Chong SY, Deng L, Mayhoo T, Fu P, Stein D, Denny T, Coffman F, Azimi N, Mahieux R, Kashanchi F. Overexpression of p21^{WAF1} in Human T-Cell Lymphotropic Virus Type 1-Infected Cells and Its Association with Cyclin A/cdk2. *J Virol* 2000; 74: 7270-7283
 - 20 Shin JY, Kim HS, Park J, Park JB, Lee JY. Mechanism for Inactivation of the KIP Family Cyclin-dependent Kinase Inhibitor Genes in Gastric Cancer Cells. *Cancer Res* 2000; 60: 262-265
 - 21 Strahl BD, Allis CD. The language of covalent histone modifications. *Nature* 2000; 403: 41-45
 - 22 Adams RL, McKay EL, Craig LM, Burdon RH. Mouse DNA methylase: methylation of native DNA. *Biochem. Biophys Acta* 1979; 561: 345-357
 - 23 Yeivin A, Razin A. Gene methylation patterns and expression. *EXS* 1993; 64: 523-568
 - 24 Baylin SB, Herman JG, Graff JR, Vertino PM, Issa JP. Alterations in DNA methylation: a fundamental aspect of neoplasia. *Adv Cancer Res* 1998; 72: 141-196
 - 25 Gu W, Roeder RG. Activation of p53 sequence-specific DNA binding by acetylation of the p53 C-terminal domain. *Cell* 1997; 90: 595-606
 - 26 Struhl K. Histone acetylation and transcriptional regulatory mechanism. *Genes Dev* 1998; 12: 599-606
 - 27 Taunton J, Hassig CA, Schreiber SL. A mammalian histone deacetylase related to the yeast transcriptional regulator Rpd3p. *Science* 1996; 272: 408-411
 - 28 Xiao H, Hasegawa T, Isobe K. p300 collaborates with Sp1 and Sp3 in p21^{WAF1/CIP1} promoter activation induced by histone deacetylase inhibitor. *J Biol Chem* 2000; 275: 1371-1376
 - 29 Xiao H, Hasegawa T, Isobe K. Both sp1 and sp3 are responsible for p21waf1 promoter activity induced by histone deacetylase inhibitor in H1H3t3 cells. *J Cell Biochem* 1999; 73: 291-302
 - 30 Sambucetti LC, Fischer DD, Zabudoff S, Kwon PO, Chamberlin H, Trogani N, Xu H, Cohen D. Histone deacetylase inhibition selectively alters the activity and expression of cell cycle proteins leading to specific chromatin acetylation and antiproliferative effects. *J Biol Chem* 1999; 274: 34940-34947
 - 31 Archer SY, Hodin RA. Histone acetylation and cancer. *Current Opin*
 - 32 Siavoshian S, Segain JP, Kornprobst M, Bonnet C, Cherbut C, Galmiche JP, Blottiere HM. Butyrate and trichostatin A effects on the proliferation/differentiation of human intestinal epithelial cells: induction of cyclin D3 and p21 expression. *Gut* 2000; 46: 507-514
 - 33 Saito A, Yamashita T, Mariko Y, Nosaka Y, Tsuchiya K, Ando T, Suzuki T, Tsuruo T, Nakanishi O. A synthetic inhibitor of histone deacetylase, MS-27-2 75, with marked *in vivo* antitumor activity against human tumors. *Proc Natl Acad Sci U S A* 1999; 96: 4592-4597
 - 34 Vettese-Dadey M, Grant PA, Hebbes TR, Crane- Robinson C, Allis CD, Workman JL. Acetylation of histone H4 plays a primary role in enhancing transcription factor binding to nucleosomal DNA *in vitro*. *EMBO J* 1996; 15: 2508-2518
 - 35 Bird AP, Wolffe AP. Methylation-induced repression-belts, braces, and chromatin. *Cell* 1999; 99: 451-454
 - 36 Wade PA, Wolffe AP. Histone acetyltransferases in control. *Curr Biol* 1997; 7: R82-R84
 - 37 Workman JL, Kingston RE. Alteration of nucleosome structure as a mechanism of transcriptional regulation. *Annu Rev Biochem* 1998; 67: 545-579
 - 38 Ng HH, Zhang Y, Hendrick B, Johnson CA, Turner BM, Erdjument-Bromage H, Tempst P, Reinberg D, Bird A. MBD2 is a transcriptional repressor belonging to the MeCP1 histone deacetylase complex. *Nat Genet* 1999; 23: 58-61
 - 39 Jeppesen P, Turner BM. The inactive X chromosome in female mammals is distinguished by a lack of histone H4 acetylation, a cytogenetic marker for gene expression. *Cell* 1993; 74: 281-289
 - 40 Kass SU, Landsberger N, Wolffe AP. DNA methylation directs a time-dependent repression of transcription initiation. *Curr Biol* 1997; 7: 157-165
 - 41 Schubeler D, Lorincz MC, Cimbor DM, Telling A, Feng YQ, Bouhassira EE, Groudine M. Genomic targeting of methylated DNA: influence of methylation on transcription, replication, chromatin structure, and histone acetylation. *Mol Cell Biol* 2000; 20: 9103-9112
 - 42 Zhang Y, Ng HH, Erdjument-Bromage H, Tempst P, Bird A, Reinberg D. An analysis of the NuRD subunits reveals a histone deacetylase core complex and a connection with DNA methylation. *Genes Devel* 1999; 13: 1924-1935
 - 43 Wade PA, Geggion A, Jones PL, Ballestar E, Aubry F, Wolffe AP. Mi-2 complex couples DNA methylation to chromatin remodeling and histone deacetylation. *Nat Genet* 1999; 23: 62-66
 - 44 Rountree MR, Bachman KE, Baylin SB. DNMT1 binds HDAC2 and a new co-repressor, DMAP1, to form a complex at replication foci. *Nat Genet* 2000; 25: 269-276
 - 45 Fuks F, Burgers WA, Brehm A, Hughes-Davies L, Kouzarides T. DNA methyltransferase DNMT1 associates with histone deacetylase activity. *Nat Genet* 2000; 24: 88-91
 - 46 Baylin SB. Tying it all together: epigenetics, genetics, cell cycle, and cancer. *Science* 1997; 277: 1948-1949
 - 47 Chuang LS, Ian HI, Koh TW, Ng HH, Xu G, Li BFL. Human DNA-(Cytosine-5) methyltransferase-PCNA complex as a target for p21^{WAF1}. *Science* 1997; 277: 1996-2000
 - 48 Nass SJ, Ferguson AT, El-Ashry D, Nelson WG, Davidson NE. Expression of DNA methyltransferase (DMT) and the cell cycle in human breast cancer cells. *Oncogene* 1999; 18: 7453-7461
 - 49 Balbin M, Hannon GJ, Pendas AM, Ferrando AA, Vizoso F, Fueyo A, Lopez-Otin C. Functional analysis of a p21^{WAF1}, CIP1, SDI1 mutant (Arg94Trp) identified in a human breast carcinoma. Evidence that the mutation impairs the ability of p21 to inhibit cyclin-dependent kinases. *J Biol Chem* 1996; 271: 15782-15786
 - 50 Malkowicz SB, Tomaszewski JE, Linnenbach AJ, Cangiano TA, Maruta Y, McGarvey TW. Novel p21^{WAF1/CIP1} mutations in superficial and invasive transitional cell carcinomas. *Oncogene* 1996; 13: 1831-1837
 - 51 Shiohara M, el-Deiry WS, Wada M, Nakamaki T, Takeuchi S, Yang R, Chen DL, Vogelstein B, Koeffler HP. Absence of WAF1 mutations in a variety of human malignancies. *Blood* 1994; 84: 3781-3784
 - 52 Maki CG, Howley PM. Ubiquitination of p53 and p21 is differentially affected by ionizing and UV radiation. *Mol Cell Biol* 1997; 17: 355-363
 - 53 Periyasamy S, Ammanamanchi S, Tillekeratne MP, Brattain MG. Repression of transforming growth factor-beta receptor type I promoter expression by Sp1 deficiency. *Oncogene* 2000; 19: 4660-4667
 - 54 Ling CC, Guo M, Chen CH, Deloherey T. Radiation-induced apoptosis: effects of cell age and dose fractionation. *Cancer Res* 1995; 55: 5207-5212
 - 55 Allan LA, Duhig T, Read M, Fried M. The p21^{WAF1/CIP1} Promoter Is Methylated in Rat-1 Cells: Stable Restoration of p53-Dependent p21^{WAF1/CIP1} Expression after Transfection of a Genomic Clone Containing the p21^{WAF1/CIP1} Gene. *Mol Cell Biol* 2000; 20: 1291-1298

- 56 Chen B, He L, Savell VH, Jenkins JJ, Parham DM. Inhibition of the interferon- γ /signal transducers and activators of transcription (STAT) pathway by hypermethylation at a STAT-binding site in the p21^{WAF1} promoter region. *Cancer Res* 2000; 60: 3290-3298
- 57 Chen B, Liu X, Savell VH, Dilday BR, Johnson MW, Jenkins JJ, Parham DM. Increased DNA methyltransferase expression in rhabdomyosarcomas. *Int J Cancer* 1999; 83: 10-140
- 58 Young JJ, Smith JR. DNA methyltransferase inhibition in normal human fibroblasts induces a p21-dependent cell cycle withdrawal. *J Biol Chem* 2001; 276: 19610-19616
- 59 Milutinovic S, Knox JD, Szyf M. DNA methyltransferase inhibition induces the transcription of the tumor suppressor p21^{WAF1/CIP1}/sdi1. *J Biol Chem* 2000; 275: 6353-6359
- 60 Fournel M, Sapieha P, Beaulieu N, Besterman JM, MacLeod AR. Down-regulation of human DNA-(cytosine-5) methyltransferase induces cell cycle regulation p16ink4A and p21^{WAF1}/Cip1 by distinct mechanisms. *J Biol Chem* 1999; 274: 24250-24256
- 61 De Marzo AM, Marchi VL, Yang ES, Veeraswamy R, Lin X, Nelson WG. Abnormal Regulation of DNA Methyltransferase Expression during Colorectal Carcinogenesis. *Cancer Res* 1999; 59: 3855-3860
- 62 Itazaki H, Nagashima K, Sugita K, Yoshida H, Kawamura Y, Yasuda Y. Isolation and structural elucidation of new cyclotetrapeptides, trapoxins A and B, having detransformation activities as antitumor agents. *J Antibiot* 1990; 12: 1524-1532
- 63 Demary K, Wong L, Spanjaard RA. Effects of retinoic acid and sodium butyrate on gene expression, histone acetylation and inhibitor of proliferation of melanoma cells. *Cancer Lett* 2001; 163:103-107
- 64 Han JW, Ahn SH, Park SH, Wang YS, Bae GU, Seo DW, Kwon HK, Hong S, Lee HY, Lee YW, Lee HW. Apicidin, a Histone deacetylase inhibitor, inhibits proliferation of tumor cells via induction of p21^{WAF1}/Cip1 and Gelsolin. *Cancer Res* 2000;60:6068-6074
- 65 DiGiuseppe JA, Weng LJ, Yu KH, Fu S, Kastan MB, Samid D, Gore SD. Phenylbutyrate-induced G1 arrest and apoptosis in myeloid leukemia cells: structure-function analysis. *Leukemia* 1999; 13: 1243-1253
- 66 Richon VM, Sandhoff TW, Rifkind RA, Marks PA. Histone deacetylase inhibitor selectively induces p21^{WAF1} expression and gene-associated histone acetylation. *Proc Natl Acad Sci U S A* 2000; 97:10014-10019
- 67 el-Deiry WS, Tokino T, Waldman T, Oliner JD, Velculescu VE, Burrell M, Hill DE, Healy E, Rees JL, Hamilton SR. Topological control of p21^{WAF1/CIP1} expression in normal and neoplastic tissues. *Cancer Res* 1995; 55: 2910-2919
- 68 Halevy O, Novitch BG, Spicer DB, Skapek SX, Rhee J, Hannon GJ, Beach D, Lassar ABL. Correlation of terminal cell cycle arrest of skeletal muscle with induction of p21 by MyoD. *Science* 1995; 267: 1018-1021
- 69 Parker SB, Eichele G, Zhang P, Rawla A, Sands AT, Bradley A, Olson EN, Harper JW, Elledge SJ. p53-independent expression of p21Cip1 in muscle and other terminally differentiating cells. *Science* 1995; 67: 1024-1027
- 70 Missero C, Calautti E, Eckner R, Chin J, Tsai LH, Livingston DM, Dotto GP. Involvement of the cell-cycle inhibitor Cip1/WAF1 and the E1A-associated p300 protein in terminal differentiation. *Proc Natl Acad Sci U S A* 1995; 92: 5451-5455
- 71 Juan LJ, Shia WJ, Chen MH, Yang WM, Seto E, Lin YS, Wu CW. Histone deacetylases specifically down-regulate p53-dependent gene activation. *J Biol Chem* 2000; 275: 20436-20443
- 72 Clark E, Santiago F, Deng L, Chong S, de la Fuente C, Wang L, Fu P, Stein D, Denny T, Lanka V, Mozafari F, Okamoto T, Kashanchi F. Loss of G1/S Checkpoint in Human Immunodeficiency Virus Type 1-Infected Cells Is Associated with a Lack of Cyclin-Dependent Kinase Inhibitor p21/Waf1. *J Virol* 2000; 74: 5040-5052
- 73 Macleod KF, Sherry N, Hannon G, Beach D, Tokino T, Kinzler K, Vogelstein B, Jacks T. p53-dependent and independent expression of p21 during cells growth, differentiation, and DNA damage. *Genes Dev* 1995; 9: 935-944
- 74 Bannister AJ, Kouzarides T. The CBP (CREB binding protein) coactivator is a histone acetyltransferase. *Nature* 1996; 384: 641-643
- 75 Parekh BS, Maniatis T. Virus infection leads to localized hyperacetylation of histones H3 and H4 at the IFN- γ promoter. *Mol Cell* 1999; 3: 125-129
- 76 Torchia J, Rose DW, Inostroza J, Kamei Y, Westin S, Glass CK, Rosenfeld MG. The transcriptional co-activator p/CIP binds CBP and mediates nuclear receptor function. *Nature* 1997; 387: 677-684
- 77 Yang X, Herrmann CH, Rice AP. The human immunodeficiency virus Tat proteins specifically associate with TAK in vivo and require the carboxy-terminal domain of RNA polymerase II for function. *J Virol* 1996; 70: 4576-4584
- 78 Ogryzko VV, Schiltz RL, Russanova V, Howard BH, Nakatani Y. The transcriptional coactivators p300 and CBP are histone acetyltransferases. *Cell* 1996; 87: 953-959
- 79 Janknecht R, Hunter T. Transcription. A growing coactivator network. *Nature* 1996; 383: 22-23
- 80 Martinez-Balbas MA, Bauer UM, Nielsen SJ, Brehm A, Kouzarides T. Regulation of E2F1 activity by acetylation. *EMBO J* 2000; 19: 662-671
- 81 Owen GI, Richer JK, Tung L, Takimoto G, Horwitz. Progesterone regulates transcription of the p21^{WAF1} cyclin-dependent kinase inhibitor gene through Sp1 and CBP/p300. *J Biol Chem* 1998; 273: 10696-10701
- 82 Snowden AW, Anderson LA, Webster GA, Perkins ND. A novel transcriptional repression domain mediates p21^{WAF1/CIP1} induction of p300 transactivation. *Mol Cell Biol* 2000; 20: 2676-2686
- 83 Candau R, Moore PA, Wang L, Barlev N, Ying CY, Rosen CA, Berger SL. Identification of human proteins functionally conserved with the yeast putative adaptor ADA2 and GCN5. *Mol Cell Biol* 1996; 16: 593-602
- 84 Yang XJ, Ogryzko VV, Nishikawa J, Howard BH, Nakatani Y. A p300/CBP-associated factor that competes with the adenoviral oncoprotein E1A. *Nature* 1996; 382: 319-324
- 85 Schiltz RL, Nakatani Y. The PCAF acetylase complex as a potential tumor suppressor. *Biochim. Biophys. Acta* 2000; 1470: M37-M53
- 86 Smith ER, Belote JM, Schiltz RL, Yang XJ, Moore PA, Berger SL, Nakatani Y, Allis CD. Cloning of Drosophila GCN5: conserved features among metazoan GCN5 family members. *Nucleic Acids Res* 1998;26:2948-2954
- 87 Mahajan MA, Park ST, Sun XH. Association of a novel GTP-binding protein, DRG, with TAL oncogenic proteins. *Oncogene* 1996; 12: 2343-2350
- 88 Peverali FA, Ramqvist T, Saffrich R, Pepperkok R, Barone MV, Phillipson L. Regulation of G1 progression of E2A and Id helix-loop-helix proteins. *EMBO J* 1994; 13: 4291-4301
- 89 Prabhu S, Ignatova A, Park ST, Sun XH. Regulation of the expression of cyclin-dependent kinase inhibitor p21 by E2A and Id proteins. *Mol Cell Biol* 1997; 17: 5888-5896
- 90 Murre C, McCaw PS, Baltimore D. A new DNA binding and dimerization motif in immunoglobulin enhancer binding, daughterless, MyoD and myc proteins. *Cell* 1989; 56: 777-783
- 91 Lania L, Majello B, De Luca P. Transcriptional regulation of the Sp family proteins. *Int J Biochem Cell Biol* 1997; 29: 1313-1323
- 92 Birnbaum MJ, van Wijnen AJ, Odgren PR, Last TJ, Suske G, Stein GS, Stein JL. Sp1 transactivation of cell cycle regulated promoters is selectively repressed by Sp3. *Biochem* 1995; 34: 16503-16508
- 93 Brandeis M, Frank D, Keshet I, Siegfried Z, Medelsohn M, Nemes A, Tempel V, Razin A, Cedar H. Sp1 elements protect a CpG island from de novo methylation. *Nature* 1994; 371: 435-438
- 94 Pagliuca A, Gallo P, Lania L. Differential role for Sp1/Sp3 transcription factors in the regulation of the promoter activity of multiple cyclin-dependent kinase inhibitor genes. *J Cell Biochem* 2000; 76: 360-367
- 95 Periyasamy S, Ammanamanchi S, Tillekeratne MP, Brattain MG. Repression of transforming growth factor-beta receptor type I promoter expression by Sp1 deficiency. *Oncogene* 2000;19:4660-4667
- 96 Hagen G, Muller S, Beato M, Suske G. Cloning by recognition site screening of two novel GT box binding proteins: A family of Sp1 related genes. *Nuclear Acids Res* 1992; 20: 5519-5525
- 97 Horvath CM, Wen Z, Darnell JE Jr. A STAT protein domain that determines DNA sequence recognition suggests a novel DNA-binding domain. *Genes Dev* 1995; 9: 984-994
- 98 Chin YE, Kitagawa M, Su WC, You ZH, Iwamoto Y, Fu XY. Cell growth arrest and induction of cyclin-dependent kinase inhibitor p21 WAF1/CIP1 mediated by STAT1. *Science* 1996; 272: 719-722
- 99 Darnell JE, Jr. STATs and gene regulation. *Science* 1997; 277: 1630-1635
- 100 Li R, Waga S, Hannon GJ, Beach D, Stillman B. Differential effects by the p21 CDK inhibitor on PCNA-dependent DNA replication and repair. *Nature* 1994; 371: 534-537
- 101 Waga S, Hannon GJ, Beach D, Stillman B. The p21 inhibitor of cyclin-dependent kinases controls DNA replication by interaction with PCNA. *Nature* 1994; 369: 574-578

Edited by Wu XN

• REVIEW •

Influencing factors of pancreatic microcirculatory impairment in acute pancreatitis

Zong-Guang Zhou, You-Dai Chen

Zong-Guang Zhou, You-Dai Chen, Department of Hepato-bilio-pancreatic Surgery & Institute of Microcirculation, West China Hospital, Sichuan University, Chengdu 610041, Sichuan Province, China

Correspondence to: Dr. Zong-Guang Zhou, Department of Hepato-bilio-pancreatic Surgery & Institute of Microcirculation, West China Hospital, Sichuan University, Chengdu 610041, Sichuan Province, China. 258836@mail.guoli.com.cn

Telephone: +86-28-5422484

Received 2001-11-02 Accepted 2001-12-05

Abstract

Pancreatic microcirculatory disturbance plays an important role in the pathogenesis of acute pancreatitis, and it involves a series of changes including vasoconstriction, ischaemia, increased vascular permeability, impairment of nutritive tissue perfusion, ischaemia/reperfusion, leukocyte adherence, hemorrhological changes and impaired lymphatic drainage. Ischaemia possibly acts as an initiating factor of pancreatic microcirculatory injury in acute pancreatitis, or as an aggravating/continuing mechanism. The end-artery feature of the intralobular arterioles suggests that the pancreatic microcirculation is highly susceptible to ischaemia. Various vasoactive mediators, as bradykinin, platelet activating factor, endothelin and nitric oxide participate in the development of microcirculatory failure.

Zhou ZG, Chen YD. Influencing factors of pancreatic microcirculatory impairment in acute pancreatitis. *World J Gastroenterol* 2002;8(3):406-412

INTRODUCTION

Acute pancreatitis remains an important surgical problem with high morbidity and mortality^[1-4]. It is not merely an injury caused by the activated pancreatic enzymes but also involves pancreatic ischaemia. Evidences in basic and clinical research suggest that disturbance of pancreatic microcirculation plays an important role in its pathophysiological processes^[5-14]. The specific local microcirculatory changes cannot be prevented merely by adequate fluid therapy. In recent years, studies with modern molecular biological tools have elucidated that many factors are involved in the development of pancreatic microcirculatory disturbance. Whether the disturbance of pancreatic microcirculation is an initiating factor or as a consequence of progressive pancreatitis is still debatable. The pathophysiological changes of pancreatic microcirculatory disturbance in acute pancreatitis are complex, they include local release of acinar enzymes^[15-25], vasoactive mediators^[26-39], vasoconstriction, increase in vascular permeability, ischaemia^[40-41], ischaemia/reperfusion, leukocyte adherence, intravascular coagulation, capillary stasis, etc., resulting in pancreatic oedema, hemoconcentration, and impaired capillary and venous drainage^[42-44], consequently leading to hemorrhagic pancreatic necrosis^[45].

ROLES OF ISCHAEMIA IN PANCREATIC MICROCIRCULATORY DISTURBANCE DURING ACUTE PANCREATITIS

Ischaemia as an initiating factor

There is a considerable evidence supporting ischaemia as an initiating

factor of pancreatic microcirculatory injury in acute pancreatitis^[46-48]. As long ago as 1862, Panum induced hemorrhagic pancreatitis by injection of wax droplets into pancreatic arteries. Later similar changes were noticed by intra-arterial injection of 8-20µm microspheres, irreversibly obstructing terminal arterioles and occluding the capillaries. While the use of larger particles only results in pancreatic oedema, because there are abundant arcade-like anastomoses between the pancreatic interlobular vessels. There is also evidence suggesting that microvascular injection of microspheres may progress to chronic active pancreatitis.

A clinical report revealed at autopsy that atheromatous thrombi embolized from the aorta into the pancreatic arteries were associated with acute pancreatitis in 10 of 12 cases. The incidence of pancreatitis in 182 patients died after cardiac surgery was 16%. There was also evidence for a high susceptibility of the pancreas to ischaemic injury in patients died of shock. A high incidence of acute pancreatitis shown after cardiopulmonary bypass operations seemed to be associated with intraoperative hypoperfusion in the splanchnic area.

By means of intravital microscopy in conjunction with technique of selected cells-labeling, direct impairments of pancreatic microcirculation in the early phase of acute pancreatitis have been observed in the experimental ischaemia induced by controlled haemorrhage or interruption of arterial blood supply to the pancreas^[49], suggesting the pancreatic microcirculation being highly susceptible to ischaemia. This is closely related to the microvasculature of pancreatic lobule; there is a single centrally-located intralobular artery as the exclusive vascular supply of each lobule, no anastomosis between the intralobular arteries and their branches exists, indicating the cause of its high susceptibility to ischaemia^[50,51].

Ischaemia as an aggravating and continuing mechanism

Temporary complete or partial ischaemia of pancreas would not cause hemorrhagic pancreatic necrosis, the slight histological and functional changes are completely reversible. However, temporary ischaemia has the potential of being transitional from edematous to necrotizing pancreatitis^[52]. While temporary arterial occlusion alone does not injure the pancreas following induction of edematous pancreatitis by duct ligation^[53] with hyperstimulation, arterial occlusion for only 15 min can result in parenchymal necrosis, suggesting that ischaemia as an aggravating factor participates in the development of acute pancreatitis.

Impairment of microcirculatory perfusion of pancreas is the consequence of the effect of various local factors, such as vasoconstriction, free radicals, intravascular coagulation, release of vasoactive mediators taking part in the whole course of acute pancreatitis (see below). Recently, ischaemia/reperfusion is considered one of the important causative factors for development of acute pancreatitis after pancreatic transplantation. It has been repeatedly demonstrated that change of pancreatic perfusion is an early event in experimental acute pancreatitis, and microcirculatory impairment in human pancreas also correlate well with the degree of ischaemic injury. These findings support the hypothesis that the microvasculature is the primary target of reperfusional injury after ischaemia.

CHANGES OF PANCREATIC MICROCIRCULATION IN ACUTE PANCREATITIS

Many indirect methods have been applied to assess the changes of pancreatic microcirculation during acute pancreatitis in previous studies^[54]. Recently, intravital fluorescence microscopy combined with the technique of separate labeled-cells and computerized image analysis system has been successfully used in the studies of pancreatic microcirculation in acute pancreatitis. Many important phenomena as vascular permeability change, vasoconstriction, capillary blood flow, functional capillary density, leukocyte-endothelium interaction, etc., have been continuously and directly observed during the course of acute pancreatitis. It is now believed that microcirculatory changes is important as well as early feature in the pathophysiology of acute pancreatitis^[55].

Vasoconstriction

The first step in the sequence of microcirculatory events in pancreatitis is the constriction of interlobular vessels, especially in the proximal segments of the interlobular arterioles and venules^[56,57]. The vasoconstriction occurring in the early phase of acute pancreatitis may cause ischaemia and stasis of the microcirculation^[58], which can be prevented by the radical scavengers, superoxide dismutase and N-(2-mercaptopropionyl)glycine in sodium taurocholate-induced pancreatitis, suggesting that vasoconstriction might be induced by free radicals. There is also great support for the concept that solutions injected into the pancreatic duct to induce biliary pancreatitis exert their effect via the interstitial route. Even at a low injection pressure of 40 cmH₂O, rupture of the ducto-acinar junction is detectable with subsequent fluid extravasation in the interstitial space, where they gain access to the pancreatic microvasculature precipitating vascular spasm. It has been noticed that segmental constriction of pancreatic arteries occurred in bile-induced pancreatitis, and of mesenteric arteries directly exposed to diluted bile. There is also pronounced damage to the pancreatic vessels resulting in haemorrhage, endothelial detachment and thrombosis, as has been shown with the taurocholate, trypsin, and trypsin-digested blood vessels. The vasotoxic effect of these substances was further substantiated by the demonstration that interstitial injection into the omentum precipitates similar changes at the injection site. The finding that stress and shock can convert oedematous to hemorrhagic experimental pancreatitis suggests that catecholamines mediators might participate in the process. Therefore, pancreatic vasoconstriction in acute pancreatitis might be relevant to a variety of factors.

Changes of permeability

The intravital microscopic findings of immediate leakage of the macromolecular plasma marker (FITC-Dextran 70) from the microvasculature into the interstitial tissue, and the scanning electron microscopic evidence of leakage of the cast material through the capillary membrane in the early phase of acute experimental pancreatitis suggest that presence of increased permeability during the disease process. Further experiments demonstrate that permeability changes precede stasis and stasis precedes leukocyte adherence^[59], suggesting that increased vascular permeability and ischaemia are the initial microcirculatory lesions in acute pancreatitis induced by sodium taurocholate leading to haemorrhagic necrosis. The non-specific detergent effect of sodium taurocholate and bile acids in general seems to be responsible for the initial changes due to the direct dissolution of cellular membranes.

Changes of nutritive tissue perfusion

Acute pancreatitis is characterized by impairment of nutritive tissue perfusion as a consequence of gradually decreased capillary blood flow

and functional capillary density^[60]. Reduction of capillary infusion volume and of functional capillary density has been observed with intravital microscopy and laser-Doppler flowmetry in the experiments of acute pancreatitis. In such experiments, capillaries are progressively excluded from perfusion starting 30min after the induction of pancreatitis, and with only few capillaries remaining perfused after 3h. At the same time, flow through the preferential pathways is maintained. Measurements of pancreatic blood flow during acute pancreatitis have ever yielded conflicting results. Some found no change or even increased blood flow, but most experiments have repeatedly demonstrated decreased total blood flow in acute pancreatitis. The perfusion values with an initial increase followed by a sharp decrease have been observed. Increased pancreatic blood flow is considered as a consequence of vasodilatation in acute inflammation. Because of the tremendous distributional disturbances of the microcirculation in the pancreas, however, measurements of total blood flow of the pancreatitis do not reflect proportionately the pathological status of different local regional perfusion within the pancreas. The pathological states, both the hyperemia and ischaemia, can be found at the same time in the different regions within the pancreas, thus emphasizing the importance of capillary blood flow measurement for accurate evaluation of microcirculatory blood flow changes. In most of the studies the degree of pancreatic hypoperfusion was found to be disproportionately more severe than the decrease in cardiac output at comparable intervals. Moreover it has been shown that a decrease in pancreatic perfusion cannot be prevented by adequate fluid therapy using Ringer's solution even though cardiovascular parameters are stabilized at the baseline level, proposing a specific mechanism of local microcirculatory ischaemic impairment^[61-63].

Impairment of ischaemia/reperfusion and leukocyte adherence

Ischaemia/reperfusion of the pancreas with impairment of the microcirculation has attracted attention both in experimental and clinical studies of acute pancreatitis^[64-73]. Ischaemia/reperfusion leads to the adherence of leukocytes to the vascular endothelium. In parallel with reduction of functional capillary density, an increase of heterogeneity of capillary perfusion has been noted. Primary capillary perfusion failure after onset of reperfusion is a characteristic microcirculatory feature of ischaemia and is called no-reflow phenomenon. Among various stimuli promoting leukocyte-endothelium interaction are ischaemia/reperfusion and formation of oxygen free radicals leading to rolling and adherence of leukocytes, the latter provoking the "reflow/paradox" phenomenon with loss of endothelial integrity and macromolecular leakage as an end result. Enhanced generation of oxygen radicals elicits ischaemia/reperfusion-induced leukocyte infiltration in the tissue, which is instrumental in the progression of acute pancreatitis. Degree of endothelial cell dysfunction and severity of leukocyte adherence is dependent upon the duration of ischaemia and reperfusion. Complete ischaemia/reperfusion of the pancreas induces extensive capillary stasis, i. e. pancreatic microcirculatory failure.

Effect of hemorrhheological changes

Since blood viscosity is the inherent resistance of blood to flow, it is probable that the hemorrhheological changes might be important to acute necrotizing pancreatitis^[74-84]. 188 Wistar rats were studied by measuring hemorrhheological and stereological parameters of pancreatic microvasculature. The results showed that increased blood viscosity, causing red blood cell aggregation with rouleaux formation, and decreased erythrocyte deformability are responsible for pancreatic microcirculatory disturbances and play an important role in the transition of oedematous pancreatitis to necrosis.

It has been noticed that the time points in the course of

experimental acute pancreatitis are extremely variable. This can be explained as investigators with various pancreatitis models, different infused substance, concentration, volume as well as intraductal pressure, the latter may be more important than the others. The high intraductal injection pressure results in an increased leakage of bile and a more generalized distribution in the interstitial space, even immediate hemorrhagic pancreatic necrosis, thus emphasizing the pathophysiological significance of experimental models in acute pancreatitis. In the low-pressure ductal perfusion model the etiological factor and the pathophysiological course are similar to those associated with the disease clinically.

VASOACTIVE MEDIATORS IN ACUTE PANCREATITIS

Bradykinin

Bradykinin probably exerts its influences upon microvessels via several pathways involving endothelial cells, including stimulating the formation and release of NO, arachidonic acid metabolites and tachykinins. Microcirculatory responses to bradykinin are biphasic: at low concentrations it causes vasodilatation, while at higher concentrations it causes vasoconstriction.

The role which bradykinin plays in microcirculatory impairment of acute pancreatitis is controversial. It was noticed that in sodium taurocholate-induced pancreatitis, the number of perfused capillaries was increased and capillary flow preserved and the mean venular leukocyte adherence decreased and histopathological change improved in icatibant (a B2 receptor antagonist)-treated rats; kinase II inhibitor captopril or exogenous bradykinin in addition to an otherwise effective dosage of icatibant resulted in microcirculatory stasis, extensive venular leukocyte adherence and severe histological damage, indicating that bradykinin may aggravate the microcirculatory disturbance^[85,86]. But another study showed that B2 receptor antagonist increased the severity of acute pancreatitis, while lys-bradykinin substituting bradykinin didn't^[87].

Platelet-activating factor(PAF)

PAF acts on microvascular diameter, permeability and leukocyte rolling, adhesion and migration through different mechanisms, including synthesis and release of NO and arachidonic acid metabolites, and upregulated expressions of ICAM-1 and CD11/CD18. Actions of PAF on microvasculature have the following features: constriction response of venules to PAF is stronger than that of the arterioles; its action on arteriolar diameter is biphasic.

It was observed that treatment with PAF receptor antagonist improved pancreatic capillary blood flow, reduced the severity of pancreatitis-associated endothelial barrier compromise and pancreatic leukocyte recruitment, suggesting that PAF is proinflammatory in pancreatitis^[88-92].

Endothelin(ET)

There are three kinds of endothelins, and endothelin-1 is predominantly expressed by vascular endothelial cells. There are three types of endothelin receptors, and ETA receptor is endothelin-1 selective, and found mainly on vascular smooth muscle cells, mediating vasoconstriction; ETB is nonselective and expressed by endothelial cells; it mediates vasodilatation through the release of NO and prostacyclin. The action of endothelin-1 on microvessels is biphasic: at low concentration, it causes vasodilatation; at higher concentration, it causes sustained vasoconstriction.

Several experiments demonstrated that endothelin-1 was involved in the microcirculatory disturbance and in the development and progression of acute pancreatitis^[93-99]. Administration of endothelin-1 after the caerulein injection decreased pancreatic blood flow significantly, aggravating microcirculatory disturbance. Topically

superfused endothelin-1 induced pancreatic microvascular deterioration and acinar cell injury similar to that induced by intraductal infusion of sodium taurocholate in rats^[100]. Studies also showed that ETA receptor antagonist is protective in microcirculatory disturbance of acute pancreatitis^[101].

Nitric oxide (NO)

NO is formed from L-arginine by NO synthase(NOS). cNOS(constitutive form) catalyzes formation of NO of physiological level. Catalytic activity of iNOS(inducible form) is stronger and lasts longer than that of cNOS, and NO of higher than physiological level is produced by iNOS. NO dilates blood vessels, but at higher concentrations it is cytotoxic.

Pancreatic NO level in acute pancreatitis may be decreased^[102] or significantly elevated in different experiments. Intravenous administration of L-arginine to rats with hemorrhagic pancreatitis improved pancreatic blood flow and a meliorated the severity of pancreatitis in a dose-dependent manner, while nitro-L-arginine infusion to the rats with edematous pancreatitis caused a decrease in pancreatic blood flow and exacerbated pancreatitis, indicating that NO is protective^[103-106]. However, some experiments showed that NO was not involved in the progression from edematous to hemorrhagic pancreatitis. Even microcirculatory changes were significantly alleviated in caerulein-induced pancreatitis pretreated with nitro-L-arginine, suggesting NO may be proinflammatory^[107]; it was found that L-arginine improved the pancreatic microcirculation but worsened the microscopic alterations within the pancreas^[108,109].

Adhesion molecules

Leukocyte-endothelial interaction is an important step in the development of acute pancreatitis. It was demonstrated by experiments that levels of ICAM-1, PECAM-1 and ELAM-1 were upregulated, and expressions of P- and E-selectin enhanced, and leukocytes became CD18-positive in acute pancreatitis^[110,111]. Immunoneutralization of adhesion molecules was proven effective in the treatment of acute pancreatitis^[112]. Administration of monoclonal antibody against ICAM-1 to rats with acute severe pancreatitis significantly enhanced capillary blood flow in the pancreas, reduced leukocyte rolling and stabilized capillary permeability^[113].

PATHOGENESIS OF MICROCIRCULATORY FAILURE IN ACUTE PANCREATITIS

The pancreatic microcirculation is impaired in acute pancreatitis^[114-124]. Capillary stasis may be due to a variety of mechanisms including hemoconcentration and intravascular coagulation, generation of oxygen free radicals in the microenvironment of the pancreatic ducto-acinar complex, increase in interstitial pressure, increase in leukocyte-endothelium interaction^[125], and local reduction of endothelial derived relaxation factor (nitrous oxide)^[126]. An acinar abnormality may be the initiating factor arising from a combination of ductal obstruction and exocrine hypersecretion followed by an increase in intraductal pressure and leakage of enzymes into the pancreatic interstitium with release of zymogen and lysozymes.

Hemoconcentration and intravascular coagulation play an additional role in the development of pancreatic ischaemia in acute pancreatitis. The increased capillary permeability is the initial feature of experimental biliary pancreatitis, resulting in loss of fluid and cells into the pancreatic interstitium induced by osmolarity shifts either in the duct or extracellular fluid^[127]. Local hemoconcentration takes place at the site of plasma sequestration, even if the systemic hematocrit is maintained at the initial level. In conjunction with the impairment of endothelium, intravascular coagulation occurs and causes a further decrease of blood fluidity. These changes are

aggravated by a systemic hypercoagulability in acute pancreatitis, probably due to thromboplastic material and activated trypsin gaining access to the systemic circulation.

The mechanism of oxygen free radical is important in acute pancreatitis of any causes^[128] and is a direct sequel of biliopancreatic reflux at the onset of acute biliary pancreatitis. Besides disintegration of cell membranes by lipid peroxidation, free radicals trigger the extravasation of granulocytes into the surrounding parenchyma representing an early lesion in acute experimental pancreatitis. The initial margination of granulocytes in the capillaries may be a contributing factor in endothelial injury and impairment of capillary perfusion. Oxygen radicals mediate depletion of pancreatic sulphhydryl compounds with changes in both lipid peroxide and oxygen radical scavengers. Serum concentrations of vitamin C, a potent antioxidant, are depleted in acute pancreatitis so that synthetic ascorbic acid derivatives have been used as a free radical scavenger.

Posts ischemic intensive adherence of leukocytes to the endothelium of the venules and adhesive leukocytes forming plaques partially occluding the lumen of the venules have been observed within the reperfusional period in the experimental acute pancreatitis. This adhesive interaction is largely confined to postcapillary venules. And it is determined by a variety of factors such as expression of adhesion molecules on leukocytes and/or endothelial cells, products of leukocyte (superoxide) and endothelial cell (nitric oxide) activation and physical forces generated by the movement of blood along the vessel wall^[129,130]. The firm adhesion of leukocytes that take place within postcapillary venules may increase the postcapillary pressure more than 200 folds, cause the passive dilatation of the capillaries and microcirculatory stasis. Many studies show that some compounds appear to be effective in reducing or abolishing leukocyte-endothelial cell adhesion, whereas some classical anti-inflammatory drugs such as indomethacin and aspirin actually promote leukocyte adhesion in the venules.

There may also be relation to lymphatic drainage^[131]. Increase in local interstitial pressure as a consequence of obstructed lymph drainage further interferes with pancreatic microperfusion due to the venous outflow impairment. In the early period of acute experimental pancreatitis, dilated lymphatic vessels are visible macroscopically, and further progress of oedema with consequent focal hemorrhagic pancreatic necrosis is possible in case of insufficient lymphatic drainage. Experiment demonstrates that an increase of thoracic duct lymph flow followed by a pronounced and prolonged reduction. Erythrocytes originating from pancreatic interstitial hemorrhages were shown to enter and obstruct the microlymphatics.

CONCLUSIONS

Recent advances in experimental research have helped witness the pathophysiology of acute pancreatitis. The phenomena of microcirculatory changes observed in acute experimental pancreatitis during the past few years gradually underlie the disturbance of the local microcirculation in acute pancreatitis, but several challenges remain. Still some questions remain unexplained concerning the mechanisms: (1) Which is the first event in the pathogenesis of acute pancreatitis? (2) Which factor determines the edematous or hemorrhagic necrotizing pancreatitis in a given experimental or clinical situation? (3) What is the role of impaired distribution of blood supply in early steps of acute pancreatitis? The potential vasoactive mediators responsible for the progression of the disease severity have largely remained subjecting to speculation and debate.

REFERENCES

- Slavin J, Ghaneh P, Sutton R, Hartley M, Rowlands P, Garvey C, Hughes M, Neoptolemos J. Management of necrotizing pancreatitis. *World J Gastroenterol* 2001;7:476-481
- Wu K, Wang BX, Wang XP. Effects of clostridium butyricum on bacterial translocation in rats with acute necrotizing pancreatitis. *Shijie Huaren Xiaohua Zazhi* 2000;8:883-886
- Tu WF, Li JS, Zhu WM, Li ZD, Liu FN, Chen YM, Xu JG, Shao HF, Xiao GX, Li A. Influence of Glutamine and caecostomy/colonic irrigation on gut bacteria/endotoxin translocation in acute severe pancreatitis in pigs. *Shijie Huaren Xiaohua Zazhi* 1999;7:135-138
- Wu CT, Li ZL, Huang XC, Zhang ZL. Effect of Chinese medicine "Qing Yi Tang" and bifidobacterium mixture on intestinal bacterial translocation following acute necrotizing pancreatitis. *Shijie Huaren Xiaohua Zazhi* 1999;7:525-528
- Banks PA. Acute pancreatitis: medical and surgical management. *Am J Gastroenterol* 1994;89(8 Suppl):S78-85
- Kelly DM, McEntee GP, Delaney C, McGeeney KF, Fitzpatrick JM. Temporal relationship of acinar and microvascular changes in caerulein-induced pancreatitis. *Br J Surg* 1993;80:1174-1176
- Bockman DE. Microvasculature of the pancreas. Relation to pancreatitis. *Int J Pancreatol* 1992;12:11-21
- Klar E. Etiology and pathogenesis of acute pancreatitis. *Helv Chir Acta* 1992;59:7-16
- Waldner H. Vascular mechanisms to induce acute pancreatitis. *Eur Surg Res* 1992;24 Suppl 1:62-67
- Wu GD, Wu CW, Xu HB. Qingyitang decoction in treatment of 42 patients with severe acute pancreatitis. *Huaren Xiaohua Zazhi* 1998;6:619-621
- Sweiry JH, Mann GE. Pancreatic microvascular permeability in caerulein-induced acute pancreatitis. *Am J Physiol* 1991;261(4 Pt 1):G685-692
- Kusterer K, Enghofer M, Zendler S, Blochle C, Usadel KH. Microcirculatory changes in sodium taurocholate-induced pancreatitis in rats. *Am J Physiol* 1991;260(2 Pt 1):G346-351
- Klar E, Endrich B, Messmer K. Microcirculation of the pancreas. A quantitative study of physiology and changes in pancreatitis. *Int J Microcirc Clin Exp* 1990;9:85-101
- Wu CT, Li ZL. Anatomy of main pancreatic duct of hybrid dog and acute pancreatitis model. *Shijie Huaren Xiaohua Zazhi* 1999;7:62-63
- Chen HM, Shyr MH, Chen MF. Gabexate mesilate improves pancreatic microcirculation and reduces lung edema in a rat model of acute pancreatitis. *J For mos Med Assoc* 1997;96:704-709
- Gong ZH, Yuan YZ, Lou KX, Tu SP, Zhai ZK, Xu JY. Effects and mechanisms of somatostatin analogues on apoptosis of pancreatic acinar cells in acute pancreatitis in mice. *Shijie Huaren Xiaohua Zazhi* 1999;7:964-966
- Li TZ, Sun SQ, Sun DL. Serological studies on the metabolism of intercellular matrix in human acute pancreatitis. *Huaren Xiaohua Zazhi* 1998;6:1082-1083
- Chen HM, Hwang TL, Chen MF. The effect of gabexate mesilate on pancreatic and hepatic microcirculation in acute experimental pancreatitis in rats. *J Surg Res* 1996;66:147-53
- Huch K, Schmidt J, Schrott W, Sinn HP, Buhr H, Herfarth C, Klar E. Hyperoncotic dextran and systemic aprotinin in necrotizing rodent pancreatitis. *Scand J Gastroenterol* 1995;30:812-816
- Nishiwaki H, Satake K, Hiura A, Umeyama K. Effects of a newly synthesized pancreatic protease inhibitor (PATM) on pancreatic microcirculation in experimental acute pancreatitis. *Gastroenterol Jpn* 1989;24:177-180
- Li ZS, Xu GM, Sun ZX, Jin ZD, Zhou XP, Xie SQ, Li P. Early ERCP and endoscopic treatment in 66 patients with acute pancreatitis. *Huaren Xiaohua Zazhi* 1998;6:150-152
- Li ZS, Qian XD, Xu GM, Sun ZX, Zou XP, Xie SQ. Preventive effect of octreotide on hyperamylasemia and pancreatitis after ERCP. *Huaren Xiaohua Zazhi* 1998;6:617-618
- Kurzanov AN, Titova GP, Vinogradov VA, Aleinik VA, Gerasimov NF. Morphofunctional changes in the pancreas in response to dalargin under normal conditions and in experimental pancreatitis. *Biull Eksp Biol Med* 1988;105:445-447
- Lehtola A, Talja M, Puolakkainen P, Nordling S, Schroder T. Peritoneal lavage combined with volume therapy in porcine hemorrhagic pancreatitis. Effects on hemodynamics, microcirculation, and peritoneal morphology. *Scand J Gastroenterol* 1987;22:559-567
- Yuan YZ, Lou KX, Gong ZH, Tu SP, Zhai ZK, Xu JY. Effects and mechanisms of emodin on pancreatic tissue EGF expression in acute pancreatitis in rats. *Shijie Huaren Xiaohua Zazhi* 2001;9:127-130
- Xia SH, Zhao XY, Guo P, Da SP. Hemocirculatory disorder in dogs with severe acute pancreatitis and intervention of platelet activating factor antagonist. *Shijie Huaren Xiaohua Zazhi* 2001;9:550-554
- Wu CT, Li ZL. Effect of DAO on intestinal damage in acute necrotizing pancreatitis in dogs. *Shijie Huaren Xiaohua Zazhi* 1999;7:64-65

- 28 Zhao HP, Wang WX, Yang CW, Shou NY. Therapeutic effects of naltrexone in plasma endotoxin in experimental acute hemorrhagic necrotizing pancreatitis of rats. *Shijie Huaren Xiaohua Zazhi* 1999;7:400-402
- 29 Qin RY, Zou SQ, Wu ZD, Qiu FZ. Effect of splanchnic vascular perfusion on production of TNF α and OFR in rats with acute hemorrhagic necrotizing pancreatitis. *Huaren Xiaohua Zazhi* 1998; 6:831-833
- 30 Hirano T, Hirano K. Thromboxane A2 receptor antagonist prevents pancreatic microvascular leakage in rats with caerulein-induced acute pancreatitis. *Int J Surg Investig* 1999;1:203-210
- 31 Bhatia M, Saluja AK, Singh VP, Frossard JL, Lee HS, Bhagat L, Gerard C, Steer ML. Complement factor C5a exerts an anti-inflammatory effect in acute pancreatitis and associated lung injury. *Am J Physiol Gastrointest Liver Physiol* 2001;280:G974-978
- 32 Bhatia M, Brady M, Zagorski J, Christmas SE, Campbell F, Neoptolemos JP, Slavin J. Treatment with neutralising antibody against cytokine-induced neutrophil chemoattractant (CINC) protects rats against acute pancreatitis associated lung injury. *Gut* 2000; 47:838-844
- 33 Leung PS, Chan WP, Nobiling R. Regulated expression of pancreatic renin-angiotensin system in experimental pancreatitis. *Mol Cell Endocrinol* 2000;166:121-128
- 34 Gomez-Cambronero L, Camps B, de La Asuncion JG, Cerda M, Pellin A, Pallardo FV, Calvete J, Sweiry JH, Mann GE, Vina J, Sastre J. Pentoxifyline ameliorates cerulein-induced pancreatitis in rats: role of glutathione and nitric oxide. *J Pharmacol Exp Ther* 2000;293: 670-676
- 35 Hirota M, Ogawa M. Shock and its mediators. *Nippon Geka Gakkai Zasshi* 1999;100:667-673
- 36 al-Eryani S, Payer J, Huorka M, Duris I. Etiology and pathogenesis of acute pancreatitis. *Bratisl Lek Listy* 1998;99:303-311
- 37 Plusczyk T, Westermann S, Rathgeb D, Feifel G. Acute pancreatitis in rats: effects of sodium taurocholate, CCK-8, and Sec on pancreatic microcirculation. *Am J Physiol* 1997;272(2 Pt 1):G310-320
- 38 Sakai Y, Hayakawa T, Kondo T, Shibata T, Kitagawa M, Sobajima H, Naruse S, Ohnishi ST. Protective effects of a prostaglandin E1 oligomer on taurocholate-induced rat pancreatitis. *J Gastroenterol Hepatol* 1992;7:591-595
- 39 Vollmar B, Waldner H, Schmand J, Conzen PF, Goetz AE, Habazettl H, Schweiberer L, Brendel W. Oleic acid induced pancreatitis in pigs. *J Surg Res* 1991;50:196-204
- 40 Lehtola A, Kivilaakso E, Puolakkainen P, Karonen SL, Lempinen M, Schroder T. Effects of dextran 70 versus crystalloids in the microcirculation of porcine hemorrhagic pancreatitis. *Surg Gynecol Obstet* 1986; 162:556-562
- 41 Kaplan MH. Pathogenesis of pancreatitis: a unified concept. *Int J Pancreatol* 1986;1:5-8
- 42 Sunamura M, Yamauchi J, Shibuya K, Chen HM, Ding L, Takeda K, Kobari M, Matsuno S. Pancreatic microcirculation in acute pancreatitis. *J Hepatobil Pancreat Surg* 1998;5:62-68
- 43 Plusczyk T, Rathgeb D, Westermann S, Feifel G. Somatostatin attenuates microcirculatory impairment in acute sodium taurocholate-induced pancreatitis. *Dig Dis Sci* 1998;43:575-585
- 44 Schmidt J, Klar E. Etiology and pathophysiology of acute pancreatitis. *Ther Umsch* 1996;53:322-332
- 45 Hoffmann TF, Leiderer R, Waldner H, Arbogast S, Messmer K. Ischemia reperfusion of the pancreas: a new *in vivo* model for acute pancreatitis in rats. *Res Exp Med (Berl)* 1995; 195:125-144
- 46 Sendur R, Pawlik WW. Vascular factors in the mechanism of acute pancreatitis. *Przegl Lek* 1996;53:41-45
- 47 Moolenaar W, Lamers CB. Cholesterol crystal embolization and the digestive system. *Scand J Gastroenterol Suppl* 1991;188:69-72
- 48 Hegewald G, Nikulin A, Gmaz-Nikulin E, Plamenac P, Barenwald G. Ultrastructural changes of the human pancreas in acute shock. *Pathol Res Pract* 1985;179:610-615
- 49 Klar E, Schrott W, Foitzik T, Buhr H, Herfarth C, Messmer K. Impact of microcirculatory flow pattern changes on the development of acute edematous and necrotizing pancreatitis in rabbit pancreas. *Dig Dis Sci* 1994;39:2639-2644
- 50 Zhou ZG, Gao XH. Morphology of pancreatic microcirculation in the monkey: light and scanning electron microscopic study. *Clin Anat* 1995; 8:190-201
- 51 Zhou Z, Zeng Y, Yang P, Cheng Z, Zhao J, Shu Y, Gao X, Yan L, Zhang Z. Structure and function of pancreatic microcirculation. *Shengwu Yiyue Gongchengxue Zazhi* 2001;18:195-200
- 52 Furukawa M, Kimura T, Sumii T, Yamaguchi H, Nawata H. Role of local pancreatic blood flow in development of hemorrhagic pancreatitis induced by stress in rats. *Pancreas* 1993;8:499-505
- 53 Plusczyk T, Westermann S, Bersal B, Menger M, Feifel G. Temporary pancreatic duct occlusion by ethibloc: cause of microcirculatory shutdown, acute inflammation, and pancreas necrosis. *World J Surg* 2001;25:432-437
- 54 Bassi D, Kollias N, Fernandez-del Castillo C, Foitzik T, Warshaw AL, Rattner DW. Impairment of pancreatic microcirculation correlates with the severity of acute experimental pancreatitis. *J Am Coll Surg* 1994;179:257-263
- 55 Banerjee AK, Galloway SW, Kingsnorth AN. Experimental models of acute pancreatitis. *B J Surg* 1994; 81:1096-1103
- 56 Klar E, Werner J. New pathophysiologic knowledge about acute pancreatitis. *Chirurg* 2000;71:253-264
- 57 Onizuka S, Ito M, Sekine I, Tsunoda T, Eto T. Spontaneous pancreatitis in spontaneously hypertensive rats. *Pancreas* 1994;9:54-61
- 58 Skoromnyi AN, Starosek VN. Hemodynamic changes in the liver, kidney, small intestine and pancreas in experimental acute pancreatitis. *Klin Khir* 1998;12:46-48
- 59 Kusterer K, Poschmann T, Friedemann A, Enghofer M, Zendler S, Usadel KH. Arterial constriction, ischemia-reperfusion, and leukocyte adherence in acute pancreatitis. *Am J Physiol* 1993; 265(1 Pt 1): G165-171
- 60 Kerner T, Vollmar B, Menger MD, Waldner H, Messmer K. Determinants of pancreatic microcirculation in acute pancreatitis in rats. *J Surg Res* 1996;62:165-171
- 61 Chen HM, Shyr MH, Ueng SW, Chen MF. Hyperbaric oxygen therapy attenuates pancreatic microcirculatory derangement and lung edema in an acute experimental pancreatitis model in rats. *Pancreas* 1998;17: 44-49
- 62 Klar E, Messmer K, Warshaw AL, Herfarth C. Pancreatic ischaemia in experimental acute pancreatitis: mechanism, significance and therapy. *Br J Surg* 1990;77:1205-1210
- 63 Knol JA, Inman MG, Strodel WE, Eckhauser FE. Pancreatic response to crystalloid resuscitation in experimental pancreatitis. *J Surg Res* 1987;43:387-392
- 64 Obermaier R, Benz S, Kortmann B, Benthues A, Ansoerge N, Hopt UT. Ischemia/reperfusion-induced pancreatitis in rats: a new model of complete normothermic *in situ* ischemia of a pancreatic tail-segment. *Clin Exp Med* 2001;1:51-59
- 65 Benz S, Bergt S, Obermaier R, Wiessner R, Pfeffer F, Schareck W, Hopt UT. Impairment of microcirculation in the early reperfusion period predicts the degree of graft pancreatitis in clinical pancreas transplantation. *Transplantation* 2001; 27:71:759-763
- 66 Mayer H, Schmidt J, Thies J, Ryschich E, Gebhard MM, Herfarth C, Klar E. Characterization and reduction of ischemia/reperfusion injury after experimental pancreas transplantation. *J Gastrointest Surg* 1999;3:162-166
- 67 von Dobschuetz E, Hoffmann T, Messmer K. Inhibition of neutrophil proteinases by recombinant serpin Lex032 reduces capillary no-reflow in ischemia/reperfusion-induced acute pancreatitis. *J Pharmacol Exp Ther* 1999;290:782-788
- 68 von Dobschuetz E, Hoffmann T, Engelschalk C, Messmer K. Effect of diaspirin cross-linked hemoglobin on normal and postischemic microcirculation of the rat pancreas. *Am J Physiol* 1999;276(6 Pt 1): G1507-1514
- 69 Vollmar B, Janata J, Yamauchi J, Wolf B, Heuser M, Menger MD. Exocrine, but not endocrine, tissue is susceptible to microvascular ischemia/reperfusion injury following pancreas transplantation in the rat. *Transpl Int* 1999;12:50-55
- 70 Benz S, Pfeffer F, Adam U, Schareck W, Hopt UT. Impairment of pancreatic microcirculation in the early reperfusion period during simultaneous pancreas-kidney transplantation. *Transpl Int* 1998;11 Suppl 1:S433-435
- 71 Benz S, Schnabel R, Morgenroth K, Weber H, Pfeffer F, Hopt UT. Ischemia/reperfusion injury of the pancreas: a new animal model. *J Surg Res* 1998;75:109-115
- 72 Hoffmann TF, Leiderer R, Harris AG, Messmer K. Ischemia and reperfusion in pancreas. *Microsc Res Tech* 1997;37:557-571
- 73 Menger MD, Bonkhoff H, Vollmar B. Ischemia-reperfusion-induced pancreatic microvascular injury. An intravital fluorescence microscopic study in rats. *Dig Dis Sci* 1996;41:823-830
- 74 Schmidt J, Huch K, Mithofer K, Hotz HG, Sinn HP, Buhr HJ, Warshaw AL, Herfarth C, Klar E. Benefits of various dextrans after delayed therapy in necrotizing pancreatitis of the rat. *Intensive Care Med* 1996; 22:1207-1213
- 75 Hotz HG, Schmidt J, Ryschich EW, Foitzik T, Buhr HJ, Warshaw AL, Herfarth C, Klar E. Isovolemic hemodilution with dextran prevents contrast medium induced impairment of pancreatic microcirculation in necrotizing pancreatitis of the rat. *Am J Surg* 1995;169:161-166

- 76 Klar E, Foitzik T, Buhr H, Messmer K, Herfarth C. Isovolemic hemodilution with dextran 60 as treatment of pancreatic ischemia in acute pancreatitis. Clinical practicability of an experimental concept. *Ann Surg* 1993;217:369-374
- 77 Yan LN, Lei ZM, Cui XZ, Chen HQ, Yang YT, Li L, Tan JS, Chen LL, Wu HB, Li KL. The role of hemorheologic disturbance in experimental acute pancreatitis. *Huaxi Yike Daxue Xuebao* 1993;24:71-74
- 78 Klar E, Mall G, Messmer K, Herfarth C, Rattner DW, Warshaw AL. Improvement of impaired pancreatic microcirculation by isovolemic hemodilution protects pancreatic morphology in acute biliary pancreatitis. *Surg Gynecol Obstet* 1993;176:144-150
- 79 Schmidt J, Fernandez-del Castillo C, Rattner DW, Lewandowski KB, Messmer K, Warshaw AL. Hyperoncotic ultrahigh molecular weight dextran solutions reduce trypsinogen activation, prevent acinar necrosis, and lower mortality in rodent pancreatitis. *Am J Surg* 1993;165:40-44
- 80 Kusterer K, Enghofer M, Poschmann T, Usadel KH. The effect of somatostatin, gabexate mesilate and dextran 40 on the microcirculation in sodium taurocholate-induced pancreatitis. *Acta Physiol Hung* 1992;80:407-415
- 81 Yan LN, Wei JJ, Wu HG, Chen HQ, Zhong GH, Li L, Chen LL, Li KL, Tan JS. The role of hemorheologic changes in the pathogenesis of acute hemorrhagic necrotizing pancreatitis. *Huaxi Yike Daxue Xuebao* 1990;21:25-29
- 82 Klar E, Herfarth C, Messmer K. Therapeutic effect of isovolemic hemodilution with dextran 60 on the impairment of pancreatic microcirculation in acute biliary pancreatitis. *Ann Surg* 1990;211:346-353
- 83 Aleksandrova NP, Petukhov EB, Riabova SS. Blood rheology and microcirculation in the dynamics of acute experimental pancreatitis. *Biull Eksp Biol Med* 1988;105:106-108
- 84 Becker H, Senninger N. Hemorrhagic pancreatitis: effect of dextran 40 and plasma on microcirculation disorders of the pancreas. *Langenbecks Arch Chir* 1985;365:57-67
- 85 Bloechle C, Kusterer K, Kuehn RM, Schneider C, Knoefel WT, Izbicki JR. Inhibition of bradykinin B2 receptor preserves microcirculation in experimental pancreatitis in rats. *Am J Physiol* 1998; 274(1 Pt 1): G42-51
- 86 Hoffmann T, Kubler J, Messmer K. Bradykinin antagonism in ischemia and reperfusion of the pancreas. *Zentralbl Chir* 1996;121:412-422
- 87 Weidenbach H, Lerch MM, Gress TM, Pfaff D, Turi S, Adler G. Vasoactive mediators and the progression from oedematous to necrotising experimental acute pancreatitis. *Gut* 1995;37:434-440
- 88 Flickinger BD, Olson MS. Localization of the platelet-activating factor receptor to rat pancreatic microvascular endothelial cells. *Am J Pathol* 1999;154:1353-1358
- 89 Foitzik T, Hotz HG, Eibl G, Hotz B, Kirchengast M, Buhr HJ. Therapy for microcirculatory disorders in severe acute pancreatitis: effectiveness of platelet-activating factor receptor blockade vs. endothelin receptor blockade. *J Gastrointest Surg* 1999;3:244-251
- 90 Wang X, Sun Z, Borjesson A, Haraldsen P, Aldman M, Deng X, Leveau P, Andersson R. Treatment with lexipafant ameliorates the severity of pancreatic microvascular endothelial barrier dysfunction in rats with acute hemorrhagic pancreatitis. *Int J Pancreatol* 1999;25: 45-52
- 91 Ji Z, Wang B, Li S. The role of platelet activating factor in mesenterioangial microcirculatory disturbance complicated with acute pancreatitis in rats. *Zhonghua Yixue Zazhi* 1995;75:139-140
- 92 Travis SP, Jewell DP. The role of platelet-activating factor in the pathogenesis of gastrointestinal disease. *Prostagl Leukot Essent Fatty Acids* 1994;50:105-113
- 93 Plusczyk T, Bersal B, Menger MD, Feifel G. Differential effects of ET-1, ET-2, and ET-3 on pancreatic microcirculation, tissue integrity, and inflammation. *Dig Dis Sci* 2001;46:1343-1351
- 94 Foitzik T, Faulhaber J, Hotz HG, Kirchengast M, Buhr HJ. Endothelin mediates local and systemic disease sequelae in severe experimental pancreatitis. *Pancreas* 2001;22:248-254
- 95 Foitzik T, Eibl G, Hotz HG, Faulhaber J, Kirchengast M, Buhr HJ. Endothelin receptor blockade in severe acute pancreatitis leads to systemic enhancement of microcirculation, stabilization of capillary permeability, and improved survival rates. *Surgery* 2000;128:399-407
- 96 Foitzik T, Eibl G, Buhr HJ. Therapy for microcirculatory disorders in severe acute pancreatitis: comparison of delayed therapy with ICAM-1 antibodies and a specific endothelin A receptor antagonist. *J Gastrointest Surg* 2000;4:240-246
- 97 Foitzik T, Hotz HG, Hot B, Kirchengast M, Buhr HJ. Endothelin-1 mediates the alcohol-induced reduction of pancreatic capillary blood flow. *J Gastrointest Surg* 1998;2:379-384
- 98 Foitzik T, Faulhaber J, Hotz HG, Kirchengast M, Buhr HJ. Endothelin receptor blockade improves fluid sequestration, pancreatic capillary blood flow, and survival in severe experimental pancreatitis. *Ann Surg* 1998;228:670-675
- 99 Liu XH, Kimura T, Ishikawa H, Yamaguchi H, Furukawa M, Nakano I, Kinjoh M, Nawata H. Effect of endothelin-1 on the development of hemorrhagic pancreatitis in rats. *Scand J Gastroenterol* 1995;30:276-282
- 100 Plusczyk T, Bersal B, Westermann S, Menger M, Feifel G. ET-1 induces pancreatitis-like microvascular deterioration and acinar cell injury. *J Surg Res* 1999; 85: 301-310
- 101 Liu X, Nakano I, Ito T, Kimura T, Nawata H. Is endothelin-1 an aggravating factor in the development of acute pancreatitis? *Chin Med J (Engl)* 1999;112:603-607
- 102 Shibuya K, Sunamura M, Yamauchi J, Takeda K, Kobari M, Matsuno S. Analysis of the derangement of the pancreatic microcirculation in a rat cerulein pancreatitis model using an intravital microscope system. *Tohoku J Exp Med* 1996; 180: 173-186
- 103 Vollmar B, Janata J, Yamauchi JJ, Menger MD. Attenuation of microvascular reperfusion injury in rat pancreas transplantation by L-arginine. *Transplantation* 1999;67:950-955
- 104 Dobosz M, Hac S, Mionskowska L, Dobrowolski S, Wajda Z. Microcirculatory disturbances of the pancreas in cerulein-induced acute pancreatitis in rats with reference to L-arginine, heparin, and procaine treatment. *Pharmacol Res* 1997;36:123-128
- 105 Dobosz M, Hac S, Wajda Z. Does nitric oxide protect from microcirculatory disturbances in experimental acute pancreatitis in rats? *Int J Microcirc Clin Exp* 1996;16:221-226
- 106 Liu X, Nakano I, Yamaguchi H, Ito T, Goto M, Koyanagi S, Kinjoh M, Nawata H. Protective effect of nitric oxide on development of acute pancreatitis in rats. *Dig Dis Sci* 1995;40:2162-2169
- 107 Dobosz M, Wajda Z, Hac S, Mysliwska J, Mionskowska L, Bryl E, Roszkiewicz A, Mysliwski A. Heparin and nitric oxide treatment in experimental acute pancreatitis in rats. *Forum (Genova)* 1998;8: 303-310
- 108 Dobosz M, Wajda Z, Hac S, Mysliwska J, Bryl E, Mionskowska L, Roszkiewicz A, Mysliwski A. Nitric oxide, heparin and procaine treatment in experimental cerulein-induced acute pancreatitis in rats. *Arch Immunol Ther Exp (Warsz)* 1999;47:155-160
- 109 Hac DS, Mionskowska L, Dobrowolski S, Dymecki D, Makarewicz W, Wajda Z. Microcirculation disorders of the pancreas in cerulein induced acute pancreatitis in rats with regard to nitrogen oxide and heparin. *Wiad Lek* 1997;50(Pt 2):108-114
- 110 Lundberg AH, Granger DN, Russell J, Sabek O, Henry J, Gaber L, Kotb M, Gaber AO. Quantitative measurement of P- and E-selectin adhesion molecules in acute pancreatitis: correlation with distant organ injury. *Ann Surg* 2000; 231: 213-222
- 111 Sunamura M, Shibuya K, Yamauchi J, Matsuno S. Microcirculatory derangement and ischemia of the pancreas. *Nippon Geka Gakkai Zasshi* 1999;100:342-346
- 112 Wang X, Sun Z, Borjesson A, Andersson R. Inhibition of platelet-activating factor, intercellular adhesion molecule 1 and platelet endothelial cell adhesion molecule 1 reduces experimental pancreatitis-associated gut endothelial barrier dysfunction. *Br J Surg* 1999;86: 411-416
- 113 Frossard JL, Saluja A, Bhagat L, Lee HS, Bhatia M, Hofbauer B, Steer ML. The role of intercellular adhesion molecule 1 and neutrophils in acute pancreatitis and pancreatitis-associated lung injury. *Gastroenterology* 1999;116:694-701
- 114 Kaska M, Pospisilova B, Slizova D. Pathomorphological changes in microcirculation of pancreas during experimental acute pancreatitis. *Hepatogastroenterology* 2000;47:1570-1574
- 115 Knoefel WT, Kollias N, Warshaw AL, Waldner H, Nishioka NS, Rattner DW. Pancreatic microcirculatory changes in experimental pancreatitis of graded severity in the rat. *Surgery* 1994;116: 904-913
- 116 Foitzik T, Bassi DG, Fernandez-del Castillo C, Warshaw AL, Rattner DW. Intravenous contrast medium impairs oxygenation of the pancreas in acute necrotizing pancreatitis in the rat. *Arch Surg* 1994;129: 706-711
- 117 Kelly DM, McEntee GP, McGeeney KF, Fitzpatrick JM. Microvasculature of the pancreas, liver, and kidney in cerulein-induced pancreatitis. *Arch Surg* 1993;128:293-295
- 118 Garcia-Cano J, Vazquez Rodriguez de Alba J, Garcia Cabezas J, Diaz-Rubio M. Acute pancreatitis in thrombotic thrombocytopenic purpura. Apropos 2 cases. *An Med Interna* 1992;9:551-553
- 119 Waldner H, Schmand J, Vollmar B, Goetz A, Conzen P, Schweiberer L, Brendel W. Pancreatic circulation in experimental biliary pancreatitis. *Langenbecks Arch Chir* 1990;375:112-118
- 120 Gress TM, Arnold R, Adler G. Structural alterations of pancreatic microvasculature in cerulein-induced pancreatitis in the rat. *Res Exp Med*

- (Berl) 1990;190:401-412
- 121 McEntee G, Leahy A, Cottell D, Dervan P, McGeeney K, Fitzpatrick JM. Three-dimensional morphological study of the pancreatic microvasculature in caerulein-induced experimental pancreatitis. *Br J Surg* 1989;76:853-855
- 122 Nishiwaki H, Satake K, Ko I, Umeyama K. Pancreatic microcirculation in acute pancreatitis of dogs. *Nippon Geka Gakkai Zasshi* 1988;89:238-244
- 123 Nuutinen P, Kivisaari L, Standertskjold-Nordenstam CG, Lempinen M, Schroder T. Microangiography of the pancreas in experimental hemorrhagic pancreatitis. *Eur J Radiol* 1986;6:187-190
- 124 Nuutinen P, Kivisaari L, Standertskjold-Nordenstam CG, Lempinen M, Schroder T. Microangiography of the pancreas in experimental oedemic and haemorrhagic pancreatitis. *Scand J Gastroenterol Suppl* 1986;126:12-17
- 125 Chen HM, Sunamura M, Shibuya K, Yamauchi JI, Sakai Y, Fukuyama S, Mikami Y, Takeda K, Matsuno S. Early microcirculatory derangement in mild and severe pancreatitis models in mice. *Surg Today* 2001;31:634-642
- 126 Menger MD, Plusczyk T, Vollmar B. Microcirculatory derangements in acute pancreatitis. *J Hepatobiliary Pancreat Surg* 2001;8:187-194
- 127 Andre EA, Costa PL, Guarita DR, Meirelles Filho JS, Laudanna AA. Changes in capillary permeability during severe experimental acute pancreatitis in rats. *Rev Hosp Clin Fac Med Sao Paulo* 1996;51:184-188
- 128 Petersson U, Kallen R, Montgomery A, Borgstrom A. Role of oxygen-derived free radicals in protease activation after pancreas transplantation in the pig. *Transplantation* 1998;65:421-426
- 129 Inagaki H, Nakao A, Kurokawa T, Nonami T, Harada A, Takagi H. Neutrophil behavior in pancreas and liver and the role of nitric oxide in rat acute pancreatitis. *Pancreas* 1997;15:304-309
- 130 Toyama MT, Lewis MP, Kusske AM, Reber PU, Ashley SW, Reber HA. Ischaemia-reperfusion mechanisms in acute pancreatitis. *Scand J Gastroenterol Suppl* 1996;219:20-23
- 131 Kul'chitskii KI, Zurnadzhi IN, Blagodarov VN, Bogdanova GI, Shchitov VS, Ponomareva VP. The lymph and blood microcirculatory beds of the pancreas in the early period of experimental acute pancreatitis. *Lik Sprava* 1994;87-89

Edited by Wu XN

Relationship between bilirubin free radical and formation of pigment gallstone

Xiang-Tao Liu, Jian Hu

Xiang-Tao Liu, Jian Hu, Department of Chemical Biology, School of Pharmaceutical Sciences, Peking University, Beijing 100083, China
Supported by the National Natural Science Foundation of China, No. 3880768 and No. 39170719

Correspondence to: Xiang-Tao Liu, Department of Chemical Biology, School of Pharmaceutical Sciences, Peking University, Beijing 100083, China. lxt421@sohu.com

Telephone: +86-010-62091539 Fax: +86-010-62015584

Received 2001-07-19 Accepted 2001-09-04

Abstract

In this paper, we summarize the main progresses made in our group in the field of the mechanism of pigment gallstone formation. It was found that after treatment with free radicals, bilirubin (BR) was changed into free radical itself, and a semiquinone free radical and a superoxide free radical bound with metal were recognized, which was detected by ESR (electron spin resonance). By the means of NMR (nuclear magnetic resonance) and IR (Infra-red spectra), it was postulated that bilirubin polymerized through the reaction between the vinyl group and the hydroxyl group under the attack of free radicals. It was also found that bilirubin free radical were liable to calcify in a kinetic study. Because of its chemical properties, bilirubin free radical was shown to be cytotoxic to hepatocyte, which was demonstrated based on the following facts: induction of phospholipid peroxidation (LPO), leakage of lactate dehydrogenase (LDH) and decrease of glutathione. As to the mechanism of bilirubin-induced cytotoxicity, it was postulated that the main target of bilirubin free radical was the cell membrane, including phospholipid and membrane bound proteins, especially spectrin, a content of cytoskeleton. Based on the results mentioned above, it was deduced that bilirubin free radical is the key factor that initiates and promotes the formation of pigment gallstone, which is consistent with other researches in recent years.

Liu XT, Hu J. Relationship between bilirubin free radical and formation of pigment gallstone. *World J Gastroenterol* 2002;8(3):413-417

INTRODUCTION

For years, gallstone has been nearly the most common illness in digestive system all over the world, especially in China^[1-9], and there are many methods to treat this illness^[10-16], including many Chinese traditional medicines. Although some therapies were successful in the end, the best way to deal with the illness is to prevent it before it occurs. So it is important to clarify the key factors that promote the formation of gallstone. Although there were lots of researches in this field that intended to discover the secrets behind the gallstone^[17-41], there are still lots of phenomena we cannot explain now.

For the mechanism of formation of pigment gallstone, the earliest suggestion came from Maki^[42]. He indicated that bacterial infection induced the hydrolysis of conjugated bilirubin and increased the level of free bilirubin, which was the critical factor for gallstone formation. However, there are many cases of gallstone without bacterial infection. Moreover, the increase of bilirubin concentration

is only an essential condition for the precipitation of bilirubin, but not enough to form stone.

In 1982, Elek *et al*^[43] reported the ESR signal of pigment gallstone. Its intensity varied linearly with quantity of bilirubin. It gave a hint that the formation of pigment gallstone was likely to be linked with free radicals. Recently, a lot of facts indicate that free radicals are the triggers or important links of many diseases. They are relative to cell damages and mutation. In view of the relationship of pigment gallstone with inflammation and accompanying damages of liver, kidney, gastrointestinal system, probably there are certain carriers of free radicals in the circulation and the free radicals cause cell damages. Based on the Elek's experiment, the carrier might be bilirubin. However, we have to illustrate:

Firstly, the attackers during inflammation are superoxide free radicals and hydroxyl radicals, then, how we can link the formation of pigment gallstone to these free radicals.

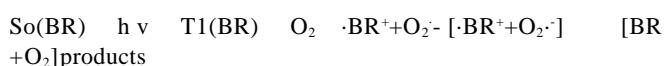
Secondly, whether or not bilirubin free radicals formed in situ during inflammation can induce cell damages and initiate the following pathological processes.

In this report, we demonstrate that bilirubin free radicals can be formed under the attack of other free radicals and induce evident cell damages. Then, the relationship between the formation of pigment gallstone and bilirubin free radicals will be discussed.

FORMATION OF BILIRUBIN FREE RADICAL AND ITS CHEMICAL NATURE

As we find, solid bilirubin absorbs oxygen reversibly when exposed to air, and meanwhile bilirubin free radicals are detectable by ESR^[44]. ESR spectra showed that the free radicals signals of solid bilirubin were composed of a semiquinone signal and a superoxide radical signal (Figure 1). The former may be formed from the carbonyl group, while the latter may be bound with a metal ion, especially the iron that might be released from the haem from which bilirubin was produced. High spin Fe (II) or Fe (III) was found to be coordinated with four tetrapyrrol nitrogens, which was the same as in haem. Various free radical sources, such as FeSO₄+EDTA, XO/XOD and ⁶⁰Co-irradiation were used to generate bilirubin free radicals. The ESR signals obtained were in accordance with those of natural pigment gallstone^[45] (Figure 2). Moreover, the ESR signals of bilirubin became diminished after treatment with free radicals scavengers, such as SOD, mannitol and vitamin C, or ligand of Fe²⁺ or Fe³⁺^[46].

The above results support a mechanism suggested by Foote for photooxidation of bilirubin^[47]: (where BR refers to bilirubin, and T1 represents the transition state of the reaction)



Bilirubin free radicals in solution were showed to be more complex than solid bilirubin free radicals. According to the ESR signals and computer simulation, it was deduced that the signals were composed of three groups of free radicals signals: $\cdot\text{H}_2\text{O}_2^{\cdot-}$, $\text{RCH}_2\cdot$ (Figure 3)^[48]. $\text{O}_2^{\cdot-}$ was from natural bilirubin, and the other two free radicals might be generated during attack of $\text{O}_2^{\cdot-}$ to C-C bond. In

some experiments, only $\cdot\text{OH}$ was trapped by DMPO, which was considered as the dismutation product of $\text{O}_2^{\cdot-}$. In experiment at 77K, semiquinone signal also could be identified just as in solid bilirubin.

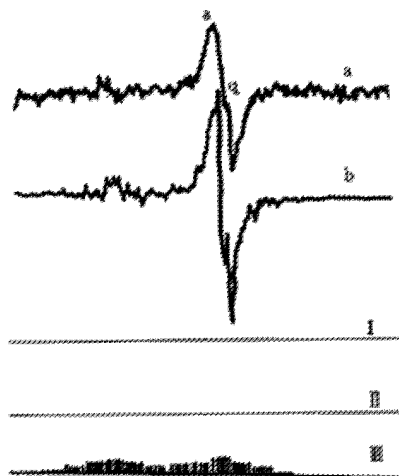


Figure 1 Simulation of ESR spectrum of bilirubin. (a) The experimental spectrum; (b): Simulating spectrum. (I) Superoxide radical; (II) Semiquinone radical; (III) Free electron of superoxideradical delocalized to tetrapyrrole (heterotropism is ignored).

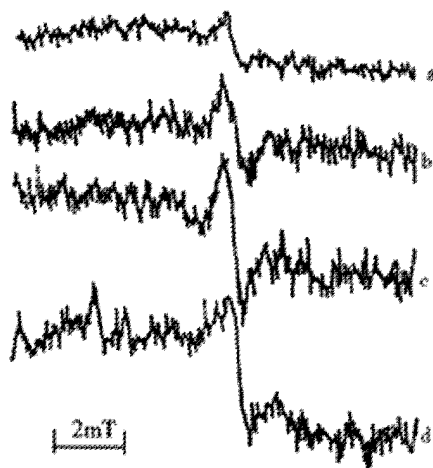


Figure 2 ESR spectra of bilirubin treated with: (a) Bilirubin(from Sigma) as control; (b) ^{60}Co (100Gy); (c) $\cdot\text{OH}$ (Fe(II)+EDTA); (d) $\text{O}_2^{\cdot-}$ (XO/XOD). The relative intensity of ESR peak is: a:b:c:d=1:2.1:2.8:3.9

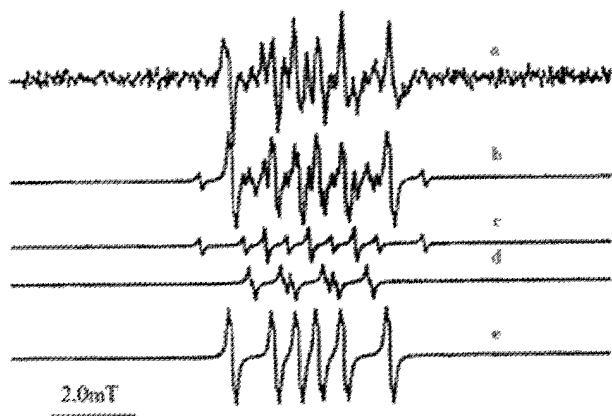


Figure 3 ESR spectra of spin-trapping of bilirubin free radical in solution. (a) DMPO-trapping spectrum of bilirubin; (b) computer simulating spectrum; (c) Simulating spectrum of DMPO-H; (d) Simulating spectrum of DMPO-OOH; (e) simulating spectrum of DMPO-CH₂R.

In conclusion, we proved that bilirubin free radicals consisted of at least semiquinone free radicals and metal bound superoxide free radicals. In solution, $\text{O}_2^{\cdot-}$ attacks bilirubin to generate $\cdot\text{H}$ and RCH_2^{\cdot} , and also dismutates into $\cdot\text{OH}$. Because of the chemical properties of bilirubin free radical, its contributions to the formation of gallstone and its effects on cells discussed below become easier to understand.

PROPERTIES OF BILIRUBIN FREE RADICAL RELEVANT TO FORMATION OF PIGMENT GALLSTONE

To explore the polymerization of bilirubin induced by free radicals, IR and NMR were used to compare the polymerization of original bilirubin or bilirubin treated with free radicals sources. The only significant variation in IR spectra was the decrease of the absorbance at 990cm^{-1} (vinyl group). If the absorbance at 1610cm^{-1} (carboxyl group) was taken as the inner reference^[49], the ratio A_{990}/A_{1610} was found to be 0.6470, 0.5646 and 0.5587 in untreated bilirubin and bilirubin treated with FeSO_4 +EDTA and ^{60}Co irradiation respectively. In NMR spectra, increase of the integral area of the methyl group (1.237ppm) and decrease of that of the vinyl group (above 5ppm) were observed (Figure 4).

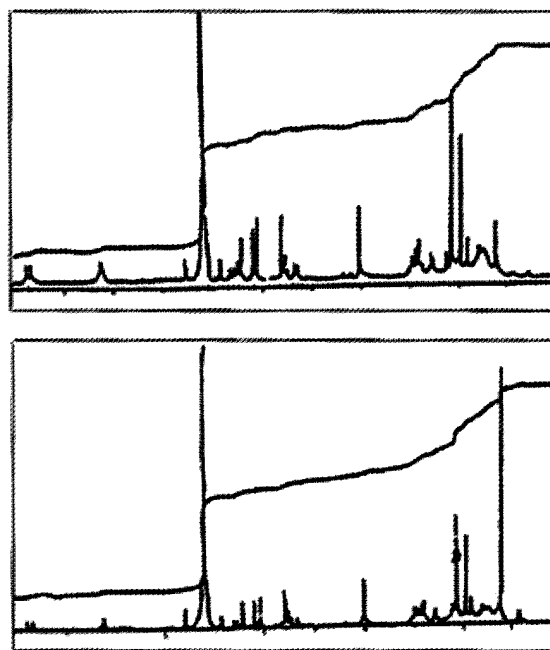


Figure 4 ^1H -NMR spectra of bilirubin. (A) commercial bilirubin (from Sigma); (B) bilirubin treated with ^{60}Co .

Thus, we postulated that bilirubin molecules polymerized through the reaction between the vinyl group and the hydroxyl group by free radicals attack. This hypothesis was consistent with William's suggestion^[50].

By means of the light scattering method, the average molecular weight of the bilirubin free radicals in DMSO solution was determined in the range 60000-80000, which was higher than that of original samples (<20000). The particle size distribution was measured by means of Coulter counter and the result showed that bilirubin free radicals became larger^[51]. A kinetic study showed that the treated bilirubin reacted with calcium ion more rapidly than the untreated sample, and the conditional solubility product was found to be lower. These results suggested that bilirubin free radicals tended to polymerize and deposit, leading to the formation of gallstone.

Based on the above results, we considered that during the gallstone formation bilirubin reacted with the active-oxygen species formed *in vivo* and was changed into free radicals, then polymerized, aggregated and calcified. This might be an important step of formation of pigment gallstone.

CYTOTOXICITY OF BILIRUBIN FREE RADICAL AND ITS CONTRIBUTION TO THE FORMATION OF PIGMENT GALLSTONE

It is well known that bilirubin is cytotoxic. In our experiments, we found that bilirubin free radicals could induce phospholipid peroxidation (LPO), lactate dehydrogenase (LDH) leakage from hepatocytes (Figure 5), and the decrease of intracellular total glutathione (GSH) and oxidized glutathione (GSSG) levels (Figure 6)^[52].

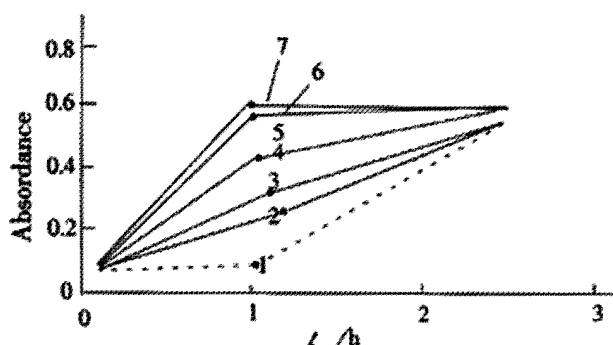


Figure 5 Leakage of lactate dehydrogenase (LDH) of hepatocyte. 1. Control; 2-7. Treated with BR_{VC} , $BR_{comm}+BSA$, BR_{comm} , BR_{Co} , BR_{Fe} , $BR_{XO/XOD}$

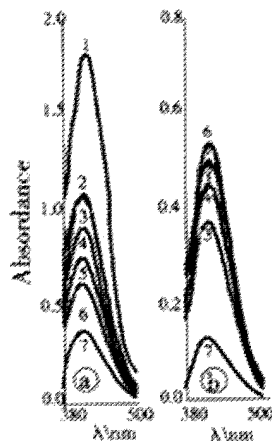


Figure 6 Absorption curve of total and oxidized glutathione level of hepatocyte. (A) Total glutathione; (B) Oxidized glutathione. 1. Control; 2-7. Treated with BR_{VC} , $BR_{comm}+BSA$, BR_{comm} , BR_{Co} , BR_{Fe} , $BR_{XO/XOD}$

The above effects can be diminished when hepatocytes were incubated with bilirubin treated with free radicals scavenger. So cytotoxicity of bilirubin might come from its chemical nature-free radical, just as what had been discussed above. In order to clarify the mechanism of bilirubin-induced cytotoxicity, we investigated effects of bilirubin free radicals on erythrocyte membrane. The SDS-PAGE results showed that after treatment of membrane with bilirubin free radicals, the integral area of band 1 and 2 decreased and some small molecular bands appeared between band 2 and 3 (Figure 7), which indicated that a part of membrane bound proteins, especially the spectrin, were degraded, then the membrane structure might be damaged. The above result was also supported by means of labeling membrane protein with fluorescamine (Figure 8)^[53]. In addition, due to the degradation of membrane bound proteins, the increase of lateral movements of

phospholipids, decrease of polarizability as well as decrease of microviscosity of erythrocyte membrane were observed by means of fluorescence polarization measurement^[54]. The studies on the reaction between membrane and bilirubin free radicals showed that the process comprised three steps: firstly, a rapid formation of an electrostatic complex between bilirubin free radicals and polar groups of phospholipid, then a slow inclusion of bilirubin into hydrophobic core of membrane, and finally an erythrocyte membrane-induced bilirubin aggregation^[55].

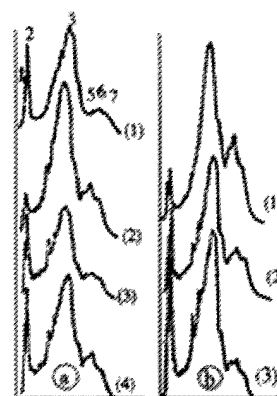


Figure 7 Scans of SDS-PAGE stained with Coomassie blue R-250. (A) 1. control, 2-4 human erythrocyte membrane treated with BR_{Co} , the irradiation doses are 100, 50, 5 (Gy) respectively; (B) human erythrocyte membrane treated with BR_{Fe} , the concentrations of 1-3 are 16.67, 13.3, 6.7 (mmol/L) respectively

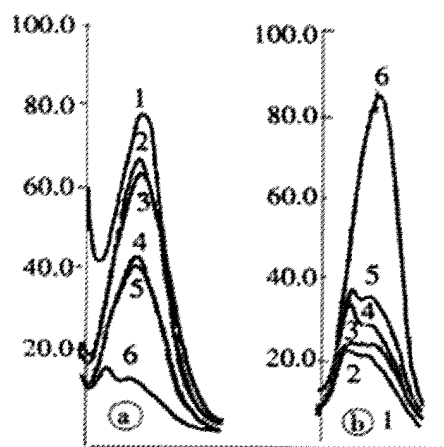


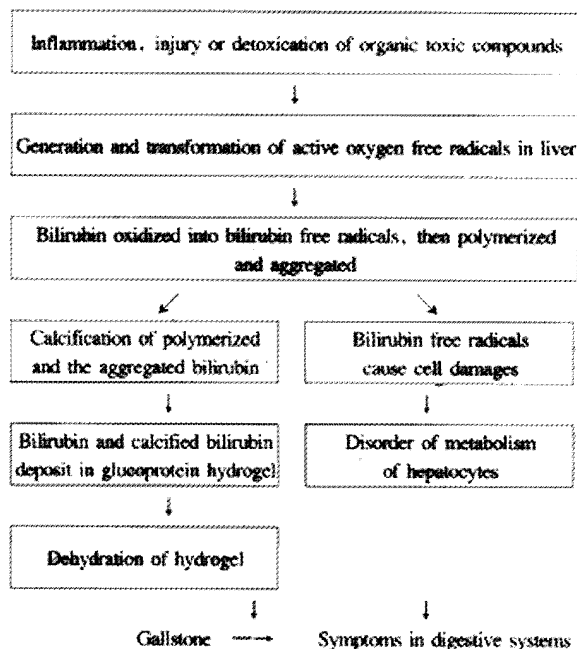
Figure 8 Fluorescence spectrum of erythrocyte proteins labeled with fluorescamine. (A) In the precipitated proteins; (B) In the supernatants. 1. control, 2. BR_{VC} , 3. BR_{comm} , 4-5. BR_{Fe}^{aa} (10 and 20 mmol/L) 6. BR_{Co} (100 Gy)

In summary, bilirubin free radicals can damage the liver cells, which can induce the change of ingredients of the bile, decrease the amount of bile acid. Meanwhile, the abnormal metabolism in hepatocyte can lead to hydrolysis of the conjugated bilirubin, increase the concentration of free bilirubin, thus make bilirubin supersaturated to the bile and promote the formation of pigment gallstone. Moreover, the cell damages caused by free radicals can also promote excretion of glucoprotein, which might act as adhesives and increase the particle size of calcium bilirubinate.

CONCLUSIONS

Based on our results, we considered that there were two ways by which bilirubin free radicals promoted the formation of pigment gallstone. On the one hand, due to the properties of free radicals, bilirubin free radicals formed *in vivo* were more liable to polymerize

and aggregate, then induced the formation of stone. On the other hand, the damages on hepatocytes induced by bilirubin free radicals also impaired the cell function, then led to the disorder of metabolism, which gave rise to the formation of stone indirectly, as well as symptoms in digestive systems. The whole process is illustrated as follows:



REFERENCES

- Zhuang XQ, Sun GH. Analysis of 91 cirrhotic patients complicated by cholelithiasis. *Xin Xiaohuabingxue Zazhi* 1994;2(Suppl 2):20
- Zhang CP, Zhang DX, Han B. The cystic diseases in liver cirrhosis. *Xin Xiaohuabingxue Zazhi* 1994;2(Suppl 2):36
- Hu ZQ, Wu DJ, Wang Y, Wang YH, Xu GN. Clinical analysis of patients with gallstones concomitant gastroduodenal diseases. *Xin Xiaohuabingxue Zazhi* 1996;4:260-261
- Chen G, Wang P, Shi JS, Qin XL. A clinical study of the relationship between gallbladder cancer and gallstone. *Xin Xiaohuabingxue Zazhi* 1997;5:321-322
- Chen P, Wang BS, He LQ. Multifactorial analysis of recurrence of cholecystolithiasis in Shanghai area. *World J Gastroenterol* 1999;5:31-33
- Tandon RK. Prevalence and type of biliary stones in India. *World J Gastroenterol* 2000;6(Suppl 3):4-5
- Jüngst D, Niemeyer A, Müller I, Zündt B, Meyer G, Wilhelm M, del Pozo R. Mucin and phospholipids determine viscosity of gallbladder bile in patients with gallstones. *World J Gastroenterol* 2001;7:203-207
- Shi JS, Ma JY, Zhu LH, Pan BR, Wang ZR, Ma LS. Studies on gallstone in China. *World J Gastroenterol* 2001;7:593-596
- Huang W, Xu BW. Percutaneous cholecystolithocentesis in 552 patients with cholelithiasis. *Xin Xiaohuabingxue Zazhi* 1994;2:96-97
- Zhong J, Wu WY. Experimental study on gandering inhibiting the development of cholesterol stone in guinea pigs. *Xin Xiaohuabingxue Zazhi* 1995;3:69-71
- Yang ZX, Zhu D, Yang YH, Meng YJ, Wang JH. Cholelitholytic effect of Chinese herb rongshiyihao through nasobiliary catheter. *Xin Xiaohuabingxue Zazhi* 1996;4:489-491
- Shi JS, Ren B, Ma QJ, Cheng L, Luo J, Meng QC, Tian HP, Han MR. Experimental study of *Artemisia capillaris* and *Radix curcumae* in preventing gallstone formation in guinea pigs. *Shijie Huaren Xiaohua Zazhi* 1998;6:564-566
- Guo ZW, Wang LF, Shi MY, An X, Deng MJ. Effects of danyihewei granule on stoneforming factors in biliary tract and prevention of postoperative stone formation. *Shijie Huaren Xiaohua Zazhi* 1999;7:132-134
- Xiang RC, Chen F, Wang KM. Synergic effect of erythromycin and CoAA on gallbladder contraction in patients with cholelithiasis. *China Natl J New Gastroenterol* 1996;2:109-111
- Zheng CQ, Li YQ, Zhao SY. Effect of single herb of li dan pai shi tang on motility of gallbladder in normal subjects. *China Natl J New Gastroenterol* 1996;2(Suppl 1):124
- Li ZS. Progress in endoscopic management of pancreas diseases. *World J Gastroenterol* 1998;4:178-180
- Zhao JT, Qi GY, Gao BS, Liang HB, Zhang CQ. Study on motility function of gallbladder in cholelithiasis patients. *Xin Xiaohuabingxue Zazhi* 1996;4:249-250
- Yin QX, Peng LY, Lu RH. Relationship between the bile ingredients and cholelithiasis in patients with liver cirrhosis. *Xin Xiaohuabingxue Zazhi* 1996;4(Suppl 5):81-82
- Shi XS, Huang MK, Wu FL. pH and calcium concentration in gallbladder and hepatic bile. *Xin Xiaohuabingxue Zazhi* 1997;5(Suppl 6):47-48
- Lü HD, Tian MG, Zhang XP, Li HL. Influence of fever on biliary elements of guinea pigs. *Xin Xiaohuabingxue Zazhi* 1997;5:703-704
- Tu XQ, Xiao YQ, Zhu XG, Xu HB, Li WM, Liu YJ. Effects of bile monoconjugated bilirubin on cholesterol nucleation. *Xin Xiaohuabingxue Zazhi* 1997;5:755-756
- Wang XY, Sun XP, Zhou Q, Yang JL, He ZY. Relationship between female hormones, blood lipids and cholelithiasis. *Huaren Xiaohua Zazhi* 1998;6(Suppl 7):216-218
- Wang CY, Yu HZ, Zhang WW. Effect of sex hormones on gallstone formation in rabbits. *Huaren Xiaohua Zazhi* 1998;6(Suppl 7):219-220
- Fang CH, Yang JZ, Kang HG. A PCR study on Hp DNA of bile, mucosa and stone in gallstones patients and its relation to stone nuclear formation. *Shijie Huaren Xiaohua Zazhi* 1999;7:233-235
- Fang CH, Yang J. A study on DNA of aerobic and anaerobic bacteria in bile, mucosa and stone in gallstone patients. *Shijie Huaren Xiaohua Zazhi* 2000;8:66-68
- Zhou LS, Shi JS, Wang ZR, Wang L. Tumor necrosis factor α in gallbladder and gallstone. *Shijie Huaren Xiaohua Zazhi* 2000;8:426-428
- Smout AJPM, vanBerge Henegouwen GP, Samsom M. Normal and disturbed motility of gallbladder and sphincter of oddi. *China Natl J New Gastroenterol* 1996;2(Suppl 1):35-37
- Chen Y, Wang LL, Xiao YX, Ni JH, Yu Y. Analysis of amino acid constituents of gallstones. *China Natl J New Gastroenterol* 1997;3:255-256
- Chen YQ, Cai D, Zhang YL, Hua TF. A comparative study of changing patterns of concanavalin A-binding proteins in early stage of cholesterol gallstone. *China Natl J New Gastroenterol* 1997;3:257-259
- Lü HD, Tian MG, Zhang XP, Li HL. Influence of fever on biliary elements of guinea pigs. *China Natl J New Gastroenterol* 1997;3:265
- Han TQ, Zhang SD, Tang WH, Jiang ZY. Bile acids in serum and bile of patients with cholesterol gallstone. *World J Gastroenterol* 1998;4:82-84
- Wu XT, Xiao LJ, Li XQ, Li JS. Detection of bacterial DNA from cholesterol gallstones by nested primers polymerase chain reaction. *World J Gastroenterol* 1998;4:234-237
- Zhao JC, Xiao LJ, Zhu H, Shu Y, Cheng NS. Changes of lipid metabolism in plasma, liver and bile during cholesterol gallstone formation in rabbit model. *World J Gastroenterol* 1998;4:337-339
- Luo XZ, Wang LS, Lin SZ. An analysis of the relationship between ultrasonography and laparoscopic cholecystectomy. *World J Gastroenterol* 1998;4(Suppl 2):83
- Lin QY, Du JP, Zhang MY, Yao YG, Li L, Cheng NS, Yan LN, Xiao LJ. Effect of apolipoprotein E gene Hha I restricting fragment length polymorphism on serum lipids in cholecystolithiasis. *World J Gastroenterol* 1999;5:228-230
- Wei JG, Wang YC, Du F, Yu HJ. Dynamic and ultrastructural study of sphincter of Oddi in early-stage cholelithiasis in rabbits with hypercholesterolemia. *World J Gastroenterol* 2000;6:102-106
- Jiao XY, Shi JS, Wang JS, Yang YJ, He P. Effects of radical cholecystectomy on nutritional and immune status in patients with gallbladder carcinoma. *World J Gastroenterol* 2000;6:445-447
- Zhou JF, Cai D, Zhu YG, Yang JL, Peng CH, Yu YH. A study on relationship of nitric oxide, oxidation, peroxidation, lipoperoxidation with chronic cholecystitis. *World J Gastroenterol* 2000;6:501-507
- Lammert F, Südfeld S, Busch N, Matern S. Cholesterol crystal binding of biliary immunoglobulin A: visualization by fluorescence light microscopy. *World J Gastroenterol* 2001;7:198-202
- Zhao JT, Qi GY, Gao BS, Liang HB, Zhang CQ. Study on motility function of gallbladder in cholelithiasis patients. *Xin Xiaohuabingxue Zazhi* 1996;4:249-250
- Zhu X. Survey of the relation between fatty liver and gallstone by ultrasonography. *Xin Xiaohuabingxue Zazhi* 1996;4:258-259
- Maki T. Pathogenesis of calcium bilirubinate gallstone. *Ann Surg* 1966;164:90-100
- Elek G, Rockenbauer A. The free radical signal of pigment gallstone. *Klinische Wochenschrift* 1982;60:33-35
- Yang ZH, Wang K, Liu XT. ESR and NMR studies of bilirubin free

- radical. *Sci China B* 1991;8:847-852
- 45 Yang ZH, Wang K, Liu XT. The nature and source of ESR signal in bilirubin. *Advances in free radical and medicine*, Atomic Energy Press, Beijing, 1991;1:309-314
 - 46 Liu XT, Sun FL, Zhao LW, Wang K, Yang ZH, Zhou YH. Polymerization, Aggregation and stable free radical formation of bilirubin induced by activ-oxygen free radical. *Chin BJ* 1990;6:437-443
 - 47 Foote CS. Photosensitized Oxidation and Singlet Oxygen: Consequences in Biological Systems. *Free Radicals in Biology*, Vol.11, Pryor, W.A., Ed., Academic Press, 1976: 3
 - 48 Liu XT, Yang ZH, Wang K, Xiao MF. Some chemical behavior of bilirubin free radical in solution. *Advances in free radical and medicine*, Atomic Energy Press, Beijing, 1991; 3: 35-42
 - 49 Rege RV, Webster CC, Ostrow JD, Carr SH, Ohkubo H. Validation of infrared spectroscopy for assessment of vinyl polymers of bile-pigment gallstones. *Biochem J* 1980;224:871-876
 - 50 William B, Dwyer KR, Kennard CH. Black pigment or polybilirubinate gallstones. *Ann Surg* 1981;193:331-333
 - 51 Liu XT, Tang B, Wang K. The interaction between calcium and bilirubin free radical in the presence of sodium cholate. *Beijing Medi Univer* 1990; 22:285-286
 - 52 Liu XT, Liu HJ, Wang K. Studies on damages of rat hepatocyte induced by bilirubin free radical. *Chin BJ* 1995; 11:71-75
 - 53 Liu XT, Wang K, Xiao MF, Shen LP. Damages of erythrocyte membrane induced by bilirubin free radicals. *Chin BJ* 1992; 8:597-601
 - 54 Liu XT, Shen LP, Wan ZH, Wang K. Effect of bilirubin free radicals on the fluidity of erythrocyte membrane. *Beijing Medi Univer* 1993; 25:369-371
 - 55 Liu XT, Wang K, Xu R. Interaction process of bilirubin free radical with erythrocyte membrane. *Advances in free radical and medicine*, Atomic Energy Press, Beijing, 1991; 3:14-21

Edited by Hu DK

• ESOPHAGEAL CANCER •

Field Population-based blocking treatment of esophageal epithelia dysplasia

Jun Hou, Pei-Zhong Lin, Zhi-Feng Chen, Zhen-Wei Ding, Shao-Sheng Li, Fan-Shu Men, Li-Ping Guo, Yu-Tong He, Chui-Yun Qiao, Chui-Lan Guo, Jian-Ping Duan, Deng-Gui Wen

Jun Hou, Zhi-Feng Chen, Yu-Tong He, Jian-Ping Duan, Deng-Gui Wen, Hebei Cancer Institute, and The Fourth Affiliated Hospital of Hebei Medical University, Shijiazhuang 050011, Hebei Province, China
Pei-Zhong Lin, Zhen-Wei Ding, Li-Ping Guo, Cancer Institute, China Academy of Medical Science, Beijing 100021
Shao-Sheng Li, Fan-Shu Men, Chui-Yun Qiao, Chui-Lan Guo, Cixian Cancer Institute, Cixian County 056500, Hebei Province, China
Supported by The National Eighth-Five-Year Scientific Championship Project No. 85-914-01-02
Correspondence to: Dr. Deng-Gui Wen, Hebei Cancer Institute, Jiankanglu 5, Shijiazhuang 050011, China. dengguiwen@hotmail.com
Telephone: +86-311-6033511 Fax: +86-311-6077634
Received 2001-12-20 Accepted 2002-02-07

Abstract

AIM: To confirm the value of blocking treatment by zenshengping (ZSP), a Chinese herb composite, and Riboflavin for esophageal epithelia dysplasia cases screened out in high risk area in northern china by exfoliative balloon cytology (EBC), so to reduce the incidence rate of esophageal cancer(EC).

METHODS: Esophageal epithelium dysplasia cases including mild esophageal epithelium dysplasia (MEED), stage one severe esophageal epithelium dysplasia (SEEDI), and stage two severe esophageal epithelium dysplasia (SEEDII) were screened out from people aged 40 years and older in the high risk area of Chixian. These cases were randomly divided into a treatment and control group. Subjects in the treatment and control groups took ZSP, riboflavin, and placebo daily for three years. EC cases registered by cancer registry and identified by EBC re-screening in the treatment and control groups were used to calculate incidence and blocking rates to demonstrate the effects of blocking medication.

RESULTS: It was found that 31.92% and 24.15% of people aged 40 years and older in Cixian could be diagnosed as MEED and SEED cases. The severity of dysplasia increased with age. ZSP had blocked EC occurrence by 47.79% after 3 year medication among the SEED cases.

CONCLUSION: ZSP can block the development from SEEDI and SEEDII to EC by 47.79%. Efforts should be made to screen and treat dysplasia cases in people aged 40 years and older in high risk areas to reduce the mortality figures.

Hou J, Lin PZ, Chen ZF, Ding ZW, Li SS, Men FS, Guo LP, He YT, Qiao CY, Guo CL, Duan JP, Wen DG. Field Population-based blocking treatment of esophageal epithelia dysplasia. *World J Gastroenterol* 2002;8(3):418-422

INTRODUCTION

The prognosis of esophageal and cardia cancer is the worst among digestive carcinomas because more than 90% of all its patients are clinically detected at advanced stages, and most of the patients can undergo only non-curative surgery due to either local tumor invasion

into the surrounding tissue or distant metastasis at the time of operation^[1-3]. The five year survival rate for clinically diagnosed EC is below 10%. On the other hand, treatment results for early digestive carcinomas are excellent. Several strategies exist for early treatment, including surgery, endoscopic resection, Chinese herbs, etc. The five year survival of early treated EC and gastric cancer patients can reach 90% or more^[4-16]. Because most EC and gastric patients have no apparent symptoms until the disease develops into advanced stages, early diagnosis at hospitals seems unrealistic presently, and early detection is undergone mostly among high risk populations in area with high incidence by means of exfoliative balloon cytology (EBC) and/or endoscopy^[17-24].

Besides treatment of early ECs such as carcinoma in situ or intramucosal carcinoma, another promising strategy of secondary prevention is receiving great interest presently. A number of researchers have demonstrated that esophageal epithelium dysplasia (EED) is a precancerous lesion which can either develop further into a more severe stage or cancer, stay unchanged, or reverse back to normal again for a period of several years or even a decade. It is therefore very promising to detect patients with EED and treat the precancerous lesions before they transform into the irreversible malignant stage in high risk populations^[25-31]. There are several techniques and chemicals or nutrients that have been reported to be effective in blocking precancerous lesions from transforming into cancer^[32-42]. Linpeizhong reported that an herb composite named Zenshengpin (ZSP) had shown an inhibitory rate of 50% after three years of medication for SEEDI and SEEDII cases^[25]. The present report came from "A Comprehensive Field Prevention and Treatment Study of Esophageal Cancer" carried out in the Chixian county of Hebei Province, which is adjacent to the Linxian county of Henan province, and also has the highest incidence rate of ECs in the world. This study was one of The National Eighth-Five-Year Scientific Championship Project. Its aim was to explore the feasibility of massive screening for EED patients among high risk people and to examine the long term effects of blocking treatment by ZSP and micronutrients in large samples of EED cases.

MATERIALS AND METHODS

Chixian is situated at 36°30" northern latitude, 114°40" eastern longitude, on the east side of the Taihang Mountain, along the Zhanghe River. Across the river to the south is the Anyang City of Henan province. Chixian county occupies an area about 951 square kilometers, and its population is 583611. There is a remarkable variation in the earth stratum of the county, with mountainous, hilly, and level land each constituting about one-third of its total area. The climate is influenced mainly by the warm mainland seasonal wind. The average temperature is 18-25°C and the waterfall is 600-700 millimeters. The major soil there is brown and light colored weed earth. Farm products include wheat, corn, millet, rice, red potato, and beans. Iron and coal are the main minerals, and coal is the main local fuel of the county.

The National Eighth-Five-Year Scientific Championship Project chose people aged 40 years and older in nine rural administrative units in the hilly part of Chixian County as the study population. The hilly

part of the county has a higher incidence rate of EC than the plain part. The nine rural administrative units were further randomly divided into two districts; a treatment and a control district. The number of the study population was 122497. They resided in 101 villages. There was no significant difference in the sex and age distribution of the study population between the treatment and control districts. In preparation for a massive EBC screen of the study population to detect EC, near esophageal cancer (NEC), MEED, SEEDI, and SEEDII cases, a county wide conference was convened by the Chixian County government for local leaders and cancer prevention professionals from the three administrative levels including the county, the rural administration unit, and the villages. At the conference, special committees were set up on each of the three administration level to be responsible for the execution of the EBC massive screen in the areas under their authority. After the conference, a forceful propaganda campaign was carried out countywide to advertise the benefits of massive EBC screenings such as early detection, early treatment and satisfactory survival results. One day prior to the screening, personal contacts with potential examinees were made by local physicians to arrange details for the screening. At the beginning of the screening, physical examination was performed by physicians to exclude persons with serious contraindication to EBC examination, then EBC examination was performed by specialists. Four slides were prepared from specimens obtained by the procedure. The slides were afterwards examined by cytologists with no knowledge about the design of the study. Diagnosis was made according to the five grade cytology classification system including grade I normal, grade II MEED, grade IIIa SEEDI, grade IIIb SEEDII, grade IV NEC, and grade V EC^[28]. A diagnosis of cancer was made only after verification by at least three cytologists. Patients initially diagnosed with grade IIIa, grade IIIb, grade IV, and grade V were reexamined by electronic endoscopy with biopsy.

Finally, 16748 people of the study population in the two districts accepted EBC screening. MEED, SEEDI, and SEEDII patients screened out from the treatment district were pre-chosen as the treatment group; while those of the MEED, SEEDI and SEEDII

cases detected from the control district were chosen to be the control group. There were 1566 cases of MEED and 1396 cases of SEED (including SEEDI and SEEDII) in the treatment group; and 3780 MEED and 2649 SEED cases in the control group. The MEED patients in the treatment group took 8 calcium tablets (CT) which were equivalent to 3 grams of caco3 and 5 milligrams of riboflavin. The SEED patients in the treatment group took 8 ZSP tablets daily. The MEED and SEED cases in the control group took 8 placebo tablets which were the same in color and size as ZSP and CT. The medication of ZSP, CT and placebo continued for three years. Half a year after initiation of the medication, EC cases diagnosed in the treatment and control groups were registered by a cancer registry constructed specifically for the study. At the end of the three year medication, EBC screening was re-initiated to identify EC cases in the treatment and control groups. EC cases registered by the registry and identified by the EBC re-screening were summarized to calculate the incidence rates for the treatment and control groups respectively.

RESULTS

Detection rates of MEED, SEEDI, SEEDII, NEC, and EC

As in Table 1, there were 179 cases of EC, 172 of NEC, 866 of SEEDII, 3179 of SEEDI, and 5346 of MEED as detected by the initial EBC screening from the 16,748 high risk participants aged 40 years and older in the treatment and control districts. The detection rates of MEED, SEEDI, SEEDII, NEC, and EC were 31.92%, 18.98%, 5.17%, 1.03%, and 1.07% respectively. As the age increased by 5 year intervals, the detection rates of MEED, SEEDI, SEEDII, NEC, and EC all increased from the lowest for the 40-year-old group to the highest for the 60-year-old group, but the amount of increase in the detection rates with increase of age was not equal for MEED, SEEDI, SEEDII, NEC, and EC. The increase was the sharpest for EC and the lowest for MEED. An odds ratio (OR) defined as the ratio of the detection rates of the 60-year-old group against that of the 40-year-old group was 5.78 for EC, 2.56 for NEC, 1.80 for SEEDII, 1.61 for SEEDI, and only 1.18 for MEED.

Table 1 Age distribution of detection rates of MEED, SEEDI, SEEDII, NEC, and EC by EBC screening

Histology Grade	Age										Total	OR	
	40-		45-		50-		55-		60-				
	<i>n</i>	Rate%	<i>n</i>	Rate%	<i>n</i>	Rate%	<i>n</i>	Rate%	<i>n</i>	Rate%			
Normal	2703	50.50	1578	43.83	1094	39.10	945	35.59	746	30.09	7021	41.92	0.60
MEED	1574	29.40	1100	31.76	928	33.17	882	33.22	862	34.77	5346	31.92	1.18
SEEDI	820	15.32	626	18.08	550	19.66	572	21.54	611	24.65	3179	19.98	1.61
SEEDII	208	3.89	151	4.36	166	5.93	167	6.29	174	7.02	866	5.17	1.80
NEC	28	0.52	39	1.13	29	1.04	43	1.62	33	1.33	172	1.03	2.56
EC	20	0.37	29	0.84	31	1.11	46	1.73	53	2.14	179	1.07	5.78
Total	5353		3463		2789		2655		2479		16748		

EBC re-screening

EBC re-screening was carried out at the end of the three year medication period to detect EC patients among the MEED, SEEDI, and SEEDII cases in the treatment and control groups. Among the 4045 SEED cases, 77 EC cases had been diagnosed and registered before EBC re-screening (Table 2). With them excluded, there were 3968 SEED cases who should have been re-screened, and in the end 2976 (75.00%) were re-examined. The re-screening completion rate for the treatment and control groups of SEED was 78.4% and 74.2% respectively. As for the 5346 MEED cases, with the 76 EC cases already diagnosed and registered prior to re-screening excluded, 3775 (71.63%) were re-screened. The re-screening rates for the MEED treatment and control groups were 75.6% and 74% respectively.

Registered EC cases and incidence rates

From half a year after initiation of ZSP and CT medication to the time of re-screening, 77 cases of EC were diagnosed and registered among the 4045 SEED cases (Table 2). The three-year incidence rate by registered EC cases alone for all of the SEED cases was 1.90% (77/4045), and for SEED in the treatment and control groups were 0.78% (11/1396) and 2.49% (66/2649) respectively. A significant difference existed between the incidence rates of the two groups ($\chi^2=14.21, P<0.01$). For the 5346 MEED cases, 76 EC patients were registered. The three year incidence rate for all of the MEED cases was 1.42% (76/5346), and was 1.14% (18/1566) and 1.54% (58/3780) for MEED in the treatment and control groups respectively.

There was no significant difference between the incidence rates of the two groups ($\chi^2=1.17, P>0.05$).

Table 2 Effect of blocking treatment of MEED and SEED cases by ZSP, CT, and PLACEBO after three year medication

Group	No. subjects	EC Diagnosed			Incidence Rates (%)	Block Rates (%)
		EBC Re-screening	Registration	Total		
Treatment	1566	10	18	28	1.79	
Control	3780	26	58	84	2.22	
Total	5346	36	76	112	2.10	19.37

SEED

Group	No. subjects	EC Diagnosed			Incidence Rates (%)	Block Rates (%)
		EBC Re-screening	Registration	Total		
Treatment	1396	17	11	28	2.01	
Control	3649	36	66	102	3.85	
Total	4045	53	77	130	3.21	47.79

Re-screened EC cases and prevalence rates

By EBC re-screening, 53 EC cases were detected from the 2976 SEED cases. The prevalence rate was 1.78% (53/2976) for all of the SEED cases combined, and was 1.61% (17/1054) and 1.87% (36/1922) for SEED cases in the treatment and control groups respectively. There was no significant difference between the prevalence rates of the two groups ($\chi^2=0.26, P>0.05$). Among the 3775 MEED cases, 36 EC cases were diagnosed by EBC re-screening, with a prevalence rate of 0.95% (36/3775) for the MEED combined, 0.89% (10/1114) for the treatment group, and 0.97% (26/2661) for the control group. There was no significant difference in the prevalence rates between the two groups ($\chi^2=0.15, P>0.05$).

Combined incidence and blocking rates

During the first three year follow-up, 242 diagnoses of EC were made by registration and re-screening from the 9,391 SEED and MEED cases, yielding a total incidence rate of 2.58% (242/9391) for SEED and MEED combined, 1.89% (56/2962) for the treatment group, and 2.89% (186/6429) for the control group. A significant difference existed between the two groups ($\chi^2=8.12, P<0.01$). A blocking rate of 34.60% calculated as $(2.89-1.89)/2.89 \times 100\%$ was obtained to assess the effects of a three year period of medication by ZSP and CT.

As in Table 2, 112 EC cases were accumulated by three year registration and EBC-re-screening from the 5346 MEED cases (76 registered and 36 screened out). An incidence rate of 2.10% (112/5346) was calculated for the whole MEED group, 1.79% (28/1566) for MEED in the treatment group, and 2.22% (84/3780) for MEED in the control group. The difference between the incidence rates of the two groups did not reach a significant level ($\chi^2=1.02, P>0.05$), and a blocking rate of 19.37% was calculated to demonstrate the effect of CT for MEED cases.

130 EC cases were diagnosed from the 4045 SEED cases by three year registration and EBC re-screening (77 registered and 53 re-screened out). The incidence rate was 3.21% for all of the SEED cases, 2.01% (28/1396) for SEED in the treatment, and 3.85% (102/2649) for SEED in the control group. The difference between the incidence rates of the two groups reached a significant level ($\chi^2=10.00, P<0.01$), and the blocking rate by ZSP for SEED was 47.79%.

Incidence and blocking rates of EC for SEEDI and SEEDII

As in Table 3, 69 EC diagnoses were made during the three year study

period among the 3179 SEEDI cases. The incidence rate was 2.17% (69/3179) for all of the SEEDI cases, 1.66% (20/1206) for SEEDI in the treatment group, and 2.48% (49/1973) for SEEDI in the control group. There was no significant difference between the incidence rates of the treatment and control group ($\chi^2=2.40, P>0.05$), and the corresponding blocking rate was 33.06%.

There were 61 EC cases diagnosed from the 866 SEEDII cases during the same period, yielding an incidence rate of 7.04% (61/866) for all of the SEEDII, 2.87% (8/279) for SEEDII in the treatment group, and 9.03% (53/587) for SEEDII in the control group. A significant difference was observed between the two incidence rates of the two groups ($\chi^2=10.00, P<0.01$), and the blocking rate of ZSP for SEEDII was 68.22%.

Table 3 Results of blocking treatment of SEEDI and SEEDII cases by ZSP and PLACEBO after three years of medication

Group	No. subjects	No. EC Diagnosed	Incidence Rates (%)	Block Rates (%)
Treatment	1206	20	1.66	
Control	1973	49	2.48	
Total	3179	69	2.17	33.06

SEEDII

Group	No. subjects	No. EC Diagnosed	Incidence Rates (%)	Block Rates (%)
Treatment	279	8	2.87	
Control	587	53	9.03	
Total	866	61	7.04	68.22

DISCUSSION

Dysplasia is an atypical state of the epithelium with a basophilic matrix, a high matrix-core ratio, and hyperheterochromatin. It is historically classified into three grades according to the degree of atypical epithelium in comparison with the basal zone as defined by the World Health Organization's International Histological Classification of Tumors^[43]. Atypical cells localized in the basal zone in MEED, while immature cells occupy more than three quadrants of the epithelium in SEEDI and SEEDII.

In this study, we found that 31.92% and 24.15% of people aged 40 years and older in Chixian could be diagnosed as MEED and SEED cases. Qiu and Yang^[44] have reported a similar dysplasia rate of 32.28% in people aged 21 years and older in Linxian, which is a neighboring County to Chixian County situated in the same Taihang Mountain area in northern China where there is the highest incidence of EC. However, the rate of dysplasia in low risk regions was only 4.78%, most of the dysplasia belonged to MEED, and the frequency of dysplasia correlated well with the regional level of ECs.

The severity of dysplasia increased with age. As in Table 1, as patients got older, their chances of being detected as one of the dysplasia states grew higher. This was true with MEED, SEED I, and SEEDII. Moreover, the extent of increase in detection rates with age was small for MEED, large for SEEDI, and still larger for SEEDII. The Odds Ratios of the detection rates of the 60-year-old group versus that of the 40-year-old group for MEED, SEEDI and SEEDII were 1.18, 1.61, and 1.80 respectively. This increase with age is remarkably similar to the increase of incidence or mortality of EC with age^[46-50], but the degree of the latter was much greater. As in Table 1, the Odds Ratio of detection rates of 60-year-olds against that of 40-year-olds grew up to 2.56 and 5.78 for NEC and EC. It may be suggested that the increase of dysplasia rates with age was small and unstable or reversible for the less severe states such as MEED, but

became fixed and remarkably large as the dysplasia progressed into more severe stages or transformed into NEC and EC.

While the chances of dysplasia increased with age, the total detection rates for MEED, SEED and SEEDII decreased from 31.92%, 18.98% to 5.17% in the direction of dysplasia development. It may suggest that although dysplasia may proceed further, only a limited portion proceeds into more severe or malignant.

Our finding and discussion so far support the notion that dysplasia belongs to a early form of carcinoma. The main difference between dysplasia and EC may be that dysplasia is an unstable or unfixed state of existence. It may develop further, but much of it will stay unchanged, or even return to normal or less severe again. Therefore, if we could detect and treat precancerous dysplasia lesions before they develop into carcinomas, then the long-term survival of ECs should dramatically improve.

The present study has focused primarily on the blocking treatment of dysplasia cases in high risk populations. The result was that ZSP blocked EC incidence rate by 47.79% after 3 years of medication for the SEED cases. In a previous National Seventh Five Research Project carried out in Linxian County, Lin found that ZSP reduced the EC transformation rate of SEED cases by 52.2% after 3 year medication^[24]. These consistent findings by a series of population-based prospective cohort studies in the same high risk area enabled us to conclude that EC is preventable on the secondary blocking treatment level, and ZSP is an effective agent to treat precancerous EC lesions in high risk areas^[51-53].

Experimental observations indicate that cancer preventive chemical agents take effect by acting on the promotion stage^[25]. The anticarcinogenicity of certain Chinese herbs is considered to share the same mechanism. In this study, the significant blocking rate of 47.79% by ZSP for the SEED cases resulted mainly from the difference in the registered incidence of EC between the treatment and control groups, as there was no significant difference in the re-screened EC incidence rates between the two groups. As we know, registered EC represents clinically diagnosed late-staged EC, while EC screened out by EBC belonged to the early asymptomatic patients. The finding that ZSP reduced only the registered three year incidence rate, but not the EBC re-screened incidence rate of EC suggests that ZSP may have blocked or delayed the appearance of clinically recognizable EC developed from SEED. In other words, ZSP acted mainly on the late stage of EC development. As in Table 3, the more remarkable blocking rate by ZSP for SEEDII versus SEEDI (68.22% versus 33.06%) also supports the idea that ZSP was effective in blocking or delaying the appearance of EC during the late stages of EC development.

In a previous comprehensive field prevention and treatment study of esophageal cancer carried out in Linxian county, Lin found that Riboflavin had no significant effect on MEED cases at the end of three years of medication, but a blocking rate of 37.0% appeared at the end of 9 year follow up^[24,25]. The result at the end of a three year medication period was the same as in the present study. Further findings will be reported by continuous observation.

In conclusion, we regard dysplasia as a precancerous lesion in people aged 40 years and older in high risk areas. Efforts should be made to screen and treat dysplasia cases before the disease transforms into the irreversible malignant state. Effective screening plus blocking treatment in high risk populations may reduce the mortality rate of EC over the long term. ZSP has been made from natural Chinese herbs which are cheap and share rich resources. Repeated demonstration of its ability will make it a promising agent for secondary prevention of EC.

REFERENCES

- Chen KN, Xu GW. Diagnosis and treatment of esophageal cancer. *Shijie Huaren Xiaohua Zazhi* 2000;8:196-202
- Liu HF, Liu WW, Fang DC. Study of the relationship between apoptosis and proliferation in gastric carcinoma and its precancerous lesion. *Shijie Huaren Xiaohua Zazhi* 1999;7:649-651
- Sherman Jr CD. Digestive carcinomas. In: Union Internationale Contre Le Cancer (UICC). Manual of clinical oncology 5. Beijing: The joint publishing house of Beijing Medical University and China Union Medical University, 1992:237-38
- Urba SG, Orringer MB, Tamayo CP, Bromberg J, Forastiere A. Concurrent preoperative chemotherapy and radiation therapy in localized esophageal adenocarcinoma. *Cancer* 1992;69:285-289
- China Ministry Of Public Health. Esophageal cancer. In: China Ministry Of Public Health, ed. Diagnosis and treatment criteria for common malignances in China 2. Beijing: The joint publishing house of Beijing Medical University and China Saint Medical University, 1991:30-31
- Wolfe WG, Anna L, Vaughn RN, Seigler HF, Hathorn JW, Leopold KA, Duhaylongsod FG, Durham NC. Survival of patients with carcinoma of the esophagus treated with combined-modality therapy. *J Thorac Cardiovasc Surg* 1993;105:749-756
- Wang ZQ, He J, Chen W, Chen Y, Zhou TS, Lin YC. Relationship between different sources of drinking water, water quality improvement and gastric cancer mortality in Changle County-A retrospective-cohort study in high incidence area. *World J Gastroenterol* 1998;4:45-47
- Sun JJ, Zhou XD, Zhou G, Liu YK. Expression of intercellular adhesive molecule-1 in liver cancer tissues and liver cancer metastasis. *World J Gastroenterol* 1998;4:202-205
- Yoneda M. Regulation of hepatic function by brain neuropeptides. *World J Gastroenterol* 1998;4:192-196
- Yu JY, Wang LP, Meng YH, Hu M, Wang JL, Bordin C. Classification of gastric neuroendocrine tumors and its clinicopathologic significance. *World J Gastroenterol* 1998;4:158-161
- Deng LY, Zhang YH, Xu P, Yang SM, Yuan XB. Expression of IL-1 β converting enzyme in 5-FU induced apoptosis in esophageal carcinoma cells. *World J Gastroenterol* 1999;5:50-52
- Xiao B, Jing B, Zhang YL, Zhou DY, Zhang WD. Tumor growth inhibition effect of hIL-6 on colon cancer cells transfected with the target gene by retroviral vector. *World J Gastroenterol* 2000;6 :89-92
- Qian SB, Chen SS. Transduction of human hepatocellular carcinoma cells with human Y-interferon gene via retroviral vector. *World J Gastroenterol* 1998;4:210-213
- Shen ZY, Xu LY, Li EM, Cai WJ, Chen MH, Shen J, Zeng Y. Telomere and telomerase in the initial stage of immortalization of esophageal epithelial cell. *World J Gastroenterol* 2002;8:357-362
- Cao WX, Qu JM, Fei XF, Zhu ZG, Yin HR, Yan M, Lin YZ. Methionine-dependence and combination chemotherapy on human gastric cancer cells *in vitro*. *World J Gastroenterol* 2002;8:230-232
- Wu K, Zhao Y, Liu BH, Li Y, Liu F, Guo J, Yu WP. RRR- α -tocopheryl succinate inhibits human gastric cancer SGC-7901 cell growth by inducing apoptosis and DNA synthesis arrest. *World J Gastroenterol* 2002;8:26-30
- Ma LS. Intensify improvement of the diagnosis and treatment level of digestive system diseases in China. *World J Gastroenterol* 1998;4 :287-293
- Gu QL, Li NL, Zhu ZG, Yin HR, Lin YZ. A study on arsenic trioxide inducing *in vitro* apoptosis of gastric cancer cell lines. *World J Gastroenterol* 2000;6 :435-437
- Zou SC, Qiu HS, Zhang CW, Hou QT. A clinical and long term follow up study of perioperative sequential triple therapy for gastric cancer. *World J Gastroenterol* 2000;6:284-287
- Chen GR, Jiang XL, Wang YP. Endoscopic treatment skill on submucosal benign tumors. *Dia Treat Dig Dis* 2001;1:43-45
- Zhang XY. Some recent works on diagnosis and treatment of gastric cancer. *World J Gastroenterol* 1999;5:1-3
- Qiao GB, Han CL, Jiang RC, Sun CS, Wang Y, Wang YJ. Overexpression of P53 and its risk factors in esophageal cancer in urban areas of Xi'an. *World J Gastroenterol* 1998;4:57-60
- Chai L, Yu SZ. Gastric cancer molecular epidemiology in Fujian Changle. *Shijie Huren Xiaohua Zazhi* 1999;7:652-655
- Lin PZ, Chen ZF, Hou J, Liu TG, Wang JX, Ding ZW, Guo LP, Li SS, Men FS, Du CL. Chemical prevention of esophageal cancer. *Zhongguo Yixue Keixue Yuan Xuebao* 1998;20:413-417
- Lin PZ, Zhang JS, Rong ZP, Han R, Xu SP, Gao RQ, Ding ZW, Wang JX, Feng HJ, Cao SG, Guo WS. Medicamentous inhibitory therapy of precancerous lesions of the esophagus-3 and 5 year inhibitory effect of ZSP, Retinamide and Riboflavin. *Zhongguo Yixue Keixue Yuan Xuebao* 1990;12:235-245
- Shen Q, Wang DL, Xiang YY, Wang C, Ren ZC, Yan AH, Ren XH, Chang FJ, Zhang JM, Ye XJ, Zhou YF, Huang M, Zhen HZ, Chai XS, Chen HM, Zhang JQ, Chang YF, Luo DS. A preliminary report of nutritional intervention in dysplasia of the esophagus. *Zhongguo Zhongliu Lichuang* 1991;18:31-35
- Hou J, Yuan FR, Li SS, Li ZY, Chen ZF. A clinical study on the treatment results of esophageal dysplasia by composite Dangsheng pill. *Zhongguo Yixue Xuebao* 1992;7:11-13
- Kitamura K, Kuwano H, Yasuda M, Sonoda K, Sumiyoshi K, Tsutsui S, Kitamura M, Sugimachi K. What is the earliest malignant lesion in the esophagus? *Cancer* 1996;77:1614-1618

- 29 Xia HK. Association between *Helicobacter pylori* and gastric cancer: current knowledge and future research. *World J Gastroenterol* 1998;4: 93-96
- 30 Tian XJ, Wu J, Meng L, Dong ZW, Shou CC. Expression of VEGF 121 in gastric carcinoma MGC803 cell line. *World J Gastroenterol* 2000;6:281-283
- 31 Assy N, Paizi M, Gaitini D, Baruch Y, Spira G. Clinical implication of VEGF serum levels in cirrhotic patients with or without portal hypertension. *World J Gastroenterol* 1999;5:296-300
- 32 Xiao ZF, Yang ZY, Zhou ZM, Yin WB, Gu XZ. Radiotherapy of double primary esophageal carcinoma. *World J Gastroenterol* 2000;6:145-146
- 33 Xiao B, Shi YQ, Zhao YQ, You H, Wang ZY, Liu XL, Yin F, Qiao TD, Fan DM. Transduction of Fas gene or Bcl-2 antisense RNA sensitizes cultured drug resistant gastric cancer cells to chemotherapeutic drugs. *World J Gastroenterol* 1998;4:421-425
- 34 Zhang QX, Dou YL, Shi XY, Ding YI. Expression of somatostatin mRNA in various differentiated types of gastric carcinoma. *World J Gastroenterol* 1998;4:48-51
- 35 Hou J, Chen ZF, Li SS, Li ZY, Yan HR. Clinical study on treatment of esophageal precancerous lesion with Cangdouwan Pill. *Zhongguo Zonglun Lingchuang* 1996;23:117-119
- 36 Wu QM, Li SB, Wang Q, Wang DH, Li XB, Liu CZ. The expression of COX-2 in esophageal carcinoma and its relation to clinicopathologic characteristic. *Shijie Huaren Xiaohua Zazhi* 2001;9:11-14
- 37 Hou J, Yan FR, Li SS, Li ZY, Chen ZF. Clinical study on the effect of Cangdouwan on esophageal precancerous lesion. *Zhongguo Zhongxiyi Jiehe Zhazhi* 1992;12:604-606
- 38 Abe M, Takahashi M. Intraoperative radiotherapy: the Japanese experience. *Int J Radiat Oncol Biol Phys* 1981;7:863-868
- 39 Swisher SG, Hunt KK, Holmes C, Zinner MJ, McFadden DW. Changes in the surgical management of esophageal cancer from 1970-1993. *The American J. Surgery* 1995;169:609-615
- 40 Tao DM, Xu YZ, Wang XH, Gu YK, Wang DY, Wang TX. Follow up of 417 cases of severe esophageal dysplasia. *Henan Zhongliuxue Zhazhi* 1997;10:38-43
- 41 Li JY, Blot LI B, Tailor, Guo WD, Wang W, Liu PQ, Zhen SF, Yang ZS, Liu FS, Sun YH, LIU SF, Wang GQ, Wang ZY, Zhang YH, Lu SX, Wu YP, Zhou XN, Shen Q, Zhang DH, Lian GT, Hu TS, Wang ZQ, Liu Y, Greenwood, Flawmeine. Preliminary reports of population-based nutritional preventive experiment of cancer and other common diseases. *Zhonghua Zhongliu Zhazhi* 1993;15:165-181
- 42 Semba S, Yokozaki H, Yamamoto S, Yasui W, Tahara E. Microsatellite instability in precancerous lesions and adenocarcinomas of the stomach. *Cancer* 1996;77:1620-1627
- 43 Correa P. Precursors of gastric and esophageal cancer. *Cancer* 1982; 50:2554-2565
- 44 Qiu SL, Yang GR. Precursor lesions of esophageal cancer in high-risk population in Henan province. *Cancer* 1988;62:551-557
- 45 Mimori K, Mori M, Tanaka S, Akiyoshi T, Sugimachi K. The overexpression of elongation factor 1 Gamma mRNA in gastric carcinoma. *Cancer* 1995;75:1446-1449
- 46 Forastiere AA, Orringer MB, Perez-Tamayo C, Urba SG, Husted S, Takasugi BJ, Zahurak M. Concurrent chemotherapy and radiation therapy followed by transhiatal esophagectomy for local-regional cancer of the esophagus. *J Clinical Oncology* 1990;8:119-127
- 47 Cao GH, Yan SM, Yuan ZK, Wu L, Liu YF. A study of the relationship between trace element Mo and gastric cancer. *World J Gastroenterol* 1998;4:55-56
- 48 Jiang YF, Yang ZH, Hu JQ. Recurrence or metastasis of HCC: Predictors, early detection and experimental antiangiogenic therapy. *World J Gastroenterol* 2000;6:61-65
- 49 Qiao YL, Hou J, Yang L, He YT, Liu YY, Li LD, Li SS, Lian SY, Ding ZW. Trend of esophageal cancer in the high risk area of Taihang mountain and prevention strategy. *Zhongguo Yixue Kei Xueyuan Xuebao* 2001;23:10-14
- 50 Inoue H, Takeshita K, Hori H, Muraoka Y, Yoneshita H, Endo M. Endoscopic mucosal resection with a cap-fitted panendoscope for esophagus, stomach, and colon mucosal lesions. *Gastrointestinal Endoscopy* 1993;39:58-64
- 51 Dong ZW, Tang PZ, Li LD. Control strategy in high risk area of esophageal cancer in China. *Zhongguo Zhongliu* 2000;9:71-73
- 52 Shen Q, Zhen HZ, Cai XS, Chen HM, Zhang JQ, Wang DL, Xiang YY, Chang YF, Luo DS, Wang C, Chang FJ. Compound riboflavin used in nutritional intervention of esophageal dysplasia- A long-term study. *Henan Zhongliuxue Zhazhi* 1991;4:1-5
- 53 Ding ZW, Gao F, Lin PZ, Wang JX, Guo LP. Long term effect of block treatment for esophageal dysplasia cases. *Zhonghua Zhongliu Zhazhi* 1999; 21:275-277

Edited by Pagliarini R

• ESOPHAGEAL CANCER •

Tumor suppressor gene p16 and Rb expression in gastric cardia precancerous lesions from subjects at a high incidence area in northern China

Yun Zhou, Shan-Shan Gao, Yong-Xin Li, Zong-Min Fan, Xin Zhao, Yi-Jun Qi, Jun-Ping Wei, Jian-Xiang Zou, Gang Liu, Li-Huo Jiao, Yong-Min Bai, Li-Dong Wang

Yun Zhou, Department of Oncology, the First Affiliated Hospital, Zhengzhou University, Zhengzhou 450052, Henan Province, China
Shan-Shan Gao, Yong-Xin Li, Zong-Min Fan, Xin Zhao, Yi-Jun Qi, Jun-Ping Wei, Jian-Xiang Zou, Gang Liu, Li-Huo Jiao, Yong-Min Bai, Li-Dong Wang, Laboratory for Cancer Research, College of Medicine, Zhengzhou University (Formerly Henan Medical University), Zhengzhou 450052, Henan Province, China
Supported by the National Natural Science Foundation of China, No. 39770296

Correspondence to: Li-Dong Wang, M.D., Laboratory for Cancer Research, College of Medicine, Zhengzhou University, Zhengzhou 450052, Henan Province China. ldwang@371.net
Telephone: +86-371-6970165 Fax: +86-371-6970165
Received 2001-07-05 Accepted 2001-07-16

Abstract

AIM: To further understand the molecular basis for gastric cardia carcinogenesis and to provide etiological clues.

METHODS: Endoscopic mucosa biopsy and histopathological examinations were made on 37 subjects from a high incidence area for both esophageal and gastric cardia carcinomas in northern China. All the biopsy samples were fixed in 850ml⁻¹ alcohol and embedded in paraffin. Each block contained one piece of tissue and was serially sectioned at 5 μ m. Immunohistochemistry (ABC) was carried out on these gastric cardia samples to determine the alterations of p16 and Rb.

RESULTS: Based on the histopathological examination there were 11 cases of chronic superficial gastritis, 12 cases of chronic atrophic gastritis and 14 cases of dysplasia. The immunostaining demonstrated different levels of unclear immunostaining of p16 and Rb in normal gastric cardia tissue and the tissues with different severity of lesions. With the lesions progressing, the positive immunostaining rates for p16 protein had a decreasing tendency. In contrast, the positive immunostaining rate for Rb protein had an increasing tendency. There was a significant negative relationship between the two parameters. Changes of p16 was CSG 11(100%), CAG 7 (58%), DYS 4(29%) and changes of Rb was CSG 2(18%), CAG 8(67%) and DYS 12(86%), ($P<0.05$).

CONCLUSION: The alterations of p16 and Rb protein may play a role in the early stages of gastric cardia carcinogenesis.

Zhou Y, Gao SS, Li YX, Fan ZM, Zhao X, Qi YJ, Wei JP, Zou JX, Liu G, Jiao LH, Bai YM, Wang LD. Tumor suppressor gene p16 and Rb expression in gastric cardia precancerous lesions from subjects at a high incidence area in northern China. *World J Gastroenterol* 2002;8(3):423-425

INTRODUCTION

Gastric cardia cancer is subject being studied. An interesting observation is that gastric cardia cancer and esophageal cancer seem to

occur together in many high-incidence areas in China, and both were referred to as esophageal cancer (EC) by the public because of the common syndrome of dysphagia^[1,2]. Histologically, esophageal and gastric cardia cancers have been considered as single clinical entity for incidence and mortality calculation in China. The molecular changes in the early stage of gastric cardia carcinogenesis have not been characterized^[3-5]. In the present study, we investigated the roles of p16 and Rb alteration in gastric cardia carcinogenesis by measuring the expression rates of p16 and Rb in normal gastric cardia tissues and the tissues with different severity of lesions from the symptom-free subjects at a high incidence area of gastric cardia cancers in Henan, northern China.

MATERIALS AND METHODS

Tissue collection and processing

Gastric cardia biopsies were taken from 37 symptom-free subjects at Huixian County and Linxian County, Henan Province, China, the high-risk areas for esophageal and gastric cardia cancers during the mass survey. All the biopsy specimens were fixed with 850ml⁻¹ alcohol, embedded with paraffin, and serially sectioned at 5 μ m. The sections were mounted onto histostick-coated slides. Three or four adjacent ribbons were collected for histopathological analysis (HE stain), and immunohistochemical staining. Histopathological diagnosis for gastric cardia epithelia was made using the previously established criteria. Based on the cellular morphological changes and tissue architecture, the gastric cardia epithelia were graded as chronic superficial gastritis (CSG), chronic atrophic gastritis (CGT) and dysplasia (DYS)^[6-9]. The polyclonal p16 antibody is rabbit antiserum against human p16 protein (Dakoco, USA). The polyclonal Rb antibody is rabbit antiserum against man Rb protein (Oncogene Science Inc., USA). After dewaxing, inactivating endogenous peroxidase activity, and blocking cross-reactivity with normal serum, we incubated the sections with a diluted solution of the primary antibodies overnight at 4°C (1:100 for p16, 1:100 for Rb). Location of the primary antibodies was achieved by subsequent application of a biotinylated anti-primary antibody, an avidin biotin complex conjugated to horseradish peroxidase, and diaminobenzidine (Vectastain Elite Kit, Dako, USA). Normal serum blocking and omission of the primary antibody were used as negative controls^[10,15].

Statistical analysis

The data were expressed as the mean \pm SD unless otherwise stated. The χ^2 test was used for histopathological and immunostaining rate evaluation ($P<0.05$ considered significant).

RESULTS

Histopathology findings

Histopathological examination showed that there were 11 cases of chronic superficial gastritis, 12 cases of chronic atrophic gastritis and 14 cases of dysplasia (Table 1). Both p16 and Rb immunostaining-positive cells were observed in different severity of lesions of gastric

cardia epithelia. In CSG, the positive immunostaining rates of p16 was much higher than that of Rb. An interesting observation is that the positive immunostaining rate of p16 was much lower than that of Rb in DYS. As the lesions of gastric cardia epithelia progressed from CSG to DYS, the positive immunostaining rates of p16 decreased significantly ($P < 0.05$), especially from CSG to CAG. However, the positive immunostaining rates of Rb increased significantly ($P < 0.05$). Correlation analysis showed significantly negative correlation between the decreasing tendency of P16 and the increasing tendency of Rb with the lesions progressing from CSG, CAG to DYS.

Table 1 Changes of p16 and Rb in gastric cardia precancerous lesions

Histological types	Number examined	P16 IHC positive ^a n (%)	Rb IHC positive ^b n (%)
CSG	11	11(100)	2(18)
CAG	12	7(58)	8(67)
DYS	14	4(29)	12(86)

^a $P < 0.05$, CSG vs CAG, CAG vs DYS; ^b $P < 0.05$, DYS vs CAG, CAG vs. CSG

DISCUSSION

Gastric cardia carcinoma (GCC) is one of the most frequent digestive malignant diseases in northern China. A remarkable epidemiological characteristic for GCC is the occurring together with esophageal cancer in the same high-incidence area (HIA). In contrast with the strikingly decreasing of incidence rate of distal gastric cancer around the world in the past two decades, especially in America and Europe, the incidence of GCC increased dramatically; the incidence of esophageal-gastric-junction cancer increased to 6 folds with a speed of 4% yearly, which was one of the fastest increasing malignant diseases, the mechanism in unclear. There are several distinct differences between GCC and distal gastric cancer with respect to epidemiology, etiological factors, histogenesis and clinical characteristics, and therefore GCC should be categorized as a distinct clinical disease. Lacking of sensitive and diagnostic biomarker and technique in early stage of GCC as well as the deficiency of effective and specific reagents for its treatment and prevention leads to its poor prognosis and higher mortality. An interesting observation in this study was that the alterations of tumor suppressor gene p16 and Rb products occurred in the early stage of gastric cardia carcinogenesis, even in CSG. With the lesions progressing from CSG, CAG to DYS, the positive immunostaining rates of p16 decreased significantly, especially from CSG to CAG. However, the positive immunostaining rates of Rb increased significantly. The positive immunostaining rate of p16 was much higher than of Rb in CSG. But, in DYS, the positive immunostaining rates of p16 was much lower than that of Rb. These results suggested that the tumor suppressor gene p16 and Rb may play different roles in the different stages of gastric cardia epithelia carcinogenesis. CAG and GYS have been considered as precancerous lesions of stomach cancer. Although the role of CSG is not clear during the gastric cardia carcinogenesis, it may provide a favorable macroenvironment for gastric carcinogenesis. The significance of CSG in the development of stomach cancer remains to be further characterized.

P16 gene, located at chromosome 9p21, is a new tumor suppressor gene, which was identified by an American molecular geneticist in 1995 and is also called multiple tumor suppressor 1 (MTS1) for its suppressing function to multiple tumors. Recent studies showed that the changes of p16 gene and its products were found in many primary tumors and cell lines^[9,11-15]. Rb gene is the first tumor suppressor gene identified by the location cloning method, located at chromosome 13p. The product of Rb is a nuclear phosphoprotein, which is distributed extensively in different kinds of tissues^[16-22]. It was considered that the cell-cycle progression normally depends on regulation by cyclins and cyclin inhibiting proteins. The overexpression of cyclins and/or the deletion of inhibiting protein could result in overworking of cell-cycle dependent kinetics (cdk),

which makes cells enter into proliferative stage. The p16 could functionally inhibit cdk activity specifically and make Rb unphosphorylated, thus preventing the cell cycle progression from G1 phase to S phase^[22-26].

Tam *et al* found that inactive Rb and/or Rb protein exist in all of the p16 over-expression cell lines, and inactive Rb protein could act directly on p16, suggesting that Rb can inhibit p16 protein expression. P16, Rb and cdk may constitute a feedback regulation circle. In the present study, a significant negative relationship between p16 and Rb protein expression was observed, which is consistent with Tam's observation^[26-33].

REFERENCES

- Zhou Q, Zou JX, Chen YL, Yu HZ, Wang LD, Li YX, Guo HQ, Gao SS, Qiu SL. Alteration of tumor suppressor gene p16 and Rb in gastric carcinogenesis. *Xin Xiaohuabingxue Zazhi* 1997;5:705-706
- Wang Y, Yang SQ, Wang ZG, Pu XD, Sun WG, Liu GZ. Significance of P16 protein expression in hepaticocellular carcinoma tissues. *Huaren Xiaohua Zazhi* 1998;6:412-414
- Quan J, Fan XG. Progress in experimental research of *Helicobacter pylori* infection and gastric carcinoma. *Shijie Huaren Xiaohua Zazhi* 1999;7:1068-1069
- Lu JG, Huang ZQ, Wu JS, Wang Q, Ma QJ, Yao X. Significance of tumor suppressor gene p16 expression in primary biliary cancer. *Shijie Huaren Xiaohua Zazhi* 2000;8:638-610
- Xiao WH, Liu WW, Lu YY, Li Z. Mutation of suppressor gene p53 in hepatocellular carcinoma. *Xin Xiaohuabingxue Zazhi* 1997;5:573-574
- Jiang HH, Liu ZM, Zuang YQ, Yang DH, Jiang YQ, Li JQ. Homozygous deletion of p16 in human gastric adenocarcinoma. *Huaren Xiaohua Zazhi* 1998;6:934-935
- Wu SH, Ma LP, Lin W, Sui YF. The relation between suppressor gene p16, p21, PRB and gastric cancer. *Shijie Huaren Xiaohua Zazhi* 1999;7:551
- Qi YJ, Wang LD, Nie Y, Cai C, Yang GY, Xing EP, Yang CS. Alteration of p16 mRNA expression in esophageal cancer tissue from patients at high incidence area in northern China. *World J Gastroenterol* 1998;4(Suppl 2):108
- Luo F, Kan B, Lei S, Yan LN, Mao YQ, Zou LQ, Yang YX, Wei YQ. Study on p53 protein and C-erbB2 protein expression in primary hepatic cancer and colorectal cancer by flow cytometry. *World J Gastroenterol* 1998;4(Suppl 2):87
- Jiao LH, Wang LD, Xing EP, Yang GY, Yang CS. Frequent inactivation of p16 and p15 expression in human esophageal squamous cell carcinoma detected by RT-PCR. *World J Gastroenterol* 1998;4(Suppl 2):105
- Tian XJ, Wu J, Meng L, Dong ZW, Shou CC. Expression of VEGF-121 in gastric carcinoma MGC803 cell line. *World J Gastroenterol* 2000;6:281-283
- Liu HF, Liu WW, Fang DC, Men RP. Expression of bcl-2 protein in gastric carcinoma and its significance. *World J Gastroenterol* 1998;4:228-230
- He SW, Shen KQ, He YJ, Xie B, Zhao YM. Regulatory effect and mechanism of gastric and its antagonists on colorectal carcinoma. *World J Gastroenterol* 1999;5:408-416
- Huang PL, Zhu SN, Lu SL, Dai SZ, Jin YL. Inhibitor of fatty acid synthase induced apoptosis in human colonic cancer cells. *World J Gastroenterol* 2000;6:295-297
- Zhou Q, Zou JX, Chen YL, Yu HZ, Wang LD, Li YX, Guo HQ, Gao SS, Qiu SL. Alteration of tumor suppressor gene p16 and Rb in gastric carcinogenesis. *China Nat J New Gastroenterol* 1997;3:265
- Yang JM, Wang RQ, Bu BG, Zhou ZC, Fang DC and Luo YH. Effect of HCV infection on expression of several cancer-associated gene products in HCC. *World J Gastroenterol* 1999;5:25-27
- Qin Y, Li B, Tan YS, Sun ZL, Zuo FQ, Sun ZF. Polymorphism of p16INK4a gene and rare mutation of p15INK4b gene exon2 in primary hepatocarcinoma. *World J Gastroenterol* 2000;6:411-414
- Li J, Yang XK, Yu XX, Ge ML, Wang WL, Zhang J, Hou YD. Overexpression of p27KIP1 induced cell cycle arrest in G1 phase and subsequent apoptosis in HCC-9204 cell line. *World J Gastroenterol* 2000;6:513-521
- Favrot M, Coll JL, Louis N, Negoescu A. Cell death and cancer: replacement of apoptotic genes and inactivation of death suppressor genes in the rapy. *Gene Ther* 1998;5:728-739
- Gao HJ, Yu LZ, Bai JF, Peng YS, Sun G, Zhao HL, Miu K, Lu XZ, Zhang XY, Zhao ZQ. Multiple genetic alterations and behavior of cellular biology in gastric cancer and other gastric mucosal lesion: *H. pylori* infection, histological types and staging. *World J Gastroenterol* 2000;6:848-854
- Huang ZM. Modern research in traditional herbal medicine Oenanthe

- Javanica. *Shijie Huaren Xiaohua Zazhi* 2001;9:1-5
- 22 Quigley EMM. Is there a pathologic basis for gastrointestinal dysotility? *World J Gastroenterol* 1998;4(Suppl 2):10-17
- 23 Zhou YA, Gu ZP, Wang XX, Ma QF, Huang LJ. Reexpression of p16-INK4a gene suppresses growth of human esophageal carcinoma cells. *Shijie Huaren Zazhi* 2001;9:877-881
- 24 Chino O, Kijima H, Nishi T, Tanaka H, Oshiba G, Kise Y, Kajiwarra H, Tsuchida T, Tanaka M, Tajima T, Makuuchi H. Clinicopathological studies of esophageal carcinoma on achalasia: analysis of carcinogenesis using histological and immunohistochemical procedures. *Anticancer Res* 2000;20 :3717-3722
- 25 Jin S, Peng Q, Lu S. Deletion of MTS1/p16 gene in human esophageal carcinoma. *Zhonghua Zhongliu Zazhi* 1998;20:9-11
- 26 Chiang PW, Beer DG, Wei WL, Orringer MB, Kurnit DM. Detection of erbB-2 amplifications in tumors and sera from esophageal carcinoma patients. *Clin Cancer Res* 1999;5:1381-1386
- 27 Schrupp DS, Matthews W, Chen GA, Mixon A, Altirki NK. Flavopiridol mediates cell cycle arrest and apoptosis in esophageal cancer cells. *Clin Cancer Res* 1998;4:2885-2890
- 28 Tang YC, Li Y, Qian GX. Reduction of tumorigenicity of SMMC27721 hepatoma cells by vascular endothelial growth factor antisense gene therapy. *World J Gastroenterol* 2001;7:22-27
- 29 Chen QP. Enteral nutrition and acute pancreatitis. *World J Gastroenterol* 2001;7:185-192
- 30 Niu WX, Qin XY, Liu H, Wang CP. Clinicopathological analysis of patients with gastric cancer in 1200 cases. *World J Gastroenterol* 2001;7:281-284
- 31 Yuan P, Sun MH, Zhang JS, Zhu XZ, Shi DR. APC and K ras gene mutation in aberrant crypt foci of human colon. *World J Gastroenterol* 2001;7:352-356
- 32 He XS, Su Q, Chen ZC, He XT, Long ZF, Ling H, Zhang LR. Expression, deletion and mutation of p16 gene in human gastric cancer. *World J Gastroenterol* 2001;7:515-521
- 33 Zhang XL, Quan QZ, Wang YJ, Jiang XL, Wang D, Li WB. Protective effects of cyclosporine A on T cell dependent ConA induced liver injury in Kunming mice. *World J Gastroenterol* 2001;7:569-571

Edited by Ma JY

• GASTRIC CANCER •

Rapid screening mitochondrial DNA mutation by using denaturing high-performance liquid chromatography

Man-Ran Liu, Kai-Feng Pan, Zhen-Fu Li, Yi Wang, Da-Jun Deng, Lian Zhang, You-Yong Lu

Man-Ran Liu, Kai-Feng Pan, Zhen-Fu Li, Yi Wang, Da-Jun Deng, Lian Zhang, You-Yong Lu, Beijing Institute for Cancer Research, Beijing Laboratory of Molecular Oncology, School of Oncology, Peking University, Beijing 100034, China
Supported by the National Key Basic Science Research Program, No. G1998051203 and National Science Foundation of China (NSFC), No. 39602526.

Correspondence to: Dr. You-Yong Lu, Peking University, School of Oncology, Beijing Institute for Cancer Research, Beijing Laboratory of Molecular Oncology, 1 Da-Hong-Luo-Chang Street, Western District, Beijing 100034, China. yongylu@public.bta.net.cn
Telephone: +86-10-66163061 Fax: +86-10-66175832
Received 2002-01-28 Accepted 2002-03-14

Abstract

AIM: To optimize conditions of DHPLC and analyze the effectiveness of various DNA polymerases on DHPLC resolution, and evaluate the sensitivity of DHPLC in the mutation screening of mitochondrial DNA (mtDNA).

METHODS: Two fragments of 16s gene of mitochondrial DNA (one of them F2 is a mutant fragment) and an A3243G mutated fragment were used to analyze the UV detection limit and determine the minimum percentage of mutant PCR products for DHPLC and evaluate effects of DNA polymerases on resolution of DHPLC. Under the optimal conditions, we analyzed the mtDNA mutations from muscle tissues of mitochondrial encephalomyopathy with lactic acidosis and stroke-like episodes (MELAS) and screened blindly for variances in D-loop region of mtDNA from human gastric tumor specimen.

RESULTS: Ten A3243G variants were detected in 12 cases of MELAS, no alterations were detected in controls and these results were consistent with the results obtained by analysis of RFLP with ApaI. We also identified 26 D-loop variances in 46 cases of human gastric cancer tissues and 38 alterations in 13 gastric cancer cell lines. The mutation of mtDNA at 80ng PCR products containing a minimum of 5% mutant sequences could be detected by using DHPLC with UV detector. Moreover, Ampli-Taq Gold polymerase was equally as good as the proofreading DNA polymerase (e.g., Pfu) in eliminating the false positive produced by Taq DNA polymerases.

CONCLUSION: DHPLC is a powerful, rapid and sensitive mutation screening method for mtDNA. Proofreading DNA polymerase is more suitable for DHPLC analysis than Taq polymerase.

Liu MR, Pan KF, Li ZF, Wang Y, Deng DJ, Zhang L, Lu YY. Rapid screening of mitochondrial DNA mutation by using denaturing high-performance liquid chromatography. *World J Gastroenterol* 2002;8(3):426-430

INTRODUCTION

A number of methods, such as PCR-SSCP, DGGE and CSGE, have been developed to screen the gene mutation. PCR-SSCP is a common method in mutation detection^[1-16]. The low resolution and reproducibility or time-cost limit their application for mutation

screening^[17-23]. Recently, a more accurate and rapid DNA screening strategy^[24-29]—Denaturing High-performance Liquid Chromatography (DHPLC) has been applied to mutation screening in human disease-related gene^[30-42] and prenatal diagnosis^[43,44].

However, there are few published data on detection of mitochondrial DNA (mtDNA) variation by DHPLC, especially in cancer. In order to detect effectively the mtDNA mutation, the optimizations of DHPLC for mtDNA mutation screening have been evaluated. The evaluation included the ultraviolet (UV) detection limit for PCR products with variant ingredients, minimal detected ratio of variant to wild type in PCR mixture. In addition, small peak was often observed preceding the chromatography profile in both amplimers of nucleus and mitochondrial genes when Taq DNA polymerases were used in PCR amplification. It may result in failure of DHPLC analysis. Therefore, we also evaluated the effect of DNA polymerases on the resolution of DHPLC in detection of heteroduplex. Basing on those analyses, we identified the mutation of A3243G substitute for patients with mitochondrial encephalomyopathy with lactic acidosis and stroke-like episodes (MELAS). Finally, the variances of D-loop in mtDNA were blindly screened by DHPLC for patients with gastric carcinoma and gastric cancer cell lines.

MATERIALS AND METHODS

Samples and DNA preparation

The specimen in this study included: (1) 12 cases of MELAS, 72 cases of other mitochondrial encephalomyopathies and 30 cases of controls. (2) 46 paired samples of gastric tumor tissues and non-tumor tissues, and 13 gastric cancer cell lines. (3) A randomly selected fragment (fragment 6: from 2616 to 2884nt) within 16s gene was selected to evaluate effect of 11 brands of DNA polymerases on resolution of DHPLC. (4) Another variant fragment (fragment 2: from 1777 to 2069nt) in 16s gene of gastric cancer cell line MKN45 was used to analyze the UV detection limit of PCR products for DHPLC. A variant sample of MELAS, whose ratio of mutant type (G) to wild type (A) at 3243 allele site was about 60 percent, was employed to determine the minimum percentage of mutant PCR products for DHPLC. The genome DNA was isolated following standard phenol/chloroform and ethanol precipitation extraction procedures.

PCR conditions and quantification of PCR products

Fragment containing A3243G mutation in mtDNA of MELAS was amplified by using one pair of oligonucleotide primers. Fragments of D-loop were amplified by using four pairs of overlapping primers described by Levin *et al*^[45]. Another pair of primers was used to amplify fragment 6 (F6) within 16s gene for assessing effect of DNA polymerases on DHPLC (Table 1). 20μL standard PCR reactive system contain genome DNA 15ng, forward and reverse primer 125nmol·L⁻¹ each, 1×buffer (Mg²⁺ 1.6μmol·L⁻¹), dNTP 37.5μmol·L⁻¹, Pfu DNA polymerase 1.5units (or Taq DNA polymerase 1 unit). PCR was performed with 32 cycles consisting of a denaturing step of 94°C for 35s, primer annealing for 50s and an elongation step of 72°C for 90s. The final step at 72°C was extended to 10min. Annealing temperature of each fragment was showed in table 1. In addition, one mutated fragment (F2), harboring in mitochondrial 16s

gene of gastric cancer cell line MKN45, was used to analyze the UV detection limit of PCR products for DHPLC and amplified by PCR protocol for 19, 21, 24, 27, 30 cycles at annealing temperature of 53°C with Pfu polymerase.

Table 1 Primer sequence, PCR Conditions and DHPLC oven temperature used in this study

Fragments	Size (bp)	Primer Sequence	Annealing temp. (°C)	DHPLC temp. (°C)	DHPLC start gradient
A3243G	494	F: cctcccttaggaaaggaca R: gcctagggttgaggttgacca	59	58	55% B ^a
D-loop F1	505	F: gctggaagatct ttaactccaccattagcacc R: ctacgcgtcgac gcgaggagtagcactcttg	65	58	58%B
D-loop F2	515	F: gctggaagatct aatcaatatccgcacaag R: ctacgcgtcgac ttaagtctgtggccagaag	65	58	58%B
D-loop F3	494	F: gctggaagatct caccctattaaccactcacg R: ctacgcgtcgac tgagattagtagtatggag	58	57	58%B
D-loop F4	585	F: gctggaagatct acaagaacccataaccaccagc R: ctacgcgtcgac acttggttaacgtgtgacc	65	58	59%B
16s-F2	292	F: atatgtaccgcaagggaaga R: ggggttctgtggcgaat	53	56	49%B
16s-G6	268	F: aataggacactgtatgaatgg R: tagttcgttgactgggtg	53	60	51 %B

^aEluent buffer B was 0.1mmol·L⁻¹ TAE, 25% acetonitrile, pH7.0.

The PCR products of mutant fragment (F2) amplified with 19-30 cycles were electrophoresed by 2% agarose gel. The agarose gel was exposed to Kodak Image Station 440CF, and the resulting signal qualified by using the Kodak 1d Image Analysis software. Values were normalized against pUC18 message. A variant sample which ratio of mutant type (G) to wild type (A) at 3243 allele site was about 60 percent and a normal blood sample were amplified respectively. Both PCR products were mixed according to ratio of mutant: wild type to be 50%, 40%, 30%, 20%, 10%, 5% and 0%.

DHPLC analysis

PCR products from gastric cancer cell lines were mixed with about 30 percent of PCR ingredients of normal blood in order to detect homozygous mutation in cell lines. Prior to DHPLC analysis, all fragments were heated to 95°C for 3min, followed by slow cooling to 45°C over 50min to form a mixture of hetero- and homoduplex. The melting temperature and optimal gradient for each fragment (Table 1) can be obtained with WAVEMAKER4.0 software with some empirical optimization. Aliquots of 3μL PCR products were automatically loaded on the DNasep column and eluted on a linear acetonitrile gradient in a 0.1mol·L⁻¹ triethylamine acetate buffer (pH 7.0) with a constant flow rate of 0.9mL·min⁻¹. Elution of DNA from the column was detected by absorbing at 260nm.

DNA sequencing

PCR products were purified by 4% PAGE gel. Direct sequencing of the PCR products was performed by use of the fluorescent terminators on an ABI Prism 377 sequencer (PE Biosystems, USA). The sequence data were checked with MITOMAP Human mtDNA "Cambridge" Sequences (<http://www.gen.emory.edu/MITOMAP/mitoseq.html>).

RESULTS

Optimization of DHPLC for mtDNA mutation detection

The UV detection limit was analyzed for PCR products with variants. The concentration of PCR products of 16s gene containing a variance from gastric cancer cell line MKN45 was about 8, 20, 40, 85 and 110ng·μL⁻¹ after amplification with 19, 21, 24, 27, 30 cycles respectively. The UV detection limit was about 80ng for the PCR products whose mutated ingredients were efficiently detected by DHPLC.

The minimal ratio of heteroduplex detected by DHPLC was studied. To investigate the sensitivity of DHPLC in detection of mtDNA variants, we used PCR products from the mutated MELAS sample to mix with normal blood amplimers based on ratio of mutant to wild type to be 50%, 40%, 30%, 20%, 10%, 5%, 1% and 0%. Our results showed that heteroduplexes were sensitively

detected by DHPLC, when the ratio (mutant:wild) range from 5% to 50% in the mixture of PCR products (Figure 1). Moreover, the chromatography profiles of DHPLC were similar when mutant products in mixture were about 10-40%. It suggested that homozygous mutation could be easily identified if 20-30% wild PCR products were added.

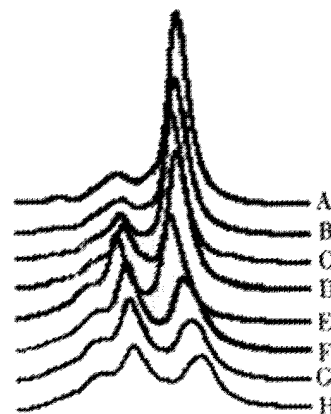


Figure 1 The minimal ratio of hetero-: homoduplex in mixture were identified by DHPLC. The composition of mutant type in PCR product mixture are 0% (A, wild type), 1% (B), 5% (C), 10% (D), 20% (E), 30% (F), 40% (G) and 50% (H) respectively. Chromatogram B has no difference to chromatogram A. Heteroduplex peak start to change in sample containing 5% variant (C). The heteroduplex can be obviously discerned in sample with 10% variant (D). Chromatogram E to H is almost similar. It indicates that about 5% mutant composition in PCR product mixture can be detected by DHPLC.

The effect of DNA polymerases on DHPLC was evaluated. A small peak was often observed preceding the main peak in most of fragments amplified by Taq DNA polymerases. In order to understand whether this was an universality or DHPLC resolution induced by Taq polymerase, we chose 6 brands of Taq, 1 type of Taq Gold and 4 kinds proofreading DNA polymerases to amplify a randomly selected fragment (F6) for DHPLC analysis. Our findings displayed that all in this study gave a broadened peak proceeding the main peak, but Taq Gold and proofreading DNA polymerases (such as Pfu and Vent) had no or tiny peak before the main peak (Figure 2). To exclude the results that were induced by polymerase buffer, we further amplified the fragment using Taq polymerase to match with Taq Gold and proofreading polymerase buffer, or Taq Gold and proofreading polymerase with Taq polymerase buffer. The results indicated that the particular small peak was only related to Taq DNA polymerase itself.

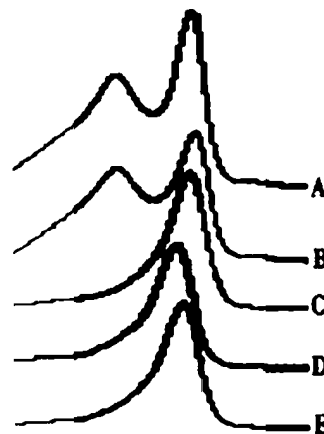


Figure 2 The universality of a broad small peak proceeding the main peak induced by Taq DNA polymerase. An extra small peak is observed preceding the eluted chromatography profile of A and B but not in chromatogram of C, D and E. Chromatogram A is a representative of products amplified by Taq DNA

polymerase. B is typical chromatography profile when Taq DNA polymerase matched with Pfu DNA polymerase buffer in PCR reaction. C and D respectively comes from amplimers amplified by Ampli-Taq Gold and Vent DNA polymerase. E is one of chromatograms coming from PCR amplification by using Pfu DNA polymerase.

Mutation screening of mtDNA

Patients with MELAS have been suggested to associate with mutation of A3243G in tRNA^{Leu}[46,47]. 10 variant cases out of 12 MELAS patients were successfully identified by DHPLC. No alterations were detected in 72 cases with other mitochondrial encephalomyopathies and 30 controls at this allele site. These results were completely consistent with results obtained by restriction endonuclease Apa I.

Basing on above results, we further screened blindly the variants of non-coding D-loop region of mtDNA in gastric cancer using 4 pairs of overlapping primers. In the primary scanning, 28 heteroduplexes were identified in gastric tumor tissues and 38 variances were distinguished in cell lines. The typical chromatograms of heteroduplexes in each fragment were showed in Figure 3. To prove the results, all of positive samples were detected repeatedly. 26 heteroduplexes in tumor group were confirmed, 2 cases were checked to be negative. The two samples were distinguished to be positive due to change of retention time in contrast with other samples, but their chromatograms were similar with wild type. The detected variant frequency of mtDNA by DHPLC was listed in table 2. Ten variant fragments were randomly chosen for direct DNA sequencing, and all of mutated fragments were confirmed.

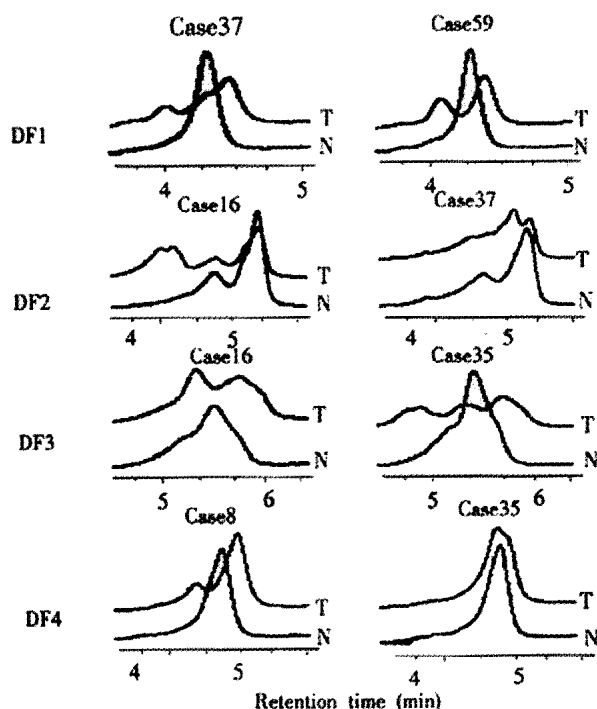


Figure 3 The representative DHPLC chromatograms of variant fragments detected blindly for patients with gastric carcinoma in D-loop of mtDNA. The chromatogram of tumor tissue is visibly different to that of its counterpart non-tumor tissue. The variant cases are listed on the top of each DHPLC chromatogram. DF1, DF2, DF3 and DF4 represent the tested fragments of D-loop respectively. T: tumor tissues; N: non-tumor tissues.

Table 2 The detected frequency of variance of mtDNA by using DHPLC

Fragments Samples	A3243G			D-loop	
	MELAS	Other Encephal ^a	Normal blood	Tumor	Cell line
Positive/total fragments	10/12	0/72	0/30	26/184	38/52
Percent (%)	83.3	0	0	14.1	73.1

DISCUSSION

Mutation detection by DHPLC is performed at a temperature sufficient to partially denature the DNA heteroduplexes. The different retention times of hetero- and homoduplex on the DNasep matrix allow for high sensitivity and rapid detection[48,49]. In generally, the heteroduplex profile is easily distinguished from homoduplex peak.

Although the present data have showed that DHPLC is a convenient and sensitive method in mutation screening[17,22,24-26,28]. It may be a challenge to mutation detection of mtDNA because of complicated heteroplasmy in mitochondria[50,51] and various types of variances in mtDNA molecule. Due to hundreds to thousands mtDNA copies in a cell[52], the ratio of a special mutant to normal mtDNA is relatively low. However, a number of various variants may co-existence in a sample. For these reasons, sensitive and rapid detecting method is needed to distinguish different types of variances in large sets of mtDNA copies. We applied DHPLC to screen the mtDNA mutation in this study. Our data showed that DHPLC was a powerful screening strategy for mtDNA mutation. Firstly, about 80ng of PCR products with variant that could be identified by DHPLC were enough to UV detection limit. The heteroduplex peak was not visible when total PCR products were less than 50ng each injection. But the homoduplex peak could be satisfactorily detected. Next, about 5 percent of mutant products in PCR mixture were effectively discerned. These results indicated that DHPLC was sensitive to distinguish those minimal special variants from a large normal mtDNA. Finally, the results were reproducible.

In detection of A3243G mutation for MELAS patients, we proved our collaborators research. Ten variant samples identified by using restriction endonuclease ApaI were all distinguished by DHPLC. Heteroduplexes of tumor tissues obtained by DHPLC were also visibly different to that of non-tumor counterpart, when DHPLC was used to screen blindly the variances of D-loop of mtDNA in gastric cancer. These results also demonstrated that DHPLC, as same as research for nuclear DNA[25-27,29,34], was a sensitive method for mtDNA mutation screening.

As mutation detection of nucleus genes, several factors must be addressed when DHPLC is employed in mtDNA screening. These factors include primer design, PCR optimization, choice of optimal melting temperature or reverse-phase gradient[29,49,53] and DNA polymerase in this study. We find Taq polymerase may influence identification of mutation for DHPLC screening. Taq DNA polymerase tends to add a deoxyribonucleotide, preferentially dATP, to the 3'-hydroxyl terminus of a blunt-ended substrate, and the high-sensitivity of the WAVE system makes it capable of registering these A-tailed products to form an extra peak. In particular, the GC-rich small fragment with high T_m is easy to be influenced. Because the selected temperature of column oven is high, the retention time of heteroduplex will be reduced and the extra small peak is prone to form a false heteroduplex peak.

The concentration of dNTP in PCR reaction is factor of DHPLC resolution for heteroduplex detection. DNA molecules bind with the DNasep cartridge via the triethylammonium acetate (TEAA). The dNTP contends with DNA in interaction with TEAA and decrease DNasep cartridge's binding sites to TEAA-DNA complex. Therefore, ability of cartridge to bind with DNA and resolution of DHPLC will be reduced. In order to obtain improved resolution of DHPLC, it is necessary to elute the cartridge by 75% acetonitrile regularly.

In conclusion, DHPLC is a powerful screening method for mtDNA mutation because of its high-throughput, automation, sensitivity and high reproducibility.

ACKNOWLEDGMENT

We thank Dr. Z.X. Wan and J.J.Zhang for kindly providing of

mtDNA from MELAS and other known mutated samples. We also thank Dr. W.G. Liu, Assistant professor, Mayo Clinic, Rochester USA, for comments on the manuscript. This work was supported by the National Key Basic Science Research Program, No. G1998051203, and National Science Foundation of China (NSFC), No. 39602526.

REFERENCES

- Deng ZL, Ma Y. Aflatoxin sufferer and p53 gene mutation in hepatocellular carcinoma. *World J Gastroenterol* 1998; 4: 28-29
- Luo D, Liu QF, Gove C, Naomov NV, Su JJ, Williams R. Analysis of N-ras gene mutation and p53 gene expression in human hepatocellular carcinomas. *World J Gastroenterol* 1998; 4: 97-99
- Peng XM, Peng WW, Yao JL. Codon 249 mutations of p53 gene in development of hepatocellular carcinoma. *World J Gastroenterol* 1998; 4:125-127
- Zhao X, Cai YY, Xie DW, Wang LD, Yang CS. Multiplex PCR SSCP: a highly effective and efficient method of mutation detection and analysis. *World J Gastroenterol* 1998; 4:106
- Peng XM, Yao CL, Chen XJ, Peng WW, Gao ZL. Codon 249 mutations of p53 gene in non-neoplastic liver tissues. *World J Gastroenterol* 1999; 5:324-326
- Weng ML, Li JG, Gao F, Zhang XY, Wang PS, Jiang XC. The mutation induced by space conditions in *Escherichia coli*. *World J Gastroenterol* 1999; 5:445-447
- Ji CY, Smith DR, Goh HS. The role and prognostic significance of p53 mutation in colorectal carcinomas. *World J Gastroenterol* 2000; 6:78
- Liu WD, Hada T, Cheng JD, Higashino K. Point mutations in E2, NS3 and NS5A of hepatitis G virus. *World J Gastroenterol* 2000; 6:41
- Qin Y, Li B, Tan YS, Sun ZL, Zuo FQ, Sun ZF. Polymorphism of p16INK4a gene and rare mutation of p15INK4b gene exon2 in primary hepatocarcinoma. *World J Gastroenterol* 2000; 6:411-414
- Wang Y, Liu H, Zhou Q, Li X. Analysis of point mutation in site 1896 of HBV precore and its detection in the tissues and serum of HCC patients. *World J Gastroenterol* 2000; 6:395-397
- Wang XJ, Yuan SL, Li CP, Iida N, Oda H, Aiso S, Ishikawa T. Infrequent p53 gene mutation and expression of the cardia adenocarcinomas from a high-incidence area of Southwest China. *World J Gastroenterol* 2000; 6:750-753
- Liu J, Chen SL, Zhang W, Su Q. P21-WAF1 gene expression with p53 mutation in esophageal carcinoma. *Shijie Huaren Xiaohua Zazhi* 2000; 8:1350-1353
- Cui J, Yang DH, Qin HR. Mutation and clinical significance of c-fms oncogene in hepatocellular carcinoma. *Shijie Huaren Xiaohua Zazhi* 2001; 9:392-395
- Fan RY, Li SR, Wu ZT, Wu X. Detection of P53 protein, K-ras and APC gene mutation in sporadic colorectal cancer tissue and exfoliative epithelial cells in stool. *Shijie Huaren Xiaohua Zazhi* 2001; 9:771-775
- He XS, Su Q, Chen ZC, He XT, Long ZF, Ling H, Zhang LR. Expression, deletion and mutation of p16 gene in human gastric cancer. *World J Gastroenterol* 2001; 7:515-521
- Yuan P, Sun MH, Zhang JS, Zhu XZ, Shi DR. APC and K-ras gene mutation in aberrant crypt foci of human colon. *World J Gastroenterol* 2001; 7:352-356
- Choy YS, Dabora SL, Hall F, Ramesh V, Niida Y, Franz D, Kasprzyk-Obara J, Reeve MP, Kwiatkowski DJ. Superiority of denaturing high performance liquid chromatography over single-stranded conformation and conformation-sensitive gel electrophoresis for mutation detection in TSC2. *Ann Hum Genet* 1999; 63:383-391
- Gross E, Arnold N, Goette J, Schwarz-Boeger U, Kiechle M. A comparison of BRCA1 mutation analysis by direct sequencing, SSCP and DHPLC. *Hum Genet* 1999; 105:72-78
- Boutin P, Vasseur F, Samson C, Wahl C, Froguel P. Routine mutation screening of HNF-1 α and GCK genes in MODY diagnosis: how effective are the techniques of DHPLC and direct sequencing used in combination? *Diabetologia* 2001; 44:775-778
- Eng C, Brody LC, Wagner TM, Devilee P, Vijg J, Szabo C, Tavtigian SV, Nathanson KL, Ostrander E, Frank TS. Interpreting epidemiological research: blinded comparison of methods used to estimate the prevalence of inherited mutations in BRCA1. *J Med Genet* 2001; 38: 824-833
- Klein B, Weirich G, Brauch H. DHPLC-based germline mutation screening in the analysis of the VHL tumor suppressor gene: usefulness and limitations. *Hum Genet* 2001; 108:376-384
- Kristensen VN, Kelefotis D, Kristensen T, Borresen-Dale AL. High-throughput methods for detection of genetic variation. *Biotechniques* 2001; 30:318-322
- Xiao WZ, Oefner PJ. Denaturing high-performance liquid chromatography: A review. *Hum Mutat* 2001;17:439-474
- O'Donovan MC, Oefner PJ, Roberts SC, Austin J, Hoogendoorn B, Guy C, Speight G, Upadhyaya M, Sommer SS, McGuffin P. Blind analysis of denaturing high-performance liquid chromatography as a tool for mutation detection. *Genomics* 1998; 52:44-49
- Arnold N, Gross E, Schwarz-Boeger U, Pfisterer J, Jonat W, Kiechle M. A highly sensitive, fast, and economical technique for mutation analysis in hereditary breast and ovarian cancers. *Hum Mutat* 1999; 14:333-339
- Hoogendoorn B, Norton N, Kirov G, Williams N, Hamshire ML, Spurlock G, Austin J, Stephens MK, Buckland PR, Owen MJ, O'Donovan MC. Cheap, accurate and rapid allele frequency estimation of single nucleotide polymorphisms by primer extension and DHPLC in DNA pools. *Hum Genet* 2000; 107:488-493
- Spiegelman JL, Mindrinos MN, Oefner PJ. High-accuracy DNA sequence variation screening by DHPLC. *Biotechniques* 2000; 29:1084-1090
- Roberts PS, Jozwiak S, Kwiatkowski DJ, Dabora SL. Denaturing high-performance liquid chromatography (DHPLC) is a highly sensitive, semi-automated method for identifying mutations in the TSC1 gene. *J Biochem Biophys Methods* 2001; 47:33-37
- Taliani MR, Roberts SC, Dukek BA, Pruthi RK, Nichols WL, Heit JA. Sensitivity and specificity of denaturing high-pressure liquid chromatography for unknown protein C gene mutations. *Genet Test* 2001; 5:39-44
- Yokomizo A, Tindall DJ, Drabkin H, Gemmill R, Franklin W, Yang P, Sugio K, Smith DI, Liu W. PTEN/MMAC1 mutations identified in small cell, but not in non-small cell lung cancers. *Oncogene* 1998; 17:475-479
- Benit P, Kara-Mostefa A, Berthelon M, Sengmany K, Munnich A, Bonnefont JP. Mutation analysis of the hamartin gene using denaturing high performance liquid chromatography. *Hum Mutat* 2000; 16: 417-421
- Gross E, Arnold N, Pfeifer K, Bandick K, Kiechle M. Identification of specific BRCA1 and BRCA2 variants by DHPLC. *Hum Mutat* 2000; 16:345-353
- Nickerson ML, Weirich G, Zbar B, Schmidt LS. Signature-based analysis of MET proto-oncogene mutations using DHPLC. *Hum Mutat* 2000; 16:68-76
- van Den Bosch BJ, de Coe RF, Scholte HR, Nijland JG, van Den Bogaard R, de Visser M, de Die-Smulders CE, Smeets HJ. Mutation analysis of the entire mitochondrial genome using denaturing high performance liquid chromatography. *Nucleic Acids Res* 2000;28:E89
- Cohn D, Mutch D, Elbendary A, Rader J, Herzog T, Goodfellow P. No evidence for BCL10 mutation in endometrial cancers with microsatellite instability. *Hum Mutat* 2001; 17:117-121
- Gross E, Kiechle M, Arnold N. Mutation analysis of p53 in ovarian tumors by DHPLC. *J Biochem Biophys Methods* 2001; 47:73-81
- Han SS, Cooper DN, Upadhyaya MN. Evaluation of denaturing high performance liquid chromatography (DHPLC) for the mutational analysis of the neurofibromatosis type 1 (NF1) gene. *Hum Genet* 2001; 109:487-497
- Kleymenova E, Walker CL. Determination of loss of heterozygosity in frozen and paraffin embedded tumors by denaturing high-performance liquid chromatography (DHPLC). *J Biochem Biophys Methods* 2001; 47:83-90
- Le Gac G, Mura C, Ferec C. Complete scanning of the hereditary hemochromatosis gene (HFE) by use of denaturing HPLC. *Clin Chem* 2001; 47:1633-1640
- Lin D, Goldstein JA, Mhatre AN, Lustig LR, Pfister M, Lalwani AK. Assessment of denaturing high-performance liquid chromatography (DHPLC) in screening for mutations in connexin 26 (GJB2). *Hum Mutat* 2001; 18:42-51
- Nicolao P, Carella M, Giometto B, Tavolato B, Cattin R, Giovannucci-Uzielli ML, Vacca M, Regione FD, Piva S, Bortoluzzi S, Gasparini P. DHPLC analysis of the MECP2 gene in Italian Rett patients. *Hum Mutat* 2001; 18:132-140
- zur Stadt U, Rischewski J, Schneppenheim R, Kabisch H. Denaturing HPLC for identification of clonal T-cell receptor gamma rearrangements in newly diagnosed acute lymphoblastic leukemia. *Clin Chem* 2001; 47:2003-2011
- Lam CW, Sin SY, Lau ET, Lam YY, Poon P, Tong SF. Prenatal diagnosis of glycogen storage disease type 1b using denaturing high performance liquid chromatography. *Prenat Diagn* 2000; 20:765-768
- Benit P, Bonnefont JP, Kara Mostefa A, Francannet C, Munnich A, Ray PF. Denaturing high-performance liquid chromatography (DHPLC)-based prenatal diagnosis for tuberous sclerosis. *Prenat Diagn* 2001; 21:279-283
- Levin BC, Cheng HY, Reeder DJ. A human mitochondrial DNA standard reference material for quality control in forensic identification, medical diagnosis, and mutation detection. *Genomics* 1999; 55:135-146
- Dubeau F, De Stefano N, Zifkin BG, Arnold DL, Shoubridge EA. Oxidative phosphorylation defect in the brains of carriers of the tRNA^{Leu} (UUR) A3243G mutation in a MELAS pedigree. *Ann Neurol* 2000; 47:

- 179-185
- 47 Sternberg D, Chatzoglou E, Laforet P, Fayet G, Jardel C, Blondy P, Fardeau M, Amselem S, Eymard B, Lombes A. Mitochondrial DNA transfer RNA gene sequence variations in patients with mitochondrial disorders. *Brain* 2001; 124:984-994
- 48 Kuklin A, Davis AP, Haefele R, Alianell G, Gjerde D, Taylor P. New paradigms in NDA polymorphism detection. *Biomed Prod* 1998; 7:90-92
- 49 Kuklin A, Munson K, Gjerde D, Haefele R, Taylor P. Detection of single-Nucleotide Polymorphisms with the WAVETM DNA fragment Analysis System. *Genet Test* 1997/98; 1:201-206
- 50 Battersby BJ, Shoubridge EA. Selection of a mtDNA sequence variant in hepatocytes of heteroplasmic mice is not due to differences in respiratory chain function or efficiency of replication. *Hum Mol Genet* 2001; 10: 2469-2479
- 51 Srivastava S, Moraes CT. Manipulating mitochondrial DNA heteroplasmy by a mitochondrially targeted restriction endonuclease. *Hum Mol Genet* 2001; 10:3093-3099
- 52 Chinnery PF, Turnbull DM. Mitochondrial DNA and disease. *Lancet* 1999; 354:17-21
- 53 Narayanaswami G, Taylor P. Improved efficiency of mutation detection by denaturing high-performance liquid chromatography using modified primers and hybridization procedure. *Genet Test* 2001; 5:9-16

Edited by Pagliarini R

• GASTRIC CANCER •

Changes of NF- κ B, p53, Bcl-2 and caspase in apoptosis induced by JTE-522 in human gastric adenocarcinoma cell line AGS cells: role of reactive oxygen species

Hong-Liang Li, Dan-Dan Chen, Xiao-Hong Li, Hai-Wei Zhang, Yan-Qing Lü, Chun-Ling Ye, Xian-Da Ren

Hong-Liang Li, Xiao-Hong Li, Yan-Qing Lü, Chun-Ling Ye, Xian-Da Ren, Department of Pharmacology, Jinan University Pharmacy College, Guangzhou 510632, Guangdong, China
Dan-Dan Chen, Department of Cardiology, First Affiliated Hospital, Zhongshan University, Guangzhou 510089, Guangdong, China
Hai-Wei Zhang, Department of Pathology, Jinan University Medical College, Guangzhou 510632, Guangdong, China

Supported by National Natural Science Foundation of China, No. 39770300, 30070873, and the Overseas Chinese Affairs Office of the State Council Foundation, No. 98-33

Correspondence to: Prof. Xian-Da Ren, Department of Pharmacology, Jinan University Pharmacy College, Guangzhou 510632, Guangdong, China. tsam@jnu.edu.cn

Telephone: +86-20-85220261

Received 2002-01-28 Accepted 2002-03-05

Abstract

AIM: To identify whether JTE-522 can induce apoptosis in AGS cells and ROS also involved in the process, and to investigate the changes in NF- κ B, p53, bcl-2 and caspase in the apoptosis process.

METHODS: Cell culture, MTT, Electromicroscopy, agarose gel electrophoresis, lucigenin, Western blot and electrophoretic mobility shift assay (EMSA) analysis were employed to investigate the effect of JTE-522 on cell proliferation and apoptosis in AGS cells and related molecular mechanisms.

RESULTS: JTE-522 inhibited the growth of AGS cells and induced the apoptosis. Lucigenin assay showed the generation of ROS in cells under incubation with JTE-522. The increased ROS generation might contribute to the induction of AGS cells to apoptosis. EMSA and Western blot revealed that NF- κ B activity was almost completely inhibited by preventing the degradation of I κ B α . Additionally, by using Western blot we confirmed that the level of bcl-2 was decreased, whereas p53 showed a great increase following JTE-522 treatment. Their changes were in a dose-dependent manner.

CONCLUSION: These findings suggest that reactive oxygen species, NF- κ B, p53, bcl-2 and caspase-3 may play an important role in the induction of apoptosis in AGS cells after treatment with JTE-522.

Li HL, Chen DD, Li XH, Zhang HW, Lü YQ, Ye CL, Ren XD. Changes of NF- κ B, p53, Bcl-2 and caspase in apoptosis induced by JTE-522 in human gastric adenocarcinoma cell line AGS cells: role of reactive oxygen species. *World J Gastroenterol* 2002;8(3):431-435

INTRODUCTION

Apoptosis is an active cell death process, which requires specific gene regulation. A critical role for p53 in the execution of some forms of apoptosis has been suggested^[1-6]. This protein is a sequence-specific DNA-binding protein, active as a transcription factor. It has been proposed that p53 may be involved in the cellular response to DNA

damage, producing arrest in the G₁ phase of the cell cycle to allow efficient repair of DNA before entry to S phase, or cell death if the damage is too large to be repaired^[7,8]. Another gene implicated in apoptosis is bcl-2. The bcl-2 gene product functions as an anti-apoptotic signal, suppressing apoptosis induced by a wide variety of stimuli, including chemotherapeutic drugs and γ radiation^[9-13]. The exact mechanism of bcl-2 in preventing apoptosis is still not clear. However, bcl-2 has been implicated in cellular control of their redox state^[14].

Previous studies have demonstrated that non-steroidal anti-inflammatory drugs (NSAIDs) given *in vivo* to rodents and human can inhibit tumor growth^[15,16]. JTE-522 is a novel NSAIDs, which is a specific inhibitor of cyclooxygenase-2 (COX-2) with significant anti-inflammatory and analgesic properties^[17]. Some reported that JTE-522 possesses strong chemopreventive activity against colon carcinogenesis^[18], but the precise mechanism by which JTE-522 inhibits colon carcinogenesis is not clear. It is often attributed to specific inhibition of arachidonic acid metabolism via coxenzymes. However, recent studies showed that the antitumor effect had little connection with NSAIDs inhibitory activity against cyclooxygenase, and was not prevented by exogenous supplementation of 16,16-dimethyl prostaglandin E₂. Several groups have shown that certain NSAIDs induce apoptosis of tumor cell line, which is associated with the generation of reactive oxygen species (ROS)^[19,20]. However, the signaling pathway leading to apoptotic cell death remains unclear.

ROS can play a central role in regulating cell proliferation and cell death. Evidence has been obtained that ROS such as superoxide and hydrogen peroxide can influence cell death triggered by internal cues (p53-mediated), external cues (TGF- β -mediated) and immunogenic signals (TNF- α)^[21,22]. In other instances, however, generation of ROS can inhibit apoptosis. Although the mechanism involved is still controversial, redox status and/or hydrogen peroxide have both been proposed as critical factors^[19]. Therefore it is possible that ROS may play a role in regulating apoptosis in gastric epithelium.

The purpose of the present study is to identify whether JTE-522 can induce apoptosis in AGS cells and ROS are also involved in the process, and to investigate the changes in NF- κ B, p53, bcl-2 and caspase in the apoptosis process.

MATERIALS AND METHODS

Cell line and reagents

Human gastric adenocarcinoma cell line AGS was provided by Cancer Institute, Zhongshan University. Cells were grown in RPMI-1640 medium and supplemented with 10% new bovine serum, penicillin G (100kU.L⁻¹) and kanamycin (0.1g.L⁻¹) at 37°C in a 5% CO₂-95% air atmosphere. Antibodies used in this study included p53, bcl-2, I κ B α and Beta actin were obtained from Santa Cruz. All other chemicals were purchased from Sigma Chemical Co (St. Louis, MO, USA).

MTT assay

AGS cells growing on 96-well plates were treated with JTE-522 (0.1 mmol/L - 1 mmol/L) for 72h, untreated cells served as a control. 10 μ L of the 2.5g.L⁻¹ stock solution of 3-[4, 5-dimethylthiazolyl]-2,

5-diphenyl-tetrazolium bromide (MTT) was added to each well. After 1h of incubation at 37°C, the medium was removed, 50µl of the extraction buffer (10% Triton-X100; 0.1mol/L HCl) was added, and plates were gently shaken for 30min at room temperature. The optical densities were measured at 570nm.

Morphological and biochemical analysis of apoptosis

Morphological changes in the nuclear chromatin of cells undergoing apoptosis were detected by electron microscopy (EM). Cells were pelleted and fixed with 30mL/L glutaraldehyde in PBS. EM analysis was performed as described previously^[23]. Oligonucleosomal cleavage of genomic DNA was detected by agarose gel electrophoresis. In brief, genomic DNA isolated as previously described^[24] was subjected to 1.5% agarose gel electrophoresis, followed by ethidium bromide staining.

Assay for reactive oxygen species production

Generation of ROS was assessed using lucigenin. AGS cells grown in 75cm² culture flasks were incubated for 6h with JTE-522 (0.1-1mmol/L) in the presence or absence of 100µmol/L pyrrolidine dithiocarbamate (PDTTC). The cells were then scraped off and washed in cold Hank's buffer. An aliquot containing 1×10⁶ cells in 100µL of Hank's buffer was mixed in microtiter wells with 100µl of lucigenin prepared at a concentration of 40µmol/L. Light emission was detected using a Berthold LB96V luminometer for 3min.

Assessment of caspase activity

Caspase-3 activity was measured using a caspase assay kit according to the supplier's instruction. In brief, caspase-3 fluorogenic substrates (Ac-DEVD-AMC or Ac-IETD-AMC) were incubated with JTE-522-treated with cell lysates for 1h at 37°C, then AMC liberated from Ac-DEVD-AMC or Ac-IETD-AMC was measured using a fluorometric plate reader with an excitation wavelength of 380nm and an emission wavelength of 420-460nm.

Western blot analysis

The cells were lysed in lysis buffer (25mmol/L hepes, 1.5% Triton X-100, 1% sodium deoxycholate, 0.1% SDS, 0.5mol/L NaCl, 5mmol/L EDTA, 50mmol/L NaF, 0.1mmol/L sodium vanadate, 1mmol/L phenylmethylsulfonyl fluoride (PMSF), and 0.1g.L⁻¹ leupeptin (pH7.8) at 4°C with sonication. The lysates were centrifuged at 15000g for 15min and the concentration of the protein in each lysate was determined with Coomassie brilliant blue G-250. Loading buffer (42mmol/L Tris-HCl, 10% glycerol, 2.3% SDS, 5% 2-mercaptoethanol and 0.002% bromophenol blue) was then added to each lysate, which was subsequently boiled for 3min and then electrophoresed on a SDS-polyacrylamide gel. Proteins were transferred to nitrocellulose and incubated sequentially with antibodies against IκBα, p53 and bcl-2 and then with peroxidase-conjugated secondary antibodies in the second reaction. Detection was performed with enhanced chemiluminescence reagent.

Electrophoretic mobility shift assay (EMSA)

Nuclear extracts were prepared from AGS cells treated with JTE-522. Synthetic double-strand oligonucleotides of consensus NF-κB binding sequence, GATCCCAACGGCAGGGGA, were end-labeled with [³²P]ATP using T4 polynucleotide kinase. Nuclear extract was incubated with the labeled probe in the presence of poly (dI-dC) in a binding buffer containing 20mM N-2-hydroxyethylpiperazine-N'-2-ethanesulfonic acid at room temperature for 30min. For supershift assays, a total of 0.2µg of antibodies against p65 subunit of NF-κB were included in the reaction. DNA-protein complexes were resolved by electrophoresis in a 5% non-denaturing polyacrylamide gel, which was dried and visualized by autoradiography.

RESULTS

Effect of JTE-522 on cell proliferation and apoptosis

AGS cells were incubated with various doses of JTE-522 for 72h. Analysis of cell viability using MTT assay showed that JTE-522 significantly inhibited cell viability. The inhibition of cell viability was dependent on the dose of JTE-522 used (Figure 1).

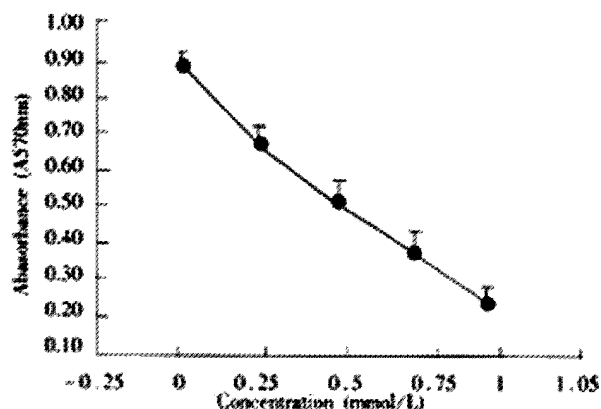


Figure 1 Effect of JTE-522 on cell growth in AGS cells. The cells were treated with various concentrations of JTE-522 for 72h. The antiproliferative effect was measured by MTT assay. Results are the means±SD from three independent determinations.

The effect was due to apoptosis as demonstrated by EM and electrophoresis of genomic DNA. JTE-522-treated cells showed compacted nuclear chromatin with finely granular masses margined against the nuclear envelope and condensed cytoplasm, the nuclear outline was convoluted and the organelles were preserved (Figure 2) and led to oligonucleosomal cleavage of genomic DNA (Figure 3), which were hallmarks of apoptosis.

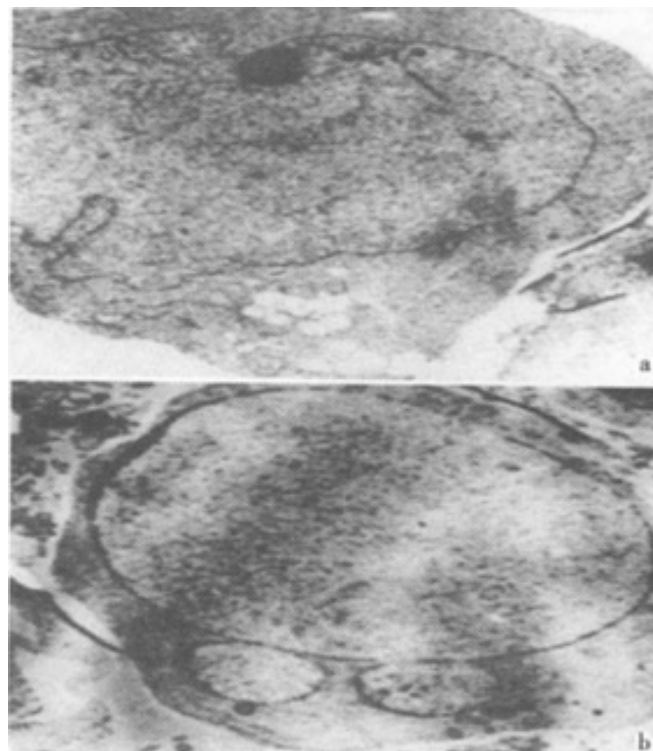


Figure 2 Electro micrographs of JTE-522-treated AGS cells. Control AGS cells (A), or treated with 1mmol/L (B) JTE-522 for 72h, were examined by EM as in "Materials and Methods". Magnification: ×4000

We next investigated whether the activation of caspase was involved in JTE-522-induced apoptosis of AGS cells. JTE-522-induced apoptosis of AGS cells was accompanied by the induction of caspases activity as demonstrated by the cleavage of Ac-DEVD-AMC and Ac-IETD-AMC, respectively (Figure 4). These results indicated that JTE-522-induced cell death of AGS cells was a typical apoptosis associated with caspase activation.

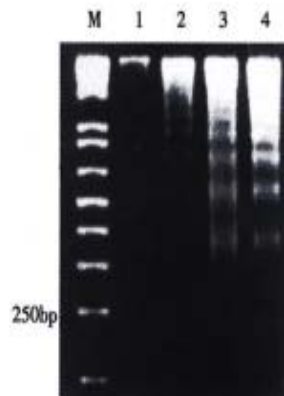


Figure 3 DNA ladder pattern formation of AGS cells. Cells treated with different concentrations of JTE-522 for 72h and the formation of oligonucleosomal fragments was determined by 1.5% agarose gel electrophoresis. M, DNA markers; lanes 1-4, AGS cells treated with 0, 0.25, 0.50, 1mmol/L of JTE-522

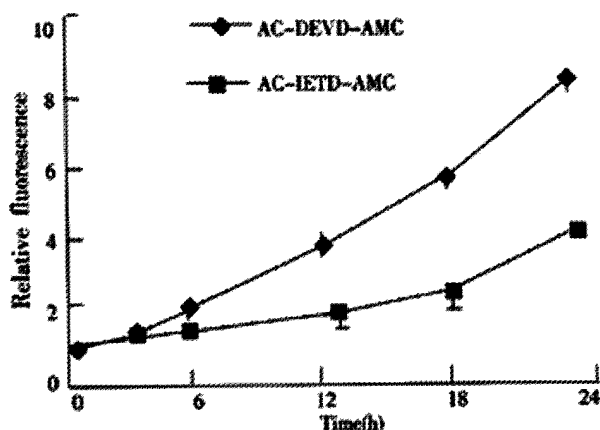


Figure 4 Activation of caspase-3 activities by JTE-522 in AGS cells for indicated time period. JTE-522 treatment (0.75mmol/L) induced cleavage of Ac-DEVD-AMC and Ac-IETD-AMC, indicating activation of caspase-3 activity, respectively

Effect of JTE-522 on the production of ROS in AGS cells

The effect of JTE-522 on the production of ROS in AGS cells, as assessed with lucigenin chemiluminescence, was shown in Figure 5. Chemiluminescence was significantly enhanced by incubation with various doses of JTE-522. This enhancement was prevented by co-incubation with PDTC at 100 μ mol/L. These results demonstrated the generation of reactive oxygen species in cells under incubation with JTE-522.

Effect of JTE-522 on the expression of p53, bcl-2, I κ B α and the activation of NF- κ B

NF- κ B plays a complex role in regulating programmed cell death. In many instances the inhibition of NF- κ B activity can sensitize cells to death inducers^[25]. In other instances, however, NF- κ B activation has been found to play an important role in the induction of apoptosis. To determine whether the treatment with JTE-522 have any effect in the NF- κ B transcriptional factors. We performed EMSA with nuclear extracts prepared from control or treated cells exposed to JTE-522 for various concentrations for 6h. The NF- κ B specific complexes found in this cell line were almost complete inhibited in comparison with untreated

cells (Figure 6A). In accordance with result, an analysis of I κ B α proteins level by Western blot demonstrated that the degradation of this protein was greatly inhibited during the apoptotic process (Figure 6B).

Additionally, by using Western blot we confirmed that the level of bcl-2 was decreased, whereas p53 showed a great increase following JTE-522 treatment. Their changes were in a dose-dependent manner (Figure 7).

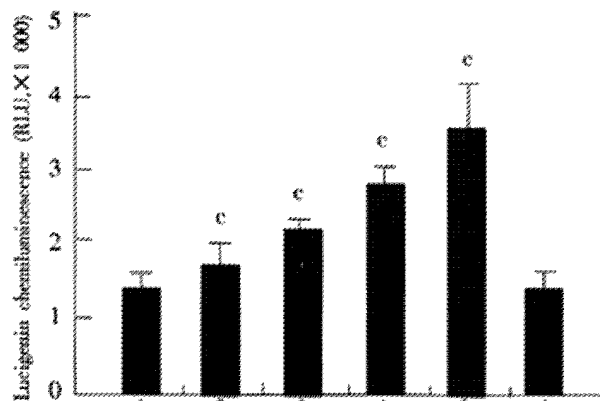


Figure 5 Effect of JTE-522 on the generation of ROS. AGS cells were incubated for 6h with JTE-522 (0.25-1mmol/L) in the presence or absence of PDTC at 100 μ mol/L. Lucigenin-associated chemiluminescence was measured for 3min with a lumirometer. (A). Lane 1: control; lane 2-5: AGS cells treated with 0.25, 0.5, 0.75, 1mmol/L of JTE-522; lane 6: JTE-522 (1mmol/L) +PDTC (100 μ mol/L) * P <0.01 vs control. Results are the means \pm SD from three independent determinations.

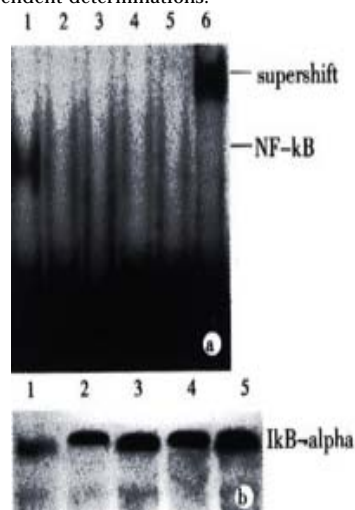


Figure 6 Effect of JTE-522 on NF- κ B binding activity and I κ B α degradation. Cells were treated with JTE-522 for 6h. Cells were harvested and EMSA was performed as described (A). Lane 1: control; lane 2-5: AGS cells treated with 0.25, 0.50, 0.75, 1mmol/L of JTE-522. The identity of DNA-complexed proteins was confirmed by supershift assays using antibodies against p65 subunit of NF- κ B (lane 6). Immunoblot analysis of I κ B α of corresponding cytosolic supernatant (B). Representative results from four independent experiments.

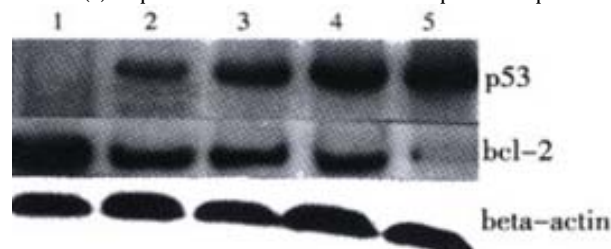


Figure 7 P53, bcl-2 protein levels in AGS cells treated with JTE-522. Cell lysates were collected and processed at 6h. The whole cellular protein was electrophoresed in SDS-PAGE gel. Western blot was performed using antibodies against p53, bcl-2. Beta actin was used as a lane-loading control. (1) control; (2) 0.25mmol/L; (3) 0.5mmol/L; (4) 0.75mmol/L; (5) 1 mmol/L. Representative results from three independent experiments.

DISCUSSION

Using cultured AGS human gastric adenocarcinoma cells, the observations described in this study demonstrate that JTE-522, a novel NSAIDs inhibits the growth of AGS cells and induces apoptosis in a concentration-dependent manner.

The onset of apoptosis is associated with the proteolytic activation of caspases. Caspases, a family of cysteine proteases, play a critical role in the execution of apoptosis^[26-31]. They are synthesized as proenzymes that are processed by self-proteolysis and/or cleavage by another protease to their active forms in cells undergoing apoptosis. Caspase-3 is a major executioner of apoptosis. It is promoted during the early stage of apoptosis and the activated form is a marker for cells undergoing apoptosis^[32]. After activation by initiators, the proform (p32) is cleaved to the active forms p20, p17, or p11, respectively^[33]. Therefore, activation of caspase-3 in AGS cells in this study not only indicated the occurrence of apoptosis, but also implied the involvement of caspase-3 in JTE-522-induced apoptosis.

ROS have been found to play a central role in regulating apoptosis in numerous instances. Given that reduced rates of apoptosis may contribute to carcinogenesis, the regulation of cellular ROS production may be an important variable in the development of neoplasias. Other studies have also suggested a potential role for ROS in cancer suppression. For example, the p53 tumor suppressor protein activates the expression of ROS-generating proteins that increase cellular ROS production and eventually trigger apoptosis^[34,35]. Increased ROS generation by chemopreventive agents may serve to compensate the lower levels of ROS generation in p53 null cells (AGS cells are p53 null)^[36,37]. Animal studies have also implicated ROS in regulating carcinogenesis. Mice with elevated levels of glutathione peroxidase are more sensitive to skin carcinogenesis than their wild type counterpart^[32]. A similar correlation has been made in the colon, where strains with higher levels of glutathione peroxidase activity have a higher cancer risk. The role of ROS in carcinogenesis is however likely to be complex given the potential mutagenicity of ROS. For example, the NSAIDs inhibition of cyclooxygenase has been proposed to suppress carcinogenesis by suppressing the production of peroxy radicals and the subsequent formation of mutagenic lipid peroxidation breakdown products^[38]. The role of ROS in carcinogenesis may depend on the relative levels of different ROS generated, and where and when they are present. However, as demonstrated in this paper, we showed that JTE-522 increased ROS generation in AGS cells, and this increased ROS generation might contribute to the induction of AGS cells to apoptosis.

The bcl-2 protooncogene is unique among cellular genes for its ability in many contexts to block apoptotic cell death. A mechanism has been proposed in which bcl-2 regulates antioxidant pathways at sites of free radical generation^[39]. The protein of bcl-2 also protects against apoptosis by blocking cytochrome C release hence this protein may have an antioxidant function^[40]. In our experiment, the expression of bcl-2 decreased, and the p53 protein upregulated following JTE-522 treatment, these changes may implies that intracellular ROS may interfere with the expression of bcl-2 and p53, thereby contributing to inducing apoptosis in AGS cells.

In studying the mechanism by which the NSAIDs influenced cell death, common effects on the transcription factor NF- κ B were noted. The NF- κ B transcription factor is ubiquitous and can be detected under its inactive form in the cytoplasm of almost all cell types^[41,42]. It suppresses the expression of cytokines, chemokines, growth factors, cell adhesion molecules, and some acute phase proteins in health and various pathological states^[43,44]. Experimental data clearly indicate that NF- κ B is a major regulator of the inflammatory reaction by controlling the expression of pro-inflammatory molecules in response to cytokines oxidatives stress and infectious agents^[45,46]. NF- κ B is maintained under such an inactive cytoplasmic form by virtue of its association with an inhibitory molecule named I κ B. I κ B α is the best

characterized member of this family. In our current work, EMSA revealed that JTE-522 inhibited NF- κ B activation. Western blot experiments demonstrated that this effect was mediated by inhibition of I κ B α degradation. Determining the role of NF- κ B in gastric carcinogenesis could help to guide the development of improved chemoprevention and treatment strategies.

In summary, JTE-522 inhibited cell growth and induced apoptosis in AGS cells. Increased ROS may play an important role in this caspase-3 mediated apoptotic process. The inhibition of NF- κ B by JTE-522 may be mediated by preventing I κ B α degradation. The precise relationship and importance of each of these factors in the apoptotic process should be established by more direct and profound analysis.

ACKNOWLEDGMENTS

We gratefully acknowledge Prof Geng-Tao Lui, Institute of Material Medica, Chinese Academy of Medical Sciences for the many helpful discussion and suggestions relating to this work; Special thanks to Chris Simmet and Pasricha Jerriment for proofreading the manuscript and for useful suggestions; Dr Cheng-Wei He for technical advice and helpful discussion; Dr Gang-Fei Peng for FCM; Dr Tao Wang for Western blot; Dr Guo-Qing Xie and Mr Hai-Nan Wang for photo processing.

REFERENCES

- Peng XM, Peng MM, Chen Q, Yao JL. Apoptosis, Bcl-2 and p53 protein expression in tissues from hepatocellular carcinoma. *Huaren Xiaohua Zazhi* 1998; 6: 834-836
- Hua JS. Effect of Hp: cell proliferation and apoptosis on stomach cancer. *Shijie Huaren Xiaohua Zazhi* 1999;7: 647-648
- Xue XC, Fang GE, Hua JD. Gastric cancer and apoptosis. *Shijie Huaren Xiaohua Zazhi* 1999;7: 359-361
- Qin LF, Wang RN. Prognostic significance of FCM DNA analysis in carcinoma of stomach. *Shanghai Dier Yike Daxue Xuebao* 1992; 12: 198-202
- Yu GQ, Zhou Q, Ding Ivan, Gao SS, Zhang ZY, Zou JX, Li YX, Wang LD. Changes of p53 protein blood level in esophageal cancer patients and normal subjects from a high incidence area in Henan, China. *World J Gastroenterol* 1998; 4: 218
- Luo D, Liu QF, Gove V, Namov NV, Su JJ, Williams R. Analysis of N-ras gene mutation and p53 gene expression in human hepatocellular carcinomas. *World J Gastroenterol* 1998; 4: 97-99
- Li HL, Zhang HW, Ren XD. Synergism between heparin and adriamycin on cell proliferation and apoptosis in human nasopharyngeal carcinoma CNE2 cells. *Acta Pharmacol sin* 2002;23:167-172
- Li HL, Ye KH, Ren XD. Heparin induced apoptosis in human nasopharyngeal carcinoma CNE2 cells. *Cell Research* 2001;11:311-315
- Qiao Q, Wu JS, Zhang J, Ma QJ, Lai DN. Expression and significance of apoptosis related gene bcl-2, bax in human large intestine adenocarcinoma. *Shijie Huaren Xiaohua Zazhi* 1999; 7: 936-938
- Yuan RW, Ding Q, Jiang HY, Qin XF, Zou SQ, Xia SS. Bcl-2, p53 protein expression and apoptosis in pancreatic cancer. *Shijie Huaren Xiaohua Zazhi* 1999; 7: 851-854
- Jiang YG, Li QF, Wang YM, Gu CH. Bcl-2/bax expression and hepatocyte apoptosis on liver tissue in tupaia with HDV/HBV infection. *Shijie Huaren Xiaohua Zazhi* 2000; 8: 625-628
- Fan XQ, Ya JG. Apoptosis in oncology. *Cell Research* 2001;11:1-7
- Zhang MH, Zhang Q, Shao BX. Effect of Bcl-2 and caspase-3 on calcium distribution in apoptosis of HL-60 cell. *Cell Research* 2000; 10: 213-20
- Kane DJ, Sarafian TA, Anton R, Hahh H, Bntler E. Bcl-2, inhibition of neural death: decreased generation of reactive oxygen species. *Science* 1993; 262: 1274-1277
- Reddy BS, Rao CV, Seibert K. Evaluation of COX-2 inhibitor for potential chemopreventive properties in colon carcinogenesis. *Cancer Res* 1996; 56: 4566-4569
- Shibata MA, Hasegawa R, Imaida K, Hagiwara A. Chemoprevention by dehydroepiandrosterone and indomethacin in a rat model of multiorgan carcinogenesis model. *Cancer Res* 1995; 55: 4870-4874
- Tomozawa S, Nagawa H, Tsuno N. Inhibition of haematogenous metastasis of colon cancer in mice by a selective COX-2 inhibitor, JTE-522. *Br J Cancer* 1999; 81: 1274-1279
- Yang ZY, Rorison KA. Cyclooxygenase-2-selective antagonists do not inhibit growth of colorectal carcinoma cell lines. *Cancer letters* 1998; 122: 25-30

- 19 Kusuvara H, Komatsu H, Sugahara K. Reactive oxygen species are involved in the apoptosis induced by NSAIDs in cultured gastric cells. *Eur J Pharmacol* 1999; 383: 331-337
- 20 Tanaka K, Pracyk JB, Takeda K, Yu ZX, Finkel T. Expression of Id1 results in apoptosis of cardiac myocytes through a redox-dependent mechanism. *J Biol Chem* 1998; 273: 25922-25828
- 21 Fridovich I. Superoxide radical and superoxide dismutases. *Annu Rev Biochem* 1995; 64: 97-112
- 22 Manna SK, Zhang HJ, Yan T, Oberley LW, Aggarwal BB. Overexpression of manganese superoxide dismutase suppress tumor necrosis factor-induced apoptosis and activation of nuclear transcription factor- κ B and AP-1. *J Biol Chem* 1998; 273: 13245-13254
- 23 Qiao L, Hanif R, Sphical E, Steven J, Rigas B. Effect of aspirin on induction of apoptosis in AGS human colon adenocarcinoma cells. *Biochem Pharmacol* 1998; 55: 53-64
- 24 Jiang ZF, Zhao Y, Hong X, Zhai ZH. Nuclear apoptosis induced by isolated mitochondria. *Cell Research* 2000; 10: 221-232
- 25 Beg AA, Baltimore D. An essential role for NF- κ B in preventing TNF- α induced cell death. *Science* 1996; 274: 787-789
- 26 Cohen GM. Caspases: the executioners of apoptosis. *Biochem J* 1997; 326: 1-6
- 27 Kumar S, Lavin MF. The ICE family of cysteine proteases as effectors of cell death. *Cell Death Differ* 1996; 3: 255-267
- 28 Salvesen GS and Dixit VM. Caspases: intracellular signaling by proteolysis. *Cell* 1997; 91: 443-446
- 29 Shen ZY, Shen J, Li QS, Chen CY, Chen JY, Zeng Y. Morphological and functional changes of mitochondria in apoptosis esophageal carcinoma cells induced by arsenic trioxide. *World J Gastroenterol* 2002;8:31-35
- 30 Du C, Fang M, Li Y, Wang X, Smac A. Mitochondrial protein that promotes cytochrome c dependent caspase activation by eliminating IAP inhibition. *Cell* 2000; 102: 43-53
- 31 Desagher S, OsenSand A, Nichols A, Eskes R, Montessuit S, Lauper S, Maundrell K, Antonsson B, Martinou JC. Bid-induced conformational cytochrome c release during apoptosis. *J Cell Biol* 1999; 144: 891-901
- 32 Schlegel J, Peters I, Orrenius S, Miller DK. Cpp32/apopain is a key interleukin 1 beta converting enzyme-like protease involved in Fas-mediated apoptosis. *J Biol Chem* 1996; 271: 1841-1844
- 33 Stennicke HR, Salvesen GS. Properties of the caspases. *Biochim Biophys Acta* 1998; 1387: 17-31
- 34 Polyak K, Xia Y, Zweier JL, Kinzler KW. A model for p53-mediated apoptosis. *Nature* 1997; 389: 300-305
- 35 Johnson TM, Yu ZX, Ferrans RA. Relative oxygen species are downstream mediators of p53-dependent apoptosis. *Proc Natl Acad Sci USA* 1996; 93: 11848-11852
- 36 Ossina NK, Cannas A, Powers VC, Gilbert EM, Tomei SR. Interferon- γ modulates a p53-independent apoptotic pathway and apoptosis-related gene expression. *J Biol Chem* 1997; 272: 16351-16357
- 37 Xu CT, Huang LT, Pan BK. Current gene therapy for stomach carcinoma. *World J Gastroenterol* 2001;7:752-759
- 38 Lu YP, Lou YR, Newmark HL, Huang MT. Enhanced skin carcinogenesis in transgenic mice with high expression of glutathione peroxidase or both glutathione peroxidase and superoxide dismutase. *Cancer Res* 1997; 57: 1468-1474
- 39 Hockenbery OM, Oltvai ZN, Yin XM, Korsmeyer SJ. Bcl-2 functions in an antioxidant pathway to prevent apoptosis. *Cell* 1993; 75: 241-251
- 40 Cai J, Jones DP. Superoxide in apoptosis: mitochondrial generation triggered by cytochrome C loss. *J Biol Chem* 1998; 273: 11401-1144
- 41 Barnes PJ, Karin M. Nuclear factor- κ B, a pivotal transcription factor in chronic inflammatory disease. *New Eng J Med* 1997; 336: 1066-1071
- 42 Huang S, Li JY, Wu J, Meng L, Shou CC. Mycoplasma infections and different human carcinomas. *World J Gastroenterol* 2001;7:266-269
- 43 Baeuerle PA, Baltimore D. NF- κ B: ten years after. *Cell* 1996; 87: 13-20
- 44 Wu YL, Sun B, Zhang XJ, Wang SN, He HY, Qiao MM, Zhong J, Xu JY. Growth inhibition and apoptosis induction of Sulindac on human gastric cancer cells. *World J Gastroenterol* 2001;7:796-800
- 45 Kipp E, Ghosh S. Inhibition of NF- κ B by sodium salicylate and aspirin. *Science* 1994; 265: 956-959
- 46 Giardina C, Boulares H, Inan MS. NSAIDs and butyrate sensitize a human colorectal cancer cell line to TNF and Fas ligation: the role of reactive oxygen species. *Biochim Biophys Acta* 1999; 1448: 425-438

Edited by Zhang JZ

• GASTRIC CANCER •

Inhibition of human telomerase in MKN-45 cell line by antisense hTR expression vector induces cell apoptosis and growth arrest

Run-Hua Feng, Zheng-Gang Zhu, Jian-Fang Li, Bin-Ya Liu, Min Yan, Hao-Ran Yin, Yan-Zhen Lin

Run-Hua Feng, Zheng-Gang Zhu, Jian-Fang Li, Bin-Ya Liu, Min Yan, Hao-Ran Yin, Yan-Zhen Lin, Shanghai Institute of Digestive Surgery, Ruijin Hospital, Shanghai Second Medical University, Shanghai 200025, China
Supported by the National Natural Science Foundation of China, No. 39770725

Correspondence to: Dr. Zheng-Gang Zhu, Shanghai Institute of Digestive Surgery, Ruijin Hospital, Shanghai Second Medical University, Shanghai 200025, China. digsurg@online.sh.cn
Telephone: +86-21-64373909 Fax: +86-21-64373909
Received 2002-01-14 Accepted 2002-02-07

Abstract

AIM: To investigate the effects of antisense human telomerase RNA (hTR) on the biologic behavior of human gastric cancer cell line: MKN-45 by gene transfection and its potential role in the gene therapy of gastric cancer.

METHODS: The hTR cDNA fragment was cloned from MKN-45 through RT-PCR and subcloned into eukaryotic expression vector (pEF6/V5-His-TOPO) in cis-direction or trans-direction by DNA recombinant methods. The constructed sense, antisense and empty vectors were transfected into MKN-45 cell lines separately by lipofectin-mediated DNA transfection technology. After drug selection, the expression of antisense hTR gene in stable transfectants and normal MKN-45 cells was detected by RT-PCR, the telomerase activity by TRAP, the apoptotic features by PI and Hoechst 33258 staining, the cell cycle distribution by flow cytometry and the population doubling time by cell counting. Comparison among the stable transfectants and normal MKN-45 cells was made.

RESULTS: The sense, antisense hTR eukaryotic expression vectors and empty vector were successfully constructed and proved to be the same as original design by restriction endonuclease analysis and sequencing. Then, they were successfully transfected into MKN-45 cell lines separately with lipofectin. The expression of antisense hTR gene was only detected in MKN-45 cells stably transfected with antisense hTR vector (named as MKN-45-ahTR) but not in the control cells. In MKN-45-ahTR, the telomerase activity was inhibited by 75%, the apoptotic rate was increased to 25.3%, the percentage of cells in the G0/G1 phase was increased to 65%, the proliferation index was decreased to 35% and the population doubling time was prolonged to 35.3 hours. However, the telomerase activity, the apoptotic rate, the distribution of cell cycle, the proliferation index and the population doubling time were not different among the control cells.

CONCLUSION: Antisense hTR can significantly inhibit telomerase activity and proliferation of MKN-45 cells and induce cell apoptosis. Antisense gene therapy based on telomerase inhibition can be a potential therapeutic approach to the treatment of gastric cancer.

Feng RH, Zhu ZG, Li JF, Liu BY, Yan M, Yin HR, Lin YZ. Inhibition of human telomerase in MKN-45 cell line by antisense hTR expression vector induces cell apoptosis and growth arrest. *World J Gastroenterol* 2002;8(3):436-440

INTRODUCTION

Gastric cancer is a very common tumor in China. More and more patients with gastric cancer can now be found in early stage because of the improvement of the technology of diagnosis^[1]. Although surgery and chemotherapy are effective for these patients with localized tumors, the prognosis of patients having advanced or metastatic tumors is not ideal^[2-6]. As a result, it is absolutely necessary to explore a novel modality of treatment. Fortunately, with the development of molecular biology, medicine is on the brink of a new era—that of molecular genetic medicine. People are now equipped with a new and powerful weapon: gene therapy which was previously only the stuff of dreams and scientific fantasy to fight against disease. Just like other kinds of cancer, the gastric cancer is now recognized as a genetic disease. The gastric cancer cells contain many genetic alterations (caused by some pathogenic agents such as *Helicobacter pylori*) which accumulate as tumor develop^[7-28]. This makes it possible to treat cancer with gene therapy^[29,30]. Because the target aimed by the gene therapy is undoubtedly the abnormal gene, thus, the task to find an effective target gene directed against by the gene therapy is becoming increasingly important and urgent. Human telomerase is a ribonucleoprotein which can add the telomeric repeats (TTAGGG) to the ends of the chromosome to maintain the telomere length using its integral RNA component (hTR) as a template^[31,32]. Initially identified in HeLa cell extracts, human telomerase has been detected in immortalised cell lines and more than 85% of tumors while normally quiescent in normal somatic cells (except for proliferative cells of renewable tissues such as activated lymphocytes)^[33-35]. It is suggested that cancer cells maybe achieve cellular immortality, an important characteristic of cancer cell, through the reactivation of telomerase^[36,37]. The seemingly essential roles of telomerase in maintaining telomere length, ensuring chromosome integrity and its nearly ubiquitous reactivation in human cancers have made telomerase a new therapeutic target for anticancer therapy^[38,39]. It was reported that HeLa cells transfected with an antisense hTR lost telomeric DNA and began to die after 23 to 26 doublings. According to a recent review, telomerase activity was also detected in 85-88% of gastric carcinomatous tissues. To gastric cancer, hTR was expressed at a higher level in the tumor than that in the corresponding mucosa and tumors with telomerase activity were generally large in size with a high frequency of lymph node metastasis. Moreover, the patients with telomerase-positive tumors shared poorer prognosis than those with telomerase-negative tumors^[40-45]. However, whether antisense gene therapy directed against telomerase will be useful in gastric cancer is so far unknown. We describe here the biologic behavior changes in MKN-45 cell line, a human gastric cell line, after transfected with antisense hTR expression vector and investigate the potential value of telomerase as a target for antisense gene therapy in gastric cancer.

MATERIALS AND METHODS

Cell Culture

MKN-45 cell, a human gastric cancer cell line, was obtained from Shanghai institute of Cell Biology, Chinese Academy of Sciences. The cells were routinely cultured in RPMI-1640 media (Gibco BRL) supplemented with 10% heat-inactivated fetal bovine serum (Gibco BRL), 100u/ml penicillin and 100u/ml streptomycin in an atmosphere consisting of 5% CO₂ in air at 37°C in a humidified incubator.

Construction of sense and antisense hTR eukaryotic expression vector

The hTR cDNA fragment was cloned from MKN-45 cell line through RT-PCR and subcloned into eukaryotic expression vector: pEF6/V5-His-TOPO vector (Invitrogen) in cis-direction or trans-direction by using DNA recombinant methods as described previously^[46]. They were all proved to be the same as original design by restriction endonuclease analysis and sequencing. The sense, antisense and empty vectors were named as pEF-hTR, pEF-ahTR and pEF-empty correspondingly.

Transfection of eukaryotic expression vector

Stable transfection of pEF-hTR, pEF-ahTR and pEF-empty was carried out by standard lipofection mediated DNA transfection method. In brief, approximately 1.5×10⁵ MKN-45 cells were transfected with 2μg vector DNA that had been complexed with 20μl lipofectin reagent (Gibco BRL). Two days after the transfection, the stable transfectants were selected by 2μg/ml blasticidin (Invitrogen) in the culture media. They were named as MKN-45-hTR, MKN-45-ahTR and MKN-45-empty correspondingly.

In addition, the pEF6/V5-His-TOPO/lacZ vector (pEF6/V5-His-TOPO vector carrying the reporter gene: lacZ gene in its multi cloning sites, provided by Invitrogen) was transfected into MKN-45 cells and selected by the same method as described above. It was named as MKN-45-lac correspondingly.

RT-PCR for detecting antisense hTR expression

Total RNA was extracted from the transfectants and normal MKN-45 cells using Trizol reagent (Gibco BRL). One microgram of total RNA was reversetranscribed with ahTR specific primer1 (5'-gaacgggccagcagctgacat-3') using THERMOSCRIPT RT-PCR system for first-strand cDNA synthesis (Gibco BRL). The RT condition was set for 65°C, 30min→85°C, 5min. Then, the cDNA was amplified with the PCR using PLATINUM Taq DNA polymerase (Gibco BRL) and employing ahTR specific primer1 and primer2 (5'-gggtgcggagggtggcct-3'). The PCR conditions were set for 94°C, 2min→94°C, 20s; 69°C, 20s; 72°C, 20s; 30 cycles→72°C, 2min. The product length is 196bp. The G6PDH was co-reversetranscribed employing G6PDH specific primer1 (5'-cgcccccttctctccctctgct-3') and co-amplified with PCR using G6PDH specific primer1 and primer2 (5'-cccgcctctgctgctgactac-3') as internal control. The product length is 247bp. Each RT-PCR product was electrophoretically separated in 2% agarose with EtBr.

β-Gal staining

The MKN-45 cells stably transfected with pEF6/V5-His-TOPO/lacZ vector were subjected to β-Gal staining by using β-Gal Staining Kit (Invitrogen) to detect whether the vector could effectively express lacZ gene.

Apoptotic features

To determine whether MKN-45-ahTR transfected with the pEF-ahTR vector displayed an apoptotic morphology, it was stained with the DNA binding fluorochrome bis (benzimidazole) trihydro-chloride, Hoechst 33258 (provided by Shanghai institute of Immunology) and observed under UV fluorescence microscope.

To determine the apoptotic rate and cell cycle distribution, the MKN-45-ahTR and control cells were stained with PI and analysed by flow cytometry.

Telomerase activity assay

Telomerase activity was measured using the commercially available TRAP_{EZE} Telomerase Detection Kit (Intergen). In brief, the cell extract was made according to the protocol provided, then 2μl of the cell extract was added to 48μl of the reaction mixture containing 10× TRAP Reaction Buffer, 50× dNTP Mix, TS Primer, TRAP Primer Mix, Taq Polymerase and dH₂O in amounts and types specified by the TRAP_{EZE} Telomerase Detection Kit. After centrifuged briefly, this mixture was incubated at 30°C for 30min to allow telomerase elongation of the TS primer and then subjected to PCR amplification in a thermal cycler for 35 cycles: 94°C for 30s; 59°C for 30s and 72°C for 30s. The product was then electrophoresed on a 12.5% non-denaturing PAGE (without urea). After electrophoresis, the gel was stained with SYBR Green I (Molecular Probes) according to the manufacturer's instructions.

Quantification of telomerase product was calculated using BIO-RAD Fluor-STM MultiImager and the formula (discussed in detail in the TRAP_{EZE} Telomerase Detection Kit instruction booklet).

$$\text{TPG}(\text{units}) = \frac{(\chi - \chi_0) / c}{(\gamma - \gamma_0) / c_R} \times 100$$

Abbreviation in the above formular is as follows: TPG, total product generated; χ , sample signal; χ_0 , heat-inactivated control; γ , 0.1 amole quantitation TSR8 control; γ_0 , 1× CHAPS Lysis Buffer only control; c , sample internal standard band; c_R , 0.1 amole quantitation TSR8 internal standard band.

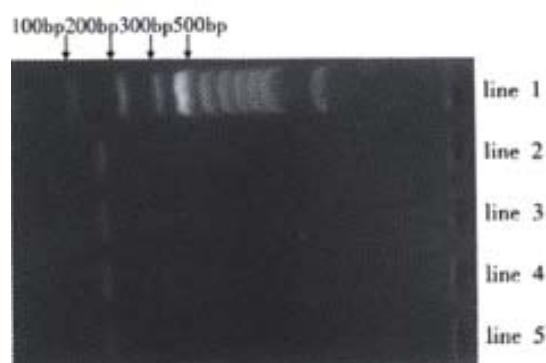
Cell growth curve and population doubling time

Cells were seeded at a density of 2×10⁵ per 25ml flask in 1.5ml of cell culture media. The number of cells per flask was counted every day for 6 days. The population doubling time of cells transfected with pEF-hTR, pEF-ahTR and pEF-empty and normal MKN-45 cells were calculated and the cell growth curve was drawn.

RESULTS

Expression of antisense hTR gene in MKN-45 cells

We transfected MKN-45 cells with pEF-hTR, pEF-ahTR and pEF-empty vector respectively, following the blasticidin selection, the drug resistant cells were collected and RT-PCR was performed with antisense hTR specific primers. We detected the ahTR specific product only in the pEF-ahTR vector transfected cells but not in the pEF-hTR, pEF-empty vector transfected cells and parental cells. However, steady state expression of G6PDH (as internal control) was observed in all cells.



Line 1: 100bp DNA Ladder (Promega), Lane 2: normal MKN-45, Lane 3: MKN-45-hTR, Lane 4: MKN-45-empty, Lane 5: MKN-45-ahTR

Figure 1 The expression of antisense hTR gene.

Only the cells transfected with pEF-ahTR expressed the antisense hTR, however, the G6PDH was detected in all samples that indicated an appropriate RT-PCR reaction.

β-Gal staining

After drug selection, nearly all MKN-45 cells stably transfected with pEF6/V5-His-TOPO/lacZ vector were stained blue by β-Gal Staining Kit while parental cells were not.

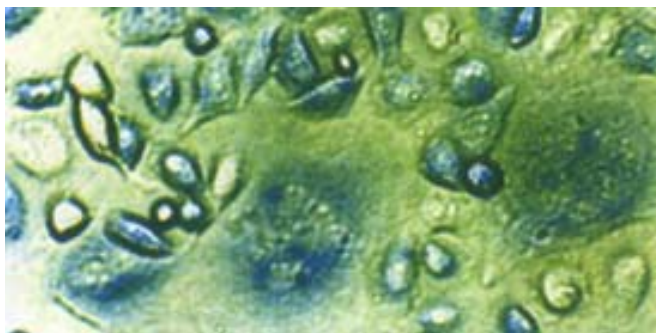
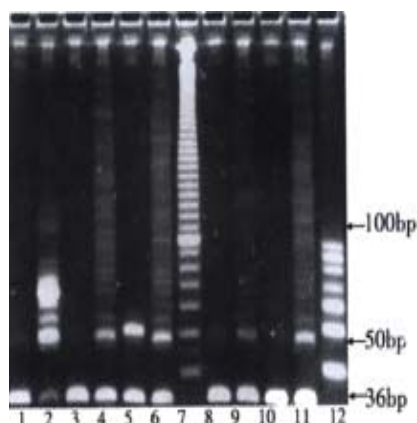


Figure 2 The result of β-Gal staining of MKN-45-lac. (×600)

Telomerase activity

We measured telomerase activity of the pEF-hTR, pEF-ahTR and pEF-empty transfected MKN-45 cells and parental cells through TRAP method described above. It was found that the level of telomerase activity in the pEF-ahTR transfected MKN-45 cells was greatly inhibited, compared with that in the parental MKN-45 cells. However, there was no difference between the level of telomerase activity in the pEF-hTR, pEF-empty transfected MKN-45 cells and parental MKN-45 cells.



Line 1: 1× CHAPS Lysis Buffer only control; Line 2: 0.1 amole quantitation TSR8 control; Line 3: MKN-45-empty heat-inactivated control; Line 4: MKN-45-empty; Line 5: MKN-45 heat-inactivated control; Line 6: MKN-45; Line 7: 10bp DNA Ladder (Gibco BRL); Line 8: MKN-45-ahTR heat-inactivated control; Line 9: MKN-45-ahTR; Line 10: MKN-45-hTR heat-inactivated control; Line 11: MKN-45-hTR; Line 12: 10bp DNA Step Ladder (Promega). **Figure 3A** Detection of telomerase activity with the telomeric repeat amplification protocol (TRAP) assay. A 36bp internal control band present in all samples indicated an appropriate polymerase chain reaction (PCR).

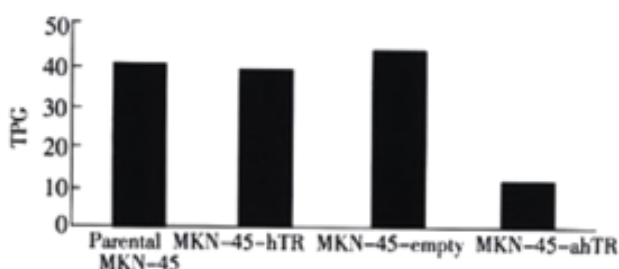


Figure 3B Comparison of telomerase activity in MKN-45-ahTR and control cells. Compared with control cells, the telomerase activity in MKN-45-ahTR was inhibited by about 75%.

Cellular effects of telomerase inhibition

As Figures 4, 5 and Table 1 showed, compared with controls cells, the MKN-45-ahTR cell displayed a longer population doubling time, an increased percentage of cells in the G0/G1 phase, a lower cell proliferation index and a higher apoptotic rate, which demonstrated that, through inhibiting telomerase activity, antisense hTR gene transfection could inhibit the proliferative capacity of NKN-45 and induce cell apoptosis.



Figure 4 Hoechst 33258 staining of MKN-45-ahTR. (×600) The cells undergoing apoptosis demonstrated apoptotic chromatin changes: blebbing, fragmentation and condensation under fluorescence microscope.

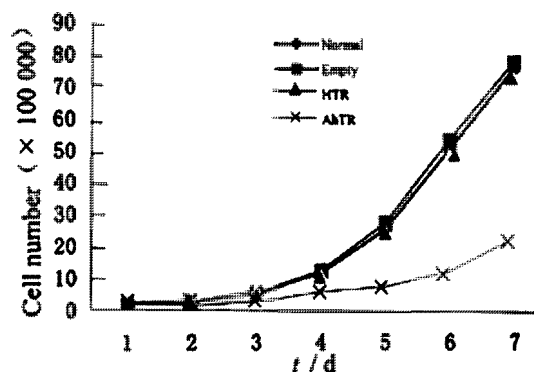


Figure 5 Cell growth curve.

Table 1 Comparison of distribution of cell cycle, cellular proliferation index, apoptotic rate, population doubling time of MKN-45-ahTR and those of control cells

	Distribution of cell cycle (%)			cell proliferation index (%)	Apoptotic rate (%)	population doubling time (hours)
	G0/G1	S	G2/M			
MKN-45-ahTR	65	34.2	0.8	35	25.3	35.3
MKN-45-hTR	55.7	37.5	6.8	44.3	0	23.2
MKN-45-empty	54.1	38.4	7.5	45.9	0	22.7
normal MKN-45	54.7	37.8	7.5	45.3	0	22.9

DISCUSSION

Compared with normal somatic cells, which reach the end of their replicative capacity after a limited number of population doubling and enter a senescence phase, the cancer cells have an unlimited replicative capacity. This important characteristic of cancer, named immortality, is gaining more and more attention, seeing that cancer cells may achieve cellular immortality through only a major pathway: activation of the telomerase^[47].

Telomerase is a unique ribonucleoprotein that can synthesize telomeric DNA onto chromosomal ends using a segment of its RNA component (hTR) as a template to compensate for the loss of telomeric repeats (TTAGGG) caused by the so-called “end-replication” problem. Recent Study demonstrated that 758 of 895 (85 %) of malignant tumors but none of 70 normal somatic tissues

expressed telomerase activity. In addition, the level of telomerase activity influences the prognosis of patient to a certain degree. For example, high level of telomerase correlates with poor clinical outcome in neuroblastoma, while patients with metastatic IV-S neuroblastoma without telomerase activity experiences spontaneous regression of tumors. These findings indicate that telomerase plays an important role in carcinogenesis and therefore undoubtedly become the basis of the widely held view of telomerase as a highly selective target for antisense gene therapy of cancer^[48].

The RNA component of telomerase (hTR) is crucial to the telomerase activity^[49-51]. Human cell lines that expressed hTR mutated in the template region generated the predicted mutant telomerase activity. In addition, recent experiments have shown that antisense gene therapy directed against telomerase RNA component (hTR) could effectively inhibit telomerase activity and induce apoptotic cell death in ovarian cancer, prostate cancer, bladder cancer, malignant gliomas and human breast epithelial cells^[52-56]. However, whether such anti-cancer effect can be obtained in human gastric cancer is still unknown. Therefore, we examined the effect of antisense hTR (ahTR) expression on the growth of human gastric cancer cell line: MKN-45 through transfection of an ahTR expression vector.

Given that whether the vector can effectively and stably express the exogenous gene it carries will directly influence the effect of antisense gene therapy. Firstly, we adopted two different methods to detect the expression of exogenous gene by the pEF6/V5-His-TOPO vector before conducting other experimental items. The first one was to detect the expression of reporter gene. pEF6/V5-His-TOPO/lacZ vector is the same as the pEF6/V5-His-TOPO vector except that the former carrying lacZ gene, a kind of widely used reporter gene, in its multi cloning sites. Usually by using β -Gal staining method, the researchers can easily detect the expression of lacZ gene through which they further evaluate the ability of the vector's promoter to express the exogenous gene. We found that nearly all cells stably transfected with pEF6/V5-His-TOPO/lacZ vector were stained blue while control cells were not. Therefore, we believed that pEF6/V5-His-TOPO/lacZ vector could effectively express the exogenous gene (lacZ gene) it carried, so did the pEF6/V5-His-TOPO vector. The second one was to detect the expression of antisense hTR gene directly through RT-PCR method. Only the cells transfected with pEF-ahTR expressing the antisense hTR gene were found. Both the results proved that pEF6/V5-His-TOPO vector could effectively express the exogenous gene, thus laying the solid fundament for the study of following experimental items.

As the results showed, the most significant conclusions we could draw from this study were that telomerase in human gastric cancer cell line: MKN-45 could be inhibited by a vector expressing mRNA complementary to the template region of hTR and that the growth of cancer cells was retarded and cell apoptosis was induced after telomerase was inhibited by this method. Therefore, our experiment clearly demonstrated that blocking the RNA component of telomerase with antisense hTR expression vector appeared to be a rational approach to the treatment of gastric cancer. The telomerase may become an ideal target for antisense gene therapy in human gastric cancer.

However, it is noticeable that not all cells transfected with antisense hTR gene underwent apoptosis, and underlying mechanism is still unknown. The possible reason is that the carcinogenesis process is complicated and the reactivation of telomerase may play an important but by no means the sole role during this process. Many oncogenes and tumor suppressor genes are also involved in tumorigenesis^[57,58]. While believed to be necessary for cancer cells to grow without limit, telomerase is not sufficient to transform a normal cell into a tumor cell. Thus, anti-cancer effect of antisense gene therapy will be more satisfactory if multitargets are aimed. For example, a recent report showed that the combination of 2-5A-anti-hTR and Ad5CMV-p53 had greater anti-tumor efficacy against all

p53-mutant glioma cells than each treatment alone^[59]. Seeing that telomerase activity and p53 dysfunction are also detected in gastric cancer^[60,61], this approach may be effective in treating gastric cancer patients too and the similar investigation is being conducted in our laboratory now.

REFERENCES

- Zhang XY. Some recent works on diagnosis and treatment of gastric cancer. *World J Gastroenterol* 1999;5:1-3
- Lin YZ, Yin HR, Zhu ZG, Lu W, Li DL, Zhang J. The surgical treatment of gastric cancer in Shanghai. *Asian J Surg* 2001;24:258-262
- Maehara Y, Kakeji Y, Oda S, Takahashi I, Akazawa K, Sugimachi K. Time trends of surgical treatment and the prognosis for Japanese patients with gastric cancer. *Br J Cancer* 2000;83: 986-991
- Borie F, Millat B, Fingerhut A, Hay JM, Fagniez PL, De Saxce B. Lymphatic involvement in early gastric cancer: prevalence and prognosis in France. *Arch Surg* 2000;135:1218-1223
- Cascinu S, Graziano F, Barni S, Labianca R, Comella G, Casaretti R, Frontini L, Catalano V, Baldelli AM, Catalano G. A phase II study of sequential chemotherapy with docetaxel after the weekly PELF regimen in advanced gastric cancer. A report from the Italian group for the study of digestive tract cancer. *Br J Cancer* 2001;84:470-474
- Valle JW. Adjuvant therapy for gastric cancer-has the standard changed? *Br J Cancer* 2001; 84: 875-877
- Liu HF, Liu WW, Fang DC, Yang SM, Wang RQ. Bax gene expression and its relationship with apoptosis in human gastric carcinoma and precancerous lesions. *Shijie Huaren Xiaohua Zazhi* 2000;8:665-668
- Fang DC, Zhou XD, Luo YH, Wang DX, Lu R, Yang SM, Liu WW. Microsatellite instability and loss of heterozygosity of suppressor gene in gastric cancer. *Shijie Huaren Xiaohua Zazhi* 1999;7:479-481
- Wang YK, Ma NX, Lou HL, Li Y, Wang L, Pan H, Zhang ZB. Relationship between P53, nm23 protein expression and lymphatic hyperplasia in gastric cancer. *Shijie Huaren Xiaohua Zazhi* 1999;7:34-36
- Takano Y, Kato Y, van Diest PJ, Masuda M, Mitomi H, Okayasu I. Cyclin D2 overexpression and lack of p27 correlate positively and cyclin E inversely with a poor prognosis in gastric cancer cases. *Am J Pathol* 2000;156:585-594
- Cui DX, Yan XJ, Su CZ. Differentially expressed genes were isolated in gastric carcinoma by optimised differential display PCR. *Shijie Huaren Xiaohua Zazhi* 1999;7:139-144
- Zhao Y, Zhang XY, Shi XJ, Hu PZ, Zhang CS, Ma FC. Clinical significance of expressions of P16, P53 proteins and PCNA in gastric cancer. *Shijie Huaren Xiaohua Zazhi* 1999;7:246-248
- Noguchi T, Muller W, Wirtz HC, Willers R, Gabbert HE. FHIT gene in gastric cancer: association with tumour progression and prognosis. *J Pathol* 1999;188:378-381
- Cui DX, Yan XJ, Zhang L, Zhao JR, Jiang M, Guo YH, Zhang LX, Bai XP, Su CZ. Screening and its clinical significance of 6 fragments of highly expressing genes in gastric cancer and precancerous mucosa. *Shijie Huaren Xiaohua Zazhi* 1999;7:770-772
- He XS, Su Q, Chen ZC, He XT, Long ZF, Ling H, Zhang LR. Expression, deletion and mutation of p16 gene in human gastric cancer. *World J Gastroenterol* 2001;7:515-521
- Liu HF, Liu WW, Fang DC, Men RP. Expression and significance of proapoptotic gene Bax in gastric carcinoma. *World J Gastroenterol* 1999; 5:15-17
- Wang B, Shi LC, Zhang WB, Xiao CM, Wu JF, Dong YM. Expression and significance of P16 gene in gastric cancer and its precancerous lesions. *Shijie Huaren Xiaohua Zazhi* 2001;9:39-42
- Ji F, Peng QB, Zhan JB, Li YM. Study of differential polymerase chain reaction of C-erbB-2 oncogene amplification in gastric cancer. *World J Gastroenterol* 1999;5:152-155
- Guo CQ, Wang YP, Liu GY, Ma SW, Ding GY, Li JC. Study on *Helicobacter pylori* infection and -p53, c-erbB-2 gene expression in carcinogenesis of gastric mucosa. *Shijie Huaren Xiaohua Zazhi* 1999;7:313-315
- Chen SY, Wang JY, Ji Y, Zhang XD, Zhu CW. Effects of *Helicobacter pylori* and protein kinase C on gene mutation in gastric cancer and precancerous lesions. *Shijie Huaren Xiaohua Zazhi* 2001;9:302-307
- Zhang Z, Yuan Y, Gao H, Dong M, Wang L, Gong YH. Apoptosis, proliferation and p53 gene expression of H. pylori associated gastric epithelial lesions. *World J Gastroenterol* 2001;7:779-782
- Wang DX, Fang DC, Li W, Du QX, Liu WW. A study on relationship between infection of *Helicobacter pylori* and inactivation of antioncogenes in cancer and pre-cancerous lesion. *Shijie Huaren Xiaohua Zazhi* 2001; 9:984-987
- Xue FB, Xu YY, Wan Y, Pan BR, Ren J, Fan DM. Association of *H. pylori* infection with gastric carcinoma: a Meta analysis. *World J Gastroenterol* 2001;7:801-804

- 24 Miehlik S, Kirsch C, Dragosics B, Gschwandler M, Oberhuber G, Antos D, Dite P, Luter J, Labenz J, Leodolter A, Malfertheiner P, Neubauer A, Ehninger G, Stolte M, Bayerdorfer E. *Helicobacter pylori* and gastric cancer: current status of the Austrian Czech German gastric cancer prevention trial (PRISMA Study). *World J Gastroenterol* 2001;7:243-247
- 25 Liu HF, Liu WW, Fang DC, Yang SM, Zhao L. Gastric epithelial apoptosis induced by *Helicobacter pylori* and its relationship with Bax protein expression. *Shijie Huaren Xiaohua Zazhi* 2000;8:860-862
- 26 Yamagata H, Kiyohara Y, Aoyagi K, Kato I, Iwamoto H, Nakayama K, Shimizu H, Tanizaki Y, Arima H, Shinohara N, Kondo H, Matsumoto T, Fujishima M. Impact of *Helicobacter pylori* infection on gastric cancer incidence in a general Japanese population: the Hisayama study. *Arch Intern Med* 2000;160:1962-1968
- 27 Zhang ZW, Farthing MJG. Molecular mechanisms of *H. pylori* associated gastric carcinogenesis. *World J Gastroenterol* 1999;5:369-374
- 28 Yao YL, Xu B, Song YG, Zhang WD. Overexpression of cyclin E in Mongolian gerbil with *Helicobacter pylori*-induced gastric precancerosis. *World J Gastroenterol* 2002;8:60-63
- 29 Yu WL, Huang ZH. Progress in studies on gene therapy for gastric cancer. *Shijie Huaren Xiaohua Zazhi* 1999;7:887-889
- 30 Xu CT, Huang LT, Pan BR. Current gene therapy for stomach carcinoma. *World J Gastroenterol* 2001;7:752-759
- 31 Chen B, Liu WW, Fang DC. An overview of current studies on telomerase. *Shijie Huaren Xiaohua Zazhi* 2001;9:441-446
- 32 Chen JL, Blasco MA, Greider CW. Secondary structure of vertebrate telomerase RNA. *Cell* 2000;100:503-514
- 33 Vasef MA, Ross JS, Cohen MB. Telomerase activity in human solid tumors. Diagnostic utility and clinical applications. *Am J Clin Pathol* 1999;112:S68-75
- 34 Feng DY, Zheng H, Fu CY, Cheng RX. An improvement method for the detection of *in situ* telomerase activity: *in situ* telomerase activity labeling. *World J Gastroenterol* 1999;5:535-537
- 35 He XX, Wang JL, Wu JL, Yuan SY, Ai L. Telomerase expression, *Hp* infection and gastric mucosal carcinogenesis. *Shijie Huaren Xiaohua Zazhi* 2000;8:505-508
- 36 Fu W, Begley JG, Killen MW, Mattson MP. Anti-apoptotic role of telomerase in pheochromocytoma cells. *J Biol Chem* 1999;274:7264-7271
- 37 Hahn WC, Stewart SA, Brooks MW, York SG, Eaton E, Kurachi A, Beijersbergen RL, Knoll JH, Meyerson M, Weinberg RA. Inhibition of telomerase limits the growth of human cancer cells. *Nat Med* 1999;5:1164-1170
- 38 Lichtsteiner SP, Lebkowski JS, Vasserot AP. Telomerase, a target for anticancer therapy. *Ann N Y Acad Sci* 1999;886:1-11
- 39 Guo Z, Yang SM. A new anti-cancer target point: progress in the studies of telomere and its inhibitors. *Shijie Huaren Xiaohua Zazhi* 1999;7:607-609
- 40 Ma JP, Zhan WH, Cai SR, Peng JS, Wang JP. Telomerase activity in gastric cancer. *Chin J Dig* 2000;1:13-16
- 41 He XX, Wang JL, Wu JL, Yuan SY, Ai L. Telomere, cellular DNA content and gastric mucosal carcinogenesis. *Shijie Huaren Xiaohua Zazhi* 2000;8:509-512
- 42 Okusa Y, Ichikura T, Mochizuki H, Shinomiya N. Clinical significance of telomerase activity in biopsy specimens of gastric cancer. *J Clin Gastroenterol* 2000; 30: 61-63
- 43 Zhang FX, Deng ZY, Zhang XY, Kang SC, Wang Y, Yu XL, Wang H, Bian XH. Telomeric length associated with prognosis in human primary and metastatic gastric cancer. *Shijie Huaren Xiaohua Zazhi* 2000; 8:153-155
- 44 Kakeji Y, Maehara Y, Koga T, Shibahara K, Kabashima A, Tokunaga E, Sugimachi K. Gastric cancer with high telomerase activity shows rapid development and invasiveness. *Oncol Rep* 2001;8:107-110
- 45 Yakoob J, Hu GL, Fan XG, Zhang Z. Telomere, telomerase and digestive cancer. *World J Gastroenterol* 1999;5:334-337
- 46 Feng RH, Li JF, Liu BY, Zhu ZG, Yin HR. hTR gene cloning from human gastric cancer cells and the construction of its sense and antisense eukaryotic expression vector. *Shijie Huaren Xiaohua Zazhi* 2001;9: 1409-1414
- 47 Shammas MA, Simmons CG, Corey DR, Reis RJS. Telomerase inhibition by peptide nucleic acids reverses "immortality" of transformed human cells. *Oncogene* 1999;18:6191-6200
- 48 Neidle S, Kelland LR. Telomerase as an anti-cancer target: current status and future prospects. *Anti-cancer drug des* 1999;14:341-347
- 49 Weilbaecher RG, Lundblad V. Assembly and regulation of telomerase. *Curr Opin Chem Biol* 1999;3:573-577
- 50 Gilley D, Blackburn EH. The telomerase RNA pseudoknot is critical for the stable assembly of a catalytically active ribonucleoprotein. *Proc Natl Acad Sci USA* 1999;96:6621-6625
- 51 Liu JP. Studies of the molecular mechanisms in the regulation of telomerase activity. *FASEB J* 1999; 13: 2091-2104
- 52 Kushner DM, Paranjape JM, Bandyopadhyay B, Cramer H, Leaman DW, Kennedy AW, Silverman RH, Cowell JK. 2-5A antisense directed against telomerase RNA produces apoptosis in ovarian cancer cells. *Gynecol Oncol* 2000;76:183-192
- 53 Kondo Y, Koga S, Komata T, Kondo S. Treatment of prostate cancer *in vitro* and *in vivo* with 2-5-A-anti-telomerase RNA component. *Oncogene* 2000;19:2205-2211
- 54 Koga S, Kondo Y, Komata T, Kondo S. Treatment of bladder cancer cells *in vitro* and *in vivo* with 2-5A antisense telomerase RNA. *Gene Ther* 2001;8:654-658
- 55 Mukai S, Kondo Y, Koga S, Komata T, Barna BP, Kondo S. 2-5A antisense telomerase RNA therapy for intracranial malignant gliomas. *Cancer Res* 2000;60:4461-4467
- 56 Herbert BS, Pitts AE, Baker SI, Hamilton SE, Wright WE, Shay JW, Corey DR. Inhibition of human telomerase in immortal human cells leads to progressive telomere shortening and cell death. *Proc Natl Acad Sci USA* 1999;96:14276-14281
- 57 Wu SH, Ma LP, Jin W, Sui YF. Tumor suppressor gene: P16, p21, PRB and gastric cancer. *Shijie Huaren Xiaohua Zazhi* 1999;7:551
- 58 Wang DX, Fang DC, Liu WW. Study on alteration of multiple genes in intestinal metaplasia, atypical hyperplasia and gastric cancer. *Shijie Huaren Xiaohua Zazhi* 2000;8:855-859
- 59 Komata T, Kondo Y, Koga S, Ko SC, Chung LWK, Kondo S. Combination therapy of malignant glioma cells with 2-5-A-antisense telomerase RNA and recombinant adenovirus p53. *Gene Ther* 2000;7: 2071-2079
- 60 Qin LJ. *In situ* hybridization of P53 tumor suppressor gene in human gastric precancerous lesions and gastric cancer. *Shijie Huaren Xiaohua Zazhi* 1999;7:494-497
- 61 Zhang L, Fu HM, Jin SZ, Huang R, Zhou CG. Overexpression of P53 and relationship between extracellular matrix and differentiation, invasion and metastasis of gastric carcinoma. *Shijie Huaren Xiaohua Zazhi* 2001;9:992-996

Edited by Zhang JZ

• GASTRIC CANCER •

Expression and function of classical protein kinase C isoenzymes in gastric cancer cell line and its drug-resistant sublines

Ying Han, Zhe-Yi Han, Xin-Min Zhou, Ru Shi, Yue Zheng, Yong-Quan Shi, Ji-Yan Miao, Bo-Rong Pan, Dai-Ming Fan

Ying Han, Zhe-Yi Han, Xin-Min Zhou, Yong-Quan Shi, Ji-Yan Miao, Dai-Ming Fan, Institute of Digestive Disease, Xijing Hospital, Fourth Military Medical University, Xi'an 710032, Shaanxi Province, China
Ru Shi, Department of Pharmacology and Reagents, Xijing Hospital, Fourth Military Medical University, Xi'an 710032, Shaanxi Province, China
Yue Zheng, the 6th Undergraduate Section, Fourth Military Medical University, Xi'an 710032, Shaanxi Province, China

Bo-Rong Pan, Oncology Center of Xijing Hospital, Fourth Military Medical University, Xi'an 710032, Shaanxi Province, China

Supported by the National Nature Science Foundation of China, No. 30030140 and No. 30000066.

Correspondence to: Dai-Ming Fan, Institute of Digestive Disease, Xijing Hospital, Fourth Military Medical University, Xi'an 710032, Shaanxi Province, China. fandaim@fmmu.edu.cn

Telephone: +86-29-3375221 Fax: +86-29-2539041

Received 2001-11-02 Accepted 2001-12-06

Abstract

AIM: To investigate the expression and function of classical protein kinase C (PKC) isoenzymes in inducing MDR phenotype in gastric cancer cells.

METHODS: Two cell lines were used in the study: gastric cancer cell SGC7901 and its drug-resistant cell SGC7901/VCR stepwise-selected by vincristine 0.3, 0.7 and 1.0mg·L⁻¹, respectively. The expression of classical PKC (cPKC) isoenzymes in SGC7901 cells and SGC7901/VCR cells were detected using immunofluorescent cytochemistry, laser confocal scanning microscope and Western blot. The effects of anti-PKC isoenzymes antibody on adriamycin accumulation in SGC7901/VCR cells were determined using flow cytometric analysis.

RESULTS: (1) SGC7901 cells exhibited positive staining of PKC-α. SGC7901/VCR cells exhibited stronger staining of PKC-α than SGC7901 cells. The higher dosage vincristine selected, the much stronger staining of PKC-α was observed on SGC7901/VCR cells. (2) Both SGC7901 and SGC7901/VCR cells exhibited positive staining of PKC-βI and PKC-βII with no significant difference. (3) Compared with SGC7901, SGC7901/VCR cells had decreased adriamycin accumulation and retention. Accumulation of adriamycin in SGC7901 was 5.21±2.56mg·L⁻¹, in SGC7901/VCR 0.3 was 0.85±0.29mg·L⁻¹, in SGC7901/VCR 0.7 was 0.81±0.32mg·L⁻¹, and in SGC7901/VCR 1.0 was 0.80±0.33mg·L⁻¹; Retention of adriamycin in SGC 7901 was 2.51±1.23mg·L⁻¹, in SGC7901/VCR 0.3 was 0.47±0.14mg·L⁻¹, in SGC7901/VCR 0.7 was 0.44±0.15mg·L⁻¹, and in SGC 7901/VCR 1.0 was 0.41±0.11mg·L⁻¹. (4) Fluorescence intensity presented adriamycin accumulation in SGC7901/VCR cells was increased from 1.14±0.36 to 2.71±0.94 when cells were co-incubated with anti-PKC-α but not with anti-PKC-βI, PKC-αII and PKCγ antibodies.

CONCLUSION: PKC-α, but not PKC-βI, PKC-βII or PKCγ, may play a role in multidrug resistance of gastric cancer cells SGC7901/VCR.

Han Y, Han ZY, Zhou XM, Shi R, Zheng Y, Shi YQ, Miao JY, Pan BR, Fan DM. Expression and function of classical protein kinase C isoenzymes in gastric cancer cell line and its drug-resistant sublines. *World J Gastroenterol* 2002;8(3):441-445

INTRODUCTION

Multi-drug resistance (MDR), the principal mechanism by which many cancers develop resistance to a variety of chemotherapeutic drugs, is a major factor in the failure of many forms of chemotherapy^[1-4]. It affects patients with numerous blood cancers and solid tumors. Cellular drug resistance is mediated by different mechanisms operating at different steps of the cytotoxic action of the drug from a decrease of drug accumulation in the cell to the abrogation of apoptosis induced by the chemical substance. Several different mechanisms will switch on in the MDR cells, but usually one major mechanism is operating. The most investigated mechanisms with known clinical significance are: (1) activation of transmembrane proteins effluxing different chemical substances from the cells, in which P-glycoprotein (P-gp) is the most known efflux pump; (2) activation of the enzymes of the glutathione detoxification system; (3) alterations of the genes and the proteins involved into the control of apoptosis (especially p53 and Bcl-2)^[5-12]. PKC comprises a family of at least 13 distinct serine/threonine kinase isoenzymes involved in signal transduction pathways that govern a wide range of physiological processes including differentiation, proliferation, gene expression, brain function, membrane transport and the organization of cytoskeletal and extracellular matrix proteins^[13-26]. Recently accumulated evidence indicates that PKC activity, especially cPKC, plays a significant role in the formation of tumor MDR. The isoenzymes possess distinct differences in localization in different cells. Within a single cell, PKC isoforms also exhibit differences in expression and function, so research on distinct function in tumor MDR of isoenzymes has important significance in screening drugs with high specificity that could reverse MDR and in disclosing the mechanism of MDR formation and its regularity of the reversion.

MATERIALS AND METHODS

Materials

Human gastric cancer cell line SGC7901 was reserved by our institute and its drug-resistant sublines SGC7901/VCR were stepwise-selected by vincristine 0.3, 0.7 and 1.0mg·L⁻¹, respectively. RPMI 1640 medium was the product of Gibco (U.S.A.). Newborn bovine serum was purchased from Hyclone (U.S.A.). Chemical drugs vincristine and adriamycin were purchased from Farmitalia Carlo Erba

(U.S.A.) and Minsheng (Hangzhou, China). Rabbit-anti-human polyclonal antibody PKC- α , PKC- β I, PKC- β II and PKC γ were the products of Santa Cruz Biotechnology. SABC immunohistochemistry kit and the HRP labeled goat-anti-rabbit IgG was purchased from Boste (Wuhan, China). FITC labeled goat-anti-rabbit IgG was purchased from Zhongshan (China).

Methods

Immunofluorescent cytochemistry The expression of PKC isoenzymes were detected by routine immunocytochemical fluorescence method^[27,28]. The procedures were as follows. Cells were maintained at 37°C in a 50mL·L⁻¹ CO₂-humidified incubator in RPMI 1640 medium supplemented with 25mmol·L⁻¹ HEPES buffer and 100mL·L⁻¹ new born bovine serum. SGC7901/VCR cells were cultured in the medium with extra adding vincristine at the concentration of 0.3, 0.7 and 1.0mg·L⁻¹, respectively. Cells at exponential phase were harvested, digested by 2.5g·L⁻¹ trypsin and then cultured on the slides in the medium described above at 37°C for further 24h; RPMI 1640 medium was then washed by PBS and cells were fixed in cold acetone for 5min; 50mL·L⁻¹ H₂O₂ was added and incubated at room temperature for 10-15min and added 3g·L⁻¹ TritonX-100 for another 15min; normal goat serum (1:10) was added and incubated at room temperature for 30min; rabbit-anti-human polyclonal antibody PKC- α , PKC- β I, PKC- β II and PKC γ (1:100) were added respectively and incubated at 4°C over night; FITC labeled goat-anti-rabbit IgG was added and incubated at 37°C for 1h; the slides were sealed by 500mL·L⁻¹ glycerin buffer and observed with a fluorescence microscope. Unrelated monoclonal antibody and PBS were used as negative controls.

Laser confocal scanning microscope The laser confocal scanning microscope protocols used were as described^[29,30]. Methods of cell culture and stain with Ab were carried out as described in immunocytochemical fluorescence method. FITC labeled goat-anti-rabbit IgG was added in the darkness and incubated at room temperature for 3h; the slides were sealed by 500mL·L⁻¹ glycerin buffer and observed with a laser confocal scanning fluorescence microscope. Unrelated monoclonal antibody and PBS were used as negative controls.

SDS-PAGE According to Chen et al and Xiao *et al*^[31-33], cells at exponential phase were harvested and washed by cold PBS and suspended in extraction buffer (50mmol·L⁻¹ Tris-Cl (pH7.5), 150mmol·L⁻¹ NaCl, 0.2mmol·L⁻¹ EDTA, 1mmol·L⁻¹ PMSF and 10g·L⁻¹ NP-40). The homogenate was heated for 5min in a boiling water bath and then centrifuged. The supernatants were harvested and the protein concentrations were assayed by Bradford method. 150 μ g total protein were electrophoresed on SDS-polyacrylamide gels with the stacking and the separating gels containing 50 and 100g·L⁻¹ acrylamide, respectively, and the gels were stained with Coomassie brilliant blue dye.

Western blot analysis According to She *et al*^[34], after SDS-PAGE, proteins were transferred onto nitrocellulose membrane under a constant current of mA for 1h. Non-specific binding sites were blocked by PBS with 50mL·L⁻¹ milk plus 1g·L⁻¹ Tween-20 at room temperature. Primary and secondary antibodies were rabbit-anti-human polyclonal antibody PKC and HRP labeled goat-anti-rabbit IgG, respectively. Films were exposed in DAB detection reagent to develop color of bands.

Flow cytometric analysis According to Jiang *et al*^[35] and Feng *et al*^[36], cells were cultured in 6-well culture plates at 37°C for 48h, adriamycin was added to the final concentration of 5mg·L⁻¹. After further culture for 1h, rabbit-anti-human polyclonal antibody against different cPKC isoenzymes was added and incubated for 40min, PBS and normal rabbit serum were used as negative controls. And then,

cells were harvested or cultured in drug-free medium for another 30 min and harvested. The harvested cells of the phases were suspended in cold PBS, intracellular adriamycin fluorescence intensity was determined by flow cytometric analysis with the stimulative and acceptant wave length at 488nm and 575nm, respectively.

Statistical analysis Data were presented as $\bar{x} \pm s$. Significant differences were determined by using ANOVA in statistical software SPSS10.0.

RESULTS

Immunofluorescent cytochemistry

To investigate the expression of PKC isoenzymes of SGC7901 cells and its drug-resistant cell subline SGC7901/VCR, immunofluorescent cytochemistry was performed. The positive signals were of fluorescent signals. Both SGC7901 cells and SGC7901/VCR cells expressed PKC- α , PKC- β I, PKC- β II and PKC γ . The expression of PKC- α was stronger in SGC7901/VCR cells than that in SGC7901 cells. There was no significant difference in the expression of PKC- β I and PKC- β II between SGC7901/VCR cells and SGC7901 cells. And the expression of PKC γ in SGC7901/VCR cells was positive as strongly as that in SGC7901 cells, and also no significant difference was found.

Laser confocal microscope analysis

PKC- α expressed in both SGC7901 cells and SGC7901/VCR cells. The positive signals were localized in cytoplasm and membrane. Compared with SGC7901 cells, the intensity of fluorescence in SGC7901/VCR cells was increased significantly when analysed by the intensity of pixel by using computer, which was 100 in SGC7901/VCR cells and 80 in SGC7901 cells.

Western blot

The expression of PKC- α was significantly higher in SGC7901/VCR cells than that in SGC7901 cells, in which expression increased with the increase of drug-dose-resistance of SGC7901/VCR cells. No significant difference was found in the expression of PKC- β I, PKC- β II and PKC γ between SGC7901/VCR cells and SGC7901 cells (Figure 1).

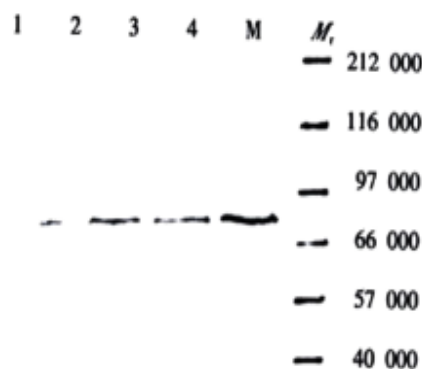


Figure 1 Western blot (detected with anti-PKC- α antibody)

Flow cytometric analysis

The effects of anti-PKC- α or β I antibody on adriamycin accumulation and retention in SGC7901/VCR cells were determined by flow cytometric analysis. When cells were cultured in drug-RPM1640, intracellular drug concentration would increase and finally stabilised at the highest plateau value, which was called adriamycin accumulation. When cells were cultured in drug-free medium, drug was effluxed from cells and subsequently, drug concentration stabilised at a lower plateau value, which was still higher than the

initial value and so called adriamycin retention. The results presented by the values of fluorescence intensity showed that adriamycin accumulation and retention decreased in SGC7901/VCR cells than that in SGC7901 cells. When co-incubated with anti-PKC- α antibody, the accumulation of adriamycin in MDR cells increased and showed partly dose-dependent effect, while PKC- β I, PKC- β II and PKC γ could not influence the ADR accumulation in SGC7901/VCR cells (Table 1,2).

Table 1 Adriamycin accumulation and retention in cells by flow cytometric analysis ($\bar{x} \pm s$ fluorescence intensity)

Adriamycin	SGC7901	SGC7901/VCR in different resistant drug dose (VCR.mg.L ⁻¹)		
		0.3	0.7	1.0
Accumulation	5.21 \pm 2.56	0.85 \pm 0.29 ^b	0.81 \pm 0.32 ^b	0.80 \pm 0.33 ^b
Retention	2.51 \pm 1.23	0.47 \pm 0.14 ^b	0.44 \pm 0.15 ^b	0.41 \pm 0.11 ^b

^bP<0.01, vs SGC7901.

Table 2 Effects of adriamycin accumulation in SGC7901/VCR cells by anti-PKC isoenzymes Ab ($\bar{x} \pm s$ fluorescence intensity)

Group	ρ (anti-PKC isoenzymes Ab)/(μ g.L ⁻¹)			
	0	25	250	500
Anti-PKC- α Ab	1.14 \pm 0.36	1.09 \pm 0.32	2.49 \pm 0.84 ^b	2.71 \pm 0.94 ^b
Anti-PKC- β IAb	1.14 \pm 0.36	1.13 \pm 0.38	1.14 \pm 0.39	1.14 \pm 0.39
Anti-PKC- α IIAb	1.14 \pm 0.36	1.14 \pm 0.38	1.14 \pm 0.40	1.14 \pm 0.39
Anti-PKC- γ Ab	1.14 \pm 0.36	1.14 \pm 0.39	1.14 \pm 0.40	1.14 \pm 0.39

^bP<0.01, vs 0 μ g.L⁻¹ anti-PKC isoenzymes Ab

DISCUSSION

The development of resistance to chemotherapeutic agents remains one of the major obstacles for successful cure of cancer patients. Tumor cells may acquire MDR in the course of exposure to various compounds that are used in modern anticancer therapy, including cytotoxic drugs and differentiating agents. Therefore, the recurrence of the disease after the initial treatment may be associated with establishment of secondary MDR in the residual tumor. Research on resistance to cancer treatment was mainly focused for 20 years on MDR. No useful method of reversing MDR, suitable for clinical use, has yet emerged from this large quantity of work. The reason could be an complicated mechanism involved in it. There are several ways for cancer cells to develop resistance or defense mechanisms against cytotoxic drugs^[37-43].

Resistance to therapy has been correlated to the presence of at least two molecular “pumps” that actively expel chemotherapeutic drugs from the tumor cells. This action thus spares tumor cells from the effects of the drug, which has to act inside the cells at the nucleus or the cytoplasm. The two pumps commonly found to confer MDR in cancer are P-gp and multidrug resistance-associated protein (MRP). But they can not explicate the phenomenon of MDR fully. It also reported that some cancer cells are resistant to signal of apoptosis and so making cell life longer might confer to the MDR phenotype.

Recent studies have indicated that the signal of phosphorylation might be an important part of MDR mechanisms. PKC isoforms are often overexpressed in disease states such as cancer and play a critical role in regulation of long term cellular events such as proliferation, differentiation and tumorigenesis. An increase in PKC activity might result in an oncogenic role and in MDR. Several studies indicate a role for PKC in the regulation of the MDR phenotype, since several PKC inhibitors are able to partially reverse MDR and inhibit P-gp phosphorylation.

The PKC family consists of several isoforms comprising three groups: classical, novel and atypical. PKC isoforms are widely

distributed in mammalian tissues and have many important physiological functions^[44-47]. cPKC subfamily shows significant specificity in tissue distribution. The isoenzymes possess distinct differences in localization in different cells. Within a single cell, PKC isoforms also exhibit differences in their distribution before and after their translocation following activation. For example, thymus cells express PKC- α and PKC- β I but not PKC- β II and PKC γ ; Cortical and medullary cells of suprarenal gland express PKC- α , while the cortical cells also express PKC- β I and PKC γ .

To date in recent years, the MDR phenotype is also associated with variation in content of PKC isoenzymes. Different isoforms possess distinct differences in expression and function in different MDR cells. It has been confirmed that sensitive cells show the phenotype of MDR when transfected with cDNA encoding PKC- α , which indicates the effect of PKC on MDR. Resistance to ADR of mouse leukemia MDR cell-line could be reversed by anti-PKC- β mAb when it was incubated with anti-PKC- α or anti-PKC- β mAb^[48-60].

This study confirmed that PKC- α , PKC- β I, PKC- β II and PKC γ were expressed in both SGC7901 cells and SGC7901/VCR cells. Our results showed that the expression of PKC- α was significantly higher in SGC7901/VCR cells than that in SGC7901 cells and the expression increased with the increase of drug-dose-resistance of SGC7901/VCR cells. There was no significant difference in the expression of PKC- β I, PKC- β II and PKC γ between SGC7901/VCR cells and SGC7901 cells. The result of flow cytometric analysis showed that ADR accumulation decreased in SGC7901/VCR cells much than that in SGC7901 cells, together with increase of the expression of PKC- α . Further study confirmed that anti-PKC- α antibody could reverse ADR accumulation in MDR cells to some degree and showed partly dose-dependent effect, while PKC- β I, PKC- β II and PKC γ could not influence the ADR accumulation in SGC7901/VCR cells. The results suggested that the formation of MDR in SGC7901/VCR cells was associated with over expression of PKC- α but not with PKC- β I, PKC- α II and PKC γ . Since isoenzymes of PKC possess only 1-10 amino acid in there pseudo substrate action site in C1 domain, research on distinct function in tumor MDR of isoenzymes has important significance in screening effective drugs with high specificity that could reverse MDR and in disclosing the mechanism of MDR formation and its regularity of the reversion. Because gastric cancer is common in China and some areas in the world^[61-80], this results may be important for further study.

REFERENCES

- 1 Yao XQ, Qing SH. Detection of multidrug resistance gene in progressive colon cancer and its significance. *Shijie Huaren Xiaohua Zazhi* 1999;7:535-536
- 2 Tu SP, Jiang SH, Qiao MM, Cheng SD, Wang LF, Wu YL, Yuan YZ, Wu YX. Effect of trichosanthin on cytotoxicity and induction of apoptosis of multiple drugs resistance cells in gastric cancer. *Shijie Huaren Xiaohua Zazhi* 2000;8:150-152
- 3 Cheng SD, Wu YL, Zhang YP, Qiao MM, Guo QS. Abnormal drug accumulation in multidrug resistant gastric carcinoma cells. *Shijie Huaren Xiaohua Zazhi* 2001;9:131-134
- 4 Zhang LJ, Chen KN, Xu GW, Xing HP, Shi XT. Congenital expression of Mdr-1 gene in tissues of carcinoma and its relation with pathomorphology and prognosis. *World J Gastroenterol* 1999;5:53-56
- 5 Zhan M, Yu D, Lang A, Li L, Pollock RE. Wild type p53 sensitizes soft tissue sarcoma cells to doxorubicin by down-regulating multidrug resistance-1 expression. *Cancer* 2001;92:1556-1566
- 6 Liu B, Staren E, Iwamura T, Appert H, Howard J. Effects of Taxotere on invasive potential and multidrug resistance phenotype in pancreatic carcinoma cell line SUIT-2. *World J Gastroenterol* 2001;7:143-148
- 7 Chen B, Zhang XY, Zhang YJ, Zhou P, Gu Y, Fan DM. Antisense to cyclin D1 reverses the transformed phenotype of human gastric cancer cells. *World J Gastroenterol* 1999;5:18-21
- 8 Liu XL, Xiao B, Yu ZC, Guo JC, Zhao QC, Xu L, Shi YQ, Fan DM. Down regulation of Hsp90 could change cell cycle distribution and increase drug sensitivity of tumor cells. *World J Gastroenterol* 1999;5:199-208

- 9 You H, Xiao B, Cui DX, Shi YQ, Fan DM. Two novel gastric cancer associated genes identified by differential display. *World J Gastroenterol* 1998;4:334-336
- 10 Xiao B, Shi YQ, Zhao YQ, You H, Wang ZY, Liu XL, Yin F, Qiao TD, Fan DM. Transduction of Fas gene or Bcl-2 antisense RNA sensitizes cultured drug resistant gastric cancer cells to chemotherapeutic drugs. *World J Gastroenterol* 1998;4:421-425
- 11 Warr JR, Bamford A, Quinn DM. The preferential induction of apoptosis in multidrug-resistant KB cells by 5-fluorouracil. *Cancer Lett* 2002;175:39-44
- 12 Roepe PD. pH and multidrug resistance. *Novartis Found Symp* 2001;240:232-247
- 13 Caruso-Neves C, Silva IV, Morales MM, Lopes AG. Cytoskeleton elements mediate the inhibition of the (Na⁺)+K⁺)atpase activity by PKC in *Rhodnius prolixus* malpighian tubules during hyperosmotic shock. *Arch Insect Biochem Physiol* 2001;48:81-88
- 14 Suga S, Wu J, Ogawa Y, Takeo T, Kanno T, Wakui M. Phorbol ester impairs electrical excitation of rat pancreatic beta-cells through PKC-independent activation of KATP channels. *BMC Pharmacol* 2001;1:3
- 15 MacDonald JF, Kotecha SA, Lu WY, Jackson MF. Convergence of PKC-dependent kinase signal cascades on NMDA receptors. *Curr Drug Targets* 2001;2:299-312
- 16 Chen L, Hahn H, Wu G, Chen CH, Liron T, Schechtman D, Cavallaro G, Banci L, Guo Y, Bolli R, Dorn GW 2nd, Mochly-Rosen D. Opposing cardioprotective actions and parallel hypertrophic effects of delta PKC and varepsilon PKC. *Proc Natl Acad Sci U S A* 2001;98:11114-11119
- 17 Kumar A, Hawkins KS, Hannan MA, Ganz MB. Activation of PKC-beta(I) in glomerular mesangial cells is associated with specific NF-kappaB subunit translocation. *Am J Physiol Renal Physiol* 2001;281:F613-619
- 18 Rivedal E, Opsahl H. Role of PKC and MAP kinase in EGF- and TPA-induced connexin43 phosphorylation and inhibition of gap junction intercellular communication in rat liver epithelial cells. *Carcinogenesis* 2001;22:1543-1550
- 19 Smith J, Yu R, Hinkle PM. Activation of MAPK by TRH Requires Clathrin-Dependent Endocytosis and PKC but Not Receptor Interaction with beta-Arrestin or Receptor Endocytosis. *Mol Endocrinol* 2001;15:1539-1548
- 20 Banan A, Fields JZ, Talmage DA, Zhang Y, Keshavarzian A. PKC-beta1 mediates EGF protection of microtubules and barrier of intestinal monolayers against oxidants. *Am J Physiol Gastrointest Liver Physiol* 2001;281:G833-847
- 21 Manier DH, Shelton RC, Sulser F. Cross-talk between PKA and PKC in human fibroblasts: what are the pharmacotherapeutic implications? *J Affect Disord* 2001;65:275-279
- 22 Boesch DM, Garvin JL. Age-dependent activation of PKC isoforms by angiotensin II in the proximal nephron. *Am J Physiol Regul Integr Comp Physiol* 2001;281:R861-867
- 23 Lum H, Podolski JL, Gurnack ME, Schulz IT, Huang F, Holian O. Protein phosphatase 2B inhibitor potentiates endothelial PKC activity and barrier dysfunction. *Am J Physiol Lung Cell Mol Physiol* 2001;281:L546-555
- 24 Shindo M, Irie K, Nakahara A, Ohigashi H, Konishi H, Kikkawa U, Fukuda H, Wender PA. Toward the identification of selective modulators of protein kinase C (PKC) isozymes: establishment of a binding assay for PKC isozymes using synthetic C1 peptide receptors and identification of the critical residues involved in the phorbol ester binding. *Bioorg Med Chem* 2001;9:2073-2081
- 25 Kim MS, Lim WK, Cha JG, An NH, Yoo SJ, Park JH, Kim HM, Lee YM. The activation of PI 3-K and PKC zeta in PMA-induced differentiation of HL-60 cells. *Cancer Lett* 2001;171:79-85
- 26 Radeff JM, Nagy Z, Stern PH. Involvement of PKC-beta in PTH, TNF-alpha, and IL-1 beta effects on IL-6 promoter in osteoblastic cells and on PTH-stimulated bone resorption. *Exp Cell Res* 2001;268:179-188
- 27 Ma X, Qiu DK, Xu J, Zeng MD. Effects of Cordyceps polysaccharides in patients with chronic hepatitis C. *Huaren Xiaohua Zazhi* 1998;6:582-584
- 28 Zhao LF, Han DW. Clinical significance of endotoxemia in liver diseases. *Shijie Huaren Xiaohua Zazhi* 1999;7:391-393
- 29 Wang CM, Huang XF, Pan BR, Dai XW, Ma FC, Zhao YM. Expression of chromogranin C/secretogranin II and pancreastatin in the pancreatic ductal carcinoma. *Huaren Xiaohua Zazhi* 1998;6:470-473
- 30 Huang XF, Wang CM, Dai XW, Pan BR, Yu LB, Fang L, Qian B, Zhao YL. Significance of cathepsin D and chromogranin A expression in human primary hepatocellular carcinomas. *Huaren Xiaohua Zazhi* 1998;6:474-478
- 31 Chen YK, Wu XB, Zhang ZY. Study on causes of serum anti-HBs positive patients with chronic liver diseases. *Huaren Xiaohua Zazhi* 1998;6:49-50
- 32 Xiao B, Shi YQ, Zhao YQ, You H, Liu XL, Fan DM. Expression of Fas gene in gastric cancer cells transduced with Fas gene. *Huaren Xiaohua Zazhi* 1998;6:400-403
- 33 Yang LJ, Sui YF, Chen ZN. Preparation and activity of conjugate of monoclonal antibody HAb18 against hepatoma F(ab')₂ fragment and staphylococcal enterotoxin A. *World J Gastroenterol* 2001;7:216-221
- 34 She FF, Su DH, Lin JY. Virulence and potential pathogenicity of coccoid *Helicobacter pylori* induced antibiotics. *World J Gastroenterol* 2001;7:254-258
- 35 Jiang XL, Quan QZ, Sun ZQ, Wang YJ, Qi F. Expression of adhesion molecules in tissues and peripheral lymphocyte of patients with ulcerative colitis. *Huaren Xiaohua Zazhi* 1998;6:54-55
- 36 Feng S, Song JD, Tian XR. Significance of proliferating cell nuclear antigen expression in colorectal carcinomas. *Huaren Xiaohua Zazhi* 1998;6:146-147
- 37 Gu SQ, Liang YY, Fan LR, Li BY, Wang DS. Co-regulative effects of the cAMP/PKA and DAG/PKC signal pathways on human gastric cancer cells during differentiation induced by traditional Chinese medicines. *China Natl J New Gastroenterol* 1997;3:50-53
- 38 Liu B, Staren E, Iwamura T, Appert H, Howard J. Effects of Taxotere on invasive potential and multidrug resistance phenotype in pancreatic carcinoma cell line SUIT-2. *World J Gastroenterol* 2001;7:143-148
- 39 Xu BH, Zhang RJ, Lu DD, Chen XD, Wang NJ. Expression of mdrl gene coded P-glycoprotein in hepatocellular carcinoma and its clinical significance. *Huaren Xiaohua Zazhi* 1998;6:783-785
- 40 Liu ZM, Shou NH. Expression significance of mdrl gene in gastric carcinoma tissue. *Shijie Huaren Xiaohua Zazhi* 1999;7:145-146
- 41 Shi YQ, Xiao B, Miao JY, Zhao YQ, You H, Fan DM. Construction of eukaryotic expression vector pBK fas and MDR reversal test of drug-resistant gastric cancer cells. *Shijie Huaren Xiaohua Zazhi* 1999;7:309-312
- 42 Liu Y, Lu MZ, Li QM, Wang YL. The expression of p53 C-myc and P-gp proteins in gastric cancer. *Xin Xiaohuabingxue Zazhi* 1997;5:585-586
- 43 Yin F, Shi YQ, Zhao WP, Xiao B, Miao JY, Fan DM. Suppression of P-gp induced multiple drug resistance in a drug resistant gastric cancer cell line by overexpression of Fas. *World J Gastroenterol* 2000;6:664-670
- 44 Kato A, Miyazaki M, Ambiru S, Yoshitomi H, Ito H, Nakagawa K, Shimizu H, Yokosuka O, Nakajima N. Multidrug resistance gene (MDR-1) expression as a useful prognostic factor in patients with human hepatocellular carcinoma after surgical resection. *J Surg Oncol* 2001;78:110-115
- 45 Kaminski MS, Zelenetz AD, Press OW, Saleh M, Leonard J, Fehrenbacher L, Lister TA, Stagg RJ, Tidmarsh GF, Kroll S, Wahl RL, Knox SJ, Vose JM. Pivotal Study of Iodine I 131 Tositumomab for Chemotherapy-Refractory Low-Grade or Transformed Low-Grade B-Cell Non-Hodgkin's Lymphomas. *J Clin Oncol* 2001;19:3918-3928
- 46 Ahlman H, Khorram-Manesh A, Jansson S, Wangberg B, Nilsson O, Jacobsson CE, Lindstedt S. Cytotoxic treatment of adrenocortical carcinoma. *World J Surg* 2001;25:927-933
- 47 Dei S, Teodori E, Garnier-Suillerot A, Gualtieri F, Scapecchi S, Budriesi R, Chiarini A. Structure-activity relationships and optimisation of the selective MDR modulator 2-(3,4-dimethoxyphenyl)-5-(9-fluorenylamino)-2-(methylethyl) pentanenitrile and its N-methyl derivative. *Bioorg Med Chem* 2001;9:2673-2682
- 48 Mansson E, Paul A, Lofgren C, Ullberg K, Paul C, Eriksson S, Albertioni F. Cross-resistance to cytosine arabinoside in a multidrug-resistant human promyelocytic cell line selected for resistance to doxorubicin: implications for combination chemotherapy. *Br J Haematol* 2001;114:557-565
- 49 Meng LH, Zhang JS, Ding J. Salvicine, a novel DNA topoisomerase II inhibitor, exerting its effects by trapping enzyme-DNA cleavage complexes. *Biochem Pharmacol* 2001;62:733-741
- 50 Chang G, Roth CB. Structure of MsbA from *E. coli*: A Homolog of the Multidrug Resistance ATP Binding Cassette (ABC) Transporters. *Science* 2001;293:1793-1800
- 51 Gill PK, Gescher A, Gant TW. Regulation of MDR1 promoter activity in human breast carcinoma cells by protein kinase C isozymes alpha and theta. *Eur J Biochem* 2001;268:4151-4157
- 52 Shtil AA, Ktitorova OV, Kakpakova ES, Holian O. Differential effects of the MDR1 (multidrug resistance) gene-activating agents on protein kinase C: evidence for redundancy of mechanisms of acquired MDR in leukemia cells. *Leuk Lymphoma* 2000;40:191-195
- 53 Matsumoto Y, Kunishio K, Nagao S. Increased phosphorylation of DNA topoisomerase II in etoposide resistant mutants of human glioma cell line. *J Neurooncol* 1999;45:37-46
- 54 Pallares-Trujillo J, Lopez-Soriano FJ, Argiles JM. Lipids: A key role in multidrug resistance? *Int J Oncol* 2000;16:783-798
- 55 van Gijn R, van Tellingen O, Haverkate E, Kettenes-van den Bosch JJ, Bult A, Beijnen JH. Pharmacokinetics and metabolism of the staurosporine

- analogue CGP 41 251 in mice. *Invest New Drugs* 1999;17:29-41
- 56 Merritt JE, Sullivan JA, Drew L, Khan A, Wilson K, Mulqueen M, Harris W, Bradshaw D, Hill CH, Rumsby M, Warr R. The bisindolylmaleimide protein kinase C inhibitor, Ro 32-2241, reverses multidrug resistance in KB tumour cells. *Cancer Chemother Pharmacol* 1999;43:371-378
 - 57 Han Y, Cao YX, Shi YQ, Fan DM. Expression of P-gp and PKC isoenzymes in multidrug resistance gastric cancer cell-line SGC7901/VCR. *Disi Junyi Daxue Xuebao* 2000;21:1454-1456
 - 58 Han Y, Shi YQ, Li L, Fan DM. Expression and function of PKC isoenzymes PKC- α and PKC- β I in gastric cancer cell-line SGC 7901 and its subline SGC7901/VCR. *Zhonghua Zhongliu Zazhi* 2001;23:103-106
 - 59 Han Y, Shi YQ, Zheng Y, Nie YZ, Zhang HB, Zhang ML, Pan BR, Fan DM. Protein kinase C is related to multidrug resistance by MGr1-Ag. *Shijie Huaren Xiaohua Zazhi* 2001;9:517-521
 - 60 Han Y, Shi YQ, Zheng Y, Zhang HB, Zhang ML, Wang CM, Fan DM. Expression and distribution of PKC isoenzymes in swelling activated multidrug resistance gastric cancer cell-line. *Zhonghua Yixue Zazhi* 2001; 81: 328-331
 - 61 Xu L, Zhang SM, Wang YP, Zhao FK, Wu DY, Xin Y. Relationship between DNA ploidy, expression of ki 67 antigen and gastric cancer metastasis. *World J Gastroenterol* 1999;5:10-11
 - 62 Wu YA, Lu B, Liu J, Li J, Chen JR, Hu SX. Consequence alimentary reconstruction in nutritional status after total gastrectomy for gastric cancer. *World J Gastroenterol* 1999;5:34-37
 - 63 Ji F, Peng QB, Zhan JB, Li YM. Study of differential polymerase chain reaction of C-erbB 2 oncogene amplification in gastric cancer. *World J Gastroenterol* 1999;5:152-155
 - 64 Zhan WH, Ma JP, Peng JS, Gao JS, Cai SR, Wang JP, Zheng ZQ, Wang L. Telomerase activity in gastric cancer and its clinical implications. *World J Gastroenterol* 1999;5:316-319
 - 65 Ji F, Wang WL, Yang ZL, Li YM, Huang HD, Chen WD. Study on the expression of matrix metallo proteinase 2Mrna in human gastric cancer. *World J Gastroenterol* 1999;5:455-457
 - 66 Wang H, Zheng MH, Zhang HB, Zhu J, He JR, Lu AG, Ji YB, Zhang MJ, Jiang Y, Yu BM, Li HW. Study on incisional implantation of tumor cells by carbon dioxide pneumo peritoneum in gastric cancer of a murine model. *World J Gastroenterol* 1999;5:544-546
 - 67 Zou SC, Qiu HS, Zhang CW, Tao HQ. A clinical and long term follow up study of peri operative sequential triple therapy for gastric cancer. *World J Gastroenterol* 2000;6:284-286
 - 68 Cai L, Yu SZ, Zhang ZF. Helicobacter pylori infection and risk of gastric cancer in Changle County, Fujian Province, China. *World J Gastroenterol* 2000;6:374-376
 - 69 Zhang FX, Zhang XY, Fan DM, Deng ZY, Yan Y, Wu HP, Fan JJ. Antisense telomerase RNA induced human gastric cancer cell apoptosis. *World J Gastroenterol* 2000;6:430-432
 - 70 Gu QL, Li NL, Zhu ZG, Yin HR, Lin YZ. A study on arsenic trioxide inducing in vitro apoptosis of gastric cancer cell lines. *World J Gastroenterol* 2000;6:435-437
 - 71 Wang ZN, Xu HM. Relationship between collagen c α expression and biological behavior of gastric cancer. *World J Gastroenterol* 2000;6:438-439
 - 72 Tu SP, Zhong J, Tan JH, Jiang XH, Qiao MM, Wu YX, Jiang SH. Induction of apoptosis by arsenic trioxide and hydroxy camptothecin in gastric cancer cells *in vitro*. *World J Gastroenterol* 2000;6:532-539
 - 73 Jiang BJ, Sun RX, Lin H, Gao YF. Study on the risk factors of lymphatic metastasis and the indications of less invasive operations in early gastric cancer. *World J Gastroenterol* 2000;6:553-556
 - 74 Deng DJ. Progress of gastric cancer etiology: Nnitrosamides in the 1990s. *World J Gastroenterol* 2000;6:613-618
 - 75 Gao HJ, Yu LZ, Bai JF, Peng YS, Sun G, Zhao HL, Miu K, Lü XZ, Zhan g XY, Zhao ZQ. Multiple genetic alterations and behavior of cellular biology in gastric cancer and other gastric mucosal lesions: *H. pylori* infection, histological types and staging. *World J Gastroenterol* 2000;6:848-854
 - 76 Miehke S, Kirsch C, Dragosics B, Gschwandler M, Oberhuber G, Antos D, Dite P, Lc]uter J, Labenz J, Leodolter A, Malfertheiner P, Neubauer A, Ehninger G, Stolte M, Bayerd rffer E. Helicobacter pylori and gastric cancer: current status of the Austrian-Czech-German gastric cancer prevention trial (PRISMA Study). *World J Gastroenterol* 2001;7:243-247
 - 77 Xu AG, Li SG, Liu JH, Gan AH. Function of apoptosis and expression of the proteins Bcl-2, p53 and C-myc in the development of gastric cancer. *World J Gastroenterol* 2001; 7:403-406
 - 78 Cai L, Yu SZ, Zhang ZF. Glutathione S-transferases M1, T1 genotypes and the risk of gastric cancer: A case control study. *World J Gastroenterol* 2001;7:506-509
 - 79 He XS, Su Q, Chen ZC, He XT, Long ZF, Ling H, Zhang LR. Expression, deletion and mutation of p16 gene in human gastric cancer. *World J Gastroenterol* 2001;7:515-521
 - 80 Fang DC, Yang SM, Zhou XD, Wang DX, Luo YH. Telomere erosion is independent of microsatellite instability but related to loss of heterozygosity in gastric cancer. *World J Gastroenterol* 2001;7:522-526

Edited by Zhang JZ

• GASTRIC CANCER •

Induction of apoptosis by TPA and VP-16 is through translocation of TR3

Su Liu, Qiao Wu, Xiao-Feng Ye, Jian-Huai Cai, Zhi-Wei Huang, Wen-Jin Su

Su Liu, Qiao Wu, Xiao-Feng Ye, Jian-Huai Cai, Zhi-Wei Huang, Wen-Jin Su, Key Laboratory of the Ministry of Education for Cell Biology and Tumor Cell Engineering, School of Life Sciences, Xiamen University, Xiamen 361005, Fujian Province, China
Supported by the National Outstanding Youth Science foundation of China (B type, 39825502); the National Natural Science Foundation of China (39880015, 30170477); the Natural Science Foundation of Fujian Province (C0110004).

Correspondence to: Dr. Qiao Wu, Key Laboratory of the Ministry of Education for Cell Biology and Tumor Cell Engineering, School of Life Sciences, Xiamen University, Xiamen 361005, Fujian Province, China. xgwu@xmu.edu.cn
Telephone: +86-592-2182542 Fax: +86-592-2086630
Received 2001-11-02 Accepted 2001-12-20

Abstract

AIM: To investigate the role of TR3 in induction of apoptosis in gastric cancer cells.

METHODS: Human gastric cancer cell line, MGC80-3, was used. Expression of TR3 mRNA and its protein was detected by Northern blot and Western blot. Localization of TR3 protein was showed by immunofluorescence analysis under laser-scanning confocal microscope. Apoptotic morphology was observed by DAPI fluorescence staining, and apoptotic index was counted among 1000 cells randomly. Stable transfection assay was carried out by Lipofectamine.

RESULTS: Treatment of MGC80-3 cells with TPA and VP-16 resulted in apoptosis, accompanied by the repression of Bcl-2 protein in a time-dependent manner. At the same time, TPA and VP-16 also up-regulated expression level of TR3 mRNA in MGC80-3 cells that expressed TR3 mRNA. When antisense-TR3 expression vector was transfected into the cells, expression of TR3 protein was repressed. In this case, TPA and VP-16 did not induce apoptosis. In addition, TPA and VP-16-induced apoptosis involved in translocation of TR3. In MGC80-3 cells, TR3 localized concentrative in nucleus, after treatment of cells with TPA and VP-16, TR3 translocated from nucleus to cytosol obviously. However, when this nuclear translocation was blocked by LMB, apoptosis was not occurred in MGC80-3 cells even in the presence of TPA and VP-16.

CONCLUSION: Induction of apoptosis by TPA and VP-16 is through induction of TR3 expression and translocation of TR3 from nucleus to cytosol, which may be a novel signal pathway for TR3, and represent the new biological function of TR3 to exert its effect on apoptosis in gastric cancer cells.

Liu S, Wu Q, Ye XF, Cai JH, Huang ZW, Su WJ. Induction of apoptosis by TPA and VP-16 is through translocation of TR3. *World J Gastroenterol* 2002;8(3):446-450

INTRODUCTION

TR3 (also termed as NGFI-B and Nur77) is an orphan receptor that belongs to the member of the steroid/thyroid/retinoid receptor superfamily^[1-3]. It is an immediate-early response gene, and its expression is rapidly induced by a variety of growth stimuli, including

growth factors, phorbol ester and cAMP-dependent pathways^[1,3-5]. Similar to other members of the superfamily, TR3 functions in nucleus as a transcriptional factor to positively or negatively regulate gene expression necessary to alter the cellular phenotype in response to the growth stimuli^[6]. We found recently that TR3 heterodimerizes with retinoid X receptor (RXR) that binds to retinoic acid receptor α (RAR α) promoter, and regulates RAR α expression that is critical to inducing apoptosis^[7]. In addition, TR3 also heterodimerizes with chicken ovalbumin upstream promoter transcription factor (COUP-TF) to inhibit COUP-TF binding to retinoic acid responsive element (RARE) through direct protein-protein interaction^[8]. These evidences suggest that TR3 can mediate diverse signals through its ability either to bind to a variety of response elements or to interact with different protein factors. However, the mechanism by which TR3 exerts its biological functions remains largely unknown.

Apoptosis, as a distinct form of cell death, is an important process that can lead to tumor regression, and suppression of apoptosis is often associated with abnormal cell survival and malignant growth^[9-15]. The involvement of TR3 in apoptosis was first demonstrated by showing that TR3 was rapidly induced by T-cell antigen receptor (TCR) signaling in immature thymocytes and T-cell hybridomas^[16,17]. Overexpression of a dominant-negative TR3 protein or inhibition of TR3 expression by antisense-TR3 inhibited TCR-induced apoptosis, whereas constitutive expression of TR3 led to massive apoptosis^[16,17]. These evidences clearly indicate that TR3 plays an important role in TCR-mediated apoptosis. The involvement of TR3 in apoptosis process is also observed in many cancer cell lines. Treatment of lung cancer cells with AHPN/CD437 strongly induced apoptosis, which was accompanied by a rapid induction of TR3. Inhibition of TR3 by antisense-TR3 effectively abolished apoptosis induction by AHPN/CD437^[18]. Rapid induction of TR3 was also found in other cancer cells after stimulation of apoptosis by a variety of apoptosis-inducing agents^[19-21]. Therefore, these observations suggest that expression of TR3 is required for induction of cell apoptosis.

How TR3 functions to regulate apoptosis in gastric cancer cells is less understood. In this study, we investigated the role of TR3 in inducing apoptosis in gastric cancer cells. The results showed that 12-O-tetradecanoylphorbol-13-acetate (TPA) and VP-16 (also called etoposide) induced apoptosis, accompanied by TR3 expression. More importantly, TR3 protein translocated from nucleus to cytosol, when apoptosis occurred by TPA or VP-16 induction. However, when the translocation was blocked by leptomycin B (LMB), apoptosis was not detected, even in the presence of apoptotic stimuli. Our findings, therefore, have drawn an inspiration that translocation of TR3 from nucleus to cytosol may be one of the essential links involved in the mechanism of apoptosis by apoptotic stimuli in gastric cancer cells.

MATERIALS AND METHODS

Cell line and culture condition

Human gastric cancer cell line, MGC80-3, was established by Cancer Research Center in Xiamen University^[22]. The cells were maintained in RPMI-1640 medium, supplemented with 10% FCS, 1 mM glutamine, and 100u/ml penicillin.

Agents

TPA and VP-16 (Sigma) are used as apoptosis stimuli that can induce apoptosis in a variety of cells, including breast cancer cells, lung cancer cells, prostate cancer cells^[23-30]. LMB is an antibiotic with anti-fungal and anti-tumor activity that was first discovered and purified from the fermentation broth and mycelia of streptomyces^[31-33]. Recently, this antibiotic has become an important tool for studying nuclear localization^[34-36].

Apoptosis analysis^[37]

MGC80-3 cells were treated with TPA and VP-16 for different time indicated in figures, trypsinized, washed with PBS, fixed in 3.7% paraformaldehyde, and then stained with 50 μ g/mL of 4,6-diamidino-2-phenylindole (DAPI, Sigma) containing 100 μ g/mL of DNase-free RNase A to facilitate the examination of nuclei under fluorescence microscope. Apoptotic cells were counted among 1000 cells randomly. The apoptotic index was a mean of three independent experiments.

Immunofluorescence analysis^[38]

MGC80-3 cells were cultured on cover glass overnight, and then treated with TPA and VP-16 as required. After washed with PBS, cells were fixed in 4% paraformaldehyde. After fixation, the cells were incubated firstly with anti-TR3 antibody (Santa Cruz), and then reacted with corresponding FITC-conjugated anti-IgG (Pharminogen) as secondary antibody. Fluorescent images were observed and analyzed under laser-scanning confocal microscope (Bio-Rad MRC-1024ES).

Western blot analysis^[38,39]

Total 50 μ g of nuclear extract was electrophoresed on 8% denaturing gel and electroblotted onto a nitrocellulose membrane. The membrane was probed with anti-TR3 antibody followed by corresponding secondary antibody. The antibody reactivity was detected with an Amersham ECL kit according to the manufacturer's instruction. For the cytosolic and nuclear fractions, the cells were suspended in 500 μ l of 10mM Tris-Cl (pH 7.8), 1% Nonidet P-40, 10mM mercaptoethanol, 0.5mM phenylmethylsulfonyl fluoride, 1 μ g/ml leupeptin and aprotinin for 2 min at 0°C, then 500 μ l of DDW was added, and the cells were allowed to swell for 2min. The cells were sheared by 10 passages through 22 gauge needle. Nuclei were recovered by centrifugation at 400Xg for 6min, and the low-speed supernatant was centrifuged at 100000g for 30min. The high-speed supernatant constituted the cytosolic fraction.

Stable transfection

Antisense-TR3 expression vector (provided kindly by Dr. Uemura, and Dr. Chang^[40]) was stably transfected into MGC80-3 cells by LipofectamineTM (Gibco/BRL) as described previously^[41], then screened with 600 μ g of G418. Expression of endogenous TR3 protein was determined by Western blot.

RESULTS

Expression of TR3 mRNA in response to apoptotic stimuli

TPA and VP-16 were both known as the apoptotic stimuli which induced apoptosis in many kinds of cancer cell lines, including the cancer cells of prostate, breast and lung^[23-30]. To determine whether these apoptotic stimuli also functioned in gastric cancer cells, a specific, DAPT staining for display of apoptotic nuclear morphology was adopted under fluorescence microscope^[38]. The observation indicated that treatment of MGC80-3 cells with TPA and VP-16 caused the classical morphological characteristics of apoptosis, including nuclear condensation and fragmentation (Figure 1A). The apoptotic index was further determined by counting 1000 cells randomly. In MGC80-3 cells, the apoptotic index was merely 3.89

%. However, the apoptotic index induced by TPA and VP-16 increased in a time-dependent manner (Figure 1B). The highest apoptotic index reached 44.33% (for TPA induction) and 32.16% (for VP-16 induction), respectively. Thus, the data demonstrated that TPA and VP-16 indeed induced apoptosis in gastric cancer cells.

Members of the Bcl-2 family were involved in the regulation of apoptotic process^[42,43]. Since TPA and VP-16 induced apoptosis significantly in MGC80-3 cells shown above, it should be interrelated with some proteins that were associated with apoptosis initiation. To investigate this possibility, expression of Bcl-2 was detected. Western blot showed that when TPA treated with cells for different time, the expression of BCL-2 protein was repressed in a time-dependent manner (Figure 1C), which was consistent with the result shown in Figure 1A and B. Similar result was seen in the cells treated with VP-16 (data not shown). This result suggested that inhibition of Bcl-2 might render MGC80-3 cells more susceptible to the apoptosis-inducing effect of TPA and VP-16.

Several evidences showed that TR3 was involved in the regulation of apoptosis in different cell types^[16,44,45]. We investigated the role of TR3 in apoptosis of MGC80-3 cells induced by TPA and VP-16. Treatment of cells with TPA and VP-16 not only induced MGC80-3 cell apoptosis and repressed its relative protein, Bcl-2 (Figure 1A-C), but also enhanced expression of TR3 mRNA obviously that was expressed at relative low level in MGC80-3 cells (Figure 1D). Taken together, these results revealed a possible link between expression of TR3 and induction of apoptosis in gastric cancer cells.

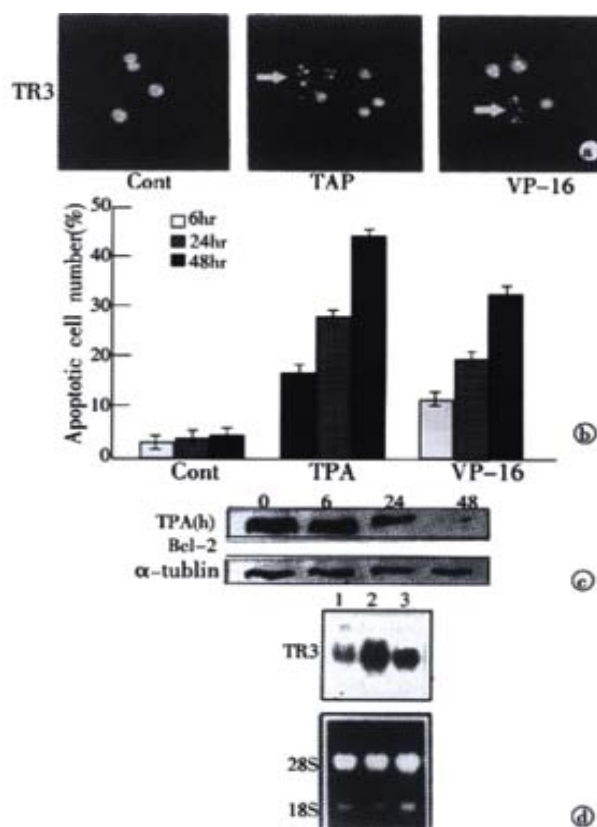


Figure 1 Induction of apoptosis and TR3 expression induced by TPA and VP-16 in MGC80-3 cells. (A) Morphological analysis of apoptotic cells. Cells treated with TPA and VP-16 for 24 hr, and then stained with DAPI. Nuclear morphology was visualized under fluorescence microscope. (B) Measure of apoptotic index by counting 1000 cells stained with DAPI under fluorescence microscope. The data shown represents mean of three independent experiments (\pm SE). (C) Analysis of Bcl-2 protein expression. Cells were treated with TPA for indicated time, and Western blot was performed as described in

materials and methods. α -tubulin was used to quantify the amount of protein used in each lane. (D) Detection of TR3 mRNA expression. Cells were treated with TPA and VP-16 for 24 hr. Preparation of total RNA and Northern blot were carried out as described in materials and methods. 18S and 28S were shown to quantify the loading RNA. Lane 1: control; Lane 2: TPA treatment; Lane 3: VP-16 treatment.

Translocation of nuclear TR3 to cytosol induced by apoptotic stimuli

It was reported recently that translocation of protein was closely associated with its biological function^[24,38,47]. To determine whether the apoptotic stimuli could cause translocation of TR3 in MGC80-3 cells, the immunofluorescent localization of TR3 protein was conducted by using correspondent TR3-specific antibody and laser-scanning confocal microscope observation. The results illustrated that in MGC80-3 cells, TR3 protein was concentrative in nucleus (Figure 2A). When treatment of TPA for 6 hr, the majority of TR3 protein was still remained in nucleus, little in cytosol. However, after 24 hr of TPA treatment, the majority of TR3 protein translocated from nucleus to cytosol, little in nucleus (Figure 2A). Similar result was also seen in the cells treated with VP-16. After treatment of 24 hr, TR3 protein almost translocated to cytosol (data not shown).

To further verify this protein translocation, the cytosolic and nuclear fractions were isolated respectively, and TR3 protein level was detected by Western blot. As shown in Figure 2B, TR3 protein was expressed in MGC80-3 cells, which located in nucleus (Figure 2B). TPA and VP-16 treatment led to down-regulation of TR3 protein in nuclear and up-regulation in cytosol with a time-dependent manner. After treatment of the cells for 6 hr with TPA and VP-16, respectively, TR3 protein was distributed both in nucleus and cytosol. However, after 24 hr treatment of TPA and VP-16, TR3 protein appeared more in cytosol and little in nucleus clearly (Figure 2B). This result was in accordance with the result shown in Fig. 2A, suggesting that translocation of TR3 protein might be associated with induction of apoptosis, which was a novel signal pathway for TPA and VP-16 to exert their biological functions.

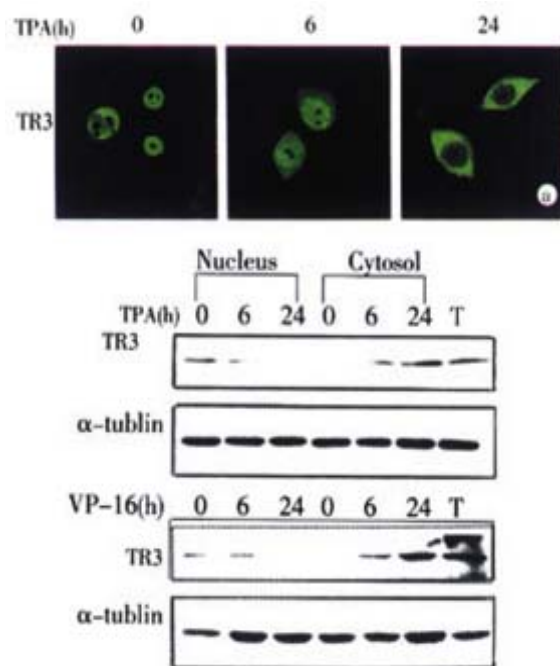


Figure 2 Translocation of TR3 protein from nucleus to cytosol in MGC80-3 cells. The cells treated with TPA for indicated time. (A) Translocation of TR3 protein observed by laser-scanning confocal microscope. TR3 protein was immunostained with anti-TR3 antibody and corresponding FITC-conjugated secondary antibody. (B) Western blot showed the translocation of TR3 protein. Nuclear and cytosolic fractions were prepared as described in materials and methods. α -tubulin was shown to quantify the loading protein. T: total protein.

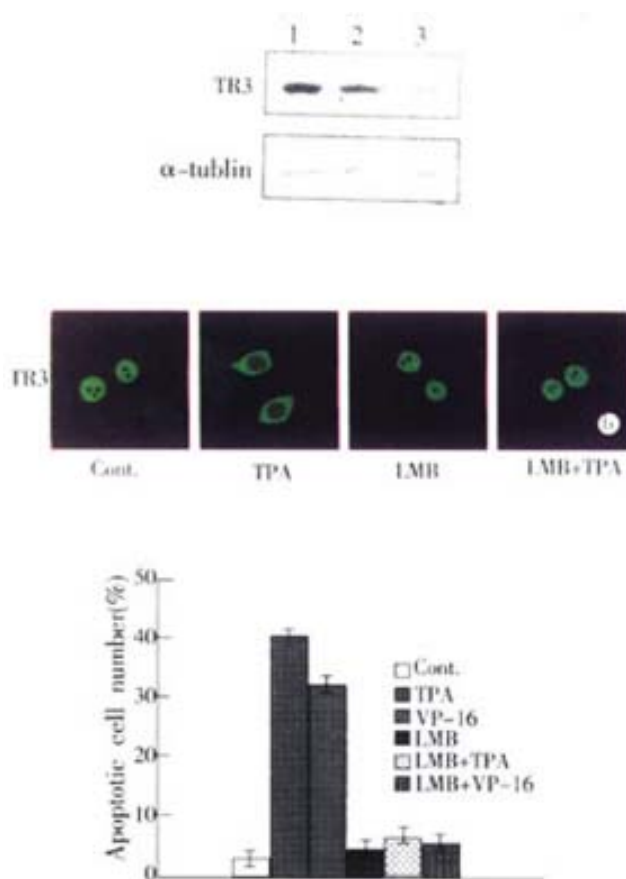


Figure 3 Inhibition of TR3 protein expression and its translocation in MGC80-3 cells. (A) Repression of TR3 protein expression by transfection of antisense-TR3 expression vector into MGC80-3 cells. Endogenous TR3 protein was determined by Western blot. Empty vector was also transfected into cells as a positive control. α -tubulin was shown to quantify the loading protein. Lane 1: protein from MGC80-3 cells; Lane 2: protein from the cells transfected with empty vector; Lane 3: protein from the cells transfected with antisense-TR3 expression vector. Inhibitory effect of LMB on TR3 protein translocation induced by TPA. The cells treated with different agents indicated as in the figure. The reaction with antibody was similar to the description in Fig. 2A. (C) Inhibitory effect of LMB on apoptosis induction by TPA and VP-16. Cells treated with different agents indicated as in the figure. Apoptotic index was measured as described in Fig. 1B.

Inhibition of both TR3 protein expression and its translocation

Since TR3 protein was expressed in MGC80-3 cells (Figure 2A, B), we transfected antisense-TR3 expression vector into the cells to determine whether inhibition of TR3 protein expression caused TPA and VP-16 fail to induce apoptosis. The stable transfection result was showed in Figure. 3A. Expression of TR3 protein was almost repressed in transfected cells, whereas TR3 protein still expressed in the cells transfected with empty vector, compared to MGC80-3 cells. In this transfected cells, TPA and VP-16 could not induce apoptosis. The apoptotic index only reached 5.14% (for TPA induction) and 4.62% (for VP-16 induction), which were less than that in MGC80-3 cells treated with TPA and VP-16 (Figure 1B) and those transfected with empty vector (apoptotic index amounted to 39.78% for TPA induction and 27.56% for VP-16 induction).

It was then necessary to probe into the intrinsic mechanism of whether there was some inevitable linkage between TR3 protein translocation and apoptosis induction. Since LMB has been used in many systems to demonstrate the nuclear localization and inhibited the export of a number of proteins, including actin, transcription factors, kinases and cell cycle regulators^[48-54], we used LMB as inhibitor to block nuclear protein TR3 export from nucleus to cytosol. In MGC80-3 cells, TR3 protein was mainly located in nucleus, after treatment of

24 hr with TPA, the most of TR3 protein was translocated from nucleus to cytosol in the absence of LMB (Figure 3B). However, in the presence of LMB, TR3 protein was remained in nucleus, although MGC80-3 cells were treated by TPA for 24 hr (Figure 3B). The similar result was also observed in VP-16 treated-cells (data not shown). According to this inhibitory result, we detected the apoptotic index to determine the relationship between translocation of TR3 protein and apoptosis induction. As shown in Figure 3C, in the presence of LMB, TPA and VP-16 did not induced apoptosis, compared with that TPA and VP-16 induced apoptosis of MGC80-3 cells obviously in the absence of LMB. Thus, preventing the nuclear TR3 protein export from nucleus to cytosol repressed TPA and VP-16's ability to induce apoptosis. The result again confirmed that translocation of TR3 protein was associated with induction of apoptosis.

DISCUSSION

The TR3 orphan receptor is required for activation-induced apoptosis of T-cell hybridomas^[16]. To gain insight into its function during apoptosis, we, in this study, analyzed the relationship between TR3 expression and its translocation and apoptosis induction in gastric cancer cells.

TR3 is an early response gene whose expression is induced by a variety of stimuli, including signals for cell survival, such as growth factors, and signals for cell death, such as TCR^[1,3-5]. To study the role of TR3 in gastric cancer cells, we used TPA and VP-16 to induce apoptosis, and found that when apoptosis occurred and its related protein Bcl-2 was inhibited by TPA and VP-16 in MGC80-3 cells, TR3 mRNA was indeed up-regulated. After transfection of antisense-TR3 expression vector into MGC80-3 cells that expressed TR3 at protein level resulted in the inhibition of TR3 protein expression. In the transfected cells, we could not detect marked apoptosis, even in the presence of TPA and VP-16 induction. The apoptotic index was only 5.14% (for TPA induction) and 4.62% (for VP-16 induction), similar to the control MGC80-3 cells with 3.89% and less than the TPA and VP-16 treated-cells with 44.33% (for TPA induction) and 32.16% (for VP-16 induction). These results indicated that TPA and VP-16 regulated apoptosis through induction of TR3 expression at both mRNA and protein levels.

TR3 functions as a nuclear transcription factor in the regulation of target gene expression^[6]. The movement of transcription factors between nucleus and cytoplasm is important in regulating its activity^[24,47]. Our observation showed that TPA and VP-16-induced apoptosis involved in translocation of TR3 protein. In MGC80-3 cells, TR3 protein localized mainly in the nucleus in which it might be associated with other nuclear proteins related to stimulation of cell proliferation, such as PKB/AKT, cFos, and AP-1^[18,55-58]. However, when cells were treated with TPA and VP-16 for 24 hours, respectively, translocation of TR3 from nucleus to cytosol was observed, with an increase protein expression of TR3 in cytosol and a decrease in nucleus in a time-dependent manner. In this case, apoptosis induced by TPA and VP-16 did happened, also in a time-dependent manner, and during this process, Bcl-2 protein, known to induce cell survival in variety of cell types^[59,60], was strongly inhibited by TPA and VP-16. In addition, when this nuclear export was blocked by LMB, apoptosis was not detected, regardless of the presence of TPA and VP-16. As a comparison, all-trans retinoic acid that could not induce TR3 translocation from nucleus to cytosol failed to induction of apoptosis in MGC80-3 cells although it could also induce TR3 expression (data not shown). Taken together, these data clearly demonstrated that induction of apoptosis by TPA and VP-16 was through the translocation of TR3 from nucleus to cytosol, which might be a novel signal pathway for apoptosis and the new function for TR3 to exert its effect on apoptosis induction. Bcl-2 may play an important role in the regulation of TPA and VP-16 -induced apoptosis.

Of course, the link between the mechanism of TR3 function and the apoptosis induction in gastric cancer cells should be studied further from other aspects.

REFERENCES

- Milbrandt J. Nerve growth factor induces a gene homologous to the glucocorticoid receptor gene. *Neuron* 1998;1:183-188
- Chang C, Kokontis J. Identification of a new member of the steroid receptor super-family by cloning and sequence analysis. *Biochem Biophys Res Commun* 1988;155:971-977
- Hazel TG, Nathans D, Lau LF. A gene inducible by serum growth factors encodes a member of the steroid and thyroid hormone receptor superfamily. *Proc Natl Acad Sci USA* 1988;85:8444-8448
- Williams GT, Lau LF. Activation of the inducible orphan receptor gene nur77 by serum growth factors: dissociation of immediate - early responses. *Mol Cell Biol* 1993;13:6124-6136
- Lim RW, Zhu CY, Stringer B. Differential regulation of primary response gene expression in skeletal muscle cell through multiple signal transduction pathways. *Biochim Biophys Acta* 1995; 126:91-100
- Williams TE, Fahrner TJ, Johnston M, Milbrandt J. Identification of the DNA binding site for NGFI-B by genetic selection in yeast. *Science* 1991;252:277-281
- Wu Q, Dawson M, Zheng Y, Hobbs PD, Agadir A, Jong L, Li Y, Liu R, Zhang XK. Inhibition of trans-retinoic acid-resistant human breast cancer cell growth by retinoid x receptor-selective retinoids. *Mol Cell Biol* 1997;17:6598-6608
- Wu Q, Li Y, Liu R, Agadir A, Lee OK, Liu Y, Zhang XK. Modulation of retinoic acid sensitivity in lung cancer cells through dynamic balance of orphan receptors nur77 and COUP-TF and their heterodimerization. *EMBO J* 1997;16:1656-1669
- Fisher DE. Apoptosis in cancer therapy: crossing the threshold. *Cell* 1994;78:539-542
- Jacobson MD, Burne JF, King MP. Bcl-2 blocks apoptosis in cells lacking mitochondrial DNA. *Nature* 1993;361:365-369
- Douglas RG, John CR. Mitochondrial and Apoptosis. *Science* 1998;8: 1309-1312
- Boldin MP, Goncharov TM, Goltsev YV. Involvement of MACH, a novel MORT1/FADD-interacting protease, in Fas/Apo1- and TNF receptor induced cell death. *Cell* 1996;85:803-815
- Enari M, Sakahira H, Yokoyama H. A caspase-activated Dnase that degrades DNA during apoptosis and its inhibitor ICAD. *Nature* 1998; 391:43-50
- Zhuang XQ, Yuan SZ, Wang XH, Lai RQ, Luo ZQ. Oncoprotein expression and inhibition of apoptosis during colorectal tumorigenesis. *China Natl J New Gastroentero* 1996; 2:3-5
- Xue XC, Fang GE, Hua JD. Gastric cancer and apoptosis. *Shijie Huaren Xiaohua Zazhi* 1999;7:359-361
- Woronicz JD, Calnan B, Ngo V, Winoto A. Requirement for the orphan steroid receptor nur77 in apoptosis of T-cell hybridomas. *Nature* 1994;367:277-280
- Liu ZG, Smith SW, McLaughlin KA, Schwartz LM, Osborne BA. Apoptotic signals delivered through the T-cell hybrid require the immediate-early gene nur77. *Nature* 1994;367:281-284
- Li Y, Agadir A, Liu R, Dawson M, John CR, Fontana JA, Bost F, Hobbs PD, Zheng Y, Chen GQ, Shroot B, Mercola D, Zhang XK. Molecular determinants of AHPN(CD437)-induced growth arrest and apoptosis in human lung cancer cell lines. *Mol Cell Biol* 1998;18:4719-4731
- Maruyama K, Tsukada T, Bandoh S, Sasaki K, Ohkura N, Yamaguchi K. Retinoic acids differentially regulate NOR-1 and its closely related orphan nuclear receptor genes in breast cancer cell line MCF-7. *Biochem Biophys Res Comm* 1997;231:417-420
- Gregg TW, Lau LF. Activation of the inducible orphan receptor gene nur77 by serum growth factors: dissociation of immediate-early and delayed-early responses. *Mol Cell Biol* 1993;13: 6124-6136
- Jeong KY, Lau LF. Involvement of JunD in transcription activation of the orphan receptor gene nur77 by nerve growth factor and membrane depolarization in PC12 cells. *Mol Cell Biol* 1994; 14:7731-7743
- Wang KH. Establishment of gastric carcinoma cell line MGC80-3 cells. *Exp Biol Sinica* 1983; 16:257-267
- Yang XJ, Chen SB, Bao JZ, Wang Y, Zhang ZB, Zhang XK, Zhang XR. Effect of HGF on etoposide-induced apoptosis. *Chin J New Gastroenterol* 1997; 5: 518-519
- Li H, Kolluri SK, Gu J, Dawson M, Cao XH, Hobbs PD, Chen GQ, Lu JS, Lin F, Xie ZH, Fontana JA, Reed JC, Zhang XK. Cytochrome C release and apoptosis induced by mitochondrial targeting of nuclear orphan receptor TR3. *Science* 2000;289:1159-1164
- Agadir A, Shealy YF, Hill DH, Zhang XK. Retinyl methyl ether down-regulates transcriptional activation by tumor promoter TPA and nuclear protooncogenes cJun and cFos. *Cancer Res* 1997; 57:3444-3450

- 26 Jia L, Patwari Y, Srinivasula SM, Neland AC, Fernandes-alnemri T, Alnemri ES, Kelsey SM. Bax translocation is crucial for the sensitivity of leukaemic cells to etoposide-induced apoptosis. *Oncogene* 2001;20: 4817-4826
- 27 Custodio BA, Cardoso MP, Madeira MC, Almeida LM. Mitochondrial permeability transition induced by the anticancer drug etoposide. *Toxicology in vitro* 2001;15:265-270
- 28 Godlewski MM, Motyl MA, Gajkowska B, Wareski P, Koronkiewicz M, Motyl T. Subcellular redistribution of BAX during apoptosis induced by anticancer drugs. *Anti-cancer drugs* 2001;12: 607-617
- 29 Kim R, Inoue H, Tanabe K, Toge T. Effect of inhibitors of cysteine and serine proteases in anticancer drug-induced apoptosis in gastric cancer cells. *Int J Oncology* 2001;18:1227-1232
- 30 Friedrich K, Wieder T, Von Haefen C, Radetzki S, Janicke R, Schulze-Osthoff K, Dorken B, Daniel PT. Overexpression of caspase-3 restores sensitivity for drug-induced apoptosis in breast cancer cell lines with acquired drug resistance. *Oncogene* 2001;20:2749-2760
- 31 Hamamoto T. Leptomycins A and B, new antifungal antibiotics. II. Structural elucidation. *J Antibiot (Tokyo)* 1983;36:646-650
- 32 Hamamoto T. Leptomycins A and B, new antifungal antibiotics. III. Mode of action on *Schizosaccharomyces pombe*. *J Antibiot (Tokyo)* 1985;38:1573-1580
- 33 Yoshida M. Effects of Leptomycin B on the cell cycle of fibroblasts and fission yeast cells. *Exp Cell Res* 1990;187:150-156
- 34 Fornerod M, Ohno M, Yoshida M, Mattaj JW. CRM1 is an export receptor for leucine-rich nuclear export signals. *Cell* 1997;90:1051-1060
- 35 Ossareh NB, Bachelier F, Dargemont C. Evidence for a role of CRM1 in signal-mediated nuclear protein export. *Science* 1997;278:141-144
- 36 Fukuda M, Asano S, Nakamura T, Adachi M, Yoshida M, Yanagida M, Nishida E. CRM1 is responsible for intracellular transport mediated by the nuclear export signal. *Nature* 1997;390:308-311
- 37 Liu Y, Lee MO, Wang HG, Li Y, Hashimoto Y, Klaus M, John CR, Zhang XK. Retinoic acid receptor (mediates the growth-inhibitory effect of retinoic acid by promoting apoptosis in human breast cancer cells. *Mol Cell Biol* 1996;16:1138-1149
- 38 Wu Q, Liu S, Ding L, Ye XF, Su WJ. PKC (translocation from mitochondria to nucleus is closely related to induction of apoptosis in gastric cancer cells. Science in China 2001, in press
- 39 Wu Q. Distinct Ways of Retinoic Acid Receptors on Inhibition of AP-1 Activity in Gastric Cancer Cells. *Chin J Biochem Mol Biol* 2001;17: 430-435
- 40 Uemura H, Chang C. Antisense TR3 orphan receptor can increase prostate cancer cell viability with etoposide. *Treatment Endocrinol* 1997;139:2329-2334
- 41 Liu S, Wu Q, Chen ZM, Su WJ. The effect pathway of retinoic acid is through regulation of retinoic acid receptor α in gastric cancer cells. *World J Gastroenterol* 2001;7:662-666
- 42 Xu AG, Li SG, Liu JH, Gan AH. The function of apoptosis and protein expression of bcl-2, p53 and C-myc in the development of gastric cancer. *World J Gastroenterol* 2000; 6(Suppl 3):27
- 43 Wang XW, Xie H. Presence of Fas and Bcl-s proteins in BEL-7404 human hepatoma cells. *World J Gastroenterol* 1998; 4:540-543
- 44 Woronicz JD, Lina A, Calnan BJ, Szychowski S, Cheng L, Winoto A. Regulation of the Nur77 orphan steroid receptor in activation-induced apoptosis. *Mol Cell Biol* 1995;15:6364-6376
- 45 Lin W, Youn HD, Liu J. Thapsigargin-induced apoptosis involves Cabin1-MEF2-mediated induction of Nur77. *Eur J Immunol* 2001;31: 1757-1764
- 46 Steff AM, Trop S, Maira M, Drouin J, Hugo P. Opposite ability of pre-TCR and alpha beta TCR to induce apoptosis. *J Immunol* 2001;166: 5044-5050
- 47 Katagiri Y, Takeda K, Yu ZX, Ferans VJ, Ozato K, Guroff G. Modulation of retinoid signaling through NGF-induced nuclear export of NGFI-B. *Nat Cell Biol* 2000;2:435-440
- 48 Wada A, Fukuda M, Mishima M, Nishida E. Nuclear export of actin novel mechanism regulating the subcellular localization of a major cytoskeletal protein. *EMBO J* 1998;17:1635-1641
- 49 Sachdev S, Hannink M. Loss of Ik(a-mediated control over nuclear import and DNA binding enables oncogenic activation of c-Rel. *Mol Cell Biol* 1998;18:5445-5456
- 50 Kudo N, Taoka H, Toda T, Yoshida M, Horinouchi S. A novel nuclear export signal sensitive to oxidative stress in the fission yeast transcription factor Pap 1. *J Biol Chem* 1999; 274:15151-15158
- 51 Huang TT, Kudo N, Yoshida M, Miyamoto S. A nuclear export signal in the N-terminal regulatory domain of Ik α controls cytoplasmic localization of inactive NF- κ B/IkBa complexes. *Proc Natl Acad Sci USA* 2000;97:1014-1019
- 52 Fukuda M, Gotoh Y, Nishida E. Interaction of MAP kinase with MAP kinase kinase: its possible role in control of nucleocytoplasmic transport of MAP kinase. *EMBO J* 1997;16:1901-1908
- 53 Engel K, Kotlyarov A, Gaestel M. Leptomycin B-sensitive nuclear export of MAPKAP kinase 2 is regulated by phosphorylation. *EMBO J* 1998;17:3363-3371
- 54 Taagepera S, McDonald D, Loeb JE, Whitaker LL, McElroy AK, Wang JYJ, Hope TJ. Nuclear-cytoplasmic shuttling of C-ABL tyrosine kinase. *Proc Natl Acad Sci USA* 1999; 95:7457-7562
- 55 Fernandez PM, Brunel F, Jimenez MA, Saez JM, Cereghini S, Zakari MM. Nuclear receptors Nor1 and NGFI-B/Nur77 play similar, albeit distinct, roles in the hypothalamo-pituitary-adrenal axis. *Endocrinology* 2000;141:2392-2400
- 56 Pekarsky Y, Hallas C, Palamarchuk A, Koval A, Bullrich F, Hirata Y, Bichi R, Letofsky J, Croce CM. AKT phosphorylates and regulates the orphan nuclear receptor Nur77. *Proc Natl Acad Sci USA* 2001;98:3690-3694
- 57 Kang HJ, Song MJ, Choung SY, Kim SJ, Lee MO. Transcriptional induction of Nur77 by indomethacin that results in apoptosis of colon cancer cells. *Biol Pharm Bull* 2000; 23:815-819
- 58 Meng AH, Ling YL, Zhang XP, Zhao XY, Zhang JL. CCCK-8 inhibits expression of TNF-alpha in the spleen of endotoxic shock rats and signal transduction mechanism of p38 MAPK. *World J Gastroenterol* 2002; 8:139-143
- 59 Dai J, Yu SX, Qi XL, Bo AH, Xu YL, Guo ZY. Expression of bcl-2 and c-myc protein in gastric carcinoma and precancerous lesions. *World J Gastroenterol* 1998; 4 (Suppl 2): 84-85
- 60 Liu HF, Liu WW, Fang DC, Men RP. Expression of bcl-2 protein in gastric carcinoma and its significance. *World J Gastroenterol* 1998; 4: 228-230

Edited by Zhang JZ

• GASTRIC CANCER •

Effect of preoperative regional artery chemotherapy on proliferation and apoptosis of gastric carcinoma cells

Hou-Quan Tao, Shou-Chun Zou

Hou-Quan Tao, Shou-Chun Zou, Department of Surgery, Zhejiang Provincial People's Hospital, Hangzhou 310014, Zhejiang Province, China
Correspondence to: Dr. Hou-quan Tao, Department of Surgery, Zhejiang Provincial People's Hospital, Hangzhou 310014, Zhejiang Province, China. houquantao@yahoo.com

Telephone: +86-571-85236842 Fax: +86-571-85131448

Received 2001-12-20 Accepted 2002-02-23

Abstract

AIM: To study the effects of preoperative regional artery chemotherapy (PRACT) in inducing growth inhibition and apoptosis of gastric carcinoma (GC) cells.

METHODS: TUNEL (terminal-deoxynucleotidyl-transferase TdT-mediated dUTP-fluorescein and labeling) method and immunohistochemical techniques were used to detect the state of apoptosis and proliferation of GC cells in histopathologic sections. A total of 110 cases of GC and 68 cases of metastatic lymph node with or without PRACT were adopted. Correlations between apoptosis index (AI), proliferation index (PI) and PRACT and prognosis were analysed.

RESULTS: The apoptosis index (AI) was significantly higher in the PRACT group ($12.5\% \pm 4.33\%$) than in the untreated group ($7.1\% \pm 3.43\%$, $P < 0.001$), whereas the proliferation index (PI) in the PRACT group ($33.8\% \pm 8.8\%$) was significantly lower than that in untreated group ($43.6\% \pm 12.8\%$, $P < 0.01$). Both AI and PI were correlated to the differentiation degree of GC in PRACT group, the AI in the differentiated group was higher than that in undifferentiated group ($P < 0.001$), but the PI was lower in the differentiated group than that of the undifferentiated group ($P < 0.01$). The AI of GC cells in metastatic lymph node was also significantly higher in the PRACT group ($7.9\% \pm 3.41\%$) than in the untreated group ($3.6\% \pm 2.93\%$, $P < 0.01$), though the PI of GC cells in metastatic lymph nodes in the PRACT group ($17.2\% \pm 6.8\%$) was significantly lower than that in the untreated group ($26.7\% \pm 9.3\%$, $P < 0.01$). The severity of histopathologic changes was significantly higher in the PRACT group than in the untreated group ($P < 0.05$). In addition, postoperative surveys demonstrated that the 5-year survival rate of GC patients in the PRACT group was significantly higher than that of patients in the untreated group ($P < 0.01$).

CONCLUSION: Preoperative regional artery chemotherapy (PRACT) showed inhibitory action on the growth of GC cells mainly through inhibiting proliferation and inducing the apoptosis of tumor cells. PRACT can improve the prognosis of GC patients also.

Tao HQ, Zou SC. Effect of preoperative regional artery chemotherapy on proliferation and apoptosis of gastric carcinoma cells. *World J Gastroenterol* 2002;8(3):451-454

INTRODUCTION

Human gastric carcinogenesis is a multistep and multifactorial process^[1-8]. In this process, the state of apoptosis and proliferation of gastric epithelium will change^[9,10]. The loss of balance between cell proliferation and apoptosis may result in tumor development and progression^[11-16]. Cell necrosis and apoptosis are two fundamental processes of tumor cell death. Apoptosis is the biological process of tumor cell death regulated by genes^[17-28]. Many (and perhaps all) agents of cancer chemotherapy effect tumor cell killing *in vitro* and *in vivo* through inducing the mechanisms of apoptosis. Many chemotherapy-induced side-effects and mass shrinkage may result from the increase of tumor cell apoptosis and the inhibition of tumor cell proliferation^[17, 29-34].

To clarify the relationship between the effects of preoperative regional artery chemotherapy (PRACT) on inhibition and killing of GC cells with apoptosis, methods of terminal-deoxynucleotidyl-transferase (TdT)-mediated dUTP-fluorescein and labeling (TUNEL) and immunohistochemical techniques were used to detect the apoptosis and proliferation of GC cells in 110 cases of GC with or without PRACT. Histopathologic changes and prognosis were also observed and compared between the two groups.

MATERIALS AND METHODS

Clinical data

110 patients with GC who underwent curative resections at Zhejiang Provincial Peoples' Hospital from Dec. 1988 to July 1996 were studied, including 68 cases with PRACT and 42 cases without PRACT. No significant difference was found in the age, sex, and TNM staging between the two groups. The surgical specimens were fixed in 10% formaldehyde solution, and paraffin embedded tissue blocks were cut into 6μm sections and mounted on glass slides. All patients had been followed up at least 5 years after operation.

Scheme of preoperative chemotherapy

Celiac arteriography was performed by precutaneous transfemoral-artery catheters according to Seldinger's method and superselective catheterization proceeded to the supplying artery of focus of lesion. Antineoplastic agents of FAP(5-FU 1.0g/m², MMC 10mg/m², CDDP 80mg/m²) or FMP(5-FU 1.0g/m², ADR 20mg/m², CDDP 80mg/m²) scheme was infused into regional artery by a single administration and thereafter surgical operation was performed in 10-14 days.

Main reagents

Terminal-deoxynucleotidyl-transferase(TdT)-mediated dUTP-fluorescein and labeling(TUNEL) kits were purchased from Boehringer Inc. and stored in -20°C for use. SP kits and PCNA monoclonal antibody were produced by Maixin Inc.(Fujian).

Histochemical detection of apoptosis

Tumor cell apoptosis was identified by the TUNEL method^[35,36]. Briefly, deparaffinized and rehydrated sections were treated with proteinase K (20mg/L in 10mmol/L Tris, pH 8.0) for 20min at room temperature and washed with 1×TBS (20mmol/L Tris, pH 7.6,

140mmol/L NaCl). After, endogenous peroxidase was inactivated by using 30ml/L hydrogen for 5min and washing with 1×TBS. Equilibration buffer was added to each section and samples were incubated at room temperature for 20min. Terminal deoxynucleotidyl transferase (TdT) enzyme in TdT labeling reaction mixture at 1:20 dilution was piped onto the sections, followed by 2h incubation at 37°C. After terminating the reaction by immersing sections into stop solution and washing with blocking buffer for 10min at room temperature, the anti-digoxigenin-peroxidase was added to the sections. NBT/BCIP solution was used for color development. Sections were counterstained by fast red. A positive control was generated by covering a specimen with DNase I(1mg/L) as the first step of the procedure. Specific positive tissue sections were used for negative controls by substituting distilled water for the TdT in the reaction mixture. Positively stained tumor cells were identified as nuclei that were blue-brown in color, and were counted in ten randomly selected fields under high power of microscope to determine the rate of apoptosis cell among all tumor cells. Apoptotic index (AI)=(the number of apoptosis cells/total number of tumor cells)×1000%.

Immunohistochemical staining for PCNA

SP immunohistochemical staining techniques were used. The primary antibody was PCNA monoclonal antibody (diluted 1:50). Before staining, the sections were microwave heated in 0.05mol·L⁻¹ citric acid solution for antigen retrieval. PBS was substituted for primary antibodies as negative control. PCNA-positive cells (proliferative cells) were observed. The proliferative index (PI) was obtained by calculating the percentage of positively stained cells evaluated for each tissue section after counting 1000 cells at ten high power fields randomly.

Comparison of pathologic histology change

In H&E staining sections, tumor cell necrosis and degeneration, endothelium change, and the degree of fibrosis were observed and compared between the PRACT group and untreated group. The degree of histopathologic change was divided into four grades from 0 to III.

Statistical analysis

Data were expressed as $\bar{x} \pm s$, and the t test or Wilcoxin test were used for statistical analysis. Survival rate was calculated by using Kaplan-Meier method and analyzed by the log-rank test. The level of significance was $P < 0.05$.

RESULTS

Comparison of tumor cell proliferation and apoptosis between PRACT and untreated groups

The main morphological characteristics of apoptosis cell consist of cell shrinkage, cytoplasmic condensation, nuclear pyknosis, cytomembrane blebbing or fragmentation, and formation of apoptotic bodies. More apoptosis and less proliferation were detected in the patients in the PRACT group. The apoptosis index (AI) of the PRACT group and untreated group was (12.5%±4.33%) and (7.1%±3.43%), respectively. The t test showed that the AI of the PRACT group was significantly higher than that of the untreated group ($P < 0.001$), whereas the proliferation index (PI) in the PRACT group (33.8%±8.8%) was significantly lower than that in untreated group (43.6%±12.8%, $P < 0.01$).

Relationship between tumor cell proliferation, apoptosis and the tumor differentiation degree in PRACT group

The pathologic diagnosis and grading of GC was determined according to the Histopathologic Standard of the Chinese National Gastric Cancer Association. GC was divided mainly into two histologic subtypes: a

differentiated type which consists of papillary and tubular adenocarcinomas, and an undifferentiated type which consists of poorly differentiated adenocarcinomas, signet ring-cell carcinomas and mucinous adenocarcinomas. Among the 68 patients with PRACT, AI of 32 tumors of the differentiated type was (14.8%±4.99%), while that of undifferentiated type tumor was only (6.6%±3.31%), AI was significantly different between the two groups ($P < 0.001$). However, the PI of 32 tumors of the differentiated type (29.6%±7.4%) was lower than that in the undifferentiated group (38.5%±11.2%, $P < 0.01$).

Effect of PRACT on proliferation and apoptosis of metastatic lymph node GC cells

Among the 62 cases with lymph node metastasis, AI of metastatic lymph node GC cells in 34 cases with PRACT was (7.9%±3.41%), and that of 28 cases without PRACT was (7.9%±2.93%). The t test indicated that there was a significant difference between two groups ($P < 0.01$). On the contrary, the PI in the metastatic lymph node GC cells in 34 cases with PRACT (17.2%±6.8%) was significantly lower than that of 28 untreated cases (26.7%±9.3%, $P < 0.01$).

Comparison of histopathologic changes between PRACT and untreated groups (Table 1)

The data are shown in Table 1. No change was marked as grade 0, I to III grade was defined change. The Wilcoxin test showed a significance difference between the two groups.

Table 1 Comparison of histopathologic changes between the PRACT group and the untreated group

Histopathologic grade	PRACT group (n=68)	Untreated group (n=42)
0	26	26 ^a
I	22	12
II	16	4
III	4	0

^a $P < 0.05$, vs I+II+III

Effect of PRACT on the survival rate of GC patients

All patients underwent curative resection and had been followed up for at least 5 years, 49 died of tumor recurrence. A postoperative survey demonstrated that the 5-year survival rate of patients with PRACT (63.2%, 43/68) was significantly higher than that of patients without PRACT (42.8%, 18/42, $P < 0.01$).

DISCUSSION

PRACT can effectively inhibit or kill cancer cells by a single administration of high concentration antineoplastic agent into the main supplying artery of the cancer focus. It can not only limit and reduced the tumor mass and improve the curative rate, but it can also act on the peri-operative area by means of drug infiltration to kill subclinical tumor foci which may exist before the operation as well as the invisible micrometastatic foci so as to increase the opportunity of curative resection^[33,37]. Many *in vitro* and *in vivo* experiments indicated that the induction of apoptosis and inhibition of proliferation are the main mechanisms of eliminating tumor cells by most chemotherapeutic agents^[17,29-34,38]. To explore the effect of PRACT on human GC cell apoptosis, TUNEL, a combined molecular biological and morphological technique, was used to investigate and compare the number of apoptotic cells in GC tissue sections as well as that in metastatic lymph node sections of the PRACT and untreated groups. This method, using an *in situ* staining technique, demonstrates not only the distribution pattern of apoptotic cells, but also the

sensitivity of the technique: it can detect very small amount of apoptotic cells, so it is widely used in cell apoptosis studies^[35,36]. Moreover, PCNA expression was detected by using an immunohistochemical technique in order to count the proliferation index.

Cell apoptosis is different from cell necrosis; the latter is a pathological form of extensive cell death under strong cell damage and it is not under gene regulation, while cell apoptosis is a normal physiological phenomenon for the active elimination of surplus cells or defective cells under strict genetic control^[29]. It plays an important role in regulating total cell amount and also in malignant disease. After gene mutation and formation of malignancy, the rate of cell apoptosis lowers significantly. It is this depletion of cell apoptosis contributing to the expansion of tumor mass; hence it is possible to treat the cancer by means of increasing the proportion of tumor cell apoptosis. Recent studies have shown that 5-Fu, MMC, CDDP, ADR and many other chemotherapeutic drugs treat cancer by inhibiting proliferation and inducing apoptosis^[29-34,39-41]. So induction of tumor cell apoptosis has already been used as an important indicator to detect the ability of chemotherapeutic drugs to inhibit tumor growth. FMC or FAP schemes composed of the aforementioned drugs are now frequently used for pre-operative chemotherapy of GC.

Our results demonstrate that: (1) The apoptosis index of GC cells in the PRACT group is significantly higher than that of the untreated group, and PI of GC cells in the PRACT group is significantly lower than that of the untreated group, indicating that PRACT has an obvious inhibition effect on GC cells. We also found that no significant necrosis was found in the rich blood supply area around the blood vessels, but instead much apoptosis was observed there, indicating that induction of apoptosis by PRACT is the main mechanism of inhibition of tumor growth. (2) Apoptosis rate is correlated with tumor differentiation degree in the PRACT group. AI of differentiated type of GC is significantly higher than that of undifferentiated type, but PI of differentiated type of GC is significantly lower than that of undifferentiated type. This may be due to the better blood supply of the differentiated type of GC^[42], allowing more chemotherapeutic drugs to be delivered to the tumor tissue to increase the induction of tumor cell apoptosis so it is more sensitive to chemotherapy. (3) AI of GC cells in metastatic lymph nodes is significantly higher in the PRACT group than that of the untreated group, and PI of GC cells in metastatic lymph nodes is significantly lower in the PRACT group than that of the untreated group, suggesting that PRACT is able to inhibit proliferation and induce apoptosis of metastatic tumor cells. This is very interesting, because lymph node metastasis and recurrence of GC are main factors influencing the overall postoperative survival rate. If the apoptotic cell proportion in metastatic lymph nodes can be increased by effective measures, the prognosis of postoperative GC patients can be improved. Our results suggest that PRACT may approach this goal. (4) With respect to the histopathologic change of GC, including cancer cell reactions, endothelium changes, and the degree of fibrosis, the degree of severity is higher in PRACT group than that in untreated group, suggesting that PRACT can lead to more structural changes of GC tissue so as to enhance the killing effect of cancer cells by chemotherapy drugs. (5) With regard to prognosis, we have showed that PRACT can increase the relapse-free survival rate of GC patients^[37]. In fact, altering the balance between apoptosis and proliferation may contribute to improving the prognosis of cancer^[43-49]. The results of this paper indicate that PRACT can induce apoptosis and inhibit proliferation of GC cells. So we suggest that PRACT is a useful therapeutic scheme for GC.

In conclusion, this study of detecting the proliferation and apoptosis of GC with or without PRACT showed significant inhibition of GC cell growth by PRACT, with its mechanism mainly through

inducing tumor cell apoptosis. PRACT can increase the survival rate of GC patients after operation.

REFERENCES

- 1 Ma JL, Liu WD, Zhang ZZ, Zhang L, You WC, Chang YS. Relationship between gastric cancer and precancerous lesions. *Huaren Xiaohua Zazhi* 1998;6:222-223
- 2 Liu WZ, Zheng X, Shi Y, Dong QJ, Xiao SD. Effect of *Helicobacter pylori* infection on gastric epithelial proliferation in progression from normal mucosa to gastric carcinoma. *World J Gastroenterol* 1998;4:246-248
- 3 Badov D, Lambert JR, Finlay M, Balazs ND. *Helicobacter pylori* as a pathogenic factor in Menetrier's disease. *Am J Gastroenterol* 1998;93:1976-1979
- 4 Tucci A, Poli L, Tosetti C, Biasco G, Grigioni W, Varoli O, Mazzoni C, Paparo GF, Stanghellini V, Caletti G. Reversal of fundic atrophy after eradication of *Helicobacter pylori*. *Am J Gastroenterol* 1998;93:1425-1431
- 5 Pan CJ, Zhong P, Huang XR, Liu KY, Wang SX. Study on the correlation between proliferation and apoptosis in atrophy and intestinal metaplasia of gastric mucosa. *Shijie Huaren Xiaohua Zazhi* 2000;8:143-146
- 6 Xia HX, Zhang GS. Apoptosis and proliferation in gastric cancer caused by *Hp* infection. *Shijie Huaren Xiaohua Zazhi* 1999;7:740-742
- 7 Lu W, Chen LY, Gong HS. PCNA and c-erbB-2 expression in gastric mucosal intestinal metaplasia with *Helicobacter pylori* infection. *Shijie Huaren Xiaohua Zazhi* 1999;7:111-113
- 8 Ishida M, Gomyo Y, Tatebe S, Ohfuji S, Ito H. Apoptosis in human gastric mucosa, chronic gastritis, dysplasia, and carcinoma: analysis by terminal deoxynucleotidyl transferase-mediated dUTP-biotin nick end labeling. *Virchows Arch* 1996;428:229-235
- 9 Wang YK, Ji XL, Ma NX. Expressions of p53 bcl-2 and c-erbB-2 proteins in precarcinomatous gastric mucosa. *Shijie Huaren Xiaohua Zazhi* 1999;7:114-116
- 10 Tu SP, Jiang SH, Tan JH, Jiang XH, Qiao MM, Zhang YP, Wu YL, Wu YX. Proliferation inhibition and apoptosis induced by arsenic trioxide on gastric cancer cell SGC-7901. *Shijie Huaren Xiaohua Zazhi* 1999;7:18-21
- 11 Anti M, Armuzzi A, Gasbarrini A, Gasbarrini G. Importance of changes in epithelial cell turnover during *Helicobacter pylori* infection in gastric carcinogenesis. *Gut* 1998;43:S27-S32
- 12 Akira K, Yoshihiko M, Tadashi K, Yoshihiro K, Keizo S. The biologic features of intramucosal gastric carcinoma with lymph node metastasis. *Surgery* 2002;131:S71-77
- 13 Martin SJ, Green DR. Apoptosis and cancer: the failure of controls on cell death and cell survival. *Crit Rev Oncol/Hematol* 1995;18:137-153
- 14 Guo YQ, Zhu ZH, Li JF. Flow cytometric analysis of apoptosis and proliferation in gastric cancer and precancerous lesion. *Shijie Huaren Xiaohua Zazhi* 2000;8:983-915
- 15 Shen YF, Zhuang H, Shen JW, Chen SB. Cell apoptosis and neoplasms. *Shijie Huaren Xiaohua Zazhi* 1999;7:267-268
- 16 Hale AJ, Smith CA, Satherland LC, Stomeman VEA, Longthorne VL, Culhane AL. Apoptosis: molecular regulation of cell death. *Eur J Biochem* 1996;236:1-26
- 17 Kimura H, Konishi K, Kaji M, Maeda K, Yabushita K, Tsuji M, Ogino H, Satomura Y, Unoura M, Miwa A. Apoptosis, cell proliferation and expression of oncogenes in gastric carcinomas induced by preoperative administration of 5-fluorouracil. *Oncol Rep* 2000;7:971-976
- 18 Liu HF, Liu WW, Fang DC, Men RP. Expression and significance of proapoptotic gene Bax in gastric carcinoma. *World J Gastroenterol* 1999;5:15-17
- 19 Liu HF, Liu WW, Fang DC, Men RP. Expression of bcl-2 protein in gastric carcinoma and its significance. *World J Gastroenterol* 1998;4:228-230
- 20 Xu AG, Li SG, Liu JH, Gan AH. Function of apoptosis and expression of the proteins Bcl-2, p53 and C-myc in the development of gastric cancer. *World J Gastroenterol* 2001;7:403-406
- 21 Guo CQ, Wang YP, Liu GY, Ma SW, Ding GY, Li JC. Study on *Helicobacter pylori* infection and -p53, c-erbB-2 gene expression in carcinogenesis of gastric mucosa. *Shijie Huaren Xiaohua Zazhi* 1999;7:313-315
- 22 Qin LJ. In situ hybridization of P53 tumor suppressor gene in human gastric precancerous lesions and gastric cancer. *Shijie Huaren Xiaohua Zazhi* 1999;7:494-497
- 23 Zhang ZW, Farthing MJG. Molecular mechanisms of *H. pylori* associated gastric carcinogenesis. *World J Gastroenterol* 1999;5:369-374
- 24 Mao LZ, Wang SX, Ji WF, Ren JP, Du HZ, He RZ. Comparative studies on p53 and PCNA expressions in gastric carcinoma between young and aged patients. *Huaren Xiaohua Zazhi* 1998;6:397-399
- 25 Wang XH, Zhang WD, Zhang YL, Zheng JZ, Sun Y. Relationship between

- Hp* infection and oncogene and tumor suppressor gene expressions in gastric cancer and precancerosis. *Huaren Xiaohua Zazhi* 1998;6:516-518
- 26 Sun YX, Chen CJ, Zhou HG, Shi YQ, Pan BR, Feng WY. Expression of c-myc and p53 in colorectal adenoma and adenocarcinoma. *Huaren Xiaohua Zazhi* 1998;6:1054-1056
- 27 Xu QW, Li YS, Zhu HG. Relationship between expression P53 protein, PCNA and CEA in colorectal cancer and lymph node metastasis. *World J Gastroenterol* 1998;4:218
- 28 Lin GY, Chen ZL, Lu CM, Li Y, Ping XJ, Huang R. Immunohistochemical study on p53, H-rasp21, c-erbB-2 protein and PCNA expression in HCC tissues of Han and minority ethnic patients. *World J Gastroenterol* 2000;6:234-238
- 29 Yusuf AH. Apoptosis and the dilemma of cancer chemotherapy. *Blood* 1997;89:1845-1853
- 30 Zain J, Huang YQ, Feng X, nierodzik ML, Li JJ, Karparkin S. Concentration-dependent dual effect of thrombin on impaired growth/apoptosis or mitogenesis in tumor cells. *Blood* 2000;95:3133-3138
- 31 Kelly JD, Williamson KE, Weir HP, McManus DT, Hamilton PW, Keane PF, Johnston SR. Induction of apoptosis by mitomycin-C in an ex vivo model of bladder cancer. *Bju Int* 2000;85:911-917
- 32 Shah SA, Potter MW, McDade TP, Ricciardi R, Perugini RA, Elliott PT, Adams J, Callery MP. 26S proteasome inhibition induces apoptosis and limits growth of human pancreatic cancer. *J Cell Biochem* 2001;82:110-122
- 33 Huang j, He X, Lin X, Zhang C, Li J. Effect of preoperative transcatheter arterial chemoembolization on tumor cell activity in hepatocellular carcinoma. *Zhonghua Yixue Zazhi* 2000;113:446-448
- 34 Wu YL, Sun B, Zhang XJ, Wang SN, He HY, Qiao MM, Zhong J, Xu JY. Growth inhibition and apoptosis induction of Sulindac on Human gastric cancer cells. *World J Gastroenterol* 2001;7:796-800
- 35 Wijsmal JH, Jonker RR, Keijzer R, van de Velde CJ, Cornelisse CJ. A new method to detect apoptosis in paraffin sections in situ end labeling of fragmented DNA. *J Histochem Cytochem* 1993;41:7-12
- 36 Kiyozuka Y, Akamatsu T, Singh Y, Ichiyoshi H, Senzaki H, Tsubura A. Optimal prefiration of cells to demonstrate apoptosis by the TUNEL method. *Acta Cytol* 1999;43:393-399
- 37 Zou SC, Qiu HS, Zhang CW, Tao HQ. A clinical and long-term follow-up study of perioperative sequential triple therapy for gastric cancer. *World J Gastroenterol* 2000;6:284-286
- 38 Hickman JA. Apoptosis induced by anticancer drugs. *Cancer metasis Rev* 1992;11:121-139
- 39 Dive C, Hickman JA. Drug-target interactive: only first step in the comitment to a programmed cell death? *Br J Cancer* 1991;64:192-196
- 40 Inada T, Ichikawa A, Igarashi S, Kubota T, Ogata Y. Effect of preoperative 5-fluorouracial on apoptosis of advanced gastric cancer. *J Surg Oncol* 1997;65:106-110
- 41 Inada T, Ichikawa A, Kubota T, Ogata Y, Moossa AR, Hoffman RM. 5-Fu-induced apoptosis correlates with efficacy against human gastric and colon cancer xenografts in nude mice. *Anticancer Res* 1997;17:1965-1971
- 42 Tao HQ, Lin YZ, Wang RN. Significance of microvessel count and vascular endotjelial growth factor expression in intestinal-type gastric carcinoma. *Zhongguo Zhongliu Linchuang* 1998;25:786-789
- 43 Shen XB, Zhao XM, Hu JG, Jin XP, Wang J. Significance of cell apoptosis and proliferation in gastric cancer. *Shejie Huaren Xiaohua Zazhi* 2000;8:1050-1052
- 44 Zhang M, Cai S, Shi D. Prognostic value of cell proliferation and apoptosis in uterine cervical cancer treated with radiation. *Zhonghua Zhongliu Zazhi* 1999;21:290-292
- 45 Xie X, Clausen OPF, De Angelis P, Boysen M. Bax expression has prognostic significance that is enhanced when combined with AgNOR counts in glottic carcinoma. *Br J Cancer* 1998;78:100-105
- 46 Rieger L, Weller M, Bornemann A, Schabet M, Dichgans J, Meyermann R. Bcl-2 family protein expression in human malignant glioma: a clinical-pathological correlative study. *J Neurol Sci* 1998;155:68-75
- 47 Re GG, Hazen-Martin DJ, EL-Bahtimi R, Brownlee NA, Willingham MC, Garvin AJ. Prognostic significance of Bcl-2 in Wilm's tumors and oncogenic protential of Bcl-Xl in rare tumor cases. *Int J Cancer* 1999;84:192-200
- 48 Ghanem MA, van der Kwast TH, Den Hollander JC, Sudaryo MK, Van den Heuvel MM, Noordzij MA, Nijman RJM, Soliman EH, van Steenbrugge GJ. The prognostic significance of apoptosis-associated protein Bcl-2, BAX, and Bcl-X in clinical nephroblastoma. *Br J Cancer* 2001;85:1557-1563
- 49 Apolinario RM, van der Valk P, de Jong JS, Deville W, van Art-Otte J, Dingemans AM, van Mourik JC, Postmus PE, Pinedo HM, Giaccone G. Prognostic value of the expression of p53, bcl-2, and bax oncoproteins, and neovascularization in patient with radically resected non-small-cell lung cancer. *J Clin Oncol* 1997;15:2456-2466

Edited by Pagliarini R

• GASTRIC CANCER •

Effects of epidermal growth factor on the growth of human gastric cancer cell and the implanted tumor of nude mice

Lu Xia, Yao-Zong Yuan, Chun-Di Xu, Yong-Pin Zhang, Ming-Ming Qiao, Jia-Xu Xu

Lu Xia, Yao-Zong Yuan, Chun-Di Xu, Yong-Pin Zhang, Ming-Ming Qiao, Jia-Xu Xu, Department of Gastroenterology, Ruijin Hospital, Shanghai Second Medical University, Shanghai 200025, China
Correspondence to: Dr. Lu Xia, Department of Gastroenterology, Ruijin Hospital, Shanghai Second Medical University, Shanghai 200025, China. xialu@126.com
Telephone: +86-21-64370045-665242 Fax: +86-21-64150773
Received 2001-09-26 Accepted 2001-10-29

Abstract

AIM: Epidermal growth factor (EGF) plays an important role in the regulation of gastrointestinal tissue growth and development, and it can stimulate epithelial proliferation, cell differentiation and growth. It has been established that the EGF can promote gastric cytoprotection and ulcer healing. But the potential ability of EGF to regulate the gastric cancer growth is unknown. This study is to investigate the influence of EGF on human gastric cancer cell and the implanted tumor growth of nude mice.

METHODS: The cell growth rates of human gastric adenocarcinoma cell lines MKN-28, MKN-45, SGC-7901 and normal human gastric epithelial cells 3T3 were assessed when incubated with recombinant human EGF (rhEGF, 0.05, 0.1, 0.5, 1.0, 10, 50, 100 mg.L⁻¹) using MTT method. The cells of MKN-28, MKN-45, SGC-7901 (gastric cancer tissue 1.5 mm³) were implanted in the BALB/cA nude mice for 10 days. The EGF was given intraperitoneally (15, 30, 60 µg.kg⁻¹) for 3 weeks. The body weights of the tumor-bearing animals and their tumor mass were measured afterwards to assess the mitogenic effect of rhEGF in the nude mice.

RESULTS: Within the concentration range of 0.05-100 mg.L⁻¹, rhEGF could increase the cell growth of normal 3T3 cells (cell growth rate 100% vs 102.8%, *P* < 0.05), but partially restrain the gastric cancer cell growth. The latter effect was related to cell differentiation. In 15-60 µg/kg rhEGF groups, the mean implanted tumor mass of MKN-28 cell were 1.75g, 1.91g, 2.08g/NS group 1.97g (*P* > 0.05), the mean tumor mass of SGC-7901 cell were 1.53g, 1.07g, 1.20g/NS group 1.07g (*P* > 0.05), and for MKN-45 cell, the tumor mass were respectively 1.92g, 1.29g, 1.77g/NS group 1.82g (*P* > 0.05). So rhEGF had no obvious effect on implanted MKN-28, SGC-7901 and MKN-45 tumor growth.

CONCLUSION: EGF has no stimulating effect on the human gastric cancer cell growth neither *in vitro* nor *in vivo*.

Xia L, Yuan YZ, Xu CD, Zhang YP, Qiao MM, Xu JX. Effects of epidermal growth factor on the growth of human gastric cancer cell and the implanted tumor of nude mice. World J Gastroenterol 2002;8(3):455-458

INTRODUCTION

Growth factors are found in a variety of adult and embryonic tissues. They are important regulators of cell differentiation and proliferation,

and play an important role in maintaining the integrity of the epithelium. They have also been implicated in malignancy. Epidermal growth factor (EGF), a single-chain polypeptide of 53 amino acid residues, is found mainly in the submandibular glands and Brunner's gland of the gastrointestinal tract. It can be combined with the specific receptor (EGF-R) of the target cell membrane^[1]. Some studies suggested that the expression of EGF-R was increased in gastric cancer tissue. It was also reported that EGF can increase the mitosis *in vitro*^[2]. Patients with EGF receptor-positive gastric cancer may have a poorer prognosis than those with EGF receptor-negative cancers. So, EGF has the function to influence the tumor cell growth. At present, the effect of EGF in this process has been unclear yet.

In this report, we seek to determine the effect of EGF on the growth of human gastric cancer cell (MKN-28, SGC-7901 and MKN-45) *in vitro*. In nude mice which underwent surgical implantation of the same gastric cancer cells, EGF was injected intraperitoneally to investigate the influence of EGF on tumor cell growth, so as to confirm the safety of EGF in the treatment of peptic ulcer^[3-14].

MATERIALS AND METHODS

Materials

Gastric cancer cell lines, MKN-28, SGC-7901 and MKN-45, are well-differentiated, moderate-differentiated and low-differentiated human adenocarcinoma cell lines respectively. 3T3 cell is normal human gastric epithelium. They are all established and characterized in our laboratory. rhEGF was obtained from Institute of Biochemistry and Cell Biology, Shanghai Institute for Biological Science, Chinese Academy of Science (100 µg/amp). 3-(4,5-dimethylthiazol-2-yl) and 5-diphenyltetrazolium bromide were the product of Fluka Chemie AG. Balb/cA nude mice: were obtained from Institute of Pharmaceutics, Shanghai Institute for Biological Science, Chinese Academy of Science. 35-40 day old, 18-20g, female. Mitomycin C (MMC) was the product of Kyowa Hakko, Japan, 2mg/Amp.

Methods

Cell cultures Human gastric cancer cells were propagated as adherent monolayers and removed from culture surfaces by treatment with trypsin, then seeded in microwells at 1×10^8 L⁻¹ in complete medium composed of RPMI 1640 and 200 mL L⁻¹ fetal bovine serum (FBS). The cells were grown in 96-well microplates of RPMI 1640 tissue culture medium supplemented with 200 mL L⁻¹ FBS at 37°C in a humidified atmosphere of 50 mL L⁻¹ CO₂ in air. After 24h incubation, the cells were then added by rhEGF at the concentration of 0.05, 0.1, 0.5, 1.0, 10, 50, 100 mg.L⁻¹ for further incubation of 72 hours. Uninoculated RPMI 1640 medium was used as a control under otherwise identical experimental procedures. At the end of cell incubation, cell numbers and their viability were determined by MTT method. Add MTT (1 g.L⁻¹) in each microwell for 4h in 37°C air. After centrifugation, 100 µL dimethyl sulfoxide (DMSO) was added into each well for 30 minutes. Absorption rate of treated and control cells was measured at 570nm (A value) for quantitative measurement of cell growth. Each test kit contained a positive control and an additional

positive control. Experimental controls were treated with DMSO only.

Tumor implantation into nude mice Gastric cancer tissue (1.5mm³) were implanted s.c. in the right dorsal area of 4-6wk old male nude mice. Animals were fed with an autoclaved diet and tap water (acidified to pH 2.5). After 10d, the animals were assigned into the rhEGF treatment groups (15,30,60µg.kg⁻¹, intraperitoneally, 5 times per week for 3wk), negative control group (saline, 2mL intraperitoneum) and positive control group(MMC, 2mg.kg⁻¹, twice every week, 6 times altogether). The body mass of Balb/cA tumor-bearing animals and their tumor weights were measured using anesthesia with ether.

Inhibitory rate (IR) of tumor growth = m(tumor)_c- m(tumor)_T/m(tumor)_c
(m(tumor)_c: mean tumor weight of negetive control group; m(tumor)_T: mean tumor weight of rhEGF treatment group).

Statistical analysis

Student's *t* test was performed to assess potentially significant differences between individual groups of observations. The test statistics were then compared with values obtained from standard two-tailed tables. A *P* value of <5% was accepted as indicating probable significance when comparing the various groups.

RESULTS

Mitogenic effects of EGF in vitro

We found that EGF had no significant growth-stimulatory effects on gastric cancer cells in a dose-dependent manner (Figure 1). The lowest cell growth rates in MKN-28, S-7901 and MKN-45 cell lines were 81.7%, 80.7% and 86.1% respectively, compared with the control at the 0.05,50,100mg.L⁻¹ of rhEGF. EGF could inhibit the cancer cell growth within the level of 0.05 to 100mg.L⁻¹. But there was no probable significance within the same group. In contrast, for the normal 3T3 cells, EGF could increase the cell growth significantly after the coinubation (*P*=0.0008). We also found that the influence of EGF on the gastric cancer cell growth was dependent on the differentiation of the cell. Under the same concentration, the inhibition was greater in well-differentiated cells.

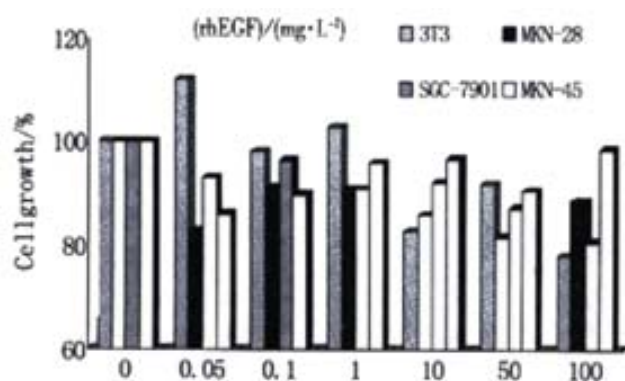


Figure 1 The effect of rhEGF on the growth of gastric cancer

Effect of EGF on the implanted tumor in nude mice

The mean tumor weight of negative control group after the study was 1.97g in MKN-28 nude mice. In MMC treatment group, the tumor weight was 0.47g (*P*<0.05). In rhEGF groups (15,30,60µg.kg⁻¹), the tumor weights were 1.75, 1.91 and 2.08g respectively. The inhibitory rate were -5.3% to 11.1%, compared with negative control group. In rhEGF60µg.kg⁻¹ group, the positive data suggested that the weight was higher than control, but the difference was not

significant. There were no significant difference compared with the negative control group (Table 1). In S-7901 and MKN-45 cell lines, the same results found indicated that intraperitoneal rhEGF treatment could not stimulate the tumor growth in nude mice within the concentration 15-30µg.kg⁻¹ (Table 2,3).

Table 1 The effect of rhEGF i.p. on the growth of MKN-28 tumor in nude mice

Group	Dosage	n	Body mass/g		Tumor mass $\bar{x} \pm s$ /g	Inhibitory rate/%	P value
			Beginning	End			
NS	0.2mL	16	17.6	22.6	1.97±0.94	—	—
MMC	2µg.kg ⁻¹	8	17.8	20.0	0.47±0.61	76.2	<0.05
RhEGF	15µg.kg ⁻¹	8	17.4	22.0	1.75±0.81	11.1	<0.05
RhEGF	30µg.kg ⁻¹	8	17.9	23.8	1.91±0.98	3.0	<0.05
RhEGF	60µg.kg ⁻¹	8	17.9	22.9	2.08±1.56	-5.3	<0.05

P value: compared with the NS group.

Table 2 The effect of rhEGF i.p. on the growth of SGC-7901 tumor in nude mice

Group	Dosage	n	Body mass/g		Tumor mass $\bar{x} \pm s$ /g	Inhibitory rate/%	P value
			Beginning	End			
NS	0.2mL	16	14.4	25.2	1.07±0.60	—	—
MMC	2µg.kg ⁻¹	8	15.2	21.7	0.66±0.29	38.6	<0.05
RhEGF	15µg.kg ⁻¹	8	15.9	25.3	1.53±0.29	-43.8	<0.05
RhEGF	30µg.kg ⁻¹	8	14.1	23.8	1.07±0.63	-0.7	<0.05
RhEGF	60µg.kg ⁻¹	8	13.4	23.9	1.20±0.47	-12.5	<0.05

P value: compared with the NS group.

Table 3 The effect of rhEGF i.p. on the growth of MKN-45 tumor in nude mice

Group	Dosage	n	Body mass/g		Tumor mass $\bar{x} \pm s$ /g	Inhibitory rate/%	P value
			Beginning	End			
NS	0.2mL	20	16.1	19.8	1.82±0.95	—	—
MMC	2µg.kg ⁻¹	10	16.2	19.7	1.07±0.42	41.1	<0.05
RhEGF	15µg.kg ⁻¹	10	16.0	20.3	1.92±1.04	-5.5	<0.05
RhEGF	30µg.kg ⁻¹	10	16.5	19.8	1.29±0.83	8.0	<0.05
RhEGF	60µg.kg ⁻¹	8	16.1	20.4	1.77±1.04	3.1	<0.05

DISCUSSION

We have examined the effect of EGF on the established cell line, MKN-28, SGC-7901 and MKN-45, derived from human gastric adenocarcinoma, both *in vitro* and *in vivo*. The results may be somewhat controversy to those formerly reported, that EGF had no obviously effect on the gastric cancer growth^[15,16]. Growth factors are components of signal transduction pathways that have a considerable spectrum of biological activity, such as control of cell proliferation, differentiation, apoptosis and transformation^[17,18]. Of these growth factors, EGF family are important agents for gastric mucosa. The EGF family include at least seven mammalian polypeptides: EGF, TGF-α, amphiregulin (AR), crypto heregulin, betacellulin and heparin-binding epidermal growth factor (HB-EGF). Except crypto and heregulin, all of these proteins have been shown to bind and activate the 170-kilodalton EGF receptor tyrosine kinase^[19,20]. They share a similar spectrum of biological activities exerted through interaction with EGF-R. EGF-R is a transmembrane glycoprotein, which can stimulate cell proliferation mainly through induction of the proto-oncogenes c-fos and c-myc, and of molecules such as polyamines. The TGF can cause morphological transformation and promote anchorage independent growth *in vitro*. Although there is no evidence of TGF secretion from nonneoplastic adult tissue, it is synthesized during fetal development and produced by many tumor tissues^[21,22]. TGF-α is frequently produced by malignant as well as normal cells and may stimulate their own proliferation. However, less is known about the role of EGF in oncogenesis^[23-25]. The importance of growth factors in the healing and oncogenesis of gastrointestinal diseases has recently received much attention. In inflamed mucosa, EGF is found predominantly in the cytoplasm of the superficial epithelial and isthmus

cells, as in the normal mucosa^[26]. In addition to providing a mitogenic stimulus, EGF may also help the proliferating cells to migrate into the superficial epithelium during the process of "cytoprotective" epithelial repair^[27].

The development of monoclonal and polyclonal antibodies against EGF has allowed studies of the localization of EGF in normal and neoplastic tissues to be performed^[28-31]. Immunocytochemical staining has shown distribution of epidermal growth factor and transforming growth factor α (TGF- α) in the gastrointestinal tract with high levels^[32-35]. Normal epithelial cells secrete such growth factors to regulate cell replacement by autocrine or paracrine mechanisms. It is speculated that these growth factors may regulate the transition rate between G2-phase and mitosis of the cell cycle^[36]. It has reported that HB-EGF is mitogenic for some types of cells, such as fibroblasts, vascular smooth muscle cells, keratinocytes and rat hepatocytes, but not endothelial cells^[37].

The mitogenic action of EGF and TGF- α *in vitro* has been reported in many gastrointestinal tissues, including esophagus, stomach and intestine, and there is little information about the association between the mucosal expression of these peptides and indices of cellular proliferation *in vivo*^[38]. It was reported that EGF immunoreactivity was present in 26-37% of gastric cancers, and the presence of EGF in gastric cancer correlated with the degree of gastric wall invasion, lymph node metastasis and disease progression^[39-42]. Although the epidermal growth factor/receptor system has been found abnormal in intestinal type gastric cancer, overexpression of EGF-R, erbB-2 and erbB-3 receptor genes was mainly found. There has been some controversy in the literature whether EGF-R overexpression related to tumor progression or to early stages of gastric carcinogenesis^[43-46]. The study had shown that overexpression of the EGF-R gene was infrequent in the metaplastic gastric mucosa. A major problem in gastric carcinogenesis is to determine the changing point from benign pre-neoplastic lesions to malignancy. There is a general agreement that this process involves different steps in cellular changes, requiring both activation and inhibition of specific genes, but there is still no evidence to support EGF or EGF-R overexpression to be a reliable marker of increased cancer risk in patients^[47-50]. The present study has sought to clarify their effect on the growth of gastric cancer cell *in vitro* and *in vivo*. In this study, we have found that there was no effect of EGF on the growth of established cell lines, MKN-28, SGC-7901, MKN-45, derived from human gastric adenocarcinoma, both *in vitro* and *in vivo*. Further study is headed to elucidate whether EGF could cause abnormal differentiation of the cells during the treatment of peptic ulcer for a long period.

REFERENCES

- 1 Playford RJ, Wright NA. Why is epidermal growth factor present in the gut lumen. *Gut* 1996;38:303-305
- 2 Maehiro K, Watanabe S, Hirose M, Iwazaki R, Miwa H, Sato N. Effects of epidermal growth factor and insulin on migration and proliferation of primary cultured rabbit gastric epithelial cells. *Gastroenterology* 1997;32:573-578
- 3 Chen BW, Wang HT, Liu ZX, Jie BQ, Ma QJ. Effect of exogenous EGF on proto-oncogene expression in experimental gastric ulcer in rats. *Shijie Huaren Xiaohua Zazhi* 1999;7:504-509
- 4 Fiorucci S, Lanfrancone L, Santucci L, Calabro A, Orsini B, Federici B, Morelli A. Epidermal growth factor modulates pepsinogen secretion in guinea pig gastric chief cells. *Gastroenterology* 1996;111:945-958
- 5 Konturek PC, Brzozowski T, Konturek SJ, Ernst H, Drozdowicz D, Pajdo R, Hahn EG. Expression of epidermal growth factor alpha during ulcer healing. *Scand J Gastroenterol* 1997; 32:6-15
- 6 Konturek PC, Ernst H, Brzozowski T. Expression of epidermal growth factor and transforming growth factor α after exposure of rat gastric mucosa to stress. *Scand J Gastroenterol* 1996;31:209-216
- 7 Hu YT, Zhen CE, Xing GZ, Zhang ML, Zhang JS, Wang DX, Lu YM. Relationship between transforming growth factor alpha, epidermal growth factor and prostaglandin E2 in patients with peptic ulcer. *Shijie Huaren Xiaohua Zazhi* 2002;10:43-47
- 8 Konturek JW, Hengst K, Konturek SJ, Domschke W. Epidermal growth factor in gastric ulcer healing by nocolprost, a stable prostaglandin E2 derivative. *Scand J Gastroenterol* 1997;32:980-984
- 9 Kang JY, Teng CH, Chen FC. Effect of capsaicin and cimetidine on the healing of acetic acid induced gastric ulceration in the rat. *Gut* 1996;38:832-836
- 10 Furukawa O, Okabe S. Cytoprotective effect of epidermal growth factor on acid-and pepsin-induced damage to rat gastric epithelial cells: roles of Na⁺/H⁺ exchangers. *J Gastroenterol Hepatol* 1997;12:353-359
- 11 Arakawa T, Watanabe T, Fukuda T, Higuchi K, Takaishi O, Yamasaki K, Kobayashi K, Tarnawski A. Indomethacin treatment during initial period of acetic acid-induced rat gastric ulcer healing promotes persistent polymorphonuclear cell-infiltration and increases future ulcer recurrence. *Dig Dis Sci* 1996;41:2055-2061
- 12 Qiu BS, Pfeiffer CJ, Wu W, Cho CH. Tungstic acid reduction of cold-resistant stress-induced ulceration in rats. *J Gastroenterol Hepatol* 1997; 12:19-23
- 13 Blandizzi C, Gherardi G, Marveggio C, Lazzeri G, Natale G, Carignani D, Colucci R, Tacca MD. Suramin enhances ethanol-induced injury to gastric mucosa in rats. *Dig Dis Sci* 1997;42:1233-1241
- 14 Miyazaki Y, Hiraoka S, Tsutsui S, Kitamura S, Shinomura Y, Matsuzawa Y. Epidermal growth factor receptor mediates stress induced expression of its ligands in rat gastric epithelial cells. *Gastroenterol* 2001;120:108-116
- 15 Ross JS, McKenna BJ. The HER-2/neu oncogene in tumors of the gastrointestinal tract. *Cancer Invest* 2001;19:554-568
- 16 Wang LD, Wilson EJ, Osburn J, Delvalle J. Epidermal growth factor inhibits carbachol-stimulated canine parietal cell function via protein kinase C. *Gastroenterology* 1996;110:469-477
- 17 Wagner S, Beil W, Westermann J, Logan R, Bock CT, Trautwein C, Bleck JS, Manns MP. Regulation of gastric epithelial cell growth by *Helicobacter pylori*: evidence for a major role of apoptosis. *Gastroenterology* 1997;113:1836-1847
- 18 Messa C, Russo F, Pricci M, Di Leo A. Epidermal growth factor and 17beta-estradiol effects on proliferation of a human gastric cancer cell line (AGS). *Scand J Gastroenterol* 2000;35:753-758
- 19 Granelli P, Fichera G, Zennaro F, Siadi C, Ruberto FD, Fregoni F, Appierto V, Buffa R, Ferrero S, Biunno I. Expression of the epidermal growth factor receptor gene in human intestinal metaplasia: a preliminary report. *Scand J Gastroenterol* 1997;32:485-489
- 20 Naef M, Yokoyama M, Friess H, Buchler MW, Korc M. Co-expression of heparin-binding EGF-like growth factor and related peptides in human gastric carcinoma. *Int J Cancer* 1996;66:315-321
- 21 Chen DL, Wang WZ, Wang JY. Epidermal growth factor prevents gut atrophy and maintains intestinal integrity in rats with acute pancreatitis. *World J Gastroenterol* 2000;6:762-765
- 22 Seno M, Tada H, Kosaka M, Sasada R, Igarashi K, Shing Y, Folkman J, Ueda M, Yamada H. Human beatcellulin, a member of the EGF family dominantly expressed in pancreas and small intestine, is fully active in a monomeric form. *Growth Factors* 1996;13:181-191
- 23 Becker KF, Keller G, Hoefler H. The use of molecular biology in diagnosis and prognosis of gastric cancer. *Surg Oncol* 2000;9:5-11
- 24 Werner M, Becker KF, Keller G, Hofler H. Gastric adenocarcinoma: pathomorphology and molecular pathology. *J Cancer Res Clin Oncol* 2001;127:207-216
- 25 Masaki T, Hatanaka Y, Nishioka M, Tokuda M, Shiratori Y, Reginfo W, Omata M. Activation of epidermal growth factor receptor kinase in gastric carcinoma: a preliminary study. *Am J Gastroenterol* 2000;95:2135-2136
- 26 Sanz-Ortega J, Steinberg SM, Moro E, Saez M, Lopez JA, Sierra E, Sanz-Espenera J, Merino MJ. Comparative study of tumor angiogenesis and immunohistochemistry for p53, c-ErbB2, c-myc and EGFR as prognostic factors in gastric cancer. *Histol Histopathol* 2000;15:455-462
- 27 Ma L, Liu ES, Chow JY, Wang JY, Cho CH. Interactions of EGF and ornithine decarboxylase activity in the regulation of gastric mucus synthesis in cigarette smoke exposed rats. *Zhonghua Binglixue Zazhi* 1999;42:137-143
- 28 Pelaez BM, Ruibal MA, Aza GJ. Gastric carcinoma: expression of c-erbB-2/neu oncoprotein, epidermal growth factor receptor, cathepsin D, progesterone receptor and tumor associated glycoprotein-72 in different histological types. *Rev Esp Enferm Dig* 1999;91:826-837
- 29 Choi JH, Kim HC, Lim HY, Nam DK, Kim HS, Yi SY, Shim KS, Han WS. Detection of transforming growth factor-alpha in the serum of gastric carcinoma patients. *Oncology* 1999;57:236-241
- 30 Hirao T, Sawada H, Koyama F, Watanabe A, Yamada Y, Sakaguchi T, Tatsumi T, Fujimoto H, Emoto K, Narikiyo M, Oridate N, Nakano H. Antisense epidermal growth factor receptor delivered by adenoviral vector blocks tumor growth in human gastric cancer. *Cancer Gene Ther* 1999;6:423-427
- 31 Hosokawa N, Yamamoto S, Uehara Y, Hori M, Tsuchiya KS. Effect of thiazinotrienomycin B, an ansamycin antibiotic, on the function of epidermal growth factor receptor in human stomach tumor cells. *J Antibiot* 1999;52:485-490

- 32 Luan F, Wang M, You W. The correlation of TGF- α , EGFR in precancerous lesions and carcinoma of stomach with PCNA expression. *Zhonghua Binglixue Zazhi* 1997;26:31-34
- 33 Koyama S, Maruyama Y, Adachi S. Expression of epidermal growth factor receptor and CD44 splicing variants sharing exons 6 and 9 on gastric and esophageal carcinomas: a two-color flow-cytometric analysis. *J Cancer Res Clin Oncol* 1999;125:47-54
- 34 Wang Q, Wu JS, Gao DM, Lai DN, Ma QJ. Expression significance of epidermal growth factor receptor and transforming growth factor α mRNA in human colorectal carcinoma. *Shijie Huaren Xiaohua Zazhi* 1999;7:590-592
- 35 Hu X, Gao J, Li Y. The amounts of inositol 1,4,5-triphosphate and its response to epidermal growth factor and laminin of carcinoma subclones with high or low metastatic potentials. *Zhonghua Yixue Zazhi* 1997;77:665-667
- 36 Tsugawa K, Yonemura Y, Hirono Y, Fushida S, Kaji M, Miwa K, Miyazaki I, Yamamoto H. Amplification of the c-met, c-erbB-2 and epidermal growth factor receptor gene in human gastric cancers: correlation to clinical features. *Oncology* 1998;55:475-481
- 37 Slesak B, Harlozinska A, Porebska I, Bojarowski T, Lapinska J, Rzeszutko M, Wojnar A. Expression of epidermal growth factor receptor family proteins (EGFR, c-erbB-2 and c-erbB-3) in gastric cancer and chronic gastritis. *Anticancer Res* 1998;18:2727-2732
- 38 Murakami N, Fukuchi S, Takeuchi K, Hori T, Shibamoto S, Ito F. Antagonistic regulation of cell migration by epidermal growth factor and glucocorticoid in human gastric carcinoma cells. *J Cell Physiol* 1998;176:127-137
- 39 Romano M, Ricci V, Popolo AD, Sommi P, Blanco CD, Bruni CB, Ventura U, Cover TL, Blaser MJ, Coffey RJ, Zarrilli R. *Helicobacter pylori* upregulates expression of epidermal growth factor-related peptides, but inhibits their proliferative effect in MKN 28 gastric mucosal cells. *J Clin Invest* 1998; 101:1604-1613
- 40 Ishikawa T, Ichikawa Y, Tarnawski A, Fujiwara Y, Fukuda T, Arakawa T, Mitsuhashi M, Shimada H. Indomethacin interferes with EGF-induced activation of ornithine decarboxylase in gastric cancer cells. *Digestion* 1998;59:47-52
- 41 Gao JH, Liang HJ, Liu WW, Fang DC, Wang ZH. Expression of C-myc gene protein and epidermal growth factor receptor in gastric mucosa pre-and post- *Helicobacter pylori* clearance. *Shijie Huaren Xiaohua Zazhi* 1999;7:1018-1019
- 42 Zarrilli R, Ricci V, Romano M. Molecular response of gastric epithelial cells to *Helicobacter pylori*-induced cell damage. *Cell Microbiol* 1999;1:93-99
- 43 He Y, Zhou J, Wu JS, Dou KF. Inhibitory effects of EGFR antisense oligodeoxynucleotide in human colorectal cancer cell line. *World J Gastroenterol* 2000;6:747-749
- 44 Masaki T, Hatanaka Y, Nishioka M, Tokuda M, Shiratori Y, Reginfo W, Omata M. Activation of epidermal growth factor receptor kinase in gastric carcinoma: a preliminary study. *Am J Gastroenterol* 2000;95: 2135-2136
- 45 Uribe JM, Barrett KE. Nonmitogenic actions of growth factors: An integrated view of their role in intestinal physiology and pathophysiology. *Gastroenterology* 1997;112:225-268
- 46 Murayama Y, Miyagawa JI, Higashiyama S, Kondo S, Yabu M, Isozaki K, Kayanoki Y, Kanayama S, Shinomura Y, Taniguchi N, Matsuzawa Y. Localization of heparin-binding epidermal growth factor in human gastric mucosa. *Gastroenterology* 1995;109:1051-1059
- 47 Filipe MJ, Osborn M, Linehan J, Sanidas E, Brito MJ, Jankowski J. Expression of transforming growth factor α , epidermal growth factor receptor and epidermal growth factor in precursor lesions to gastric carcinoma. *British J Cancer* 1995;71:30-36
- 48 Yashi W, Oue N, Kuniyasu H, Ito R, Tahara E, Yokozaki H. Molecular diagnosis of gastric cancer: present and future. *Gastric Cancer* 2001; 4:113-121
- 49 Saikawa Y, Kubota T, Otani Y, Kitajima M, Modlin IM. Cyclin D1 antisense oligonucleotide inhibits cell growth stimulated by epidermal growth factor and induces apoptosis of gastric cancer cells. *Jpn J Cancer Res* 2001;92:1102-1109
- 50 Garcia I, Vizoso F, Andicoechea A, Raigoso P, Verez P, Alexandre E, Garcia-Muniz JL, Allende MT. Clinical significance of epidermal growth factor receptor content in gastric cancer. *Int J Biol Markers* 2001;16:183-188

Edited by Zhang JZ

• LIVER CANCER •

P53 immunohistochemical scoring: an independent prognostic marker for patients after hepatocellular carcinoma resection

Lun-Xiu Qin, Zhao-You Tang, Zeng-Chen Ma, Zhi-Quan Wu, Xin-Da Zhou, Qing-Hai Ye, Yuan Ji, Li-Wen Huang, Hu-Liang Jia, Hui-Chuan Sun, Lu Wang

Lun-Xiu Qin, Zhao-You Tang, Zeng-Chen Ma, Zhi-Quan Wu, Xin-Da Zhou, Qing-Hai Ye, Yuan Ji, Li-Wen Huang, Hu-Liang Jia, Hui-Chuan Sun, Lu Wang, Liver Cancer Institute and Zhongshan Hospital, Fudan University, Shanghai, China

Supported by the Key Project of Medical Development in Shanghai, the National Science Funding for Young Scientists (No. 30000075), and Fund for Leading Specialty of Shanghai Metropolitan Bureau of Public Health
Correspondence to: Zhao-You Tang, M.D., Professor & Chairman, Liver Cancer Institute & Zhongshan Hospital, Fudan University, 136 Yi Xue Yuan Road, Shanghai 200032, China. zytang@srcap.stc.sh.cn
Telephone: +86-21-64037181

Received 2001-09-26 Accepted 2001-10-29

Abstract

AIM: To confirm if p53 mutation could be a routine predictive marker for the prognosis of hepatocellular carcinoma (HCC) patients.

METHODS: Two hundreds and forty-four formalin-fixed paraffin-embedded tumor samples of the patients with HCC receiving liver resection were detected for nuclear accumulation of p53. The percent of P53 immunoreactive tumor cells was scored as 0 to 3+ in P53 positive region (<10% -, 10-30% +, 31-50% ++, >50% +++). Proliferating cell nuclear antigen (PCNA) and some clinicopathological characteristics, including patients' sex, preoperative serum AFP level, tumor size, capsule, vascular invasion (both visual and microscopic), and Edmondson grade were also evaluated.

RESULTS: In univariate COX hazard regression model analysis, tumor size, capsule status, vascular invasion, and p53 expression were independent factors that were closely related to the overall survival (OS) rates of HCC patients. The survival rates of patients with 3+ for p53 expression were much lower than those with 2+ or + for p53 expression. Only vascular invasion ($P<0.05$) and capsule ($P<0.01$) were closely related to the disease-free survival (DFS) of HCC patients. In multivariate analysis, p53 overexpression (RI 0.5456, $P<0.01$) was the most significant factor associated with the OS rates of patients after HCC resection, while tumor size (RI 0.5209, $P<0.01$), vascular invasion (RI 0.5271, $P<0.01$) and capsule (RI-0.8691, $P<0.01$) were also related to the OS. However, only tumor capsular status was an independent predictive factor ($P<0.05$) for the DFS. No significant prognostic value was found in PCNA-I, Edmondson's grade, patients' sex and preoperative serum AFP level.

CONCLUSION: Accumulation of p53 expression, as well as tumor size, capsule and vascular invasion, could be valuable markers for predicting the prognosis of HCC patients after resection. The quantitative immunohistochemical scoring for P53 nuclear accumulation

might be more valuable for predicting prognosis of patients after HCC resection than the common qualitative analysis.

Qin LX, Tang ZY, Ma ZC, Wu ZQ, Zhou XD, Ye QH, Ji Y, Huang LW, Jia HL, Sun HC, Wang L. P53 immunohistochemical scoring: an independent prognostic marker for patients after hepatocellular carcinoma resection. *World J Gastroenterol* 2002;8(3):459-463

INTRODUCTION

Liver cancer has been ranked the 2nd cancer killer in China since 1990s. The age-standardized mortality rate in China is as high as 34.7/10⁵, which accounts for 53% of all liver cancer deaths worldwide^[1]. Although many advances in its clinical study have been made, a definitive subset is cured by surgery only, and encouraging long-term survival of patients have been obtained in some clinical centers, the overall dismal outcome of patients with hepatocellular carcinoma (HCC) have not been completely changed^[2,3]. Lack of control of metastatic foci and recurrence is the most prevalent cause of death in patients with HCC, and it is important to identify the factors that predispose patients to death. Much effort has been made to predict HCC behavior, but there is still lack of specific prognostic indicators.

Prognostic factors in HCC conventionally consist of staging with the tumor node metastasis system (TNM) and grading by tumor cellular differentiation. With new discoveries in the cancer biology, pathological and biological factors of HCC in relation to prognosis have been studied quite extensively. Morphological features of the tumor, both gross and histological, are found to be significantly associated with tumor recurrence and patient survival. A complementary approach is to analyze the HCC for molecular markers with prognostic significance with reference to the recurring possibility and survival time. A large number of molecular biological factors have been shown to be associated with the invasiveness of HCC, and have potential prognostic significance, e.g. c-erbB-2, uPA, PAI-I, VEGF, CDKN2 and p53 mutations, p53 antibody, H-ras, mdm-2, TGF α , EGFR, VEGF, bFGF, PD-ECGF, MMP-2, ICAM-1 are positively related to HCC invasiveness, whereas nm23-H1, Kai-1, TIMP-2, Integrin α 5 and E-cadherin are negatively relative factors^[4]. Although a great amount of markers have been tried, a routine biomarker for prediction of prognosis of HCC is not yet available.

As early as in 1995, we found that p53 mutations were related to the invasiveness of HCC. Thereafter, we performed immunohistochemical staining for p53 overexpression in the surgical specimen of HCC patients treated in our institute, to see if p53 mutation could be a routine predictive marker for the prognosis of HCC patients. In the present study, we reviewed the results of the studies over the past 5 years, and evaluated whether nuclear accumulation of p53 would be a feasible prognostic marker in the routine diagnostic evaluation of HCC, in particular, to analyze the relationship between p53 overexpression and survival of patients with HCC.

MATERIALS AND METHODS

Tumor samples and HCC patients

Totally, 256 consecutive patients with HCC were enrolled in this study. All of them were surgically treated in the Liver Cancer Institute of Fudan University (former Liver Cancer Institute of Shanghai Medical University), Shanghai, China in the years 1996-1999. Except for 12 cases without informative follow-up data, 244 cases were reviewed, which included 197 male (80.7%) and 47 female (19.3%). The mean age was 50.4 (15-76) years. All specimens were formalin-fixed, paraffin-embedded, which were proved to be hepatocellular carcinoma (HCC). Some histological characteristics including the states of capsule, vascular invasion (both visual and microscopic), cell differentiation were reviewed by one pathologist. The mean tumor size was 5.9 (1-16)cm, ≤ 5 cm in 131 cases (53.7%), >5 cm but ≤ 8 cm 56 cases (23.0%), and >8 cm 57 cases (23.3%). The tumor of 128 cases (52.5%) had no capsule, and 116 cases (47.5%) were well-capsulated. The Edmondson grade distribution was grade I in 7 (2.9%) cases, Grade II-III in 235 (96.3%) cases, and grade IV in 2 (0.8%) cases. Vascular invasion was found in 69 cases (28.3%), which included visual tumor thrombi in portal vein in 31 cases and microvascular invasion in 38 cases. Obvious evidence of liver cirrhosis was found in 217 (88.9%) cases, no cirrhosis in 27 (11.1%) cases. Two hundred and twenty-two cases (91%, 222/244) were followed up. The mean follow-up time was 21.6 (2.2-49) months.

Immunohistochemistry

A standard indirect immunoperoxidase protocol was used for immunohistochemistry (ABC-Elite; Vector Laboratories, Inc., Burlingame, CA). Monoclonal anti-p53, PCNA antibodies (Dako) were used for detection of p53 and PCNA, respectively (1:200 dilution in PBS containing 1% bovine serum albumin and 0.1% Triton X-100). A high-temperature (20 minutes in a pressure cooker) treatment procedure with antigen unmasking solution (Vector Laboratories, Inc.) was used to enhance the staining. The primary antibody was omitted for negative controls.

We used the percentage of p53-positive tumor nuclei in all major foci of cancer as p53 immunohistochemical scoring system. The percent of p53 immunoreactive tumor cells was scored as 0 to 3+ in p53 positive regions. Nuclear p53 expression in $\geq 10\%$ of tumor cells was scored as aberrant overexpression, $<10\%$ -, 10%-30% +, 31%-50% ++, and $>50\%$ +++.

The patients' sex, serum AFP level, and the pathological characteristics of tumor, including tumor size, capsule, vascular invasion (both visual and microscopic), Edmondson grade, etc. were also evaluated.

Statistical analyses

The log-rank test, Kaplan-Meier analysis and univariate and multivariate Cox regression modeling were used for evaluation of contribution of the variables to relapse and disease-specific survival. Overall and disease-free survival rates were calculated with the Life-Table method, and the survival time was calculated from the operative date. The survival curves were estimated by Kaplan-Meier analysis. The prognostic significance of these markers was analyzed using the log-rank test. A Cox regression analysis was performed to show the relationship of the markers studied with the overall and disease-free survival rates of the HCC patients, and to identify the prognostic factors of the HCC patient after operation. The results were correlated with clinicopathological parameters and the prognosis evaluated by uni- and multi-variate analysis using local control, freedom from distant metastasis, disease-free survival, and overall survival as endpoints.

RESULTS

The 1-, 3- and 5-year overall survival rates of the 244 cases of HCC patients studied were 81.9%, 57.6% and 48.7%, respectively. And, the 1-, 3- and 5-year disease-free survival rates were 55.2%, 38.3%, and 32.2%, respectively. p53 immunohistochemical staining was heterogeneous in the HCC tissues, and nuclear staining for p53 were found in 112 of the 222 (50.5%) cases. The 1-, 3- and 5-year overall survival rates of the HCC patients with positive p53 nuclear accumulation were 81.2% (91/112), 50.9% (57/112), and 33.0% (37/112), while those of the HCC patients with negative p53 expression were 88.8%, 66.3% and 60.6%, respectively. Furthermore, among the patients with positive P53 expression, those with 3+ ($>50\%$) for P53 immunohistochemical scoring had a poorest prognosis, their 1-, and 3-year overall survival rates were only 38.5%, and 12.3%, which were much lower than those with 2+ (60.0% and 46.7%, respectively) and those with + (83.5% and 57.3%, respectively). Therefore, the score of P53 overexpression was adversely related to the survival rates of HCC patients (Table 1).

Table 1 Relationship between some clinicopathological parameters and overall survival rates of HCC patients (a univariate analysis)

Parameters	n	Overall survival rates %		
		1-year	3-year	5-year
P53 expression				
-	110	88.8	66.3	60.6
+	86	83.5	57.3	42.9
++	13	60.0	46.7	
+++ ^b	13	38.5	12.3	
Tumors size (cm)				
<=5cm	122	92.6	69.0	55.8
>5, <=8cm	50	78.0	63.0	55.1
>8cm ^b	50	60.0	23.9	
Vascular invasion				
No	160	88.7	68.5	60.7
Microscopic	36	80.6	47.0	
Visual	26	42.3	7.5	
Capsule				
No	112	74.0	42.0	26.4
Well ^b	110	90.5	75.9	75.9

^bP<0.01

The overall survival rates of patients after radical resection of small HCC (≤ 5 cm) were higher than those >5 cm and ≤ 8 cm in diameter. The 3-year survival rate of those with tumor >8 cm in diameter (23.9%) was much lower than those with tumor ≤ 8 cm in diameter (63.0%) (Table 1). The 1- and 3-year overall survival rates of the HCC patients with vascular invasion (both visual and microscopic) were 64.5% (42/62) and 30.6% (19/62), respectively. The patients with visual tumor thrombi in portal vein had a poorer prognosis, their 1- and 3-year overall survival rates were only 42.3% (11/26) and 7.5% (2/26), respectively. No 5-year survival was found. The 1-year, 3-year, and 5-year overall survival rates of patients without vascular invasion were 88.7%, 68.5%, and 60.7%, respectively, which were much higher than those with vascular invasion (P<0.01). A similar situation was also found with disease-free survival (Table 1). The 1-, 3-, and 5-year overall survival rates of patients with well-capsulated HCC were 90.5%, 75.9%, and 75.9%, respectively, while those of the patients without tumor capsule were 74.0%, 42.0%, and 26.4% Table. No significant relationship

between the PCNA-LI, Edmondson grade, patients' sex, or serum AFP level, and overall or disease-free survival rates was found ($P>0.05$).

In univariate Cox hazard regression model analysis, tumor size, capsule status, vascular invasion, p53 expression were independent factors that were closely related to the overall survival rates of HCC patients, while no obvious relationship was found between the PCNA ($P>0.05$) expression and the overall survival. Only vascular invasion ($P=0.0187$) and tumor capsule ($P=0.0059$) were closely related to the disease-free survival of HCC patients, no obvious relationship was found between p53, PCNA status and the disease-free survival (Tables 1, 2).

Similarly, in multivariate analysis, the p53 (RI 0.5456, $P<0.01$) was the most significant factor associated with the overall survival rates of HCC patients after resection. Tumor size (RI 0.5209, $P<0.01$), vessel invasion (RI 0.5271, $P<0.01$) and capsule (RI-0.8691, $P<0.01$) were also related to the overall survival. For the disease-free survival, tumor capsule status remained the only independent predictive factor ($P<0.05$, Table 3). No significant prognostic value was found in the PCNA-LI, Edmondson grade, or patients' sex, serum AFP level for the overall or disease-free survival both in univariate and multivariate Cox analyses.

Table 2 Parameters affecting the disease-free survival rates of HCC patients (a univariate analysis)

Patients (a univariate analysis)				
Parameters	n	Disease-free survival rates (%)		
		1-year	3-year	5-year
Vascular invasion				
No	116	93.9	64.6	54.2
Yes ^a	22	72.7	37.0	
Capsule				
No	57	82.3	44.9	44.9
Yes ^b	81	96.3	73.2	

^a $P<0.05$, ^b $P<0.01$, vs No.

Table 3 Relationship between some clinicopathological parameters and overall survival rates of HCC patients (a multivariate analysis)

	Correlation coefficient	Wald	Standard error	P
P53 expression	0.55	18.88	0.13	<0.01
Tumor size	0.52	14.97	0.13	<0.01
Vascular invasion	0.53	11.85	0.15	<0.01
Tumor capsule	-0.87	10.30	-0.10	<0.01

DISCUSSION

It is difficult to predict the prognosis of patients with HCC, because so far, there is no any specific marker for that yet. Assessment of the clinicopathological and biological malignancy of HCC may help predict outcome. Some pathological features, such as size of the tumor, vascular invasion, fibrous capsule infiltration, and intrahepatic metastasis are thought as prognostic factors for HCC^[5]. New invasiveness scoring system has been proposed based on the items such as venous invasion, tumor capsule, intrahepatic spreading, etc. In our previous report, tumor size was the most important factor for the prognosis of HCC patients and postoperative recurrence possibility^[3]. In this study, in univariate Cox hazard regression model analysis, tumor size, capsule status, and vascular invasion were independent factors which were closely related to both of the overall and disease-free survival rates of HCC patients. Similarly, in multivariate analysis, they were also independent prognostic factors for the overall survival, and the tumor capsule status and vascular invasion were predictive factors for disease-free survival. All these further confirmed

the significance of pathological characteristics of tumor itself in the survival of HCC patients, and the importance of early detection, early diagnosis and early treatment of HCC.

Some biomarkers such as the tumor DNA content, P53 protein expression, proliferating cell nuclear antigen (PCNA) labeling index, and argyrophilic proteins of nuclear organizer regions were used as markers of biological malignancy. P53 protein plays a central role in cellular responses, including cell-cycle arrest and cell death in response to DNA damage. p53 dysfunction can induce abnormal cell growth, increased cell survival, genetic instability, and drug resistance. p53 mutations occur in approximately half of human cancers. Associations of p53 mutation or positive immunohistochemical stain with higher grade and more advanced stage are common. p53 mutation has been found related to advanced tumor stage in cancers of endometrium, cervix, ovary, liver, prostate and bladder, indicating that for these tumors p53 mutation may be a late event contributing to tumor progression^[6]. And p53 mutation has been reported to be a strong marker predicting an increased risk of local relapse, treatment failure, and overall and disease-free survival in many kinds of human carcinomas, such as breast^[7-11], colon-recta^[12,13], esophagus^[14], head and neck^[15], lung^[16-18], ovarian^[19], as well as sarcoma^[20]. An increased intracellular concentration of the P53 protein, although not identical to, is sometimes seen in tumors with p53 mutation and correlated with poor prognosis in some tumors. Several studies have shown a relationship between the nuclear accumulation of p53 protein and poor disease-free and overall survival of prostate cancer^[21,22], and oral cancer^[23]. Detection of micrometastasis of the regional lymph nodes of ovarian cancer by immunohistochemical staining of P53 protein may be useful in predicting the prognosis of patients with stage I or II epithelial ovarian cancer^[24]. The presence of serum anti-p53 antibody has also been found to be associated with survival of patients with breast cancer, ovarian cancer, and hepatocellular carcinoma, and colorectal cancer^[25,26]. However, there is still a great controversy as to whether alteration of the p53 gene adversely affects the survival of cancer patients. Many reports failed to show the independent prognostic value of p53 in the carcinomas of tongue^[27], breast^[28-30], stomach^[31], lung^[32], ovarian^[33], bladder^[34,35], colorectal^[36], and non-Hodgkin's lymphoma^[37].

In a similar situation, there are controversial results about the relationship between the p53 overexpression or p53 gene mutation and the prognosis of HCC patients. It was shown that p53 mutation was involved in determining the dedifferentiation, the proliferative activity, tumor progression^[38], and closely related to the invasiveness of HCC^[4], which might also influence the postoperative course. Mutations of p53 gene or positive immunostaining for mutant P53 protein expression could be used as a significant indicator of poor prognosis^[39-41]. Serum anti-p53 antibody could also be a useful prognostic factor for patients with HCC^[42]. However, many studies showed that neither the immunohistochemical detection of p53 expression, nor the serum anti-p53 antibodies had a significant prognostic value for outcome of patients with HCC^[43-45].

In this study, nuclear staining for P53 was found in 112 of the 222 (50.5%) cases, which was similar to the previous study. The 3-year and 5-year overall survival rates of the HCC patients with positive P53 nuclear accumulation were much lower than those of the HCC patients with negative P53 expression. Its significance was even better than that of the factors such as tumor size, vascular invasion and tumor capsule, though they were also related to the overall survival. Therefore, the score of P53 overexpression was adversely related to the survival rates of HCC patients. These indicated that p53 mutation or nuclear accumulation of p53 expression could be a valuable marker for predicting the prognosis of HCC patients after resection. Among the patients with positive P53 expression, those

with 3+ (>50%) for P53 immunohistochemical scoring had a poorest prognosis, their 1-, and 3-year overall survival rates were only 38.5% and 12.3%, respectively, which were much lower than those with 2+ (60.0% and 46.7%) and those with + (83.5% and 57.3%). Therefore, the quantitative immunohistochemical scoring for P53 expression might be more valuable than the common qualitative analysis for P53 expression for predicting the prognosis of HCC patients.

Proliferating cell nuclear antigen (PCNA) labeling index has been thought as another marker of biological malignancy. A correlation between PCNA-LI and recurrent time and rate was reported. PCNA-LI could be a valuable prognostic marker for HCC. However, in this study, no correlation between PCNA-LI and overall or disease-free survival was found.

In summary, HCC is one of the most common cancers in China. Although great advances in its clinical study have been made, metastatic recurrence is the most prevalent cause of death in patients with HCC. Over the past few years, much effort has been made on this target, including predicting HCC behavior^[46-60]. In this study, through the retrospective review of the 244 HCC patients, we found that accumulation of p53 expression as well as tumor size, capsule or vascular invasion could be a valuable marker for predicting the prognosis of HCC patients after resection. The quantitative immunohistochemical scoring for P53 nuclear accumulation might be more valuable than the common qualitative analysis for P53 expression for predicting prognosis of patients after HCC resection.

REFERENCES

- Pisani P, Parkin M, Bray F, Ferlay J. Estimates of the worldwide mortality from 25 cancers in 25 cancers in 1990. *Int J Cancer* 1999;83: 18-29
- Greenlee RT, Hill-Harmon MB, Murray T, Thun M. Cancer Statistics, 2001. *CA Cancer J Clin* 2001;51:15-36
- Tang ZY. Hepatocellular carcinoma-Cause, treatment and metastasis. *World J Gastroenterol* 2001;7:445-454
- Tang ZY, Qin LX, Wang XM, Zhou G, Liao Y, Weng Y, Jiang XP, Lin ZY, Liu KD, Ye SL. Alterations of oncogenes, tumor suppressor genes and growth factors in hepatocellular carcinoma: with relation to tumor size and invasiveness. *Chin Med J* 1998;111:313-318
- Poon RT, Fan ST, Ng IO, Lo CM, Liu CL, Wong J. Different risk factors and prognosis for early and late intrahepatic recurrence after resection of hepatocellular carcinoma. *Cancer* 2000;89:500-507
- Greenblatt MS, Bennett WP, Hollstein M, Harris CC. Mutations in the p53 tumor suppressor gene: Clues to cancer etiology and molecular pathogenesis. *Cancer Res* 1994;54:4855-4878
- Overgaard J, Yilmaz M, Guldberg P, Hansen LL, Alsner J. TP53 mutation is an independent prognostic marker for poor outcome in both node-negative and node-positive breast cancer. *Acta Oncol* 2000; 39:327-333
- Zellars RC, Hilsenbeck SG, Clark GM, Allred DC, Herman TS, Chamness GC, Elledge RM. Prognostic value of p53 for local failure in mastectomy-treated breast cancer patients. *J Clin Oncol* 2000;18: 1906-1913
- Takahashi M, Tonoki H, Tada M, Kashiwazaki H, Furuuchi K, Hamada J, Fujioka Y, Sato Y, Takahashi H, Todo S, Sakuragi N, Moriuchi T. Distinct prognostic values of p53 mutations and loss of estrogen receptor and their cumulative effect in primary breast cancers. *Int J Cancer* 2000;89:92-99
- Blaszyk H, Hartmann A, Cunningham JM, Schaid D, Wold LE, Kovach JS, Sommer SS. A prospective trial of midwest breast cancer patients: a p53 gene mutation is the most important predictor of adverse outcome. *Int J Cancer* 2000;89:32-38
- Sirvent JJ, Fortuno-Mar A, Olona M, Orti A. Prognostic value of p53 protein expression and clinicopathological factors in infiltrating ductal carcinoma of the breast. A study of 192 patients. *Histol Histopathol* 2001;16:99-106
- Bouzourene H, Gervaz P, Cerottini JP, Benhattar J, Chaubert P, Saraga E, Pampallona S, Bosman FT, Givel JC. p53 and Ki-ras as prognostic factors for Dukes' stage B colorectal cancer. *Eur J Cancer* 2000;36:1008-1015
- Kahlenberg MS, Stoler DL, Rodriguez-Bigas MA, Weber TK, Driscoll DL, Anderson GR, Petrelli NJ. p53 tumor suppressor gene mutations predict decreased survival of patients with sporadic colorectal carcinoma. *Cancer* 2000;88:1814-1819
- Ireland AP, Shibata DK, Chandrasoma P, Lord RV, Peters JH, DeMeester TR. Clinical significance of p53 mutations in adenocarcinoma of the esophagus and cardia. *Ann Surg* 2000;231:179-187
- Tamas L, Kraxner H, Mechtler L, Repassy G, Ribari O, Hirschberg A, Szentkuti G, Jaray B, Szentirmay Z. Prognostic significance of P53 histochemistry and DNA histogram parameters in head and neck malignancies. *Anticancer Res* 2000;20:4031-4037
- Gemba K, Ueoka H, Kiura K, Tabata M, Harada M. Immunohistochemical detection of mutant p53 protein in small-cell lung cancer: relationship to treatment outcome. *Lung Cancer* 2000;29:23-31
- Murakami I, Hiyama K, Ishioka S, Yamakido M, Kasagi F, Yokosaki Y. p53 gene mutations are associated with shortened survival in patients with advanced non-small cell lung cancer: an analysis of medically managed patients. *Clin Cancer Res* 2000;6:526-530
- Mitsudomi T, Hamajima N, Ogawa M, Takahashi T. Prognostic significance of p53 alterations in patients with non-small cell lung cancer: a meta-analysis. *Clin Cancer Res* 2000;6:4055-4063
- Shahin MS, Hughes JH, Sood AK, Buller RE. The prognostic significance of p53 tumor suppressor gene alterations in ovarian carcinoma. *Cancer* 2000;89:2006-2017
- de Alava E, Antonescu CR, Panizo A, Leung D, Meyers PA, Huvos AG, Pardo-Mindan FJ, Healey JH, Ladanyi M. Prognostic impact of P53 status in Ewing sarcoma. *Cancer* 2000;89:783-792
- Borre M, Stausbol-Gron B, Overgaard J. p53 accumulation associated with bcl-2, the proliferation marker MIB-1 and survival in patients with prostate cancer subjected to watchful waiting. *J Urol* 2000;164:716-721
- Leibovich BC, Cheng L, Weaver AL, Myers RP, Bostwick DG. Outcome prediction with p53 immunostaining after radical prostatectomy in patients with locally advanced prostate cancer. *J Urol* 2000; 163:1756-1760
- Osaki T, Kimura T, Tatemoto Y, Dapeng L, Yoneda K, Yamamoto T. Diffuse mode of tumor cell invasion and expression of mutant p53 protein but not of p21 protein are correlated with treatment failure in oral carcinomas and their metastatic foci. *Oncology* 2000;59:36-43
- Suzuki M, Ohwada M, Saga Y, Kohno T, Takei Y, Sato I. Micrometastatic p53-positive cells in the lymph nodes of early stage epithelial ovarian cancer: prognostic significance. *Oncology* 2001;60: 170-175
- Shiota G, Ishida M, Noguchi N, Oyama K, Takano Y, Okubo M, Katayama S, Tomie Y, Harada K, Hori K, Ashida K, Kishimoto Y, Hosoda A, Suou T, Kanbe T, Tanaka K, Nosaka K, Tanida O, Kojo H, Miura K, Ito H, Kaibara N, Kawasaki H. Circulating p53 antibody in patients with colorectal cancer: relation to clinicopathologic features and survival. *Dig Dis Sci* 2000;45:122-128
- Vogl FD, Frey M, Kreienberg R, Runnebaum IB. Autoimmunity against p53 predicts invasive cancer with poor survival in patients with an ovarian mass. *Br J Cancer* 2000;83:1338-1343
- Kantola S, Parikka M, Jokinen K, Hyrynkanis K, Soini Y, Alho OP, Salo T. Prognostic factors in tongue cancer - relative importance of demographic, clinical and histopathological factors. *Br J Cancer* 2000; 83:614-619
- Ferrero JM, Ramaioli A, Formento JL, Francoual M, Etienne MC, Peyrottes I, Ettore F, Leblanc-Talent P, Namer M, Milano G. P53 determination alongside classical prognostic factors in node-negative breast cancer: an evaluation at more than 10-year follow-up. *Ann Oncol* 2000;11:393-397
- Bergh J. Clinical studies of p53 in treatment and benefit of breast cancer patients. *Endocr Relat Cancer* 1999;6:51-59
- Reed W, Hannisdal E, Boehler PJ, Gundersen S, Host H, Marthin J. The prognostic value of p53 and c-erb B-2 immunostaining is over-rated for patients with lymph node negative breast carcinoma: a multivariate analysis of prognostic factors in 613 patients with a follow-up of 14-30 years. *Cancer* 2000;88:804-813
- Kaye PV, Radebold K, Isaacs S, Dent DM. Expression of p53 and p21waf1/cip1 in gastric carcinoma: lack of inter-relationship or correlation with prognosis. *Eur J Surg Oncol* 2000;26:39-43
- Schiller JH, Adak S, Feins RH, Keller SM, Fry WA, Livingston RB, Hammond ME, Wolf B, Sabatini L, Jett J, Kohman L, Johnson DH. Lack of prognostic significance of p53 and K-ras mutations in primary resected non-small-cell lung cancer on E4592: a Laboratory Ancillary Study on an Eastern Cooperative Oncology Group Prospective Randomized Trial of Postoperative Adjuvant Therapy. *J Clin Oncol* 2001;19:448-457
- Gadducci A, Cianci C, Cosio S, Carnino F, Fanucchi A, Buttitta F, Conte PF, Genazzani AR. p53 status is neither a predictive nor a prognostic variable in patients with advanced ovarian cancer treated with a paclitaxel-based regimen. *Anticancer Res* 2000;20:4793-4799
- Gontero P, Casetta G, Zitella A, Ballario R, Pacchioni D, Magnani C, Muir GH, Tizzani A. Evaluation of P53 protein overexpression, Ki67 proliferative activity and mitotic index as markers of tumour recurrence in superficial transitional cell carcinoma of the bladder. *Eur Urol* 2000;38:

- 287-296
- 35 Fleshner N, Kapusta L, Ezer D, Herschorn S, Klotz L. p53 nuclear accumulation is not associated with decreased disease-free survival in patients with node positive transitional cell carcinoma of the bladder. *J Urol* 2000;164:1177-182
- 36 Gallego MG, Acenero MJ, Ortega S, Delgado AA, Cantero JL. Prognostic influence of p53 nuclear overexpression in colorectal carcinoma. *Colon Rectum* 2000;43:971-975
- 37 Nieder C, Petersen S, Petersen C, Thames HD. The challenge of p53 as prognostic and predictive factor in Hodgkin's or non-Hodgkin's lymphoma. *Ann Hematol* 2001;80:2-8
- 38 Itoh T, Shiro T, Seki T, Nakagawa T, Wakabayashi M, Inoue K, Okamura A. Relationship between p53 overexpression and the proliferative activity in hepatocellular carcinoma. *Int J Mol Med* 2000;6:137-142
- 39 Jeng KS, Sheen IS, Chen BF, Wu JY. Is the p53 gene mutation of prognostic value in hepatocellular carcinoma after resection? *Arch Surg* 2000;135:1329-1333
- 40 Sugo H, Takamori S, Kojima K, Beppu T, Futagawa S. The significance of p53 mutations as an indicator of the biological behavior of recurrent hepatocellular carcinomas. *Surg Today* 1999;29:849-855
- 41 Hayashi H, Sugio K, Matsumata T, Adachi E, Takenaka K, Sugimachi K. The clinical significance of p53 gene mutation in hepatocellular carcinomas from Japan. *Hepatology* 1995;22:1702-1707
- 42 Shiota G, Kishimoto Y, Suyama A, Okubo M, Katayama S, Harada K, Ishida M, Hori K, Suou T, Kawasaki H. Prognostic significance of serum anti-p53 antibody in patients with hepatocellular carcinoma. *J Hepatol* 1997;27:661-668
- 43 Tangkijvanich P, Janchai A, Charuruks N, Kullavanijaya P, Theamboonlers A, Hirsch P, Poovorawan Y. Clinical associations and prognostic significance of serum anti-p53 antibodies in Thai patients with hepatocellular carcinoma. *Asian Pac J Allergy Immunol* 2000;18:237-243
- 44 Saffroy R, Lelong JC, Azoulay D, Salvucci M, Reynes M, Bismuth H, Debuire B, Lemoine A. Clinical significance of circulating anti-p53 antibodies in European patients with hepatocellular carcinoma. *Br J Cancer* 1999;79:604-610
- 45 Terris B, Laurent-Puig P, Belghitti J, Degott C, Henin D, Flejou JF. Prognostic influence of clinicopathologic features, DNA-ploidy, CD44H and p53 expression in a large series of resected hepatocellular carcinoma in France. *Int J Cancer* 1997;74:614-619
- 46 Tang ZY, Sun FX, Tian J, Ye SL, Liu YK, Liu KD, Xue Q, Chen J, Xia JL, Qin LX, Sun HC, Wang L, Zhou J, Li Y, Ma ZC, Zhou XD, Wu ZQ, Lin ZY, Yang BH. Metastatic human hepatocellular carcinoma models in nude mice and cell line with metastatic potential. *World J Gastroenterol* 2001;7:597-601
- 47 Li Y, Tang ZY, Ye SL, Liu YK, Chen J, Xue Q, Chen J, Gao DM, Bao WH. Establishment of cell clones with different metastatic potential from the metastatic hepatocellular carcinoma cell line MHCC97. *World J Gastroenterol* 2001;7:630-636
- 48 Niu Q, Tang ZY, Ma ZC, Qin LX, Zhang LH. Serum vascular endothelial growth factor is a potential biomarker of metastatic recurrence after curative resection of hepatocellular carcinoma. *World J Gastroenterol* 2000;6:565-568
- 49 Wu ZQ, Fan J, Qiu SJ, Zhou J, Tang ZY. The value of postoperative hepatic regional chemotherapy in prevention of recurrence after radical resection of primary liver cancer. *World J Gastroenterol* 2000;6:131-133
- 50 Wang Q, Lin ZY, Feng XL. Alterations in metastatic properties of hepatocellular carcinoma cell following H-ras oncogene transfection. *World J Gastroenterol* 2001;7:335-339
- 51 Jiang YF, Yang ZH, Hu JQ. Recurrence or metastasis of HCC: predictors, early detection and experimental antiangiogenic therapy. *World J Gastroenterol* 2000;6:61-65
- 52 Cao XY, Liu J, Lian ZR, Clayton M, Hu JL, Zhu MH, Fan DM, Feitelson M. Cloning of differentially expressed genes in human hepatocellular carcinoma and nontumor liver. *World J Gastroenterol* 2001;7:579-582
- 53 Hou L, Li Y, Jia YH, Wang B, Xin Y, Ling MY. Molecular mechanism about lymphogenous metastasis of hepatocarcinoma cells in mice. *World J Gastroenterol* 2001;7:532-536
- 54 Fan ZR, Yang DH, Cui J, Qin HR, Huang CC. Expression of insulin-like growth factor II and its receptor in hepatocellular carcinogenesis. *World J Gastroenterol* 2001;7:285-288
- 55 Xu J, Mei MH, Zeng SE, Shi QF, Liu YM, Qin LL. Expressions of ICAM and its mRNA in sera and tissues of patients with hepatocellular carcinoma. *World J Gastroenterol* 2001;7:120-125
- 56 Huang XF, Wang CM, Dai XW, Li ZJ, Pan BR, Yu LB, Qian B, Fang L. Expressions of chromogranin: A and cathepsin D in human primary hepatocellular carcinoma. *World J Gastroenterol* 2000;6:693-698
- 57 Mei MH, Xu J, Shi QF, Yang JH, Chen Q, Qin LL. Clinical significance of serum intercellular adhesion molecule 1 detection in patients with hepatocellular carcinoma. *World J Gastroenterol* 2000;6:408-410
- 58 Qin Y, Li B, Tan YS, Sun ZL, Zuo FQ, Sun ZF. Polymorphism of p16INK4a gene and rare mutation of p15INK4b gene exon2 in primary hepatocarcinoma. *World J Gastroenterol* 2000;6:411-414
- 59 Kong XB, Yang ZK, Liang LJ, Huang JF, Lin HL. Overexpression of Pglycoprotein in hepatocellular carcinoma and its clinical implication. *World J Gastroenterol* 2000;6:134-135
- 60 Lin GY, Chen ZL, Lu CM, Li Y, Ping XJ, Huang R. Immunohistochemical study on p53, H-ras/p21, c-erbB2 protein and PCNA expression in HCC tissues of Han and minority ethnic patients. *World J Gastroenterol* 2000;6:234-238

Edited by Ma JY

• LIVER CANCER •

Antitumor activities of human autologous cytokine-induced killer (CIK) cells against hepatocellular carcinoma cells *in vitro* and *in vivo*

Fu-Sheng Wang, Ming-Xu Liu, Bing Zhang, Ming Shi, Zhou-Yun Lei, Wen-Bing Sun, Qing-You Du, Ju-Mei Chen

Fu-Sheng Wang, Ming-Xu Liu, Bing Zhang, Ming Shi, Zhou-Yun Lei, Wen-Bing Sun, Qing-You Du, Ju-Mei Chen, Division of Biological Engineering, Beijing Institute of Infectious Diseases, Beijing 100039, China
Wen-Bing Sun, Department of Surgery, Beijing Hospital of Infectious Diseases, Beijing 100039, China

Supported by Science and Technology Development Foundation of Beijing Institute of Infectious Diseases, No.01Z094

Correspondence to: Dr. Fu-Sheng Wang, Division of Biological Engineering, Beijing Institute of Infectious Diseases, 26 Fengtai Road, Beijing 100039, China. fswang@public.bta.net.cn

Telephone: +86-10-66933332 Fax: +86-10-63831870

Received 2001-04-11 Accepted 2002-02-25

Abstract

AIM: To characterize the anticancer function of cytokine-induced killer cells (CIK) and develop an adoptive immunotherapy for the patients with primary hepatocellular carcinoma (HCC), we evaluated the proliferation rate, phenotype and the antitumor activity of human CIK cells from healthy donors and HCC patients *in vitro* and *in vivo*.

METHODS: Peripheral blood mononuclear cells (PBMC) from healthy donors and patients with primary HCC were incubated *in vitro* and induced into CIK cells in the presence of various cytokines such as interferon-gamma (IFN- γ), interleukin-1 (IL-1), IL-2, and monoclonal antibody (mAb) against CD3. The phenotype and characterization of CIK cells were identified by flow cytometric analysis. The cytotoxicity of CIK cells was determined by ^{51}Cr release assay.

RESULTS: The CIK cells were shown to be a heterogeneous population with different cellular phenotypes. The percentage of CD3 $^{+}$ /CD56 $^{+}$ positive cells, the dominant effector cells, in total CIK cells from healthy donors and HCC patients, significantly increased from 0.1-0.13% at day 0 to 19.0-20.5% at day 21 incubation, which suggested that the CD3 $^{+}$ CD56 $^{+}$ positive cells proliferated faster than other cell populations of CIK cells in the protocol used in this study. After 28 day *in vitro* incubation, the CIK cells from patients with HCC and healthy donors increased by more than 300-fold and 500-fold in proliferation cell number, respectively. CIK cells originated from HCC patients possessed a higher *in vitro* antitumor cytotoxic activity on autologous HCC cells than the autologous lymphokine-activated killer (LAK) cells and PBMC cells. In *in vivo* animal experiment, CIK cells had stronger effects on the inhibition of tumor growth in Balb/c nude mice bearing BEL-7402-producing tumor than LAK cells (mean inhibitory rate, 84.7% vs 52.8%, $P < 0.05$) or PBMC (mean inhibitory rate, 84.7% vs 37.1%, $P < 0.01$).

CONCLUSION: Autologous CIK cells are of highly efficient cytotoxic effector cells against primary hepatocellular carcinoma cells and might serve as an alternative adoptive therapeutic strategy for HCC patients.

Wang FS, Liu MX, Zhang B, Shi M, Lei ZY, Sun WB, Du QY, Chen JM. Antitumor activities of human autologous cytokine-induced killer (CIK) cells against hepatocellular carcinoma cells *in vitro* and *in vivo*. *World J Gastroenterol* 2002;8(3):464-468

INTRODUCTION

Cytokine-induced killer (CIK) cells are the major histocompatibility complex-unrestricted cytotoxic lymphocytes and generated by incubation of peripheral blood monocytes (PBMC) in the presence of various types of cytokines such as CD3 monoclonal antibody, interleukin-2 (IL-2), interleukin-1 (IL-1) and interferon-gamma^[1]. CIK cells are the population of heterogenous effector cells possessing enhanced cytotoxicity and a higher proliferation rate as compared with lymphokine-activated killer (LAK) and tumor infiltrating lymphocytes (TIL) cells. The high anti-tumor activity of CIK cells is mainly due to the high proliferation of double CD3 $^{+}$ and CD56 $^{+}$ positive cells^[2-5]. Some reports indicated that CIK cells, other than LAK and TIL cells, can be efficiently employed as an adjuvant in anticancer immunotherapeutic strategy for the eradication of residual cancer cells and prevention or delay of tumor relapse^[6-9].

Hepatocellular carcinoma (HCC) is the malignant transformation of hepatocytes and is a common complication of chronic hepatitis mainly caused by hepatitis B virus (HBV) and hepatitis C virus (HCV) infection in China^[10]. The mechanisms underlying the malignant transformation of hepatocytes are not well defined. Many driving factors including the persistent hepatitis B or C virus infections, host immunological and genetic factors might have been involved in the process. For example, a failure to mount an efficient immune response to HCC cells, either because of selective defects or immune tolerance in the host immune system or because of tumor interference with a function(s) of immune cells, could account for the inability of HCC patients to block the pathogenesis of HCC occurrence^[11-18]. In attempt to characterize the anticancer function of CIK cells and develop an alternative adoptive immunotherapy for the patients with primary HCC, we evaluated the proliferation rate and phenotype of CIK cells from healthy donors and primary HCC patients. Furthermore, we compared the cytotoxic activity and antitumor effects of major effector CIK cells with double CD3 $^{+}$ and CD56 $^{+}$ positive markers against the primary and secondary HCC *in vitro* cell culture system and *in vivo* tumor-bearing mice model.

MATERIALS AND METHODS

Reagents and cell lines

RPMI1640 and DMEM medium, recombinant human IL-1 α , IL-2, interferon gamma (IFN- γ), TNF- α and monoclonal antibody against the CD3 surface antigen (mAb CD3) were all purchased from Gibco Co. The Flt-3 ligand, mouse anti-human FITC-conjugated CD3 and CD56 monoclonal antibodies were obtained from BD-Pharmingen and Fetal calf serum (FCS) from Hyclone. BEL7402 is human HCC cell line kept in liquid nitrogen in our laboratory.

Cell separation

The patients with primary HCC and healthy donors were submitted to cytophoresis after their writing contents were signed. An enriched peripheral blood mononuclear cells (PBMC) product was collected using the specific program of the Cobe Spectra blood separator. Cells were resuspended in phosphate buffered saline (PBS) without calcium and magnesium. The separation of PBMC was performed as previously described^[2,19-21]. The concentrated PBMC cells were used immediately for CIK cell culture.

Generation of cytokine-induced killer (CIK) cells

CIK cells were generated as described previously^[2,3,22,23]. Briefly, non-adherent Ficoll-separated human peripheral blood mononuclear cells were prepared and incubated in RPMI1640 medium containing 100ml·L⁻¹ FCS and various types of cytokines added according to the reported protocol with minor modifications^[23]. The final concentrations of the cytokines and antibody added were as follows: IL-2, 1000×10³U·L⁻¹; IL-1, 100×10³U·L⁻¹; IFN-γ, 100×10³U·L⁻¹; mAb CD3, 50μg·L⁻¹. Cells were incubated at 37°C in a humidified atmosphere of 50ml·L⁻¹ CO₂ and fed every 3 days in fresh complete medium with 100ml·L⁻¹ FCS and various types of cytokines at 0.5×10⁶cells·L⁻¹.

Immunofluorescent staining of effector cells

Starting PBMC, LAK or CIK effector cells were stained with various types of FITC- or PE-conjugated mouse mAb's against human surface antigens. Antibodies used included anti-CD3, anti-CD4, anti-CD16, anti-CD56 and anti-TCR-α/β, anti-TCR-γ/δ (all from Becton Dickinson, Beijing, China). Five ×10⁵ of cells were incubated with a optimal amount of antibody at 4°C for 30min. To remove excessive antibody, the incubation mixture was centrifuged at 250×g for 10min. The pellet was resuspended in PBS containing 2ml·L⁻¹ of human AB serum and treated as described before^[21]. Stained cells were washed and analyzed with FACScaliber (Becton Dickinson) in our laboratory.

Isolation of primary HCC cells from patients

Fresh liver cancer tissues were obtained from the HCC patients at the department of Surgery in our hospital and immediately immersed in sterilized PBS (pH 7.0) solution containing penicillin, 100×10³U·L⁻¹; streptomycin, 100×10³U·L⁻¹ and gentamycin, 500×10³U·L⁻¹ for 1h at room temperature, then washed with PBS for three times. The liver cancer tissues were cut into small pieces (1-2mm³ in size), and digested with 37°C-rewarm serum-free medium with 1.25g·L⁻¹ of collagenase-V for 2h. In order to separate them into single cell suspension, all the digested pieces of tissues were filtered through the 200 mesh of sterilized copper wire bag. The single cell suspension was further isolated by Percoll gradient centrifugation. Finally, the resuspended cells in DMEM medium with 200ml·L⁻¹ FCS were the primary HCC cells.

Cytotoxic effects of CIK cells by ⁵¹Cr release assay

⁵¹Cr release cytotoxic assays were performed as reported previously^[24]. Briefly, one ×10⁶ of human primary HCC cells were incubated with culture medium containing 7.4MBq of ⁵¹Cr solution at 37°C for one hour. The labeling cells were washed with PBS solution for three times and added to 96-well culture plates at 2×10⁴cells/well. CIK cells were incubated with tumor cells at various ratios of effector cells to target cells as 6.25 : 1, 12.5 : 1, 25 : 1 and 50 : 1. After 4h incubation, all cells were collected by centrifugation and an aliquot of supernatant was counted in a gamma counter. The percentage of specific release was calculated as described^[25].

Inhibitory Effects of CIK cells on HCC in tumor-bearing nude mice models

In pilot experiments, 1.5×10⁶ of BEL-7402 cells injected subscapularly could produce solid tumor in Balb/c nude mice at the tenth day with 100% of incidence rate. The Balb/c nude mice used in the study were randomly divided into four groups treated with physical solution, PBMC, LAK and CIK cells, respectively. The nude mice received 3.0Gy of whole body irradiation and injected subscapularly with 5×10⁶ BEL-7402 cells, which were at the stage of exponential growth (designated as day 0). On day 1, 0.25mL of 1×10⁷ effector cells such as CIK, PBMC or LAK cells were injected locally where tumor cells were inoculated for 6 consecutive days. In controls, the nude mice received 0.25mL physical solution. The size of tumor was recorded every other day. The solid tumors were peeled off after the nude mice were dislocated by killing them on the 35th day.

Statistical analysis

The Wilcoxon matched-pairs test was used to analyze for statistical significance. The P value less than 0.05 was considered as significant difference.

RESULTS

Proliferation and phenotype of CIK cells

Figure 1A and B show the proliferation of CIK cells from healthy donors and patients with primary HCC at different incubation days. During cell generation, there was a steady increase in both the absolute number and the percentage of CD3⁺/CD56⁺ cells, e.g. the percentage of CD3⁺/CD56⁺ cells was 7.5% on 14d and 51.3% on 56d of in vitro incubation, respectively. After 14d in vitro incubation, the number of total incubated CIK cells increased significantly (500 fold from 8.07×10⁵ to 1.02×10⁸). The majority (as high as 82%±6.4%) of these cells were positive for TCR-α/β. Cells expressing TCR-γ/δ were relatively rare (4.5%±2.6%). The proliferation capability of PBMC obtained from normal donors was slightly higher than that of PBMC obtained from the HCC patients. The percentage of double CD3⁺/CD56⁺ positive cells varied during CIK cell generation. The percentage of CD3⁺/CD56⁺ positive cells in total CIK cells from healthy donors and HCC patients significantly increased from 0.1-0.13% at day 0 to 18.95-20.5% at day 21, which suggested that the CD3⁺ CD56⁺ positive cells proliferated faster than other populations of CIK cells in the protocol used in this study.

In peripheral blood, 24.2% of CD56⁺ cells coexpressed CD3⁺ as compared to 36.2% in LAK cell cultures and 76% in CIK cell cultures (Figure 2). Conversely, only 17.8% and 42.1% of CD3⁺ cells in peripheral blood and LAK cells coexpressed CD56⁺, whereas 76.6% of CIK CD3⁺ cells coexpressed CD56⁺. At d 28 of CIK cell generation, the percentage of CD3⁺ cells coexpressing CD56⁺ increased to 82.4%.

Table 1 Phenotype of CIK cells and cytotoxic activity of CIK subsets

Subset	Percentage positively of CIK	LU/10 ⁶ cell stained cells	Cell number ×10 ⁶	Total LU per culture
CIK		43.6±4.8	712±24.3	29,074
TCR-α/β	82.0±6.4	20.6±3.8	583±41.6	12,088
CD56	30.4±5.6	78.4±6.9	214±70.3	13,948
CD16	15.8±5.4	60.4±6.0	89±40.9	4106

Note: Total LU per culture was calculated by multiplying the number of LU per million cells by the total number of cells.

Effect of different sera on CIK proliferation

When CIK cells were incubated in RPMI1640 medium containing 100 ml·L⁻¹ of fetal calf serum or 100ml·L⁻¹ human AB serum or free-

serum medium, respectively, they exhibited different growth curves (Figure 3). CIK cells had the highest proliferation rate in human AB serum-containing medium, the lowest in serum-free medium. The proliferated numbers of CIK cells increased by 500 fold in human AB serum-containing medium, 450 fold increase in fetal calf serum-containing medium, and 50-60 fold in free-serum medium, respectively.

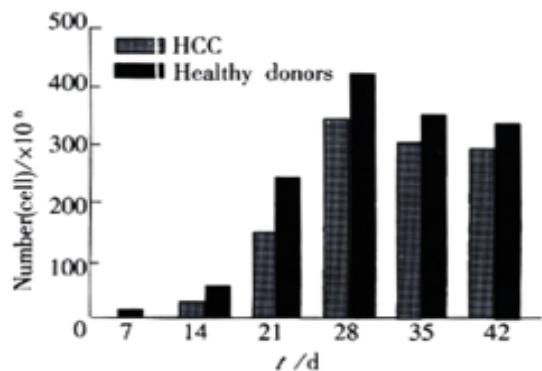


Figure 1A Proliferation of CIK cells *in vitro* culture system

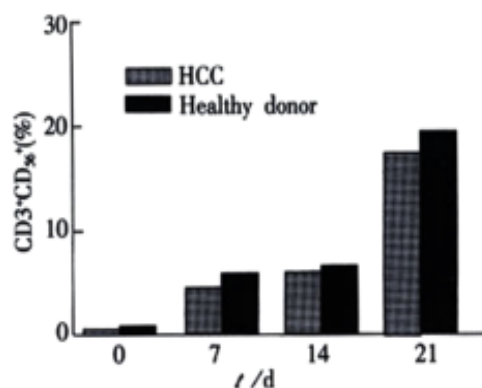


Figure 1B The percentages of double CD3⁺ CD56⁺ positive cells at various incubation time *in vitro* culture system

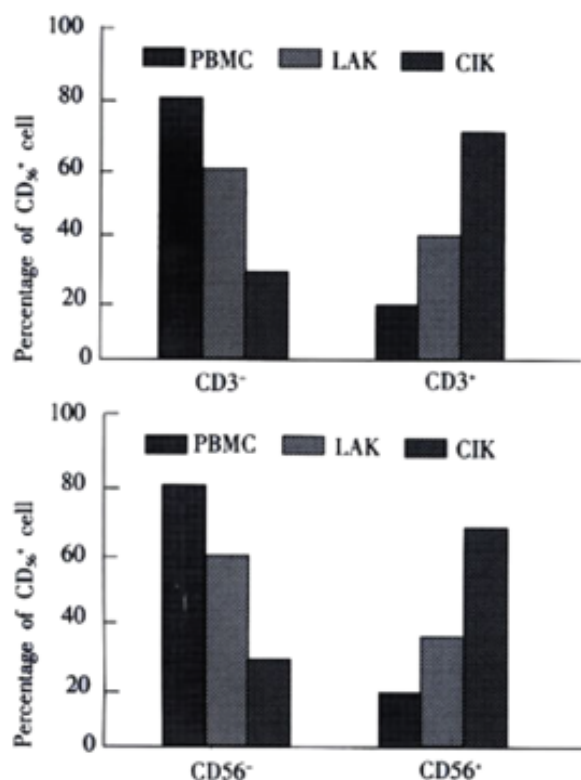


Figure 2 Subsets of CIK cells from patients with primary HCC. CIK cells were

counterstained for CD3 and CD56 at day 12 of CIK generation and the percentage of positively stained cells was determined by flow cytometry. PBMC and LAK were stained like CIK cells. LAK cells were used at day 6 of generation. Upper. CD56⁺ subsets of CIK cells, LAK, PBMC. Subsets of CD56⁺ cells were compared to the total number of CD56⁺ cells. The figure represents data from three different experiments. Results are presented as mean value \pm SEM. Lower. CD3⁺ subsets of CIK cells, LAK, PBMC. Subsets of CD3⁺ cells were compared to the total number of CD3⁺ cells. The figure represents data from three different experiments. Results are presented as mean value \pm SEM.

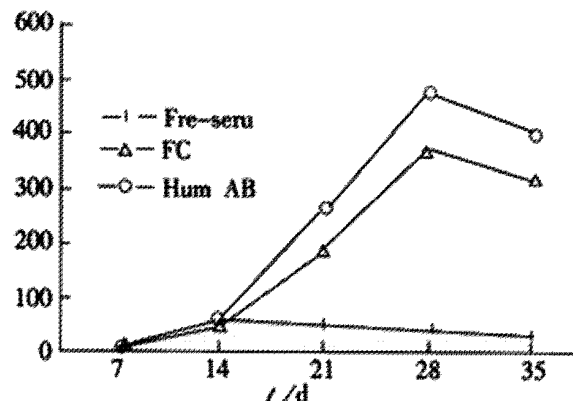


Figure 3 Effects of different culture system on growth of CIK cells

Cytotoxic activity of CIK cells on primary HCC cells

The CIK cell subpopulations were tested for cytotoxicity against the HCC cells as measured by ⁵¹Cr release. The primary HCC cells were used as the target cells and the CIK cells from the same patients with HCC as the effector cells. Both of them at various ratios of effector cells to target cells were mixed together for evaluation of the cytotoxic activity of CIK cells. CD3⁺/CD56⁺ T cells were identified to be the major cytolytic effectors, as previously reported, the CD3⁺/CD56⁺ subpopulation of CIK cells exhibited maximum ⁵¹Cr release cytotoxicity toward target cells (Figure 4) with the increased ratio of effector and target cells, the cytotoxic effects of CIK cells correspondingly became stronger. In controls, PBMC cells only showed a weaker cytotoxic effect on primary HCC cells compared with CIK cells, and maintained at a lower platform level even if the ratio of effector and target cells increased.

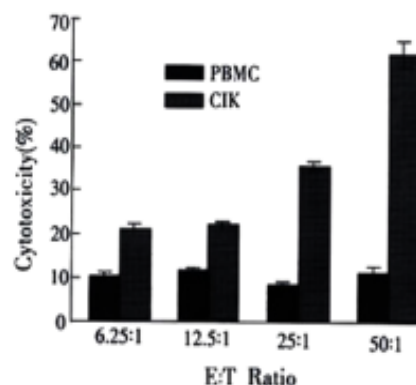


Figure 4 Cytotoxic activity of CIK, PBMC cells against primary HCC cells

Inhibitory effects of CIK cells on HCC in tumor-bearing nude mice

Inhibitory effects of CIK cells on HCC cells in tumor-bearing nude mice are summarized in Table 2. In CIK-treated group, 15 nude mice were inoculated with tumor cells and received treatment of CIK cells for six day consecutively. Tumorigenesis was found in ten of fifteen (66.7%) nude mice. However, tumorigenesis was formed in all the mice in PBMC and LAK treated groups. Furthermore, the tumor size was smaller and limited in the mice of CIK-treated group as compared with those in the mice of PBMC- and LAK-treated groups. There was an obvious difference between the CIK group and LAK group

($P<0.05$), and between CIK group and PBMC group ($P<0.01$), which suggest that CIK cells have a great priority of inhibitory effects on tumorigenesis in tumor-bearing nude mice as compared with LAK cells.

Table 2 Inhibitory effects of CIK, PBMC and LAK cells on HCC cells in tumor-bearing nude mice

Group	n	Tumor/g	Tumorigenesis (%)	Inhibitory rate (%)
Control	9	2.10±0.41	100	0
PBMC	11	1.32±0.27	100	37.1
LAK	11	0.99±0.33	100	52.8
CIK	15	0.32±0.31	66.7	84.7 ^{ab}

^a $P<0.05$ vs LAK group, ^b $P<0.01$ vs PBMC group.

DISCUSSION

In this study, we found that autologous CIK cells had a higher proliferation rate and enhanced cytotoxic activity compared with lymphokine-activated killer cells^[5,26,27]. The CIK cells from the primary HCC patients had a lower proliferation ability than that from the healthy donors though no obvious difference was found in the phenotype and components of CIK cells between the two groups. Interestingly, the cytotoxic activity of CIK cells from healthy donors was proved to be stronger than that from the patients with primary HCC. This results might reflect the functions of CIK cells in HCC patients is probably inhibited to some extent by itself, which is consistent with the fact that there is a decreased function of peripheral blood dendritic cells in patients with primary HCC^[28,29]. Whether the dysfunctional dendritic cells led to the decreased proliferation and function of CIK cells? Martin *et al* reported that CIK cells significantly increased the cytotoxic activity after co-cultured with autologous dendritic cells, and they considered this phenomenon to be induced by IL-12 cytokine secretion from dendritic cells and cell-cell interactions between the two population^[5].

Though LAK cells recognize and kill target cells by a non-MHC restricted mechanism in the same way like CIK cells, the CIK cells were found to have the greatest lytic activity^[5]. Our results suggested that the CIK effector cells are the subpopulation coexpressing CD3⁺/CD56⁺ phenotypes, which supported the facts that CIK cells possessed a higher proliferation rate and higher antitumor cytotoxic activity in vitro than LAK cells^[26,30,31].

Immunological effector cells involved in cell-mediated cytotoxicity, such as CIK cells, cytotoxic T lymphocytes (CTLs) and natural killer (NK) cells, possess cytoplasmic granules that are involved in target cell death. These granules contain a pore-forming protein called perforin or cytolytic, a family of serine esterases (granzymes), lysosomal enzymes, and proteoglycan molecules. The cytolysis of tumor cells produced by CIK effector cells might be mediated by the local direct exocytosis of cytoplasmic granules that penetrate the cell membrane of the bound target cell. Stimulation of CIK cells with tumor cells or anti-CD3 mAb is sufficient for exocytosis of cytotoxic material. The detailed mechanism by which these effector cells recognize tumor cell targets has remained elusive. However, leukocyte function associated antigen-1 (LFA-1) and intercellular adhesion molecule-1 (ICAM-1) appears to be involved. CIK cells do not express the CD16 (Fc receptor) surface molecule, and therefore do not participate in antibody-dependent cellular cytotoxicity (ADCC). The CD3⁺/CD56⁺ cell subpopulation is derived from T cells. The cytotoxic effects of CIK cells against tumor cell targets are blocked by antibodies against the adhesion receptor LFA-1 and its counter receptor, ICAM-1, indicating that the adhesion molecule LFA-1 responsible for cellular interaction is necessary for CIK cell-mediated cytotoxicity. Cognate tumor cell targets could also induce BLT esterase release from CIK cells. These observations showed that the cellular interaction involving LFA-1 is important for cytolysis of target cells by the CIK cells. The mechanism of exocytosis of cytoplasmic granules leading to cytolysis of the target

cell is still unclear. Based on the previous reports, the pathway by which CIK cells can kill target cells, is probably dependent on LFA-1, which probably leads to a granule-dependent cytolysis and is usually the dominant one and accounts for CIK cell cytotoxicity against HCC target cells mediated by CIK recognition structures. Identification of the putative CIK receptors for tumor cell targets as well as other cell surface molecules involved in these cytotoxicity mechanisms will be extremely useful for further understanding of non-MHC-restricted lymphocyte cytotoxicity against tumor cells^[5,21,32, 33].

Our study showed that the human CIK cells could eradicate 84.7% of the established human hepatoma tumor in nude mice and had no toxic side effects, which is consistent with the reports described before^[5,30,31]. In addition, CIK cells have an important property of efficiently killing the resistant tumor cells with overexpression of p-glycoprotein^[33,34]. Recent studies proved that the activity of CIK cells killing tumor cells in a non-MHC restricted way could be enhanced by co-culture with dendritic cells or by using the bispecific antibody. In summary, CIK cells may have a major impact on the adoptive immunotherapeutic protocols for patients with primary HCC^[35,36].

REFERENCES

- Zoll B, Lefterova P, Csapai M, Finke S, Trojanek B, Ebert O, Micks B, Roig K, Fehlinger M, Schmidt-Wolf GD, Huhn D, Schmidt-Wolf IG. Generation of cytokine-induced killer cells using exogenous interleukin-2, -7, or -12. *Cancer Immunol Immunother* 1998; 47: 221-226
- Du QY, Wang FS, Xu DP, Liu H, Lei ZY, Liu MX, Wang YD, Chen JM and Wu CT. Cytotoxic effects of CIK against hepatocellular carcinoma cells in vitro. *Shijie Huaren Xiaohua Zazhi* 2000; 8: 863-866
- Maki G. Ex vivo purging of stem cell autografts using cytotoxic cells. *J Hematother Stem Cell Res* 2001;10:545-551
- Lu PH, Negrin RS. A novel population of expanded human CD3⁺CD56⁺ cells derived from T cells with potent in vivo anti-tumor activity in mice with potent severe combined immunodeficiency. *J Immunol* 1994; 153: 1687-1696
- Marten A, Renoth S, von Lilienfeld-Toal M, Buttgerit P, Schakowski F, Glasmacher A, Sauerbruch T, Schmidt-Wolf IG. Enhanced lytic activity of cytokine-induced killer cells against multiple myeloma cells after co-culture with idiotype-pulsed dendritic cells. *Haematologica* 2001; 86:1029-1037
- Shi Y, Yu J, Cen X, Zhu P, Ma M. Large-capacity expanded cytotoxic-induced killer cells and its cytotoxic activity. *Shengwu Yixue Gongchengxue Zazhi* 2001; 18:94-96
- Alvarnas JC, Linn YC, Hope EG, Negrin RS. Expansion of cytotoxic CD3⁺ CD56⁺ cells from peripheral blood progenitor cells of patients undergoing autologous hematopoietic cell transplantation. *Biol Blood Marrow Transplant* 2001; 7:216-222
- Hoffman DM, Gitlitz BJ, Belldgrun A, Figlin RA. Adoptive cellular therapy. *Semin Oncol* 2000; 27: 221-233
- Andreesen R, Hennemann B, Krause SW. Adoptive immunotherapy of cancer using monocyte-derived macrophages: rationale, current status, perspectives. *J Leukoc Biol* 1998; 64: 419-426
- Zhou HG, Gu GW. Study of molecular epidemiology in hepatocellular carcinoma in China. *Shijie Huaren Xiaohua Zazhi* 1998; 6:432-434
- Chen HB, Zhang JK, Huang ZL, Sun JL, Zhou YQ. Effects of cytokines on dendritic cells against human hepatoma cell line. *Shijie Huaren Xiaohua Zazhi* 1999;7:191-193
- Li MS, Yuan AL, Zhang WD, Liu SD, Lu AM, Zhou DY. Dendritic cells induce the enhancement of immune reactions against hepatocellular carcinoma cells in vitro. *Shijie Huaren Xiaohua Zazhi* 1999;7:161-163
- Ma CH, Sun WS, Cao YL, Zhang LN, Song J. Coinhibitory effect of recombinant tumor necrosis factor α and mutant interleukin-2 on H7402. *Huaren Xiaohua Zazhi* 1998;6:97-98
- He P, Tang ZY, Ye SL, Liu BB. Relationship between expression of a fetoprotein messenger RNA and some clinical parameters of human hepatocellular carcinoma. *World J Gastroenterol* 1999;5:111-115
- Lee JH, Ku JL, Park YJ, Lee KU, Kim WH, Park JG. Establishment and characterization of four human hepatocellular carcinoma cell lines containing hepatitis B virus DNA. *World J Gastroenterol* 1999;5:289-295
- Kong XB, Yang ZK, Liang LJ, Huang JF, Lin HL. Overexpression of P-glycoprotein in hepatocellular carcinoma and its clinical implication. *World J Gastroenterol* 2000; 6:134-135
- Yang DH, Zhang MQ, Du J, Xu C, Liang QM, Mao JF, Qin HR, Fan ZR. Inhibitory effect of IGF- α antisense RNA on malignant phenotype of hepatocellular carcinoma. *World J Gastroenterol* 2000;6:266-267
- Bian HJ, Chen ZN, Deng JL. Direct technetium-99m labeling of anti-hepatoma monoclonal antibody fragment: a radioimmunoconjugate for hepatocellular carcinoma imaging. *World J Gastroenterol* 2000;6:348-352

- 19 Schmidt-Wolf GD, Negrin RS, Schmidt-Wolf IG. Activated T cells and cytokine-induced CD3+CD56+ killer cells. *Ann Hematol* 1997; 74: 51-56
- 20 Finke S, Trojanek B, Lefterova P, Csipai M, Wagner E, Kircheis R, Neubauer A, Huhn D, Wittig B, Schmidt-Wolf IG. Increase of proliferation rate and enhancement of antitumor cytotoxicity of expanded human CD3⁺ CD56⁺ immunologic effector cells by receptor-mediated transfection with the interleukin-7 gene. *Gene Ther* 1998; 5: 31-39
- 21 Ren H, Xing SX, Xu HW, Song YH, Shang XZ, Zhou GS, Tian JX, Li DJ. Initial Study on proliferation of CIK cells and their antitumor activity *in vitro* and *in vivo*. *Zhongguo Zhongliu Shengwu Zhiliao Zazhi* 1999; 6: 17-21
- 22 Zoll B, Lefterova P, Ebert O, Huhn D, Von Ruecker A, Schmidt-Wolf IG. Modulation of cell surface markers on NK-like T lymphocytes by using IL-2, IL-7 or IL-12 *in vitro* stimulation. *Cytokine* 2000;12:1385-1390
- 23 Schmidt-Wolf IG, Finke S, Trojanek B, Denkena A, Lefterova P, Schwella N, Heuft HG, Prange G, Korte M, Takeya M, Dorbic T, Neubauer A, Wittig B, Huhn D. Phase I clinical study applying autologous immunological effector cells transfected with the interleukin-2 gene in patients with metastatic renal cancer, colorectal cancer and lymphoma. *Br J Cancer* 1999; 81:1009-1016
- 24 Carlens S, Gilljam M, Chambers BJ, Aschan J, Guven H, Ljunggren HG, Christensson B, Dilber MS. A new method for *in vitro* expansion of cytotoxic human CD3-CD56⁺ natural killer cells. *Hum Immunol* 2001;62:1092-1098
- 25 Hoyle C, Bangs CD, Chang P, Kamel O, Mehta B, Negrin RS. Expansion of Philadelphia chromosome-negative CD3⁺CD56⁺ cytotoxic cells from chronic myeloid leukemia patients: *in vitro* and *in vivo* efficacy in severe combined immunodeficiency disease mice. *Blood* 1998; 92: 3318-3327
- 26 Zhang JK, Chen HB, Sun JL, Zhou YQ. Effect of dendritic cells on LPAK cells induced at different times in killing hepatoma cells. *Shijie Huaren Xiaohua Zazhi* 1999;7:673-675
- 27 Xiao LF, Luo LQ, Zou Y, Huang SL. Study of the phenotype of PBLs activated by CD28/CD80 and CD2/CD58 and acting with hepatoma cells and the restricted usage of TCR V α gene subfamily. *Shijie Huaren Xiaohua Zazhi* 1999;7:1044-1046
- 28 Kakumu S, Ito S, Ishikawa T, Mita Y, Tagaya T, Fukuzawa Y, Yoshioka K. Decreased function of peripheral blood dendritic cells in patients with hepatocellular carcinoma with hepatitis B and C virus infection. *J Gastroenterol Hepatol* 2000; 15:431-436
- 29 Ninomiya T, Akbar SM, Masumoto T, Horiike N, Onji M. Dendritic cells with immature phenotype and defective function in the peripheral blood from patients with hepatocellular carcinoma. *J Hepatol* 1999;31:323-331
- 30 Flieger D, Kufer P, Beier I, Sauerbruch T, Schmidt-Wolf IG. A bispecific single-chain antibody directed against EpCAM/CD3 in combination with the cytokines interferon alpha and interleukin-2 efficiently re-targets T and CD3+CD56⁺ natural-killer-like T lymphocytes to EpCAM-expressing tumor cells. *Cancer Immunol Immunother* 2000; 49:441-448
- 31 Muller M, Scheffold C, Lefterova P, Huhn D, Neubauer A, Schmidt-Wolf IG. Potential of autologous immunologic effector cells for prediction of progression of disease in patients with chronic myelogenous leukemia. *Leuk Lymphoma* 1998; 31:335-341
- 32 Verneris MR, Kornacker M, Mailander V, Negrin RS. Resistance of *ex vivo* expanded CD3+CD56⁺ T cells to Fas-mediated apoptosis. *Cancer Immunol Immunother* 2000; 49:335-345
- 33 Schmidt-Wolf IG, Lefterova P, Johnston V, Scheffold C, Csipai M, Mehta BA, Tsuruo T, Huhn D, Negrin RS. Sensitivity of multidrug-resistant tumor cell lines to immunologic effector cells. *Cell Immunol* 1996; 169: 85-90
- 34 Wang FS, Kobayashi H, Liang KW, Ohnuma T, Holland FJ. Retrovirus-mediated transfer of anti-MDR1 ribozymes fully restores chemosensitivity of P-glycoprotein-expressing human lymphoma cells. *Human Gene Therapy* 1999; 10: 1185-1195
- 35 Toporski J, Gorczynska E, Kalwak K, Turkiewicz D, Nowakowska B, Ryczan R, Boguslawska-Jaworska J. Double haploidentical transplantation of hematopoietic progenitor cells in a boy with myelodysplastic syndrome. *Pediatr Hematol Oncol* 1999;16:257-261
- 36 Lefterova P, Marten A, Buttgerit P, Weineck S, Scheffold C, Huhn D, Schmidt-Wolf IG. Targeting of natural killer-like T immunologic effector cells against leukemia and lymphoma cells by reverse antibody-dependent cellular cytotoxicity. *J Immunother* 2000; 23:304-310

Edited by Ma JY

• LIVER CANCER •

The promoting molecular mechanism of alpha-fetoprotein on the growth of human hepatoma Bel7402 cell line

Meng-Sen Li, Ping-Feng Li, Shi-Peng He, Guo-Guang Du, Gang Li

Meng-Sen Li, Department of Biochemistry, Hainan Medical College, Haikou 571101, Hainan Province, China

Ping-Feng Li, Guo-Guang Du, Gang Li, Department of Biochemistry and Molecular Biology, Health Science Center, Peking University, Beijing 100083, China

Shi-Peng He, Department of Biophysics, Health Science Center, Peking University, Beijing 100083, China

Supported by National Natural Science Foundation of China, No. 39760077

Correspondence to: Gang Li and Ping-Feng Li, Department of Biochemistry and Molecular Biology, Health Science Center, Peking University, Beijing 100083, China. ligang55@263.net or 55ligang@163.com
Telephone: +86-10-62092454

Received 2002-01-26 Accepted 2002-03-05

Abstract

AIM: The goal of this study was to characterize the AFP receptor, its possible signal transduction pathway and its proliferative functions in human hepatoma cell line Bel 7402.

METHODS: Cell proliferation enhanced by AFP was detected by MTT assay, ^3H -thymidine incorporation and S-stage percentage of cell cycle analysis. With radioactive labeled ^{125}I -AFP for receptor binding assay; cAMP accumulation, protein kinase A activity were detected by radioactive immunosorbent assay and the change of intracellular free calcium ($[\text{Ca}^{2+}]_i$) was monitored by scanning fluorescence intensity under TCS-NT confocal microscope. The expression of oncogenes N-ras, p53, and p21^{ras} in the cultured cells *in vitro* were detected by Northern blotting and Western blotting respectively.

RESULTS: It was demonstrated that AFP enhanced the proliferation of human hepatoma Bel 7402 cell in a dose dependent fashion as shown in MTT assay, ^3H -thymidine incorporation and S-phase percentage up to 2-fold. Two subtypes of AFP receptors were identified in the cells with Kds of $1.3 \times 10^{-9} \text{ mol.L}^{-1}$ and $9.9 \times 10^{-8} \text{ mol.L}^{-1}$ respectively. Pretreatment of cells with AFP resulted in a significant increase (625%) in cAMP accumulation. The activity of protein kinase A activity were increased up to 37.5, 122.6, 73.7 and 61.2% at treatment time point 2, 6, 12 and 24 hours. The level of intracellular calcium were elevated after the treatment of alpha-fetoprotein and achieved to 204% at 4min. The results also showed that AFP (20 mg.L^{-1}) could upregulate the expression of N-ras oncogenes and p53 and p21^{ras} in Bel 7402 cells. In the later case, the alteration were 81.1%(12h) and 97.3%(12h) respectively compared with control.

CONCLUSION: These results demonstrate that AFP is a potential growth factor to promote the proliferation of human hepatoma Bel 7402 cells. Its growth-regulatory effects are mediated by its specific plasma membrane receptors coupled with its transmembrane signaling transduction through the pathway of cAMP-PKA and intracellular calcium to regulate the expression of oncogenes.

Li MS, Li PF, He SP, Du GG, Li G. The promoting molecular mechanism of alpha-fetoprotein on the growth of human hepatoma Bel7402 cell line. *World J Gastroenterol* 2002;8(3):469-475

INTRODUCTION

Alpha-fetoprotein (AFP) is an oncofetal protein normally produced in the fetal liver and yolk sac, whose higher serum level is a useful marker for hepatocellular carcinoma and yolk sac tumors. Although the physicochemical and structural properties of this 70-kDa glycoprotein have been largely documented, its pathophysiological functions were limited in *in vitro* studies. In the last decade, the growth regulatory properties of AFP have aroused interest as a result of studies involving ontogenetic and oncogenic growth in both cell culture and animal models^[1-3]. A myriad of studies has now described that AFP is capable of regulating growth in ovarian, placental, uterine, hepatic phagocyte, bone marrow, and lymphatic cells^[4] in addition to various neoplastic cells^[5]. This suggests that AFP is not merely a fetal form of albumin-like carrier protein and a marker for cancer and fetal disorders, but should rather now be considered as a potential factor associated with the regulation of growth, differentiation, regeneration, apoptosis and transformation in both ontogenetic and oncogenic growth processes. Although it is currently thought that a 62- to 67-kDa membrane protein on the surface of monocytes and phagocytes is specific for AFP binding^[6,7], the properties of the binding sites were still unknown in most tumor cell lines. Furthermore, few studies have focused on its intracellular signaling events and gene expression. The goal of this study is to characterize the AFP receptor, its possible signal transduction pathway and its proliferative functions in human hepatoma Bel 7402 cells.

MATERIALS AND METHODS

Reagents

Purified AFP was from Sigma (USA). Monoclonal antibody against AFP (anti-AFP) was prepared in this laboratory and used to block AFP. The cAMP kit and Na^[125I] were purchased from Amersham, UK. Fluo-3 AM was from BIORAD (USA). Monoclonal antibodies for p53 and p21 were purchased from MBI (USA).

Purification of human AFP Human AFP was prepared as previously described^[8]. Briefly, human cord blood AFP was precipitated by ammonium sulphate and passed through an anti-AFP affinity chromatography column. AFP-positive fractions were collected and concentrated. The purity of prepared AFP was 92.7% as determined by sodium dodecyl sulfate-polyacrylamide gel electrophoresis. The protein was stored at -80°C until use.

Effect of AFP on the cell proliferation Total 1.5×10^4 cells per well of Bel 7402 cells were plated into 96-well plates and cultured in RPMI 1640 medium supplemented with 10% fetal calf serum (FCS) at 37°C in a humidified atmosphere of 5% CO₂ for 48h. The cultures were replaced with medium without FCS for another 24h, and treated with different concentration of AFP ($1-80 \text{ mg.L}^{-1}$) for 48h. The effects of AFP on the proliferation of cells were measured by MTT assay and ^3H -Thymidine incorporation, which were performed following a regular procedure.

Effect of AFP on the cell cycle First, 3×10^4 cells per well of Bel 7402 cells were plated into 6-well plates. Culture and AFP treatment were then performed as described above. After being treated

for 24h, the cells were digested with 0.25% trypsin/0.02% EDTA and washed three times with PBS. A final density of 1×10^6 cells in 1ml was added 20 μ l (10mg.mL⁻¹) RNase (Promega USA) solution and incubated at 37°C for 30min. The effects of AFP on the cell cycle were detected with flow cytometry.

AFP receptor binding assay Bel-7402 cells were maintained in a humidified atmosphere of 5% CO₂ at 37°C in RPMI-1640 medium supplemented with 10% FCS. The cells were initially depleted of serum for 12h and then washed with cold medium. Resuspended cells were passed through a 300-mesh screen and adjusted to 1×10^6 cells per ml. ¹²⁵I-AFP was radioiodinated by the iodogen method and run through a column of Sephadex-G25 to remove free ¹²⁵I. The specific activity of ¹²⁵I-AFP was 2715 Ci per mmol and the purity of radioactivity ratio was 99.4%. Each reaction contained 7 $\times 10^5$ cells, ¹²⁵I-AFP of 5 $\times 10^4$ cpm and different concentrations of non-labeled AFP (0.25-64.5ng). The reaction was triplicated and performed at 4°C for 2h. All samples were collected onto glassfiber membrane (presaturated with 0.5% albumin) and washed three times with 15ml of PBS. The radioactivity of ¹²⁵I was detected by a γ -counter. Human serum albumin (HSA) as a non-labeled ligand was utilized for measuring IC₅₀. The parameters of binding were ed using a program of Radioligand Binding Assay of Receptors (RBA).

Extraction and measurement of cAMP The cells were adjusted to 4 $\times 10^4$ cells per ml and cultured in 24 well plates. After 24h incubation, the cells were collected and resuspended in the medium supplemented with 0.1% egg albumin and 25mmol.L⁻¹ of HEPES (pH 7.4) and 2mmol.L⁻¹ IBMX (3-methyl-1-isobutyl-xanthine) at 37°C for 15min. AFP (20mg.L⁻¹) and/or anti-AFP (40mg.L⁻¹) was added into each well respectively for 4h. Extraction of cAMP was performed according to the method described by Iwashia^[9]. In short, the supernatant was removed and replaced with 1ml of cold PBS per well. After wash, the pellet was frozen in -80°C for 30min and then 0.5ml of HCl (0.05N) was added into each well for another 30min. The samples were thawed and spun at 10000g for 5min. The supernatants were lyophilized, and the content of cAMP was measured by the radio immunoassay following the instruction of cAMP assay kit.

Determination of protein kinase A activity Total 4 $\times 10^5$ cells per well were cultured in 24-well plates for 48h, changed to fresh medium without FCS for another 24h, and then treated with either AFP (20mg.L⁻¹), anti-AFP (40mg.L⁻¹) or AFP (20mg.L⁻¹) plus anti-AFP (40mg.L⁻¹) respectively. After 2, 6, 12 and 24h treatment, the cells were washed and resuspended in 1ml PBS. The measurement of PKA activity has been described by Plet^[10]. Briefly, 40 μ l of cell extract was mixed with 160 μ l of the reaction mixture at the final concentration of 20mmol.L⁻¹ Tris-HCl (pH 7.5), 5mmol.L⁻¹ MgCl₂, 0.25g.L⁻¹ BSA, 0.5g.L⁻¹ histone, 2 $\times 10^{-7}$ mol.L⁻¹ ATP (γ -³²P ATP, 3.7 $\times 10^4$ Bq) and 8.0 μ mol.L⁻¹ cAMP at 37°C for 10min. Followed by incubation on ice for 5min, the reaction mixture was filtered through Whatmen GF/C filter, washed with 10% TCA-2% phosphoric acid and 5% TCA for 30min. The radioactivities were measured by a liquid scintillation counter, and PKA activity was expressed as pmol value of ³²P in histone catalyzed by per mg protein per min.

Determination of intracellular calcium concentration The cell suspension was dispensed into specific culture plates at a density of 2 $\times 10^4$ cells per ml and incubated at 37°C in a humidified atmosphere of 5% CO₂ for 48h. The supernatant was removed and replaced with medium without FCS for 6h, followed by washing three times with Hank's solution. The measurement of intracellular calcium concentration has been described by Tsugorka and Petti *et al*^[11,12]. Briefly, the cells were loaded with 10ml of Fluo-3AM in Hank's solution at a final concentration of 5 μ mol.L⁻¹ and incubated at 37°C

for 30min. After washing 3 times with Hank's solution, either AFP (20mg.L⁻¹) or anti-AFP (40mg.L⁻¹) was loaded into each well. The change of intracellular free calcium ([Ca²⁺]_i) was monitored by scanning fluorescence intensity under TCS-NT confocal microscopy every 10s.

RNA isolation and Northern blotting Cells were treated with either AFP (20mg.L⁻¹), anti-AFP (40mg.L⁻¹) or AFP (20mg.L⁻¹) plus anti-AFP(40mg.L⁻¹) for 24h. Total cellular RNA was isolated from cell lines with TRIzol reagent(Promega, Madison,WI, U.S.A) according to the manufacturer's protocol. RNA (10-20 μ g/lane),quantitated by absorbance at 260nm, and fractionated by eletrophoresis through a 1% formaldehyde agarose gel, and the fractionated RNA was transferred(in 20 \times SSC) to nitrocellulose membranes(Millipore corporation Bedford, MA; U.S.A), by standard procedure^[13] These membranes were hybridized with a ³²P labeled probe and washed using standard protocol. The membranes were then exposed to X-ray film at -70°C for varying periods of time.

Western blot analysis Cells were treated with either AFP (20mg.L⁻¹), anti-AFP (40mg.L⁻¹) or AFP (20mg.L⁻¹) plus anti-AFP(40mg.L⁻¹) for 24h. After three times wash, the cells in each reaction were lysed in 10 μ l of lysis buffer containing 0.2% Triton X-100, 500mmol.L⁻¹ NaCl, 500mmol.L⁻¹ sucrose, 1mmol.L⁻¹ EDTA, 0.15mmol.L⁻¹ spermine, 0.5mmol.L⁻¹ spermidine, 10mmol.L⁻¹ HEPES (pH 8.0), 200 μ mol.L⁻¹ phenylmethylsulfonyl fluoride, 2mg leupeptin.L⁻¹, 2mg pepstatin.L⁻¹, 24 IU aprotinin.ml⁻¹ and 7mmol.L⁻¹ γ -mercaptoethanol. 40 μ g proteins were subjected to sodium dodecyl sulfate-polyacrylamide gel electrophoresis (SDS-PAGE) and transferred to PVDF membrane for immunodetection. SDS- PAGE molecular weight markers (Bio-Rad) verified the correct location of the visualized bands. The membranes were blocked in 5% nonfat milk (w/v) in PBS-Tween, then probed with anti-p53 or anti-p21 and followed by secondary antibodies (goat anti-mouse Ig-alkaline phosphatase). Immunoreactive proteins were detected using color development system (NBT/BCIP).

Statistical analysis Data were analyzed by t test and expressed as mean \pm SD based on 3 or 4 independent experiments.

RESULTS

Effect of AFP on the cell proliferation

Pretreating Bel 7402 cells with AFP (1-80mg.L⁻¹) resulted in a dose-dependent increase in cell proliferation (Figure 1). The increase was about 2-fold at a dose of 80mg.L⁻¹ as compared to the control (0mg.L⁻¹). The effects of AFP (20mg.L⁻¹) on cell proliferation could be blocked by anti-AFP (40mg.L⁻¹) which was observed both in MTT assay and ³H-Thymidine incorporation (Figure 2). The increase was not observed in the HSA-treated group and non-treatment control. Flow cytometric analysis showed that AFP (20mg.L⁻¹) pretreatment increased the S phase cell population by 59.3% of Bel 7402 cells (Table 1).

Table 1 The effects of AFP on the cell cycle progression. Bel 7402 cells maintained in RPMI 1640 medium were respectively treated with either AFP (20mg.L⁻¹), anti-AFP (40mg.L⁻¹), AFP (20mg.L⁻¹) + anti-AFP (40mg.L⁻¹) or HSA (20mg.L⁻¹) for 24 hours. The effects of AFP on the cell cycle progression were analyzed by flow cytometry. The data represented the mean values of four independent experiments performed each in triplicate

Groups	G ₁ (%)	S (%)	G ₂ +M (%)
Conrtol	37.0 \pm 3.0	42.7 \pm 2.8	19.2 \pm 1.8
AFP	20.3 \pm 1.6 ^a	68.0 \pm 4.2 ^a	12.7 \pm 1.3 ^a
AFP+anti-AFP	32.0 \pm 2.1	48.8 \pm 2.51	9.2 \pm 1.3
anti-AFP	34.61 \pm 1.9	45.8 \pm 2.5	19.6 \pm 1.9
HSA	36.9 \pm 4.3	43.2 \pm 2.6	19.9 \pm 2.4

^aP<0.05 vs control group

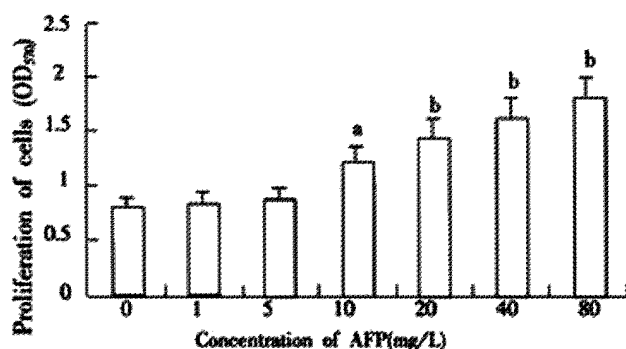


Figure 1 The effects of different concentration of AFP on the proliferation of cells. Bel 7402 cells were incubated with different concentrations of AFP for 48h and the cell proliferation was measured by MTT assay. The data represented the mean values of six independent experiments performed each in triplicate. ^a $P < 0.05$ and ^b $P < 0.01$ vs control (0mol.L⁻¹).

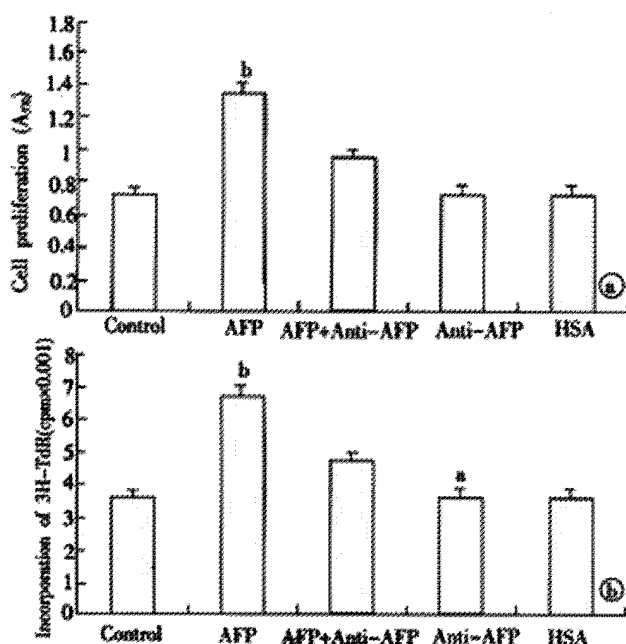


Figure 2 The blockage of anti-AFP to the effect of AFP on the proliferation of cells. A. The data of MTT assay. B. The data of ³H-TdR incorporation. The cells were respectively treated with either AFP (20mg.L⁻¹), anti-AFP (40mg.L⁻¹), AFP (20mg.L⁻¹) + anti-AFP (40mg.L⁻¹) or HSA (20mg.L⁻¹) for 48h. (MTT assay) or 18h (³H-TdR incorporation). The data represented the mean value of four independent experiments performed each in triplicate. ^a $P < 0.05$ and ^b $P < 0.01$ vs control (0mol.L⁻¹).

Distribution of AFP receptor on the membranes of Bel 7402 cells

The binding sites of AFP on the surface of the cells and K_d values were calculated based on Scatchard plot analysis of ¹²⁵I-AFP. Scatchard analysis showed that there were two classes of receptors with different affinities on Bel 7402 cells. As for Bel 7402 cells, K_{D1} with 89400 sites per cell was 1.3×10^{-9} mol.L⁻¹ and K_{D2} with 582000 sites per cell was 9.9×10^{-8} mol.L⁻¹ (Figure 3). To indicate a higher affinity of the binding sites for AFP, IC₅₀ was calculated to achieve 50% inhibition. More than two fold of HSA were needed compared with AFP (data not shown), which indicated a higher affinity for the binding sites on the surface of cells to AFP.

Effect of AFP on intracellular camp

AFP markedly elevated the concentration of cAMP up to 625% in Bel 7402 cells (Figure 4). Anti-AFP could not alter the concentrations of

cAMP when added alone, but it reversed the effect of AFP. As a control, HSA did not influence the content of cAMP.

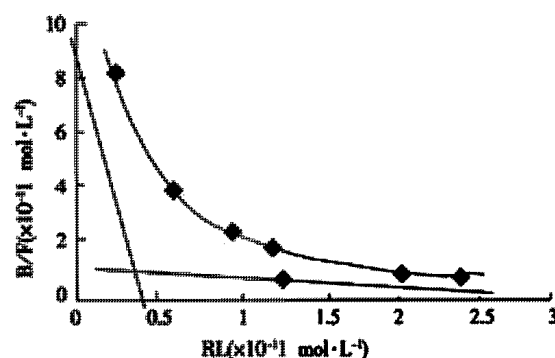


Figure 3 Scatchard analysis of ¹²⁵I-AFP binding to Bel 7402 cells. The properties of AFP receptor in Bel 7402 cells was detected with receptor binding assay and analyzed by a program of Radioligand Binding Assay of Receptor. The data were selected from three independent experiments.

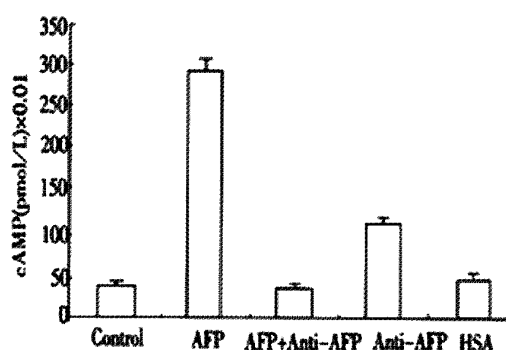


Figure 4 The effects of AFP on the cAMP concentration in cytosol of human hepatoma Bel 7402 cells. 4×10^4 cells were respectively treated with AFP (20mg.L⁻¹), anti-AFP (40mg.L⁻¹), AFP (20mg.L⁻¹) + anti-AFP (40mg.L⁻¹) or HSA (20mg.L⁻¹). The data represented the mean values of four independent experiments performed each in triplicate. ^b $P < 0.01$ vs control (0mol.L⁻¹).

Effect of AFP on PKA activity

The activities of PKA in the cytosol of Bel 7402 cells were obviously elevated after being treated with AFP (20mg.L⁻¹) for 2, 6, 12 or 24h (Figure 5). The activities of PKA were increased up to 37.5, 122.6, 73.7 and 61.2% in Bel 7402 cells at each time point. The peak value was achieved at 6h and then declined gradually, but still maintained a higher activity for several hours. Anti-AFP or HSA alone did not affect the activity of PKA in Bel 7402 cells, but anti-AFP could block the effects of AFP on the activity of PKA.

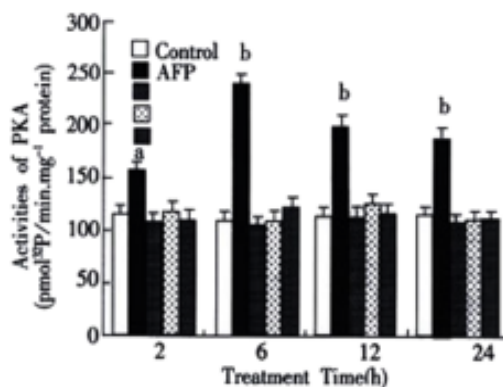


Figure 5 The effects of AFP on the activity of PKA in Bel 7402 cells. 4×10^5 cells per ml were respectively treated with either AFP (20mg.L⁻¹), anti-AFP (40mg.L⁻¹), AFP (20mg.L⁻¹) + anti-AFP (40mg.L⁻¹) or HAS (20mg.L⁻¹) for different time and the activities of intracellular PKA were then detected. The data represented the mean values of four independent experiments performed each in triplicate. ^a $P < 0.05$ and ^b $P < 0.01$ vs control (0mol.L⁻¹).

Determination of intracellular $[Ca^{2+}]_i$ release

Figures 6A1-5 and figure 6B showed that AFP increased the intracellular $[Ca^{2+}]_i$ after treatment of 2, 4, 6, 8 and 10 min in Bel 7402 cells. The

peak was achieved at treatment time 4 min (increment 204.1% in Bel 7402 cells). Anti-AFP and HSA did not change the content of $[Ca^{2+}]_i$ in either cell type. However, anti-AFP could reverse the effect of AFP.

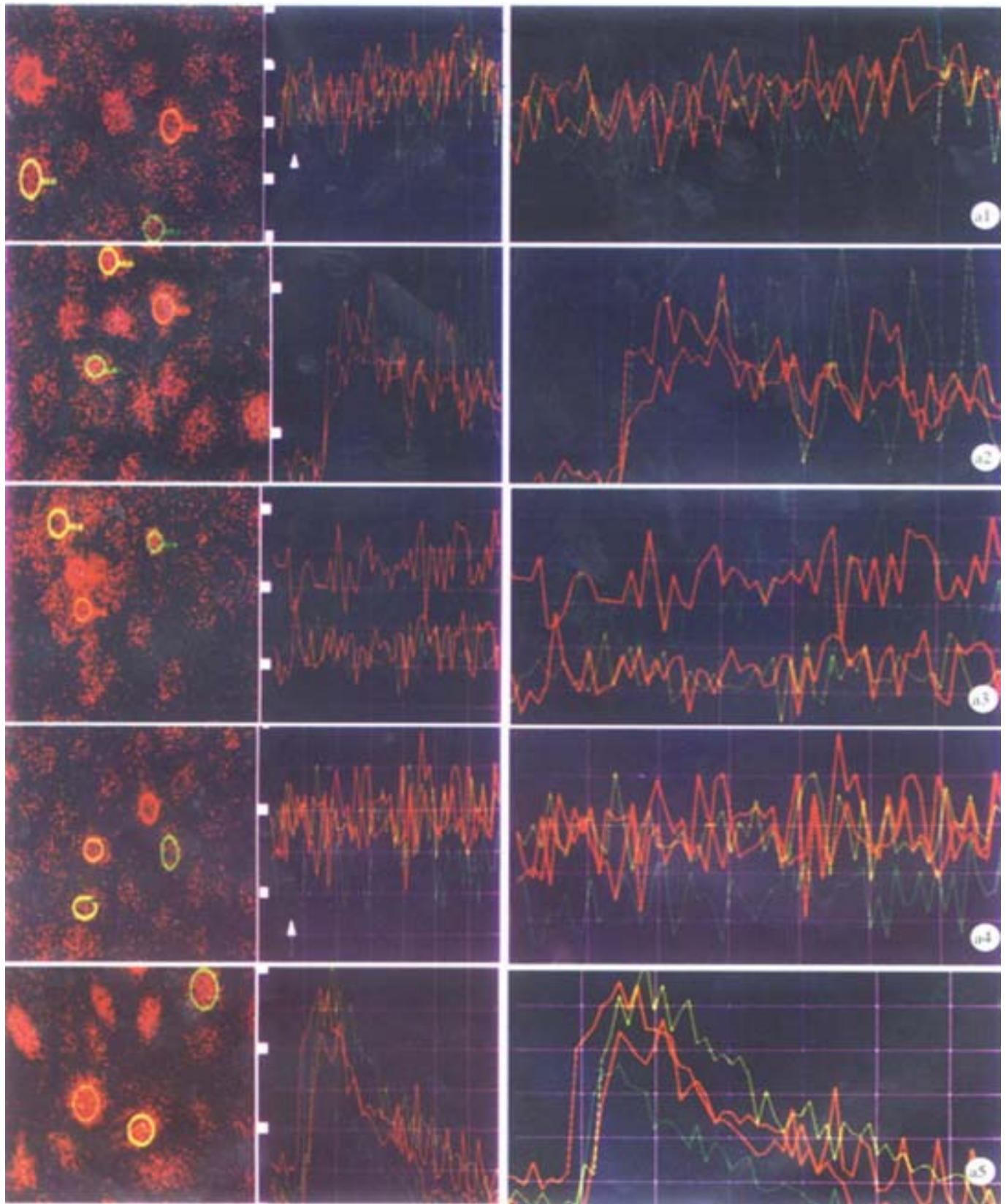


Figure 6A The change of Ca^{2+} concentration in human hepatoma Bel7402 cells was measured by confocal microscopic scanning. Cells were incubated with $5\mu\text{mol.L}^{-1}$ fluo-3/AM at 37°C for 30min and then stimulated with Hank's. (1) AFP(20mg.L^{-1}); (2) HSA(20mg.L^{-1}); (3) Anti-AFP; (40mg.L^{-1}); (4) or AFP(20mg.L^{-1}) + Anti-AFP(40mg.L^{-1}); (5) The arrow indicate the stimulated time point.

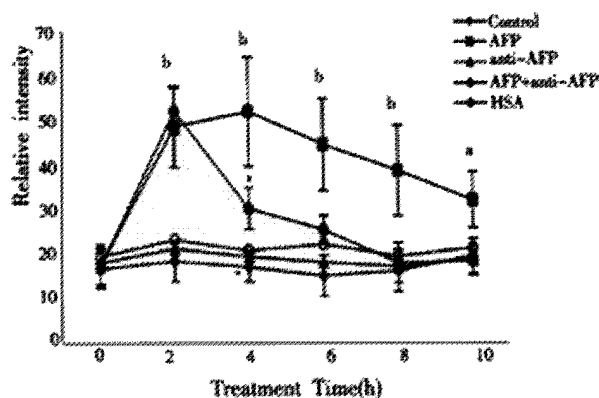


Figure 6B The graph shows the scanning results. The data represented as the mean value of 10 cells \pm s. * $P < 0.05$ and $^b P < 0.01$ vs control (0 mol.L^{-1})

Expression of p53 and p21 proteins

The results in Figure 8 demonstrated the overexpression of mutant p53 and p21 protein in AFP-treated group in Bel 7402 cells. Anti-AFP could reverse the upregulated effects of AFP on the expression of p53 and p21 genes. HSA could not influence the amount of these proteins. Each graph was selected from 3 similar results.

Expression of N-ras mRNA

The results in Figure 7 demonstrated the overexpression of N-ras mRNA in AFP-treated group in the Bel 7402 cells. Anti-AFP could reverse the upregulated effects of AFP on the expression of N-ras mRNA. HSA could not influence the mRNA amount of the oncogene. Each graph was selected from 3 similar results.

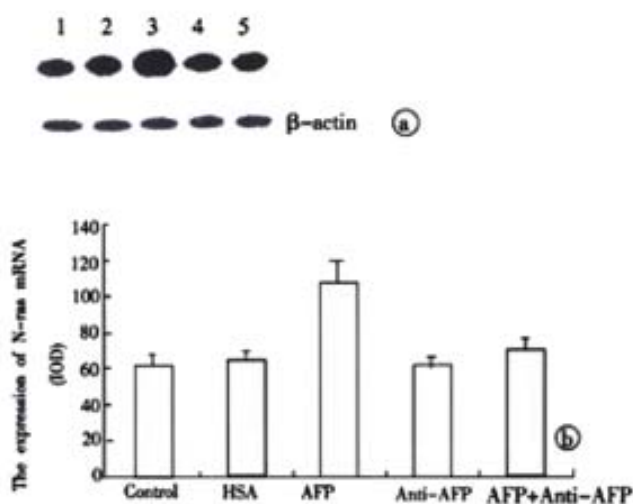


Figure 7 The effects of AFP on the expression of N-ras mRNA in Bel 7402 cells. 1×10^5 cells were respectively treated with AFP (20 mg.L^{-1}), anti-AFP (40 mg.L^{-1}), AFP (20 mg.L^{-1}) + anti-AFP (40 mg.L^{-1}) or HSA (20 mg.L^{-1}) for 12 hours and expression of N-ras mRNA was detected by Northern blot assay. Lane 1: control group; Lane 2: HSA treated group; Lane 3: AFP treated group; Lane 4: anti-AFP treated group; Lane 5: AFP plus anti-AFP treated group. The data was selected from 3 independent experiments. A: Autoradiograph of Northern blot. B: Quantitated by densitometric scanning of N-ras mRNA expression blot in Bel7402 cells (relative IOD units). The columns represent the means of triplicate determinations \pm s.

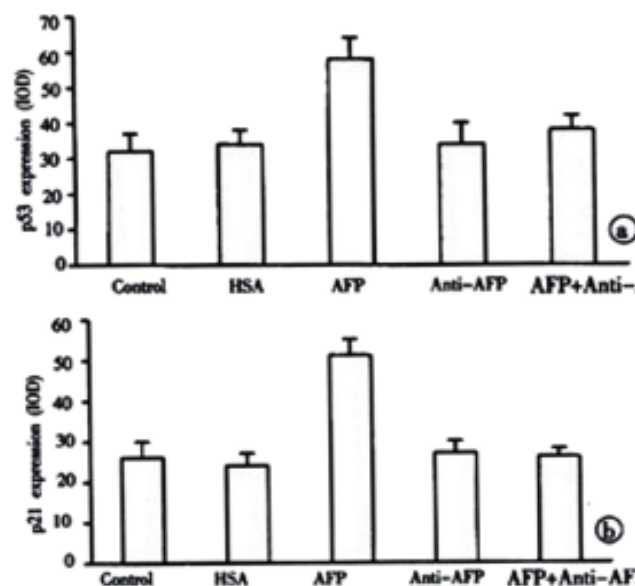
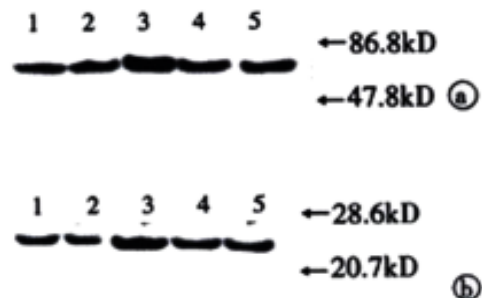


Figure 8 The effects of AFP on the expression of p53 (A) and p21 (B) proteins in Bel 7402 cells. 1×10^5 cells were respectively treated with AFP (20 mg.L^{-1}), anti-AFP (40 mg.L^{-1}), AFP (20 mg.L^{-1}) + anti-AFP (40 mg.L^{-1}) or HSA (20 mg.L^{-1}) for 24 hours and the expression of p53 and p21 protein were detected by Western blot assay. Lane 1: control group; lane 2: HSA treated group; lane 3: AFP treated group; lane 4: anti-AFP treated group; lane 5: AFP plus anti-AFP treated group. The data was selected from 3 independent experiments. A: p53; B: p21. The columns represent the means of triplicate determinations \pm s.

DISCUSSION

AFP is an onco-developmental gene product. In the adult, AFP is highly expressed during liver regeneration and hepatocarcinogenesis and used as a maker for the diagnosis of hepatocellular carcinoma^[14-16]. The regulation and activation on the expression of the AFP gene have been extensively investigated^[17-21]. Although less data indicated AFP could causes apoptosis in tumor cells^[22,23], the data from most current research demonstrate that AFP is enhancer in tumor growth. The downregulation of expression of alpha-fetoprotein is able to induce the suppression of growth of malignant hepatocyte cell^[24-26]. Although the biological role of AFP in cell growth has been reported^[27-29], the properties of the AFP receptor as well as the subsequent events after AFP binding were still undefined. Our data indicate that a specific AFP receptor does exist in a human tumor cell line, Bel 7402 cells. There were two kinds of receptors with different affinities in Bel 7402 cells ($K_D: 10^{-9}$ and $10^{-8} \text{ mol.L}^{-1}$), which was consistent with similar experiments that characterized the K_D of binding protein in monocytes in the range of 10^{-11} - $10^{-7} \text{ mol.L}^{-1}$ ^[6,30]. The AFP-binding protein possibly containing the AFP-receptor has been isolated from human

embryos and human breast cancer tissue^[31].

Based on the results of MTT assay, ³H-thymidine incorporation and flow cytometry analysis, as well as the enhanced expression of mutant p53 and p21 and expression of protooncogenes N-ras mRNA, AFP appears to be a potential growth promoting factor.

Since the albumin and AFP genes are similar in structure, they are believed to be derived from a common ancestral gene, even in the same albuminoid gene family. In all our AFP studies, none of the results showed that human serum albumin (HSA) as a control was able to alter the parameters of cell proliferation although it can non-specifically bind to the cell surface.

Little information on the effect of AFP on signal transduction was available. The present experiments demonstrated that intracellular cAMP was significantly elevated 7 fold in Bel 7402 cells. PKA activities were also increased. This indicates that a cAMP-dependent protein kinase pathway is involved in the effects of AFP on the tumor cells, even though some data from other laboratory indicated that the alteration of activity of PKC affected only liver gene expression rather than cell growth in fetal hepatocytes^[32]. Other experiments for the relationship between AFP and message has been tested^[33].

In addition, the results of intracellular calcium showed that AFP markedly increased intracellular [Ca²⁺]_i. It has been reported that Bcl-2 suppresses apoptosis by inhibiting calcium activation of the permeability transition of mitochondria^[34] and the inhibition of calcium influx was related to the suppression of lymphoma cell-line proliferation^[35]. Furthermore, a reciprocal regulation between calcium signaling and hypertrophic growth has been identified^[36]. According to these findings, a higher intracellular [Ca²⁺]_i elicited by AFP may play a role in tumorigenesis.

Although growing evidence has confirmed the effects of AFP on the growth of tumor cells, little work has focused on the subsequent events in the nucleus. The impacts of overexpression of protooncogenes N-ras, mutant p53, p21 and other genes on tumor growth have been largely documented^[37-41]. In the present experiment, mutant p53 and p21 protein were over produced under the treatment of AFP, which was consistent with similar work^[42,43]. It suggested that the mechanism by which elevated levels of mutant p53 and p21 proteins might be involved in AFP-induced oncogenesis.

The pattern inducing the hepatocarcinogenesis is multimodal^[44,45], but the effect of AFP on the growth of tumor has been confirmed. Based on our experiments, the functional mechanism of AFP on the growth of tumors may be attributed, at least in part, to receptor-mediated cAMP pathway and/or calcium signaling resulting in overexpression of certain genes. The clarification of the mechanism will provide a possibility for the gene therapy of liver tumor^[46-48]. Further investigations on the function of AFP may shed further light on the mechanism of AFP action.

ACKNOWLEDGMENT

This work was supported by National Natural Science Foundation of China (1.39760077). We wish to thank Lei Hu, M.D., PhD, Northwestern University, Chicago, USA, for critical reading of the manuscript.

REFERENCES

- Mizejewski GJ, Warner AS. Alpha-fetoprotein can regulate in the uterus of the immature and adult ovariectomized mouse. *J Reprod Fert* 1989; 85: 177-185
- Keel BA, Eddy KB, Cho S, May JV. Synergistic action of purified alpha-fetoprotein and growth factors on the proliferation of porcine granulosa cells in monolayer culture. *Endocrinology* 1991; 129: 217-225
- Wang W, Alpert E. Downregulation of phorbol 12-myristate 13-acetate-induced tumor necrosis factor-alpha and interleukin-1 beta production and gene expression in human monocytic cells by human alpha-fetoprotein. *Hepatology* 1995; 22: 921-928
- Mizejewski GJ. Alpha-fetoprotein as a biologic response modifier: relevance to domain and subdomain structure. *Proc Soc Exp Biol Med* 1997; 215: 333-362
- Dudich E, Semenkova L, Gorbatova E, Dudich I, Khromykh L, Tatulov E, Grechko G, Sukhikh G. Growth-regulative activity of human alpha-fetoprotein for different types of tumor and normal cells. *Tumour Biol* 1998; 19: 30-40
- Suzuki Y, Zeng CQ, Alpert E. Isolation and characterization of a specific alpha-fetoprotein receptor on human monocytes. *J Clin Invest* 1992; 90: 1530-1536
- Moro R, Tamaoki T, Wegmann TG, Longnecker BM, Laderoute MP. Monoclonal antibodies directed against a widespread oncofetal antigen: The alpha-fetoprotein receptor. *Tumor Biol* 1993; 14: 116-130
- Nish S, Hiral H. Purification of human, dog and rabbit α -fetoprotein by immunoabsorbents of sepharose couple with anti- human α -fetoprotein. *Biochem et Biophysica ACTA* 1972; 278: 293-298
- Iwashita S, Mitsui KI, Shoji-kasai Y. cAMP-mediated modulation of signal transduction of epidermal growth factor (EGF) receptor system in human epidermoid carcinoma A431 cells. *J Biol Chem* 1990; 265: 10702-10708
- Plet A, Evain-Brion D, Gerbaud P, Anderson WB. Retinoic acid-induced rapid loss of nuclear cyclic AMP-dependent protein kinase in teratocarcinoma cells. *Cancer Res* 1987; 47: 5831-5834
- Tsugorka A, Roise E, Blatter LA. Imaging elementary events of calcium release in skeletal cells. *Science* 1995; 269: 1723-1726
- Petti EJ, Hallett MB. Early Ca²⁺ signaling events in neutrophils detected by rapid confocal laser scanning. *Biochem J* 1995; 310: 445-448
- Sambrook J, Fritsch EF, Maniatis T. Molecular cloning: A laboratory manual, 2nd edition. *Cold spring harbor* 1989; 18:60-75
- Tu DG, Wang ST, Chang TT, Chiu NT, Yao WJ. The value of serum tissue polypeptide specific antigen in the diagnosis of hepatocellular carcinoma. *Cancer* 1999; 85: 1039-1043
- Sell S, Xu KL, Huff WE, Kabena LF, Harvery RB, Dunsford HA. Aflatoxin exposure produces serum alphafetoprotein elevations and marked oval cell proliferation in young male Pekin ducklings. *Pathology* 1998; 30: 34-39
- Yuasa T, Yoshiki T, Ogawa O, Tanaka T, Isono T, Mishina M, Higuchi K, Okada Y, Yoshida O. Detection of alpha-fetoprotein mRNA in seminoma. *J Androl* 1999; 20: 336-340
- Chen H, Egan JO, Chiu JF. Regulation and activities of alpha-fetoprotein. *Crit Rev Eukaryot Gene Expr* 1997; 7: 11-41
- Ohguchi S, Nakatsukasa H, Higashi T, Ashida K, Nouse K, Ishizaki M, Hino N, Kobayashi Y, Uematsu S, Tsuji T. Expression of alpha-fetoprotein and albumin genes in human hepatocellular carcinomas: limitations in the application of the genes for targeting human hepatocellular carcinoma in gene therapy. *Hepatology* 1998; 27: 599-607
- Ishikawa H, Nakata K, Tsuruta S, Nakao K, Kato Y, Tamaoki T, Eguchi K. Differential regulation of albumin gene expression by heparin-binding epidermal growth factor-like growth factor in alpha-fetoprotein-producing and -nonproducing human hepatoma cells. *Tumour Biol* 1999; 20: 130-138
- Abelev GI, Eraiser TL. Cellular aspects of alpha-fetoprotein reexpression in tumors. *Semin Cancer Biol* 1999; 9: 95-107
- Magge TR, Cai Y, El-Houseini ME, Locker J, Wan YJ. Retinoic acid mediates down-regulation of the alpha-fetoprotein gene through decreased expression of hepatocyte nuclear factors. *J Biol Chem* 1998; 273: 30024-30032
- Dudich I, Tokhtamysheva N, Semenkova L, Dudich E, Hellman J, Korpela T. Isolation and structural and functional characterization of two stable peptic fragments of human alpha-fetoprotein. *Biochemistry* 1999; 38: 10406-10414
- Dudich E, Semenkova L, Dudich I, Gorbatova E, Tokhtamysheva N, Tatulov E, Nikolaeva M, Sukhikh G. alpha-fetoprotein causes apoptosis in tumor cells via a pathway independent of CD95, TNFR1 and TNFR2 through activation of caspase-3-like proteases. *Eur J Biochem* 1999; 266: 750-761
- Zhang M, Gong Y, Assy N, Minuk GY. Increased GABAergic activity inhibits alpha-fetoprotein mRNA expression and the proliferative activity of the HepG2 human hepatocellular carcinoma cell line. *J Hepatol* 2000; 32:85-91
- Hamamoto R, Kamihira M, Iijima S. Growth and differentiation of cultured fetal hepatocytes isolated various developmental stages. *Biosci Biotechnol Biochem* 1999; 63: 395-401
- Gruppiso PA, Bienieki TC, Faris RA. The relationship between differentiation and proliferation in late gestation fetal rat hepatocytes. *Pediatr Res* 1999; 46: 14-19
- Wang XW, Xie H. Alpha-fetoprotein enhances the proliferation of human hepatoma cell in vitro. *Life Science* 1999; 64: 17-23
- Wang XW, Xu B. Stimulation of tumor-cell growth by alpha-fetoprotein. *Int J Cancer* 1998; 75: 596-599
- Koide N, Nishio A, Igarashi J, Kajikawa S, Adachi W, Amano J. Alpha-fetoprotein-producing gastric cancer: histochemical analysis of cell proliferation, apoptosis, and angiogenesis. *Am J Gastroenterol* 1999; 94: 1658-1663
- Torres JM, Geuskens M, Uriel J. Activated human T lymphocytes express albumin binding proteins which cross-react with alpha-fetoprotein. *Eur J*

- Cell Biol* 1992; 57: 222-228
- 31 Kanevsky VY, Pozdnyakova LP, Aksenova OA, Severin SE, Katukov VY, Severin ES. Isolation and characterization of AFP-binding proteins from tumor and fetal human tissues. *Biochem Mol Biol Int* 1997; 41: 1143-1151
 - 32 Roncero C, Ventura JJ, Sanchez A, Bois JB, Mesa ML, Thomassin H, Danan JL, Benito M, Fabregat I. Phorbol esters down-regulate alpha-fetoprotein gene expression without affecting growth in fetal hepatocytes in primary culture. *Biochim Biophys Acta* 1998; 1402: 151-164
 - 33 Benassayag C, Rigourd V, Mignot TM, Hassid J, Leroy MJ, Robert B, Civel C, Grange G, Dallot E, Tanguy J, Nunez EA, Ferre F. Does high polyunsaturated free fatty acid level at the feto-maternal interface alter steroid hormone message during pregnancy? *Prostagl Leukot Essent Fatty-Acids* 1999; 60: 393-399
 - 34 Murphy RC, Schneider E, Kinnally KW. Overexpression of Bcl-2 suppresses the calcium activation of a mitochondrial megachannel. *FEBS Lett* 2001; 497: 73-76
 - 35 Anesini C, Ferraro G, Lopez P, Borda E. Different intracellular signals coupled to the antiproliferative action of aqueous crude extract from *Larrea divaricata* Cav. and nor-dihydroguaiaretic acid on a lymphoma cell line. *Phytomedicine* 2001; 8: 1-7
 - 36 Kline R, Jiang T, Xu X, Rybin VO, Steinberg SF. Abnormal calcium and protein kinase C-epsilon signaling in hypertrophied atrial tumor myocytes (AT-1 cells). *Am J Physiol Heart Circ Physiol* 2001; 280: H2761-2769
 - 37 Kirla R, Salminen E, Huhtala S, Nuutinen J, Talve L, Haapasalo H, Kalim H. Prognostic value of the expression of tumor suppressor genes p53, p21, p16 and prb, and Ki-67 labelling in high grade astrocytomas treated with radiotherapy. *J Neurooncol* 2000; 46: 71-80
 - 38 Yuen PW, Lam KY, Choy JT, Ho WK, Wei WI. Clinicopathological significance of p53 and p21 expression in the surgical treatment of laryngeal carcinoma. *Anticancer Res* 2000; 20: 4863-4866
 - 39 Komarova EA, Christov K, Faerman AI, Gudkov AV. Different impact of p53 and p21 on the radiation response of mouse tissues. *Oncogene* 2000; 19: 1791-1798
 - 40 Kumar DD, Kubota H, Tabara H, Kotoh T, Monden N, Igarashi M, Kohno H, Nagasue N. nm23 in the primary and metastatic sites of gastric carcinoma. Relation to AFP-producing carcinoma. *Oncology* 1999; 56: 122-128
 - 41 Yamamoto H, Fujimoto J, Okamoto E, Furuyama J, Tamaoki T, Hashimoto TT. Suppression of growth of hepatocellular carcinoma by sodium butyrate *in vitro* and *in vivo*. *Int J Cancer* 1998; 76: 897-902
 - 42 Liu Z, Liu G, Zhang S. Reversing effect of dimethyl-4,4'-dimethoxy-5,6,5',6'-dimethylenedioxybiphenyl-2,2'-dicarboxylate (DDB) on the phenotypes of human hepatocarcinoma cells line. *Cancer Lett* 1996; 108: 67-72
 - 43 Mazume H, Nakata K, Hida D, Hamasaki K, Tsuruta S, Nakao K, Kato Y, Eguchi K. Effect of simvastatin, a 3-hydroxy-3-methylglutaryl coenzyme A reductase inhibitor, on alpha-fetoprotein gene expression through interaction with the ras-mediated pathway. *J Hepatol* 1999; 30: 904-910
 - 44 Feng DY, Zheng H, Tan Y, Cheng XR. Effect of phosphorylation of MAPK and Stat3 and expression of c-fos and c-jun proteins on hepatocarcinogenesis and their clinical significance. *World J Gastroenterol* 2001; 7: 33-36
 - 45 Sun BH, Zhang J, Wang BJ, Zhao XP, Wang YK, Yu ZQ, Yang DL, Hao LJ. Analysis of *in vivo* patterns of caspase 3 gene expression in primary hepatocellular carcinoma and its relationship to p21^{WAF1} expression and hepatic apoptosis. *World J Gastroenterol* 2000; 6: 356-360
 - 46 Ishikawa H, Nakata K, Mawatari F, Ueki T, Tsuruta S, Ido A, Nakao K, Kato Y, Ishii N, Eguchi K. Utilization of variant-type of human alpha-fetoprotein promoter in gene therapy targeting for hepatocellular carcinoma. *Gene Ther* 1999; 6: 465-470
 - 47 Ohguchi S, Nakatsukasa H, Higashi T, Ashida K, Nouse K, Ishizaki M, Hino N, Kobayashi Y, Uematsu S, Tsuji T. Expression of alpha-fetoprotein and albumin genes in human hepatocellular carcinomas: limitations in the application of the genes for targeting human hepatocellular carcinoma in gene therapy. *Hepatology* 1998; 27: 599-607
 - 48 Moskaleva EY, Posypanova GA, Shmyrev II, Rodina AV, Muizhnek EL, Severin ES, Katukov VY, Luzhkov YM, Severin SE. Alpha-fetoprotein-mediated targeting-a new strategy to overcome multidrug resistance of tumour cells *in vitro*. *Cell Biol Int* 1997; 21: 793-799

Edited by Pagliarini R and Zhang JZ

• LIVER CANCER •

Influence of hepatic arterial blockage on blood perfusion and VEGF, MMP-1 expression of implanted liver cancer in rats

Wei-Jian Guo, Jie Li, Wan-Long Ling, Yong-Rui Bai, Wen-Zhu Zhang, Yu-Fan Cheng, Wen-Hua Gu, Jun-Yan Zhuang

Wei-Jian Guo, Jie Li, Wan-Long Ling, Wen-Hua Gu, Jun-Yan Zhuang, Department of Oncology, Xinhua Hospital of Shanghai Second Medical University, Shanghai 200092, China
Yong-Rui Bai, Department of Radiotherapy, Xinhua Hospital of Shanghai Second Medical University, Shanghai 200092, China
Wen-Zhu Zhang, Yu-Fan Cheng, Department of Pathology, Xinhua Hospital of Shanghai Second Medical University, Shanghai 200092, China
Supported by Science and Technology Development Fund of Shanghai Municipality, No. 004119086
Correspondence to: Wei-Jian Guo, Department of Oncology, Xinhua Hospital of Shanghai Second Medical University, 1665 Kongjiang Road, Shanghai 200092, China. guoweijian1@sohu.com
Received 2001-08-09 Accepted 2001-10-22

Abstract

AIM: To investigate the influence of hepatic arterial blockage on blood perfusion of transplanted cancer in rat liver and the expression of vascular endothelial growth factor (VEGF) and matrix metalloproteinase-1 (MMP-1), and to explore the mechanisms involved in transarterial embolization (TAE)-induced metastasis of liver cancer preliminarily.

METHODS: Walker 256 carcinosarcoma was transplanted into rat liver to establish the liver cancer model. Hepatic arterial ligation (HAL) was used to block the hepatic arterial blood supply and simulate TAE. Blood perfusion of tumor in control, laparotomy control, and HAL group was analyzed by Hoechst 33342 labeling assay, the serum VEGF level was assayed by ELISA, the expression of VEGF and MMP-1 mRNA was detected by in situ hybridization.

RESULTS: Two days after HAL, the number of Hoechst 33342 labeled cells which represent the blood perfusion of tumor directly and hypoxia of tumor indirectly in HAL group decreased significantly compared with that in control group (329 ± 29 vs 384 ± 19 , $P < 0.01$). The serum VEGF level in the HAL group increased significantly as against that of the control group ($93 \text{ ng} \cdot \text{L}^{-1} \pm 44 \text{ ng} \cdot \text{L}^{-1}$ vs $55 \text{ ng} \cdot \text{L}^{-1} \pm 19 \text{ ng} \cdot \text{L}^{-1}$, $P < 0.05$). The expression of VEGF and MMP-1 mRNA in the tumor tissue of the HAL group increased significantly compared with that of the control and the laparotomy control groups ($P < 0.05$). The blood perfusion data of the tumor, represented by the number of Hoechst 33342 labeled cells, showed a good linear inverse correlation with the serum VEGF level ($r = -0.606$, $P < 0.05$) and the expression of VEGF mRNA in the tumor tissue ($r = -0.338$, $P < 0.01$).

CONCLUSION: Blockage of hepatic arterial blood supply results in decreased blood perfusion and increased expression of metastasis-associated genes VEGF and MMP-1 of transplanted liver cancer in rats. Decreased blood perfusion and hypoxia may be the major cause of up-regulated expression of VEGF.

Guo WJ, Li J, Ling WL, Bai YR, Zhang WZ, Cheng YF, Gu WH, Zhuang JY. Influence of hepatic arterial blockage on blood perfusion and VEGF, MMP-1 expression of implanted liver cancer in rats. *World J Gastroenterol* 2002;8(3):476-479

INTRODUCTION

Primary liver cancer (PLC) is one of the most common cancers in Asia. Patients with PLC usually have very poor prognoses, and the overall 5-year survival rate was not more than 5% worldwide^[1-3]. Surgery is considered as the only potential cure. However, the resection rate for PLC is only 10%-30%. Transarterial embolization (TAE) is one of the main non-surgical treatments for liver cancer in Asia via selectively blocking of the hepatic arterial blood supply of the tumor. However, a prospective controlled study showed that TAE enhanced the rate of lung metastases and accelerated metastases in patients with PLC^[4]. Other reports also showed that preoperative TAE for resectable PLC or TAE after curative resection of PLC could result in intrahepatic recurrence or extrahepatic metastasis, and a shorter survival^[5,6]. Metastases induced by TAE will undoubtedly reduce the long-term efficacy of TAE for PLC, but the mechanisms responsible for that have not been previously reported and there is no good method to inhibit metastasis.

In the present study, we have observed the influence of hepatic arterial ligation (HAL) which simulate TAE on metastasis related genes expression in Walker 256 tumor transplanted in rat liver to explore the mechanisms involved in TAE-induced metastasis of liver cancer preliminarily.

MATERIALS AND METHODS

Tumor model and treatment schedule

An implanted liver cancer model was obtained from Shanghai Medical Industry Research Institute, China. Male pathogen-free Wistar rats, weighing 100-120g, were anesthetized with pentobarbital sodium (40mg/kg). Following midline laparotomy, Walker 256 carcinosarcoma (about 1 mm^3) was implanted into one hepatic lobe of the rat. Seven days later, the rats that developed tumors were divided randomly into 3 groups: a control group without any treatment ($n=8$), a laparotomy control group ($n=4$) which underwent laparotomy only, and a HAL group ($n=8$). In the HAL group, after anesthesia and laparotomy, the proper hepatic artery was ligated by a sewing line.

Staining of perfused vessels with Hoechst 33342

The perfusion marker Hoechst 33342 (Sigma, USA) was dissolved in sterile saline immediately before use. Two days after HAL, all rats from all three groups were anesthetized and then their abdominal cavity was opened. The inferior vena cava was punctured to collect 0.5mL blood and to inject 0.2mL Hoechst 33342 (at a concentration of $6.25 \text{ g} \cdot \text{L}^{-1}$). The hepatic lobes bearing tumor were excised 1min after injection of Hoechst 33342 to prevent diffusion of Hoechst 33342 into adjacent non-perfused vascular structures. Hoechst 33342 is removed very rapidly from the circulation (half-time of 2min) and is very stable, once bound to DNA. Thus, Hoechst 33342 specifically labels the nuclei of endothelial cells and nuclei of the cells adjacent to the vessel walls, thereby delineating the perfused vessels^[7-9]. The tumors were excised and frozen in liquid nitrogen and then stored at -80°C until tumors were sectioned. Frozen sections ($5 \mu\text{m}$) were cut and Hoechst 33342 labeled cells were visualized and photographed

under a fluorescence microscope equipped with a camera with 365nm excitation and 420nm emission filters showing blue fluorescence. Four high power fields under the fluorescence microscope were photographed and Hoechst 33342 labeled cells were counted. The mean number of labeled cells reflected the blood perfusion of tumor and has been shown to be inversely related to the level of hypoxia in tumor^[7].

In situ hybridization (ISH) detection

ISH kits (Boster, China) were used to detect vascular endothelial growth factor (VEGF) and matrix metalloproteinase-1 (MMP-1) mRNA expression. Experiments were performed following the manufacturer's instructions. Briefly, frozen sections (5 μ m) were taken from the tumor and fixed with 40g·L⁻¹ polyformaldehyde in PBS (0.1mol·L⁻¹) for 30min, then digested in pepsin for 3min at 37°C. The material was prehybridized for 2h and then hybridized with Digoxin labeled probe overnight at 40°C. After hybridization, sections were washed with 2 \times SSC, 0.2 \times SSC, and then incubated with rabbit anti-Digoxin antibody, biotinylated secondary antibody IgG, SABC. Slides were stained with DAB and studied under a light microscope equipped with a camera. A positive stain should be present as intracytoplasmic. The level of mRNA expression was evaluated by two of the authors on blinded sections and was expressed as a positive staining rate.

Serum VEGF assay with ELISA

Blood samples collected from the inferior vena cava of rats were pooled, coagulated, and centrifuged at 1000 \times g for 10min. After the serum was aspirated, the VEGF level was assayed with an ELISA kit (MEGA, USA). Experiments were performed following the manufacturer's instructions.

Statistical analysis

The number of Hoechst 33342 labeled cells, the percentage of positive staining cells of ISH detection, and the serum VEGF level were expressed as mean \pm SD. The difference between mean values were compared by Student's *t* test. A *P* value less than 0.05 was considered to be statistically significant. Linear regression was used for the correlation assessment. Statistical analyses were performed using SPSS software.

RESULTS

Blood perfusion of tumor

The mean number of Hoechst 33342 labeled cells represents the blood perfusion of tumor, and indirectly represents the level of hypoxia in tumor. The lower number of labeled cells suggests an impaired blood perfusion and a higher level of hypoxia in tumor. The mean number of Hoechst 33342 labeled cells in the control, the laparotomy control, and the HAL groups were 384 \pm 19, 369 \pm 27, and 329 \pm 29, respectively. The number of labeled cells in the HAL group decreased significantly compared with that in the control and the laparotomy control groups (*P*<0.05, Table 1 and Figure 1). This suggests a decreased blood perfusion and a more serious hypoxia of tumor after HAL.

VEGF and MMP-1 mRNA expression

ISH showed both VEGF and MMP-1 mRNA expressed in the implanted tumor of control and laparotomy control groups. There was no significant difference between these two groups (*P*>0.05). The expression of VEGF and MMP-1 in the HAL group was elevated significantly compared with values in the control and the laparotomy control groups (*P*<0.05). Results of their expression in the different groups are shown in Table 1, and Figures 2 and 3.

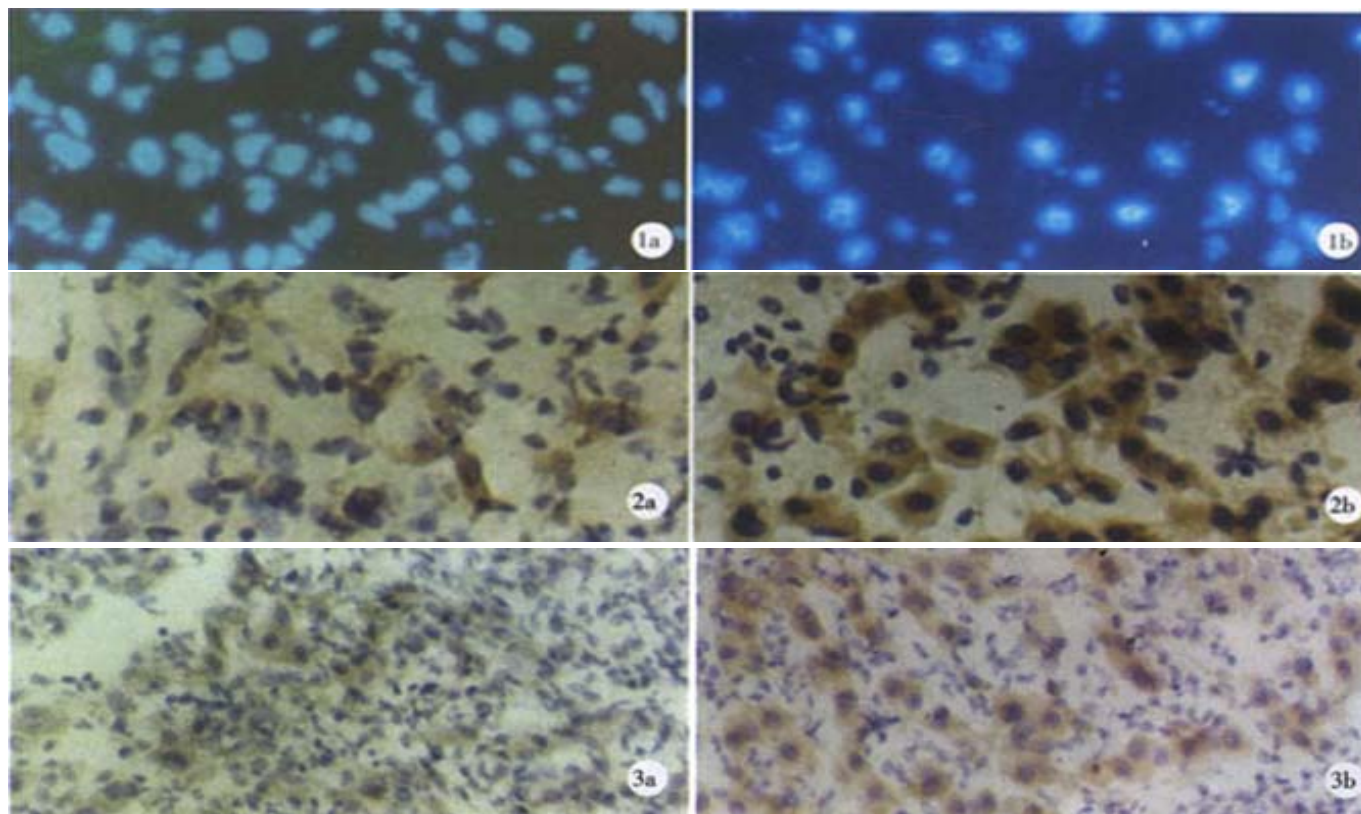


Figure 1 Hoechst 33342 labeled cells. A: Control animals; B: HAL group, decreased number of labeled cells means decreased vascular supply.
Figure 2 VEGF mRNA in hybridization. A: Low expression in tumor of control animals; B: HAL group, a higher VEGF expression.
Figure 3 MMP-1 mRNA in hybridization. A: Low expression in tumor of control animals; B: HAL group, a higher MMP-1 expression.

Serum VEGF level

The serum VEGF level was $55\text{ng}\cdot\text{L}^{-1}\pm 19\text{ng}\cdot\text{L}^{-1}$ in the control group, and $70\text{ng}\cdot\text{L}^{-1}\pm 40\text{ng}\cdot\text{L}^{-1}$ in the laparotomy control group, which was elevated slightly, but not significantly, as compared to the control group. While in the HAL group, the level of serum VEGF was $93\text{ng}\cdot\text{L}^{-1}\pm 44\text{ng}\cdot\text{L}^{-1}$, which was elevated significantly when compared with the control group ($P<0.05$, Table 1).

Table 1 Number of Hoechst labeled cells, serum VEGF, and VEGF, MMP-1 mRNA expression in tumor ($\bar{x}\pm s$)

Groups	n	Hoechst 33342 labeled cells	Serum VEGF ($\text{ng}\cdot\text{L}^{-1}$)	VEGF mRNA	MMP-1 mRNA
Control	8	384 ± 19	55 ± 19	0.34 ± 0.14	0.24 ± 0.17
Laparotomy control	4	369 ± 27	70 ± 40	0.19 ± 0.17	0.30 ± 0.02
HAL	8	$329\pm 29^{\text{bc}}$	$93\pm 44^{\text{a}}$	$0.51\pm 0.15^{\text{ad}}$	$0.47\pm 0.11^{\text{bc}}$

^a $P<0.05$, ^b $P<0.01$ vs control group; ^c $P<0.05$, ^d $P<0.01$ vs laparotomy control group.

Correlation between blood perfusion and VEGF, MMP-1 expression

There was a positive correlation between the serum VEGF level and the expression level of VEGF mRNA in tumor tissue ($r=0.206$, $P<0.05$). The blood perfusion data of tumor, represented by number of Hoechst 33342 labeled cells, showed a good linear inverse correlation with the serum VEGF level ($r=-0.606$, $P<0.05$) and VEGF mRNA expression in tumor tissue ($r=-0.338$, $P<0.01$). These data suggest that deteriorating blood perfusion and increased hypoxia of tumor correlated with a higher level of VEGF expression. There was no linear correlation between the number of Hoechst 33342 labeled cells and MMP-1 mRNA expression in tumor tissue.

DISCUSSION

TAE is an excellent debulking procedure and destroys malignant cells by selectively blocking the blood perfusion of the liver cancer. However, TAE can not block the blood supply of liver cancer and eliminate tumor cells completely, because the liver cancer receives the blood supply not only from the hepatic artery, but also from the port vein. Besides, it has been found that TAE could promote metastases of liver cancer^[4-6]. Thus, the long-term efficacy of TAE was disappointing: the 5-year survival rate was not above 20%^[10-14]. Even in several prospective randomized trials, TAE failed to improve significantly the survival of patients with PLC^[15,16]. Currently, the mechanisms involved in TAE-induced metastases of PLC are unknown. Understanding the mechanisms will facilitate the development of methods for blocking metastases and promoting long-term efficacy of TAE for treatment of liver cancer.

In recent years, many *in vitro* studies showed that hypoxia could enhance the metastatic ability of cancer cells by different mechanisms. It was reported that hypoxia stimulated carcinoma cell invasiveness by way of up-regulation of urokinase receptor expression^[17,18]. Hypoxia is the most important stimulus for the up-regulation of VEGF, one of the key cytokines for angiogenesis^[19-21]. Hypoxia could also induce the expression of other genes that promote angiogenesis and metastasis, such as basic fibroblast growth factor (bFGF) and angiogenin in tumor cells^[22-24]. Rofstad *et al*^[25] found that hypoxia could induce metastasis of human melanoma cells via VEGF-mediated angiogenesis. *In vivo* research also suggested that hypoxia may be one of the important stimuli of metastases. Hypoxia of tumor correlated with the expression of VEGF^[26-29], which was found to be correlated with metastases of the tumor and poor prognosis^[30-34]. Hypoxia in the squamous cell carcinoma of the uterine cervix with lymph node metastases was more serious than that in the carcinoma without lymph node metastases^[35]. Thus, we hypothesized that the inefficient vascular supply after TAE would result in hypoxia of some of the liver cancer cells, as it blocks the blood supply incompletely. We also suggest that hypoxia caused by

TAE may induce metastasis-associated factors, such as VEGF mediated metastases of liver cancer. It was found that the serum VEGF level in patients with liver cancer elevated 7 days after TAE therapy^[36]. In the present study, we blocked the hepatic arterial blood supply of implanted cancer in rat liver by HAL to simulate TAE therapy, and found that the blood perfusion decreased. This appears to suggest a more serious hypoxia. The expression of VEGF, both in serum and in tumor tissue, increased 2 days after the blockage of the arterial blood supply. Furthermore, we found that there was an inverse correlation between the blood perfusion of tumor and the serum VEGF level or VEGF mRNA expression in tumor tissues. These data indicate that hypoxia after HAL may be the major cause of the elevated expression of VEGF. The results of our study provide evidence for our hypothesis preliminarily. The hypoxia after TAE should be detected directly by hypoxyprobe-1^[37,38], and if the hypoxia and expression of VEGF play a direct role in the mechanisms involved in TAE-induced metastases of liver cancer requires further studies. MMP is a secreted or transmembrane protein that is capable of digesting extracellular matrix and basement membrane and was associated with invasion and metastases of human tumor, such as hepatocellular carcinoma and colon cancer^[39-46]. It has been found that hypoxia could increase cellular invasiveness by inducing the expression of MMP^[47-50]; but there was no report about the change of MMP expression in liver cancer after TAE or HAL therapy. In the present study, we found that the expression of MMP-1 in tumor tissue increased 2 days after the blockage of the arterial blood supply, but there was no linear correlation between the blood perfusion of the tumor and MMP-1 mRNA expression in tumor tissue. Which is the cause of elevated MMP-1 expression and whether it played a direct role in the mechanisms involved in TAE-induced metastasis need further study.

In conclusion, the blood perfusion of implanted liver cancer in rats decreases and the expression of metastases-associated genes VEGF and MMP-1 increases after blockage therapy of the hepatic arterial blood supply. Decreased blood supply and hypoxia may be the main cause of VEGF expression. A more complete understanding of the mechanisms involved in TAE-induced metastasis may lead to an enhancement of the long-term effects of TAE on liver cancer.

ACKNOWLEDGMENT

We would like to thank Mrs. Margaret-Hiatt Rosen, Director of Admission, the Mead School, Stamford, USA, for her correction of the English translation of the paper.

REFERENCES

- 1 Faivre J, Forman D, Esteve J, Obradovic M, Sant M. Survival of patients with primary liver cancer, pancreatic cancer and biliary tract cancer in Europe. EUROCARE Working Group. *Eur J Cancer* 1998; 34: 2184-2190
- 2 Chen J, Sankaranarayanan R, Li W. Population-based survival analysis of primary liver cancer in a high-incidence area-Qidong, China during 1972-1991. *Zhonghua Yufang Yixue Zazhi* 1997; 31: 149-152
- 3 El-Serag HB, Mason AC, Key C. Trends in survival of patients with hepatocellular carcinoma between 1977 and 1996 in the United States. *Hepatology* 2001; 33: 62-65
- 4 Lion TC, Shih SC, Kao CR. Pulmonary metastasis of hepatocellular carcinoma associated with transarterial chemoembolization. *J Hepatol* 1995; 23: 563-568
- 5 Hanazaki K, Kajikawa S, Shimozaawa N, Mihara M, Shimada K, Hiraguri M, Koide N, Adachi W, Amano J. Survival and recurrence after hepatic resection of 386 consecutive patients with hepatocellular carcinoma. *J Am Coll Surg* 2000; 191: 381-388
- 6 Lai EC, Lo CM, Fan ST, Liu CL, Wong J. Postoperative adjuvant chemotherapy after curative resection of hepatocellular carcinoma: a randomized controlled trial. *Arch Surg* 1998; 133: 183-188
- 7 Rijken PF, Bernsen HJ, Peters JP, Hodgkiss RJ, Raleigh JA, van der Kogel AJ. Spatial relationship between hypoxia and the (perfused) vascular network in a human glioma xenograft: a quantitative multi-parameter analysis. *Int J Radiat Oncol Biol Phys* 2000; 48: 571-582
- 8 Bernsen HJ, Rijken PF, Hagemeier NE, van der Kogel AJ. A quantitative analysis of vascularization and perfusion of human glioma xenografts at different implantation sites. *Microvasc Res* 1999; 57: 244-257
- 9 Durand RE, Raleigh JA. Identification of nonproliferating but viable

- hypoxic tumor cells *in vivo*. *Cancer Res* 1998; 58: 3547-3550
- 10 Ueno K, Miyazono N, Inoue H, Nishida H, Kanetsuki I, Nakajo M. Transcatheter arterial chemoembolization therapy using iodized oil for patients with unresectable hepatocellular carcinoma: evaluation of three kinds of regimens and analysis of prognostic factors. *Cancer* 2000; 88: 1574-1581
- 11 Poon RT, Ngan H, Lo CM, Liu CL, Fan ST, Wong J. Transarterial chemoembolization for inoperable hepatocellular carcinoma and postresection intrahepatic recurrence. *J Surg Oncol* 2000; 73: 109-114
- 12 Savastano S, Miotto D, Casarrubea G, Teso S, Chiesura-Corona M, Feltrin GP. Transcatheter arterial chemoembolization for hepatocellular carcinoma in patients with Child's grade A or B cirrhosis: a multivariate analysis of prognostic factors. *J Clin Gastroenterol* 1999; 28: 334-340
- 13 Sithinamsuwan P, Piratvisuth T, Tanomkiat W, Apakupakul N, Tongyoo S. Review of 336 patients with hepatocellular carcinoma at songklanagarind hospital. *World J Gastroenterol* 2000; 6: 339-343
- 14 Guo WJ, Yu EX. Evaluation of combined therapy with chemoembolization and irradiation for large hepatocellular carcinoma. *Br J Radiol* 2000; 73: 1091-1097
- 15 Pelletier G, Ducreux M, Gay F, Lubinski M, Hagege H, Dao T, Van Steenberghe W, Buffet C, Rougier P, Adler M, Pignon JP, Roche A. Treatment of unresectable hepatocellular carcinoma with lipiodol chemoembolization: a multicenter randomized trial. *Groupe CHC. J Hepatol* 1998; 29: 129-134
- 16 Bruix J, Llovet JM, Castells A, Montana X, Bru C, Ayuso MDC, Vilana R, Rodes J. Transarterial embolization versus symptomatic treatment in patients with advanced hepatocellular: results of a randomized, controlled trial in a single institution. *Hepatology* 1998; 27: 1578-1583
- 17 Graham CH, Forsdike J, Fitzgerald CJ, Macdonald-Goodfellow S. Hypoxia-mediated stimulation of carcinoma cell invasiveness via up-regulation of urokinase receptor expression. *Int J Cancer* 1999; 80: 617-623
- 18 Kroon ME, Koolwijk P, van der Vecht B, van Hinsbergh VW. Urokinase receptor expression on human microvascular endothelial cells is increased by hypoxia: implications for capillary-like tube formation in a fibrin matrix. *Blood* 2000; 96: 2775-2783
- 19 Gunningham SP, Currie MJ, Han C, Turner K, Scott PA, Robinson BA, Harris AL, Fox SB. Vascular endothelial growth factor-B and vascular endothelial growth factor-C expression in renal cell carcinomas: regulation by the von Hippel-Lindau gene and hypoxia. *Cancer Res* 2001; 61: 3206-3211
- 20 Rossler J, Breit S, Havers W, Schweigerer L. Vascular endothelial growth factor expression in human neuroblastoma: up-regulation by hypoxia. *Int J Cancer* 1999; 81: 113-117
- 21 Vasir B, Aiello LP, Yoon KH, Quickel RR, Bonner-Weir S, Weir GC. Hypoxia induces vascular endothelial growth factor gene and protein expression in cultured rat islet cells. *Diabetes* 1998; 47: 1894-1903
- 22 Le YJ, Corry PM. Hypoxia-induced bFGF gene expression is mediated through the JNK signal transduction pathway. *Mol Cell Biochem* 1999; 202: 1-8
- 23 Hartmann A, Kunz M, Kstlin S, Gillitzer R, Toksoy A, Brcker EB, Klein CE. Hypoxia-induced up-regulation of angiogenin in human malignant melanoma. *Cancer Res* 1999; 59: 1578-1583
- 24 Brahimi-Horn C, Berra E, Pouyssegur J. Hypoxia: the tumor's gateway to progression along the angiogenic pathway. *Trends Cell Biol* 2001; 11: S32-36
- 25 Rofstad EK, Danielsen T. Hypoxia-induced metastasis of human melanoma cells: involvement of vascular endothelial growth factor-mediated angiogenesis. *Br J Cancer* 1999; 80: 1697-1707
- 26 Fukumura D, Xu L, Chen Y, Gohongi T, Seed B, Jain RK. Hypoxia and acidosis independently up-regulate vascular endothelial growth factor transcription in brain tumors *in vivo*. *Cancer Res* 2001; 61: 6020-6024
- 27 Cvetkovic D, Movsas B, Dicker AP, Hanlon AL, Greenberg RE, Chapman JD, Hanks GE, Tricoli JV. Increased hypoxia correlates with increased expression of the angiogenesis marker vascular endothelial growth factor in human prostate cancer. *Urology* 2001; 57: 821-825
- 28 Dunst J, Stadler P, Becker A, Kuhn T, Lautenschlager C, Molls M, Haensgen G. Tumor hypoxia and systemic levels of vascular endothelial growth factor (VEGF) in head and neck cancers. *Strahlenther Onkol* 2001; 177: 469-473
- 29 Laderoute KR, Alarcon RM, Brody MD, Calaoagan JM, Chen EY, Knapp AM, Yun Z, Denko NC, Giaccia AJ. Opposing effects of hypoxia on expression of the angiogenic inhibitor thrombospondin 1 and the angiogenic inducer vascular endothelial growth factor. *Clin Cancer Res* 2000; 6: 2941-2950
- 30 Ishigami SI. Predictive value of vascular endothelial growth factor in metastasis and prognosis of human colonrectal cancer. *Br J Cancer* 1998; 78: 1379-1384
- 31 O-charoenrat P, Rhys-Evans P, Eccles SA. Expression of vascular endothelial growth factor family members in head and neck squamous cell carcinoma correlates with lymph node metastasis. *Cancer* 2001; 92: 556-568
- 32 Fujimoto J, Sakaguchi H, Aoki I, Khatun S, Tamaya T. Clinical implications of expression of vascular endothelial growth factor in metastatic lesions of ovarian cancers. *Br J Cancer* 2001; 85: 313-316
- 33 Niu Q, Tang ZY, Ma ZC, Qin LX, Zhang LH. Serum vascular endothelial growth factor is a potential biomarker of metastatic recurrence after curative resection of hepatocellular carcinoma. *World J Gastroenterol* 2000; 6: 565-568
- 34 Harada Y, Ogata Y, Shirouzu K. Expression of vascular endothelial growth factor and its receptor KDR (kinase domain-containing receptor)/Flk-1 (fetal liver kinase-1) as prognostic factors in human colorectal cancer. *Int J Clin Oncol* 2001; 6: 221-228
- 35 Sundfor K, Lyng H, Rofstad EK. Tumour hypoxia and vascular density as predictors of metastasis in squamous cell carcinoma of the uterine cervix. *Br J Cancer* 1998; 78: 822-827
- 36 Suzuki H, Mori M, Kawaguchi C, Adachi M, Miura S, Ishii H. Serum vascular endothelial growth factor in the course of transcatheter arterial embolization of hepatocellular carcinoma. *Int J Oncol* 1999; 14: 1087-1090
- 37 Raleigh JA, Chou SC, Bono EL, Thrall DE, Varia MA. Semiquantitative immunohistochemical analysis for hypoxia in human tumors. *Int J Radiat Oncol Biol Phys* 2001; 49: 569-574
- 38 Shabsigh A, Ghafar MA, de la Taille A, Burchardt M, Kaplan SA, Anastasiadis AG, Buttyan R. Biomarker analysis demonstrates a hypoxic environment in the castrated rat ventral prostate gland. *J Cell Biochem* 2001; 81: 437-444
- 39 Jiang YF, Yang ZH, Hu JQ. Recurrence or metastasis of HCC, predictors, early detection and experimental antiangiogenic therapy. *World J Gastroenterol* 2000; 6: 61-65
- 40 Ogata Y, Miura K, Ohkita A, Nagase H, Shirouzu K. Imbalance between matrix metalloproteinase 9 and tissue inhibitor of metalloproteinases 1 expression by tumor cells implicated in liver metastasis from colorectal carcinoma. *Kurume Med J* 2001; 48: 211-218
- 41 Ohnishi Y, Tajima S, Ishibashi A. Coordinate expression of membrane type-matrix metalloproteinases-2 and 3 (MT2-MMP and MT3-MMP) and matrix metalloproteinase-2 (MMP-2) in primary and metastatic melanoma cells. *Eur J Dermatol* 2001; 11: 420-423
- 42 Ghilardi G, Biondi ML, Mangoni J, Leviti S, DeMonti M, Guagnellini E, Scorza R. Matrix metalloproteinase-1 promoter polymorphism 1G/2G is correlated with colorectal cancer invasiveness. *Clin Cancer Res* 2001; 7: 2344-2346
- 43 O-Charoenrat P, Rhys-Evans PH, Eccles SA. Expression of matrix metalloproteinases and their inhibitors correlates with invasion and metastasis in squamous cell carcinoma of the head and neck. *Arch Otolaryngol Head Neck Surg* 2001; 127: 813-820
- 44 Nordqvist AC, Smurawa H, Mathiesen T. Expression of matrix metalloproteinases 2 and 9 in meningiomas associated with different degrees of brain invasiveness and edema. *J Neurosurg* 2001; 95: 839-844
- 45 Ye S, Dhillon S, Turner SJ, Bateman AC, Theaker JM, Pickering RM, Day I, Howell WM. Invasiveness of cutaneous malignant melanoma is influenced by matrix metalloproteinase 1 gene polymorphism. *Cancer Res* 2001; 61: 1296-1298
- 46 Yamamoto H, Itoh F, Iku S, Adachi Y, Fukushima H, Sasaki S, Mukaiya M, Hirata K, Imai K. Expression of matrix metalloproteinases and tissue inhibitors of metalloproteinases in human pancreatic adenocarcinomas: clinicopathologic and prognostic significance of matrilysin expression. *J Clin Oncol* 2001; 19: 1118-1127
- 47 Yamanaka M, Ishikawa O. Hypoxic conditions decrease the mRNA expression of proalpha1(I) and (III) collagens and increase matrix metalloproteinases-1 of dermal fibroblasts in three-dimensional cultures. *J Dermatol Sci* 2000; 24: 99-104
- 48 Canning MT, Postovit LM, Clarke SH, Graham CH. Oxygen-mediated regulation of gelatinase and tissue inhibitor of metalloproteinases-1 expression by invasive cells. *Exp Cell Res* 2001; 267: 88-94
- 49 Koong AC, Denko NC, Hudson KM, Schindler C, Swiersz L, Koch C, Evans S, Ibrahim H, Le QT, Terris DJ, Giaccia AJ. Candidate genes for the hypoxic tumor phenotype. *Cancer Res* 2000; 60: 883-887
- 50 Himelstein BP, Koch CJ. Studies of type IV collagenase regulation by hypoxia. *Cancer Lett* 1998; 124: 127-133

• LIVER CANCER •

The point mutation of p53 gene exon7 in hepatocellular carcinoma from Anhui Province, a non HCC prevalent area in China

Hu Liu, Yuan Wang, Qing Zhou, Shu-Yu Gui, Xu Li

Hu Liu, Yuan Wang, Qing Zhou, Laboratory of Molecular Biology and Department of Biochemistry, Anhui Medical University, Hefe 230032i, Anhui Province, China

Shu-Yu Gui, Department of Respiratory Disease, the First Affiliated Hospital of Anhui Medical University, Hefe 230022, Anhui Province, China

Xu Li, Department of Infectious Disease, the First Affiliated Hospital of Anhui Medical University, Hefe 230022, Anhui Province, China

Supported by the Natural Science Foundation of Anhui Province, No. 99044312(WY) and No.9741006(LX) and Natural Science Foundation of Anhui Educational Commission, No.JL-97-077(WY).

Correspondence to: Yuan Wang, Laboratory of Molecular Biology, Anhui Medical University, Hefe 230032, Anhui Province, China. wangyuan@mail.hf.ah.cn

Telephone: +86-551-5161140

Received 2001-12-20 Accepted 2002-01-24

Abstract

AIM: In hepatocellular carcinoma (HCC) prevalent areas of China, the point mutation of p53 exon7 is highly correlated with Hepatitis B virus(HBV) infection and aflatoxin B intake. While in non-HCC-prevalent areas of China, these factors are not so important in the etiology of HCC. Therefore, the point mutation of p53 exon7 may also be different than that in HCC-prevalent areas of China. The aim of this study is to investigate the status and carcinogenic role of the point mutation of p53 gene exon7 in hepatocellular carcinoma from Anhui Province, a non-HCC-prevalent area in China.

METHODS: PCR,PCR-SSCP and PCR-RFLP were applied to analyze the homozygous deletion and point mutation of p53 exon7 in HCC samples from Anhui, which were confirmed by DNA sequencing and Genbank comparison.

RESULTS: In the 38 samples of hepatocellular carcinoma, no homozygous deletion of p53 exon7 was detected and point mutations of p53 exon7 were found in 4 cases, which were found to be heterozygous mutation of codon 249 with a mutation rate of 10.53%(4/38). The third base mutation(GiúT) of p53 codon 249 was found by DNA sequencing and Genbank comparison.

CONCLUSION: The incidence of point mutation of p53 codon 249 is lower in hepatocellular carcinoma and the heterozygous mutation of p53 exon7 found in these patients only indicate that they have genetic susceptibility to HCC. p53 codon 249 is a hotspot of p53 exon7 point mutation, suggesting that the point mutation of p53 exon 7 may not play a major role in the carcinogenesis of HCC in Anhui Province, a non-HCC-prevalent area in China.

Liu H, Wang Y, Zhou Q, Gui SY, Li X. The point mutation of p53 gene exon7 in hepatocellular carcinoma from Anhui Province, a non HCC prevalent area in China. *World J Gastroenterol* 2002;8(3):480-482

INTRODUCTION

Hepatocellular carcinoma is one of the most common cancers in the world. Abnormalities of p53 are the most frequent genetic alterations in human cancers, and the role and mechanism of p53 gene mutations have been well studied in many types of cancer^[1-3]. Genetic analysis of 26 HCC samples from North America and Europe revealed a high incidence of an AGG→AGT transversional changes in codon 249 of the p53 gene; and recently exon7 has been proven a hotspot of p53 gene mutation^[4-6]. Zhang *et al*^[4] reported the high relationship between HBVx gene and codon 249 mutation of the p53 gene in HCC-prevalence areas in China. Our previous studies have also indicated that hepatitis B virus infection is an important risk factor for HCC^[7]. These data indicate that p53 mutations generally occur in the process of HCC carcinogenesis in HCC-prevalent area in China. However, further mutation analyses will be necessary to clarify the status of p53 mutations for HCC in non-HCC-prevalent areas in China.

In this study, we analyzed p53 exon 7 point mutation in HCCs from non-HCC-prevalent areas in China using the polymerase chain reaction(PCR), PCR-single-strand conformational polymorphism (PCR-SSCP), PCR-restriction fragment length polymorphism (PCR-RFLP) and DNA sequencing analysis.

MATERIALS AND METHODS

Specimens

The surgical specimens of HCC were collected from the First Affiliated Hospital of Anhui Medical University, which were confirmed by pathological diagnosis and stored at -80°C. The patients were born in and permanent residents of different places of the Anhui Province, China.

PCR of p53 exon7

DNA was extracted from tissues with standard proteinase K-phenol/chloroform methods^[9]. The primers for p53 gene exon7 amplification were designed according to the sequence of p53 exon7 published^[4,5]. 3'primer(GW-XI-1C): 5'CTT GCC ACA GGT CTC CCC AA,5'primer (GW-XI-1D): 5' TGT GCA GGG TGG CAA GTG GC; CDK4 as a control, 3'primer(GW-IV-1K): 5'GGA GGT CGG TAC CAG AGT G,5'primer(GW-IV-1J): 5'CAT GTA GAC CAG GAC AGG. Into 100ng of DNA template of each sample was added PCR reaction solution (10mmol/L Tris, 50mmol/L KCl, 2mmol/L MgCl₂, 0.001% Gelatin, 200mmol/L dNTPs, 6% DMSO and 0.5mmol/L primers). Hotstart was performed: 97°C 5min; chilled on ice at once. 0.9U of Taq polymerase was added, which was diluted with 1×PCR buffer for each sample. Ran PCR: 94°C 30s, 60°C 30s, 72°C 30s, 35 cycles in all and checked with 2% agarose gel electrophoresis stained with ethidium bromide. The result of homozygous deletion should be the one with no specific band of p53 exon7 while its counterpart of CDK4 appeared.

PCR-SSCP of p53 exon7^[1]

8μl of PCR products were aspirated, into which was added equal volumes of deionized formamide and 4μl of DNA loading buffer (0.25% bromophenol blue, 0.25% xylene cyanol FF, 30% glycerol).

They were mixed well, boiled for 5min, and then chilled on ice for 3min. The samples (20 μ l in volume) were loaded into separate wells. Samples were run in an 8% non-denaturing polyacrylamide gel at 80V for 5 hrs. The gel was taken off from the electrophoresis apparatus and readied for silver staining. The gel was submerged in 5% ethanol for 5min; 3min in 1% HNO₃; 20min in 0.012mol·L⁻¹ AgNO₃; washed with dd-H₂O for about 10 sec; developed with 0.28mol·L⁻¹ Na₂CO₃; fixed with 10% acetic acid; and finally washed with dd-H₂O. When the bands appeared, photos were taken and the gel was dried with Slab Gel Dryer or wrapped with a membrane and air dried for several days. Na₂CO₃ was changed 2-4 times when the developing solution turned black.

Restrictive endonuclease digestion of p53 exon7 and Restrictive enzyme mapping

Into each restrictive endonuclease system was added 2 μ l of 10 \times Buffer C, 2 μ l of DTT(1%), 2 μ l of BSA(1%) and 0.25 μ l of HaeIII(20U· μ l⁻¹). The total volume was brought up to 20 μ l with PCR products. They were incubated at 37°C for 3hrs and checked with an 8% non-denaturation polyacrylamide gel, electrophoresed at 40V for 4hrs and developed with silver staining^[8] as described above.

DNA sequencing of PCR products

The sample of p53 exon7 mutation was confirmed by PCR-SSCP and RFLP and PCR products of p53 exon7 were sent the to Bioasia Biotechnololy Company, Shanghai, China for DNA sequencing with ABI 377 automatic DNA sequencer.

RESULTS

PCR of p53 exon7

With 100ng of genomic DNA extracted from surgical HCC tissue as template, p53 exon7 and CDK4 genes were amplified with different specific primers in separate tubes. The products were checked with 2% agarose gel electrophoresis. The results showed that the products amplified with each pair of specific pairs were of the same length with that reported in the literature(Figure 1). No homozygous deletion of p53 exon7 was found in any HCC surgical sample.



Figure 1 Agarose gel electrophoresis of PCR products of p53 exon7. A: 1-6. PCR products of p53 exon7 amplified from HCC genomic DNA 710bp DNA ladder; B: 1-6. PCR products of CDK4 gene amplified from HCC genomic DNA as control

PCR-SSCP of p53 exon7

Point mutations of p53 exon7 were found in 4 cases out of the 38 samples of HCC examined. No.1, 6 and 9 sample had point mutations of p53 exon7 (Figure 2).

PCR-RFLP of the codon 249 of p53 exon7

With PCR-RFLP, we found that 4 samples have heterozygous point mutation of p53 codon 249, which has a band of 150bp in addition to wild type bands(40, 60, and 90bp) as shown by agarose/EB gel electrophoresis(Figure 3). However, no homozygous point mutation was found among these samples, which would have had bands of 40bp and 150bp. We found that those samples which have point mutation of p53 codon 249 was the same samples that were found to have point mutation of p53 exon 7 by PCR-SSCP.

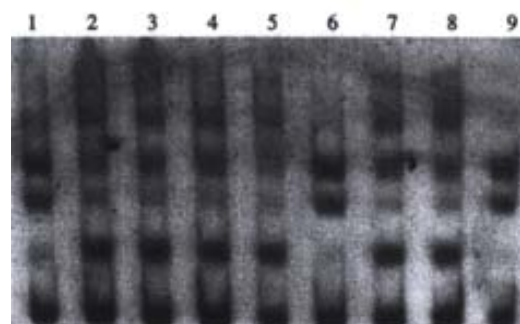


Figure 2 PCR-SSCP of p53 exon7 Samples of 1,6,9 have point mutations of p53 exon7 Samples of 2,3,4,5,7,8 don't have point mutations of p53 exon7

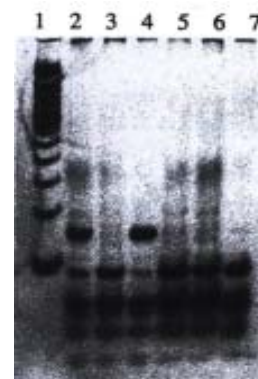


Figure 3 PCR-RFLP of p53 codon249. 1. 100bp DNA ladder; 2 and 4: heterozygous point mutation of p53 codon249; 3, 5, 6 and 7: p53 Exon7 wild type.

DNA sequencing

One sample that has been found by PCR-SSCP to have point mutation of p53 exon7 was randomly chosen for DNA sequencing. The DNA sequencing result is shown in the following graph. The sequence was compared with that published by the Genbank (gbAF136270.1 HOMOTSP1), which shows that a point mutation exists in p53 codon 249 with ggAc taken place of ggCc (Figure 4,5).

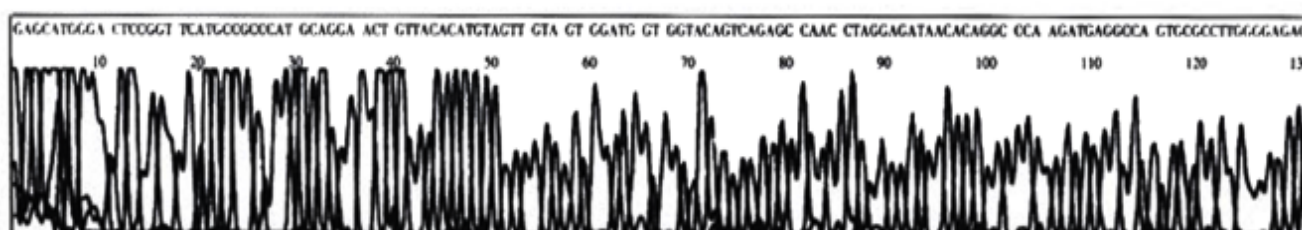


Figure 4 Sequencing of p53 exon 7 PCR product

• LIVER CANCER •

Effect of Nimesulide on proliferation and apoptosis of human hepatoma SMMC-7721 cells

Geng Tian, Jie-Ping Yu, He-Sheng Luo, Bao-Ping Yu, Hui Yue, Jian-Ying Li, Qiao Mei

Geng Tian, Jie-Ping Yu, He-Sheng Luo, Bao-Ping Yu, Hui Yue, Jian-Ying Li, Qiao Mei, Gastroenterology department, Renmin hospital of Wuhan university, Wuhan 430060, Hubei Province, China

Correspondence to: Jie-Ping Yu, Gastroenterology department, Renmin hospital of Wuhan university, 238Jie-fang Road, Wuhan 430060, Hubei Province, China. tg3030330@sina.com

Telephone: +86-27-88077184

Received 2001-11-15 Accepted 2002-01-15

Abstract

AIM: Cyclooxygenase-2 (COX-2) has been suggested to be associated with carcinogenesis. We sought to investigate the effect of the selective COX-2 inhibitor, Nimesulide on proliferation and apoptosis of SMMC-7721 human hepatoma cells.

METHODS: This study was carried out on the culture of hepatic carcinoma SMMC-7721 cell line. Various concentrations of Nimesulide (0, 200 μ mol/L, 300 μ mol/L, 400 μ mol/L) were added and incubated. Cell proliferation was detected with MTT colorimetric assay, cell apoptosis by electron microscopy, flow cytometry and TUNEL.

RESULTS: Nimesulide could significantly inhibit SMMC-7721 cells proliferation dose-dependent and in a dependent manner compared with that of the control group. The duration lowest inhibition rate produced by Nimesulide in SMMC-7721 cells was 19.06%, the highest inhibition rate was 58.49%. After incubation with Nimesulide for 72h, the most highest apoptosis rate and apoptosis index of SMMC-7721 cells comparing with those of the control were $21.20\% \pm 1.62\%$ vs $2.24\% \pm 0.26\%$ and 21.23 ± 1.78 vs 2.01 ± 0.23 ($P < 0.05$).

CONCLUSION: The selective COX-2 inhibitor, Nimesulide can inhibit the proliferation of SMMC-7721 cells and increase apoptosis rate and apoptosis index of SMMC-7721 cells. The apoptosis rate and the apoptosis index are dose-dependent. Under electron microscope SMMC-7721 cells incubated with 300 μ mol and 400 μ mol Nimesulide show apoptotic characteristics. With the clarification of the mechanism of selective COX-2 inhibitors, These COX-2 selective inhibitors can become the choice of prevention and treatment of cancers.

Tian G, Yu JP, Luo HS, Yu BP, Yue H, Li JY, Mei Q. Effect of Nimesulide on proliferation and apoptosis of human hepatoma SMMC-7721 cells. *World J Gastroenterol* 2002;8(3):483-487

INTRODUCTION

Hepatic carcinoma was one of most common malignant tumors in China. Its death rate was the third among all cancers, second to gastric carcinoma and lung carcinoma. Although there is a progress in diagnosis and treatment of hepatic carcinoma, its prognosis is still poor. Investigating its pathogenesis and finding new diagnostic and treatment methods is important. Recent epidemiological studies indicate an inverse relationship between the risk of colorectal cancer

and intake of NSAIDs. NSAIDs could reduce the incidence of gastric carcinoma and pancreatic carcinoma. It could inhibit tumor cells proliferation and induce apoptosis^[1-4]. Cyclooxygenases (COXS) are key enzymes in the conversion of arachidonic acid to prostaglandins and other eicosanoids. Recently two isoforms of the enzyme have been identified. COX-1 is constitutively expressed in a number of cell types, whereas the isoform designated COX-2 is inducible by a variety of factors, as cytokines, growth factors, and tumor promoters. Some studies have suggested that COX-2, but not COX-1, was involved in colon carcinogenesis and might thus be the target of chemopreventive effect by the COX inhibitor, nonsteroidal anti-inflammatory drugs. The effects of COX-2 on inflammation, precancerous conditions and cancers have been delineated^[42-47]. To date the effects of Nimesulide on the growth and apoptosis of human hepatoma cell line SMMC-7721 in vitro have not been analyzed, and that is the aim of this study.

MATERIALS AND METHODS

RPMI 1640 medium is a product of CIBCO; Nimesulide and MTT were from Sigma; In situ cell death detection kit was from Boehringer Mannheim, Germany; 96-well plates were from Costar.

Cell lines and culture

Human hepatoma SMMC-7721 cells were obtained from the Wuhan University Center for type culture collection. The cells were grown as monolayers in RPMI1640 medium supplemented with 10% fetal calf serum (FCS, Gibco) and incubated at 37°C in the humidified incubator with 5% CO₂ in air.

Assay of cell proliferation

The SMMC-7721 cells were seeded at 5×10^4 /ml density in 96-well plates 200 μ l cell suspension per well. Each group had four wells with a non-treated group as control. When the cells anchored to the plates, various concentrations (0, 200 μ mol/L, 300 μ mol/L, 400 μ mol/L) of Nimesulide were added and the slides were incubated at 37°C, 5% CO₂ for 5 days. In order to maintain Nimesulide concentrations, we changed the culture medium (included various concentrations of Nimesulide) every day. When the cells described above were cultured for 48h, 72h, 96h, 120h, 0.5% MTT 20 μ l was added to each well and cultured for another 4h. The supernatant was discarded and dimethyl sulfoxide (DMSO) 200 μ l added. When the crystals were dissolved, the optical density (OD) value of the slides was read on an enzyme-labeled Minireader II at 492nm. Cellular proliferation inhibition rate (CPIR) was calculated using the following equation: $CPIR = (1 - \text{average OD value of experimental group} / \text{average OD value of control group}) \times 100\%$

Electron microscopic observation

The SMMC-7721 cells were seeded in culture flasks. Four culture bottles were divided into normal group and control group. When the cells were anchored to the plates, various concentrations (0, 200 μ mol/L, 300 μ mol/L, 400 μ mol/L) of Nimesulide were added and the cells incubated at 37°C, 5% CO₂ for 3 days. Then hepatoma cells were

digested by 0.25% trypsinase and collected. After rinsing with PBS, the cells were fixed with 2.5% glutaraldehyde for 30min and washed with PBS. After routine embedding and sectioning, the cells were observed by Hitachi H-600 electronic microscope.

Flow cytometric analysis

The SMMC-7721 cells were seeded in culture flasks. The culture bottles were divided into normal and three control groups. Each group had three culture bottles. When the cells were anchored to the plates, various concentrations (0,200 μ mol/L,300 μ mol/L,400 μ mol/L) of Nimesulide were added and the cells incubated at 37°C, 5% CO₂ for 3 days. Then each group of cells were washed with PBS, trypsinized and fixed with 70% ethanol at -20°C for 30 minutes. Fixed cells were incubated with IP/Rnase solution for 15 minutes and 10⁶ cells of each culture bottle were harvested and analyzed with FACScan Becton Dickeyson Flow Cytometer.

In situ apoptotic cell death detection by TUNEL

A TUNEL kit (Boehringer Mannheim, IN) was used to detect DNA fragmentation, the characteristic of apoptotic cell death. The SMMC-7721 cells were seeded in culture flasks. Culture bottles were divided into normal and three control groups. Each group had three culture bottles. When the cells were anchored to the plates, various concentrations (0,200 μ mol/L,300 μ mol/L,400 μ mol/L) of Nimesulide were added and the cells incubated at 37°C, 5% CO₂ for 3 days. In order to maintain Nimesulide concentrations, we changed the culture medium (including various concentrations of Nimesulide) every day. After having been cultured for 3 days, each culture bottle cells were scraped and centrifuged 800r/min for 5 minutes. Then the deposited cells were smeared and air-dried. Following the manufacturer's directions, smears were incubated with the TUNEL reaction mixture for 60min at 37°C and then with converter-POD for 30min. The DAB-substrate solution was added to the smears and kept at room temperature until positive signal appeared. Then they were dried and analyzed under light microscope.

Under light microscope, the TUNEL positive nuclei were stained brown. Selecting 5 fields randomly (the number of cells in each field >1000).

Apoptosis index (AI)=(number of apoptotic cells/ the number of cells in each field) ×100%.

Statistical analysis

Statistical analysis was performed using the student's t test and analysis of variance. $P<0.05$ was considered significant.

RESULTS

Effect of Nimesulide in various concentrations on the growth of SMMC-7721

We analyzed the effects of Nimesulide on cell proliferation in cultured human hepatoma cell line SMMC-7721 after 5 days of treatment. Nimesulide, a selective COX inhibitor, produced a dose-dependent inhibition of cells growth (Table 1 and Figure 1). The lowest inhibition rate produced by Nimesulide in SMMC-7721 cells was 19.06%, the highest being 58.49%.

Morphology observation

Under the electron microscope, SMMC-7721 cells exhibited characteristics of apoptosis including plasma membrane blebbing, cytoplasmic condensation, pyknotic nuclei, condensed chromatin and apoptotic bodies. Compared with control groups, 300 μ mol/L and 400 μ mol/L groups cells had many more cells with apoptotic characteristics (Figure 2).

Table 1 Inhibition effect of Nimesulide on proliferation and growth in hepatic carcinoma cell line SMMC-7721

Nimesulide Concentrations (μ mol/L)	OD Value			
	the 2 nd day	the 3 rd day	the 4 th day	the 5 th day
0	1.039±0.066	1.516±0.117	2.142±0.072	2.467±0.080
200	0.841±0.027 ^a	1.109±0.231 ^a	1.416±0.080 ^a	1.341±0.021 ^a
300	0.796±0.019 ^a	1.002±0.274 ^a	1.101±0.028 ^a	1.243±0.168 ^a
400	0.581±0.164 ^a	0.825±0.016 ^a	0.943±0.032 ^a	1.024±0.026 ^a

^a $P<0.05$ vs control group

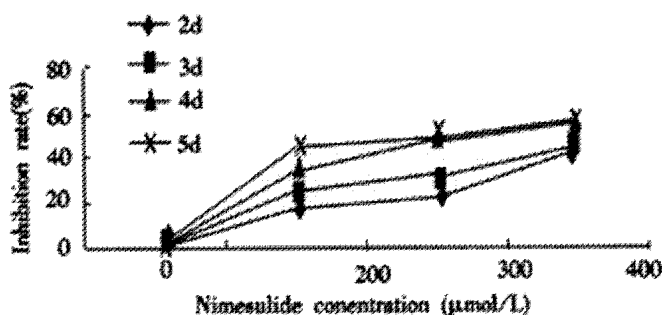


Figure 1 Inhibition rate of Nimesulide on proliferation of SMMC-7721 cells. Cells were incubated with 200 μ mol/L,300 μ mol/L,400 μ mol/L Nimesulide for 2d,3d,4d,5d respectively.



Figure 2 Transmission electron micrograph of SMMC-7721 cells treated with Nimesulide at the concentration of 300 μ mol/L for 72h. The picture showed early change of apoptosis, the nuclear chromatin condensation.

Flow-cytometry analysis of cell apoptosis

The peak value appearing before the G₁ peak is called apoptotic peak. As shown in Figure 3 and Table 2, the apoptotic peak and rate increased with increasing concentrations of Nimesulide. Furthermore, Nimesulide induced cells apoptosis in a dose and time-dependent manner ($P<0.01$).

Table 2 Apoptosis rate of SMMC-7721 cells induced by Nimesulide

Nimesulide concentration (μ mol/L)	Apoptosis rate (%)
0	2.24±0.26
200	7.42±0.43 ^b
300	9.84±1.54 ^b
400	21.20±1.62 ^b

^b $P<0.01$ vs control group

Analysis of apoptosis by TUNEL

As shown in Figure 4 and Table 3, the apoptotic index increased with increase of Nimesulide concentrations which what appeared to be dose-dependent relationship in the alone groups ($P<0.05$).

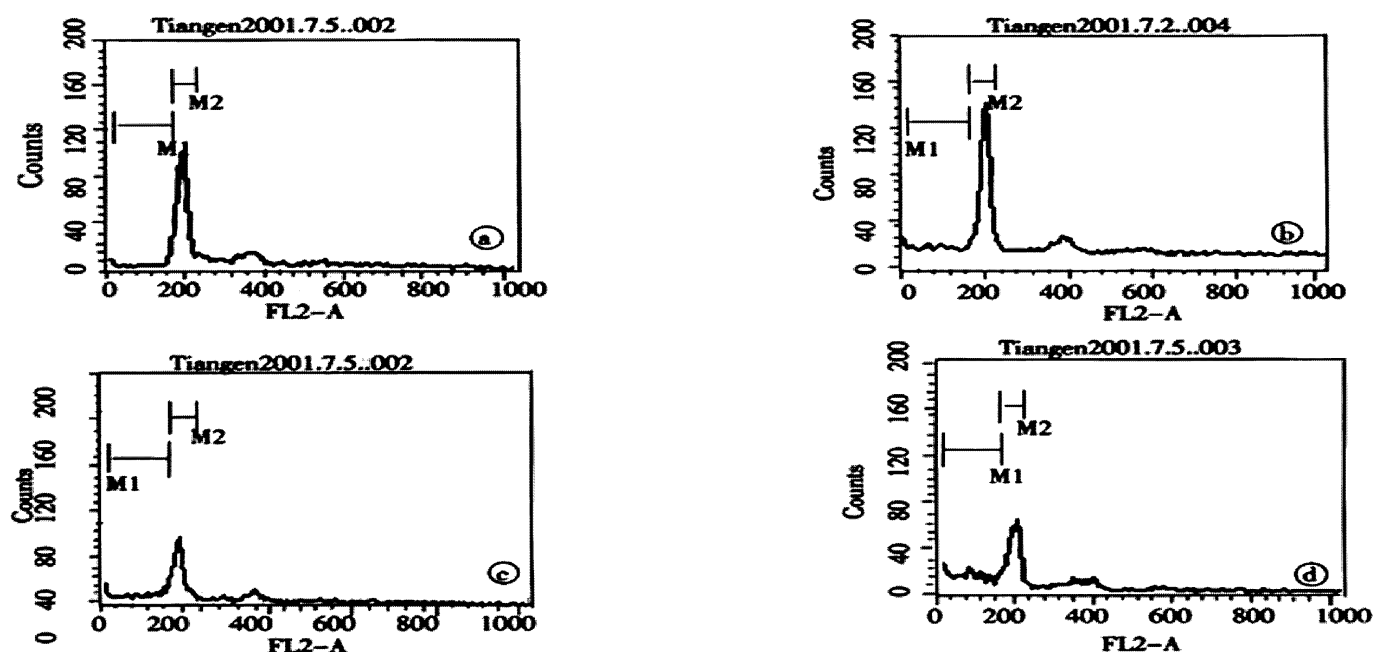


Figure 3 Cell apoptosis was determined by flow-cytometry, SMMC-7721 cells were treated with Nimesulide at various concentrations (0, 200, 300, 400 $\mu\text{mol/L}$ respectively A to D).

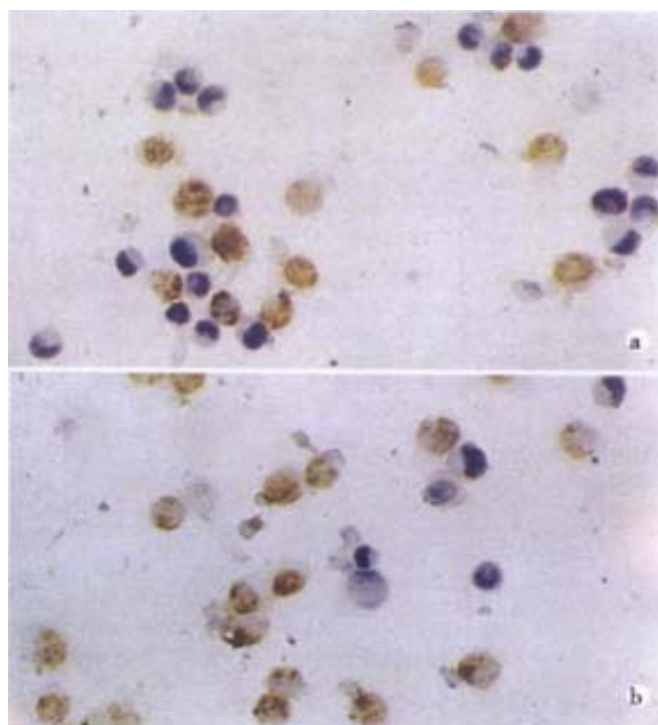


Figure 4 TUNEL stain showed SMMC-7721 cells apoptosis. SMMC-7721 cells were treated with Nimesulide at various concentrations (300, 400 $\mu\text{mol/L}$ A and B).

Table 3 Apoptosis index of SMMC-7721 cells induced by Nimesulide

Nimesulide concentration ($\mu\text{mol/L}$)	Apoptosis index (%)
0	2.016 \pm 0.23
200	7.64 \pm 0.34 ^a
300	10.14 \pm 1.42 ^a
400	21.23 \pm 1.78 ^a

^a $P < 0.05$ vs control group

DISCUSSION

It had been shown that selective COX-2 inhibitors inhibited tumor cells proliferation and induced tumor cells apoptosis, in colon and prostate carcinoma cell lines^[48,49]. To date, their effects on human hepatoma SMMC-7721 cell lines have not yet been studied. The aim of this study was to investigate the effect of Nimesulide, a selective COX inhibitor, on the proliferation and apoptosis of SMMC-7721 cell lines. The results indicated that various concentrations of Nimesulide could change the morphology of SMMC-7721 cells and inhibit SMMC-7721 cells proliferation obviously in a dose and time-dependent manner. Nimesulide could induce SMMC-7721 cells apoptosis and cause death in a dose-dependent manner. The precise mechanism by which selective COX-2 inhibitors inhibit tumor cells growth and induce tumor cells apoptosis was not been clearfield. The available data supported the two hypotheses.

Some studies indicate that COX-2 is a key enzyme in the conversion of arachidonic acid to prostaglandins. Selective COX-2 inhibitors can decrease prostaglandins biosynthesis, and prostaglandins can inhibit cell-mediated immunity, which enables the tumor cells escaping the host-immunity^[50,51]; PGs also can conjugate with PPAR α and activate cell proliferation passage of signal conduction, promote cells proliferation^[52]; PGs can also inhibit cells apoptosis and cause cells division uncontrollable, thus accelerating tumor genesis^[53,54]; the effects of COX-2 inhibitors might involve prostaglandin biosynthesis. Some studies indicated that the effects of COX-2 were not related to COX-2 expression and PGs. Hanif *et al.*^[55] verified that NASIDs (nonselective COX inhibitors) could induce apoptosis of colon carcinoma cell line HCT-15. HCT-15 cells have no COX gene transcription, and does not produce PGs. When adding exogenous PGs to the HCT-15 cells, it could not reverse the induction of HCT-15 cells apoptosis by NASIDs.

On the whole, Nimesulide, a selective COX-2 inhibitor, can inhibit the growth of hepatoma cells and induce tumor cells apoptosis. With the clarification of the mechanism of selective COX-2 inhibitors, These COX-2 selective inhibitors can become the choice of prevention and treatment of cancers.

ACKNOWLEDGMENT

I would like to thank my wife and all those who provided assistance for this study.

REFERENCES

- Gao HJ, Yu LZ, Sun G, Miu K, Bai JF, Zhang XY, Lü XZ, Zhao ZQ. The expression of COX-2 in gastric carcinoma and paracancerous tissues. *Shijie Huaren Xiaohua Zazhi* 2000;8:578-579
- Wu HP, Wu KCH, Li L, Yao LP, Lan M, Wang X, Fan DM. Cloning of human cyclooxygenase-2 (Hcox-2) encoded gene and the study of gastric cancer cell transfected with its antisense vector. *Shijie Huaren Xiaohua Zazhi* 2000;8: 1211-1217
- Gao HJ, Yu LZ, Bai JF, Peng YS, Sun G, Zhao HL, Miu K, Lü XZ, Zhang XY, Zhao ZQ. Multiple genetic alterations and behavior of cellular biology in gastric cancer and other gastric mucosal lesions: *H. pylori* infection, histological types and staging. *World J Gastroenterol* 2000;6:848-854
- Wu QM, Li SB, Wang Q, Wang DH, Li XB, Liu CZ. The expression of COX-2 in esophageal carcinoma and its relationship to clinicopathologic characteristic. *Shijie Huaren Xiaohua Zazhi* 2001; 9: 11-14
- Sun B, Wu YL, Zhang XJ, Wang SN, He HY, Qiao MM, Zhang YP, Zhong J. Effects of Sulindac on growth inhibition and apoptosis induction in human gastric cancer cells. *Shijie Huaren Xiaohua Zazhi* 2001; 9:997-1002
- Zhuang ZH, Wang LD. Non-steroidal anti-inflammatory drug and digestive tract tumors. *Shijie Huaren Xiaohua Zazhi* 2001;9:1050-1053
- Shen ZX, Cao G, Sun J. The effect of COX-2 mRNA expression in colorectal cancer tissues. *Shijie Huaren Xiaohua Zazhi* 2001;9:1082-1084
- Mann M, Sheng H, Shao J, Williams CS, Pisacane PI, Sliwowski MX, DuBois RN. Targeting cyclooxygenase 2 and HER-2/neu pathways inhibit colorectal carcinoma growth. *Gastroenterology* 2001; 120: 1713-1739
- Glinghammar B, Rafter J. Colonic luminal contents induce cyclooxygenase 2 transcription in human colon carcinoma cells. *Gastroenterology* 2001; 120: 401-410
- Wallace JL, McKnight W, Reuter BK, Vergnolle N. NSAID-induced gastric damage in rats: requirement for inhibition of both cyclooxygenase 1 and 2. *Gastroenterology* 2000; 119: 706-714
- Callejas NA, Bosca L, Williams CS, DuBOIS RN, Martin-Sanz P. Regulation of cyclooxygenase 2 expression in hepatocytes by CCAAT/enhancer-binding proteins. *Gastroenterology* 2000; 119: 493-501
- Zhang Z, DuBois RN. Par-4, a proapoptotic gene is regulated by NSAIDs in human colon carcinoma cells. *Gastroenterology* 2000; 118: 1012-1017
- Shirvani VN, Ouatu-Lascar R, Kaur BS, Omary MB, Triadafilopoulos G. Cyclooxygenase 2 expression in Barrett's esophagus and adenocarcinoma: Ex vivo induction by bile salts and acid exposure. *Gastroenterology* 2000;118:487-496
- Shattuck-Brandt RL, Varilek GW, Radhika A, Yang F, Washington MK, DuBois RN. Cyclooxygenase 2 expression is increased in the stroma of colon carcinomas from IL-10(-/-) mice. *Gastroenterology* 2000; 118:337-345
- Sinicropo FA, Lemoine M, Xi L, Lynch PM, Cleary KR, Shen Y, Frazier ML. Reduced expression of cyclooxygenase 2 proteins in hereditary nonpolyposis colorectal cancers relative to sporadic cancers. *Gastroenterology* 1999; 117: 350-358
- Fu S, Ramanujam KS, Wong A, Fantry GT, Drachenberg CB, James SP, Meltzer SJ, Wilson KT. Increased expression and cellular localization of inducible nitric oxide synthase and cyclooxygenase 2 in *Helicobacter pylori* gastritis. *Gastroenterology* 1999; 116: 1319-1329
- Bosch-Marce M, Claria J, Titos E, Masferrer JL, Altuna R, Poo JL, Jimenez W, Arroyo V, Rivera F, Rodes J. Selective inhibition of cyclooxygenase 2 spares renal function and prostaglandin synthesis in cirrhotic rats with ascites. *Gastroenterology* 1999; 116: 1167-1175
- Klimp AH, Hollema H, Kempinga C, van der Zee AG, de Vries EG, Daemen T. Expression of cyclooxygenase-2 and inducible nitric oxide synthase in human ovarian tumors and tumor-associated macrophages. *Cancer Res* 2001; 61: 7305-7309
- Lal G, Ash C, Hay K, Redston M, Kwong E, Hancock B, Mak T, Kargman S, Evans JF, Gallinger S. Suppression of intestinal polyps in Msh2-deficient and non-Msh2-deficient multiple intestinal neoplasia mice by a specific cyclooxygenase-2 inhibitor and by a dual cyclooxygenase-1/2 inhibitor. *Cancer Res* 2001; 61: 6131-6136
- Subbarayan V, Sabichi AL, Llansa N, Lippman SM, Menter DG. Differential expression of cyclooxygenase-2 and its regulation by tumor necrosis factor-alpha in normal and malignant prostate cells. *Cancer Res* 2001; 61: 2720-2726
- Oshima M, Murai N, Kargman S, Arguello M, Luk P, Kwong E, Taketo MM, Evans JF. Chemoprevention of intestinal polyposis in the Apcdelta716 mouse by rofecoxib, a specific cyclooxygenase-2 inhibitor. *Cancer Res* 2001; 61: 1733-1740
- Shiotani H, Denda A, Yamamoto K, Kitayama W, Endoh T, Sasaki Y, Tsutsumi N, Sugimura M, Konishi Y. Increased expression of cyclooxygenase-2 protein in 4-nitroquinoline-1-oxide-induced rat tongue carcinomas and chemopreventive efficacy of a specific inhibitor, nimesulide. *Cancer Res* 2001; 61: 1451-1456
- Boudreau MD, Sohn KH, Rhee SH, Lee SW, Hunt JD, Hwang DH. Suppression of tumor cell growth both in nude mice and in culture by n-3 polyunsaturated fatty acids: mediation through cyclooxygenase-independent pathways. *Cancer Res* 2001; 61: 1386-1391
- Denkert C, Kobel M, Berger S, Siegert A, Leclere A, Trefzer U, Hauptmann S. Expression of cyclooxygenase 2 in human malignant melanoma. *Cancer Res* 2001; 61: 303-308
- Taylor MT, Lawson KR, Ignatenko NA, Marek SE, Stringer DE, Skovan BA, Gerner EW. Sulindac sulfone inhibits K-ras-dependent cyclooxygenase-2 expression in human colon cancer cells. *Cancer Res* 2000; 60: 6607-6610
- Williams CS, Watson AJ, Sheng H, Helou R, Shao J, DuBois RN. Celecoxib prevents tumor growth *in vivo* without toxicity to normal gut: lack of correlation between *in vitro* and *in vivo* models. *Cancer Res* 2000; 60: 6045-6051
- Souza RF, Shewmake K, Beer DG, Cryer B, Spechler SJ. Selective inhibition of cyclooxygenase-2 suppresses growth and induces apoptosis in human esophageal adenocarcinoma cells. *Cancer Res* 2000; 60: 5767-5772
- Grubbs CJ, Lubet RA, Koki AT, Leahy KM, Masferrer JL, Steele VE, Kelloff GJ, Hill DL, Seibert K. Celecoxib inhibits N-butyl-N-(4-hydroxybutyl)-nitrosamine-induced urinary bladder cancers in male B6D2F1 mice and female Fischer-344 rats. *Cancer Res* 2000; 60: 5599-5602
- Jacoby RF, Seibert K, Cole CE, Kelloff G, Lubet RA. The cyclooxygenase-2 inhibitor celecoxib is a potent preventive and therapeutic agent in the min mouse model of adenomatous polyposis. *Cancer Res* 2000; 60: 5040-5044
- Joki T, Heese O, Nikas DC, Bello L, Zhang J, Kraeft SK, Seyfried NT, Abe T, Chen LB, Carroll RS, Black PM. Expression of cyclooxygenase 2 (COX-2) in human glioma and *in vitro* inhibition by a specific COX-2 inhibitor, NS-398. *Cancer Res* 2000; 60: 4926-4931
- Attiga FA, Fernandez PM, Weeraratna AT, Manyak MJ, Patierno SR. Inhibitors of prostaglandin synthesis inhibit human prostate tumor cell invasiveness and reduce the release of matrix metalloproteinases. *Cancer Res* 2000; 60: 4629-4637
- Marrogi A, Pass HI, Khan M, Metheny-Barlow LJ, Harris CC, Gerwin BI. Human mesothelioma samples overexpress both cyclooxygenase-2 (COX-2) and inducible nitric oxide synthase (NOS2): *in vitro* antiproliferative effects of a COX-2 inhibitor. *Cancer Res* 2000; 60: 3696-3700
- Cahlin C, Gelin J, Delbro D, Lonnroth C, Doi C, Lundholm K. Effect of cyclooxygenase and nitric oxide synthase inhibitors on tumor growth in mouse tumor models with and without cancer cachexia related to prostanoids. *Cancer Res* 2000; 60: 1742-1749
- Masferrer JL, Leahy KM, Koki AT, Zweifel BS, Settle SL, Woerner BM, Edwards DA, Flickinger AG, Moore RJ, Seibert K. Antiangiogenic and antitumor activities of cyclooxygenase-2 inhibitors. *Cancer Res* 2000; 60: 1306-1311
- Reddy BS, Hirose Y, Lubet R, Steele V, Kelloff G, Paulson S, Seibert K, Rao CV. Chemoprevention of colon cancer by specific cyclooxygenase-2 inhibitor, celecoxib, administered during different stages of carcinogenesis. *Cancer Res* 2000; 60: 293-297
- Mohammed SI, Knapp DW, Bostwick DG, Foster RS, Khan KN, Masferrer JL, Woerner BM, Snyder PW, Koki AT. Expression of cyclooxygenase-2 (COX-2) in human invasive transitional cell carcinoma (TCC) of the urinary bladder. *Cancer Res* 1999; 59: 5647-5650
- Molina MA, Sitja-Arnau M, Lemoine MG, Frazier ML, Sinicropo FA. Increased cyclooxygenase-2 expression in human pancreatic carcinomas and cell lines: growth inhibition by nonsteroidal anti-inflammatory drugs. *Cancer Res* 1999; 59: 4356-4362
- Tucker ON, Dannenberg AJ, Yang EK, Zhang F, Teng L, Daly JM, Soslow RA, Masferrer JL, Woerner BM, Koki AT, Fahey TJ 3rd. Cyclooxygenase-2 expression is up-regulated in human pancreatic cancer. *Cancer Res* 1999; 59: 987-990
- Chan G, Boyle JO, Yang EK, Zhang F, Sacks PG, Shah JP, Edelstein D, Soslow RA, Koki AT, Woerner BM, Masferrer JL, Dannenberg AJ. Cyclooxygenase-2 expression is up-regulated in squamous cell carcinoma of the head and neck. *Cancer Res* 1999; 59: 991-994
- Zimmermann KC, Sarbia M, Weber AA, Borchard F, Gabbert HE, Schror K. Cyclooxygenase-2 expression in human esophageal carcinoma. *Cancer Res* 1999;59:198-204
- Koga H, Sakisaka S, Ohishi M, Kawaguchi T, Taniguchi E, Sasatomi K, Harada M, Kusaba T, Tanaka M, Kimura R, Nakashima Y, Nakashima

- O, Kojiro M, Kurohiji T, Sata M. Expression of cyclooxygenase-2 in human hepatocellular carcinoma: relevance to tumor dedifferentiation. *Hepatology* 1999; 29: 688-696
- 42 Nanji AA, Jokelainen K, Fotouhinia M, Rahemtulla A, Thomas P, Tipoe GL, Su GL, Dannenberg AJ. Increased severity of alcoholic liver injury in female rats: role of oxidative stress, endotoxin, and chemokines. *Am J Physiol Gastrointest Liver Physiol* 2001; 281: G1348-1356
- 43 Ganey PE, Barton YW, Kinser S, Sneed RA, Barton CC, Roth RA. Involvement of cyclooxygenase-2 in the potentiation of allyl alcohol-induced liver injury by bacterial lipopolysaccharide. *Toxicol Appl Pharmacol* 2001; 174: 113-121
- 44 Miyamoto T, Ogino N, Yamamoto S, Hayaishi O. Purification of prostaglandin endoperoxide synthetase from bovine vesicular gland microsomes. *J Bio Chem* 1976; 251:2629-2636
- 45 Simmons DL, Levy DB, Yannoni Y, Erikson RL. Identification of Phorbol ester-repressible v-src- inducible gene. *Proc Natl Acad Sci USA* 1989;86:1178-1182
- 46 Tian G, Yu JP, Luo HS, Yu BP, Li JY. The expression and effect of cyclo oxygenases-2 in acute hepatic injury. *Shijie Huaren Xiaohua Zazhi* 2002;10:24-27
- 47 Tian G, Yu JP, Luo HS, Yu BP, Li JY. The effect of COX-2 and oxidant stress in acute hepatic injury. *Yixue Yanjiusheng Xuebao* 2002; 6; 165-169
- 48 Elder DJE, Halton DE, Hague A, Paraskeva C. Induction of apoptotic cell death in human colorectal carcinoma cell lines by a cyclooxygenase-2 (COX-2) selective nonsteroidal anti-inflammatory drug: independence from COX-2 protein expression. *Clin Cancer Res* 1997; 3:1679-1683
- 49 Liu X H, Yao S, Kirschenbaum A, Levine AC. NS398, a selective cyclooxygenase inhibitor induces apoptosis and downregulates bcl-2 expression in LNCap cells. *Cancer Res* 1998; 58:4245-4249
- 50 Yang VW, Shields JM, Hamilton SR, Spannhake EW, Hubbard WC, Hyind LM, Robinson R, Giardiello FM. Size-dependent increased in prostanoid levels in adenomas of patients with familial adenomatous polyposis. *Cancer Res* 1998;58:1750-1753
- 51 Votila P. The role of cyclic AMP and oxygen intermediates in the inhibition of cellular immunity in cancer. *Cancer Immunot Immunother* 1996;43: 1-9
- 52 Parker J, Kaplon MK, Alvarez CJ, Krishnaswamy G. Prostaglandin H synthase expression is variable in human colorectal adenocarcinoma cell lines. *Exp cell Res* 1997;236: 321-329
- 53 Sheng H, Shao JY, Morrow JD, Beauchamp RD, Dubois RN. Modulation of apoptosis and BCL-2 expression by prostaglandin E2 in human colon cancer cells. *Cancer Res* 1998;58: 362-366
- 54 Orlov SN, Thorin-Trescases N, Dulin No. Activation of cAMP signaling transiently inhibits apoptosis in vascular smooth muscle cell in a site upstream of caspase-1. *Cell Death Differ* 1999;6:661-672
- 55 Hanif R, Pittas A, Feng Y, Koutsos MI, Qiao L, Staiano-Coico L, Shiff SI, Rigas B. Effects of nonsteroidal anti-inflammatory drugs on proliferation and on induction of apoptosis in colon cancer cells by prostaglandin-independent pathway. *Biochem Pharmacol* 1996; 52:237-245

Edited by Wu XN

• LARGE INTESTINAL CANCER •

Reduction of the incidence and mortality of rectal cancer by polypectomy: a prospective cohort study in Haining County

Shu Zheng, Xi-Yong Liu, Ke-Feng Ding, Lin-Bo Wang, Pei-Lin Qiu, Xin-Feng Ding, Yong-Zhou Shen, Gao-Fei Shen, Qi-Rong Sun, Wei-Dong Li, Qi Dong, Su-Zhan Zhang

Shu Zheng, Xi-Yong Liu, Qi Dong, Cancer Institute, Zhejiang University, 88 Jiefang Road, HangZhou 310009, Zhejiang Province, China
Ke-feng Ding, Lin-Bo Wang, Pei-Lin Qiu, Su-Zhan Zhang, The 2nd affiliated Hospital, Medical School of Zhejiang University, 88 Jiefang Road, HangZhou 310009, Zhejiang Province, China
Xin-Feng Ding, Yong-Zhou Shen, Gao-Fei Shen, Qi-Rong Sun, Wei-Dong Li, Haining Cancer Institute, Haining 314400, Zhejiang Province, China
Supported by The 7th 5-year National Medical Strategic Science and Technology Plan, No. 75-61-02-17; The 8th 5-year National Medical Strategic Science and Technology Plan, No. 85-914-01-09
Correspondence to: Shu Zheng, Cancer Institute, Zhejiang University, 88 Jiefang Road, HangZhou 310009, Zhejiang Province, China. zhengshu@mail.hz.zj.cn
Telephone: +86-571-87783868 Fax: +86-571-87214404
Received 2001-12-20 Accepted 2002-02-07

Abstract

AIM: To reduce the incidence and mortality of rectal cancer and address the hypothesis that colorectal cancer often arise from precursor lesion(s), either adenomas or non-adenomatous polyps, by conducting a population-based mass screening for colorectal cancer in Haining County, Zhejiang, PRC.

METHODS: From 1977 to 1980, physicians screened the population of Haining County using 15cm rigid endoscopy. Of over 240000 participants, 4076 of them were diagnosed with precursor lesions, either adenomas or non-adenomatous polyps, which were then removed surgically. All individuals with precursor lesions were followed up and reexamined by endoscopy every two to five years up to 1998.

RESULTS: After the initial screening, 953 metachronous adenomas and 417 non-adenomatous polyps were detected and removed from the members of this cohort. Further, 27 cases of colorectal cancer were detected and treated. Log-rank tests showed that the survival time among those cancer patients who underwent mass screening increased significantly compared to that of other colorectal cancer patients ($P < 0.0001$). According to the population-based cancer registry in Haining County, age-adjusted incidence and mortality of rectal cancer decreased by 41% and 29% from 1977-1981 to 1992-1996, respectively. Observed cumulative 20-year rectal cancer incidence was 31% lower than the expected in the screened group; the mortality due to rectal cancer was 18% lower than the expected in the screened group.

CONCLUSION: Mass screening for rectal cancer and precursor lesions with proctoscopy in the general population and periodical following-up with routine endoscopy for high-risk patients may decrease both the incidence and mortality of rectal cancer.

Zheng S, Liu XY, Ding KF, Wang LB, Qiu PL, Ding X, Shen YZ, Shen GF, Sun QR, Li WD, Dong Q, Zhang SZ. Reduction of the incidence and mortality of rectal cancer by polypectomy: a prospective cohort study in Haining County. *World J Gastroenterol* 2002;8(3):488-492

INTRODUCTION

Colorectal cancer is the second most common cause of death from cancer in the United States^[1,2] and the fifth in mainland of China^[3]. Dietary modification and non-steroidal anti-inflammatory drugs (NSAID) may reduce the risk of colorectal cancer^[4-6]. Nevertheless, few of the Chinese people have benefited from these chemoprevention strategies so far. Recently, the results of several randomized controlled trial showed that fecal occult blood testing (FOBT) based on mass screening might reduce the mortality caused by colorectal cancer in general population^[7-9]. Unfortunately, the incidence of colorectal cancer could not be reduced by this protocol.

As reviewed by Potter^[10-13], colorectal cancer is a result of accumulation of multiple genetic alterations within the epithelial cells. The concept of the adenoma-to-carcinoma is well accepted, and describes a stepwise progression from normal colorectal epithelium to adenoma, and to carcinoma^[14-16]. The adenomatous polyps, the precursor lesion resulted from epithelial cell hyperproliferation and crypt dysplasia, have malignant potential. Progression from precursor lesions to colorectal cancer is a multi-step process that requires ten to fifteen years^[15]. Approximately 30-60% of patients with a history of adenomas will develop a metachronous adenoma within three to five years after their initial polypectomy^[17,18]. Therefore, it has been hypothesized that removing colorectal polyps might change the natural history of colorectal cancer; mass screening and following up with endoscopy might reduce the incidence and mortality of colorectal cancer. Nevertheless, evidence for the effectiveness of colonoscopy is indirect, since no large trials with mortality endpoints have been conducted to evaluate the efficacy of screening for colorectal cancer with colonoscopy^[19-21].

According to census survey of death causes in 1970 in China, more than 66% of colorectal cancers were found in the rectum^[22-24]. It is suggested that about 60% of colorectal cancer could be effective by screening with proctoscopy in China. To prove above hypothesis, we conducted a population-based mass screening with 15cm rigid endoscopy in Haining County, PRC from 1977 to 1980. Results presented herein are based on findings at the initial screening as well as 20 years of follow-up examinations in those individuals with precursor lesions.

MATERIALS AND METHODS

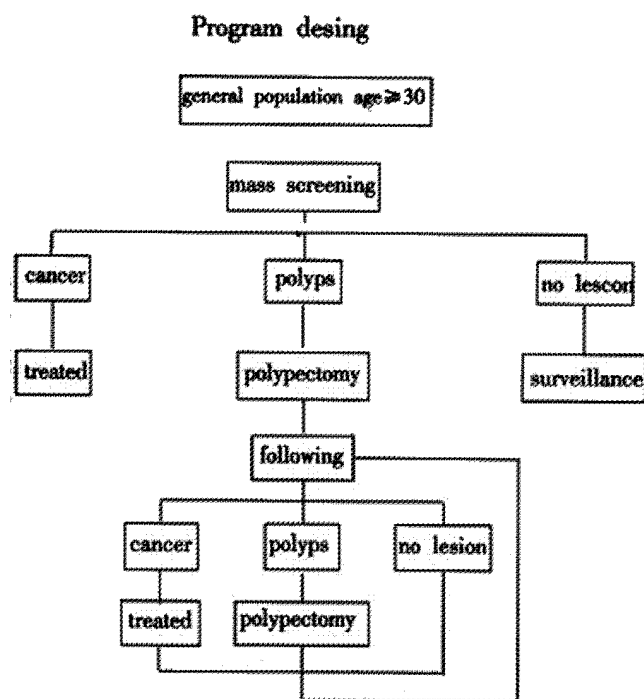
Study design was described in Figure 1. The high-risk population with rectal polyps was identified by proctoscopy through a general population-based mass-screening program, and followed with endoscopy periodically. All detectable polyps including adenomatous or non-adenomatous polyps were removed.

As previously described in detail^[25,26], population-based screenings with 15cm rigid endoscopy was conducted from 1977 to 1978 in Haining County, a rural community located in the eastern part of China. Only residents in Haining County who were at least 30 years old were eligible for the screenings. The screening team includes

epidemiologist, physician, pathologist, surgeon and investigators, who had been trained before starting the program. We screened 186234 of the 223866 eligible individuals (83% response rate), of which 2815 were found carrying polyps and/or adenomas. The detectable adenoma and/or polyp were surgically removed thereafter. All individuals with precursor lesions were eligible for follow-up endoscopic screenings, which were performed in the years of 1979-1980, 1981, 1983, 1987, 1993 and 1998. In addition, of the 53987 volunteers who aged 30 or over screened during 1979-1980's following-up, polyps and/or adenomas were detected and removed in 1,261 individuals. These patients were eligible for follow-up endoscopic screenings in 1982, 1984, 1988, 1994 and 1998. Due to technological advances in screening methods during this time period, all screenings after 1985 were performed with 60cm flexible sigmoidoscopy rather than 15cm rigid endoscopy.

Pathologic material was reviewed independently by three senior pathologists using standard criteria developed by the World Health Organization (WHO). A final diagnosis was made when at least two of the pathologists agreed on the patient's diagnosis. The age distribution of patients from both screenings is presented in Table 1. Table 2 lists the pathologic features of the initial polyp or adenoma for each patient; for patients with more than one adenoma or polyp, the most advanced lesion is listed.

Cancer mortality data was collected since 1974, and Cancer incidence data was available since 1977 by the population-based cancer registry in Haining County. The International Classification of Disease (ICD-9) was employed by the registry for site-specific histologic classification. Population estimates were based on the periodic censuses, with age- and sex-specific annual estimates derived by linear inter- and extrapolation for the remaining years. Rates for each period are age-adjusted to the world standard population using the direct method for each 5-year age group. From 1974 to 1976, before mass screening program carried out, the adjusted mortality of colon and rectum cancer was 2.66 and 4.20 per 100000 respectively. From 1977 to 1996, histologic confirmation was available for 94.4% of the 1005 incident colorectal cancer cases and 92.3% of the 735 deaths due to colorectal cancer.



Note: Polyps include adenomatous polyps and non-adenomatous polyps. All polyps would be removed when detected by endoscopy examiner.

Figure 1 Design for mass screening and following-up with endoscopy

Table 1 Age distribution of two groups of high-risk populations with polyps

Age Group	1 ^a		2 ^b		Total(%)
	Male(%)	Female(%)	Male(%)	Female(%)	
30-	644(36.6)	440(41.6)	287(34.4)	181(37.2)	1 552(38.1)
40-	452(25.7)	270(25.6)	226(27.1)	100(23.7)	1 049(25.8)
50-	434(24.7)	237(22.4)	204(24.4)	99(23.5)	974(23.9)
60-	164(9.3)	89(8.4)	99(11.9)	37(27.2)	389(9.6)
70-	64(3.7)	21(2.0)	19(2.3)	5(1.2)	109(2.7)
Total	1758	1057	835	422	4072

^a1: high-risk population with history of polyps identified during 1977-1978; ^b2: High-risk population identified in 1980. The age of 4 participants is unknown

Table 2 Pathologic features of initial polyps of two groups of high-risk populations

Pathologic Diagnosis	First group		Second group		Total	
	n	%	n	%	n	%
Adenoma	1485	52.88	876	69.47	2361	58.02
Tubular	1352	48.15	843	66.85	2195	53.94
Tubulovillous	104	3.70	31	2.46	135	3.32
Villous	19	0.68	2	0.16	21	0.52
Non-adenomatous	1326	47.22	382	30.29	1708	41.98
Mucosal	596	21.23	95	7.53	691	16.98
Juvenile	183	6.52	95	7.53	278	6.83
Hyperplastic	113	4.02	72	5.71	185	4.55
Inflammatory	90	3.21	4	0.32	94	2.31
Schistosomiasis	326	11.61	115	9.12	441	10.84
Lymphoid	10	0.36	1	0.08	11	0.27
Other	8	0.28	0	0.00	8	0.20
No pathologic diag	7	0.25	3	0.24	10	0.25
Total	2815		1261		4076	

RESULTS

From 1979 to 1998, patients diagnosed with adenomas and/or polyps during the first screening have been followed up six times. Of 2815 cases with polyps, 20.5% of them participated whole six times endoscopy examination, and 89.6% finished at least three times. While those patients diagnosed at the group of volunteers have been re-screened five times, and 82.5% of them were re-examined at least two times. Table 3 summarizes the expected and observed incidence rates of adenomas, polyps and colorectal cancer for both groups. After the initial screening, 953 metachronous adenomas and 417 non-adenomatous polyps were detected and removed from members of this cohort. Further, 27 cases of colorectal cancer were detected and treated, we analyzed data collected by the cancer registry of Haining County, Zhejiang Province, PR China. Both rectum cancer incidence and mortality were decreased steadily from 1977 to 1996 (Table 3). The age and sex adjusted incidence rates of rectal cancer decreased from 7.27 per 100000 (1977-1981) to 3.71 per 100000 (1992-1996), and mortality was decreased from 4.20 per 100000 (1974-1976) to 2.98 per 100 000 (1992-1996). Thus, age-adjusted incidence and mortality of rectal cancer decreased by 41% and 29% respectively. Nevertheless, both adjusted incidence rates and mortality of colon cancer increased slightly at the same period.

Table 3 Output of following with endoscopy among high-risk population with history of polyps

Year	Expected n	Observed n (%)	Adenoma n (%)	Non-adenomatous n (%)	Colorectal cancer (1/100000)
1st group					
1979	2803	2197(78.38)	178(8.10)	104(4.73)	6(273.10)
1981	2763	1592(57.62)	61(3.83)	27(1.70)	4(251.26)
1983	2719	2147(78.96)	108(5.03)	33(1.54)	2(93.15)
1987	2689	2408(89.52)	191(7.93)	96(4.00)	4(166.11)
1993	2388	1475(61.77)	121(8.20)	52(3.53)	4(271.19)
1998	2207	1020(46.22)	95(9.31)	17(1.67)	4(392.16)
2nd group					
1982	1253	461(36.79)	17(3.69)	6(1.30)	0(0.00)
1984	1235	1056(85.51)	49(4.64)	26(2.46)	0(0.00)
1988	1183	931(78.70)	64(6.87)	20(2.15)	0(0.00)
1994	1097	479(43.66)	33(6.68)	17(3.55)	3(626.30)
1998	1040	486(46.73)	36(7.41)	17(3.50)	0(0.00)
Total		1425	2953(6.68)	417(2.93)	27(189.45)

^aFollowing with 60cm flexible sigmoidoscopy since 1987

Cumulative 20-year incidence and mortality caused by colon and rectal cancers are presented in Figures 2,3 and table 4. Figure 2 shows the incidence of colon and rectal cancers in those individuals aged 30 years and older in the mass screening in 1977. Figure 3 shows mortality caused by colon and rectal cancer in the screened population (those aged 30 years and older in 1977). According to incidence and mortality of age and sex sub-group during 1977 to 1981, we calculated the annual expected rate of sub-group for this cohort population from 1977 to 1996, and then 20-year cumulative incidence and mortality. Observed cumulative 20-year rectal cancer incidence was 31% lower than expected in the screened group; mortality caused by rectal cancer was 18% lower than expected in the screened group. There is no significant difference of incidence and mortality of colon cancer almost between observed and expected. Results showed incidence and mortality were only reduced in the rectal cancer, but not colon cancer.

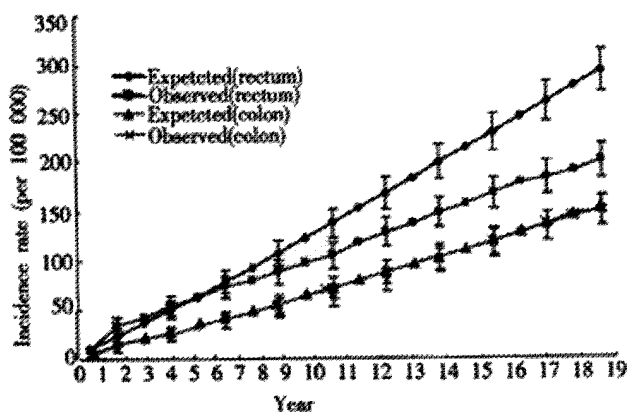


Figure 2 The Expected and Observed Twenty-year Cumulative Incidence of Colon and Rectum Cancer

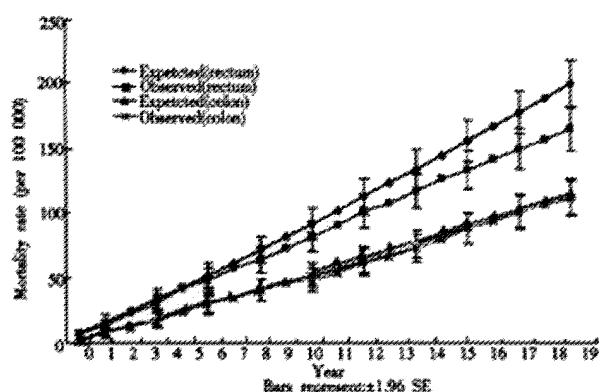


Figure 3 The Expected and Observed Twenty-year Cumulative mortality of Colon and Rectum Cancer

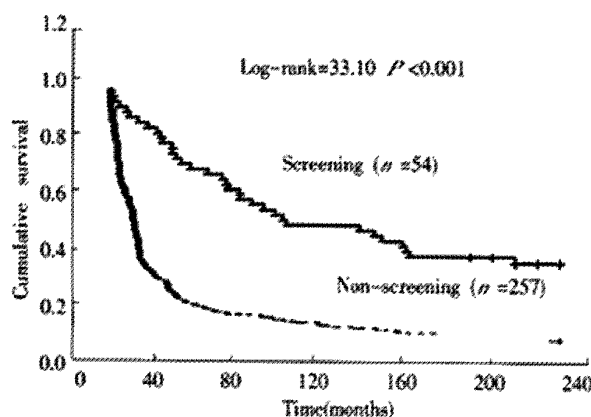


Figure 4 Survival curve (Kaplan-Meier) of rectal cancer diagnosed during 1977-1982

During the initial screenings, 54 cases of colorectal adenocarcinomas were detected and treated. Survival analyses showed that patients with rectal cancers detected during the screenings had significantly longer survival time than rectal cancers identified in patients who were not included in the mass screenings at the same period (log-rank=27.12; $P<0.001$) (See Figure 4). The mean age of screened rectal cancer patients was 57 years (SD=12.8) while the mean age of non-screened rectal cancer patients was 59 years (SD=12.1). The median survival time of screened patients was 133 months (95% CI=56-210mos.) compared with only 14 months (95% CI=11-15 mos.) in non-screened patients. Excluded the leading time bias, the median survival time for screened patients was prolonged by 7.9 years.

DISCUSSION

In the 1980's, it was suggested that population-wide screening with fecal occult blood test (FOBT) was not cost-effective^[27,28]. However, more recent analyses suggest that FOBT-based screening can reduce colorectal cancer mortality^[29-32]. Mandel and colleagues at the Mayo Clinic in Minnesota conducted a randomized screening of over 46,000 individuals^[33,34]. Participants were randomized to annual or biannual FOB test group and a control group. The cumulative 18-year colorectal cancer mortality was reduced by 33% in the annually screened group and 21% in the biennially screened group compared to the control group. It is important to note that although FOBT may be important in early detection of colorectal cancer, this test does not affect the underlying process of neoplastic transformation in the large bowel. In addition, the use of a rehydrated hemoccult test instead of an unrehydrated hemoccult test increased test sensitivity but decreased test specificity resulting in over 10% of participants undergoing colonoscopy exam at each screening. Moreover, a total of 38% of the screened group had at least one colonoscopy during the entire study period. It was proposed by Lang and colleagues that approximately one third to one half of the observed reduction in mortality found in Mandel's study was the result of chance selection for colonoscopy rather than the FOBT itself^[35-37]. Another two randomized screening trials using unrehydrated hemoccult test every two years resulted in only 4% of the test group requiring colonoscopy, yet reduced colorectal cancer mortality by 15-18%^[39-43]. However, no evidence showed incidence rate has been reduced from colorectal cancer by FOBT-based mass screening.

The population-wide mass screenings were conducted from 1977-1980 among 246252 residents of Haining County aged 30 years or older. The overall participation rates were 83%. A total of 54 cases of rectal cancer were detected and treated. Overall survival in these patients was significantly increased compared to non-screened rectal cancer patients (log-rank=33.4; $P<0.0001$). Excluding leading time bias, the survival time was prolonged by almost 8 years in screened patients. In addition, 4076 patients with newly discovered adenomas and/or nonadenomatous polyps were treated by polypectomy and followed with periodic examinations through 1998. During follow-up, 953 metachronous adenomas and 417 nonadenomatous polyps were detected and removed; an additional 27 colorectal cancers, 12 of which were carcinoma in situ, were diagnosed and treated. According to the Haining County Cancer Registry, from 1977 to 1996 both age- and sex-adjusted colorectal cancer incidence and mortality decreased by 41% and 29% respectively. Further, cumulative 20-year observed incidence and mortality from rectal cancer in the screened population decreased by 31% and 18%, respectively. If interest, incidence rates of rectal cancer in Shanghai, PRC (located 120km from Haining) increased by 11.3% in males and 6.0% in females from 1972 to 1994^[44,45]. Chinese official data showed from 1973-1975 to 1990-1992, age and sex adjusted mortality caused by colorectal cancer increase by 3.61% in urban and decrease by 5.22% in rural population of China^[3]. Above evidence supported that

both incidence and mortality of rectal cancer decreased in Haining due to the population-wide mass screening and following-up with endoscopy to high-risk population.

Winawer and colleagues reported a 76-90% reduction in colorectal cancer incidence in 1418 adenoma patients who underwent periodic colonoscopy after initial polypectomy compared to age-, sex-, and polyp-size-adjusted control groups. Further, follow-up colonoscopy performed three years after initial colonoscopy detection and removal was found to be as effective as follow-up colonoscopy performed after only one or two years. Thus, it is suggested that a screening interval of three years is sufficient following colonoscopic removal of newly diagnosed adenomas^[15,16]. Anyway, our results showed only 31% reduction of incidence of rectal cancer through population-wide mass screening with proctoscopy. It is suggested that there are other pathways besides except of adenoma pathway.

These results suggest that colorectal cancer may be prevented by mass screening with FOBT or endoscopy. Further, removal of precursor lesions may slow or halt the natural history of rectal neoplasms. Our data suggest that mass screening by endoscopy can reduce the incidence and mortality of colorectal cancer. Screening guidelines for asymptomatic individuals suggest that all individuals aged 50 years or older may be benefited by periodic digital rectal examinations, stool guaiac and/or colonoscopy. For patients without adenomas or polyps, these exams should be repeated every three to five years, while patients with precursor lesions should be re-examined for new lesions after one year^[46-48]. Data from cancer statistics of United States indicated that approximately 60% of colorectal cancers are found in the distal colon or rectum^[49,50]. However, according to 1980's report by the Research Team in China, 80% of colorectal cancers are found in the distal colon or rectum, with up to 66% in the rectum alone^[24]. Therefore, it was suggested that mass screening and following up with sigmoidoscopy periodically might be more cost-effective than colonoscopy in China.

REFERENCES

- Landis SH, Murray T, Bolden S, Wingo PA. Cancer Statistics, 1999. *CA Cancer J Clin* 1999;49:8-31
- Landis SH, Murray T, Bolden S, Wingo PA. Cancer statistics, 1998. *CA Cancer J Clin* 1998;48:6-29
- Li LD, Lu FZ, Zhang SW, Mu R, Sun Xd, Wangpu XM, Sun J, Zhou YS, Ouyang NH, Rao KQ, Chen YD, Sun AM, Sun AM, Xue ZF, Xia Y. Analyses of variation trend and short term detection of Chinese malignant tumor mortality during twenty years. *Zhong guo Zhongliu* 1997;19:3-9
- Gupta RA, Dubois RN. Colorectal cancer prevention and treatment by inhibition of cyclooxygenase-2. *Nature Rev Cancer* 2001;1:11-21
- Cruz-Correa M, Hyland LM, Romans KE, Booker SV, Giardiello FM. Long-term treatment with sulindac in familial adenomatous polyposis: a prospective cohort study. *Gastroenterology* 2002;122:641-645
- Gwyn K, Sinicrope FA. Chemoprevention of colorectal cancer. *Am J Gastroenterol* 2002;97:13-21
- Mandel JS, Church TR, Bond JH, Ederer F, Geisser MS, Mongin SJ, Snover DC, Schuman LM. The effect of fecal occult-blood screening on the incidence of colorectal cancer. *N Engl J Med* 2000;343:1603-1607
- Robinson MH, Rodrigues VC, Hardcastle JD, Chamberlain JO, Mangham CM, Moss SM. Faecal occult blood screening for colorectal cancer at Nottingham: details of the verification process. *J Med Screen* 2000;7:97-98
- Jorgensen OD, Kronborg O, Fenger C. A randomised study of screening for colorectal cancer using faecal occult blood testing: results after 13 years and seven biennial screening rounds. *Gut* 2002;50:29-32
- Potter JD. Colorectal cancer: Molecules and Populations. *J Natl Cancer Inst* 1999;91:916-932
- Slattery ML, Potter JD, Ma KN, Caan BJ, Leppert M, Samowitz W. Western diet, family history of colorectal cancer, NAT2, GSTM-1 and risk of colon cancer. *Cancer Causes Control* 2000;11:1-8
- Borugian MJ, Sheps SB, Whittemore AS, Wu AH, Potter JD, Gallagher RP. Carbohydrates and colorectal cancer risk among Chinese in North America. *Cancer Epidemiol Biomarkers Prev* 2002;11:187-193
- Ulrich CM, Kampman E, Bigler J, Schwartz SM, Chen C, Bostick R, Fosdick L, Beresford SA, Yasui Y, Potter JD. Colorectal adenomas and the C677T MTHFR polymorphism: evidence for gene-environment interaction? *Cancer Epidemiol Biomarkers Prev* 1999;8:659-668
- Markowitz AJ, Winawer SJ. Screening and surveillance for colorectal cancer. *Semin Oncol* 1999;26:485-498
- Winawer SJ. Natural history of Colorectal Cancer. *Am J Med* 1999;106:3S-6S
- Winawer SJ, Zauber AG. The advanced adenoma as the primary target of screening. *Gastrointest Endosc Clin N Am* 2002;12:1-9
- Bedenne L, Faiver J, Boutron MC. Adenoma-carcinoma sequence or "de novo" carcinogenesis? A study of adenoma remnants in a population-based series of large bowel cancer. *Cancer* 1992;69:833-838
- Bedenne L, Jouve JL. Monitoring colorectal cancer after surgical resection. *Presse Med* 1999;28:651-656
- Smith RA, Cokkinides V, von E, Levin B, Cohen C, Runowicz CD, Sener S, Saslow D, Eyre HJ. American Cancer Society. American Cancer Society guidelines for the early detection of cancer. *CA Cancer J Clin* 2002;52:8-22
- Smith RA, von Eschenbach AC, Wender R, Levin B, Byers T, Rothenberger D, Brooks D, Creasman W, Cohen C, Runowicz C, Saslow D, Cokkinides V, Eyre H. ACS Prostate Cancer Advisory Committee, ACS Colorectal Cancer Advisory Committee, ACS Endometrial Cancer Advisory Committee. American Cancer Society guidelines for the early detection of cancer: update of early detection guidelines for prostate, colorectal, and endometrial cancers. Also: update 2001—testing for early lung cancer detection. *CA Cancer J Clin* 2001;51:38-75;77-80
- Byers T, Levin B, Rothenberger D, Dodd GD, Smith RA. American Cancer Society guidelines for screening and surveillance for early detection of colorectal polyps and cancer: update 1997. American Cancer Society Detection and Treatment Advisory Group on Colorectal Cancer. *CA Cancer J Clin* 1997;47:154-160
- Zheng S. Early detection and early diagnosis for colorectal cancer. *Shiyong Zhongliu* 1987;4:129-131
- Yu H, Zheng S, Cai XH, Wu JM, Qiu PL, Zhu WX. Evaluation of RPHA fecal occult blood test in screening for colorectal cancer. *Zhonghua Zhongliu Zazhi* 1990;12:108-111
- Zheng S, Yu H, Zhang SZ, Yong G, Sun QR, Zhou L, Liu XY, Li WD. Evaluation of digestive malignant tumor screening methods. *Shiyong Zhongliu Zazhi* 1996; 11:188-189
- Yang G, Zheng W, Sun QR, Shu XO, Li WD, Yu H, Shen GF, Shen YZ, Potter JD, Zheng S. Pathologic Features of Initial Adenoma as Predictors for Metachronous adenomas of the rectum. *J Natl Cancer Inst* 1998;9:1661-1665
- Sun QR. Dynamic Observation on 2815 cases of recto-anal adenoma and polyps for 10 years. *Zhonghua Waikexue Zazhi* 1992;9:561-566
- Eddy DM, Nugent FW, Eddy JF, Collier J, Gilbertsen V, Gottlieb LS, Rice R, Sherlock P, Winawer S. Screening for colorectal cancer in a high-risk population: result of a mathematical model. *Gastroenterology* 1987;92:682-692
- Bat L, Pines A, Ron E, Niv Y, Arditi E, Shemesh E. A community-based program of colorectal screening in an asymptomatic population: evaluation of screening tests and compliance. *Am J Gastroenterol* 1986;81:647-651
- Bond JH. Fecal occult blood test screening for colorectal cancer. *Gastrointest Endosc Clin N Am* 2002;12:11-21
- La VC. Fecal occult blood screening for colorectal cancer: open issues. *Ann Oncol* 2002;13:31-34
- Burke CA, Tadikonda L, Machicao V. Fecal occult blood testing for colorectal cancer screening: use the finger. *Am J Gastroenterol* 2001;96:3175-3177
- Bolin TD, Lapsley HM, Korman MG. Screening for colorectal cancer: what is the most cost-effective approach? *Med J Aust* 2001;174:298-301
- Mandel JS, Church TR, Bond JH, Ederer F, Geisser MS, Mongin SJ, Snover DC, Schuman LM. The effect of fecal occult-blood screening on the incidence of colorectal cancer. *N Engl J Med* 2000;343:1603-1607
- Mandel JS. Colorectal cancer screening. *Cancer Metastasis Rev* 1997;16:263-279
- Lang CA, Ransohoff DF. What can we conclude from the randomized controlled trials of fecal occult blood test screening? *Eur J Gastroenterol Hepatol* 1998;10:199-204
- Lang CA, Ransohoff DF. Fecal occult blood screening for colorectal cancer. Is mortality reduced by chance selection for screening colonoscopy? *JAMA* 1994;271:1011-1013
- Ransohoff DF, Lang CA. Using colonoscopy to screen for colorectal cancer. *Am J Gastroenterol* 1994;89:1765-1766
- Mapp TJ, Hardcastle JD, Moss SM, Robinson MH. Survival of patients with colorectal cancer diagnosed in a randomized controlled trial of faecal occult blood screening. *Br J Surg* 1999;86:1286-1291
- Robinson MH, Hardcastle JD, Moss SM, Amar SS, Chamberlain JO, Armitage NC, Scholefield JH, Mangham CM. The risks of screening: data from the Nottingham randomised controlled trial of faecal occult blood screening for colorectal cancer. *Gut* 1999;45:588-592
- Moss SM, Hardcastle JD, Coleman DA, Robinson MH, Rodrigues VC.

- Interval cancers in a randomized controlled trial of screening for colorectal cancer using a faecal occult blood test. *Int J Epidemiol* 1999;28:386-390
- 41 Rasmussen M, Kronborg O, Fenger C, Jorgensen OD. Possible advantages and drawbacks of adding flexible sigmoidoscopy to hemoccult-II in screening for colorectal cancer. A randomized study. *Scand J Gastroenterol* 1999;34:73-78
- 42 Kjeldsen BJ, Kronborg O, Fenger C, Jorgensen OD. The pattern of recurrent colorectal cancer in a prospective randomised study and the characteristics of diagnostic tests. *Int J Colorectal Dis* 1997;12:329-334
- 43 Kronborg O, Fenger C, Olsen J, Jorgensen OD, Sondergaard O. Randomized population study of screening for intestinal cancer with Hemoccult-II. *Ugeskr Laeger* 1997;159:4977-4981
- 44 Ji BT, Devesa SS, Chow WH, Jin F, Gao YT. Colorectal cancer incidence trends by subsite in urban Shanghai, 1972-1994. *Ca Epid Bio Prev* 1998; 7: 661-666
- 45 Jin F, Devesa SS, Chow WH, Zheng W, Ji BT, Fraumeni JF Jr, Gao YT. Cancer incidence trends in urban Shanghai, 1972-1994: an update. *Int J Cancer* 1999; 83: 435-440
- 46 Liu XY, Zheng S, Yang G, YU H, Zhou L, Zhang X, Sun QR, Shen GF, Shen YZ, Ding XF. Evaluation of the application of the optimized colorectal cancer screening protocol in high-risk population. *Zhongliu Fangzhi Yanjiu* 1997;24:197-199
- 47 Zheng S. Progress in colorectal cancer research in China. *Zhongguo Zhongliu Linchuang* 1998;25:225-228
- 48 Zheng S. Recent study on colorectal cancer in China. *Chin Med J* 1996; 109:179-192
- 49 Greenlee RT, Murray T, Bolden S, Wingo PA. Cancer statistics, 2000. *CA Cancer J Clin* 2000;50:7-33
- 50 Ries LA, Wingo PA, Miller DS, Howe HL, Weir HK, Rosenberg HM, Vernon SW, Cronin K, Edwards BK. The annual report to the nation on the status of cancer, 1973-1997, with a special section on colorectal cancer. *Cancer* 2000;88:2398-2424

Edited by Pagliarini R

• LARGE INTESTINAL CANCER •

Effects of ursolic acid and oleanolic acid on human colon carcinoma cell line HCT15

Jie Li, Wei-Jian Guo, Qing-Yao Yang

Jie Li, Wei-Jian Guo, Department of Oncology, Cancer Center, Xin Hua Hospital, Shanghai Second Medical University, Shanghai 200092, China
Qing-Yao Yang, Department of Biology, Shanghai Teachers University, Shanghai 200234, China

Correspondence to: Dr. Jie Li, Department of Oncology, Cancer Center, Xin Hua Hospital, Shanghai Second Medical University, Shanghai 200092, China. ljee@citiz.net

Telephone: +86-21-65010796 Fax: +86-21-65010796

Received 2001-12-20 Accepted 2002-02-07

Abstract

AIM: Ursolic acid (UA) and oleanolic acid (OA) are triperpene acids having a similar chemical structure and are distributed widely in plants all over the world. In recent years, it was found that they had marked anti-tumor effects. There is little literature currently available regarding their effects on colon carcinoma cells. The present study was designed to investigate their inhibitory effects on human colon carcinoma cell line HCT15.

METHODS: HCT15 cells were cultured with different drugs. The treated cells were stained with hematoxylin-eosin and their morphologic changes observed under a light microscope. The cytotoxicity of these drugs was evaluated by tetrazolium dye assay. Cell cycle analysis was performed by flow cytometry (FCM). Data were expressed as means \pm SEM and Analysis of variance and Student's *t*-test for individual comparisons.

RESULTS: Twenty-four to 72h after UA or OA 60 μ mol/L treatment, the numbers of dead cells and cell fragments were increased and most cells were dead at the 72nd hour. The cytotoxicity of UA was stronger than that of OA. Seventy-eight hours after 30 μ mol/L of UA or OA treatment, a number of cells were degenerated, but cell fragments were rarely seen. The IC_{50} values for UA and OA were 30 and 60 μ mol/L, respectively. Proliferation assay showed that proliferation of UA and OA-treated cells was slightly increased at 24h and significantly decreased at 48h and 60h, whereas untreated control cells maintained an exponential growth curve. Cell cycle analysis by FCM showed HCT15 cells treated with UA 30 and OA 60 for 36h and 72h gradually accumulated in G_0/G_1 phase (both drugs $P < 0.05$ for 72h), with a concomitant decrease of cell populations in S phase (both drugs $P < 0.01$ for 72h) and no detectable apoptotic fraction.

CONCLUSION: UA and OA have significant anti-tumor activity. The effect of UA is stronger than that of OA. The possible mechanism of action is that both drugs have an inhibitory effect on tumor cell proliferation through cell-cycle arrest.

Li J, Guo WJ, Yang QY. Effects of ursolic acid and oleanolic acid on human colon carcinoma cell line HCT15. *World J Gastroenterol* 2002;8(3):493-495

INTRODUCTION

Ursolic acid (UA) and oleanolic acid (OA) are triperpene acids having a similar chemical structure and are distributed widely in plants

all over the world^[1-20]. They are of interest to scientists because of their biological activities. OA has antifungal^[21,22], insecticidal^[23], anti-HIV^[24,25], diuretic^[26], complement inhibitory^[27], blood sugar depression^[28] and gastrointestinal transit modulating^[29] activities. UA and OA also possess liver-protection^[30-33] and anti-inflammatory effects^[34-37]. In recent years, it was found that they had marked anti-tumor effects and exhibited cytotoxic activity toward many cancer cell line in culture^[38-44]. Concerning their effects on colon carcinoma cells, there is little available so far in the current literature. The present study was designed to investigate their inhibitory effects on the human colon carcinoma cell line HCT15.

MATERIALS AND METHODS

Drugs and reagents

UA and OA were gifts from Professor Qing-Yao Yang, Department of Biology, Shanghai Teachers University. UA was extracted from *Catharantus roseus* L. with purity 99%, and OA from *Ziziphus jujuba* Mill. with purity 98%. The drugs were dissolved in 100% ethanol and then diluted 10 times with RPMI-1640 as the working solution, the final concentration of ethanol being less than 2%. Me^a-2SO was purchased from the Sigma Company (USA).

Cell line and culture medium

HCT15 had been introduced from the NCI (USA) and was cultured and kept in this laboratory. The culture medium used was RPMI-1640 with 10% BSA (Huamei BG, Co Ltd, China).

Cell morphology observation

The morphology of the live cells was observed with an inverted microscope and the live and dead cells were identified after 1% Trypan blue staining^[45]. Cell smear was stained with hematoxylin-eosin (HE). Cytotoxicity identification with tetrazolium dye assay (MTT) 1.8×10^4 cells were inoculated to each of the 3 parallel wells on a 96-well plate and cultured overnight. Different concentrations of UA and OA were added with a final volume of 0.2mL and cultured for 72 more hours. MTT 20 μ L (5g/L) was added to each well. 4h later samples were centrifuged and the supernatant was discarded. 180 μ L Me₂SO was added and the 570nm absorbance was read. The mean value of each concentration (3 well) was obtained. Experiments were repeated three times^[46].

The inhibition rate (%) = (1 - average rate of the treated/average of the control) \times 100

Flowcytometric detection of cell cycle

Cell cycle was determined by flowcytometric assays^[47]. To 1ml of cell suspension with a concentration of 1×10^8 /L, 30 μ mol/L UA and OA 60 μ mol/L were added. The cells were collected after being cultured for 36h and 72h, respectively. Collected cells were treated with absolute alcohol, then with 1% Triton X-100 (Sigma, USA) for 10min at room temperature. The samples were centrifuged, and the supernatant discarded. 0.01% Rnase was added and samples were shaken for 10min in a 37°C water bath. Samples were stained with 0.05% propidium iodide for 10min in 4°C in darkness. The cell cycle distribution was detected with flowcytometer (Model FACSCALIBAR, B.D., USA) and 10000 cells were analyzed with MODFIT software.

Data analysis

Data are displayed as percentage of control condition. Data were expressed as means \pm SEM and Analysis of variance and Student's *t*-test for individual comparisons. $P < 0.05$ was considered statistically significant.

RESULTS

Changes in cell morphology

When HCT15 cells were treated with UA 60 μ mol/L for 24 hours, a number of cells were found dead with a lot of cellular fragments. Among the intact cells, the dead ones accounted for more than 30%. Seventy-two hours later, the number of cells decreased significantly and the remaining cells became shrunken with disappearance of cellular refraction. On the smear stained with HE, a large amount of cellular fragments could be found. When treated with OA 60 μ mol/L for 24 hours, a few cells were dead. There were relatively large amounts of cellular fragments and the dead cells accounted for about 15% at 72 h. Within 72 hours of either UA or OA treatment at a concentration of 30 μ mol/L, a percentage of the cells became rugate at the periphery with blurred cellular borders. There was no obvious cell fragmentation. Relatively large amount of degenerated cells could be seen on HE stained smear, but degenerated cells with OA were markedly less than that with UA.

The cytotoxicity

Cell viability was significantly decreased by treatment of UA and OA for 72 h in a dose-dependent manner. Their IC_{50} were 30 μ mol/L for UA and 60 μ mol/L for OA (Figure 1). Proliferation assay showed that proliferation of UA and OA-treated cells slightly increased at 24 h and significantly decreased at 48 h and 60 h, whereas untreated control cells maintained exponential growth curves (Figure 2).

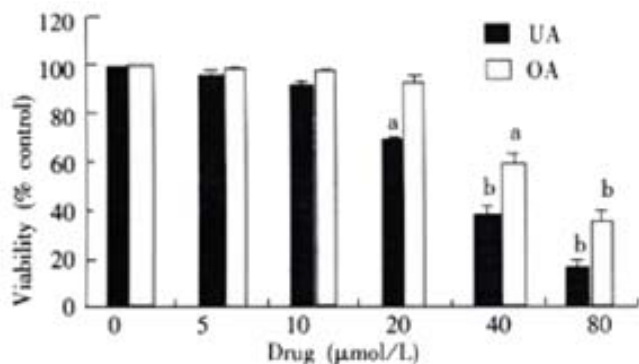


Figure 1 Effects of UA and OA on viability of colon carcinoma cell line. Relative cell viability was assessed by MTT assays. HCT15 cells were treated with various concentrations of UA and OA, respectively for 48 h. Data points represent mean values of 3 replicates, with bar indicating SEM. ^a $P < 0.05$, ^b $P < 0.01$ vs control.

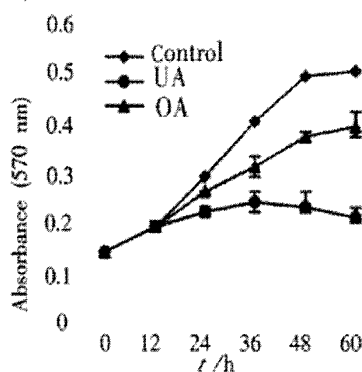


Figure 2 Effects of UA and OA on proliferation of HCT15 cells. HCT15 cells were treated with 30 μ mol/L UA and OA, respectively. The absorbance of 570 nm means the amount of living cells. Data points represent mean values of 3 replicates, with bar indicating SEM. $P < 0.05$, $P < 0.01$ vs control.

Change in cell cycle

When treated the HCT15 cells with different doses of UA and OA for different times, the cell cycle obtained by FCM were as shown in Table 1. HCT15 cells treated with UA 30 μ mol/L and OA 60 μ mol/L for 12 h and 48 h gradually accumulated in G_0/G_1 phase, with a concomitant decrease of cell population in S phase and no detectable apoptotic fraction.

Table 1 The cell cycle distribution of colon carcinoma cell line HCT15 treated with UA and OA ($n=3$ $\bar{x} \pm s$)

Cell cycle	Control		UA (30 μ mol/L)		OA (60 μ mol/L)	
	36h	72h	36h	72h	36h	72h
G_0+G_1	62 \pm 7	50 \pm 7	70 \pm 6	81 \pm 10 ^a	68 \pm 9	76 \pm 6 ^a
S	31 \pm 5	42 \pm 8	22 \pm 4 ^a	9 \pm 3 ^b	26 \pm 4	12 \pm 3 ^b
G_2+M	7 \pm 2	8 \pm 2	8 \pm 3	10 \pm 2	6 \pm 1	12 \pm 2

^a $P < 0.05$, ^b $P < 0.01$ vs control.

DISCUSSION

UA and OA both belong to pentacyclic triterpenoid acids. They have a similar molecular structure, but have different sites of the methyl group on the E loop: if the methyl group at C_{19} of UA is moved to C_{20} , it becomes OA. They are distributed widely in plants. In Korean traditional medicine, UA was used in anti-tumor therapy for a long time. Recently, it has been indicated in and outside China that UA and OA have a definitive antitumor activity by various routes^[48-50].

This paper observed the anti-tumor activity of UA and OA on the HCT15 cells with some preliminary studies on their mechanism of action. With concentrations higher than their IC_{50} , there was obvious cell death and fragmentation. With the IC_{50} concentration, a few cell fragments were found, but cell death was also obvious. To investigate the effects of UA and OA on the viability of HCT15 cells, HCT15 viability was assessed by MTT assay. In addition, we performed a proliferation assay to identify the anti-proliferation effect of UA and OA. The results showed that cell viability was significantly decreased in a concentration-dependent manner and proliferation was markedly inhibited by both drugs. It was shown that both drugs possessed an inhibitory effect on HCT15 cells. The activity was significantly stronger with UA than with OA. According to changes in HCT15 cell morphology, UA and OA have a direct cytotoxic effect on HCT15 cells. Also it has been reported that UA exhibited both cytotoxic and cytostatic activity in A431 human epidermoid carcinoma cells^[48] and OA has a cytotoxic activity against many cancer cell lines^[43]. After incubation of the HCT15 cells with UA or OA for different times, the cell cycle was notably changed. When treated with IC_{50} concentration for 36 and 72 hours, the G_0/G_1 phase cells were gradually increased, with a concomitant decrease of cell population in S phase and no detectable apoptotic fraction. This result was in accordance with an inhibitory effect of UA and OA on HCT15 cells proliferation. These observations suggest that UA and OA may be involved in the action of the G_0/G_1 checkpoint and inhibition of DNA replication. Some studies have supported this inference. They have found that oleanane-type triterpenoids had inhibitory effects on DNA polymerase beta and DNA topoisomerases^[51,52]. Many papers have demonstrated that UA can induce apoptosis^[53,54]. But in the present study FCM assays showed that no apoptotic fraction in treated HCT15 cells. It is worth studying this further by using other methods of detecting apoptosis.

In conclusion, UA and OA have a definite anti-tumor activity on HCT15 cells. The effect of UA is stronger than that of OA. The possible mechanism of action is that both drugs have an inhibitory effect on tumor cell proliferation through cell-cycle arrest.

The toxicity of UA and OA is low and their distribution in plants is extensive. Besides their anti-tumor activity, they also possess immuno-regulatory and liver-protective effects. Therefore, they have

a bright future in clinical application. Further investigation to explore their potential in tumor treatment may prove to be worthwhile.

REFERENCES

- Zhu N, Sheng S, Sang S, Jhoo JW, Bai N, Karwe MV, Rosen RT, Ho CT. Triterpene Saponins from Debittered Quinoa (*Chenopodium quinoa*) Seeds. *J Agric Food Chem* 2002;50:865-867
- Takeoka G, Dao L, Teranishi R, Wong R, Flessa S, Harden L, Edwards R. Identification of three triterpenoids in almond hulls. *J Agric Food Chem* 2000;48:3437-3439
- Upadhyay RK, Pandey MB, Jha RN, Singh VP, Pandey VB. Triterpene glycoside from *Terminalia arjuna*. *J Asian Nat Prod Res* 2001;3:207-212
- Si J, Gao G, Chen D. Chemical constituents of the leaves of *Crataegus scabrifolia* (Franch.) Rehd. *Zhongguo Zhongyao Zazhi* 1998;23:422-432
- Guo XM, Zhang L, Quan SC, Hong YH, Sun LN, Liu MZ. Isolation and identification of Triterpenoid compounds in the fruits of *Chaenomeles lagenaria* (Loisel.) Koidz. *Zhongguo Zhongyao Zazhi* 1998;23:546-547
- Wang YP, Zhu ZY, Wang CF, Yang JS. Determination of oleanolic acid and total saponins in *Aralia* L. *Zhongguo Zhongyao Zazhi* 1998;23:518-521
- Shi LF, Cai Z, Wu GT, Yang ST, Ma Y. RP-HPLC determination of water-soluble active constituents and oleanolic acid in the fruits of *Ligustrum lucidum* Ait. collected from various areas. *Zhongguo Zhongyao Zazhi* 1998;23:77-79
- Ding H, Wang Y, Wang SY, You WY. Quantitative determination of ursolic acid in *Herba cynomorii* by ultraviolet spectrophotometry. *Zhongguo Zhongyao Zazhi* 1998 ;23:102-103, inside back cover
- Zhou FX, Liang PY, Zhou Q, Qin ZQ. Chemical constituents of the stem and root of *Syzygium buxifolium* Hook. Et Arn. *Zhongguo Zhongyao Zazhi* 1998;23:164-165
- Kamel MS, Mohamed KM, Hassanean HA, Ohtani K, Kasai R, Yamasaki K. Acylated flavonoid glycosides from *Bassia muricata*. *Phytochemistry* 2001;57:1259-1262
- Akbar E, Riaz M, Malik A. Ursene type nortriterpene from *Debregeasia salicifolia*. *Fitoterapia* 2001;72:382-385
- Siddiqui BS, Sultana I, Begum S. Triterpenoidal constituents from *Eucalyptus camaldulensis* var. *obtusata* leaves. *Phytochemistry* 2000;54:861-865
- Prasad D, Juyal V, Singh R, Singh V, Pant G, Rawat MSM. A new secoiridoid glycoside from *Lonicera angustifolia*. *Fitoterapia* 2000;71:420-424
- Hou AJ, Yang H, Jiang B, Zhao QS, Lin ZW, Sun HD. A new ent-kaurane diterpenoid from *Isodon phyllostachys*. *Fitoterapia* 2000;71:417-419
- Ye WC, Zhang QW, Liu X, Che CT, Zhao SX. Oleanane saponins from *Gymnema sylvestre*. *Phytochemistry* 2000;53:893-899
- Setzer WN, Setzer MC, Bates RB, Jackes BR. Biologically active triterpenoids of *Syncarpia glomulifera* bark extract from Paluma, north Queensland, Australia. *Planta Med* 2000;66:176-177
- Nguyen LH, Harrison LJ. Xanthenes and triterpenoids from the bark of *Garcinia vilsbiana*. *Phytochemistry* 2000;53:111-114
- Perez-Camino MC, Cert A. Quantitative determination of hydroxy pentacyclic triterpene acids in vegetable oils. *J Agric Food Chem* 1999; 47:1558-1562
- Chang CW, Wu TS, Hsieh YS, Kuo SC, Chao PD. Terpenoids of *Syzygium formosanum*. *J Nat Prod* 1999;62:327-328
- Vo DH, Yamamura S, Ohtani K, Kasai R, Yamasaki K, Nguyen TN, Hoang MC. Oleanane saponins from *Polyscias fruticosa*. *Phytochemistry* 1998;47:451-457
- Tang HQ, Hu J, Yang L, Tan RX. Terpenoids and flavonoids from *Artemisia species*. *Planta Med* 2000;66:391-393
- Jeong TS, Hwang EI, Lee HB, Lee ES, Kim YK, Min BS, Bae KH, Bok SH, Kim SU. Chitin synthase II inhibitory activity of ursolic acid, isolated from *Crataegus pinnatifida*. *Planta Med* 1999;65:261-263
- Marquina S, Maldonado N, Garduno-Ramirez ML, Aranda E, Villarreal ML, Navarro V, Bye R, Delgado G, Alvarez L. Bioactive oleanolic acid saponins and other constituents from the roots of *Viguiera decurrens*. *Phytochemistry* 2001;56:93-97
- Kashiwada Y, Nagao T, Hashimoto A, Ikeshiro Y, Okabe H, Cosentino LM, Lee KH. Anti-AIDS agents 38. Anti-HIV activity of 3-O-acyl ursolic acid derivatives. *J Nat Prod* 2000;63:1619-1622
- Ma C, Nakamura N, Hattori M, Kakuda H, Qiao J, Yu H. Inhibitory effects on HIV-1 protease of constituents from the wood of *Xanthoceras sorbifolia*. *J Nat Prod* 2000;63:238-242
- Alvarez ME, Maria AO, Saad JR. Diuretic activity of *Fabiana patagonica* in rats. *Phytother Res* 2002;16:71-73
- Assefa H, Nimrod A, Walker L, Sindelar R. Enantioselective synthesis and complement inhibitory assay of A/B-ring partial analogues of oleanolic acid. *Bioorg Med Chem Lett* 2001;11:1619-1623
- Yoshikawa M, Matsuda H. Antidiabetogenic activity of oleanolic acid glycosides from medicinal foodstuffs. *Biofactors* 2000;13:231-237
- Li Y, Matsuda H, Yoshikawa M. Effects of oleanolic acid glycosides on gastrointestinal transit and ileus in mice. *Bioorg Med Chem* 1999;7:1201-1205
- Yim TK, Wu WK, Pak WF, Ko KM. Hepatoprotective action of an oleanolic acid-enriched extract of *Ligustrum lucidum* fruits is mediated through an enhancement on hepatic glutathione regeneration capacity in mice. *Phytother Res* 2001;15:589-592
- Saraswat B, Visen PK, Agarwal DP. Ursolic acid isolated from *Eucalyptus tereticornis* protects against ethanol toxicity in isolated rat hepatocytes. *Phytother Res* 2000;14:163-166
- Latha PG, Panikkar KR. Modulatory effects of *ixora coccinea* flower on cyclophosphamide-induced toxicity in mice. *Phytother Res* 1999;13: 517-520
- Jeong HG. Inhibition of cytochrome P450 2E1 expression by oleanolic acid: hepatoprotective effects against carbon tetrachloride-induced hepatic injury. *Toxicol Lett* 1999;105:215-222
- Ismaili H, Tortora S, Sosa S, Fkih-Tetouani S, Ildirissi A, Della Loggia R, Tubaro A, Aquino R. Topical anti-inflammatory activity of *Thymus wilddenowii*. *J Pharm Pharmacol* 2001;53:1645-1652
- Giner-Larza EM, Manez S, Recio MC, Giner RM, Prieto JM, Cerda-Nicolas M, Rios JL. Oleanonic acid, a 3-oxotriterpene from *Pistacia*, inhibits leukotriene synthesis and has anti-inflammatory activity. *Eur J Pharmacol* 2001;428:137-143
- Ryu SY, Oak MH, Yoon SK, Cho DI, Yoo GS, Kim TS, Kim KM. Anti-allergic and anti-inflammatory triterpenes from the herb of *Prunella vulgaris*. *Planta Med* 2000;66:358-360
- Baricevic D, Sosa S, Della Loggia R, Tubaro A, Simonovska B, Krasna A, Zupancic Topical anti-inflammatory activity of *Salvia officinalis* L. leaves: the relevance of ursolic acid. *J Ethnopharmacol* 2001;75:125-132
- Li J, Xu LZ, Zhu WP, Zhang TM, Li XM, Jin AP, Huang KM, Li DL, Yang QY. Effects of ursolic acid and oleanolic acid on Jurkat lymphoma cell line *in vitro*. *Zhongguo Aizheng Zazhi* 1999; 9:395-397
- Hollosy F, Idei M, Csorba G, Szabo E, Bokonyi G, Seprodi A, Meszaros G, Szende B, Keri G. Activation of caspase-3 protease during the process of ursolic acid and its derivative-induced apoptosis. *Anticancer Res* 2001;21:3485-3491
- Rios MY, Gonzalez-Morales A, Villarreal ML. Sterols, triterpenes and biflavonoids of *Viburnum juncundum* and cytotoxic activity of ursolic acid. *Planta Med* 2001;67:683-684
- Martin-Cordero C, Reyes M, Ayuso MJ, Toro MV. Cytotoxic triterpenoids from *Erica andevalensis*. *Z Naturforsch [C]* 2001;56:45-48
- Lauthier F, Taillet L, Trouillas P, Delage C, Simon A. Ursolic acid triggers calcium-dependent apoptosis in human Daudi cells. *Anticancer Drugs* 2000;11:737-745
- Ko HH, Yen MH, Wu RR, Won SJ, Lin CN. Cytotoxic isoprenylated flavans of *Broussonetia kazinoki*. *J Nat Prod* 1999;62:164-166
- Cha HJ, Park MT, Chung HY, Kim ND, Sato H, Seiki M, Kim KW. Ursolic acid-induced down-regulation of MMP-9 gene is mediated through the nuclear translocation of glucocorticoid receptor in HT1080 human fibrosarcoma cells. *Oncogene* 1998;16:771-778
- Mascotti K, McCullough J, Burger SR. HPC viability measurement: trypan blue versus acridine orange and propidium iodide. *Transfusion* 2000; 40:693-696
- Li J, Xu LZ, He KL, Guo WJ, Zheng YH, Xia P, Chen H. Reversal effects of norgestrol acetate on multidrug resistance in adriamycin-resistant MCF7 breast cancer cell line. *Breast Cancer Res* 2001; 3:253-263
- Cao WX, Cheng QM, Fei XF, Li SF, Yin HR, Lin YZ. A study of preoperative methionine-depleting parenteral nutrition plus chemotherapy in gastric cancer patients. *World J Gastroenterol* 2000; 6:255-258
- Hollosy F, Meszaros G, Bokonyi G, Idei M, Seprodi A, Szende B, Keri G. Cytostatic, cytotoxic and protein tyrosine kinase inhibitory activity of ursolic acid in A431 human tumor cells. *Anticancer Res* 2000;20:4563-4570
- Choi CY, You HJ, Jeong HG. Nitric oxide and tumor necrosis factor- α production by oleanolic acid via nuclear factor- κ B activation in macrophages. *Biochem Biophys Res Commun* 2001;288:49-55
- Subbaramaiah K, Michaluart P, Sporn MB, Dannenberg AJ. Ursolic acid inhibits cyclooxygenase-2 transcription in human mammary epithelial cells. *Cancer Res* 2000;60:2399-2404
- Wada S, Iida A, Tanaka R. Screening of triterpenoids isolated from *Phyllanthus flexuosus* for DNA topoisomerase inhibitory activity. *J Nat Prod* 2001;64:1545-1547
- Deng JZ, Starck SR, Hecht SM. DNA polymerase beta inhibitors from *Baeckea gunniana*. *J Nat Prod* 1999;62:1624-1626
- Choi BM, Park R, Pae HO, Yoo JC, Kim YC, Jun CD, Jung BH, Oh GS, So HS, Kim YM, Chung HT. Cyclic adenosine monophosphate inhibits ursolic acid-induced apoptosis via activation of protein kinase A in human leukemic HL-60 cells. *Pharmacol Toxicol* 2000;86:53-58
- Kim DK, Baek JH, Kang CM, Yoo MA, Sung JW, Chung HY, Kim ND, Choi YH, Lee SH, Kim KW. Apoptotic activity of ursolic acid may correlate with the inhibition of initiation of DNA replication. *Int J Cancer* 2000;87:629-636

• LARGE INTESTINAL CANCER •

TGF β_1 expression and angiogenesis in colorectal cancer tissue

Bin Xiong, Ling-Ling Gong, Feng Zhang, Ming-Bo Hu, Hong-Yin Yuan

Bin Xiong, Ling-Ling Gong, Feng Zhang, Ming-Bo Hu, Hong-Yin Yuan, Department of Oncology, Affiliated Zhongnan Hospital of Wuhan University, Wuhan 430071, Hubei Province, China
Supported by Hubei province Natural Science Foundation, No.2000J054
Correspondence to: Dr. Bin Xiong, Department of Oncology, Affiliated Zhongnan Hospital of Wuhan University, Wuhan 430071, Hubei, Province, China. xbxh@public.wh.hb.cn
Telephone: +86-27-87325716
Received 2001-07-19 Accepted 2001-08-23

Abstract

AIM: Transforming growth factor(TGF) β_1 is involved in a variety of important cellular functions, including cell growth and differentiation, angiogenesis, immune function and extracellular matrix formation. However, the role of TGF β_1 as an angiogenic factor in colorectal cancer is still unclear. We investigate the relationship between transforming growth factor β_1 and angiogenesis by analyzing the expression of transforming growth factor(TGF) β_1 in colorectal cancer, as well as its association with VEGF and MVD.

METHODS: The expression of TGF β_1 , VEGF, as well as MVD were detected in 98 colorectal cancer by immunohistochemical staining. The relationship between the TGF β_1 expression and VEGF expression, MVD was evaluated. To evaluate the effect of TGF β_1 on the angiogenesis of colorectal cancers.

RESULTS: Among 98 cases of colorectal cancer, 37 were positive for TGF β_1 (37.8%), 36 for VEGF (36.7%), respectively. The microvessel counts ranged from 19 to 139.8, with a mean of 48.7 (standard deviation, 21.8). The expression of TGF β_1 was correlated significantly with the depth of invasion, stage of disease, lymph node metastasis, VEGF expression and MVD. Patients in T3-T4, stage III-IV and with lymph node metastasis had much higher expression of TGF β_1 than patients in T1-T2, stage I-II and without lymph node metastasis ($P < 0.05$). The positive expression rate of VEGF (58.3%) in the TGF- β_1 positive group is higher than that in the TGF- β_1 negative group (41.7%, $P < 0.05$). Also, the microvessel count (54 ± 18) in TGF- β_1 positive group is significantly higher than that in TGF- β_1 negative group (46 ± 15 , $P < 0.05$). The microvessel count in tumors with both TGF- β_1 and VEGF positive were the highest (58 ± 20 , 36-140, $P < 0.05$). Whereas that in tumors with both TGF- β_1 and VEGF negative were the lowest (38 ± 16 , 19-60, $P < 0.05$).

CONCLUSION: TGF β_1 might be associated with tumor progression by modulating the angiogenesis in colorectal cancer and TGF β_1 may be used as a possible biomarker.

Xiong B, Gong LL, Zhang F, Hu MB, Yuan HY. TGF β_1 expression and angiogenesis in colorectal cancer tissue. *World J Gastroenterol* 2002;8(3):496-498

INTRODUCTION

Angiogenesis is essential for tumor growth and metastasis^[1-6]. An association between poor prognosis and increase in microvascular

density (MVD) of tumor has been reported in certain tumors^[5-10]. This neoangiogenesis depends on the production of angiogenic factors by tumor cells and normal cells^[7-15]. Vascular endothelial growth factor (VEGF) also plays a key role in angiogenesis of tumor^[3-20], but the role of transforming growth factor- β_1 is not clear yet. Now the expression of TGF- β_1 and VEGF, MVD were detected in 98 colorectal cancer by immunohistochemical staining, in order to investigate the correlation of TGF- β_1 and angiogenesis in colorectal cancer.

MATERIALS AND METHODS

Patients

All total of 98 colorectal adenocarcinoma patients who had undergone surgical resection in the Affiliated Zhongnan Hospital of Wuhan University (Wuhan) from July 1998 to December 2000 were included. There were 53 male and 45 female, with an age range from 23 to 74 years (mean, 56 ± 11.2 years). Among the 98 adenocarcinoma patients, 17 were well differentiated, 47 moderately differentiated and 34 poorly differentiated. According to Dukes stage criteria, 34 cases were stage I, 29 stage II, 30 stage III and 5 stage IV.

Methods

Immunohistochemistry All the tissue specimens were fixed in 100 mL L^{-1} neutral formalin and embedded in paraffin. Five-micrometer-thick sections were treated with xylene, dehydrated in ethanol. Tissue sections were washed three times in 0.05 mol L^{-1} PBS, incubated in endogenous peroxidase blocking solution. Non-specific antibody binding was blocked by pretreatment with PBS containing 5 g L^{-1} bovine serum albumin. Sections were then rinsed in PBS and incubated overnight at 4°C with diluted anti-TGF β_1 protein polyclonal antibody, anti-VEGF protein polyclonal antibody and anti-CD34 protein monoclonal antibody. These steps were performed using immunostain kit according to the manufacturers instructions. PBS was used as substitutes of protein antibody for negative control groups. The sections were examined under light microscopy. Anti-TGF β_1 protein polyclonal antibody were purchased from Bosden Co (Wuhan). Anti-VEGF protein polyclonal antibody, anti-CD34 protein monoclonal antibody, and S-P detection kit were purchased from Fuzhou Maixin Co. Anti-TGF β_1 protein polyclonal antibody was diluted to 1:100. Anti-VEGF protein polyclonal antibody and anti-CD34 protein monoclonal antibody were impromptu type.

Results Positive signal was located in the cytoplasm or/and cell membrane. Immunoreactivity was graded as follows: +, $\geq 10\%$ stained tumor cells; -, $< 10\%$ stained tumor cells^[21-23]. The microvessel counting procedures have been described in the published studies^[21-24]. Briefly, the stained sections were screened at a magnification of $\times 100$ ($\times 10$ objective and $\times 10$ ocular lens) under a light microscope to identify the 3 regions of the section with the highest microvessel density. Microvessels were counted in these areas at a magnification of $\times 200$, and the average numbers of microvessels were recorded. The average number is known as MVD of the tumor.

Statistical analysis The difference between each group was analyzed by Chi-square test and correlativity. Significant difference was taken of $P < 0.05$.

RESULTS

TGF β_1 expression in colorectal cancer and clinicopathologic findings

TGF β_1 was localized mainly in the cytoplasm and cell membrane of the tumor cells (Figure 1). TGF β_1 expression was detected in 37 tumors (37.8%). The correlation between TGF β_1 expression and the clinicopathologic findings was shown in Table 1. The expression of TGF β_1 was correlated significantly with the depth of invasion, stage of disease and lymph node metastasis. Patients in T3-T4, stage III-IV and with lymph node metastasis had much higher TGF β_1 than patients in T1-T2, stage I-II and without lymph node metastasis ($P < 0.05$). The expression of TGF β_1 was not correlated with age, gender and differentiation degree of the tumor.

Relationship between TGF β_1 expression, VEGF expression and MVD

VEGF was localized mainly in the cytoplasm and cell membrane of the tumor cells (Figure 2). VEGF expression was detected in 36 tumors (36.7%), and TGF- β_1 expression was correlated closely with VEGF expression (Table 1). The positive expression rate of VEGF (58.3%) in the positive TGF- β_1 group was higher than that in the negative TGF- β_1 group (41.7%, $P < 0.05$).

The number of the microvessel counts in all cases were 19-140 (\pm s, 49 ± 22). Moreover, the microvessel counts were 54 ± 18 in TGF- β_1 positive tumors and 46 ± 15 in TGF- β_1 negative tumors ($P < 0.05$, Table 1). TGF- β_1 expression, VEGF expression and MVD were significantly correlated one another ($r = 0.5816$, 0.2619 and 0.5182 , respectively, $P < 0.05$). The microvessel counts in tumors with both positive TGF- β_1 and VEGF were the highest (58 ± 20 , 36-140; $P < 0.05$). The microvessel counts in tumors with both negative TGF- β_1 and VEGF were the lowest (38 ± 16 , 19-60; $P < 0.05$). The microvessel counts in tumors with positive TGF β_1 and negative VEGF were 25-128 (49 ± 18), and that in tumors with negative TGF β_1 and positive VEGF were 31-133 (50 ± 20), lower than that in tumors with both positive TGF- β_1 and VEGF ($P < 0.05$).

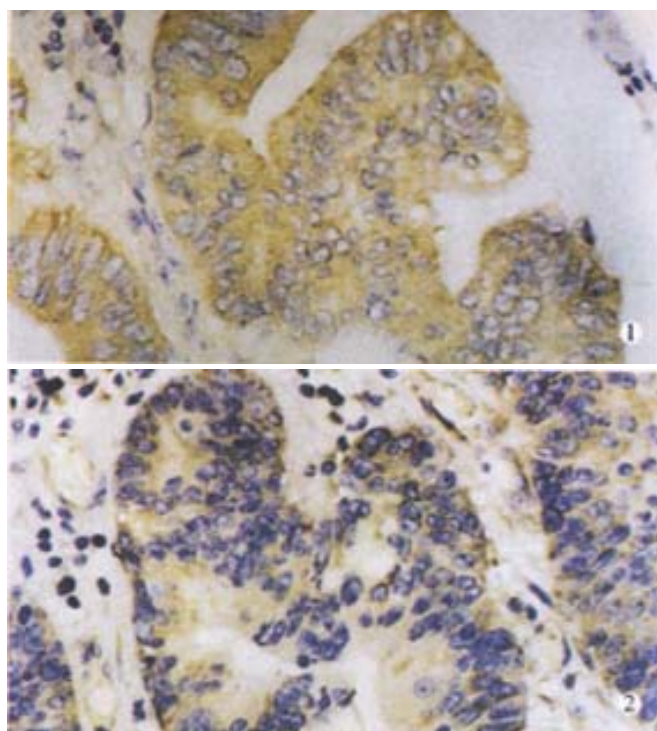


Figure 1 TGF β_1 mainly in cytoplasm and membrane of tumor cells, $\times 400$
Figure 2 VEGF expression mainly in cytoplasm and membrane of tumor cell, $\times 400$

Table 1 Relationship between expression of TGF β_1 and clinicopathologic findings

Clinic-pathologic parameters	TGF β_1 expression(%)	
	Positive(n=37)	Negative(n=61)
Male	20 (37.8)	33 (62.3)
Female	17 (37.8)	28 (62.2)
Age (y)	55 \pm 13	57 \pm 12
Histology: differentiation		
Well	9(52.9)	8 (47.1)
Moderate	15 (31.9)	32 (68.1)
Poor	13 (38.2)	21 (61.8)
Depth of invasion		
T1-T2	17 (28.3)	43 (71.7)
T3-T4	20 (52.6)	18 (47.4) ^a
Lymph node metastasis		
Present	18 (51.4)	17 (48.6)
Absent	19 (30.2)	44 (69.8) ^a
Dukes Stage		
I	8 (23.5)	26 (76.5)
II	9 (31.1)	20 (68.9)
III+IV	20 (57.1)	15 (42.9) ^a
VEGF expression		
Positive	21 (58.3)	15 (41.7)
Negative	16 (25.8)	46 (74.2) ^a
MVD ($\bar{x} \pm s$)	54 \pm 18	46 \pm 15 ^a

^a $P < 0.05$, vs positive

DISCUSSION

The process of angiogenesis is the outcome of an imbalance between positive and negative angiogenic factors produced by both tumor cells and normal cells. Numerous angiogenic factors have been described. Of these, VEGF play a key role in the angiogenesis in the colorectal cancer^[3-25]. VEGF is a multi-functional cytokine, and has direct relationship with angiogenesis. The factors that regulate VEGF expression in tumor and non-tumor cells have now been elucidated^[20-31]. The TGF β s represent a family of multifunctional cytokines that modulate the growth and function of many cells, including those with malignant transformation. The over-expression of TGF β_1 has been reported in tissue from patients with different carcinoma, and is believed to play a role in tumor transformation and progression, as well as in tumor regression^[23-33]. Studied the correlation of TGF β_1 and angiogenesis of gastric cancer, and found TGF β_1 might regulate angiogenesis through an up-regulation of the expression of VEGF. A direct correlation between TGF β_1 expression and microvessel counts had not been identified in the current study^[20-30]. TGF β_1 has no relationship with VEGF expression in breast cancer tissue, but is correlated with the expression of platelet-derived growth factor, and co-regulate angiogenesis^[20-24]. The modulating mechanisms of TGF β_1 in angiogenesis are not entirely the same in different type of tumor.

The role of TGF β_1 in angiogenesis of colorectal cancer is not identified yet. This study found that the expression of VEGF and MVD in positive TGF β_1 group are significantly higher than that in TGF β_1 negative group. The expression of TGF β_1 is significantly positively correlated with the expression of VEGF. It demonstrated that TGF β_1 may be correlated indirectly with angiogenesis through an up-regulation of the expression of VEGF. The expression of TGF β_1 is also significantly positively correlated with MVD in colorectal cancer.

It demonstrates that TGF β_1 may modulate angiogenesis directly or indirectly through up-regulating the expression of other angiogenic factors. The microvessel counts in tumors that were both positive TGF- β_1 and VEGF were the highest of all. It demonstrates that TGF- β_1 and VEGF may co-modulate the angiogenesis.

TGF β_1 expression was detected in 37 tumors (37.8%). The expression of TGF β_1 was correlated significantly with the depth of invasion, stage of disease and lymph node metastasis. Patients in T3-T4, stage III-IV and with lymph node metastasis had much higher expression of TGF β_1 than patients in T1-T2, stage I-II and without lymph node metastasis ($P < 0.05$).

REFERENCES

- Grunstein J, Roberts WG, Mathieu-Costello O, Hanahan D, Johnson RS. Tumor-derived expression of vascular endothelial growth factor is a critical factor in tumor expansion and vascular function. *Cancer Res* 1999; 59:1592-1598
- Karpanen T, Egeblad M, Karkkainen MJ, Kubo H, Yla-Herttuala S, Jaattela M, Alitalo K. Vascular endothelial growth factor C promotes tumor lymphangiogenesis and intralymphatic tumor growth. *Cancer Res* 2001;61:1786-1790
- Siemeister G, Schirner M, Weindel K, Reusch P, Menrad A, Marme D, Martiny-Baron G. Two independent mechanisms essential for tumor angiogenesis: inhibition of human melanoma xenograft growth by interfering with either the vascular endothelial growth factor receptor pathway or the tie-2 pathway. *Cancer Res* 1999; 59: 3185-3191
- Masood R, Ca J, Zheng T, Smith DL, Hinton DR, Gill PS. Vascular endothelial growth factor(VEGF) is an autocrine growth factor for VEGF receptor-positive human tumors. *Blood* 2001;98:1904-1913
- Leenders W, Altena MV, Lubsen N, Rutter D, Waa RDI. *In vivo* activities of mutants of vascular endothelial growth factor(VEGF) with differential *in vitro* activities. *Int J Cancer* 2001;91: 327-333
- Veikkola T, Karkkainen M, Claesson-Welsh L, Alitalo K. Regulation of angiogenesis via vascular endothelial growth factor receptors. *Cancer Res* 2000;60: 203-212
- Teraoka H, Sawada T, Nishihara T, Yashiro M, Ohira M, Ishikawa T, Nishini H, Hirakawa K. Enhanced VEGF production and decreased immunogenicity induced by TGF β -1 promote liver metastasis of pancreatic cancer. *British J Cancer* 2001;85:612-617
- Wu RS, Meade-Tollin L, Besselse D, Seftor E, Katsanis E, McEarchern JA, Koble JJ, Mack V, Arteaga CL, Dumout N, Mary JC, Akporiaye ET. Invasion and metastasis of a mammary tumor involve TGF β signaling. *Int J Cancer* 2001; 91: 76-82
- Ying YQ, Zhou X, Wu P, Huang WB. Significance of TGF- α and TGF- β_1 expressions in the tissue of colorectal cancer. *Shijie Huaren Xiaohua Zazhi* 2001;9:223-225
- Wang SM, Wu JS, Yao X, He ZS, Pan BR. Effect of TGF α , EGFR anti-sense oligodeoxynucleotides on colon cancer cell line. *Shijie Huaren Xiaohua Zazhi* 1999;7:522-524
- Wang CH, Zhang XM, Zhan M, Tang FX. TGF- β and its receptor expression in human colorectal cancer. *Shijie Huaren Xiaohua Zazhi* 2001;9:462-463
- Yu BM, Zhao R. Molecular biology of colorectal carcinoma. *Shijie Huaren Xiaohua Zazhi* 1999;7:173-175
- Yang JH, Rao BJ, Wang Y, Tu XH, Zhang LY. Clinical significance of detecting the circulating cancer cells in peripheral blood from colorectal cancer. *Shijie Huaren Xiaohua Zazhi* 2000;8:187-189
- Jia L, Chen TX, Sun JW, Na ZM, Zhang HH. Relationship between microvessel density and proliferating cell nuclear antigen and prognosis in colorectal cancer. *Shijie Huaren Xiaohua Zazhi* 2000;8:74-76
- Maehara YB, Kakeji Y, Kabashima A, Emi Y, Watanabe A, Akazawa K, Baba H, Kohnoe S, Sugimachi K. Role of transforming growth factor- β_1 in invasion and metastasis in gastric carcinoma. *J Clin Oncol* 1999;17:607-614
- Rodeck V, Nishiyama J, Mauriel A. Independent regulation of growth and Smad-mediated transcription by TGF- β in human melanoma cells. *Cancer Res* 1999;59:547-550
- Shyr M, Sheen C, Han SC, Chin WS, Hock CE, Wei JC. Serum levels of TGF- β_1 in patients with breast cancer. *Arch Surg* 2001;13:937-940
- Shim KS, Kim KH, Han WS, Park EB. Elevated serum levels of transforming growth factor- β_1 in patients with colorectal carcinoma. *Cancer* 1999;85:554-561
- Kadambi A, Carreira CM, Yun CO, Padera TP, Dolmans DE, Carmeliet P, Fukumura D, Jain RK. Vascular endothelial growth factor (VEGF)-C differentially affects tumor vascular function and leukocyte recruitment: role of VEGF-receptor 2 and host VEGF-A. *Cancer Res* 2001; 61: 2404-2408
- Saito H, Tsujitani S, Oka S, Kondo A, Lkeguchi M, Maeta M, Kaibara N. The expression of transforming growth factor- β_1 is significantly correlated with the expression of vascular endothelial growth factor and poor prognosis of patients with advanced gastric carcinoma. *Cancer* 1999;86:1455-1462
- Zhuang ZH, Chen YL, Wang CD, Chen YG. Expression of TGF β_1 and TGF β receptor in gastric carcinoma and precancerous lesions. *Shijie Huaren Xiaohua Zazhi* 1999;7: 507-509
- Xiong B, Yuan HY, Hu MB, Zhang F. Serum levels of transforming growth factor- β_1 correlating with T cell subsets and natural killer cell activity in colorectal cancer. *Shijie Huaren Xiaohua Zazhi* 2001;9:1194-1195
- Ariazi EA, Satomi Y, Ellis MJ, Haag JD, Shi W, Sattler CA, Gould MN. Activation of the transforming growth factor β signaling pathway and induction of cytostasis and apoptosis in mammary carcinomas treated with the anticancer agent perillyl alcohol. *Cancer Res* 1999;59:1917-1928
- Liu DH, Zhang W, Su YP, Zhang XY, Huang YX. Constructions of eukaryotic expression vector of sense and antisense VEGF165 and its expression regulation. *Shijie Huaren Xiaohua Zazhi* 2001; 9:886-891
- Wan SM, Sun SH, Deng MD, Ge QL, Yang YJ. TGF- β_1 and PDGF-A expression in gastric cancer tissue and prognosis. *Shijie Huaren Xiaohua Zazhi* 2002;10: 36-39
- Si XH, Yang LJ. Extraction and purification of TGF β and its effect on the induction of apoptosis of hepatocytes. *World J Gastroenterol* 2001; 7: 527-531
- Wu K, Liu BH, Zhao DY, Zhao Y. Effect of vitamin E succinate on expression of TGF- β_1 , C-Jun and JNK1 in human gastric cancer SGC-7901 cells. *World J Gastroenterol* 2001;7:83-87
- Liu F, Liu JX, Cao ZC, Li BS, Zhao CY, Kong L, Zhen Z. Relationship between TGF- β_1 , serum indexes of liver fibrosis and hepatic tissue pathology in patients with chronic liver diseases. *Shijie Huaren Xiaohua Zazhi* 1999; 7: 519-521
- Liu XP, Song SB, Li G, Wang DJ, Zhao HL, Wei LX. Correlations of microvessel quantitation in colorectal tumors and clinicopathology. *Shijie Huaren Xiaohua Zazhi* 1999; 7: 37-39
- Huang YX, Zhang GX, Lu MS, Fan GR, Chen NL, Wu GH. Increased expression of transforming growth factor- β_1 in hepatocellular carcinoma. *Huaren Xiaohua Zazhi* 1999; 7: 150-152
- Yan JC, Chen WB, Ma Y, Shun XH. Expression of vascular endothelial growth factor in liver tissues of hepatitis B. *Huaren Xiaohua Zazhi* 1999; 7: 837-840
- Xiang DD, Wei YL, Li JF. Molecular mechanism of TGF- β_1 on Ito cell. *Huaren Xiaohua Zazhi* 1999; 7: 980-981
- Ma XM, Wang YL, Pan BR. Progress in VEGF studies. *Huaren Xiaohua Zazhi* 1999; 7: 895-896

Edited by Wu XN

• VIRAL LIVER DISEASES •

Full-length core sequence dependent complex-type glycosylation of hepatitis C virus E2 glycoprotein

Li-Xin Zhu, Jing Liu, Ying-Chun Li, Yu-Ying Kong, Caroline Staib, Gerd Sutter, Yuan Wang, Guang-Di Li

Li-Xin Zhu, Jing Liu, Ying-Chun Li, Yu-Ying Kong, Yuan Wang, Guang-Di Li, Institute of Biochemistry and Cell Biology, Shanghai Institutes for Biological Sciences, Chinese Academy of Sciences, Shanghai 200031, China
Caroline Staib, Gerd Sutter, GSF-Institut für Molekulare Virologie, Trogerstr. 4b, 81675 München, Germany. The first two authors contributed equally to this paper.

Supported by the National 863 High Technology Foundation of China, No.863-102-07-02-02, No.2001AA215171 and the project CHN 98/112 (WTZ-Internationales Büro des BMBF).

Correspondence to: Yuan Wang and Guang-Di Li, Institute of Biochemistry and Cell Biology, Shanghai Institutes for Biological Sciences, Chinese Academy of Sciences, 320 Yue-Yang Road, Shanghai 200031, China. wangyuan@server.shcnc.ac.cn

Telephone: +86-21-64374430 Fax: +86-21-64338357

Received 2001-12-05 Accepted 2002-01-23

Abstract

AIM: To study HCV polyprotein processing is important for the understanding of the natural history of HCV and the design of vaccines against HCV. The purpose of this study is to investigate the affection of context sequences on hepatitis C virus (HCV) E2 processing.

METHODS: HCV genes of different lengths were expressed and compared in vaccinia virus/T7 system with homologous patient serum S94 and mouse anti-serum M_{E2116} raised against *E.coli*-derived E2 peptide, respectively. Deglycosylation analysis and GNA (*Galanthus nivalus*) lectin binding assay were performed to study the post-translational processing of the expressed products.

RESULTS: E2 glycoproteins with different molecular weights (~75kDa and ~60kDa) were detected using S94 and M_{E2116}, respectively. Deglycosylation analysis showed that this difference was mainly due to different glycosylation. Endo H resistance and its failure to bind to GNA lectin demonstrated that the higher molecular weight form (75kDa) of E2 was complex-type glycosylated, which was readily recognized by homologous patient serum S94. Expression of complex-type glycosylated E2 could not be detected in all of the core-truncated constructs tested, but readily detected in constructs encoding full-length core sequences.

CONCLUSION: The upstream conserved full-length core coding sequence was required for the production of E2 glycoproteins carrying complex-type N-glycans which reacted strongly with homologous patient serum and therefore possibly represented more mature forms of E2. As complex-type N-glycans indicated modification by Golgi enzymes, the results suggest that the presence of full-length core might be critical for E1/E2 complex to leave ER. Our data may contribute to a better understanding of the processing of HCV structural proteins as well as HCV morphogenesis.

Zhu LX, Liu J, Li YC, Kong YY, Staib C, Sutter G, Wang Y, Li GD. Full-length core sequence dependent complex-type glycosylation of hepatitis C virus E2 glycoprotein. *World J Gastroenterol* 2002;8(3):499-504

INTRODUCTION

Hepatitis C virus (HCV), the major cause of post-transfusion and community-acquired non-A, non-B hepatitis^[1,2], is a member of the Flaviviridae family^[3]. This virus has a positive-sense, single stranded RNA genome of about 9.6 kb, which encodes a polyprotein precursor of about 3000 amino acids. The polyprotein is further processed into various precursors and mature viral proteins^[4,5]. The structural proteins are encoded in the order NH₂-core-E1-E2-P7, which are processed into core (C), E1, E2, and P7 by host membrane-associated signal peptidase(s)^[6-11]. The downstream nonstructural region is processed by a viral metalloprotease and a viral serine protease located at the N-terminus of NS3^[12-17]. The core protein is thought to constitute the viral capsid with E1 and E2 being the virus envelope proteins. Numerous studies have shown that E1 and E2 are heavily glycosylated and associate to form a noncovalent heterodimeric complex^[9,10,18,19]. E1 and E2 are believed to be type I transmembrane proteins with an N-terminal glycosylated ectodomain and a C-terminal hydrophobic anchor.

The lack of an efficient *in vitro* cell culture system for productive HCV propagation^[20-27] and low levels of HCV particles in the liver tissues or blood of infected patients^[28,29] have hampered the study of native viral proteins. Fortunately, a variety of prokaryotic and eukaryotic expression systems have proved useful for the production and characterization of HCV encoded proteins^[8,9,11,30-32]. However, diverse findings have been reported, regarding the molecular weights of E2, which most likely is a reflection of the differences in efficiency of HCV polyprotein processing and post-translational modification achieved in the particular systems^[7-9,11,17-19,30]. In this study, the E2 expression of recombinant plasmids carrying various length of HCV C-E1-E2 coding sequences was analyzed in the vaccinia virus/bacteriophage T7 RNA polymerase expression system^[33]. The results suggest that the upstream conserved core coding sequence is required for the production of E2 glycoproteins carrying complex-type N-glycans which react strongly with homologous patient serum and therefore possibly represent more mature forms of E2.

MATERIALS AND METHODS

Cells and viruses

Human HeLa (ATCC #CCL-2) and monkey BS-C-1 (ATCC #CCL-26) cells were maintained in Dulbecco's modified essential medium (DMEM/HG) supplemented with 5% heat inactivated fetal calf serum (FCS) at 37°C in a 5% CO₂ atmosphere. Recombinant vaccinia virus vTT7 that expresses the bacteriophage T7 RNA polymerase gene under the control of vaccinia virus early/late promoter P7.5 was generated and propagated as previously described^[34]. PFU (plaque forming unit) titration was performed on BS-C-1 cell monolayers.

Plasmid constructions

The vaccinia virus/T7 promoter expression vector pTM1 was kindly provided by Bernard Moss (NIH, Bethesda, USA) and all of the expression plasmids carrying HCV cDNA encoding structural proteins described below were derived from pTM1. Figure 1 depicts the HCV gene fragment in the expression plasmids. Plasmids pCEH-2 (1-730)

and pEH containing HCV C, E1 and E2 gene of subtype 1b^[35] (GENBANK accession #D10934) were described previously^[34]. Briefly, cDNA sequences encoding HCV polyprotein amino acids 192 to 730 were inserted into pTM1 to obtain pEH. HCV sequences encoding complete C were fused with the E1/E2 sequences of pEH to result in plasmid pCEH-2(1-730). The latter plasmid served as basis for PCR cloning to generate plasmids pCE1(1-341), ptCEH-2(108-730), ptCEH-2(120-730), ptCEH-2(137-730), ptCEH-2(156-730), ptCEH-2(167-730), pCEH-2(1-661) and pTM1/EH(192-661) for the expression of 5' or/and 3' truncated HCV sequences encoding HCV polyprotein amino acids as indicated by numbers in parenthesis. Plasmid pC-E2H(1-195/394-661) was generated by deleting E1 coding sequences from pCEH-2(1-661) and linking polyprotein amino acids aa194 and aa394 together. Authenticity of HCV cDNA sequences in all constructed plasmids was confirmed by automatic sequencing.

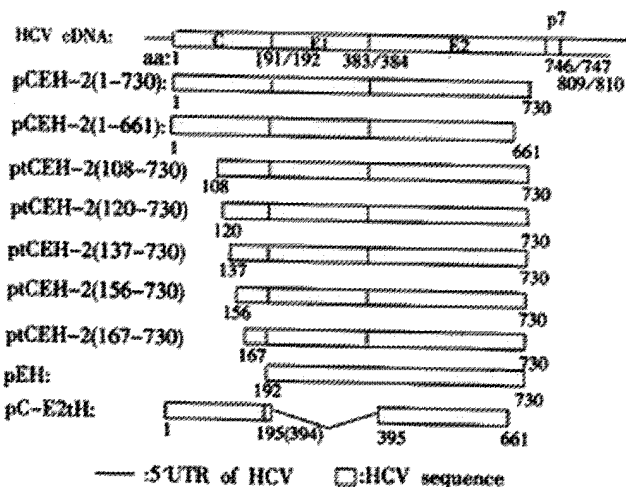


Figure 1 Schematic maps of HCV coding sequences inserted into the plasmid pTM1 and expressed under transcriptional control of the bacteriophage T7 pol promoter. Numbers refer to amino acids of the HCV polyprotein.

Transient expression of recombinant genes using vaccinia virus/T7 RNA polymerase (VV-T7pol)

HeLa cells grown to 80% confluency were infected with recombinant vaccinia virus vTT7 at a multiplicity of infection (MOI) of 10 PFU per cell to allow for production of recombinant T7 RNA polymerase. At 2h post-infection, the inoculum was removed and DNA of pTM1 based expression plasmids was transfected using DOTAP liposomal transfection reagent as described by the manufacturer (Roche Molecular Biochemicals, Mannheim). After 24 hours of incubation, infected/transfected cells were washed twice with PBS, harvested by scraping, pelleted upon brief centrifugation, and resuspended in a small volume of PBS. Cell lysates were prepared by adding SDS-PAGE sample loading buffer and stored at -80°C until further analysis.

Western blot analysis

Cell lysates were separated by reductive SDS-PAGE and then transferred onto nitrocellulose membranes (Schleicher & Schuell). Blocking was done using 5% fat-free milk powder. For immunodetection of HCV proteins, blots were incubated with primary antibodies, washed, and incubated with 1000 fold diluted HRP-protein A (Sigma). The membranes were then washed again and reactive proteins were detected using the ECL system (Amersham Pharmacia Biotech) according to the manufacturers' instructions. The primary antibodies used in this study include: anti-HCV human serum S94 at a dilution of 1:500 (kindly provided by Wang, Y., Beijing

University, China), anti-HCV human serum S268 at a dilution of 1:500 (kindly provided by Lu Z., Shanghai Ruijin Hospital, China), anti-E2 mouse polyclonal antibody M_{E2116}^[36] at a dilution of 1:300 (raised against E. Coli-derived HCV E2 polypeptide aa450 to 565), and anti-E1 rabbit polyclonal antibody R_{E1135-C} at a dilution of 1:250 (raised against an E. coli-derived C-terminally truncated HCV E1 fragment).

Characterization of N-glycans on expressed E2 glycoproteins

For deglycosylation analysis, cell pellets were directly lysed in denaturing buffer provided by the manufacturer and digested with PNGase F (NEB) or Endo H (NEB) for 2 hours at 37°C.

The type of N-glycans on expressed E2 glycoproteins was also analyzed by testing its ability to bind to GNA (Galanthus nivalus) lectin. HeLa cells infected with vTT7 and transfected with pCEH-2(1-730) were collected by scraping, washed in cold PBS, and then lysed with lysis buffer (50mM Tris-HCl [pH8.0], 150mM NaCl, 0.5% Nonidet P-40, 1mM PMSF). After centrifugation at 10000g, the supernatant was allowed to bind to GNA-agarose (Sigma). The flow-through fraction was collected and the gel matrices were washed with lysis buffer. Bound proteins were eluted with 1M α -D-mannopyranoside (Sigma) in lysis buffer. Samples were then analyzed by Western-blotting.

RESULTS

Detection of E2 glycoproteins of different Molecular Weights using antibodies of distinct origins

The hybrid vaccinia virus/T7 bacteriophage RNA polymerase expression system was used to study the expression of the HCV structural proteins. The transient expression products of plasmids pCEH-2(1-730) and pCEH-2(1-661), which contain HCV cDNA encoding the structural region terminating at amino acid 730 and 661 of the polyprotein respectively, were analyzed by Western blot using polyclonal mouse serum M_{E2116} raised against E.coli-derived E2 protein^[36]. E2 products with apparent molecular weights (MWs) of ~60kDa and ~50kDa were detected for pCEH-2(1-730) and pCEH-2(1-661) respectively (Figure 2, lane 1, 3). The apparent molecular weights were higher than calculated values, which, along with the heterogeneous appearance of the detected bands, suggested that these were glycosylated expression products. The lower molecular weight of the E2 species obtained from expression of pCEH-2(1-661) in comparison to pCEH-2(1-730) was consistent with the introduced truncation at the 3' end of the E2 coding sequences leading to the loss of 70 amino acids in the recombinant polypeptide backbone.

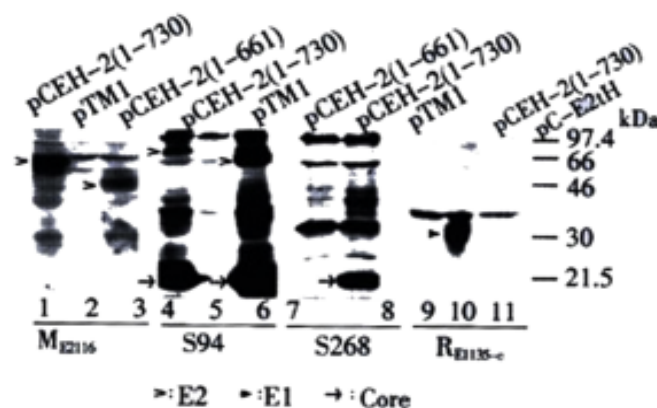


Figure 2 Detection of E2 glycoprotein species of different molecular masses. Transient expression products were analyzed by Western blot with antibodies of distinct origin: mouse polyclonal antibody M_{E2116} (lane 1, 2, 3); HCV patient serum S94 (lane 4, 5, 6); HCV patient serum S268 (lane 7, 8); rabbit polyclonal antibody R_{E1135-C} (lane 9, 10, 11). Empty vector pTM1 was used as the negative control. HCV-specific protein bands are indicated by arrowheads. The plasmids used for transfection are indicated at the top of the lanes.

The expression products were also analyzed with HCV patient serum S94. Multiple prominent bands were detected for pCEH-2(1-730) and pCEH-2(1-661), but not for vector plasmid pTM1, representing expressed HCV structure proteins and possibly some precursors. The bands of ~75 kDa and ~66 kDa (Figure 2, lane 4, 6), which again consistent with the different length of E2 coding sequence in both plasmids, should represented the E2 proteins, although their MWs were higher than that detected by M_{E2116} . It is worth noting that the analyzed HCV cDNA originated from the same patient from whom S94 was collected. The core antigen and some precursors of expression products could also be detected by another HCV patient serum S268, but we could not detect the E2-specific 75kDa band (Figure 2, lane 8), which could be attributed to the high variability of the E2 glycoprotein^[37, 38].

The antibody dependent detection of different E2 glycoprotein species was surprising. To rule out that the E2 bands of higher MW is the uncleaved E1-E2 precursors, the expression products from pCEH-2(1-730) were analyzed with anti-E1 rabbit sera. A heavy band of about 30kDa was detected, possibly representing multiple forms of E1 proteins (Figure 2, lane 10), while no E1-specific band with higher MW was detected. Another possible explanation could be that E2 polypeptides of varying sizes were synthesized due to incomplete or irregular processing of the polyprotein. This hypothesis was abandoned when we subjected recombinant proteins to deglycosylation with PNGase F prior to Western blot analysis with mouse polyclonal antibody M_{E2116} . After PNGase F treatment, only one E2-specific band with apparent molecular weight of 30 kDa was detected for pCEH-2(1-661) expression products, while an E2-specific doublet band of 33/34 kDa was detected for pCEH-2(1-730) expression products (Figure 3), which is consistent with the MWs of calculated E2 polypeptide backbones. It suggests that difference of the MWs of E2 species detected by M_{E2116} and S94 from the same transient expression products (pCEH-2(1-730): ~60kDa and ~75kDa, pCEH-2(1-661): ~50kDa and ~66kDa) is mainly due to different N-glycosylation. The detection of a E2 peptide doublet with pCEH-2(1-730) but not with pCEH-2(1-661) is in agreement with the fact that E2 contains a PKR-eIF2 α phosphorylation site (PKR: RNA-activated protein kinase) at aa659-670^[39], which is largely deleted in the pCEH-2(1-661) construct.

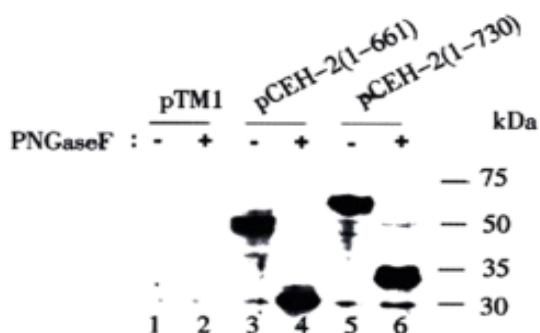


Figure 3 Deglycosylation analysis of the expressed HCV E2 proteins with PNGase F. Transient expression products were subjected to Western blot analysis with M_{E2116} as the primary antibody. pTM1 transfected cells were used as control. The plasmids used for transfection are indicated at the top of the lanes. Samples incubated with deglycosylation buffer were run in parallel. +: samples digested with PNGase F, -: samples incubated with PNGase F reaction buffer.

Altogether, the above results suggest that the 75kDa and 66kDa bands detected by S94 are HCV E2 glycoproteins of heavier glycosylation and thus higher molecular weight.

M_{E2116} - and S94-reactive E2 glycoproteins carried different types of N-glycans

Since M_{E2116} - and S94-reactive E2 species had polypeptide backbones

of the same size, the difference in apparent molecular weight and antibody reactivity could only be attributed to differences in the degree and/or type of glycosylation. The glycan type on different E2 species expressed from pCEH-2(1-730) was then analyzed by testing their sensitivity to PNGase F and Endo H. PNGase F hydrolyzes all types of N-glycan chains from glycopeptides and glycoproteins unless they carry α -1-3 linked core fucose residues present in insect and plant glycoproteins^[40], while Endo H cleaves only high mannose structures and hybrid structures on N-linked oligosaccharides of glycoproteins^[41]. Figure 4A shows that the M_{E2116} -reactive E2 species was sensitive to both PNGase F and Endo H digestion. The S94-reactive E2 species disappeared after PNGase F digestion (Figure 4B). It was difficult to detect the deglycosylated E2 with S94 after PNGase F treatment, because there were multiple HCV polyprotein precursor proteins of about 30000 reacted strongly with S94 and unglycosylated E2 seemed to react weakly with S94 (unpublished data). However, the highly glycosylated, S94-reactive E2 band remained after Endo H digestion (Figure 4B). The glycan type of different E2 species expressed from pCEH-2(1-730) were also analyzed by testing their ability to bind to GNA lectin. GNA is specific for the non-reducing end of α -D-mannosyl residue of glycoconjugate and therefore can be used to probe the presence of high mannose type or hybrid type glycans on glycoproteins^[42, 43]. The M_{E2116} -reactive E2 species could quantitatively bind to and be eluted from GNA-agarose, whereas no obvious binding could be demonstrated for S94-reactive E2 species (Figure 5).

The resistance of S94-reactive E2 glycoprotein species to Endo H digestion together with the fact that it could not bind to GNA indicates that the S94-reactive E2 protein carries complex-type glycans.

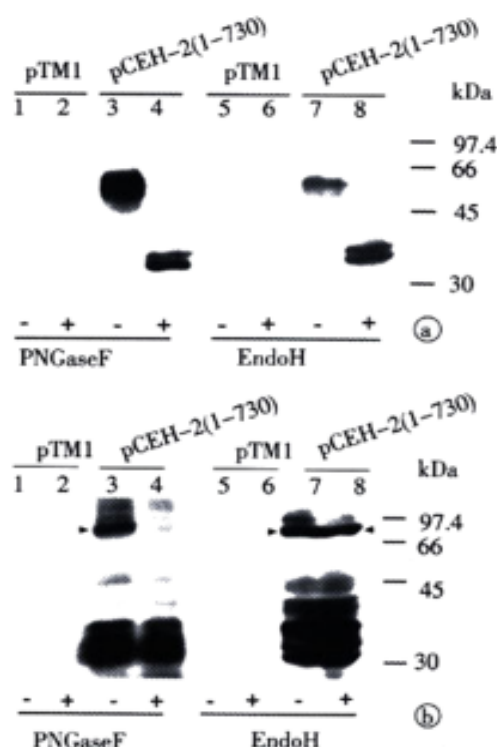


Figure 4 Different sensitivities of two glycosylated E2 species to PNGase F and Endo H. Transient expression products of pCEH-2(1-730) were digested with PNGase F or Endo H, respectively. The digested samples were analyzed by Western blot with M_{E2116} (A) and S94 (B). Empty vector pTM1 was used as negative control.

Samples incubated with deglycosylation buffer were run in parallel. +: samples digested with Endoglycosidase, -: samples incubated with Endoglycosidase reaction buffer. The plasmids used for transfection are indicated at the top of the lanes. Endoglycosidases used in this study are indicated at the bottom of the lanes. S94-reactive E2 proteins are indicated by arrowheads.

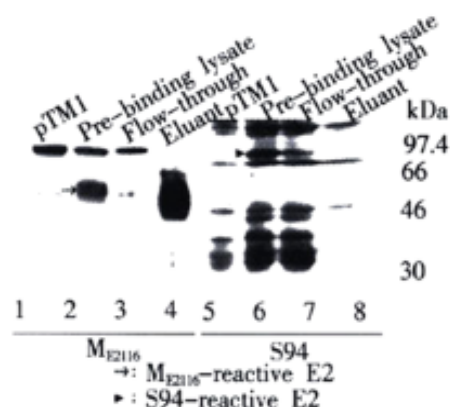


Figure 5 Different ability of differently glycosylated E2 species to bind to GNA-agarose. HeLa cells infected with vT7 and transfected with pCEH-2(1-730) were collected, washed and lysed with lysis buffer. The cleared supernatant was then allowed to bind to GNA-agarose. The gel beads were washed and eluted with 1M α -D-mannopyranoside in lysis buffer. Pre-binding lysate, flow-through and eluate fractions were analyzed by Western blot analysis. HeLa cells infected with vT7 and transfected with pTM1 were served as negative control. The sera used as primary antibodies are indicated at the bottom of the lanes. E2 proteins are indicated by arrowheads.

HCV core sequence dependent formation of complex-glycosylated E2

We also assessed if co-expression of core or E1 coding sequences had any effect on the production of the E2 proteins, which was readily recognized by homologous patient serum S94. A set of expression plasmids containing HCV cDNAs with various deletions in the core sequence (ORF starting at aa108, aa120, aa137, aa151, or aa167, respectively) were constructed. The lysates from vT7-infected and plasmid DNA transfected HeLa cells were analyzed by Western blot with either the mouse anti-serum M_{E2116} or the patient serum S94 (Figure 6).

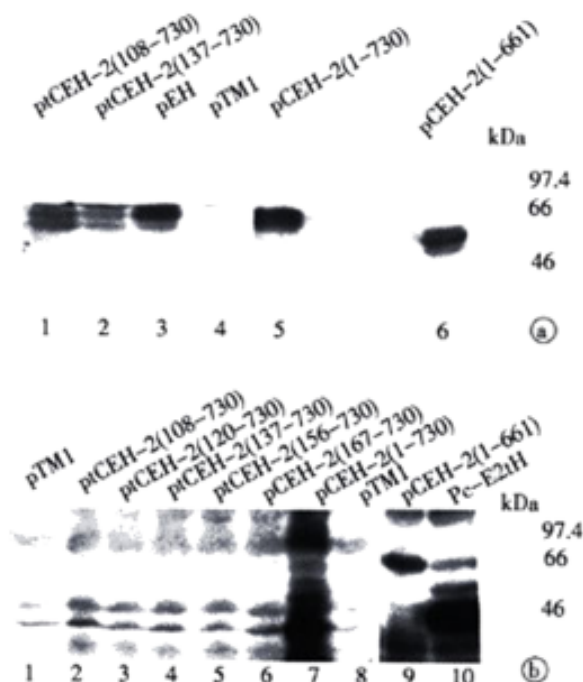


Figure 6 Requirement of the core sequence for the expression of complex-type glycosylated E2. Expression products of differently truncated HCV structural genes were analyzed by Western blot analysis. Blots were probed with M_{E2116} (A) or with S94 (B). Empty vector pTM1 was used as negative control. The plasmids used for transfection are indicated at the top of the lanes.

When using mouse antibody M_{E2116} , recombinant E2 of ~ 60 kDa and ~ 50 kDa could be detected upon expression of all constructs tested (Figure 6A). Patient serum S94 allowed detection of E2 for pCEH-2(1-730) and pCEH-2(1-661) with full-length core coding sequences (Figure 6B, lanes 7, 9), similar to that described in Figure 2. In contrast, no E2 products could be visualized after expression of constructs containing no or only partial core sequences (Figure 6B, lanes 1-6). Interestingly, deletion of E1 coding sequences had no significant effect on the synthesis of S94 detectable E2 protein (Figure 6B, lane 10). These results suggest that the presence of complete HCV core sequence is crucial for the expression and/or post-translational processing of the complex-type glycosylated form of E2.

DISCUSSION

In this study, various constructs of HCV cDNAs placed under transcriptional control of the bacteriophage T7 promoter were transiently expressed using vaccinia virus/T7 system. Upon characterization of the HCV gene products with different antibodies, two species of E2 with different MWs were identified in the expression products of the same plasmid. The high molecular weight forms of E2 were readily recognized by a patient serum, but displayed weak reactivity with antibodies raised against E. coli derived E2. These high molecular weight forms of E2 were not likely produced from inefficient proteolytical processing at the E1/E2 boundary as these proteins were not stained with E1-specific antibodies. Efficient processing at E1/E2 was confirmed by deglycosylation analysis. The difference of the MWs of E2 species detected by S94 and by M_{E2116} was therefore mainly due to different N-glycosylation. The S94-reactive E2 glycoproteins, which were resistant to Endo H digestion and could not bind to GNA, carry complex-type glycans.

The specific recognition of the complex-type glycosylated E2 but not the high-mannose-type glycosylated E2 by homologous patient serum S94 suggested that the former could be a better representation of native E2 proteins on HCV virions. Similar results were also reported by Inudoh *et al*^[44]. By comparing the reactivity of complex-type glycosylated E2 and the high-mannose-type glycosylated E2 with different patient sera, they demonstrated that the former is superior in diagnosing HCV infection. Their results and our results reported here are in concordance with the finding that E2 protein on patient derived virions contained complex-type sugars indicating Golgi-specific modification^[45].

Expression of full-length or C-terminally truncated envelop proteins in eukaryotic cells has demonstrated that E1 and E2 are retained within the ER membrane system due to the presence of ER-retention signals in the C-termini of both envelope proteins^[46-50]. However, recent study indicates that HCV E2 proteins could also present in the Golgi apparatus of the stably transfected cell line expressing HCV C-E1-E2-NS2 fragment. A possible explanation could be that Martire *et al*^[51] used an HCV gene fragment including full-length core sequences in their study while structural protein sequences without full-length core sequences were used to study the localization of envelop proteins. The results reported here demonstrated that the complex-type glycosylated, possibly more mature form of E2 is only detectable upon co-expression of the complete HCV core coding sequence. Deletion of the first 107 N-terminal core amino acid residues was obviously sufficient to abrogate production of complex-glycosylated E2. This result suggest that the core protein might allow for targeting the envelope glycoproteins to Golgi-specific modification, which could be a key step in the morphogenesis of HCV virions. HCV-like particles were observed when HCV cDNA encoding whole core, E1 and E2 was expressed in baculovirus-insect expression system^[52]. After binding of core to the E1-E2 complex statically located on the ER membrane, virus-like particles might be formed and the conformation of E1-E2 complex changed, which could result in the abrogation of the ER-retention

signal for the E1-E2 complex. Then the virus-like particles might migrate along the secretion pathway, where E2 (and E1) proteins undergo more complex glycosylation by the Golgi enzymes.

In summary, upon expression of recombinant HCV core, E1, and E2 sequences, the E2 proteins of different glycosylations could be identified. The complex-glycosylated E2 protein might represent a more mature form of E2 and its formation required the conserved core coding sequences. Our data may contribute to a better understanding of the processing of HCV structural proteins as well as HCV morphogenesis.

ACKNOWLEDGMENT

We thank Wang, Y. and Lu, Z. for providing the HCV clones and the HCV specific patient sera.

REFERENCES

- Choo QL, Kuo G, Weiner AJ, Overby LR, Bradley DW, Houghton M. Isolation of a cDNA clone derived from a blood-borne non-A, non-B viral hepatitis genome. *Science* 1989; 244: 359-362
- Kuo G, Choo QL, Alter HJ, Gitnick GL, Redeker AG, Purcell RH, Miyamura T, Dienstag JL, Alter MJ, Stevens CE, Tegtmeier GE, Bonino F, Colombo M, Lee WS, Kuo C, Berger K, Shuster JR, Overby LR, Bradley DW, Houghton M. An assay for circulating antibodies to a major etiologic virus of human non-A, non-B hepatitis. *Science* 1989; 244: 362-364
- Major ME, Feinstone SM. The molecular virology of hepatitis C. *Hepatology* 1997; 25: 1527-1538
- Choo QL, Richman KH, Han JH, Berger K, Lee C, Dong C, Gallegos C, Coit D, Medina-Selby A, Barr PJ, Weiner AJ, Bradley DW, Kuo G, Houghton M. Genetic organization and diversity of the hepatitis C virus. *Proc Natl Acad Sci USA* 1991; 88: 2451-2455
- Houghton M, Weiner A, Han J, Kuo G, and Choo QL. Molecular biology of hepatitis viruses: implications for diagnosis, development and control of viral disease. *Hepatology* 1991; 14: 381-388
- Harada S, Watanabe Y, Takeuchi K, Suzuki T, Katayama T, Takebe Y, Saito I, Miyamura T. Expression of processed core protein of hepatitis C virus in mammalian cells. *J Virol* 1991; 65: 3015-3021
- Hijikata M, Kato N, Ootsuyama Y, Nakagawa M, Shimotohno K. Gene mapping of the putative structural region of the hepatitis C virus genome by *in vitro* processing analysis. *Proc Natl Acad Sci USA* 1991; 88: 5547-5551
- Lanford RE, Notvall L, Chavez D, White R, Frenzel G, Simonsen C, Kim J. Analysis of hepatitis C virus capsid, E1 and E2/NS1 proteins expressed in insect cells. *Virology* 1993; 197: 225-235
- Ralston R, Thudium K, Berger K, Kuo C, Gervase B, Hall J, Selby M, Kuo G, Houghton M, Choo QL. Characterization of hepatitis C virus envelop glycoprotein complexes expressed by recombinant vaccinia viruses. *J Virol* 1993; 67: 6753-6761
- Selby MJ, Choo QL, Berger K, Kuo G, Glazer E, Eckart M, Lee C, Chien D, Kuo C, Houghton M. Expression, identification and subcellular localization of the proteins encoded by the hepatitis C viral genome. *J Gen Virol* 1993; 74:1103-1113
- Spaete RR, Alexander D, Rugroden ME, Choo QL, Berger K, Crawford K, Kuo C, Leng S, Lee C, Ralston R, Thudium K, Tung JW, Kuo G, Houghton M. Characterization of the hepatitis C virus E2/NS1 gene product expressed in mammalian cells. *Virology* 1992; 188: 819-830
- Grakoui A, McCourt DW, Wychowski C, Feinstone SM, Rice CM. A second hepatitis C virus-encoded proteinase. *Proc Natl Acad Sci USA* 1993; 90: 10583-10587
- Hijikata M, Mizushima H, Akagi T, Mori S, Kakiuchi N, Kato N, Tanaka T, Kimura K, Shimotohno K. Two distinct proteinase activities required for the processing of a putative nonstructural precursor protein of hepatitis C virus. *J Virol* 1993; 67: 4665-4675
- Eckart MR, Selby M, Masiarz F, Lee C, Berger K, Crawford K, Kuo C, Kuo G, Houghton M, Choo QL. The hepatitis C virus encodes a serine protease involved in processing of the putative nonstructural proteins from the viral polyprotein precursor. *Biochem Biophys Res Commun* 1993; 192: 399-406
- Grakoui A, McCourt DW, Wychowski C, Feinstone SM, Rice CM. Characterization of the hepatitis C virus-encoded serine proteinase: determination of proteinase-dependent polyprotein cleavage sites. *J Virol* 1993; 67: 2832-2843
- Manabe S, Fuke I, Tanishita O, Kaji C, Gomi Y, Yoshida S, Mori C, Takamizawa A, Yosida I, Okayama H. Production of nonstructural proteins of hepatitis C virus requires a putative viral protease encoded by NS3. *Virology* 1994; 198: 636-644
- Tomei L, Failla C, Santolini E, De Francesco R, La Monica N. NS3 is a serine protease required for processing of hepatitis C virus polyprotein. *J Virol* 1993; 67: 4017-4026
- Grakoui A, Wychowski C, Lin C, Feinstone SM, Rice CM. Expression and identification of hepatitis C virus polyprotein cleavage products. *J Virol* 1993; 67: 1385-1395
- Matsuura Y, Suzuki T, Suzuki R, Sato M, Aizaki H, Saito I, Miyamura T. Processing of E1 and E2 glycoprotein of hepatitis C virus expressed in mammalian and insect cells. *Virology* 1994; 205: 141-150
- Hiramatsu N, Dash S, Gerber MA. HCV cDNA transfection to HepG2 cells. *J Viral Hepat* 1997; 4 Suppl 1: 61-67
- Seipp S, Mueller HM, Pfaff E, Stremmel W, Theilmann L, Goeser T. Establishment of persistent hepatitis C virus infection and replication *in vitro*. *J Gen Virol* 1997; 78: 2467-2476
- Rumin S, Berthillon P, Tanaka E, Kiyosawa K, Trabaud MA, Bizollon T, Gouillat C, Gripon P, Guguen-Guillouzo C, Inchauspe G, Trepo C. Dynamic analysis of hepatitis C virus replication and quasispecies selection in long-term cultures of adult human hepatocytes infected *in vitro*. *J Gen Virol* 1999; 80: 3007-3018
- Lohmann V, Korner F, Koch J, Herian U, Theilmann L, Bartenschlager R. Replication of subgenomic hepatitis C virus RNAs in a hepatoma cell line. *Science* 1999; 285: 110-113
- Song ZQ, Hao F, Min F, Ma QY, Liu GD. Hepatitis C virus infection of human hepatoma cell line 7721 *in vitro*. *World J Gastroenterol* 2001; 7: 685-689
- Bartenschlager R, Lohmann V. Novel cell culture systems for the hepatitis C virus. *Antiviral Res* 2001; 52: 1-17
- Lohmann V, Korner F, Dobierzewska A, Bartenschlager R. Mutations in hepatitis C virus RNAs conferring cell culture adaptation. *J Virol* 2001; 75: 1437-1449
- Pietschmann T, Lohmann V, Rutter G, Kurpanek K, Bartenschlager R. Characterization of cell lines carrying self-replicating hepatitis C virus RNAs. *J Virol* 2001; 75: 1252-1264
- Ni YH, Chang MH, Lue HC, Hsu HY, Wang MJ, Chen PJ, Chen DS. Posttransfusion hepatitis C virus infection in children. *J Pediatr* 1994; 124: 709-713
- Luengrojanakul P, Vareesangthip K, Chainuvati T, Murata K, Tsuda F, Tokita H, Okamoto H, Miyakawa Y, Mayumi M. Hepatitis C virus infection in patients with chronic liver disease or chronic renal failure and blood donors in Thailand. *J Med Virol* 1994; 44: 287-292
- Hsu HH, Donets M, Greenberg HB, Feinstone SM. Characterization of hepatitis C virus structural proteins with a recombinant baculovirus expression system. *Hepatology* 1993; 17: 763-771
- Yan BS, Liao LY, Leou K, Chang YC, Syu WJ. Truncating the putative membrane association region circumvents the difficulty of expressing hepatitis C virus protein E1 in *Escherichia coli*. *J Virol Methods* 1994; 49: 343-351
- Zhu LX, Kong YY, Wang Y, Li GD. Effect of downstream sequence on the cleavage of envelop protein 1 signal sequence in hepatitis C virus. *Acta Biochim Biophys Sin* 2001; 33: 682-686
- Moss B, Elroy-Stein O, Mizukami T, Alexander WA, Fuerst TR. New mammalian expression vectors. *Nature* 1990; 348: 91-92
- Li Y, Li G, Kong Y, Wang Y, Wang Y, Wen Y. Expression of structural proteins of hepatitis C virus (HCV) in mammalian cells. *Science in China (Series C)* 1998; 41: 47-55
- Wang Y, Okamoto H, Tsuda F, Nagayama R, Tao QM, Mishiro S. Prevalence, genotypes and isolate (HC-C2) of hepatitis C virus in Chinese patients with liver disease. *Journal of Medical Virology* 1993; 40: 254-260
- Liu J, Zhu L, Zhang X, Lu M, Kong Y, Wang Y, Li G. Expression, purification, immunological characterization and application of *E. coli*-derived hepatitis C virus E2 proteins. *Biotechnology and Applied Biotechnology* 2001; 34: 109-119
- Hijikata M, Kato N, Ootsuyama Y, Nakagawa M, Ohkoshi S, Shimotohno K. Hypervariable regions in the putative glycoprotein of hepatitis C virus. *Biochem Biophys Res Commun* 1991; 175: 220-228
- Weiner AJ, Brauer MJ, Rosenblatt J, Richman KH, Tung J, Crawford K, Bonino F, Saracco G, Choo QL, Houghton M, Han JH. Variable and hypervariable domains are found in the regions of HCV corresponding to the flavivirus envelope and NS1 proteins and the pestivirus envelope glycoproteins. *Virology* 1991; 180: 842-848
- Taylor DR, Shi ST, Romano PR, Barber GN, Lai MMC. Inhibition of the interferon-inducible protein kinase PKR by HCV E2 protein. *Science* 1999; 285: 107-110
- Tarentino AL, Gomez CM, Plummer TH. Deglycosylation of asparagine-linked glycans by peptide:N-glycosidase F. *Biochemistry* 1985; 24: 4665-4671
- Tai T, Yamashita K, Ogata-Arakawa M, Koide N, Muramatsu T. Structural studies of two ovalbumin glycopeptides in relation to the endo-beta-N-acetylglucosaminidase specificity. *J Biol Chem* 1975; 250: 8569-8575
- Kaku H, Goldstein IJ. Snowdrop lectin. *Methods Enzymol* 1989; 179: 327-331

- 43 Shibuya N, Berry JE, Goldstein JJ. One-step purification of murine IgM and human alpha 2-macroglobulin by affinity chromatography on immobilized snowdrop bulb lectin. *Arch Biochem Biophys* 1988; 267: 676-680
- 44 Inudoh M, Nyunoya H, Tanaka T, Hijikata M, Kato N, Shimotohno K. Antigenicity of hepatitis C virus envelope proteins expressed in Chinese hamster ovary cells. *Vaccine* 1996; 14: 1590-1596
- 45 Sato K, Okamoto H, Aihara S, Hoshi Y, Tanaka T, Mishiro S. Demonstration of sugar moiety on the surface of HCV recovered from the circulation of infected humans. *Virology* 1993; 196: 354-357
- 46 Cocquerel L, Duvet S, Meunier JC, Pillez A, Cacan R, Wychowski C, Dubuisson J. The transmembrane domain of hepatitis C virus glycoprotein E1 is a signal for static retention in the endoplasmic reticulum. *J Virol* 1999; 73: 2641-2649
- 47 Flint M, McKeating JA. The C-terminal region of the hepatitis C virus E1 glycoprotein confers localization within the endoplasmic reticulum. *J Gen Virol* 1999; 80: 1943-1947
- 48 Duvet S, Cocquerel L, Pillez A, Cacan R, Verbert A, Moradpour D, Wychowski C, Dubuisson J. Hepatitis C virus glycoprotein complex localization in the endoplasmic reticulum involves a determinant for retention and not retrieval. *J Biol Chem* 1998; 273: 32088-32095
- 49 Cocquerel L, Meunier JC, Pillez A, Wychowski C, Dubuisson J. A retention signal necessary and sufficient for endoplasmic reticulum localization maps to the transmembrane domain of hepatitis C virus glycoprotein E2. *J Virol* 1998; 72: 2183-2191
- 50 Mottola G, Jourdan N, Castaldo G, Malagolini N, Lahm A, Serafini-Cessi F, Migliaccio G, Bonatti A. New determinant of endoplasmic reticulum localization is contained in the juxtamembrane region of the ectodomain of hepatitis C virus glycoprotein E1. *J Biol Chem* 2000; 275: 24070-24079
- 51 Martire G, Viola A, Iodice L, Lotti LV, Gradini R, Bonatti S. Hepatitis C virus structural proteins reside in the endoplasmic reticulum as well as in the intermediate compartment/cis-Golgi complex region of stably transfected cells. *Virology* 2001; 280: 176-182
- 52 Baumert TF, Ito S, Wong DT, Liang TJ. Hepatitis C virus structural proteins assemble into viruslike particles in insect cells. *J Virol* 1998; 72: 3827-3836

Edited by Schmid R and Pang LH

• VIRAL LIVER DISEASES •

DNA immunization with fusion genes encoding different regions of hepatitis C virus E2 fused to the gene for hepatitis B surface antigen elicits immune responses to both HCV and HBV

Jing Jin, Jian-Ying Yang, Jing Liu, Yu-Ying Kong, Yuan Wang, Guang-Di Li

Jing Jin, Jian-Ying Yang, Jing Liu, Yu-Ying Kong, Yuan Wang, Guang-Di Li, Institute of Biochemistry and Cell Biology, Shanghai Institutes for Biological Sciences, Chinese Academy of Science, Shanghai 200031, China
Supported by the National High-Technology Program of China, No. 863-102-07-02-02

Correspondence to: Yuan Wang and Guang-Di Li, Institute of Biochemistry and Cell Biology, Shanghai Institutes for Biological Sciences, Chinese Academy of Sciences, 320 Yue-Yang Road, Shanghai 200031, China. wangyuan@server.shnc.ac.cn
Telephone: +86-21-64374430 Ext 5326 Fax: +86-21-64338357
Received 2001-12-05 Accepted 2002-01-23

Abstract

AIM: Both Hepatitis B virus (HBV) and Hepatitis C virus (HCV) are major causative agents of transfusion-associated and community-acquired hepatitis worldwide. Development of a HCV vaccine as well as more effective HBV vaccines is an urgent task. DNA immunization provides a promising approach to elicit protective humoral and cellular immune responses against viral infection. The aim of this study is to achieve immune responses against both HCV and HBV by DNA immunization with fusion constructs comprising various HCV E2 gene fragments fused to HBsAg gene of HBV.

METHODS: C57BL/6 mice were immunized with plasmid DNA expressing five fragments of HCV E2 fused to the gene for HBsAg respectively. After one primary and one boosting immunizations, antibodies against HCV E2 and HBsAg were tested and subtyped in ELISA. Splenic cytokine expression of IFN- γ and IL-10 was analyzed using an RT-PCR assay. Post-immune mouse antisera also were tested for their ability to capture HCV viruses in the serum of a hepatitis C patient *in vitro*.

RESULTS: After immunization, antibodies against both HBsAg and HCV E2 were detected in mouse sera, with IgG2a being the dominant immunoglobulin sub-class. High-level expression of INF- γ was detected in cultured splenic cells. Mouse antisera against three of the five fusion constructs were able to capture HCV viruses in an *in vitro* assay.

CONCLUSION: The results indicate that these fusion constructs could efficiently elicit humoral and Th1 dominant cellular immune responses against both HBV S and HCV E2 antigens in DNA-immunized mice. They thus could serve as candidates for a bivalent vaccine against HBV and HCV infection. In addition, the capacity of mouse antisera against three of the five fusion constructs to capture HCV viruses *in vitro* suggested that neutralizing epitopes may be present in other regions of E2 besides the hypervariable region 1.

Jin J, Yang JY, Liu J, Kong YY, Wang Y, Li GD. DNA immunization with fusion genes encoding different regions of hepatitis C virus E2 fused to the gene for hepatitis B surface antigen elicits immune responses to both HCV and HBV. *World J Gastroenterol* 2002;8(3):505-510

INTRODUCTION

Both Hepatitis B virus (HBV) and Hepatitis C virus (HCV) are major causative agents of transfusion-associated and community-acquired hepatitis worldwide^[1,2]. It is estimated that there are 250 million HBV carriers in the world and more than 10% of chronically infected HBV patients eventually develop cirrhosis and hepatocellular carcinoma^[3]. About 2-3% of the world population are HCV carriers. More than 70% of HCV infections become chronic, among which 5-20% progress to liver cirrhosis and hepatocellular carcinoma^[4,5]. Available HBV vaccines have proven to be safe and effective in preventing HBV infection. However, high costs, exclusion of some escape mutants and neonatal intolerance are eliminating their wide use^[6]. So far, no vaccine is available against HCV infection. IFN- γ treatment is the only useful therapy available. However, only 20-30% of treated patients develop long-term responses^[7]. Therefore, HBV and HCV infections pose a worldwide health threat and the development of uniformly effective vaccines of affordable prices is an urgent task.

DNA immunization, which allows the *de novo* synthesis of antigens in host's cells, is able to elicit protective humoral and cellular immune responses in several animal models of viral infection^[8-10]. The cellular context for *de novo* synthesized proteins to achieve proper maturation is a particularly important advantage for proteins such as those constituting viral envelopes whose maturation requires the help of additional cellular factors. Increasing data showed that DNA immunization against HBsAg elicited strong humoral and cellular immune responses that protect chimpanzees against the challenge with HBV. Moreover, DNA immunization in transgenic mice expressing HBsAg in the liver resulted in the clearance of HBsAg and long-term control of transgene expression, suggesting that DNA immunization is a potential tool in the treatment of HBV chronic carriers^[11-15]. DNA immunization with HCV E2 protein that was believed to carry the major neutralization epitopes of HCV^[16] also was studied in several animal models including primates^[17-21]. These studies demonstrated that DNA immunization with HCV E2 elicited strong humoral and cellular immune responses in various animals, though it did not elicit sterilizing immunity in chimpanzees against the challenge with a monoclonal homologous virus. The DNA immunization did appear to modify the infection and might have prevented the progression to chronicity, suggesting that DNA vaccine could be a promising approach for HCV treatment.

The objective of this research was to simultaneously stimulate immune responses against both HBV and HCV by DNA immunization with fusion constructs comprising of various HCV E2 gene fragments fused to the HBsAg gene of HBV. HBsAg carries all the information required for membrane translocation, particle assembly and secretion from mammalian cells. We have previously shown that HBsAg carrying HBV preS1 (21-47) at its truncated carboxyl terminal end could present the preS1 epitope on the surface of the chimeric particle and induce preS1 specific antibodies in mice^[22-24]. Moreover, humoral and cellular immune responses were successfully induced via

direct injection of the plasmid containing the HBsAg-preS1 fusion gene^[15]. These data indicated that gene fragments of proper size could be fused to the C-terminal of HBsAg without affecting particle assembly and secretion, and were capable of inducing immune responses against both HBsAg and the fused epitope. Although the epitopes on envelope protein E2 are not very clear yet, there have been some successful experiments to determine the immune determinants^[25-27]. Based on these previous findings, five fragments of HCV-E2 were selected in the hydrophilic region of E2 protein and fused to the truncated 3' end of HBsAg gene. The humoral and cellular immune responses of the plasmids expressing fusion proteins were evaluated. Furthermore, virus-capture ability of antibodies against those HCV-E2 fragments was also examined. The results are opening a new approach to the development of a bivalent vaccine against HBV and HCV, and lead to a better understanding of the immunological property of HCV-E2.

MATERIALS AND METHODS

Expression plasmids

Five HCV E2 gene fragments (A to E) were amplified from pUC18/E (E1-E2 gene of HCV genome type 1b inserted in pUC18)^[28] with following primers:

Fragment	Sense Primer	Antisense Primer
A(384-413)	P1 CGGCGTTGTATACACACCTACG	P2 TGGGAATTCAAAGCTGGATTTTCT
B(414-443)	P3 GAAATCGTATACGTGAACACCA	P4 CCGAATTCAGTAGAACAGCGCG
C(460-489)	P5 CATGGCCGTATACCGCTCCATTG	P6 GTCGAATTCAGTAGTCCAGCA
D(490-519)	P7 TTGCTGGGTATACCCACCTCGA	P8 GAGAATTCAGTCTGCCACCAC
E(529-549)	P9 GGTGGGGGTATACGATCGCTC	P10 TACGAATTCACCAAGTGCCTGCGG

AccI and *EcoRI* sites were introduced in sense and antisense primers, respectively. After digestion with *AccI* and *EcoRI*, PCR products were inserted downstream from the HBV S gene in pcDNA3S^[29] to obtain pcDNA3SE2-A, pcDNA3SE2-B, pcDNA3SE2-C, pcDNA3SE2-D and pcDNA3SE2-E (Figure 1). A fragment coding for amino acids 384 to 649 of HCV-E2 was also amplified from pUC18/E with primers P11 (5'-CCGGCGGATCCATGAACACC-3') and P12 (5'-GCGAATTCATCCTCGAGTCCAG-3'). PcDNA3E2 was constructed by inserting this PCR product digested with *Bam*HI and *EcoRI* into the MCS of pcDNA3 (Figure 1).

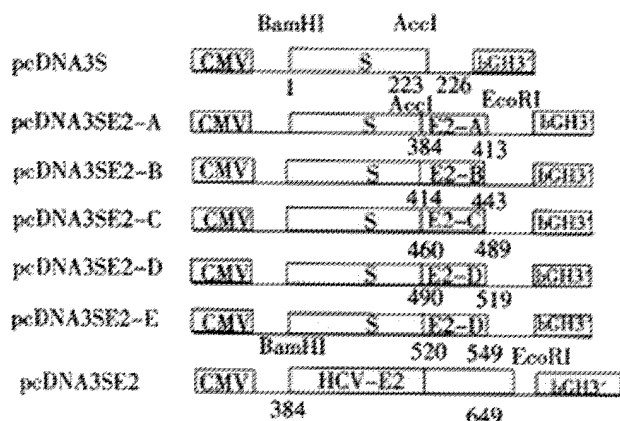


Figure 1 Schematic diagram of the expression plasmids. The coordinates below the bars refer to the corresponding amino acid residues of HBV surface antigen (HBsAg) and HCV E2 protein. The fusion genes were under the control of CMV immediate early promoter in pcDNA3. Bovine growth hormone (bGH) 3'-untranslated sequences were used as polyadenylation signals.

ELISA for transiently expressed HBV surface antigen

COS-M6 cells were maintained in Dulbecco's Modified Eagle's

medium (DMEM) supplemented with 5% fetal calf serum (Gibco, BRL, USA). 10µg of plasmid DNA and 5µg of an internal control pSK110, which expresses β-galactosidase, were transfected into 5×10⁵ COS-M6 cells by calcium phosphate co-precipitation method. Forty-eight hours after transfection, cells and media were collected. The activity of β-galactosidase in cell lysate obtained by cycles of freezing and thawing was analyzed to normalize the variation of transfection efficiency among different samples. HBsAg in cell lysates and media was determined with a commercial ELISA kit (Sino-American Co., Shanghai, China). The kit was adapted for quantitative measurements of HBsAg using purified yeast derived HBsAg (National Vaccine and Serum Institute, Beijing, China) as potency standard. Results were presented as means of three independent experiments^[23,30].

Western Blotting of transiently expressed products

HeLa cells were maintained in DMEM supplemented with 5% fetal calf serum. To enhance the expression level of fusion genes, cells were first infected with vaccinia virus vTT7 that expresses T7 RNA polymerase at a M.O.I. of 10 pfu per cell^[31]. Two hours post-infection, 1-2×10⁵ cells were transfected with 10µg of plasmid DNA by calcium phosphate method. Eighteen hours after transfection, cells were collected and cell lysate was electrophoresed on a 12.5% SDS-PAGE and subsequently electro-blotted onto nitrocellulose membrane. After blocking for 1h with 5% powdered lipid-free milk in PBST (PBS containing 0.1% Tween 20), the membrane was incubated with anti-HBs McAb H116 (kindly provided by Dr. E. Hildt, Munich, Germany) or anti-HCV E2 (450-565) polyclonal antiserum RE2-116^[32], followed by incubation with HRP conjugated secondary antibody (Dako Co., Denmark). Signals were detected by enhanced chemi-luminescence (ECL) blotting analysis system (Amersham-Pharmacia Co., UK).

DNA immunization of mice

C57BL/6 (H-2^b) mice were purchased from Shanghai Laboratory Animal Center. Groups of five female mice, 6-8 weeks old, were injected with 100µg of expression plasmids into regenerated tibialis anterior (TA) muscles 5 days after treatment of 100µl 10⁻⁵mol/l cardiotoxin (Sigma, USA)^[15,29]. Four weeks later, the mice were boosted in the same way.

Serologic tests

Sera were collected by tail bleeding at different time points pre-and post-injection and assayed for anti-HBs and anti-HCV-E2 by ELISA. Microwell plates were coated with serum derived HBsAg particles^[29] (Kehua Co., Shanghai, China), or 0.1µg/well HCV-E2 (385-565) expressed in *E. Coli*^[32]. After blocking with 5% powdered lipid-free milk in PBST (PBS containing 0.1% Tween 20), serial two-fold dilutions of sera were added. The bound antibodies were detected with HRP-conjugated rabbit anti-mouse IgG (1:1000) (Dako Co., Denmark) after extensive washing with PBST. Sera from mice immunized with pcDNA3 vector at 1 in 20 dilution were used as negative controls. A positive result was defined as an absorbance value of great than twice the absorbance of negative control with a cutoff of 0.050. Seroconversion was defined as giving a positive reading at 1:20 dilution. Antibody titres of pooled seroconverted animal sera were set as the highest dilution giving a positive reading (end-point dilution method)^[22,32].

To type the subclasses of IgG, mouse sera of each group were collected 6 weeks after the first immunization, and the titers of IgG1 and IgG2a antibodies assayed individually by a similar end-point dilution method, using the HRP-conjugated rabbit anti-mouse IgG1 and IgG2a (Serotec Co., Oxford, UK) for detection.

Splenic cytokine expression test

Expression of IFN- γ and IL-10 were assayed semi-quantitatively as described^[33,34]. Mice were killed 10 weeks after the first injection and spleens were removed aseptically. The single cell suspensions of the splenocytes were prepared and maintained in DMEM supplemented with 5% fetal calf serum and 5×10^{-5} M β -ME at a density of 10^7 cells per well. Cells were stimulated with 0.5 μ g/ml rDNA yeast derived HBsAg (National Vaccine and Serum Institute, Beijing, China), followed by culture at 37°C. At 0, 24, 48 hr post-stimulation, splenic cells were sampled. Total RNA was extracted with Trizol (Gibco, BRL, USA) and reverse transcribed with random hexamer primers (New England Biolabs Inc, Beverly, USA.). Messenger RNAs for IFN- γ and IL-10 were semi-quantitated by competitive RT-PCR^[33,34]. Splenic cells from mice immunized with pcDNA3 and mitogen ConA (5 μ g/ml) served as a negative and a positive control respectively.

Analysis of the virus capture capability of immune sera

The virus capture capability of antibodies in immune sera was assessed according to the method of affinity capture RT-PCR (AC-RT-PCR) detection of HEV in patient stool specimens^[35] with a few modifications. Briefly, 0.5ml microcentrifuge tubes were coated with 50 μ l goat anti-mouse IgG F(ab')₂ (0.02 μ g/ μ l, Jackson ImmunoResearch Laboratories, Inc., West Grove, USA), capped and incubated at room temperature for 1hr. After blocking with 5% powdered lipid-free milk in PBST for 15 min at 37°C and overnight at 4°C, tubes were aspirated and washed with 150 μ l PBST. The mouse sera were adjusted to same titre of 1:80 by dilution with PBS, to avoid the variations of the results caused by different antibody titers in different samples. Tubes were subsequently loaded with 25 μ l properly diluted mouse immune sera and 25 μ l HCV-RNA-PCR-positive patient's serum (1.6×10^7 HCV genome Equivalent [Geq] per ml, provided by Dr. X. Zhang, Ruijin Hospital, Shanghai, China) diluted 1:50 in PBS. The mixtures were mixed gently and incubated for 1 hr at room temperature and overnight at 4°C. Tubes were then washed three times with 150 μ l wash buffer (25 mM Tris-HCl pH8.0, 75mM KCl, 2.5mM MgCl₂). Captured virus was detected with a commercial HCV PCR testing kit (Sino-American Co., Shanghai, China) which specifically amplifies a 225 bp fragment in the 5' UTR of HCV RNA. HCV which was captured directly by a conformation specific monoclonal antibody (McAb) against HCV-E2, 219A2, (kindly provided by Dr. S. Abrignani, IRIS, Siena, Italy) was used as positive control.

RESULTS

Transient expression of HBsAg-HCV E2 fusion proteins Five expression plasmids containing the HCV-E2 coding sequences (corresponding to amino acids 384-413, 414-443, 460-489, 490-519, 529-549) fused to the 3' end of HBV-S gene were constructed as described in "Materials and Methods". COS-M6 cells were then transfected with these plasmids respectively.

Forty-eight hours post-transfection, the presence of HBsAg fusion protein in the cell lysates and culture media was measured with HBsAg ELISA. HBsAg was detected in both the cell lysates and culture media, indicating that the fusion constructs were able to express and secrete HBsAg efficiently (Figure 2).

Expressed HBsAg and HCV-E2 fusion proteins were also evaluated by Western Blot. They were separated by SDS-PAGE gel, followed by incubation with HBsAg specific McAb H116 (Figure 3A). Compared with HBsAg expressed by pcDNA3S (Figure 1), which contained the major surface gene of HBV only and displayed 24000 and 27000 protein bands for the unglycosylated and glycosylated forms respectively (Figure 3A, lane1)^[29], all the fusion antigens showed slower migratory bands (27000 and 29000), indicating

successful expression of the fusion proteins. Two fusion constructs SE2-B (414-443) and SE2-D (490-519) displayed additional bands at 31000, which might result from multi-glycosylation. Expressed fusion proteins SE2-C (460-489), SE2-D (490-519) and SE2-E (529-549) were also incubated with polyclonal antibody RE2-116. The band pattern in the Western Blots (Figure 3B) was consistent with that in Figure 3A, suggesting that these fusion proteins possess both HBV-S and HCV-E2 antigenicity. SE2-A(384-413) and SE2-B(414-443) were not assayed for HCV-E2, since they did not locate in the reactive region (450-565) of RE2-116. By contrast, the non-fused truncated E2(384-649) (Figure 1) displayed only a single band as large as the expected unglycosylated product (Figure 3B, lane 1).

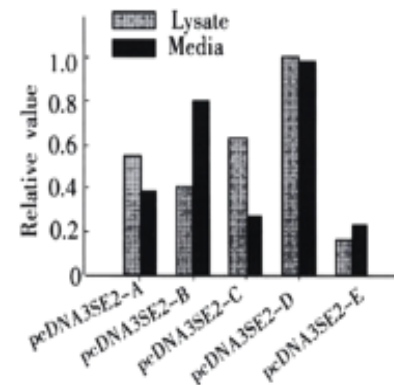


Figure 2 Comparison of the expression and secretion level of fusion proteins in COS cells.

pcDNA3SE2-A, pcDNA3SE2-B, pcDNA3SE2-C, pcDNA3SE2-D, pcDNA3SE2-E are the plasmids expressing HBsAg fused with different HCV E2 fragments. The HBsAg in the culture medium (gray) and cell lysates (black) was measured by a commercial ELISA kit (Sino-American Co., Shanghai, China). Results were presented as means of three independent experiments (see Materials and Methods). The amount of HBsAg expressed by pcDNA3SE2-D in cell lysates was arbitrarily taken as 1.0.

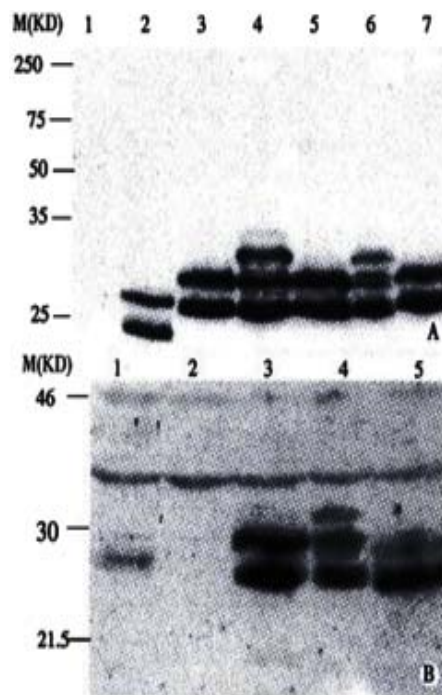


Figure 3 Characterization of the fusion antigens transiently expressed in HeLa cells by Western blotting.

After separation by a 12.5% SDS-PAGE, the proteins were blotted onto a nitrocellulose membrane and incubated with (A) anti-S McAb (H166, 1:300 diluted), (B) anti-HCV E2 (450-565) polyclonal antiserum RE2-116 (1:500 diluted) respectively. (A) lane 1-7, fusion proteins expressed by pcDNA3, pcDNA3S, pcDNA3SE2-A, pcDNA3SE2-B, pcDNA3SE2-C, pcDNA3SE2-D and pcDNA3SE2-E respectively. (B) lane 1-5, fusion proteins expressed by pcDNA3SE2-C, pcDNA3SE2-D, pcDNA3SE2-E respectively.

Humoral responses to fusion antigens in DNA-immunized mice

C57BL/6 mice were injected with HCV-E2 and HBV-S fusion constructs. As shown in Table 1, the immunized mice produced antibodies against both HBsAg and HCV-E2 after the first injection, and the seroconversion rate increased quickly after the boost, reaching 100% at week 6 or 8. Antibodies were still detectable after 24 weeks. Impressively, the anti-HCV E2 antibody titers elicited in mice immunized with fusion constructs were much higher than that induced in mice injected with pcDNA3E2 (up to 40 fold difference), which contained non-fused HCV E2(384-649). Compared with the humoral response induced by pcDNA3S, all the fusion constructs were able to induce equivalent or slightly smaller anti-HBs antibody responses.

Subsets of IgG against both HBsAg and HCV-E2 were also determined. The IgG profiles specific to HBsAg indicated the obvious predominance of IgG2a (Figure 4A), while IgG profiles specific to HCV-E2 varied among different constructs (Figure 4B). Only pcDNA3SE2-A and pcDNA3SE2-D induced predominant IgG2a against HCV-E2, suggesting that the T helper responses elicited against these two fragments were Th1 dominant.

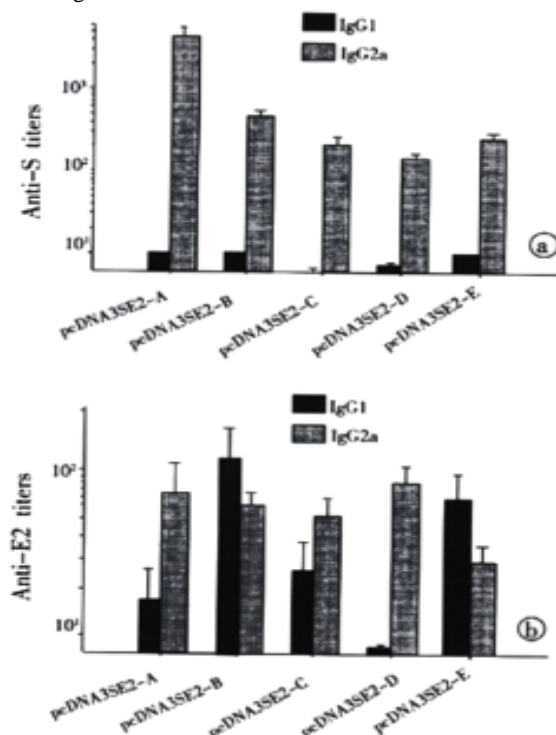


Figure 4 IgG subtypes profile of antibodies against HBsAg and HCV E2. Sera collected from mice 6 weeks after boosting were assayed for the IgG1 and IgG2a antibodies against HBsAg and HCV E2. For each group of 5 mice, titers of IgG1 and IgG2a antibodies were determined individually by serial two-fold dilution titration methods using HRP-conjugated rabbit anti-mouse IgG1 and IgG2a (Serotec Co., Oxford, UK) for detection. (as described in Materials and Methods). The arithmetic mean \pm standard deviation (SD) ($n=5$) is shown. (A) Anti-HBs, (B) Anti-HCV E2.

Expression of cytokines in the cultured splenic cells from DNA-immunized mice

After the *in vitro* stimulation of splenic cells derived from immunized mice, expressions of cytokines were analyzed by competitive RT-PCR. 24 hrs post-stimulation with rDNA yeast derived HBsAg (National Vaccine and Serum Institute, Beijing, China), high levels of IFN- γ were detected in the splenic cells from the mice immunized with pcDNA3SE2-A, pcDNA3SE2-B, pcDNA3SE2-C and pcDNA3SE2-E (Figure 5). The IL-10 expression was also detectable, but weaker than IFN- γ expression.

Table 1A Sero-conversion Ratios and Titres of Anti-HBsAg in DNA Immunized Mice

Weeks	DNAImmunogen					
	pcDNA3S	pcDNA3SE2-A	pcDNA3SE2-B	pcDNA3SE2-C	pcDNA3SE2-D	pcDNA3SE2-E
0 ^a	(0/5)	(0/5)	(0/5)	(0/5)	(0/5)	(0/5)
2	(5/5)	(1/5)	(1/5)	(1/5)	(1/5)	(2/5)
4 ^b	1280 ^c (5/5)	1280(4/5)	640(2/5)	320(2/5)	320(2/5)	320(4/5)
6	10240(5/5)	10240(5/5)	5120(4/5)	5120(4/5)	5120(5/5)	2560(5/5)
8	5120(5/5)	5120(5/5)	5120(5/5)	5120(5/5)	5120(5/5)	5120(5/5)
10	5120(5/5)	5120(5/5)	2560(4/5)	2560(5/5)	2560(5/5)	5120(5/5)
16	1280(5/5)	1280(5/5)	640(4/5)	320(5/5)	640(5/5)	80(5/5)
24	1280(5/5)	1280(5/5)	640(4/5)	320(5/5)	640(5/5)	80(5/5)

Note: Groups of mice ($n=5$) were injected i.m. with the respective plasmids, and anti-HBsAg antibody titers were measured at different time points by ELISA. Sera from mice immunized with pcDNA3 vector were used as negative controls and showed no reactivity with any coated antigens (data not shown). For sero-conversion, 1:20 starting dilution were assayed and the sera giving positive reading were taken as converted one. To determine antibody titers, serial two-fold dilutions of pooled seroconverted immune sera were incubated in antigen-coated wells. A positive result was defined as an absorbance value of greater than twice the absorbance of the negative control with a cutoff of 0.050(also see Materials and Methods). At week 2 only sero-conversion testing was performed at 1:20 dilution. ^athe first immunization; ^bthe second immunization (boost); ^c(n/n); sero-conversion ratio, numbers of sero-converted mice relative to the total number tested; ^dtiter; reciprocal of the two-fold dilution factor at end point; pools of seroconverted sera from test groups were tested.

Table 1B Sero-conversion Ratios and Titres of Anti-HCV-E2 in DNA Immunized Mice

Weeks	DNAImmunogen					
	pcDNA3S	pcDNA3SE2-A	pcDNA3SE2-B	pcDNA3SE2-C	pcDNA3SE2-D	pcDNA3SE2-E
0 ^a	(0/5)	(0/5)	(0/5)	(0/5)	(0/5)	(0/5)
2	(1/5)	(2/5)	(1/5)	(1/5)	(1/5)	(1/5)
4 ^b	40 ^c (2/5)	320(3/5)	160(1/5)	320(3/5)	320(2/5)	320(1/5)
6	160(5/5)	640(5/5)	640(5/5)	2560(5/5)	2560(5/5)	5120(4/5)
8	880(5/5)	640(5/5)	320(5/5)	5120(5/5)	5120(5/5)	5120(4/5)
10	80(5/5)	160(5/5)	320(5/5)	5120(5/5)	5120(5/5)	5120(4/5)
16	80(5/5)	80(5/5)	160(5/5)	160(5/5)	320(5/5)	80(4/5)
24	40(5/5)	40(5/5)	80(5/5)	80(5/5)	160(5/5)	40(4/5)

Note: Groups of mice ($n=5$) were injected i.m. with the respective plasmids, and seroconversion ratio and anti-HCV E2 antibody titers were measured at different time points by ELISA. With the exception of coating antigen (E2 (385-565)), all experimental procedures were the same as described in Table 1A. ^athe first immunization; ^bthe second immunization (boost); ^c(n/n); sero-conversion ratio, numbers of sero-converted mice relative to the total number tested; ^dtiter; reciprocal of the two-fold dilution factor at end point, pools of positive sera from test groups were tested.

Virus-capture ability of antisera from DNA-immunized mice

To test the virus-capture capability of antibodies elicited in response to DNA immunization, affinity-capture-RT-PCR (AC-RT-PCR) was performed as described in "Materials and Methods". The HCV virions bound to anti-HCV-E2 were detected by nested RT-PCR to amplify a specific fragment in the 5'-UTR of HCV genome. The results indicated that immune sera of mice immunized with pcDNA3SE2-A, pcDNA3SE2-B and pcDNA3SE2-D were able to capture HCV virions in the serum of a hepatitis C patient *in vitro* (Figure 6).

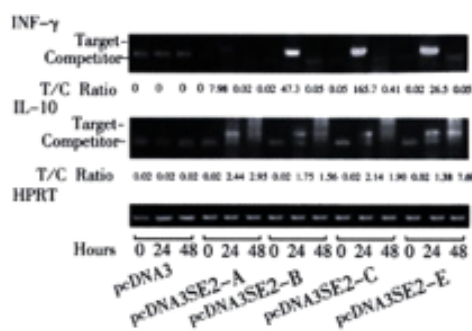


Figure 5 IFN- γ and IL-10 mRNA expression. mRNA was isolated from splenic cells of immunized mice after stimulation with HBsAg for 0, 24, 48 hours. IFN- γ and IL-10 mRNA expression was

determined by semi-quantitative RT-PCR after standardization of the cDNA concentration by amplification of HPRT. Level of expression is indicated as ratio of target to competitor, calculated from densitometric analysis of their PCR products. (High ratio indicates high expression of target mRNA).

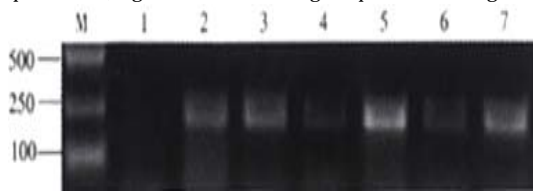


Figure 6 Detection of HCV captured by mouse antisera by nested RT-PCR. After immuno-capture of HCV from hepatitis C patient serum (1.6×10^7 HCV GEq per ml) by antisera from groups of mice immunized with pcDNA3, pcDNA3SE2-A, pcDNA3SE2-B, pcDNA3SE2-C, pcDNA3SE2-D and pcDNA3SE2-E (lane 1 to lane 6), viruses were detected by nested RT-PCR using the HCV RT-PCR testing kit (Sino-America Co., Shanghai, China). Lane 7, the positive control using McAb against HCV E2 to capture HCV. Lane M, molecular markers.

DISCUSSION

In this report, five fusion constructs comprising various fragments within the hydrophilic region of HCV-E2 fused to the 3' end of the S gene of HBV were constructed. The immune responses of mice to immunization with these fusion constructs indicated that all five constructs were able to elicit strong antibody responses against both HBsAg and HCV-E2. Importantly, antibody typing showed the HBsAg specific Th1 like responses, which were consistent with the high levels of IFN- γ expression in cultured spleen cells from the immunized mice after stimulation with HBsAg. The IgG subtype responses to HCV-E2 also showed E2 specific Th1 like responses to E2-A and E2-D. Since Th1 like response is essential for triggering a wide range of cellular responses against infectious agents, including NK cell responses, CTL responses and inflammatory reactions, the results of the DNA immunization with our fusion plasmids suggest a promising strategy to clear both HBV and HCV in the host.

The excellent vaccine potential of our constructs may be ascribed to the use of HBsAg as a carrier. HBsAg has the advantage of assembling into large secretable particles, which form a virus-like polymeric structure that enhances antigenic stability and provides a high-density presentation to antigen-presenting cells (APC). HBsAg has been used successfully as vaccine carrier to present various antigens^[15,23,29,36,37]. The successful immune responses to both HBV S and HCV E2 in these reports support our preliminary observation that antigens of a proper size fused to C-terminal of HBsAg could be successfully presented without affecting the immunogenicity of HBsAg. Moreover, our fusion constructs were able to elicit higher levels of antibody responses to HCV E2, compared to pcDNA3E2 that encodes only a truncated HCV-E2 (384-649). This of course suggests that fusion to HBsAg may help these fragments to be presented more effectively to APCs, and hence induce stronger humoral responses against HCV-E2. These fusion constructs may turn out to be promising candidates for the vaccines against HCV and HBV.

It is well established that the intact E2 glycoproteins expressed alone or together with E1 (E1-E2 heterodimer) are retained in the endoplasmic reticulum^[38] and that E2 proteins expressed in mammalian cells without the signal sequence at the C-terminus of E1 are not glycosylated^[39]. Consistently, we also observed that the truncated E2 (384-649) was expressed in unglycosylated form in mammalian cells. However, the use of HBsAg as carrier seems to give rise to expression of fusion proteins carrying HCV-E2 epitopes in glycosylated and secretable form, which emphasizes the advantage of HBsAg as a carrier. Notably, two products, SE2-B and SE2-D expressed by pcDNA2SE2-B and pcDNA3SE2-D, produced an additional 31000 glycosylated form, suggesting that in addition to the glycosylation site in HBsAg, some sites in fragment B and D also may be glycosylated. Since glycosylation is a decisive factor for biological molecules to carry out correct biological functions, the additional glycosylation of the fusion constructs may elicit immune responses similar to that of natural

infections by the HCV. This may be an additional reason that our constructs are able to elicit strong immune responses.

The results presented here also suggest that the DNA immunization with different HCV E2 fragments fused to HBsAg may be a useful approach to screen for epitopes or immune determinants on HCV-E2. Nakano *et al.*^[18] inserted different regions of HCV E2 into the preS2 region of HBV surface protein, and evaluated the humoral immune responses of these fusion constructs via DNA immunization. Their study also suggest that fusion constructs of E2 with HBsAg might be an efficient way to identify restricted immunogenic domains within E2. In our study, each of the chosen E2 fragments contained only 30 amino acids, it provides a possibility to study the antigenic domains of HCV E2 more precisely. Antibody responses and IgG subtype typing against these E2 fragments suggest that B- and T- epitopes were present in fragment D(490-519). Furthermore, the results of virus-capture assay showed that HCV virions in the serum of a hepatitis C patient could be captured by immune sera against SE2-A, SE2-B and SE2-D *in vitro*. In particular, antibodies against fragment D exhibited the strongest ability to capture HCV virions. Because the ability of antibodies to bind viruses is a prerequisite for neutralizing viruses *in vivo* and preventing bodies from being infected, our data suggest that besides HVR1-containing fragment A, fragments B and D probably also harbour neutralizing epitopes. So far, only HVR1 has been confirmed to be an important epitope^[40-48] whose corresponding antibody can neutralize the binding of HCV-E2 to susceptible cells *in vitro*, and prevent HCV infection after *in vitro* neutralization^[42,43]. Recently, correlation between circulating antibodies against HVR1 and resolution of chronic hepatitis C has been confirmed^[49]. However, the high variability of HVR1 interferes with the development of HVR1-based vaccines. Some researchers suggested that there may be B-cell epitopes located downstream from HVR1^[17,18,50]. Rosa *et al.*^[43] speculated that there may be at least one additional neutralizing epitope located somewhere other than HVR1 of HCV E2, this was based on the finding that HVR-1 peptide failed to completely block the binding of HCV to susceptible cells. Our results suggest that potential neutralizing epitopes may be present within fragments B (414-443) and D (490-519) that are downstream from HVR1. Since fragments B and D are relatively more conservative than HVR1, it would seem that vaccines containing fragments B and/or D may be more promising than that containing only HVR1. Further studies on these neutralizing epitopes are under way, which hopefully will lead to a better understanding of the immunological property of HCV E2, and facilitate the design of efficient HCV vaccines.

ACKNOWLEDGMENT

The authors are grateful to Dr. E. Hildt for providing monoclonal antibody (McAb) H166, Dr. S. Abrignani for McAb 219A2, Dr. Yuan ZH for HRP-Rabbit antibody against mouse IgG1 and IgG2a, Dr. Zhang XX for HCV patient serum and Qu D for her help in cytokine test.

REFERENCES

- 1 Choo QL, Kuo G, Weiner AJ, Overby LR, Bradley DW, Houghton M. Isolation of a cDNA clone derived from a blood-borne non-A, non-B viral hepatitis genome. *Science* 1989;244:359-362
- 2 Kuo G, Choo QL, Alter HJ, Gitnick GL, Redeker AG, Purcell RH, Miyamura T, Dienstag JL, Alter MJ, Stevens CE. An assay for circulating antibodies to a major etiologic virus of human non-A, non-B hepatitis. *Science* 1989;244:362-364
- 3 Tiollais P, Buendia MA. Hepatitis B virus. *Sci Am* 1991;264:48-54
- 4 Alter MJ, Margolis HS, Krawczynski K, Judson FN, Mares A, Alexander WJ, Hu PY, Miller JK, Gerber MA, Sampliner RE. The natural history of community-acquired hepatitis C in the United States: the Sentinel Counties chronic non-A, non-B hepatitis study team. *N Engl J Med* 1992;327:1899-1905
- 5 Saito I, Miyamura T, Ohbayashi A, Harada H, Katayama T, Kikuchi S, Watanabe Y, Koi S, Onji M, Ohta Y. Hepatitis C virus infection is associated with the development of hepatocellular carcinoma. *Proc Natl Acad Sci USA* 1990;87:6547-6549
- 6 Thanavala Y. Novel approaches to vaccine development against HBV. *J Biotechnol* 1996;44:67-73

- 7 Fried MW, Sambrook J. Therapy of hepatitis C. *Semin Liver Dis* 1995; 15:82-91
- 8 Wayne CL, Michael B. DNA Vaccine. *Crit Rev Immunol* 1998;18:449-484
- 9 Donnelly JJ, Ulmer JB, Liu MA. Immunization with DNA. *J Immunol Meth* 1994;176:145-152
- 10 McDonnell WM, Askari FK. DNA Vaccines. *N Engl J Med* 1996;334:42-45
- 11 Davis HL, Michel ML, Whalen RG. DNA-based immunization induces continuous secretion of hepatitis B surface antigen and high levels of circulating antibody. *Human Mol Genetics* 1993;2:1847-1851
- 12 Michel ML, Davis HL, Schleef M, Mancini M, Tiollais P, Whalen RG. DNA-mediated immunization to the hepatitis B surface antigen in mice: Aspects of the humoral response mimic hepatitis B viral infection in humans. *Proc Natl Acad Sci USA* 1995;92:5307-5311
- 13 Mancini M, Davis H, Tiollais P, Michel ML. DNA-based immunization against the envelope proteins of the hepatitis B virus. *J Biotechnol* 1996;44:47-57
- 14 Mancini M, Hadchouel M, Davis HL, Whalen RG, Tiollais P, Michel ML. DNA-mediated immunization in a transgenic mouse model of the hepatitis B surface antigen chronic carrier state. *Proc Natl Acad Sci USA* 1996;93:12496-12501
- 15 Hui J Y, Mancini M, Li G D, Wang Y, Tiollais P, Michel M-L. Immunization with a plasmid encoding a modified hepatitis B surface antigen carrying the receptor binding site for hepatocytes. *Vaccine* 1999;17:1771-1778
- 16 Choo QL, Kuo G, Ralston R, Weiner A, Chien D, Van Nest G, Han J, Berger K, Thudium K, Kuo C. Vaccination of chimpanzees against infection by the hepatitis C virus. *Proc Natl Acad Sci USA* 1994;91:1294-1298
- 17 Tedeschi V, Akatsuka T, Shih JWK, Battagay M, Feinstone SM. A specific antibody response to HCV E2 elicited in mice by intramuscular inoculation of plasmid DNA containing coding sequences for E2. *Hepatology* 1997;25:459-462
- 18 Nakano I, Maertens G, Major ME, Vitvitski L, Dubuisson J, Fournillier A, De Martynoff G, Trepo C, Inchauspe G. Immunization with plasmid DNA encoding hepatitis C virus envelope E2 antigenic domains induces antibodies whose immune reactivity is linked to the injection mode. *J Virol* 1997;71:7101-7109
- 19 Fornis X, Emerson SU, Tobin GJ, Mushahwar IK, Purcell RH, Bukh J. DNA immunization of mice and macaques with plasmids encoding hepatitis C virus envelope E2 protein expressed intracellularly and on the cell surface. *Vaccine* 1999;17:1992-2002
- 20 Fournillier A, Depla E, Karayiannis P, Vidalin O, Maertens G, Trepo C, Inchauspe G. Expression of noncovalent hepatitis C virus envelope E1-E2 complexes is not required for the induction of antibodies with neutralizing properties following DNA immunization. *J Virol* 1999;73:7497-7504
- 21 Fornis X, Payette PJ, Ma X, Satterfield W, Eder G, Mushahwar IK, Govindarajan S, Davis HL, Emerson SU, Purcell RH, Bukh J. Vaccination of chimpanzees with plasmid DNA encoding the hepatitis C virus (HCV) envelope E2 protein modified the infection after challenge with homologous monoclonal HCV. *Hepatology* 2000;32:618-25
- 22 Xu X, Li GD, Kong YY, Yang HL, Zhang ZC, Cao HT, Wang Y. A modified hepatitis B virus surface antigen with the receptor-binding site for hepatocytes at its C-terminus: Expression, antigenicity and immunogenicity. *J Gen Virol* 1994;75:3673-3677
- 23 Hui JY, Li GD, Kong YY, Wang Y. Expression and characterization of chimeric hepatitis B surface antigen particles carrying preS epitopes. *J Biotechnol* 1999;72:49-59
- 24 Yang JY, Jin J, Kong YY, Wei J, Zhang ZC, Li GD, Wang Y, Yuan HY, Li YY. Purification and characterization of recombinant hepatitis B virus surface antigen SS1 expressed in *Pichia pastoris*. *Acta Biochem Biophys Sin* 2000;32:503-508
- 25 Koshy R, Inchauspe G. Evaluation of hepatitis C virus protein epitopes for vaccine development. *Trends Biotechnol* 1996;149:364-369
- 26 Fournillier A, Nakano I, Vitvitski L, Depla E, Vidalin O, Maertens G, Trepo C, Inchauspe G. Modulation of immune responses to hepatitis c virus envelope E2 protein following injection of plasmid DNA using single or combined delivery routes. *Hepatology* 1998;28:237-244
- 27 Lee JW, Kim KM, Jung SH, Lee KJ, Choi EC, Sung YC, Kang CY. Identification of a domain containing B-cell epitopes in hepatitis C virus E2 glycoprotein by using mouse monoclonal antibodies. *J Virol* 1999;73:11-18
- 28 Wang Y, Okamoto H, Tsuda F, Naqayama R, Tao QM, Mishiro S. Prevalence, genotypes, and an isolate (HC-C2) of Hepatitis C Virus in Chinese patients with liver disease. *J Med Virol* 1993;40:254-260
- 29 Hui JY, Li GD, Kong YY, Yuan Wang. DNA-based immunization against hepatitis B surface antigen carrying preS epitopes. *Chinese Sci Bull* 1999;44:620-623
- 30 Feng Y, Kong YY, Wang Y, Qi GR. Intracellular inhibition of the replication of hepatitis B virus by hammerhead ribozyme. *J Gastroenterol Hepatol* 2001;16:1125-1130
- 31 Fuerst TR, Niles EG, Studier FW, Moss B. Eukaryotic transient-expression system based on recombinant vaccinia virus that synthesizes bacteriophage T7 RNA polymerase. *Proc Natl Acad Sci USA* 1986;83:8122-8126
- 32 Liu J, Zhu LX, Zhang XX, Lu M, Kong YY, Wang Y, Li GD. Expression, purification, immunological characterization and application of *Escherichia coli*-derived hepatitis C virus E2 proteins. *Biotechnol Appl Biochem* 2001;34:109-119
- 33 Sun B, Wells J, Goldmuntz E, Silver P, Remmers EF, Wilder RL, Caspi RR. A simplified, competitive RT-PCR method for measuring rat IFN- γ mRNA expression. *J Immunol Methods* 1996;195:139-148
- 34 Sun B, Rizzo LZ, Sun SH, Chan CC, Wiggert B, Wilder RL, Caspi RR. Genetic susceptibility to experimental autoimmune uveitis involves more than a predisposition to generate a T helper-1-like or a T helper-2-like response. *J Immunol* 1997;159:1004-1011
- 35 He JK, Binn LN, Caudill JD, Asher LV, Longer CF, Innis BL. Antiserum generated by DNA vaccine binds to hepatitis E virus (HEV) as determined by PCR and immune electron microscopy (IEM): application for HEV detection by affinity-capture RT-PCR. *Virus Res* 1999;62:59-65
- 36 Prange R, Werr M, Birkner M, Hilfrich R, Streeck RE. Properties of modified hepatitis B virus surface antigen particles carrying preS epitopes. *J Gen Virol* 1995;76:2131-2140
- 37 Major ME, Vitvitski L, Mink MA, Schleier M, Whalen RG, Trepo C, Inchauspe G. DNA-based immunization with chimeric vectors for the induction of immune responses against the Hepatitis C virus nucleocapsid. *J Virol* 1995;69:5798-5805
- 38 Duvet S, Cocquerel L, Pillez A, Cacan R, Verbert A, Moradpour D, Wychowski C, Dubuisson J. Hepatitis C virus glycoprotein complex localization in the endoplasmic reticulum involves a determinant for retention and not retrieval. *J Biol Chem* 1998;273:32088-32095
- 39 Saito T, Sherman GJ, Kurokohchi K, Guo ZP, Donets M, Yu MY, Berzofsky JA, Akatsuka T, Feinstone SM. Plasmid DNA-based immunization for hepatitis C virus structural proteins: immune responses in mice. *Gastroenterology* 1997;112:1321-1330
- 40 Weiner AJ, Geysen HM, Christopherson C, Hall JE, Mason TJ, Saracco G, Bonino F, Crawford K, Marion CD, Crawford KA. Evidence for immune selection of hepatitis C virus (HCV) putative envelope glycoprotein variants: potential role in chronic HCV infections. *Proc Natl Acad Sci USA* 1992;89:3468-3472
- 41 Zibert A, Schreier E, Roggendorf M. Antibodies in human sera specific to hypervariable region 1 of hepatitis C virus can block viral attachment. *Virology* 1995;208:653-661
- 42 Scarselli E, Cerino A, Esposito G. Occurrence of antibodies reactive with more than one variant of the putative envelope glycoprotein (gp70) hypervariable region 1 in viremic hepatitis C virus-infected patients. *J Virol* 1995;69:4407-4412
- 43 Rosa D, Campagnoli S, Moretto C, Guenzi E, Cousens L, Chin M, Dong C, Weiner AJ, Lau JY, Choo QL, Chien D, Pileri P, Houghton M, Abrignani S. A quantitative test to estimate neutralizing antibodies to the hepatitis C virus: cytofluorimetric assessment of envelope glycoprotein 2 binding to target cells. *Proc Natl Acad Sci USA* 1996;93:1759-1763
- 44 Farci P, Shimoda A, Wong D, Cabezon T, De Gioannis D, Strazzer A, Shimizu Y, Shapiro M, Alter HJ, Purcell RH. Prevention of hepatitis C virus infection in chimpanzees by hyperimmune serum against the hypervariable region 1 of the envelope 2 protein. *Proc Natl Acad Sci USA* 1996;93:15394-15399
- 45 Zibert A, Dudziak P, Schreier E, Roggendorf M. Characterization of antibody response to hepatitis C virus protein E2 and significance of hypervariable region 1-specific antibodies in viral neutralization. *Arch Virol* 1997;142:523-534
- 46 Esumi M, Ahmed M, Zhou YH, Takahashi H, Shikata T. Murine antibodies against E2 and hypervariable region 1 cross-reactively capture Hepatitis C virus. *Virology* 1998;251:158-164
- 47 Watanabe K, Yoshioka K, Ito H, Ishigami M, Takagi K, Utsunomiya S, Kobayashi M, Kishimoto H, Yano M, Kakumu S. The hypervariable region 1 protein of Hepatitis C virus broadly reactive with sera of patients with chronic Hepatitis C has a similar amino acid sequence with the consensus sequence. *Virology* 1999;264:153-158
- 48 Shang DZ, Zhai WW, Allain JP. Broadly cross-reactive, high-affinity antibody to hypervariable region 1 of the Hepatitis C virus in rabbits. *Virology* 1999;258:396-405
- 49 Ishii K, Rosa D, Watanabe Y, Katayama T, Harada H, Wyatt C, Kiyosawa K, Aizaki H, Matsuura Y, Houghton M, Abrignani S, Miyamura T. High titers of antibodies inhibiting the binding of envelope to human cells correlate with natural resolution of chronic hepatitis C. *Hepatology* 1998;28:1117-1120
- 50 Mink MA, Benichou S, Madaule P, Tiollais P, Prince AM, Inchauspe G. Characterization and mapping of a B-cell immunogenic domain in hepatitis C virus glycoprotein using a yeast peptide library. *Virology* 1994;200:246-255

• BASIC RESEARCH •

Effects of Yigan Decoction on proliferation and apoptosis of hepatic stellate cells

Xi-Xian Yao, You-Wei Tang, Dong-Mei Yao, He-Ming Xiu

Xi-Xian Yao, Dong-Mei Yao, Department of Gastroenterology, The Second Hospital of Hebei Medical University, Shijiazhuang 050000, Hebei Province, China

You-Wei Tang, He-Ming Xiu, Department of Geriatrics, Bethune International Peace Hospital, Shijiazhuang 050082, Hebei Province, China

Supported by Hebei Province Administration Bureau of TCM, No. 200001

Correspondence to: Dr. Xi-Xian Yao, Department of Gastroenterology, The Second Hospital of Hebei Medical University, Shijiazhuang 050000, Hebei Province, China. yaioxian@263.net

Telephone: +86-311-7814356

Received 2001-06-03 Accepted 2001-12-08

Abstract

AIM: To investigate the effects of Chinese herb Yigan Decoction on proliferation and apoptosis of the hepatic stellate cells (HSC) *in vitro*.

METHODS: The study *in vitro* was carried out in the culture of HSC lines. Various concentrations of Yigan Decoction were added and incubated. Cell proliferation was detected with MTT colorimetric assay. Cell apoptosis was detected by electron microscopy, flow cytometry and TUNEL.

RESULTS: The proliferation of HSC was inhibited by Yigan Decoction, which depending on dose and time significantly. The HSC proliferation rates of groups at the end concentrations 144 and 72(g·L⁻¹) were 21.62% and 40.54% respectively, significantly lower than that of normal control group ($P < 0.01$). The HSC proliferation rates of groups at the end concentrations 36, 18 and 9(g·L⁻¹) were 54.05%, 45.95% and 51.35% respectively, lower than that of control group ($P < 0.05$). When the end concentration was 4.5g·L⁻¹, the proliferation rate was 83.78%, which appeared no significant differences compared with control group. At the same concentrations of 18g·L⁻¹, the inhibitory effects of Yigan Decoction at 24h, 48h and 72h time point were observed, the effects were time-dependent, and reached a peak at 72h. Meanwhile, it was showed that the inducing effects of Yigan Decoction on HSC apoptosis were dose-dependent and time-dependent. The apoptosis index(AI) was detected by TUNEL. After Yigan Decoction had been incubated for 48h at the end concentration of 18g·L⁻¹, the AI (14.5±3.1)% was significantly higher than that of control group (4.3±1.3)% ($P < 0.01$). When visualized under transmission electron microscopy, some apoptotic stellate cells were found, i.e. dilated endoplasmic reticulum, irregular nuclei, chromatin condensation and heterochromatin ranked along inside of nuclear membrane. By flow cytometry detection, after HSC was treated with Yigan Decoction at different concentrations of 36, 18 and 9(g·L⁻¹) for 48 h, AI (%) were 13.3±3.2, 10.7±2.7 and 10.1±2.5 respectively, which were significantly higher than that of control group(4.1±1.9) ($P < 0.01$). At the same concentration of 18g·L⁻¹ for 24h, 48h and 72h, AI (%) were 9.3±1.8, 10.7±2.7 and 14.6±4.3 respectively, which were significantly higher than that of control group ($P < 0.01$).

CONCLUSION: Yigan Decoction could significantly inhibit HSC proliferation and increase the apoptosis index of HSC dose-dependently and time-dependently, which may be related to its mechanism of antifibrosis.

Yao XX, Tang YW, Yao DM, Xiu HM. Effects of Yigan Decoction on proliferation and apoptosis of hepatic stellate cells. *World J Gastroenterol* 2002;8(3):511-514

INTRODUCTION

As the mechanisms of hepatic fibrosis have been gradually clarified and thus, many attempts to treat hepatic fibrosis have been made recently. But up to date there is still no effective way to treat hepatic fibrosis^[1]. Recent insights^[2-11] into the molecular pathogenesis of hepatic fibrosis and the efficacy of TCM have provided hope for the foreground of successful therapy, such as compound 861^[12], Kangxianfang^[13], Fuzhenghuayu decoction^[14-16], Ganyanping^[17] etc. Yigan Decoction, which was designed in our lab, was used in clinical setting for nearly twenty years. Our clinical practice has revealed that it has a marked curative effect on treating chronic liver diseases^[18]. Hepatic sinusoidal cells such as the hepatic stellate cells (HSC), endothelial cells or Kupffer cells are deeply involved in hepatic fibrogenesis or fibrolysis. Recent studies have made their morphology and functions clear. A wealth of evidence now indicates that HSC is the key to produce fibrosis which served as the major source of fibrillar and nonfibrillar matrix proteins. Quiescent HSC synthesize low levels of matrix proteins, but as a result of injury, HSC could be proliferated and transformed to myofibroblast, a process termed activation^[4]. So to inhibit HSC activation and proliferation and induce apoptosis of the activated HSC is one of the most important strategies for preventing and curing liver fibrosis. HSC cultured in uncoated plastic plates *in vitro* spontaneously undergo activation and share the similar features of cell activation *in vivo*^[19]. This culture-induced activation has been extensively studied as a model of the activation secondary to liver fibrogenesis. In order to testify the action of Yigan Decoction on liver fibrosis and investigate its mechanism, the effects of Chinese herb Yigan Decoction on the proliferation and apoptosis of HSC *in vitro* were observed.

MATERIALS AND METHODS

Cell culture

HSC lines (CFSC) (established by Professor Greenwel) were provided by Southwest Hospital, Third Military Medical University. The phenotype was activated HSC^[20, 21]. Cells were cultured in RPMI1640 (Gibco) medium plus 100mL⁻¹ fetal calf serum, penicillin 1×10⁵U·L⁻¹ and streptomycin 100mg·L⁻¹, and kept in a controlled atmosphere (5% CO₂) incubator at 37°C.

Drug treatment

Yigan Decoction consists of Radix Salviae Miltiorrhizae, Radix Angelicae Sinensis, Radix Paeoniae Rubra and Hirudo, etc. The decoction was made by Hebei Institute of Gastroenterology, containing 0.72g of crude herbs in each milliliter. Exponentially growing cells were seeded in plates for 24h and treated with Yigan Decoction at

various concentrations (144, 72, 36, 18, 9 and $4.5\text{g}\cdot\text{L}^{-1}$) for 24h, 48h and 72h, respectively. The cells not treated with this drug served as control cells.

Dose-dependent effects of Yigan Decoction on cell proliferation

Colorimetric MTT assays^[23] were used to observe cell proliferation. HSC were incubated in 96 well plates. The concentration of cells was modulated to $1\times 10^8\cdot\text{L}^{-1}$. After cultured for 24h, Yigan Decoction was added in different concentrations such as 144, 72, 36, 18, 9 and $4.5\text{g}\cdot\text{L}^{-1}$ for 48h. Each group was arranged three duplicate wells. After the supernatant was extracted and 0.05% MTT solution 10 μL was added to all wells for 4h, DMSO 100 μL was added for coloration. After a few minutes at room temperature to ensure that all crystals were dissolved, the optic-metric density (OD) was read on ELISA reader at test wavelength of 570nm and referent wavelength of 630nm.

Time-dependent effects of Yigan Decoction on cell proliferation

The cultured cells were grown up to logarithmic growth phase, digested with $2.5\text{g}\cdot\text{L}^{-1}$ trypsin. The concentration of cells was modulated to $1\times 10^8\cdot\text{L}^{-1}$. HSC were incubated in 24 well plates. Each well was added with 1mL. After being cultured for 24h, Yigan Decoction (50 μL) was added into wells at the same end concentration of $18\text{g}\cdot\text{L}^{-1}$. Cell proliferation was observed at different times, i.e., 24h, 48h and 72h after the herb was treated, each was arranged three duplicate wells. The number of HSC was counted at the end of each time.

Apoptosis examined by TUNEL

In situ cell death detection kits were purchased from Boehringer Mannheim Company, Germany. The cells were adjusted to a density of 2×10^3 cells/ cm^2 , added to 24-well plates with cover glass-slides in 0.5mL each well. After being incubated with Yigan Decoction at the end concentration of $18\text{g}\cdot\text{L}^{-1}$ for 48h, the glass slides were taken out, rinsed, fixed and stained. The negative control with omission of TUNEL enzyme was designed according to the manufacturer's manual. The cells stained with dark brown nucleus were considered as positive cells. Ten optical fields, about 500-1000 cells were selected randomly and counted in each glass-slide under the high magnification ($\times 400$) microscope. Apoptosis Index (AI) = (apoptotic cells/ total cells) $\times 100\%$.

Apoptosis examined by transmission electron microscopy

HSC were treated with Yigan Decoction at the end concentration of $18\text{g}\cdot\text{L}^{-1}$ for 48h. Then the cells were centrifugated and fixed in glutaraldehyde for observation of transmission electron microscopy.

Apoptosis examined by flow cytometry

HSC were treated with Yigan Decoction at the end concentration of 36, 18 and $9\text{g}\cdot\text{L}^{-1}$ for 24h, 48h and 72h. Cells were digested by $2.5\text{g}\cdot\text{L}^{-1}$ trypsin, washed by PBS, fixed by cold ethanol at 4°C and dyed with PI (propidium iodide), and then were analyzed by flow cytometry.

Statistics

Results were expressed as mean \pm SD ($\bar{x}\pm s$). Differences between groups and differences over times were analyzed using analysis of variance and Newman-Keuls methods where appropriate. *P* values less than 0.05 were considered to be statistically significant.

RESULTS

Dose-dependent inhibitory effects of Yigan Decoction on cell proliferation

Yigan Decoction could significantly inhibit HSC proliferation dose-dependently compared with the control group (Table 1). The

inhibitory effects of groups at concentrations of 144 and $72\text{g}\cdot\text{L}^{-1}$ were stronger than those of groups at concentrations of 36, 18 and $9\text{g}\cdot\text{L}^{-1}$, and no obvious inhibitory effect was found at the herb concentration of $4.5\text{g}\cdot\text{L}^{-1}$.

Time-dependent inhibitory effects of Yigan Decoction on cell proliferation

At the end concentration of $18\text{g}\cdot\text{L}^{-1}$, HSC were significantly inhibited compared with control group. The number of cells was manually counted. The effect was time-dependent, and reached a peak at 72h ($P<0.01$) (Table 2).

Apoptosis of HSC induced by Yigan Decoction examined by TUNEL

Based on the above results that Yigan Decoction could inhibit HSC proliferation at concentrations of $9\text{--}144\text{g}\cdot\text{L}^{-1}$ from 24h to 72h, we selected the $18\text{g}\cdot\text{L}^{-1}$ of Yigan Decoction and 48h affecting period as experimental conditions so as to better compare with the results of the herb on HSC lines. After Yigan Decoction had been incubated for 48h, the AI $22.5\pm 7.1\%$ was significantly higher than that of control group $4.3\pm 1.3\%$ ($P<0.01$). Apoptotic cell is characterized by compaction of nuclear chromatin and condensation of cytoplasm. By TUNEL stain the most condensed cells demonstrated evidence of DNA fragmentation and were strongly stained (Figure 1, arrowed).

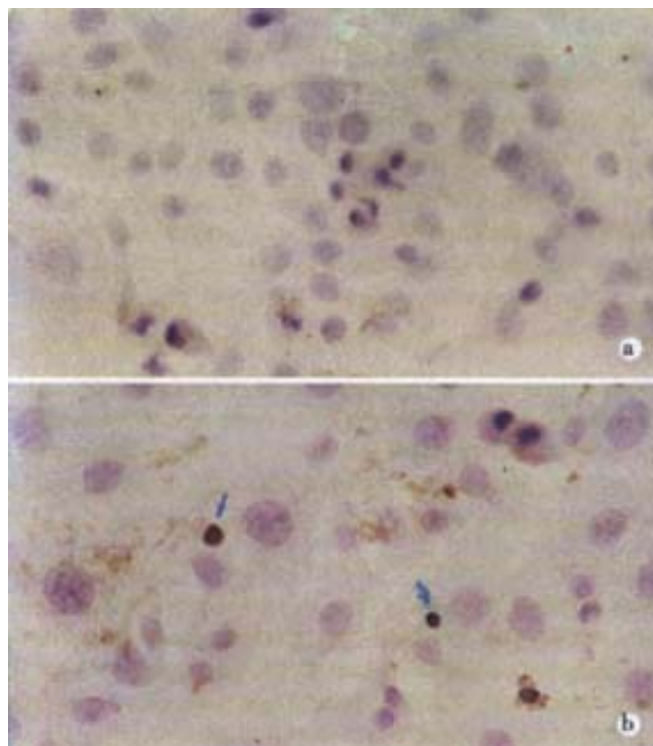


Figure 1 (A) Control HSC (TUNEL $\times 400$). (B) Apoptotic cell characterized by compaction of nuclear chromatin and condensation of cytoplasm (TUNEL $\times 400$). By TUNEL stain the most condensed cells demonstrated evidence of DNA fragmentation and were strongly staining (iu).

Apoptosis of HSC induced by Yigan Decoction examined by transmission electron microscopy

After 24~48h treatment of Yigan Decoction, we visualized under inverted microscopy. Small rounded cells were observed on the surface of the monolayer. These cells could be displaced by agitation of the tissue culture plate, demonstrating that they were very loosely adherent to the monolayer and that some were detached and floating in the culture supernatant (Figure 2). These features are compatible with HSC that have undergone programmed cell death or apoptosis^[24].

When visualized under transmission electron microscopy, the apoptotic HSC were found, i.e. dilated endoplasmic reticulum, irregular nuclei, chromatin condensation and heterochromatin ranked along inside of nuclear membrane. All of these features are characteristic of apoptosis and distinguish programmed cell death from necrosis (Figure 3).

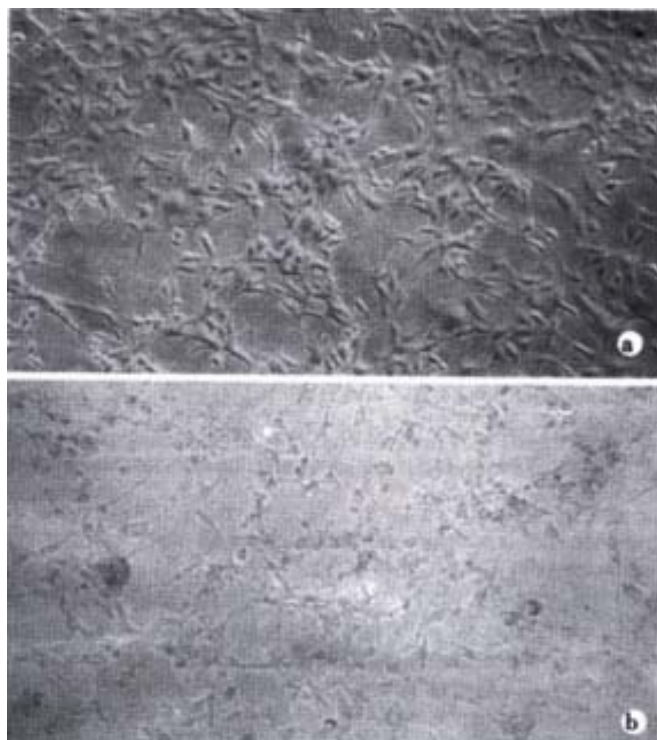


Figure 2 Morphological changes of HSC observed by light microscopy treated by Yigan Decoction. (A) Untreated cells ($\times 200$); (B) some HSC got round, detached and floating in the culture supernatant after exposure to $18\text{g}\cdot\text{L}^{-1}$ Yigan Decoction for 48h ($\times 100$).

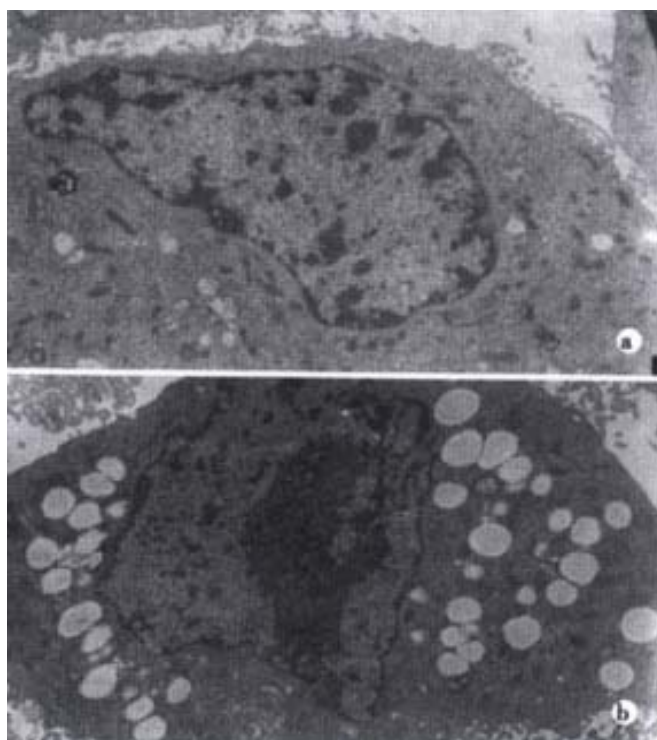


Figure 3 Ultrastructures of HSC with or without treatment with Yigan Decoction. Following 48h treatment of Yigan Decoction, dilated endoplasmic reticulum, irregular nuclei, chromatin condensation and heterochromatin ranked along inside of nuclear membrane could be found (A $5000\times$). Untreated cells (B $5000\times$).

Apoptosis examined by flow cytometry

After HSC were treated with Yigan Decoction at different concentrations of 36, 18 and $9(\text{g}\cdot\text{L}^{-1})$ for 48h, the apoptosis rate was significantly higher than that of control group ($P<0.01$) (Table 3). Our experiments showed that Yigan Decoction could increase the apoptosis rate dose-dependently and time-dependently compared with the control group. (Table 3 and 4, Figure 4).

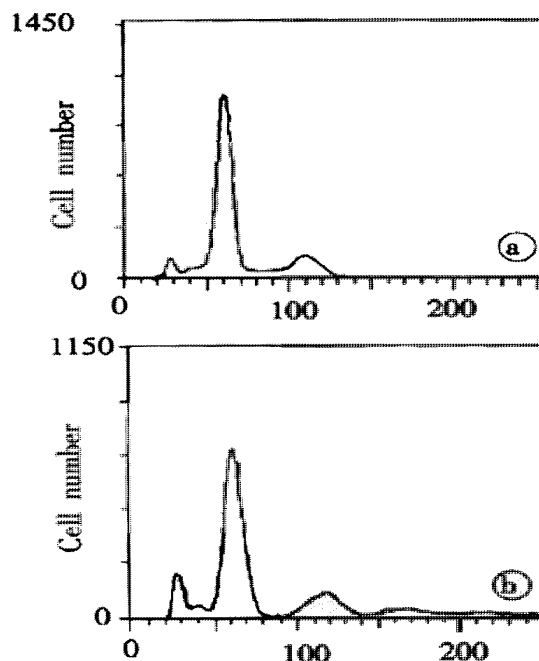


Figure 4 Flow cytometry changes. (A) Control group. (B) Yigan Decoction group.

Table 1 Effects of Yigan Decoction on HSC proliferation ($\bar{x}\pm s$)

Groups	Herb concentrations ($\text{g}\cdot\text{L}^{-1}$)	ODs	proliferation rates (%)
Yigan Decoction	144	0.08 ± 0.02^b	21.62
	72	0.15 ± 0.04^b	40.54
	36	0.20 ± 0.03^a	54.05
	18	0.17 ± 0.02^a	45.95
	9	0.19 ± 0.05^a	51.35
	4.5	0.31 ± 0.04	83.78
Control		0.37 ± 0.03	100

^a $P<0.05$, ^b $P<0.01$ vs control group.

Table 2 Effects of Yigan Decoction on HSC proliferation ($\times 10^3\cdot\text{L}^{-1}$) ($\bar{x}\pm s$)

Groups	24h	48h	72h
Control	1.440 ± 0.124	2.288 ± 0.178	2.335 ± 0.146
Yigan Decoction	1.203 ± 0.112	1.258 ± 0.098^b	1.359 ± 0.079^b

^b $P<0.01$ vs control group.

Table 3 Apoptosis indexes of Yigan Decoction on HSC ($\bar{x}\pm s$)

Groups	Herb concentrations ($\text{g}\cdot\text{L}^{-1}$)	apoptosis indexes (%)
Yigan Decoction	36	13.3 ± 3.2^b
	18	10.7 ± 2.7^b
	9	10.1 ± 2.5^b
Control		4.1 ± 1.9

^b $P<0.01$ vs control group.

Table 4 Time-dependent effects of Yigan Decoction on HSC apoptosis ($\bar{x}\pm s$)

Groups	24h	48h	72h
Control	4.5 ± 1.3	7.1 ± 1.9	8.0 ± 1.8
Yigan Decoction	9.3 ± 1.8^b	10.7 ± 2.7^b	14.6 ± 4.3^b

^b $P<0.01$ vs control group.

DISCUSSION

Recent studies have found clearly the key role of HSC in developing liver fibrosis. HSC could activate, proliferate and largely synthesize various components of extracellular matrix in chronic liver disease, that would lead to liver fibrosis^[22]. Studies suggest that HSC numbers are controlled by apoptosis in addition to proliferation during progressive fibrosis and particularly during recovery from fibrosis. The key event in the process of injury-fibrosis-recovery sequence is the loss of activated HSC mediated by apoptosis^[23]. Therefore to induce apoptosis of activated HSC is one of the most important therapeutic strategies for liver fibrosis. Recent evidence has demonstrated that a mechanism to eliminate activated HSC in culture and in animal models is inducing apoptosis. Interestingly, activated HSC are more sensitive to some mechanisms of apoptosis than quiescent HSC. Such a mechanism may serve in the future to eliminate the undesirable activated HSC without affecting their normal quiescent counterpart.

The CFSC used in present study is activated HSC. So it shared some features with activated HSC *in vivo* and could be used as a desirable cell model for the test of antifibrotic drugs. Although the desirable antifibrotic drugs have not been found up to now, some herbal decoctions have been reported to prevent fibrogenesis effectively, showing a good prospect of using Chinese herbs in treating chronic liver diseases^[24]. It was reported that Radix Salviae Miltiorrhizae (RSM) can inhibit fibroblast cells^[25]. RSM can prevent liver fibrosis if it is used for a long time^[26]. Large doses of RSM can activate collagenase and help reduce extracellular matrix. The level of P III P and laminin were decreased in patients with liver disease after treatment of RSM. Studies demonstrated that long-term treatment of RSM for 10-12wk can reduce portal vein, spleen diameters and blood flow, but the velocity of blood flow did not change^[27]. These results demonstrated the advantage of Chinese herbs in treating chronic hepatic diseases. Yigan Decoction, one of formally produced herbs, could prevent extracellular matrix production and deposit in CCl₄ induced rat liver fibrosis^[28], and improve fibrotic liver structure and liver function in patients with chronic hepatitis or cirrhosis^[18]. It is mainly composed of RSM, Radix Angelicae Sinensis (RAS), Radix Paeoniae Rubra and Hirudo, which have the actions of promoting blood circulation, removing blood stasis, shrinking the liver and spleen.

The present results suggest that Yigan Decoction could significantly inhibit HSC proliferation and increase the apoptosis rate of HSC dose-dependently and time-dependently compared with the control group ($P < 0.01$). After Yigan Decoction had been incubation for 48h, the apoptosis rate of HSC was 27.5% compared with 7.1% in the control group ($P < 0.01$). Our findings strongly suggest that inhibition of HSC proliferation and induction of HSC apoptosis may play an important role in the antifibrotic actions of Yigan Decoction. Our data may provide a new idea for the future development of therapeutic antifibrotic strategies by means of traditional Chinese medicine.

The antifibrotic effect of Yigan Decoction has been well proved by the results of experimental and clinical studies. However, Chinese herbs have very complicated components and their metabolisms are not well clarified yet. There's still a long way to go. With the ever-increasing in-depth studies about the pharmacodynamics, pharmacokinetics, reasonable combinations of drugs, the best preparation form and dosages of each herb and courses, Yigan Decoction is expected to be an effective antihepatofibrotic drug.

REFERENCES

- Brenner DA. Therapeutic strategy for liver fibrosis. *J Gastroenterol Hepatol* 1999; 14(Suppl.): A279-A280

- Wu CH. Fibrodynamics-elucidation of the mechanisms and sites of liver fibrogenesis. *World J Gastroenterol* 1999; 5: 388-390
- Liu CH, Hu YY, Wang XL, Liu P, Xu LM. Effect of salvianolic acid-A on NIH/3T3 fibroblast proliferation, collagen synthesis and gene expression. *World J Gastroenterol* 2000; 6: 361-364
- Friedman SL. The cellular basis of hepatic fibrosis. Mechanisms and treatment strategies. *N Engl J Med* 1993; 328: 1828-1835
- Liu SR, Gu HD, Li DG, Lu HM. A comparative study of fat storing cells and hepatocytes in collagen synthesis and collagen gene expression. *Xin Xiaohuabingxue Zazhi* 1997; 5: 761-762
- Gu SW, Luo KX, Zhang L, Wu AH, He HT, Weng JY. Relationship between ductile proliferation and liver fibrosis of chronic liver disease. *Shijie Huaren Xiaohua Zazhi* 1999; 7: 845-847
- Yan JC, Ma Y, Chen WB, Shun XH. Dynamic observation on liver fibrosis and cirrhosis of hepatitis B. *Huaren Xiaohua Zazhi* 1998; 6: 699-702
- Wang Y, Gao Y, Huang YQ, Yu JL, Fang SG. Gelatinase A proenzyme expression in the process of experimental liver fibrosis. *Shijie Huaren Xiaohua Zazhi* 2000; 8: 165-167
- Lu LG, Zeng MD, Li JQ, Qiu DK, Hua J, Fan ZP. Expression of intercellular adhesion molecular-1 by activated hepatic stellate cells. *Huaren Xiaohua Zazhi* 1998; 6: 567-569
- Wang X, Chen YX, Xu CF, Zhao GN, Huang YX, Wang QL. Relationship between tumor necrosis factor- α and liver fibrosis. *World J Gastroenterol* 1998; 4: 18
- Cheng ML, Wu YY, Huang KF, Luo TY, Ding YS, Lu YY, Liu RC, Wu J. Clinical study on the treatment of liver fibrosis due to hepatitis B by IFN- α 1 and traditional medicine preparation. *World J Gastroenterol* 1999; 5: 267-269
- You H, Wang BE, Wang TL, Ma XM, Zhang J. Proliferation and apoptosis of hepatic stellate cells and effects of compound 861 on liver fibrosis. *Zhonghua Ganzangbing Zazhi* 2000; 8: 78-80
- Wu JG, Li XY. Clinical studies of Kangxianfang in treating liver cirrhosis. *Xin Xiaohuabingxue Zazhi* 1997; 5: 303-304
- Hu YY, Liu C, Liu P, Gu HT, Ji G, Wang XL. Anti-fibrosis and anti-peroxidation of lipid effects of Fuzhenghuayu decoction on rat liver induced by CCl₄. *Xin Xiaohuabingxue Zazhi* 1997; 5: 485-486
- Gu HT, Hu YY, Xu LM, Liu P, Liu C. Pathological observation on effects of Fuzhenghuayu decoction on rat liver induced by CCl₄. *Zhongxiyi Jiehe Ganbing Zazhi* 1997; 7: 224-226
- Liu P, Liu C, Xu LM, Xue HM, Liu CH, Zhang ZQ. Effects of Fuzhenghuayu 319 recipe on liver fibrosis in chronic hepatitis B. *World J Gastroenterol* 1998; 4: 348-353
- Du LJ, Tang WX, Dan ZL, Zhang WY, Li SB. Protective effect of Ganyanping on CCl₄ induced liver fibrosis in rats. *Huaren Xiaohua Zazhi* 1998; 6: 21-22
- Yao XX, Fu YL, Li XL, Jia YP, An ZC, Zhang XZ. Therapeutic effect of Yigan Decoction on chronic hepatitis: a multi-center observation of 324 cases. *Hebei Yixueyuan Xuebao* 1989; 10: 231-233
- Friedman SL. Cellular sources of collagen and regulation of collagen production in liver. *Sem in Liver Dis* 1990; 10: 20-29
- Zhu YH, Hu DR. Establishment and application of hepatic stellate cells. *Shijie Huaren Xiaohua Zazhi* 1999; 7: 348-349
- Denizot F, Lang R. Rapid colorimetric assay for cell growth and survival. Modifications to the tetrazolium dye procedure giving improved sensitivity and reliability. *J Immunol Methods* 1986; 89: 271-277
- Bissell DM, Friedman SL, Maher JJ, Roll FJ. Connective tissue biology and hepatic fibrosis: Report of a conference. *Hepatology* 1990; 11: 488-498
- Iredale JP, Benyon RC, Pickering J, McCullen M, Northrop M, Pawley S, Hovell C, Arthur MJ. Mechanisms of spontaneous resolution of rat liver fibrosis. *J Clin Invest* 1998; 102: 538-549
- Jia KM. Pay more attention to the study of the treatment of hepatitis B. *Zhonghua Neike Zazhi* 2000; 39: 797-798
- Yao XX, Li XT, Li YW, Zhang XY. Clinical and experimental study of Radix Salviae Miltiorrhizae and other Chinese herbs of blood-activating and stasis-eliminating effects on hemodynamics of portal hypertension. *Zhonghua Xiaohua Zazhi* 1998; 18: 24-27
- Yao XX, Cui DL, Sun YF, Li XT. Clinical and experimental study of effect of Radix Salviae Miltiorrhizae and other blood-activating and stasis-eliminating Chinese herbs on hemodynamics of portal hypertension. *World J Gastroenterol* 1998; 4: 439-442
- Li XT, Bai WY, Wang HM, Yao XX. Study of effects of Radix salviae miltiorrhizae on portal hypertension in experimental cirrhotic dogs. *Xin Xiaohuabingxue Zazhi* 1997; 5: 421-422
- Yao XX, Tang YW, Yao DM, Xiu HM. Effect of Yigan Decoction on the expression of type I, III collagen proteins in experimental hepatic fibrosis in rats. *Shijie Huaren Xiaohua Zazhi* 2001; 9: 263-267

• BASIC RESEARCH •

Salvia miltiorrhiza monomer IH764-3 induces hepatic stellate cell apoptosis via caspase-3 activation

Xiao-Lan Zhang, Li Liu, Hui-Qing Jiang

Xiao-Lan Zhang, Li Liu, Hui-Qing Jiang, Department of Gastroenterology, The Second Hospital of Hebei Medical University, Shijiazhuang 050000 Hebei Province, China

Supported by Fund of the Scientific and Technical Department of Hebei Province, No. 01276134

Correspondence to: Professor Hui-Qing Jiang, Department of Gastroenterology, The Second Hospital of Hebei Medical University, Shijiazhuang 050000, Hebei Province, China. huiqingj@heinfo.net
Telephone: +86-311-7046901 Ext. 6513

Received 2001-12-20 Accepted 2002-01-23

Abstract

AIM: To investigate the effects of IH764-3 on HSC apoptosis, and the expression of caspase-3 protein in HSC apoptotic process.

METHODS: HSCs were cultured in medium with different IH764-3 doses ($10\mu\text{g}\cdot\text{mL}^{-1}$, $20\mu\text{g}\cdot\text{mL}^{-1}$, $30\mu\text{g}\cdot\text{mL}^{-1}$, $40\mu\text{g}\cdot\text{mL}^{-1}$) and without IH764-3, and HSC proliferation was quantitatively measured by ^3H -thymidine incorporation. The morphological changes of HSCs were observed with transmission electron microscope after exposure to the dose of $40\mu\text{g}\cdot\text{mL}^{-1}$ of IH764-3 for 48 hr. The apoptosis rates were detected by annexin V/PI and TdT-mediated dUTP nick end labeling (TUNEL). The expression of caspase-3 protein was determined by flow cytometry.

RESULTS: (1) HSC proliferation rates induced with different IH764-3 doses ($10\mu\text{g}\cdot\text{mL}^{-1}$, $20\mu\text{g}\cdot\text{mL}^{-1}$, $30\mu\text{g}\cdot\text{mL}^{-1}$, $40\mu\text{g}\cdot\text{mL}^{-1}$) were significantly reduced compared with that of the control group ($P<0.01$). (2) With the doses above, IH764-3 dose-dependently produced HSC apoptosis rates of 6.7% (9.4%), 9.3% (21.6%), 15.1% (27.2%) and 19.0% (28.4%) respectively, by annexin V and PI-labeled flow cytometry assay (or TUNEL), while it was only 2.3% (6.7%) in the control. (3) The expression of caspase-3 protein in IH764-3 groups was significantly higher than that of the control ($P<0.05$).

CONCLUSION: Within the dose range used in present study, IH764-3 can inhibit HSC proliferation, as well as enhance HSC apoptosis. Furthermore, IH764-3 can significantly increase the caspase-3 protein expression.

Zhang XL, Liu L, Jiang HQ. Salvia miltiorrhiza monomer IH764-3 induces hepatic stellate cell apoptosis via caspase-3 activation. *World J Gastroenterol* 2002;8(3):515-519

INTRODUCTION

Hepatic fibrosis occurs as a result of the accumulation of excess extracellular matrix (ECM) around the hepatic sinus and portal vein^[1-19]. Activated hepatic stellate cells (HSCs) are the main source of ECM in the process of hepatic fibrosis. Therefore, HSCs play a central role in the hepatic fibrogenesis^[20-34]. Either proliferation or apoptosis of HSCs or both may affect the population of HSCs^[35-39]. Recent studies have shown that apoptosis is the main process to eliminate the activated HSCs during the resolution of hepatic fibrosis^[40-42]. To induce the apoptosis of HSCs, therefore, might be an

important strategy for the hepatic fibrosis therapy^[43-45].

Chinese herbal medicine Salviae Miltiorrhiza, which can improve circulatory status and eliminate stasis, exhibits a series of important pharmacological effects on anti-inflammation, antioxidation, and inhibiting the platelet aggregation^[46-49]. IH764-3, extracted from Salviae Miltiorrhiza, preserves all of these beneficial effects. Furthermore, in recent studies, it has been documented that IH764-3 could play an important role in anti-fibrosis, inhibiting the proliferation of HSCs and the synthesis of collagens^[47,50]. However, there are few reports so far concerns about the effects of IH764-3 on HSC apoptosis and its mechanisms. In present study, we therefore used annexin-V/PI double labeling flow cytometry, TUNEL and transmission electron microscope to examine the effects of IH764-3 on HSC apoptosis. Meanwhile, the effects of IH764-3 on the expression of caspase-3 protein during HSC apoptosis were also observed.

MATERIALS AND METHODS

Materials

HSC line CFSC was established and kindly provided by Prof. Greenwel in America, which phenotype was activated HSCs, and derived from the CCl₄-induced cirrhotic rat^[51]. RPMI-1640 medium was purchased from GIBCO Co. Fetal calf serum was from Four Season Green Biological Co, Hangzhou, China. IH764-3 was kindly provided by Prof. Chun-Zheng Yang from Hematopathy Institute, Chinese Academy of Medical Science. ^3H -TdR was from Isotope Institute, Chinese Academy of Atomic Energy. Annexin-V cell apoptosis assay kit was purchased from Baosai Biological Technology Co, Beijing. TUNEL assay kit was from Boster Biological Engineering Co, Wuhan, China. Caspase-3 assay kit was from CLONTECH Co, USA. Goat anti-mouse FITC-IgG was the product of Microorganism Institute, Academy of Military Medical Sciences, China. Other reagents were analytically pure.

Methods

Cell culture The HSCs were thawed and plated in RPMI-1640 medium containing $100\text{mL}\cdot\text{L}^{-1}$ fetal calf serum, $100\text{KU}\cdot\text{L}^{-1}$ penicillin, $100\text{mg}\cdot\text{L}^{-1}$ streptomycin, $4\text{mmol}\cdot\text{L}^{-1}$ L-glutamine and $0.1\text{mmol}\cdot\text{L}^{-1}$ HEPES. Cells were kept in culture at 37°C in a $50\text{mL}\cdot\text{L}^{-1}$ CO₂ atmosphere and 100% humidity. The HSCs were digested with 0.25% trypsin and subcultured from one to three when the cells proliferated into a full monolayer. The first change of the culture medium was made about 24 hr after subculturing, and then the cells were subcultured again about 72 hr. Experiments were carried out while the cells were in exponential growth phase. Cells were plated in 25cm^2 plastic flasks at a density of $2\times 10^5\cdot\text{L}^{-1}$ or onto 96-well plates at a density of $5\times 10^6\cdot\text{L}^{-1}$. When the cells were nearly 100% confluent, they were continued to incubate for another 12 hr in serum-free RPMI-1640 culture medium. At that time most of the cells were in G₀ phase, they were divided into different groups. The dose-response studies were performed using different doses of IH764-3 ($10\mu\text{g}\cdot\text{mL}^{-1}$, $20\mu\text{g}\cdot\text{mL}^{-1}$, $30\mu\text{g}\cdot\text{mL}^{-1}$ and $40\mu\text{g}\cdot\text{mL}^{-1}$) and lasted for 12-48 hr, while the time-response studies were carried out at the timepoints of 12, 24, 48 and 72 hr with the dose of $30\mu\text{g}\cdot\text{mL}^{-1}$ of IH764-3.

Inhibition of cell proliferation assays HSCs were plated to triplicate wells in a 96-well plate with the concentration of $5 \times 10^3 \cdot \text{mL}^{-1}$. When the cells were nearly 100% confluent, they were cultured in serum-free medium for 12 hr. Then the medium was replaced with fresh medium containing 2% fetal calf serum and different IH764-3 doses, 1.11×10^4 Bq ^3H -Thymidine was added to each well. After 24 hr of incubation, HSCs were collected onto filter membrane and baked 1 hr at 100°C . The radioactivity (cpm) was determined with the beta-scintillation counter (Beckman). The inhibition of HSC proliferation was expressed by inhibitory rate, which was calculated as: inhibition rate = [(cpm of control group - cpm of IH764-3 group) / cpm of control group] $\times 100\%$.

Apoptosis detection The following methods were used to detect apoptosis: (1) Transmission electron microscope: After exposure to the dose of $40 \mu\text{g} \cdot \text{mL}^{-1}$ of IH764-3 for 48 hr, cells were trypsinized, collected, washed with PBS and centrifuged at 1200g for 10 min. The cell pellet was fixed in 4% glutaral for 2 hr, 1% osmium acid for 1 hr and dehydrated gradually, then stained by uranium acetic acid and lead citromalic acid. The cells were observed with transmission electron microscope and the ultrastructural changes were recorded. (2) Annexin-V/PI labeling to detect apoptotic rate^[52]: Briefly, the trypsinized HSCs were washed twice with PBS, stained with annexin-V (10L) and PI (5 μL) for 10 min, and the apoptotic rate was quantified by FACSCalibur flow cytometry (Becton Dickinson Inc.) at 488 nm wavelength. More than 1×10^4 cells were detected, and the results were analyzed with Modfit LT software. The stained cells were divided into three subgroups: The cells in V⁻/PI⁻ subgroup were survived cells which membrane was intact, The cells in V⁺/PI⁻ subgroup were apoptotic cells which membrane intact but with phosphatidylserine translocation; The cells in V⁺/PI⁺ subgroup were necrotic cells which membrane was impairment and with phosphatidylserine translocation. (3) Determination of apoptosis by TUNEL method: After trypsinization and collection, cells were fixed with 4% paraformaldehyde for 30 min. Apoptosis was assayed by TUNEL method. Briefly, the cells were incubated with proteinase K (5 $\mu\text{L} \cdot \text{mL}^{-1}$) at 37°C for 5 min, labeled by TdT and digoxin-d-UTP at 4°C in a humidified chamber to stay overnight, anti-digoxin antibody was added. After being incubated at 37°C for 30 min, the cells were stained with diaminobenzidine (DAB). Apoptotic cells presented as brownish stain in the nucleus, but we should pay special attention to distinguish the stained DNA fragments in cytoplasm due to some nuclear leakage. At least 500 cells were examined and the rate of apoptotic cells was calculated as the percentage of stained-cell per 100 cells.

Determination of Caspase-3 expression Trypsinized cells were washed in PBS, and fixed at 4°C in 70% ethanol overnight. Fixed cells were precipitated and washed in PBS. Cells (6×10^5) were suspended in 0.5 mL permeable buffer diluted by PBS, and subsequently incubated with anti-Caspase-3 antibody, FITC-labeled goat anti-rat IgG antibody (1:20)^[53], then cells were washed with PBS, assayed by flow cytometer. The relative quantity of the protein was expressed by Fluorescence index (FI).

Statistical analysis

Data were expressed as $\bar{x} \pm s$. One-way analysis of variance was used for multiple comparisons, and Newman-Keuls test and χ^2 test were used for intra-groups comparisons. *P* values less than 0.05 were considered to be statistically significant.

RESULTS

Effect of IH764-3 on proliferation of HSCs

Compared with the control group, IH764-3 had a significant inhibitory effect on ^3H -TdR incorporation; the inhibition was dose-dependent (Table 1).

Table 1 The effect of IH764-3 on ^3H -TdR incorporation ($\bar{x} \pm s$)

Dosage ($\mu\text{g} \cdot \text{mL}^{-1}$)	Cpm	Inhibitory rate (%)
0	19749 \pm 7222	
1	018339 \pm 5344	7.1
2	014147 \pm 1850 ^b	28.4
3	09125 \pm 916 ^b	53.8
4	05313 \pm 426 ^b	73.1

^b*P* < 0.01 vs control

Morphological changes

The shape of cells incubated with $30 \mu\text{g} \cdot \text{mL}^{-1}$ or $40 \mu\text{g} \cdot \text{mL}^{-1}$ of IH764-3 for 6 hr changed from stellate or shuttle to spherical, and the intercellular space was increased. 12 hr later, the cells began to detach from the plate and it is more remarkable at 24 hr. With the transmission electron microscope, the decreased volume, condensed chromatin and decreased nucleocytoplasmic ratio of apoptotic cell were noted. Some cells showed typical apoptotic changes: the pyknosis and margination of the nuclear chromatin. Moreover, the nuclei fragment, annular or crescent body, cytoplasm vacuoles and swollen Mitochondria were also observed. Some cells were karyolysis and turn into the specific apoptotic bodies (Figure 1).

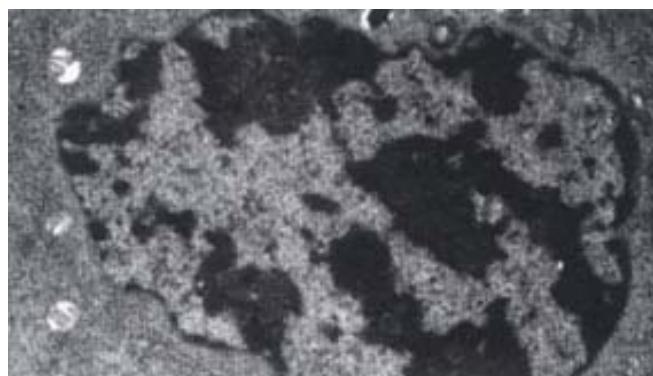


Figure 1 The apoptotic cells in $40 \mu\text{g} \cdot \text{mL}^{-1}$ IH764-3 for 48 hr (TEM 10000 \times) Apoptotic cells became small, the chromatin condensed

Annexin-V/PI combined labeling flow cytometry

The rate of apoptosis was both dose-dependent and time-dependent (Table 2A, 2B). For the $40 \mu\text{g} \cdot \text{mL}^{-1}$ group at 24 hr and $30 \mu\text{g} \cdot \text{mL}^{-1}$ group at 48-72 hr, the apoptotic cells presented worse progressive changes, most of the cells were V⁺/PI⁺ subclass, namely necrosis. The necrotic rate was 21.0-31.3%. Figure 2A, 2B.

Table 2A Apoptotic rates of HSCs exposed IH764-3 with different doses by Annexin-V/PI (%)

Time	doses	0 $\mu\text{g} \cdot \text{mL}^{-1}$	10 $\mu\text{g} \cdot \text{mL}^{-1}$	20 $\mu\text{g} \cdot \text{mL}^{-1}$	30 $\mu\text{g} \cdot \text{mL}^{-1}$	40 $\mu\text{g} \cdot \text{mL}^{-1}$
12hr		0.3	2.2	3.7	6.7	15.1
48hr		2.3	6.7	9.3	15.1	19.7

Table 2B Percentage of apoptotic HSCs exposed to IH764-3 ($30 \mu\text{g} \cdot \text{mL}^{-1}$) at different timepoints by Annexin-V/PI (%)

Time	0hr	12hr	24hr	48hr	72hr
Apoptosis rate	0.3	6.7	10.3	15.1	19.6

Detection of HSC apoptosis by TUNEL

After exposure of HSCs to different dose of IH764-3, the apoptotic indexes in experimental group by TUNEL assay at 48 hr were 9.4%

$\pm 2.6\%$ ($10\mu\text{g}\cdot\text{mL}^{-1}$), $21.6\pm 5.5\%$ ($20\mu\text{g}\cdot\text{mL}^{-1}$), $27.2\pm 6.2\%$ ($30\mu\text{g}\cdot\text{mL}^{-1}$) and $28.4\pm 6.5\%$ ($40\mu\text{g}\cdot\text{mL}^{-1}$), respectively, which were significantly higher than that in control group ($6.7\pm 0.6\%$, $P<0.01$) (Figure 3).

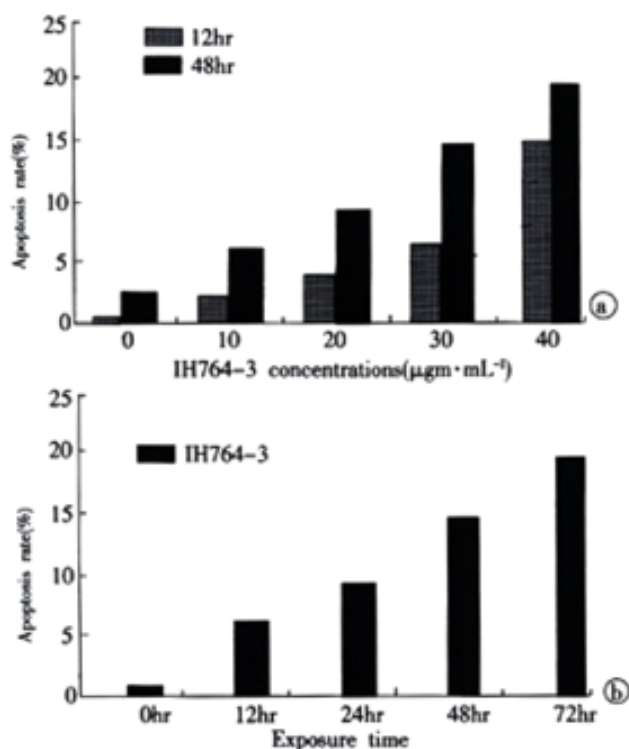


Figure 2 apoptosis rates of HSCs exposed to IH764-3. (A) dose-dependent; (B) time-dependent with the concentration of $30\mu\text{g}\cdot\text{mL}^{-1}$ of IH764-3.

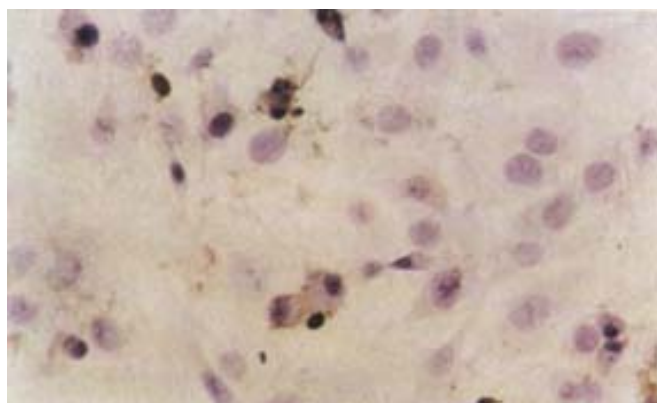


Figure 3 The apoptotic cells in $30\mu\text{g}\cdot\text{mL}^{-1}$ IH764-3 for 48hr(TUNEL10×40)

IH764-3 induced caspase-3 protein Expression in HSCs

With the given doses, IH764-3 could increase Caspase-3 protein expression dose-dependently. There was also a positive relationship between Caspase-3 protein expression and apoptosis rate (Table 3).

Table 3 Fluorescence index of caspase-3 protein in HSCs ($\bar{x}\pm s$)

Dosage ($\mu\text{g}\cdot\text{mL}^{-1}$)	Caspase-3	P value
0	175.6 \pm 22.5	
10	215.1 \pm 26.9	<0.01
20	231.6 \pm 28.6	<0.01
30	304.7 \pm 30.7	<0.01
40	338.9 \pm 32.1	<0.01

DISCUSSION

The dynamic balance between the cell proliferation and apoptosis plays a key role in growth, development and maintenance of physiological functions of individuals. Once the balance is broken, varieties of pathological and pathophysiological changes will take place. HSCs are the major cells that produce ECM components and proliferated significantly in hepatic fibrosis^[36]. It has been considered that apoptosis may play at least a partial role in reducing HSC population and decreasing the production of ECM components in hepatic fibrosis, thus triggering the process of HSC apoptosis is perhaps an important strategy to resolve the hepatic fibrosis^[45,54]. IH764-3, an extract of *Salviae Miltiorrhiza*, has been proved to be an effective agent for anti-hepatic fibrosis in animal model. However, up to the present, whether its anti-fibrotic mechanism was related to the induction of HSC apoptosis or not has not been elucidated yet.

Cell apoptosis, which is different from necrosis, is an initiative cell death process that activates endogenous DNA endonuclease, with the morphological characteristics of pyknosis and the chromatin margination to become lump or crescent bodies. Then cytoplasm condenses and cell shrinks, which finally forms apoptotic bodies. However, the cell membrane is integrated and the organelles keep intact. In present study, a great deal of typical apoptotic cells was found on plates treated with IH764-3, which demonstrated that IH764-3 did trigger the HSC apoptosis.

Apoptosis is a dynamic developing process that can be divided into early phase, metaphase and late phase. It has been reported that flow cytometry is the most sensitive method to examine apoptosis^[52,53]. In early apoptotic phase, the translocation of phosphatidylserine, which has high affinity to Annexin-V, from the inner leaflet to the outer layer of the plasma membrane, could be easily recognized by Annexin-V labeling method. Moreover, when combining with PI stain, it could also distinguish from necrotic cells. In this study, we found that IH764-3 could dose-dependently induce apoptosis at 12 and 48 hr timepoints, the apoptotic rate was 2.2% in $10\mu\text{g}\cdot\text{mL}^{-1}$ group and 15.1% in $40\mu\text{g}\cdot\text{mL}^{-1}$ group. In $30\mu\text{g}\cdot\text{mL}^{-1}$ group, the apoptotic rate was time-dependent. In $40\mu\text{g}\cdot\text{mL}^{-1}$ group at 24hr and $30\mu\text{g}\cdot\text{mL}^{-1}$ group at 48-72hr, the apoptotic cells presented progressive worse advanced changes, most of the cells became necrotic, the necrotic rate reached 21.0-31.3%. Similar changes were also observed with transmission electron microscope. Thus it could be concluded that low doses of IH764-3 mainly induced apoptosis, while in high doses, it could not only induce apoptosis, but also necrosis.

The remarkable biochemical characteristic of apoptosis is the genome DNA fragmentation. This is because the activated endogenous endonuclease can degrade the connected DNA between nucleosomes into 180-200bp oligonucleotide fragments. With terminal deoxynucleotidyl transferase, utilizing exogenous biotin-labeled-free nucleotides, the free nucleotides in 3' terminal can be catalyzed to get together in a non template-dependent manner, making the break nickings of DNA is labeled. Therefore, we used TUNEL method as another way to prove the apoptosis further. The results showed that apoptosis indexes in IH764-3 groups were higher than that of the control. Furthermore, the indexes were dose-dependent in IH764-3 groups. All of the above demonstrated that IH764-3 could induce HSC apoptosis in time and dose-dependent manner, but the signal transduction process remains unclear.

Caspase-3, a key proteinase in apoptosis pathway, is one of the proteases in cysteine aspartic acid specific proteases family, and is also called as cysteine proteases P32. It splits the peptide bond at asparagic residue of specific motif sequence in substrate protein. The activated caspase-3 may cause apoptosis^[55] and results in what we saw the apoptotic signs under microscope. Caspase-3 can split inhibitory caspase activated deoxyribonuclease (ICAD) into CAD^[56,57], which

degrades DNA in nucleus.

To examine the possible mechanism of HSC apoptosis induced by IH764-3, we observed the expression of caspase-3 protein. The results showed that IH764-3 from $10\mu\text{g}\cdot\text{mL}^{-1}$ to $40\mu\text{g}\cdot\text{mL}^{-1}$ could increase the expression of caspase-3 protein. The more the apoptosis developed, the more the caspase-3 protein expressed. So we deduced that HSC apoptosis induced by IH764-3 was mediated by caspase-3 activation. Increased expression of caspase-3 protein was possibly one of the mechanisms in HSC apoptosis induced by IH764-3. Any reagents that increase caspase-3 protein expression might have a potential possibility to become new drugs to treat patients with hepatic fibrosis^[58].

ACKNOWLEDGEMENTS

The authors wish to thank Professor Greenwel for his kindly providing the cell line and Professor Chun-zheng Yang for presenting IH764-3. We also thank Dr Hong-Qun Liu and Dr Shuang Chen for their critical reading of the manuscript.

REFERENCES

- Jiang HQ, Zhang XL. Progress in the study of pathogenesis in hepatic fibrosis. *Shijie Huaren Xiaohua Zazhi* 2000;8:687-689
- Wu CH. Fibrodynamics-elucidation of the mechanisms and sites of liver fibrogenesis. *World J Gastroenterol* 1999;5:388-390
- Wang JY, Zhang QS, Guo JS, Hu MY. Effects of glycyrrhetic acid on collagen metabolism of hepatic stellate cells at different stages of liver fibrosis in rats. *World J Gastroenterol* 2001;7:115-119
- Du WD, Zhang YE, Zhai WR, Zhou XM. Dynamic changes of type α_1 , III and IV collagen synthesis and distribution of collagen-producing cells in carbon tetrachloride-induced rat liver fibrosis. *World J Gastroenterol* 1999;5:397-403
- Friedman SL. Molecular mechanisms of hepatic fibrosis and principles of therapy. *J Gastroenterol* 1997;32:424-430
- Shapiro SD, Senior RM. Matrix metalloproteinase: matrix degradation and more. *Am J Respir Cell Mol Biol* 1999;20:1100-1102
- Massova I, Kotra LP, Fridman R, Mobashery S. Matrix metalloproteinases: structure, evolution, and diversification. *FASEB J* 1998;12:1075-1095
- Benyon RC, Hovell CJ, Gaca MD, Jones EH, Iredale JP, Arthur MJ. Progelatinase A is produced and activated by rat hepatic stellate cells and promotes their proliferation. *Hepatology* 1999;30:977-986
- Knittel T, Mehde M, Kobold D, Saile B, Dinter C, Ramadori G. Expression patterns of matrix metalloproteinases and their inhibitors in parenchymal and non-parenchymal cells of rat liver: regulation by TNF- α and TGF- β 1. *J Hepatol* 1999;30:48-60
- Bai WY, Yao XX, Feng LY. The study status of liver fibrosis. *Shijie Huaren Xiaohua Zazhi* 2000;8:1267-1268
- Bahr MJ, Vincent KJ, Arthur MJ, Fowler AV, Smart DE, Wright MC, Clark IM, Benyon RC, Iredale JP, Mann DA. Control of the tissue inhibitor of metalloproteinases-1 promoter in culture-activated rat hepatic stellate cells: regulation by activator protein-1 DNA binding proteins. *Hepatology* 1999;29:839-848
- Liu HL, Li XH, Wang DY, Yang SP. Matrix metalloproteinase-2 and tissue inhibitor of metalloproteinase-1 expression in fibrotic rat liver. *World J Gastroenterol* 2000;6:881-884
- Greenwel P, Dominguez-Rosales JA, Mavi G, Rivas-Estilla AM, Rojkind M. Hydrogen peroxide: a link between acetaldehyde-elicited α 1(I) collagen gene up-regulation and oxidative stress in mouse hepatic stellate cells. *Hepatology* 2000;31:109-116
- Friedman SL. Cytokines and fibrogenesis. *Semin Liver Dis* 1999;19:129-140
- Weng HL, Cai WM, Liu RH. Animal experiment and clinical study of effect of gamma-interferon on hepatic fibrosis. *World J Gastroenterol* 2001;7:42-48
- Yao XX. Diagnosis and treatment of hepatic fibrosis. *Shijie Huaren Xiaohua Zazhi* 2000;8:681-689
- Xiang DD, Li QF, Wang YM, Wang YF. The effect of vitamin E emulsion on procollagen III and matrix metalloproteinases-1 mRNA in hepatic stellate cells. *Shijie Huaren Xiaohua Zazhi* 1999;7:1085
- Svegliati-Baroni G, Ridolfi F, Di Sario A, Saccomanno S, Bendia E, Benedetti A, Greenwel P. Intracellular signaling pathways involved in acetaldehyde-induced collagen and fibronectin gene expression in human hepatic stellate cells. *Hepatology* 2001;33:1130-1140
- Chen PS, Zhan WR, Zhang YE, Zhang JS. The effect of hypoxia on collagen and matrix metalloproteinase hepatic stellate cells. *Shijie Huaren Xiaohua Zazhi* 2000;8:586-587
- Pinzani M, Marra F, Carloni V. Signal transduction in hepatic stellate cells. *Liver* 1998;18:2-13
- Huang GC, Zhang JS. Signal transduction in activated hepatic stellate cells. *Shijie Huaren Xiaohua Zazhi* 2001;9:1056-1060
- Carloni V, Pinzani M, Giusti S, Romanelli RG, Parola M, Bellomo G, Failli P, Hamilton AD, Sebt SM, Laffi G, Gentilini P. Tyrosine phosphorylation of focal adhesion kinase by PDGF is dependent on ras in human hepatic stellate cells. *Hepatology* 2000;31:131-140
- Zhu YH, Hu DR. The establishment and application of hepatic stellate cell lines. *Shijie Huaren Xiaohua Zazhi* 1999;7:348-349
- Zhu YH, Hu DR, Nie QH, Liu GD, Tan ZX. Study on activation and c-fos, c-jun expression of *in vitro* cultured human hepatic stellate cells. *Shijie Huaren Xiaohua Zazhi* 2000;8:299-302
- Huang GC, Zhang JS, Zhang YE. Effects of retinoic acid on proliferation, phenotype and expression of cyclin-dependent kinase inhibitors in TGF- β 1-stimulated rat hepatic stellate cells. *World J Gastroenterol* 2000;6:819-823
- Potter JJ, Rennie-Tankersley L, Anania FA, Mezey E. A transient increase in c-myc precedes the transdifferentiation of hepatic stellate cells to myofibroblast-like cells. *Liver* 1999;19:135-144
- Xiang DD, Wei YL, Li QF. Molecular mechanism of transforming growth factor β 1 on Ito cell. *Shijie Huaren Xiaohua Zazhi* 1999;7:980-981
- Lu LG, Zeng MD, Li JQ, Qiu DK, Hua J, Fan ZP. Expression of intercellular adhesion molecule-1 and hepatic stellate cell activation. *Shijie Huaren Xiaohua Zazhi* 1998;6:567-569
- Tang YW, Yao XX. The regulated role of Hepatocarcinoma cell in hepatic stellate cell activation. *Shijie Huaren Xiaohua Zazhi* 2001;9:202-204
- Huang X, Li DG, Wang ZR, Wei HS, Cheng JL, Zhan YT, Zhou X, Xu QF, Li X, Lu HM. Expression changes of activin A in the development of hepatic fibrosis. *World J Gastroenterol* 2001;7:37-41
- Liu C, Liu P, Liu CH, Zhu XQ, Ji G. Effects of Fuzhenghuayu decoction on collagen synthesis of cultured hepatic stellate cells, hepatocytes and fibroblasts in rats. *World J Gastroenterol* 1998;4:548-549
- Wei HS, Li HM, Li DG, Zhan YT, Wang ZR, Huang X, Cheng JL, Xu QF. The regulatory role of AT1 receptor on activated HSCs in hepatic fibrogenesis: effects of RAS inhibitors on hepatic fibrosis induced by CCl $_4$. *World J Gastroenterol* 2000;6:824-828
- Vasilidou V, Lee J, Pappa A, Petersen DR. Involvement of p65 in the regulation of NF-kappa B in rat hepatic stellate cells during cirrhosis. *Biochem Biophys Res Commun* 2000;273:546-550
- Kato R, Kamiya S, Ueki M, Yajima H, Ishii T, Nakamura H, Katayama T, Fukui F. The fibronectin-derived antitumor peptides suppress the myofibroblastic conversion of rat hepatic stellate cells. *Exp Cell Res* 2001;265:54-63
- Lu P, Luo HS, Yu BP. Apoptosis and liver diseases. *Shijie Huaren Xiaohua Zazhi* 2000;8:1157-1159
- Gressner AM. The cell biology of liver fibrogenesis-an imbalance of proliferation, growth arrest and apoptosis of myofibroblasts. *Cell Tissue Res* 1998;292:447-452
- Liu WB, Wang JY. NF-kB and apoptosis of hepatic stellate cells. *Shijie Huaren Xiaohua Zazhi* 2001;9:1054-1055
- Lang A, Schoonhoven R, Tuva S, Brenner DA, Rippe RA. Nuclear factor kappa B in proliferation, activation, and apoptosis in rat hepatic stellate cells. *J Hepatol* 2000;33:49-58
- Saile B, Matthes N, Knittel T, Ramadori G. Transforming growth factor β and tumor necrosis factor β inhibit both apoptosis and proliferation of activated rat hepatic stellate cells. *Hepatology* 1999;30:196-202
- Gong W, Pecci A, Roth S, Lahme B, Beato M, Gressner AM. Transformation-dependent susceptibility of rat hepatic stellate cells to apoptosis induced by soluble Fas ligand. *Hepatology* 1998;28:492-502
- Iwamoto H, Sakai H, Tada S, Nakamura M, Nawata H. Induction of apoptosis in rat hepatic stellate cells by disruption of integrin-mediated cell adhesion. *J Lab Clin Med* 1999;134:83-89
- Iredale JP, Benyon RC, Pickering J, McCullen M, Northrop M, Pawley S, Hovell C, Arthur MJ. Mechanisms of spontaneous resolution of rat liver fibrosis. Hepatic stellate cell apoptosis and reduced hepatic expression of metalloproteinase inhibitors. *J Clin Invest* 1998;102:538-549
- Fischer R, Schmitt M, Bode JG, Haussinger D. Expression of the peripheral-type benzodiazepine receptor and apoptosis induction in hepatic stellate cells. *Gastroenterology* 2001;120:1212-1226
- Issa R, Williams E, Trim N, Kendall T, Arthur MJ, Reichen J, Benyon RC, Iredale JP. Apoptosis of hepatic stellate cells: involvement in resolution of biliary fibrosis and regulation by soluble growth factors. *Gut* 2001;48:548-557
- Cales P. Apoptosis and liver fibrosis: antifibrotic strategies. *Biomed Pharmacother* 1998;52:259-263
- Yang CZ, Liu RL, Liu J. The role of IH764-3 in prolyl hydroxyl of

- collagen biosynthesis. *Zhongguo Yixue Kexueyuan Xuebao* 1993;15:364-368
- 47 Wasser S, Ho JM, Ang HK, Tan CE. Salvia Miltiorrhiza reduces experimentally induced hepatic fibrosis in rats. *J Hepatol* 1998;29:760-771
 - 48 Liu CH, Hu YY, Wang XL, Liu P, Xu LM. Effects of salvianolic acid-A on NIH/3T3 fibroblast proliferation, collagen synthesis and gene expression. *World J Gastroenterol* 2000;6:361-364
 - 49 Cheng ML, Liu SD. The basic study and clinical research on hepatic fibrosis. 1st ed. Beijing: People's Medical Publishing House 1996:228-283
 - 50 Chen YX, Li S, Fan LY, Kong XT, Yang CZ, Yu BL. The experiment study of effect on hepatic fibrosis by Salvia Miltiorrhiza monomer IH764-3. *Zhonghua Yixue Zazhi* 1998;78:636-637
 - 51 Greenwel P, Schwartz M, Rossas M, Peyrol S, Grimaud JA, Rojkind M. Characterization of fat-storing cell lines derived from normal and CCl₄-cirrhotic livers. *Lab Invest* 1991;65:644-653
 - 52 Boersma AW, Nooter K, Oostrum RG, Stoter G. Quantification of apoptotic cells with fluorescein isothiocyanate-labeled annexin V in chinese hamster ovary cell cultures treated with cisplatin. *Cytometry* 1996;24:123-130
 - 53 Zuo LF. Flow cytometry and biomedicine. *Shenyang: Liaoning Sci Technol Publ House* 1996;213-267
 - 54 Iredale JR. Hepatic Stellate Cell Behavior during Resolution of Liver Injury. *Semin Liver Dis* 2001;21:427-436
 - 55 Nagata S. Apoptosis by death factor. *Cell* 1997;88:355-365
 - 56 Enari M, Talanian RV, Wong WW, Nagata S. Sequential activation of ICE-like and CPP32-like proteases during Fas-mediated apoptosis. *Nature* 1996;380:723-726
 - 57 Sakahira H, Enari M, Nagata S. Cleavage of CAD inhibitor in CAD activation and DNA degradation during apoptosis. *Nature* 1998;391:96-99
 - 58 Wright MC, Issa R, Smart DE, Trim N, Murray GI, Primrose JN, Arthur MJP, Iredale JP, Mann DA. Gliotoxin Stimulates the Apoptosis of Human and Rat Hepatic Stellate Cells and Enhances the Resolution of Liver Fibrosis in Rats. *Gastroenterology* 2001;121:685-698

Edited by Zhu L

• BASIC RESEARCH •

Effect of Maotai liquor in inducing metallothioneins and on hepatic stellate cells

Ming-Liang Cheng, Jun Wu, Hai-Qin Wang, Lie-Ming Xue, Ying-Zhi Tan, Liu Ping, Cheng-Xiu Li, Neng-Hui Huang, Yu-Mei Yao, Lan-Zheng Ren, Lan Ye, Ling Li, Mei-Lin Jia

Ming-Liang Cheng, Jun Wu, Hai-Qin Wang, Yu-Mei Yao, Department of Infectious Diseases, Affiliated Hospital, Guiyang Medical College, Guiyang 550004, Guizhou Province, China

Lie-Ming Xue, Ying-Zhi Tan, Liu Ping, Shanghai University of Traditional Chinese Medicine, Shanghai 200020, China

Cheng-Xiu Li, Neng-Hui Huang, Lan-Zheng Ren, Lan Ye, Ling Li, Mei-Lin Jia, Department of pharmacology, Guiyang Medical College, Guiyang 550004, Guizhou Province, China

Supported by The primary sciences and technology project of Guizhou province, No. 19992015

Correspondence to: Ming-Liang Cheng, Professor Department of Infectious Diseases, Affiliated Hospital, Guiyang Medical College, Guiyang 550004, Guizhou Province, China. chengml@21cn.com

Telephone: +86-851-6782199(H), +86-851-6855119 Ext. 3263 (O)

Received 2002-05-02 Accepted 2002-05-25

Abstract

AIM: To explore the possible mechanism why drinking Maotai liquor dose not cause hepatic fibrosis.

METHODS: After being fed with Maotai for 56 days consecutively, the male SD rats were decolated for detecting the biological indexes, and the livers were harvested to examine the liver indexes and the level of hepatic metallothioneins (MT). Hepatic stellate cells (HSC) proliferation and collagen generation were also observed.

RESULTS: Hepatic MT contents were $216.0\text{ng}\cdot\text{g}^{-1}\pm 10.8\text{ng}\cdot\text{g}^{-1}$ in the rats of Maotai group and $10.0\text{ng}\cdot\text{g}^{-1}\pm 2.8\text{ng}\cdot\text{g}^{-1}$ in the normal control group, which was increased obviously in Maotai group ($P<0.05$). In the rats with grade CCL₂ poisoning induced by Maotai, hepatic MT content was $304.8\text{ng}\cdot\text{g}^{-1}\pm 12.1\text{ng}\cdot\text{g}^{-1}$ whereas in the controls with grade CCL₄ poisoning, it was $126.4\text{ng}\cdot\text{g}^{-1}\pm 4.8\text{ng}\cdot\text{g}^{-1}$ ($P<0.05$). MDA was $102.0\text{nmol}\cdot\text{g}^{-1}\pm 3.4\text{nmol}\cdot\text{g}^{-1}$ in Maotai group and $150.8\text{nmol}\cdot\text{g}^{-1}\pm 6.7\text{nmol}\cdot\text{g}^{-1}$ in the control group ($P<0.05$). When both of the groups were suffering from grade CCL₄ poisoning, hepatic MT contents was negatively correlated with MDA ($r=-0.8023$, $n=20$, $P<0.01$). The 570nmA values of each tube with HSC regeneration at concentrations of 0, 10, 50, 100, and 200g·L⁻¹ of Maotai were 0.818, 0.742, 0.736, 0.72, 0.682, and 0.604, respectively. From the concentration of 10g·L⁻¹, Maotai began to show obvious inhibitory effects against HSC, and the inhibition was concentration-dependent ($P<0.05$, $P<0.01$). Type I collagen contents in HSC were 61.4, 59.9, 50.1, 49.2, 48.7, 34.4μg·g⁻¹ at concentrations of 0, 10, 50, 100, and 200g·L⁻¹ of Maotai. At the concentration of 100-200g·L⁻¹, Maotai had obvious inhibitory effect against the secretion of type I collagen ($P<0.05$). Gene expression analysis was conducted on cells with Maotai concentrations of 0, 50, 100g·L⁻¹ respectively and the ash values of β-actin gene expression were 0.88, 0.74, and 0.59, respectively, suggesting that at the concentration of 100g·L⁻¹, Maotai could obviously inhibit gene expression of type I procollagen ($P<0.05$), but the effect was not obvious at the concentration of 50g·L⁻¹ ($P>0.05$). At the concentration of

10g·L⁻¹, HSC growth *in vitro* inhibition rates were 16.4 ± 2.3 in Maotai group and -8.4 ± 2.3 in the control group ($P<0.05$).

CONCLUSION: Maotai liquor can increase metallothioneins in the liver and inhibit the activation of HSC and the synthesis of collagen in many aspects, which might be the mechanism that Maotai liquor interferes in the hepatic fibrosis.

Cheng ML, Wu J, Wang HQ, Xue LM, Tan YZ, Ping L, Li CX, Huang NH, Yao YM, Ren LZ, Ye L, Li L, Jia ML. Effect of Maotai liquor in inducing metallothioneins and on hepatic stellate cells. *World J Gastroenterol* 2002; 8(3):520-523

INTRODUCTION

Long term alcohol abusing may result in alcoholic liver diseases, and the volume and duration of drinking has a close relationship with alcoholic liver diseases^[1-5]. According to recent studies, the main cause of alcoholic hepatic injury^[6-12] is due to acetaldehyde and hydroxy free radicals oxidized from alcohol which can injure the hepatocytes and activate the lipid peroxidation. The necrosis, inflammation, alcohol, its metabolites and lipid peroxidation are all able to activate Kupffer cells to secrete many cytokines which in turn activate hepatic stellate cells to produce various components of extracellular matrix (ECM). When a large amount of ECM is deposited in the liver, it will lead to hepatic fibrosis^[13-18]. Now many studies have demonstrated that metallothionein (MT) has the cytoprotective effect of clearing away the oxygen-derived free radicals^[19-24]. It is found^[25,26] that alcohol can induce the increase of metallothionein in rats liver, but the mechanism has not been elucidated. MT is endogenous anti-injury substance and plays a role in the defence of stress reaction^[27]. Maotai liquor has its unique brewing technique, at the same time, there are multiple microorganisms in the special geographical situations which are able to absorb abundant amino acids, vitamins and many essential microelements^[28]. It was reported by Li Xinyan *et al* that drinking Maotai liquor 150g for ten years daily did not result in significant damage to the liver, moreover, it could help protect one's health. Epidemiological study showed that no one died of liver disease in those workers who had drunk Maotai liquor for about 30 years. No obvious hepatic fibrosis or cirrhosis of liver was found in the epidemiological study of 99 workers who had a long history of drinking, or in the pathological examination of their liver needle biopsies nor were they seen in rats fed with Maotai liquor for a successive 56 days^[28]. In order to explore the effect of Maotai liquor on the liver, we observed its effect on hepatic stellate cell proliferation *in vitro*, collagen generation, gene expression and growth of human hepatic stellate cells, and the effect of Maotai liquor in inducing metallothioneins in the rats liver and the relationship between it and CCL₄ hepatic injury were also studied in order to demonstrate the possible mechanism in the inhibition on the hepatic fibrosis.

MATERIALS AND METHODS

Materials

Male SD rats, weighing (300±20)g, were purchased from the

Experimental Animal Center of the Third Military Medical University, Chongqing, China. Maotai liquor (530 ± 2) g·L⁻¹, was produced by Guizhou Maotai Distillery with bar code 6902952880026 provided by Section 4 of Guizhou Oil & Foodstuff Export and Import Company. MT standard was provided by Dr. Jie Liu in National Institute of Environmental Health Sciences, U. S. A. 3-[4,5-dimethylthiazol]-2,5-diphenyltetrazolium bromide. MTT were bought from Sigma Co., U. S. A.; trypsin was purchased from Difco. U. S. A and; 199 culture medium and MEM culture medium without calcium are the products of Gibco Co., U. S. A; newborn bovine serum (NBS) was produced by Shanghai Huamei Co.; type I rat tail collagen standard (diluted slowly with Na²-2CO₃/NaHCO₃ to 10 -200ng·L⁻¹) and rabbit anti-rat type I collagen antibody (diluted 1:500 with 0.01mol·L⁻¹ PBS) were products of Cambiolem Co.; horseradish peroxidase marker labeled goat anti-rabbit antibody (IgG-HRP, diluted 1:1000 with PBS containing 100ml·L⁻¹ NBS) was purchased from Hua Mei Company; Total protein determination agent (dcproteinassag) was the product of Biorad Co., U. S. A.; RT-PCR reaction agent and PCR marker were purchased from Promega Co.; diethylpyrocarbonate, guanidine sulfocyanate, saturated mixture of phenol and chloroform, and agarose were bought from Shanghai Sangon Co. Freezing High-speed Centrifuge (1.0R, 22R), CO₂ incubator and ultra low temperature freezer were purchased from German Heraeus Co.; inverted microscope was produced by Japanese Olympus Co.; thermostat water bath, thermostat water bath vibrator were produced by Shanghai Medical Equipment Factory; Labsystems Multiskan MS Enzyme Marker Device, was produced in Finland; Danbury CT ultrasonic membrane breaker was the product of Sonicsmaterials Co.; 90mm culture plate, 60mm culture plate, 6-well, 24-well, and 96-well culture plate were the products of Danish Nunc Co.; Beck Wallac 1410 Liquid Scintillation Counter was the product of Beckman Co. U. S. A; Watson-Marlow 101U Constant current pump was produced in U. S. A.

Effect of maotai liquor on liver MT of rats

Forty SD male rats were divided into two groups averagely. 20 rats were fed with Maotai liquor at 2mL·kg⁻¹ diluted 1:1 by distilled water once everyday for 56 days. The other 20 rats in the control group were fed with saline at the same volume. After all rats had been fed for the last time, 10 rats of each group were given mixture of CCl₄ and olive oil in a volume ratio of 1:1 at 2.5mL·kg⁻¹. All rats were sacrificed after the last feed to get blood for testing biological indexes, to calculate liver indexes by liver quantity, and to determine the content of MT in the liver by saturation method of Cd- hemoglobin, and the lipid peroxidation product of aldehyde measured by the method of thiobarbiturate.

Isolation and culture of hepatic stellate cells (HSC)

HSC were isolated by in situ perfusion. The test of cell proliferation was done by MTT. When monolayer HSC appeared in the 96-well culture plate, they were cultured in the medium containing Maotai liquor with different concentration of 1-400mg·L⁻¹ and 50g·L⁻¹ NBS for 18 hours, then 20μL MTT (5g·L⁻¹) was added in each well and continued the culture for 4 hours. After that, suspension was removed and the plate was aired, then 100μL acid isopropanol with 0.05mol·L⁻¹ HCl was added to each well, little black crystals were dissolved by agitating which formed the steady purple solution. The absorbance (A) in each well was determined by ELSIA at the wave-length of 570nm. There were 4 well in each sample. When the subculturing HSC grew into full monolayer in the 24-well culture plate, then they were cultured in the medium containing Maotai liquor with different concentration from 1mg·L⁻¹ to 400mg·L⁻¹ and 50g·L⁻¹ NBS for 24 hours.

Determination of type I collagen and total protein

After the culture was ended, it was centrifugated at 450×g at 4°C for 20 minutes. Both the suspension and cell layer were collected separately. The collected cells were dissolved by 0.2mol·L⁻¹ NaOH 0.5ml in each well and washed with 0.5ml double distilled water. Ultrasonic membrane-breaking was done for 10s at 40°C. Type I collagen in the suspension was determined by ELISA (the enzyme labelling plate was coated with type I collagen standard and samples at different concentration were kept overnight at 4°C; then IgG-HRP was used for incubation after they bound to type I collagen antibody; pyrocatechol oxidation was used for staining, and value A was obtained at 492nm wavelength by Labsystem ELISA equipment, which automatically calculated the standard curve and contents of each specimen.). Total protein in the cell layer was determined by DC protein assay kit.

Semiquantitative RT-PCR

Total RNA was isolated from HSC by phenol-chloroform extraction and isopropanol precipitation. The primer of procollagenβ1(I) was synthesized, purified and evaluated by Shanghai Sangon Company (See Table 1). One μg of total RNA was reversely transcribed according to the instructions of the RT-PCR Kit at 48°C for 45min. The PCR mixture contained 50pmol·L⁻¹ primer of procollagen β1[I] or GAPDH, 1μL 10mmol·L⁻¹ dNTPs, 2μL 25mmol·L⁻¹ MgSO₄, 5 units AMV reverse transcriptase, 5 units Tfl DNA polymerase and 10mL AMV/Tfl buffer. The PCR conditions included an initial denaturation-2min at 94°C, 30 cycles consisting of (a) 30s denaturation at 94°C;(b)1 min primer annealing at 60°C; (c) 2min elongation at 38°C; and one final step of 7min at 68°C. The PCR product or DNA marker mixed with 5μL loading buffer were electrophoresed on a 1.5% agarose gel, visualized by UV and quantified densitometrically. Procollagenβ1[I], pre-albumin, or hydroxyproline expression was calculated by determining the ratio of Procollagen α1[I], relative to β-actin mRNA.

Table 1 Primer sequence and expected PCR product length

Primer designation	Sequence	Product length
α1(I)upstream	CACCCTCAAGAGCCTGAGTC	253bp
α1(I)downstream	GTT CGGGCTGATGTACCAGT	
β-actin upstream	ACATCTGCTGGAAGGTGGAC	163bp
β-actin downstream	GGTACCACCATGTACCCAGG	

The effect of Maotai liquor on human HSC

80000 human HSC cells were inoculated in each well in the 96-well plate, and they were cultured in the DMEM medium with 100mL·L⁻¹ FBS at 37°C in a humidified atmosphere containing 5% CO₂ for 24 hours. Then they were continuously cultured in the DMEM medium with 20mL·L⁻¹ FBS for 24hours. At last they were cultured in the medium containing different concentration of Maotai liquor (Maotai liquor was diluted to 0.5g·L⁻¹, 1g·L⁻¹, 5g·L⁻¹, 10g·L⁻¹, 50g·L⁻¹ by DMEM medium with 20mL·L⁻¹ FBS or alcohol). Cells cultured in the DMEM medium with 20mL·L⁻¹ FBS was used as the control. After they were cultured for 20 hours, 20μL MTT (5g·L⁻¹) was added in each well and the culture continued for 4 hours more. Then the medium was removed, 100μL acid isopropanol with 0.05mol·L⁻¹ HCl was added in each well, after little black crystals were dissolved, value A was obtained at 570nm wavelength by Labsystem ELISA equipment and the inhibiting rate of cell proliferation was calculated.

Statistics analysis

Data were analyzed by *t* test and *q* test.

RESULTS

Effect of Maotai liquor on rats liver MT content

Maotai liquor could induce the MT in rats liver to increase to 22 times of its original level (See Table 2). It is thought that lipid peroxidation of cell membrane and the intracellular accumulation of Ca^{2+} are the important links of hepatocellular damage. In the control group, MDA in the liver was obviously increased after they were intoxicated by CCl_4 , merely Maotai liquor did not influence MDA in rats' liver. MT in rats fed with Maotai liquor when intoxicated by CCl_4 was increased obviously more than those rats they were not fed with Maotai liquor, but MDA was decreased. There was a negative relationship between MT and MDA in rats liver intoxicated by CCl_4 in the control and trial group ($r=-0.8023$, $n=20$, $P<0.01$).

Table 2 The effect of Maotai liquor on MT and MDA in rats liver ($n=10$, $\bar{x}\pm s$)

Group	MT($\text{ng}\cdot\text{g}^{-1}$)	MDA($\text{ng}\cdot\text{g}^{-1}$)
Control group	10.0 \pm 2.8	60.2 \pm 3.1
Maotai liquor group	216.0 \pm 10.8 ^b	60.1 \pm 2.4
CCl_4 Group	126.4 \pm 4.8 ^b	150.8 \pm 6.7 ^b
CCl_4 + Maotai liquor group	304.8 \pm 12.1 ^{bd}	102.0 \pm 3.44 ^{bd}

^b $P<0.01$, vs control group; ^d $P<0.01$, vs CCl_4 group (analysis of variance and q test)

Effect of Maotai liquor on rats' HSC

We normally obtained $(3-5)\times 10^7$ HSC from one rat. Lipid droplets in the primary HSC were obvious, but during the course of culture, lipid droplets decreased. And as they were passaged, HSC became extended, and looked like myofibroblasts. Each concentration of Maotai liquor had no effect on the shape of HSC. The absorbance (A) at 570nm of HSC in the medium with 0mg·L⁻¹, 10mg·L⁻¹, 50mg·L⁻¹, 100mg·L⁻¹ and 200mg·L⁻¹ Maotia liquor were 0.818, 0.742, 0.736, 0.72, 0.682 and 0.604, respectively. From the concentration of 10g·L⁻¹, Maotai liquor had obvious inhibiting effect on the proliferation of HSC, and the effect was enhanced with the increase of the concentration of Maotai liquor ($P<0.05$, $P<0.01$). The content of type I collagen of HSC in the medium with 0mg·L⁻¹, 10mg·L⁻¹, 50mg·L⁻¹, 100mg·L⁻¹ and 200mg·L⁻¹ Maotia liquor were 61.4 $\mu\text{g}\cdot\text{g}^{-1}$, 59.9 $\mu\text{g}\cdot\text{g}^{-1}$, 49.2 $\mu\text{g}\cdot\text{g}^{-1}$, 50.1 $\mu\text{g}\cdot\text{g}^{-1}$, 48.7 $\mu\text{g}\cdot\text{g}^{-1}$ and 34.4 $\mu\text{g}\cdot\text{g}^{-1}$, respectively. The 100-200g·L⁻¹ Maotai liquor had obvious inhibiting effect on the secretion of type I collagen ($P<0.05$). The analysis of gene expression of HSC in the 0mg·L⁻¹, 50mg·L⁻¹ and 100mg·L⁻¹ Maotia liquor group showed that the relative density of β -actin ($n=3$) analyzed by computer were 0.88, 0.74 and 0.59, respectively. The result showed that 100g·L⁻¹ Maotia liquor could significantly inhibit the gene expression of type I procollagen ($P<0.05$), but 50g·L⁻¹ Maotia liquor did not have such effect ($P>0.05$).

Table 3 The effect of Maotai liquor on HSC of human ($n=3$, $\bar{x}\pm s$)

Group	Inhibiting Rate of HSC
Alcohol group (10g·L ⁻¹)	-8.4 \pm 2.3
Maotai liquor group (0.5g·L ⁻¹)	-4.52 \pm 0.3
Maotai liquor group (1g·L ⁻¹)	12.4 \pm 10.4 ^b
Maotai liquor group (5g·L ⁻¹)	17.4 \pm 1.6 ^b
Maotai liquor group (10g·L ⁻¹)	16.4 \pm 2.3 ^b

^b $P<0.01$, vs alcohol group

Effect of Maotai liquor on the growth of HSC (See Table 3)

There were three experiment groups in our study: blank control group, control group and trial group. First alcohol was diluted to 530

g·L⁻¹ (the same concentration as Maotai liquor) and then it was dispensed to different concentrations which was the same as Maotai liquor. We used 0.5g·L⁻¹, 1g·L⁻¹, 5g·L⁻¹ and 10g·L⁻¹ Maotai liquor to study the different inhibiting effect on HSC. Our result showed that there was a significant difference between the 10g·L⁻¹ alcohol group and 10g·L⁻¹ Maotai group ($P<0.01$). That was Maotai liquor had a significant inhibiting effect on the proliferation of HSC, but alcohol did not have such effect.

DISCUSSION

MT is a low molecular weight metal-binding protein with rich cysteine existing widely in the biosphere and can be induced *in vivo* by many factors^[29-32]. MT is also a non-enzyme protein which has bioactive functions of binding heavy metals, clearing free radicals, anti-oxidation and cytoprotection. It is now the most powerful bioactive substance which can remove free radicals. In recent years, a lot of research studies show that MT can protect hepatic cells from injury and be helpful in repairing hepatocytes without inducing hepatic fibrosis^[33-38]. Induced by Maotai liquor, the increased MT in rats' liver was able to decrease the lipid peroxidation product of MDA in the liver intoxicated by CCl_4 . Our result showed that there was a negative correlation between MT and MDA in the liver and it proved that Maotai liquor was able to induce MT to antagonize the effect poisoning by CCl_4 . It may be one of the possible mechanisms in explaining why long term drinking proper volume of Maotai would not cause hepatic fibrosis or cirrhosis.

Hepatic fibrosis is an important pathologic process resulted from many chronic liver diseases and may process to liver cirrhosis. It is also the key point that many chronic liver diseases are hard to cure completely. Many investigations showed that the activation of HSC is the key point in the pathological process of hepatic fibrosis. HSC was activated by many pathological factors so that alterations in the phenotype and function of HSC happened. HSC was highly proliferated and secreted a large amount of extracellular matrix deposited in the liver which would result in hepatic fibrosis. Collagen was the most important component in the extracellular matrix^[46-48]. The degree of increase of collagen was type I>type III>type IV. The cell proliferation and the enhanced generation of collagen were the main characteristics of activation of HSC. [³H]thymidine incorporation was able to reflect the cell division and proliferation. In the inhibiting experiments of different concentration of Maotai liquor in both HSC from rats and HSC from human beings showed that Maotai liquor had a concentration-dependent inhibiting effect on the proliferation of HSC. The generation of collagen was that first the collagen gene was transcribed and then translated into procollagen and the product secreted in the extracellular matrix. Our experiment showed that Maotai liquor had inhibiting effect on the expression of collagen gene and the secretion of collagen protein, but 10g·L⁻¹ alcohol had no such inhibiting effect. All those showed that Maotai liquor could inhibit the activation of HSC in many links. The inhibiting effect of Maotai liquor in the activation of HSC and the generation of collagen may be the possible reasons why Maotai liquor can interfere with the process of hepatic fibrosis.

REFERENCES

- 1 Tang TH. Recent studies of alcoholic liver diseases. *Shijie Huaren Xiaohua Zazhi* 2000;8:56
- 2 Lin H, Lu M, Zhang YX, Wang BY, Fu BY. Induction of a rat model of alcoholic liver diseases. *Shijie Huaren Xiaohua Zazhi* 2001;9:24-28
- 3 Wu J, Liu RC, Li J, Wang WL, Hu L, Yang QZ, Liang YD, Lu YY, Cheng ML, Ding YS. To study the risk factors of hepatic cirrhosis in viral hepatitis and hepatic fibrosis. *Cina Public Health* 1999;15:394
- 4 Wu J, Cheng ML, Ding YS, Liu RC, Li J, Wang WL, Hu L. Five years follow-up survey of risk factor of virus hepatic cirrhosis. *Shijie Huaren Xiaohua Zazhi* 2000;8:1365-1367
- 5 Wei L, Tao QM. Interactions between alcohol and hepatitis C. *Shijie*

- Huaren Xiaohua Zazhi 1998;6: 539-541
- 6 Sun YN. Recent studies in pathogenesis of alcoholic liver diseases. *GuowaiYiyao. Xiaohuaxi Jibing Fengece* 1999;19:97-101
- 7 Bo AH, Tian CS, Xue GP, Du JH, Xu YL. Morphology of immune and alcoholic liver diseases in rats. *Shijie Huaren Xiaohua Zazhi* 2001;9:157-160
- 8 Lu XY. Mechanism of free radicals on liver injury induced by ethanol. *Xin xiaohuabingxue Zazhi* 1997;5: 200-202
- 9 Fan JG, Zeng MD, Wang GL. Pathogenesis of fatty liver. *Shijie Huaren Xiaohua Zazhi* 1999;7:5-7
- 10 Anania FA, Womack L, Jiang M, Saxena NK. Aldehydes potentiate alpha(2)(I) collagen gene activity by JNK in hepatic stellate cells. *Free Radic Biol Med* 2001;15:30:846-857
- 11 Ruoyu Ni, Maria Anna Leo, Zhao JB, Charles S. Toxicity of β -carotene and its exacerbation by acetaldehyde in HepG2 cells. *Alcohol and Alcoholism* 2001; 36: 281-285
- 12 Zima T, Fialova L, Mestek O, Janebova M, Crkovska J, Malbohan I, Stipek S, Mikulikova L, Popov P. Oxidative stress, metabolism of ethanol and alcohol-related diseases. *J Biomed Sci* 2001;8:59-70
- 13 Fan JG, Zeng MD, Hong J, Li JQ, Qiu DK. Effects of free unsaturated fatty acids on proliferation of L-02 and HLF cell lines and synthesis of extracellular matrix. *Shijie Huaren Xiaohua Zazhi* 1998;6:502-6504
- 14 Lu LG, Zeng MD, Li JQ, Fan JG, Hua J, Fan ZP, Dai N, Qiu DK. Effect of arachidonic acid and linoleic acid on proliferation of rat hepatic stellate cells. *Shijie Huaren Xiaohua Zazhi* 1999; 7:10-12
- 15 Wu J, Zern MA. Hepatic stellate cells: a target for the treatment of liver fibrosis. *J Gastroenterol* 2000;35:665-672
- 16 Zeng MD. Fatty liver New challenge in domain of liver disease. *Zhonghua Ganzhangbing Zazhi* 2000; 8: 69
- 17 Wang Q, ren GX, Qi Z, Li ML, Song X. Evaluation of serological assay for the detection of liver fibrosis in the patients with liver diseases caused by alcohol. *Huaren Xiaohua Zazhi* 1998;6: 364-365
- 18 Lü XH, Xie YH, Fu BY, Liu CR, Wang BY. Dynamic expression of tissue inhibitor of metalloproteinase 1 in alcoholic liver disease in rats. *Shijie Huaren Xiaohua Zazhi* 2001;9:29-33
- 19 Qiu BS, Wang Y, Hu ML, Xu LY. Study on Prevention of ZnMT against membrane damage induced by MeHg. *Guangdong Weiliang Yuansu Kexue* 1999; 6: 15-181006-446X
- 20 himura N, Miyabara Y, Suzuki JS, Sato M, Aoki Y, Satoh M, Yonemoto J, Tohyama C. Induction of metallothionein in the livers of female Sprague-Dawley rats treated with 2,3,7,8-tetrachlorodibenzo-p-dioxin. *Life Sci* 2001;69:1291-1303
- 21 Park JD, Liu Y, Klaassen CD. Protective effect of metallothionein against the toxicity of cadmium and other metals(I). *Toxicology* 2001; 163:93-100
- 22 Wright J, George S, Martinez-Lara E, Carpena E, Kindt M. Levels of cellular glutathione and metallothionein affect the toxicity of oxidative stress in an established carp cell line. *Mar Environ Res* 2000;50: 503-508
- 23 Zaroogian G, Jackim E. In vivo metallothionein and glutathione status in an acute response to cadmium in Mercenaria brown cells. *Comp Biochem Physiol C Toxicol Pharmacol* 2000;127:251-261
- 24 Fabisiak JP, Pearce LL, Borisenko GG, Tyhurina YY, Tyurin VA, Razzack J, Lazo JS, Pitt BR, Kagan VE. Bifunctional anti/prooxidant potential of metallothionein: redox signaling of copper binding and release. *Antioxid Redox Signal* 1999;1:349-364
- 25 Zhou J, Cheng S. Metallothionein and Medicine. *Shengli Kexue Jinzhan* 1995;26:29
- 26 Cheng YY, Wang DL, Jiang YG, Gu JF, Wang YY. Effect of stress on the levels of metallothionein and mineral elements in Rats. *Yingyang Xuebao* 1996;18: 317-321
- 27 Tang CS, Li ZP, Su JY. Metallothionein is an endogenous protection factor against cell damage. *Beijing Yikedaxue Xuebao* 1989;21:108
- 28 Xiao Y. Preliminary explanation of the mechanism which the long-term drinking of Guizhou maotai will not induce liver fibrosis. *Zhonghua Yixue Zazhi* 2001;81:6284
- 29 Yang YX, Liu JY. Studies on zinc-induced metallothionein synthesis in rabbits. *Weiliangyuansu Yu Jiankangyanjiu* 1996;13:1-2
- 30 Zhang WQ, Tie JK, Shen HM, Xu GS, Ru BG. A preliminary study on the induction of metallothionein in rats with Aluminum administration by different ways. *Zhonghua Yufangyixue Zazhi* 1998;32:153-155
- 31 Dai JG, Yang S, Chen JH. Influence of calcium and zinc in the synthesis of hepatic metallothionein in mice. *Weisheng Dulixue Zazhi, Zhongguo Gonggong weisheng* 1997;13:95-96
- 32 Yang S, Dai JG, Chen JH. Influence of calcium and cadmium in the synthesis of hepatic metallothionein in mice. *Weisheng Dulixue Zazhi* 1996;10: 4-5
- 33 Yang S, Dai JG, Chen JH. The interaction of zinc and cadmium in the synthesis of hepatic metallothionein in mouse. *Nanjing Yikedaxue Xuebao* 1996; 16: 57-59
- 34 Nong JX, He QR, Wang SP. Relationship between metallothionein and cadmium-induced liver and kidney injury. *Shiyong Yufang Yixue* 1999;6: 177-179
- 35 He QR, Wang SP. Effects of CCl₄-induced hepatic damage on cadmium nephrotoxicity in rats. *Zhonghua Laodongweisheng Zhiyebing Zazhi* 1998;16:30-33
- 36 Mitsuyoshi H, Nakashima T, Sumida Y, Yoh T, Nakajima Y, Ishikawa H, Inaba K, Sakamoto Y, Okanoue T, Kashima K. Ursodeoxycholic acid protects hepatocytes against oxidative injury via induction of antioxidants. *Biochem Biophys Res Commun* 1999;263:537-542
- 37 Sato S, Shimizu M, Hosokawa T, Saito T, Okabe M, Niioka T, Kurasaki M. Distribution of zinc-binding metallothionein in cirrhotic liver of rats administered zinc. *Pharmacol Toxicol* 2000;87:292-296
- 38 Sato M, Sasaki M, Hojo H. Antioxidative roles of metallothionein and manganese superoxide dismutase induced by tumor necrosis factor-alpha and interleukin-6. *Arch Biochem Biophys* 1995;316:738-744
- 39 Lu LG, Zeng MD, Li JQ, Qiu DK, Hua J, Fan ZP. Expression of intercellular adhesion molecule 1 by activated hepatic stellate cell. *Shijie Huaren Xiaohua Zazhi* 1998; 6: 576-569
- 40 Zhu YH, Hu DR, Nie QH, Liu GD, Tan ZX. Study on activation and c-fos, c-jun expression of in vitro cultured human hepatic stellate cells. *Shijie Huaren Xiaohua Zazhi* 2000;8:299-302
- 41 Wang YD, Jia LW, Li CM. Hepatic content of collagens and laminin in rat model of experimental liver fibrosis. *World J Gastroenterol* 2000;6:73
- 42 Xiang DD, Wei YL, Li QF. The molecular mechanism in the effects of TGF- β 1 on Ito cell. *Shijie Huaren Xiaohua Zazhi* 1999;7:980-981
- 43 Qing JP, Jiang MD. The feature and regulation of liver stellate cell in relation with liver fibrosis. *Shijie Huaren Xiaohua Zazhi* 2001;9:801-804
- 44 Zhu YH, Hu DR, Nie QH, Liu GD, Tan ZX. Study on activation and c-fos, c-jun expression of in vitro cultured human hepatic stellate cells. *Shijie Huaren Xiaohua Zazhi* 2000;8:299-302
- 45 Lu LG, Zeng MD, Li JQ, Hua J, Fan JG, Fan ZP, Qiu DK. Effect of lipid on proliferation and activation of rat hepatic stellate cells (I). *World J Gastroenterol* 1998;4:497-499
- 46 Cheng ML, Liu SD. The basic study and clinical research on hepatic fibrosis. *Renmin Weisheng Chubanshe*, 1996;1: 30-45
- 47 Lu X, Liu CH, Xu GF, Chen WH, Liu P. Successive observation of laminin and collagen IV on hepatic sinusoid during the formation of liver fibrosis in rats. *Shijie Huaren Xiaohua Zazhi* 2001;9:260-262
- 48 Wang Y, Gao Y, Yang JZ. Gene expression of collagenase in experimental liver fibrosis. *Shijie Huaren Xiaohua Zazhi* 1999;7:1004-1006

Edited by Wu XN

• BASIC RESEARCH •

Characteristics and mechanism of enzyme secretion and increase in $[Ca^{2+}]_i$ in Saikosaponin(I) stimulated rat pancreatic acinar cells

Yi Yu, Wen-Xiu Yang, Hui Wang, Wen-Zheng Zhang, Bao-Hua Liu, Zhi-Yong Dong

Yi Yu, Wen-Xiu Yang, Hui Wang, Wen-Zheng Zhang, Bao-Hua Liu, Zhi-Yong Dong, Department of Biophysics, Nankai University, Tianjin, 300071, China

Presented at the Third East Asian Biophysics Symposium, Kyongju, Korea, May 22-26, 2000

Supported by National Natural Science Foundation of China, No. 39770910

Correspondence to: Wen-xiu Yang, Department of Biophysics, School of Physics, Nankai University, Tianjin 300071, China. yangwenx@public.tpt.tj.cn

Telephone: +86-22-23501491 Fax: +86-22-23501490

Received 2001-12-05 Accepted 2002-02-19

Abstract

AIM: This investigation was to reveal the characteristics and mechanism of enzyme secretion and increase in $[Ca^{2+}]_i$ stimulated by saikosaponin(I) [SA(I)] in rat pancreatic acini.

METHODS: Pancreatic acini were prepared from male Wistar rats. Isolated acinar cells were suspended in Eagle's MEM solution. After adding drugs, the incubation was performed at 37°C for a set period of time. Amylase of supernatant was assayed using starch-iodide reaction. Isolated acinar single cell was incubated with Fura-2/AM at 37°C, then cells were washed and resuspended in fresh solution and attached to the chamber. Cytoplasm $[Ca^{2+}]_i$ of a single cell was expressed by fluorescence ratio F340/F380 recorded in a Nikon PI Ca^{2+} measurement system.

RESULTS: Rate course of amylase secretion stimulated by SA(I) in rat pancreatic acini appeared in bell-like shape. The peak amplitude increased depended on SA(I) concentration. The maximum rate responded to 1×10^{-5} mol/L SA(I) was 13.1-fold of basal and the rate decreased to basal level at 30 min. CCK-8 receptor antagonist Bt_2 -cGMP markedly inhibited amylase secretion stimulated by SA(I) and the dose-effect relationship was similar to that by CCK-8. $[Ca^{2+}]_i$ in a single acinar cell rose to the peak at 5 min after adding 5×10^{-6} mol/L SA(I) and was 5.1-fold of basal level. In addition, there was a secondary increase after the initial peak. GDP could inhibit both the rate of amylase secretion and rising of $[Ca^{2+}]_i$ stimulated by SA(I) in a single pancreatic acinar cell.

CONCLUSION: SA(I) is highly efficient in promoting the secretion of enzymes synthesized in rat pancreatic acini and raising intracellular $[Ca^{2+}]_i$. Signaling transduction pathway of SA(I) involves activating special membrane receptor and increase in cytoplasm $[Ca^{2+}]_i$ sequentially.

Yi Y, Yang WX, Wang H, Zhang WZ, Liu BH, Dong ZY. Characteristics and mechanism of enzyme secretion and increase in $[Ca^{2+}]_i$ in Saikosaponin(I) stimulated rat pancreatic acinar cells. *World J Gastroenterol* 2002;8(3):524-527

INTRODUCTION

Bupleurum, one kind of traditional Chinese Drug, have a variety of roles in clinical practice. Our pharmacological investigations have indicated Bupleurum has significant promoting effect on enzyme

secretion in rat pancreatic acini^[1], Saikosides is the compound of the active Saikosaponin component in Bupleurum. The kinetics of enzyme secretion stimulated by Saikosides in a dose-dependent manner can be divided into first phase of high-potency secretion and later phase of low-potency secretion. The accumulation of enzyme secretion stimulated by 200 mg/L Saikosides with 30 min incubation is 6.5 folds of the basal level^[2]. Based on the results of separation, purification and identification for Saikosides^[3], we have compared the activities of nine kinds of Saikosaponins. Saikosaponin(I) [SA(I)] has the best effect of promoting secretion. The promoting effect of SA(I) increase in a dose-dependent manner, and the enzyme release stimulated by 5×10^{-5} mol/L SA(I) is 9.5 folds of basal^[4,5].

Cholecystokinin (CCK) and Carbachol (CCh) are two important secretagogues for enzyme secretion from pancreatic acini. The promoting response associated with CCK-8 is in a dose-dependent manner, and high concentrations of CCK have submaximal amylase release. Furthermore, the relative potency of CCK to mobilize intracellular Ca^{2+} is dependent on the concentration of CCK-8. At low concentration of CCK-8 (10^{-12} mol/L- 10^{-11} mol/L), it induces a series of transient increase in $[Ca^{2+}]_i$ termed "Ca²⁺ oscillations", and high concentration of CCK-8 evokes the single peak of $[Ca^{2+}]_i$ ^[6-8]. Cellular signaling transduction pathway of increase in $[Ca^{2+}]_i$ evoked by CCK-8, involves activating G protein coupled receptors by CCK-8 binding its receptor, producing inositol 1,4,5-triphosphate (IP₃) and diacylglycerol (DAG) by activating the phospholipase C (PLC), and releasing Ca^{2+} from endoplasmic reticulum (ER) by activating the IP₃ receptor^[9-14]. Increase in $[Ca^{2+}]_i$ evoked by CCK-8 and CCh not only result from ER, but from influx of extracellular Ca^{2+} ^[15-17]. Recently, it was shown that both activated PKC and elevated intracellular Ca^{2+} mediate activation of NF- κ B and *mob-1* expression by supraphysiological CCK^[18,19]. Our investigations have indicated Saikosides is also a significant Ca^{2+} -mobilizing secretagogue. The kinetics of $[Ca^{2+}]_i$ induced by Saikosides varied with two peaks, and promotion of Saikosides on pancreatic exocrine could be correlative with the kinetics of $[Ca^{2+}]_i$. The effect of 200 mg/L Saikosides was reduced by 35% and the second peak of $[Ca^{2+}]_i$ dramatically declined in Ca^{2+} -free medium^[2]. These results showed that increase in $[Ca^{2+}]_i$ evoked by SA(I) include both Ca^{2+} release from the intracellular Ca^{2+} pool and subsequent influx of Ca^{2+} through plasmic membrane.

In order to elucidate the characteristics and mechanism of enzyme secretion and increase in $[Ca^{2+}]_i$ in SA(I) stimulated rat pancreatic acinar cells, here we report an analysis in rate kinetics of SA(I) stimulated amylase secretion, Characteristics of ligand-receptor binding and kinetics of $[Ca^{2+}]_i$ evoked by SA(I) in a single cell as well as the effects of guanosine-5'-diphosphate trisodium salt (GDP) on amylase secretion and $[Ca^{2+}]_i$.

MATERIALS AND METHODS

Materials

Cholecystokinin-8 (CCK-8), Carbachol (CCh), Dibutylguanosine-3',

5'-cyclic monophosphate (Bt_2 -cGMP), Guanosine-5'-diphosphate trisodium salt (GDP), Fura2-AM, Collagenase IA, soybean trypsin inhibitor were from Sigma Chemical Co (St. Louis, MO); Other chemicals were from Tianxiangren Bio. Co. Ltd. (Beijing, China). Saikosaponin I was separated and identified by the School of Pharmaceutical Science, Beijing University.

Methods

Preparation of isolated acini Isolated pancreatic acini were prepared by the method of Duan from male Wistar rat (200-250g) that had been fasted overnight^[20]. Individual Acini were prepared by 0.3g/L collagenase digestion at 37°C and purified by centrifugation through the Eagle's MEM containing 4% bovine serum albumin. The isolated acini were then allowed to resuspend at 37°C for 30min in HEPES-buffered Ringer solution supplemented with 11.1mmol/L glucose, minimal Eagle's amino acids medium and 0.1g/L soybean trypsin inhibitor and were through gas with 1000mL/L O_2 .

Measurement of amylase release Acini were suspended in Eagle's MEM solution. After adding the drug, the incubation was performed at 37°C for a set period of time. Then the supernatant was removed and assayed for amylase. Amylase release was expressed at the ratio of the content of amylase released into the medium during the incubation to the total content. The total amylase content was estimated by measuring the amylase activity present in the acini broken at the beginning of the incubation.

Detection of cytosolic free Ca^{2+} concentration According to the method of Cui *et al.*^[21] briefly, isolated acini were incubated with 5×10^{-6} mol/L Fura-2/AM at 37°C for 40min and then washed and resuspended in fresh physiological salt solution. Isolated acini were attached to Sykus-Moor perfusion chamber and continuously superfused by a buffer medium containing agonist at 1ml/min. Stimulus was introduced by changing perfusion buffer containing relevant chemicals. Inlet perfusion buffer was pre-warmed to 37°C in a water bath. Fluorescence ratios of f340/f380 were recorded in a Nikon PI Ca^{2+} measurement system, with a pin-hole size of 0.5 focused onto the apical portion of a single acinar cell within acinar formation or formations, and a Nikon neutral density filter (#8) was placed in the excitation light path.

Statistical analysis Values of each group were expressed as $\bar{x} \pm s$. Group comparison was performed using student's *t* test. $P < 0.05$ was considered significant.

RESULTS

Rate dynamics of amylase secretion in SA(I) stimulated pancreatic acini

Under the different stimulation of 1×10^{-6} mol/L, 5×10^{-6} mol/L and 1×10^{-5} mol/L SA(I) in pancreatic acini, the amylase release accumulation from acini within 37°C incubation at different time were detected. Rate course of amylase release was obtained by differential analytics of enzyme accumulation with a computer program (Figure 1). The kinetics of rate-time effect could be divided into two phases, named by increasing phase and declining phase. With the concentration of SA(I) increasing, secreting rate rose more quickly and reached the higher peak, then it fell into basal level soon. The maximum rates of amylase secretion stimulated by 1×10^{-6} mol/L, 5×10^{-6} mol/L and 1×10^{-5} mol/L SA(I) were 3.2-fold, 7.4-fold, and 13.1-fold of basal, corresponding time at 16.5min, 14.5min, 12.5min. Those data indicated that though the SA(I) stimulated enzyme release obviously, the main promoting effect of SA(I) took place in the 20min after adding the drug, and promoting action disappeared at 30min.

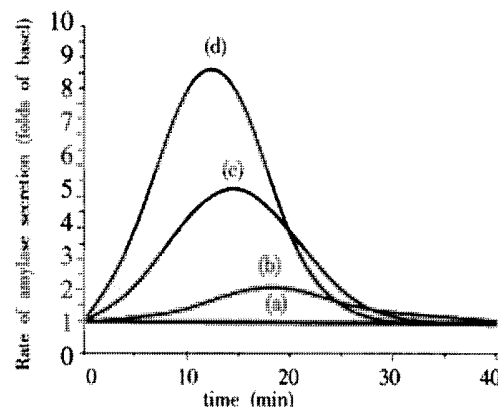


Figure 1 Rate kinetics of amylase secretion stimulated by SA(I) in the rat pancreatic acini. The results were expressed at the ratio of amylase secretion during the incubation to the basal secretion. a: basal value was standardized as 1, b: 1×10^{-6} mol/L SA(I), c: 5×10^{-6} mol/L SA(I), d: 1×10^{-5} mol/L SA(I). The values represented the $\bar{x} \pm s$ from four independent experiments.

Dose-response of inhibition of receptor antagonist on amylase secretion stimulated by SA(I)

In order to explore whether SA(I) stimulated signal was transduced through the effect of membranous receptor, the effects of CCK-8 receptor antagonist Bt_2 -cGMP and CCh receptor antagonist atropine on SA(I) stimulated amylase secretion had been studied. In Table 1, enzyme secretion induced by SA(I) was markedly depressed by Bt_2 -cGMP. The inhibitory effects of Bt_2 -cGMP on action of SA(I) and CCK-8 had similar characteristics of dose-effect relationship. Amylase secretion stimulated by secretagogues decreased within the medium containing 1×10^{-7} mol/L Bt_2 -cGMP ($^aP < 0.05$). With increasing concentration of Bt_2 -cGMP, the inhibition was enhanced ($^bP < 0.01$). 1×10^{-4} mol/L Bt_2 -cGMP decreased action of SA(I) and CCK-8 by 31.3% and 34.4% respectively.

In Table 2, atropine was observed to depress amylase secretion stimulated by CCh ($^bP < 0.01$). 1×10^{-5} mol/L atropine eliminated the promoting effect of CCh, but had no apparent inhibition on the that of SA(I) at 1×10^{-8} mol/L- 1×10^{-5} mol/L atropine range ($P > 0.05$).

Table 1 Effect of different concentrations of Bt_2 -cGMP on amylase secretion stimulated by SA(I) and CCK-8

Bt_2 -cGMP concentration (mol/L)	Amylase release (% of total)	
	1×10^{-8} mol/L CCK-8	5×10^{-6} mol/L SA(I)
Control	19.5±1.6	31.0±2.1
1×10^{-7}	17.8±1.9 ^a	27.4±2.5 ^a
1×10^{-6}	15.6±2.0 ^b	25.6±1.4 ^b
1×10^{-5}	14.0±1.2 ^b	23.1±1.8 ^b
1×10^{-4}	12.8±1.7 ^b	21.2±0.9 ^b

Rat pancreatic acini were incubated with either 1×10^{-8} mol/L CCK-8 or 5×10^{-6} mol/L SA(I) in adding different concentrations of Bt_2 -cGMP medium. After 30min, the incubation was stopped and the content of amylase in the supernatant was assayed. The values represented the $\bar{x} \pm s$ from 4 separate experiments. ^a $P < 0.05$, ^b $P < 0.01$ vs control.

Table 2 Effect of different concentrations of atropine on amylase secretion stimulated by SA(I) and CCh

Atropine concentration (mol/L)	Amylase release (% of total)	
	1×10^{-5} mol/L CCh	5×10^{-6} mol/L SA(I)
Control	15.2±1.3	30.8±3.3
1×10^{-8}	11.6±1.6 ^b	27.9±11.4
1×10^{-7}	10.5±1.2 ^b	25.1±7.4
1×10^{-6}	8.8±1.3 ^b	27.5±6.9
1×10^{-5}	8.3±1.6 ^b	25.5±6.2

Rat pancreatic acini were incubated with either 1×10^{-5} mol/L CCh or 5×10^{-6} mol/L SA(I) in adding different concentration of atropine medium. After 30min, the incubation stopped and the content of amylase in the supernatant was assayed. The values represent the $\bar{x} \pm s$ from 4 separate experiments. ^a $P < 0.05$, ^b $P < 0.01$ vs control.

Dynamics of SA(I) and CCK-8 evoked $[Ca^{2+}]_i$ in single pancreatic acinar cell

The time courses of SA(I) and CCK-8 evoked $[Ca^{2+}]_i$ in a single pancreatic acinar cell were shown in Figure 2. 1×10^{-9} mol/L CCK-8 induced a monophasic $[Ca^{2+}]_i$ spike resulting in an increase of 4.2 folds from basal and declined to basal speedily. 5×10^{-6} mol/L SA(I) evoked $[Ca^{2+}]_i$ gradually increased within 5 min after addition of SA(I), and peak of $[Ca^{2+}]_i$ was 5.0 folds of basal. Unlike CCK, $[Ca^{2+}]_i$ rose again after falling, caused a diphasic Ca^{2+} spike.

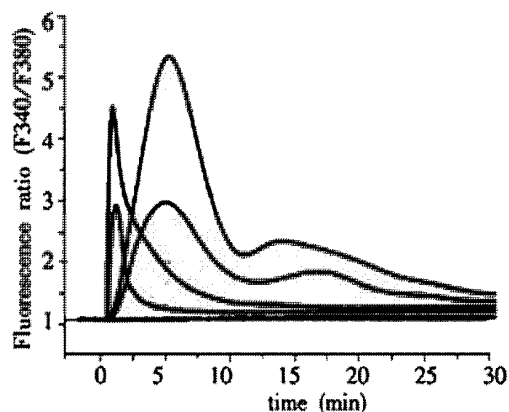


Figure 2 Kinetics of SA(I) and CCK-8 evoked $[Ca^{2+}]_i$ and effects of GDP in a single rat pancreatic acinar cell. $[Ca^{2+}]_i$ were expressed by Fluorescence ratio F340/F380. a. 1×10^{-9} mol/L CCK-8; b. 1×10^{-9} mol/L CCK-8 + 5×10^{-3} mol/L GDP; c. 5×10^{-6} mol/L SA(I); d. 5×10^{-6} mol/L SA(I) + 5×10^{-3} mol/L GDP; e. Base. Time 0 is determined by the time of adding drug.

Effects of GDP on dynamics of amylase secretion rate and $[Ca^{2+}]_i$ induced by SA(I) in pancreatic acini

Figure 3 illustrated the effects of GDP on rate change of amylase release stimulated by SA(I). GDP could inhibit the rate of amylase secretion stimulated by 5×10^{-6} mol/L SA(I), whose rate-time curve of amylase secretion was similar to that of SA(I) in configuration, but addition of 5×10^{-3} mol/L GDP decreased the maximal rate by 54%. These data suggested GDP mainly inhibited high-potency phase of amylase secretion stimulated by SA(I).

In the kinetic experiments of $[Ca^{2+}]_i$ induced by SA(I) and CCK-8 in a single pancreatic acinar cell (Figure 2), addition of 5×10^{-3} mol/L GDP inhibited 1×10^{-9} mol/L CCK-8-induced $[Ca^{2+}]_i$ peak amplitude by 39%, with similar dynamic characteristics of $[Ca^{2+}]_i$. Addition of 5×10^{-3} mol/L GDP caused diphasic spike of $[Ca^{2+}]_i$ induced by 5×10^{-6} mol/L SA(I) decrease either, this resulted in a 44% decrease of initial Ca^{2+} peak, but a secondary increase in $[Ca^{2+}]_i$ still appeared.

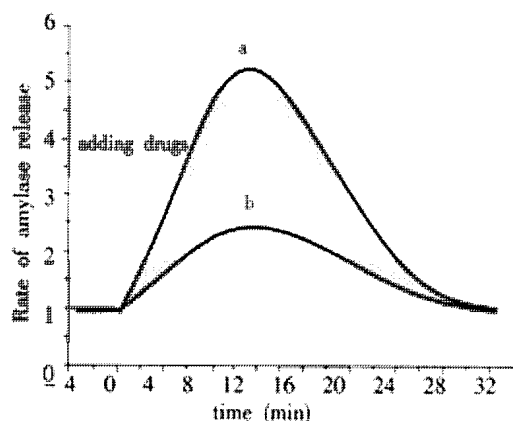


Figure 3 Inhibitory of GDP on rate course of SA(I) stimulated amylase secretion in rat pancreatic acini (base secretion rate is normalized as 1.0). a. 5×10^{-6} mol/L SA(I); b. 5×10^{-6} mol/L SA(I) + 5×10^{-3} mol/L GDP. The data points represent from four separate experiments

DISCUSSION

A series of investigation for amylase secretion stimulated by Bupleurum and its effective components show that they have the rapid and high-potency ability of promoting pancreatic acini enzyme secretion and the validity of reversing functional disorder of pancreas exocrine. From the analysis of rate kinetics of amylase secretion stimulated by SA(I) (Figure 1), within 15 min following adding SA(I), the rate of amylase secretion increased rapidly, then gradually decreased and returned to basal level at 30 min. It indicates that different from CCK to enhance the synthesis of protein^[22,23], the main effect of SA(I) is to hasten secretion of the exocrine protein synthesized and accumulated in granules.

To determine whether the stimulating signal of SA(I) on acinar cells is transduced by binding to the receptor on the cellular membrane, is the first task in the investigation of its mechanism of action. It is known that physiological functions of CCK-8 and CCh are mediated by specific types of receptors now termed the CCK_A and M₃ receptors. CCK_A and M₃ receptors belong to the receptors of G protein-coupled superfamily which transduce the stimulating signal by generation of intracellular second messengers, primarily IP₃ and DAG^[9-11,14,24]. We compared the effects of CCK-8 and CCh receptor antagonist, Bt₂-cGMP and atropine, on amylase secretion caused by SA(I) (Table 1, 2), the results showed that atropine had no detectable influence on the action of SA(I). Moreover, the dose-effect relationships of inhibition of Bt₂-cGMP on SA(I) and CCK-8 were similar. The results suggested that interaction between SA(I) and its membrane receptor initiated intracellular signaling transduction. The receptor of SA(I) has similar characteristics as that of CCK-8. To clarify the detail machinery of receptor of SA(I) will require further study.

As mentioned in our previous papers^[25], the rising dynamics of mean intracellular $[Ca^{2+}]_i$ induced by SA(I) in rat pancreatic acinar cells could produce two peaks. When pancreatic acini were incubated in Ca^{2+} -free medium, in the second step, $[Ca^{2+}]_i$ did not rise and fell to the basal level gradually, and the second peak disappeared. The finding demonstrated the Ca^{2+} release from intracellular Ca^{2+} pool resulted in the first $[Ca^{2+}]_i$ peak, and second $[Ca^{2+}]_i$ peak depending on the extracellular Ca^{2+} influx in sequence. In the present experiments of single acinar cell $[Ca^{2+}]_i$ was concordant with our previous report, 1×10^{-9} mol/L CCK-8 could cause a large transient increase in $[Ca^{2+}]_i$. But it is different from CCK-8 that the change of $[Ca^{2+}]_i$ caused by SA(I) had relatively slow rate and higher peak value. In addition, there was a secondary increase after the initial peak of $[Ca^{2+}]_i$. The data suggested SA(I) had a different mechanism from that of CCK inducing Ca^{2+} release from ER and might be through more signaling transduction pathways to initiate the intracellular calcium mobilization and subsequent extracellular calcium influx. So the intracellular increase in $[Ca^{2+}]_i$ caused by SA(I) could maintain a longer time course. These mechanisms correlated with high-potency effect of SA(I) on pancreatic exocrine. It is now known that the changes of intracellular calcium play a key role in many functions of cells. Recently, several reports showed that the spatio-temporal patterns of the intracellular calcium carried the Ca^{2+} signals to regulate gene expression and cell differentiation^[26-29]. The specificity of Ca^{2+} signal is somewhat more acute in polarized secretory cells such as pancreatic acinar cells^[30-32]. These researches suggest that such pattern of Ca^{2+} signal induced by SA(I) in our present studies may offer specific signal to modulate enzymes secretion in pancreatic acinar cells.

In addition, GDP could cause obvious decrease of amylase secretion and increase in $[Ca^{2+}]_i$ induced by SA(I). GDP mainly inhibited the early peak of $[Ca^{2+}]_i$ and high-potency phase of secretion stimulated by SA(I). The decrease of $[Ca^{2+}]_i$ anticipated the inhibition of amylase secretion in sequence (Figure 2,3). Several

investigators had reported that the increase in intracellular level of GDP could cause the inhibition of G-protein activity in pancreatic acini^[33-35]. These G-proteins, including both ras-like small GTP-binding proteins and heterotrimeric G-proteins, had important role on the release of intracellular calcium and amylase secretion stimulated by secretagogues^[14, 36-40]. More experimental data are required whether intracellular signal of stimulatory effect of SA(I) transducing to down stream through activation of G protein coupling receptor.

In summary, the results presented in this study prove that SA(I) has high-potency in stimulating the amylase secretion in rat pancreatic acini and its main effect is to promote exocytosis of enzymes synthesized by the cells. The transmembrane signal of SA(I) is transduced through interaction with its membrane receptor. Subsequently, $[Ca^{2+}]_i$ is increased by intracellular Ca^{2+} release and extracellular Ca^{2+} influx, so as to enhance the function of cellular enzyme secretion.

REFERENCES

- Chen XQ, Yang WX, Xu WS, Yang F, Kong D, Wu XZ. Stimulative action of bupleurum chinensis on amylase secretion from pancreatic acini and its dependence on Ca^{2+} . *Zhongguo Zhongxiyi Jiehe Zazhi* 1997;17:211-212
- Yang WX, Yu Y, Yao HQ, Zhao YY, Liang H. Kinetics of enzyme secretion and $[Ca^{2+}]_i$ in pancreatic acini stimulated by Saikosides. *Zhongguo Xueshu Qikan Wenzhai (Keji Kuaibao)* 1999;5:1185-1186
- Liang H, Zhao YY, Qi HY, Huang J, Zhang RY. A new saikosaponin from bupleurum DC. *Yaoxue Xuebao* 1998; 33:37-41
- Yang WX, Yu Y, Yao HQ, Wang H, Zhao YY, Liang H. Comparative research of enzyme secretion in pancreatic acini stimulated by saikosaponins. *Zhongguo Xueshu Qikan Wenzhai (Keji Kuaibao)* 1999;5: 1529-1530
- Yang WX, Yu Y, Zhao YY, Liang H, Wang H, Zhou J. The characteristics of saikosaponin-stimulated pancreatic acini protein secretion and effects of Ca^{2+} . *Nankai Daxue Xuebao* 2000;33:41-44
- Tsunoda T, Stuenkel EL, Williams JA. Oscillatory mode of calcium signaling in rat pancreatic acinar cells. *Am J Physiol* 1990; 258: C147-C155
- Williams JA, Blevins GT. Cholecystokinin and regulation of pancreatic acinar cell function. *Physiol Rev* 1993;73:709-723
- Giovanna T, Zhang BX, Xu X, Muallem S. Compartmentalization of Ca^{2+} signaling and Ca^{2+} pools in pancreatic acini. *J Bio Chem* 1994;269: 29621-29628
- Muallem S, Beeker TG. Relationship between hormonal, GTP and $Ins(1,4,5)P_3$ -stimulated Ca^{2+} uptake and release in pancreatic acinar cells. *Biochem J* 1989;263:333-339
- Yasuhiro T, Chung O. The regulatory site of functional GTP binding protein coupled to the high affinity cholecystokinin receptor and phospholipase A2 pathway is on the G- β subunit of Gq protein in pancreatic acini. *Biochem Biophys Res Com* 1995;211:648-655
- Berridge MJ. Inositol trisphosphate and calcium signaling. *Nature* 1993;361:315-325
- Takashi K, Shunsuke S, Shinji K, Toyohiko H, Chohei S, Junji K. Cholecystokinin receptor occupation and cholecystokinin-induced calcium mobilization in the early phase in rat pancreatic acini. *Biochem Biophys Acta* 1991;1094:231-237
- Xu X, Zeng WZ, Muallem S. Regulation of inositol 1,4,5-trisphosphate-activated Ca^{2+} channel by activation of G protein. *J Bio Chem* 1996; 271:11737-11744
- Verspohl EJ, Herrmann K. Involvement of G proteins in the effect of Carbachol and Cholecystokinin in rat pancreatic islets. *Am J Physiol* 1996;271:E65-E72
- Hurley TW, Ronald WB. Regulating transient and sustained changes of cytosolic Ca^{2+} in rat pancreatic acini. *Am J Physiol* 1990; 258:C54-C61
- Stephen JP, Mari SSP. Cyclic GMP mediates the agonist-stimulated increase in plasma membrane calcium entry in the pancreatic acinar cell. *J Bio Chem* 1990; 265: 12846-12853
- Anna G, Stephen P. Nitric oxide production regulates cGMP formation and calcium influx in pancreatic acinar cells. *Am J Physiol* 1994; 266:G350-G356
- Han B, Logsdon C. CCK stimulates mob-1 expression and NF- κ B activation via protein kinase C and intracellular Ca^{2+} . *Am J Physiol Cell Physiol* 2000; 278: C344-C351
- Gukovsky I, Gukovskaya AS, Blinman TA, Zaninovic V, Pandol SJ. Early NF-kappaB activation is associated with hormone-induced pancreatitis. *Am J Physiol* 1998; 275:G1402-G1414
- Duan RD, Wagner ACC, Yule DI, Williams JA. Multiple inhibitory effects of genistein on stimulus-secretion coupling in rat pancreatic acini. *Am J Physiol* 1994; 266: G303-G310
- Cui ZJ, Kanno T. Cholecystokinin analog JMV-180-induced intracellular calcium oscillations are mediated by inositol 1,4,5-trisphosphate in rat pancreatic acini. *Zhongguo Yaoli Xuebao* 2000;21: 377-380
- Bragado MJ, Groblewski GE, Williams JA. Regulation of protein synthesis by cholecystokinin in rat pancreatic acini involves PHAS-I and the p70 S6 kinase pathway. *Gastroenterology* 1998; 115:733-742
- Bragado MJ, Tashiro M, Williams JA. Regulation of the initiation of pancreatic digestive enzyme protein synthesis by Cholecystokinin in rat pancreas *in vivo*. *Gastroenterology* 2000; 119:1731-1739
- Talkad VD, Potto RJ, Metz DC, Turner RJ, Fortune KP, Bhat ST, Gardner JD. Characterization of the three different states of the cholecystokinin(CCK) receptor in pancreatic acini. *Biochem Biophys Acta* 1994;1224:103-116
- Yang WX, Yu Y, Zhang WZ, Wang H, Li XD, Zhao YY, Liang H. Inhibitory role of GDP on saikosaponin(I) stimulated enzyme secretion and rising of $[Ca^{2+}]_i$ in rat pancreatic acini. *Acta Pharmacol Sin* 2001;22: 669-672
- Bootman MD, Lipp P, Berridge MJ. The organisation and functions of local Ca^{2+} signals. *J Cell Sci* 2001; 114: 2213-2222
- Dotmentsch RE, Xu K, Lewis RS. Calcium oscillation increase the efficiency and specificity of gene expression. *Nature* 1998; 392: 933
- Kummer U, Olsen LF, Dixon CJ, Green AK, Bornberg-Bauer E, Baier G. Switching from simple to complex oscillations in calcium signaling. *J Biophys* 2000; 79:1188-1195
- West AE, Chen WG, Dalva MB, Dolmetsch RE, Kornkauer JM, Shaywitz AJ, Takasa MA, Tao X, Greenberg ME. Calcium regulation of neuronal gene expression. *Proc Natl Acad Sci USA* 2001; 98:11024
- Xu X, Zeng WZ, Diaz J, Muallem S. Spatial compartmentalization of Ca^{2+} signaling complexes in pancreatic acini. *J Biol Chem* 1996; 271: 24684-24690
- James W. Putney, Pharmacology of Capacitative Calcium Entry. *Mol Interv* 2001; 1: 84-94
- Shuttleworth TJ. Intracellular Ca^{2+} signalling in secretory cells. *J Exp Biol* 1997; 200: 303-314
- Padfield PT, Ding TG, Jamieson TD. Ca^{2+} -dependent amylase secretion from pancreatic acinar cells occurs without activation of phospholipase C linked-G-proteins. *Biochem Biophys Res commun* 1991;174:536-541
- Gasman S, Chasserot-Golaz S, Popoff MR, Aunis D, Bader MF. Involvement of Rho GTPases in calcium-regulated exocytosis from adrenal chromaffin cells. *J Cell Sci* 1999; 112: 4763-4771
- Rosales J, Ernst JD. GTP-dependent permeabilized neutrophil secretion requires a freely diffusible cytosolic protein. *J Cell Biochem* 2000; 80:37-45
- Ohnishi H, Mine T, Shibata H, Ueda N, Tsuchida T, Fujita T. Involvement of Rab4 in regulated exocytosis of rat pancreatic acini. *Gastroenterology* 1999; 116:943-952
- Dabrowski A, Vanderkuur JA, Carter-Su C, Williams JA. Cholecystokinin stimulates formation of Shc-Grb2 complex in rat pancreatic acinar cells through a protein kinase C-dependent mechanism. *J Biochem* 1996;271:27125-27129
- Ohnishi H, Samuelson LC, Yule DI, Ernst SA, Williams JA. Overexpression of Rab3D enhances regulated amylase secretion from pancreatic acini of transgenic mice. *J Clin Invest* 1997;100: 3044-3052
- Padfield PJ, Panesar N. The two phases of regulated exocytosis in permeabilized pancreatic acini are modulated differently by heterotrimeric G Proteins. *Biochem Biophys Res Com* 1998;245:332-336
- Nozu F, Tsunoda Y, Ibitayo AI, Bitar KN, Owyang C. Involvement of RhoA and its interaction with protein kinase C and Src in CCK-stimulated pancreatic acini. *Am J Physiol* 1999;276: G915-G923

Edited by Wu XN

• BASIC RESEARCH •

Effect of endotoxin on portal hemodynamic in rats

Xiang-Jun Bi, Min-Hu Chen, Jing-Hui Wang, Jie Chen

Xiang-Jun Bi, Min-Hu Chen, Jing-Hui Wang, Jie Chen, Department of Gastroenterology, First Affiliated Hospital, Sun Yat-sen University, Guangzhou 510089, Guangdong Province, China
Correspondence to: Xiang-Jun Bi, Department of Gastroenterology, First Affiliated Hospital, Sun Yat-sen University, Guangzhou 510089, Guangdong Province, China. bixj@gzsums.edu.cn
Telephone: +86-20-87334343

Received 2001-10-19 Accepted 2001-11-18

Abstract

AIM: To study the effects of endotoxin on portal hemodynamic of normal and noncirrhotic portal hypertensive rats.

METHODS: Normal rats were intraperitoneally injected with 0.1, 0.25, 0.5, 1.0, 2.0, 4.0 mg·kg⁻¹ of lipopolysaccharide (LPS) respectively, portal vein ligation (PVL) and intrahepatic portal occlusion (IPO) rats as well as sham-operated rats were treated with an intraperitoneal injection of 1.0 mg·kg⁻¹ of LPS, the portal vein pressure (PVP), portal venous flow (PVF), inferior vena cava pressure (IVCP) and portal vein resistance (PVR) were detected 4 hours after injection.

RESULTS: PVF of the 5 groups of rats accepting intraperitoneal injection of LPS were increased from 14.0 to 18.0, 22.2, 26.2, 34.8, 39.6, 38.8 mL·min⁻¹ 4 hours after injection of LPS ($P < 0.01$). PVP of the 4 groups of rats accepting more than 0.1 mg/kg·b.w of LPS was increased from 1.04 to 1.25, 1.50, 1.80, 1.95, 2.05 kPa ($P < 0.01$). The increments of PVF and PVP were in a dose-dependent manner of LPS. PVR of the 5 groups of rats was decreased from 51 to 42, 44, 48, 45, 44, 47 kPa·min·L⁻¹ ($P < 0.05$) and no dose-dependent manner was observed. PVF of PVL, IPO and sham-operated rats increased from 22.6 to 32.8, 22.0 to 28.0, 14.0 to 34.8 mL·min⁻¹ ($P < 0.01$), and PVP increased from 1.86 to 2.24, 1.74 to 1.95, 1.04 to 1.80 kPa ($P < 0.01$), PVR decreased from 71 to 61, 67 to 61, 52 to 44 kPa·min·L⁻¹ after intraperitoneal injection of 1 mg·kg⁻¹ of LPS. The increments of PVF and PVP of PVL and IPO rats were significantly less than the sham-operated rats ($P < 0.01$). There was no significant difference between the amounts of PVR decreased in the two groups of PHT model rats and sham-operated rats ($P > 0.05$) after intraperitoneal injection 1 mg·kg⁻¹ of LPS.

CONCLUSION: Endotoxin could prompt portal hypertension of the normal and noncirrhotic portal hypertensive rats by increasing portal blood flow mainly.

Bi XJ, Chen MH, Wang JH, Chen J. Effect of endotoxin on portal hemodynamic in rats. *World J Gastroenterol* 2002;8(3):528-530

INTRODUCTION

Endotoxin is lipopolysaccharide (LPS), a component of the outer membrane of the Gram-negative bacteria, which is released from the Gram-negative bacterial cell wall. Its functional component is lipid

A. Many researchers have discovered that endotoxemia can lead to an alteration of systemic hemodynamics and some organs' blood circulation such as the lungs, liver and kidney^[1-4]. However, some researchers have displayed evidence against a role for endotoxin in the hyperdynamic circulation of rats with prehepatic portal hypertension^[5]. The activation of endotoxin occurs through a series of vaso modulators such as nitric oxide (NO), endothelin and others^[4-11]. These vaso modulators could modulate portal venous flow (PVF), portal vein resistance (PVR) and/or portal vein pressure (PVP). In patients suffering from liver cirrhosis with PHT, endotoxemia is often present and might contribute to the development of liver cirrhosis and PHT^[12-14]. Whether or not PHT models without liver cirrhosis are more sensitive to endotoxin is still unclear^[15,16]. Little has been done to study the effects of various dosages of LPS on portal hemodynamics. So, to detect what role endotoxin plays in PHT, we designed the following experiments to discover the effects of various dosages of LPS on the portal hemodynamics of both normal rats as well as non-cirrhosis PHT rats.

MATERIALS AND METHODS

Animals

Female Sprague Dawley rats weighing 200-250g were obtained from the Laboratory Animal Center of Sun Yat-sen University, and fed with standard rat chow. (1) Surgery was performed as in Yachida's method^[17]. Under penbarbital (50 mg·kg⁻¹, intraperitoneal injection) anesthesia, the portal vein was isolated and a single ligature placed around both the portal vein and a 16-gauge needle. The needle was ligated together with the portal vein and immediately removed to allow the portal vein to expand to the limit imposed by the ligature. A catheter was inserted through the mesentery vein into the portal vein and another into the inferior vena cava. Pressure transducers (Philips CM 130) recorded PVP and IVCP. PVF was recorded with an electromagnetic flow meter (Nihonkohden). The abdomen was closed and the rats were allowed to recover for 2 wks. In sham-operated rats, surgery consisted of dissection and visual inspection of the portal vein without ligature. (2) Surgery was performed as in Li's *et al*^[18] method. Under penbarbital anesthesia as above, microspheres (about 2×10^4 each time) of Sephadex LH-20 (Pharmacia) were injected into the mesentery vein; injection was repeated 5 times. The portal venous and vena cava pressure were recorded as above. The abdomen was closed and the rats were allowed to recover for 2 wks. Sham-operated rats above were used as a control.

Effects of LPS on portal hemodynamics

Normal rats were divided into seven groups, each group containing five rats. Rats were intraperitoneally injected with LPS (from *Escherichia coli* serotype, Sigma) at dosages of 0.1, 0.25, 0.5, 1.0, 2.0, 4.0 mg·kg⁻¹ respectively. Equivalent volumes of saline were intraperitoneally injected as a control. 4h later, anesthesia and operation were manipulated as above. A catheter was inserted through mesentery vein into portal vein and another catheter into the inferior vena cava. Pressure transducers (Philips CM 130) recorded PVP and IVCP. PVF was recorded with an electromagnetic flow meter (Nihonkohden). PVF, PVP and IVCP were checked four hours after injection and PVR was determined according to the formula: $PVR = (PVP - IVCP) / PVF$.

PHT rats were divided into PVL, IPO model, and sham-operated groups, each group containing ten rats, and then divided at random into two groups of five rats. PVL, IPO and sham-operated rats were each intraperitoneally injected with LPS at the dose of $1.0\text{mg}\cdot\text{kg}^{-1}$. The other PVL, IPO and sham-operated rats were intraperitoneally injected equivalent volumes of saline as control. PVF, PVP and IVCP were checked as above 4h after injection and PVR was determined according to the formula: $\text{PVR}=(\text{PVP}-\text{IVCP})/\text{PVF}$.

The alteration of portal hemodynamics of the noncirrhotic and sham-operated rats after injection of LPS was analyzed. The means and increment percentages of PVF, PVP, and PVR of the PVL and IPO groups were compared with that of the sham-operated group.

Statistical analysis

Data were expressed as $\bar{x}\pm s$. Statistical analysis between groups was made by means of the student's unpaired *t* test by means of SPSS10.0 software, with $P<0.05$ being regarded as statistically significant.

RESULTS

Portal hemodynamic of model rats after operation

Just after portal vein ligation, PVF averaged $10.8\text{mL}\cdot\text{min}^{-1}$, PVP increased to 1.85kPa and PVR increased to $142\text{kPa}\cdot\text{min}\cdot\text{L}^{-1}$. Two weeks after operation, PVF, PVP and PVR averaged $22.6\text{mL}\cdot\text{min}^{-1}$, 1.86kPa and $71\text{kPa}\cdot\text{min}\cdot\text{L}^{-1}$. After finishing portal vein occlusion, PVF averaged $9.6\text{mL}\cdot\text{min}^{-1}$, PVP increased to 2.05kPa and PVR $180\text{kPa}\cdot\text{min}\cdot\text{L}^{-1}$. Two weeks after operation, PVF, PVP and PVR averaged $22\text{mL}\cdot\text{min}^{-1}$, 1.74kPa and $67\text{kPa}\cdot\text{min}\cdot\text{L}^{-1}$. PVP of the models was significantly increased the moment after operation and 2 wks after operation ($P<0.01$).

Effects of LPS on portal hemodynamic

PVF of all the groups of rats accepting intraperitoneal injection of LPS was significantly increased 4h after injection ($P<0.01$). Except for the group of rats accepting intraperitoneal injection of $0.1\text{mg}\cdot\text{kg}^{-1}$ of LPS ($P>0.05$), the other groups of rats were all significantly increased in PVP 4h after injection ($P<0.01$). PVF and PVP increased in a dose-dependent manner with increasing LPS concentration. Except for the group of rats accepting intraperitoneal injection of $0.5\text{mg}\cdot\text{kg}^{-1}$ of LPS ($P>0.05$), the other groups of rats were all decreased in PVR 4h after injection ($P<0.05$) and no dose-dependent manner of LPS was observed (Table 1).

Table 1 Effects of LPS on portal hemodynamics

Dose of LPS ($\text{mg}\cdot\text{kg}^{-1}$)	PVF ($\text{mL}\cdot\text{min}^{-1}$)	<i>P</i>	PVP (kPa)	<i>P</i>	PVR ($\text{kPa}\cdot\text{min}\cdot\text{L}^{-1}$)	<i>P</i>
0.00	14.0 ± 0.44		1.04 ± 0.020		51	
0.10	18.0 ± 0.44	0.000	1.05 ± 0.022	0.743	42	0.001
0.25	22.2 ± 0.66	0.000	1.25 ± 0.026	0.000	44	0.003
0.50	26.2 ± 0.80	0.000	1.50 ± 0.015	0.000	48	0.086
1.00	34.8 ± 0.80	0.000	1.80 ± 0.023	0.000	45	0.003
2.00	39.6 ± 0.74	0.000	1.95 ± 0.035	0.000	44	0.001
4.00	38.8 ± 0.33	0.000	2.05 ± 0.022	0.000	47	0.008

Compare rats accepting intraperitoneal injection of various doses of LPS with rats not accepting LPS.

Effects of endotoxin on portal hemodynamic of PHT models

PVF and PVP of sham-operated rats increased from $14.0\text{mL}\cdot\text{min}^{-1}$ and 1.04kPa to $34.8\text{mL}\cdot\text{min}^{-1}$ and 1.80kPa . PVR decreased from $52\text{kPa}\cdot\text{min}\cdot\text{L}^{-1}$ to $44\text{kPa}\cdot\text{min}\cdot\text{L}^{-1}$ 4h after intraperitoneal injection of $1\text{mg}\cdot\text{kg}^{-1}$ of LPS. PVF of PVL and IPO model rats increased to $32.8\text{mL}\cdot\text{min}^{-1}$ and $28.0\text{mL}\cdot\text{min}^{-1}$ respectively; PVP increased to 2.24kPa and 1.95kPa respectively; and PVR decreased to $61\text{kPa}\cdot\text{min}\cdot\text{L}^{-1}$

and $61\text{kPa}\cdot\text{min}\cdot\text{L}^{-1}$ respectively. In the three groups of rats, intraperitoneal injection $1\text{mg}\cdot\text{kg}^{-1}$ of LPS significantly changed PVF, PVP and PVR ($P<0.01$, Table 2).

The percentages of PVF increase in the PVL, IPO and sham-operated groups of rats were 45.1%, 27.3%, and 148.6% respectively. PVP increased 20.4%, 12.1%, and 73.1% respectively. PVR increased -14.1%, -9.0%, and -15.4% respectively (Table 3). The increase of PVF and PVP in the two groups of PHT model rats were significantly different from sham-operated rats ($P<0.01$). There was no significant difference between the decrease of PVR in the two groups of PHT model rats and sham-operated rats ($P>0.05$ Table 3).

Table 2 Effects of LPS on portal hemodynamics of sham-operated and PHT rats

Group	PVF ($\text{mL}\cdot\text{min}^{-1}$)	PVP (kPa)	PVR ($\text{kPa}\cdot\text{min}\cdot\text{L}^{-1}$)
Portal vein ligation	32.8 ± 1.6	2.24 ± 0.073	61
Control	22.6 ± 1.7	1.86 ± 0.044	71
Intrahepatic portal occlusion	28.0 ± 2.1	1.95 ± 0.054	61
Control	22.0 ± 2.1	1.74 ± 0.037	67
Sham-operated	34.8 ± 0.7	1.80 ± 0.046	44
Control	14.0 ± 0.4	1.04 ± 0.039	52

Table 3 Alteration of portal hemodynamics of the noncirrhotic and sham-operated rats after injection of LPS

Group	PVF ($\text{mL}\cdot\text{min}^{-1}$)	Increment (%)	PVP (kPa)	Increment (%)	PVR (kPa· min·ml ⁻¹)	Increment (%)
PVL	10.2 ± 0.8	45.13	0.38 ± 0.047	20.43	-10	-14.08
IPO	6.4 ± 1.14	27.27	0.21 ± 0.026	12.07	-10	-8.96
Sham- operated	20.8 ± 0.84	148.57	0.76 ± 0.038	73.08	-8	-15.38

DISCUSSION

Portal hypertension (PHT) is mainly due to two factors, PVF and PVR. Increase of PVF could lead to portal congestion, and PVR could prevent portal output and lead to portal gore. PHT is apt to be associated with a series of cytokines and vasodilators^[19]. Endotoxin could enhance synthesis of a series of vasoconstrictors such as endothelins, as well as a series of vasodilators such as nitric oxide (NO). These modulators are able to adjust portal and systemic hemodynamics functionally. Across the cell's membrane, NO could spread to smooth muscle cells, enhance synthesis of cyclic guanosine monophosphate (cGMP), and consequently decrease intracellular Ca^{2+} concentrations, thus inducing vasorelaxation^[11]. NO could also increase cardiac output and lower the vessel's reaction to vasoconstrictors, causing systemic and splanchnic hyperdynamic circulation^[20,21]. Our research proved LPS could increase PVF of normal and noncirrhotic portal hypertensive rats and that this increase was associated with the dosage of LPS, which demonstrated increasing PVF was an important factor to form PHT. Endotoxemia could modulate the intrahepatic portal vessel and consequently alter the resistance of the intrahepatic portal vessel^[23, 24]. Endotoxin signals hepatic cells to secrete a series of cytokines such as tumor necrosis factor (TNF α) and endothelin and consequently enhances synthesis and deposition of collagens^[25-27]. Endothelin has been reported to be able to induce constriction of the smooth muscle cells of the hepatic vasculature^[28]. Endothelin can also prompt hepatic stellate cells (HSC) to proliferate and constrict^[29]. Endotoxin was thought to increase PVP by the ways above. However, endotoxin-induced increase of NO synthesized by inducible nitric oxide synthase could lead to vasorelaxation and lower the vessel's response to vasoconstrictors, which might account for the increase of PVR. Yokoyama reported the liver maintains its microcirculatory flow by vascular remodeling from the hepatic arterial vasculature following PVL^[30], which might induce the decrease of PVR in noncirrhotic

PHT rats. This research shows the PVR of normal and noncirrhotic PHT rats decreased after intraperitoneal injection of LPS, which demonstrated effectively that increasing PVF was the main factor to forming PHT.

PHT models moderate PVP through a new balance of vasoconstrictors and vasodilators^[1]. PHT model rats were reported to be sensitive to LPS^[15] by means of portal vein ligation. But Chu suggested some evidence against a role for endotoxin in the hyperdynamic circulation of rats with prehepatic portal hypertension^[5]. Our experiments show that after intraperitoneal injection of LPS, PVF and PVP of PVL and IPO model rats increased significantly less than that of sham-operated rats ($P < 0.01$). Another report found artery vessel of PVL rats more blunt to LPS and the increment of NOS was significantly less than sham-operated rats^[16], which might act as an explanation of our results. We would perform research with vasoconstrictors and vasodilators to further demonstrate our results.

REFERENCES

- Liu F, Li JX, Li CM, Leng XS. Plasm endothelin in patients with vasodilator in cirrhotic patients. *World J Gastroenterol* 2001; 7: 126-127
- Xu KD, Liu TF, Cing X. Significance of detection of plasm nitric oxide, endothelin, endotoxin in patients with liver cirrhosis. *World J Gastroenterol* 1998; 4(Suppl 2): 64
- Qin RY, Zou SQ, Wu ZD, Qiu FZ. Influence of splanchnic vascular infusion on the content of endotoxins in plasma and the translocation of intestinal bacteria in rats with acute hemorrhage necrosis pancreatitis. *World J Gastroenterol* 2000;6:577-580
- Mu Y, Shen YZ, Chu YF. Effects of tetrandrine on gastric mucosa and liver in portal hypertensive rats. *China Natl J New Gastroenterol* 1997;3:192-194
- Chu CJ, Lee FY, Wang SS, Chang FY, Lin HC, Lu RH, Wu SL, Chan CC, Tai CC, Lai IN, Lee SD. Evidence against a role for endotoxin in the hyperdynamic circulation of rats with prehepatic portal hypertension. *J Hepatol* 1999; 30: 1105-1111
- Zhang GL, Wang YH, Teng HL, Lin ZB. Effects of aminoguanidine on nitric oxide production induced by inflammatory cytokines and endotoxin in cultured rat hepatocytes. *World J Gastroenterol* 2001;7:331-334
- Feng ZJ, Feng LY, Sun ZM, Song M, Yao XX. Expression of nitric oxide synthase protein and gene in the splanchnic organs of liver cirrhosis and portal hypertensive rats. *World J Gastroenterol* 2000;6(Suppl 3):33
- Zhang GF, Zhang MA, Chen YR, Wang L. The roles of endothelin and nitric oxide in gastric mucosa injuries in rats with endotoxemia. *Shijie Huaren Xiaohua Zazhi* 2000;8(Suppl8):24
- Liu BH, Chen HS, Zhou JH, Xiao N. Effects of endotoxin on endothelin receptor in hepatic and intestinal tissues after endotoxemia in rats. *World J Gastroenterol* 2000;6:298-300
- Horie Y, Kato S, Ohki E, Tamai H, Ishii H. Role of endothelin in endotoxin-induced hepatic microvascular dysfunction in rats fed chronically with ethanol. *J Gastroenterol Hepatol* 2001;16:916-922
- Horie Y, Kimura H, Kato S, Ohki E, Tamai H, Yamagishi Y, Ishii H. Role of nitric oxide in endotoxin-induced hepatic microvascular dysfunction in rats chronically fed ethanol. *Alcohol Clin Exp Res* 2000; 24: 845-851
- Goulis J, Patch D, Burroughs AK. Bacterial infection in the pathogenesis of variceal bleeding. *Lancet* 1999; 353: 139-142
- Jia JB, Han DW, Xu RL, Gao F, Zhao LF, Zhao YC, Yan JP, Ma XH. Effect of endotoxin on fibronectin synthesis of rat primary cultured hepatocytes. *World J Gastroenterol* 1998;4:329-331
- Yang JM, Han DW, Xie CM, Liang QC, Zhao YC, Ma XH. Endotoxins enhance hepatocarcinogenesis induced by oral intake of thioacetamide in rats. *World J Gastroenterol* 1998;4:128-132
- Perez del Pulgar S, Pizcueta P, Engel P, Bosch J. Enhanced monocyte activation and hepatotoxicity in response to endotoxin in portal hypertension. *J Hepatol* 2000; 32: 25-31
- Heller J, Sogni P, Tazi KA, Chagneau C, Poirel O, Moreau R, Lebrec D. Abnormal regulation of aortic NOS2 and NOS3 activity and expression from portal vein-stenosed rat after lipopolysaccharide administration. *Hepatology* 1999; 30: 698-704
- Yachida S, Ikeda K, Kaneda K, Goda F, Maeba T, Maeta H. Preventive effect of preoperative portal vein ligation on endotoxin-induced hepatic failure in hepatectomized rats is associated with reduced tumour necrosis factor alpha production. *Br J Surg* 2000; 87: 1382-1390
- Li XN, Benjamin IS, Alexander B. A new rat model of portal hypertension induced by intraportal injection of microspheres. *World J Gastroenterol* 1998; 4: 66-69
- Perez del Pulgar S, Pizcueta P, Engel P, Bosch J, Rodas J. Neutrophil adhesion is impaired in the mesentery but not in the liver sinusoids of portal hypertensive rats. *Am J Physiol Gastrointest Liver Physiol* 2001; 280: G1351-1319
- Roberts LR, Kamath PS. Pathophysiology of variceal bleeding. *Gastrointest Endosc Clin N Am* 1999; 9: 167-174
- Wiest R, Groszmann RJ. Nitric oxide and portal hypertension: its role in the regulation of intrahepatic and splanchnic vascular resistance. *Semin Liver Dis* 1999; 19: 411-426
- Huang YQ, Xiao SD, Mo JZ, Zhang DZ. Effects of nitric oxide synthesis in hibitor in long/term treatment on hyperdynamic circulatory state in cirrhotic rats. *World J Gastroenterol* 2000;6(Suppl3):31
- Bauer M, Bauer I, Sonin NV, Kresge N, Baveja R, Yokoyama Y, Harding D, Zhang JX, Clemens MG. Functional significance of endothelin B receptors in mediating sinusoidal and extrasinusoidal effects of endothelins in the intact rat liver. *Hepatology* 2000; 31: 937-947
- Gandhi CR, Kuddus RH, Nemoto EM, Murase N. Endotoxin treatment causes an upregulation of the endothelin system in the liver: amelioration of increased portal resistance by endothelin receptor antagonism. *J Gastroenterol Hepatol* 2001; 16: 61-69
- Cho JJ, Hoher B, Herbst H, Jia JD, Raehl M, Hahn EG, Riecken EO, Schappan D. An oral endothelin-A receptor antagonist blocks collagen synthesis and deposition in advanced rat liver fibrosis. *Gastroenterology* 2000; 118: 1169-1178
- Wang X, Chen YX, Xu CF, Zhao GN, Huang YX, Wang QL. Relationship between tumor necrosis factor- α and liver fibrosis. *World J Gastroenterol* 1998;4:18
- Chu YK, Wu JS, Ma QJ, Gao DM, Wang X. Plasm TNF- α levels during the formation of liver cirrhosis and portal hypertension in rats. *Huaren Xiaohua Zazhi* 1998;6:755-756
- Garcia PJ, Zhang JX, Sonin N, Nakanishi K, Clemens MG. Ischemia/reperfusion induces an increase in the hepatic portal vasoconstrictive response to endothelin-1. *Shock* 1999; 11: 325-329
- Petrowsky H, Schmandra T, Lorey T. Endothelin-induced contraction of the portal vein in cirrhosis. *Eur Surg Res* 1999; 31: 289-296
- Yokoyama Y, Baveja R, Sonin N. Hepatic neovascularization after partial portal vein ligation: novel mechanism of chronic regulation of blood flow. *Am J Physiol Gastrointest Liver Physiol* 2001;280:G21-31

Edited by Pagliarini R

• BASIC RESEARCH •

The role of endotoxin, TNF- α , and IL-6 in inducing the state of growth hormone insensitivity

Ping Wang, Ning Li, Jie-Shou Li, Wei-Qin Li

Ping Wang, Ning Li, Jie-Shou Li, Wei-Qin Li, Medical College of Nanjing University, Research Institute of General Surgery, Jinling Hospital, Nanjing 210002, Jiangsu Province, China

Supported by the key project of the tenth-five foundation of PLA, No. 01Z011.

Correspondence to: Ping Wang, Research Institute of General Surgery, Jinling Hospital, 305 Zhong Shan East Road, Nanjing 210002, Jiangsu Province, China. wpmd@yahoo.com

Telephone: +86-25-4826808 Ext 58067

Received 2001-12-05 Accepted 2002-01-28

Abstract

AIM: Critical illnesses such as sepsis, trauma, and burns cause a growth hormone insensitivity, which leads to an increased negative nitrogen balance. Endotoxin is generously released into blood under these conditions and stimulates the production of proinflammatory cytokines such as TNF- α , IL-6, and IL-1, which may play a very important role in inducing the growth hormone insensitivity. The objective of this current study was to investigate the role of endotoxin, TNF- α and IL-6 in inducing the growth hormone insensitivity at the receptor and post-receptor levels.

METHODS: Spague-Dawley rats were injected with endotoxin, TNF- α , and IL-6, respectively and part of rats injected with endotoxin was treated with exogenous somatotropin simultaneously. All rats were killed at different time points. The expression of IGF-I, GHR, SOCS-3 and β -actin mRNA in the liver was detected by RT-PCR and the GH levels were measured by radioimmunoassay, the levels of TNF- α and IL-6 were detected by ELISA.

RESULTS: There was no significant difference in serum GH levels between experimental group and control rats after endotoxin injection, however, liver IGF-I mRNA expression had been obviously down-regulated in endotoxemic rats. Liver GHR mRNA expression also had a predominant down-regulation after endotoxin injection. The lowest regulation of liver IGF-I mRNA expression occurred at 12h after LPS injection, being decreased by 53% compared with control rats. For GHR mRNA expression, the lowest expression occurred at 8h and had a 81% decrease. Although SOCS-3 mRNA was weakly expressed in control rats, it was strongly up-regulated after LPS injection and had a 7.84 times increase compared with control rats. Exogenous GH could enhance IGF-I mRNA expression in control rats, but it did fail to prevent the decline in IGF-I mRNA expression in endotoxemic rats. Endotoxin stimulated the production of TNF- α and IL-6, and the elevated IL-6 levels was shown a positive correlation with increased SOCS-3 mRNA expression. The liver GHR mRNA expression was obviously down-regulated after TNF- α iv injection and had a 40% decrease at 8h, but the liver SOCS-3 mRNA expression was the 4.94 times up-regulation occurred at 40min after IL-6 injection.

CONCLUSION: The growth hormone insensitivity could be induced by LPS injection, which was associated with down-

regulated GHR mRNA expression at receptor level and with up-regulated SOCS-3 mRNA expression at post-receptor level. The in vivo biological activities of LPS were mediated by TNF- α and IL-6 indirectly, and TNF- α and IL-6 may exert their effects on the receptor and post-receptor levels respectively.

Wang P, Li N, Li JS, Li WQ. The role of endotoxin, TNF- α , and IL-6 in inducing the state of growth hormone insensitivity. *World J Gastroenterol* 2002;8(3):531-536

INTRODUCTION

Infection especially severe intra-abdominal infection is characterized by catabolic status associated with severe protein loss and negative nitrogen balance^[1-7]. Meantime, the levels of many important hormones such as glucocorticoid, insulin and growth hormone (GH) do not decline, but their biological activities have reduced obviously. Critical illnesses such as sepsis, trauma and burns can usually cause a elevated level of growth hormone at early stage, however the insulin-like growth factor I (IGF-I), which is a growth hormone-dependent growth factor that inhibits protein breakdown, has been showing decreased predominantly, this phenomenon indicating a status of growth hormone insensitivity^[8-12]. In this condition, the administration of high doses of recombinant human growth hormone could not improve negative nitrogen balance, in contrary, it may lead to other metabolic disorders and result in increased morbidity and mortality^[13].

Endotoxin is generously released into blood under the infected condition and stimulates the production of proinflammatory cytokines such as TNF- α , IL-6, and IL-1^[14-18], which play very important roles in inducing the GH insensitivity. The GH insensitivity can occur at receptor and post-receptor levels, the receptor level associates with down-regulated GHR mRNA expression^[19, 20]; the post-receptor insensitivity mainly occurs on the intracellular signal transduction pathway of growth hormone. Recent studies have suggested that the SOCS protein family, especially SOCS-3 play a very important role on this level^[21, 22]. In this study, we investigated whether the GH insensitivity could be induced by LPS, TNF- α and IL-6 iv injection, and what kind of roles they played.

MATERIALS AND METHODS

Animals

All experimental procedures were carried out in compliance with the appropriate institutional and national ethical guidelines for work with laboratory animals. 156 adolescent male Spague-Dawley rats (240-260g) were obtained from animal center of Jinling Hospital (Nanjing, China). They were given free access to food and water for three days before experiments.

Endotoxin and cytokines preparation

Escherichia coli lipopolysaccharide (LPS; serotype O111:B4 phenol extract), obtained from Sigma Chemical (St. Louis, MO), was resuspended in sterile endotoxin-free saline to obtain 4mg/ml

solutions. The recombinant rat TNF- α and IL-6 provided by Peppo Tech EC Ltd (London, England), were resuspended in sterile endotoxin-free saline to obtain 100000U/ml solutions. Human growth hormone, kindly provided by Serono, was resuspended in sterile endotoxin-free saline to obtain a 1mg/ml solution.

Experimental protocols

Male Spague-Dawley rats (provided by Animal Center of Jingling Hospital), weighing 250 ± 10 g, were given free access to food and water for three days before experiments. Rats were anesthetized with ether and received LPS, GH, TNF- α , IL-6, and saline injection. LPS, TNF- α , and IL-6 were administered through superficial dorsal veins of penis and GH was injected subcutaneously. All rats were killed at different time points; blood of rats with LPS injected was collected and centrifuged at 500g for 10min at 4°C to collect serum. Livers were removed, flash-frozen in liquid nitrogen, and stored at -80°C until homogenate preparation and RNA extraction.

Effect of endotoxin on liver expression of IGF-I, GHR, and SOCS-3 mRNA

After the 3-day adaptation period, 42 rats were randomly divided into laboratory group ($n=36$) and control group ($n=6$), LPS ($7.5\text{mg}\cdot\text{kg}^{-1}$ iv) was administered to the laboratory group, every six rats were killed at 1h, 2h, 4h, 8h, 12h, and 24h after injection. The control rats were given intravenous saline.

Effect of GH on liver expression of IGF-I, GHR, and SOCS-3 mRNA along with endotoxin injection

After 3-day adaptation period, 24 rats were divided into 4 groups (6 rats/group). The first group received one injection of LPS ($7.5\text{mg}\cdot\text{kg}^{-1}$ iv) and one injection of saline (sc), the second group received one injection of GH ($1.5\text{mg}\cdot\text{kg}^{-1}$ sc) and one injection of saline (iv), the third group received one injection of LPS ($7.5\text{mg}\cdot\text{kg}^{-1}$ iv) and one injection of GH ($1.5\text{mg}\cdot\text{kg}^{-1}$ sc), the fourth group received two injections of saline. All rats were killed at 10h after injection.

Effects of TNF- α and IL-6 on liver expression of GHR and SOCS-3 mRNA

After the 3-day adaptation period, 102 rats were randomly divided into laboratory group ($n=96$) and control group ($n=6$). Rat recombinant TNF- α and IL-6 ($100000\text{U}/\text{kg}\cdot\text{wt}$) were injected through the same pathway and every six rats were killed after 20min, 40min, 1h, 2h, 4h, 8h, 12h and 24h. The control rats were given intravenous saline.

Analysis of mRNA by RT-PCR

Fresh-frozen liver samples were homogenized and total RNA was performed using TRIZOL Reagent (Biobasic Inc, Scarborough, Ontario, Canada). With Access RT-PCR system kit (Promega Corporation, Madison, WI), the cDNA synthesis and amplification was done in one tube following the manufacture's instructions. In brief, $1\mu\text{g}$ RNA, $1\mu\text{M}$ primers for SOCS-3, GHR, IGF-I and β -actin were added to each reaction mixture respectively, which included 0.2mM dNTP, 1mM MgSO_4 , AMV reverse transcriptase 5U, Tfl DNA polymerase 5U, and AMV/Tfl 5 \times buffer 10 μL . The reaction final volume was 50 μL and was covered with 30 μL mineral oil. RT-PCR reaction was run in the following procedures: (1)Reverse transcription: 48°C for 45min, 1 cycle. (2)AMV RT inactivation and RNA/cDNA/primers denaturation: 94°C for 2min, 1 cycle. (3) Second strand cDNA synthesis and PCR amplification: denaturation 94°C for 30s, annealing 60°C for 1min, extension 68°C for 2min, 28 cycles for SOCS-3 and 21 cycles for GHR and IGF-I, β -actin as intra-control to be amplified along with SOCS-3, GHR and IGF-I. (4)

Final extension: 68°C for 7min, 1 cycle. 5 μL each RT-PCR reaction was electrophoresed in a 1.7% Metaphor agarose (FMC Bioproducts, Rockland, ME) gel and stained with ethidium bromide. Products of RT-PCR reactions were photographed and analyzed by densitometry. The expression of IGF-I, GHR, and SOCS-3 mRNA in laboratory group is represented as a percentage or times compared with their expression in control group.

Polymerase chain reaction primers were as follows: IGF-I sense, (5') CAC ATC TCT TCT ACC TGG CAC TC (3'); IGF-I antisense, (5') GGA TGG AAC GAG CTG ACT TTG TA (3'), to give a 270 base pair product; GHR sense, (5') CTG GGT TGA GTT CAT TGA GCT GGA T (3'); GHR antisense, (5') TGT AGA GGG GAG TTG GTG GGT TGA C (3'), to give a 394 base pair product; SOCS-3 sense, (5') ACC AGC GCC ACT TCT TCA CG (3'); and SOCS-3 antisense, (5') GTG GAG CAT CAT ACT GAT CC (3'), to give a 450 base pair product; β -actin sense, (5') CAT TTC CGG TGC ACG ATG GAG (3'); β -actin antisense, (5') GCC ATC CTG CGT CTG GAC CTG (3'), to give a 599 base pair production. All primers spanned at least one intron of genomic DNA.

Serum levels of GH, TNF- α and IL-6

Blood was obtained from the inferior vena cava at the time of sacrifice. Serum growth hormone levels was measured by radioimmunoassay according to manufacture's instructions (Northern Isotope Co, Beijing, China). Serum samples were analyzed for TNF- α and IL-6 content by enzyme-linked immunosorbent assay according to manufacture's instructions (BioSource International, Camarillo, CA).

Statistics analysis

All data are expressed as means \pm SEM. Correlation between data was analyzed with linear regression. Comparisons between two groups were performed using an unpaired Student's t test. Differences were considered statistically significant when $P < 0.05$.

RESULTS

Levels of serum growth hormone after endotoxin injection

The levels of serum growth hormone at each time points after LPS injection had no significant difference compared with control rats, it maintained a relatively stable status (Table 1).

Table 1 Serum GH levels in LPS injected rats at different time points and control rats

	<i>n</i>	GH levels(ng/ml)
Control	6	2.19 ± 0.48
1h	6	1.85 ± 0.37^a
2h	6	1.95 ± 0.45^a
4h	6	1.76 ± 0.27^a
8h	6	1.79 ± 0.27^a
12h	6	1.77 ± 0.20^a
24h	6	1.79 ± 0.55^a

^aStatistically no difference compared with control rats.

Liver IGF-I mRNA expression

Liver IGF-I mRNA expression had already declined by 25% vs. control rats at 8 hours. On the time of 12 hours, we observed the lowest level of expression, which was a 53% decrease compared with control rats. It did not recover to the normal level and had a 15% reduction at 24 hours (Figure 1A, 1B). Although exogenous GH administration in control rats significantly enhanced the liver IGF-I mRNA expression, it did fail to prevent its decline in endotoxemic rats (Figure 1C).

Liver GHR mRNA expression

Liver GHR mRNA expression had already down-regulated by 45% at 2 hours after LPS injection, the lowest regulation occurred at 8 hours, which was a 89% decrease compared with control rats. After 24 hours, it did not recover to the normal level and had a 44% decrease (Figure 2A, 2B). the exogenous GH administration had no effect on the liver GHR mRNA expression in control and endotoxemic rats (Figure 2C).

Liver SOCS-3 mRNA expression

The liver SOCS-3 mRNA was weakly expressed in control rats, however, it was strongly up-regulated by 7.84 times *vs.* control rats at 1 hour after LPS injection. This level was maintained at 2 hours and it still had a 1.8 times increase at 24 hours (Figure 3A, 3B). the exogenous GH infusion had no effect on the liver SOCS-3 mRNA expression in control and endotoxemic rats (Figure 3C).

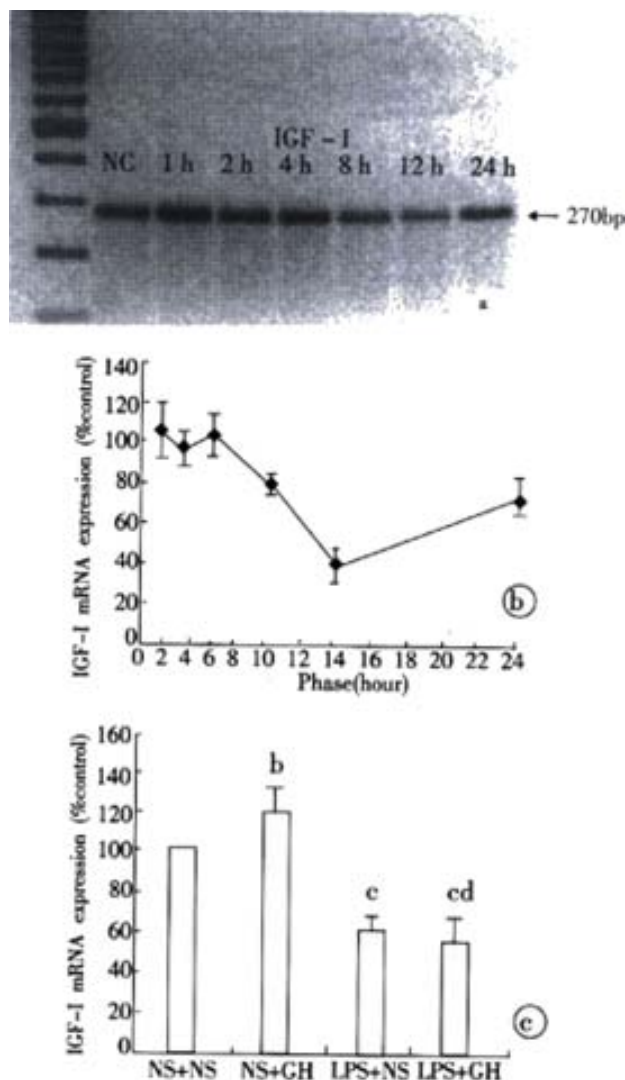


Figure 1 (A, B) Liver IGF-I mRNA expression response to endotoxin injection at different time points. (C) Liver IGF-I mRNA expression after single GH injection and endotoxin injection along with or without GH injection. ^b*P*<0.05 compared with NS+NS group, ^c*P*<0.01 *vs* NS+NS group, ^d*P*>0.05 compared with LPS+NS group. NS as saline injection.

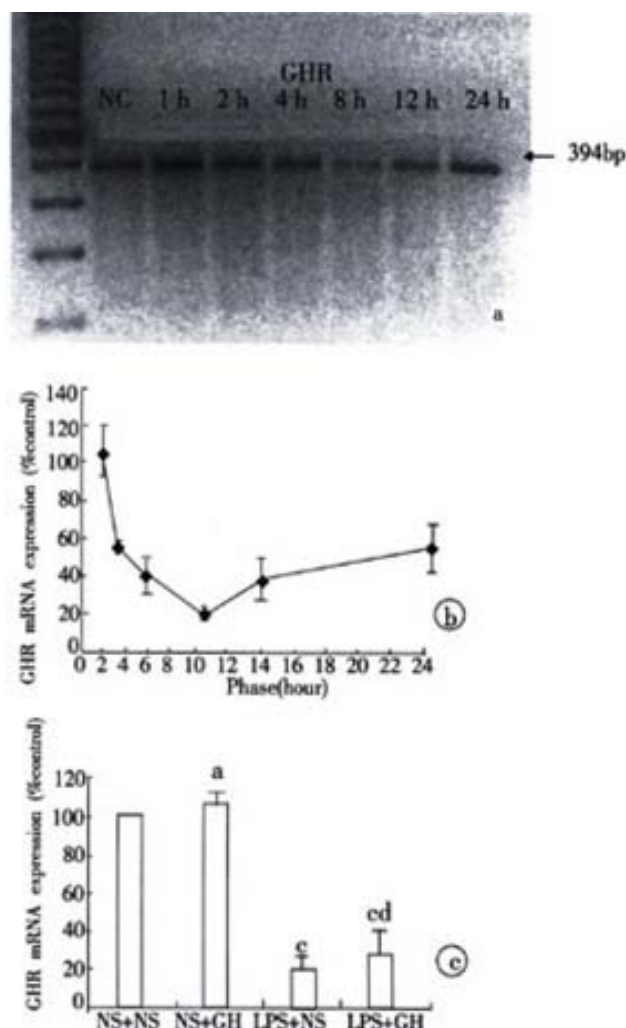


Figure 2 (A, B) Liver GHR mRNA expression responded to endotoxin injection at different time points. (C) Liver GHR mRNA expression after single GH injection and endotoxin injection along with or without GH injection. ^a*P*>0.05 compared with NS+NS group, ^c*P*<0.01 *vs* NS+NS group, ^d*P*>0.05 compared with LPS+NS group. NS as saline injection.

Levels of serum TNF- α and IL-6 after LPS injection and the correlation between liver SOCS-3 mRNA expression and IL-6 concentration

The TNF- α level was increased rapidly after LPS injection, but it decreased obviously from the second hour and returned to the normal level at 4h. The IL-6 level was also elevated rapidly after LPS injection; it got to the highest level at 2h and then decreased gradually (Table 2). Linear regression analysis was shown a positive correlation of IL-6 with liver SOCS-3 mRNA expression ($r=0.935$, $P<0.01$).

Table 2 Serum TNF- α and IL-6 levels in LPS injected rats at different time points and control rats

	<i>n</i>	TNF- α levels(pg/ml)	IL-6 levels(pg/ml)
Control	6	<20	<8
1h	6	342.80 \pm 50.01	1438.74 \pm 323.07
2h	6	75.81 \pm 11.50	1678.03 \pm 126.57
4h	6	<20	1332.67 \pm 120.95
8h	6	<20	142.59 \pm 48.07
12h	6	<20	48.75 \pm 10.57
24h	6	<20	46.82 \pm 11.64

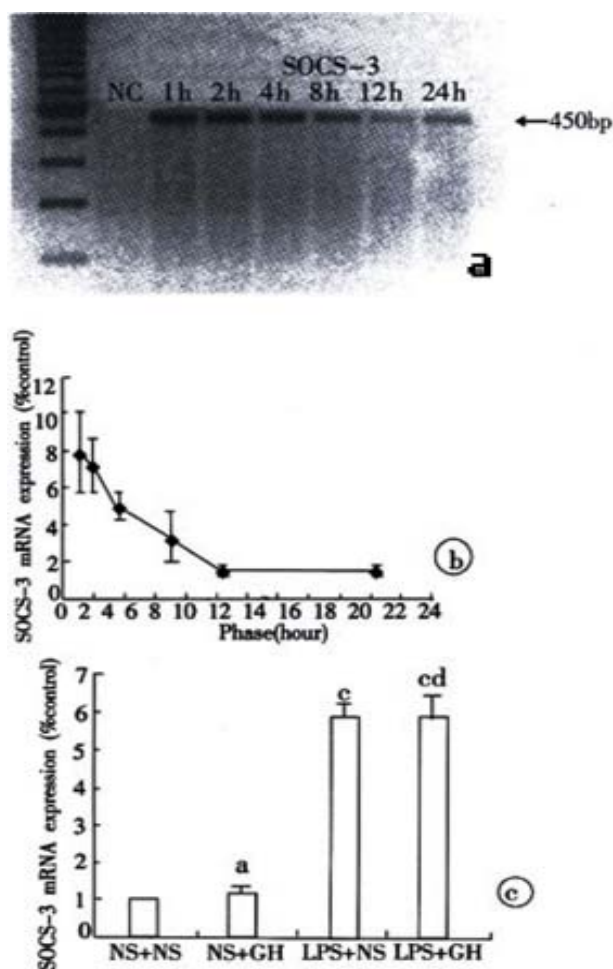


Figure 3 (A, B) Liver SOCS-3 mRNA expression response to endotoxin injection at different time points. (C) Liver SOCS-3 mRNA expression after endotoxin injection along with or without GH injection. ^a $P > 0.05$ compared with NS+NS group, ^c $P < 0.01$ vs NS+NS group, ^d $P > 0.05$ compared with LPS+NS(7.5) group. NS as saline injection.

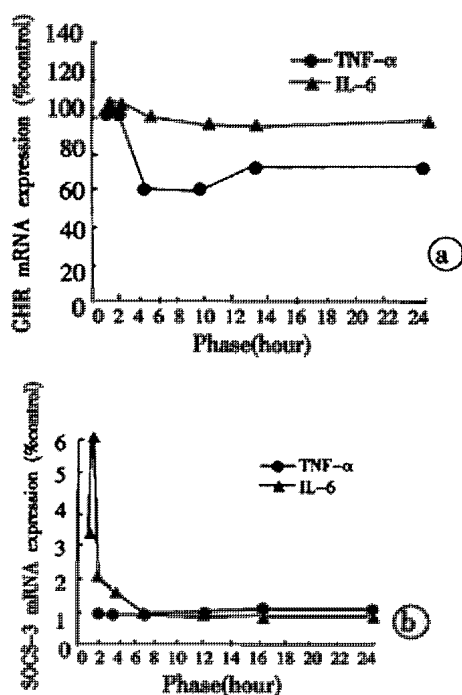


Figure 4 Liver GHR(A) and SOCS-3(B) mRNA expression response to TNF-α and IL-6 iv injection at different time points.

Effects of TNF-α and IL-6 on liver expression of GHR and SOCS-3 mRNA

The liver GHR mRNA expression after TNF-α injection had already down-regulated at 4 hours and it reached the lowest level at 8 hours, which was a 40% decrease compared with control rats. At 24 hours, a 27% reduction still existed. The IL-6 injection had no effect on the liver GHR mRNA expression at different time points (Figure 4A). The liver SOCS-3 mRNA had weak expressions at all time points after TNF-α injection, no difference could be found compared with control rats. The IL-6 injection was able to up-regulate rapidly the liver SOCS-3 mRNA expression, the latter showing a 2.73 times increase at 20 minutes and the highest level occurred at 40 minutes with a 4.94 times increase compared with control rats (Figure 4B).

DISCUSSION

In this report, using an experimental method of *E. coli* endotoxin infusion in laboratory rats, we have found endotoxin-induced growth hormone insensitivity. At 12 hours after LPS injection, there was no difference in serum growth hormone concentration between the experimental and control rats, however, the liver IGF-I mRNA expression had already declined obviously. In control rats, the liver IGF-I mRNA expression was up-regulated by 25% after exogenous GH administration, but in endotoxemic rats, GH did fail to prevent the decline in liver IGF-I mRNA expression. Several groups have observed that decreased IGF-I may result from a state of GH insensitivity. Ross *et al*^[8] reported low circulating IGF-I levels in critically ill patients despite elevated GH secretion. More recently, the study^[19] showed that after a single injection of LPS in rats, plasma IGF-I level remained low despite the fact that GH level had returned to normal value. In agreement with these authors, our study support the possibility that the GH insensitivity maybe one of the important factors for the reduced liver IGF-I mRNA expression after LPS injection.

Growth hormone insensitivity can occur at receptor and post receptor levels, on the receptor level GH insensitivity is associated with the reduced GHR numbers on target cell surface^[19,20]. Because of the shorter half-life of liver GHR (30-40min)^[23] and the decreased liver GHR mRNA expression by endotoxin, these led to the reduced GHR synthesis. Our results shown that liver GHR mRNA expression was obviously down-regulated after LPS injection, manifested that LPS had effect on the receptor level GH insensitivity indeed.

The factor of post-receptor level GH insensitivity has caused more and more attention recently, and it is associated with a novel family of suppressor of cytokine signalling (SOCS) which includes eight members (SOCS-1 to SOCS-7 and CIS) that act in a classical negative feedback loop to regulate cytokine signal transduction^[24-29]. SOCS-3 is a strong inhibitor on growth hormone intracellular signal transduction^[30-32].

Once growth hormone binds to its receptor, the intracellular signal transduction is activated through JAK-STAT pathway^[33,34]. The first activated tyrosine kinase is JAK2, which promotes the tyrosyl phosphorylation of both JAK2 itself and signal transducer and activator of transcription 5b (STAT 5b). Phosphorylated STAT 5b causes its dimerization and then the dimerized STAT 5b translocates into the nucleus, where it binds with high affinity to the promoters of various target genes and then activates the gene transcription such as IGF-I. SOCS-3 can block the GH intracellular JAK/STAT-dependent signaling pathway at different levels^[35-44], including competitively inhibits the phosphorylation of STAT 5b. Binds to GHR and leads to the degradation of GHR-JAK2 compound directly or indirectly through Elongin B and Elongin C, in the end the JAK2 kinase loses its activity. Through binding to GHR, SOCS-3 can inhibit the JAK2 kinase activity directly. Our experiment observed that after LPS injection, liver SOCS-3 mRNA expression was rapidly up-regulated with a 7.84 times increase at 1 hour compared with the weak expression in control rats, this

indicating that LPS induced the production of post-receptor GH insensitivity.

The *in vivo* biological activities of LPS are largely mediated by the production of proinflammatory cytokines such as tumor necrosis factor- α (TNF- α), interleukin-1 β (IL-1 β), and IL-6^[45-50], which is illustrated in our experiment by the marked stimulation of the secretion of TNF- α and IL-6 in blood. TNF- α and IL-6 had different roles in inducing the GH insensitivity, TNF- α injection leading to a reduced expression of liver GHR mRNA, and IL-6 being associated with the up-regulated SOCS-3 mRNA expression after injection. The elevated IL-6 levels stimulated by LPS had significant positive correlation with the increased liver SOCS-3 mRNA expression induced by LPS.

The mechanisms of TNF- α -induced GHR mRNA suppression was mostly mediated by inhibition of Sp transactivator binding to the L2 promoter of GHR gene^[51], the other way might be associated with some other cytokines stimulated by TNF- α , such as IL-1^[52]. Both IL-6 and GH, belonging to the cytokine receptor superfamily, can transduce their signal from cell surface to nucleus through the same JAK-STAT pathway^[53-55]. Hence, the elevated IL-6 levels stimulated by LPS promoted the increased expression of SOCS-3 mRNA, which not only had a negative feedback to IL-6 biological activities, but also inhibited the GH intracellular signal transduction^[56-60].

In summary, our study observed that the growth hormone insensitivity could be induced by endotoxin, which suggested that the endotoxin played a very important role in inducing the GH insensitivity. The endotoxin not only had predominant effect on the GHR gene expression, but also induced the phenomenon of negative feedback loop at post-receptor level. The toxic effect of endotoxin was mostly mediated by TNF- α and IL-6 indirectly, and TNF- α mainly had effect on the receptor gene expression, but for IL-6, it mainly caused the negative feedback loop at post-receptor level.

REFERENCES

- Wu XN. Current concept of pathogenesis of severe acute pancreatitis. *World J Gastroenterol* 2000;6:32-36
- Wu XN. Treatment revisited and factors affecting prognosis of severe acute pancreatitis. *World J Gastroenterol* 2000;6:663-665
- Zhang JJ, Dong WF, Zhu ZY. The clinical significance and rational evaluation of early nutritional support in severe head-injured patients. *World J Gastroenterol* 2000;6(Suppl3):20
- Chen QP. Enteral nutrition and acute pancreatitis. *World J Gastroenterol* 2001;7:185-192
- Mitch WE, Bailey JL, Wang X, Jurkovitz C, Newby D, Price SR. Evaluation of signals activating ubiquitin-proteasome proteolysis in a model of muscle wasting. *Am J Physiol* 1999;276:C1132-C1138
- Breuille D, Voisin L, Contrepois M, Arnal M, Rose F, Obled C. A sustained rat model for studying the long-lasting catabolic state of sepsis. *Infect Immun* 1999;67:1079-1085
- Voisin L, Breuille D, Combaret L, Pouyet C, Taillandier D, Aurousseau E, Obled C, Attia D. Muscle wasting in a rat model of long-lasting sepsis results from the activation of lysosomal, Ca²⁺-activated, and ubiquitin-proteasome proteolytic pathways. *J Clin Invest* 1996;97:1610-1617
- Ross BJM, Chew SL. Acquired growth hormone resistance. *Eur J Endocrinol* 1995; 132:655-660
- Bhutta ZA, Bang P, Karlsson E, Hagenas L, Nizami SQ, Soder O. Insulin-like growth factor I response during nutritional rehabilitation of persistent diarrhoea. *Arch Dis Child* 1999;80:438-442
- Vary TC, Dardevet D, Grizard J, Voisin L, Buffiere C, Denis P, Breuille D, Obled C. Differential regulation of skeletal muscle protein turnover by insulin and IGF-I after bacteremia. *Am J Physiol* 1998;275:E584-E593
- Bjarnason R, Wickelgren R, Hermansson M, Hammarqvist F, Carlsson B, Carlsson LMS. Growth hormone treatment prevents the decrease in insulin-like growth factor I gene expression in patients undergoing abdominal surgery. *J Clin Endocrinol Metab* 1998;83:1566-1572
- Hobler SC, Williams AB, Fischer JE, Hasselgren PO. IGF-I stimulates protein synthesis but does not inhibit protein breakdown in muscle from septic rats. *Am J Physiol* 1998;274:R571-R576
- Takala J, Roukonen E, Webster NR, Nielsen MS, Zandstra DF, Vundelinckx G, Hinds CJ. Increased mortality associated with growth hormone treatment in critically ill adults. *N Eng J Med* 1999;341:785-792
- Wang JY, Wang XL, Liu P. Detection of serum TNF- α , IFN- γ , IL-6 and IL-8 in patient with hepatitis B. *World J Gastroenterol* 1999;5:38-40
- Sanlioglu S, Williams CM, Samavati L, Butler NS, Wang G, McCray PB, Ritchie TC, Hunninghake GW, Zandi E, Engelhardt JF. Lipopolysaccharide induces rac1-dependent reactive oxygen species formation and coordinates tumor necrosis factor- α secretion through IKK regulation of NF- κ B. *J Biol Chem* 2001;276:30188-30198
- Ebong SJ, Goyyert SM, Nemzek JA, Kim J, Bolgos GL, Remick DG. Critical role of CD14 for production of proinflammatory cytokines and cytokine inhibitors during sepsis with failure to alter morbidity or mortality. *Infect Immun* 2001;69:2099-2106
- Krakauer T. Suppression of endotoxin- and staphylococcal exotoxin-induced cytokines and chemokines by a phospholipase C inhibitor in human peripheral blood mononuclear cells. *Clin Diagn Lab Immunol* 2001;8:449-453
- Massoudy P, Zahler S, Becker BF, Braun SL, Barankay A, Meisner H. Evidence for inflammatory responses of the lungs during coronary artery bypass grafting with cardiopulmonary bypass. *Chest* 2001;119:31-36
- Defalque D, Brandt N, Ketelslegers JM, Thissen JP. GH insensitivity induced by endotoxin injection is associated with decreased liver GH receptors. *Am J Physiol* 1999;276:E565-E572
- Hermansson M, Wickelgren RB, Hannarquist F, Bjarnason R, Wennstrom I, Wernerman J, Carlsson B, Carlsson LM. Measurement of human growth hormone receptor messenger ribonucleic acid by a quantitative polymerase reaction-based assay: demonstration of reduced expression after elective surgery. *J Clin Endocrinol Metab* 1997;82:421-428
- Nicholson SE, Hilton DJ. The SOCS protein: a new family of negative regulators of signal transduction. *J Leuko Biol* 1998;63:665-668
- Alexander WS, Starr R, Metcalf D, Nicholson SE, Farley A, Elefanti AG, Brysha M, Kile BT, Richardson R, Baca M, Zhang JG, Willson TA, Viney EM, Sprigg NS, Rakar S, Corbin J, Mifsud S, Dirago L, Cary D, Nicola NA, Hilton DJ. Suppressors of cytokine signaling (SOCS): negative regulators of signal transduction. *J Leukoc Biol* 1999;66:588-592
- Frick GP, Tai LR, Baumbach WR, Goodman HM. Tissue distribution, turnover, and glycosylation of the long and short growth hormone receptor isoforms in rat tissues. *Endocrinology* 1998;139:2824-2830
- Kreba DL, Hilton DJ. SOCS proteins: negative regulators of cytokine signaling. *Stem Cells* 2001;19:378-387
- Stoiber D, Kovarik P, Cohnsey S, Johnston JA, Steinlein P, Decker T. Lipopolysaccharide induces in macrophages the synthesis of the suppressor of cytokine signaling 3 and suppresses signal transduction in response to the activating factor IFN- γ . *J Immunol* 1999;163:2640-2647
- Pezet A, Favre H, Kelly PA, Edery M. Inhibition and restoration of prolactin signal transduction by suppressor of cytokine signaling. *J Biol Chem* 1999;274:24497-24502
- Bjerkbak C, Haschimi KE, Frantz JD, Flier JS. The role of SOCS-3 in leptin signaling and leptin resistance. *J Biol Chem* 1999;274:30059-30065
- Hilton DJ, Richardson RT, Alexander WS, Viney EM, Willson TA, Sprigg NS, Starr R, Nicholson SE, Metcalf D, Nicola NA. Twenty proteins containing a C-terminal SOCS box form five structural classes. *Proc Natl Acad Sci USA* 1998;95:114-119
- Gisselbrecht S. The CIS/socs proteins: a family of cytokine-inducible regulators of signaling. *Euro Cytokine Network* 1999;10:463-470
- Mao Y, Ling PR, Fitzgibbons TP, McCowen KC, Frick GP, Bistrrian BR, Smith RJ. Endotoxin-induced inhibition of growth hormone receptor signaling in rat liver *in vivo*. *Endocrinology* 1999;140:5505-5515
- Petra TE, Amilcar FM, Anneli SE, Lena S, Gunnar N. Growth hormone regulation of SOCS-2, SOCS-3, and CIS messenger ribonucleic acid expression in the rat. *Endocrinology* 1999;140:3693-3704
- Adams TE, Hansen JA, Starr R, Nicola NA, Hilton DJ, Billestrup N. Growth hormone preferentially induces the rapid, transient expression of SOCS-3, a novel inhibitor of cytokine receptor signaling. *J Biol Chem* 1998;273:1285-1287
- Argetsinger LS, Christin CS. Mechanism of signaling by growth hormone receptor. *Physiol Rev* 1996;74:1089-1107
- Han Y, Leaman DW, Watling D, Rogers NC, Groner B, Kerr IM, Wood WI, Stark GR. Participation of JAK and STAT proteins in growth hormone-induced signaling. *J Biol Chem* 1996;271:5947-5952
- Hansen JA, Lindberg K, Hilton DJ, Nielsen JH, Billestrup N. Mechanism of inhibition of growth hormone receptor signaling by suppressor of cytokine signaling proteins. *Mol Endocrinol* 1999;13:1832-1843
- Ram PA, Waxman DJ. SOCS/CIS protein inhibition of growth hormone-stimulated STAT5 signaling by multiple mechanisms. *J Biol Chem* 1999;274:35553-35561
- Zhang JG, Farley A, NicholSEN SE, Willson TA, Zugarot LM, Simpsont RJ, Moritz RL, Cary D, Richardson R, Hausmann G, Kile BJ, Kent SBH, Alexander WS, Metcalf D, Hilton DJ, Nicola NA, Baca M. The conserved SOCS box motif in suppressors of cytokine signaling binds to elongin B and C and may couple bound proteins to proteasomal degradation. *Proc Natl Acad Sci USA* 1999;96:2071-2076
- Biosclair YR, Wanf JR, Shi JR, Hurst KR, Ooi GT. Role of the suppressor of cytokine signaling-3 in mediating the inhibitory effects of

- interleukin-1 β on the growth hormone-dependent transcription of the acid-labile subunit gene in liver cells. *J Biol Chem* 2000;275:3841-3847
- 39 Schaefer F, Chen Y, Tsao T, Nouri P, Rabkin R. Impaired JAK-STAT signal transduction contributes to growth hormone resistance in chronic uremia. *J Clin Invest* 2001;108:467-475
- 40 Kamizono S, Hanada T, Yasukawa H, Minoguchi S, Kato R, Minoguchi M, Hattori K, Hatakeyama S, Yada M, Morita S, Kitamura T, Kato H, Nakayama K, Yoshimura A. The SOCS box of SOCS-1 accelerates ubiquitin-dependent proteolysis of TEL-JAK2. *J Biol Chem* 2001;276:12530-12538
- 41 Ram PA, Waxman DJ. Role of the cytokine-inducible SH2 protein CIS in desensitization of STAT5b signaling by continuous growth hormone. *J Biol Chem* 2000;275:39487-39496
- 42 Sasaki F, Yasukawa I, Shouda T, Kitamura T, Dikic I, Yoshimura A. CIS3/SOCS-3 suppresses erythropoietin(EPO) signaling by binding the EPO receptor and JAK2. *J Biol Chem* 2000;275:29338-29347
- 43 Cohnsey SJ, Sanden D, Cacalano NA, Yoshimura A, Mui A, Migone TS, Johnston JA. SOCS-3 is tyrosine phosphorylated in response to interleukin-2 and suppresses STAT5 phosphorylation and lymphocyte proliferation. *Mol Cell Biol* 1999;19:4980-4988
- 44 Song MM, Shuai K. The suppressor of cytokine signaling (SOCS)1 and SOCS3 but not SOCS2 proteins inhibit interferon-mediated antiviral and antiproliferative activities. *J Biol Chem* 1998;273:35056-35062
- 45 Dinarello CA. proinflammatory cytokines. *Chest* 2000;118:503-508
- 46 Iwagaki A, Porro M, Pollack M. Influence of synthetic antiendotoxin peptides on lipopolysaccharide(LPS) recognition and LPS-induced proinflammatory cytokine responses by cell expressing membrane-bound CD14. *Infect Immun* 2000;68:1655-1663
- 47 Zhao B, Brauner A, Li YH, Normark S. Expression of and cytokine activation by Escherichia coli curli fibers in human sepsis. *J Infect Diseases* 2000;181:602-612
- 48 Bruggen TVD, Jenhuis SN, Raaij EV, Verhouf J, Asbeck BSV. Lipopolysaccharide-induced tumor necrosis factor alpha production by human monocytes involves the Raf-1/MEK1-MEK2/ERK1-ERK2 pathway. *Infect Immun* 1999;67:3824-3829
- 49 Soltys J, Quinn MT. Modulation of endotoxin- and enterotoxin-induced cytokine release by in vivo treatment with β -(1,6) branched β -(1,3)-glucan. *Infect Immun* 1999;67:244-252
- 50 Thissen JP, Verniers J. Inhibition by interleukin-1 β and tumor necrosis factor- β of the insulin-like growth factor I messenger ribonucleic acid response to growth hormone in rat hepatocyte. *Endocrinology* 1997;138:1078-1084
- 51 Denson LA, menon RK, Shaufl A, Bajwa HS, Williams CR, Karpen SJ. TNF- α downregulates murine hepatic growth hormone receptor expression by inhibiting Sp1 and Sp3 binding. *J Clin Invest* 2001; 107:1451-1458
- 52 Wolf M, Bohm S, Brand M, Kreymann G. Proinflammatory cytokines interleukin-1 β and tumor necrosis factor- α inhibit growth hormone stimulation of insulin-like growth factor I synthesis and growth hormone receptor mRNA levels in cultured rat liver cells. *Eur J Endocrinol* 1996;135:729-737
- 53 Heinrich PC, Behrmann I, Newen GM, Schaper F, Graeve L. Interleukin-6-type cytokines signaling through the gp130/Jak/STAT pathway. *Biochem J* 1998;334:297-314
- 54 Kishimoto T, Akira S, Narazaki M, Taga T. Interleukin-6 family of cytokines and gp130. *Blood* 1995;86:1243-1254
- 55 Chen TS, wang LH, Farrar WL. Interleukin 1 activates androgen receptor-mediated gene expression through a signal transducer and activator of transcription 3-dependent pathway in LNCap prostate cancer cells. *Cancer Res* 2000;60:2132-2135
- 56 Paul C, Seilliez I, Thissen JP, Cam AL. Regulation of expression of the rat SOCS-3 gene in hepatocytes by growth hormone, interleukin-6 and glucocorticoids. *Eur J Biochem* 2000;267:5849-5857
- 57 Narazaki M, Fujimoto M, Matsumoto T, Morita Y, Saito H, Kajita T, Yashizaki K, Naka T, Kishimoto T. Three distinct domains of SSI-1/SOCS-1/JAB protein are required for its suppression of interleukin-6 signaling. *Proc Natl Acad Sci USA* 1998;95:13130-13134
- 58 Nicholson SE, Willson TA, Farley A, Starr R, Zhang JG, Baca M, Alexander WS, Metcalf D, Hilton DJ, Nicola NA. Mutational analyses of the SOCS proteins suggest a dual domain requirement but distinct mechanisms for inhibition of LIF and IL-6 signal transduction. *EMBO J* 1999;18:375-385
- 59 Terstegen L, Gatsios P, Bode JG, Schaper F, Heinrich PC, Graeve L. The inhibition of interleukin-6-dependent STAT activated protein kinases depends on tyrosine 795 in the cytoplasmic tail of glycoprotein 130. *J Biol Chem* 2000;275:18810-18817
- 60 Schmitz J, Weissenbach M, Haan S, Heinrich PC, Schaper F. SOCS-3 exerts its inhibitory function on interleukin-6 signal transduction through the SHP2 recruitment site of gp130. *J Biol Chem* 2000;275:12848-12856

Edited by Zhao P

• BASIC RESEARCH •

Distribution of constitutive nitric oxide synthase in the jejunum of adult rat

Yan-Min Chen, Zhong-Ming Qian, Jian Zhang, Yan-Zhong Chang, Xiang-Lin Duan

Yan-Min Chen, Jian Zhang, Yan-Zhong Chang, Xiang-Lin Duan, Life Science College, Hebei Normal University, Shijiazhuang 050016, Hebei Province, China

Zhong-Ming Qian, Department of Applied Biology and Chemical Technology, The Hong Kong Polytechnic University, Hung Hom, Kowloon, Hong Kong

Supported by Natural Science Foundation of Hebei Province; Education Department Foundation of Hebei Province. No. 2002136.

Correspondence to: Xiang-Lin Duan, Life Science College, Hebei Normal University, Shijiazhuang 050016, Hebei Province, China. dxlzh@sj-user.he.cninfo.net

Telephone: +86-311-6049941 Ext.86480 Fax: +86-311-5828784

Received 2002-01-11 Accepted 2002-01-28

Abstract

AIM: To study the distribution of the constitutive nitric oxide synthase (NOS) in the jejunum of adult rat.

METHODS: The distribution of endothelial NOS (eNOS) was detected by immunohistochemistry. Immunofluorescence histochemical dual staining technique were used for studying the distribution of neuronal NOS (nNOS) and eNOS. The dual stained slides were observed under a confocal laser scanning microscope.

RESULTS: Positive neuronal NOS (nNOS) and endothelial NOS (eNOS) cells were found to be distributed in lamina propria of villi, and the epithelial cell was not stained. eNOS was mainly located in submucosal vascular endothelia, while nNOS was mainly situated in myenteric plexus. Some cells in the villi had both nNOS and eNOS. More than 80% of the cells were positive for both nNOS and eNOS, the rest cells were positive either for nNOS or for eNOS.

CONCLUSION: The two constitutive nitric oxide synthases are distributed differently in the jejunum of rat. nNOS distributed in myenteric plexus is a neurotransmitter in the non-adrenergic non-cholinergic (NANC) inhibitory nerves. eNOS distributed in endothelial and smooth muscle cells of blood vessels plays vasodilator role. eNOS and nNOS are coexpressed in some cells of lamina propria of villi. NO generated by those NOS is very important in the physiological and pathological process of small intestine.

Chen YM, Qian ZM, Zhang J, Chang YZ, Duan XL. Distribution of constitutive nitric oxide synthase in the jejunum of adult rat. *World J Gastroenterol* 2002;8(3):537-539

INTRODUCTION

Nitric oxide (NO) is an intercellular and endocellular signal molecule, and has an important role in the physiological process of intestine. For example, NO can regulate muscular contraction and blood circulation of the intestine^[1,2]. Nitric oxide synthase (NOS) is widely distributed in the intestine, and has several isoforms, such as constitutive nitric oxide synthase (nNOS and eNOS) and inducible NOS (iNOS)^[3]. In previous studies, NOS was mostly located in small intestine and could be shown by enzyme cytochemistry, but different isoforms of NOS^[4-8] could not be distinguished. In order to study the characteristics and distribution of NOS,

immunohistochemistry and immunofluorescence histochemical dual staining technique were used to investigate the distribution of the constitutive nitric oxide synthase (NOS) in the jejunum of adult rat, to provide morphological basis of digestive physiology.

MATERIALS AND METHODS

Specimens

Segments (1-2cm) of the jejunum were removed from decapitated male Sprague-Dawley rats (250-300g) and placed immediately in a fixative consisting of 4% paraformaldehyde and 0.1 M phosphate buffer (PB, pH7.4). The fixed jejunum segments were rinsed for at least 12h at 4°C in 0.1 M PB (pH7.2) containing 30% sucrose, and then cryostat sections were made at 6µm thickness and mounted onto glass slides.

Reagents

Rabbit anti-rat eNOS antibody and SP kit were purchased from Beijing Zhongshan Biotechnical Company. Mouse anti-rat nNOS antibody, FITC-conjugated anti-mouse IgG and PE-conjugated anti-rabbit IgG were purchased from Wuhan Boster Biological Technology Company.

Immunohistochemistry

Immunohistochemical staining for eNOS was performed using SP technique with the following procedure.

(1)The slides were washed in 0.01 M phosphate-buffered saline (PBS). Endogenous peroxidase was blocked by 0.3% H₂O in methanol for 25 minutes, followed by incubation in normal goat serum for 30 minutes at room temperature. (2)The slides were incubated with a 1 : 75 dilution of the primary rabbit anti-rat eNOS antibody for 12 hour at 4°C. A biotin-streptavidin detection system was employed with diaminobenzidine as the chromogen. (3)Then the slides were washed with PBS and incubated with a reagent (biotinylated anti-immunoglobulin) for 60 minutes at 37°C. After rinsing in PBS, the slides were incubated with the peroxidase-conjugated streptavidin label for 60 minutes at 37°C, and incubated with diaminobenzidine and H₂O₂ for 5 minutes. Finally the sections were counterstained with hematoxylin.

Immunofluorescence histochemical dual-staining technique

The slides were incubated with normal goat serum for 30 minutes, followed by incubation with rabbit anti-rat eNOS antibody and mouse anti-rat nNOS antibody for 48 hour at 4°C. Then, These were washed with PBS and incubated with FITC-conjugated anti-mouse IgG and PE-conjugated anti-rabbit IgG for 24 hour at 4°C. After rinsing in PBS, the slides were observed under a confocal laser scanning microscope (MR/A₂, Nikon). Excitation of FITC and PE were 488 and 495 nm respectively, emission of FITC and PE were 525 and 578 nm. 0.01 M PBS was used as a substitute for primary antibody for negative control groups.

RESULTS

Immunohistochemistry showed that eNOS was localized in the cytoplasm solely. eNOS was distributed mainly in the endothelia of submucosa vessels. Part of the smooth muscle of submucosa vessels was also positive

for eNOS (Figure 1). There were strongly positive substances in the cells of lamina propria of the villi, and in the cells near the striated border of villous epithelia. The epithelial cells were unstained (Figure 2).

Under the confocal laser scanning microscope, the positive substances of nNOS labeled by FITC were green, and those of eNOS

labeled by PE were red. The positive substances of nNOS were distributed mainly in myenteric plexus, rarely in the submucosal plexus (Figure 3). In the lamina propria of the villi, more than 80% of the cells were positive for both nNOS and eNOS, the rest of them were positive either for nNOS or for eNOS (Figure 4 and 5).

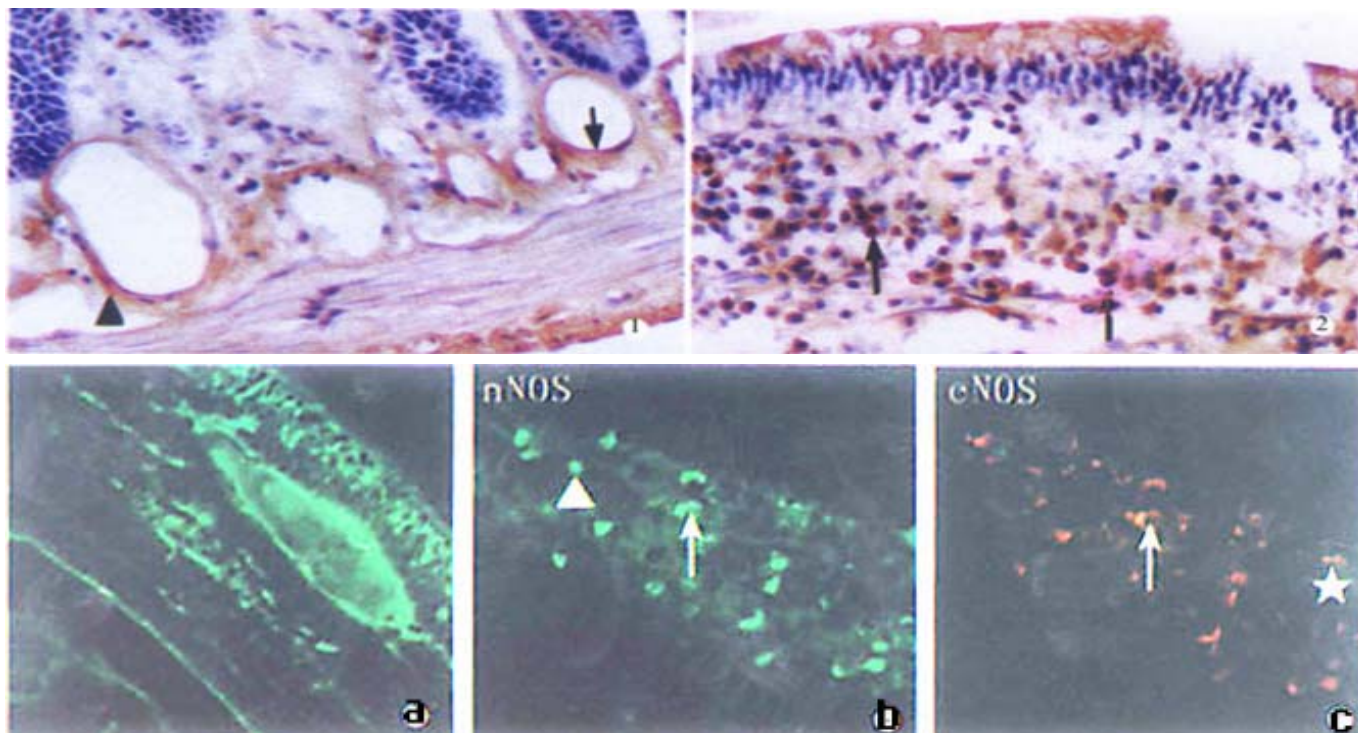


Figure 1 Immunohistochemical stain of eNOS in jejunal submucosa, showing the positive endothelium(↑) and microvascular smooth muscle(▲). ×170

Figure 2 Immunohistochemical stain of eNOS in jejunal villi, showing the positive cell in the proper layer(↑). ×170

Figure 3-4-5 Immunofluorescence histochemical double-stain in jejunum observed under a confocal laser scanning microscope, fig3 showing the positive substances of nNOS were distributed mainly in myenteric plexus. ×350 fig4 and fig5 showing the nNOS-positive cell(▲), the eNOS-positive cell(★) and double-stained cell(↑) in the proper layer of villi. ×250

DISCUSSION

The two constitutively expressed, Ca^{2+} -dependent NOS isoforms previously identified in neurons (nNOS) and endothelial cells (eNOS) are now known to be distributed more widely^[9-11]. eNOS is found in cardiac myocytes^[12,13], epithelial cells^[14-16], human platelets^[17] and various neurons, particularly the pyramidal neurons of the hippocampus, where it is coexpressed with nNOS^[18]. nNOS is found in the cytoskeleton of fast-contracting skeletal muscle fibers^[19]. In our study, we found nNOS and eNOS were coexpressed in some cells of lamina propria of the villi. NO generated by those cells plays an important role in absorption and protection of microvasculature. Inhibition of endogenous NOS by N_G -nitro-L-arginine methyl ester (L-NAME) caused secretion of water and ions, and this secretion was reversed by administration of the NOS substrate L-arginine^[20]. Previous studies indicated that norepinephrine^[21, 22], somatostatin^[23], and neuropeptide Y^[24] increased ileal water and ion absorption at a similar magnitude to that observed with L-arginine. It is consistent with the hypothesis that endogenous NO has a proabsorptive influence in the intestine in the basal state. Furthermore, endogenous NO can reduce the vascular albumin leakage provoked by lipopolysaccharide (LPS)^[25] and maintain microvascular integrity^[26-29].

Our study showed that nNOS was distributed mainly in the myenteric plexus, rarely in submucosal plexus. Recent pharmacological and physiological studies demonstrated that NO is a neurotransmitter in the non-adrenergic non-cholinergic (NANC)

inhibitory nerves of the gut^[30-34]. During nerve stimulation, NO generated by nNOS in nerve terminals regulates the release of vasoactive intestinal polypeptide (VIP) when diffuses to muscle cells to participate in muscle relaxation^[35-38]. Teng *et al*^[39] found eNOS was selectively expressed in rabbit gastric and human intestinal smooth muscle cells. In turn, VIP acts on smooth muscle cells to generate NO. The NO formed in the muscle cells constitutes the predominant component (60-80%) of NO formed during nerve stimulation.

Using NOS histochemistry and endothelial cell immunohistochemistry, Nichols *et al*^[40] provided the first anatomic evidence of NOS in both endothelial and smooth muscle cells of submucosal blood vessels in the intestines of rat and human, but he could not distinguish the isoform. We found eNOS was distributed in the endothelial and smooth muscle cells of submucosal blood vessels. This particular localization of eNOS was unexpected since only the inducible isoform of NOS had been reported in the vascular smooth muscle cells^[41-44]. These anatomical data strongly supported the proposed vasodilator role of NO in the mammalian gastrointestinal tract. There is both basal and stimulated release of NO from the endothelium. Stimulated NO release is affected by certain antagonists (acetylcholine, ATP, or bradykinin) or by physical stimuli such as fluid shear stress^[45-49] or low arterial PO_2 ^[50]. Vascular smooth muscle-derived NO behaves as an autocrine factor that plays a role in modulation of vasodilator tone and represents a reserve pool of NOS, which may be required when the tissue is under a local stress. The

source of NO within the vascular wall, either intimal or medial, should be a consideration in future studies in terms of the relative contribution of these sources to vasodilator tone in the gut wall.

REFERENCES

- Eskandari MK, Kalff JC, Billiar TR, Lee KK, Bauer AJ. LPS-induced muscularis macrophage nitric oxide suppresses rat jejunal circular muscle activity. *Am J Physiol* 1999;277:G478-486
- Konomi H, Meedeniya AC, Simula ME, Toouli J, Saccone GT. Characterization of circular muscle motor neurons of the duodenum and distal colon in the Australian brush-tailed possum. *J Comp Neurol* 2002;443:15-26
- Peng X, Wang SL. Nitric oxide and gastrointestinal movement. *Shijie Huaren Xiaohua Zazhi* 1998; 6:445-446
- Peng X, Feng JB, Wang SL. Distribution of nitric oxide synthase in stomach wall in rats. *World J Gastroenterol* 1999;5:92
- Nichols K, Staineds W, Krantis A. Nitric oxide synthase distribution in the rat intestine: a histochemical analysis. *Gastroenterology* 1993; 105:1651-1661
- Bagyanszki M, Roman V, Fekete E. Quantitative distribution of NADPH-diaphorase-positive myenteric neurons in different segments of the developing chicken small intestine and colon. *Histochem J* 2000;32:679-684
- Peng X, Feng JB, Wang SL. Nitric oxide synthase distribution in myenteric plexus of rat digestive tract. *Shijie Huaren Xiaohua Zazhi* 1998;6:250-252
- Wilhelm M, Batori Z, Pasztor I, Gabriel R. NADPH-diaphorase positive myenteric neurons in the ileum of guinea-pig, rat, rabbit and cat: a comparative study. *Eur J Morphol* 1998;36:143-152
- Bredt DS, Hwang PM, Glatt CE, Lowenstein C, Reed RR, Snyder SH. Cloned and expressed nitric oxide synthase structurally resembles cytochrome P-450 reductase. *Nature* 1991;351:714-718
- Busconi L, Michel T. Endothelial nitric oxide synthase: N-terminal myristoylation determines subcellular localization. *J Biol Chem* 1993; 268:8410-8413
- Marsden PA, Schappert KT, Chen HS, Flowers M, Sundell CL, Wilcox JN, Lamas S, Michel T. Molecular cloning and characterization of human endothelial nitric oxide synthase. *FEBS Lett* 1992;307:287-293
- Feron O, Belhassen L, Kobzik L, Smith TW, Kelly RA, Michel T. Endothelial nitric oxide synthase targeting to caveolae: specific interactions with caveolin isoforms in cardiac myocytes and endothelial cells. *J Biol Chem* 1996;271:22810-22814
- Balligand JL, Kobzik L, Xan XQ, Kaye DM, Belhassen L, O'hera DS, Kelly RA, Smith TW, Michel T. Nitric oxide-dependent parasympathetic signaling is due to activation of constitutive endothelial nitric oxide synthase in cardiac myocytes. *J Biol Chem* 1995;270:14582-14586
- Kobzik L, Bredt DS, Lowenstein CJ, Drazen J, Gaston B, Sugarbaker D, Stamler JS. Nitric oxide synthase in human and rat lung: immunocytochemical and histochemical localization. *Am J Respir Cell Mol Biol* 1993;9:371-377
- Lamas S, Marsden PA, Li GK, Tempst P, Michel T. Endothelial nitric oxide synthase: molecular cloning and characterization of a distinct constitutive enzyme isoform. *Proc Natl Acad Sci* 1992;89:6348-6352
- Shaul PW, North AJ, Wu LC, Wells LB, Brannon TS, Lau KS, Michel T, Margraf LR, Star RA. Endothelial nitric oxide synthase is expressed in cultured human bronchial epithelium. *J Clin Invest* 1994;94:2231-2236
- Sase K, Michel T. Expression of constitutive endothelial nitric oxide synthase in human blood platelets. *Life Sci* 1995;57:2049-2055
- Dinerman JL, Dawson TM, Schell J, Snowman A, Snyder SH. Endothelial nitric oxide synthase localized to hippocampal pyramidal cells: implications for synaptic plasticity. *Proc Natl Acad Sci USA* 1994;91:4214-4218
- Nakane M, Schmidt HW, Pollock JS, Forseman U, Murad F. Cloned human brain nitric oxide synthase is highly expressed in skeletal muscle. *FEBS Lett* 1993;316:175-180
- Barry MK, Aloisi JD, Pickering SP, Yeo CJ. Nitric oxide modulates water and electrolyte transport in the ileum. *Ann Surg* 1994;219:382-388
- Yano CJ, Couse NF, Antiohos C, Zinner MJ. The effect of norepinephrine on intestinal transport and perfusion pressure in the isolated perfused rabbit ileum. *J Surg Res* 1988;44:617-624
- Yao CJ, Couse NF, Zinner MJ. Discrimination between alpha1 and alpha2 adrenergic receptors in the isolated perfused ileum. *Surgery* 1988;104:130-136
- Anthone GJ, Bastidas JA, Orandle MS, Yao CJ. Direct proabsorptive effect of octreotide on ionic transport in the small intestine. *Surgery* 1990;108:1136-1142
- Anthone GJ, Orandle MS, Wang BH, Yao CJ. Neuropeptide Y induced intestinal absorption: mediation by α_2 -adrenergic receptors. *Surgery* 1991;110:1132-1138
- Crouser ED, Julian MW, Weinstein DM, Fahy RJ, Bauer JA. Endotoxin-induced ileal mucosal injury and nitric oxide dysregulation are temporally dissociated. *Am J Respir Crit Care Med* 2000;161:1705-1712
- László F, Morschl E, Pávó I, Whittle BJR. Nitric oxide modulates the gastrointestinal plasma extravasation following intraabdominal surgical manipulation in rats. *Eur J Pharmacol* 1999;375:211-215
- Iwashita E, Miyahara T, Hino K, Tokunaga T, Wakisaka H, Sawazaki Y. High nitric oxide synthase activity in endothelial cells in ulcerative colitis. *J Gastroenterol* 1995;30:551-554
- Tan B, He SY, Deng HW, Li YJ. Effect of quercetin on adhesion of platelets to microvascular endothelial cells *in vitro*. *Acta Pharmacol Sin* 2001;22:851-856
- Laszlo F, Whittle BJ, Moncada S. Time-dependent enhancement or inhibition of endotoxin-induced vascular injury in rat intestine by nitric oxide synthase inhibitors. *Br J Pharmacol* 1994;111:1309-1315
- Takeuchi T, Nioka S, Yamaji M, Okishio Y, Ishii T, Nishio H, Takatsuji K, Hata F. Decrease in participation of nitric oxide in nonadrenergic, noncholinergic relaxation of rat intestine with age. *Jpn J Pharmacol* 1998;78:293-302
- Nakao K, Takahashi T, Utsunomiya J, Owyang C. Extrinsic neural control of nitric oxide synthase expression in the myenteric plexus of rat jejunum. *J Physiol* 1998;507:549-560
- Shah S, Nathan L, Singh R, Fu YS, Chaudhuri G. E2 and not P4 increases NO release from NANC nerves of the gastrointestinal tract: implications in pregnancy. *Am J Physiol Regul Integr Comp Physiol* 2001;280:R1546-1554
- Shah S, Hobbs A, Singh R, Cuevas J, Ignarro LJ, Chaudhuri G. Gastrointestinal motility during pregnancy: role of nitrergic component of NANC nerves. *Am J Physiol Regul Integr Comp Physiol* 2000; 279:R1478-1485
- Correia NA, Oliveira RB, Ballejo G. Pharmacological profile of nitrergic nerve-, nitric oxide-, nitrosoglutathione- and hydroxylamine-induced relaxations of the rat duodenum. *Life Sci* 2000;68:709-717
- Vittoria A, Costagliola A, Carrese E, Mayer B, Cecio A. Nitric oxide-containing neurons in the bovine gut, with special reference to their relationship with VIP and galanin. *Arch Histol Cytol* 2000;63:357-368
- Simula ME, Brookes SJ, Meedeniya AC, Toouli J, Saccone GT. Distribution of nitric oxide synthase and vasoactive intestinal polypeptide immunoreactivity in the sphincter of Oddi and duodenum of the possum. *Cell Tissue Res* 2001;304:31-41
- Ekelund M, Ekblad E. Intestinal adaptation in atrophic rat ileum is accompanied by supersensitivity to vasoactive intestinal peptide, pituitary adenylate cyclase-activating peptide and nitric oxide. *Scand J Gastroenterol* 2001;36:251-257
- Konturek SK, Konturek PC. Role of nitric oxide in the digestive system. *Digestion* 1995;56:1-13
- Teng B, Murthy KS, Kuemmerle JF, Grider JR, Sase K, Michel T, Makhoul GM. Expression of endothelial nitric oxide synthase in human and rabbit gastrointestinal smooth muscle cells. *Am J Physiol* 1998; 275:G342-351
- Nichols K, Staines W, Rubin S, Krantis A. Distribution of nitric oxide synthase activity in arterioles and venules of rat and human intestine. *Am J Physiol* 1994; 267:G270-275
- Charpie JR, Webb RC. Vascular myocyte-derived nitric oxide is an autocrine that limits vasoconstriction. *Biochem Biophys Res Commun* 1993;194:763-768
- Hirafuji M, Tsunoda M, Machida T, Hamaue N, Endo T, Miyamoto A, Minami M. Reduced expressions of inducible nitric oxide synthase and cyclooxygenase-2 in vascular smooth muscle cells of stroke-prone spontaneously hypertensive rats. *Life Sci* 2002;70:917-926
- Teng X, Li D, Catravas JD, Johns RA. C/EBP-beta mediates iNOS induction by hypoxia in rat pulmonary microvascular smooth muscle cells. *Circ Res* 2002;90:125-127
- Teng X, Zhang H, Snead C, Catravas JD. Molecular mechanisms of iNOS induction by IL-1 beta and IFN-gamma in rat aortic smooth muscle cells. *Am J Physiol Cell Physiol* 2002;282:C144-152
- Busse R, Mulsch A. Endothelium-derived relaxing factor: nitric oxide. *Mol Aspects Inflam* 1991;42:189-205
- Busse R, Mulsch A, Fleming I, Hecker M. Mechanisms of nitric oxide release from the vascular endothelium. *Circulation* 1993;87(Suppl.V):18-26
- Ignarro LJ, Wood KS, Fukuto JM. Continuous basal formation of endothelium-derived relaxing factor and muscle-derived relaxing factor, both of which are nitric oxide. *J Cardiovasc Pharmacol* 1991;17(suppl.3):S229-S233
- Lamontagne D, Pohl U, Busse R. Mechanical deformation of vessel wall and shear stress determine the basal EDRF release in the intact coronary vascular bed. *Circ Res* 1992;70:123-130
- Pohl U, Holtz J, Busse R, Bassenge E. Crucial role of endothelium in the vasodilator response to increased flow *in vivo*. *Hypertension* 1986;8:37-44
- Pohl U, Busse R. Hypoxia stimulates the release of endothelium-derived relaxant factor. *Am J Physiol* 1989;256(Heart Circ Physiol 25):H1595-H1600

• BASIC RESEARCH •

Evidences for vagus nerve in maintenance of immune balance and transmission of immune information from gut to brain in STM-infected rats

Xi Wang, Bai-Ren Wang, Xi-Jing Zhang, Zhen Xu, Yu-Qiang Ding, Gong Ju

Xi Wang, Bai-Ren Wang, Zhen Xu, Yu-Qiang Ding, Gong Ju, Institute of Neuroscience, Fourth Military Medical University, Xi'an 710032, Shaanxi Province, China

Xi-Jing Zhang, Department of Anesthesiology, Xi Jing Hospital, Fourth Military Medical University, Xi'an 710032, Shaanxi Province, China
Supported by National Natural Science Foundation, No. 39830130

Correspondence to: Gong Ju, Institute of Neurosciences, The Fourth Military Medical University, Xi'an, P.R. China. jugong@fmmu.edu.cn
Telephone: +86-29-3374557 Fax: +86-29-3246270

Received 2001-11-02 Accepted 2001-11-27

Abstract

AIM: To determine whether *Salmonella Typhimurium* (STM) in gastrointestinal tract can induce the functional activation of brain, whether the vagus nerve involves in signaling immune information from gastrointestinal tract to brain and how it influences the immune function under natural infection condition.

METHODS: Animal model of gastrointestinal tract infection in the rat was established by an intubation of *Salmonella Typhimurium* (STM) into stomach to mimic the condition of natural bacteria infection. Subdiaphragmatic vagotomy was performed in some of the animals 28 days before infection. The changes of Fos expression visualized with immunohistochemistry technique in hypothalamic paraventricular nucleus (PVN) and supraoptic nucleus (SON) were counted. Meanwhile, the percentage and the Mean Intensities of Fluorescent (MIFs) of CD4+ and CD8+ T cells in peripheral blood were measured by using flow cytometry (FCM), and the pathological changes in ileum and mesenteric lymph node were observed in HE stained sections.

RESULTS: In bacteria-stimulated groups, inflammatory pathological changes were seen in ileum and mesenteric lymph node. The percentages of CD4+ T cells in peripheral blood were decreased from $42\% \pm 4.5\%$ to $34\% \pm 4.9\%$ ($P < 0.05$) and MIFs of CD8+ T cells were also decreased from 2.9 ± 0.39 to 2.1 ± 0.36 ($P < 0.05$) with STM stimulation. All of them proved that our STM-infection model was reliable. Fos immunoreactive (Fos-ir) cells in PVN and SON increased significantly with STM stimulation, from 189 ± 41 to 467 ± 62 ($P < 0.05$) and from 64 ± 21 to 282 ± 47 ($P < 0.05$) individually, which suggested that STM in gastrointestinal tract induced the functional activation of brain. Subdiaphragmatic vagotomy attenuated Fos expression in PVN and SON induced by STM, from 467 ± 62 to 226 ± 45 ($P < 0.05$) and from 282 ± 47 to 71 ± 19 ($P < 0.05$) individually, and restored the decreased percentages of CD4+ T cells induced by STM from $34\% \pm 4.9\%$ to original level $44\% \pm 6.0\%$ ($P < 0.05$). In addition, subdiaphragmatic vagotomy itself also decreased the percentages of CD8+ T cells (from $28\% \pm 3.0\%$ to $21\% \pm 5.9\%$, $P < 0.05$) and MIFs of CD4+ (from 6.6 ± 0.6 to 4.9 ± 1.0 , $P < 0.05$) and CD8+ T cells (from 2.9 ± 0.39 to 1.4 ± 0.34 , $P < 0.05$). Both of them

manifested the important role of vagus nerve in transmitting immune information from gut to brain and maintaining the immune balance of the organism.

CONCLUSION: Vagus nerve does involve in transmitting abdominal immune information into the brain in STM infection condition and play an important role in maintenance of the immune balance of the organism.

Wang X, Wang BR, Zhang XJ, Xu Z, Ding YQ, Ju G. Evidences for vagus nerve in maintenance of immune balance and transmission of immune information from gut to brain in STM-infected rats. *World J Gastroenterol* 2002;8(3):540-545

INTRODUCTION

It has been suggested in recent studies that the vagus nerve, the tenth cranial nerve, might play an important role in transmitting immune information into the brain^[1-5]. However, this conclusion is based on the experiments in which cytokines, endotoxins or exotoxins were usually used as immune stimulators through intraperitoneal or intravenous injection. All these immune stimulations, however, are non-natural and the role of vagus in natural infection condition has not been established yet. *Salmonella Typhimurium* (STM) belongs to the group B of *Salmonella*. It can infect both human beings and animals through gastrointestinal tract and leads to a local or general infection by inhibiting the host immune system^[6]. Thus, in the current experiments we introduced *Salmonella Typhimurium* (STM) into stomach to mimic the natural bacteria infection in gastrointestinal tract and to reassess the role of vagus in transmission of immune signal by subdiaphragmatic vagotomy. The production of c-fos, an immediately early gene, has been used as a morphological marker of functionally activated brain neurons^[7-15]. In the present study we observed the STM-induced Fos expression in hypothalamic paraventricular nucleus (PVN) and supraoptic nucleus (SON) and the effect of vagotomy. We also studied the importance of integrity of vagus nerve in the balance of T cell subpopulations.

MATERIALS AND METHODS

Animals

Adult male Sprague Dawley albino rats (180-210g, offered by Animal Center, Fourth Medical University) were used. Rats were housed individually in a temperature-controlled room in a natural light/dark cycle, with food and water available freely. The animals were trained for adaptation to handling and gastric intubation before the following procedures started.

Procedures

Subdiaphragmatic vagotomy Rats were anesthetized with pentobarbital sodium (40mg/kg, i.p.) and subjected to a complete subdiaphragmatic vagotomy ($n=10$) or sham operation ($n=10$). Briefly, after laparotomy, the two trunks of vagus were identified under an operating microscope. Both trunks were cut off close to the

diaphragm. For sham vagotomy, the vagus was similarly exposed but was not cut. After surgery, a recovery period of 28 days was allowed.

Preparation of STM Wild strain of STM (offered by Laboratory of Bacteria, Xijing Hospital, Fourth Medical University) was preserved in freeze-dried powder before use. In order to enhance the pathogenicity of the bacteria, STM were sub-cultured in mice abdomen (Kunming mice offered by Animal Center, Fourth Medical University) for 3 times and then the number of the bacteria was adjusted to 10^{10} /ml for use.

Intubation of STM Rats ($n=20$) were divided into 4 groups randomly, 5 for each. Group 1, saline(NS) + sham operation; 2, NS + vagotomy; 3, STM + sham operation; 4, STM + vagotomy. Food was taken away from the rats 24h prior to intubating STM or saline. After anesthetized with ether, all rats were intubated with 30g/L NaHCO_3 300 μl to neutralize gastric acid. Then the animals of groups 3 and 4 were gastrically intubated with STM (10^{10} in saline, 1ml) and in the others (Groups 1 and 2) 1 ml of saline were given.

Perfusion and Sectioning After intubation for 22h, all rats were deeply anesthetized with pentobarbital (80mg/kg) and 1ml of blood was taken via heart as quickly as possible. The rats were then perfused transcardially with saline 100ml followed by 4% paraformaldehyde in 0.1M phosphate buffer (PB) 500ml, pH 7.4, at 4°C. Blood was anti-coagulated with heparin. Brains, part of ileum and mesenteric lymph node were taken out and cryoprotected in 20% sucrose in 0.1 M PB overnight at 4°C. Frontal sections in 50 μm -thickness were cut through whole brains with a microtome and collected in cold cryoprotectant and stored at -20°C until immunohistochemistry processing. Serial ileum and mesenteric lymph node sections in 5 μm -thickness were cut with a cyostat and mounted onto slides coated with gelatin and stored at -20°C until histochemistry processing.

HE staining of ileum and mesenteric lymph node sections Slides of ileum and mesenteric lymph node were immersed successively in dimethylbenzene (10min \times 2), graded ethanol (100% 5min \times 2, 95% 2min, 80% 2min, 70% 2min and distilled water 2min), Harris hematoxylin (5-10min) and 10% acid ethanol for several seconds. After rinsed with tap water for 30min, slides were immersed again successively in distilled water (10-30min), graded ethanol (70%, 80%, and 95% 2min for each), 0.5% eosin (5-10min), 95% ethanol from several seconds to minutes, 100% ethanol (5min \times 2) and dimethylbenzene (10min \times 2). At last, the slides were sealed with gum and observed under a light microscope (Olympus B \times 60).

Flow cytometry (FCM) of blood T Cell Blood CD4+ and CD8+ T lymphocytes were labeled by using indirect immunofluorescent labeling method. First, 80 μl of anti-coagulated blood was incubated with mice anti rat CD4 mAb (1:100, Serotec company) or 15 μl of mice anti rat CD8 mAb (1:100, Serotec company) for 30min at 4°C, then with 40 μl of goat anti mice IgG-FITC (1:100, Serotec company) after washing twice with 0.01Mol/L Phosphate-buffered saline (PBS). FCM was used to detect the percentages and the Mean Intensities of Fluorescence (MIFs) of CD4+ and CD8+ T cells.

Immunohistochemistry of Brain Sections ABC immunohistochemical technique was used to detect Fos-immunoreactive (Fos-ir) cells in brain. One-in-five of brain sections were incubated with primary antibody raised from rabbit against Fos protein (Sigma Inc.) at a dilution of 1:3000. After incubation at room temperature for 36h, sections were rinsed with 0.01Mol/L Phosphate-buffered saline (PBS) (10min \times 3) and then incubated with biotinylated secondary antibody against rabbit IgG (Sigma Inc, diluted at 1:500) at room temperature for 4h. After rinsing with 0.01Mol/L PBS (10min \times 3), sections were incubated with avidin-biotin-horseradish peroxidase

(1:500, Sigma Inc.) at room temperature for 2h. The reaction product was visualized with amine nickel sulfate-enhanced 3,3'-diaminobenzidine (DAB) method. The sections were dehydrated in graded ethanol, cleared with dimethylbenzene, and coverslipped with gum.

Counting of Fos-ir cells Sections of hypothalamus were observed with a light microscope (Olympus BX60). The number of Fos-ir cells was quantified by counting immunostained nuclei in PVN or SON at two consecutive typical sections with an image analysis system (Leica Quantimet 570 C). The number of Fos-positive nuclei in PVN or SON was the group mean \pm SE.

Statistical analyses All data were expressed as mean \pm SE and were analyzed by one-way ANOVA. Post hoc analysis was done by using the Student-Newman-Keuls (SNK) multiple comparison test. A value of $P<0.05$ was considered significant.

RESULTS

HE staining

Inflammation change was seen in ileum and mesenteric lymph node in the rats stimulated with STM. There are numerous bacilli in ileum cavity in the infected rats. The structure of the villus of the infected ileum was destroyed (Figure E2), part of epithelial cells were scaled, and many neutrophil, red blood cell and fibroblast infiltrated into the villus. At the same time, secondary lymphoid folliculi appeared in mesenteric lymph node (Figure E4). Figures.E1 and E3 show the normal tissue image of the villus and mesenteric lymph node in saline-treated rat.

FCM

Table 1 shows the percentages and MIFs of CD4+and CD8+ T cells in every group.

Figure1 A shows that subdiaphragmatic vagotomy itself in normal animals had no evident effect on the percentages of CD4+ T cells, but the stimulation of STM itself in sham-operated animals decreased the percentages of CD4+ T cells from $42\% \pm 4.5\%$ to $34\% \pm 4.9\%$ ($P<0.05$) and after subdiaphragmatic vagotomy the decreased percentages of CD4+ T cells in STM stimulated rats restored from $34\% \pm 4.9\%$ to $44\% \pm 6.0\%$, the level of non- STM stimulated rats ($P<0.05$).

Figure1 B shows that subdiaphragmatic vagotomy itself in NS+operation animals decreased MIFs of CD4+ T cells from 6.6 ± 0.6 to 4.9 ± 1.0 ($P<0.05$), indicating the inhibition of subdiaphragmatic vagotomy to CD4+ T cells.

Figure1 C and Figure1 D show that subdiaphragmatic vagotomy itself in normal rats decreased the percentages of CD8+ T cells (from $28\% \pm 3.0\%$ to $21\% \pm 5.9\%$, $P<0.05$) as well as MIFs of CD8+ T cells (from 2.9 ± 0.39 to 1.4 ± 0.34 , $P<0.05$). STM stimulation itself in sham-operated rats also depressed the percentages of CD8+ T cells (from $28\% \pm 3.0\%$ to $21\% \pm 5.9\%$, $P>0.05$) and MIFs of CD8+ T cells (from 2.9 ± 0.39 to 2.1 ± 0.36 , $P<0.05$). Subdiaphragmatic vagotomy in STM-challenged rats aggravated the inhibition of STM to the percentages of CD8+ T cells (from $23\% \pm 2.0\%$ to $17\% \pm 5.8\%$, $P<0.05$) and MIFs of CD8+ T cells (from 2.1 ± 0.36 to 1.1 ± 0.06 , $P<0.05$).

Table 1 Percentages (%) and MIF of CD8+ and CD4+ T cells ($\bar{x} \pm s$)

	NS+sham	NS+vagotomy	STM+sham	STM+vagotomy
CD4	42 \pm 4.5	46 \pm 4.6	34 \pm 4.9 ^b	44 \pm 6.0 ^a
CD4 MIF	6.6 \pm 0.6	4.9 \pm 1.0 _b	6.8 \pm 1.1	6.1 \pm 1.0
CD8	28 \pm 3.0	21 \pm 5.9 ^b	23 \pm 2.0	17 \pm 5.8 ^a
CD8 MIF	2.9 \pm 0.39	1.4 \pm 0.34 ^b	2.1 \pm 0.36 ^b	1.1 \pm 0.06 ^a

^a $P<0.05$ vs STM+sham; ^b $P<0.05$ vs NS+sham

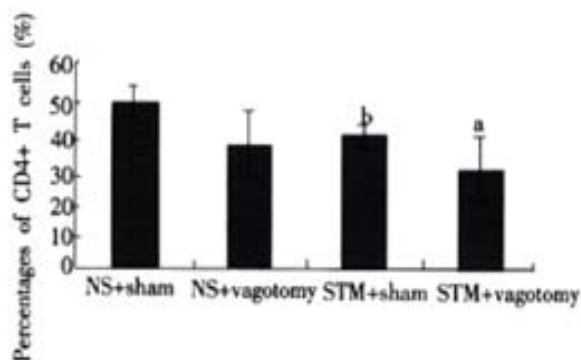


Figure 1A Percentages of blood CD4+ T cells. ^a $P < 0.05$ vs. STM+sham, ^b $P < 0.05$ vs NS+sham

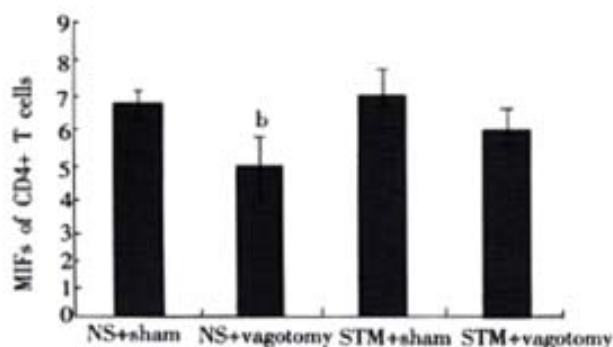


Figure 1B The Mean Intensities of Fluorescence (MIFs) of blood CD4+ T cells. ^b $P < 0.05$ vs NS+sham

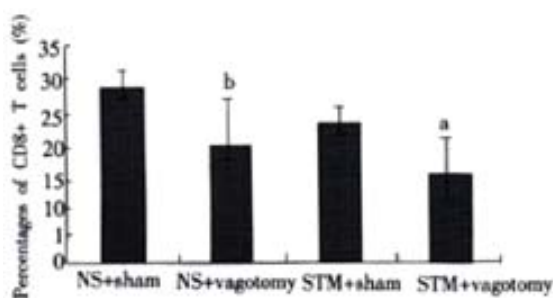


Figure 1C Percentages of blood CD8+ T cells. ^a $P < 0.05$ vs STM+sham, ^b $P < 0.05$ vs NS+sham

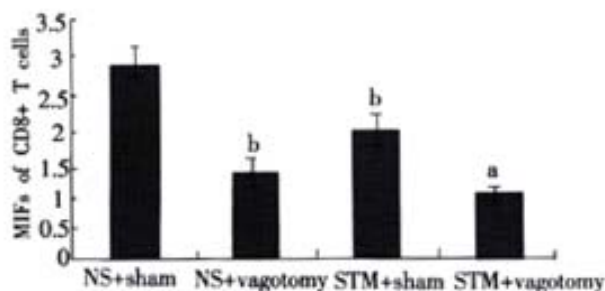


Figure 1D The Mean Intensities of Fluorescence (MIFs) of blood CD8+ T cells. ^a $P < 0.05$ vs STM+sham; ^b $P < 0.05$ vs NS+sham

Immunohistochemistry

Table 2 shows the number of Fos-ir cells in PVN and SON in each group. The numbers of Fos-ir cells in PVN and SON of STM+sham-operated rats increased significantly compared with that of NS+sham from 189 ± 41 to 467 ± 62 ($P < 0.05$) and from 64 ± 21 to 282 ± 47 ($P < 0.05$) individually (Figures.E5, E6, E9, E10). The positive neuron distributed in both magnocellular and parvocellular portions of

PVN as well as dorsal and ventral parts of SON. Fos expressions were attenuated in PVN and SON in the rats of STM+vagotomy group compared with that of STM+sham group from 467 ± 62 to 226 ± 45 ($P < 0.05$) and from 282 ± 47 to 71 ± 19 ($P < 0.05$) individually (Figures. E6, E7, E10, E11), but it was still higher than that of saline-treated animal (189 ± 41 and 64 ± 21 individually). There was no significant changes of Fos expression in NS + vagotomy rats compared with NS + sham rats (Figures.E5, E8, E9, E12).

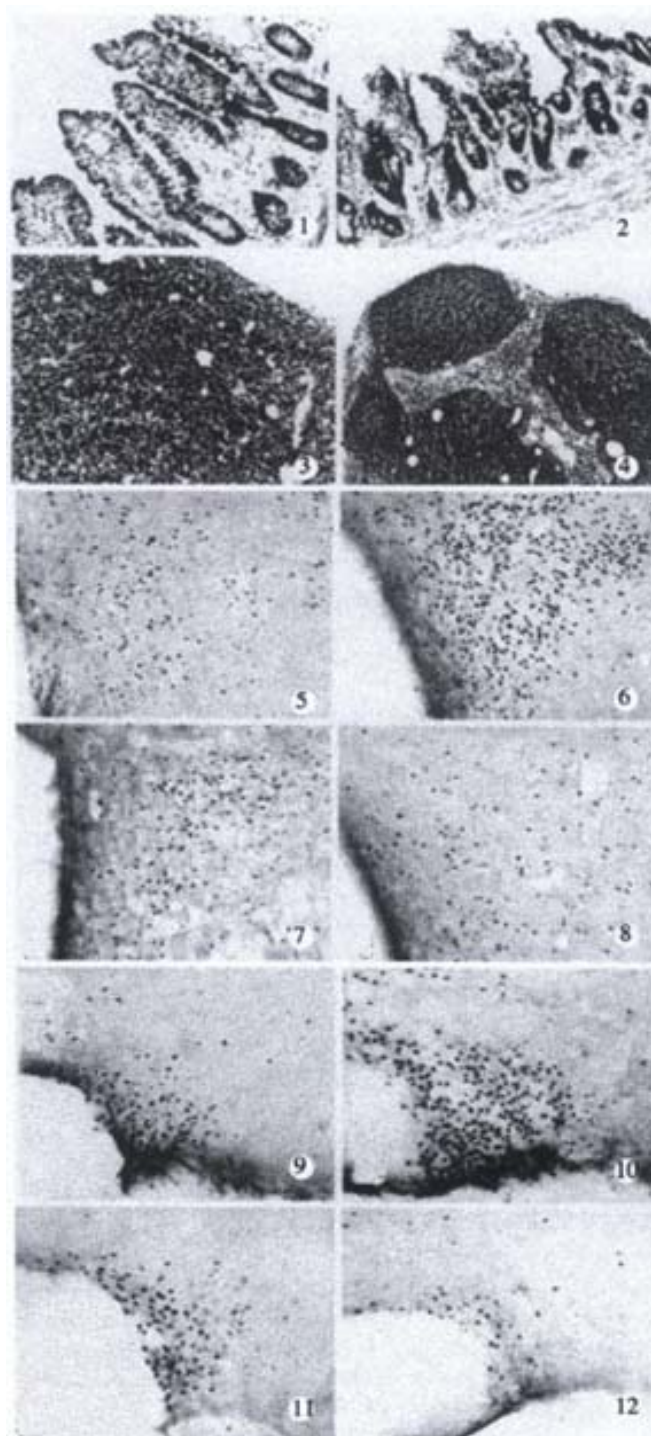


Figure 2 In Figures E 1 and 3 show the normal structures of the villus and mesenteric lymph node in saline-injected rats; 2 and 4 show the villus and mesenteric lymph node in STM-challenged rats. 5 and 9 show Fos expression in PVN and SON respectively in NS + sham rats; 6 and 10 show Fos expressions in PVN and SON respectively in STM + sham rat; 7 and 11 show Fos expressions in PVN and SON respectively in STM + vagotomy rat; 8 and 12 show Fos expressions in PVN and SON respectively in NS + vagotomy rat. $\times 50$

Table 2 Numbers of Fos-ir Cells in PVN and SON ($\bar{x} \pm s$)

	NS + sham	NS + vagotomy	STM + sham	STM + vagotomy
PVN	189±41	131±38	467±62 ^a	226±45 ^b
SON	64±21	49±22	282±47 ^a	71±19 ^b

^a*P*<0.05 vs NS + Sham; ^b*P*<0.05 vs STM + sham

DISCUSSION

More and more evidences have shown that there is a complicated bidirectional inter-relationship between nervous system and immune system^[4,16-23]. Immune signals produced during antigen challenge can be transmitted into central nervous system (CNS) and influence the function of the latter. In turn, CNS can modulate the activity of immune system. However, it is still an unsolved problem up to now how the immune signals are transmitted into CNS. Two of hypotheses have been proposed^[1-4]: one is through humoral route and the other, via neural pathway. Among the neural pathways the vagus nerve in transferring peripheral immune signals into CNS has been paid more attention to^[1-5,24,25]. A large amount of evidences indicate that vagus plays an important role in surveying the peripheral immune information into CNS. For example, subdiaphragmatic vagotomy inhibits a series of brain-mediated responses to peripheral administration of lipopolysaccharide (LPS), IL-1 β or TNF- β , such as induction of IL-1 β mRNA within mice brain^[26,27], activation of hypothalamic corticotropin-releasing hormone neurons and ACTH secretion^[28,29], LPS-induced fever in guinea pigs^[30], Fos immunoreactivity in primary afferent neurons of the vagus^[31], the inhibition of social exploration^[32], a monophasic fever^[33], the hyperalgesia^[34,35] etc. Administration of IL-1 β in hepatic portal vein induced afferent discharges of hepatic branch of vagus, but the discharges disappeared in vagotomy rats^[36]. Nucleus tractus solitarius lesions attenuated the first fever peak induced by intraperitoneal injection of IL-1 β ^[37]. All of the above mentioned experiments indicate that intact vagus is necessary for transmitting the immune information from periphery, especially from peritoneal cavity, to the brain. According to the anatomical structure of vagus, the abdominal organs such as liver, stomach, intestines, lymph node, etc. are innervated mostly by subdiaphragmatic vagus and the vagus contains important visceral sensory afferent fibers from abdominal organs^[38,39]. Thus, we conjecture that subdiaphragmatic vagus may play an important role in transmitting the abdominal immune information into the brain and is important in maintaining immune balance.

All the immune challenges used in previous studies were bacterial toxins such as LPS or immune cytokines injected intraperitoneally or intravenously. In this experiment we established a rat model of gastrointestinal tract infection by STM intubation to mimic the natural infection and a subdiaphragmatic vagotomy was performed to further observe the role of vagus in immune signal transmission. According to aetiology, STM can invade intestinal mucosa and largely reproduce, and then further spread into the drained mesenteric lymph nodes and disseminate via the bloodstream^[40]. STM is an intracellular Gram-negative bacterial pathogen that infects both phagocytic and non-phagocytic cells^[6,40-43]. It can inhibit the host immune system and cause a range of diseases including enteric fever and gastroenteritis^[6]. It has been reported that the depletion of either CD4⁺ or CD8⁺ T cells by STM impairs their ability to transfer protective immunity to virulent *S. typhimurium*^[6]. These studies indicate that CD4⁺ and CD8⁺ T cells act synergistically to control infection with virulent *S. typhimurium*^[6,44,45]. In our experiment the villus of the infected ileum was destroyed, part of epithelial cells scaled, and the number of neutrophils, red blood cells as well as fibroblasts increased in the villus. At the same time, secondary lymphoid folliculus stimulated with STM emerged in mesenteric lymph nodes. The percentages of

CD4⁺ and CD8⁺ T cells and MIFs of CD8⁺ T cells of peripheral blood were all inhibited, which was consistent with the previous reports. These changes induced by STM suggest that our STM infection model was reliable.

The result showed that in NS+sham rats Fos proteins expressed in a few of PVN and SON neurons, which suggests that in normal condition some PVN and SON neurons are active, and may be related to the modulation of routine metabolic activities. After being stimulated with STM the number of Fos-ir cells significantly increased in PVN and SON. It indicated that these cells were activated by STM-challenge. It is well known that CNS, especially hypothalamus, involves in modulation of acute immune reaction^[46]. PVN and SON, which are two most important nuclei in hypothalamus related to autonomic function, are mainly composed of three kinds of neurons neurochemically: oxytocinergic, vasopressinergic and CRH neurons^[46]. All of these three kinds of neurons can involve in neuroimmunomodulation^[46]. Yang *et al.*^[46] reported that, as the neuroimmunomodulation integrating center, hypothalamic PVN modulates the immune function through three pathways: The first is CRH -ACTH-adrenal cortex axis, the second is oxytocin neuroendocrine pathway, and the third is PVN-spinal cord sympathetic preganglionic projection. Although we can't determine which kind of neurons were activated in this experiment since we did not apply double-labeling technique to identify them, we proposed from the observation of distribution of Fos positive neurons in the subnuclei of PVN and SON that, maybe, all these three kind neurons were activated.

But, how the immune signals are transmitted into the brain is an important and unsolved question. Is it through vagus or humoral pathway, or both of them? What we focused on in the present study was the role of vagus in the sensation and transmission of immune signals to brain. So, we severed subdiaphragmatic vagus to observe whether the Fos expressions in PVN and SON induced by STM infection and the T cell subpopulation were influenced. After subdiaphragmatic vagotomy, Fos expressions in PVN and SON were attenuated. At the same time we found that the decreased percentage of CD4⁺ T cells in STM-infected rats restored after subdiaphragmatic vagotomy. These results indicate the importance of intact subdiaphragmatic vagus in signaling immune information from abdominal organs to CNS. We tend to conclude from our results that subdiaphragmatic vagus does play a role in transferring immune information into brain during the abdominal inflammatory phase.

However, the detailed mechanism about how vagus nerve senses the immune stimulation and transfers it into electric signal is still not fully understood. It is known that macrophages, dendritic cells, and other immune cells detect and present antigens and respond by releasing proinflammatory mediators, such as IL-1 β , IL-6 and TNF- α ^[23,47,48]. Goehler *et al.*^[47] found that between the fibers of abdominal vagus there exist immune cells which can produce IL-1 β . IL-1 β acts to both coordinating the peripheral immune response and signaling the CNS^[49]. The globe cells of vagus paraganglia near liver hilus could be stained by biotinylated IL-1 receptor antagonist^[50] and by anti rat IL-1 receptor type I antibody^[51], which suggested the possibility for vagus to sense the local IL-1. We^[51] and others^[52] also have reported that the primary sensory neurons in nodose ganglia of vagus contain IL-1 receptor protein and mRNA, which indicates that vagus nerve probably can sense IL-1 directly.

It is necessary to point out that vagus is definitely not the only route for immune signal getting into the brain, since it is found in the present study that although the number of STM stimulation-induced Fos expressed neurons in hypothalamus is attenuated after vagotomy, the number is still higher than that in control. So the humoral pathways or other nerves may also involve in the immune signals transmission in some degree, which still needs further study.

Our results also showed that subdiaphragmatic vagotomy itself decreased the percentages of CD8⁺ T cells and MIFs of CD4⁺ and CD8⁺ T cells, which indicated the importance of intact vagus in maintaining the host immune balance. This is also accordant with our previous study^[53]. As we know that CD4⁺ and CD8⁺ T cells are necessary in clearing STM^[6,54,55]. Vagotomy inhibits the subpopulation of T cells, which is a disadvantage to STM clearance and only aggravate the inhibition to CD4⁺ and CD8⁺ T cells induced by STM. How does the vagus influence the phenotype of lymphatic cells? Vagus contains both afferent and efferent fibers innervating abdomen. The former can transmit abdominal information into CNS and the latter innervates some immune organs or immune cells, such as abdominal lymph node. When we cut off subdiaphragmatic vagotomy, on the one hand, the abdominal immune information can't be transmitted into the brain; on the other hand, the brain can't influence the abdominal immune organizations via vagus. We suppose that this is probably the answer.

In summary, subdiaphragmatic vagus is able to signal immune information from abdomen into the brain and intact vagus is necessary in maintaining the host immune balance.

REFERENCES

- Maier SF, Goehler LE, Fleshner M, Watkins LR. The role of the vagus in cytokine-to-brain communication. *Ann N Y Acad Sci* 1998; 840: 289-300
- Goehler LE, Gaykema RPA, Hansen MK, Anderson K, Maier SF, Watkins LR. Vagal immune-to-brain communication: a visceral chemosensory pathway. *Auton Neurosci: Basic & Clinical* 2000; 85: 49-59
- Dantzer R, Konsman PJ, Bluthé RM, Kelley KW. Neural and humoral pathways of communication from the immune system to the brain: parallel or convergent? *Auton Neurosci: Basic & Clinical* 2000; 85: 60-65
- Watkins LR, Maier SF, Goehler LE. Cytokine-to-brain communication: a review & analysis of alternative mechanisms. *Life Sci* 1995; 57: pp1011-1026
- Wang X, Wang BR, Ju G. The role of the vagus nerve in transmitting immune information into the brain. *Shanghai Mianyixue Zazhi* 2000; 20:192-194
- Lo WF, Ong H, Metcalf ES, Soloski MJ. T cell responses to Gram-negative intracellular bacterial pathogens: A role for CD8⁺ T cells in immunity to Salmonella infection and the involvement of MHC class Ib molecules. *J Immunol* 1999; 162: 5398-5406
- Stephen MS, Frank RS. Early response genes as markers of neuronal activity and growth factor action. *Adv in Neurol* 1993; 59: 273-284
- Xu ZC, Jiang XH. Advance and development of Early response genes in neuroscience research. *Shengli Kexue Jinzhan* 1997; 28: 49-51
- Wang X, Wang BR, Duan XL, Ju G. The basal expression of Fos in the rat under the normal life situation. *Zhongguo Shenjing Jiepouxue Zazhi* 2000; 16: 353-358
- Matsunaga W, Takamata A, Bun H, Nakashima T. LPS-induced Fos expression in oxytocin and vasopressin neurons of the rat hypothalamus. *Brain Res* 2000; 858: 9-18
- Zhang X, Ju G. The induction and display of c-fos oncogene. *Shengli Kexue Jinzhan* 1991; 22: 299-303
- Arnold FJL, Bueno MDL, Shiers H, Hancock DC, Evan GI, Herbert J. Expression of c-fos in regions of the basal limbic forebrain following intracerebroventricular corticotropin-releasing factor in unstressed or stressed male rats. *Neurosci* 1992; 51: pp377-390
- Imaki T, Shhibasaki T, Hotta M, Demura H. Intracerebroventricular administration of corticotropin-releasing factor induces c-fos mRNA expression in brain regions related to stress responses: comparison with pattern of c-fos mRNA induction after stress. *Brain Res* 1993; 616: 114-125
- Morgan JJ, Cohen DR, Hempstead JL, Curran T. Mapping patterns of c-fos expression in the central nervous system after seizure. *Science* 1987; 237: 192-197
- Hare AS, Clarke G, Tolchard S. Bacterial lipopolysaccharide-induced changes in FOS protein expression in the rat brain: correlation with thermoregulatory changes and plasma corticosterone. *J Neuroendocrinol* 1995; 7: 791-799
- Borovikova LV, Lvanona S, Zhang M, Yang H, Botchkina GI, Watkins LR, Wang H, Abumrad N, Eaton JW, Tracey JK. Vagus nerve stimulation attenuates the systemic inflammatory response to endotoxin. *Nature* 2000; 405: 458-462
- Erricsson A, Arias C, Sawchenko PE. Evidence for an intramedullary prostaglandin-dependent mechanism in the activation of stress-related neuroendocrine circuitry by intravenous interleukin-1. *J Neurosci* 1997; 17: 7166-7179
- Ivanov AI, Kulchitsky VA, Sugimoto N, Simons CT, Romanovsky AA. Does the formation of lipopolysaccharide tolerance require intact vagal innervation of the liver? *Auton Neurosci: Basic and Clinical* 2000; 85: 111-118
- Downing JEG, Miyan JA. Neural immunoregulation: emerging roles for nerves in immune homeostasis and disease. *Immunol Today* 2000; 21: 281-289
- Roth J, Souza GEP. Fever induction pathways: evidence from responses to systemic or local cytokine formation. *Braz J Med Biol Res* 2001; 34: 301-314
- Watkins LR, Maier SF. Implications of immune-to-brain communication for sickness and pain. *Proc Natl Acad Sci* 1999; 96: pp7710-7713
- Shanks N, Windle RJ, Perks PA, Harbuz MS, Jessop DS, Ingram CD, Lighman SL. Early-life exposure to endotoxin alters hypothalamic-pituitary-adrenal function and predisposition to inflammation. *Proc Natl Acad Sci* 2000; 97: 5645-5650
- Ling YL, Meng AH, Zhao XY, Shan BE, Zhang JL, Zhang XP. Effect of cholecystokinin on cytokines during endotoxic shock in rats. *World J Gastroenterol* 2001; 7: 667-671
- Romanovsky AA. Thermoregulatory manifestations of systemic inflammation: lessons from vagotomy. *Auton Neurosci: Basic and Clinical* 2000; 85: 39-48
- Blatteis CM, Li SX. Pyrogenic signaling via vagal afferents: what stimulates their receptors? *Auton Neurosci: Basic and Clinical* 2000; 85: 66-71
- Laye S, Bluthé RM, Kent S, Combe C, Medina C, Parnet P, Kelley K, Dantzer R. Subdiaphragmatic vagotomy blocks induction of IL-1 β mRNA in mice brain in response to peripheral LPS. *Am J Physiol* 1995; 268:R1327-R1331
- Hansen MK, Taishi P, Chen Z, Krueger JM. Vagotomy blocks the induction of interleukin-1 (IL-1) mRNA in the brain of rats in response to systemic IL-1. *J Neurosci* 1998; 18: 2247-2253
- Gaykema RPA, Dijkstra I, Tilders RJH. Subdiaphragmatic vagotomy suppresses endotoxin-induced activation of hypothalamic corticotropin-releasing hormone neurons and ACTH secretion. *Endocrinol* 1995; 136: 4717-4720
- Kapcala LP, He RJ, Gao Y, Pieper JO, Detolla LJ. Subdiaphragmatic vagotomy inhibits intra-abdominal interleukin-1 β stimulation of adrenocorticotropin secretion. *Brain Res* 1996; 728: 247-254
- Sehic E, Blatteis CM. Blockade of lipopolysaccharide-induced fever by subdiaphragmatic vagotomy in guinea pigs. *Brain Res* 1996; 726: 160-166
- Gaykema RPA, Goehler LE, Tilders FJ, Bol J GJM, McGorry M, Fleshner M, Maier SF, Watkins LR. Bacterial endotoxin induces Fos immunoreactivity in primary afferent neurons of the vagus. *Neuroimmunomodulation* 1998; 5: 234-240
- Luheshi GN, Bluthé RM, Rushorforth D, Mulcahy N, Konsman JP, Goldbach M, Dantzer R. Vagotomy attenuates the behavioural but not the pyrogenic effects of interleukin-1 in rats. *Auton Neurosci: Basic and Clinical* 2000; 85: 127-132
- Romanovsky AA, Simons CT, Szekely M, Kulchitsky VA. The vagus nerve in the thermoregulatory response to systemic inflammation. *Am J Physiol* 1997; 273: R407-R413
- Watkins LR, Wiertelak EP, Goehler LE, Smith KP, Martin D, Maier SF. Characterization of cytokine-induced hyperalgesia. *Brain Res* 1994; 654: 15-26
- Watkins LR, Goehler LE, Reiton J, Brewer MT, Maier SF. Mechanisms of tumor necrosis factor- α (TNF- α) hyperalgesia. *Brain Res* 1995; 692: 244-250
- Nijima A. The afferent discharges from sensors for interleukin 1 β in the hepatoportal system in the anesthetized rat. *J Auton Nerv Sys* 1996; 61: 287-291
- Gordon FJ. Effect of nucleus tractus solitarius lesions on fever produced by interleukin-1 β . *Auton Neurosci: Basic and Clinical* 2000; 85: 102-112
- Berthoud HR, Neuhuber WL. Functional and chemical anatomy of the afferent vagal system. *Auton Neurosci: Basic & Clinical* 2000; 85: 1-17
- Dou DB, Cai G. Regulation of the stomach motility function. *Shijie Huaren Xiaohua Zazhi* 1999; 7: 353-354
- Niedergang F, Sirard JC, Blanc CT, Kraehenbuhl JP. Entry and survival of Salmonella Typhimurium in dendritic cells and presentation of recombinant antigens do not require macrophage-specific virulence factors. *Proc Natl Acad Sci* 2000; 97: 14650-14655
- Portillo FGD, Finlay B. Salmonella invasion of nonphagocytic cells induces formation of macropinosomes in the host cell. *Infect and Immun* 1994; 62: p4641-4645

- 42 Cookson BT, Bevan MJ. Identification of a natural T cell epitope presented by Salmonella-infected macrophages and recognized by T cells from orally immunized mice. *J Immunol* 1997; 158: 4310-4319
- 43 Weinstein DL, Carsiotis M, Lissner CR, O'Brien AD. Flagella help Salmonella typhimurium survive within murine macrophages. *Infect and Immun* 1984; 46: p819-825
- 44 Tite JP, Dougan G, Chatfield SN. The involvement of tumor necrosis factor in immunity to Salmonella infection. *Infect and Immun* 1991; 147: 3161-3164
- 45 Nauciel C. Role of CD4⁺ T cells and T-independent mechanisms in acquired resistance to Salmonella typhimurium infection. *Infect and Immun* 1990; 145: 1265-1269
- 46 Yang H, Wang L, Ju G. Evidence for hypothalamic paraventricular nucleus as an integrative center of neuroimmunomodulation. *Neuroimmunomodulation* 1997; 4: 120-127
- 47 Goehler LE, Gaykema RPA, Nguyen KT, Lee JE, Tilders FJH. Interleukin-1 β in immune cells of the abdominal vagus: a link between the immune and nervous system? *J Neurosci* 1999; 19: 2799-2806
- 48 Xia B. Pathogeny and mechanism of inflammatory bowel disease. *Shijie Huaren Xiaohua Zazhi* 2001; 9: 245-250
- 49 Maier SF, Wiertelak EP, Martin D, Wakins LR. Interleukin-1 mediates the behavioral hyperalgesia produced by lithium chloride and endotoxin. *Brain Res* 1993; 623: 321-324
- 50 Goehler LE, Relton JK, Dripps D, Kiechle R, Tartaglia N, Maier SF, Watkins LR. Vagal paranganglia bind biotinylated interleukin-1 receptor antagonist: a possible mechanism for immune-to-brain communication. *Brain Res Bul* 1997; 43: 357-364
- 51 Wang X, Wang BR, Duan XL, Liu HL, Ju G. The expression of IL-1 receptor type I in nodose ganglion and vagal paranganglion in the rat. *Zhongguo Shenjing Kexue Zazhi* 2000; 16: 90-93
- 52 Ek M, Kurosawa M, Lundeborg T, Ericsson A. Activation of vagal afferents after intravenous injection of interleukin-1 β : role of endogenous prostaglandins. *J Neurosci* 1998; 18: 9471-9479
- 53 Wang X, Cao YX, Wang BR, Xu Z, Jin L, Duan XL, Ju G. The influence of subdiaphragmatic vagotomy on CD4⁺/CD8⁺ T cells in peripheral blood. *Xibao Fenzi Yu Mianyixue Zazhi* 2000; 16: 230-231
- 54 Mesorley SJ, Cookson BT, Jenkins MK. Characterization of CD4⁺ T cells responses during natural infection with Salmonella typhimurium. *J Immunol* 2000; 164: 986-993
- 55 Sandrine P, Paolo TB, Marika P, Charles N. Th1 response in Salmonella typhimurium-infected mice with a high or low rate of bacterial clearance. *Infect and Immun* 1997; 65: 4509-4514

Edited by Hu DK

• BASIC RESEARCH •

Relationship between lymphocyte apoptosis and endotoxin translocation after thermal injury in rats

Pei-Yuan Xia, Jiang Zheng, Hong Zhou, Wen-Dong Pan, Xiao-Jian Qin, Guan-Xia Xiao

Pei-Yuan Xia, Department of Pharmacy and Clinical Pharmacology, Southwestern Hospital, Third Military Medical University, Chongqing 400038, China
Jiang Zheng, Hong Zhou, Wen-Dong Pan, Xiao-Jian Qin, Guan-Xia Xiao, Institute of Burn Research, Southwestern Hospital, Third Military Medical University, Chongqing 400038, China

Supported by the National Basic Research Priorities Programme of China, No. G199905403

Correspondence to: Pei-Yuan Xia, M. D., ph. D., Department of Pharmacy and Clinical Pharmacology, Southwestern Hospital, Third Military Medical University, Chongqing 400038, China. xiapy61@mail.tmmu.com.cn

Received 2001-11-02 Accepted 2001-12-04

Abstract

AIM: To investigate the relationship between lymphocyte apoptosis in peripheral blood, spleen and mesenteric lymph nodes (MLN) and endotoxin translocation after thermal injury in rats.

METHODS: In a Wistar rat model inflicted with 30% TBSA III degree scalding, serum LPS levels in portal vein and vena cava were quantified by tachypleus amebocyte lysate (TAL) technique. The analysis of peripheral blood lymphocyte was employed in situ Cell Death Detection Kit and evaluated by flow cytometry. Apoptotic lymphocytes in paraffin-embedded spleen and MLN sections were examined by histologic analysis, in situ deoxynucleotidyl transferase dUTP nick-end labeling (TUNEL) and peroxidase (POD) staining. The images were taken by Coolcd camera system, and the count and optical density value (transmission light) of apoptotic lymphocytes were analyzed with software Spot and Imagine proplus 4.10a(IPP4.10a).

RESULTS: In the period of 3 to 48 postburn hours (PBHs) serum LPS level ($\times 10^3$ EU·L⁻¹) in portal vein (2.11 ± 0.02 , 5.66 ± 0.20 , 3.70 ± 0.22 , 2.56 ± 0.28 , 0.90 ± 0.11) was higher than that in vena cava (0.63 ± 0.01 , 1.53 ± 0.18 , 0.83 ± 0.32 , 0.52 ± 0.12 , 0.23 ± 0.02 , $P < 0.01$), but both increased sharply in postburn rats ($P < 0.01$) and reached a peak at 6 PBH. Analysis of apoptotic lymphocytes showed that the proportion (%) of postburn apoptotic cells was much higher than that in healthy rats (8.34 ± 1.53 , 8.13 ± 1.81 , 20.77 ± 3.94 , 23.90 ± 3.92 , 11.23 ± 1.35 and 13.26 ± 2.09 at 3, 6, 12, 24, 48 and 72 PBH, respectively, $vs 3.99 \pm 1.72$, $P < 0.01$), especially after 6 PBH. The concentrations of lymphocytic apoptosis at 12 and 24 PBH were markedly higher than that at other time points. Meantime, few apoptotic lymphocytes were found in normal MLN, but increased postburn obviously (3 ± 1 $vs 546 \pm 83$, 285 ± 39 , 149 ± 30 , 58 ± 10 , 36 ± 11 and 33 ± 9 in turn, $P < 0.01$), especially at 3 PBH, whereas apoptotic lymphocytes were concentrated in splenic cortex before the burn and decreased obviously during 72 PBHs (499 ± 186 $vs 12 \pm 8$, 19 ± 15 , 12 ± 7 , 100 ± 15 , 123 ± 25 and 226 ± 26 in turn, $P < 0.01$) though a slight rise was found in the medulla after 24 PBH. Optical density of apoptotic lymphocytes was significantly reduced in spleen in the 24 PBHs and raised in MLN during 48 PBHs than that prior to the burn, respectively.

CONCLUSION: Gut-origin LPS is a major cause of endotoxemia taken place early in rats following severe thermal injury and could induce extensive lymphocyte apoptosis in blood and MLN, which suggests an immunosuppression state could follow the initial injury and favors a septic state based on apoptotic mechanism.

Xia PY, Zheng J, Zhou H, Pan WD, Qin XJ, Xiao GX. Relationship between lymphocyte apoptosis and endotoxin translocation after thermal injury in rats. *World J Gastroenterol* 2002;8(3):546-550

INTRODUCTION

Endotoxin or lipopolysaccharide (LPS) is a major cause of the local inflammation and septic shock and has been shown to impair host immune defense^[1-10]. With the experimental endotoxemia or sepsis in C3H/HeN (endotoxin-sensitive) mice, it was demonstrated in recent studies that LPS could cause thymic atrophy and bring about the increased apoptotic lymphocytes in thymus, spleen and gut-associated lymphatic tissue^[11-13]. Since the lymphocytes appear essential to both competent immune function and to the control of inflammatory response^[14,15], the lymphocyte apoptosis induced by LPS may play important roles in the development and regulation of the immune system, especially in the gut-dysfunction situations induced by sepsis or severe injuries. Endotoxemia in the patients with severe injury has been suggested to be an important factor in the systemic inflammatory response syndrome (SIRS)^[16,17]. It was found in the previous *in-vivo* study that gut-origin endotoxemia following the intestinal mucosal barrier dysfunction could occur in early postburn period and lead to the injury of systemic organs such as lungs, liver etc^[18,19]. Although the exact routes by which translocating LPS reach the blood and systemic organs are not known with certainty, most researchers believed that LPS was capable of translocating from the gut via both the mesenteric lymphatics and the portal blood^[20]. Because the mesenteric lymph nodes (MLN) receives its lymphatic drainage from the small intestine, cecum and proximal colon, we believed that MLN should be a major site and pathway of translocated gut-origin LPS. However, little has been known about lymphocyte apoptosis in circulating blood and MLN induced by endotoxin translocation after thermal injury and the relationship between them.

The present experiments were performed in severe scalded rats to determine the effects of gut-origin LPS translocation on the apoptosis of lymphocytes in circulating blood, spleen and MLN, and to investigate the relationship between them.

MATERIALS AND METHODS

Animals and reagents

Forty-two adult Wistar rats weighing 235-345g were randomly distributed in the normal control and 6 thermal injury groups, i.e. 3, 6, 12, 24, 48 and 72h after scalding. Each group contained 6 animals (half males and half females). Rats in the thermal injury groups were inflicted with 30% total burn surface area (TBSA) III degree scalding on their back after anesthetized with 30mg/kg of

intraperitoneal pentobarbital. Then under general anesthesia at the different time points after the thermal injury, the blood of rats' portal vein and vena cava were collected for LPS test and the isolation of peripheral blood lymphocyte, respectively. MLN and spleen were harvested by aseptic manipulation and fixed in 10mL·L⁻¹ paraformaldehyde solution (pH 7.4) for 24h. All chemicals used in this study were purchased from Sigma Chemical Co. (USA) unless specified otherwise. Endotoxin-free glassware and plasticware were prepared by baking at 250°C for 1.5h and radiating with ⁶⁰Co, respectively.

Determination of serum LPS levels in portal vein and vena cava

Sera were obtained from the blood samples of portal vein and vena cava by clotting for 60min on ice and then centrifuged at 2500g at 4°C for 5min respectively, filtered, aliquoted, and frozen at -70°C. After all serum samples were collected, the serum LPS levels were determined with a commercially available kit for tachypleus amebocyte lysate (TAL) technique (Zhanjiang A & C Biological Ltd, Zhanjiang, China) according to the manufacture's guidelines.

Isolation and preparation of lymphocyte

Lymphocyte in the heparinized blood from vena cava were isolated by density gradient centrifugation using ficoll-hypaque (d=1.077) followed by two washing steps in phosphate buffered saline (PBS) and lysis of residual erythrocytes using nine volumes of an ice-cold isotonic ammonium chloride solution (NH₄Cl 155mmol·L⁻¹, KHCO₃ 10mmol·L⁻¹, EDTA 0.1mmol·L⁻¹) to one volume of cell pellet at 4°C for 7min^[21]. Lymphocytes were greater than 98% as analyzed by microscopy using Hemacolor staining (Merk, Germany). Cell viability was greater than 97% as assessed by the trypan blue exclusion test. Isolated lymphocytes were maintained in a glass bottle in RPMI 1640-medium without fetal calf serum (endotoxin-free; Gibco BRL, Life Technologies, USA) at a concentration of 1×10⁹ cells·L⁻¹ in 5mL·L⁻¹ CO₂ at 37°C for 2h to exclude macrophage before the analysis of apoptosis. Then the cells were collected by centrifugation and washed twice in PBS.

Flow cytometric analysis of apoptotic lymphocyte

The analysis of apoptotic lymphocytes was performed by an in situ Cell Death Detection Kit, Fluorescein (Roche, Germany). The procedures in brief was according to the manufacture's guidelines as follows: lymphocyte were suspended and fixed with 40mL·L⁻¹ paraformaldehyde solution (pH 7.4), rinsed in PBS twice, and incubated in permeabilization solution (1 g·L⁻¹ Triton X-100 in 1 g·L⁻¹ sodium citrate) for 2min on ice. The cells were again rinsed in PBS, centrifuged and incubated in terminal deoxynucleotidyl transferase (TdT)-mediated dUTP nick end labeling (TUNEL) reaction mixture for 1h at 37°C in a humidified atmosphere at dark. Then cells were rinsed in PBS again. TUNEL fluorescence of individual nuclei in a final volume of 500μL cells solution was analyzed by an FACS Calibur (Becton Dickinson, USA), while gating on physical parameters was enacted to exclude cell debris. A minimum of 10000 events were counted per sample. The results were reported as the percentage of hypodiploid (fragmented) nuclei reflecting the relative proportion of apoptotic cells.

Analysis of apoptotic lymphocytes in spleen and MLN

Paraffin-embedded spleen and MLN tissue were cut into sections of 5μm and mounted on Vectabond Reagent slides, deparaffinized and rehydrated through xylene, graded ethanol to distilled water. Then the tissue sections were pre-treated with 20mg·L⁻¹ proteinase K for 30min, and analyzed with an in situ Cell Death Detection Kit, POD (Roche, USA) according to the manufacture's guidelines. Each

experiment set up by TUNEL reaction mixture without terminal transferase served as negative control. The images were taken by Coolcd camera system, and the count and optical density (OD) value of apoptotic lymphocytes were analyzed with software Spot and Imagine proplus 4.10a (IPP 4.10). The counts and optical density values (transmission light) of TUNEL-POD positive lymphocytes in spleen and MLN were determined in three high-resolution fields selected randomly in the area concentrated positive apoptotic lymphocytes and two thousand cells per field were counted per slides.

Statistical analysis

All the data was analyzed by Student's *t* test and expressed as $\bar{x} \pm s$. The statistical difference $P < 0.05$ was considered as significantly and $P < 0.01$ as very significant.

RESULTS

Serum LPS in portal vein and vena cava increased after thermal injury

Serum LPS levels in portal vein and vena cava increased sharply postburn ($P < 0.01$) and reached to a peak level at 6 PBH and decreased thereafter. LPS level in portal vein was higher than that in the vena cava ($P < 0.01$) in the period of 3 to 48 PBHs, but both decreased to near control level at 72 PBH (Figure 1).

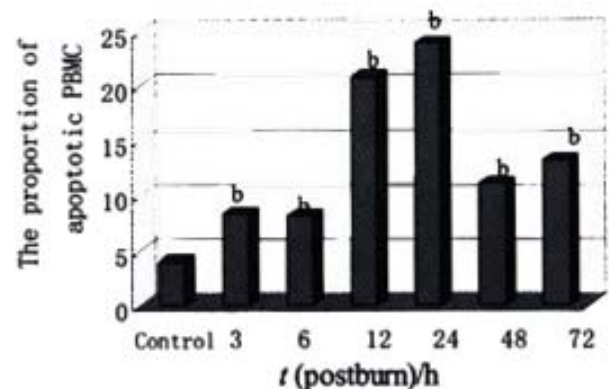


Figure 1 Comparison of the LPS levels postburn in portal vein and in vena cava. ^b $P < 0.01$, vs control; ^c $P < 0.01$, portal vein vs vena cava

Apoptosis of lymphocytes

Lymphocytes isolated from the circulation of healthy rats exhibited a low proportion of apoptotic cells at (3.99±1.72)%, but increased obviously during the whole postburn period of the experiment ($P < 0.01$), especially after 6 PBH. The concentrations of lymphocytic apoptosis at 12 and 24 PBH were markedly higher than that at other time points (Figure 2,3).

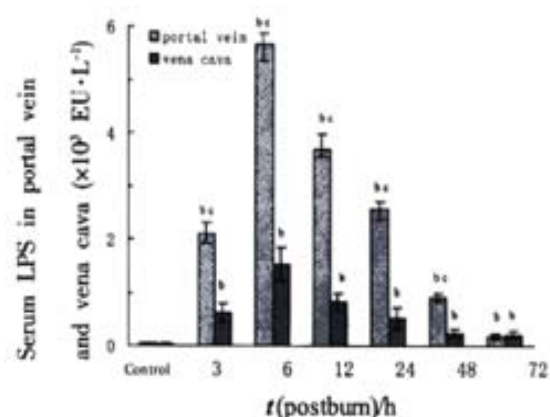


Figure 2 The relative proportions of apoptotic lymphocytes postburn. ^b $P < 0.01$, vs control

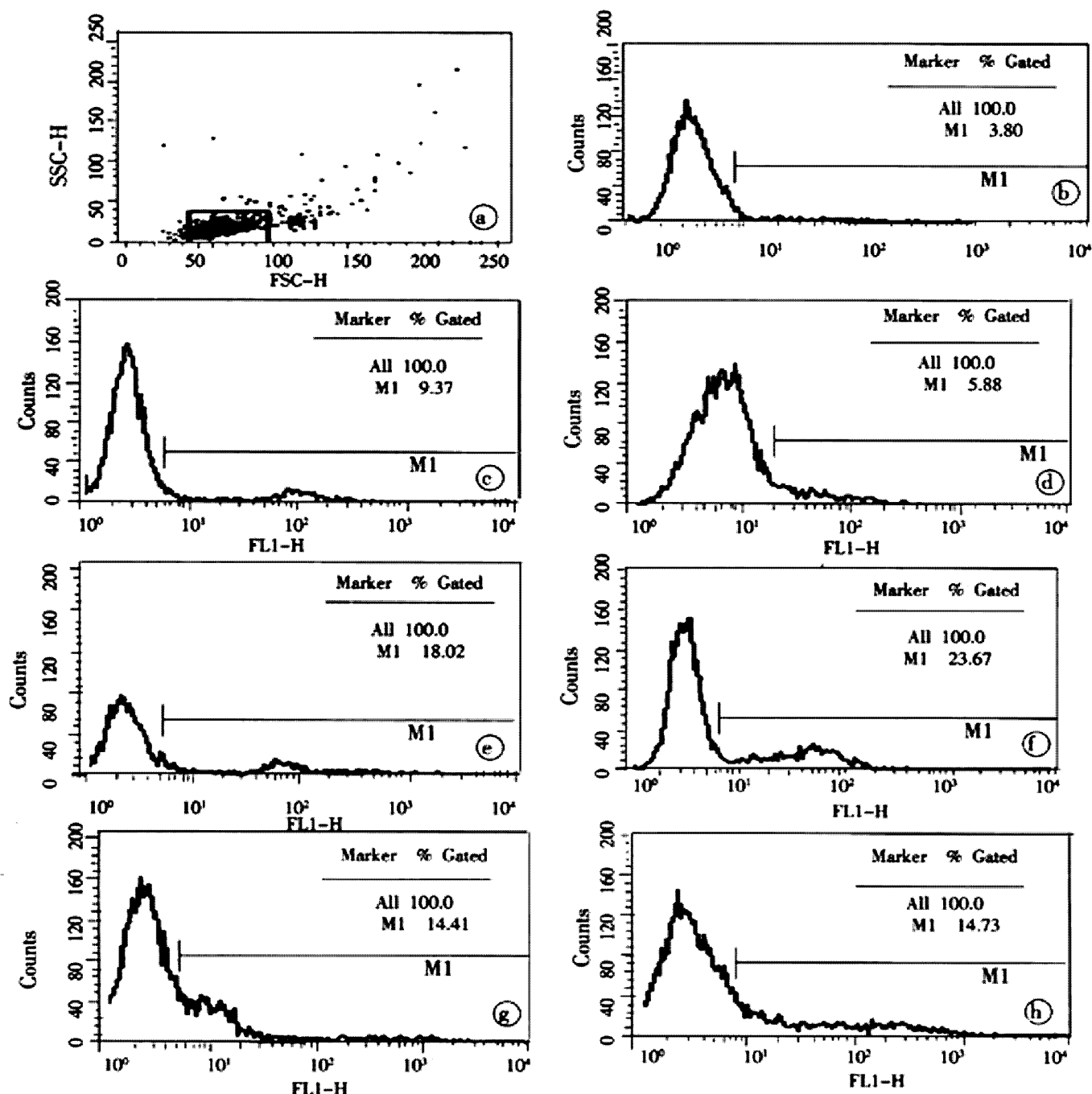


Figure 3 The results of typical flow cytometric analysis of postburn apoptotic lymphocytes. a, b, c, d, e, f, g and h were the relative proportion of apoptotic lymphocytes isolated from one rat in the control and group 3, 6, 12, 24, 48 and 72 PBH, respectively.

Apoptotic lymphocytes in spleen and MLN

It was shown by the results of TUNEL-POD staining and the counts of apoptotic lymphocytes that the apoptotic cells were few in normal MLN (Figure 4a), but increased postburn obviously ($P < 0.01$), especially at 3 PBH (Figure 4b, Table 1). Opposite to MLN, apoptotic lymphocytes were concentrated in spleen cortex before burn (Figure 4c), but decreased obviously during 3 to 72 PBHs ($P < 0.01$) though a slight rise was found in the medulla after 24 PBH (Figure 4d, Table 1). Since the principle of TUNEL-POD is to label the fragmented genomic DNA, the biochemical hallmark of apoptotic cell, the color density of nuclei staining could indirectly reflect the extent of DNA fragmentation. Optical density of TUNEL-POD staining in apoptotic lymphocytes was significantly reduced in spleen in the 24 PBHs, but raised in MLN during 48 PBHs than that before burn, respectively (Table 2).

Table 1 Apoptotic lymphocyte counts in 2000 total cells of spleen and MLN

Tissue	Healthy control	t(postburn)/h					
		3	6	12	24	48	72
Spleen	499±186	12±8 ^b	19±15 ^b	12±7 ^b	100±15 ^b	123±25 ^b	226±26 ^b
MLN	3±1	546±83 ^b	285±39 ^b	149±30 ^b	58±10 ^b	36±11 ^b	33±9 ^b

^b $P < 0.01$, vs control

Table 2 The optical density values(transmission light) of TUNEL-POD positive lymphocytes in spleen and MLN

Tissue	Healthy control	t(postburn)/h					
		3	6	12	24	48	72
Spleen	0.54±0.03	0.30±0.02 ^b	0.35±0.12 ^b	0.36±0.03 ^b	0.36±0.02 ^b	0.44±0.19	0.52±0.12
MLN	0.24±0.06	0.83±0.16 ^b	0.96±0.25 ^b	0.62±0.16 ^b	0.45±0.04 ^b	0.35±0.07 ^b	0.29±0.04

^b $P < 0.01$, vs control

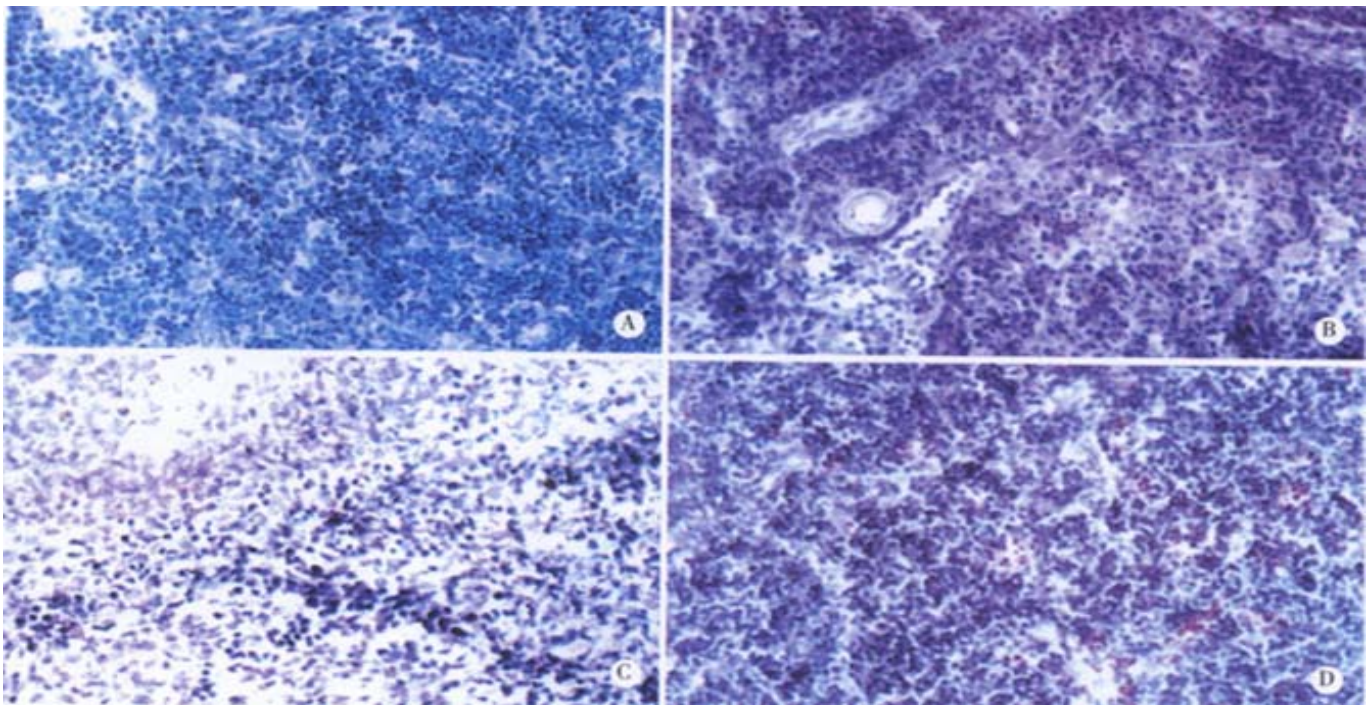


Figure 4 Apoptotic lymphocytes in spleen and MLN. (TUNEL-POD staining $\times 400$, the nuclei stained brown are positive apoptotic cells). a: MLN from the healthy rat; b: MLN from the rat at 3 PBH; c: Spleen from the healthy rat; d: Spleen from the rat 24 PBH.

DISCUSSION

Translocation of gut bacteria and endotoxin is a common situation after severe trauma, probably as a consequence of loss of physical integrity of the mucosal barrier, increments in permeability, or impaired local immune function resulted from ischemia-reperfusion injury of intestine. The gut-origin LPS translocated to the portal circulation or gut lymphatics has been thought to subsequently initiate a septic process leading to the development of SIRS^[22]. In this study, the LPS levels in portal vein and vena cava increased sharply after the severe thermal injury (Figure 1) indicating that endotoxin could enter the blood circulation in the early period of trauma and might be a main cause of endotoxemia.

The gastrointestinal tract contains numerous immune effector and regulatory cells of lymphoid and myeloid origin that are thought to play a critical role in host defense against enteric infections^[23]. And at a systemic level, the lymphocytes, through the production of regulatory cytokines, are important in mediating and controlling the host immune response. This was well illustrated by the spontaneous appearance of gastrointestinal inflammatory disease in a number of animals deficient in different cytokines, including IL-2 and IL-10, etc^[24-26]. Thus, the increased lymphocyte apoptosis in circulatory blood and gut-associated lymphoid tissues must impair the balance between the functions of host defense and immune tolerance in the gut immune system^[27,28]. The observation presented here provided some evidence that local and systemic pathologic lymphocyte apoptosis following an initial event of injury could impair the immune system. In the scalded rats, the counts of apoptotic lymphocytes in peripheral blood and MLN increased dramatically during the whole 72 PBHs, and reached a peak level at 12-24 PBHs and 3 PBH, respectively (Figure 2,3, 4, Table 1, 2). The results of lymphocyte apoptosis in MLN were consistent with that reported by Mongini *et al*^[22]. Moreover, It was surprised to observe the apoptotic lymphocytes in the spleen decreased obviously after thermal injury in this study (Figure 4, Table 1, 2) though splenic lymphocyte seemed to be less sensitive to apoptosis triggered by LPS

and oxidative stress^[11,12,29]. Specifically, we also found that splenic apoptotic lymphocytes were located mainly in the cortex in healthy rats, but being present in the medulla after thermal injury. The implications of these results are unclear. During normal lymphocyte development, immature lymphocytes are located in the cortex and migrate to the medulla in the course of maturation. The depletion of cortical lymphocytes by apoptosis may be one mechanism of eliminating potentially autoreactive immune cells^[22]. As for the decreased splenic apoptotic lymphocytes in the scalded rats, whether it is a reaction induced by the lymphocyte apoptosis in peripheral blood remains to be clarified.

Taking that both change tendency of lymphocyte apoptosis and serum LPS level after thermal injury into consideration, it was found that the peak level of lymphocyte apoptosis appeared earlier in MLN and much later in circulatory blood than that of LPS in the blood. The results indicated that MLN was an advanced station in the routing of the LPS translocation and suggested that the translocation of gut-origin LPS was a major factor of lymphocyte apoptosis in rats with severe burn injury. Furthermore, LPS translocated into the blood could lead to a further breakdown of gut immune barrier and thus accelerate the entrance of enteric bacteria and their toxins into the circulation^[30] and result in an immunosuppressive state due to the induction of lymphocyte apoptosis^[14,22,31]. This might explain why the peak level of apoptotic lymphocytes came forth much later in circulatory blood than that in MLN.

In addition to our observations in the present study, thymocyte and mucosal lymphocyte apoptosis after thermal injury had been recently reported^[32,33]. Although in these two studies the increased lymphocyte apoptosis in thymus and gut-associated lymphoid tissue seemed mainly due to the increased corticosterone concentration in plasma and in the lymphoid tissue, the presence of lymphocyte apoptosis in the peripheral blood, thymus and gut-associated lymphoid tissue following injury could explain the immunosuppressive state following such injury. In fact, decreased lymphocyte apoptosis in

sepsis can improve survival by overexpression of Bcl-2 in transgenic mice^[34]. In summary, we can reach the conclusion that an immunosuppression state could follow the initial injury and favor a septic state based on apoptotic mechanism, and that the immunosuppressive state after the thermal injury can be the event induced by translocation of gut-origin LPS and bacteria spreading to other tissues, and which in turn causes a recurrence of sepsis.

REFERENCES

- Bouchon A, Facchetti F, Weigand MA, Colonna M. TREM-1 amplifies inflammation and is a crucial mediator of septic shock. *Nature* 2001; 410: 1103-1107
- Yi JH, Ni RY, Luo DD, Li SL. Intestinal flora translocation and overgrowth in upper gastrointestinal tract induced by hepatic failure. *World J Gastroenterol* 1999;5:327-329
- Wray GM, Foster SJ, Hinds CJ, Thiernemann C. A cell wall component from pathogenic and non-pathogenic gram-positive bacteria (peptidoglycan) synergises with endotoxin to cause the release of tumour necrosis factor- α , nitric oxide production, shock, and multiple organ injury/dysfunction in the rat. *Shock* 2001; 15: 135-142
- Zhu L, Yang ZC, Li A, Cheng DC. Protective effect of early enteral feeding on postburn impairment of liver function and its mechanism in rats. *World J Gastroenterol* 2000;6:79-83
- Schultz MJ, Olszyna DP, de-Jonge E, Verbon A, van-Deventer SJ, van-der-Poll T. Reduced ex vivo chemokine production by polymorphonuclear cells after in vivo exposure of normal humans to endotoxin. *J Infect Dis* 2000; 182: 1264-1267
- Fu WL, Xiao GX, Yue XL, Hua C, Lei MP. Tracing method study of bacterial translocation in vivo. *World J Gastroenterol* 2000;6:153-155
- Liu BH, Chen HS, Zhou JH, Xiao N. Effects of endotoxin on endothelin receptor in hepatic and intestinal tissues after endotoxemia in rats. *World J Gastroenterol* 2000; 6:298-300
- Zuo GQ, Gong JP, Liu CA, Li SW, Wu XC, Yang K, Li Y. Expression of lipopolysaccharide binding protein and its receptor CD14 in experimental alcoholic liver disease. *World J Gastroenterol* 2001;7:836-840
- Heagy W, Hansen C, Nieman K, Cohen M, Richardson C, Rodriguez JL, West MA. Impaired ex vivo lipopolysaccharide-stimulated whole blood tumor necrosis factor production may identify "septic" intensive care unit patients. *Shock* 2000; 14: 271-277
- Zhang GL, Wang YH, Teng HL, Lin ZB. Effects of aminoguanidine on nitric oxide production induced by inflammatory cytokines and endotoxin in cultured rat hepatocytes. *World J Gastroenterol* 2001; 7: 331-334
- Zhang YH, Takahashi K, Jiang GZ, Kawai M, Fukada M, Yokochi T. In vivo induction of apoptosis (programmed cell death) in mouse thymus by administration of lipopolysaccharide. *Infect Immun* 1993; 61: 5044-5048
- Manhart N, Vierlinger K, Habel O, Bergmeister LH, Gotzinger P, Sautner T, Spittler A, Boltz-Nitulescu G, Marian B, Roth E. Lipopolysaccharide causes atrophy of Peyer's patches and an increased expression of CD28 and B7 costimulatory ligands. *Shock* 2000; 14: 478-483
- Wang SD, Huang KJ, Lin YS, Lei HY. Sepsis-induced apoptosis of the thymocytes in mice. *J Immunol* 1994;152:5014-5021
- Hotchkiss RS, Swanson PE, Freeman BD, Tinsley KW, Cobb JP, Matuschak GM, Buchman TG, Karl IE. Apoptotic cell death in patients with sepsis, shock, and multiple organ dysfunction. *Crit Care Med* 1999; 27: 1230-1251
- Hotchkiss RS, Chang KC, Swanson PE, Tinsley KW, Hui JJ, Klender P, Xanthoudakis S, Roy S, Black C, Grimm E, Aspiotis R, Han Y, Nicholson DW, Karl IE. Caspase inhibitors improve survival in sepsis: a critical role of the lymphocyte. *Nat Immunol* 2000; 1: 496-501
- Pape HC, Remmers D, Grotz M, Schedel I, von-Glinski S, Oberbeck R, Dahlweit M, Tscherne H. Levels of antibodies to endotoxin and cytokine release in patients with severe trauma: does posttraumatic dysregulation contribute to organ failure? *J Trauma* 1999; 46: 907-913
- Crespo E, Macias M, Pozo D, Escames G, Martin M, Vives F, Guerrero JM, Acuna-Castroviejo D. Melatonin inhibits expression of the inducible NO synthase II in liver and lung and prevents endotoxemia in lipopolysaccharide-induced multiple organ dysfunction syndrome in rats. *FASEB J* 1999; 13: 1537-1546
- Hotchkiss RS, Schmiege RE, Swanson PE, Freeman BD, Tinsley KW, Cobb JP, Karl IE, Buchman TG. Rapid onset of intestinal epithelial and lymphocyte apoptotic cell death in patients with trauma and shock. *Crit Care Med* 2000; 28: 3207-3217
- Goris RJA, Bebbler IPT, Mollen RMH, Koopman JP. Dose selective decontamination of the gastrointestinal tract prevent multiple organ failure. *Arch Surg* 1991; 126: 561-562
- Alexander JW, Gianotti L, Pyles T, Carey MA, Babcock GF. Distribution and survival of *Escherichia coli* translocating from the intestine after thermal injury. *Ann Surg* 1991; 213: 558-567
- Ertel W, Keel M, Infanger M, Ungethüm U, Steckholzer U, Trentz O. Circulating mediators in serum of injured patients with septic complications inhibit neutrophil apoptosis through up-regulation of protein-tyrosine phosphorylation. *J Trauma* 1998; 44: 767-775
- Mongini C, Ruybal PH, Garcia RH, Mocetti E, Escalada A, Christiansen S, Argibay P. Apoptosis in gut-associated lymphoid tissue: a response to injury or a physiologic mechanism? *Transplant Proc* 1998; 30: 2673-2676
- Malstrom C, James S. Inhibition of murine splenic and mucosal lymphocyte function by enteric bacterial products. *Infect Immun* 1998; 66: 3120-3127
- Sadlack B, Merz H, Schorle H, Schimpl A, Feller AC, Horak I. Ulcerative colitis-like disease in mice with a disrupted interleukin-2 gene. *Cell* 1993; 75: 253-261
- Kulkarni AB, Huh CG, Becker D, Geiser A, Lyght M, Flanders KC, Roberts AB, Sporn MB, Ward JM. Transforming growth factor (1 null mutation in mice causes excessive inflammatory response and early death. *Proc Natl Acad Sci USA* 1993; 90: 770-774
- Kuhn R, Lohler J, Rennick D, Rajewsky K, Muller W. Interleukin-10-deficient mice develop chronic enterocolitis. *Cell* 1993; 75: 263-274
- Ayala A, Xu YX, Ayala CA, Sonefeld DE, Karr SM, Evans TA, Chaudry IH. Increased mucosal B-lymphocyte apoptosis during polymicrobial sepsis is a Fas ligand but not an endotoxin-mediated process. *Blood* 1998; 91: 1362-1372
- Andjelic S, Khanna A, Suthanthiran M, Nikolic ZJ. Intracellular Ca²⁺ elevation and cyclosporin A synergistically induce TGF- β 1-mediated apoptosis in lymphocytes. *J Immunol* 1997; 158: 2527-2534
- Freeman BD, Reaume AG, Swanson PE, Epstein CJ, Carlson EJ, Buchman TG, Karl IE, Hotchkiss RS. Role of CuZn superoxide dismutase in regulating lymphocyte apoptosis during sepsis. *Crit Care Med* 2000; 28: 1701-1708
- Navaratnam RLN, Morris SE, Traber DL, Flynn J, Woodson L, Linares H, Herndon DN. Endotoxin (LPS) increased mesenteric vascular Resistance (MVR) and bacterial translocation. *J Trauma* 1990; 30: 1104-1115
- Kurita-Ochiai T, Fukushima K, Ochiai K. Butyric acid-induced Apoptosis of murine thymocytes, splenic T cells, and human jurkat T cells. *Infect Immun* 1997; 65: 35-41
- Fukuzuka K, Edwards CK 3rd, Clare-Salzer M, Copeland EM 3rd, Moldawer LL, Mozingo DW. Glucocorticoid and Fas ligand induced mucosal lymphocyte apoptosis after burn injury. *J Trauma* 2000; 49: 710-716
- Nakanishi T, Nishi Y, Sato EF, Ishii M, Hamada T, Inoue M. Thermal injury induces thymocyte apoptosis in the rat. *J Trauma* 1998; 44: 143-148
- Hotchkiss RS, Swanson PE, Knudson CM, Chang KC, Cobb JP, Osborne DF, Zollner KM, Buchman TG, Korsmeyer SJ, Karl IE. Overexpression of Bcl-2 in transgenic mice decreases apoptosis and improves survival in sepsis. *J Immunol* 1999; 162: 4148-4150

Edited by Wu XN

• BASIC RESEARCH •

Expression of CD14 protein and its gene in liver sinusoidal endothelial cells during endotoxemia

Jian-Ping Gong, Li-Li Dai, Chang-An Liu, Chuan-Xin Wu, Yu-Jun Shi, Sheng-Wei Li, Xu-Hong Li

Jian-Ping Gong, Chang-An Liu, Chuan-Xin Wu, Yu-Jun Shi, Sheng-Wei Li, Xu-Hong Li, Department of General Surgery, the Second College of Clinical Medicine & the Second Affiliated Hospital of Chongqing University of Medical Science, Chongqing, 400010, China

Li-Li Dai, Department of Digestive Disease, the Second College of Clinical Medicine & the Second Affiliated Hospital of Chongqing University of Medical Science, Chongqing, 400010, China

Supported by the National Natural Science Foundation of China, No. 39970719, 30170919

Correspondence to: Dr Jian-Ping Gong, Department of General Surgery, the Second College of Clinical Medicine & the Second Affiliated Hospital of Chongqing University of Medical Science, 74 Linjiang Road, Chongqing 400010, China. gongjianping11@hotmail.com

Telephone: +86-23-85541610 Fax: +86-23-63822815

Received 2001-11-15 Accepted 2001-12-10

Abstract

AIM: To observe expression of CD14 protein and CD14 gene in rat liver sinusoidal endothelial cells (LSECs) during endotoxemia, and the role of CD14 protein in the activation of lipopolysaccharide (LPS)-induced LSECs.

METHODS: Wistar rat endotoxemia model was established first by injection of a dose of LPS (5mg/kg, *Escherichia coli* O111:B4) via the tail vein, then sacrificed after 0h, 3h, 6h, 12h, and 24h, respectively. LSECs were isolated from normal and LPS-injected rats by an in situ collagenase perfusion technique. The isolated LSECs were incubated with rabbit anti-rat CD14 polyclonal antibody, then stained with goat anti rabbit IgG conjugated fluorescein isothiocyanate (FITC) and flow cytometric analysis (FCM) was performed. The percentage and mean fluorescence intensity (MFI) of CD14-positive cells were taken as the indexes. LSECs were collected to measure the expression of CD14 mRNA by in situ hybridization analysis. The isolated LSECs from normal rats were incubated firstly with anti-CD14 antibody, then stimulated with different concentrations of LPS, and the supernatants of these cells were then collected for measuring the levels of tumor necrosis factor (TNF)- α and Interleukin (IL)-6 with ELISA.

RESULTS: In rats with endotoxemia, LSECs displayed a strong MFI distinct from that of control rats. CD14 positive cells in rats with endotoxemia were 54.32%, 65.83%, 85.64%, and 45.65% at 3h, 6h, 12h, and 24h respectively, there was significant difference when compared to normal group of animals (4.45%) ($P < 0.01$). The expression of CD14 mRNA in isolated LSECs was stronger than that in control rats. In LPS group, the levels of TNF- α and IL-6 were $54 \pm 6 \text{ ng} \cdot \text{L}^{-1}$, $85 \pm 9 \text{ ng} \cdot \text{L}^{-1}$, $206 \pm 22 \text{ ng} \cdot \text{L}^{-1}$, $350 \pm 41 \text{ ng} \cdot \text{L}^{-1}$, $366 \pm 42 \text{ ng} \cdot \text{L}^{-1}$ and $103 \pm 11 \text{ ng} \cdot \text{L}^{-1}$, $187 \pm 20 \text{ ng} \cdot \text{L}^{-1}$, $244 \pm 26 \text{ ng} \cdot \text{L}^{-1}$, $290 \pm 31 \text{ ng} \cdot \text{L}^{-1}$, and $299 \pm 34 \text{ ng} \cdot \text{L}^{-1}$, respectively at different concentration points. In anti-CD14 group, the levels of TNF- α and IL-6 were $56 \pm 5 \text{ ng} \cdot \text{L}^{-1}$, $67 \pm 8 \text{ ng} \cdot \text{L}^{-1}$, $85 \pm 10 \text{ ng} \cdot \text{L}^{-1}$, $113 \pm 12 \text{ ng} \cdot \text{L}^{-1}$, $199 \pm 22 \text{ ng} \cdot \text{L}^{-1}$ and $104 \pm 12 \text{ ng} \cdot \text{L}^{-1}$, $125 \pm 12 \text{ ng} \cdot \text{L}^{-1}$, $165 \pm 19 \text{ ng} \cdot \text{L}^{-1}$, $185 \pm 21 \text{ ng} \cdot \text{L}^{-1}$, and $222 \pm 23 \text{ ng} \cdot \text{L}^{-1}$, respectively at

different concentration points. There was significant difference between the two groups ($P < 0.01$).

CONCLUSION: LSECs can synthesize CD14 protein and express CD14 gene during endotoxemia. CD14 protein plays an important role in the activation of LPS-induced LSECs. This finding has important implications for the understanding of the mechanisms by which LPS may injure liver sinusoidal endothelial cells during sepsis.

Gong JP, Dai LL, Liu CA, Wu CX, Shi YJ, Li SW, Li XH. Expression of CD14 protein and its gene in liver sinusoidal endothelial cells during endotoxemia. *World J Gastroenterol* 2002;8(3):551-554

INTRODUCTION

Lipopolysaccharide (LPS) has been shown to play a key role in the pathogenesis of severe sepsis and septic shock caused by gram-negative bacteria. LPS stimulates monocytes and macrophages to release proinflammatory mediators, such as tumor necrosis factor (TNF)- α and interleukins^[1-10]. Recent studies have reported that LPS-binding protein (LBP) and LPS receptor CD14 mediate responses of activated monocytes, macrophages and other cells to LPS^[11-13]. CD14 is a 55-kDa glycoprotein with multiple leucine-rich repeats and was first described as a myeloid differentiation antigen^[14]. CD14 has been identified as receptor for complexes of LPS and LBP. It is known that CD14 is linked to the cell membrane by a glycosylphosphatidylinositol anchor in myeloid lineage cells, and it plays a pivotal role in the activation of LPS-induced monocytes and macrophages^[15, 16]. But it is not yet clear whether CD14 is expressed by vascular endothelial cells. Indeed, it has been generally accepted that endothelial cells do not express CD14^[17]. Soluble CD14 (sCD14) is thought to facilitate LPS-induced activation of endothelial cells^[18]. However, recent studies have shown that endothelial cells are sensitive to low concentration of LPS and anti-CD14 antibodies can block endothelial cell activation even in the absence of serum, which is an observation inconsistent with the concept that endothelial cells do not express CD14^[19]. Our aim was to demonstrate that liver sinusoidal endothelial cells (LSECs) synthesize CD14 protein and express CD14 gene in rats with endotoxemia, and the role of CD14 protein in the activation of LPS-induced LSECs.

MATERIALS AND METHODS

Reagents

LPS (*Escherichia coli* O111: B4) and collagenase (type IV) were purchased from Sigma Chemical Company (St. Louis, Mo.). A rabbit anti-rat CD14 polyclonal antibody was purchased from Santa Cruz Biotechnology (Santa Cruz, Calif). Fluorescein isothiocyanate (FITC)-IgG were purchased from Zhongshan Biotechnology Company (Beijing, China). In situ hybridization analysis kit of CD14 mRNA was purchased from Boshide Biotechnology Company (Wuhan, China).

Animals

Male Wistar rats, which were pathogen-free and weighed

approximately 225g each, were purchased from the Animal Center of Chongqing University of Medical Science. The rats were exposed each day to 12h of light and darkness respectively. Rodent chow and water were provided ad libitum. Experimental protocols were approved by the Institutional Care and Use Committee of Chongqing University of Medical Science.

The endotoxemia model of animals

The Wistar rat endotoxemia model was established as described previously^[20]. In brief, animals were injected with a dose of LPS (5mg/kg, Escherichia coli O111: B4) via the tail vein, then the sacrificed after 3h, 6h, 12h, and 24h, respectively. There were six rats at each time point. Other six rats were used as control group (0h).

LSECs isolation

LSECs were isolated from normal and LPS-injected rats by an in situ collagenase perfusion technique, modified as described previously^[21]. In brief, livers were removed after a portal vein perfusion with Hanks' balanced salt solution (HBSS) and the homogenate was digested in a solution of 0.5% collagenase. LSECs were separated from other nonparenchymal cells by two cycles of differential centrifugation (50×g for 2min) and further purified over a 30% Percoll gradient. LSECs purity exceeded 90% as assessed by light microscopy, and viability was typically greater than 95% as determined by trypan blue exclusion assay.

Determination of CD14 mRNA by in situ hybridization

In situ hybridization was performed as described previously^[22]. Positive result: positive location was blue.

Flow cytometric analysis

Expression of CD14 protein in LSECs was examined by flow cytometric analysis as described previously^[23]. In brief, LSECs were incubated with rabbit anti-rat CD14 polyclonal antibody (1ug/ml) after washing, and then cells were incubated with goat anti-rabbit immunoglobulin G labeled with FITC. After being washed three times, 10000 cells were analyzed by flow cytometry (Coulter, USA), and the percentage and mean fluorescence intensity (MFI) of CD14-positive cells were taken as the indexes.

Blocking test of anti-CD14 antibody

To determinate the role of CD14 in the activation of LPS-induced LSECs, LSECs were isolated from normal rats. These cells were harvested and adjusted to a concentration of 1×10^6 /ml/well and were divided into two groups. Group of LPS: LSECs were incubated at different concentrations of LPS (0, 0.01ug/ml, 1ug/ml, 10ug/ml, and 100ug/ml). Group of anti-CD14 antibody blockade: LSECs were pre-incubated for 30min with 0.2ml CD14 antibody (1:100 dilution) before different concentrations of LPS were added. Supernatants were then collected for measuring the levels of TNF- α and IL-6 with ELISA.

Statistical analysis

All results were expressed as mean \pm SEM. Statistical differences between means were determined by using Student's *t* test. The value of $P < 0.01$ was considered significant.

RESULTS

Binding of FITC to LSECs

To confirm expression of CD14 on LSECs, we examined the binding of FITC to the cells. CD14 positive cells were 4.45% in rats of normal group. But in rats with endotoxemia, CD14 positive cells were 54.32%, 65.83%, 85.64%, and 45.65% at 3 h, 6 h, 12 h, and 24 h

respectively after stimulation of LPS, which were significant different when compared with normal group of animals ($P < 0.01$) (Figure 1).

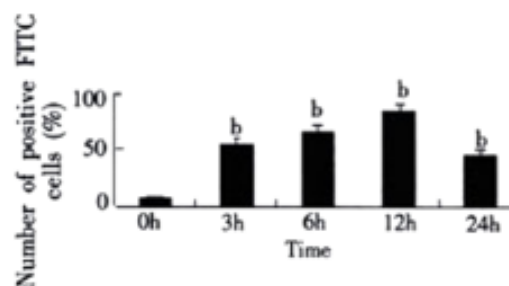


Figure 1 The percentage of positive FITC cells. ^b $P < 0.01$ vs 0h

Expression of CD14 gene in LSECs

We postulated that LSECs could express CD14 mRNA during endotoxemia. In order to examine the cell-specific expression of CD14 mRNA, freshly isolated and purified LSECs were analyzed by in situ hybridization with a riboprobe specific for rat CD14. Our analysis showed that LSECs from controls had no detectable level of CD14 mRNA. LPS treatment increased the level of CD14 mRNA in LSECs, inducing expression as early as 3h after LPS treatment. The expression of CD14 gene increased with time, reaching a maximum induction by 12h after treatment of LPS, and subsequently declined to low level by 24h.

Results of blocking test

In LPS group, with increasing of LPS concentrations, the levels of TNF- α and IL-6 in supernatant of LSECs also increased. In group of anti-CD14 antibody blockade, productions of TNF- α and IL-6 in supernatants of LSECs were obviously inhibited by Ab against CD14 when compared with LPS group ($P < 0.01$). (Figure 2 and 3)

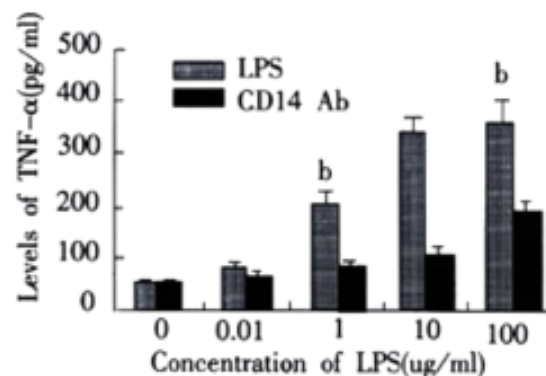


Figure 2 Effect of CD14 Ab on production of TNF- α in supernatants of LSECs. ^b $P < 0.01$ vs CD14 Ab

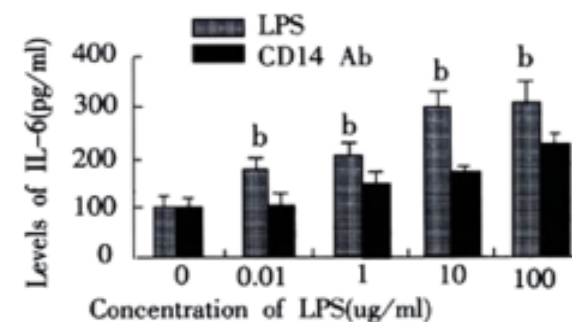


Figure 3 Effect of CD14 Ab on production IL-6 in supernatants of LSECs. ^b $P < 0.01$ vs CD14 Ab

DISCUSSION

CD14 as a key LPS signaling molecule was first reported to be expressed in monocyte-macrophage system^[4,12,23]. Recent works have showed that the CD14 antigen is expressed in many types of cells and tissues^[20, 24-32]. But it is not yet clear whether vascular endothelial cells could synthesize CD14 protein and express CD14 gene. Beekhuizen *et al* reported endothelial cells did not express CD14. With method of in situ hybridization, Fearn *et al*^[24] found that endothelial cells did not express CD14 protein. Wang *et al*^[18] considered that sCD14 was thought to facilitate LPS-induced activation of endothelial cells. But, Lee *et al*^[33] found CD14-negative murine pre-B cells (70Z/3), which were unresponsive to low concentrations of LPS (0.1ng/ml) even in the presence of serum, showed responses to LPS when transfected with CD14. Surprisingly, anti-CD14 antibody blocked endothelial cell activation by LPS even in the absence of serum, which is an observation inconsistent with the concept that endothelial cells do not express CD14 protein.

In this experiment, we selected LSECs to represent vascular endothelial cells as targets of our experiment, and determined whether LSECs could synthesize CD14 protein and express CD14 gene. We found: (1)LSECs from normal rats did not synthesize CD14 protein and express CD14 gene, but the synthesis and expression of CD14 were markedly upregulated by LPS during endotoxemia, accompanied with the expression of CD14 mRNA, which showed that CD14 protein in LSECs was not passively acquired from serum. (2)Anti-CD14 antibody could block LSECs activation by LPS in the absence of serum, which further indicated that LSECs could synthesize and express CD14 molecules.

Why were our findings different from previously published data that endothelial cells were CD14 negative? We think there were a few possibilities: (1)many authors used routine passaging of multiple culture of human vascular endothelial cells (HUVEC) or HUVEC purchased from tissue culture laboratories to observe whether these cells expressed CD14, but these cells might lose CD14 gene when they were cultured at multiple passages. Jersmann *et al*^[34] reported when HUVEs were cultured at passages 3 to 5, these cells were indistinguishable from passage 1 HUVEC in a number of properties and displayed normal morphology and viability and response to TNF to the same extent as passage 1 cells. However, unlike passage 1 cells, HUVEC that had undergone multiple passing expressed extremely low amounts of CD14 protein. We used freshly isolated primary rat LSECs to study the expression of CD14 and found they could obviously synthesize and express CD14 during endotoxemia. (2) LSECs were different from other endothelial cells in location, construction, and function. LSECs are located in hepatic sinus and stimulated by LPS from gut via portal vein blood, so these cells have their property which are different from other endothelial cells^[35]. (3) The choice of Ab against CD14 for the flow cytometric analysis may have been an additional explanation for the previously reported lack of CD14 on the endothelial cells' surface. Jersmann *et al*^[34] stained HUVEC with five different primary mAbs (MY4, 2D-15C, TUK4, LeuM3, and Rmo52) against CD14, and found only MY4 and TUK4 produced a positive stain and MY4 was the most effective mAb for detection of CD14 expression in endothelial cells. We stained LSECs with rabbit anti-rats primary antibody against CD14 from Santa Cruz Biotechnology and found this Ab against CD14 was effective for detecting the expression of CD14 protein. As expression of CD14 in animals is probably different from that in humans, further investigation of the expression of CD14 among animals is going on actively in our laboratory.

REFERENCES

- Gong JP, Liu CA, Wu CX, Li SW, Shi YJ, Li XH. Nuclear factor kB activity in patients with acute severe cholangitis. *World J Gastroenterol* 2002; 8:346-349
- Gong JP, Wu CX, Liu CA, Li SW, Shi YJ, Yang K, Li Y, Li XH. Intestinal damage mediated by Kupffer cells in rats with endotoxemia. *World J Gastroenterol* 2002; 8: press
- Gong JP, Liu CA, Wu CX, Li SW, Shi YJ, Yang K, Li Y, Li XH. Liver sinusoidal endothelial cell injury by neutrophils in rats with acute obstructive cholangitis. *World J Gastroenterol* 2002; 8:342-345
- Heumann D, Adachi Y, Roy DL, Ohno N, Yadomae T, Glauser MP, Calandra T. Role of plasma, lipopolysaccharide-binding protein, and CD14 in response of mouse peritoneal exudate macrophages to endotoxin. *Infect Immun* 2001; 69: 378-385
- Merkel SM, Alexander S, Zufall E, Oliver JD, Huet-Hudson YM. Essential role for estrogen in protection against *Vibrio vulnificus*-induced endotoxic shock. *Infect Immun* 2001; 69: 6119-6122
- Rabeih L, Irinopoulou T, Cholley B, Haeflner-Cavillon N, Carreno MP. Gram-positive and Gram-negative bacteria do not trigger monocyte cytokine production through similar intracellular pathways. *Infect Immun* 2001; 69: 4590-4599
- Fry DE. Sepsis syndrome. *Am Surg* 2000; 66:126-132
- Hotchkiss RS, Karl IE. Cytokine blockade in sepsis are two better than one? *Crit Care Med* 2001; 29: 671-672
- Mathurin P, Deng QG, Keshavarzian A, Choudhary S, Holmes EW, Tsukamoto H. Exacerbation of alcoholic liver injury by enteral endotoxin in rats. *Hepatology* 2000; 32:1008-1017
- Parker SJ, Watkins PE. Experimental models of gram-negative sepsis. *Br J Surg* 2001; 88:22-30
- Nanbo A, Nishimura H, Muta T, Nagasawa S. Lipopolysaccharide stimulates HepG2 human hepatoma cells in the presence of lipopolysaccharide-binding protein via CD14. *Eur J Biochem* 1999; 260: 183-191
- Gutsmann T, Muller M, Carroll SF, Mackenzie RC, Wiese A, Seydel U. Dual role of lipopolysaccharide (LPS)-binding protein in neutralization of LPS and enhancement of LPS-induced activation of mononuclear cells. *Infect Immun* 2001; 69: 6942-6950
- Hiki N, Berger D, Mimura Y, Frick J, Dentener MA, Buurman WA, Seidelmann M, Kaminishi M, Beger HG. Release of endotoxin-binding proteins during major elective surgery: role of soluble CD14 in phagocytic activation. *World J Surg* 2000; 24: 499-506
- Ulevitch RJ, Tobias PS. Receptor-dependent mechanisms of cell stimulation by bacterial endotoxin. *Annu Rev Immunol* 1995; 13: 437-457
- Enomoto N, Yamashina S, Kono H, Schemmer P, Rivera CA, Enomoto A, Nishiura T, Nishimura T, Brenner DA, Thurman RG. Development of a new, simple rat model of early alcohol-induced liver injury based on sensitization of Kupffer cells. *Hepatology* 1999; 29: 1680-1689
- Li SW, Gong JP, Wu CX, Shi YJ, Liu CA. Lipopolysaccharide induced synthesis of CD14 proteins and its gene expression in hepatocytes during endotoxemia. *World J Gastroenterol* 2002; 8: 124-127
- Kono H, Wheeler MD, Rusyn I, Lin M, Seabra V, Rivera CA, Bradford BU, Forman DT, Thurman RG. Gender differences in early alcohol-induced liver injury: role of CD14, NF-kB, and TNF- α . *Am J Physiol* 2000; G652-661
- Wong PM, Chung SW, Sultzner BM. Genes, receptors, signals and responses to lipopolysaccharide endotoxin. *Scand J Immunol* 2000; 51: 123-127
- Von Asmuth EJU, Dentener MA, Baxil V, Bouma MG, Leeuwenberg JFM, Buurman WA. Anti-CD14 antibodies reduce responses of cultured human endothelial cells to endotoxin. *Immunology* 1993; 80: 78-83
- Gong JP, Xu MQ, Li K, Zhu J, Han BL. Expression of CD14 in Kupffer cells induced by lipopolysaccharide. *Di-San Junyi Daxue Xuebao* 2001; 23: 425-428
- Gong JP, Han BL. Technique of isolation, culture and identification of liver cells. *Shijie Huaren Xiaohua Zazhi* 1999; 7:417-419
- Fearn C, Loskutoff DJ. Role of tumor necrosis factor alpha in induction of murine CD14 gene expression by lipopolysaccharide. *Infect Immun* 1997; 65: 4822-4831
- Gong JP, Han BL. Effects of CD14 in LPS mediating activation of Kupffer cells. *Shijie Huaren Xiaohua Zazhi* 1999; 7:875-877
- Fearn C, Kravchenko VV, Ulevitch RJ, Loskutoff DJ. Murine CD14 gene expression *in vivo*: extramylloid synthesis and regulation by lipopolysaccharide. *J Exp Med* 1995; 181: 857-866
- Li SW, Wu CX, Shi YJ, Liu CA. Lipopolysaccharide upregulates expression of CD14 gene and CD14 proteins of hepatocytes in rats. *Chin J Hepatol* 2001; 9:103-105
- Zuo GQ, Gong JP, Liu CA, Li SW, Wu XC, Yang K, Li Y. Expression of lipopolysaccharide binding protein and its receptor CD14 in experimental alcoholic liver disease. *World J Gastroenterol* 2001; 6: 836-840
- Jiang Q, Akashi S, Miyake K, Petty HR. Cutting edge: lipopolysaccharide induces physical proximity between CD14 and toll-like

- receptor 4 (TLR4) prior to nuclear translocation of NF-kB. *J Immunol* 2000; 165:3541-3544
- 28 Ikejima K, Enomoto N, Seabra V, Ikejima A, Brenner DA, Thurman RG. Pronase destroys the lipopolysaccharide receptor CD14 on Kupffer cells. *Am J Physiol* 1999; 276: G591-G598
- 29 Scott MG, Vreugdenhil ACE, Buurman WA, Hancock REW, Gold MR. Cutting edge: cationic antimicrobial peptides block the binding of lipopolysaccharide (LPS) to LPS binding protein. *J Immunol* 2000; 164:549-553
- 30 Asea A, Kraeft SK, Kurt-Jones EA, Stevenson MA, Chen LB, Fixberg RW, Koo GC, Calderwood SK. HSP70 stimulates cytokine production through a CD14-dependant pathway, demonstrating its dual role as a chaperone and cytokine. *Nature Med* 2000; 6:435-442
- 31 Haziot A, Hijiya N, Gangloff SC, Silver J, Goyert SM. Induction of a novel mechanism of accelerated bacterial clearance by lipopolysaccharide in CD14-deficient and Toll-like receptor 4-deficient mice. *J Immunol* 2001; 166:1075-1078
- 32 Perea PY, Mayadas TN, Takeuchi O, Akira S, Zaks-Zilberman, Goyert SM, Vogel SN. CD11b/CD18 acts in concert with CD14 and toll-like receptor (TLR) 4 to elicit full lipopolysaccharide and taxol-inducible gene expression. *J Immunol* 2001; 166: 574-581
- 33 Lee JD, Kato K, Tobias PS, Kirkland TN, Ulevitch RJ. Transfection of CD14 into 70Z/3 cells dramatically enhances the sensitivity to complexes of lipopolysaccharide (LPS) and LPS binding protein. *J Exp Med* 1992; 175: 1697-1703
- 34 Jersmann HPA, Hii CST, Hodge GL, Ferrante AF. Synthesis and surface expression of CD14 by human endothelial cells. *Infect Immun* 2001; 69: 479-485
- 35 Bone-Larson CL, Simpson KJ, Colletti LM, Lukacs NW, Chen SC, Lira S, Kunkel S, Hogaboam CM. The role of chemokines in the immunopathology of the liver. *Immunol Rev* 2000; 177: 8-20

Edited by Hu DK

• BASIC RESEARCH •

The effects of anisodamine and dobutamine on gut mucosal blood flow during gut ischemia/reperfusion

Sen Hu, Zhi-Yong Sheng

Sen Hu, Zhi-Yong Sheng, Burns Institute, 304th Hospital of PLA, Beijing 100037, China

Supported by the Tenth Five-Year Key Project of PLA, No.01L081
Correspondence to: Dr Sen Hu, Burns Institute, 304th Hospital of PLA, 51 Fu Cheng Road, Beijing 100037, China

Telephone: +86-10-66867397 Fax: +86-10-68429998

Received 2002-01-26 Accepted 2002-02-20

Abstract

AIM: To determine if anisodamine is able to augment mucosal perfusion during gut I/R ischemia-reperfusion.

METHODS: A jejunal sac was formed in Sprague Dawley rat. A Laser Doppler probe and a tonometer were inserted into the sac which was filled with saline. The superior mesenteric artery was occluded (SMAO) for 60 minutes followed by 90 minutes of reperfusion. At the end of 60 minutes of SMAO, either 0.2mg/kg of anisodamine or dobutamine was injected into the jejunal sac. Laser Doppler mucosal blood flow and regional PCO_2 (PrCO_2) measurements were made.

RESULTS: Mucosal blood flow was significantly increased at 30, 60 and 90 minutes of reperfusion (R_{30}, R_{60}, R_{90}) when intraluminal anisodamine or dobutamine was present compared to intraluminal saline only ($44 \pm 3.3\%$ or $48 \pm 4.1\%$ vs $37 \pm 2.6\%$ at R_{30} , $57 \pm 5.0\%$ or $56 \pm 4.7\%$ vs $45 \pm 2.7\%$ at R_{60} , $64 \pm 3.3\%$ or $56 \pm 4.2\%$ vs $48 \pm 3.4\%$ at R_{90} , respectively $P < 0.05$). Blood flow changes were also reflected by lowering of jejunal PrCO_2 measurements after intraluminal anisodamine or dobutamine compared with that of the saline controls ($41 \pm 3.1\text{mmHg}$ or $44 \pm 3.0\text{mmHg}$ vs $49 \pm 3.7\text{mmHg}$ at R_{30} , $38 \pm 3.7\text{mmHg}$ or $40 \pm 2.1\text{mmHg}$ vs $47 \pm 3.8\text{mmHg}$ at R_{60} , $34 \pm 2.1\text{mmHg}$ or $39 \pm 3.0\text{mmHg}$ vs $46 \pm 3.4\text{mmHg}$ at R_{90} , respectively, $P < 0.05$). Most interesting finding was that there were significantly higher mucosal blood flow and lower jejunal PrCO_2 in anisodamine group than those in dobutamine group at 90 minutes of reperfusion ($64 \pm 3.3\%$ vs $56 \pm 4.2\%$ for blood flow or $34 \pm 2.1\text{mmHg}$ vs $39 \pm 3.0\text{mmHg}$ for PrCO_2 , respectively, $P < 0.05$), suggesting that anisodamine had a more lasting effect on mucosal perfusion than dobutamine.

CONCLUSION: Intraluminal anisodamine and dobutamine can augment mucosal blood flow during gut I/R and alleviate mucosal acidosis. The results provided beneficial effects on the treatment of splanchnic hypoperfusion following traumatic or burn shock.

Hu S, Sheng ZY. The effects of anisodamine and dobutamine on mucosal blood flow during gut ischemia/reperfusion. *World J Gastroenterol* 2002;8(3):555-557

INTRODUCTION

With remarkable advancement in our understanding of shock and greater ability to resuscitate patients from shock, few people today died of hypovolemic shock. However there still exists an inadequate

splanchnic perfusion, especially gut ischemia, despite apparent normalization of global hemodynamic parameters. Clinical and experimental studies have implicated gut hypoperfusion as an important inciting event which contributes to gut origin sepsis and multiple organ dysfunction^[1-10]. To improve gut perfusion, thus averting compensated shock, is still an important goal of resuscitation of shock^[11,12]. Anisodamine and dobutamine are commonly used as antishock drugs, as they can improve the microcirculation flow and splanchnic perfusion^[13-16]. Anisodamine, an anticholinergic drug extract from a Chinese herb *Anisodus tanguticus*, also processes many other beneficial effects such as inhibition of thromboxane synthesis and protection of cell from reperfusion injury^[17-20]. Some researches indicated that anisodamine and dobutamine augmented gut perfusion during the shock^[21,22], but there was no report concerning their intraluminal effects on mucosal blood flow and metabolism in the gut. The purpose of this study is to investigate the effects of local administration of anisodamine and dobutamine on mucosal blood flow and PrCO_2 in a gut ischemia-reperfusion (I/R) rat model.

MATERIALS AND METHODS

Animal model

Male Sprague-Dawley rats weighing 350-450 grams were employed after acclimatization to the experimental environment. Rats were fasted overnight but allowed free access to water. Anesthesia was induced and maintained with 2% isoflurane and body temperature maintained at 37°C by the use of a warming blanket. Through an upper midline laparotomy, a segment of jejunum measuring 16cm in length was isolated 5cm distal to the ligament of Treitz with preservation of its mesentery. The isolated loop was closed at both ends with 3-0 silk ligatures^[23,24]. The superior mesenteric artery (SMA) was isolated at its origin and clamped for 60 minutes, followed by release of the clamp and restoration of blood to the intestine for 90 minutes to produce gut ischemia and reperfusion injury (I/R injury). At the time of release of the clamp, either 0.2mg/kg of anisodamine or dobutamine was injected into the jejunal sac. At the conclusion of the experiment, cardiac puncture and exsanguination were used to achieve euthanasia.

Animals were divided into three groups: Group one ($n=15$): I/R + anisodamine + saline; group two ($n=15$): I/R + dobutamine + saline and group three ($n=10$): I/R + saline as control.

Measurement of mucosal blood flow

A Teflon-coated laser optic flow probe (Peri flux PF409, flexible probe with 0.25mm fiber separation) was inserted through a small enterotomy at the proximal end of the jejunal sac and it was positioned along the antimesenteric border of the jejunum to the center of the sac. Mucosal blood flow was continuously recorded with a laser Doppler flow monitor (Peri Flux 4001 Master; Perimed, Jaarnfalla, Sweden). Blood flow measurements using Laser Doppler flow meters are not absolute but rather indicate flow in arbitrary perfusion units. Measurements were taken as the average flow over a five-minute period following an initial 30 minute period of stabilization. The quality of the signal was monitored by visualization on the computer screen so that motion artifact and noise were excluded from measurement^[25,26].

Measurement of PCO₂ (PrCO₂)

In the same animal, a 5F saline tonometer was inserted through a small enterotomy at the distal end of the sac and positioned to the center of the sac. The system was allowed to equilibrate for 30 minutes at which time a baseline PrCO₂ measurement was obtained by discarding the first 0.3ml saline from the tonometer balloon and using the remaining 0.7ml for analysis (model 1610 pH/blood gas analyzer, Milano, Italy). Regional PCO₂ (PrCO₂) was calculated using the following formula: PrCO₂=measure PCO₂×EF. EF=equilibration factor, and based on the equilibration period for saline which gained from the handbook^[27-29].

Doppler measurements and PrCO₂ determinations were made every 30 minutes throughout the experimental period.

Statistics

Data were reported as mean ±SEM and were analyzed by one-way analysis of variance (ANOVA) or student *t* test, significance was set at *P*<0.05.

RESULTS

Laser doppler flow

Table 1 showed the effects of anisodamine and dobutamine on gut mucosal blood flow. Laser Doppler baseline flow (arbitrary units) was not different among groups. Flow dropped significantly during ischemia, with a reduction to 12% of baseline level, but notably not down to zero. With reperfusion, flow increased over time in all groups (*P*<0.05) but did not reach baseline by 90 minutes. When compared to saline group, mucosal blood flow were higher in the anisodamine and dobutamine groups (*P*<0.05) throughout the reperfusion period. Blood flow was also significantly higher at 90 minutes after reperfusion in anisodamine group compared with dobutamine animals (*P*<0.05).

Table 1 Effects of anisodamine and dobutamine on gut mucosal blood flow (%)

Goups	B	I ₆₀	R ₃₀	R ₆₀	R ₉₀
Anisodamine	98±3.8	14±3.9	44±3.3 ^{ab}	57±5.0 ^{ab}	64±3.3 ^{abc}
Dobutamine	100±5.2	18±2.1	48±4.1 ^{ab}	56±4.7 ^{ab}	56±4.2 ^{ab}
Saline	103±6.9	16±3.4	37±2.6 ^a	45±2.7 ^a	48±3.4 ^a

Mean ± SEM; **P*<0.05, vs I₆₀; ^b*P*<0.05, vs saline; ^c*P*<0.05, vs Dobutamine; B, baseline; I₆₀, ischemia 60 minutes; R₃₀, reperfusion 30 minutes; R₆₀, reperfusion 60 minutes; R₉₀, reperfusion 90 minutes.

Tonometry PrCO₂

Table 2 depicts jejunal PrCO₂ during I/R. Jejunal PrCO₂ did not differ in baseline among the groups, but it was significantly increased at 60 minutes of ischemia in all groups, amounting to 204% of baseline level. With reperfusion, PrCO₂ dropped over time in all groups (*P*<0.05), but did not reach the baseline. When compared with saline group, PrCO₂ values were lower in the anisodamine and dobutamine groups (*P*<0.05) throughout reperfusion period. There were no significant differences between anisodamine group and dobutamine animals at 30 and 60 minutes of reperfusion, but by 90 minutes of reperfusion anisodamine administration resulted in a significantly lower PrCO₂ than dobutamine (*P*<0.05).

Table 2 Effects of anisodamine and dobutamine on PrCO₂ (mm Hg)

Goups	B	I ₆₀	R ₃₀	R ₆₀	R ₉₀
Anisodamine	28±2.2	55±3.9	41±3.1 ^{ab}	38±3.7 ^{ab}	34±2.1 ^{abc}
Dobutamine	31±3.8	61±7.8	44±3.0 ^a	40±2.1 ^{ab}	39±3.0 ^{ab}
Saline	26±2.5	57±5.4	49±3.7	47±3.8 ^a	46±3.4 ^a

Mean ± SEM; **P*<0.05, vs I₆₀; ^b*P*<0.05, vs saline; ^c*P*<0.05, vs Dobutamine; B, baseline; I₆₀, ischemia 60 minutes; R₃₀, reperfusion 30 minutes; R₆₀, reperfusion 60 minutes; R₉₀, reperfusion 90 minutes

DISCUSSION

Both laboratory and clinical studies have demonstrated that splanchnic perfusion remains significantly impaired following resuscitation in traumatic, hemorrhagic and septic shock^[30-33]. Intravital video microscopic studies by Flynn *et al*^[34,35] have shown that although inflow and premucosal arterioles return to normal after resuscitation from hemorrhagic shock, there is a progressive arteriolar constriction resulting in a decrease in blood flow. There have been few reports about effects of intraluminal vasoactive agents on gut mucosal blood flow during both ischemia and reperfusion. It has been demonstrated that dobutamine could augment gut microcirculatory blood flow in septic shock^[36,37]. Observation in extensively burned patients by Sheng, *et al*^[22] have shown that intravenous administration of anisodamine 12 hours postburn resulted in a significant elevation in gastric pH and decrease in plasma level of TNF. In a porcine model of 30% TBSA full-thickness burn, anisodamine (0.4mg/kg) infused intravenously for one hour could increase portal blood flow, and it showed a positive correlation with intestinal pH^[38]. The use of Laser Doppler-measured tissue perfusion is a reliable technique that has been validated in the assessment of gastrointestinal mucosal blood flow, and the results were shown to correlate with other techniques of measurement of local blood flow^[33,38]. Recently, its use as a clinical tool for assessing jejunal mucosal perfusion had also been demonstrated^[39]. In this study with advanced Laser Doppler technique, we further demonstrated the beneficial effect of anisodamine on gut mucosal perfusion during I/R injury in comparison with dobutamine. The results showed that intraluminal anisodamine or dobutamine did increase mucosal blood flow throughout reperfusion as compared to intraluminal saline only. Blood flow augmentation was reflected by lower jejunal PrCO₂ measurements with intraluminal anisodamine or dobutamine. The most interesting finding was that there were significantly lower jejunal PrCO₂ and higher mucosal blood flow in anisodamine group than those in dobutamine at 90 minutes of reperfusion, suggesting that anisodamine had a more lasting effect on mucosal perfusion than dobutamine.

Tissue CO₂ gas tonometry provides an indirect measurement of perfusion and/or mucosal metabolic stress. Gastric tonometry, in particular, has been suggested as a tool to monitor splanchnic perfusion in experimental animals and critically ill patients^[40-43]. Though studies have demonstrated low gastric intramucosal pH (pHi) is a good predictor of poor outcome in critically ill patients, no improvement in outcome has been ascertained when patients are resuscitated based on the results of gastric tonometry^[44-46]. In this study we used 5F gut tonometry, in which the air pocket can be matched with rat small bowel sac, and the results are more accurate than gastric tonometry in detecting gut perfusion and metabolism^[47-50]. In our study significant increases in gut PrCO₂ following gut I/R were found, which could be markedly reduced by intraluminal anisodamine or dobutamine. These results might suggest that anisodamine or dobutamine is capable of augmenting mucosal blood flow, thus improving gut mucosal metabolism.

In conclusion, we have demonstrated in this laboratory model of gut ischemia and reperfusion that intraluminal anisodamine or dobutamine could augment mucosal blood flow, alleviate mucosal acidosis, improve metabolism in mucosal cell. These results provided reliable evidence to clinicians to adopt anisodamine or dobutamine in the treatment of splanchnic hypoperfusion, especially gut mucosal blood flow reduction following traumatic or burn shock.

REFERENCES

- Heithan TH, Kone BC, Mercer DW, Moody FG, Weisbrodt NW, Moore FA. Postinjury multiple organ failure: The role of the gut. *Shock* 2001; 15:1-10
- Moore FA. The role of the gastrointestinal tract in postinjury multiple organ

- failure. *Am J Surg* 1999;178:449-453
- 3 Zhang LY, Wang ZG, Zhu PF, Qin HJ. Gut barrier function disturbance posterior to hemorrhagic shock resuscitation in rats. *Shijie Huaren Xiaohua Zazhi* 2001;9:767-770
- 4 Hu S, Sheng ZY, Zhou BT, Guo ZR, Lu JY, Xue LB, Jin H, Sun XQ, Sun SR, Li JY, Lu Y. Study on delay two-phase multiple organ dysfunction syndrome. *Chin Med J* 1998;111:101-108
- 5 Hu S, Sheng ZY, Zhou BT, Xue LB, Jin H, Lu Y, Lin HY. Experimental study on hemodynamic changes in the development of multiple organ dysfunction syndrome. *Zhongguo Weizhongbing Jijiu Yixue* 1996;8:707-709
- 6 Reed LL, Mangano R, Martin M, Hochman M, Kocka F, Barrett J. The effect of hypertonic saline resuscitation on bacterial translocation after hemorrhagic shock in rats. *Surgery* 1991;110:685-690
- 7 Tamion F, Richard V, Lyoumi S, Daveau M, Bonmarchand G, Leroy T, Thuillez C, Lebreton JP. Gut ischemia and mesenteric synthesis of inflammatory cytokines after hemorrhagic or endotoxic shock. *Am J physiol* 1997;273:G314-G321
- 8 Moore EE, Moore FA, Franciose RJ, Kim FJ, Biffl, Banerjee A. Postischemia gut serves as a priming bed for circulating neutrophils that provoke multiple organ failure. *J Trauma* 1994;37:881-887
- 9 Magnotti LJ, Upperman JS, Xu DZ, Lu Q, Deitch EA. Gut derived mesenteric lymph but not portal blood increases endothelial cell permeability and promotes lung injury after hemorrhagic shock. *Ann Surg* 1998;228:518-527
- 10 Schmidt H, Secchi A, Wellmann R, Bach A, Bohrer H, Gebhard MM, Martin E. Effect of endotoxemia on intestinal villus microcirculation in rats. *J Surg Res* 1996;61:521-526
- 11 Fiddian-Green RG, Haglund U, Gutierrez, Shoemaker WC. Goals for the resuscitation on shock. *Crit Care Med* 1993;21:S25-S31
- 12 Friedman G, Silva E, Vincent JL. Has the mortality of septic shock changed with time? *Crit Care Med* 1998;26:2078-2086
- 13 Martin C, Viviani X, Arnaud S, Viallet R, Rougon T. Effects of norepinephrine plus dobutamine or norepinephrine alone on left ventricular performance of septic shock patients. *Crit care Med* 1999;27:1708-1713
- 14 Hoogenberg K, Smit AJ, Girbes AJ. Effects of low-dose dopamine on renal and systemic hemodynamics during incremental norepinephrine infusion in healthy volunteers. *Crit Care Med* 1998;26:260-265
- 15 Backer DD, Zhang HB, Cherkhaoui S, Borgers M, Vincent JL. Effects of dobutamine on hepato-splanchnic hemodynamics in an experimental model of hyperdynamic endotoxic shock. *Shock* 2001;15:208-214
- 16 Yang XH. Mechanism of the protective effect of anisodamine in gut ischemia injury. *Zhongguo Bingli Shengli Zazhi* 1988;4:134-136
- 17 Huang YS, Li A, Yang ZC. Roles of thromboxane and its inhibits anisodamine in burn shock. *Burns* 1990;16:249-253
- 18 Shi LB, Peng SY, Meng XY, Liu YB, Peng CH. The role of platelet activating factor in hepatic ischemia-reperfusion injury and the protective effect of anisodamine. *Zhongguo Weizhongbing Jijiu Yixue* 2001;13:220-222
- 19 Jang CG, Yang GT, Tang Y. Influence of Anisodamine on neuronal apoptosis after cerebral reperfusion in the rats. *Zhongguo Jijiu Zazhi* 2001;21:131-133
- 20 Meng XK, Shi LB, Peng SY, Peng CH, Wu YL, Sheng HW. Experimental study of anisodamine against hepatic ischemia-reperfusion injury. *Zhongguo Jijiu Yixue* 2001;21:4-6
- 21 Joly LM, Monchi M, Cariou A. Effects of dobutamine on gastric mucosal perfusion and hepatic metabolism in patients with septic shock. *Am J Respir Crit Care Med* 1999;160:1983-1986
- 22 Sheng ZY, Gao WY, Guo ZR, He LX. Anisodamine restores bowel circulation in burn shock. *Burns* 1997;23:142-146
- 23 Wilson TH. Methods. IN: Wilson TH, ed. *Intestinal Absorption*. Philadelphia: W. B. Saunders Co 1962:20-39
- 24 Hu S, Kozar RA, Moore FA, Sheng ZY. Enteral feeding of glucose increases intestinal mucosal blood flow during intestinal ischemia/reperfusion injury. *Zhonghua Shaoshang Zazhi* 2001;17:139-141
- 25 Wang P, Zhou M, Cioffi WG, Bland KI, Zheng F, Chaudry IH. Is prostacyclin responsible for producing the hyperdynamic response during early sepsis? *Crit Care Med* 2000;28:1534-1539
- 26 Elizalde JJ, Hernandez C, Liach J, Monton C, Bordes JM, Pique JM, Torres A. Gastric intramucosal acidosis in mechanically ventilated patients: role of mucosal blood flow. *Crit Car Med* 1998;26:827-832
- 27 Dawson AM, Trenchard D, Guz A. Small bowel tonometer: assessment of small gut mucosal oxygen tension in dog and man. *Nature* 1965; 206: 943-945
- 28 Heinonen PO, Jousela IT, Blomqvist KA. Validation of air tonometric measurement of gastric regional concentration of CO₂ in critically ill septic patients. *Intensive Care Med* 1977;23:524-529
- 29 McKinley BA, Marvin RG, Moore FA. Gastric and intestinal mucosal regional PCO₂ following shock resuscitation: changes with small intestinal enteral feeding. *Shock* 1999;11:S72-73
- 30 Fiddian-Green RG. Associations between intramucosal acidosis in the gut and organ failure. *Crit Care Med* 1993;21:S103-107
- 31 Grossie B, Weisbrodt NW. Inhibition of small intestinal transit by ischemia/reperfusion in the rat. *Dig Dis Sci* 1998;43:1585-1587
- 32 Wang P, Shou M, Rana MW. Differential alterations in microvascular perfusion in various organs during early and late sepsis. *Am J Physiol* 1992;263:G38-G43
- 33 Wang P, Hauptman JG, Chaudry IH. Hemorrhage produces depression in microvascular blood flow that persists despite fluid resuscitation. *Circ Shock* 1990;32:307-318
- 34 Flynn WJ, Cryer HG, Garrison RH. Pentoxifylline restores intestinal microvascular blood flow during resuscitated hemorrhagic shock. *Surgery* 1991;110:350-356
- 35 Flynn WJ, Gosche JR, Garrison RN. Intestinal blood flow is restored with glutamine or glucose infusion after hemorrhage. *J Surg Res* 1992;52:499-504
- 36 Gutierrez G, Clark C, Brown K SD, Price K, Ortiz L, Nelson C. Effect of dobutamine on oxygen consumption and gastric intramucosal pH in septic patients. *Am J Respir Crit Care Med* 1994;150:324-329
- 37 Nevriere R, Chagnon JL, Vallet B, Lebleu N, Marechal X, Mathieu D, Wattel F, Dupuis B. Dobutamine improves gastrointestinal mucosal blood flow in a porcine model of endotoxic shock. *Crit Care Med* 1997; 25:1371-1377
- 38 Gao WY, Sheng ZY, Gou ZR, He LX, Xiong DX, Song HF, Zhang SX, Ma NS, Chang GY. Protective effect of anisodamine on intestine in the early period of burn shock. *Jiefangjun Yixue Zazhi* 1995;20:88-91
- 39 Thoren A, Elam M, Ricksten S. Differential effects of dopamine, dopexamine, and dobutamine on jejunal mucosal perfusion early after cardiac surgery. *Crit Care Med* 2000;28:2338-2343
- 40 Temmesfeld-Wollbrück B, Szalay A, Olschewski H. Advantage of buffered solutions or automated capnometry in air-filled balloons for use in gastric tonometry. *Intensive Care Med* 1997;23:423-427
- 41 Knudson G, Bermudez KM, Doyle CA, Mackersie RC, Hopf HW, Morabito D. Use of tissue oxygen tension measurements during resuscitation from hemorrhagic shock. *J Trauma* 1997;42:608-611
- 42 Hu S, Sheng ZY, Zhou BT, Xue LB, Jin H. Changes in gastrointestinal intramucosal pH in goats resuscitated from hypovolemic shock. *Zhongguo Weizhongbing Jijiu Yixue* 1997;9:708-710
- 43 Marik P, Lorenzana A. Effect of tube feeding on the measurement of gastric intramucosal pH. *Crit Care Med* 1996;24:1498-1500
- 44 Gomersall CD, Joynt GM, Freebairn RC, Hung V, Buckley CA, Oh TE. Resuscitation of critically ill patients based on the results of gastric tonometry: A prospective, randomized, controlled trial. *Crit Care Med* 2000;28:607-614
- 45 Kirton OC, Windsor J, Wedderburn R, Hudson-Civetta J, Shatz DV, Mataragas NR, Civetta JM. Failure of splanchnic resuscitation in the acutely injured trauma patient correlates with multiple organ-system failure and length of stay in the ICU. *Chest* 1998;113:1064-1069
- 46 Ivatury RR, Simon RJ, Islam S, Fuego A, Rohman M, Stahl WM. A prospective randomized study of resuscitation after major trauma: Global oxygen transport induces versus organ-specific gastric mucosal pH. *J Amer Col Surg* 1996;183:145-154
- 47 Walley KR, Friesen BP, Humer MF, Phang PT. Small bowel tonometry is more accurate than gastric tonometry in detecting gut ischemia. *J Appl Physiol* 1998;85:1770-1777
- 48 Barry B, Mallick A, Hartley G, Bodenham, Vucevic M. Comparison of air tonometry with gastric tonometry using saline and other equilibrating fluids: an in vivo and in vitro study. *Intensive Care Med* 1998; 24:777-784
- 49 Noone RB, Bolden JE, Mythen NG, Vaslef SN. Comparison of the response of saline tonometry and an automated gas tonometry device to a change in CO₂. *Crit Care Med* 2000;28:3728-3733
- 50 Thorburn K, Hatherill M, Roberts PC, Durward A, Tibby SM, Murdoch IA. Evaluation of the 5-French saline paediatric gastric tonometer. *Intensive Care Med* 2000;26:973-980

Edited by Wu XN

• CLINICAL RESEARCH •

Presence and density of common bile duct microlithiasis in acute biliary pancreatitis

Maciej Kohut, Andrzej Nowak, Ewa Nowakowska-Dulawa, Tomasz Marek

Maciej Kohut, Andrzej Nowak, Ewa Nowakowska-Dulawa, Tomasz Marek, Department of Gastroenterology, Central Clinical Hospital, Silesian Academy of Medicine, Katowice, Poland

Supported by Silesian Medical Academy scientific grants - NN-4-173-94, NN-1-161-95, NN-4-200-96, NN-1-248-97

Correspondence to: Maciej Kohut, Department of Gastroenterology, Silesian Academy of Medicine, Medyków 14,40 - 752 Katowice, Poland. maciej.2250177@pharmanet.com.pl

Telephone: +48-32-7894401 Fax: +48-32-2523119

Received 2002-01-11 Accepted 2002-03-07

Abstract

AIM: Common bile duct microlithiasis (CBDM) is found in majority of patients with acute biliary pancreatitis (ABP) and no CBD stones in fluoroscopy during urgent ERCP. It is unclear, however, whether CBDM is a cause or the result of the disease. This prospective study was done to investigate the presence and density of CBDM in patients with ABP, when endoscopic retrograde cholangiopancreatography (ERCP) was done in different periods from the onset of the disease.

METHODS: One hundred fifty one consecutive patients with ABP and no CBDS on ERCP, performed as an urgent (<24h of admission) procedure, (101 - with gallbladder stones, 50 post-cholecystectomy patients), treated during last 4 years were prospectively included to the study. The presence and density of CBDM (cholesterol monohydrate crystals-CMCs and calcium bilirubinate granules-CBGs) in bile collected directly from common bile duct during ERCP was prospectively calculated according to Juniper and Burson criteria. High density of crystals was considered, when we found >10CMCs and/or >25 clusters of CBGs on 1 slide.

RESULTS: CBD microlithiasis was present in given number of patients: on d1-30/34 (88.2%), on d2 41/49 (83.7%), on d3-23/33 (69.6%), on d4-7-24/35 (68.6%) [*P* for trend=0.018]. In patients with CBD microlithiasis the high density of crystals was observed in given number of patients: on d1-27/30 (90%), on d2-34/41 (82.9%), on d3-18/23 (78.3%), on d4-7-16/24 (66.7%) [*P* for trend=0.039].

CONCLUSION: In patients with ABP and no CBDS on ERCP, CBD microlithiasis is observed in the majority of patients, especially during the first day of the disease. Density of CBD microlithiasis is the highest in the first day of the disease. This suggests that CBD microlithiasis can be the cause and not the result of ABP.

Kohut M, Nowak A, Nowakowska-Dulawa E, Marek T. Presence and density of common bile duct microlithiasis in acute biliary pancreatitis. *World J Gastroenterol* 2002;8(2):558-561

INTRODUCTION

Some cases of acute biliary pancreatitis (ABP) are due to the biliary microcrystals (microlithiasis). The pathogenesis of acute pancreatitis (AP) produced by biliary crystals is unknown. It is probably related to the temporary impaction or migration of very small stones or

clusters of crystals at the level of the ampoule of Vater. The mechanism of such pancreatitis is presumably the same as that when "normal size" biliary stones are impacted in the ampoule of Vater in the onset of the disease^[1,2]. Literature on this problem started with simple case reports^[3-5]. In the end of 1980's and the beginning of 1990's some larger series of patients with acute pancreatitis possibly associated with biliary sludge or microlithiasis were presented^[1,6-10]. However, most of patients presented in these papers suffered from acute pancreatitis classified as so called "idiopathic" pancreatitis, as they do not bear gallbladder sludge, gallbladder stones and they did not have the history of cholecystectomy.

The methodology of these reports was based on the microscopic bile examination (MBE), which was a widely used technique in the diagnosis of gallstone disease before the advent of modern imaging procedures such as ultrasonography^[11,12]. Almost all authors studied gallbladder bile obtained after stimulated gallbladder contractions via either blindly or endoscopically placed tube at the level of the papilla of Vater. Even in one of the best papers by Lee *et al*^[6] the common bile duct bile has been investigated only in less than half of the patients. In the rest of cases the stimulated gallbladder bile was the matter of study. The minority of authors studied the bile obtained directly from the biliary tree on ERCP or via the T-tube placed in common bile duct during cholecystectomy with choledochotomy^[13,14].

To our knowledge the study of common bile duct microlithiasis (CBDM) in patients with gallbladder stones or prior cholecystectomy and no CBD stones on ERCP is scanty^[13,14]. In our previous paper we have found CBDM in vast majority of ABP cases (76%)^[15]. One can argue, however, that the CBD microlithiasis can be the result and not the cause of the disease-CBD microlithiasis can be produced in the biliary tree due to the obstructed outflow of bile. This cholestasis can be related to the compression of distal common bile duct stone made by swollen pancreatic head during acute pancreatitis. Thus, we conducted the study of the presence and density of CBD microlithiasis in patients with ABP and no CBD stones on ERCP performed in the different periods from the onset of the disease. The aims of our work were to study the presence of CBD microlithiasis in different periods from the onset of the acute biliary pancreatitis, and the density of CBD microlithiasis in patients with microlithiasis in different periods from the onset of acute biliary pancreatitis.

MATERIALS AND METHODS

Materials

The study had been performed between September 1993 and January 1997 in the Department of Gastroenterology of the Silesian Academy of Medicine in Katowice, which is the reference centre for gastrointestinal diseases for approximately 4 million inhabitants area. Informed consent was obtained from all the subjects. Protocol of the study was approved by the local Ethics Committee in February 1993.

Methods

ERCP was done urgently - up to 24 hours of admission. Only patients with no more than 7 days from the onset of ABP were included to the study. We included patients with gallbladder stones or patients previously cholecystectomized. Patients without suspected biliary pathology [e.g. with pancreas divisum or with metabolic

(hyperlipidaemia) acute pancreatitis] were excluded. Patients with alcoholic pancreatitis were also excluded. The diagnostic criteria for ABP were (both criteria must be present): (1) Typical clinical picture (epigastric pain), elevated levels of pancreatic enzymes (exceeding at least 3 times upper normal range), typical patterns of pancreatitis in abdominal imaging methods (ultrasonography, CT-scan), and (2) History of gallstones (e.g. cholecystectomy), positive laboratory criteria of biliary etiology of acute pancreatitis according to Goodman *et al*^[16], gallstones on ultrasonography.

After the cannulation of the orifice of the ampoule of Vater was verified and the diagnostic catheter was placed in the common bile duct by injection of contrast medium (Meglumine diazotriacetate, Uropolinum, Polfa, Poland), the examiner confirmed that there were no "macroscopic" bile duct stones on fluoroscopy and X-ray films. Then the CBD bile was collected by manual suction through the standard ERCP catheters (Olympus and Boston Scientific companies) to the sterile syringe attached to the proximal end of the catheter. Approximately 5mL of bile was achieved from every patient. All the following procedures were done in the sterile conditions. Immediately after the collection the bile sample was divided into two parts of the same volume. One part was examined immediately, while the second one was incubated in the temperature of 37°C for 24h. The presence of biliary microlithiasis was recorded as the combined result from both microscopic bile examinations. We established the diagnosis of CBD microlithiasis when at least we found crystals (immediately after incubation or on both microscopic bile examinations). The patients did not receive any antibiotic treatment prior to ERCP that can influence microscopic bile examination due to the drug precipitation in the bile.

The sample of bile was centrifuged 12 000 r·min⁻¹ for 10 min. Centrifugation enables to separate bile from the contrast medium we used during ERCP. The contrast medium floated over the bile after centrifugation. The sediment found on the bottom of the bile was than examined under direct and polarising light microscope, equipped with a heating stage. The same was done on the next day with the second portion of incubated bile. Three slides with bile sediment were examined for each sample. We prospectively used criteria of Juniper and Burson for counting crystals, as shown in Table 1^[17]. Cholesterol monohydrate crystals (CMC) were identified on the basis of their rhomboid shape and their birefringence under cross - polarisation. Calcium bilirubinate granules (CBG) were identified on the basis of their reddish - brown colour and tendency to aggregate^[17]. The number of crystals were graded as 1 - 4 when present and 0 when absent. Grades 1 - 4 corresponded to the grades specified by Juniper and Burson^[17]. A positive result (at once, after incubation or both) for CMCs was taken if graded 1 - 4, and for CBGs if graded 3 - 4 (> 25 crystals per slide). The diagnosis of high density of crystals was done only if we have found > 10 CMCs and/or > 25 CBGs per one slide - as proposed by Juniper and Burson^[17]. These criteria were derived directly from the original paper of Juniper and Burson, who discovered, that some cases with small number of calcium bilirubinate granules (graded 1 and 2, < 25 crystals per slide) were healthy and did not present cholelithiasis. All the bile samples were examined by one of the investigators, who were unaware of any clinical information.

The data were prospectively collected in the purpose-made database and analysed with the statistical package STATISTICA 5.0PL. The results are expressed as $\bar{x} \pm s$. Unpaired t Student tests (Fisher's exact test - two-sided or Mann-Whitney's test when needed) and chi - 2 test when appropriate were used for statistical analyses. The level < 0,05 was considered as statistically significant.

RESULTS

Demographic clinical and biochemical data of all the patients are shown in Table 2. The comparison of the characteristics of the

patients with and without microlithiasis is given in the Table 3. There were no differences in the sex, mean age, the presence of gallbladder stones, mean BMI, mean levels of biochemical cholestasis (bilirubin, alkaline phosphatase and alanine transaminase) of patients in both subgroups. Presence and density of common bile duct microlithiasis (CBDM) in patients with acute biliary pancreatitis and no CBD stones on ERCP done in different periods from the onset of the disease are presented in Figures 1 and 2, respectively. The results showed statistically significant decrease in the presence of microlithiasis, when the patient moved away from the onset of acute biliary pancreatitis. We observed also the fall in the presence of high density of microlithiasis. The highest density was in the first day of acute biliary pancreatitis, falling down in next days of the disease. These results also achieved the statistical significance.

Table 1 System of Juniper and Burson for counting microlithiasis^[4]

Number of crystals per one slide	Grading
<10	+
10-25	++
25-40	+++
>40	++++

Table 2 Demographic, clinical and biochemical data of all patients with no common bile duct stones on ERCP

All cases		
Number of patients		
151		
Sex (M : F)		
49 : 102		
Age (years) ($\bar{x} \pm s$)		
53.9(± 15.7)		
Number of cases with gallbladder stones		
101		
Number of cases with prior cholecystectomy		
50		
Number of cases with Goodman's criteria of		
129		
ABP present (at least 1 criterion)		
Biochemical		
values (range, mean and SD)	Bilirubin ($\mu\text{mol}\cdot\text{L}^{-1}$)	17-3065 4.57(± 44.03)
	Alkaline phosphatase ($\text{IU}\cdot\text{L}^{-1}$)	57-556216.5(± 115.3)
	Alanine transaminase ($\text{IU}\cdot\text{L}^{-1}$)	16-1335351.2(± 252.8)

Normal levels of liver enzymes in our lab:

- Bilirubin <17 $\mu\text{mol}\cdot\text{L}^{-1}$)
- Alkaline phosphatase <110 $\text{IU}\cdot\text{L}^{-1}$)
- ALT <40 $\text{IU}\cdot\text{L}^{-1}$)

Table 3 Demographic, clinical and biochemical features of patients in relation to the diagnosis of common bile duct microcrystals (Fischer's s exact test or U Mann-Whitney's test when needed)

Feature	Microcrystals present (n=118)	Microcrystals absent (n=33)	P
Women	91	11	0.066
Men	27	22	0.066
Age[years] (mean)	52.4	54.2	0.623
Gallbladder stones present	81	20	0.770
BMI (mean)	27.8	28.7	0.490
Number of cases with Goodman's criteria of ABP present (at least 1 criterion)	106	23	0.670
Bilirubin [$\text{mol}\cdot\text{L}^{-1}$] (mean)	54.4	49.3	0.607
Alkaline phosphatase [$\text{IU}\cdot\text{L}^{-1}$] (mean)	213.7	178.9	0.148
Alanine transaminase [$\text{IU}\cdot\text{L}^{-1}$] (mean)	350.4	383.4	0.577

Results of microscopic bile examination (types of detected crystals) are shown in Figure 3. Calcium bilirubinate granules present alone (50% of cases with microlithiasis) were found the most frequently on MBE (Figure 3). CBGs together with CMCs were present in 43.2% cases with microlithiasis. Cholesterol monohydrate crystals were present alone only in 6.8% of patients with microlithiasis. We did not record any case of microspherulites.

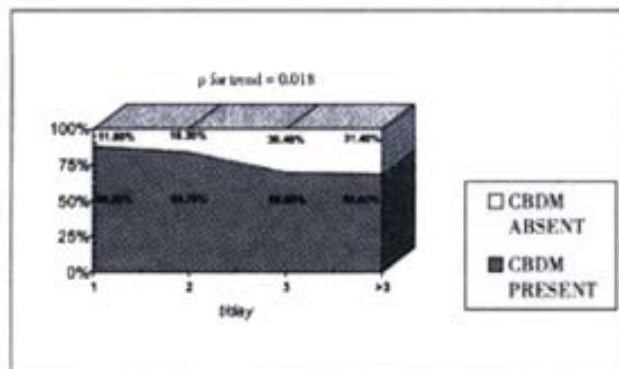


Figure 1 The presence of common bile duct microlithiasis (CBDM) in patients with acute biliary pancreatitis in different periods from the onset of the disease. (Fischer's exact test or Mann-Whitney's test when needed).

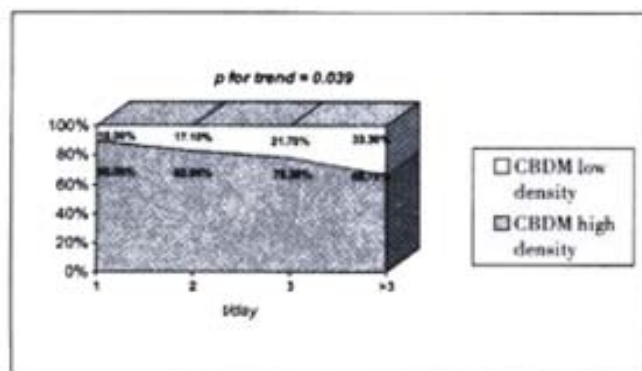


Figure 2 The density of common bile duct microlithiasis (CBDM) in patients with crystals on ERCP in different periods from the onset of the disease. (Fischer's exact test or Mann-Whitney's test when needed).

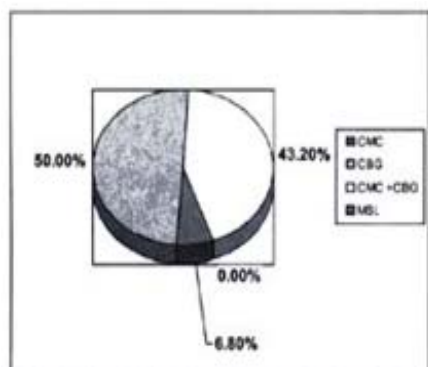


Figure 3 Types of detected microcrystals.
CMC - cholesterol monohydrate crystals
CBG - calcium bilirubinate granules
MSL - microspherulites

DISCUSSION

Duodenal bile fractions was microscopically checked since decades in search for gallstone disease^[11, 12, 17]. This method has shown the sensitivity and specificity around 70-90%. The microscopic examination of stimulated gallbladder bile collected via the tube, placed either under radiological guidance or endoscope in the duodenum at the level of the papilla has been shown to be reliable in the diagnosis of gallstone disease as well^[18, 19]. Both methods of

MBE had lost its attractivity after the advent of ultrasonographic examination of the gallbladder and bile ducts. However, the bile is still examined in some patients, especially with acute pancreatitis of uncertain origin^[1,3,4-10]. Common bile duct bile has been microscopically examined in patients with endoscopically placed naso - biliary tube or surgically placed T - tube in CBD^[13]. Sensitivity of 100% of such microscopic examination for CBD stones recognition was reported^[13].

In another study common bile duct bile was obtained directly from the duct during ERCP^[14]. We have shown the sensitivity of 85% in the diagnosis of choledocholithiasis^[14] and the same methodology was used in this study.

Our study was designed to find out the presence and density of CBD microlithiasis in patients with acute biliary pancreatitis and no CBD stones on ERCP, when ERCP was done in different periods from the onset of the ABP. ABP was diagnosed according to the typical abdominal symptoms of acute pancreatitis, ultrasound and CT changes of pancreatic gland and the presence of gallbladder stones or prior cholecystectomy. All the patients presented also a significant (more than $2 \times N$) elevation of at least one of biochemical markers of cholestasis (alkaline phosphatase, alanine transaminase, and bilirubin).

ERCP is one of the diagnostic standards in choledocholithiasis. This method can give false (positive and negative) results, but the sensitivity and specificity of the method is believed to be above 90-95%^[20]. In this respect, we can exclude almost all cases with CBD stones during fluoroscopy with high confidence that our group of patients contains really no cases with CBD stones.

No one of the tested biochemical parameters achieved statistical significance as a marker of microcrystals (Table 2). Similar values of biochemical data in patients with or without microlithiasis can be explained by the finding of signs of recent stone passage through the papilla of Vater in some patients. Swollen papilla with enlarged (usually quite easy to cannulate) reddish orifice, sometimes with a drop of blood, were found on ERCP in some ABP patients, mostly without microlithiasis. In these patients elevated biochemical markers were seen, as in patients with microlithiasis and without recent passage signs. The absence of microlithiasis in patients with signs of recent passage of stone may be explained so called "flushing out" mechanism after decompression of bilio - pancreatic duct system. This deserves further studies.

Microcrystals within the biliary tree are present intermittently^[19]. We observed very high percentage of microlithiasis in studied group of patients with ABP. This can be explained by the fact that majority of cases were admitted and ERCP performed on first three days of the disease. In previous studies, done few weeks or even months after the acute episode of acute pancreatitis, the percentage of cases with microlithiasis was lower^[3,5,7-9,11,12,18].

The main idea behind our study was to exclude the biliary microlithiasis as the result of acute pancreatitis. The presented results confirmed our presumption, that the percentage of cases with microlithiasis fell down, when the beginning of the acute pancreatitis was becoming distant. The percentage of patients with high density of microlithiasis also falls down with time. We can speculate that the high density microlithiasis was potentially more harmful in the sense, that it can easily aggregate at the level of the orifice of the ampoule of Vater, leading to the obstruction of the outflow of pancreatic juice. It suggests, that microlithiasis is the cause and not the result of the acute pancreatitis.

Results of microscopic bile examinations, found in this study (Figure 3), confirm previous observation, that calcium bilirubinate granules (CBG) are more frequently found in patients with AP^[1, 6, 7]. CBG were present alone (50%) or in association with CMC (43.2%) of all cases with microlithiasis. CMC were found alone in only 6.8% of cases. Previously CMCs were also less frequently found in endoscopically obtained duodenal bile, than in gallbladder bile in the same patient^[21].

In our opinion one important etiopathogenetic conclusion comes from the study: microlithiasis can provoke acute biliary pancreatitis. Crystals can irritate the papilla, leading to inflammation of the papilla and obstructed outflow of pancreatic juice. If very high percentage of patients with microcrystals is present in the first day of ABP and if the high percentage of high density microlithiasis is also present in the first day of the disease, it seems logical to perform next step - the investigation of the influence of endoscopic sphincterotomy in such patients.

List of abbreviations

ABP	- acute biliary pancreatitis
CBD	- common bile duct
CBDS	- common bile duct stones
CBDM	- common bile duct microlithiasis
CMCs	- cholesterol monohydrate crystals
CBGs	- calcium bilirubinate granules
ERCP	- endoscopic retrograde cholangiopancreatography

Meetings presentations

Parts of this work were presented as abstracts during:

1. 6th United Gastroenterology Week, Birmingham, UK, 18-23 October 1997 (Gut 1997; 41 (3): P241).
2. DDW, New Orleans, USA 17-20 May 1998 (Gastrointest Endosc 1998; 47: AB 124).
3. 11th World Congress of Gastroenterology, Vienna, Austria 6-11 September 1998 (Digestion 1998; 54: 494: 3441).

REFERENCES

- 1 Ros E, Navarro S, Bru C, Garcia-Puges A, Valderrama R. Occult microlithiasis in "idiopathic" acute pancreatitis-prevention of relapses by cholecystectomy or ursodeoxycholic acid therapy. *Gastroenterology* 1991; 101:1701-1709
- 2 Acosta JM, Pellegrini CA, Skinner DB. Aetiology and pathogenesis of acute biliary pancreatitis. *Surgery* 1980; 88: 118-124
- 3 Perrota G, Pugliese G, Esposito R. Acute pancreatitis and biliary microlithiasis. A study of biliary sediment. *G Chir* 1989; 10: 646-648
- 4 Block MA, Priest RJ. Acute pancreatitis related to grossly minute stones in a radiographically normal gallbladder. *Am J Dig Dis* 1967; 12: 945-948
- 5 Negro P, Flati G, Flati D. Occult gallbladder microlithiasis causing acute recurrent pancreatitis. *Acta Chir Scand* 1984; 150: 503-506
- 6 Lee SP, Nichols JF, Park HZ. Biliary sludge as a cause of acute pancreatitis. *N Eng J Med* 1992; 326: 589-593
- 7 Neoptolemos JP, Davidson BR, Winder AF, Vallance D. Role of duodenal bile crystals analysis in the investigation of "idiopathic" pancreatitis. *Br J Surg* 1988; 75: 450-453
- 8 Reyez-Lopez A, Mino-Fugerolas G, Costan-Rodero G, Perez-Rodriguez E, Montero-Alvarez JL, Cabrera D. Value of duodenal drainage in the etiologic diagnosis of acute pancreatitis. *Rev Esp Enferm Dig* 1993; 83: 363-366
- 9 Bel FJ, Aparisis L, Garcia-Tell G, Rosello J, Rodrigo J. Biliary drainage in the diagnosis of microlithiasis. Value in acute idiopathic pancreatitis and in patients with pain in the right hypochondrium. *Rev Esp Enferm Dig* 1994; 85: 343-347
- 10 Humbert P, Casals A, Boix J. Usefulness of microscopic study of the duodenal bile in the diagnosis of pancreatitis of unknown cause. *Rev Esp Enferm* 1989; 75: 471-474
- 11 Lyon BBV. Diagnosis and treatment of diseases of the gallbladder and biliary ducts. *Am J Med Assoc* 1919; 73: 980-986
- 12 Bockus HL, Shay H, Willard JM. Comparison of bile drainage and cholecystography in gallstone disease with special reference to bile microscopy. *J Am Med Assoc* 1931; 96: 311-317
- 13 Agarwal DK, Choudhuri G, Saraswat VA, Negi TS. Utility of biliary microscopic analysis in predicting composition of common bile stones. *Scand J Gastroenterol* 1994; 29: 352-354
- 14 Buscail L, Escourrou J, Delvaux M, Guimbaud R, Nicolet T, Freximos J. Microscopic examination of bile directly collected during endoscopic cannulation of the papilla. Utility in patients with suspected microlithiasis. *Dig Dis Sci* 1992; 37: 116-120
- 15 Nowak A, Kohut M, Nowakowska-Dulawa E, Marek TA, Kaczor R. Common bile duct microlithiasis in patients with acute biliary pancreatitis and no CBD stones on ERCP. *Digestion* 1998; 59: 494
- 16 Goodman AJ, Neoptolemos JP, Carr-Locke DL, Finlay DB, Fossard DP. Detection of gallstones after acute pancreatitis. *Gut* 1985; 26: 125-132
- 17 Juniper K, Burson EN. Biliary tract studies II. The significance of biliary crystals. *Gastroenterology* 1957; 32: 175-211
- 18 Abbas A, Baumann R, Schutlz JF. Cristaux de cholesterol et lithiase biliaire. Interet de l' etude de la bile recueillie par tubage duodenal. *Gastroenterol Clin Biol* 1984; 8: 454-457
- 19 Marks JW, Bonorris G. Intermittency of cholesterol crystals in duodenal bile from gallstone patients. *Gastroenterology* 1984; 87: 622-627
- 20 Prat F, Amouyal G, Amouyal G, Pelletier G, Choury AD, Buffet C, Etienne JP. Prospective controlled study of endoscopic ultrasonography and endoscopic retrograde cholangiography in patients with suspected common bile duct lithiasis. *Lancet* 1996; 346: 75-79
- 21 Janowitz P, Swobodnik W, Weschler JG, Zoller A, Kuhn K, Ditschuneit H. Comparison of gallbladder bile and endoscopically obtained duodenal bile. *Gut* 1990; 31: 1407-1410

Edited by Pan BR and Zhang JZ

• CLINICAL RESEARCH •

HCV-specific cytokine induction in monocytes of patients with different outcomes of hepatitis C

Rainer P. Woitas, Uwe Petersen, Dirk Moshage, Hans H. Brackmann, Bertfried Matz, Tilman Sauerbruch, Ulrich Spengler

Rainer P. Woitas, Uwe Petersen, Dirk Moshage, Tilman Sauerbruch, Ulrich Spengler, Department of Internal Medicine I, University of Bonn, 53105 Bonn, Germany

Hans H. Brackmann, Institute of Experimental Hematology, University of Bonn, 53105 Bonn, Germany

Bertfried Matz, Institute of Medical Microbiology and Immunology, University of Bonn, 53105 Bonn, Germany

Correspondence to: Dr. Rainer P. Woitas, Medizinische Klinik, Poliklinik I, -Allgemeine Innere Medizin-, Universität Bonn, Sigmund-Freud-Strasse 25, D-53105 Bonn, Germany. woitas@uni-bonn.de

Received 2002-03-12 Accepted 2002-04-25

Abstract

AIM: Cytokine release by macrophages critically determines the type of immune response to an antigen. Therefore, we studied hepatitis C virus (HCV)-specific induction of interleukins-1 β , -10, -12 (IL-1 β , IL-10, IL-12), and tumor necrosis factor- α (TNF- α) in monocytes.

METHODS: Intracellular cytokine expression was studied by flow cytometry in 23 patients with chronic hepatitis C, 14 anti-HCV seropositives without viremia and 11 controls after stimulation of peripheral blood mononuclear cells with recombinant core, NS3, NS4, NS5a and NS5b proteins.

RESULTS: Patients with HCV viremia revealed greater spontaneous expression of IL-1 β , TNF- α , and IL-10. Furthermore, greater than twofold higher IL-10 expression was induced by the HCV antigens in chronic hepatitis C than in the other two groups ($P < 0.05$). In contrast, neither IL-12 nor TNF- α was induced preferentially.

CONCLUSION: In chronic hepatitis C antigen-specific cytokine induction in monocytes is apparently shifted towards predominant IL-10 induction - not counterbalanced by antiviral type 1 cytokines. This may contribute to persistent viral replication.

Woitas RP, Petersen U, Moshage D, Brackmann HH, Matz B, Sauerbruch T, Spengler U. HCV-specific cytokine induction in monocytes of patients with different outcomes of hepatitis C. *World J Gastroenterol* 2002;8(3):562-566

INTRODUCTION

Resistance or susceptibility to viral infections is critically linked to cytokine release, which can be polarized towards a type 1 (IFN- γ , TNF- α , IL-2) or type 2 (IL-4, IL-10, IL-13) pattern in helper as well as cytotoxic T lymphocytes^[1]. Type 1 and type 2 T lymphocytes are not derived from different lineages but develop from the same precursors, and their differentiation is influenced by the environment during priming. The most important signals are cytokines themselves: IL-12 produced by activated macrophages is the principal cytokine

inducing type 1 responses, whereas the development of type 2 T lymphocytes is induced by IL-4 and IL-10.

Hepatitis C virus (HCV) infection frequently leads to persistent viral replication, which may be facilitated by selective alterations in the host's immune response^[2]. In this context, studies of T cell functions in patients with chronic hepatitis C have indicated an inappropriately low production of antiviral type 1 cytokines in response to HCV antigens^[3-7] possibly facilitating persistent infection. However, it is not clear, whether the imbalance in the cytokine pattern is due to direct alterations of T cell function or a consequence of altered T cell priming. Because of their critical role for the type of immune reaction triggered in response to an antigen, we used flow cytometric detection of intracytoplasmic cytokines to study at the single cell level the HCV-specific induction of IL-1 β , IL-10, IL-12 and TNF- α in peripheral blood monocytes.

MATERIALS AND METHODS

Patients

Three groups of patients were included into this study: Group 1 consisted of 23 patients with chronic hepatitis C (male, $n=20$; female, $n=3$; median age 33, range 21-61), elevated liver enzymes and detectable HCV-RNA in the serum. The mean virus load was 6.3×10^6 copies/mL (SD 1.0×10^6 copies/mL) (QuantiplexTM HCV RNA 2.0 assay, Chiron, Emeryville, CA). Group 2 consisted of 14 carefully selected patients with previous HCV infection (male, $n=12$; female, $n=2$; median age 28.5, range 18-63), who had consistently normal aminotransferases without detectable viral RNA on repeated examination over at least 2 years. Finally, 11 anti-HCV negative volunteers (male, $n=5$; female, $n=6$; median age 30, range 24-66) served as a control group (group 3).

There were no significant differences between the two anti-HCV groups with respect to total immunoglobulin levels, and all were free from cryoglobulins or autoantibodies. None of the individuals in this study had hepatitis B virus or human immunodeficiency virus co-infection. The study was approved by the local ethical committee and conformed to the ethical guidelines of the 1975 Declaration of Helsinki.

Diagnosis of HCV Infection

HCV antibodies were detected with a microparticle enzyme immunoassay (MEIA) (AxSYM, Abbott, Wiesbaden, Germany) according to the instructions of the manufacturer. Positive results were confirmed by dot immunoassay (Matrix, Abbott, Wiesbaden, Germany). HCV RNA was detected with a nucleic acid purification kit (Viral Kit, Qiagen, Hilden, Germany) followed by reverse transcription and nested polymerase chain reaction as described elsewhere^[8]. Quantitative determination of HCV RNA copies was done via branched DNA technology (Chiron, Emeryville, CA). In group 1, genotypes of the infecting HCV strains were determined by the INNO-LiPA HCV II test (Innogenetics, Zwijndrecht, Belgium) except one patient, who could not be genotyped. This group revealed

the following isolates: 1a ($n=8$), 1b ($n=9$), 2b ($n=1$), 3a ($n=1$), and mixed ($n=3$; genotypes 1b/2b; 2a/2c; 4c/4d).

Patients of group 2 were characterized by genotype-specific antibodies to NS4 (Murex, Abbott Wiesbaden, Germany). Serotypes 1 and 4 were found in 10 and 1 patients, respectively. Three patients had indeterminate serotypes.

HCV antigens

The purified recombinant proteins [r-core (truncated): aa 1-115, r-NS3: aa 1007-1534, r-NS4: aa 1616-1862, r-NS5: aa 2007-2268] derived from the HCV-1 prototype sequence^[9] were purchased from Mikrogen, Munich, Germany. The bacterial lipopolysaccharide content of the proteins was between 4.0-20 pg/ μ g recombinant protein as determined by the Limulus assay. Lipopolysaccharide from *E. coli* OH101 (Sigma, Munich, Germany) was used in the control experiments.

Antibodies

Fluorescein isothiocyanate (FITC)- and phycoerythrin (PE)-labelled antibodies were purchased from the following companies: FITC- and PE-labelled -anti-CD14 (mouse IgG2b, clone MÖP9) from Becton Dickinson (Heidelberg, Germany); FITC- and PE-labelled anti-IL-1 β (mouse IgG1, clone H9.5) was purchased by Holtzel Diagnostica (Cologne, Germany). Anti-IL-10/PE (rat IgG2a, clone JES3-19F1), anti-IL-12/PE (mouse IgG1, clone C11.5.14), anti-TNF- α /PE (mouse IgG1, clone MAb11) as well as appropriate isotype controls from Pharmingen (Hamburg, Germany). Unlabelled mAbs for blocking experiments were purchased from Pharmingen (Hamburg, Germany) except for IL-1 β that was a gift of Holtzel Diagnostica (Cologne, Germany).

Cells and cell culture

PBMC (1.1×10^6 /ml) isolated from fresh EDTA blood by Ficoll density-gradient centrifugation (Biochrom, Berlin, Germany) were resuspended in low endotoxin level culture medium (RPMI 1640, Biochrom, Berlin, Germany) containing 10% autologous human serum, 100 units/ml penicillin, 100 units/ml streptomycin and incubated at 37°C with 5% CO₂ in 96 well microtiter plates (Sarstedt, Berlin, Germany) in the presence of recombinant HCV proteins (1 μ g/ml) or LPS (10-200 ng/ml). Kinetic experiments showed that the antigen-specific cytokine induction indicated a maximum after 12 hours of stimulation. Further experiments revealed 1.0 μ M monensin (Sigma, Munich Germany) for 12 hours to be optimal to enhance the signal/noise ratio as well as to exclude relevant toxicity^[10-12].

Dual-colour flow cytometry for immunophenotyping and intracytoplasmic staining of cytokines

CD14 and intracytoplasmic cytokines were detected by direct immunofluorescence using a paraformaldehyde (PFA)-saponin procedure with 4% PFA as fixative and 0.2% saponin for permeabilisation. In brief, cultured cells were washed twice in Hank's balanced salt solution (HBSS) (Gibco, Eggenstein, Germany) and stained for the surface markers (20 minutes incubation at 4°C in the dark). After one further wash, the cells were fixed in ice cold HBSS containing 4% PFA for 5 minutes and washed again. Cells were resuspended in HBSS containing 0.2% saponin (saponin buffer). Then cytokine specific antibodies diluted in saponin buffer were added at a concentration of 0.5-3.0 μ g/ml and incubated for 30 minutes at room temperature in the dark. Cells were washed in saponin buffer and analyzed by dual-colour flow cytometry on a FACS Sort

flowcytometer (Becton Dickinson, Heidelberg, Germany). Forward and side scatter as well as gating for CD14⁺ cells were used to identify monocytes. The data were analyzed with the CellQuest (software (Becton Dickinson) after counting 5000 CD14⁺ cells. All experiments were performed in triplicate.

To ensure specificity of the cytokine staining procedures, the binding of each mAb was blocked with an excess of unlabelled mAb.

Statistics

Results are given as median and range. Differences between the groups were analyzed by the Kruskal-Wallis test, Mann-Whitney *U* test and Wilcoxon signed rank test, as appropriate. All calculations were performed on a personal computer with Statview 4.5 software (Abacus Concepts inc., Berkeley CA, USA). *P* values <0.05 were regarded as significant.

RESULTS

Using flowcytometric detection of intracytoplasmic cytokines in combination with CD14 staining, we were able to specifically measure spontaneous as well as HCV antigen-induced production of IL-1 β , IL-10, IL-12 and TNF- α in peripheral blood monocytes (Figure 1). Following stimulation with LPS, intracytoplasmic expression of the cytokines did not show statistically significant differences between the study groups for the cytokines with the exception of IL-1 β , which was higher in patients with chronic hepatitis C when compared to the controls (Table 1). Cytokine production after 12 hours of HCV-specific stimulation together with the corresponding spontaneous and LPS-induced production is summarized in Table 1.

With respect to spontaneous production of IL-1 β , TNF- α , IL-10, and IL-12, there was considerable individual variability which was most pronounced in the group with chronic hepatitis C. The numbers of monocytes with detectable spontaneous production of IL-12 were low in general (0.1-5.1%) and on average not significantly different between the three study groups. In contrast, average numbers with detectable spontaneous production of IL-1 β , TNF- α , and IL-10 were higher in patients with chronic hepatitis C than in aviremic anti-HCV seropositives. However, due to considerable inter-individual variations, these differences between the groups reached statistical significance only for IL-1 β and IL-10 ($P<0.05$).

Antigen-specific stimulation of peripheral blood mononuclear cells resulted in increased numbers of monocytes with production of IL-1 β , TNF- α , IL-10, and IL-12 in each study group for most of the tested HCV proteins (Table 1). However, after stimulation with the HCV proteins core, NS3, NS4, NS5a, and NS5b, the numbers of IL-1 β and IL-10 producing monocytes were at least twofold higher in patients with chronic hepatitis C than in aviremic anti-HCV seropositives and the controls ($P<0.05$ for each HCV protein). In contrast, statistically significant differences ($P<0.05$) in the numbers of TNF- α and IL-12 producing monocytes between patients with chronic hepatitis C and the other groups were only seen after stimulation with HCV core and NS5b (Table 1). The marked difference in the balance between IL-1 β and IL-10 producing monocytes, and TNF- α and IL-12 producing ones among the patients with chronic hepatitis C is illustrated in Figure 2, which shows the stimulation experiments with recombinant NS4 as a representative example. Since stimulation of monocytes was performed in the presence of T cells, we undertook control experiments with untouched isolated monocytes. When these purified monocytes were stimulated with HCV antigens or LPS, the cells showed a similar behaviour although the number of cytokine producing macrophages was strongly reduced compared to the PBMC assays (data not shown).

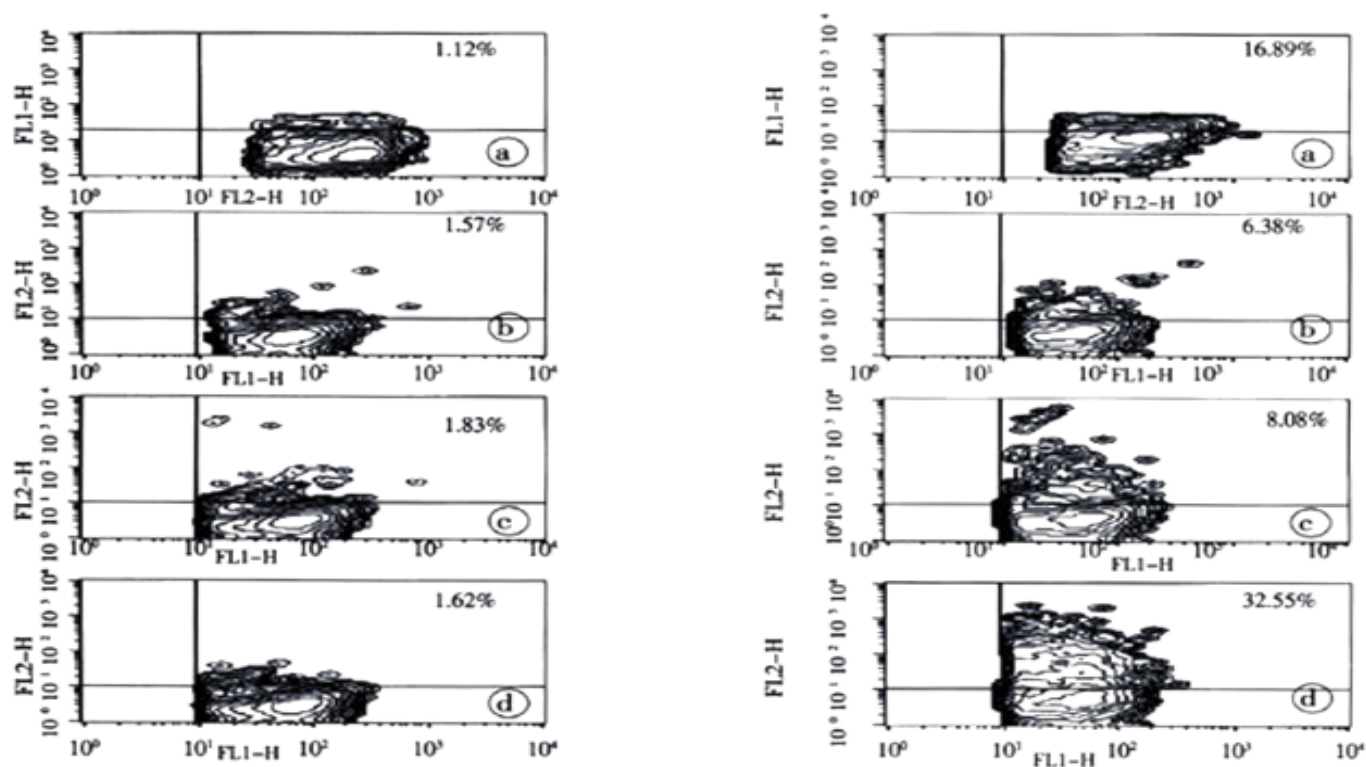


Figure 1 Contour plots of cytokine expression in CD14⁺ cells. These contour plots show representative experiments for the detection of spontaneous expression (buffer control, left column) and HCV NS5b-induced expression (1 μ g/mL, right column) of IL-1 β (a), IL-10 (b), IL-12 (c) and TNF- α (d) in peripheral blood CD14⁺ monocytes of patient # 23 with chronic hepatitis C at 12 hours of incubation.

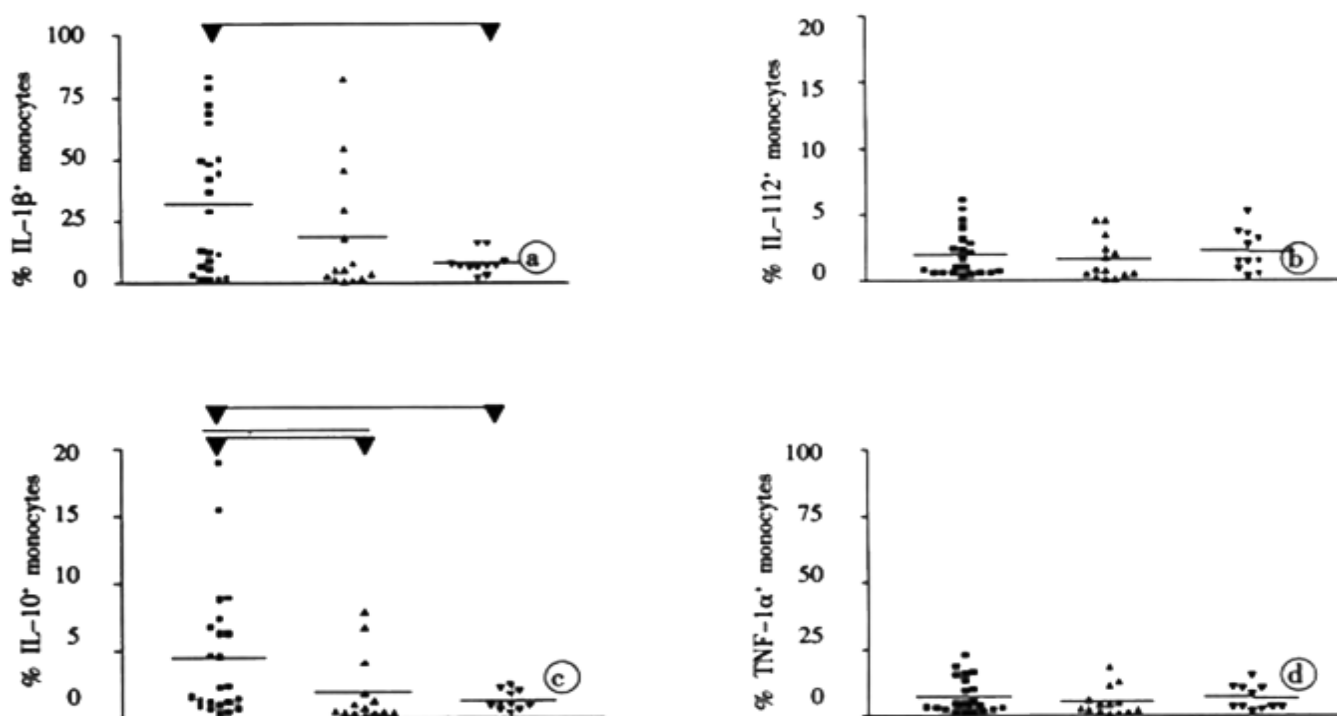


Figure 2 Induction of cytokines by the HCV NS4 protein. The graph displays the fractions of IL-1 β (a), IL-10 (b), IL-12 (c) and TNF- α (d) producing monocytes 12 hours after stimulation with recombinant NS4 protein (1 μ g/mL) for patients with chronic hepatitis C (filled squares), aviremic anti-HCV seropositives (upward triangles), and non-HCV related controls (downward triangles). Each dot represents the mean percentage of a single patient obtained from triplicate experiments. The horizontal bar gives the mean of each group.

Table 1 CD14⁺ monocytes with detectable intracellular cytokine expression

	Chronic hepatitis C (n=23)		Aviremic anti-HCV seropositives (n=14)		Controls (n=11)	
	% CD14 ⁺ monocytes	§ Significance	% CD14 ⁺ monocytes	§ Significance	% CD14 ⁺ monocytes	§ Significance
IL-1 β						
Spontaneous expression	13.6 [0.3-82.1]	a, b	1.9 [0.4-65.5]		2.1 [0.6-4.7]	
Expression after stimulation with						
Core	21.5 [0.9-84.8]	a, b, c	3.1 [0.1-69.6]	c	2.8 [0.6-8.3]	
NS3	42.0 [1.1-91.1]	a, b, c	7.0 [0.6-71.8]	c	6.1 [1.6-31.6]	c
NS4	28.3 [0.4-82.4]	a, b, c	4.6 [0.2-81.8]		6.2 [1.6-15.5]	c
NS5a	34.3 [0.4-87.2]	a, b, c	3.3 [0.1-77.8]	c	8.3 [1.7-14.5]	c
NS5b	27.6 [1.7-89.9]	a, b, c	6.2 [0.8-75.3]	c	4.8 [0.8-30.3]	
LPS	55.5 [7.6-96.5]	b	36.2 [4.0-97.0]		24.1 [9.4-48.7]	
IL-10						
Spontaneous expression	1.4 [0.2-8.6]	a, b	0.4 [0.1-6.1]		0.7 [0.1-1.3]	
Expression after stimulation with						
Core	2.6 [0.3-24.4]	a, b, c	0.6 [0.1-8.3]	c	1.0 [0.2-1.8]	
NS3	2.4 [0.2-20.2]	a, b, c	0.8 [0.2-9.8]	c	0.8 [0.2-2.3]	c
NS4	2.0 [0.2-18.8]	a, b, c	0.5 [0.0-7.7]		0.9 [0.2-2.1]	c
NS5a	2.0 [0.2-16.9]	a, b, c	0.7 [0.1-7.9]	c	1.0 [0.1-3.2]	c
NS5b	3.7 [0.1-22.4]	a, b, c	0.7 [0.1-12.6]	c	0.7 [0.2-5.4]	
LPS	12.4 [0.2-39.8]		6.4 [0.3-25.0]		6.0 [0.5-19.1]	
IL-12						
Spontaneous expression	0.8 [0.2-5.1]		0.5 [0.2-3.1]		0.6 [0.1-2.3]	
Expression after stimulation with						
Core	2.0 [0.2-8.1]	a	0.7 [0.1-3.1]		1.1 [0.3-3.2]	
NS3	1.8 [0.5-16.3]	c	1.1 [0.2-5.3]	c	1.6 [0.2-12.2]	c
NS4	1.0 [0.3-6.1]	c	0.8 [0.8-4.5]		4.5 [0.3-5.2]	c
NS5a	1.5 [0.3-9.1]	c	0.8 [0.1-3.7]	c	1.5 [0.2-3.7]	c
NS5b	2.2 [0.3-40.1]	b,c	1.0 [0.3-5.2]	c	0.9 [0.2-6.1]	
LPS	18.7 [0.7-61.8]		6.2 [0-12.7]		11.8 [2.4-33.5]	
TNF- α						
Spontaneous expression	3.2 [0.1-39.5]		0.8 [0.2-12.0]		1.3 [0.4-3.4]	
Expression after stimulation with						
Core	6.9 [0.3-51.3]	b, c	1.5 [0.1-12.8]	c	1.7 [0.3-6.1]	c
NS3	5.4 [0.2-40.7]		2.9 [0.4-16.4]	c	3.7 [0.9-23.3]	c
NS4	3.1 [0.2-21.9]		2.7 [0.1-17.7]	c	2.9 [1.1-14.6]	c
NS5a	4.30 [0.1-22.7]		1.8 [0.2-11.1]	c	4.0 [1.3-8.3]	c
NS5b	10.9 [0.7-53.8]	a, b, c	2.3 [0.4-23.2]	c	2.0 [0.9-9.6]	c
LPS	35.0 [1.50-91.2]		21.3 [1.5-51.4]		31.5 [12.1-47.9]	

§ Significances:

 a= P <0.05 Chronic HCV infection vs. aviremic anti-HCV seropositives (Kruskal-Wallis test and Mann-Whitney U test)

 b= P <0.05 Chronic HCV infection vs. Controls (Kruskal-Wallis test and Mann-Whitney U test)

 c= P <0.05 Stimulated vs. spontaneous cytokine expression (Wilcoxon signed rank test)

Data are given as median+ range.

DISCUSSION

Impaired function of macrophages has been described repeatedly in infection with HCV and also the closely related Dengue virus^[13-17]. Our study adds to these observation that in chronic hepatitis C altered macrophage function may also comprise the pattern of cytokines produced in response to HCV antigens. Of note, the various cytokines appeared to be involved differentially. Despite considerable individual variability, we found significantly greater average numbers of monocytes with spontaneous IL-1 β and IL-10 production in patients with chronic hepatitis than that in aviremic anti HCV seropositives or the HCV-naïve controls. This finding appears to be compatible with in vivo pre-activation of the monocytes from patients with chronic hepatitis C. However, the numbers of monocytes with spontaneous IL-12 production did not reveal any conspicuous differences between our study groups. Thus far, studies on the cytokine production in hepatitis C have produced conflicting results for macrophages, mainly because monocytes were assessed only indirectly by measuring cytokines in the supernatants of peripheral blood mononuclear cells after stimulation with mitogen or LPS. This flowcytometric study is the first investigation, which provides HCV-specific data for monocytes at the single cell level in a more or less physiological environment that enables natural interactions to take place between the monocytes and other peripheral blood mononuclear cells, e.g. CD4⁺ T lymphocytes. Control experiments with untouched isolated monocytes showed that these interactions were crucial for an effective cytokine induction. Despite similar behaviour after stimulation the amount of cytokine

producing macrophages was strongly reduced (data not shown). With the flowcytometric approach, we could demonstrate that the numbers of IL-1 β ⁺ and IL-10⁺ monocytes increased significantly upon stimulation with the HCV antigens, whereas a similar induction of TNF- α and IL-12 was not observed.

After exposure to the HCV proteins a slight increase in the number of monocytes with expression of IL-1 β , TNF- α , IL-10, and IL-12 was also seen in the HCV-naïve control group. This finding most likely indicates a non-specific stimulatory effect of the HCV antigens on the monocytes, probably due to small amounts of contaminating endotoxin. Compared to this non-specific effect this results indicate marked (2-7 fold) antigen-specific induction of IL-1 β and IL-10 in response to all HCV antigens, but a less prominent induction of IL-12 and TNF- β in response to HCV core and NS5b in the group with chronic hepatitis C.

Similar responses were occasionally seen in few patients of our aviremic anti-HCV seropositive group. However, we cannot exclude completely that HCV replication below the detection limit of PCR technique was present in some of these patients, despite the fact that the group of aviremic anti-HCV seropositives was selected carefully to ensure that these patients had gained immune-mediated control of their HCV infection. Thus persistent low level viremia might be an explanation for the occasional altered cytokine responses in this group.

In general, our findings are in line with a previous report by Kakumu *et al.*, who reported increased IL-10 levels but unaltered IL-12 production in mononuclear cells of patients with chronic hepatitis

C^[18]. Furthermore, increased spontaneous TNF- α expression in patients with chronic hepatitis C is in line with previous work published by Kishihara and co-workers^[19]. As our flowcytometric approach enabled interactions between the monocytes and other immunoregulatory cells, which are important for the generation of antigen-specific responses, it was not unexpected that our results differed from those studies, which used purified monocytes^[20]. Thus, we could not confirm reduced numbers of IL-1 β and TNF- α monocytes in chronic hepatitis C, as has been reported for purified monocytes from patients with chronic hepatitis C by Mendoza and co-workers^[21].

The reasons for altered macrophage functions in chronic hepatitis C are unclear at present. Although HCV RNA has been detected in macrophages of a variable proportion of patients with chronic hepatitis C^[22], the reported percentages of HCV-RNA positive monocytes seem to be too low as to explain the altered cytokine induction by a direct infection of the monocytes^[23]. Persistent antigenic stimulation due to chronic hepatitis C viremia provides a better alternative explanation. For instance, continued production of HCV antigens may lead to the formation of antigen-antibody complexes, which can bind to Fc γ receptors on immunocompetent cells. Fc γ receptor ligation on monocytes will then result in reversal of macrophage pro-inflammatory responses as IL-10 up-regulation together with a reciprocal inhibition of IL-12 production can result from such Fc γ receptor triggering^[24]. Likewise, the blunted TNF- α responses observed in our *in vitro* stimulation experiments are likely to reflect altered immunoregulation, because loss of inducible TNF- α secretion has been well documented in pre-activated monocytes^[25].

Irrespective of the underlying cause, altered cytokine production by macrophages in chronic hepatitis C is likely to have important functional consequences. The high proportion of macrophages, which produce IL-1 β either spontaneously or after antigen-specific challenge may indicate that these macrophages are pre-conditioned towards pro-inflammatory reactions. However, proinflammatory cytokines required for efficient antiviral responses such as IL-12 and TNF- α show blunted responses to the HCV antigens. On the contrary, cytokine production appeared to be markedly biased towards IL-10 already at the level of the macrophages. Due to the pivotal role of monocytes and macrophages for the initiation of immune responses, the uniform up-regulation of IL-10 in response to HCV antigens, not counterbalanced by IL-12, may explain poor HCV-specific type I cytokine responses, which have been observed repeatedly in chronic hepatitis C^[3-7]. Thus, altered cytokine production by monocytes and macrophages might contribute to HCV persistence, because these cells may not support sufficiently effective antiviral immune responses.

ACKNOWLEDGMENTS

We gratefully acknowledge Eva-Maria Althausen, Department of Internal Medicine I and Bettina Kochan, Institute of Medical Microbiology and Immunology for excellent technical assistance. This work was supported by a generous grant of the Joachim Kuhlmann AIDS-Stiftung.

REFERENCES

- Abbas AK, Murphy KM, Sher A. Functional diversity of helper T lymphocytes. *Nature* 1996; 383:787-793
- Cerny A, Chisari FV. Pathogenesis of chronic hepatitis C: immunological features of hepatic injury and viral persistence. *Hepatology* 1999; 30:595-601
- Lechmann M, Woitas RP, Langhans B, Kaiser R, Ihlenfeldt HG, Jung G, Sauerbruch T, Spengler U. Decreased frequency of HCV core-specific peripheral blood mononuclear cells with type 1 cytokine secretion in chronic hepatitis C. *J Hepatol* 1999; 31:971-978
- Malaguarnera M, Di Fazio I, Laurino A, Pistone G, Restuccia S, Trovato BA. Decrease of interferon gamma serum levels in patients with chronic hepatitis C. *Biomed Pharmacother* 1997; 51:391-396
- Osna N, Silonova G, Vilgert U, Hagina E, Kuse V, Giedraitis V, Zvirbliene A, Mauricas M, Sochnev A. Chronic hepatitis C: T-helper1/T-helper2 imbalance could cause virus persistence in peripheral blood. *Scand J Clin Lab Invest* 1997; 57:703-710
- Reiser M, Marousis CG, Nelson DR, Lauer G, Gonzalez-Peralta RP, Davis GL, Lau JY. Serum interleukin 4 and interleukin 10 levels in patients with chronic hepatitis C virus infection. *J Hepatol* 1997; 26:471-478
- Woitas RP, Lechmann M, Jung G, Kaiser R, Sauerbruch T, Spengler U. CD30 induction and cytokine profiles in hepatitis C virus core-specific peripheral blood T lymphocytes. *J Immunol* 1997; 159:1012-1018
- Woitas RP, Rockstroh JK, Beier I, Jung G, Kochan B, Matz B, Brackmann HH, Sauerbruch T, Spengler U. Antigen-specific cytokine response to hepatitis C virus core epitopes in HIV/hepatitis C virus-coinfected patients. *Aids* 1999; 13:1313-1322
- Choo QL, Kuo G, Weiner AJ, Overby LR, Bradley DW, Houghton M. Isolation of a cDNA clone derived from a blood-borne non-A, non-B viral hepatitis genome. *Science* 1989; 244:359-362
- Tartakoff AM. Perturbation of the structure and function of the Golgi complex by monovalent carboxylic ionophores. *Methods Enzymol* 1983; 98:47-59
- Jung T, Schauer U, Heusser C, Neumann C, Rieger C. Detection of intracellular cytokines by flow cytometry. *J Immunol Methods* 1993; 159:197-207
- Pickler LJ, Singh MK, Zdravski Z, Treer JR, Waldrop SL, Bergstresser PR, Maino VC. Direct demonstration of cytokine synthesis heterogeneity among human memory/effector T cells by flow cytometry. *Blood* 1995; 86:1408-1419
- Bain C, Fatmi A, Zoulim F, Zarski JP, Trepo C, Inchauspe G. Impaired allostimulatory function of dendritic cells in chronic hepatitis C infection. *Gastroenterology* 2001; 120:512-524
- Kanto T, Hayashi N, Takehara T, Tatsumi T, Kuzushita N, Ito A, Sasaki Y, Kasahara A, Hori M. Impaired allostimulatory capacity of peripheral blood dendritic cells recovered from hepatitis C virus-infected individuals. *J Immunol* 1999; 162:5584-5591
- Mathew A, Kurane I, Green S, Vaughn DW, Kalayanarooj S, Suntayakorn S, Ennis FA, Rothman AL. Impaired T cell proliferation in acute dengue infection. *J Immunol* 1999; 162:5609-5615
- Hiasa Y, Horiike N, Akbar SM, Saito I, Miyamura T, Matsuura Y, Onji M. Low stimulatory capacity of lymphoid dendritic cells expressing hepatitis C virus genes. *Biochem Biophys Res Commun* 1998; 249:90-95
- Auffermann-Gretzinger S, Keffe EB, Levy S. Impaired dendritic cell maturation in patients with chronic, but not resolved, hepatitis C virus infection. *Blood* 2001; 97:3171-3176
- Kakumu S, Okumura A, Ishikawa T, Iwata K, Yano M, Yoshioka K. Production of interleukins 10 and 12 by peripheral blood mononuclear cells (PBMC) in chronic hepatitis C virus (HCV) infection. *Clin Exp Immunol* 1997; 108:138-143
- Kishihara Y, Hayashi J, Yoshimura E, Yamaji K, Nakashima K, Kashiwagi S. IL-1 beta and TNF-alpha produced by peripheral blood mononuclear cells before and during interferon therapy in patients with chronic hepatitis C. *Dig Dis Sci* 1996; 41:315-321
- Cella M, Scheidegger D, Palmer-Lehmann K, Lane P, Lanzavecchia A, Alber G. Ligation of CD40 on dendritic cells triggers production of high levels of interleukin-12 and enhances T cell stimulatory capacity: T-T help via APC activation. *J Exp Med* 1996; 184:747-752
- Mendoza EC, Paglieroni TG, Zeldis JB. Decreased phorbol myristate acetate-induced release of tumor necrosis factor-alpha and interleukin-1 beta from peripheral blood monocytes of patients chronically infected with hepatitis C virus. *J Infect Dis* 1996; 174:842-844
- Bouffard P, Hayashi PH, Acevedo R, Levy N, Zeldis JB. Hepatitis C virus is detected in a monocyte/macrophage subpopulation of peripheral blood mononuclear cells of infected patients. *J Infect Dis* 1992; 166:1276-1280
- Mellor J, Haydon G, Blair C, Livingstone W, Simmonds P. Low level or absent *in vivo* replication of hepatitis C virus and hepatitis G virus/GB virus C in peripheral blood mononuclear cells. *J Gen Virol* 1998; 79:705-714
- Sutterwala FS, Noel GJ, Salgame P, Mosser DM. Reversal of proinflammatory responses by ligating the macrophage Fc gamma receptor type I. *J Exp Med* 1998; 188:217-222
- Haas JG, Baeuerle PA, Riethmuller G, Ziegler-Heitbrock HW. Molecular mechanisms in down-regulation of tumor necrosis factor expression. *Proc Natl Acad Sci USA* 1990; 87:9563-9567

• CLINICAL RESEARCH •

Coinfection of TT virus and response to interferon therapy in patients with chronic hepatitis B or C

Yung-Chih Lai, Ruey-Tyng Hu, Sien-Sing Yang, Chi-Hwa Wu

Yung-Chih Lai, Ruey-Tyng Hu, Sien-Sing Yang, Chi-Hwa Wu, Liver Unit, Department of Internal Medicine, Cathay General Hospital, Taipei, Taiwan
Correspondence to: Sien-Sing Yang, MD, Liver Unit, Cathay General Hospital, 280 Jen-Ai Rd., Sec. 4, Taipei, Taiwan 106. yangss@seed.net.tw
Telephone: +886-2-2708-2121 Ext. 3121

Received 2002-03-30 Accepted 2001-05-25

Abstract

AIM: To investigate the serum positive percentage of TT virus (TTV) in patients with chronic hepatitis B or C and the response of the coinfecting TTV to interferon (IFN) during IFN therapy for chronic hepatitis B and C.

METHODS: We retrospectively studied the serum samples of 70 patients with chronic hepatitis who had received IFN- α therapy from January 1997 to June 2000, which included 40 cases of hepatitis B and 30 hepatitis C. All the patients had been followed up for at least 6 months after the end of IFN therapy. The serum TTV DNA was detected using the polymerase chain reaction (PCR) before and every month during the course of IFN treatment.

RESULTS: TTV infection was detected in 15% (6/40) of the chronic hepatitis B group and 30% (9/30) of the chronic hepatitis C group. Loss of serum TTV DNA during IFN therapy occurred in 3 of 6 patients (50%) and 6 of 9 (67%) of hepatitis B and C groups, respectively. Seronegativity of TTV was found all during the first month of IFN therapy in the 9 patients. There was no correlation between the seroconversion of TTV and the biochemical changes of the patients.

CONCLUSION: TTV is not infrequently coinfecting in patients with chronic hepatitis B and C in Taiwan, and more than half of the TTV infections are IFN-sensitive. However, the loss of serum TTV DNA does not affect the clinical course of the patients with chronic hepatitis B or C.

Lai YC, Hu RT, Yang SS, Wu CH. Coinfection of TT virus and response to interferon therapy in patients with chronic hepatitis B or C. *World J Gastroenterol* 2002;8(3):567-570

INTRODUCTION

In 1997, a novel DNA virus was isolated from a patient with post-transfusion hepatitis of unknown etiology in Japan, and was designated as TT virus (TTV) after the initials of the index patient^[1]. From then on TTV has been studied worldwide. Now we know that TTV genome is non-enveloped, circular, single-stranded DNA and comprises 3,852 bases with a particle size of 30-50nm. These findings suggest that TTV is closely related to the Circoviridae^[2,3].

In the original studies from Japan, the agent was found in 34/290 (12%) of healthy donors, compared to 9/19 (47%) of patients with fulminant non-A to G hepatitis and 41/90 (46%) with non-A-G chronic liver disease^[2]. In 72 patients with chronic liver disease in the United Kingdom, TTV DNA was demonstrated in 18 cases (25%), compared to 10% of 30 cases of healthy controls^[4]. Chronic liver

disease caused by hepatitis B virus (HBV) and hepatitis C virus (HCV) infection is common in Taiwan^[5,6] and interferon (IFN) has been used for the treatment of chronic infections. Therefore, we aimed to study the serum positive percentage of TTV infection in such patients who had received IFN therapy and also to see the response of TTV to IFN during the course of the treatment.

MATERIALS AND METHODS

Patients

We retrospectively studied the frozen-stored serum samples from the patients who had received IFN therapy for chronic hepatitis B and C at Cathay General Hospital from January 1997 to June 2000.

For chronic hepatitis B, we only included the cases with both positive HBsAg (Auszyme, Abbott Lab., North Chicago, IL) and positive HBeAg [HBe (rDNA) EIA, Abbott Lab.]. Hepatitis C was confirmed with positive results for the anti-HCV antibody (Murex anti-HCV, version III, Murex Diagnostics Ltd., Dartford, England). All the cases had elevated serum alanine transaminase (ALT) levels for more than 6 months and had had at least three documented occasions of levels higher than twice the upper limit of normal (<35 IU/L), at least 1 month apart, and within 6 months prior to enrollment. All the patients underwent liver biopsy within 1 month before the start of IFN treatment. The diagnosis of chronic liver disease was based on clinical and pathological results. Serum samples taken from the patients were stored at -70°C until use.

None of our patients was alcoholic, an intravenous drug abuser or homosexual. None had received hepatotoxic drugs, herbal medicine or immuno-suppressive therapy within the 6 months prior to IFN therapy. Patients with metabolic liver diseases including hemochromatosis, Wilson's disease or α -1 anti-trypsin deficiency and autoimmune hepatitis were excluded by clinical and laboratory examinations. None had decompensated liver function (prolonged prothrombin time >3 seconds, serum total bilirubin >3.0 mg/dl, or serum albumin <3.0 gm/dl), chronic renal failure, clotting abnormalities, or serious neurological disorders. Those who coinfecting with both HBV and HCV were also excluded. Informed consent for the IFN therapy and examinations, including virological assays, was obtained from all the patients.

Laboratory assays

The patients underwent blood biochemical tests every week for the initial 4 weeks and every 2 weeks thereafter during the treatment until 24 weeks. After the end of the treatment, the patients were followed up at 4-week intervals for 12 months.

Serum samples from hepatitis C patients were examined for HCV RNA using reverse transcription-nested polymerase chain reaction (PCR) with primers for the 5'-noncoding region of HCV RNA. Genotyping of HCV RNA was assayed by PCR with type-specific primers^[7]. Serum HBV DNA was quantified with the use of a signal amplified solution hybridization antibody capture assay (Hybrid capture system, Digene, Gaithersburg, MD, USA). The presence of serum HCV RNA or HBV DNA was determined before the initiation of IFN therapy, at the end of therapy, and at 24 weeks after the completion of therapy.

Detection of TTV DNA

Serum TTV DNA was determined in specimens before the initiation of IFN therapy and regularly checked every 1 month during the course of the treatment. TTV DNA was examined using the PCR method with nested primers as previously described^[8]. Briefly, DNA was extracted from 100 μ L of serum using a QIAMP blood kit (QIAGEN Ltd., Crawley, UK) and resuspended in 50 μ L of elution buffer. For the first round of PCR, 25 μ L of reaction mixture containing 2 μ L of the cDNA sample, 1 \times PCR buffer (10mM tris-HCl pH 9.0, 50mM KCl, 1.5mM MgCl₂, 0.01% gelatin, and 0.1% Triton X-100), 10mM of each dNTP, 100ng of each outer primer T-1 (sense: 5'-ACA GAC AGA GGA GAA GGC AAC ATG-3') and T-2 (anti-sense: 5'-CTA CCT CCT GGC ATT TTA CC-3'), and 1 unit of Taq DNA polymerase was amplified in a thermal cycler (Perkin-Elmer Cetus, Norwalk, CT) for 30 cycles. One microliter of the PCR products was re-amplified for another 30 cycles with 100ng of inner primers, T-3 (sense: 5'-GGC AAC ATG TTA TGG ATA GAC TGG-3') and T-4 (anti-sense: CTG GCA TTT TAC CAT TTC CAA AGT T-3'). The amplified products were separated by 3% agarose gel electrophoresis and stained with ethidium bromide.

Interferon therapy

For the patients with chronic hepatitis B, 10 million units (mu) of recombinant interferon alfa-2b (Intron A, Schering-Plough, Co. Kenilworth, NJ, USA) was subcutaneously administered three times weekly for 24 weeks. For those with hepatitis C, 4.5 million units of recombinant alfa-2a (Roferon-A, F. Hoffmann-La Roche Ltd., Basle, Switzerland) was used subcutaneously three times a week for 24 weeks. The response to IFN was classified into two patterns according to the serum ALT level. Patient who had normalized serum ALT level (<35 IU/L) during therapy and remained constant for up to 6 months after the end of therapy was considered to have a biochemical sustained response. Non-sustained response was defined as serum ALT level that could not be normalized either at the end of therapy or during the follow-up period. The virological sustained response was defined as the absence of HBV DNA and HBeAg for hepatitis B, HCV RNA for hepatitis C and TTV DNA for TTV infection at 6 months after the end of therapy.

Statistical analysis

Data were analyzed by Student's *t* test, Chi-squared test with Yates' correction or Fisher's exact test where appropriate. All statistical tests were two-sided. A *P* value of less than 0.05 was considered significant.

RESULTS

The sera of 70 patients were studied, which included 40 patients with chronic hepatitis B and 30 patients with chronic hepatitis C (Table 1). The difference of ages between the two groups was statistically significant (*P*<0.001). In those with chronic hepatitis B, the mean age was 33 years; whereas in the chronic hepatitis C group, it was 41 years. As for the gender distribution and serum ALT levels, there was no statistically significant difference between the two groups.

Serum TTV DNA could be detected in 6 cases (15%) of chronic hepatitis B and 9 cases (30%) of chronic hepatitis C. However, the difference was not statistically significant (*P*=0.130) (Table 1).

During IFN therapy loss of serum TTV DNA was found in 3 of 6 (50%) TTV-positive patients with chronic hepatitis B and 6 of 9 (67%) TTV-positive patients with chronic hepatitis C (Table 2). Because this was a retrospective study and the doses of IFN used for chronic hepatitis B and C were different, we could not compare the rate of TTV disappearance between the two groups. Of interest,

disappearance of serum TTV DNA occurred during the first 4 weeks of IFN therapy in all the 9 cases despite the regimen of treatment or the type of chronic viral hepatitis (Table 2). In addition, serum ALT levels did not change when TTV disappeared from the serum. Serum TTV DNA was still examined every 4 weeks after the cessation of IFN therapy in the 9 cases of TTV seroconversion and had continued for 24 weeks. There was no case having the re-emergence of TTV DNA during this follow-up period.

Disappearance of TTV occurred in different genotypes of chronic hepatitis C (1a: 1/1 case, 1b: 3/5 cases, 2a: 1/2 cases, 2b: 1/1 case.). However, the number of cases was small.

In the group of chronic hepatitis B, 10 patients had virological persistent response to IFN therapy, and all the 10 patients also had biochemical persistent response. Whereas, only one patient (1/3 cases) with virological persistent response of TTV DNA had biochemical persistent response (Table 3). If we further exclude the patient with concomitant loss of HBV DNA, HBeAg and TTV DNA, none of the patients (0/2 cases) with TTV virological persistent response had biochemical persistent response.

In the group of chronic hepatitis C, all the 7 patients with virological persistent response of HCV RNA to IFN therapy had biochemical persistent response, and 2 patients (2/6 cases) with virological sustained response of TTV DNA had biochemical persistent response (Table 4). Nevertheless, none of the patients (0/4 cases) of TTV virological sustained response had biochemical persistent response after exclusion of 2 patients of concomitant loss of TTV DNA and HCV RNA.

Table 1 Demographic data and serum positive percentage of TTV in the two groups

Type	Sex (M/F)	Age (yr)	ALT (IU/L)	TTV DNA	
				No.Positive	%
B ^a (n=40)	29/11	33±8 ^c	133±65	6	15
C ^b (n=30)	24/6	41±9	121±60	9	30

^aChronic hepatitis B group. ^bChronic hepatitis C group. ^c*P*<0.001.

Table 2 Loss of serum TTV DNA during IFN therapy in the two groups

	Time of IFN Therapy (weeks)						Total
	4	8	12	16	20	24	
B ^a	3	0	0	0	0	0	3
C ^b	6	0	0	0	0	0	6

Data are presented as case number. ^aChronic hepatitis B group. ^bChronic hepatitis C group.

Table 3 Relationship between viral and biochemical responses in the group of chronic hepatitis B

	Virological SR	
	HBV (n=10)	TTV (n=3)
Biochemical SR (+)	10	1
Biochemical SR (-)	0	2

SR: sustained response, *P*=0.038, by Fisher's exact test

Table 4 Relationship between viral and biochemical responses in the group of chronic hepatitis C

	Virological SR	
	HCV (n=7)	TTV (n=6)
Biochemical SR (+)	7	2
Biochemical SR (-)	0	4

SR: sustained response, *P*=0.021, by Fisher's exact test

DISCUSSION

Epidemiologic studies have confirmed that TTV is a parenterally transmitted agent as demonstrated by donor-recipient linkage in transfused patients and by a high prevalence among hemophiliacs and intravenous drug abusers^[9-11]. In general, TTV is common in populations at risk of infection with blood-borne viruses^[2,12-14]. Many hepatitis viruses share the same modes of transmission, thus multiple viral infections may occur in a given patient^[15].

Coinfection of TTV has been observed frequently in patients with chronic hepatitis B or C^[4]. Chronic infection of hepatitis B or C virus is common in Taiwan. Thus, we made use of such patients who underwent interferon treatment to study the TT virus. In our series TTV DNA was detected in 15% of chronic hepatitis B and 30% of chronic hepatitis C, which were comparable to the results of Kao *et al*^[16], (22% and 37%, respectively) and apparently higher than that (10%) of healthy adults in Taiwan^[8]. In a prior study by Naoumov *et al*, TTV infection was detected in 21% of 33 patients with chronic hepatitis C and 20% of 10 patients with chronic hepatitis B^[4]. In Thailand, Tanaka *et al*, also found that 36% of 59 patients with HBsAg (+) and 36% of 10 patients with HCV RNA (+) had TTV infection^[17]. Several other studies also reported that the serum positive rates of TTV DNA in the patients with chronic hepatitis C, and the range was 20-46%^[18-20]. The variation might be due to the different primers used for the detection of TTV DNA. These results imply that HBV, HCV, and TTV may share common modes of transmission^[16].

The interferons possess antiproliferative, antiviral and immunomodulant properties^[21]. Extensive clinical trials have confirmed the efficacy of recombinant interferon-alfa for patients with chronic hepatitis B, C and D^[22-26]. However, because the causal role of TTV in liver disease has not been established, there is only a few papers which studied the response of TTV to IFN therapy. Taking advantage of previous research of IFN therapy for chronic hepatitis B and C, we were able to retrospectively study the prevalence of TTV in these patients and to see the response of TTV to IFN treatment. In our study, loss of serum TTV DNA during IFN therapy was noted in 50% (3/6) of chronic hepatitis B and 67% (6/9) of chronic hepatitis C. Regrettably, the comparison of these results was not feasible because this was a retrospective study and the doses of IFN used in two groups were different. Kao *et al*^[16], had similar results and they found that 41% (17/41) of patients with HCV and TTV coinfection lost serum TTV DNA at 24 weeks after the end of IFN therapy for chronic hepatitis C. Virological sustained response of TTV DNA after IFN therapy was detected to be 40-55% in patients coinfecting with chronic hepatitis C according to the recently published reports^[18-20, 27]. These findings suggest that TTV was actually vulnerable and responsive to IFN therapy. In addition, all the 9 IFN-responsive cases in our series lost their TTV DNA within the first 4 weeks of IFN therapy. This kind of seroconversion occurred in the same way in both hepatitis B and C groups, but we need more cases to further observe and confirm this phenomenon. With the results above, we know that TTV could be divided into 2 types according to the response to IFN therapy: IFN-sensitive and IFN-resistant. For the IFN-sensitive virus, the 4-week course of IFN therapy was enough to cause the seronegativity of TTV DNA. Moreover, virological sustained response could be achieved in all the 9 IFN-sensitive cases.

TTV was detected in patients with different genotypes of chronic hepatitis C. Loss of serum TTV DNA during IFN therapy occurred in all the genotypes in our study. The conversion rate between each genotype could not be compared because the number of patients was not enough. Nevertheless, the loss of serum TTV DNA during IFN therapy did not seem to be associated with the genotype of HCV.

Investigations of TTV showed considerable diversity among different isolates. The genetic diversity has continued to expand as

more and more isolates have been studied^[2,4,12]. The different response patterns to IFN therapy must be related to the genetic diversity. Comparison of partial viral DNA nucleotide sequences and phylogenetic analysis done by Chayama *et al*^[27] showed that viral strains that had a high identity to the prototype virus were more resistant to IFN than those showing low nucleotide sequence identity. The variants with multiple substitutions in the genomic sequence were more apt to be eliminated by IFN. Further analysis with new genotyping assays will reveal more information in this field.

During the course of IFN treatment, we did not find any correlation between the seroconversion of TTV DNA and the change of serum ALT levels. Although TTV was sensitive to IFN therapy in many subjects, the improvement in ALT levels after IFN therapy was not attributable to the eradication of TTV but rather to that of HCV or HBV. The disappearance of TTV DNA had no effect on the biochemical response to IFN therapy^[18,20]. According to such results, TTV may lack pathogenicity or clinical association with liver disease in these patients, which is consistent with the conclusions of many other reports^[4,8,28,29].

In summary, the serum positive percentage of TTV in chronic hepatitis B or C in our series was not low. During the IFN therapy for chronic hepatitis B or C, disappearance of coinfecting TTV occurred in more than half of the patients. IFN-sensitive TTV usually lost its DNA during the first month of treatment. Genotyping of TTV might further clarify the cause of diverse responses to IFN therapy. The finding that the disappearance of TTV DNA did not affect the clinical course of chronic hepatitis favors the null hypothesis of no significant association of TTV with liver disease.

REFERENCES

- 1 Nishizawa T, Okamoto H, Konishi K, Yoshizawa H, Miyakawa Y, Mayumi M. A novel DNA virus (TTV) associated with elevated transaminase levels in posttransfusion hepatitis of unknown etiology. *Biochem Biophys Res Commun* 1997; 241:92-97
- 2 Okamoto H, Nishizawa T, Kato N, Ukita M, Ikeda H, Iizuka H. Molecular cloning and characterization of a novel DNA virus (TTV) associated with posttransfusion hepatitis of unknown etiology. *Hepatology Research* 1998; 10:1-16
- 3 Mushahwar IK, Erker JC, Muerhoff AS, Leary TP, Simon JN, Birkenmeyer LG. Molecular and biophysical characterization of TT virus; evidence for a new virus family infecting humans. *Proc Natl Acad Sci USA* 1999; 96:3177-3182
- 4 Naoumov N, Petrova EP, Thomas MG, Williams R. Presence of a newly described human DNA virus (TTV) in patients with liver disease. *Lancet* 1998; 352:195-197
- 5 Chen DS. Hepatitis B virus infection, its sequelae, and prevention in Taiwan. In: Okuda K, Ishak KG, editors. *Neoplasm of the liver*. Tokyo: Springer Verlag 1987; 71-80
- 6 Chen DS, Kao G, Sung JL, Lai MY, Sheu JC, Chen PJ. Hepatitis C virus infection in an area hyperendemic for hepatitis B and chronic liver disease: the Taiwan experience. *J Infect Dis* 1990; 162: 817-822
- 7 Kao JH, Chen PJ, Yang PM, Lai MY, Sheu JC, Wang TH. Interfamilial transmission of hepatitis C virus: the important role of infections between spouses. *J Infect Dis* 1992; 166: 900-903
- 8 Kao JH, Chen W, Hsiang SC, Chen PJ, Lai MY, Chen DS. Prevalence and implication of TT virus infection: minimal role in patients with non-A-E hepatitis in Taiwan. *J Med Virol* 1999; 59: 307-312
- 9 Yang SS, Wu CH, Chen TH, Huang YY, Huang CS. TT viral infection through blood transfusion: retrospective investigation on patients in a prospective study of post-transfusion hepatitis. *World J Gastroenterol* 2000; 6: 53-56
- 10 Desai SM, Muerhoff AS, Leary TP. Prevalence of TT virus infection in US blood donors and populations at risk for acquiring parenterally transmitted viruses. *J Infect Dis* 1999; 179:1242-1244
- 11 MacDonald DM, Scott GR, Clutterbuck D. Infrequent detection of TT virus infection in intravenous drug users, prostitutes, and homosexual men. *J Infect Dis* 1999; 179:686-689
- 12 Hohne M, Berg T, Muller AR, Schreier E. Detection of sequences of TT virus, a novel DNA virus, in German patients. *J Genl Virol* 1998; 79:2761-2764
- 13 Poovorawan Y, Theamboonlers A, Jantaradsamee P, Kaew-in N, Hirsch P, Tangkitvanich P. Hepatitis TT virus infection in high-risk groups.

- Infection* 1998; 26:355-358
- 14 Takayama S, Yamazaki S, Matsuo S, Sugii S. Multiple infection of TT virus (TTV) with different genotypes in Japanese hemophiliacs. *Biochem Biophys Res Commun* 1999; 256: 208-211
- 15 Pontisso P, Ruvoletto MG, Fattovich G, Chemello L, Galloini A, Ruol A. Clinical and virological profiles in patients with multiple hepatitis virus infections. *Gastroenterology* 1993; 105:1529-1533
- 16 Kao JH, Chen W, Chen PJ, Lai MY, Chen DS. TT virus infection in patients with chronic hepatitis B or C: influence on clinical, histological and virological features. *J Med Virol* 2000; 60: 387-392
- 17 Tanaka H, Okamoto H, Luengrojanakul P, Chainuvati T, Tsuda F, Tanaka T. Infection with an unenveloped DNA virus (TTV) associated with posttransfusion non-A to G hepatitis in hepatitis patients and healthy blood donors in Thailand. *J Med Virol* 1998; 56: 234-238
- 18 Watanabe H, Saito T, Kawamata O, Shao L, Aoki M, Terui Y. Clinical implication of TT virus superinfection in patients with chronic hepatitis C. *Am J Gastroenterol* 2000;95:1776-1780
- 19 Akahane Y, Sakamoto M, Miyazaki Y, Okada S, Inoue T, Ukita M. Effect of interferon on a nonenveloped DNA virus (TT virus) associated with acute and chronic hepatitis of unknown etiology. *J Med Virol* 1999;58:196-200
- 20 Hagiwara H, Hayashi N, Mita E, Oshita M, Kobayashi I, Iio S. Influence of transfusion-transmitted virus infection on the clinical features and response to interferon therapy in Japanese patients with chronic hepatitis C. *J Viral Hepat* 1999;6:463-469
- 21 Baron S, Tying SK, Fleischmann WR, Coppenhaver DH, Niesel DW, Klimpel GR. The interferons: mechanisms of action and clinical applications. *JAMA* 1991; 266: 1375-1383
- 22 Hoofnagle JH. Therapy of acute and chronic viral hepatitis. *Adv Intern Med* 1994; 39:241-275
- 23 Woo MH, Burnakis TG. Interferon alfa in the treatment of chronic viral hepatitis B and C. *Ann Pharmacother* 1997; 31: 330-337
- 24 Di Bisceglie AM, Fong TL, Fried MW, Swain MG, Baker B, Korenman J. A randomized controlled trial of recombinant alpha-interferon therapy for chronic hepatitis B. *Am J Gastroenterol* 1993; 88:1887-1892
- 25 Poynard T, Bedossa P, Chevallier M, Mathurin P, Lemonnier C, Trepo C. A comparison of three interferon alfa-2b regimens for the long-term treatment of chronic non-A, non-B hepatitis. *N Engl J Med* 1995; 332: 1457-1462
- 26 Iino S, Hino K, Kuroki T, Suzuki H, Yamamoto S. Treatment of chronic hepatitis C with high-dose interferon alpha-2b. A multicenter study. *Dig Dis Sci* 1993; 38: 612-618
- 27 Chayama K, Kobayashi M, Tsubota A, Kobayashi M, Arase Y, Suzuki Y. Susceptibility of TT virus to interferon therapy. *J Gen Virol* 1999;80: 631-634
- 28 Kanda T, Yokosuka O, Ikeuchi T. The role of TT virus infection in acute viral hepatitis. *Hepatology* 1999; 29: 1905-1908. Utsunomiya S, Yoshioka K, Wakita T, Seno H, Takagi K, Ishigami M. TT virus infection in hemodialysis patients. *Am J Gastroenterol* 1999; 94: 3567-3570

Edited by Zhang JZ

• CLINICAL RESEARCH •

Epidemiological and histopathological study of relevance of Guizhou Maotai liquor and liver diseases

Jun Wu, Ming-Liang Cheng, Guo-Hao Zhang, Rong-Wei Zhai, Neng-Hui Huang, Cheng-Xiu Li, Tian-Yong Luo, Shuang Lu, Zhi-Qin Yu, Yu-Mei Yao, Ying-Ying Zhang, Lan-Zhen Ren, Lan Ye, Ling Li, Hui-Na Zhang

Jun Wu, Ming-Liang Cheng, Tian-Yong Luo, Shuang Lu, Zhi-Qin Yu, Yu-Mei Yao, Ying-Ying Zhang, Department of Infectious Diseases, Affiliated Hospital, Guiyang Medical College, Guiyang 550004, Guizhou Province, China
Guo-Hao Zhang, Hospital of Doutai Distillery, Renhuai 563000, Guizhou Province, China

Rong-Wei Zhai, Shanghai university of Medical Sciences, Shanghai 200025, China
Neng-Hui Huang, Cheng-Xiu Li, Lan-Zhen Ren, Lan Ye, Ling Li, Hui-Na Zhang, Department of pharmacology, Guiyang Medical College, Guiyang 550004, Guizhou Province, China

Supported by The primary sciences and technology project of Guizhou province., No. 19992015

Correspondence to: Jun Wu, Department of Infectious Diseases, Affiliated Hospital, Guiyang Medical College, Guiyang 550004, Guizhou Province, China. wuwuj@21cn.com

Telephone: +86-851-6702233(H), +86-851-6855119 Ext.3263 (O)

Received 2002-05-02 Accepted 2002-05-25

Abstract

AIM: To explore the relevance of Maotai liquor and liver diseases.

METHODS: Epidemiological study was conducted on groups of subjects, each consisting of 3 subjects from the Maotai liquor group consisting of 99 individuals and one from the non-alcoholic control group consisting of 33 individuals. Liver biopsy was performed on 23 volunteers from Guizhou Maotai Distillery who had a constant and long history of drinking Maotai liquor. Experimental histopathological study was conducted as follows: sixty male Wistar rats were divided into 3 groups randomly and fed with Maotai liquor, ordinary white wine, and physiological saline respectively for a period of 8 and 12 weeks. The rats were sacrificed in batches, then serum ALT, AST, TBil, and AKP were measured. Rat livers were harvested to measure the liver indexes, GSH, and MDA. Histopathological examinations were also performed. Another eighty mice were randomly divided into 4 groups and fed with Maotai (at different dosages of 10 ml·kg⁻¹ and 20 ml·kg⁻¹), ethanol, and physiological saline. The animals were sacrificed after 4 weeks and serum ALT was determined. Then the livers were harvested and liver indexes and MDA were measured.

RESULTS: The incidence rate of hepatic symptoms, splenomegaly, liver function impairment, reversal of Albumin/Globulin and increased diameter of portal veins in the Maotai liquor group were 1.0%(1/99), 1.0%(1/99), 1.0%(1/99), 1.0%(1/99), 0(0/99) and 0(0/99), 0(0/99), 0(0/99), 0(0/99), 0(0/99), respectively. There was no significant difference between the Maotai group and the non-alcoholic control group ($P>0.05$). Various degree of fatty infiltration of hepatocytes was found in the 23 volunteers receiving liver biopsy, but there was no obvious hepatic fibrosis or cirrhosis. A comparison was made between the Maotai liquor group and the ordinary white wine group. It was found that hepatic MDA in rats and mice were 0.33 ± 0.10 and 0.49 ± 0.23 respectively in Maotai group and 0.61 ± 0.22 and 0.66 ± 0.32 in the ordinary white wine group; MDA had an obvious decrease in the Maotai liquor group ($P<0.05$);

hepatic GSH were $0.12\text{mg}\cdot\text{g}^{-1}\pm0.06\text{mg}\cdot\text{g}^{-1}$ in rats of the Maotai liquor group and $(0.08\pm0.02)\text{mg}\cdot\text{g}^{-1}$ in white wine group, it was obviously increased in the Maotai liquor group ($P<0.05$). After the 20 rats had been fed with ordinary white wine for 8 weeks consecutively, disarranged hepatocyte cords, fatty infiltration of hepatocytes, and fibrous septa of varying widths due to hepatic connective tissues proliferation were observed; after 12 weeks, the fibrous tissue proliferation continued and early cirrhosis appeared. Compared with the ordinary white wine group, fatty infiltration was observed in the 8-week and 12-week groups, but no necrosis or fibrosis or cirrhosis was found in the Maotai liquor group ($P<0.05$).

CONCLUSION: Maotai liquor may cause fatty liver but not hepatic fibrosis or cirrhosis, and it can strengthen lipid peroxidation in the liver.

Wu J, Cheng ML, Zhang GH, Zhai RW, Huang NH, Li CX, Luo TY, Lu S, Yu ZQ, Yao YM, Zhang YY, Ren LZ, Ye L, Li L, Zhang HN. Epidemiological and histopathological study of relevance of Guizhou Maotai liquor and liver diseases. *World J Gastroenterol* 2002;8(3):571-574

INTRODUCTION

Alcohol can cause fatty liver, hepatitis and liver cirrhosis^[1-5]. A lot of research showed that there was a close relationship between liver diseases and alcohol content of liquor. If one drinks ardent spirits 80 to 150g daily for more than ten years, he will get alcoholic hepatitis, hepatic fibrosis, liver cirrhosis and even hepatocellular carcinoma^[6-13]. Maotai liquor has a very unique brewing technique which is different from that for ordinary white wine, and there are multiple microorganisms in the special geographical situations which are able to absorb abundant amino acids, vitamins and many essential microelements^[14], so the taste of Maotai is very sweet and pure. A study on 40 individuals reported by Li et al showed that drinking Maotai liquor more than 150g daily for ten years would not cause liver injury. Our previous study showed that Maotai liquor was able to induce increase of metallothioneins(MT), inhibit the proliferation of hepatic stellate cell (HSC) and generation of collagen and enhance the effect of antioxidation^[15]. Our study has initially interpreted the anti-fibrosis mechanism of Maotai liquor. A study was conducted on groups of subjects from Guizhou Maotai Distillery, each consisting of 3 subjects from the Maotai liquor group of 99 individuals who had a constant and long history of drinking Maotai liquor and one from the non-alcoholic control group of 33 individuals. Liver biopsy was performed on some of them and liver biopsy and serological tests in rats and mice fed with Maotai liquor were performed in order to explore the effect of Maotai liquor has on the liver.

MATERIALS AND METHODS

Materials

One hundred and thirty two individuals from Guizhou Maotai Distillery, aged from 30 to 60 years old, were divided into Maotai

liquor group consisting of 99 individuals and non-alcoholic control group consisting of 33 individuals. All members of the Maotai liquor group have the capacity for liquor of more than 250g.d⁻¹ and drinking history of longer than ten years. There was no significant difference between the two groups in sex and age. The male Wistar rats weighing (300±20)g were employed in this study (Provided by Experimental Animal center, the Third Military Medical University); the mice of Kunming species weighing (22±2)g (Provided by Experimental Animal center, Guiyang Medical College) were also used. Maotai liquor of (530±2)g·L⁻¹ was produced by Guizhou Maotai Distillery, China, whose code bar was 6902952880026; the ordinary white wine of (530±2)g·L⁻¹ was provided by the Fourth Department of Guizhou Food Export and Import Company.

Methods

Questionnaires were prepared in advance including sex, age, drinking history (capacity and duration), history of liver diseases, and history of gastropathy, etc. Physical examination, abdominal B ultrasound (the size of liver and spleen, diameter of portal vein), serum ALT, A/G, LN and HA were also done at the same time. Liver biopsy was performed in twenty three volunteers from the Maotai group, the liver tissue was fixed by formalin of 40g·L⁻¹, embedded by paraffin, sectioned and stained by HE. Sixty male Wistar rats were randomly divided into Maotai liquor group, ordinary white wine group and normal control group. Rats in the wine group were fed with 2mL·kg⁻¹ Maotai liquor and 2mL·kg⁻¹ ordinary white wine both of which were diluted one fold by distilled water, and in the control group were fed with the same volume of saline. All rats were fed once everyday continuously for 8 weeks, and after the last feed, 15 rats were fasted for 20 hours and then sacrificed to get blood for testing serum ALT, AST, TBil and AKP were tested, and Rat livers were harvested to measure the liver indexes, GSH, MDA, the liver tissue was embedded, sectioned and stained with HE. The remaining 5 rats in each group were sacrificed for histopathological examination after fed for 12 weeks. Eighty mice (40male, 40female) were randomly divided into 4 groups [two Maotai groups (at different dosage of 1 mL·kg⁻¹ and 2 mL·kg⁻¹), ethanol group, and physiological saline group]. Mice were fed with dosage of 1 mL·kg⁻¹ and 2 mL·kg⁻¹ Maotai in the two Maotai groups respectively. In the ethanol group, mice were fed (with) 53 g·L⁻¹ ethanol at dosage of 1 mL·kg⁻¹, they were fed once everyday for 4 weeks. After the last feed, the mice were killed to measure serum ALT, the liver indexes and MDA. Questionnaires were done by special messenger, and were examined and verified by persons in charge of the study.

Statistic analysis

The data were analyzed by *t* test and χ^2 test.

RESULTS

Epidemiologic analysis

The 98 individuals who had a long history of wine drinking had no symptoms abnormal, signs or liver function; only one who had a history of hepatitis showing cirrhosis of liver. He had symptoms of liver disease, splenomegaly, lightly increase of ALT and reversed A/G. There was no increase in the diameter of portal vein trunk in those individuals, compared with that of the control group, ($P>0.05$). None of those who had a history of drinking Maotai for more than 30 years died of liver diseases. (See Table 1). There was a slight increase of serum LN, but a significant increase of HA, ($P<0.05$) (See Table 2). All twenty three individuals in the Maotai group who had biopsy had varying degrees of fatty infiltration of hepatocytes. One of them had slight necrosis, but none had obvious hepatic fibrosis or cirrhosis of liver, in compared with that of the white wine group ($P<0.05$).

Experimental study in rats

Neither Ordinary white wine nor Maotai liquor had obvious effect on ALT, AST, TBil, ALP and liver indexes in rats fed for 8 weeks, compared to the normal control group. There was no significant difference between them ($P>0.05$) (See Table 3); but Maotai liquor was able to increase the level of GSH and decrease the level of liver MDA (See Table 4). There were no obvious pathologic changes in rat liver of the normal control group (See figure 1). In the ordinary white wine group, all twenty rats had disarrangement of hepatocyte cords, fatty infiltration and hyperplasia of fibrous tissue which formed the fibrous septa (See Figure 2) after they had been fed for 8 weeks. The fibrous tissue had further hyperplasia in the rats of the 12-week group and there were also signs of early cirrhosis of liver (See figure 3). But after the Maotai group had been fed for 8 weeks and 12 weeks, all rats had fatty infiltration, 17 were mild degree and 3 were moderate degree; all were devoided of necrosis of hepatocytes, hepatic fibrosis and cirrhosis ($P<0.05$) (See figure 4,5) when compared with that of the white wine group.

Table 1 Epidemiologic study of the Relationship between Guizhou Maotai liquor and Liver Diseases

	Group	Number	Positive	
			Number	Rate (%)
History of	Maotai Group	99	1	1.0
liver disease	Control Group	33	0	0
Symptoms of	Maotai Group	99	1	1.0
liver disease	Control Group	33	0	0
Hepatomegaly	Maotai Group	99	15	15.2
	Control Group	33	3	9.1
Splenomegaly	Maotai Group	99	1	1.0
	Control Group	33	0	0
Abnormal ALT	Maotai Group	99	1	1.0
	Control Group	33	0	0
Reversed A/G	Maotai Group	99	1	1.0
	Control Group	33	0	0
Portal trunk	Maotai Group	99	0	0
widening	Control Group	33	0	0

Table 2 Serum ALT, LN, and HA in Maotai Group ($\bar{x}\pm s$)

Group	<i>n</i>	ALT(nkat·L ⁻¹)	LN(μg·L ⁻¹)	HA(μg·L ⁻¹)
Control Group	33	683±150	88±24	106±32
Maotai Group	99	650±100	132±71 ^a	293±194 ^a

^a $P<0.05$, vs control group

Table 3 The effect of Maotai wine to the liver function of rats ($n=20$, $\bar{x}\pm s$)

Group	Serum biochemical index				Liver index and biochemical index		
	ALT (nkat·L ⁻¹)	AST (nkat·L ⁻¹)	Tbil (nmol·L ⁻¹)	AKP (nkat·L ⁻¹)	Index (g·kg ⁻¹)	GSH (mg·g ⁻¹)	MDA (A)
Saline	517±233	300±150	12.68±6.47	350±217	27.93±8.64	0.06±0.01	0.66±0.24
Ordinary	567±167	300±67	13.54±2.50	433±67	29.19±4.41	0.08±0.02	0.61±0.22
white wine							
Maotai wine	533±183	283±133	11.54±6.20	450±133	27.81±2.11	0.12±0.06 ^a	0.33±0.10 ^a

^a $P<0.05$, vs control group

Table 4 The effect of Maotai wine to the liver function of mice ($n=20$, $\bar{x}\pm s$)

Group	Dosage (mL·kg ⁻¹)	ALT (nkat·L ⁻¹)	liver index (mg·g ⁻¹)	MDA (A)
Saline	10	316±83	40.34±7.54	0.69±0.21
Alcohol	10	333±83	40.96±7.21	0.66±0.32
Maotai wine	10	383±133	43.8±8.79	0.49±0.23 ^a
Maotai wine	20	250±100	39.48±3.84	0.46±0.12 ^a

^a $P<0.05$, vs control group

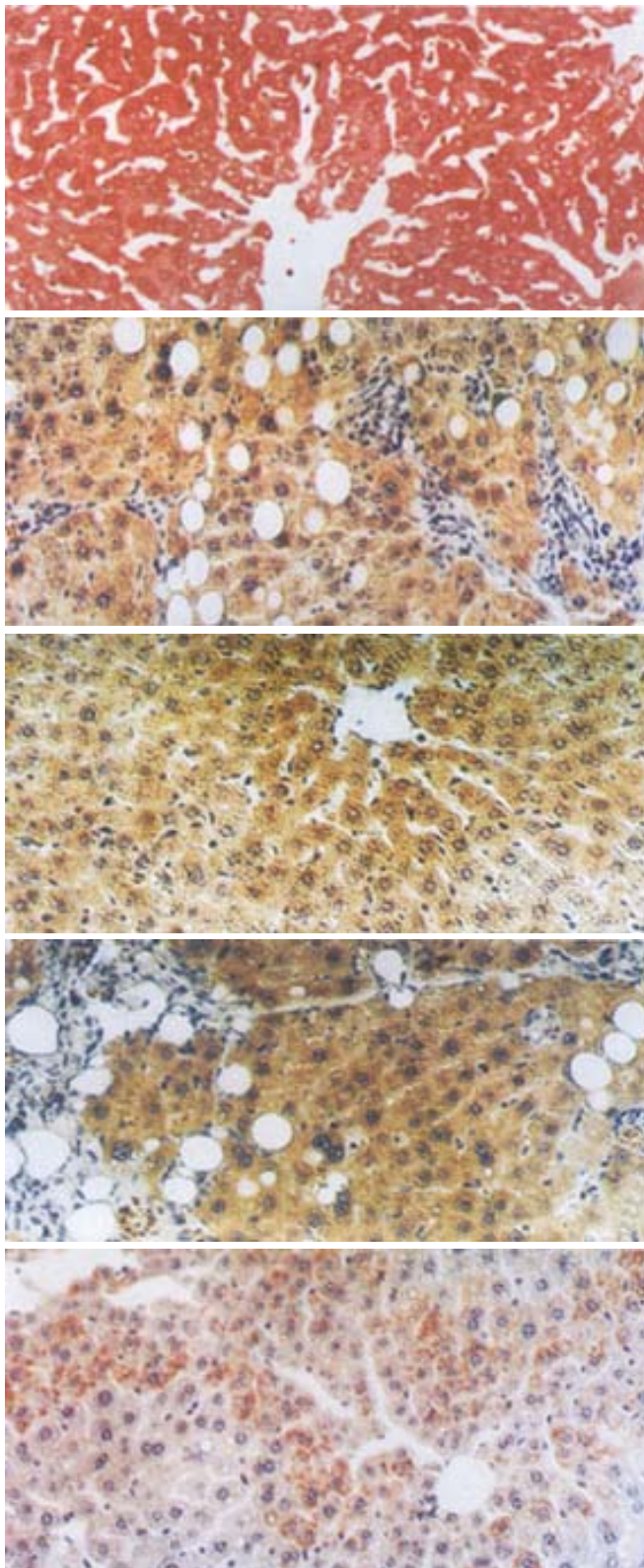


Figure 1 Normal liver tissue, hepatic cords were well arranged, the structure of hepatic lobule were intact. (HE.×200)

Figure 2 After fed with alcohol for 8 weeks, disorganized hepatic cords, fatty infiltration, mesenchymal hyperplasia, and fibrosis could be seen. (HE.×200)

Figure 3 After fed with alcohol for 12 weeks, there were fatty infiltration of hepatocytes, hyperplasia of connective tissue, and early manifestation of cirrhosis. (HE.×200)

Figure 4 After fed with Maotai liquor for 8 weeks, there were a few infiltrating inflammatory cells, normally arranged hepatic cords, liver sinusoids were dilated and lipid droplet could be seen in hepatocytes. (HE.×200)

Figure 5 After fed with alcohol for 12 weeks, brown changes and lipid droplet could be obviously seen in hepatocytes. (HE.×200)p

DISCUSSION

About 40% of those who drank 150g ardent spirits every day would have fatty liver and alcoholic hepatitis^[15]. Alcoholic fatty liver diseases can be manifested as fatty liver, alcoholic hepatitis, hepatic fibrosis and cirrhosis of liver, frequently they are overlapping. And fatty liver can proceed to hepatic fibrosis via inflammatory progress. The varying pathology of alcoholic fatty liver diseases have similar pathogenesis in hepatic fibrosis and cirrhosis^[16-22]. They are mainly caused by activation of HSC, resulting in excessive deposition and relatively insufficient degradation of ECM. Alcohol, acetaldehyde, lipid, fatty acids, etc can activate and stimulate Kupffer cells to secrete many cytokines which activate HSC to produce various components of ECM, as collagen, laminin, and hyaluronic acid, etc.

In recent years, studies have shown alcohol has direct damage effect to the hepatocytes^[23-32]. Alcohol can be oxidized to acetaldehyde with elimination hydroxy free radicals, which causes lipid peroxidation, hepatocytic damage and apoptosis. Lipid peroxidation and its metabolic products malondialdehyde (MDA) and free radicals have strong cellular toxicity^[33-37]. GSH^[38-44] being an antioxidant is able to inhibit lipid peroxidation, and is also involved in hepatic detoxication, thus it can process cytoprotective effect. MT is a low molecular weight metal-binding protein rich in thioaminopropionic acid. Studies in recent years showed that MT has the effects of eliminating hydroxy free radicals and other oxidation products, being also protective^[45-49].

Hepatic pathological changes of human being and animals show that Maotai liquor can lead to fatty infiltration in the liver, but no obvious hepatic fibrosis or cirrhosis of liver. Similar findings were shown in epidemiological study, B mode ultrasound and liver biopsy in the Maotai liquor group. One died of liver diseases in this group.

By contrast, various widths of fibrous septa and cirrhosis can be seen in the liver of rats fed ordinary white wine. Why is fatty infiltration in which Maotai liquor group dose not lead to liver fibrosis and cirrhosis of liver? The answer is that Maotai liquor was able to lower the MDA level in the rats and mice liver and increase the level of liver GSH as comparing with those in the ordinary white wine group, $P < 0.05$. It also showed that Maotai liquor had the inhibitory effect on lipid peroxidation and was cytoprotective. Moreover, study in vitro showed that Maotai liquor could increase MT which was the most powerful bioactive substance of scavenging free radicals and antagonizing liver damage. Maotai liquor may also inhibit the activation of hepatic stellate cells and generation of collagen.

Our study revealed that Maotai liquor was able to elevate the level of workers' serum LN and HA in Maotai liquor group vs. ordinary white wine group, ($P < 0.05$). It may be related with the activation of hepatic stellate cells (HSC) by ethanol, acetaldehyde, lipid and fatty acid. The elevation of LN was mild, but HA was very obvious whose reason may be that the serum level of HA was related with the ability of hepatic secretion and the renal excretion. In the acute hepatic injury caused by alcohol, inflammation and drugs, the level of serum HA may be very high, but it only points at a possible hepatic fibrosis or the early stage of hepatic fibrosis because researches show that the level of HA is not very high, even normal, in the late stage of hepatic fibrosis^[50].

As one of the three most famous distilled spirits of the world, Maotai liquor was brewed with open solid state fermentation in a special geographical environment, so it has formed its own style which is hard for others to imitate. According to the analysis of the nutritive component in Maotai liquor in recent years, in every 100 ml Maotai Liquor, there were 18mg protein, 6667 u superoxide dismutase (SOD), 0.06 mg vitamin B₁, 0.1 mg vitamin B₂ and 1.19 mg vitamin C, 0.022 mg manganese (Mn), 0.026 mg copper (Cu), 0.42 mg iron (Fe), 1.0 mg potassium (Ka), and <0.005 mg zinc (Zn); 4.7 mg methanol, 4.7 mg aldehyde compounds. And there were also 18 kinds of amino acids and 6 kinds of essential amino acids

except acimeton and tryptophan which were never found in the Jiang flavor white wine before Maotai. There were SOD and multiple human essential microelements in Maotai liquor, especially rich in Fe, Mn and Cu. The components of methanol, benzene and aldehyde were much lower than it was ruled in the international standard.

REFERENCES

- Cheng ML, Liu SD. The basic study and clinical research on hepatic fibrosis. *Renmin Weisheng Chubanshe* 1996;84-86
- Sun YN. Recency studies in Pathogenesis of alcoholic liver diseases. *Guowai Yiyao. Xiaohuaxi Jibing Fengce* 1999;19:97-101
- Fan JG, Zeng MD, Wang GL. Pathogenesis of fatty liver. *Shijie Huaren Xiaohua Zazhi* 1999;7:5-7
- Tang TH. Recent studies of alcoholic liver diseases. *Shijie Huaren Xiaohua Zazhi* 2000;8:56
- Miyano S, Maeyama S, Iwaba A, Ogata S, Koike J, Kishi M, Uchikoshi T. A clinicopathological study of acute hepatitis in heavy drinkers, unrelated to hepatitis A, B, or C viruses. *Alcohol Clin Exp Res* 2001;25:69S-74S
- Wu J, Liu RC, Li J, Wang WL, Hu L, Yang QZ, Liang YD, Lu YY, Cheng ML, Ding YS. To study the risk factors of hepatic cirrhosis in hepatitis virus and hepatic fibrosis. *Cina Public Health* 1999;15:394
- Wu J, Cheng ML, Ding YS, Liu RC, Li J, Wang WL, Hu L. Five years follow-up survey of risk factor of virus hepatic cirrhosis. *Shijie Huaren Xiaohua Zazhi* 2000;8:1365-1367
- Pan RM, Shao XD. Clinical characteristics of alcoholic liver disease. *World J Gastroenterol* 1998;4:95-96
- Huang Z, Tian DL, Yuan AH. Experimental animal models with alcoholic liver diseases. *Huaren Xiaohua Zazhi* 1998;6:712-713
- Liu WW. Etiological studies of hepatocellular carcinoma. *Shijie Huaren Xiaohua Zazhi* 1999;7:93-95
- Gu GW, Zhou HG. New concept in etiology of liver cancer. *Huaren Xiaohua Zazhi* 1998;6:185-187
- Pan RM, Shao XD. Clinical characteristics of alcoholic liver disease. *World J Gastroenterol* 1998;4:95-96
- Bellentani S, Saccoccio G, Costa G, Tiribelli C, Mancu F, Sodde M, Croce LS, Sasso F, Pozzato G, Cristianini G, Brandi G. Drinking habits as co-factors of risk for alcohol induced liver damage. *Gut* 1997;41:845-850
- Xiao Y. Preliminary explanation of the mechanism which long term drinking of Guizhou maotai will not incur liver fibrosis. *Zhonghua Yixue Zazhi* 2001;81:628
- Wang JY. Clinical Epidemiology of fatty liver. *Zhonghua Ganzangbing Zazhi* 2000;8:115
- Fan JG, Zeng MD, Hong J, Li JQ, Qiu DK. Effects of free unsaturated fatty acids on proliferation of L-02 and HLF cell lines and synthesis of extracellular matrix. *Shijie Huaren Xiaohua Zazhi* 1998;6:502-504
- Sun DL, Sun SQ, Li TZ, Lu XL. Serologic study on extracellular matrix metabolism in patients with viral liver cirrhosis. *Huaren Xiaohua Zazhi* 1999;0:55-56
- Lü XH, Xie YH, Fu BY, Liu CR, Wang BY. Dynamic expression of tissue inhibitor of metalloproteinase 1 in alcoholic liver disease in rats. *Shijie Huaren Xiaohua Zazhi* 2001;9:29-33
- Lu LG, Zeng MD, Li JQ, Fan JG, Hua J, Fan ZP, Dai N, Qiu DK. Effect of arachidonic acid and linoleic acid on proliferation of rat hepatic stellate cells. *Shijie Huaren Xiaohua Zazhi* 1999; 7:10-12
- Kishore R, McMullen MR, Nagy LE. Stabilization of tumor necrosis factor α mRNA by chronic ethanol: role of A+U rich elements and p38 mitogen activated protein kinase signaling pathway. *J Biol Chem* 2001;10
- Wu J, Zern MA. Hepatic stellate cells: a target for the treatment of liver fibrosis. *J Gastroenterol* 2000;35:665-672
- Anania FA, Womack L, Jiang M, Saxena NK. Aldehydes potentiate α (2)(I) collagen gene activity by JNK in hepatic stellate cells. *Free Radic Biol Med* 2001; 30:846-857
- Ruoyu Ni, Maria Anna Leo, Jingbo Zhao and Charles S. Toxicity of α -carotene and its exacerbation by acetaldehyde in HepG2 cells. *Alcohol and Alcoholism* 2001; 36: 281-285
- Zhang B, Zhang DF, Ren H. Resistance of Bcl-2 adenovirus vector to HepG2 cell apoptosis induced by ethanol. *Zhonghua Ganzangbing Zazhi* 2000;8:215-217
- Slukvin II, Boor PJ, Jerrells TR. Initiation of alcoholic fatty liver and hepatic inflammation with a specific recall immune response in alcohol-consuming C57Bl/6 mice. *Clin Exp Immunol* 2001;125:123-133
- Deaciuc IV, Nikolova-Karakashian M, Fortunato F, Lee EY, Hill DB, McClain CJ. Apoptosis and dysregulated ceramide metabolism in a murine model of alcohol-enhanced lipopolysaccharide hepatotoxicity. *Alcohol Clin Exp Res* 2000;24:1557-1565
- Lu LG. Hepatic sieve and fatty liver. *Zhonghua Ganzangbing Zazhi* 2000;8:115
- Lin H, Lü M, Zhang YX, Wang BY, Fu BY. Induction of a rat model of alcoholic liver diseases. *Shijie Huaren Xiaohua Zazhi* 2001;9:24-28
- Bo AH, Tian CS, Xue GP, Du JH, Xu YL. Morphology of immuno and alcoholic liver diseases in rats. *Shijie Huaren Xiaohua Zazhi* 2001;9:157-160
- Yang CF, Chen XM, Liu J, Zheng WX, Chang W. Study of the effect of alcohol on liver lipid peroxidation in the rat. *Xiandai Yufang Yixue* 1996;23:141-143
- MacDonald GA, Bridle KR, Ward PJ, Walker NI, Houghlum K, George DK, Smith JL, Powell LW, Crawford DH, Ramm GA. Lipid peroxidation in hepatic teatosis in humans is associated with hepatic fibrosis and occurs predominately in acinar zone 3. *J Gastroenterol Hepatol* 2001;16:599-606
- Zima T, Fialova L, Mestek O, Janebova M, Crkovska J, Malbohan I, Stipek F, Mikulikova L, Popov P. Oxidative stress, metabolism of ethanol and alcohol-related diseases. *J Biomed Sci* 2001;8:59-70
- Lu XY. Mechanism of free radicals on liver injury induced by ethanol. *Xin Xiaohuabingxue Zazhi* 1997;5: 200-202
- Degoul F, Sutton A, Mansouri A, Cepanec C, Degott C, Fromenty B, Beaugrand M, Valla D, Pessayre D. Homozygosity for alanine in the mitochondrial targeting sequence of superoxide dismutase and risk for severe alcoholic liver disease. *Gastroenterology* 2001;120:1468-1474
- Poli G. Pathogenesis of liver fibrosis: role of oxidative stress. *Mol Aspects Med* 2000;21:49-98
- Mutlu-Turkoglu U, Dogru-Abbasoglu S, Aykac-Toker G, Mirsal H, Beyazyurek M, Uysal M. Increased lipid and protein oxidation and DNA damage in patients with chronic alcoholism. *J Lab Clin Med* 2000;136:287-291
- French SW. Intragastric ethanol infusion model for cellular and molecular studies of alcoholic liver disease. *J Biomed Sci* 2001;8:20-27
- Tang YP, Yang GZ, Lu HL, Tu YQ, Zhang Y. Effects of external glutathione in protection against organ injury after infection. *Zunyi Yixueyuan Xuebao* 1999;22: 85-87
- Shi JS, Sheng MP, Li F. protection from DEN carcinogenesis by glutathione in rat hepatoma model. *Zunyi Yixueyuan Xuebao* 1998; 21:1-5
- Dai DW, Wu SM, Qi QE, Li M, Chen HJ, Chai W. Effects of glutamine on intracellular reduced glutathione in cultured human intestinal epithelial cells with anoxia/reoxygenation. *Zhonghua Binglischengli Zazhi* 1999;15: 128-130
- Li J, Tu BQ, Yang TS, Liu JJ, Jia FM. Alteration of glutathione in RBC in patients with liver cirrhosis and its clinical significance. *Xinxiaohua Zazhi* 1996;4:18-19
- Sun GY, Liu WW. Free radicals and Digestive system neoplasms. *Huaren Xiaohua Zazhi* 1998;6:272-273
- Soltys K, Dikdan G, Koneru B. Oxidative stress in fatty livers of obese Zucker rats: rapid amelioration and improved tolerance to warm ischemia with tocopherol. *Hepatology* 2001;34:13-18
- Yu JC, Jiang ZM, Li DM. Glutamine: a precursor of glutathione and its effect on liver. *World J Gastroenterol* 1999;5:143-146
- Nishimura N, Miyabara Y, Suzuki JS, Sato M, Aoki Y, Satoh M, Yonemoto J, Tohyama C. Induction of metallothionein in the livers of female Sprague-Dawley rats treated with 2,3,7,8-tetrachlorodibenzo-p-dioxin. *Life Sci* 2001;69:1291-1303
- Park JD, Liu Y, Klaassen CD. Protective effect of metallothionein against the toxicity of cadmium and other metals(1). *Toxicology* 2001; 163:93-100
- Wright J, George S, Martinez-Lara E, Carpena E, Kindt M. Levels of cellular glutathione and metallothionein affect the toxicity of oxidative stressors in an established carp cell line. *Mar Environ Res* 2000;50: 503-508
- Zaroogian G, Jackim E. In vivo metallothionein and glutathione status in an acute response to cadmium in *Mercenaria mercenaria* brown cells. *Comp Biochem Physiol C Toxicol Pharmacol* 2000;127:251-261
- Fabisiak JP, Pearce LL, Borisenko GG, Tyhurina YY, Tyurin VA, Razzack J, Lazo JS, Pitt BR, Kagan VE. Bifunctional anti/prooxidant potential of metallothionein: redox signaling of copper binding and release. *Antioxid Redox Signal* 1999;1:349-364
- Kong XT. Early Diagnosis of hepatic fibrosis. *Zhonghua Ganzangbing Zazhi* 2000;8:241-242

Edited by Wu XN

• CLINICAL RESEARCH •

Clinical significance of plasma D-dimer and von Willebrand factor levels in patients with ulcer colitis

Gang Xu, Ke-Li Tian, Guo-Ping Liu, Xue-Jun Zhong, Shao-Ling Tang, Yan-Ping Sun

Gang Xu, Guo-Ping Liu, Xue-Jun Zhong, Shao-Ling Tang, Yan-Ping Sun, Department of Gastroenterology, Chinese PLA 456 Hospital of PLA, Jinan 250031, Shandong Province, China

Ke-Li Tian, Department of Biochemistry, Shandong University, Jinan 250062, Shandong Province, China

Correspondence to: Gang Xu, Institute of Gastroenterology, First Military Medical University, Guangzhou 510515, Guangdong Province, China. gangxujn@263.net

Telephone: +86-20-85141544

Received 2001-09-14 Accepted 2001-10-29

Abstract

AIM: To investigate the levels of D-dimer(DD) and von Willebrand factor(vWF) and the relationship between DD and vWF in ulcerative colitis(UC) patients.

METHODS: A total of 29 plasma specimens were obtained from patients with ulcerative colitis (male 13, female 16), aged 21-47 years (33 ± 11). Disease activity was assessed by Truelove-Writeria. Patients with a score of above 5 were regarded as having active colitis. Twenty healthy people(male 12, female 8), aged 19-53 years(31 ± 14), served as normal controls. Blood samples were taken from an antecubital vein puncture. Blood(1.8 mL) was injected into the tubes containing sodium citrate (0.13 mmol/L). The plasma was obtained by centrifugation at $3000\text{ r}\cdot\text{min}^{-1}$ for 10 min, and stored at $-80\text{ }^{\circ}\text{C}$ until assayed by ELISA.

RESULTS: The mean plasma levels of DD and vWF in active UC patients were significantly higher than those of the controls (0.69 ± 0.41 vs 0.27 ± 0.11 , $P<0.01$; 143 ± 46 vs 103 ± 35 , $P<0.01$). The mean plasma levels of DD in the patients with active disease were higher than those with inactive disease(0.69 ± 0.41 vs 0.48 ± 0.29 , $P<0.05$). The levels of vWF were not different between active and inactive patients. DD levels were positively related to vWF levels($r=0.574$, $P<0.01$). There was no significant difference between levels of DD and vWF and the scope of disease and sex of the patients.

CONCLUSION: vWF is an important feature and a good marker of UC; intravascular thrombus and endothelial cell dysfunction were found in UC patients; and the combined test of DD and vWF is helpful to distinguish the activity of the UC patients.

Xu G, Tian KL, Liu GP, Zhong XJ, Tang SL, Sun YP. Clinical significance of plasma D-dimer and von Willebrand factor levels in patients with ulcer colitis. *World J Gastroenterol* 2002;8(3):575-576

INTRODUCTION

The pathogenesis of ulcerative colitis(UC) is still unknown^[1,2]. Some studies suggested that intestinal vascular injury caused by intramural vascular thrombosis or vasculitis was considered as a potential pathogenetic mechanism of inflammatory bowel disease. The D-Dimer (DD) is known to be a special fibrin degradation product, which is used as an index of fibrin turnover and intravascular

thrombogenesis^[3]. von willebrand factor(vWF) is released from endothelial cells, which is used as a marker for endothelial damage^[4]. In this study, we investigated the change of DD and vWF levels in UC patients and the relationship between these two markers.

MATERIALS AND METHODS

Patients

A group of 29 patients (male 13, female 16), aged 21-47 years(33 ± 11), were diagnosed by routine clinical, radiologic, endoscopic and histologic means(excluding heart and brain vessel diseases, diabetes and other diseases that affect blood coagulation). Disease activity was assessed by Truelove-Writeria. Patients with a score of above 5 were regarded as having active colitis. Meanwhile 20 healthy people(male 12, female 8), aged 19-53 years (31 ± 14), served as normal controls.

Measurement of plasma DD and vWF levels

Blood samples were taken from an antecubital vein puncture. Blood (1.8 mL) was injected into the tubes containing sodium citrate(0.13 mmol/L). The plasma was obtained by centrifugation at $3000\text{ r}\cdot\text{min}^{-1}$ for 10 min, and stored at $-80\text{ }^{\circ}\text{C}$ until assayed by ELISA(The Sun Biotechnology Company, Fujian, China).

Statistical analysis

Statistical analysis of mean value of DD and vWF levels were made by Student's *t* test and Student -Newman-keuls's test. $P<0.05$ was considered to be significant.

RESULTS

DD and vWF levels in patients with UC

The mean plasma levels of DD and vWF in active UC patients were significantly higher than those of the controls ($P<0.01$, Table 1). The mean plasma levels of DD in the patients with active disease were higher than that of inactive disease ($P<0.05$). The levels of vWF had no difference between active and inactive patients. DD levels was positively related to vWF levels($r=0.574$, $P<0.01$).

Table 1 Changes of DD and vWF levels in patients with UC ($\bar{x}\pm s$)

	<i>n</i>	DD(mg/l)	vWF(%)
controls	20	0.27 ± 0.11	102.75 ± 34.91
UC active	17	0.69 ± 0.41^{ab}	142.71 ± 45.96^a
Inactive	12	0.48 ± 0.29^a	135.00 ± 26.25^a

^a $P<0.01$, vs control; ^b $P<0.05$, vs inactive

Table 2 The levels of DD and vWF in different sex and scope of disease ($\bar{x}\pm s$)

	<i>n</i>	DD(mg/l)	vWF (%)
Sex			
Male	13	0.58 ± 0.11	142.84 ± 42.85
Female	16	0.55 ± 0.15	138.75 ± 36.75
Scope of disease			
Rectum-sigmoid	15	0.58 ± 0.27	137.11 ± 36.87
Left-side	9	0.59 ± 0.26	138.78 ± 42.22
Colon	5	0.63 ± 0.41	143.60 ± 51.60

DD and vWF levels in gender of disease and scope of disease

DD and vWF levels seemed to be increased with the scope of disease gradually, but differences were not significant with different scope of disease. There was no statistical difference between males and females (Table 2).

DISCUSSION

Von willebrand factor(vWF) is a high molecular weight multimeric glycoprotein, synthesized and released by vascular endothelial cells and megakaryocytes. It has two functions: firstly, this glycoprotein carries factor VIII in the circulation and is required for factor VIII stability in the plasma. Serving as the carrier for factor VIII, vWF may also coordinate formation of the fibrin rich thrombus at the site of endothelial cell injury; secondly, this glycoprotein may mediate initial platelet adhesion to the subendothelium by linking to specific platelet membrane receptors and to constituents of subendothelial connective tissues. This is pertinent to the damage of the vascular endothelium^[5]. Most of plasma vWF is derived from endothelial cells rather than from platelets under normal circumstances, suggesting that vWF is a good marker of endothelial dysfunction^[6,7]. Clinically, in vitro and animal studies support the concept that increased levels of circulating vWF reflect endothelial cell damage or injury^[8]. Elevated vWF levels have been demonstrated in the patients with inflammatory vascular disease and associated disorders, including rheumatoid arthritis, systemic sclerosis, systematic lupus erythematosus, Felty's syndrome, giant cell arteritis and polyarteritis nodosa. Intestinal vascular injury caused by intramural vascular thrombosis or vasculitis is considered as a potential pathogenetic mechanism of inflammatory bowel disease. We investigated the role of vascular injury in the pathogenesis of UC by examining the levels of plasma vWF. The results showed that vWF levels were more significantly raised in the active or inactive patients with UC, as compared with the controls. The levels of vWF were unrelated to the scope of the disease, and there was no statistical difference between males and females. Our results confirmed and extended those of other investigators^[9], showing that concentration of circulation vWF is elevated in UC patients. Our results supported the hypothesis that intestinal endothelial cell damage was an important feature of UC and proved that vWF was a good marker of UC.

It is well known that DD is a marker of ongoing intravascular thrombogenesis. In the previous researches, DD test was established as a useful aid in the diagnosis of the deep-vein thrombosis of the lower limbs and pulmonary embolism^[10]. Some reports showed higher DD levels in patients with coronary artery disease, Sickle cell disease, systemic lupus erythematosus, several sorts of neoplasms^[11,12] and acute pancreatitis^[13]. Weber's results showed that DD levels were higher in patients with UC^[14]. Our results showed significantly higher DD levels in patients with UC, both in active and inactive patients, as compared with the controls. It confirmed the presence of intravascular thrombus in UC patients. Thus anticoagulant treatment, with either warfarin or heparin, may have a positive influence on UC.

Several reports indicated that DD is used as a marker of

inflammation. Elevated level is a well-established marker of acute-phase reaction and may reflect the presence of inflammation^[12,15]. Our results showed that DD levels were significantly higher in patients with active UC than those with inactive UC, but there was no statistical difference in vWF levels between active and inactive UC patients. There was positive correlation between vWF and DD, we therefore, proposed that the combined test of DD and vWF is helpful to distinguish the activity of the UC patients.

REFERENCES

- 1 Cui HF, Jiang XL. Treatment of corticosteroids-resistant ulcerative colitis with oral low molecular weight heparin. *World J Gastroenterol* 1999;5:448-450
- 2 Das KM, Farag SA. Current medical therapy of inflammatory bowel disease. *World J Gastroenterol* 2000; 6:483-489
- 3 Danesh J, Whincup P, Walker M, Lennon L, Thomson A, Appleby P, Rumley A, Lowe GD. Fibrin D-dimer and coronary heart disease: prospective study and meta-analysis. *Circulation* 2001;103:2323-2327
- 4 Goldsmith I, Kumar P, Carter P, Blann AD, Patel RL, Lip GY. Atrial endocardial changes in mitral valve disease: a scanning electron microscopy study. *Am Heart J* 2000; 140: 777-845
- 5 Jager A, van-Hinsbergh VW, Kostense PJ, Emesis JJ, Nijpels G, Dekker JM, Heine RJ, Bouter LM, Stehouwer CD. Increased levels of soluble vascular cell adhesion molecule 1 are associated with risk of cardiovascular mortality in type 2 diabetes: the Hoorn study. *Diabetes* 2000; 49:485-491
- 6 Feng D, Bursell SE, Clermont AC, Lipinska I, Aiello LP, Laffel L, King GL, Tofler GH. von Willebrand factor and retinal circulation in early-stage retinopathy of type 1 diabetes. *Diabetes care* 2000;23:1694-1698
- 7 Albornoz L, Alvarez D, Otero JC, Gadano A, Salviu J, Gerona S, Sorroche P, Villamil A, Mastai R. von Willebrand factor could be an index of endothelial dysfunction in patients with cirrhosis: relationship to degree of liver failure and nitric oxide levels. *J Hepatol* 1999;30:451-455
- 8 Makris TK, Stavroulakis GA, Dafni UG, Gialeraki AE, Krespi PG, Hatzizacharias AN, Tsoukala CG, Vythoulkas JS, Kyriakidia MK. ACE/DD genotype is associated with hemostasis balance disturbances reflecting hypercoagulability and endothelial dysfunction in patients with untreated hypertension. *Am Heart J* 2000;140:760-765
- 9 Meucci G, Pareti F, Vecchi M, Saibeni S, Bressi C, Franchis R. Serum von Willebrand factor levels in patients with inflammatory bowel disease are related to systemic inflammation. *Scand J Gastroenterol* 1999;34:287-290
- 10 Righimi M, Goehring C, Bounameaux H, Perrier A. Effects of age on the performance of common diagnostic tests for pulmonary embolism. *Am J Med* 2000;109:357-361
- 11 Blackwell K, Haroon Z, Broadwater G, Berry D, Harris L, Iglehart JD, Dewhirst M, Greenberg C. Plasma D-dimer levels in operable breast cancer patients correlate with clinical stage and axillary lymph node status. *J Clin Oncol* 2000; 18:600-608
- 12 Kohno I, Inuzuka K, Itoh Y, Nakahara K, Eguchi Y, Sugo T, Soe G, Sakata Y, Murayama H, Matsuda M. A monoclonal antibody specific to the granulocyte-derived elastase-fragment D species of human fibrinogen and fibrin: its application to the measurement of granulocyte-derived elastase digests in plasma. *Blood* 2000;95:1721-1728
- 13 Xu G, Zhong XJ, Guo WM, Sui RL, Tang SL, Sun YP. D-dimer and von Willebrand factor levels in acute pancreatitis patients. *Shijie Huaren Xiaohua Zazhi* 1999;7:1088-1089
- 14 Weber P, Husemann S, Vielhaber H, Zimmer KP, Nowak-Gottl U. Coagulation and fibrinolysis in children, adolescents, and young adults with inflammatory bowel disease. *J Pediatr Gastroenterol Nutr* 1999;28: 418-422
- 15 Kim SB, Chi HS, Park JS, Hong CD, Yang WS. Effect of increasing serum albumin on plasma D-dimer, von Willebrand factor, and platelet aggregation in CAPD patients. *Am J Kidney Dis* 1999;33:312-317

Edited by Ma JY

Hepatitis C and HIV co-infection: a review

Irena Maier, George Y. Wu

Irena Maier, George Y. Wu, Department of Medicine, Division of Gastroenterology-Hepatology University of Connecticut Health Center, Farmington, CT, USA

Correspondence to: George Y. Wu, M.D., Ph.D, Department of Medicine Division of Gastroenterology-Hepatology, University of Connecticut Health Center, Rm. AM-045, 263 Farmington Avenue, Farmington, CT 06030-1845, USA. wu@nso.uchc.edu

Telephone: +1-860-679-3158 **Fax:** +1-860-679 3159

Received 2002-06-27 **Accepted** 2002-07-04

Abstract

Co-infection with hepatitis C virus and human immunodeficiency virus is common in certain populations. Among HCV (+) persons, 10 % are also HIV (+), and among HIV (+) persons, 25 % are also HCV (+). Many studies have shown that in intravenous drug users, co-infection prevalence can be as high as 90-95 %. There is increasing evidence supporting the concept that people infected with HIV have a much more rapid course of their hepatitis C infection. Treatment of co-infection is often challenging because highly active anti-retroviral therapy (HAART) therapy is frequently hepatotoxic, especially in the presence of HCV. The purpose of this review is to describe the effects that HIV has on hepatitis C, the effects that hepatitis C has on HIV, and the treatment options in this challenging population.

Maier I, Wu GY. Hepatitis C and HIV co-infection: a review. *World J Gastroenterol* 2002; 8(4):577-579

INTRODUCTION

Hepatitis C is an RNA flavivirus that infects 4 million people in the United States making up approximately 1.8 % of the population, and 150-200 million worldwide. In persons with HIV, its prevalence is estimated to be approximately 50 %^[1]. Main sources for transmission include IV drug use, transfusion of blood products prior to screening, and to a lesser extent sexual intercourse and needle sticks. It is almost universal among hemophiliacs who received transfusions prior to July 1992^[2]. HCV is the leading indication for liver transplantation in the U.S. today, and is responsible for approximately 10 000 deaths per year. It is estimated that by 2 015, HCV will be responsible for 40 000 deaths per year.

Seventy to eighty percent of acute HCV infections become chronic. Approximately 25 % of these patients develop end stage cirrhosis after 20 to 25 years, and 1 to 4 % of patients with cirrhosis develop hepatoma each year. The median time to cirrhosis is about 19 years. Once cirrhosis is present, the risk of hepatoma increases dramatically. The median time to develop hepatoma is about 29 years. Factors that promote progression of HCV include: alcohol intake, age over 45 at the time of infection, HIV co-infection, male gender, and co-infection with hepatitis B or other viruses. HIV infection and alcohol consumption are independently associated with accelerated progression of fibrosis^[3].

Potential mechanisms of HCV-induced liver disease include direct cellular toxicity, immune-mediated toxicity, viral replication, immune selection, and role of cryoglobulins. In patients that are immunosuppressed, there is an increased rate of viral replication and an increased progression rate of HCV.

The diagnosis of HCV is made by an ELISA test, which is sensitive and specific. In immunosuppressed persons, however, there may be a false negative test in the presence of hepatitis C viremia. Therefore, in a high risk HIV patient who has a negative antibody test, a quantitative PCR is also recommended^[2].

The standard treatment for persons who do not have HIV is combination therapy consisting of interferon alfa and ribavirin. Should this be the standard of care in HIV positive patients as well? The approach to the co-infected patient is somewhat more complicated.

HCV/HIV CO-INFECTION

Epidemiology

Not all HIV (+) persons are at risk for HIV. Of HCV (+) persons, approximately 10% are also HIV (+), and of HIV (+) persons, approximately 25% are also HCV (+)^[4-6]. Table 1^[7] shows the incidence of HCV and HIV infection by special population.

Table 1^[7] The incidence of HCV and HIV infection by special population

	% HCV Infection	% HIV
IV Drug Users	60%	31%
Homosexual Men	Unclear	47%
Heterosexual Men	20%	10%
Transfusion <1992	7-20%	2%
Occupational	<1%	<1%
Unknown	10%	9%

Table 2^[11] Similarities and differences of HCV and HIV

Statistics	HCV	HIV
U.S. Infected	4 million	1 million
Globally Infected	60-180 million	45 million
Primary transmission	Blood	Sex
Treatment Cure	Yes (40%)	No
T 1/2	2.3	6.4
Daily Replication	10 ¹² -10 ¹³	10 ⁹ -10 ¹⁰
Mutation Rates	10 ⁻³ -10 ⁻⁴	10 ⁻³ -10 ⁻⁴

In developed countries, the majority of HIV positive persons who acquired infection by IV drug use (IDU) are co-

infected with HCV^[8]. In many studies, more than 90-95 % of IV drug users are co-infected. Only 4-8 % of gay men who are HIV (+) are also HCV (+)^[9], since HCV is not as easily transmitted by sexual contact. If a patient has both HIV and HCV infection, that patient will be more likely to transmit HIV compared with HCV through heterosexual contact. The presence of HIV may increase the risk of acquiring HCV, as seen in some studies^[10]. Two to 10% of women co-infected with HIV/HCV transmitted HCV to their newborns. The risk of transmission was directly related to the degree of HCV viremia. Also, HIV transmission is more likely in mothers with high HCV-RNA levels. Table 2^[11] lists some statistics for HCV and HIV.

Natural history

In infections with HCV alone, the host cell-mediated immune response often determines the long term outcome. It has been evident that HIV makes the course of HCV infection more rapid and that end stage liver disease is the leading cause of death in HIV patients. It is thought that the more rapid progression of HCV in co-infected patients is due to a weakened cellular immune response. The estimated mean interval from HCV infection to development of cirrhosis is significantly shorter for patients co-infected with HIV (7 vs 30 years)^[12-15]. Co-infected patients have higher levels of HCV RNA than HCV-only infected patients. Titers usually correlate with the CD4 count^[16]. Viral load is considered to be a predictor of response to therapy, but HCV viral loads in HCV-only infected patients cannot be compared to HIV/HCV patients with any prediction to outcome of treatment. Patients with HIV/HCV infection may also have more severe liver damage (higher score of piecemeal necrosis and a higher stage of fibrosis) than those without HIV infection^[17-19].

However, the impact that HCV has upon HIV disease progression is less clear. Some studies have reported a significantly faster HIV progression (predominantly in hemophiliac patients infected with HCV genotype 1)^[20], while others showed no impact. IL-10 has been proposed to decrease inflammation in HCV patients. It also should be noted that patients that have HIV naturally have lower levels of IL-10, which may explain the observed accelerated liver disease in co-infected patients^[21].

Treatment options

HIV patients have been living longer making the HCV infection a pressing problem^[22]. Regarding treatment of HCV in co-infected patients, the main factor in deciding who should be treated is the CD4 count. Patients with CD4 counts greater than 500 have been found to have response rates not significantly different from patients without HIV. Patients with CD4 counts less than 200 have been shown to have no significant response. Hence, therapy in those cases is not recommended. Patients with CD4 counts less than 500, but greater than 200 have intermediate response rates^[17]. Accordingly, patients are generally treated with HAART first to optimize the immune system before initiating anti-HCV therapy.

Interferon

Interferon monotherapy for hepatitis C in patients with HIV, without AIDS, is similar to that observed in patients with HCV alone. Periodic monitoring of CD4 count is warranted since up to 80 % of the patients treated had significant reductions in the absolute CD4 count^[23].

Interferon plus ribavirin

Standard treatment in co-infected patients with satisfactory CD4 counts is to treat the HCV with interferon alfa plus ribavirin for 24 weeks^[24-27]. If the quantitative HCV RNA PCR is negative at the 24 week point, then treatment should be continued for an additional 24 weeks (for a total of 48 weeks). However, if the PCR is positive at 24 weeks, the risks of continuing treatment are likely to outweigh benefits of the regimen^[23].

Further treatment options

Pegylated interferon is an alternative to interferon plus ribavirin that seems to provide similar treatment efficacy without the ribavirin side effects^[28,29].

There are no definitive data on pegylated interferon and ribavirin in co-infected patients, but preliminary reports suggest a further increase in the sustained viral response rate compared to standard thrice weekly interferon plus ribavirin^[30]. It is likely that the dependence of response rates on CD4 counts will likely be similar to standard interferon-ribavirin.

Liver toxicity is a potential problem with all of the HAART medications^[1]. There is a higher rate of hepatotoxicity in co-infected patients who are being treated with HAART therapy. Of the protease inhibitors, several sources cite Ritonavir as the most liver toxic. Ritonavir trough levels are often twice as high in patients with HCV infection. Indinavir can cause severe hyperbilirubinemia in patients with HCV co-infection. Nelfinavir and Saquinavir are the safest among protease inhibitors in patients with compromised liver function. Among the NNRTIs, Nevirapine frequently causes elevation in transaminases, while Efavirenz is least likely to cause liver toxicity^[31].

Ribavirin may interact with selected nucleoside reverse transcriptase inhibitors (AZT, ddi, d4T) and reduce their anti-HIV activity due to interference with intracellular phosphorylation. If AZT is given concomitant with ribavirin, there is an increased incidence of anemia and complete blood counts should be carefully monitored^[32].

Future challenges

In order to maximize therapeutic efficacy, we will need to determine the immunological defect that is responsible for the diminished cellular immune response to HCV in HIV/HCV co-infected patients. It will be of value to determine the mechanism causing the defect that leads to an increase in hepatotoxicity in anti-retroviral drugs so that drug therapy can be better managed. Hepatotoxicity can possibly be decreased by manipulating the chemical structures of some of these medications. More studies need to be done on the interactions between HIV and HCV in man.

REFERENCES

- 1 **Dodig M.** Hepatitis C and human immunodeficiency virus co-infections. *J Clin Gastroenterol* 2001;**33**:367-374
- 2 **Troisi CL,** Hollinger FB, Hoots WK, Contant C, Gill J, Ragni M, Parmley R, Sexauer C, Gomperts E, Buchanan G. A multicenter study of viral hepatitis in a United States hemophilic population. *Blood* 1993;**81**:412-418
- 3 **Papaevangelou V,** Pollack H, Rochford G, Kokka R, Hou Z, Chernoff D, Hanna B, Krasinski K, Borkowsky W. Increased transmission of vertical hepatitis C virus (HCV) infection to human immunodeficiency virus (HIV) - infected infants of HIV - and HCV - co-infected women. *J Infect Dis* 1998;**178**:1047-1052
- 4 **Wright TL,** Hollander H, Pu X, Held MJ, Lipson P, Quan S, Polito A, Thaler MM, Bacchetti P, Scharschmidt BF.

- Hepatitis C in HIV-infected patients with and without AIDS: Prevalence and relationship to patient survival. *Hepatology* 1994;**20**:1152-1155
- 5 **Bonacini M.** Hepatitis C in patients with human immunodeficiency virus infection: diagnosis, natural history, meta-analysis of sexual and vertical transmission, and therapeutic issues. *Arch Intern Med* 2000;**160**:3365-3373
 - 6 **Ockenga J.** Hepatitis B and C in HIV-infected patients. Prevalence and prognostic value. *J Hepatol* 1997;**27**:18-24.
 - 7 **Bower W.** The Epidemiology of Hepatitis C Virus and HIV. Report from Conference on HIV/HCV Co-infection: Part 1, Session2: Co-infection, October 11, 2001
 - 8 **Stark K,** Schreier E, Muller R, Wirth D, Driesel G, Bienzle U. Prevalence and determinants of anti-HCV seropositivity and of HCV genotype among intravenous drug users in Berlin. *Scand J Infect Dis* 1995;**27**:331-337
 - 9 **Bodsworth NJ,** Cunningham P, Kaldor J, Donovan B. Hepatitis C virus infection in a large cohort of homosexually active men: Independent associations with HIV-1 infection and injecting drug use but not sexual behavior. *Genitourin Med* 1996;**72**:118-122
 - 10 **Eyster ME,** Alter HJ, Aledort LM, Quan S, Hatzakis A, Goedert JJ. Heterosexual co-transmission of hepatitis C virus (HCV) and human immunodeficiency virus (HIV). *Ann Intern Med* 1991;**115**:764-768
 - 11 **Stapleton J.** Basic Virology of HIV and HCV: Parallels and Contrasts? Report from Conference on HIV/HCV Coinfection: Part 1, Session 5, October 11,2001
 - 12 **Pol S,** Lamorthe B, Thi NT, Thiers V, Carnot F, Zylberberg H, Berthelot P, Brechot C, Nalpas B. Retrospective analysis of the impact of HIV infection and alcohol use on chronic hepatitis C in a large cohort of drug users. *J Hepatol* 1998;**28**:945-950
 - 13 **Benhamou Y,** Di Martino V, Bochet M, Colombet G, Thibault V, Liou A, Katlama C, Poynard T. The MultivirC Group. Factors affecting liver fibrosis in human immunodeficiency virus – and hepatitis C virus – co-infected patients: Impact of protease inhibitor therapy. *Hepatology* 2001;**34**:283-287
 - 14 **Soto B,** Sanchez-Quijano A, Rodrigo L, del Olmo JA, Garcia-Bengoechea M, Hernandez-Quero J, Rey C, Abad MA, Rodriguez M, Sales Gilabert M, Gonzalez F, Miron P, Caruz A, Relimpio F, Torronteras R, Leal M, Lissen E. Human immunodeficiency virus infection modifies the natural history of chronic parenterally-acquired hepatitis C with an unusually rapid progression to cirrhosis. *J Hepatol* 1997;**26**:1-5
 - 15 **Benhamou Y,** Bochet M, Di Martino V, Charlotte F, Azria F, Coutellier A, Vidaud M, Bricaire F, Opolon P, Katlama C, Poynard T. Liver fibrosis progression in human immunodeficiency virus and hepatitis C virus co-infected patients. *Hepatology* 1999;**30**:1054-1058
 - 16 **Beld M,** Penning M, Lukashov V, McMorro M, Roos M, Pakker N, van den Hoek A, Goudsmit J. Evidence that both HIV and HIV-induced immunodeficiency enhance HCV replication among HCV seroconverters. *Virology* 1998;**244**:504-512
 - 17 **Garcia-Samaniego J,** Soriano Y, Castilla J, Bravo R, Moreno A, Carbo J, Iniguez A, Gonzalez J, Munoz F. Influence of hepatitis C virus genotypes and HIV infection on histological severity of chronic hepatitis C. The hepatitis/HIV Spanish Study Group. *Am J Gastroenterol* 1997;**92**:1130-1134
 - 18 **Allory Y,** Charlotte F, Benhamou Y, Opolon P, Le Charpentier Y, Poynard T. Impact of human immunodeficiency virus infection on the histological features of chronic hepatitis C: A case-control study. The MULTIVIRC group. *Hum Pathol* 2000;**31**:69-74
 - 19 **Causse X,** Payen JL, Izopet J, Babany G, Girardin MF. Does HIV-infection influence the response of chronic hepatitis C to interferon treatment? A French multicenter prospective study. *J Hepatol* 2000;**32**:1003-10
 - 20 **Dieterich DT.** Hepatitis C virus and human immunodeficiency virus: clinical issues in co-infection. *Am J Med* 1999;**107**:79S-84S
 - 21 **Koziel M.** Immune responses Against HIV and HCV: What Lessons Can We Learn From These Different Viruses? Report from Conference on HIV/HCV Coinfection: Part2, Session7, October11,2001
 - 22 **Poles MA.** Hepatitis C virus/human immunodeficiency virus co-infection: clinical management issues. *Clin Infect Dis* 2000;**31**:154-161
 - 23 **Soriano V,** Garcia-Samaniego J, Bravo R, Gonzalez J, Castro A, Castilla J, Martinez-Odriozola P, Colmenero M, Carballo E, Suarez D, Rodriguez-Pinero FJ, Moreno A, del Romero J, Pedreira J, Gonzalez-Lahoz J. Interferon alpha for the treatment of chronic hepatitis C in patients infected with human immunodeficiency virus. Hepatitis – HIV Spanish Study Group. *Clin Infect Dis* 1996;**23**:585-591
 - 24 **Landau A.** Efficacy and safety of combination therapy with interferon-alpha 2b and ribavirin for chronic hepatitis C in HIV-infected patients. *AIDS* 2000;**14**:839-844
 - 25 **Sherman KE.** Diagnosis and management of the HCV/HIV – co-infected patient. *AIDS Clin Care* 2002;**14**:39-48
 - 26 **Soriano V.** Interferon plus ribavirin for chronic hepatitis C in HIV-infected patients. *AIDS* 2000;**14**:2409-2410
 - 27 **Nasti G.** Chronic hepatitis C in HIV infection: feasibility and sustained efficacy of therapy with interferon alpha-2b and ribavirin. *AIDS* 2001;**15**:1783-1787
 - 28 **Schiffman M,** Pockros PJ, Reddy RK. A controlled, randomized, multicenter, descending dose phase II trial of pegylated interferon alfa-2A (PEG) vs standard interferon alfa-2A (IFN) for treatment of chronic hepatitis C. *Gastroenterology* 1999;**116**:A1275
 - 29 **Zeuzem S,** Feinman SV, Rasenack J, Heathcote EJ, Lai MY, Gane E, O'Grady J, Reichen J, Diago M, Lin A, Hoffman J, Brunda MJ. Peginterferon alfa-2a in patients with chronic hepatitis C. *N Engl J Med* 2000;**343**:1666-1672
 - 30 **Sulkowski MS,** Reindollar R, Yu J. Pegylated interferon alfa-2A (Pegasys) and ribavirin combination therapy for chronic hepatitis C: A phase II open label study. *Gastroenterology* 2000;**118**:A950
 - 31 **Bonacini M.** Management issues in patients co-infected with hepatitis C and HIV. *AIDS Read* 2002;**12**:19-21
 - 32 **Sulkowski MS,** Thomas DL, Chaisson RE, Moore RD. Hepatotoxicity associated with antiretroviral therapy in adults infected with human immunodeficiency virus and the role of hepatitis C or B virus infection. *JAMA* 2000;**283**:74-80

Edited by Zhang JZ

• GASTRIC CANCER •

Profiling of differentially expressed genes in human Gastric carcinoma by cDNA expression array

Lian-Xin Liu, Zhi-Hua Liu, Hong-Chi Jiang, Xin Qu, Wei-Hui Zhang, Lin-Feng Wu, An-Long Zhu, Xiu-Qin Wang, Min Wu

Lian-Xin Liu, Hong-Chi Jiang, Xin Qu, Wei-Hui Zhang, Lin-Feng Wu, An-Long Zhu, Department of Surgery, the First Clinical College, Harbin Medical University, Harbin 150001, Heilongjiang Province, China

Lian-Xin Liu, Zhi-Hua Liu, Xiu-Qin Wang, Min Wu, National Laboratory of Molecular Oncology, Department of Cell Biology, Cancer Institute, Chinese Academy of Medical Science & Peking Union Medical College, Beijing 100021, China

Support by China Key Program on Basic Research, Grant Number: Z19-01-01-02; Chinese Climbing Project No.18; Youth Natural Scientific Foundation of Heilongjiang Province

Correspondence to: Dr. Lian-Xin Liu, Department of Surgery, the First Clinical College, Harbin Medical University, No.23 Youzheng Street, Nangang District, Harbin 150001, Heilongjiang Province, China. liulianxin@sohu.com

Telephone: +86-451-3668999 Fax: +86-451-3670428

Received 2002-07-08 Accepted 2002-07-19

Abstract

AIM: To investigate the expression of cancer related genes in gastric carcinoma (GC) through the use of Atlas Human Cancer Array membranes with 588 well-characterized human genes related to cancer and tumor biology.

METHODS: Hybridization of cDNA blotting membrane was performed with ³²P-labeled cDNA probes synthesized from RNA isolated from gastric carcinoma and adjacent noncancerous gastric epithelial tissue. AtlasImage, which is a software specific to array, was used to analyze the result.

RESULTS: The differentially expression cell cycle/growth regulator in GC showed a stronger tendency toward cell proliferation with 2.7-fold up-regulation of CK1. The promoter genes of apoptosis were down-regulated, including caspase-8 precursor, caspase-9 and caspase-10. Among the oncogene/tumor suppressor genes, ABL2 was down-regulated. In addition, some genes were up-regulated, including matrix metalloproteinase 2 (MMP-2), MMP-16 (MT3-MMP), SKY, CD9 and semaphorin V. A number of genes were down-regulated, including neuroendocrine-dlg (NE-dlg), retinoic acid receptor gamma and tumor suppressor DCC colorectal. In general, The expression of the cancer progression genes were up-regulated, while the expression of anti-cancer progression genes were down-regulated.

CONCLUSION: Investigation of these genes should help to disclose the molecular mechanism of the onset, progression and prognosis of GC. Several genes are reported herein to be altered in GC for the first time. The quick and high-throughout method of profiling gene expression by cDNA array provides us with an overview of key factors that may involved in GC, and may aid the study of GC carcinogenesis and provide molecular targets for diagnosis and therapy. The precise

relationship between the altered genes and gastric carcinogenesis is a matter for further investigation.

Liu LX, Liu ZH, Jiang HC, Qu X, Zhang WH, Wu LF, Zhu AL, Wang XQ, Wu M. Profiling of differentially expressed genes in human Gastric carcinoma by cDNA expression array. *World J gastroenterol* 2002; 8(4):580-585

INTRODUCTION

Gastric carcinoma (GC) is one of the most common malignant tumors worldwide, which ranks the first in frequency among human cancer in China^[1]. However, the molecular mechanism underlying GC are currently unknown. Some genes may play a significant role in carcinogenesis, such as p53, bcl-2, bax, and *c-myc*^[2-4]. However, these genetic changes do not precisely reflect the biological nature of tumor cells or the clinical characteristics of GC patients.

Tumor development and progression involves a cascade of genetic alterations. Techniques frequently used to study gene expression alterations, such as Reverse Transcription Polymerase Chain Reaction (RT-PCR), Differential Display Polymerase Chain Reaction (DD-PCR) and Northern blot analysis, have their limitations: some need large amounts of RNA, others are time-consuming and can only study a small number of genes simultaneously. Hence, analysis of expression profiles of a large number of genes in clinical GC material is an essential step toward clarifying the detailed mechanisms of carcinogenesis and discovering target molecules for the development of novel therapeutic drugs.

The cDNA microarray technology, which has recently undergone rapid development, enables investigators to study the gene expression profile and gene activation of thousands of genes and sequences^[5,6]. This technique allows the large-scale comparison of multiple genes in a single hybridization and has been used successfully to explore the gene expression profile of various carcinomas and diseases^[7-11].

In this study, we used cDNA expression microarray technology containing 588 genes related to carcinoma to analyze genes that are differentially expressed in human GC and normal gastric epithelial tissues. This large body of information not only furthers our understanding of the mechanism of carcinogenesis but also reveals novel features of known genes and identifies potential candidates for GC diagnosis and therapy.

MATERIALS AND METHODS

Tissues and specimens

Sixteen pairs of GC and corresponding noncancerous gastric epithelial tissue were obtained with informed consent from patients who underwent gastrectomy at the First Clinical College of Harbin Medical University and Cancer Hospital of Chinese Academy of Medical Science. Tumor tissue was

dissected from the resected specimen. The normal tissue block was taken from the distal resection margin. The specimens were immediately frozen in liquid nitrogen. Histopathological classification was performed by a single pathologist.

RNA isolation and purification

Total RNA were obtained by extracting frozen tissues in Trizol (Life Technologies Inc., Gaithersburg, MD, USA) according to the manufacturer's instructions. Normal gastric epithelial tissue and GC tissue were morsellated and homogenized in Trizol solution (1ml/100mg). Homogenates were incubated for 15 min on ice, and then a 1/5 volume of chloroform was added to the homogenates. After vigorous agitation for 5 min, the inorganic phase was separated by centrifugation at 12000×g for 20 min at 4 °C. RNA were then precipitated in the presence of 1 volume of isopropanol and centrifuged at 10 000×g for 15 min at 4 °C. RNA pellets were washed with 70 % ice-cold ethanol and then dissolved in diethyl pyrocarbonate (DEPC) – treated H₂O. Total RNA concentration and quantity was assessed by absorbency at 260nm using a Nucleic Acid and Protein Analyzer (BECKMAN 470, USA).

cDNA microarray membrane

Atlas Human Cancer cDNA Expression Array (7742-1) was purchased from Clontech Laboratories Inc(Palo Alto, USA). The membrane contained 10ng of each gene-specific cDNA from 588 known genes and 9 housekeeping genes(Figure 1A). Several plasmid and bacteriophage DNAs and blank spots are also included as negative and blank controls to confirm hybridization specificity. The cancer-related genes analyzed in this study are divided into six groups: (A)cell cycle regulators, growth regulators intermediate filament markers; (B) apoptosis, oncogenes, and tumor suppressors; (C) DNA damage response/repair and recombination; cell fate and development; and receptors; (D) cell adhesion and motility; and angiogenesis; (E) invasion regulators and cell-cell interactions; (F) growth factors and cytokines. A complete list of the 588 genes with the array positions and GeneBank accession number spotted on the array is available at Clontech's web site (<http://www.clontech.com>).

cDNA synthesis , labeling and purification

Total RNA was reverse-transcribed into cDNA and labeled with α -³²P dCTP using Superscript™ Preamplification system for First Strand cDNA Synthesis (Life Technologies, Gaithersburg, MD, USA). Before labeling, 5 µg total RNA of each type was treated with 2 µl DNase I (10 units/µl, Boehringer Mannheim, Mannheim, Germany), 1 µl RNasin (40 units/µl, Promega, Madison, WI, USA) at 37 °C for 15 min to remove contaminated DNA. For each labeling, the treated 5 µg total RNA was raised in volume to 6 µl with diethyl pyrocarbonate (DEPC)-treated H₂O and first incubated with 4 µl oligo dT (0.5 µg/µl, Life Technologies, Gaithersburg, MD, USA) at 70 °C for 10 min. Then, 6 µl 5× first strand reaction buffer, 1 µl 0.1 M DTT (Life Technologies, Gaithersburg, MD, USA), 1.5 µl dNTP mixture containing dATP, dGTP, dTTP at 20 µM (Promega, Madison, WI, USA), 10 µl α -³²P dCTP (10 µCi/µl, NEN Life Science, Boston, MA, USA) and 1.5 µl SuperScript II reverse transcriptase (200 units/µl, Life Technologies, Gaithersburg, MD, USA) were added and incubated at 37 °C for 90 min. The labeled first strand cDNA probes were purified by Spin 200 column (Clontech, Palo Alto, CA, USA) to remove the unincorporated nucleotides. After purification, labeled cDNAs were denatured in a boiling water bath for 3 min before use.

Membrane hybridization and exposure

Five milliliters ExpressHyb hybridization solution (Clontech, Palo Alto, CA, USA) and 5 µg Cot-1 DNA (Life Technologies, Gaithersburg, MD, USA) were added to the tube containing Atlas human cancer cDNA expression array, which were pre-hybridized at 68 °C for 2 h. Then different incubated probes were added to different tubes and hybridization was performed at 68 °C for 18 h in rolling bottles. The membranes were washed twice at 68 °C in 2 × SSC, 0.1 % SDS for 20 min, once at 50 °C in 1 × SSC, 0.5 % SDS for 20 min , once at room temperature in 0.5 × SSC, 1% SDS for 20 min and 0.5 × SSC10 min. Membrane were then exposed to X-ray films (Fuji Films, Tokyo, Japan) at -70 °C for 24-48 h.

Images and analysis

The images were scanned with Fluor-S MultiImager (Bio-Rad, Hercules, CA, USA) and saved as TIFF format files. The TIFF images were imported into the AtlasImage analysis software Version 1.01 a (Clontech, Palo Alto, CA, USA) and analyzed step by step with the guide. Housekeeping gene Ubiquitin was selected for normalization, because its expression was constant in cancer array hybridization system. Then the normalized intensity of each spot representing a unique gene expression level was acquired. Genes were considered to be up-regulated when the intensity ratio was ≥ 1.5 and the difference was $\geq 10\ 000$ between the expressions of GC tissues and normal gastric tissues.

RESULTS

Using a cDNA expression microarray technique we established the expression profile of 588 genes, selected from different areas of cancer research, in human GC and normal gastric tissue (Figure 1B, 1C). No signals were visible in the blank spots and negative control spots indicating that the Atlas human cancer array hybridization was highly specific. The housekeeping genes' density were very similar at the same time which indicate that the results were credible (Figure 1B,1C). We used the housekeeping gene, Ubiquitin, to normalize the intensities. The color image of the difference between GC and normal gastric tissue was produced by AtlasImage array software (Figure 1D) . The comparison results analyzed by AtlasImage software showed that there were 63 genes altered, 8 were up-regulated and 55 down-regulated in GC versus normal gastric tissue, using the criteria that the ratio was=1.5 or the difference was=10 000 (Table 1). There were pronounced differences in the gene expression profile between the two tissues.

DISCUSSION

In this study, we have explored the gene expression profiles in human GC and adjacent noncancerous normal gastric tissues using Atlas human cancer array which contains 588 genes that were classified according to their function to be relevant for cancer. cDNA array technology is used to examine simultaneously the expression of specific genes on a single hybridization. Although human genome projects have generated large-scale sequence data for millions of genes, the biological functions of such genes remain to be clarified. It is very important to define differential gene expression profiles of tumors and normal tissues before understanding the functional significance of specific gene products. Although expression analysis techniques such as Differential Display Polymerase Chain Reaction (DD-PCR), northern blot, and serial analysis of gene expression (SAGE) and RT-PCR have been widely used in the past, these studies are time-consuming and can only be used to deal with a limited number of genes.

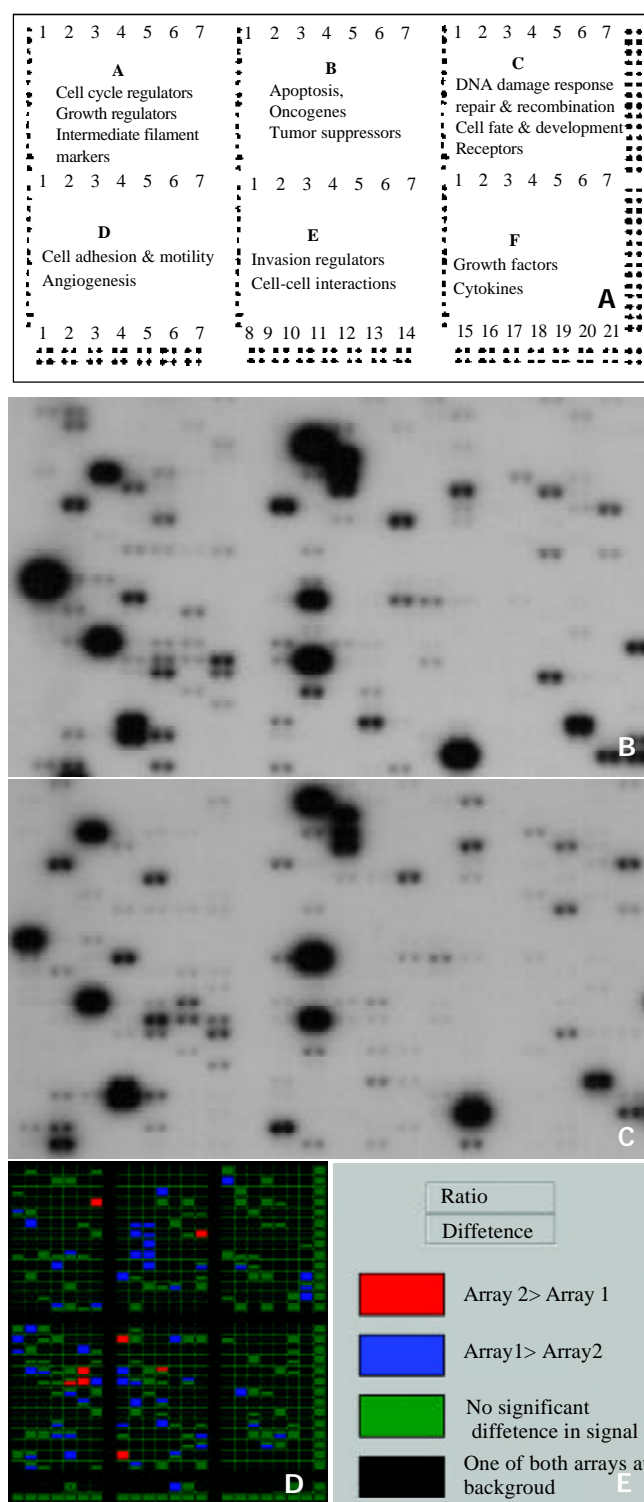


Figure 1 Parallel analysis of gene expression profiles in human gastric carcinoma and adjacent normal gastric mucosa. The schematic diagram of Atlas human cancer expression array contains 588 cancer-related human cDNA spotted as duplicates. Nine housekeeping genes are spotted at the bottom line to serve as positive controls. Dark grey spots at the outer end of the array represent genomic DNA spots, which serve as orientation marks (A). Atlas human cancer cDNA expression array (Clontech, USA) was hybridized with 32 P-labeled cDNA probes obtained from total RNA of human gastric carcinoma (B) and adjacent normal gastric tissues (C). The colorful compare diagram between human gastric carcinoma and adjacent normal gastric tissues was got when you aligned two arrays to AtlasImage Grid Templates and adjusted the alignments and background calculations (D). Definitions of colors in the array comparison were showed (E).

Table 1 Genes differentially expressed between HCC and adjacent noamal liver tissues generated by atlasImage software (Version 1.01a)

Gene	Ratio	Differ-ence	Protein/gene
B2f		-42675	TRAF6
E2h	0.171	-31204	T-plasminogen activator (T-PA)
B3h	0.444	-31180	caspase-8 precursor;MACH; FLICE;(CAP4) (CASP8)
D1b	0.334	-30676	byglycan
B3i	0.445	-30287	caspase-9 precursor; ICE-LAP6; apoptotic protease MCH-6
B2g	0.493	-28449	TRAF-interacting protein (TRIP)
B3g		-27610	caspase-8 precursor; MCH-5 isoform alpha
E4j	0.346	-27534	CDC42 GTPase-activating protein
C7m	0.336	-27032	retinoid X receptor beta (RXR-beta)
B1k	0.438	-26170	serine/threonine protein kinase NIK;
B3j	0.486	-25940	ICE-like apoptotic protease 4 precursor; caspase-10
B3f		-25206	caspase-7 precursor; apoptotic protease MCH-3; LICE2
F2g	0.428	-23730	endothelin ET2
D2a	0.176	-22099	collagen type VIII alpha-1
D7f	0.47	-21445	PLGF 1 & 2 precursor (placenta growth factor)
C7l	0.593	-21145	retinoic acid receptor gamma
A4j	0.326	-20847	extracellular signal-regulated kinase 6(ERK6) (ERK5)
E5b	0.299	-20388	rho GDP-dissociation inhibitor 1
E2f	0.638	-20244	extracellular matrix metalloproteinase inducer emmprin
D4j	0.624	-20147	integrin beta7
D2n	0.646	-17013	TENASCIN-R
F4l	0.626	-16150	interleukin-6 (IL-6) precursor; BSF-2; interferon beta-2;
B5l	0.633	-16122	proto-oncogene rhoA multidrug resistance protein;
B7j	0.639	-15630	tyrosine-protein kinase ABL2; tyrosine kinase ARG (ABL)
E7l	0.721	-15615	ephrin type-B receptor 2 precursor; tyrosine-protein eph-3
E1f	0.318	-15559	MMP-9; gelatinase B
B2i	0.245	-15356	CD40 receptor associated factor 1 (CRAF1)
D5g	0.569	-15106	ezzrin (cytovillin 2)
E7k		-14688	ephrin type-B receptor 1 precursor ; NET
E1j		-14540	MMP-13; collagenase-3
A2f	0.403	-14368	serine/threonine protein kinase PITALRE
D5m	0.38	-14156	tumor suppressor DCC colorectal
E1e	0.3	-13906	MMP-8; collagenase-2
D2e	0.295	-13706	collagen type XVIII alpha
D2m	0.624	-12991	tenascin-C
F3j	0.77	-12411	transcription factor ETR103;early growth response protein 1
C2j	0.648	-12053	Rad
F5k	0.68	-11371	leukocyte interferon-gamma (IFN-gamma)
D5k	0.643	-11064	ninjurin-1
C7k	0.356	-11056	retinoic acid receptor epsilon; retinoic acid receptor beta-2
C1b	0.392	-10834	ataxia telangiectasia (ATM)
D4k	0.799	-10645	integrin beta8
D1c		-10630	CD34
D3e	0.798	-10529	vitronectin precursor; serum spreading factor;
B4c	0.347	-10506	WSL-LR +WSL-S1+WSL-S2+TRAMP (Apo-3)
D6c	0.264	-10460	semaphorin E
E2n	0.483	-9167	low-density lipoprotein receptor-related protein 1 precursor
E5m	0.351	-8076	truncated-cadherin;H-cadherin;heart-cadherin
A4n	0.363	-7958	stress-activated protein kinase JNK3 ; JNK3;
A5i	0.282	-7204	E2F-3
E6f	0.287	-7197	neuroendocrine-dlg (NE-dlg);
A1e	0.343	-7043	cell division protein kinase 5; kinase PSSALRE
E4h	0.419	-6025	rhoHP1
D6h	0.451	-4647	LAR
A7n	0.466	-4426	desmin
E4e	2.185	4701	RAS-related C3 botulinum toxin substrate 1 (P21-RAC2)
D5f	1.447	10249	CD9
B7g	2.841	11419	SKY (DTK) (TYRO3) (RSE)
A7d	2.705	13394	type II cytoskeletal 11 keratin;cytokeratin 1 (K1; CK 1)
D6f	2.772	14015	semaphorin-1
D6e	3.182	15879	semaphorin V
E1b	3.079	15956	MMP-2; gelatinase A
E1m	2	17032	MMP-16 (MT3-MMP)

The microarray technique was first reported in 1995 by Schena *et al*^[5] and allows the simultaneous parallel expression analysis of thousands of genes. There is considerable interest in the potential application of cDNA microarray analysis for gene expression profiles in human cancers^[12]. Such information might be useful for tumor classification, for elucidation of key factor in tumors and for the identification of genes which might be useful for diagnostic purposes or as therapeutic targets^[13-15]. The Atlas Human cDNA Expression system provides a convenient and quick method for simultaneously profiling the expression of 588 genes related to cancer at the same time.

Among the genes showing differential expression in human GC, compared with the adjacent normal gastric tissue, several different classes of genes were up-regulated. Cytokeratin 1 (CK1), which is an intermediate filament protein, has a 2.7-fold up-regulation. The cytokeratins assembly *in vivo*, with obligatory heterologous dimeric combinations of different cytokeratins from each of the two major groups, comprising together more than 20 different individual cytokeratins. The keratin polypeptide expression common to all melanoma cells include K1 protein expression. A measure of keratin expression universality in malignant melanoma cells may have implications regarding their invasive and metastatic behaviors^[16]. However it has never been reported in GC. Sky is a member of a subfamily of related receptor tyrosine kinases. Sky may function as a cell adhesion molecule and mediate cell-to-cell or cell-matrix interactions between hematopoietic cells and their respective microenvironments^[17]. CD9 belongs to the tetraspanin superfamily of cell-surface proteins that span the membrane four times, forming two extracellular loops^[18]. A low CD9 expression by tumors of the lung may be associated with poor prognosis^[19]. Although the expression of CD9 was markedly down-regulated in basal cell carcinoma^[20], it was up-regulated in GC. CD9 was found to be useful for prognosis of patients with colorectal cancer^[21] or pancreatic cancer^[22]. CD9 gene is a useful indicator of a poor prognosis in breast cancer patients^[23].

Matrix metalloproteinases (MMPs) are members of a multigene family of zinc- and calcium-dependent enzymes involved in the degradation of numerous extracellular matrix (ECM) components^[24,25]. MMP-2 and MT3-MMP were up-regulated in GC. MMP-2 may initiate and promote angiogenesis^[26] and is considered to play a critical role in cell migration and invasion^[27]. It is also thought to play an important role in tumour progression^[28]. It has been reported that some kinds of malignant tumor tissues, including lung and stomach carcinomas, contain activated MMP-2^[29]. MT3-MMP plays a role in extracellular matrix (ECM) turnover by activating proMMP-2 and also by acting directly on ECM macromolecules^[30].

As described above, numerous genes were up-regulated, however more genes were down-regulated. Caspases are essential components of the mammalian cell death machinery. Caspase-8,9 and 10 were all down-regulated in GC. Caspase-9 is the member of the apoptotic protease cascade that is triggered by cytochrome c and dATP^[31]. Caspase-9 in the presence of cytochrome c and dATP can form an initiating complex for an apoptotic protease cascade^[32]. Activated caspase-9 in turn cleaves and activates caspase-3, -6 and -7 zymogens^[33]. Activation of the above caspases is blocked by a dominant negative form of caspase-9^[32]. The Fas/APO-1-receptor associated cysteine protease Mch5 (caspase-8), a member of the interleukin-1 β -converting enzyme family, is believed to be the enzyme responsible for activating a protease cascade after Fas-receptor ligation, leading to cell

death^[34,35]. A total of eight different isoforms of caspase-8 have been described. Only two of the caspase-8 isoforms (caspase-8/a and caspase-8/b) were predominantly expressed in cells of different origin. Both isoforms were recruited to the CD95 death-inducing signaling complex and were activated upon CD95 stimulation with similar kinetics^[36]. Caspase-10 is involved in CD95 and p55 signal transduction. Caspase-10 is recruited to both the CD95 and p55 tumor necrosis factor receptor signaling complexes in a FADD-dependent manner^[37] and may be responsible for activation of the ICE-like proteases^[38].

Retinoic acid receptors (RARs) are members of the steroid/thyroid hormone receptor superfamily. RARs serve as ligand-activated transcription factors^[39]. RARs are found in all tissues but predominantly in the developing fetus, dividing tumor cells and adult skin^[40]. Retinoic acid (RA) exerts its effects by differentially regulating its own receptor gene expression, including RAR alpha, beta, and gamma^[41]. RAR-gamma selectively binding retinoids are potent inhibitors of breast cancer cell proliferation alone and in combination with interferon-gamma (IFN-gamma)^[42]. RAR-gamma plays a critical role in mediating growth suppression by RA in ovarian cancer cells^[43]. Reduced endogenous RAR gamma expression may contribute to the malignant phenotype of human NB^[44]. RAR-gamma plays a critical role in a genetic switch between melanocytes and melanoma and induction of ligand-dependent apoptosis^[45]. It is still not known if RAR plays a similar role in GC.

The DCC (deleted in colorectal cancer) gene was originally identified as a candidate tumour suppressor gene in colonic carcinogenesis on the basis of allelic losses in chromosome 18q.21 in 70 % of colon cancers. DCC appears likely to play a significant role in differentiation, cell fate determination, and migration in the nervous system and perhaps other tissues as well^[46]. Absence of DCC expression however is not associated with colonic tumour progression^[47,48].

Neuroendocrine-Dlg (NE-Dlg, neuronal and endocrine dig) is a member of the discs-large-related (DLG) subfamily of the membrane-associated guanylate kinase-related proteins^[49]. NE-dlg is a human homolog of the *Drosophila* discs large (dlg) tumor suppressor protein^[50]. The NE-dlg appears to be critical for synaptogenesis, acting as a site-specific organizational center for integral membrane proteins and their downstream signaling molecules associated with the cytoskeleton^[50]. NE-Dlg directly interacts with the colorectal tumor suppressor gene adenomatous polyposis coli (APC), suggesting that it may play a role in regulating cell proliferation in epithelial cells^[50].

In conclusion, our study demonstrates that cDNA array is a powerful tool to explore gene expression profiles in cancer. The genes described in this study should therefore be a valuable resource for basic research, into molecular mechanism of carcinogenesis and the progression and prognosis of tumors. In addition, the clinical application of this work, may include the development of new diagnostic markers and the identification of novel therapeutic strategies for GC.

ACKNOWLEDGMENTS

We thank Dr. Michael Kelly (Department of Surgery, St. George Hospital, University of New South Wales, Sydney, Australia) for his review of the manuscript and helpful suggestions.

REFERENCE

- 1 **Deng DJ**. progress of gastric cancer etiology: N-nitrosamides 1999s. *World J Gastroenterol* 2000;**6**:613-618
- 2 **Baba H**, Korenaga D, Kakeji Y, Haraguchi M, Okamura T,

- Maehara Y. DNA ploidy and its clinical implications in gastric cancer. *Surgery* 2002;**131**:S63-70
- 3 **Xu AG**, Li SG, Liu JH, Gan AH. Function of apoptosis and expression of the proteins Bcl-2, p53 and C-myc in the development of gastric cancer. *World J Gastroenterol* 2001;**7**:403-406
- 4 Liu HF, Liu WW, Fang DC, Men RP. Expression and significance of proapoptotic gene Bax in gastric carcinoma. *World J Gastroenterol* 1999;**5**:15-17
- 5 **Schena M**, Shalon D, Davis RW, Brown PO. Quantitative monitoring of gene expression patterns with a complementary DNA microarray. *Science* 1995;**270**:467-470
- 6 **Wang K**, Gan L, Jeffery E, Gayle M, Gown AM, Skelly M, Nelson PS, Ng WV, Schummer M, Hood L, Mulligan J. Monitoring gene expression profile changes in ovarian carcinomas using cDNA microarray. *Gene* 1999;**229**:101-108
- 7 **Ross DT**, Scherf U, Eisen MB, Perou CM, Rees C, Spellman P, Iyer V, Jeffrey SS, Van de Rijn M, Waltham M, Pergamenschikov A, Lee JC, Lashkari D, Shalon D, Myers TG, Weinstein JN, Botstein D, Brown PO. Systematic variation in gene expression patterns in human cancer cell lines. *Nat Genet* 2000;**24**:227-235
- 8 **Khan J**, Simon R, Bittner M, Chen Y, Leighton SB, Pohida T, Smith PD, Jiang Y, Gooden GC, Trent JM, Meltzer PS. Gene expression profiling of alveolar rhabdomyosarcoma with cDNA microarrays. *Cancer Res* 1998;**58**:5009-5013
- 9 **Lu J**, Liu Z, Xiong M, Wang Q, Wang X, Yang G, Zhao L, Qiu Z, Zhou C, Wu M. Gene expression profile changes in initiation and progression of squamous cell carcinoma of esophagus. *Int J Cancer* 2001;**91**:288-294
- 10 **Kallioniemi OP**. Biochip technologies in cancer research. *Ann Med* 2001;**33**:142-147
- 11 **Khan J**, Saal LH, Bittner ML, Chen Y, Trent JM, Meltzer PS. Expression profiling in cancer using cDNA microarrays. *Electrophoresis* 1999;**20**:223-229
- 12 **Hu YC**, Lam KY, Law S, Wong J, Srivastava G. Identification of differentially expressed genes in esophageal squamous cell carcinoma (ESCC) by cDNA expression array: overexpression of Fra-1, Neogenin, Id-1, and CDC25B genes in ESCC. *Clin Cancer Res* 2001;**7**:2213-2221
- 13 **Selaru FM**, Zou T, Xu Y, Shustova V, Yin J, Mori Y, Sato F, Wang S, Oлару A, Shibata D, Greenwald BD, Krasna MJ, Abraham JM, Meltzer SJ. Global gene expression profiling in Barrett's esophagus and esophageal cancer: a comparative analysis using cDNA microarrays. *Oncogene* 2002;**21**:475-478
- 14 **Unger MA**, Rishi M, Clemmer VB, Hartman JL, Keiper EA, Greshock JD, Chodosh LA, Liebman MN, Weber BL. Characterization of adjacent breast tumors using oligonucleotide microarrays. *Breast Cancer Res* 2001;**3**:336-341
- 15 **Rew DA**. DNA microarray technology in cancer research. *Eur J Surg Oncol* 2001;**27**:504-508
- 16 **Katagata Y**, Aoki T, Hozumi Y, Yoshida T, Kondo S. Identification of K1/K10 and K5/K14 keratin pairs in human melanoma cell lines. *J Dermatol Sci* 1996;**13**:219-227
- 17 **Crosier PS**, Hall LR, Vitas MR, Lewis PM, Crosier KE. Identification of a novel receptor tyrosine kinase expressed in acute myeloid leukemic blasts. *Leuk Lymphoma* 1995;**18**:443-449
- 18 **Maecker HT**, Todd SC, Levy S. The tetraspanin superfamily: molecular facilitators. *FASEB J* 1997;**11**:428-442
- 19 **Adachi M**, Taki T, Konishi T, Huang CI, Higashiyama M, Miyake M. Novel staging protocol for non-small-cell lung cancers according to MRP-1/CD9 and KAI1/CD82 gene expression. *J Clin Oncol* 1998;**16**:1397-1406
- 20 **Okochi H**, Kato M, Nashiro K, Yoshie O, Miyazono K, Furue M. Expression of tetra-spans transmembrane family (CD9, CD37, CD53, CD63, CD81 and CD82) in normal and neoplastic human keratinocytes: an association of CD9 with alpha 3 beta 1 integrin. *Br J Dermatol* 1997;**137**:856-863
- 21 **Mori M**, Mimori K, Shiraishi T, Haraguchi M, Ueo H, Barnard GF, Akiyoshi T. Motility related protein 1 (MRP1/CD9) expression in colon cancer. *Clin Cancer Res* 1998;**4**:1507-1510
- 22 **Sho M**, Adachi M, Taki T, Hashida H, Konishi T, Huang CL, Ikeda N, Nakajima Y, Kanehiro H, Hisanaga M, Nakano H, Miyake M. Transmembrane 4 superfamily as a prognostic factor in pancreatic cancer. *Int J Cancer* 1998;**79**:509-516
- 23 **Huang CI**, Kohno N, Ogawa E, Adachi M, Taki T, Miyake M. Correlation of reduction in MRP-1/CD9 and KAI1/CD82 expression with recurrences in breast cancer patients. *Am J Pathol* 1998;**153**:973-983
- 24 **Polette M**, Birembaut P. Membrane-type metalloproteinases in tumor invasion. *Int J Biochem Cell Biol* 1998;**30**:1195-1202
- 25 **Reynolds JJ**. Collagenases and tissue inhibitors of metalloproteinases: a functional balance in tissue degradation. *Oral Dis* 1996;**2**:70-76
- 26 **Sang QX**. Complex role of matrix metalloproteinases in angiogenesis. *Cell Res* 1998;**8**:171-177
- 27 **Nagase H**. Cell surface activation of progelatinase A (proMMP-2) and cell migration. *Cell Res* 1998;**8**:179-186
- 28 **Rooprai HK**, McCormick D. Proteases and their inhibitors in human brain tumours: a review. *Anticancer Res* 1997;**17**:4151-4162
- 29 **Ueno H**, Nakamura H, Inoue M, Imai K, Noguchi M, Sato H, Seiki M, Okada Y. Expression and tissue localization of membrane-types 1, 2, and 3 matrix metalloproteinases in human invasive breast carcinomas. *Cancer Res* 1997;**57**:2055-2060
- 30 **Matsumoto S**, Katoh M, Saito S, Watanabe T, Masuho Y. Identification of soluble type of membrane-type matrix metalloproteinase-3 formed by alternatively spliced mRNA. *Biochim Biophys Acta* 1997;**1354**:159-170
- 31 **Li P**, Nijhawan D, Budihardjo I, Srinivasula SM, Ahmad M, Alnemri ES, Wang X. Cytochrome c and dATP-dependent formation of Apaf-1/caspase-9 complex initiates an apoptotic protease cascade. *Cell* 1997;**91**:479-489
- 32 **Pan G**, Humke EW, Dixit VM. Activation of caspases triggered by cytochrome c *in vitro*. *FEBS Lett* 1998;**426**:151-154
- 33 **Srinivasula SM**, Ahmad M, Fernandes-Alnemri T, Alnemri ES. Autoactivation of procaspase-9 by Apaf-1-mediated oligomerization. *Mol Cell* 1998;**1**:949-957
- 34 **Yuan J**. Transducing signals of life and death. *Curr Opin Cell Biol* 1997;**9**:247-251
- 35 **Muzio M**, Salvesen GS, Dixit VM. FLICE induced apoptosis in a cell-free system. Cleavage of caspase zymogens. *J Biol Chem* 1997;**272**:2952-2956
- 36 **Scaffidi C**, Medema JP, Krammer PH, Peter ME. FLICE is predominantly expressed as two functionally active isoforms, caspase-8/a and caspase-8/b. *J Biol Chem* 1997;**272**:26953-26958
- 37 **Vincenz C**, Dixit VM. Fas-associated death domain protein interleukin-1beta-converting enzyme 2 (FLICE2), an ICE/Ced-3 homologue, is proximally involved in CD95- and p55-mediated death signaling. *J Biol Chem* 1997;**272**:6578-6583
- 38 **Srinivasula SM**, Ahmad M, Fernandes-Alnemri T, Litwack G, Alnemri ES. Molecular ordering of the Fas-apoptotic pathway: the Fas/APO-1 protease Mch5 is a CrmA-inhibitable protease that activates multiple Ced-3/ICE-like cysteine proteases. *Proc Natl Acad Sci U S A* 1996;**93**:14486-14491
- 39 **Repa JJ**, Berg JA, Kaiser ME, Hanson KK, Strugnell SA, Clagett-Dame M. One-step immunoaffinity purification of

- recombinant human retinoic acid receptor gamma. *Protein Expr Purif* 1997;**9**:319-330
- 40 **Sharma RP**, Kim YW. Localization of retinoic acid receptors in anterior-human embryo. *Exp Mol Pathol* 1995;**62**: 180-189
 - 41 **Wan YJ**, Cai Y, Magee TR. Retinoic acid differentially regulates retinoic acid receptor-mediated pathways in the Hep3B cell line. *Exp Cell Res* 1998;**238**:241-247
 - 42 **Widschwendter M**, Daxenbichler G, Culig Z, Michel S, Zeimet AG, Mortl MG, Widschwendter A, Marth C. Activity of retinoic acid receptor-gamma selectively binding retinoids alone and in combination with interferon-gamma in breast cancer cell lines. *Int J Cancer* 1997;**71**:497-504
 - 43 **Wu S**, Zhang D, Zhang ZP, Soprano DR, Soprano KJ. Critical role of both retinoid nuclear receptors and retinoid-X-receptors in mediating growth inhibition of ovarian cancer cells by all-trans retinoic acid. *Oncogene* 1998;**17**:2839-2849
 - 44 **Marshall GM**, Cheung B, Stacey KP, Camacho ML, Simpson AM, Kwan E, Smith S, Haber M, Norris MD. Increased retinoic acid receptor gamma expression suppresses the malignant phenotype and alters the differentiation potential of human neuroblastoma cells. *Oncogene* 1995;**11**:485-491
 - 45 **Spanjaard RA**, Ikeda M, Lee PJ, Charpentier B, Chin WW, Eberlein TJ. Specific activation of retinoic acid receptors (RARs) and retinoid X receptors reveals a unique role for RARgamma in induction of differentiation and apoptosis of S91 melanoma cells. *J Biol Chem* 1997;**272**:18990-18999
 - 46 **Fearon ER**. DCC: is there a connection between tumorigenesis and cell guidance molecules? *Biochim Biophys Acta* 1996;**1288**:M17-23
 - 47 **Nigro JM**, Cho KR, Fearon ER, Kern SE, Ruppert JM, Oliner JD, Kinzler KW, Vogelstein B. Scrambled exons. *Cell* 1991;**64**:607-613
 - 48 **Reymond MA**, Dworak O, Remke S, Hohenberger W, Kirchner T, Kockerling F. DCC protein as a predictor of distant metastases after curative surgery for rectal cancer. *Dis Colon Rectum* 1998;**41**:755-760
 - 49 **Ciardiello F**, Dono R, Kim N, Persico MG, Salomon DS. Expression of cripto, a novel gene of the epidermal growth factor gene family, leads to *in vitro* transformation of a normal mouse mammary epithelial cell line. *Cancer Res* 1991;**51**:1051-1054
 - 50 **Baldassarre G**, Romano A, Armenante F, Rambaldi M, Paoletti I, Sandomenico C, Pepe S, Staibano S, Salvatore G, De Rosa G, Persico MG, Viglietto G. Expression of teratocarcinoma-derived growth factor-1 (TDGF-1) in testis germ cell tumors and its effects on growth and differentiation of embryonal carcinoma cell line NTERA2/D1. *Oncogene* 1997;**15**:927-936

Edited by Kelly MD

• GASTRIC CANCER •

The expression of hTERT mRNA and cellular immunity in gastric cancer and precancerosis

Xi-Xian Yao, Lei Yin, Zhong-Cheng Sun

Xi-Xian Yao, Lei Yin, Department of Digestive Medicine, the 2nd Hospital of Hebei Medical University, Shijiazhuang 050000, Hebei Province, China

Zhong-Cheng Sun, The Traditional Chinese Medical College of Hebei Medical University, Shijiazhuang 050081, Hebei Province, China

Supported by Science and Technology Fund, Governmental Department of Health, Hebei Province, No.2K007

Correspondence to: Professor Xi-Xian Yao, Department of Digestive Medicine, the 2nd Hospital of Hebei Medical University, Shijiazhuang 050000, Hebei Province, China. yaioxian@263.net

Telephone: +86-311-7046901 Ext. 8631, 8632

Received 2001-06-03 **Accepted** 2001-12-08

Abstract

AIM: To observe the expression of Human telomerase reverse transcriptase (hTERT) in gastric carcinomas and precancerosis lesions, to evaluate the immune state of such patients, and to then study the clinical significance of hTERT and immune state for the diagnosis, treatment and prognosis of gastric cancer.

METHODS: In situ hybridization was used to detect the expression of hTERT mRNA in 116 endoscopic of gastric mucosa. Analyzed tissue samples were as follows: 30 cases of chronic superficial gastritis (CSG), 44 of precancerosis lesions (including 27 of chronic atrophic gastritis, 8 of adenomatous polyp and 9 of gastric ulcer) and 42 of gastric cancer (GC). In addition, the T lymphocyte subsets (CD3⁺, CD4⁺, CD8⁺, CD4⁺/CD8⁺) and natural killer cells (NK) in peripheral blood were determined by flow cytometric analysis (FCM) in 30 cases of CSG, 27 of precancerosis (chronic atrophic gastritis, CAG), and 42 of GC. The data were compared with those of normal control (NC).

RESULTS: The detected positive rate of hTERT varied as follows: 86 % (36/42) in GC, 36 % (16/44) in precancerosis lesions and 0 % (0/30) in CSG. The expression of hTERT mRNA was not associated with patient gender, tumor location, macroscopic type, lymph node metastasis, or degree of differentiation. It was found that the CD3⁺, CD4⁺ of the CSG group were lower than that of NC ($P < 0.05$). Meanwhile, the T lymphocyte subsets (CD3⁺, CD4⁺, CD4⁺/CD8⁺ ratio) and NK cells of CAG were remarkably lower than that of NC and CSG groups ($P < 0.05-0.01$). Values of T cells and NK cells of the GC group were significantly abnormal when compared with the CAG group ($P < 0.05-0.01$). Furthermore, with tumor progression, the function of T cells was weakened gradually.

CONCLUSION: The expression of telomerase may be a crucial step in gastric carcinogenesis and increased hTERT mRNA may serve as a novel marker for diagnosis of GC. The immune state of patients with GC and precancerosis was somewhat depressed, which indi-

cates the importance of cellular immunological assays in cancer patients.

Yao XX, Yin L, Sun ZC. The expression of hTERT mRNA and cellular immunity in gastric cancer and precancerosis. *World J Gastroenterol* 2002; 8(4):586-590

INTRODUCTION

There are many factors that contribute to gastric carcinogenesis^[1-10]. Currently, telomerase has been a major focus^[11-23]. Telomerase activation is associated with an early stage of stomach carcinogenesis^[24-33]. Human telomerase reverse transcriptase (hTERT) has been identified as a catalytic subunit of human telomerase. Recent studies have demonstrated a close correlation between telomerase activity and hTERT expression^[32-41]. In this study, *in situ* hybridization (ISH) was used to detect hTERT expression in patients with GC and precancerosis, which could help us better understand the role of telomerase in the carcinogenesis and development of GC.

In the meantime, many studies have suggested that immune responses to tumor cells play an important role in GC^[42-54]. We detected tumor specific lymphocytes (T lymphocytes) and nonspecific natural killer (NK) cells in order to clarify the correlation between cell mediated immunity and the clinicopathologic factors of GC.

MATERIALS AND METHODS

Tissue samples

Gastroscopic removal tissues were obtained from the second affiliated Hospital of Hebei Medical University from January 2 000 to July 2 000. Totally, 116 gastroscopic samples were analyzed. The patients (mean age, 48.3 years; range, 40-56 years) are as follows: 42 cases of GC, 44 chronic gastritis with atypical hyperplasia (including 27 of CAG, 8 of adenomatous polyp and 9 of gastric ulcer), and 30 CSG. In case selection, the disease of liver, circulatory, endocrinopathy and rheumatic systems were excluded. The gastroscopic samples were fixed into formalin with 1 % DEPC to prevent mRNA degradation. For FCM of T lymphocytes and NK cells, 1ml samples of venous blood from each patient was put into a heparinized tube. The value of T lymphocytes and NK cells of 20 blood donors in the same age range were run as NC.

hTERT assay

ISH was carried out by using an hTERT ISH Detection Kit (produced by Wuhan Boster Biological Technology Ltd.). The antisense poly-oligonucleotide probe was digoxin-labeled.

Formalin-fixed, paraffin-embedded samples were cut at 5 μ m and adhered to poly-l-lysine treated slides. Samples were deparaffinized and rehydrated through a graded series of ethanol, and endogenous peroxidase was blocked using 3 % hydrogen peroxide for 10 min. The slides were digested with pepsin at 37 degrees for 15-20 min. 20 μ l of probe was hybridized

to each slide for 16-20 h at 40 degrees. After hybridization, excess probe was removed by washing in $2\times$ SSC at 37 degrees. Tissue sections were preblocked for 20 min with blocking reagent, then the primary antibody (rabbit anti-digoxin antibody) was added for 60 min at 37 degrees. After washing with 0.5 M PBS three times at 5 min each, the slides were incubated with the secondary goat anti-rabbit immunoglobulin (IgG) antibody conjugated with biotin for 20 min at 37 degrees, then washed with 0.5 M PBS again as previously described. Samples were next incubated with SABC for 20 min at room temperature and rinsed with 0.5M PBS for four times at 5 min each. The reaction products of peroxidase were visualized by incubation with chromogen diaminobenzidine for 15-20 min. Finally, the slides were counterstained for nuclei by haematoxylin stain. A negative control was prepared for each sample using a hybridization solution without probe. The positive signals of hTERT mRNA expression were stains with the color of brown-yellow located in cell plasma. The average percentage of positive cells was determined in at least 5 areas at $\times 400$ and assigned to one of four categories: (-)-negative or equivocal staining; (+)-weak positive, cells were stained in 1-25%; (++)-middle positive, cells were stained in 25-50 %; and (+++)-strong positive expression, cells were stained over 50 %.

Flow cytometric analysis of cellular immunity

The heparinized venous blood samples were made into suspensions of single cells, then plated in reaction tubes. Monoclonal antibodies of mature T cells ($CD3^+$), $T_H(CD4^+)$, $T_s(CD8^+)$, and NK cells(CD^+) were added, then shaken into a well-distributed solution. The solution was incubated for 30 min at room temperature, then rinsed with distilled water for 10 min. The cells were collected after centrifugation at 1000 rpm for 10 min and kept at 4 degrees. Measurement of T cells and NK cells was performed by using a FACSCalibur flow cytometer (Becton Dickinson).

Statistical analyses

The χ^2 test was used for statistical analysis of the frequency of positive hTERT among each group. The data of T cells and NK cells were expressed as mean \pm standard deviation ($\bar{x}\pm s$), and the differences between the value of different groups were analysed by the *t* test. The criterion of significance was set at $P<0.05$.

RESULTS

Expression levels of hTERT

The positive signals of hTERT mRNA expression were brown-yellow stains located in the cell plasma. (Figure 1 and 2). The expression levels of hTERT in different gastric mucosae are summarized in Table 1. There was no hTERT mRNA expression in CSG (0/30). Positive hTERT was detected in 16 of 44 (36 %) of precancerous lesions and 36 of 42 (86 %) GC.

Carcinomas exhibited positive hTERT significantly more frequently than did precancerous lesions ($P<0.05$, by χ^2 test). The positive rate of three groups with dysplasia of CAG, adenomatous polyps (AP) and gastric ulcers (GU) are 37 % (10 of 27), 38 % (3 of 8) and 33 % (3 of 9) respectively. There was no significant difference among the three groups ($P>0.05$). Positive rate of early-stage GC and advanced-stage GC are 88 % (7 of 8) and 85 % (29/34) respectively. There was no significant difference between the two groups ($P>0.05$). We also grouped the cancer patients by gender, tumour location, macroscopic type, histological grade, and lymph node

metastasis, and found the positive rates of hTERT were not correlated with these clinicopathological factors.

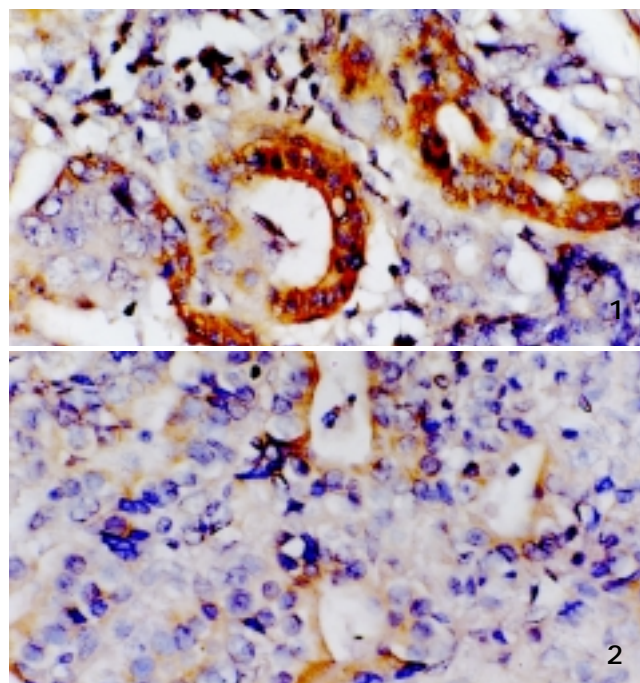


Figure 1 Positive signal of hTERT in gastric adenocarcinoma, localized in plasma. ISH, $\times 400$

Figure 2 Weak positive signal of hTERT in precancerous lesions, localized in plasma. ISH, $\times 400$

Table 1 The expression of hTERT mRNA in 116 cases of gastric mucosae

groups	n	hTERT mRNA			positive(%)
		+	++	+++	
CSG	30	0	0	0	0
CAG	27	10	0	0	37
AP	8	2	1	0	38
GU	9	3	0	0	33
GC	42	15	18	3	86

The detection results of T cells and NK cells

The results are summarized in Tables 2 and 3.

Table 2 T lymphocyte subsets and NK cells in different gastric disease ($\bar{x}\pm s$)

groups	n	CD3 ⁺ (%)	CD4 ⁺ (%)	CD8 ⁺ (%)	CD4 ⁺ /CD8 ⁺	NK
NC	20	68.0 \pm 2.0	39.9 \pm 4.5	27.1 \pm 4.5	1.4 \pm 0.2	21.4 \pm 3.7
CSG	30	61.6 \pm 4.4 ^a	35.9 \pm 3.3 ^a	26.7 \pm 4.2	1.4 \pm 0.1	20.1 \pm 5.1
CAG	27	57.6 \pm 3.1 ^{ac}	33.5 \pm 2.8 ^{ac}	26.8 \pm 2.8	1.2 \pm 0.1 ^{bd}	13.5 \pm 3.4 ^{bd}
GC	42	53.4 \pm 10.6 ^e	29.4 \pm 7.6 ^e	35.6 \pm 8.6 ^e	0.9 \pm 0.4 ^e	9.4 \pm 4.4 ^f

^a $P<0.05$, ^b $P<0.01$ vs NC ^c $P<0.05$ ^d $P<0.01$ vs CSG; ^e $P<0.05$, ^f $P<0.01$ vs CAG

Table 3 T lymphocyte subsets and NK cells in different stages of gastric cancer ($\bar{x} \pm s$)

groups	n	CD3 ⁺ (%)	CD4 ⁺ (%)	CD8 ⁺ (%)	CD4 ⁺ /CD8 ⁺	NK
tumor gross type						
early	8	57.5±5.5	32.1±9.1	28.2±10.0	1.1±0.6	8.7±3.9
advanced	34	52.9±9.8 ^b	26.8±6.0 ^b	35.5±8.1	0.8±0.3 ^a	9.6±4.5
lymph node metastasis						
without	13	57.3±7.8	31.2±7.4	32.4±8.5	1.1±0.4	9.7±4.7
with	29	52.5±10.1 ^c	25.7±5.8 ^c	36.7±8.1	0.7±0.3 ^c	9.2±4.3

^a $P < 0.05$, ^b $P < 0.01$ vs early-stage cancer; ^c $P < 0.05$ vs the cancer patients without lymph node metastasis

The results of T cells examination were as follows: (1) The values of CD3⁺ and CD4⁺ in CSG were significantly lower than that in NC ($P < 0.05$ *t* test). CD8⁺ and CD4⁺/CD8⁺ ratio were slightly lower in CSG than in NC, but the change was not significant ($P > 0.05$). (2) The values of CD3⁺, CD4⁺, CD4⁺/CD8⁺ in CAG were significantly lower compared with CSG and NC ($P < 0.05-0.01$). There was no significant change in CD8⁺ ($P > 0.05$). (3) Compared with CAG, all the values of T cells had remarkable changes ($P < 0.05-0.01$). (4) The values of CD3⁺, CD4⁺, and CD4⁺/CD8⁺ in advanced cancer were remarkably lower than in early-stage cancers ($P < 0.05-0.01$). (5) The values of CD3⁺, CD4⁺, and CD4⁺/CD8⁺ in the cancer patients with lymph node metastasis were significantly lower than that of cancer patients without lymph node metastasis ($P < 0.05$).

The results of NK cell examination were as follows: (1) There was no significant difference between CSG and NC ($P > 0.05$). (2) The value of NK was significantly lower in CAG than in CSG ($P < 0.01$). (3) The value of NK is also significantly lower in GC than in CAG ($P < 0.01$). (4) There was no significant difference between early-stage cancer and advanced cancer ($P > 0.05$). The value of NK was not associated with lymph node metastasis ($P > 0.05$).

DISCUSSION

Most current studies have proposed that reactivation of telomerase is a critical step in tumorigenesis^[24-41]. There is a close correlation between hTERT and telomerase activity^[32,33]. Several researchers have reported high levels of hTERT expression in malignant tissues but not in non-malignant tissues by using ISH techniques^[14,15,34]. In this study, we used the ISH method to analyze the localization of hTERT mRNA expression in formalin-fixed, paraffin-embedded tissues and got similar results as those previously reported. High levels of hTERT expression were found in the plasma of most carcinoma cells (Figure 1), and the positive rate was 86 %. hTERT expression also increased in precancerous lesions with the positive rate of 36 %, most of them were weakly positive (Figure 2). No expression was observed in CSG. There is great significance among the three groups above ($P < 0.01$). Very high levels of hTERT were detected in 7 of 8 early-stage GC (88 %), which is remarkably greater than that of the precancerous group (36 %). These data indicate that hTERT overexpression may be not only an early event but also a critical step in carcinogenesis of the stomach. Our result is good evidence that telomerase can be an important marker for diagnosis of early-stage cancers.

It is now almost axiomatic that host immunological reaction is an important factor in resistance to tumors. Immunological cells, either sensitized or nonspecifically activated, are considered necessary to inhibit or kill tumor cells^[42-54]. The

cell-mediated immunity (CMI) in contact with tumor cells plays an important role in host immune defense of GC patients. Immune response to cancer cells may be mediated mainly by T lymphocyte subsets and nonspecific natural killer (NK) cells. Many studies indicate that T lymphocyte activity is correlated closely with carcinogenesis and development of GC. Critically, the T_H/T_S ratio is a more important index to evaluate the state of cellular immunity and anti-tumor activity^[46-50]. NK cells are the main components of nonspecific immune surveillance, which is capable of killing tumor cells without being sensitized previously, and makes up the first defense line to eliminate cancer cells^[51-53]. In order to realize the importance of immune state in the process of gastric carcinogenesis, we used FCM to detect the mature T lymphocyte, T_H , T_S , T_H/T_S , and NK cells in peripheral blood, whose superficial markers are CD3⁺, CD4⁺, CD8⁺, CD4⁺/CD8⁺, and CD(16+56)⁺, respectively.

Our results suggested that T lymphocyte subsets and NK cells have significant changes in every stage of the progression from normal gastric mucosa to GC: (1) In NC the values are as follows: CD3⁺, 68.02±2.01; CD4⁺, 39.89±4.50; CD8⁺, 27.14±4.51; CD4⁺/CD8⁺, 1.42±0.21; and NK, 21.44±3.74. (2) CD3⁺ (61.61±4.39) and CD4⁺ (35.92±3.30) in CSG were significantly lower than that of NC, which indicated that CSG patients not only had the infiltrating lymphocytes in local pathological change but also had a remarkable imbalance in the T cell immunity of the host body. In the CAG group, CD3⁺ (57.55±3.13), CD4⁺ (33.54±2.82), CD4⁺/CD8⁺ (1.22±0.13), and NK (13.48±3.44) were all remarkably decreased, which indicated the cellular immunity of CAG patients had a distinct abnormality. In the GC group, CD3⁺ (53.37±10.55), CD4⁺ (29.37±7.61), CD4⁺/CD8⁺ (0.90±0.39) and NK (9.40±4.38) became much lower than ever. Furthermore, the impairment of cellular immunity became more and more critical with tumor progression and metastasis (Table 3). All these results indicated: (1) The state of cellular immunity of patients with GC was correlated with prognosis. The deficiency of cellular immunity may play an important role in the continuing growth and metastasis of GC; and (2) Using a combination of immunotherapy with other modalities, e.g. chemotherapy or radiation, may lead to effective antitumor therapy.

Reports regarding the relationship between hTERT and local pathological lesions, and the cellular immunity of the host in the process of gastric carcinogenesis are still rare. We found that hTERT had a certain expression in precancerous lesions while the immunity state of most of those patients decreased. In early-stages of GC, the expression of hTERT had remarkably increased and the cellular immunity had decreased at the same time. These situations are worthy of more attention. According to previous studies, the main mechanism of cellular immunological insufficiency of GC patients is that tumor cells can produce a large amount of immunosuppressive factors. Before the metamorphoses of precancerous cells, the components of their antigens have had the characteristics of cancer cells in the process of transition from precancerous to cancer. Such cells can also produce immunosuppressive factors to impair host's cellular immunity. Thus, the insufficiency of the immune system may lead the cancer to worsen, which may cause a vicious cycle. It has been demonstrated that telomerase activation is a crucial step in gastric carcinogenesis. When the expression of telomerase changes the antigenic components of cells in the process of gastric carcinogenesis, then can cancer cells avoid immune surveillance? When telomerase activation affects the role of apoptosis, can this cause T cell or NK cell damage? Such questions need further research. Discussing such questions will

be helpful to realize the mechanism of further reduction of cellular immunity in the process of carcinogenesis and cancer proliferation, and also will provide good prospects of gene therapy which combine anti-tumor telomerase and immunotherapy.

REFERENCES

- Zhang XY.** Some recent works on diagnosis and treatment of gastric cancer. *World J Gastroenterol* 1999;**5**:1-3
- Xue XC,** Fang GE, Hua JD. Gastric cancer and apoptosis. *Shijie Huaren Xiaohua Zazhi* 1999;**7**:359-361
- Liu C,** Shun ZY, Wei MY, Ying NY. Fish sauce and gastric cancer: an ecological study in Fujian Province, China. *World J Gastroenterol* 2000;**6**:572-576
- Zhuang ZH,** Chen YL, Wang CD, Chen YG. Expression of TGF-1 and TGF- β receptor 1 in gastric carcinoma and precancerous lesions. *Shijie Huaren Xiaohua Zazhi* 1999;**7**:507-509
- Wu YA,** Lu B, Liu J, Li J, Chen JR, Hu SX. Consequence alimentary reconstruction nutritional status after total gastrectomy gastric cancer. *World J Gastroenterol* 1999;**5**:34-37
- Zhou HP,** Wang X, Zhang NZ. Early apoptosis in intestinal and diffuse gastric carcinomas. *World J Gastroenterol* 2000;**6**:898-901
- Liu HF,** Liu WW, Fang DC, Men RF, Wang ZH. Apoptosis and its relationship with Fas ligand expression in gastric carcinoma and its precancerous lesion. *Shijie Huaren Xiaohua Zazhi* 1999;**7**:561-563
- Bi GT,** Yong HY, Zheng LG, Gang WO, Kui Z. Ascorbic acid secretion in the human stomach and the effect of gastrin. *World J Gastroenterol* 2000;**6**:704-708
- Liu HF,** Liu WW, Fang DC. Study of the relationship between apoptosis and proliferation in gastric carcinoma and its precancerous lesion. *Shijie Huaren Xiaohua Zazhi* 1999;**7**:649-651
- Shou CZ,** Hua SQ, Cheng WZ, Hou QT. A clinical and long-term follow-up study of peri-operative sequential triple therapy for gastric cancer. *World J Gastroenterol* 2000;**6**:284-286
- Guan JL,** Zhang JP, Zhou TH. Relationship between telomerase, *Helicobacter pylori* and stomach cancer. *Shijie Huaren Xiaohua Zazhi* 2000;**8**:910-911
- Yang SM,** Fang DC, Luo YH, Lu R, Liu WW. Telomerase activity in gastroenterological submucous tumors and its clinical significance. *Shijie Huaren Xiaohua Zazhi* 1998;**6**:765-767
- Ma JP,** Cai SR, Zhan WH. Telomerase activity in human gastric carcinoma by TRAP silver stain assay. *Zhonghua Weichang Waike Zazhi* 1998;**1**:103-105
- Hiyama E,** Yokoyama H, Kitadai Y, Tahara E, Tahara H, Ide T, Haruma K, Yasui W, Kajiyama G, Tagara EC. *In situ* mRNA Hybridization Technique for Analysis of Human Telomerase RNA in Gastric Precancerous and Cancerous Lesions. *Jpn J Cancer Res* 1998;**89**:1187-1194
- Yasui W,** Tahara H, Tahara E, Fujimoto J, Nakayama J, Ishikawa F, Ide T, Tahara E. Expression of Telomerase Catalytic Component, Telomerase Reverse Transcriptase, in Human Gastric Carcinomas. *Jpn J Cancer Res* 1998;**89**:1099-1103
- Tahara H,** Kuniyasu H, Yokozaki H, Yasui WW, Shay J, Ide T, Tahara E. Telomerase activity in preneoplastic and neoplastic gastric and colorectal lesions. *Clin Cancer Res* 1995;**1**:1245-1251
- Ahn MJ,** Noh YH, Lee YS, Lee JH, Chung TJ, Kim IS, Choi IY, Kim SH, Lee JS, Lee KH. Telomerase Activity and its Clinicopathological Significance in Gastric Cancer. *Eur J Cancer* 1997;**33**:1319-1313
- Maruyama Y,** Hanai H, Fujita M, Kaneko E. Telomere Length and Telomerase Activity in Carcinogenesis of the Stomach. *Jpn J Clin Oncol* 1997;**27**:216-220
- Hiyama E,** Yokoyama T, Tatsumoto N, Hiyama K, Imamura Y, Murakami Y, Kodama T, Piatyszek MA, Shay JW, Matsuura Y. Telomerase activity in gastric cancer. *Cancer Res* 1995;**55**:3258-3262
- He XX,** Wang JL, Wu JL, Yuan SY, Ai L. Telomere, cellular DNA content and gastric mucosal carcinogenesis. *Shijie Huaren Xiaohua Zazhi* 2000;**8**:509-512
- Zhang FX,** Zhang XY, Fan DM, Yan Y, Xu ZK. Telomerase activity in gastric cancer and precancerous. *Disi Junyi Daxue Xuebao* 1998;**19**:457-459
- Yang SM,** Fang DC, Luo YH, Wang ZH, Lu R, Liu WW. Telomerase Activity in Gastric Mucosa From Endoscopy. *Zhonghua Xiaohua Neijing Zazhi* 1997;**14**:298-300
- He XX,** Wang JL, Wu JL, Yuan SY, Ai L. Telomerase expression, Hp infection and gastric mucosal carcinogenesis. *Shijie Huaren Xiaohua Zazhi* 2000;**8**:505-508
- Naka K,** Yokozaki H, Yasui W, Tahara H, Tahara E, Tahara EC. Effect of Antisense Human Telomerase RNA Transfection on the Growth of Human Gastric Cancer Cell Lines. *Biochem Biophys Res Commun* 1999;**255**:753-758
- Zhang FX,** Deng ZY, Zhang XY, Dang SC, Wang Y, Yu XL, Wang H, Bian XH. Telomeric length associated with prognosis in human primary and metastatic gastric cancer. *Shijie Huaren Xiaohua Zazhi* 2000;**8**:153-155
- Kuniyasu H,** Domen T, Hamamoto T, Yokozaki H, Yasui W, Tahara H, Tahara E. Expression of human telomerase RNA is an early event of stomach carcinogenesis. *Jpn J Cancer Res* 1997;**88**:103-107
- Jong HS,** Park YI, Kim S, Sohn JH, Bang YJ, Kim NK. Up-Regulation of Human Telomerase Catalytic Subunit during Gastric Carcinogenesis. *Cancer* 1999;**86**:559-565
- Yasui W,** Tahara E, Tahara H, Fujimoto J, Naka K, Nakayama J, Ishikawa F, Ide T, Tahara E. Immunohistochemical Detection of Human Telomerase Reverse Transcriptase in Normal Mucosa and Precancerous Lesions of the Stomach. *Jpn J Cancer Res* 1999;**90**:589-595
- Yang SM,** Fang DC, Luo YH, Lu R, Liu WW. Effect of antisense gene to human telomerase reverse transcriptase on telomerase activity and expression of apoptosis-associated gene. *Shijie Huaren Xiaohua Zazhi* 2002;**10**:149-152
- Wang W,** Luo HS, Yu BP. Expression of human telomerase reverse transcriptase gene and c-myc protein in gastric carcinogenesis. *Shijie Huaren Xiaohua Zazhi* 2002;**10**:258-261
- Chiu CP,** Dragowska W, Kim NW, Vaziri H, Yui J, Thomas TE, Harley CB and Lansdrop PM. Differential Expression of Telomerase Activity in Hematopoietic Progenitors from Adult Human Bone Marrow. *Stem Cell* 1996;**14**:239-248
- Nakamura TM,** Morin GB, Chapman KB, Weinrich SL, Andrews WH, Lingner J, Harley B, Cech TR. Telomerase catalytic subunit homologs from fission yeast and human. *Science* 1997;**277**:955-959
- Luo F,** Sun JL, Ren DM, Cai D, Shen M. Effect of hyperthermia on telomerase activity and genes expression in human gastric cancer cell line. *Shijie Huaren Xiaohua Zazhi* 2001;**9**:1261-1264
- Yao XX,** Yin L, Zhang JY, Bai WY, Li YM, Sun ZC. hTERT expression and cellular immunity in gastric cancer and precancerous. *Shijie Huaren Xiaohua Zazhi* 2001;**9**:508-512
- Meng ZQ,** Guo WJ, Yu EX, Song MZ, Huang WX. Inhibition of telomerase activity and induced apoptosis of liver cancer cell SMMC-7721 by drug serum of Jianpi Liqi herbs. *Shijie Huaren Xiaohua Zazhi* 2000;**8**:879-882
- Suda T,** Isokawa O, Aoyagi Y, Nomoto M, Tsukada K, Shimizu T, Suzuki Y, Naito A, Igarashi H, Yanagi M, Takahashi T and Asakura H. Quantitation of Telomerase Activity in Hepatocellular Carcinoma: A Possible Aid for a Prediction of Recurrent Diseases in the Remnant Liver. *Hepatology* 1998;**27**:402-406
- Fang XM,** Yu JP, Luo HS. Relationship between hTERT

- and P16 gene expressions and telomerase activity in colorectal cancer. *Shijie Huaren Xiaohua Zazhi* 2002;**10**:12-14
- 38 **Shen ZY**, Xu LY, Li EM, Cai WJ, Chen MH, Shen J, Zeng Y. Telomere and telomerase in the initial stage of immortalization of esophageal epithelial cell. *World J Gastroenterol* 2002;**8**:357-362
- 39 **Feng RH**, Li JF, Liu BY, Zhu ZG, Yin HR. hTR gene cloning from human gastric cancer cells and the construction of its sense and antisense eukaryotic expression vector. *Shijie Huaren Xiaohua Zazhi* 2001;**9**:1409-1414
- 40 **Nakashio K**, Kitamoto M, Tahara H, Nakanishi T, IDE T, Kajiyama G. Significance of telomerase activity in the diagnosis of small differentiated hepatocellular carcinoma. *Int J Cancer* 1997;**74**:141-147
- 41 **Yang JL**, Fang DC, Yang SM, Luo YH, Lu R, Luo KL, Liu WW. Construction of sense and antisense hTR eukaryotic expression vector. *Shijie Huaren Xiaohua Zazhi* 2000;**8**:491-493
- 42 **Xin Y**, Zhao FK, Zhang SM, Wu DY, Wang YP, Xu L. Relationship between CD44v6 expression and prognosis in gastric carcinoma patients. *Shijie Huaren Xiaohua Zazhi* 1999;**7**:210-214
- 43 **Chen ZF**, Deng CS, Xia B, Zhu YQ, Zeng J, Gong LL. Expression of heat shock protein 60, CD44 splice variant V6 in human gastric cancer. *Shijie Huaren Xiaohua Zazhi* 2001;**9**:988-991
- 44 **Morgner A**, Miehle S, Stolte M, Neubauer A, Alpen B, Thiede C, Klann H, Hierlmeier FX, Ell C, Ehninger G, Bayerdiffer E. Development of early gastric cancer 4 and 5 years after complete remission of Helicobacter pylori associated gastric low grade marginal zone B cell lymphoma of MALT type. *World J Gastroenterol* 2001;**7**:248-253
- 45 **Nagashima S**, Kashii Y, Torsten E, Reichert, Yoshinori Suminami, Tadamichi Suzuki and Thereasa L. Whiteside. Human Gastric Carcinoma Transduced with the IL-2 Gene Increased Sensitivity to Immune Effector Cells *In Vitro* and *In Vivo*. *Int J Cancer* 1997;**72**:174-183
- 46 **Kume T**, Oshima K, Yamashita Y, Shirakusa T, Kikuchi M. Relationship between Fas-ligand expression on carcinoma cell and cytotoxic T-lymphocyte response in lymphoepithelioma-like cancer of the stomach. *Int J Cancer* 1999;**84**:339-343
- 47 **Zhong LM**, Li JY, Xiao GX, Chen DD. The relationship between lymphocyte immune function and lipid peroxidative injury in gastric cancer patients. *Chin J Gen Surg* 2000;**15**:361-363
- 48 **Bai DJ**, Yang GL, Yuan HY, Li Y, Wang K. Effects of cimetidine on T lymphocyte subsets in perioperative gastrointestinal cancer patients. *Shijie Huaren Xiaohua Zazhi* 2000;**8**:147-149
- 49 **Zhang H**, Ren XL, Yao XX. T lymphocyte subsets, nitric oxide, hexosamine and Helicobacter pylori infection in patients with chronic gastric diseases. *Shijie Huaren Xiaohua Zazhi* 1999;**7**:127-129
- 50 **Nie ZH**, Zhu Y, Zhang M, Feng FB, Chen Y, Wang BZ, Geng YL, Chen XZ. Relationship of T lymphocyte subsets in peripheral blood with gastric mucosal active inflammation, Gas and SS contents in patients with duodenal ulcer. *Shijie Huaren Xiaohua Zazhi* 1999;**7**:338-340
- 51 **Ishigami S**, Natsugoe S, Tokuda K, Nakajo A, Che X, Iwashige H, Aridome K, Holita S, Aikou T. Prognostic Value of Intratumoral Natural Killer Cells in Gastric Carcinoma. *Cancer* 2000;**88**:577-583
- 52 **Zhou YM**, Lan ZF, Zhao JC. Detection of Cell-Mediated Immunity of Patients with Chronic Atrophic Gastritis Patients and Gastric Cancer Patients. *Zhongliu Fangzhi Yanjiu* 1999;**26**:104-105
- 53 **Adachi T**, Hinoda Y, Nishimori I, Adachi M, Imai K. Increased Sensitivity of Gastric Cancer Cells to Natural Killer and Lymphokine-Activated killer Cells by Antisense Suppression of N-Acetylgalactosaminyltransferase. *J Immunol* 1997;**159**:2645-2646
- 54 **Mi JQ**, Zhang ZH and Shen MC. Significance of CD44v6 protein expression in gastric carcinoma and precancerous lesions. *Shijie Huaren Xiaohua Zazhi* 2000;**8**:156-158

Edited by Pagliarini R

• GASTRIC CANCER •

Relationship between the expression of iNOS, VEGF, tumor angiogenesis and gastric cancer

Zheng-Jun Song, Ping Gong, Yu-E Wu

Zheng-Jun Song, Ping Gong, Yu-E Wu, Department of Gastroenterology, First Affiliated Hospital of Xi'an Jiaotong University, Xi'an 710061, Shaanxi Province, China

Correspondence to: Dr. Zheng-Jun Song, Department of Gastroenterology, First Affiliated Hospital of Xi'an Jiaotong University, Xi'an 710061, Shaanxi Province, China. gongp828@sohu.com

Telephone: 029-3077073

Received 2002-01-11 **Accepted** 2002-02-07

Abstract

AIM: To investigate the relationship between the expression of inducible nitric oxide synthase (iNOS), vascular endothelial growth factor (VEGF), the microvascular density (MVD) and the pathological features and clinical staging of gastric cancer.

METHODS: Immunohistochemical staining was used for detecting the expression of iNOS and VEGF in 46 resected specimens of gastric carcinoma; the monoclonal antibody against CD34 was used for displaying vascular endothelial cells, and MVD was detected by counting of CD34-positive vascular endothelial cells.

RESULTS: Of 46 resected specimens of gastric carcinoma, the rates of expressions of iNOS and VEGF were 58.70% and 76.09%, respectively, and MVD averaged 55.59 ± 19.39 . Judged by the standard TNM criteria, the rate of expression of iNOS in stage IV (84.46%) was higher than those in stage I, II, III (Fish exact probabilities test, $P=0.019, 0.023$ and 0.033 , respectively); the rates of expression of VEGF in stage III, IV (76.0%, 92.31%, respectively) were higher than those in stage I, II (Fish exact probabilities test, $P=0.031, 0.017, 0.022$ and 0.019). MVDs in stage III, IV ($64.72 \pm 14.96, 67.09 \pm 18.29$, respectively) were higher than those in stage I, II ($t=2.378, 4.015, 2.503$ and $2.450, P<0.05, P<0.001, P<0.001, P<0.05$, respectively). In 37 gastric carcinoma specimens with lymph node metastasis, MVD (68.69 ± 18.07) and the rates of expression of iNOS and VEGF (70.27%, 83.78%, respectively) were higher than those in the specimens with absence of metastasis ($t=2.205, c^2=6.3587, c^2=6.2584, P<0.01, P<0.05, P<0.05$, respectively). MVD and the expressions of iNOS and VEGF were not correlated to the location, size or grade of tumor, nor with the depth of invasion of tumor; MVDs in the positive iNOS and VEGF specimens ($59.88 \pm 18.02, 58.39 \pm 17.73$, respectively) were higher than those in the negative iNOS and VEGF specimens ($c^2=6.3587$ and $6.1574, P<0.05, P<0.05$, respectively); thus the expressions of iNOS and VEGF was correlated to MVD, but the expression of iNOS was not correlated to that of VEGF. In addition, of the 46 surviving patients, the 5-year survival rate of patients with positive iNOS or VEGF tumors was significantly less than that of patients with negative iNOS- or VEGF tumors ($c^2=4.3842$ and $5.4073, P<0.05, P<0.05$, respectively).

CONCLUSION: The expressions of iNOS and VEGF are closely related to tumor angiogenesis, and are involved in the advancement and the lymph node metastasis; thus MVD and the expressions of iNOS and VEGF may serve indexes for evaluating staging of gastric carcinoma and forecasting its risk of metastasis, which will help establish a comprehensive therapeutical measure of post-operative patients and provide a new approach to tumor therapy.

Song ZJ, Gong P, Wu YE. Relationship between the expression of iNOS, VEGF, tumor angiogenesis and gastric cancer. *World J Gastroenterol* 2002;8(4):591-595

INTRODUCTION

Gastric carcinoma, as one of the most common human malignant tumor, ranks worldwide as the first leading cause of gastrointestinal cancer-related mortality. In China, it now ranks the second. It had been shown that tumor angiogenesis played an important role in its growth, invasion, metastasis and recurrence^[1-9]. We studied the relationship between the expression of iNOS, VEGF, MVD and the pathological features, lymph node metastasis and clinical staging of gastric carcinoma, and evaluated the relationship between tumor angiogenesis and the expression of iNOS, VEGF as well as the relationship between tumor angiogenesis and the advancement and the metastasis of gastric cancer using immunohistochemical staining method in order to reveal the biological features of iNOS and VEGF, which will contribute to further understanding of oncogenesis and provide a new approach to tumor therapy.

MATERIALS AND METHODS

Materials

The resected specimens from 46 cases of gastric cancer confirmed pathologically were obtained from our hospital from January 1999 to October 2000. Of these, 35 patients were male, and 11 female, with a mean age of 56.96 ± 11.26 (32 to 78). All of them had not received any radiotherapy or chemotherapy. Among these specimens, 8 were situated in the upper third of the stomach, 13 in the middle third, and 25 in the lower third. Histologically, they were classified by the WHO criteria, 5 were highly differentiated adenocarcinoma, 10 moderately-differentiated, 28 poorly-differentiated, 2 undifferentiated, and 1 was gastric mucous adenocarcinoma. As regards to the size of cancer, 2 were <3 cm, 18.3-5 cm, 26 >5 cm. 34 tumors invaded to the serosa and 12 tumors did not. By TNM staging of UICC, 2 cases were in stage I, 6 in stage II, 25 in stage III, and 13 in stage IV. Only 37 cases had local lymph node metastasis.

Reagents and methods

Antibody against iNOS was purchased from Wu Han Boster Co. Ltd; antibodies against VEGF and CD34 and ready-to-use

SP immunohistochemical reagent box were purchased from FuJian Maxin Co. Ltd. Formalin-fixed, paraffin-embedded surgical specimens from 46 cases of gastric carcinoma were available and sliced sequentially with a thickness of 4 μm . The slices carrying the detected antigen were dyed with SP immunohistochemical staining method, and those in the control group were dyed according to the above method, with the first antibody substituted by PBS.

Statistical methods

The data were presented as $\bar{x} \pm s$; numerical variable by the chi-square test; enumeration data by t test; the differences of these groups were compared by analysis of variance.

RESULTS

The cytoplasm of the gastric cancer cells staining brown granules were identified to be positive iNOS or VEGF, and the slices were graded respectively according to the density and the percentage of positively stained gastric carcinoma cells into score 0,1,2 or 3. If the sum of two scores was 0-2, the slice would be considered as the negative iNOS or VEGF; whereas 3-6, it would be considered as positive iNOS or VEGF. When the cytoplasm of theirs stained brown or brownish yellow, vascular endothelial cells were CD34- positive; the microvessels were counted according to the number of single endothelial cell or endothelial cell cluster showing brownish yellow granules in the cytoplasm. The slices were observed first microscopically under the low power ($\times 40$), then selected the most dense area of microvessel under the high power ($\times 200$, the surface area of every vision field being 0.785 mm^2), and the number of microvessel in 3 vision fields were counted and took the average as MVD of this specimen^[10].

The relationship between the expressions of iNOS and VEGF, MVD and pathological features of gastric carcinoma

The positive iNOS and VEGF stained were located at brownish yellow stained granules in the cytoplasm. The positive expression rate of iNOS was 58.7% (27/46) and that of VEGF was 76.09% (35/46). In addition, the positive expression of CD34 was mainly presented at brownish yellow or brownish granules in the cytoplasm of vascular endothelial cell. In all cases, MVD was 20.7 to 81.7 per vision field of high power with an average of 55.59 ± 19.39 .

As shown in Table 1, MVD and the rate of expression of iNOS in gastric carcinoma tissue had no significant differences among the site, the size, the degree of differentiation and the depth of invasion of gastric cancer. MVD and the rate of expression of iNOS in cases having lymph node metastasis was significantly higher than those having no lymph node metastasis ($t=2.205$, $\chi^2=6.3587$, $P<0.05$, $P<0.05$, respectively). The rate of expression of VEGF in the gastric carcinoma tissue also had no significant differences among the site, the size, the degree of differentiation of gastric cancer. The rate of expression of VEGF in the gastric carcinomas invading serosa was higher than that failed to invade serosa ($\chi^2=6.2584$, $P<0.05$). Likewise, the rate of expression of VEGF in cases having lymph node metastasis was significantly higher than cases having no lymph node metastasis ($\chi^2=6.1574$, $P<0.05$).

The relationship between the expression of iNOS, VEGF, MVD and TNM staging of gastric carcinoma

As shown in Table 2, the rates of expression of iNOS, VEGF, MVD, the tumor angiogenesis were all related to the clinical staging of gastric carcinoma, and increased with the progression of disease.

Table 1 The relationship between the expressions of iNOS and VEGF, MVD and pathological features of gastric carcinoma

Pathological characteristics	MVD ($\bar{x} \pm s$)	positive iNOS (%)	positive VEGF (%)	total
Site of gastric cancer lesion				
Upper one third	61.50 ± 14.50	5(62.50)	4(50.0)	8
Middle one third	59.82 ± 16.54	8(61.54)	10(76.92)	13
Lower one third	54.52 ± 20.01	14(56.00)	21(84.0)	25
Size of tumor				
< 3 cm	61.50 ± 20.51	1(50.0)	2(100.0)	2
3~5cm	59.78 ± 16.58	11(61.11)	14(77.78)	18
> 5cm	54.86 ± 17.99	15(57.69)	19(73.08)	26
Depth of invasion				
Invading serosa	62.35 ± 32.97	22(64.71)	29(85.29) ^c	34
Not invading serosa	55.15 ± 18.28	5(41.67)	6(50.0)	12
Metastasis of lymph nodes				
Positive	68.69 ± 18.07^a	26(70.27) ^b	31(83.78) ^d	37
Negative	54.40 ± 14.23	3(33.33)	4(44.44)	9
Degree of differentiation*				
Well differentiated	49.49 ± 20.10	10(66.67)	11(73.33)	15
Poorly differentiated	59.24 ± 16.80	17(54.84)	24(77.42)	31

Note: *Well differentiated cancer cells include highly and moderately differentiated ones; poorly differentiated cancer cells include poorly differentiated and undifferentiated ones and mucous adenocarcinoma. ^a $P<0.01$ ($t=2.205$), vs MVD in cases having no lymph node metastasis; ^b $P<0.05$ ($\chi^2=6.3587$), vs the rate of expression of iNOS in cases having no lymph node metastasis; ^c $P<0.05$ ($\chi^2=6.2584$), vs the rate of expression of VEGF in gastric carcinomas not invading to serosa; ^d $P<0.05$ ($\chi^2=6.1574$), vs the rate of expression of VEGF in cases having no lymph node metastasis.

Table 2 The relationship between the expression of iNOS, VEGF, MVD and TNM staging of gastric carcinoma

Clinical staging	<i>n</i>	Expression of iNOS (%)	Expression of VEGF (%)	MVD ($\bar{x} \pm s$)
Stage I	2	1(50.0)	1(50.0)	51.00 ± 7.0^d
Stage II	6	2(33.33)	3(50.0)	47.66 ± 8.71^e
Stage III	25	13(52.0)	19(76.0) ^b	64.72 ± 14.96^f
Stage IV	13	11(84.62) ^a	12(92.31) ^c	76.09 ± 18.29^g

^a $P<0.05$, (Fish exact probabilities test, $P=0.019$, 0.023 and 0.033), vs the rate of expression of iNOS in stage I, II and III, respectively; ^b $P<0.05$ (Fish exact probabilities test, $P=0.031$ and 0.017), vs the rates of expression of VEGF in stage I and II, respectively; ^c $P<0.05$ (Fish exact probabilities test, $P=0.022$ and 0.019), vs the rates of expression of VEGF in stage I and II, respectively; ^d $P<0.05$ ($t=2.378$, vs MVD in stage III; $P<0.001$ ($t=4.015$), vs MVD in stage IV; $P<0.001$ ($t=2.503$), vs MVD in stage I; ^e $P<0.05$ ($t=2.450$), vs MVD in stage I.

The relationship between MVD and the rates of expression of iNOS and VEGF

The above results show that MVD (59.88 ± 18.02) in the iNOS-

positive gastric tissue was higher than that (49.64 ± 12.06) in the iNOS-negative one ($t=3.980, P<0.05$); and MVD (58.39 ± 17.73) in the VEGF-positive gastric tissue was higher than that (45.43 ± 18.21) in the VEGF-negative one ($t=4.098, P<0.05$), suggesting that the expressions of iNOS and VEGF were related to MVD and tumor angiogenesis.

The relationship between the expressions of iNOS and VEGF and the prognosis of gastric carcinoma

As shown in Table 3, among 46 patients, the 5-year survival rate of the patients with iNOS- or VEGF-positive tumors was significantly less than that of the patients with iNOS- or VEGF-negative tumors ($\chi^2=4.3842$ and $5.4073, P<0.05, P<0.05$, respectively).

Table 3 The relationship between the expressions of iNOS and VEGF and the prognosis of gastric carcinoma

	n	survival period		rate of five-year survival
		< 5 years	> 5 years	(%)
iNOS expression				
Positive	27	22	5	18.52 ^a
Negative	19	10	9	47.37
VEGF expression				
Positive	35	30	5	14.29 ^b
Negative	11	5	6	54.55

^a $P<0.05, (\chi^2=4.3842)$, vs the iNOS-negative gastric cancer patients;

^b $P<0.05, (\chi^2=5.4073)$, vs the VEGF-negative gastric cancer patients.

DISCUSSION

MVD is related to the increase of the risk of metastasis and/or the decrease of survival period of gastric carcinoma patients^[11], and being a reliable index of tumor angiogenesis^[12]. In the present study, we labeled the vascular endothelial cells with monoclonal antibody against CD34 and detected MVD in all specimens by immunohistochemical staining method, and finally found MVD averaging 55.59 ± 19.39 per vision field of high power, indicating active tumor angiogenesis. In addition, MVD in the specimens having lymph node metastasis was significantly higher than that having no metastasis, suggesting that increase of MVD and tumor angiogenesis in gastric carcinomas might result in cancer cells entering into the blood circulation, and the lymph node metastasis could be promoted when the gastric cancer cells invade lymphatic vessels. In 46 resected gastric cancer specimens, MVDs in stage III and IV were significantly higher than those in stage I and II ($t=2.378, 4.015, 2.503$ and $2.450, P<0.05, P<0.001, P<0.001, P<0.05$, respectively), indicating MVD was closely related to clinical staging of gastric carcinoma, and MVD and tumor angiogenesis increased with the invasion of gastric cancer. This result reveals MVD may reflect the advancement of gastric carcinoma and the extent of tumor angiogenesis and metastasis^[13], thus it can serve an important index forecasting the prognosis of gastric cancer^[5, 14].

It is shown that the expression of iNOS in most tumor tissue is higher than that in the normal one^[15]; Nitric oxide produced through iNOS induction may increase the vascular permeability and accelerate the nutrient supply of tumor tissue and finally promote the tumor growth^[16, 17]. In this study, we found that the rate of expression of iNOS of gastric carcinoma in stage IV

was higher than those in stage I, II and III (Fisher exact probabilities test, $P=0.019, 0.023$ and 0.033 , respectively), revealing the expression of iNOS of gastric cancer increased with staging of the cancer, and was higher in late stage^[18], the higher the expression of iNOS of gastric cancer, the more the advancement and the worse the prognosis^[19, 20]. We also found that the rate of expression of iNOS of gastric carcinoma in those having lymph node metastasis was higher than that having no metastasis ($\chi^2=6.3587, P<0.05$), suggesting the significant increase of its expression in the gastric cancer tissue can promote its lymph node metastasis.

VEGF plays an important role in each stage of tumor angiogenesis^[21, 22], and its over expression is closely related to clinical staging, lymph node metastasis and recurrence of gastric carcinoma^[23, 24]. In the present study, we found that the rate of expression of VEGF was related to the depth of invasion, it was higher in gastric cancers with the invasion of serosa than in gastric cancers without that ($\chi^2=6.2584, P<0.05$), indicating VEGF may contribute to the invasive growth of gastric carcinoma, and is relevant to the lymph node metastasis^[28]. These are corroborated in stage III or IV lesions. These results show the over expression of VEGF in the gastric cancer tissue has prognostic significance^[25-47].

VEGF produced by tumor cell can bind with the surface acceptor of vascular endothelial cell, and promote the production of nitric oxide that can transmit messages between the cells and induce tumor angiogenesis^[48, 49]. This study showed that the rates of expressions of iNOS and VEGF of gastric cancer were related to MVD ($t=3.980$ and $4.098, P<0.05, P<0.05$, respectively), indicating iNOS and VEGF were closely related to tumor angiogenesis^[50, 51], and might be important factors involved in gastric carcinoma angiogenesis. Moreover, iNOS and VEGF and their effects on angiogenesis can promote the lymph node metastasis and the prognosis, thus iNOS, VEGF and MVD may all serve important indexes reflecting the biological behaviors, advancement and prognosis of gastric carcinoma.

In conclusion, active angiogenesis exists in the gastric cancer tissue, and MVD is closely relevant to lymph node metastasis, clinical staging and advancement of gastric carcinoma and may act as a valuable index of gastric cancer prognosis; the rates of expressions of iNOS and VEGF in gastric carcinoma are higher than those in the normal gastric tissue, and are related to lymph node metastasis and clinical staging, suggesting they are involved in the advancement and metastasis of gastric cancer which are relevant to its prognosis^[52]; the rates of expressions of iNOS and VEGF in the gastric cancer tissue are closely related to MVD, and they may be important factors involved in gastric carcinoma angiogenesis, thus iNOS, VEGF and MVD can act as important indexes reflecting the biological behaviors, advancement and prognosis of gastric cancer. In addition, further study on the mechanism of their regulation will probably offer a new approach to anticancer treatment.

REFERENCES

- 1 Folkman J. What is the evidence that tumors are angiogenesis dependent? *J Natl Cancer Inst* 1990; **82**: 4-6
- 2 Tao H, Lin Y, Yin H. Prognostic value of tumor vascularity in gastric carcinoma. *Zhonghua Waike Zazhi* 1998; **36**: 307-309
- 3 Koga J, Kakeji Y, Sumiyoshi Y, Kimura Y, Shibahara K, Emi Y, Maehara Y, Sugimachi K. Angiogenesis and macrophage infiltration in Borrmann type IV gastric cancer. *Fukuoka Igaku Zasshi* 2001; **92**: 334-339
- 4 Che X, Hokita S, Natsugoe S, Tanabe G, Baba M, Takao S, Aikou T. Tumor angiogenesis related to growth pattern and lymph node metastasis in early gastric cancer. *Chin*

- Med J* 1998;**111**:1090-1093
- 5 **Erenoglu C**, Akin ML, Uluutku H, Tezcan L, Yildirim S, Batkin A, Erenoglu C, Akin ML, Uluutku H, Tezcan L, Yildirim S, Batkin A. Angiogenesis predicts poor prognosis in gastric carcinoma. *Dig Surg* 2000;**17**:581-586
 - 6 **Shimoyama S**, Kaminishi M. Increased angiogenin expression in gastric cancer correlated to cancer progression. *J Cancer Res Clin Oncol* 2000;**126**:468-474
 - 7 **Yoshikawa T**, Yanoma S, Tsuburaya A, Kobayashi O, Sairenji M, Motohashi H, Noguchi Y. Angiogenesis inhibitor, TNP-470, suppresses growth of peritoneal disseminating foci. *Hepatogastroenterology* 2000;**47**:298-302
 - 8 **Xiangming C**, Hokita S, Natsugoe S, Tanabe G, Baba M, Takao S, Kuroshima K, Aikou T. Angiogenesis as an unfavorable factor related to lymph node metastasis in early gastric cancer. *Ann Surg Oncol* 1998;**5**:585-589
 - 9 **Maehara Y**, Hasuda S, Abe T, Oki E, Kakeji Y, Ohno S, Sugimachi K. Tumor angiogenesis and micrometastasis in bone marrow of patients with early gastric cancer. *Clin Cancer Res* 1998;**4**:2129-2134
 - 10 **Weidner N**, Folkman J, Pozza F, Bevilacqua P, Allred EN, Moore DH, Meli S, Gasparini G. Tumor angiogenesis: a new significant and independent prognostic indicator in early state breast carcinoma. *J Natl Cancer Inst* 1992;**84**:1875-1887
 - 11 **Stakey JR**, Crowle PR, Taubenberger S. Mast-cell-deficient W/W^v mice exhibit a decreased rate of tumor angiogenesis. *Int J Cancer* 1988;**42**:48-52
 - 12 **Fukumura D**, Jain R K. Role of nitric oxide in angiogenesis and microcirculation in tumors. *Cancer Metastasis Rev* 1998;**17**:77-89
 - 13 **Zhang W**, Yang H, Han S. The effect of ectopic HCG on microvessel density in gastric carcinoma. *Zhonghua Zhongliu Zazhi* 1998;**20**:351-353
 - 14 **Araya M**, Terashima M, Takagane A, Abe K, Nishizuka S, Yonezawa H, Irinoda T, Nakaya T, Saito K. Microvessel count predicts metastasis and prognosis in patients with gastric cancer. *J Surg Oncol* 1997;**65**:232-236
 - 15 **Son HJ**, Kim YH, Park DI, Kim JJ, Rhee PL, Paik SW, Choi KW, Song SY, Rhee JC. Interaction between cyclooxygenase-2 and inducible nitric oxide synthase in gastric cancer. *J Clin Gastroenterol* 2001;**33**:383-388
 - 16 **Maeda H**, Akaike Y. Nitric oxide and oxygen radical in infection, inflammation and cancer. *Biochemistry* 1998;**63**:854-856
 - 17 **Nicotera P**, Bonfoco E, Brune B. Mechanisms for nitric oxide-induced cell death. *Adv Neuroimmunol* 1997;**5**:411-420
 - 18 **Rajnakova A**, Mochhala S, Goh PM, Ngoi S. Expression of nitric oxide synthase, cyclooxygenase, and p53 in different stages of human gastric cancer. *Cancer Lett* 2001;**172**:177-185
 - 19 **Koh E**, Noh SH, Lee YD, Lee HY, Han JW, Lee HW, Hong S. Differential expression of nitric oxide synthase in human stomach cancer. *Cancer Lett* 1999;**146**:173-180
 - 20 **Doi C**, Noguchi Y, Marat D, Saito A, Fukuzawa K, Yoshikawa T, Tsuburaya A, Ito T. Expression of nitric oxide synthase in gastric cancer. *Cancer Lett* 1999;**144**:161-167
 - 21 **Folkman J**. Tumor angiogenesis: Therapeutic implication. *N Eng J Med* 1971;**285**:1182-1186
 - 22 **Liu DH**, Zhang XY, Fan DM, Huang YX, Zhang JS, Huang WQ, Zhang YQ, Huang QS, Ma WY, Chai YB, Jin M. Expression of vascular endothelial growth factor and its role in oncogenesis of human gastric carcinoma. *World J Gastroenterol* 2001;**7**:500-505
 - 23 **Tao HQ**, Lin YZ, Wang RN. Significance of vascular endothelial growth factor messenger RNA expression in gastric cancer. *World J Gastroenterol* 1998;**4**:10-13
 - 24 **Konno H**, Baba M, Tanaka T, Kamiya K, Ota M, Oba K, Shoji A, Kaneko T, Nakamura S. Overexpression of vascular endothelial growth factor is responsible for the hematogenous recurrence of early-stage gastric carcinoma. *Eur Surg Res* 2000;**32**:177-181
 - 25 **Ichikura T**, Tomimatsu S, Ohkura E, Mochizuki H. Prognostic significance of expression of vascular endothelial growth factor (VEGF) and VEGF-C in gastric carcinoma. *J Surg Oncol* 2001;**78**:132-137
 - 26 **Kido S**, Kitadai Y, Hattori N, Haruma K, Kido T, Ohta M, Tanaka S, Yoshihara M, Sumii K, Ohmoto Y, Chayama K. Interleukin 8 and vascular endothelial growth factor: prognostic factors in human gastric carcinomas? *Eur J Cancer* 2001;**37**:1482-1487
 - 27 **Lisconi P**, Malugani F, Bonfanti A, Bucovec R, Secondino S, Brivio F, Ferrari-Bravo A, Ferrante R, Vigore L, Rovelli F, Mandala M, Viviani S, Fumagalli L, Gardani GS. Abnormally enhanced blood concentrations of vascular endothelial growth factor (VEGF) in metastatic cancer patients and their relation to circulating dendritic cells, IL-12 and endothelin-1. *J Biol Regul Homeost Agents* 2001;**15**:140-144
 - 28 **Yonemura Y**, Fushida S, Bando E, Kinoshita K, Miwa K, Endo Y, Sugiyama K, Partanen T, Yamamoto H, Sasaki T. Lymphangiogenesis and the vascular endothelial growth factor receptor (VEGFR)-3 in gastric cancer. *Eur J Cancer* 2001;**37**:918-923
 - 29 **Lu M**, Jiang Y, Wang R. The relationship of vascular endothelial growth factor and angiogenesis to the progression of gastric carcinoma. *Zhonghua Binglixue Zazhi* 1998;**27**:278-281
 - 30 **Kabashima A**, Maehara Y, Kakeji Y, Sugimachi K. Overexpression of vascular endothelial growth factor C is related to lymphogenous metastasis in early gastric carcinoma. *Oncology* 2001;**60**:146-150
 - 31 **Kimura H**, Konishi K, Nukui T, Kaji M, Maeda K, Yabushita K, Tsuji M, Miwa A. Prognostic significance of expression of thymidine phosphorylase and vascular endothelial growth factor in human gastric carcinoma. *J Surg Oncol* 2001;**76**:31-36
 - 32 **Maehara Y**, Kabashima A, Koga T, Tokunaga E, Takeuchi H, Kakeji Y, Sugimachi K. Vascular invasion and potential for tumor angiogenesis and metastasis in gastric carcinoma. *Surgery* 2000;**128**:408-416
 - 33 **Konno H**, Baba M, Tanaka T, Kamiya K, Ota M, Oba K, Shoji A, Kaneko T, Nakamura S. Overexpression of vascular endothelial growth factor is responsible for the hematogenous recurrence of early-stage gastric carcinoma. *Eur Surg Res* 2000;**32**:177-181
 - 34 **Mori A**, Arii S, Furutani M, Mizumoto M, Uchida S, Furuyama H, Kondo Y, Gorrin-Rivas MJ, Furumoto K, Kaneda Y, Imamura M. Soluble Flt-1 gene therapy for peritoneal metastases using HVJ-cationic liposomes. *Gene Ther* 2000;**7**:1027-1033
 - 35 **Sakatani T**, Okamoto E, Tsujitani S, Ikeguchi M, Kaibara N, Ito H. Expressions of thymidine phosphorylase (dThdPase) and vascular endothelial growth factor on angiogenesis in intestinal-type gastric carcinoma. *Oncol Rep* 2000;**7**:831-836
 - 36 **Yoshikawa T**, Tsuburaya A, Kobayashi O, Sairenji M, Motohashi H, Yanoma S, Noguchi Y. Plasma concentrations of VEGF and bFGF in patients with gastric carcinoma. *Cancer Lett* 2000;**153**:7-12
 - 37 **Maeda K**, Kang SM, Onoda N, Ogawa M, Kato Y, Sawada T, Chung KH. Vascular endothelial growth factor expression in preoperative biopsy specimens correlates with disease recurrence in patients with early gastric carcinoma. *Cancer* 1999;**86**:566-571
 - 38 **Yonemura Y**, Endo Y, Fujita H, Fushida S, Ninomiya I, Bandou E, Taniguchi K, Miwa K, Ohoyama S, Sugiyama K, Sasaki T. Role of vascular endothelial growth factor C expression in the development of lymph node metastasis in gastric cancer. *Clin Cancer Res* 1999;**5**:1823-1829
 - 39 **Kimura H**, Konishi K, Kaji M, Maeda K, Yabushita K, Tsuji M, Miwa A. Highly aggressive behavior and poor prognosis of small cell carcinoma in the stomach: flow cytometric and immunohistochemical analysis. *Oncol Rep* 1999;**6**:767-772
 - 40 **Tomoda M**, Maehara Y, Kakeji Y, Ohno S, Ichiyoshi Y, Sugimachi K. Intratumoral neovascularization and growth

- pattern in early gastric carcinoma. *Cancer* 1999;**85**:2340-2346
- 41 **Hyodo I**, Doi T, Endo H, Hosokawa Y, Nishikawa Y, Tanimizu M, Jinno K, Kotani Y. Clinical significance of plasma vascular endothelial growth factor in gastrointestinal cancer. *Eur J Cancer* 1998;**34**:2041-2045
 - 42 **Maeda K**, Kang SM, Onoda N, Ogawa M, Sawada T, Nakata B, Kato Y, Chung YS, Sowa M. Expression of p53 and vascular endothelial growth factor associated with tumor angiogenesis and prognosis in gastric cancer. *Oncology* 1998;**55**:594-599
 - 43 **Saito H**, Tsujitani S, Kondo A, Ikeguchi M, Maeta M, Kaibara N. Expression of vascular endothelial growth factor correlates with hematogenous recurrence in gastric carcinoma. *Surgery* 1999;**125**:195-201
 - 44 **Kraft A**, Weindel K, Ochs A, Marth C, Zmija J, Schumacher P, Unger C, Marne D, Gastl G. Vascular endothelial growth factor in the sera and effusions of patients with malignant and nonmalignant disease. *Cancer* 1999;**85**:178-187
 - 45 **Maeda K**, Kang SM, Ogawa M, Onoda N, Sawada T, Nakata B, Kato Y, Chung YS, Sowa M. Combined analysis of vascular endothelial growth factor and platelet-derived endothelial cell growth factor expression in gastric carcinoma. *Int J Cancer* 1997;**74**:545-550
 - 46 **Takita M**, Onda M, Tokunaga A. Immunohistochemical demonstration of angiogenic growth factors and EGF receptor in hepatic metastases and primary human gastric cancer. *Nippon Ika Daigaku Zasshi* 1998;**65**:358-366
 - 47 **Kabashima A**, Maehara Y, Kakeji Y, Sugimachi K. Overexpression of vascular endothelial growth factor C is related to lymphogenous metastasis in early gastric carcinoma. *Oncology* 2001;**60**:146-150
 - 48 **Ziche M**, Morbidelli L, Choudhuri R, Zhang HT, Donnini S, Granger HJ, Bicknell R. Nitric oxide synthase lies downstream from vascular endothelial growth factor-induced but not basic fibroblast growth factor-induced angiogenesis. *J Clin Invest* 1997;**99**:2625-2634
 - 49 **Takahashi Y**, Cleary KR, Mai M, Kitadai Y, Bucana CD, Ellis LM, Takahashi Y, Cleary KR, Mai M, Kitadai Y, Bucana CD, Ellis LM. Significance of lessel and Vascular endothelial growth factor and its receptor cdk7 in intestinal tpe gastril cancer. *Cancer Res* 1996;**2**:1679-1684
 - 50 **Yamamoto S**, Yasui W, Kitadai Y, Yokozaki H, Haruma K, Kajiyama G, Tahara E. Expression of vascular endothelial growth factor in human gastric carcinomas. *Pathol Int* 1998;**48**:499-506
 - 51 **Takahashi Y**, Ellis LM, Ohta T, Mai M. Angiogenesis in poorly differentiated medullary carcinoma of the stomach. *Surg Today* 1998;**28**:367-372
 - 52 **Maeda K**, Kang SM, Onoda N, Ogawa M, Kato Y, Sawada T, Chung KH. Vascular endothelial growth factor expression in preoperative biopsy specimens correlates with disease recurrence in patients with early gastric carcinoma. *Cancer* 1999;**86**:566-571

Edited by Wu XN

• GASTRIC CANCER •

The role of KDR in the interactions between human gastric carcinoma cell and vascular endothelial cell

Juan Ren, Lei Dong, Cang-Bao Xu, Bo-Rong Pan

Juan Ren, Department of Oncological Radiotherapy, First Hospital of Xi'an Jiaotong University, Xi'an 710061, Shaanxi Province, China
Lei Dong, Department of Gastroenterology, Second Hospital of Xi'an Jiaotong University, Xi'an 710004, Shaanxi Province, China
Cang-Bao Xu, Department of Pathophysiology, Lund University, Sweden

Bo-Rong Pan, Oncology Center, Xijing Hospital, Fourth Military Medical University, Xi'an 710032, Shaanxi Province, China

Correspondence to: Dr. Juan Ren, Department of Oncological Radiotherapy, First Hospital, Xi'an Jiaotong University Xi'an 710061, Shaanxi Province, China. renjuan88@163.net

Telephone: +86-29-3058229 **Fax:** +86-29-4333028

Received 2002-03-19 **Accepted** 2002-04-20

Abstract

AIM: To study the interactions between human gastric carcinoma cell (HGCC) and human vascular endothelial cell (HVEC), and the role of KDR in these interactions.

METHODS: Antisense oligodeoxynucleotide (ASODN) specific to KDR gene was devised and added to the culture medium of HGCC and HVEC. After the action of ASODN, the proliferation of two cells was measured by MTT method. The role of KDR in regulating the proliferation of two kinds of cells was known through observing the effect of ASODN on them. The conditioned mediums (CMs) of HGCC and HVEC were prepared. The CM of one kind of cell was added acting on the other kind of cell, then the cell proliferation was measured by MTT. After the action of ASODN or CM, the cellular expression of KDR gene was detected with *in situ* hybridization (ISH) for mRNA level and with immunohistochemical staining for protein level. ABC-ELISA was used to detect hVEGF in the CMs of two cells.

RESULTS: KDR ASODN could specifically inhibit the proliferation of HGCC and HVEC significantly. The growth inhibitory rate amounted to 55.35 % and 54.83 %, respectively ($P < 0.01$). HGCC and HVEC could secrete a certain level of hVEGF (92.06 ± 1.69 ng/L, 77.70 ± 8.04 ng/L). The CM of HGCC could significantly stimulate the growth (2.70 ± 0.01 times) and KDR gene expression of HVEC ($P < 0.01$) while the CM of HVEC could significantly inhibit the growth (52.97 ± 0.01 %) and KDR gene expression of HGCC ($P < 0.01$).

CONCLUSION: KDR plays a key role in regulating the proliferation of HGCC and HVEC. There exist complicated interactions between HGCC and HVEC. HGCC can significantly stimulate the growth of HVEC while HVEC can significantly inhibit the growth of HGCC. KDR is involved in the interactions between them.

Ren J, Dong L, Xu CB, Pan BR. The role of KDR in the interactions between human gastric carcinoma cell and vascular endothelial cell. *World J Gastroenterol* 2002; 8(4):596-601

INTRODUCTION

There exist many kinds of cells besides tumor cell in the solid neoplasm. The relations among all kinds of cells are very complicated. These cells depend on each other and contribute together to the genesis, development, invasion and metastasis of tumor. During the tumor angiogenesis and hematogenous metastasis, there exist complicated interactions between tumor cell (TC) and vascular endothelial cell (VEC). In the pre-angiogenesis, how does TC induce VEC to establish the tumor vascular system? How does TC influence the proliferation, degeneration, morphogenesis and functions of its neighbouring VEC? On the other hand, the interactions between the two cells play a role in the tumor hematogenous metastasis. There exist some complicated mechanisms in these processes. The study of tumor angiogenesis mainly focuses on the interactions among the vascular component cells while the study of tumor metastasis mainly focuses on the interactions between TC and its surrounding stroma. Seldom does anyone notice the interactions between TC and VEC. To better understand some mechanisms in gastric carcinoma angiogenesis and hematogenous metastases, we select human gastric carcinoma cell (HGCC) and human vascular endothelial cell (HVEC) to study their interrelations and some factors in these interactions^[1]. Conditioned mediums (CMs) of HGCC and HVEC were prepared. The CM of one kind of cell was added to the other kind of cell, then the cell proliferation was measured by MTT. Many studies have found that KDR, VEGF receptor 2, played an important role in regulating the biological functions of TC and VEC. In order to make clear the role of KDR in regulating the growth of HGCC and HVEC, antisense oligodeoxynucleotide (ASODN) specific to KDR mRNA was devised and was added acting on the two cells^[2,3]. There has been no one to devise KDR ASODN up to now. After the action of CM, the expression of KDR gene was detected. The purpose is to probe into the interactions between HGCC and HVEC and if KDR is involved in the interactions.

MATERIALS AND METHODS

Materials

Cell line HGCC line SGC7901 and HVEC line Eahy926 were employed. The expression of KDR on two cells was (++) .

KDR antisense oligodeoxynucleotide (ASODN) and the action of KDR ASODN ASODN, sense oligodeoxynucleotide (SODN) and mismatch oligodeoxynucleotide (MODN) specific to KDR mRNA were designed by the software "Primer 3". The sequence of ASODN was: 5' CAC CTT GCT CTG CAT CCT G 3', The sequence of SODN was 5' CAG GAT GCA GAG CAA GGT G 3', The sequence of MODN was 5' CAC TTT GAT CTA CAC CCT G 3'; The way of KDR ASODN action: cells were placed in serum free medium for growth arresting. At different periods, ASODN in different doses and culture medium with serum were added at the same time. After different periods: the proliferation of cell was measured by MTT. The cell without the action of ODN was taken as control.

Methods

Preparing CM, measuring activity of conditioned medium (CM) and measuring level of hVEGF

Cells in different confluent states were washed twice with PBS, then 3 mL culture medium was added to the cells. The medium what was taken as CM was collected after different periods. After the growth of HGCC and HVEC was arrested for 24 h and 6 h respectively, CM was added. The proliferation of cell was measured by MTT after different culturing periods. The cell without the action of CM was taken as control. The level of hVEGF in CMs of two cells was measured by ABC-ELISA kit(Jingmei, Beijing).

MTT (methyl tetrazolium colorimetry) 20 μ L MTT solution (5 g/L) was added to 200 μ L medium in each well of 96 well plate. 4 h later, the supernant was discarded, 150 μ L DMSO (Dimethylsulphoxide) was added. After the crystal was dissolved completely, absorption spectrum was measured at 490 nm in the enzyme linked immunosorbent assay meter. The inhibitory rate of cell proliferation = $[1 - (\text{the mean } A \text{ of experimental group} / \text{The mean } A \text{ of control group})] \times 100\%$

Detecting the expression of KDR gene After the action of KDR ASODN or the action of CM of one kind of cell on the other kind of cell, the expression of KDR gene was measured by *in situ* hybridization for KDR mRNA level and immunohistochemical staining for KDR protein level. Probe for KDR mRNA was designed by the software "Primer 3". The sequence is 5' GGT AGG AGA GGA TAT CCA GCC TG 3'; Probe labeling and *in situ* hybridization (ISH) were carried on according to the manuals of the Dig Oligodexynucleotide Tailing Kit and Dig Detection Kit (Boehringer Mannheim, Germany) respectively. PBS was substituted for anti-Dig-Ap as negative control. Immunohistochemical staining for KDR protein on the cells was carried on according to the manual of the SABC Kit (Huamei, Henang). KDR polyclonal antibody (Santa cruz, USA) was diluted 1:100. Secondary mouse-anti-rat antibody (Huamei, Henang) was diluted 1:25. PBS was substituted for primary antibody as negative control. The sections were analyzed for A value in the image analysis apparatus.

Statistical analysis

t test was used to compare the means.

RESULTS

Effects of KDR ASODN on the proliferation of HGCC and HVEC

KDR ASODN inhibited the proliferation of HGCC and HVEC significantly. It produced effects in 0.5-1 μ mol/L and 3-6 h later. The cell proliferation inhibitory rate could amount to more than 50 %. The inhibitory rate was related to the dose and action periods (Table 1, 2).

Difference between the effects of KDR ASODN and SODN, MODN on HGCC, HVEC

There existed significant difference between the effects of KDR ASODN and SODN, MODN on the proliferation of HGCC and HVEC (Table 3).

Effects of KDR ASODN on the expression of KDR gene in HGCC and HVEC

Through ISH for detecting KDR mRNA level and immunohistochemical staining for KDR protein level, it was found that KDR ASODN inhibited the expression of KDR gene in HGCC and HVEC significantly (Table 4) (Figure 1).

Table 1 Dose-effect of KDR ASODN on HGCC and HVEC for 48 h ($n=8$, $\bar{x} \pm s$)

KDR ASODN dose / (μ mol/L)	Inhibitory rate of cell proliferation(%)	
	HGCC	HVEC
0(control)	0	0
0.5	21.32 ^b	0
1	28.31 ^b	15.33 ^b
5	34.56 ^b	30.53 ^b
10	45.59 ^b	39.67 ^b
15	55.35 ^b	54.83 ^b
20	50.74 ^b	48.79 ^b

^b $P < 0.01$ vs control.

Table 2 Time-effect of 15 μ mol/L KDR ASODN on HGCC and HVEC ($n=8$, $\bar{x} \pm s$)

KDR ASODN action time/h	Inhibitory rate of cell proliferation(%)	
	HGCC	HVEC
0(control)	0	0
3	16.41 ^b	0
6	18.99 ^b	6.67 ^b
12	28.96 ^b	10.36 ^b
24	38.90 ^b	37.52 ^b
48	55.35 ^b	54.83 ^b
72	50.45 ^b	46.18 ^b

^b $P < 0.01$ vs control.

Table 3 Difference between the effects of KDR ASODN and SODN, MODN ($n=8$, $\bar{x} \pm s$)

Types of KDR ODN	Inhibitory rate of cell proliferation(%)	
	HGCC	HVEC
No ODN(control)	0	0
ASODN	45.07 ^b	31.18 ^b
SODN	3.15 ^d	2.61 ^d
MODN	2.88 ^d	2.02 ^d

^b $P < 0.01$, vs control. ^d $P < 0.01$, vs ASODN group.

Table 4 Expression of KDR mRNA and protein in HGCC and HVEC after the action of KDR ASODN ($n=8$, $\bar{x} \pm s$)

action of KDR ASODN	A of HGCC		A of HVEC	
	mRNA	protein	mRNA	protein
Before(control)	0.35 \pm 0.03	0.33 \pm 0.02	0.37 \pm 0.03	0.34 \pm 0.03
After	0.16 \pm 0.02 ^b	0.15 \pm 0.02 ^b	0.16 \pm 0.02 ^b	0.15 \pm 0.02 ^b

^b $P < 0.01$, vs control.

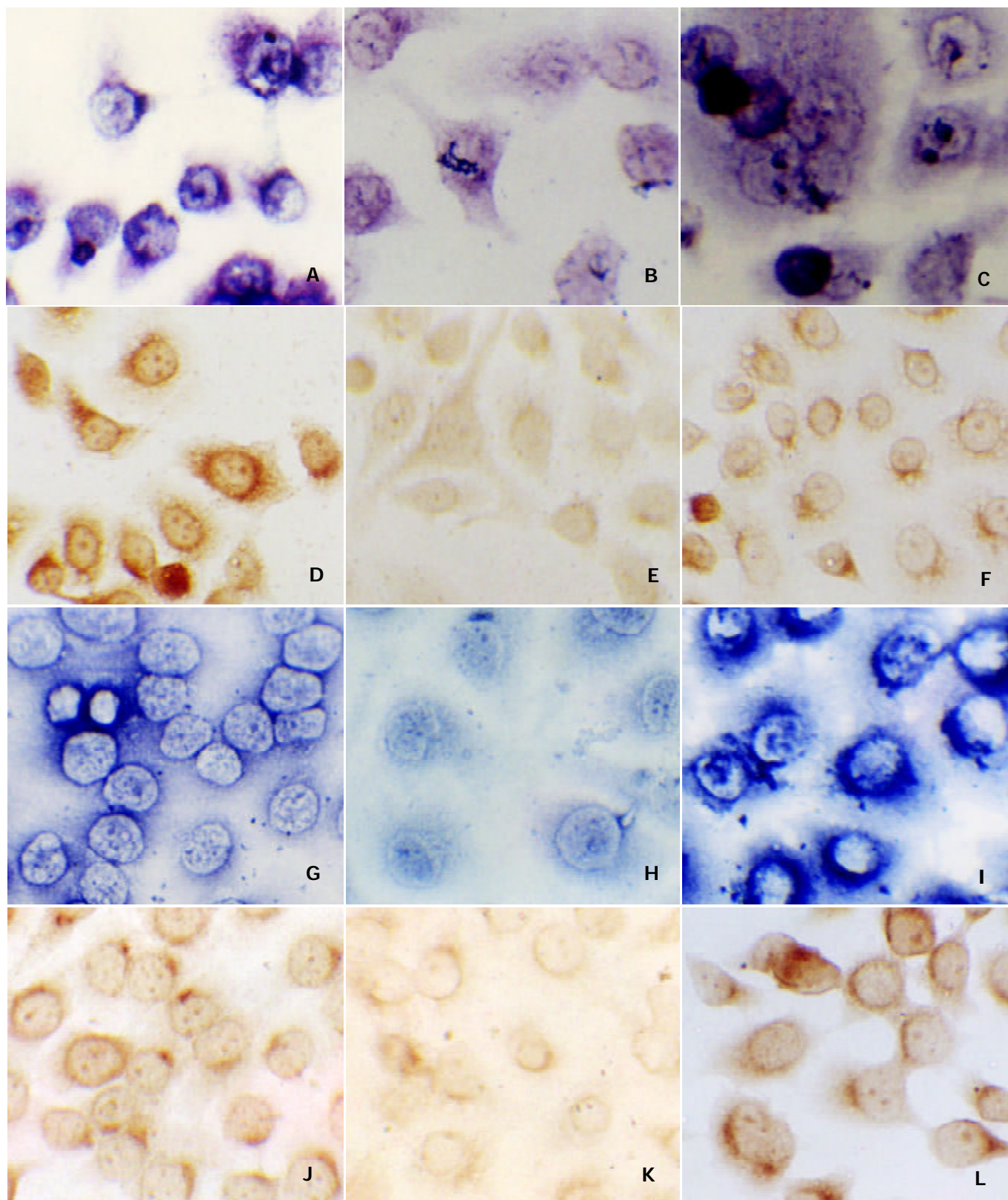


Figure 1 Expression of KDR gene in HGCC and HVEC before and after the action of KDR ASODN and CM
 A. KDR mRNA in HGCC (Control) (*in situ* hybridization); B. KDR mRNA in HGCC after the action of KDR ASODN (*in situ* hybridization); C. KDR mRNA in HGCC after the action of CM of HVEC (*in situ* hybridization); D. KDR protein in HGCC (Control) (immunohistochemical staining); E. KDR protein in HGCC after the action of KDR ASODN (immunohistochemical staining); F. KDR protein in HGCC after the action of CM of HVEC (immunohistochemical staining); G. KDR mRNA in HVEC (Control) (*in situ* hybridization); H. KDR mRNA in HVEC after the action of KDR ASODN (*in situ* hybridization); I. KDR mRNA in HVEC after the action of CM of HGCC (*in situ* hybridization); J. KDR protein in HVEC (Control) (immunohistochemical staining); K. KDR protein in HVEC after the action of KDR ASODN (immunohistochemical staining); L. KDR protein in HVEC after the action of CM of HGCC (immunohistochemical staining)

Effect of conditioned medium of gastric carcinoma cell on vascular endothelial cell The conditioned medium of HGCC could stimulate the proliferation of HVEC ($^aP < 0.05$ vs no-CM action

group) significantly. The stimulation effect was related to the CMs of different cell confluent state, different preparing periods, different volume fraction and different action periods (Table 5, 6).

Table 5 Different dose-time-effects of CMs of subconfluent and confluent HGCC on HVEC ($n=8$, $\bar{x} \pm s$)

CM volume fraction	A of CM group / A of control group									
	100%CM		80%CM		50%CM		30%CM		10%CM	
t / h cell confluent state	subconfluent	confluent	subconfluent	confluent	subconfluent	confluent	subconfluent	confluent	subconfluent	confluent
24	2.38±0.01 ^a	1.29±0.00 ^{ab}	2.70±0.01 ^a	1.55±0.02 ^{ab}	2.21±0.01 ^a	1.49±0.02 ^{ab}	2.10±0.03 ^a	1.44±0.01 ^{ab}	1.92±0.02 ^a	1.11±0.01 ^{ab}
48	1.60±0.01 ^a	1.22±0.01 ^{ab}	1.54±0.01 ^a	1.33±0.02 ^{ab}	1.38±0.02 ^a	1.23±0.02 ^{ab}	1.37±0.02 ^a	1.21±0.01 ^{ab}	1.31±0.01 ^a	1.15±0.02 ^{ab}
72	0.89±0.00	0.85±0.00	0.99±0.01	1.03±0.01	1.07±0.01 ^a	1.11±0.01 ^a	1.27±0.01 ^a	1.01±0.00 ^b	1.01±0.00	1.15±0.01 ^a

^a $P < 0.05$ vs No-CM action group, ^b $P < 0.05$ vs subconfluent group.

Table 6 Different dose-time-effect of CMs of different preparing periods of confluent HGCC on HVEC ($n=8$, $\bar{x} \pm s$)

CM volume fraction	A of CM group / A of control group									
	100%CM		80%CM		50%CM		30%CM		10%CM	
t / h Preparing periods	24hCM	48hCM	24hCM	48hCM	24hCM	48hCM	24hCM	48hCM	24hCM	48hCM
24	1.29±0.01 ^a	1.38±0.01 ^{ab}	1.55±0.02 ^a	1.39±0.01 ^{ab}	1.49±0.01 ^a	1.38±0.01 ^{ab}	1.44±0.02 ^a	1.30±0.01 ^{ab}	1.11±0.01 ^a	1.00±0.01 ^b
48	1.22±0.01 ^a	1.11±0.02 ^{ab}	1.33±0.01 ^a	1.14±0.02 ^{ab}	1.23±0.01 ^a	1.03±0.01 ^b	1.21±0.01 ^a	1.03±0.01 ^b	1.15±0.01 ^a	1.02±0.01 ^b
72	0.85±0.01	0.78±0.00	0.99±0.01	0.92±0.00	1.07±0.02 ^a	1.14±0.01 ^{ab}	1.27±0.01 ^a	1.20±0.01 ^{ab}	1.15±0.01 ^a	1.16±0.01 ^a

^a $P < 0.05$ vs No-CM action group, ^b $P < 0.05$ vs preparing for 24 hCM group.

Effect of conditioned medium of vascular endothelial cell on gastric carcinoma cell

The conditioned medium of HVEC could inhibit the proliferation of HGCC ($^aP < 0.05$ vs no-CM action group) significantly. The inhibitory effect was related to the different cell confluent states and different volume fractions (Table 7).

Table 7 Effects of CMs of subconfluent and confluent HVEC on HGCC for 48 h ($n=8$, $\bar{x} \pm s$)

Volume fraction	Inhibitory rate of cell proliferation(%)	
	CM of subconfluent HVEC	CM of confluent HVEC
100%CM	52.97±0.01 ^a	31.62±0.02 ^{ab}
80%CM	54.26±0.01 ^a	30.46±0.01 ^{ab}
50%CM	23.46±0.01 ^a	19.00±0.01 ^{ab}
30%CM	21.70±0.00 ^a	2.13±0.01 ^b
10%CM	14.36±0.00 ^a	1.61±0.00 ^b

^a $P < 0.05$ vs No-CM action group; ^b $P < 0.05$ vs subconfluent group

Expression of KDR gene in HVEC before and after the action of HGCC CM

The mRNA level(A value of *in situ* hybridization) before and after the action of HGCC CM was (0.37±0.03), (0.48±0.01^b) respectively ($^bP < 0.01$ vs before the action). The protein level (A value of immunohistochemical staining) before and after

the action of HGCC CM was (0.34±0.03), (0.48±0.02^b) respectively, ($^bP < 0.01$ vs before the action). So, after the CM of HGCC acted on HVEC, the expression level of KDR gene in HVEC was increased significantly (Figure 1).

Expression of KDR gene in HGCC before and after the action of HVEC CM

The mRNA level(A value of *in situ* hybridization) before and after the action of HVEC CM was (0.35±0.03), (0.22±0.02^b) respectively. The protein level(A value of immunohistochemical staining) before and after the action of HVEC CM was (0.33±0.03), (0.23±0.02^b) respectively, ($^bP < 0.01$ vs before the action). So, after the CM of HVEC acted on HGCC, the expression level of KDR gene in HGCC was inhibited significantly (Figure 1).

The hVEGF levels in the CMs of HGCC and HVEC

The hVEGF level in the CMs of HGCC and HVEC was (92.06±1.69 ng/L), (77.70±8.04 ng/L) respectively.

DISCUSSION

An important advance in oncology is that the importance of the tumor angiogenesis in the tumor genesis, growth and metastases, and the importance of the vascular targeting therapy in the tumor treatment have been proved. One of the most important factors in the tumor angiogenesis is vascular endothelium growth factor(VEGF). VEGF can promote and maintain the establishment of tumor vascular system. And it can promote the tumor growth directly. VEGF can induce the mitogenesis and chemotaxis of vascular endothelial cell(VEC)

and tumor cell(TC) intensely. Almost all types of TC and tumor VEC can secrete VEGF. But the expression of VEGF in the normal tissue is very low. In the four VEGF receptors, R₂: KDR is the main receptor which gives play to VEGF functions, while other receptors play little role in cell growth. KDR is highly expressed on the TC and tumor VEC while lowly expressed on the normal tissues. In order to make clear the role of KDR in regulating the growth of HGCC and HVEC, We devised the antisense oligodeoxynucleotide(ASODN) specific to KDR mRNA. There has been no one to devise KDR ASODN up to now. The results showed that KDR ASODN could inhibit the growth and expression of KDR gene of HGCC and HVEC significantly. There was a great difference between the effects of ASODN and SODN, MODN. The CMs of two cells had a certain level of *h*VEGF. This illustrated that KDR ASODN could really enter into the cells and specifically block the expression of KDR gene to interrupt the self-scrine and parascrine growth-stimulation pathway of VEGF. The results showed that VEGF and its receptor KDR played a key role in regulating the proliferation of HGCC and HVEC.

In the human solid neoplasm, there exist many kinds of cells besides the tumor cell, such as: interstitial cell, immunocyte and vascular cell. They depend on each other to contribute to the tumor genesis, development, invasion and metastasis. The interactions among them are complicated. During the tumor angiogenesis and tumor hematogenous metastasis, both VEC and TC contribute to finishing the pathology processes. The interactions between them act in close coordination in establishing tumor vascular system and finishing hematogenous metastasis. There exist very complicated interrelations between TC and VEC. In the pre-angiogenesis, how does TC induce VEC to establish the tumor vascular system? That is, how does TC influence the proliferation, degeneration, morphogenesis and functions of its neighboring VEC? Or, how does VEC influence these characters of its neighboring TC? These are all unclear. On the other hand, the interactions between two cells are involved in the tumor infiltration and hematogenous metastasis. Tumor vascular provides the passage for tumor infiltration and metastasis. The integrated vascular endothelium is the barrier to the tumor infiltration and metastasis. How do these two kinds of cells interact reciprocally to render the tumor cell to adhere to and destroy the vascular endothelium to enter vascular lumen and damage it again to enter stroma? There exist some complicated mechanisms in this process. The study of tumor angiogenesis mainly focuses on the interactions among the vascular component cells while the study of tumor invasion and metastasis mainly focuses on the interactions between TC and surrounding stroma. Seldom has anyone noticed the interactions between TC and VEC. The relations between TC and VEC are not clear. Studies on this aspect are very few. Studies abroad always choose melanoma, glioblastoma, cephalo-cervical squamous carcinoma and hepatocellular carcinoma [4-19], but not gastric carcinoma as the target research yet. And the results are also controversial. We have not found anyone who studies gastric carcinoma yet. There are lots of studies on gastric carcinoma [20-45], but seldom in this aspect. To better understand some mechanisms in gastric carcinoma angiogenesis and hematogenous metastases, we select HGCC and HVEC to study their interrelations and the mechanisms. Considering the results showed that KDR was an important regulator to the growth of HGCC and HVEC, we study the role of KDR in the interactions between the two cells.

Results showed that CMs of HGCC with different confluent state, different preparing periods, different volume fraction and

different action periods stimulated the growth of HVEC significantly. The activity of CM of subconfluent cell was stronger than that of CM of confluent cell. The activity of CM preparing for 24 h was stronger than that of CM preparing for 48 h. After the nutrition exhaustion was replenished, the more of the volume fraction, the stronger of the activity. This is consistent with the results of some studies. Someone found CM of bladder carcinoma stimulated the growth of HVEC. Others found that cephalo-cervical squamous carcinoma cell stimulated the growth of HVEC through secreting FGF and VEGF. But there were other contrary viewpoints. Zhao found bladder carcinoma cell inhibited the growth of HVEC through a 10-16bp tRNA fragment. Albini found some kinds of tumor cells inhibited HVEC to form vascular through secreting IFN- γ . There was also a neutral objection: TC has little effect on the proliferation of HVEC. Some researchers found that although TC had no effect on the growth of HVEC, TC could change morphology of HVEC or its sensitivity to TNF- α . We think these different results are due to different cell types. Results showed that HGCC could secrete a certain level of *h*VEGF. CM of HGCC could up-regulate the expression of KDR gene in HVEC. It illustrated that KDR played an important role in the growth-stimulation of HGCC to HVEC. It needs further study to show if there exist other factors and mechanisms involved in this effect of HGCC on HVEC.

Our results also showed that CM of HVEC could significantly inhibit the growth of HGCC. The activity of CM of subconfluent cell was stronger than that of CM of confluent cell. After the nutrition exhaustion was replenished, the more of the volume fraction, the stronger of the activity. We do not know what this inhibition means exactly. Maybe in the tumor angiogenesis, the inhibition could prevent HGCC to occupy the place of vascular or participate into the vascularization. Then the stimulation of vascular system to growth of gastric carcinoma is not through the direct interaction between HGCC and HVEC, but the establishment of the vascular system passes nutrition to HGCC and excretes its metabolism waste. HVEC also secreted a certain level of *h*VEGF and VEGF could stimulate the proliferation of HGCC. But CM of HVEC inhibited the growth of HGCC and the KDR gene expression in HGCC. Although HVEC produced growth-stimulator, VEGF, HVEC could interrupt the role of VEGF on HGCC through reducing the level of its main functional receptor, KDR. It illustrated that KDR play an important role in the growth-inhibition of HVEC to HGCC. Whether HVEC secretes some other growth-inhibiting factors to inhibit the proliferation of HGCC or not needs further study.

REFERENCES

- 1 **Ren J**, Dong L, Xu CB, Pan BR, Li MZ. Interactions between the human gastric carcinoma cell and vascular endothelial cell. *Shijie Huaren Xiaohua Zazhi* 2001; **9**: 1254-1260
- 2 **Ren J**, Dong L, Xu CB. Effect of KDR antisense oligodeoxynucleotide on the human gastric carcinoma cell. *Di-si Junyi Daxue Xuebao* 2002; **23**: 333-336
- 3 **Ren J**, Dong L, Xu CB. Effect of KDR ASODN on the human vascular endothelial cell. *Jichu Yixue Yu Linchuang* 2002; **8**: in press.
- 4 **Von BC**, Hayen W, Hartmann A, Mueller KW, Allolio B, Nehls V. Endothelial capillaries chemotactically attract tumor cells. *J Pathol* 2001; **193**: 267-376
- 5 **Okamoto H**, Ohigashi H, Nakamori S, Ishikawa O, Imaoka S, Mukai M, Kusama T, Fuji H. Reciprocal functions of liver tumor cells and endothelial cells. Involvement of endothelial cell migration and tumor cell proliferation at a primary site in distant metastasis. *Eur Surg Res* 2000; **32**: 374-379

- 6 **Moreno A**, Villar ML, Camara C, Luque R, Cespon C, Gonzalez-PP, Roy G, Lopez JJ. Interleukin-6 dimers produced by endothelial cells inhibit apoptosis of B-chroniclymphocytic leukemia cells. *Blood* 2001; **97**:242-249
- 7 **Brandvold KA**, Neiman P, Ruddell A. Angiogenesis is an early event in the generation of myc-induced lymphomas. *Oncogene* 2000; **19**: 2780-2785
- 8 **De BES**, Rosati S, Jacobs S, Kamps WA, Vellenga E. Increased bone marrow vascularization in patients with acute myeloid leukaemia: a possible role for vascular endothelial growth factor. *Br J Haematol* 2001; **113**:296-304
- 9 **Hewett PW**. Identification of tumor-induced changes in endothelial cell surface protein expression: an *in vitro* model. *Int J Biochem Cell Biol* 2001; **33**:325-335
- 10 **Luo J**, Guo P, Matsuda K, Truong N, Lee A, Chun C, Cheng SY, Kore M. Pancreatic cancer cell-derived vascular endothelial growth factor is biologically active *in vitro* and enhances tumorigenicity *in vivo*. *Int J Cancer* 2001; **92**:361-369
- 11 **Witt C J**, Gabel S P, Meisinger J. Interrelationship between protein phosphatase-2A and cytoskeletal architecture during the endothelial cell response to soluble products produced by human head and neck cancer. *Otolaryngol Head Neck Surg* 2000; **122**:721-727
- 12 **Kuroda K**, Miyata K, Tsutsumi Y. Preferential activity of wild-type and mutant tumor necrosis factor- α against tumor-derived endothelial like cells. *Jpn J Cancer Res* 2000; **91**:59-67
- 13 **Shemirani B**. Head and Neck squamous cell carcinoma lines produce biologically active angiogenic factors. *Oral Oncol* 2000; **36**: 61-66
- 14 **Beierle EA**, Strande LF, Berger AC, Chen MK. VEGF is upregulated in a neuroblastoma and hepatocyte coculture model. *J Surg Res* 2001; **97**:34-40
- 15 **Vidal Vanaclocha F**, Fantuzzi G, Mendoza L. IL-18 regulated IL-1 β dependent hepatic melanoma metastasis via vascular cell adhesion molecule-1. *Proc Natl Acad Sci USA* 2000; **97**:734-739
- 16 **Aoki M**, Kanamori M, Yudoh K, Ohmori K, Yasuda T, Kimura T. Effects of vascular endothelial growth factor and E-selectin on angiogenesis in the murine metastatic RCT sarcoma. *Tumour Biol* 2001; **22**:239-246
- 17 **Liu W**, Davis DW, Ramirez K, McConkey DJ, Ellis LM. Endothelial cell apoptosis is inhibited by a soluble factor secreted by human colon cancer cells. *Int J Cancer* 2001; **92**: 26-30
- 18 **Albini A**, Marchisone C, Del Grosso F. Inhibition of angiogenesis and vascular tumor growth by interferon-producing cells: A gene therapy approach. *Am J Pathol* 2000; **156**:1381-1393
- 19 **Kamada H**, Tsutsumi Y, Kihira T. *In vitro* remodeling of tumor vascular endothelial cells using conditioned medium from various tumor cells and their sensitivity to TNF- α . *Biochem Biophys Res Commun* 2000; **268**:809-813
- 20 **Wu K**, Zhao Y, Liu BH, Li Y, Liu F, Guo J, Yu WP. RRR- α -tocopheryl succinate inhibits human gastric cancer SGC-7901 cell growth by inducing apoptosis and DNA synthesis arrest. *World J Gastroenterol* 2002; **8**:26-30
- 21 **Wang X**, Lan M, Shi YQ, Lu J, Zhong YX, Wu HP, Zai HH, Ding J, Wu KC, Pan BR, Jin JP, Fan DM. Differential display of vincristine-resistance-related genes in gastric cancer SGC7901 cell. *World J Gastroenterol* 2002; **8**:54-59
- 22 **Yao YL**, Xu B, Song YG, Zhang WD. Overexpression of cyclin E in Mongolian gerbil with *Helicobacter pylori*-induced gastric precancerosis. *World J Gastroenterol* 2002; **8**:60-63
- 23 **Yang SM**, Fang DC, Luo YH, Lu R, Liu WW. Effect of antisense gene to human telomerase reverse transcriptase on telomerase activity and expression of apoptosis-associated gene. *Shijie Huaren Xiaohua Zazhi* 2002; **10**:149-152
- 24 **Zheng ZH**, Xun XJ, Qiu GR, Liu YX, Wang MX, Sun KL. E-cadherin gene mutation in precancerous condition, early and advanced stage of gastric cancer. *Shijie Huaren Xiaohua Zazhi* 2002; **10**:153-156
- 25 **Wang W**, Luo HS, Yu BP. Expression of human telomerase reverse transcriptase gene and c-myc protein in gastric carcinogenesis. *Shijie Huaren Xiaohua Zazhi* 2002; **10**:258-261
- 26 **Li JY**, Yu JP, Luo HS, Yu BP, Huang JA. Effects of nonsteroidal anti-inflammatory drugs on the proliferation and cyclooxygenase activity of gastric cancer cell line SGC7901. *Shijie Huaren Xiaohua Zazhi* 2002; **10**:262-265
- 27 **Xue FB**, Xu YY, Wan Y, Pan BR, Ren J, Fan DM. Association of *H. pylori* infection with gastric carcinoma: a Meta analysis. *World J Gastroenterol* 2001; **7**:801-804
- 28 **Liu DH**, Zhang XY, Fan DM, Huang YX, Zhang JS, Huang WQ, Zhang YQ, Huang QS, Ma WY, Chai YB, Jin M. Expression of vascular endothelial growth factor and its role in oncogenesis of human gastric carcinoma. *World J Gastroenterol* 2001; **7**:500-505
- 29 **Cai L**, Yu SZ, Zhang ZF. Glutathione S-transferases M1, T1 genotypes and the risk of gastric cancer: A case-control study. *World J Gastroenterol* 2001; **7**:506-509
- 30 **He XS**, Su Q, Chen ZC, He XT, Long ZF, Ling H, Zhang LR. Expression, deletion and mutation of p16 gene in human gastric cancer. *World J Gastroenterol* 2001; **7**:515-521
- 31 **Fang DC**, Yang SM, Zhou XD, Wang DX, Luo YH. Telomere erosion is independent of microsatellite instability but related to loss of heterozygosity in gastric cancer. *World J Gastroenterol* 2001; **7**:522-526
- 32 **Cui JH**, Krueger U, Henne-Bruns D, Kremer B, Kalthoff H. Orthotopic transplantation model of human gastrointestinal cancer and detection of micrometastases. *World J Gastroenterol* 2001; **7**:381-386
- 33 **Ni CR**. Expression significance of GST- π , P-gp, Top II and nm23H1 in gastric carcinoma. *Shijie Huaren Xiaohua Zazhi* 2001; **9**:897-901
- 34 **Wang X**, Zhao YQ, Fan DM. Construction and expression of gastric cancer MG7 mimic epitope fused to heat shock protein 70. *Shijie Huaren Xiaohua Zazhi* 2001; **9**:892-896
- 35 **Liu DH**, Zhang W, Su YP, Zhang XY, Huang YX. Constructions of eukaryotic expression vector of sense and antisense VEGF-165 and its expression regulation. *Shijie Huaren Xiaohua Zazhi* 2001; **9**:886-891
- 36 **Liu WC**, Mu HX, Ren J, Zhang XY, Pan BR. Anti tumor activity of defensin on gastric cancer cell line *in vitro*. *Shijie Huaren Xiaohua Zazhi* 2001; **9**:622-626
- 37 **Han Y**, Shi YQ, Zheng Y, Nie YZ, Zhang HB, Zhang ML, Pan BR, Fan DM. Protein kinase C is related to multidrug resistance induced by Mdr1Ag. *Shijie Huaren Xiaohua Zazhi* 2001; **9**:517-521
- 38 **Kong XD**, Zhang SZ, Hu JK, Xiao CY, Sun Y, Xia QJ. Abnormalities of p15 gene and protein expression in gastric cancers. *Shijie Huaren Xiaohua Zazhi* 2001; **9**:513-516
- 39 **Yao XX**, Yin L, Zhang JY, Bai WY, Li YM, Sun ZC. hTERT expression and cellular immunity in gastric cancer and precancerosis. *Shijie Huaren Xiaohua Zazhi* 2001; **9**:508-512
- 40 **Chen SY**, Wang JY, Ji Y, Zhang XD, Zhu CW. Effects of *Helicobacter pylori* and protein kinase C on gene mutation in gastric cancer and precancerous lesions. *Shijie Huaren Xiaohua Zazhi* 2001; **9**:302-307
- 41 **Cheng SD**, Wu YL, Zhang YP, Qiao MM, Guo QS. Abnormal drug accumulation in multidrug resistant gastric carcinoma cells. *Shijie Huaren Xiaohua Zazhi* 2001; **9**:131-134
- 42 **Wang B**, Shi LC, Zhang WB, Xiao CM, Wu JF, Dong YM. Expression and significance of p16 gene in gastric cancer and its precancerous lesions. *Shijie Huaren Xiaohua Zazhi* 2001; **9**:39-44
- 43 **Liu HF**, Liu WW, Fang DC. Effect of combined anti Fas mAb and IFN- γ on the induction of apoptosis in human gastric carcinoma cell line SGC-7901. *Shijie Huaren Xiaohua Zazhi* 2000; **8**:1361-1364
- 44 **Gao MX**, Zhang NZ, Ji CX. Estrogen receptor and PCNA in gastric carcinomas. *Shijie Huaren Xiaohua Zazhi* 2000; **8**: 1117-1120
- 45 **Xia JZ**, Zhu ZG, Liu BY, Yan M, Yin HR. Significance of immunohistochemically demonstrated micrometastases to lymph nodes in gastric carcinomas. *Shijie Huaren Xiaohua Zazhi* 2000; **8**:1113-1116

Edited by Pang LH

Expression of sphingosine kinase gene in the interactions between human gastric carcinoma cell and vascular endothelial cell

Juan Ren, Lei Dong, Cang-Bao Xu, Bo-Rong Pan

Juan Ren, Department of Oncological Radiotherapy, First Hospital of Xi'an Jiaotong University, Xi'an 710061, Shaanxi Province, China
Lei Dong, Department of Gastroenterology, Second Hospital of Xi'an Jiaotong University, Xi'an 710004, Shaanxi Province, China

Cang-Bao Xu, Department of Pathophysiology, Lund University, Sweden

Bo-Rong Pan, Oncology Center, Xijing Hospital, Fourth Military Medical University, Xi'an 710032, Shaanxi Province, China

Correspondence to: Dr. Juan Ren, Department of Oncological Radiotherapy, First Hospital, Xi'an Jiaotong University Xi'an 710061, Shaanxi Province, China. renjuan88@163.net

Telephone: +86-29-3058229 **Fax:** +86-29-4333028

Received 2002-03-29 **Accepted** 2002-04-20

Abstract

AIM: To study the interactions between human gastric carcinoma cell (HGCC) and human vascular endothelial cell (HVEC), and if the expression of sphingosine kinase (SPK) gene was involved in these interactions.

METHODS: The specific inhibitor to SPK, dimethyl sphingosine (DMS), was added acting on HGCC and HVEC, then the cell proliferation was measured by MTT. The conditioned mediums (CMs) of HGCC and HVEC were prepared. The CM of one kind of cell was added to the other kind of cell, and the cell proliferation was measured by MTT. After the action of CM, the cellular expression of SPK gene in mRNA level was detected with *in situ* hybridization (ISH).

RESULTS: DMS could almost completely inhibit the proliferation of HGCC and HVEC. The growth inhibitory rates could amount to 97.21 %, 83.42 %, respectively ($P < 0.01$). The CM of HGCC could stimulate the growth of HVEC (2.70 ± 0.01 , $P < 0.01$) while the CM of HVEC could inhibit the growth of HGCC (52.97 ± 0.01 %, $P < 0.01$). There was no significant change in the mRNA level of SPK gene in one kind of cell after the action of the CM of the other kind of cell.

CONCLUSION: SPK plays a key role in regulating the proliferation of HGCC and HVEC. There exist complicated interactions between HGCC and HVEC. HGCC can significantly stimulate the growth of HVEC while HVEC can significantly inhibit the growth of HGCC. The expression of SPK gene is not involved in the interactions.

Ren J, Dong L, Xu CB, Pan BR. Expression of sphingosine kinase gene in the interactions between human gastric carcinoma cell and vascular endothelial cell. *World J Gastroenterol* 2002;8(4):602-607

INTRODUCTION

There exist many kinds of cells besides tumor cells in the solid neoplasm. These cells depend on each other and contribute together to the genesis, development, invasion and metastasis of tumor. The relations among all kinds of cells are very

complicated. During the tumor angiogenesis and hematogenous metastasis, there exist complicated interactions between tumor cell (TC) and vascular endothelial cell (VEC)^[1]. In the pre-angiogenesis, how does TC induce VEC to establish the tumor vascular system? On the other hand, the interactions between the two cells play a role in the tumor hematogenous metastasis. There exist some complicated mechanisms in these processes. The study of tumor angiogenesis mainly focuses on the interactions among the vascular component cells while the study of tumor metastasis mainly focuses on the interactions between TC and its surrounding stroma. Seldom does anyone notice the interactions between TC and VEC. To better understand some mechanisms in human gastric carcinoma angiogenesis and hematogenous metastasis, we selected human gastric carcinoma cell (HGCC) and human vascular endothelial cell (HVEC) to study the interactions between HGCC and HVEC and some mechanisms involved in these actions. Sphingosine kinase (SPK) is a newly found important kinase in regulating many biological functions of most kinds of cells. SPK can induce the synthesis of extracellular transmitter and intracellular second messenger, sphingosine-1-phosphate (SPP). To determine whether SPK took part in regulating the proliferation of HGCC and HVEC, the specific inhibitor to SPK, dimethyl sphingosine (DMS), was acted on the two cells^[2]. The present study aims to probe into the interrelationships between HGCC and HVEC and if the expression of SPK gene was involved in these effects. The cell proliferation and the expression of SPK mRNA were measured after the action of the conditioned medium (CM) of the other kind of cell.

MATERIALS AND METHODS

Materials

Cell line HGCC line SGC7901 and HVEC line Eahy926 were employed.

Methods

Conditioned medium (CM) preparation, the ways of the actions of CM and DMS Cells in different confluent states were washed twice with PBS, then 3 mL culture medium was added to the cells. The medium what was taken as CM was collected after different periods. Cells were placed in serum free medium for growth arresting. After the growth of HGCC and HVEC was arrested for 24 h and 6 h respectively, the CM of the other kind of cell was added to the cell. The cell proliferation was measured by MTT after different culturing periods. The cell without the action of CM was taken as control. The action way of DMS was as same as the way of CM. The cell without the action of DMS was taken as control.

MTT (methyl tetrazolium colorimetry) 20 μ L MTT solution (5 g/L) was added to 200 μ L medium in each well of 96 well plate. 4h later, the supernant was discarded, 150 μ L DMSO was added in. After the crystal was dissolved completely, absorption spectrum (A) was measured at 490 nm in the enzyme linked immunosorbent assay meter. The inhibitory rate of cell

proliferation = $[1 - (\text{the mean } A \text{ of experimental group} / \text{The mean of control group})] \times 100\%$

Detecting the expression of SPK gene After the action of CM of the other kind of cell, the cellular expression of SPK gene was detected by *in situ* hybridization (ISH) for mRNA level. There has been no antibody to SPK available up to now, so that it is impossible to detect the level of SPK protein. Probe specific to SPK mRNA was designed with the software “Primer 3”. The sequence of SPK probe is 5’ ATA TAC CAA GTA GGG GCA TTC ATA CTC 3’; Probe labeling and ISH were carried on according to the manual of the Dig Oligonucleotide Tailing Kit and Dig Detection Kit (Boehringer Mannheim, Germany) respectively. PBS was substituted for anti-Dig-Ap as negative control. The sections were analyzed for A value in the image analysis apparatus.

Statistical analysis

t test was used to compare the means.

RESULTS

Effects of DMS on the proliferation of HGCC and HVEC

DMS could almost completely inhibit the proliferation of HGCC and HVEC. The growth inhibitory rates could amount to 97.21 % and 83.42 % respectively ($^bP < 0.01$ vs control). DMS could produce effects in 1 $\mu\text{mol/L}$ and 3 h later. The inhibitory rate was related to the dose and action periods. 10 $\mu\text{mol/L}$ DMS inhibited the proliferation of HGCC significantly, and the effect was increasing by leaps and bounds when the dose was from 3.5 $\mu\text{mol/L}$ to 5 $\mu\text{mol/L}$ or the action period was from 24 h to 48 h. 25 $\mu\text{mol/L}$ DMS inhibited the growth of HVEC significantly, and the effect was increasing by leaps and bounds when the dose was from 10 $\mu\text{mol/L}$ to 15 $\mu\text{mol/L}$ or the action period was from 48 h to 72 h (Table 1, 2).

Table 1 Dose-effect of DMS on HGCC and HVEC for 48 h ($n=8$, $\bar{x} \pm s$)

DMS dose/ ($\mu\text{mol/L}$)	Inhibitory rate of cell proliferation(%)	
	HGCC	HVEC
0(control)	0	0
1	12.33 ^b	5.61 ^b
2	17.53 ^b	11.11 ^b
3.5	31.31 ^b	17.77 ^b
5	54.68 ^b	18.41 ^b
7.5	64.34 ^b	19.82 ^b
10	80.68 ^b	31.02 ^b
15	89.04 ^b	65.76 ^b
20	92.67 ^b	76.02 ^b
25	95.91 ^b	82.32 ^b
30	97.21 ^b	83.42 ^b

^b $P < 0.01$ vs control.

Table 2 Time-effect of 10 $\mu\text{mol/L}$ DMS on HGCC and HVEC ($n=8$, $\bar{x} \pm s$)

DMS action periods / h	Inhibitory rate of cell proliferation(%)	
	HGCC	HVEC
0(control)	0	0
3	9.11 ^b	5.18 ^b
6	13.46 ^b	7.05 ^b
12	20.18 ^b	11.12 ^b
24	41.98 ^b	19.52 ^b
48	80.68 ^b	31.02 ^b
72	93.55 ^b	56.44 ^b

^b $P < 0.01$ vs control.

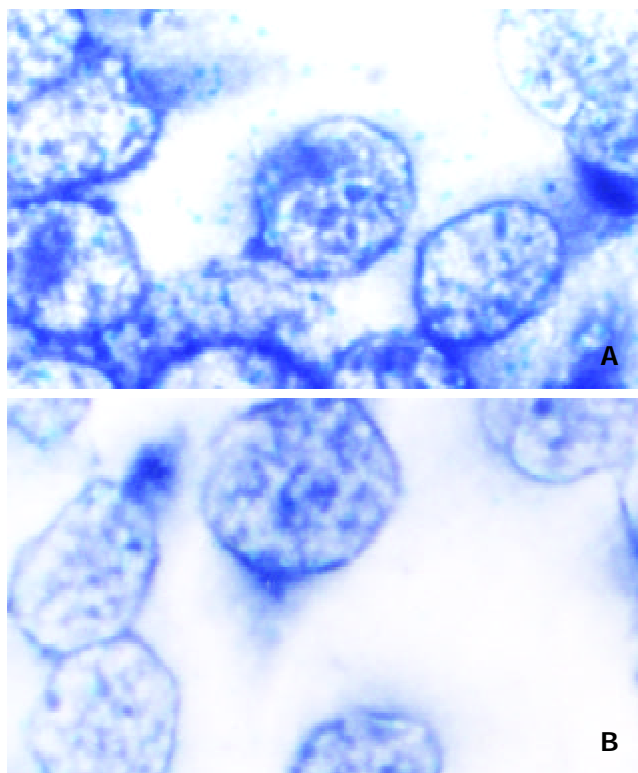


Figure 1 Expression of SPK mRNA in HVEC after the action of the CM of HGCC. a: SPK mRNA in HVEC without the action of CM of HGCC (Control) (*in situ* hybridization); b: SPK mRNA in HVEC after the action of CM of HGCC (*in situ* hybridization)

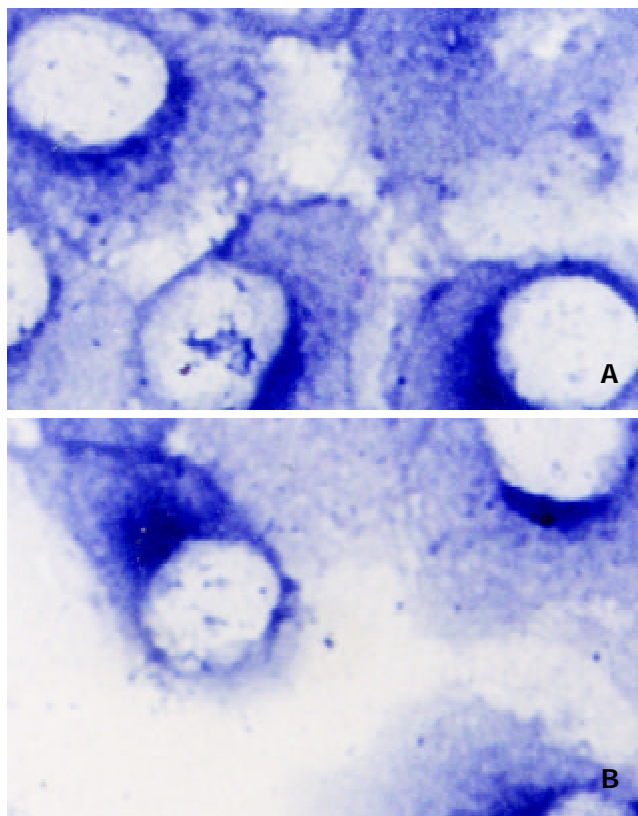


Figure 2 Expression of SPK mRNA in HGCC after the action of the CM of HVEC. a: SPK mRNA in HGCC without the action of CM of HVEC (Control) (*in situ* hybridization); b: SPK mRNA in HGCC after the action of CM of HVEC (*in situ* hybridization)

Table 3 Different dose-time-effects of CMs of subconfluent and confluent HGCC on HVEC ($n=8$, $\bar{x}\pm s$)

CM volume fraction	A of CM group / A of control group									
	100%CM		80%CM		50%CM		30%CM		10%CM	
t / h	cell	confluent	state	subconfluent	confluent	subconfluent	confluent	subconfluent	confluent	subconfluent
24	2.38±0.01 ^a	1.29±0.00 ^{ab}	2.70±0.01 ^a	1.55±0.02 ^{ab}	2.21±0.01 ^a	1.49±0.02 ^{ab}	2.10±0.03 ^a	1.44±0.01 ^{ab}	1.92±0.02 ^a	1.11±0.01 ^{ab}
48	1.60±0.01 ^a	1.22±0.01 ^{ab}	1.54±0.01 ^a	1.33±0.02 ^{ab}	1.38±0.02 ^a	1.23±0.02 ^{ab}	1.37±0.02 ^a	1.21±0.01 ^{ab}	1.31±0.01 ^a	1.15±0.02 ^{ab}
72	0.89±0.00	0.85±0.00	0.99±0.01	1.03±0.01	1.07±0.01 ^a	1.11±0.01 ^a	1.27±0.01 ^a	1.01±0.00 ^b	1.01±0.00	1.15±0.01 ^a

^a $P<0.05$ vs No-CM action group, ^b $P<0.05$ vs subconfluent group.

Table 4 Different dose-time-effect of CMs of different preparing periods of confluent HGCC on HVEC ($n=8$, $\bar{x}\pm s$)

CM volume fraction	A of CM group / A of control group									
	100%CM		80%CM		50%CM		30%CM		10%CM	
t / h	Preparing	periods	24hCM	48hCM	24hCM	48hCM	24hCM	48hCM	24hCM	48hCM
24	1.29±0.01 ^a	1.38±0.01 ^{ab}	1.55±0.02 ^a	1.39±0.01 ^{ab}	1.49±0.01 ^a	1.38±0.01 ^{ab}	1.44±0.02 ^a	1.30±0.01 ^{ab}	1.11±0.01 ^a	1.00±0.01 ^b
48	1.22±0.01 ^a	1.11±0.02 ^{ab}	1.33±0.01 ^a	1.14±0.02 ^{ab}	1.23±0.01 ^a	1.03±0.01 ^b	1.21±0.01 ^a	1.03±0.01 ^b	1.15±0.01 ^a	1.02±0.01 ^b
72	0.85±0.01	0.78±0.00	0.99±0.01	0.92±0.00	1.07±0.02 ^a	1.14±0.01 ^{ab}	1.27±0.01 ^a	1.20±0.01 ^{ab}	1.15±0.01 ^a	1.16±0.01 ^a

^a $P<0.05$ vs No-CM action group, ^b $P<0.05$ vs preparing for 24 hCM group.

Effect of conditioned medium of gastric carcinoma cell on vascular endothelial cell

The conditioned medium of HGCC could stimulate the proliferation of HVEC (^a $P<0.05$ vs no-CM action group) significantly. The stimulation effect was related to the different cell confluent states, different preparing periods, different volume fractions and different action periods (Table 3,4).

Effect of conditioned medium of vascular endothelial cell on gastric carcinoma cell

The conditioned medium of HVEC could inhibit the proliferation of HGCC significantly (^b $P<0.01$ vs no-CM action group). The inhibitory effect was related to the different cell confluent states and different volume fractions (Table 5).

Table 5 Effects of CMs of subconfluent and confluent HVEC on HGCC for 48 h ($n=8$, $\bar{x}\pm s$)

Volume fraction	Inhibitory rate of cell proliferation(%)	
	CM of subconfluent HVEC	CM of confluent HVEC
100%CM	52.97±0.01 ^a	31.62±0.02 ^{ab}
80%CM	54.26±0.01 ^a	30.46±0.01 ^{ab}
50%CM	23.46±0.01 ^a	19.00±0.01 ^{ab}
30%CM	21.70±0.00 ^a	2.13±0.01 ^b
10%CM	14.36±0.00 ^a	1.61±0.00 ^b

^a $P<0.05$ vs No-CM action group; ^b $P<0.05$ vs subconfluent group.

Expression of SPK gene in HVEC before and after the action of HGCC CM

The mRNA level (A value of *ISH*) in HVEC before and after the

action of HGCC CM were (0.265±0.016), (0.264±0.021) respectively. There was no significant difference between them. So, after the CM of HGCC acted on HVEC, the expression level of SPK gene in HVEC had no significant change (Figure 1).

Expression of SPK gene in HGCC before and after the action of HVEC CM

The mRNA level (A value of *ISH*) in HGCC before and after the action of HVEC CM were (0.244±0.016), (0.243±0.018) respectively. There was no significant difference between them. So, after the CM of HVEC acted on HGCC, the expression level of SPK gene in HGCC had not been significantly changed (Figure 2).

DISCUSSION

In the human solid neoplasm, there exist many kinds of cells besides the tumor cell, such as: interstitial cell, immunocyte and vascular cell. They depend on each other to contribute to the tumor genesis, development, invasion and metastasis. There exist complicated interactions among these cells. During tumor angiogenesis and tumor hematogenous metastasis, both vascular endothelial cell (VEC) and tumor cell (TC) contribute to finishing the pathology processes. The interactions between VEC and TC act in close coordination in establishing tumor vascular system and finishing hematogenous metastasis. There are very complicated interrelations between TC and VEC. In the pre-angiogenesis, how does TC induce VEC to establish the tumor vascular system? That is, how does TC influence the proliferation, degeneration, morphogenesis and functions of its neighboring VEC? Or, how does VEC influence these characters of its neighboring TC? These are all unclear. On the other hand, the interactions between two cells are involved in the tumor infiltration and hematogenous metastasis. Tumor vascular provides the passage for tumor infiltration and metastasis. The integrated vascular endothelium is the barrier

to the tumor infiltration and metastasis. How do these two kinds of cells interact reciprocally to render tumor cell to adhere to and destroy the vascular endothelium to enter vascular lumen and damage it again to enter stroma? There exist some complicated mechanisms in this process. The study of tumor angiogenesis mainly focuses on the interactions among the vascular component cells while the study of tumor invasion and metastasis mainly focuses on the interactions between TC and surrounding stroma. Seldom has anyone noticed the interactions between TC and VEC. The relations between TC and VEC are not clear. Studies on this aspect are very few. Studies abroad always choose melanoma, glioblastoma, cephalo-cervical squamous carcinoma and hepatocellular carcinoma^[3-18], but not gastric carcinoma as the target research yet. And the results are also controversial. We have not found anyone who studies gastric carcinoma yet. There are lots of studies on gastric carcinoma^[19-29], but seldom in this aspect. To better understand some mechanisms in gastric carcinoma angiogenesis and hematogenous metastases, we select human gastric carcinoma cell(HGCC) and human vascular endothelial cell(HVEC) to study their interrelations and the mechanisms.

Results in this study showed that CMs of HGCC with different confluent states, different preparing periods, different volume fractions and different action periods could all stimulate the growth of HVEC significantly. The activity of CM of subconfluent cell was stronger than that of CM of confluent cell. The activity of CM preparing for 24 h was stronger than that of CM preparing for 48 h. After the nutrition exhaustion was replenished, the more of the volume fraction, the stronger of the activity. This is consistent with the results of some studies. Someone found CM of bladder carcinoma stimulated the growth of HVEC. Others found that cephalo-cervical squamous carcinoma cell stimulated the growth of HVEC through secreting FGF and VEGF. But there were other contrary viewpoints. Zhao found bladder carcinoma cell inhibited the growth of HVEC through a 10-16bp fragment of tRNA. Albini found some kinds of TCs inhibited HVEC to form vascular through secreting IFN- γ . There was also a neutral objection: TC has little effect on the proliferation of HVEC. Some researchers found that although TC had no effect on the growth of HVEC, TC could change morphology of HVEC or its sensitivity to TNF- α . We think these different results are due to different cell types. Our results also showed that CM of HVEC could inhibit the growth of HGCC significantly. The activity of CM of subconfluent cell was stronger than that of CM of confluent cell. After the nutrition exhaustion was replenished, the more of the volume fraction, the stronger of the activity. We do not know what this means exactly. Maybe in the tumor angiogenesis, this inhibition could prevent HGCC to occupy the place of vascular or participate into the vascularization. Then the stimulation of vascular system to the growth of gastric carcinoma is not through the direct interactions between HGCC and HVEC, but through the establishment of the vascular system that passes nutrition to TC and excretes its metabolism waste. Whether HVEC secretes some growth-inhibiting factors to inhibit the proliferation of HGCC or not needs further study.

Sphingosine 1-phosphate(SPP) is a newly found important extracellular transmitter and intracellular second messenger. SPP regulates many biological functions of most kinds of cells through taking part in several signal transduction pathways which include MAPK/ERK(mitogen activated protein kinase/extracellular regulating kinase, MAPK/ERK)pathway, CAMP signal transduction pathway, Ca^{2+} /CaM(Calmodulin, CaM) pathway and phospholipase D pathway. The functions of SPP

include: regulating the proliferation, morphology, migration, adhesion and apoptosis of cells, maintaining the structure of the endothelium and epithelium, regulating vasculogenesis, regulating the cardiovascular function, regulating the intracellular level of Ca^{2+} and K^{+} , regulating tumor metastasis and so on^[29-39]. The synthesis of SPP depends on the activation of sphingosine kinase(SPK). The activation of SPK is closely related to the survival and function of cells^[40-49]. Lots of factors can activate SPK such as PDGF(platelet derived growth factor, PDGF) and Fc receptors. The concentrations of SPK in the plasma and serum are 200 nM, 500 nM respectively. There are several phosphorylated sites and combination sites for Ca^{2+} and CaM in the SPK sequence. The sequence of SPK is highly conservative from yeast, protozoon to mammal. The activity of SPK can be detected in the cytoplasm and cell membrane. The functions of SPK are somewhat similar to the functions of PLC(phospholipase C, PLC). To define the role of SPK in regulating the proliferation of HGCC and HVEC, the specific inhibitor to SPK, DMS, was added to the two cells. Results showed that DMS could almost completely inhibit the proliferation of HGCC, HVEC and DMS could produce effects in 1 $\mu\text{mol/L}$ and 3 h later. This illustrated that the regulation of DMS on the proliferation of two cells was prompt, sensitive and striking. Considering SPK was an important regulator to the growth of HGCC and HVEC, we studied the role of SPK in the interactions between these two cells. We found that the expression of SPK mRNA in one kind of cell with no significant change after the action of the CM of the other kind of cell. This showed that the expression of SPK gene didn't involve in the interactions between two cells. Maybe the regulation of one cell on the other cell is through some other factors or pathways. It needs further study to define the other mechanisms involved in the interrelationships between HGCC and HVEC.

REFERENCES

- 1 **Ren J**, Dong L, Xu CB, Pan BR, Li MZ. Interactions between the human gastric carcinoma cell and vascular endothelial cell. *Shijie Huaren Xiaohua Zazhi* 2001; **9**: 1254-1260
- 2 **Ren J**, Dong L, Xu CB. Role of sphingosine-1-phosphate in regulating the proliferation of human gastric carcinoma cell and vascular endothelial cell. *Xi'an Yike Daxue Xuebao* 2001; **6**:527-531
- 3 **Von BC**, Hayen W, Hartmann A, Mueller KW, Allolio B, Nehls V. Endothelial capillaries chemotactically attract tumor cells. *J Pathol* 2001; **193**:367-376
- 4 **Okamoto H**, Ohigashi H, Nakamori S, Ishikawa O, Imaoka S, Mukai M, Kusama T, Fuji H. Reciprocal functions of liver tumor cells and endothelial cells. Involvement of endothelial cell migration and tumor cell proliferation at a primary site in distant metastasis. *Eur Surg Res* 2000; **32**: 374-379
- 5 **Moreno A**, Villar ML, Camara C, Luque R, Cespon C, Gonzalez-PP, Roy G, Lopez JJ. Interleukin-6 dimers produced by endothelial cells inhibit apoptosis of B-chronic lymphocytic leukemia cells. *Blood* 2001; **97**:242-249
- 6 **Brandvold K A**, Neiman P, Ruddell A. Angiogenesis is an early event in the generation of myc-induced lymphomas. *Oncogene* 2000; **19**: 2780-2785
- 7 **De BES**, Rosati S, Jacobs S, Kamps WA, Vellenga E. Increased bone marrow vascularization in patients with acute myeloid leukaemia: a possible role for vascular endothelial growth factor. *Br J Haematol* 2001; **113**:296-304
- 8 **Hewett PW**. Identification of tumor-induced changes in endothelial cell surface protein expression: an *in vitro*

- model. *Int J Biochem Cell Biol* 2001; **33**:325-335
- 9 **Luo J**, Guo P, Matsuda K, Truong N, Lee A, Chun C, Cheng SY, Kore M. Pancreatic cancer cell-derived vascular endothelial growth factor is biologically active *in vitro* and enhances tumorigenicity *in vivo*. *Int J Cancer* 2001; **92**:361-369
- 10 **Witt C J**, Gabel S P, Meisinger J. Interrelationship between protein phosphatase-2A and cytoskeletal architecture during the endothelial cell response to soluble products produced by human head and neck cancer. *Otolaryngol Head Neck Surg* 2000; **122**:721-727
- 11 **Kuroda K**, Miyata K, Tsutsumi Y. Preferential activity of wild-type and mutant tumor necrosis factor- α against tumor-derived endothelial like cells. *Jpn J Cancer Res* 2000; **91**:59-67
- 12 **Shemirani B**. Head and Neck squamous cell carcinoma lines produce biologically active angiogenic factors. *Oral Oncol* 2000; **36**: 61-66
- 13 **Beierle EA**, Strande LF, Berger AC, Chen MK. VEGF is upregulated in a neuroblastoma and hepatocyte coculture model. *J Surg Res* 2001; **97**:34-40
- 14 **Vidal Vanaclocha F**, Fantuzzi G, Mendoza L. IL-18 regulated IL-1 β dependent hepatic melanoma metastasis via vascular cell adhesion molecule-1. *Proc Natl Acad Sci USA* 2000; **97**:734-739
- 15 **Aoki M**, Kanamori M, Yudoh K, Ohmori K, Yasuda T, Kimura T. Effects of vascular endothelial growth factor and E-selectin on angiogenesis in the murine metastatic RCT sarcoma. *Tumour Biol* 2001; **22**:239-246
- 16 **Liu W**, Davis DW, Ramirez K, McConkey DJ, Ellis LM. Endothelial cell apoptosis is inhibited by a soluble factor secreted by human colon cancer cells. *Int J Cancer* 2001; **92**: 26-30
- 17 **Albini A**, Marchisone C, Del Grosso F. Inhibition of angiogenesis and vascular tumor growth by interferon-producing cells: A gene therapy approach. *Am J Pathol* 2000; **156**:1381-1393
- 18 **Kamada H**, Tsutsumi Y, Kihira T. *In vitro* remodeling of tumor vascular endothelial cells using conditioned medium from various tumor cells and their sensitivity to TNF- α . *Biochem Biophys Res Commun* 2000; **268**:809-813
- 19 **Wu K**, Zhao Y, Liu BH, Li Y, Liu F, Guo J, Yu WP. RRR- α -tocopheryl succinate inhibits human gastric cancer SGC-7901 cell growth by inducing apoptosis and DNA synthesis arrest. *World J Gastroenterol* 2002; **8**:26-30
- 20 **Wang X**, Lan M, Shi YQ, Lu J, Zhong YX, Wu HP, Zai HH, Ding J, Wu KC, Pan BR, Jin JP, Fan DM. Differential display of vincristine-resistance-related genes in gastric cancer SGC7901 cell. *World J Gastroenterol* 2002; **8**:54-59
- 21 **Yao YL**, Xu B, Song YG, Zhang WD. Overexpression of cyclin E in Mongolian gerbil with *Helicobacter pylori*-induced gastric precancerosis. *World J Gastroenterol* 2002; **8**: 60-63
- 22 **Yang SM**, Fang DC, Luo YH, Lu R, Liu WW. Effect of antisense gene to human telomerase reverse transcriptase on telomerase activity and expression of apoptosis-associated gene. *Shijie Huaren Xiaohua Zazhi* 2002; **10**:149-152
- 23 **Zheng ZH**, Xun XJ, Qiu GR, Liu YX, Wang MX, Sun KL. E-cadherin gene mutation in precancerous condition, early and advanced stage of gastric cancer. *Shijie Huaren Xiaohua Zazhi* 2002; **10**:153-156
- 24 **Wang W**, Luo HS, Yu BP. Expression of human telomerase reverse transcriptase gene and c-myc protein in gastric carcinogenesis. *Shijie Huaren Xiaohua Zazhi* 2002; **10**:258-261
- 25 **Li JY**, Yu JP, Luo HS, Yu BP, Huang JA. Effects of nonsteroidal anti-inflammatory drugs on the proliferation and cyclooxygenase activity of gastric cancer cell line SGC7901. *Shijie Huaren Xiaohua Zazhi* 2002; **10**:262-265
- 26 **Xue FB**, Xu YY, Wan Y, Pan BR, Ren J, Fan DM. Association of *H. pylori* infection with gastric carcinoma: a Meta analysis. *World J Gastroenterol* 2001; **7**:801-804
- 27 **Liu DH**, Zhang XY, Fan DM, Huang YX, Zhang JS, Huang WQ, Zhang YQ, Huang QS, Ma WY, Chai YB, Jin M. Expression of vascular endothelial growth factor and its role in oncogenesis of human gastric carcinoma. *World J Gastroenterol* 2001; **7**:500-505
- 28 **Cai L**, Yu SZ, Zhang ZF. Glutathione S-transferases M1, T1 genotypes and the risk of gastric cancer: A case-control study. *World J Gastroenterol* 2001; **7**:506-509
- 29 **He XS**, Su Q, Chen ZC, He XT, Long ZF, Ling H, Zhang LR. Expression, deletion and mutation of p16 gene in human gastric cancer. *World J Gastroenterol* 2001; **7**:515-521
- 30 **Boguslawski G**, Grogg JR, Welch Z, Ciechanowicz S, Sliva D, Kovala AT, McGlynn P, Brindley DN, Rhoades RA, English D. Migration of vascular smooth muscle cells induced by sphingosine 1-phosphate and related lipids: potential role in the angiogenic response. *Exp Cell Res* 2002; **274**:264-274
- 31 **Mora A**, Sabio G, Risco AM, Cuenda A, Alonso JC, Soler G, Centeno F. Lithium blocks the PKB and GSK3 dephosphorylation induced by ceramide through protein phosphatase-2A. *Cell Signal* 2002; **14**:557-562
- 32 **Shekar S**, Tumaney AW, Rao TJ, Rajasekharan R. Isolation of Lysophosphatidic Acid Phosphatase from Developing Peanut Cotyledons. *Plant Physiol* 2002; **128**:988-996
- 33 **Broomhead JN**, Ledoux DR, Bermudez AJ, Rottinghaus GE. Chronic effects of fumonisin B1 in broilers and turkeys fed dietary treatments to market age. *Poult Sci* 2002; **81**:56-61
- 34 **Melendez AJ**, Allen JM. Phospholipase D and immune receptor signalling. *Semin Immunol* 2002; **14**:49-55
- 35 **Itakura A**, Tanaka A, Aioi A, Tonogaito H, Matsuda H. Ceramide and sphingosine rapidly induce apoptosis of murine mast cells supported by interleukin-3 and stem cell factor. *Exp Hematol* 2002; **30**:272-278
- 36 **Han X**. Characterization and direct quantitation of ceramide molecular species from lipid extracts of biological samples by electrospray ionization tandem mass spectrometry. *Anal Biochem* 2002; **302**:199-212
- 37 **Mei J**, Holst LS, Landstrom TR, Holm C, Brindley D, Manganiello V, Degerman E. C(2)-ceramide influences the expression and insulin-mediated regulation of cyclic nucleotide phosphodiesterase 3B and lipolysis in 3T3-L1 adipocytes. *Diabetes* 2002; **51**: 631-637
- 38 **Maruyama W**, Oya-Ito T, Shamoto-Nagai M, Osawa T, Naoi M. Glyceraldehyde-3-phosphate dehydrogenase is translocated into nuclei through Golgi apparatus during apoptosis induced by 6-hydroxydopamine in human dopaminergic SH-SY5Y cells. *Neurosci Lett* 2002; **321**:29-32
- 39 **Ryu Y**, Takuwa N, Sugimoto N, Sakurada S, Usui S, Okamoto H, Matsui O, Takuwa Y. Sphingosine-1-phosphate, a platelet-derived lysophospholipid mediator, negatively regulates cellular Rac activity and cell migration in vascular smooth muscle cells. *Circ Res* 2002; **90**: 325-332
- 40 **Melendez AJ**, Allen JM. Phospholipase D and immune receptor signaling. *Semin Immunol* 2002; **14**: 49-55
- 41 **Melendez AJ**, Khaw AK. Dichotomy of Ca²⁺ signals triggered by different phospholipid pathways in antigen stimulation of human mast cells. *J Biol Chem* 2002; [epub

- ahead of print]
- 42 **Chin TY**, Hwang HM, Chueh SH. Distinct effects of different calcium-mobilizing agents on cell death in NG108-15 neuroblastoma X glioma cells. *Mol Pharmacol* 2002; **61**: 486-494
- 43 **McCaig C**, Perks CM, Holly JM. Signalling pathways involved in the direct effects of IGFBP-5 on breast epithelial cell attachment and survival. *J Cell Biochem* 2002; **84**: 784-794
- 44 **Vann LR**, Payne SG, Edsall LC, Twitty S, Spiegel S, Milstien S. Involvement of sphingosine kinase in TNF- α stimulated tetrahydrobiopterin biosynthesis in C6 glioma cells. *J Biol Chem* 2002; [epub ahead of print]
- 45 **Xia P**, Wang L, Moretti PA, Albanese N, Chai F, Pitson SM, D'Andrea RJ, Gamble JR, Vadas MA. Sphingosine Kinase Interacts with TRAF2 and Dissects Tumor Necrosis Factor- α Signaling. *J Biol Chem* 2002; **277**: 7996-8003
- 46 **Ancellin N**, Colmont C, Su J, Li Q, Mittereder N, Chae SS, Stefansson S, Liao G, Hla T. Extracellular export of sphingosine kinase-1 enzyme. Sphingosine 1-phosphate generation and the induction of angiogenic vascular maturation. *J Biol Chem* 2002; **277**: 6667-6675
- 47 **Alemanly R**, Kleuser B, Ruwisch L, Danneberg K, Lass H, Hashemi R, Spiegel S, Jakobs KH, Meyer zu Heringdorf D. Depolarisation induces rapid and transient formation of intracellular sphingosine-1-phosphate. *FEBS Lett* 2001; **509**: 239-244
- 48 **Pitson SM**, Moretti PA, Zebol JR, Vadas MA, D'Andrea RJ, Wattenberg BW. A point mutant of human sphingosine kinase 1 with increased catalytic activity. *FEBS Lett* 2001; **509**: 169-173
- 49 **Rosenfeldt HM**, Hobson JP, Maceyka M, Olivera A, Nava VE, Milstien S, Spiegel S. EDG-1 links the PDGF receptor to Src and focal adhesion kinase activation leading to lamellipodia formation and cell migration. *FASEB J* 2001; **15**: 2649-2659

Edited by Zhao P

• GASTRIC CANCER •

Effect of jianpiyiwei capsule on gastric precancerous lesions in rats

Xue-Ying Shi, Feng-Zhi Zhao, Xin Dai, Lian-Sheng Ma, Xiu-Yu Dong, Jie Fang

Xue-Ying Shi, Feng-Zhi Zhao, Xin Dai, Lian-Sheng Ma, Xiu-Yu Dong, Jie Fang, Department of Pathology, Peking University, School of Basic Medical Sciences, Beijing, 100083 China

Feng-Zhi Zhao, Xin Dai, Jie Fang, Department of Pathology, Dongzhimen Affiliated Hospital, Beijing University of Traditional Chinese Medicine, Beijing 100700, China

Lian-Sheng Ma, Taiyuan Research & Treatment Center for Digestive Diseases, Taiyuan 030001, Shanxi Province, China

Xiu-Yu Dong, Department of Gastroenterology, Third School of Clinical Medicine, Peking University, School of Medical Sciences, Beijing 100083, China

Correspondence to: Dr. Lian-Sheng Ma, Taiyuan Research & Treatment Center of Digestive Disease, 77 Shuangta Xiejie, Taiyuan 030001, Shanxi Province China. wjcd@public.bta.net.cn

Telephone: +86-10-85381892 **Fax:** +86-10-85381893

Received 2002-04-09 **Accepted** 2002-06-15

Abstract

AIM: To evaluate the therapeutic effect of compound Chinese drugs, Jianpiyiwei capsule (JPYW) on gastric precancerous lesions in rats and to explore its mechanism of action.

METHODS: Model of gastric precancerous lesions was constructed in male Wistar rats: a metal spring was inserted and fixed through pyloric sphincter. One week after recovery, each rat was given 50-60 °C hot paste containing 150 g/L NaCl 2 mL orally, twice a week for 15 weeks. Then 10 normal and 11 model rats were anaesthetized, after the measurement of gastric mucosa blood flow (GMBF), the rats were killed and the mucosal hexosamines and malonic dialdehyde (MDA) were measured. The morphological changes of gastric mucosa were observed macroscopically and microscopically, and by an automatic imaging analysis system. Other rats were treated with JPYW 1.5 g/kg·d⁻¹ or 4.5 g/kg·d⁻¹, or distilled water as negative control respectively (*n*=10 in each group). After 12 weeks, all the rats were examined as above.

RESULTS: The gastric mucosa of model rats showed chronic atrophic gastritis with dysplasia and intestinal metaplasia (IM), GMBF and hexosamine content were reduced significantly and MDA was increased as compared to the normal group (*P*<0.01). After 12 weeks treatment, the pathological changes of the negative control group became worsened, while in JPYW treated groups the changes were modified with significant increase of GMBF and reduction of MDA, although the hexosamine concentration increased only mildly.

CONCLUSION: JPYW increases GMBF and reduces MDA content in gastric mucosa and has therapeutic effects on gastric precancerous lesions.

Shi XY, Zhao FZ, Dai X, Ma LS, Dong XY, Fang J. Effect of jianpiyiwei capsule on gastric precancerous lesions in rats. *World J Gastroenterol* 2002; 8(4):608-612

INTRODUCTION

Jianpiyiwei capsule (JPYW), a compound Chinese drug, has the effect of replenishing *qi* (vital energy) and invigorate the spleen, promoting blood flow and regulating the stomach function. This study investigates the therapeutic effect of JPYW on gastric precancerous lesions in rats, and tries to elucidate its mechanism of action in part.

MATERIALS AND METHODS

Male Wistar rats, weighed 250 g to 300 g, were purchased from the Laboratory Animal Center, Chinese Academy of Medical Science. The rats were housed in an air-conditioned animal room at 25±2 °C and 60 % humidity with food and water available *ad libitum*, and drinking water was changed every day.

The establishment of gastric precancerous lesions in rats was modified according to Zhao's method^[1] with modification: a metal spring was inserted and fixed through pyloric sphincter. One week after recovery, each rat was given 50-60 °C hot paste containing 150g/L NaCl 2 mL orally, twice a week for 15 weeks. Then, all the survived rats were divided randomly into 4 groups: (1) model group (*n*=11), (2) negative control (*n*=10), (3) small dose JPYW group (*n*=10), (4) large dose JPYW group (*n*=10). Group 1 rats were killed 16 weeks after the operation, group 2-4 were given diluted water 2 mL/d, JPYW 1.5g/kg·d⁻¹ or JPYW 4.5g/kg·d⁻¹, separately, 6 times per week for 12 weeks. Moreover, a group of normal rats (*n*=10) were raised for 16 weeks and killed together with group 1.

Gastric mucosa blood flow (GMBF) assays

Before the rats were killed, they were forbidden from food except drinking freely for 24 hours, then they were anaesthetized. After incision of the abdominal wall, an ultrasonic detective probe was put to the junction between antrum pylori and corpus ventriculi in gastric curvature of stomach through an incision at the provetriculus, and the voltage number were read to represent the relative level of GMBF.

Morphological study

After the detection of GMBF, the rat was killed and stomach was removed and cut off through the greater curvature, washed by physiological saline and residual liquid was absorbed. The whole stomach was first observed in gross, and then the gastric mucosa of posterior wall was scraped off and frozen to -20 °C immediately for the detection of hexosamines and malonic dialdehyde (MDA). The anterior wall was fixed in 10 % neutral buffered formalin over 24 hours, then were cut into 2 mm-wide pieces, all the pieces were embedded in paraffin. 5 μm sections, stained with hematoxylin and eosin and with alcian blue, periodic acid-schiff and high iron diamine (AB-PAS/HID), were examined under light microscopy.

Quantitative histologic evaluations were performed using

an automatic imaging analysis system (produced by Beijing University of Aeronautics and Astronautics). Ten cases of each group were selected for the morphometric measurements, including: (1) thickness of glandular layer *vs* thickness from surface to the end of muscular layer of mucosa (T_1/T_2 , five low visual fields in corpus ventriculi and 5 in antrum pylori for each section), (2) nuclear area *vs* cytoplasm area of epithelioglandular cells(N/C), (3) intra-cavity periphery of a gland *vs* the diameter of the circle whose area was equal to the glandular cavity(P_1/D_1), (4) periphery of basal coil in a gland *vs* the diameter of the circle whose area was equal to the gland (P_2/D_2). (2)-(4), each measured 10 middle visual fields in one section.

Hexosamines and MDA assays

The achievement of gastric mucosa has been described as above. The hexosamine content in gastric mucosa was detected according to Neuhaus' s method^[2], and the measurement of MDA by thiobarbituric acid method.

Statistical analysis

Numerical values were expressed as $\bar{x} \pm s$. Comparisons of data between groups were performed with *student's t* test or χ^2 test. $P < 0.05$ was considered significant.

RESULTS

Effects of JPYW on the morphological changes of gastric precancerous lesions in rats

Gross examination of stomach in model and negative control groups showed thinning and paleness of gastric mucosa, with disarrayed plicae and small white nodules, while in the normal groups it was pink, moistened and smooth. In JPYW treated groups, the gross change of gastric mucosa was only modest as compared with negative control group, especially in 4.5 g/Kg·d⁻¹ group ($P < 0.05$ or 0.01) (Table 1).

Histopathology of gastric mucosa in the model and the negative control groups revealed increased incidence of chronic superficial gastritis (CSG), chronic atrophic gastritis (CAG), intestinal metaplasia (IM) and gastric mucosa dysplasia, as compared with normal and JPYW treated groups ($P < 0.05$ or 0.01)(Table 2,). AB-PAS/HID staining showed both complete and incomplete IM (Figure 1).

Data by automatic image pattern analysis were shown in table 3. The ratios of T_1/T_2 , representing the degree of mucosal atrophy, were greatly reduced in model and negative control groups both at the gastric body and the antrum, and ratios of N/C, P_1/D_1 , P_2/D_2 representing the degree of dysplasia, were increased more prominently in those two groups as compared with normal group ($P < 0.01$). In JPYW treated groups, all the ratios approached normal, although there were still some difference between 1.5g/Kg·d⁻¹ group and normal ($P < 0.05$ or 0.01). (Table 3)

Table 1 Effects of JPYW on macroscopical changes of gastric precancerous lesions in rats

group	n	erosion / ulceration	Disarrayed plicae	thinning of mucosa	white nodules	xanthochromia of mucosa
normal	10	0	0	1	0	0
model	11	6 ^b	7 ^b	9 ^b	9 ^b	5 ^a
negative	10	6 ^a	6 ^a	9 ^b	10 ^b	5 ^a
1.5 g/Kg·d ⁻¹	10	2	1 ^{ce}	3 ^{cf}	3 ^{cf}	1 ^{ce}
4.5 g/Kg·d ⁻¹	10	0 ^{de}	0 ^{de}	1 ^{df}	2 ^{df}	0

n: number; normal: normal group; model: model group; negative: negative control group; 1.5 g/Kg·d⁻¹: JPYW 1.5 g/

Kg·d⁻¹ group; 4.5 g/Kg·d⁻¹:JPYW 4.5 g/Kg·d⁻¹ group ^a $P < 0.05$, ^b $P < 0.01$, *vs* normal group; ^c $P < 0.05$, ^d $P < 0.01$, *vs* model group; ^e $P < 0.05$, ^f $P < 0.01$, *vs* negative control group.

Table 2 Effects of JPYW on histological changes of gastric pre-cancerous lesions in rats

group	n	CSG	CAG	dysplasia	IM
normal	10	1	0	0	0
model	11	11 ^b	10 ^b	8 ^b	3
negative	10	10 ^b	10 ^b	8 ^b	5 ^b
1.5 g/Kg·d ⁻¹	10	3 ^{df}	5 ^{ae}	2 ^{ce}	1
4.5 g/Kg·d ⁻¹	10	2 ^{df}	1 ^{df}	1 ^{df}	0 ^e

n: number; normal: normal group; model: model group; negative: negative control group; 1.5 g/Kg·d⁻¹: JPYW 1.5g/Kg·d⁻¹ group; 4.5 g/Kg·d⁻¹:JPYW 4.5 g/Kg·d⁻¹ group ^a $P < 0.05$, ^b $P < 0.01$, *vs* normal group; ^c $P < 0.05$, ^d $P < 0.01$, *vs* model group; ^e $P < 0.05$, ^f $P < 0.01$, *vs* negative control group.

Table 3 Automatic imaging pattern analysis effects of JPYW ($\bar{x} \pm s$, n=10)

group	T_1/T_2 in gastric body	T_1/T_2 in antrum	N/C	P_1/D_1	P_2/D_2
normal	10.6±2.0	5.9±1.0	0.54±0.02	3.53±0.08	3.43±0.07
model	1.9±0.4 ^b	1.3±0.2 ^b	0.75±0.04 ^b	4.18±0.09 ^b	3.69±0.08 ^b
negative	1.8±0.5 ^b	1.1±0.1 ^{bc}	0.78±0.02 ^{bc}	4.39±0.10 ^{bd}	3.95±0.08 ^{bd}
1.5 g/Kg·d ⁻¹	4.3±0.6 ^{bdf}	3.1±0.7 ^{bdf}	0.62±0.02 ^{bdf}	3.62±0.09 ^{bdf}	3.55±0.06 ^{bdf}
4.5 g/Kg·d ⁻¹	8.9±1.8 ^{df}	5.3±0.9 ^{df}	0.55±0.03 ^{df}	3.57±0.07 ^{df}	3.46±0.07 ^{df}

normal: normal group; model: model group; negative: negative control group; 1.5 g/Kg·d⁻¹: JPYW 1.5 g/Kg·d⁻¹ group; 4.5 g/Kg·d⁻¹:JPYW 4.5 g/Kg·d⁻¹group ^a $P < 0.05$, ^b $P < 0.01$, *vs* normal group; ^c $P < 0.05$, ^d $P < 0.01$, *vs* model group; ^e $P < 0.05$, ^f $P < 0.01$, *vs* negative control group.

Table 4 Effects of JPYW on GMBF and the gastric mucosal hexosamines and MDA contents ($\bar{x} \pm s$)

group	n	GMBF(mV)	Hexosamines(mg/g)	MDA(μmol/g)
normal	10	0.29±0.05	6.8±1.1	46±25
model	11	0.17±0.04 ^b	4.8±0.7 ^b	374±49 ^b
negative	10	0.18±0.04 ^b	4.9±0.8 ^b	419±43 ^{bc}
1.5g/Kg·d ⁻¹	10	0.27±0.07 ^{de}	5.2±1.2 ^b	312±56 ^{bce}
4.5g/Kg·d ⁻¹	10	0.29±0.05 ^{de}	5.6±0.9 ^{ac}	271±40 ^{bce}

n: number; normal: normal group; model: model group; negative: negative control group; 1.5g/Kg·d⁻¹: JPYW 1.5g/Kg·d⁻¹ group; 4.5 g/Kg·d⁻¹:JPYW 4.5 g/Kg·d⁻¹ group ^a $P < 0.05$, ^b $P < 0.01$, *vs* normal group; ^c $P < 0.05$, ^d $P < 0.01$, *vs* model group; ^e $P < 0.05$, ^f $P < 0.01$, *vs* negative control group.

Effects of JPYW on GMBF

The GMBF in model group was reduced more obviously than that in the normal group ($P < 0.01$). After 12wk treatment, there was no increase of GMBF in negative control group, but great improvements were seen in JPYW treated groups as compared with model or negative control group ($P < 0.01$). (Table 4)

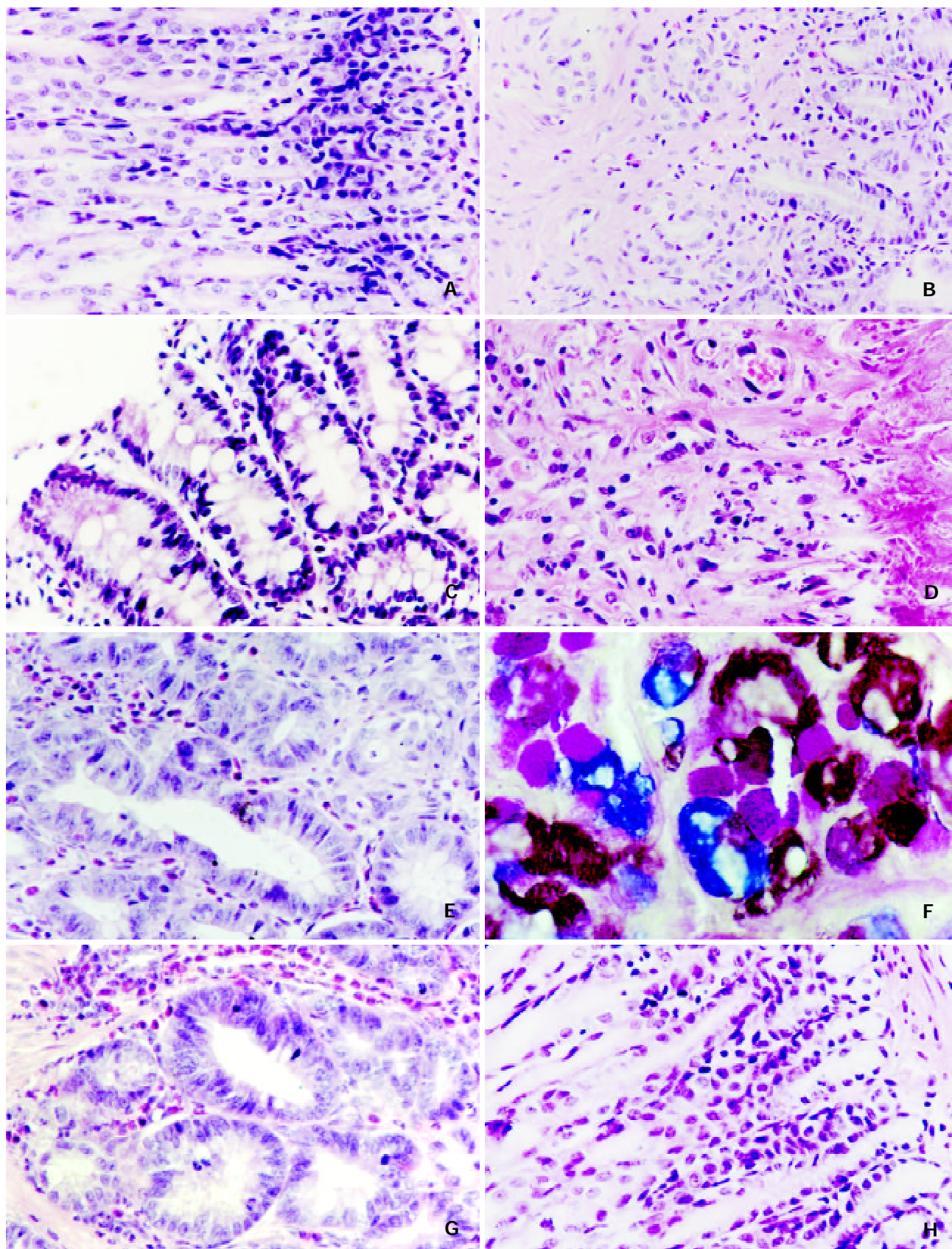


Figure 1(A-D) Effects of JPYW on histological changes of gastric precancerous lesions in rats A: Morphology of gastric mucosa in normal rat. HE 100× B-D Show the histologic changes of gastric mucosa in model group, B: CAG HE 100×, C: IM without dysplasia HE 100×, D: ulcer HE 100×.

Figure 1(E-F) Effects of JPYW on histological changes of gastric precancerous lesions in rats E-F Show the histologic changes of gastric mucosa in model group, E: Moderate dysplasia with IM HE 100×, F: Incomplete IM AB-PAS/HID 200× G: Moderate to severe dysplasia in gastric mucosa in negative control group HE 100× H: The histological figure of gastric mucosa in JPYW 4.5g/Kg·d⁻¹ group is close to normal HE 100×

Effects of JPYW on gastric mucosal contents of hexosamines and MDA

In the model group, the gastric mucosa hexosamine content was lower and MDA was higher than that in the normal group. After 12 wk treatments, no differences were seen between them in the negative control group and model group, yet in 4.5 g/Kg·d⁻¹ group there was some increase in hexosamine content, significant difference was still present when compared with normal group ($P < 0.05$). Moreover, the MDA content in JPYW treated groups was greatly reduced ($P < 0.05$ or 0.01). (Table 4)

DISCUSSION

Although the over all incidence of gastric cancer has steadily declined in the western world^[3], it is still the most common fatal malignancy in China^[4], therefore the treatment of gastric precancerous lesions should be one of the important measures for preventing gastric cancer.

Since 1988 Correa and his colleagues proposed a human model of gastric carcinogenesis, which is gastric cancer develops through a complex sequence of events from normal mucosa to superficial gastritis, chronic atrophic gastritis, IM, dysplasia and finally to intestinal type gastric cancer, numerous studies have found genetic alterations in gastric precancerous lesions and supported the hypothesis^[5-10]. But the etiology of gastric precancerous lesions has not been fully elucidated. Many factors are thought to have close relations to gastric carcinogenesis, such as a diet high in salt^[11,12] and starch^[13], consumption of high temperature food^[14], *Helicobacter pylori* (HP) infection^[15-19], drinking alcohol^[19,20], smoking^[20,21] and bile reflux^[21-23].

Some experimental studies have shown that the high-salt diet may potentiate HP-associated carcinogenesis in mice by inducing proliferation, pit cell hyperplasia, and glandular atrophy^[24], and 50-week bile reflux may cause gastric cancer in rats^[25]. In this article, we establish a model of gastric precancerous lesions in rats by inserted a metal spring through gastric pylorus sphincter and given hot paste containing high concentration of NaCl, which lead to the development of precancerous gastric lesions. The typical feature of this model are glandular atrophy, lamina propria infiltration of chronic inflammatory cells, thickening of muscularis mucosa, glandular dysplasia and IM, simulating human gastric precancerous lesions. JPYW was found to have obvious effects on gastric precancerous lesions in rats with thickening of gastric mucosa and decreased incidence of dysplasia and IM that firmly supported our hypothesis that JPYW has therapeutic effects on gastric precancerous lesions.

GMBF is an important part of mucosal defense system, bringing oxygen and nutrients to the mucosal cells, against penetration of carcinogenesis into gastric mucosa^[26], maintaining the structure and function of the stomach and is closely associated with the pathogenesis and the healing of gastrointestinal lesions^[27]. In the JPYW treated groups, the GMBF recovered to normal, which indicates that the increase of GMBF may be one of the mechanisms of JPYW on gastric precancerous lesions.

Etiologic studies find that blood levels of natural antioxidants in patients with gastric precancerous lesions or cancer are much lower than healthy people^[28] and low level of dietary vitamin C may contribute to the progression of precancerous lesions to gastric cancer^[29], whereas a dietary high intake of antioxidants may lower the risk for gastric cancer^[30]. Farinati *et al.*^[31] reported that there was an oxidative DNA damage accumulation with mutagenic and carcinogenic

potential in chronic gastritis. MDA content, an metabolite of lipid peroxidant, were found higher in gastric mucosa of patients with HP gastritis^[32] and in N-methyl-N'-nitro-N-nitrosoguanidine induced gastric cancer in rats^[33]. In our experiment, the MDA content of gastric mucosa in the model rats increased significantly, which implied that the free radicals participated in the occurrence of gastric precancerous lesions. And the reduction of mucosal MDA content in JPYW treated groups indicates that JPYW has a protective action on gastric mucosa.

We also noticed that the hexosamines content, which partially represented the function of gastric mucosal barrier^[34] decreased obviously in gastric mucosa of model rats, and only increased slightly in JPYW treated groups with absence of statistical differences. This suggests that the therapeutic effects of JPYW in gastric precancerous lesions dose not involve hexosamine content.

In conclusion, JPYW has therapeutic effects on gastric precancerous lesions, it increases GMBF and reduces mucosal MDA content which may also play a role in its mechanism of action.

REFERENCES

- 1 Zhao FZ, Lu XF, Dai X, Bu YM, Zhang XC, Shi XY, Fang J, Dong JH, Tian DL, Ma QS, Qin LM, Wang ZC, Yang YF. Effects of three decoctions on histopathologic changes, pH and total cholic acid of gastric juice in experimental chronic gastritis in rats. *Zhongguo Zhongyao Zazhi* 1995; **20**:488-492
- 2 Neuhaus OW, Letzring M. Determination of hexosamines in conjunction with electrophoresis on starch. *Anal Chem* 1957; **29**: 1230-1233
- 3 Palli D. Epidemiology of gastric cancer: an evaluation of available evidence. *J Gastroenterol* 2000; **35**(suppl): 1284-1289
- 4 Sun X, Mu R, Zhou Y, Dai X, Qiao Y, Zhang S, Huangfu X, Sun J, Li L, Lu F. 1990-1992 mortality of stomach cancer in China. *Zhonghua Zhongliu Zazhi* 2002; **24**:4-8
- 5 Wang YK, Ji XL, Ma NX. Relationship between morphology of gastric mucosa dysplasia and the expression of p53, Bcl-2 and c-erbB-2. *Shijie Huaren Xiaohua Zazhi* 1999; **7**: 114-116
- 6 Gong C, Mera R, Bravo JC, Buiz B, Diaz-Escamilla K, Fantham ET, Correa P, Hunt JD. K-ras mutations predict progression of preneoplastic gastric lesions. *Cancer Epidemiol Biomarkers Prev* 1999; **8**:167-171
- 7 Dai J, Yu SX, Qi XL, Bo AH, Xu YL, Guo ZY. Expression of bcl-2 and c-myc protein in gastric carcinoma and precancerous lesions. *World J Gastroenterol* 1998; **4**(suppl 2): 84-85
- 8 Wu MS, Shun CT, Wang HP, Lee WJ, Wang TH, Lin JT. Loss of pS2 protein expression is an early event of intestinal-type gastric cancer. *Jpn J Cancer Res* 1998; **89**:278-282
- 9 Kim JJ, Baek MJ, Kim L, Kim NG, Lee YC, Song SY, Noh SH, Kim H. Accumulated frameshift mutation at coding nucleotide repeats during the progression of gastric carcinoma with microsatellite instability. *Lab Invest* 1999; **79**: 1113-1120
- 10 Toru H, Yokozaki H, Kitadai Y, Tahara E, Tahara H, Ide T, Haruma K, Yasui W, Kajiyama G. *In situ* mRNA hybridization technique for analysis of telomerase RNA in gastric precancerous and cancerous lesions. *Jpn J Cancer Res* 1998; **89**: 1187-1194
- 11 Ward MH, Lopez-Carrillo L. Dietary factors and the risk of gastric cancer in Mexico city. *Am J Epidemiol* 1999; **149**: 925-932
- 12 Ye WM, Yi YN, Luo RX, Zhou TS, Lin RT, Chen GD. Diet and gastric cancer: a case-control study in Fujian Province,

- China. *World J Gastroenterol* 1998; **4**:516-518
- 13 **Munoz N**, Plummer M, Vivas J, Moreno V, De-Sanjosé S, Lopaze G, Oliver W. A case-control study of gastric cancer in Venezuela. *Int J Cancer* 2001; **93**:417-423
- 14 **Mathew A**, Gangadharan P, Varghese C, Nair MK. Diet and stomach cancer: a case-control study in South India. *Eur J Cancer Prev* 2000; **9**:89-97
- 15 **Honda S**, Fujioka T, Tokieda M, Satoh R, Nishizono A, Nasu M. Development of *Helicobacter pylori*-induced gastric carcinoma in mongolian gerbils. *Cancer Res* 1998; **58**:4255-4259
- 16 **Zarrilli R**, Ricci V, Romano M. Molecular response of gastric epithelial cells to *Helicobacter pylori*-induced cell damage. *Cell Microbiol* 1999; **1**:93-99
- 17 **Zhang L**, Jiang Y, Pan KF, Lui WD, Ma JL, Zhou T. Infection of *H. Pylori* with cagA⁺ strain in a high-risk area of gastric cancer. *Huaren Xiaohua Zazhi* 1998; **6**:40-41
- 18 **Jablonska M**, Chlumska A. Genetic factors in the development of gastric precancerous lesions—a role of *Helicobacter pylori*? *J Physiol-Paris* 2001; **95**:477-481
- 19 **You WC**, Zhang L, Gail MH, Ma JL, Chang YS, Blot WJ, Li JY, Zhao CL, Liu WD, Li HQ, Hu YR, Bravo JC, Correa P, Xu GW, Fraumeni JF. *Helicobacter pylori* infection, garlic intake and precancerous lesions in a Chinese population at low risk of gastric cancer. *Int J Epidemiol* 1998; **27**:941-944
- 20 **De Stefani E**, Boffetta P, Carzoglio J, Mendilaharsu S, Deneo-Pellegrini H. Tobacco smoking and alcohol drinking as risk factors for stomach cancer: a case-control study in Uruguay. *Cancer Causes Control* 1998; **9**:321-329
- 21 **Barrios A**. Biliary gastritis as a precancerous lesion. *Anaerobe* 1999; **5**:385-390
- 22 **Lorusso D**, Linsalata M, Pezzolla F, Berloco P, Osella AR, Guerra V, Di-Leo A, Demma I. Duodenogastric reflux and mucosal polyamines in the non-operated stomach and in the gastric remnant after Billroth II gastric resection. A role in gastric carcinogenesis? *Anticancer Res* 2000; **20**:2197-2201
- 23 **Zullo A**, Rinaldi V, Hassan C, Lauria V, Attili AF. Gastric pathology in cholecystectomy patients: role of *Helicobacter pylori* and bile reflux. *J Clin Gastroenterol* 1998; **27**:335-338
- 24 **Fox JG**, Dangler CA, Taylor NS, King A, Koh TJ, Wang TC. High-salt diet induces gastric epithelial hyperplasia and parietal cell loss, and enhances *Helicobacter pylori* colonization in C57BL/6 mice. *Cancer Res* 1999; **59**:4823-4828
- 25 **Miwa K**, Fujimura T, Hasegawa H, Kosaka T, Miyata R, Miyazaki I, Hattori T. Is bile or are pancreaticoduodenal secretions related to gastric carcinogenesis in rats with reflux through the pylorus?. *J Cancer Res Clin Oncol* 1992; **118**:570-574
- 26 **Srobye H**, Westby J, Ovrebo K, Kvinnsland S, Svanes K. Role of blood flow in protection against penetration of carcinogens into normal and healing rat gastric mucosa. *Dig Dis Sci* 1995; **40**:2509-2515
- 27 **Kawano S**, Tsuji S. Role of mucosal blood flow: a conceptual review in gastric mucosal injury and protection. *J Gastroenterol Hepatol* 2000; **15**(suppl):D1-6
- 28 **Beno I**, Klvanova J, Magalova T, Brtkova A. Blood levels of natural antioxidants in gastric and colorectal precancerous lesions and cancers in Slovakia. *Neoplasma* 2000; **47**:37-40
- 29 **You WC**, Zhang L, Gail MH, Chang YS, Liu WD, Ma JL, Li JY, Jin ML, Hu YR, Yang CS, Blaser MJ, Correa P, Blot WJ, Fraumeni JF, Xu GW. Gastric dysplasia and gastric cancer: *Helicobacter pylori*, serum vitamin C, and other risk factors. *J Natl Cancer Inst* 2000; **92**:1607-1612
- 30 **Ekstrom AM**, Serafini M, Nyren O, Hansson LE, Ye W, Wolk A. Dietary antioxidant intake and the risk of cardia cancer and noncardia cancer of the intestinal and diffuse types: a population-based case-control study in Sweden. *Int J Cancer* 2000; **87**:133-140
- 31 **Farinati F**, Cardin R, Degan p, Rugge M, Mario FD, Bonvicini P, Naccarato R. Oxidative DNA damage accumulation in gastric carcinogenesis. *Gut* 1998; **42**:351-356
- 32 **Drake IM**, Mapstone NP, Schorah CJ, White KL, Chalmers DM, Dixon MF, Axon AT. Reactive oxygen species activity and lipid peroxidation in *Helicobacter pylori* associated gastritis: relation to gastric mucosal ascorbic acid concentrations and effect of *H. pylori*. *Gut* 1998; **42**:768-771
- 33 **Sun GY**, Liu WW, Zhou ZQ, Fang DC, Men RF, Luo YH. Free radicals in development of experimental gastric carcinoma and precancerous lesions induced by N-methyl-N'-nitro-N-nitrosoguanidine in rats. *Huaren Xiaohua Zazhi* 1998; **6**:219-221
- 34 **Zhang H**, Yao HS. Studies of *Hp* infection NO and hexosamine content and immune function in chronic gastric disease. *Huaren Xiaohua Zazhi* 1998; **6**:1092-1093

Edited by Wu XN

• GASTRIC CANCER •

Expression of focal adhesion kinase and $\alpha 5$ and $\beta 1$ integrins in carcinomas and its clinical significance

Jian-Min Su, Lu Gui, Yi-Ping Zhou, Xi-Liang Zha

Jian-Min Su, Yi-Ping Zhou, Department of Chemistry, FuDan University, Shanghai 200032, China

Lu Gui, Department of Pathology, Jinshan Hospital, FuDan University Medical Center, Shanghai 200032, China

Xi-Liang Zha, Department of Biochemistry, FuDan University Medical Center, Shanghai 200032, China

Supported by National Natural Science Foundation of China, No. 39970373 and the grant from the Science Committee of Shanghai, No. 00JC14042

Correspondence to: Xi-Liang Zha, Department of Biochemistry, FuDan University Medical Center, 138 Yixueyuan Road, Shanghai 200032, China. xlzha@shmu.edu.cn

Telephone: +86-21-64041900-2312 or 2696

Received 2002-01-11 **Accepted** 2002-02-09

Abstract

AIM: To detect the expression pattern of FAK (focal adhesion kinase) and integrin $\alpha 5$ and $\beta 1$ subunits in different kinds of cancerous tissues and to study their correlation with clinicopathological data including tumor type, grade and lymph node status. **METHODS:** Using an immunohistochemical technique, we examined the expression of FAK and integrin $\alpha 5$ and $\beta 1$ subunits in cancerous and noncancerous tissues obtained from 75 patients with gastric carcinomas, 21 colorectal carcinomas, 16 hepatocellular carcinomas, 20 uterocervical carcinomas, and 20 breast carcinomas.

RESULTS: The staining of FAK was stronger in cancerous than in noncancerous areas. Enhanced expression of FAK was detected in poor-differentiated carcinoma of the stomach and colorectum. Tumors with lymph node metastases had more FAK protein than those without metastases. In addition, the deeper the extent of tumor infiltration, the higher the FAK expression. The expression of integrin $\alpha 5$ and $\beta 1$ subunits was lower in cancerous areas than in noncancerous areas, but it was higher in well-differentiated cancerous tissues than in poor differentiated tissues. The relationship between the expression of integrin $\alpha 5$ and $\beta 1$ subunits and infiltration or metastasis was not significant. Cancerous tissues with stronger FAK expression (++ or +++) also had a higher expression of integrin $\alpha 5$ and $\beta 1$ subunits in the tumor and its unaffected margins.

CONCLUSION: FAK is a better marker for carcinogenesis and the progression of cancer than integrin $\alpha 5$ or $\beta 1$ subunit, and it may be not only a transformation-linked enzyme but also a progression-linked enzyme.

Su JM, Gui L, Zhou YP, Zha XL. Expression of focal adhesion kinase and $\alpha 5$ and $\beta 1$ integrins in carcinomas and its clinical significance. *World J Gastroenterol* 2002; 8(4):613-618

INTRODUCTION

In recent years, much attention has focused on cell adhesion molecules. These studies have shown that adhesion molecules

affect cell behaviors and mediate signal transduction, especially in cancer cells. Integrins are a large family of cell surface receptors that are found in many animal species^[1]. They can affect signal transduction, cell proliferation, differentiation, survival and apoptosis, cell cycle and invasion and metastasis of carcinoma cells^[2-7]. Previous studies have provided a better understanding of the signaling pathways activated by integrins in adherent cells^[1]. As integrins bind to the extra cellular matrix (ECM), they become clustered in the plane of the cell membrane and activate a variety of non-receptor protein tyrosine kinases (PTKs), such as FAK, Abl, Syk and Src-family PTKs^[7-13]. Upon activation of FAK, a number of focal adhesion components, such as paxillin, tensin, Shc and P130cas, are phosphorylated and activate the ERK2/MAPK signaling pathway network^[13-20]. Therefore, FAK may play a central role in integrin-stimulated signaling events^[20], but it is a precondition that integrins bind to the ECM and cluster in the plane of the cell membrane. Integrin expression has been studied^[21-34], but studies on the expression integrin $\alpha 5$ and $\beta 1$ subunits and FAK in gastric cancer and uterocervical cancer are rare. Furthermore, the correlation between integrin and FAK expression has not been studied, and the difference of integrin or FAK expression among these five kinds of cancer has not been reported either.

In the present study, the authors used an immunohistochemical technique to examine the expression of integrin $\alpha 5$ and $\beta 1$ subunits and FAK in gastric cancer, colorectal cancer, hepatocellular carcinomas, uterocervical cancer, and breast cancer. In addition, the authors correlated the expression of FAK and integrin $\alpha 5$, and $\beta 1$ subunits with clinicopathologic data, including tumor differentiation, infiltration and metastasis.

MATERIALS AND METHODS

Specimens

Tissue samples were obtained from 75 cases of gastric carcinoma (40 males and 35 females), 21 colorectal cancer (11 males and 10 females), 16 hepatocellular carcinomas (10 males and 6 females), 20 uterocervical cancer, and 20 breast cancer that had undergone total or partial resection in Tumor Hospital, Shanghai Medical University from Jan. 1995 to Jan. 1996. Patient age ranged from 20 to 85 years old. Of the specimens, 51 cases of gastric cancer, 16 colorectal cancer, 16 hepatocellular carcinomas, 18 uterocervical cancer and 17 breast cancer were with unaffected margins. The specimens were fixed in 4 % methanol solution, embedded in wax, and cut in 5 μ m serial sections.

Reagents

Antibodies used in this study were as follows: rabbit anti-mouse FAK polyclonal antibody, biotinylated sheep anti-rabbit IgG, and biotinylated sheep anti-mouse IgG from Santa Cruz Biotechnology, Inc. (California, U.S.A.). Monoclonal mouse antibodies directed against human integrin $\alpha 5$ subunit and human integrin $\beta 1$ subunit were provided by Dr. Mingzhe Zheng at University of Washington, Seattle, U.S.A

Immunohistochemistry

Immunohistochemical staining was performed using the avidin-biotin-peroxidase technique^[35]. Anti-FAK antibody was diluted into 1:100, anti- $\alpha 5$ 1:15, and anti- $\beta 1$ 1:80. The avidin-biotin-peroxidase reagent kit was purchased from Vector Laboratories Inc.

A semiquantitative evaluation system was used to determine antigen expression in tissue samples^[36]. Expression was graded on the following scale: negative reaction, (-); mild positive, (+); moderate positive, (++); strong positive, (+++). Evaluation of cell-surface and cytoplasmic staining was performed independently by two of the authors. In the occasional instance of disagreement, the slide was reviewed by the third observer, and a consensus opinion was obtained. The protein expression was correlated with tumor grades, which was in accordance with WHO classification.

Statistical analysis

was performed by using the χ^2 test. A *P* value of <0.05 was considered significant.

RESULTS

Expression of FAK and integrin subunits $\alpha 5$ and $\beta 1$ in human gastric carcinomas

The expression patterns of the integrin subunits $\alpha 5$ and $\beta 1$ and FAK in the 75 cases of gastric carcinomas and 51 unaffected margins are summarized in Table 1. Of the 51 unaffected margin specimens, only 2 (4 %) showed moderate (++) FAK, others showed either negative or minimal FAK, but 39 (76 %) cases showed moderate (++) or strong (+++) integrin $\alpha 5$ immunoreactivity (Figure 1 A), and 43 (85 %) showed moderate (++) or strong (+++) integrin $\beta 1$ immunoreactivity. Of the 75 cancer specimens, 43 (57 %) samples showed moderate (++) or strong (+++) FAK immunoreactivity (Figure 3 A), 22 (30 %) samples had moderate integrin $\alpha 5$ immunoreactivity, and 19 (25 %) showed moderate integrin immunoreactivity. None of 75 cancer specimens showed strong immunoreactivity (+++) and neither integrin $\alpha 5$ nor $\beta 1$ subunit. In contrast with 51 unaffected margin specimens, 35 (69 %) carcinoma specimens had reduced $\alpha 5$ immunoreactivity, 43 (85 %) had reduced $\beta 1$ immunoreactivity, and 46 (90 %) had increased FAK immunoreactivity. So a significant difference was found between gastric carcinomas and their unaffected margins in the expression of FAK, integrin $\alpha 5$, and $\beta 1$ subunit.

When FAK expression was compared with histopathological and clinical parameters, the authors found that 30 (68 %) of 44 cases of poorly-differentiated cancer showed moderate or strong immunoreactivity, however, only 13 (42 %) of 31 well-differentiated cancer showed moderate or strong; Of the 59 deep or full stratum invasive cancer, 40 (68 %) showed moderate or strong, and only 3 (23 %) of 16 superficial or mucous invasive cancer showed moderate or strong; 30 (77 %) of 39 cases with lymph node metastasis showed moderate or strong, but 13 (36 %) of 36 cases without lymph node metastasis showed moderate or strong activity. So, a significant association was found between enhanced expression of FAK and poor differentiation, deep invasion, and lymph node metastasis of gastric carcinomas.

In addition, of the 44 cases of poorly-differentiated cancer, 36 (81.8 %) showed negative or minimal $\alpha 5$ and 37 (84 %) showed negative or minimal $\beta 1$, of the 31 moderate or well differentiated cancers, 17 (55 %) showed negative or minimal $\alpha 5$ and 19 (61 %) showed negative or minimal $\beta 1$. Reduced expression of subunit $\alpha 5$ and $\beta 1$ was significantly associated with poorly-differentiated carcinomas, but not with invasion and lymph node metastasis.

Finally, the authors found that 30 of the 43 gastric

carcinomas with high FAK expression (++ or +++) had over expression of integrin subunit $\alpha 5$ and $\beta 1$ in the tumor tissues and unaffected margin of the same specimens.

Expression of FAK and integrin subunits $\alpha 5$ and $\beta 1$ in human colorectal carcinomas

The expression patterns of the integrin subunits $\alpha 5$ and $\beta 1$ and FAK in the 21 colorectal carcinomas and 16 unaffected margins are summarized in Table 2.

Table 1 Expression of FAK and integrin subunits $\alpha 5$ and $\beta 1$ in human gastric carcinomas and their relation to clinical and histological variables

	FAK		Integrin $\alpha 5$		Integrin $\beta 1$	
	-/+	++/+++	-/+	++/+++	-/+	++/+++
Type of tissues						
Unaffected margin specimen	49	2	12	39	8	43
Gastric carcinoma	32	43	53	22	56	19
	<i>P</i> <0.01		<i>P</i> <0.01		<i>P</i> <0.01	
Differentiation						
Poor	14	30	36	8	37	7
Moderate or well	18	13	17	14	19	12
	<i>P</i> <0.05		<i>P</i> <0.05		<i>P</i> <0.01	
Extent of invasion						
Mucosa or superficial stratum	13	3	11	5	12	4
Deep or full stratum	19	40	42	17	44	15
	<i>P</i> <0.01		NS		NS	
Metastasis						
Absent	23	13	26	10	29	7
Present	19	30	27	12	27	12
	<i>P</i> <0.01		NS		NS	

NS: No significant

Table 2 Expression of FAK and integrin subunits $\alpha 5$ and $\beta 1$ in human colorectal carcinomas and their relation to clinical and histological variables

	FAK		Integrin $\alpha 5$		Integrin $\beta 1$	
	-/+	++/+++	-/+	++/+++	-/+	++/+++
Type of tissues						
Unaffected margin specimen	15	1	8	8	5	11
Gastric carcinoma	8	13	17	4	13	8
	<i>P</i> < 0.01		<i>P</i> < 0.01		<i>P</i> < 0.01	
Differentiation						
Poor	2	9	9	2	7	4
Moderate or well	6	4	8	2	6	4
	<i>P</i> < 0.05		NS		NS	
Extent of invasion						
Mucosa or superficial stratum	4	0	3	1	2	2
Deep or full stratum	4	13	14	3	11	16
	<i>P</i> < 0.01		NS		NS	
Metastasis						
Absent	6	4	9	2	9	2
Present	2	9	8	2	4	6
	<i>P</i> < 0.01		NS		<i>P</i> <0.05	

NS: No significant

In contrast with 16 unaffected margin specimens, 10 (62 %) carcinoma specimens had reduced $\alpha 5$ immunoreactivity (Figure1 B), 6 (37 %) had reduced $\beta 1$ immunoreactivity (Figure2A,2B), and 13 (81 %) had increased FAK immunoreactivity(Figure3 B). So a significant difference was found between colorectal carcinomas and their unaffected margins in the expression of FAK, integrin $\alpha 5$, and $\beta 1$ subunit.

When FAK expression was compared with histopathological and clinical parameters, A significant association was also found between over expression of FAK and poor differentiation, deep invasion, and present lymph node metastasis of colorectal carcinomas.

In addition, low expression of subunit $\alpha 5$ and $\beta 1$ was significantly associated with poorly-differentiated colorectal carcinomas, but not with invasion and metastasis.

Expression of FAK and integrin subunits $\alpha 5$ and $\beta 1$ in human hepatocellular carcinomas

The expression patterns of the integrin subunits $\alpha 5$ and $\beta 1$ and FAK in the 16 hepatocellular carcinomas and their unaffected margins are summarized in Table 3.

Table 3 Expression of FAK and integrin subunits $\alpha 5$ and $\beta 1$ in human hepatocellular carcinomas and their relation to clinical and histological variables

	FAK		Integrin $\alpha 5$		Integrin $\beta 1$	
	-/+	++/+++	-/+	++/+++	-/+	++/+++
Type of tissues						
Unaffected margin specimen	15	1	3	13	1	15
Hepatocellular carcinoma	4	12	11	5	10	6
	$P < 0.01$		$P < 0.01$		$P < 0.01$	
Differentiation						
Poor	1	7	8	0	7	1
Moderate or well	2	5	3	5	4	5
	$P < 0.05$		$P < 0.01$		$P < 0.05$	

In contrast with 16 unaffected margin specimens, 11 (69 %) carcinoma specimens had reduced $\alpha 5$ immunoreactivity, 7 (44 %) had reduced $\beta 1$ immunoreactivity, and 11 (69 %) had increased FAK immunoreactivity. So a significant difference was found between hepatocellular carcinomas and their unaffected margins in the expression of FAK, integrin $\alpha 5$ and $\beta 1$ subunit.

When these protein expression was compared with the degree of differentiation the authors found a significant association between these protein expression of FAK and poor differentiation in hepatocellular carcinomas.

Expression of FAK and integrin subunits $\alpha 5$ and $\beta 1$ in human uterocervical carcinomas

The expression patterns of the integrin subunits $\alpha 5$ and $\beta 1$ and FAK in the 20 uterocervical carcinomas and 18 unaffected margins are summarized in Table 4. Comparing with 18 unaffected margin specimens, 13 (72 %) carcinoma specimens had reduced $\alpha 5$ immunoreactivity, 14 (78 %) had reduced $\beta 1$ immunoreactivity, and 3 (17 %) had increased FAK immunoreactivity. So the positive percentage of integrin $\alpha 5$ or $\beta 1$ had a significant difference between carcinomas and their unaffected margins. That of FAK was not apparent.

A significant association was not found between increased expression of FAK and poor differentiation or deep invasion of uterocervical carcinomas. Reduced expression of subunit $\alpha 5$ and $\beta 1$ was significantly associated with poor differentiated carcinomas, but not with invasion.

Expression of FAK and integrin subunits $\alpha 5$ and $\beta 1$ in human breast carcinomas

The expression patterns of the integrin subunits $\alpha 5$ and $\beta 1$ and FAK in the 20 breast carcinomas and 17 unaffected margins are summarized in Table 4. Similarly, the increased FAK expression was significantly associated with breast carcinogenesis and lymph node metastasis of breast carcinomas. Reduced expression of subunit $\alpha 5$ and $\beta 1$ was significantly associated with breast carcinogenesis and poorly-differentiated carcinomas, but not with lymph node metastasis. In contrast with 17 unaffected margin specimens, 14 (82 %) carcinoma specimens had reduced $\alpha 5$ immunoreactivity, 16 (94 %) had reduced $\beta 1$ immunoreactivity, and 14 (82 %) had increased FAK immunoreactivity.

Table 4 Expression of FAK and integrin subunits $\alpha 5$ and $\beta 1$ in human uterocervical carcinomas and their relation to clinical and histological variables

	FAK		Integrin $\alpha 5$		Integrin $\beta 1$	
	-/+	++/+++	-/+	++/+++	-/+	++/+++
Type of tissues						
Unaffected margin specimen	18	0	13	5	9	9
adenocarcinoma	9	1	9	9	1	9
Squamous carcinoma	10	0	10	0	9	1
	$P > 0.05$		$P > 0.05$		$P > 0.05$	
Differentiation						
Poor	9	1	10	0	9	1
Moderate or well	10	0	9	1	9	1
	$P > 0.05$		$P > 0.05$		$P > 0.05$	
Extent of invasion						
Mucosa or superficial stratum	5	0	5	0	4	1
Deep or full stratum	14	1	14	1	14	1
	$P > 0.05$		NS		NS	

NS: No significant

Table 5 Expression of FAK and integrin subunits $\alpha 5$ and $\beta 1$ in human breast carcinomas and their relation to clinical and histological variables

	FAK		Integrin $\alpha 5$		Integrin $\beta 1$	
	-/+	++/+++	-/+	++/+++	-/+	++/+++
Type of tissues						
Unaffected margin specimen	17	0	8	9	6	11
Breast carcinoma	10	10	20	0	20	0
	$P < 0.01$		$P < 0.05$		$P < 0.01$	
Metastasis						
Absent	9	3	12	0	12	0
Present	1	7	8	0	8	0
	$P < 0.01$		NS		$P > 0.05$	

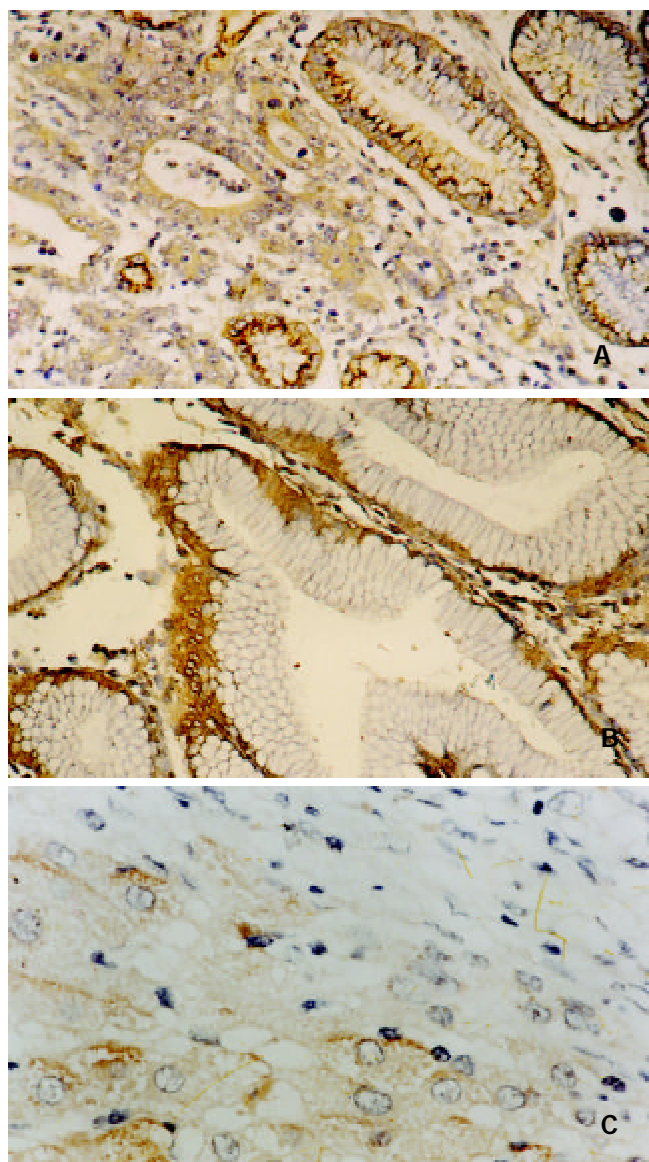


Figure 1 Integrin $\alpha 5$ subunit expressed in carcinoma and unaffected margin tissues, ABC-DAB, $\times 400$

A. Positive expression of integrin $\alpha 5$ subunit in unaffected margin tissues of gastric carcinoma.
B. Positive expression of integrin $\alpha 5$ subunit in unaffected margin tissues of colorectal carcinoma.
C. Positive expression of integrin $\alpha 5$ subunit in unaffected margin tissues of hepatocellular carcinoma.

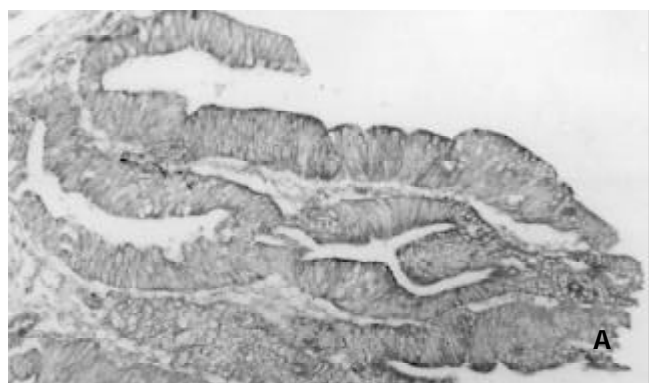


Figure 2 A. Positive expression of integrin $\beta 1$ subunit in unaffected margin tissues of colorectal carcinoma, ABC-DAB, $\times 100$.

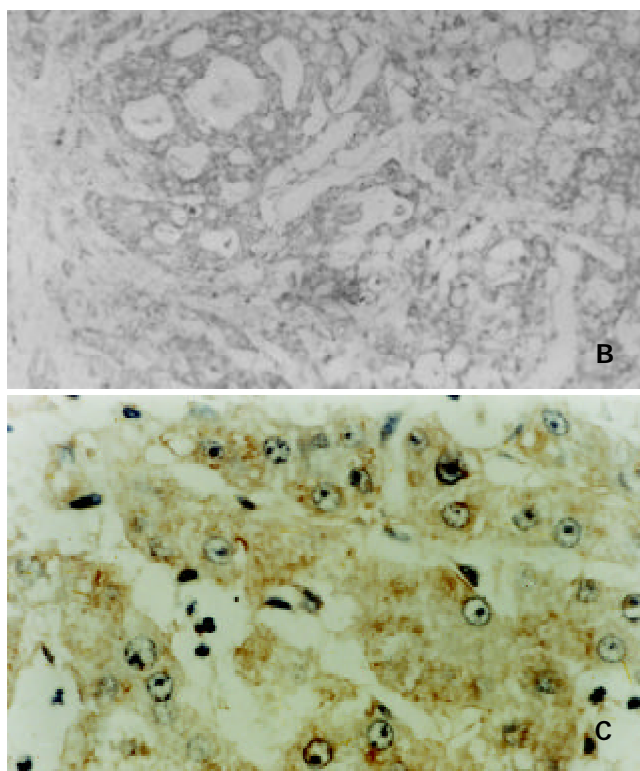


Figure 2 Integrin $\beta 1$ subunit expressed in carcinoma and unaffected margin tissues

B. Negative expression of Integrin $\beta 1$ subunit in colorectal carcinoma specimen, ABC-DAB, $\times 200$.
C. Positive expression of integrin $\beta 1$ subunit in unaffected margin tissues of hepatocellular carcinoma, ABC-DAB, $\times 400$.

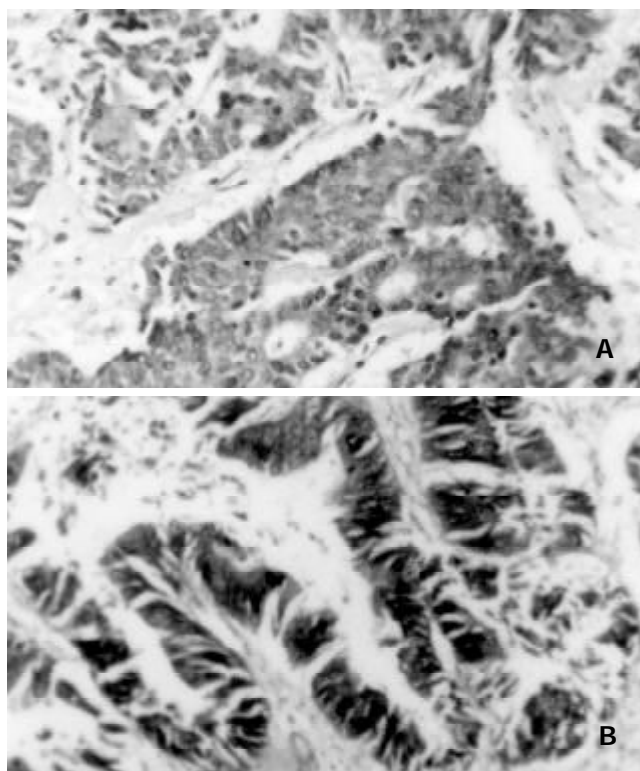


Figure 3 FAK expressed in carcinoma tissues, ABC-DAB, $\times 400$

A. Positive expression of FAK in gastric carcinoma.
B. Positive expression of FAK in colorectal carcinoma.

NS: No significant

DISCUSSION

This study indicated that the expression of the FAK antigen was lower in unaffected noncancerous margin tissues than in carcinoma tissues, whereas expression of integrin $\alpha 5$ and $\beta 1$ subunits was higher in unaffected margin than in carcinoma tissues. The quantity of all three proteins related to the degree of differentiation of the cancer. The reasons for these findings are complex. First, the contents of fibronectin and laminin in the ECM is lower in normal tissues than in cancerous counterparts. However, the fibroblast is stimulated by cancer cells to produce more matrix proteins thereby increasing the concentration of matrix proteins^[37]. Second, the increased expression of integrin $\alpha 5$ and $\beta 1$ subunits in preliminary cancer tissue make the matrix proteins relatively much more deficient. Under these conditions, FAK can exist in a state with high tyrosine-phosphorylated on the Tyr-397/Src SH2 binding site^[30-42]. However, the Src-family PTKs are not significantly associated with FAK that has only low levels of kinase activity and its expression is reduced^[13, 20, 43-45]. In unaffected margin tissues, the negative regulators of integrin-stimulated signaling events include the FAK-associated PTP, PTEN and the p130cas that all reduced the kinase activity of FAK^[46-48]. The quantity of matrix proteins is increased in the ECM of cancerous tissue. Integrins bind to the ECM, and become clustered in the plane of the cell membrane where they increase FAK tyrosine phosphorylation and kinase activity. Src-PTKs can significantly associate with FAK. Since FAK kinase activity is important for the FAK-enhanced increase in Src-PTK activity^[49] and Src-PTKs can also phosphorylate FAK within the kinase activation loop (Tyr-576 and Tyr-577) to promote maximal FAK kinase activity, the transient complex formed between FAK and Src after integrin stimulation of cells may lead to the maximal activation of both PTKs^[38, 50]. The survival signals are continually magnified, and cells with overexpression of FAK can inhibit the effects of PTEN on PI3-K activity and partially inhibit its effects on PIP₃ levels, Akt phosphorylation and cell apoptosis^[51]. Cells proliferate extensively. Therefore the authors believe overexpression of FAK is required for carcinogenesis. The reduced expression of integrin $\alpha 5, \beta 1$ subunit in carcinomas does not decrease the FAK kinase activity. Ca²⁺, PKC and Phorbol 12-myristate 13-acetate (PMA), can also increase FAK kinase activity^[20].

This study indicates that the relationship between integrin $\alpha 5, \beta 1$ subunits and metastasis is not significant in cancer cells, whereas FAK expression is significantly associated with metastasis or invasiveness. The process of cancer invasion or metastasis is complex, and involves attachment of the cancer cell to the ECM, decomposition of the ECM by proteases, and migration of cancer cells. The integrin subunits that aid cell adhesion are reduced in cancerous tissue, but integrin subunits that relate to cell migration are increased or constant^[52]. On the basis of these findings, the expression of a single integrin subunit may not correlate with metastasis, but FAK is different because it can associate with integrin $\beta 2, \beta 3$ and some α subunits^[20, 53]. Several other cellular stimuli that generate signals through either G-protein linked receptors, transmembrane growth factor receptors or other unknown mechanisms can increase the level of FAK tyrosine phosphorylation in cells^[20]. Thus, FAK may play a central role in signaling events stimulated by integrin or other molecules.

This study also indicates that the quantity change of integrin $\alpha 5, \beta 1$ and their related signal molecule FAK is relate to the type of cancer. For integrin $\alpha 5$, breast carcinoma (82 %) had the most reduced expression, then uterocervical carcinoma

(72%), gastric carcinoma (69 %), hepatocellular carcinoma (69 %), colorectal carcinoma (62 %) successively. For integrin $\alpha 1$, breast carcinoma (94 %) also had the most reduced expression, then gastric carcinoma (85 %), uterocervical carcinoma (78 %), hepatocellular carcinoma (44 %), colorectal carcinoma (37 %) successively. For FAK, gastric carcinoma (90 %) had the most increased expression, then colorectal carcinoma (80 %), breast carcinoma (80 %), hepatocellular carcinoma (69 %), uterocervical carcinoma (37 %) successively. From the above data, the authors find that the changes of integrin $\alpha 1$ and FAK is much more related with the type of cancer.

In summary, the authors have shown in the present study that expression of FAK is more significantly associated with carcinogenesis, differentiation and metastasis than that of integrin $\alpha 5$ and $\beta 1$ subunits. FAK may be not only a transformation-linked enzyme but also a progression-linked enzyme. The level of FAK expression might be a valuable marker for the carcinogenesis and progression of some types of carcinoma. The expression of integrin $\alpha 5, \beta 1$ and FAK is relate to the type of cancer.

ACKNOWLEDGMENTS

We are grateful to Dr. Ming-Zhe Zheng, University of Washington, Washington, USA, for providing the integrin antibody and to the Pathology Department of the Cancer Hospital of Shanghai Medical University for providing surgical specimens. We also thank Mrs. Xiu-Fong Zhang and Mrs. Yue-Zheng Dai for their instruction in preparing this manuscript.

REFERENCES

- 1 **Filippo GG**, Erkki R. Integrin signaling. *Science* 1999; **285**:1028-1032
- 2 **Hynes RO**. Integrins: versatility, modulation and signaling in cell adhesion. *Cell* 1992; **69**:11-15
- 3 **Juliano RL**, Haskill S. Signal transduction from the extracellular matrix. *J Cell Biol* 1993; **120**: 577-585
- 4 **Erkki R**. Integrins as signaling molecules and targets for tumor therapy. *Kidney Int* 1997; **51**:1413-1417
- 5 **Brooks PC**, Montgomery AMP, Rosenfeld M. Integrin $\alpha_v \beta_3$ antagonists promote tumor regression by inducing apoptosis of angiogenic blood vessels. *Cell* 1994; **79**:1157-1164
- 6 **Blau HM**, Baltimore D. Differentiation requires continuous regulation. *J Cell Biol* 1991; **112**: 781-783
- 7 **Judith AV**, David AC. Integrins and cancer. *Curr Opin Cell Biol* 1996; **8**: 724-730
- 8 **Miyamoto S**, Teramoto H, Gutkind JS, Yamada KM. Integrins can collaborate with growth factors for phosphorylation of receptor tyrosine kinases and MAP kinase activation: roles of integrin aggregation and occupancy of receptors. *J Cell Biol* 1996; **135**(6 Pt 1): 1633-1642
- 9 **Schaller MD**, Sasaki T. Differential signaling by the focal adhesion kinase and cell adhesion kinase beta. *J Biol Chem* 1997; **272**: 25319-25325
- 10 **Guan JL**. Role of focal adhesion kinase in integrin signaling. *Int J Biochem Cell Biol* 1997; **29**: 1085-1096
- 11 **Hanks SK**, Polte TR. Signaling through focal adhesion kinase. *Bioessays* 1997; **19**: 137-145
- 12 **Parsons JT**, Parsons SJ. Src family protein tyrosine kinases: cooperating with growth factor and adhesion signaling pathways. *Curr Opin Cell Biol* 1997; **9**: 187-192
- 13 **Schlaepfer DD**, Hunter T. Integrin signalling and tyrosine phosphorylation: just the FAKs? *Trends Cell Biol* 1998; **8**: 151-157
- 14 **Bellis SL**, Miller JT, Turner CE. Characterization of tyrosine phosphorylation of paxillin in vitro by focal adhesion kinase. *J Biol Chem* 1995; **270**: 17437-17441
- 15 **Schaller MD**, Parsons JT. pp125FAK-dependent tyrosine phosphorylation of paxillin creates a high-affinity binding site for Crk. *Mol Cell Biol* 1995; **15**: 2635-2645
- 16 **Tachibana K**, Urano T, Fujita H, Ohashi Y, Kamiguchi K,

- Iwata S, Hirai H, Morimoto C. Tyrosine phosphorylation of Crk-associated substrates by focal adhesion kinase: A putative mechanism for the integrin-mediated tyrosine phosphorylation of Crk-associated substrates. *J Biol Chem* 1997; **272**: 29083-29090
- 17 **Vuori K**, Hirai H, Aizawa S, Ruoslahti E. Introduction of p130Cas signaling complex formation upon integrin-mediated cell adhesion: a role for Src family kinases. *Mol Cell Biol* 1996; **16**: 2606-2613
- 18 **Hamasaki K**, Mimura T, Morino N, Furuya H, Nakamoto T, Aizawa S, Morimoto C, Yazaki Y, Hirai H, Nojima Y. Src kinase plays an essential role in integrin-mediated tyrosine phosphorylation of Crk-associated substrate p130Cas. *Biochem Biophys Res Commun* 1996; **222**: 338-343
- 19 **Sakai R**, Nakamoto T, Ozawa K, Aizawa S, Hirai H. Characterization of the kinase activity essential for tyrosine phosphorylation of p130Cas in fibroblasts. *Oncogene* 1997; **14**: 1419-1426
- 20 **Schlaepfer DD**, Hauck CR and Sieg DJ. Signaling through focal adhesion kinase. *Progress Biophys Mol Biol* 1999; **71**: 435-478
- 21 **Markku M**, Roberto C, Elizabeth W. Distribution of VLA integrin in solid tumors. *Am J Path* 1993; **142**:1009-1018
- 22 **Stamp GWH**, Pignatelli M. Distribution of b1, a1, a2 and a3 integrin chains in basal cell carcinomas. *J Path* 1991; **163**:307-313
- 23 **Pignatelli M**, Andrewm H, Gordon WHS. Low expression of b1, a2, and a3 subunits of VLA integrins in malignant mammary tumours. *J Path* 1991; **165**:25-32
- 24 **Pignatelli M**, Smith MEF, Bodmer WF. Low expression of collagen receptors in moderate and poorly differentiated colorectal adenocarcinomas. *Br J Cancer* 1990; **61**:636-638
- 25 **Karin K**, Peter S, Laurence B. Expression of VLA-a2, VLA-a6, and VLA-b1 chains in normal mucosa and adenomas of the colon, and in colon carcinomas and their liver metastases. *Am J Path* 1991; **138**:741-750
- 26 **Monica L**, Raymond W, Judith S. Expression of the VLA b1 integrin family in bladder cancer. *Am J Path* 1994; **144**: 1016-1022
- 27 **Maragou P**, Bazopoulou KE, Panotopoulou E, Kakarantza AE, Sklavounou AA, Kotaridis S. Alteration of integrin expression in oral squamous cell carcinomas. *Oral Dis* 1999; **5**: 20-26
- 28 **Shinohara M**, Nakamura S, Sasaki M, Kurahara S, Ikebe T, Harada T, Shirasuna K. Expression of integrins in squamous cell carcinoma of the oral cavity correlations with tumor invasion and metastasis. *Am J Clin Pathol* 1999; **111**: 75-88
- 29 **Hakkinen L**, Kainulainen T, Salo T, Grenman R, Larjava H. Expression of integrin alpha9 subunit and tenascin in oral leukoplakia, lichen planus, and squamous cell carcinoma. *Oral Dis* 1999; **5**: 210-217
- 30 **Gonzalez MA**, Pinder SE, Wencyk PM, Bell JA, Elston CW, Nicholson RI, Robertson JF, Blamey RW, Ellis IO. An immunohistochemical examination of the expression of E-cadherin, alpha- and beta/gamma-catenins, and alpha2- and beta1-integrins in invasive breast cancer. *J Pathol* 1999; **187**: 523-529
- 31 **Nejjari M**, Hafdi Z, Dumortier J, Bringuier AF, Feldmann G, Scoazec JY. Alpha6beta1 integrin expression in hepatocarcinoma cells: regulation and role in cell adhesion and migration. *Int J Cancer* 1999; **83**: 518-525
- 32 **Sordat I**, Bosman FT, Dorta G, Rousselle P, Aberdam D, Blum AL, Sordat B. Differential expression of laminin-5 subunits and integrin receptors in human colorectal neoplasia. *J Pathol* 1998; **185**: 44-52
- 33 **Ensinger C**, Obrist P, Bacher SC, Mikuz G, Moncayo R, Riccabona G. Beta 1-Integrin expression in papillary thyroid carcinoma. *Anticancer Res* 1998; **18**: 33-40
- 34 **Tagliabue E**, Ghirelli C, Squicciarini P, Aiello P, Colnaghi MI, Menard S. Prognostic value of alpha 6 beta 4 integrin expression in breast carcinomas is affected by laminin production from tumor cells. *Clin Cancer Res* 1998; **4**: 407-410
- 35 **Cui J**, Zhou XD, Liu YK, Tang ZY, Zile MH. Abnormal Beta-catenin gene expression with invasiveness of primary hepatocellular carcinoma in China. *World J Gastroenterol* 2001; **7**:542-546
- 36 **Su JM**, Zhou YP, Zha XL. E-Cadherin expression in four kinds of carcinomas and their relations to differentiation and metastasis. *Chin J Cancer Res* 2001; **13**: 1-5
- 37 **Saiki I**, Makabe T, Yoneda J, Murata J, Ishizaki Y, Kimizuka F, Kato I, Azuma I. Inhibitory effect of fibronectin and its recombinant polypeptides on the adhesion of metastatic melanoma cells to laminin. *Jpn J Cancer Res* 1991; **82**:1113-1118
- 38 **Calalb MB**, Polte TR, Hanks SK. Tyrosine phosphorylation of focal adhesion kinase at sites in the catalytic domain regulates kinase activity: a role for Src family kinases. *Mol Cell Biol* 1995; **15**: 954-963
- 39 **Calalb MB**, Zhang X, Polte TR, Hanks SK. Focal adhesion kinase tyrosine-861 is a major site of phosphorylation by Src. *Biochem Biophys Res Commun* 1996; **228**: 662-668
- 40 **Schwartz MA**, Schaller MD, Ginsberg MH. Integrins: emerging paradigms of signal transduction. *Annu Rev Cell Dev Biol* 1995; **11**:549-11599
- 41 **Schlaepfer DD**, Hunter T. Evidence for *in vivo* phosphorylation of the Grb2 SH2-domain binding site on focal adhesion kinase by Src-family protein-tyrosine kinases. *Mol Cell Biol* 1996; **16**: 5623-5633
- 42 **Richardson A**, Shannon JD, Adams RB, Schaller MD, Parsons J. Identification of integrin-stimulated sites of serine phosphorylation in FRNK, the separately expressed C-terminal domain of focal adhesion kinase: a potential role for protein kinase A. *Biochem J* 1997; **324**: 141-149
- 43 **Chan PY**, Kanner SB, Whitney G, Aruffo A. A transmembrane-anchored chimeric focal adhesion kinase is constitutively activated and phosphorylated at tyrosine residues identical to pp125FAK. *J Biol Chem* 1994; **269**: 20567-20574
- 44 **Wary KK**, Mainiero F, Isakoff SJ, Marcantonio EE, Giancotti FG. The adaptor protein Shc couples a class of integrins to the control of cell cycle progression. *Cell* 1996; **87**: 733-743
- 45 **Lin TH**, Aplin AE, Shen Y, Chen Q, Schaller M, Romer L, Aukhil I, Juliano RL. Integrin-mediated activation of MAP kinase is independent of FAK: evidence for dual integrin signaling pathways in fibroblasts. *J Cell Biol* 1997; **136**: 1385-1395
- 46 **Tamura M**, Gu J, Matsumoto K, Aota S, Parsons R, Yamada KM. Inhibition of cell migration, spreading and focal adhesions by tumor suppressor PTEN. *Science* 1998; **280**: 1614-1617
- 47 **Garton AJ**, Burnham MR, Bouton AH, Tonks NK. Association of PTP-PEST with the SH3 domain of p130cas; a novel mechanism of protein tyrosine phosphatase substrate recognition. *Oncogene* 1997; **15**: 877-885
- 48 **Shen Y**, Schneider G, Cloutier JF, Veillette A, Schaller MD. Direct association of protein-tyrosine phosphatase PTP-PEST with paxillin. *J Biol Chem* 1998; **273**: 6474-6481
- 49 **Schlaepfer DD**, Hunter T. Focal adhesion kinase overexpression enhances ras-dependent integrin signaling to ERK2/mitogen-activated protein kinase through interactions with and activation of c-Src. *J Biol Chem* 1997; **272**: 13189-13195
- 50 **Schlaepfer DD**, Hanks H, Hunter T, Peter VDG. Integrin-mediated signal transduction linked to Ras pathway by GRB2 binding to focal adhesion kinase. *Nature* 1994; **372**: 786-791
- 51 **Masohito T**, Jianguo G, Erik HJD, Takahisa T, Shingo M, Kenneth MY. PTEN interactions with focal adhesion kinase and suppression of the extracellular matrix-dependent phosphatidylinositol 3-kinase/Akt. Cell survival pathway. *J Biol Chem* 1999; **274**: 20693-20703
- 52 **Zha XL**. *Structure and Function of Biomacromolecules*. In: (Chen HL) eds Cell adhesion molecule. Shanghai: Shanghai Med University 1999:123-142
- 53 **Lilley L**, Paul EH, Martin AS, Mark HG, Sanford JS. Integrin signaling roles for the cytoplasmic tails of albb3 in the tyrosine phosphorylation of pp125FAK. *J Cell Sci* 1995; **108**: 3817-3825

Edited by Zhang JZ

• GASTRIC CANCER •

Identification of tumor associated single-chain Fv by panning and screening antibody phage library using tumor cells

Yong-Zhan Nie, Feng-Tian He, Zhi-Kui Li, Kai-Chun Wu, Yun-Xin Cao, Bao-Jun Chen, Dai-Ming Fan

Yong-Zhan Nie, Feng-Tian He, Zhi-Kui Li, Kai-Chun Wu, Yun-Xin Cao, Bao-Jun Chen, Dai-Ming Fan, Institute of Digestive Diseases, Xijing Hospital, Fourth Military Medical University, Xi'an 710032, Shaanxi Province, China

Supported by the National "863" Strategy for Science (102-10-01-06) and National Natural Science Foundation of China, No. 39525020

Correspondence to: Dai-Ming Fan, Institute of Digestive Diseases, Xijing Hospital, Fourth Military Medical University, Changle West Road, Xi'an 710032, Shaanxi Province, China. fandaim@fmmu.edu.cn

Telephone: +86-29-2539041 **Fax:** +86-29-2539041

Received 2001-06-12 **Accepted** 2001-09-14

Abstract

AIM: To study the feasibility of panning and screening phage-displaying recombinant single-chain variable fragment (ScFv) of anti-tumor monoclonal antibodies for fixed whole cells as the carriers of mAb-binding antigens.

METHODS: The recombinant phage displaying libraries for anti-colorectal tumor mAb MC3Ab, MC5Ab and anti-gastric tumor mAb MGD1 was constructed. Panning and screening were carried out by means of modified fixation of colorectal and gastric tumor cells expressed the mAb-binding antigens. Concordance of binding specificity to tumor cells between phage clones and parent antibodies was analyzed. The phage of positive clones was identified with competitive ELISA, and infected by *E.coli* HB2151 to express soluble ScFv.

RESULTS: The ratio of positive clones to MC3-ScF-MC5-ScFv and MGD1-ScFv were 60 %, 24 % and 30 %. MC3-ScFv had M_r 32 000 confirmed by Western blot. The specificity to antigen had no difference between 4 positive recombinant phage antibodies and MC3Ab.

CONCLUSION: The modified process of fixing whole tumor cells is efficient, convenient and feasible to pan and screen the phage-displaying ScFv of anti-tumor monoclonal antibodies.

Nie YZ, He FT, Li ZK, Wu KC, Cao YX, Chen BJ, Fan DM. Identification of tumor associated single-chain Fv by panning and screening antibody phage library using tumor cells. *World J Gastroenterol* 2002; 8(4) :619-623

INTRODUCTION

Tumor specific or associated antibodies *in vivo* diagnosis and treatment in tumor patients have been sought recently^[1-4]. Most tumor-specific or tumor-associated antibodies have been obtained by the approach to immunizing animals with tumor cells, which inevitably cause allergic reaction against animal antibodies^[5,6]. To miniaturize animal antibodies is an efficient way to decrease the rejection and allergy reaction. Gene

engineering methods, especially phage display(PD), have great advantages^[7-9]. It is the best way that purified tumor antigens (TA) were coated to capture recombinant antibodies in phage antibody library^[10-12]. Unfortunately, many TA corresponding to tumor specific antibodies have not yet been isolated and purified, even not yet identified^[13,14]. It hinders the production of miniaturizing tumor-specific antibodies specific to un-isolated TA. It was speculated that the whole tumor cells which expressed TA might have been considered for replacement of TA. However, It was reported that the panning and screening of PD was non-specific by means of replacing TA with whole tumor cells^[8]. This could be attributed to the much lower antigen density and much complicated antigens. Nevertheless, significant progress on the methods has been made, allowing the utilization of PD using whole tumor cells^[15,16]. But this utilization is just limited to screen new unknown recombinant antibodies. In this study, we modified the fixing conditions of whole cells for panning and screening phage libraries constructed for the unique monoclonal antibodies such as anti-colon cancer MC3, MC5mAb and anti-gastric cancer MGD1 mAb^[13,17-21], and cell ELISA for screening ScFv clone. The results were satisfactory.

MATERIALS AND METHODS

Cell lines

Gastric tumor cell lines^[2, 10] KATO-III, AGS, MKN-45, GC803, SGC7901, colorectal tumor cell lines W480, HT-29, CoCa-2, and human fibroblast cells were grown in RPMI 1640 or DMEM supplemented with 100 mL⁻¹ new born bovine serum (NBS). All cell lines were grown adherently except KATO-III.

Construction of phage ScFv libraries

mRNA was isolated from the corresponding antibodies hybridoma cells. VH and VL cDNA were amplified with RT-PCR and linked with ScFv by linker DNA to form ScFc DNA, which then were inserted into plasmid PCANBSE. Plasmid DNA was transformed into *E.coli* strain TG1. ScFv-phage was induced by superinfection with helper phage M13KO7.

Cells fixation

The fixed cells were used for libraries panning and as antigens of cell ELISA. Methods reported by Ridgway *et al*^[8] were used with the following modifications. Fixation of suspending cells: the cells were washed with PBS, resuspended, and transferred to 96-well enzyme-labeled plates at $(4-5) \times 10^5$ cells/well. The volume of cell suspension was no less than 300 μ l each well. Otherwise, the cells would be distributed unevenly during centrifugation. The plates were centrifuged for 12 min at 1 200 r \cdot min⁻¹, and the supernatants were discarded immediately without disturbing the pellets. The plates were allowed to dry at 37 °C for 15-20 min. Into each well, 2.5 g \cdot L⁻¹ glutaraldehyde prepared with 60 μ l of 0.1 mol \cdot L⁻¹ PBS was added. Twelve min later, the fixative solution was discarded. The cells were washed 5 times by PBS. The plates were blocked with 100

g·L⁻¹ skimmed milk powder overnight at 4 °C. Coating of suspending cells for library panning: the cells were plated into 6-well plates at (1-1.5)×10⁷ cells/well. The cell suspension volume was no less than 7mL in each well. The rest procedures were as described above. Fixation of adherent cells: the cells were plated into 96-well plates at 0.2×10⁴ cells/well. The cells were allowed to incubate 48-72 h. When the cells were 80 % confluent, the medium was removed. The plates were washed twice with prewarmed PBS and dried at 37 °C for 20 min. The cells were fixed for 8 min as described above.

Detection of intracellular peroxidase

The fixed cells were divided into 2 groups. Cells in one group were treated with 3 mL·L⁻¹ H₂O₂ prepared with methanol and washed 3 times with PBS. The plates were blocked with 50 g·L⁻¹ skimmed milk powder overnight at 4 °C (or 37 °C for 2h). Cells in another group were treated with blocking solution directly. After the blocking solution was removed, the plates were washed 3 times with PBS containing 0.5 g·L⁻¹ Tween20, and OPD substrate(50 µl/ well) was added to develop color. thirty min later, the color development was terminated with 2 mol·L⁻¹ sulfuric acid. A490 were read. The well without substrate was designed as background control. Negative control and blank control were also designed.

Panning of phage libraries

The TG1 recombinant phage antibodies and soluble ScFv secreted by *E.coli* HB2151 were obtained according to the kit instructions (Pharmacia Biotech)^[7]. Wash the 6 well plate coated with tumor cells three times with PBS, empty it completely after each wash. Fill the plate completely with blocking buffer to block any remaining sites on the plate surface. Incubate at room temperature for 1 h. Wash the flask three times with PBS, and empty it completely after each wash. Prepare 14 mL of blocking buffer containing 1 mL·L⁻¹ thimerosal or 100 mL·L⁻¹ sodium azide as a preservative. Dilute the 16 mL of PEG-precipitated recombinant phage with 14 mL of blocking buffer and incubate at room temperature for 10-15 min. Add 20 mL of the diluted recombinant phage to the plate and incubate for 2 h at 37°C. Wash the plate 20 times with PBS and 20 times with PBS containing 10 mL·L⁻¹ Tween 20. Empty the plate completely each time. To isolate colonies for small-scale rescue, reinfect *E. coli* TG1 cells with bound phage directly in the panning vessel and plate the reinfected cells. Subsequent rounds of panning are to be performed. Add the entire 10 mL of log-phase TG1 cells to the flask or panning vessel. Incubate with shaking at 37 °C for 1 h. Transfer the entire 10 mL from the panning vessel into a sterile 50 mL disposable polypropylene centrifuge tube. To the cell suspension, add ampicillin to 0.1 g·L⁻¹, and glucose to a final concentration of 200 g·L⁻¹. Also add 4×10¹⁰ pfu of M13KO7 volume of stock to add=4×10¹³ pfu÷M13KO7 pfu/L. Incubate the culture for 1 h at 37°C with shaking. Sediment the cells by centrifugation and complete the rescue. The selection procedure was repeated 4 times before isolated clones were tested by ELISA.

Cell ELISA

Detection of parent antibodies activity^[22,23]: cellular endogenous peroxidase activity was rather low, so treatment of cells with H₂O₂ was unnecessary. The procedures were as follows. mAb were added to the blocked wells (50 µl/well). The plates stood for 1h at 37°C. The cells were washed 5 times by PBST. fifty µL horseradish peroxidase (HRP) conjugated sheep anti-mice IgG was added to each blocked well. The plates stood for 1h

at 37 °C. Cells were washed 5 times with PBST. OPD substrate (50 µl/well) was added to develop color. Ten to twenty min later, A490 was read. Normal mice IgG and PBS served as negative and blank controls respectively.

Screening of recombinant phage antibodies or recombinant soluble ScFv clones: recombinant phage antibodies (M13KO7 as negative control) or soluble antibodies bearing anti-E-tag label protein displayed on phage served as the first antibody. Incubation condition was set as 2h at room temperature, gently shaking at 120 r·min⁻¹ with cradle. Correspondently, rabbit anti-M13-HRP polyclonal antibody (1:5 000, Pharmacia) or mouse anti-E-tag IgG (1:1000, Pharmacia) were chosen as the second antibody, for the latter sheep anti-mouse IgG HRP, should be used. The rest procedures were as described above.

Concordance of the specificity to tumor cells between the positive recombinant phage clones and parent mAb: the blocked cells were coated as described above (including tumor cells or normal cells expressing antigen highly, lowly and blankly). Pairs of ScFv and parent antibodies were added to all cell plates respectively. A values for each well were read by the same method. Correlation coefficient was obtained through correlation analysis^[24-26].

Competitive ELISA

The aim was to screen positive clones with high affinity^[27-29]. The cells were coated as described previously. ScFv-phage supernatants or recombinant soluble ScFv (50 µl/well) were added to plates after co-incubation with 1/4 volume of 200 g·L⁻¹ skimmed milk powder for 15min. The plates stood for 1hr at 37 °C. Twenty-five µl corresponding mAb was added to each well. After standing for 1h at 37 °C, the plates were washed. Fifty µl HRP conjugated sheep anti-mouse IgG were added to each well. After standing for 1 h at 37 °C, the plates were washed 5 times with PBST. 50 µl OPD substrate were added to each well to develop color. A490 were read 10-20 min later. M13KO7 served as negative control. Inhibition rate (%)=1-(A490 for experimental well/A490 for control well)×100%.

Western blot

Routine methods were applied^[30-33].

Statistical methods

The data were analyzed with SPSS software package.

RESULTS

Detection of parent antibody activity with cell ELISA

The least dilution for MC3mAb was 25 mg·L⁻¹, for MC5mAb was 50 mg·L⁻¹, and for MGD1mAb was 12.5mg·L⁻¹. A490 were all more than 0.600, indicating that the mAb used in the experiment were active.

Construction of the ScFv antibody libraries

The VH, VL and ScFv DNAs were about 340, 320 and 750 bp respectively(Figures 1,2).

Panning of phage libraries with coated cells

When suspending cells were plated, if the cell suspensions adding to each well were not enough (<5 mL) or the cell number in each well was too many (>2×10⁷ cells/well), the cells would be distributed unevenly during centrifugation. In 4 outer wells, the cells were found to be distributed in a half-moon shape, which was inconvenient for next fixation and panning steps. To avoid the above problems, we added no less than 7 mL cell

suspensions to each well with $(1-1.5) \times 10^7$ cells/well, and speeded centrifugation to $1\,200\text{ r} \cdot \text{min}^{-1}$ gradually. The TG1 containing recombinant phage recovered after 4 rounds of panning were plated on SOB-AG (A: ampicillin ,G: glucose). After 14 h, dense clones were observed.

Screening of recombinant phage antibodies or recombinant soluble clones with cell ELISA

Sixty clones were selected randomly from each panned library. The positive clones, whose A490 were over 0.300 (positive control), were counted. The ratio of positive clones were obtained. Soluble expression of *E.coli*. HB2151 was carried out using the positive clones. Its positive rate was determined by cell ELISA and Western blot. The result is shown in Table 1.

Concordance of binding specificity of phage library and parent antibody to tumor cells

Taking MC3-ScFv clone19 as example, the binding specificity of ScFv and parent antibody MC3 to AGS, SW480, SGC7901 fibroblasts were analyzed as shown in Table 2. A490 of parent antibodies were set as Y axis, and that of ScFv as X axis. Correlation analysis revealed $r = 0.991, P < 0.01$, primarily indicating the concordance of binding specificity of MC3-ScFv clone 19 and parent antibody to tumor cells. Other clones of MC3-ScFv displayed similar characteristics to MC3-ScFv clone 19.

Table 1 Ratio of positive recombinant phage antibody clone and soluble ScFv

	Recombinant phage antibodies		Soluble ScFv	
	Ratio of positive clone (%)	Ratio of competitive clone (%)	Ratio of positive clone (%)	Ratio of competitive clone (%)
MC3 ScFv	60	8	30	8
MC5 ScFv	24	6	18	4
MGD1 ScFv	30	4	10	4

Table 2 Concordance for MC3-ScFv-19 and it's parental mAb specificity to cells

Cell lines	MC3-ScFv 19	MC3 Ab
AGS	1.403 ± 0.132	0.929 ± 0.187
SW480	0.921 ± 0.201	0.647 ± 0.132
SGC7901	0.257 ± 0.045	0.259 ± 0.078
Fibroblast	0.325 ± 0.106	0.297 ± 0.056

Screening of positive ScFv clones with competitive ELISA

Inhibition rate over 30 % was put as criteria^[8]. Positive clones from all libraries were obtained as shown in Table 1. As an example ,inhibition rates of 4 positive recombinant phage MC3 antibodies were 56.2 %, 53.6 %, 49.7% and 46.7 %. And inhibition rates of their soluble ScFvs were 41.5 %, 36.9 %, 33.7 % and 21.6 % respectively.

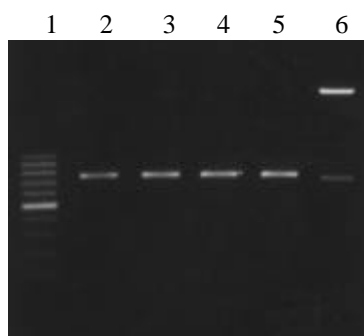
Western blot

Soluble products expressed by *E.coli*. HB2151 were all about M_r 32 000, consistent with the expected molecule weight of soluble ScFv. The result is shown in Figure 3.



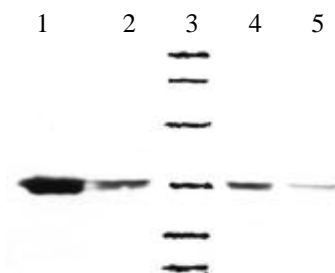
Lane 1: 100bp DNA ladder (100-1 000 bp); lane 2, 4,6: VL DNA; lane 3,5,7: VH DNA; lane 8: VH DNA marker(2.7 kb, 350 bp)

Figure 1 VH and VL DNA amplified by RT-PCR



Lane 1: 100bp DNA ladder (100-1 000 bp); lane 2, 3,4,5: MC5, MC3, MGD1, MGD1 ScFv DNA; lane 6 ScFv DNA marker (2.7 kb, 750 bp)

Figure 2 ScFv DNA amplified by RT-PCR



1,2,4,5: Four posotive clones of MC3 ScFv, 3: Low molecular weight marker(14.4, 20.1, 31.0, 43.0, 66.2, 97.4)KD

Figure 3 Western blotting of soluble MC3-ScFv clones

DISCUSSION

Phage display (PD) has many advantages in preparing minimized mouse and man antibodies. But the operation has met great difficulties due to severe conditions. The most difficult to satisfy is purified antigen, which is necessary for library panning and clone screening^[32-35]. Recently, whole cells have been used in PD to obtain tumor-associated or tumor-specific antibodies. The results are encouraging. Kupsch *et al*^[32] obtained human melanoma specific antibody by panning of a phage library using melanoma cells as negative screening, peripheral mononuclear cells as negative screening. Ridgway *et al*^[8] cloned a human anti-CD55 ScFv by subtractive panning of a phage library using tumor and nontumor cells. In their studies,

they panned the known libraries to obtain new tumor specific ScFv, so most possible integrity of tumor antigen should have been retained, so they used live cells in panning and cell ELISA. However, the procedures were complicated, and the specialized equipments were required. Particularly, only tumor-associated membrane antigens could be obtained, as for intracellular antigens, the method was powerless^[36-38]. The defects could be avoided by using fixed cells. But fixation procedures could destroy antigens partially, resulting in loss of some information. In the present report, we have studied the amenability of fixed cells to phage panning in PD technique.

Since development of mAb technique in the 1980s, many tumor specific or associated mAb have been cloned. However, most tumor antigens have not been identified and purified, and most mouse mAb had great molecular weight, and heterogeneity, which limited the application^[39-42]. So, it is necessary to minimize some specific mAb. We constructed recombinant phage displaying libraries for anti-colorectal tumor mAb MC3Ab, MC5Ab and anti-gastric tumor mAb MGD1. Panning was carried out using fixed coated colorectal and gastric tumor cell lines. The positive recombinant phage clones were screened by means of cell ELISA. The concordance of the specificity to tumor cells with parent mAb was analyzed. The affinity of positive clones with tumor antigens was detected with competitive ELISA. The molecules and product amounts were determined by Western blot. All results suggested that fixed cells could be used to panning tumor-associated mouse ScFv using PD.

However, only the following conditions were satisfactory, it successful manipulation was confirmed. Activity of antigen should not be influenced during cell fixation procedures^[43-45]. If the structure of antigen determinant cluster were changed during the fixation procedures, the fixation procedures should be modified or the fixative should be changed. We got satisfactory results using coating cells and cell ELISA with the following modifications. Cell lines highly expressing target antigens were used. Adherently or half-adherently grown cells were used because they easily plated and distributed evenly after plating. Fixation with glutaraldehyde could be half shortened. Cell lines highly expressing endogenous peroxidase were excluded to avoid destruction of lipoprotein antigens caused by methanol and H₂O₂ blocking^[46-48]. So previous detection of endogeneous peroxidase activity of cell lines is very important; Fixation condition with glutaraldehyde should be modified. Kupsch *et al*^[32] recommended that the cells should be fixed with glutaraldehyde at concentration of 5 g · L⁻¹ for 30 min in cell ELISA. But we found that the results were more satisfactory with glutaraldehyde at concentration of 2.5 g · L⁻¹ for 12 min for suspending cells and for 9min for adherent cells. Other precise conditions, such as centrifugation condition of suspending cells, drying prior to fixation, should also be paid great attention to^[49,50]. Application limits: Firstly, fixed cells could be applied to minimization and gene engineering of known mouse mAb. The phage libraries were constructed by using hybridoma. Panning of phage libraries and screening of positive clones were feasible theoretically and practically by using cell lines which strongly expressed these mAb-binding antigens. Secondly, fixed cells might be also applied to panning of large human, mouse phage libraries to obtain unknown tumor specific antibodies. Although fixation procedures might destroy antigens partially so as to lose some information, application of live cells also had disadvantages, such as unfeasibility of screening of intracellular antigens. In present study, gastric tumor specific antigen corresponding to MDG1-ScFv did belong to intracellular antigens, which further indicating the amenability of the fixed cells.

ACKNOWLEDGMENT

We would like to thank Prof. Bo-Rong Pan from Oncology Center, Xijing Hospital for his great contributions to this article.

REFERENCES

- 1 **McCall AM**, Shahied L, Amoroso AR, Horak EM, Simmons HH, Nielson U, Adams GP, Schier R, Marks JD, Weiner LM. Increasing the affinity for tumor antigen enhances bispecific antibody cytotoxicity. *J Immunol* 2001; **166**:6112-6117
- 2 **Zhang XY**. Some recent works on diagnosis and treatment of gastric cancer. *World J Gastroenterol* 1999; **5**:1-3
- 3 **Fan DM**, Xiao B, Shi YQ, Ming F, Qiao TD, Chen BJ, Chen Z. A novel cDNA fragment associated with gastric cancer drug resistance was screened out from a library by monoclonal antibody MGr-1. *World J Gastroenterol* 1998; **4**(suppl 2):110-111
- 4 **Ji F**, Wang WL, Yang ZL, Li YM, Huang HD, Chen WD. Study on the expression of matrix metalloproteinase-2 mRNA in human gastric cancer. *World J Gastroenterol* 1999; **5**:455-457
- 5 **Zhou C**, Jiang M, Xu L, Zhen Y. Construction and secretory expression of single-chain Fv fragment M97 with therapeutic potential against tumor invasion and metastasis. *Zhongguo Yixue Kexueyuan Xuebao* 1998; **20**:81-88
- 6 **Liu HF**, Liu WW, Fang DC, Men RP. Expression and significant of proapoptotic gene Bax in gastric carcinoma. *World J Gastroenterol* 1999; **5**:15-17
- 7 **Adams GP**, Schier R. Generating improved single-chain Fv molecules for tumor targeting. *Immunol Methods* 1999; **231**:249-260
- 8 **Ridgway JB**, Ng E, Kern JA, Lee J, Brush J, Goddard A, Carter P. Identification of a human Anti-CD55 single-chain Fv by subtractive panning of a phage library using tumor and nontumor cell lines. *Cancer Res* 1999; **59**:2718-2723
- 9 **Rozemuller H**, Chowdhury PS, Pastan I, Kreitman RJ. Isolation of new anti-CD30 scFvs from DNA-immunized mice by phage display and biologic activity of recombinant pseudomonas exotoxin produced by fusion with truncated pseudomonas exotoxin. *Int J Cancer* 2001; **92**:861-870
- 10 **Roovers RC**, van der Linden E, de Bruine AP, Arends JW, Hoogenboom HR. *In vitro* characterisation of a monovalent and bivalent form of a fully human anti Ep-CAM phage antibody. *Cancer Immunol Immunother* 2001; **50**:51-59
- 11 **Powers DB**, Amersdorfer P, Poul M, Nielsen UB, Shalaby MR, Adams GP, Weiner LM, Marks JD. Expression of single-chain Fv-Fc fusions in *Pichia pastoris*. *J Immunol Methods* 2001; **251**:123-135
- 12 **Yuan Y**, Cong W, Xu RT, Wang XJ, Gao H. Gastric cancer screening in 16 villages of Zhuanghe region: a high risk area of stomach cancer in China. *World J Gastroenterol* 1998; (Suppl 2):111-112
- 13 **Shi YQ**, Xiao B, Miao JY, Zhao YQ, You H, Fan DM. Construction of eukaryotic expression vector pBK-fas and MDR reversal test of drug-resistant gastric cancer cells. *Shijie Huaren Xiaohua Zazhi* 1999; **7**:309-312
- 14 **Wei TY**, Wei MX, Yang SM. Significance of expression of cyclin D1, P16 and preneoplastic lesion tissues. *Shijie Huaren Xiaohua Zazhi* 2000; **8**:234-235
- 15 **Van E**, Kruif W, Germeraad WT, Berendes P, Ropke C, Platenburg PP, Logtenberg T. Subtractive isolation of phage-displayed single-chain antibodies to thymic stromal cells by using intact thymic fragments. *Proc Natl Acad Sci USA* 1997; **94**:3903-3908
- 16 **Cai XH**, Garen A. Comparison of fusion phage libraries displaying V_H single-chain Fv antibody repertoire of a vaccinated melanoma patient as a source of melanoma-specific targeting molecules. *Proc Natl Acad Sci USA* 1997; **94**:9261-9266
- 17 **Guo JC**, Li JC, Fan DM, Qiao TD, Zhang XY. Regulation of HSP70 expression in human gastric cancer cell line SGCT901 by gene transfection. *Shijie Huaren Xiaohua Zazhi* 1999; **7**:773-776

- 18 **Liu HF**, Liu WW, Fang DC, Liu FX, He GY. Clinical significance of Fas antigen expression in gastric carcinoma. *World J Gastroenterol* 1999; **5**:90-91
- 19 **Chao CY**, Lie J, Fan DM. Immunohistochemical study of monoclonal antibody MGD-1 in gastric carcinoma. *Histopathology* 1989; **15**:523-529
- 20 **Xiao B**, Shi YQ, Zhao YQ, You H, Wang ZY, Liu XL, Yin F, Qiao TD, Fan DM. Transduction of Fas gene or bcl-2 antisense RNA sensitizes cultured drug resistant gastric cancer cells to chemotherapeutic drugs. *World J Gastroenterol* 1998; **4**:421-425
- 21 **Cao GD**, Wang SW, Wu SS, Li HF, Zhang WG. Retrovirus mediated antisense RNA to bcl-2 alter the biological behavior of stomach carcinoma MGC-803 cell lines. *World J Gastroenterol* 1998; **4**(suppl 2):45-48
- 22 **Luo ZB**, Luo YH, Lu R, Jim HY, Zhang PB, Xu CP. Immunohistochemical study on dendritic cells in gastric mucosa of patients with gastric cancer and precancerous lesions. *Shijie Huaren Xiaohua Zazhi* 2000; **8**:400-402
- 23 **Xu SH**, Feng JG. Relationship between CD44 in the peripheral blood of patients with colorectal cancer and clinico-pathological features. *Shijie Huaren Xiaohua Zazhi* 2000; **8**:432-435
- 24 **Zhang J**, Wang WL, Li Q, Qiao Q. Expression and significance of transforming growth factor- α and its receptor in human primary hepatocellular carcinoma. *Shijie Huaren Xiaohua Zazhi* 1999; **7**:939-941
- 25 **Du DW**, Zhou YX, Feng ZH, Li GY, Yao ZQ. Study on immunization of anti subcutaneous transplanting tumor induced by gene vaccine. *Shijie Huaren Xiaohua Zazhi* 1999; **7**: 955-957
- 26 **Zheng CS**, Wang WL, Reng WD, Hu PZ, Chai YB, Ma FC. Promotion of apoptosis of SMMC7721 cells by Bcl-2 ribozyme. *Shijie Huaren Xiaohua Zazhi* 2000; **8**:417-419
- 27 **Wang CD**, Chen YL, Wu T, Liu YR. Association between low expression of somatostatin receptor II gene and lymphoid metastasis in patients with gastric cancer. *Shijie Huaren Xiaohua Zazhi* 1999; **7**:864-866
- 28 **Han FC**, Yan XJ, Hou Y, Xiao LY, Guo YH, Su CZ. Gold immunochromatographic assay for anti-Helicobacter pylori antibody. *Shijie Huaren Xiaohua Zazhi* 1999; **7**:743-746
- 29 **Cui DX**, Yan XJ, Zhang L, Zhao JR, Jiang M, Guo YH, Zhang LX, Bai XP, Su CZ. Screening and its clinical significance of 6 fragments of highly expressing genes in gastric cancer and precancerous mucosa. *Shijie Huaren Xiaohua Zazhi* 1999; **7**:770-773
- 30 **Wang YF**, Wu XN, Zhang XQ, Chen XF. Circulating soluble intercellular adhesion molecule-1 and vascular cell adhesion molecule-1 in patients with gastric cancer. *Shijie Huaren Xiaohua Zazhi* 1998; **6**:1017-1019
- 31 **Sun YX**, Chen CJ, Zhou HG, Shi YQ, Pan BR, Feng WY. Expression of c-myc and p53 in colorectal adenoma and adenocarcinoma. *Shijie Huaren Xiaohua Zazhi* 1998; **6**:1054-1056
- 32 **Kupsch JM**, Tidman NH, Kang NV, Truman H, Hamilton S, Patel N, Newton Bishop JA, Leigh IM, Crowe JS. Isolation of human-specific antibodies by selection of an antibody phage library on melanoma cells. *Clin Cancer Res* 1999; **5**: 925-931
- 33 **Tordsson JM**, Ohlsson LG, Abrahmsen LB, Karlstrom PJ, Lando PA, Brodin TN. Phage-selected primate antibodies fused to superantigens for immunotherapy of malignant melanoma. *Cancer Immunol Immunother* 2000; **48**:691-702
- 34 **Marty C**, Scheidegger P, Ballmer-Hofer K, Klemenz R, Schwendener RA. Production of functionalized single-chain Fv antibody fragments binding to the ED-B domain of the B-isoform of fibronectin in *Pichia pastoris*. *Protein Expr Purif* 2001; **21**:156-164
- 35 **Sakai A**. Inhibition of endothelial cell adhesion molecule expression with SJC13, an azaindolizine derivative, *in vitro*. *Inflamm Res* 1996; **45**:224-229
- 36 **Goel A**, Colcher D, Baranowska-Kortylewicz J, Augustine S, Booth BJ, Pavlinkova G, Batra SK. Genetically engineered tetravalent single-chain Fv of the pancarcinoma monoclonal antibody CC49: improved biodistribution and potential for therapeutic application. *Cancer Res* 2000; **60**: 6964-6971
- 37 **Kang N**, Hamilton S, Odili J, Wilson G, Kupsch J. In vivo targeting of malignant melanoma by 125Iodine- and 99mTechnetium-labeled single-chain Fv fragments against high molecular weight melanoma-associated antigen. *Clin Cancer Res* 2000; **6**:4921-4931
- 38 **Kuan CT**, Wikstrand CJ, Archer G, Beers R, Pastan I, Zalutsky MR, Bigner DD. Increased binding affinity enhances targeting of glioma xenografts by EGFRvIII-specific scFv. *Int J Cancer* 2000; **88**:962-969
- 39 **Tur MK**, Huhn M, Sasse S, Engert A, Barth S. Selection of scFv phages on intact cells under low pH conditions leads to a significant loss of insert-free phages. *Biotechniques* 2001; **30**:404-408
- 40 **Goel A**, Augustine S, Baranowska-Kortylewicz J, Colcher D, Booth BJ, Pavlinkova G, Tempero M, Batra SK. Single-Dose versus fractionated radioimmunotherapy of human colon carcinoma xenografts using 131I-labeled multivalent CC49 single-chain fvs. *Clin Cancer Res* 2001; **7**:175-184
- 41 **Khare PD**, Shao-Xi L, Kuroki M, Hirose Y, Arakawa F, Nakamura K, Tomita Y, Kuroki M. Specifically targeted killing of carcinoembryonic antigen (CEA)-expressing cells by a retroviral vector displaying single-chain variable fragmented antibody to CEA and carrying the gene for inducible nitric oxide synthase. *Cancer Res* 2001; **61**:370-375
- 42 **Boldicke T**, Tesar M, Griesel C, Rohde M, Grone HJ, Waltenberger J, Kollet O, Lapidot T, Yayon A, Weich H. Anti-VEGFR-2 scFvs for cell isolation. Single-chain antibodies recognizing the human vascular endothelial growth factor receptor-2 (VEGFR-2/flk-1) on the surface of primary endothelial cells and preselected CD34+ cells from cord blood. *Stem Cells* 2001; **19**:24-36
- 43 **Matsumura R**, Umemiya K, Goto T, Nakazawa T, Ochiai K, Kagami M, Tomioka H, Tanabe E, Sugiyama T, Sueishi M. Interferon gamma and tumor necrosis factor alpha induce Fas expression and anti-Fas mediated apoptosis in a salivary ductal cell line. *Clin Exp Rheumatol* 2000; **18**:311-318
- 44 **Yuan QA**, Yu WY, Huang CF. Construction and expression of a hepatocellular carcinoma specific rodent and its humanized single-chain Fv fragments in *Escherichia coli*. *Shengwu Gongcheng Xuebao* 2000; **16**:86-90
- 45 **Ozaki H**, Ishii K, Horiuchi H, Arai H, Kawamoto T, Okawa K, Iwamatsu A, Kita T. Cutting edge: combined treatment of TNF-alpha and IFN-gamma causes redistribution of junctional adhesion molecule in human endothelial cells. *J Immunol* 1999; **163**:553-557
- 46 **Ohizumi I**, Tsunoda S, Taniguchi K, Saito H, Esaki K, Koizumi K, Makimoto H, Wakai Y, Matsui J, Tsutsumi Y, Nakagawa S, Utoguchi N, Ohsugi Y, Mayumi T. Identification of tumor vascular antigens by monoclonal antibodies prepared from rat-tumor-derived endothelial cells. *Int J Cancer* 1998; **77**:561-566
- 47 **Takami S**, Yamashita S, Kihara S, Ishigami M, Takemura K, Kume N, Kita T, Matsuzawa Y. Lipoprotein(a) enhances the expression of intercellular adhesion molecule-1 in cultured human umbilical vein endothelial cells. *Circulation* 1998; **97**:721-728
- 48 **Strindhall J**, Lundblad A, Pahlsson P. Interferon-gamma enhancement of E-selectin expression on endothelial cells is inhibited by monensin. *Scand J Immunol* 1997; **46**:338-343
- 49 **Yamaguchi M**, Suwa H, Miyasaka M, Kumada K. Selective inhibition of vascular cell adhesion molecule-1 expression by verapamil in human vascular endothelial cells. *Transplantation* 1998; **65**:756-757
- 50 **Zund G**, Nelson DP, Neufeld EJ, Dzus AL, Bischoff J, Mayer JE, Colgan SP. Hypoxia enhances stimulus-dependent induction of E-selectin on aortic endothelial cells. *Proc Natl Acad Sci U S A* 1996; **93**:7075-7080

Edited by Ma JY

• LIVER CANCER •

Clinical short-term results of radiofrequency ablation in liver cancers

Hong-Chi Jiang, Lian-Xin Liu, Da-Xun Piao, Jun Xu, Min Zheng, An-Long Zhu, Shu-Yi Qi, Wei-Hui Zhang, Lin-Feng Wu

Hong-Chi Jiang, Lian-Xin Liu, Da-Xun Piao, Jun Xu, An-Long Zhu, Wei-Hui Zhang, Lin-Feng Wu, Department of Surgery, the First Clinical College, Harbin Medical University, Harbin 150001, Heilongjiang Province, China

Min Zheng, Department of Ultrasound Diagnosis, the First Clinical College, Harbin Medical University, Harbin 150001, Heilongjiang Province, China

Shu-Yi Qi, Second Inpatient Department, the First Clinical College, Harbin Medical University, Harbin 150001, Heilongjiang Province, China

Support by Youth Natural Scientific Foundation of Heilongjiang Province, Youth Natural Scientific Foundation of Harbin and Heilongjiang Province Education Government Grant

Correspondence to: Dr. Lian-Xin Liu, Department of Surgery, the First Clinical College, Harbin Medical University, 23 Youzheng Street, Nangang District, Harbin 150001, Heilongjiang Province, China. liulianxin@sohu.com

Telephone: +86-451-3668999 **Fax:** +86-451-3670428

Received 2002-06-20 **Accepted** 2002-07-04

and system diseases (1 at 7 month, 1 at 9 month, and 1 at 12 month), 1 patients died from cardiovascular shock, but no RFA-related death. At a median follow-up of 10 months (range, 1-24 months), 6 patients (16.7 %) had recurrences at an RFA site, and 20 patients (56.7 %) remained clinically free of disease.

CONCLUSION: RF ablation appears to be an effective, safe, and relatively simple procedure for the treatment of unresectable liver cancers. The rate and severity of complications appear acceptable. However, further study is necessary to assess combination with other therapies, long-term recurrence rates and effect on overall survival.

Jiang HC, Liu LX, Piao DX, Xu J, Zheng M, Zhu AL, Qi SY, Zhang WH, Wu LF. Clinical short-term results of radiofrequency ablation in liver cancers. *World J Gastroenterol* 2002;8(4):624-630

Abstract

AIM: To study local therapeutic efficacy, side effects, and complications of radiofrequency ablation (RFA), which is emerging as a new method for the treatment of patients with hepatocellular carcinoma (HCC) with cirrhosis or chronic hepatitis and metastatic liver cancer.

METHODS: Thirty-six patients with primary and secondary liver cancers (21 with primary hepatocellular carcinoma, 12 with colorectal cancer liver metastases and 3 with other malignant liver metastases), which were considered not suitable for curative resection, were included in this study. They were treated either with RFA (RITA2000, Mountain View, California, USA) percutaneously ($n=20$) or intraoperatively ($n=16$). The procedures were performed using the ultrasound guidance. The quality of RFA was based on monitoring of equipments and subject feeling of the practitioners. Patients treated with RFA was followed according to clinical findings, radiographic images, and tumor markers.

RESULTS: Thirty-six patients underwent RFA for 48 nodules. RFA was used to treat an average 1.3 lesions per patient, and the median size of treated lesions was 2.5 cm (range, 0.5-9 cm). The average hospital stay was 5.6 days overall (2.8 days for percutaneous cases and 7.9 days for open operations). Seven patients underwent a second RFA procedure (sequential ablations). Sixteen HCC patients with a high level of alpha fetoprotein (AFP) and 9 colorectal cancer liver metastases patients with a high level of serum carcinoembryonic antigen (CEA) have a great reduction benefited from RFA. Four (11.1 %) patients had complications: one skin burn; one postoperative hemorrhage; one cholecystitis and one hepatic abscess associated with percutaneous ablations of a large lesion. There were 4 deaths: 3 patients died from local

INTRODUCTION

Hepatocellular carcinoma (HCC) is one of the most common solid cancers in the world, with an annual incidence estimated to be at least one million new patients, especially in Eastern Asian and South African^[1]. Furthermore, the liver is second only to lymph nodes as a common site of metastasis from other solid cancers, particularly in patients with colorectal adenocarcinoma^[2]. Surgical resection of HCC, colorectal cancer hepatic metastases, and patients with other types of primary tumors with liver-only metastases can result in significant long-term survival benefit in 20 % to 35 % of patients^[3-5]. However, the majority of hepatic cancers are not suitable for curative resection at the time of diagnosis. Only 5 % to 15 % of newly diagnosed HCC or colorectal cancer liver metastasis patients undergo a potentially curative resection. Difficulties related to surgical resection are those of the size, site, number of tumors, adjacent to vascular and biliary structures, extrahepatic involvement, poor general condition, and poor liver function especially in HCC with inadequate functional hepatic reserve related to coexistent cirrhosis^[6,7]. Thus, for the majority of patients with primary or metastatic hepatic malignancies who are not candidates for surgical resection, novel treatment approaches to control and potentially cure the unresectable tumors in the liver must be explored. In the last few years, minimal invasive techniques have become available for destruction of hepatic carcinomas. These include percutaneous ethanol injection (PEI), hepatic arterial embolization and thermoablation with cryoprobes, microwave, laser or radiofrequency^[8-18].

Radiofrequency ablation (RFA) is a relatively new procedure for treatment of hepatic tumors not amenable to resection. RFA employs a high-frequency alternating current to cause thermal coagulation and protein denaturation. The procedure is carried out using a needle electrode connected to a radiofrequency generator. As ions attempt to follow the

change in direction of the alternating current, there is frictional heating within the tissue. The result is a coagulative necrosis of the targeted tissue. Previous studies have employed both imaging studies and pathologic evaluation of ablated lesions to show complete tumor eradication^[19-28].

The purpose of this analysis was to evaluate our initial experience with RFA of hepatic tumors, and examine the associated complications and local recurrence rate. Although the number of patients is limited and the follow-up is short, we provide some insight for the future wider application of this method.

MATERIALS AND METHODS

Patients

The study was performed with approval from the institutional ethics committees at the First Clinical College of Harbin Medical University. Informed consent was obtained from all patients at the time of enrollment.

Between January 2000 and December 2001, 36 consecutive patients (22 men, 14 women; mean age, 48.1 years; age range, 35-74 years) with HCC and liver metastases underwent the RF procedure. Twenty-one patients suffered HCC and 3 was recurrent HCC. Twelve patients got liver metastases from colorectal carcinoma, 2 patients from breast cancers, 1 from gastric carcinoma. The cirrhosis, which existed not only in HCC but also in liver metastases, were in 26 patients. It was related to hepatitis B in 15 patients, related to hepatitis C in 3, related to hepatitis B or C in 6 and related to alcohol use in 2. The Child-Pugh class of cirrhosis was determined in each patient, and at the time of the ablation procedure, Twenty-five patients were judged to have Child-Pugh class A; and 11 class B. Pathologic result of HCC was obtained by means of ultrasonographically (US) guided biopsy with a 21-gauge cutting needle or viral hepatitis or cirrhosis history with a high level of AFP. Biopsy was not performed in patients in whom US and CT findings consistently indicated HCC and AFP levels were more than 200 ng/mL (>200 µg/L). The pathologic result of liver metastases was got by the same way and a history of primary colorectal carcinoma or other cancer with an increasing of CEA and other serum makers. Biopsy was only performed in patients in whom US and CT findings not consistently indicated metastasis and CEA levels were normal. The characteristics of 36 patients treated with RFA are summarized in Table 1.

All the patients had been examined by three experienced surgeon and were considered to be unsuitable for surgical intervention. Patients with coexistent morbidity-related poor life expectancy, multinodular or diffuse intrahepatic tumor, extrahepatic spread, portal thrombosis, Child-Pugh class C cirrhosis, refractory ascites, prothrombin activity less than 50 %, or a platelet count lower than $50 \times 10^9/L$ were excluded from this study.

Before enrollment, the stage of intrahepatic disease was determined by using US and contrast material-enhanced spiral computed tomography (CT) in all the patients. Selective hepatic angiography and magnetic resonance (MR) images were acquired in 11 patients. Dual-phase spiral CT was performed with injection of 150 mL of contrast. Selective hepatic angiography and MR were only conducted in patients whose images of ultrasound and CT were not clear. The size and location of the HCC nodules were assessed with Couinaud nomenclature by means of consensus between at least two observers who compared the images obtained with each of the radiological techniques.

All patients who underwent RF ablation, the following

serologic values were measured before treatment and 24 hours, 48 hours, 7 days, and 1 month after treatment, including AFP, CEA, CA19-9, transaminases, alkaline phosphatase, bilirubin, electrolytes, hemoglobin, fibrinogen, haptoglobin, creatinine, prothrombin activity, and complete blood cell count.

Table 1 Characteristics of 36 patients treated with radiofrequency ablation

Characteristics ^a	HCC	CLM	OLM
No. of patients	21	12	3
No. of nodules	28	17	3
Mean age	45.9(35-70)	52.3(41-74)	50.6(48-54)
Male/Female	15/6	9/3	0/3
Child-Pugh cirrhosis			
Class A	11	11	3
Class B	10	1	0
Class C	0	0	0
Positive HBsAg	10	4	1
Positive Antibody against Hepatitis C	2	1	0
Positive HBsAg and Hepatitis C	6	0	0
Lesion size			
< 3.0 cm	15	10	2
>3.0 cm and <5.0 cm	8	4	1
>5.0 cm	5	3	0
Serum AFP > 200 µg/L	20	1	0
Serum CEA > 20 µg/L	1	12	0

^aHCC=Hepatocellular carcinoma, CLM=Colorectal cancer liver metastases, OLM=Other malignancies liver metastases, AFP=α-fetoprotein, CEA= carcinoembryonic antigen

Equipments

Multielectrode, 15-gauge and radiofrequency probes, which was expandable by 8 hooks, were supplied by RITA Medical Systems (Mountain View, California). The hook-shaped retractable electrodes are deployed to a maximum diameter of 5.0 cm. The probe is insulated to within 1 cm of the tip to prevent cauterization along the shaft. Each electrode tip contains a thermistor that allows temperature monitoring in the tissue around the needle. The radiofrequency generator (RITA Medical Systems) delivers a 460 kHz continuous unmodulated sinusoidal waveform in the monopolar output mode (50-150 W). A computer (IBM ThinkPad, USA) with dedicated software (Micro Interactive, USA) connected to the generator recorded the power delivered, impedance values, thermistor temperatures, and timing of each procedure.

RFA procedures

The percutaneous procedure was performed in a hospital procedure room by one radiologist, one surgeon and one nurse. One hour before treatment, the patient received an orally administered sedative and an intravenously administered analgesic. The patient was monitored continuously before, during, and after the procedure. A 20-cm-long, 15-gauge and multielectrode RF probe with an expansion at 2, 3, 4, 5 cm (Starburst XL, RITA, California, USA) was used to deliver

RF energy. Grounding was achieved by attaching a dispersive pad with a surface area greater than 400 cm² to each of the patient's thighs. The patients were under local anesthesia induces by using 10 ml of 1 % Lidocaine injected from the skin into the peritoneum along the predetermined puncture line. The electrode was then attached to a 460-kHz RF generator.

Celiotomy was performed if the percutaneous method was not feasible or the lesions located near diaphragm and major hepatic vessel or bile ducts. The lesions were identified by a combination of manual palpation and handheld intraoperative ultrasonography. During the period of RFA using open laprotomy, Pringle's occlusion was applied to increase the effectiveness by preventing heat conduction from surrounding vessels.

All procedures were under the guidance of ultrasound. During lesion ablation, a thermocouple embedded in the electrode tip continuously measured the local temperature. Tissue impedance was monitored continuously by means of circuitry incorporated in the generator. For each treatment session, a single RF probe was positioned at the center of the tumor less than 3 cm in diameter. Otherwise, RF probe was introduced into a 1.0 cm deep position from the center of the lesion more than 3.0 cm diameter. Following satisfactory deployment of the multiple array, the initial power was applied at 50W and then increased in 10W increments at 1, 2, 3, and 4 minutes to a maximum power of 90W. Power and tissue impedance was monitored continuously from the RF generator. Treatment started automatically when the temperatures of each tips were above 95 °C. Treatment continued until power "roll-off" occurred, indicating a precipitous drop in power output as tissue impedance increased markedly from coagulative necrosis. Before took out the probe, the ablation of the puncture line was necessary to prevent tumor cell metastasis.

During energy deposition, a hyperechoic patch due to vaporization and cavitation effects was observed around the electrode tip; the patch progressively increased to cover all of the neoplastic area or a larger area. Several minutes after the end of treatment, the hyperechoic patch cleared and was replaced by a hyperechoic ring, which was usually smaller. RF energy was applied for 10-12 minutes. After RF therapy, patients were hospitalized for 2-3 days for percutaneous, whereas were 7-10 days in open celiotomy, unless complications necessitated longer hospitalization.

Effectiveness of RFA

All treatment sessions were completed within 1 month after the beginning of the therapies. Dynamic CT was performed 1 week and 1 month after the initial treatments. The CT scans were interpreted by the same radiologist. When a nonenhancing area with a diameter equal to or greater than that of the treated nodule was detected, tumor necrosis was considered to be complete. When nodule enhancement was seen at dynamic CT, tumor necrosis was considered to be incomplete. Additional RFA was performed in nodules that showed incomplete necrosis at dynamic CT performed 1 week after the initial treatment. The therapeutic effect was evaluated with dynamic CT 1 month after the initial treatment, and when no enhancing lesion was seen, the therapeutic effect was considered to be complete. When nodule enhancement was still seen, the therapeutic effect was considered to be incomplete and one more procedure was offered to these patients.

Follow-up dynamic CT was performed every 3 months. A newly appeared and enhanced lesion in or near the treated nodule or an enlargement of the treated nodule was considered to be residual foci of the disease. The follow-up periods ranged from 1 to 24 months (mean, 10 months).

RESULT

Therapeutic efficacy

The results of RF treatment, according to tumor size and pathology, are summarized in Table 2. Seven lesions required repeat treatment within 1 month after the initial ablation, and one lesion was re-treated after 6 months of follow-up owing to the identification of small foci of persistent viable tumor that were undetectable at the previous examination. Overall, when compared with tumor pathology, tumor size was highly significant in predicting treatment success. Tumors less than 3.0 cm in diameter were fully ablated once with recurrence. Tumors 3.1-5.0 cm in diameter were more successfully treated significantly than those greater than 5.0 cm in diameter. At 6-month follow-up, abnormal α -fetoprotein levels normalized (<20 ng/mL [20 μ g/L]) in 6 of 21 patients, decreased in 10 patients, and increased in 5 patients. CEA levels normalized in 4 of 12 patients, decreased in 5 patients, and increased in 2 patients. There were 4 deaths: 3 patients died from local and system diseases (1 at 7 month, and 1 at 9 month and 1 at 12 month), and 1 patients died from cardiovascular shock.

Table 2 Summary of results of RFA in liver cancers

Results ^a	HCC			CLM			OLM		
	<3.0cm	>3.0cm	>5.0cm	<3.0cm	>3.0cm	>5.0cm	<3.0cm	>3.0cm	>5.0cm
	<5.0cm			<5.0cm			<5.0cm		
Nodules necrosis	16	5	3	9	4	2	0	2	1
Retreated nodulars	0	2	2	1	0	1	0	0	0
Normal AFP	5	1	0	1	0	0	0	0	0
Decreased AFP	6	2	1	0	0	0	0	0	0
Normal CEA	0	1	0	3	0	0	0	0	0
Decreased CEA	0	0	0	3	1	1	0	0	0

^aHCC=Hepatocellular carcinoma, CLM=Colorectal cancer liver metastases, OLM=Other malignancies liver metastases, AFP= α -fetoprotein, CEA=carcinoembryonic antigen

Imaging findings

A rim of hyperattenuation surrounding the region of coagulated tumor was apparent in the majority of cases during the portal phase of contrast enhancement on CT scans obtained 24 hours after RF treatment. This was attributed to reactive hyperemia rather than residual viable tumor and disappeared progressively on subsequent follow-up studies. Thickening of the hepatic capsule was sometimes observed on CT scans obtained 1 month after ablation and beyond, particularly when the tumor was located close to the surface of the liver. This finding also progressively disappeared on subsequent follow-up studies.

Immediately following RF therapy, treated areas of tumor appeared as areas of hypoattenuation, compared with both surrounding liver and residual tumor. However, tumor size was unchanged, compared with pretreatment tumor size, regardless of treatment response. On subsequent follow-up CT scans, areas of successfully treated tumor remained either unchanged in size or diminished at unpredictable rates.

Although the diameter of the hyperechoic focus seen during treatment was used to guide the duration of RF application, and grossly corresponded to the diameter of necrosis demonstrated at CT, conventional US was not used for the evaluation of therapeutic response. This was principally

because of the heterogeneous and variable extent of hyperechogenicity observed after treatment (Figure 1,2).

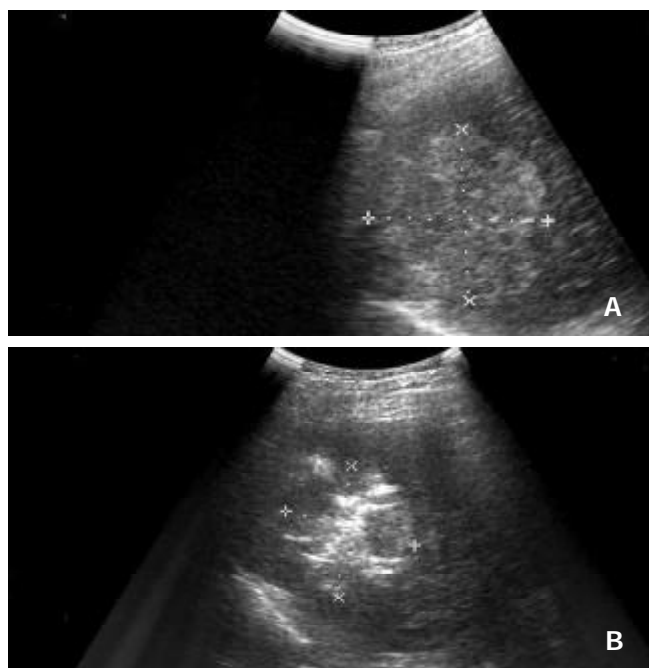


Figure 1 (A) Intercostal oblique sonogram shows a 5.7cm diameter nodular HCC in segment 8. (B) The RF electrode has been placed in the lesion, and the electrode tip is recognizable as an echogenic area in the tumor. Sonogram obtained after several minutes of energy deposition shows a hyperechoic patch around the electrode tip.

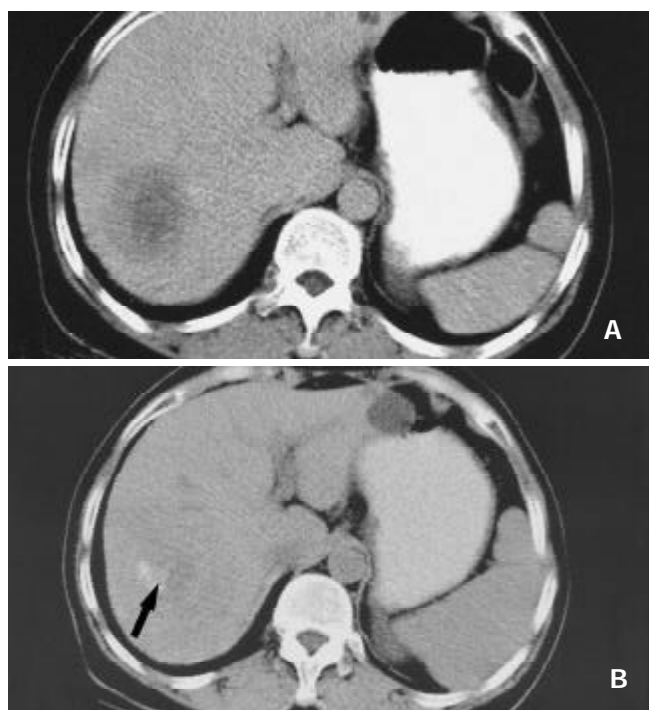


Figure 2 Nearly complete necrosis in a large HCC located in segment 7 and treated with RF therapy in a 57-year-old colorectal cancer liver metastases. (A) CT scan obtained prior to therapy demonstrates a large, 5.3 cm nodules. (B) CT scan obtained 6 months after RF therapy shows nearly complete tumor necrosis. A small hypervascularized area of viable neoplastic tissue (arrow) remains at the posteromedial aspect of the tumor.

Side effects

The majority of patients treated with the use of sedation or analgesia had mild or moderate pain during the percutaneous procedure. This disappeared 1-2 days following the cessation of RF application. However, in 2 cases, propofol and additional analgesia with assisted ventilation were administered to complete the procedure. In 1 of 25 patients, RF application had to be interrupted temporarily because of severe pain and transfer to open operation. In the majority of patients, a small asymptomatic right pleural effusion that lasted for less than 1 month was observed.

In the majority of patients, transaminase levels increased two to nine times over baseline during the first 3 days following therapy. Moreover, a slight increase in leukocytes and bilirubin and a decrease in platelets were observed. All of these test results returned to baseline levels by 7 days following RF ablation. No significant changes in other test results were observed.

Complications

Four (11.1%) patients had complications: one liver abscess; one skin burn; one postoperative hemorrhage and one cholecystitis.

Major complications

One 51 year old patient with cirrhosis and diabetes and two hepatocellular carcinoma nodules of 5.0 and 2.5 cm diameter had a liver abscess (2.7 %). On day 15 after the procedure, this patient had fever with leukocytosis. US showed a big liver abscess in the remnant of big tumor. The patient was treated successfully with percutaneous drainage of the abscess. This complication was attributed to a break in sterile technique and not to the application of RF. As a result of this complication, however, antibiotic prophylaxis with 1 000 mg of ceftriaxone sodium (Rocephin, Roche, Shanghai, China) is currently administered to all patients.

Minor complications

One (2.7 %) of 36 patients developed self-limited intraperitoneal hemorrhage (the appearance of peritoneal effusion with an associated 1-2 g/dL decrease in serum hemoglobin). This patient did not require blood transfusion or other interventions. Another had a mild cholecystitis with a severe leukocytosis. The patient had been given antibiotic for 5 days and recovered quickly. One patient got a skin burn due to incorrectly grounding for not attaching the dispersive pad to skin in the early stage of performing RFA. None of these complications required further treatment, although hospital discharge was delayed.

DISCUSSION

The management of HCC and liver metastases is challenging. HCC and liver metastases from other solid tumors are major causes of morbidity and cancer-related death worldwide. The poor prognosis of HCC is underscored by a mortality index of 0.94. That is mean that 94 % of the patients diagnosed with HCC will die as a result of this disease^[1]. Similarly, the development of solid tumor liver metastases is frequently a sign of rapidly death if not be treated. Although resection of primary or metastatic hepatic lesions can be curative in some cases, most patients have unresectable tumors. Unfortunately, systemic chemotherapy is rarely effective and often associated with significant toxicity, with few complete responses and rare long-term progression-free survival, and usually do not

significantly improve overall patient survival^[29-31]. As previously noted, the majority of patients with primary or metastatic liver tumors are not candidates for resection; however, because potentially curative or palliative benefit may be derived from destruction of the liver tumors, in situ ablative techniques like PEI, cryoablation and RFA were developed.

The mechanism of RF is that a high-frequency alternating current (100 to 500 kHz), mostly 460 kHz, passes from an uninsulated electrode tip into the surrounding tissues and causes ionic vibration as the ions attempt to follow the change in the direction of the rapidly alternating current. This ionic vibration causes frictional heating of the tissues surrounding the electrode, rather than the heat being generated from the probe itself. The goal of RFA is to achieve local temperatures so that tissue destruction occurs. In general, thermal damage to cells begins at 42 °C, with exposure times required for cell death at this temperature ranging from 3 to 50 hours depending on the nature of the tissue. As the temperature is increased, there is an exponential decrease in the exposure time needed for cellular destruction. At temperatures above 60 °C, intracellular proteins including collagen denature, the lipid bilayer melts and cell death becomes inevitable. Thermal coagulation begins at 70 °C and tissue desiccation at 100 °C, producing coagulation necrosis of tumor tissue and surrounding hepatic parenchyma. Tissue heating also drives extracellular and intracellular water out of the tissue and results in further destruction of the tissue due to coagulative necrosis^[19,20,32-34].

The first probe used in RF was a monopolar which only destroyed 1.5 cm tissues in diameter. Advances in RF technology led to the development of monopolar and bipolar tissue ablation devices designed to destroy larger areas of tissue, particularly malignant tumors. For tumor ablation, a needle electrode is placed in the tumor via a percutaneous or intraoperative approach, and an indifferent dispersive electrode pad is applied to the patient's outer skin surface, much like the grounding pads used for hemostatic electrocautery during surgical procedures. The final size of the sphere of heat-ablated tissue is proportional to the square of the radiofrequency current, also known as the radiofrequency power density. The radiofrequency power delivered via a monopolar electrode decreases in proportion to the square of the distance from the electrode. Therefore, the tissue temperature falls rapidly with increasing distance away from the electrode. The zone of tissue necrosis can be increased to 2.0 to 3.0 cm by the use of bipolar needle electrodes. New needles have been developed with multiple array hook electrodes used in our patients. The needle electrode shaft is placed into the tumor with the array retracted. Using real-time ultrasound guidance, the array is then deployed from the needle tip into the tumor. These deployed multiple array hooks create a series of electrodes with a diameter up to 5 cm, across which the radiofrequency current can be passed. Using a radiofrequency current generator with a 50 to 150 watt power output for 5 to 15 minutes, a 4.0 to 5.0 cm diameter tumor, can be ablated with 3.5 cm diameter hook electrodes fully deployed. In larger tumors, the needle electrode can be repositioned and the hook electrodes redeployed to create overlapping zones of coagulative necrosis to produce complete ablation of the tumor and a surrounding rim of hepatic parenchyma^[35-38].

RF thermal ablation has proved to be safe and effective for the treatment of hepatic tumors in patients who are considered to be unsuitable for surgical intervention and recently has attracted much attention. It has some merits compared with the other percutaneous techniques: The treatment time is shorter than that with the more popular

percutaneous ethanol injection^[39], the thermal lesions are larger than those obtained with a microwave electrode^[40], and it is less expensive and easier to perform than interstitial laser photocoagulation, in which multiple fiber insertions are always required^[41], and it is more safer and lower complications than cryotherapy^[42].

HCC with cirrhosis responded best to treatment with RFA than liver metastases. Large lesions over 3 cm were treated showing lesion stability on CT scan and a dramatic fall in AFP levels. The reason for a good response in this group of tumors is probably due to the characteristic features of hepatocellular carcinomas, which offer better heat conduction. It is clear that RFA is a useful primary therapy in patients with unresectable HCC, especially in cases with a poor liver reserve from cirrhosis and with multiple and deep-seated lesions. Prior experience treating small HCC described the "oven effect"^[39], whereby cirrhotic liver surrounding individual HCC nodules acts as a thermal insulator that increases tissue heating during RF therapy. The results of this study further support the importance of this effect.

Colorectal liver metastases are usually hard. Patients with colorectal liver metastases usually have no cirrhosis, and as they have good liver reserve, most patients without extrahepatic spread are suitable for liver resection. Unresectability is commonly due to extensive multiple, bilateral disease or central lesions. For patients with colorectal metastases, we found that those with large liver deposits over 5 cm in diameter often required two applications of RFA because of the large diameter in relation to the radius of the thermal coagulation.

The local recurrence rate in the present study was 19.5 %. Previous studies have reported highly variable local recurrence rates associated with RFA, ranging from 0 % to 100 %. Curley *et al*^[43] reported a local recurrence rate of 1.8 % in one of the largest series published to date. In our experience, local recurrences were evident at a median follow-up time of 6 months and were associated with ablation of larger tumors. It is possible that the rate of local recurrence may be reduced by specific interventions. For example, newer probes have been developed to produce larger spheres of coagulation necrosis. We are now more likely to deploy the electrode in several overlapping ablation sites to encompass tumors greater than 5 cm in diameter. For larger tumors requiring more than one deployment, we have used open operation to perform the procedure and prolonged the acting time. Selective use of the Pringle maneuver in patients with larger tumors or tumors in the vicinity of large vessels may provide larger zones of ablation. Additionally, based on our limited experience, repeat RFA seems to be well tolerated.

However, recurrence in the liver is frequently accompanied by extrahepatic disease, and careful preoperative staging is essential to select patients who could potentially benefit from repeat RFA. More recently, it has been understood that HCC is a multifocal disease in due time. In other words, the first lesion to be detected is only the prelude to other neoplasms. For this reason, we believe that it is appropriate to offer repeat RFA for selected patients with isolated hepatic recurrence^[44-46].

There is growing interest in applying RFA technology via minimally invasive approaches. Some have reported on the use of percutaneous and laparoscopic RFA procedures. In suitable patients, the percutaneous approach can be performed without general anesthesia. The laparoscopic approach can be used to evaluate for extrahepatic disease and spare the patient a laparotomy. However there are limitations with the more minimally invasive approaches, so patients must be carefully selected. We do not have experience with laparoscopic

procedures for RFA, and long-term follow-up is necessary to determine whether this approach is equivalent to an open procedure. We have limited experience with percutaneous RFA. Difficult localization of the lesion under transcutaneous ultrasound guidance was thought to be the cause of failure. Few data are available regarding long-term follow-up of patients undergoing percutaneous RFA. Major complications, such as bilioperitoneum, intrahepatic abscesses, acute thrombosis of the portal vein, and a death related to necrosis of the diaphragm have been reported following percutaneous RFA. We have been hesitant to perform percutaneous RFA except in cases of relatively small tumors that are well within the hepatic parenchyma, away from adjacent organs. The potential for inadvertent ablation of the diaphragm, colon, stomach or other organs is an important consideration. In our experience, there is one patient who have liver abscess after percutaneous RFA due to instrict sterilization. But, minimal invasive do have less harm to patients with cancers, especially in HCC with cirrhosis and late-stage liver metastases. We have chosen to perform RFA as a percutaneous procedure in the vast majority of cases. We therefore believe that the decision to perform percutaneous ablation should be a multidisciplinary effort^[47,48].

Resection or ablation of liver tumors will not cure most patients with primary or metastatic malignant disease, although long-term disease-free survival rates of 20 % to 40 % .We are very encouraged by our initial experience with RFA as a treatment for malignant liver tumors because it is safe, well-tolerated, associated with few complications, and usually effective in controlling grossly or ultrasonographically evident in liver tumors. If there are a combination of cryotherapy, percutaneous ethanol injection, RFA with regional and systemic chemotherapy, such a multimodality treatment approach will reduce hepatic and extrahepatic recurrence rates, and thus enhance long-term survival rates.

REFERENCES

- 1 **Qin LX**, Tang ZY. The prognostic significance of clinical and pathological features in hepatocellular carcinoma. *World J Gastroenterol* 2002;**8**:193-199
- 2 **Weiss L**, Grundmann E, Torhorst J, Hartveit F, Moberg I, Eder M, Fenoglio-Preiser CM, Napier J, Horne CH, Lopez MJ. Hematogenous metastatic patterns in colonic carcinoma: an analysis of 1541 necropsies. *J Pathol* 1986;**50**:195-203
- 3 **Yamanaka N**, Okamoto E, Oriyama T, Fujimoto J, Furukawa K, Kawamura E, Tanaka T, Tomoda F. A prediction scoring system to select the surgical treatment of liver cancer. Further refinement based on 10 years of use. *Ann Surg* 1994;**219**:342-346
- 4 **Nagorney DM**, van Heerden JA, Ilstrup DM, Adson MA. Primary hepatic malignancy: surgical management and determinants of survival. *Surgery* 1989;**106**:740-748
- 5 **Fong Y**, Cohen AM, Fortner JG, Enker WE, Turnbull AD, Coit DG, Marrero AM, Prasad M, Blumgart LH, Brennan MF. Liver resection for colorectal metastases. *J Clin Oncol* 1997;**15**:938-946
- 6 **Calvet X**, Bruix J, Bru C, Gines P, Vilana R, Sole M, Ayuso MC, Bruguera M, Rodes J. Natural history of hepatocellular carcinoma in Spain. 5 years experience in 249 cases. *J Hepato* 1990;**10**:311-317
- 7 **Buscarini L**, Fornari F, Canaletti R, Sbolli G, Civardi G, Cavanna L, Di Stasi M. Diagnostic aspects and follow-up of 174 cases of hepatocellular carcinoma. Second report. *Oncology* 1991;**48**:26-30
- 8 **Zhou XD**, Tang ZY, Yu YQ, Ma ZC. Clinical evaluation of cryosurgery in the treatment of primary liver cancer. Report of 60 cases. *Cancer* 1988;**61**:1889-1892
- 9 **McGahan JP**, Browning PD, Brock JM, Tesluk H. Hepatic ablation using radiofrequency electrocautery. *Invest Radiol* 1990;**5**:267-270
- 10 **Onik GM**, Atkinson D, Zemel R, Weaver ML. Cryosurgery of liver cancer. *Semin Surg Oncol* 1993;**9**:309-317
- 11 **Castells A**, Bruix J, Bru C, Fuster J, Vilana R, Navasa M, Ayuso C, Boix L, Visa J, Rodes J. Treatment of small hepatocellular carcinoma in cirrhotic patients: a cohort study comparing surgical resection and percutaneous ethanol injection. *Hepatology* 1993;**18**:1121-1126
- 12 **Kotoh K**, Sakai H, Sakamoto S, Nakayama S, Satoh M, Morotomi I, Nawata H. The effect of percutaneous ethanol injection therapy on small solitary hepatocellular carcinoma is comparable to that of hepatectomy. *Am J Gastroenterol* 1994;**89**:194-198
- 13 **Livraghi T**, Giorgio A, Marin G, Salmi A, de Sio I, Bolondi L, Pompili M, Brunello F, Lazzaroni S, Torzilli G. Hepatocellular carcinoma and cirrhosis in 746 patients: long-term results of percutaneous ethanol injection. *Radiology* 1995;**197**:101-108
- 14 **Seki T**, Wakabayashi M, Nakagawa T, Itho T, Shiro T, Kunieda K, Sato M, Uchiyama S, Inoue K. Ultrasonically guided percutaneous microwave coagulation therapy for small hepatocellular carcinoma. *Cancer* 1994;**74**:817-825
- 15 **Murakami R**, Yoshimatsu S, Yamashita Y, Matsukawa T, Takahashi M, Sagara K. Treatment of hepatocellular carcinoma: value of percutaneous microwave coagulation. *Am J Roentgenol* 1995;**164**:1159-1164
- 16 **Higuchi T**, Kikuchi M, Okazaki M. Hepatocellular carcinoma after transcatheter hepatic arterial embolization. *Cancer* 1994;**73**: 2259-2267
- 17 **Sato M**, Watanabe Y, Ueda S, Iseki S, Abe Y, Sato N, Kimura S, Okubo K, Onji M. Microwave coagulation therapy for hepatocellular carcinoma. *Gastroenterology* 1996;**110**:1507-1514
- 18 **Shibata T**, Murakami T, Ogata N. Percutaneous microwave coagulation therapy for patients with primary and metastatic hepatic tumors during interruption of hepatic blood flow. *Cancer* 2000;**88**:302-311
- 19 **Rossi S**, Di Stasi M, Buscarini E, Quaretti P, Garbagnati F, Squassante L, Paties CT, Silverman DE, Buscarini L. Percutaneous RF interstitial thermal ablation in the treatment of hepatic cancer. *Am J Roentgenol* 1996;**167**:759-768
- 20 **Solbiati L**, Ierace T, Goldberg SN, Sironi S, Livraghi T, Fiocca R, Servadio G, Rizzatto G, Mueller PR, Del Maschio A, Gazelle GS. Percutaneous US-guided RF tissue ablation of liver metastasis: results of treatment and follow-up in 16 patients. *Radiology* 1997;**202**:195-203
- 21 **Livraghi T**, Goldberg SN, Monti F, Bizzini A, Lazzaroni S, Meloni F, Pellicano S, Solbiati L, Gazelle GS. Saline-enhanced radio-frequency tissue ablation in the treatment of liver metastases. *Radiology* 1997;**202**:205-210
- 22 **Solbiati L**, Goldberg SN, Ierace T, Livraghi T, Meloni F, Dellanoce M, Sironi S, Gazelle GS. Hepatic metastasis: percutaneous radio-frequency ablation with cooled-tip electrodes. *Radiology* 1997;**205**:367-373
- 23 **Rossi S**, Buscarini E, Garbagnati F, Di Stasi M, Quaretti P, Rago M, Zangrandi A, Andreola S, Silverman D, Buscarini L. Percutaneous treatment of small hepatic tumors by an expandable RF needle electrode. *Am J Roentgenol* 1998;**170**: 1015-1022
- 24 **Curley SA**, Izzo F, Delrio P, Ellis LM, Granchi J, Vallone P, Fiore F, Pignata S, Daniele B, Cremona F. Radiofrequency ablation of unresectable primary and metastatic hepatic malignancies. *Ann Surg* 1999;**230**:1-8
- 25 **Dodd GD 3rd**, Soulen MC, Kane RA, Livraghi T, Lees WR, Yamashita Y, Gillams AR, Karahan OI, Rhim H. Minimally

- invasive treatment of malignant hepatic tumors: at the threshold of a major breakthrough. *Radio Graphics* 2000;**20**:9-27
- 26 **Parikh AA**, Curley SA, Fornage BD, Ellis LM. Radiofrequency ablation of hepatic metastases. *Semin Oncol* 2002;**29**:168-182
- 27 **Goldberg SN**, Gazelle GS, Solbiati L, Rittman WJ, Mueller PR. Radiofrequency tissue ablation: increased lesion diameter with a perfusion electrode. *Acad Radiol* 1996;**3**:636-644
- 28 **Goldberg SN**, Solbiati L, Hahn PF, Cosman E, Conrad JE, Fogle R, Gazelle GS. Radio-frequency tumor ablation using a clustered electrode technique: results in animals and patients with liver metastases. laboratory and clinical experience in liver metastases. *Radiology* 1998;**209**:371-379
- 29 **Docì R**, Gennari L, Bignami P, Montalto F, Morabito A, Bozzetti F, Bonalumi MG. Morbidity and mortality after hepatic resection of metastases from colorectal cancer. *Br J Surg* 1995;**82**:377-381
- 30 **Jamison RL**, Donohue JH, Nagorney DM, Rosen CB, Harmsen WS, Ilstrup DM. Hepatic resection for metastatic colorectal cancer results in cure for some patients. *Arch Surg* 1997;**132**:505-510
- 31 **Stangl R**, Altendorf-Hofmann A, Charnley RM, Scheele J. Factors influencing the natural history of colorectal liver metastases. *Lancet* 1994;**343**:1405-1410
- 32 **McGahan JP**, Brock JM, Tesluk H, Gu WZ, Schneider P, Browning PD. Hepatic ablation with use of radio-frequency electrocautery in the animal model. *J Vasc Interv Radiol* 1992;**3**:291-297
- 33 **McGahan JP**, Griffey SM, Budenz RW, Brock JM. Percutaneous ultrasound-guided radiofrequency electrocautery ablation of prostate tissue in dogs. *Acad Radiol* 1995;**2**:61-65
- 34 **Goldberg SN**, Gazelle GS, Dawson SL, Rittman WJ, Mueller PR, Rosenthal DI. Tissue ablation with radiofrequency: effect of probe size, gauge, duration, and temperature on lesion volume. *Acad Radiol* 1995;**2**:399-404
- 35 **Goldberg SN**, Gazelle GS, Halpern EF, Rittman WJ, Mueller PR, Rosenthal DI. Radiofrequency tissue ablation: importance of local temperature along the electrode tip exposure in determining lesion size and shape. *Acad Radiol* 1996;**3**:212-218
- 36 **Goldberg SN**, Gazelle GS, Dawson SL, Rittman WJ, Mueller PR, Rosenthal DI. Tissue ablation with radiofrequency using multiprobe arrays. *Acad Radiol* 1995;**2**: 670-674
- 37 **Miao Y**, Ni Y, Mulier S, Wang K, Hoey MF, Mulier P, Penninckx F, Yu J, De Scheerder I, Baert AL, Marchal G. Ex vivo experiment on radiofrequency liver ablation with saline infusion through a screw-tip cannulated electrode. *J Surg Res* 1997;**71**:19-24
- 38 **Goldberg SN**, Solbiati L, Hahn PF, Cosman E, Conrad JE, Fogle R, Gazelle GS. Large-volume tissue ablation with radio frequency by using a clustered, internally cooled electrode technique: laboratory and clinical experience in liver metastases. *Radiology* 1998;**209**:371-379
- 39 **Livraghi T**, Goldberg SN, Lazzaroni S, Meloni F, Solbiati L, Gazelle GS. Small hepatocellular carcinoma: treatment with radio-frequency ablation versus ethanol injection. *Radiology* 1999;**210**:655-661
- 40 **Shibata T**, Iimuro Y, Yamamoto Y, Maetani Y, Ametani F, Itoh K, Konishi J. Small hepatocellular carcinoma: comparison of radio-frequency ablation and percutaneous microwave coagulation therapy. *Radiology* 2002;**223**:331-337
- 41 **Heisterkamp J**, van Hillegersberg R, Ijzermans JN. Interstitial laser coagulation for hepatic tumours. *Br J Surg* 1999;**86**:293-304
- 42 **Bilchik AJ**, Wood TF, Allegra D, Tsioulis GJ, Chung M, Rose DM, Ramming KP, Morton DL. Cryosurgical ablation and radiofrequency ablation for unresectable hepatic malignant neoplasms: a proposed algorithm. *Arch Surg* 2000;**135**:657-664
- 43 **Curley SA**, Izzo F, Ellis LM, Nicolas Vauthey J, Vallone P. Radiofrequency ablation of hepatocellular cancer in 110 patients with cirrhosis. *Ann Surg* 2000;**232**: 381-391
- 44 **Pearson AS**, Izzo F, Fleming RY, Ellis LM, Delrio P, Roh MS, Granchi J, Curley SA. Intraoperative radiofrequency ablation or cryoablation for hepatic malignancies. *Am J Surg* 1999;**178**:592-599
- 45 **Scudamore CH**, Lee SI, Patterson EJ, Buczkowski AK, July LV, Chung SW, Buckley AR, Ho SG, Owen DA. Radiofrequency ablation followed by resection of malignant liver tumors. *Am J Surg* 1999;**177**: 411-417
- 46 **Rossi S**, Garbagnati F, Lencioni R, Allgaier HP, Marchiano A, Fornari F, Quaretti P, Tolla GD, Ambrosi C, Mazzaferro V, Blum HE, Bartolozzi C. Percutaneous radio-frequency thermal ablation of nonresectable hepatocellular carcinoma after occlusion of tumor blood supply. *Radiology* 2000;**17**:119-126
- 47 **Livraghi T**, Goldberg SN, Lazzaroni S, Meloni F, Ierace T, Solbiati L, Gazelle GS. Hepatocellular carcinoma: radio-frequency ablation of medium and large lesions. *Radiology* 2000;**214**:761-768
- 48 **Wong SL**, Edwards MJ, Chao C, Simpson D, McMasters KM. Radiofrequency ablation for unresectable hepatic tumors. *Am J Surg* 2001;**182**:552-557

Edited by Zhang JZ

Intergrin gene expression profiles of human hepatocellular carcinoma

Lian-Xin Liu, Hong-Chi Jiang, Zhi-Hua Liu, Jing Zhou, Wei-Hui Zhang, An-Long Zhu, Xiu-Qin Wang, Min Wu

Lian-Xin Liu, Hong-Chi Jiang, Wei-Hui Zhang, An-Long Zhu, Department of Surgery, the First Clinical College, Harbin Medical University, Harbin 150001, Heilongjiang Province, China

Lian-Xin Liu, Zhi-Hua Liu, Jing Zhou, Xiu-Qin Wang, Min Wu, National Laboratory of Molecular Oncology, Department of Cell Biology, Cancer Institute, Chinese Academy of Medical Science & Peking Union Medical College, Beijing 100021, China

Support by China Key Program on Basic Research, Grant Number: Z19-01-01-02; Chinese Climbing Project No.18; Youth Natural Scientific Foundation of Heilongjiang Province

Correspondence to: Professor Zhi-Hua Liu, National Laboratory of Molecular Oncology, Cancer Institute, Chinese Academy of Medical Science & Peking Union Medical College, Panjiayuan, Chaoyang District, Beijing 100021, China. liulianxin@sohu.com

Telephone: +86-451-3668999 Fax: +86-451-3670428

Received 2002-05-03 Accepted 2002-06-15

Abstract

AIM: To investigate gene expression profiles of intergrin genes in hepatocellular carcinoma (HCC) through the usage of Atlas Human Cancer Array membranes, semi-quantitative reverse transcription polymerase chain reaction (RT-PCR) and Northern blot.

METHODS: Hybridization of cDNA array membrane was performed with α ^{32}P -labeled cDNA probes synthesized from RNA isolated from hepatocellular carcinoma and adjacent non-cirrhotic liver. AtlasImage, which is a software specific to array, was used to analyze the result. RT-PCR of 24 pairs specimen and Northern blot of 4 pairs specimen were used to confirm the expression pattern of some intergrin genes identified by Atlas arrays hybridization.

RESULTS: Among 588 genes spotted in membrane, 17 genes were related to intergrin. Four genes were up-regulated, such as intergrin alpha8, beta1, beta7 and beta8 in HCC. Whereas there were no genes down-regulated in HCC. RT-PCR and Northern blot analysis of intergrin beta1 gene gave results consistent with cDNA array findings.

CONCLUSION: Investigation of these intergrin genes should help to disclose the molecular mechanism of the cell adhesion, invasive and metastasis of HCC. A few genes are reported to have changed in HCC for the first time. The quick and high-throughout method of profiling gene expression by cDNA array provides us overview of key factors that may involved in HCC, and may find the clue of the study of HCC metastasis and molecular targets of anti-metastasis therapy. The precise relationship between the altered genes and HCC is a matter of further investigation.

Liu LX, Jiang HC, Liu ZH, Zhou J, Zhang WH, Zhu AL, Wang XQ, Wu M. Intergrin gene expression profiles of human hepatocellular carcinoma. *World J Gastroenterol* 2002; 8(4):631-637

INTRODUCTION

Hepatocellular carcinoma (HCC) is one of the most common malignant tumors worldwide, which ranks eighth in frequency among human cancer especially in Asia, Africa and South Europe, accounting for an estimated one million deaths annually. Men are afflicted at least twice as often as women. Although HCC ranks eighth in frequency among cancers worldwide, it is the sixth among men and eleventh among women^[1]. It is one of the few human cancers for which an underlying etiology can be identified in most cases, and has a background of chronic inflammatory liver diseases caused by viral infection that induces cirrhosis^[2]. HCC is unusual in patients with primary biliary cirrhosis but common when cirrhosis is secondary to chronic viral hepatitis^[3,4]. However, it is not clear how this disorders result in HCC. Some tumor suppressor genes, such as RB and p53, may play a significant role in hepatocarcinogenesis^[5,6]. Besides this, growth factor including transforming growth factor- α (TGF- α) have been implicated in the development of HCC^[7]. It is early-stage metastasis that causes lower 5-year survival rate. However, these genetic changes do not precisely reflect the biological nature of cancer cells or the clinical characteristics of HCC patients. So, the molecular mechanism of metastasis of HCC is currently unknown. Cell adhesion and migration are fundamental properties of the metastasis. Changes in cell adhesion and migration are very important in the formation of tumors, and invasion and metastasis by neoplasms^[8].

The integrin family of cell adhesion receptors plays a fundamental role in the processes involved in cell division, differentiation and movement. The extracellular domains of integrin alpha/beta heterodimers mediate cell-matrix and cell-cell contacts while their cytoplasmic tails associate with the cytoskeleton. Integrins are capable of transducing information in a bidirectional manner and the beta subunit is now recognized to play an important role in this process. Recent studies have led to the identification of a ligand-binding region on the beta subunit similar to that already characterized on some alpha subunits, and sequences in the cytoplasmic tails of the beta subunits that interact with cytoskeletal and signaling components. Adhesive events can also play a role in the progression of all four major classes of human disease--neoplastic, inflammatory, traumatic and infectious--and the specific nature of integrin adhesion mechanisms make them an attractive target for therapy^[9].

Tumor development and progression involves a cascade of genetic alterations. Techniques frequently used to study gene expression alterations, such as RT-PCR, differential display PCR and Northern blot analysis, have their limitations: some need large amounts of RNA, others are time-consuming and can only study a small number of genes simultaneously. Hence, analysis of the expression profiles of a large number of genes in clinical HCC materials is an essential step toward clarifying the detailed mechanisms of metastasis and discovering target molecules for the development of novel therapeutic drugs.

The cDNA microarray technology, recently developed,

enables investigators to study the gene expression profile and gene activation in thousands of genes and sequences^[10-15]. This technique allows the large-scale comparison of multiple genes in a single hybridization and has been used successfully to explore the gene expression profiles in some kinds of carcinomas and other diseases^[16-20].

In this study, we used cDNA expression microarray technology containing 17 intergrin genes related to cell adhesion and invasion that are differentially expressed in human HCC. This large body of information not only furthers an understanding of the mechanism of metastasis but also reveals novel features of intergrin genes and identifies potential candidates for cancer metastasis detection and HCC therapy.

MATERIAL AND METHODS

Tissues and specimen

Twenty-four pairs of primary HCC and corresponding noncancerous liver tissues without cirrhosis were obtained with informed consent from patients who underwent hepatectomy at the First Clinical College of Harbin Medical University and Cancer Hospital of Chinese Academy of Medical Science. Cancerous and noncancerous tissues were enucleated separately from the tumorous and nontumorous part of resected liver. The normal tissue block was from the distal incision tissue. Histopathological diagnosis and classification were performed by the same pathologist. The specimen were immediately frozen in liquid nitrogen.

RNA isolation and purification

Total RNA were extracted from frozen tissues in Trizol (Life Technologies Inc, Gaithersburg, MD) according to the manufacturer's instructions. Normal liver tissues and HCC tissues were made in spices and homogenized in Trizol solution (1 ml/100 mg). Homogenates were incubated for 15 min on ice, and then a 1/5 volume of chloroform was added to the homogenates. After vigorous agitation for 5 min, the inorganic phase was separated by centrifugation at 12 000×g for 20 min at 4 °C. RNA were then precipitated in the presence of 1 volume of isopropanol and centrifuged at 10 000×g for 15 min at 4 °C. RNA pellets were washed with 70 % ice-cold ethanol and then dissolved in diethyl pyrocarbonate (DEPC) - treated H₂O. Total RNA concentration and quantity was assessed by absorbency at 260 nm using an Nucleic Acid and Protein Analyzer (Beckman 470, USA).

cDNA microarray

Atlas human cancer cDNA expression array (7742-1) were purchased from Clontech Laboratories Inc (Palo Alto, USA). The membrane contained 10 ng of each gene-specific cDNA from 588 known genes and 9 housekeeping genes. Several plasmid and bacteriophage DNAs and blank spots are also included as negative and blank controls to confirm hybridization specificity. These genes analyzed in this study related to cell adhesion and motility, including laminin, collagen, fibronectin and intergrin. A complete list of the intergrin genes with the array positions and GeneBank accession number spotted on the array is available at Clontech's web site (<http://www.clontech.com>).

cDNA synthesis, labeling and purification

Total RNA was reverse-transcribed into cDNA and labeled with α -³²P dCTP using Superscript™ Preamplification System for First Strand cDNA Synthesis (Life Technologies, Gaithersburg, MD). Before labeling, 5 μ g total RNA of each

sample was treated with 2 μ l DNase I (10 units/ μ l, Boehringer Mannheim, Germany), 1 μ l RNasin (40 units/ μ l, Promega, Madison, USA) at 37 °C for 15 min to remove contaminated DNA. For each labeling, the treated 5 μ g total RNA was raised in volume to 6 μ l with diethyl pyrocarbonate (DEPC)-treated H₂O and first incubated with 4 μ l oligo dT (0.5 μ g/ μ l, Life Technologies, USA) at 70 °C for 10 min. Then, 6 μ l 5×first strand reaction buffer, 1 μ l 0.1 M DTT (Life Technologies, Gaithersburg, MD), 1.5 μ l dNTP mixture containing dATP, dGTP, and dTTP at 20 μ M (Promega, Madison, USA), 10 μ l α -³²P dCTP (10 μ Ci/ μ l, NEN Life Science, Boston, MA) and 1.5 μ l SuperScript II reverse transcriptase (200 units/ μ l, Life Technologies, USA) were added and incubated at 37 °C for 90 min. The labeled first strand cDNA probes were purified by Spin 200 column (Clontech, Palo Alto, CA) to remove the unincorporated nucleotides. After purification, labeled cDNAs were denatured in a boiling water bath for 3 min before use.

Membrane hybridization and exposure

Five milliliters ExpressHyb hybridization solution (Clontech, Palo Alto, CA) and 5 μ g Cot-1 DNA (Life Technologies, USA) were added to the tube containing Atlas human cancer cDNA expression array, which was pre-hybridized at 68 °C for 2 hr. Then different incubated probes were added to different tubes and hybridization was performed at 68 °C for 18 hr in a rolling bottle. The membranes were washed twice at 50 °C in 2×SSC, 0.1 % SDS for 20 min, once at 68 °C in 1×SSC, 0.5 % SDS for 20 min, once at room temperature in 0.5×SSC, 1 % SDS for 20 min and 0.5×SSC 10 min. Membrane were then exposed to X-ray films (Fuji Films, Tokyo, Japan) at -70 °C for 1-3 days.

Image and Analysis

The images were scanned with Fluor-S MultiImager (Bio-Rad, Hercules, CA) and saved as TIFF format files. The TIFF images were imported into the AtlasImage analysis software Version 1.01 a (Clontech, Palo Alto, CA) and analyzed step by step with the guide. Housekeeping genes Ubiquitin and GAPDH were selected for normalization, because their expression was constant in cancer array hybridization system. Then the normalized intensity of each spot representing a unique gene expression level was acquired. Genes were considered to be up-regulated when the intensity ratio was ≥ 1.5 and the difference was $\geq 10\,000$ between the expression of HCC tissues and normal liver tissues.

Semi-quantitative RT-PCR

To confirm the cDNA array results, semi-quantitative RT-PCR of 24 pairs of HCC tissues and normal liver tissues was performed for intergrin beta1 displaying expression alterations. Five micrograms of total RNA in each hybridization sample was used to synthesize the first strand cDNA with SuperScript Preamplification System For First Strand cDNA Synthesis kit (Life Technologies, USA). Then 1 μ l product was used as the template to amplify specific fragments in a 25 μ l reaction mixture under the following conditions: denaturation at 95 °C (3 min); 22 cycles of 94 °C (25 sec), 60 °C (25 sec) and 72 °C (45 sec); then 72 °C extension (3 min). In each PCR reaction, primers for the human glyceraldehyde-3-phosphate dehydrogenase (GAPDH) gene were used as an internal control. GAPDH, which is considered a housekeeping gene, showed similar expression levels by cDNA array analysis for the control and tumor samples. The 5 μ l RT-PCR reaction product was analyzed by electrophoresis on a 1.5 % agarose gel. The electrophoresis images were scanned by Fluor-S MultiImager

(Bio-Rad, USA) and the original intensity of every specific band was quantified with the software Multi-Analyst (Bio-Rad, USA). The data were compared after being normalized by the intensity of GAPDH. After normalization, the adjusted intensities were calculated for the amplified gene products, and the ratios were calculated. The sequences of the PCR primer pairs of intergrin beta1 and GAPDH were designed using Primer3 Internet software program. (Whitehead Institute, Boston ,USA). Their specificity was confirmed by a BLAST Internet software assisted search for a nonredundant nucleotide sequence database (National Library of Medicine, Bethesda, MD, USA).

Primer sequences were as follows: GAPDH, forward primer 5'-ACCACAGTCCATGCCATCAC-3' and reverse primer 5'-TCCACCACCCTGTTGCTGTA-3'; Intergrin beta1, forward primer 5'-GGAGTCAGGCAAATGCTCTC-3' and reverse primer 5'-GCTAAGGCCACTTCTGCATC-3'.

Northern blot

RNAs of HCC and normal liver tissues were separated by electrophoresis in a 1.5 % agarose gel containing 2.2M formaldehyde in pairs then transferred onto a nylon membrane (Zeta-Probe, Bio-Rad, USA) by capillary action under 10×SSPE. RNA was permanently attached to the membrane by UV illumination for 150 s (GS Gene Linker, Bio-Rad, USA). RNA intactness was estimated by comparing the intensities of the 28S and 18S ribosomal RNA bands. Hybridization was performed overnight in a rolling bottles containing 8ml of hybridization buffer (5×SSPE, 5×Denhardt's solution, 0.5 % SDS, 0.2 mg/ml heat-denatured salmon sperm DNA, and 50 % formamide) and the hybridization probe that was obtained by PCR amplification. The primers were as follow: β -actin, forward primer 5'-CGTCTGGACCTGGCTGGCCGGGACC-3' and reverse primer 5'-CTAGAAGCATTTGCGGTGGACGATG-3'; Intergrin beta1, forward primer 5'-GTGTGGCCCAAGACA GTTCT-3' and reverse primer 5'-GGTTACCCACCTCT GACT-3'. α -³²P-labeled cDNA probes were synthesized using Primer-a-Gene Random Labeling Kit (Promega, USA) and following the protocol.

The membranes were washed twice at room temperature in 2 × SSPE, 0.1 % SDS for 10 min, once at 42 °C in 1 × SSPE, 0.1 % SDS for 15 min and once at 50 °C in 0.5×SSPE, 0.1 % SDS for 20 min. Membrane were then exposed to X-ray films (Fuji Films, Tokyo, Japan) at -70 °C for 24-48 h.

RESULTS

Atlas human cancer cDNA microarray expression profile

Using a cDNA expression microarray technique we established the expression profile of intergrin genes selected from different areas of cancer research in human HCC and normal liver tissues (Figure 1A, 1B). No signals were visible in the blank spots (G1,G8,G15) and negative control spots (G2-4,G9-11,G16-18) indicating that the Atlas human cancer array hybridization was highly specific. The housekeeping genes' intensities were very similar at the same time, which indicatea that the results were credible (Figure 1A,1B). Two housekeeping genes, Ubiquitin and GAPDH, were used to normalize the intensities. The color image of the difference between HCC and normal liver tissue was produced by AtlasImage array software (Figure 1C) . The comparative analysis by AtlasImage software showed that there were 4 intergrin genes changed, all of them up-regulated in HCC versus normal liver tissues, based on the criteria that the ratio was ≥ 1.5 or the difference was $\geq 10\,000$ (Table 1). There

were significant differences in the intergrin gene expression profile between the two tissues.

Table 1 Intergrin genes differentially expressed between HCC and adjacent noamal liver tissues generated by atlasImage software (Version 1.01a)

Gene	Ratio	Difference	Protein/gene
D4b	1.476895	12673	integrin alpha 8 (ITGA8)
D4e	1.507798	4363	integrin beta 1 (ITGB1)
D4j	1.997615	23003	integrin beta 7 precursor (ITGB7)
D4k	2.065331	23938	integrin beta 8 precursor (ITGB8)

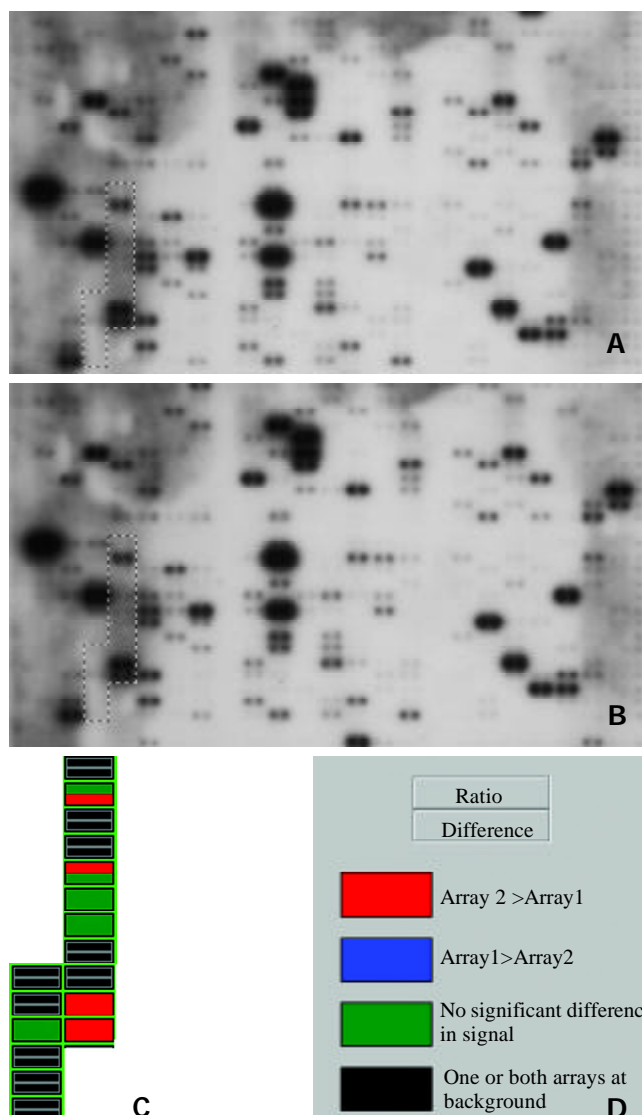


Figure 1 Parallel analysis of intergrin gene expression in human hepatocellular carcinoma and adjacent normal liver tissues. Atlas human cancer cDNA expression array (Clontech, USA) is hybridized with ³²P-labeled cDNA probes obtained by RT-PCR from total RNA of human hepatocellular carcinoma (A) and adjacent normal liver tissues (B). The intergrin gene region is marked in the photo. The colorful comparative diagram between human hepatocellular carcinoma and adjacent normal liver tissues is obtained when one aligns two arrays to AtlasImage Grid Templates and adjusts the alignments and background calculations (C). Definitions of colors in the array comparison are showed (D).

Semi-quantitative RT-PCR

RT-PCR was performed in twenty four paired tissues in to verify accuracy and universality of the hybridization data. RT-PCR data of intergrin beta1 agreed well with hybridization data after normalization by comparing the band intensities. Among the 24 paired tissues, RT-PCR results of 18 pairs of specimen were identical to the microarray results (Figure 2).

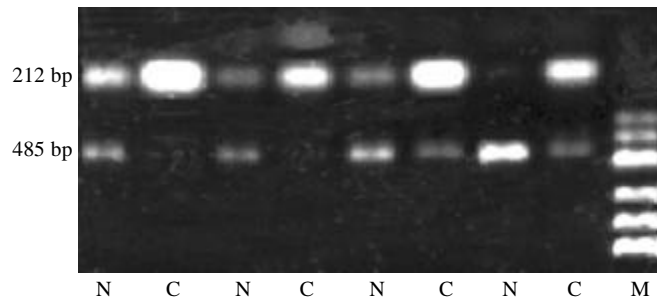


Figure 2 Partial semi-quantitative RT-PCR results for Intergrin beta1 in 24 paired tissues. A total of 10 μ l RT-PCR products are electrophoresed on 2% agarose gel containing ethidium bromide. The level of GAPDH is used as an internal control. (RT-PCR, reverse transcription- polymerase chain reaction; N, adjacent noamal liver tissue; C, human hepatocellular carcinoma tissue; GAPDH, glyceraldehyde-s-phosphate dehydrogenase; M, pUC Mix Maker)

Northern Hybridization

Northern hybridization was performed in four paired tissues to verify accuracy of the microarray hybridization data. Northern hybridization data of 4 genes agreed well with microarray hybridization. Among the 4 paired tissues, the northern hybridization results of 4 genes further meant that the Atlas human cancer cDNA microarray data were reliable and comparable (Figure 3).

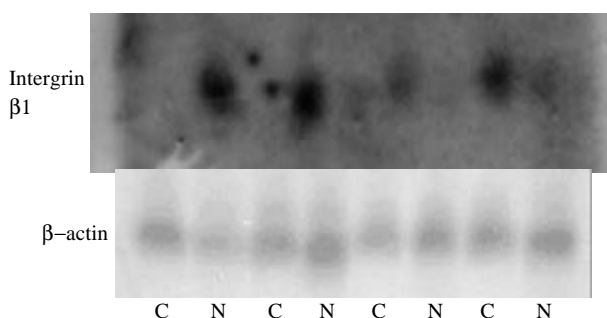


Figure 3 Nothern blot analysis of Intergrin beta1, which differentially express in human hepatocellular carcinoma and adjacent normal liver tissues, to confirm the Atlas human cancer cDNA expression array. Four paired cases are used to determine these genes expression patterns. Twenty μ g RNA is analyzed on a 1.2% denaturing agrose gel and tansfer onto a nylon membrane. 32 P-labeled cDNA probes for these genes are hybridized to the RNA-bloted membranes. After stringent washes, membranes are exposed to X-ray film overnight at -70°C . The same membranes are rehybridized with human β -actin for an RNA loading control. (C, human hepatocellular carcinoma tissue; N, adjacent noamal liver tissue)

DISCUSSION

In this study, we have investigated the gene expression profiles in human HCC and adjacent noncancerous liver tissues using Atlas human cancer array which contains 17 genes that were

classified according to intergrin. cDNA array technology is used to examine simultaneously the expression of specific genes on a single hybridization. Although human genome project has generated a large-scale sequence data for a great number of genes, the biological functions of such genes remain to be deciphered. It is very important to define differential gene expression profiles of tumors and normal tissues before understanding the functional significance of specific gene products. Although expression analysis techniques such as differential display polymerase chain reaction (DD-PCR), northern blot, and serial analysis of gene expression (SAGE) and RT-PCR have been widely used in the past, these studies are time-consuming and can only be used to deal with a limited number of genes. Thus a systematic approach to examine large number of genes simultaneously is required. Microarray techniques have been developed in this condition^[21].

Microarray technique was firstly reported in 1995 by Schena and Brown^[10], which allows simultaneous parallel expression analysis of thousands of genes. There is considerable interest in the potential application of cDNA microarray analysis for gene expression profiles in human cancers^[22]. Such information might be useful for tumor classification, elucidation of key factors in tumor metastasis, and identification of genes which might be useful for diagnostic purposes or as therapeutic targets^[23-25]. The analytical principle of human cDNA expression array is based on reverse northern blot hybridization. DNA fragments representing human genes are immobilized in duplicate onto a nylon membrane. Each cDNA fragment is 200-500 bp long and is selected as a unique sequence. This sequence is without a poly(A) tail, repetitive elements or homologous sequence to avoid cross-hybridization and nonspecific binding of a cDNA probe. α - ^{32}P or α - ^{33}P labeled cDNA probes generated by RT-PCR of total or messenger RNA samples are then hybridized to a microarray membrane. The hybridization image can be obtained by autoradiography after a high-stringency wash. The final result will be exported by a specific software designed to analyze the membrane^[26,27].

All intergrin genes identified were up-regulated in human HCC. Integrins are cell surface receptors that mediate the physical and functional interactions between a cell and its surrounding extracellular matrix (ECM). Expressed as heterodimers, the specific alpha or beta chains that constitute the integrin receptor determine the repertoire of ECM proteins to which a specific integrin may bind. While classically, the role ascribed to integrins has been that of anchoring cells to the ECM, the more contemporary spectrum of integrin function greatly exceeds that of mere cell adhesion. Recent reports have demonstrated that the interaction between the ECM and cell surface integrins leads to intracellular signaling events that affect cell migration, proliferation, and survival, which in the context of neoplastic cells, can translate directly into the malignant phenotype. Indeed, the role of specific integrins in tumorigenesis has been demonstrated in numerous cancer types. Integrins are a major family of cell adhesion molecules involved in cell-cell and cell-extracellular matrix interactions^[28].

Each integrin is a heterodimeric glycoprotein composed of an alpha and a beta subunit. Intergrin beta7 was mainly reported in hematology. The beta 7 chain of integrin forms heterodimers with the alpha 4 or alpha E chains. Mature B cells express alpha4 beta7, which is a receptor for vascular cell adhesion molecule-1 and fibronectin^[29]. The alpha4 beta7 integrin acts as a gut homing receptor. High levels of beta 7 mRNA was restricted to intra-epithelial mucosa T-lymphocytes^[30,31]. Beta 7 integrins have been implicated in

the autoimmune process in rheumatoid arthritis^[32]. It also involved in hematologic tumors that $\alpha 4\beta 7$ ligand in the adhesion of in vivo activated multiple myeloma blood B cell adhesion to bone marrow fibroblasts. The adhesion properties distinguish them from normal B cells. Although the malignant status of these cells is as yet undefined, their adhesion properties implicate multiple myeloma blood B cells in migratory spread of the disease^[33].

Integrin beta8 subunit mRNA has been shown to be expressed at higher levels in the central nervous system than in other organs^[34]. The present study demonstrates that $\alpha \nu \beta 8$ is a growth-inhibitory molecule and provides the first evidence for an *in vivo* function of the divergent integrin subunit $\beta 8$ ^[35,36] and $\beta 8$ integrin subunit is growth inhibitory in epithelial cells and that the divergent $\beta 8$ cytoplasmic domain is sufficient to confer growth inhibition. It was not known why integrin beta8 were up-regulated in HCC.

Integrin alpha 8 subunit always associates with beta1 subunit. Integrin beta-1 is essential for epithelial-mesenchymal interactions and can interact with a number of alpha subunits. The integrin alpha 8 beta 1 has been reported to bind to fibronectin, vitronectin, tenascin-C and osteopontin in cell adhesion or neurite outgrowth assays^[37-39]. Integrin alpha8 beta1 may help regulate kidney development and other morphogenetic processes^[40]. Mice with a mutation in the alpha8 gene do not express the integrin alpha8 beta1 and exhibit profound deficits in kidney morphogenesis^[39]. Alpha 8 beta 1 mediates neurite outgrowth of embryonic sensory and motor neurons on tenascin-C extracellular matrix protein^[41]. The integrin family consists of a series of related alpha beta heterodimers involved in a variety of cell-matrix and cell-cell adhesion functions.

Integrin beta1 is essential for epithelial-mesenchymal interactions and can interact with a number of alpha subunits^[42]. Cell adhesion to fibronectin can be mediated by the interaction of an integrin (alpha 5 beta 1) with the Arg-Gly-Asp-Ser (RGDS)-containing cell adhesion region of fibronectin. The beta 1 subunit plays an important role in binding and assembly of exogenous fibronectin, perhaps by participation in the organization, regeneration, or cycling of the assembly site rather than by a direct interaction with fibronectin^[43]. Alpha 5 beta 1 and alpha 2 beta 1 integrins play an important role in transducing mechanical stimuli into intracellular signals. The integrin alpha 4 beta 1 (also known as very late antigen-4, VLA4) interacts with the immunoglobulin superfamily member vascular cell adhesion molecule-1 (VCAM-1), and with an alternatively spliced form of fibronectin^[44]. The integrin alpha 3 beta 1 is a multiligand extracellular matrix receptor (VLA-3) found in many cell types. It may function as a receptor for fibronectin, laminin, collagen and also for ladsin, epiligrin and entactin^[45,46].

To investigate the role of integrins in HCC invasion, we analyzed the relationship between the expression and activity of beta1 integrins. Some studies showed that different types of HCC cells showed various levels of constitutive activity of beta1 integrins as assessed by the TS2/16 requirement in cell adhesion. Remarkably, as a result of in vitro chemoinvasion assay, the levels of constitutive activity of beta1 integrins correlated with the invasive ability of HCC cells^[47]. A new human HCC cell line with a highly metastatic potential was established from subcutaneous xenograft of a metastatic model of human HCC in nude mice (LCI-D20) by means of alternating cell culture in vitro and growth in nude mice, which has a high integrin^[48]. But there was still another result showed integrins beta 1 down-regulated in poorly differentiated HCC, whereas relatively high activity in metastatic tumors and the presence of all integrins in cirrhotic liver^[49]. Most results

showed neoplastic progression of HCCs may be correlated with an aberrant expression of adhesion molecules^[50]. Our results showed magnificent up-regulation in HCC compared with adjacent normal liver tissues.

Members of the beta 1 subfamily of integrins contribute to cell adhesion, cytoskeletal organization and signal transduction processes. In some transformed cell lines and tumors, a correlation has been established between the level of expression of the beta 1 and neoplastic behavior. In other instances, normal and neoplastic tissues differ in beta 1 integrin expression or sub-cellular distribution. The level of expression of beta 1 integrins in tumor cells may affect tumor growth properties in several ways, including: (a) effects on anchorage dependence of growth; (b) direction of signaling processes; (c) organization of the extracellular matrix and presentation of matrix bound growth factors; (d) effects on the functions of host defense cells. Thus the interplay between integrin expression and tumor behavior is complex and might be viewed as a series of interactive feedback loops rather than in terms of a straightforward cause and effect relationship^[51].

In conclusion, our study demonstrated that cDNA array is a powerful tool to explore gene expression profiles in cancer. The integrin genes described in this study should therefore provide valuable resources not only for basic research, such as molecular mechanism of metastasis, progression and prognosis, but also for clinical application, such as development of new diagnostic markers and identification of therapeutic intervention in human HCC.

ACKNOWLEDGMENTS

We thank Drs. Jian-Hua Zhao, Xin Li, Guo-Ping Li, Heng Zhang, Fang Ding, Ai-Ping Luo, Hui-Xin Wang, for their excellent technical assistance and Professor David DL Morris and Dr. Steven Gan Department of Surgery, St. George Hospital of (University of New South Wales, Sydney, Australia) for their review of the manuscript and helpful suggestions.

REFERENCE

- 1 **Tang ZY**. Hepatocellular carcinoma-Cause, treatment and metastasis. *World J Gastroenterol* 2001; **7**: 445-454
- 2 **Schafer DF**, Sorrell MF. Hepatocellular carcinoma. *Lancet* 1999; **353**: 1253-1257
- 3 **Hanley AJ**, Choi BC, Holowaty EJ. Cancer mortality among Chinese migrants: a review. *Int J Epidemiol* 1995; **24**: 255-265
- 4 **Qin LX**, Tang ZY. The prognostic significance of clinical and pathological features in hepatocellular carcinoma. *World J Gastroenterol* 2002; **8**: 193-199
- 5 **Naka T**, Toyota N, Kaneko T, Kaibara N. Protein expression of p53, p21WAF1, and Rb as prognostic indicators in patients with surgically treated hepatocellular carcinoma. *Anticancer Res* 1998; **18**: 555-564
- 6 **Montesano R**, Hainaut P, Wild CP. Hepatocellular carcinoma: from gene to public health. *J Natl Cancer Inst* 1997; **89**: 1844-1851
- 7 **Collier JD**, Guo K, Gullick WJ, Bassendine MF, Burt AD. Expression of transforming growth factor alpha in human hepatocellular carcinoma. *Liver* 1993; **13**: 151-155
- 8 **Van Waes C**. Cell adhesion and regulatory molecules involved in tumor formation, hemostasis, and wound healing. *Head Neck* 1995; **17**: 140-147
- 9 **Green LJ**, Mould AP, Humphries MJ. The integrin beta subunit. *Int J Biochem Cell Biol* 1998; **30**: 179-184

- 10 **Schena M**, Shalon D, Davis RW, Brown PO. Quantitative monitoring of gene expression patterns with a complementary DNA microarray. *Science* 1995; **270**: 467-470
- 11 **DeRisi J**, Penland L, Brown PO, Bittner ML, Meltzer PS, Ray M, Chen Y, Su YA, Trent JM. Use of a cDNA microarray to analyse gene expression patterns in human cancer. *Nat Genet* 1996; **14**: 457-460
- 12 **Ramsay G**. DNA chips: state-of-the art. *Nat Biotechnol* 1998; **16**: 40-44
- 13 **Cole KA**, Krizman DB, Emmert-Buck MR. The genetics of cancer-a 3D model. *Nat Genet* 1999; **21**(1 Suppl): 38-41
- 14 **Afshari CA**, Nuwaysir EF, Barrett JC. Application of complementary DNA microarray technology to carcinogen identification, toxicology, and drug safety evaluation. *Cancer Res* 1999; **59**: 4759-4760
- 15 **Kallioniemi OP**. Biochip technologies in cancer research. *Ann Med* 2001; **33**: 142-147
- 16 **Wang K**, Gan L, Jeffery E, Gayle M, Gown AM, Skelly M, Nelson PS, Ng WV, Schummer M, Hood L, Mulligan J. Monitoring gene expression profile changes in ovarian carcinomas using cDNA microarray. *Gene* 1999; **229**: 101-108
- 17 **Ross DT**, Scherf U, Eisen MB, Perou CM, Rees C, Spellman P, Iyer V, Jeffrey SS, Van de Rijn M, Waltham M, Pergamenschikov A, Lee JC, Lashkari D, Shalon D, Myers TG, Weinstein JN, Botstein D, Brown PO. Systematic variation in gene expression patterns in human cancer cell lines. *Nat Genet* 2000; **24**: 227-235
- 18 **Khan J**, Simon R, Bittner M, Chen Y, Leighton SB, Pohida T, Smith PD, Jiang Y, Gooden GC, Trent JM, Meltzer PS. Gene expression profiling of alveolar rhabdomyosarcoma with cDNA microarrays. *Cancer Res* 1998; **58**: 5009-5013
- 19 **Lu J**, Liu Z, Xiong M, Wang Q, Wang X, Yang G, Zhao L, Qiu Z, Zhou C, Wu M. Gene expression profile changes in initiation and progression of squamous cell carcinoma of esophagus. *Int J Cancer* 2001; **91**: 288-294
- 20 **Hu YC**, Lam KY, Law S, Wong J, Srivastava G. Identification of differentially expressed genes in esophageal squamous cell carcinoma (ESCC) by cDNA expression array: overexpression of Fra-1, Neogenin, Id-1, and CDC25B genes in ESCC. *Clin Cancer Res* 2001; **7**: 2213-2221
- 21 **Khan J**, Saal LH, Bittner ML, Chen Y, Trent JM, Meltzer PS. Expression profiling in cancer using cDNA microarrays. *Electrophoresis* 1999; **20**: 223-229
- 22 **Selaru FM**, Zou T, Xu Y, Shustova V, Yin J, Mori Y, Sato F, Wang S, Olaru A, Shibata D, Greenwald BD, Krasna MJ, Abraham JM, Meltzer SJ. Global gene expression profiling in Barrett's esophagus and esophageal cancer: a comparative analysis using cDNA microarrays. *Oncogene* 2002; **21**: 475-478
- 23 **Unger MA**, Rishi M, Clemmer VB, Hartman JL, Keiper EA, Greshock JD, Chodosh LA, Liebman MN, Weber BL. Characterization of adjacent breast tumors using oligonucleotide microarrays. *Breast Cancer Res* 2001; **3**: 336-341
- 24 **Sgroi DC**, Teng S, Robinson G, LeVangie R, Hudson JR Jr, Elkahoul AG. In vivo gene expression profile analysis of human breast cancer progression. *Cancer Res* 1999; **59**: 5656-5661
- 25 **Ono K**, Tanaka T, Tsunoda T, Kitahara O, Kihara C, Okamoto A, Ochiai K, Takagi T, Nakamura Y. Identification by cDNA microarray of genes involved in ovarian carcinogenesis. *Cancer Res* 2000; **60**: 5007-5011
- 26 **Schulze A**, Downward J. Navigating gene expression using microarrays--a technology review. *Nat Cell Biol* 2001; **3**: E190-195
- 27 **Rew DA**. DNA microarray technology in cancer research. *Eur J Surg Oncol* 2001; **27**: 504-508
- 28 **Uhm JH**, Gladson CL, Rao JS. The role of integrins in the malignant phenotype of gliomas. *Front Biosci* 1999; **4**: D188-199
- 29 **Manie SN**, Astier A, Wang D, Phifer JS, Chen J, Lazarovits AI, Morimoto C, Freedman AS. Stimulation of tyrosine phosphorylation after ligation of beta7 and beta1 integrins on human B cells. *Blood* 1996; **87**: 1855-1861
- 30 **Shaw SK**, Cepek KL, Murphy EA, Russell GJ, Brenner MB, Parker CM. Molecular cloning of the human mucosal lymphocyte integrin alpha E subunit. Unusual structure and restricted RNA distribution. *J Biol Chem* 1994; **269**: 6016-6025
- 31 **Parker CM**, Cepek KL, Russell GJ, Shaw SK, Posnett DN, Schwarting R, Brenner MB. A family of beta 7 integrins on human mucosal lymphocytes. *Proc Natl Acad Sci U S A* 1992; **89**: 1924-1928
- 32 **Jorgensen C**, Couret I, Canovas F, Bologna C, Brochier J, Reme T, Sany J. In vivo migration of tonsil lymphocytes in rheumatoid synovial tissue engrafted in SCID mice: involvement of LFA-1. *Autoimmunity* 1996; **24**: 179-185
- 33 **Masellis-Smith A**, Belch AR, Mant MJ, Pilarski LM. Adhesion of multiple myeloma peripheral blood B cells to bone marrow fibroblasts: a requirement for CD44 and alpha4beta7. *Cancer Res* 1997; **57**: 930-936
- 34 **Nishimura SL**, Boylen KP, Einheber S, Milner TA, Ramos DM, Pytela R. Synaptic and glial localization of the integrin alphavbeta8 in mouse and rat brain. *Brain Res* 1998; **791**: 271-282
- 35 **Clarke AS**, Lotz MM, Chao C, Mercurio AM. Activation of the p21 pathway of growth arrest and apoptosis by the b4 integrin cytoplasmic domain. *J Biol Chem* 1995; **270**: 22673-22676
- 36 **Cambier S**, Mu DZ, O'Connell D, Boylen K, Travis W, Liu WH, Broaddus VC, Nishimura SL. A Role for the Integrin $\alpha v \beta 8$ in the Negative Regulation of Epithelial Cell Growth. *Cancer Res* 2000; **60**: 7084-7093
- 37 **Varnum-Finney B**, Venstrom K, Muller U, Kypta R, Backus C, Chiquet M, Reichardt LF. The integrin receptor alpha 8 beta 1 mediates interactions of embryonic chick motor and sensory neurons with tenascin-C. *Neuron* 1995; **14**: 1213-1222
- 38 **Denda S**, Reichardt LF, Muller U. Identification of osteopontin as a novel ligand for the integrin alpha8 beta1 and potential roles for this integrin-ligand interaction in kidney morphogenesis. *Mol Biol Cell* 1998; **9**: 1425-1435
- 39 **Denda S**, Muller U, Crossin KL, Erickson HP, Reichardt LF. Utilization of a soluble integrin-alkaline phosphatase chimera to characterize integrin alpha 8 beta 1 receptor interactions with tenascin: murine alpha 8 beta 1 binds to the RGD site in tenascin-C fragments, but not to native tenascin-C. *Biochemistry* 1998; **37**: 5464-5474
- 40 **Muller U**, Wang D, Denda S, Meneses JJ, Pedersen RA, Reichardt LF. Integrin alpha8beta1 is critically important for epithelial-mesenchymal interactions during kidney morphogenesis. *Cell* 1997; **88**: 603-613
- 41 **Hartner A**, Schocklmann H, Prols F, Muller U, Sterzel RB. Alpha8 integrin in glomerular mesangial cells and in experimental glomerulonephritis. *Kidney Int* 1999; **56**: 1468-1480
- 42 **Sonnenberg A**, Gehlsen KR, Aumailley M, Timpl R. Isolation of alpha 6 beta 1 integrins from platelets and adherent cells by affinity chromatography on mouse laminin fragment E8 and human laminin pepsin fragment. *Exp Cell Res* 1991; **197**: 234-244
- 43 **Fogarty FJ**, Akiyama SK, Yamada KM, Mosher DF. Inhi-

- bition of binding of fibronectin to matrix assembly sites by anti-integrin (alpha 5 beta 1) antibodies. *J Cell Biol* 1990; **111**: 699-708
- 44 **Takada Y**, Murphy E, Pil P, Chen C, Ginsberg MH, Hemler ME. Molecular cloning and expression of the cDNA for alpha 3 subunit of human alpha 3 beta 1 (VLA-3), an integrin receptor for fibronectin, laminin, and collagen. *J Cell Biol* 1991; **115**: 257-266
- 45 **Kikkawa Y**, Akaogi K, Mizushima H, Yamanaka N, Umeda M, Miyazaki K. Stimulation of endothelial cell migration in culture by ladsin, a laminin-5-like cell adhesion protein. *In Vitro Cell Dev Biol Anim* 1996; **32**: 46-52
- 46 **Carter WG**, Ryan MC, Gahr PJ. Epiligrin, a new cell adhesion ligand for integrin alpha 3 beta 1 in epithelial basement membranes. *Cell* 1991; **65**: 599-610
- 47 **Masumoto A**, Arao S, Otsuki M. Role of beta1 integrins in adhesion and invasion of hepatocellular carcinoma cells. *Hepatology* 1999; **29**:68-74
- 48 **Tian J**, Tang ZY, Ye SL, Liu YK, Lin ZY, Chen J, Xue Q. New human hepatocellular carcinoma (HCC) cell line with highly metastatic potential (MHCC97) and its expressions of the factors associated with metastasis. *Br J Cancer* 1999; **81**:814-821
- 49 **Jaskiewicz K**, Chasen MR. Differential expression of transforming growth factor alpha, adhesions molecules and integrins in primary, metastatic liver tumors and in liver cirrhosis. *Anticancer Res* 1995; **15**: 559-562
- 50 **Patriarca C**, Roncalli M, Gambacorta M, Cominotti M, Coggi G, Viale G. Patterns of integrin common chain beta 1 and collagen IV immunoreactivity in hepatocellular carcinoma. Correlations with tumour growth rate, grade and size. *J Pathol* 1993; **171**: 5-11
- 51 **Juliano RL**. The role of beta 1 integrins in tumors. *Semin Cancer Biol* 1993; **4**: 277-283

Edited by Zhang JZ

Overexpression of *p28/gankyrin* in human hepatocellular carcinoma and its clinical significance

Xiao-Yong Fu, Hong-Yang Wang, Lu Tan, Shu-Qin Liu, Hui-Fang Cao, Meng-Chao Wu

Xiao-Yong Fu, Hong-Yang Wang, Shu-Qin Liu, Hui-Fang Cao, International Co-operation Laboratory on Signal Transduction, Eastern Hepatobiliary Surgery Institute, the Second Military Medical University, 200438, Shanghai, China

Lu Tan, Department of pathology, Eastern hepatobiliary surgery hospital, the Second Military Medical University, 200438, Shanghai, China

Meng-Chao Wu, Department of clinical surgery, Eastern hepatobiliary surgery hospital, the Second Military Medical University, 200438, Shanghai, China

Supported by the Chinese National Distinguished Young Scholar Awards, No. 39825114, Chinese National Key Project of Basic Research, No. G1998051210 and the Key Project of the Chinese National Natural Science Foundation, No. 39830080.

Correspondence to: Dr. Hong-Yang Wang, International Co-operation Laboratory on Signal Transduction, Eastern Hepatobiliary Surgery Institute, the Second Military Medical University, 200438, Shanghai, China. hywangk@online.sh.cn

Telephone: +86-21-25070856 **Fax:** +86-21-65566851

Received 2002-03-11 **Accepted** 2002-04-20

Abstract

AIM: To investigate the expression of *p28/gankyrin* gene and its role in the carcinogenetic process of human hepatocellular carcinoma (HCC).

METHODS: 64 specimens of HCC and para-carcinoma tissues, 22 specimens of non-tumor liver tissues (7 normal, 15 cirrhosis), 10 specimens of normal human tissues and 5 hepatoma cell lines were studied for the expression of *p28/gankyrin* by Northern blot. The expression of *p28/gankyrin* protein was detected immunohistochemically by using the specific polyclonal antibody.

RESULTS: Northern blot analysis indicated that the expression of *p28/gankyrin* mRNA was intensively distributed in brain and heart, weakly in lung, spleen and muscle, undetectable in digestive system including liver, pancreas, stomach, small and large intestines. *p28/gankyrin* mRNA was absent in normal liver, weakly detected in liver cirrhosis and in 18 of 64 para-carcinoma liver tissues. In contrast, the expression of *p28/gankyrin* mRNA was intensively detected in all 5 hepatoma cell lines tested, markedly increased in 57 of 64 and moderately increased in 5 of 64 HCC samples. In comparison with liver cirrhosis and para-carcinoma liver tissues, the average expression of *p28/gankyrin* mRNA in HCC was increased 3.6- (2.901 ± 0.507 vs 0.805 ± 0.252, $P < 0.05$) and 5.2-fold (2.901 ± 0.507 vs 0.557 ± 0.203, $P < 0.01$), respectively. In addition, *p28/gankyrin* mRNA expression level was higher in HCC with portal vein tumor thrombus and microscopic hepatic vein involvement ($P = 0.021$ and $P = 0.047$, respectively). The overexpression of *p28/gankyrin* protein in HCC was targeted in hepatic tumor cells, not in bile duct cells and other interstitial cells.

CONCLUSION: Overexpression of *p28/gankyrin* in HCC

plays an important role and contributes to the metastasis potential in the process of carcinogenesis. *p28/gankyrin* may become a specific biological tissue marker for the pathological diagnosis of HCC.

Fu XY, Wang HY, Tan L, Liu SQ, Cao HF, Wu MC. Overexpression of *p28/gankyrin* in human hepatocellular carcinoma and its clinical significance. *World J Gastroenterol* 2002;8(4):638-643

INTRODUCTION

Human primary hepatocellular carcinoma (HCC) is one of the most common types of malignant cancer in Asia and Africa where hepatitis virus infection and exposure to specific liver carcinogens are prevalent^[1-4]. HCC has ranked second in cancer mortality in China since the 1990s and is increasing in frequency among males in many countries^[5,6]. Although the major viral and environmental risk factors for HCC development have been unraveled^[7,8], the oncogenic pathways leading to malignant transformation of liver cells have long remained obscure^[9]. It has been widely reported that some tumor suppressor genes such as *p53* and *p16^{INK4A}* play a vital role in the development of HCC^[10-13], while few oncogenes that control growth behavior or metastatic potential of HCC have been underscored.

p28 gene was initially cloned in human cDNA library by comparing the amino-acid sequence of a subunit isolated from the purified bovine erythrocyte PA700 complex with protein structures in databases of Homo-Protein cDNA Bank^[14-16]. *p28* protein is one of the non-ATPase subunits of PA700 (also called 19 S complex), a 700 kDa multisubunit regulatory complex of the human 26 S proteasome^[17]. Intriguingly, *p28* protein contained six conserved motifs known as 'ankyrin repeats'^[18-20], implying that this subunit may contribute to interaction of the 26 S proteasome with other proteins. Recently, another gene named '*gankyrin*' was cloned by cDNA subtractive hybridization in HCC and its sequence is identical to *p28* gene^[21]. Because of the putative proteasome connection, the oncogenic effect of *p28/gankyrin* in HCC may be associated with the ubiquitin-proteasome pathway^[22-24]. So far, the mechanism of up-regulation of *p28/gankyrin* in HCC is still unknown.

In order to elucidate the role of *p28/gankyrin* in carcinogenesis of HCC and its correlation with clinical parameters, the following study was carried out.

MATERIALS AND METHODS

Sample collection and processing

All 64 HCC specimens and their para-carcinoma tissues (more than 2 cm away from the focus), were sampled from 64 patients who had undergone curative hepatectomy (58 men and 6 women; mean age 46.4 ± 10.5 years). Patients who had received radiotherapy or chemotherapy before hepatectomy were excluded. Non-tumor liver tissues were obtained from

22 patients who had received hepatic hemangioma surgery. Ten different types of human normal tissues were from 2 men of accidental deaths. They were all cases from 1999 to 2000 in Eastern Hepatobiliary Surgery Hospital in Shanghai, China. Informed consent was obtained from all patients for subsequent use of their resected tissues. These specimens were immediately dissected into small pieces under aseptic condition within half an hour, quickly-frozen and preserved in liquid nitrogen before subsequent procedures. The specimens used for immunohistochemistry (IHC) were routinely processed, formalin-fixed and paraffin-embedded, at least 2 serial paraffin sections of 4 mm-6 mm thick were made, one for hematoxylin and eosin (HE) staining and the other for *p28/gankyrin* protein detection.

Cells lines

A series of cell lines (ATCC, Rockville, MD) were investigated in this study, including HepG2 (ATCC HB-8065), HuH-7, SK-Hep-1 (ATCC HTB-52), Chang liver (ATCC CCL-13), and a human fetal hepatocyte cell line WRL 68 (ATCC CL-48). They were maintained, as specified by the suppliers, in Dulbecco's modified Eagle medium or other recommended mediums supplemented with 10% fetal bovine serum at 37 °C in a humidified atmosphere of 5% CO₂ in air.

Northern blot analysis of *p28/gankyrin* transcript

Preparation and labeling of the probe Polymerase chain reaction (PCR) of a human fetal liver cDNA library (provided by Max-Planck Institute) was performed in a final volume of 50 µl containing all four dNTPs (each at 200 µmol/L), 1.25 mmol/L MgCl₂, 2.5 units of Taq (TaKaRa Biotech, Dalian, China) and each primer at 0.5 µmol/L. The following temperature program was used: 1 cycle at 94 °C for 5 min, 35 cycles at 94 °C for 40 s, 52 °C for 30 s and 72 °C for 55 s, followed by a final extension at 72 °C for 8 min. Primers used for amplification were human *p28/gankyrin* sense primer corresponding to nucleotides 2-19 (5' - GCGGATCCAGTAGTTGCTGGGACAGC-3'), and antisense primer complementary to nucleotides 830-847 (5' - GCGAATTCGGAACAAGAGTCAACATG-3') with the BamHI and EcoRI restriction sites at their 5' strand ends respectively. The PCR product was cloned into pcDNA3.1 vector (Invitrogen, Groningen, Netherlands) to generate the clone full.hup28.pcDNA3.1, which was confirmed by sequencing with an automatic DNA sequencer (ABI model 3700). The purified PCR product was labeled with α-³²P-dATP by a random primer labeling method as described^[25] with Prime-a-Gene Labeling System (Promega, Madison, WI).

RNA extraction and preparation of the hybridization membrane Samples subjected to RNA analysis were isolated from surgical specimens of HCC and the para-carcinoma liver tissues of 64 patients and from a series of non-tumor liver samples, normal human tissues and hepatoma cell lines by the acid guanidinium thiocyanate-phenol-chloroform extraction method as previously described^[26]. Total RNA (40mg) was denatured and separated by electrophoresis in a 1.0 % agarose gel containing 2.2 mol/L formaldehyde and then transferred to nitrocellulose membranes (BA85, Schleicher Schuell, Germany). The membranes were dried in a vacuum drying oven at 80 °C for 2 h and sealed in a plastic bag for use.

Northern blot analysis Hybridization of the membranes was performed by using the labeled *p28/gankyrin* cDNA as the probe at 42 °C for 20 h in a solution containing 50 % formamide, 5×SSC, 0.1 % SDS and 5× Denhardt's after the membranes had been pre-hybridized in the same solution with 0.1 mg/ml salmon sperm DNA at 42 °C for 4 h. After this hybridization,

the membranes were rinsed in stringent conditions (65 °C for 30 min in a washing buffer of 0.1×SSC and 0.1 % SDS) and then exposed to Kodak X-ray film at -80 °C for 14 days. The expression level of mRNA was normalized with ethidium bromide-stained 18 s rRNA as internal standard and analyzed by Phosphor Imager (FLA 2000, Fujifilm, Japan).

Immunohistochemical analysis of *P28/Gankyrin* protein

Preparation of the polyclonal antibody A polyclonal antibody against *p28/gankyrin* protein (226 amino acid) was prepared. Briefly, a 683-bp fragment from nucleotide 2 to 684 (amino acid 1-221) was generated by PCR and subcloned into the fusion expression vector pPROEX-HTb (Gibco/BRL Life Technologies, NY) using *Bam*HI and *Xho*I. The expression vector was then transformed into competent *Escherichia coli* DH5a for induction of 6×histidine-fused protein with 0.6 mmol/L isopropyl-1-thio-β-D-galactopyranoside (IPTG) at 37 °C for 3 h. The cells were harvested and lysed with ice-cold TS buffer containing 50 mmol/L Tris-HCl (pH 8.0), 150 mmol/L NaCl, 1 mg/ml lysozyme, 5 mmol/L EDTA, 0.5 mmol/L phenylmethylsulfonyl fluoride, 0.2 mg/L aprotinin and 1 % Triton X-100. The lysates were purified by affinity chromatography with Ni-NTa agarose column (Qiagen, Germany) and identified by electrophoresis on a 10 % SDS-PAGE gel. The purified fusion protein emulsified with Freund's adjuvant (Gibco/BRL Life Technologies, NY) was used to immunize two New Zealand rabbits (male, 2.5-3.0 kg) for preparation of the polyclonal antibody. Antibody valence was determined by double immunodiffusion test on 1 % agar gel. For the specificity, affinity chromatography was applied to purify the antibody from the immune sera by an antigen column.

Immunohistochemical staining *p28/gankyrin* protein was detected in HCCs, para-carcinoma liver tissues and SK-Hep1 cell line by using peroxidase-labeled secondary antibody two-step IHC technique with the DAKO EnVision system (DAKO Corporation, carpinteria, USA). All paraffin embedded samples were deparaffined and rehydrated, and the SK-Hep1 cells cultured on coverslips were fixed in 4 % polyformalin for 30 min, then pretreated with citrate buffer (0.01 mol/L citric acid: pH 6.0) for 15 min at 100 °C in a microwave oven. After being treated with 0.3 % H₂O₂ for 10 min to block the endogenous peroxidase, the sections were incubated with 10 % fetal calf serum for 30 min to reduce nonspecific binding, and then the primary *p28/gankyrin* antibody was applied to the sections at 4 °C overnight. The sections were subsequently incubated with horseradish peroxidase (HR) -labeled goat anti-rabbit immunoglobulin for 30 min, followed by incubation with prepared liquid 3,3'-diaminobenzidine (DA) + substrate-chromogen solution for 10 min at room temperature. Finally, the sections were counterstained with hematoxylin. The negative controls were conducted by substituting rabbit normal serum for the primary antibody to verify the possibility of false-positive responses from the secondary antibody.

Clinical data and histopathological parameters

The following variables were evaluated: age, sex, HBsAg, accompanying cirrhosis, serum α-fetoprotein (AFP) level, tumor size, satellite nodules, formation of tumor capsule, fibrous capsular infiltration, portal vein tumor thrombus, microscopic invasion of the tumor into hepatic vein, and histological grade of HCC according to Edmonson and Steiner's classification^[27].

Statistical analysis

Data of *p28/gankyrin* mRNA levels were presented as means

\pm SD. Significance of differences was assessed by analysis of variance (ANOVA) or Student's *t*-test. *P* values of ≤ 0.05 were considered statistically significant.

RESULTS

Clinical profiles and histopathologic examination

64 patients with primary HCC were recruited in this study, including 58 males and 6 females with ages ranging from 24 to 74 years (mean, 46.4 ± 10.5 years). Serum anti-hepatitis B virus was detected in 45 (70.3%) of 64 patients and positive anti-hepatitis C virus in serum was found in 6 (18.8%) of 32 patients examined. 50 (78.1%) patients showed increased serum AFP level and levels above 1000 mg/L were observed in 29 of them. Histopathologically, 47 of 64 HCCs and 15 of 22 non-tumor liver tissues displayed cirrhosis. Among the 46 patients with fibrocapsule formation around HCC, 21 had broken through and 19 of them had microscopic hepatic vein involvement. Portal vein tumor thrombus was found in 18 (28.1%) patients and 32 (50.0%) patients had satellite nodules in primary HCC. According to Edmonson and Steiner's classification, 20 (31.3%) and 44 (68.7%) patients were classified to grade I-II group and grade III-IV group, respectively.

Tissue distribution of *p28/gankyrin* mRNA

Northern blot analysis showed that *p28/gankyrin* was expressed as one single transcript of 1.5 kb, corresponding well with the size of the cloned cDNA (Figure 1 A). *p28/gankyrin* was strongly expressed in brain and heart, whereas weaker expression was found in lung and spleen. Faint signals were discerned in muscle, but no signals were observed in digestive system including liver, pancreas, stomach, small and large intestine.

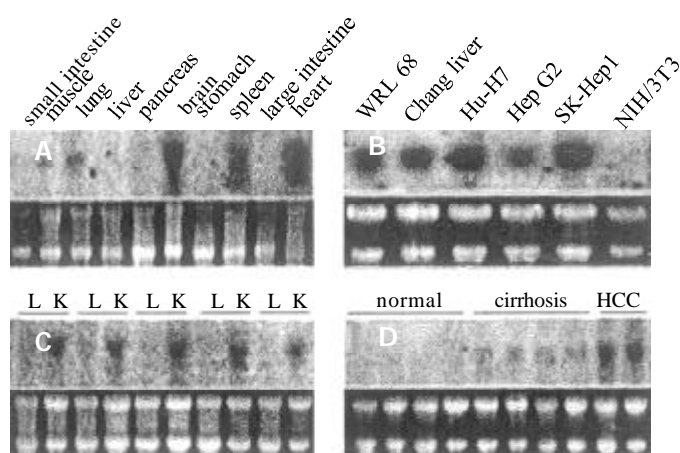


Figure 1 Northern blot of *p28/gankyrin* in a series of human normal tissues, hepatoma cell lines, HCC and non-tumor liver tissues. (A) *p28/gankyrin* expression in ten different normal adult human tissues. (B) *p28/gankyrin* expression in five hepatoma cell lines and NIH/3T3 cell. (C) *p28/gankyrin* expression in HCC and para-carcinoma liver tissues. L indicates the para-carcinoma liver tissues, and K indicates the HCC tissues. (D) Comparison of *p28/gankyrin* expression in normal human liver tissues, liver cirrhosis and HCC tissues. Each bottom panel showed equal amount of total RNA loading as indicated in 28s and 18s rRNA.

p28/gankyrin expression in hepatoma cell lines

In the 5 human hepatoma cell lines, *p28/gankyrin* mRNA was detected as the expected size with various expression levels

(Figure 1 B). It was expressed strongly in SK-Hep1, weakly in HepG2 and no expression has been found in NIH/3T3 cell line.

p28/gankyrin expression in HCC, para-carcinoma and non-tumor liver tissues

p28/gankyrin mRNA expression levels were higher in the 64 HCC samples than in the para-carcinoma tissues (Figure 1 C). *p28/gankyrin* mRNA levels were markedly increased in 57 of 64 (89.1%), moderately increased in 5 of 64 (7.8%) HCC samples. In the remaining two HCC samples, *p28/gankyrin* mRNA was expressed at the same level as the para-carcinoma liver tissues. In contrast, *p28/gankyrin* mRNA expression was weakly detected in 18 of 64 (28%) and was below the level of detection in 46 of 64 (72%) para-carcinoma liver samples. In 22 non-tumor liver samples, *p28/gankyrin* was absent in 7 normal livers and weakly present in 15 liver cirrhosis tissues (Figure 1D). Densitometric analysis of all northern blots indicated that compared with liver cirrhosis and para-carcinoma liver tissues, the average expression of *p28/gankyrin* mRNA in HCC was increased by 3.6- $(2.901 \pm 0.507$ vs 0.805 ± 0.252 , $P < 0.05$) and 5.2-fold (2.901 ± 0.507 vs 0.557 ± 0.203 , $P < 0.01$), respectively (Figure 2A).

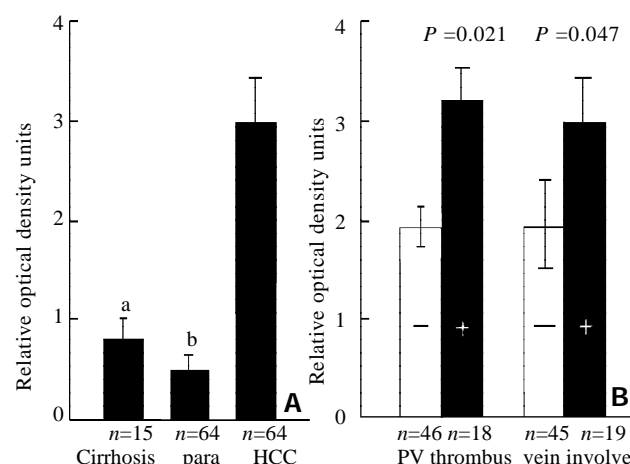


Figure 2 Densitometric analysis. The ratio of the optical density of *p28/gankyrin* mRNA to the corresponding 18 S rRNA signals was calculated and expressed as means \pm SD. (A) Comparison of *p28/gankyrin* expression in human liver cirrhosis, para-carcinoma liver tissues and HCCs. ^aThe expression in HCCs was significantly higher than that in liver cirrhosis ($P < 0.05$). ^bThe expression in HCCs was significantly higher than that in para-carcinoma liver tissues ($P < 0.01$). (B) Clinicopathological significance of *p28/gankyrin* expression in HCCs. *p28/gankyrin* mRNA levels were significantly higher ($P = 0.021$) in portal vein thrombus group than in non-thrombus group, higher ($P = 0.047$) in microscopic hepatic vein involvement group than in non-hepatic vein involvement group.

Correlation of *p28/gankyrin* mRNA expression with clinicopathological parameters

Comparison of clinical profiles of HCC patients with *p28/gankyrin* mRNA expression was summarized in Table 1. From these results, age, sex, HBsAg, and accompanying cirrhosis were not significantly correlated with the expression levels of *p28/gankyrin* ($P > 0.05$). Relationships of *p28/gankyrin* mRNA expression with histopathological parameters were listed in Table 2. These results showed that there were no significant correlation between *p28/gankyrin* mRNA expression and various parameters, including serum AFP level, tumor size, satellite nodules, formation of tumor capsule, fibrous capsular

infiltration, and histological grade of HCC. However, it was noted that *p28/gankyrin* mRNA levels (Figure 2B) were significantly higher ($P=0.021$) in portal vein thrombus group ($n=18$) than in non-thrombus group ($n=46$), higher ($P=0.047$) in microscopic hepatic vein involvement group ($n=19$) than in non-hepatic vein involvement group ($n=45$). This fact implies that tumors with high levels of *p28/gankyrin* mRNA expression tend to be more metastatic than those with low levels.

Immunohistochemical examination

Immunohistochemistry was performed in HCCs and corresponding para-carcinoma liver tissues to determine the exact cellular site of *p28/gankyrin* protein. *p28/gankyrin* was moderately to intensely present in the cytoplasm of most hepatocytes in HCC tissues, while nuclear immunostaining was also occasionally observed (Figure 3A). In para-carcinoma liver tissues, *p28/gankyrin* was weakly present in the cytoplasm of hepatocytes (Figure 3B). The histospecific expression of *p28/gankyrin* was absent in the bile duct cells, blood vein endometrial cells and other interstitial cells in liver tissues (Figure 3C). In SK-Hep1 cell line immunostaining, *p28/gankyrin* was mainly present in the cytoplasm, while occasionally in the nucleus (Figure 3D).

Table 2 Clinicopathological features of patients with HCC: comparison with *p28* mRNA expression

Variables	<i>n</i>	mRNA level ^a	Df	<i>p</i> -value ^b
Serum AFP (ng/ml)			62	0.330
<25	14	2.439±0.362		
25~1000	21	2.469±0.273		
>1000	29	2.821±0.389		
Tumor size (cm)			62	0.124
<5	21	2.393±0.206		
5~10	27	2.852±0.468		
>10	16	3.001±0.652		
Capsule formation			62	0.242
Positive	46	2.661±0.421		
Negative	18	3.016±0.460		
Fibrous capsular infiltration			44	0.240
Positive	21	2.833±0.636		
Negative	25	2.513±0.226		
Hepatic vein involvement			62	0.047
Positive	19	3.726±0.306		
Negative	45	2.442±0.532		
Satellite nodules			62	0.243
Absent	32	2.467±0.209		
Present	32	2.931±0.554		
Portal vein thrombus			62	0.021
Absent	46	2.390±0.230		
Present	18	3.971±0.384		
Histological grade ^c			62	0.466
I-II	20	2.809±0.538		
III-IV	44	2.859±0.655		

Abbreviations: serum AFP, serum alpha-fetoprotein.

^aResults were expressed as the mean±standard deviation.

^b*p*-value was based on the analysis of variance (ANOVA) or Student's *t*-test, variances were adjusted by Bartlett's method.

^cAccording to Edmonson and Steiner's classification.

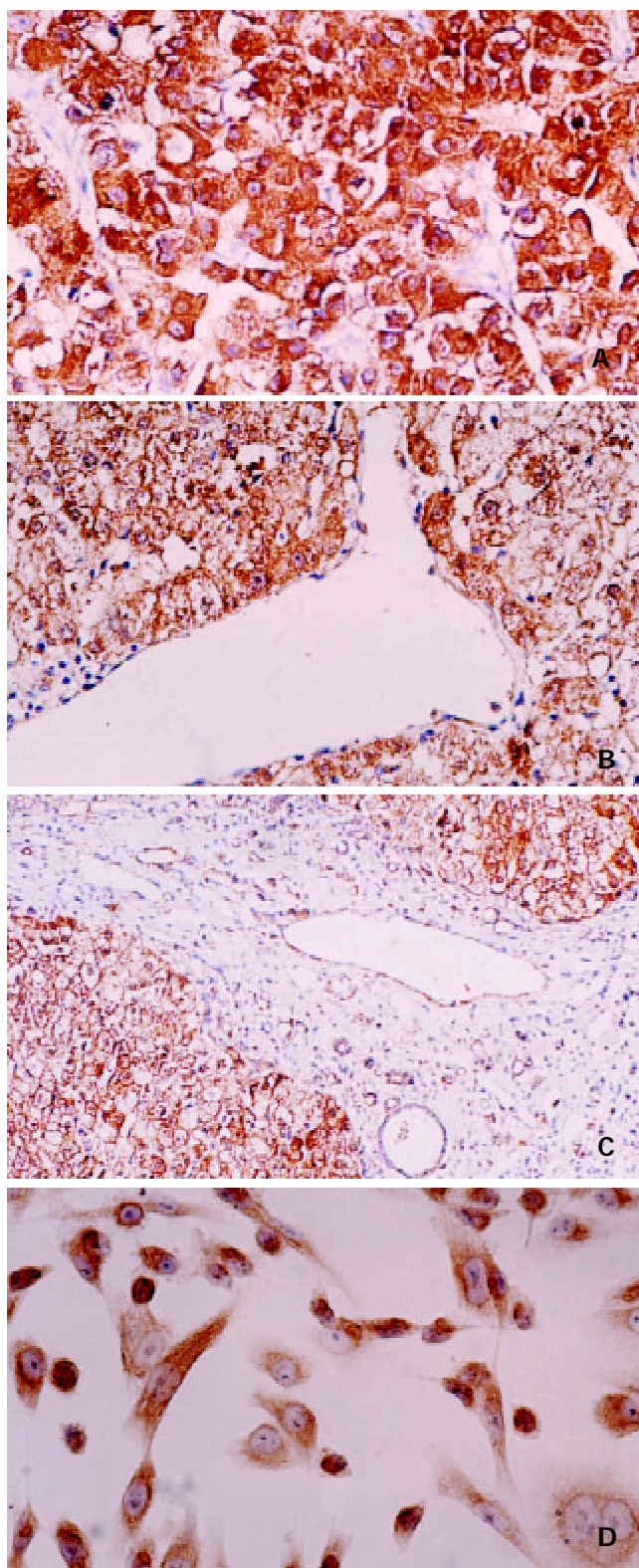


Figure 3 Immunohistochemical staining of *P28/Gankyrin* in HCC, para-carcinoma liver tissue and SK-Hep1 cell line (A) *p28/gankyrin* was moderately to intensely present in the cytoplasm of most hepatocytes in HCC tissue, and occasionally present in the nucleus of hepatocytes. (B) In contrast, *p28/gankyrin* was weakly present in the cytoplasm of hepatocytes in para-carcinoma liver tissue. (C) *p28/gankyrin* protein signals were specifically present in the cytoplasm of hepatocytes, while absent in bile duct cells, blood vein endometrial cells and other interstitial cells. (D) In SK-Hep1 cells, *p28/gankyrin* was mostly located in cytoplasm and occasionally in the nucleus.

Table 1 Clinical profiles of patients with HCC: comparison with *p28* mRNA expression

Variables	<i>n</i>	mRNA level ^a	Df	<i>p</i> -value ^b
Age (years)			62	0.231
<40	18	2.910±0.695		
40~60	35	2.790±0.367		
>60	11	1.673±0.546		
Sex			62	0.401
Male	58	2.734±0.422		
Female	6	2.650±0.238		
HBsAg			62	0.269
Positive	45	2.919±0.426		
Negative	19	2.317±0.362		
Cirrhosis			62	0.180
Absent	17	3.157±0.885		
Present	47	2.631±0.301		

Abbreviations: HBsAg, hepatitis B surface antigen.

^a Results were expressed as the mean ± standard deviation.

^b *p*-value was based on the analysis of variance (ANOVA) or Student's *t*-test, variances were adjusted by Bartlett's method.

DISCUSSION

p28/gankyrin gene has been identified recently as an oncogene expressed in HCC and its up-regulation is not related to the grade or stage of the tumors^[21]. However, the above mentioned study did not address the potential importance of normal or cirrhosis liver, in the context of high *p28/gankyrin* expression observed in HCC, nor did it investigate *p28/gankyrin* mRNA expression with respect to histopathological parameters of HCC. In the present study, *p28/gankyrin* mRNA expression was examined in the normal liver, liver cirrhosis, and HCC. *p28/gankyrin* mRNA was absent in normal liver samples, weakly expressed in liver cirrhosis samples and intensively expressed in 62 of 64 (96.8 %) HCC samples compared with the para-carcinoma liver tissues by northern blot analysis. These findings indicate that *p28/gankyrin* is a useful biological marker of HCC and plays an important role in the process of liver carcinogenesis.

Interestingly, *p28/gankyrin* mRNA levels were significantly higher in HCCs with portal vein tumor thrombosis than in those without. Microscopic hepatic vein involvement is also an important correlated parameter with regard to *p28/gankyrin* mRNA expression. It is well known that hepatocellular carcinoma has a strong propensity to invade vessel and duct systems^[28-30]. Rapid invasion and metastasis of HCC seriously hold back the clinical therapy and also significantly affect the prognosis of patients with HCC, as well as HCC recurrence after surgery^[31-33]. According to our study, *p28/gankyrin* may play a significant role in the promotion of metastatic potential in HCC. Though the detailed mechanism of the promotion role of *p28/gankyrin* in HCC metastasis is currently under investigation, more valuable clinical management of HCC can be applied by the evaluation of *p28/gankyrin* expression combined with other effective markers.

In the present study, *p28/gankyrin* was highly expressed in human brain and heart, weakly expressed in lung, spleen and muscle, suggesting that *p28/gankyrin* has a physiological role in these tissues. However, *p28/gankyrin* mRNA was not detected in human digestive system including liver, pancreas,

stomach, small and large intestines. This result indicates that *p28/gankyrin* expression may be developmentally heterogeneous. Up-regulation of *p28/gankyrin* mRNA in liver where it is normally absent correlates significantly with the occurrence of HCC, which is like the alteration of serum AFP levels in patients with HCC^[34,35]. This incident implies that to understand the mechanism of liver carcinogenesis promoted by *p28/gankyrin*, the involvement of *p28/gankyrin* in liver development process should be considered.

p28/gankyrin was strongly expressed in SK-Hep1 cells, while weakly in HepG2 cells. It should be noted that SK-Hep1, not HepG2, has the tumorigenic potential when inoculated in nude mice^[36]. Thus, the higher expression of *p28/gankyrin* in SK-Hep1, to some extent, contributes to the cell tumorigenesis. This conclusion coincides well with our experiment that *p28/gankyrin* caused cell transformation after being transfected into NIH/3T3 cells (data not shown).

By using our specific polyclonal antibody against *p28/gankyrin* protein, the cellular localization of *p28/gankyrin* expression in HCC was determined. *p28/gankyrin* protein was mainly localized in the cytoplasm of hepatocytes, from weakly in hepatocytes of para-carcinoma cirrhosis liver to intensively in hepatocytes of HCC. Occasionally, the nuclear localization of *p28/gankyrin* in malignant hepatocytes of HCC was also observed. It is interesting that *p28/gankyrin* protein can not be detected in bile duct cells, blood vein endometrial cells and other interstitial cells in liver tissues. The prospective application of *p28/gankyrin* in clinical pathological diagnosis as a specific tissue marker should be investigated further by collecting more examination data and statistical analysis.

In conclusion, *p28/gankyrin* mRNA is markedly overexpressed in HCC compared with para-carcinoma liver, normal liver or liver cirrhosis. In addition, in HCC, *p28/gankyrin* mRNA expression correlates significantly with metastasis potential of this cancer. The *p28/gankyrin* protein is particularly highly expressed in the hepatocytes of HCC. These findings suggest that *p28/gankyrin* plays an important role in the carcinogenesis of HCC by influencing tumor metastasis behavior and that it may serve as a new specific tissue marker for the pathological diagnosis of HCC.

REFERENCES

- 1 Teo EK, Fock KM. Hepatocellular carcinoma: an Asian perspective. *Dig Dis* 2001; **19**: 263-268
- 2 Yu MC, Yuan JM, Govindarajan S, Ross RK. Epidemiology of hepatocellular carcinoma. *Can J Gastroenterol* 2000; **14**: 703-709
- 3 Guo SP, Wang WL, Zhai YQ, Zhao YL. Expression of nuclear factor-kappa B in hepatocellular carcinoma and its relation with the X protein of hepatitis B virus. *World J Gastroenterol* 2001; **7**: 340-344
- 4 Sylla A, Diallo MS, Castegnaro J, Wild CP. Interactions between hepatitis B virus infection and exposure to aflatoxins in the development of hepatocellular carcinoma: a molecular epidemiological approach. *Mutat Res* 1999; **428**: 187-196
- 5 Tang ZY. Hepatocellular carcinoma-cause, treatment and metastasis. *World J Gastroenterol* 2001; **7**: 445-454
- 6 Shea KA, Fleming LE, Wilkinson JD, Wohler-Torres B, McKinnon JA. Hepatocellular carcinoma incidence in Florida. Ethnic and racial distribution. *Cancer* 2001; **91**: 1046-1051
- 7 Yu MW, Chiu YH, Yang SY, Santella RM, Chern HD, Liaw YF, Chen CJ. Cytochrome P450 1A1 genetic polymorphisms and risk of hepatocellular carcinoma among chronic hepatitis B carriers. *Br J Cancer* 1999; **80**: 598-603
- 8 Zondervan PE, Wink J, Alers JC, IJzermans JN, Schalm

- SW, de Man RA, van Dekken H. Molecular cytogenetic evaluation of virus-associated and non-viral hepatocellular carcinoma: analysis of 26 carcinomas and 12 concurrent dysplasias. *J Pathol* 2000; **192**: 207-215
- 9 **Feitelson MA**, Sun B, Satioglu Tufan NL, Liu J, Pan J, Lian Z. Genetic mechanisms of hepatocarcinogenesis. *Oncogene* 2002; **21**: 2593-2604
 - 10 **Hsu IC**, Metcalf RA, Sun T, Welsh JA, Wang NJ, Harris CC. Mutational hotspot in the p53 gene in human hepatocellular carcinoma. *Nature* 1991; **350**: 427-428
 - 11 **Liu H**, Wang Y, Zhou Q, Gui SY, Li X. The point mutation of p53 gene exon7 in hepatocellular carcinoma from Anhui Province, a non HCC prevalent area in China. *World J Gastroenterol*. 2002; **8**: 480-482
 - 12 **Liew CT**, Li HM, Lo KW, Leow CK, Chan JY, Hin LY, Lau WY, Lai PB, Lim BK, Huang J, Leung WT, Wu S, Lee JC. High frequency of p16^{INK4A} gene alterations in hepatocellular carcinoma. *Oncogene* 1999; **18**: 789-795
 - 13 **Jin M**, Piao Z, Kim NG, Park C, Shin EC, Park JH, Jung HJ, Kim CG, Kim H. p16 is a major inactivation target in hepatocellular carcinoma. *Cancer* 2000; **89**: 60-68
 - 14 **DeMartino GN**, Moomaw CR, Zagnitko OP, Proske RJ, Chu-Ping M, Afendis SJ, Swaffield JC, Slaughter CA. PA700, an ATP-dependent activator of the 20S proteasome, is an ATPase containing multiple members of a nucleotide-binding protein family. *J Biol Chem* 1994; **269**: 20878-20884
 - 15 **Kato S**, Sekine S, Oh SW, Kim NS, Umezawa Y, Abe N, Yokoyama-Kobayashi M, Aoki T. Construction of a human full-length cDNA bank. *Gene* 1994; **150**: 243-250
 - 16 **Hori T**, Kato S, Saeki M, DeMartino GN, Slaughter CA, Takeuchi J, Toh-e A, Tanaka K. cDNA cloning and functional analysis of p28(Nas6p) and p40.5(Nas7p), two novel regulatory subunits of the 26S proteasome. *Gene* 1998; **216**: 113-122
 - 17 **Baumeister W**, Walz J, Zuhl F, Seemuller E. The proteasome: paradigm of a self-compartmentalizing protease. *Cell* 1998; **92**: 367-380
 - 18 **Michaely P**, Bennett V. The ANK repeat: a ubiquitous motif involved on macromolecular recognition. *Trends Cell Biol* 1992; **2**: 127-129
 - 19 **Bork P**. Hundreds of ankyrin-like repeats in functionally diverse proteins: mobile modules that cross phyla horizontally? *Proteins* 1993; **17**: 363-374
 - 20 **Venkataramani R**, Swaminathan K, Marmorstein R. Crystal structure of the CDK4/6 inhibitory protein p18INK4c provides insights into ankyrin-like repeat structure/function and tumor-derived p16INK4 mutations. *Nat Struct Biol* 1998; **5**: 74-81
 - 21 **Higashitsuji H**, Itoh K, Nagao T, Dawson S, Nonoguchi K, Kido T, Mayer RJ, Arii S, Fujita J. Reduced stability of retinoblastoma protein by gankyrin, an oncogenic ankyrin-repeat protein overexpressed in hepatomas. *Nature Med* 2000; **1**: 96-99
 - 22 **Wang J**, Sampath A, Raychaudhuri P, Bagchi S. Both Rb and E7 are regulated by the ubiquitin proteasome pathway in HPV-containing cervical tumor cells. *Oncogene* 2001; **20**: 4740-4749
 - 23 **Ciechanover A**. The ubiquitin-proteasome pathway: on protein death and cell life. *EMBO J* 1998; **17**: 7151-7160
 - 24 **Spataro V**, Norbury C, Harris AL. The ubiquitin-proteasome pathway in cancer. *Br J Cancer* 1998; **77**: 448-455
 - 25 **Sambrook J**, Fritsch EF, Maniatis T. Molecular cloning. In: *A laboratory manual*. 2nd eds. New York: Cold Spring Harbor Laboratory Press, 1989: 502-506
 - 26 **Chomczynski P**, Sacchi N. Single-step method of RNA isolation by acid guanidinium thiocyanate-phenol-chloroform extraction. *Anal Biochem* 1987; **162**: 156-159
 - 27 **Edmonson HA**, Steiner PE. Primary carcinoma of the liver. A study of 100 cases among 48,900 necropsies. *Cancer* 1954; **7**: 462-503
 - 28 **Yuki K**, Hirohashi S, Sakamoto M, Kanai T, Shimosato Y. Growth and spread of hepatocellular carcinoma. A review of 240 consecutive autopsy cases. *Cancer* 1990; **66**: 2174-2179
 - 29 **Toyosaka A**, Okamoto E, Mitsunobu M, Oriyama T, Nakao N, Miura K. Intrahepatic metastases in hepatocellular carcinoma: evidence for spread via the portal vein as an efferent vessel. *Am J Gastroenterol* 1996; **91**: 1610-1615
 - 30 **Ikeda Y**, Matsumata T, Adachi E, Hayashi H, Takenaka K, Sugimachi K. Hepatocellular carcinoma of the intrabiliary growth type. *Int Surg* 1997; **82**: 76-78
 - 31 **Tung-Ping Poon R**, Fan ST, Wong J. Risk factors, prevention, and management of postoperative recurrence after resection of hepatocellular carcinoma. *Ann Surg* 2000; **232**: 10-24
 - 32 **Yamanaka J**, Yamanaka N, Nakasho K, Tanaka T, Ando T, Yasui C, Kuroda N, Takata M, Maeda S, Matsushita K, Uematsu K, Okamoto E. Clinicopathologic analysis of stage II-III hepatocellular carcinoma showing early massive recurrence after liver resection. *J Gastroenterol Hepatol* 2000; **15**: 1192-1198
 - 33 **Poon RT**, Fan ST, Ng IO, Lo CM, Liu CL, Wong J. Different risk factors and prognosis for early and late intrahepatic recurrence after resection of hepatocellular carcinoma. *Cancer* 2000; **89**: 500-507
 - 34 **Izumi R**, Shimizu K, Kiriya M, Hashimoto T, Urade M, Yagi M, Mizukami Y, Nonomura A, Miyazaki I. Alpha-fetoprotein production by hepatocellular carcinoma is prognostic of poor patient survival. *J Surg Oncol* 1992; **49**: 151-155
 - 35 **Nomura F**, Ohnishi K, Tanabe Y. Clinical features and prognosis of hepatocellular carcinoma with reference to serum alpha-fetoprotein levels. Analysis of 606 patients. *Cancer* 1989; **64**: 1700-1707
 - 36 **Marra CA**, de Alaniz MJ. Incorporation and metabolic conversion of saturated and unsaturated fatty acids in SK-Hep1 human hepatoma cells in culture. *Mol Cell Biochem* 1992; **117**: 107-118

Edited by Pang LH

• LIVER CANCER •

Subcellular daunorubicin distribution and its relation to multidrug resistance phenotype in drug-resistant cell line SMMC-7721/R

Jia-Yin Yang, Hua-You Luo, Qi-Yuan Lin, Zi-Ming Liu, Lu-Nan Yan, Ping Lin, Jie Zhang, Shong Lei

Jia-Yin Yang, Hua-You Luo, Qi-Yuan Lin, Zi-Ming Liu, Lu-Nan Yan, Department of General Surgery, West China Hospital, Sichuan University, Chengdu 610044, Sichuan Province, China

Ping Lin, Cancer Research Institution, West China Hospital, Sichuan University, 610044, Sichuan Province, China

Jie Zhang, Department of Confocal Laser Scanning Microscopy, West China Hospital, Sichuan University, 610044, Sichuan Province, China
Shong Lei, Cancer Biotechnological Treatment Center, West China Hospital, Sichuan University, 610044, Sichuan Province, China

Supported by the grant from National Nature Science Foundation of China, No. 39770723

Correspondence to: Dr. Jia-Yin Yang, Department of General surgery, First Affiliated Hospital, Zhejiang University College of Medicine, Hangzhou 310003, China. yjy7429@hotmail.com

Telephone: +86-571-87033324 **Fax:** +86-571-87236570

Received 2002-03-25 **Accepted** 2002-04-09

Abstract

AIM: To investigate the correlation between subcellular daunorubicin distribution and the multidrug resistance phenotype in drug-resistant cell line SMMC-7721/R.

METHODS: The multidrug resistant cell line SMMC-7721/R, a human hepatocellular carcinoma cell line, was established. Antisense oligonucleotides (AS-ODN) were used to obtain different multidrug resistance phenotypes by inhibiting the expression of *mdr1* gene and/or multidrug resistance-related protein gene (*mrp*) using Lipofectamine as delivery agent. Expression of *mdr1* and *mrp* genes was evaluated by RT-PCR and Western blotting. Intracellular daunorubicin (DNR) concentration was measured by flow cytometry. Subcellular DNR distribution was analyzed by confocal laser scanning microscopy. Adriamycin (ADM) and DNR sensitivity was examined by MTT method.

RESULTS: Low level expression of *mdr1* and *mrp* mRNAs and no expression of P-Glycoprotein(P-gp) and multidrug resistance-related protein (*P₁₉₀*) were detected in parental sensitive cells SMMC-7721/S, but over-expression of these two genes was observed in drug-resistant cell SMMC-7721/R. The expression of *mdr1* and *mrp* genes in SMMC-7721/R cells was down-regulated to the level in the SMMC-7721/S cells by AS-ODN. Intracellular DNR concentration in SMMC-7721/S cells was 10 times higher than that in SMMC-7721/R cells. In SMMC7721/S cells intracellular DNR distributed evenly in the nucleus and cytoplasm, while in SMMC-7721/R cells DNR distributed in a punctate pattern in the cytoplasm and was reduced in the nucleus. DNR concentration in SMMC-7721/R cells co-transfected with AS-ODNs targeting to *mdr1* and *mrp* mRNAs recovered to 25 percent of that in SMMC7721/R cells. Intracellular DNR distribution pattern in drug-resistant cells treated by AS-ODN was similar to drug-sensitive cell, and the cells resistance index (RI) to DNR and ADM decreased at most from 88.0 and 116.0 to 4.0

and 2.3, respectively. Co-Transfection of two AS-ODNs showed a stronger synergistic effect than separate transfection.

CONCLUSIONS: P-gp and *P₁₉₀* are two members mediating MDR in cell line SMMC7721/R. Intracellular drug concentration increase and subcellular distribution change are two important factors in multidrug resistance (MDR) formation. The second factor, drugs transport by P-gp and *P₁₉₀* from cell nucleus to organell in cytoplasm, may play a more important role.

Yang JY, Luo HY, Lin QY, Liu ZM, Yan LN, Lin P, Zhang J, Lei S. Subcellular daunorubicin distribution and its relation to multidrug resistance phenotype in drug-resistant cell line SMMC-7721/R. *World J Gastroenterol* 2002;8(4):644-649

INTRODUCTION

Multidrug resistance (MDR) remains a significant obstacle for cancer chemotherapy. The MDR observed in many cell lines is most commonly accompanied with overexpression of one or both of the members of the ATP-binding cassette superfamily of transport proteins, P-glycoprotein (P-gp) and multidrug resistance-related protein(*Mrp*, *P₁₉₀*)^[1-7]. P-gp or *P₁₉₀* acts as an energy-dependent outward transport pump, removing drugs from the cytoplasm and from the plasma membrane, thereby decreasing intracellular drug accumulation^[8-12].

Human hepatocellular carcinoma drug-resistant cell line SMMC7721/R showed a strong multidrug resistance to DNR and other anthracycline, and overexpression of P-gp and *P₁₉₀* was observed in this cell line. Previous studies suggested that subcellular drug distribution contributing to cells drug resistance may be mostly mediated by P-gp and/or *P₁₉₀* in many other cell lines^[13-20]. But there is no direct evidence suggesting the role of these two pump proteins in MDR of SMMC7721/R. In order to understand MDR phenotype and mechanism in SMMC7721/R, based on previous studies of antisense technology related to *mdr1* gene and *mrp* gene, we used laser scanning confocal microscopy to evaluate the intracellular distribution of DNR and then explored the correlation of intracellular drug(DNR) transportation and distribution with multidrug resistance phenotype.

MATERIALS AND METHODS

Cell lines and culture conditions

Human hepatocellular carcinoma cell line SMMC-7721 was provided by Cancer Research Institution, West China Hospital of Sichuan University. Drug-resistance cell line was established by the stepwise selection with increasing concentration of ADM as previously described^[21]. The ADM gradually increased from 0.005 µg/ml to 0.1 µg/ml.

Cells were grown in RPMI 1640 medium supplemented with 10 % fetal calf serum in a 5 % CO₂ atmosphere at 37 °C.

Materials

Phosphorothioate antisense oligonucleotides(AS-ODN): targeting to *mdr1* start codon region (AS-ODN/*mdr1*): 5' - CCA TCC CGA CCT CGC GCT CC-3' [22], targeting to *mrp* coding region (AS-ODN/*mrp*): 5' -TGC TGT TCG TGC CCC CGC CG-3' [23]. Control oligonucleotide (AS-ODN/nonsense) was a 20-mer nonsense phosphorothioate oligonucleotide. All oligonucleotides were synthesized by Life Technologies Inc, USA. Lipofectamine, TRIzol, RT-PCR kit, and primers were also purchased from Life Technologies Inc. Lumi-Light^{PLUS} Western Blotting Kit was purchased from Boehringer Mannheim, German. Antibodies against *mdr1*/P-gp and *mrp*/P₁₉₀ were from Santa Cruz, USA. DNR was purchased from Minalo Inc, Italy.

Treatment of cells with AS-ODNs

The experimental protocols were similar to those previously described [22,24]. Briefly, cells (5 × 10⁵) were seeded in a 25 ml flask at 1 × 10⁵ cells/ml and grown to 75 % confluence. Cells were transfected with 1.5 nmol of AS-ODN with 50 ml of Lipofectamine. Cells were harvested at different times after transfection for analysis.

Detection of drug sensitivity of cells by MTT [25,26]

Cells were exposed to drug at 37 °C for 2 h, then were washed and seeded (50 000 cells/ml) in 96-well microplates for 72 h. MTT (20 µl, 2.5 mg/ml) was added to each well for 3 h. Medium was discarded and 150 µl of DMSO were added to each well. Optical densities were measured at 490nm (A₄₉₀). The tumor cells living ratio (TCL) was determined according to the formula: $TCL = A_{490\text{experiment}} / A_{490\text{control}} \times 100\%$. The 50 % inhibitory concentration (IC₅₀) was calculated according to concentration-TCL curve. Resistance index (RI) was calculated using the formula: $RI = IC_{50\text{drug resistant cells}} / IC_{50\text{parent cells}}$.

Measurement of *mdr1* and *mrp* mRNAs by RT-PCR

Primers *mrp*: 5' -TGA AGG ACT TCG TGT CAG CC-3', 5' -GTC CATGAT GGT GTT GAG CC-3'; *mdr1*: 5' -GGC TCC GAT ACA TGG TTT TCC-3', 3' -TTC AGT GCG ATC TTC CCA GC-5'. β_2 -microglobulin(β_2 M): 5' -ACC CCC ACT GAA AAA GAT GA-3', 5' -ATC TTC AAA CCT CCA TGA TG-3'.

β_2 M expression was used as control for the amount of RNA used. Total RNA from cells was extracted using TRIzol. The effect of AS-ODN was studied after 24 h pre-incubation with AS-ODN and Lipofectamine. *Mrp*, *mdr1*, and β_2 M RNA transcripts were detected using RT-PCR as described before [27,28]. An aliquot of each reaction mixture was then analyzed by electrophoresis on 2 % agarose gel. Densitometry was performed using UVP gel image analysis system (BIO-RAD, USA) and the ratio between the target and control PCR products was determined by dividing the densitometric volume of the target band by that of the control band.

Measurement of cell expression of P-gp and P₁₉₀ with western blotting

The expression of the two proteins was detected according to the manufacturer's instructions of Lumi-Light^{PLUS} Western Blotting Kit. The concentrations of the primary antibodies against P-gp and P₁₉₀ were 1 µg/ml and 2 µg/ml, respectively. The concentrations of the secondary antibodies were both 0.4 µg/ml.

Observation of intracellular DNR distribution by confocal laser scanning microscopy (CLSM)

The experimental procedures were similar to those previously described [29-31]. Cells (1 × 10⁵) were seeded to 960 mm² petri dish with a slide inside and incubated in a 5 % CO₂ atmosphere at 37 °C. After cells had reached 75 % confluence, normal medium was replaced with serum-free RPMI 1640 medium and cells were incubated with DNR at 2 µg/ml for 1 h. The effect of AS-ODN was studied after 72 h pre-incubation with AS-ODN and Lipofectamine. After two washes with PBS and addition of drug free medium cells grown on slides were examined with CLSM (MRC-1024ES, BIO-RAD Inc., USA). Cover-slips were mounted on slides, supported and sealed on lacquer tiers to prevent compression and drying out. Intracellular drug fluorescence was observed using the 488 nm laser line for excitation and the filter that allows measurement of emitted light above 515 nm.

Detection of intracellular DNR concentration by flow cytometry (FCM)

Cells (1 × 10⁵) were seeded into 25 ml flask and grown to 95 % confluence. They were then dissociated with pancreatin and suspended in serum-free medium. DNR was added to a final concentration of 2 µg/ml and incubated for 1 h at 37 °C. After two washes with PBS each sample was divided into 3 tubes to be analyzed by FCM [32] (Elite ESP, Coulter Inc., USA). Results were expressed as the ratio of fluorescence intensity values between each experimental sample and control sample of SMMC7721/R cells without treatment.

RESULTS

Drug sensitivity

As shown in Table 1, the parental sensitive cells SMMC7721/S were highly sensitive to DNR and ADM. However, the drug resistant cells SMMC7721/R were 88-fold resistant to DNR and 116-fold to ADM, respectively, when compared with SMMC7721/S cells. Resistance index(RI) to DNR and ADM in SMMC7721/R cells co-transfected of AS-ODN/*mdr1* (0.5 µmol/L) and AS-ODN/*mrp* (0.5 µmol/L) decreased from 88 and 116 to 4 and 2.3, respectively. Treatment with separate AS-ODN/*mdr1* or AS-ODN/*mrp* showed a lesser reversal effect on MDR than co-transfection of these two AS-ODNs. Nonsense oligonucleotides did not affect the drug resistance in SMMC7721/R cells.

Table 1 Effect of AS-ODN on drug sensitivity of cells ($\bar{x} \pm s$)

Cells	IC ₅₀ (mg/L)		RI	
	DNR	ADM	DNR	ADM
SMMC-7721/S	0.003±0.0006	0.004±0.0008	1.0	
SMMC-7721/R	0.264±0.0094	0.463±0.0254	88.0	116.0
AS-ODN/ <i>mdr1</i>	0.094±0.0065	0.079±0.0014	31.4	19.8
AS-ODN/ <i>mrp</i>	0.072±0.0002	0.097±0.0009	24.0	24.3
SMMC-7721/R+	0.012±0.0011	0.009±0.0007	4.00	2.3
AS-ODN/ <i>mdr1</i> + <i>mrp</i>				
SMMC-7721/R+	0.245±0.0110	0.451±0.0187	81.7	112.8
AS-ODN/nonsense				

Values(IC₅₀) represent the mean ± standard deviation of at least three experiments and value(RI) represent the mean of three experiments. All values were calculated as described in MATERIALS AND METHODS. The concentration of each AS-ODN is 0.5 µmol/L and the treatment time is 72 hours.

Expression of *mdr1* gene and *mrp* gene

As shown by RT-PCR, The amplification products of *mrp*, *mdr1*, and β_2M were 256bp, 168bp, and 120 bp, respectively. Over-expression of *mrp* and *mdr1* mRNAs were detected in SMMC7721/R, but low level mRNA expression in SMMC7721/S was observed. The mRNA expression in SMMC7721/R cells treated with AS-ODN decreased to the level of SMMC7721/S (Figure 1).

No P-gp and P₁₉₀ were detected in parental cells SMMC7721/S. Over-expression of P-gp and P₁₉₀ was observed in drug resistant cells SMMC7721/R. Treatment of SMMC7721/R with AS-ODNs inhibited the expression of P-gp and P₁₉₀ (Figure 2).

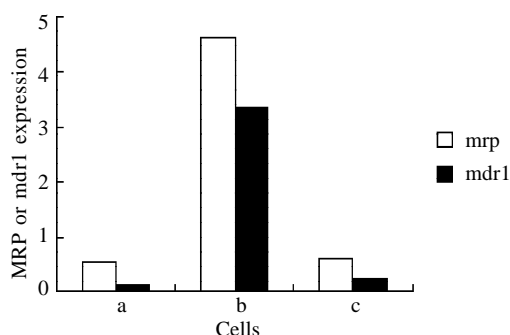


Figure 1 Quantification of PCR. The ratio between the *mdr1* or *mrp* and β_2M gene is expressed as described in MATERIALS AND METHODS. (a. parental cell-SMMC7721/S; b. SMMC7721/R; c. SMMC7721/R incubated with 0.5 μ mol/L AS-ODN for 24 hours)

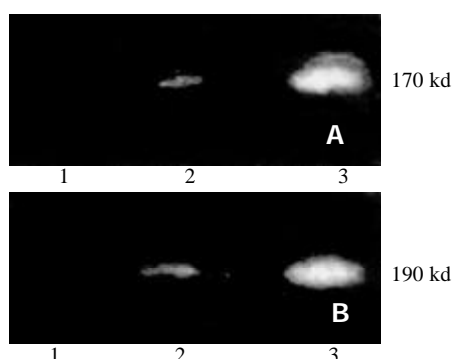


Figure 2 Expression of P-gp and P₁₉₀ analyzed with Western blot. (a) immunoblotted with anti-P-gp antibody; (b) immunoblotted with anti-P₁₉₀ antibody. 1. parental cell-SMMC7721/S; 2. SMMC7721/R treated by AS-ODN (0.5 μ mol/L, 72 hours); 3. SMMC7721/R.

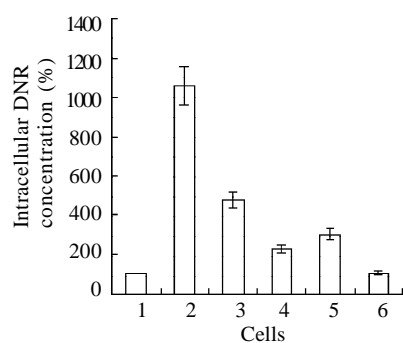


Figure 3 Intracellular DNR concentrations in cells treated with antisense oligonucleotides. The concentration of each AS-ODN is 0.5 mmol/L and the treatment time is 72 hours. Data are the mean \pm standard deviation of three independent experiments. (1. SMMC7721/R; 2. SMMC7721/S; 3. SMMC7721/R treated with AS-ODN/*mdr1*+*mrp*; 4. SMMC7721/R treated with AS-ODN/*mdr1*; 5. SMMC7721/R treated by AS-ODN/*mrp*; 6. SMMC7721/R treated with AS-ODN/nonsense.)

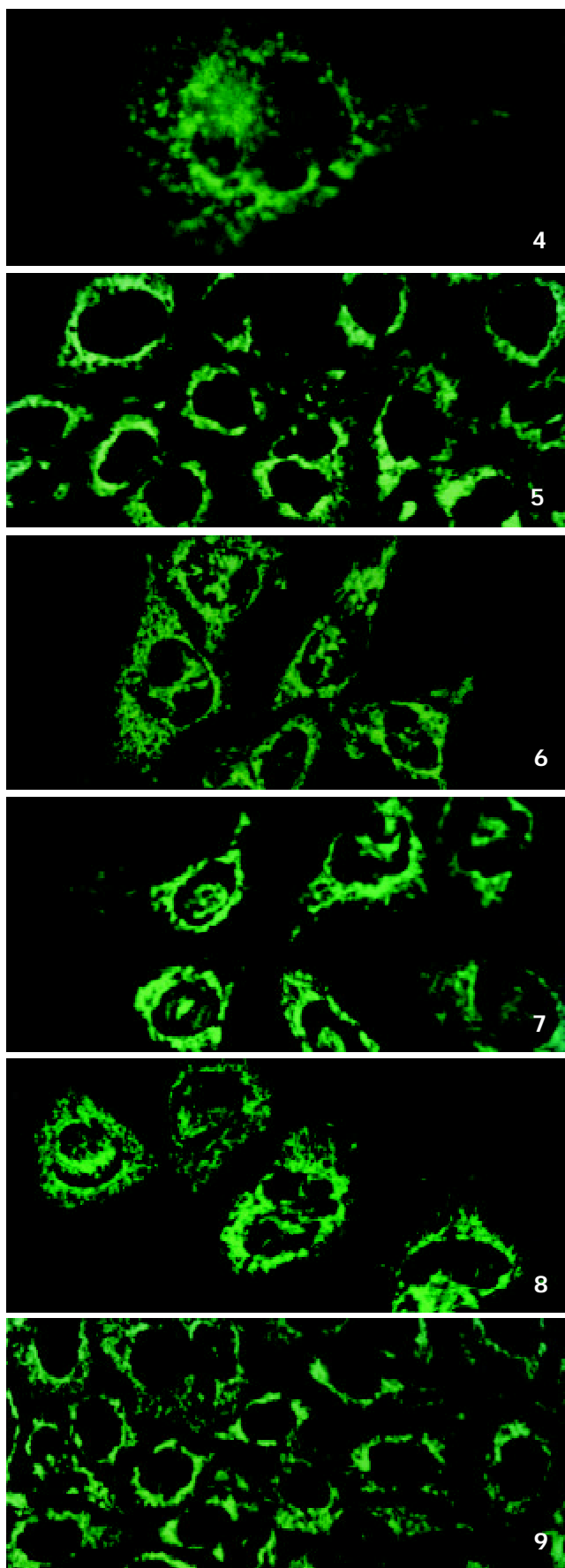


Figure 4 Intracellular DNR distribution in parental sensitive cells SMMC7721/S.

Figure 5 Intracellular DNR distribution in drug-resistant cells SMMC7721/R.

Figure 6 Intracellular DNR distribution in drug-resistant cells SMMC7721/R pre-treated with AS-ODN/mdr1 and AS-ODN/mrp. Each AS-ODN concentration is 0.5 $\mu\text{mol/L}$ and the treatment time is 72 hours.

Figure 7 Intracellular DNR distribution in drug-resistant cells SMMC7721/R pre-treated with AS-ODN/mdr1 (0.5 $\mu\text{mol/L}$) for 72 hours.

Figure 8 Intracellular DNR distribution in drug-resistant cells SMMC7721/R treated with AS-ODN/mrp (0.5 $\mu\text{mol/L}$) for 72 hours.

Figure 9 Intracellular DNR distribution in drug-resistant cells SMMC7721/R treated with nonsense oligonucleotides (0.5 $\mu\text{mol/L}$) for 72 hours.

Intracellular accumulation of DNR

Intracellular concentration of drugs in drug-resistant cells reduced to 10 percent of that in parental cells SMMC7721/S. Co-transfection of AS-ODN/mdr1+mrp up-regulated intracellular drug concentration to 4 times of that in SMMC7721/R cells. The up-regulation effect of separate transfection of AS-ODN/mdr1 or AS-ODN/mrp was much less than co-transfection (Figure 3).

Subcellular distribution of DNR

In parental cells SMMC7721/S DNR fluorescence mainly located in the nucleus and was diffusely present in the cytoplasm (Figure 4). In drug-resistant cells SMMC7721/R, DNR fluorescence retained in the perinuclear zone and in peripheral punctate vesicles, with little or no drug in the nuclear zone (Figure 5).

In SMMC7721/R cells incubated separately with AS-ODN/mrp or AS-ODN/mdr1 for 72 h, the subcellular distribution of DNR was similar to parental cells SMMC7721/S, with less intranuclear fluorescence intensity than in SMMC7721/S cells. Cells transfected separately with AS-ODN/mrp or AS-ODN/mdr1 did not show any difference in subcellular DNR distribution (Figure 7 and Figure 8). Co-transfection of AS-ODN/mdr1 and AS-ODN/mrp caused more drugs accumulation in nuclear than that in cells incubated separately with either AS-ODN (Figure 6). Nonsense oligonucleotides did not affect the drug subcellular distribution pattern in drug-resistant cells SMMC7721/R (Figure 9).

DISCUSSION

It has been reported that parental SMMC7721 cells have no or low level expression of mdr1/P-gp and mrp/P₁₉₀. However, over-expression of P-gp and P₁₉₀ was observed in drug-resistant cells SMMC7721/R, which was confirmed in our study.

In order to obtain cell line with different multidrug resistance phenotypes, we made use of the specificity of antisense oligonucleotides in down-regulating gene expression to specifically block mdr1/P-gp or mrp/P₁₉₀ function. Antisense technology is increasingly becoming a reliable tool for manipulation of gene expression and rapidly moving into the therapeutic arena^[33-47]. Down-regulation of expression of mdr1 mRNA/P-gp and mrp mRNA/P₁₉₀ by AS-ODN was observed and accompanied with recovery of drug sensitivity in SMMC7721/R cells. Drug-resistant SMMC7721/R cells co-transfected with AS-ODN/mrp and AS-ODN/mdr1 showed 50-fold drug sensitivity to ADM, when compared with drug-resistant cells SMMC7721/R.

The fluorescence emitted by anthracycline DNR, a substrate of P-gp and P₁₉₀, can be detected by FCM and CSLM^[14,17,31,48,51]. There is a good correlation between intracellular drug concentration and cells drug sensitivity^[8,16,49,50,52,53]. In our studies, FCM data enforced the opinion that reduction of

intracellular drug concentration results in increase of drug resistance in cells. Intracellular DNR concentration in cell line SMMC7721/R decreased to 10 percent of that in SMMC7721/S and meanwhile resistance to ADM and DNR increased by 116 times and 88 times respectively than that of SMMC7721/S. Co-transfection of AS-ODN/mrp and AS-ODN/mdr1 only restored intracellular DNR concentration to 40 percent of that of SMMC7721/S. Inconsistently, the drug resistance to DNR was reduced from 88-fold to 4-fold and to ADM from 116-fold to 2.3-fold when compared with SMMC7721/S. These data indicate that some other factors must play a more important role in MDR mechanism besides the reduction of intracellular drug accumulation. The mechanism focused in recently is modified drug localization^[13,51,54]. We used CSLM technology to explore this interesting point.

In our studies, we observed that in cell line SMMC7721/S DNR fluorescence distributed evenly in the nucleus and cytoplasm, while in cell line SMMC7721/R DNR distributed in a punctate pattern in the cytoplasm and was reduced in the nucleus. Transfection of AS-ODN changed the the subcellular DNR distribution pattern in SMMC7721/S cells to that in SMMC7721/R cells. This observation indicates that P-gp or P₁₉₀ not only pumps DNR out of cells, but also transports DNR from nuclear to cytoplasm and into some organelles such as Golgi apparatus. As P-gp or P₁₉₀ probably locates in cell membrane, nuclear membrane, Golgi apparatus, or endoplasmic reticulum^[13,54-59], the actions of these two proteins may cause reduction of intracellular and intranuclear drug concentration and drug accumulation in some organelles. The combined effect may prevent the targeting of the drugs to nucleus, which reduces cell death even if the total amount of drugs inside the cells was not dropped significantly. Golgi apparatus is widely believed to be the organelle which holds the drugs^[54,59]. Previous studies found that there were some differences in subcellular drug distribution pattern between different cell lines in which MDR phenotype was mediated by P-gp and by P₁₉₀^[49]. However, we did not observe such phenomenon in the present study.

Our studies suggest that after the potent inhibition of P-gp or P₁₉₀ expression by AS-ODN intracellular drug concentration was increased and subcellular drug distribution changed, which leads to the reversal of multidrug resistance in cell line SMMC7721/R. Therefore, we believe that over-expression of P-gp and/or P₁₉₀ is an important mechanism in mediating MDR in cell line SMMC7721/R.

Although co-transfection of AS-ODNs targeting the two genes didn't enhance the inhibitory effect on expression of P-gp or P₁₉₀ when compared with separate transfection of either AS-ODN, the synergistic effects of the two AS-ODNs on reduction of intracellular or intranuclear drugs and on recovery of cell drug sensitivity were much more prominent than separate transfection. This finding indicates that MDR in SMMC7721/R is mediated at least by both P-gp and P₁₉₀. The combination of MDR reversal methods against these proteins is effective in drug-resistant cells.

REFERENCES

- 1 **van Brussel JP**, van Steenbrugge GJ, Romijn JC, Schroder FH, Mickisch GH. Chemosensitivity of prostate cancer cell lines and expression of multidrug resistance-related proteins. *Eur J Cancer* 1999;**35**:664-671
- 2 **Liu ZM**, Shou NH. Expression significance of mdr1 gene in gastric carcinoma tissue. *Shijie Huaren Xiaohua Zazhi* 1999;**7**:145-146
- 3 **Ning XX**, Wu KC, Shi YQ, Wang X, Zhao YQ, Fan DM.

- Construction and expression of gastric cancer MG7 mimic epitope fused to heat shock protein 70. *Shijie Huaren Xiaohua Zazhi* 2001;**9**:892-896
- 4 **Leith CP**, Kopecky KJ, Chen IM, Eijdem L, Slovak ML, McConnell TS, Head DR, Weick J, Grever MR, Appelbaum FR, Willman CL. Frequency and clinical significance of the expression of the multidrug resistance proteins MDR1/P-glycoprotein, MRP1, and LRP in acute myeloid leukemia: a Southwest Oncology Group Study. *Blood* 1999;**94**:1086-1099
- 5 **Zhang LJ**, Chen KN, Xu GW, Xing HP, Shi XT. Congenital expression of mdr-1 gene in tissues of carcinoma and its relation with pathomorphology and prognosis. *World J Gastroenterol* 1999;**5**:53-56
- 6 **Yin F**, Shi YQ, Zhao WP, Xiao B, Miao JY, Fan DM. Suppression of P-gp induced multiple drug resistance in a drug resistant gastric cancer cell line by overexpression of Fas. *World J Gastroenterol* 2000;**6**:664-670
- 7 **Liu B**, Staren E, Iwamura T, Appert H, Howard J. Effects of Taxotere on invasive potential and multidrug resistance phenotype in pancreatic carcinoma cell line SUIT-2. *World J Gastroenterol* 2001;**7**:143-148
- 8 **Ferlini C**, Distefano M, Pignatelli F, Lin S, Riva A, Bombardelli E, Mancuso S, Ojima I, Scambia G. Antitumour activity of novel taxanes that act at the same time as cytotoxic agents and P-glycoprotein inhibitors. *Br J Cancer* 2000;**83**:1762-1768
- 9 **Wada H**, Saikawa Y, Niida Y, Nishimura R, Noguchi T, Matsukawa H, Ichihara T, Koizumi S. Selectively induced high MRP gene expression in multidrug-resistant human HL60 leukemia cells. *Exp Hematol* 1999;**27**:99-109
- 10 **Benderra Z**, Morjani H, Trussardi A, Manfait M. Characterization of H⁺-ATPase-dependent activity of multidrug resistance-associated protein in homoharringtonine-resistant human leukemic K562 cells. *Leukemia* 1998;**12**:1539-1544
- 11 **Tkaczyk-Gobis K**, Tarasiuk J, Seksek O, Stefanska B, Borowski E, Garnier-Suillerot A. Transport of new non-cross-resistant antitumor compounds of the benzoperimidine family in multidrug resistant cells. *Eur J Pharmacol* 2001;**413**:131-141
- 12 **Heijn M**, Hooijberg JH, Scheffer GL, Szabo G, Westerhoff HV, Lankelma J. Anthracyclines modulate multidrug resistance protein (MRP) mediated organic anion transport. *Biochim Biophys Acta* 1997;**1326**:12-22
- 13 **Larsen AK**, Escargueil AE, Skladanowski A. Resistance mechanisms associated with altered intracellular distribution of anticancer agents. *Pharmacol Ther* 2000;**85**:217-229
- 14 **Borg AG**, Burgess R, Green LM, Scheper RJ, Liu Yin JA. P-glycoprotein and multidrug resistance-associated protein, but not lung resistance protein, lower the intracellular daunorubicin accumulation in acute myeloid leukaemic cells. *Br J Haematol* 2000;**108**:48-54
- 15 **Okumura H**, Chen ZS, Sakou M, Sumizawa T, Furukawa T, Komatsu M, Ikeda R, Suzuki H, Hirota K, Aikou T, Akiyama SI. Reversal of P-glycoprotein and multidrug-resistance protein-mediated drug resistance in KB cells by 5-O-benzoylated taxinine K. *Mol Pharmacol* 2000;**58**:1563-1569
- 16 **Manciu L**, Chang X, Riordan JR, Buyse F, Ruyschaert JM. Nucleotide-induced conformational changes in the human multidrug resistance protein MRP1 are related to the capacity of chemotherapeutic drugs to accumulate or not in resistant cells. *FEBS Lett* 2001;**493**:31-35
- 17 **Gong Y**, Wang Y, Chen F, Han J, Miao J, Shao N, Fang Z, Ou Yang R. Identification of the subcellular localization of daunorubicin in multidrug-resistant K562 cell line. *Leuk Res* 2000;**24**:769-774
- 18 **Chou KM**, Paul Krapcho A, Hacker MP. Impact of the basic amine on the biological activity and intracellular distribution of an aza-anthrapyrazole: BBR 3422. *Biochem Pharmacol* 2001;**62**:1337-1343
- 19 **Mankhetkorn S**, Teodori E, Garnier-Suillerot A. Partial inhibition of the P-glycoprotein-mediated transport of anthracyclines in viable resistant K562 cells after irradiation in the presence of a verapamil analogue. *Chem Biol Interact* 1999;**121**:125-140
- 20 **Hirsch-Ernst KI**, Ziemann C, Rustenbeck I, Kahl GF. Inhibitors of mdr1-dependent transport activity delay accumulation of the mdr1 substrate rhodamine 123 in primary rat hepatocyte cultures. *Toxicology* 2001;**167**:47-57
- 21 **Yu LF**, Zhang YP, Qiao MM, Wu YL. Establishment and characterization of vincristine-resistant MKN28/VCR, MKN45/VCR of human gastric cancer cell lines. *Shijie Huaren Xiaohua Zazhi* 2001;**9**:297-301
- 22 **Alahari SK**, DeLong R, Fisher MH, Dean NM, Villet P, Juliano RL. Novel chemically modified oligonucleotides provide potent inhibition of P-glycoprotein expression. *J Pharmacol Exp Ther* 1998;**286**:419-428
- 23 **Stewart AJ**, Canitrot Y, Baracchini E, Dean NM, Deeley RG, Cole SP. Reduction of expression of the multidrug resistance protein (MRP) in human tumor cells by antisense phosphorothioate oligonucleotides. *Biochem Pharm* 1996;**51**:461-469
- 24 **Motomura S**, Motoji T, Takanashi M, Wang YH, Shiozaki H, Sugawara I, Aikawa E, Tomida A, Tsuruo T, Kanda N, Mizoguchi H. Inhibition of P-glycoprotein and recovery of drug sensitivity of human acute leukemic blast cells by multidrug resistance gene (mdr1) antisense oligonucleotides. *Blood* 1998;**91**:3163-3171
- 25 **Cao WX**, Ou JM, Fei XF, Zhu ZG, Yin HR, Yan M, Lin YZ. Methionine-dependence and combination chemotherapy on human gastric cancer cells in vitro. *World J Gastroenterol* 2002;**8**:230-232
- 26 **Liu B**, Staren E, Iwamura T, Appert H, Howard J. Taxotere resistance in SUIT Taxo tere resistance in pancreatic carcinoma cell line SUIT 2 and its sublines. *World J Gastroenterol* 2001;**7**:855-859
- 27 **Chen WX**, Li YM, Yu CH, Cai WM, Zheng M, Chen F. Quantitatively analysis of transforming growth factor beta 1 mRNA in patients with alcoholic liver disease. *World J Gastroenterol* 2002;**8**:379-381
- 28 **Gong JP**, Wu CX, Liu CA, Li SW, Shi YJ, Li XH, Peng Y. Liver sinusoidal endothelial cell injury by neutrophils in rats with acute obstructive cholangitis. *World J Gastroenterol* 2002;**8**:342-345
- 29 **Shen ZY**, Shen WY, Chen MH, Shen J, Cai WJ, Yi Z. Nitric oxide and calcium ions in apoptotic esophageal carcinoma cells induced by arsenite. *World J Gastroenterol* 2002;**8**:40-43
- 30 **Wang JP**, Duan GR, Zhao YL, Du DW. Effect of P16 gene expression in growth of human hepatic carcinoma cell line 7721 with confocal microscopic analysis. *Shijie Huaren Xiaohua Zazhi* 2000;**8**:767-770
- 31 **Cheng SD**, Wu YL, Zhang YP, Qiao MM, Guo QS. Abnormal drug accumulation in multidrug resistant gastric carcinoma cells. *Shijie Huaren Xiaohua Zazhi* 2001;**9**:131-134
- 32 **Gao F**, Yi J, Shi GY, Li H, Shi XG, Tang XM. The sensitivity of digestive tract tumor cells to As₂O₃ is associated with the inherent cellular level of reactive oxygen species. *World J Gastroenterol* 2002;**8**:36-39
- 33 **Agrawal S**. Importance of nucleotide sequence and chemical modifications of antisense oligonucleotides. *Biochim Biophys Acta* 1999;**1489**:53-68
- 34 **Gleave ME**, Miyake H, Zellweger T, Chi K, July L, Nelson C, Rennie P. Use of antisense oligonucleotides targeting the antiapoptotic gene, clusterin/testosterone-repressed prostate message 2, to enhance androgen sensitivity and chemosensitivity in prostate cancer. *Urology* 2001;**58**:39-49
- 35 **Wang L**, Chen L, Walker V, Jacob TJ. Antisense to MDR1 mRNA reduces P-glycoprotein expression, swelling-activated Cl⁻ current and volume regulation in bovine ciliary epithelial cells. *J Physiol* 1998;**511**:33-44
- 36 **Nie QH**, Cheng YQ, Xie YM, Zhou YX, Cao YZ. Inhibiting

- effect of antisense oligonucleotides phosphorothioate on gene expression of TIMP-1 in rat liver fibrosis. *World J Gastroenterol* 2001;**4**:363-369
- 37 **Agarwal N**, Gewirtz AM. Oligonucleotide therapeutics for hematologic disorders. *Biochim Biophys Acta* 1999; **1489**: 85-96
- 38 **Giraud-Panis M**, Leng M. Transplatin-modified oligonucleotides as modulators of gene expression. *Pharmacol Ther* 2000;**85**:175-181
- 39 **Wang XW**, Yuan JH, Zhang RG, Guo LX, Xie Y, Xie H. Antihepatoma effect of alpha fetoprotein antisense phosphorothioate oligodeoxynucleotides *in vitro* and in mice. *World J Gastroenterol* 2001;**7**:345-351
- 40 **Tang YC**, Li Y, Qian GX. Reduction of tumorigenicity of SMMC27721 hepatoma cells by vascular endothelial growth factor antisense gene therapy. *World J Gastroenterol* 2001;**7**:22-27
- 41 **He Y**, Zhou J, Wu JS, Dou KF. Inhibitory effects of EGFR antisense oligodeoxynucleotide in human colorectal cancer cell line. *World J Gastroenterol* 2000;**6**:747-749
- 42 **Zhang L**, Li SN, Wang XN. CEA and AFP expression in human hepatoma cells transfected with antisense IGF-I gene. *World J Gastroenterol* 1998;**4**:30-32
- 43 **Zhong S**, Wen SM, Zhang DF, Wang QL, Wang SQ, Ren H. Sequencing of PCR amplified HBV DNA pre-c and c regions in the 2.2.15 cells and antiviral action by targeted antisense oligonucleotide directed against sequence. *World J Gastroenterol* 1998;**4**:434-436
- 44 **Zhang FX**, Zhang XY, Fan DM, Deng ZY, Yan Y, Wu HP, Fan JJ. Antisense telomerase RNA induced human gastric cancer cell apoptosis. *World J Gastroenterol* 2000;**6**:430-432
- 45 **Liu DH**, Zhang XY, Fan DM, Huang YX, Zhang JS, Huang WQ, Zhang YQ, Huang QS, Ma WY, Chai YB, Jin M. Expression of vascular endothelial growth factor and its role in oncogenesis of human gastric carcinoma. *World J Gastroenterol* 2001;**7**:500-505
- 46 **Gu ZP**, Wang YJ, Li JG, Zhou YA. VEGF₁₆₅ antisense RNA suppresses oncogenic properties of human esophageal squamous cell carcinoma. *World J Gastroenterol* 2002;**8**:44-48
- 47 **Xiao B**, Shi YQ, Zhao YQ, You H, Wang ZY, Liu XL, Yin F, Qiao TD, Fan DM. Transduction of Fas gene or Bcl-2 antisense RNA sensitizes cultured drug resistant gastric cancer cells to chemotherapeutic drugs. *World J Gastroenterol* 1998;**4**:421-425
- 48 **Ferrao P**, Sincock P, Cole S, Ashman L. Intracellular P-gp contributes to functional drug efflux and resistance in acute myeloid leukaemia. *Leuk Res* 2001;**25**:395-405
- 49 **Gong YP**, Liu T, Jia YQ, Qin L, Deng CQ, Yang RY. Comparison of Pgp- and MRP-mediated multidrug resistance in leukemia cell lines. *Int J Hematol* 2002;**75**:154-160
- 50 **Benderra Z**, Trussardi A, Morjani H, Villa AM, Doglia SM, Manfait M. Regulation of cellular glutathione modulates nuclear accumulation of daunorubicin in human MCF7 cells overexpressing multidrug resistance associated protein. *Eur J Cancer* 2000;**36**:428-434
- 51 **Hayes JH**, Soroka CJ, Rios-Velez L, Boyer JL. Hepatic sequestration and modulation of the canalicular transport of the organic cation, daunorubicin, in the Rat. *Hepatology* 1999;**29**:483-493
- 52 **Chou TC**, Depew KM, Zheng YH, Safer ML, Chan D, Helfrich B, Zatorska D, Zatorski A, Bornmann W, Danishefsky SJ. Reversal of anticancer multidrug resistance by the ardeemins. *Proc Natl Acad Sci U S A* 1998;**95**: 8369-8374
- 53 **Courtois A**, Payen L, Vernhet L, de Vries EG, Guillouzo A, Fardel O. Inhibition of multidrug resistance-associated protein (MRP) activity by rifampicin in human multidrug-resistant lung tumor cells. *Cancer Lett* 1999;**139**:97-104
- 54 **Belhoussine R**, Morjani H, Millot JM, Sharonov S, Manfait M. Confocal scanning microspectrofluorometry reveals specific anthracycline accumulation in cytoplasmic organelles of multidrug-resistant cancer cells. *J Histochem Cytochem* 1998;**46**:1369-1376
- 55 **Zhang JT**. Determinant of the extracellular location of the N-terminus of human multidrug-resistance-associated protein. *Biochem J* 2000;**348**:597-606
- 56 **Laupeze B**, Amiot L, Bertho N, Grosset JM, Lehne G, Fauchet R, Fardel O. Differential expression of the efflux pumps P-glycoprotein and multidrug resistance-associated protein in human monocyte-derived dendritic cells. *Hum Immunol* 2001;**62**:1073-1080
- 57 **Meschini S**, Calcabrini A, Monti E, Del Bufalo D, Stringaro A, Dolfini E, Arancia G. Intracellular P-glycoprotein expression is associated with the intrinsic multidrug resistance phenotype in human colon adenocarcinoma cells. *Int J Cancer* 2000;**87**:615-628
- 58 **Demeule M**, Jodoin J, Gingras D, Beliveau R. P-glycoprotein is localized in caveolae in resistant cells and in brain capillaries. *FEBS Lett* 2000;**466**:219-224
- 59 **Kipp H**, Arias IM. Newly synthesized canalicular ABC transporters are directly targeted from the Golgi to the hepatocyte apical domain in rat liver. *J Biol Chem* 2000; **275**:15917-15925

Edited by Bo XN

Metallothionein expression in hepatocellular carcinoma

Geng-Wen Huang, Lian-Yue Yang

Geng-Wen Huang, Lian-Yue Yang, Department of General Surgery, Xiangya Hospital, Central South University, Changsha 410008, Hunan Province, China

Supported by the Science Fund of Department of Science and Technology of Hunan Province, No. 98ssy1008

Correspondence to: Dr. Geng-Wen Huang, Department of General Surgery, Xiangya Hospital, Central South University, Changsha 410008, Hunan Province, China. hgw21@163.net

Telephone: +86-731-4350637

Received 2001-12-05 **Accepted** 2002-02-07

Abstract

AIM: To investigate the expression of metallothioneins (MTs), which were recently thought to have close relationship with tumors, in human hepatocellular carcinoma.

METHODS: Histological specimens of 35 cases of primary human hepatocellular carcinoma with para-neoplastic liver tissue and 5 cases of normal liver were stained for MTs with monoclonal mouse anti-MTs serum (E9) by the immunohistochemical ABC technique.

RESULTS: MTs were stained in the 35 cases of HCC, including 6 cases negative (17.1 %), 23 weakly positive (65.7 %), and 6 strongly positive (17.1 %). But MTs were stained strongly positive in all the five cases of normal liver and 35 cases of para-neoplastic liver tissue. The differences of MTs expression between HCC and normal liver tissue or para-neoplastic liver tissue were highly significant ($P < 0.01$). The rate of MTs expression in HCC grade I was 100 percent, higher than that in grade II (81 %) and grade III and IV (78 %). But the differences were not significant ($P > 0.05$). No obvious correlations between MTs expression in HCC and tumor size, clinical stage or serum alpha fetoprotein concentration were found ($P > 0.05$).

CONCLUSION: Decrease of MTs expression in HCC may play a role in carcinogenesis of HCC. MTs are stained heterogeneously in HCC. We can choose the anticancer agents according to the MTs concentration in HCC, which may improve the results of chemotherapy for HCC.

Huang GW, Yang LY. Metallothionein expression in hepatocellular carcinoma. *World J Gastroenterol* 2002; 8(4):650-653

INTRODUCTION

Metallothioneins (MTs) are a family of low-molecular weight, cysteine rich proteins which are widely distributed in various species. MTs are thought to be involved in heavy-metal detoxification, intracellular trace elements storage and scavenging free radicals. Recently, emerging data suggest that MTs have close relationship with tumors. They might play important roles in carcinogenic and apoptotic process and differentiation of tumor cells^[1-12]. And besides, MTs are attributed to affording tumor cells resistance to some important chemotherapeutic agents^[13]. This study is aimed to examine

MTs expression in human hepatocellular carcinoma (HCC) and to explore its biological and clinical significance.

MATERIALS AND METHODS

Clinical material

The clinical information and pathological specimens from 35 patients, whose liver tumors were removed at XiangYa Hospital from 1998 to 2000, were analyzed. All the cases were reviewed to confirm the pathological diagnosis of HCC. All the 35 specimens of HCC contained their corresponding para-neoplastic liver tissue. The ages of patients ranged from 31 to 71 years, with a mean \pm SD of 49.92 ± 9.32 years. 33 were men and 2 women. According to Edmonson pathologic grading, there were 5 cases of grade I, 16 grade II and 14 grade III-IV. According to the clinical staging of UICC, there were 22 cases of stage II, 5 stage III and 8 stage IV. All the cases had positive HBsAg. This study also included 5 cases of normal liver tissue, around the hepatic hemangioma excised also in XiangYa Hospital.

Immunohistochemical determination of MTs

All the specimens were fixed in 10 % buffered formalin and embedded in paraffin. Five-micrometre thick sections were cut from the tissue blocks, mounted onto glass slides and were used for staining. ABC technique was adopted. Briefly, 5 μ m sections were deparaffinized and rehydrated first, and then were immersed in 3 % H_2O_2 with methanol for 30 minutes to remove the endogenous peroxidase activity. Sections were further incubated with 10 % normal goat serum for 1 hour, followed by incubation with monoclonal mouse anti-MTs serum (E9) (1:50) at 4 °C overnight. The sections were then washed in phosphate buffer solution (PBS) (0.01M, pH 7.2) and they were sequentially incubated with: (1) biotinylated goat anti-mouse IgG, and (2) avidin-biotin horseradish peroxidase complex following the manufacturers' instruction (ABC kit, BOSTER Ltd. Wuhan). Staining was developed by immersing slides in 0.05 % 3,3'-diaminobenzidine tetrahydrochloride (DAB) with 0.33 % hydrogen peroxide. All slides were counterstained with haematoxylin, dehydrated and mounted. PBS substituted for the primary antibody was used as the negative control. According to the proportion of positively stained cells, a grade was given from I to III, with Grade I indicating less than one third of cells stained and Grade III indicating more than two thirds of cells stained. The intensity of MTs expression was also graded and given a grade for 0 to II, with Grade 0 indicating no staining, and Grade II indicating the greatest intensity of staining. A weighted score was then generated to semiquantify the MTs expression level in the tissue by multiplying the MTs intensity score with the proportion of the positively stained tumors cells. A weighted score of zero indicated no MTs staining (-), more than 3 indicated strongly positive MTs staining (++) and that between zero and 3 indicated weakly positive MTs staining (+)^[14].

Statistical analysis

The data were expressed semiquantitatively. Ridit test was used to determine the difference. The results were considered statistically significant when $P < 0.05$.

RESULTS

All negative control slides showed no staining for MTs, demonstrating the specificity of the monoclonal antibody E9. Strongly positive MTs immunoreactivity was observed in all the five control normal liver sections, mostly in cytoplasm with a few in nucleus. All the surrounding connective tissues, including blood vessels and bile ducts were negative for MTs staining. Twenty-nine of 35 HCC showed positive MTs staining, including 6 strongly positive (17.1 %) (Figure 1), 23 weakly positive (65.7 %) (Figure 2) and 6 negative (17.1 %) (Figure 3). MTs expressed strongly in all the para-neoplastic liver tissue. The differences of MTs expression between HCC and para-neoplastic liver tissue or normal liver tissue were highly significant (Table 1, $P<0.01$).

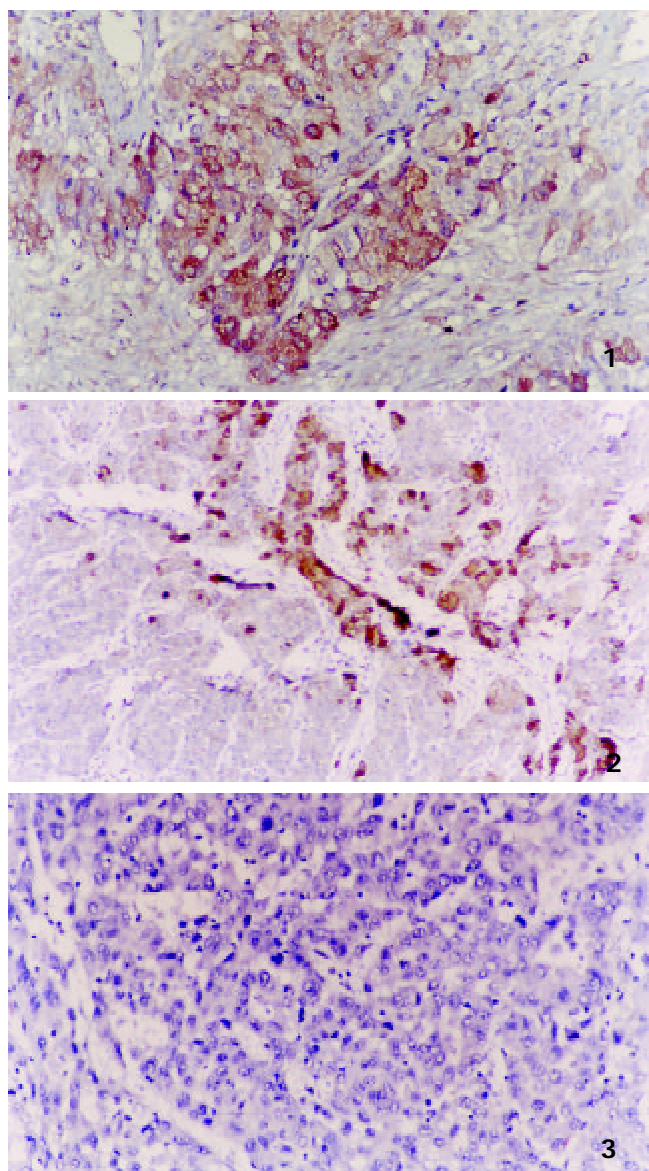


Figure 1 Strongly positive staining of MTs in hepatocellular carcinoma ABC $\times 200$

Figure 2 Weakly positive staining of MTs in hepatocellular carcinoma ABC $\times 200$

Figure 3 Negative staining of MTs in hepatocellular carcinoma ABC $\times 200$

The positive ratio of MTs expression in grade I of HCC was 100 %, higher than that in grade II (81 %) and grade III and IV (78 %). But the differences did not reached the level of

significance ($P>0.05$). In addition, the differences of MTs expression in HCC with different clinical stages, tumor sizes and serum alpha fetoprotein concentration were not significant either (Table 2).

Table 1 Levels of MTs expression in HCC, para-neoplastic and normal liver tissues

	<i>n</i>	MTs score		
		-	+	++
HCC	35	6	23	6
Para-neoplastic tissue ^b	35	0	0	35
Normal liver tissue ^b	5	0	0	5

^b $P<0.01$, vs HCC

Table 2 Correlation between MTs expression and clinicopathologic data of HCC

	MTs score			
	<i>n</i>	-	+	++
Pathologic grade				
Grade I	5	0	3	2
Grade II	16	3	10	3
Grade III-IV	14	3	10	1
Clinical stage				
Stage I-II	22	5	14	3
Stage III-IV	13	1	9	3
Size (mm)				
≤50	9	3	6	0
>50	26	3	17	6
AFP concentration (ng/ml)				
≤50	13	3	6	4
>50	22	3	17	2

DISCUSSION

Recently, much attention was paid to the association between MTs and tumors. Available information suggested that MTs might play important roles in carcinogenic and apoptotic process of some tumors^[1-13,15-20]. Using immunohistochemical staining method, MTs have been localized intensively in various types of human tumors in organs and tissues such as skin, kidneys, prostate, testes, gallbladder, colon, breast and endometrium^[15-32]. It was mainly attributed to loss of control of the transcription of MTs genes, which was caused by activation of some oncogenes, such as Ha-ras, in tumor cells^[33]. However, the potential roles of MTs in carcinogenic process was not yet well understood^[34]. Several pieces of evidence suggested that MTs could combine with and sequester those carcinogenic substances in cells. When the cells were invaded by the carcinogenic substances, many protective processes were activated to scavenge those substances. Elevation of MTs may be one of the processes^[35-40]. But not all the tumors contained

elevated MTs^[41], such as HCC. In this study, the authors have detected MTs expression in 35 cases of HCC and their corresponding para-neoplastic liver tissue and 5 cases of normal liver tissue. The results showed that MTs were strongly positive in all the normal liver tissue and para-neoplastic liver tissue, considerably higher than those in HCC tissue, which conformed to the finding of Deng^[14]. MTs are functional proteins in liver tissue, which is involved in heavy metal detoxification. The down-regulation of MTs expression in HCC suggested that these cells probably have different proliferative or differentiated characteristics as compared to the surrounding normal hepatocytes, and MTs may be a marker of hepatocellular differentiation. In addition, this down-regulation might play a role in carcinogenic process of HCC. MTs are one of the most important intracellular free radicals scavengers, and oxidative injury may be one of the most important causes of gene mutation. As a result, this down-regulation of MTs expression might cause accretion of oxidative in cells, which might lead to activating some oncogenes or inactivating some tumor-suppressor genes^[38-40].

Several other studies have also shown that the MTs levels may be related to the degree of differentiation of tumor cells. For example, using immunohistochemical staining method, a distinct difference between seminoma and nonseminoma of human testicular tumors was found^[21]. Well-differentiated seminoma showed little or no staining for MTs while less differentiated nonseminoma (embryonic carcinoma) strongly expressed MTs. MTs overexpression in human breast carcinoma, colorectal carcinoma, esophageal carcinoma, osteosarcoma, endometrial carcinoma and melanoma tended to correlate with poor prognosis^[19,24-42]. In this study, the positive rate of MTs expression in grade I of HCC is 100 percent, higher than grade II (81 %) and grade III and IV (78%), but the differences have not reach the level of significance. So the genuine relationship between MTs and differentiation of HCC remains to be further investigated.

Resistance to antineoplastic agents is one of the major obstacles to curative therapy of HCC. The development of this resistance has been explained by several factors, including increased DNA repair processes and expression of MDR gene^[43]. In 1998, Kelley *et al*^[44] found that tumor cell lines with acquired resistance to the antineoplastic agent cisplatin overexpressed MTs and demonstrated cross-resistance to other electrophilic anticancer agents, such as melphalan, chlorambucil. Furthermore, cells transfected with bovine papilloma virus expression vectors containing DNA encoding human MTs were resistant to electrophilic anticancer drugs mentioned above, but not to 5-fluorouracil or vincristine. Thus, overexpression of MTs represented one mechanism of resistance to a subset of clinically important anticancer drugs. Those results were substantiated by a series of other experiments^[45-49]. The mechanism that MTs were involved in drug resistance might be that MTs in tumor cells could combine with those electrophilic anticancer drugs and prevent them from acting on their targets, such as DNA. In this study, we have shown that MTs expressed heterogeneously in HCC, including 6 cases with strong expression, 23 with weak expression and 6 negative. The authors therefore assumed that resistance to electrophilic antineoplastic agents in a portion of HCC might be related to MTs expression in tumor tissue.

Thus, anticancer agents could be chosen according to the levels of MTs expression in order to improve the efficiency of chemotherapy for HCC. For example, electrophilic antineoplastic agents were used in the treatment of HCC without MTs and non-electrophilic antineoplastic agents were used in HCC containing high levels of MTs. However, the

effect of this design remains to be determined. Recently, a gene therapy by transactivating MTs to the chemoresistant tumour cells to reverse the chemoresistance have been reported^[50]. In the near future, oncologists are really able to use the knowledge about MTs in overcoming cancer.

The down-regulation of MTs expression in HCC might play roles in carcinogenesis of HCC, but its biological and clinical significance is still uncertain. A further understanding of the association between MTs expression and resistance to anticancer agents should facilitate the chemotherapy for HCC.

REFERENCES

- 1 **Takaba K**, Saeki K, Suzuki K, Wanibuchi H, Fukushima S. Significant overexpression of metallothionein and cyclin D1 and apoptosis in the early process of rat urinary bladder carcinogenesis induced by treatment with N-butyl-N-(4-hydroxybutyl) nitrosamine or sodium L-ascorbate. *Carcinogenesis* 2000; **21**: 691-700
- 2 **Jayasurya A**, Bay BH, Yap WM, Tan NG, Tan BK. Proliferative potential in nasopharyngeal carcinoma: correlations with metallothionein expression and tissue zinc levels. *Carcinogenesis* 2000; **21**: 1809-1812
- 3 **Hiura T**, Khalid H, Yamashita H, Tokunaga Y, Yasunaga A, Shibata S. Immunohistochemical analysis of metallothionein in astrocytic tumors in relation to tumor grade, proliferative potential, and survival. *Cancer* 1998; **83**: 2361-2369
- 4 **Abdel-Mageed AB**, Agrawal KC. Activation of nuclear factor kappaB: potential role in metallothionein-mediated mitogenic response. *Cancer Res* 1998; **58**: 2335-2338
- 5 **Aloia TA**, Harpole DH Jr, Reed CE, Allegra C, Moore MB, Herndon JE, D'Amico TA. Tumor marker expression is predictive of survival in patients with esophageal cancer. *Ann Thorac Surg* 2001; **72**: 859-866
- 6 **Jayasurya A**, Bay BH, Yap WM, Tan NG. Correlation of metallothionein expression with apoptosis in nasopharyngeal carcinoma. *Br J Cancer* 2000; **82**: 1198-1203
- 7 **Zhang XH**, Takenaka I. Incidence of apoptosis and metallothionein expression in renal cell carcinoma. *Br J Urol* 1998; **81**: 9-13
- 8 **Joseph MG**, Banerjee D, Kocha W, Feld R, Stitt LW, Cherian MG. Metallothionein expression in patients with small cell carcinoma of the lung: correlation with other molecular markers and clinical outcome. *Cancer* 2001; **92**: 836-842
- 9 **Hishikawa Y**, Kohno H, Ueda S, Kimoto T, Dhar DK, Kubota H, Tachibana M, Koji T, Nagasue N. Expression of metallothionein in colorectal cancers and synchronous liver metastases. *Oncology* 2001; **61**: 162-167
- 10 **Ebert MP**, Gunther T, Hoffmann J, Yu J, Miehls S, Schulz HU, Roessner A, Korc M, Malfertheiner P. Expression of metallothionein II in intestinal metaplasia, dysplasia, and gastric cancer. *Cancer Res* 2000; **60**: 1995-2001
- 11 **Jin R**, Chow VT, Tan PH, Dheen ST, Duan W, Bay BH. Metallothionein 2A expression is associated with cell proliferation in breast cancer. *Carcinogenesis* 2002; **23**: 81-86
- 12 **Tan Y**, Sinniah R, Bay BH, Singh G. Metallothionein expression and nuclear size in benign, borderline, and malignant serous ovarian tumours. *J Pathol* 1999; **189**: 60-65
- 13 **Cherian MG**, Howell SB, Imura N, Klaassen CD, Koropatnick J, Lazo JS, Waalkes MP. Role of metallothionein in carcinogenesis. *Toxicol Appl Pharmacol* 1994; **126**: 1-5
- 14 **Deng DX**, Chakrabarti S, Waalkes MP, Cherian MG. Metallothionein and apoptosis in primary hepatocellular carcinoma and metastatic adenocarcinoma. *Histopathology* 1998; **32**: 340-347
- 15 **Tuzel E**, Kirkali Z, Yorukoglu K, Mungan MU, Sade M. Metallothionein expression in renal cell carcinoma: subcellular localization and prognostic significance. *J Urol*

- 2001; **165**: 1710-1713
- 16 **Ishii K**, Usui S, Yamamoto H, Sugimura Y, Tatematsu M, Hirano K. Decreases of metallothionein and aminopeptidase N in renal cancer tissues. *J Biochem* 2001; **129**: 253-258
- 17 **Naito S**, Koga H, Yokomizo A, Sakamoto N, Kotoh S, Nakashima M, Kiue A, Kuwano M. Molecular analysis of mechanisms regulating drug sensitivity and the development of new chemotherapy strategies for genitourinary carcinomas. *World J Surg* 2000; **24**: 1183-1186
- 18 **Janssen AM**, van Duijn W, Oostendorp-Van De Ruit MM, Kruidenier L, Bosman CB, Griffioen G, Lamers CB, van Krieken JH, van De Velde CJ, Verspaget HW. Metallothionein in human gastrointestinal cancer. *J Pathol* 2000; **192**: 293-300
- 19 **Jin R**, Bay BH, Chow VT, Tan PH, Lin VC. Metallothionein 1E mRNA is highly expressed in oestrogen receptor-negative human invasive ductal breast cancer. *Br J Cancer* 2000; **83**: 319-323
- 20 **Ioachim EE**, Kitsiou E, Carassavoglou C, Stefanaki S, Agnantis NJ. Immunohistochemical localization of metallothionein in endometrial lesions. *J Pathol* 2000; **191**: 269-273
- 21 **Chin JL**, Banerjee D, Kadhim SA, Kontozoglou TE, Chauvin PJ, Cherian MG. Metallothionein in testicular germ cell lines and drug resistance. *Cancer* 1993; **72**: 3029-3035
- 22 **Kuo T**, Lo SK. Immunohistochemical metallothionein expression in thymoma: correlation with histological types and cellular origin. *Histopathology* 1997; **30**: 243-248
- 23 **Shukla VK**, Aryya NC, Pitale A, Pandey M, Dixit VK, Reddy CD, Gautam A. Metallothionein expression in carcinoma of the gallbladder. *Histopathology* 1998; **33**: 154-157
- 24 **Zelger B**, Hittmair A, Schir M, Ofner C, Ofner D, Fritsch PO, Bocker W, Jasani B, Schmid KW. Immunohistochemically demonstrated metallothionein expression in malignant melanoma. *Histopathology* 1993; **23**: 257-264
- 25 **Goulding H**, Jasani B, Pereira H, Reid A, Galea M, Bell JA, Elston CW, Robertson JF, Blamey RW, Nicholson RA. Metallothionein expression in human breast cancer. *Br J Cancer* 1995; **72**: 968-972
- 26 **Douglas-Jones AG**, Schmid KW, Bier B, Horgan K, Lyons K, Dallimore ND, Moneypenny IJ, Jasani B. Metallothionein expression in duct carcinoma in situ of the breast. *Hum Pathol* 1995; **26**: 217-222
- 27 **Uozaki H**, Horiuchi H, Ishida T, Iijima T, Imamura T, Machinami R. Overexpression of resistance-related proteins (metallothioneins, glutathione-S-transferase pi, heat shock protein 27, and lung resistance-related protein) in osteosarcoma. Relationship with poor prognosis. *Cancer* 1997; **79**: 2336-2344
- 28 **Sens MA**, Somji S, Garrett SH, Beall CL, Sens DA. Metallothionein isoform 3 overexpression is associated with breast cancers having a poor prognosis. *Am J Pathol* 2001; **159**: 21-26
- 29 **Jasani B**, Schmid KW. Significance of metallothionein overexpression in human tumours. *Histopathology* 1997; **31**: 211-214
- 30 **Rossen K**, Haerslev T, Hou-Jensen K, Jacobsen GK. Metallothionein expression in basaloid proliferations overlying dermatofibromas and in basal cell carcinomas. *Br J Dermatol* 1997; **136**: 30-34
- 31 **Zhang XH**, Jin L, Sakamoto H, Takenaka I. Immunohistochemical localization of metallothionein in human prostate cancer. *J Urol* 1996; **156**: 1679-1681
- 32 **Giuffre G**, Barresi G, Sturniolo GC, Sarnelli R, D'Inca R, Tuccari G. Immunohistochemical expression of metallothionein in normal human colorectal mucosa, in adenomas and in adenocarcinomas and their associated metastases. *Histopathology* 1996; **29**: 347-354
- 33 **Schmidt CJ**, Hamer DH. Cell specificity and an effect of ras on human metallothionein gene expression. *Proc Natl Acad Sci USA* 1986; **83**: 3346-3350
- 34 **Abdel-Mageed AB**, Agrawal KC. Activation of nuclear factor kappaB: potential role in metallothionein-mediated mitogenic response. *Cancer Res* 1998; **58**: 2335-2338
- 35 **Ioachim EE**, Goussia AC, Agnantis NJ, Machera M, Tsianos EV, Kappas AM. Prognostic evaluation of metallothionein expression in human colorectal neoplasms. *J Clin Pathol* 1999; **52**: 876-879
- 36 **Sutoh I**, Kohno H, Nakashima Y, Hishikawa Y, Tabara H, Tachibana M, Kubota H, Nagasue N. Concurrent expressions of metallothionein, glutathione S-transferase-pi, and P-glycoprotein in colorectal cancers. *Dis Colon Rectum* 2000; **43**: 221-232
- 37 **Hishikawa Y**, Koji T, Dhar DK, Kinugasa S, Yamaguchi M, Nagasue N. Metallothionein expression correlates with metastatic and proliferative potential in squamous cell carcinoma of the oesophagus. *Br J Cancer* 1999; **81**: 712-720
- 38 **McCluggage WG**, Maxwell P, Hamilton PW, Jasani B. High metallothionein expression is associated with features predictive of aggressive behaviour in endometrial carcinoma. *Histopathology* 1999; **34**: 51-55
- 39 **Rossmann TG**, Goncharova EI. Spontaneous mutagenesis in mammalian cells is caused mainly by oxidative events and can be blocked by antioxidants and metallothionein. *Mutat Res* 1998; **402**: 103-110
- 40 **Zhang B**, Satoh M, Nishimura N, Suzuki JS, Sone H, Aoki Y, Tohyama C. Metallothionein deficiency promotes mouse skin carcinogenesis induced by 7,12-dimethylbenz[a]anthracene. *Cancer Res* 1998; **58**: 4044-4046
- 41 **Duncan EL**, Reddel RR. Downregulation of metallothionein-IIA expression occurs at immortalization. *Oncogene* 1999; **18**: 897-903
- 42 **Florianczyk B**, Grzybowska L. Metallothionein levels in cell fractions from breast cancer tissues. *Acta Oncol* 2000; **39**: 141-143
- 43 **Xu BH**, Zhang RJ, Lu DD, Chen XD, Wang NJ. Expression of mdrl gene coded pglycoprotein in hepatocellular carcinoma and its clinical significance. *Huaren Xiaohua Zazhi* 1998; **6**: 783-785
- 44 **Kelley SL**, Basu A, Teicher BA, Hacker MP, Hamer DH, Lazo JS. Overexpression of metallothionein confers resistance of anticancer drugs. *Science* 1988; **241**: 1813-1815
- 45 **Kondo Y**, Kuo SM, Watkins SC, Lazo JS. Metallothionein localization and cisplatin resistance in human hormone-independent prostatic tumor cell lines. *Cancer Res* 1995; **55**: 474-477
- 46 **Miyazaki H**, Naitoh Y, Nakahashi Y, Yanagitani S, Kuno K, Ueno Y, Okajima A, Inoue K. Induction of metallothionein isoforms in rat hepatoma cells by various anticancer drugs. *J Biochem* 1998; **124**: 65-71
- 47 **Shnyder SD**, Hayes AJ, Pringle J, Archer CW. P-glycoprotein and metallothionein expression and resistance to chemotherapy in osteosarcoma. *Br J Cancer* 1998; **78**: 757-759
- 48 **Moriyama-Gonda N**, Igawa M, Shiina H, Wada Y. Heat-induced membrane damage combined with adriamycin on prostate carcinoma PC-3 cells: correlation of cytotoxicity, permeability and P-glycoprotein or metallothionein expression. *Br J Urol* 1998; **82**: 552-559
- 49 **Kikuchi Y**, Hirata J, Yamamoto K, Ishii K, Kita T, Kudoh K, Tode T, Nagata I, Taniguchi K, Kuwano M. Altered expression of gamma-glutamylcysteine synthetase, metallothionein and topoisomerase I or II during acquisition of drug resistance to cisplatin in human ovarian cancer cells. *Jpn J Cancer Res* 1997; **88**: 213-217
- 50 **Vandier D**, Calvez V, Massade L, Gouyette A, Mickley L, Fojo T, Rixe O. Transactivation of the metallothionein promoter in cisplatin-resistant cancer cells: a specific gene therapy strategy. *J Natl Cancer Inst* 2000; **92**: 642-647

Edited by Zhang JZ

• LIVER CANCER •

HLA class I expression in primary hepatocellular carcinoma

Jian Huang, Mei-Ying Cai, Da-Peng Wei

Jian Huang, Mei-Ying Cai, Da-Peng Wei, Immunology Department, West China University of Medical Sciences, Chengdu 610044, Sichuan Province, China

Supported by the National Natural Science Foundation of China, No.30070855

Correspondence to: Jian Huang, Bioinfo Tech Incorporated Company, 10F Zhuangsen No.8 Dongsheng Street, Chengdu 610015, Sichuan Province, China. huangjian@bioinfochina.com

Telephone: +86-28-6260468-243 **Fax:** +86-28-6698350

Received 2001-06-03 **Accepted** 2002-02-16

Abstract

AIM: To investigate whether CTL vaccine therapy is suitable for primary hepatocellular carcinoma (HCC) from the viewpoint of HLA class I antigens expression.

METHODS: The immunocytochemistry, image analysis, flow cytometry, and labeled streptavidin biotin (LSAB) method of immunohistochemistry were applied respectively to study 4 HCC cell lines (e.g. Alexander, HepG2, SMMC-7721, and QGY-7703) cultured *in vitro* and 6 frozen tissue specimens of HCC.

RESULTS: The positive control cell line Raji had very strong positive staining. Most mitotic and nonmitotic cells of the 4 HCC cell lines had various intensity of HLA class I antigens expression. The negative control cell K562 and the control slides of all the cell lines had no positive staining. In the 6 HCC specimens immunohistochemically studied, histological normal hepatocytes had no or very weak positive staining and the liver sinus had very strong positive staining. Most HCC cells in the sections from the 6 HCC specimens had strong positive HLA class I antigens staining. The positive staining was located in the cytoplasm, the perinuclear area, and at the cell membrane of the liver cancer cells. Flow cytometry also revealed that Raji and those 4 HCC cell lines had strong HLA class I antigens expression, which was confirmed quantitatively by the image analysis. It showed that the objective grayscale values of Raji and those 4 HCC cell lines were significantly different from that of K562 (Raji 114.04 ± 10.94 , Alexander 165.97 ± 5.35 , HepG2 167.02 ± 12.60 , QGY-7703 161.46 ± 7.13 , SMMC-7721 165.93 ± 5.21 , K562 244.89 ± 4.60 , $P < 0.01$). Significant differences were also found between Raji and the 4 HCC cell lines.

CONCLUSION: HCC cells express HLA class I antigens strongly. From this point of view, the active specific immunotherapy of CTL vaccine is suitable and practicable for HCC.

Huang J, Cai MY, Wei DP. HLA class I expression in primary hepatocellular carcinoma. *World J Gastroenterol* 2002; 8(4): 654-657

INTRODUCTION

The immunity of cytotoxic T lymphocyte (CTL) is crucial for

anti-tumor immune response. Tumor cells expressing MHC class I antigens is a necessary molecular basis and requirement for effective presentation, recognition, and cytotoxicity. Many tumors do decrease or lack MHC class I antigens to escape from immune surveillance. The monitoring of MHC class I antigens expression in tumors, therefore, is undoubtedly helpful to decide which immune strategy is suitable for a given tumor [1]. Therefore, it is necessary to start a preliminary investigation on the HLA class I antigens expression of HCC tissues *in vivo* and corresponding cell lines cultured *in vitro* before the design and construction of CTL vaccine against HCC.

MATERIALS AND METHODS

Main reagents

Mouse anti human HLA-ABC mAb, DAKO Corp; FITC labeled mouse anti human HLA-ABC mAb, Beckman Coulter Corp; biotin labeled goat anti mouse IgG and HRP-labeled streptavidin, from Beijing Zhongshan Corp; avidin biotin blocking system, Wuhan Boster Corp.

Cell lines and specimens

The erythromyeloid cell line K562 and the Burkitts' lymphoma cell line Raji were used as HLA class I antigens negative and positive control cells respectively [2,3]. The human HCC cell lines Alexander [4], HepG2 [5], SMMC-7721, and QGY-7703 were all kept and passed by our group. The cells above were maintained in complete PRMI 1640 medium at 37 degrees in a incubator with 5 % CO₂. Fifteen pathological specimens were obtained from surgically resected tissues of patients with HCC in the First Affiliated Hospital of West China University of Medical Sciences. The specimens were frozen immediately in liquid nitrogen. Four 1 mm consecutive frozen sections were prepared and stored at -70 degrees. HE Staining was done by the routine method.

Immunocytochemistry and immunohistochemistry

HCC cell lines were grown on the glass slides until confluence and then fixed and washed. Some slides were coated with the fixed and washed Raji and K562 cells. The frozen sections were also fixed and washed. The endogenous peroxidase on the slides and sections were inactivated, and the slides and sections were blocked by normal goat serum. Additionally, the endogenous biotin in the frozen sections was blocked. The slides and sections were incubated with 50 µl of 1:100 diluted mouse anti-HLA-ABC mAb or 50 µl PBS as control at 37 degrees in humid box for 1h and then were washed twice with PBS for 5 min each time. Next, 50 µl of 1:200 diluted biotin labeled goat-anti mouse IgG was added. After being incubated for 30 min and washed as before, 50 µl of 1:200 diluted HRP labeled streptavidin was added. The following incubation and washing was exactly the same as above. Finally, 50 µl of DAB working solution was added for color reaction under the microscopical

scrutiny. The reaction was stopped with tap water rinse. The slides and sections were then counterstained with hematoxylin as routine assay.

Image analysis

The slides were focused under photographic microscope and the 24 bit true color images at a resolution 768×576 were captured in real time by the JVC TK-C1381 digital camera. The captured images were read into the Mias-2000 Medical Images Analyzer. The objective grayscale was obtained through color HSV splitting and half binary quantifying. The data were assessed by Newman-Keuls method of *q* test using statistical package PEMS2.1 for *Medical Statistics of Chinese Medical Encyclopedia*. Values of $P < 0.05$ were considered statistically significant.

Flow cytometry

Cells were washed twice with PBS at 1200 r/min for 5 min per time. Then the cell concentration was adjusted to 1×10^6 Entries/ml and incubated with 10 μ l of 1:10 diluted FITC labeled mouse anti HLA-ABC or mouse IgG as negative control at room temperature for 30 min. At last, cells were washed once and detected by Elite-ESP flow cytometer.

RESULTS

Routine HE stain

Raji and K562 cells were round in shape. QGY-7703, Alexander and HepG2 seem to be polygonal. SMMC-7721 cells were spindly. All the cell lines above had evident features of tumor cells, which were heterogeneous in nuclear size. Mononuclear tumor giant cells were commonly seen in these cell lines. In addition, binuclear or multinuclear, normal or abnormal mitotic tumor cells were frequent in QGY-7703, HepG2 and SMMC-7721. Ten of 15 specimens from patients clinically, were diagnosed as HCC pathologically in corresponding paraffin sections by the Pathological Department. The left 5 specimens were excluded from this study, which were confirmed to be combined hepatocholangiocellular carcinoma, cholangiocellular carcinoma, nodular cirrhosis, secondary liver cancer from nasopharyngeal carcinoma and colon cancer, respectively. In comparison between the HE stain of frozen sections with that of paraffin sections, HCC cells could be found in only 6 of the 10 paraffin sections corroborated specimens. The remained 4 frozen specimens without HCC cells, possibly due to the failure of sampling HCC tissue, were also excluded from this study.

Immunocytochemistry and immunohistochemistry

Positive staining of HLA class I antigens appeared brown in color. Raji cells had very strong positive staining. Most mitotic and nonmitotic cells of the 4 HCC cell lines have various intensity of HLA class I antigens expression. The positive staining of HLA class I antigens was located in the cytoplasm, the perinuclear area, and at the cell membrane, but none in K562 and the control slides of all the cell lines (Figures 1, 2). In the 6 HCC specimens studied immunohistochemically, histologically normal hepatocytes had no or very weak positive staining and the liver sinus had very strong positive staining. Most HCC cells in the sections from the 6 HCC specimens had strong positive staining of HLA class I antigens, which were located in the cytoplasm, the perinuclear area, and at the

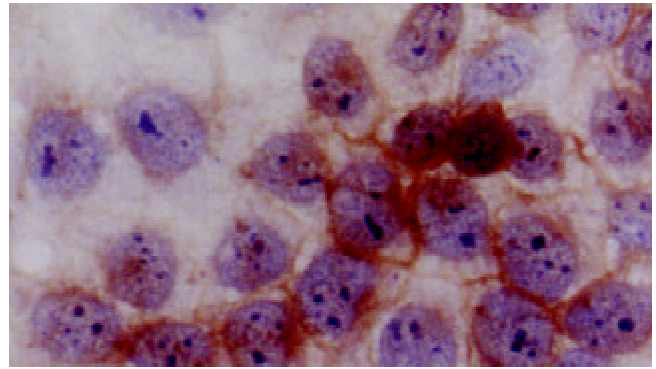


Figure 1 Positive staining of HLA- I antigens at QGY-7703 cell membrane. LSAB×350

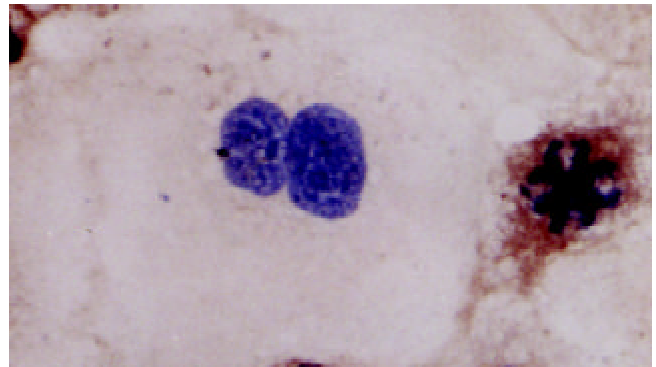


Figure 2 Positive staining of HLA- I antigens in cytoplasm of dividing Alexander cells. LSAB×350

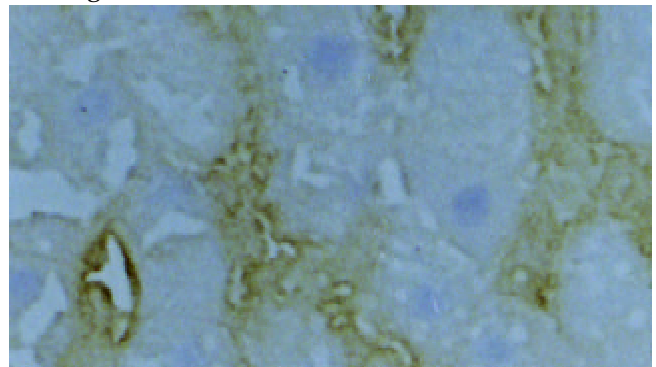


Figure 3 Negative staining of histologically normal liver cells and intensive positive staining within sinusoids. LSAB×100

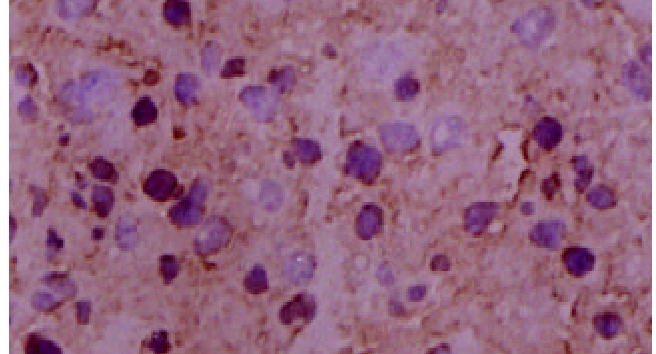


Figure 4 Positive staining of hepatocellular carcinoma cells

LSAB×100

Image analysis

The image analysis of HLA class I antigens expressions in the slides showed that the objective grayscale values of Raji and those 4 HCC cell lines were significantly different from that of K562 ($P<0.01$). Significant differences were also found between Raji and the 4 HCC cell lines (Table 1).

Table 1 Grayscale value comparison of HLA- I antigens among different cell lines

Tumor cell lines	n	Grayscale value ($\bar{x}\pm s$)
Raji	7	114.04±10.94 ^a
Alexander	7	165.97±5.35 ^{ab}
HepG2	7	167.02±12.60 ^{ab}
QGY-7703	7	161.46±7.13 ^{ab}
SMMC-7721	7	165.93±5.21 ^{ab}
K562	7	244.89±4.60

^a $P<0.01$ vs K562; ^b $P<0.01$ vs Raji.

Flow cytometry

The positive control Raji cells had strong fluorescence intensity, but Raji cells incubated with FITC labeled mouse IgG had very weak fluorescence. Fluorescence intensities of QGY-7703, Alexander, HepG2, and SMMC-7721 were very high. Some cells of the 4 cell lines had equal or even higher fluorescence intensities than those of Raji. The negative control cells K562 had very weak fluorescence intensity of HLA class I antigens, the irrelevant fluorescence stain of K562 was also weak (Figures 5, 6).

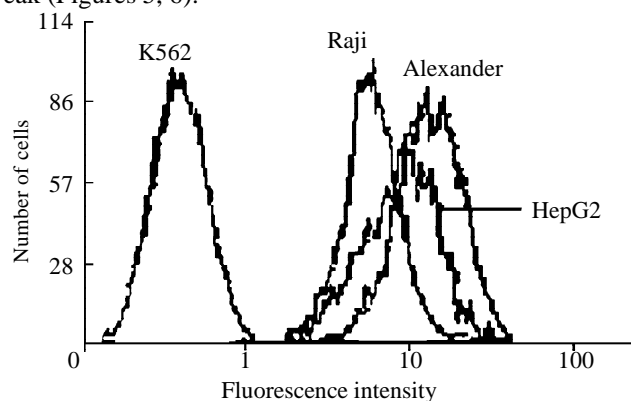


Figure 5 Flow cytometric histogram comparison of HLA- I antigens among K562, Raji, Alexander, HepG2 cell lines SMMC-7721

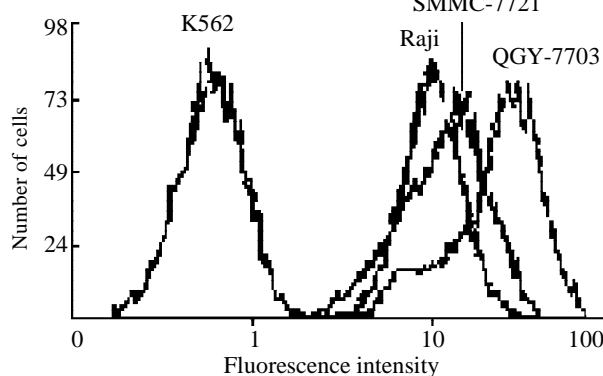


Figure 6 Flow cytometric histogram comparison of HLA- I

antigens among K562, Raji , SMMC-7721, QGY-7703 cell lines

DISCUSSION

HCC, one of the most common cancers, is the second cancer killer in China, and its mortality rate tends to increase year by year. About 11 000 of Chinese die of HCC annually. This number covers approximately half of the world population who die of HCC. At present, the overall curative effect of HCC is far from satisfaction. More than 2/3 of the HCC patients were found inoperable. The surgically treated patients have to face the challenge that how to clear away the residual cells to prevent metastasis and relapse. Because of serious side effects of radiotherapy and chemotherapy, new therapy is urgent clinically to be searched and developed so as to improve the curative effect of HCC. In recent years, studies of CTL vaccines against HCC have become frontiers of HCC immunotherapy [6-8]. The expression of MHC class I antigens is essential in CTL cytotoxicity. For example, the killing activity of mouse AFP specific CTL to mouse HCC cell lines Hepa1-6 and BWIC3, which express few MHC class I antigens, is much lower than that of MHC class I antigens positive EL4 cells [6]. Thus, whether HCC is suitable for CTL vaccine therapy depends to a great extent on the HLA class I antigens expression status of HCC cells.

Although a few studies have reported that liver cancer cells in HCC tissue or cultured *in vitro* have strong HLA class I antigens expression [2,3,9-12], few are aimed at Chinese. A Chinese research group, however, have initiated a study involving the expression of HLA-ABC on hepatocarcinoma. Our results of Alexander and HepG2 are consistent with results of other groups [2,3,10-13]. HCC cell lines QGY-7703 and SMMC-7721 have been established from HCC tissues of Chinese patients and frequently used in studies in China. Our results of these two cell lines indicate that both of them have strong HLA class I antigens expression. In addition, we found that mitotic HCC cells also strongly express HLA class I antigens. This phenomenon was not reported before, indicating that the corresponding specific CTL may kill the mitotic liver cancer cells. Our investigation on frozen specimens from 6 Chinese HCC patients shows that most liver cancer cells in the HCC tissue have strong HLA class I antigens expression. This is also consistent with the results of other groups [2,9,13]. It is worth paying attention to the articles of Paterson *et al* [9]. They reported that liver cancer cells in a handful of HCC specimens (4/70, 5.7%) did not express HLA class I antigens. However, this is not found in our study, possibly due to the limited amount of the specimens studied in our present study.

The results in our studies also indicate that in histologically normal liver HLA class I antigens were mainly expressed on liver sinusoidal lining cells rather than on hepatocytes. This is consistent with the results of several other groups [2,9,14]. The reason why the phenomenon that histologically normal hepatocytes have no or only weak HLA class I antigens expression though liver cancer cells strongly express HLA class I antigens, may be related to the unique lymphocytes distribution in liver and NK-cell escape [1,15,16]. About 31 % of the liver resident lymphocytes are NK cells [15]. Therefore, re-expression or enhanced expression of HLA class I antigens on HCC cells would be helpful for inhibiting the nonspecific cytotoxicity of NK cells. However, the cause of above phenomenon and its immunobiological implications remain to be explained by further studies.

In brief, the results of this study and other research groups indicate, from viewpoint of HLA class I antigens expression, that CTL vaccine therapy is suitable and practicable for HCC. This would provide *in vivo* and *in vitro* experimental basis for

the follow-up study of CTL vaccine design and construction.

REFERENCES

- 1 **Ruiz-Cabello F**, Garrido F. HLA and cancer: from research to clinical impact. *Immunol Today* 1998; **19**: 539-542
- 2 **Sung CH**, Hu CP, Hsu HC, Ng AK, Chou CK, Ting LP, Su TS, Han SH, Chang CM. Expression of class I and class II major histocompatibility antigens on human hepatocellular carcinoma. *J Clin Invest* 1989; **83**: 421-429
- 3 **Wadee AA**, Paterson A, Coplan KA, Reddy SG. HLA expressions in hepatocellular carcinoma cell lines. *Clin Exp Immunol* 1994; **97**: 328-333
- 4 **Alexander JJ**, Bey EM, Geddes EM, Lecatsas G. Establishment of continuously growing cell line from primary carcinoma of the liver. *S Afr Med J* 1976; **50**: 2124-2128
- 5 **Aden DP**, Fogel A, Plokin S, Damjanov I, Knowles BB. Controlled synthesis of HBsAg in a differentiated human liver carcinoma-derived cell line. *Nature* 1979; **282**: 615-616
- 6 **Vollmer CM Jr**, Eilber FC, Butterfield LH, Ribas A, Disette VB, Koh A, Montejo LD, Lee MC, Andrews KJ, McBride WH, Glaspy JA, Economou JS. Alpha-fetoprotein-specific genetic immunotherapy for hepatocellular carcinoma. *Cancer Res* 1999; **59**: 3064-3067
- 7 **Butterfield LH**, Koh A, Meng W, Vollmer CM, Ribas A, Disette V, Lee E, Glaspy JA, McBride WH, Economou JS. Generation of human T-cell responses to an HLA-A2.1-restricted peptide epitope derived from alpha-fetoprotein. *Cancer Res* 1999; **59**: 3134-3142
- 8 **Butterfield LH**, Meng WS, Koh A, Vollmer CM, Ribas A, Disette VB, Faull K, Glaspy JA, McBride WH, Economou JS. T cell responses to HLA-A*0201-restricted peptides derived from human alpha-fetoprotein. *J Immunol* 2001; **166**: 5300-5308
- 9 **Paterson AC**, Sciort R, Kew MC, Callea F, Dusheiko GM, Desmet VJ. HLA expressions in human hepatocellular carcinoma. *Br J Cancer* 1988; **57**: 369-373
- 10 **Paroli M**, Carloni G, Franco A, De Petrillo G, Alfani E, Perrone A, Barnaba V. Human hepatoma cells expressing MHC antigens display accessory cell function, dependence on LFA-1/ICAM-1 interaction. *Immunology* 1994; **82**: 215-221
- 11 **Tatsumi T**, Takehara T, Katayama K, Mochizuki K, Yamamoto M, Kanto T, Sasaki Y, Kasahara A, Hayashi N. Expression of costimulatory molecules B7-1 (CD80) and B7-2 (CD86) on human hepatocellular carcinoma. *Hepatology* 1997; **25**: 1108-1114
- 12 **Kurokohchi K**, Carrington M, Mann D, Simonis TB, Alexander-Miller MA, Feinstone SM, Akatsuka T, Berzofsky JA. Expression of HLA class I molecules and the transporter associated with antigen processing in hepatocellular carcinoma. *Hepatology* 1996; **23**: 1181-1188
- 13 **Zhai SH**, Liu JB, Zhu P, Wang YH. CD54, CD80, CD86 and HLA-ABC expressions in liver cirrhosis and hepatocarcinoma. *Shijie Huaren Xiaohua Zazhi* 2000; **8**: 292-295
- 14 **Franco A**, Barnaba V, Natali P, Balsano C, Musca A, Balsano F. Expression of class I and class II Major histocompatibility complex antigens on human hepatocytes. *Hepatology* 1988; **8**: 449-454
- 15 **Doherty DG**, O'Farrelly C. Innate and adaptive lymphoid cells in the human liver. *Immunol Rev* 2000; **174**: 5-20
- 16 **Luo DZ**, Vermijlen D, Ahishali B, Triantis V, Plakoutsi G, Braet F, Vanderkerken K, Wisse E. On the cell biology of pit cells, the liver-specific NK cells. *World J Gastroenterol* 2000; **6**: 1-11

Edited by Ma JY

• LIVER CANCER •

Role and limitation of FMPSPGR dynamic contrast scanning in the follow-up of patients with hepatocellular carcinoma treated by TACE

Fu-Hua Yan, Kang-Rong Zhou, Jie-Min Cheng, Jian-Hua Wang, Zhi-Ping Yan, Reng-Rong Da, Jia Fan, Yuan Ji

Fu-Hua Yan, Kang-Rong Zhou, Jie-Min Cheng, Jian-Hua Wang, Zhi-Ping Yan, Reng-Rong Da, Department of Radiology, Zhongshan Hospital, Fudan University, Shanghai 200032, China

Jia Fan, Department of Hepatobiliary-surgery, Zhongshan Hospital, Fudan University, Shanghai 200032, China

Yuan Ji, Department of Pathology, Zhongshan Hospital, Fudan University, Shanghai 200032, China

Supported by Clinical Important Item of Chinese Health Ministry, No. 97030220

Correspondence to: Dr Fu-Hua Yan, Zhongshan Hospital, Fudan University, 180 Fenglin Road, Shanghai 200032, China. yanfuhua@yahoo.com

Telephone: +86-21-64041990 Ext. 2453 **Fax:** +86-21-64037258

Received 2001-12-05 **Accepted** 2002-02-07

Abstract

AIM: To evaluate the role and limitation of fast multiplanar spoiled gradient-recalled (FMPSPGR) MR dynamic contrast scanning in the follow-up of patients with HCC treated by transarterial chemoembolization (TACE).

METHODS: Twenty-two patients with 24 HCC lesions confirmed by biopsy or surgical resection underwent MR imaging in 4-9wks after TACE with a superconducting 1.5 T MR scanner, including SE T₁WI, T₂WI and FMPSPGR dynamic contrast scanning. The signal intensities of all lesions on SE T₁WI, T₂WI and the enhancement patterns on FMPSPGR dynamic contrast scanning were observed, and the comparison was made between MRI findings and pathological results in all the cases.

RESULTS: Of the 24 lesions, the signal intensities were various on SE T₁WI and T₂WI. On T₁WI, 13 lesions appeared as hyperintense, 4 lesions were isointense and the other 7 lesions were hypointense. Histologically, hyperintense lesions showed on T₁WI were viable tumor or hemorrhage; isointensities were coagulative necrosis or inflammatory infiltration; hypointensities were tumor, liquefied necrosis, coagulative necrosis or inflammatory infiltration. On T₂WI, 15 lesions appeared as hyperintense, 3 lesions were isointense and the other 6 lesions were hypointense. Hyperintense lesions showed on T₂WI were residuals of viable tumor, hemorrhage, liquefied necrosis or inflammatory infiltration; isointense lesions were residuals of viable tumor or inflammatory infiltration; hypointense lesions were coagulative necrosis. On FMPSPGR dynamic contrast scanning, 18 of the 24 lesions enhanced on early-phase dynamic scanning corresponding to residuals of viable tumor and the other 6 lesions had no enhancement at this phase because complete necrosis were seen in the histologic examination. On delayed-phase dynamic scanning, 6 lesions had permanent enhancement appeared as inhomogeneous hyperintensity and both residuals of viable tumor and inflammatory infiltration were found by histologic examination. 18 lesions were hypointense

at this phase and 8 of them coexisted with peripheral ring-like enhancement of the lesions resulting from viable tumors or inflammatory infiltration.

CONCLUSION: FMPSPGR MR dynamic contrast scanning can reflect the pathologic changes of HCC treated by TACE. Especially, early-phase dynamic scanning can evaluate accurately residuals of viable tumor and necrosis in HCC lesions. FMPSPGR dynamic contrast scanning is useful in the follow-up of patients with HCC treated by TACE combined with SE T₁WI and T₂WI, but it is difficult to differentiate peripheral viable tumors from inflammatory infiltration.

Yan FH, Zhou KR, Cheng JM, Wang JH, Yan ZP, Da RR, Fan J, Ji Y. Role and limitation of FMPSPGR dynamic contrast scanning in the follow-up of patients with hepatocellular carcinoma treated by TACE. *World J Gastroenterol* 2002; 8(4):658-662

INTRODUCTION

Hepatocellular carcinoma (HCC) is a malignancy prevalent in the Asia countries. Surgical resection is the first choice for the treatment, but this option is not always possible because of coexisting severe cirrhosis, multiple lesions and other conditions not suitable for surgery. In case of unresectable HCC, transarterial chemoembolization (TACE) has been one of the widely used and effective treatment methods and demonstrated great potential in improving survival time, especially, it has been proved to be more effective in combination with percutaneous ethanol injection, Chinese traditional medicine or laser thermal ablation, etc.^[1-31]. Since TACE is difficult to kill the tumor cells for once completely, the treatment efficacy of TACE was influenced by many factors, such as the size of tumors, blood supply and the ultra-selectivity of the catheter etc. It is very important to assess objectively the viability and necrosis of the tumors after TACE in HCC, and to take further treatment to improve the general therapeutic effects and the survival rate. Magnetic resonance imaging (MRI) has been a useful modality in the diagnosis of HCC, especially fast multiplanar spoiled gradient recalled (FMPSPGR) sequence dynamic contrast scanning could reflect sufficiently the blood supply of HCC^[32-39]. The therapeutic effects of TACE in HCC were evaluated with MRI in this study, and the role and limitation of FMPSPGR dynamic contrast scanning in the follow-up of patients with HCC treated by TACE were discussed.

MATERIALS AND METHODS

Twenty-two cases with massive or nodular types of HCC were collected from Sept. 1997 to May 1999. All cases were confirmed by biopsy ($n=19$) or surgical resection after TACE ($n=3$).

Transarterial chemoembolization was performed by selectively introducing a catheter into the hepatic artery and injecting antitumor agents (5-FU 1 000 mg, Cisplatin 80 mg

or Bioroubixing 60-70 mg). Subsequently, the peripheral embolization of the tumors was done with 38 % ultrafluid iodized oil (Lipiodol) (10-25 ml) mixed with Mitomycin 16-20 mg, then the central embolization of the tumors was done with 3-5 strips of gelatine sponge (0.1-0.2 cm × 1 cm).

MRI was performed in 4-9 wk after TACE with a superconducting 1.5 T MR scanner (GE Medical Systems Milwaukee, WI), including T₁WI (TR/TE=500-700 ms/14-16 ms) and T₂WI (TR/TE=2 000-4 000 ms/30-90 ms) and FMPSPGR dynamic contrast MRI (Matrix 256×128, thickness 7 mm, gap 3 mm, TR/TE Flip Angle=100-150 ms/1.6~4.6 ms/60°-90°). Three to four repeated acquisitions were obtained at 25 s, 60 s, 90 s and 180 s respectively following power injection of 15-20 ml (0.15 mmol/kg) of Gd-DTPA (gadopentetic dimeglumine, Magnevist, Shering Pharmaceutical Ltd.) via antecubital vein.

Nineteen cases underwent biopsy with the CT guidance. The other 3 cases underwent surgical resection after TACE. The MRI images of all cases were read and analyzed by 2 experienced radiologists. The comparison of MRI images between before and after TACE was done in 6 cases. The comparison was also done between MRI findings and pathological results in all cases.

RESULTS

A total of 24 lesions were identified in the 22 cases of HCC. The size of the lesions ranged 3.9-8.2 cm in diameter, with average 5.3 cm (Figure 1).

Findings of HCC after TACE on SE sequence were showed in Table 1.

Table 1 Findings of HCC after TACE on SE sequence

SE sequence	signal intensity			
	hyperintensity		isointensity	
	homogeneity	inhomogeneity	homogeneity	inhomogeneity
T ₁ WI	9	4	4	2
T ₂ WI	3	12	3	3

Table 2 Comparison of MR findings on SE sequence with pathology

SE sequence	signal intensity	Pathological changes
T ₁ WI	hyperintensity	viable tumors, hemorrhage
	isointensity	viable tumors, coagulative necrosis, inflammatory infiltration
	hypointensity	viable tumors, coagulative necrosis, liquefied necrosis, inflammatory infiltration
	hyperintensity	viable tumors, hemorrhage, liquefied necrosis, inflammatory infiltration
	hypointensity	viable tumors, inflammatory infiltration
T ₂ WI	isointensity	viable tumors, inflammatory infiltration
	hypointensity	coagulative necrosis

Table 3 Comparison of MR findings on FMPSPGR sequence with pathology

FMPSPGR sequence	enhancement	pathological changes
enhanced early phase	enhanced area	viable tumors
	no enhanced area	necrosis
	enhanced area	viable tumors, inflammatory infiltration
enhanced late phase	no enhanced area	viable tumors, necrosis
	peripheral ring-like enhancement	viable tumors, inflammatory infiltration
	peripheral ring-like enhancement	viable tumors, inflammatory infiltration

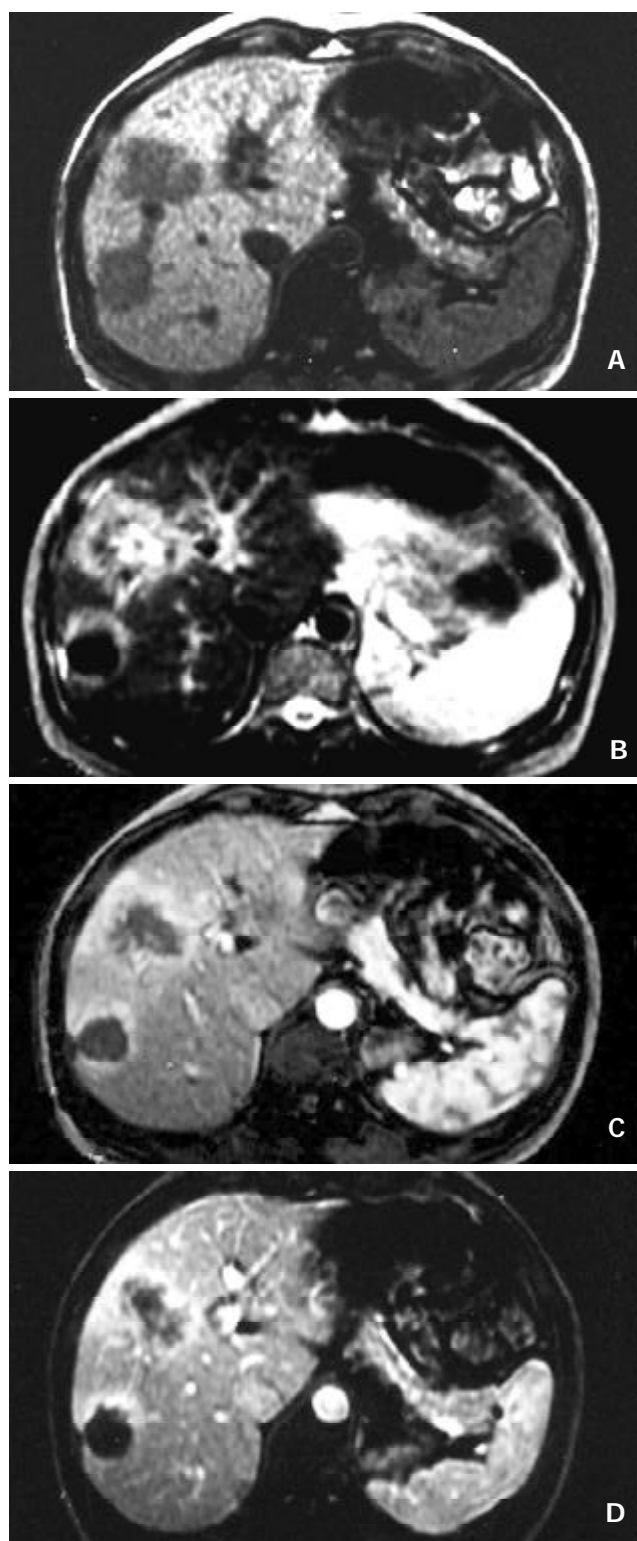


Figure 1 HCC after TACE. A T₁WI shows two hypointense lesions in the right anterior and posterior lobe. B T₂WI shows that the central coagulative necrosis of the right posterior lesion is hypointense and the peripheral residuals of viable tumors is hyperintense. The right anterior lesion is inhomogeneous intensity with liquefied necrosis (central higher hyperintensity), coagulative necrosis (punctual hypointensity) and peripheral residuals of viable tumors (peripheral hyperintensity). C FMPSPGR dynamic contrast early phase scanning shows that both of liquefied necrosis and coagulative necrosis have no enhancement and peripheral residuals of viable tumors enhanced. D The peripheral residuals of viable tumors have permanent enhancement at the dynamic contrast late phase.

Findings of HCC after TACE on FMPSPGR sequence

Eighteen lesions were enhanced at the dynamic early phase, in which one of the lesions revealed homogeneous hyperintensity, and the other 17 were inhomogeneous hyperintense. 6 lesions showed no enhancement on this phase. At the late phase of contrast scanning, 6 lesions were still inhomogeneous hyperintense, 18 hypointense and 10 homogeneous hypointensity, and peripheral ring-like enhancement of the tumors were seen in 8 lesions.

Comparison of MR findings with pathology was showed at Table 2-3

The MRI findings corresponding to the results of pathology showed that complete necrosis was seen in 6 lesions and various degrees of necrosis coexisted with viable tumors were seen in 17 lesions, except one. Peripheral ring-like enhancement of tumors seen on the FMPSPGR dynamic contrast late phase scanning, could be difficult to be differentiated viable tumors from inflammatory infiltration because of the limitation of bioptic spots.

DISCUSSION

TACE has been applied in unresectable HCC as an efficient therapy to improve the survival rate and also as a preoperative modality in some HCC patients to make the tumors diminution and then underwent surgical resection^[5-31]. Since TACE is difficult to kill all the tumor cells for once completely, so it is generally used repeatedly. It is needed to evaluate the viability and necrosis of HCC accurately for optimally choosing the further proper managing methods. Angiography is an effective method for evaluating HCC lesions treated with TACE. It could reflect sufficiently the blood supply of viable tumors and demonstrate the blood supply of lateral circulation of HCC. But angiography is an invasive technique and therefore is not suitable for routine follow-up in such patients^[40,41]. CT could be considered as a routine modality to judge the efficacy of TACE. It could demonstrate accurately the size, shape, location of the lesions, intrahepatic metastatic nodules and the distribution of lipiodol in the tumors and provide valuable imaging information to determinate the interval of TACE^[42-49]. Generally, the homogeneous and complete deposition of lipiodol within the lesions would indicate the high degree necrosis of the tumors, but it is difficult to judge the viability and necrosis of the tumors correctly, due to the inhomogeneous deposition, because lipiodol negative area doesn't actually represent the viability of the tumors. The necrosis within the lesions before TACE was also lipiodol negative area. On the other hand, the viable tumors could be enhanced on the CT contrast scanning, but the enhancement area within the lesions could also be affected by artifacts of the high concentrations of lipiodol, making it difficult to evaluate the therapeutic efficiency objectively.

Several authors considered that MR was valuable in the evaluation of therapeutic efficiency of TACE, especially on SE T₂WI, most of viable tumors were hyperintense and the coagulative necrosis within the tumors considered as a positive response to TACE were hypointense^[50-58]. But this results showed that the signal intensity of the tumors after TACE were variable on the SE T₁WI and T₂WI, but all of viable tumors, hemorrhage, liquefied necrosis and inflammatory infiltration could also result in hyperintensity on the T₂WI. Therefore it was difficult to assess the viable tumors of HCC after TACE by conventional SE imaging. However, it was reliable to judge coagulative necrosis on T₂WI, especially the changes during the process of intratumor hemorrhage after TACE presenting

as hyperintensity and then turned in to coagulative necrosis presenting hypointensity. This study also demonstrated that it was significant to compare the signal intensity of HCC on T₂WI before and after TACE to evaluate the degree of coagulative necrosis. The original hyperintensity of HCC turned to hypointensity indicated the presence of coagulative necrosis after TACE.

FMPSPGR dynamic contrast scanning plays a very important role in the detection and characterization of HCC. It is possible to obtain the high quality images of whole liver during a single breath-hold with rapid acquisition. It could demonstrate accurately the blood supply of tumors and reveal the contrast enhancement patterns of HCC. HCC is hypervascular and enhanced rapidly and obviously at the dynamic early phase scanning and declined at the late phase^[33-39]. This results showed that FMPSPGR dynamic contrast scanning also had a great value in the evaluation of therapeutic efficacy of TACE. The residual viable tumors were showed as rapid enhanced portions within the lesions, homogeneous or inhomogeneous, when necrotic portions had no enhancement at the contrast early phase scanning. At the late phase scanning, the enhancement of the most lesions became hypointensity, and just a few lesions showed persistent enhancement. Pathologically, both viable tumors and inflammatory infiltration could present such changes, so the contrast early phase scanning was more reliable in the evaluation of viable tumors, combined by with conventional SE sequence, and more accurate to assess the viability and the necrosis of tumors and useful in the followed up of HCC patients after TACE.

This study has some limitation in which all MR images based on histological specimens, but false positivity or false negativity may be present because of the factors in sampling.

REFERENCES

- 1 **Qin LX**, Tang ZY. The prognostic significance of clinical and pathological features in hepatocellular carcinoma. *World J Gastroenterol* 2002; **8**: 193-199
- 2 **Wu MC**, Shen F. Progress in research of liver surgery in China. *World J Gastroenterol* 2000; **6**: 773-776
- 3 **Fan J**, Wu ZQ, Tang ZY, Zhou J, Qiu SJ, Ma ZC, Zhou XD, Ye SL. Multimodality treatment in hepatocellular carcinoma patients with tumor thrombi in portal vein. *World J Gastroenterol* 2001; **7**: 28-32
- 4 **Tang ZY**. Hepatocellular carcinoma-cause, treatment and metastasis. *World J Gastroenterol* 2001; **7**: 445-454
- 5 **Parks RW**, Garden OJ. Liver resection for cancer. *World J Gastroenterol* 2001; **7**: 766-771
- 6 **Chen MS**, Li JQ, Zhang YQ, Lu LX, Zhang WZ, Yuan YF, Guo YP, Lin XJ, Li GH. High-dose Iodized oil transcatheter arterial chemoembolization for patients with large hepatocellular carcinoma. *World J Gastroenterol* 2002; **8**: 74-78
- 7 **Palma LD**. Diagnostic imaging and interventional therapy of hepatocellular carcinoma. *Br J Radiol* 1998; **71**: 808-818
- 8 **Livraghi T**. Treatment of hepatocellular carcinoma by interventional methods. *Eur. Radiol* 2001; **11**: 2207-2219
- 9 **Gattoni F**, Dova S, Ulenghi CM. Three-year follow-up of 62 cirrhotic patients with hepatocellular carcinoma treated with chemoembolization. *Minerva Chir* 2000; **55**: 31-37
- 10 **Luo YQ**, Wang Y, Chen H, Wu MC. Effect of post-operative survival rate with pre-operative transcatheter arterial chemoembolization in the patients with resectable hepatocellular carcinoma. *Shijie Huaren Xiaohua Zazhi* 2001; **9**: 468-469
- 11 **Zangos S**, Mack MG, Straub R, Engelmann K, Eichler K, Balzer J, Vogl TJ. Transarterial chemoembolization (TACE) of liver metastases. A palliative therapeutic approach.

- Radiology* 2001; **41**: 84-90
- 12 **Tu SP**, Wu DM, Yuan YZ, Wu YL, Jiang SH, Wu XX. Treatment of hepatocellular carcinoma by transcatheter arterial chemoembolization with hydroxycamptothecin. *Shijie Huaren Xiaohua Zazhi* 1999; **7**: 158-160
 - 13 **Cao W**, Wang ZM, Liang ZH, Zhang HX, Wang YQ, Guan Y, Li WX, Pan BR. Effects of angiogenesis inhibitor TNP-470 with lipiodol in arterial embolization of liver cancer in rabbits. *Shijie Huaren Xiaohua Zazhi* 2000; **8**: 629-632
 - 14 **Jia XC**, Tian JM, Wang ZT, Chen D, Ye H, Liu Q, Yang JJ, Sun F, Lin L, Lu JP, Wang F, Cheng HY. A retrospective review on interventional treatment of 10000 cases of liver cancer. *Shijie Huaren Xiaohua Zazhi* 1998; **6**: 2-3
 - 15 **Wang HL**, Zhao XX, Chen RP, Jing RF, Zhang XP. Treatment of hepatocellular carcinoma by hepatic arterial chemoembolization in 58 cases. *Xin Xiaohua Bingxue Zazhi* 1996; **4**: 471
 - 16 **Zheng CS**, Feng GS, Zhou RP, Liang B, Liang HP, Zhen J, Yu JM, Liu H. Hepatic arterial infusion chemotherapy and embolization in the treatment of primary hepatic carcinoma. *China Natl J New Gastroenterol* 1997; **3**: 104-107
 - 17 **Lencioni R**, Paolicchi A, Moretti M, Pinto F, Armillotta N, Di Giulio M, Cicorelli A, Donati F, Cioni D, Bartolozzi C. Combined transcatheter arterial chemoembolization and percutaneous ethanol injection for the treatment of large hepatocellular carcinoma: local therapeutic effect and long-term survival rate. *Eur Radiol* 1998; **8**: 439-444
 - 18 **Pacella CM**, Bizzarri G, Cecconi P, Caspani B, Maggnolfi F, Bianchini A, Anelli V, Pacella S, Rossi Z. Hepatocellular carcinoma: long-term results of combined treatment with laser thermal ablation and transcatheter arterial chemoembolization. *Radiology* 2001; **219**: 669-678
 - 19 **Fan J**, Teng GJ, He SC, Guo JH, Yang DP, Weng GY. Arterial chemoembolization for hepatocellular carcinoma. *World J Gastroenterol* 1998; **4**: 33-37
 - 20 **Li L**, Wu PH, Li JQ, Zhang WZ, Lin HG, Zhang YQ. Segmental transcatheter arterial embolization for primary hepatocellular carcinoma. *World J Gastroenterol* 1998; **4**: 511-512
 - 21 **Pelletier G**, Ducreux M, Gay F, Luboinski M, Hagege H, Dao T, Van Steenberghe W, Buffet C, Rougier P, Adler M, Pignon JP, Roche A. Treatment of unresectable hepatocellular carcinoma with lipiodol chemoembolization: a multicenter randomized trial. Group CHC. *J Hepatol* 1998; **29**: 129-134
 - 22 **Allgaier HP**, Deibert P, Olschewski M, Spamer C, Blum U, Gerok W, Blum HE. Survival benefit of patients with inoperable hepatocellular carcinoma treated by a combination of transarterial chemoembolization and percutaneous ethanol injection---a single-center analysis including 132 patients. *Int J Cancer* 1998; **79**: 601-605
 - 23 **Wang JH**, Lin G, Yan ZP, Wang XL, Cheng JM, Li MQ. Stage II surgical resection of hepatocellular carcinoma after TAE: a report of 38 cases. *World J Gastroenterol* 1998; **4**: 133-136
 - 24 **Bruix J**, Llovet JM, Castells A, Montana X, Bru C, Ayuso MC, Vilana R, Rodes J. Transarterial embolization versus symptomatic treatment in patients with advanced hepatocellular carcinoma: results of a randomized, controlled trial in a single institution. *Hepatology* 1998; **27**: 1578-1583
 - 25 **Huang J**, He X, Lin X, Zhang C, Li J. Effect of preoperative transcatheter arterial chemoembolization on tumor cell activity in hepatocellular carcinoma. *Chin Med J* 2000; **113**: 446-448
 - 26 **Kuyvenhoven JPh**, Lamers CB, van Hoek B. Practical management of hepatocellular carcinoma. *Scand J Gastroenterol Suppl* 2001; **234**: 82-87
 - 27 **Koda M**, Murawaki Y, Mitsuda A, Oyama K, Okamoto K, Idobe Y, Suou T, Kawasaki H. Combination therapy with transcatheter arterial chemoembolization and percutaneous ethanol injection alone for patients with small hepatocellular carcinoma: a randomized control study. *Cancer* 2001; **92**: 1516-1524
 - 28 **Poyanli A**, Rozanes I, Acunas B, Sencer S. Palliative treatment of hepatocellular carcinoma by chemoembolization. *Acta Radiol* 2001; **42**: 602-607
 - 29 **Loewe C**, Cejna M, Schoder M, Thurnher MM, Lammer J, Thurnher SA. Arterial embolization of unresectable hepatocellular carcinoma with use of cyanoacrylate and lipiodol. *J Vasc Interv Radiol* 2002; **13**: 61-69
 - 30 **Alsowmely AM**, Hodgson HJ. Non-surgical treatment of hepatocellular carcinoma. *Aliment Pharmacol Ther* 2002; **16**: 1-15
 - 31 **Dohmen K**, Shirahama M, Shigematsu H, Miyamoto Y, Torii Y, Irie K, Ishibashi H. Transcatheter arterial chemoembolization therapy combined with percutaneous ethanol injection for unresectable large hepatocellular carcinoma: an evaluation of the local therapeutic effect and survival rate. *Hepatogastroenterology* 2001; **48**: 1409-1415
 - 32 **Zhou KR**, Yan FH. Imaging diagnosis of micro liver cancer in China. *Shijie Huaren Xiaohua Zazhi* 2001; **9**: 733-736
 - 33 **Oi H**, Murakami T, Kim T, Matsushita M, Kishimoto H, Nakamura H. Dynamic MR imaging and early-phase helical CT for detecting small intrahepatic metastases of hepatocellular carcinoma. *AJR* 1996; **166**: 369-374
 - 34 **Siegelman ES**, Outwater EK. MR imaging techniques of the liver. *RCNA* 1998; **36**: 263-329
 - 35 **Fernandez MP**, Redvanly RD. Primary hepatic malignant neoplasms. *RCNA* 1998; **36**: 333-348
 - 36 **Yan FH**, Zhou KR, Shen JZ, Zeng MS, Yang J, Wu D, Gong JS, Shi WB. The comparative study of the enhancement patterns of SHCC with dynamic MRI and dynamic CT. *Zhonghua Zhongliu Zazhi* 2001; **23**: 413-416
 - 37 **Yan FH**, Zhou KR, Wu D, Yang J, Gong JS, Shen JZ. Evaluation of dynamic enhanced fast multiplanar spoiling gradient-recalled in the diagnosis of small hepatocellular carcinoma. *Zhonghua Ganzangbing Zazhi* 2001; **9**: 139-141
 - 38 **Yan FH**, Yang J, Zeng MS, Zhou KR. Comparative study of spiral CT, dynamic MRI and US for diagnosis of small hepatocellular carcinoma. *Zhongguo Yixue Jisuanji Chengxiang Zazhi* 1997; **3**: 20-24
 - 39 **Onaya H**, Itai Y. MR imaging of hepatocellular carcinoma. *Magn Reson Imaging Clin N Am* 2000; **8**: 757-768
 - 40 **Tsui EY**, Chan JH, Cheung YK, Cheung CC, Tsui WC, Szeto MI, Lau KW, Yuen MK, Luk SH. Evaluation of therapeutic effectiveness of transarterial chemoembolization for hepatocellular carcinoma: correlation of dynamic susceptibility contrast-enhanced echoplanar imaging and hepatic angiography. *Clin Imaging* 2000; **24**: 210-216
 - 41 **Gattoni F**, Dova S, Tonolini M, Uslenghi CM. Study of the liver and the portal venous system with digital rotational angiography. *Radiol Med (Torino)* 2001; **101**: 118-124
 - 42 **Choi BI**, Kim HC, Han JK, Park JH, Kim ST, Lee HS, Kim CY, Han MC. Therapeutic effect of transcatheter oil chemoembolization therapy for encapsulated nodular hepatic carcinoma: CT and Pathologic findings. *Radiology* 1992; **182**: 709-713
 - 43 **Takayasu K**, Arii S, Matsuo N, Yoshikawa M, Ryu M, Takasal K, Sato M, Yamanaka N, Shimamura Y, Ohto M. Comparison of CT findings with resected specimens after chemoembolization with iodized oil for hepatocellular carcinoma. *AJR* 2000; **175**: 699-704
 - 44 **Vogl TJ**, Trapp M, Schroeder H, Mack M, Schuster A, Schmi J, Neuhaus P, Felix R. Transarterial chemoembolization for hepatocellular carcinoma: volumetric and morphologic CT criteria for assessment of prognosis and therapeutic success-results from a liver transplantation center. *Radiology* 2000; **214**: 349-357
 - 45 **Katyal S**, Oliver JH, Peterson MS, Chang PJ, Baron RL, Can BI. Prognostic significance of arterial phase CT for prediction of response to transcatheter arterial chemoembolization in unresectable hepatocellular carcinoma: a retrospective analysis. *AJR* 2000; **175**: 1665-1672
 - 46 **Lencioni R**, Pinto F, Armillotta N, Giulio M, Gaeta P, Di

- Candio G, Marchi S, Bartolozzi C. Intrahepatic metastatic nodules of hepatocellular carcinoma detected at lipiodol-CT: imaging-pathologic correlation. *Abdom Imaging* 1997; **22**: 253-258
- 47 **Marcato N**, Abergel A, Alexandre M, Boire JY, Darcha C, Duchene B, Chipponi J, Boyer L, Viallet JF, Bommelaer G. Hepatocellular carcinoma in cirrhosis: semeiology and performance of magnetic resonance imaging and lipiodol computed tomography. *Gastroenterol Clin Biol* 1999; **23**: 114-121
- 48 **Catalano O**, Esposito M, Sandomenico F, Nunziata A, Siani A. Multiphasic helical computed tomography of hepatocarcinoma. Assessment after chemoembolization. *Radiol Med (Torino)* 2000; **99**: 456-460
- 49 **Sze DY**, Razavi MK, So SK, Jeffrey RB Jr. Impact of multidetector CT hepatic arteriography on the planning of chemoembolization treatment of hepatocellular carcinoma. *AJR* 2001; **177**: 1339-1345
- 50 **Castrucci M**, Sironi S, Cobelli F De, Salvioni M, Del Maschio A. Plain and gadolinium-DTPA-enhanced MR imaging of hepatocellular carcinoma treated with transarterial chemoembolization. *Abdom Imaging* 1996; **21**: 488-494
- 51 **Ito K**, Honjo K, Fujita T, Matsui M, Awaya H, Matsumoto T, Matsunaga N, Nakaanishi T. Therapeutic efficacy of transcatheter arterial chemoembolization for hepatocellular carcinoma: MRI and pathology. *JCAT* 1995; **19**: 198-203
- 52 **Yamashita Y**, Yoshimatsu S, Sumi M, Harada M, Takahashi M. Dynamic MR imaging of hepatoma by transcatheter arterial embolization therapy. Aseessment of treatment effect. *Acta Radiol* 1993; **34**: 303-308
- 53 **De Santis M**, Torricelli P, Cristani A, Cioni G, Montanar N, Sardini C, Ventura E, Romagnoli R. MRI of hepatocellular carcinoma before and after transcatheter chemoembolization. *JCAT* 1993; **17**: 901-908
- 54 **Bartolozzi C**, Lencioni R, Caramella D, Falaschi F, Cioni R, DiCoscio G. Hepatocellular carcinoma: CT and MR features after transcatheter arterial chemoembolization and percutaneous ethanol injection. *Radiology* 1994; **191**: 123-128
- 55 **De Santis M**, Alborino S, Tartoni PL, Torricelli P, Casolo A, Romagnoli R. Effects of Lipiodol retention on MRI signal intensity from hepatocellular carcinoma and surrounding liver treated by chemoembolization. *Eur Radiol* 1997; **7**: 10-16
- 56 **Semelka RC**, Worawattanakul S, Mauro MA, Bernard SA, Cance WG. Malignant hepatic tumors: changed on MRI after hepatic arterial chemoembolization-preliminary findings. *J Magn Reson Imaging* 1998; **8**: 48-56
- 57 **Kubota K**, Hira N, Nishikawa T, Fujiwara Y, Murata Y, Ito S, Yoshida D, Yishida S. Evaluation of hepatocellular carcinoma after treatment with transcatheter arterial chemoembolization: comparison of Lipiodol-CT, power Doppler sonography, and dynamic MRI. *Abdom Imaging* 2001; **26**: 184-190
- 58 **Chan JH**, Tsui EY, Luk SH, Yuen MK, Cheung YK, Wong KP. Detection of hepatic tumor perfusion following transcatheter arterial chemoembolization with dynamic susceptibility contrast-enhanced echoplanar imaging. *Clin Imaging* 1999; **23**: 190-194

Edited by Zhang JZ

• LARGE INTESTINAL CANCER •

Arterial chemotherapy of 5-fluorouracil and mitomycin C in the treatment of liver metastases of colorectal cancer

Lian-Xin Liu, Wei-Hui Zhang, Hong-Chi Jiang, An-Long Zhu, Lin-Feng Wu, Shu-Yi Qi, Da-Xun Piao

Lian-Xin Liu, Wei-Hui Zhang, Hong-Chi Jiang, An-Long Zhu, Lin-Feng Wu, Da-Xun Piao, Department of Surgery, the First Clinical College, Harbin Medical University, Harbin 150001, Heilongjiang Province, China

Shu-Yi Qi, Department of VIP, the First Clinical College, Harbin Medical University, Harbin 150001, Heilongjiang Province, China

Supported by Youth Natural Scientific Foundation of Heilongjiang Province and Harbin

Correspondence to: Dr Lian-Xin Liu, Department of Surgery, the First Clinical College, Harbin Medical University, No.23 Youzheng Street, Nangang District, Harbin 150001, Heilongjiang Province, China. liulianxin@sohu.com

Telephone: +86-451-3668999 Fax: +86-451-3670428

Received 2002-07-20 Accepted 2002-07-25

Abstract

AIM: Regional chemotherapy using hepatic artery catheters is a good method of treating patients with colorectal cancer liver metastases. We investigated the survival of patients with liver metastases from colorectal cancer using 5-fluorouracil (5-FU) and mitomycin C through implantable hepatic arterial infusion port.

METHODS: Seventy-five patients with inoperable liver metastases from colorectal cancer were included between March, 1992 and November, 2001. We placed implantable hepatic arterial catheter (HAC) port by laparotomy. 5-FU, 1 000 mg/m²/d continuous infusion for five days every four weeks, was delivered in the hepatic arterial catheter through the port. Mitomycin C, 30 mg/m²/d infusion in the first day every cycle through the port. Response to the treatment was evaluated by serial determinations of plasma CEA and imaging techniques consisting of computerized tomography and sonography of liver.

RESULTS: Sixty-eight were performed hepatic artery chemotherapy and fifty-six were followed up among seventy-five HAC patients. Twenty-six patients (46.4 %) have responded and 4 complete remission were achieved. Eight patients (14.3 %) had stable liver metastases. Twenty-two patients (39.3 %) were progressed with increased tumor size and number. Twenty-nine patients (51.8 %) had a decreased serum CEA level, while 10 patients (17.9 %) were stable and 17 patients (30.4 %) had an increased serum CEA level. There were no operative death in this series. Complications, which occurred in 18 patients (32.1 %), were as followed: hepatic artery thrombosis in 11, Upper gastric and intestinal bleeding in 3, liver abscess in 1, pocket infection in 1, cholangitis in 1, and hepatic artery pseudo-aneurysm in one patient.

CONCLUSION: Combined infusion of 5-FU and mitomycin C by hepatic artery catheter port is an effective treatment for liver metastases from colorectal cancer.

The high response and lower complication rates prove the adjuvant treatment of colorectal cancer with this treatment.

Liu LX, Zhang WH, Jiang HC, Zhu AL, Wu LF, Qi SY, Piao DX. Arterial chemotherapy of 5-fluorouracil and mitomycin C in the treatment of liver metastases of colorectal cancer. *World J Gastroenterol* 2002; 8(4):663-667

INTRODUCTION

Colorectal cancer is one of the leading causes of cancer-related mortality in China^[1-29]. Approximately half of the patients undergoing apparently curative resection will die within 5 years because of recurrent disease, mostly with liver metastases^[30]. Liver was the only site affected in 50 % of these patients. Synchronous hepatic metastases are detected in 20 % of patients under bowel resection, while metachronous disease occurs in another 30 %^[31-33]. However about 5-20 % of patients with colorectal hepatic metastases undergo resection with curative intention, resulting in a five year survival of 20-40 %. The one-year and three-year survivals of untreated patients with liver metastases are 31 % and 2.6 %, respectively^[34-36]. Most liver metastases were unresectable because of the number, size, position of tumors and general conditions unsuitable for liver resection.

Unfortunately, the results of conventional systemic chemotherapy have been disappointing. Single-agent 5-fluorouracil (5-FU), which has been used for many years to treat metastatic colorectal cancer, has a response rate of approximately less than 20 %. The addition of mitomycin C produces higher response rates with a trend towards increase survival and probably similar results can be achieved with high dose 5-FU alone^[37,38].

As most drugs have a steep dose-dependent curve, it is a basic pharmacokinetic principle that if one can increase drug delivery to tumors then increased response rates can be achieved. An alternative approach to the therapy of liver metastases is therefore to deliver the drug intra-arterially^[39,40]. Hepatic artery catheter chemotherapy is a therapeutic possibility for unresectable liver metastases for many years. The rationale for Hepatic artery catheter chemotherapy is based on the fact that liver metastases over 1 cm derive most their blood supply from hepatic artery. The other rationale is the high first pass hepatic extraction of the drug used for this approach. Both factors make high local drug concentrations with reduced systemic toxicity and allow treatment with relatively high dosages compared to intravenous treatment^[41,42].

We report our experience of an intra-arterial combined use of 5-FU and mitomycin C in patients with unresectable colorectal liver metastases. The aim of this approach was firstly achieve high response with combination of drugs.

MATERIALS AND METHODS

Patients

Seventy-five patients (43 male, 32 female) with a median age of 58.3 years (range 31-76) with multifocal colorectal metastases confined to the liver and not suitable to surgical resection and other regional ablation which include radio frequency ablation, ethanol injection, cryotherapy and laser ablation, were included in the study between January 1992 and November 2001. Seventeen patients had synchronous and 58 patients had metachronous liver metastases. Preoperative assessment included computerized tomography(CT) scan of abdomen and pelvis, either radiographic or CT examination of the chest and colonoscopy of bowel to exclude extrahepatic disease. Some patients were undergone Positron Emission Tomography (PET) recently. Selective superior mesenteric angiography was performed before surgery to define hepatic arterial anatomy in some patients. Histological confirmation of the presence of liver metastases was obtained by ultrasound guided fine needle biopsy or fine needle biopsy in laparotomy before implantation of hepatic artery catheter port. Blood test including hematology, liver function, renal function and CEA were performed before operation.

Hepatic artery catheter port

Patients underwent a laparotomy and the hepatic artery catheter (HAC) was positioned in the ligated gastroduodenal artery with the catheter tip located at the junction of the gastroduodenal and common hepatic artery, thereby gaining access to the hepatic arterial flow. The other end was connected to a subcutaneous infusion port placed over the left costal margin. A cholecystectomy was routinely performed to prevent potential chemical cholecystitis during chemotherapy. Various surgical maneuvers were used in patients with aberrant hepatic arterial anatomy, which include position the catheter in other artery and bypass of hepatic artery with artificial vessels. Adequate perfusion of the liver was confirmed at the time of operation with a test of blue dye. The port was flushed with heparinized saline(1 000 μ ml).

Chemotherapy

All patients received continuously hepatic arterial 5-FU and mitomycin C perfusion using an ambulatory pump. Patients received 1 000 mg/m²/d 5-FU in 12 hours for five days every 4 weeks. thirty mg/m² mitomycin C was perfused in 2 hours after the use of 5-FU in first day every cycle. Ten microgram of dexamethasone was given before perfusion everyday. Cimetidine and Losec were prescribed as prophylaxis against gastroduodenal ulceration. Haemological and biochemical toxicity were assessed every 2 weeks and graded according to WHO toxicity criteria. In patients with significant side effects, the subsequent dose was delayed until recovery.

Study parameters

Evaluation of the HAC were performed every two cycles by CT scan or ultrasound of liver and serum CEA, while a chest film or CT and blood test were also made. Completed response was defined as the disappearance of all tumor. Partial response was defined as a >50 % decrease of the lesion size and number. Progressive response was defined as a >25 % increase in any measurable lesion or the appearance of a new lesion. Stable response was defined as <25 % increase and <50 % decrease of the lesion. The decisions of further treatment were made after 6 cycles intra-arterial chemotherapy. Patients who progressed were offered alternative treatment. Patient whose catheters were thrombosis or unusable because other

complications but had complete, partial and stable response, were commenced on an intravenous chemotherapy using 5-FU and mitomycin C.

Statistical analysis

Time to progression and overall survival were estimated by Kaplan-Meier survival curves using SPSS. Seven patients, which were not regularly performed chemotherapy due to the toxicity or rejected chemotherapy, were excluded from the study. Twelve patients were not follow up in time and accurately were not included in this study.

RESULTS

Treatment and survival

Of the 75 patients, four patients rejected intra-arterial 5-FU and mitomycin C chemotherapy. Three patients would not continue the chemotherapy because of the severe toxicity of cytotoxic drugs, although many procedures were performed. During 68 patients who continued at least 6 cycles of chemotherapy, twelve patients were not completely and accurately followed up. So, only fifty-six patients were treated and studied. The median number of cycles received were 10 (range 6-25). Median follow up were 21 months (range 8-37months). Forty-one patients have died till the close day of follow up. Predicted median survival from the time of catheter insertion was 15 months (Figure 1).

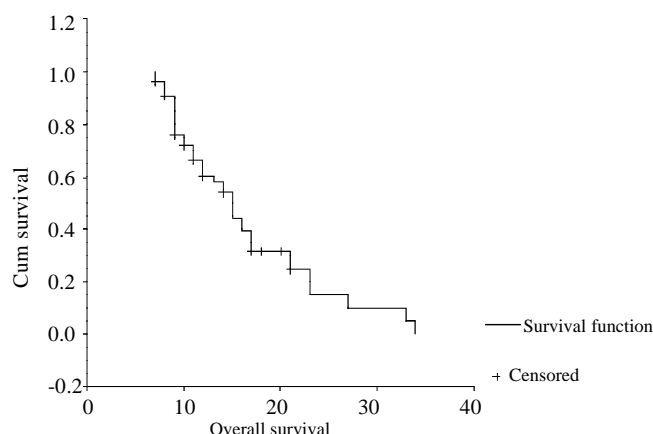


Figure 1 Kaplan-Meier survival curve. Median survival 15 months

Response

Response is expression as best response during the course of intra-arterial treatment. Twenty-six patients(46.4 %) were responded, of whom, 4 had complete response and 22 had partial response. Eight patients(14.3 %) were stable, whereas 22 patients(39.3 %) were progressed. Twenty-nine patients(51.8 %) had a decreased serum CEA level, while 10 patients(17.9 %) were stable and 17 patients(30.4 %) had an increased serum CEA level. There were no operative death in this series.

Complications

Hepatic artery thrombosis (in 11 patients, 19.8 %) is the complications most frequently observed in patients with HAC. The presenting symptoms of this complications were abdominal pain and obstruction of the catheter. It was confirmed by angiography in 6 patients and by Doppler ultrasound examination in 5 patients. Upper gastric and intestinal bleeding were present in 3 patients, which due to perforation of gastric and duodenal ulceration at surgery in 2 patients and duodenal ulceration bleeding at gastroscopy in 1 patient. There were all performed before 1995 when we did

not use blue dye. There were one patient presented with high fever after intra-arterial chemotherapy. She was diagnosed liver abscess by CT scan of liver and cured by ultrasound guide drainage. One patients which has a pocket infection has healed after intravenous antibiotics and drainage. One patients with cholangitis has to move the catheter and port. There are still one bleeding ulcer due to hepatic artery pseudo-aneurysm at surgery.

DISCUSSION

When colorectal cancer metastasises to liver, the prognosis becomes very awful. More than fifty percent colorectal cancer liver metastases patients will died in six months. For this reason, various treatment have been attempted, which include HAC, radio frequency ablation^[44], cryotherapy^[45], ethanol injection^[46], systemic chemotherapy^[47] and radiotherapy^[48]. As most cytotoxic drugs have a steep dose-dependence response curve: the higher the concentration of the drug, the higher the antitumor effects^[39]. Hepatic artery catheter chemotherapy emerged in this condition. Besides this, metastatic tumors in the liver derived their blood supply mainly from the hepatic artery (90-95 %). HAC can directly perfuse the chemotherapy to liver metastases from colorectal cancer. The drugs will result in a prolonged exposure of high concentration to the tumors, while reducing the systemic side effects following the metabolism of the drug in the liver. HAC were undertaken more than 30 years for these reasons^[49-51].

There are some studies compared intra-arterial chemotherapy with conventional systemic chemotherapy showed consistently higher response rates in patients receiving intra-arterial chemotherapy^[49]. In the United Kingdom, Patients were randomized to receive intra-arterial through a totally implantable infusion device; in the latter group 20 % patients were given systemic chemotherapy. Survival was significantly longer in the intra-arterial group (median survival 405days compared with 226days). The intra-arterial group also had a better quality of life than those received systemic chemotherapy^[52]. Other study showed that the response rate was 43 % in the intra-arterial group compared with 9 % in the systemic chemotherapy group. Furthermore, the intra-arterial group showed a significant increase in survival of one year(64 % compared with 44 %) and two years (23 % compared with 13 %). Other studies also showed a higher response rates in intra-arterial chemotherapy than that in systemic chemotherapy^[53].

In all studies, 5-FU and FUDR were chosen for the arterial route of administration. As 84-99 % of FUDR is extracted by the liver on first pass, it seemed logical to use FUDR to achieve the dual objective of high levels within the tumor and low plasma levels, thereby increasing the probability of the tumor's response while minimizing the systemic toxicity^[54]. But 55 % of patients using FUDR in the UK and French studies developed extra-hepatic progression, suggesting that these patients may have had occult extra-hepatic disease at the time of entry into the trial or during the intra-arterial chemotherapy. The lower plasma level of drugs have been misplaced. But, 5-FU which has a lower hepatic extraction rather than FUDR, allowed the drug to "spill over" into the systemic circulation^[55]. Mitomycin C is also a valuable drug for the systemic chemotherapy in colorectal cancer. In this way, we hoped to maximize the response rates within the liver but also to suppress the development of extrahepatic metastases by combined use of 5-FU and mitomycin C. It seemed likely that both of these objectives could be achieved with a response rate of 46.4 %. At the same time, systemic toxicity was relatively mild and no chemical hepatitis or biliary sclerosis developed as that in

FUDR.

Imaging and CEA are good markers in follow up of patients. Serum CEA determinations were the most sensitive indicator of tumor regression or recurrence and proceed changes in the imaging test by at least 1-2 months. Angiography CT(CTA) seems to be the most sensitive to change in tumor size and find new metastases. Sonography is the cheapest way to follow up.

Although there are some complications in HAC, it is still a feasible method for colorectal cancer liver metastases. Most complications was related to the technique of surgery and care of patients^[55]. Meticulous attention to ligation of all vessels that would cause gastroduodenal misperfusion can eliminate gastritis, duodenitis, and gastroduodenal ulceration related to HAC chemotherapy^[56]. The intraoperative blue injection are necessary to confirm total hepatic perfusion and to rule out any gastroduodenal misperfusion. Gastroscopy investigation of the gastroduodenal perfusion of blue injected through the port is very important before initiating HAC chemotherapy. Displacement of the catheter tip into the hepatic artery often leads to thrombosis of the artery. Dismal migration of the catheter into the gastroduodenal artery may cause vessel or catheter occlusion, hemorrhage, aneurysm, and rupture of the gastroduodenal artery^[57]. These complications were all emerged in the early stage of this procedure when we did not have so much experience to avoid these. Liver abscess and infection of port were due to unstrictly sterilize procedure which can be avoided at all.

In conclusion, HAC 5-FU and mitomycin C chemotherapy is better than systemic chemotherapy and other combination of drugs in colorectal cancer liver metastases, which were not suitable for surgery, cryotherapy, radio frequency ablation and other adjunctive therapy, although there are still 39.3 % patients progression and some complications, some of them were dangerous.

REFERENCES

- 1 **Xiong B**, Gong LL, Zhang F, Hu MB, Yuan HY. TGF β_1 expression and angiogenesis in colorectal cancer tissue. *World J Gastroenterol* 2002;**8**:496-498
- 2 **Zheng S**, Liu XY, Ding KF, Wang LB, Qiu PL, Ding X, Shen YZ, Shen GF, Sun QR, Li WD, Dong Q, Zhang SZ. Reduction of the incidence and mortality of rectal cancer by polypectomy: a prospective cohort study in Haining County. *World J Gastroenterol* 2002;**8**:488-492
- 3 **Wan J**, Zhang ZQ, Zhu C, Wang MW, Zhao DH, Fu YH, Zhang JP, Wang YH, Wu BY. Colonoscopic screening and follow-up for colorectal cancer in the elderly. *World J Gastroenterol* 2002;**8**:267-269
- 4 **Zhao B**, Wang ZJ, Xu YF, Wan YL, Li P, Huang YT. Report of 16 kindreds and one kindred with hMLH1 germline mutation. *World J Gastroenterol* 2002;**8**:263-266
- 5 **Wu BP**, Xiao B, Wan TM, Zhang YL, Zhang ZS, Zhou DY, Lai ZS, Gao CF. Construction and selection of the natural immune Fab antibody phage display library from patients with colorectal cancer. *World J Gastroenterol* 2001;**7**:811-815
- 6 **Cai Q**, Sun MH, Lu HF, Zhang TM, Mo SJ, Xu Y, Cai SJ, Zhu XZ, Shi DR. C linicopathological and molecular genetic analysis of 4 typical Chinese HNPCC families. *World J Gastroenterol* 2001;**7**:805-810
- 7 **Zhu JW**, Yu BM, Ji YB, Zheng MH, Li DH. Upregulation of vascular endothelial growth factor by hydrogen peroxide in human colon cancer. *World J Gastroenterol* 2002;**8**:153-157
- 8 **Sun K**, Jin BQ, Feng Q, Zhu Y, Yang K, Liu XS, Dong BQ. Identification of CD226 ligand on colo205 cell surface. *World J Gastroenterol* 2002;**8**:108-113

- 9 **Zhang YL**, Zhang ZS, Wu BP, Zhou DY. Early diagnosis for colorectal cancer in China. *World J Gastroenterol* 2002;**8**: 21-25
- 10 **Luo MJ**, Lai MD. Identification of differentially expressed genes in normal mucosa, adenoma and adenocarcinoma of colon by SSH. *World J Gastroenterol* 2001; **7**: 726-731
- 11 **Yi J**, Wang ZW, Cang H, Chen YY, Zhao R, Yu BM, Tang XM. P16 gene methylation in colorectal cancers is associated with Duke's staging. *World J Gastroenterol* 2001;**7**: 722-725
- 12 **Makin GB**, Breen DJ, Monson JRT. The impact of new technology on surgery for colorectal cancer. *World J Gastroenterol* 2001;**7**:612-621
- 13 **Li XG**, Song JD, Wang YQ. Differential expression of a novel colorectal cancer differentiation-related gene in colorectal cancer. *World J Gastroenterol* 2001; **7**: 551-554
- 14 **Wang LP**, Liang K, Shen Y, Yin WB, Hans G, Zeng YJ. Neutron-induced apoptosis of HR8348 cells in vitro. *World J Gastroenterol* 2001;**7**:435-439
- 15 **Zheng CX**, Zhan WH, Zhao JZ, Zheng D, Wang DP, He YL, Zheng ZQ. The prognostic value of preoperative serum levels of CEA, CA19-9 and CA72-4 in patients with colorectal cancer. *World J Gastroenterol* 2001;**7**:431-434
- 16 **Li XW**, Ding YQ, Cai JJ, Yang SQ, An LB, Qiao DF. Studies on mechanism of Sialy Lewis-X antigen in liver metastases of human colorectal carcinoma. *World J Gastroenterol* 2001;**7**:425-430
- 17 **Cui JH**, Krueger U, Henne-Bruns D, Kremer B, Kalthoff H. Orthotopic transplantation model of human gastrointestinal cancer and detection of micrometastases. *World J Gastroenterol* 2001;**7**:381-386
- 18 **Yuan P**, Sun MH, Zhang JS, Zhu XZ, Shi DR. APC and K-ras gene mutation in aberrant crypt foci of human colon. *World J Gastroenterol* 2001;**7**:352-356
- 19 **Deng YC**, Zhen YS, Zheng S, Xue YC. Activity of boanmycin against colorectal cancer. *World J Gastroenterol* 2001;**7**:93-97
- 20 **Peng ZH**, Xing TH, Qiu GQ, Tang HM. Relationship between Fas/FasL expression and apoptosis of colon adenocarcinoma cell lines. *World J Gastroenterol* 2001; **7**: 88-92
- 21 **Wu BP**, Zhang YL, Zhou DY, Gao CF, Lai ZS. Microsatellite instability, MMR gene expression and proliferation kinetics in colorectal cancer with familial predisposition. *World J Gastroenterol* 2000;**6**:902-905
- 22 **He Y**, Zhou J, Wu JS, Dou KF. Inhibitory effects of EGFR antisense oligodeoxynucleotide in human colorectal cancer cell line. *World J Gastroenterol* 2000;**6**:747-749
- 23 **Jia XD**, Han C. Chemoprevention of tea on colorectal cancer induced by dimethylhydrazine in Wistar rats. *World J Gastroenterol* 2000;**6**:699-703
- 24 **Guo WJ**, Zhou GD, Wu HJ, Liu YQ, Wu RG, Zhang WD. Glutathione S-transferase-pi in colorectal cancer cells. *World J Gastroenterol* 2000;**6**:454-455
- 25 **Wang YX**, Ruan CP, Li L, Shi JH, Kong XT. Clinical significance of changes of perioperative T cell and expression of its activated antigen in colorectal cancer patients. *World J Gastroenterol* 1999;**5**:181-182
- 26 **Hu JY**, Wang S, Zhu JG, Zhou GH, Sun QB. Expression of B7 costimulation molecules by colorectal cancer cells reduces tumorigenicity and induces anti-tumor immunity. *World J Gastroenterol* 1999;**5**:147-151
- 27 **Tan W**, Lin DX, Xiao Y, Kadlubar FF, Chen JS. Chemoprevention of 2-amino-1-methyl-6-phenylimidazo [4,5-b]pyridine-induced carcinogen-DNA adducts by Chinese cabbage in rats. *World J Gastroenterol* 1999;**5**:138-142
- 28 **Liu QZ**, Tuo CW, Wang B, Wu BQ, Zhang YH. Liver metastasis models of human colorectal carcinoma established in nude mice by orthotopic transplantation and their biologic characteristic. *World J Gastroenterol* 1998;**4**:409-411
- 29 **Hu JY**, Su JZ, Pi ZM, Zhu JG, Zhou GH, Sun QB. Radioimmunoimaging of colorectal cancer using ^{99m}Tc labeled monoclonal antibody. *World J Gastroenterol* 1998; **4**: 303-306
- 30 **Taylor I**, Gillams AR. Colorectal liver metastases: alternatives to resection. *J R Soc Med* 2000 ; **93**: 576-579
- 31 **Bleiberg H**, Hendlitz A. Advanced colorectal cancer treatment in Europe: what have we achieved? *Anticancer Drugs* 2002;**13**:461-471
- 32 **Lujan HJ**, Plasencia G, Jacobs M, Viamonte M 3rd, Hartmann RF. Long-term survival after laparoscopic colon resection for cancer: complete five-year follow-up. *Dis Colon Rectum* 2002;**45**:491-501
- 33 **Jass JR**, Young J, Leggett BA. Evolution of colorectal cancer: change of pace and change of direction. *J Gastroenterol Hepatol* 2002;**17**:17-26
- 34 **Wudel LJ**, Chapman WC, Shyr Y, Davidson M, Jeyakumar A, Rogers SO Jr, Allos T, Stain SC. Disparate outcomes in patients with colorectal cancer: effect of race on long-term survival. *Arch Surg* 2002;**137**:550-554
- 35 **Dizon DS**, Kemeny NE. Intrahepatic arterial infusion of chemotherapy: clinical results. *Semin Oncol* 2002;**29**:126-135
- 36 **Ponz D**. Prevention and chemoprevention of colorectal neoplasms. *Dig Liver Dis* 2002;**34**:59-69
- 37 **Kemeny NE**, Ron IG. Hepatic arterial chemotherapy in metastatic colorectal patients. *Semin Oncol* 1999;**26**:524-535
- 38 **McCarthy M**. Arterial chemotherapy improves survival after hepatic metastases. *Lancet* 1999;**353**:1771
- 39 **Ensminger WD**. Intrahepatic arterial infusion of chemotherapy: pharmacologic principles. *Semin Oncol* 2002;**29**:119-125
- 40 **van Riel JM**, van Groenigen CJ, Giaccone G, Pinedo HM. Hepatic arterial chemotherapy for colorectal cancer metastatic to the liver. *Oncology* 2000;**59**:89-97
- 41 **Aldrighetti L**, Arru M, Angeli E, Venturini M, Salvioni M, Ronzoni M, Caterini R, Ferla G. Percutaneous vs. surgical placement of hepatic artery indwelling catheters for regional chemotherapy. *Hepatogastroenterology* 2002;**49**:513-517
- 42 **Howell JD**, Warren HW, Anderson JH, Kerr DJ, McArdle CS. Intra-arterial 5-fluorouracil and intravenous folinic acid in the treatment of liver metastases from colorectal cancer. *Eur J Surg* 1999;**165**:652-658
- 43 **Aldrighetti L**, Arru M, Ronzoni M, Salvioni M, Villa E, Ferla G. Extrahepatic biliary stenoses after hepatic arterial infusion (HAI) of floxuridine (FUDR) for liver metastases from colorectal cancer. *Hepatogastroenterology* 2001; **48**:1302-1307
- 44 **Liu LX**, Jiang HC, Piao DX. Radiofrequency ablation of liver cancers. *World J Gastroenterol* 2002;**8**:393-399
- 45 **Sotsky TK**, Ravikumar TS. Cryotherapy in the treatment of liver metastases from colorectal cancer. *Semin Oncol* 2002;**29**:183-191
- 46 **Livraghi T**. Guidelines for treatment of liver cancer. *Eur J Ultrasound* 2001;**13**:167-176
- 47 **Biasco G**, Gallerani E. Treatment of liver metastases from colorectal cancer: what is the best approach today? *Dig Liver Dis* 2001;**33**:438-444
- 48 **Malik U**, Mohiuddin M. External-beam radiotherapy in the management of liver metastases. *Semin Oncol* 2002;**29**: 196-201
- 49 **Lygidakis NJ**, Sgourakis G, Dedemadi G, Safioleus MC, Nestoridis J. Regional chemoimmunotherapy for nonresectable metastatic liver disease of colorectal origin. A prospective randomized study. *Hepatogastroenterology* 2001; **48**:1085-1087
- 50 **Zanon C**, Grosso M, Clara R, Alabiso O, Chiappino I, Miraglia S, Martinotti R, Bortolini M, Rizzo M, Gazzera

- C. Combined regional and systemic chemotherapy by a mini-invasive approach for the treatment of colorectal liver metastases. *Am J Clin Oncol* 2001;**24**:354-359
- 51 van Riel JM, van Groenigen CJ, Albers SH, Cazemier M, Meijer S, Bleichrodt R, van den Berg FG, Pinedo HM, Giaccone G. Hepatic arterial 5-fluorouracil in patients with liver metastases of colorectal cancer: single-center experience in 145 patients. *Ann Oncol* 2000;**11**:1563-1570
- 52 **Allen-Mersh TG**, Earlam S, Fordy C, Abrams K, Houghton J. Quality of life and survival with continuous hepatic-artery floxuridine infusion for colorectal liver metastases. *Lancet* 1994;**344**:1255-1260
- 53 **Howell JD**, McArdle CS, Kerr DJ, Buckles J, Ledermann JA, Taylor I, Gallagher HJ, Budden J. A phase II study of regional 2-weekly 5-fluorouracil infusion with intravenous folinic acid in the treatment of colorectal liver metastases. *Br J Cancer* 1997;**76**:1390-1393
- 54 **Pelosi E**, Bar F, Battista S, Bello M, Bucchi MC, Alabiso O, Molino G, Bisi G. Hepatic arterial infusion chemotherapy for unresectable confined liver metastases: prediction of systemic toxicity with the application of a scintigraphic and pharmacokinetic approach. *Cancer Chemother Pharmacol* 1999; **44**:505-510
- 55 **Kemeny N**, Fata F. Hepatic-arterial chemotherapy. *Lancet Oncol* 2001;**2**:418-428
- 56 **Fiorentini G**, De Giorgi U, Giovanis P, Guadagni S, Cantore M, Marangolo M. International Society of Regional Cancer Treatment and Societa Italiana di Terapie Integrate Locoregionali in Oncologia. Intra-arterial hepatic chemotherapy (IAHC) for liver metastases from colorectal cancer: need of guidelines for catheter positioning, port management, and anti-coagulant therapy. *Ann Oncol* 2001; **12**:1023
- 57 **Eid A**, Reissman P, Zamir G, Pikarsky AJ. Reconstruction of replaced right hepatic artery, to implant a single-catheter port for intra-arterial hepatic chemotherapy. *Am Surg* 1998; **64**:261-262

Edited by Yan T

• LARGE INTESTINAL CANCER •

Loss of heterozygosity on long arm of chromosome 22 in sporadic colorectal carcinoma

Chong-Zhi Zhou, Zhi-Hai Peng, Fang Zhang, Guo-Qiang Qiu, Lin He

Chong-Zhi Zhou, Zhi-Hai Peng, Fang Zhang, Guo-Qiang Qiu, Department of General Surgery, Shanghai First People Hospital, Shanghai 200080, China

Lin He, Shanghai Institutes for Biological Science, Chinese Academy of Science, Shanghai 200031, China

Supported by the National Natural Science Foundation of China, No. 30080016

Correspondence to: Dr. Zhi-Hai Peng, Department of General Surgery, Shanghai First People Hospital, 85 Wujin Road, Shanghai 200080, China. pengpzhb@online.sh.cn

Telephone: +86-021-63240090 Ext. 3102

Received 2001-11-02 **Accepted** 2001-11-29

Abstract

AIM: The loss of heterozygosity (LOH) on tumor suppressor genes is believed to play a key role in carcinogenesis of colorectal cancer. In this study, we analyzed the LOH at 5 loci on the long arm of chromosome 22 in sporadic colorectal cancer to identify additional loci involved in colorectal tumorigenesis.

METHODS: Five polymorphic microsatellite markers were analyzed in 83 cases of colorectal and normal DNA by PCR. PCR products were electrophoresed on an ABI 377 DNA sequencer; Genescan 3.1 and Genotype 2.1 software were used for LOH scanning and analysis. Comparison between LOH frequency and clinicopathological data were performed by χ^2 test. $P < 0.05$ was considered as statistically significant.

RESULTS: The average LOH frequency on chromosome 22q was 28.38 %. The region between markers D22S280 and D22S274 (22q12.2-q13.33) exhibited relatively high LOH frequency. The two highest LOH loci with frequencies of 35.09 % and 34.04 % was identified on D22S280 (22q12.2-12.3) and D22S274 (22q13.32-13.33). 8 cases showed LOH at all informative loci, suggesting that one chromosome 22q had been completely lost. On D22S274 locus, LOH frequency of rectal cancer was 50 % (9/18), which was higher than that of proximal colon cancer (12 %, 2/17) ($P=0.018$). The frequency of distal colon cancer was 42 % (5/12), also higher than that of proximal colon cancer. But there was no statistical significance. Putting both the tumors in distal colon and rectum together into consideration, the frequency, 47 % (14/30), was higher than that of proximal colon cancer ($P=0.015$), suggesting the mechanism of carcinogenesis was different in both groups.

CONCLUSIONS: This study provided evidence for the involvement of putative tumor suppressor genes related to the sporadic colorectal carcinoma on chromosome 22q. The tumor-suppressor-gene(s) might locate on the 22q12.2-12.3 and/or 22q13.32-13.33.

Zhou CZ, Peng ZH, Zhang F, Qiu GQ, He L. Loss of heterozygosity on long arm of chromosome 22 in sporadic colorectal carcinoma. *World J Gastroenterol* 2002;8(4):668-673

INTRODUCTION

Colorectal cancer is one of the three leading causes of worldwide cancer mortality. The progression of the cancer is thought to result from an accumulation of genetic alteration at numerous loci controlling growth and proliferation. As a model for both multistep and multipathway carcinogenesis, colorectal neoplastic progression provides paradigms of both oncogenes and tumor suppressor genes^[1,2]. The loss of heterozygosity (LOH) on tumor suppressor genes is believed to be one of the key steps to carcinogenesis of colorectal cancer^[3]. The loss of one allele at a specific locus is caused by a deletion mutation or loss of a chromosome from a chromosome pair^[4]. When this occurs at a tumor suppressor gene locus where one of the alleles is already abnormal, it can result in neoplastic transformation. In colorectal cancers, frequent allelic loss has been identified in chromosome 5q (30 %), 8p (40 %), 17p (75-80 %), 18q (80 %), and 22q (20-30 %)^[5,6]. Indeed, much has been published on tumor suppressor genes APC, p53, and DCC, which have been localized to chromosome 5q, 17p, and 18q, respectively. The LOH analysis became an effective way to find informative loci and then to find candidate tumor suppressor genes^[7,8]. In this study we analyzed the LOH at 5 loci on chromosome 22 in sporadic colorectal cancer to identify additional loci involved in colorectal tumorigenesis.

MATERIALS AND METHODS

Materials

This study was based on 83 consecutively collected tumors, including 40 males and 43 females, from unrelated patients with colorectal cancer, treated at the surgical department in Shanghai First people's hospital, China, between 1998 and 1999. The patients' ages ranged from 31 to 84 years with a median of 66. All patients were confirmed by pathology, and were staged by Dukes criterion. Dukes stage A, B, C, D were 8, 21, 40, 14 cases respectively. Well-differentiated adenocarcinoma was 23 cases, moderate differentiated adenocarcinoma was 39, poorly differentiated adenocarcinoma was 6 and mucinous adenocarcinoma was 15. HNPCC patients were ruled out by Amsterdam criteria^[9,10]. Each patient gave his or her informed consent for the use of his or her tissue in this study.

Methods

DNA Extraction The cancerous and adjacent normal tissues were fresh frozen within 30 min after removed. These tissues were then cut into cubes of approximately 2 mm³ and immediately frozen in liquid nitrogen. DNA was extracted using standard methods with proteinase K digestion and phenol/chloroform purification.

Microsatellite Markers and PCR Five fluorescence-labeled primers for polymorphic microsatellite markers (PE Applied Biosystems Foster city CA, USA), at a density of approximately

one marker every 8 cM (Figure 1), was used to amplify matched pairs of normal and tumor DNAs for LOH analysis.

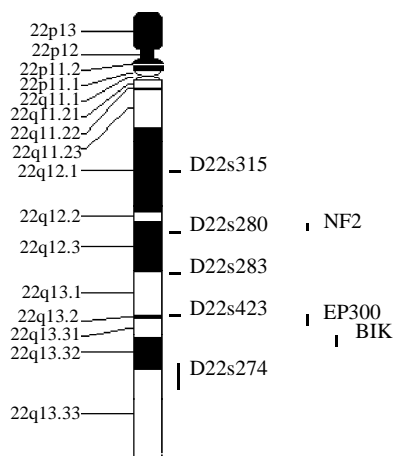


Figure 1 Microsatellite markers and the colorectal cancer related candidate tumor suppressor genes on the long arm of chromosome 22

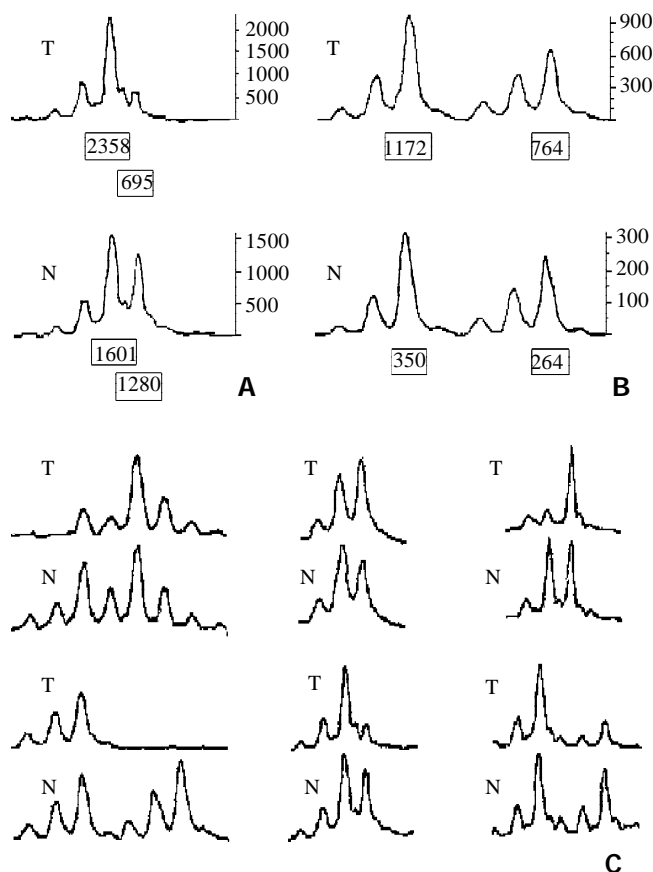


Figure 2 A: The typical peak of LOH: Allele ratio = $(T1/T2)/(N1/N2) = (2358/695)/(1601/1280) = 2.7 > 1.5$; B: The peak of normal (no LOH): Allele ratio = $(T1/T2)/(N1/N2) = (1172/764)/(350/264) = 1.15$; C: Various kinds of typical peaks of LOH
T: Tumor N: Normal

Polymorphic microsatellite markers were analyzed in each patient's tumor and normal DNAs by PCR (GeneAmp PCR System 9700, PE Applied Biosystems Foster city CA, USA). PCR conditions^[11] were as follows: 5 μ l total volume with approximately 1.4 ng of DNA as a template with 10 \times standard buffer, 0.3 μ l Mg^{2+} , 0.8 μ l deoxynucleotide triphosphates, 0.3

unit of Hot-start taq polymerase and 0.06 ml of each oligonucleotide primer, with the forward primer fluorescence labeled with HEX, FAM or NED. Cycling conditions consisted of 3 stages: an initial denaturation at 96 degrees for 12 min in Stage I; 14 cycles each at 94 degrees for 20 sec, 63-56 degrees for 1min (0.5 degrees decreased per cycle), 72 degrees for 1 min in Stage II; 35 cycles each at 94 degrees for 20 sec, 56 degrees for 1 min, 72 degrees for 1 min in stage III.

LOH Analysis A portion of each PCR product (0.5 μ l) was combined with 0.1 μ l of Genescan 500 size standard (PE Applied Biosystems Foster city CA, USA) and 0.9 μ l of formamide loading buffer. After denaturation at 96 degrees for 5 min, products were electrophoresed on a 5 % polyacrylamide gels on an ABI 377 DNA sequencer (PE Applied Biosystems Foster city CA, USA) for 3 hours. Genotype 2.1 software displayed individual gel lanes as electropherograms with a given size, height, and area for each detected fluorescent peak. Stringent criteria were used to score the samples. Alleles were defined as the two highest peaks within the expected size range. A ratio of T1:T2/N1:N2 of less than 0.67 or greater than 1.50 was scored as a loss of heterozygosity (Figure 2). Most amplification of normal DNA produced two PCR products indicating heterozygosity. A single fragment amplified from normal DNA (homozygote) and those PCR reactions in which fragments were not clearly amplified were scored as not informative. The LOH frequency of a locus was equal to the ratio of the number between allelic loss and informative cases. The average LOH frequency of chromosome 22 long arm was the average value of each locus LOH frequency.

Statistics analysis

Comparison between LOH and clinicopathological data were performed by χ^2 test. $P < 0.05$ was considered as statistically significant.

RESULTS

LOH of 5 microsatellite markers on chromosome 22q

The average LOH frequency at chromosome 22 q was 28.38 %. The region between markers D22S280 and D22S274 (22q12.2-q13.33) exhibited relatively high LOH frequency, the two highest LOH loci with frequencies of 35.09 % and 34.04 % was identified on D22S280 (22q12.2-12.3) and D22S274 (22q13.32-13.33). Of these 83 cases, 8 cases had behaved LOH in all informative loci, suggesting that one chromosome 22q had been completely lost (Table 1-2).

Table 1 LOH frequency of 5 microsatellite markers on the long arm of chromosome 22

Locus	Location	LOH case	Normal case	LOH rate (%)	Informative rate (%)
D22S315	22q12.1	12	56	17.65	81.93
D22S280	22q12.2-12.3	20	37	35.09	68.67
D22S283	22q12.3-13.1	17	43	28.33	72.29
D22S423	22q13.2	15	41	26.79	67.47
D22S274	22q13.32-13.33	16	31	34.04	56.63

The relationship of clinicopathological features and LOH on chromosome 22

On D22S274 locus, LOH frequency of rectal cancer was 50 % (9/18), which was higher than that of proximal colon cancer (12 %, 2/17) ($P = 0.018$). The frequency of distal colon cancer

was 42 % (5/12), which was also higher than the frequency of proximal colon cancer. But there was no statistical significance. Putting both the tumors in distal colon and rectum together into consideration, the frequency, 47 % (14/30), was higher than that

of proximal colon cancer ($P=0.015$). There was no association between LOH of each marker on chromosome 22q and other clinicopathological data (patient sex, age, tumor size, growth pattern or Dukes stage). It indicated that LOH of 22q was a

Table 2 Clinicopathological features of 8 cases of sporadic colorectal carcinoma who behaved LOH in all informative loci

No	Gender	Age	Location	Gross Pattern	Size (cm)	Differentiation	Dukes stage
125	Female	52	Sigmoid Colon	Ulcerative	5.5×4	Moderately	A
128	Male	70	Descending Colon	Ulcerative	4×4.5	Moderately	C
134	Female	70	Ascending Colon	Massive	5×5.5	Moderately	C
137	Female	76	Sigmoid Colon	Ulcerative	6×6	Moderately	C
138	Female	66	Rectum Colon	Ulcerative	3×3	Well	A
210	Female	41	Ascending Colon	Massive	5×4	Well	A
220	Female	79	Ascending Colon	Massive	7×4	Well	B
223	Male	63	Rectum	Encroaching	6×6.5	Moderately	D

Table 3 The relationship between clinicopathological features and LOH of 5 loci on chromosome 22

		D22S315		D22S280		D22S283		D22S423		D22S274	
		N	L	N	L	N	L	N	L	N	L
Gender	Male	28	6	19	7	21	7	22	5	13	8
	Female	28	6	18	13	22	10	19	10	18	8
Age	>60	41	9	24	19	31	15	30	11	22	13
	≤60	15	3	13	1	12	2	11	4	9	3
Location	Proximal Colon	21	4	13	7	18	5	14	6	15	2
	Distal Colon	13	4	12	4	11	5	12	6	7	5 ^b
	Rectum	22	4	12	9	14	7	15	3	9	9 ^a
Gross Pattern	Massive	23	4	16	8	19	7	16	6	11	5
	Ulcerative	21	7	15	9	14	7	18	7	14	9
	Encroaching	12	1	6	3	10	3	7	2	6	2
Size	≥5(cm)	25	7	14	11	20	8	18	10	17	5
	<5(cm)	31	5	23	9	23	9	23	5	14	11
LN Metastasis	LN(+)	36	9	26	13	31	11	26	11	24	7
	LN(-)	20	3	11	7	12	6	15	4	7	9
Differentiation	Well	15	3	8	6	13	3	11	5	7	5
	Moderately	28	3	17	10	19	10	24	5	15	7
	Poorly	3	3	4	2	3	1	1	2	3	3
	Mucinous	10	3	8	2	8	3	5	3	6	1
Dukes stage	A	3	3	1	3	3	2	3	2	2	4
	B	17	1	10	4	9	4	12	2	5	5
	C	26	4	18	11	22	9	19	7	16	5
	D	10	4	8	2	9	2	7	4	8	2

^a $P=0.018$, the LOH frequency of rectal cancer vs. that of proximal colon cancer

^b $P=0.015$, the LOH frequency of cancer in distal colon and rectum vs. that of proximal colon cancer

DISCUSSION

During tumorigenesis, loss of the wild-type allele (inherited from the non-mutation-carrying parents) is frequently observed at the appropriate locus. To date, loss of heterozygosity (LOH) on tumor suppressor genes plays a key role in colorectal cancer transformation^[3]. And LOH analysis of sporadic colorectal cancer can promote the discovery of unknown tumor suppressor genes^[7,8]. In this study, LOH scanning was carried out in 83 sporadic colorectal cancer samples with 5 highly polymorphic markers and analyzed by Genotyper software,

that is, by the ratio of the fluorescence intensity of allele, with an effort to identifying additional loci involved in colorectal tumorigenesis.

In this study, the average LOH frequency of chromosome 22q is 28.38 %, which is consistent with previous observations^[5,6]. D22S280 (22q12.2-12.3) and D22S274 (22q13.32-13.33) exhibited highest LOH frequency, indicating that colon cancer related tumor suppressor gene(s) located in this region and perhaps near D22S280 or/and D22S274. The previous study showed that 22q13.1-13.3 behaved high LOH frequency in

sporadic colorectal cancer^[12,13]. This study is consistent with the finding, and also showed that 22q12.2-12.3 existed obvious LOH phenomenon, which was similar to the pancreatic adenocarcinomas^[14].

By database referring, there are three candidate tumor-suppressor genes related to colon cancer, NF2 (22q12.2)^[15], EP300 (22q13)^[16], NBK/BIK (22q13.3)^[17] on 22q12.2-13.33. NF2 gene was confirmed to be a tumor-suppressor-gene in neurofibromatosis type 2 syndrome^[18-21]. And NF2 gene inactivation was also reported in NF2-associated tumor and some sporadic cancer^[22-28]. NF2 gene encodes a 587-amino acid protein with striking similarity to several members of the ERM family of proteins proposed to link cytoskeletal components with proteins in the cell membrane, including moesin, ezrin, and radixin. Because of the resemblance to these 3 proteins, Trofatter *et al* called the NF2 gene product merlin^[29]. Stokowski *et al*^[30] found that 80 % of the merlin mutants significantly altered cell adhesion by causing cells to detach from the substratum. They stated that such changes in cell adhesion might be an initial step in the pathogenesis of NF2. And some scholars also studied the relationship between NF2 gene and sporadic colorectal cancer and found that NF2 gene was probably involved in some colorectal tumors, but was not the critical chromosome 22q tumor suppressor gene involved in colon tumorigenesis^[31,32]. The results of this study suggested that there might be colon cancer related candidate tumor-suppressor-gene(s) on 22q12.2 and NF2 was the only known tumor-suppressor-gene in this region. So it was needed to evaluate the effect of NF2 gene on colorectal carcinogenesis, and the new tumor suppressor gene involved in colon tumorigenesis can not be excluded absolutely. There were 2 putative tumor-suppressor genes on 22q13.2-13.31, EP300 and NBK/BIK^[33]. P300 is the number of the retinoblastoma protein family. Stein *et al*^[34] supposed that p300 acted as a tumor suppressor firstly. Recently, Hasan *et al*^[35] proposed the p300 might participate in chromatin remodeling at DNA lesion sites to facilitate proliferating cell nuclear antigen (PCNA) function in DNA repair synthesis. Muraoka *et al*^[36] raised the possibility that inactivation of EP300 gene was involved in the genesis or progression of colorectal cancer. And Gayther *et al*^[37] described EP300 mutations that predicted a truncated protein in 6 (3 %) of 193 epithelial cancers analyzed and provided the first evidence that it behaved as a classic tumor suppressor gene. But EP300 mutation was rare in colorectal cancer tissue. So Castells *et al*^[12] presumed that NBK/BIK gene, a proapoptotic BCL-2 family member^[38-41], acted as a candidate gene in that region. However, SSCP sequencing analysis excluded mutations of this gene. The results of this study showed that the LOH frequency was also high on 22q13, especial on 22q13.32-13.33, suggesting that colorectal cancer associated candidate tumor-suppressor genes are likely to locate on chromosome 22q13.

Yana *et al*^[13] indicated that loss of heterozygosity correlated with Dukes staging. Iino *et al*^[42] suggested that allelic loss on 22q was significantly associated with the presence of lymph node metastasis. However, Castells *et al*^[12] did not support their opinion. This result also agreed with Castells' study and suggested that there was no association between LOH of each marker on chromosome 22q and Dukes staging. However, we found on D22S274 locus, LOH frequency of rectal cancer was higher than that of proximal colon cancer. And the frequency of the tumors in distal colon and rectum was also higher than that of the tumors in proximal colon cancer. Now it was admitted that the mechanism of carcinogenesis in distal colon was different from that in proximal colon^[43-45]. And the mechanism in rectal cancer was also different from that in the

common phenomenon in sporadic colorectal cancer (Table 3). proximal colon^[46]. Distal colonic cancer displayed a higher frequency of 17p and 18q allelic loss, p53 accumulation^[47], *c-myc* expression and aneuploidy^[48]. Right-sided tumors are more often diploid^[48] and of the microsatellite instability (MSI) phenotype. Rectal cancers showed significantly more expression of p53 than that in proximal colon cancer^[46], which was similar with distal colonic cancer. This study showed the D22S274 LOH was more frequent in distal colon and rectal cancer than in proximal colon ones, which proved the mechanism of carcinogenesis in distal colon and rectum was not completely same as that in the proximal colon.

Allelic loss on chromosome 22q is present not only in colorectal cancer but also in carcinomas of the ovary (55 %)^[49-52], breast (40 %)^[53-55], pancreatic endocrine (30 %)^[27], oral cavity (40 %)^[56], stomach^[57], liver^[58], lung^[59], head and neck^[60], and insulinoma^[61]. After microsatellite DNA analysis, several attempts were made to identify a region of deletion and eventually the tumor suppressor genes responsible for these neoplasms. Allelic deletions were restricted to D22S274 (22q13) marker in oral squamous cell carcinoma^[56]. Handel-Fernandez *et al* found that LOH region presented between marker D22S444 and D22S922 (22q13.2-q13.3), indicating the locations of tumor suppressor genes that may contribute to the development of pancreatic cancer^[14]. Considering these results, it is tempting to hypothesize that the same putative tumor suppressor genes might be involved in these different neoplastic processes. Further LOH scanning with high-density microsatellite markers in the region and the study of the relationship between these genes and the carcinogenesis of sporadic colorectal cancer may provide much more genetic information and find the potential tumor suppressor genes.

REFERENCES

- 1 Fearon ER, Vogelstein B. A genetic model for colorectal tumorigenesis. *Cell* 1990; **61**:759-767
- 2 Hardy RG, Meltzer SJ, Jnkowski JA. ABC of colorectal cancer: Molecular basis for risk factors. *BMJ* 2000; **321**:886-889
- 3 Kataoka M, Okabayashi T, Johira H, Nakatani S, Nakashima A, Takeda A, Nishizaki M, Orita K, Tanaka N. Aberration of p53 and DCC in gastric and colorectal cancer. *Oncol Rep* 2000; **7**:99-103
- 4 Lengauer C, Kinzler KW, Vogelstein B. Genetic instabilities in human cancers. *Nature* 1998; **396**: 643-649
- 5 Vogelstein B, Fearon ER, Kern SE, Hamilton SR, Preisinger AC, Nakamura Y, White R. Allelotype of colorectal carcinomas. *Science* 1989; **244**:207-211
- 6 Weber TK, Conroy J, Keitz B, Rodriguez-Bigas M, Petrelli NJ, Stoler DL, Anderson GR, Shows TB, Nowak NJ. Genome-wide allelotyping indicates increased loss of heterozygosity on 9p and 14q in early age of onset colorectal cancer. *Cytogenet Cell Genet* 1999; **86**:142-147
- 7 Baker SJ, Fearon ER, Nigro JM, Hamilton SR, Preisinger AC, Jessup JM, vanTuinen P, Ledbetter DH, Barker DF, Nakamura Y, White R, Vogelstein B. Chromosome 17 deletions and p53 gene mutations in colorectal carcinomas. *Science* 1989; **244**:217-221
- 8 Kinzler KW, Nilbert MC, Vogelstein B, Bryan TM, Levy DB, Smith KJ, Preisinger AC, Hamilton SR, Hedge P, Markham A, Carlson M, Joslyn G, Groden J, White R, Miki Y, Miyoshi Y, Nishisho I, Nakamura Y. Identification of a gene located at chromosome 5q21 that is mutated in colorectal cancers. *Science* 1991; **251**:1366-1370
- 9 Vasen HF, Mecklin JP, Khan PM, Lynch HT. The International Collaborative Group on Hereditary Non-Polyposis Colorectal Cancer (ICG-HNPCC). *Dis Colon Rectum* 1991; **34**:424-425

- 10 **Vasen HF**, Watson P, Mecklin JP, Lynch HT. New clinical criteria for hereditary nonpolyposis colorectal cancer (HNPCC, Lynch syndrome) proposed by the International Collaborative group on HNPCC. *Gastroenterology* 1999; **116**: 1453-1456
- 11 **Peng Z**, Ling Y, Bai S, Tang H, Zhou C, Qiu G, Liu W, He L, Xie KP. Loss of heterozygosity on chromosome 3 in sporadic colorectal carcinoma. *Zhonghua Yixue Zazhi* 2001; **81**: 336-339
- 12 **Castells A**, Ino Y, Louis DN, Ramesh V, Gusella JF, Rustgi AK. Mapping of a target region of allelic loss to a 0.5-cM interval on chromosome 22q13 in human colorectal cancer. *Gastroenterology* 1999; **117**:831-837
- 13 **Yana I**, Kurahashi H, Nakamori S, Kameyama M, Nakamura T, Takami M, Mori T, Takai S, Nishisho I. Frequent loss of heterozygosity at telomeric loci on 22q in sporadic colorectal cancers. *Int J Cancer* 1995; **17**:60:174-177
- 14 **Handel-Fernandez ME**, Nassiri M, Arana M, Perez MM, Fresno M, Nadji M, Vincek V. Mapping of genetic deletions on the long arm of chromosome 22 in human pancreatic adenocarcinomas. *Anticancer Res* 2000; **20**:4451-4456
- 15 **Arai E**, Ikeuchi T, Karasawa S, Tamura A, Yamamoto K, Kida M, Ichimura K, Yuasa Y, Tonomura A. Constitutional translocation t(4;22)(q12;q12.2) associated with neurofibromatosis type 2. *Am J Med Gene* 1992; **44**: 163-167
- 16 **Eckner R**, Ewen ME, Newsome D, Gerdes M, DeCaprio JA, Lawrence JB, Livingston DM. Molecular cloning and functional analysis of the adenovirus E1A-associated 300-kD protein (p300) reveals a protein with properties of a transcriptional adaptor. *Genes Dev* 1994; **8**:869-884
- 17 **Verma S**, Budarf ML, Emanuel BS, Chinnadurai G. Structural analysis of the human pro-apoptotic gene Bik: chromosomal localization, genomic organization and localization of promoter sequences. *Gene* 2000; **254**: 157-162
- 18 **Seizinger BR**, Rouleau G, Ozelius LJ, Lane AH, George-Hyslop P, Huson S, Gusella JF, Martuza RL. Common pathogenetic mechanism for three tumor types in bilateral acoustic neurofibromatosis. *Science* 1987; **236**:317-319
- 19 **Evans DGR**, Trueman L, Wallace A, Collins S, Strachan T. Genotype/phenotype correlations in type 2 neurofibromatosis (NF2): evidence for more severe disease associated with truncating mutations. *J Med Genet* 1998; **35**:450-455
- 20 **Legoux P**, Legrand MF, Ollagnon E, Lenoir G, Thomas G, Zucman-Rossi J. Characterisation of 16 polymorphic markers in the NF2 gene: application to hemizygosity detection. *Hum Mutat* 1999; **13**: 290-293
- 21 **Bruder CEG**, Hirvela C, Tapia-Paez I, Fransson I, Segraves R, Hamilton G, Zhang XX, Evans DG, Wallace AJ, Baser ME, Zucman-Rossi J, Hergersberg M. High resolution deletion analysis of constitutional DNA from neurofibromatosis type 2 (NF2) patients using microarray-CGH. *Hum Molec Genet* 2001; **10**: 271-282
- 22 **Kluwe L**, Mautner VF. Mosaicism in sporadic neurofibromatosis 2 patients. *Hum Molec Genet* 1998; **7**: 2051-2055
- 23 **Kluwe L**, Friedrich RE, Hage C, Lindenau M, Mautner VF. Mutations and allelic loss of the NF2 gene in neurofibromatosis 2-associated skin tumors. *J Invest Derm* 2000; **114**: 1017-1021
- 24 **Fukasawa T**, Chong JM, Sakurai S, Koshiishi N, Ikeno R, Tanaka A, Matsumoto Y, Hayashi Y, Koike M, Fukayama M. Allelic loss of 14q and 22q, NF2 mutation, and genetic instability occur independently of c-kit mutation in gastrointestinal stromal tumor. *Jpn J Cancer Res* 2000; **91**:1241-1249
- 25 **Gutmann DH**, Hirbe AC, Haipek CA. Functional analysis of neurofibromatosis 2 (NF2) missense mutations. *Hum Mol Genet* 2001; **10**: 1519-1529
- 26 **Cheng JQ**, Lee WC, Klein MA, Cheng GZ, Jhanwar SC, Testa JR. Frequent mutations of NF2 and allelic loss from chromosome band 22q12 in malignant mesothelioma: evidence for a two-hit mechanism of NF2 inactivation. *Genes Chromosomes Cancer* 1999; **24**: 238-242
- 27 **Schulze KM**, Hanemann CO, Muller HW, Hanenberg H. Transduction of wild-type merlin into human schwannoma cells decreases schwannoma cell growth and induces apoptosis. *Hum Mol Genet* 2002; **11**: 69-76
- 28 **Quezado MM**, Middleton LP, Bryant B, Lane K, Weiss SW, Merino MJ. Allelic loss on chromosome 22q in epithelioid sarcomas. *Hum Pathol* 1998; **29**:604-608
- 29 **Trofatter JA**, MacCollin MM, Rutter JL, Murrell JR, Duyao MP, Parry DM, Eldridge R, Kley N, Menon AG, Pulaski K, Haase VH, Ambrose CM, Munroe D, Bove C, Haines JL, Martuza RL, MacDonald ME, Seizinger BR, Short MP, Buckler AJ, Gusella JF. A novel moesin-, ezrin-, radixin-like gene is a candidate for the neurofibromatosis 2 tumor suppressor. *Cell* 1993; **72**: 791-800
- 30 **Stokowski RP**, Cox DR. Functional analysis of the neurofibromatosis type 2 protein by means of disease-causing point mutations. *Am J Hum Genet* 2000; **66**: 873-891
- 31 **Arakawa H**, Hayashi N, Nagase H, Ogawa M, Nakamura Y. Alternative splicing of the NF2 gene and its mutation analysis of breast and colorectal cancers. *Hum Mol Genet* 1994; **3**: 565-568
- 32 **Rustgi AK**, Xu L, Pinney D, Sterner C, Beauchamp R, Schmidt S, Gusella JF, Ramesh V. Neurofibromatosis 2 gene in human colorectal cancer. *Cancer Genet Cytogenet* 1995; **84**:24-26
- 33 **Zou Y**, Peng H, Zhou B, Wen Y, Wang SC, Tsai EM, Hung MC. Systemic tumor suppression by the proapoptotic gene bik. *Cancer Res* 2002; **62**:8-12
- 34 **Stein RW**, Corrigan M, Yaciuk P, Whelan J, Moran E. Analysis of E1A-mediated growth regulation functions: binding of the 300-kilodalton cellular product correlates with E1A enhancer repression function and DNA synthesis-inducing activity. *J Virol* 1990; **64**:4421-4427
- 35 **Hasan S**, Hassa PO, Imhof R, Hottiger MO. Transcription coactivator p300 binds PCNA and may have a role in DNA repair synthesis. *Nature* 2001; **410**: 387-391
- 36 **Muraoka M**, Konishi M, Kikuchi-Yanoshita R, Tanaka K, Shitara N, Chong JM, Iwama T, Miyaki M. p300 gene alterations in colorectal and gastric carcinomas. *Oncogene* 1996; **12**: 1565-1569
- 37 **Gayther SA**, Batley SJ, Linger L, Bannister A, Thorpe K, Chin SF, Daigo Y, Russell P, Wilson A, Sowter HM, Delhanty JDA, Ponder BAJ, Kouzarides T, Caldas C. Mutations truncating the EP300 acetylase in human cancers. *Nature Genet* 2000; **24**: 300-303
- 38 **Boyd JM**, Gallo GJ, Elangovan B, Houghton AB, Malstrom S, Avery BJ, Ebb RG, Subramanian T, Chittenden T, Lutz RJ, Chinnadurai G. Bik, a novel death-inducing protein shares a distinct sequence motif with Bcl-2 family proteins and interacts with viral and cellular survival-promoting proteins. *Oncogene* 1995; **11**: 1921-1928
- 39 **Han J**, Sabbatini P, White E. Induction of apoptosis by human Nbk/Bik, a BH3-containing protein that interacts with E1B 19K. *Molec Cell Biol* 1996; **16**: 5857-5864
- 40 **Radetzki S**, Kohne CH, von Haefen C, Gillissen B, Sturm I, Dorken B, Daniel PT. The apoptosis promoting Bcl-2 homologues Bak and Nbk/Bik overcome drug resistance in Mdr-1-negative and Mdr-1-overexpressing breast cancer cell lines. *Oncogene* 2002; **21**:227-238
- 41 **Marshansky V**, Wang X, Bertrand R, Luo H, Duguid W, Chinnadurai G, Kanaan N, Vu MD, Wu J. Proteasomes modulate balance among proapoptotic and antiapoptotic Bcl-2 family members and compromise functioning of the electron transport chain in leukemic cells. *J Immunol* 2001; **166**:3130-3142
- 42 **Iino H**, Fukayama M, Maeda Y, Koike M, Mori T, Takahashi T, Kikuchi-Yanoshita R, Miyaki M, Mizuno S, Watanabe S. Molecular genetics for clinical management of colorectal carcinoma. 17p, 18q, and 22q loss of heterozygosity and decreased DCC expression are correlated with the metastatic potential. *Cancer* 1994; **73**:1324-1331
- 43 **Buflin JA**. Colorectal cancer: evidence for distinct genetic categories based on proximal or distal tumor location. *Ann*

- Intern Med* 1990; **113**: 779-788
- 44 **Distler P**, Holt PR. Are right- and left-sided colon neoplasms distinct tumors? *Dig Dis* 1997; **15**:302-311
 - 45 **Lindblom A**. Different mechanisms in the tumorigenesis of proximal and distal colon cancers. *Curr Opin Oncol* 2001; **13**: 63-69
 - 46 **Kapiteijn E**, Liefers GJ, Los LC, Kranenbarg EK, Hermans J, Tollenaar RA, Moriya Y, van de Velde CJ, van Krieken JH. Mechanisms of oncogenesis in colon versus rectal cancer. *J Pathol* 2001; **195**:171-178
 - 47 **Soong R**, Grieu F, Robbins P, Dix B, Chen D, Parsons R, House A, Iacopetta B. p53 alterations are associated with improved prognosis in distal colonic carcinomas. *Clin Cancer Res* 1997; **3**: 1405-1411
 - 48 **Lanza G Jr**, Maestri I, Dubini A, Gafa R, Santini A, Ferretti S, Cavazzini L. p53 expression in colorectal cancer: relation to tumor type, DNA ploidy pattern and short-term survival. *Am J Clin Pathol* 1996; **105**:604-612
 - 49 **Bryan EJ**, Watson RH, Davis M, Hitchcock A, Foulkes WD, Campbell IG. Localization of an ovarian cancer tumor suppressor gene to a 0.5-cM region between D22S284 and CYP2D, on chromosome 22q. *Cancer Res* 1996; **56**: 719-721
 - 50 **Englefield P**, Foulkes WD, Campbell IG. Loss of heterozygosity on chromosome 22 in ovarian carcinoma is distal to and is not accompanied by mutations in NF2 at 22q12. *Br J Cancer* 1994; **70**: 905-907
 - 51 **Lin H**, Pizer ES, Morin PJ. A frequent deletion polymorphism on chromosome 22q13 identified by representational difference analysis of ovarian cancer. *Genomics* 2000; **69**:391-394
 - 52 **Bryan EJ**, Thomas NA, Palmer K, Dawson E, Englefield P, Campbell IG. Refinement of an ovarian cancer tumour suppressor gene locus on chromosome arm 22q and mutation analysis of CYP2D6, SREBP2 and NAGA. *Int J Cancer* 2000; **87**:798-802
 - 53 **Allione F**, Eisinger F, Parc P, Noguchi T, Sobol H, Birnbaum D. Loss of heterozygosity at loci from chromosome arm 22Q in human sporadic breast carcinomas. *Int J Cancer* 1998; **75**:181-186
 - 54 **Iida A**, Kurose K, Isobe R, Akiyama F, Sakamoto G, Yoshimoto M, Kasumi F, Nakamura Y, Emi M. Mapping of a new target region of allelic loss to a 2-cM interval at 22q13.1 in primary breast cancer. *Genes Chromosomes Cancer* 1998; **21**: 108-112
 - 55 **Castells A**, Gusella JF, Ramesh V, Rustgi AK. A region of deletion on chromosome 22q13 is common to human breast and colorectal cancers. *Cancer Res* 2000; **60**: 2836-2839
 - 56 **Miyakawa A**, Wang XL, Nakanishi H, Imai FL, Shiiba M, Miya T, Imai Y, Tanzawa H. Allelic loss on chromosome 22 in oral cancer: possibility of the existence of a tumor suppressor gene on 22q13. *Int J Oncol* 1998; **13**: 705-709
 - 57 **Sud R**, Wells D, Talbot IC, Delhanty JD. Genetic alterations in gastric cancers from British patients. *Cancer Genet Cytogenet* 2001; **126**:111-119
 - 58 **Takahashi K**, Kudo J, Ishibashi H, Hirata Y, Niho Y. Frequent loss of heterozygosity on chromosome 22 in hepatocellular carcinoma. *Hepatology* 1993; **17**:794-799
 - 59 **Nishioka M**, Kohno T, Takahashi M, Niki T, Yamada T, Sone S, Yokota J. Identification of a 428-kb homozygously deleted region disrupting the SEZ6L gene at 22q12.1 in a lung cancer cell line. *Oncogene* 2000; **19**:6251-6260
 - 60 **Poli-Frederico RC**, Bergamo NA, Reis PP, Kowalski LP, Zielenska M, Squire JA, Rogatto SR. Chromosome 22q a frequent site of allele loss in head and neck carcinoma. *Head Neck* 2000; **22**:585-590
 - 61 **Wild A**, Langer P, Ramaswamy A, Chaloupka B, Bartsch DK. A novel insulinoma tumor suppressor gene locus on chromosome 22q with potential prognostic implications. *J Clin Endocrinol Metab* 2001; **86**:5782-5787

Edited by Zhang JZ

• LARGE INTESTINAL CANCER •

Transforming growth factor- β 1 in invasion and metastasis in colorectal cancer

Bin Xiong, Hong-Yin Yuan, Ming-Bo Hu, Feng Zhang, Zheng-Zhuan Wei, Ling-Ling Gong, Guo-Liang Yang

Bin Xiong, Hong-Yin Yuan, Ming-Bo Hu, Feng Zhang, Zheng-Zhuan Wei, Ling-Ling Gong, Guo-Liang Yang, Department of Oncology, Affiliated Zhongnan Hospital of Wuhan University, Wuhan 430071, Hubei Province, China

Supported by Hubei Province Natural Science Foundation, No. 2000J054

Correspondence to: Dr. Bin Xiong, Department of Oncology, Affiliated Zhongnan Hospital of Wuhan University, Wuhan 430071, Hubei Province, China. xbxh@public.wh.hb.cn

Telephone: +86-27-87325716

Received 2001-08-08 **Accepted** 2001-09-20

Abstract

AIM: To investigate the role of TGF β 1 in invasion and metastasis in colorectal cancer by analysing TGF β 1 correlated with depth of tumor invasion, stage and metastasis.

METHODS: Serum TGF β 1 levels were determined in 50 patients with colorectal cancer and 30 healthy volunteers using a TGF β 1 enzyme-linked immunosorbent assay. TGF β 1 expression in primary and lymph node metastatic lesions were detected in 98 cases of colorectal cancer by immunohistochemical staining and *in situ* hybridization.

RESULTS: Serum levels of TGF β 1 in patients with colorectal cancer ($40 \pm 18 \text{ mg} \cdot \text{L}^{-1}$) were significantly higher than those in the healthy control group ($19 \pm 8 \text{ mg} \cdot \text{L}^{-1}$), $P < 0.05$. Elevated levels of serum TGF β 1 were found in 60 % of patients with colorectal cancer when the mean $+2 \text{ s}$ was used as the upper limit of the normal range ($35.1 \text{ mg} \cdot \text{L}^{-1}$). Increases in serum TGF β 1 levels were significantly associated with Duke's stage ($P < 0.05$), but there was no significant difference between Duke's stage B patients and Duke's stage C patients. In the cytoplasm of cancer cells, TGF β 1 was immunostained in 37.8 % (37/98) of colorectal cancer, and this expression was confirmed by *in situ* hybridization. Among 35 cases of colorectal cancer with lymph node metastatic lesions, TGF β 1 positive staining was found in 18 (51.4 %) cases of primary tumor, and 25 (71.4 %) cases with lymph node metastatic lesions, respectively. Of 17 cases with no staining in the primary lesion, 7 (41.2%) cases showed TGF β 1 staining in the metastatic lesion. Serum TGF β 1 levels and TGF β 1 expression in colorectal cancer tissues were correlated significantly with depth of tumor invasion, stage and metastasis. Patients in stage C-D, T3-T4 and with metastasis had significantly higher TGF β 1 levels than patients in stage A-B, T1-T2 and without metastasis ($P < 0.05$).

CONCLUSION: These results suggest that transforming growth factor- β 1 is closely related to the invasion and metastasis of colorectal cancer. It increased the

invasive and metastatic potential of tumor by altering a tumor microenvironment. TGF β 1 may be used as a possible biomarker.

Xiong B, Yuan HY, Hu MB, Zhang F, Wei ZZ, Gong LL, Yang GL. Transforming growth factor- β 1 in invasion and metastasis in colorectal cancer. *World J Gastroenterol* 2002; 8(4):674-678

INTRODUCTION

The incidence of colorectal cancer has become high in China and its biology is a hot topic of research^[1-44]. Tumor invasion and metastasis are complex processes in which cancer cells detach from the original tumor mass to establish metastatic foci at distant sites. Metastatic cells characteristically lose growth inhibitory responses, undergo alteration in adhesiveness and demonstrate enhanced production of enzymes that can degrade extracellular matrix components. Since it is the development of metastatic disease that is primarily responsible for cancer mortality, an understanding of the mechanisms that facilitate metastatic tumor progression is of great importance^[1]. Transforming growth factor (TGF)- β 1 is a 25-kd polypeptides. This growth factor regulates cell growth and differentiation in both normal and transformed cells. TGF- β 1 was found to inhibit the growth of normal and neoplastic cells. Resistance to the negative growth-regulating properties of TGF- β 1 has been observed in epithelial and mesenchymal tumors. Tumor cell lines that lack TGF- β receptors lose responsiveness to TGF- β 1, and the escape of cells from TGF- β 1 mediated negative regulation is linked to tumor progression^[45]. Colorectal cancer is one of the most malignant neoplasms. TGF- β 1 plays a crucial role in tumor extension. We examined the expression of TGF- β 1 in primary and lymph node metastatic lesions in colorectal cancer, as well as serum TGF- β 1 levels in the peripheral veins. Our objective is to determine the clinical significance of TGF- β 1 in advance of colorectal cancer.

MATERIALS AND METHODS

Patients

Serum TGF- β 1 assays were performed in 50 patients treated from July 1999 to June 2000. There were 32 men and 18 women, and their age ranged from 23 to 74 years (means, 53 ± 11 years). According to Duke's staging criteria, 9 cases were stage I, 18 stage II, 18 stage III and 5 stage IV. Thirty healthy volunteers were selected as control group among whom there were 17 men and 13 women. Their age ranged from 20 to 56 years (means, 45 ± 8 years).

A total of 98 colorectal adenocarcinoma patients (including the 50 patients above) who had undergone surgical resection in the Affiliated Zhongnan Hospital of Wuhan University (Wuhan, China) from July 1998 to December 2000, TGF β 1 and TGF β R II immunohistochemical staining and *in situ* hybridization were performed. There were 53 men and 45 women, and their age ranged from 23 to 74 years (means,

56 \pm 11 years). Among 98 patients, 17 were well differentiated adenocarcinoma, 47 moderately differentiated adenocarcinoma and 34 poorly differentiated adenocarcinoma. According to Duke's staging criteria, 34 cases were stage I, 29 stage II, 30 stage III and 5 stage IV.

Methods

Preparation of serum sample and TGF β 1 assay Two mL of blood sample, collected from the peripheral vein before surgery, were stored for approximately 3 h at 4 °C until the samples were centrifuged. Blood samples were centrifuged at 3 000 g for 20 min. The serum was separated and stored frozen at -70 °C until the time of analysis. TGF β 1 was assayed using human TGF β 1 enzyme-linked immunoabsorbent assay kits. The ELISA kits were obtained from Quantikine Co. of USA. The TGF β 1 assay was performed according to the methods outlined in the package insert. Standard samples of 200 μ g were added to each well, and incubated for 3 h at room temperature. After complete wash of each well, 200 μ l TGF β 1 conjugate was added to each well and these were incubated for 1.5 h at room temperature. We repeated the aspiration/wash and added 200 μ l of substrate solution to each well and incubated for 20 min. Finally, we added 50 μ l of stop solution and absorbances in each well were measured using a spectrophotometric plate reader at a wavelength of 490 nm. To determine the TGF- β 1 concentration in each sample, we first calculated the average absorbance value in each set of duplicates. Serum levels of TGF- β 1 were calculated from linear regression equation.

Immunohistochemistry All the tissue specimens were fixed in 100 mL \cdot L⁻¹ neutral formalin and embedded in paraffin. Five-um thick sections were xylene dehydrated in ethanol. Tissue sections were washed three times in 0.05 mol \cdot L⁻¹ PBS, and incubated in endogenous peroxidase blocking solution. Non-specific antibody binding was blocked by pretreatment with PBS containing 5g \cdot L⁻¹ bovin serum albumin. Sections were then rinsed in PBS and incubated overnight at 4 °C with diluted anti-TGF β 1 and anti-TGF β R II protein polyclonal antibody. The steps were performed using Immunostain kit according to the manufacturer's instructions. PBS was used as substitutes of protein antibody for negative control groups. The sections were examined under light microscopy. Anti-TGF β 1 and anti-TGF β R II protein polyclonal antibody were purchased from Bosden Comp. (Wuhan, China). S-P detection kit was purchased from Fuzhou Maixin Comp. (Fuzhou, China). Anti-TGF β 1 and anti-TGF β R II protein polyclonal antibody were diluted to 1:100.

In situ hybridization All the tissue specimens were fixed in 100 mL \cdot L⁻¹ neutral formalin and embedded in paraffin. Six-um thick sections were xylene dehydrated in ethanol, and digested with 10 mg \cdot L⁻¹ proteinase for 10 min. Sections were washed in 0.5 mol \cdot L⁻¹ PBS for 15 min. They were incubated overnight at 37 °C with the 500 μ g \cdot L⁻¹ digoxigenin-labeled RNA probe in hybridization buffer. After hybridization, sections were washed in 2 \times SSC for 10 min at 37 °C and finally in 0.2 \times SSC for 15 min at 37 °C. Sections were incubated with alkaline phosphatase-conjugated anti-digoxigenin antibody for 60 min at 37 °C. The steps were performed using in situ hybridization kit according to the manufacturer's instructions. The kits were purchased from Bosden Comp. (Wuhan, China).

TGF β 1 *in situ* hybridization probe sequences were:

- (1)5-CGTTTCACCAGCTCCATGTCGATGGTCTTGCAAT-3'
(2)5-CTTGATTTTAATCTCTGCAAGCGCAGCTCTGCACG-3'

(3)5-TTGGTATCCAGGGCTCTCCGGTGCCGTGAGCTGTG-3'

Statistical analysis

The difference between each group was analyzed by Chi-square test and correlativity. The limit of significant difference was $P < 0.05$.

RESULTS

Serum TGF β 1 levels in patients with colorectal cancer

Serum TGF β 1 levels in patients with colorectal cancer (40.4 \pm 17.6 μ g \cdot L⁻¹) were significantly higher than in normal controls (19.2 \pm 8.0 μ g \cdot L⁻¹), $P < 0.01$. Elevated levels of serum TGF β 1 were found in 60 % of patients with colorectal cancer when the mean +2 s was used as the upper limit of the normal range (35.1 μ g \cdot L⁻¹, Figure 1). Increased in serum TGF β 1 levels were significantly associated with Duke's stage ($P < 0.05$), but there was no significant difference between Duke's stage B patients and Duke's stage C patients. Serum levels of TGF β 1 were 29.2 \pm 7.3 μ g \cdot L⁻¹ in Duke's stage A patients, 39.5 \pm 11.9 μ g \cdot L⁻¹ in Duke's stage B patients, 43.1 \pm 15.8 μ g \cdot L⁻¹ in Duke's stage C patients, and 57.8 \pm 16.2 μ g \cdot L⁻¹ in Duke's stage D patients. Serum levels of TGF β 1 in each stage were significantly higher than those in the control group (Figure 2). Serum levels of TGF β 1 were not correlated with age, gender, tumor size and differentiation degree of tumor.

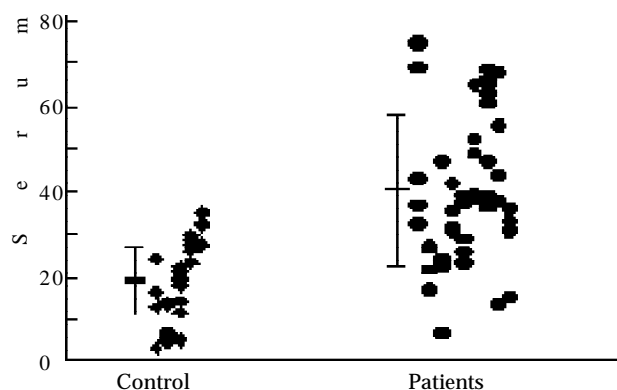


Figure 1 Serum TGF β 1 in patients with colorectal cancer. Bars represent mean \pm standard deviation.

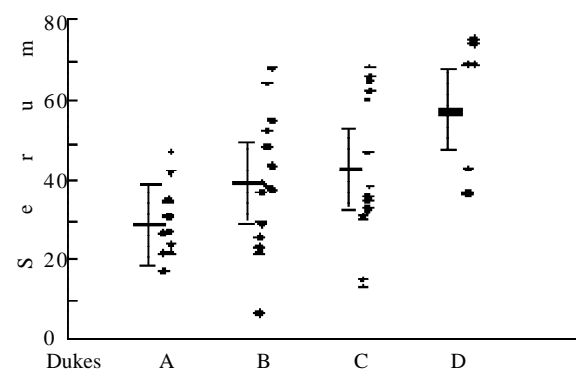


Figure 2 Serum TGF β 1 in patients with colorectal cancer according to Duke's stage. Bars represent mean \pm standard deviation.

TGF β 1 and TGF β R II Expression in colorectal cancer tissue The TGF β 1 and TGF β R II protein were stained mainly in the cytoplasm and cell membrane of cancer cells, as shown in Figures 3 and 4. Staining was classified as negative if less than 10 % of the cells were positive and as positive if more than 10 % were positive^[2]. Thirty-seven (37.8 %) of 98 tissues from colorectal cancer patients were positive for TGF β 1

staining and forty-six (46.9 %) were positive for TGF β R II staining. The expression of TGF β 1 and TGF β R II was correlated significantly with the depth of invasion, stage of disease and metastasis (lymph node and distant metastasis). Patients in T₃-T₄, stage C-D and with metastasis had significantly higher expression of TGF β 1 than patients in T₁-T₂, stage A-B and without metastasis ($P < 0.05$). Patients in T₃-T₄, stage C-D and with metastasis had significantly lower expression of TGF β R II than patients in T₁-T₂, stage A-B and without metastasis ($P < 0.05$). The expression of TGF β 1 and TGF β R II was not correlated with age, gender, tumor size and differentiation degree of tumor (Table 1).

Table 1 Clinicopathologic characteristics of colorectal cancer with expression of TGF β 1 and TGF β R II

Variables	<i>n</i>	TGF β 1-positive		TGF β R II-positive	
		<i>n</i> (%)		<i>n</i> (%)	
Age(yrs)	≥50	60	24(40.0)	30(50.0)	
	<50	38	13(34.2)	16(42.1)	
Sex	Male	53	20(41.5)	25(53.7)	
	Female	45	17(31.0)	21(37.9)	
Tumor size	<5cm	56	21(37.5)	24(42.9)	
	≥5cm	42	16(38.1)	22(52.4)	
Histology					
Well-diff. ade	17	9(52.9)		11(64.7)	
Mode-diff. ade	47	15(31.9)		19(40.4)	
Poor-diff. ade	34	13(38.2)		16(47.1)	
Depth of invasion					
T ₁ -T ₂	60	17(28.3)		33(55.0)	
T ₃ -T ₄	38	20(52.6) ^a		13(34.2) ^a	
Metastasis	Present	35	18(51.4)	11(31.4)	
	Absent	63	19(30.2) ^a	35(55.6) ^a	
Stage	A	34	8(23.5)	23(67.7)	
	B	29	9(31.1)	13(44.8)	
	C+D	35	20(57.1) ^a	10(28.6) ^a	

^a $P < 0.05$, T₁-T₂ vs T₃-T₄, Present vs Absent, A, B vs C+D

TGF β mRNA expression in colorectal cancer tissue

The expression of TGF β 1 mRNA in 50 colorectal cancer tissues was examined. The degree of staining was prominent in cases of TGF β 1 positive immunohistochemical staining, but it was rare for negative cases of immunohistochemical staining. The pattern of distribution of TGF β 1 mRNA is the same as immunohistochemical staining (Figure 5).

Relationship of TGF β 1 expression between primary and lymph node metastatic lesions Among 35 cases of colorectal cancer with lymph node metastatic lesions, the TGF β 1 positive rate was 51.4 % (18/35) for primary lesions and 71.4 % (25/35) for metastatic lesions in the lymph nodes. Of 17 cases with no staining in the primary lesion, 7 cases (41.2 %) showed TGF β 1 staining in the metastatic lesion (Figure 6).

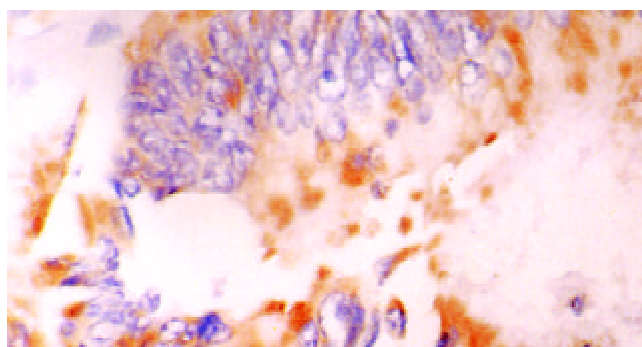


Figure 3 TGF β 1 staining in cytoplasm of cancer cells. $\times 400$

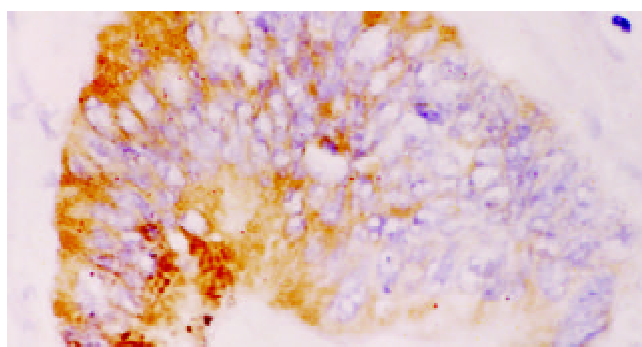


Figure 4 TGF β R II staining in cytoplasm of cancer cells. $\times 400$

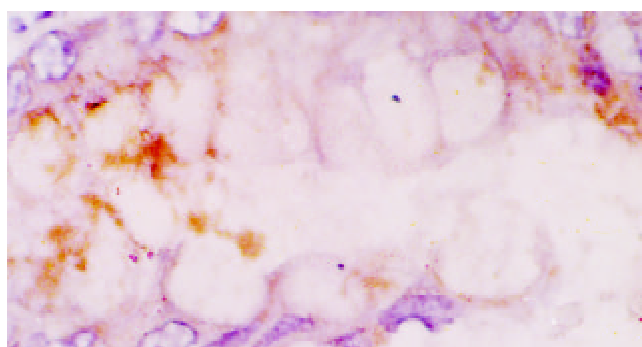


Figure 5 TGF β 1 mRNA expression in colorectal cancer *in situ* hybridization. $\times 400$

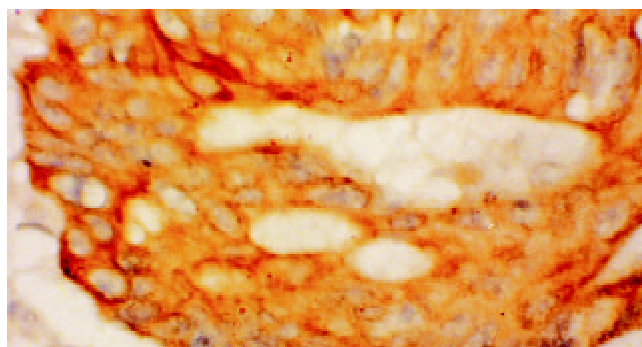


Figure 6 TGF β 1 Expression in lymph node metastatic lesions. $\times 400$

DISCUSSION

TGF β 1 has been found to be overexpressed locally in many tumors, and is believed to play a role in tumor transformation and progression, as well as in tumor regression^[46-48]. Although

TGF β 1 acts as a potent inhibitor of cell growth and tumor progression, loss of this negative regulation can lead to tumor development. TGF β 1 switches to a growth stimulator with tumor progression. Growth inhibition is replaced in many tumors by the opposite response, growth stimulation. This paradoxical switch in the responsiveness of tumor cell to TGF β 1 during neoplastic progression may be due to the inactivation of the TGF β 1 signaling pathway such as mutations in the type 2 TGF β receptor gene or through reduced expression and increase of blood supply to a tumor mass and inhibition of immunologic mechanisms involved in tumor identification and cytolysis. In cases of breast cancer, expression of TGF β 1 was positively associated with invasion and metastasis. Maehara *et al*^[45] reported that the expression of TGF β 1 in gastric cancer cells was closely related to infiltrative growth of the cancer and to the higher rate of lymph node metastasis.

We found that TGF β 1 levels in the serum of patients with colorectal cancer were significantly elevated compared with normal controls. TGF β 1 was overexpressed in colorectal cancer tissue compared with normal colorectal mucosa. Elevated serum levels of TGF β 1 and over-expression of TGF β 1 in colorectal cancer tissue were correlated significantly with invasion and metastasis of colorectal cancer. Patients in T₃-T₄, stage C-D and with metastasis had significantly higher expression of TGF β 1 in tumor tissue and TGF β 1 levels in the serum than patients in T₁-T₂, stage A-B and without metastasis ($P < 0.05$). The expression of TGF β 1 in tumor tissue and TGF β 1 levels in the serum were not correlated with age, gender and differentiation degree of tumor. Shim *et al*^[49] reported that patients of colorectal cancer in stage C-D had significantly higher expression of TGF β 1 in tumor tissues and TGF β 1 levels in the serum than patients in stage A-B ($P < 0.05$). TGF β 1 in colorectal cancer patients may be associated with disease progression. Among 35 cases of colorectal cancer with lymph node metastasis lesions, the TGF β 1 positive rate was 51.4 % (18/35) for primary lesions and 71.4 % (25/35) for metastatic lesions in the lymph nodes. Of 17 cases with no staining in the primary lesion, 7 cases (41.2 %) showed TGF β 1 staining in the metastatic lesion. The preferential expression of TGF β 1 in lymph node metastases suggests a clonal selection of tumor cells with TGF β 1 expression, specific for the higher potential of lymph node metastasis in tumor advance, and TGF β 1 plays a role related to the malignant progression of colorectal cancer. We also found that TGF β R II expression was significantly lower in colorectal cancer tissues than in normal mucosa. The expression of TGF β R II in tumor tissues of Patients in T₃-T₄, stage C-D and with metastasis was significantly lower than that in patients in T₁-T₂, stage A-B and without metastasis ($P < 0.05$). The expression of TGF β R II in tumor tissues was not correlated with age, gender and differentiation degree of tumor. The lower expression of TGF β R II in colorectal cancer may be associated with disease progression. In our previous study^[50,51], we found that TGF β 1 expression was correlated significantly with angiogenesis in colorectal cancer tissues and inhibition of immunologic mechanisms involved in tumor identification and cytolysis. TGF β 1 is closely related to the invasion and metastasis of colorectal cancer, and it may be used as a possible biomarker.

REFERENCES

- 1 Mceachern JA, Koble JJ, Mack V, Arteaga CL, Dumout N, Mary JC, Akporiaye ET. Invasion and metastasis of a mammary tumor involve TGF β signaling. *Int J Cancer* 2001;**91**: 76-82
- 2 Xiao B, Jing B, Zhang YL, Zhou DY, Zhang WD. Tumor growth inhibition effect of hIL-6 on colon cancer cells transfected with the target gene by retroviral vector. *World J Gastroenterol* 2000;**6**:89-92
- 3 Huang PL, Zhu SN, Lu SL, Dai SZ, Jin YZ. Inhibitor of fatty acid synthase induced apoptosis in human colonic cancer cells. *World J Gastroenterol* 2000;**6**:295-297
- 4 Xie B, He SW, Wang XD. Effect of gastrin on protein kinase and its subtype in human colon cancer cell line SW 480. *World J Gastroenterol* 2000;**6**:304-306
- 5 Guo WJ, Zhong ZD, Wu HJ, Liu YQ, WuRG, Zhang WD. Ultrastructural localization of glutathione s-transferase-pi in human colorectal cancer cells. *World J Gastroenterol* 2000;**6**:454-455
- 6 Yuan P, Sun MH, Zhang JS, Zhu XZ, Shi DR. APC and K-ras gene mutation in aberrant crypt foci of human colon. *World J Gastroenterol* 2001;**7**:352-356
- 7 Zheng CX, Zhan WH, Zhao JZ, Zheng D, Wang DP, He YL, Zheng ZQ. The prognostic value of preoperative serum levels of CEA CA19-9 and CA72-4 in patients with colorectal cancer. *World J Gastroenterol* 2001;**7**:431-434
- 8 Peng ZH, Xing TH, Qiu GQ, Tang HM. Relationship between Fas/FasL expression and apoptosis of colon adenocarcinoma cell lines. *World J Gastroenterol* 2001;**7**:88-92
- 9 Li XG, Song JD, Wang YQ. Differential expression of a novel colorectal cancer differentiation-related gene in colorectal cancer. *World J Gastroenterol* 2001;**7**:551-554
- 10 Wang W, Luo HS, Yu BP. Telomerase and colorectal cancer. *Shijie Huaren Xiaohua Zazhi* 2000;**8**:800-802
- 11 Ying YQ, Zhou G, Wu P, Huang WB. Significance of TGF- α and TGF- β 1 expressions in the tissue of colorectal cancer. *Shijie Huaren Xiaohua Zazhi* 2001;**9**:223-225
- 12 Xie B, He SW, Wang DK. Inhibition of neomycin on gastrin-stimulating cell proliferation of human colon cell line SW480. *Shijie Huaren Xiaohua Zazhi* 1999;**7**:249-251
- 13 Qiao Q, Wu JS, Zhang J, Ma QJ, Lai DN. Expression and significance of apoptosis related gene bcl-2, bax in human large intestine adenocarcinoma. *Shijie Huaren Xiaohua Zazhi* 1999;**7**:936-938
- 14 Jiang HY, Qing SH. Research on related factors with lymph node metastasis of colorectal cancer. *Shijie Huaren Xiaohua Zazhi* 1999;**7**:982-984
- 15 Wang Q, Wu JS, Lai DN, Ma QJ, Pan BR. Expression and significance of p16 protein in colorectal carcinoma. *Shijie Huaren Xiaohua Zazhi* 1999;**7**:1047-1048
- 16 Cao JB, Li SR. Relation between human papilloma virus and colorectal cancer. *Shijie Huaren Xiaohua Zazhi* 1999;**7**:1070-1071
- 17 Zhang LL, Zheng ZS, Zhang YL, Wu BP, Guo W, Liu XX, Zhou DY. Microsatellite instability in multiple primary colorectal cancers. *Shijie Huaren Xiaohua Zazhi* 1999;**7**:397-399
- 18 Li M, Wang H, Yu BM, Zheng MH. Effect of p53 gene mutation and tumor markers on the prognosis of patients with colorectal cancer. *Shijie Huaren Xiaohua Zazhi* 1999;**7**:425-426
- 19 Wang SM, Wu JS, Yao X, He ZS, Pan BR. Effect of TGF α , EGFR anti-sense oligodeoxynucleotides on colon cancer cell line. *Shijie Huaren Xiaohua Zazhi* 1999;**7**:522-524
- 20 Li WS, Li JS. Surgical treatment of left colon carcinoma obstruction. *Shijie Huaren Xiaohua Zazhi* 1999;**7**:533-534
- 21 Yao XQ, Qing SH. Detection of multidrug resistance gene in progressive colon cancer and its significance. *Shijie Huaren Xiaohua Zazhi* 1999;**7**:535-536
- 22 Fan YF, Huang ZH. Progress in the studies of gene therapy for colorectal cancer. *Shijie Huaren Xiaohua Zazhi* 2001;**9**:427-430
- 23 Wang CH, Zhang XM, Zhan M, Tang FX, Li L. TGF- β and its receptor expression in human colorectal cancer. *Shijie Huaren Xiaohua Zazhi* 2001;**9**:462-3
- 24 Fan RY, Li SR, Wu ZT, Wu X. Detection of p53 protein, k-ras and APC gene mutation in sporadic colorectal cancer tissue and exfoliative epithelial cell in stool. *Shijie Huaren Xiaohua Zazhi* 2001;**9**:771-775

- 25 **Sheng ZX**, Chao G, Sun J. Clinical significance of Cox-2 mRNA expression in colorectal cancer tissue. *Shijie Huaren Xiaohua Zazhi* 2001;**9**:1082-1083
- 26 **Yu BM**, Zhao R. Molecular biology of colorectal carcinoma. *Shijie Huaren Xiaohua Zazhi* 1999;**7**:173-175
- 27 **Deng YC**, Zhen YS, Zheng S, Xue YC. Activity of boanmycin against colorectal cancer. *World J Gastroenterol* 2001;**7**:93-97
- 28 **Bai DJ**, Yang GL, Yuan HY, Li Y, Wang K. Effect of cimetidine on T-lymphocyte subsets in perioperative gastrointestinal cancer patients. *Shijie Huaren Xiaohua Zazhi* 2000;**8**:147-149
- 29 **Yang JH**, Rao BQ, Wang Y, Tu XH, Zhang LY, Chen SH, Ou-Yong XN, Dai XH. Clinical significance of detecting the circulating cancer cells in peripheral blood from colorectal cancer. *Shijie Huaren Xiaohua Zazhi* 2000;**8**:187-189
- 30 **Li SR**. Early diagnosis of colorectal cancer. *Shijie Huaren Xiaohua Zazhi* 2001;**9**:780-782
- 31 **Sheng JQ**, Chen ZM. Colorectal cancer related gene in the screen of colorectal cancer. *Shijie Huaren Xiaohua Zazhi* 2001;**9**:783-785
- 32 **Gu F**, Lu YM. Treatment of colorectal adenoma. *Shijie Huaren Xiaohua Zazhi* 2001;**9**:785-786
- 33 **Han RY**. Early endoscopic diagnosis of colorectal cancer. *Shijie Huaren Xiaohua Zazhi* 2001;**9**:789-790
- 34 **Han YY**. Endoscopic treatment of colorectal cancer. *Shijie Huaren Xiaohua Zazhi* 2001;**9**:790-792
- 35 **Wang YB**, Yang ZX. Routine diagnosis of colorectal cancer. *Shijie Huaren Xiaohua Zazhi* 2001;**9**:792-793
- 36 **Ma Q**, Zhang ZS, Wang QY. Reverse of multidrug resistance to colorectal cancer. *Shijie Huaren Xiaohua Zazhi* 2001;**9**:822-825
- 37 **Gu HP**, Ni CR, Zhan RZ. Relationship of expression of CD15, CD44V6 and nm23H1 mRNA with metastasis and prognosis of colon carcinoma. *Shijie Huaren Xiaohua Zazhi* 2000;**8**:887-891
- 38 **Zha R**, Yu BM, Zhang GC, Zheng MH, Li DH, Huang L, Zhou HZ. Effect of selenium on immunity and anti-oxidative functions in patients with colorectal carcinoma. *Shijie Huaren Xiaohua Zazhi* 2000;**8**:1013-1016
- 39 **Jia L**, Chen TX, Sun JW, Na ZM, Zhang HH. Relationship between microvessel density and proliferating cell nuclear antigen and prognosis in colorectal cancer. *Shijie Huaren Xiaohua Zazhi* 2000;**8**:74-76
- 40 **Ji DJ**, Cao Y, Zhang YL, Jiang B, Yu N, Feng FC, Zhou DY. Synchronous studies on variation of p53 gene transcriptions and expression in HT-29, Lovo cells. *Shijie Huaren Xiaohua Zazhi* 2000;**8**:77-79
- 41 **Zhao R**, Zhang GC, Yu BM, Zheng MH, Li DH, Zhu YM, Hu BY. Effect of selemin on T lymphocyte against colonic cancer cells. *Shijie Huaren Xiaohua Zazhi* 2000;**8**:80-83
- 42 **Cao JB**, Li SR, Zhu QP, Gu SY, Li YJ, Chen ZM, Zhang HG. The study of relationship between human papillomavirus and colorectal cancer. *Shijie Huaren Xiaohua Zazhi* 2000;**8**:111-112
- 43 **Chen J**, Gu GG, Ling WH, Luo YH. Microsatellite instability in 46 cases with non-hereditary colorectal cancer. *Shijie Huaren Xiaohua Zazhi* 2000;**8**:350-352
- 44 **Wang ZW**, Cheng RX, Zhou GJ, Shen HD, Chon YQ. CK20 mRNA expression in the peripheral blood of colorectal cancer patients. *Shijie Huaren Xiaohua Zazhi* 2000;**8**:818-820
- 45 **Maehara Y**, Kakeji Y, Kabashima A. Role of transforming growth factor- β 1 in invasion and metastasis in gastric carcinoma. *J Clin Oncol* 1999;**17**:607-614
- 46 **Rodeck V**, Nishiyama J, Mauriel A. Independent regulation of growth and Smad-mediated transcription by TGF- β in human melanoma cells. *Cancer Res* 1999;**53**:547-550
- 47 **Shyr M**, Sheen C, Han SC, Chin WS, Hock CE, Wei JC. Serum levels of TGF- β 1 in patients with breast cancer. *Arch Surg* 2001;**136**:937-940
- 48 **Farina AR**, Coppa A, Tiberio A, Turco A, Colletta G, Mackay AR. TGF- β 1, enhances the invasiveness of human MDA-MB-231 breast cancer cells by up-regulating urokinase activity. *In J Cancer* 1998;**75**:721-730
- 49 **Shim K S**, Kim K H, Han WS, Park E B. Elevated serum levels of transforming growth factor- β 1 in patients with colorectal carcinoma. *Cancer* 1999;**85**:554-561
- 50 **Xiong B**, Yuan HY, Zhang F, Hu MB, Yang GL. The expression of transforming growth factor β 1 in colorectal cancer and its relation to angiogenesis. *World J Gastroenterol* 2002;**8**:496-498
- 51 **Xiong B**, Yuan HY, Hu WB, Ydan T, Yang GD. Serum levels of transforming growth factor- β 1 correlating with T cell subsets and natural killer cell activity in colorectal cancer. *Shijie Huaren Xiaohua Zazhi* 2001;**9**:1194-1195

Edited by Ma JY

• VIRAL HEPATITIS •

Clinical observation of salvianolic acid B in treatment of liver fibrosis in chronic hepatitis B

Ping Liu, Yi-Yang Hu, Cheng Liu, Da-Yuan Zhu, Hui-Ming Xue, Zhi-Qiang Xu, Lie-Ming Xu, Cheng-Hai Liu, Hong-Tu Gu, Zhi-Qing Zhang

Ping Liu, Yi-Yang Hu, Cheng Liu, Hui-Ming Xue, Zhi-Qiang Xu, Lie-Ming Xu, Cheng-Hai Liu, Hong-Tu Gu, Shanghai University of Traditional Chinese Medicine, Shanghai 200032, China
Da-Yuan Zhu, Shanghai Institute of Metabolic Diseases, Chinese Academy of Sciences, Shanghai 200031, China

Zhi-Qing Zhang, the 4th Huaiyin City Hospital, Huaian City, 223000, Jiangsu Province, China

Supported by the National 9th Five-Year Breakthrough Scientific Project, No. 96-906-08-02

Correspondence to: Dr. Ping Liu, Professor of medicine, Shanghai University of Traditional Chinese Medicine Institute of Liver Diseases, 530 Lingling Rd, Shanghai 200032, China. liuliver@online.sh.cn

Telephone: +86-21-5423-1109 **Fax:** +86-21-6403-6889

Received 2001-10-21 **Accepted** 2001-12-20

Abstract

AIM: To evaluate the clinical efficacy of *salvianolic acid B* (SA-B) on liver fibrosis in chronic hepatitis B.

METHODS: Sixty patients with definite diagnosis of liver fibrosis with hepatitis B were included in the trial. Interferon- γ (IFN- γ) was used as control drug. The patients took orally SA-B tablets or received muscular injection of IFN- γ in the double blind randomized test. The complete course lasted 6 months. The histological changes of liver biopsy specimen before and after the treatment were the main evidence in evaluation, in combination with the results of contents of serum HA, LN, IV-C, P-III-P, liver ultrasound imaging, and symptoms and signs.

RESULTS: Reverse rate of fibrotic stage was 36.67 % in SA-B group and 30.0 % in IFN- γ group. Inflammatory alleviating rate was 40.0 % in SA-B group and 36.67 % in IFN- γ group. The average content of HA and IV-C was significantly lower than that before treatment. The abnormal rate also decreased remarkably. Overall analysis of 4 serological fibrotic markers showed significant improvement in SA-B group as compared with the IFN- γ group. Score of liver ultrasound imaging was lower in SA-B group than in IFN- γ group (HA 36.7 % vs 80 %, IV-C 3.3 % vs 23.2 %). Before the treatment, ALT AST activity and total bilirubin content of patients who had regression of fibrosis after oral administration of SA-B, were significantly lower than those of patients who had aggravation of fibrosis after oral administration of SA-B. IFN- γ showed certain side effects (fever and transient decrease of leukocytes, occurrence rates were 50 % and 3.23 %), but SA-B showed no side effects.

CONCLUSION: SA-B could effectively reverse liver fibrosis in chronic hepatitis B. SA-B was better than IFN- γ in reduction of serum HA content, overall decrease of 4 serum fibrotic markers, and decrease of ultrasound imaging score. Liver fibrosis in chronic hepatitis B with slight liver injury was more suitable to SA-B in anti-fibrotic treatment. SA-B showed no obvious side effects.

Liu P, Hu YY, Liu C, Zhu DY, Xue HM, Xu ZQ, Xu LM, Liu CH, Gu HT, Zhang ZQ. Clinical observation of salvianolic acid B in treatment of liver fibrosis in chronic hepatitis B. *World J Gastroenterol* 2002; 8(4):679-685

INTRODUCTION

Radix Salviae Miltiorrhizae (Sm) can activate blood circulation and resolve stasis and is a commonly used herb clinically^[1]. Sm was applied to the late-stage schistosomiasis cirrhosis and splenomegaly at first time in 1958^[2]. Later Dr. Yu used its injection to treat hepatitis B at the early-stage cirrhosis^[3], the biopsy examination before and after treatment identified that Sm could effectively alleviate the pathological changes of liver fibrosis. *Salvianolic acid B* (SA-B), a major water soluble component in Sm^[4], protected the tetrachloride carbon (CCl₄) induced fibrosis in rats, and reversed dimethylnitrosamine (DMN) induced liver fibrosis in rats. It could prevent liver cell injury, inhibit proliferation of hepatic stellate cells (HSC) and collagen production *in vitro*^[5-9]. Based on the stable preparation procedures and long-term toxic test on rats, we used SA-B tablets and interferon- γ (IFN- γ) injection as control drug in the double blind randomized clinical trial^[10-16]. The liver biopsy examination before and after treatment was used as a major evaluation standard, assisted by serum fibrotic markers, liver ultrasound imaging, liver function test, symptoms and dynamic observation of regular test of blood, urine, and renal function, in order to study the clinical efficacy, indications, and side effects of SA-B in liver fibrosis with chronic hepatitis B.

SUBJECTS AND METHODS

Subjects

Patients having liver fibrosis with chronic hepatitis B were included in the trial. Initially 77 patients were involved, but 17 of them were not included in the final analysis because of following reasons: 1) 4 patients showed no obvious liver fibrosis in their first liver biopsies; 2) 7 patients failed to undertake their second liver biopsies; and 3) 6 patients' liver specimen were too small to make pathological examination.

Before and after the treatment, the liver biopsy specimens of 60 patients were in accordance to pathological diagnosis 30 patients in SA-B group, 28 males and 2 females and 30 patients in IFN- γ group, 28 males and 2 females. The age in SA-B group was 36.1 ± 9 years, and in IFN- γ group 35.1 ± 7.8 years. Duration of hepatitis B in SA-B group was 3.9 ± 3.2 years, and 3.6 ± 4.6 years in IFN- γ group. There was no significant difference in grade and stage of pathological examinations between two groups before treatment.

Diagnostic criteria

History: The patient had a history of hepatitis B or HBsAg carrier and still had the symptoms and signs of hepatitis and

abnormal liver function when included in the trial. Etiological marker: HBsAg was positive. Ultrasound imaging: In accordance to the ultrasound images of chronic hepatitis B. Liver biopsy examination: Definite pathological diagnosis of liver fibrosis. The fibrotic stage was S1-S4. Symptoms: Pain in the hepatic region, general fatigue, anorexia and abdominal distention. Signs: Hepatomegaly, splenomegaly, hepatic facies, palmar erythema, vascular spiders.

Criteria to enroll subjects

Age: 18-60 years, in accordance to the diagnostic criteria for liver fibrosis in hepatitis B. Histological fibrotic stage was S1-S4.

Criteria to exclude subjects

(1) Over 60, or less than 18 years of age. Patient in pregnancy or in breast feeding period. (2) Complicated with hepatitis C or other hepatic viral infection; suspicion of autoimmune hepatitis; and drug hepatitis or alcoholic hepatitis. (3) Decompensated post-hepatic cirrhosis. (4) Severe complications of cardiovascular systems, renal, or hematopoietic system; mental diseases. (5) Failure to achieve twice liver biopsy or failure to make pathological diagnosis with liver biopsy specimens. Patients meeting any one of the above criteria were excluded from the trial.

Group and administration

Grouping The patients were divided into two groups based on their randomized number they received.

Drug The double blind randomized method was used. SA-B tablet (30 mg/tablet) and placebo tablet (made of excipient), having same package and labels, were named Gan Xian Ling I and Gan Xian Ling II respectively. All the tablets were prepared by the Shanghai Institute of Drug, Chinese Academy of Sciences. Interferon- γ injection (IFN- γ , 1MU/injection) and placebo injection (made of substrate without IFN- γ activity) having the same package and labels were named IFN- γ I and IFN- γ II respectively. Injections were provided by the Shanghai Clone Biological High Technology Limited Company (Product NO.980508, revelation after treatment).

Drug administration Double blinded method was used in drug administration. The group I patients were orally administered with Gan Xian Ling I tablet, 2 tablets t.i.d for 6 months. And patient had muscular injection of IFN- γ -I once a day in the first month and then once every other day in the following five months. The group II patients were administrated with Gan Xian Ling II and IFN- γ -II. The usage was the same as in group I.

Regular items observed

Recording and observation of symptoms and signs Patient's symptoms and signs were recorded in detail using "Clinical Observation Table" once a month before and during the treatment.

Etiological markers of hepatitis B HBV marker: ELISA, the kit was obtained from Shanghai Ke Hua Company. HBV-DNA: PCR, the kit was from Hua Mei Company (PCR-HT420III).

Liver function The patient had liver function examination (Tai Er Kang Automatic Biochemical Instrument) every month during the treatment, including contents of serum proteins, total bilirubin, direct bilirubin, and activities of ALT (Alanine Aminotransferase) and AST (Aspartate Aminotransferase). The kit was a product of Shanghai Ke Hua-Dong Ling Diagnostic Instrument Company.

Liver ultrasound imaging Specific professional technicians

were assigned to do the ultrasound imaging of liver, gallbladder and spleen (HITACHIEUB-410 type) for the patients and made records. Based on the literature, rate and score each item (liver surface, liver parenchyma, liver edge, intra-hepatic vessels)^[17], Table 1.

Table 1 Ultrasound image scoring for liver fibrosis

Items	1	2	3
Liver surface	Normal (smooth)	Irregular	Waved-shaped (or serrated)
Liver edge	Normal (sharp)	Blunt at tip	Blunt at the edge
Liver parenchyma	Normal (even)	Rough	Nodular(or patch-like)
Intra-hepatic vessels	Normal (clear)	Elusive	Unevenly narrow, wide,thick or thin

Serum fibrotic markers The serum from each patient was collected before, during, and after treatment and stored at -70 °C. All the serum specimens, at one time, were examined by Shanghai Changzheng Hospital (PLA Clinical Immune Center) in a blinded manner. Hyaluronic acid (HA): radioimmunoassay, the kit was from Shanghai Navy Medical Institute. Laminin (LM): radioimmunoassay, the kit was from Shanghai Navy Medical Institute. Type IV Collagen (C-IV): ELISA, the kit was from Shanghai Seng Xiong Technology Enterprise Company. Type-III-procollagen-N-peptide (P-III-P): radioimmunoassay, the kit was from Shanghai Oren Diagnostic Instrument Limited Company.

Histopathological examination of liver

Each patient had percutaneous liver biopsy guided by ultrasound imaging within one week before and after treatment. The liver biopsy specimens were fixed by 10 % formalin and embedded by paraffin according to the routine procedures. HE stain: sections (4 μ m) were routinely HE stained. Collagen stain: double stain reticular fibers and collagen fibers by Gorden-Sweet method and Masson trichrome method.

Sections with HE stain and collagen stain and pathological diagnosis were made by three pathologists in a blinded manner, according to "1995 National Prevention and Treatment Plan of Viral Hepatitis"^[18,19] (inflammatory grades and fibrotic stages were determined when more than two pathologists reached the same diagnosis).

Side effects and security

Negative response of each patient was carefully observed and recorded during treatment. Each patient received EKG, renal function examination, regular blood test and regular urine test before, during and after treatment.

Images and analysis

Radit analysis was used for rank data of pathological grades and stages. *t*-test or analysis for variance was used for measurement data and χ^2 test for enumeration data.

RESULTS

Correlation between serum fibrotic markers and pathological changes of liver fibrosis

The serum fibrotic markers were generally consistent with the valuation of stages and grades (Tables 2 and 3, Figures 1 and 2). Although the standard deviation of markers (individual difference) was large, combined use of HA, P-III-P and IV-C was much better and serum LM content was in normal ranges.

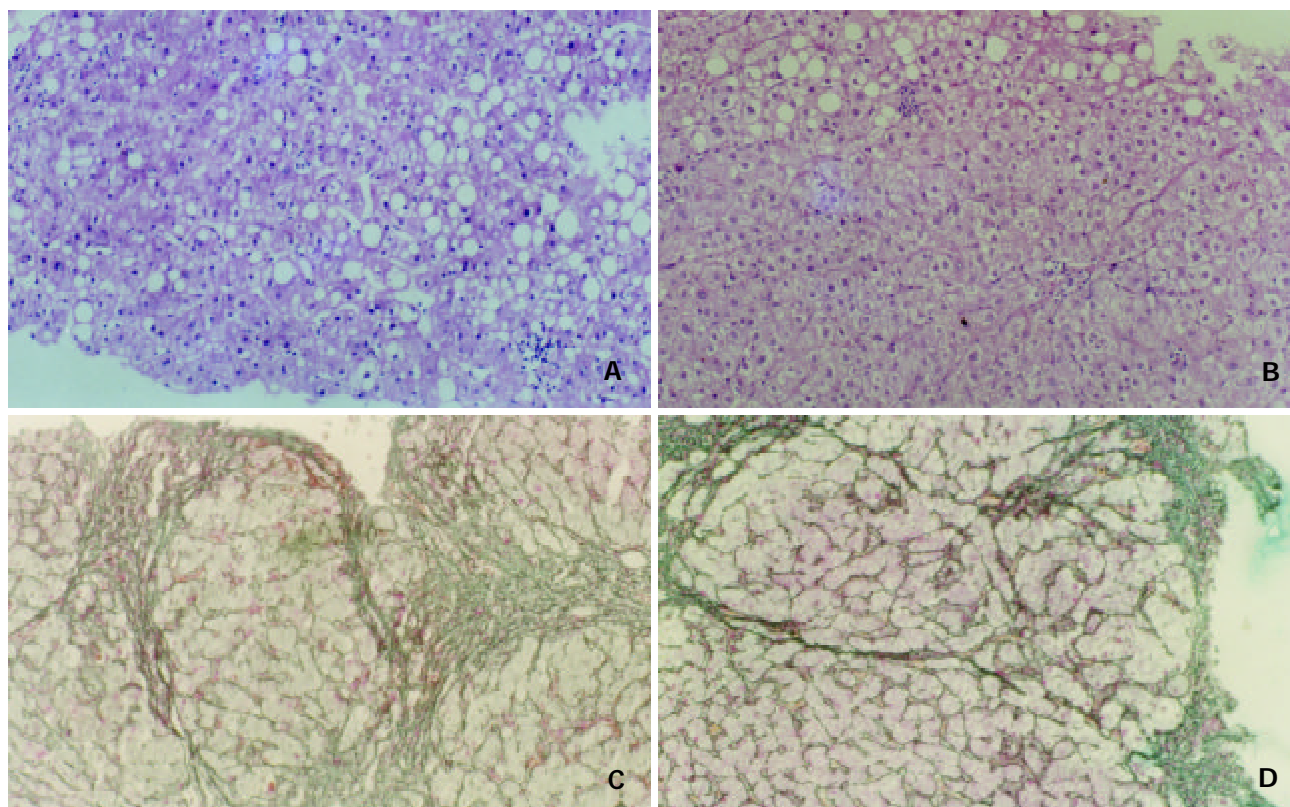


Figure 1 Histological changes of liver biopsy specimens before and after treatment in IFN- γ group:

A: First liver biopsy (G3, HE stain, $\times 100$) before treatment; B: Second liver biopsy (G3, HE stain, $\times 100$) after treatment; C: First liver biopsy (S4, collagen stain, $\times 100$) before treatment; D: Second liver biopsy (S3, GS stain, $\times 100$) after treatment.

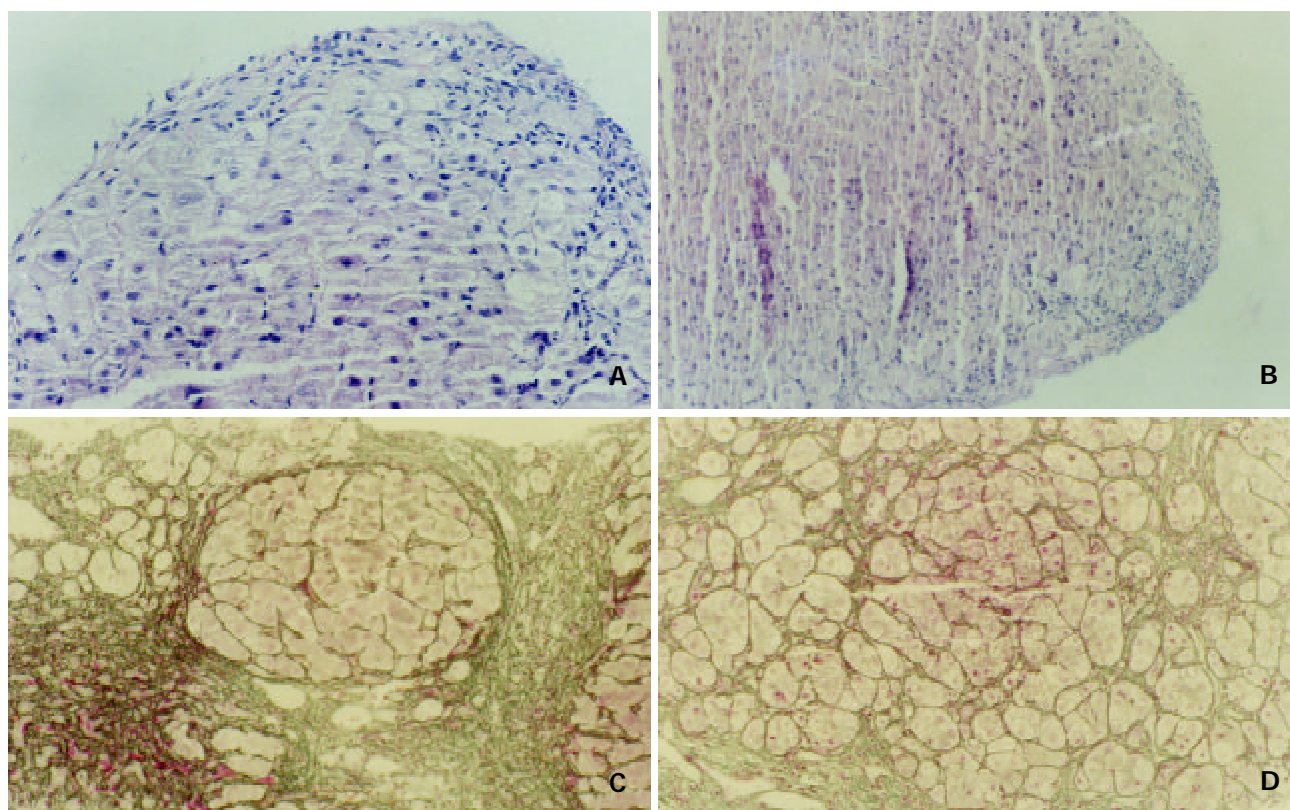


Figure 2 Histological changes of liver biopsy specimens before and after treatment in SA-B group:

A: First liver biopsy (G3, HE stain, $\times 100$) before treatment; B: Second liver biopsy (G3, HE stain, $\times 100$) after treatment; C: First liver biopsy (S4, collagen stain, $\times 100$) before treatment; D: Second liver biopsy (S3, collagen stain, $\times 100$) after treatment.

Table 2 Correlation between serum fibrotic markers and fibrotic stages

Stages(n)	HA($\mu\text{g/L}$)	LM($\mu\text{g/L}$)	IV-C($\mu\text{g/L}$)	PIIIP($\mu\text{g/L}$)
S0 (4)	103 \pm 67.6	116 \pm 34.8	232 \pm 148	6.7 \pm 2.3
S1 (14)	156 \pm 175	103 \pm 30	129 \pm 92 ^{a,c}	7.4 \pm 3.1 ^{a,c}
S2 (31)	197 \pm 175	99 \pm 26.5	178 \pm 138	8.5 \pm 4.1 ^a
S3 (35)	252 \pm 243	107 \pm 22	227 \pm 123	10.8 \pm 4.9
S4 (36)	239 \pm 176	108 \pm 22.6	232 \pm 158	13 \pm 7.8

^a $P<0.05$, vs S4; ^c $P<0.05$, S3.**Table 3** Correlation between serum fibrotic markers and inflammatory grades

Grades(n)	HA($\mu\text{g/L}$)	LM($\mu\text{g/L}$)	IV-C($\mu\text{g/L}$)	PIIIP($\mu\text{g/L}$)
G0 (1)	96	106	212	9.2
G1 (14)	136 \pm 161 ^{a,c}	119 \pm 26	146 \pm 92 ^a	6.38 \pm 2.4 ^{a,c}
G2 (35)	165 \pm 158 ^a	96 \pm 22	178 \pm 128 ^a	7.71 \pm 3.7 ^{a,c}
G3 (49)	258 \pm 216	105 \pm 25	211 \pm 129	12 \pm 5.85
G4 (21)	276 \pm 202	107 \pm 24	276 \pm 178	14 \pm 7.44

^a $P<0.05$, vs S4; ^c $P<0.05$, S3.

Changes of liver fibrotic stages and inflammatory grades

Based on the liver fibrotic stages and inflammatory grades before and after treatment, it was rated as improved (alleviated by ≥ 1 stage), stable, or deteriorated (≥ 1 stage). The improvement rates of inflammatory grades and fibrotic stages were 40.0 % and 36.67 % respectively in SA-B group, which were slightly higher than in IFN- γ group (36.67 % and 30.0 %). Deterioration rates were 16.7 % and 20.0 % in SA-B group, which were much lower than in IFN- γ group (20.0 % and 30.0 %). There was no significant difference between the two groups. Fibrotic stages of 4 patients in SA-B group decreased by 2 stages after treatment. But there was none in IFN- γ group.

Changes of serum fibrotic markers

There was no significant differences in serum HA, LM and P-III-P contents between the two groups before treatment. But the serum IV-C content in SA-B group was obviously higher than that in IFN- γ group before treatment. The average content of serum HA in SA-B group decreased remarkably after treatment ($P<0.05$), and decreased in IFN- γ group, but with no significant difference. The abnormal rate of serum HA content in SA-B decreased from 80 % to 36.67 % ($P<0.05$). But there was no significant difference in the changes of abnormal rate of serum HA content in IFN- γ group. Serum IV-C content decreased remarkably in SA-B group after treatment ($P<0.05$), but it increased in IFN- γ group. There was no significant difference in serum LM and P-III-P contents before and after treatment in both groups. Overall, the first three markers of 9 patients in SA-B group were lowered by ≥ 30 % after treatment, but of only one patient in IFN- γ group (Tables 4-6).

Changes of serum liver function

There was no difference in liver function (Alb, globulin, Serum ALT, AST and GGT activities, serum total and direct bilirubin) between the two groups before treatment. Alb was within normal ranges but globulin was much higher than the normal before treatment in both groups. Alb increased significantly after

treatment in IFN- γ group ($P<0.05$), but had no change in SA-B group. There was no significant change of globulin before and after treatment in both groups. The abnormally high ALT activities before the treatment in SA-B group decreased significantly in the first month ($P<0.05$) and maintained at low levels in the following months of the treatment. In terms of individual subject, ALT activities of 14 patients (46.67 %) in IFN- γ group and 7 patients (23.33 %) in SA-B group continued to increase after treatment, but with no significant difference between the two groups ($P<0.05$), (Table 7). AST activities decreased after treatment in both groups, but without significant difference (Table 8).

GGT activities decreased after treatment in both groups, without significant difference. Serum total and direct bilirubin content in both groups were close to the upper limit of normal ranges. Total bilirubin contents decreased after treatment in both groups without significant difference. Direct bilirubin contents decreased significantly after treatment in both groups. The remarkable decrease of direct bilirubin in SA-B group started in the 3rd treatment.

Changes of liver ultrasound imaging

There was no obvious change of portal veins and splenic veins before and after treatment in the two groups. SA-B showed an improving tendency based on the score of ultrasound imaging. The scores of only two patients in SA-B group rose (deterioration). But scores of 11 patients increased in the control group. There was significant difference between the two groups ($P<0.05$), (Table 9).

Table 4 Serum HA, LM, IV-C and PIIIP contents before, during and after treatment

		HA($\mu\text{g/L}$)	LM($\mu\text{g/L}$)	IV-C($\mu\text{g/L}$)	PIIIP($\mu\text{g/L}$)
IFN- γ group	Before	250 \pm 210	94 \pm 27	112 \pm 64	10.4 \pm 5.0
	During	225 \pm 248	110 \pm 22	219 \pm 143	10.2 \pm 4.4
	After	185 \pm 172	104 \pm 26	212 \pm 105	8.0 \pm 2.8
SA-B group	Before	267 \pm 211	103 \pm 17	294 \pm 155	13.2 \pm 8.1
	During	219 \pm 243	117 \pm 21	248 \pm 164	11.9 \pm 4.9
	After	169 \pm 183 ^a	118 \pm 24	190 \pm 142 ^{b,c}	9.7 \pm 5.3

^a $P<0.05$, ^b $P<0.01$, vs before treatment; ^c $P<0.05$, vs during treatment.**Table 5** Abnormal rates of serum fibrotic markers before and after treatment (abnormal rate(%) = number of abnormal cases/total cases)

Groups		HA $>110\mu\text{g/L}$	LN $>132\mu\text{g/L}$	IV-C $>140\mu\text{g/L}$	PIIIP $\geq 5\mu\text{g/L}$
IFN- γ	Before	21/30(70%)	1/30(3.33%)	6/30(20.0%)	20/29(68.97%)
	After	17/30(56.7%)	3/30(10.0%)	20/30(66.7%)	25/29(86.2%)
SA-B	Before	24/30(80%)	1/30(3.33%)	24/30(80.0%)	26/28(92.86%)
	After	11/30(36.67%) ^a	7/30(23.23%)	15/30(50.0%) ^a	25/28(89.29%)

^a $P<0.05$, vs before treatment.**Table 6** Decrease of 4 serum fibrotic markers >30 % after treatment in two groups

Groups	Total number	Decrease of 3 markers >30 %	Decrease of 2 markers >30 %	Decrease of 1 marker >30 %
IFN- γ	30	1(3.33%)	6(20%)	13(43.33%)
SA-B	30	9(30%)	7(23.33%)	7(23.33%)

^a $P<0.05$, vs IFN- γ

Table 7 Change of ALT activities before and after treatment *n* (%)

Group	Recovered	Decreased (>50%)	Decreased (<50%)	Stable	Increased
IFN- γ	6(20)	4(13.33)	4(13.33)	2(6.67)	14(46.67)
SA-B	6(20)	5(16.67)	8(26.67)	4(13.33)	7(23.33) ^a

^a $P<0.05$, vs IFN- γ .**Table 8** Change of AST activities before and after treatment *n* (%)

Group	Recovered	Decreased (>50%)	Decreased (<50%)	Stable	Increased
IFN- γ	8(26.67)	3(10.0)	4(13.33)	4(13.33)	11(36.67)
SA-B	7(23.33)	2(6.67)	4(13.33)	5(16.67)	12(40.00)

Table 9 Change of ultrasound image scoring

Groups	<i>n</i>	Before treatment	After treatment	Improved <i>n</i> (%)	Deteriorated <i>n</i> (%)
IFN- γ	29	5.38 \pm 1.52	5.75 \pm 1.45	4(13.79)	11(37.93)
SA-B	30	5.10 \pm 1.52	4.70 \pm 1.44	9(30)	2(6.67) ^a

Comparison of χ^2 test between two groups, ^a $P<0.05$

Changes of serum viral markers

HBsAg of each patient in both groups was positive before treatment. No changes happened for HBsAg/anti-HBs after treatment. HBV-DNA of 4 patients in each group became negative after treatment. HBeAg of 13 patients in IFN- γ group and of 15 patients in SA-B group were positive before treatment. But after treatment, 4 patients in IFN- γ group and 3 patients in SA-B group became negative. And at the same time, 2 patients in each group were positive in anti-HBe.

Changes of symptoms and signs

After 6 months treatment, major symptoms and signs such as anorexia, general fatigue, weakness and soreness in lumbar regions and knees, insomnia, yellow urine and hypochondriac pain were remarkably relieved in both groups.

Side effects and safety

The results of EKG, renal function, regular blood test and regular urine test showed no change during the treatment in SA-B group. There were no side effects or negative responses in SA-B group. Fifteen patients in IFN- γ group had fever at the beginning of the treatment. One patient was unable to tolerate the side effect, thus terminating the trial. The other patients succeeded in finishing the clinical trial after the disappearance of fever. One patient in IFN- γ group had transient decrease of leukocytes. Under careful observation, the patient recovered after treatment (without stopping drug administration or using special treatment). No other side effect was noticed.

Analysis of factors affecting anti-fibrotic treatment effect

Histopathological fibrotic stages before and after treatment were the evidence for evaluating the drug efficacy. It was divided into improved, stable and deteriorated groups. The analysis of liver function and serum fibrotic markers before treatment showed that the effect of SA-B in anti-fibrosis was related to the level of liver injury before treatment. The patient having regression of fibrosis after treatment had much lower ALT and AST activities and total bilirubin content before treatment than those having aggravation of fibrosis after

treatment. There was no obvious correlation among the above factors in IFN- γ group (Tables 10 and 11).

Table 10 Correlation between change of fibrotic stages before and after treatment, liver function and serum fibrotic markers before treatment in SA-B group

Items	Improved(<i>n</i> =11)	Unchanged(<i>n</i> =13)	Deteriorated (<i>n</i> =6)
Albumin(g/L)	40 \pm 4.4	39.3 \pm 6.5	39.5 \pm 3.0
Globulin(g/L)	31.1 \pm 6.7	33.9 \pm 6.9	30.9 \pm 8.5
ALT(U)	64 \pm 41 ^a	108 \pm 83	201 \pm 155
AST(U)	48 \pm 29 ^b	73 \pm 55 ^a	155 \pm 108
GGT(U)	72 \pm 44	99 \pm 47	96 \pm 54
Total bilirubin(mMol)	14.9 \pm 3.9 ^b	15.0 \pm 6.6 ^a	21 \pm 10
Direct bilirubin(mMol)	2.9 \pm 1.7	3.1 \pm 2.3	5.0 \pm 4.0
HA(μ g/L)	172 \pm 110	292 \pm 188	386 \pm 330
LN(μ g/L)	106 \pm 10	107 \pm 21	91 \pm 18
IV-C(μ g/L)	248 \pm 88	352 \pm 176	284 \pm 164
PIIIP(μ g/L)	10.2 \pm 6.8	14.8 \pm 7.3	15 \pm 10.2

Compared with elevation of stages, ^a $P<0.05$, ^b $P<0.01$ **Table 11** Correlation between change of fibrotic stages before and after treatment, liver function and serum fibrotic markers before treatment in IFN- γ group

Items	Improved(<i>n</i> =9)	Unchanged(<i>n</i> =12)	Deteriorated (<i>n</i> =9)
Albumin(g/L)	39.9 \pm 5.0	40.8 \pm 4.6	40.6 \pm 6.7
Globulin(g/L)	28.1 \pm 4.6	30.7 \pm 4.0	31.9 \pm 5.3
ALT activities(U)	94 \pm 56	79 \pm 51	171 \pm 286
AST activities(U)	77 \pm 53	56 \pm 33	80 \pm 73
GGT activities(U)	76 \pm 41	76 \pm 48	81 \pm 40
Total bilirubin(mMol)	13.4 \pm 7.6	16.5 \pm 6.4	18.9 \pm 7.0
Direct bilirubin(mMol)	3.0 \pm 2.2	3.6 \pm 2.5	3.3 \pm 2.0
HA(μ g/L)	219 \pm 230	284 \pm 246	237 \pm 145
LM(μ g/L)	97 \pm 34	87 \pm 18	102 \pm 30
IV-C(μ g/L)	128 \pm 84	104 \pm 56	92 \pm 32
PIIIP(μ g/L)	12.0 \pm 6.2	9.1 \pm 5.5	10.9 \pm 2.3

DISCUSSION

The hepatic fibrosis is the important pathological feature of chronic liver diseases, which is characterized by HSC activation and the overproduction of extracellular matrix^[20-36]. Therefore, inhibition or reversion of hepatic fibrosis is one of the main therapeutic strategies^[37-50]. In this study, we found the SA-B effect on liver fibrosis in hepatitis B for the first time, through the double blind trial with IFN- γ as control drug and the observation of liver histopathology, serum fibrotic markers, liver function, liver ultrasound imaging, and symptoms and signs before and after treatment.

SA-B could effectively reverse fibrosis in hepatitis B

The 10th International Congress of Gastroenterology, Los Angeles, September 1994 suggested the etiological base in terms of the diagnosis of chronic hepatitis, making inflammatory grading criteria according to the severity of histological inflammatory necrosis and fibrotic stage standards according to the level of liver fibrosis. Currently liver biopsy is still the "Gold Standard" for scoring fibrosis. But the great

difference in the same liver specimens limited the value of biopsy, making it difficult to evaluate the fibrosis generally and correctly. Liver ultrasound imaging could reflect the specific images of fibrosis. Semi-quantitative evaluation of liver fibrosis and cirrhosis was simple and easily accessible. It was beneficial in the general evaluation of fibrosis, but it failed to precisely reflect the anti-fibrotic effect of the drug because of the insufficiency of quantitative determination. At the same time, multiple factors would affect serum fibrotic markers in the evaluation. It was favorable to combine multiple methods in evaluation. Total 120 biopsy specimens before and after treatment showed that serum fibrotic markers generally rose with the aggravation of fibrotic stages and inflammatory degrees. But the dispersion degree was large. The correlation was better in HA, IV-C and P-III-P. And LM was generally within the normal ranges.

Adapting to the current situation in diagnosis of liver fibrosis, histological fibrotic stages before and after treatment were fundamental in the evaluation of the efficacy in this trial. Improvement rates of fibrotic stages and inflammatory grades were 36.67 % (11/30) and 40 % (12/30) in SA-B group, and were 30 % (9/30) and 36.67 % (11/30) in IFN- γ group, with no significant differences between the two groups. Fibrotic stages of 4 patients decreased more than 2 stages in SA-B group, but none in IFN- γ group. HA and IV-C contents decreased significantly after treatment in SA-B group ($P < 0.05$). The abnormal rate of HA was lowered from 80 % to 36.67 % in SA-B group ($P < 0.05$). In the overall analysis of 4 serum fibrotic marker, 9 patients (30 %) in SA-B group had simultaneous decrease of 3 markers, better than one patient in IFN- γ group. Scores of liver ultrasound imaging with 2 patients in elevation in SA-B group was better than in IFN- γ group with 11 patients in elevation, with significant difference. General analysis of liver biopsy, serum fibrotic markers and ultrasound imaging showed superior effect of SA-B to IFN- γ .

There was no significant change in HBV antigen and antibody systems after treatment in both groups. Anti-fibrotic effect of SA-B or IFN- γ was not related to anti-viral effect. Both drugs were favorable in the relief of symptoms and signs.

Factors affecting anti-fibrotic effect of SA-B

After categorizing the changes of histological fibrotic stages, we analyzed the factors affecting anti-fibrotic effect of SA-B through the analysis of serum fibrotic markers and liver functions before treatment. Before treatment, ALT and AST activities and total bilirubin contents in fibrosis improvement group were significantly lower than those in fibrosis aggravation group. The effect was not related to the contents of serum fibrotic markers before treatment. Severity of liver inflammatory injury was the major factor affecting the anti-fibrotic effect of SA-B. SA-B had a satisfactory effect in regression of fibrosis with minor liver injury prior to treatment, but had no favorable results for severe liver injury prior to treatment. The fibrotic stage was not the major factor affecting the anti-fibrotic effect. There was no relationship in IFN- γ group. The result was instructive in the clinical application of SA-B. It was good anti-fibrotic effect in the treatment of fibrosis patients with minor inflammatory injury.

No side effects or toxicity of SA-B

There was no obvious negative response in SA-B group during the whole treatment. It showed high security in the 6-month administration. Fever and transient decrease of leukocytes were noticed in IFN- γ group. The rate of fever occurrence was 50 %, but it did not affect the completion of the whole treatment.

REFERENCES

- 1 **Xu DS**. Dan Shen (Radix Salviae Miltorrhizae): Biology and Application. Beijing Science Press, 1990
- 2 **Wu YS**, Yang CH, Jiang JF. Primary report of radix salviae miltorrhizae in treatment of late-stage schistosomiasis and splenomegaly. *Zhonghua Yixue Zazhi* 1958;542-545
- 3 **Yu YX**, Yang HQ, Zhu LZ, Cao L, Liu ZL, Zhu LR, Zhang EK, Tian YM, Shen HC, Teng SC. Clinical trial of large-dose radix salviae miltorrhizae in treatment of liver fibrosis. *Shanghai Zhongyiyao Zazhi* 1994; 8-10
- 4 **Chen ZX**, Gu WH, Huang HZ, Yang XM, Sun CJ, Chen WZ, Dong YL, Ma HL. Research of water soluble salvianolic acids in radix salviae miltorrhizae. *Yaoli Tongbao* 1981; **16**: 24-25
- 5 **Liu P**, Mizoguchi Y, Morisawa S. Anti-fibrotic effect of magnesium- salvianolic acid B on liver fibrosis rat. *Zhongguo Yiyao Xuebao* 1993; **8**: 65-67
- 6 **Hu YY**, Liu P, Liu C, Gu HT, Liu CH, Ji G. Influence of extracts from radix salviae miltorrhizae on CCl₄ and DMN induced liver fibrosis rat. *Shanghai Zhongyiyao Zazhi* 1999;7-10
- 7 **Liu P**, Liu NM, Xu LM, Hu YY, Ji G, Liu C. Effect of salvianolic acid B in direct protection of liver cells of original generation rat damaged by CCl₄ in vitro. *Zhongguo Zhongyao Zazhi* 1997; **22**: 303-305
- 8 **Liu P**, Mizoguchi Y, Morisawa S. Effect of magnesium lithospermate B on D-galactosamine induced liver injury rat. *Zhongguo Zhongyiyao Zazhi* 1995; **1**: 291-293
- 9 **Xu LM**, Liu C, Liu P. Effect of salvianolic acid B on regeneration, form and extra-cellular matrix synthesis of liver lipocytes of second generation rat. *Zhonghua Ganzangbing Zazhi* 1996; **4**: 86-89
- 10 **Jiang SL**, Yan XX, Shun YF. The treatment of hepatic fibrosis. *Shijie Huaren Xiaohua Zazhi* 2000; **8**: 684-686
- 11 **Rockey DC**, Chung JJ. Interferon gamma inhibits lipocyte activation and extracellular matrix mRNA expression during experimental liver injury: implications for treatment of hepatic fibrosis. *J Invest Med* 1994; **42**: 660-70
- 12 **Pancr V**, Wolowczuk I, Guerret S, Copin MC, Delanoye A, Capron A, Aurialt C. Protective effect of rSm28GST-specific T cells in schistosomiasis: role of gamma interferon. *Infect Immun* 1994; **62**: 3723-3730
- 13 **Grossman HJ**, White D, Grossman VL, Bhathal PS. Effect of interferon gamma on intrahepatic haemodynamics of the cirrhotic rat liver. *J Gastroenterol Hepatol* 1998; **13**: 1058-1060
- 14 **Oide H**, Watanabe S, Sato N. The effect of interferon gamma on hepatic haemodynamics. *J Gastroenterol Hepatol* 1998; **13**: 975-976
- 15 **Hoffmann KF**, Caspar P, Cheever AW, Wynn TA. IFN-gamma, IL-12, and TNF-alpha are required to maintain reduced liver pathology in mice vaccinated with Schistosoma mansoni eggs and IL-12. *J Immunol* 1998; **161**: 4201-4210
- 16 **Bai WY**, Yan XX, Feng LY. Recent progression of hepatic fibrosis research. *Shijie Huaren Xiaohua Zazhi* 2000; **8**: 1267-1268
- 17 **Xu YQ**, Wang BE, Cao HG. Ultrasound imaging diagnosis of liver fibrosis. *Zhonghua Ganzangbing Zazhi* 1998; **6**: 245
- 18 Proposal of prevention and treatment of viral hepatitis (temporary). *Zhonghua Neike Zazhi* 1995; **34**: 788-791
- 19 **Wang TL**, Zhang TH. Development of pathological category of viral hepatitis. *Zhonghua Binglixue Zazhi* 1996; **25**: 67-69
- 20 **Jian HQ**, Zhang XL. The mechanisms of hepatic fibrosis. *Shijie Huaren Xiaohua Zazhi* 2000; **8**: 687-689
- 21 **Chen WH**, Liu P, Xu GF, Lu X, Xiong WG, Li FH, Liu CH. Role of lipid peroxidation in liver fibrogenesis induced by dimethylnitrosamine. *Shijie Huaren Xiaohua Zazhi* 2001; **9**: 645-648
- 22 **Liu C**, Chen W, Liu P, Wang Z, Hu Y, Liu C. Changes of lipid peroxidation in liver fibrogenesis induced by dimethylnitrosamine and drugs' intervention. *Zhonghua Ganzangbing Zazhi* 2001; **9**: 18-20
- 23 **Neubauer K**, Saile B, Ramadori G. Liver fibrosis and al-

- tered matrix synthesis. *Can J Gastroenterol* 2001; **15**: 187-193
- 24 **Paradis V**, Perlemuter G, Bonvoust F, Dargere D, Parfait B, Vidaud M, Conti M, Huet S, Ba N, Buffet C, Bedossa P. High glucose and hyperinsulinemia stimulate connective tissue growth factor expression: a potential mechanism involved in progression to fibrosis in nonalcoholic steatohepatitis. *Hepatology* 2001; **34**: 738-744
- 25 **Schneiderhan W**, Schmid-Kotsas A, Zhao J, Grunert A, Nussler A, Weidenbach H, Menke A, Schmid RM, Adler G, Bachem MG. Oxidized low-density lipoproteins bind to the scavenger receptor, CD36, of hepatic stellate cells and stimulate extracellular matrix synthesis. *Hepatology* 2001; **34**: 729-737
- 26 **Benyon RC**, Arthur MJ. Extracellular matrix degradation and the role of hepatic stellate cells. *Semin Liver Dis* 2001; **21**: 373-384
- 27 **Vaillant B**, Chiaramonte MG, Cheever AW, Soloway PD, Wynn TA. Regulation of hepatic fibrosis and extracellular matrix genes by the Th response: new insight into the role of tissue inhibitors of matrix metalloproteinases. *J Immunol* 2001; **167**: 7017-7026
- 28 **Breitkopf K**, Lahme B, Tag CG, Gressner AM. Expression and matrix deposition of latent transforming growth factor beta binding proteins in normal and fibrotic rat liver and transdifferentiating hepatic stellate cells in culture. *Hepatology* 2001; **33**: 387-396
- 29 **Bruck R**, Genina O, Aeed H, Alexiev R, Nagler A, Avni Y, Pines M. Halofuginone to prevent and treat thioacetamide-induced liver fibrosis in rats. *Hepatology* 2001; **33**: 379-386
- 30 **Watanabe T**, Niioka M, Hozawa S, Kameyama K, Hayashi T, Arai M, Ishikawa A, Maruyama K, Okazaki I. Gene expression of interstitial collagenase in both progressive and recovery phase of rat liver fibrosis induced by carbon tetrachloride. *J Hepatol* 2000; **33**: 224-235
- 31 **Nakamura T**, Sakata R, Ueno T, Sata M, Ueno H. Inhibition of transforming growth factor beta prevents progression of liver fibrosis and enhances hepatocyte regeneration in dimethylnitrosamine-treated rats. *Hepatology* 2000; **32**: 247-255
- 32 **Castera L**, Hartmann DJ, Chapel F, Guettier C, Mall F, Lons T, Richardet JP, Grimbirt S, Morassi O, Beaugrand M, Trinchet JC. Serum laminin and type IV collagen are accurate markers of histologically severe alcoholic hepatitis in patients with cirrhosis. *J Hepatol* 2000; **32**: 412-418
- 33 **Brenner DA**, Waterboer T, Choi SK, Lindquist JN, Stefanovic B, Burchardt E, Yamauchi M, Gillan A, Rippe RA. New aspects of hepatic fibrosis. *J Hepatol* 2000; **32**: 32-38
- 34 **Benyon RC**, Iredale JP. Is liver fibrosis reversible? *Gut* 2000; **46**: 443-446
- 35 **Levy MT**, Trojanowska M, Reuben A, Friedman SL. Evaluation of fibrosis and hepatitis C. *Am J Med* 1999; **107**: 27S-30S
- 36 **Friedman SL**. Molecular regulation of hepatic fibrosis, an integrated cellular response to tissue injury. *J Biol Chem* 2000; **275**: 2247-2250
- 37 **Angelico M**, Di Paolo D, Trinito MO, Petrolati A, Araco A, Zazza S, Lionetti R, Casciani CU, Tisone G. Failure of a reinforced triple course of hepatitis B vaccination in patients transplanted for HBV-related cirrhosis. *Hepatology* 2002; **35**: 176-181
- 38 **Lim KN**, Casanova RL, Boyer TD, Bruno CJ. Autoimmune hepatitis in African Americans: presenting features and response to therapy. *Am J Gastroenterol* 2001; **96**: 3390-3394
- 39 **Moreau R**, Asselah T, Codat B, De Kerguenec C, Pessione F, Bernard B, Poynard T, Binn M, Grange JD, Valla D, Lebre D. Comparison of the effect of terlipressin and albumin on arterial blood volume in patients with cirrhosis and tense treated by paracentesis: a randomised pilot study. *Gut* 2002; **50**: 90-94
- 40 **Riley TR**, Bhatti AM. Preventive strategies in chronic liver disease: part II, cirrhosis. *Am Fam Physician* 2001; **64**: 1735-1740
- 41 **Rajan S**, Liebman HA. Treatment of hepatitis C related thrombocytopenia with interferon alpha. *Am J Hematol* 2001; **68**: 202-209
- 42 **Border WA**, Noble N. Maximizing hemodynamic-independent effects of angiotensin II antagonists in fibrotic diseases. *Semin Nephrol* 2001; **21**: 563-572
- 43 **Freeze HH**. Congenital disorders of glycosylation and the pediatric liver. *Semin Liver Dis* 2001; **21**: 501-516
- 44 **Tolan DJ**, Davies MH, Millson CE. Fibrosing cholestatic hepatitis after liver transplantation in a patient with hepatitis C and HIV infection. *N Engl J Med* 2001; **345**: 1781
- 45 **Simeonova PP**, Gallucci RM, Hulderman T, Wilson R, Kommineni C, Rao M, Luster MI. The role of tumor necrosis factor-alpha in liver toxicity, inflammation, and fibrosis induced by carbon tetrachloride. *Toxicol Appl Pharmacol* 2001; **177**: 112-120
- 46 **Di Martino V**, Rufat P, Boyer N, Renard P, Degos F, Martinot-Peignoux M, Matheron S, Le Moing V, Vachon F, Degott C, Valla D, Marcellin P. The influence of human immunodeficiency virus coinfection on chronic hepatitis C in injection drug users: a long-term retrospective cohort study. *Hepatology* 2001; **34**: 1193-1199
- 47 **Bini EJ**, Weinshel EH, Generoso R, Salman L, Dahr G, Pena-Sing I, Komorowski T. Impact of gastroenterology consultation on the outcomes of patients admitted to the hospital with decompensated cirrhosis. *Hepatology* 2001; **34**: 1089-1095
- 48 **Romagnuolo J**, Jhangri GS, Jewell LD, Bain VG. Predicting the liver histology in chronic hepatitis C: how good is the clinician? *Am J Gastroenterol* 2001; **96**: 3165-3174
- 49 **Angulo P**, Jorgensen RA, Lindor KD. Incomplete response to ursodeoxycholic acid in primary biliary cirrhosis: is a double dosage worthwhile? *Am J Gastroenterol* 2001; **96**: 3152-3157
- 50 **Nakamuta M**, Ohta S, Tada S, Tsuruta S, Sugimoto R, Kotoh K, Kato M, Nakashima Y, Enjoji M, Nawata H. Dimethyl sulfoxide inhibits dimethylnitrosamine-induced hepatic fibrosis in rats. *Int J Mol Med* 2001; **8**: 553-560

Edited by Ma JY

• VIRAL HEPATITIS •

Genetic evolution of structural region of hepatitis C virus in primary infection

Song Chen, Yu-Ming Wang

Song Chen, Yu-Ming Wang, Department of Infectious Diseases, Southwest Hospital, Third Military Medical University, Chongqing 400038, China

Supported by the Natural Science Foundation of China, No. 3987069

Correspondence to: Song Chen, Department of Infectious Diseases, Southwest Hospital, Third Military Medical University, 30 Gaotanyan Zhengjie, Shapingba District, Chongqing 400038, China. a65427757@hotmail.com

Telephone: +86-23-687754141

Received 2001-09-26 **Accepted** 2001-11-27

Abstract

AIM: To investigate the dynamics of hepatitis C virus (HCV) variability through putative envelope genes during primary infection and the mechanism of viral genetic evolution in infected hosts.

METHODS: Serial serum samples prospectively collected for 12 to 34 months from a cohort of acutely HCV-infected individuals were obtained, and a 1-kb fragment spanning E1 and the 5' half of E2, including Thirty-three cloned cDNAs representing each specimen were assessed by a method that combined a single-stranded conformational polymorphism (SSCP) and heteroduplex analysis (HDA) method to determine the number of clonotypes hypervariable region, was amplified by reverse transcriptase PCR and cloned. Nonsynonymous mutations per nonsynonymous site (dn), synonymous mutations per synonymous site (ds), dn/ds ratio and genetic distances within each sample were evaluated for intrahost evolutionary analysis.

RESULTS: Quasispecies complexity and sequence diversity were lower in early samples and a further increase after seroconversion, although ds value in the envelope genes was higher than dn value during primary infection. The trend, pronounced in most of samples, toward lower ds values in the E1 than in the 5' portion of E2. Quasispecies complexity was higher and E2 dn/ds ratio was a trend toward higher value in later samples during persistent viremia. We also found individual features of HCV genetic evolution in different subjects who were infected with different HCV genotypes.

CONCLUSION: Mutations of actively replicating virus arise stochastically with certain functional constraints. A complexity quasispecies exerted by a combination of either neutral evolution or selective forces shows clear differences in individuals, and associated with HCV persistence.

Chen S, Wang YM. Genetic evolution of structural region of hepatitis C virus in primary infection. *World J Gastroenterol* 2002; 8(4):686-693

INTRODUCTION

Hepatitis C virus (HCV) is an important cause of morbidity and mortality worldwide [1,2]. Infection with HCV becomes chronic in >80 % of the cases and is a major cause of liver cirrhosis [3] and hepatocellular carcinoma [4]. In fact, HCV-related end-stage liver disease is now the leading reason for liver transplantation. HCV has also been linked to extrahepatic diseases, such as cryoglobulinemia and glomerulonephritis [5].

One of the important characteristics of HCV is that its genome exhibits significant genetic heterogeneity as a result of the accumulation of mutations during viral replication. This high mutation rate, which is characteristic of RNA viruses, can be attributed to an error-prone RNA-dependent RNA polymerase that lacks proofreading activity [6]. Several different genotypes have been described [7]. Analogous to other RNA viruses, HCV circulates in an infected individual as a population of closely related, yet heterogeneous, sequences: the quasispecies [7-11]. The distribution of mutations has been reported to be uneven but the basis of this variability is unexplained [12]. A hot-spot for mutation is described within the genome encoding a portion of E2 termed the hypervariable region (HVR), which encodes neutralizing epitopes [13,14]. It is postulated that genetic variation, translated into protein variability results in the production of HCV quasispecies. Interaction between host and virus selects those quasispecies better adapted to survival.

To date, the vast majority of studies describing HCV quasispecies evolution in humans have focused on the HVR1 of the HCV genome. In contrast, there have been very few longitudinal analyses of multiple HCV genes or entire structural genes in infected humans. Previous studies tracking multiple HCV genomic regions over time have been restricted to variations in few clones from infected individuals, and correlation with viral persistence [32]. We recently developed a method combining heteroduplex analysis (HAD) and single-stranded conformational polymorphism (SSCP) analysis (referred to herein as the HDA+SSCP method) that could assess genetic complexity with high sensitivity (ability to discriminate between distinct sequences) and specificity (chance that clones detected as distinct truly represent distinct sequences) and that could provide accurate estimates of genetic diversity in a previous investigation by sampling a sufficiently large number of cloned cDNAs [15]. In the prospective study we investigated the genomic complexity of HCV by HDA+SSCP method of structural gene sequences in serial serum from HCV-infected individuals. In order to detect evidence of selection of HCV mutation by the host, we compared the frequency of mutations resulting in amino acid substitutions (nonsynonymous) with those that are "silent" at the protein level (synonymous).

MATERIALS AND METHODS

Patients

As a part of a prospective study of acute HCV infection, serial serum samples were obtained from individuals in the ALIVE

cohort of injection drug abusers (IDUs) in Chongqing. These samples were tested for antibodies to HCV by using the second-generation HCV enzyme immunoassay. Individuals were identified as seroconverters when a sample tested positive following at least one negative result. For all HCV seroconverters, The presence of HCV RNA was evaluated in sera collected 6 months before seroconversion, at seroconversion, and during subsequent semiannual visits (median of 7). HCV RNA were detected by a quantitative reverse transcriptase PCR (RT-PCR) assay (AMPLICOR HCV MONITOR; Roche Diagnostic Systems, Branchburg, N. J.), the linear range of which was determined to be 500 to 500 000 copies per ml of serum by our and other laboratories^[16,17]. Liver tests, including Alanine aminotransferase (ALT) levels in serum, performed at the first clinical examination and repeated during follow-up. Hepatitis B surface antigen, anti-HBc, anti-HBe and anti-HIV Ig M were negative in all subjects. The genome subtype was determined as described previously^[18]. Clinical and virological backgrounds of the subjects studied are summarized in Table 1.

Table 1 Molecular, biochemical, and serological characterization of the nine HCV primary infections

Subject	Sample	Age(yr)/ Sex	Duration of infection (month)	Log ₁₀ [HCV RNA] ^a	ALT level (IU/ml) ^b	Result of ELISA ^c
A		28/F				
	A1		0	7.12	116	Neg
	A2		8	6.90	69	Pos
	A3		12	6.58	92	Pos
B		30/M				
	B1		0	7.27	110	Neg
	B2		6	6.50	35	Pos
	B3		29	5.70	37	Pos
C		33/M				
	C1		0	6.41	41	Pos
	C2		24	5.25	23	Pos
	C3		34	5.14	10	Pos

^a Number of HCV RNA molecules per ml plasma. Time zero is the time where the first sample was available; other time are times after time zero. ^b Normal value, < 40 IU/ml. ^c ELISA: neg, negative; pos, positive.

METHODS

Envelope region amplification HCV RNA characterization was based on examination of 33 cloned cDNAs spanning the 1 025-nucleotide (nt) region thought to encode envelope protein E1 and a segment of E2, including HVR1. Total RNA was extracted from 100 µl serum by using 500 µl Trizol LS Reagent (Life Technologies, Gaithersburg, Md.) at room temperature, followed by chloroform extraction and isopropanol precipitation in the presence of 20 µg glycogen (Boehringer Mannheim, Indianapolis, Ind.). The RNA pellet was washed with 75 % (vol/vol) ethanol and then air dried briefly and redissolved in 50 µl diethyl pyrocarbonate-treated water with 10 mM dithiothreitol (Promega, Madison, Wis.) and 5 U of RNasin ribonuclease inhibitor (Promega). After incubation at 65°C for 5 min, 5 µl purified RNA was used to generate cDNA in a 20-µl reaction mixture at 37°C for 1 h with 20 U of

Moloney murine leukemia virus RT (Promega) and first-round PCR reverse primer. The entire 20-µl cDNA synthesis reaction mixture was used for the first-round PCR in a 25-µl reaction mixture containing 0.75 U Expand HF polymerase mixture (Boehringer Mannheim, Indianapolis, Ind.), 1.5 mM MgCl₂, 0.2 mM concentration of deoxynucleoside triphosphates, and 500 µM concentrations of primers. The primers were outer forward (837 to 862; 5' - GCAACAGGGAAYYTDCCGGTGCTC-3'), outer reverse (2020 to 1998; 5' - TTCATCCASGTRCAVCCRAACCA-3'), inner forward (846 to 874; 5' - AAYYTRCCCGGTGCTCYT TYTCTA-3'), and inner reverse (1882 to 1857; 5' - GTGAAR CARTACACYGGRCCRCANAC-3'). Degenerate bases are indicated with standard codes of the international union of Pure and applied chemistry. Nucleotide positions are numbered according to the HCV-J6 sequence. One microliter of the first-round reaction mixture was added to the second-round PCR, which had the same reagents as in the first round except for primers. Thermal-cycling conditions for the inner and outer reactions were denaturation for 120 s at 94 °C, followed by 35 cycles of 45 s at 94 °C, 45 s at 60 °C, and 120 s at 72 °C (during the last 25 cycles, the elongation time was increased by 20 s per cycle).

Cloning of cDNA and complexity analysis of 33 cloned cDNAs by gel shift The 1-kb HCV cDNA product was ligated into vector pT-adv and used to transform *Escherichia coli* TOP 10F' competent cells (TA Cloning kit; CLONTECH Laboratories, Inc.). Transformants were detected per manufacturer's protocol, and cloning efficiency was >90 %.

Polyacrylamide gel electrophoresis (8 %) was carried out with the addition of 15 % (W/V) urea to increase the resolution. For each subject, the gel shift patterns of 33 cloned cDNAs were examined by amplifying a 573-bp region spanning HVR1 and by using a nonradioactive method that detects distinct variants within a sample by using a combination of heteroduplex analysis (HDA) and single-stranded conformational polymorphism (SSCP) on a single gel (HDA+SSCP)^[15]. Sequences obtained from the serial passage were analyzed by using a divergent variant from the acute-phase sample from each subject. A clonotype is defined as two or more cloned cDNAs that have indistinguishable patterns of electrophoretic migration by HAD+SSCP. The complexity of the quasispecies was characterized by the clonotype ratio, calculated as the number of clonotypes divided by 33, the number of cloned cDNAs examined. The clonotype ratio therefore varies from 0.03 (homogenous) to 1 (highly complex).

Nucleotide sequencing To examine each subject's quasispecies for signature sequences (motifs uniquely shared by a group of sequences) and for evolutions in the sensitivity of the HDA+SSCP method, a subset of cloned cDNAs was identified. For each subject, at least two cloned cDNAs were selected for sequencing based on gel shift patterns: one from the majority clonotype, another from each clonotype consisting of more than 10 % of the 33 cloned cDNAs examined, and the cloned cDNA with the largest heteroduplex gel shift. Sequences were positively determined from the M13 reverse primer and negatively from T7 promoter binding sites of plasmid clones by using a PRISM 377 DNA Sequencer (version 3.3; Applied Biosystems, Inc., Foster City, Calif.). Sequences were assembled by using the ESEE3s program, and primer sequences were removed.

Phylogenetic analysis DNA distance matrices were calculated by using the DNADIST program, maximum-likelihood, with a transition-to-transversion ratio of 4.25^[19], and phylogenetic trees were generated by the Neighbor-joining program with

random addition. Subtype reference sequences used for phylogenetic analysis had the following accession numbers: 1a, M62321; 1b, D10934; 2a, D00944; 2b, D10988; 3a, D17763; 4a, Y11604; 5a, Y13184; 6a, Y12083.

The proportion of nonsynonymous substitutions per potential nonsynonymous site (dn) and synonymous substitutions per potential synonymous site (ds) were calculated by the method of Nei and Gojobori [20].

Statistical analysis Quantitative values were compared by using the Student's *t* test, the Kruskal Wallis test or the analysis of the variance when necessary. *P* values lower than 0.05 were considered significant. All statistical calculations were performed using the SPSS for Windows, version 8.0 software package.

RESULTS

Clonotypes detected by HDA+SSCP method

For each subject, use of a common cDNA clone to drive the HDA+SSCP gels permitted comparison of clonotypes among specimens. Among 99 cloned cDNAs from acute-Cphase specimens, 16 distinct patterns (clonotypes) were identified, in which five clonotypes were observed in two subjects each, and six clonotypes detected in subject C. However, acute and chronic samples from three individuals each shared no clonotype.

The quasispecies complexity was examined by assessing 33 cDNA clones from each specimen using the clonotype ratio. E2/HVR1 clonotype ratio values obtained for the samples from three individuals at each time point, ranging from 0.15 to 0.63, was plotted in Table 2. No trends were observed as clonotype ratio values changed with the changes in circulating viral load, serum ALT level (Figure 1).

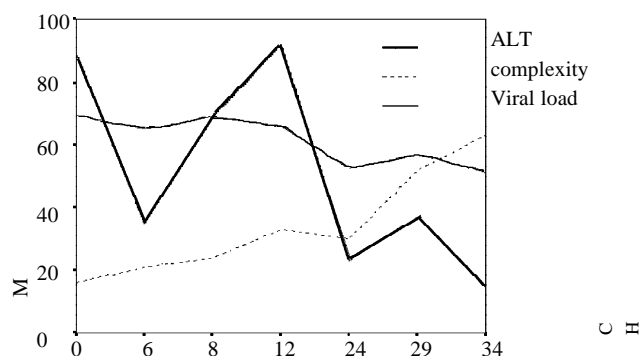


Figure 1 Changes in HCV viral load, ALT level, and HCV-E2 sequence clonotype ratio at serial samples from six individuals with HCV infection.

Initial sequence analysis

Using HDA+SSCP to select representative cloned cDNAs, 18 distinct cloned cDNAs were identified for sequencing. All such sequences were 1 022 bp, except for the sequences of single variants from subject F, which had a 1-bp deletion. To determine the genetic identity of cDNA clones of the same clonotype, two representative sequences representing the majority clonotype were compared for each specimen. There were eighteen differences among 14 pairs of 573-bp sequences (99.7 %). The ten sporadic substitutions were probably artifactual, occurring at a frequency of 4.1×10^{-5} sporadic substitutions per site per PCR cycle, similar the error rate of *Taq* during amplification of homogeneous sequences [21]. For each majority clonotype, one of the two sequences was free of sporadic substitutions and was used in all subsequent analyses to represent that clonotype. In addition, no two cloned cDNAs

identified as being distinct by HDA+SSCP analysis had identical sequences. Therefore, the HDA+SSCP method is both highly sensitive and specific in detecting differences among cDNA clones, as previously reported.

Phylogenetic analysis revealed that two subjects' sequence (A and B) clustered with 3b, while those of another (C) clustered with subtype 1b (Figure 3).

Quasispecies complexity and the outcome of acute infection

In each pair of samples from the same individual, the complexity of the quasispecies assessed using the clonotype ratio increased with time from seroconversion, both during the acute phase and also during the chronic phase (Figure 1). Quasispecies complexity correlated with estimated duration of HCV infection ($r = 0.931$, $P < 0.01$).

Table 2 Characteristics of samples and results of SSCP/HDA*

Sample	Genotype	Clonotype distribution**	No. of clonotypes	ratio
A1	3b	27,3,1,1,1	5	0.15
A2		15,7,5,2,1,1,1,1	8	0.24
A3		12,8,4,2,1,1,1,1,1,1	11	0.33
B1	3b	21,7,2,1,1	5	0.15
B2		19,7,2,2,1,1,1	7	0.21
B3		10,4,4,2,1,1,1,1,1,1,1,1,1	17	0.52
C1	1b	17,11,2,1,1,1	6	0.18
C2		8,4,4,2,2,1,1,1,1,1	10	0.30
C3		7,4,2,2,2,1,1,1,1,1,1,1,1,1,1,1,1,1,1,1,1	21	0.63

*Clonotype, a group of electrophoretically indistinguishable cloned cDNAs; clonotype ratio, the number of clonotypes divided by 33, the number of clones examined; **Each number represents a clonotype; the value indicates the number of cloned cDNAs assigned to that clonotype by the SSCP/HDA method

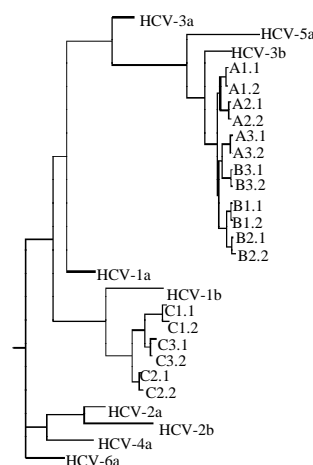


Figure 2 Unrooted tree showing the diversity of 372-nt E2/HVR1 sequences cloned from IDUs with HCV subtype 3b (A, B) and 1b (C). Identifiers correspond to those in Table 1, followed by the timing of the specimen (as defined in Materials and Methods). Representative sequences obtained from the GenBank database are shown in bold type. The number and line at the bottom denote the proportion of nucleotides substituted for a given horizontal branch length. The dendrogram was produced using Neighbor-joining program in the PHYLIP suite of programs.

A group:

171

GCSFSIFLLALFSLCTCPASGLEHNRNASGLYILTNDSCNSIVYEADDEVILHLP GCVPCTATGNQTSCWTPVSP TVAVRHPGATTASIRNHVDMLVG

```

-----T-----H-----
-----T-----K-----D-----S-----G-----
-----K-----D-----S-----G-----
-----Y-T-V-----V-----Y-----V-----
-----Y-T-V-----V-----Y-----V-----

```

AATLCCALYIGDLGCGAVFLVGQAFTFRPRRHITVQTCNCSIYPGHISGHRMAWDMMMNWSIPAIGLLISHLMRLPQTFFDLVIGAHWGV MAGLAYFSM

```

-----S-----
-----S-V-----A-----V-----R-----IT-----
-----S-V-----A-----T-----
-----S-V-----Q-----L-----
-----S-V-----Q-----L-----

```

← F1 384 E2 →

QGNWAKVCIVLIMFSGVDAGTHITGGAAAYSTSGLASLFTQGPQNLHLVNSNGSWHINSTALSCNDSLNTGFIAGLIVHHKFNSTGCPARMSSCKP

```

-----S-----V-----
-----G-----S-Y-S-S-RTA-FV-SP-Q-----N-----F-Y-----S-K-----
-----G-----N-Y-S-R-FV-SP-Q-----N-----F-Y-----S-KY-----
-----G-----T-Y-SDA-RTAK-IT-S-Q-----N-I-----F-Y-----
-----G-----T-Y-N-A-RTAK-IT-S-Q-----N-I-----F-Y-----

```

HVR1

511

ITAFKQGWGSLKDVNISGPSEDRPYCWHPYPPRCDTVQALKVCGPVYCF (A1.1)

```

----- (A1.2)
-----E-----T-M-S-----R-IE-PT----- (A2.1)
-----E-----T-M-S-----R-IE-PT-M----- (A2.2)
-----T-----S-S-N-SE----- (A3.1)
-----T-----S-S-N-SE----- (A3.2)

```

B group.

171

GCSFSIFLLALFSLCTCPASGLEHNRNTSGLYILTNDSCNKSIVYEADDVILHSPGCVPCTATGNQTSCWTPVSP TVAVRYPGATTASIRGHVDMLVG

```

-----K-----V-----
-----Q-----
-----Q-----M-----
-----G-----Q-----H-----M-----
-----Q-----M-----

```

AATLCSALYVGDLGCGAVFLVGQAFTFRPRRHATVQTCNCSIYPGHISGHRMAWDMMMNWSIPAIGLLVSHLMRLPQTFFDLVTGAHWGV MAGLAYFSM

```

-----I-----
-----V-----I-----I-----
-----I-----T-----I-----
-----I-----I-----V-----
-----I-----I-----V-----

```

← E1 384 E2 →

QGNWAKVGIVLIMFSGVDAGTYTTGGSAARSASGLVGLFSSGPQQNLHLVNSNGSWHINSTALNCNDSLNTGFIAGLIFYHKNSTGCPDRMSRCKP

```

-----R-----
-----T-HT-TF-R-P-S-Q-----S-----I-----SA-S-R-----
-----T-HT-TF-P-S-Q-----S-----I-L-SA-S-----
-----T-T-S-NMG-A-ITN-T-R-Q-T-----I-----I-----A-S-----
-----T-S-NVG-G-ITN-T-R-Q-T-----I-----I-----A-S-----

```

HVR1

511

ITAFEQGWGSLTDVNVSGSSEDRPYCWHPYPPRCPETVKAPTVCGPVYCF (B1.1)

```

----- (B1.2)
-----K-K-I-P-----N-Q----- (B2.1)
-----K-K-I-P-----N----- (B2.2)
-----D-I-----N-Q-L----- (B3.1)
-----D-----N-L----- (B3.2)

```

C group:

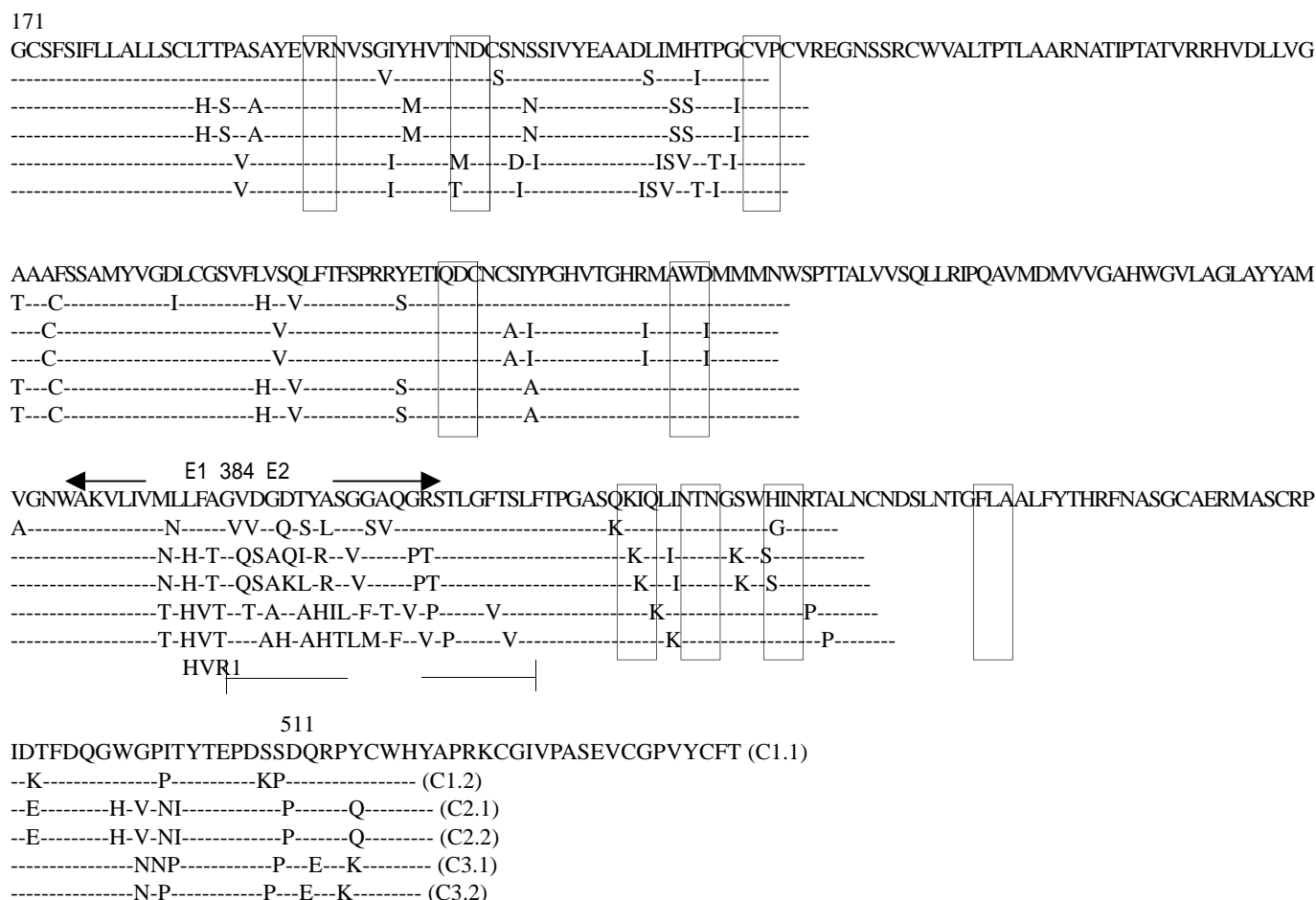


Figure 3 Alignment of inferred amino acid sequences for the majority clonotype and each clonotype from each subjects A, B, F at different time points. In the last column, an alphabetical label is given for each subject. Period indicate identity to the amino acid at that position in the first sequence. Position of the E1 and E2 region are indicated above the alignment, whereas that of HVR1 is indicated below the alignment at the N terminus of E2. potential N-linked glycosylation site are boxed. For each subject, numbers indicate the different clones obtained.

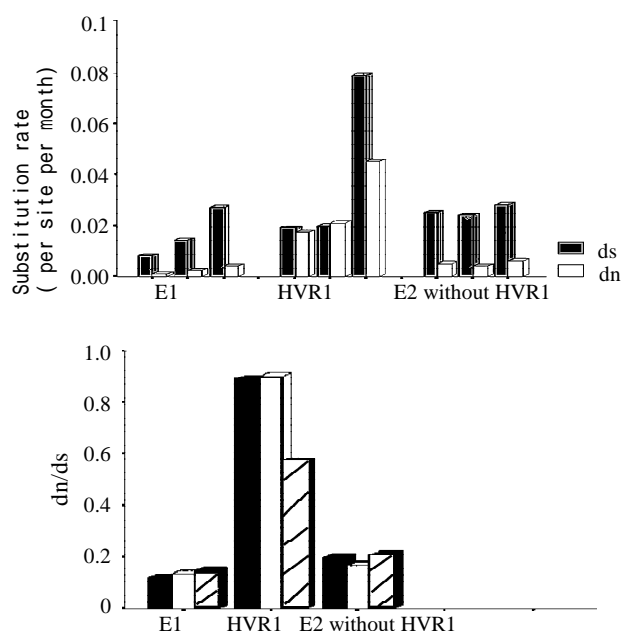


Figure 4 ds and dn, and dn/ds for acute-phase samples and persistent-phase samples from three individuals with HCV infection. In each panel, The individuals are presented in the order A, B.

Detailed analysis of sequences from serial passages

Figure 3 shows the amino acid alignment of the sequences derived from the cloned E2/HVR1 and the flanking E1 subfragment obtained from the three individuals and highlights the nonsynonymous changes. A phylogenetic study of these sequences (Figure 2) revealed that sequences from two individuals (A and B) tended to cluster tightly, segregated away from clusters of sequences from the individual C. For individuals A and B, the sequences from samples A1 to A3 or B1 to B3 maintained a low mean intrasample genetic distance: 0.0009 (A1), 0.0131 (A2), 0.0089 (A3), and 0.0014 (B1), 0.0054 (B2), 0.0046 (B3), respectively. The sequences found in the samples from individual C displayed a greater intrasample distance with late sample (C3 [collected 34 months after C1]) documenting a sharp increase (0.0214). An additional intrasample parameter evaluated in this study was the proportion of nonsynonymous substitutions per potential nonsynonymous site (dn) and synonymous substitutions per potential synonymous site (ds); It is shown in Figure 4 that ds values in the E1 region are lower than ones in E2/HVR1 at the samples from all individuals. There is the trend, observed during serial passages in three individuals, toward higher intersample dn/ds ratios in the E2/HVR1 than in E1, although

intersample dn/ds ratio were less than 1.0 with except for individual C (Figure 4). These data principally document that (i) early sequences have a low genetic divergence (oligoclonal profile), (ii) the dynamics and extent of the host selective pressure may differ among different individuals with different HCV genotypes, (iii) there are segmental effects of selective pressure on the envelope region of HCV genome.

DISCUSSION

Sequence analysis of cDNA clones derived from PCR products from individual patients has provided important information on the genetic variability of HCV HVR1 [22-29]. However, taking into account the quasispecies nature of HCV infection and the marked heterogeneity of patients with chronic HCV infection, sequence analysis of a large number of clones would be necessary for accurate assessment of viral evolution in individuals, but because of the effort and expense, published studies obtain sequence information from a small number of colonies per subject. To overcome this potentially serious limitation, HDA and SSCP assays have been developed and proposed as means of reducing sequence analyses [30-32]. Electrophoretic analysis of SSCP has been more expedient, but its sensitivity (ability to identify distinct clones) is limited and it does not provide an estimate of genetic distance [33,34]. Heteroduplex analysis (HDA) is also convenient and provides information on both genetic complexity and distance [35-43]. However, HDA alone may not be sufficiently sensitive. Because the HVR1 PCR product is less than 200 base, the distance between heteroduplexes and homoduplex does not accurately reflect the degree of heterogeneity [30]. Our approach is a method for measuring HCV quasispecies complexity that combines HDA and SSCP in a single gel visualized with UV light. Furthermore, we repeated studies using a larger region in the exposed portion of the envelope 2 gene. Similar sensitivity to the HVR1 has been shown. The method was sensitive and specific for detecting clonotypes, and the number of clonotypes detected correlated strongly with sequence diversity when 33 cloned cDNA are assessed [15].

Artificial 'minor' quasispecies can result from *Taq* polymerase-derived errors introduced during amplification [21] or from selection during amplification and cloning procedures [44]. In this study, PCR artifacts have been minimized by the use of thermostable polymerases with proofreading function; selection phenomena are not also considered, because the cloning efficiency is very high (>90 %) and defective sequences (deletion or stop codons) are not detected. It is important that the variability of the E1 and E2/HVR1 sequences in each sample was limited to segregating polymorphisms, suggesting that the nucleotide substitutions in these sequences are spontaneous mutations.

The current study principally document that low quasispecies complexity and intrasample genetic divergence was observed in the first samples collected from these three individuals, before a specific humoral immune response was elicited, or soon after antibody production, suggests that in its early phase HCV infection may be an oligoclonal event. Despite the vulnerability of IDUs to HCV multiple transmission through a variety of unknown routes, we found on evidence of mixed HCV genotype infection, neither did we find higher quasispecies complexity or genetic distance values in the first samples from the IDU compared to the blood donor (do not shown). Sequencing of inserted E1 and E2/HVR1 clones derived from all three subjects shows that variation in sequences of the minority variants involved single-nucleotide

substitutions from majority variant, accounting for the tight clustering of sequences seen in a dendrogram. These data are consistent with quasispecies evolution from a single HCV founder strain and again point to the rarity of multiple HCV carriage in IDUs [45]. Meanwhile, We note that there were differences in quasispecies complexity and diversity in the circulation before and early after the appearance of antibody. In individual A with subtype-3b infection, there was only a single change in the E2/HVR1 region in the first sample (before seroconversion), and the variants that subsequently emerged possessed more changes suggesting that these and the dominant variant belong to one monophyletic group. By contrast, there was multiple substitution in the E2/HVR1 region in the first sample (early after seroconversion) from individual C with subtype-1b infection. Such a disparity in genetic complexity of HCV in samples at the acute stage of infection has been noted in a previous study of three patients with acute hepatitis C [23]. Data from our study suggest that difference in viral quasispecies complexity and diversity in early samples could be due to a variety of factors, including whether effective humoral responses or cellular responses have been triggered, or possibly the subtype. However, it is possible that mixed infections are in fact common but that one subtype prevails and the other becomes undetectable. It would be feasible to apply the HAD+SSCP procedure to larger numbers of serum samples to confirm the absence or paucity of multiple infection in IDUs or patient subgroup. This confirmation would imply that vaccination programs employing live, attenuated HCV vaccines might be more effective in preventing primary HCV infections than inactivated, subunit, or epitope vaccines would be.

From a mechanistic perspective, variation with the HCV genome is assumed to be caused by random mutation and selection of variants which are most fit to propagate in a given host [46,47]. Generally, synonymous changes are often thought to represent a molecular clock, independent of external pressure and expected to occur at a rate proportional to the organism's reproductive rate. Whereas nonsynonymous changes are selected by immune pressure [47]. The results shown in Figure 4 are the trend, pronounced in most of samples, toward lower ds values in the E1 than in the 5' portion of E2. Lower ds values in the 5' half of E1 than in a 3' segment of E2 have been detailed in recent studies [24,51,52]. Lower ds values may indicate that E1 region has some constraints on synonymous variation, such as RNA secondary structure or binding sites for factors that regulate replication or translation. However, In protein-coding regions, multiple forces affect the balance between fixation of silent (synonymous) mutations versus those that alter amino acid sequence (nonsynonymous). In the present study, HVR1 variation during 6-8 months of infection did not reveal a common pattern of increasing diversity within each subject, though later sequences did diverge from earlier ones, indicating the action of selective forces. In addition, there is the trend, also pronounced in a longitudinal study of three subjects each, toward higher dn/ds ratios (as a surrogate indicator for immune pressure) in the E2/HVR1 than in E1. These results suggest that selective pressure acts differently on different genomic regions. Since the high mutation rate within the hypervariable regions of HCV E2 or the V loops Of HIV gp120 could be explained by the fact that these regions are free of structural constraints, a role for the HVR1 of HCV (and other viruses) as decoy antigen has recently been proposed, stimulating a strong immune response so that a early response to a highly immunogenic region might suppress or delay the response to other less-dominant epitopes, resulting in a diversion of the immune response away from more-conserved regions [48-50], but in some cases, is ineffective for viral clearance [51].

In conclusion, HDA+SSCP assay facilitates rapid and reliable assessment of HCV quasispecies diversity. Combined with nucleotide-sequencing procedure, it provides evidence that different dynamics of quasispecies evolution is associated with viral features and its fitness for individual environments. Mutations of actively replicating virus arise stochastically with certain functional constraints. In a longitudinal study of three subjects, HVR1 variation during the first 8 months of infection did not reveal a common pattern of increasing diversity within each subject, though later sequences did diverge from earlier one. We were unable to identify an envelope sequence motif that predicts the outcome of primary infection.

REFERENCES

- 1 **Meier V**, Mihm S, Braun PW, Ramadori G. HCV-RNA positivity in peripheral blood mononuclear cells of patients with chronic HCV infection: does it really mean viral replication. *World J Gastroenterol* 2001; **7**: 228-234
- 2 **Braun PW**, Meier V, Braun F, Ramadori G. Combination of "low-dose" ribavirin and interferon alfa-2a therapy followed by interferon alfa-2a monotherapy in chronic HCV infected non-responders and relapsers after interferon alfa-2a monotherapy. *World J Gastroenterol* 2001; **7**: 222-227
- 3 **Tong MJ**, El-Fara NS, Reikes AR, Co RL. Clinical outcomes after transfusion-associated hepatitis C. *N Engl J Med* 1995; **332**: 1463-1466
- 4 **Villano SA**, Vlahov D, Nelson KE, Cohn S, Thomas DL. Persistence of viremia and the importance of long-term follow-up after acute hepatitis c infection. *Hepatology* 1999; **29**: 908-914
- 5 **Hoofnagle JH**. Hepatitis C: the clinical spectrum of disease. *Hepatology* 1997; **26**: 15s-20s
- 6 **Chung RT**, He W, Saquib A, Contreras AM, Xavier RJ, Chawla A, Wang TC, Schmidt EV. Hepatitis C virus replication is directly inhibited by IFN-alpha in a full-length binary expression system. *Proc Natl Acad Sci USA* 2001; **98**: 9847-9852
- 7 **Chen S**, Wang YM, Li CM, Fang YF. Molecular epidemiology of HCV infection in intravenous drug abusers. *Shijie Huaren Xiaohua Zazhi* 2001; **9**: 526-528
- 8 **Kato N**, Ootsuyama Y, Tanaka T, Nakagawa M, Nakazawa T, Muraio K, Ohkoshi S, Hijikata M, Shimotohno K. Marked sequence diversity in the putative envelope proteins of hepatitis C viruses. *Virus Res* 1992; **22**: 107-123
- 9 **Martell M**, Esteban JI, Quer J, Genesee J, Weiner A, Esteban R, Guardia J, Gomez J. Hepatitis C virus (HCV) circulates as a population of different but closely related genomes: quasispecies nature of HCV genome distribution. *J Virol* 1992; **66**: 3225-3229
- 10 **Allain JP**, Dong Y, Vandamme AM, Moulton V, Salemi M. Evolutionary rate and genetic drift of hepatitis C virus are not correlated with the host immune response: studies of infected donor-recipient clusters. *J Viral* 2000; **74**: 2541-2549
- 11 **Forns X**, Purcell H, Bukh J. Quasispecies in viral persistence and pathogenesis of hepatitis C virus. *Trends Microbiol* 1999; **7**: 402-409
- 12 **Bukh J**, Miller RH, Purcell HR. Genetic heterogeneity of hepatitis C virus: quasispecies and genotypes. *Semin Liver Dis* 1995; **15**: 41-63
- 13 **Weiner AJ**, Brauer MJ, Rosenblatt J, Richman KH, Tung J, Crawford K, Bonino F. Variable and hypervariable domains are found in the regions of HCV corresponding to the flavivirus envelope and NS1 proteins and the pestivirus envelope glycoproteins. *Virology* 1991; **180**: 842-848
- 14 **Weiner AJ**, Geysen HM, Christopherson C, Hall EJ, Mason TJ, Saracco G, Bonino F. Evidence for immune selection of hepatitis C Virus (HCV) putative envelope glycoprotein variants: potential role in chronic HCV infections. *Proc Natl Acad Sci USA* 1992; **89**: 3468-3472
- 15 **Wang YM**, Ray SC, Laeyendecker O, Ticehurst RJ, Thomas D. Assessment of hepatitis C virus sequence complexity by electrophoretic mobilities of both single- and double-stranded DNAs. *J Clin Microbiol* 1998; **36**: 2982-2989
- 16 **Wang PZ**, Nie QH, Zhang ZW, Bai XG. Quantitative study of HCV RNA in different population of hepatitis C virus infection. *Shijie Huaren Xiaohua Zazhi* 2000; **8**: 1247-1250
- 17 **Park Y**, Lee KO, Oh MJ, Chai YG. Distribution of genotypes in the 5' untranslated region of hepatitis C virus in Korea. *J Med Microbiol* 1998; **47**: 643-647
- 18 **Smith DB**, Simmonds P. Characteristics of nucleotide substitution in the hepatitis C virus genome: constraints on sequence change in coding regions at both ends of the genome. *J Mol Evol* 1997; **45**: 238-246
- 19 **Nei M**, Gojobori T. Simple methods for estimating the numbers of synonymous and nonsynonymous nucleotide substitutions. *Mol Biol Evol* 1986; **3**: 418-426
- 20 **Smith DB**, McAllister J, Casino C and Simmonds P. Virus 'quasispecies': making a mountain out of a molehill? *J Gen Virol* 1997; **78**: 1511-1519
- 21 **Honda M**, Kaneko S, Sakai A, Unoura M, Murakami S, Kobayashi K. Degree of diversity of hepatitis C virus quasispecies and progression of liver disease. *Hepatology* 1994; **20**: 1144-1151
- 22 **Manzin A**, Solforosi L, Petrelli E, Macarri G, Tosone G, Piazza M, Clementi M. Evolution of hypervariable region 1 of hepatitis C virus in primary infection. *J Virol* 1998; **72**: 6271-6276
- 23 **McAllister J**, Casino C, Davidson F, Power J, Lawlor E, Yap PL, Simmonds P, Smith DB. Long-term evolution of the hypervariable region of hepatitis C virus in a common-source-infected cohort. *J Virol* 1998; **72**: 4893-4905
- 24 **Ni YH**, Chang MH, Chen PJ, Lin HH, Hsu HY. Evolution of hepatitis C virus quasispecies in mothers and infants infected through mother-to-infant transmission. *J Hepatol* 1997; **26**: 967-974
- 25 **Faci P**, Shimonda A, Wang D, Cabezu T, De-Gioannis D, Strazzere A, Shimizu Y, Shapiro M, Alter HJ, Purcell RH. Prevention of hepatitis C virus infection in chimpanzees by hyperimmune serum against the hypervariable region 1 of the envelope 2 protein. *Proc Natl Acad Sci USA* 1996; **93**: 15394-15399
- 26 **Okamoto H**, Kojima M, Okada SI, Yoshizawa H, Iizuka H, Tanaka T, Muchmore EE, Ito Y, Mishira S. Genetic drift of hepatitis C virus during an 8.2 year infection in a chimpanzee: variability and stability. *Virology* 1992; **190**: 894-899
- 27 **Sakamoto N**, Enomoto N, Kurosaki M, Marumo F, Sato C. Sequential change of the hypervariable region of the hepatitis C virus genome in acute infection. *J Med Virol* 1994; **42**: 103-108
- 28 **Weiner AJ**, Thaler MM, Crawford K, Ching K, Kansopon J, Chien DY, Hall JE, Hu F, Houghton M. A unique predominant hepatitis C virus variant found in an infant born to a mother with multiple variants. *J Virol* 1993; **67**: 4365-4368
- 29 **Lee JH**, Stripf T, Roth WK, ZeuZem S. Non-isotopic detection of hepatitis C virus quasispecies by single strand conformation polymorphism. *J Med Virol* 1997; **53**: 245-251
- 30 **Moribe T**, Hayashi N, Kanazawa Y, Mita E, Fusamoto H, Negi M, Kaneshige T, Igimi H, Kamada T, Uchida K. Hepatitis C viral complexity detected by single-strand conformation polymorphism and response to interferon therapy. *Gastroenterology* 1995; **108**: 789-795
- 31 **Sullivan DG**, Wilson JJ, Carithers RLJ, Perkins JD, Gretch DR. Multigene tracking of hepatitis C virus quasispecies after liver transplantation: correlation of genetic diversification in the envelope region with asymptomatic or mild disease patterns. *J Virol* 1998; **72**: 10036-10043
- 32 **Cotton RG**. Current methods of mutation detection. *Mutat Res* 1993; **285**: 125-144
- 33 **Carrington M**, Millter T, White M, Gerrard B, Stewart C, Dean M, Mann D. Typing of HLA-DQA1 and DQB1 using

- DNA single-stranded conformational polymorphism. *Hum Immun* 1992; **33**: 208-212
- 34 **Calvo PL**, Kansopon J, Sra K, Quan S, Dinello R, Guaschino R, Calabrese G, Danielle F, Brunatto MR, Bonino F, Massaro L, Polito A, Houghton M, Weiner AJ. Hepatitis C virus heteroduplex tracking assay for genotype determination reveals diverging genotype 2 isolates in Italian hemodialysis patients. *J Clin Microbiol* 1998; **36**: 227-233
- 35 **Delwart EL**, Shpaer EG, Louwagie J, McCutchan FE, Graz M, Rubsamen WH, Mullins JJ. Genetic relationships determined by a DNA heteroduplex mobility assay: analysis of HIV-1 env genes. *Science* 1993; **262**: 1257-1261
- 36 **Chen S**, Wang YM, Fang YF, Wu ZJ. Genetic complexity of the envelope region 2 (E2) of hepatitis C virus in HCV-infected individuals. *Zhonghua Weishengwuxue He Mianyixue Zazhi* 2001; **21**: 397-399
- 37 **Gavier B**, Martinez-Gonzalez MA, Riezu-Boj JJ, Lasarte JJ, Garcia N, Civeira MP, Prieto J. Viremia after one month of interferon therapy predicts treatment outcome in patients with chronic hepatitis C. *Gastroenterology* 1997; **113**: 1647-1653
- 38 **Gretch DR**, Polyak SJ, Wilson JJ, Carithers RL, Jr., Perkins JD, Corey L. Tracking hepatitis C virus quasispecies major and minor variants in symptomatic and asymptomatic liver transplant recipients. *J Virol* 1996; **70**: 7622-7631
- 39 **Kreis S**, Whistler T. Rapid identification of measles virus strains by the heteroduplex mobility assay. *Virus Res* 1997; **47**: 197-203
- 40 **Nelson JAE**, Fiscus SA, Swanstrom R. Evolutionary variants of the human immunodeficiency virus type 1 V3 region characterized by using a heteroduplex tracking assay. *J Virol* 1997; **71**: 8750-8758
- 41 **Polyak SJ**, Faulkner G, Carithers RL, Corey L, Gretch DR. Assessment of hepatitis C virus quasispecies heterogeneity by gel shift analysis: correlation with response to interferon therapy. *J Infect Dis* 1997; **175**: 1101-1107
- 42 **Wilson JJ**, Polyak SJ, Day TD, Gretch DR. Characterization of simple and complex hepatitis C virus quasispecies by heteroduplex gel shift analysis: correlation with nucleotide sequencing. *J Gen Virol* 1995; **76**: 1763-1771
- 44 **Forns X**, Bukh J, Purcell RH, Emertson SU. How *Escherichia coli* can bias the results of molecular cloning: preferential selection of defective genomes of hepatitis C virus during the cloning procedure. *Proc Natl Acad Sci USA* 1997; **94**: 13909-13914
- 45 **Harris KA**, Teo CG. Diversity of hepatitis C virus quasispecies evaluated by denaturing gradient gel electrophoresis. *Clin Diagn Lab Immunol* 2001; **8**: 62-73
- 46 **Kato N**, Ootsuyama Y, Tanaka T, Nakagawa M, Nakazawa T, Muraio K, Ohkoshi S, Hijikata M, Shimotohno K. Humoral immune response to hypervariable region 1 of the putative envelope glycoprotein (gp70) of hepatitis C virus. *J Virol* 1993; **67**: 3923-3930
- 47 **Gojobori T**, Morijama EN, Kimura M. Molecular clock of viral evolution, and the neutral theory. *Proc Natl Acad Sci USA* 1990; **87**: 10015-10018
- 48 **Zhang L**, Diaz RS, Ho DD, Mosley JW, Busch MP, Mayer A. Host-specific driving force in human immunodeficiency virus type 1 evolution in vivo. *J Virol* 1997; **71**: 2555-2561
- 49 **Wyatt R**, Sullivan N, Thali M, Repke H, Ho D, Robinson J, Posner M, Sodroski J. Functional and immunologic characterization of human immunodeficiency virus type 1 envelope glycoproteins containing deletions of the major variable regions. *J Virol* 1993; **67**: 4557-4565
- 50 **Garrity RR**, Rimmelzwaan G, Minassian A, Tsai WP, Lin G, de-Jong JJ, Goudsmit J, Nara PL. Refocusing neutralizing antibody response by targeted dampening of an immunodominant epitope. *J Immunol* 1997; **159**: 279-289
- 51 **Ray SC**, Wang YM, Laeyendecker O, Ticehurst JR, Villano SA, Thomas DL. Acute hepatitis C virus structural gene sequences as predictors of persistent viremia: hypervariable region 1 as a decoy. *J Virol* 1999; **73**: 2938-2946
- 52 **Smith DB**, Simmonds P. Characteristics of nucleotide substitution in the hepatitis C virus genome: constraints on sequence change in coding regions at both ends of the genome. *J Mol Evol* 1997; **45**: 234-246

Edited by Ma JY

• VIRAL HEPATITIS •

Activity of HDV ribozymes to trans-cleave HCV RNA

Yue-Cheng Yu, Qing Mao, Chang-Hai Gu, Qi-Fen Li, Yu-Ming Wang

Yue-Cheng Yu, Qing Mao, Chang-Hai Gu, Qi-Fen Li, Yu-Ming Wang, Institute of Infectious Diseases of Chinese PLA, Southwest Hospital, Third Military Medical University, Chongqing 400038, China
Supported by the National Natural Science Foundation of China, No.39600031

Correspondence to: Dr. Yue-Cheng Yu, Institute of Infectious Diseases of Chinese PLA, Southwest Hospital, Third Military Medical University, Chongqing 400038, China. yuechengyu212001@163.net

Telephone: +86-23-68754147 **Fax:** +86-23-68754142

Received 2001-11-02 **Accepted** 2001-11-27

Abstract

AIM: To explore whether HDV ribozymes have the ability to trans-cleave HCV RNA.

METHODS: Three HDV genomic ribozymes were designed and named RzC1, RzC2 and RzC3. The substrate RNA contained HCV RNA 5'-noncoding region and 5'-fragment of C region (5'-NCR-C). All the ribozymes and HCV RNA 5'-NCR-C were obtained by transcription in vitro from their DNA templates, and HCV RNA 5'-NCR-C was radiolabelled at its 5'-end. Under certain pH, temperature, appropriate concentration of Mg^{2+} and deionized formamide, these ribozymes were respectively or simultaneously mixed with HCV RNA 5'-NCR-C and reacted for a certain time. The trans-cleavage reaction was stopped at different time points, and the products were separated with polyacrylamide gel electrophoresis (PAGE), displayed by autoradiography. Percentage of trans-cleaved products was measured to indicate the activity of HDV ribozymes.

RESULTS: RzC1 and RzC2 could trans-cleave 26 % and 21.8 % of HCV RNA 5'-NCR-C under our reaction conditions with $2.5 \text{ mol} \cdot \text{L}^{-1}$ deionized formamide respectively. The percentage of HCV RNA 5'-NCR-C trans-cleaved by RzC1, RzC2 or combined usage of the three ribozymes increased with time, up to 24.9 %, 20.3 % and 37.3 % respectively at 90 min point. Almost no product from RzC3 was observed.

CONCLUSION: HDV ribozymes are able to trans-cleave specifically HCV RNA at certain sites under appropriate conditions, and combination of several ribozymes aiming at different target sites can trans-cleave the substrate more efficiently than using only one of them.

Yu YC, Mao Q, Gu CH, Li QF, Wang YM. Activity of HDV ribozymes to trans-cleave HCV RNA. *World J Gastroenterol* 2002; 8(4):694-698

INTRODUCTION

Ribozymes are sorts of small RNAs which have catalytic activity, and some of them can bind specifically through Watson-Crick base pairs with and trans-cleave substrate RNA in appropriate target sites^[1-4]. Hammerhead ribozymes and hairpin ribozymes have been tried widely to cleave many target RNAs, such as pathogenic microbes RNA^[5-10], oncogene mRNA^[11-15] and other kinds of pathogenity-associated functional mRNA^[16-18]. A great deal of experiments have demonstrated that these

ribozymes, if well-designed, could be applied as antiviral or antitumor gene therapeutic drugs. Yet there are still few researches showing whether HDV ribozymes, owning a kind of pseudoknot-like secondary structure, have the ability to kill pathogenic virus or not. HDV ribozymes include genomic ribozymes (g.Rz) and antigenomic ribozymes (ag.Rz), of them the latter is duplicate intermediates of HDV^[19,20]. This study was to evaluate the ability of g.Rz to trans-cleave HCV RNA at molecular levels.

MATERIALS AND METHODS

Reagents

All the cDNA of ribozymes were synthesized in a DNA synthesizer and purified with $160 \text{ g} \cdot \text{L}^{-1}$ denatured (7 mol·L⁻¹ urea) polyacrylamide gel electrophoresis in Shanghai Sangon Bioengineering Company. Plasmid pHCV-neo was kindly provided by Dr. Wang working in our institute. Polymerase chain reaction (PCR) reagents and T7 transcription kit (RibomaxTM) were purchased from Sino-American Bioengineering Company. Agarose Gel DNA Purification Kit, calf intestinal alkaline phosphatase (CIP) and T4 polynucleotide kinase were bought from Boehringer Mannheim Co. $\gamma\text{-}^{32}\text{P}\text{-ATP}$ was the product of Beijing Yuhui Co, and KODAK X-ray film was chosen to do autoradiography.

Preparation of template for transcription of substrate in vitro

pHCV-neo contains full length of HCV RNA 5'-NCR (341nt), translation-initiating codon AUG and 5'-fragment of C region (90nt). Sequence of HCV RNA 5'-NCR-C has been proved to be identical with that of HCV strains isolated from Chinese people reported by Bi et al. pHCV-neo has T7 phage promoter sequence ahead of HCV cDNA. Transcription template of HCV RNA 5'-NCR-C was prepared by the PCR method. The upper primer was T7 phage promoter sequence: 5'-TAA TAC GAC TCA TAG-3', and the reversed primer identified with the sequence from 413th to 383th nucleotide (nt) of HCV genome: 5'-GCGGGATCCCCGGAACCTTGACGTCCTG-3' (the italic letter was cleavage site of BamHI designed for future cloning). Route PCR process was adopted. PCR products were purified by Agarose Gel DNA Purification Kit, and the unpaired A at 3' end was cut off with Klenow enzyme. All these procedures were made according to the kit guidebook. After that, PCR products were regained by phenol (pH8.0)/chloroform/isoamyl alcohol (volume ratio 25:24:1) extraction, precipitated with ethanol, and redissolved with RNAase-free water.

Design of ribozymes and preparation of their transcription templates

Based on the structure of our formerly reported g.Rz55, we designed here three kinds of HCV RNA-targeting g.Rzs named RzC1, RzC2 and RzC3 respectively. The target sequences and their location in HCV RNA 5'-NCR-C are shown in Table 1. Routine PCR process was adopted to prepare the transcription templates of the ribozymes. PCR templates were formerly synthesized cDNA of these ribozymes. The upper primer contained T7 phage promoter

sequence (Italic letters): 5'-TAATACGACTCACTATAG TCTAGAGTCCCAGCCTCCTCGCTGGC-3', and the reversed primer was 5'-CTCGGATCCGTCCTCCATTCGCCATTCCG AAGAATGTTGCCC-3'. Purification of PCR products and treatment of their 3'-end were the same as that mentioned above.

Table 1 Target sequences and their location in HCV RNA 5'-NCR-C

Target sequence	Location in HCV RNA 5' NCR-C	Ribozyme
5'...CGU ↓ GCAGCCU...3'	107-113 nt	RzC1
5'...GUU ↓ GGGUCG...3'	268-274 nt	RzC2
5'...CAU ↓ GAGCACG...3'	345-351 nt	RzC3

Transcription *in vitro*

Each transcription reaction was done under 37 °C for 4 h, with a total volume of 20 µl, containing template DNA 1.5 µg, rNTP (preservation concentration 25 mmol·L⁻¹) 6 µl, 5× transcription buffer 4 µl, T7 RNA polymerase 2 µl (preservation concentration 1 µ·µl⁻¹). Digestion of DNA templates, purification and quantification of transcription products were executed according to the kit guidebook.

Radiolabel of substrate RNA at 5'-end

Phosphate at the 5'-end of substrate RNA was deleted with CIP, then the substrate RNA was radiolabelled at the 5'-end with T4 polynucleotide kinase and γ-³²P-ATP. After that, substrate RNA was purified by routine phenol (pH4.5)/chloroform/ isoamyl alcohol (volume ratio 25:24:1) extraction, precipitated with ethanol, and redissolved with RNAase-free water and then quantified, and stored at -20 °C. All operations were made according to the guidelines.

Trans-cleavage reaction and measurement of effects-time relationship

Trans-cleavage reaction was done under conditions with or without deionized formamide having a final concentration of 2.5 mol·L⁻¹. Each reaction system contained radiolabelled substrate RNA 50 nmol·L⁻¹, ribozymes 5 µmol·L⁻¹, Tris·Cl (pH7.5) 50 mmol·L⁻¹, with a total volume of 10 µL. The standard reaction protocol was as follows: heat the tube containing the reaction mixtures to 95 °C for 3 min → place on ice for 10 min → dip into 37 °C water for another 10 min → add prewarmed MgCl₂ to the final concentration of 20 mmol·L⁻¹ → keep the reaction temperature at 37 °C for 2 h → separate reaction products by electrophoresis on a 80 g·L⁻¹ polyacrylamide gel containing 7 mol·L⁻¹ urea → display the products by autoradiography at -70 °C (the X-ray film was exposed for 0.5 µs beforehand) for about 24 h → measure A value of the images with Gel Documentation-Analyzing Systems (Gel Doc™ 2000, Bio-Rad) and then calculate the percentage of substrate cleaved by the ribozymes.

Under the optimized cleavage conditions, following reactions were made in four tubes containing 15 µl mixtures each, of which three reactions were designed for each ribozyme to trans-cleave the target RNA, separately, and the fourth reaction for all the three ribozymes to trans-cleave the substrate RNA simultaneously and cooperatively. The reaction procedures were the same as that mentioned above, except that after MgCl₂ was added to the mixtures, the reactions were terminated at 10, 30 and 90 min time points. Five µL solution was removed from each tube at different time points for investigating the effects-time relationship.

Percentage of cleavage (%) = A value of cleaved substrate RNA / (A value of cleaved substrate RNA + A value of uncleaved substrate RNA) × 100%

RESULTS

Effects of the ribozymes to trans-cleave substrate RNA under different conditions

Transcription templates of RzC1, RzC2, RzC3 and HCV RNA 5'-NCR-C were proven to be obtained successfully by 20 g·L⁻¹ agarose gel electrophoresis. The ribozymes and substrate RNA were successfully synthesized by transcription *in vitro* known from 80 g·L⁻¹ denatured (7 mol·L⁻¹ urea) polyacrylamide gel electrophoresis.

According to the design, HCV RNA 5'-NCR-C should be trans-cleaved into 106nt (5' product) and 324nt (3' product) fragments by RzC1, 267nt and 163nt fragments by RzC2, and 344nt and 86nt fragments by RzC3. As HCV RNA 5'-NCR-C was radiolabelled at its 5'-end, only the 5'-products were displayed in X-ray films after autoradiography. The results showed that RzC1 and RzC2 are able to trans-cleave HCV RNA 5'-NCR-C under the selected reaction conditions, and the length of their cleavage products was set in accordance with the design. Percentage of substrate RNA cleaved by RzC1 and RzC2 under the conditions without deionized formamide at 2 h time point was 4.2 % and 3.5 %, respectively. With the addition of deionized formamide to the trans-cleavage reaction systems to a final concentration of 2.5 mol·L⁻¹, percentage of cleaved substrate RNA reached up to 26 % and 21.8 %, respectively at the same time point (Figure 1). It was surprising that under both conditions with or without deionized formamide, RzC3 almost had no trans-cleavage activity to HCV RNA 5'-NCR-C. Based on the whole experiment, we think that the reaction conditions with deionized formamide was better than that without it, thus being adopted in the future investigations.

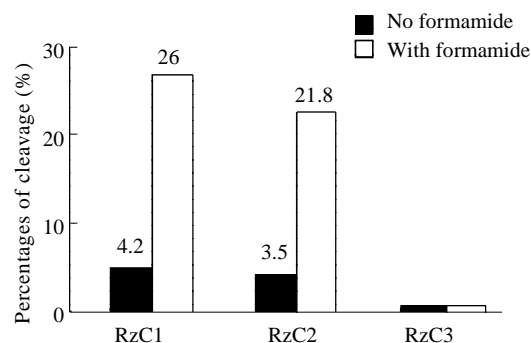


Figure 1 Effects of RzC1, RzC2 and RzC3 to trans-cleave HCV RNA 5'-NCR-C under different conditions (results came from image analysis).

Roles of the three ribozymes to trans-cleave substrate RNA at different time points

Under the optimized reaction conditions, fragments of HCV RNA 5'-NCR-C trans-cleaved by RzC1 and RzC2 were produced at the fixed time points (Figures 2 and 3). When the three ribozymes were added to one tube to trans-cleave HCV RNA 5'-NCR-C simultaneously, images of 106nt and 267nt fragments corresponding to the cleavage products of RzC1 and RzC2 respectively were observed in the same X-ray film (Figure 4), yet no marked image of 344nt fragment meaning the substrate RNA cleaved by RzC3 turned up at the same time.

Effects-time relationship of the ribozymes to trans-cleave substrate RNA

Percentage of cleaved substrate RNA by RzC1 and RzC2 was

6.1% and 4.6 % at 10 min time point, 14.0 % and 11.7 % at 30 min time point, and 24.9 % and 20.3 % at 90 min time point respectively. These results showed that the percentage of RzC1 and RzC2 to trans-cleave HCV RNA 5' -NCR-C increased with time. At the same time, nearly no effects of RzC3 to trans-cleave HCV RNA 5' -NCR-C was observed. The percentage of these ribozymes to trans-cleave HCV RNA 5' -NCR-C in one tube turned out to be 8.4 % at 10 min, 19.5 % at 30 min and 37.3 % at 90 min time point respectively (Figure 5). These results demonstrated that the combination of ribozymes aiming at different target sites could be applied to cleave substrate RNA more efficiently than using only one of them.

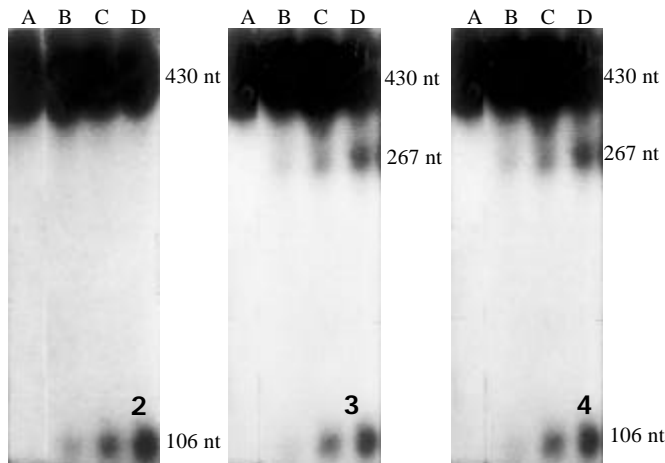


Figure 2 Results of trans-cleavage by RzC1. A: HCV RNA 5' -NCR-C in the system without ribozymes; B,C,D: Results of HCV RNA 5' -NCR-C trans-cleaved by RzC1 10, 30 and 90 min time points, respectively.

Figure 3 Results of trans-cleavage by RzC2. A: HCV RNA 5' -NCR-C in the system without ribozymes; B,C,D: Results of HCV RNA 5' -NCR-C trans-cleaved by RzC2 at 10, 30 and 90 min time points, respectively.

Figure 4 Results of trans-cleavage by combination of RzC1, RzC2 and RzC3. A: HCV RNA 5' -NCR-C in the system without ribozymes; B,C,D: Results of HCV RNA 5' -NCR-C trans-cleaved by the ribozymes at 10, 30 and 90 min time points, respectively.

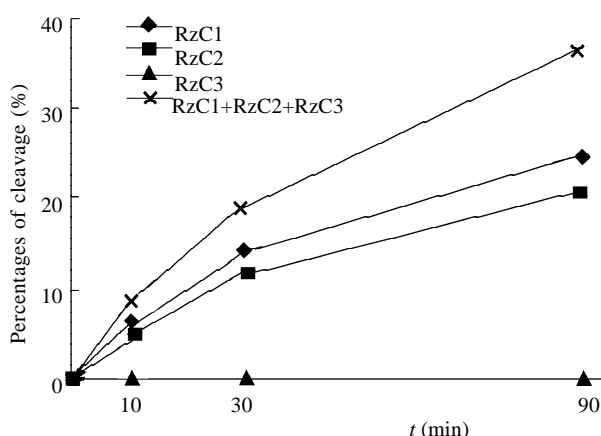


Figure 5 Effects-time relationship of RzC1, RzC2 and RzC3 to trans-cleave HCV RNA 5' -NCR-C.

DISCUSSION

HDV ribozymes were first reported for their self-cleavage activity, also named cis-cleavage, which meant splicing reaction occurring within the catalytic RNA molecule itself, i.e. intramolecular cleavage^[19,21]. Several years later, it was found that a self-cleavage HDV ribozyme could also be divided into

two parts, one part ("ribozyme" component) still maintained the catalytic activity and the other part (homologous "substrate" component) could be cleaved by the former intermolecularly when they were taken together again. This kind of intermolecular cleavage was called trans-cleavage, and the "ribozyme" components having trans-cleavage activity were usually described as trans-HDV ribozymes^[22]. Our previous studies have shown that trans-HDV genomic ribozyme g.Rz55 was able to trans-cleave its homologous substrate S87 with a percentage of about 69 % under conditions Tris-Cl 50 mmol·L⁻¹ (pH7.5) and MgCl₂ 20 mmol·L⁻¹^[23]. In recent years, some researches have found that the substrate-binding region of trans-HDV ribozymes might be changeable to some extent^[24]. These findings are the theoretical and experimental bases for reconstruction and application of HDV ribozymes to trans-cleave HCV RNA 5' -NCR-C.

Many studies have shown that HDV ribozymes owned a kind of special pseudoknot-like secondary structure which was different from that of hammerhead ribozymes and hairpin ribozymes^[25-29], so did their requirements to the target sequences of substrate RNA^[30-36]. Roy *et al.* reported that trans-ag.Rz was able to cleave 814nt HDAg mRNA efficiently at several target sites, and concluded that all the sequences having the characteristic of 5' ...R₄R₃R₂Y₋₁↓G₁N₂N₃(A/C/U)₄N₅N₆N₇...3' (R=A or G, Y=U or C) in HDAg mRNA might be the most possible sites to be cleaved by trans-ag.Rz^[37]. The results are of significant value to design trans-g.Rz, because the secondary structure of g.Rz and ag.Rz is similar.

Five principles have been abided by during our selection of target sites of trans-g.Rz in HCV RNA 5' -NCR-C. Firstly, the target sequence was in accordance with the basic requirements of g.Rz, i.e., the first base G at 3' -end of the cleavage site was designed to form G-U wobble pair with the g.Rz. Secondly, the best first base at 5' -end of the cleavage site in substrate RNA was U. It should be noted that at any time G must not be selected when determine the first base at 5' -end of the cleavage site, and also it is necessary to avoid that more than two consecutive C located at 5' -end of the cleavage site. Thirdly, the more G-C or C-G base pair in the 7bp target sequences, the better for the ribozymes to bind the substrate. Fourthly, regions forming long intramolecular Watson-Crick base pairs in the reported HCV RNA 5' -NCR-C secondary structure were avoided as possible as it could. Finally, target sequences were located in the important functional regions of HCV RNA 5' -NCR-C such as internal ribosome entry site (IRES) and translation-initiating codon. These were the most important basic principles to design trans-HDV ribozymes and determine the target sites to be cleaved.

According to the theories and rules mentioned above, we tried to design trans-genomic ribozymes RzC1, RzC2 and RzC3 to cleave their heterologous substrate RNA, i.e. HCV RNA. The results showed that under the optimized cleaving reaction conditions, RzC1 and RzC2 exhibited the ability to trans-cleave HCV RNA 5' -NCR-C, and the percentage of cleaved substrate were increased with time, up to 24.9 % and 20.3 % respectively at 90 min time point. Combination of all these ribozymes resulted in 37.3 % substrate RNA to be cleaved at the same reaction conditions and time. From these results, we got to know that rationally designed trans-HDV ribozymes had the activity to cleave HCV RNA 5' -NCR-C which was the heterologous substrate to such ribozymes, and the cleavage effects could be improved by applying different trans-HDV ribozymes to cleave HCV RNA at multiple target sites simultaneously.

In comparison of the self-cleavage and trans-cleavage

activity of HDV ribozymes at natural target sites in homologous substrate RNA and other target sites in HDV mRNA, the activity of RzC1 and RzC2 to trans-cleave HCV RNA 5' -NCR-C was a little lower, and RzC3 had almost no cleavage activity. By comparing the sequences and structure of RzC1, RzC2 and RzC3 to cis-HDV ribozymes and trans-HDV ribozymes reported by others, and the differences among the target RNAs, we suppose that the possible reasons may lie in several respects. Firstly, the target sites in HCV RNA 5' -NCR-C and the structure of trans-HDV ribozymes should be further optimized by more methods. For example, the calculation and application of the free energies required for forming pseudoknot and binding of ribozyme to substrate^[38], or other strategies to map the accessible sites in substrate for ribozyme to bind^[39,40]. Secondly, it is likely that the activity of trans-HDV ribozymes might be weakened if the A-U or U-A base pair just adjoined the G-U wobble pair when A-U or U-A and C-G or G-C base pairs co-existed in the binding regions of ribozymes and substrate RNA. Thirdly, the special secondary structure of HCV RNA 5' -NCR-C might impede the cleavage activity of trans-HDV ribozymes^[31,41]. Fourthly, other sequences at both ends of trans-HDV ribozymes might diminish their cleavage activity^[42]. Finally, different reaction conditions such as the kind of buffer might significantly influence the cleavage effects sometimes^[43]. Certain denaturing agents such as deionized formamide in an appropriate concentration may reduce the formation of complex secondary structure of substrate RNA, thus improve the trans-cleavage activity to some extent^[41]. A suitable pH of solution was very important for the trans-cleavage to occur too, and pH7.0-7.5 was commonly used during researches *in vitro*. Divalent cations such as Mg²⁺, Ca²⁺ and Mn²⁺ could bind and interact with the ribozymes' phosphate-pentose skeleton full of negative charges^[44,45], thus facilitating the ribozymes to fold into and maintain active structure, and/or take part in trans-cleavage reaction directly^[46-49].

HCV is an important pathogenic factor of chronic hepatitis, and related to the formation of cirrhosis and occurrence of hepatocarcinoma or cholangiocarcinoma^[50]. Finding new ways to control HCV infection is difficult but necessary. IRES and translation-initiating codon of HCV RNA are usually chosen as the trans-cleave target sequences not only because they are the important functional regions, but also they are very conservative in each HCV variant^[51]. As a result, ribozymes aiming at the two regions will have a universal cleavage effects on all of the HCV variants. Effects of HDV ribozymes to trans-cleave HCV RNA 5' -NCR-C at extracellular molecular levels are not completely in accordance with that exhibited intracellularly, because intracellular conditions and factors that influence the ribozyme activity are far more complicated than the extracellular ones. On the other hand, HDV ribozymes are the only kind of viral ribozymes which exist in mammalian cells naturally, especially in human hepatocytes. Based on these opinions and facts, it is expected that the intracellular location and cleavage activity of HDV ribozymes might be more efficient than that of hammerhead ribozymes and hairpin ribozymes, thus it is necessary and valuable to assess the roles of HDV ribozymes in trans-cleaving HCV RNA intracellularly.

REFERENCES

- Curtis EA**, Bartel DP. The hammerhead cleavage reaction in monovalent cations. *RNA* 2001; **7**: 546-552
- Lilley DM**. Structure, folding and catalysis of the small nucleolytic ribozymes. *Curr Opin Struct Bio* 1999; **9**: 330-338
- Tanner NK**. Ribozymes: The characteristic and properties of catalytic RNAs. *FEMS Microbio Rev* 1999; **33**: 257-275
- Welch PJ**, Barber JR, Wong-Staal F. Expression of ribozymes in gene transfer systems to modulate target RNA levels. *Curr Opin Biotechnol* 1998; **9**: 486-496
- Jia ZS**, Zhou YX, Lian JQ, Feng ZH, Li YG, Zhang WB. Computerized design of hepatitis C virus RNA-directed hammerhead ribozymes. *Shijie Huaren Xiaohua Zazhi* 1999; **7**: 300-302
- Li JG**, Zhou YX, Lian JQ, Jia ZS, Feng ZH. Inhibitory effect of ribozyme on HBeAg in human HCC cells. *Shijie Huaren Xiaohua Zazhi* 1999; **7**: 28-30
- Weinberg M**, Passman M, Kew M, Arbuthnot P. Hammerhead ribozyme-mediated inhibition of hepatitis B virus X gene expression in cultured cells. *J Hepatol* 2000; **33**: 142-151
- de-Feyter R**, Li P. Technology evaluation: HIV ribozyme gene therapy. Gene Shears Pty Ltd. *Curr Opin Mol Ther* 2000; **2**: 332-335
- Cagnon L**, Rossi JJ. Downregulation of the CCR5 beta-chemokine receptor and inhibition of HIV-1 infection by stable VA1-ribozyme chimeric transcripts. *Antisense Nucleic Acid Drug Dev* 2000; **10**: 251-261
- Han S**, Wu Z, Yang H, Wang R, Yie Y, Xie L, Tien P. Ribozyme-mediated resistance to rice dwarf virus and the transgene silencing in the progeny of transgenic rice plants. *Transg Res* 2000; **9**: 195-203
- Zhang CS**, Wang WL, Peng WD, Hu PZ, Chai YB, Ma FC. Promotion of apoptosis of SMMC-7721 cells by Bcl-2 ribozyme. *Shijie Huaren Xiaohua Zazhi* 2000; **8**: 417-419
- Lui VW**, He Y, Huang L. Specific down-regulation of HER-2/neu mediated by a chimeric U6 hammerhead ribozyme results in growth inhibition of human ovarian carcinoma. *Mol Ther* 2001; **3**: 169-177
- Ludwig A**, Saretzki G, Holm PS, Tiemann F, Lorenz M, Emrich T, Harley CB, von-Zglinicki T. Ribozyme cleavage of telomerase mRNA sensitizes breast epithelial cells to inhibitors of topoisomerase. *Cancer Res* 2001; **61**: 3053-3061
- Kijima H**, Scanlon KJ. Ribozyme as an approach for growth suppression of human pancreatic cancer. *Mol Biotechnol* 2000; **14**: 59-72
- Tokunaga T**, Tsuchida T, Kijima H, Okamoto K, Oshika Y, Sawa N, Ohnishi Y, Yamazaki H, Miura S, Ueyama Y, Nakamura M. Ribozyme-mediated inactivation of mutant K-ras oncogene in a colon cancer cell line. *Br J Cancer* 2000; **83**: 833-839
- Hu WY**, Fukuda N, Nakayama M, Kishioka H, Kanmatsuse K. Inhibition of vascular smooth muscle cell proliferation by DNA-RNA chimeric hammerhead ribozyme targeting to rat platelet-derived growth factor A-chain mRNA. *J Hypertens* 2001; **19**: 203-212
- Leavitt MC**, Yu G, Zhou C, Barber JR. Inhibition of interleukin-1beta (IL-1beta) production in human cells by ribozymes against IL-1beta and IL-1beta converting enzyme (ICE). *Antisense Nucleic Acid Drug Dev* 2000; **10**: 409-414
- LaVail MM**, Yasumura D, Matthes MT, Drenser KA, Flannery JG, Lewin AS, Hauswirth WW. Ribozyme rescue of photoreceptor cells in P23H transgenic rats: long-term survival and late-stage therapy. *Proc Natl Acad Sci USA* 2000; **97**: 11488-11493
- Yu YC**, Gu CH, Mao Q, Li QF, Wang YM. *In vitro* self-cleavage activity of hepatitis delta virus ribozymes with different length and its significance. *Shijie Huaren Xiaohua Zazhi* 2000; **8**: 39-41
- Diegelman AM**, Kool ET. Mimicry of the hepatitis delta virus replication cycle mediated by synthetic circular oligodeoxynucleotides. *Chem Biol* 1999; **6**: 569-576
- Wadkins TS**, Shih I, Perrotta AT, Been MD. A pH-sensitive RNA tertiary interaction affects self-cleavage activity of the HDV ribozymes in the absence of added divalent metalion. *J Mol Biol* 2001; **305**: 1045-1055
- Shih IH**, Been MD. Ribozyme cleavage of a 2,5-phosphodiester linkage: mechanism and a restricted divalent metal-ion requirement. *RNA* 1999; **5**: 1140-1148
- Yu YC**, Gu CH, Mao Q, Li QF, Wang YM. Trans-cleavage

- activity of hepatitis delta virus ribozymes. *J Med Coll PLA* 2000; **15**: 237-239
- 24 **Nishikawa F**, Roy M, Fauzi H, Nishikawa S. Detailed analysis of stem I and its 5' and 3' neighbor regions in the trans-acting HDV ribozyme. *Nucleic Acids Res* 1999; **27**: 403-410
- 25 **Wilson TJ**, Zhao ZY, Maxwell K, Kontogiannis L, Lilley DM. Importance of specific nucleotides in the folding of the natural form of the hairpin ribozyme. *Biochemistry* 2001; **40**: 2291-2302
- 26 **Pinard R**, Lambert D, Heckman JE, Esteban JA, Gundlach CW, Hampel KJ, Glick GD, Walter NG, Major F, Burke JM. The hairpin ribozyme substrate binding-domain: a highly constrained D-shaped conformation. *J Mol Biol* 2001; **307**: 51-65
- 27 **Zhao ZY**, Wilson TJ, Maxwell K, Lilley DM. The folding of the hairpin ribozyme: dependence on the loops and the junction. *RNA* 2000; **6**: 1833-1846
- 28 **Michiels PJ**, Schouten CH, Hilbers CW, Heus HA. Structure of the ribozyme substrate hairpin of Neurospora VS RNA: a close look at the cleavage site. *RNA* 2000; **6**: 1821-1832
- 29 **Fedor MJ**. Structure and function of the hairpin ribozyme. *J Mol Biol* 2000; **297**: 269-291
- 30 **Nakano S**, Chadalavada DM, Bevilacqua PC. General acid-base catalysis in the mechanism of a hepatitis delta virus ribozyme. *Science* 2000; **287**: 1493-1497
- 31 **Ferre-D'Amare AR**, Doudna JA. Crystallization and structure determination of a hepatitis delta virus ribozyme: use of the RNA-binding protein U1A as a crystallization module. *J Mol Biol* 2000; **295**: 541-556
- 32 **Matysiak M**, Wrzesinski J, Ciesiolka J. Sequential folding of the genomic ribozyme of the hepatitis delta virus: structural analysis of RNA transcription intermediates. *J Mol Biol* 1999; **291**: 283-294
- 33 **Wadkins TS**, Perrotta AT, Ferre-D'Amare AR, Doudna JA, Been MD. A nested double pseudoknot is required for self-cleavage activity of both the genomic and antigenomic hepatitis delta virus ribozymes. *RNA* 1999; **5**: 720-727
- 34 **Mercure S**, Lafontaine D, Ananvoranich S, Perreault J. Kinetic analysis of delta ribozyme cleavage. *Biochemistry* 1998; **37**: 16975-16982
- 35 **Walter NG**, Chan PA, Hampel KJ, Millar DP, Burke JM. A base change in the catalytic core of the hairpin ribozyme perturbs function but not domain docking. *Biochemistry* 2001; **40**: 2580-2587
- 36 **Perez-Ruiz M**, Barroso-DelJesus A, Berzal-Herranz A. Specificity of the hairpin ribozyme. Sequence requirements surrounding the cleavage site. *J Biol Chem* 1999; **274**: 29376-29380
- 37 **Roy G**, Ananvoranich S, Perreault J. Delta ribozyme has the ability to cleave in trans an mRNA. *Nucleic Acids Res* 1999; **27**: 942-948
- 38 **Isambert H**, Siggia ED. Modeling RNA folding paths with pseudoknots: application to hepatitis delta virus ribozyme. *Proc Natl Acad Sci USA* 2000; **97**: 6515-620
- 39 **Wrzesinski J**, Legiewicz M, Ciesiolka J. Mapping of accessible sites for oligonucleotide hybridization on hepatitis delta virus ribozymes. *Nucleic Acids Res* 2000; **28**: 1785-1793
- 40 **Nyholm T**, Andang M, Bandholtz A, Maijgren C, Persson B, Hotchkiss G, Fehniger TE, Larsson S, Ahrlund-Richter L. Interaction between hammerhead ribozyme and RNA substrates measured by a surface plasmon resonance biosensor. *J Biochem Biophys Methods* 2000; **44**: 41-57
- 41 **Ferre-D'Amare AR**, Doudna JA. RNA folds: insights from recent crystal structures. *Annu Rev Biophys Biomol Struct* 1999; **28**: 57-73
- 42 **Chadalavada DM**, Knudsen SM, Nakano S, Bevilacqua PC. A role for upstream RNA structure in facilitating the catalytic fold of the genomic hepatitis delta virus ribozyme. *J Mol Biol* 2000; **301**: 349-367
- 43 **Perrotta AT**, Shih I, Been MD. Imidazole rescue of a cytosine mutation in a self-cleaving ribozyme. *Science* 1999; **286**: 123-126
- 44 **Maderia M**, Hunsicker LM, DeRose VJ. Metal-phosphate interactions in the hammerhead ribozyme observed by 31P NMR and phosphorothioate substitutions. *Biochemistry* 2000; **39**: 12113-12120
- 45 **Butcher SE**, Allain FH, Feigon J. Determination of metal ion binding sites within the hairpin ribozyme domains by NMR. *Biochemistry* 2000; **39**: 2174-2182
- 46 **Wittberger D**, Berens C, Hammann C, Westhof E, Schroeder R. Evaluation of uranyl photocleavage as a probe to monitor ion binding and flexibility in RNAs. *J Mol Biol* 2000; **300**: 339-352
- 47 **Nishikawa F**, Nishikawa S. Requirement for canonical base pairing in the short pseudoknot structure of genomic hepatitis delta virus ribozyme. *Nucleic Acids Res* 2000; **28**: 925-931
- 48 **Hunsicker LM**, DeRose VJ. Activities and relative affinities of divalent metals in unmodified and phosphorothioate-substituted hammerhead ribozymes. *J Inorg Biochem* 2000; **80**: 271-281
- 49 **Hammann C**, Cooper A, Lilley DM. Thermodynamics of ion-induced RNA folding in the hammerhead ribozyme: an isothermal titration calorimetric study. *Biochemistry* 2001; **40**: 1423-1429
- 50 **Liu XF**, Zou SQ, Qiu FZ. Construction of HCV-core gene vector and its expression in cholangiocarcinoma. *World J Gastroenterol* 2002; **8**: 135-138
- 51 **Kruger M**, Beger C, Li QX, Welch PJ, Tritz R, Leavitt M, Barber JR, Wong-Staal F. Identification of eIF2B gamma and eIF2 gamma as cofactors of hepatitis C virus internal ribosome entry site-mediated translation using a functional genomics approach. *Proc Natl Acad Sci USA* 2000; **97**: 8566-8571

Edited by Ma JY

• VIRAL HEPATITIS •

Detection of enteroviruses and hepatitis a virus in water by consensus primer multiplex RT-PCR

Jun-Wen Li, Xin-Wei Wang, Chang-Qing Yuan, Jin-Lai Zheng, Min Jin, Nong Song, Xiu-Quan Shi, Fu-Huan Chao

Jun-Wen Li, Xin-Wei Wang, Chang-Qing Yuan, Jin-Lai Zheng, Min Jin, Nong Song, Xiu-Quan Shi, Fu-Huan Chao, Department of Environment and Health, Institute of Health and Environmental Medicine of Tianjin, 1 Da Li Road, Tianjin 300050, China

Supported by Natural Science Foundation of China, No. 39570609

Correspondence to: Dr. Jun-Wen Li, Department of Environment and Health, Institute of Health and Environmental Medicine of Tianjin, 1 Da Li Road, Tianjin 300050, China. junwenli@eyou.com

Telephone: +86-22-84655345 **Fax:** +86-22-23328809

Received 2002-01-28 **Accepted** 2002-03-14

Abstract

AIM: To develop a rapid detection method of enteroviruses and Hepatitis A virus (HAV).

METHODS: A one-step, single-tube consensus primers multiplex RT-PCR was developed to simultaneously detect Poliovirus, Cocksackie virus, Echovirus and HAV. A general upstream primer and a HAV primer and four different sets of primers (5 primers) specific for Poliovirus, Cocksackie virus, Echovirus and HAV cDNA were mixed in the PCR mixture to reverse transcript and amplify the target DNA. Four distinct amplified DNA segments representing Poliovirus, Cocksackie virus, Echovirus and HAV were identified by gel electrophoresis as 589-, 671-, 1084-, and 1128bp sequences, respectively. Semi-nested PCR was used to confirm the amplified products for each enterovirus and HAV.

RESULTS: All four kinds of viral genome RNA were detected, and producing four bands which could be differentiated by the band size on the gel. To confirm the specificity of the multiplex PCR products, semi-nested PCR was performed. For all the four strains tested gave positive results. The detection sensitivity of multiplex PCR was similar to that of monoplex RT-PCR which was 24 PFU for Poliovirus, 21 PFU for Cocksackie virus, 60 PFU for Echovirus and 105 TCID₅₀ for HAV. The minimum amount of enteric viral RNA detected by semi-nested PCR was equivalent to 2.4 PFU for Poliovirus, 2.1 PFU for Cocksackie virus, 6.0 PFU for Echovirus and 10.5 TCID₅₀ for HAV.

CONCLUSION: The consensus primers multiplex RT-PCR has more advantages over monoplex RT-PCR for enteric viruses detection, namely, the rapid turnaround time and cost effectiveness.

Li JW, Wang XW, Yuan CQ, Zheng JL, Jin M, Song N, Shi XQ, Chao FH. Detection of enteroviruses and hepatitis A virus in water by consensus primer multiplex RT-PCR. *World J Gastroenterol* 2002; 8(4):699-702

INTRODUCTION

Enteroviruses include Poliovirus, Cocksackie virus and Echo virus. Enteroviruses and HAV can bring about many diseases^[1].

The enteroviruses and HAV transmit through water or foods and constitute a risk to public health, even when their concentrations are very low. Therefore, to establish a set of fast and dependable technique for detecting enteroviruses and HAV in water is of great importance for preventing outbreak of virus diseases through water and, at the same time laying a foundation for working out virology sanitation standards for drinking water.

The traditional technique for detecting viruses at present is cell culture^[2] and it is characterized by its large water volume treated and high sensitivity. Normally viruses can be cultured and reproduced even if there is only one infectious virus existing in water. But the technique also has some shortcomings: (1) it needs great efforts and is time-consuming. There are high technical demands on cell culture and its result is unstable. It takes more than 3 days from inoculating virus to the time when visible pathological cell change effect (PCE) appears. For HAV, there is no pathological cell change effect and it takes 6-8 weeks to carry out the test. (2) it is poor in specificity. It is impossible to draw a clear identification among enteroviruses on the basis of pathological cell changes.

In recent years, PCR has been adopted extensively in detecting enterovirus or HAV in environment owing to its high specificity and simpler operation^[1,3-5]. But it also has its shortcomings. Firstly, the sensitivity is low. Although PCR itself possesses high sensitivity and it can pick out even there is only one virus, its sensitivity still does not come up to the standards for testing virus in water because the size of added samples is extremely small (about 10 ml). Even the viruses in the water are concentrated, the volume is still too large for PCR. Secondly, the testing capability is inconsistent with infectivity of the virus. It is unable to decide whether the virus is infectious even if the result is positive. Besides, conventional PCR can only detect one type of virus at one time. There are many types of viruses in water so it can't meet the needs of practical application. Tsai *et al*^[6] used multiplex-PCR to detect poliovirus, hepatitis A virus and rotavirus at one time. Their technique requires more primers and these primers interfere with each other, making it more difficult to test the viruses over three types. Zoll *et al*^[7] employed general primer PCR to detect enterovirus but their method can only show whether there is existence of enterovirus or not. It can not distinguish the types of viruses.

The combination of the cell culture with PCR technique is implemented organically in our study for the purpose of setting up a set of fast and dependable methods for testing viruses in water. This method can either preserve the advantages of the cell culture and PCR technique or overcome the shortcomings of each technique. Our technique is basically divided into three steps: first, to make collection and recovery of viruses in water; second, to make short-term cultivation of viruses; and third, to detect viral nucleic acid using multiplex-PCR and identified by semi-nested PCR.

MATERIALS AND METHODS

Viruses and viruses assays

Plaque-purified Poliovirus type 1, strain LSc, Cox B1,3 and 4 or Echo 7,9,11,12 virus were used as the model for the enteroviruses that may be present in the water. These viruses were grown and assayed by using African green monkey kidney (Vero) cells as previously described^[1]. The viruses were titrated by the plaque method and expressed as plaque-forming units (PFU). The NJ-3 strain of HAV (Institute of Military Medical Research of Nanjing) was adopted to the human hepatoma cell line PLC/PRF/5 by serial passages. The HAV antigen was detected by ELISA method.

Virus seeding

A virus mixture containing 1.0×10^5 PFU of Poliovirus type 1, strain LSc, Cox B₃ or Echo 9 virus, and 1.0×10^5 TCID₅₀ of HAV was seeded into 10 liters of water samples. The seeded and unseeded samples were concentrated by electropositive filter media particle as described previously by Jun-Wen Li, and the recovery of seeded viruses was 88.7 %^[8]. The final concentrates were 1.0 ml, if needed, which was cultured for three days for HAV or one day for other enteroviruses. The sensitivities of RT-PCR were evaluated with the ten-fold dilutions of HAV or other enteroviruses which were made with HPLC grade water.

RNA extraction and purification

Viral genome RNA was extracted and purified by the TRIzol Reagent kit (Life Technologies) according to the manufacturer's recommendation, and the RNA was stored at -20 °C for future analysis.

Primers

The consensus primer of enteroviruses was from the 5' non-coding region because of their presence in many enteroviruses serotypes^[7,9]; the specific primers for enteric viruses, including HAV, were selected from the 5' coding region; and the semi-nested PCR primers were designed within the fragment of the first PCR products. The information of primers was summarized in Table 1.

Table 1 Nucleotide sequences and positions of primers

Primers	Sequence(5'-3')	Position	band sizes (bp)
CE(+)	ATTGGATTGGCCATCCGGTG	620-639	
P(-)1	TCCACCACCACCCTCTCGACTC	1169-1190	571
P(-)2	GCATTACACTGTACGTGCAC	1271-1290	671
C(-)1	CACCAACACCCATACCTGCA	1470-1489	870
C(-)2	GCGCACATTGGCGCAATTGTG	1683-1703	1084
E(-)1	CGCACCCCATCTCAGCTTCA	1330-1349	730
E(-)2	TTCATTGTGGCAAACCTTGA	1727-1747	1128
H(-)	CCAATCTCCTGATCCAAAGC	1557-1577	
H(+1)	AACCCTACACCTTTCCAACA	1146-1165	432
H(+2)	GATTCACTTGCAGATTGGC	989-1008	589

+, upstream primer, -; downstream primer, 1: semi-nested primer; 2: the first PCR primer, CE; general primer, P: primers of Polioviruses; C: primers of Coxsackie viruses; E: primers of Echoviruses; H: primers of HAV

One-step, single-tube multiplex PCR

2-10 µl of purified viral RNAs were added in a final 100 µl containing 1×PCR buffer with 1.5 mM MgCl₂, 0.2mM each of dNTP, 0.2 µM each of the primers, 10 U Rnase inhibitor, 5mM of DTT, 1 µl of mixture of reverse transcriptase and DNA polymerase. RT was carried out at 50 °C for 30 min. This was followed by an initial denaturation at 94 °C for 3 min, and 30 PCR cycles of denaturation at 94 °C for 0.5 min, annealing at 60 °C for 0.5 min and extension at 68 °C for 1 min with a fixed ramp time of 3 seconds for each cycle^[10].

Semi-nested PCR

The semi-nested PCR was carried out on a final 50 µl containing 1×PCR buffer with 2.5 mM MgCl₂, 0.2 mM each of dNTP, 0.2 µM each of primers, 1 µl of the first PCR product and 2.5U of *Taq* polymerase. This was followed by an initial denaturation at 94 °C for 3 min, and 30 PCR cycles of denaturation at 94 °C for 0.5 min, annealing at 60 °C for 0.5 min and extension at 68 °C for 1 min^[12,13].

Analysis of PCR products

10 µl of each amplified product was electrophoresed on a 1.5 % agarose gel in 1×TBE buffer containing 0.5 µg/ml ethidium bromide. The amplified bands were directly visualized under UV light^[7,14].

RESULTS

Specificities of the primers

First, only one kind of viral RNA extracted from cell culture was tested in the multiplex PCR with all the primers. It is shown that only one amplicon was yielded, which was in agreement with the information on the designed primers (results not shown).

Secondly, two kinds of viral RNA were added to the multiplex PCR, it is expected that there were two PCR products on the gel which were conformed to the theoretical results (Figure1).

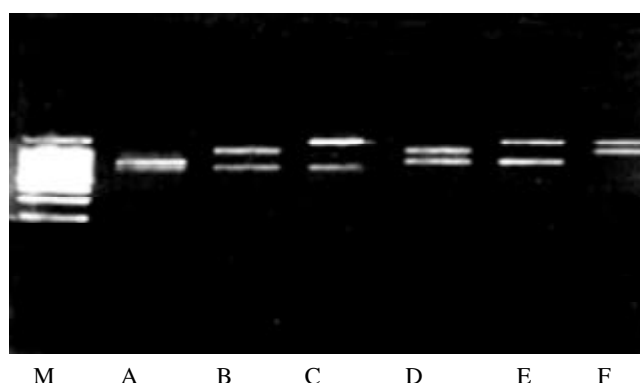
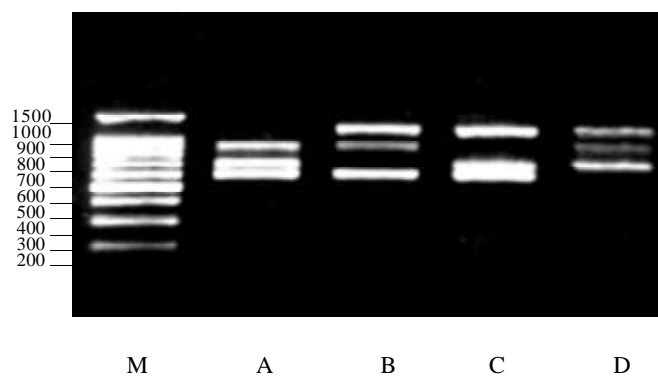


Figure1 PCR products of two types of viruses
M:DNA ladder,A: HAV and PV, B: HAV and CV,C: HAV and EV; D: PV and CV, E: PV and EV,F: CV and EV

Thirdly, three kinds of viral RNA were tested in the multiplex PCR, and given similar results (Figure2).

Fourthly, all four kinds of viral genome RNA were detected, and produced four bands which could be differentiated by the band size on the gel (Figure 3).

To confirm the specificity of the multiplex PCR products, semi-nested PCR was performed. For all the four strains tested gave positive results (Figure 4).



M:DNA ladder,A: HAV,PV and CV; B: HAV,CV and EV; C: HAV,PV and EV;D: PV,CV and EV

Figure2 PCR products of three types of viruses

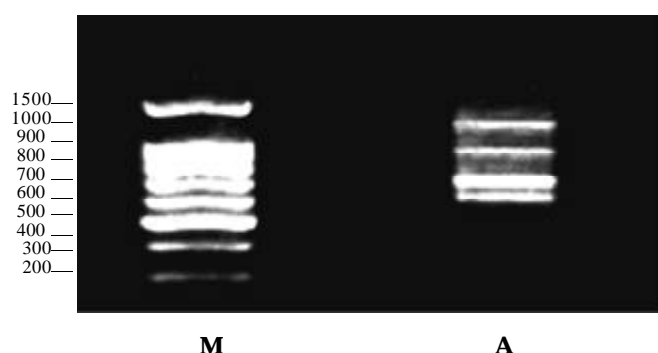


Figure3 PCR products of four types of viruses
M:DNA ladder,A: poliovirus 1(671bp), Coxsackie virus B3 (1084bp), Echo virus 9(1128bp),and HAV(589bp)

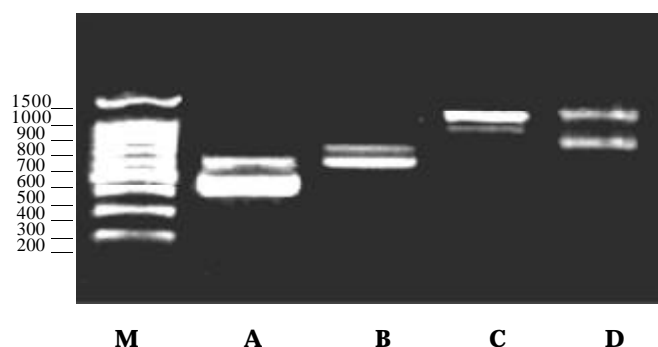


Figure4 Semi-nested PCR products of four types of viruses
M:DNA ladder,A: HAV(589,432bp) ,B: Poliovirus 1(671,571bp), C: Coxsackie virus B3(1084,870bp), D: Echo virus 9(1128,730bp)

Sensitivity of PCR

The detection sensitivity of multiplex PCR was similar to that of monoplex RT-PCR which was 24 PFU for Poliovirus, 21 PFU for Coxsackie virus, 60 PFU for Echovirus and 105 TCID₅₀ for HAV. The minimum amount of enteric viral RNA detected by semi-nested PCR was equivalent to 2.4 PFU for Poliovirus, 2.1 PFU for Coxsackie virus, 6.0 PFU for Echovirus and 10.5 TCID₅₀ for HAV (Table 2). The method achieved a 10 folds higher sensitivity than that of multiplex PCR.

Detection of viral genome after concentration

A tap water with and without seeding enteroviruses were collected for testing. Viruses added in the 10 liters of water which were not concentrated in primary could not be detected by

the multiplex PCR or semi-nested PCR, even when 200-1 000 PFU or TCID₅₀ of viruses were seeded. However, viruses seeded in the waters which were concentrated with electropositive filter media could be detected by multiplex PCR and semi-nested PCR and obtained the similar sensitivity with that from cell cultures.

50 liters of tap water, or river water, or 5 liters of sewage, or 10 liters of ocean water were concentrated with electropositive filter media, and the virus RNAs were extracted from the concentrates. The multiplex PCR and semi-nested PCR were used to amplify the enteric viruses RNA. It is found that only Poliovirus RNA could be detected from the concentrate from 50 liters river water, other enteroviruses were not detected.

Table 2 Sensitivity of semi-nested-PCR for different viruses

Viruses	Virus concentration (PFU)				
	10 ³	10 ²	10 ¹	10 ⁰	10 ⁻¹
Poliovirus	+	+	+	+(2.4)	-
Coxsackie virus B3	+	+	+	+(2.1)	-
Echovirus 9	+	+	+	+(6.0)	-
Three viruses	+	+	+(10.5)	-	-

DISCUSSION

In our studies, cell culture and PCR are combined together to improve the detection sensitivity and specificity. For the cell culture method, it has the advantages of large volume of testing water and high sensitivity. Viable viruses can be fostered and reproduced even if there is existence of only one type. But it is poor in specificity^[15]. Types of virus can't be distinguished according to pathological changes cell and immunology method is needed to make further identifications. So it is heavy, complicated and time consuming (at least 3 days; it will take 6-8 weeks to identify hepatitis A virus) to implement the test. As for PCR, it has the advantages of high specificity and simpler operation. But its sensitivity can't come up to the testing standards owing to its small testing size, and the same positive results are obtained no matter the virus is infectious or not so long as nucleic acid is complete. The improved cell culturing-PCR technique combines the high sensitivity of cell culture with the high specificity of PCR together, and avoids the shortcomings of low specificity and long testing period of cell culture, only two or four days are needed to detect Poliovirus, Coxsackie virus, Echovirus or HAV (cell culture for one or three days), thus two thirds testing time of cell culture is saved. Furthermore, cell culture dilutes the substances which play inhibiting effect on PCR in water, which further improves the sensitivity of PCR. In addition, this technique is only used to test the infectious viruses in water, hence inconsistency of PCR results with actual infectivity can be avoided^[16].

The accuracy and reliability are ensured by using semi-nested PCR to identify PCR products. The techniques used at present to determine PCR products are Southern hybridization, PCR- dependent DNA fingerprint pattern, nucleic acid sequencing and nested PCR, etc.^[3,4,6]. Southern blot is poor in sensitivity and very complicated to handle^[17-24]. It is generally taken as tool enzyme in molecule cloning and demands enzyme chip points existing in the expanded segment; DNA fingerprint pattern is poor in specificity with unstable results; nucleic acid sequencing is complicated, costly and low in efficiency; while

nested PCR has many strong points. It is not only good in specificity and sensitivity but also easy to handle and is low in price^[4,25]; semi-nested PCR has similar principles and functions as that of nested PCR. It further cuts down the cost by saving a strip of primer.

The general primer multiplex-PCR is established for detection of four kinds of enteroviruses in our studies. There were many shortcomings in the researches prior to ours, such as, only one virus can be detected at one time using conventional PCR so it can't meet the needs of practical application; Tsai *et al*^[6] used multiplex-PCR to detect Poliovirus, Hepatitis A virus and Rotavirus at one time. Their technique required more primers and these primers interfere with each other, making it more difficult to test viruses for three types or more; Zoll *et al*^[7] employed general primer PCR technique to detect Poliovirus, Cocksackie virus, Echo virus and new enterovirus. But their method can only show whether there is existence of enterovirus or not. It can not distinguish the types of virus and is impossible to detect hepatitis A virus. Namely, general primer multiplex-PCR combines the general primer with multiplex PCR, giving consideration to the strong points of the two techniques and overcoming the weak points of each. Six primers are used in one reacting tube and four types of enteroviruses can be detected in one reaction while in conventional PCR, eight strips of primer are required.

The incidence of Poliovirus in developing countries is 4% while in developed countries, the infection of Poliovirus is of less clinical significance but it is generally used as an indicating virus in water^[25,11]. Cocksackie virus and Echo virus can lead to diseases such as aseptic meningitis, viral myocarditis, diarrhea etc. Because group A Cocksackie virus is hard to culture and the virus source is very difficult to ensure, it is not tested hereon. To sum up, the technique can be used to detect Poliovirus, group B Cocksackie virus, Echo virus and Hepatitis A virus. Nearly all viruses can be detected among enteroviruses except group A Cocksackie virus.

REFERENCES

- 1 Egger D, Pasamontes L, Ostermayer M and Bienz K. Reverse transcription multiplex PCR for differentiation between Polio- and enteroviruses from clinical and environmental samples. *J Clin Microbiol* 1995;**33**:1442-1447
- 2 Reynolds KA, Gerba CP, Pepper IL. Detection of infectious enteroviruses by an integrated cell culture-PCR. *Appl Environ Microbiol* 1996;**62**: 1424-1427
- 3 Chapman NM, Tracy S, Gauntt CJ, Fortmueller U. Molecular detection and identification of enteroviruses using enzymatic amplification and nucleic acid hybridization. *J Clin Microbiol* 1990;**28**:843-850
- 4 Guyader FL, Dubois E, Menard D, Pommepuy M. Detection of hepatitis A virus, rotavirus, and enterovirus in naturally contaminated shellfish and sediment by reverse transcription-semi-nested PCR. *Appl Environ Microbiol* 1994;**60**:3665-3671
- 5 Gantzer G, Senouci S, Maul A, Levi Y, Schwartzbrodm L. Enterovirus genomes in wastewater: concentration on glass wool and glass power and detection by RT-PCR. *J Virol Methd* 1997;**65**:265-271
- 6 Tsai YL, Tran B, Sangermano LR, Palmer CJ. Detection of poliovirus, HAV, and rotavirus from sewage and ocean water by triplex RT-PCR. *Appl Environ Microbiol* 1994;**60**: 2400-2407
- 7 Zoll GJ, Melchers WJG, Kopecka H, Jambroes G, van der Poel HJA, Galama JMD. General primer-mediated polymerase chain reaction for detection of enteroviruses: application for diagnostic routine and persistent infections. *J Clin Microbiol* 1992;**30**:160-165
- 8 Li JW, Wang XW, Rui QY, Song N, Zhang FG, Ou YC, Chao FH. A new and simple method for concentration of enteric viruses from water. *J Virol Mehtds* 1998;**74**:99-108
- 9 Sheng DL. Current Protocols for Molecular Biology(1st edition). Beijing: Senior Education Press, 1993 :147-149
- 10 Sellner LN, Coelen RJ, Mackenzie JS. A one-tube, one manipulation RT-PCR reaction for detection of Ross River virus. *J Virol Methods* 1992;**40**: 255-264
- 11 Abraham R, Chonmaitree T, McCombs J, Prabhakar B, Verde PTL, Ogra PL. Rapid detection of poliovirus by RT-PCR: application for differentiation between poliovirus and nonpoliovirus enterovirus. *J Clin Microbiol* 1993;**31**:395-399
- 12 Yu QF. Modern Stanitary Microbiology(1st edition). Beijing: People Medical Press, 1995:54-66
- 13 Li JW, Zhang FG, Chao FH, Wang XW, Song N, Wang FY. Detection of enteroviruses by semi-nested RT-PCR. *Zhong guo Weisheng Jianyan Zazhi* 1996;**6**: 125- 127
- 14 Yang DL, Wang BC. DNA Amplification and Applification in Medicine. Jinan: Shangdong Science and Technological Press, 1992:74-79
- 15 Seah CLK, Chow VTK, Tan HC, Chan YC. Rapid, single RT-PCR typing of dengue viruses using five NS3 gene primers. *J Virol Methods* 1995;**51**: 193- 200
- 16 Straub TM, Pepper IL, Gerba CP. Comparison of PCR and cell culture for detection of enteroviruses in sludge-amended field soils and determination of their transport. *Appl Environ Microbiol* 1995;**61**:2066-2068
- 17 Shieh YSC, Wait D, Tai L, Sobsey MD. Methods to remove inhibitors in sewage and other fecal wastes for enterovirus detection by the PCR. *J Virol Methods* 1995;**54**:51-66
- 18 Moore NJ, Margolin AB. Evaluation of radioactive and nonradioactive gene probes and cell culture for detection of poliovirus in water samples. *Appl Environ Microbiol* 1993;**59**: 3145-3146
- 19 Williams SJ, Schwer C, Krishnarao ASM, Heid C, Karger BL, Williams PM. Quantitative competitive PCR: analysis of amplified products of the HIV-1 gag gene by capillary electrophoresis with laser-induced fluorescence detection. *Anal Bioch* 1996;**236**:146- 152
- 20 Doktycz MJ, Hurst GB, Goudarzi SH, McLuckey SA, Tang K, Chen H, Uziel M, Jacobson KB, Woychik RP, Buchanan MV. Analysis of PCR-amplified DNA products by mass spectrometry using matrix-assisted laser desorption and electrospray: current status. *Anal Bioch* 1995;**230**: 205- 214
- 21 Li JW, Zhang FG, Chao FH, Wang XW, Song N. Detection of HAV by one-step, one-tube RT-PCR. *Zhongguo Wei sheng Jianyan Zazhi* 1996;**6**: 63- 65
- 22 Ma JF, Gerba CP, Pepper IL. Increased sensitivity of poliovirus detection in tap water concentrates by RT-PCR. *J Virol Methods* 1995;**55**: 295- 302
- 23 Xiong ZG, Laird PW. COBRA: a sensitive and quantitative DNA methylation assay. *Nucleic Acid Res* 1997;**25**: 2532-2534
- 24 Xun ZX. Current Biochemical Theory and Research Technology(1st edition). Beijing: Military Medical Sciences Press, 1995: 422-424
- 25 Tilston P, Corbitt G. A single tube nested PCR for the detection of hepatitis C virus RNA. *J Virol Methd* 1995;**53**: 121-129

Edited by Wu XN

• *H. pylori* •

Follow up of serial urea breath test results in patients after consumption of antibiotics for non-gastric infections

Wai-Keung Leung, Lawrence Cheung-Tsui Hung, Carrie Ka-Li Kwok, Rupert Wing-Loong Leong,
Daniel Kwok-Keung Ng, Joseph Jao-Yiu Sung

Wai-Keung Leung, Lawrence Cheung-Tsui Hung, Rupert Wing-Loong Leong, Joseph Jao-Yiu Sung, Department of Medicine & Therapeutics, Prince of Wales Hospital, the Chinese University of Hong Kong, Shatin, Hong Kong, China

Carrie Ka-Li Kwok, Daniel Kwok-Keung Ng, Department of Paediatrics, Kwong Wah Hospital, Kowloon, Hong Kong, China

Correspondence to: Dr. Wai K. Leung, Department of Medicine & Therapeutics, Prince of Wales Hospital, Shatin, N.T., Hong Kong, China. wkleung@cuhk.edu.hk

Telephone: +852-2632-3140 **Fax:** +852-2637-3852

Received 2002-06-29 **Accepted** 2002-07-11

Abstract

AIM: The widespread use of antibacterial therapy has been suggested to be the cause for the decline in the prevalence of *Helicobacter pylori* infection. This study examine the serial changes of urea breath test results in a group of hospitalized patients who were given antibacterial therapy for non-gastric infections.

METHODS: Thirty-five hospitalized patients who were given antibacterial therapy for clinical infections, predominantly chest and urinary infections, were studied. Most (91 %) patients were given single antibiotic of either a penicillin or cephalosporin group. Serial ¹³C-urea breath tests were performed within 24 hours of initiation of antibiotics, at one-week and at six-week post-therapy. *H. pylori* infection was diagnosed when one or more urea breath tests was positive.

RESULTS: All 35 patients completed three serial urea breath tests and 26 (74 %) were *H. pylori*-positive. Ten (38 %) *H. pylori*-infected patients had at least one negative breath test results during the study period. The medium delta ¹³C values were significantly lower at baseline (8.8) than at one-week (20.3) and six-week (24.5) post-treatment in *H. pylori*-positive individuals ($P=0.022$). Clearance of *H. pylori* at six-week was only seen in one patient who had received anti-helicobacter therapy from another source.

CONCLUSION: Our results suggested that one-third of *H. pylori*-infected individuals had transient false-negative urea breath test results during treatment with antibacterial agent. However, clearance of *H. pylori* infection by regular antibiotic consumption is rare.

Leung WK, Hung LC-T, Kwok CK-L, Leong RW-L, Ng DK-K, Sung JJ-Y. Follow up of serial urea breath test results in patients after consumption of antibiotics for non-gastric infections. *World J Gastroenterol* 2002; 8(4):703-706

INTRODUCTION

The rediscovery of *Helicobacter pylori* in 1984 had revolutionized our understanding of gastroduodenal diseases [1].

This bacterium is now generally considered to be the most important cause of peptic ulcer diseases, gastric adenocarcinoma and MALT lymphoma of the stomach^[2, 3]. Unless given appropriate antibiotic treatment, most infected individuals will remain infected throughout their lifetime. Spontaneous clearance of infection, particularly in adult, is rare^[4, 5].

Interestingly, recent epidemiological studies suggest a gradual reduction in the prevalence of *H. pylori* infection, particularly in developed countries^[4]. This decline in *H. pylori* prevalence is accompanied by a parallel reduction in the incidence of gastric carcinoma^[6]. The reason for this decrease remains unknown for the moment but widespread use of antibiotics in the community has been speculated to be an important cause for this decline. This study sought to determine the serial changes of urea breath test in patients after taking antibacterial agents given for conditions other than *H. pylori* infection. The aim is to elucidate the effects of antibacterial agents on urea breath test results and determine whether antibacterial therapy given for concomitant infections would result in clearance of *H. pylori* infection.

MATERIALS AND METHODS

Study design

Patients who were hospitalized for clinical infections, other than gastrointestinal tract infection, and requiring the use of antibiotics were recruited. The prescription of antibacterial agent was at the discretion of the attending clinicians. Patients were excluded if they were pregnant, had previous gastric surgery, had previously received anti-helicobacter treatment, or had been using acid-suppressive agents or antibiotics in the recent six weeks. For all eligible patients, informed consent was obtained from the patients or their parents. Since it is unethical to delay or withhold anti-bacterial therapy, urea breath test was performed as soon as possible but usually performed after the initiation of the antibacterial agents. All urea breath tests, however, should be performed within 24 hours of admission. Subsequent urea breath tests were repeated at one-week and at six-week after the completion of antibiotics. Drug history during the study period, including acid suppressive therapies and antibiotics, was recorded. All patients diagnosed with *H. pylori* infection were offered *H. pylori* eradication therapy at the conclusion of this study. The study protocol was approved by the Clinical Research Ethics Committees of the Chinese University of Hong Kong and the Kwong Wah Hospital of Hong Kong SAR.

¹³C urea breath test

¹³C-urea breath test (UBT) was performed in all patients, adult or children, following the same protocol. All patients were fasted for a minimum of four hours and were then given a citric acid test meal to delay gastric emptying. A 75-mg ¹³C-urea tablet dissolved in water was then given. Breath samples

were collected before the test meal and 30 minutes after the ingestion of the urea solution. Two devices, a 10-ml glass tube and a sealed aluminum bag, were used for collection of exhaled air. The difference in $^{13}\text{CO}_2$ between the two breath samples was analyzed by both the isotope ratio mass spectrometry (Europa Scientific, Crewe, UK) and the infrared spectrometer (FANci2, Fischer Analysen Instrumente, Leipzig, Germany). A concordant delta $^{13}\text{CO}_2$ value greater than 5 was regarded as a positive result as described previously [7].

Determination of *H. pylori* infection status

Since none of these patients had indication for endoscopy, *H. pylori* infection status was determined by the non-invasive urea breath test. Patients were classified as *H. pylori*-positive when one or more of the three consecutive breath test results tested positive. This was based on the assumptions that urea breath test was accurate in diagnosing *H. pylori* infection, and that natural acquisition of *H. pylori* infections was extremely rare [4,5]. Serology test (ASSURE; Genelabs Diagnostics, Singapore) was used in patients with three consecutive negative urea breath tests for the detection of IgG anti-*Helicobacter* antibody to rule out the possibility of false negative breath test results. This serology test has been previously validated in our population [8].

Statistics

All statistical analysis was performed by GraphPad Prism version 2.01 (San Diego, CA, USA). Comparisons of the delta ^{13}C values among the three consecutive urea breath tests were made by Kruskal-Wallis test. Post-hoc analysis was performed by Dunn's multiple comparison test.

RESULTS

Patients' characteristics

A total of 35 patients were examined in this study (median age=66 years, range 5-81; 13 male and 22 female). Two study subjects were less than 18 years of age. The primary diagnoses of these patients were chest infection ($n=20$), urinary tract infection ($n=12$) and other infections ($n=3$). Thirty-two (91 %) patients received a single antibiotic whereas three (9 %) received two antibacterial agents during the hospitalization period. All patients received a one- to two-week course of standard dose penicillin ($n=20$) or cephalosporin ($n=15$) during the study period. Intravenous route was initially given in 25 (71 %) patients whereas the rest received oral antibiotics throughout the hospitalizations. One patient also received a course of anti-*Helicobacter* therapy from his primary care physicians during the follow up period.

Urea breath test

All 35 patients completed the three consecutive urea breath tests. By using the pre-defined criterion, 26 (74 %) patients were considered to be *H. pylori*-positive. None of the remaining 9 patients with negative breath tests had anti-*Helicobacter* antibody detected.

The serial breath test results of the study patients were given in Table 1. Ten (29 %) *H. pylori*-positive patients had at least one negative urea breath test results during the study period. Of these 10 patients, 7 had the first test result negative whereas the second and/or third test was (were) positive. Two patients had a single negative test result at one-week post-treatment. Among the 26 *H. pylori*-positive patients, only one was found to have a negative test result at six-week post-antibiotic treatment. However, this patient had been prescribed a one-

week course of proton-pump inhibitor-based triple therapy for dyspepsia by his primary care practitioner two weeks after discharge from hospital. It thus appeared that the apparent clearance of *H. pylori* was attributed to the specific anti-*Helicobacter* therapy instead of the first course of antimicrobial agent.

Table 1 Results of serial urea breath tests in the study patients

Baseline	UBT		No. of patients
	1-wk post-antibacterial therapy	6-wk post-antibacterial therapy	
Neg	Neg	Neg	9
Neg	Neg	Pos	1
Neg	Pos	Pos	6
Pos	Neg	Pos	2
Pos	Pos	Neg	1*
Pos	Pos	Pos	16
		Total	35

*This patient was given specific anti-*Helicobacter* therapy between second and third urea breath tests by his primary care physicians. Pos=positive; Neg=negative

For all *H. pylori* infected patients, the median delta $^{13}\text{CO}_2$ values taken at baseline, one-week and six-week post-treatment were 8.8, 20.3 and 24.5 respectively ($P=0.022$). Post-hoc analysis showed that the median value measured at baseline was significantly lower than at six-week post treatment ($P<0.05$). On the other hand, the difference between the first and second urea breath tests did not reach statistical significance (Figure 1).

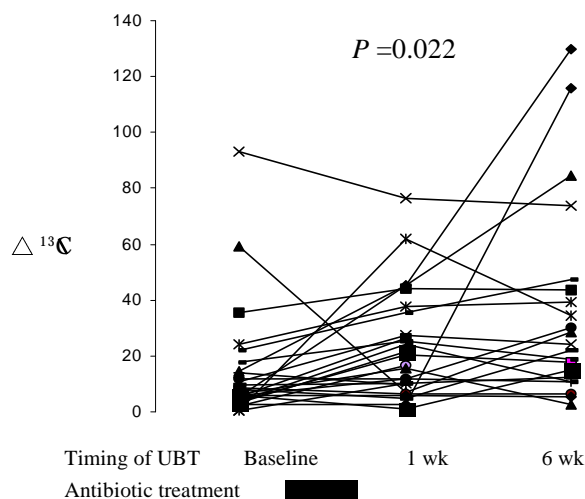


Figure 1 Changes in the delta ^{13}C values ($\Delta^{13}\text{C}$) of urea breath tests after consumption of antibiotics in *H. pylori*-infected patients. The broad line indicated the duration of antibiotics consumption. A delta ^{13}C value of greater than 5 was regarded as a positive result. There was a significant difference between the median delta ^{13}C values taken at baseline, one-week and six-week post treatment ($P=0.022$). Post-hoc analysis showed that only the difference between the first and the third urea breath tests reached statistical significance ($P<0.05$).

All patients who had a transient negative urea breath test result were given antibiotics by the intravenous route whereas

10 (56 %) of the *H. pylori*-infected patients with persistent positive breath test results received intravenous antibiotics ($P = 0.05$). On the other hand, the choice and duration of antibiotic therapy did not correlate with false negative breath test results.

DISCUSSION

Urea breath test is considered to be the best non-invasive test for diagnosis of *H. pylori* infection, which is useful in both diagnosis and post-treatment testing. However, it can be potentially influenced by drugs that cause suppression of *H. pylori* and hence, its urease activity. In this regard, the proton pump inhibitor is the drug that is most extensively examined. Laine et al showed that 33 % of *H. pylori*-infected patients had a negative breath test result when receiving standard dose of lansoprazole for the treatment of gastro-esophageal reflux disease^[9]. The breath test results returned positive in all patients at 14-day after stopping the treatment. Although antibiotic combinations are used in the treatment of *H. pylori*, the effect of concomitant antibacterial agents given for other conditions, usually single drug, on urea breath test results has not been evaluated.

In this study, we prospectively studied the serial changes of urea breath tests in a small group of hospitalized patients who were given antibiotics for infections other than *H. pylori*. Despite the small number of patients examined, the results of this study could provide insights into the effects of antibacterial therapy on urea breath test results and hence *H. pylori* statuses post-treatment. Unlike proton pump inhibitor with limited choices and relatively well-defined standard doses, the choices of antibiotics and the duration of therapy are highly variable. Most of our study subjects suffered from chest or urinary tract infections and were given a 1-2 week course of penicillin or cephalosporin. As shown by our results, antibacterial agents frequently (38 %) caused false-negative breath test results in *H. pylori*-infected individuals. This was best illustrated by the significantly lower delta $^{13}\text{CO}_2$ value of first test results while receiving antibacterial treatment. This transient suppression occurred within 24 hours of antibiotics treatment and could last for more than one-week post-treatment. Nevertheless, none of the study subjects, except the one who had received specific anti-*Helicobacter* treatment, had a persistent negative breath test at 6-week.

This observation is important for three reasons. First, the widespread use of antibiotics in the community for various infections have been speculated to be a major reason for the decline in prevalence of *H. pylori* infection and possibly the decline in gastric cancer incidences worldwide. This is supported by a recent epidemiological study that demonstrated a reduced risk of gastric cancer among patients who were given antibiotic prophylaxis for hip replacement surgery^[10]. Their protective effect is presumably due to the serendipitous eradication of *H. pylori* by the antibiotics, which leads to subsequent reduction in the risk of development of gastric cancer. However, if one looks into the rate of disappearance of anti-*Helicobacter* antibody in patients who were given antibiotics, it was not significantly higher than control suggesting that the reduction in cancer incidences may not be directly related to the clearance of *H. pylori*, at least from serological point of view. In the present study, clearance of *H. pylori* after a single course of antibiotic is rare. Despite the *in vitro* sensitivity of *H. pylori*, the eradication rate of a single standard dose of antibacterial agent is extremely low, particularly with the use of penicillin and cephalosporin groups.

Previous data showed that the best single therapy for *H. pylori* is clarithromycin^[11]. Nonetheless, the use of two-week high dose clarithromycin (2 gram per day) could only achieve eradication of *H. pylori* in about one-third of the patients^[11]. In practice, the success of eradication is low without acid suppressive agent such as proton pump inhibitors or bismuth compounds^[12]. The second importance of this study is the potential risk of inducing acquired resistance with repeated exposure to antimicrobial agent. Exposure of *H. pylori* to antimicrobial agents without eliminating the bacteria poses a major risk of inducing acquired resistance. This may offer a plausible explanation for the rising incidence of antibiotic resistance in countries where there is high consumption of antibiotics^[13-15]. The third reason for the importance of this paper would be that treatment of antibiotics affect diagnostic accuracy of UBT.

The prevalence of *H. pylori* infection in this study (74 %) is much higher than previously reported in local dyspeptic patients. This is most likely due to random effect in study involving small number of patients. Ideally, baseline urea breath test should be performed prior to the administration of antibiotics and biopsy-based diagnosis should be used for the proper documentation of *H. pylori* status, but for ethnical reasons, these problems are difficult to overcome. However, we have performed serology tests in patients who had negative urea breath tests to detect presence of anti-*Helicobacter* antibody. Thus, the chance of misclassifying *H. pylori*-positive patient as negative would be minimal.

In conclusion, this study showed that over one-third of patients had a transient suppression of urease activity and hence, false-negative urea breath test results during treatment with antibacterial agents. This usually reverts back to normal at six-week post treatment and thus, testing for *H. pylori* should be postponed accordingly. On the other hand, spontaneous clearance of *H. pylori* by antibacterial agent given for other conditions is extremely rare, and could not account for the fall in prevalence of *H. pylori* in most developed countries.

REFERENCES

- 1 **Warren JR**, Marshall B. Unidentified curved bacilli in the stomach of patients with gastritis and peptic ulceration. *Lancet* 1984;**1**:1311-1315
- 2 **Anonymous**. NIH Consensus Conference. *Helicobacter pylori* in peptic ulcer disease. NIH Consensus Development Panel on *Helicobacter pylori* in Peptic Ulcer Disease. *Helicobacter pylori* in peptic ulcer disease. *JAMA* 1994;**272**: 65-69
- 3 **Anonymous**. Current European concepts in the management of *Helicobacter pylori* infection. The Maastricht Consensus Report. European *Helicobacter Pylori* Study Group. *Gut* 1997;**41**:8-13
- 4 **Xia HH**, Talley NJ. Natural acquisition and spontaneous elimination of *Helicobacter pylori* infection: clinical implications. *Am J Gastroenterol* 1997;**92**:1780-1787
- 5 **Kumagai T**, Malaty HM, Graham DY, Hosogaya S, Misawa K, Furihata K, Ota H, Sei C, Tanaka E, Akamatsu T, Shimizu T, Kiyosawa K, Katsuyama T. Acquisition versus loss of *Helicobacter pylori* infection in Japan: Results from an 8-year birth cohort study. *J Infect Dis* 1998;**178**: 717-721
- 6 **Pisani P**, Parkin DM, Bray F, Ferlay J. Estimates of the worldwide mortality from 25 cancers in 1990. *Int J Cancer* 1999;**83**:18-29
- 7 **Leung WK**, Chan FKL, Falk MS, Suen R, Sung JY. Comparison of two rapid whole-blood tests for *Helicobacter py-*

- lori* infection in Chinese patients. *J Clin Microbiol* 1998;**36**: 3441-3442
- 8 **Hung CT**, Leung WK, Chan FKL, Sung JY. Comparison of two new rapid serology tests for diagnosis of *Helicobacter pylori* infection in Chinese patients. *Digest Liver Dis* 2002;**34**:111-115
- 9 **Laine L**, Estrada R, Trujillo M, Knigge K, Fennerty MB. Effect of proton-pump inhibitor on diagnostic testing for *Helicobacter pylori*. *Ann Intern Med* 1998;**129**:547-550
- 10 **Akre K**, Signorello LB, Engstrand L, Bergstrom R, Larsson S, Eriksson BI, Nyren O. Risk for gastric cancer after antibiotic prophylaxis in patients undergoing hip replacement. *Cancer Res* 2000;**60**:6376-6380
- 11 **Leung WK**, Graham DY. Clarithromycin for *Helicobacter pylori* infection. *Exp Opin Pharmacother* 2000;**1**:507-514
- 12 **Lind T**, Megraud F, Unger P, Bayerdorffer E, O' morain C, Spiller R, Veldhuyzen Van Zanten S, Bardhan KD, Hellblom M, Wrangstadh M, Zeijlon L, Cederberg C. The MACH2 study: role of omeprazole in eradication of *Helicobacter pylori* with 1-week triple therapies. *Gastroenterology* 1999;**116**:248-253
- 13 **Megraud F**. Epidemiology and mechanism of antibiotic resistance in *Helicobacter pylori*. *Gastroenterology* 1998;**115**: 1278-1282
- 14 **Osato MS**, Reddy R, Reddy SG, Penland RL, Malaty HM, Graham DY. Pattern of primary resistance of *Helicobacter pylori* to metronidazole or clarithromycin in the United States. *Arch Intern Med* 2001;**161**:1217-1220
- 15 **Kim JJ**, Reddy R, Lee M, Kim JG, El-Zaatari FA, Osato MS, Graham DY, Kwon DH. Analysis of metronidazole, clarithromycin and tetracycline resistance of *Helicobacter pylori* isolates from Korea. *J Antimicrob Chemother* 2001;**47**:459-461

Edited by Zhang JZ

• BASIC RESEARCH •

Stimulation of p38 MAPK by hormonal preconditioning with atrial natriuretic peptide

Alexandra K. Kiemer, Stefanie Kulhanek-Heinze, Tobias Gerwig, Alexander L. Gerbes, Angelika M. Vollmar

Alexandra K. Kiemer, Stefanie Kulhanek-Heinze, Tobias Gerwig, Angelika M. Vollmar, Department of Pharmacy, Center of Drug Research, University of Munich, Germany

Alexandra K. Kiemer, Stefanie Kulhanek-Heinze, Tobias Gerwig, Alexander L. Gerbes, Department of Medicine II, Klinikum Grosshadern, University of Munich, Germany

Supported by the Deutsche Forschungsgemeinschaft (DFG: Ge 576/14-2 and FOR 440/1-2: KI 702/2). A.K.K. is a recipient of the "Bayerischer Habilitationsförderpreis".

Correspondence to: Alexandra K. Kiemer, Ph.D., Department of Pharmacy, Center of Drug Research, Butenandtstr. 5-13, 81377 Munich, Germany. alexandra.kiemer@cup.uni-muenchen.de

Telephone: +49-89-2180-7165 **Fax:** +49-89-2180-7170

Received 2002-05-20 **Accepted** 2002-06-03

Abstract

AIM: Stress-activated signaling pathways responsible for hepatic ischemia reperfusion injury and their modulation by protective interventions are widely unknown. Preconditioning of rat livers with Atrial Natriuretic Peptide (ANP) attenuates ischemia reperfusion injury (Gerbes et al. *Hepatology* 1998, 28: 1309-1317). Since ANP has recently been shown to be a regulator of the p38 MAPK pathway in endothelial cells (Kiemer et al. *Circ Res* 2002, 90:874-881), aim of this study was to investigate activities of MAPK during ischemia and reperfusion and effects of ANP on MAPK.

METHODS: Rat livers were perfused with KH-buffer in the presence or absence of ANP for 20 min, kept in cold UW solution for 24 h, and reperfused for up to 120 min. Activities of p38 MAPK and JNK was determined by *in vitro* phosphorylation assays using MBP and *c-jun* as substrates. After SDS/PAGE electrophoresis, gels were quantified by phosphorimaging.

RESULTS: Activity of p38 MAPK in control organs decreased in the course of ischemia and reperfusion by 85%, whereas ANP increased p38 activity by up to 30-fold. JNK activation of control livers increased in the course of ischemia and reperfusion by up to three-fold. This increase in JNK activity was slightly elevated in ANP preconditioned organs.

CONCLUSION: This work represents a systematic investigation of MAPK activation during liver ischemia and reperfusion. Employing ANP, for the first time a pharmacological approach to modulate these central signal transduction molecules is presented.

Kiemer AK, Kulhanek-Heinze S, Gerwig T, Gerbes AL, Vollmar AM. Stimulation of p38 MAPK by hormonal preconditioning with Atrial Natriuretic Peptide. *World J Gastroenterol* 2002;8(4): 707-711

INTRODUCTION

Ischemia reperfusion (I/R) injury is the main cause of severe complications following liver transplantation^[1,2]. Therefore, measures to reduce I/R injury are of highest clinical interest. However, there is still incomplete understanding of the pathomechanisms leading to I/R injury and of signalling pathways responsible for protective interventions.

Mitogen activated protein kinases (MAPK) are dually phosphorylated serine/threonine protein kinases (for review see^[3,4]). They regulate an extensive range of cellular processes including gene transcription, cytoskeletal organization, metabolic homeostasis, cell growth, and apoptosis^[3,4]. They represent signalling molecules which can be activated by various cellular stresses and cytokines and which therefore play a crucial role in the stress response^[5]. Their role in the stress response, however, either detrimental or protective, seems to strongly depend on the system looked at^[6].

In mammalian cells, three closely related parallel cascades of MAPK are known, the p38 MAPK, the *c-jun* N-terminal kinase (JNK), as well as the extracellular signal-regulated protein kinases p42/p44 (ERK)^[4]. ERKs are critical regulators of gene transcription in cell proliferation and differentiation, while JNK and p38 pathways seem to be involved in cellular responses to environmental stresses and inflammatory cytokines^[3].

Several groups have observed activation of MAPK in the course of *warm* ischemia and reperfusion^[7-11] whereas there is only limited information on activation of MAPK after *cold* ischemic storage^[12-14]. However, these reports show controversial data on the activation pattern of MAPK.

Since recent data show that protective preconditioning strategies, such as whole animal heat shock^[15,16] or short time hypoxic^[17] or ischemic preconditioning^[18,19] significantly activate stress-activated MAPKs, these kinases are suggested as central signal transduction pathways mediating protection from I/R injury. Therefore, we felt that a systematic investigation of MAPK activation after cold ischemic storage should lead to a more complete understanding of their role in I/R injury. Moreover, the potential pharmacological modulation of MAPK by the hepatoprotective Atrial Natriuretic Peptide (ANP) should be investigated. This cardiovascular hormone has previously been shown to attenuate I/R injury after both *warm*^[20] and *cold*^[21] ischemia of the rat liver. Protection conveyed by ANP involves the attenuated activation of pro-inflammatory transcription factors and the reduced expression of TNF- α ^[22] as well as induction of heat shock proteins^[23]. The initial signalling events responsible for the protective potential of hormonal preconditioning by ANP, however, are still unknown. ANP has recently been reported by us and others as a regulator of the p38 MAPK cascade^[24,25]. By investigating an effect of ANP on MAPK activation, an information on signalling events potentially involved in liver protection should be obtained.

MATERIALS AND METHODS

Materials

Rat ANP 99-126 was purchased from Calbiochem/Novabiochem, Bad Soden, Germany. [γ^{32} P]-ATP (3000 Ci/mmol) was from Amersham Pharmacia (Braunschweig, Germany); Complete[®] was from Roche (Heidelberg, Germany). Recombinant *c-jun* 1-79, polyclonal rabbit anti-p38, and anti-JNK antibodies were purchased from Calbiochem-Novabiochem (Bad Soden, Germany). Protein A-agarose, myelin basic protein, and all other materials were from Sigma, Deisenhofen, Germany.

Methods

Liver perfusion Male Sprague-Dawley rats weighing 250-300 g were purchased from SAVO (Kisslegg, Germany) and housed in a climatized room with a 12-hour light-dark cycle. The animals had free access to chow (Standard-Diet, Altromin 1314 Lage, Germany) and water up to the time of the experiments. After anaesthetizing the animals with pentobarbital (50 mg/kg body weight, intraperitoneally), the portal vein was cannulated and the livers were perfused *in situ* with hemoglobin-free and albumin-free, bicarbonate-buffered Krebs-Henseleit (KH) solution (pH 7.4, 37 °C) gassed with 95% O₂ and 5% CO₂. The perfusion medium was pumped through the livers with a membrane pump at a constant flow rate of 3.0-3.5 ml \times min⁻¹ \times g liver⁻¹ in a non-recirculating fashion. After 10 min controlling the stability of the system, ANP (200 nM) was added to the perfusate for 20 min, livers were then perfused with 30 ml of cold (4 °C) University of Wisconsin (UW) solution for 1 min. Then the organs were kept in 150 ml UW solution at 4 °C for 24 h. Following the period of ischemia, livers of each group were reperfused with KH buffer for 2 h. At the indicated times, i.e. before ischemia, at the end of ischemia and after 45 and 120 min of reperfusion livers were snap-frozen and stored at -85 °C until further analysis. Five independent experiments were performed.

The "Principles of laboratory animal care" (NIH publication No 86-23, revised 1985) as well as the German Law on the Protection of Animals were followed. The study was registered with the local animal welfare committee.

Immunoprecipitation and in vitro phosphorylation assay

Tissue lysates were prepared from frozen liver sections. Briefly, tissue samples (100 μ g) were homogenized in ice-cold lysis buffer (containing 2 mM EDTA, 137 mM NaCl, 10% glycerol, 2 mM tetrasodium pyrophosphate, 20 mM Tris, 1% Triton[®] \times -100, 20 mM sodium glycerophosphate, 10 mM sodium fluoride, 2 mM sodium vanadate, 1 mM PMSF, 1 \times Complete[®]) with a dounce homogenizer, and centrifuged at 11 180 \times g for 10 min at 4 °C. Aliquots of the supernatant were taken for determination of protein concentrations and the tissue extract was frozen at -85 °C. The protein concentrations were estimated after the method of Pierce. Equal amounts of protein were incubated with the respective antibody (1.5 μ l of anti-p38, 3 μ l of anti-JNK; polyclonal rabbit antibodies, Calbiochem-Novabiochem, Bad Soden, Germany) shaking for 2 h. Afterwards immunoprecipitation was performed with protein A agarose (5 μ l) shaking overnight at 4 °C. After centrifugation (11 180 \times g, 4 min, 4 °C) the precipitates were washed three times with lysis buffer and once with kinase buffer (containing 20 mM Hepes pH 7.5, 20 mM MgCl₂, 25 mM sodium glycerophosphate, 100 μ M sodium vanadate, 2 mM DTT). Immunoprecipitates were resuspended in 20 μ l of kinase buffer, 3 μ l of substrate solution (1 mg/300 μ l MBP for p38, Sigma, Deisenhofen, Germany and 1 mg/ml of recombinant *c-jun* 1-

79, Calbiochem-Novabiochem, Bad Soden, Germany) and a 10 μ l volume of ATP mix was added, containing kinase buffer with 10 mCi/ml [γ^{32} P]-ATP, (3 000 Ci/mmol, Amersham, Braunschweig, Germany), 5 mM ATP and 2 M MgCl₂. The reaction mixture was incubated at 30 °C for 20 min shaking. Phosphorylation was stopped by the addition of 6 μ l 5 \times Laemmli buffer and heating for 3 min at 90 °C. 30 μ l of the reaction mixture were resolved in a 12% (MBP) or 15% (*c-jun*) SDS polyacrylamide gel in a Laemmli system at 200 V. Band intensities were quantified by phosphorimaging (Packard, Meriden, USA). Ratio of digital light units (DLU) of respective values vs. controls were determined.

Statistical analysis

Data are expressed as means \pm SEM of three to five independent experiments. A *P* value of < 0.05 was considered significant (unpaired student's *t* test, Graph Pad Prism, version 3.02).

RESULTS

MAPK activities in the course of ischemia and reperfusion

At the end of cold ischemic storage for 24 h rat livers displayed a significantly reduced activation of p38 MAPK activity (Figure 1). The p38 activity even further decreased in the course of reperfusion and at the end of the 120 min reperfusion period displayed only 15% of pre-ischemic values (Figure 1).

The *c-jun* N-terminal kinase (JNK) was activated in the reperfusion period (up to 3-fold). No increase of *c-jun* phosphorylation could be measured at the end of ischemia (Figure 2).

Influence of ANP on MAPK activities

When rat livers were pre-conditioned by adding 200 nM of ANP to the pre-ischemic perfusion buffer the livers displayed a completely different pattern of MAPK activities. At the end of the preconditioning period ANP treated organs displayed a tremendous increase in p38 activity by 12-fold (Figure 3). In the course of the experiment the p38 activity even further increased compared to the respective control organs (Figure 3).

ANP did not affect JNK activity during preconditioning. However, ANP-pretreated organs showed elevated post-ischemic JNK activities (Figure 4).

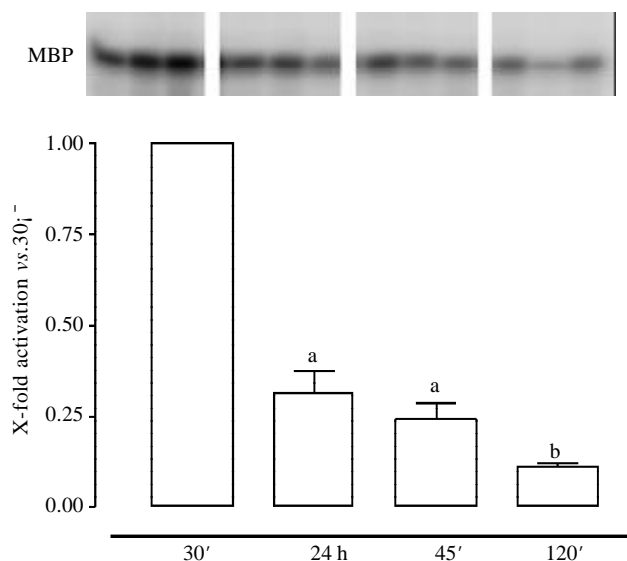


Figure 1 p38 MAPK activities in the course of ischemia and reperfusion. Livers were perfused through the portal vein with KH-buffer and snap frozen at 30 min, after 24 h of ischemic

storage in UW solution (4°C), and after 45 and 120 min of reperfusion. Deep-frozen organs were lysed and assayed for p38 MAPK activity as described under “Materials and Methods”. Determination of density light units was performed by phosphorimaging and values for the respective time points are expressed as ratio vs. values for pre-ischemic (30 min) organs. Bars show means \pm SEM of three independent perfusion experiments. ^a $P < 0.05$ and ^b $P < 0.01$: statistically different from pre-ischemic 30 min controls.

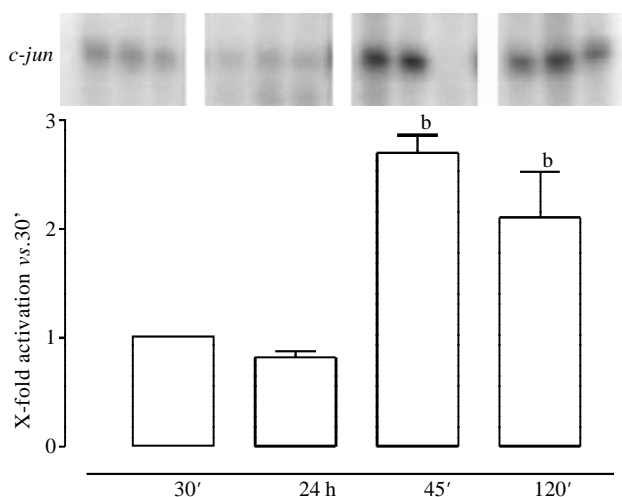


Figure 2 JNK activities in the course of ischemia and reperfusion. Isolated perfused rat livers were snap frozen at 30 min, after 24 h of ischemic storage in UW solution (4°C), and after 45 and 120 min of reperfusion. Deep-frozen organs were lysed and assayed for MAPK activity as described under “Materials and Methods”. Determination of density light units was performed by phosphorimaging and values for the respective time points are expressed as ratio vs. values for pre-ischemic (30 min) organs. Bars show means \pm SEM of three independent perfusion experiments. ^b $P < 0.01$: statistically different from pre-ischemic 30 min controls.

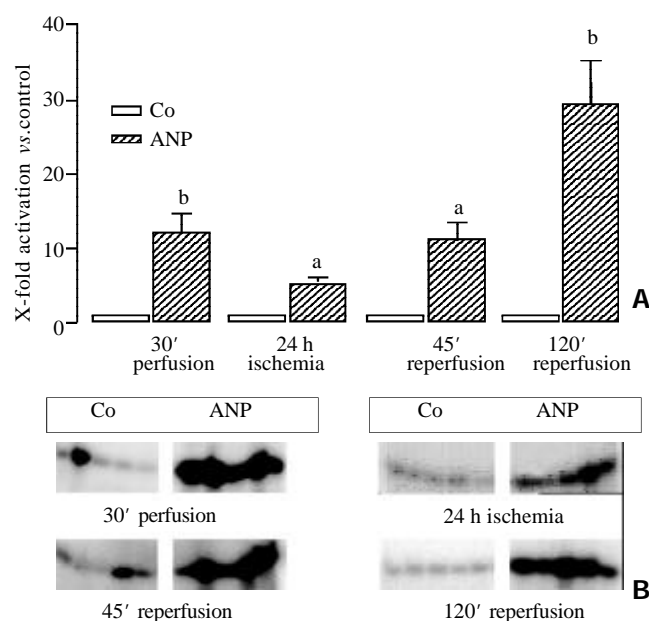


Figure 3 ANP increases the activity of p38 MAPK in the course of ischemia and reperfusion. Livers perfused with KH-buffer in the presence or absence of ANP (200 nM) underwent 24 h of cold ischemic storage and were snap frozen at the respective time points. p38 MAPK activity was determined as described under “Materials and Methods”. Density light units were determined by phosphorimaging and values for ANP-treated

organs were divided by mean values for control organs at the respective time points. Panel A: Bars show means \pm SEM of five independent perfusion experiments with ^a $P < 0.05$ and ^b $P < 0.01$: statistically different from controls at the respective time point. Panel B: Data show representative autoradiograms.

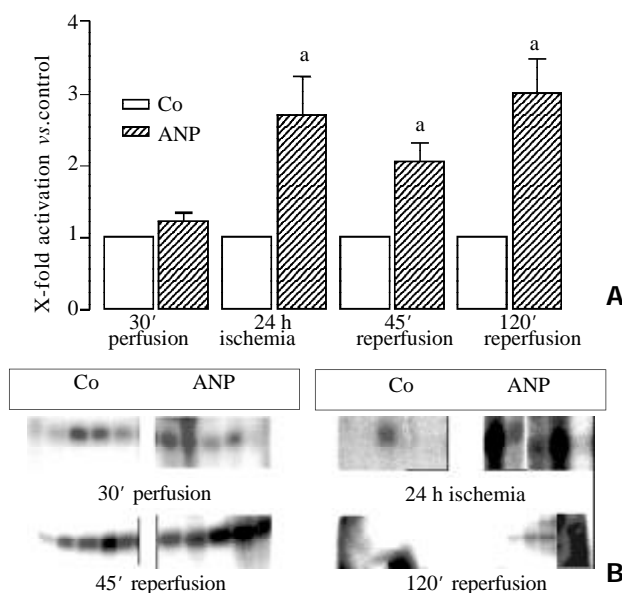


Figure 4 ANP and JNK activity. Isolated perfused livers were either left untreated or preconditioned with ANP (200 nM) for 20 min. After 24 h of ischemia and up to 120 min of reperfusion JNK activity was determined as described under “Materials and Methods”. Determination of density light units was performed by phosphorimaging and values for ANP-treated organs were divided by mean values for control organs at the respective time points. Panel A: Bars show means \pm SEM of five independent perfusion experiments with ^a $P < 0.05$: statistically different from controls at the respective time point. Panel B: Data show representative autoradiograms.

DISCUSSION

This work represents a systematic characterization of the stress-activated p38 MAPK and JNK activities during ischemia and reperfusion of the isolated perfused rat liver. The following results were obtained: (I) p38 shows a decreasing activity in the whole course of ischemia and reperfusion whereas (II) JNK is only activated during reperfusion. (III) Even more importantly, our paper reports for the first time that preconditioning with Atrial Natriuretic Peptide exerts a tremendous increase of p38 MAPK activation but shows no effect on JNK.

Our data on the time course of MAPK activation during cold ischemia and reperfusion adds further information to the increasing discussion on the role of p38 MAPK during I/R. Decreased p38 activity at the end of cold ischemia was also seen by Iesalnieks *et al.*^[14] using a rat liver transplantation model, but not in the work of the Brenner group which reported no change of p38 activity^[12]. After transplantation activation^[14] as well as no effect on p38 MAPK^[12] has been demonstrated. Since p38 is referred to as a stress-induced MAPK^[5] the decline of p38 MAPK activities we observed in ischemia as well as reperfusion might surprise. However, p38 activity might not solely reflect a stress response, but also mediate the induction of protective mechanisms.

For JNK convincing evidence is available that this MAPK is stimulated in the course of reperfusion. The data presented

here are supported by several other observations of increased activity of JNK during reperfusion for models of both cold^[12,14] and warm^[7] ischemic livers.

Taken together, MAPK are affected by I/R. The differences between our data and other work most likely reflect the different experimental set-up and therefore different basal MAPK activities and time dependency of activation.

The most important question arising from this discussion is the role of MAPKs in I/R injury. To address this question known protective strategies have to be examined for their effect on MAPKs during I/R. Up to now, these kinds of studies in the liver are quite rare. The outcome of our work, namely that preconditioning with ANP leads to a striking increase of p38 MAPK activities but is without effect on JNK, is therefore of great importance. Both hyperthermic^[26] as well as ischemic^[18,19] preconditioning have also been shown to represent protective strategies against I/R injury. Both JNK and p38 MAPK were reported to be activated by hyperthermia^[15,18] and a short time ischemic period of 10 min as used for ischemic preconditioning^[18,19] was shown to activate JNK^[8].

Our data point to p38 MAPK activation as a central signal transduction pathway of hepatoprotection during I/R. Hypoxic preconditioning of hepatocytes has recently been shown to also activate p38 MAPK^[17], thus supporting our assumption. For the heart, in fact, activation of p38 is reported to be a key signal in protection by ischemic preconditioning^[27]. Moreover, the hepatoprotective action of CO has very recently been reported to be exerted *via* p38 MAPK activation^[28].

ANP must be administered at least 20 min before ischemia in order to protect against I/R injury of the rat liver^[21]. Thus, the strong activation of p38 MAPK at the end of the preconditioning period *i.e.* before ischemia is suggested to be the crucial step in mediating hepatoprotection by ANP.

The meaning of increased MAPK activities by ANP at the end of reperfusion periods is less easy to explain. The augmented MAPK activities might simply reflect the increased number of vital hepatocytes in ANP preconditioned liver as compared to untreated tissue.

In summary, our data represent a systematic investigation of stress-activated MAPK in the course of ischemia and reperfusion. Second and even more importantly the pharmacological activation of MAPK as a mediator of preconditioning was achieved by the administration of the cardiovascular hormone ANP. The observation that protective strategies such as pre-treatment with ANP profoundly interact with the MAPK signalling cascade suggests them as crucial mediators of preconditioning.

ACKNOWLEDGEMENT

We thank Ingrid Liß for excellent technical assistance.

REFERENCES

- 1 **Bilzer M**, Gerbes AL. Preservation injury of the liver: mechanisms and novel therapeutic strategies. *J Hepatol* 2000;**32**:508-515
- 2 **Jaeschke H**. Preservation injury: mechanisms, prevention and consequences. *J Hepatol* 1996;**25**:774-780
- 3 **Cobb MH**. MAP kinase pathways. *Prog Biophys Mol Biol* 1999;**71**:479-500
- 4 **Widmann C**, Gibson S, Jarpe MB, Johnson GL. Mitogen-activated protein kinase: conservation of a three-kinase module from yeast to human. *Physiol Rev* 1999; **79**:143-180
- 5 **Kyriakis JM**, Avruch J. Mammalian mitogen-activated protein kinase signal transduction pathways activated by stress and inflammation. *Physiol Rev* 2001;**81**:807-869
- 6 **Cross TG**, Scheel-Toellner D, Henriquez NV, Deacon E, Salmon M, Lord JM. Serine/threonine protein kinases and apoptosis. *Exp Cell Res* 2000;**256**:34-41
- 7 **Bendinelli P**, Piccoletti R, Maroni P, Bernelli-Zazzera A. The MAP kinase cascades are activated during post-ischemic liver reperfusion. *FEBS Lett* 1996;**398**:193-197
- 8 **Onishi I**, Tani T, Hashimoto T, Shimizu K, Yagi M, Yamamoto K, Yoshioka K. Activation of c-Jun N-terminal kinase during ischemia and reperfusion in mouse liver. *FEBS Lett* 1997;**420**:201-204
- 9 **Zwacka RM**, Zhang Y, Zhou W, Halldorson J, Engelhardt JF. Ischemia/reperfusion injury in the liver of BALB/c mice activates AP-1 and nuclear factor kappaB independently of IkappaB degradation. *Hepatology* 1998;**28**:1022-1030
- 10 **Onishi I**, Shimizu K, Tani T, Hashimoto T, Miwa K. JNK activation and apoptosis during ischemia-reperfusion. *Transplant Proc* 1999;**31**:1077-1079
- 11 **Crenesse D**, Gugenheim J, Hornoy J, Tornieri K, Laurens M, Cambien B, Lenegrat G, Cursio R, De Souza G, Auburger P, Heurteaux C, Rossi B, Schmid-Alliana A. Protein kinase activation by warm and cold hypoxia-reoxygenation in primary-cultured rat hepatocytes-JNK(1)/SAPK (1) involvement in apoptosis. *Hepatology* 2000;**32**:1029-1036
- 12 **Bradham CA**, Stachlewitz RF, Gao W, Qian T, Jayadev S, Jenkins G, Hannun Y, Lemasters JJ, Thurman RG, Brenner DA. Reperfusion after liver transplantation in rats differentially activates the mitogen-activated protein kinases. *Hepatology* 1997;**25**:1128-1135
- 13 **Bradham CA**, Schemmer P, Stachlewitz RF, Thurman RG, Brenner DA. Activation of nuclear factor-kappaB during orthotopic liver transplantation in rats is protective and does not require Kupffer cells. *Liver Transplantation and Surgery* 1999;**5**:282-293
- 14 **Iesalnieks I**, Rentsch M, Lengyel E, Mirwald T, Jauch K, Beham A. JNK and p38MAPK are activated during graft reperfusion and not during cold storage in rat liver transplantation. *Transplant Proc* 2001;**33**:931-932
- 15 **Bendinelli P**, Piccoletti R, Maroni P, Bernelli-Zazzera A. The liver response to in vivo heat shock involves the activation of MAP kinases and RAF and the tyrosine phosphorylation of Shc proteins. *Biochem Biophys Res Commun* 1995;**216**:54-61
- 16 **Maroni P**, Bendinelli P, Zuccorononno C, Schiaffonati L, Piccoletti R. Cellular signalling after in vivo heat shock in the liver. *Cell Biol Int* 2000;**24**:145-152
- 17 **Carini R**, De Cesaris MG, Splendore R, Vay D, Domenicotti C, Nitti MP, Paola D, Pronzato MA, Albano E. Signal pathway involved in the development of hypoxic preconditioning in rat hepatocytes. *Hepatology* 2001;**33**:131-139
- 18 **Fung JJ**. Ischemic preconditioning: Application in clinical liver transplantation. *Liver Transpl* 2001;**7**:300-301
- 19 **Arai M**, Thurman RG, Lemasters JJ. Ischemic preconditioning of rat livers against cold storage-reperfusion injury: Role of nonparenchymal cells and the phenomenon of heterologous preconditioning. *Liver Transpl* 2001;**7**:292-299
- 20 **Bilzer M**, Witthaut R, Paumgartner G, Gerbes AL. Prevention of ischemia/reperfusion injury in the rat liver by atrial natriuretic peptide. *Gastroenterology* 1994;**106**:143-151
- 21 **Gerbes AL**, Vollmar AM, Kiemer AK, Bilzer M. The guanylate cyclase-coupled natriuretic peptide receptor: a new target for prevention of cold ischemia-reperfusion damage of the rat liver. *Hepatology* 1998;**28**:1309-1317
- 22 **Kiemer AK**, Vollmar AM, Bilzer M, Gerwig T, Gerbes AL. Atrial Natriuretic Peptide reduces expression of TNF- α mRNA during reperfusion of the rat liver upon decreased activation of NF-kappaB and AP-1. *J Hepatol* 2000;**33**:236-246

- 23 **Kiemer AK**, Gerbes AL, Bilzer M, Vollmar AM. The atrial natriuretic peptide and cGMP: novel activators of the heat shock response in rat livers. *Hepatology* 2002;**35**:88-94
- 24 **Tsukagoshi H**, Shimizu Y, Kawata T, Hisada T, Shimizu Y, Iwamae S, Ishizuka T, Iizuka K, Dobashi K, Mori M. Atrial natriuretic peptide inhibits tumor necrosis factor- α production by interferon- γ -activated macrophages via suppression of p38 mitogen-activated protein kinase and nuclear factor- κ B activation. *Regul Pept* 2001;**99**:21-29
- 25 **Kiemer AK**, Weber NC, Fürst R, Bildner N, Kulhanek-Heinze S, Vollmar AM. Inhibition of p38 MAPK activation *via* induction of MKP-1: Atrial Natriuretic Peptide reduces TNF- α -induced actin polymerisation and endothelial permeability. *Circ Res* 2002;**90**:874-881
- 26 **Terajima H**, Enders G, Thiaener A, Hammer C, Kondo T, Thiery J, Yamamoto Y, Yamaoka Y, Messmer K. Impact of hyperthermic preconditioning on postischemic hepatic microcirculatory disturbances in an isolated perfusion model of the rat liver. *Hepatology* 2000;**31**:407-415
- 27 **Nakano A**, Cohen MV, Downey JM. Ischemic preconditioning: from basic mechanisms to clinical applications. *Pharmacol Ther* 2000;**86**:263-275
- 28 **Amersi F**, Shen XD, Anselmo D, Melinek J, Iyer S, Southard DJ, Katori M, Volk HD, Busuttil RW, Buelow R, Kupiec-Weglinski JW. Ex vivo exposure to carbon monoxide prevents hepatic ischemia/reperfusion injury through p38 MAP kinase pathway. *Hepatology* 2002;**35**:815-823

Edited by Zhang JZ

• BASIC RESEARCH •

Anti-inflammatory effect of cholecystokinin and its signal transduction mechanism in endotoxic shock rat

Ai-Hong Meng, Yi-Ling Ling, Xiao-Peng Zhang, Jun-Lan Zhang

Ai-Hong Meng, Yi-Ling Ling, Jun-Lan Zhang, Department of Pathophysiology, Hebei Medical University, Shijiazhuang 050017, Hebei Province, China

Xiao-Peng Zhang, Department of Cardiothoracic Surgery, Hebei Provincial People's Hospital, Shijiazhuang 050071, Hebei Province, China

Supported by the Health Committee of Hebei Province, No.2k002, the Science and Technology Department of Hebei Province, No.01276410D, and the Natural Science Foundation of Hebei Province, No.302490

Correspondence to: Professor Yi-Ling Ling, Department of Pathophysiology, Hebei Medical University, Shijiazhuang 050017, Hebei Province, China. lingyl20@sina.com.cn

Telephone: +86-311-6052263

Received 2002-03-13 **Accepted** 2002-04-23

Abstract

AIM: To study the anti-inflammatory effects of cholecystokinin-octapeptide (CCK-8) on lipopolysaccharide (LPS)-induced endotoxic shock (ES) and further investigate its signal transduction pathways involving p38 mitogen-activated protein kinase (MAPK) and I κ B- α .

METHODS: Eighty-four rats were divided randomly into four groups: LPS (8 mg \cdot kg⁻¹, iv) induced ES; CCK-8 (40 mg \cdot kg⁻¹, iv) pretreatment 10 min before LPS (8 mg \cdot kg⁻¹); CCK-8 (40 μ g \cdot kg⁻¹, iv) or normal saline (control) groups. The inflammatory changes of lung and spleen, phagocytic function of alveolar macrophage, quantification of inflammatory cells in bronchoalveolar lavage (BAL) were investigated in rats by using hematoxylin and eosin (HE) staining, phagocytosis of *Candida albicans* and differential cell counting. Nitric oxide (NO) production in serum, lung and spleen was measured with the Griess reaction. The mechanism involving p38 MAPK and I κ B- α signal pathways was investigated by Western blot.

RESULTS: Inflammatory changes of lung and spleen induced by LPS were alleviated by CCK-8, the increase of NO induced by LPS in serum, lung and spleen was significantly inhibited and the neutrophil infiltration in BAL was significantly reduced by CCK-8. The number of neutrophils was $(52 \pm 10) \times 10^6$ cells \cdot L⁻¹ in LPS group, while it decreased to $(18 \pm 4) \times 10^6$ cells \cdot L⁻¹ in CCK-8+LPS ($P < 0.01$). The phagocytic rate of CCK-8 group increased to $(62.49 \pm 9.49) \%$, compared with control group $(48.16 \pm 14.20) \%$, $P < 0.05$. The phagocytosis rate was $(85.14 \pm 4.64) \%$ in LPS group, which reduced to $(59.33 \pm 3.14) \%$ in CCK-8+LPS group ($P < 0.01$). The results of phagocytosis indexes showed similar changes. CCK-8 may play an important role in increasing the expression of p38 MAPK and decreasing the degradation of I κ B- α in lung and spleen of ES rats.

CONCLUSION: CCK-8 can result in anti-inflammatory

effects, which may be related to activation of p38 MAPK and inhibition on the degradation of I κ B- α .

Meng AH, Ling YL, Zhang XP, Zhang JL. Anti-inflammatory effect of cholecystokinin and its signal transduction mechanism in endotoxic shock rat. *World J Gastroenterol* 2002; 8(4):712-717

INTRODUCTION

Lipopolysaccharide (LPS), a main component of Gram-negative bacterial endotoxin^[1], is the leading cause of sepsis or endotoxic shock (ES), and when administered experimentally to animals, it results in the same inflammatory response mimically. Physical stress such as infection can stimulate proinflammatory cytokine production and release. The overproduction of these cytokines has been postulated to contribute to the development of tissue injury^[2]. The pathogenesis of inflammatory sepsis is also linked to the overproduction of nitric oxide (NO), a potentially toxic molecule, being possibly responsible in part for the cytotoxicity of the inflammatory process^[3]. Nuclear factor (NF)- κ B is a heterodimeric protein complex containing two members of the rel family of transcription factors, p50 and p65. At rest, the heterodimeric NF- κ B complex is located in the cytoplasm bound to an inhibitory factor, I κ B. Upon stimulation, I κ B- α is phosphorylated and proteolytically degraded or processed by proteasomes and other proteases. Free NF- κ B then translocates into the nucleus where it binds to various gene promoter regions controlling the expression of various pro-inflammatory and proliferative agents^[4]. NO augments the activation of NF- κ B in macrophages and, therefore, may play a role in producing a positive cycle of inflammation^[5]. One of the earliest responses to LPS is activation of the mitogen-activated protein kinase (MAPK) homolog p38. The p38 MAPK is involved in intracellular signals that regulate a variety of cellular responses during inflammation^[6]. A slightly later cellular response to LPS is the activation of NF- κ B, which does not require p38 kinase activity^[7].

Cholecystokinin (CCK), a component from the gastrin-CCK family, first isolated from hog intestine, shows a widespread distribution in different organs and tissues. The sulfated carboxy-terminal octapeptide (CCK-8), isolated from the central nervous system and digestive tract, is the predominant active form. CCK-8 possessed both excitatory and inhibitory action on contractile activity of different regions of stomach in guinea pigs^[8]. CCK-8 could antagonize the elimination of morphine on the potentiations of ACh to duodenal activities^[9]. Besides the effects on the digestive tract, other biological actions of CCK-8 have been observed, for instance appetite inhibition and so on^[10,11]. In the spleen, CCK-8 is formed in high abundance in the white pulp where it appears to surround cell clusters. It seems that CCK-8 increases the secretion of immunoglobulins *in vivo*^[12], whereas it inhibits Molt-4 lymphoblast proliferation^[13] and modulates mitogen-

induced lymphoproliferation and intracellular calcium mobilization *in vitro*^[14,15]. CCK-8, a chemoattractant for human monocytes and rat macrophages^[16], enhancing human eosinophil chemotaxis induced by PAF and LTB₄ in allergic patient^[17] is a negative modulator of several murine macrophage and human neutrophil functions^[18,19].

Our previous *in vivo* and *in vitro* study demonstrated that CCK-8 could protect animals from ES^[20,21], which was related to its inhibitory effect on the overproduction of proinflammatory cytokines^[22] and on the transcription of TNF- α ^[23]. In the present study, the effects of CCK-8 on NO production, inflammatory changes of lung and spleen induced by LPS and phagocytic function of rat alveolus macrophage and further on the p38 MAPK and I κ B- α expression in lung and spleen were investigated.

MATERIALS AND METHODS

Materials

CCK-8 (sulfated), LPS (*E.coli* LPS, serotype 0111:B4), leupeptin, pepstatin A, Triton X-100 and p38 monoclonal antibody were all purchased from Sigma, RPMI-1640 from GibcoBrl, aprotinin from Boehringer, I κ B- α polyclonal antibody from Santa Cruz. All other reagents used were of analytic grade.

Methods

Animal preparation^[22] Sprague-Dawley rats (150-200 g BW, Experimental Animal Center of Hebei Province) were randomly assigned to four groups injected different agents via tail vein. For group receiving LPS, a bolus dose (8mg/kg) of LPS was injected into the tail vein. For group of CCK-8+LPS, a bolus dose (40 μ g/kg) of CCK-8 was administered 10 min before the injection of LPS. Negative control animals received saline. CCK-8 (40 μ g/kg) was also administered alone in the other group.

Sample collection Animals were sacrificed at 2 h, 6 h or 12 h, spleen and lung were rapidly excised and rinsed of blood, and blood was taken and centrifuged to collect serum. The samples were stored at -80°C for analysis of NO content. Additional groups of animals were sacrificed at 30 min and their lungs and spleens excised were analyzed for p38 MAPK and I κ B- α expression.

Histological examination Rats were treated as described in animal preparation and sacrificed at 2 h, 6 h or 12 h after LPS administration. Lung and spleen were sliced into pieces and preserved in 10 % formalin. Tissue samples were embedded in paraffin, cut into 5- μ m sections, and then assessed by routine staining with hematoxylin and eosin (HE) and examined by light microscopy.

Nitrate/nitrite analysis The samples (serum, spleen, lung) collected 2 h, 6 h or 12 h were analyzed. Tissues were homogenized with PBS (4°C, pH 7.2, 100 mg tissue/ml) and centrifuged at 12 000 rpm, 10 min. Supernatants and serum were assayed NO content based on the Griess reaction, which consists of measurement of stable end breakdown products of NO such as nitrite that are considered to be reliable markers for NO formation. The nitrite was converted to a deep purple compound and absorbance was read at 550 nm, and nitrite concentration was determined using NaNO₂ standards.

Phagocytic function Two hours after injection of LPS, bronchus alveolus lavage fluid (BALF) was obtained and macrophages were isolated from BALF by centrifugation (1 500 rpm, 10 min)^[6]. Being washed with normal saline (NS), the cells were resuspended in RPMI-1640, adjusted to 10⁶/ml and incubated

for 2 h. The adherent monolayer was washed with RPMI-1640 and then aliquots of *Candida albicans* (2 \times 10⁷ cells/ml medium), previously in water bath (100°C) for 30 min were added. After 60 min of incubation, the plates were washed with NS, fixed and stained and the number of yeasts ingested per 100 macrophages was counted. Phagocytosis rate and phagocytosis index were calculated according to the following equation:

Phagocytosis rate (%) = (macrophages with yeasts ingested / total macrophages) %

Phagocytosis index = number of *Candida albicans* ingested / number of macrophages with *Candida albicans* ingested

Quantification of inflammatory cells Neutrophil influx was determined in the BALF samples obtained 2 h by differential cell counting. Total whole cell counts were obtained in BALF. The cells were smeared on slides and stained with Wrights-Giemsa stain. Three differential counts on 200 cells per slide were performed and the percentage of macrophages/monocytes, lymphocytes and neutrophils were determined.

Western blot Lung and spleen were excised 30 min after injection of LPS. Tissues were homogenized in a buffer containing 50 mM Tris (pH7.5), 150 mM NaCl, 1 % TritonX-100, 0.5% deoxycholic acid, 0.1 % sodium dodecyl sulfate, 1 mM phenylmethylsulfonyl fluoride (PMSF), 10 mM NaF, 1mM sodium vanadate and a 40 μ g/ml protease inhibitor cocktail and centrifuged at 18 000 rpm, 4 °C, 10 min. Supernatants were fractionated on 12 % SDS-polyacrylamide gels, transferred to poly (vinylidene difluoride) membranes, and incubated with phospho-specific anti-p38 MAPK or I κ B- α polyclonal antibody. Being washed three times in T-PBS, membranes were incubated in horseradish peroxidase-linked secondary antibody for 1 h at room temperature. Membranes were again washed three times with T-PBS and stained with diaminobenzidine (DAB).

Statistical analysis Data were reported as $\bar{x} \pm s$. Statistical differences between values from different groups were determined by one way ANOVA and Newman-Keuls *q* test. Significance was set at *P*<0.05.

RESULTS

CCK-8 alleviated inflammatory changes induced by LPS

Lung and spleen were harvested at 2 h, 6 h or 12 h. There were structural injury in LPS group and alleviated changes in CCK-8+LPS group at 2 h, while more significant changes at 6 h and 12 h. The lung of LPS-stimulated rats demonstrated widened septa of alveoli, diffuse infiltration and migration of acute inflammatory cells (PMN) accompanied by atrophied or disappeared alveoli, and slight alveolar atelectasis or emphysema. While in CCK-8+LPS group, the inflammatory changes were evident, but to a lesser extent. The spleen of LPS-stimulated rats showed hyperaemia in spleen sinusoids with concentrated red blood cells (RBC) and PMN, while it changes to a lesser extent in CCK-8+LPS group. There was not much difference between CCK-8 group and control group (Figure 1).

CCK-8 inhibited NO production

Studies of LPS-induced NO production in spleen, lung and serum showed increase in either nitrate or nitrite levels at 2 h, 6 h or 12 h after LPS administration. Significant increase was observed at 6 h, compared with that in control animals. CCK-8 produced inhibitory effect on increase of NO content induced by LPS (Table 1).

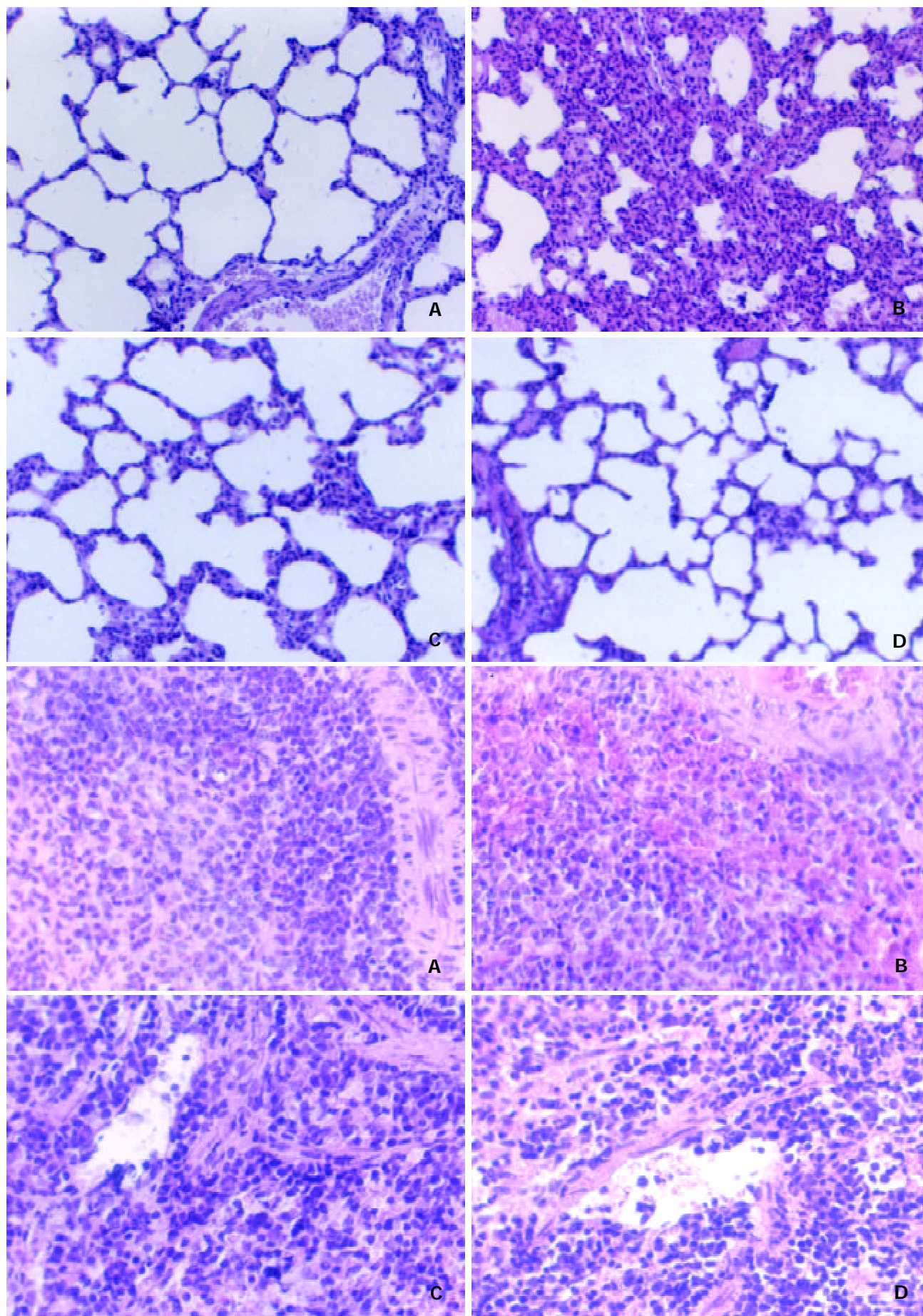


Figure 1 CCK-8 alleviated pulmonary (upper, $\times 100$) and spleen (lower, $\times 200$) structural injury 6 h after LPS administration. A. Control group. B. LPS group. C. CCK-8+LPS group. D. CCK-8 group. Plate depicts a representative field from one of three rats.

Table 1 Inhibitory effect of CCK-8 on LPS stimulated nitrite production in serum, lung and spleen ($n=6$)

Group	2 h	6 h	12 h
Serum ($\mu\text{mol} \cdot \text{L}^{-1}$)			
Control	36.8 ± 2.2	39.2 ± 3.2	33.8 ± 4.1
LPS	78.2 ± 7.4^b	250.9 ± 19.6^b	302.9 ± 41.2^b
CCK-8+LPS	48.5 ± 5.3^d	124.8 ± 4.9^{bd}	
CCK-8	37.3 ± 2.3	32.4 ± 6.6	
Lung ($\mu\text{mol} \cdot \text{g}^{-1}$)			
Control	48.9 ± 7.6	47.2 ± 4.7	51.2 ± 6.1
LPS	117.5 ± 6.7^b	140.6 ± 24.1^b	186.6 ± 8.3^b
CCK-8+LPS	81.9 ± 10.8^{bd}	114.8 ± 8.3^{bd}	
CCK-8	52.6 ± 5.6	44.0 ± 2.3	
Spleen ($\mu\text{mol} \cdot \text{g}^{-1}$)			
Control	53.9 ± 5.6	48.5 ± 9.0	49.8 ± 6.1
LPS	71.3 ± 8.9^b	74.7 ± 4.2^a	63.5 ± 3.8^a
CCK-8+LPS	59.6 ± 3.3^c	46.5 ± 11.0^d	
CCK-8	45.0 ± 2.9	42.7 ± 2.3	

^a $P < 0.05$, ^b $P < 0.01$ vs Control, ^c $P < 0.05$, ^d $P < 0.01$ vs LPS

Phagocytic function changes

Phagocytosis of alveolar macrophages isolated from BALF 2 h after LPS administration was increased significantly, the phagocytosis index increased from 2.43 ± 0.71 (Control) to 3.80 ± 0.60 ($P < 0.05$). CCK-8 showed an inhibitory effect on the LPS-induced increase of *Candida albicans* phagocytosis by macrophage. The phagocytosis index in CCK-8+LPS group reduced to 2.21 ± 0.14 , $P < 0.05$. While the phagocytosis rate of CCK-8 group was $(62.49 \pm 9.49)\%$, which was higher than control group $(48.16 \pm 14.20)\%$, $P < 0.05$ (Figure 2).

Changes of inflammatory cells

Compared with Control, significant increase of BAL neutrophils was observed in LPS group, The number increased from $(1 \pm 0.2) \times 10^6$ cells $\cdot \text{L}^{-1}$ to $(52 \pm 10) \times 10^6$ cells $\cdot \text{L}^{-1}$, $P < 0.01$. It decreased to $(18 \pm 4) \times 10^6$ cells $\cdot \text{L}^{-1}$, $P < 0.01$, in CCK-8+LPS group compared with LPS group.

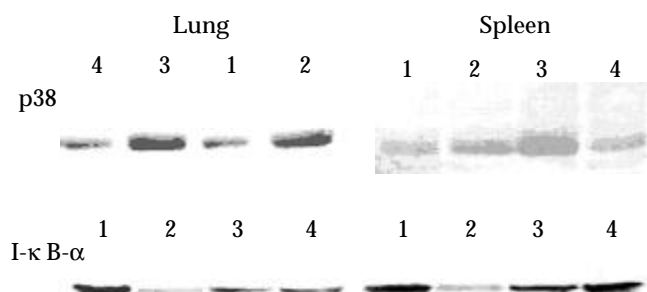


Figure 3 p38 MAPK (A) was activated by LPS and enhanced by CCK-8 in rat lung (left) or spleen (right) using Western blotting. Degradation of IκB-α in lung and spleen following LPS administration was observed and pre-administration of CCK-8 could reduce its degradation. These figures are representative of three different experiments. 1. Normal control, 2. LPS ($8 \text{ mg} \cdot \text{kg}^{-1}$), 3. CCK-8 ($40 \mu\text{g} \cdot \text{kg}^{-1}$)+LPS, 4. CCK-8

Western blot

Significant phosphorylation of p38 MAPK was observed in lung and spleen of endotoxic rats 30 min post LPS administration. CCK-8 can enhance LPS-induced phosphorylation of p38 MAPK significantly. Phosphorylation of p38 MAPK was also observed in animals receiving normal saline or CCK-8. The degradation of IκB-α in lung and spleen following LPS administration was observed, while the procedure of pre-administration of CCK-8 could reduce its degradation (Figure 3).

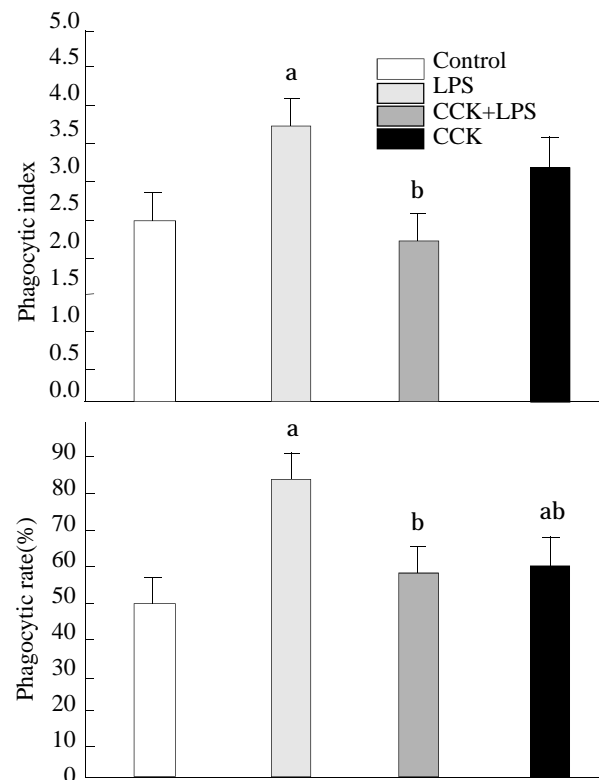


Figure 2 Effect of CCK-8 on LPS-induced increase of phagocytic capacity of *Candida albicans* by alveolar macrophages isolated 2 h after LPS administration.

^a $P < 0.05$ vs Control, ^b $P < 0.01$ vs LPS.

DISCUSSION

Some studies examined *ex vivo* measures of immune function stimulated by LPS or CCK-8. While *ex vivo* determinations of immune function are useful, and yield important information concerning the status of the immune system, there is the concern that *ex vivo* stimulation of immune cells may not be naturalistic and consequently be of limited value when immunocompetence is assessed in a whole organism. Thus another approach which has been used to assess immunological status in laboratory animals, is to examine their ability to respond to an *in vivo* challenge with bacterial LPS^[24]. Macrophages are the sources of proinflammatory cytokines^[25]. Inflammatory mediators like cytokines, NO and reactive oxygen species are released by activated macrophages from various sources, including spleen and lung. NO is particularly important as a vasodilator but also participates in immunologic reactions, including the ability of macrophages to kill tumor cells and bacteria^[26]. Some of the deleterious effects of LPS on organ function have been attributed to NO^[27]. CCK-8 exerts an inhibitory effect on the overproduction of proinflammatory cytokines induced by LPS, which suggested its functions of anti-inflammatory effect^[22]. In addition, CCK-8 inhibits LPS-

induced increase of NO, which may be related to its inhibition on inducible NO synthase^[28]. In contrast, our data do not support the idea that CCK-8 may be mediating the anti-inflammatory effects by the production of NO, to which anti-inflammatory effects also have been described^[29].

Members of the MAPK cascade are considered to play key roles in signal transduction pathways activated by a wide range of stimuli. The three best characterized members of this growing family of serine/threonine kinases are extracellular signal-regulated kinase (ERK), *c-jun* N-terminal kinase (JNK) and p38. Active MAPK are responsible for the phosphorylation of a variety of effector proteins including several transcription factors^[30]. P38 may help reduce organ destruction while inhibition of p38 during induction of cerulein pancreatitis leads to the occurrence of acinar necrosis^[31]. Recent evidence from other systems indicates that p38 activation can indeed be protective. Thus, p38 is reportedly important for protection observed after ischemic precondition in myocardial cells and it is evidenced that p38 may exert protective effects via its substrate MAPKAPK2 (MAPK activated protein kinase 2)^[32,33]. Activated p38 inhibited iNOS induction, which may be due to the ability of p38 to inhibit LPS-induced JNK activation^[34,35]. The anti-inflammatory effects of CCK-8 seem to involve the p38 MAPK pathway. The mechanism by which CCK-8 modulates the p38 MAPK remains unclear at this time. Sodium salicylate suppress TNF- α production, activates p38 MAPK and inhibits both ERK1/ERK2 and SAPK/JNK MAPKs in LPS-stimulated macrophages. Additionally, it has been shown that p38 activation is required for I κ B-mediated inhibition of NF- κ B^[36]. It was reported that LPS-induced production of TNF- α was regulated mainly, but not exclusively, through the p38 MAPK pathway^[37-40]. Other signal pathway may be involved. Induction of tolerance by sublethal hemorrhage (SLH) is dependent of p38 MAPK activation and this intracellular signal may be a necessary step in the initiation of the cellular reprogramming associated with tolerance. The normal activation of p38 MAPK is preserved in response to a "second insult" with LPS despite an attenuation in TNF production by tolerant cell^[41].

NF- κ B plays an important role in physiologic and pathologic conditions as an inducible nuclear factor. NF- κ B/Rel have been implicated in the inflammatory response. Degradation of I κ B- α proteins frees NF- κ B proteins, which then translocate into the nucleus, where they activate transcription^[42]. Another study from our laboratory showed CCK-8 inhibited the increased activity of NF- κ B induced by LPS in lung of rats, which may be related to its anti-inflammatory effect.

CCK-8 inhibits phagocytic function of alveolar macrophages isolated 2 h after LPS administration. *In vivo*, this would prevent the excess accumulation of phagocytic cells in the inflamed area, and thereby decrease the phagocytic process. This may be related to its anti-inflammatory effect. Interestingly, CCK-8 itself increases the phagocytic process compared with control. The result indicated that CCK-8 may play different immunoregulatory role in different conditions^[43]. The development of tissue damage in shock is closely associated with the release of an ever-increasing number of mediators and accumulation of neutrophils at the sites of infection or injury^[44]. CCK-8 alleviated the accumulation of neutrophils in BALF, which may be related to its protecting effect on lung of ES rats.

The results of the present study show that administration of CCK-8 prevents inflammatory changes in lung and spleen of rats and attenuates increase of NO and inflammatory cells induced by LPS. Moreover, CCK-8 inhibits LPS-induced

increase of macrophage phagocytic function while itself increases phagocytic function. CCK-8 enhances the expression of p38 MAPK while reduces the degradation of I κ B- α induced by LPS, which may be involved in the signal transduction pathway.

REFERENCES

- 1 **Fan K**. Regulatory effects of lipopolysaccharide in murine macrophage proliferation. *World J Gastroenterol* 1998; **4**:137-139
- 2 **Molina PE**, Abumrad NN. Differential effects of hemorrhage and LPS on tissue TNF- α , IL-1 and associate neuro-hormonal and opioid alterations. *Life Sci* 2000; **66**:399-409
- 3 **Zhang GL**, Wang YH, Teng HL, Lin ZB. Effects of aminoguanidine on nitric oxide production induced by inflammatory cytokines and endotoxin in cultured rat hepatocytes. *World J Gastroenterol* 2001; **7**: 331-334
- 4 **Chen F**, Casanova V, Shi X, Demers LM. New insights into the role of nuclear factor- κ B, a ubiquitous transcription factor in the initiation of diseases. *Clin Chem* 1999; **45**: 7-17
- 5 **Kang JL**, Lee K, Casanova V. Nitric oxide up-regulates DNA-binding activity of nuclear factor- κ B in macrophages stimulated with silica and inflammatory stimulants. *Mol Cell Biochem* 2000; **215**:1-9
- 6 **Ohashi N**, Matsumori A, Furukawa Y, Ono K, Okada M, Iwasaki A, Miyamoto T, Nakano A, Sasayama S. Role of p38 mitogen-activated protein kinase in neointimal hyperplasia after vascular injury. *Arterioscler Thromb Vasc Biol* 2000; **20**:2521-2526
- 7 **Garrett TA**, Rosser MFN, Raetz CRH. Signal transduction triggered by lipid A-like molecules in 70Z/3 pre-B lymphocyte tumor cells. *Biochimica et Biophysica Acta* 1999; **1437**: 246-256
- 8 **Li W**, Zheng TZ and Qu SY. Effect of cholecystokinin and secretin on contractile activity of isolated gastric muscle strips in guinea pigs. *World J Gastroenterol* 2000; **6**:93-95
- 9 **Xu MY**, Lu HM, Wang SZ, Shi WY, Wang XC, Yang DX, Yang CX, Yang LZ. Effect of devazepide reversed antagonism of CCK-8 against morphine on electrical and mechanical activities of rat duodenum *in vitro*. *World J Gastroenterol* 1998; **4**:524-526
- 10 **De la Fuente M**, Carrasco M, Del Rio M, Hernanz A. Modulation of murine lymphocyte functions by sulfated cholecystokinin octapeptide. *Neuropeptides* 1998; **32**:225-233
- 11 **Du YP**, Zhang YP, Wang SC, Shi J and Wu SH. Function and regulation of cholecystokinin-octapeptide, α -endorphin and gastrin in anorexic infantile rats treated with ErBao Granules. *World J Gastroenterol* 2001; **7**: 275-280
- 12 **Alverdy J**, Stern E, Poticha S, Baunoch D, Adrian T. Cholecystokinin modulates mucosal immunoglobulin A function. *Surgery* 1997; **122**:386-393
- 13 **Tang SC**, Braunsteiner H, Wiedermann C. Regulation of human T lymphoblast growth by sensory neuropeptides: Augmentation of cholecystokinin-induced inhibition of Molt-4 proliferation by somatostatin and vasoactive intestinal peptide *in vitro*. *Immunol Lett* 1992; **34**:237-242
- 14 **Elitsur Y**, Luck GD. The inhibition effect of cholecystokinin in human colonic lamina propria lymphocyte proliferation, and reversal by the cholecystokinin receptor antagonist L-364817. *Neuropeptides* 1991; **20**:41-47
- 15 **McMillen MA**, Ferrara A, Adrian TE, Margolis DS, Schaefer HC, Zucker KA. Cholecystokinin effect on human lymphocyte ionized calcium and mitogenesis. *J Surg Res* 1995; **58**:149-158
- 16 **Sacerdote P**, Ruff MR, Pert CB. Cholecystokinin and the immune system: Receptor-mediated chemotaxis of human and rat monocytes. *Peptides* 1988; **9** (suppl.1): 29-34
- 17 **Numao T**, Agrawal DK. Neuropeptides modulate human

- eosinophil chemotaxis. *J Immunol* 1992; **149**: 3309-3315
- 18 **De la Fuente M**, Campos M, Del Rio M, Hernanz A. Inhibition of murine peritoneal macrophage functions by sulfated cholecystokinin octapeptide. *Regul Pept* 1995; **55**:47-56
- 19 **Carrasco M**, Del Rio M, Hernanz A, De La Fuente M. Inhibition of human neutrophil functions by sulfated and nonsulfated cholecystokinin octapeptides. *Peptides* 1997; **18**:415-422
- 20 **Ling YL**, Huang SS, Wang LF, Wan M, Hao RL. Cholecystokinin-octapeptide (CCK-8) reverses experimental endotoxin shock. *Shengli Xuebao* 1996; **48**:390-394
- 21 **Meng AH**, Ling YL, Wang DH, Gu ZY, Li SJ, Zhu TN. Cholecystokinin-octapeptide alleviates tumor necrosis factor- α induced changes in rabbit pulmonary arterial reactivity and injuries of endothelium *in vitro*. *Shengli Xuebao* 2000; **52**:502-506
- 22 **Ling YL**, Meng AH, Zhao XY, Shan BE, Zhang JL, Zhang XP. Effect of cholecystokinin on cytokines during endotoxin shock in rats. *World J Gastroenterol* 2001; **7**: 667-671
- 23 **Meng AH**, Ling YL, Zhang XP, Zhao XY, Zhang JL. CCK-8 inhibits expression of TNF- α in the spleen of endotoxin shock rats and signal transduction mechanism of p38 MAPK. *World J Gastroenterol* 2002; **8**: 139-143
- 24 **Connor TJ**, Kelly JP, McGee M, Leonard BE. Methylenedioxymethamphetamine (MDMA; Ecstasy) suppresses IL-1 α and TNF- α secretion following an *in vivo* lipopolysaccharide challenge. *Life Sci* 2000; **67**:1601-1612
- 25 **Wu XN**. Current concept of pathogenesis of severe acute pancreatitis. *World J Gastroenterol* 2000; **6**:32-36
- 26 **Wu GH**, Zhang YW, Wu ZH. Modulation of postoperative immune and inflammatory response by immune-enhancing enteral diet in gastrointestinal cancer patients. *World J Gastroenterol* 2001; **7**: 357-362
- 27 **Mailman D**, Guntuku S, Bhuiyan MB, Murad F. Organ sites of lipopolysaccharide-induced nitric oxide production in the anesthetized rat. *Nitric Oxide* 2001; **5**: 243-51
- 28 **Meng AH**, Ling YL, Wang DH, Gu ZY, Li SJ, Zhu TN. Role of nitric oxide in cholecystokinin-octapeptide alleviation of tumor necrosis factor- α induced changes in rabbit pulmonary arterial reactivity. *Shengli Xuebao* 2001; **53**:478-482
- 29 **Derijard B**. Independent human MAP kinase signal transduction pathways defined by MEK and MKK isoforms. *Science* 1995; **267**:682-685
- 30 **Widmann C**, Gibson S, Jarpe MB, Johnson GL. Mitogen activated protein kinase: conservation of a three kinase module from yeast to human. *Physiol Rev* 1999; **79**:143-180
- 31 **Fleischer F**, Dabew R, G ke B, Wagner ACC. Stress kinase inhibition modulates acute experimental pancreatitis. *World J Gastroenterol* 2001; **7**: 259-265
- 32 **Weinbrenner C**, Liu GS, Cohen MV, Downey JM. Phosphorylation of tyrosine 182 of p38 mitogen activated protein kinase correlates with the protection of preconditioning in the rabbit heart. *J Mol Cell Cardiol* 1997; **29**:2383-2391
- 33 **Nakano A**, Baines CP, Kim SO. Ischemic preconditioning activates MAPKAPK2 in the isolated rabbit heart: evidence for involvement of p38 MAPK. *Circ Res* 2000; **86**:144-151
- 34 **Chan ED**, Morris KR, Belisle JT, Hill P, Remigio LK, Brennan PJ, Riches DW. Induction of inducible nitric oxide synthase-NO* by lipoarabinomannan of Mycobacterium tuberculosis is mediated by MEK1-ERK, MKK7-JNK, and NF-kappaB signaling pathways. *Infect Immun* 2001; **69**:2001-2010
- 35 **Chan ED**, Riches DW. IFN-gamma + LPS induction of iNOS is modulated by ERK, JNK/SAPK, and p38 (mapk) in a mouse macrophage cell line. *Am J Physiol Cell Physiol* 2001; **280**:C441-450
- 36 **Vittimberga FJ**, McDade TP, Perugini RA, Callery MP. Sodium salicylate inhibits macrophage TNF- α production and alters MAPK activation. *J Surg Res* 1999; **84**:143-149
- 37 **Geppert TD**, Whitehurst CE, Thompson P, Beutler B. Lipopolysaccharide signals activation of tumor necrosis factor biosynthesis through the ras/raf-1/MEK/MAPK pathway. *Mol Med* 1994; **1**: 93-103
- 38 **Badger AM**. Pharmacological profile of SB203580, a selective inhibitor of cytokine suppressive binding protein/p38 kinase, in animal models of arthritis, bone resorption, endotoxin shock and immune function. *J Pharm Exp Ther* 1996; **279**: 1453-1461
- 39 **Wysk M**, Yang D, Lu HT, Flavell RA, Davis RJ. TNF-induced cytokine expression mediated by the p38 MAP kinase activator MKK3. *Proc Nat Acad Sci USA* 1999; **96**:3763-3768
- 40 **Haddad EB**, Birrell M, McCluskie K, Ling A, Webber SE, Foster ML, Belvisi MG. Role of p38 MAP kinase in LPS-induced airway inflammation in the rat. *Bri J Pharmacol* 2001; **132**:1715-1724
- 41 **Mendez C**, Jaffray C, Wong V, Salhab KF, Kramer AA, Carey LC, Norman JG. Involvement of p38 mitogen-activated protein kinase in the induction of tolerance to hemorrhagic and endotoxin shock. *J Surg Res* 2000; **91**:165-170
- 42 **Guo SP**, Wang WL, Zhai YQ, Zhao YL. Expression of nuclear factor- κ B in hepatocellular carcinoma and its relation with the X protein of hepatitis B virus. *World J Gastroenterol* 2001; **7**:340-344
- 43 **Carrasco M**, Hernanz A, De La Fuente M. Effect of cholecystokinin and gastrin on human peripheral blood lymphocyte functions, implication of cyclic AMP and interleukin 2. *Regul Pept* 1997; **70**: 135-142
- 44 **Wu RQ**, Xu YX, Song XH, Chen LJ, Meng XJ. Adhesion molecule and proinflammatory cytokine gene expression in hepatic sinusoidal endothelial cells following cecal ligation and puncture. *World J Gastroenterol* 2001; **7**: 128-130

Edited by Zhao P

• BASIC RESEARCH •

Effect of cholecystokinin octapeptide on tumor necrosis factor α transcription and nuclear factor- κ B activity induced by lipopolysaccharide in rat pulmonary interstitial macrophages

Bin Cong, Shu-Jin Li, Yu-Xia Yao, Gui-Jun Zhu, Yi-Ling Ling

Bin Cong, Shu-Jin Li, Yi-Ling Ling, Department of Pathophysiology, Hebei Medical University, Shijiazhuang 050017, Hebei Province, China

Yu-Xia Yao, Molecular Biological Laboratory, Hebei Medical University, Shijiazhuang 050017, Hebei Province, China

Gui-jun Zhu, Department of chest surgery, The Fourth Hospital, Hebei Medical University, Shijiazhuang 050017, Hebei Province, China

Supported by Natural Science Foundation of Hebei Province, No. 300322

Correspondence to: Bin Cong, Department of Pathophysiology, Hebei Medical University, Shijiazhuang 050017, Hebei Province, China. congbinbc@sina.com

Telephone: +86-311-6044121, ext 5874.

Received 2002-04-04 **Accepted** 2002-05-17

Abstract

AIM: To elucidate the anti-inflammatory mechanism of an intestinal neuropeptide, sulfated cholecystokinin octapeptide (sCCK-8), the effects of sCCK-8 on lipopolysaccharide (LPS)-induced tumor necrosis factor α (TNF- α) mRNA expression and NF- κ B activity in pulmonary interstitial macrophages (PIMs) were studied.

METHODS: PIMs from rat were stimulated with LPS ($1\text{mg} \cdot \text{L}^{-1}$) in the presence or absence of sCCK-8 (10^{-8} - $10^{-6}\text{mol} \cdot \text{L}^{-1}$) or/and CCK receptor antagonist proglumide ($2\text{mg} \cdot \text{L}^{-1}$). The expression of TNF- α mRNA was assayed by reverse transcription polymerase chain reaction (RT-PCR) at 3h of the stimulation, and nuclear factor- κ B (NF- κ B) binding activity was analyzed by electrophoretic mobility shift assay (EMSA) at 1 h of stimulation. The I κ B- α protein level in the cytoplasm at 30 min of the stimulation was detected by Western blot.

RESULTS: sCCK-8, at concentrations from $10^{-8}\text{mol} \cdot \text{L}^{-1}$ to $10^{-6}\text{mol} \cdot \text{L}^{-1}$ obviously inhibited LPS-induced TNF- α mRNA expression and NF- κ B binding activity in a dose-dependent manner, $P < 0.05$, $P < 0.01$. Stimulation PIMs with LPS resulted in a reduction of I κ B- α protein level, $P < 0.01$, which was elevated by sCCK-8, $P < 0.05$. The effects of sCCK-8 on NF- κ B activity and I κ B protein level were attenuated by CCK receptor antagonist proglumide, $P < 0.01$.

CONCLUSION: sCCK-8 inhibits LPS-induced TNF- α mRNA expression by regulating NF- κ B activity in rat PIMs, which is mediated through CCK receptors and inhibiting

I κ B- α degradation. This represents one of the anti-inflammatory mechanisms of sCCK-8.

Cong B, Li SJ, Yao YX, Zhu GJ, Ling YL. Effect of cholecystokinin octapeptide on tumor necrosis factor α transcription and nuclear factor- κ B activity induced by lipopolysaccharide in rat pulmonary interstitial macrophages. *World J Gastroenterol* 2002; 8(4): 718-723

INTRODUCTION

Interactions between the central nervous system (CNS) and the immune system, particularly through neuropeptides, are of growing interest. Due to the abundant autonomic innervation and extensive lymphoid compartment localized in the gastrointestinal tract, a number of neuropeptides with observed and potential immunomodulatory effects have been isolated from gut tissues^[1]. These intestinal neuropeptides with immunomodulatory effects include growth hormone^[2], somatostatin^[3], vasoactive intestinal peptide (VIP)^[4,5], calcitonin gene-related peptide (CGRP)^[6], neuropeptide Y^[7,8], neurotensin^[9], and cholecystokinin (CCK)^[10].

CCK is discovered initially in the gut with the function of contracting gallbladder, and subsequently localized in the central and peripheral nervous system^[10]. CCK is identified as several different size of the peptide including 4, 8, 33, 39, and 58 amino acid forms. The sulfated carboxy-terminal octapeptide (sCCK-8) is the biologically predominant active form localized in the small intestine, blood and CNS^[10]. In the last decade few studies have investigated the relation between CCK and immune cells. Okahata *et al*^[11] demonstrated CCK immunoreactivity in peripheral blood leukocytes. Data from several labs suggest that CCK mediates an increase in intracellular calcium in human peripheral blood mononuclear cells and T lymphocyte cell line^[12,13]. sCCK-8 can inhibit the mobility capacity and the mitogen-induced lymphocytic proliferation, but can increase the adherence and the spontaneous proliferation of lymphocytes^[14,15]. In addition, sCCK-8 is a negative modulator of several functions of murine peritoneal macrophages and human neutrophils including the production of superoxide anion, phagocytosis and mobility^[16-18]. Interestingly, sCCK-8 causes an *in vitro* inhibition of lipopolysaccharide (LPS)-induced TNF- α production, sCD14 release and mCD14 expression in rat pulmonary interstitial macrophages (PIMs)^[19]. Consistently, the production of proinflammatory cytokines including TNF- α , IL-1 α , and IL-6 in endotoxin shock (ES) rat was also inhibited by sCCK-8 *in vivo*^[20,21]. These results suggested that sCCK-8 has anti-inflammatory effect to some extent, a new field about the biological action of CCK, which was also confirmed by a

morphological observation that sCCK-8 clearly lessened the inflammatory lesions in lung, spleen and liver tissues in ES rat^[22].

It is well known that transcriptional factor NF- κ B plays a pivotal role in LPS-induced TNF- α gene expression and involved in the inflammatory response^[23]. To elucidate the anti-inflammatory mechanism of sCCK-8, we investigated the effects of sCCK-8 on TNF- α mRNA expression and NF- κ B activity in the present study.

MATERIALS AND METHODS

Materials

Collagenase IA, LPS (*E. Coli* 0111: B4), sCCK-8 and proglumide were obtained from Sigma (St. Louis, MO). RPMI-1640 culture medium and TRIzol reagents were obtained from Gibco BRL (Gercy-Pontoise, France). Avian myeloblastosis virus reverse transcriptase and Gel shift assay system were purchased from Promega (Madison, WI). Taq DNA polymerase was obtained from Sangon (Shanghai, China). Coomassie brilliant blue G250 assay kit was purchased from JianCheng Biotechnology (Nanjing, China). An anti-I κ B α polyclonal antibody (C-21) was purchased from Santa Cruz (Santa Cruz, CA.) and horseradish peroxidase (HRP)-conjugated IgG was from Zhongshan Biotechnology (Beijing, China). Female, specific pathogen-free Sprague-Dawley rats (weighting 180-220 g BW) were obtained from Experimental Animal Center of Hebei Province.

Preparation of rat PIMs

PIMs were isolated from perfused rat lungs with a collagenase digestion technique, modified as Wizemann *et al*^[24] described. Alveoli were lavaged 12 to 14 times with 4 °C phosphate-buffered saline (PBS) containing 0.6 mmol \cdot L⁻¹ EDTA (PBS-EDTA) to remove alveolar macrophages. Lung vessels were perfused with 100 ml PBS-EDTA to remove the monocytes and other blood cells. Then the lung tissues were cut into 500 μ m slices followed by digestion in 175 U \cdot ml⁻¹ collagenase IA containing 0.1 g \cdot L⁻¹ DNase and 100 ml \cdot L⁻¹ fetal bovine serum (FBS) in a shaking 37 °C water bath for 60 min. The suspension was then filtered through 30 μ m mesh. After washing 2 times (400 \times g, 4 °C, 10 min) with PBS, the cells were resuspended in RPMI-1640 medium containing 15 ml \cdot L⁻¹ FBS, 100 U \cdot ml⁻¹ penicillin, and 100 μ g \cdot ml⁻¹ streptomycin and incubated for 2 h at the conditions of 37 °C and 50 ml \cdot L⁻¹ CO₂. Nonadherent cells were removed by gentle washing with warm medium. Remaining adherent cells contained more than 93 % PIMs and the contamination by polymorphonuclear leukocytes and alveolar macrophages was less than 7 %. PIMs viability was greater than 95 %, determined by trypan blue exclusion assay. PIMs (1 \times 10⁶) were plated on to culture dishes. After washing 3 times with serum-free medium, PIMs were stimulated with LPS (1 mg \cdot L⁻¹), in the presence or absence of sCCK-8 (10⁻⁸-10⁻⁶ mol \cdot L⁻¹) or/and the CCK receptor antagonist proglumide (2 mg \cdot L⁻¹) for indicated time.

Semi-quantitative RT-PCR for the detection of TNF- α

To determine whether sCCK-8 affect TNF- α transcription, PIMs were stimulated with LPS in the presence or absence of 10⁻⁸-10⁻⁶ mol \cdot L⁻¹ sCCK-8 for 3 h. Total cellular RNA was prepared with TRIzol reagents. cDNA was synthesized from 4 μ g of the total RNA by extension of random primers with avian myeloblastosis virus reverse transcriptase. PCR of the cDNA was performed in a final volume of 25 μ l containing 2 mmol \cdot L⁻¹ MgCl₂, 4 units Taq DNA polymerase, and 25 pmol specific primers. Amplification of the house-keeping enzyme

glyceraldehydes-3-phosphate dehydrogenase (GADPH) was always involved to serve as control of reaction efficacy. The PCR was performed at the conditions of denaturation for 45 s at 94 °C, annealing for 45 s at 48 °C for TNF- α and 55 °C for GADPH, extension for 45 s at 72 °C, and at the end of 35 cycles, further extension for 5 min at 72 °C. The primers were TNF- α sense, 5' -CCAACAAGGAGGAGAAGT-3' ; TNF- α antisense, 5' -GTATGAAGTGGCAAATCG-3' (323bp). The synthesized PCR products were separated by electrophoresis on a 20 g \cdot L⁻¹ agarose gel and analyzed by Gel-Pro analyzer version 3.1 software (Media Cybernetics). The ratio of arbitrary unit (AU, $D_{area} \cdot D_{density}$) of target genes over GADPH was used for expressing the relative level of mRNA expression.

Electrophoretic Mobility Shift Assay (EMSA) for NF- κ B activity

PIMs were stimulated with LPS in the presence or absence of sCCK-8 for 1 h. Nuclear extracts were prepared essentially as described by Liu *et al*^[25]. Cells were washed with PBS, lysed with five-pellet volume of buffer A containing 10 mmol \cdot L⁻¹ HEPES (pH 7.9), 10 mmol \cdot L⁻¹ KCl, 1.5 mmol \cdot L⁻¹ MgCl₂, 0.5 mmol \cdot L⁻¹ DTT, 0.5 mmol \cdot L⁻¹ PMSF, and 5 ml \cdot L⁻¹ NP-40 and centrifuged for 10 min at 1 850 \times g. Then the pellets were resuspended with three-pellet volume of buffer B (same as buffer A, but without NP-40) and incubated on ice for 10 min. The cells were centrifuged for 15 min at 3 000 \times g to pellet the nuclei. Nuclear pellets were extracted by gently resuspending the nuclei in two third-nuclei pellet volume of buffer C (20 mmol \cdot L⁻¹ HEPES (pH 7.9), 10 mmol \cdot L⁻¹ KCl, 1.5 mmol \cdot L⁻¹ MgCl₂, 200 ml \cdot L⁻¹ glycerol, 0.2 mmol \cdot L⁻¹ EDTA, 0.5 mmol \cdot L⁻¹ DTT, and 0.5 mmol \cdot L⁻¹ PMSF) and one third-nuclei pellet volume of buffer D (same as buffer C but with 400 mmol \cdot L⁻¹ KCl). After the nuclei were shaken in buffer C plus buffer D for 60 min on ice, the supernatants were collected by centrifugation at 15 000 \times g for 30 min at 4 °C. Protein concentration was determined using Coomassie brilliant blue G250 assay kit. Double-stranded deoxyoligonucleotides containing the NF- κ B consensus recognition site (5'-AGTTGAGGGGACTTTCCAGG-3') were end labeled with [γ -³²P]ATP using T4 polynucleotide kinase and purified with ethanol precipitation. The nuclear proteins (10 μ g per lane) were incubated with the radiolabeled probe DNA (3.5 pmol, 10 μ Ci) in the presence of 1 mmol \cdot L⁻¹ MgCl₂, 0.5 mmol \cdot L⁻¹ EDTA, 0.5 mmol \cdot L⁻¹ DTT, 50 mmol \cdot L⁻¹ NaCl, 10 mmol \cdot L⁻¹ Tris-HCl (pH 7.5), 0.05 μ g poly(dI-dC), and 40 ml \cdot L⁻¹ glycerol in a final volume of 10 μ l. Binding reactions were then incubated at room temperature for 30 min. The DNA-protein complexes were separated on a 6 % nondenaturing polyacrylamide gel. The gel was then dried and visualized by autoradiography at -80 °C.

Western blot analysis for I κ B α protein level

PIMs were stimulated with LPS in the presence or absence of sCCK-8 for 30 min. Cytoplasmic protein was extracted using lysis buffer containing 100 mmol \cdot L⁻¹ HEPES, 10 ml \cdot L⁻¹ Triton X-100, 1 mmol \cdot L⁻¹ EDTA, 10 mmol \cdot L⁻¹ DTT, and 1 mmol \cdot L⁻¹ PMSF. The lysate was centrifuged 20 000 \times g for 15 min at 4 °C after ice bath for 15 min. The supernatant was collected and the protein concentration was determined using Coomassie brilliant blue G250 assay kit. Each sample of 100 mg protein was separated on a SDS-10 % polyacrylamide gel and transferred to nitrocellulose membrane. The membrane was sequentially blocked in TBS containing 20 g \cdot L⁻¹ milk

and then incubated with $2 \mu\text{g} \cdot \text{mL}^{-1}$ I κ B α antibody C-21 (Santa Cruz) overnight, washed, and further incubated with a goat anti-rabbit IgG horseradish peroxidase-conjugated secondary antibody. Blocking and secondary antibody incubation each lasted 1 h at 37 °C. After several washes, the membrane was developed with DAB. Semi-quantitative analysis of immunoreactivity were measured by Gel-Pro analyzer software, and the results were expressed as AU ($D_{\text{area}} \cdot D_{\text{density}}$).

Statistical analysis

Data were presented as $\bar{x} \pm s$ and compared with ANOVA and least significant difference test using SPSS statistical program. A level of $P < 0.05$ was considered statistically significant.

RESULTS

sCCK-8 inhibited LPS-induced TNF- α mRNA expression

Increase in TNF- α mRNA was observed 3 h after stimulating PIMs with $1 \text{ mg} \cdot \text{L}^{-1}$ LPS ($P < 0.01$), and the increase was about 3.1 fold. However in the PIMs co-incubated by LPS and sCCK-8, TNF- α mRNA expression level was obviously lowered in comparison with LPS group ($P < 0.05$, $P < 0.01$). The inhibitory rate of 10^{-8} , 10^{-7} and $10^{-6} \text{ mol} \cdot \text{L}^{-1}$ sCCK-8 was 19 %, 41 % and 33 % respectively. TNF- α mRNA expression level was not affected by sCCK-8 alone ($P > 0.05$) (Figure 1).

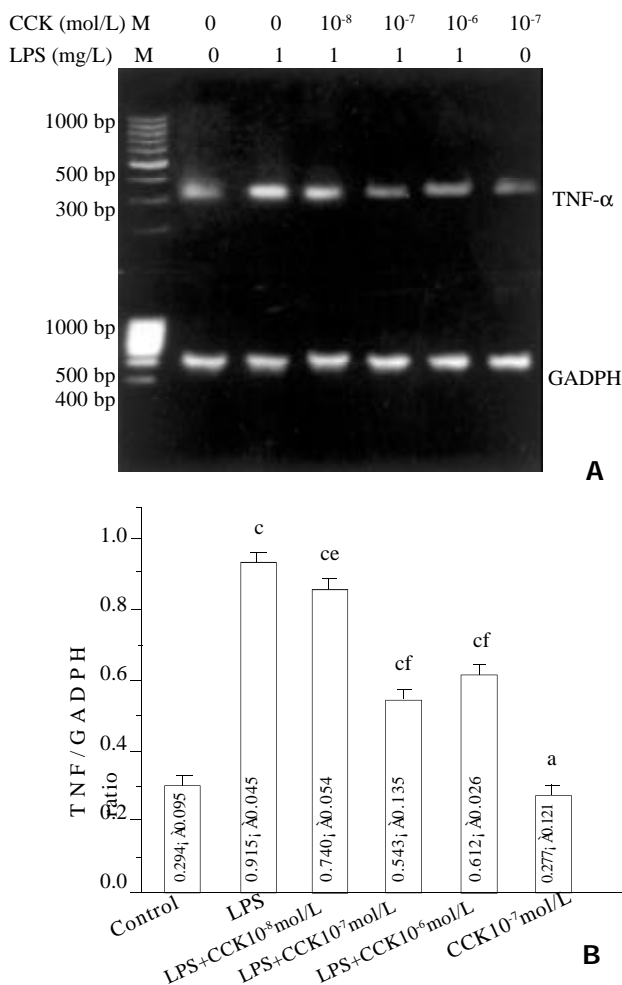


Figure 1 sCCK-8 inhibited LPS-induced TNF- α mRNA expression in PIMs in a dose-dependent manner. A: Representative pictures of three experiments of RT-PCR. B: Relative level of TNF- α mRNA expression. $n=3$, $\bar{x} \pm s$, $^aP > 0.05$, $^cP < 0.01$ vs control, $^eP < 0.05$, $^fP < 0.01$ vs LPS.

sCCK-8 inhibited LPS-induced NF- κ B binding activity

The NF- κ B binding activity was significantly higher in PIMs stimulated with $1 \text{ mg} \cdot \text{L}^{-1}$ LPS in comparison with unstimulated cells ($P < 0.01$), and additional treatment with sCCK-8 markedly reduced the binding activity in a dose-dependent manner. sCCK-8 at the concentrations of 10^{-8} , 10^{-7} , and $10^{-6} \text{ mol} \cdot \text{L}^{-1}$ inhibited LPS-induced NF- κ B binding activity by 34 %, 93 % and 100 % respectively ($P < 0.05$, $P < 0.01$). The effect of sCCK-8 was abrogated by proglumide ($P < 0.01$). sCCK-8 alone had no effect on the NF- κ B binding activity ($P > 0.05$). The binding specificity was confirmed by using homologous (NF- κ B) and nonhomologous (AP-2) oligonucleotides as competitors (Figure 2).

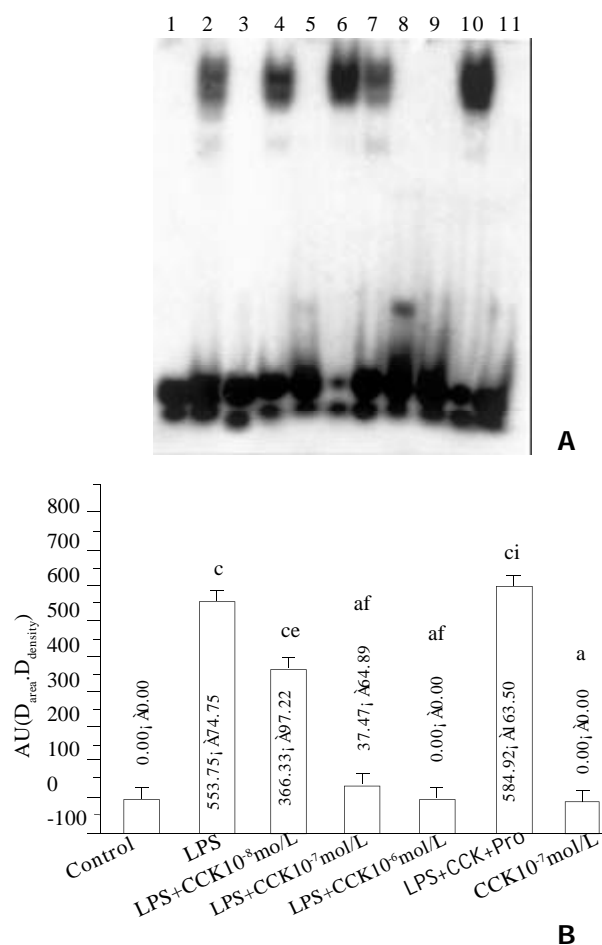


Figure 2 sCCK-8 inhibited LPS-induced NF- κ B binding in PIMs in a dose-dependent manner through CCK receptor. A: Representative autoradiography picture of three experiments of EMSA. Lane 1, negative control; lane 2, positive control; lane 3, ^{32}P -labeled NF- κ B Oligo plus unlabeled NF- κ B Oligo (competitor); lane 4, ^{32}P -labeled NF- κ B Oligo plus unlabeled AP-2 Oligo (noncompetitor); lane 5, control; lane 6, LPS; lane 7, LPS+CCK $10^{-8} \text{ mol} \cdot \text{L}^{-1}$; lane 8, LPS+CCK $10^{-7} \text{ mol} \cdot \text{L}^{-1}$; lane 9, LPS+CCK $10^{-6} \text{ mol} \cdot \text{L}^{-1}$; lane 10, LPS+CCK+proglumide; lane 11, CCK $10^{-7} \text{ mol} \cdot \text{L}^{-1}$. B: Densitometry of EMSA showing decreased NF- κ B binding in PIMs treated with sCCK-8. $n=3$, $\bar{x} \pm s$, $^aP > 0.05$, $^cP < 0.01$ vs control, $^eP < 0.05$, $^fP < 0.01$ vs LPS, $^iP < 0.01$ vs LPS+CCK $10^{-7} \text{ mol} \cdot \text{L}^{-1}$.

sCCK-8 increased I κ B α protein level

The I κ B α protein level in PIMs markedly decreased at 30 min of LPS incubation ($P < 0.01$), sCCK-8 at concentrations of 10^{-8} - $10^{-6} \text{ mol} \cdot \text{L}^{-1}$ clearly increased I κ B α protein level in

PIMs exposure to LPS ($P < 0.05$). The effect was dose dependent and was attenuated by proglumide ($P < 0.01$). sCCK-8 alone had no effect on the κ B α protein level ($P > 0.05$) (Figure 3).

Proglumide	0	0	0	0	0	0	2 mg/L
CCK(mol/L)	0	0	10^{-8}	10^{-7}	10^{-6}	10^{-7}	0
LPS(mg/L)	0	1	1	1	0	0	0

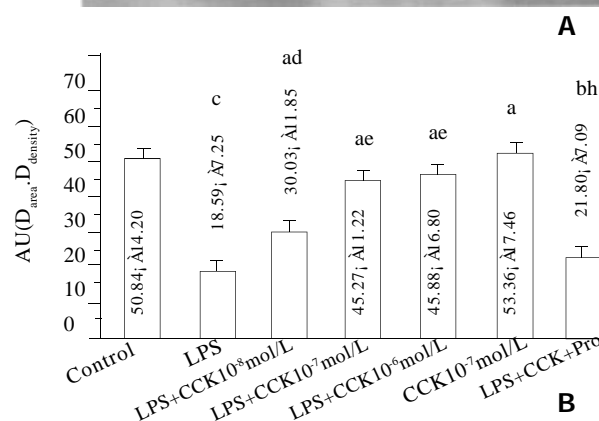


Figure 3 sCCK-8 increased I κ B α protein level at 30 min after LPS stimulation in a dose-dependent manner in PIMs. A: Representative Western blot of three experiments. B: Normalized total protein of I κ B α immunoreactivity. $n=3$, $\bar{x} \pm s$, ^a $P > 0.05$, ^b $P < 0.05$, ^c $P < 0.01$ vs control; ^d $P > 0.05$, ^e $P < 0.05$, ^f $P < 0.01$ vs LPS; ^g $P < 0.05$ vs LPS+CCK10⁻⁷ mol \cdot L⁻¹.

DISCUSSION

As an intestinal neuropeptide, sCCK-8 not only protects gastric mucosa against alcohol-induced injury^[26-28], but also is a potent protective agent against acute lung injury by LPS^[22,29]. It obviously reduced the pulmonary artery hypertension and lessened the inflammatory lesion in lung tissues of ES rats^[22,29]. We investigated the effect of sCCK-8 on PIMs since these cells play an important role in the inflammatory response to LPS in the lung. Recently, it was reported that treating rats with LPS resulted in a significant increase in production of reactive oxygen intermediates by PIMs, but not by alveolar macrophages (AM). This treatment also markedly enhanced phagocytosis only in PIMs and caused a significant increase in chemotaxis of PIMs towards C5a. These data demonstrated that PIMs play a role in the inflammatory response of the lung to acute endotoxemia^[24]. In this study we showed that incubation of rat PIMs with sCCK-8 caused a decrease in LPS-induced TNF- α mRNA expression level in a dose-dependent manner, which suggested that the inhibitory effect of sCCK-8 on TNF- α production occurred at a transcriptional level.

It is well known that transcriptional factor NF- κ B plays a pivotal role in LPS-induced TNF- α gene expression^[23,30]. The present study indicated that sCCK-8 inhibited NF- κ B binding activity in PIMs response to LPS in a dose-dependent manner, which was consistent with our results in the previous *in vivo* study that sCCK-8 inhibited NF- κ B activity in ES rat lung tissues^[31]. These results demonstrated that NF- κ B might be the upstream mechanism of the inhibitory effect of sCCK-8 on LPS-induced TNF- α mRNA expressions. Because NF- κ B activation can lead to enhanced expression of

proinflammatory cytokines, chemokines, inflammatory enzymes such as inducible NO synthase (iNOS) and cyclooxygenase (COX-2), adhesion molecules and inflammatory receptors^[23,30,32,33], modulation of NF- κ B activation may provide a direct way of inhibiting inflammatory mediators^[34]. Directing drug discovery efforts towards NF- κ B activation rather than towards any one of its many target genes could produce a much greater therapeutic benefit by inhibiting expression of the constellation of NF- κ B-induced pro-inflammatory genes^[35]. Several anti-inflammatory drugs, including corticosteroids, the non-steroidal cyclooxygenase inhibitor sulindac, the benzophenanthridine alkaloid sanguinarine, aspirin and salicylate have all been shown to inhibit NF- κ B activation at different stages^[35]. Corticosteroids inhibit NF- κ B by upregulating the expression of its inhibitor I κ B, which displaces DNA-bound NF- κ B and restores the latent cytoplasmic I κ B-NF- κ B complex^[35,36]. Sulindac^[37], aspirin and salicylate^[38] specifically inhibit I κ B kinase activity, and it has also been demonstrated that sanguinarine inhibits NF- κ B activation at the level of I κ B phosphorylation^[39]. In this study, we first demonstrated that the inhibitory effect of sCCK-8 on NF- κ B activity was an important signal transduction mechanism of its anti-inflammatory effect. This can also explain the anti-ES role of sCCK-8^[22], because NF- κ B acts as an important transcriptional factor in the pathogenesis of ES.

Activation of NF- κ B is triggered by phosphorylation of an inhibitory subunit, I κ B. In unstimulated cells, NF- κ B is sequestered in the cytoplasm through interaction with I κ B α and I κ B β inhibitory proteins. In response to proinflammatory stimuli (eg LPS, cytokines, viruses), I κ B is first phosphorylated in its N-terminal domain by a large multikinase complex, then polyubiquitinated, and finally degraded by the proteasome. The released NF- κ B complex translocates into the nucleus where it will initiate gene transcription upon binding its cognate DNA motifs in regulatory segments of TNF- α gene and other target genes involved in inflammatory and immune process^[40]. To elucidate the upstream mechanism of sCCK-8 inhibiting NF- κ B activity, we further detected whether sCCK-8 affected I κ B α protein level with method of Western blot. And the results demonstrated that the decreased I κ B α protein level in LPS-stimulated PIMs was elevated by sCCK-8 in a dose-dependent manner. The increase in I κ B α protein level could be the result of decreased degradation, increased synthesis, or a combination of these two mechanisms. Because we detected the elevation of I κ B α protein level at 30 min of LPS and sCCK-8 incubation, it was not likely that there could be *de novo* protein synthesis in such short time. So the increase of I κ B α protein level was caused by its diminished degradation, suggesting that sCCK-8 inhibited the degradation of I κ B α , and subsequently abrogated the translocation to nucleus of NF- κ B. However, recently few studies showed that in pancreatic cells, supraphysiological concentrations of CCK (10^{-7} mol \cdot L⁻¹) induced chemokine expression through the activation of NF- κ B^[41,42]. CCK (10^{-7} mol \cdot L⁻¹) also induced the degradation of I κ B α in pancreatic cells^[41]. So treatment rats with the supraphysiological concentrations of CCK analogue caerulein led to an acute inflammatory response resembling aspects of clinically important disease acute pancreatitis and it had been used to duplicate the experimental model of acute pancreatitis^[41,42]. In our study, the same concentrations of CCK-8 (10^{-7} mol \cdot L⁻¹) showed significant inhibitory effect on NF- κ B activation and I κ B α degradation in LPS-stimulated PIMs, but had no effect on them in the unstimulated PIMs. This discrepancy may be

due to the specificity of the role of CCK in different cells. It is reported that stimulation murine peritoneal macrophages and human neutrophils with CCK led to an inhibition of protein kinase C (PKC) activity^[16,18], yet it caused an activation of PKC in rat pancreatic cells^[41,42].

Recent data demonstrated the presence of CCK receptors on human monocytes^[43] and lymphocytes^[44,45]. Our laboratory reported that the pulmonary macrophages expressed CCK receptor detected by *in situ* hybridization and *in situ* RT-PCR^[46]. In this study, we found that a CCK receptor antagonist proglumide blocked the effects of sCCK-8 on NF- κ B binding activity and I κ B protein level, indicating that the roles of sCCK-8 were mediated through CCK receptor. Yet the signal transduction mechanisms between CCK receptor and I κ B remain to be further determined.

In this study, the concentration of sCCK-8 that showed a distinct effect on LPS-induced TNF- α mRNA expression and NF- κ B activity was from 10^{-8} to 10^{-6} mol \cdot L $^{-1}$. However, sCCK-8 alone, at a concentration of 10^{-7} mol \cdot L $^{-1}$ had no effect on the above functions of the resting PIMs. Similarly, De la Fuente *et al*^[16] reported that several functions of resting mouse peritoneal macrophages were inhibited by sCCK-8 at the lower concentrations of 10^{-10} - 10^{-8} mol \cdot L $^{-1}$ but not the higher concentration of 10^{-6} mol \cdot L $^{-1}$. They considered that the lower response to higher concentrations of sCCK-8 might be ascribed to a process of cell desensitization, which is characteristic of sequestration and/or down-regulation of CCK receptor. We reported that LPS up-regulated the expression of CCK receptor^[47], so LPS activating PIMs rather than resting PIMs could response to higher concentration of sCCK-8.

In conclusion, our results show that sCCK-8 reduces LPS-induced TNF- α production at transcriptional level by inhibiting NF- κ B activity, and the inhibitory effect of NF- κ B activity is mediated through the decrease of I κ B degradation, which represents one of the anti-inflammatory mechanisms of sCCK-8.

REFERENCES

- 1 Jonsdottir IH. Special feature for the Olympics: effects of exercise on the immune system: neuropeptides and their interaction with exercise and immune function. *Immunol Cell Biol* 2000;**78**:562-570
- 2 Heemskerk VH, Daemen MA, Buurman WA. Insulin-like growth factor-1 (IGF-1) and growth hormone (GH) in immunity and inflammation. *Cyto Gro Fac Rev* 1999;**10**:5-14
- 3 Corsi MM, Fulgenzi A, Tiengo M, Pravettoni G, Gaja G, Ferrero ME. Effect of somatostatin on beta-endorphin release in rat experimental chronic inflammation *Life sci* 1999;**64**:2247-2254
- 4 Leceta J, Gomariz RP, Carmen M, Abad C, Ganea D, Delgado M. Receptors and transcriptional factors involved in the anti-inflammatory activity of VIP and PACAP. *Ann N Y Acad Sci* 2000;**921**:92-102
- 5 Ganea D, Delgado M. Neuropeptides as modulators of macrophage functions. Regulation of cytokine production and antigen presentation by VIP and PACAP. *Arch Immunol Ther Exp* 2001;**49**:101-110
- 6 Cadieux A, Monast NP, Pomerleau F, Fournier A, Lanoue C. Bronchoprotector properties of calcitonin gene-related peptide in guinea pig and human airways. Effect of pulmonary inflammation *Am J Res Cri Care Med* 1999;**159**:235-243
- 7 Dela Fuente M, Del Rio M, Medina S. Changes with aging in the modulation by neuropeptide Y of murine peritoneal macrophage functions. *J Neuroimmunol* 2001;**116**:156-167
- 8 Elenkov IJ, Wilder RL, Chrousos GP, Vizi ES. The sympathetic nerve--an integrative interface between two supersystems: the brain and the immune system. *Pharmacol Rev* 2000;**52**:595-638
- 9 Feldberg RS, Cochrane DE, Carraway RE, Brown E, Sawyer R, Hartunian M, Wentworth D. Evidence for a neurotensin receptor in rat serosal mast cells. *Inflamm Res* 1998;**47**:245-250
- 10 Crawley JN, Corwin RL. Biological actions of cholecystokinin. *Peptides* 1994;**15**:731-755
- 11 Okahata H, Nishi Y, Muraki K, Sumii K, Yukitaka M, Tomofusa U. Gastrin/cholecystokinin-like immunoreactivity in human blood cells. *Life Sci* 1985;**36**:369-373
- 12 Sacerdote P, Breda M, Barcellini W, Meroni PL, Panerai AE. Age-related changes of beta-endorphin and cholecystokinin in human and rat mononuclear cells. *Peptides* 1991;**12**:1353-1356
- 13 Akiyoshi J, Yamauchi C, Furuta M, Katsuragi S, Kohno Y, Yamamoto Y, Miyamoto M, Tsutsumi T, Isogawa K, Fujii I. Relationship between SCL-90, Maudsley Personality Inventory and CCK4-induced intracellular calcium response in T cells. *Psychiatry Res* 1998;**81**:381-386
- 14 Medina S, Rio MD, Cuadra BD, Guayerbas N, Fuente MD. Age-related changes in the modulatory action of gastrin-releasing peptide, neuropeptide Y and sulfated cholecystokinin octapeptide in the proliferation of murine lymphocytes. *Neuropeptides* 1999;**33**:173-179
- 15 Dela Fuente M, Carrasco M, Del Rio M, Hernanz A. Modulation of murine lymphocyte functions by sulfated cholecystokinin octapeptide. *Neuropeptides* 1998;**32**:225-233
- 16 Dela Fuente M, Campos M, Del Rio M, Hernanz A. Inhibition of murine peritoneal macrophage functions by sulfated cholecystokinin octapeptide. *Regul Pept* 1995;**55**:47-56
- 17 Dela Fuente M, Medina S, Del Rio M, Ferrandez MD, Hernanz A. Effect of aging on the modulation of macrophage functions by neuropeptides. *Life Sci* 2000;**67**:2125-2135
- 18 Carrasco M, Del Rio M, Hernanz A, De la Fuente M. Inhibition of human neutrophil functions by sulfated and nonsulfated cholecystokinin octapeptides. *Peptides* 1997;**18**:415-422
- 19 Li SJ, Cong B, Yan YL, Yao YX, Ma CL, Ling YL. Cholecystokinin octapeptide inhibits the in vitro expression of CD14 in rat pulmonary interstitial macrophage induced by lipopolysaccharide. *Chin Med J* 2002;**115**:276-279
- 20 Ling YL, Meng AH, Zhao XY, Shan BE, Zhang JL, Zhang XP. Effect of cholecystokinin on cytokines during endotoxemic shock in rats. *World J Gastroenterol* 2001;**7**:667-671
- 21 Meng AH, Ling YL, Zhang XP, Zhao XY, Zhang JL. CCK-8 inhibits expression of TNF- α in the spleen of endotoxemic shock rats and signal transduction mechanism of p38 MAPK. *World J Gastroenterol* 2002;**8**:139-143
- 22 Ling YL, Huang SS, Wang LF, Zhang JL, Wan M, Hao RL. Cholecystokinin octapeptide reverses experimental endotoxin shock. *Shengli Xuebao* 1996;**48**:390-394
- 23 Christman JW, Lancaster LH, Blackwell TS. Nuclear factor kappa B: a pivotal role in the systemic inflammatory response syndrome and new target for therapy. *Intensive Care Med* 1998;**24**:1131-1138
- 24 Witzemann TM, Laskin DL. Enhanced phagocytosis, chemotaxis, and production of reactive oxygen intermediates by interstitial macrophages following acute endotoxemia. *Am J Respir Cell Mol Biol* 1994;**11**:358-365
- 25 Liu S, Khemlani LS, Shapiro RA, Johnson ML, Liu K, Geller DA, Watkins SC, Goyert SM, Billiar TR. Expression of CD14 by hepatocytes: upregulation by cytokines during endotoxemia. *Infect Immun* 1998;**66**:5089-5098
- 26 Mercer DW, Cross JM, Smith GS, Miller TA. Protective action of gastrin-17 against alcohol-induced gastric injury in the rat: role in mucosal defense. *Am J Physiol* 1997;**273**:G365-G373
- 27 Mercer DW, Cross JM, Chang L, Lichtenberger LM. Bombesin prevents gastric injury in the rat: role of gastrin.

- Dig Dis Sci* 1998;**43**: 826-833
- 28 **Mercer DW**, Smith GS, Miller TA. Cyclooxygenase inhibition attenuates cholecystokinin-induced gastroprotection. *Dig Dis Sci* 1998;**43**:468-475
- 29 **Ling YL**, Cong B, Gu ZY, Li SJ, Zhou XH. Inhibitory effect of cholecystokinin octapeptide on pulmonary arterial hypertension during endotoxemic shock. *Zhongguo Xueshu Qikan Wenzhai* 2000; **6**:890-892
- 30 **Baeuerle PA**, Baltimore D. NF- κ B: ten years after. *Cell* 1996;**87**:13-20
- 31 **Cong B**, Ling YL, Gu ZY. Effect of cholecystokinin octapeptide on lipopolysaccharide-induced increase of NF- κ B activity in rat lung tissues (Abstract). *Zhongguo Bingli Shengli Zazhi* 2000;**16**:991-991
- 32 **Goldring CE**, Reveneau S, Pinard D, Jeannin JF. Hyporesponsiveness to lipopolysaccharide alters the composition of NF- κ B binding to the regulatory regions of inducible nitric oxide synthase gene. *Eur J Immunol* 1998; **28**:2960-2970
- 33 **Barnes PJ**, Adcock IM. NF- κ B: a pivotal role on asthma and a new target for therapy. *Trends in Pharmacol Sci* 1997; **18**:46-50
- 34 **Zhang GL**, Ghosh S. Toll-like receptor - mediated NF- κ B activation: a phylogenetically conserved paradigm in innate immunity. *J Clin Invest* 2001; **107**: 13-19
- 35 **Emery JG**, Ohlstein EH, Jaye M. Therapeutic modulation of transcription factor activity. *Trends in Pharmacol Sci* 2001; **22**:233-240
- 36 **Barnes PJ**. Anti-inflammatory actions of glucocorticoids: molecular mechanisms. *Clin Sci (Lond)* 1998;**94**:557-572
- 37 **Yamamoto Y**, Yin MJ, Lin KM, Gaynor RB. Sulindac inhibits activation of the NF- κ B pathway. *J Biol Chem* 1999; **274**:27307-27314
- 38 **Yin MJ**, Yamamoto Y, Gaynor RB. The anti-inflammatory agents aspirin and salicylate inhibit the activity of I κ B kinase- β . *Nature* 1998;**396**:77-80
- 39 **Chaturvedi MM**, Kumar A, Darnay BG, Chainy GB, Agarwal S, Aggarwal BB. Sanguinarine (pseudochelerythrine) is a potent inhibitor of NF- κ B activation, α phosphorylation, and degradation. *J Biol Chem* 1997; **272**: 30129-30134
- 40 **Baeuerle PA**. I κ B- NF- κ B structures: at the interface of inflammation control. *Cell* 1998;**95**:729-731
- 41 **Tando Y**, Algul H, Wagner M, Weidenbach H, Adler G, Schmid RM. Caerulein-induced NF- κ B/Rel activation requires both Ca^{2+} and protein kinase C messengers. *Am J Physiol* 1999;**277**:G678-686
- 42 **Han B**, Logsdon CD. CCK stimulates mob-1 expression and NF-kappaB activation via protein kinase C and intracellular Ca^{2+} . *Am J Physiol Cell Physiol* 2000;**278**:C344-351
- 43 **Schmitz F**, Schrader H, Otte J, Schmitz H, Stuber E, Herzig K, Schmidt WE. Identification of CCK-B/gastrin receptor splice variants in human peripheral blood mononuclear cells. *Regul Pept* 2001; **101**:25-33
- 44 **Cuq P**, Gross A, Terraza A, Fourmy D, Clerc P, Dornand J, Magous R. mRNAs encoding CCKB but not CCKA receptors are expressed in human T lymphocytes and Jurkat lymphoblastoid cells. *Life Sci* 1997; **61**:543-555
- 45 **Dornand J**, Serge R, Francoise M, Jean-Pierre B, Suzanne C, Jean F, Richard M. Gastrin-CCK-B type receptors on human T lymphoblastoid Jurkat cells. *Am J Physiol* 1995; **268**:G522-529
- 46 **Cong B**, Ling YL, Zuo M. In situ RT-PCR detection of cholecystokinin receptor gene expression in rat lung tissues (Abstract). *Zhongguo Bingli Shengli Zazhi* 1998; **14**:335-335
- 47 **Cong B**, Ling YL, Gu ZY. The expression of cholecystokinin receptor A and B gene in rat lung tissues (Abstract). *Zhongguo Bingli Shengli Zazhi* 1997;**13**:55-55

Edited by Zhao M

• BASIC RESEARCH •

Hyposmotic membrane stretch potentiated muscarinic receptor agonist-induced depolarization of membrane potential in guinea-pig gastric myocytes

Lin Li, Nan-Ge Jin, Lin Piao, Ming-Yu Hong, Zheng-Yuan Jin, Ying Li, Wen-Xie Xu

Lin Li, Nan-Ge Jin, Lin Piao, Zheng-Yuan Jin, Ying Li, Wen-Xie Xu, Department of Physiology, Yanbian University College of Medicine, Yanji 133000, Jilin Province, China

Ming-Yu Hong, Wen-Xie Xu, Center of experiment, Affiliated Hospital of Yanbian University College of Medicine, Yanji 133000, Jilin Province, China

Supported by the National Natural Science Foundation of China, No. 39860031.

Correspondence to: Dr. Wen-Xie Xu, Department of Physiology, Yanbian University College of Medicine, Juzi 121, Yanji 133000, Jilin Province, China. wenxiexu@ybu.edu.cn

Telephone: +86-433-2660586 **Fax:** +86-433-2659795

Received 2002-04-09 **Accepted** 2002-04-27

Abstract

AIM: To investigate the relationship between hyposmotic membrane stretch and muscarinic receptor agonist-induced depolarization of membrane potential in antral gastric circular myocytes of guinea-pig.

METHODS: Using whole cell patch-clamp technique recorded membrane potential and current in single gastric myocytes isolated by collagenase.

RESULTS: Hyposmotic membrane stretch hyperpolarized membrane potential from $-60.0\text{mV} \pm 1.0\text{mV}$ to $-67.9\text{mV} \pm 1.0\text{mV}$. TEA (10mmol/L), a nonselective potassium channel blocker significantly inhibited hyposmotic membrane stretch-induced hyperpolarization. After KCl in the pipette and NaCl in the external solution were replaced by CsCl to block the potassium current, hyposmotic membrane stretch depolarized the membrane potential from $-60.0\text{mV} \pm 1.0\text{mV}$ to $-44.8\text{mV} \pm 2.3\text{mV}$ ($P < 0.05$), and atropine (1 $\mu\text{mol/L}$) inhibited the depolarization of the membrane potential. Muscarinic receptor agonist Carbachol depolarized membrane potential from $-60.0\text{mV} \pm 1.0\text{mV}$ to $-50.3\text{mV} \pm 0.3\text{mV}$ ($P < 0.05$) and hyposmotic membrane stretch potentiated the depolarization. Carbachol induced muscarinic current (I_{ech}) was greatly increased by hyposmotic membrane stretch.

CONCLUSION: Hyposmotic membrane stretch potentiated muscarinic receptor agonist-induced depolarization of membrane potential, which is related to hyposmotic membrane stretch-induced increase of muscarinic current.

Li L, Jin NG, Piao L, Hong MY, Jin ZY, Li Y, Xu WX. Hyposmotic membrane stretch potentiated muscarinic receptor agonist-induced depolarization of membrane potential in guinea-pig gastric myocytes. *World J Gastroenterol* 2002; 8 (4):724-727

INTRODUCTION

In gastrointestinal smooth muscle, stretch is a very important physiological stimulation. However, the first quantitative electrophysiological evidence about such a myogenic response

emerged until an experiment was done that the recordings of tension and intracellular membrane potential were simultaneously carried out in the rabbit taenia coli^[1,2,4]. It has been demonstrated that when the muscle was stretched the tension relates closely to the depolarization of the membrane potential and the frequency of the action potential^[1-4], but the mechanism is not very clear that how stretch excited cell membrane and caused smooth muscle contraction. It is well known that muscarinic current is nonselective cation current which can depolarize membrane potential^[5,6] and contribute to calcium influx^[7]. In our previous study we found that mechanical stretch increased the voltage-dependent calcium current^[8-10], and Kirber *et al*^[11,12] reported that stretch activated ion channel (SACs) existed in gastric myocytes. In gut smooth muscle muscarinic current is very important for regulating motility of smooth muscle, but the relationship is not clear between muscarinic current and membrane stretch. In 1997, Waniishi *et al*^[13] reported that hyposmotic membrane stretch increased muscarinic current in guinea-pig ileum. But the relationship of mechanical stretch and muscarinic receptor agonist-induced depolarization of membrane potential is not clear in gastric smooth muscle. Thus in this study, the relationship between hyposmotic membrane stretch and muscarinic receptor agonist-induced depolarization of membrane potential was investigated in antral gastric circular myocytes of guinea-pig.

MATERIALS AND METHODS

Preparation of cells

Guinea-pigs (obtained from the Experimental Animal Department of Norman Bethune University, Certificate No 10-6 004) of either sex weighing 300-350 g were anaesthetized by urethane (50 mg/kg). The antral part of the stomach was promptly excised and equilibrated in a Ca^{2+} -free solution which was oxygenated, then the circular muscle layer was separated from the muscle layer and dissected into small segments (1×4 mm). These segments were kept in a modified Kraft-Bruhe (K-B) medium at 4 °C for 15 minutes. Then they were incubated at 36 °C in 4ml digestion medium (Ca^{2+} -free PSS) containing 0.1 % collagenase (II), 0.1 % dithioerythritol, 0.15 % trypsin inhibitor and 0.2 % bovine serum albumin for 25-35 min. Then the softened muscle segments were transferred into the modified K-B medium, and single cells were dispersed by gentle agitation with a wide-bored fire-polished glass pipette. Isolated gastric myocytes were kept in modified K-B medium at 4 °C until use.

Electrophysiological recording

Isolated cells were transferred to a small chamber (0.1 ml) on the stage of an inverted microscope (IX-70 Olympus, Japan) for 10-15 min to settle down, and continuously superfused with isosmotic physiologic salt solution (PSS) by gravity (2-3 ml/min). Glass pipettes with a resistance of 2-5 M Ω were used to make a giga seal of 5-10 G Ω . Whole-cell currents and

Membrane potential were recorded with an Axopatch 1-D patch-clamp amplifier (Axon Instrument, USA) polygraph (RM 6200, Nihon Kohden, Tokyo, Japan).

Drugs and solutions

Ca²⁺-free PSS containing (in mmol/L) NaCl 134.8, KCl 4.5, glucose 5, and N-[2-hydroxyethyl] piperazine- N-[2-ethanesulphonic acid] (HEPES) 10 was adjusted to pH 7.4 with Tris [hydroxymethyl] aminomethane (TRIZMA). Modified K-B solution containing (in mmol/L) L-glutamate 50, KCl 50, taurine 20, KH₂PO₄ 20, MgCl₂·6H₂O 3, glucose 10, HEPES 10 and egtazic acid 0.5 was adjusted to pH 7.40 with KOH. Isosmotic solution containing (in mmol/L) NaCl 80, KCl 4.5, MgCl₂·6H₂O 1, CaCl₂·2H₂O 2, glucose 5, HEPES 10, sucrose 110, was adjusted to pH 7.4 with Tris; CsCl 99, HEPES 10, Sucrose 90, was adjusted to pH 7.40 with tris. Hyposmotic solution containing (in mmol/L) NaCl 80, KCl 4.5, MgCl₂·6H₂O 1, CaCl₂·2H₂O 2, glucose 5, HEPES 10 was adjusted to pH 7.40 with tris; CsCl 99, HEPES 10, was adjusted to pH 7.40 with Tris. Pipette solution containing (in mmol/L) K-aspartic acid 110, Mg-ATP 5, MgCl₂·6H₂O 1, KCl 20, EGTA 10, di-tris-creatine phosphate 2.5, disodium-creatine phosphate 2.5, HEPES 5, pH was adjusted to 7.30 with KOH; CsCl 135, Na₂ATP 3, MgCl₂ 3, di-tris-creatine phosphate 2.5, disodium-creatine phosphate 2.5, HEPES 5, EGTA 0.5 was adjusted to pH 7.30 with tris. Tetraethylammonium (TEA), Carbachol (CCh) and Atropine were made up as stock solutions (1mol/L, 10 mmol/L and 1μmol/L respectively). All drugs in this experiment were purchased from Sigma (USA).

Hyposmotic membrane stretch

Cells were superfused with normal and hypotonic solution.

Data analysis

Data were expressed as $\bar{x} \pm s$. Statistical significance was estimated by paired *t*-test. $P < 0.05$ were considered to be statistically significant.

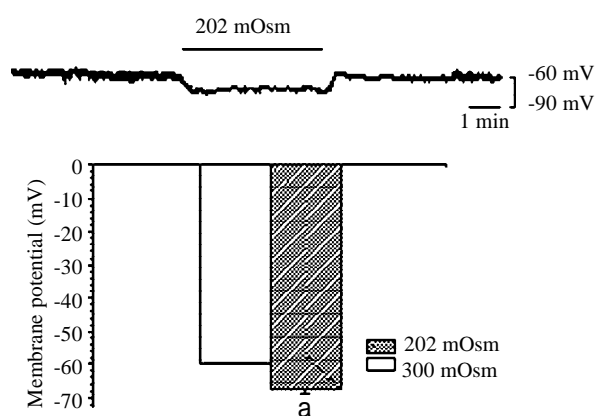


Figure 1 Effect of hyposmotic membrane stretch on membrane potential ($^aP < 0.05$ vs control).

RESULTS

Effect of hyposmotic membrane stretch on membrane potential

Membrane current was clamped by the conventional whole-cell patch clamp configuration and membrane potential was modulated to about -60.0 mV, so that it is close to resting potential of the gastric myocyte. After being superfused with hyposmotic solution (202 mOsm), the membrane potential

hyperpolarized from -60.0 ± 1.0 mV to -67.9 ± 1.0 mV in a few seconds, and the amplitude of polarization was increased by 13.4 ± 1.6 % (Figure 1, $n = 10$, $P < 0.05$). TEA, a nonspecific potassium channel blocker (10 mmol/L) significantly inhibited the hyperpolarization induced by hyposmotic membrane stretch, the membrane potential depolarized from -70.9 ± 2.2 mV to -65.7 ± 1.6 mV, inhibited from 100 % of control to 47.8 ± 6.6 % ($n = 7$, $P < 0.05$, Figure 2). In the condition of KCl in the pipette and NaCl in the external solution were replaced by CsCl to block the potassium current, hyposmotic membrane stretch depolarized membrane potential from -60.0 ± 1.0 mV to -44.8 ± 2.3 mV ($n = 5$, $P < 0.05$, Figure 3).

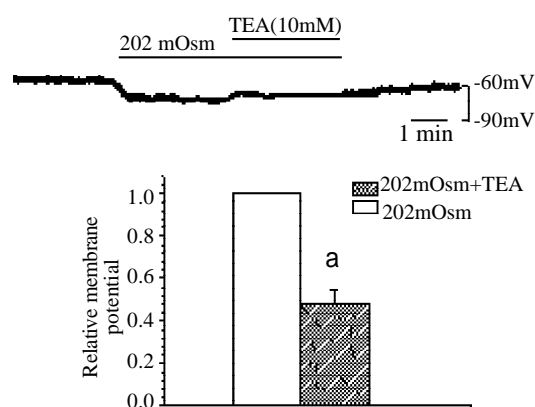


Figure 2 Effect of TEA on membrane potential caused by hyposmotic membrane stretch ($^aP < 0.05$ vs control).

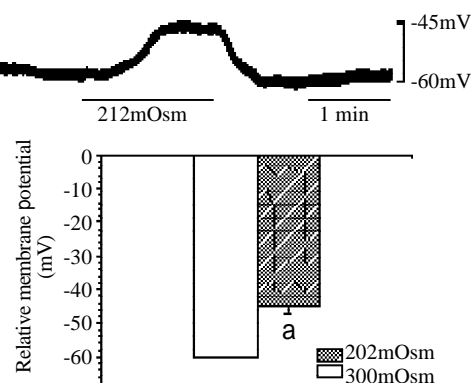


Figure 3 Hyposmotic membrane stretch induced depolarization of membrane potential in the solution including CsCl ($^aP < 0.05$ vs control).

Effects of hyposmotic membrane stretch on muscarinic receptor agonist-induced depolarization of membrane potential

Potassium current was still blocked by CsCl, muscarinic receptor agonist carbachol depolarized membrane potential from -60.0 ± 1.0 mV to -50.3 ± 0.3 mV and hyposmotic membrane stretch potentiated the depolarization of the membrane potential from -50.3 ± 0.3 mV to -37.3 ± 1.8 mV, the potentiated percentage is 239.4 ± 10.6 % ($n = 3$, $P < 0.05$, Figure 4). When the membrane potential depolarized by hyposmotic membrane stretch, atropine (1μmol/L) inhibited the depolarization, the membrane potential hyperpolarized from -47.3 ± 2.4 mV to -53.0 ± 1.9 mV, inhibited from 100 % of control to 47.6 ± 4.7 % ($n = 4$, $P < 0.05$, Figure 5).

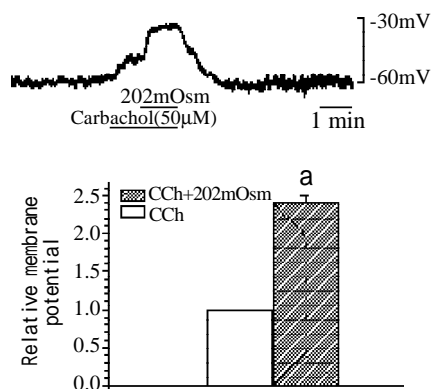


Figure 4 Hypotonic membrane stretch increased the depolarization of membrane potential induced by CCh in the solution including CsCl ($^aP < 0.05$ vs control).

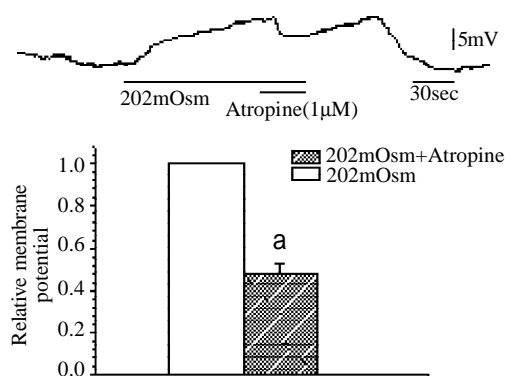


Figure 5 The effect of Atropine on membrane potential hyperpolarized by hypotonic membrane stretch in the solution including CsCl ($^aP < 0.05$ vs control).

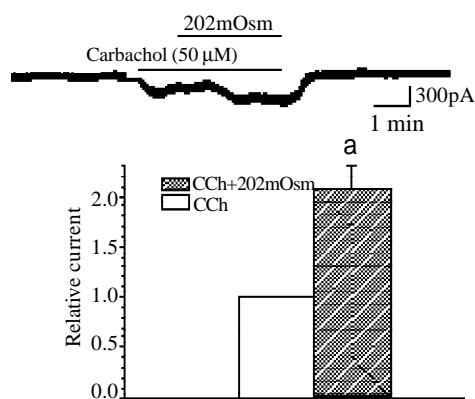


Figure 6 Hypotonic membrane stretch increased the amplitude of the current induced by Carbachol ($^aP < 0.05$ vs control).

Effect of hypotonic membrane stretch on muscarinic current

In conventional whole-cell patch clamp configuration, membrane potential was clamped at -20 mV, inward current was induced by carbachol and the mean value was 183.3 ± 30.7 pA. Hypotonic membrane stretch significantly increased muscarinic current induced by carbachol from 183.3 ± 30.7 pA to 383.3 ± 73.8 pA, and the increased percentage is $206.9 \pm 23.4\%$ ($n=4$, $P < 0.05$, Figure 6).

DISCUSSION

The simple and main method of stretching cell membrane is hypotonic cell swelling, in this study, we applied hypotonic cell swelling to investigate the relationship between hypotonic membrane stretch and muscarinic receptor agonist-induced depolarization of membrane potential. In present study, we observed that hypotonic membrane stretch hyperpolarized membrane potential; TEA, a nonselective potassium channel blocker significantly inhibited hypotonic membrane stretch-induced hyperpolarization. After KCl in the pipette and NaCl in the external solution were replaced by CsCl to block the potassium current, hypotonic membrane stretch depolarized the membrane potential, and atropine inhibited the depolarization of the membrane potential. Muscarinic receptor agonist carbachol depolarized membrane potential and hypotonic membrane stretch potentiated the depolarization; carbachol induced muscarinic current (I_{CCh}) was greatly increased by hypotonic membrane stretch.

It must be mentioned here that we have applied hypotonic membrane stretch which is not same as mechanical stretch under physiological condition, but it is the common method for stretching cell membrane now. It is well known that almost every kind of cells are able to regulate their volume so that they are still in the normal physiological condition^[14,15]. In this experiment, hypotonic cell swelling is inevitable to elicit the reaction resist to volume increase, so calcium sensitive potassium channels were activated and have potassium and chloride ion efflux to decrease cell volume, our previous studies have proved it^[16,17]. In this work, hypotonic membrane stretch includes two kinds of stimulation, one is cell volume increase; the other is cell membrane stretch, so it is inevitable to activate potassium channel. However, the focus of our study is the relationship between membrane stretch and muscarinic receptor agonist-induced depolarization of membrane potential, so we blocked potassium current to observe depolarization induced by muscarinic receptor agonist clearly. When the cell superfused with hypotonic solution, the membrane potential was hyperpolarized, but in the condition of KCl in the pipette and NaCl in the external solution were replaced by CsCl to block the potassium current, hypotonic membrane stretch depolarized membrane potential. Therefore the hyperpolarization induced by hypotonic stress related to activation of potassium channel which is very important mechanism in cell volume regulation. In gut smooth muscle, stretch is very important physiological stimulation, the stretch caused smooth muscle contraction. There are two theories about the mechanism of stretch-induced smooth muscle contraction, one is nervous mechanism; the other is muscular mechanism. But the ionic channel event in muscular mechanism is not very clear. It is reported that stretch activated channel (SACs) were activated by membrane stretch in gastric myocyte, and this channel is not voltage dependent and nonselective cation^[18,19]. Our previous study found that hypotonic membrane stretch increased L-type calcium current and it is related to cytoskeleton in gastric myocytes of guinea-pig^[8,9]. Waniishi *et al*^[13] observed that hypotonic membrane stretch increase carbachol-induced muscarinic nonselective cation current obviously in ileum smooth muscle of guinea-pig. In present study, hypotonic membrane stretch potentiated carbachol-induced depolarization of membrane potential and M receptor blocker, atropine significantly inhibited hypotonic membrane stretch-induced depolarization. Since in the condition of clamping membrane potential, hypotonic membrane stretch significantly increased carbachol-induced muscarinic current, so hypotonic membrane stretch via increasing muscarinic

current potentiated carbachol-induced depolarization of membrane potential.

Acetylcholine is very important for regulating gastrointestinal smooth muscle motility. When the muscarinic receptor is activated by acetylcholine, it not only releases the calcium from the calcium store through the G-protein pathway^[20], but also activates a nonselective cation channel which can depolarize the membrane potential. Activation of the muscarinic receptor operated channel is followed by the entry of the cations such as calcium, and it induces the contraction of the muscle eventually. Our results demonstrated that in the gut myocytes, the mechanical stretch is probably one of the important mechanisms of regulating the muscarinic receptor operated channel. Therefore when the stomach is distended by food in physiological condition, gastric tonic contraction is potentiated via long and short- vagus nerve reflex, in another way, stretch may be potentiated the effect of vagus nerve on gastric tonic contraction through increasing muscarinic current. Since hyposmotic membrane stretch potentiates carbachol-induced depolarization through increasing muscarinic current, it may be also one mechanism in smooth muscle contraction caused by stretch.

REFERENCES

- 1 **Bülbring E**, Kuriyama H. The effect of adrenaline on the smooth muscle of guinea-pig taenia coli in relation to the degree of stretch. *J Physiol (Lond)* 1963; **169**: 198-212
- 2 **Coburn RF**. Stretch-induced membrane depolarization in ferret trachealis smooth muscle cells. *J Appl Physiol* 1987; **62**: 2320-2325
- 3 **Harder DR**. Pressure dependent membrane depolarization in cat middle cerebral artery. *Circ Res* 1984; **55**: 197-202
- 4 **Harder DR**, Gilbert R, Lombard JH. Vascular muscle cell depolarization and activation in renal arteries on elevation of transmural pressure. *Am J Physiol* 1987; **253**: F778-781
- 5 **Inoue R**, Isenberg G. Effect of membrane potential on acetylcholine-induced inward current in guinea-pig ileum. *J Physiol (Lond)* 1990; **424**: 57-71
- 6 **Chen S**, Inoue R, Ito Y. Pharmacological characterization of muscarinic receptor-activated cation channels in guinea-pig ileum. *Br J Pharmacol* 1993; **109**: 793-801
- 7 **Kim SJ**, Koh EM, Kang TM, Kim YC, So I, Isenberg G, Kim KW. Ca^{2+} influx through carbachol-activated non-selective cation channels in guinea-pig gastric myocytes. *J Physiol (Lond)* 1998; **513**: 749-760
- 8 **Xu WX**, Kim SJ, Kim SJ, So I, Kang TM, Rhee JC, Kim KW. Effect of stretch on calcium channel currents recorded from the antral circular myocytes of guinea-pig stomach. *Pflügers Arch* 1996; **432**: 159-164
- 9 **Xu WX**, Kim SJ, So I, Kim KW. Role of actin microfilament in osmotic stretch-induced increase of voltage-operated calcium channel current in guinea-pig gastric myocytes. *Pflügers Arch*, 1997; **434**: 502-504
- 10 **Xu WX**, Li Y, Wu LR, Li ZL. Effects of different kinds of stretch on voltage-dependent calcium current in antral circular smooth muscle cells of the guinea-pig. *Acta physiol Sini* 2000; **52**: 69-74
- 11 **Kirber MT**, Walsh JV Jr, Singer JJ. Stretch-activated ion channels in smooth muscle: a mechanism for the initiation of stretch-induced contraction. *Pflügers Arch* 1988; **412**: 339-345
- 12 **Kirber MT**, Agustin GH, Bowman DS, Fogarty KE, Tuft RA, Singer JJ, Fay FS. Multiple pathways responsible for the stretch-induced increase in Ca^{2+} concentration in toad stomach smooth muscle cells. *J Physiol* 2000; **524**: 3-17
- 13 **Waniishi Y**, Inoue R, Ito Y. Preferential potentiation by hypotonic cell swelling of muscarinic cation current in guinea pig ileum. *Am J Physiol* 1997; **272**: C240-C253
- 14 **Baumagar CM**, Feher JJ. Osmosis and the regulation of cell volume. In: Sperelakis N (ed) *Cell Physiol Source Book* 1995:194-211
- 15 **Hoffmann EK**, Simonsen LO. Membrane mechanisms in volume and pH regulation in vertebrate cells *Physiol Rev.* 1989; **69**: 315-382
- 16 **Piao L**, Li Y, Li L, Jin NG, Li ZL, Xu WX. The involvement of calcium mobilization in the calcium-activated potassium currents activated by hyposmotic swelling in gastric antral circular myocytes of the guinea-pig. *JJP* 2001; **51**: 223-230
- 17 **Piao L**, Li Y, Li L, Xu WX. Increment of calcium-activated and delayed rectifier potassium current by hyposmotic swelling in gastric antral circular myocytes of guinea pig. *Acta Pharmacol Sin* 2001; **22**: 566-572
- 18 **Xu WX**, Kim SJ, So I, Kang TM, Rhee JC, Kim KW. Volume-sensitive chloride current activated by hyposmotic swelling in antral gastric myocytes of the guinea-pig. *Pflügers Arch* 1997; **435**: 9-19
- 19 **Davis MJ**, Donovitz JA, Hood JD. Stretch-activated single-channel and whole cell currents in vascular smooth muscle cells. *Am J Physiol* 1992; **262**: C1083-C1088
- 20 **Komori S**, Kawai M, Takewaki T, Ohashi H. GTP-binding protein involvement in membrane currents evoked by carbachol and histamine in guinea-pig ileal muscle. *J Physiol Lond* 1992; **450**: 105-126

Edited by Zhao M

• BASIC RESEARCH •

Hepatoprotective role of *ganoderma lucidum* polysaccharide against BCG-induced immune liver injury in mice

Guo-Liang Zhang, Ye-Hong Wang, Wei Ni, Hui-Ling Teng, Zhi-Bin Lin

Guo-Liang Zhang, Ye-Hong Wang, Wei Ni, Hui-Ling Teng, Zhi-Bin Lin, Department of Pharmacology, School of Basic Medical Sciences, Beijing University, Beijing 100083, China

Supported by the National Natural Science Foundation of China, No.39770861, No. 30171097; Beijing University Center For Human Disease Genomics Research Foundation, No. 2000-A-1; and JANSSEN Science Research Foundation

Presented at the third international symposium on hepatology, Hangzhou, China, 18-23 October, 2001

Correspondence to: Dr. Guo-Liang Zhang, Department of Pharmacology, School of Basic Medical Sciences, Beijing University, Beijing 100083, China. yuankui@public.bta.net.cn

Telephone: +86-10-62091421 Fax: +86-10-62015681

Received 2002-03-12 Accepted 2002-04-23

Abstract

AIM: To examine the effect of *ganoderma lucidum* polysaccharide (GLP) on the immune liver injury induced by BCG infection, and investigate the relationship between degrees of hepatic damage and NO production in mice.

METHODS: Immune hepatic injury was markedly induced by BCG-pretreatment (125 mg·kg⁻¹, 2-week, iv) or by BCG-pretreatment plus lipopolysaccharide (LPS, 125 mg·kg⁻¹, 12-hour, iv) in mice *in vivo*. Hepatocellular damage induced by BCG-pretreated plus inflammatory cytokines mixture (CM), which was included TNF- α , IL-1 β , IFN- γ and LPS in culture medium *in vitro*. Administration of GLP was performed by oral or incubating with culture medium at immune stimuli simultaneity. Liver damage was determined by activity of alanine aminotransferase (ALT) in serum and in hepatocytes cultured supernatant, by liver weight changes and histopathological examination. NO production in the cultured supernatant was determined by the Griess reaction. Moreover, inducible nitric oxide synthase (iNOS) protein expression was also examined by immunohistochemical method.

RESULTS: Immune hepatic injury was markedly induced by BCG or BCG plus inflammatory cytokines in BALB/c mice *in vivo* and *in vitro*. Under BCG-stimulated condition, augment of the liver weight and increase of the serum/supernatant ALT level were observed, as well as granuloma forming and inflammatory cells soakage were observed by microscopic analysis within liver tissues. Moreover, NO production was also increased by BCG or/and CM stimuli in the culture supernatant, and a lot of iNOS positive staining was observed in BCG-prestimulated hepatic sections. Application of GLP significantly mitigated hepatic tumefaction, decreased ALT enzyme release and NO production in serum/supernatant, improved the pathological changes of chronic and acute inflammation induced by BCG-stimuli in mice. Moreover, the immunohistochemical result showed that GLP inhibited iNOS protein expression in BCG-immune hepatic damage model.

CONCLUSION: The present study indicates that NO participates in immune liver injury induced by *Mycobacterium bovis* BCG infection. The mechanisms of protective roles by GLP for BCG-induced immune liver injury may be due to influence NO production in mice.

Zhang GL, Wang YH, Ni W, Teng HL, Lin ZB. Hepatoprotective role of *ganoderma lucidum* polysaccharide against BCG-induced immune liver injury in mice. *World J Gastroenterol* 2002;8(4):728-733

INTRODUCTION

Ganoderma lucidum polysaccharide (GLP) is an important pharmacological ingredient extracted from fruit bodies and mycelium of mushroom *Ganoderma Lucidum* (Fr.) Karst. It has been extensively documented that GLP can improve the damage induced by specific and nonspecific immunity responses^[1,2]. In our laboratory recently studies, it was confirmed that GLP enhanced phagocytosis of intraperitoneal macrophage, inhibited the growth of implanted Sarcoma 180 and HL-60 tumor cells *in vitro*^[3-5]. However, the regulating mechanism of GLP in the immune response remain unknown. On the other hand, hepatitis is a prevalent disease in the Chinese population. It has been recognized that the immune factors, such as virus/parasite infection, autoimmune stimuli, etc., were the dominant reasons of hepatic damage in hepatitis^[6-10]. But the commonly used model of liver injury induced by chemicals does not accurately represent the clinical situation^[11, 12]. Therefore, It is required that development of new therapy drugs depends primarily on the availability of animal models relevant to human hepatitis or hepatocellular immune damage.

In the recently studies, *Mycobacterium bovis* bacillus Calmette-Guerin (BCG) infection has been proven to induce immune hepatic injury in rodent animal^[13,14]. In this pathological model, the releases of hepatic endogenous cytokines, such as TNF- α , IFN- γ and IL-1 β were observed *in vivo*^[15-17]. Moreover, in our laboratory previously experiment, it has been observed that inflammatory cytokines including TNF- α and IL-1 β stimulated NO production in the primary cultured rat hepatocytes *in vitro*^[18], but the influence of GLP in this immune damage model and the exact function of NO production in the presence of inflammatory stimuli have not been elucidated yet. Therefore, the present study was performed to determine the effects of GLP on the BCG-stimulated immune liver injury *in vitro* and *in vivo*, and to investigate the possible mechanism of the influence induced by GLP in this immune response.

MATERIALS AND METHODS

Reagents

Following reagents were purchased from Sigma Chemical Co.: collagenase (Type IV, 340 kU·g⁻¹), bovine insulin, and lipopolysaccharide (LPS, *E.coli*.0111:B4). Other materials were obtained from the following sources: kit for determining

serum and culture supernatant alanine transaminase (ALT) was from Beijing Institute of Biological Products (Beijing); *Mycobacterium tuberculosis* Bacille Calm  tte-Gu  rin (BCG) vaccine was from the National Vaccine and Serum Institute (Beijing); human recombinant (rh) tumor necrosis factor-   (TNF-  ), interleukin-1 beta (IL-1  ), interferon-gamma (IFN-  ) were from Academy of Military Medical Sciences (Beijing), and Dulbecco's modified Eagle's medium (DMEM) from Gibco BRL; *Ganoderma lucidum* polysaccharide (GLP) was isolated from mycelium of *Ganoderma lucidum* and provided by the Department of Phytochemistry, College of Pharmacy, Beijing University^[5]. For using immunohistochemistry, iNOS polyclonal antibody (rabbit anti-mouse immunoglobulin) was purchased from Beijing Zhong-Shan Biotechnology co., LTD.

Animals treatment and liver damage induction

Male BALB/c mice weighing 18-22g (6-8 weeks old), were provided by Experimental Animal Center, Beijing University. Immune hepatic injury was induced by intravenous injection of BCG (125 mg   kg⁻¹) for two weeks, or induced by LPS (125   g   kg⁻¹) for 12 hours at BCG-pretreated 14day later^[13,19]. Control group mice were treated by same volume of phosphate buffered saline (PBS). After animals were BCG-pretreated 7 days, the different concentrations (25 mg   kg⁻¹, 50 mg   kg⁻¹, 100 mg   kg⁻¹ and 200 mg   kg⁻¹, respectively) of GLP were intragastric administered once at everyday within succedent one week. At immune stimulating 2 weeks later, mice were killed by cervical dislocation, blood was collected and centrifuged at 3000 rpm for 5 min. Serum was obtained at the supernatant for mensuration enzyme level. Liver samples were removed rapidly for histopathological and immunohistochemical examination.

Hepatocyte isolation and culture

Hepatocytes were harvested from control mice or BCG-pretreated for 2 weeks mice using an *in situ* collagenase perfusion technique^[20]. After inhalation anesthesia, the abdomen of the animals was opened and shaved, the portal vein was exposed and cannulated. Then the liver was perfused at 37   C *in situ* first with a calcium-free phosphate-buffered saline solution (PBS) with 6-8 mL/min velocity of flow. This perfusion was continued for 5 min, then it was switched to 0.5 g   L⁻¹ collagenase and 10 g   L⁻¹ bovine albumin in PBS buffer for 15 min. The liver was removed and the cells were combed gently in tissue culture medium. Hepatocytes were pelleted, washed, and separated from nonparenchymal cells by differential centrifugation at 50   g. Viability of cells exceeded 85 % as determined by trypan blue exclusion. Hepatocytes were plated onto 6-well plastic tissue-culture plates (1    10⁹ cells   L⁻¹ in each well). Medium in the control consisted of DMEM with L-arginine (0.5 mmol   L⁻¹), insulin (1 mmol   L⁻¹), Hepes (15mmol   L⁻¹), L-glutamine, penicillin, streptomycin, and 100 mL   L⁻¹ low-endotoxin newborn calf serum. After overnight incubation, the medium was changed with a cytokines mixture (CM) containing LPS (10 mg   L⁻¹), IL-1   (10 KU   L⁻¹), TNF-   (500 KU   L⁻¹) and IFN-   (100 KU   L⁻¹). Other experimental conditions included addition of GLP, at the different concentrations (50 mg   L⁻¹ or 200 mg   L⁻¹), to the CM. After primary cultures were maintained for 24 h at 37   C in 50 mL   L⁻¹ CO₂, hepatocytes or cultured supernatants were collected for nitrite and ALT activity assays^[21].

Assay for hepatocellular enzyme release and NO production

As a marker of hepatocytes necrosis, activity of alanine aminotransferase (ALT) was spectrophotometrically measured using a determining kit in serum and culture supernatants, at

520 nM in the presence of   -ketoglutarate, aspartate, NADH and malate dehydrogenase, as described^[19]. The amount of NO production in the serum and the culture supernatants were determined as its stable oxidative product, nitrite, by an automated procedure based on the Griess reaction, as previously described^[20].

Histopathological and immunohistochemical examination

Livers were removed, fixed overnight in 10 % buffered formalin, and paraffin-embedded. Six-micrometer sections were stained with hematoxylin-eosin for histological evaluation. Immunohistochemical staining for iNOS protein expression was carried out using rabbit polyclonal antibodies to iNOS on cryostat sections (five-micrometer). The sections were incubated with peroxidase-labeled rabbit anti-mouse immunoglobulin for 1 hour. After another wash in PBS, the sections were stained with AEC for several minutes to develop the color and washed in water. Each experiment was repeated two to three times with similar results. Three random sections of each liver were examined^[19].

Statistics analysis

Data were presented with $\bar{x} \pm s$, Statistical analysis was performed using ANOVA. Differences were judged to be statistically significant when the *P* value was less than 0.05.

RESULTS

Effect of *Ganoderma lucidum* polysaccharide (GLP) on the liver weight and the activity of serum alanine transaminase (ALT) in BCG-induced immune hepatic injury in mice *in vivo*

Compared with the control of group, BCG-pretreatment markedly induced hepatic damage (Table 1). The augment of the liver weight and the serum ALT level were observed after BCG-administrated 2 weeks in mice (*P*<0.01). Furthermore, application of inflammatory lipopolysaccharides (LPS) for BCG-pretreated mice induced serum ALT activity further higher than that BCG-treated alone in mice (*P*<0.05), but the liver weights were not further increased than that BCG-stimulated only groups. On the other hand, under the presence of BCG stimuli conditions, administration of CLP decreased the liver weight within the range of 50 mg   kg⁻¹ (*P*<0.05) to 200 mg   kg⁻¹ (*P*<0.01), simultaneously, serum ALT release were significantly decreased by GLP treatment in a dose-dependent manner within the similar range of concentrations (*P*<0.05).

Table 1 Effect of *Ganoderma lucidum* polysaccharide (GLP) on the weight of liver and the activity of serum alanine transaminase (ALT) in BCG-induced immune hepatic injury in mice ($\bar{x} \pm s$)

Group	Liver weight (g)	ALT (U�� L ⁻¹)
Control	0.99��0.16	22.03��10.99
BCG (125 mg�� kg ⁻¹)	1.79��0.24 ^b	245.18��41.03 ^b
BCG (125 mg�� kg ⁻¹) + LPS (125 ��g�� kg ⁻¹)	1.84��0.14 ^b	285.88��23.81 ^{b,c}
BCG (125 mg�� kg ⁻¹) + GLP (25mg�� kg ⁻¹)	1.78��0.20 ^b	236.86��27.94 ^b
BCG (125 mg�� kg ⁻¹) + GLP (50mg�� kg ⁻¹)	1.57��0.18 ^{b,c}	189.81��43.99 ^{b,c}
BCG (125 mg�� kg ⁻¹) + GLP (100mg�� kg ⁻¹)	1.28��0.20 ^{b,d}	178.78��13.16 ^{b,d}
BCG (125 mg�� kg ⁻¹) + GLP (200mg�� kg ⁻¹)	1.41��0.43 ^{b,c}	208.18��27.93 ^{b,c}

^a*P*<0.05, ^b*P*<0.01 compared with control. ^c*P*< 0.05, ^d*P*< 0.01 compared with BCG-pretreated group. *n*=9 mice (liver weight groups) or 10 mice (ALT groups).

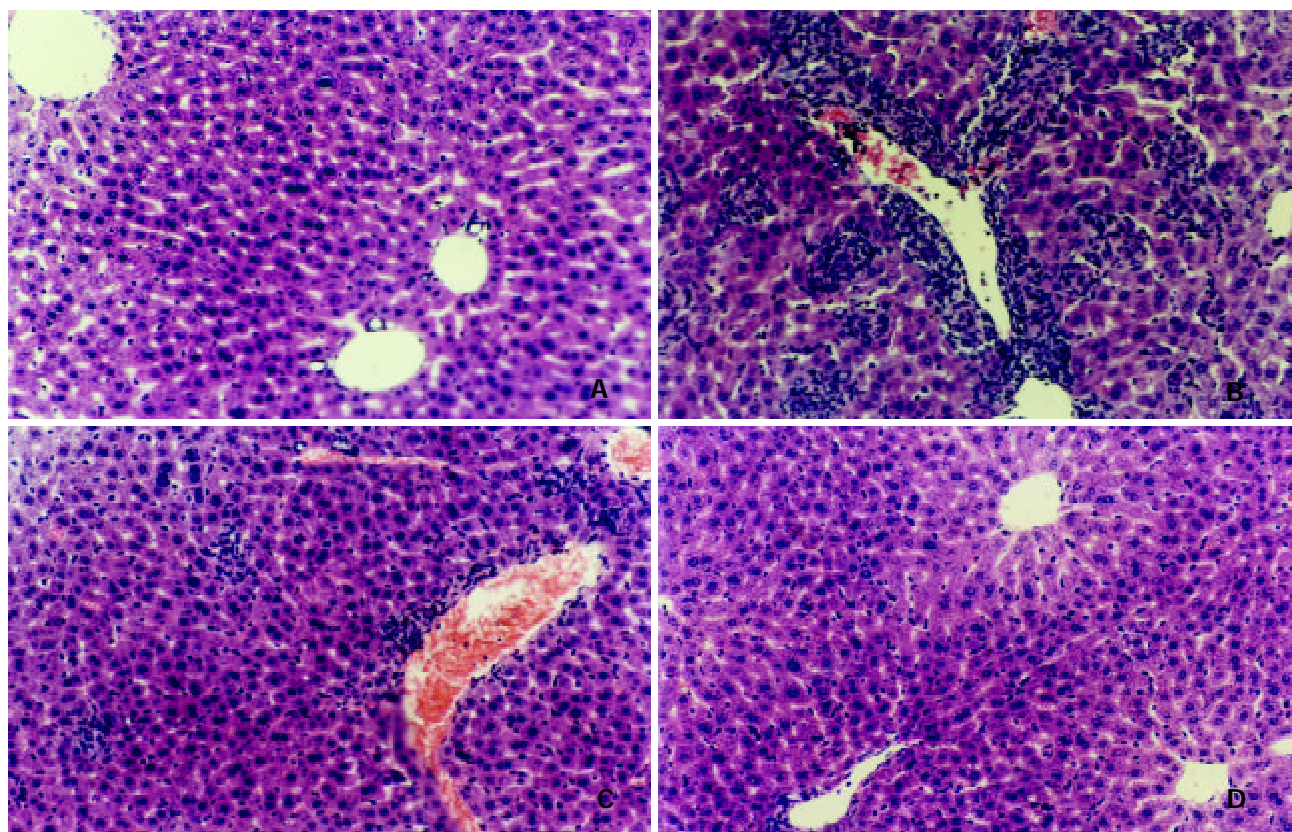


Figure 1 Histological changes of BCG-induced immune hepatic injury in the presence or absence of *Ganoderma lucidum* polysaccharide (GLP) in mice. Hematoxylin and eosin. Mice were treated with (A) control, (B) Bacille Calmette-Guérin (BCG, $125 \text{ mg} \cdot \text{kg}^{-1}$, 2 weeks), (C) BCG plus lipopolysaccharides (LPS, $125 \text{ } \mu\text{g} \cdot \text{kg}^{-1}$, 12hr), (D) BCG plus GLP ($100 \text{ mg} \cdot \text{kg}^{-1}$), as described in Materials and Methods. (Original magnification $200\times$)

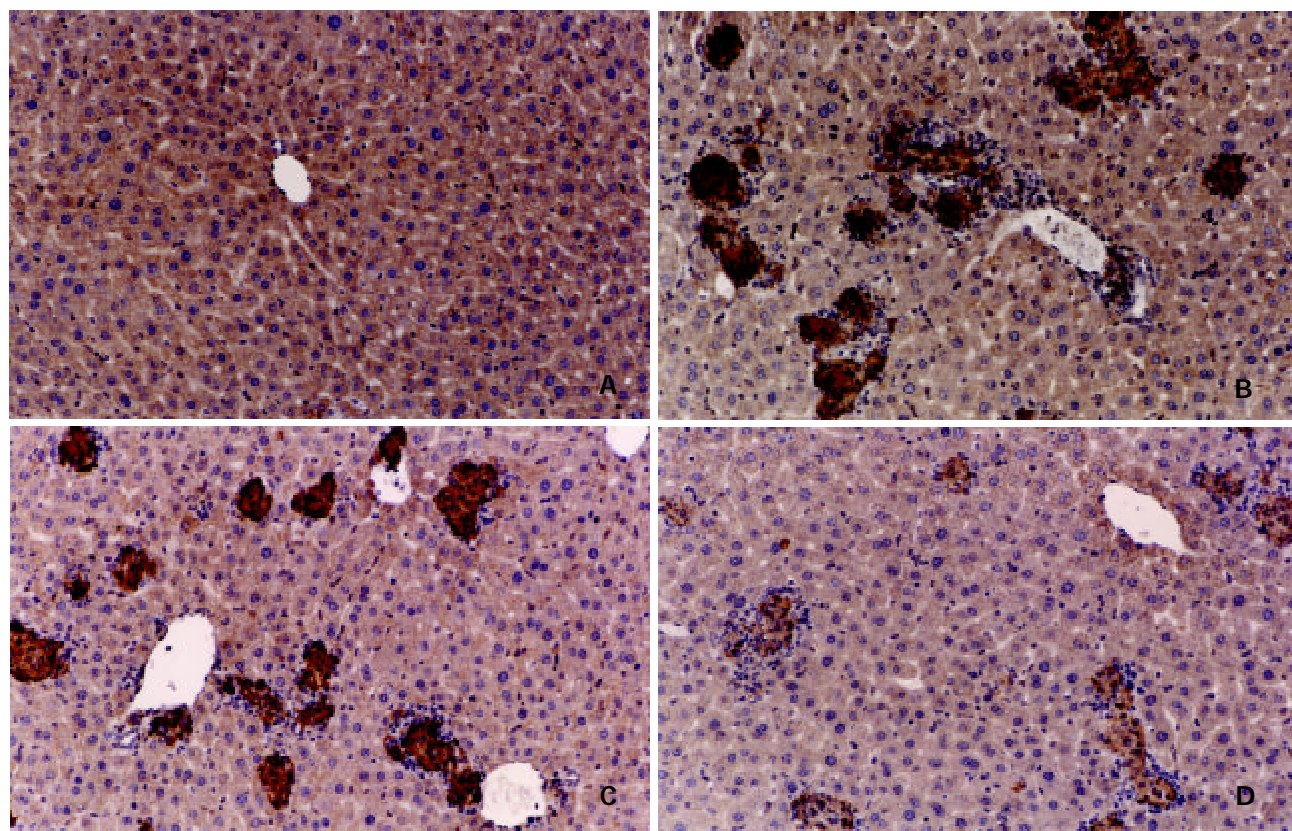


Figure 2 Immunohistochemical examination of inducible nitric oxide synthase (iNOS) protein expression stimulated by BCG in the presence or absence of *Ganoderma lucidum* polysaccharide (GLP) in mice. (Original magnification $200\times$). Mice were treated with (A) control, (B) Bacille Calmette-Guérin (BCG, $125 \text{ } \mu\text{g} \cdot \text{kg}^{-1}$, 2 weeks), (C) BCG plus lipopolysaccharides (LPS, $125 \text{ mg} \cdot \text{kg}^{-1}$, 12hr), (D) BCG plus GLP ($100 \text{ mg} \cdot \text{kg}^{-1}$), as described in Materials and Methods.

Effect of *Ganoderma lucidum* polysaccharide (GLP) on the pathohistological changes in BCG-stimulated hepatic tissues in mice *in vivo*

As shown in Figure 1, opposing with the results of control group, BCG-stimulated group were observed markedly changes of liver histologic structure (Figure 1-B), for example, infiltration within liver lobules by inflammatory cells, extensive hepatocytes hypertrophy, nuclear narrow, and granulation and vacuolization of the hepatocyte cytoplasm were observed in the liver section. Moreover, treatment with BCG plus LPS for mice resulted in more severe histological changes including thrombosis in the central hepatic vein and hemorrhage in the liver parenchyma (Figure 1-C). Granulomas formation, a marker of chronic hepatitis fibrosis, were significantly increased by BCG-stimulated hepatic tissues (Table 2, $P<0.01$). But in the presence of BCG condition, the result showed that LPS was not triggered more the granuloma forming, on the contrary, triggered more fearful hepatic tissues hemorrhage (Figure 1 B-C).

On the other hand, the results of histological examination shown that GLP ($100\text{ mg}\cdot\text{kg}^{-1}$) alleviated hepatic damage in BCG-induced acute inflammation, such as markedly decrease of infiltration within liver lobules by inflammatory cells, nuclear narrow, etc. in the observed liver section (Figure 1-D). Moreover, granulomas formation were also decreased by GLP treatment at concentration range from $100\text{ mg}\cdot\text{kg}^{-1}$ to $200\text{ mg}\cdot\text{kg}^{-1}$ ($P<0.01$).

Table 2 Effect of *Ganoderma lucidum* polysaccharide (GLP) on the granuloma formation (numbers/microscopic view) in BCG-pretreated mice hepatic histological slides. ($\bar{x}\pm s$)

Group	Granulomas
Control	0
BCG ($125\text{ mg}\cdot\text{kg}^{-1}$)	64.67 ± 4.97^b
BCG ($125\text{ mg}\cdot\text{kg}^{-1}$) + LPS ($125\text{ }\mu\text{g}\cdot\text{kg}^{-1}$)	54.40 ± 4.93^b
BCG ($125\text{ mg}\cdot\text{kg}^{-1}$) + GLP ($50\text{ mg}\cdot\text{kg}^{-1}$)	60.00 ± 4.24^b
BCG ($125\text{ mg}\cdot\text{kg}^{-1}$) + GLP ($100\text{ mg}\cdot\text{kg}^{-1}$)	$4.00\pm 1.22^{b,d}$
BCG ($125\text{ mg}\cdot\text{kg}^{-1}$) + GLP ($200\text{ mg}\cdot\text{kg}^{-1}$)	$36.80\pm 5.81^{b,d}$

^a $P<0.05$, ^b $P<0.01$ compared with control. ^c $P<0.05$, ^d $P<0.01$ compared with BCG-pretreated group. $n=5$ microscopic views.

Effects of *Ganoderma lucidum* polysaccharide (GLP) on the ALT activity and NO production induced by BCG in the presence or absence of cytokines mixture (CM) in primary cultured mice hepatocytes *in vitro*

The result of this part of experiment shown that inflammatory cytokines increased NO production and ALT release into the supernatant in the primary cultured hepatocytes prestimulated by BCG ($P<0.01$, Table 3). In the absence of cytokines condition, addition of CLP only had not influence on the activity of ALT enzyme and NO production in BCG-pretreated cultured supernatant ($P>0.05$). Whereas, in the presence of inflammatory cytokines plus BCG prestimuli condition, ALT activity and NO production were markedly inhibited by application of GLP ($P<0.01$).

CM (Cytokines mixture): IL-1 β $10\text{ KU}\cdot\text{L}^{-1}$, TNF α $500\text{ KU}\cdot\text{L}^{-1}$, and IFN γ $100\text{ KU}\cdot\text{L}^{-1}$ plus LPS $10\text{ mg}\cdot\text{L}^{-1}$; Cultured hepatocytes were harvested from control group, BCG-prestimulated group *in vivo*, and BCG plus CM-stimulated group *in vitro*, respectively, in the absence or presence of GLP for 24 h; Amount of nitrite and activity of ALT in the supernatant were assayed 24 h after start of stimulation *in vitro*.

Table 3 Effects of *Ganoderma lucidum* polysaccharide (GLP) on the alanine transaminase (ALT) activity and nitrite (NO_2^-) production induced by BCG-prestimulating in the presence or absence of cytokines mixture (CM) in primary cultured mice hepatocytes *in vitro* ($\bar{x}\pm s$)

Group	ALT ($\text{U}\cdot\text{L}^{-1}$)	NO_2^- ($\mu\text{mol}\cdot\text{L}^{-1}$)
Control	11.52 ± 1.41^b	1.41 ± 0.72^a
BCG	17.87 ± 3.41	3.52 ± 1.72
BCG + GLP ($50\text{ mg}\cdot\text{L}^{-1}$)	21.30 ± 2.87	3.95 ± 1.27
BCG + GLP ($200\text{ mg}\cdot\text{L}^{-1}$)	18.03 ± 2.24	3.24 ± 1.08
BCG + Cytokines Mixture (CM)	46.34 ± 4.17^b	13.53 ± 5.58^b
BCG + CM + GLP ($50\text{ mg}\cdot\text{L}^{-1}$)	$23.98\pm 6.33^{a,d}$	4.11 ± 2.26^d
BCG + CM + GLP ($200\text{ mg}\cdot\text{L}^{-1}$)	20.61 ± 3.74^d	3.49 ± 1.38^d

^a $P<0.05$, ^b $P<0.01$ compared with BCG-pretreated group; ^c $P<0.05$, ^d $P<0.01$ compared with BCG+CM group. $n=7$ mice. (3 wells for each treatment in each experiment).

Effect of *Ganoderma lucidum* polysaccharide (GLP) on the inducible nitric oxide synthase (iNOS) protein expression in BCG-stimulated mice hepatic tissues *in vivo*

To confirm the possible mechanism about hepatoprotective role of GLP against BCG-stimulated in mice, the correlativity between iNOS expression and immune hepatic damage were investigated. As shown in the results of immunohistochemistry, compared with control group mice, there was a lot of iNOS positive brown stained agglomerate observed in BCG-stimulated hepatic section (Figure 2 A-B). But consisted with the results of granuloma forming, there were not more the iNOS expression induced by LPS in the presence of BCG stimuli condition (Figure 2-C). On the contrary, treatment of GLP significantly inhibited iNOS protein expression under similar BCG-stimulated condition (Figure 2-D).

DISCUSSION

In the present experiment, the results shown that the administration of GLP was effective against acute and chronic hepatic inflammation induced by BCG-immunostimuli in mice. Administration of GLP significantly decreased serum or supernatant ALT level in BCG-caused acute inflammatory response *in vivo* and *in vitro*. Histological changes, such as hemorrhage and necrosis in hepatic lobules, inflammatory infiltration of lymphocytes and kupffer cells around the central vein, were simultaneously improved by the treatment of GLP. These results were consistent with that GLP showed anti-inflammatory and antioxidative activities in the previous other laboratory observed results^[22]. Moreover, pathohistological examination also showed that GLP decreased the granuloma formation, which is popularly considered as the first step of fibrillar repair in the chronic inflammatory process^[23-26]. This result suggested that GLP may be not only as an anti-inflammatory agent, but also may be used as an antifibrotic therapy for hepatocirrhosis.

To investigate the possible mechanisms of the hepatic protective effect of GLP in the immune-stimulated condition, we further detected NO production in primary cultured hepatocytes and iNOS protein expression in the BCG-stimulated hepatic tissues^[27-30]. The results shown that GLP alone had no effect on the production of NO in the cultured hepatocytes. In the presence of BCG condition, cytokines

mixture (CM) including TNF- α , IFN- γ , and LPS, significantly increased the NO production. When combined with GLP, this effect had been remarkably reversed. At the same time point, GLP also attenuated the increase of ALT activity in inflammatory cytokines-stimulated hepatocytes *in vitro*. It has been recognized that NO is produced by cNOS and/or iNOS in mice liver^[31-37]. The results of immunohistochemistry shown that GLP effect on NO production is mainly through iNOS under immunological stimuli condition. The results of this study suggested that although the exact mechanism of action of GLP on such macrophage/lymphocyte properties of granulomas remain unknown, nevertheless, it might be related to NO production induced by cytokines^[38-42]. Therefore, inhibition of NO production is partly the mechanisms of GLP protective effect on the immunological injured liver.

In summary, the present study indicates that NO participates in immune liver injury induced by *Mycobacterium bovis* BCG infection. Furthermore, the mechanisms of protective roles by GLP for BCG-induced immune liver injury in mice may be due to influence NO production. However, further study is needed to understand the exact mechanisms of the antihepatotoxic activity and the free radical scavenging activity of GLP. The clinical applicability of GLP remains to be established.

REFERENCES

- 1 **Bao XF**, Liu CQ, Fang J, Li XY. Structural and immunological studies of a major polysaccharide from spores of *Ganoderma lucidum* (Fr.) Karst. *Carbohydr Res* 2001; **332**: 67-74
- 2 **Cheung WM**, Hui WS, Chu PW, Chiu SW, Ip NY. *Ganoderma* extract activates MAP kinases and induces the neuronal differentiation of rat pheochromocytoma PC12 cells. *FEBS Lett* 2000; **486**: 291-296
- 3 **Ma L**, Lin ZB. Effects of *Ganoderma* polysaccharides on IL-2 production by mouse splenocytes *in vitro*. *J Beij Med Univ* 1991; **23**: 412-417
- 4 **Lei LS**, Lin ZB. Effect of *Ganoderma* polysaccharides on T cell subpopulations and production of interleukin 2 in mixed lymphocyte response. *Acta Pharmaceutica Sinica* 1992; **27**: 331-335
- 5 **Zhang QH**, Lin ZB. The antitumor activity of *Ganoderma lucidum* (Curt.:Fr.) P. Karst. (Ling Zhi) (Aphyllphoromy cetideae) polysaccharides is related to tumor necrosis factor- α and interferon- γ . *Inter J Med Mushrooms* 1999; **1**: 207-215
- 6 **Ouyang EC**, Wu CH, Walton C, Promrat K, Wu GY. Transplantation of human hepatocytes into tolerized genetically immunocompetent rats. *World J Gastroenterol* 2001; **7**: 324-330
- 7 **Guo SP**, Wang WL, Zhai YQ, Zhao YL. Expression of nuclear factor- κ B in hepatocellular carcinoma and its relation with the X protein of hepatitis B virus. *World J Gastroenterol* 2001; **7**: 340-344
- 8 **You J**, Zhuang L, Tang BZ, Yang WB, Ding SY, Li W, Wu RX, Zhang HL, Zhang YM, Yan SM, Zhang L. A randomized controlled clinical trial on the treatment of Thymosin-a 1 versus interferon- α in patients with hepatitis B. *World J Gastroenterol* 2001; **7**: 411-414
- 9 **Li XW**, Ding YQ, Cai JJ, Yang SQ, An LB, Qiao DF. Studies on mechanism of Sialy Lewis-X antigen in liver metastases of human colorectal carcinoma. *World J Gastroenterol* 2001; **7**: 425-430
- 10 **Liu BH**, Chen HS, Zhou JH, Xiao N. Effects of endotoxin on endothelin receptor in hepatic and intestinal tissues after endotoxemia in rats. *World J Gastroenterol* 2000; **6**: 298-300
- 11 **Cheng JL**, Tong WB, Liu BL, Zhang Y, Yan Z, Feng BF. Hepatitis C virus in human B lymphocytes transformed by Epstein-Barr virus *in vitro* by in situ reverse transcriptase-polymerase chain reaction. *World J Gastroenterol* 2001; **7**: 370-375
- 12 **Zhuang L**, You J, Tang BZ, Ding SY, Yan KH, Peng D, Zhang YM, Zhang L. Preliminary results of Thymosin-a 1 versus interferon- α treatment in patients with HBe-AG negative and serum HBV DNA positive chronic hepatitis B. *World J Gastroenterol* 2001; **7**: 407-410
- 13 **Carpenter E**, Fray L, Gormley E. Antigen-specific lymphocytes enhance nitric oxide production in *Mycobacterium bovis* BCG-infected bovine macrophages. *Immunol Cell Biol* 1998; **76**: 363-368
- 14 **Wang GS**, Liu GT. Role of nitric oxide in immunological liver damage in mice. *Biochem Pharmacol* 1995; **49**: 1277-1281
- 15 **Bai XY**, Jia XH, Cheng LZ, Gu YD. Influence of IFN-2b and BCG on the release of TNF and IL-1 by Kupffer cells in rats with hepatoma. *World J Gastroenterol* 2001; **7**: 419-421
- 16 **Erb KJ**, Kirman J, Delahunt B, Chen WX, Gros GL. IL-4, IL-5 and IL-10 are not required for the control of *M. Bovis*-BCG infection in mice. *Immunol Cell Biol* 1998; **76**: 41-46
- 17 **Ugaz EMA**, Pinheiro SR, Guerra JL, Palermo-Neto J. Effects of prenatal diazepam treatment on *Mycobacterium bovis*-induced infection in hamsters. *Immunopharmacology* 1999; **41**: 209-217
- 18 **Zhang GL**, Lin ZB. Effects of cytokines on the endotoxin stimulated nitric oxide production in the primary cultured rat hepatocytes. *Beijing Yike Daxue Xuebao* 1998; **30**: 180-182
- 19 **Zhang GL**, Lin ZB, Zhang B. Effects of selective inducible nitric oxide synthase inhibitor on immunological hepatic injury in rat. *Zhanghua Yixue Zazhi* 1998; **78**: 540-543
- 20 **Zhang GL**, Lin ZB. Dinoprostone potentiates cytokines and lipopolysaccharides to induce nitric oxide production in cultured rat hepatocytes. *Acta Pharmacol Sinica* 1999; **20**: 262-266
- 21 **Zhang GL**, Wang YH, Teng HL, Lin ZB. Effects of aminoguanidine on the nitric oxide production induced by inflammatory cytokines and endotoxin in cultured rat hepatocytes. *World J Gastroenterol* 2001; **7**: 331-334
- 22 **Lee JM**, Kwon H, Jeong H, Lee JW, Lee SY, Baek SJ, Surh YJ. Inhibition of lipid peroxidation and oxidative DNA damage by *Ganoderma lucidum*. *Phytother Res* 2001; **15**: 245-249
- 23 **Nie QH**, Cheng YQ, Xie YM, Cao YZ. Inhibiting effect of antisense oligonucleotides phosphorothioate on gene expression of TIMP-1 in rat liver fibrosis. *World J Gastroenterol* 2001; **7**: 363-369
- 24 **Huang YQ**, Xiao SD, Mo JZ, Zhang DZ. Effects of nitric oxide synthesis inhibitor in long term treatment on hyperdynamic circulatory state in cirrhotic rats. *World J Gastroenterol* 2000; **6** (Suppl 3): 31
- 25 **Feng ZJ**, Feng LY, Sun ZM, Song M, Yao XX. Expression of nitric oxide synthase protein and gene in the splanchnic organs of liver cirrhosis and portal hypertensive rats. *World J Gastroenterol* 2000; **6** (Suppl 3): 33
- 26 **Vernia S**, Beaune P, Coloma J, Lopez-Garcia PM. Differential sensitivity of rat hepatocyte CYP isoforms to self-generated nitric oxide. *FEBS Lett* 2001; **488**: 59-63
- 27 **Wang JH**, Redmond HP, Wu QD, Bouchier-Hayes D. Nitric oxide mediates hepatocyte injury. *Am J Physiol* 1998; **275**: G1117-G1126
- 28 **Alexander B**. The role of nitric oxide in hepatic metabolism. *Nutrition* 1998; **14**: 376-390
- 29 **Kaibori M**, Sakitani K, Oda M, Kamiyama Y, Masu Y, Nishizawa M, Ito S, Okumura T. Immunosuppressant FK506 inhibits inducible nitric oxide synthase gene expression at a step of NF- κ B activation in rat hepatocytes. *J Hepatol* 1999; **30**: 1138-1145
- 30 **McCafferty DM**, Mudgett JS, Swain MG, Kubes P. Inducible nitric oxide synthase plays a critical role in resolving intestinal inflammation. *Gastroenterology* 1997; **112**: 1022-1027
- 31 **Moriyama A**, Tabaru A, Unoki H, Abe S, Masumoto A, Otsuki M. Plasma nitrite/nitrate concentrations as a tumor marker for hepatocellular carcinoma. *Clinica Chimica Acta* 2000; **296**: 181-191
- 32 **Hara H**, Mitani N, Adachi T. Inhibitory effect of nitric oxide on the induction of cytochrome P450 3A4 mRNA by 1,

- 25-dihydroxyvitamin D3 in Caco-2 cells. *Free Rad Res* 2000; **33**: 279-285
- 33 **Yu J**, Guo F, Ebert MPA, Malfertheiner P. Expression of inducible nitric oxide synthase in human gastric cancer. *World J Gastroenterol* 1999; **5**: 430-431
- 34 **Ji XL**, Shen MS, Yin T. Liver inflammatory pseudotumor or parasitic granuloma? *World J Gastroenterol* 2000; **6**: 458-460
- 35 **Heneka MT**, Loschmann PA, Gleichmann M, Weller M, Schulz JB, Wullner U, Klockgether T. Induction of nitric oxide synthase and nitric oxide-mediated apoptosis in neuronal PC12 cells after stimulation with tumor necrosis factor- α / lipopolysaccharide. *J Neurochem* 1998; **71**: 88-94
- 36 **Liu SH**, Tzeng HP, Kuo ML, Lin-Shiau SY. Inhibition of inducible nitric oxide synthase by b-lapachone in rat alveolar macrophages and aorta. *Br J Pharmacol* 1999; **126**: 746-750
- 37 **Vos TA**, Gouw AS, Klok PA, Havinga R, Goor H, Huitema S, Roelofsen H, Kuipers F, Jansen P, Moshage H. Differential effects of nitric oxide synthase inhibitors on endotoxin-induced liver damage in rats. *Gastroenterology* 1997; **113**: 1323-1333
- 38 **Tzeng E**, Billiar TR, Williams DL, Li J, Lizonova A, Kovacs I, Kim YM, Pa P. Adenovirus-mediated inducible nitric oxide synthase gene transfer inhibits hepatocyte apoptosis. *Surgery* 1998; **124**: 278-283
- 39 **Nomura T**, Ohtsuki M, Matsui S, Sumi-Ichinose C, Nomura H, Hagino Y. Nitric oxide donor NOR3 inhibits ketogenesis from oleate in isolated rat hepatocytes by a cyclic GMP-independent mechanism. *Pharmacol Tox* 1998; **82**: 40-46
- 40 **Imagawa J**, Yellon DM, Baxter GF. Pharmacological evidence that inducible nitric oxide synthase is a mediator of delayed preconditioning. *Br J Pharmacol* 1999; **126**: 701-708
- 41 **Tuncat B**, Uludag O, Altug S, Abacoglu N. Effects of nitric oxide synthase inhibition in lipopolysaccharide-induced sepsis in mice. *Pharmacol Res* 1998; **38**: 405-411
- 42 **Ohmori H**, Egusa H, Ueura N, Matsumoto Y, Kanayama N, Hikida M. Selective augmenting effects of nitric oxide on antigen-specific IgE response in mice. *Immunopharmacology* 2000; **46**: 55-63

Edited by Pang LH

• BASIC RESEARCH •

Apoptosis of rat hepatic stellate cells induced by anti-focal adhesion kinase antibody

Xiao-Jing Liu, Li Yang, Hong-Bin Wu, Ou Qiang, Ming-Hui Huang, Ying-Ping Wang

Xiao-Jing Liu, Ou Qiang, Ming-Hui Huang, Laboratory of Department of Internal Medicine, West China Hospital, Sichuan University, Chengdu 610041, Sichuan Province, China

Li Yang, Yi-Ping Wang, Department of Gastroenterology of West China Hospital, Sichuan University, Chengdu 610041, Sichuan Province, China

Hong-Bin Wu, Laboratory of Department of Surgery, West China Hospital, Sichuan University, Chengdu 610041, Sichuan Province, China

Supported by the National Natural Science Foundation of China, No.39800054

Correspondence to: Xiao-Jing Liu, Laboratory of Department of Internal Medicine, West China Hospital, Sichuan University, 37 Wainan Guoxueshang, Chengdu 610041, Sichuan Province, China. xiaojingliu67@hotmail.com

Received 2001-09-26 **Accepted** 2001-10-29

Abstract

AIM: To explore the role of focal adhesion kinase (FAK) in the apoptosis in culture-activated rat hepatic stellate cells (HSCs) using a specific anti-FAK antibody.

METHODS: Rat HSCs were prepared from Wistar rats by *in situ* perfusion of collagenase and pronase and single-step density Nycodenz gradient. Culture-activated HSCs were serum-starved and treated with the anti-FAK antibodies for 24, 48 or 72 h. The apoptosis of HSC was detected by DNA-fragment assay, flow cytometry and caspase-3 activity determination. The expression of tissue inhibitor of metalloproteinase-1 (TIMP-1) mRNA was assessed by reverse transcription polymerase chain reaction (RT-PCR).

RESULTS: The experiment showed that anti-FAK antibodies induced apoptosis of culture-activated rat HSCs. This phenomenon displayed the classical features of apoptotic cell death (DNA fragmentation, cell cycle analysis) after treated with 30 mg·L⁻¹ FAK antibody for 72 h, and accompanied by a significant increase of caspase-3 activity (1208±76) vs (309±28) nmol·min⁻¹·g⁻¹, *t*=208.5, *P*<0.05. Meanwhile, treatment with the FAK antibody in HSCs could markedly decrease the TIMP-1 mRNA expression (0.07±0.01 vs 0.38±0.03, *t*=2.72, *P*<0.05).

CONCLUSION: FAK plays an important role in the survival of HSCs and the specific anti-FAK antibody could induce the apoptosis in rat HSCs.

Liu XJ, Yang L, Wu HB, Qiang O, Huang MH, Wang YP. Apoptosis of rat hepatic stellate cells induced by anti-focal adhesion kinase antibody. *World J Gastroenterol* 2002; 8(4):734-738

INTRODUCTION

Focal adhesion kinase (FAK) is a non-receptor tyrosine ubiquitously expressed in cells. It was initially shown to be the initiator of focal adhesion formation in adherent cells, after its binding to integrins which induce its autophosphorylation^[1].

However, it can also be activated by a great variety of other stimuli being able to act on different intracellular signaling, and neuropeptides^[2-4]. Its autophosphorylation is followed by a submembranous localization which is crucial for the biological roles of FAK, including cell spreading, migration, proliferation, survival and prevention of apoptosis^[5-7]. Proteolytic cleavage of FAK by caspase-3 has been reported during growth factor deprivation-induced apoptosis in human umbilical vein endothelial cells^[8], which implies an association between FAK and apoptosis^[9,10]. The pathologic basis of hepatic cirrhosis is fibrosis and hepatic stellate cells (HSC) are presently regarded as one of the key cell types involved in the progression of liver fibrosis^[11-13]. The perpetuation of HSC activation leads to an increased number of collagen-producing cells and finally to the accumulation of extracellular matrix (ECM)^[14-16]. Therefore, the strategy for terminating the proliferation of activated HSC by apoptosis might be an exciting therapy for patients with chronic liver injury and fibrosis^[17-19].

FAK has also been shown to play an important role in the HSC activation^[20]. PLC γ recruitment by FAK during HSC adhesion is an important process implicating a link between integrin and PDGF-mediated signal pathways to regulate HSC adhesion and mobility^[21]. An adherence dependent pp125FAK-paxillin signaling pathway in fibroblasts inhibited damage-induced apoptosis^[22]. Thus, we hypothesized that the modulation of biological roles of FAK by a neutralizing anti-FAK antibody might stop the fibroproliferative response and induce apoptosis in HSC.

MATERIALS AND METHODS

Materials

Male Wistar rats were obtained from the Experimental Animal Center of West China Medical Center of Sichuan University (West China University of Medical Sciences, Chengdu, Sichuan). Dulbecco's modified medium (DMEM), Trypsin-EDTA and new born calf serum (CS) were from GibcoBRL (Maryland, USA). Pronase, Collagenase B and DNAase I were from Roche Molecular Biochemicals, (Mannheim, Germany). Nycodenz was from Sigma (ST. Louis, USA). Antibodies to Desmin, α -smooth muscle actin (α -SMA) were obtained from Dako (Glostrup, Denmark). Affinity-purified polyclonal antibody to FAK (epitope mapping at the carboxy terminus of focal adhesion kinase) were purchased from Santa Cruz (Santa Cruz, USA). The caspase-3 cellular activity assay kit was purchased from CalBiochem-Novabiochem Corporation (San Diego, USA).

Methods

HSC isolation and apoptosis induction HSCs were isolated from male Wistar rats by *in situ* pronase-collagenase perfusion and single-step Nycodenz gradient^[23]. The cells were seeded at a density of $1.5 \times 10^5/\text{cm}^2$ on glass coverslips in 6-well culture plate or 100-mm dishes (Falcon) and maintained in DMEM containing 200 ml·L⁻¹ heat-inactivated new-born calf serum. The purity of HSC preparations was assessed by

intrinsic vitamin A autofluorescence and immunocytochemistry with antibody against desmin. The viability of the cells was evaluated by the Trypan blue dye exclusion test. The purity and viability of the primary cells exceeded 90 % and 95 %, respectively. Therefore, HSC cultured on uncoated plastic dishes spontaneously acquired an activated phenotype, characterized by expression of α -SMA and by loss of vitamin A droplets^[24,25]. After reaching confluency (about 10-14 d after plating), activated HSC were detached by incubation with trypsin, and split in a 1:2 ratio. Experiments were performed on cells between the second and 5th passages using 3 independent cell lines, and the purity of activated HSC exceeded 98 %. HSC (5×10^6) were plated in uncoated plastic dishes for 4 h and the medium was changed to serum-free DMEM for 24 h to synchronize the HSC in the G₁ phase of the cell cycle^[26]. The antibodies against FAK was filter-sterilized and added to the serum-free DMEM medium containing 1 g·L⁻¹ bovine serum albumin (the final concentration of anti-FAK antibodies was 30 mg·L⁻¹). The analysis of apoptosis was carried out after 24-72 h of incubation with the antibodies. The serum-free DMEM medium containing the antibodies was changed every 24 h.

Analysis of DNA fragmentation HSC from the anti-FAK antibodies treated was pooled for DNA fragmentation analysis. A DNA fragmentation assay was performed as described previously^[27]. In brief, HSC was gently lysed for 30 min at 48 °C in a buffer containing 5 mmol·L⁻¹ Tris buffer (pH7.4), 20 mmol·L⁻¹ EDTA, and 5 ml·L⁻¹ Triton X-100. After centrifugation at 15 000r·min⁻¹ for 15 min, supernatants containing soluble fragmented DNA were collected and treated with RNAase (20 mg·L⁻¹), followed by proteinase K (20 mg·L⁻¹) digestion. DNA fragments were precipitated in 990ml·L⁻¹ ethanol. Samples were then electrophoresed on a 20g·L⁻¹ agarose gel, visualized with 1 g·L⁻¹ ethidium bromide and photographed under short-wave ultraviolet light.

Flow cytometry Cell viability was determined using trypan blue dye exclusion, and the existence of apoptotic cells was confirmed as well by the appearance of a sub-G₀/G₁ peak fraction in the cell cycle analysis^[28]. For the cell cycle analysis, ethanol-fixed cells were stained with propidium iodide (50 mg·L⁻¹) in the presence of RNase A (100 mg·L⁻¹), and then analyzed using the fluorescence-activated cell sorter (FACS, Coulter, EPICS ELITE ESP model), with a cell cycle analysis program.

Cellular caspase-3 activity determination The cellular caspase-3 activity assay from Calbiochem-Novabiochem Corporation measures the colorimetric reaction of the cleavage of the amino acid motif DEVD, thereby releasing the chromophorep-nitroanilide^[29]. Following phosphate-buffered saline washing, cell lysate was prepared according to the manufactures' instructions. The level of caspase-3 enzymatic activity on the cell lysate is directly proportional to the color reaction that was quantitated spectrophotometrically at a wavelength of 405 nm, using a microplate reader for 96 wells (Bio Rad, model 550). And the total protein content of each cell lysate was determined by the Coomassie dye binding assay (Bradford method). Data were corrected for background (no substrate or no cell lysate) and caspase-3 activities were expressed as nmol·min⁻¹·g⁻¹ of protein.

TIMP-1 mRNA detection by RT-PCR The total RNA was isolated from HSC using Trizol reagent (Life Technologies, Inc, USA), precipitated in ethanol and resuspended in sterile RNAase-free water for storage at -70 °C, as described previously^[30]. One-step reverse transcription-polymerase chain reaction (RT-PCR) was performed according to the method of the supplier (Titan™ one tube RT-PCR kit, Roche Molecular

Biochemicals). Primers for rat tissue inhibitors metalloproteinase-1 (TIMP-1) and GAPDH were designed using the Primer3 program from Whitehead Institute for Biomedical Research (Cambridge, MA, USA)^[31], synthesized and purified by HPLC in Gibco BRL Custom Primers (HongKong). Primer sequences were as follows: TIMP-1 sense, 5'-GAC CTG GTC ATA AGG GCT AAA-3'; antisense, 5'-GCC CGT GAT GAG AAA CTC TTC ACT-3'; GAPDH sense, 5'-ACC ACA GTC CAT GCC ATC AC-3'; antisense, 5'-TCC ACC ACC CTG TTG CTG TA-3', and the expected size was 216 bp and 452 bp respectively. One microgram RNA was added to each reaction and the RT-PCR was performed in the following steps: reverse-transcription was performed at 50 °C for 30 min; and amplification was performed in a thermal controller (model PTC-100, MJ Research, Watertown, USA) for 35cycles (denaturation at 94 °C for 1 min, annealing at 56 °C for 1 min and extension at 72 °C for 1 min), and 10 min at 72 °C for final extension after the last cycle. 5 μ l of the PCR products was analyzed by 20 g·L⁻¹ agarose gel electrophoresis with TAE buffer at 80V for 40 min, visualized with ethidium bromide and photographed under UV light. The semi-quantitative analysis was performed. TIMP-1/GAPDH quotient is the indication of TIMP-1. Experiments were performed at least three times with similar results.

Statistical analysis

Results of cell cycle analysis were expressed as percentage of total examined cells and statistical analysis was performed by χ^2 test. Other results were expressed as $\bar{x} \pm s$. Differences between means were analyzed with Student *t* test for paired samples. A value of *P*<0.05 was considered statistically significant.

RESULTS

DNA fragmentation assay

We investigated the role of FAK in the survival of HSC to rescue cells from apoptosis. An antibody to FAK that could inhibit its activation was used to test this hypothesis. This antibody binds to the COOH-terminal region of FAK, which contains the targeting sequence that is required for efficient recruitment of FAK to the focal adhesion^[22, 32, 33]. HSC was treated with 30 mg·L⁻¹ anti-FAK antibodies in DMEM without serum. Genomic DNA fragment analysis performed 48-72 h after treatment demonstrating an oligonucleosomal DNA ladder for the treated cells, and the cells after treatment for 24 h showed minimal DNA ladder whereas the control cells in DMEM without the antibodies displayed no DNA degradation (Figure 1).

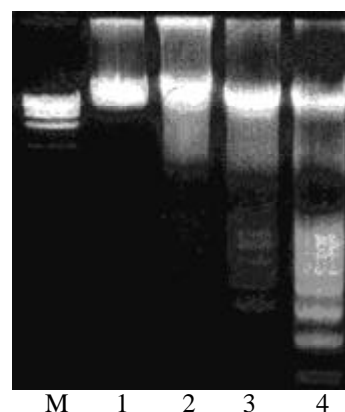


Figure 1 Oligonucleosomal genomic DNA fragmentation. Lane M: DNA marker of PBR322; Lane 1: Control HSCs; Lane 2, 3, 4: HSC treated with anti-FAK antibodies for 24, 48 or 72 h.

Flow cytometry

A predominant sub-G₁ population (39.8 %) characteristic of apoptosis was observed in anti-FAK antibodies treated HSCs for 72 hours by propidium iodide staining and flow cytometric analysis, while the control cells only had a (5.2 %) sub-G₁ population (Figure 2). There was significant difference between these two groups (39.8 % vs 5.2 %, $\chi^2=1716.4$, $P<0.001$). And a significant sub-G₁ population (16.5 %) was also observed in anti-FAK antibodies treated HSCs for 48 hours, while the control cells only had a (3.1 %) sub-G₁ population (16.5 % vs 3.1 %, $\chi^2=507.8$, $P<0.001$). However, there was no significant difference between the 24-hour treatment and controls (3.1 % vs 2.7 %, $\chi^2=1.4$, $P>0.05$).

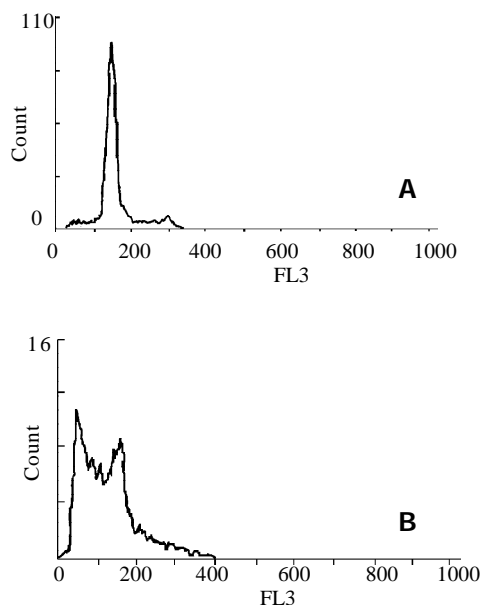


Figure 2 Flow cytometric analysis of HSCs.

A: Control HSC; B: HSC treated with anti-FAK antibodies for 72 h showed the presence of a hypodiploid (sub-G₁) fraction, indicating DNA degradation.

Cellular caspase-3 activity

Anti-FAK antibodies -induced apoptosis was accompanied by a significant time-dependent increase of caspase-3 activity (Table 1).

Table 1 Caspase-3 activation in HSCs by anti-FAK antibodies (n=6)

Groups	Caspase-3 activity (nmole·min ⁻¹ ·g ⁻¹)
Control (24 h)	36.5±12.6
Treatment (24 h)	41.9±15.3
Control (48 h)	110.7±18.6
Treatment (48 h)	233.5±25.9 ^a
Control (72 h)	36.5±12.6
Treatment (72 h)	1208.5±76.4 ^a

^a $P<0.05$, vs control (233.5±25.9 vs 110.7±18.6, $t=33.9$, $P<0.05$; 1208.5±76.4 vs 36.5±12.6, $t=208.5$, $P<0.05$)

Effect of anti-FAK antibody on the expression of TIMP-1 in HSCs

To evaluate whether the anti-FAK antibody affects the expression of TIMP-1 in HSCs, RT-PCR analysis was performed to detect the gene expression level of TIMP-1 after the treatment with anti-FAK antibodies in HSC. The mRNA

expression levels of cells that treated with the antibodies for 72 h was remarkably decreased as against that of the controls (0.07 ± 0.01 vs 0.38 ± 0.03 , $P<0.05$, Figure 3). But there was no significant difference between the cells treated with the antibodies for 48 h or 24 h and their controls ($P>0.05$).

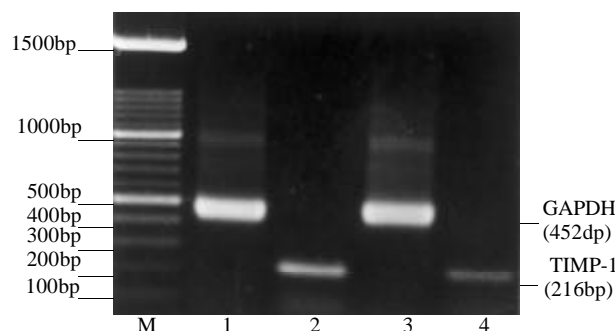


Figure 3 Electrophoresis analysis of RT-PCR product.

Lane M: 100bp DNA ladder; Lane 1, 2: amplified from cDNA from the control HSCs; Lane 3, 4: amplified from cDNA from HSCs treated with anti-FAK antibodies for 72 h. The positive bands of 452bp and 216bp represented GAPDH and TIMP-1 respectively. Lane 4 showed decreased expression of TIMP-1 in HSC compared with lane 2.

DISCUSSION

Liver fibrosis is characterized by an accumulation of extracellular matrix protein that impairs normal function with severity. It represents the common end point of the majority of chronic liver injuries. Ultimately, it results in distortion of the liver architecture (cirrhosis) which is associated with disturbance of liver function and significant morbidity and mortality^[34-37]. At the cellular level there is now a wealth of evidence indicating that HSC represents the pivot of the fibrotic process. In the injured liver and during culture, quiescent HSCs transform from a retinoid rich pericyte-like cell to a myofibroblast-like cells (MFB). This so-called “activation” is associated with a loss of vitamin A droplets, increased proliferation, and sensitivity towards endothelins, increased production of ECM proteins, in addition to multiple alterations in gene expression^[11-15]. Activation and transformation of HSCs into MFB may be viewed as a “wound-healing response”, however, little is known about the termination of this process, while HSC is abundant in the diseased liver tissue during fibrogenesis, and resolution of liver fibrogenesis is associated with reduced number of HSC. In the recovery from liver injury, apoptotic HSC was detected in parallel to a reduction in the total number of HSC within the liver tissue and an essential element of this recovery process is apoptosis of activated HSC^[17-19]. Apoptosis (or programmed cell death) is the controlled mechanism by which cells are eliminated from tissue without eliciting an inflammatory response. Apoptosis of HSC may therefore play a central role in the resolution of fibrosis by eliminating the source of both the neomatrix and the metalloproteinase (collagenase) inhibitors and thereby facilitating net matrix degradation. Therefore, promoting HSC apoptosis may be a viable method to facilitate matrix degradation in fibrotic liver, thereby manipulating the fibrotic process. An understanding of the control of HSC apoptosis is important precisely because regulating this process may provide a novel therapeutic approach to the treatment of advanced hepatic fibrosis^[18-20].

Anchorage of cells to the ECM is mediated by integrins^[38], which not only mediated cell adhesion but also initiate

intracellular signal transduction^[39]. A family of nonreceptor tyrosine kinases, composed of FAK, proline-rich tyrosine kinase (PYK-2), and integrin-linked kinase complex with the intracellular domain of integrins, leading to activation of various signaling pathways subsequent to integrin stimulation. Since the initial discovery and characterization of FAK, a number of different functions have been proposed for this unusual tyrosine kinase. FAK plays a pivotal role in transducing survival signals mediated by engagement of integrins with the ECM, enabling the cell to enter the cell cycle, thereby preventing apoptosis^[1,40]. In rat HSCs, a soluble RGD peptide that blocks attachment to fibronectin and vitronectin triggered apoptosis in the serum-free condition, suggesting that integrin-mediated events can regulate death decisions in HSC^[27]. Furthermore, the authors^[27] reported that RGD peptides reduce the phosphorylation of FAK in HSC. Therefore in the current study we have described the role of FAK in the apoptosis in HSC.

Recently, a potential role for FAK in the suppression of apoptosis has been suggested in different cell types^[7,41]. This study showed that anti-FAK antibodies induced apoptosis of culture-activated rat HSCs. This phenomenon displayed the classical features of apoptotic cell death (DNA fragmentation, cell cycle analysis), and accompanied by a significant increase of caspase-3 activity. Caspases, a family of the interleukin-1 β converting enzyme (ICE) family of cysteine proteases, are key intracellular mediators of apoptosis^[42,43]. Caspase-3, also known as CPP32, Yama or apopain, is one of the principle caspases found in apoptotic cells^[44]. Our observations suggest that induction of apoptosis in HSCs by anti-FAK antibodies may through the caspase-3 activation.

The data presented in this paper demonstrate that treatment of HSC with anti-FAK antibodies decreased the expression of TIMP-1 mRNA. Matrix metalloproteinases (MMP) and their specific inhibitors (TIMP) are thought to play an essential role in liver injury associated with tissue remodeling^[45-47], and it was reported that antisense oligonucleotides directed to TIMP-1 had some anti-hepatic fibrosis effect in the experimental immune hepatic rat models^[48]. MMP or their inhibitors (TIMP) have been suggested to regulate apoptosis, and TIMP-1 inhibits cell death induced by hydrogen peroxide, adriamycin, or X-ray radiation^[49]. It has recently shown that recovery from established experimental fibrosis can occur through the apoptosis of HSCs and is associated with reductions in liver collagen and expression of the TIMP-1 and TIMP-2^[47]. Furthermore, FAK signaling pathway plays a pivotal role in the secretion of MMPs^[50]. Therefore, the anti-FAK antibody regulated apoptotic pathway in HSCs might be triggered by interference with the TIMP-1 function.

In conclusion, integrin-ECM interactions influence apoptosis in rat HSC, and FAK is required for transducing survival signals from ECM in HSC. Our experiment provided a link between FAK and caspase-3, the expression of TIMP-1 and HSC survival. Thus the regulation of apoptosis may be very important in HSC biology.

REFERENCES

- Schaller MD.** Biochemical signals and biological responses elicited by the focal adhesion kinase. *Biochim Biophys Acta* 2001; **1540**: 1-21
- Ben Mahdi MH,** Andrieu V, Pasquier C. Focal adhesion kinase regulation by oxidative stress in different cell types. *IUBMB Life* 2000; **50**: 291-299
- Schlaepfer DD,** Hauck CR, Sieg DJ. Signaling through focal adhesion kinase. *Prog Biophys Mol Biol* 1999; **71**: 435-478
- Monteiro HP,** Gruia-Gray J, Peranovich TM, de Oliveira LC, Stern A. Nitric oxide stimulates tyrosine phosphorylation of focal adhesion kinase, Src kinase, and mitogen-activated protein kinase in murine fibroblasts. *Free Radic Biol Med* 2000; **28**: 174-182
- Zachary I,** Glikli G. Signaling transduction mechanisms mediating biological actions of the vascular endothelial growth factor family. *Cardiovasc Res* 2001; **49**: 568-581
- Parsons JT,** Martin KH, Slack JK, Taylor JM, Weed SA. Focal adhesion kinase: a regulator of focal adhesion dynamics and cell movement. *Oncogene* 2000; **19**: 5606-5613
- Gauthier R,** Harnois C, Drolet JF, Read JC, Vezina A, Vachon PH. Human intestinal epithelial cell survival: differentiation state-specific control mechanisms. *Am J Physiol Cell Physiol* 2001; **280**: C1540-1554
- Abu-Ghazaleh R,** Kabir J, Jia H, Lobo M, Zachary I. Src mediates stimulation by vascular endothelial growth factor of the phosphorylation of focal adhesion kinase at tyrosine 861 and migration and anti-apoptosis in endothelial cells. *Biochem J* 2001; **360**: 255-264
- van de Water B,** Nagelkerke JF, Stevens JL. Dephosphorylation of focal adhesion kinase (FAK) and loss of focal contacts precede caspase-mediated cleavage of FAK during apoptosis in renal epithelial cells. *J Bio Chem* 1999; **274**: 13328-13337
- Sonoda Y,** Matsumoto Y, Funakoshi M, Yamamoto D, Hanks SK, Kasahara T. Anti-apoptotic role of focal adhesion kinase (FAK) induction of inhibitor-of-apoptosis proteins and apoptosis suppression by the overexpression of FAK in a human leukemic cell line, HL-60. *J Biol Chem* 2000; **275**: 16309-16315
- Albanis E,** Friedman SL. Hepatic fibrosis. Pathogenesis and principles of therapy. *Clin Liver Dis* 2001; **5**: 315-334
- Zhu YH,** Hu DR, Nie QH, Liu GD, Tan ZX. Study on activation and *c-fos*, *c-jun* expression of *in vitro* cultured human hepatic stellate cells. *Shijie Huaren Xiaohua Zazhi* 2000; **8**: 299-302
- Eng FJ,** Friedman SL. Fibrogenesis I. New insight into hepatic stellate cell activation: the simple becomes complex. *Am J Physiol* 2000; **279**: G7-G11
- Friedman SL.** Molecular regulation of hepatic fibrosis, an integrated cellular response to tissue injury. *J Biol Chem* 2000; **275**: 2247-2250
- Huang GC,** Zhang JS. Intercellular signal transduction of activated hepatic stellate cells. *Shijie Huaren Xiaohua Zazhi* 2001; **9**: 1056-1060
- Du WD,** Zhang YE, Zhai XM. Dynamic changes of type I, III and IV collagen synthesis and distribution of collagen-producing cells in carbon tetrachloride-induced rat liver fibrosis. *World J Gastroenterol* 1999; **5**: 397-403
- Wright MC,** Issa R, Smart DE, Trim N, Murray GI, Primrose JN, Arthur MJ, Iredale JP, Mann DA. Gliotoxin stimulates the apoptosis of human and rat hepatic stellate cells and enhance the resolution of liver fibrosis in rats. *Gastroenterology* 2001; **121**: 685-698
- Kato R,** Kamiya S, Ueki M, Yajima H, Ishii T, Nakamura H, Katayama T, Fukai F. The fibronectin-derived antiadhesive peptides suppress the myofibroblastic conversion of rat hepatic stellate cells. *Exp Cell Res* 2001; **265**: 54-63
- Issa R,** Williams E, Trim N, Kendall T, Arthur MJ, Reichen J, Benyon RC, Iredale JP. Apoptosis of hepatic stellate cells: involvement in resolution of biliary fibrosis and regulation by soluble growth factors. *Gut* 2001; **48**: 548-557
- Britton RS,** Bacon BR. Intracellular signaling pathways in stellate cell activation. *Alcohol Clin Exp Res* 1999; **23**: 922-925
- Carloni V,** Pinzani M, Giusti S, Romanelli RG, Parola M, Bellomo G, Failli P, Hamilton AD, Sebt SM, Laffi G, Gentilini P. Tyrosine phosphorylation of focal adhesion kinase by PDGF is dependent on ras in human hepatic stellate cells. *Hepatology* 2000; **31**: 131-140
- Harrington EO,** Smeglin A, Newton J, Ballard G, Rounds

- S. Protein tyrosine phosphatase-dependent proteolysis of focal adhesion complexes in endothelial cell apoptosis. *Am J Physiol Lung Cell Mol Physiol* 2001; **280**: L342-L353
- 23 **Tang YW**, Yao XX. Regulating effect of HCC cells on the activation of stellate cells. *Shijie Huaren Xiaohua Zazhi* 2001; **9**: 202-204
- 24 **Huang GL**, Zhang JS, Zheng YE. Effects of retinoic acid on proliferation, phenotype and expression of cyclin dependent kinase inhibitors in TGFb1 stimulated rat hepatic stellate cells. *World J Gastroenterol* 2000; **6**: 819-823
- 25 **Wang JY**, Zhang QS, Guo JS, Hu MY. Effects of glycyrrhetic acid on collagen metabolism of hepatic stellate cells at different stages of liver fibrosis in rats. *World J Gastroenterol* 2001; **7**: 115-119
- 26 **Davis PK**, Ho A, Dowdy SF. Biological methods for cell-cycle synchronization of mammalian cells. *Biotechniques* 2001; **30**: 1322-1326
- 27 **Iwamoto H**, Sakai H, Tada S, Nakamuta M, Nawata H. Induction of apoptosis in rat hepatic stellate cells by disruption of integrin-mediated cell adhesion. *J Lab Clin Med* 1999; **134**: 83-89
- 28 **Guo YQ**, Zhu ZH, Li JF. Flow cytometric analysis of apoptosis and proliferation in gastric cancer and precancerous lesion. *Shijie Huaren Xiaohua Zazhi* 2000; **8**: 983-987
- 29 **Fischer R**, Schmitt M, Bode JG, Haussinger D. Expression of the peripheral-type benzodiazepine receptor and apoptosis induction in hepatic stellate cells. *Gastroenterology* 2001; **120**: 1212-1226
- 30 **Jiang YF**, Yang ZH, Hu JQ. Recurrence or metastasis of HCC: predictors, early detection and experimental antiangiogenic therapy. *World J Gastroenterol* 2000; **6**: 61-65
- 31 **Rozen S**, Skaletsky H. Primer 3 on the WWW for general users and for biologist programmers. *Methods Mol Biol* 2000; **132**: 365-386
- 32 **Hauck CR**, Sieg DJ, Hsia DA, Loftus JC, Gaarde WA, Monia BP, Schlaepfer DD. Inhibition of focal adhesion kinase expression or activity disrupts epidermal growth factor-stimulated signaling promoting the migration of invasive human carcinoma cells. *Cancer Res* 2001; **61**: 7079-7090
- 33 **Nolan K**, Lacoste J, Parsons JT. Regulated expression of focal adhesion kinase-related nonkinase, the autonomously expressed C-terminal domain of focal adhesion kinase. *Mol Cell Biol* 1999; **19**: 6120-6129
- 34 **Battaller R**, Brenner DA. Hepatic stellate cells as a target for the treatment of liver fibrosis. *Semin Liver Dis* 2001; **21**: 437-451
- 35 **Cheng ML**, Wu YY, Huang KF, Luo TY, Ding YS, Lu YY, Liu RC, Wu J. Clinical study on the treatment of liver fibrosis due to hepatitis B by INF- α_1 and traditional medicine preparation. *World J Gastroenterol* 1999; **5**: 267-269
- 36 **Wang FS**, Wu ZZ. Current situation in studies of gene therapy for liver cirrhosis and liver fibrosis. *Shijie Huaren Xiaohua Zazhi* 2000; **8**: 371-373
- 37 **Yao XX**. Diagnosis and treatment of liver fibrosis. *Shijie Huaren Xiaohua Zazhi* 2000; **8**: 681-689
- 38 **Aoudjit F**, Vuori K. Integrin signaling inhibits paclitaxel-induced apoptosis in breast cancer cells. *Oncogene* 2001; **20**: 4995-5004
- 39 **Van der Flier A**, Sonnenberg A. Function and interactions of integrins. *Cell Tissue Res* 2001; **305**: 285-298
- 40 **Oktay M**, Wary KK, Dans M, Birge RB, Giancotti FG. Integrin-mediated activation of focal adhesion kinase is required for signaling to Jun NH₂-terminal kinase and progression through the G₁ phase of the cell cycle. *J Cell Biol* 1999; **145**: 1461-1469
- 41 **Xu LH**, Yang X, Bradham CA, Brenner DA, Baldwin AS Jr, Craven RJ, Cance WG. The focal adhesion kinase suppresses transformation-associated, anchorage-independent apoptosis in human breast cancer cells. Involvement of death receptor-related signaling pathways. *J Biol Chem* 2000; **275**: 30597-30604
- 42 **Leist M**, Jaattela M. Four deaths and a funeral: from caspases to alternative mechanisms. *Nat Rev Mol Cell Biol* 2001; **2**: 589-598
- 43 **Suzuki A**, Shiraki K. Tumor cell "dead or alive": caspase and survivin regulate cell death, cell cycle and cell survival. *Histol Histopathol* 2001; **16**: 583-593
- 44 **Springer JE**, Nottingham SA, McEwen ML, Azbill RD, Jin Y. Caspase-3 apoptotic signaling following injury to the central nervous systems. *Clin Chem Lab Med* 2001; **39**: 299-307
- 45 **McCrudden R**, Iredale JP. Liver fibrosis, the hepatic stellate cell and tissue inhibitors of metalloproteinases. *Histol Histopathol* 2000; **15**: 1159-1168
- 46 **Knittel T**, Mehde M, Grundmann A, Saile B, Scharf JG, Ramadori G. Expression of matrix metalloproteinases and their inhibitors during hepatic tissue repair in the rat. *Histochem Cell Biol* 2000; **113**: 443-453
- 47 **Arthur MJ**. Fibrogenesis II. Metalloproteinases and their inhibitors in liver fibrosis. *Am J Physiol Gastrointest Liver Physiol* 2000; **279**: G245-G249
- 48 **Nie QH**, Cheng YQ, Xie YM, Zhou YX, Cao YZ. Inhibiting effect of antisense oligonucleotides phosphorothioate on gene expression of TIMP-1 rat liver fibrosis. *World J Gastroenterol* 2001; **7**: 363-369
- 49 **Li G**, Fridman R, Kim HR. Tissue inhibitor of metalloproteinase-1 inhibits apoptosis of human breast epithelial cells. *Cancer Res* 1999; **59**: 6267-6275
- 50 **Sein TT**, Thant AA, Hiraiwa Y, Amin AR, Sohara Y, Liu Y, Matsuda S, Yamamoto T, Hamaguchi M. A role for FAK in the concanavalin A-dependent secretion of matrix metalloproteinases-2 and 9. *Oncogene* 2000; **19**: 5539-5542

Edited by Ma JY

• BASIC RESEARCH •

Effects of the tyrosine protein kinase inhibitor genistein on the proliferation, activation of cultured rat hepatic stellate cells

Xiao-Jing Liu, Li Yang, Yong-Qiu Mao, Qiong Wang, Ming-Hui Huang, Yi-Ping Wang, Hong-Bin Wu

Xiao-Jing Liu, Ming-Hui Huang, Laboratory of Department of Internal Medicine, West China Hospital, Sichuan University, Chengdu 610041, Sichuan Province, China

Li Yang, Qiong Wang, Yi-Ping Wang, Department of Gastroenterology of West China Hospital, Sichuan University, Chengdu 610041, Sichuan Province, China

Yong-Qiu Mao, Center for Cancer Biotherapy of West China Hospital, Sichuan University, Chengdu 610041, Sichuan Province, China

Hong-Bin Wu, Laboratory of Department of Surgery, West China Hospital, Sichuan University, Chengdu 610041, Sichuan Province, China
Supported by the National Natural Science Foundation of China, No.39800054

Correspondence to: Xiao-Jing Liu, Laboratory of Department of Internal Medicine, West China Hospital, Sichuan University, 37 Wainan Guoxueshang, Chengdu 610041, Sichuan Province, China. xiaojingliu67@hotmail.com

Received 2002-01-25 **Accepted** 2002-03-05

Abstract

AIM: Hepatic stellate cell (HSC) plays a pivotal role in liver fibrosis and is considered as the therapeutic target for the treatment of hepatic fibrosis. Tyrosine protein kinase plays an important role in the proliferation, activation of HSC. The purpose of the study is to investigate the effects of the tyrosine protein kinase inhibitor genistein on the proliferation and activation of cultured rat HSC.

METHODS: Rat HSC were isolated from Wistar rats by *in situ* perfusion of collagenase and pronase and single-step density Nycodenz gradient. Culture-activated HSC were serum-starved and incubated with 10^{-9} to 10^{-5} mol/L concentration of genistein for 24, 48 or 72 h. In PDGF-induced HSC proliferation, HSC were stimulated with $10 \text{ mg} \cdot \text{L}^{-1}$ PDGF-BB for 15 min, and then treated with genistein for the same time. Cell proliferation was measured by MTT assay and based on flow cytometric analysis of cell cycle. The α -smooth muscle actin (α -SMA) expression in HSC was studied with confocal laser microscopy and flow cytometry. *c-fos*, *c-jun* and cyclin D₁ expression in HSC was also detected by flow cytometry.

RESULTS: Genistein inhibited basal and PDGF-induced proliferation of HSC at the concentration of 10^{-8} to 10^{-5} mol/L, and treatment with 10^{-7} mol/L concentration of genistein for 48 h inhibited the HSC proliferation significantly (the inhibition rate was 70.3 %, $P < 0.05$). Immunofluorescence detected by confocal laser microscopy and flow cytometry showed that treatment with 10^{-7} mol/L genistein for 48 h suppressed the expression of α -SMA significantly in HSC (the specific fluorescence intensity were 60.2 ± 21.5 vs 35.3 ± 11.6 and 12.8 ± 10.4 vs 9.54 ± 6.39 , respectively, both $P < 0.05$). The intensity of *c-fos*, *c-jun* and cyclin D₁ expression of HSCs treated with 10^{-7} mol/L genistein for 48 h was also significantly decreased compared with the controls.

CONCLUSION: Genistein influences proliferation of HSC, suppresses the expression of α -SMA in HSC and

inhibits the intensity of *c-fos*, *c-jun* and cyclin D₁ expression of HSCs. Genistein has therapeutic potential against liver fibrosis.

Liu XJ, Yang L, Mao YQ, Wang Q, Huang MH, Wang YP, Wu HB. Effects of the tyrosine protein kinase inhibitor genistein on the proliferation, activation of cultured rat hepatic stellate cells. *World J Gastroenterol* 2002; 8(4):739-745

INTRODUCTION

Hepatic stellate cells (HSC) are liver mesenchymal cells located in the space of Disse, in close contact with hepatocytes and sinusoidal endothelial cells. In normal liver tissue, they are responsible for vitamin A storage and metabolism. During liver fibrogenesis, HSC undergo a process of activation by acquiring a myofibroblast-like phenotype characterized by increased proliferation and extracellular matrix component synthesis^[1-3]. It is known that several cytokine can stimulate HSC proliferation (such as PDGF^[4], EGF and bFGF) and collagen synthesis (TGF- β_1) in activated HSCs^[5-7]. In addition, the activated cells express substantial amounts of α -smooth muscle actin (α -SMA) and show strong contracting activity. Taken together, HSC have been postulated to play critical roles in the development of fibrosis of the liver that was injured by viral infection, alcohol and various drugs^[8-11]. Therefore, it is important to find out some agents that block HSC activation, a prerequisite to liver fibrosis.

During culture of HSC in a medium supplemented with serum, they spontaneously undergo activation. This culture-induced activation has been extensively studied as a model of the activation secondary to liver fibrogenesis. This *in vitro* model is useful to understand the molecular mechanism underlying the activation and/or inactivation of HSC in injured liver. In this context, interferons^[12], nitrovasodilators^[13], relaxin^[14] and pentoxifylling^[15] have been shown to inhibit the activation of cultured HSC. Molecular mechanism for the activation of HSC was found to involve intracellular signal cascades and transcriptional regulation of certain genes^[16-19].

Recently, tyrosine protein kinase (TPK) signaling pathways were reported to play an important role in the activation of HSC^[20]. TPK are involved in signal transduction pathways that control cell proliferation and differentiation and they may be classified into two general groups: (a) membrane receptor tyrosine protein kinases, including EGF-, PDGF-, CFS-, IGF- and insulin receptor^[21], and (b) non-receptor linked and cytosolic tyrosine protein kinase^[22]. Receptor tyrosine kinase that mediate HSC proliferation include the PDGF receptors^[4, 23].

Among many polypeptide growth factors potentially involved in chronic liver inflammation, PDGF, a dimer of two chain referred to as A-chain and B-chain, has been shown to the most potent mitogen for cultured HSC isolated from rat, mouse or human liver^[24]. Of the three possible dimeric forms of PDGF (AA, AB and BB), PDGF-BB had been shown to be the most potent in stimulating HSC growth and relative

intracellular signaling, in agreement with a predominant expression of PDGF-R β (or type B) subunits as compared with the expression of PDGF-R α (or type A) subunits in activated HSC. Importantly, co-distribution of PDGF with cells expressing the relative receptor subunits (α and β) has been clearly shown after chronic liver tissue damage^[23], thus, confirming a functional role of this polypeptide mitogen in the development of hepatic fibrosis.

PDGF receptors are tyrosine protein kinases that are activated by dimerization and autophosphorylation after ligand stimulation. The phosphorylated tyrosine can then associate with intracellular signaling molecules including phospholipase C γ (PLC γ), phosphatidylinositol 3'-kinase (PI-3K), Src, Grb2-Sos, and Ras-GTPase activating protein. In particular, the attention was focused on PDGF-induced activation of three major pathways recently shown to be highly relevant for transducing the mitogenic effect of this polypeptide mitogen, namely PI-3K, extracellular signal regulated kinase (ERK) and changed in intracellular calcium concentration ($[Ca^{2+}]_i$)^[25, 26].

In the past decade many efforts were made to develop drugs that inhibit the tyrosine kinase receptors and their intracellular signal transduction pathway^[26]. Inhibition of PDGF-R receptor tyrosine kinase activity has been reported for tyrphostin classes of compounds^[27]. Tyrphostins are small molecules designed to inhibit tyrosine kinases either through competition for substrates or through adenosine triphosphate binding. Iwamoto *et al*^[28] had shown that Tyrphostin AG1295 reduced the proliferation response of HSC, and their findings suggested a new strategy for the prevention of liver fibrosis with inhibitors of tyrosine kinase receptors. However, whether TPK inhibitors other than tyrphostin also have such effects on HSC is not known. Furthermore, the molecular mechanism by which TPK inhibitors suppress the activation of HSC also remains uncovered.

Genistein (4,5,7-trihydroxyisoflavone), a soybean-derived isoflavone, is a TPK inhibitor that attenuates growth factor- and cytokine-stimulated proliferation of both normal and cancer cells. Extensive epidemiological, *in vitro*, and animal studies have been performed, and most studies indicated that genistein has beneficial effects on a multitude of human disorders, including cancers, cardiovascular diseases, osteoporosis, and postmenopausal symptoms^[29-31]. Although genistein has been shown to dose-dependently inhibit natural and PDGF-BB-induced proliferation and DNA synthesis of aortic smooth muscle cells from stroke-prone spontaneously hypertensive rats^[32], it is unknown whether genistein could inhibit the proliferation of activated HSC. The aim of the present study was to investigate the effects of genistein on basal and PDGF-induced HSC proliferation and activation of HSC.

MATERIALS AND METHODS

Materials

Male Wister rats were obtained from Experimental Animal Center of West China Medical Center of Sichuan University (West China University of Medical Sciences, Chengdu, Sichuan). Genistein and Nycodenz were obtained from Sigma (ST. Louis, USA). Dulbecco's modified medium (DMEM), trypsin-EDTA and new-born calf serum (CS) were from GibcoBRL (Maryland, USA). Pronase, Collagenase B and DNAase I were from Roche Molecular Biochemicals, (Mannheim, Germany). Monoclonal Antibodies to Desmin, μ -smooth muscle actin (α -SMA) were obtained from Dako (Glostrup, Denmark). Monoclonal antibody to phosphotyrosine containing protein (p-Tyr), polyclonal antibodies to cyclinD₁,

c-fos and *c-jun* were purchased from Santa Cruz Biotechnology (Santa Cruz, USA).

Methods

HSC isolation and culture HSC were isolated from male Wister rats by *in situ* pronase, collagenase perfusion and single-step Nycodenz gradient according to our previous report^[33]. The cells were seeded at a density of $1.5 \times 10^5/\text{cm}^2$ on glass coverslips in 6-well culture plate or 100-mm dishes (Falcon) and maintained in DMEM containing $20 \text{ mL} \cdot \text{L}^{-1}$ heat-inactivated new-born calf serum (CS). The purity of HSC preparations was assessed by intrinsic vitamin A autofluorescence and immunocytochemistry with antibody against desmin. The viability of the cells was evaluated by the Trypan blue dye exclusion test. The purity and viability of the primary cells exceeded 90 % and 95 %, respectively. Therefore, HSC were cultured on uncoated plastic dishes where they spontaneously acquired an activated phenotype, characterized by expression of α -SMA and by loss of vitamin A droplets^[34, 35]. After reaching confluency (about 10-14 days after plating), activated HSC were detached by incubation with trypsin, and split in a 1:2 ratio. Experiments were performed on cells between the second and 5th passages using 3 independent cell lines, and the purity of activated HSC exceeded 98 %.

Cell viability and proliferation assay The HSC were plated at densities of $2 \times 10^4/\text{ml}$ in 24-well plates and incubated for various time periods and various concentrations with genistein. The viability of cells was analyzed by light microscope, Trypan blue staining^[35]. The proliferation of HSC was assessed with 3-(4,5-dimethylthiazol-2-yl)-2,5-diphenyltetrazolium (MTT), as described^[36], using cell cultured in 96-well plates. The HSC were plated at a density of 2000 cells/well in 96-well tissue culture dishes and allowed to grow for 24 hrs in DMEM containing $20 \text{ mL} \cdot \text{L}^{-1}$ CS under standard tissue culture conditions. After three cell washes with phosphate-buffered saline (PBS), the growth of HSCs was arrested by adding DMEM medium without serum for 24 h. First, HSC were incubated with a concentration of 0 (control) or 10^{-9} to 10^{-5} mol/L genistein in fresh DMEM medium without serum and allowed to grow for 24, 48 or 72 h. Second, in PDGF-BB ($10 \mu\text{g} \cdot \text{L}^{-1}$), proliferation of HSC was induced for 15 min and cells were incubated with a concentration of 0 (control) or 10^{-9} to 10^{-5} mol/L genistein for 24, 48 or 72 h. Four replicates were used for each experimental point. Absorbance values for cell-free wells were subtracted from all values.

Cell cycle analyze by flow cytometry After 24 h of serum deprivation, HSC were stimulated with or without $10 \mu\text{g} \cdot \text{L}^{-1}$ PDGF-BB for 15 min and treated with genistein. At the indicated time, HSC were harvested by trypsin-EDTA, washed twice with PBS, and fixed in $700 \text{ mL} \cdot \text{L}^{-1}$ ethanol overnight at 4°C . After washing once with PBS, fixed cells were stained with propidium iodide ($50 \text{ mg} \cdot \text{L}^{-1}$) in the presence of RNase A ($100 \text{ mg} \cdot \text{L}^{-1}$), and the cell cycle distribution was analyzed using the FACScan (Coulter, EPICS ELITE ESP model), with a cell cycle analysis program.

Immunofluorescence and confocal laser microscopy Rat HSC were cultured on glass cover slips in DMEM medium containing $20 \text{ mL} \cdot \text{L}^{-1}$ CS for 24 h, left in serum-free DMEM medium for an additional 24 h, and then incubated with genistein (10^{-9} - 10^{-5} mol/L) for 24, 48 or 72 h. In PDGF treatment, genistein was added after incubated with PDGF-BB ($10 \mu\text{g} \cdot \text{L}^{-1}$) for 15 min. The cells were fixed with $4 \text{ mg} \cdot \text{L}^{-1}$ buffered paraformaldehyde with a pH of 7.4 for 20 min and then permeabilized for 10 min with PBS containing $0.1 \text{ mg} \cdot \text{L}^{-1}$ Triton X-100. The cells were then stained for indirect

immunofluorescence using either a monoclonal antibody against α -SMA diluted 1:100 in PBS or a monoclonal antibody against phospho-tyrosine containing protein diluted 1:50 in PBS as primary antibodies. A goat anti-mouse fluorescein isothiocyanate (FITC)-conjugated affinity-purified antibody was used as secondary antibodies at 1:200 dilution in PBS. Cells were analyzed with a laser scanner confocal microscope Bio-Rad MRC 1024ES equipped with a Nikon (Tokyo, Japan) Diaphot inverted microscope.

Immunofluorescent detection of α -SMA, cyclinD₁, *c-fos* and *c-jun* by flow cytometry Rat HSC were cultured in plastic 100 mm dishes (Nunc) in DMEM medium containing 20 mL \cdot L⁻¹ CS for 24 h, left in serum-free DMEM medium for an additional 24 h, and then incubated with Genistein (10^{-9} - 10^{-5} mol/L) for 24, 48 or 72 h. After treatment, the cells were detached by trypsin and fixed with 4 mg \cdot L⁻¹ buffered paraformaldehyde with a pH of 7.4 for 20 min and then permeabilized for 10 min with PBS containing 0.1 mg \cdot L⁻¹ Triton X-100. The cells were then stained for indirect immunofluorescence using either a monoclonal antibody against α -SMA diluted 1:50 in PBS or a polyclonal antibody against cyclin D₁, *c-fos* and *c-jun* diluted 1:50 in PBS as primary antibodies. A goat anti-mouse fluorescein isothiocyanate (FITC)-conjugated affinity-purified antibody and a goat anti-rabbit FITC-conjugated antibody were used as secondary antibodies at 1:200 dilution in PBS. Cells were analyzed on a FACScan (Coulter, EPICS ELITE ESP model) to determine the expression of α -SMA, cyclin D₁, *c-fos* and *c-jun*.

Statistical analysis

Results of cell cycle analyze were expressed as percentage of total examined cells and statistical analysis was performed by χ^2 test. Other results were expressed as $\bar{x} \pm s$. Differences between means were analyzed with student *t* test for paired samples. A value of $P < 0.05$ was considered statistically significant.

RESULTS

Effects of genistein on the viability of HSC

In order to determine toxic effects of genistein on rat HSC, they were treated for 3 days with concentration from 10^{-9} to 10^{-5} mol/L of genistein and analyzed by light microscope and trypan blue staining. Genistein concentration of 1×10^{-5} mol/L or lower concentrations had no detectable effects on the cellular morphology or Trypan blue staining.

Effects of Genistein on the proliferation of HSC

First, we observed effects of genistein on the proliferation of cultured HSC. As shown in Figure 1, genistein inhibited proliferation of HSC at the concentration of 10^{-8} to 10^{-5} mol/L, and treatment with 10^{-7} mol/L concentration of genistein for 48 h inhibited the HSC proliferation significantly (the inhibition rate was 70.3 %, and the absorbance value was 0.042 ± 0.014 vs 0.151 ± 0.055 , $t = 3.51$, $P < 0.05$).

Second, in PDGF-BB-induced proliferation of HSC, the effective concentration for significant inhibition was 10^{-7} mol/L as shown in Figure 1.

Similar results were obtained with the cell cycle analyze in HSC. As shown in Figure 2, A and B, the percentages of S phase in HSCs of control or PDGF-BB stimulated groups were 24 % and 40.1 % respectively. In contrast, genistein treatment led to a significant inhibition of new DNA synthesis, and the percentages of S phase in HSCs of 10^{-7} mol/L concentration of genistein treated for 48 h were 16.3 % and 19.9 % respectively (Figure 2, C and D). (24% vs 16.3% , $\chi^2 = 53.01$, $P < 0.01$; 40.1% vs 19.9% , $\chi^2 = 240.1$, $P < 0.01$).

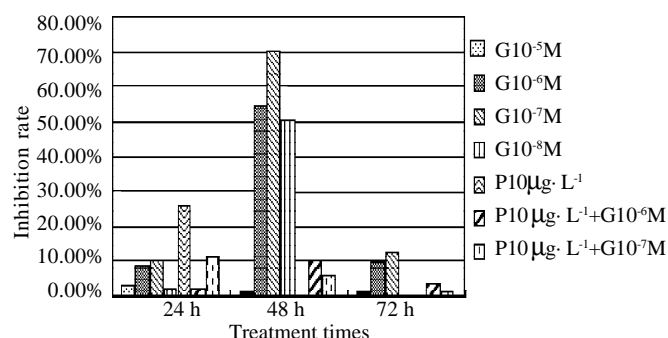


Figure 1 Genistein inhibited the basal and PDGF-BB induced proliferation of HSCs. Cell proliferation was measured by MTT incorporation

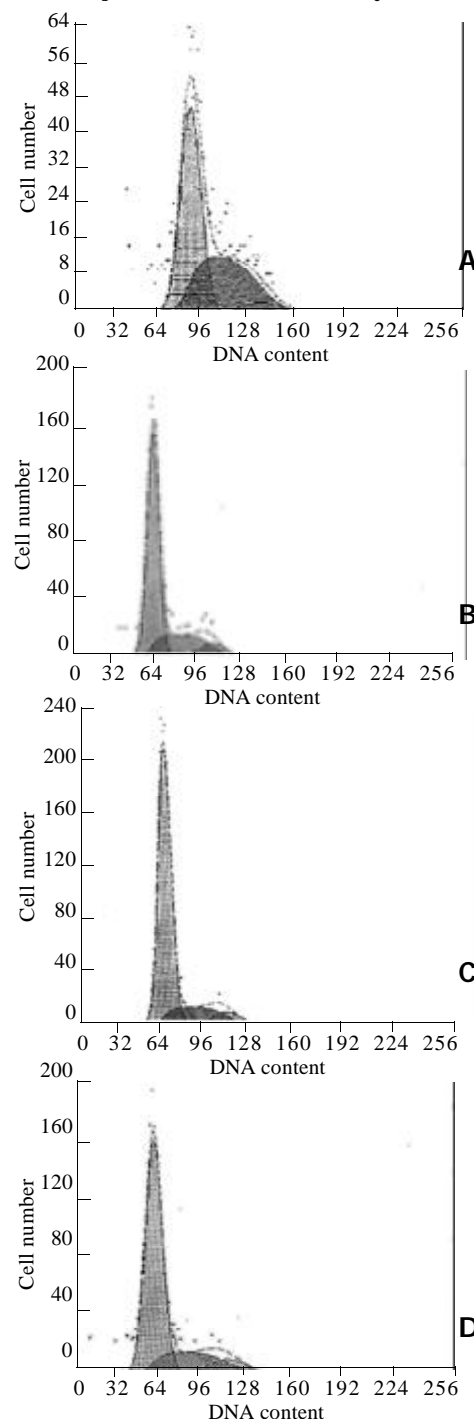


Figure 2 Flow cytometric analysis of cell cycle of HSC. (A) Control HSC; (B) HSCs stimulated with 10 μ g \cdot L⁻¹ PDGF-BB for 15 min; (C) HSC treated with 10⁻⁷ mol/L genistein for 48 h; (D) HSC stimulated with 10 μ g \cdot L⁻¹ PDGF-BB for 15 min and then incubated with 10⁻⁷ mol/L genistein for 48 h.

Effects of genistein of the expression of α -SMA in HSC

Smooth muscle α -actin has been accepted for use as one of the indicator of activated HSCs. Immunofluorescence detecting by confocal laser microscopy showed that treatment with 10^{-7} mol/L genistein for 48 h suppressed the expression of α -SMA significantly (the specific fluorescence intensity was 60.2 ± 21.5 vs 35.3 ± 11.6 , $t=12.45$, $P<0.01$, Figure3). And this observation was also confirmed by detecting the immunofluorescence expression of α -SMA in HSC by flow cytometry, as shown in Figure 4 and Table 1.

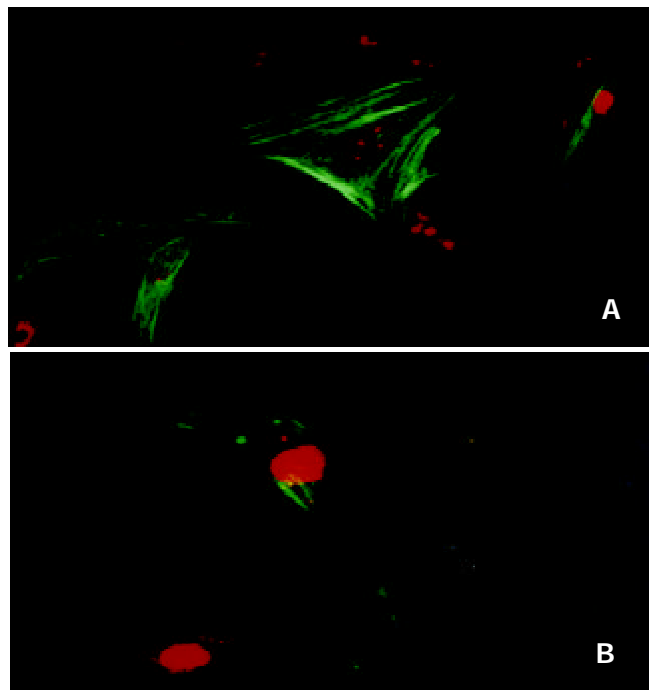


Figure 3 Immunofluorescence detection of α -SMA in HSC by confocal laser microscopy ($\times 600$). (A) Strong staining was observed in control HSC; (B) only a few cells were stained when HSC treated with 10^{-7} mol/L genistein for 48 h

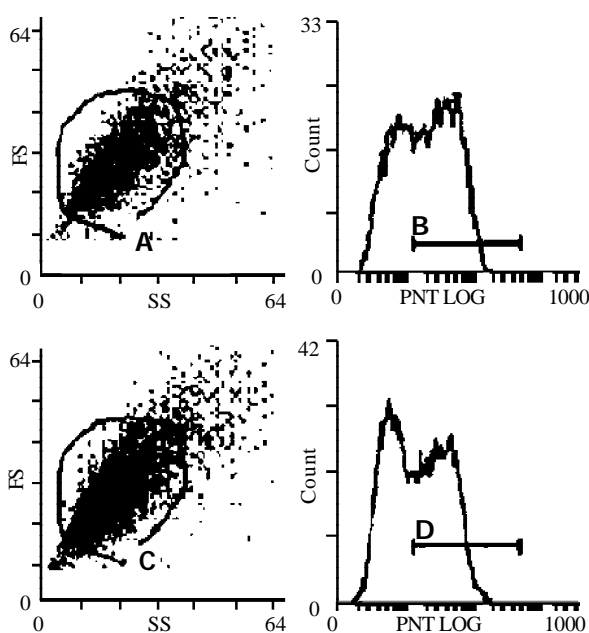


Figure 4 Flow cytometric analysis of α -SMA in HSC. (A,B) control HSC (C,D) HSC treated with 10^{-7} mol/L genistein for 48 h. showed significant decreased fluorescence intensity ($P<0.05$).

Effects of genistein on tyrosine phosphorylation in HSCs

Immunofluorescence detecting by confocal laser microscopy showed that PDGF-BB stimulated the tyrosine phosphorylation significantly after $10 \mu\text{g} \cdot \text{L}^{-1}$ PDGF-BB incubated with HSC for 15 min (the specific fluorescence intensity was 27.1 ± 18.8 vs 66.5 ± 36.3 , $t=14.65$, $P<0.05$); but treatment with 10^{-7} mol/L genistein for 48 h suppressed the expression of tyrosine phosphorylation significantly (the specific fluorescence intensity was 66.5 ± 36.3 vs 46.6 ± 16.4 , $t=7.39$, $P<0.05$, Figure5).

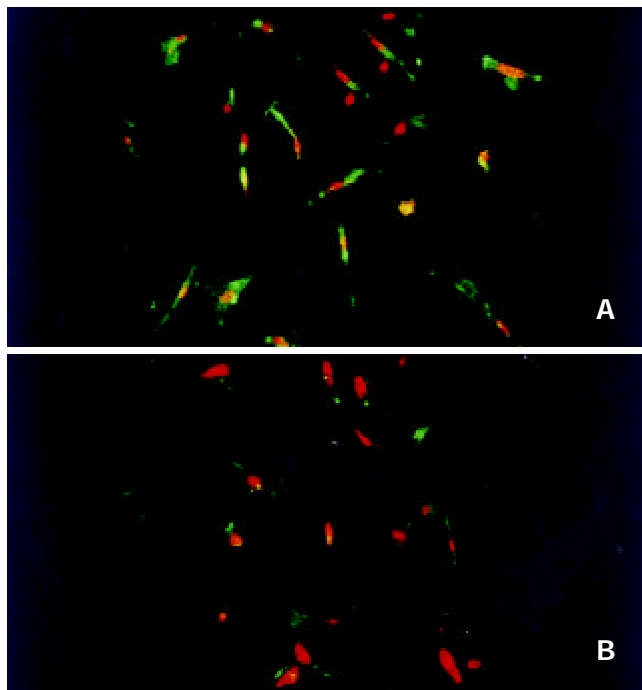


Figure 5 Immunofluorescence detection of the expression of tyrosine phosphorylation in HSC by confocal laser microscopy ($\times 200$). (A) HSC stimulated with $10 \mu\text{g} \cdot \text{L}^{-1}$ PDGF-BB for 15 min showed a strong staining for phosphotyrosine containing protein; (B) HSCs stimulated with $10 \mu\text{g} \cdot \text{L}^{-1}$ PDGF-BB for 15 min and then incubated with 10^{-7} mol/L genistein for 48 h showed significant decreased fluorescence intensity for phosphotyrosine containing protein.

Table 1 Flow cytometric analysis of α -SMA, *c-fos*, *c-jun* and cyclin D₁ expression in HSCs (the specific fluorescence intensity)

Groups	HSC control for 24hrs	10^{-7} mol/Lgenistein treated for 24 hrs	t test	HSC control for 48 hrs	10^{-7} mol/Lgenistein treated for 48 hrs	t test
α -SMA Detected	6.15 ± 4.03	5.01 ± 3.30	$t=15.39$	12.8 ± 10.4	9.54 ± 6.39	$t=15.03$
cell numbers (n)	4857	5086	$P<0.05$	2940	3985	$P<0.05$
<i>c-fos</i> Detected	19.4 ± 7.55	16.3 ± 5.74	$t=20.64$	14.7 ± 5.68	12.1 ± 4.18	$t=18.68$
cell numbers (n)	3122	7649	$P<0.05$	2412	2917	$P<0.05$
<i>c-jun</i> Detected	17.22 ± 5.49	15.69 ± 4.77	$t=13.32$	7.99 ± 4.11	6.74 ± 2.05	$t=3.20$
cell numbers (n)	3454	5100	$P<0.05$	6589	4194	$P<0.05$
cyclinD ₁ Detected	25.6 ± 11.1	24.0 ± 9.98	$t=10.23$	5.76 ± 2.05	3.00 ± 1.05	$t=66.32$
cell numbers (n)	8604	9569	$P<0.05$	5615	5584	$P<0.05$

Effects of genistein on expression of *c-fos*, *c-jun* and cyclin D₁

The expression of *c-fos*, *c-jun* and cyclin D₁ were remarkably lower in HSCs that incubated with 10^{-7} mol/L genistein for 48 hrs than in the controls, as shown in Table 1 and Figure 6.

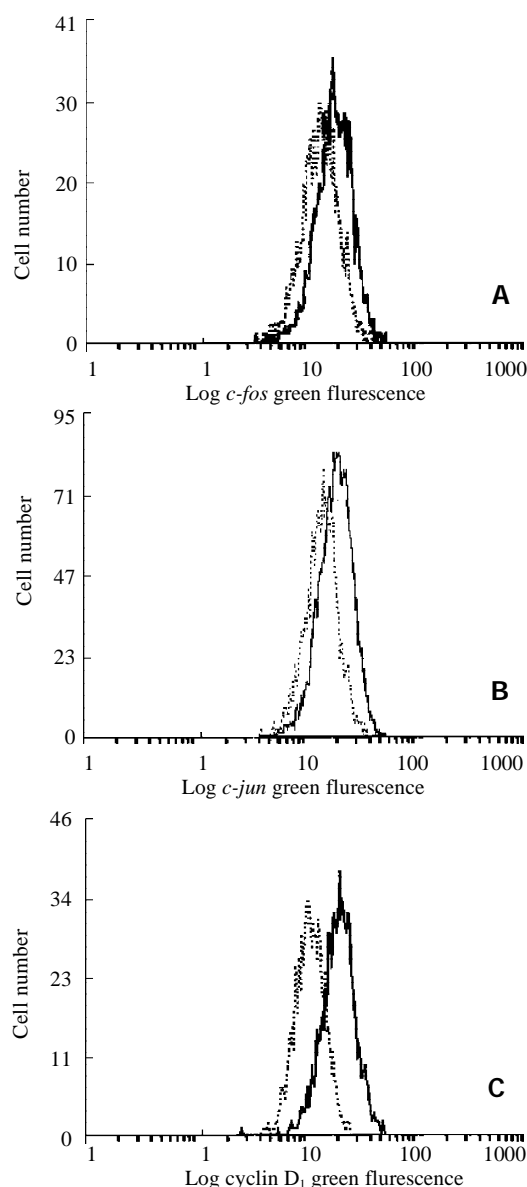


Figure 6 Flow cytometric analysis of *c-fos* (A), *c-jun* (B) and cyclin D₁ (C) expression in HSC. - indicated the control HSC and - indicated HSC treated with 10^{-7} mol/L genistein for 48h.

DISCUSSION

Genistein—a soy derived isoflavone has recently attracted much attention of the medical scientific community. This compound was found to be a potent agent in both prophylaxis and treatment of cancer as well as other chronic diseases. In addition to its proposed actions on prevention cancer, genistein has recently been shown to have antitumor, anti-oxidant and anti-inflammatory effects^[29, 30]. The great interest that has focused on genistein led to the identification of numerous intracellular targets of its action in the live cells. It was reported^[37] that six flavonoids (fisetin, quercetin, apigenin, phloretin, hesperatin and chalcone) inhibited the proliferation of HSCs, but the underlying mechanisms responsible for their effects are not yet completely understood. And little is known about the effects of genistein on the HSCs, the cell type primarily involved in hepatic fibrogenesis. Therefore we used an *in vitro* model in which the activation and proliferation of HSCs were induced by growth on plastic dishes to study the effects of genistein on HSCs and its possible mechanisms.

This culture-induced activation process showed, as far as known, all features of the *in vivo* process. The present report describes that genistein influences several aspects of the HSC activation. It diminishes proliferation, decreases the expression of α -SMA, *c-fos*, *c-jun* and cyclin D₁ and these effects of genistein are not due to a toxic cell damage.

In this study, we observed the effect of genistein on the proliferation of activated HSCs. We found that 10^{-8} to 10^{-5} mol/L concentration of genistein not only inhibited the basal proliferation of activated HSC, but also inhibited the proliferation of HSCs induced by PDGF-BB. Inhibition of proliferation of HSCs by genistein is not surprising, because reduced cell growth by genistein has been extensively reported. The activated HSCs express receptors for various growth factors, such as PDGF^[23,38], IGF^[39], and bFGF^[40], which are receptor tyrosine protein kinases (RTKs) that have been implicated in HSCs proliferation. One mechanism how genistein might influence the proliferation of HSCs might be the down-regulation of the RTKs in the membrane of HSCs.

In mammalian cells, the Ras/ERK pathway directs signals to the immediate-early genes, such as *c-fos*, *c-jun* and other co-regulated genes. *c-fos* has been reported to function by forming homodimer alone or heterodimer with *c-jun*, which forms the dimeric transcription factor complex activator protein-1 (AP-1)^[41, 42]. Recently, it has been demonstrated that the mitogen activated protein kinase (MAPK) family, including *c-jun* NH₂-terminal kinase (JNK) and ERK, plays an important role in the HSC cellular response to stress^[43]. Acetaldehyde, the major active metabolite of alcohol, is known to stimulate α I (I) collagen production in HSC in a JNK-dependent pathway^[44]. *C-fos* and *c-jun*, two important terminals of various signal transduction pathways and important nuclear factors involved in regulating cytokine gene expression, have been reported to express in activated human HSCs^[45]. Recent evidence showed that genistein significantly attenuated the hydrogen peroxide-induced proliferation in aortic smooth muscle cells and *c-jun* gene expression^[46], and the inhibition of *c-fos* expression, AP-1 transactivation and ERK phosphorylation may contribute to the growth-inhibitory effect of genistein in some breast cell types^[47]. The results of our experiments showing an inhibition of *c-fos* and *c-jun* expression by genistein further support an effect of this drug on the activated Ras/ERK pathway, including downstream nuclear events leading to HSC cell proliferation.

Another interesting finding is that genistein reduced the protein level of cyclin D₁, a cell cycle related protein. Proliferation of eukaryotic cells is generally controlled at stages from G₁ to S transition phases. G₁ cyclins include three forms of cyclin D (D₁, D₂ and D₃) and cyclin E that associate with either cdk2, cdk4 or cdk6, and cyclin D₁, D₂, and D₃ are markers for G₁ phase^[48]. It was reported that administration of genistein to rats with a acute renal injury decreased the activation of ERK, and the induction of cyclin D₁ was also prevented by this treatment^[49]. The present study showed that genistein decreased the cellular level of cyclin D₁, and this notion was consistent with the results obtained by cell cycle analyze and MTT assay.

Genistein examined in the present study also inhibited the expression of α -SMA in HSCs. Expression of α -SMA is reported to be regulated by the discoidin domain receptor 2 (DDR2), a tyrosine kinase receptor expressed in mesenchymal tissue whose ligand is fibrillar collagen^[50]. In general, HSC undergoing proliferation concomitantly express α -SMA^[1-3]. Inhibitors for HSC activation, such as candesartan and perindopril^[51], the semisynthetic analogue of fumagillin TNP-

470^[52], interferon^[12] and a selective ROCK inhibitor, Y27632^[53], block both cellular proliferation and expression of α -SMA. Therefore, proliferation and expression of α -SMA in HSC seem to be triggered by the same signal transduction pathway, although so far a detailed analysis has been lacking. Perhaps, growth-stimulatory signals involve the activation of positive transcription factors in the 5' -flanking region of α -SMA gene. However, the molecular mechanism by which genistein inhibits the expression of α -SMA in HSC should be further studied.

In summary, the present report showed that genistein regulated the proliferation and the expression of α -SMA, *c-fos*, *c-jun* and the cell cycle protein D₁, thereby modulating functions of HSC. This effect appears partially mediated by a reduction of PDGF-stimulated ERK activity as well as of other intracellular pathways. The mechanisms of action of genistein include its role as weak estrogens, inhibitor of TPK-dependent signal transduction processes and as cellular antioxidants^[30, 54]. Findings^[55, 56] suggest that estradiol is a potent inhibitor of HSC activation and transformation, and it suppressed the induction of hepatic fibrosis. So the effects of genistein to HSCs may also include its weak estrogens role. Because HSCs play pathological roles in inflammation and fibrosis of the liver, therapeutic potential of genistein to hepatic fibrosis should be studied further.

REFERENCES

- Eng FJ, Friedman SL. Fibrogenesis I. New insight into hepatic stellate cell activation: the simple becomes complex. *Am J Physiol* 2000; **279**: G7-G11
- Friedman SL. Molecular regulation of hepatic fibrosis, an integrated cellular response to tissue injury. *J Biol Chem* 2000; **275**: 2247-2250
- Albanis E, Friedman SL. Hepatic fibrosis. Pathogenesis and principles of therapy. *Clin Liver Dis* 2001; **5**: 315-334
- Kinnman N, Gorla O, Wendum D, Gendron MC, Rey C, Poupon R, Housset C. Hepatic stellate cell proliferation is an early platelet-derived growth factor-mediated cellular event in rat cholestatic liver injury. *Lab Invest* 2001; **81**: 1709-1716
- Xiang DD, Wei YL, Li QF. Molecular mechanism of transforming growth factor β_1 on Ito cell. *Shijie Huaren Xiaohua Zazhi* 1999; **7**: 980-981
- Liu F, Liu JX. Role of transforming growth factor β_1 in hepatic fibrosis. *Shijie Huaren Xiaohua Zazhi* 2000; **8**: 86-88
- Liu F, Wang XM, Liu JX, Wei MX. Relationship between serum TGF- β_1 of chronic hepatitis B and hepatic tissue pathology and hepatic fibrosis quantity. *Shijie Huaren Xiaohua Zazhi* 2000; **8**: 528-531
- Battaller R, Brenner DA. Hepatic stellate cells as a target for the treatment of liver fibrosis. *Semin Liver Dis* 2001; **21**: 437-451
- Wang FS, Wu ZZ. Current situation in studies of gene therapy for liver cirrhosis and liver fibrosis. *Shijie Huaren Xiaohua Zazhi* 2000; **8**: 371-373
- Dai WJ, Jiang HC. Advances in gene therapy of liver cirrhosis, a review. *World J Gastroenterol* 2001; **7**: 1-8
- Yao XX. Diagnosis and treatment of liver fibrosis. *Shijie Huaren Xiaohua Zazhi* 2000; **8**: 681-689
- Cheng ML, Wu YY, Huang KF, Luo TY, Ding YS, Lu YY, Liu RC, Wu J. Clinical study on the treatment of liver fibrosis due to hepatitis B by IFN- α and traditional medicine preparation. *World J Gastroenterol* 1998; **4**: 329-331
- Failli P, DeFRANCO RM, Caligiuri A, Gentilini A, Romanelli RG, Marra F, Batignani G, Guerra CT, Laffi G, Gentilini P, Pinzani M. Nitrovasodilators inhibit platelet-derived growth factor-induced proliferation and migration of activated human stellate cells. *Gastroenterology* 2000; **119**: 479-492
- Williams EJ, Benyon RC, Trim N, Hadwin R, Grove BH, Arthur MJ, Unemori EN, Iredale JP. Relaxin inhibits effective collagen deposition by cultured hepatic stellate cells and decreases rat liver fibrosis *in vivo*. *Gut* 2001; **49**: 577-583
- Wu YA, Kong XT. Anti-hepatic fibrosis effect of pentoxifylling. *Shijie Huaren Xiaohua Zazhi* 1999; **7**: 265-266
- Huang GC, Zhang JS. Intercellular signal transduction of activated hepatic stellate cells. *Shijie Huaren Xiaohua Zazhi* 2001; **9**: 1056-1060
- Svegliati-Baroni G, Didolfi F, Di Sario A, Saccomammo S, Bendia E, Benedetti A, Greenwel P. Intracellular signaling pathways involved in acetaldehyde-induced collagen and fibronectin gene expression in human hepatic stellate cells. *Hepatology* 2001; **33**: 1130-1140
- Lang A, Brenner DA. Gene regulation in hepatic stellate cell. *Ital J Gastroenterol Hepatol* 1999; **31**: 173-179
- Pinzani M, Marra F. Cytokine receptors and signaling in hepatic stellate cells. *Semin Liver Dis* 2001; **21**: 397-416
- Carlioni V, Pinzani M, Giusti S, Romanelli RG, Parola M, Bellomo G, Failli P, Hamilton AD, Sebt SM, Laffi G, Gentilini P. Tyrosine phosphorylation of focal adhesion kinase by PDGF is dependent in ras in human stellate cells. *Hepatology* 2000; **31**: 131-140
- Lamorte L, Park M. The receptor tyrosine kinases: role in cancer progression. *Surg Oncol Clin N Am* 2001; **10**: 271-288
- Martin GS. The hunting of the Src. *Nat Rev Mol Cell Biol* 2001; **2**: 467-475
- Robino G, Parola M, Marra F, Caligiuri A, De Franco RM, Zamara E, Bellomo G, Gentilini P, Pinzani M, Dianzani MU. Interaction between 4-hydroxy-2, 3-alkenals and the platelet-derived growth factor-beta receptor. Reduced tyrosine phosphorylation and downstream signaling in hepatic stellate cells. *J Biol Chem* 2000; **275**: 40561-40567
- Kinnman N, Hultcrantz R, Barbu V, Rey C, Wendum D, Roupon R, Housset C. PDGF-mediated chemoattraction of hepatic stellate cells by bile duct segments in cholestatic liver injury. *Lab Invest* 2000; **80**: 697-707
- Betsholtz C, Karlsson L, Lindahl P. Developmental roles of platelet-derived growth factors. *Bioessays* 2001; **23**: 494-507
- Ostman A, Heldin CH. Involvement of platelet-derived growth factor in disease: development of specific antagonists. *Adv Cancer Res* 2001; **80**: 1-38
- Morin MJ. From oncogene to drug: development of small molecule tyrosine kinase inhibitors as anti-tumor and anti-angiogenic agents. *Oncogene* 2000; **19**: 6574-6583
- Iwamoto H, Nakamuta M, Tada S, Sugimoto R, Enjoji M, Nawata H. Platelet-derived growth factor receptor tyrosine kinase inhibitor AG1295 attenuates rat hepatic stellate cell growth. *J Lab Clin Med* 2000; **135**: 406-412
- Goldwyn S, Lazinsky A, Wei H. Promotion of health by soy isoflavones: efficacy, benefit and safety concerns. *Grug Metabol Drug Interact* 2000; **17**: 261-289
- Polkowski K, Mazurek AP. Biological properties of genistein. A review of in vitro and in vivo data. *Acta Pol Pharm* 2000; **57**: 135-155
- Wang HK. The therapeutic potential of flavonoids. *Expert Opin Investig Drugs* 2000; **9**: 2103-2119
- Pan W, Ikeda K, Takebe M, Yamori Y. Genistein, daidzein and glycitein inhibit growth and DNA synthesis of aortic smooth muscle cells from stroke-prone spontaneously hypertensive rats. *J Nutri* 2001; **131**: 1154-1158
- Liu XJ, Yang L, Wu HB, Qiang O, Huang MH, Wang YP. Apoptosis induction of rat hepatic stellate cells by anti-focal adhesion kinase antibody. *World J Gastroenterol* 2002; **8**: (Accepted)
- Huang GL, Zhang JS, Zheng YE. Effects of retinoic acid on proliferation, phenotype and expression of cyclin dependent kinase inhibitors in TGF β 1 stimulated rat hepatic stellate cells. *World J Gastroenterol* 2000; **6**: 819-823
- Wang JY, Zhang QS, Guo JS, Hu MY. Effects of glycyrrhetic acid on collagen metabolism of hepatic stellate cells at different stages of liver fibrosis in rats. *World J*

- Gastroenterol* 2001; **7**: 115-119
- 36 **Faouzi S**, Lepreux S, Bedin C, Dubuisson L, Balabaud C, Bioulac-Sage P, Desmouliere A, Rosenbaum J. Activation of cultured rat hepatic stellate cells by tumoral hepatocytes. *Lab Invest* 1999; **79**: 485-493
 - 37 **Zhang M**, Zhang JP, Ji HT, Wang JS, Qian DH. Effect of six flavonoids on proliferation of hepatic stellate cells *in vitro*. *Acta Pharmacol Sin* 2000; **21**: 253-256
 - 38 **Di-Sario A**, Svegliati Baroni G, Bendia E, Ridolfi F, Saccomanno S, Ugili L, Trozzi L, Marzoni M, Jezequel AM, Macarri G, Benedetti A. Intracellular pH regulation and Na⁺/H⁺ exchange activity in human stellate cells: effect of platelet-derived growth factor, insulin-like growth factor 1 and insulin. *J Hepatol* 2001; **34**: 378-385
 - 39 **Svegliati-Baroni G**, Ridolfi F, Di Sario A, Casini A, Marucci L, Gaggiotti G, Orlandoni P, Macarri G, Perego L, Benedetti A, Folli F. Insulin and insulin-like growth factor-1 stimulate proliferation and type I collagen accumulation by human hepatic stellate cells: differential effects on signal transduction pathways. *Hepatology* 1999; **29**: 1743-1751
 - 40 **Fibbi G**, Pucci M, Grappone C, Pellegrini G, Salzano R, Casini A, Milani S, Del Rosso M. Functions of the fibrinolytic system in human Ito cells and its control by basic fibroblast and platelet-derived growth factor. *Hepatology* 1999; **29**: 868-878
 - 41 **Thomson S**, Mahadevan LC, Clayton AL. MAPK kinase-mediated signaling to nucleosomes and immediate-early gene induction. *Semin Cell Dev Biol* 1999; **10**: 205-214
 - 42 **Schinelli S**, Zanassi P, Paolillo M, Wang H, Feliciello A, Gallo V. Stimulation of endothelin B receptors in astrocytes induces camp response element-binding protein phosphorylation and c-fos expression via multiple mitogen-activated protein kinase signaling pathways. *J Neurosci* 2001; **21**: 8842-8853
 - 43 **Reeves HL**, Dack CL, Peak M, Burt AD, Day CP. Stress-activated protein kinases in the activation of rat hepatic stellate cells in culture. *J Hepatol* 2000; **32**: 465-472
 - 44 **Chen A**, Davis BH. The DNA binding protein BTEB mediates acetaldehyde-induced, jun-N-terminal kinase-dependent alpha1 (I) collagen gene expression in rat hepatic stellate cells. *Mol Cell Biol* 2000; **20**: 2818-2826
 - 45 **Zhu YH**, Hu DR, Nie QH, Liu GD, Tan ZX. Study on activation and c-fos, c-jun expression of in vitro cultured human hepatic stellate cells. *Shijie Huaren Xiaohua Zazhi* 2000; **8**: 299-302
 - 46 **Jin N**, Hatton ND, Harrington MA, Xia X, Larsen SH, Rhoades RA. H₂O₂-induced egr-1, fra-1 and c-jun gene expression is mediated by tyrosine kinase in aortic smooth muscle cells. *Free Radic Biol Med* 2000; **29**: 736-746
 - 47 **Dampier K**, Hudson EA, Howells LM, Manson MM, Walker RA, Gescher A. Difference between human breast cell lines in susceptibility towards growth inhibition by genistein. *Br J Cancer* 2001; **85**: 618-624
 - 48 **Lu B**, Dai YM. Abnormal cycle regulation of cells in the HCC. *Shijie Huaren Xiaohua Zazhi* 2001; **9**: 205-208
 - 49 **Ishizuka S**, Yano T, Hagiwara K, Sone M, Nihei H, Ozasa H, Horikawa S. Extracellular signal-regulated kinase mediates renal regeneration in rats with myoglobinuric acute renal injury. *Biochem Biophys Res Commun* 1999; **254**: 88-92
 - 50 **Olaso E**, Labrador P, Wang L, Ikeda K, Eng FJ, Klein R, Lovett DH, Lin HC, Friedman SL. DDR2 receptor regulates fibroblast proliferation and migration through extracellular matrix by transcriptional activation of MMP-2. *J Biol Chem* 2001; **26** [epub ahead of print]
 - 51 **Yoshiji H**, Kuriyama S, Yoshii J, Ikenaka Y, Noguchi R, Nakatani T, Tsujinoue H, Fukui H. Angiotensin-II type I receptor interaction is a major regulator for liver fibrosis development in rats. *Hepatology* 2001; **34**: 745-750
 - 52 **Wang YQ**, Ikeda K, Ikebe T, Hirakawa K, Sowa M, Nakatani K, Kawada N, Kaneda K. Inhibition of hepatic stellate cell proliferation and activation by the semisynthetic analogue of fumagillin TNP-470 in rats. *Hepatology* 2000; **32**: 980-989
 - 53 **Tada S**, Iwamoto H, Nakamuta M, Sugimoto R, Enjoji M, Nakashima Y, Nawata H. A selective ROCK inhibitor, Y27632, prevents dimethylnitrosamine-induced hepatic fibrosis in rats. *J Hepatol* 2001; **34**: 529-536
 - 54 **Barnes S**, Boersma B, Patel R, Kirk M, Darley-Usmar VM, Kim H, Xu J. Isoflavonoids and chronic disease: mechanisms of action. *Biofactors* 2000; **12**: 209-215
 - 55 **Shimizu I**, Mizobuchi Y, Yasuda M, Shiba M, Ma YR, Horie T, Liu F, Ito S. Inhibitory effect of oestradiol on activation of rat hepatic stellate cells *in vivo* and *in vitro*. *Gut* 1999; **44**: 127-136
 - 56 **Yasuda M**, Shimizu I, Shiba M, Ito S. Suppressive effects of estradiol on dimethylnitrosamine-induced fibrosis of the liver in rats. *Hepatology* 1999; **29**: 719-727

Edited by Pagliarini R

• BASIC RESEARCH •

Immunologic role of nitric oxide in acute rejection of golden hamster to rat liver xenotransplantation

Tong-Jin Diao, Tong-Ye Yuan, You-Lin Li

Tong-Jin Diao, Tong-Ye Yuan, You-Lin Li, Department of General Surgery and Hepatobiliary Surgery, the Chinese PLA Navy 401 Hospital Qingdao 266071, China

Correspondence to: Tong-Jin Diao, Department of General surgery and Hepatobiliary Surgery, Chinese PLA 401th Navy Hospital, Qingdao 266071, Shandong Province, China. diao tongjin@hotmail.com
Telephone: +86-532-5811737

Received 2001-07-19 **Accepted** 2002-06-15

Abstract

AIM: To evaluate the immunologic role and expression significances of nitric oxide(NO), nitric oxide synthase (NOS), and its isoenzyme in acute rejection to liver xenografts from golden hamster in rat.

METHODS: Liver transplantations were randomly divided into five groups($n=6-9$): isografts (group I); xenografts (group II); xenografts plus cyclosporine treatment (group III), xenografts plus cyclophosphamide treatment combined with splenectomy (group IV), and xenografts using cyclophosphamide in combination with splenectomy (group V) and xenografts using splenectomy in addition to cyclophosphamide and cyclosporine treatments (group V). The levels of ALT, TNF- α , and nitric oxide production (NOx) in serum of recipients were examined, and expressions of type II (iNOS) and type III (cNOS) nitric oxide synthase (NOS)-inducible NOS (iNOS) and constitutive NOS (cNOS) were observed by NADPH diaphorase histochemical and immunohistochemical staining.

RESULTS: The level of serum ALT, activity of serum TNF- α and systemic levels of NO metabolite in groups II and IV were higher than those of groups I and V (serum ALT, 2416 ± 475 , 2540 ± 82.5 nkat.L $^{-1}$ vs $(556.8 \pm 43.5, 677.30 \pm 38.2)$ nkat.L $^{-1}$, $P < 0.01$; (serum TNF- α , 353.5 ± 16.1 , 444.6 ± 28.1 ng.L $^{-1}$ vs $38.5 \pm 5.2, 52.0 \pm 5.7$) ng.L $^{-1}$, $P < 0.01$; (serum NOx $514.6 \pm 18.1, 336.0 \pm 43.0$ nmol.g $^{-1}$, vs $26.1 \pm 5.7, 27.7 \pm 6.0$) nmol.g $^{-1}$, $P < 0.01$). Cyclosporine in group III can repress the cellular immune response and the synthesis of nitric oxide and the expression of NO synthase, but not prolong the liver xenograft survival. The over-expression of NOS, iNOS and cNOS in liver xenograft rejection in groups II and IV were detected by NADPH diaphorase histochemical and immunohistochemical staining.

CONCLUSION: The degrees of acute rejection can be effectively repressed in golden hamster to rat liver xenografts with splenectomy and cyclosporine. Nitric oxide metabolites, and nitric oxide synthase and its isoenzymes, above all inducible NOS (iNOS) can be used as potential diagnostic markers for acute rejection in liver transplantation. The cellular localization of nitric oxide varies according to the immunologic status of liver xenografts, thus thinking that hepatocyte derived nitric oxide may be protective

in the hyporesponsive state, but hepatic injury is likely triggered by centrilobular iNOS expression in the superresponsive state.

Diao TJ, Yuan TY, Li YL. Immunologic role of nitric oxide in acute rejection of golden hamster to rat liver xenotransplantation. *World J Gastroenterol* 2002; 8(4):746-751

INTRODUCTION

Immune rejection remains an impediment to its overall clinical success in orthotopic liver transplantation, and acute rejection is seriously harmful to the grafts and recipients. Besides clinical symptoms and signs, histological analysis of biopsy remains the most useful tool for assessing the severity of rejection, but the liver graft may have been severely damaged at this time. It is an urgent issue of the moment to study the mechanisms of acute rejection and search for special early markers of diagnosis in liver transplantation. The cellular immunity has been testified to be a chief mechanism in rejecting liver transplantation^[1-8].

In recent years, as an endothelium-derived relaxing factor (EDRF), nitric oxide (NO), which is a highly reactive free radical with a multitude of organ specific regulatory functions, has received a tremendous amount of attention within the realm of organ transplantation^[9-11], for it can induce directly specific and nonspecific immunity of the body^[12]. While a great deal of research has centered upon its cellular and molecular biology and pharmacology, little is known about NO's contribution to overall organ physiology or pathophysiology. In organ transplantation, NO has been postulated to possess immunomodulatory functions. However, it remains unknown whether NO is immunosuppressive or immunostimulatory. In addition, does NO have a role in immunologic function within the settings of acute rejection, chronic rejection, or hyporesponsiveness? Our previous studies suggested that the beneficial effects of hepatic nitric oxide on the reperfusion injury in the rat orthotopic liver transplantation (OLT) by supplementing NO pathway or inhibiting the endothelium NOS with NG Nitro-L-arginine methyl ester (L-NAME)^[13-15]. It was reported that hepatocyte-derived NO may be protective in the hyporesponsive state. However, Jsoe *et al*^[16] reported recently that a selective iNOS inhibitor attenuated ischemia-reperfusion injury in the pig liver, suggesting that NO produced by iNOS has a cytotoxic rather than a hepatoprotective effect on the hepatic warm I/R injury. As a result, further investigation regarding the immunologic role of NO in acute rejection in OLT is warranted. Our aim was to investigate the immunologic role of nitric oxide and expressing significance of NOS and its isoenzyme in acute rejection of golden hamster to rat liver xenografts.

MATERIALS AND METHODS

Materials

Male Wistar rats weighing 180-260 g purchased from Shanghai Experimental Animal Centre, Chinese Academy of Sciences,

and female golden hamsters weighing 150–200 g, purchased from the Shanghai Municipal Institute of Family Planning were used as donors and recipients respectively. All animals were maintained on a 12 h light/dark cycle and fed commercially available rat chow and had free access to water. Nitroblue tetrazolium and β -NADPH reduced nicotinamide adenine dinucleotide phosphate, rabbit antimouse iNOS(NOS II) and cNOS (NOSIII) polyclonal antibody were obtained from Sigma.

Methods

Experimental Design All animals were randomly divided into five groups($n=6-9$):Group I (isografts) both donors and recipients were Wistar rats; Group II, in which Wistar rats and golden hamsters served as donors and recipients respectively, is xenografts in acute rejection;GroupIII was subjected to orthotopic liver xenotransplantation treated with cyclosporine (30 mg/kg.d),served as cellular immunosuppressive group; Group IV was xenografts using cyclophosphamide (40 mg/kg. d) in combination with splenectomy,as humoral immunity defeat group; and group V was xenografts using splenectomy,cyclosporine and cyclo-phosphamide as double immunosuppressive group.

Orthotopic liver transplantation Orthotopic liver transplantation (OLT) was performed according to Harihara's three Cuff technique with minor modifications as previously reported^[17,18], in which the suprahepatic vena cava (SVC) was reconstructed by the Cuff method, along with the infrahepatic inferior vena cava (IVC) and the portal vein.The bile duct was internally stented with a polyethylene stent. The splenectomy was simultaneously carried out in the grafted recipients.

Specimen measurement The blood samples were obtained *via* the tail vein at the days 3, 5, 7, 10, 14, and so on postoperatively, or *via* portal vein or infrahepatic IVC in the recipient being killed or its liver tissue being biopsied, and then centrifuged by 3 000 r·min⁻¹ at 4 °C for 10 min. The upper serum after snap-frozen was immediately stored at -80 °C refrigerator before determination of nitric oxide metabolite production by the improved Griess' s method, aspartate aminotransferase(AST),and α -tumor necrosis factor(TNF- α)according to MTT. The inferior lobe of right liver biopsy was carried out with methoxyfluorane anesthesia in groups II,III and IV5, 14 and 21days after postoperation .The samples were instantly stored in liquid nitrogen, and kept frozen at -80 °C refrigerator.

Histopathology Sections of the grafted liver were fixed in 100 mL·L⁻¹ formalin and prepared with haematoxylin and eosin stain for routine light microscopy.

Histochemical staining for NO synthase (NADPH diaphorase staining) The grafted liver specimens were fixed in 40 g·L⁻¹ paraformal-dehyde and 4 g·L⁻¹ picric and in 0.1 mol·L⁻¹ sodium phosphate buffer,pH7.4,for 4 h at 4 °C. Subsequently,specimens were frozen at -80 °C until cutting the sections. Cryostat sections were immersed for 10 min in 0.1 mol·L⁻¹ phosphate buffer,pH8.0, and were incubated for 40 min at 37 °C in prewarmed solution consisting of 0.1 mol·L⁻¹ phosphate buffer,pH8.0;3 g·L⁻¹ Triton X-100;0.5 mmol·L⁻¹ nitroblue tetrazolium; and 1.0 mmol·L⁻¹ NADPH. After washing in 0.1 mol·L⁻¹ phosphate buffer,pH7.4,the sections were dehydrated with graded alcohol(70,80,95 and 100 mL·L⁻¹). Slides were rinsed in PBS and counter stained with fast red for 2 min, and cover slips were mounted on microscopic glass slides. Areas with a positive reaction for NADPH diaphorase were stained dark blue in cytoplasm, and in red nucleus^[19-23].

Immunohistochemistry Immunohistochemical methods were used to detect the expressions of inducible NOS (iNOS)and

constitutive NO synthase(cNOS) with specific polyclonal antibody against cNOS or iNOS by the avidin-biotin complex method using an ABC immunostaining kit (Vector Labs, Burlingame, Calif)Areas with a positive reaction were stained pale brown .

Statistical analysis Data are presented as means \pm standard errors of the means ($\bar{x} \pm s$).Comparisons among different groups of samples were made by two-tailed test χ^2 test and *F* test. A value of *P*<0.05 was considered to be statistically significant.

RESULTS

Survival

The Survival of recipient in groups II,III and IV ,in which no significant alteration was found(6.9 ± 0.4 , 7.3 ± 1.0 d, 7.0 ± 0.6 d, respectively) significantly lowered as compared with that of groups I and V , the difference being not statistically significant(48.5 ± 20.7 d vs 37.1 ± 9.9 d, *P*>0.05,Table 1).

Biochemical parameters(Table 1)

Following OLT, serum samples were assayed for ALT,TNF- α and NO on 3,7 and 14 postoperative days (Table 1).The serum values for ALT and TNF- α in groups II and IV were 4-11 times greater than those of groups I and V (*P*<0.01, vs groups I and V).The serum levels of NO metabolites (NOx) in groups II and IV were 12-20 times greater than in groups I , III and V .

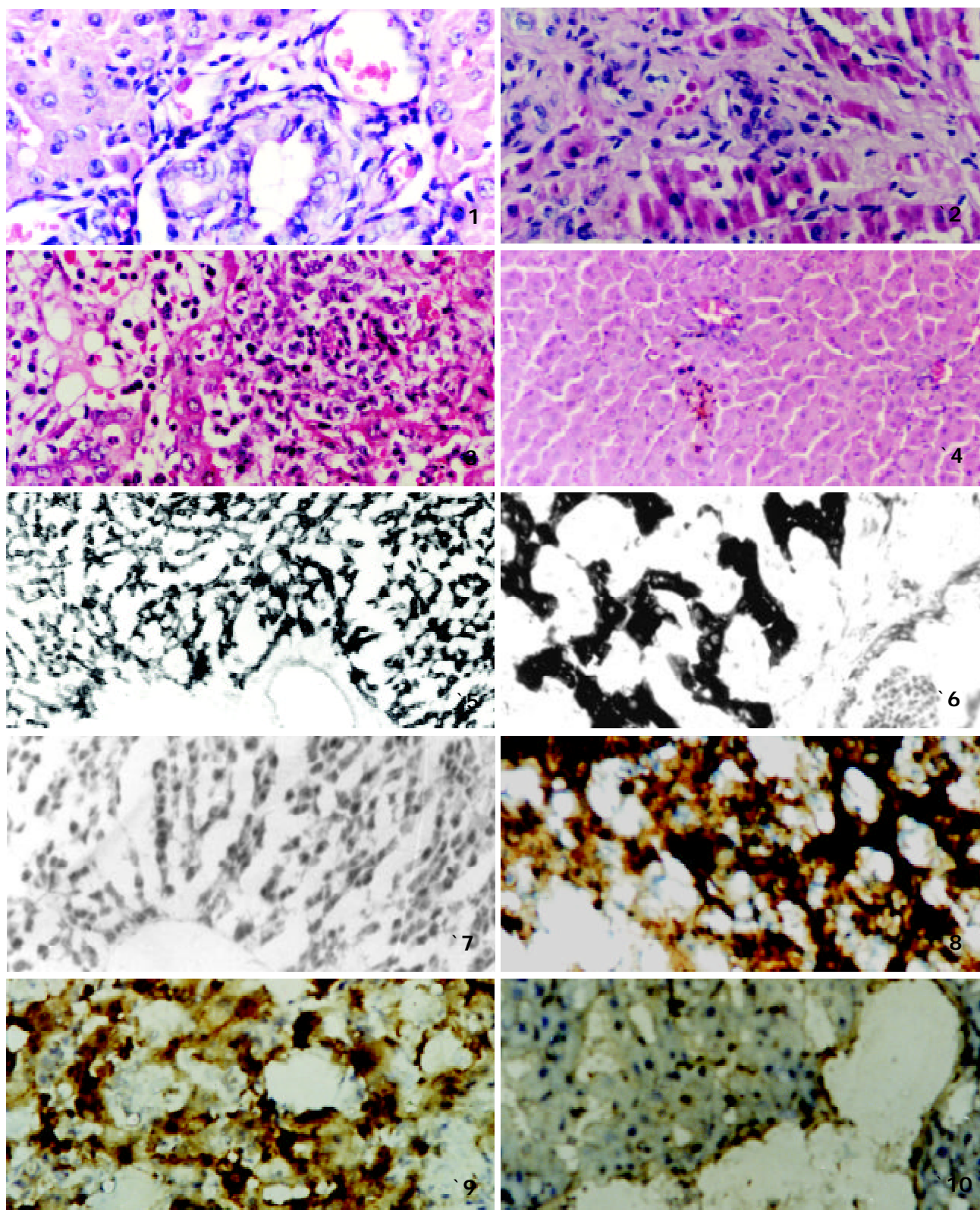
Table 1 Effects of biochemical parameters and recipient survival on cellular and/or humoral immunosuppression in rat liver transplantation

Group	Serum ALT (nkat·L ⁻¹)	Serum TNF- α (ng·L ⁻¹)	Serum NO \bar{x} (nmol·g ⁻¹)	Survival (d)
I	556.8 \pm 43.5	38.5 \pm 5.2.	26.0 \pm 5.7	48.5 \pm 27.7
II	2416 \pm 475 ^b	353.5 \pm 16.1 ^b	514.6 \pm 18.1 ^b	6.9 \pm 0.4 ^b
III	2550 \pm 55.6 ^b	66.0 \pm 2.9	41.5 \pm 3.6	7.3 \pm 1.0 ^b
IV	2540 \pm 82.5 ^b	44.6 \pm 28.1 ^b	336.0 \pm 43.0 ^b	7.0 \pm 0.6 ^b
V	677.30 \pm 38.2	52.0 \pm 5.7	27.7 \pm 6.0	37.1 \pm 9.9

^b*P*<0.01, vs I and V groups.

Histopathology

Histological examination of the grafted liver in groups I and V revealed almost normal liver sinusoidal architecture with the exception of complication of the secondary infections such as subhepatic abscess of cholangiojejunal fistula, pneumonia, etc. (Figures 1,2).Acute rejection appeared in heterogeneous OLT group II ,histological examination demonstrated only a small amount of cellular infiltrates in sinusoid areas by the 3rd postoperative day; inflammatory cell infiltration was increased significantly by the 5th postoperative day; diffuse polymorphonuclear and mononuclear cell infiltration, massive necrosis of hepatocytes and hepatic parenchymal interstitial hemorrhage were found by the 7th postoperative day (Figure 3). In group III,cyclosporine decreased significantly cellular infiltration,but severe hepatocyte necrosis and cyclophosphamide greatly attenuated hepatic necrosis and interstitial hemorrhage,yet cellular infiltration still remained the principal feature. In group V of xenografts using splenectomy,cyclophosphamide and cyclosporine, the architecture of the hepatic lobule was well preserved ,with no hepatocyte necrosis, and a small amount of cellular infiltrates only in the portal areas (Figure 4).



Figures 1,2 Liver tissue from isograft (Group I)complicated with subhepatic abscess of cholangiojejunal fistula at 14 d post-transplantation and with pneumonia at 94 d post-transplantation. HE $\times 66$

Figure 3 Liver tissue from acutely rejecting liver xenograft(Group II)at 7 d post-transplant HE $\times 66$

Figure 4 Liver tissue from xenograft (Group V) with double immunosuppressive action at 14d post-transplantation. HE $\times 33$

Figures5, 6 NADPH diaphorase histochemocal staining in acutely rejecting liver xenografts (Group II) at 2,7 d post-transplantation . NADPH-d $\times 33$, $\times 66$

Figure 7 NO synthase in liver xenograft (Group V) with double immunosuppressive action at 14d post-transplantation,showing negative NO synthase. NADPH-d $\times 33$

Figures 8,9 iNOS and cNOS in acutely rejecting rat orthotopic liver xenograft (Group II) at 7 d post-transplantation. ABC $\times 66$

Figure10 cNOS in liver xenograft (Group V) with double immunosuppressive action at 14d post-transplantation. ABC $\times 33$

NADPH diaphorase and immunohistochemical staining findings

Expressions of nitric oxide synthase (NOS) in grafted liver tissue were detected by NADPH diaphorase staining methods. A small amount of NOS positive expressions in group I was localized to vascular endothelium and hepatocytes. The expression levels of NOS in groups II, III and IV were obviously increased by the 2nd postoperative day, dominantly localized to hepatocyte and hepatic sinusoidal lining cells. The expression time of NOS was earlier at least two days than that of pathological damage (Figure 5). The intensity of NO synthase staining by the 5th-7th postoperative day was strongest in both the portal inflammatory infiltrate and hepatocytes showing purple dark blue precipitation (Figure 6). In contrast, the intensity of NO synthase signal in group V was significantly weaker than that of groups II, III and IV (Figure 7).

The immunohistochemical staining findings for grafted liver tissue demonstrated that a small amount of signal intensity of constitutive NO synthase was present in the grafted liver tissues in group I, but no expression of inducible NO synthase. In contrast, the intensity of both cNOS and iNOS, in groups II, III and IV was significantly greater than in group I (Figures 8, 9). There was no significant difference in the staining intensity of both cNOS and iNOS between groups I and V (Figure 10).

DISCUSSION

Recently, the postoperative immunosurveillance after organ transplantation has received a tremendous amount of attention. It has been reported that the occurrence rate of rejection in clinical liver transplantation was still as high as 48-77 %, the liver allotransplants do not undergo hyperacute rejection even if the liver is transplanted in a crossmatch positive or ABO mismatched recipient. Acquiring easily immunologic tolerance, livers grafted between widely disparate species can be more easily accepted than other grafted organs such as heart, kidney etc, which were rapidly lost because of hyperacute rejection mediated by humoral immunity, the recipient of liver xenografts can even survive for days. Hamster-to-rat liver xenotransplantation (HORLT), as a concordant heterotopic liver transplantation, undergo acute rejection mediated by cellular and humoral immunity^[14]. Although the small amount of antibody titer was found in hamster-to-rat cardiac transplantation after recipient's splenectomy, the survival of recipient prolonged significantly. In contrast, the survival of liver xenograft failed to prolong significantly, though the antibody titer still was not high in hamster-to-rat liver xenotransplantation subjected to splenectomy. Our results demonstrated that the combined treatment with splenectomy and cyclophosphamide due to depressing humoral immune response could reduce significantly humoral antibody formation, and lighten the hepatocyte necrosis, and completely eliminate interstitial hemorrhage, but it failed to ameliorate infiltrating cells and the expression of NO synthase in liver xenografts, and prolong the xenograft survival. However, cyclosporine could obviously depress the cellular immunity to decreased cellular infiltration, but severe hepatocyte necrosis and hemorrhage remained unchanged, thus failed to prolong xenograft survival and to improve liver functions. Only the double immunosuppression of the combined treatment with splenectomy, cyclophosphamide, and cyclosporine completely repressed the rejection of liver xenografts, significantly reduced antibody formation and infiltrating cells, eliminated the grafted liver function and prolong xenograft survival.

Nitric oxide (NO) is a highly reactive and commonly

synthesized free radical with a multitude of organ specific regulatory functions. Within the realm of solid organ transplantation, NO has been the focus of attention. Discordant reports have appeared regarding the functional role of NO in systemic physiology and pathophysiology^[24-35]. In organ transplantation, elevated systemic levels of NO metabolites always accompany the acute rejection of heart^[36-37], lung^[38-39], liver^[40-41], renal^[42], pancreas^[43-44], and small bowel^[45] allografts in both humans and rats. The potential hepatoprotective or hepatotoxic effects of NO, however, have yet to be clarified, especially, the role of NO and sites of synthesis in the immunologic states following organ transplantation. Our preliminary studies confirmed that hepatocyte NO production may be hepatoprotective in state of free radical production in hamster-to-rat liver xenografts. Monitoring of NO levels has been suggested as a clinical diagnostic means for initiation of intervention in transplantation management. Nitric oxide synthesis is an important component of nonspecific defense synthesis for a number of pathogens. Until recently, the pathway for induction of iNOS was presumed to be initiated by macrophage cytokine elaboration or lipopolysaccharide from gram-negative bacteria. The present knowledge suggests that specific and nonspecific immunity is mediated by iNOS. Therefore, nonreticulo-endothelial cells, such as hepatocytes, containing iNOS, may play an unrecognized role in immunity. The exact roles of NO in liver xenograft rejection are still not clear. Although NO, possessing diverse functions, such as regulation of local blood as an endothelium-derived relaxing factor, inhibition of platelet aggregation, and attenuation of neutrophil adherence, as a natural extracellular scavenger of superoxide anions, NO was considered to have cytoprotective effects against the rejection of liver xenograft, and cytotoxic and cytostatic effector functions through the nitrosylation and inhibition of cellular enzymes critical to mitochondrial respiration and DNA synthesis^[48-51]. However, the role of NO in oxidative stress mediated injury, has been controversial. It was reported that iNOS mRNA in rat heart transplantation was present in the inflammatory infiltrate but not within the cardiac myocytes. In our study, the expression of iNOS in liver xenotransplantation was identified in both hepatocytes and portal inflammatory cells. Therefore, the exact role of NO in liver xenograft acute rejection remains to be further studied using both a selective iNOS inhibitor (aminoguanidine hemisulfate) and a relatively selective iNOS inhibitor. Recent studies demonstrated that intraportal administration of aminoguanidine hemisulfate, a selective iNOS inhibitor, significantly suppressed nitric oxide production and serum aspartate aminotransferase after reperfusion, inhibited nitrotyrosine expression and attenuated hepatic damage^[10]. Protective or injuring effects of NO may depend upon the relative local concentrations of NO and accompany of biologic modifiers such as IL-1, TNF- α or INF- γ . The process of acute rejection, which may be organ specific with respect to its biochemical mediators, is determined not only by the properties of inflammatory infiltrates, but also by the response of the parenchymal cells within the specific graft.

Our study also demonstrated that the serum levels of NO metabolites (NO_x) in unmodified xenografts (group II) and xenografts using double-immunosuppressive action (group V). The cellular immunosuppressant using cyclosporine alone can repress the expression and synthesis of nitric oxide without improvement of graft survival. The efficacy of cyclosporine having the suppression of specific activated T cells, as an immunosuppressant for organ transplantation and severe refractory autoimmune diseases, increased its clinical

application. Our study revealed that cyclosporine treatment resulted in inhibition of iNOS expression and consequently reduces iNOS enzyme activity during acute liver xenograft rejection. Unfortunately, cyclosporine administration is associated with renal vasoconstriction and vascular injury, which is thought to be a major pathophysiologic factor in chronic CSA-induced nephro-toxicity. Cyclosporine has been shown to generate superoxide through an as-yet-unclarified alteration of cytochrome P-450-dependent mixed function oxidases, the primary pathway of CSA metabolism. *In vitro*, superoxide has been demonstrated to enhance inactivation of NO released from endothelial cells. It was reported that NO maintains a protective function with vasoconstricting effect to CSA. In addition, NADPH diaphorase and immunohistochemical staining findings in this study indicate that nitric oxide synthase (NOS) and its isoenzyme, especially iNOS could be used as potential diagnostic markers for acutely rejecting orthotopic liver transplantation. In conclusion, the degrees of acute rejection with double immunosuppressive action using spleenectomy, cyclophosphamide and cyclosporine can be effectively repressed in golden hamster to rat liver xenografts. The elevated systemic levels of NO metabolites and the overexpression of NO synthase and its isoenzymes, especially iNOS, accompanying the acute rejection of liver xenotransplantation can be used as potential diagnostic markers for acute rejection. The cellular localization of nitric oxide varies according to the immunologic status of liver xenografts, thus hepatocyte derived nitric oxide may be considered protective in the hyporesponsive state, but hepatic injury is likely triggered by centrilobular iNOS overexpression in the superresponsive state.

REFERENCES

- 1 **Diao TJ**, Li YL. Immunosurveillance role of nitric oxide and nitric oxide synthase in the acute rejection of hamster to rat concordant orthotopic liver xenotransplantation. *Zhonghua Ganzangbing Zazhi* 2001; **9**:96-97
- 2 **Xu JM**, Xu SY, Mei Q, Ding CH, Zhou AW. Role of the inhibitory effect of melatonin on nitric oxide production in immunological liver injury in mice. *Zhongguo Yaolixue Tongbao* 1998; **14**: 533-535
- 3 **Wang GS**. Studies on the role of nitric oxide and tumor necrosis factor in immunological liver injury in mice and effects of new anti-hepatitis compounds on the liver injury. *Shengli Kexue Jinzhan* 1996; **27**: 47-49
- 4 **Wang GS**, Liu GT. Role of nitric oxide on the immunological liver injury in mice. *Zhonghua Yixue Zazhi* 1996; **76**: 203-206
- 5 **Zhang GL**, Lin ZB, Zhang B. Effects of selective inducible nitric oxide synthase inhibitor on immunological hepatic injury in rat. *Zhonghua Yixue Zazhi* 1998; **78**: 540-543
- 6 **Guo SM**, Deng SH, Chen CX, Liu B. Serum nitric oxide levels and natural killer cell activity in patients with chronic liver diseases. *Anhui Yike Daxue Xuebao* 1999; **34**: 201-202
- 7 **Zhang XL**, Qin YZ, Han XL. The expression of inducible nitric oxide synthase in T-cell-dependent liver injury in mice induced by concanavalin. *Zhonghua Chuanranbing Zazhi* 1998; **16**: 212-215
- 8 **Teng SL**, Wu XR, Xi L. Effect of nitric oxide and free radicals on acute liver injury in rats. *Shijie Huaren Xiaohua Zazhi* 1999; **7**:222-223
- 9 **Huang YQ**, Xiao SD, Zang DZ, Mo JZ. Effects of erythropoietin or nitric oxide synthesis inhibitor on hyperdynamic circulatory state in cirrhotic rats. *Zhonghua Yixue Zazhi* 1998; **78**: 139-142
- 10 **Diao TJ**, Wu MC, Yao XP. Nitric oxide and rejection of liver transplantation. *Gandanyi Waike Zazhi* 1997; **9**:185-187
- 11 **Diao TJ**, Wu MC, Yao XP. Nitric oxide and ischemia reperfusion injury. *Gandanyi Waike Zazhi* 1999; **11**:219-221
- 12 **Zhang H**, Yao HS. Studies of *Hp* infection NO and hexosamine content and immune function in chronic gastric diseases. *Huaren Xiaohua Zazhi* 1998; **6**:1092-1093
- 13 **Diao TJ**, Yao XP, Ji B, Yang JM, Wu MC, Zhang SG. Effects of L-arginine during ischemia-reperfusion injury in rat orthotopic liver transplantation. *Shijie Huaren Xiaohua zazhi* 1998; **6**:291-295
- 14 **Diao TJ**, Yao XP, Yin CC, Li DM, Yang JM, Wu MC. Expression of intracellular adhesion molecule -1 (ICAM-1) during cold ischemia reperfusion injury in rat orthotopic liver transplantation. *Zhonghua Yixue Zazhi* 1999; **79**:814-815
- 15 **Diao TJ**, Deng LH, Li DM, Yao XP, Yang JM, Wu MC. Functional roles of nitric oxide pathway during ischemia-reperfusion injury in the rat orthotopic liver transplantation. *Jichu Yixue yu Linchuang* 2000; **20**:48-55
- 16 **Isobe M**, Katsuramaki T, Hirata K, Kimura H, Nagayama M, Matsuno T. Beneficial Effects of inducible nitric oxide synthase inhibitor on reperfusion injury in the pig liver. *Transplantation* 1999; **68**:803-813
- 17 **Diao TJ**, Yao XP, Ji B, Yang JM, Wu MC, Zhang SG. Improvement of the surgical procedure and prevention of the complications in hamster to rat liver xenotransplantation using the three-cuff technique. *Gandanyi Waike Zazhi* 1998; **10**:100-103
- 18 **Diao TJ**, Yao XP, Ji B, Yang JM, Wu MC, Zhang SG, Tan JW. The operative improved methods in model of rat orthotopic liver transplantation. *Gandanyi Waike Zazhi* 1999; **7**:10-12
- 19 **Zhou YK**, Cong WM, Qian GX, Wang Y, Cai ZF, Ding JM, Wu MC. Expression of nitric oxide synthase in human hepatocellular carcinoma and cirrhotic liver tissue and its clinical significance. *Zhonghua Gandan Waike Zazhi* 1999; **5**: 17-19
- 20 **Chen G**, Gong HY, Zhou SQ, Chen Z. Expression of inducible nitric oxide synthase in hepatocyte during infection of abdominal cavity. *Shijie Huaren Xiaohua zazhi* 1999; **7**:704-705
- 21 **Lei YN**, Song TS, Hu SL. A double staining study of acetylcholinesterase and nitric oxide synthase on myenteric plexus of rat ileum. *Zhongguo Zuzhihuaxue yu Xibaohuaxue Zazhi* 1998; **7**: 100-103
- 22 **Peng X**, Feng JB, Wang SL. Nitric oxide synthase distribution in myenteric plexus of rat digestive tract. *Huaren Xiaohua zazhi* 1998; **6**: 250-252
- 23 **Huang YQ**, Xiao SD, Zang DZ, Mo JZ, Li RR, Peng YS. Study on the localization of nitric oxide synthase in esophagus of cirrhotic rats. *Zhonghua Xiaohua Zazhi* 1998; **18**: 86-88
- 24 **Guan HG**, Chen XR, Qian HX, Lu GC, Cao W. Expression of endothelin-1 and nitric oxide synthase mRNA in gastric mucosa of rats with cirrhosis and portal hypertensive gastropathy after disconnection. *Zhonghua Yixue Zazhi* 1998; **78**:702-703
- 25 **Guo JS**, Gu YL, Wang JY, Cao ZX. Expression and activity patterns of iNOS and eNOS in acetic acid induced gastric ulcers in rats. *Shijie Huaren Xiaohua Zazhi* 2001; **9**:288-292
- 26 **Zhang GF**, Zhang MA, Chen YR, Wang L. Role of endothelium and nitric oxide on the blood endotoxin of rat gastric mucosa injuries. *Shijie Huaren Xiaohua Zazhi* 2000; **8**(suppl):24
- 27 **Zeng JZ**, Zhang WD, Liu XX, Zhang ZS, Zhang YL, Zhou DY. Significance and role of tyrosine kinase and nitric oxide synthase active transformation in the gastric mucosa injuries and repairs. *Shijie Huaren Xiaohua Zazhi* 2000; **8**:354-355
- 28 **Wang DR**, Chen J, Li JM, Zhang ZG. Expression of inducible nitric oxide synthase and *Hp* infection in chronic gastritis and peptic ulcer. *Huaren Xiaohua Zazhi* 1998; **6**:597-599
- 29 **Yan HM**, Li YK. Progress in studies on nitric oxide in chronic gastritis. *Shijie Huaren Xiaohua Zazhi* 1999; **7**:355-356
- 30 **Wu JW**, Luo JY, Gong J, Jiang Y. The role of nitric oxide during the small intestinal migrating motor complex. *Zhonghua Xiaohua Zazhi* 1999; **19**: 82-84

- 31 **Zang HY**, Wu ZY, Chen ZP. Nitric oxide synthase and hyperdynamic circulation of portal hypertension. *Zhonghua Shiyanzhizhi* 1999; **16**: 284-285
- 32 **Huang YQ**, Xiao SD, Zhang DZ, Mo JZ. Effects of nitric oxide and IL-8 on hyperdynamic circulatory state in cirrhotic patients. *Huaren Xiaohua Zazhi* 1998; **6**: 1079-1081
- 33 **Wang Q**, Huang JF. Expression of eNOS and IL-10 gene in signal transduction for liver regeneration. *Zonghua Waike Zazhi* 1998; **36**: 522-524
- 34 **Chen G**, Liu B, Cai XM, Gu CH. Clinical significance of changes of endothelin and nitric oxide levels in peripheral blood of patients with severe hepatitis. *Shijie Huaren Xiaohua Zazhi* 1999; **7**: 122-124
- 35 **Cooper M**, Lindholm P, Pieper G, Seibel R, Moore G, Nakanishi A, Dembny K, Komorowski R, Johnson C, Adams M, Roza A. Myocardial nuclear factor- κ B activity and nitric oxide production in rejection cardiac allografts. *Transplantation* 1998; **66**: 838-844
- 36 **Menon SG**, Zhao LP, Xu SX, Samlowski WE, Shelby J, McGregor J, Bapry WH. Relative importance of cytotoxic T lymphocytes and nitric oxide-dependent cytotoxicity in contractile dysfunction of rejecting murine cardiac allografts. *Transplantation* 1998; **66**: 413-419
- 37 **Romero M**, Garcia-Monzon C, Clemente G, Salcedo M, Alvarez E, Majano PL, Moreno-Otero R. Intrahepatic expression of inducible nitric oxide synthase in acute liver allograft rejection: evidence of modulation by corticosteroids. *Liver-Transplantation* 2001; **7**: 16-21
- 38 **Wang XF**, Lewis DA, Kim HK, Tazelaar HD, Park YS, McGregor CGA, Miller VM. Alterations in mRNA for inducible and endothelial nitric oxide synthase and plasma nitric oxide with rejection and/or infection of allotransplanted. *lungs Transplant* 1998; **66**: 567-572
- 39 **Soccal PM**, Jani A, Chang S, Leonard CT, Pavlakis M, Doyle R. Inducible nitric oxide synthase transcription in human lung transplantation. *Transplantation* 2000; **70**: 384-385
- 40 **Van-der-Hoeven J A**, Lindell S, Van-suylichem PT, Vos T, Groothuis GG, Moshage H, Ploeg RJ. Extended preservation and effect of nitric oxide production in liver transplantation. *Transpl Int* 1998; **11**: 171-173
- 41 **Roth E**. The impact of L-arginine-nitric oxide metabolism on ischemia/reperfusion injury. *Curr Opin Clin Nutr Metab Care* 1998; **1**: 97-99
- 42 **Garcia-Criado FJ**, Eleno N, Santos Benito F, Valdunciel JJ, Reverte M, Lozano-Sanchez FS, Ludena MD, Gomez-Alonso A, Lopez-Novoa JM. Protective effect of exogenous nitric oxide on the renal function and inflammatory response in a model of ischemia-reperfusion. *Transplantation* 1998; **66**: 982-990
- 43 **Vollmar B**, Janata J, Yamauchi JJ, Menger MD. Attenuation of microvascular reperfusion injury in rat pancreas transplantation by L-arginine. *Transplantation* 1999; **67**: 950-955
- 44 **Benz S**, Schnabel R, Weber H, Pfeffer F, Wiesne R, Breitenbuch PV, Nizze H, Schareck W, Hot U R. The nitric oxide donor sodium nitroprusside is protective in ischemia/reperfusion injury of the pancreas. *Transplantation* 1998; **66**: 994-999
- 45 **Zhao ZQ**, Zhu WX, Liu FL, Zhang L. Changes and implication of oxygen free radical in intestinal ischemia-reperfusion of dogs. *Shijie Huaren Xiaohua Zazhi* 2001; **9**: 921-924
- 46 **Diao TJ**, Li WH, Wu MC, Yao XP, Yang JM, Li DM, Ji B, Li FC. Cellular localization of nitric oxide synthase during acute rejection in golden hamster to rat orthotopic liver xenotransplantation. *Shijie Huaren Xiaohua Zazhi* 1999; **7**: 855-860
- 47 **Diao TJ**, Li YL, Zhao XD, Li DM, Yao XP, Yang JM, Wu MC. The function of nitric oxide in acute rejection of golden hamster to rat orthotopic liver xenotransplantation and studies of NADPH-diaphorase histochemistry. *Gandanyai Waike Zazhi* 2000; **12**: 193-197
- 48 **Chen XH**, Li ZZ, Bao MS, Zheng HX. Effect of nitric oxide on liver ischemia reperfusion injury in rats *in vivo*. *Shijie Huaren Xiaohua Zazhi* 1999; **7**: 295-297
- 49 **Zhao ZL**, Zhang YS, Yu JL, Gao Y. Research status *in quo* on the liver donor preservation and reperfusion injuries. *Shijie Huaren Xiaohua Zazhi* 2001; **9**: 74-77
- 50 **Zang ZC**, Ji ZH, Huang ZQ, Meng XJ. Roles of nitric oxide and TXA₂/PGI₂ on the liver ischemia reperfusion injuries. *Shijie Huaren Xiaohua Zazhi* 2001; **9**: 452-453
- 51 **Zhang QH**, Cai D, Chen ZY, Hou LD, Gu JH, Zhao JC. Changes of inflammatory mediator in dog liver transplantation. *Gandan Waike Zazhi* 1998; **6**: 247-248

Edited by Ma JY

• BASIC RESEARCH •

The anabolic effects of recombinant human growth hormone and glutamine on parenterally fed, short bowel rats

Yan Gu, Zhao-Han Wu

Yan Gu, Zhao-Han Wu, Department of General Surgery, Zhongshan Hospital, Fudan University, Shanghai 200032, China

Correspondence to: Yan Gu, Department of General Surgery, Shanghai Ninth People's Hospital, Shanghai Second Medical University, Shanghai 200011, China. gu-yan@yeah.net

Telephone: +86-21-63138341

Received 2002-01-14 **Accepted** 2002-02-09

Abstract

AIM: To evaluate the metabolic effects associated with administration of rhGH and/or Gln in parenterally fed, short-bowel rats.

METHODS: Forty SD rats subjected to 75 % intestinal resection and maintained with parenteral nutrition were randomly divided into 4 groups as follows: -rhGH, -Gln; -rhGH, +Gln; +rhGH, -Gln; +rhGH, +Gln. Body weight and nitrogen balance were evaluated daily. After 6 days of PN, rats were killed, various organs were dissected and weighted, the carcasses were used for analysis of body composition. Serum GH and IGF-1 were determined by RIA method.

RESULTS: Weight loss in rats with rhGH (17.4 ± 12.8 g) and rhGH+Gln (23.8 ± 3.5 g) was significantly less than rats with PN alone (29.6 ± 6.9 g) and rats with Gln-supplemented PN (31.85 ± 12.8 g), $P < 0.05$. The accumulated NB in rats with rhGH (1252.9 ± 294.3 mg N/d) and rhGH+Gln (1261.7 ± 85.5 mg N/d) was significantly greater than those with PN alone (704.8 ± 379.0 mg N/d) and with Gln-supplemented PN (856.7 ± 284.4 mg N/d), $P < 0.05$. The absolute weight of gastrocnemius muscle in rats with rhGH (2683.9 ± 341.6 mg) and rhGH+Gln (2579.1 ± 359.5 mg) was greater than those with PN alone (2176.3 ± 167.1 mg) and with Gln-supplemented PN (2141.9 ± 353.6 mg). Although the absolute weight of remnant small intestine itself was not significantly different in 4 experimental groups, the weight/length of the segments was greater in rats with rhGH and/or Gln (48.7 ± 5.5 , 52.7 ± 4.1 and 67.4 ± 5.3 respectively) than those with PN alone (47.8 ± 5.0), there were synergistic effects between rhGH and Gln in improvement of the weight/length of remnant small intestine, $P < 0.05$. Analyses of body carcass composition showed that a higher percentage of carcass weight as protein and a lower percentage of carcass weight as fat were occurred in rats with rhGH (20.8 ± 4.0 , 6.0 ± 2.6) and rhGH+Gln (21.3 ± 2.4 , 4.4 ± 1.5) than those with PN alone (16.4 ± 2.4 , 9.2 ± 3.7) and with Gln-supplemented PN (17.8 ± 3.0 , 6.3 ± 2.0), rhGH had significant effects on alteration of body composition, $P < 0.05$. Serum GH and IGF-1 concentration in rats with rhGH (5.221 ± 0.8 and 425.1 ± 19.2 ng/ml respectively) and rhGH+Gln (5.507 ± 1.0 and 461.1 ± 49.9 ng/ml respectively) were greater than those with PN alone (3.327 ± 1.7 and 325.8 ± 29.6 ng/ml respectively) and with Gln-supplemented PN (3.433 ± 0.1 and 347.7 ± 55.7 ng/ml respectively), $P < 0.01$.

CONCLUSION: rhGH significantly improves the anabolism in parenterally fed, short bowel rats, anabolic effect with Gln is less dramatic, there is no synergistic effect between rhGH and Gln in improvement of whole body anabolism. IGF-1 plays an important part in growth-promoting effects of rhGH.

Gu Y, Wu ZH. The anabolic effects of recombinant human growth hormone and glutamine on parenterally fed, short bowel rats. *World J Gastroenterol* 2002;8(4):752-757

INTRODUCTION

Short bowel syndrome follows therapeutic massive small bowel resection, following such surgery, affected patients often require long-term parenteral nutrition (PN) to provide adequate nutrition to meet the needs of the body^[1-2]. However, long-term experience with conventional PN is unable to increase or even maintain body protein, the anabolic response to PN is often suboptimal because of the concomitant presence of catabolism and/or alterations in the hormonal regulation of metabolism^[3-4]. Thus the efficacy of treatment with anabolic opsonins, such as growth factors, glutamine (Gln) is currently under the investigation^[5-7]. But few studies have made direct comparisons of the metabolic response to rhGH vs. Gln in the body. The objective of the present study was to evaluate the relative anabolic and metabolic effects associated with administration of rhGH, Gln and the combination of rhGH and Gln during PN in short-bowel rats and to gain insight regarding potential mechanism mediating the anabolic effects of these factors.

MATERIALS AND METHODS

Animals and experimental design

Forty male Sprague-Dawley rats weighing 180-220 g were housed and underwent an acclimatization period of 7 days. After overnight fasting, they were anesthetized with 0.5 % pentobarbital (40 mg/kg) shortly before surgery. Two operations were performed: 1, placement of PN catheter in the superior vena cava via the external jugular vein; 2, 75 % small intestinal resection. After operation, the rats were placed in individual metabolic cages^[8].

The experimental design was a randomized complete block with four treatment groups arranged in a 2×2 factorial design as follows: -rhGH, -Gln; -rhGH, +Gln; +rhGH, -Gln; +rhGH, +Gln. The final sample size was 10 rats per group. In addition, an orally fed, nonoperated, age-matched group ($n=8$) was included to serve as reference for determination of net changes in total body content of protein, water and fat. After surgery, on day 0 only saline was provided through the catheter. From day 1 to day 6, PN solution was given and water was provided ad libitum. Rats received rhGH and/or Gln for 6 days, during which PN provided the sole source of nutrition.

At the end of the experiment, the rats were reanesthetized and laparotomy was performed under sterile conditions. Blood was collected by cardiac puncture, and thymus, heart, lung, spleen, liver, kidney, adrenal, testis and gastrocnemius muscles were dissected, weighted, frozen and stored at -70°C . The entire gastrointestinal tract was removed, flushed with cold saline, the wet weight of stomach, remnant small intestine (from pylorus to cecum), and cecum was recorded. The length of remnant small intestine segment was also determined. After removal of the above tissues, carcass weights were recorded and carcasses were stored at -70°C for body composition analysis.

Recombinant human growth hormone (rhGH)

rhGH (Saizen) was provided by Serono Singapore Pte. Ltd, Singapore. The dose of rhGH was $1\text{ U/kg}\cdot\text{d}$ ($0.33\text{ mg/kg}\cdot\text{d}$) administered once a day as a subcutaneous injection over a hind limb beginning on day 1 and continued for 6 days. Sham saline injection was given to rats not treated with rhGH^[9].

Compositions of PN solution

The PN solution was prepared aseptically using 7 % Vamine (SSPC), 50 % dextrose, 20 % Intralipid (SSPC), vitamins, trace elements and electrolytes. Gly-Gln (Pharmacia & Upjohn Co. Germany) was added to the Gln-PN solution and Gly-Ala-Ser-Pro was added to the standard PN solution to equalize the total nitrogen to 8.62 g/L in both solutions. All rats received $166.4\text{ Kcal/kg}\cdot\text{d}$ and $1.4\text{ g N/kg}\cdot\text{d}$ parenterally with an infusion pump. Compositions of the Gln-PN and standard PN are shown in Table 1.

Table 1 Compositions of Gln-PN and standard-PN solution (100ml)

	Gln-PN	Standard-PN
50 % Dextrose (ml)	33	33
20 % Intralipid (ml)	17	17
7 % Vamine (ml)	30	30
17.54 % Gly-Gln (ml)	16	0
Gly-Ala-Ser-Pro (ml)	0	16
10 % KCL (ml)	1	1
10 % NaCL (ml)	1	1
Addamel(SSPC) (ml)	1	1
Soluvit(SSPC) (ml)	1	1
Non-protein Calories (Kcal)	104	104
Total nitrogen (g)	0.862	0.862

Body composition

Body composition analysis was performed on rat carcasses to determine the percent composition of water, protein and fat^[10,11]. Total carcass water was determined by freeze-drying the carcasses to obtain a constant dry carcass weight and then subtracting it from total carcass weight. The freeze-dried carcasses were then homogenized, and aliquots of dried rat homogenate were assayed for nitrogen and lipid concentrations^[10]. Carcass nitrogen concentration was determined by micro-Kjeldahl analysis of 0.50 g dried rat homogenate^[12], and carcass protein concentration was calculated by multiplying carcass nitrogen concentration by 6.25. carcass lipid concentration was determined by extracting 1.0 g dried rat homogenate with 2:1 (v/v) Chloroform-methanol, and then determine lipid concentration gravimetrically^[10].

Nitrogen balance

Nitrogen contents of urine samples were determined by micro-Kjeldahl procedure^[12]. Daily nitrogen balance (NB) was determined by subtracting 24-hour urinary nitrogen from daily nitrogen intake, which was calculated from the volume of PN solution given. Accumulated NB was calculated by subtracting 6-day urinary nitrogen from 6-day nitrogen intake.

Serum GH and IGF-1 determination

Serum GH and IGF-1 concentrations were determined by radioimmunoassay in the isotope laboratory of Zhongshan Hospital^[13]. Plasma IGF-1 was assayed with the DSL-2900 rat IGF-1 RIA kit (Diagnostic systems laboratories, Inc. USA), serum GH was assayed with the human GH RIA kit (Beifang biological technical institute, Beijing, China).

Statistical analysis

Data were analyzed by one-or two-way analysis of variance (ANOVA) using the Stata 5.0 program. The four PN groups in the factorial arrangement were compared in a two-way ANOVA, the reference group was excluded from the two-way ANOVA. Group means determined by the least-significant difference technique were considered significantly different at $P<0.05$. Values were expressed as means \pm SE.

RESULTS

Body weight and body composition

Changes in body weight are summarized in Figure 1. There were no significant differences in body weight at the time of surgery and when PN was initiated, $P>0.05$. After 6 days of PN, rats given rhGH weighted significantly more than rats given without rhGH. Compared to the weight before the surgery, weight loss in rats with rhGH ($17.4\pm12.18\text{ g}$) and rhGH+Gln ($23.8\pm3.46\text{ g}$) was significantly less than those with PN alone ($29.6\pm6.89\text{ g}$) and with Gln-supplemented PN ($31.8\pm12.75\text{ g}$), $P<0.05$.

Results of body composition analysis are shown in Table 2. There were no significant differences in the absolute amount and percentage of water among the groups, $P>0.05$; the absolute amount of body fat in rats with rhGH+Gln was significantly decreased compared to those with PN alone and Gln-supplemented PN; however, rats with rhGH and rhGH + Gln showed a somewhat increase in the absolute amount and proportion of the body protein. rhGH had significant effects on alteration of body fat and body protein, $P<0.05$. Gln had no such effects, and there were no significant synergistic effects between rhGH and Gln in changes of body composition, $P>0.05$.

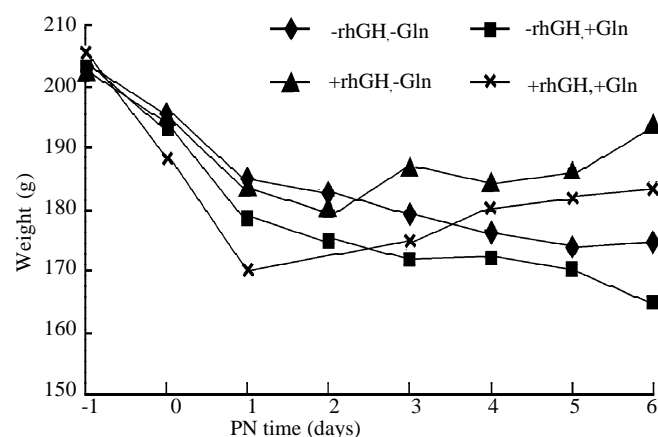


Figure 1 Daily changes in body weight in rats with PN

Table 2 Body composition of short-bowel rats maintained with PN and given rhGH and/or Gln

	Carcass Water		Carcass Fat		Carcass Protein	
	g	%	g	%	g	%
-rhGH						
-Gln	74.4±9.9	66.9±3.8	8.5±3.9	9.2±3.7	17.9±3.2	16.4±2.4
+Gln	71.0±12.9	68.8±3.4	6.0±1.7	6.3±2.0	18.2±2.5	17.8±3.0
+rhGH						
-Gln	76.5±14.5	71.0±6.2	5.4±2.3	6.0±2.6	22.2±3.0	20.8±4.0
+Gln	65.1±3.2	68.9±1.0	4.7±1.5 ^a	4.4±1.5	20.3±3.1	21.3±2.4
Reference	77.7±2.3	73.1±1.0	7.2±1.7	7.6±1.9	18.0±1.8	16.9±1.5
two-way ANOVA						
Gln	NS	NS	0.0332	NS	NS	NS
rhGH	NS	NS	0.0153	0.0296	0.0134	0.0035
Gln+rhGH	NS	NS	NS	NS	NS	NS

^a $P < 0.05$ vs rats with PN alone, Gln-supplemented PN and reference rats. Reference group was not included in 2-way analysis of variance (ANOVA).

Table 3 Organ and tissue weights of rats maintained with PN and given rhGH and/or Gln

	reference	-rhGH, -Gln	-rhGH, +Gln	+rhGH, -Gln	+rhGH, +Gln
Thymus (mg)	392.2±76.1	376.9±88.5	412.9±85.9	376.3±50.8	355.1±41.7
Heart (mg)	693.6±89.9	652.8±106.4	649.4±78.4	624.7±35.3	615.2±102.8
Lung (mg)	1086.1±143.7	1213.8±205.6	1032.3±137.2 ^b	1318.7±168.2 ^a	1067.9±119.9
Liver (mg)	8515.2±1201.7	7722.0±540.1	7819.5±1005.5	9608.9±884.7 ^c	8180.5±556.6
Spleen (mg)	493.2±56.1	669.8±99.9 ^d	467.8±153.8	589.7±112.1	580.3±93.3
Stomach (mg)	1067.5±156.8	1115.7±111.9	1087.1±181.4	1171.6±75.9	1216.9±171.9
Remnant intestine(mg)	1688.9±228.9	1658.0±264.9	1632.2±242.0	1679.0±270.9	1632.2±242.0
Weight/length of remnant intestine		47.8±5.0	48.7±5.5	52.7±4.1	67.4±5.3 ^e
Cecum (mg)	724.9±61.3	628.2±90.4	620.8±130.2	548.0±147.5	608.6±80.3
Kidney (mg)	1747.2±265.7	1468.6±178.4	1485.9±208.2	1602.1±157.6	1408.1±62.6
Adrenal (mg)	54.5±8.2	42.7±11.4	48.0±8.9	47.1±3.8	44.1±7.7
Testis (mg)	2434.4±279.1	2385.1±164.8	2100.4±293.5	2383.2±397.8	2123.0±289.4
gastrocnemius muscles (mg)	2551.4±279.2 ^f	2176.3±167.1	2141.9±353.6	2683.9±341.6 ^f	2579.1±359.5 ^f

^a $P < 0.05$ vs rats with rhGH+Gln and reference rats; ^b $P < 0.05$ vs rats with rhGH and PN alone; ^c $P < 0.05$ vs rats with PN alone, Gln-supplemented PN and rhGH+Gln; ^d $P < 0.05$ vs rats with Gln-supplemented PN and reference rats; ^e $P < 0.05$ vs rats with PN alone and Gln-supplemented PN; ^f $P < 0.05$ vs rats with PN alone and Gln-supplemented PN.

Daily and accumulated nitrogen balance

Changes in daily nitrogen balance were shown in Figure 2. the improvements in daily NB was significantly higher in rats with rhGH and rhGH+Gln than those with PN alone and Gln-supplemented PN from day 4-6, $P < 0.05$. the accumulated NB in rats with rhGH (1252.9±294.3 mg N/d) or rhGH+Gln (1261.7±85.5 mg N/d) was significantly greater than those with PN alone (704.8±379.0 mg N/d) and with Gln-supplemented PN (856.7±284.4 mg N/d), $P < 0.05$. rhGH had significant effects on changes of NB, $P < 0.01$, action of Gln was not significant statistically and there were no synergistic effects between rhGH and Gln.

Organ and tissue weights

The absolute weights of thymus, heart, lung, liver, spleen, stomach, remnant small intestine, cecum, kidney, adrenal, testis and gastrocnemius muscles are shown in table 3. Treatment with rhGH significantly increased the absolute weight of the gastrocnemius muscles compared to those not given rhGH, $P < 0.01$, whereas Gln showed no significantly effect on the weight of this muscle tissue, $P > 0.05$, there was no evidence of an additive effect of rhGH and Gln on the weight of gastrocnemius muscles. Although rhGH or Gln didn't affected the absolute weight of the remnant small intestine, the ratio of weight/length was greater in rats treated with Gln, rhGH and rhGH+Gln than

those with PN alone (2-way ANOVA contrasting 4 experimental groups, $P=0.019$, 0.012 and 0.018 respectively), there were synergistic effects between rhGH and Gln in the increase of the weight/length of the remnant small intestine. Lung, liver and spleen weights were increased in rats treated with rhGH, others were not significantly affected by rhGH and/or Gln, $P>0.05$.

Serum GH and IGF-1 concentrations

Rats treated with rhGH or rhGH+Gln showed significantly higher serum concentrations of GH and IGF-1 than those treated without rhGH, $P<0.05$. Plasma GH and IGF-1 concentrations increased by 61 % and 42 % in rats with rhGH application respectively. There was no significant difference in concentrations of GH and IGF-1 between rats treated with PN alone and those treated with Gln-supplemented PN and between rats treated with rhGH and those treated with rhGH+Gln, $P>0.05$. Plasma GH and IGF-1 concentrations were unaffected by Gln administration. See Figure 3.

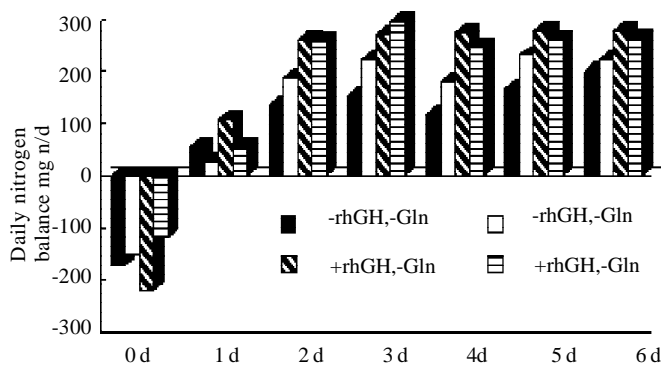


Figure 2 Daily changes of nitrogen balance in rats with PN

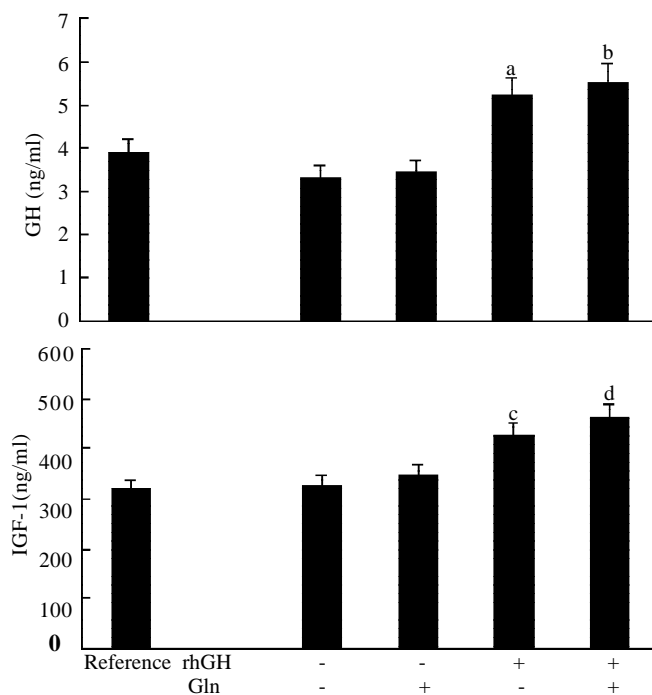


Figure 3 Concentrations in serum of GH and IGF-1 in rats maintained with PN and given rhGH and/or Gln for 6 days after massive intestinal resection. $^aP<0.05$ vs rats with Gln-

supplemented PN and reference rats; $^bP<0.05$ vs rats with PN alone and rats with Gln-supplemented PN; $^cP<0.05$ vs rats with PN alone and reference rats; $^dP<0.05$ vs rats with PN alone, Gln-supplemented PN and reference rats.

DISCUSSION

Massive small bowel resection results in a marked decrease in the total surface area available for the absorption of luminal nutrients^[14,15]. Affected patients often require long-term parenteral nutrition to provide adequate protein, energy and other essential nutrients to meet the needs of the body^[16]. Although this approach attenuates protein losses, PN alone is often unable to increase or even maintain body protein^[17], thus administration of rhGH and Gln have been of great interest in both of human and animal research in recent years^[18-23]. Our experimental design provides new information about the relative anabolic and metabolic effects of rhGH vs. Gln and about interactive effects associated with simultaneous administration of these factors during PN.

Changes in body weight and nitrogen balance reflect the efficacy of PN^[24]. We find in our study that PN alone doesn't reserve the weight loss and nitrogen catabolism induced by short-bowel. Coinfusion of rhGH in short-bowel rats significantly reduced the weight loss and nitrogen catabolism as demonstrated by a significantly decrease in nitrogen excretion and significantly greater weight gain compared with rats without receiving rhGH, there is no significant difference between rats with rhGH and with rhGH+Gln. The anabolic effects of Gln in rats given PN without rhGH were less dramatic compared with rats with PN alone in terms of increased weight gain and decreased nitrogen excretion. Body composition analysis further confirmed that increases in carcass weights and nitrogen retention with rhGH were due to retention of carcass protein rather than fat or water retention. Gln had no significant effects on body composition. Our results demonstrated that the administration of rhGH could result in significant anabolic effects on body growth and improve the efficiency of PN.

GH is anabolic in protein metabolism^[25-27]. Treatment with rhGH significantly increased the absolute weights of gastrocnemius muscles compared with those not given rhGH, whereas weights of thymus, heart, kidney, stomach, remnant small intestine, cecum, adrenal, testis were not affected by rhGH. Gln showed no significant effect on the weight of tissues mentioned above. This specific anabolic effects of rhGH may reflect differences in the distribution of GH receptors within various organs and tissues^[28,29]. As skeletal muscle is the main effectors of GH action^[11], stimulation of rhGH on skeletal muscle is more prominent compared to other organs. In our experiment, although we didn't observe a rhGH and/or Gln effect on weights of small intestine, the ratio of weights/length of small intestine increased with rhGH and/or Gln administration, there is evidence of synergy, i.e., statistical interaction, between rhGH and Gln. Our studies of adaptation of the remnant small intestine in short-bowel rats also supported a synergistic response to rhGH and Gln^[8]. Gln is the principal fuel utilized by the small intestine and is an essential precursor for purine and pyrimidine synthesis required for DNA biosynthesis and cell division in the intestinal mucosa^[30-32]. Thus a constant supply of Gln to the intestinal mucosa in short-bowel is required and mandatory^[33-35]. GH is another growth factor that may influence compensation of the small intestinal remnant^[36-38]. Although opinions differ^[39], GH is supposed to vigorously stimulate intestinal adaptation, it is suggested that GH takes part in the maintenance of the structure and function of the intestinal mucosa^[40-42]. This study provides additional

evidence that simultaneous treatment with rhGH and Gln is more anabolic than administration of either rhGH or Gln alone in the remnant small intestine. In addition, in our study we find liver, spleen and lung weights increased with rhGH, but as the weight of these organs were easily affected by the deposited blood, further research is still needed to understand the effects of rhGH on these organs.

IGF-1 is an important peptide growth factor^[43]. GH induces IGF-1 synthesis in the liver, which is thought to be the primary source of circulating IGF-1, and in many tissues with GH receptors including intestinal tissues^[44-48]. IGF-1 has diverse regulatory functions, including stimulation of DNA and RNA synthesis, tissue amino acid uptake, and cellular protein accrual^[49-51]. In our studies, circulating GH and IGF-1 concentrations were increased accordingly in rats treated with rhGH and with rhGH + Gln. However, supplemental Gln alone did not alter circulating GH or IGF-1 concentrations. Given the current experimental conditions, we may confirm in our study that the growth-promoting effects of rhGH are due to induction of IGF-1 production, enhanced IGF-1 synthesis contributes to the anabolic effects of rhGH.

In summary, our results indicate that treatment with rhGH during PN produced a whole body growth response that appeared to be mediated by greater concentrations of IGF-1, action of Gln is less dramatic, and there is no synergistic effect on the body anabolism between rhGH and Gln.

REFERENCES

- Sundaram A**, Koutkia P, Apovian CM. Nutritional management of short bowel syndrome in adults. *J Clin Gastroenterol* 2002;**34**:207-220
- Robinson MK**, Ziegler TR, Wilmore DW. Overview of intestinal adaptation and its stimulation. *Eur J Pediatr Surg* 1999;**9**:200-206
- Ziegler TR**, Rombeau JL, Young LS, Fong Y, Marano M, Lowry SF, Wilmore DW. Recombinant human growth hormone enhances the metabolic efficacy of parenteral nutrition: a double blind, randomized controlled study. *J Clin Endocrinol Metab* 1992;**74**:865-873
- Wilmore DW**. Growth factors and nutrients in the short bowel syndrome. *J Parenter Enteral Nutr* 1999; **23**: S117-120
- Byrne TA**, Morrissey TB, Gatzen C, Benfell K, Nattakom TV, Scheltinga MR, LeBoff MS, Ziegler TR, Wilmore DW. Anabolic therapy with growth hormone accelerates protein gain in surgical patients requiring nutritional rehabilitation. *Annals of Surgery* 1993;**218**:400-418
- Howarth GS**, Shoubridge CA. Enhancement of intestinal growth and repair by growth factors. *Curr Opin Pharmacol* 2001;**1**:568-574
- Biolo G**, Iscra F, Bosutti A, Toigo G, Ciochi B, Geatti O, Gullo A, Guarnieri G. Growth hormone decreases muscle glutamine production and stimulates protein synthesis in hypercatabolic patients. *Am J Physiol Endocrinol Metab* 2000; **279**:E323-332
- Gu Y**, Wu ZH, Xie JX, Jin DY, Zhuo HC. Effects of rhGH and Gln supplemented parenteral nutrition on intestinal adaptation in short-bowel rats. *Clinical Nutrition* 2001;**20**: 159-166
- Gu Y**, Wu ZH, Jin DY. Metabolic effects of recombinant human growth hormone in parenteral fed, short-bowel rats. *J Shanghai Med Univ* 2000; **27**: 117-120
- Yang H**, Grahn M, Schalch DS, Ney DM. Anabolic effects of IGF-1 coinjected with total parenteral nutrition in dexamethasone-treated rats. *Am J Physiol (Endocrinol Metab)* 1994;**266**:E690-E698
- Lo HC**, Hinton PS, Peterson CA, Ney DM. Simultaneous treatment with IGF-1 and GH additively increases anabolism in parenterally fed rats. *Am J Physiol (Endocrinol Metab)* 1995;**269**:E368-E376
- Concon JM**, Soltess D. Rapid micro Kjeldahl digestion of cereal grains and other biological materials. *Anal Biochem* 1973;**53**:35-41
- Gosling JP**. A decade of development in immunoassay methodology. *Clin Chem* 1990;**36**:1408-1427
- Schwartz MZ**, Maeda K. Short bowel syndrome in infants and children. *Pediatr Clin North Am* 1985;**32**:1265-1279
- Dudrick SJ**, Latifi R, Fosnocht DE. Management of the short bowel syndrome. *Surg Clin North Am* 1997;**71**:625-643
- Vanderhoof JA**, Burkley KT, Antoson DL. Potential for mucosal adaptation following massive small bowel resection in 3-week-old versus 8-week-old rats. *J Pediatr Gastroenterol Nutr* 1983;**2**:672-676
- Wilmore DW**. Catabolic illness-strategies for enhancing recovery. *N Eng J Med* 1991;**325**:695-702
- Haque SM**, Chen K, Usui N, Iiboshi Y, Okuyama H, Masunari A, Cui L, Nezu R, Takagi Y, Okada A. Alanine-glutamine dipeptide-supplemented parenteral nutrition improves intestinal metabolism and prevent increased permeability in rats. *Ann Surg* 1996;**223**:334-341
- Frankel WL**, Zhang W, Afonso J, Klurfeld DM, Don SH, Laitin E, Deaton D, Furth EE, Pietra GG, Naji A. Glutamine enhancement of structure and function in transplanted small intestine in the rat. *JPEN* 1993;**17**:47-55
- Gomez de Segura IA**, Aguilera MJ, Codesal J, Codoceo R, De-Miguel E. Comparative effects of growth hormone in large and small bowel resection in the rat. *J Surg Res* 1996; **62**:5-10
- Byrne TA**, Persinger RL, Young LS, Ziegler TR, Wilmore DW. A new treatment for patients with short-bowel syndrome. *Ann Surg* 1995;**3**:243-255
- Hammarqvist F**, Sandgren A, Andersson K, Essen P, McNurlan MA, Garlick PJ, Wernerman J. Growth hormone together with glutamine-containing total parenteral nutrition maintains muscle glutamine levels and results in a less negative nitrogen balance after surgical trauma. *Surgery* 2001;**129**:576-586
- Scolapio JS**. Treatment of short-bowel syndrome. *Curr Opin Clin Nutr Metab Care* 2001;**4**:557-560
- Edens NK**, Gil KM, Elwyn DH. The effects of varying energy and nitrogen intake on nitrogen balance, body composition, and metabolic rate. *Clin Chest Med* 1986;**7**:3-17
- Gatzen C**, Scheltinga MR, Kimbrough TD, Jacobs DO, Wilmore DW. Growth hormone attenuates the abnormal distribution of body water in critically ill surgical patients. *Surgery* 1992;**112**:181-187
- Petersen SR**, Holaday NJ, Jeevanandam M. Enhancement of protein synthesis efficiency in parenterally fed trauma victims by adjuvant recombinant human growth hormone. *J Trauma* 1994;**36**:726-733
- Mjaaland M**, Unneberg K, Larsson J, Nilsson L, Revhaug A. Growth hormone after abdominal surgery attenuated forearm glutamine, alanine, 3-methylhistidine, and total amino acid efflux in patients receiving total parenteral nutrition. *Ann Surg* 1993;**217**:413-422
- Tissen JP**, Ketelslegers JM, Underwood LE. Nutritional regulation of the IGFs. *Endocrinol Rev* 1994;**15**:80-101
- Flint DJ**, Garden MJ. Influence of growth hormone deficiency on growth and body composition in rats, site-specific effects upon adipose tissue development. *J Endocrinol* 1993;**137**:203-211
- Klimberg VS**, Souba WW, Salloum RM. Intestinal glutamine metabolism after massive short-bowel resection. *Am J Surg* 1990;**159**:27-33
- Boelens PG**, Nijveldt RJ, Houdijk AP, Meijer S, van Leeuwen PA. Glutamine alimentation in catabolic state. *J Nutr* 2001;**131**:2569S-2577S
- Van Acker BA**, Hulsewe KW, Wagenmakers AJ, von Meyenfeldt MF, Soeters PB. Response of glutamine me-

- tabolism to glutamine-supplemented parenteral nutrition. *Am J Clin Nutr* 2000;**72**:790-795
- 33 **Wilmore DW.** The effect of glutamine supplementation in patients following elective surgery and accidental injury. *J Nutr* 2001;**131**:2543S-2549S
 - 34 **Powell-Tuck J,** Jamieson CP, Bettany GE, Obeid O, Fawcett HV, Archer C, Murphy DL. Adouble blind, randomised, controlled trial of glutamine supplementation in parenteral nutrition. *Gut* 1999;**45**:82-88
 - 35 **Sacks GS.** Glutamine supplementation in catabolic patients. *Ann Pharmacother* 1999;**33**:348-354
 - 36 **Zhou X,** Li YX, Li N, Li JS. Glutamine enhances the gut-trophic effect of growth hormone in rat after massive small bowel resection. *J Surg Res* 2001;**99**:47-52
 - 37 **Schulman DI,** Hu CS, Duckett G, Lavallee-Grey M. Effects of short-term growth hormone therapy in rats undergoing 75% small intestinal resection. *J Pediatr Gastroenterol Nutr* 1992;**14**:3-11
 - 38 **Chen K,** Nezu R, Inoue M, Wasa M, Iiboshi Y, Fukuzawa M, Kamata S, Takagi Y, Okada A. Beneficial effects of growth hormone combined with parenteral nutrition in the management of inflammatory bowel disease: An experimental study. *Surgery* 1997;**14**:212-218
 - 39 **Peterson CA,** Carey HV, Hinton PL, Lo HC, Ney DM. GH elevates serum IGF-1 levels but does not alter mucosal atrophy in parenterally fed rats. *Am J Physiol* 1997; **272**: G1100-1108
 - 40 **Zhou X,** Li YX, Li N, Li JS. Effect of bowel rehabilitative therapy on structural adaptation of remnant small intestine: animal experiment. *World J Gastroenterol* 2001;**7**: 66-73
 - 41 **Fadrique B,** Lopez JM, Bermudez R, Gomez de Segura IA, Vazquez I, De Miguel E. Growth hormone plus high protein diet promotes adaptation after massive bowel resection in aged rats. *Exp Gerontol* 2001;**36**:1727-1737
 - 42 **Durant M,** Gargosky S, Dahlstrom K, Fang R, Hellman B JR, Castillo R. The role of growth hormone in adaptation to massive small intestinal resection in rats. *Pediatr Res* 2001;**49**:189-196
 - 43 **Ney DM.** Effects of insulin-like growth factor-I and growth hormone in models of parenteral nutrition. *JPEN J Parenter Enteral Nutr* 1999;**23**(6 Suppl):S184-189
 - 44 **Rotacin P.** Structure, evolution, expression and regulation of insulin-like growth factor 1 and 2. *Growth factor* 1991;**5**: 3-18
 - 45 **Winesett DE,** Ulshen MH, Hoyt EC, Mohapatra NK, Fuller CR, Lund PK. Regulation and localization of the insulin-like growth factor system in small bowel during altered nutrient status. *Am J Physiol* 1995;**268**:G631-640
 - 46 **Bornfeldt KE,** Arnqvist HJ, Enberg B, Mathews LS, Norstedt G. Regulation of insulin-like growth factor-I and growth hormone receptor gene expression by diabetes and nutritional state in rat tissues. *J Endocrinol* 1989; **122**: 651-656
 - 47 **Noguchi T.** Protein nutrition and insulin-like growth factor system. *Br J Nutr* 2000;**84**:S241-244
 - 48 **Davey HW,** Xie T, McLachlan MJ, Wilkins RJ, Waxman DJ, Grattan DR. STAT5b is required for GH-induced liver IGF-I gene expression. *Endocrinology* 2001;**142**:3836-3841
 - 49 **Noda T,** Iwakiri R, Fujimoto R, Matsuo S, Aw TY. Programmed cell death induced by ischemia-reperfusion in rat intestinal mucosa. *Am J Physiol* 1998;**274**:G270-276
 - 50 **Gosteli-Peter MA,** Winterhalter KH, Schmid C, Froesch ER, Zapf J. Expression and regulation of insulin-like growth factor-1 (IGF-1) and IGF-binding protein messenger ribonucleic acid levels in tissues of hypophysectomized rats infused with IGF-1 and growth hormone. *Endocrinology* 1994;**135**:2558-2567
 - 51 **Bornfeldt KE,** Arnqvist HJ, Norstedt G. Regulation of insulin-like growth factor-1 and growth hormone receptor by diabetes and nutritional states in rat tissues. *J Endocrinology* 1991;**129**:1201-1206

Edited by Pagliarini R

• CLINICAL RESEARCH •

Modified techniques of heterotopic total small intestinal transplantation in rats

Xiao-Ting Wu, Jie-Shou Li, Xiao-Fei Zhao, Wen Zhuang, Xie-Lin Feng

Xiao-Ting Wu, Wen Zhuang, Xie-Lin Feng, Department of General Surgery, West China Hospital, Sichuan University, Chengdu 610041, Sichuan Province, China

Jie-Shou Li, Research Institute of General Surgery, Nanjing General Hospital of PLA, Clinical School of Medical College, Nanjing University, Nanjing 210002, Jiangsu Province, China

Xiao-Fei Zhao, Sichuan Reproductive Health Institute, Chengdu 610041, Sichuan Province, China

Supported by the State Education Commission Research Foundation for Scientists Returning from Abroad (1997) 436.

Correspondence to: Professor Xiao-Ting Wu, Department of General Surgery, West China Hospital, Sichuan University, 37 Guo Xue Rd., Chengdu 610041, Sichuan Province, China. wxt1@yahoo.com

Telephone: +86-28-85422479 **Fax:** +86-28-85582944

Received 2001-06-02 **Accepted** 2001-10-30

Abstract

AIM: To establish a successful model of heterotopic total small intestinal transplantation (SIT) in rats in order to reduce the complications and increase the survival rate.

METHODS: A total of 196 Wistar rats underwent heterotopic SIT with microsurgical technique. Technical modifications included shortening fasting time and supplying energy before surgery, administering optimal volume of crystalloid fluid to the donor and recipient during surgical procedures, reducing mechanical and ischemic injuries to donor intestine, revascularizing small intestinal graft with a combination of conventional aorta to aorta anastomosis and a cuffed portal vein to left renal vein anastomosis which resulted in an acceptably short warm ischemic time, and also an adequate blood supply and drainage of the graft.

RESULTS: The average time for the donor surgery was 86min±20min, the mean operative time for the recipient was 115min±20min and warm ischemia time was shortened to 40min±5min. There was a shorter revascularizing time of the graft, the abdominal aorta (AA) to AA anastomosis being 21min±10min, and the cuffed portal vein (PV) to the renal vein anastomosis being 5min±5min. The one-week survival rate of 98 rats with SIT was 88.78% (87/98), without thrombosis and stenosis of anastomosis. The longest survival time of recipient rats was more than 389 days after SIT, the rats were maintaining normal weight, with perfect intestinal function and intact intestinal histology.

CONCLUSION: These modified techniques for SIT would remarkably reduce the complications and improve survival rate in rats, which provided a potentially more consistent and practical model for experimental and clinical studies.

Wu XT, Li JS, Zhao XF, Zhuang W, Feng XL. Modified techniques of heterotopic total small intestinal transplantation in rats. *World J Gastroenterol* 2002; 8(4):758-762

INTRODUCTION

Since Monchick and Russel^[1] established the model of small intestinal transplantation (SIT) in 1971, much modification and development have been achieved^[2-11]. However, the technical complexity and high mortality have hindered the wide use of this valuable model^[12-24]. Parallel to our clinical SIT practice, we have successfully established a stable and practical model of heterotopic SIT with fewer complications and higher survival rate using the modified techniques.

MATERIALS AND METHODS

Animals

One hundred and ninety-six male adult Wistar inbred strain rats weighing between 180g and 310g (Shanghai Laboratory Animal Center of Academy of Sciences of China) were used as donors and recipients. Housed and fed at the Animal Center of Nanjing University, the rats were put accustomed to the environment for at least 7 days before surgery. The donor and recipient were paired according to the similar body weight.

Preoperational care and anesthesia

All the donor and recipient rats stayed fasting in metabolic cages with no access to water but allowed to drink 5% glucose normal saline added with 160 000U/L gentamycin ad libitum for 10 h-12 h. The rats were anesthetized with an intraperitoneal injection of 1% ketamine (1mL/100g) supplemented with the 1/4 primitive dose of ketamine as required.

Donor operation

Lactated Ringer's solution with 2.5g/L Cefazomelin was infused via the penile vein by micropump (Perfusor Secura FT, B. Braun Melsunge AF, Germany) at 4 ml/h. The abdomen was opened using a "⊥" -shaped incision, and the jejunum was cut at 1cm away from the Treitz's ligament and ileum at 2 cm proximal to ileocecal valve. The entire colon was removed. The portal vein (PV) was separated from pancreas. The segment of abdominal aorta (AA) containing the superior mesenteric artery (SMA) was mobilized by ligating and dividing the lumbar artery. The lumbar arteries from the AA were meticulously ligated with 8-0 nylon sutures to minimize bleeding between the celiac and left renal artery. The left renal vessels were then ligated. The dissected AA was ligated below the left renal artery. The celiac artery was ligated, followed by the ligation of the pyloric vein and splenic vein. Five to eight ml 2.5g/L Cefazomelin in saline was injected into the small intestine through the upper end of the jejunum. The AA was cannulated with a fine polyethylene catheter and the PV was cut off near hepatic hilum. The graft was perfused in situ with 2-3 ml 4 °C lactate Ringer's solution containing 125 000U/L heparin by micropump at 40 ml/h until the graft intestine and mesentery turned pale, and the fluid in the PV became clear. At last, the intestine and its vascular supply including a part of AA were removed en bloc. Under operational microscope and

in lactated Ringer's solution ice-water bath, the PV end was placed into a polyethylene cuff tube and its end part of endothelium was turned over to cover the end of cuff tube. The PV end and cuff tube were fixed with 6-0 silk sutures. Hence, the round orifice of the PV was exactly in the center of the cuff tube (Figure 1). The small intestinal graft was stored in lactated Ringer's solution at 4 °C^[25-27].

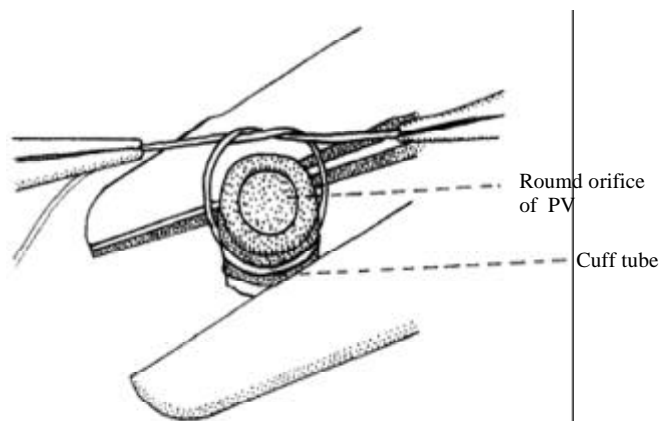


Figure 1 Fix cuff tub of PV

Recipient operation

Anesthesia and intravenous infusion for the recipient were the same as for the donors. The abdomen was opened via a midline incision from the ensisternum to the bladder level. The left ureter and renal artery were ligated. The left renal vein was dissected. The pedicle near renal hilum was ligated and the ligating suture was left as a tractor after removal of the left kidney. Segment of the recipient's abdominal AA (0.6-1.0 cm) was mobilized below the vessels to the left kidney. Under operating microscope ($\times 10$ amplification), the AA of the adventitia membrane of the anterior wall was removed and opened via a longitudinal arteriotomy. The lumen was flushed with low molecular dextran solution. The donor's small intestine was picked up from the ice water, surrounded by a gauze sponge packed with ice crystals, and then placed onto the right flank of the rats. The arterial anastomosis was performed first. After ensuring that the artery was not twisted, an end-to-side anastomosis was performed using continuous 9-0 non-traumatic nylon suture. The posterior wall was anastomosed from the inside of the vessels. The anterior wall of the arterial anastomosis was sutured externally. Each lateral wall of the artery was sutured with 8-10 sutures. The end of the left renal vein of the recipient was opened with a longitudinal incision. Two 9-0 nylon stay sutures were placed at the lateral sides of the anastomosis as a self-retaining retractor. The upper and lower sides of the incision were hauled by the pedicle ligating suture and microtweezer respectively. The cuffed PV of the small intestinal graft was inserted into the left renal vein of the recipient to revascularize the heterotopic small intestinal graft. The anastomosis was fixed with 5-0 silk suture (Figure 2). The left renal venous clamp was released first, followed by the clamps over and beneath the AA anastomosis, and the blood supply of the small intestinal graft was recovered. The arterial anastomosis was compressed lightly with a dry sponge for 1 to 2 min after reperfusion and then usually the oozing blood could be easily stopped. If blood was spouting from the arterial anastomosis, it should be quickly repaired with interruptive sutures. For the purpose of warm and flush, 20 mL warm saline was instilled in the peritoneal cavity. The small intestinal graft was put in order, and placed

onto the left flank of the rats. Both ends of the graft were exteriorized as stomas. The stomas were sutured with four 7-0 silk sutures between the host peritoneum and the seromuscular layer of the graft and four 5-0 silk sutures between the skin and the everted mucosa of the graft (Figure 3). The abdomen was closed using two layers of 1-0 silk continuous sutures.

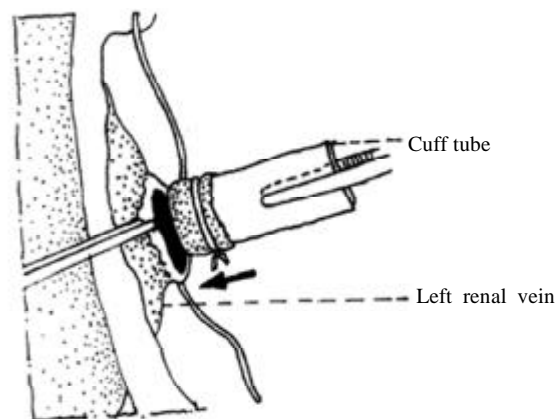


Figure 2 PV to left renal vein anastomosis

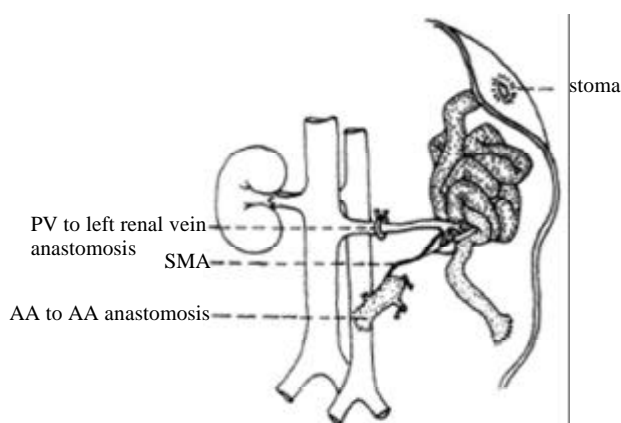


Figure 3 Heterotopic total small intestinal transplantation in rats

RESULTS

Operated by one person, the average time for the donor surgery was 86 ± 20 min, and 115 ± 20 min for the recipient and the average warm ischemic time being 40 ± 5 min. There was a shorter revascularization time of the graft, the AA to AA anastomosis was 21 ± 10 min, and the cuffed PV to the renal vein anastomosis was 5 ± 5 min. Sixteen rats which died from anesthetic accidents and hemorrhage during operation were not included in the statistical data. Among the 98 heterotopic whole small intestinal transplantation, 11 rats died in 6 days, the autopsy verified 2 cases of arterial anastomotic hemorrhage, 3 cases of the native small intestinal dysfunction, 4 cases of infection of abdominal cavity, and 2 cases of the pulmonary complications (Figure 4). There was no gross or microscopic evidence of either vascular occlusion in any of the grafts or stoma-related complications. The one-week survival rate was 88.7% (87/98). The rats recovered vigor and vitality after the operative day. The shape and color of the transplanted small intestines were nearly the same as the native intestines from the tenth day. The longest survival time of recipient rats was more than 389 days after SIT when the data were collected. They maintained normal weight, perfect intestinal function and intact intestinal histology.

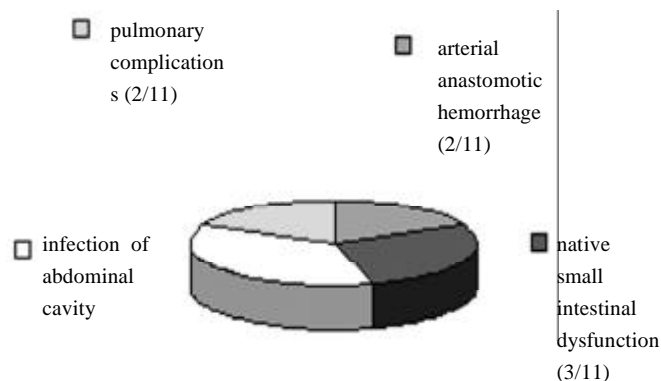


Figure 4 Cause of death in SIT rats

DISCUSSION

SIT of the rat remains a microsurgical technique which is difficult to manage. According to the need of clinical SIT practice, we used Wistar inbred strain rats as donors and recipients to practise heterotopic SIT, so that the model would not be affected by immune responses^[28-40]. Following the modified methods of Zhong *et al*^[2] and Kiyozaki *et al*^[3], we have accumulated a great and original experience with reducing complications and increasing survival rate in rats.

Enhancement of operative tolerance

Shortening fasting time Both donor and recipient rats were placed in metabolic cages and kept fasting before surgery, without eatable cushion and dirt. The fasting time was shortened from 48 h (donors) and 24 h (recipients) respectively to less than 12 h, a satisfying result could be achieved through this management, only a little bile and bowel fluid were found in the small intestinal graft by surgery. The rats received 5% glucose normal saline *ad libitum* before surgery for a supplement of water, salt and energy.

Intravenous infusion Hypovolemic shock was the most common cause of postoperative death in SIT rats because of hemorrhage, evaporation and loss of bowel fluid^[15]. The total blood volume of rats was about 5.5-6.5 ml/100 g body weight, if the loss of blood exceeded 3 mL, ischemic damage of small intestinal graft would occur in donors, and death would happen in recipients. Besides improving dissecting and anastomotic techniques to reduce bleeding, continuous infusion with lactated Ringer's solution via penile vein could keep blood pressure stable during surgery and increase survival rate. If there was a mass bleeding or blockage in intravenous infusion during surgical procedure, rats were given 4-5 ml (2 ml/100 g body weight) of 5% glucose normal saline via back subcutaneous injections after SIT. Fatal pulmonary edema and heart failure could be caused by overdose solution or fast infusion, so the infusion should be controlled to an optimum volume, never excessive.

Improvement in the vitality of small intestinal graft The quality of donor organ affected directly the result of transplantation. This is especially true for the small intestinal graft, which is much liable to mechanical and ischemic injuries during the procedure. The recipient rat "stupor" or "no vitality" or failure to death within 1 d-2d after SIT mostly occurred due to the quality of small intestinal graft. During the whole harvest procedure, the non-traumatic techniques should be adopted, a gauze sponge with saline was used to mobilize the graft gently

instead of holding or clamping with hand and microtweezer, and not to toss and turn the graft repeatedly so as to avoid damage. Because of the "┐" - shaped incision, the small intestinal graft dissected from the colon could be easily placed into abdominal cavity to reduce the exposure and vaporization damage. As vigorous intra-luminal irrigation and graft perfusion directly damaged the microcirculation of the graft^[41-44], we changed the method of perfusion from parting body to *in situ* graft perfusion in living donors and significantly reduced the volume of intra-luminal irrigation from 50-70 ml^[1] to 5-8 ml. The small intestine was put in order before graft perfusion, then the solution in the gut lumen could easily flow out. The speed of irrigation was not quickened till the intra-luminal solution flowed out, avoiding over-distention of the donor small intestine. The volume of graft perfusion *in situ* was reduced from 12-20 ml^[1] to 3-5 ml. The speed and volume of perfusion were accurately controlled by micropump instead of gravity, the graft perfusion was complete and the damage was reduced to minimum. Ischemic injury due to hypovolemic shock during the harvesting was often neglected by surgeons. For example, early ligation of the pyloric and splenic vein rapidly caused splanchnic venous congestion leading to shock^[2]. Therefore, we performed this procedure just prior to perfusion and after ligation of the celiac artery to avoid graft blood flow reduction. We also minimized ischemic injury to the donor small intestine by meticulous ligation of the lumbar vessels to avoid unnecessary blood loss, early ligation of the distal AA to improve perfusion of the graft and intravenous administration of 6-8 ml of lactated Ringer's solution to supply blood volume and improve blood circulation of the small intestinal graft during the surgery. A shorter warm ischemic time was very important for the improvement of graft vitality, the warm ischemic time in our experiment was almost controlled in 40 min. If the time was too long, the normal blood circulation could not be recovered, the result of transplantation would be seriously affected, which appeared as the graft edema, segmental venous stasis, congestion and extremely thin enteric fluid.

Improvement of recipient surgical procedure

It was critical that there was an adequate blood flow from the SMA to the graft and out through the PV smoothly. Based on Zhong^[2] and Kiyozaki^[3] surgery procedure, we refined some techniques. The blood flow of the inferior vena cava (IVC) was not blocked during surgery, so the blood circulation was not interrupted. The cuff technique was used with a cuffed anastomosis of the donor PV to the recipient left renal vein, the whole procedure of anastomosis spent about 5 min. Since the cuff tube was sculpted from a polyethylene tube with 2.3 mm in outer diameter and 1.8 mm in inner diameter, there was a larger and standard anastomosis. Furthermore, the endangium of the cuffed PV was well overturned, there was no any exposed anastomotic material in the venous lumen. So the unobstructed rate was much higher, none of rats died of the venous anastomotic complication. The AA column with SMA of the graft was anastomosed end to side to the AA of the recipient, the anastomotic bore was bigger and shapeable, so the anastomosis could be in progress smoothly without any tension. We used low molecular dextran solution without heparin to rinse the anastomosis, the damage to the endothelium was slighter^[45-46], and the chance of anastomotic stenosis and thrombosis was greatly reduced^[47-50]. These improved techniques resulted in an adequate blood flow to the graft without acute and chronic graft ischemia and the survival rate of the transplanted rat was obviously increased. It was true

that removal of one kidney did not increase the mortality in our experiment yet. After removal of one kidney, the remained kidney usually has a capacity to compensate. The adaptation may take place within 12-24 h and reach the largest degree during 1-2 wk. There was no an obvious disadvantage effect on physiological function and some experimental researches such as the absorptive function and permeability of transplanted small intestine could be studied on the model without any inconvenient.

In conclusion, our results suggested that applying these modified techniques would remarkably reduce the complications and improve survival rate in rats, the transplanted small intestine had a long-term fine function, this provided a potentially more consistent and practical model meeting the need of experimental and clinical studies.

REFERENCES

- 1 **Monchik GJ**, Russell PS. Transplantation of small bowel in the rat: technical and immunological considerations. *Surgery* 1971;**70**:693-702
- 2 **Zhong R**, Grant D, Sutherland F, Wang PZ, Chen HF, Lo S, Stiller C, Duff J. Refined technique for intestinal transplantation in the rat. *Microsurgery* 1991;**12**:268-274
- 3 **Kiyozaki H**, Kobayashi E, Toyama N, Miyata M. Segmental small bowel transplantation in the rat: comparison of lipid absorption between jejunal and ileal grafts. *JPEN* 1996;**20**:67-70
- 4 **Schraut WH**, Abraham VS, Lee KKW. Portal versus caval venous drainage of small bowel allografts: technical and metabolic consequences. *Surgery* 1986;**99**:193-198
- 5 **Lee KKW**, Schraut WH. Structure and function of orthotopic small bowel allografts in rats treated with cyclosporine. *Am J Surg* 1986;**151**:55-60
- 6 **Kimura K**, Money SR, Jaffe BM. The effects of size and site of origin of intestinal grafts on small-bowel transplantation in the rat. *Surgery* 1987;**101**:618-622
- 7 **Fujiwara H**, Raju S, Grogan JB, Lewin JR, Johnson WW. Total orthotopic small bowel allotransplantation in the dog. Features of atypical rejection and graft-versus-host reaction. *Transplantation* 1987;**44**:747-753
- 8 **Kimura K**, LaRosa CA, Money SR, Jaffe BM. Segmental intestinal transplantation in rats with resected entire small bowel, ileocecal valve, and cecum. *J Surg Res* 1988;**45**:349-356
- 9 **Kaneko H**, Hancock W, Schweizer RT. Progress in experimental porcine small-bowel transplantation. *Arch Surg* 1989;**124**:587-592
- 10 **Kimura K**, LaRosa CA, Blank MA, Jaffe BM. Successful segmental intestinal transplantation in enterectomized pigs. *Ann Surg* 1990;**211**:158-164
- 11 **Li N**, Li JS, Liao CX, Li YS, Wu XH. Successful segmental small bowel allotransplantation in pigs. *Chin Med J* 1993;**106**:187-190
- 12 **Zhong R**, Grant D, Black R, Stiller C, Duff J. Combined small bowel and kidney transplantation in the rat. *Transplantation Proceedings* 1989;**21**:2907-2908
- 13 **Schroeder P**, Sandforth F, Gundlach M, Deltz E, Thiede A. Functional adaptation of small intestinal mucosa after syngeneic and allogeneic orthotopic small bowel transplantation. *Transplantation Proceedings* 1989;**21**:2887-2889
- 14 **Martinelli GP**, Knight RK, Kaplan S, Racelis D, Dikman SH, Schanzer H. Small bowel transplantation in the rat. Effect of pretransplant blood transfusions and cyclosporine on host survival. *Transplantation* 1988;**45**:1021-1026
- 15 **Zhong R**, Wang P, Chen H, Sutherland F, Duff J, Grant D. Surgical techniques for orthotopic intestinal transplantation in the rat. *Transplantation Proceedings* 1990;**22**:2443-2444
- 16 **Schweizer E**, Gundlach M, Gassel HJ, Deltz E, Schroeder P. Effects of two-step small bowel transplantation on intestinal morphology and function. *Transplantation Proceedings* 1991;**23**:688
- 17 **Frankel WL**, Zhang W, Afonso J, Klurfeld DM, Don SH, Laitin E, Deaton D, Furth EE, Pietra GG, Naji A, Rombeau JL. Glutamine enhancement of structure and function in transplanted small intestine in the rat. *JPEN* 1993;**17**:47-55
- 18 **Harnel RP Jr**. A simplified technique of small intestinal transplantation in the rat. *J Pediatr Surgery* 1984;**19**:400-403
- 19 **Sigalet DL**, Kneteman NN, Fedorak RN, Kizilisik T, Madsen KE, Thomson AB. Small intestinal function following syngeneic transplantation in the rat. *J Surg Res* 1996;**61**:379-384
- 20 **Price BA**, Cumberland NS, Clark CL, Pockley AG, Wood RFM. Evidence that orthotopic transposition following rat heterotopic small bowel transplantation corrects overgrowth of potentially pathogenic bacteria. *Transplantation* 1996;**61**:649-651
- 21 **Winkelaar GB**, Smith LJ, Martin GR, Sigalet DL. Fat absorption after small intestinal transplantation in the rat. *Transplantation* 1997;**64**:566-571
- 22 **Raofi V**, Fontaine MJ, Mihalov ML, Holman DM, Dunn TB, Vitello JM, Asolati M, Kumins NH, Benedetti E. Comparison of jejunal and ileal surveillance biopsies in a porcine model of intestinal transplantation. *Transplantation* 1999;**68**:188-191
- 23 **Li YS**, Li JS, Li N. Surgical technique for intestinal transplantation in rats. *Huaren Xiaohua Zazhi* 1998;**6**:667-669
- 24 **Li YX**, Li JS, Li N. Improved technique of vascular anastomosis for small intestinal transplantation in rats. *World J Gastroenterol* 2000;**6**:259-262
- 25 **Li YS**, Li JS, Li N, Jiang ZW, Zhao YZ, Li NY, Liu FN. Evaluation of various solutions for small bowel graft preservation. *World J Gastroenterol* 1998;**4**:140-143
- 26 **Luther B**, Lehmann C, David H, Klinnert J. Preservation of isolated intestinal segments using the University of Wisconsin solution. *Transplantation Proceedings* 1991;**23**:2459
- 27 **Zhang S**, Kokudo Y, Nemoto EM, Todo S. Biochemical evidence of mucosal damage of intestinal grafts during cold preservation in University of Wisconsin, Euro-Collins, and lactated Ringer's solutions. *Transplantation Proceedings* 1994;**26**:1494-1495
- 28 **Hatcher PA**, Deaton DH, Bollinger RR. Transplantation of the entire small bowel in inbred rats using cyclosporine. *Transplantation* 1987;**43**:478-484
- 29 **Grant D**, Zhong R, Gunn H, Duff J, Garcia B, Keown P, Wijsman J, Stiller C. Graft-versus-host disease associated with intestinal transplantation in the rat. Host immune function and general histology. *Transplantation* 1989;**48**:545-549
- 30 **de Bruin RW**, Saat RE, Heineman E, Jeekel J, Marquet RL. The effect of cyclosporine A in small-bowel transplantation in rats is dependent on the rat strain combination used. *Transplantation Proceedings* 1990;**22**:2472-2473
- 31 **Wang M**, Qu X, Stepkowski SM, Chou TC, Kahan BD. Beneficial effect of graft perfusion with anti-T cell receptor monoclonal antibodies on survival of small bowel allografts in rat recipients treated with brequinar alone or in combination with cyclosporine and sirolimus. *Transplantation* 1996;**61**:458-464
- 32 **Alessiani M**, Spada M, Dionigi P, Arbustini E, Regazzi M, Fossati GS, Zonta A. Combined immunosuppressive therapy with tacrolimus and mycophenolate mofetil for small bowel transplantation in pigs. *Transplantation* 1996;**62**:563-567
- 33 **Yin DP**, Sankary HN, Williams J, Krieger N, Fathman CG. Induction of tolerance to small bowel allografts in high-responder rats by combining anti-CD4 with CTLA4Ig. *Transplantation* 1996;**62**:1537-1539
- 34 **Fryer J**, Grant D, Jiang J, Metrakos P, Ozcay N, Ford C,

- Garcia B, Behme R, Zhong R. Influence of macrophage depletion on bacterial translocation and rejection in small bowel transplantation. *Transplantation* 1996;**62**:553-559
- 35 **Toogood GJ**, Rankin AM, Tam PK, Morris PJ, Dallman MJ. The immune response following small bowel transplantation: I. An unusual pattern of cytokine expression. *Transplantation* 1996;**62**:851-855
- 36 **Koide S**, McVay LD, Frankel WL, Behling CA, Zhou ED, Shimada T, Zhang W, Rombeau JL. Increased expression of tissue cytokines in graft-versus-host disease after small bowel transplantation in the rat. *Transplantation* 1997;**64**:518-524
- 37 **Ozday N**, Fryer J, Grant D, Freeman D, Garcia B, Zhong R. Budesonide, a locally acting steroid, prevents graft rejection in a rat model of intestinal transplantation. *Transplantation* 1997;**63**:1220-1225
- 38 **Toogood GJ**, Rankin AM, Tam PK, Morris PJ, Dallman MJ. The immune response following small bowel transplantation. II. A very early cytokine response in the gut-associated lymphoid tissue. *Transplantation* 1997;**63**:1118-1123
- 39 **Mueller AR**, Platz KP, Heckert C, Hausler M, Guckelberger O, Schuppan D, Lobeck H, Neuhaus P. The extracellular matrix: an early target of preservation/reperfusion injury and acute rejection after small bowel transplantation. *Transplantation* 1998;**65**:770-776
- 40 **Johnsson C**, Bengtsson M, Tufveson G. Recipient-reactive antibodies occur during development of acute graft-versus-host reaction after small bowel transplantation. *Transplantation* 1996;**62**:343-346
- 41 **van Oosterhout JMA**, de Boer HH, Jerusalem CR. Small bowel transplantation in the rat: the adverse effect of increased pressure during the flushing procedure of the graft. *J Surg Res* 1984;**36**:140-146
- 42 **Cicalese L**, Caraceni P, Nalesnik MA, Borle AB, Schraut WH. Oxygen free radical content and neutrophil infiltration are important determinants in mucosal injury after rat small bowel transplantation. *Transplantation* 1996;**62**:161-166
- 43 **Sugitani A**, Bauer AJ, Reynolds JC, Halfter WM, Nomoto M, Starzl TE, Todo S. The effect of small bowel transplantation on the morphology and physiology of intestinal muscle: a comparison of autografts versus allografts in dogs. *Transplantation* 1997;**63**:186-194
- 44 **Kaihara S**, Egawa H, Inomata Y, Uemoto S, Asonuma K, Tanaka K. Serotonin as a useful parameter for cold and warm ischemic injury in small bowel transplantation. *Transplantation* 1997;**64**:405-410
- 45 **Buckley RC**, Davidson SF, Das SK. The role of various antithrombotic agents in microvascular surgery. *Br J Plast Surg* 1994;**47**:20-23
- 46 **Cox GW**, Runnels S, Hsu HS, Das SK. A comparison of heparinised saline irrigation solutions in a model of microvascular thrombosis. *Br J Plast Surg* 1992;**45**:345-348
- 47 **Davidson SF**, Brantley SK, Talbot PJ, Das SK. A functional model of microvascular thrombosis. *Plast Reconstr Surg* 1990;**86**:579-581
- 48 **Khoury RK**, Cooley BC, Kenna DM, Edstrom LE. Thrombosis of microvascular anastomoses in traumatized vessels: fibrin versus platelets. *Plast Reconstr Surg* 1990;**86**:110-117
- 49 **Davidson SF**, Brantley SK, Das SK. Comparison of single-dose antithrombotic agents in the prevention of microvascular thrombosis. *J Hand Surg* 1991;**16**:585-589
- 50 **Buckley RC**, Davidson SF, Das SK. Effects of ketorolac tromethamine (Toradol) on a functional model of microvascular thrombosis. *Br J Plast Surg* 1993;**46**:296-299

Edited by Ma JY

• CLINICAL RESEARCH •

Ultrasonic aspiration hepatectomy for 136 patients with hepatocellular carcinoma

Wei Wu, Xin-Bao Lin, Jian-Min Qian, Zhen-Ling Ji, Zao Jiang

Wei Wu, Xin-Bao Lin, Institute of Acoustics, Ultrasonic Medical Electronics Research Group, State Key Laboratory of Modern Acoustics, Nanjing University, Nanjing 210093, Jiangsu Province, China

Jian-Min Qian, The first Affiliated Hospital of Nanjing Medical University, Nanjing 210029, Jiangsu Province, China

Zhen-Ling Ji, Zao Jiang, The Affiliated Zhongda Hospital of Southeast University, Nanjing 210009, Jiangsu Province, China

Correspondence to: Wei Wu, Institute of Acoustics, Ultrasonic Medical Electronics Research Group, State Key Laboratory of Modern Acoustics, Nanjing University, Nanjing 210093, Jiangsu Province, China. weiwu-cs@sohu.com

Telephone: +86-25-3272447

Received 2001-06-19 **Accepted** 2001-07-16

Abstract

AIM: To study the operative injury, post-operative complications, the hospitalization time, the post-operative survival rate of ultrasonic aspiration hepatectomy with a domestic new type of ultrasonic surgical device in comparison with that of conventional techniques of hepatectomy.

METHODS: A total 136 patients with hepatocellular carcinoma (HCC, including 12 patients in 1991 and 124 consecutive patients from July 1995 to December 2000) underwent ultrasonic aspiration in liver resection (group T) and 179 HCC patients received conventional hepatectomy during the corresponding period (group C). The results of the two groups were compared statistically.

RESULTS: There was no significant difference in the mean operation time between group T (152 ± 11 min) and C (144 ± 11 min). No operation or hospital death occurred in both groups. In group T, the mean volumes of bleeding (463 ± 15 ml) and blood transfusion (381 ± 12 ml) were markedly less than those in group C (557 ± 20 ml, and 507 ± 18 ml, respectively, $P < 0.05$). The mean hospitalization time of group T (8.9 ± 0.6 d) was markedly shorter than that of group C (11.7 ± 0.6 d) ($P < 0.05$). The incidence of complications in group T was markedly lower than in group C, post-operative jaundice occurred in 4/136 and 31/179, respectively ($P < 0.05$), liver failure in 0/136 and 2/179, cholorrhea in 0/136 and 6/179, hydrothorax in 21/136 and 39/179 ($P < 0.05$), ascites in 9/136 and 54/179, respectively ($P < 0.05$). There was no significant difference in the 1-year survival rate between the two groups ($P > 0.05$), while the 3-year survival rate of group T (64.2 %) increased markedly as compared with that of group C (55.7 %) ($P < 0.01$).

CONCLUSION: The ultrasonic aspiration hepatectomy with a domestic new type of ultrasonic surgical device could evidently reduce the operative injury and post-operative complications, shorten the hospitalization time and prolong the survivals of HCC patients.

Wu W, Lin XB, Qian JM, Ji ZL, Jiang Z. Ultrasonic aspiration hepatectomy for 136 patients with hepatocellular carcinoma. *World J Gastroenterol* 2002; 8 (4):763-765

INTRODUCTION

Hepatocellular carcinoma (HCC) is common in China^[1-10], and its treatment is not satisfactory so far^[11-17]. The first choice of treatment for HCC is hepatectomy, but the resectability is only about 4-20 %^[18-25]. Therefore, it is important to improve the technique of liver resection and to increase the resectability. The invention of ultrasonic surgical device (also called ultrasound scalpel) is a breakthrough in medical field since the 1980 s, it was also one of the developing hotspots in the surgery. The reason for its attention is that when compared with electric surgery unit, laser and microwave as well as other methods^[26-36], it has many advantages including less lesion for the tissue in or around the operating field, less bleeding (or no bleeding), clear operating field, less operating risk, high security and more convenient to operate^[37-40]. Since the 1990s, ultrasonic aspiration hepatectomy has been popularized in many European and American countries, and is now a standard technique of hepatosurgery^[41]. Our study on 136 ultrasonic aspiration hepatectomies indicated that ultrasonic aspiration hepatectomy could reduce operative injury and the incidence of the major operative complication markedly. In the meantime, it could shorten the duration of hospitalization, reduce the blood transfusion during the operation, and raise the survival rate.

MATERIALS AND METHODS

Materials

From April 1991 to December 2000, we observed randomly (completely random design) 136 primary liver carcinoma patients (group T) treated by ultrasonic aspiration hepatectomy and 179 primary liver carcinoma patients (group C) treated by conventional technique. The ages of patients in group T and C were 13-72 years (mean 57 ± 15 years) and 19-74 years (mean 55 ± 16 years), respectively. There were 14 and 21 patients with intrahepatic metastasis in the group T and C, respectively (Table 1). NTY-300 multifunctional ultrasonic surgical device (made in China) was used. The equipment was composed of main unit that could work in multi frequency, several kinds of hand-pieces and control keyboard. It had multifunction of ultrasonic cutting, aspiration, and liposuction. The basic principle was that the computer device of the mainframe could produce electric signal ranging from 19 to 35kHz of frequency, and the signal was amplified by power amplifier, then sent to the hand-piece after impedance conversion by the output isolating transformer, thus producing ultrasonic vibration. At the same time, the sampling circuit could feed back the working status of the hand-piece to the computer device judging whether it was falling in the best working frequency. And the computer could modulate it automatically to assure that the portable therapeutic head fell in suitable resonance frequency to give

the maximal ultrasound energy output. There are several simple control keys for manual operation on the control panel. And the corresponding parameters were displayed on the display monitor.

Table 1 Clinical data of patients included in this study

Main parameter	Common hepatectomy (n=179)	Ultrasonic aspiration hepatectomy (n=136)
Mean age (yrs)	55±16	57±15
M/F	166/13	128/8
T B/ (μmolL ⁻¹)	17.4±1.4	16.4±1.5
D B/ (μmolL ⁻¹)	3.1±0.3	3.0±0.3
ALB/ (gL ⁻¹)	40.0±7.0	42.4±7.4
ALT/ (nkatL ⁻¹)	667.0±49.8	538.1±51.2
AST/ (nkatL ⁻¹)	602.6±50.8	566.3±40.0
TT/ (g L ⁻¹)	78.62±7.85	73.32±8.26
Size of tumor		
T≤2cm	84	67
2cm≤T≤5cm	59	44
5cm≥T	36	25
Location		
Right	40	32
Tri-liver lobe	3	2
Left tri-liver lobe	8	5
VIII segment	19	16
Others	109	81
Number of tumor		
1	135	102
2	38	27
≥3	6	7

Methods

The bilateral subcostal approach, extended to the right as far as the midaxillary line, to the left as far as the lateral margin of the rectus muscle, and medially upwards the xiphoid process of the sternum (Mercedes incision) or a right subcostal incision extended along the median line (Invested-L incision) is the classic approach. JM-II retractor (made in China) was routinely used for opening the abdominal wall. In the first stage the ligaments around the lobe to be resected were dissected until the lobe was mobilized. The liver to be resected was demarcated by cautery, and stitched to block the local blood supply. The ultrasonic aspirator was utilized in hepatoparenchyma dissection. Liver cells were broken and emulsified, and aspirated out of body. The intrahepatic canaliculi were exposed and can be dissected and ligated. The oozing sites were controlled by conventional methods.

Statistical treatment

t-test and χ^2 test were used.

RESULTS

There was no significant difference in the mean operation time between groups T (152±11min) and C (144±11min). No operation or hospital death of patients occurred in both groups. In group T, the mean volumes of bleeding (463±15 ml) and blood transfusion (381±12 ml) were markedly less than those in group C (557±20 ml, and 507±18 ml, respectively, $P<0.05$). The mean hospitalization time of group T (8.9±0.6 d) was markedly shorter than that of group C (11.7±0.6 d), ($P<0.05$).

The incidence of complications in the group T was significantly lower than in group C. There was no significant difference in the 1-year survival rate between the two groups ($P>0.05$), while the 3-year survival rate of group T (64.2 %) increased markedly as compared with that of group C (55.7 %), (Table 2).

Table 2 Comparison of operation and treatment conditions between the two groups

Main parameter	Common hepatectomy (n=179)	Ultrasonic aspiration hepatectomy (n=136)
Operation time/min	144±11	152±11
Bleeding volume/ml	557±20	463±15 ^a
Transfusion volume/ml	507±18	381±12 ^a
Hospitalization day	11.7±0.6	8.9±0.6 ^a
Liver failure	2	0
Postoperative jaundice	31	4 ^a
Cholorrhea	6	0
Hydrothorax	39	21 ^a
Ascites	54	9 ^a
1-year survival rate	92.5%	94.8%
3-year survival rate	55.7%	64.2% ^b

^a $P<0.05$, ^b $P<0.01$, vs Common hepatectomy.

DISCUSSION

In the ultrasonic aspiration hepatectomy, semisolid liver tissue is broken and emulsified under the conjugated effects of ultrasonic shock acceleration and high-velocity liquid jet, and then is aspirated out by suction. Since most liver cancer patients (>90%) in China are complicated with liver cirrhosis [3-10], some researchers considered that it was difficult for the cirrhosis liver tissues containing plenty of connective tissue to be unbroken by ultrasonic knife. In fact, ultrasonic knife is just a common name, whose main function is not tissue-cut, but to expose intrahepatic canaliculi after breaking the cellular elements. For the intrahepatic fibrous tissue, the routine operative technique should be used [18-25].

Our data indicated that ultrasonic aspiration hepatectomy could significantly reduce the operative injury and the incidence of complication and shorten the mean hospitalization time by 3-4 days. Because of less blood transfusion required and tumor manipulation avoided in the operation, the 3-year survival rate of group T was higher than that of group C. The main technical advantages of this clinical application included (1) by the conventional operative procedure tissues are dissected with fingers, scissors or knife handle, and some fine canaliculi could not be exposed readily, so it is hard to avoid operative injury, which resulted in more bleeding during or after operation and higher incidence of cholorrhea. Ultrasonic knife can aspirate the liver tissues around the incision, the blood vessel and bile duct remained. The operators could ligate the vessel and bile duct perfectly, so cholorrhea and hematorrhea after operation may be avoided. (2) ultrasonic knife is actually a kind of ultrasonic aspirator. According to the principle that the highly hydrated tissues could be emulsified easily, ultrasonic knife could aspirate the cellular debris out of body, but it cannot replace the conventional operative technique. (3) since the main blood vessel and bile duct injuries can be avoided in the operation, the tumor near portahepatis can be cut off, thus it raises the resectability of liver cancer. Our first patient treated with this procedure was a 13 year old child with a tumor encroached on the first and second portahepatis. The pathologic diagnosis after operation was

hepatocellular carcinoma. The patient has been remained well and alive up to 10 years. In the 136 operations, there were 64 complicated operations, 32 right liver lobe resections, 16 VIII liver segment resections, 5 tri-liver lobe resections, and 2 left tri-liver lobe resections. (4)local block of blood flow could reduce bleeding in operation and assure the safety of hepatectomy^[2,8], which is important in saving blood resources and accelerating the rehabilitation of patient. (5)ultrasonic aspiration hepatectomy with no demand to block the portahepatis, is especially suitable for the patients with impairment of liver function so as to avoid further injuries to liver parenchyma.

REFERENCES

- 1 **Lin NF**, Tang J, Hoteyi SM. Study on environmental etiology of high incidence areas of liver cancer in China. *World J Gastroenterol* 2000; **6**: 572-576
- 2 **Gu GW**, Zhou HG. New concept in etiology of liver cancer. *Shijie Huaren Xiaohua Zazhi* 1998; **6**:185-187
- 3 **Yu SZ**, Dong CH. Risk identification, assessment and control of primary hepatocellular cancer. *Huaren Xiaohua Zazhi* 1998; **6**:1026-1029
- 4 **Jiang XL**, Pan BR, Ma JY, Ji ZH, Ma LS. Gastroenterologies in the beginning of new century---review and prospect. *Shijie Huaren Xiaohua Zazhi* 2000; **8**:1161-1176
- 5 **Tang ZY**. Hepatocellular carcinoma cause, treatment and metastasis. *World J Gastroenterol* 2001; **7**:445-454
- 6 **Wu MC**. Clinical research advances in primary liver cancer. *World J Gastroenterol* 1998; **4**:471-474
- 7 **Liu JP**, Peng WW, Li MD, Li QF. Clinical significance of serum and liver β -2 microglobulin in patients with various types of HBV infection. *Huaren Xiaohua Zazhi* 1998; **6** (Suppl 7):195-197
- 8 **Liao HY**, Lang ZW, Zhu RP, Cui BN, Li XM, Li Y, Weng L. The study of infection on hepatitis G virus in the tissue of hepatocellular carcinoma. *Shijie Huaren Xiaohua Zazhi* 1998; **6**(suppl 7):401
- 9 **Yuan FP**, Huang PS, Wang Y, Gong HS. Relationship between EBV infection in Fujian HCC and HBV and P53 protein expression. *Shijie Huaren Xiaohua Zazhi* 1999; **7**:491-493
- 10 **Deng ZL**, Ma Y, Yuan L, Teng PK. The importance of hepatitis C as a risk factor for hepatocellular carcinoma in Guangxi. *World J Gastroenterol* 2000; **6**(suppl 3):75
- 11 **Zhang BH**, Liu Y, Qian GX, Chen H, Wu MC. The prognostic significance of detection of AFPmRNA and AFP after HCC resected. *Huaren Xiaohua Zazhi* 1998; **6**(suppl 7):125-126
- 12 **Wu ZQ**, Fan J, Qiu SJ, Zhou J, Tang ZY. The value of post-operative hepatic regional chemotherapy in prevention of recurrence after radical resection of primary liver cancer. *World J Gastroenterol* 2000; **6**:131-133
- 13 **Ji W**, Ma KS, Dong JH, Huang XL, He ZP. The stage II hepatectomy on hepatic cancer after selective portal vein embolization. *Shijie Huaren Xiaohua Zazhi* 2001; **9**:1209-1210
- 14 **Yamanaka J**, Yumauaka N, Nakasho K, Tanaka T. Clinicopathologic analysis of stageII-III hepatocellular carcinoma showing early massive recurrence after liver resection. *J Gastroenterol Hepatol* 2000; **15**:1192-1198
- 15 **Dai YM**, Chen H, Wang NJ, Ni CR, Cong WM, Zhang SP. Clinicopathologic risk factors and prognostic evaluation in hepatocellular carcinoma recurrence after surgery. *Xin Xiaohuabingxue Zazhi* 1997; **5**:439-441
- 16 **Sun WB**. Further decrease the fatality rate in aged patients undergoing hepatobiliary surgery. *Huaren Xiaohua Zazhi* 1998; **6**:61-63
- 17 **Kobayashi T**, Kubota K, Takayama T, Makauchi M. Telomerase activity as a predictive marker for recurrence of hepatocellular carcinoma after hepatectomy. *Am J Surg* 2001; **181**:284-288
- 18 **Tang ZY**. Advances in clinical research of hepatocellular carcinoma in China. *Huaren Xiaohua Zazhi* 1998; **6**:1013-1016
- 19 **Zhang J**, Zhang JR. Surgical treatment of liver metastatic neoplasms. *Shijie Huaren Xiaohua Zazhi* 1999; **7**:414
- 20 **Vallet C**, Martinet O, Mosimann F. Surgical treatment of hepatic metastases. *Rev Med Suisse Romande* 2001; **121**:119-124
- 21 **Zhou XD**, Tang ZY, Yang BH, Lin ZY, Ma ZC, Ye SL, Wu ZQ, Fan J, Qin LX, Zheng BH. Experience of 1000 patients who underwent hepatectomy for small hepatocellular carcinoma. *Cancer* 2001; **91**:1479-1486
- 22 **Patiutko IuI**, Sagaidak IV, Kotelnikov AG, Badaliau KhV, Tumanian AO. Current approaches to surgical treatment of liver tumors. *Vopr Oukol* 1998; **44**:580-583
- 23 **Liu CL**, Fan ST, Lo CM, Tung PR, Wong J. Anterior approach for major right hepatic resection for large hepatocellular carcinoma. *Ann Surg* 2000; **232**:25-31
- 24 **Wu MC**, Shen F. Progress in research of liver surgery in China. *World J Gastroenterol* 2000; **6**:773-776
- 25 **Wu ZQ**, Fan J, Qiu SJ, Zhou J, Ma ZC, Zhou XD, Tang ZH. An approach for difficult hepatectomy-retrograde hepatectomy in 29 patients with liver malignant tumor. *Hepatogastroenterol* 1999; **46**:1140-1144
- 26 **Savvier E**, Castaing D. Use of a water-jet dissector during hepatectomy. *Ann Chir* 2000; **125**:370-375
- 27 **Asahara T**, Dohi K, Nakahara H, Katayama K, Itamoto T, Sugino K, Moriwaki K, Shiroyama K, Azuma K, Ito K, Shimamoto F. Laparoscopy-assisted hepatectomy for a large tumor of the liver. *Hiroshima J Med Sci* 1998; **47**:163-166
- 28 **Chen HY**, Ker CG, Juan CC, Lo HW. Laparoscopic subsegmentectomy for hepatocellular carcinoma with cirrhosis: a case report. *Kaohsiung J Med Sci* 2000; **16**:582-586
- 29 **Gertsch P**, Pelloni A, Guerra A, Krpo A. Initial experience with the harmonic scalpel in liver surgery. *Hepatogastroenterology* 2000; **47**:733-736
- 30 **Yamashita Y**, Sakai T, Maekawa T, Watanabe K, Iwasaki A, Shirakusa T. Thoracoscopic transdiaphragmatic microwave coagulation therapy for a liver tumor. *Surg Endosc* 1998; **12**:1254-1258
- 31 **Jia YC**, Tian JM, Wang ZT, Chen D, Ye H, Liu Q, Yang JJ, Sun F, Lin L, Lu JP, Wang F, Cheng HY. A retrospective review on interventional treatment of 10000 cases of liver cancer. *Huaren Xiaohua Zazhi* 1998; **6**:2-3
- 32 **Tu SP**, Wu DM, Yuan YZ, Wu YL, Jiang SH, Wu YX. Treatment of hepatocellular carcinoma by transcatheter arterial chemoembolization with hydroxycamptothecin. *Shijie Huaren Xiaohua Zazhi* 1999; **7**:158-160
- 33 **Cheng SZ**, Zhang JH, Cheng YJ. Relative analization in the effects of percutaneous injecting several agents into hepatic neoplasmo. *Shijie Huaren Xiaohua Zazhi* 2000; **8** (suppl 8):88
- 34 **Fan J**, Ten GJ, He SC, Guo JH, Yang DP, Weng GY. Arterial chemoembolization for hepatocellular carcinoma. *World J Gastroenterol* 1998; **4**:33-37
- 35 **Huang DZ**, Wu YD, Song XQ, Hu XH, Kang P. United treatment with iodine-125 oil embolism and local radioactive therapy on hepatic carcinoma. *Shijie Huaren Xiaohua Zazhi* 2001; **9**:1198-1201 (in Chinese)
- 36 **Fan J**, Wu ZQ, Tang ZY, Zhou J, Qiu ST, Ma ZC, Zhou XD, Ye SL. Multimodality treatment in hepatocellular carcinoma patients with tumor in portal vein. *World J Gastroenterol* 2001; **7**:28-32
- 37 **Yamamoto Y**, Ikai I, Kume M, Sakai Y, Yamauchi A, Shinohara H, Morimoto T, Shimahara Y, Yamamoto M, Yamaoka Y. New simple technique for hepatic parenchymal resection using a Cavitron Ultrasonic Surgical Aspirator and bipolar cautery equipped with a channel for water dripping. *World J Surg* 1999; **23**: 1032-1037
- 38 **Trupka A**, Hallfeldt K, Kalteis T, Schmidbauer S, Schweiberer L. Open and laparoscopic liver resection with a new ultrasound scalpel. *Chirurg* 1998; **69**: 1352-1356
- 39 **Kokudo N**, Kimura H, Yamamoto H, Seki M, Ohta H, Matsubara T, Takahashi T. Hepatic parenchymal transection using ultrasonic coagulating shears: a preliminary report. *J Hepatobiliary Pancreat Surg* 2000; **7**: 295-298
- 40 **Ouchi K**, Mikuni J, Sugawara T, Ono H, Fujiya T, Matsubara Y, Kakugawa Y, Yamanami H, Nakagawa K. Hepatectomy using an ultrasonically activated scalpel for hepatocellular carcinoma. *Dig Surg* 2000; **17**: 138-142
- 41 **Fan ST**, Lai ECS, Lo CM, Chu KM, Liu CL, Wong J. Hepatectomy with an ultrasonic dissector for hepatocellular carcinoma. *Br J Surg* 1996; **83**:117-120

Edited by Ma JY

• CLINICAL RESEARCH •

Endoscopic dilation of esophageal stricture without fluoroscopy is safe and effective

Yong-Guang Wang, Thian-Lok Tio, Nib Soehendra

Yong-Guang Wang, Department of Endoscopic Surgery, Peking University People's Hospital, 100034 Beijing, China

Thian Lok Tio, Division of GI, Department of Medicine, Georgetown University Hospital, Washington DC, USA

Nib Soehendra, Department of Interdisciplinary Endoscopy, University Hospital Eppendorf, Hamburg, Germany

Correspondence to: Yong-Guang Wang MD, PhD, Department of Endoscopic Surgery, Peking University People's Hospital, Beijing 100034, China. endowang@sina.com

Telephone: +86-10-66510952 **Fax:** +86-10-66510952

Received 2000-09-21 **Accepted** 2000-09-29

Abstract

AIM: Endoscopic dilation of esophageal strictures is a commonly performed procedure in the management of dysphagia. The procedure is usually done with fluoroscopic guidance. The aim of this study was to assess the use of Tracer guide wire in conjunction with Savary-Gilliard dilators in the dilation of tight esophageal strictures without fluoroscopy.

METHODS: Fifty-five patients with significant dysphagia from strictures due to a variety of causes were dilated endoscopically. The procedure consisted of two parts. First, a guidewire was passed using endoscopic guidance, and then, dilation was performed without fluoroscopy. A modified Tracer wire was employed and was particularly effective in negotiating very tight esophageal strictures, in which the lumen is less than 6 mm. In general, the "Rule of Three" and "2-3 sessions in 10 days, maximum dilation up to 42 French" rules were followed. 401 dilations in a total of 55 patients (malignant strictures 30, benign 25) in 177 sessions were carried out.

RESULTS: The guide wire placement and Savary-Gilliard dilation were successfully performed without fluoroscopy, and improvement of dysphagia was achieved in all patients. Esophageal plastic stent (out diameter 40 French) was placed in five patients with malignant stricture-three of them with tracheo-esophageal fistula.

CONCLUSION: Dilation using Tracer guide wire without fluoroscopy is safe and effective in treatment of even very tight esophageal strictures.

Wang YG, Tio TL, Soehendra N. Endoscopic dilation of esophageal stricture without fluoroscopy is safe and effective. *World J Gastroenterol* 2002;8(4):766-768

INTRODUCTION

Dilation of esophageal strictures is a commonly performed procedure used to relieve dysphagia due to malignant or benign stenotic lesions. In clinical practice, fluoroscopy is recommended for monitoring the position of the guide wire and dilator^[1-6]. Some authors, however, believe that fluoroscopy is not necessary for Maloney dilation in chronic esophageal strictures^[7,8]. Recently, Fleischer^[9] and Kadakia^[10] reported that

esophageal dilation with polyvinyl bougies using a marked guide wire without fluoroscopy was safe. The aim of this study to describe our preliminary experience using a modified Tracer guide wire (MTGW) and marked Savary-Gilliard dilators without the use of fluoroscopy.

MATERIALS AND METHODS

Patients

Between September 1994 and February 1996, 55 consecutive patients (40 males, 15 females, from 10 to 80 years old, median age 58 years) with esophageal strictures were referred to our unit for dilation because of persistent or recurrent dysphagia. Whether a stenosis was benign or malignant, stenosis was ascertained using endoscopy and biopsy. There were 25 benign lesions and 30 malignant tumors. The diagnoses are summarized in Table 1. The strictures were classified by us into five grades according to clinical symptoms of dysphagia and endoscopic findings. The grading system is summarized in Table 2. Grade III and grade IV strictures (lumen less than 6 mm) are considered as very tight esophageal strictures (VTES). All of our patients had various degrees of dysphagia. Total of 177 sessions of dilation were performed for 55 patients who had various degrees of dysphagia prior to each session. 28 sessions (15.8 %) of dilation were carried out for grade I strictures, 99 (55.9 %) for grade II and 50 (28.3 %) for VETS. X-ray studies of the geography of the strictures were performed for each case before treatment.

Table 1 The Etiology of esophageal strictures

Malignant	n	Benign	n
Esophageal Cancer		Anastomotic stenosis	13
Upper	3	Postoperative stenosis	2
Middle	11	Caustic stricture	2
Lower	7	Achalasia	5
Esophageal stump ca	5	Esophagitis	2
Anastomotic ca	2	External compression	1
Lung ca	2		
Total	30		25

Table 2 The Classification of esophageal strictures

Grades	Passage (can eat)	Endoscopy* (can pass)	Lumen diameter
0	Normal diet(+)	Standard one(+)	>12mm
I	Solid diet (+)	GIF-XQ/240(+)	9-12mm
II	Half liquid (+)	GIF-XP (+)	6-9mm
III	Liquid diet(+)	GIF-XP (-)	<6mm
IV	Water (+)/(-)	Tracer wire(+)**	<1mm

*Endoscopy: used Olympus endoscope. **Tracer wire (Wilson-Cook Medical Inc.) is 300cm length with markers.

Instruments

Examinations were performed usually with Olympus GIF-XP 20 gastroscope (Olympus Corp, Tokyo, Japan). Dilation was performed with market Savary-Gilliard dilators and a modified Tracer guide wire (0.035", 300 cm length, with markers,) (Wilson-Cook Medical Inc. Winston-Salem, NC. USA).

Technique

If the stricture could be passed with a paediatric endoscope, the guidewire was placed under endoscopic guidance. Thereafter, dilation was performed without fluoroscopy. For very tight esophageal strictures, the Tracer guide wire was used by us as a path-finder and also for Savary-Gilliard dilation without fluoroscopy. The technique is as follows: 1) Under endoscopic guidance, the VTES is approached. The Tracer guide wire is gently inserted through the stricture until the wire has been advanced more than 70 cm (for normal anatomy) without strong resistance having been encountered. (2) Keeping the wire in place, the scope is withdrawn. The scope can be re-inserted alongside the wire. (3) The VTES is dilated over the Tracer wire starting with a 15 French or 21 French dilator using the markers on the wire and also on the dilators for guidance, or under endoscopic control. (4) Post the final dilation with a size 27 French or 33 French, the paediatric gastroscope is passed through the dilated lumen into the stomach.

In general, the "rule of three-dilator size increased step by step and dilation times is no more than three for each session" and "the rule of 2-3 sessions in 10 days, with maximum dilation up to 42 French" were followed. All procedures were performed without intravenous sedation, although local oropharyngeal anesthesia was given.

RESULTS

A total of 401 dilations in 55 patients in 177 sessions was done. The grade of benign and malignant stenosis before dilation was summarized in Table 3. The success rate for both placement of the guide wire and dilation was 100 % without use of fluoroscopy. There were no major complications (Table 4).

Table 3 The grade before dilation (177 sessions / 55 patients)

Grade	Sessions	%
0	0	0
I	28	15.8
II	99	55.9
III & IV	50	28.3

Table 4 Adverse events and complications induced by the guide wire placement or dilation without fluoroscopic control

Complications	n	(%, 401 dilations)
Superficial mucosal tear	3	0.75
Tracheal intubation of Tracer	1	0.25
Severe hemorrhage	0	
Perforation	0	
Sepsis	0	
Death	0	

The Tracer wire was successfully used to pass the VTES. The diameters of Savary-Gilliard dilators employed in this study were 15 French dilators in 3.8 %, 21 Fr. in 14.2 %, 27 Fr. and 33 Fr. dilators in 56.1 %, 38 Fr. in 15.7 %, 42 Fr. in 5.9 % and 45 Fr. (only be used for patients with achalasia) in 4.3 %. The average number of dilators per session was 2.7. Esophageal plastic stent (outer diameter 40 Fr., Wilson-Cook Medical Inc. NC.) was placed over the Olympus GIF-XP endoscope for five malignant strictures after being dilated up to 42 Fr. without fluoroscopic guidance. Three of them had strictures associated with tracheo-esophageal fistulae. There were no procedure-induced serious complications such as perforation, bleeding, sepsis and death. One patient with tracheo-esophageal fistula developed a dry cough during insertion of the wire. The wire was withdrawn and then reinserted successful without further event. Superficial mucosal tear was found in one patient with a post-myotomy stricture performed for achalasia (grade II stricture, 4.0 cm on length) after 42 Fr. dilation, and in one patient with an alkali induced corrosive stricture involving the entire length of the esophagus (grade II to III) after 33 Fr. dilation. In both cases the superficial tears healed spontaneously 3-5 days later.

DISCUSSION

Successful esophageal dilation involves both successful placement of the guide wire and dilation. This study demonstrates that Savary-Gilliard dilation can be successful without fluoroscopic control. There were no serious procedure-induced complications. All 55 unselected consecutive patients had significant dysphagia due to different types of esophageal pathology. Symptom relief was achieved in all patients.

The results are similar to that reported by Fleischer in a series of 100 patients and Kadakia in a series of 68 patients. In these two studies, the endoscope could be passed through the stricture in most patients and the tip of the marked Savary-Gilliard wire was placed under endoscopic view. However, the endoscope was impassable in 5 % and 29.4 % respectively. For these cases, fluoroscopy was required. The passage of the marked Savary-Gilliard wire for VTES, especially for malignant ones with tracheo-esophageal fistula and abnormal anatomy of the esophagus, such as angulation and diverticulum, is both difficult and hazardous without the aid of the fluoroscopy. Instead of marked Savary-Gilliard wire, we used the modified Tracer wire. The Tracer wire has a very soft and flexible tip which is considered atraumatic. The wire is hydrophilically coated on its distal 60 cm making it very slippery when wet. It can be passed through the stricture easily without trauma and be coiled in the stomach. Esophageal or stomach perforation could not be induced with the coil-able and atraumatic wire tip. During insertion of the wire, if there is resistance or if the patient starts coughing (which indicates that the wire is inserted into trachea through the fistula), the wire should be withdrawn and reinsertion performed. The proximal part (240 cm) of the wire is Teflon coated making it stiff enough to have a dilator passed over it, and also is marked for control of the procedures. Our study shows that the Tracer wire is very safe as a "path-finder" for VTES. Furthermore, Savary-Gilliard dilation can be performed immediately without exchange to a standard Savary-Gilliard guidewire. This is different from the techniques reported by Ling *et al*^[11] and Mohandas *et al*^[12]. In order to prevent complications, the "rule of three" popularized by Boyce (4) was followed by us. Dilation should be terminated when resistance is encountered during three consecutive dilations. Our experience suggests that in

long (>3.0 cm), subglottic, caustic strictures and in lesions of stump esophagus, the rule should not be employed. We agree that experience can teach how much resistance is significant during dilation. The maximum size of dilator used is a very important factor in avoiding complications. It has been suggested that the maximum size be at most 48 French^[3]. Based on our experiences, we believe that maximum dilation up to 42 French is sufficient for the Chinese population. This guarantees a normal diet and also reduces the risks associated with the procedure. In addition, in anastomotic strictures, the Tracer wire should be used when the endoscope can not be passed. In conclusion, the marked Savary-Gilliard dilator via a marked Tracer guide wire without fluoroscopy is safe and effective. Adequate placement of a guide wire prior to dilation is crucial in achievement of successful dilation.

REFERENCES

- 1 **Cotton PB**, Williams CP. Practical gastrointestinal endoscopy. 3rd ed. *Oxford: Blackwell Sci Pub* 1990;59-61
- 2 **Geenen JE**, Fleischer DE, Waye JD. Techniques in therapeutic endoscopy. 2nd ed. *New York: Gower Med Pub* 1992; 2:9-11
- 3 **Bennett JR**, Hunt RH. Therapeutic endoscopy and radiology of the gut. 2nd ed. *New York: Chapman and Hall Med* 1990:19-20
- 4 **Boyce HW**. Esophageal dilation. *Gastroenterol Endosc News* 1986;1-3
- 5 **Cheng YS**, Shang KZ, Zhuang QX, Li MH, Xu JR, Yang SX. Interentiongal therapy and cause of esophageal benign stricture. *Huaren Xiaohua Zazhi* 1998;**6**:791-794
- 6 **Pan X**, Chen CR, Gao TS, Huang JZ, Wang YP. Endoscopic dilation for patients with esophago cardiac stricture using domestic dilator. *Xin Xiaohuabingxue Zazhi* 1997;**5** (suppl 6):57-58
- 7 **Ho SB**, Case O, Katsman RJ, Lipschultz EM, Metzger RJ, Onstad GR, Silvis SE. Fluoroscopy is not necessary for Maloney dilation of chronic esophageal strictures. *Gastrointest Endosc* 1994;**40**:11-14
- 8 **Bailey AD**, Golder F. Can clinicians accurately assess esophageal dilation without fluoroscopy? *Am J Gastroenterol* 1989; **84**:373-375
- 9 **Fleischer DE**, Benjamin SB, Cattau EL, Jr Collen MJ, Lewis JH, Jaffee MH, Zeman RK A marked guidewire facilitates esophageal dilation. *Am J Gastroenterol* 1989; **84**:359-361
- 10 **Kadakia SC**, Cohan CF, Starnes EC. Esophageal dilation with polyvinyl bougies using a guidewire markings without the aid of fluoroscopy. *Gastrointest Endosc* 1991;**37**:183-187
- 11 **Vargas-Tank L**, Ovalle L, Fernandez C, Mella B, Estay R, del Solar MP, Soto JR. Use a very flexible guide wire to permit dilation of complex malignant strictures of the esophagus. *Gastrointest Endosc* 1995;**40**:8-10
- 12 **Mohandas KM**, Swaroop VS, Desai DC. Dilation of difficult gastrointestinal strictures using a modified wire-guided technique. *Endoscopy* 1995;**27**:446-448

Edited by Pagliarini R

Chromosomal aberrations related to metastasis of human solid tumors

Lun-Xiu Qin

Lun-Xiu Qin, Liver Cancer Institute and Zhongshan Hospital, Fudan University, Shanghai, China

Correspondence to: Lun-Xiu Qin, MD, PhD, Professor of Surgery, Liver Cancer Institute & Zhongshan Hospital, Fudan University, 136 Yi Xue Yuan Road, Shanghai 200032, China. lxqin@zshospital.com

Telephone: +86-21-64041990 Ext 2914 **Fax:** +86-21-64037181

Received 2002-06-11 **Accepted** 2002-06-25

Abstract

The central role of sequential accumulation of genetic alterations during the development of cancer has been firmly established since the pioneering cytogenetic studies successfully defined recurrent chromosome changes in specific types of tumor. In the course of carcinogenesis, cells experience several genetic alterations that are associated with the transition from a preneoplastic lesion to an invasive tumor and finally to the metastatic state. Tumor progression is characterized by stepwise accumulation of genetic alterations. So does the dominant metastatic clone. Modern molecular genetic analyses have clarified that genomic changes accumulate during the development and progression of cancers. In comparison with the corresponding primary tumor, additional events of chromosomal aberrations (including gains or allelic losses) are frequently found in metastases, and the incidence of combined chromosomal alterations in the primary tumor, plus the occurrence of additional aberrations in the distant metastases, correlated significantly with decreased postmetastatic survival. The deletions at 3p, 4p, 6q, 8p, 10q, 11p, 11q, 12p, 13q, 16q, 17p, 18q, 21q, and 22q, as well as the over-representations at 1q, 8q, 9q, 14q and 15q, have been found to associate preferentially with the metastatic phenotype of human cancers. Among of them, the deletions on chromosomes 8p, 17p, 11p and 13p seem to be more significant, and more detail fine regions of them, including 8p11, 8p21-12, 8p22, 8p23, 17p13.3, 11p15.5, and 13q12-13 have been suggested harboring metastasis-suppressor genes. During the past decade, several human chromosomes have been functionally tested through the use of microcell-mediated chromosome transfer (MMCT), and metastasis-suppressor activities have been reported on chromosomes 1, 6, 7, 8, 10, 11, 12, 16, and 17. However, it is not actually known at what stage of the metastatic cascade these alterations have occurred. There is still controversial with the association between the chromosomal aberrations and the metastatic phenotype of cancer. As the progression of human genome project and the establishment of more and more new techniques, it is hopeful to make clear the genetic mechanisms involved in the tumor metastasis in a not very long future, and provide new clues to predicting and controlling the metastasis.

Qin LX. Chromosomal aberrations related to metastasis of human solid tumors. *World J Gastroenterol* 2002; 8(5):769-776

INTRODUCTION

The central role of sequential accumulation of genetic alterations during the development of cancer has been firmly established since the pioneering cytogenetic studies successfully defined recurrent chromosome changes in specific types of tumor. In the course of carcinogenesis, cells experience several genetic alterations (including gains and deletions) that are associated with the transition from a preneoplastic lesion to an invasive tumor and finally to the metastatic state. High frequency of chromosomal deletions elicited as losses of heterozygosity (LOH) is a hallmark of genomic instability in cancer. Functional losses of tumor suppressor genes caused by LOH at defined regions during clonal selection for growth advantage define the minimally lost regions as their likely locations on chromosomes. LOH is elicited at the molecular or cytogenetic level as a deletion, a gene conversion, single or double homologous and nonhomologous mitotic recombinations, a translocation, chromosome breakage and loss, chromosomal fusion or telomeric end-to-end fusions, or whole chromosome loss with or without accompanying duplication of the retained chromosome. Because of the high level of specificity, LOH has recently become invaluable as a marker for diagnosis and prognosis of cancer^[1].

Many new molecular cytogenetic techniques, including various kinds of fluorescent in situ hybridization (FISH), comparative genomic hybridization (CGH), allelic imbalance (AI) and genotyping analyses, single nucleotide polymorphism (SNP) analysis, etc., have been established in recent years. These new techniques allow positional identification of gains and losses of DNA sequences in the entire tumor genome. These analytic approaches, particularly CGH and AI analysis, have already been applied over a wide range of tumor specimens, cell lines, and archival materials to define chromosomal imbalances. Molecular genetic analyses with these new strategies have clarified that genomic changes accumulate during the development and progression of cancers. A considerable amount of genetic alterations on solid tumors has been accumulated during the past few years.

Tumor progression is characterized by stepwise accumulation of genetic alterations. The dominant metastatic clone is also characterized by an accumulation of genetic alterations, but it is not actually known at what stage of the metastatic cascade these alterations have occurred. In comparison with the corresponding primary tumor, additional events of chromosomal aberrations (including gains or allelic losses) are frequently found in metastases and the incidence of combined chromosomal alterations in the primary tumor, plus the occurrence of additional aberrations in the distant metastases, correlated significantly with decreased postmetastatic survival. It is hypothesized that the occurrence of additional genetic aberrations is either involved in termination of dormancy of micrometastatic tumor cells at distant organ sites or acquired during further progression of metastases. However, only a few indications as to which genetic alterations among the multitude of changes might be

preferentially associated with the metastatic phenotype^[2-8].

During the past decade, several human chromosomes have been functionally tested through the use of microcell-mediated chromosome transfer (MMCT), and metastasis-suppressor activities have been reported on chromosomes 1, 6, 7, 8, 10, 11, 12, 16, and 17. Such functional studies, combined with positional and expression-based gene cloning techniques, have enabled the identification of KAI1, KISS-1, MKK4/SEK1, and BRMS1 as metastasis-suppressor genes^[9]. In this paper, we will review the chromosomal aberrations associated with the metastatic phenotype of solid tumor.

CHROMOSOME 8

Alterations of human chromosome 8p have been commonly detected in many tumor types^[10-12]. Some studies have shown that loss of 8p is associated with the advance of tumors, and plays an important role in the tumor progression of many tumors including colorectal^[13], bladder^[14,15], breast^[10] and liver cancers^[16]. Recently, some studies have also shown that loss of 8p may be associated with the metastasis of laryngeal carcinoma^[17], bladder cancer^[18], renal cell carcinoma^[19], colorectal carcinoma^[20], lung cancer^[21], mantle cell lymphoma (MCL)^[22], and the poor prognosis of colorectal cancer patients^[23]. Bockmuhl *et al* found that 8p23 allelic loss was an independent prognostic marker for disease-free interval, and was associated with poor prognosis in head and neck squamous cell carcinoma and could be useful in refining diagnosis of these tumors^[24]. So, 8p might harbor one or more tumor suppressor genes that are important in the progression, especially in the metastasis of cancers, which was confirmed by irradiated MMCT technique^[25, 26].

The presence of at least three tumor suppressor or metastasis suppressor genes loci on 8p (8p21, 8p22, and 8p23) that may be cooperative events has been suggested in HCC and ovarian cancer^[12,27]. Several candidate tumor suppressor genes have been mapped to 8p including DLC-1(8p21.3-22)^[28], FEZ1 gene (8p22)^[29] and liver-related putative tumor suppressor (LTPS) gene (8p23)^[30]. However, alterations of these genes may occur as an early event in the development of cancer, and their association with the metastasis is not confirmed^[31]. Oba *et al.* found two putative tumor suppressor genes on chromosome 8p might play different roles, deletions on 8p22-p21.3 play an important role in tumor differentiation, while an 8p21.1-p21.2 deletion plays a role in the progression and metastasis of prostate cancer^[32]. Allelic loss at 8p22 was associated with higher tumor grade, and no tumor that retained heterozygosity for markers at 8p22 had metastasized to distant organs, whereas a substantial portion of tumors that lost alleles in that region had done so. These imply that loss or inactivation of tumor-suppressing activity encoded on 8p contributes to malignancy and to the metastatic potential of bladder cancers^[18]. Arai's results suggest that putative tumor suppressor genes, which may be involved in the metastatic process of colorectal cancer, are located on chromosomes 8p21-22. Allelic losses in these regions are possible risk factors for early lymph node metastasis^[33]. Nihei *et al*^[26] used a functional positional cloning strategy to define the region harboring the metastasis suppressor gene in 8p21-12, and localized it to a 60-kb cloned region.

Chromosome 8p deletion is also one of the recurrent chromosomal aberrations in HCC that are common detected either by CGH or by microsatellite analysis^[34-36]. In our previous study, we compared the differences of genomic alterations between matched primary and metastatic HCC by CGH, and found that the majority of chromosomal aberrations in both primary and metastatic lesions of HCC were consistent with those in previous reports. The most interesting finding in this

study is the deletion of 8p which was detected in 8 metastatic lesions but only in 3 corresponding primary HCC, 5 cases of HCC acquired deletion on 8p as they progressed to metastatic stage, although some differences of genomic alterations between primary and its corresponding metastatic lesion were also found. These suggest that 8p may harbor one or more tumor suppressor genes that are important in the HCC progression especially in the tumor metastasis^[37]. This result was confirmed in the metastatic model of HCC and its cell line^[38]. Recently, in another genome-wide microsatellite analysis, deletion on chromosome 8p was further proved to be related to progression and metastasis of HCC, and 8p23.3, 8p11.2 were two likely regions harboring metastasis-related genes^[39].

CHROMOSOME 17

The frequency of allele loss on 17p has been correlated significantly with prognostic features such as the number and size of liver secondaries, the depth of invasion, metastasis to the lymph nodes, and venous invasion of cancers^[40-42]. Multiple regression analysis identified the numerical aberrations of chromosome 17 as independent significant determinants of lymph node metastasis. A similar result is also found in HCC. LOH on 17p13 of HCC correlates with the stage, portal invasion, intrahepatic metastasis, and nuclear morphometry of cancer cells. These suggest that the LOH on 17p13 is closely connected to the progression of HCC^[43].

p53 is an important TSG on 17p13.1, and its aberration has been linked to the development and progress of human cancers including HCC^[44]. However, in addition to 17p13.1, many studies showed that the frequently deleted region was 17p13.3^[45-49]. The minimum region of LOH on chromosome 17p13.3 in HCC has been defined within the region between D17S643 and D17S1574. Moreover, D17S926 in the minimum region of LOH has the highest frequency of LOH, and its sequencing analysis has been accomplished. In this region, 6 novel genes have been characterized. One of them is designated HCC suppressor 1 (HCCS1)^[45]. Our recent study showed that the AI ratio of chromosome 17p was as high as 74-87 % in primary lesions, and 73-87 % in metastasis lesions of HCC. Moreover, high level of AI was also identified in 17p11.2-12 (74-87 %). A 20cM segment within 17p11.2-13.1 was found related to metastasis phenotype, with the highest increased-grade AI (28-44 %) in metastatic lesions^[39]. All these suggested that in addition to the p53 gene at 17p13.1, an as yet unidentified TSG(s) residing at 17p13.3 might play a role in development, progression and metastasis of HCC.

Discontinuous portions of human chromosome 17 (D17S952-D17S805, D17S930-D17S797, and D17S944-qter) that together suppress the metastatic ability of AT6.1 Dunning rat prostatic cancer cells when introduced via MMCT have been identified^[50,51]. PCR and Southern blot analyses demonstrated that three of the four markers on 17p13, including HIC1 and TP53, and 12 of the 13 markers in 17q21-23, including BRCA1 and the metastasis-suppressor gene NME1 (nm23), were not retained in this region^[50]. AT6.1 microcell hybrids containing this portion of chromosome 17 were tested in vivo in spontaneous metastasis assays. Spontaneous metastasis is measured by the ability of tumor cells to form a locally growing tumor at the site of injection and disseminate to and grow at secondary sites thereafter. At the experimental end point, the number of overt surface metastases observed in the lungs from mice with AT6.1-17 tumors was reduced 15- to 30-fold compared with lungs from mice bearing parental AT6.1 tumors^[50]. This suppression could be due to the inhibition of any step within the metastatic cascade. A series

of in vivo experiments were conducted, and no evidence was found to suggest that there is a decrease in the number and/or viability of tumor cells colonizing the lung^[51]. Development of overt metastases was associated with loss of the metastasis-suppressor region of chromosome 17^[10,52,53].

CHROMOSOME 1

Frequent allelic losses on the short arm of chromosome 1 have been observed in a wide variety of human tumors. Allelic loss at 1p22-p31 was correlated with lymph node metastasis. Alterations of one or more tumor suppressor genes at 1p22-p31 may play a role at late stages of carcinogenesis, especially with regard to local progression and lymph node metastasis^[54]. There may be at least two distinct tumor suppressor genes inactivated by allelic deletion on 1p36.1 and 1p36.3, respectively^[55].

Amplification of 1q was also commonly detected in esophageal carcinoma, breast cancer, and colon cancer^[56-58]. Gain of 1q might be one of the early genetic changes in HCC since it was one of the most commonly detected alterations in HCC^[59, 60]. In most cases, the gain of 1q involved whole long arm. However, in our previous study, high copy number amplification on 1q was detected in 4 primary and 6 metastatic HCC with a minimum amplification region at 1q12-q22. Most interestingly, in two cases amplification of 1q12-q22 was only detected in metastatic HCC. This imply that overexpression of an oncogene(s) at 1q12-q22 confers a selective advantage in HCC. High copy number amplification of 1q12-22 may only occur in late stage of HCC and provide more advantage of growth selection. This suggests that 1q might harbor one or more oncogenes related to the development or progression of many cancers. Moreover, this provides us a candidate minimum amplification region on 1q12-q22 for further study to clone genes related to the development and progression of HCC^[37]. A correlation of metastatic events with an increase in the copy number of genes located at 1q, in particular at 1q21-q23 is also found in renal clear cell carcinomas^[61]. And more, an insertion of chromosome 13 material in the short arm of chromosome 1 has been only observed in micrometastatic cells^[62].

CHROMOSOME 6

Highly frequent loss of 6q is found in many kinds of solid tumors, and is considered later events associated with tumor progression, and is thought to confer metastatic potential to the carcinomas (such as in biliary tract, etc.)^[63]. Yoshida *et al.* introduced an intact chromosome 6 into the highly metastatic C8161 human melanoma cells by MMCT. Parental cells formed tumors in every mouse given an intradermal injection of 1×10^6 cells, and more than 90 % of the mice developed regional lymph node and lung metastases. In contrast, chromosome 6-C8161 hybrids (neo6/C8161) were still tumorigenic, but completely suppressed for metastasis. Intravenous injection of neo6/C8161 cells also did not produce metastases. Introduction of a version of chromosome 6 with deletions on the long arm allowed refinement of the metastasis-suppressor locus to a 40-megabase (Mb) region represented by chromosomal bands 6q16.3-q23. The neo6/C8161 cells were still locally invasive, and cells were even detected in efferent vessels. This finding implied that the step(s) in the metastatic cascade inhibited by introduction of chromosome 6 occurred subsequent to intravasation^[9,64-71]. Shirasaki *et al.*^[72] found that inactivation of a tumor suppressor gene(s) mapping to 6q16.3-q23 by deletion or mutation coupled with LOH may lead to the down-regulation of a putative metastasis suppressor gene, KiSS1.

CHROMOSOME 10

LOH on chromosome 10q is found associated with tumour progression in SCC, SCLC, and prostate cancer. It may become a useful genetic marker in the assessment of the malignant potential and a potential genetic discriminator between progressors and nonprogressors after radical surgery of these tumour types^[73,74]. Deletions on chromosome 10q25-q26 is responsible for the metastatic phenotype of squamous cell carcinomas in head and neck^[75], and colorectal carcinomas^[76], which may play a particular pathogenetic role in the metastatic process. One gene, LAPSER1 [an LZTS1(or FEZ1)-related gene] maps within a subregion of human chromosome 10q24.3 that has been reported to be deleted in various cancers, including prostate tumors, as frequently as the neighboring PTEN locus. This gene is involved in the regulation of cell growth, loss of its function may contribute to the development of cancer^[77].

A telomerase repressor gene may be located on 10p15.1 by deletion mapping using MMCT, radiated microcell fusion (RMF), FISH and STS analysis. 10p15.1 harbors a gene involved in repression of telomerase RNA component in human somatic cells and each putative repressormay act independently^[78].

CHROMOSOME 11

A strong relationship between LOH at chromosome 11q23.3 and the presence of extensive tumor plugs in lymphovascular spaces (LVS) has been demonstrated, which suggests that genes at this locus may regulate vasculoinvasion. Patients with LOH at 11q23.3 are significantly more likely to have disease recurrence than patients without LOH at 11q23.3. Although unlikely to have an impact early in carcinogenesis, tumor-suppressor genes located in the region of 11q23.3 appear to be important in tumor progression, facilitating lymphovascular space invasion and, by inference, spread to lymph nodes in squamous cell carcinoma of the cervix^[79] and melanoma^[80]. Deletion on 11q22-qter, together with the gains of 8q23-qter and 20q was observed in tumors metastatic to the lymph nodes. Gains of 8q23-qter and 20q and loss of 11q22-qter allow the prediction of lymph node metastasis^[81]. LOH at 11q13.1-5, the region around the MEN1 locus, may be valuable in predicting the invasiveness of pituitary adenomas^[82]. However, Pairwise found metastasizing tumors are characterized by overrepresentations on chromosomes 11q13 and 22q, and deletions on 18q^[83].

The centromeric part of chromosome segment 11p15.5 contains a region of frequent allele loss in many adult solid malignancies. This region, called LOH11A, is lost in 75 % of lung cancers and is thought to contain a gene that may function as a metastasis suppressor. Genetic complementation studies have shown suppression of the malignant phenotype including reduction of metastasis formation. Bepler *et al.* constructed a high-resolution physical map and contig over 1.4 Mb that includes the beta-hemoglobin gene cluster and the gene for the large subunit of ribonucleotide reductase (RRM1). Through sequencing and computerized analysis, we determined that this region contains an unusually large number of transposable elements, which suggests that double-stranded DNA breaks occur frequently here. Twenty-two putative genes were identified. Because of its location at the site of maximal allele loss in the 650-kb LOH11A region and previous functional studies, RRM1 is the most likely candidate gene with metastasis suppressor function. The malignant phenotype results from a relative loss of function rather than a complete loss^[84]. Two distinct tumor suppressor loci on chromosome 11p15, one is between D11S1318 and D11S4088 (approximately 500 kb)

within 11p15.5, a second, critical region of LOH spans the markers D11S1338-D11S1323 (approximately 336 kb) at 11p15.5-p15.4, may contribute to tumor progression and metastasis in breast cancer and lung cancer^[85,86]. The human SRBC gene (hSRBC), a candidate tumor suppressor gene, is mapped to chromosome region 11p15.5-p15.4, close to marker D11S1323, at which frequent LOH has been observed in sporadic breast, lung, ovarian, and other types of adult cancers as well as childhood tumors^[87]. Introduction of human chromosome 11 by MMCT could suppress MDA-MB-435 breast carcinoma cell metastasis^[88]. One important metastasis-suppressor gene, KAI1, maps to 11p11.2-p13.

CHROMOSOME 13

LOH of 13q is a common event in oncogenesis and/or progression of oral SCC and larynx carcinoma, and significant correlation between LOH of 13q14.3 and lymph node metastasis is found. These suggest the existence of a new suppressor gene near D13S273-D13S176 loci which may play a role in these events^[18,89]. Allelotype analysis of whole chromosomes showed that allelic loss at 13q12-13 of the primary ESC was closely associated with lymph node metastasis, and unidentified tumor suppressor gene(s) in this region might be involved^[90]. The high LOH rate for different microsatellite markers in and around the putative TSG locus C13 on chromosome 13q13 has been found^[91]. However, Hyytinen et al. found that gain of the 13q12-q13 chromosomal region as well as losses of 4, 6q24-qter, 20p and 21q were associated with androgen independence and tumorigenicity with additional changes correlating with metastasis^[92].

CHROMOSOME 14

Significantly more LOH events at markers D14S62 and D14S51 in primary breast cancers from patients with lymph node-negative disease than these with lymph node-positive disease were found, suggesting the presence of a gene in this region that affects metastatic potential. Analysis of small interstitial or terminal deletions in the tumors of six especially informative patients with lymph node-negative disease places the putative metastasis-related gene in a 1490-kilobase region near D14S62. LOH in the D14S62 region may impede the process of metastasis. Therefore, the D14S62 region LOH profile may have prognostic implications, and the isolation of the metastasis-related gene(s) in this region may lead to better diagnosis and treatment of breast cancer^[93]. This unusual observation suggests that, whereas the LOH of this region promotes primary breast cancer formation, some gene(s) mapping to this 1.6-Mb region is rate-limiting for breast cancer metastasis. Thus, if primary breast cancers delete this region, their ability to metastasize decreases. To identify this gene(s), Martin *et al*^[94] physically mapped this area of chromosome 14q, confirmed the position of two known genes and 13 other expressed sequence tags into this 1.6-Mb region. One of these, the metastasis-associated 1 (MTA1) gene, previously identified as a metastasis-promoting gene, mapped to the center of our 1.6-Mb target region. Thus, MTA1 represents a strong candidate for this breast cancer metastasis-promoting gene.

CHROMOSOME 16

Genomic aberration at the chromosome 16q arm is one of the most consistent abnormalities observed by LOH and CGH analyses in human prostate cancer, suggesting that there are tumor suppressor or metastasis suppressor genes encoded by

this chromosomal region. When the MMCT hybrid cells containing whole human chromosome 16 were injected, the number of metastatic lesions in the lung was significantly reduced as much as 99 % on average. Therefore, chromosome 16 has a strong activity to suppress the metastatic ability of AT6.1 cells while it did not affect the tumorigenesis and tumor growth rate. A PCR analysis of various microcell hybrid clones with sequence-tagged site markers indicates that the metastasis suppressor activity is located in the q24.2 region of chromosome 16. These suggest that there is a metastasis suppressor gene in this region that may play an important role in the progression of prostate cancer^[95]. Deletion of chromosome 16q23-24 appears in a high frequency in metastases of prostate cancer. The strong correlations suggest that they may be important risk factors, contributing to the metastatic potential of the tumor^[96-98]. The presence of putative tumor-suppressor genes on chromosome 16q23.2-24.1 has been suggested by LOH analysis in several cancer types. The candidate gene WWOX/FOR has been mapped within this region^[99-101].

CHROMOSOME 18

Deletion on 18p is shown as one of the most frequent losses in metastasizing tumors in primary larynx tumor^[102]. Two distinct minimum regions of AI on 18q have been identified. The first region is between the genetic markers D18S1119 and D18S64. The second region lies more distal on the long arm of the chromosome and is between the genetic markers D18S848 and D18S58. Significantly higher AI was found in the metastatic samples, which is consistent with 18q losses occurring late in tumor progression^[103]. Detailed deletion mapping in these tumors identified a distinct commonly deleted region within a 5-cM interval in 18q21.1. The primary tumors had either no detectable abnormality of chromosome 18 or the region involving LOH was limited while the metastatic foci showed more frequent and extended allelic losses on this chromosome. These suggest that inactivation of one or more putative tumor suppressor genes on 18q21 other than DCC and DPC4 plays an important role in the progression of human prostate cancer^[104]. Loss of 18q in metastatic and locally recurrent tumors, but not in primary tumors from the same patients, suggests that a tumor suppressor gene in this region may be important in the progression of breast cancer, squamous cell carcinoma, etc.^[7,105,106].

OTHERS

In addition, loss of 9p and gains of 17q and Xq are other genomic changes which frequently occurred in metastases but not in the corresponding primary tumor^[19].

The deletions at 3p12-p14, 3p21, 4p15-p16, 6q24-qter, 8p22-p23, 10q21-qter and 21q22, as well as the over-representations at 1q21-q25, 8q, 9q34, 14q12 and 15q12-q15, occurred significantly more often in the metastatic tumour group^[107]. Areas of deletion predominantly or completely common to the colorectal and the metastatic tumour were detected on chromosomes 5q, 8p, 17p, 18q, and 22q. Preferential loss in metastatic tumours was observed on chromosomal arm 3p^[108]. Chu *et al*^[109] compared the genetic abnormalities specifically associated with varying metastatic potential of prostate cancer cell lines by CGH, and found that PC3M-LN4, the derivative line that produced significantly larger metastatic tumors in the lymph nodes and had higher incidences of distant metastases, had a specific gain of 1q21-q22 and losses of 10q23-qter and 18q12-q21. LNCaP-LN3, a derivative line that had a significantly higher incidence of

lymph node metastases and produced significantly larger metastatic tumors in the lymph nodes, had specific losses of 16q23-qter and 21q.

A strong association between 12p12-13 LOH and distant metastasis has been found, which raises the possibility that mutational inactivation of a gene at 12p12-13, possibly p27/kip1, plays a pivotal role in the development of metastatic disease^[110, 111].

LOH of 19q13 was associated with overall survival in local-regional International Neuroblastoma Staging System stages 1, 2, and 3 patients and was specifically present in tumors at the site of recurrence^[112].

The gain of chromosome 20 may be available as a genetic marker for the diagnosis or prediction of liver metastasis^[113, 114].

The Xq25 region harbors a putative tumor suppressor gene whose inactivation in breast cancer is associated with tumor progression and metastasis. LOH at this region, therefore, potentially could be used as a prognostic marker for disease development^[115].

QUESTIONS AND PROSPECTS

There is still controversial with the association between the chromosomal aberrations and the metastatic phenotype of cancer. Some reports showed the frequencies of the most common aberrations were relatively similar in primary tumors and metastases, but no aberrations specific to metastases were detected^[116]. And more, among of the chromosomes mentioned above, which one plays the most important role in the metastatic process. Based on the published data and the author's experience, chromosomes 8 and 17 should be paid more attention to. To date, combined analyses of the different aberrations of various chromosomal regions would be much more valuable in predicting the metastatic potential and prognosis of human solid tumors^[8]. As the progression of human genome project and the establishment of more and more new techniques, it is hopeful that the genetic mechanisms involved in the tumor metastasis could be made clear in a not very long future, and provide new clues to predicting and controlling the metastasis.

REFERENCES

- 1 **Thiagalingam S**, Foy RL, Cheng KH, Lee HJ, Thiagalingam A, Ponte JF. Loss of heterozygosity as a predictor to map tumor suppressor genes in cancer: molecular basis of its occurrence. *Curr Opin Oncol* 2002;**14**:65-72
- 2 **Bockmuhl U**, Petersen S, Schmidt S, Wolf G, Jahnke V, Dietel M, Petersen I. Patterns of chromosomal alterations in metastasizing and nonmetastasizing primary head and neck carcinomas. *Cancer Res* 1997;**57**: 5213-5216
- 3 **Schwendel A**, Langerck H, Reichel M, Schrock E, Ried T, Dietel M, Petersen I. Primary small-cell lung carcinomas and their metastases are characterized by a recurrent pattern of genetic alterations. *Int J Cancer* 1997;**74**: 86-93
- 4 **Nishizaki T**, Devries S, Chew K, Goodson IIIWK, Ljung BM, Thor A, Waldman FM. Genetic alterations in primary breast cancers and their metastases: direct comparison using modified comparative genomic hybridization. *Genes Chromosome Cancer* 1997;**19**: 267-272
- 5 **Cobaleda C**, Perez-Losada J, Sanchez-Garcia I. Chromosomal abnormalities and tumor development: from genes to therapeutic mechanisms. *Bio Essays* 1998;**20**: 922-930
- 6 **Adeyinka A**, Mertens F, Idvall I, Bondeson L, Ingvar C, Mitelman F, Pandis N. Different patterns of chromosomal imbalances in metastasizing and non-metastasizing primary breast carcinomas. *Int J Cancer* 1999;**84**:370-375
- 7 **Hampl M**, Hampl JA, Reiss G, Schackert G, Saeger HD, Schackert HK. Loss of heterozygosity accumulation in primary breast carcinomas and additionally in corresponding distant metastases is associated with poor outcome. *Clin Cancer Res* 1999;**5**:1417-1425
- 8 **Choi SW**, Choi JR, Chung YJ, Kim KM, Rhyu MG. Prognostic implications of microsatellite genotypes in gastric carcinoma. *Int J Cancer* 2000;**89**:378-383
- 9 **Yoshida BA**, Sokoloff MM, Welch DR, Rinker-Schaeffer CW. Metastasis-Suppressor Genes: a Review and Perspective on an Emerging Field. *J Natl Cancer Inst* 2000;**92**:1717-1730
- 10 **Yokota T**, Yoshimoto M, Akiyama F, Sakamoto G, Kasumi F, Nakamura Y, Emi M. Localization of a tumor suppressor gene associated with the progression of human breast carcinoma within a 1-cM interval of 8p22-p23.1. *Cancer* 1999;**85**:447-452
- 11 **Perincheri G**, Bukurov N, Nakajima K, Chang J, Hooda M, Oh BR, Dahiya R. Loss of two new loci on chromosome 8 (8p23 and 8q12-13) in human prostate cancer. *Int J Oncol* 1999;**14**:495-500
- 12 **Wright K**, Wilson PJ, Kerr J, Do K, Hurst T, Khoo SK, Ward B, Chenevix-Trench G. Frequent loss of heterozygosity and three critical regions on the short arm of chromosome 8 in ovarian adenocarcinomas. *Oncogene* 1998;**17**:1185-1188
- 13 **Takanishi DM Jr**, Kim SY, Kelemen PR, Yaremko ML, Kim AH, Ramesar JE, Horrigan SK, Montag A, Michelassi F, Westbrook CA. Chromosome 8 Losses in Colorectal Carcinoma: Localization and Correlation With Invasive Disease. *Mol Diagn* 1997;**2**:3-10
- 14 **Muscheck M**, Sukosd F, Pesti T, Kovacs G. High density deletion mapping of bladder cancer localizes the putative tumor suppressor gene between loci D8S504 and D8S264 at chromosome 8p23.3. *Lab Invest* 2000;**80**:1089-1093
- 15 **Wagner U**, Bubendorf L, Gasser TC, Moch H, Gorog JP, Richter J, Mihatsch MJ, Waldman FM, Sauter G. Chromosome 8p deletions are associated with invasive tumor growth in urinary bladder cancer. *Am J Pathol* 1997;**151**: 753-759
- 16 **Emi M**, Fujiwara Y, Ohata H, Tsuda H, Hirohashi S, Koike M, Miyaki M, Monden M, Nakamura Y. Allelic loss at chromosome band 8p21.3-p22 is associated with progression of hepatocellular carcinoma. *Genes Chromosomes Cancer* 1993;**7**:152-157
- 17 **Kujawski M**, Sarlomo-Rikala M, Gabriel A, Szyfter K, Knuutila S. Recurrent DNA copy number losses associated with metastasis of larynx carcinoma. *Genes Chromosomes Cancer* 1999;**26**:253-257
- 18 **Ohgaki K**, Iida A, Ogawa O, Kubota Y, Akimoto M, Emi M. Localization of tumor suppressor gene associated with distant metastasis of urinary bladder cancer to a 1-Mb interval on 8p22. *Genes Chromosomes Cancer* 1999;**25**:1-5
- 19 **Bissig H**, Richter J, Desper R, Meier V, Schraml P, Schaffer AA, Sauter G, Mihatsch MJ, Moch H. Evaluation of the clonal relationship between primary and metastatic renal cell carcinoma by comparative genomic hybridization. *Am J Pathol* 1999;**155**:267-274
- 20 **Parada LA**, Maranon A, Hallen M, Tranberg KG, Stenram U, Bardi G, Johansson B. Cytogenetic analyses of secondary liver tumors reveal significant differences in genomic imbalances between primary and metastatic colon carcinomas. *Clin Exp Metastasis* 1999;**17**:471-479
- 21 **Petersen S**, Aninat-Meyer M, Schluns K, Gellert K, Dietel M, Petersen I. Chromosomal alterations in the clonal evolution to the metastatic stage of squamous cell carcinomas of the lung. *Br J Cancer* 2000;**82**:65-73
- 22 **Martinez-Climent JA**, Vizcarra E, Sanchez D, Blesa D, Marugan I, Benet I, Sole F, Rubio-Moscardo F, Terol MJ, Climent J, Sarsotti E, Tormo M, Andreu E, Salido M, Ruiz MA, Prosper F, Siebert R, Dyer MJ, Garcia-Conde J. Loss of a novel tumor suppressor gene locus at chromosome 8p is associated with leukemic mantle cell lymphoma. *Blood*

- 2001;**98**:3479-3482
- 23 **Halling KC**, French AJ, McDonnell SK, Burgart LJ, Schaid DJ, Peterson BJ, Moon-Tasson L, Mahoney MR, Sargent DJ, O'Connell MJ, Witzig TE, Farr GH Jr, Goldberg RM, Thibodeau SN. Microsatellite Instability and 8p Allelic Imbalance in Stage B2 and C Colorectal Cancers. *J Natl Cancer Inst* 1999;**91**:1295-1303
- 24 **Bockmuhl U**, Ishwad CS, Ferrell RE, Gollin SM. Association of 8p23 deletions with poor survival in head and neck cancer. *Otolaryngol Head Neck Surg* 2001;**124**:451-455
- 25 **Nihei N**, Kouprina N, Larionov V, Oshima J, Martin GM, Ichikawa T, Barrett JC. Mapping of metastasis suppressor gene(s) for rat prostate cancer on the short arm of human chromosome 8 by irradiated microcell-mediated chromosome transfer. *Genes Chromosomes Cancer* 1996;**17**:260-268
- 26 **Nihei N**, Kouprina N, Larionov V, Oshima J, Martin JM, Ichikawa T, Barrett JC. Functional evidence for a metastasis suppressor gene for rat prostate cancer within a 60-kilobase region on human chromosome 8p21-p12. *Cancer Res* 2002;**62**:367-370
- 27 **Pineau P**, Nagai H, Prigent S, Wei Y, Gyapay G, Weissenbach J, Tiollais P, Buendia MA, Dejean A. Identification of three distinct regions of allelic deletions on the short arm of chromosome 8 in hepatocellular carcinoma. *Oncogene* 1999;**18**:3127-3134
- 28 **Yuan BZ**, Miller MJ, Keck CL, Zimonjic DB, Thorgeirsson SS, Popescu NC. Cloning, characterization, and chromosomal localization of a gene frequently deleted in human liver cancer (DLC-1) homologous to rat RhoGAP. *Cancer Res* 1998;**58**:2196-2199
- 29 **Ishii H**, Baffa R, Numata SI, Murakumo Y, Rattan S, Inoue H, Mori M, Fidanza V, Alder H, Croce CM. The FEZ1 gene at chromosome 8p22 encodes a leucine-zipper protein, and its expression is altered in multiple human tumors. *Proc Natl Acad Sci USA* 1999;**96**:3928-3933
- 30 **Liao C**, Zhao MJ, Song H, Uchida K, Yokoyama KK, Li TP. Identification of the gene for a novel liver-related putative tumor suppressor at a high-frequency loss of heterozygosity region of chromosome 8p23 in human hepatocellular carcinoma. *Hepatology* 2000;**32**:721-727
- 31 **Park WS**, Lee JH, Park JY, Jeong SW, Shin MS, Kim HS, Lee SK, Lee SN, Lee SH, Park CG, Yoo NJ, Lee JY. Genetic analysis of the liver putative tumor suppressor (LPTS) gene in hepatocellular carcinomas. *Cancer Lett* 2002;**178**:199-207
- 32 **Oba K**, Matsuyama H, Yoshihiro S, Kishi F, Takahashi M, Tsukamoto M, Kinjo M, Sagiya K, Naito K. Two putative tumor suppressor genes on chromosome arm 8p may play different roles in prostate cancer. *Cancer Genet Cytogenet* 2001;**124**:20-26
- 33 **Arai T**, Akiyama Y, Yamamura A, Hosoi T, Shibata T, Saitoh K, Okabe S, Yuasa Y. Allelotype analysis of early colorectal cancers with lymph node metastasis. *Int J Cancer* 1998;**79**:418-423
- 34 **Guan XY**, Fang Y, Sham JS, Kwong DL, Zhang Y, Liang Q, Li H, Zhou H, Trent JM. Recurrent chromosome alterations in hepatocellular carcinoma detected by comparative genomic hybridization. *Genes Chromosomes Cancer* 2000;**29**:110-116
- 35 **Li SP**, Wang HY, Li JQ, Zhang CQ, Feng QS, Huang P, Yu XJ, Huang LX, Liang QW, Zeng YX. Genome-wide analyses on loss of heterozygosity in hepatocellular carcinoma in Southern China. *J Hepatol* 2001;**34**:840-849
- 36 **Wang G**, Zhao Y, Liu X, Wang L, Wu C, Zhang W, Liu W, Zhang P, Cong W, Zhu Y, Zhang L, Chen S, Wan D, Zhao X, Huang W, Gu J. Allelic loss and gain, but not genomic instability, as the major somatic mutation in primary hepatocellular carcinoma. *Genes Chromosomes Cancer* 2001;**31**:221-227
- 37 **Qin LX**, Tang ZY, Sham JS, Ma ZC, Ye SL, Zhou XD, Wu ZQ, Trent JM, Guan XY. The association of chromosome 8p deletion and tumor metastasis in human hepatocellular carcinoma. *Cancer Res* 1999;**59**:5662-5665
- 38 **Qin LX**, Tang ZY, Ye SL, Liu Y K, Ma ZC, Zhou XD, Wu ZQ, Lin ZY, Sun FX, Tian J, Guan XY, Pack SD, Zhuang ZP. Chromosome 8p deletion is associated with metastasis of human hepatocellular carcinoma when high and low metastatic models are compared. *J Cancer Res Clin Oncol* 2001;**127**:482-488
- 39 **Zhang LH**, Qin LX, Ma ZC, Ye SL, Liu YK, Ye QH, Wu X, Huang W, Tang ZY. Identification of allelic imbalances regions related to metastasis of hepatocellular carcinoma: Comparison between matched primary and metastatic lesions in 22 patients by genome-wide microsatellite analysis. *Int J Cancer* 2002 (submitted)
- 40 **Ding SF**, Delhanty JD, Zografos G, Michail NE, Dooley JS, Habib NA. Chromosome allele loss in colorectal liver metastases and its association with clinical features. *Br J Surg* 1994;**81**:875-878
- 41 **Terada R**, Yasutake T, Yamaguchi E, Hisamatsu T, Nakamura S, Ayabe H, Tagawa Y. Higher frequencies of numerical aberrations of chromosome 17 in primary gastric cancers are associated with lymph node metastasis. *J Gastroenterol* 1999;**34**:11-17
- 42 **Hampel M**, Hampel JA, Schwarz P, Frank S, Hahn M, Schackert G, Saeger HD, Schackert HK. Accumulation of genetic alterations in brain metastases of sporadic breast carcinomas is associated with reduced survival after metastasis. *Invasion Metastasis* 1998;**18**:81-95
- 43 **Suzuki K**, Hirooka Y, Tsujitani S, Yamane Y, Ikeguchi M, Kaibara N. Relationship between loss of heterozygosity at microsatellite loci and computerized nuclear morphometry in hepatocellular carcinoma. *Anticancer Res* 2000;**20**:1257-1262
- 44 **Park NH**, Chung YH, Youn KH, Song BC, Yang SH, Kim JA, Lee HC, Yu E, Lee YS, Lee SG, Kim KW, Suh DJ. Close correlation of p53 mutation to microvascular invasion in hepatocellular carcinoma. *J Clin Gastroenterol* 2001;**33**:397-401
- 45 **Zhao X**, Li J, He Y, Lan F, Fu L, Guo J, Zhao R, Ye Y, He M, Chong W, Chen J, Zhang L, Yang N, Xu B, Wu M, Wan D, Gu J. A novel growth suppressor gene on chromosome 17p13.3 with a high frequency of mutation in human hepatocellular carcinoma. *Cancer Res* 2001;**61**:7383-7387
- 46 **Nagai H**, Pineau P, Tiollais P, Buendia MA, Dejean AH. Comprehensive allelotyping of human hepatocellular carcinoma. *Oncogene* 1997;**14**:2927-2933
- 47 **Boige V**, Laurent-Puig P, Fouchet P, Flejou JF, Monges G, Bedossa P, Bioulac-Sage P, Capron F, Schmitz A, Olschwang S, Thomas G. Concerted nonsyntenic allelic losses in hyperplastic hepatocellular carcinoma as determined by a high-resolution allelotype. *Cancer Res* 1997;**57**:1986-1990
- 48 **Piao Z**, Park C, Park JH, Kim H. Allelotype analysis of hepatocellular carcinoma. *Int J Cancer* 1998;**75**:29-33
- 49 **Charroux B**, Pellizzoni L, Perkinson RA, Yong J, Shevchenko A, Mann M, Dreyfuss G. Gemin4. A novel component of the SMN complex that is found in both gems and nucleoli. *J Cell Biol* 2000;**148**:1177-1186
- 50 **Chekmareva MA**, Hollowell CM, Smith RC, Davis EM, LeBeau MM, Rinker-Schaeffer CW. Localization of prostate cancer metastasis-suppressor activity on human chromosome 17. *Prostate* 1997;**33**:271-280
- 51 **Rinker-Schaeffer CW**, Hawkins AL, Ru N, Dong J, Stoica G, Griffin CA. Differential suppression of mammary and prostate cancer metastasis by human chromosomes 17 and 11. *Cancer Res* 1994;**54**:6249-6256
- 52 **Chekmareva MA**, Kadkhodai MM, Hollowell CM, Kim H, Yoshida BA, Luu HH. Chromosome 17-mediated dormancy of AT6.1 prostate cancer micrometastases. *Cancer Res* 1998;**58**:4963-4969
- 53 **Kim HL**, Griend DJ, Yang X, Benson DA, Dubauskas Z, Yoshida BA, Chekmareva MA, Ichikawa Y, Sokoloff MH, Zhan P, Karrison T, Lin A, Stadler WM, Ichikawa T, Rubin MA, Rinker-Schaeffer CW. Mitogen-activated protein kinase kinase 4 metastasis suppressor gene expression is

- inversely related to histological pattern in advancing human prostatic cancers. *Cancer Res* 2001;**61**:2833-2837
- 54 **Tsukamoto K**, Ito N, Yoshimoto M, Kasumi F, Akiyama F, Sakamoto G, Nakamura Y, Emi M. Allelic loss on chromosome 1p is associated with progression and lymph node metastasis of primary breast carcinoma. *Cancer* 1998;**82**:317-322
 - 55 **Araki D**, Uzawa K, Watanabe T, Shiiba M, Miyakawa A, Yokoe H, Tanzawa H. Frequent allelic losses on the short arm of chromosome 1 and decreased expression of the p73 gene at 1p36.3 in squamous cell carcinoma of the oral cavity. *Int J Oncol* 2002;**20**:355-360
 - 56 **Du Plessis L**, Dietzsch E, Van Gele M, Van Roy N, Van Helden P, Parker MI, Mugwanya DK, De Groot M, Marx MP, Kotze MJ, Speleman F. Mapping of novel regions of DNA gain and loss by comparative genomic hybridization in esophageal carcinoma in the Black and Colored populations of South Africa. *Cancer Res* 1999;**59**:1877-1883
 - 57 **Guan XY**, Meltzer PS, Dalton WS, Trent JM. Identification of cryptic sites of DNA sequence amplification in human breast cancer by chromosome microdissection. *Nat Genet* 1994;**8**:155-161
 - 58 **Ried T**, Knutzen R, Steinbeck R, Blegen H, Schrock E, Heselmeyer K, du Manoir S, Auer G. Comparative genomic hybridization reveals a specific pattern of chromosomal gains and losses during the genesis of colorectal tumors. *Genes Chromosomes Cancer* 1996;**15**:234-245
 - 59 **Marchio A**, Meddeb M, Pineau P, Danglot G, Tiollais P, Bernheim A, Dejean A. Recurrent chromosomal abnormalities in hepatocellular carcinoma detected by comparative genomic hybridization. *Genes Chromosomes Cancer* 1997;**18**:59-65
 - 60 **Wong N**, Lai P, Lee SW, Fan S, Pang E, Liew CT, Sheng Z, Lau JW, Johnson PJ. Assessment of genetic changes in hepatocellular carcinoma by comparative genomic hybridization analysis: relationship to disease stage, tumor size, and cirrhosis. *Am J Pathol* 1999;**154**:37-43
 - 61 **Gronwald J**, Storkel S, Holtgreve-Grez H, Hadaczek P, Brinkschmidt C, Jauch A, Lubinski J, Cremer T. Comparison of DNA gains and losses in primary renal clear cell carcinomas and metastatic sites: importance of 1q and 3p copy number changes in metastatic events. *Cancer Res* 1997;**57**:481-487
 - 62 **Hosch S**, Kraus J, Scheunemann P, Izbicki JR, Schneider C, Schumacher U, Witter K, Speicher MR, Pantel K. Malignant potential and cytogenetic characteristics of occult disseminated tumor cells in esophageal cancer. *Cancer Res* 2000;**60**:6836-6840
 - 63 **Shiraishi K**, Okita K, Harada T, Kusano N, Furui T, Kondoh S, Oga A, Kawauchi S, Fukumoto Y, Sasaki K. Comparative genomic hybridization analysis of genetic aberrations associated with development and progression of biliary tract carcinomas. *Cancer* 2001;**91**:570-577
 - 64 **Nakao K**, Shibusawa M, Ishihara A, Yoshizawa H, Tsunoda A, Kusano M, Kurose A, Makita T, Sasaki K. Genetic changes in colorectal carcinoma tumors with liver metastases analyzed by comparative genomic hybridization and DNA ploidy. *Cancer* 2001;**91**:721-726
 - 65 **Miele ME**, Robertson G, Lee JH, Coleman A, McGary CT, Fisher PB, Lugo TG, Welch DR. Metastasis suppressed, but tumorigenicity and local invasiveness unaffected, in the human melanoma cell line MeJuSo after introduction of human chromosomes 1 or 6. *Mol Carcinog* 1996;**15**:284-299
 - 66 **You J**, Miele ME, Dong C, Welch DR. Suppression of human melanoma metastasis by introduction of chromosome 6 may be partially due to inhibition of motility, but not to inhibition of invasion. *Biochem Biophys Res Commun* 1995;**208**:476-484
 - 67 **Miele ME**, De La Rosa A, Lee JH, Hicks DJ, Dennis JW, Steeg PS, Welch DR. Suppression of human melanoma metastasis following introduction of chromosome 6 is independent of NME1 (Nm23). *Clin Exp Metastasis* 1997;**15**:259-265
 - 68 **Welch DR**, Goldberg SF. Molecular mechanisms controlling human melanoma progression and metastasis. *Pathobiology* 1997;**65**:311-330
 - 69 **Welch DR**, Chen P, Miele ME, McGary CT, Bower JM, Stanbridge EJ, Weissman BE. Microcell-mediated transfer of chromosome 6 into metastatic human C8161 melanoma cells suppresses metastasis but does not inhibit tumorigenicity. *Oncogene* 1994;**9**:255-262
 - 70 **Miele ME**, Jewett MD, Goldberg SF, Hyatt DL, Morelli C, Gualandi F, Rimessi P, Hicks DJ, Weissman BE, Barbanti-Brodano G, Welch DR. A human melanoma metastasis-suppressor locus maps to 6q16.3-q23. *Int J Cancer* 2000;**86**:524-528
 - 71 **Goldberg SF**, Harms JF, Quon K, Welch DR. Metastasis-suppressed C8161 melanoma cells arrest in lung but fail to proliferate. *Clin Exp Metastasis* 1999;**17**:601-607
 - 72 **Shirasaki F**, Takata M, Hatta N, Takehara K. Loss of expression of the metastasis suppressor gene KiSS1 during melanoma progression and its association with LOH of chromosome 6q16.3-q23. *Cancer Res* 2001;**61**:7422-7425
 - 73 **Petersen S**, Wolf G, Bockmuhl U, Gellert K, Dietel M, Petersen I. Allelic loss on chromosome 10q in human lung cancer: association with tumour progression and metastatic phenotype. *Br J Cancer* 1998;**77**:270-276
 - 74 **Alers JC**, Rochat J, Krijtenburg PJ, Hop WC, Kranse R, Rosenberg C, Tanke HJ, Schroder FH, van Dekken H. Identification of genetic markers for prostatic cancer progression. *Lab Invest* 2000;**80**:931-942
 - 75 **Bockmuhl U**, Petersen S, Schmidt S, Wolf G, Jahnke V, Dietel M, Petersen I. Patterns of chromosomal alterations in metastasizing and nonmetastasizing primary head and neck carcinomas. *Cancer Res* 1997;**57**:5213-5216
 - 76 **Bardi G**, Parada LA, Bomme L, Pandis N, Johansson B, Willen R, Fenger C, Kronborg O, Mitelman F, Heim S. Cytogenetic findings in metastases from colorectal cancer. *Int J Cancer* 1997;**72**:604-607
 - 77 **Cabeza-Arvelaiz Y**, Thompson TC, Sepulveda JL, Chinault AC. LAPSER1: a novel candidate tumor suppressor gene from 10q24.3. *Oncogene* 2001;**20**:6707-6717
 - 78 **Miura N**, Onuki N, Rathi A, Virmani A, Nakamoto S, Kishimoto Y, Murawaki Y, Kawasaki H, Hasegawa J, Oshimura M, Travis WD, Gazdar AF. hTR repressor-related gene on human chromosome 10p15.1. *Br J Cancer* 2001;**85**:1510-1514
 - 79 **O'sullivan MJ**, Rader JS, Gerhard DS, Li Y, Trinkaus KM, Gersell DJ, Huettner PC. Loss of heterozygosity at 11q23.3 in vasculoinvasive and metastatic squamous cell carcinoma of the cervix. *Hum Pathol* 2001;**32**:475-478
 - 80 **Herbst RA**, Mommert S, Casper U, Podewski EK, Kiehl P, Kapp A, Weiss J. 11q23 allelic loss is associated with regional lymph node metastasis in melanoma. *Clin Cancer Res* 2000;**6**:3222-3227
 - 81 **Tada K**, Oka M, Tangoku A, Hayashi H, Oga A, Sasaki K. Gains of 8q23-qter and 20q and loss of 11q22-qter in esophageal squamous cell carcinoma associated with lymph node metastasis. *Cancer* 2000;**88**:268-273
 - 82 **Nam DH**, Song SY, Park K, Kim MH, Suh YL, Lee JI, Kim JS, Hong SC, Shin HJ, Park K, Eoh W, Kim JH. Clinical significance of molecular genetic changes in sporadic invasive pituitary adenomas. *Exp Mol Med* 2001;**33**:111-116
 - 83 **Welkoborsky HJ**, Bernauer HS, Riazimand HS, Jacob R, Mann WJ, Hinni ML. Patterns of chromosomal aberrations in metastasizing and nonmetastasizing squamous cell carcinomas of the oropharynx and hypopharynx. *Ann Otol Rhinol Laryngol* 2000;**109**:401-410
 - 84 **Bepler G**, O'briant KC, Kim YC, Schreiber G, Pitterle DM. A 1.4-Mb high-resolution physical map and contig of chromosome segment 11p15.5 and genes in the LOH11A metastasis suppressor region. *Genomics* 1999;**55**:164-175
 - 85 **Karnik P**, Paris M, Williams BR, Casey G, Crowe J, Chen P. Two distinct tumor suppressor loci within chromosome

- 11p15 implicated in breast cancer progression and metastasis. *Hum Mol Genet* 1998;**7**:895-903
- 86 **Bepier G**, Fong KM, Johnson BE, O'Briant KC, Daly LA, Zimmerman PV, Garcia-Blanco MA, Peterson B. Association of chromosome 11 locus D11S12 with histology, stage, and metastases in lung cancer. *Cancer Detect Prev* 1998;**22**:14-19
- 87 **Xu XL**, Wu LC, Du F, Davis A, Peyton M, Tomizawa Y, Maitra A, Tomlinson G, Gazdar AF, Weissman BE, Bowcock AM, Baer R, Minna JD. Inactivation of human SRBC, located within the 11p15.5-p15.4 tumor suppressor region, in breast and lung cancers. *Cancer Res* 2001;**61**:7943-7949
- 88 **Phillips KK**, Welch DR, Miele ME, Lee JH, Wei LL, Weissman BE. Suppression of MDA-MB-435 breast carcinoma cell metastasis following the introduction of human chromosome 11. *Cancer Res* 1996;**56**:1222-1227
- 89 **Ogawara K**, Miyakawa A, Shiba M, Uzawa K, Watanabe T, Wang XL, Sato T, Kubosawa H, Kondo Y, Tanzawa H. Allelic loss of chromosome 13q14.3 in human oral cancer: correlation with lymph node metastasis. *Int J Cancer* 1998;**79**:312-317
- 90 **Harada H**, Tanaka H, Shimada Y, Shinoda M, Imamura M, Ishizaki K. Lymph node metastasis is associated with allelic loss on chromosome 13q12-13 in esophageal squamous cell carcinoma. *Cancer Res* 1999;**59**:3724-3729
- 91 **Fiedler U**, Ehlers W, Meye A, Fussel S, Faller G, Schmidt U, Wirth MP. LOH analyses in the region of the putative tumour suppressor gene C13 on chromosome 13q13. *Anticancer Res* 2001;**21**:2341-2350
- 92 **Hyttinen ER**, Thalmann GN, Zhau HE, Karhu R, Kallioniemi OP, Chung LW, Visakorpi T. Genetic changes associated with the acquisition of androgen-independent growth, tumorigenicity and metastatic potential in a prostate cancer model. *Br J Cancer* 1997;**75**:190-195
- 93 **O'Connell P**, Fischbach K, Hilsenbeck S, Mohsin SK, Fuqua SA, Clark GM, Osborne CK, Allred DC. Loss of heterozygosity at D14S62 and metastatic potential of breast cancer. *J Natl Cancer Inst* 1999;**91**:1391-1397
- 94 **Martin MD**, Fischbach K, Osborne CK, Mohsin SK, Allred DC, O'Connell P. Loss of heterozygosity events impeding breast cancer metastasis contain the MTA1 gene. *Cancer Res* 2001;**61**:3578-3580
- 95 **Mashimo T**, Watabe M, Cuthbert AP, Newbold RF, Rinker-Schaeffer CW, Helfer E, Watabe K. Human chromosome 16 suppresses metastasis but not tumorigenesis in rat prostatic tumor cells. *Cancer Res* 1998;**58**:4572-4576
- 96 **Pan Y**, Matsuyama H, Wang N, Yoshihiro S, Haggarth L, Li C, Tribukait B, Ekman P, Bergerheim US. Chromosome 16q24 deletion and decreased E-cadherin expression: possible association with metastatic potential in prostate cancer. *Prostate* 1998;**36**:31-38
- 97 **Li C**, Berx G, Larsson C, Auer G, Aspenblad U, Pan Y, Sundelin B, Ekman P, Nordenskjold M, van Roy F, Bergerheim US. Distinct deleted regions on chromosome segment 16q23-24 associated with metastases in prostate cancer. *Genes Chromosomes Cancer* 1999;**24**:175-182
- 98 **Caligo MA**, Polidoro L, Ghimenti C, Campani D, Cecchetti D, Bevilacqua G. A region on the long arm of chromosome 16 is frequently deleted in metastatic node-negative breast cancer. *Int J Oncol* 1998;**13**:177-182
- 99 **Driouch K**, Prydz H, Monese R, Johansen H, Lidereau R, Frengen E. Alternative transcripts of the candidate tumor suppressor gene, WWOX, are expressed at high levels in human breast tumors. *Oncogene* 2002;**21**:1832-1840
- 100 **Paige AJ**, Taylor KJ, Taylor C, Hillier SG, Farrington S, Scott D, Porteous DJ, Smyth JF, Gabra H, Watson JE. WWOX: a candidate tumor suppressor gene involved in multiple tumor types. *Proc Natl Acad Sci USA* 2001;**98**:11417-11422
- 101 **Bednarek AK**, Keck-Waggoner CL, Daniel RL, Laflin KJ, Bergsagel PL, Kiguchi K, Brenner AJ, Aldaz CM. WWOX, the FRA16D gene, behaves as a suppressor of tumor growth. *Cancer Res* 2001;**61**:8068-8073
- 102 **Kujawski M**, Aalto Y, Jaskula-Sztul R, Szyfter W, Szmeja Z, Szyfter K, Knuutila S. DNA copy number losses are more frequent in primary larynx tumors with lymph node metastases than in tumors without metastases. *Cancer Genet Cytogenet* 1999;**114**:31-34
- 103 **Padalecki SS**, Troyer DA, Hansen MF, Saric T, Schneider BG, O'Connell P, Leach RJ. Identification of two distinct regions of allelic imbalance on chromosome 18Q in metastatic prostate cancer. *Int J Cancer* 2000;**85**:654-658
- 104 **Ueda T**, Komiya A, Emi M, Suzuki H, Shiraishi T, Yatani R, Masai M, Yasuda K, Ito H. Allelic losses on 18q21 are associated with progression and metastasis in human prostate cancer. *Genes Chromosomes Cancer* 1997;**20**:140-147
- 105 **Nishizaki T**, DeVries S, Chew K, Goodson WH 3rd, Ljung BM, Thor A, Waldman FM. Genetic alterations in primary breast cancers and their metastases: direct comparison using modified comparative genomic hybridization. *Genes Chromosomes Cancer* 1997;**19**:267-272
- 106 **Frank CJ**, McClatchey KD, Devaney KO, Carey TE. Evidence that loss of chromosome 18q is associated with tumor progression. *Cancer Res* 1997;**57**:824-827
- 107 **Petersen S**, Aninat-Meyer M, Schluns K, Gellert K, Dietel M, Petersen I. Chromosomal alterations in the clonal evolution to the metastatic stage of squamous cell carcinomas of the lung. *Br J Cancer* 2000;**82**:65-73
- 108 **Blaker H**, Graf M, Rieker RJ, Otto HF. Comparison of losses of heterozygosity and replication errors in primary colorectal carcinomas and corresponding liver metastases. *J Pathol* 1999;**188**:258-262
- 109 **Chu LW**, Pettaway CA, Liang JC. Genetic abnormalities specifically associated with varying metastatic potential of prostate cancer cell lines as detected by comparative genomic hybridization. *Cancer Genet Cytogenet* 2001;**127**:161-167
- 110 **Kibel AS**, Faith DA, Bova GS, Isaacs WB. Loss of heterozygosity at 12P12-13 in primary and metastatic prostate adenocarcinoma. *J Urol* 2000;**164**:192-196
- 111 **Luu HH**, Zagaja GP, Dubauskas Z, Chen SL, Smith RC, Watabe K, Ichikawa Y, Ichikawa T, Davis EM, Le Beau MM, Rinker-Schaeffer CW. Identification of a novel metastasis-suppressor region on human chromosome 12. *Cancer Res* 1998;**58**:3561-3565
- 112 **Mora J**, Cheung NK, Chen L, Qin J, Gerald W. Loss of heterozygosity at 19q13.3 is associated with locally aggressive neuroblastoma. *Clin Cancer Res* 2001;**7**:1358-1361
- 113 **Nanashima A**, Yamaguchi H, Yasutake T, Sawai T, Kusano H, Tagawa Y, Nakagoe T, Ayabe H. Gain of chromosome 20 is a frequent aberration in liver metastasis of colorectal cancers. *Dig Dis Sci* 1997;**42**:1388-1393
- 114 **Balazs M**, Adam Z, Treszl A, Begany A, Hunyadi J, Adany R. Chromosomal imbalances in primary and metastatic melanomas revealed by comparative genomic hybridization. *Cytometry* 2001;**46**:222-232
- 115 **Piao Z**, Malkhosyan SR. Frequent loss Xq25 on the inactive X chromosome in primary breast carcinomas is associated with tumor grade and axillary lymph node metastasis. *Genes Chromosomes Cancer* 2002;**33**:262-269
- 116 **Tarkkanen M**, Huuhtanen R, Virolainen M, Wiklund T, Asko-Seljavaara S, Tukiainen E, Lepantalo M, Elomaa I, Knuutila S. Comparison of genetic changes in primary sarcomas and their pulmonary metastases. *Genes Chromosomes Cancer* 1999;**25**:323-331

Edited by Zhang JZ

• ESOPHAGEAL CANCER •

Identification of differentially expressed proteins between human esophageal immortalized and carcinomatous cell lines by two-dimensional electrophoresis and MALDI-TOF-mass spectrometry

Xing-Dong Xiong, Li-Yan Xu, Zhong-Ying Shen, Wei-Jia Cai, Jian-Min Luo, Ya-Li Han, En-Min Li

Xing-Dong Xiong, Jian-Min Luo, En-Min Li, Department of Biochemistry and Molecular Biology, Shantou University Medical College, Shantou 515031, Guangdong Province, China

Li-Yan Xu, Zhong-Ying Shen, Wei-Jia Cai, Department of Pathology, Shantou University Medical College, Shantou 515031, Guangdong Province, China

Ya-Li Han, Department of Biology, Shantou University, Shantou 515031, Guangdong Province, China

Supported by National Natural Science Foundation of China, NO. 39900069, NO.30170428; Guangdong Provincial Natural Science Foundation, NO.990799, NO.010431; Guangdong provincial College Natural Science Foundation, NO.200033; Guangdong provincial medical Scientific Foundation, NO.A2001419 and Research and Development Foundation of Shantou University, NO.L0004, NO.L00012.

Corresponding to: Dr. En-Min Li, Department of Biochemistry and Molecular Biology, Shantou University Medical College, 22 Xinling Road, Shantou 515031, Guangdong Province, China. nmli@21cn.com
Telephone: +86-754-8532720

Received 2002-05-18 **Accepted** 2002-06-27

Abstract

AIM: To identify the differentially expressed proteins between the human immortalized esophageal epithelial cell line (SHEE) and the malignant transformed esophageal carcinoma cell line (SHEEC), and to explore new ways for studying esophageal carcinoma associated genes.

METHODS: SHEE and SHEEC cell lines were used to separate differentially expressed proteins by two-dimensional electrophoresis. The silver-stained 2-D gels was scanned with EDAS290 digital camera system and analyzed with the PDQuest 6.2 Software. Six spots in which the differentially expressed protein was more obvious were selected and analyzed with matrix-assisted laser desorption/ionization time of flying mass spectrometry (MALDI-TOF-MS).

RESULTS: There were 107 ± 4.58 and 115 ± 9.91 protein spots observed in SHEE and SHEEC respectively, and the majority of these spots between the two cell lines matched each other ($r=0.772$), only a few were expressed differentially. After analyzed by MALDI-TOF-MS and database search for the six differentially expressed proteins, One new protein as well as other five sequence-known proteins including RNPEP-like protein, human rRNA gene upstream sequence binding transcription factor, uracil DNA glycosylase, Annexin A2 and p300/CBP-associated factor were preliminarily identified.

CONCLUSION: These differentially expressed proteins might play an importance role during malignant

transformation of SHEEC from SHEE. The identification of these proteins may serve as a new way for studying esophageal carcinoma associated genes.

Xiong XD, Xu LY, Shen ZY, Cai WJ, Luo JM, Han YL, Li EM. Identification of differentially expressed proteins between human esophageal immortalized and carcinomatous cell lines by two-dimensional electrophoresis and MALDI-TOF-mass spectrometry. *World J Gastroenterol* 2002; 8(5): 777-781

INTRODUCTION

Since Wilkins and Williams first proposed the concept of "Proteome" in 1994, the studies on tumor proteome have been made mighty advances^[1]. It is expected to find new special tumor markers and clone their associated genes via separating and identifying the tumor differentially expressed proteins by the proteomic approach to reveal the tumor pathogenesis and carry out the gene therapy^[2-6].

Esophageal carcinoma is one of the most common malignant tumors in China^[7-19], and its etiology and pathogenesis remain to be determined^[20-23]. Recent studies are mainly focused on the relationship between the change of oncogenes/suppressor oncogenes and esophageal carcinoma. However, there is no strong evidence to indicate that these oncogenes and suppressor oncogenes, including myc, ras, EGFR, int-2, cyclin D1, p53, Rb, p16, MCC, APC which are cloned originally from other kinds of tumors, are closely related to the esophageal carcinoma^[24-28]. Therefore, it is necessary to clone the new oncogenes or suppressor oncogenes, which might have an more intimate relationship with esophageal tumor pathogenesis, directly from esophageal carcinoma tissues or cells.

In recent years, it has been increasingly concerned about the roles of the human papilloma virus (HPV) played in the esophageal carcinogenesis^[29-32]. In our previous work, we transfected human embryonic esophageal mucosa cells with HPV18 E6E7 genes, and established an immortalized epithelial cell line SHEE^[33,34]. The SHEE cells were further exposed to the tumor promoter (12-O-tetradecanoyl-phorbol-13-acetate, TPA) to be induced malignant transformation, and from which a human embryonic esophageal epithelial carcinoma cell line SHEEC was then established^[35,36]. These studies not only provided the evidence for the close relationship between HPV and the esophageal carcinogenesis, but also established a reliable model for studying the molecular mechanisms of esophageal carcinogenesis, and cloning new esophageal carcinoma associated genes. In the present study, the differential expression of proteins between SHEE and SHEEC was investigated by the proteomic approach including two-

dimensional electrophoresis and MALDI-TOF-MS, which might serve as a new way for studying esophageal carcinoma associated genes.

MATERIALS AND METHODS

Cell culture

SHEE and SHEEC were cultured in MEM medium (Gibco) supplemented with 100 ml/L fetal bovine serum (100 u/ml penicillin, 100 u/ml streptomycin) and incubated at 37 °C in humidified atmosphere of 50 ml/L CO₂ incubator.

Whole soluble protein extraction and pre-treatment

To obtain whole soluble protein, the experimental procedures in *Molecular cloning* (2nd ed.) were employed^[37]. Briefly, when the cultured cells grew into a full monolayer, they were washed with ice-cold phosphate-buffer saline (PBS) three times and then treated with cold buffer containing 50 mmol/L Tris-HCl, pH8.0, 150 mmol/L NaCl, 1 % Triton X-100, 100 µg/ml Phenylmethylsulfonyl fluoride (PMSF) for 20 min at 4 °C. The broken cells were collected with a scraper and centrifuged at 12 000 g for 5 min. The supernatant, which contained the whole soluble proteins, was added to Micro Bio-Spin® chromatography columns, and the purified sample was obtained after centrifugation at 1 000g for 4 min. Protein concentrations were determined by Bradford method (BIOPhotometer, Eppendorf). The sample aliquots were stored at -20 °C until used.

Two-dimensional electrophoresis

Two-dimensional electrophoresis was carried out by using the Mini-PROTEAN II 2-D apparatus (Bio-Rad). 70 µg of the whole soluble proteins were mixed with the rehydration solution containing 8 mol/L Urea, 4 % CHAPS, 10 mmol/L DTT, 0.2 % (w/v) IPG buffer (pH3-10, liner) to a total volume of 125 µl. The mixture was pipetted into IPG strip tray channels. Both the rehydration and focusing were performed in the same focusing tray. IPG dry strips (pH3-10, 7 cm) were lowered onto the mixture with the gel side down, and then covered with mineral oil. The rehydration and isoelectric focusing (IEF) were done as follows: 1) rehydration for 12-14h, 0V; 2) 250V, 30 min; 3) 250V to 4 000V, 2 h; 4) 4 000V, 5 h. All the procedures above were performed at 20 °C. After IEF separation, the strips were immediately equilibrated for 2×10 min with 6 mol/L Urea, 0.375 mol/L Tris-HCl (pH8.8), 2 % SDS and 20 % glycerol. In the first equilibration solution, 2 % (w/v) DTT was included, and 2.5 % (w/v) iodoacetamide was added in the second equilibration. Then the IPG strips were placed on a 1.0 mm thick, 12 % SDS-PAGE gel and sealed with 1 % LowMelt agarose. Electrophoresis was carried out at a constant voltage (40 mV/gel) until the bromophenol blue frontier reached the bottom of the gels about 0.5 cm. After electrophoresis, the SDS-PAGE gels were stained with silver stain plus kit (Bio-Bad).

Image acquisition and analysis

Image scanning for the silver-stained 2-D gels was performed with EDAS290 digital camera system (Kodak) and image analysis with the PDQuest 6.2 Software (Bio-Rad). To get reliable results, three gels were employed for each cell line. After the background subtraction, spot detection and match, one standard gel for each cell line was obtained. These standard gels were then matched to yield information about the spots of differentially expressed proteins.

Protein identification by MALDI-TOF-MS

Six spots in which the differentially expressed protein was more obvious in each cell line were cut out from the gel. After washed with 300 µl milliQ water for 15 min, each protein spot was decolorized with the successive action of 50 µl of 15 mmol/L Potassium ferricyanide and 50 mmol/L sodium thiosulphate for 5-10 min. The faded gel pieces were dried in a vacuum centrifuge tube for 5 min. The cysteine reduction and alkylation were performed as incubated with 10 mmol/L DTT, 100 mmol/L NH₄HCO₃ at 56 °C for 1 h in the dark. The gel pieces were then dried again and incubated with 50 mmol/L fresh iodoacetamide in 100 mmol/L NH₄HCO₃ at room temperature for 30 min. Thereafter the gel pieces were rehydrated in digestion buffer containing 20 µl of 12.5 µg/ml modified trypsin and 20 mmol/L NH₄HCO₃ for 30 min in ice. The excess liquid was removed and the gel pieces were digested continuously at 30 °C overnight(>16 h). The resulting peptide mixture was extracted from the digested solution by centrifugation and then resuspended in 10 µl of 50 % CH₃CN and 0.1 % trifluoroacetic acid (TFA) for 10min at 30 °C on a shaking platform. Peptide mass maps were generated by Applied Biosystems Voyager System 6192 MALDI-TOF-mass spectrometry (ABI, USA). Peptide masses were analyzed using the MS-Fit search program (<http://prospector.ucsf.edu/ucshtml4.0u/msfit.htm>).

RESULTS

2-D map and image analysis

The whole soluble proteins of SHEE and SHEEC were extracted in one step and desalted with Micro Bio-Spin® chromatography columns, which made the 2-D electrophoretic patterns a much higher quality (to be published). Three pairs of gels from different batches of SHEE and SHEEC were analyzed for the purpose of quantitative and qualitative comparison with the software PDQuest6.2. There were 107±4.58 and 115±9.91 protein spots observed in SHEE and SHEEC respectively, and the majority of these spots between the two cell lines matched each other ($r=0.772$), only a few were expressed differentially. Six spots in which the differentially expressed protein was more obvious were selected and analyzed with MALDI-TOF-MS. The spot 1 was only expressed in the samples of SHEEC and absent in that of SHEE. In contrast, the spots 2 to 6 were merely observed in the SHEE samples. These six spots were marked with arrows at the corresponding site in Figure 1.

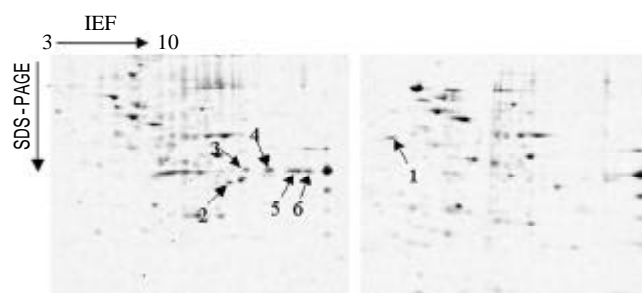


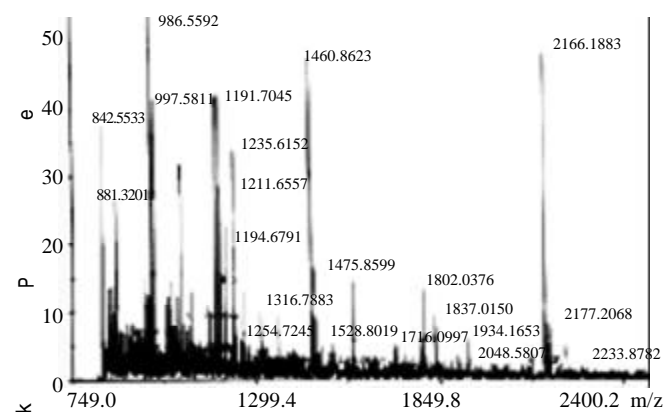
Figure 1 The differentially expressed protein spots observed in SHEE (left) and SHEEC (right) two-dimensional gels samples

Table 1 Protein identified by mass spectrometry

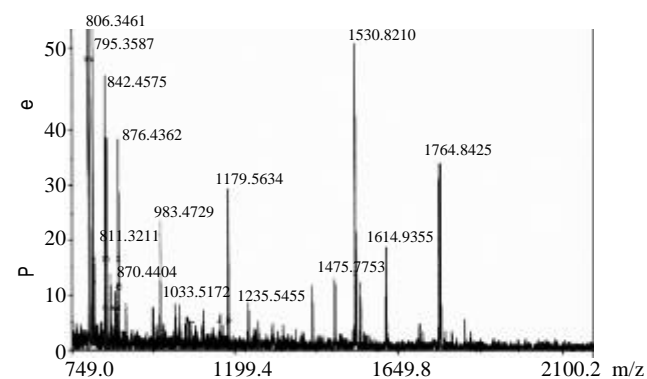
Spot No.	Accession No (NCBI nr)	Theoretic M_r	Theoretic pI	Intensity Matched(%)	Length(AA)	expression	Protein name
1	10719660	55549	4.8	10%	494	↑	RNPEP-like protein
2	1916615	75940	8.8	44%	654	↓	ribosomal RNA gene upstream sequence binding transcription factor
3	35053	35493	8.2	27%	331	↓	uracil DNA glycosylase
4	16306978	38618	7.6	47%	339	↓	annexin A2
5	7428977	92928	9.2	44%	832	↓	p300/CBP-associated factor
6	NEW PROTEIN	-	-	-	-	↓	-

MALDI-TOF-MS analysis and protein identification

The proteins contained in the six spots were identified respectively by MALDI-TOF-MS on the basis of peptide mass matching; In this way, the peptide mass fingerprinting map for each protein spot was obtained as show in Figure 2. The experimental data revealed that the protein in spot 6 was with an unknown sequence (Figure 3), and its characteristics remains to be investigated. The identified protein names, accession numbers, as well as the number of the matching peptide, the theoretical M_r and pI values, i.e. for each protein spot were listed in Table 1.



Mode of operation: Reflector Extraction mode: delayed
 Accelerating voltage: 20000 V
 Acquisition mass range: 750-3500Da Number of laser shots: 150/spectrum Laser intensity: 2233

Figure 2 The MALDI-TOF mass spectrum map of protein spot 1

Mode of operation: Reflector Extraction mode: delayed
 Accelerating voltage: 20000 V
 Acquisition mass range: 750-3000Da Number of laser shots: 200/spectrum Laser intensity: 2224

Figure 3 The MALDI-TOF mass spectrum map of protein spot 6**DISCUSSION**

The investigation of differentially expressed proteins that occurred during the generation and development of tumors is a new effective way to study tumor associated genes^[38,39]. In the present study, we preliminarily studied several of the differentially expressed proteins between SHEE and SHEEC with two-dimensional electrophoresis and MALDI-TOF-mass spectrometry. By comparing the reference proteins or peptides, five sequence-known proteins and a novel sequence-unknown protein, which expressed more differentially in the course of malignant transformation of esophageal epithelial cells, were identified for the first time. It is therefore further indicated that the methods adopted in the present study could provide a new way to study esophageal carcinoma associated genes.

RNPEP-like protein being composed of 494 amino acid residues has 49 % identity with aminopeptidase B in amino acid sequence^[40]. As judged by the parameters such as the numbers and intensity of peptide matching peak, the sequence coverage of matching peptide, as well as the theoretical and approximate values of M_r and pI , RNPEP-like protein was considered as the much higher expression in SHEEC cells. However, the significance of its overexpression in SHEEC remains unknown.

Human rRNA gene upstream sequence binding transcription factor (hUBF) is a critical element in the regulation of rRNA transcription, which performs its function by binding to the rRNA gene upstream regulator sequence (-200 to -107 and -45 to 20)^[41]. In our present work, it has been shown that the down-regulation of hUBF expression was obvious in the course of malignant transformation of SHEE, which might be the results of alterations in the regulation mechanism of rRNA gene transcription occurred in the malignant transformation of the human immortalized esophageal epithelial cells. In addition, whether or not the fact that diminished hUBF expression has been found in the well-differentiated teratocarcinoma cells^[42] related hUBF to the neoplastic differentiation, remain to be investigated.

Uracil DNA glycosylase (UDG) is an enzyme for the DNA repairment. It can hydrolyse the N-glycosidic bond connecting the base to the deoxyribose and release free uracil base and DNA with an abasic site as its products^[43]. Moon and his associates^[44] found that the uracil DNA glycosylase gene (UNG) in sporadic glioblastomas had a point mutation in exon 3, and concluded that the genetic alterations of UNG might play an important role in the development of primary glioblastomas. In our study, the UDG expression shows absent or too low to be detected after SHEE malignantly transformed into SHEEC, which means that there might exist repairing deficiencies for the damaged DNA in the course of malignant transformation of the human immortalized esophageal epithelial cells.

Annexin A2 belongs to the family of annexins that bind to phospholipids in a calcium-dependent manner. So far at least 13 annexin family members have been found. There are four repeats of a 70 amino acid motif and a variable N-terminal end contained in all these annexin family members. According to lots of investigations, the annexins seem to be involved in various biological processes including endocytosis, exocytosis, the phospholipase A2 inhibition as well as ion channel and protein kinase C activity^[45,46]. In recent years, it has been found that the annexin I was overexpressed in some kinds of malignant tumors such as human hepatocellular^[47] and pulmonary carcinomas^[48], which suggests that some of the annexin family members might relate to the carcinogenesis. Moreover, Chetcuti and his associates^[49] found that the annexin II was expressed in the normal and benign hyperplastic prostate tissue, and absent in all prostate cancer specimens. These results indicated that different members of the annexin family may have varied roles in the development and progression of tumors. The fact that the annexin A2 was expressed in SHEE but absent in SHEEC in our research indicates that annexin A2 might play a role of suppressor oncogene during malignant transformation of the human immortalized esophageal epithelial cells.

The p300/CBP-associated factor (P/CAF) that possessed intrinsic histone acetylase activity could regulate the gene expression of various sequence-specific factors that are involved in cell growth and/or differentiation including CREB, c-Jun, Fos and c-Myb through promoter-specific histone acetylation. Yang *et al*^[50] found that the expression of P/CAF in HeLa cells could block the cell-cycle progression from G1 to S phase, and counteract the mitogenic activity of adenoviral oncoprotein E1A. The P/CAF expression was absent in the esophageal carcinoma cells found in our study suggests that the P/CAF might play a role in the suppressing of the esophageal carcinoma development.

REFERENCES

- 1 **Li F**, Guan YJ, Chen ZC. Proteomics in cancer research. *Shengwu Huaxue Yu Shengwu Wuli Jinzhan* 2001; **28**: 164-167
- 2 **Sarto C**, Frutiger S, Cappellano F, Sanchez JC, Doro G, Catanzaro F, Hughes GJ, Hochstrasser DF, Mocarelli P. Modified expression of plasma glutathione peroxidase and manganese superoxide dismutase in human renal cell carcinoma. *Electrophoresis* 1999; **20**: 3458-3466
- 3 **Vercoutter-Edouart AS**, Lemoine J, Le-Bourhis X, Louis H, Boilly B, Nurcombe V, Revillion F, Peyrat JP, Hondermarck H. Proteomic analysis reveals that 14-3-3sigma is down-regulated in human breast cancer cells. *Cancer Res* 2001; **61**: 76-80
- 4 **Yanagida M**, Miura Y, Yagasaki K, Taoka M, Isobe T, Takahashi N. Matrix assisted laser desorption/ionization-time of flight-mass spectrometry analysis of proteins detected by anti-phosphotyrosine antibody on two-dimensional-gels of fibroblast cell lysates after tumor necrosis factor-alpha stimulation. *Electrophoresis* 2000; **21**: 1890-1898
- 5 **Vercoutter-Edouart AS**, Czeszak X, Crepin M, Lemoine J, Boilly B, Le-Bourhis X, Peyrat JP, Hondermarck H. Proteomic detection of changes in protein synthesis induced by fibroblast growth factor-2 in MCF-7 human breast cancer cells. *Exp Cell Res* 2001; **262**: 59-68
- 6 **Zhan XQ**, Chen ZC, Guan YJ, Li C, He CM, Liang SP, Xie JY, Chen P. Analysis of human lung squamous carcinoma cell line NCI-H520 proteome by two-dimensional electrophoresis and MALDI-TOF-mass spectrometry. *Ai zheng* 2001; **20**: 575-582
- 7 **Shen ZY**, Xu LY, Li EM, Cai WJ, Chen MH, Shen J, Zeng Y. Telomere and telomerase in the initial stage of immortalization of esophageal epithelial cell. *World J Gastroenterol* 2002; **8**: 357-362
- 8 **Shen ZY**, Shen WY, Chen MH, Shen J, Cai WJ, Zeng Y. Mitochondria, calcium and nitric oxide in the apoptotic pathway of esophageal carcinoma cells induced by As₂O₃. *Int J Mol Med* 2002; **9**: 385-390
- 9 **Chen KN**, Xu GW. Diagnosis and treatment of esophageal cancer. *Shijie Huaren Xiaohua Zazhi* 2000; **8**: 196-202
- 10 **Shen ZY**, Shen WY, Chen MH, Shen J, Cai WJ, Yi Z. Nitric oxide and calcium ions in apoptotic esophageal carcinoma cells induced by arsenite. *World J Gastroenterol* 2002; **8**: 40-43
- 11 **Shen ZY**, Shen J, Li QS, Chen CY, Chen JY, Zeng Y. Morphological and functional changes of mitochondria in apoptotic esophageal carcinoma cells induced by arsenic trioxide. *World J Gastroenterol* 2002; **8**: 31-35
- 12 **Shen ZY**, Xu LY, Li C, Cai WJ, Shen J, Chen JY, Zeng Y. A comparative study of telomerase activity and malignant phenotype in multistage carcinogenesis of esophageal epithelial cells induced by human papillomavirus. *Int J Mol Med* 2001; **8**: 633-639
- 13 **Shen ZY**, Shen J, Cai WJ, Hong C, Zheng MH. The alteration of mitochondria is an early event of arsenic trioxide induced apoptosis in esophageal carcinoma cells. *Int J Mol Med* 2000; **5**: 155-158
- 14 **Shen ZY**, Tan LJ, Cai WJ, Shen J, Chen C, Tang XM, Zheng MH. Arsenic trioxide induces apoptosis of esophageal carcinoma *in vitro*. *Int J Mol Med* 1999; **4**: 33-37
- 15 **Hao MW**, Liang YR, Liu YF, Liu L, Wu MY, Yang HX. Transcription factor EGR-1 inhibits growth of hepatocellular carcinoma and esophageal carcinoma cells lines. *World J Gastroenterol* 2002; **8**: 203-207
- 16 **Gu ZP**, Wang YJ, Li JG, Zhou YA. VEGF₁₆₅ antisense RNA suppresses oncogenic properties of human esophageal squamous cell carcinoma. *World J Gastroenterol* 2002; **8**: 44-48
- 17 **Su M**, Lu SM, Tian DP, Zhao H, Li XY, Li DR, Zheng ZC. Relationship between ABO blood groups and carcinoma of esophagus and cardia in Chaoshan inhabitants of China. *World J Gastroenterol* 2001; **7**: 657-661
- 18 **Wu MY**, Chen MH, Liang YR, Meng GZ, Yang HX, Zhuang CX. Experimental and clinic-opathologic study on the relationship between transcription factor Egr-1 and esophageal carcinoma. *World J Gastroenterol* 2001; **7**: 490-495
- 19 **Xiao ZF**, Yang ZY, Zhou ZM, Yin WB, Gu XZ. Radiotherapy of double primary esophageal carcinoma. *World J Gastroenterol* 2000; **6**: 145-146
- 20 **Yang SM**, Wang TJ, Li BY, Wu YH, Ye ZS. Detection of telomerase activity in malignant neoplasms and nonmalignant epithelial tissues of human esophagus. *World J Gastroenterol* 2000; **6**(Suppl 3): 45
- 21 **Wang DX**, Li W. Advanced on pathogenesis of esophageal cancer. *Shijie Huaren Xiaohua Zazhi* 2000; **8**: 1029-1030
- 22 **Hu SP**, Yang HS, Shen ZY. Study on etiology of esophageal carcinoma: retrospect and prospect. *Zhongguo Aizheng Zazhi* 2001; **11**: 171-174
- 23 **Deng LY**, Zhang YH, Xu P, Yang SM, Yuan XB. Expression of IL 1beta converting enzyme in 5-FU induced apoptosis in esophageal carcinoma cells. *World J Gastroenterol* 1999; **5**: 50-52
- 24 **Zou JX**, Wang LD, Shi ST, Yang GY, Xue ZH, Gao SS, Li YX, Yang CS. p53 gene mutations in multifocal esophageal precancerous and cancerous lesions in patients with esophageal cancer in high-risk northern China. *Shijie Huaren Xiaohua Zazhi* 1999; **7**: 280-284
- 25 **Liu J**, Chen SL, Zhang W, Su Q. P21-WAF1 gene expression with P53 mutation in esophageal carcinoma. *Shijie Huaren Xiaohua Zazhi* 2000; **8**: 1350-1353
- 26 **Wei ZB**, Wang LB, Tian BS, Wang JL, Sun XF, Wei JP, Liu N, Wang JH. Lugol' 27 s staining with p53 oncoproteins in detecting early esophageal cancer. *Shijie Huaren Xiaohua Zazhi* 2001; **9**: 495-498
- 27 **Zhou YA**, Gu ZP, Wang XN, Ma QF, Huang LJ. Re-ex-

- pression of p16-INK4 α gene suppresses growth of human esophageal carcinoma cells. *Shijie Huaren Xiaohua Zazhi* 2001; **9**: 877-881
- 28 **Wang LD**, Zhou Q, Wei JP, Yang WC, Zhao X, Wang LX, Zou JX, Gao SS, Li YX, Yang CS. Apoptosis and its relationship with cell proliferation, p53, Waf1p21, bcl-2 and c-myc in esophageal carcinogenesis studied with a high-risk population in northern China. *World J Gastroenterol* 1998; **4**: 287-293
 - 29 **Chen HB**, Chen L, Zhang JK, Shen ZY, Su ZJ, Cheng SB, Chew EC. Human papillomavirus 16 E6 is associated with the nuclear matrix of esophageal carcinoma cells. *World J Gastroenterol* 2001; **7**: 788-791
 - 30 **Lavergne D**, de-Villiers EM. Papillomavirus in esophageal papillomas and carcinomas. *Int J Cancer* 1999; **80**: 681-684
 - 31 **Ma QF**, Jiang H, Feng YQ, Wang XP, Zhou YA, Liu K, Jia ZL. Detection of human papillomavirus DNA in squamous cell carcinoma of the esophagus. *Shijie Huaren Xiaohua Zazhi* 2000; **8**: 1218-1224
 - 32 **Zhang J**, Yan XJ, Yan QJ, Duan J, Hou Y, Su CZ. Cloning and expression of HPV16 L₂ DNA from esophageal carcinoma in *E. coli*. *Shijie Huaren Xiaohua Zazhi* 2001; **9**: 273-278
 - 33 **Shen ZY**, Xu LY, Chen XH, Cai WJ, Shen J, Chen JY, Huang TH, Zeng Y. The genetic events of HPV-immortalized esophageal epithelium cells. *Int J Mol Med* 2001; **8**: 537-542
 - 34 **Shen ZY**, Cen S, Cai WJ, Teng ZP, Shen J, Hu Z, Zeng Y. immortalization of human fetal esophageal epithelial cells induced by E6 and E7 genes of human papilloma virus 18. *Zhonghua Shiyen He Linchuang Bingduxue Zazhi* 1999; **13**: 121-124
 - 35 **Shen ZY**, CAI WJ, Shen J, Xu JJ, Cen S, Teng ZP, Hu Z, Zeng Y. Human papilloma virus 18E6E7 in synergy with TPA induced malignant transformation of human embryonic esophageal epithelial cells. *Bingdu Xuebao* 1999; **15**: 1-5
 - 36 **Shen ZY**, Cen S, Shen J, Cai WJ, Xu JJ, Teng ZP, Hu Z, Zeng Y. Study of immortalization and malignant transformation of human embryonic esophageal epithelial cells induced by HPV18 E6E7. *J Cancer Res Clin Oncol* 2000; **126**: 589-594
 - 37 **Sambrook J**, Fritsch EF, Maniatis T (Ed). *Molecular cloning a Laboratory Manual*, 3th ed. Jin DY, Li MF, trans-ed, Beijing, China: *Sci Pub* 1998: 872-873
 - 38 **Li J**, Tan C, Xiang Q, Zhang XM, Ma J, Li WF, Wang JR, Yang JB, Liang SP, Li GY. Search for differentially expressed proteins involved in the treatment of Human Nasopharyngeal Carcinoma Cells with NGX6 using two-dimensional electrophoresis and mass spectrometry. *Shengwu Huaxue Yu Shengwu Wuli Jinzhan* 2001; **28**: 573-577
 - 39 **Yu LR**, Zeng R, Shao XX, Wang N, Xu YH, Xia QC. Identification of differentially expressed proteins between human hepatoma and normal liver cell lines by two-dimensional electrophoresis and liquid chromatography-ion trap mass spectrometry. *Electrophoresis* 2000; **21**: 3058-3068
 - 40 **Horikawa Y**, Oda N, Cox NJ, Li X, Orho-Melander M, Hara M, Hinokio Y, Lindner TH, Mashima H, Schwarz PE, del-Bosque-Plata L, Horikawa Y, Oda Y, Yoshiuchi I, Colilla S, Polonsky KS, Wei S, Concannon P, Iwasaki N, Schulze J, Baier LJ, Bogardus C, Groop L, Boerwinkle E, Hanis CL, Bell GI. Genetic variation in the gene encoding calpain-10 is associated with type 2 diabetes mellitus. *Nat. Genet* 2000; **26**: 163-175
 - 41 **Chan EKL**, Imai H, Hamel JC, Tan EM. Human autoantibody to RNA polymerase I transcription factor hUBF. Molecular identity of nucleolus organizer region autoantigen NOR-90 and ribosomal RNA transcription upstream binding factor. *J Exp Med* 1991; **174**: 1239-1244
 - 42 **Datta PK**, Budhiraja S, Reichel RR, Jacob ST. Regulation of ribosomal RNA gene transcription during retinoic acid-induced differentiation of mouse teratocarcinoma cells. *Exp Cell Res* 1997; **231**: 198-205
 - 43 **Pearl LH**. Structure and function in the uracil-DNA glycosylase superfamily. *Mutat Res* 2000; **460**: 165-181
 - 44 **Moon YW**, Park WS, Vortmeyer AO, Weil RJ, Lee YS, Winters TA, Zhuang Z, Fuller BG. Mutation of the uracil DNA glycosylase gene detected in glioblastoma. *Mutat Res* 1998; **421**: 191-196
 - 45 **Han EK**, Tahir SK, Cherian SP, Collins N, Ng SC. Modulation of paclitaxel resistance by annexin IV in human cancer cell lines. *Br J Cancer* 2000; **83**: 83-88
 - 46 **Dubois T**, Oudinet JP, Mira JP, Russo-Marie F. Annexins and protein kinase C. *Biochem Biophys Acta* 1996; **1313**: 290-294
 - 47 **Masaki T**, Tokuda M, Ohnishi M, Watanabe S, Fujimura T, Miyamoto K, Itano T, Matsui H, Arima K, Shirai M, Maeba T, Sogawa K, Konishi R, Taniguchi K, Hatanaka Y, Hatase O, Nishioka M. Enhanced expression of the protein kinase substrate annexin I in human hepatocellular carcinoma. *Hepatology* 1996; **24**: 72-81
 - 48 **Xie L**, Ying WT, Zhang KT, Xiang XQ, Qian XH, Wang YZ, Wu DC. Identification of bronchial epithelial neoplastic transformation related protein ANX1-human by two-dimensional electrophoresis and mass spectrometry. *Zhongguo Shengwu Huaxue Yu Fenzi Shengwu Xuebao* 2000; **16**: 569-573
 - 49 **Chetcuti A**, Margan SH, Russell P, Mann S, Millar DS, Clark SJ, Rogers J, Handelsman DJ, Dong Q. Loss of annexin II heavy and light chains in prostate cancer and its precursors. *Cancer Res* 2001; **61**: 6331-6334
 - 50 **Yang XJ**, Ogryzko VV, Nishikawa J, Howard BH, Nakatani Y. A p300/CBP-associated factor that competes with the adenoviral oncoprotein E1A. *Nature* 1996; **382**: 319-324

Edited by Zhu L

• GASTRIC CANCER •

The effects of vitamin E succinate on the expression of *c-jun* gene and protein in human gastric cancer SGC-7901 cells

Yan Zhao, Kun Wu, Wei Xia, Yu-Juan Shan, Li-Jie Wu, Wei-Ping Yu

Yan Zhao, Kun Wu, Wei Xia, Yu-Juan Shan, Li-Jie Wu, Department of Nutrition and Food Hygiene, Public Health School, Harbin Medical University, Harbin 150001, Heilongjiang Province, China

Wei-Ping Yu, Genetics Institute, Texas University of USA, Austin, USA
Supported by National Natural Science Foundation of China, No. 39870662

Correspondence to: Prof. Kun Wu, Department of Nutrition and Food Hygiene, Public Health School, Harbin Medical University, Harbin 150001, Heilongjiang Province, China. wukun@public.hr.hl.cn
Telephone: +86-451-3648665

Received 2002-03-11 **Accepted** 2002-04-20

Abstract

AIM: To investigate the effects of vitamin E succinate (VES) on the expression of *c-jun* gene and protein in human gastric cancer SGC-7901 cells.

METHODS: After SGC-7901 cells were treated with VES at different doses (5, 10, 20 mg·L⁻¹) at different time, reverse transcription-PCR technique was used to detect the level of *c-jun* mRNA; Western Blot was applied to measure the expression of *c-jun* protein.

RESULTS: After the cells were treated with VES at 20 mg·L⁻¹ for 3 h, the expression rapidly reached its maximum that was 3.5 times of UT control ($P < 0.01$). The level of *c-jun* mRNA was also increased following treatment of VES for 6 h. However, the expression after treatment of VES at 5 mg·L⁻¹ for 24 h was 1.6 times compared with UT control ($P < 0.01$). Western blot analysis showed that the level of *c-jun* protein was obviously elevated in VES-treated SGC-7901 cells at 20 mg·L⁻¹ for 3 h. The expression of *c-jun* protein was gradually increased after treatment of VES at 20 mg·L⁻¹ for 3, 6, 12 and 24 h, respectively, with an evident time-effect relationship.

CONCLUSION: The levels of *c-jun* mRNA and protein in VES-treated SGC-7901 cells were increased in a dose- and time-dependent manner; the expression of *c-jun* was prolonged by VES, indicating that *c-jun* is involved in VES-induced apoptosis in SGC-7901 cells.

Zhao Y, Wu K, Xia W, Shan YJ, Wu LJ, Yu WP. The effects of vitamin E succinate on the expression of *c-jun* gene and protein in human gastric cancer SGC-7901 cells. *World J Gastroenterol* 2002; 8(5):782-786

INTRODUCTION

RRR- α -tocopheryl succinate (vitamin E succinate, VES), a derivative of natural vitamin E, has been shown to be a potent growth inhibitor of various cancer cell types *in vitro* and *in vivo*^[1-7]. Growth inhibition by VES is attributed to cell cycle blockage^[4,8-10], induced cellular differentiation^[11,12], increased expression of biologically active transforming growth factor-

β s (TGF- β s) and their type II cell surface receptors^[11,13,14] and the induction of apoptosis^[15-18]. VES is noteworthy not only for its antiproliferative effects on tumor cells, but also for its non-toxic effect on normal cell types.

Gastric cancer is one of the most common tumors in China^[19-28]. Up to date, the exact mechanisms of tumorigenesis is still unclear, but our previous studies showed that VES can block cell cycle, arrest DNA synthesis and induce apoptosis in human gastric cancer SGC-7901 cells, therefore inhibiting the cell growth^[29-32]. In addition, our *in vivo* research in our laboratory demonstrated that VES inhibited benzo(a)pyrene (B(a)P)-induced forestomach carcinogenesis in female mice^[33]. The exact mechanisms of apoptosis are not clearly known, but we found that VES can secrete and activate biologically active TGF- β and then TGF- β increases the kinase activity of *c-jun* N-terminal kinase (JNK) followed by phosphorylation of *c-jun*, and finally activated *c-jun* triggers apoptosis in human gastric cancer SGC-7901 cells^[34]. In this study, the expression of *c-jun* mRNA was detected using reverse-transcription polymerase chain reaction (RT-PCR) technique and the level of *c-jun* protein was measured using western blot in order to further investigate the mechanisms of VES-triggered apoptosis.

MATERIALS AND METHODS

Materials

VES was purchased from Sigma Co. Ltd. RPMI 1640 media and TRIzol total RNA isolation kit were obtained from Gibco BRL, TITANIUM™ one-step RT-PCR kit from Clontech. Inc. *c-jun* (H79) rabbit polyclonal antibody was from Santa Cruz Biotechnologies.

Methods

Cell culture Human gastric cancer cell lines SGC-7901 were maintained in RPMI 1640 medium supplemented with 100 mL·L⁻¹ fetal calf serum (FCS), 100 kU·L⁻¹ penicillin, 100 mg·L⁻¹ streptomycin and 2 mmol·L⁻¹ L-glutamine under 50 mL·L⁻¹ CO₂ in a humidified incubator at 37 °C. SGC-7901 cells were incubated for different time periods in the presence of VES at 5, 10 and 20 mg·L⁻¹ (VES was dissolved in absolute ethanol and diluted in RPMI 1640 complete condition media correspondingly to a final concentration of VES and 1 mL·L⁻¹ ethanol), succinic acid, vitamin E and ethanol equivalents as vehicle (VEH) control and condition media only as untreated (UT) control.

RT-PCR After SGC-7901 cells were treated with VES for 3, 6 and 24 h, respectively, total cellular RNA was isolated by using TRIzol Reagent according to the manufacturer's instructions. The concentration and purity of total RNA were determined by DU^R 640 nucleic acid and protein analyzer (Beckman, USA). One-step RT-PCR was carried out following the manufacturer's instructions. RT-PCR mixture was heated 1h at 50 °C for reverse transcription and 5 min at 95 °C for pre-denaturation, then into 34 PCR cycles of 30 s at 94 °C for

denaturation, 30 s at 60 °C for annealing, 30 s at 72 °C for extension in PTC-100 programmable thermal controller (MJ Research, USA). The corresponding fragment of *c-jun* gene was amplified with specific primers synthesized^[35]. β -actin gene was designed as an internal standard with purpose to remove false negative outcome (Table 1).

Table 1 Nucleotide sequence and size of the expected PCR products for oligonucleotide primers used for RT-PCR

Genes	Sequence	Size (bp)
<i>c-jun</i>	Upstream: 5'-GGA AAC GAC CTT CTA TGA CGA GCC C-3'	315
	Downstream: 5'-GAA CCC CTC CTG CTC ATC TGT CAG G-3'	
β -actin	Upstream: 5'-GTG GGC CGC TCT AGG CAC CAA-3'	540
	Downstream: 5'-CTC TTT GAT GTC ACG CAC GAT TTC-3'	

The amplified products were separated in 20 g·L⁻¹ agarose gel stained with ethidium bromide. After electrophoresis, the gel was observed and photographed under ultraviolet reflector. The density and area of each band were analyzed using Chemilmager™ 4000 Digital System (Alpha Innotech Corporation, USA).

Western blot SGC-7901 cells treated with VES were harvested, washed in PBS and lysed in lysis buffer containing 150 mmol·L⁻¹ NaCl, 1 mL·L⁻¹ NP-40, 5 mg·L⁻¹ sodium deoxycholate, 1 g·L⁻¹ SDS, 50 mmol·L⁻¹ Tris (pH 7.4), 1 mmol·L⁻¹ DTT, 0.5 mmol·L⁻¹ Na₃VO₄, 10 mmol·L⁻¹ phenylmethylsulfonyl fluoride (PMSF), 10 mg·L⁻¹ trypsin, 10 mg·L⁻¹ aprotinin and 5 mg·L⁻¹ leupeptin. Following the centrifugation of 12 000×g for 30 min at 4 °C, the amount of protein in the supernatant was determined using Biorad DC protein assay. Equal amount of protein was separated on 10 % SDS-PAGE and transferred to nitrocellulose filter (Gibco BRL, USA) overnight. Blocked with 50 g·L⁻¹ defatty milk, the filter was incubated with *c-jun* (H79) rabbit polyclonal antibody and horseradish peroxidase-conjugated IgG, finally developed with DAB.

Statistical analysis

The data were expressed as $\bar{x} \pm s$. Statistical analysis was performed using student's *t*-test. *P*<0.05 was considered significant.

RESULTS

Effect of VES on the expression of *c-jun* mRNA in SGC-7901 cells

1 μ g of total cellular RNA from groups of control, succinate, vitamin E, VES at 5, 10 and 20 mg·L⁻¹ was added to amplify *c-jun* and β -actin genes by RT-PCR. Baseline expression of *c-jun* mRNA was observed in SGC-7901 cells (Figure 1). After the cells were treated with VES at 20 mg·L⁻¹ for 3 h, the expression rapidly reached its maximum that was 3.5 times of UT control (*P*<0.01). The level of *c-jun* mRNA was also increased following treatment of VES for 6 h. However, the expression after treatment of VES at 5 mg·L⁻¹ for 24 h was 1.6-fold increase compared with UT control (*P*<0.01), while there was no significant difference between 10 and 20 mg·L⁻¹ VES groups and UT control group (Table 2).

Effect of VES on the expression of *c-Jun* protein in SGC-7901 cells

Western blot analysis showed that the level of c-Jun protein was obviously elevated in VES-treated SGC-7901 cells at 20

mg·L⁻¹ for 3 h in a significant dose-dependent manner (Figure 2A, 2B). Meanwhile, compared with the cells in UT control group, the VES-treated cells at 20 mg·L⁻¹ exhibited 1.8-, 2.0-, 2.3- and 2.8-fold increases in the expression of *c-jun* protein for 3, 6, 12 and 24h, respectively, with an evident time-effect relationship (Figure 3A,3B).

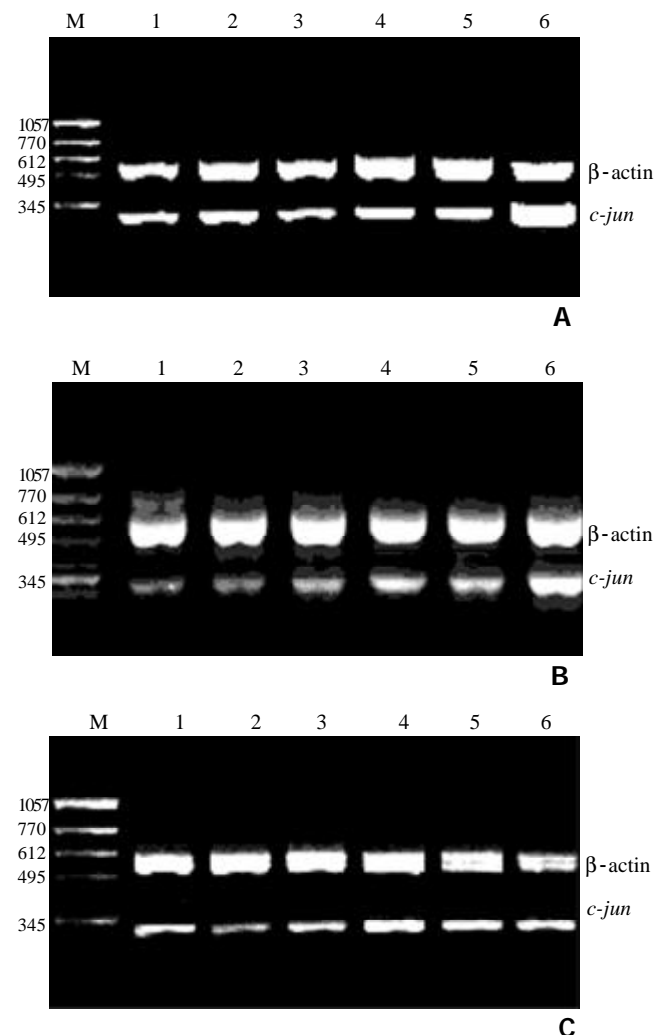


Figure 1 Effect of VES on the expression of *c-jun* mRNA in SGC-7901 cells for different time points by RT-PCR. A: treatment of VES for 3 h; B: treatment of VES for 6 h; C: treatment of VES for 24 h. 1: UT control; 2: succinate; 3: vitamin E; 4: VES at 5 mg·L⁻¹; 5: VES at 10 mg·L⁻¹; 6: VES at 20 mg·L⁻¹; M: molecular weight marker.

Table 2 The relative expression of *c-jun* mRNA in SGC-7901 cells (*n*=6, $\bar{x} \pm s$)

Groups	Ratio of <i>c-jun</i> /β-actin		
	3h	6h	24h
UT control	0.469±0.092	0.432±0.095	0.368±0.104
succinate	0.426±0.082	0.408±0.078	0.361±0.083
vitamin E	0.514±0.101	0.430±0.081	0.367±0.075
5mg·L ⁻¹ VES	0.550±0.115	0.621±0.086 ^b	0.584±0.097 ^b
10mg·L ⁻¹ VES	0.471±0.086	0.584±0.101 ^a	0.421±0.077
20mg·L ⁻¹ VES	1.663±0.109 ^b	0.905±0.099 ^b	0.411±0.094

^a*P*<0.05, ^b*P*<0.01, vs UT control.

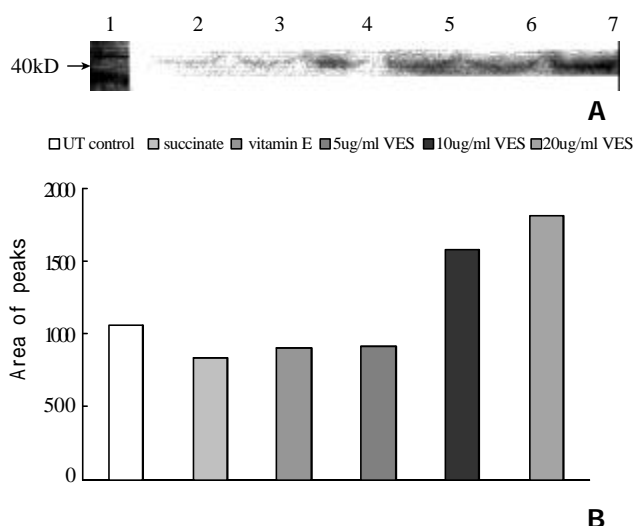


Figure 2 The expression of *c-jun* protein in SGC-7901 cells following treatment of VES for 3h. Lane1: Molecular weight marker; Lane2: UT control; Lane3: succinate; Lane4: vitamin E; Lane5: VES at 5 mg·L⁻¹; Lane6: VES at 10 mg·L⁻¹; Lane7: VES at 20 mg·L⁻¹.

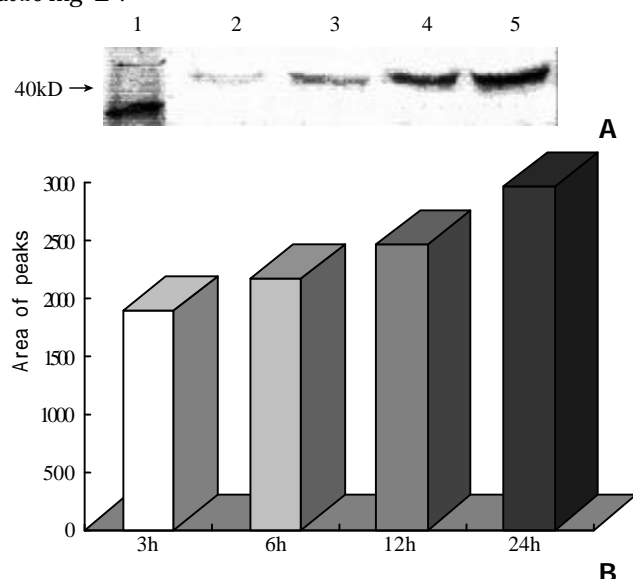


Figure 3 The expression of *c-jun* protein in SGC-7901 cells following treatment of VES at 20 mg·L⁻¹ for different time points. Lane1: Molecular weight marker; Lane2: 3 h; Lane3: 6 h; Lane4: 12 h; Lane5: 24 h

DISCUSSION

The oncogene, *c-jun*, belongs to an immediate early gene and can be rapidly and transiently induced in response to multiple extracellular stimuli^[36-38]. The product of *c-jun* gene is a nuclear transcription factor, an important composition of activation protein 1 (AP-1) dimmers, involved in signal transduction and regulation of many kinds of genes^[39-41].

Transcription of *c-jun* mRNA rises after exposure of cells to a number of treatment including ultraviolet, irradiation, heat shock, H₂O₂, TNF- α and other apoptosis-associated factors^[42-46]. In addition to this transcriptional mode of regulation, *c-jun* activity can also be modulated directly at the protein level. In certain cell types, induction of *c-jun* is observed during apoptosis. There is some evidence that prolonged expression of *c-jun* in selected vulnerable cells suggests neuronal cell death^[47].

Apoptosis is an innate program of cell suicide that is required for removal of unnecessary or damaged cells from bodily structures. Apoptosis is complex and regulated by a variety of factors^[48-58]. Previous studies showed that the induction of apoptosis in tumor cells is one of the important mechanisms of VES-induced cell growth inhibition^[59-61]. In the present study, the expression of *c-jun* mRNA and protein was measured in human gastric cancer SGC-7901 cells treated with VES at different doses for different time points. We found that the expression of *c-jun* mRNA was evidently promoted after 3 h of VES treatment at 20 mg·L⁻¹ and reduced to the normal level after 24 h of treatment; whereas in the case of VES treatment at 5 mg·L⁻¹, that was also increased after 3 h and remained a high level after 24 h. The data above showed that the *c-jun* activation was enhanced and prolonged by VES, therefore indicating that *c-jun* is involved in VES-triggered apoptosis in SGC-7901 cells. The results from western blot analysis showed that the level of *c-jun* protein was elevated following SGC-7901 cells were treated with VES at different doses for 3 h and with VES at 20 mg·L⁻¹ for different time in a dose- and time-dependent manner.

The diversity of signals and signaling pathways that are directed toward *c-jun* is also reflected in the biological responses, in which the transcription factors have been implicated. It is reported that the mainly biological functions of *c-jun* are blockage of cell cycle and induction of apoptosis^[62-64]. The study presented here demonstrated that VES can obviously increase the expression of *c-jun* mRNA and protein in human gastric cancer SGC-7901 cells, implicating that *c-jun* is involved in VES-induced apoptosis.

REFERENCES

- 1 Fariss MW, Merson MH, O Hara TM. The selective antiproliferation effects of α -tocopheryl hemisuccinate and cholesteryl hemisuccinate on murine leukemia cells result from the action of the intact compounds. *Cancer Res* 1994; **54**:3346-3357
- 2 Ottino P, Duncan JR. Effect of α -tocopheryl succinate on free radical and lipid peroxidation levels in BL6 melanoma cells. *Free Radical Biol Med* 1997; **22**:1145-1151
- 3 Israel K, Sanders BG, Kline K. RRR- α -Tocopheryl Succinate inhibits the proliferation of human prostatic tumor cells with defective cell cycle /differentiation pathway. *Nutr Cancer* 1995; **24**:161-169
- 4 Turley JM, Ruscetti FW, Kim SJ, Fu T, Gao FV, Rirchenall-Roberts MC. Vitamin E succinate inhibits proliferation of BT-20 human breast cancer cells: increased binding of cyclin A negatively regulates E2F transactivation activity. *Cancer Res* 1997; **57**:2668-2675
- 5 Neuzil J, Weber T, Gellert N, Weber C. Selective cancer cell killing by α -tocopheryl succinate. *Br J Cancer* 2000; **84**: 87-89
- 6 Pussinen PJ, Lindner H, Glatter O, Reicher H, Kostner GM, Wintersperger A, Malle E, Sattler W. Lipoprotein-associated α -tocopheryl-succinate inhibits cell growth and induces apoptosis in human MCF-7 and HBL-100 breast cancer cells. *Biochim Biophys Acta* 2000; **1485**:129-144
- 7 Malafa MP, Neitzel LT. Vitamin E succinate promotes breast cancer tumor dormancy. *J Surg Res* 2000; **93**:163-170
- 8 Kline K, Sanders BG. RRR- α -tocopheryl succinate inhibition of lectin-induced T cell proliferation. *Nutr Cancer* 1993; **19**:241-252
- 9 Yu W, Sanders BG, Kline K. Modulation of murine EL-4 thymic lymphoma cell proliferation and cytokine production by Vitamin E succinate. *Nutr Cancer* 1996; **25**:137-149
- 10 Kline K, Yu W, Sanders BG, Vitamin E. Mechanisms of Action as Tumor Cell Growth Inhibitors. *Cancer and Nutrition*. K.N. Prasad and W.C. Cole (Eds). IOS Press 1998:

- 37-53
- 11 **Kline K**, Yu W, Zhao B, Turley JM, Sanders BG. Vitamin E Succinate: Mechanisms of action as tumor cell growth inhibitor. In: *Nutrients in Cancer Prevention and Treatment*. Prasad KN, Santamaria L and Williams RM (eds). Totowa, NY:Humana 1995:39-56
- 12 **Kim SJ**, Bang OS, Lee YS, Kang SS. Production of inducible nitric oxide is required for monocytic differentiation of U937 cells induced by vitamin E-succinate. *J Cell Sci* 1998;**111**:435-441
- 13 **Simmons-Menchaca M**, Qian M, Yu W, Sanders BG, Kline K. RRR- α -Tocopheryl succinate inhibits DNA synthesis and enhances the production and secretion of biologically active transforming growth factor- β by avian retrovirus-transformed lymphoid cells. *Nutr Cancer* 1995; **24**:171-185
- 14 **Ariazi EA**, Satomi Y, Ellis MJ. Activation of the transforming growth factor beta signaling pathway and induction of cytostasis and apoptosis in mammary carcinomas treated with the anticancer agent perillyl alcohol. *Cancer Res* 1999;**59**:1917-1928
- 15 **Turley JM**, Fu T, Ruscetti FW, Mikovits JA, Bertolette DC, Birchenall-Roberts MC. Vitamin E succinate induces Fas-mediated apoptosis in estrogen receptor-negative human breast cancer cells. *Cancer Res* 1997;**57**:881-890
- 16 **Yu W**, Israel K, Liao QY, Aldaz CM, Sanders BG, Kline K. Vitamin E succinate (VES) induces Fas sensitivity in human breast cancer cells: role for Mr 43,000 Fas in VES-triggered apoptosis. *Cancer Res* 1999;**59**:953-961
- 17 **Yu W**, Liao QY, Hantash FM, Sanders BG, Kline K. Activation of extracellular signal-regulated kinase and c-Jun-NH₂-terminal kinase but not p38 mitogen-activated protein kinases is required for RRR- α -tocopheryl succinate-induced apoptosis of human breast cancer cells. *Cancer Res* 2001;**61**:6569-6576
- 18 **Neuzil J**, Weber T, Schroder A, Lu M, Ostermann G, Gellert N, Mayne GC, Olejnicka B, Negre-Salvayre A, Sticha M, Coffey RJ, Weber C. Induction of cancer cell apoptosis by α -tocopheryl succinate: molecular pathways and structural requirements. *FASEB J* 2001;**15**:403-415
- 19 **Hua JS**. Effect of Hp: cell proliferation and apoptosis on stomach cancer. *Shijie Huaren Xiaohua Zazhi* 1999;**7**:647-648
- 20 **Zhu ZH**, Xia ZS, He SG. The effects of ATRA and 5Fu on telomerase activity and cell growth of gastric cancer cells in vitro. *Shijie Huaren Xiaohua Zazhi* 2000;**8**:669-673
- 21 **Xia JZ**, Zhu ZG, Liu BY, Yan M, Yin HR. Significance of immunohistochemically demonstrated micrometastases to lymph nodes in gastric carcinomas. *Shijie Huaren Xiaohua Zazhi* 2000;**8**:1113-1116
- 22 **Tu SP**, Zhong J, Tan JH, Jiang XH, Qiao MM, Wu YX, Jiang SH. Induction of apoptosis by arsenic trioxide and hydroxy camptothecin in gastric cancer cells in vitro. *World J Gastroenterol* 2000;**6**:532-539
- 23 **Cai L**, Yu SZ, Zhang ZF. *Helicobacter pylori* infection and risk of gastric cancer in Changde County, Fujian Province, China. *World J Gastroenterol* 2000;**6**:374-376
- 24 **Yao XX**, Yin L, Zhang JY, Bai WY, Li YM, Sun ZC. hTERT expression and cellular immunity in gastric cancer and precancerosis. *Shijie Huaren Xiaohua Zazhi* 2001;**9**:508-512
- 25 **Xu AG**, Li SG, Liu JH, Gan AH. Function of apoptosis and expression of the proteins Bcl-2, p53 and *c-myc* in the development of gastric cancer. *World J Gastroenterol* 2001;**7**:403-406
- 26 **Liu DH**, Zhang XY, Fan DM, Huang YX, Zhang JS, Huang WQ, Zhang YQ, Huang QS, Ma WY, Chai YB, Jin M. Expression of vascular endothelial growth factor and its role in oncogenesis of human gastric carcinoma. *World J Gastroenterol* 2001;**7**:500-505
- 27 **Wang X**, Lan M, Shi YQ, Lu J, Zhong YX, Wu HP, Zai HH, Ding J, Wu KC, Pan BR, Jin JP, Fan DM. Differential display of vincristine-resistance-related genes in gastric cancer SGC7901 cell. *World J Gastroenterol* 2002;**8**:54-59
- 28 **Cao WX**, Ou JM, Fei XF, Zhu ZG, Yin HR, Yan M, Lin YZ. Methionine-dependence and combination chemotherapy on human gastric cancer cells in vitro. *World J Gastroenterol* 2002;**8**:230-232
- 29 **Wu K**, Ren Y, Guo J. The effects of vitamin E succinate on the cyclic regulation protein of human gastric cancer cells. *Weisheng Dulixue Zazhi* 1998;**12**:203-207
- 30 **Liu BH**, Wu K, Zhao DY. Inhibition of human gastric carcinoma cell growth by vitamin E succinate. *Weisheng Yanjiu* 2000;**29**:172-174
- 31 **Wu K**, Guo J, Shan YJ, Liu BH. The effects of vitamin E succinate on apoptosis in human gastric cancer. *Weisheng Dulixue Zazhi* 1999;**13**:84-90
- 32 **Liu BH**, Wu K. Study on the growth inhibition of Vitamin E Succinate in human gastric cancer cell. *Aibian Jibian Tubian* 2000;**12**:79-81
- 33 **Wu K**, Shan YJ, Zhao Y, Yu JW, Liu BH. Inhibitory effects of RRR- α -tocopheryl succinate on bezo(a)pyrene (B(a)P)-induced forestomach carcinogenesis in female mice. *World J Gastroenterol* 2001;**7**:60-65
- 34 **Wu K**, Liu BH, Zhao DY, Zhao Y. The effect of vitamin E succinate on the expression of TGF- β 1, *c-jun* and JNK1 in human gastric cancer SGC-7901 cells. *World J Gastroenterol* 2001;**7**:83-87
- 35 **Tetens F**, Kliem A, Tscheudschilsuren G, Navarrete Santos A, Fischer B. Expression of proto-oncogenes in bovine preimplantation blastocysts. *Anat embryol* 2000;**201**:349-355
- 36 **Feng DY**, Zheng H, Tan Y, Cheng RX. Effect of phosphorylation of MAPK and Stat3 and expression of *c-fos* and *c-jun* proteins on hepatocarcinogenesis and their clinical significance. *World J Gastroenterol* 2001;**7**:33-36
- 37 **Leppa S**, Saffrich R, Ansorge W, Bohmann D. Differential regulation of c-Jun by ERK and JNK during PC12 cell differentiation. *EMBO J* 1998;**17**:4404-4413
- 38 **Zhu YH**, Hu DR, Nie QH, Liu GD, Tan ZX. Study on activation and *c-fos*, *c-jun* expression of in vitro cultured human hepatic stellate cells. *Shijie Huaren Xiaohua Zazhi* 2000;**8**:299-302
- 39 **Guo YS**, Hellmich MR, Wen XD, Townsend CM. Activator protein-1 transcription factor mediates bombesin-stimulated cyclooxygenase-2 expression in intestinal epithelial cells. *J Biol Chem* 2001;**276**:22941-22947
- 40 **Herdegen T**, Waetzig V. AP-1 proteins in the adult brain: facts and fiction about effectors of neuroprotection and neurodegeneration. *Oncogene* 2001;**20**:2424-2437
- 41 **Yuen MF**, Wu PC, Lai VCH, Lau JYN, Lai CL. Expression of *c-myc*, *c-fos*, and *c-jun* in hepatocellular carcinoma. *Cancer* 2001;**91**:106-112
- 42 **Schroeter H**, Spencer JPE, Rice-Evans C, Williams RJ. Flavonoids protect neurons from oxidized low-density-lipoprotein-induced apoptosis involving *c-jun* N-terminal kinase (JNK), *c-jun* and caspase-3. *Biochem J* 2001;**358**:547-557
- 43 **Jiang LX**, Fu XB, Sun TZ, Yang YH, Gu XM. Relationship between oncogene *c-jun* activation and fibroblast growth factor receptor expression of ischemia reperfusion intestine in rats. *Shijie Huaren Xiaohua Zazhi* 1999;**7**:498-500
- 44 **Fan M**, Goodwin ME, Birrer MJ, Chambers TC. The *c-jun* NH₂-terminal protein kinase/AP-1 pathway is required for efficient apoptosis induced by vinblastine. *Cancer Res* 2001;**61**:4450-4458
- 45 **Kondo T**, Matsuda T, Kitano T, Takahashi A, Tashima M, Ishikura H, Umehara H, Domae N, Uchiyama T, Okazaki T. Role of *c-jun* expression increased by heat shock and ceramide-activated caspase-3 in HL-60 cell apoptosis. *J Biol Chem* 2000;**275**:7668-7676
- 46 **Potapova O**, Basu S, Mercola D, Holbrook NJ. Protective role for c-Jun in the cellular response to DNA damage. *J Biol Chem* 2001;**276**:28546-28553
- 47 **Behrens A**, Sabapathy K, Graef I, Cleary M, Crabtree GR, Wagner EF. Jun N-terminal kinase 2 modulates thymocyte apoptosis and T cell activation through *c-jun* and nuclear factor of activated T cell (NF-AT). *Proc Natl Acad Sci U S A* 2001;**98**:1769-1774

- 48 **Ashkenazi A**, Dixit VM. Apoptosis control by death and decoy receptors. *Curr Opin Cell Biol* 1999;**11**:255-260
- 49 **Behrens A**, Sibilio M, Wagner EF. Amino-terminal phosphorylation of *c-jun* regulates stress-induced apoptosis and cellular proliferation. *Nat Genet* 1999;**66**:211-216
- 50 **Sun BH**, Zhao XP, Wang BJ, Yang DL, Hao LJ. FADD and TRADD expression and apoptosis in primary human hepatocellular carcinoma. *World J Gastroenterol* 2000;**6**:223-227
- 51 **Wu K**, Guo J, Shan YJ. Inhibitory effects of VES on the growth of human squamous gastric carcinoma cells. In: Johnson IT and Fenwick GR(eds), *Dietary anticarcinogens and antimutagens-Chemical and biological aspects*. RS· C, UK: Athenaeum Press 2000:304-307
- 52 **Zhao Y**, Wu K. Cell death molecule Fas/CD95 and apoptosis. *Aibian Jibian Tubian* 2001;**13**:55-58
- 53 **Wei XC**, Wang XJ, Chen K, Zhang L, Liang Y, Lin XL. Killing effect of TNF-related apoptosis inducing ligand regulated by tetracycline on gastric cancer cell line NCI-N87. *World J Gastroenterol* 2001;**7**:559-562
- 54 **Smaele ED**, Zazzeroni F, Papa S, Nguyen DU, Jin R, Jones J, Cong R, Franzoso G. Induction of gadd45 β by NF- κ B downregulates pro-apoptotic JNK signaling. *Nature* 2001;**414**:308-313
- 55 **Wu YL**, Sun B, Zhang XJ, Wang SN, He HY, Qiao MM, Zhong J, Xu JY. Growth inhibition and apoptosis induction of Sulindac on Human gastric cancer cells. *World J Gastroenterol* 2001;**7**:796-800
- 56 **Li HL**, Chen DD, Li XH, Zhang HW, Lü YQ, Ye CL, Ren XD. Changes of NF- κ B, p53, Bcl-2 and caspase in apoptosis induced by JTE-522 in human gastric adenocarcinoma cell line AGS cells: role of reactive oxygen species. *World J Gastroenterol* 2002;**8**:431-435
- 57 **Tao HQ**, Zou SC. Effect of preoperative regional artery chemotherapy on proliferation and apoptosis of gastric carcinoma cells. *World J Gastroenterol* 2002;**8**:451-454
- 58 **Tian G**, Yu JP, Luo HS, Yu BP, Yue H, Li JY, Mei Q. Effect of Nimesulide on proliferation and apoptosis of human hepatoma SMMC-7721 cells. *World J Gastroenterol* 2002;**8**:483-487
- 59 **Yu W**, Simmons MM, You H. RRR- α -Tocopheryl Succinate induction of prolonged activation of *c-Jun* amino-terminal kinase and *c-Jun* during induction of apoptosis in human MDA-MB-435 breast cancer cells. *Mol Carcinog* 1998;**22**:247-267
- 60 **Yu W**, Sanders BG, Kline K. RRR- α -tocopheryl succinate inhibits EL4 thymic lymphoma cell growth by inducing apoptosis and DNA synthesis arrest. *Nutr Cancer* 1997;**27**:92-101
- 61 **Kogure K**, Morita M, Nakashima S, Hama S, Tokumura A, Fukuzawa K. Superoxide is responsible for apoptosis in rat vascular smooth muscle cells induced by α -tocopheryl hemisuccinate. *Biochim Biophys Acta* 2001;**1528**:25-30
- 62 **Leppa S**, Bohmann D. Diverse functions of JNK signaling and *c-Jun* in stress response and apoptosis. *Oncogene* 1999;**18**:6158-6162
- 63 **Jiang LX**, Fu XB, Sun TZ, Yang YH, Gu XM. Relationship between oncogene *c-jun* activation and fibroblast growth factor receptor expression of ischemia reperfusion intestine in rats. *Shijie Huaren Xiaohua Zazhi* 1999;**7**:498-500
- 64 **Teng CS**. Differential expression of *c-Jun* proteins during mullerian duct growth and apoptosis: caspase-related tissue death blocked by diethylstilbestrol. *Cell Tissue Res* 2000;**302**:377-385

Edited by Pang LH

• GASTRIC CANCER •

Mutation analysis of APC gene in gastric cancer with microsatellite instability

Dian-Chun Fang, Yuan-Hui Luo, Shi-Ming Yang, Xiao-An Li, Xian-Long Ling, Li Fang

Dian-Chun Fang, Yuan-Hui Luo, Shi-Ming Yang, Xiao-An Li, Xian-Long Ling, Li Fang, Department of Gastroenterology, Southwest Hospital, Third Military Medical University, Chongqing 400038, China

Supported by the National Natural Science Foundation of China, No. 30070043, and "10.5" Scientific Research Foundation of Chinese PLA, No. 01Z075.

Correspondence to: Dian-Chun Fang, M.D., Ph.D. Southwest Hospital, Third Military Medical University, Chongqing 400038, China. fangdianchun@hotmail.com

Telephone: +86-23-68754624 **Fax:** +86-23-68754124

Received 2002-03-13 **Accepted** 2002-04-29

Abstract

AIM: To evaluate the role of APC mutation in gastric carcinogenesis and to correlate APC mutation with microsatellite instability (MSI) in gastric carcinomas.

METHODS: APC mutation was measured with multiplex PCR, denaturing gradient gel electrophoresis and DNA sequencing; and MSI was analyzed by PCR-based methods.

RESULTS: Sixty-eight cases of sporadic gastric carcinoma were studied for APC mutation at exon 15 and MSI. APC mutations were detected in 15 (22.1 %) gastric cancers. Frequency of APC mutation (33.3 %) in intestinal type of gastric cancer was significantly higher than that in diffuse type (13.1 %, $P < 0.05$). On the contrary, no association was observed between APC mutation and tumor size, differentiation, depth of invasion, metastasis or clinical stages. Using five microsatellite markers, MSI in at least one locus was detected in 17 of 68 (25 %) of the tumors analyzed. APC mutations were all detected in MSI-L (only one locus, $n=9$) or MSS (tumor lacking MSI or stable, $n=51$), but no mutation was found in MSI-H (≥ 2 loci, $n=8$).

CONCLUSION: APC mutation is involved in carcinogenesis of intestinal type of gastric cancer and is independent of MSI phenotype but related to the LOH pathway in gastric cancer.

Fang DC, Luo YH, Yang SM, Li XA, Ling XL, Fang L. Mutation analysis of APC gene in gastric cancer with microsatellite instability. *World J Gastroenterol* 2002;8(5):787-791

INTRODUCTION

The mechanisms of carcinogenesis in the gastric mucosa remain unclear. Adenomatous polyposis coli or APC, has been characterized as a tumor suppressor gene and considered a "gatekeeper" because alterations in this gene occur as an early event in the neoplastic transformation^[1-3]. The APC gene was first identified in the germline of individuals with the condition known as familial adenomatous polyposis or FAP^[4] and has been shown to play a role in the development of sporadic

colorectal cancer^[5,6]. Studies have attempted to characterize the mutation of APC in sporadic gastric cancer^[7-10] and in a limited number of familial gastric cancer^[11,12]. It has been found that inactivation of APC plays a role in the development of some gastric cancers, particularly very well differentiated adenocarcinomas and signet-ring cell carcinomas^[13,14], and that the mutations of the APC gene, similar to those in colorectal tumorigenesis, occur during the early stages of gastric adenoma development^[15,16].

Genetic instability is strongly involved in neoplastic transformation and progression^[17]. In gastrointestinal carcinomas, such genetic instability may be classified into two different forms in which hypermutability occurs either by means of chromosomal instability or microsatellite instability (MSI)^[18-23]. MSI represents an important new form of genetic alteration characterized by widespread instability in repetitive nucleotide sequences. MSI has been found in the majority of tumors associated with hereditary non-polyposis colorectal cancer (HNPCC)^[24,25] in which germ-line mutation occurs within the mismatch repair genes hMSH2, hMLH1, hPMS2 or hMSH6^[26-28]. Mutations of the transforming growth factor type β receptor gene (TGF- β R II), and BAX gene are strongly correlated with MSI^[29-31]. MSI is also a distinctive feature in about 10-15 % of sporadic colorectal tumors and to a varying degree in tumors of other organs, including the stomach^[32-34]. Although mutations of APC have been reported in gastric cancer, less clear, however, is the relevance of APC mutation as a potential factor in MSI-positive gastric cancer. The aim of the present study is to correlate APC mutation with MSI in gastric carcinomas.

MATERIALS AND METHODS

Tissue samples

Sixty-eight cancer and corresponding normal tissues were obtained from surgically resected gastric carcinoma in Southwest Hospital. Each specimen was frozen immediately and stored at -80°C until analyzed. A $5\mu\text{m}$ section was cut from each tissue and stained with hematoxylin/eosin in order to confirm whether the cancer cells in tissues were predominant or not. Genomic DNA was isolated by standard proteinase-K digestion and phenol-chloroform extraction protocols. Of the 68 patients with gastric cancer, 45 were men and 23 were women with an age range of 30-76 years (mean age of 56.2 years at diagnosis). None of the patients included in the present series had a family history suggestive of HNPCC and had received chemotherapy or radiation therapy.

Multiplex PCR

Multiplex PCR was utilized in order to visualize the product of several regions simultaneously. Singleplex PCR was also used to help confirm cases and for regions that were difficult to amplify. Multiplex PCR analysis of APC exon 15 was performed using primers with a GC clamp (Table 1). Genomic DNA (100-400 ng), 0.25 μM primer for multi-primer reaction,

1×buffer, 1.5 mM MgCl₂, 0.25 mM of each dNTPs, and 0.1 U/μl Amplitaq Gold were combined in 10 μl reaction. The PCR reaction consisted of a denaturation step at 95 °C for 12 minutes followed by 32 cycles of 40 seconds at 94 °C, 60 seconds at 49 °C, and 90 seconds at 72 °C. Elongation occurred through 10 minutes at 72 °C, 10 minutes at 98 °C, 30 minutes at 50 °C and 30 minutes at 37 °C.

Denaturing gradient gel electrophoresis (DGGE)

DGGE analysis was performed for scanning mutations at 15 exon of APC gene. 8 μl of each sample was loaded on the gels consisting of 10 % polyacrylamide and 10-60 % urea-formamide. The gels were run at 90V for 17 hours in tanks of buffer at 50 °C. Gels were stained with 0.5× Sybr Green I and Sybr Green II for 20 minutes and visualized by UV transillumination. Heteroduplex samples were further analyzed by manual sequencing.

Manual sequencing

Samples were amplified for sequencing with PCR primers that did not include the GC clamp (Appendix A). The PCR reaction included 200-400 ng of genomic DNA, 0.25 μM primer, 1×buffer, 1.5mM MgCl₂, 0.25mM of each dNTPs, and 2.5U Amplitaq Gold were combined in a 10 μl reaction. The PCR reaction consisted of a denaturation step at 94 °C for 3 minutes followed by 35 cycles of 60 seconds at 94 °C, 60 seconds at 55 °C, and 60 seconds at 72 °C. A final extension step included 10 minutes at 72 °C. 1.5 % agarose gels were run at 150V to confirm the existence of PCR product. The product was purified following the instructions of the Wizard PCR Preps DNA Purification System (Promega, Madison, WI). Following the purification process, the product was run on a 1.5 % agarose gel at 150V to verify the product. Sequencing was performed following the instruction of the system. The film was read independently by two individuals according to the APC sequence.

Table 1 Primer Sequences used in APC mutation analysis

Exon	GC Clamp	Primer Sequences	Size (bp)
15.1	2/0	F-TTCAGGCAAATCCTAAGAGA/R-TTGAGCCAGGAGACATAATA	329
15.2	0/2	F-GGAATCTCATGGCAAATAGG/R-TCATCATGTCGATTGGTGTGTC	284
15.3	2/0	F-AGCAAAGTCTCTATGGTGAT/R-TGACACTTCTTCCATGACTT	387
15.4	0/2	F-CTACCATCCAGCAACAGAAA/R-TGGCATAAGGCATAGAACAT	312
15.5	2/0	F-AAGCTCTGCTGCCCATACAC/R-CTAGGTCGGCTGGGTATTGA	282
15.6	2/5	F-CTTATGCCAAATTAGAATAC/R-ACTGCTCATCTGAATATTTA	306
15.7	7/5	F-ATGATGGAGAACTAGATACA/R-ATCAGTGCTCTCAGTATAAA	253
15.8	2/5	F-AAGACCCAAACACATAATAG/R-TAATTGGTAGGCTTATCATC	327
15.9	2/0	F-AAATCGAGTGGGTTCTAATC/R-TTCTCACTGCTTGAAGACAT	355
15.10	2/6	F-CAGCCTATTGATTATAGTTT/R-AACATATTGGAGTATCTTCT	344
15.11	2/0	F-TTAACCAAGAAACAATACAG/R-CTTCGCTCACAGGATCTT	320
15.12	2/0	F-GGAAGCAGATTCTGCTAATA/R-ATAGTGTTTCAGGTGGACTTT	287
15.13	2/5	F-AGAATCAGCCAGGCACAAAG/R-CATGGTTTGTCCAGGGCTAT	310
15.14	2/6	F-TGGTAAGTGGCATTATAAGC/R-AGTATCAGCATCTGGAAGAA	279
15.15	5/2	F-AAACCAAGCCAGAAGTACCT/R-AGGCTGCTCTGATTCTGTTT	335
15.16	2/5	F-CGATGAGCCATTTATACA/R-TTTCGTTTACGTGATGAC	291
15.17	4/2	F-ATTATTTCTGCCATGCCAAC/R-TTCGATTGTTAGATCACTTA	300
15.18	2/6	F-TGCCACGGGTGTATTGTGTT/R-TTTCCTTTGGGCATAGCAG	351
15.19	4/2	F-GGTGATATTCTTGCAGAATG/R-CACGTGCTCTATATTCAGTA	250
15.20	2/0	F-GAAACCAACTTCACCAGTAA/R-AATAGGCGTGTAATGATGAG	378
15.21	2/0	F-AGTCCCAAATAATGAAGAT/R-GATTGTTGGTTGGAGGTTAG	342
15.22	2/6	F-GCTAAAGTTACCAGCCACAC/R-TTGGTCAATGTCACTGAGAG	
15.23	2/0	F-CCAGTCATCCAAAGACATAC/R-CAACAGGTCATCTTCAGAGT	
15.24	2/5	F-TCACAGGGAGAACCAAGTAA/R-TTGCACCTTCCTGAATAGC	
15.25	2/3	F-ATGGGTGGCATATTAGGTGA/R-TCGTGGGCGCTTTATTACTTG	

GC clamp: 1=CGCCCCGCGCGCCCCGCGCCCGTCCCGCGCGCCCCGCGCCG;

2=CGCCCCGCGCGCCCCGCGCCCGGCCCCGCGCCCCGCGCCG;

3=CG; 4=GCGCG; 5=CGTCCCG; 6=GCGCCCGTCCCGCGCCG;

7=CGCCCCGCGCGCCCCGCGCCCGTCCCGCGCGCCCCGCGCCGCGCCG

MSI detection

MSI analyses included five microsatellite markers: BAT25, BAT26, BAT40, D2S123, and D5S346. PCR was performed as previously described^[35]. MSI was defined as the presence of band shift in the tumor DNA that was not present in the corresponding normal DNA. Based on the number of mutated MSI markers in each tumor, carcinomas were characterized as MSI-H if they manifested instability at two or more markers, MSI-L if unstable at only one marker, and MSS if they showed no instability at any marker.

Statistical analysis

Chi-square test with Yates' correction was used. A *P* value <0.05 was considered significant.

RESULTS

Multiplex PCR and DGGE were used to scan the mutation at the exon 15 of APC in 68 gastric cancers (Figure 1). The samples that showed alterations by DGGE were further analyzed through manual sequencing (Figure 2). APC mutations were detected in 15 samples (22.1%) held APC mutations that lead to premature protein truncation (Table 2). The truncation of the protein occurred as a result of a stop codon created through a base pair change, an insertion, or a deletion.

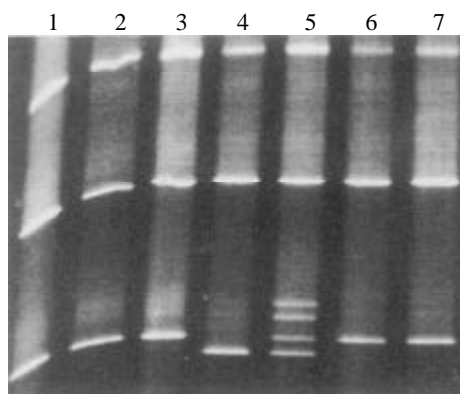


Figure 1 Abnormal four-band patterns in lane 5 after multiplex PCR and denaturing gradient gel

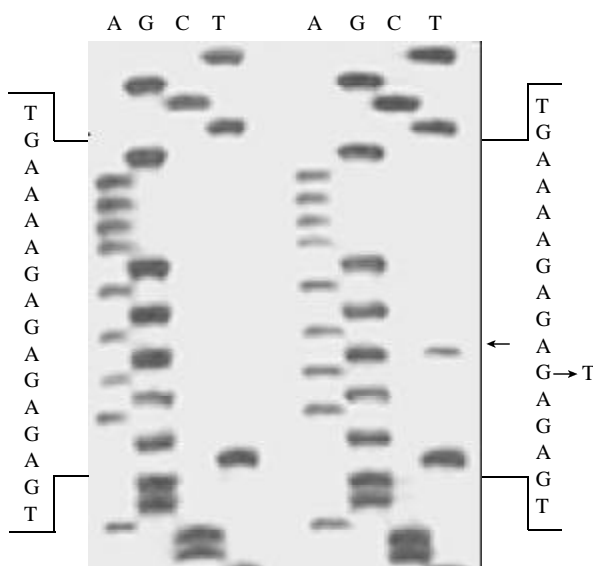


Figure 2 DNA sequencing shows a G→T change at 1464 codon

We compared mutation of exon 15 of APC gene in gastric cancer with various clinicopathological parameters including tumor size, differentiation, TNM status, clinical stage and Lauren's types. Table 3 shows the association of mutations of APC to the clinicopathological parameters of 68 gastric carcinomas. Mutations of APC gene were observed more common in intestinal type than in diffuse type tumors (*P*<0.05).

Alterations of electrophoretic patterns of PCR products of five microsatellite markers were compared between tumor and normal DNA in each patient. MSI affecting at least one locus was observed in 17 (25 %) of 68 tumors, among which eight (11.8 %) were MSI-H, nine (13.2 %) were MSI-L, and fifty-one (75 %) were MSS. Table 4 shows the association of mutations of APC to MSI of 68 gastric carcinomas. Three mutations were found in 9 tumors with MSI-L and 12 were found in 51 tumors with MSS, and no mutation was found in 8 tumors with MSI-H.

Table 2 APC mutation in 12 gastric carcinomas

Exon region	Nucleotide alteration	Nucleotide location	Codon number
15.4	C→A	2883	940
15.5	insA	2866	935
15.10	del A	3835 or 3836	1258
15.11	del AAAA	3981	1307
15.12	del AAAGA	3988	1309
15.12	G→T	4010	1317
15.13	delT	4146	1362
15.13	delGT	4254	1398
15.13	delT	4282	1407
15.14	C→T	4410	1450
15.14	G→T	4452	1464
15.15	delAG	4455	1465
15.19	insCT	5326	1755
15.21	insT	5596	1845
15.22	delG	5940	1960

Table 3 The relationship between the APC mutation and clinicopathological parameters

Parameters	No. of cases	APC mutation
Size		
<5cm	31	7
>5cm	37	8
Differentiation		
Well	14	4
Moderate	20	6
Poor	28	3
Mucinous	6	2
Lauren classification		
Intestinal type	30	10 ^a
Diffuse type	38	5
Serosal invasion		
Absent	30	6
Present	38	9
Metastasis		
Absent	33	8
Present	35	7
Clinical stage		
I and II	36	9
III and IV	32	6

^a*P*<0.05 vs diffuse type

Table 4 The relationship between MSI and APC mutation

MSI status	No. of cases	APC mutation
MSI-H	8	0
MSI-L	9	2
MSS	51	13

DISCUSSION

Mutations of APC gene has been shown to play an important role in colorectal tumorigenesis. A germline mutation in APC contributes significantly to the development of colitis-associated neoplasia^[36]. In the current study, we investigated mutations of the APC gene in 68 gastric carcinomas obtained surgically. Mutations at exon 15 of APC gene were detected in 22.1 % of gastric cancers. This finding is similar to the previous studies^[14,15]. This proportion may be an underestimate because the mutation of exons 1 through 14 were not detected in this study. Previous investigations have found that the 5' half of APC holds the majority of the germline mutations^[3,37]. The mutations identified in the study were spread throughout the exon 15 of APC sequence. Sequencing analysis confirmed that the mutations resulted in truncation of the gene products or in an amino acid change. The APC gene encodes a large protein with multiple cellular functions and interactions. Mutations in this gene would lead to alterations in signal transduction of cell, differentiation, mediation of intercellular adhesion, stabilization of the cytoskeleton and possibly regulation of the cell cycle and apoptosis^[38,39]. Our results imply that APC plays a crucial role in gastric carcinogenesis, as was observed in colorectal carcinogenesis.

In the current study, we did not find an obvious relationship between the APC mutation and tumor size, depth of invasion, node metastasis or clinical stages, indicating a limited role of the APC mutation in predicting prognosis of gastric carcinomas. This finding is in agreement with the recently published data on cholangiocarcinoma and breast cancer^[40,41]. Gastric carcinomas can be divided into "intestinal" type and "diffuse" type. The intestinal type of gastric cancer is the predominant type in elderly population at high risk and preceded by well-defined precancerous lesions, such as intestinal metaplasia and atrophic gastritis. The diffuse type is relatively more frequent in low risk populations and is not as often preceded by intestinal metaplasia. A distinct genetic pathway exists in gastric carcinogenesis of different histological subtypes and their tumor progression^[42-45]. Increased beta-catenin mRNA levels and mutational alterations of the APC and beta-catenin gene were present in intestinal type gastric cancer^[46,47], whereas epigenetic inactivation of E-cadherin via promoter hypermethylation may be an early critical event in the development of undifferentiated tumors^[48-51]. In this study, marked difference in APC mutation was noted in gastric cancer by histological type. APC mutations were significantly more frequent in intestinaltype gastric cancers as compared with diffusetype gastric cancers, suggesting that APC gene is not only a predisposing gene in colorectal cancer but also a predisposing gene in intestinal type of gastric cancer. The mutation of APC gene may be considered makers for intestinal or colonic differentiation. The mutation of APC in the majority of intestinal type cancers also supports the theory that these cancers result from transformation of intestinal metaplasia.

There is evidence that MSI cancer comprises distinctive MSI-H and MSI-L categories^[14]. MSI-H cancers are distinguished clinicopathologically and in their spectrum of genetic alterations from cancers showing MSI-L and MSS cancers^[14]. Our previous studies indicated that MSI-H gastric cancers often show lower frequency of LOH of APC, MCC and DCC genes than do MSI-L and MSS cancers^[1]. In present study, 15 APC mutations were all detected in MSI-L and MSS, but no mutation was found in those showing MSI-H. This result indicates that APC is mutational target in MSI-L and MSS tumor cells and support the notion that APC mutation-positive tumors may identify an alternative pathway which is probably

different from MSI-related phenomenon observed in HNPCC. Our analysis of APC mutation should further provide some clues to the molecular mechanisms underlying the profound genomic instability in the MSI and LOH pathway for gastric carcinoma.

REFERENCES

- 1 **Groden J**, Gelbert L, Thliveris A, Nelson L, Robertson M, Joslyn G, Samowitz W, Spirio L, Carlson M, Burt R, Leppert M, White R. Mutational analysis of patients with adenomatous polyposis: identical inactivating mutations in unrelated individuals. *Am J Hum Genet* 1993;**52**:263-272
- 2 **Kinzler KW**, Vogelstein B. Lessons from hereditary colorectal cancer. *Cell* 1996;**87**:159-170
- 3 **Mulkens J**, Poncin J, Arends JW, De Goeij AF. APC mutations in human colorectal adenomas: analysis of the mutation cluster region with temperature gradient gel electrophoresis and clinicopathological features. *J Pathol* 1998;**185**:360-365
- 4 **Groden J**, Thliveris A, Samowitz W, Carlson M, Gelbert L, Albertsen H, Joslyn G, Stevens J, Spirio L, Robertson M, Saxgeant L, Krapcho K, Wolff E, Burt R, Hughes JP, Warrington J, McPherson J, Wasumuth J, Passlier DL, Abderrahim H, Cohen D, Leppert M, White R. Identification and characterization of the familial adenomatous polyposis coli gene. *Cell* 1991;**66**:589-600
- 5 **van Wyk R**, Slezak P, Kotze MJ, Jaramillo E, Koizumi K, Grobelaar JJ. Multiple APC mutations in sporadic flat colorectal adenomas. *Eur J Hum Genet* 1999;**7**:928-932
- 6 **Abraham SC**, Wu TT, Klimstra DS, Finn LS, Lee JH, Yeo CJ, Cameron JL, Hruban RH. Distinctive molecular genetic alterations in sporadic and familial adenomatous polyposis-associated pancreaticoblastomas: frequent alterations in the APC/beta-catenin pathway and chromosome 11p. *Am J Pathol* 2001;**159**:1619-1627
- 7 **Horii A**, Nakatsuru S, Miyoshi Y, Ichii S, Nagase H, Kato Y, Yanagisawa A, Tsuchiga E, Nakamura Y. The APC gene, responsible for familial adenomatous polyposis, is mutated in human gastric cancer. *Cancer Res* 1992;**52**:3231-3233
- 8 **Sud R**, Wells D, Talbot IC, Delhanty JD. Genetic alterations in gastric cancers from British patients. *Cancer Genet Cytogenet* 2001;**126**:111-119
- 9 **Sud R**, Talbot IC, Delhanty JD. Infrequent alterations of the APC and MCC genes in gastric cancers from British patients. *Br J Cancer* 1996;**74**:1104-1108
- 10 **McKie AB**, Filipe MI, Lemoine NR. Abnormalities affecting the APC and MCC tumour suppressor gene loci on chromosome 5q occur frequently in gastric cancer but not in pancreatic cancer. *Int J Cancer* 1993;**55**:598-603
- 11 **Kusano M**, Kakiuchi H, Mihara M, Itoh F, Adachi Y, Ohara M, Hosokawa M, Imai K. Absence of microsatellite instability and germline mutations of E-cadherin, APC and p53 genes in Japanese familial gastric cancer. *Tumour Biol* 2001;**22**:262-268
- 12 **White S**, Bubb VJ, Wyllie AH. Germline APC mutation (Gln1317) in a cancer-prone family that does not result in familial adenomatous polyposis. *Genes Chromosomes Cancer* 1996;**15**:122-128
- 13 **Ebert MP**, Fei G, Kahmann S, Muller O, Yu J, Sung JJ, Malfertheiner P. Increased beta-catenin mRNA levels and mutational alterations of the APC and beta-catenin gene are present in intestinal-type gastric cancer. *Carcinogenesis* 2002;**23**:87-91
- 14 **Nakatsuru S**, Yanagisawa A, Ichii S, Tahara E, Kato Y, Nakamura Y, Horii A. Somatic mutation of the APC gene in gastric cancer: frequent mutations in very well differentiated adenocarcinoma and signet-ring cell carcinoma. *Hum Mol Genet* 1992;**1**:559-563
- 15 **Tamura G**, Maesawa C, Suzuki Y, Tamada H, Satoh M, Ogasawara S, Kashiwaba M, Satodate R. Mutations of the APC gene occur during early stages of gastric adenoma development. *Cancer Res* 1994;**54**:1149-1151
- 16 **Nakatsuru S**, Yanagisawa A, Furukawa Y, Ichii S, Kato Y, Nakamura Y, Horii A. Somatic mutations of the APC gene in precancerous lesion of the stomach. *Hum Mol Genet* 1993;**2**:1463-1465

- 17 **Lengauer C**, Kinzler KW, Vogelstein B. Genetic instability in colorectal cancers. *Nature* 1997;**386**: 632-637
- 18 **Thibodeau SN**, Bren G, Schaid D. Microsatellite instability in cancer of the proximal colon. *Science* 1993;**260**:816-819
- 19 **Ionov Y**, Peinado MA, Malkhosyan S, Shibata D, Perucho M. Ubiquitous somatic mutations in simple repeated sequences reveal a new mechanism for colonic carcinogenesis. *Natre* 1993;**363**:558-561
- 20 **Vogelstein B**, Fearon ER, Hamilton SR, Kern SE, Preisinger AC, Leppert M, Nakamura Y, White R, Smits AM, Bos JL. Genetic alterations during colorectal tumor development. *N Engle J Med* 1988;**319**:525-532
- 21 **Fearon ER**, Vogelstein B. A genetic model for colorectal tumorigenesis. *Cell* 1990;**61**:759-767
- 22 **Jen J**, Kim H, Piantadosi S, Liu ZF, Levitt RC, Sistonen P, Kinzler KW, Vogelstein B, Hamilton SR. Allelic loss of chromosome 18q and prognosis in colorectal cancer. *N Engl J Med* 1994;**331**:213-221
- 23 **White RL**. Tumor suppressing pathways. *Cell* 1998;**92**:591-592
- 24 **Aaltonen LA**, Peltomaki P, Leach FS, Sistonen P, Pylkanen L, Mecklin JP, Jarvinen H, Powell SM, Jen J, Hamilton SR. Clues to the pathogenesis of familial colorectal cancer. *Science* 1993;**260**:812-816
- 25 **Wu BP**, Zhang YL, Zhou DY, Gao CF, Lai ZS. Microsatellite instability, MMR gene, expression, and proliferation kinetics in colorectal cancer with familial predisposition. *Word J Gastroenterol* 2000; **6**:902-905
- 26 **Bronner CE**, Baker SM, Morrison PT, Warren G, Smith LG, Lescoe MK, Kane M, Earabino C, Lipford J, Lindblom A. Mutation in the DNA mismatch repair gene homologue hMLH1 is associated with hereditary non-polyposis colon cancer. *Nature* 1994;**368**:258-261
- 27 **Papadopoulos N**, Nicolaides NC, Liu B, Parsons R, Lengauer C, Palombo F, D' Arrigo A, Markowitz S, Willson JK, Kinzler KW. Mutations of GTBP in genetically unstable cells. *Science* 1995;**268**:1915-1917
- 28 **Wang Q**, Lasset C, Desseigne F, Saurin JC, Maugard C, Navarro C, Ruano E, Descos L, Trillet-Lenoir V, Bosset JF, Puisieux A. Prevalence of germline mutations of hMLH1, hMSH2, Hpms1, hPMS2, and hMSH6 genes in 75 French kindreds with nonpolyposis colorectal cancer. *Hum Genet* 1999;**105**:79-85
- 29 **Markowitz S**, Wang J, Myeroff L, Parsons R, Sun L, Lutterbaugh J, Fan RS, Zborowska E, Kinzler KW, Vogelstein B. Inactivation of the type II TGF-Beta receptor in colon cancer cells with microsatellite instability. *Science* 1995;**268**:1336-1338
- 30 **Rampino N**, Yamamoto H, Ionov Y, Li Y, Sawai H, Reed JC, Perucho M. Somatic frameshift mutations in the BAX gene in colon cancers of the microsatellite mutator phenotype. *Science* 1997;**275**:967-969
- 31 **Souza RF**, Appel R, Yin J, Wang S, Smolinski KN, Abraham JM, Zou TT, Shi YQ, Lei J, Cottrell J, Cymes K, Biden K, Simms L, Leggett B, Lynch PM, Frazier M, Powell SM, Harpaz N, Sugimura H, Young J, Meltzer SJ. Microsatellite instability in the insulin-like growth factor II receptor gene in gastrointestinal tumors. *Nat Genet* 1996;**14**:255-257
- 32 **Jass JR**, Do KA, Simms LA, Iino H, Wynter C, Pillay SP, Searle J, Radford-Smith G, Young J, Leggett B. Morphology of sporadic colorectal cancer with DNA replication errors. *Gut* 1998;**42**:673-679
- 33 **Chung YJ**, Park SW, Song JM, Lee KY, Seo EJ, Choi SW, Rhyu MG. Evidence of genetic progression in human gastric carcinomas with microsatellite instability. *Oncogene* 1997;**15**:1719-1726
- 34 **Potocnik U**, Glavac D, Golouh R, Ravnik-Glavac M. Causes of microsatellite instability in colorectal tumors: implications for hereditary non-polyposis colorectal cancer screening. *Cancer Genet Cytogenet* 2001;**126**:85-96
- 35 **Fang DC**, Yang SM, Zhou XD, Wang DX, Luo YH. Telomere erosion is independent of microsatellite instability but related to loss of heterozygosity in gastric cancer. *World J Gastroenterol* 2001;**7**:522-526
- 36 **Cooper HS**, Everley L, Chang WC, Pfeiffer G, Lee B, Murthy S, Clapper ML. The role of mutant Apc in the development of dysplasia and cancer in the mouse model of dextran sulfate sodium-induced colitis. *Gastroenterology* 2001;**121**:1407-1416
- 37 **Toyooka M**, Konishi M, Kikuchi-Yanoshita R, Iwama T, Miyaki M. Somatic mutations of the adenomatous polyposis coli gene in gastroduodenal tumors from patients with familial adenomatous polyposis. *Cancer Res* 1995;**55**:3165-3170
- 38 **Zhang T**, Otevrel T, Gao Z, Ehrlich SM, Fields JZ, Boman BM. Evidence that APC regulates survivin expression: a possible mechanism contributing to the stem cell origin of colon cancer. *Cancer Res* 2001;**61**:8664-8667
- 39 **Fearnhead NS**, Britton MP, Bodmer WF. The abc of apc. *Hum Mol Genet* 2001;**10**:721-733
- 40 **Cong WM**, Bakker A, Swalsky PA, Raja S, Woods J, Thomas S, Demetris AJ, Finkelstein SD. Multiple genetic alterations involved in the tumorigenesis of human cholangiocarcinoma: a molecular genetic and clinicopathological study. *J Cancer Res Clin Oncol* 2001;**127**:187-192
- 41 **Yuan ZQ**, Begin LR, Wong N, Brunet JS, Trifiro M, Gordon PH, Pinsky L, Foulkes WD. The effect of the I1307K APC polymorphism on the clinicopathological features and natural history of breast cancer. *Br J Cancer* 1999;**81**:850-854
- 42 **Wu MS**, Chang MC, Huang SP, Tseng CC, Sheu JC, Lin YW, Shun CT, Lin MT, Lin JT. Correlation of histologic subtypes and replication error phenotype with comparative genomic hybridization in gastric cancer. *Genes Chromosomes Cancer* 2001;**30**:80-86
- 43 **Wu MS**, Shun CT, Wang HP, Sheu JC, Lee WJ, Wang TH, Lin JT. Genetic alterations in gastric cancer: relation to histological subtypes, tumor stage, and *Helicobacter pylori* infection. *Gastroenterology* 1997;**112**:1457-1465
- 44 **Endoh Y**, Sakata K, Tamura G, Ohmura K, Ajioka Y, Watanabe H, Motoyama T. Cellular phenotypes of differentiated-type adenocarcinomas and precancerous lesions of the stomach are dependent on the genetic pathways. *J Pathol* 2000;**191**:257-263
- 45 **Ohmura K**, Tamura G, Endoh Y, Sakata K, Takahashi T, Motoyama T. Microsatellite alterations in differentiated-type adenocarcinomas and precancerous lesions of the stomach with special reference to cellular phenotype. *Hum Pathol* 2000;**31**:1031-1035
- 46 **Ebert MP**, Fei G, Kahmann S, Muller O, Yu J, Sung JJ, Malfertheiner P. Increased beta-catenin mRNA levels and mutational alterations of the APC and beta-catenin gene are present in intestinal-type gastric cancer. *Carcinogenesis* 2002;**23**:87-91
- 47 **Park WS**, Oh RR, Park JY, Lee SH, Shin MS, Kim YS, Kim SY, Lee HK, Kim PJ, Oh ST, Yoo NJ, Lee JY. Frequent somatic mutations of the beta-catenin gene in intestinal-type gastric cancer. *Cancer Res* 1999;**59**:4257-4049
- 48 **Tamura G**, Sato K, Akiyama S, Tsuchiya T, Endoh Y, Usuba O, Kimura W, Nishizuka S, Motoyama T. Molecular characterization of undifferentiated-type gastric carcinoma. *Lab Invest* 2001;**81**:593-538
- 49 **Becker KF**, Atkinson MJ, Reich U, Becker I, Nekarda H, Siewert JR, Hoffer H. E-cadherin gene mutations provide clues to diffuse type gastric carcinomas. *Cancer Res* 1994;**54**:3845-3852
- 50 **Ascano JJ**, Frierson H Jr, Moskaluk CA, Harper JC, Roviello F, Jackson CE, El-Rifai W, Vindigni C, Tosi P, Powell SM. Inactivation of the E-cadherin gene in sporadic diffuse-type gastric cancer. *Mod Pathol* 2001;**14**:942-949
- 51 **Machado JC**, Oliveira C, Carvalho R, Soares P, Berx G, Caldas C, Seruca R, Carneiro F, Sobrinho-Simoes M. E-cadherin gene (CDH1) promoter methylation as the second hit in sporadic diffuse gastric carcinoma. *Oncogene* 2001;**20**:1525-1528

Edited by Ma JY

• GASTRIC CANCER •

Effects of Chinese Jianpi herbs on cell apoptosis and related gene expression in human gastric cancer grafted onto nude mice

Ai-Guang Zhao, Hai-Lei Zhao, Xiao-Jie Jin, Jin-Kun Yang, Lai-Di Tang

Ai-Guang Zhao, Hai-Lei Zhao, Jin-Kun Yang, Lai-Di Tang,
Department of Oncology, Longhua Hospital, Shanghai University of
Traditional Chinese Medicine, Shanghai 200032, China

Xiao-Jie Jin, Renji Hospital, Shanghai Second Medical University,
Shanghai 200032, China

Supported by Shanghai High-Education Bureau Research Fund, No.
98QN72

Correspondence to: Dr. Ai-Guang Zhao, Department of Oncology,
Longhua Hospital, Shanghai University of Traditional Chinese Medicine,
725 Wanping Nanlu, Shanghai 200032, China. aiguang@hotmail.com

Telephone: +86-21-64385700 **Fax:** +86-21-64398310

Received 2002-05-02 **Accepted** 2002-06-09

Abstract

AIM: To explore the mechanism of the Sijunzi decoction and another Chinese herbal recipe (SRRS) based mainly on the Sijunzi decoction in treatment of gastric cancer.

METHODS: A human gastric adenocarcinoma cell line SGC-7901 grafted onto nude mouse was used as the animal model. The mice were divided into 3 groups, one control and the two representative experimental conditions. Animals in the two experimental groups received either Sijunzi decoction or SRRS over a 40-day period starting at 1st day after grafting. Control animals received saline on an identical schedule. Animals were killed 41 days after being grafted. The effect of therapy was assessed by two ways: (1) tumor size was periodically measured during the life of the animals; (2) tumor weight was determined by a electron balance immediately after the animals killed. For detection of apoptotic cells, apoptotic indices(AI) were examined by the terminal deoxynucleotidyl transferase-mediated deoxyuridine triphosphate fluorescence nick end labeling (TUNEL) method. Morphological alterations were observed with electron microscopy. S-P immunohistochemical method was used to detect the expression of Ki-67 in xenografts. Expression of bcl-2 and p53 was semiquantitatively detected using a reverse transcriptase-polymerase chain reaction (RT-PCR) technique.

RESULTS: When compared with controls, tumor growth (size and weight) was significantly inhibited by treatment with the Sijunzi decoction ($P<0.05$) or SRRS ($P<0.01$). The tumor inhibitory rate in the Sijunzi decoction group was 34.33 % and SRRS group 46.53 %. AI of human gastric cancer xenografts in nude mice was significantly increased to 16.24 ± 3.21 % using TUNEL method and 11.38 ± 6.46 % by FACScan in the Sijunzi decoction group compared with the controls (TUNEL: 2.63 ± 1.03 %, $P<0.01$; FACScan: 7.15 ± 1.32 %, $P<0.05$). SRRS group was also found a significantly increased AI by using TUNEL method and flow cytometry analysis compared with the controls (TUNEL: 13.18 ± 3.05 %, $P<0.05$; FACScan: 11.58 ± 5.71 % ($P<0.05$). Under electron microscope, cell shrinkage, nuclear chromatin condensation,

formation of membrane blebs and apoptotic bodies were frequently observed in Sijunzi decoction group and SRRS group. The average labeling index (LI) for Ki-67 in SRRS group was significantly decreased to 8.43 ± 2.22 % compared with the control group (10.37 ± 4.91 %) ($P<0.05$). The average labeling index for Ki-67 in sijunzi decoction group was 7.95 ± 2.54 % which was lower than that of the control group, but showed no significance ($P=0.07$). The expression level of p53 mRNA was lower in both Sijunzi decoction group and SRRS group than that in control group ($P<0.05$; $P<0.01$). The expression of bcl-2 mRNA was also decreased in SRRS group compared with the control ($P<0.01$).

CONCLUSION: The inhibition of gastric cancer cell growth *in vivo* by Chinese Jianpi herbs and SRRS is related to induction of the cell apoptosis which may be involved in aberrant expression of p53 and bcl-2 genes

Zhao AG, Zhao HL, Jin XJ, Yang JK, Tang LD. Effects of Chinese Jianpi herbs on cell apoptosis and related gene expression in human gastric cancer grafted onto nude mice. *World J Gastroenterol* 2002; 8(5):792-796

INTRODUCTION

Apoptosis plays a crucial role in the proliferation and turnover of cells in various tumors. It has been clear that its extent is often enhanced in tumor by many anticancer drugs^[1-5], such as cytotoxic drugs^[6], hormone^[1], or some Chinese herbal medicine^[7-10]. In clinic studies, some Chinese Jianpi herbs had been proved to have effect on malignant tumors, especially on gastric and colorectal tumors^[11-13]. Among these herbs we found that Codonopsis pilosula (Franch) Nannf., Atractylodes macrocephala koidz. and the Sijunzi Decoction might suppress gastric carcinoma cell proliferation and cause tumor cell loss and the nuclear condensation *in vitro*^[14]. The Sijunzi Decoction and another Chinese herbal recipe SRRS of deheat-toxin, softening hard lumps and dissolving phlegm enhance apoptosis of human gastric cancer xenografts in nude mice^[15]. Based on previous studies, we examined the apoptotic indices of human gastric cancer grafted onto nude mice after the treatment with Sijunzi Decoction and SRRS and investigate the underlying mechanism of the tumor suppressive effect of these Chinese Jianpi herbs.

MATERIALS AND METHODS

Materials

Animal models Thirty 6-7 weeks old female BALB/C-nu/nu mice (weight 18-22 g) and a human gastric carcinoma cell line SGC-7901 were obtained from Shanghai Tumor Institute (No.01842). The animals were subcutaneously grafted with the SGC-7901 cell. The tumor transplantation procedure was described previously^[15].

Drugs The Sijunzi Decoction is composed of Codonopsis pilosula (Franch) Nannf., Atractylodes macrocephala koidz, Poria cocos (Schw.) Wolf, Glycyrrhiza uralensis Fisch. The concentration of the Sijunzi Decoction was 160 g/L; SRRS is composed of Atractylodes macrocephala koidz., Poria cocos(Schw.) Wolf, Sargentodoxa cuneata(Oliv.) Rehd. Et Wils., Prunella vulgaris L. And etc. The concentration of the SRRS decoction was 240 g/L.

Experimental schedule After grafting the mice were randomly divided into 3 groups, one control and the two experimental groups assigned to receive the Sijunzi Decoction or SRRS. Each animal in the two experimental groups was given 0.5 mL of the Sijunzi Decoction or SRRS by gastric perfusion every day over a 40-day period beginning at 1st day after grafting. The control animals received normal saline according to the same schedule. Animals were killed 41 days after being grafted.

Methods

Tumor growth The effect of therapy was assessed by two ways: (1)tumor size was measured twice a week by multiplying two perpendicular diameters. (2)tumor weight was determined immediately by electron balance after the animals were killed.

Apoptosis For detection of apoptotic cells, apoptotic indices were examined by the terminal deoxynucleotidyl transferase-mediated deoxyuridine triphosphate fluorescence nick end labeling (TUNEL) method^[16-18] and flow cytometry analysis. Morphological alterations were observed with electron microscope. (1)TUNEL: *In situ cell death detection Kit POD* (ISCCD, BOEHRINGER MANNHEIM) was used to detect the apoptotic cell. The procedures was according to protocol of the kit and the other references. The positive cells were identified, counted and analyzed under the light microscope. Non-necrotic zone was selected in the tissue section and images were sent to computer by AEC camera (Grundig Electronic Co. Ltd., Germany). 10 image at least 1000 cells were selected on the screen, positive ratio analyzed by KS400 Video Image Digital Analysis System (ZEISS, Germany). (2)Electron microscopy: Some of specimens in each group were fixed with 2.5 % glutaraldehyde. Semi-thin and ultra-thin sections were cut and viewed with scanning electron microscope. The characteristics of cell apoptosis showed nuclear chromatin condensation, peripheral masses of condensed chromatin with enclosed membrane or crescent. The nuclear membrane is complete. There is little or no swelling of mitochondria or other organelles. (3) Flow cytometry analysis: Propidium iodide (PI) staining^[19-21] was used for flow cytometric detection of

apoptosis. 10⁶ cells from each of the sample were treated with RNase and stained with PI. The apoptotic cells having DNA strand breaks that had been labeled were measured on a flow cytometer (FACSCalibur, Becton Dickinson, USA). The data from 10⁶ cells/sample were collected, stored, and analyzed using CELLQUEST (Becton Dickinson USA) and ModFIT LT for mac V1.01 software (Becton Dickinson, USA).

Cell proliferation The level of expression of Ki-67 was used as a marker of cell proliferation. In present study Ki-67 was measured by S-P immunohistochemical method.

Expression of bcl-2 and p53 mRNA The Expression of p53 (5-8 exons) and bcl-2 was semiquantitatively detected using RT-PCR technique^[22-24]. A β -actin was used as an internal standard. Sequences of the primers used for RT-PCR analysis are described in Table 1. Total cellular RNA was isolated from tumor tissues using the acid-guanidium-phenol-chloroform technique. The RNA extracted from each sample was qualified by agarose gel electrophoresis and ethidium bromide staining and the amount of RNA was determined by electrophotometry A:260/280. The extracted RNA was converted to first strand cDNA with AMV reverse transcriptase (Promega). p53 and β -actin were amplified by polymerase chain reaction consisting of stage one: 2 minutes of denaturation at 94 °C before addition of Taq DNA polymerase; stage two: 1 minute of denaturation at 94 °C, 1 minute of primer annealing at 56 °C, and 1 minute of extension at 72 °C (Taq DNA polymerase, Shanghai Sangon Biology Engineering Technique Service Co. Ltd.). Gene expression of bcl-2 was also analyzed by RT-PCR, in the same manner except for annealing at 55 °C. The cyclor of PCR gene amplification is from Omn-E (Hybaid). Each reaction tube contained: 1.5 μ l 25mM MgCl₂+2.5 μ l 10 \times PCR buffer +0.5 μ l 10mM dNTP +1 μ l \times 2 20 pmol/ μ l p53 or bcl-2 primers or β -actin primers (primer concentration: 0.8 μ M) +2 μ l cDNA +0.5 μ l Taq (2.5-5U/ μ l) +16 μ l ddH₂O. Quantitative analysis: After the amplification step was completed, equal amounts (5 μ l) of PCR produces were loaded onto each lane of 1.7 % agarose gels and electrophoresed. FR-200UV/WHITE ANALYSIS (Shanghai Fu Ri Science & Technology Co. Ltd., China) took the image of electrophoresis with β -actin as internal standard, and FR-980 biological electrophoresis analysis system (Shanghai Fu Ri Science & Technology Co. Ltd., China) was used to analyze the quantity of nuclear acid.

Statistical analysis

The results were expressed as $\bar{x} \pm s$ and significant difference was assessed by Student's *t* test.

Table 1 Sequences of primers for amplified cDNA of the p53,bcl-2 and β -actin

Primers		Sequences	Combining sites	Amplifiers
p53	Sense	5'-GGAGGTTGTGAGGCGCTGC-3	645bp-663bp	311bp
	Antisense	5'-CACGCACCTCAAAGCTGTTC-3	936bp-955bp	
bcl-2	Sense	5'-CAGCTGCACCTGACGCCCTT-3'	1810bp-1829bp	191bp
	Antisense	5'-GCCTCCGTATCCTGGATCC-3'	2021bp-2040bp	
β -actin	Sense	5'-AGCGGGAAATCGTGCCTGAC-3	665bp-674bp	471bp
	Antisense	5'-ACTCCTGCTTGCTGATCCACATC-3	1103bp-1125bp	

Table 2 Chinese Jianpi herbs-induced effects on gastric cancer cell SGC-7901 ($\bar{x} \pm s$)

Treatment	Tumor weight/g (n)	Tumor size/mm ³ (n)	Percentage of control/%	Apoptotic index(AI)/%		ki-67/%
				TUNEL (n)	FACScan (n)	
Sijunzi Decoction	0.66 \pm 0.16(9) ^a	371.81 \pm 52.51(9) ^a	34.33	16.24 \pm 3.21(9) ^b	11.38 \pm 6.46(9) ^a	7.95 \pm 2.54(9) ^c
SRRS	0.54 \pm 0.23(9) ^b	322.66 \pm 126.14(9) ^b	46.53	13.18 \pm 3.05(8) ^a	11.58 \pm 5.71(8) ^a	8.43 \pm 2.22(8) ^b
Control	1.01 \pm 0.32(10)	603.61 \pm 263.39(10)		2.63 \pm 1.03(10)	7.51 \pm 1.32(10)	10.37 \pm 4.91(10)

^aP<0.05, ^bP<0.01, ^cP=0.070 vs control *t* test.

RESULTS

Chinese Jianpi herbs-induced effects on tumor growth

Each one case that the xenograft emerged later was eliminated in Sijunzi decoction group and SRRS group. Compared with the control group, tumor growth (size and weight) was significantly inhibited by treatment with the Sijunzi decoction ($P<0.05$) or SRRS ($P<0.01$). The tumor inhibitory rate of the sijunzi decoction group was 34.33 % and that in the SRRS group was 46.53 % (Table 2).

Chinese Jianpi herbs-induced effects on tumor cell apoptosis

Apoptotic index (AI) of xenografts in nude mice was significantly increased to 16.24 ± 3.21 % using TUNEL method and 11.38 ± 6.46 % FACScan in the Sijunzi decoction treatment group, compared with the controls (TUNEL: 2.63 ± 1.03 %, $P<0.01$; FACScan: 7.15 ± 1.32 %, $P<0.05$). SRRS group was also found a significantly increased AI by using TUNEL method and flow cytometry analysis compared with the controls (TUNEL: 13.18 ± 3.05 %, $P<0.05$; FACScan: 11.58 ± 5.71 %, $P<0.05$). But there was no significant difference between Sijunzi decoction group and SRRS group by using either TUNEL method or flow cytometry analysis. Under electron microscope cell shrinkage, nuclear chromatin condensation, formation of membrane blebs and apoptotic bodies were frequently observed in Sijunzi decoction group and SRRS group (Table 2).

Chinese Jianpi herbs-induced effects on tumor cell proliferation

The average labeling index for Ki-67 (LI) in SRRS treatment group (8.43 ± 2.22 %) was significantly lower than that in the control group (10.37 ± 4.91 %) ($P<0.01$). The average labeling index for Ki-67 in sijunzi decoction group was 7.95 ± 2.54 % which was lower than that of the control group, but showed no significance as the P value was 0.07 (Table 2).

Chinese Jianpi herbs-induced genetic effects

Expression of p53 (exons 5-8) and bcl-2 was semiquantitatively detected with β -actin used as an internal standard. The expression level of p53 mRNAs was 0.36 ± 0.27 , significantly lower in Sijunzi decoction group than that in control group (0.69 ± 0.20) ($P<0.05$), in SRRS group (0.19 ± 0.18) also significantly lower than that in control group ($P<0.01$). The expression of bcl-2 mRNA in SRRS group (0.33 ± 0.23) was decreased, compared with the control (0.81 ± 0.40) ($P<0.01$). In Sijunzi decoction group the expression of bcl-2 (0.41 ± 0.15) slightly decreased, compared with the control, but no statistics difference existed ($P=0.071$) (Table 3, Figure 1).

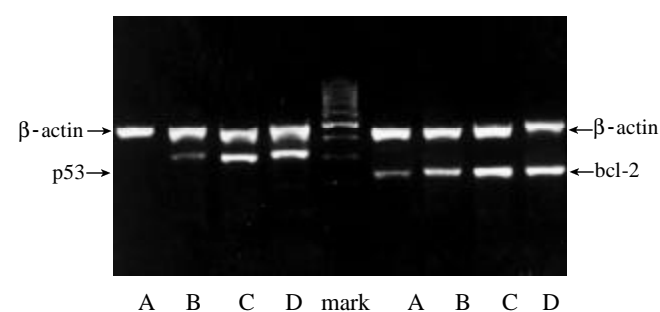


Figure 1 p53,bcl-2 mRNA expression in SGC-7901 grafted onto nude mice after treatment of Chinese Jianpi herbs by RT-PCR analysis. Lane A: SRRS group, Lane B: Sijunzi decoction group, Lane C: control group, Lane D: control group.

Table 3 Chinese Jianpi herbs-induced genetic effects ($\bar{x}\pm s$)

Treatment	p53(exons 5-8)	bcl-2
Sijunzi Decoction	$0.36\pm0.27(8)^a$	$0.41\pm0.15(8)^c$
SRRS	$0.19\pm0.18(9)^b$	$0.33\pm0.23(9)^b$
Control	$0.69\pm0.20(9)$	$0.81\pm0.40(9)$

^a $P<0.05$, ^b $P<0.01$, ^c $P=0.071$ vs control t test.

DISCUSSION

Despite its declining incidence, the gastric carcinoma remains one of the most common cause of cancer-related death in the world^[25-27]. At present gastric carcinoma is still detected later in most patients throughout the world, and even with curative resection, they remain at a high risk of relapse. Thus, there is a great need for effective adjuvant therapy for patients with gastric carcinoma^[28-30]. Our previous clinic paired comparative studies suggested that Chinese herbal recipe SRRS have therapeutic effects on advanced gastric cancer, with increasing the surviving period of the patients, improving the life quality, and decreasing the metastasis and recurrence rates after operation^[12,14]. Because of its lower toxic side-effect compared with chemical therapy, it is worth to make a further research on its anti-cancer mechanism.

As the other malignant tumor, gastric carcinoma is not only a disease with abnormal cell proliferation and differentiation, but also a disease with abnormal apoptosis^[5,31-35]. The enhanced induction of apoptosis in human gastric carcinoma cells can be observed after treatment with 5-Fluorouracil^[36], Cisplatin^[37], arsenous oxide^[38], etc. These data suggest that inducing cancer cell apoptosis may be a therapeutic method for gastric carcinoma. The present study indicated that tumor growth was significantly inhibited by treatment with the Sijunzi decoction or SRRS. TUNEL method and cytometry analysis clarified that Sijunzi decoction and SRRS enhanced apoptosis. The results suggest that the inhibition of gastric cancer cells *in vivo* by Jianpi herbs described here is related to inducing apoptosis. Immunohistochemical staining for Ki-67 showed that SRRS inhibited cell proliferation. So the inhibition of gastric cancer by SRRS is also related to suppressing the proliferation.

Apoptosis is a complex, tightly regulated, and active cellular process whereby individual cells are triggered to undergo self-destruction in a manner that will neither injure neighboring cells nor elicit any inflammatory reaction^[1,39-42]. Various triggering factor initiate corresponding proteo-lysis cascade reaction depending on mitochondrion or APO-1/FAS/CD95 receptor mediate apoptotic pathways^[40,43]. There are many oncogenes and tumor suppressor gene products in the regulation and execution of apoptosis. Among them are p53, Rb, myc, ras, raf, etc^[23,40,41,44,45]. p53, because of its role in apoptosis, has earned the name "guardian of the genome". It monitors the state of DNA, and in case of DNA damage, stalls the cell cycle. This takes place through the induction of CIP/WAF1/p21. In the absence of phosphorylated, active cyclin-dependent kinases, also another regulator of the cell cycle, Rb, remains inactive(unphosphorylated), and, hence, the cell cycle halts. This then leads to activation of DNA repair machinery. If the DNA repair fails, p53 takes over again and triggers apoptosis in a process that involves upregulation of the apoptotic-inducing bax and down-regulation of the apoptotic bcl-2^[23]. p53 also upregulates KILLER/DR5, a 45-kd apoptosis-inducing member of the tumor necrosis factor receptor family. Analogous to the APO-1/FAS/CD95 receptor

system, its activation also lead to a caspase activation^[37]. Thus p53 is known as one of the essential genes for cells to undergo apoptosis. In gastric cancer, mutant p53 expression decreased cancer cell apoptosis, p53 mutant provided selective growth superiority to the tumor cell. In our investigation we adopt the human gastric cancer cell line SGC-7901 which has point mutation in exon 6 codon 204 GAG→GCG coding Glu→Ala, which expresses mutant p53^[46,47]. RT-PCR detected p53 mRNA level was significantly lower in Sijunzi decoction group than that in control group. The expression level of p53 mRNA in SRRS group was also significantly lower than that in control group. The data suggest that these two recipes composed of Jianpi herbs induce SGC-7901 cancer cell apoptosis by down-regulation of mutant p53 mRNA expression.

We also detected apoptosis-inhibiting member of the bcl-2 family^[41,44]: bcl-2 mRNA. The expression of bcl-2 mRNA was decreased in SRRS group, compared with the control. In Sijunzi decoction group the expression of bcl-2 was slightly decreased compared with the control, but there was no statistics difference. It suggested that SRRS could suppress bcl-2 expression, but it was not stronger for than that of Sijunzi decoction. bcl-2 is the epitome of an antiapoptotic or survival gene. Attesting to its role in an apoptosis checkpoint, it counteracts apoptosis initiated by quite disparate signals, such as chemotherapeutic drugs, oxidative stress, viral infections, and p53. In gastric carcinoma, bcl-2 over-expressed at both protein and mRNA level in many cases^[48].

In our study SRRS and Sijunzi decoction down-regulated the expression of p53 mRNA and SRRS also decrease the expression of bcl-2 mRNA in SGC-7901 cancer cell undergoing apoptosis. We inferred that p53 and bcl-2 may be involved in the regulation of these Chinese Jianpi herbs inducing gastric cancer cell SGC-7901 apoptosis. The interaction contact of p53 and bcl-2 in SRRS or Sijunzi decoction inducing apoptosis needs further investigation.

REFERENCES

- Kerr JFR**, Winterford CM, Harmon BV. Apoptosis Its significance in cancer and cancer therapy. *Cancer* 1994; **73**: 2013-2026
- Lu XP**, Li BJ, Chen SL, Lu B, Jiang NY. Effect of chemotherapy or targeting chemotherapy on apoptosis of colorectal carcinoma. *Shijie Huaren Xiaohua Zazhi* 1999; **7**: 332-334
- Liang WJ**, Huang ZY, Ding YQ, Zhang WD. Lovo cell line apoptosis induced by cycloheximide combined with TNF α . *Shijie Huaren Xiaohua Zazhi* 1999; **7**:326-328
- Kong XP**, Zou QY, Li RB, Zheng PL, Yang LP, Jin SW. Apoptosis of neoplasm cell lines induced by hepatic peptides extracted from sucking porcine hepatocytes. *World J Gastroenterol* 1999; **5**:435-439
- Majno G**, Joris I. Apoptosis, oncosis, and necrosis an overview of cell death. *AM J Pathol* 1995; **146**: 3-15
- Wu JY**, Zhou XF, Jiang WX, Wang JL, Yang F, Cai XS, Zhang ZG. Effects of chemotherapeutic drugs on Bcl-2, p53 and Ki67 expression of gastric cancer. *Shijie Huaren Xiaohua Zazhi* 1999; **7**:589
- Tu SP**, Jiang SH, Qiao MM, Cheng SD, Wang LF, Wu YL, Yuan YZ, Wu YX. Effect of trichosanthin on cytotoxicity and induction of apoptosis of multiple drugs resistance cells in gastric cancer. *Shijie Huaren Xiaohua Zazhi* 2000; **8**: 150-152
- Zhu XQ**, Wang GS, Zhang XJ, Zhao Q. Apoptosis of human liver cancer EBL-7404 cells induced by traditional Chinese medicine Sodium Asafetide. *Shijie Huaren Xiaohua Zazhi* 1999; **7**:715-716
- Fan RY**, Ma L. Apoptosis of gastric cancer SGC-7901 cell induced by free radical. *Shijie Huaren Xiaohua Zazhi* 1999; **7**:807-808
- Xu AG**, Li SG, Liu JH, Shen JG, Gan AH. Apoptois of gastric cancer induced by Huangshen capsule and mechanism of nitrous oxide. *Shijie Huaren Xiaohua Zazhi* 1999; **7**:364-365
- Shen HX**, Chen L, Zhou SJ, Chen YQ, Fan Y, Lu LP. Clinical and experimental study on therapeutic effect of compound shenqitang on gastric carcinoma. *Shijie Huaren Xiaohua Zazhi* 1998; **6**: 837-840
- Qiu JX**, Jia JS, Yang JK, Zheng J, Zheng JG, Tang LD, Wang N, Shen KP, Pang HF, Ji GR, Qin DP, Li YM, Zhou XY, Luo XX, Liu MS, Qiu ZF, Cao LH, Dong MZ. Probing into the treatment of advanced stage of stomach carcinoma mainly by spleen-strengthening method. *Zhongyi Zazhi* 1992; **33**:23-25
- Wang GT**, Zhu JS, Xu WY, Wang Y, Zhou AG. Clinical and experimental studies on FuZheng anti-cancer granula combined with chemotherapy in advanced gastric cancer. *Shijie Huaren Xiaohua Zazhi* 1998; **6**:214-218
- Qiu JX**, Tang LD, Zuo JP, Gao WP, Chen FZ. Study on mechanism of herbal medicines for strengthening spleen in treatment of malignant tumor of digestive tract. *Shanghai Zhongyiyao Zazhi* 1987; **6**:45-47
- Zhao AG**, Yang JK, Zhao HL, Liu LK. Chinese Jianpi herbs induce apoptosis of human gastric cancer grafted onto nude mice. *Shijie Huaren Xiaohua Zazhi* 2000; **8**: 737-740
- Gavrieli Y**, Sherman Y, Ben-Sasson SA. Identification of programmed cell death in situ via specific labeling of nuclear DNA fragmentation. *J Cell Biol* 1992; **119**:493-501
- Zhang XL**, Liu L, Jiang HQ. Salvia miltiorrhiza monomer IH764-3 induces hepatic stellate cell apoptosis via caspase-3 activation. *World J Gastroenterol* 2002; **8**: 515-519
- Li J**, Wang WL, Wang WY, Liu B, Wang BY. Apoptosis in human hepatocellular carcinoma by terminal deoxynucleotidyl transferase mediate dUTP-FITC nick end labeling. *Shijie Huaren Xiaohua Zazhi* 1998; **6**: 491-494
- Nicoletti I**, Migliorati G, Pagliacci MC, Grignani F, Riccardi C. A rapid and simple method for measuring thymocyte apoptosis by propidium iodide staining and flow cytometry. *J Immunol Methods* 1991; **139**:271-279
- Gong J**, Traganos F, Darzy kiewicz Z. A selective procedure for DNA extraction from apoptotic cells applicable for gel electrophoresis and flow cytometry. *Anal Biochem* 1994; **218**:314-319
- Darzynkiewicz Z**, Bruno S, Bino GD, Gorczyca W, Hotz MA. Features of apoptotic cells measured by flow cytometry. *Cytometry* 1992; **13**: 795-808
- Kondo S**, Shinomura Y, Kanayama S, Higashimoto Y, Kiyohara T, Zushi S, Kitamura S, Ueyama H, Matsuzawa Y. Modulation of apoptosis by endogenous Bcl-x_L expression in MKN-45 human gastric cancer cells. *Oncogene* 1998; **17**: 2585-2591
- Miyashita T**, Krajewski S, Krajewska M, Wang HG, Lin HK, Liebermann DA, Hoffman B, Reed JC. Tumor suppressor p53 is a regulator of bcl-2 and bax gene expression *in vitro* and *in vivo*. *Oncogene* 1994; **9**:1799-1805
- Yamamoto M**, Maehara Y, Sakaguchi Y, Kusumoto T, Ichiyoshi Y, Sugimachi K. Transforming growth factor- β 1 induces apoptosis in gastric cancer cells through a p53-independent pathway. *Cancer Supplement* 1996; **77**:1628-1633
- Otsuji E**, Yamaguchi T, Sawai K, Hagiwara A, Taniguchi H, Takahashi T. Recent advances in surgical treatment have improved the survival of patients with gastric carcinoma. *Cancer* 1998; **82**: 1233-1237
- Nakajima T**, Nashimoto A, Kitamura M, Kito T, Iwanaga T, Okabayashi K, Goto M. Adjuvant mitomycin and fluorouracil followed by oral uracil plus tegafur in serosa-negative gastric cancer: a randomised trial. *Gastric Cancer Surgical Study Group. Lancet* 1999; **354**: 273-277
- Cirera L**, Balil A, Batiste-Alentorn E, Tusquets I, Cardona

- T, Arcusa A, Jolis L, Saigi E, Guasch I, Badia A, Boleda M. Randomized clinical trial of adjuvant mitomycin plus tegafur in patients with resected stage III gastric cancer. *J Clin Oncol* 1999; **17**: 3810-3815
- 28 **Hermans J**, Bonenkamp JJ, Boon MC, Bunt AMG, Ohyama S, Sasako M, Van de Velde CJH. Adjuvant therapy after curative resection for gastric cancer: Meta-analysis of randomized trials. *J Clin Oncol* 1993; **11**: 1441-1447
- 29 **Shimada K**, Ajani JA. Adjuvant therapy for gastric carcinoma patients in the past 15 years. *Cancer* 1999; **86**: 1657-1668
- 30 **Shimoyama S**, Shimizu N, Kaminishi M. Type-oriented intraoperative and adjuvant chemotherapy and survival after curative resection of advanced gastric cancer. *World J Surg* 1999; **23**: 284-292
- 31 **Pan CJ**, Zhong P, Huang XR, Liu KY, Wang SX. Study on the correlation between proliferation and apoptosis in atrophy and intestinal metaplasia of gastric mucosa. *Shijie Huaren Xiaohua Zazhi* 2000; **8**: 143-146
- 32 **Wagner S**, Beil W, Westermann J, Logan RPH, Bock CT, Trautwein C, Bleck JS, Manns MP. Regulation of gastric epithelial cell growth by *Helicobacter pylori* infection for a major role of apoptosis. *Gastroenterology* 1997; **113**: 1836-1847
- 33 **Ikeguchi M**, Cai J, Yamane N, Maeta M, Kaibara N. Clinical significance of spontaneous apoptosis in advanced gastric adenocarcinoma. *Cancer* 1999; **85**: 2329-2335
- 34 **Liu HF**, Liu WW, Fang DC, Men RF, Wang ZH. Apoptosis and its relationship with Fas ligand expression in gastric carcinoma and its precancerous lesion. *Shijie Huaren Xiaohua Zazhi* 1999; **7**: 561-563
- 35 **Xiao B**, Xiao LC, Lai ZS, Zhang YL, Zhang ZS, Zhang WD. Experimental study of the inhibition effect of Zhenailong on the growth of gastric cancer *in vitro*. *Shijie Huaren Xiaohua Zazhi* 1999; **7**: 951-954
- 36 **Sugamura K**, Makino M, Shirai H, Kimura O, Maeta M, Itoh H, Kaibara N. Enhanced induction of apoptosis of human gastric carcinoma cells after preoperative treatment with 5-Fluorouracil. *Cancer* 1997; **79**: 12-17
- 37 **Muller M**, Wilder S, Bannasch D, Israeli D, Lehlbach K, Min LW, Friedman SL, Galle PR, Stremmel W, Oren M, Krammer PH. p53 activates the CD95 (APO-1/Fas) gene in response to DNA damage by anticancer drugs. *J Exp Med* 1998; **188**: 2033-2045
- 38 **Tu SP**, Jiang SH, Tan JH, Jiang XH, Qiao MM, Zhang YP, Wu YL, Wu, YX. Proliferation inhibition and apoptosis induction by arsenic trioxide on gastric cancer SGC-7901. *Shijie Huaren Xiaohua Zazhi* 1999; **7**: 18-21
- 39 **Brown JM**, Wouters BG. Apoptosis, p53, and tumor cell sensitivity to anticancer agents. *Cancer Res* 1999; **59**: 1391-1399
- 40 **Green DR**. Apoptotic pathways: the roads to ruin. *Cell* 1998; **94**: 695-698
- 41 **Soini Y**, Paakko P, Lehto VP. Histopathological evaluation of apoptosis in cancer. *Am J Pathol* 1998; **153**: 1041-1053
- 42 **Pan G**, Ni J, Wei YF, Yu GL, Gentz R, Dixit VM. An Antagonist Decoy Receptor and a Death Domain-Containing Receptor for TRAIL. *Science* 1997; **277**: 815-818
- 43 **Ashkenazi A**, Dixit VM. Death Receptors: Signaling and Modulation. *Science* 1998; **281**: 1305-1308
- 44 **Reed JC**. Bcl-2 and the regulation of programmed cell death. *J Cell Biol* 1994; **124**: 1-6
- 45 **Arends MJ**, McGregor AH, Wyllie AH. Apoptosis is inversely related to necrosis and determines net growth in tumors bearing constitutively expressed myc, ras, and HPV oncogenes. *Am J Pathol* 1994; **144**: 1045-1057
- 46 **Zhang QY**, Lu YY, Li Z, Li WM, Cui JT, Xie SH, Deng DR. P53 gene mutation in Chinese gastric carcinoma cell lines. *Shengwu Huaxue Zazhi* 1995; **11**: 311-315
- 47 **Buchman VL**, Chumakov PM, Ninkina NN, Samarina OP, Georgiev GP. A variation in the structure of the protein-coding region of the human p53 gene. *Gene* 1988; **70**: 245-252
- 48 **Kondo S**, Shinomura Y, Kanayama S, Higashimoto Y, Miyagawa JI, Minami T, Kiyohara T, Zushi S, Kitamura S, Isozaki K, Matsuzawa Y. Over-expression of bcl-x_L gene in human gastric adenomas and carcinomas. *Int J Cancer* 1996; **68**: 727-730

Edited by Zhang JZ

• LIVER CANCER •

DNA-PKcs subunits in radiosensitization by hyperthermia on hepatocellular carcinoma hepG₂ cell line

Zhao-Chong Zeng, Guo-Liang Jiang, Guo-Min Wang, Zhao-You Tang, Walter J. Curran, George Iliakis

Zhao-Chong Zeng, Department of Radiation Oncology, Zhongshan Hospital, Fudan University, Shanghai, 200032, China

Guo-Liang Jiang, Department of Radiation Oncology of Cancer Hospital, Fudan University, Shanghai, 200032, China

Guo-Min Wang, Department of Urology, Zhongshan Hospital, Fudan University, Shanghai, 200032, China

Zhao-You Tang, Liver Cancer Institute, Fudan University, Shanghai, 200032, China

Zhao-Chong Zeng, Walter J. Curran, George Iliakis, Department of Radiation Oncology of Kimmel Cancer Center, Thomas Jefferson University, Philadelphia, PA 19107, USA

Correspondence to: Dr. Zhao-Chong Zeng, Department of Radiation Oncology, Zhongshan Hospital, Fudan University, Shanghai, 200032, China. zeng@guomai.sh.cn

Telephone: +86-21-64041990 Ext. 2763 **Fax:** +86-21-64037181

Received 2001-08-24 **Accepted** 2001-08-28

Abstract

AIM: To investigate the role of DNA-PKcs subunits in radiosensitization by hyperthermia on hepatocellular carcinoma HepG₂ cell lines.

METHODS: Hep G₂ cells were exposed to hyperthermia and irradiation. Hyperthermia was given at 45.5 °C. Cell survival was determined by an *in vitro* clonogenic assay for the cells treated with or without hyperthermia at various time points. DNA DSB rejoining was measured using asymmetric field inversion gel electrophoresis (AFIGE). The DNA-PKcs activities were measured using DNA-PKcs enzyme assay system.

RESULTS: Hyperthermia can significantly enhance irradiation-killing cells. Thermal enhancement ratio as calculated at 10 % survival was 2.02. The difference in radiosensitivity between two treatment modes manifested as a difference in the α components and the almost same β components, which α value was considerably higher in the cells of combined radiation and hyperthermia as compared with irradiating cells (1.07 Gy⁻¹ versus 0.44 Gy⁻¹). Survival fraction showed 1 logarithm increase after an 8-hour interval between heat and irradiation, whereas DNA-PKcs activity did not show any recovery. The cells were exposed to heat 5 minutes only, DNA-PKcs activity was inhibited at the nadir, even though the exposure time was lengthened. Whereas the ability of DNA DSB rejoining was inhibited with the increase of the length of hyperthermic time. The repair kinetics of DNA DSB rejoining after treatment with Wortmannin is different from the hyperthermic group due to the striking high slow rejoining component.

CONCLUSION: Determination with the cell extracts and the peptide phosphorylation assay, DNA-PKcs activity was inactivated by heat treatment at 45.5 °C, and could not

restore. Cell survival is not associated with the DNA-PKcs inactivity after heat. DNA-PKcs is not a unique factor affecting the DNA DSB repair. This suggests that DNA-PKcs do not play a crucial role in the enhancement of cellular radiosensitivity by hyperthermia.

Zeng ZC, Jiang GL, Wang GM, Tang ZY, Curran WJ, Iliakis G. DNA-PKcs subunits in radiosensitization by hyperthermia on hepatocellular carcinoma hepG₂ cell line. *World J Gastroenterol* 2002; 8(5):797-803

INTRODUCTION

Hepatocellular carcinoma (HCC) remains one of the most difficult tumors to treat^[1-15]. About 90 % of patients are unresectable at presentation because of tumor size, location, or underlying parenchymal disease^[16-20]. Those patients are sometimes recommended to receive non-surgical therapies, including radiotherapy^[21-28], radiofrequency hyperthermia^[29,30], or the hyperthermia as an adjuvant to radiation in the treatment of local and regional disease^[31]. Thermoradiotherapy currently offers the most significant advantages in the treatment of certain types of cancer^[32]. Numerous uncontrolled studies have been performed in which comparable lesions were treated with either radiation alone or combined with hyperthermia^[33]. Although many of these studies are difficult to evaluate, they give strong evidence that adjuvant heat treatment increases the probability of complete response and, consequently, tumor control. The cause of this radiosensitization has not been firmly established, however, in part this sensitization is thought to be through inhibition of repair of radiation induced DNA damage^[34-36]. The mode of this repair inhibition is still unclear. Protein denaturation and aggregation appear to be the most relevant process underlying the biological effects of hyperthermia.

Several studies have shown that hyperthermia could inhibit both recovery of radiation induced potentially lethal radiation damage (PLD) and sublethal damage (SLD)^[37]. Such inhibition was dependent on the time, temperature, and sequence of hyperthermia treatment. It was shown that polymerase β may be one of the mechanisms involved in thermo-radiosensitization^[38]. In addition, DNA-dependent protein kinase (DNA-PKcs) plays a central role in the repair of DSB^[39]. DNA-PKcs is a complex consisting of three proteins: Ku70 and Ku80 and the catalytic subunit, DNA-PKcs^[39]. The Ku70 and Ku80 proteins are involved in binding to the DNA ends at DSB and this binding activates the DNA-PKcs^[39]. A possible mechanism for hyperthermic radiosensitization is mediated through the heat lability of Ku subunits of DNA-PKcs^[40]. To support this mechanism, we have used Hep G₂ cells to study the relationship of DNA-PKcs activity in thermal radiosensitization and the kinetics of DNA DSB rejoining with the time after irradiation, addressing the main question that the role of DNA-PKcs subunits in thermal radiosensitization.

MATERIALS AND METHODS

Cell culture

HepG₂ cell line was obtained from the American Type Culture Collection (ATCC) and was grown in MEM medium supplemented with 100×10^3 U·L⁻¹ penicillin, 100 mg·L⁻¹ streptomycin, and 100 ml·L⁻¹ fetal calf serum at 37 °C in a humidified incubator, at an atmosphere of 50 ml·L⁻¹ CO₂ and 950 ml·L⁻¹ air. Cells were maintained in a phase of nearly logarithmic growth by subculturing every 4 days at an initial concentration of 2×10^5 cells in T-25 tissue culture flasks for both clonogenic assay and DNA DSB rejoining studies, 2×10^6 cells in T-75 tissue culture flasks for determination of DNA-PKcs activity. The cells were passed several times through a 20-gauge needle in syringe to make the clamp cells single in each subculturing.

Hyperthermia treatment

Hyperthermia was carried out by sealing cell cultures grown in tissue culture flasks with parafilm and immersing the flasks into a temperature control waterbath (± 0.05 °C). The continuous heating experiments ranged from 5 to 30 minutes at an interval of 5 minutes. After heating at 45.5 °C, flasks were put into ice for 10 minutes for the DNA DSB rejoining and DNA-PKcs activity studies, or a 37 °C waterbath for 5 minutes to equilibrate to 37 °C for clonogenic assay. At this point, if required, the flasks were irradiated on the ice.

Radiation treatment

Cells in flasks were irradiated using a Pantak X-ray machine operated at 320 kV, 10 mA with a 2 mm Al filter (effective photon energy about 90 kV), at a dose rate of 2.7 Gy·Min⁻¹. Dosimetry was performed with a Victoreen dosimeter which was used to calibrate an in-field ionization monitor.

Clonogenic survival

Cells were trypsinized at 37 °C for 10 minutes, and pipetted 7 times to keep the clamp cells to be single cell suspension using 20-gauge needle and 5 ml syringe in 5 ml medium. The single cell suspension was adjusted and seeded into 60-mm tissue culture dishes at various densities aiming at 20-200 colonies per dish. Cells were irradiated at room temperature in 5 mL medium and were immediately kept at 37 °C, 50 ml·L⁻¹ CO₂ incubator for 13 days. Cells were stained with crystal violet and colonies of more than 50 cells were counted. The radiation results presented for heat plus X-rays were corrected for the cell killing caused by heat alone.

Induction and repair of DNA DSB

Cells for DNA DSB repair experiments were labeled with 3.7MBq·L⁻¹ ¹⁴C-thymidine plus 2.5 μmol·L⁻¹ cold thymidine for the entire period of growth. The cells were used 3 days later as the concentration reached 1×10^6 cells/T-25 flask. When indicated by the experimental protocol, cells were treated with 20 μmol·L⁻¹ Wortmannin for 1 hour or hyperthermia at 45.5 °C for various times before irradiation. Cells were cooled to 4 °C prior to irradiation and were irradiated on ice. After irradiation, the medium was replaced with fresh growth medium pre-warm at 42 °C to rapidly restore to 37 °C, and then cells were quickly returned to the incubator at 37 °C to allow for repair. Cells were prepared for DNA DSB analysis at various time intervals thereafter.

After completion of the repair time interval, cells were trypsinized for 90 minutes in ice for the first 4 hours, and 10 minutes at 37 °C at later points. The cells were collected with 5 ml cold medium, centrifuged at 4 °C, and washed with 5 ml

cold serum-free medium. The cells were resuspended in 165 μl cold serum-free medium. This cell suspension was mixed with an equal volume of 10 g·L⁻¹ agarose (InCert agarose, FMC) to reach a concentration of 3×10^9 cells·L⁻¹. The cell-agarose suspension was then pipetted into a 3 mm diameter glass tubes and placed into ice to allow for solidification. The solidified cell-agarose suspension was extruded from the glass tubes and cut into 3 × 5 mm cylindrical blocks containing approximately 1.5×10^5 cells/block^[41]. Blocks were then placed in lysis buffer containing 10 mmol·L⁻¹ Tris, pH 8.0, 50 mmol·L⁻¹ NaCl, 0.5 mol·L⁻¹ EDTA, 2 g·L⁻¹ N-Lauryl Sarcosyl (NLS), 0.1 g·L⁻¹ proteinase E & O, and incubated first at 4 °C for 45 minutes and then at 50 °C for 16-18 hours. Following lysis, agarose blocks were washed for 1 hour at 37 °C in a buffer containing 10 mmol·L⁻¹ Tris, pH 8.0 and 0.1 mol·L⁻¹ EDTA, and were then treated for 1 hour at 37 °C in the same buffer, at pH 7.5, with 0.1 g·L⁻¹ RNAase A. Cells from identically treated non-irradiated cultures were also processed at pre-defined times to determine the signal generated by non-irradiated cells as background. For dose response, a similar protocol was also employed to determine the induction of DNA DSB except that in this case cells were embedded in agarose prior to irradiation with various doses on the ice, and were lysed immediately thereafter.

Pulsed-field gel electrophoresis

Asymmetric field inversion gel electrophoresis (AFIGE) was carried out in 5 g·L⁻¹ Seakem agarose (FMC), cast in the presence of 0.5 mg·L⁻¹ ethidium bromide, in 0.5 × TBE (45 mmol·L⁻¹ Tris, pH 8.2, 45 mmol·L⁻¹ Boric Acid, 1 mmol·L⁻¹ EDTA) at 10 °C for 40 hours. During this time, cycles of 1.25 V·cm⁻¹ for 900 seconds in the direction of DNA migration alternated with cycles of 5.0 V·cm⁻¹ for 75 seconds in the reverse direction. The agarose gels were quantified to estimate DNA damage by means of a PhosphorImager (Molecular Dynamics). Gels were dried and exposed to radiation-sensitive screens for 48-96 hours. DNA DSB was quantitated by calculating the fraction of activity released (FAR) from the well into the lane in irradiated and non-irradiated samples. The FAR measured in non-irradiated cells (background) was subtracted from the results shown with irradiated cells. Gel images were obtained either by photographing ethidium bromide-stained gels under UV light, or from the PhosphorImager.

Repair kinetics were fitted assuming two exponential components of rejoining according to the equation $\text{FAR} = A e^{-bt} + C e^{-dt}$ ^[42]. The first term in the equation was fitted to the slow and the second to the fast component of rejoining. Fitting was achieved using the non-linear regression analysis routines of a commercially available software package (SAS). Parameters A and C describe the amplitudes, and parameter b and d and the rate constants of the slow and the fast components of rejoining, respectively. From these parameters the half-time for the rejoining of the slow and the fast components were calculated as $t_{50, \text{fast}} = \ln 2/b$, and $t_{50, \text{slow}} = \ln 2/d$, respectively. The fraction of DSB rejoined by fast kinetics was calculated as $F_{\text{fast}} = A/A+C$ and $F_{\text{slow}} = C/A+C$.

Determination of DNA-PKcs activity

Cell extract preparation: Cells (2×10^6) were grown in the T-75 tissue culture flask for 5 days. After treatment, about 30×10^6 cells were collected in cold PBS after being trypsinized at 37 °C for 10 minutes, centrifuged at 4 °C, and resuspended with 1 mL cold PBS and transferred to Eppendorf tube. After spun 1 500 r·min⁻¹ for 5 minutes at 4 °C, PBS was replaced with 0.5 ml (about 4 volumes of cells) hypotonic buffer containing 10 mmol·L⁻¹ HEPES KOH pH 7.9 at 4 °C, 5 mmol·L⁻¹

KCl, 1.5 mmol·L⁻¹ MgCl₂, 20 mmol·L⁻¹ b-Glu, 0.2 mmol·L⁻¹ phenylmethylsulfonyl fluoride (PMSF), 0.5 mmol·L⁻¹ dithiothreitol (DTT). The cells were put on ice for 10 minutes, frozen in liquid nitrogen and thawed for 3 cycles, adjusted salt being 50 mmol·L⁻¹ KCl in hypotonic buffer (16 µl, 1.6 mol·L⁻¹ KCl), and allowed to stay for 10 minutes on ice. After centrifugation (40 minutes at 14 000 r·min⁻¹ at 4 °C), cytoplasm extract was obtained from the collection of supernatants. Nuclei were resuspended with 50 mmol·L⁻¹ KCl hypotonic buffer (100 ml), the salt was adjusted to 400 mmol·L⁻¹ KCl with 3 mol·L⁻¹ KCl in the buffer (13 µl), mixed in the cold room (4 °C) for 30 minutes. After centrifuged at 14 000 r·min⁻¹ for 15 minutes at 4 °C, nucleic extract was obtained from the collection of supernatants. Protein concentration of both cytoplasm and nucleic extracts were determined using Bio-Rad protein II assay.

Activity assay of DNA-PKcs: In 1.5 ml microfuge tube, the reaction buffer was set up on ice in a mixture containing 4 µl 5X kinase buffer (250 mmol·L⁻¹ HEPES, pH 7.5, 50 mmol·L⁻¹ MgCl₂, 1 mmol·L⁻¹ EGTA, 5 mmol·L⁻¹ DTT), 2 µl 10X substrate peptide (2 mmol·L⁻¹), 2 µl 10X sonicated calf thymus DNA (100 mg·L⁻¹), 2 µl (7.4 MBq·L⁻¹) of (γ-³²P) ATP. In this reaction buffer mixture, an equal volume (5 µg in 10 µl) of nucleic extract was added and mixed quickly. The optimal incorporation time was found to be 15 minutes at 30 °C. After incubation, the reaction was terminated with 20 µl stop solution (300 g·L⁻¹ acetic acid, 1 mmol·L⁻¹ ATP). Out of 40 µml reaction mixture, 20 µl was spotted on Watermann P81 phosphocellulose paper, and washed 4 times with 150 g·L⁻¹ acetic acid for 15 minutes each time. The filters were placed in scintillation vials, and the adsorbed radioactivity was quantitated. To calculate the specific activity of (γ-³²P) ATP, we removed 5 µl from any two reaction tubes, and added to scintillation vial to count. Calculation of the specific activity of (γ-³²P) ATP in cpm/pmol is shown as follows (40/5) × X/10 000 = X/1 250 [40 is the sum of the reaction volume (20 µL) + stop buffer (20 µl), 5 is the volume (µl) used for the specific activity of (γ-³²P) ATP, X is the average counts, and 10 000 is the number of pmoles of ATP in the reaction]. Calculation of incorporated ATP (pmol) is (CPM_{reaction with DNA} - CPM_{reaction without DNA}) / The specific activity of [γ-³²P] ATP in 10¹²cpm·mol⁻¹.

RESULTS

The survival curves of HepG₂ cell exposure to X-ray combined with or without hyperthermia are shown in Figure 1A and B. The mean dose of survival fraction at 2 Gy (SF₂) was 0.230±0.033 for the group of radiation alone, and 0.148±0.043 for the radiation combined with hyperthermia group. The linear-quadratic model $S=e^{-\alpha D-\beta D^2}$ was applied to describe the survival data in Figure 1, where S is the fraction of cells surviving a dose D, and α and β are constants. The α and β values are 0.805±0.037 Gy⁻¹ and 0.072 ± 0.012 Gy⁻² for the group of radiation alone, and 0.950 ± 0.018 Gy⁻¹ and 0.010 ± 0.001 Gy⁻² for the group of radiation combined with hyperthermia. The α/β ratios are 11.2 Gy and 97 Gy for the groups of radiation alone and combination modes, respectively. Thermal enhancement ratio as calculated at 10 % survival (TER₁₀) was 2.02. The difference in radiosensitivity between these two groups can be interpreted as being due to some phenomena, which manifest as a difference in the components.

Figure 1B shows the survival curves for cells exposed for various periods of time to 45.5 °C. The combination of hyperthermia with 3 Gy X-ray significantly improved the

killing effects in comparison of hyperthermia alone. Figure 1C shows a combination of hyperthermia at 45.5 °C for 15 minutes first and then 3 Gy of X-rays. When the time intervals between hyperthermia and radiation in existence, the cell survival increased with the time interval increase within 8 hours, but no significant change was observed 8 hours later.

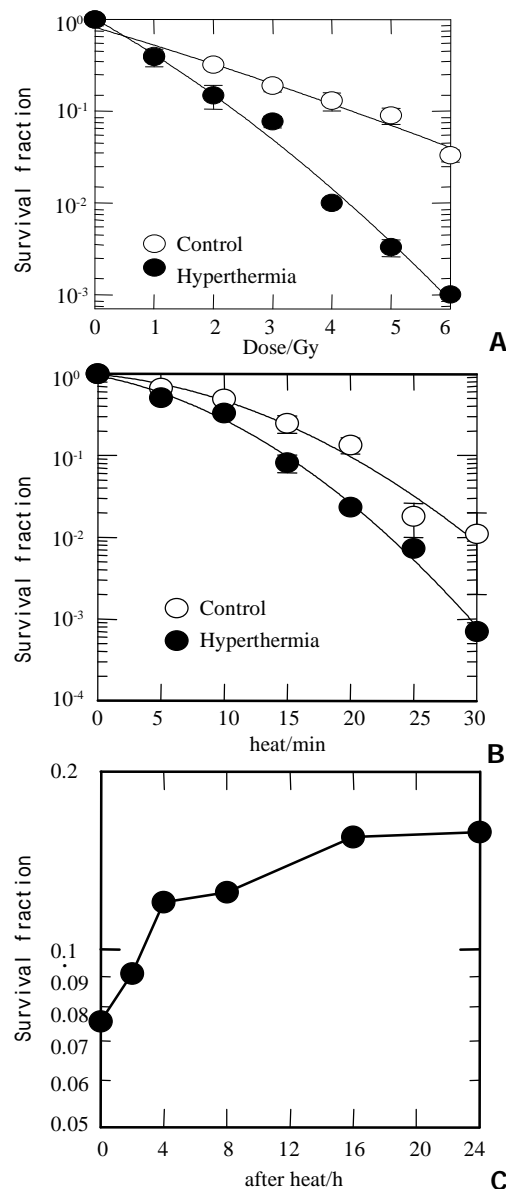


Figure 1 Survival fraction of HepG₂. A: Exposure to X-rays combined with (close circles) or without (open circles) 45.5 °C for 15 minutes; B: Heat-induced clonogenic cell death as a function of time combined with (close circles) or without (open circles) 3 Gy of X-rays; C: Irradiated with 3 Gy of X-rays at different hours after heat of 15 minutes at 45.5 °C.

The DNA-PKcs activity was measured before and after irradiation with 40 Gy X-ray, or hyperthermia for 20 minutes at 45.5 °C, or both. All of DNA-PKcs values were expressed with both relative percentage at left side and pmol at right of figures in this paper. Figure 2A shows that DNA-PKcs activity was inhibited by about 70 % at heating. Radiation stimulated DNA-PKcs activity increased about 30 % in the cells treated with or without hyperthermia at the 2nd hour. In order to determine whether the level of DNA-PKcs activity recovers its activity after hyperthermia, the time point was extended to 24 hours to correspond to clonogenic survival in Figure 1C.

As shown in Figure 2B, no restore was found in DNA-PKcs activity up to 24 hours. The DNA-PKcs activity was inhibited after the cells exposed to heat at 45.5 °C for 5 minutes (Figure 2C). The DNA-PKcs activity remained at almost the same level despite the hyperthermic time extending.

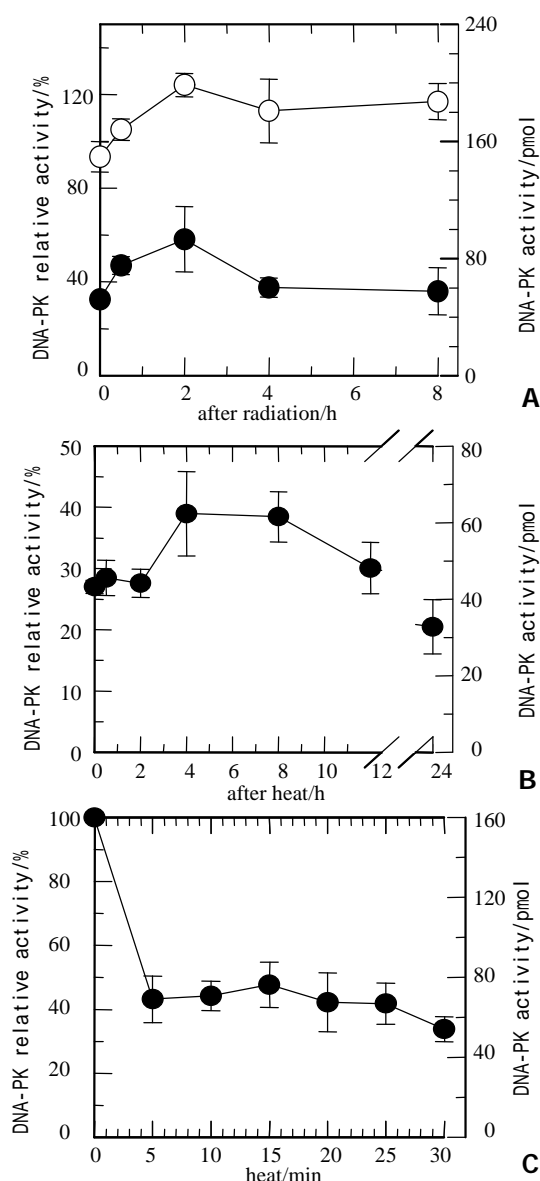


Figure 2 DNA-PKcs activity of HepG2 cells. A: Cells were heated at 45.5 °C for 20 minutes and then received 40 Gy of X-rays (closed circles) or irradiated with 40 Gy of X-rays only (open circles). At various periods, DNA-PKcs activity in heated cells was inhibited, and kept at low level about 30 %. The DNA-PKcs activity in both groups showed slight increase; B: After heated at 45.5 °C for 20 minutes, DNA-PKcs activity was still inhibited at various periods; C: DNA-PKcs activity was inhibited after exposure to heat at 45.5 °C for 5 minutes, even though the heat time was prolonged, DNA-PKcs activity levels still remained unchanged.

To understand the role of DNA-PKcs subunits in radiosensitization by hyperthermia, induction of X-ray induced DNA DSB was measured by AFIGE. Figure 3 shows the dose response curves for Hep G₂ cells receiving radiation combined with or without hyperthermia. The upper panel shows a typical gel scanned with ¹⁴C-TdR, while the lower panel shows the quantitative data as described in the Methods. The FAR, a measure of DNA DSB presence, increased almost linearly with

dose up to 30 Gy but bended downward at higher doses. Similar increases in FAR as a function of dose were observed in radiation alone or combined with hyperthermia, suggesting similar yields of DNA DSB.

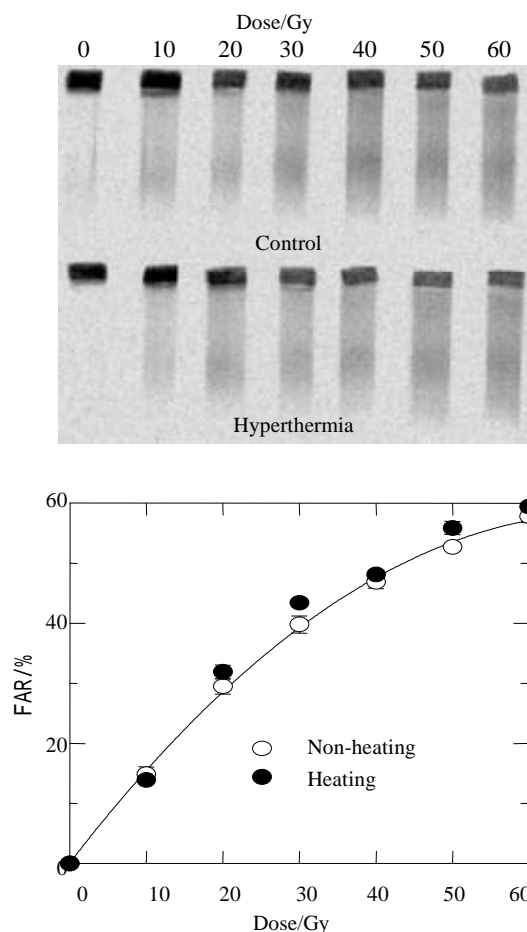


Figure 3 Dose response curves for Hep G₂ cells received radiation combined with or without hyperthermia. The upper panel shows a typical gel scanned with ¹⁴C-TdR, while the lower panel shows quantitative data as described in the Methods. The FAR increases almost linearly with dose up to 30 Gy but bends downward at higher doses. Similar increases in FAR as a function of dose are observed in radiation alone or combined with hyperthermia, suggesting similar yields of DNA DSBs.

The rate of rejoining of radiation-induced DNA DSB was subsequently examined to determine whether differences in repair between radiation alone and combined with hyperthermia for different periods of time account for the results shown in Figure 2A that the DNA-PKcs activity was inhibited after heat. Figure 4 shows that DNA DSB repairs kinetics in Hep G₂ cells. Cells were irradiated with 40 Gy and prepared for AFIGE after various periods of incubation at 37 °C to allow for repair. The upper panel in the Figure shows a typical AFIGE gel, while the lower panel shows its quantification as described in the Methods. The rejoining of DNA DSB decreased with increasing the lengths of hyperthermic time at 45.5 °C. Table 1 shows that the half-time for rejoining of the fast components was shorter in the control group or exposure to heat for 5 minutes than the exposure to longer time (15 and 20 minutes). However, the half-time of slow components in both control and hyperthermic groups were almost the same which ranged between 7 and 9 hours.

Wortmannin inhibits the entire family of PI-3 kinases and probably also other cellular kinases. To evaluate the

contribution of DNA-PKcs to Wortmannin-induced inhibition of DNA DSB rejoining, we searched for Wortmannin treatment, which is able to compare heat-induced inhibition of DNA DSB rejoining. Figure 5 indicates the kinetics of DNA DSB rejoining after treatment with Wortmannin. We found that the slow rejoining component is strikingly high. The deficiency of DNA DSB rejoining was found in Wortmannin treatment cells after 2 hours. These results are different from those in hyperthermic groups.

Table 1 The half-time and fraction of DNA DSB rejoining by fast and slow kinetics

	$T_{50,fast}$	$T_{50,slow}$	F_{fast}	F_{slow}
Control	0.49	7.07	0.80	0.20
5 min	0.33	4.15	0.44	0.56
15 min	0.92	9.37	0.49	0.51
20 min	1.25	9.24	0.30	0.70
20 mmol · L ⁻¹ Wort.	0.87	7×10^8	0.44	0.56

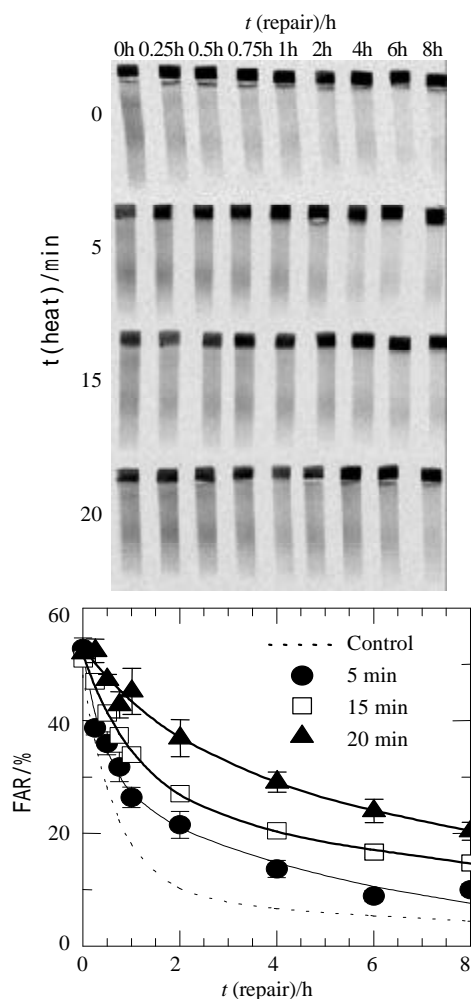


Figure 4 DNA DSBs repair kinetics in Hep G2 cells. Cells were irradiated with 40 Gy and prepared for AFAGE after various periods of incubation at 37 °C to allow for repair. The upper panel in the Figure shows a typical AFAGE gel, while the lower panel shows its quantification as described in the materials and Methods. The rejoining of DNA DSBs was decreasing with the increase of the lengths of hyperthermic time at 45.5 °C.

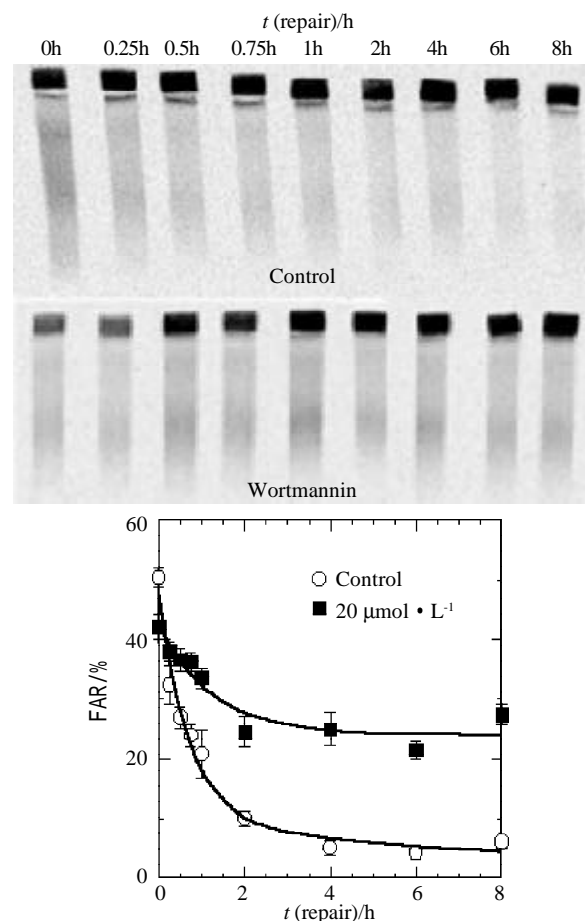


Figure 5 The kinetics of DNA DSBs rejoining after treatment with Wortmannin. The slow rejoining component is strikingly high. The deficiency of DNA DSBs rejoining was found in Wortmannin treatment cells after 2 hours.

DISCUSSION

Tumors of liver are among the most common malignancies in the world. Primary hepatocellular carcinoma was the second most common cancer and the leading cause of cancer deaths behind gastric cancer in China. Surgical resection has been accepted as the only curative therapy for primary liver cancer. Unfortunately, most patients were surgically unresectable^[1-28]. Hyperthermia^[29,30], radiation therapy^[21-28], or combination of both^[31,32] were introduced as an alternative therapeutic approach. The cause of this radiosensitization has not been firmly established.

The inhibition of DNA-PKcs by hyperthermia has been demonstrated in several studies^[40, 43,44]. In our series, DNA-PKcs activity was inhibited by about 60 % after hyperthermia at 45.5 °C for 5 minutes, and no significant change was found after increasing hyperthermia time. This result is similar to other reports^[40, 43]. Interestingly, the rejoining of DNA DSB was decreasing with the increase of the hyperthermic time at 45.5 °C. The decrease of DNA DSB repair did not correspond proportionally to the heat inhibited DNA-PKcs activity which was kept at a same low activity level between 5 and 30 minutes. This means DNA-PKcs is not critical for DNA DSB repair in heat.

The activity of DNA-PKcs depends upon the presence of double-stranded DNA ends, and is based on the similarity of their DNA-binding properties, and Ku was identified as the DNA-targeting component of this protein complex^[45-51]. This can be used to explain the fact that DNA-PKcs activity increased by about 30 % at the 2nd hour after 40 Gy X-ray irradiation, which produced plenty of DNA DSB. After

hyperthermia at 45.5 °C for 15 minutes, DNA-PKcs activity was stable at a low level (30 %) up to 24 hours. We are eager to know whether the low level DNA-PKcs affects the clonogenic survival. The results showed that the effects of thermal radiosensitization were lowered, even though DNA-PKcs activity did not restore. This indicated that there was no correlation between thermal inactivation of DNA-PKcs and radiosensitization by heat.

Wortmannin is a fungal metabolite originally characterized as an irreversible inhibitor of PI3K-like family including DNA-PKcs^[52]. The inhibition of DNA-PKcs by Wortmannin could increase the slow rejoining component, resulting in deficiency of DNA DSB repair. The kinetics of DNA DSB rejoining in hyperthermia groups different from that treated with wortmannin, inhibited the DNA-PKcs activity. This confirms that DNA DSB repair is not completely affected by DNA-PKcs, other factors might also involve in the repair.

DNA-PKcs is not critical for radiosensitization by heat. What might explain the synergistic interaction between heat and radiation? One possibility is that homologous recombination may impair after heat shock, but the contribution of this repair pathway in mammalian cells seems limited^[53]. Another possibility is that heat-induced loss of activity of DNA repair enzymes other than DNA-PKcs has been observed and proposed previously as the mechanism that underlies DNA repair inhibition and radiosensitization. These enzymes include DNA polymerases^[37], ATM system^[54], ATR system^[38], etc. Motsumoto found recently that heating up to 90 minutes affected only marginally DNA-PKcs activity in four different human cell lines (results not published). The contradictory results are due to the methods of measurement, which can not distinguish between inhibition of ATM and DNA-PKcs as the substrate, and peptide is good for both kinases.

In clonogenic assay, the difference in radiosensitivity between radiation and thermal radiation groups manifested as α difference in the α components. The dose range over which the linear component dominates in a linear-quadratic (LQ) survival relationship depends on the relative values of α and β : the higher the relative value of α , the more linear response at low doses and the less sensitive it is to dose fraction^[55]. In hyperthermia group, the α/β ratio is high, with no detectable influence of the quadratic function over the first two decades of reduction in cell survival, implying that accumulation of sublethal injury plays a negligible role in cell killing by thermal radiosensitization clinically^[56]. From these results, we can deduce that heat inhibits the repair of radiation-induced single-strand breaks and radiation-induced chromosome aberrations. This inability to repair molecular damage translates into the inability to repair both sublethal damage and potentially lethal damage produced by radiation.

In conclusion, when the DNA-PKcs activity was determined using the cell extracts and the peptide phosphorylation assay, DNA-PKcs activity was inactivated by heat treatment at 45.5 °C, and could not restore. Cell survival is not associated with the DNA-PKcs inactivity after heat. DNA-PKcs is not a unique factor affecting DNA DSB repair. This suggests DNA-PKcs does not play a crucial role in the enhancement of cellular radiosensitivity by hyperthermia.

REFERENCES

- 1 **Niu Q**, Tang ZY, Ma ZC, Qin LX, Zhang LH. Serum vascular endothelial growth factor is a potential biomarker of metastatic recurrence after curative resection of hepatocellular carcinoma. *World J Gastroenterol* 2000;**6**:565-568
- 2 **Fan J**, Wu ZQ, Tang ZY, Zhou J, Qiu SJ, Ma ZC, Zhou XD, Ye SL. Multimodality treatment in hepatocellular carcinoma patients with tumor thrombi in portal vein. *World J Gastroenterol* 2001;**7**:28-32
- 3 **Rabe C**, Pilz T, Klostermann C, Berna M, Schild HH, Sauerbruch T, Caselmann WH. Clinical characteristics and outcome of a cohort of 101 patients with hepatocellular carcinoma. *World J Gastroenterol* 2001;**7**:208-215
- 4 **Wu MC**, Shen F. Progress in research of liver surgery in China. *World J Gastroenterol* 2001;**6**:773-776
- 5 **Yip D**, Findlay M, Boyer M, Tattersall MH. Hepatocellular carcinoma in central Sydney: a 10-year review of patients seen in a medical oncology department. *World J Gastroenterol* 1999;**5**:483-487
- 6 **Lu MD**, Chen JW, Xie XY, Liang LJ, Huang JF. Portal vein embolization by fine needle ethanol injection: experimental and clinical studies. *World J Gastroenterol* 1999;**5**:506-510
- 7 **Jiang YF**, Yang ZH, Hu JQ. Recurrence or metastasis of HCC: predictors, early detection and experimental antiangiogenic therapy. *World J Gastroenterol* 2000;**6**:61-65
- 8 **Wu ZQ**, Fan J, Qiu SJ, Zhou J, Tang ZY. The value of post-operative hepatic regional chemotherapy in prevention of recurrence after radical resection of primary liver cancer. *World J Gastroenterol* 2000;**6**:131-133
- 9 **Sithinamsuwan P**, Piratvisuth T, Tanomkiat W, Apakupakul N, Tongyoo S. Review of 336 patients with hepatocellular carcinoma at Songklanagarind hospital. *World J Gastroenterol* 2000;**6**:339-343
- 10 **Tang ZY**, Sun FX, Tian J, Ye SL, Liu YK, Liu KD, Xue Q, Chen J, Xia JL, Qin LX, Sun HC, Wang L, Zhou J, Li Y, Ma ZC, Zhou XD, Wu ZQ, Lin ZY, Yang BH. Metastatic human hepatocellular carcinoma models in nude mice and cell line with metastatic potential. *World J Gastroenterol* 2001;**7**:597-601
- 11 **Bramhall SR**, Minford E, Gunson B, Buckels JAC. Liver transplantation in the UK. *World J Gastroenterol* 2001;**7**:602-611
- 12 **Li Y**, Tang ZY, Ye SL, Liu YK, Chen J, Xue Q, Chen J, Gao DM, Bao WH. Establishment of cell clones with different metastatic potential from the metastatic hepatocellular carcinoma cell line MHCC97. *World J Gastroenterol* 2001;**7**:630-636
- 13 **Tang ZY**. Hepatocellular carcinoma-cause, treatment and metastasis. *World J Gastroenterol* 2001;**7**:445-454
- 14 **Wang JH**, Lin G, Yan ZP, Wang XL, Cheng JM, Li MQ. Stage II surgical resection of hepatocellular carcinoma after TAE: a report of 38 cases. *World J Gastroenterol* 1998;**4**:133-136
- 15 **Li L**, Wu PH, Li JQ, Zhang WZ, Lin HG, Zhang YQ. Segmental transcatheter arterial embolization for primary hepatocellular carcinoma. *World J Gastroenterol* 1998;**4**:511-512
- 16 **Zheng N**, Ye SL, Sun RX, Zhao Y, Tang ZY. Effects of cryopreservation and phenylacetate on biological characters of adherent LAK cells from patients with hepatocellular carcinoma. *World J Gastroenterol* 2002;**8**:233-236
- 17 **Qin LX**, Tang ZY, Ma ZC, Wu ZQ, Zhou XD, Ye QH, Ji Y, Huang LW, Jia HL, Sun HC, Wang L. P53 immunohistochemical scoring: an independent prognostic marker for patients after hepatocellular carcinoma resection. *World J Gastroenterol* 2002;**8**:459-463
- 18 **Qin LX**, Tang ZY. The prognostic molecular markers in hepatocellular carcinoma. *World J Gastroenterol* 2002;**8**:385-392
- 19 **Zhang G**, Long M, Wu ZZ, Yu WQ. Mechanical properties of hepatocellular carcinoma cells. *World J Gastroenterol* 2002;**8**:243-246
- 20 **Zhao WH**, Ma ZM, Zhou XR, Feng YZ, Fang BS. Prediction of recurrence and prognosis in patients with hepatocellular carcinoma after resection by use of CLIP score. *World J Gastroenterol* 2002;**8**:237-242
- 21 **Zeng ZC**, Tang ZY, Wu ZQ, Ma ZC, Fan J, Qin LX, Zhou J, Wang JH, Wang BL, Zhong CS. Phase I clinical trial of oral furtulon and combined hepatic arterial chemoembolization and radiotherapy in unresectable primary liver cancers, including clinicopathologic study. *Am J Clin Oncol* 2000;**23**:449-454

- 22 **Zeng ZC**, Tang ZY, Liu KD, Lu JZ, Xie H, Yao Z. Improved long-term survival for unresectable hepatocellular carcinoma (HCC) with a combination of surgery and intrahepatic arterial infusion of ¹³¹I-anti-HCC mAb. Phase I/II clinical trials. *J Cancer Res Clin Oncol* 1998;**124**:275-80
- 23 **Zeng ZC**, Tang ZY, Liu KD, Yu YQ, Yang BH, Cai XJ, Xie H, Cao SL. Observation of changes in peripheral T-lymphocyte subsets by flow cytometry in patients with liver cancer treated with radioimmunotherapy. *Nucl Med Commun* 1995;**16**:378-385
- 24 **Liu H**, Wang Y, Zhou Q, Gui SY, Li X. The point mutation of p53 gene exon7 in hepatocellular carcinoma from Anhui Province, a non HCC prevalent area in China. *World J Gastroenterol* 2002;**8**:480-482
- 25 **Zeng ZC**, Tang ZY, Liu KD, Lu JZ, Cai XJ, Xie H. Human anti-(murine Ig) antibody responses in patients with hepatocellular carcinoma receiving intrahepatic arterial ¹³¹I-labeled Hepama-1 mAb. Preliminary results and discussion. *Cancer Immunol Immunother* 1994;**39**:332-336
- 26 **Zeng ZC**, Tang ZY, Xie H, Liu KD, Lu JZ, Chai XJ, Wang GF, Yao Z, Qian JM. Radioimmunotherapy for unresectable hepatocellular carcinoma using ¹³¹I-Hepama-1 mAb: preliminary results. *J Cancer Res Clin Oncol* 1993;**119**:257-259
- 27 **Liu LX**, Jiang HC, Piao DX. Radiofrequency ablation of liver cancers. *World J Gastroenterol* 2002;**8**:393-399
- 28 **Seong J**, Keum KC, Han KH, Lee DY, Lee JT, Chon CY, Moon YM, Suh CO, Kim GE. Combined transcatheter arterial chemoembolization and local radiotherapy of unresectable hepatocellular carcinoma. *Int J Radiation Oncol Biol Phys* 1999;**43**:393-397
- 29 **Tang ZY**, Yu YQ, Zhou XD, Ma ZC, Yang BH, Lin ZY, Lu JZ, Liu KD, Fan Z, Zeng ZC. Treatment of unresectable primary liver cancer: with reference to cytoreduction and sequential resection. *World J Surg* 1995;**19**:47-52
- 30 **Nagata Y**, Hiraoka M, Nishimura Y, Masunaga S, Mitumori M, Okuno Y, Fujishiro M, Kanamori S, Horii N, Akuta K, SaSai K, Abe M, Fukuda Y. Clinical results of radiofrequency hyperthermia for malignant liver tumor. *Int J Radiat Oncol Biol Phys* 1997;**38**:359-365
- 31 **Seong J**, Lee HS, Han KH, Chon CY, Suh Co, Kim GE. Combined treatment of radiotherapy and hyperthermia for unresectable hepatocellular carcinoma. *Yonsei Med J* 1994;**35**:252-259
- 32 **Sneed PK**, Stauffer PR, McDermott MW, Diederich CJ, Lamborn KR, Prados MD, Chang S, Weaver KA, Spry L, Malec M, Lamb SA, Voss B, Davis RL, Wara WM, Larson DA, Phillips TL, Gutin PH. Survival benefit of hyperthermia in a prospective randomized trial of brachytherapy boost ? hyperthermia for glioblastoma multiforme. *Int J Radiat Oncol Biol Phys* 1998;**40**:287-295
- 33 **Hall EJ**. Hyperthermia. In: Hall EJ., eds. Radiobiology for the radiologist. Philadelphia: J B Lippincott 1994: 278-281
- 34 **Iliakis G**, Seamer R. A DNA double-strand break repair-deficient mutant of CHO cells shows reduced radiosensitization after exposure to hyperthermic temperatures in the plateau phase of growth. *Int J Hyperthermia* 1990;**6**:801-812
- 35 **El-Awady RA**, Dikomey E, Dahm-Daphi J. Heat effects on DNA repair after ionising radiation: Hyperthermia commonly increases the number of non-repaired double-strand breaks and structural rearrangements. *Nucleic Acids* 2001;**29**:1960-1966
- 36 **Kampinga HH**, Dikomey E. Hyperthermic radiosensitization: mode of action and clinical relevance. *Int J Radiat Biol* 2001;**77**:399-408
- 37 **Raaphorst GP**. Recovery of sublethal radiation damage and its inhibition by hyperthermia in normal and transformed mouse cells. *Int J Radiat Oncol Biol Phys* 1992;**22**:1035-1041
- 38 **Raaphorst GP**, Feeley MM. Hyperthermia radiosensitization in human glioma cells comparison of recovery of polymerase activity, survival, and potentially lethal damage repair. *Int J Radiat Oncol Biol Phys* 1994;**29**:133-139
- 39 **Smith GCM**, Jackson SP. The DNA-dependent protein kinase. *Genes Devel* 1999;**13**:916-934
- 40 **Matsumoto Y**, Suzuki N, Sakai K, Morimatsu A, Hirano K, Murofushi H. A possible mechanism for hyperthermic radiosensitization mediated through hyperthermic lability of Ku subunits in DNA-dependent protein kinase. *Biochem Biophys Res Commun* 1997;**234**:568-572
- 41 **Iliakis G**, Metzger L, Denko N, Stamato TD. Detection of DNA double strand breaks in synchronous cultures of CHO cells by means of asymmetric field inversion gel electrophoresis. *Int J Radiat Biol* 1991;**59**:321-341
- 42 **Metzger L**, Iliakis G. Kinetics of DNA double strand breaks throughout the cell cycle as assayed by pulsed field gel electrophoresis in CHO cells. *Int J Radiat Biol* 1991;**59**:1325-1339
- 43 **Ihara M**, Suwa A, Komatsu K, Shimasaki T, Okaichi K, Hendrickson EA, Okumura Y. Heat sensitivity of double-stranded DNA-dependent protein kinase activity. *Int J Radiat Biol* 1999;**75**:253-258
- 44 **Woudstra EC**, Konings A.WT, Jeggo PA, Kampinga HH. Role of DNA-PKcs subunits in radiosensitization by hyperthermia. *Radiat Res* 1999;**152**:214-218
- 45 **Gottlieb TM**, Jackson SP. The DNA-dependent protein kinase: Requirement of DNA ends and association with Ku antigen. *Cell* 1993;**72**:131-142
- 46 **Wang H**, Zeng ZC, Bui TA, Sonoda E, Takata M, Takeda S, Iliakis G. Efficient rejoining of radiation-induced DNA double-strand breaks in vertebrate cells deficient in genes of the RAD52 epistasis group. *Oncogene* 2001;**20**:2212-2224
- 47 **Wang H**, Zeng ZC, Perrault AR, Cheng X, Qin W, Iliakis G. Genetic evidence for the involvement of DNA ligase IV in the DNA-PK-dependent pathway of non-homologous end joining in mammalian cells. *Nucleic Acids Res* 2001;**29**:1653-1660
- 48 **Hu B**, Zhou XY, Wang X, Zeng ZC, Iliakis G, Wang Y. The radioresistance to killing of A1-5 cells derives from activation of the Chk1 pathway. *J Biol Chem* 2001;**276**:17693-17698
- 49 **Wang H**, Zeng ZC, Bui TA, DiBiase SJ, Qin W, Xia F, Powell SN, Iliakis G. Nonhomologous end-joining of ionizing radiation-induced DNA double-stranded breaks in human tumor cells deficient in BRCA1 or BRCA2. *Cancer Res* 2001;**61**:270-277
- 50 **Asaad NA**, Zeng ZC, Guan J, Thacker J, Iliakis G. Homologous recombination as a potential target for caffeine radiosensitization in mammalian cells: reduced caffeine radiosensitization in XRCC2 and XRCC3 mutants. *Oncogene* 2000;**19**:5788-5800
- 51 **DiBiase SJ**, Zeng ZC, Chen R, Hyslop T, Curran WJ Jr, Iliakis G. DNA-dependent protein kinase stimulates an independently active, nonhomologous, end-joining apparatus. *Cancer Res* 2000;**60**:1245-1253
- 52 **Wymann MP**, Bulgarelli-Leva G, Zvelebil MJ, Pirola L, Vanhaesebroeck B, Waterfield MD, and Panayotou G. Wortmannin inactivates phosphoinositide 3-kinase by covalent modification of Lys-802, a residue involved in the phosphate transfer reaction. *Molec Cell Biol* 1996;**16**:1722-1733
- 53 **Roth DB**, Wilson JH. Relative rates of homologous and nonhomologous recombination in transfected DNA. *Proc Natl Acad Sci USA* 1985;**82**:3355-3359
- 54 **Suzuki K**, Kodama S, Watanabe M. Recruitment of ATM protein to double strand DNA irradiated with ionizing radiation. *J Biol Chem* 1999;**274**:25571-25575
- 55 **Withers HR**, McBride WH. Biologic basis of radiation therapy. In: Perez C, Brady L.W., eds: Principles & Practice of Radiation Oncology. Philadelphia, Lippincott-Raven 1998:91
- 56 **Hall EJ**. Hyperthermia. In: Hall EJ., eds. Radiobiology for the radiologist. Philadelphia: J B Lippincott 1994:271-272

Edited by Ma JY

• LIVER CANCER •

Association of hTcf-4 gene expression and mutation with clinicopathological characteristics of hepatocellular carcinoma

Ying Jiang, Xin-Da Zhou, Yin-Kun Liu, Xin Wu, Xiao-Wu Huang

Ying Jiang, Xin-Da Zhou, Yin-Kun Liu, Xin Wu, Xiao-Wu Huang, Liver Cancer Institute, Zhong Shan Hospital, Fudan University, Shanghai 200032, China

Supported by National Natural Science Foundation of China, No. 30070743

Correspondence to: Dr. Xin-Da Zhou, Liver Cancer Institute, Zhong Shan Hospital, Fudan University, 136 Yi Xue Yuan Road, Shanghai 200032, China. czjy@yahoo.com

Telephone: +86-21-64041990-2736 **Fax:** +86-21-64037181

Received 2002-02-13 **Accepted** 2002-05-26

Abstract

AIM: Hepatocellular carcinoma(HCC) is a significant health problem in China. But the molecular mechanisms of HCC remains unclear. APC/ β -Catenin/Tcf signaling pathway, also known as Wnt pathway, plays a critical role in the development and oncogenesis. As little is known about the alteration of human T-cell transcription factor-4 (hTcf-4) gene in HCC, it is of interest to study the expression and mutation of hTcf-4 gene in HCC and the relationship between hTcf-4 gene and progression of HCC.

METHODS: Reverse transcription-polymerase chain reaction (RT-PCR) method was used to detect the expression of hTcf-4 mRNA in 32 HCC and para-cancerous tissues and 5 normal liver tissues. PCR-single strand conformation polymorphism (PCR-SSCP) method was used to detect the mutation of hTcf-4 exons 1, 4, 9 and 15 in HCC. The correlation of expression and mutation of the hTcf-4 gene with clinicopathological characteristics of HCC was also analyzed.

RESULTS: RT-PCR showed that the expression rate of hTcf-4 mRNA in HCC, para-cancerous tissues and normal liver tissues was 90.6 %, 71.9 % and 80 %, respectively. The gene expression level in tumor was 0.71 ± 0.13 , much higher than that in para-cancerous liver 0.29 ± 0.05 and normal liver 0.26 ± 0.05 ($P < 0.001$), although there was no significant difference in gene expression level between para-cancerous tissues and normal liver ($P > 0.05$). Furthermore, hTcf-4 gene expression was closely associated with tumor capsule status and intrahepatic metastasis of HCC. On SSCP, 2 of 32 cases of HCC (6.25 %) displayed characteristic mutational mobility shifts in exon 15 of the hTcf-4 gene. No abnormal shifting bands were observed in para-cancerous tissues.

CONCLUSION: The high expression level of hTcf-4 in HCC, especially in tumors with metastasis, suggests that the over-expression of hTcf-4 gene may be closely associated with development and progression of HCC, but the mutation of this gene seemed to play less important role in this respect.

Jiang Y, Zhou XD, Liu YK, Wu X, Huang XW. Association of hTcf-4 gene expression and mutation with clinicopathological characteristics of hepatocellular carcinoma. *World J Gastroenterol* 2002;8(5):804-807

INTRODUCTION

Recent work has shown that APC/ β -Catenin/Tcf pathway, also known as Wnt signaling pathway, plays a key role in regulation of development and growth of the cells^[1-3]. The alteration of APC/ β -Catenin/Tcf pathway leading to cancer has been described. In differentiated cells, the cytoplasmic level of β -catenin is maintained very low through degradation by the ubiquitin-proteasome pathway, whereby serine and threonine residues in exon 3 are phosphorylated by GSK3 β ^[4-6] and ubiquitinated by binding to proteins such as APC, axin and conductin^[7-11]. In experiments with colorectal cancer and melanoma cell lines, dysfunction of APC resulted in stabilization of β -catenin and binding of excess β -catenin to Tcf/Lef to activate transcription in the nucleus^[12-16]. Furthermore, in cell lines having no APC mutations, mutations of the β -catenin gene that altered amino acid residues representing potential GSK3 β phosphorylation sites could confer resistance to degradation and lead to intracellular accumulation of β -catenin^[12,17,18]. Activated cytoplasmic β -catenin, probably bound to Tcf/Lef, is thought to migrate into the nucleus and stimulate transcription of downstream genes in a constitutive manner^[12,13]. However, recent studies focused mainly on the relationship between cancers and mutations of APC and β -catenin gene, and little is known about the change of human T-cell transcription factor-4 (hTcf-4) gene in tumors, especially about its expression and mutation in hepatocellular carcinoma (HCC). To further understanding the role of the APC/ β -Catenin/Tcf pathway in HCC, the present study examined expression and mutation of the hTcf-4 gene in HCC by reverse transcription-polymerase chain reaction (RT-PCR) and PCR-single strand conformation polymorphism (PCR-SSCP).

MATERIALS AND METHODS

Patients

Thirty-two fresh HCC specimens and the para-cancerous tissues and 5 normal liver tissues were analyzed. All specimens were obtained from patients who underwent surgery for HCC or hemangioma between 1999 and 2000 at Liver Cancer Institute, Fudan University, and stored frozen at -70 °C until use. The diagnosis was confirmed by pathological examination. The patients with HCC consisted of 12 women and 20 men with the mean age of 56 years and range from 16 to 75 years. Of the 32 patients, 16 showed abnormal serum concentration of alpha-fetoprotein (AFP) ($>20 \mu\text{g/L}$), 18 had macronodular cirrhosis (cirrhotic nodules measured at least 0.3 cm in greatest dimension) and 14 had micronodular cirrhosis (cirrhotic nodules measured $<0.3 \text{ cm}$). HCC was large in 17 patients ($>5 \text{ cm}$ in greatest dimension) and small in 15 patients ($\leq 5 \text{ cm}$). Macroscopically poorly encapsulated tumors were found in 18 patients (56 %) and cancerous thrombi in portal vein or intrahepatic metastasis were found in 15 patients (47 %).

RNA Extraction and RT-PCR

Total RNA was isolated from tissues using Trizol Reagent (Life

Technologies, Inc.) according to the manufacturer's protocol. A 3- μ g aliquot of total RNA from each specimens was reverse-transcribed into single-strand cDNA using oligo (dT)₁₅ primer and Superscript II (Life Technologies, Inc.). Each single-strand cDNA was diluted for subsequent PCR amplification of hTcf-4 and β -actin with the latter used as an internal quantitative control. The PCR was carried out in a reaction volume of 25 μ l for 5 min at 95 °C for initial denaturing, followed by 25 (for β -actin) or 30 (for hTcf-4) cycles of 94 °C for 40 s, 60 °C for 40 s, and 72 °C for 40 s on the Gene Amp PCR system 9 600 (Perkin-Elmer Corp.). The primer sequences used for amplification were 5'-CTTCCTTCCTGGGCATGGAG-3' and 5'-TGGAGGGGCGGA CTCGTCA-3' for β -actin and 5'-TGTACCCAATCACGACAGGA-3' and 5'-GCCAGCTCGTAGTATTTTCGC -3' for hTcf-4. PCR products were resolved in 2 % agarose gels and visualized by staining with ethidium bromide. To quantify PCR products, the bands representing amplified products were analyzed by Pharmacia Biotect Image MASTER VDS.

PCR-SSCP-silver staining

DNA was isolated from tissues using a DNA extraction kit (BBST Corporation) according to the manufacturer's protocol. The primers of PCR amplification of exons 1, 4, 9 and 15 of hTcf-4 were as follows: 5'-AATTGCTGCTGGTGGGTGA-3' and 5'-CCCGAGGGGCTTTT CCTA-3' for exon 1 (234bp); 5'-GAACGCTTTGATTTGGTTTC-3' and 5'-GCTTCAGAATCTCTTGCCT-3' for exon 4 (124bp); 5'-GATTCTGACGATTTACACAG-3' and 5'-GCTACGAAGAAGGTGAGAA-3' for exon 9 (196bp) and 5'-CGACCCACCATTTGTGTTGTA-3' and 5'-AAAGGCCTCGCAGTGGAAT-3' for exon 15 (144bp). The PCR reaction was performed by denaturation at 94 °C for 40s, annealing at 60 °C for 40s and extension at 72 °C for 40s for 30 cycles using 2.5 units of Taq DNA polymerase (BBST Corporation) per 25 μ l reaction volume. The PCR products were detected on 2 % agarose gels. SSCP analysis was performed as follows: 15 μ l of PCR sample plus 20 μ l of formamide loading dye (95 % formamide, 0.05 % bromophenol blue, 10 mmol/L EDTA) were boiled for 10 min, snap-frozen on ice and electrophoresed on a 12 % non-denaturing polyacrylamide gel at 300 V for 5 min, then 120 V for 3-4 h, depending on the size of PCR fragment. Silver Staining for SSCP consisted of fixation in 10 % alcohol for 5 min, sensitizing in 1 % HNO₃ for 5 min, washing twice with distilled water for 2 min, silver reaction (silver nitrate 0.25 g, formaldehyde 50 μ l, topped up with distilled water to 100 ml) for 10 min, washing with distilled water for 10s, developing (anhydrous sodium carbonate 6.0 g, formaldehyde 200 μ l, 10 % sodium thiosulfate 20 μ l, topped up with distilled water to 200 ml) for 10 min, stopping in 10 % glacial acetic acid for 10 min and anhydration in absolute alcohol for 2 min.

Statistical analysis

The statistical differences between different groups were analyzed by Student t-test or One-Way ANOVA. A value of $P < 0.05$ was considered significant. All data were disposed by SPSS9.0 statistical software.

RESULTS

Expression of hTcf-4 mRNA in HCC specimens, para-cancerous tissues and normal liver tissues

2 % Agarose gel electrophoresis showed a 406bp hTcf-4 fragment by RT-PCR amplification from normal liver tissues,

para-cancerous tissues and HCC tissues. The hTcf-4 mRNA amplification was successful in 29 of 32 HCC tissues (90.6 %), 23 of 32 para-cancerous liver tissues (71.9 %) and 4 of 5 normal liver tissues (80 %). The expression level was 0.71 ± 0.13 in tumor, much higher than that in para-cancerous liver (0.29 ± 0.05 , $P < 0.001$) and normal liver (0.26 ± 0.05 , $P < 0.001$) (Figure1). However, there was no significant difference in hTcf-4 expression level between para-cancerous tissues and normal liver tissues ($P > 0.05$).

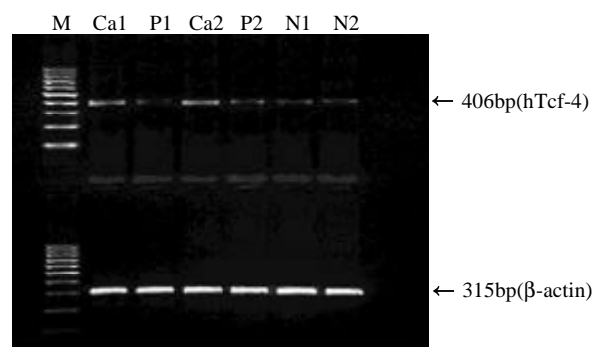


Figure1 Expression of hTcf-4 and β -actin mRNA in HCC (Ca), para-cancerous tissue (P) and normal liver (N). Semiquantitative RT-PCR analysis revealed that the expression level of hTcf-4 gene in HCC was much higher than that in para-cancerous tissues and normal livers. M: 100bp DNA Ladder

The relationship between hTcf-4 mRNA expression and clinicopathological features of the patients

Statistical analysis showed that the expression level of hTcf-4 mRNA in poorly encapsulated tumors and in tumors with intrahepatic metastasis was much higher than that in well encapsulated tumors and in tumors without metastasis ($P < 0.05$). However, no significant difference in hTcf-4 mRNA level was observed with variants of serum AFP levels, liver cirrhosis degree and tumor size (Table 1).

Table1 The relationship between hTcf-4 mRNA expression and clinicopathological features of the patients

	<i>n</i>	hTcf-4/ β -actin	<i>P</i>
AFP			
$\leq 20 \mu\text{g/L}$	16	0.71 ± 0.14	>0.05
$> 20 \mu\text{g/L}$	16	0.67 ± 0.12	
Cirrhotic nodules			
$< 0.3\text{cm}$	14	0.75 ± 0.11	>0.05
$\geq 0.3\text{cm}$	18	0.67 ± 0.14	
Tumor size			
$\leq 5\text{cm}$	15	0.66 ± 0.13	>0.05
$> 5\text{cm}$	17	0.76 ± 0.12	
Capsule			
well capsule	14	0.61 ± 0.10	<0.05
poor capsule	18	0.79 ± 0.10	
Metastasis			
Yes	15	0.78 ± 0.12	<0.05
No	17	0.66 ± 0.12	

N: number; Yes: tumors with cancerous thrombi in portal vein or intrahepatic metastasis; No: tumors without cancerous thrombi in portal vein and intrahepatic metastasis.

Detection of mutation by PCR-SSCP-silver staining

Abnormal SSCP migration bands were detected in exon 15 of the hTcf-4 gene from 2 of 32 tumor tissues (6.25 %), compared with the mobility pattern of the para-cancerous liver, demonstrating that there existed mutation in the exon 15. Among these two cases, one was complicated by portal vein thrombosis and the other had tumor without metastasis. The mobility pattern of PCR products from exons 1, 4, and 9 of the hTcf-4 gene was not altered (Figure 2).

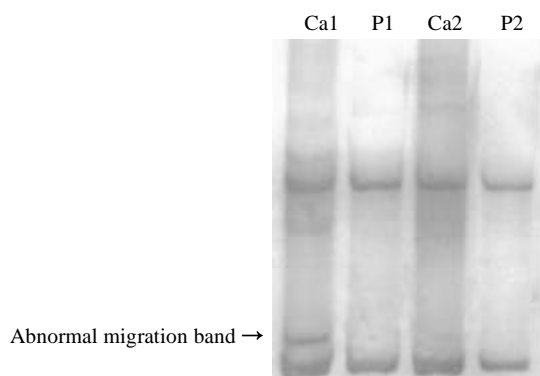


Figure 2 SSCP analysis of hTcf-4 exon 15 in HCC (Ca) and para-cancerous liver (P). Lane 1, abnormal SSCP pattern detected in exon 15 of patient 1, compared with the pattern of exon 15 from the corresponding para-cancerous liver in lane 2. Lane 3, normal SSCP pattern of exon 15 from patient 2, compared with the pattern of exon 15 from the corresponding para-cancerous liver in lane 4.

DISCUSSION

The Tcf-4 gene is a member of the APC/ β -Catenin/Tcf pathway that is well known to play a crucial role in many developmental processes and human carcinogenesis^[19-27]. Mapping to chromosome band 10q25.3^[28], Tcf-4 encodes a transcription factor that interacts functionally with β -catenin to transactivate target genes^[29-31]. Morin has recently shown that the nuclei of colon carcinoma cell lines contain constitutively active Tcf-4/ β -catenin complexes as a direct consequence of either loss of function of the tumor suppressor protein APC or gain of function by mutations in β -catenin itself^[12]. This is believed to result in the uncontrolled transcription of Tcf target genes, leading to transformation of colon epithelial cells and initiation of polyp formation. High level of hTcf-4 expression has been identified in colon cancer, mammary carcinoma and a variety of colorectal cancer cells^[21,29]. Tcf factors have also been reported as tumor inducers which aberrantly activate their target genes, now known as the *c-myc* gene and cyclin D1 gene, in many types of cancer^[30-32]. It has been reported that *c-myc* gene and cyclin D1 gene had a high expression level in HCC and were implicated in tumor progression and metastasis with the unclear mechanism^[33-39]. Therefore, it is important to elucidate the internal link between APC/ β -Catenin/Tcf pathway and liver cancer. Our present studies showed that the level of hTcf-4 expression in cancer tissues was much higher than that in para-cancerous tissues and normal liver tissues ($P < 0.001$). Moreover, we found that hTcf-4 gene expression was closely correlated with the integrity of tumor capsule and intrahepatic metastasis of HCC but not with serum AFP levels, liver cirrhosis degree and tumor size, suggesting that hTcf-4 expression was associated with invasion and metastasis of

HCC. This may be due to interaction between Tcf and E-cadherin. Huber *et al.* reported that the complex of Tcf and δ -catenin in the nucleus binds to the E-cadherin gene promoter and down-regulates E-cadherin gene transcription^[40]. On the other hand, loss of E-cadherin expression can contribute to the up-regulation of Tcf- β -Catenin pathway in human cancers^[41]. As a result, the role of E-cadherin in cell-cell adhesion is reduced, which may contribute to the metastatic potential of tumor cells.

With regard to the relationship between Tcf-4 mutations and tumor, Duval *et al.*^[42] reported that 50 % of human MSI-H (high frequency microsatellite instability) colorectal cell lines and 39 % of MSI-H colorectal primary tumors were found to have a 1-bp deletion in an (A)₉ repeat within the coding region of this gene. The (A)₉ repeat normally codes for several isoforms that could serve as modulators of Tcf-4 transcriptional activity. The deletion of one nucleotide in this repeat could change Tcf-4 transactivating properties by modifying the respective proportions of the different isoforms. In addition, one frameshift mutation in the β -Catenin binding domain (exon 1), one missense mutation in exon 4 and six nonsense or frameshift mutations localized in the 3' part of the gene were detected in a series of 24 colorectal cancer cell lines^[43]. The latter alterations interfered with the Tcf-4 capacity to interact with COOH-terminal binding protein that was implicated in the repression of the Tcf family transcriptional activity. As a result, the Tcf-4 transcriptional activity was enhanced. This indicated that the mutation of Tcf could be an important event during colorectal carcinogenesis by modifying Wnt signaling. In our experiment, we used PCR-SSCP-silver staining analysis to detect mutation of hTcf-4 exons 1, 4, 9 and 15 from human liver cancer tissues. The sensitivity of this method is generally high and greater than 80 % of mutations in most DNA fragments of 300 bp or shorter can be detected since variation of DNA sequence often results in a shift in electrophoretic mobility, which is believed to be caused by sequence-dependent alteration in the tertiary structure of single-stranded DNA. We found SSCP variants in exon 15 of 2 HCC cases (6.25%) only, of which one was complicated by portal vein thrombosis and the other originated from the tumor tissue without metastasis. It seemed that, unlike in colorectal tumor, hTcf-4 mutation may play less important role in HCC and was irrelevant to invasion and metastasis of HCC. Therefore, the enhanced transcriptional activity of hTcf-4 due to aberrant mRNA expression may be the key to HCC occurrence and development. Further study on structure and function of hTcf-4 and its interaction with oncogenes should contribute to clarification of the mechanism of liver carcinogenesis and may provide the theoretical principle for the gene therapy.

REFERENCES

- 1 Smalley MJ, Dale TC. Wnt signalling in mammalian development and cancer. *Cancer Metastasis Rev* 1999;18:215-230
- 2 Li B, Mackay DR, Dai Q, Li TWH, Nair M, Fallahi M, Schonbaum CP, Fantes J, Mahowald AP, Waterman ML, Fuchs E, Dai X. The LEF1/ β -catenin complex activates *mov1*, a mouse homolog of *Drosophila* *ovo* required for epidermal appendage differentiation. *Proc Natl Acad Sci USA* 2002; 99:6064-6069
- 3 Barker N, Morin PJ, Clevers H. The yin-yang of TCF/ β -Catenin signaling. *Adv Cancer Res* 2000; 77:1-24
- 4 Rubinfeld B, Albert I, Porfiri E, Fiol C, Munemitsu S, Polakis P. Binding of GSK3 β to the APC- β -catenin complex and regulation of complex assembly. *Science* 1996; 272:1023-1026

- 5 **Willert K**, Shibamoto S, Nusse R. Wnt-induced dephosphorylation of axin releases β -catenin from the axin complex. *Genes Dev* 1999;**13**:1768-1773
- 6 **van Noort M**, Meeldijk J, van der Zee R, Destree O, Clevers H. Wnt signaling controls the phosphorylation status of β -catenin. *J Biol Chem* 2002;**277**:17901-17905
- 7 **Hinoi T**, Yamamoto H, Kishida M, Takada S, Kishida S, Kikuchi A. Complex formation of adenomatous polyposis coli gene product and axin facilitates glycogen synthase kinase-3 β -dependent phosphorylation of β -catenin and down-regulates β -catenin. *J Biol Chem* 2000;**275**:34399-34406
- 8 **Rubinfeld B**, Albert I, Porfiri E, Munemitsu S, Polakis P. Loss of β -catenin regulation by the APC tumor suppressor protein correlates with loss of structure due to common somatic mutations of the gene. *Cancer Res* 1997;**57**:4624-4630
- 9 **Hamada F**, Tomoyasu Y, Takatsu Y, Nakamura M, Nagai S, Suzuki A, Fujita F, Shibuya H, Toyoshima K, Ueno N, Akiyama T. Negative regulation of Wingless signaling by D-axin, a Drosophila homolog of axin. *Science* 1999;**283**:1739-1742
- 10 **Sakanaka C**, Weiss JB, Williams LT. Bridging of β -catenin and glycogen synthase kinase-3 β by axin and inhibition of β -catenin-mediated transcription. *Proc Natl Acad Sci USA* 1998;**95**:3020-3023
- 11 **Behrens J**, Jerchow BA, Wurtele M, Grimm J, Asbrand C, Wirtz R, Kuhl M, Wedlich D, Birchmeier W. Functional interaction of an axin homolog, conductin, with β -catenin, APC, and GSK3 β . *Science* 1998;**280**:596-599
- 12 **Morin PJ**, Sparks AB, Korinek V, Barker N, Clevers H, Vogelstein B, Kinzler KW. Activation of β -catenin-Tcf signaling in colon cancer by mutations in β -catenin or APC. *Science* 1997;**275**:1787-1790
- 13 **Behrens J**, Kries JP, Kühl M, Bruhn L, Wedlich D, Grosschedl R, Birchmeier W. Functional interaction of β -catenin with the transcription factor LEF-1. *Nature* 1996;**382**:638-642
- 14 **Rimm DL**, Caca K, Hu G, Harrison FB, Fearon ER. Frequent nuclear/cytoplasmic localization of β -catenin without exon 3 mutations in malignant melanoma. *Am J Pathol* 1999;**154**:325-329
- 15 **Murakami T**, Toda S, Fujimoto M, Ohtsuki M, Byers HR, Etoh T, Nakagawa H. Constitutive activation of Wnt/ β -catenin signaling pathway in migration-active melanoma cells: role of LEF-1 in melanoma with increased metastatic potential. *Biochem Biophys Res Commun* 2001;**288**:8-15
- 16 **Kobayashi M**, Honma T, Matsuda Y, Suzuki Y, Narisawa R, Ajioka Y, Asakura H. Nuclear translocation of β -catenin in colorectal cancer. *Br J Cancer* 2000;**82**:1689-1693
- 17 **Iwao K**, Nakamori S, Kameyama M, Imaoka S, Kinoshita M, Fukui T, Ishiguro S, Nakamura Y, Miyoshi Y. Activation of the β -catenin gene by interstitial deletions involving exon 3 in primary colorectal carcinomas without adenomatous polyposis coli mutations. *Cancer Res* 1998;**58**:1021-1026
- 18 **Sparks AB**, Morin PJ, Vogelstein B, Kinzler KW. Mutational analysis of the APC/ β -catenin/Tcf pathway in colorectal cancer. *Cancer Res* 1998;**58**:1130-1134
- 19 **Lee YJ**, Swencki B, Shoichet S, Shivdasani RA. A possible role for the high mobility group box transcription factor Tcf-4 in vertebrate gut epithelial cell differentiation. *J Biol Chem* 1999;**274**:1566-1572
- 20 **Cho EA**, Dressler GR. TCF-4 binds β -catenin and is expressed in distinct regions of the embryonic brain and limbs. *Mech Dev* 1998;**77**:9-18
- 21 **Barker N**, Huls G, Korinek V, Clevers H. Restricted high level expression of Tcf-4 protein in intestinal and mammary gland epithelium. *Am J Pathol* 1999;**154**:29-35
- 22 **El-Tanani M**, Barraclough R, Wilkinson MC, Rudland PS. Metastasis-inducing DNA regulates the expression of the osteopontin gene by binding the transcription factor Tcf-4. *Cancer Res* 2001;**61**:5619-5629
- 23 **Nilbert M**, Rambech E. β -catenin activation through mutation is rare in rectal cancer. *Cancer Genet Cytogenet* 2001;**128**:43-45
- 24 **El-Tanani M**, Barraclough R, Wilkinson MC, Rudland PS. Regulatory region of metastasis-inducing DNA is the binding site for T cell factor-4. *Oncogene* 2001;**20**:1793-1797
- 25 **Duval A**, Iacopetta B, Ranzani GN, Lothe RA, Thomas G, Hamelin R. Variable mutation frequencies in coding repeats of TCF-4 and other target genes in colon, gastric and endometrial carcinoma showing microsatellite instability. *Oncogene* 1999;**18**:6806-6809
- 26 **Fukushima H**, Yamamoto H, Itoh F, Horiuchi S, Min Y, Iku S, Imai K. Frequent alterations of the β -catenin and TCF-4 genes, but not of the APC gene, in colon cancers with high-frequency microsatellite instability. *J Exp Clin Cancer Res* 2001;**20**:553-559
- 27 **Saeki H**, Tanaka S, Tokunaga E, Kawaguchi H, Ikeda Y, Maehara Y, Sugimachi K. Genetic alterations in the human Tcf-4 gene in Japanese patients with sporadic gastrointestinal cancers with microsatellite instability. *Oncology* 2001;**61**:156-161
- 28 **Duval A**, Busson-Leconiat M, Berger R, Hamelin R. Assignment of the TCF-4 gene (TCF7L2) to human chromosome band 10q25.3. *Cytogenet Cell Genet* 2000;**88**:264-265
- 29 **Korinek V**, Barker N, Morin PJ, van Wichen D, de Weger R, Kinzler KW, Vogelstein B, Clevers H. Constitutive transcriptional activation by a β -Catenin-Tcf complex in APC-/- colon carcinoma. *Science* 1997;**275**:1784-1787
- 30 **He TC**, Sparks AB, Rago C, Hermeking H, Zawel L, da Costa LT, Morin PJ, Vogelstein B, Kinzler KW. Identification of *c-myc* as a target of the APC pathway. *Science* 1998;**281**:1509-1512
- 31 **Shutman M**, Zhurinsky J, Simcha I, Albanese C, D'Amico M, Pestell R, Ben-Ze'ev A. The cyclin D1 gene is a target of the β -catenin/LEF-1 pathway. *Proc Natl Acad Sci USA* 1999;**96**:5522-5527
- 32 **Roose J**, Clevers H. TCF transcription factors: molecular switches in carcinogenesis. *Biochim Biophys Acta* 1999;**874**:M23-37
- 33 **Kawate S**, Fukusato T, Ohwada S, Watanuki A, Morishita Y. Amplification of *c-myc* in hepatocellular carcinoma: correlation with clinicopathologic features, proliferative activity and p53 overexpression. *Oncology* 1999;**57**:157-163
- 34 **De Miglio MR**, Simile MM, Muroli MR, Pusceddu S, Calvisi D, Carru A, Seddaiu MA, Daino L, Deiana L, Pascale RM, Feo F. Correlation of *c-myc* overexpression and amplification with progression of preneoplastic liver lesions to malignancy in the poorly susceptible Wistar rat strain. *Mol Carcinog* 1999;**25**:21-29
- 35 **Qin LX**, Tang ZY. The prognostic molecular markers in hepatocellular carcinoma. *World J Gastroenterol* 2002;**8**:385-392
- 36 **Zhang YJ**, Chen SY, Chen CJ, Santella RM. Polymorphisms in cyclin D1 gene and hepatocellular carcinoma. *Mol Carcinog* 2002;**33**:125-129
- 37 **Deane NG**, Parker MA, Aramandla R, Diehl L, Lee WJ, Washington MK, Nanney LB, Shyr Y, Beauchamp RD. Hepatocellular carcinoma results from chronic cyclin D1 overexpression in transgenic mice. *Cancer Res* 2001;**61**:5389-5395
- 38 **Joo M**, Kang YK, Kim MR, Lee HK, Jang JJ. Cyclin D1 overexpression in hepatocellular carcinoma. *Liver* 2001;**21**:89-95
- 39 **Sato Y**, Itoh F, Hareyama M, Satoh M, Hinoda Y, Seto M, Ueda R, Imai K. Association of cyclin D1 expression with factors correlated with tumor progression in human hepatocellular carcinoma. *J Gastroenterol* 1999;**34**:486-493
- 40 **Huber O**, Bierkamp C, Kemle R. Cadherins and catenins in development. *Curr Opin Cell Biol* 1996;**8**:685-691
- 41 **Gottardi CJ**, Wong E, Gumbiner BM. E-cadherin suppresses cellular transformation by inhibiting β -catenin signaling in an adhesion-independent manner. *J Cell Biol* 2001;**153**:1049-1060
- 42 **Duval A**, Gayet J, Zhou XP, Iacopetta B, Thomas G, Hamelin R. Frequent frameshift mutations of the TCF-4 gene in colorectal cancers with microsatellite instability. *Cancer Res* 1999;**59**:4213-4215
- 43 **Duval A**, Rolland S, Tubacher E, Bui H, Thomas G, Hamelin R. The human T-cell transcription factor-4 gene: structure, extensive characterization of alternative splicings, and mutational analysis in colorectal cancer cell lines. *Cancer Res* 2000;**60**:3872-3879

• LIVER CANCER •

Preparation of monoclonal antibody against apoptosis-associated antigens of hepatoma cells by subtractive immunization

Lian-Jun Yang, Wen-Liang Wang

Lian-Jun Yang, Wen-Liang Wang, Department of Pathology, Institute of Cancer Research, The Fourth Military Medical University (FMMU), Xian 710032, Shaanxi Province, China

Supported by Army Science Foundation, No.98M111

Correspondence to: Wen-liang Wang, Department of Pathology, Institute of Cancer Research, FMMU, Xi'an 710032, Shaanxi province, China. wliwang@fmmu.edu.cn

Telephone: +86-29-3284284 **Fax:** +86-29-3284284

Received 2002-10-21 **Accepted** 2002-04-20

Abstract

AIM: To elucidate the expression of the apoptosis-associated molecules in human primary hepatocellular carcinoma (HCC) cells, and prepare the monoclonal antibodies (mAb) against the apoptosis-associated antigens of HCC cells.

METHODS: Human HCC cell line HCC-9204 cells were induced apoptosis with 60 mL · L⁻¹ ethanol for 6 h and their morphological changes were observed by transmission electron microscope. The cell DNA fragmentations were detected by Terminal Deoxynucleotidyl transferase-mediated dUTP nick end labeling (TUNEL) assay, and the cell DNA contents by flow cytometry. Ten mice were immunized with ethanol-induced apoptotic HCC-9204 cells with the method of subtractive immunization, while the other 10 mice used as the control were immunized by the routine procedures. The tail blood of all the mice were prepared after the last immunization, and the produced antibodies were determined by the immunocytochemical ABC staining. The splenic cells of the mice whose tail blood sera-HCC-9204 cells serum reactions were most different between the apoptotic and the non-apoptotic were prepared and fused with the mouse myeloma cell line SP2/0 cells. The positive antibodies were selected by ELISA assay. The fusion rates of hybridoma cells and the producing rates of antibodies were calculated. The fused cells that secreted candidate objective antibody were cloned continually with the of limited dilution method, and then selected and analyzed further by the immunocytochemical ABC staining. The chromosomes of the cloned hybridoma cells that secreted objective mAb and the mAb immunoglobulin (Ig) subtype of the prepared mAb were also determined. The molecular mass of the mAb associated antigen was analyzed by Western blot assay.

RESULTS: HCC-9204 cells treated with 60 mL · L⁻¹ ethanol for 6 h, manifested obvious apoptotic morphological changes, the majority of the cells were TUNEL-positive, and the sub-G1 apoptotic peak was evident. There were 2 mice in the experimental group whose tail blood serum reacted strongly with the apoptotic HCC-9204 cells, but weakly with their non-apoptotic counterparts. In the fusion rates of hybridoma cells as well as the producing rates of the antibody described above, there did not show significant difference between the experimental and the control group, but weakly with

non-apoptotic HCC-9204. However, the total producing rate of antibodies in the experimental group was significantly lower compared with the control ($P < 0.01$), and so was the producing rate of the antibodies which reacted strongly with both apoptotic and non-apoptotic HCC-9204 cells ($P < 0.01$). After cloned continually for several times the cell that produce mAb which reacted strongly with the nuclei of ethanol-induced apoptotic HCC-9204 cells, but very weakly with that of non-apoptotic cells was selected out. Chromosome analysis revealed that the selected cell was with the universal characteristics of the monoclonal hybridoma cells which secreted mAb, and the Ig subtype of the prepared mAb was IgG1. The molecular mass of this mAb associated antigen of was about 75 ku.

CONCLUSION: Subtractive immunization is a useful method to prepare the mAb against the apoptosis-associated antigens of cells. The expression of some molecules increases to some extent in HCC-9204 cells in the process of apoptosis induced by low-concentration ethanol. The mAb that may be against ethanol-induced apoptosis-associated antigens of HCC cells was successfully prepared and primarily identified.

Yang LJ, Wang WL. Preparation of monoclonal antibody against apoptosis-associated antigens of hepatoma cells by subtractive immunization. *World J Gastroenterol* 2002;8(5):808-814

INTRODUCTION

Apoptosis is a process of active programmed cell death (PCD), which can be regulated by many kinds of biological factors encoded by a lot of mammalian genes^[1-16]. There is not only the increase or decrease of the expression of some already-existed proteins in the process of apoptosis, but also the production and presentation of some new apoptosis-associated molecules that do not express in non-apoptotic cells^[17-20]. Currently, the knowledge about apoptosis-associated molecules is still limited. The conventional process to discover new apoptosis-associated molecules is to clone and sequence the apoptosis-associated genes of cells by the methods such as differentiated PCR and phage display first, and then perform the experiments to study the function of the expressed product of the candidate apoptosis-associated genes^[21-25]. Preparing the antibodies against the associated antigens of apoptotic cells is also a very hopeful way to investigate apoptosis-associated molecules. There are already some reports about the successful preparation of the polyclonal antibodies against apoptosis-associated molecules while their antigens are unclear and even monoclonal antibodies (mAb) at the condition that their associated antigens are specific^[19, 26, 27]. However, there has been no report until now about preparing the mAb against apoptosis-associated antigens at the condition that its associated antigens are still unspecific. In the present study, some mice were immunized by the method of subtractive immunization, and the splenic cells of the effectively immunized mice were fused

with mouse myeloma cells to prepare the mAb against the apoptosis-associated antigens of human primary hepatocellular carcinoma (HCC) cells, so as to elucidate the expression of the apoptosis-associated molecules of HCC cells and investigate the methodology and feasibility to prepare mAb against the apoptosis-associated molecules of cells at the condition that the associated antigens are not clear.

MATERIALS AND METHODS

Cells, animals and main reagents

Human HCC cell line HCC-9204 was established previously by our department. Balb/c mouse myeloma cell line SP2/0 was kindly provided by Mrs. Su-Zhen Zhang, Department of Genetic and Developmental biology of our university. Ten-wk old female Balb/c mice were provided by Experimental Animals Center of our university. Cyclophosphamide (CP), PEG4000, HT (The compound of hypoxanthine and thymidine), HAT (The compound of hypoxanthine, aminopterin and thymidine), 3,3'-diaminobenzidine tetrahydrochloride (DAB), 3-aminopropyltriethoxysilane (APES), propidium iodide (PI), colchicine and Giemsa were the products of Sigma Chemical Co., USA. RNase A was the product of Promega Co., USA. HRP-labeled sheep anti-mouse IgG mAb was the product of Dako Co., USA. Terminal Deoxynucleotidyl transferase-mediated dUTP nick end labeling (TUNEL) kit was the product of Boehringer Mannheim Co., Germany. Immunohistochemical ABC kit was the product of Vector Laboratories Inc., USA. Mouse hybridoma immunoglobulin (Ig) subtyping kit was the product of Roche Molecular Biochemicals, USA.

Apoptosis induction and detection

Apoptosis induction HCC-9204 cells at log phase were cultured with RPMI1640 medium containing 60 mL·L⁻¹ ethanol for 6 h to induce cellular apoptosis, and non-treated HCC-9204 cells was used as control.

Electron microscope observation The cells were fixed in glutaraldehyde, fixed further in osmium tetroxide, dehydrated and embedded in epikote. The sections were ultra thin, stained doubly with uranyl acetate and lead citrate, and observed with transmission electron microscope (JEC Co., Japan).

TUNEL assay^[28] The cells cultured on cover slips were fixed in formol, and then put into penetrating solution (1 g·L⁻¹ sodium citrate containing 1 g·L⁻¹ Triton X-100) and reacted at 4 °C for 2 min. The cells were stained with TUNEL reaction solution contained FITC-labeled nucleotide and deoxynucleotide terminal transferase at 37 °C for 60 min, and then observed with fluorescence microscope.

DNA contents analysis The cells were fixed in 700 mL·L⁻¹ cold ethanol. RNase A (1 g·L⁻¹) was added into the suspending solution of cells and reacted at 37 °C for 30 min. Then PI (0.1 g·L⁻¹) was added with the four times volume of that of the above solution and reacted at 4 °C for 30 min. The DNA contents of different cell cycles were analyzed with flow cytometer (Coulter Co., USA).

Methods of antibody detection

ELISA assay The cells adhered to 96-well culture plate with polylysine were fixed in 0.2 mL·L⁻¹ glutaraldehyde. The supernatant of the culture medium of hybridoma cells were used as the primary antibody, and the PBS as its negative control. The HRP-labeled sheep anti-mouse IgG mAb was used as the second antibody. The indirect ELISA assay was performed with the standard procedures. Optical absorbance (A) was measured at 490 nm with ELISA detector (Bio-Rad Co., USA).

Immunocytochemical staining^[29] The cells cultured on cover slips were fixed in 950 mL·L⁻¹ ethanol. The supernatant of the culture medium of hybridoma cells was used as the primary antibody, and the PBS as its negative control. The immunocytochemical ABC staining was performed with routine procedures illuminated by the protocol of Vector Laboratories Inc.

Subtractive immunization for mice

Twenty Balb/c mice were divided randomly into 2 groups. The ten mice in the experimental group were immunized firstly with the non-apoptotic HCC-9204 cells at log phase through cavum abdominis. Then the mice were injected with CP (0.1 g·kg⁻¹ body mass) into the cavum abdominis at 10 min, 24 h and 48 h respectively after the first immunization. At the 14th, 21st and 28th d after the first immunization, the mice were further immunized with the ethanol-induced apoptotic HCC-9204 cells through the same route. The ten mice in the control group were immunized with the ethanol-induced apoptotic HCC-9204 cells through cavum abdominis for 3 times at an interval of 2 wk. The tail blood sera of animals in both group were respectively prepared after the last immunization, and the immunocytochemical ABC staining was performed as described above to detect the production of antibodies.

Cell fusion and cloning

The mice whose tail blood sera-HCC-9204 cells reactions were most different between the apoptotic and the non-apoptotic were selected from the experimental group. The splenic cells of the selected mice were prepared at the 3rd day after the last immunization, and fused with SP2/0 cells at log phase promoted by PEG4000. Two 96-well culture plates were used for every mouse. The fused cells were cultured continually with RPMI1640 medium containing HAT and HT. Five d later, the culture wells where the monoclonal hybridoma cells were growing were marked and the producing rate of the clones, i. e. the fusion rate, of hybridoma cells was calculated. When the growing hybridoma cells had covered about 1/2 of the bottom area of a culture well, the antibodies that reacted strongly with ethanol-induced apoptotic HCC-9204 cells, but weakly with the non-apoptotic were selected by the ELISA assay as described earlier and the producing rate of antibodies was calculated. The data was statistically analyzed by χ^2 test. The interested cells were cloned continually by the method of limited dilution, selected and analyzed further by the immunocytochemical ABC staining.

Identification of the characteristic of mAb

Chromosomes of hybridoma cells The cells cultured on cover slips were treated with colchicine and stained with Giemsa by the routine procedures. One hundred hybridoma cells at metaphase were counted and observed.

Ig subtype of mAb The detection and analysis of the Ig subtype of mAb was performed with standard procedures illuminated by the protocol of Roche Molecular Biochemicals.

Molecular mass of mAb-associated antigen Some ethanol-induced apoptotic and non-apoptotic HCC-9204 cells were burst and shattered respectively by ultrasonic and the proteins of cells were prepared by the routine methods. Then SDS-PAGE was performed. The supernatant of the culture medium of hybridoma cells that secreted objective mAb was used as the primary antibody. HRP-labeled sheep anti-mouse IgG mAb was used as the second antibody. The proteins in the gel of SDS-PAGE were transferred to colloxylin filter film by Western blot system (Bio-Rad Co., USA) and stained following the protocol of Bio-Rad Co.. The color was developed with freshly dispensed DAB.

RESULTS

Detection of apoptotic cells

Electron microscope observation The majority of the cells treated with $60 \text{ mL} \cdot \text{L}^{-1}$ ethanol for 6 h showed cellular pyknosis and were densely stained. The processes and microvilli on the cell surface decreased significantly or even disappeared. Granular, crescent or cricoid nuclei (Figure 1), chromatin margination, as well as cytoplasm bubbling were observed. Endoplasmic reticulum expanded and its vacuolation occurred in some cells.

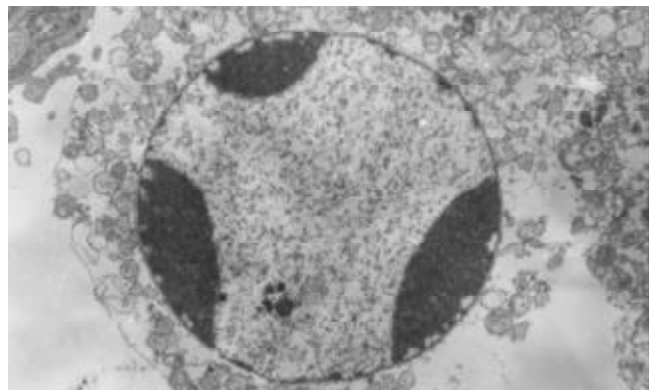


Figure 1 Morphological changes of HCC-9204 cells treated with $60 \text{ mL} \cdot \text{L}^{-1}$ ethanol for 6 h TEM $\times 6000$

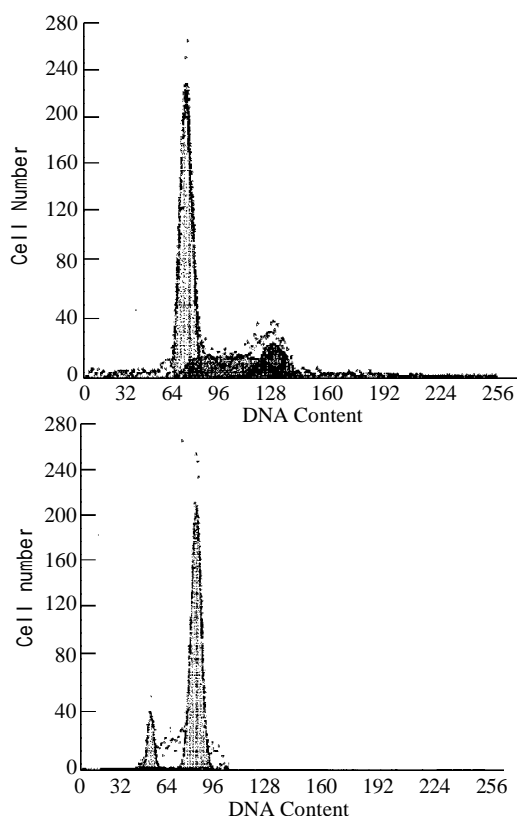


Figure 3 DNA contents of HCC-9204 cells treated with $60 \text{ mL} \cdot \text{L}^{-1}$ for 6 h. A: Non-treated HCC-9204 cells; B: HCC-9204 cells treated with $60 \text{ mL} \cdot \text{L}^{-1}$ ethanol for 6 h

TUNEL assay

The positive signal of TUNEL reaction was green or yellow in color within the round, oval, crescent or cricoid, nuclei of cells. The majority of the apoptotic cells in the experimental group were TUNEL-positive (Figure 2).

DNA contents analysis

Compared with that in the control of non-treated HCC-9204 cells, there was obvious sub-G1 apoptotic peak in the experimental group (Figure 3).

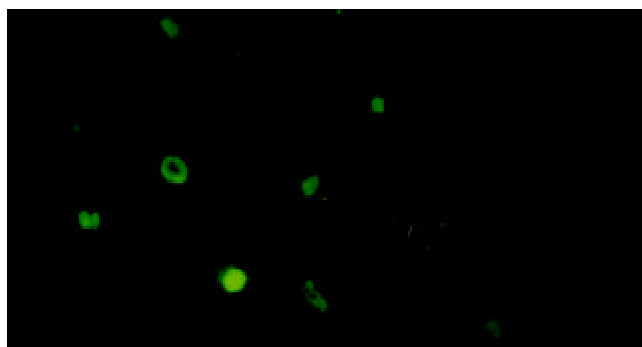


Figure 2 Detection of HCC-9204 cells treated with $60 \text{ mL} \cdot \text{L}^{-1}$ ethanol for 6 h by TUNEL assay $\times 200$

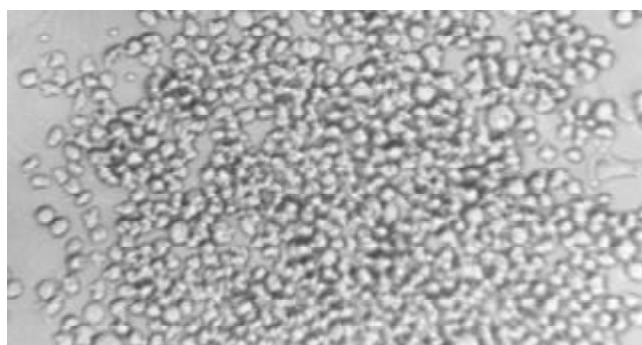


Figure 4 Monoclonal hybridoma cells growing in culture well. $\times 100$

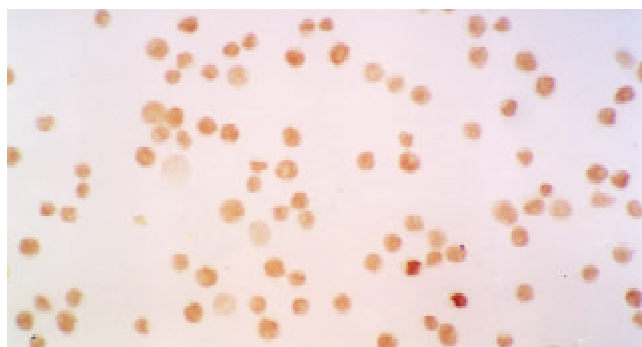


Figure 5 Immunocytochemical localization of the prepared mAb in HCC-9204 cells treated with $60 \text{ mL} \cdot \text{L}^{-1}$ ethanol for 6 h. ABC $\times 200$

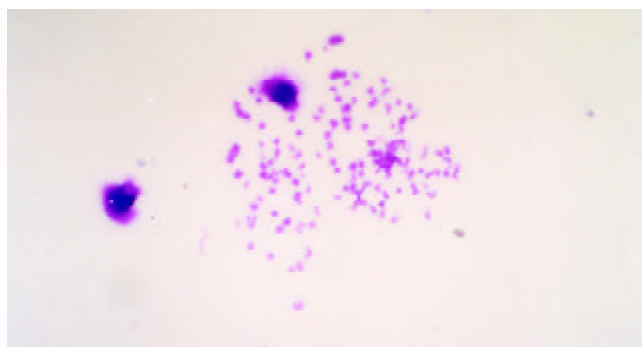


Figure 6 The chromosomes of the hybridoma cells which secrete objective mAb. $\times 400$

Table 1 The fusion rates of hybridoma cells and the producing rates of antibodies

Group	Fusion wells/Incubated wells (Fusion rate)	I(I/Fusion wells)	II(II/Fusion wells)	III(III/Fusion wells)	(I+II+III) (I+II +III)/ Fusion wells)
Experiment	241/384(62.8%)	46(19.1%) ^a	5(2.0%)	0(0%)	51(21.2%) ^a
Control	262/384(68.2%)	101(38.5%)	4(1.5%)	1(0.4%)	106(40.5%)

^a $P < 0.01$ vs Control. I: The wells whose antibodies reacted strongly with both apoptotic and non-apoptotic cells; II: The wells whose antibodies reacted strongly with apoptotic cells, but weakly with non-apoptotic cells (Difference is >8 times); III: The wells whose antibodies reacted weakly with apoptotic cells, but strongly with non-apoptotic cells (Difference is >8 times).

Subtractive immunization for mice

The tail blood sera of 8 mice in the experimental group and 10 mice in the control reacted strongly with both apoptotic and non-apoptotic HCC-9204 cells. However, the tail blood sera of the 2 other mice in the experimental group reacted strongly with apoptotic, but weakly with non-apoptotic HCC-9204 cells.

Cell fusion and cloning

Monoclonal hybridoma cells were growing in many wells of the culture plates at the 5th d after cell fusion (Figure 4).

In the fusion rate of hybridoma cells, as well as the producing rate of the antibodies that reacted strongly with apoptotic, but weakly with non-apoptotic HCC-9204 cells, there did not show significant difference between the experimental and the control group. The total producing rate of antibodies in the experimental group was significant. However, lower compared with that in the control group ($P < 0.01$), and so was the producing rate of the antibodies that reacted strongly with both apoptotic and non-apoptotic HCC-9204 cells ($P < 0.01$, Table 1).

An mAb that reacted strongly with the nuclei of ethanol-induced apoptotic, but very weakly with that of non-apoptotic HCC-9204 cells was obtained after the hybridoma cells which secreted candidate objective mAb had been cloned continually for several times (Figure 5).

Characteristic identification of mAb

Chromosomes of hybridoma cells The number of the chromosomes in the hybridoma cells which secreted objective mAb was 83 - 105, their modal number was 94 - 98, and the majority of the chromosomes were the type of terminal centromere, which is consonant with the universal characteristics of the hybridoma cells which secrete mAb (Figure 6).

Ig subtype of mAb The subtype Ig of the prepared mAb was IgG1.

Molecular mass of mAb-associated antigen The molecular mass of the prepared mAb associated antigen was about 75 ku (Figure 7).

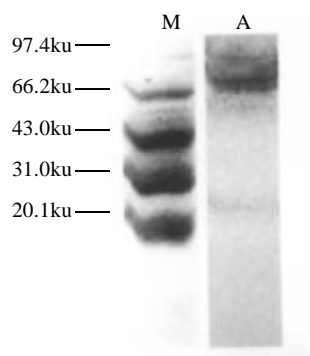


Figure 7 The molecular mass of the associated antigen of the prepared mAb. M: Standard molecular mass; A: HCC-9204 cells treated with $60 \text{ mL} \cdot \text{L}^{-1}$ ethanol for 6 h

DISCUSSION

To investigate the changes of the apoptosis-associated molecules on cell surface and the production of new antigens in the process of apoptosis is important in many fields of biomedical studies such as the mechanism of signal transduction and molecular regulation in cells and cellular immunology, *etc.*, and many mammalian gene-encoded proteins can induce or suppress apoptosis in a variety of cell types^[1-16]. It was discovered previously by the method of 2-dimensional gel electrophoresis that there are 17 new proteins, whose molecular mass are 12 - 80 ku, expressed in some cell types undergoing apoptosis induced by the transfection of wild-type *p53*^[17]. A mitochondrial membrane protein 7A6 expresses only in some kinds of apoptotic but not in non-apoptotic cells, and its mAb has been used in the detection of apoptosis in some cell types^[19, 26, 30-32]. The facts cited above indicate that in the process of apoptosis, there exists not only the up or down-regulation of some proteins expressed already in non-apoptotic cells, but also the production of new proteins that did not exist in non-apoptotic cells.

Low-concentration ethanol can induce apoptosis in some cell types such as T lymphocytes, natural killer cells, macrophage, neutrophils, nerve cells, reproduction stem cells, mucosa epithelial cells, salivary gland cells, osteoblast, thyroid epithelial cells, leukemia cells, hepatocytes and HCC cells, *etc.*^[33-40]. The results of present study showed that the majority of the HCC-9204 cells treated with $60 \text{ mL} \cdot \text{L}^{-1}$ ethanol for 6 h manifested marked morphological changes of apoptosis, the majority of the cells were TUNEL-positive, and the sub-G1 apoptotic peak detected by flow cytometry was obvious, suggested that low-concentration ethanol could induce apoptosis obviously in HCC-9204 cells and the model of ethanol-induced apoptosis in HCC cells was established successfully. The previous study with SDS-PAGE and folium scan in our laboratory have revealed that at least 7 kinds of new proteins whose molecular mass are more than 67 ku expressed in the HCC-9204 cells treated with $60 \text{ mL} \cdot \text{L}^{-1}$ ethanol for 6 h but not in non-apoptotic cells. It is well known that HCC is a common malignant tumor in China and some other places in the world, and its oncogenesis and development are related with apoptosis^[41-60]. Therefore the ethanol-induced apoptotic HCC-9204 cells were used as antigen to prepare mAb against the apoptosis-associated antigens of HCC cells in this experiment.

Most of the proteins encoded by apoptosis-associated genes express only instantaneously in cells, and the quantity of the expressed products of apoptosis-associated genes is usually very little. The general procedures of the routine of immunization for the preparation of mAb are that the mice were further immunized twice respectively with the same antigen as the first immunization at an interval of 2 wk. In our previous studies, more than ten rabbits have been immunized with ethanol-induced apoptotic HCC-9204 cells by routine immunization procedures, there was no rabbit found whose

ear blood serum reacted strongly with apoptotic, but weakly with non-apoptotic cells. There is also no mouse whose tail blood serum reacted differently with apoptotic and non-apoptotic cells in all the 10 mice used as control in this experiment. The those results suggest that the antibodies against cell apoptosis-associated antigens are difficult to be prepared by the routine immunization procedures because of the interference of the large amounts of antigens not associated with apoptosis in the apoptotic cells.

Subtractive immunization is a special method of differentiated immunization used for the preparation of antibodies when the antigen components are complicated, unclear or cannot be extracted and purified^[61-65]. The mechanism of subtractive immunization is that when certain antigens induce the immunoreaction of a animal body, the lymphocytes will proliferate, and the cells in split phase are prone to be selectively killed by the drug containing alkyls such as CP that is in common use in the procedures of subtractive immunization. When the same antigen is injected into the animal body again after the first immunization, the immunoreaction to the antigen is suppressed. CP can effectively inhibit the production of the antibodies against non-objective components of the antigen, but the production of objective antibodies cannot be influenced obviously, and neither are the fusion rates of hybridoma cells. Therefore the selection workload in the process of preparing mAb could reduce remarkably. The standard procedures of subtractive immunization are as the followings. Firstly, 2 groups of mixed antigens A and B whose components were similar were prepared. There is objective antigen in group A, but no objective antigen in group B. Secondly, group B is firstly used to immunize some animals. At the meantime, the immunized animals are treated with CP, or CP is injected 10 min, 24 h and 48 h later. Thirdly, the animals are further immunized with group A for 3 times respectively at an interval of 1 wk. At this time, the immunoreaction of the animal body to the common components of group A and group B is suppressed. Therefore the interference of non-objective antigens to the preparation of objective mAb is wakened or even may be eliminated, the immunoreaction to the objective antigens in group A is enhanced relatively, and the probability to obtain specific mAb increases significantly^[48].

There were 2 mice whose tail blood sera reacted strongly with ethanol-induced apoptotic HCC-9204 cells, but weakly with non-apoptotic HCC-9204 cells in 10 mice immunized by subtractive immunization in this experiment, indicating that there are certain antigens which express strongly in apoptotic cells, but weakly or even do not express in non-apoptotic cells in the process of HCC cells apoptosis. The subtractive immunization is therefore a useful method to prepare the antibodies against the apoptosis-associated antigens of cells. The preferable results obtained only in 20 % (2 / 10) of the mice immunized by subtractive immunization, suggesting that there is obvious individual difference in the effect of subtractive immunization with CP. In order to get ideal effect, more mice are needed to be immunized in an experiment. The fusion rate of hybridoma cells in the experimental group did not differ distinctly from that in the control group, but the total producing rate of antibodies was lower significantly than that in the control group, suggesting that CP can suppress remarkably the production of antibodies while the fusion rate of hybridoma cells is not greatly influenced. The producing rate of the antibodies which reacted strongly with both apoptotic and non-apoptotic cells in the experimental group is significantly lower than that in the control, whereas there is no remarkable difference on the producing rate of the antibodies which reacted

strongly with apoptotic, but weakly with non-apoptotic cells between the two groups, indicating that CP had partly suppressed the production of the antibodies against non-objective antigens to some extent, but not influenced that of the antibodies against objective antigens. The subtractive immunization can significantly decrease the selection workload in the process of preparing mAb when the antigen of mAb is unknown.

The mAb whose associated antigen located within the nucleus of ethanol-induced apoptotic HCC-9204 cells and reacted weakly with non-apoptotic HCC-9204 cells was prepared successfully and identified primarily in this experiment, which is consistent with some previous reports that injecting apoptotic cells into the cavum abdominis of mice can lead to the production of anti-nucleus antibodies^[66]. The results of Western blot analysis revealed that the molecular mass of the associated antigen of this mAb was about 75 ku, which is consistent with the result of our previous study that new proteins whose molecular mass are more than 67 ku are discovered in 60 mL·L⁻¹ ethanol-induced apoptotic HCC-9204 cells. The associated antigen of the mAb prepared in this experiment is the certain molecule that expresses in the nucleus of HCC-9204 cells and may be related with the ethanol-induced apoptosis. No antibody that reacted strongly with apoptotic cells, but completely absent with non-apoptotic cells is obtained in this experiment, suggesting that the antibodies against new apoptosis-associated antigens that do not exist in non-apoptotic cells is difficult to be prepared by the method of cell fusion used in this experiment. Low-concentration ethanol can not only induce apoptosis in HCC-9204 cells, but may also suppresses their proliferation and startup the expression of some molecules related with some other effect of ethanol on cells. The relationship between the mAb prepared in this experiment and its associated antigen and apoptosis in HCC cells is still to be determined and should be studied further. This experiment gives us a hopeful prospect to discover some new apoptosis-associated molecules in HCC cells.

REFERENCES

- 1 **Hengartner MO**. The biochemistry of apoptosis. *Nature* 2000; **407**:770-776
- 2 **Simon HU**. Regulation of eosinophil and neutrophil apoptosis-similarities and differences. *Immunol Rev* 2001; **179**:156-162
- 3 **Si XH**, Yang LJ. Extraction and purification of TGF β and its effect on the induction of apoptosis hepatocytes. *World J Gastroenterol* 2001; **7**:527-531
- 4 **Holtman M J**, Green JM, Jayaraman S, Arch RH. Regulation of T cell apoptosis. *Apoptosis* 2000; **5**:459-471
- 5 **Afford S**, Randhawa S. Apoptosis. *Mol Pathol* 2000; **53**: 55-63
- 6 **Yuan YZ**, Gong ZH, Lou KX, Tu SP, Zhai ZK, Xu JY. Involvement of apoptosis of alveolar epithelial cells in acute pancreatitis associated lung injury. *World J Gastroenterol* 2000; **6**:920-924
- 7 **Schuchmann M**, Galle PR. Apoptosis in liver disease. *Eur J Gastroenterol Hepatol* 2001; **13**:785-790
- 8 **Zang GQ**, Zhou XQ, Yu H, Xie Q, Zhao GM, Wang B, Guo Q, Xiang YQ, Liao D. Effect of hepatocyte apoptosis induced by TNF α on acute severe hepatitis in mouse models. *World J Gastroenterol* 2000; **6**:688-692
- 9 **Ruvolo PP**, Deng X, May WS. Phosphorylation of Bcl2 and regulation of apoptosis. *Leukemia* 2001; **15**:515-522
- 10 **Zhang FX**, Zhang XY, Fan DM, Deng ZY, Yan Y, Wu HP, Fan JJ. Antisense telomerase RNA induced human gastric cancer cell apoptosis. *World J Gastroenterol* 2000; **6**:430-432

- 11 **Dikranian K**, Ishimaru MJ, Tenkova T, Labruyere J, Qin YQ, Ikonomidou C, Olney JW. Apoptosis in the *in vivo* mammalian forebrain. *Neurobiol Dis* 2001; **8**:359-379
- 12 **Neurath MF**, Finotto S, Fuss I, Boirivant M, Galle PR, Strober W. Regulation of T-cell apoptosis in inflammatory bowel disease: to die or not to die, that is the mucosal question. *Trends Immunol* 2001; **22**:21-26
- 13 **Geng YJ**. Biologic effect and molecular regulation of vascular apoptosis in atherosclerosis. *Curr Atheroscler Rep* 2001; **3**:234-242
- 14 **Piliponsky AM**, Levi-Schaffer F. Regulation of apoptosis in mast cells. *Apoptosis* 2000; **5**:435-441
- 15 **Schmitz I**, Kirchhoff S, Krammer PH. Regulation of death receptor-mediated apoptosis pathways. *Int J Biochem Cell Biol* 2000; **32**:1123-1136
- 16 **Gompel A**, Somai S, Chaouat M, Kazem A, Kloosterboer HJ, Beusman I, Forgez P, Mimoun M, Rostene W. Hormonal regulation of apoptosis in breast cells and tissues. *Steroids* 2000; **65**:593-598
- 17 **Maxwell SA**. Two-dimensional gel analysis of p53-mediated changes in protein expression. *Anticancer Res* 1994; **14**:2549-2556
- 18 **Pawlowski K**, Pio F, Chu Z, Reed JC, Godzik A. PAAD - a new protein domain associated with apoptosis, cancer and autoimmune diseases. *Trends Biochem Sci* 2001; **26**:85-87
- 19 **Zhang C**, Ao Z, Seth A, Schlossman SF. A mitochondrial membrane protein defined by a novel monoclonal antibody is preferentially detected in apoptotic cells. *J Immunol* 1996; **157**:3980-3987
- 20 **Rovere P**, Sabbadini MG, Vallinoto C, Fascio U, Recigno M, Crosti M, Ricciardi- Castagnoli P, Balestrieri G, Tincani A, Manfredi AA. Dendritic cell presentation of antigens from apoptosis cells in a proinflammatory context. *Arthritis Rheum* 1999; **42**:1412-1420
- 21 **Cohen O**, Kimchi A. DAP-kinase: from functional gene cloning to establishment of its role in apoptosis and cancer. *Cell Death Differ* 2001; **8**:6-15
- 22 **Lo KW**, Zhang Q, Li M, Zhang M. Apoptosis-linked gene product ALG-2 is a new member of the calpain small subunit subfamily of Ca²⁺-binding proteins. *Biochemistry* 1999; **38**: 7498-7508
- 23 **Rao RM**, Dharmarajan AM, Rao AJ. Cloning and characterization of an apoptosis-associated gene in the human placenta. *Apoptosis* 2000; **5**:53-60
- 24 **Suzuki T**, Nishiyama K, Yamamoto A, Inazawa J, Iwaki T, Yamada T, Kanazawa I, Sakaki Y. Molecular cloning of a novel apoptosis-related gene, human Nap1 (NCKAP1), and its possible relation to Alzheimer disease. *Genomics* 2000; **63**:246-254
- 25 **Xiang H**, Wang J, Mao YW, Li DW. HTERT can function with rabbit telomerase RNA: regulation of gene expression and attenuation of apoptosis. *Biochem Biophys Res Commun* 2000; **278**:503-510
- 26 **Zhang C**, Xu Y, Gu J, Schlossman SF. A cell surface receptor defined by a mAb mediates a unique type of cell death similar to oncosis. *Proc Natl Acad Sci USA* 1998; **95**:6290-6295
- 27 **Chang MK**, Bergmark C, Laurila A, Horkko S, Han KH, Friedman P, Dennis EA, Witztum JL. Monoclonal antibodies against oxidized low-density lipoprotein bind to apoptotic cells and inhibit their phagocytosis by elicited macrophages: Evidence that oxidation-specific epitopes mediate macrophage recognition. *Proc Natl Acad Sci USA* 1999; **96**:6353-6358
- 28 **Ben-Sasson SA**. Identification of programmed cell death *in situ* via specific labeling of nuclear DNA fragmentation. *J Cell Biol* 1992; **119**:493-501
- 29 **Si XH**. Expression of cell cycle-associated proteins CDK4, p27 and E2F-1 in chondrosarcoma of the jaws. *Chin J Dent Res* 2001; **3**:40-43
- 30 **Koester SK**, Roth P, Mikulka WR, Schlossman SF, Zhang C, Bolton WE. Monitoring early cellular responses in apoptosis is aided by the mitochondrial membrane protein-specific monoclonal antibody. *Cytometry* 1997; **29**:306-312
- 31 **Yaguchi M**, Miyazawa K, Otawa M, Katagiri T, Nishimaki J, Uchida Y, Iwase O, Gotoh A, Kawanishi Y, Toyama K. Vitamin K2 selectively induces apoptosis of blastic cells in myelodysplastic syndrome: flow cytometric detection of apoptotic cells using APO2.7 monoclonal antibody. *Leukemia* 1998; **12**:1392-1397
- 32 **Carthy CM**, Granville DJ, Jiang H, Levy JG, Rudin CM, Thompson CB, McManus BM, Hunt DW. Early release of mitochondrial cytochrome c and expression of mitochondrial epitope 7A6 with a porphyrin-derived photosensitizer: Bcl-2 and Bcl-xL overexpression do not prevent early mitochondrial events but still depress caspase activity. *Lab Invest* 1999; **79**: 953-965
- 33 **Neuman MG**, Shear NH, Cameron RG, Katz G, Tiribelli C. Ethanol-induced apoptosis *in vitro*. *Clin Biochem* 1999; **32**:547-555
- 34 **Nanji AA**. Apoptosis and alcoholic liver disease. *Semin Liver Dis* 1998; **18**:187-190
- 35 **Baisch H**, Bollmann H, Bornkessel S. Degradation of apoptotic cells and fragments in HL-60 suspension cultures after induction of apoptosis by camptothecin and ethanol. *Cell Prolif* 1999; **32**:303-319
- 36 **Zhu Q**, Meisinger J, Emanuele NV, Emanuele MA, LaPaglia N, Van Thiel DH. Ethanol exposure enhances apoptosis within the testes. *Alcohol Clin Exp Res* 2000; **24**: 1550-1556
- 37 **De la Monte SM**, Ganju N, Banerjee K, Brown NV, Luong T, Wands JR. Partial rescue of ethanol-induced neuronal apoptosis by growth factor activation of phosphoinositol-3-kinase. *Alcohol Clin Exp Res* 2000; **24**:716-726
- 38 **Singhal PC**, Patel P, Nahar N, Franki N, Kapasi A, Reddy K, Shah N, Nwakoby IE, Mehrotra B. Ethanol-induced neutrophil apoptosis is mediated through nitric oxide. *J Leukoc Biol* 1999; **66**:930-936
- 39 **Singhal PC**, Reddy K, Ding G, Kapasi A, Franki N, Ranjan R, Nwakoby IE, Gibbons N. Ethanol-induced macrophage apoptosis: the role of TGF-beta. *J Immunol* 1999; **162**: 3031-3036
- 40 **Oberdoerster J**, Rabin RA. NGF-differentiated and undifferentiated PC12 cells vary in induction of apoptosis by ethanol. *Life Sci* 1999; **64**:PL267-272
- 41 **Cui J**, Zhou XD, Liu YK, Tang ZY, Zile MH. Abnormal β -catenin gene expression with invasiveness of primary hepatocellular carcinoma in China. *World J Gastroenterol* 2001; **7**:542-546
- 42 **Valente M**, Calabrese F. Liver and apoptosis. *Ital J Gastroenterol Hepatol* 1999; **31**:73-77
- 43 **Cao XY**, Liu J, Lian ZR, Clayton M, Hu JL, Fan DM, Feitelson M. Cloning of differentially expressed genes in human hepatocellular carcinoma and nontumor liver. *World J Gastroenterol* 2001; **7**:579-582
- 44 **Rabe C**, Pilz T, Klostermann C, Berna M, Schild HH, Sauerbruch T, Caselmann WH. Clinical characteristics and outcome of a cohort of 101 patients with hepatocellular carcinoma. *World J Gastroenterol* 2001; **7**:208-215
- 45 **Neuman MG**. Apoptosis in disease of the liver. *Crit Rev Clin Lab Sci* 2001; **38**:109-166
- 46 **Yang LJ**, Sui YF, Chen ZN. Preparation and activity of conjugate of monoclonal antibody HAB18 against hepatoma F(ab'), fragment and staphylococcal enterotoxin A. *World J Gastroenterol* 2001; **7**:216-221
- 47 **Fan ZR**, Yang DH, Cui J, Qin HR, Huang CC. Expression of insulin-like growth factor and its receptor in hepatocellular carcinogenesis. *World J Gastroenterol* 2001; **7**:285-288
- 48 **Guo WP**, Zhang HX, Wang ZM, Wang YQ, Ni DH, Li WX, Guan Y. DSA analysis of hepatic arteriovenous fistula concurrent with hepatic cancer and its clinical significance. *World J Gastroenterol* 2000; **6**:872-876
- 49 **Tang ZY**. Hepatocellular carcinoma-cause, treatment and

- metastasis. *World J Gastroenterol* 2001; **7**: 445-454
- 50 **Chen YP**, Liang WF, Zhang L, He HT, Luo KX. Transfusion transmitted virus infection in general populations and patients with various liver diseases in south China. *World J Gastroenterol* 2000; **6**:738-741
- 51 **Xu HY**, Yang YL, Guan XL, Song G, Jiang AM, Shi LJ. Expression of regulating apoptosis gene and apoptosis index in primary liver cancer. *World J Gastroenterol* 2000; **6**:721-724
- 52 **Huang XF**, Wang CM, Dai XW, Li ZJ, Pan BR, Yu LB, Qian B, Fang L. Expressions of chromogranin A and cathepsin D in human primary hepatocellular carcinoma. *World J Gastroenterol* 2000; **6**:693-698
- 53 **Liu NF**, Tang J, Mohamed Ismael HS. Study on environmental etiology of high incidence areas of liver cancer in China. *World J Gastroenterol* 2000; **6**:572-576
- 54 **Niu Q**, Tang ZY, Ma ZC, Qin LX, Zhang LH. Serum vascular endothelial growth factor is a potential biomarker of metastatic recurrence after curative resection of hepatocellular carcinoma. *World J Gastroenterol* 2000; **6**:565-568
- 55 **Shen LJ**, Zhang ZJ, Qu YM, Zhang HX, Huang R, He Y, Wang MJ, Xu GS. Computed morphometric analysis and expression of alpha fetoprotein in hepatocellular carcinoma and its related lesion. *World J Gastroenterol* 2000; **6**:415-416
- 56 **Qin Y**, Li B, Tan YS, Sun ZL, Zuo FQ, Sun ZF. Polymorphism of p16INK4a gene and rare mutation of p15INK4b gene exon2 in primary hepatocarcinoma. *World J Gastroenterol* 2000; **6**:411-414
- 57 **Mei MH**, Xu J, Shi QF, Yang JH, Chen Q, Qin LL. Clinical significance of serum intercellular adhesion molecule 1 detection in patients with hepatocellular carcinoma. *World J Gastroenterol* 2000; **6**:408-410
- 58 **Sun BH**, Zhang J, Wang BJ, Zhao XP, Wang YK, Yu ZQ, Yang DL, Hao LJ. Analysis of in vivo patterns of caspase 3 expression in primary hepatocellular carcinoma and its relationship to p21WAF1 expression and hepatic apoptosis. *World J Gastroenterol* 2000; **6**:356-360
- 59 **Zhu HZ**, Ruan YB, Wu ZB, Zhang CM. Kupffer cell and apoptosis in experimental HCC. *World J Gastroenterol* 2000; **6**:405-407
- 60 **Li J**, Yang XK, Yu XX, Ge ML, Wang WL, Zhang J, Hou YD. Overexpression of p27KIP1 induced cell cycle arrest in G1 phase and subsequent apoptosis in HCC 9204 cell line. *World J Gastroenterol* 2000; **6**:513-521
- 61 **Vareckova E**, Betakova T, Mucha V, Solarikova L, Kostolansky F, Waris M, Russ G. Preparation of monoclonal antibodies for the diagnosis of influenza A using different immunization protocols. *J Immunol Methods* 1995; **180**:107-116
- 62 **Xu J**, Rodriguez D, Kim JJ, Brooks PC. Generation of monoclonal antibodies to cryptic collagen sites by using subtractive immunization. *Hybridoma* 2000; **19**:375-385
- 63 **Denegre JM**, Ludwig ER, Mowry KL. Localized maternal proteins in *Xenopus* revealed by subtractive immunization. *Dev Biol* 1997; **192**:446-454
- 64 **BelAiba RS**, Baril P, Chebloune Y, Tabone E, Boukerche H. Identification and cloning of an 85-kDa protein homologous to RING3 that is upregulated in proliferating endothelial cells. *Eur J Biochem* 2001; **268**:4398-4407
- 65 **Trefzer U**, Rietz N, Chen Y, Audring H, Herberth G, Siegel P, Reinke S, Koniger P, Wu S, Ma J, Liu Y, Wang H, Sterry W, Guo Y. SM5-1: a new monoclonal antibody which is highly sensitive and specific for melanocytic lesions. *Arch Dermatol Res* 2000; **292**: 583-589
- 66 **Mevorach D**, Zhou JL, Song X, Elkon KB. Systemic exposure to irradiated apoptotic cells induces autoantibody production. *J Exp Med* 1998; **188**:387-392

Edited by Zhu L

• LIVER CANCER •

Significance of cyclooxygenase-2 expression in human primary hepatocellular carcinoma

De-Kai Qiu, Xiong Ma, Yan-Shen Peng, Xiao-Yu Chen

De-Kai Qiu, Xiong Ma, Yan-Shen Peng, Xiao-Yu Chen, Shanghai Institute of Digestive Diseases, Renji Hospital, Shanghai Second Medical University, Shanghai, 200001, China

Correspondence to: Dr. De-Kai Qiu, Shanghai Institute of Digestive Diseases, Renji Hospital, Shanghai Second Medical University, 145 Shandong (z) Road, Shanghai, 200001, China. dekaqiu@sh163.net
Telephone: +86-21-63200874 **Fax:** +86-21-63266027

Received 2001-12-20 **Accepted** 2002-02-09

Abstract

AIM: To clarify the significance of cyclooxygenase-2 (COX-2) expression in human primary hepatocellular carcinoma (HCC) and adjacent nontumorous tissues.

METHODS: The COX-2 protein and mRNA were investigated in 27 HCC tissues with adjacent nontumorous tissues, and 5 histologically normal liver tissues, using immunohistochemistry and in situ hybridization.

RESULTS: The well-differentiated HCC expressed COX-2 protein (5.68 ± 1.19) more strongly than moderated HCC (3.43 ± 1.98) and poor differentiated HCC (3.33 ± 1.50) ($P < 0.05$ respectively), adjacent nontumorous tissues (4.93 ± 1.05) and normal liver tissues (3.20 ± 1.92) ($P < 0.01$ respectively); More intensive staining of COX-2 in adjacent nontumorous tissues was observed than that in normal liver tissues ($P < 0.05$). There was no significant difference among adjacent nontumorous tissues, moderately differentiated HCC and poorly differentiated HCC ($P > 0.05$). The expression of COX-2 mRNA was observed in the cytoplasm of the cells of HCC and of the hepatocytes in adjacent nontumorous tissues in which COX-2 protein was positive.

CONCLUSION: The overexpression of COX-2 in well-differentiated HCC suggests that COX-2 may play a role in the early stages of hepatocarcinogenesis.

Qiu DK, Ma X, Peng YS, Chen XY. Significance of cyclooxygenase-2 expression in human primary hepatocellular carcinoma. *World J Gastroenterol* 2002; 8(5):815-817

INTRODUCTION

Cyclooxygenase (COX) is the rate-limiting enzyme involved in the conversion of arachidonic acid to prostaglandin H_2 , the precursor of various compounds including prostaglandins, prostacyclin and thromboxanes. Two COX genes, COX-1 and COX-2, have been identified, which share greater than 60 % identity at the amino acid level. COX-1 is constitutively expressed in a number of cell types, whereas COX-2 is inducible by a variety of factors such as mitogen, cytokines, growth factor, and tumor promoters^[1]. The expression of COX-2 is significantly increased in various types of carcinoma. There

is also sufficient evidence indicating that selective COX-2 inhibitors produce effective prevention of carcinogenesis and that these compounds act by inducing of apoptosis of various cancer cells. These findings suggest that COX-2 may be involved in carcinogenesis and/or progression of certain types of human malignancies^[2]. In this study, we examined the expression of COX-2 in human primary hepatocellular carcinoma (HCC) and adjacent nontumorous tissues.

MATERIALS AND METHODS

Tissue samples

HCC tissue and adjacent nontumorous liver tissues were obtained from 27 patients with hepatic tumor, who received hepatectomy at Renji hospital. Five specimens of grossly normal liver tissues from the area surrounding benign angiomas were used as controls. Specimens were fixed in 10 % neutral formalin and embedded in paraffin.

Histology

Serial 5-um sections were stained with hematoxylin and eosin. Each HCC was histologically graded into one of three categories: well-differentiated, moderately differentiated, or poorly differentiated, according to the criteria proposed by the Liver Cancer Study Group of Japan^[3]. The tumor tissues consisted of 11 well-differentiated, 7 moderately differentiated, and 9 poorly differentiated HCCs, and the nontumorous sites consisted of 3 chronic hepatitis and 24 cirrhosis.

Immunohistochemistry

Immunohistochemical staining was performed on serial sections at room temperature, using the peroxidase method with the polyclonal antibody against human COX-2 (Santa Cruz Co.). The sections were deparaffinized in xylene and rehydrated through graded alcohol, immersed the sections in 3 % hydrogen peroxide for 10 minutes to inactivate endogenous peroxidases, then were incubated for 10 minutes with 10 % normal swine serum in Tris-buffered saline to block non-specific binding, subsequently incubated overnight at 4 °C with relevant antibody. The following day, the sections were incubated with biotinylated anti-mouse IgG (Maxim Biotech Inc. USA) for 45 minutes, followed by peroxidase-conjugated streptavidin (Maxim Biotech Inc.). The chromogenic reaction was developed with diaminobenzidine for 10 minutes, and all sections were counterstained with hematoxylin. In controls, the primary antibody was omitted.

The intensity of staining for COX-2 in HCC tissues and nontumorous adjacent tissues was scored in each specimen on a scale of 0 to 3, in which 0=negative staining, 1=weakly positive staining, 2=moderately positive staining, and 3=strongly positive staining. The percentage of positive cells in each specimen was estimated and scored on a scale of 0 to 4, in which 0=negative, 1=positive staining in 1 % to 25 % of cells counted, 2, in 26 % to 50 %; 3, in 51 % to 75 %; and 4, in 76 % to 100 %. Each section was evaluated for the sum of these two parameters.

In Site Hybridization

Deparaffinized sections of liver tissue were treated with proteinase K (70 mg/ml) for 30 minutes at 37 °C, followed by fixation with paraformaldehyde (0.4 %, 20 minutes). Sections were prehybridized for 1-hour, then hybridized at 55 °C overnight with digoxigenin-labeled (labeling-kit: Boehringer Mannheim) fragments of COX-2 (Cayman Chemical). After extensive washing of the tissue section, hybridization was visualized using anti-digoxigenin, alkaline phosphatase-conjugated antibody and NBT/BCIP.

Statistical analysis

Data are presented as the mean \pm SD. Statistical significances were assessed using Mann-Whitney's *U* test. Significance was accepted when $P < 0.05$.

RESULTS

In immunohistochemical analysis, cytoplasmic staining for COX-2 was observed in HCC cells and nontumorous hepatocytes. The distribution of positive cells was mostly extensive, and occasionally focal or scattered. Different histological grades of HCC demonstrated different immunoreactivity for COX-2. A significantly high expression level of COX-2 (5.68 ± 1.19) was found in well-differentiated HCC, compared with that of normal tissue (3.20 ± 1.92), adjacent nontumorous tissues (4.93 ± 1.05) ($P < 0.01$, respectively), moderately differentiated HCC (3.43 ± 1.98) and poorly differentiated HCC (3.33 ± 1.50) ($P < 0.05$, respectively). More intensive staining of COX-2 in adjacent nontumorous tissues was observed than that in normal liver tissues ($P < 0.05$). There is no significant difference among adjacent nontumorous tissue, moderately differentiated HCC and poorly differentiated HCC ($P > 0.05$, respectively) (Figure 1). The expression of COX-2 mRNA was observed in the cytoplasm of the cells of HCC and of the hepatocytes in adjacent nontumorous tissues in which COX-2 protein was positive.

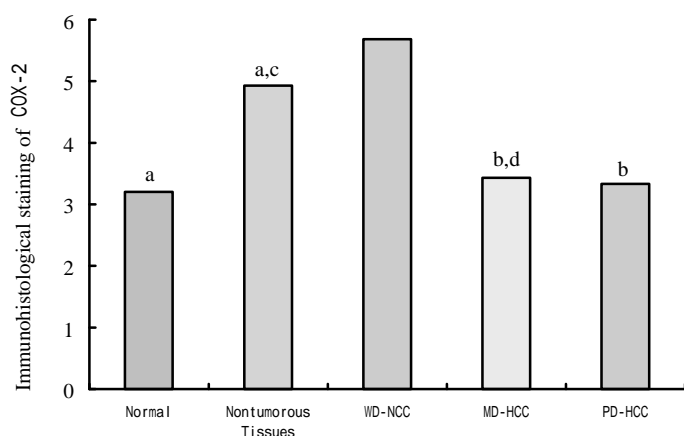


Figure1 Immunohistochemical staining scores of COX-2 in normal, adjacent nontumorous and HCC tissues. (^a $P < 0.01$ vs WD-HCC; ^b $P < 0.05$ vs WD-HCC; ^c $P < 0.05$ vs normal.)

DISCUSSION

Primary HCC is one of the most common tumors in China. The prognosis of HCC is generally poor, and the 5-year survival rate is limited to 25-39 % after surgery^[4]. The present study showed that a significantly increased expression of COX-2 was observed in HCC, suggesting that COX-2 was being involved in hepatocarcinogenesis. Of interest, a profound expression of COX-2 was demonstrated in well-differentiated

HCC. It is known that early HCC is usually a well-differentiated carcinoma and then gradually changes into a poorly differentiated phenotype during tumor progression^[5]. In this context, it is suggested that COX-2 may be associated with the early process of the progression of HCCs. This result is consistent with those reported by Koga^[6].

Recent studies have highlighted the relevance of COX-2 in human carcinogenesis. Epidemiological studies indicate that NSAIDs lead to a regression of colonic polyps in patients with familial adenomatous polyposis. NSAIDs are also known to reduce the risk of colorectal cancers, breast and lung cancers^[7]. There is also a sufficient evidence from animal studies indicating that selective COX-2 inhibitors produce effective prevention of carcinogenesis. Introduction of COX-2 cDNA into colon carcinoma cells facilitated growth. COX-2 appears to prevent apoptosis because selective COX-2 inhibitors induced apoptosis in various cell culture systems^[8]. Furthermore, it was shown that COX-2 promoted angiogenesis in malignant cells^[9]. COX-2 mRNA and protein were recently found to be expressed in human colon carcinoma^[10] and gastric carcinoma^[11]. However, COX-2 protein was not expressed in human breast carcinoma or in human basal cell carcinoma. These observations have suggested that overexpression of COX-2 in carcinomas is not the universal event in carcinogenesis but may be specific. Recently, Kondo *et al*^[12] showed that increased expression of COX-2 in nontumor liver tissue was associated with shorter disease-free survival in patients with hepatocellular carcinoma. Clinicopathological survey indicated a significant correlation between COX-2 expression and differentiated carcinoma. Moreover, high COX-2 expression in nontumorous tissue was significantly correlated with the presence of active inflammation. These findings suggest that COX-2 expression in nontumorous tissue may play a positive role in relapse of HCC after surgery.

Recent chemopreventive strategies for colon carcinogenesis have focused on using COX inhibitors, resulting in interesting data from animal models^[13]. Denda *et al*^[14] demonstrated that administration of NSAIDs suppressed cirrhosis and subsequent formation of HCC in the choline-deficient L-amino acid-defined rat model. The present finding of increased COX-2 expression in well-differentiated HCC tissues encourages chemopreventive studies for primary HCC. To clarify whether COX-2 is a principle enzyme involved in liver carcinogenesis, *in vivo* animal studies should be performed using a specific COX-2 inhibitor.

REFERENCES

- 1 Eberhart CE, Du Bois RN. Eicosanoids and the gastrointestinal tract. *Gastroenterology* 1995; **109**: 285-301
- 2 Eberhart CE, Coffey RJ, Radhika A, Giardiello FM, Ferrenbach S, DuBois RN. Up-regulation of cyclooxygenase 2 gene expression in human colorectal adenomas and adenocarcinomas. *Gastroenterology* 1994; **107**: 1183-1188
- 3 Liver Cancer Study Group of Japan. Primary liver cancer in Japan. Clinicopathologic features and results of surgical treatments. *Ann Surg* 1990; **211**: 277-287
- 4 Colombo M. Hepatocellular carcinoma. *J Hepatol* 1992; **15**: 225-236
- 5 Sugihara S, Nakashima O, Kojiro M, Majima Y, Tanaka M, Tanikawa K. The morphologic transition in hepatocellular carcinoma. A comparison of the individual histologic features disclosed by ultrasound-guided fine-needle biopsy with autopsy. *Cancer* 1992; **70**: 1488-1492
- 6 Koga H, Sakisaka S, Ohishi M, Kawaguchi T, Taniguchi E, Sasatomi K, Harada M, Kusaba T, Tanaka M, Kimura R, Nakashima Y, Nakashima O, Kojiro M, Kurohiji T, Sata

- M. Expression of cyclooxygenase-2 in human hepatocellular carcinoma: relevance to tumor dedifferentiation. *Hepatology* 1999; **29**:688-696
- 7 **Schreinemachers DM**, Everson RB. Aspirin use and lung, colon, and breast cancer incidence in a prospective study. *Epidemiology* 1994; **5**: 138-146
- 8 **Liu XH**, Yao S, Kirschenbaum A, Levine AC. NS398, a selective cyclooxygenase-2 inhibitor, induces apoptosis and down-regulates bcl-2 expression in LNCaP cells. *Cancer Res* 1998; **58**: 4245-4249
- 9 **Tsuji M**, Kawano S, Tsuji S, Sawaoka H, Hori M, DuBois RN. Cyclooxygenase regulates angiogenesis induced by colon cancer cells. *Cell* 1998;**93**:705-716
- 10 **Sano H**, Kawahito Y, Wilder RL, Hashiramoto A, Mukai S, Asai K, Kimura S, Kato H, Kondo M, Hla T. Expression of cyclooxygenase-1 and -2 in human colorectal cancer. *Cancer Res* 1995;**55**:3785-3789
- 11 **Ristimaki A**, Honkanen N, Jankala H, Sipponen P, Harkonen M. Expression of cyclooxygenase-2 in human gastric carcinoma. *Cancer Res* 1997; **57**: 1276-1280
- 12 **Kondo M**, Yamamoto H, Nagano H, Okami J, Ito Y, Shimizu J, Eguchi H, Miyamoto A, Dono K, Umeshita K, Matsuura N, Wakasa K, Nakamori S, Sakon M, Monden M. Increased expression of COX-2 in nontumor liver tissue is associated with shorter disease-free survival in patients with hepatocellular carcinoma. *Clin Cancer Res* 1999; **5**: 4005-4012
- 13 **Boolbol SK**, Dannenberg AJ, Chadburn A, Martucci C, Guo XJ, Ramonetti JT, Abreu-Goris M, Newmark HL, Lipkin ML, DeCosse JJ, Bertagnolli MM. Cyclooxygenase-2 overexpression and tumor formation are blocked by sulindac in murine model of familial adenomatous polyposis. *Cancer Res* 1996; **56**:2556-2560
- 14 **Denda A**, Endoh T, Kitayama W, Tang Q, Noguchi O, Kobayashi Y, Akai H, Okajima E, Tsujiuchi T, Tsutsumi M, Nakae D, Konishi Y. Inhibition by piroxicam of oxidative DNA damage, liver cirrhosis and development of enzyme-altered nodules caused by a choline-deficient, L-amino acid defined diet in rats. *Carcinogenesis* 1997; **18**: 1921-1930

Edited by Zhao P

Dear editors:

We found some data errors in our paper entitled "Alteration of AFP-mRNA level detected in blood circulation during liver resection for HCC and its significance", which was published in World J Gastroenterol 2002 October; 8(5):818-821. All authors have made a decision to retract this paper from your journal and all databases as soon as possible.

We are so sorry about it.

Thank you very much.

Best regards,

Xiaoping Chen

2007-11-12

• LIVER CANCER •

Expression of p53 and C-myc genes and its clinical relevance in the hepatocellular carcinomatous and pericarcinomatous tissues

Zhao-Shan Niu, Bo-Kian Li, Mei Wang

Zhao-Shan Niu, Bo-Kian Li, Department of Pathology, Medical College of Qingdao University, Qingdao 266021, Shandong Province, China
Mei Wang, Department of Foreign languages, Qingdao institute of Architecture and Engineering, Qingdao 266033, Shandong Province, China

Supported by the scientific research fundation of Shandong Provincial Education Committee (J94,K26)

Correspondence to: Zhao-Shan Niu, Department of Pathology, Medical College of Qingdao University, 38 Dengzhou Road, Qingdao 266021, Shandong Province, China. nzxmxh@public.qd.sd.cn

Telephone: +86-532-3812410

Received 2002-03-15 **Accepted** 2002-04-13

Abstract

AIM: To investigate the possible roles of p53 and C-myc genes in the primary hepatocellular carcinogenesis and the relationship between the liver hyperplastic nodule (LHN) and hepatocellular carcinoma (HCC).

METHODS: The expression of p53 and C-myc genes was detected immunohistochemically in 73 and 60 cases of HCC and pericarcinomatous tissues, respectively.

RESULTS: The positive expression of p53 in HCC was significantly higher than that in pericarcinomatous tissues ($P < 0.05$). In pericarcinomatous tissues, the p53 expression was observed only in LHN, but not in liver cirrhosis (LC) and normal liver tissues. The positive expression rate of C-myc in HCC or LHN was significantly higher than that in LC or normal liver tissues ($P < 0.05$ and $P < 0.01$), however, no significant difference was found between HCC and LHN ($P > 0.05$). The positive expression rate of p53 and C-myc in HCC was correlated with the histological differentiation, that in the poorly differentiated was significantly higher than that in well differentiated samples ($P < 0.05$).

CONCLUSION: The overexpression of p53 and C-myc genes might play a role in the carcinogenesis of HCC; And LHN seems a preneoplastic lesion related to hepatocarcinogenesis; No evidence supports that LC contribute directly to the hepatocarcinogenesis.

Niu ZS, Li BK, Wang M. Expression of p53 and C-myc genes and its clinical relevance in the hepatocellular carcinomatous and pericarcinomatous tissues. *World J Gastroenterol* 2002;8(5):822-826

INTRODUCTION

Primary hepatocellular carcinoma (HCC) is one of the most common malignant tumors in China^[1-11], and the incidence of HCC reported has apparently increased in recent years. Despite

a variety of therapeutic strategies, HCC remains a significant cause of cancer death. Therefore, to study the HCC pathogenesis is of the utmost importance to the prevention and treatment of this disease. With the advancement of HCC study, it becomes clear that the biologic behavior of HCC is closely related with the overactivation of the oncogenes and the inactivation of the tumor suppressor genes^[12,13].

In the present study, the immunohistochemical LSAB (labelled streptavidin biotin) method was used to detect the expression of p53 and C-myc genes in HCC and pericarcinomatous tissues, in order to investigate the possible roles of these genes played in the HCC carcinogenesis, and to find out the relationship between the liver hyperplastic nodule and HCC. In addition, the relationship between the expression of p53 and C-myc genes and clinicopathological parameters of HCC was preliminarily investigated.

MATERIALS AND METHODS

Materials

HCC specimens of 100 cases obtained from surgical resections or biopsies performed at the Affiliated Hospital of Medical College of Qingdao University, China. Of these patients, 76 were male and 24 female with an average of 50.4 years. None of the patients had received chemo- or radio-therapy before resection. We randomly selected 73 and 60 cases of HCC to detect the expression of p53 and C-myc genes respectively owing to the limitation of antibodies. The specimens for detecting p53 were classified into 4 grades according to Edmondson's grading criteria, 4 specimens were in grade I, 24 in grade II, 39 in grade III, and 6 in grade IV. All 73 specimens contained pericarcinomatous tissues, in which including 39 liver hyperplastic nodules (LHN), 35 liver cirrhosis (LC) and 10 normal liver tissues. Among the specimens for detecting C-myc gene, 4 were in grade I, 17 in grade II, 30 in grade III, and 9 in grade IV. All 60 specimens contained pericarcinomatous tissues, in which including 37 LHN, 30 LC and 12 normal liver tissues.

Methods

All specimens were routinely processed, alcohol-fixed and paraffin-embedded. Serial paraffin sections of 4 μ m thickness were cut and used for hematoxylin and eosin (HE) and immunohistochemical stains. Immunohistochemical LSAB method was used to detect p53 and C-myc genes. Anti-p53 monoclonal antibody DO-7, anti-C-myc monoclonal antibody and LSAB kits were purchased from Dako Co. Before staining, the sections were heated with microwave in 0.05 mol \cdot L⁻¹ citric acid solution for antigen retrieval. In each staining, a known p53 or C-myc positive section was added as the positive control, and PBS was used as the substitute of the first antibody for the negative control.

Analysis of immunohistochemical staining

Cells with brown granules under microscope were regarded as positive. The criteria for the evaluation of the p53 expression in the present study were as follows: the positive nuclei number was semiquantitatively evaluated by counting that in 8-10 randomly-chosen medium power ($\times 100$ magnification), and the four degrees of the p53 expression were considered as: negative (-), no positive cells; weak positive (+), the positive cells $<10\%$; moderately positive (+ +), the positive cells between $10\text{--}50\%$; strong positive (+ + +), the positive cells $>50\%$. For the evaluation of C-myc expression, the percentage of positively stained cells was employed as an index, which was obtained from counting 500 cells at more than 5 high power fields for each section, and classified into 4 grades: grade I, the positive cells between $1\text{--}25\%$; grade II, the positive cells $26\text{--}50\%$; grade III, the positive cells $51\text{--}75\%$; grade IV, the positive cells $76\text{--}100\%$. No positive cells were scored negative (-).

Statistical analysis

Results were analysed by χ^2 test. Differences at $P < 0.05$ were considered to be statistically significant.

RESULTS

Expression of p53 gene in HCC and its pericarcinomatous tissue

The positive staining for p53 gene expressed as brown granules, which was mainly located in the cell nuclei of tumor cells (Figure 1). The staining intensity and extent varied among tumors, different tumor regions and individual tumor cells. Immunostaining of p53 protein was negative in all tumor stroma, bile duct epithelia, LC and normal liver tissues. A few p53 weakly positive cells were found in LHN (Figure 2). The significant difference existed between HCC and LHN (χ^2 value 10.57, $P < 0.01$), and so did between LHN and LC (χ^2 value 6.94, $P < 0.01$) (Table 1).

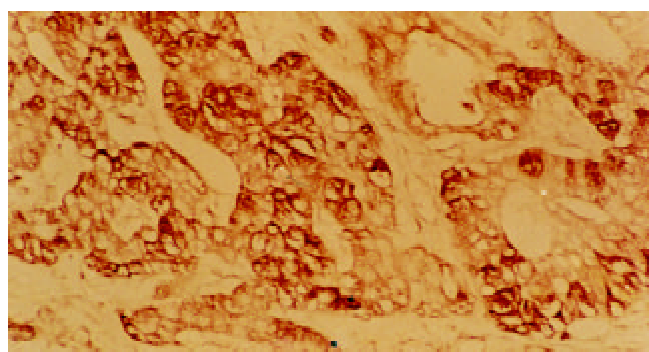


Figure 1 The positive expression of p53 gene in HCC. LSAB $\times 200$

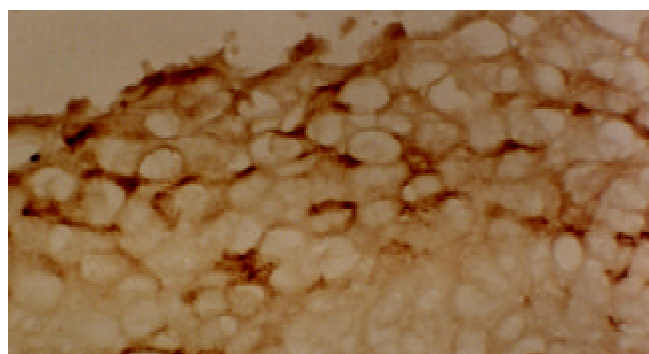


Figure 2 The positive expression of p53 gene in LHN. LSAB $\times 200$

Expression of C-myc gene in HCC and its pericarcinomatous tissue

The positive staining for C-myc gene was also expressed as brown granules, which was distributed mainly in cell nuclei, partly in cytoplasm. Although the expression rate of C-myc was higher in LHN than that in HCC, the statistical significance did not reach (χ^2 value 0.05, $P > 0.05$). The expression of C-myc gene in HCC and LHN was significantly higher than that in LC (χ^2 values 4.38, 4.51, $P < 0.05$). In HCC (Figure 3) and LHN (Figure 4) showing strong expression of C-myc, the positive-staining cells were distributed dominantly in a diffused pattern; whereas in LC (Figure 5) showing weak expression of C-myc, they preferred in a focalized pattern. The expression of C-myc was negative in normal liver tissues (Table 2).

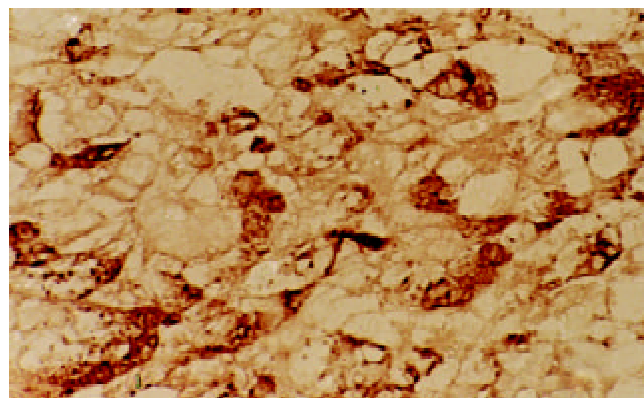


Figure 3 The positive expression of C-myc gene in HCC. LSAB $\times 200$

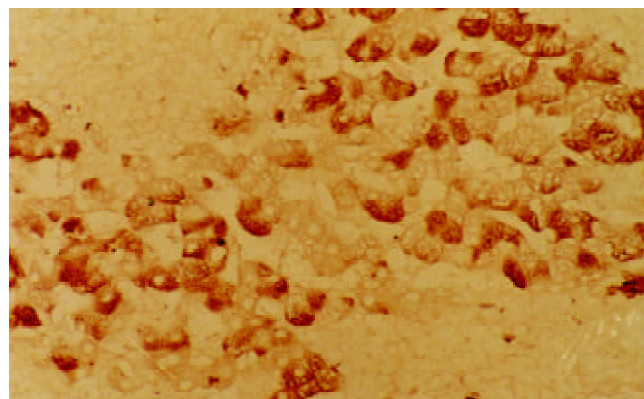


Figure 4 The positive expression of C-myc gene in LHN. LSAB $\times 200$

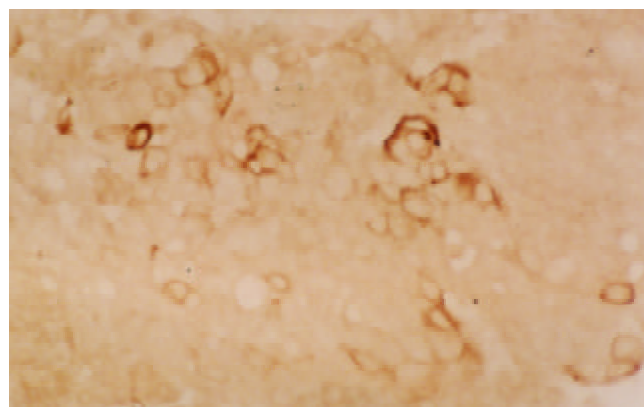


Figure 5 The positive expression of C-myc gene in LC. LSAB $\times 200$

Table 1 Expression of p53 gene in HCC and its pericarcinomatous tissue

Histological type	n	Expression of p53 gene				Positive rate (%)
		-	+	++	+++	
HCC	73	37	12	19	5	49.3
LHN	39	32	7	0	0	17.9
LC	35	35	0	0	0	0
Normal liver tissues	17	17	0	0	0	0

Table 2 Expression of C-myc gene in HCC and its pericarcinomatous tissue

Histological type	n	Expression of C-myc gene					Positive rate (%)
		-	grade I	grade II	grade III	grade IV	
HCC	60	37	0	2	9	12	38.3
LHN	37	22	1	3	3	8	40.5
LC	30	25	4	1	0	0	16.7
Normal liver tissues	12	12	0	0	0	0	0

The relationship between the expression of p53 and C-myc genes and histological grade of HCC

There were varieties of positive rates of p53 and C-myc genes in different HCC histological grades of HCC, with a close relationship between the genes expression and the tumor differentiation. The positive rates of p53 expression in Edmondson's grading III and IV and Edmondson's grading I and II were 60 % (27/45), 32.1 % (9/28), respectively, which manifested a significant difference (χ^2 value 5.36, $P < 0.05$); The positive rates of C-myc expression in Edmondson's grading III and IV and Edmondson's grading I and II were 48.7 % (19/39), 19 % (4/21), respectively, their differences were also significant (χ^2 value 5.08, $P < 0.05$) (Table 3).

Table 3 The relationship between the expression of p53 and C-myc genes and histological grade of HCC

Edmondson's grading	Expression of p53 gene		Expression of C-myc gene	
	Negative	Positive	Negative	Positive
I	4	0	3	1
II	15	9	14	3
III	18	21	18	12
IV	0	6	2	7

Correlation between p53 and C-myc protein expressions and HCC clinicopathological parameters

No significant relation was found between p53 or C-myc gene expression and patient age, sex and tumor size ($P > 0.05$).

DISCUSSION

The p53 gene is one of the most important tumor suppressor genes determined so far^[14-19]. In recent years, it has been found that the p53 protein seems not express in the benign and preneoplastic lesions, and that there was no obvious relation between the p53 protein and carcinogenesis^[20]. However, in the present study, the positive rate of p53 protein staining in LHN was 17.9 %, which coincided basically with some results in literature^[21-25]. The facts that the p53 protein expressed low in LHN and high in HCC, indicate that the high expression of p53 protein is probably associated with the cancerous transformation of hepatocytes, the early event in the carcinogenesis of HCC. It has been proved that wild type p53 protein can induce cell apoptosis whereas the mutant p53 protein can inhibit cell apoptosis and promote cell transformation and proliferation, resulting in carcinogenesis^[26-30]. The p53 protein confirmed by immunohistochemical staining was considered as the mutation type^[31]. Therefore, we speculate that p53 protein may exert its carcinogenic effect in the early stage of carcinogenesis on hepatocytes by two ways: (1) As described above, the mutant p53 protein might be associated with cell rapid proliferation and cell transformation, which ultimately results in hepatocellular carcinogenesis; (2) with the increase of the mutant p53 expression, and its inhibiting effect on apoptosis there will be an abnormal in cell numbers, which may eventually initiate the hepatocellular carcinogenesis. In addition, our results indicated that there existed a close relationship between the p53 gene expression and tumor cell differentiation in HCC, which suggests that the expression of p53 gene might serve as an index for the judgement of HCC malignant degree and its clinical prognosis.

It has been reported that the inept expression of C-myc gene correlated with carcinogenesis^[23,32,33]. However, some authors held that the overexpression of C-myc gene could not be observed until the hepatocytes had thoroughly transformed into malignancy in the late stage of HCC, which reflected the continuous proliferation of tumor cells^[34-36]. On the contrary, most experiments demonstrated the expression of C-myc in HCC and its pericarcinomatous tissue^[24,37]. In the present study, the expression of C-myc gene was observed both in LHN and LC with varied degree and LHN was similar to HCC in the expression of C-myc, which were coincident with the results of others and suggests that the overexpression of C-myc gene occurs in the early phase of HCC formation, and correlates with preneoplastic transformation and proliferation. Our results also indicated that the expression of C-myc gene in HCC was related to the cell differentiation, which suggests that C-myc gene expression may exist in the sequential process of hepatocarcinogenesis, and be related to the phase of hepatocarcinogenesis.

In the present study, the expression of p53 gene in LHN was similar to that in HCC to some extent and the overexpression of C-myc gene was seen in both samples. The mutation of p53 gene that may lead to cell malignization, thus may reflect the alterations in different biologic state of LHN, and suggest that LHN is probably in the process of malignant transformation and in relation to hepatocarcinogenesis. In the present study the expression of C-myc gene in LHN had no significant difference from that in HCC, which reveals that parts of LHN were actually in the preneoplastic state or might be cancerous though they seemed normal in histology. Some study indicated that the increased oncogene expression brought cells into a state of active proliferation that resulted in an increased frequency of mutation^[38]. This suggests that the overexpression of C-myc gene may make LHN be transformed

malignantly. Another study showed that not all altered hepatocyte foci manifested abnormal expression of C-myc in the early stage of experimental HCC and the high expression of C-myc was only seen in the poorly differentiated foci^[39]. It shows that the overexpression of C-myc gene may relate to the tumor's differentiation. Therefore, the overexpression of C-myc gene may be responsible for the low differentiation of LHN. It has been postulated that C-myc products might serve as a valid index for identifying preneoplastic lesion of HCC, the foci overexpressed C-myc were in danger of carcinogenesis^[24,33]. However, few research reports till now have been found on the relationship between LHN and HCC. The present study thus provides a new possible way to diagnose HCC at earliest possible stage, which is of great importance in improving the prognosis because early diagnosis usually means high curability.

For many years, it has been generally considered that LC was closely associated with HCC and hepatocarcinogenesis. According to carcinogenic hypothesis on oncogene, at least two activated oncogenes are required—namely, the ras gene which was representative of transforming gene and the C-myc representative of immortalizing gene. Only when the two sorts of oncogenes function coordinately can stock-cultured cells be transformed malignantly. In the present study, we found that the expression rate of C-myc protein in LC was 26.7 %, but, the expression intensity of C-myc in LC was significantly less than that in LHN. Our previous studies have indicated that there was no mutation of the ras gene in LC, and that the expression of c-erbB-2 oncogene was negative in LC, indicating that there are no mutation and activation of c-erbB-2 in LC, that is, it is impossible in this situation for malignant transformation. In addition, according to the present study, there was no mutation of p53 in LC, suggesting that LC does not necessarily link with hepatocarcinogenesis. Alcohol is the major cause of cirrhosis in European countries and the United States, responsible for 60 to 70 percent of all cases of cirrhosis, but it only infrequently leads to HCC; carbon tetrachloride can lead to LC rather than HCC. However, the reason why the ratio of HCC accompanied by LC in China is obviously higher than that in European countries and the United States perhaps lies in HBV infections, there is not a cause and effect but a accompanying relationship between LC and HCC. The significance of C-myc expression in LC remains to be investigated.

What requires a special explanation is that the LHN used in the present study is totally different from the nodules in LC. We noticed that though the majority of the LHN developed from LC, it is a cell population that differs from LC in properties and proliferative patterns. Although the liver cell cords in LC are in disarray, the hepatocytes are primarily arranged in a single line, most of which are normal in morphology; However, the hepatocytes in LHN grow by expansion, one nodule primarily contains a sort of cells, and in mixed cell nodules there exists a clear margin between the cellgroups, suggesting the nodules are of clone origin.

As to the relationship between the expression of p53 and C-myc genes and clinicopathological parameters of HCC, we found that there was no link of p53 or C-myc gene expression with patient age, sex and tumor size, which was in accordance with the previous reports^[40]. Some studies indicated that the overexpression of p53 or C-myc was closely related to the prognosis of HCC^[18,33,41-50], which was not our results have not yet confirmed that p53 or C-myc gene expression is directly associated with the prognosis of HCC. However, in the present study, the low expression of p53 gene and the overexpression of C-myc gene were found in LHN. It can be deduced that

although normal in histology, LHN is surely abnormal in gene expression. Whether the phenomenon has a tie with the recurrence of HCC after resection needs to be further studied.

REFERENCES

- 1 **Sithinamsuwan P**, Piratvisuth T, Tanomkiat W, Apakupakul N, Tongyoo S. Review of 336 patients with hepatocellular carcinoma at Songklanagarind Hospital. *World J Gastroenterol* 2000; **6**:339-343
- 2 **Sun BH**, Zhang J, Wang BJ, Zhao XP, Wang YK, Yu ZQ, Yang DL, Hao LJ. Analysis of in vivo patterns of caspase 3 gene expression in primary hepatocellular carcinoma and its relationship to p21WAF1 expression and hepatic apoptosis. *World J Gastroenterol* 2000; **6**:356-360
- 3 **Xu HY**, Yang YL, Guan XL, Song G, Jiang AM, Shi LJ. Expression of regulating apoptosis gene and apoptosis index in primary liver cancer. *World J Gastroenterol* 2000; **6**:721-724
- 4 **Feng DY**, Zheng H, Tan Y, Cheng RX. Effect of phosphorylation of MAPK and Stat3 and expression of c-fos and c-jun proteins on hepatocarcinogenesis and their clinical significance. *World J Gastroenterol* 2001; **7**:33-36
- 5 **Cui J**, Yang DH, Bi XJ, Fan ZR. Methylation status of c-fms oncogene in HCC and its relationship with clinical pathology. *World J Gastroenterol* 2001; **7**:136-139
- 6 **Fan ZR**, Yang DH, Cui J, Qin HR, Huang CC. Expression of insulin-like growth factor II and its receptor in hepatocellular carcinogenesis. *World J Gastroenterol* 2001; **7**:285-288
- 7 **Wang Q**, Lin ZY, Feng XL. Alterations in metastatic properties of hepatocellular carcinoma cell following H-ras oncogene transfection. *World J Gastroenterol* 2001; **7**:335-339
- 8 **Tang ZY**. Hepatocellular carcinoma: cause, treatment and metastasis. *World J Gastroenterol* 2001; **7**:445-454
- 9 **Cao XY**, Liu J, Lian ZR, Clayton M, Hu JH, Zhu MH, Fan DM, Feitelson M. Differentially expressed genes in hepatocellular carcinoma induced by woodchuck hepatitis B virus in mice. *World J Gastroenterol* 2001; **7**:575-578
- 10 **Zhou XD**, Tang ZY, Yang BH, Lin ZY, Ma ZC, Ye SL, Wu ZQ, Fan J, Qin LX, Zheng BH. Expression of 1000 patients who underwent hepatectomy for small hepatocellular carcinoma. *Cancer* 2001; **91**:1479-1486
- 11 **Chen X**, Cheung ST, So S, Fan ST, Barry C, Higgins J, Lai KM, Ji J, Dudoit S, Ng IO, Van De Rijn M, Botstein D, Brown PO. Gene expression patterns in human liver cancers. *Mol Biol Cell* 2002; **13**:1929-1939
- 12 **Yang JM**, Wang RQ, Bu BG, Zhou ZC, Fang DC, Luo YH. Effect of hepatitis C virus infection on expression of several cancer-associated gene products in hepatocellular carcinoma. *World J Gastroenterol* 1999; **5**:25-27
- 13 **Bian JC**, Shen FM, Shen L, Wang TR, Wang XH, Chen GC, Wang JB. Susceptibility to hepatocellular carcinoma associated with null genotypes of GSTM1 and GSTT1. *World J Gastroenterol* 2000; **6**:228-230
- 14 **Lin GY**, Chen ZL, Lu CM, Li Y, Ping XJ, Huang R. Immunohistochemical study on p53, H-rasp21, c-erbB-2 protein and PCNA expression in HCC tissues of Han and minority ethnic patients. *World J Gastroenterol* 2000; **6**:234-238
- 15 **Wang XJ**, Yuan SL, Li CP, Iida N, Oda H, Aiso S, Ishikawa T. Infrequent p53 gene mutation and expression of the cardia adenocarcinomas from a high incidence area of Southwest China. *World J Gastroenterol* 2000; **6**:750-753
- 16 **Xu AG**, Li SG, Liu JH, Gan AH. Function of apoptosis and expression of the proteins Bcl-2, p53 and C-myc in the development of gastric cancer. *World J Gastroenterol* 2001; **7**:403-406
- 17 **Fei SJ**, Chen YL, Lin IF, Chen SM, Liu GZ. Expression of ras, p21, and p53 in gastric cancer and precancerous lesions. *Shijie Huaren Xiaohua Zazhi* 2001; **9**:465-466

- 18 **Steele RJ**, Thompson AM, Hall PA, Lane DP. The p53 tumour suppressor gene. *Br J Surg* 1998; **85**:1460-1467
- 19 **Prives C**, Hall PA. The p53 pathway. *J Pathol* 1999; **187**: 112-126
- 20 **Qin LL**, Su JJ, Li Y, Yang C, Ban KC, Yian RQ. Expression of IGF- II, p53, p21 and HbxAg in precancerous events of hepatocarcinogenesis induced by AFB1 and/or HBV in tree shrews. *World J Gastroenterol* 2000; **6**:138-139
- 21 **Yang JM**, Han DW, Liang QC, Zhao JL, Hao SY, Ma XH, Zhao YC. Effects of endotoxin on expression of ras, p53 and bcl-2 oncoprotein in hepatocarcinogenesis induced by thioacetamide in rats. *China Natl J New Gastroenterol* 1997; **3**: 213-217
- 22 **Martins C**, Kedda MA, Kew MC. Characterization of six tumor suppressor genes and microsatellite instability in hepatocellular carcinoma in southern African blacks. *World J Gastroenterol* 1999; **5**:470-476
- 23 **Cai DW**, Gao CZ, Wang NJ. C-myc gene and p53 protein expression in human primary liver carcinoma. *Zhonghua Binglixue Zazhi* 1994; **23**: 100-103
- 24 **Yang SB**, Wang MW, You WD, Lu YL, Chen K, Yu G. Overexpression of C-myc and p53 gene in human hepatocellular carcinoma-a study with immunohistochemistry and in situ hybridization. *Zhonghua Zhongliu Zazhi* 1995; **17**:415-417
- 25 **Kang YK**, Kim CJ, Kim WH, Kim HO, Kang GH, Kim YI. p53 mutation and overexpression in hepatocellular carcinoma and dysplastic nodules in the liver. *Virchows Arch* 1998; **432**: 27-32
- 26 **Lane DP**, Lu X, Hupp T, Hall PA. The role of the p53 protein in the apoptotic response. *Philos Trans R Soc Lond B Biol Sci* 1994; **345**: 277-280
- 27 **Terada T**, Nakanuma Y. Expression of apoptosis, proliferating cell nuclear antigen, and apoptosis-related antigens (bcl-2, C-myc, Fas, Lewis(y) and p53) in human cholangiocarcinomas and hepatocellular carcinomas. *Pathol Int* 1996; **46**:764-770
- 28 **Hall PA**. p53: The challenge of linking basic science and patient management. *Oncologist* 1998; **3**: 218-224
- 29 **Yuen MF**, Wu PC, Lai VC, Lau JY, Lai CL. Expression of c-myc, c-fos, and c-jun in hepatocellular carcinoma. *Cancer* 2001; **91**:106-112
- 30 **Feng DY**, Zheng H, Shen M, Cheng RX, Yan YH. Regulation of p53 and bcl-2 proteins to apoptosis and cell proliferation in liver cirrhosis and hepatocellular carcinoma. *Hunan Yi ke Daxue Xuebao* 1999; **24**:325-328
- 31 **Hall PA**. p53 in tumor pathology: can we trust immunohistochemistry? -revisited. *J Pathol* 1994; **172**:1-4
- 32 **Ninomiya I**, Yonemura Y, Matsumoto H, Sugiyama K, Kamata T, Miwa K, Miyazaki I, Shiku H. Expression of C-myc gene product in gastric carcinoma. *Oncology* 1991; **48**:149-153
- 33 **Kawate S**, Fukusato T, Ohwada S, Watanuki A, Morishita Y. Amplification of c-myc in hepatocellular carcinoma: correlation with clinicopathologic features, proliferative activity and p53 overexpression. *Oncology* 1999; **57**:157-163
- 34 **Li DC**, Liu TH, Wang DT. Expression of cellular oncogenes in human primary liver cell carcinoma. *Zhonghua Binglixue Zazhi* 1990; **19**:116-118
- 35 **Su TS**, Lin LH, Lui WY, Chang CM, Chou CK, Ting LP, Hu CP, Han SH, Peng FK. Expression of c-myc gene in human hepatoma. *Biochem Biophys Res Commun* 1985; **15**: 264-268
- 36 **Beer DG**, Schwarz M, Sawada N, Pitot HC. Expression H-ras and C-myc protooncogenes in isolated r-glutamyl transpeptidase-positive rat hepatocytes and in hepatocellular carcinoma induced by diethylnitrosamine. *Cancer Res* 1986; **46**: 2435-2441
- 37 **Ling CQ**, Qian Y, Zhao JA, Jin Y. Expression of C-myc IGF-II gene and cyclinD1 in experimental hepatocarcinogenesis. *Shijie Huaren Xiaohua Zazhi* 2001; **9**: 1452-1453
- 38 **Lian ZR**, Wu MC, Gu JR, Xu GW, Xu L, Zhou SX. HBV status and expression of ets-2, IGF- II, C-myc and N-ras in human hepatocellular carcinoma and adjacent nontumorous tissues-a comparative study. *Zhonghua Zhongliu Zazhi* 1991; **13**: 5-8
- 39 **Lin YZ**, Ding L, Chen JY. The expression of C-myc, N-ras mRNA and its relations to the differentiation of preneoplastic altered hepatocytes. *Zhonghua Zhongliu Zazhi* 1993; **15**:97-100
- 40 **Ng IO**, Chung LP, Tsang SW, Lam CL, Lai EC, Fan ST, Ng M. p53 gene mutation spectrum in hepatocellular carcinomas in Hong Kong Chinese. *Oncogene* 1994; **9**: 985-990
- 41 **Wang D**, Shi JQ. Overexpression and mutations of tumor suppressor gene p53 in hepatocellular carcinoma. *China Natl J New Gastroenterol* 1996; **15**:161-164
- 42 **Li JQ**, Zhang CQ, Feng KT. PCNA, p53 protein and prognosis in primary liver cancer. *China Natl J New Gastroenterol* 1996; **2**:220-222
- 43 **Qin LX**, Tang ZY. The prognostic molecular markers in hepatocellular carcinoma. *World J Gastroenterol* 2002; **8**: 385-392
- 44 **Qin LX**, Tang ZY, Ma ZC, Zhou XD, Ye QH, Ji Y, Huang LW, Jia HL, Sun HC, Wang L. p53 immunohistochemical scoring: an independent prognostic marker for patients after hepatocellular carcinoma resection. *World J Gastroenterol* 2002; **8**: 459-463
- 45 **Ng IO**, Lai EL, Chan AS, So MK. Overexpression of p53 in hepatocellular carcinoma: A clinicopathological and prognostic correlation. *J Gastroenterol Hepatol* 1995; **10**: 250-255
- 46 **Yano M**, Asahara T, Dohi K, Mizuho T, Iwamoto KS, Seyama T. Close correlation between a p53 or hMSH2 gene mutation in the tumor and survival of hepatocellular carcinoma patients. *Int J Oncol* 1999; **14**:447-451
- 47 **Sugo H**, Takamori S, Kojima K, Beppu T, Futagawa S. The significance of p53 mutations as an indicator of the biological behavior recurrent hepatocellular carcinomas. *Surg Today* 1999; **29**:849-855
- 48 **Shen LL**, Qiu DK, Fang JY, Zhang TF, Yang JM, Chen SS, Xiao SD. Correlation between hypomethylation of c-myc and c-N-ras oncogenes and pathological changes in human hepatocellular carcinoma. *Zhonghua Zhongliu Zazhi* 1997; **19**:173-176
- 49 **Jiang WS**, Lu QM, Pan GZ. P53 gene mutation in hepatocellular carcinoma. *Zhonghua Waikexue Zazhi* 1998; **36**:531-532
- 50 **Fang Y**, Huang BJ, Liang QW, Li HM, Huang CW. Clinical significance of c-myc oncogene amplification in primary hepatocellular carcinoma by interphase fluorescence in situ hybridization. *Zhonghua Binglixue Zazhi* 2001; **30**:180-182

Edited by Zhu L

• LIVER CANCER •

Telomerase inhibition and telomere loss in BEL-7404 human hepatoma cells treated with doxorubicin

Ru-Gang Zhang, Li-Xia Guo, Xing-Wang Wang, Hong Xie

Ru-Gang Zhang, Li-Xia Guo, Xing-Wang Wang, Hong Xie, Department of Biotherapy, Institute of Biochemistry and Cell Biology, Shanghai Institutes for Biological Sciences, the Chinese Academy of Sciences, Shanghai 200031, China

Correspondence to: Prof. Hong Xie, Department of Biotherapy, Institute of Biochemistry and Cell Biology, Shanghai Institutes for Biological Sciences, the Chinese Academy of Sciences, Shanghai 200031, China. xiehong@sunm.shnc.ac.cn

Telephone: +0086-21-64735609 **Fax:** +86-21-34010138

Received 2002-02-28 **Accepted** 2002-07-06

Abstract

AIM: To study the effects of doxorubicin on telomerase activity and telomere length in hepatocellular carcinoma.

METHODS: Telomerase activity was assayed with a non-radioisotopic quantitative telomerase repeat amplification protocol-based method. The effect of doxorubicin (DOX) on the growth of BEL-7404 human hepatoma cells was determined by microculture tetrazolium assay. Mean telomere length (terminal restriction fragment) was detected by Southern blot method. The expression of telomerase subunits genes was investigated by RT-PCR. Cell apoptosis and cell cycle distribution were evaluated by flow cytometry.

RESULTS: Telomerase activity was inhibited in a dose and time-dependent manner in BEL-7404 human hepatoma cells treated with DOX for 24, 48 or 72 h in concentrations from 0.156 to 2.5 μ M which was correlated with the inhibition of cell growth. No changes were found in the mRNA expression of three telomerase subunits (hTERT, hTR and TP1) after drug exposure for 72 h with indicated concentrations. The cells treated with DOX showed shortened mean telomere length and accumulated at the G₂/M phase. However, there was almost no effects on cell apoptosis by DOX.

CONCLUSION: The telomerase inhibition and the telomere shortening by DOX may contribute to its efficiency in the treatment in hepatocellular carcinoma.

Zhang RG, Guo LX, Wang XW, Xie H. Telomerase inhibition and telomere loss in BEL-7404 human hepatoma cells treated with doxorubicin. *World J Gastroenterol* 2002; 8(5):827-831

INTRODUCTION

Telomeres form the ends of eukaryotic chromosomes consisting of an array of tandem repeats of hexanucleotide 5'-TTAGGG-3'. Telomeres protect the chromosomes from DNA degradation, end-to-end fusions, rearrangements and maintain nuclear structure^[1]. Human telomerase is a ribonucleoprotein complex, composed of a catalytic reverse transcriptase subunit (hTERT), an RNA component (hTR) that serves as a template for the synthesis of telomeric repeats, and an associated protein

subunit (TP1)^[2-4]. It adds telomeric repeats to the 3' end of telomeric DNA. This telomere stabilization by telomerase can lead to unlimited cell proliferation.

Hepatocellular carcinoma (HCC), one of the most common malignancies in the world especially in Asia and Africa, is an aggressive cancer. It causes approximately 250 000 deaths annually^[5]. It was reported that HCC exhibited a high incidence of telomerase activity and that the activity increased in accordance with the HCC degree of histological undifferentiation which was absent in normal liver tissue^[6,7]. Other reports revealed that hTERT expression was the rate-limiting determinant of HCC telomerase activity^[8-10].

Doxorubicin (DOX), an antitumor antibiotic, can intercalate into base pairs of DNA and generate toxic oxygen free radicals, which not only causes single-or double-strand DNA breaks but also damages a variety of necessary macromolecules such as proteins, lipids and RNA^[11]. DOX is one of the most efficient chemotherapy agents in the treatment of HCC, and its total efficiency rate can be up to 44 %^[12]. However, the relationship between the efficiency of DOX and telomerase activity in HCC has not yet been elucidated. In the present study, we investigated the effects of DOX on the telomerase activity and telomere length in BEL-7404 human hepatoma cells.

MATERIALS AND METHODS

Cell and culture condition

BEL-7404 human hepatoma cell line from Cell Bank of Chinese Academy of Sciences^[13], was cultured in RPMI-1640 medium (Gibco) supplemented with 10 % heat-inactivated newborn calf serum, at 37 °C in a humidified CO₂ incubator containing 5 % CO₂ and 95 % air.

Drug

DOX (Sigma) was dissolved in RPMI-1640 to the final concentration of 5mM and stored at 4 °C.

Assessment of cell proliferation

An MTT assay was conducted to determine the cell proliferation. Cells were seeded at 1×10^4 cells/well in a 96-well plate and incubated overnight. The drug was added to the cultured cells with the final concentrations from 0.156 μ M to 2.5 μ M and culturing further for another 24, 48 or 72 h respectively. Following culture, the cells were incubated with 800 mg/L 3-(4,5-dimethylthiazol-2-yl)-2,5-diphenyltetrazolium bromide (MTT, Sigma), which was used to assay the activity of mitochondrial dehydrogenases. Four hours later, 10 % sodium dodecyl sulphate - 5 % isobutanol-0.12 % hydrochloric acid solution was added to solubilize the formazan product. The plate was then incubated at 37 °C for another 12 h. The absorbance at 570 nm was measured with a model 550 microplate reader (Bio-Rad). The percent of cell growth inhibition was expressed as: (A-B)/A \times 100 %, where A was the absorbance value from the controls and B was that from the experimental cells.

Telomerase assay

Telomerase activity was assayed with PCR-based telomeric repeat amplification protocol (TRAP) as previously described^[14, 15]. Cells were collected and washed with PBS, lysed in 1×3-[(3-cholamidopropyl) dimethylammonio]-1-propanesulfonic acid (CHAPS, Sigma) buffer, incubated on ice for 30 min, and centrifuged at 12 000 g for 30 min. The protein concentration was determined by Coomassie Protein Assay. Each of TRAP reactions contained 1 µg of total protein. The reaction mixture [20 mM Tris-HCl (pH 8.3), 1.5 mM MgCl₂, 63 mM KCl, 0.005 % Tween-20, 1mM EGTA, 50 µM of each dNTPs and 0.1 µg TS (5' - AATCCGTCGAGC AGAGTT-3')] was incubated at 30 °C for 30 min, heated at 94 °C for 5 min. Then 0.1 µg of return primer ACX(5' - GCGCGG[CTTACC]₃CTAACC-3'), 0.1 µg of internal control primer NT(5' -ATCGCTTCTCGGCCTTTT-3'), 0.01 aM of internal control template TSNT(5' -AATCCGTCGAGC AGAGTTAAAGGCCGAGAAGCGAT-3') and 2 units Taq DNA polymerase (Promega) were added. The reaction mixture was then subjected to 28 PCR cycles: 94 °C for 30s and 60 °C for 30 s. PCR products were separated by electrophoresis on 12 % nondenaturing polyacrylamide gels and stained with SYBR Green I (FMC) for 15 min, visualized and analyzed by UVP system. In every experiment, a negative control (1 µl CHAPS lysis buffer) was included. All of experiments were repeated at least twice. The relative telomerase activity was quantified by the formula: TP=[(A/B)/(A cell control/ B cell control)]×100 Where TP=total product, A=total intensity of telomerase product (50 bp,56 bp,62 bp.), and B=intensity of internal control (36 bp).

RT-PCR

Total cellular RNA was extracted from cells using Trizol (Life Technologies, Inc.) according to the instructions of the manufacturer. In each reaction, 1 µg of total RNA was reverse transcribed into cDNA using M-Mlv reverse transcriptase (Promega). Primer sets used to amplify specific sequences were 5' -CGGAAGAGTGCTCTGGAGCAA-3' and 5' -GGATGAAGCGGAGTCGGA-3' for hTERT (146 bp); 5' -TCTAACCCTAACTGAGAAGGGCGTAG-3' and 5' -GTTTGCTCTAGAATGAACGGTGGAAAG-3' for hTR (126 bp); 5' -TCAAGCCAAACCTGAATCTGAG-3' for TP1 (264 bp); 5' -GTGGGGCGCCCCAGGCACCA-3' and 5' -GTCCTTAATGTCACGCACGATTTC-3' for β-actin (539 bp). The PCR conditions of hTERT and TP1 were 94 °C, 45s; 60 °C, 45 s; 72 °C, 90 s for 31 and 29 cycles, respectively. And the PCR conditions of hTR and β-actin were 94 °C, 45 s; 55 °C, 45 s; 72 °C, 90 s for 28 and 22 cycles, respectively^[2].

Telomere length assay

Genomic DNA samples were prepared as described^[16]. Cells were lysed and proteins were digested in 10 mM Tris-HCl (pH 8.0), 100 mM NaCl, 25 mM EDTA, 0.5 % SDS, 0.1 mg/ml proteinase K at 48 °C overnight. Following two extractions with phenol and one with chloroform, DNA was precipitated with ethanol and dissolved in 10 mM Tris-HCl (pH 8.0) and 1 mM EDTA (TE). Telomere length was detected using TeloTAGGG telomere length assay (Roche) according to the manufacturer's protocol. For each sample, 1 µg of genomic DNA was digested with Rsa I/Hinf I (Sigma), separated on a 0.8 % agarose gel, transferred to a nylon membrane (Amersham Hybond-N⁺), and hybridized with a telomere specific digoxigenin(DIG)-labeled probe, incubated with anti-DIG-alkaline phosphatase and detected by chemiluminescence. The blotted signal was divided into 30 equidistant intervals from 1.9 to 21.2 kilobases to calculate mean telomere length

(terminal restriction fragment, TRF) using the formula $TRF = \frac{\sum (OD_i)}{\sum (OD_i/L_i)}$, where OD_i was the chemiluminescent signal and L_i was the length of the TRF fragment at position i^[17].

Flow cytometry analysis of cell cycle and apoptosis

The cells were harvested and resuspended in the solution containing 40mM sodium citrate, 250mM sucrose and 5 % DMSO. The suspension was stored at -20 °C for 20 min, then thawed rapidly at room temperature and centrifuged to collect the cells. The cells were resuspended in a solution containing RNase A (5×10⁴ unit/g, 50 mg/L) and 20 mg/L propidium iodide (PI). The cell cycle distribution and apoptosis were determined by the fluorescence of individual cells measured with flow cytometry^[18].

RESULTS AND DISCUSSION

Inhibition of telomerase activity

Telomerase activity was inhibited in a dose and time-dependent manner in BEL-7404 human hepatoma cells treated with DOX (Figure 1A). To analyze the telomerase inhibition on the gene expression level, cells treated with DOX for 72 h were employed to study the telomerase mRNA expressions of its three major gene components, hTERT, hTR and TP1, using RT-PCR. Results showed that no changes were observed in the mRNA expression pattern of these subunits after the DOX exposure for 72 h with indicated concentrations (Figure 1B).

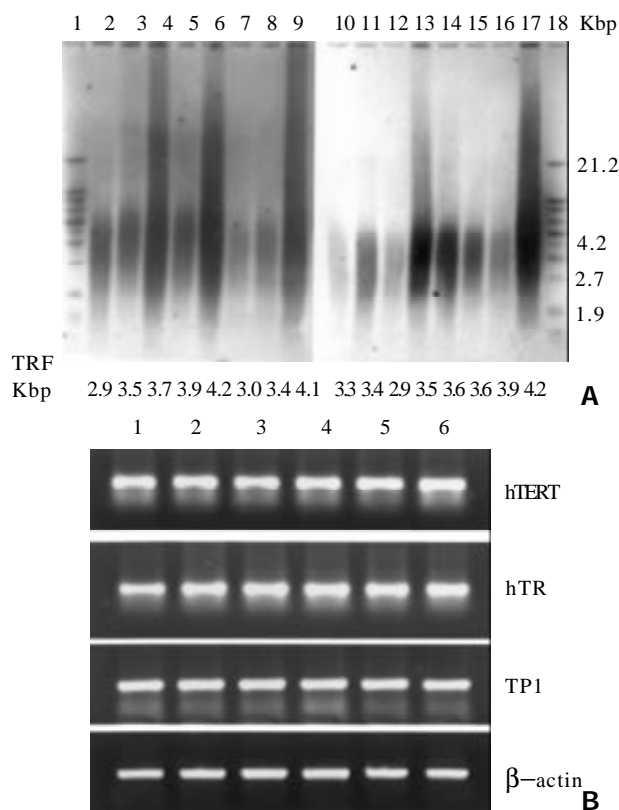


Figure 1 Telomerase inhibition by DOX in BEL-7404 human hepatoma cells. **(A)** Inhibition of telomerase activity by DOX in a dose and time-dependent manner in BEL-7404 human hepatoma cells. Lane 1, negative control; Lane 2, cell control; Lane 3–7, telomerase activity in presence of DOX for 24 h (2.5, 1.25, 0.625, 0.313 and 0.156 µM); Lane 8–12, telomerase activity in presence of DOX for 48 h (2.5, 1.25, 0.625, 0.313 and 0.156 µM); Lane 13–17, telomerase activity in presence of DOX for 72 h (2.5, 1.25, 0.625, 0.313 and 0.156 µM). All experiments were repeated at least twice and representative results were shown here. **(B)** RT-PCR analysis of hTERT, hTR and TP1 mRNA expression with DOX treatment for 72 h in a concentration range from 0.156

to 2.5 μM . Lane 1, cell control; Lane 2, 2.5 μM ; Lane 3, 1.25 μM ; Lane 4, 0.625 μM ; Lane 5, 0.313 μM ; Lane 6, 0.156 μM . β -actin was used as standard. Amplified sequences for hTERT, hTR, TP1 and β -actin are 146, 126, 264 and 539 bp, respectively.

The first report on the telomerase inhibition by DOX was presented by Zhu *et al.*, regarding the SW480 colon carcinoma cells^[19]. However, the opposite observations were reported later, in which authors found no effect of DOX on telomerase regulation in nasopharyngeal cancer, testicular cancer and squamous cell carcinoma^[20-22]. In this study, we found that the DOX treatment inhibited the telomerase activity in a dose and time-dependent manner in BEL-7404 human hepatoma cells. Considering the different results above, We think that this kind of inhibition might be cell-type specific and may be correlated with the clinical different efficiency of DOX in the treatment of different kinds and stages of tumors.

Abundant evidence indicated that the regulation of telomerase was multifactorial in mammalian cells and involves telomerase gene expression, post-translational protein-to-protein interactions, and protein phosphorylation^[23]. However, there was no information regarding three telomerase subunits expression affected by DOX in Zhu's study^[18]. In our investigation, there were no changes found in the expression of hTERT, hTR or TP1 mRNA. This indicated that the telomerase inhibition by DOX might be indirect with its antibiotic activity (eg.J damaging of necessary macromolecules).

Shortening of mean telomere length

Mean telomere length of BEL-7404 human hepatoma cells was decreased by the DOX treatment (Figure 2). Here, we believe that this is the first report regarding the shortening of telomere length by DOX treatment in BEL-7404 human hepatoma cells.

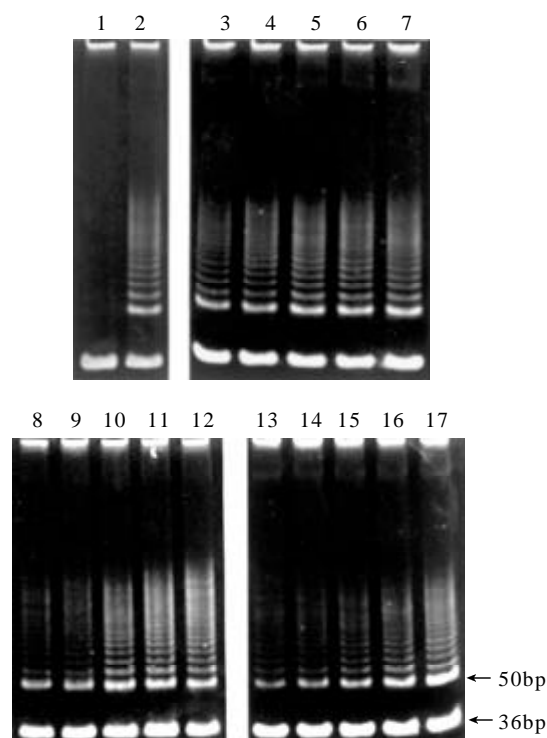


Figure 2 Shortening of mean telomere length (terminal restriction fragments, TRF) in DOX treated BEL-7404 human hepatoma cells. Lane 1 and 18, molecular marker; Lane 17, cell control; Lane 2 – 6, DOX treated for 72 h (2.5, 1.25, 0.625, 0.313 and 0.156 μM); Lane 7 – 11: DOX treated for 48 h (2.5, 1.25, 0.625, 0.313 and 0.156 μM); Lane 12–16: DOX treated for 24 h (2.5, 1.25, 0.625, 0.313 and 0.156 μM).

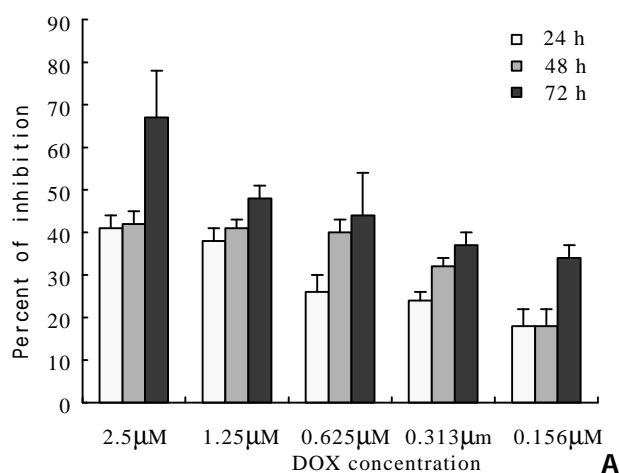
Compared with normal cells and some other carcinoma cells (such as HeLa cells), the mean telomere length of BEL-7404 human hepatoma cells is relatively short. As a result, the hepatoma cells are sensitive to telomere shortening, which may account, at least in part, for their chemosensitivity. Results from telomere shortening by cisplatin indicate that the nucleotide-excision repair system and cell division dynamics might be involved in the telomere shortening process, which make the process showing in a non-dose or time dependent manner^[24]. We assume that both of the factors may likewise participate in telomere shortening by DOX, because DOX can intercalate into DNA base pairs and result in non-dose or time dependent manner of telomere shortening.

Accumulation of cell cycle in G₂/M phase

The cell growth inhibition and cell cycle progression during DOX treatment were monitored in the present study to correlate these effects with telomerase activity inhibition and telomere loss. The growth of BEL-7404 cells was inhibited by DOX, which was indicated in (Figure 3 A). Following exposure to DOX, the hepatoma cells were accumulated in G₂/M phase, which revealed by flow cytometry (Figure 3 B). There were no marked changes observed in cell apoptosis in the experimental cells exposure to DOX for 24, 48 or 72 h with the concentrations from 0.156 to 2.5 μM , compared with the control cell.

Zhu *et al.*^[19] attributed the reduction in telomerase activity by DOX to the accumulation of cell cycle in G₂/M phase. But Holt *et al.*^[25] found that telomerase inhibition did not correlate with the cell cycle arrested at G₂/M phase but with the increasing in cell death. In present study, the cell apoptosis did not increase markedly compared with the control. Our previous research has also showed that antisense oligonucleotide to telomerase RNA component accumulated the cell cycle in G₂/M phase^[26]. The present observation confirmed the reports above, which indicated that telomerase inhibition was correlated with the cell cycle arrested at G₂/M phase.

Previously, Ishibashi *et al.*^[24] have reported that telomere loss in HeLa cells associated with the apoptosis induced by cisplatin. However, in our investigation the percent of cell apoptosis did not change markedly (Figure 3 B), although the mean telomere length was reduced by DOX. In BEL-7404 human hepatoma cells, we previously found that the cell apoptosis occurred when the mean telomere length reached to about 1.7Kb^[27]. In this study, the mean telomere did not reach to this critical length, and the apoptosis had not been induced which was consistent with the previous observation. Therefore, we deduce that telomere shortening may not be correlated with the apoptosis.



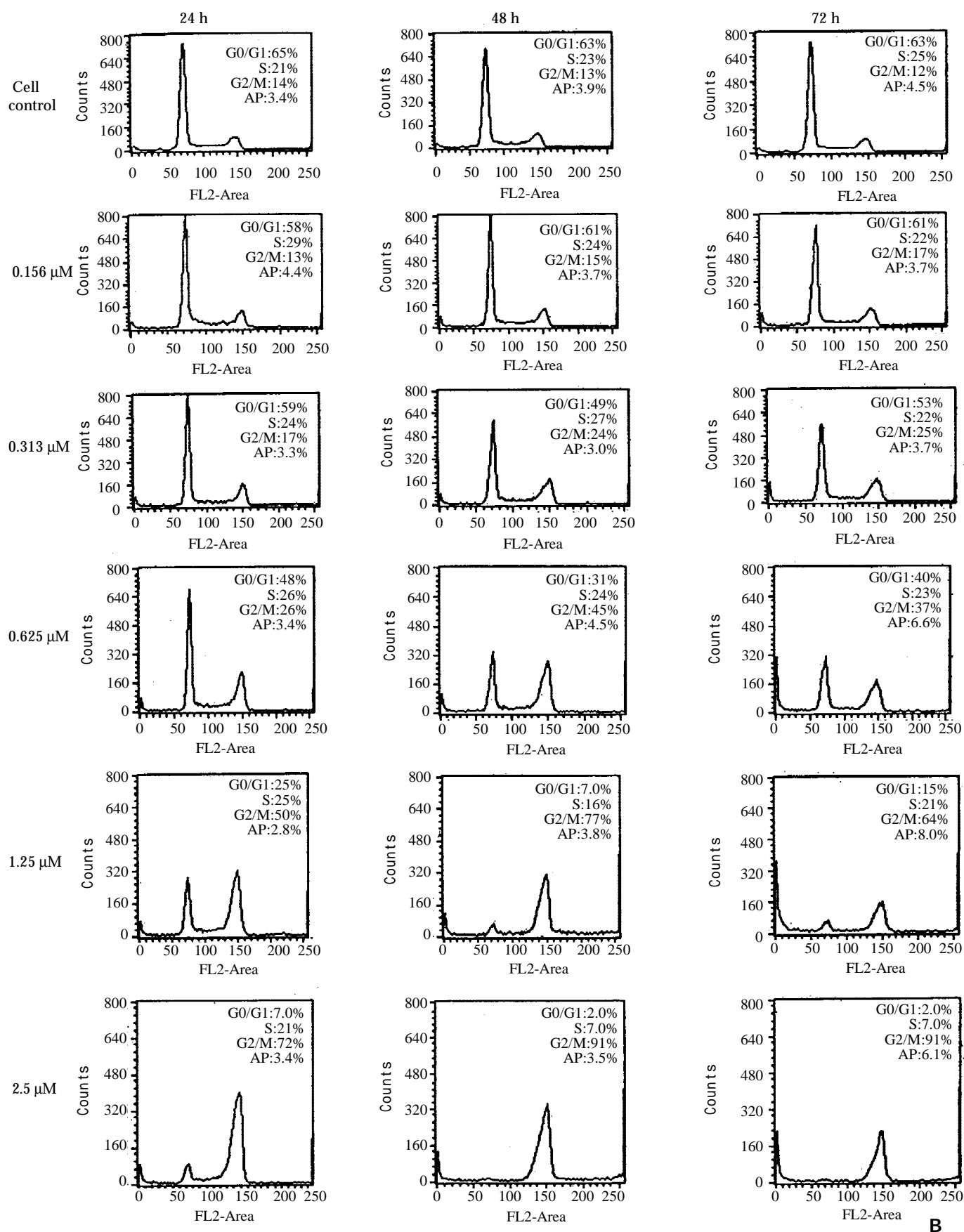


Figure 3 Effects of DOX on cell growth, cell cycle and cell apoptosis in BEL-7404 human hepatoma cells.

(A) Growth inhibition of BEL-7404 human hepatoma cells treated with DOX. Each value represents mean \pm SD from triplicate wells. **(B)** Cell cycle distribution and apoptosis in DOX treated BEL-7404 human hepatoma cells, analyzed by flow cytometry. Cell cycle was arrested at G₂/M with the treatment of DOX. Histograms of DNA contents of untreated cell control and treated with 0.156, 0.313, 0.625, 1.25 and 2.5 μ M were shown. Cells were maintained in the presence of DOX for 24, 48, and 72 h without a change in medium and collected at the times indicated. AP means the percent of apoptosis.

Many studies have shown that the telomerase activity was correlated with the cell growth^[28]. Our finding also revealed a good correlation between the inhibition of telomerase activity and the reduction in cell growth. However, in this study, the cell growth inhibition was mainly the result of cell cycle arrest, but not the increasing of cell apoptosis.

In conclusion, we found that telomerase activity was inhibited in a dose and time - dependent manner and mean telomere length was decreased by the treatment of DOX in BEL-7404 human hepatoma cells. This process correlated with the cell growth inhibition and the cell cycle accumulation in G₂/M phase. The present study indicates that the telomerase inhibition and the telomere shortening by DOX may contribute to its efficiency in the treatment of HCC.

REFERENCES

- 1 **Yakoob J**, Hu GL, Fan XG, Zhang Z. Telomere, telomerase and digestive cancer. *World J Gastroenterol* 1999; **5**:334-337
- 2 **Nakamura TM**, Morin GB, Chapman KB, Weinrich SL, Andrews WH, Linger J, Harley CW, Cech TR. Telomerase catalytic subunit homologs from fission yeast and human. *Science* 1997; **277**: 955-959
- 3 **Feng J**, Funk WD, Wang SS, Weinrich SL, Avilion AA, Chiu CP, Adams RR, Chang E, Allsopp RC, Yu J, Le S, West M, Harley CB, Andrews WH, Greider CW, Villeponteau B. The RNA component of human telomerase. *Science* 1995; **269**: 1236-1241
- 4 **Harrington L**, McPhail T, Mar V, Zhou W, Oulton R, Bass MB, Arruda I, Robinson MO. A mammalian telomerase-associated protein. *Science* 1997; **275**: 973-977
- 5 **Wang XW**, Yuan JH, Zhang RG, Guo LX, Xie Y, Xie H. Antihepatoma effect of alpha-fetoprotein antisense phosphorothioate oligodeoxyribonucleotides in vitro and in mice. *World J Gastroenterol* 2001; **7**: 345-351
- 6 **Tahara H**, Nakanishi T, Kitamoto M, Nakashio R, Shay JW, Tahara E, Kajiyama G, Ide T. Telomerase activity in human liver tissues: comparison between chronic liver disease and hepatocellular carcinomas. *Cancer Res* 1995; **55**: 2734-2736
- 7 **Nakashio R**, Kitamoto M, Tahara H, Nakanishi T, Ide T, Kajiyama G. Significance of telomerase activity in the diagnosis of small differentiated hepatocellular carcinoma. *Int J Cancer* 1997; **74**: 141-147
- 8 **Kawakami Y**, Kitamoto M, Nakanishi T, Yasui W, Tahara E, Nakayama J, Ishikawa F, Tahara H, Ide T, Kajiyama G. Immunohistochemical detection of human telomerase reverse transcriptase in human liver tissues. *Oncogene* 2000; **19**: 3888-3893
- 9 **Takahashi S**, Kitamoto M, Takaishi H, Aikata H, Kawakami Y, Nakanishi T, Shimamoto F, Tahara E, Tahara H, Ide T, Kajiyama G. Expression of telomerase component genes in hepatocellular carcinomas. *Eur J Cancer* 2000; **36**: 496-502
- 10 **Toshikuni N**, Nouse K, Higaashi T, Nakatsukasa H, Onishi T, Kaneyoshi T, Kobayashi Y, Kariyama K, Yamamoto K, Tsuji T. Expression of telomerase-associated protein 1 and telomerase reverse transcriptase in hepatocellular carcinoma. *Br J Cancer* 2000; **82**: 833-837
- 11 **Liu XL**, Xiao B, Yu ZC, Guo JC, Zhao QC, Xu L, Shi YQ, Fan DM. Down-regulation of Hsp90 could change cell cycle distribution and increase drug sensitivity of tumor cells. *World J Gastroenterol* 1999; **5**:199-208
- 12 **Han R**. Primary hepatocellular carcinoma. In: Chemoprevention and drug therapy of cancer. *Peking: Peking Med University Press*, 1991:591-592
- 13 **Wang XW**, Xie H. Presence of Fas and Bcl-2 proteins in BEL-7404 human hepatoma cells. *World J Gastroenterol* 1998; **4**: 540-543
- 14 **Zhang RG**, Wang XW, Yuan JH, Guo LX, Xie H. Using a non-radioisotopic, quantitative TRAP-based method detecting telomerase activities in human hepatoma cells. *Cell Res* 2000; **10**: 71-77
- 15 **Zhan WH**, Ma JP, Peng JS, Gao JS, Cai SR, Wang JP, Zheng ZQ, Wang L. Telomerase activity in gastric cancer and its clinical implications. *World J Gastroenterol* 1999; **5**: 316-319
- 16 **Counter CM**, Avilion AA, Lefevre CE, Stewart NG, Greider CW, Harley CB, Bacchetti S. Telomere shortening associated with chromosome instability is arrested in immortal cells which express telomerase activity. *EMBO J* 1992; **11**: 1921-1929
- 17 **Ulaner GA**, Hu JF, Vu TH, Giudice LC, Hoffman AR. Tissue-specific alternate splicing of human telomerase reverse transcriptase (hTERT) influences telomere lengths during human development. *Int J Cancer* 2001; **91**:644-649
- 18 **Yuan JH**, Zhang RP, Zhang RG, Guo LX, Wang XW, Luo D, Xie Y, Xie H. Growth-inhibiting effects of taxol on human liver cancer in vitro and in nude mice. *World J Gastroenterol* 2000; **6**: 210-215
- 19 **Zhu X**, Kumar R, Mandal M, Sharma N, Sharma HW, Dhingra U, Sokoloski J A, Hsiao R, Narayanan R. Cell cycle - dependent modulation of telomerase activity in tumor cells. *Proc Natl Acad Sci USA* 1996; **93**: 6091-6095
- 20 **Ku WC**, Cheng AJ, Wang TCV. Inhibition of telomerase activity by PKC inhibitors in human nasopharyngeal cancer cells in culture. *Biochem Biophys Res Commun* 1997; **241**: 730-736
- 21 **Burger AM**, Double JA, Newell DR. Inhibition of telomerase activity by cisplatin in human testicular cancer cells. *Eur J Cancer* 1997; **33**: 638-644
- 22 **Mese H**, Ueyama Y, Suzuki A, Nakayama S, Sasaki A, Hamekama H, Matsumura T. Inhibition of telomerase activity as a measure of tumor cell killing by cisplatin in squamous cell carcinoma cell line. *Chemotherapy* 2001; **47**:136-142
- 23 **Liu JP**. Studies of the molecular mechanisms in the regulation of telomerase activity. *FASEB J* 1999; **13**: 2091-2104
- 24 **Ishibashi T**, Lippard SJ. Telomere loss in cells treated with cisplatin. *Proc Natl Acad Sci USA* 1998; **95**: 4219-4223
- 25 **Holt SE**, Aisner DL, Shay JW, Wright WE. Lack of cell cycle regulation of telomerase activity in human cells. *Proc Natl Acad Sci USA* 1997; **94**: 10687-10692
- 26 **Zhang RG**, Wang XW, Yuan JH, Xie H. Human hepatoma cell telomerase activity inhibition and cell cycle modulation by its RNA component antisense oligodeoxyribonucleotides. *Zhongguo Yaoli Xuebao* 2000; **21**: 673-678
- 27 **Zhang RG**, Wang XW, Guo LX, Xie H. Growth inhibition of BEL-7404 human hepatoma cells by expression of mutant telomerase reverse transcriptase. *Int J Cancer* 2002; **97**: 173-179
- 28 **Greider CW**. Telomerase activity, cell proliferation, and cancer. *Proc Natl Acad Sci USA* 1998; **95**: 90-92

Edited by Zhu L

• LIVER CANCER •

Apoptosis of hepatoma cells SMMC-7721 induced by *Ginkgo biloba* seed polysaccharide

Qun Chen, Gui-Wen Yang, Li-Guo An

Gui-Wen Yang, Li-Guo An, Department of Biology, Shandong Normal University, Jinan 250014, Shandong Province, China

Qun Chen, Department of Biology & Chemistry, Huainan Teachers College, Huainan 232001, Anhui Province, China

Correspondence to: Dr. Li-Guo An, The Provincial Key Laboratory, Department of Biology, Shandong Normal University, Jinan, 250014, Shandong Province, China. anlg@sdnu.edu.cn

Telephone: +86-531-2966142

Received 2001-11-02 **Accepted** 2001-12-03

Abstract

AIM: To study the apoptosis of hepatoma cells SMMC-7721 induced by polysaccharide isolated from *Ginkgo biloba* seed.

METHODS: *Ginkgo biloba* seed polysaccharide (GBSP) was isolated by ethanol fractionation of *Ginkgo biloba* seed and purified by Sephadex G-200 chromatography. The purity of GBSP was verified by reaction with iodine-potassium iodide and ninhydrin and confirmed by UV spectrophotometer, cellulose acetate membrane electrophoresis and Sepharose 4B gel filtration chromatography. The Scanning Electron Microscope (SEM) and Flow Cytometry (FCM) were used to examine the SMMC-7721 cells with and without GBSP treatment at 500 mg/ml for 36 h.

RESULTS: GBSP product obtained was of high purity with the average molecular weight of 1.86×10^5 . Quantitative analysis of SMMC-7721 cells *in vitro* with FCM showed that the percentages of G₂-M cells without and with GBSP treatment were $17.01 \pm 1.28\%$ and $11.77 \pm 1.50\%$ ($P < 0.05$), the debris ratio of the cells were $0.46 \pm 0.12\%$ and $0.06 \pm 0.06\%$ ($P < 0.01$), and the apoptosis ratio of cells was $3.84 \pm 0.55\%$ and $9.13 \pm 1.48\%$ ($P < 0.01$) respectively. Following GBSP treatment, microvilli of SMMC-7721 cells appeared thinner and the number of spherical cells increased markedly. Most significantly, the apoptosis bodies were formed on and around the spherical cells treated with GBSP.

CONCLUSION: GBSP could potentially induce the apoptosis of SMMC-7721 cells.

Chen Q, Yang GW, An LG. Apoptosis of hepatoma cells SMMC-7721 induced by *Ginkgo biloba* seed polysaccharide. *World J Gastroenterol* 2002; 8(5):832-836

INTRODUCTION

Ginkgo biloba L., also named after white-seed tree and gongsun tree, is one of the immemorial gymnosperm of the mesozoic era. It is regarded as a living fossil and is also best known for its pharmaceutical value. According to Pen-ts' so Kan-mu (i.e. Compendium of Materia Medica), *Ginkgo biloba* L. can help cure about 20 different diseases. More recently, it has been widely accepted that flavonoid and terpeneand are the effective

components of leaves of *Ginkgo biloba*^[1-5] for treating cardiovascular and nervous system diseases, scavenging free radicals and antioxidating, etc.^[6-11]. Water-soluble polysaccharides of *Ginkgo biloba* leaves, endocarp, seeds and cultured cells were isolated and purified and their structures and some biological activities such as immunoregulation, antineoplastic action, scavenging free radicals and antioxidating were identified^[12-16]. Furthermore, *in vivo* and *in vitro* induction of apoptosis of cancer cells by polysaccharides has been reported lately^[17-22]. However, there was no report about the effects on apoptosis of tumor cells by polysaccharides isolated from *Ginkgo biloba* L. except from *Ginkgo biloba* endocarp^[23]. In this study, high-purity polysaccharide was extracted from *Ginkgo biloba* seeds and the apoptotic effect of *Ginkgo biloba* seed polysaccharides (GBSP) on hepatoma cell line SMMC-7721 was investigated by scanning electron microscope (SEM) and flow cytometry (FCM).

MATERIALS AND METHODS

Materials

High-quality *Ginkgo biloba* seeds (i.e. milkwhite color, equal weight, and smooth surface without mildew) were purchased from Jianlian Chinese Traditional Medicine Store in Jinan, Shandong Province. Hepatoma cell line SMMC-7721 was obtained from Shanghai Cell Institute, China Academy of Sciences. Culture medium RPMI1640 was obtained from Gibco Co. (USA). Sephadex G-200, Sepharose 4B, monose as standard, calf serum and propidium iodide (PI) were obtained from Sigma Co. (USA).

Isolation and purification of GBSP

Ginkgo biloba seeds of 200 g were crushed into fine particles and extracted with 3000 ml of distilled water for 8 hours at 75 °C for 3 times. The extracts were pooled, concentrated to 30 % of the original volume in a rotary evaporator at 45 °C and then centrifuged at 3000 rpm for 15 min. The supernatant was collected and added with 3 volumes of 95 % ethanol to precipitate the polysaccharide. Following centrifugation at 4000 rpm for 15 min, the polysaccharide pellet was dissolved in appropriate volume of distilled water completely, dialyzed with distilled water and decontaminated by means of Sevag to remove protein. The polysaccharide was then freeze-dried, re-dissolved in salt solution and purified further by Sephadex G-200 chromatography. The purity of the resulting GBSP was analyzed by Sepharose 4B gel filtration chromatography and cellulose acetate membrane electrophoresis^[24].

Culture of SMMC-7721 cells and treatment with GBSP^[25-28]

The SMMC-7721 cells were grown to logarithmic phase of proliferation, washed 3 times with culture medium RPMI1640 and collected at a concentration of 10^6 cells /ml. This cell suspension was then aliquoted into 6 culture bottles and cultured at 37 °C and 5 % CO₂ (CO₂ incubator, MCO-17AC, SANYO, Japan) for 24h. For cultures that were prepared for

SCM test, cover slips were placed into bottles in advance. After the cells stuck on the walls of culture bottles, GBSP solution made up with culture medium was added into 3 of 6 culture bottles at the final concentration of 500 mg/ml. The other 3 culture bottles were added with equal volume of culture medium. The cells were cultured for further 36 h under the same conditions.

Flow Cytometry^[29-31]

Supernatants of the cultures were discarded and SMMC-7721 cells with and without GBSP treatment were collected by digestion with pancreatin followed by centrifugation. PI was added to the cells for 15 min to label DNA. FCM (FACS/420, Becton Dickinson, USA) was used to analyze cell cycles and apoptosis ratios.

Scanning Electron Microscopy^[32-33]

Supernatants of the cultures were discarded and SMMC-7721 cells stuck on the cover slips with and without GBSP treatment were examined by SEM (S-570, Hitachi, Japan).

RESULTS

Characterization of GBSP

One of the objectives of this work was to obtain high-purity GBSP product from the *Ginkgo biloba* seeds. The purity of GBSP was first tested by reactions with iodine-potassium iodide and ninhydrin respectively. The results of these two reactions were negative, indicating absence of starch and protein in the GBSP product obtained. The reaction of GBSP with Molish reagent was positive, indicating that the GBSP product was composed of monose. The GBSP solution was then analyzed by UV absorption (UV-1200, The Second Beijing Optical Instrument Manufactory, China). As shown in Figure 1, there were no peaks at wavelengths of 260nm and 280nm on the UV spectrum, indicating that the GBSP product was not contaminated with nucleic acid and protein. The purity of GBSP was further analyzed by Sepharose 4B gel filtration chromatography and cellulose acetate membrane electrophoresis. The elution profile of Sepharose 4B was a single symmetrical peak (Figure 2). The cellulose acetate membrane electrophoresis displayed a single stripe of GBSP on the membrane. These indicated that the present GBSP was of high purity. The average molecular weight of the GBSP was 1.86×10^5 based on the linear calibration curve derived from Sephadex G-200 chromatography, as shown in Figure 3.

G₂-M cell ratio with and without GBSP treatment

The percentages of G₂-M cells without and with GBSP treatment were $17.01\% \pm 1.28\%$ and $11.77\% \pm 1.50\%$ ($P < 0.05$) respectively (Figures 4, 5 and Table). This indicated that GBSP inhibited the proliferation of SMMC-7721 cells.

Table 1 The cycles and apoptosis ratios of SMMC-7721 cell with and without GBSP treatment

GBSP treatment (mg/ml)	Number of culture bottles tested	G ₂ -M cell ratio (%)	Apoptosis cell ratio (%)	Debris ratio (%)
0	3	17.01 ± 1.28	3.84 ± 0.55	0.46 ± 0.12
500	3	11.77 ± 1.50^a	9.13 ± 1.48^b	0.06 ± 0.06^b

^a $P < 0.05$, ^b $P < 0.01$ vs control group (*t* test)

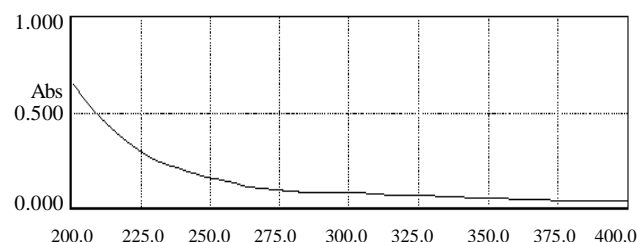


Figure 1 The UV spectrum adsorption curve of GBSP from 200nm to 400nm

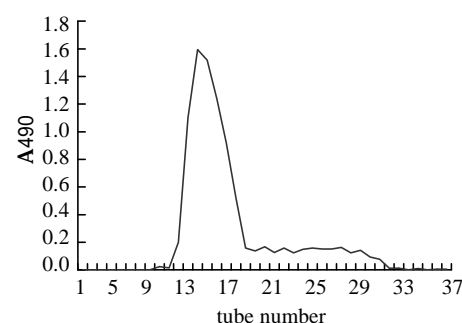


Figure 2 The profile of Sepharose 4B gel filtration chromatography

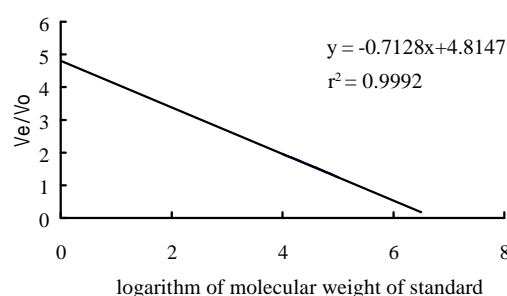


Figure 3 Standard linear calibration curve of Sephadex G-200 chromatography

Apoptosis ratio of the SMMC-7721 cell with and without GBSP treatment

The apoptosis ratio of SMMC-7721 cells without GBSP treatment was $3.84 \pm 0.55\%$ (Figure 4 and Table 1). After GBSP treatment, the apoptosis ratio increased to $9.13 \pm 1.48\%$ ($P < 0.01$ vs control group) (Figure 5 and Table 1). The debris ratio of the cells without and with GBSP treatment was $0.46 \pm 0.12\%$ and $0.06 \pm 0.06\%$, respectively ($P < 0.01$) (Figures 4, 5 and Table 1). These results showed that GBSP could induce and promote the apoptosis of SMMC-7721 cells, rather than kill SMMC-7721 cells directly.

Morphology of the SMMC-7721 cell with and without GBSP treatment

The morphology of SMMC-7721 cells with and without GBSP treatment was studied by SEM. The majority of SMMC-7721 cells without GBSP treatment was of shuttle shape (Figure 6) and small proportion of cells was of spherical shape. Close examination revealed dense microvilli on the surface of the cells, and occasionally, 2 to 3 protuberances were also observed on the cell surface. After the treatment of GBSP, these microvilli became thinner, protuberances disappeared (Figure 7) and number of spherical cells increased markedly. These spherical cells shrunk

so that their volume decreased and wrinkles were formed on their surface. Most significantly, apoptosis bodies were formed on and around the spherical cells (Figure 7). These observations suggest that GBSP could induce apoptosis in hepatoma cell line SMMC-7721, consistent with the results of FCM analysis.

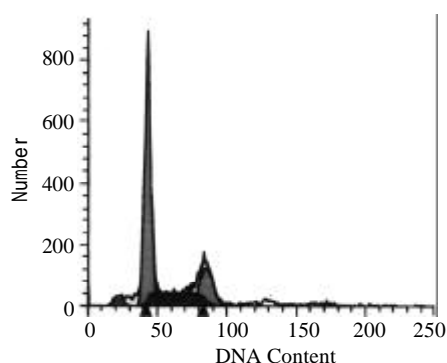


Figure 4 In the absence of GBSP treatment, the apoptosis ratio of SMMC-7721 cells was $3.84 \pm 0.55\%$, the cells debris was $0.46 \pm 0.12\%$ and the percentage of G2-M cells was $17.01 \pm 1.28\%$.

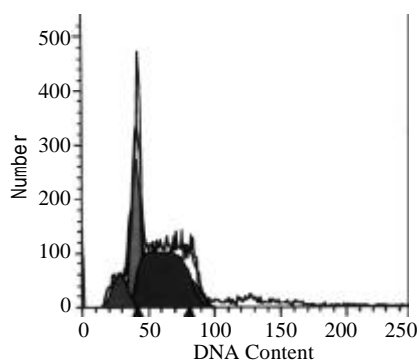


Figure 5 In the presence of GBSP treatment, the apoptosis ratio of SMMC-7721 cells was $9.13 \pm 1.48\%$, the cells debris was $0.06 \pm 0.06\%$, and the percentage of G2-M cells was $11.77 \pm 1.50\%$.



Figure 6 The majority of SMMC-7721 cells were of shuttle shape without GBSP treatment ($\times 2500$)

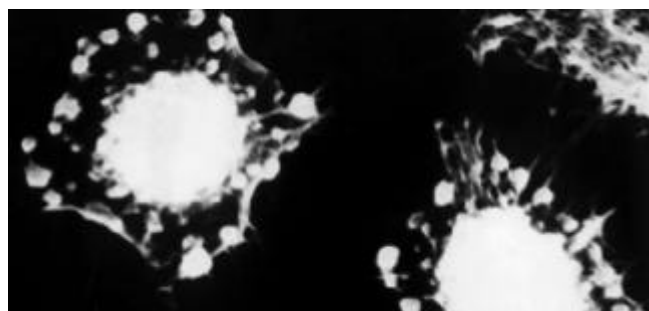


Figure 7 There were more spherical SMMC-7721 cells after GBSP treatment ($\times 2200$). These cells shrunk and apoptosis bodies were formed on and around them.

DISCUSSION

The expansion of neoplasma is associated with inhibition of apoptosis of tumor cells. There is evidence that high expression of the inhibition gene bcl-2 led to inactivation of the tumor suppression gene p53^[34-45]. When apoptosis was inhibited, tumour cells would not be eliminated in time *in vivo* and, therefore, would proliferate and diffuse more rapidly. At present, drugs such as VP-16, ADR, MTX, and Hydroxyl urea etc. are commonly used in clinical chemotherapy. These agents interfere with growth, metabolism and proliferation processes of the cells so that the apoptosis of tumour cells can be induced^[46-48]. However, like most of chemotherapeutic medicines, they have cytotoxic side-effects which cause damage to normal cells while killing neoplasma cells.

Experiments showed that ingredients of Chinese herbal medicine could induce apoptosis in tumour cells. For example, β -elemi-olefin, arabinose-cytidine and etoposide could induce apoptosis in leukemia cell line^[49-55]. It was also reported that polysaccharides isolated from Chinese herbs could inhibit the growth of tumour by activating immune system *in vivo* rather than killing tumour cells directly^[56,57]. In this *in vitro* study, we found that GBSP could effectively inhibit division of the SMMC-7721 cells and, meanwhile, induced apoptosis in hepatoma cell line SMMC-7721. Although *Ginkgo biloba* seed has been mainly used for treatment of asthma for over hundred years, it has not been known to have anti-tumour activity. The results of our present study provided valuable data for exploring the clinical application of GBSP for cancer therapy.

REFERENCES

- 1 **Liebgott T**, Miollan M, Berchadsky Y, Drieu K, Culcasi M, Pietri S. Complementary cardioprotective effects of flavonoid metabolites and terpenoid constituents of Ginkgo biloba extract (EGb 761) during ischemia and reperfusion. *Basic Res Cardiol* 2000; **95**:368-377
- 2 **Bastianetto S**, Zheng WH, Quirion R. The Ginkgo biloba extract (EGb 761) protects and rescues hippocampal cells against nitric oxide-induced toxicity: involvement of its flavonoid constituents and protein kinase C. *J Neurochem* 2000; **74**:2268-2277
- 3 **Kim SJ**, Lim MH, Chun IK, Won YH. Effects of flavonoids of Ginkgo biloba on proliferation of human skin fibroblast. *Skin Pharmacol* 1997; **10**:200-205
- 4 **Wojcicki J**, Gawronska-Szklarz B, Bieganski W, Patalan M, Smulski HK, Samochowiec L, Zakrzewski J. Comparative pharmacokinetics and bioavailability of flavonoid glycosides of Ginkgo biloba after a single oral administration of three formulations to healthy volunteers. *Mater Med Pol* 1995; **27**:141-146
- 5 **Oyama Y**, Fuchs PA, Katayama N, Noda K. Myricetin and quercetin, the flavonoid constituents of Ginkgo biloba extract, greatly reduce oxidative metabolism in both resting and Ca(2+)-loaded brain neurons. *Brain Res* 1994; **28**: 125-129
- 6 **Shen L**, Cui Y. Effects of the leaf of Ginkgo biloba L. extract on blood rheology in animals. *Zhongguo Zhongyao Zazhi* 1998; **23**: 622-623
- 7 **Logani S**, Chen MC, Tran T, Le T, Raffa RB. Actions of Ginkgo Biloba related to potential utility for the treatment of conditions involving cerebral hypoxia. *Life Sci* 2000; **67**: 1389-1396
- 8 **Tadano T**, Nakagawasai O, Tan-no K, Morikawa Y, Takahashi N, Kisara K. Effects of ginkgo biloba extract on impairment of learning induced by cerebral ischemia in mice. *Am J Chin Med* 1998; **26**:127-132

- 9 **McKenna DJ**, Jones K, Hughes K. Efficacy, safety, and use of ginkgo biloba in clinical and preclinical applications. *Altern Ther Health Med* 2001; **7**:70-86,88-90
- 10 **Yao Z**, Drieu K, Papadopoulos V. The Ginkgo biloba extract EGb 761 rescues the PC12 neuronal cells from beta-amyloid-induced cell death by inhibiting the formation of beta-amyloid-derived diffusible neurotoxic ligands. *Brain Res* 2001; **889**: 181-190
- 11 **Smith PF**, MacLennan K, Darlington CL. The neuroprotective properties of the Ginkgo biloba leaf: a review of the possible relationship to platelet-activating factor (PAF). *J Ethnopharmacol* 1996; **50**: 131-139
- 12 **Chen Q**, Yang GW, An LG. Isolation, Purification and Analysis of a Polysaccharide from the Ginkgo biloba Seed. *Zhongguo Yaoxue Zazhi* 2002; **37**: 331-333
- 13 **Kraus J**. Water-soluble polysaccharides from Ginkgo biloba leaves. *Phytochemistry* 1991; **30**: 3017-3020
- 14 **Jin JQ**, Ding DN, Bian XL, Dong HY, Ge G. The study of chemical and scavenging action to hydroxyl free radical of polysaccharides of Ginkgo biloba leaf. *Xian Yike Daxue Xuebao* 2000; **21**:417-419
- 15 **Song LY**, Ma WX, Yu RM, Kan QM, Yao XS. Studies on the biological activities of polysaccharides from the cell cultures and the leaves of Ginkgo biloba. *Zhongguo Shenghua Yaowu Zazhi* 1999; **20**: 278-280
- 16 **Zhao SQ**, Li F, Sun YM. Research progress of the exopleura of Ginkgo biloba L. *Wuhan Zhiwuxue Yanjiu* 2000; **18**:515-518
- 17 **Lin X**, Cai YJ, Li ZX, Liu ZL, Yin SF, Zhao JC. Cladonia furcata polysaccharide induced apoptosis in human leukemia K562 cells. *Acta Pharmacol Sin* 2001; **22**: 716-720
- 18 **Fullerton SA**, Samadi AA, Tortorelis DG, Choudhury MS, Mallouh C, Tazaki H, Konno S. Induction of apoptosis in human prostatic cancer cells with beta-glucan (Maitake mushroom polysaccharide). *Mol Urol* 2000; **4**: 7-13
- 19 **Sogawa K**, Yamada T, Sumida T, Hamakawa H, Kuwabara H, Matsuda M, Muramatsu Y, Kose H, Matsumoto K, Sasaki Y, Okutani K, Kondo K, Monden Y. Induction of apoptosis and inhibition of DNA topoisomerase-I in K-562 cells by a marine microalgal polysaccharide. *Life Sci* 2000; **66**: 227-231
- 20 **Sogawa K**, Matsuda M, Okutani K. Induction of apoptosis by a marine microalgal polysaccharide in a human leukemic cell line. *J Mar Biotechnol* 1998; **6**: 241-243
- 21 **Sogawa K**, Yamada T, Muramatsu Y, Sumida T, Hamakawa H, Oda H, Miyake H, Tashiro S, Matsuda M, Matsumoto K, Okutani K. Decrease of nuclear protein phosphatase 1 activity and induction of mitotic arrest and apoptosis by a marine microalgal polysaccharide in human myeloid leukemia U937 cells. *Res Commun Mol Pathol Pharmacol* 1998; **99**: 267-282
- 22 **Kim HS**, Kacew S, Lee BM. *In vitro* chemopreventive effects of plant polysaccharides (Aloe barbadensis miller, Lentinus edodes, Ganoderma lucidum and Coriolus versicolor). *Carcinogenesis* 1999; **20**: 1637-1640
- 23 **Xu AH**, Jia SQ, Chen HS, Zhou ZY, Zhu YQ. Studies of Ginkgo biloba endocarp polysaccharides inhibiting liver cancer and inducing apoptosis of liver cancer cells in mice. *Zhongyao Xinyao Yu Lincuang Yaoli* 2001; **12**: 340-341
- 24 **Cao PR**, Wu ZD, Wang RC. Isolation, purification and analysis of a polysaccharide PA3DE from the fruit bodies of *Flammulina velutipes* (Curt. ex Fr.) Sing. *Acta Biochimica et Biophysica Sinica* 1989; **21**: 152-156
- 25 **Jiang SM**, Xiao ZM, Xu ZH. Inhibitory activity of polysaccharide extracts from three kinds of edible fungi on proliferation of human hepatoma SMMC-7721 cell and mouse implanted S180 tumor. *World J Gastroenterol* 1999; **5**: 404-407
- 26 **Tian G**, Yu JP, Luo HS, Yu BP, Yue H, Li JY, Mei Q. Effect of Nimesulide on proliferation and apoptosis of human hepatoma SMMC-7721 cells. *World J Gastroenterol* 2002; **8**: 483-487
- 27 **Cui M**, Zhang HJ, An LG. Tumor growth Inhibition by polysaccharide from *Coprinus comatus*. *Shijie Huaren Xiaohua Zazhi* 2002; **10**:287-290
- 28 **Yang JQ**, Yang LY, Zhu HC. Mitomycin C-induced apoptosis of human hepatoma cell. *Shijie Huaren Xiaohua Zazhi* 2001; **9**:268-272
- 29 **Xia PY**, Zheng J, Zhou H, Pan WD, Qin XJ, Xiao GX. Relationship between lymphocyte apoptosis and endotoxin translocation after thermal injury in rats. *World J Gastroenterol* 2002; **8**: 546-550
- 30 **Yao XX**, Tang YW, Yao DM, Xiu HM. Effects of Yigan Decoction on proliferation and apoptosis of hepatic stellate cells. *World J Gastroenterol* 2002; **8**: 511-514
- 31 **Tao HQ**, Zou SC. Effect of preoperative regional artery chemotherapy on proliferation and apoptosis of gastric carcinoma cells. *World J Gastroenterol* 2002; **8**:451-454
- 32 **Zhang XL**, Liu L, Jiang HQ. Salvia miltiorrhiza monomer IH764-3 induce s hepatic stellate cell apoptosis via caspase-3 activation. *World J Gastroenterol* 2002; **8**: 515-519
- 33 **Chen XJ**, Ai ZL, Liu ZS. Apoptosis: a study on mechanism of injuries in human hepatocyte induced by mitomycin. *Shijie Huaren Xiaohua Zazhi* 2000; **8**:746-750
- 34 **Xu AG**, Li SG, Liu JH, Gan AH. Function of apoptosis and expression of the proteins Bcl-2, p53 and C-myc in the development of gastric cancer. *World J Gastroenterol* 2001; **7**:403-406
- 35 **Li HL**, Chen DD, Li XH, Zhang HW, Lu YQ, Ye CL, Ren XD. Changes of NF-kB, p53, Bcl-2 and caspase in apoptosis induced by JTE-522 in human gastric adenocarcinoma cell line AGS cells: role of reactive oxygen species. *World J Gastroenterol* 2002; **8**: 431-435
- 36 **Wang LD**, Zhou Q, Wei JP, Yang WC, Zhao X, Wang LX, Zou JX, Gao SS, Li YX, Yang CS. Apoptosis and its relationship with cell proliferation, p53, Waf1p21, bcl-2 and c-myc in esophageal carcinogenesis studied with a high-risk population in northern China. *World J Gastroenterol* 1998; **4**: 287-293
- 37 **Xu HY**, Yang YL, Guan XL, Song G, Jiang AM, Shi LJ. Expression of regulating apoptosis gene and apoptosis index in primary liver cancer. *World J Gastroenterol* 2000; **6**: 721-724
- 38 **Keith FJ**, Bradbury DA, Zhu YM, Russell NH. Inhibition of bcl-2 with antisense oligonucleotides induces apoptosis and increases the sensitivity of AML blasts to Ara-C. *Leukemia* 1995; **9**: 131-138
- 39 **Ibrado AM**, Huang Y, Fang G, Liu L, Bhalla K. Overexpression of Bcl-2 or Bcl-xL inhibits Ara-C-induced CPP32/Yama protease activity and apoptosis of human acute myelogenous leukemia HL-60 cells. *Cancer Res* 1996; **56**:4743-4748
- 40 **Bullock G**, Ray S, Reed JC, Krajewski S, Ibrado AM, Huang Y, Bhalla K. Intracellular metabolism of Ara-C and resulting DNA fragmentation and apoptosis of human AML HL-60 cells possessing disparate levels of Bcl-2 protein. *Leukemia* 1996; **10**: 1731-1740
- 41 **Wu YL**, Sun B, Zhang Xj, Wang SN, He HY, Qiao MM, Zhong J, Xu JY. Growth inhibition and apoptosis induction of Sulindac on Human gastric cancer cells. *World J Gastroenterol* 2001; **7**: 796-800
- 42 **Zhang LX**, Zhang L. Apoptosis, apoptotic regulation genes and their relationship with Atrophic gastritis. *Shijie Huaren Xiaohua Zazhi* 2002; **10**: 581-583
- 43 **Lu P**, Luo HS, Yu BP. Hepatocellular apoptosis and its apoptosis-regulating gene in rat liver fibrosis model. *Shijie Huaren Xiaohua Zazhi* 2001; **9**: 165-169
- 44 **Wang JM**, Zou Q, Zou SQ. Bcl-2 and Bax expressions and

- apoptosis in rat liver with obstructive jaundice. *Shijie Huaren Xiaohua Zazhi* 2001; **9**: 911-914
- 45 **Liu HF**, Liu WW, Fang DC, Gao JH, Wang ZH. Apoptosis and proliferation induced by *Helicobacter pylori* and its association with p53 protein expression in gastric epithelial cells. *Shijie Huaren Xiaohua Zazhi* 2001; **9**: 1265-1268
- 46 **Liu S**, Wu Q, Ye XF, Cai JH, Huang ZW, Su WJ. Induction of apoptosis by TPA and VP-16 is through translocation of TR3. *World J Gastroenterol* 2002; **8**: 446-450
- 47 **Lee JU**, Hosotani R, Wada M, Doi R, Kosiba T, Fujimoto K, Miyamoto Y, Mori C, Nakamura N, Shiota K, Imamura M. Mechanism of apoptosis induced by cisplatin and VP-16 in PANC-1 cells. *Anticancer Res* 1997; **17**: 3445-3450
- 48 **Ogretmen B**, Safa AR. Down-regulation of apoptosis-related bcl-2 but not bcl-xL or bax proteins in multidrug-resistant MCF-7/Adr human breast cancer cells. *Int J Cancer* 1996; **67**: 608-614
- 49 **Zou L**, Liu W, Yu L. beta-elemene induces apoptosis of K562 leukemia cells. *Zhonghua Zhongliu Zazhi* 2001; **23**: 196-198
- 50 **Yu C**, Wang Z, Dent P, Grant S. MEK1/2 inhibitors promote Ara-C-induced apoptosis but not loss of Delta psi(m) in HL-60 cells. *Biochem Biophys Res Commun* 2001; **286**: 1011-1018
- 51 **Zhou J**, Chen Y, Li C. Ara-c induced apoptosis in human myeloid leukemia cell line HL-60. *Zhonghua Zhongliu Zazhi* 1997; **19**: 107-110
- 52 **Chen Y**, Zhou J, Li C, Wang B, Li H. Effect of concurrent use of rh-IL-3 and rh-GM-CSF on apoptosis of HL-60 cells induced by Ara-C. *J Tongji Med Univ* 1997; **17**: 13-17
- 53 **Yang H**, Wang X, Yu L. The antitumor activity of elemene is associated with apoptosis. *Zhonghua Zhongliu Zazhi* 1996; **18**: 169-172
- 54 **Ren X**, Wang D, Li H. Study on electrochemical behavior of HL-60 cells during the etoposide-inducing apoptosis. *Zhonghua Xueyexue Zazhi* 1999; **20**: 82-84
- 55 **Jin ML**, Zhang P, Ding MX, Yun JP, Chen PF, Chen YH, Chew YQ. Altered expression of nuclear matrix proteins in etoposide induced apoptosis in HL-60 cells. *Cell Res* 2001; **11**: 125-134
- 56 **Wang JZ**, Tsumura H, Shimura K, Ito H. Antitumor activity of polysaccharide from a Chinese medicinal herb, *Acanthopanax giraldii* Harms. *Cancer Lett* 1992; **65**: 79-84
- 57 **Wang JC**, Hu SH, Su CH, Lee TM. Antitumor and immunoenhancing activities of polysaccharide from culture broth of *Herichium* spp. *Kaohsiung J Med Sci* 2001; **17**: 461-467

Edited by Liu HX

• LARGE INTESTINAL CANCER •

Analysis for phenotype of HNPCC in China

Yong-Mao Song, Shu Zheng

Yong-Mao Song, Department of Oncology, 2nd Affiliated Hospital, Medical College, Zhejiang University, Hangzhou 310009, Zhejiang Province, China

Shu Zheng, Cancer Institute, Zhejiang University, Hangzhou 310009, Zhejiang Province, China

Correspondence to: Professor Shu Zheng, Cancer Institute, Zhejiang University, 88 Jiefang Road, Hangzhou 310009, Zhejiang Province, China. zsym@mail.hz.zj.cn

Telephone: +86-571-87214404 **Fax:** +86-571-87214404

Received 2002-06-03 **Accepted** 2002-06-12

Abstract

AIM: The aims of this study were to identify the clinicopathological features of Chinese HNPCC families and to evaluate the value of criteria for suspected HNPCC (sHNPCC) in clinical diagnosis.

METHODS: According to the follow-up records, 54 HNPCC families (including 12 ICG-HNPCC families and 42 sHNPCC families) were screened out from patients with colorectal cancers (CRCs), operated upon in 2nd Affiliated Hospital of Zhejiang University from 1984 to 2001. Clinical data of probands and tumor spectrum in these families were listed and analyzed.

RESULTS: (1) Mean age, proportion of colonic cancer, poorly differentiated cancer, multiple CRCs and Dukes' A+B of the probands in ICG-HNPCC and sHNPCC kindred were 39ys and 47.5ys, 75 % and 62 %, 0 and 12.8 %, 16.7 % and 14.3 %, 58.3 % and 81 %, respectively. Compared with sporadic colorectal cancers, probands from ICG-HNPCC and sHNPCC families were obviously different at age of onset ($P=0.025$ and 0.031), tumor location ($P=0.001$ and 0.000), differentiation ($P=0.002$ and 0.011) and development of multiple tumors ($P=0.014$ and 0.002). (2) A total of 178 malignant neoplasms were found in 54 HNPCC families, including 139 colorectal cancers. Besides of colorectal cancer, extracolonic tumors occurred in stomach, endometrium, hepatobiliary system, and so on (8 gastric cancers, 6 endometrial cancers, 6 hepatobiliary system cancers and 19 others) can also be seen in Chinese ICG-HNPCC and sHNPCC families.

CONCLUSION: (1) Chinese HNPCC families have specific clinicopathological features, such as early onset, predilection for the involvement of colon, tendency of multiple CRCs, development of extracolonic tumors and well differentiation. (2) The criteria for suspected HNPCC is useful in clinical diagnosis and management of HNPCC.

Song YM, Zheng S. Analysis for phenotype of HNPCC in China. *World J Gastroenterol* 2002; 8(5): 837-840

INTRODUCTION

Colorectal cancer (CRC) is one of the most common malignant tumors. Various factors and mechanisms are involved in the

development of CRC^[1-5]. In recent years, much progress has been made in the studies of CRC^[6-13], but its morbidity is still rising^[14,15]. It has been thought that one-third of CRC have a genetic background. Hereditary nonpolyposis colorectal cancer (HNPCC) is a common autosomal dominant colorectal disorder with special clinicopathological features^[16]. In clinic, it is diagnosed by Amsterdam criteria^[17]: (1) three or more relatives with histologically verified colorectal cancer, one of whom is the first-degree to the other two; (2) colorectal cancer affecting at least two generations; and (3) one or more colorectal cancer cases diagnosed before the age of 50. Families fulfilling Amsterdam criteria were named as ICG-HNPCC in this study. As the criteria are too rigid for small families and it excludes extracolonic cancers associated with HNPCC, the Korean Hereditary Colorectal Cancer Registry designated the term "suspected HNPCC"^[18] and designed its criteria for the families who do not fulfill Amsterdam criteria but in whom a genetic basis for colorectal cancer is strongly suspected. The criteria for suspected HNPCC are as following: (1) vertical transmission of colorectal cancer or at least two siblings affected with colorectal cancer in a family and (2) development of multiple colorectal tumors (including adenomas), or at least one colorectal cancer case diagnosed before the age 50, or development of extracolonic cancer in family member. Families fulfilling these criteria were named as sHNPCC in this paper. The criteria were accepted by the International Collaborative Group (ICG) on HNPCC for international collaborative studies. It^[19] had been reported that ICG-HNPCC and suspected HNPCC have the similar molecular basis and genetic background. In China, there is still no systematic research on ICG-HNPCC or sHNPCC. Therefore, it is necessary and urgent to find out the characteristics of HNPCC in Chinese populations.

In this study we were to find out clinical phenotype of Chinese HNPCC families and to evaluate whether the criteria for suspected HNPCC is useful in clinical diagnosis and management of HNPCC.

MATERIALS AND METHODS

According to the follow-up records, 54 probands from HNPCC families (including 12 ICG-HNPCC families and 42 sHNPCC families) were screened out from patients with colorectal cancers operated upon in 2nd Affiliated Hospital of Zhejiang University from 1984 to 2001. Their clinicopathological features were compared with those of sporadic CRCs operated upon in the hospital^[20]. There were 34 male and 20 female, age ranged from 19-76ys (average 45.7), 35 cases of colonic cancer and 19 cases of rectal cancer. The tumor spectrums in these families were also analyzed. All patients were diagnosed by Amsterdam criteria or criteria for suspected HNPCC.

All data were analyzed by software STATISTICA 5.0. A value of $P<0.05$ is considered to be statistically significant.

RESULTS

Clinicopathological features of Chinese HNPCC families

Data of 54 probands with HNPCC and sporadic CRCs were listed in Table 1. From Table 1, we found that mean age of the probands of 12 ICG-HNPCC families was 39ys, proportion of

colonic cancer, well differentiated cancer, poorly differentiated cancer, mucinous tumor, Dukes' A+B and multiple CRCs were 75 %, 54.5 %, 0 %, 8.3 %, 58.3 % and 16.7 % respectively. For the probands of 42 sHNPCC families were 47.5ys, 62 %, 30.8 %, 12.8 %, 21.4 %, 81 % and 14.3 % respectively. Compared with sporadic colorectal cancers, probands from ICG-HNPCC families were obviously different at mean age ($P=0.025$), tumor site ($P=0.001$), tumor differentiation ($P=0.002$) and multiple tumors ($P=0.014$). Similar result was obtained when compared probands of sHNPCC families to sporadic cases: there were obviously different at mean age ($P=0.031$), tumor site ($P=0.000$), tumor differentiation ($P=0.011$) and multiple tumors ($P=0.002$).

Table 1 Clinical data of 54 probands

Parameters		ICG-HNPCC	sHNPCC	Total	Sporadic CRC
Sex	male	6(50%)	14(33.3%)	20(37%)	319(43%)
	female	6(50%)	28(66.7%)	34(63.0%)	423(57%)
Mean age		39y	47.5y	45.7y	56y
tumor site	colon	9(75.0%)	26(62.0%)	35(64.8%)	226(30.5%)
	rectum	3(25.0%)	16(38.0%)	19(35.2%)	516(69.5%)
Dukes' stage	A+B	7(58.3%)	34(81.0%)	41(75.9%)	347(47.8%)
	C+D	5(41.7%)	8(19.0%)	13(24.1%)	380(52.2%)
Differentiation	high	6(54.5%)	12(30.8%)	18(36.0%)	89(15.3%)
	moderate	5(45.5%)	22(56.4%)	27(54.0%)	397(68.1%)
	poorly	0	5(12.8%)	5(10.0%)	97(16.6%)
Pathology	mucinous tumors	1(8.3%)	9(21.4%)	10(18.5%)	159(21.4%)
	Non-mucinous tumors	11(91.7%)	33(78.6%)	44(81.5%)	583(78.6%)
Multiple CRCs		2(16.7%)	6(14.3%)	8(14.8%)	25(3.4%)

Except mean age ($P=0.035$), there was no obvious statistical difference between probands of ICG-HNPCC and sHNPCC families, in clinicopathological features: tumor site ($P=0.402$), Dukes' stage ($P=0.106$), tumor differentiation ($P=0.147$), Pathology ($P=0.303$) and multiple tumors ($P=0.838$).

Tumor spectrum in HNPCC families

A total of 178 malignant neoplasms were found in 54 HNPCC families including 139 colorectal cancers, 8 gastric cancers, 6 endometrial cancers, 6 hepatobiliary cancers and 19 others. In 12 ICG-HNPCC families, there were 53 tumors, including 47 CRCs, and each family had 3.92 CRCs patients. In 42 sHNPCC families, there were 125 tumors, including 92 CRCs, and each family had 2.19 CRCs patients. Except CRCs, carcinomas of stomach, endometrium, hepatobiliary system and urologic system were the most common extracolonic malignancies in HNPCC families. Extracolonic malignancies were less in ICG-HNPCC than those in sHNPCC.

Table 2 Tumor spectrum in HNPCC families

Organs	ICG-HNPCC	sHNPCC	Total
CRCs	47	92	139
Stomach	1	7	8
Endometrium	0	6	6
Hepatobiliary system	2	4	6
Lymphatic/hemato-poieticsystem	1	1	2
Esophage	0	2	2
Breast	0	1	1
Urologic system	0	5	5
Pancreas	1	0	1
Others	1	7	8
Total	53	125	178

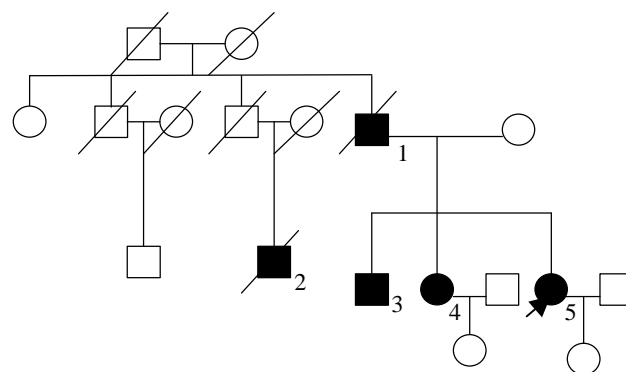


Figure 1 Pedigree of an ICG-HNPCC family.

1: father of proband, with CRC in 64ys, dead; 2: son of proband's uncle, with liver cancer, dead; 3: little brother of proband, with colonic polyps; 4: little sister of proband, with colonic cancer in 40ys, with gastric cancer 1 year later, alive; 5: arrow indicates the proband, 48ys, with colonic cancer, alive.

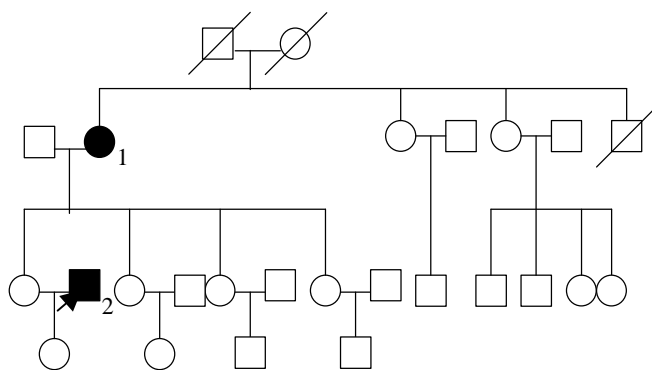


Figure 2 Pedigree of an sHNPCC family. 1: mother of proband, with CRC in 55ys, alive(80ys); 2: arrow indicates the proband, 38ys, with rectal cancer, alive.

DISCUSSION

In 1913, Warthin first described some families with an excess of colorectal, uterine and gastric cancers. It took more than half a century before Lynch undertook the task of collecting data that led to accurate description of these cancer-prone families^[21]. According to the absence or presence of extracolonic malignancies, these families were divided into Lynch I syndrome and Lynch II syndrome^[22]. Later, the syndrome was specifically called HNPCC. So HNPCC is also called Lynch syndrome.

HNPCC is an autosomal dominant disorder with special clinicopathological features^[23-27], early onset (average <45ys), high frequency of cancers in proximal colon (60-70 %), excess of synchronous (18.1 %) and metachronous (24.2 %) tumors, development of extracolonic malignancies, excess of mucinous (30-40 %) and poorly differentiated tumors (23-39 %). It is often diagnosed by Amsterdam criteria, but the criteria is too strict for little families with strong genetic basis for CRCs, then sHNPCC criteria will be useful.

Mo^[28] had described 10 Chinese HNPCC kindred. Among 10 kindred, patients had a mean age of 44.8ys and showed an excess of multiple CRCs (20.2%), a high frequency of cancers in colon (82.3 %). Zhao^[29] got the similar results. In our study, compared with sporadic CRCs, 12 probands of ICG-HNPCC kindred showed special features, such as early onset ($P<0.05$),

predilection for involvement of colon ($P<0.05$) and tendency of multiple CRCs ($P<0.05$). They also had well but not poorly differentiated appearance (proportion of well differentiated cancer, poorly differentiated cancer, mucinous tumors and Dukes' A+B were 54.5 %, 0, 8.3 % and 58.3 % respectively). Perhaps it was due to the small sample of our study or the racial difference.

For the families who do not fulfill Amsterdam criteria but in whom a genetic basis for colorectal cancer is strongly suspected, sHNPCC criteria were used. It was proved that sHNPCC had the similar genetic background with ICG-HNPCC^[19]. In our study, 42 probands of sHNPCC kindred had the similar clinicopathological features with ICG-HNPCC, early onset (mean age 47.5ys), predilection for involvement of colon (62 %), tendency of multiple CRCs (14.3 %) and well differentiation appearance.

No obvious difference was found between ICG-HNPCC and sHNPCC in their clinicopathological features ($P>0.05$), except the mean age ($P<0.05$). This difference might be due to the limited cases studied. According to phenotype of Chinese ICG-HNPCC and sHNPCC, it indicated that they might have similar genetic background. The criteria for sHNPCC will be helpful for clinical diagnosis and treatment of HNPCC.

Except CRCs, extracolonic tumors were often seen in HNPCC kindred^[30-41], such as cancers of ovary, brain, small bowel, urologic system, breast, larynx, stomach, pancreas and biliary system as well as leukemia, lymphoma, soft tissue sarcoma, desoid tumor and cutaneous tumors. Gastric cancer, endometrial cancer, carcinomas of hepatobiliary system were the most common extracolonic malignancies. In our study, gastric cancer, endometrial cancer, carcinomas of hepatobiliary system and urologic system were the four common extracolonic malignancies. Cancers of esophagus, breast, pancreas, leukemia and lymphoma were also seen in Chinese HNPCC kindreds. We also found that extracolonic malignancies were less seen in ICG-HNPCC than those in sHNPCC, perhaps it was due to the limited cases studied.

Our results suggest that both ICG-HNPCC and sHNPCC families in China had the clinicopathological features, early onset, predilection for involvement of colon, tendency of multiple CRCs, extracolonic tumors and well differentiated appearance. They might have the similar genetic background. In recent years, Chinese families are becoming smaller and smaller due to the practising of family planning^[42]. So criteria for sHNPCC will become more and more useful in clinical diagnosis of HNPCC. Now in China, establishment of HNPCC registry, genetic counseling and surveillance of high-risk asymptomatic family members are important and necessary. Endoscopic surveillance is recommended if any tumor found in some cases, and prophylactic operation is suggested^[43-49].

REFERENCES

- Vogelstein B**, Fearon ER, Hamilton SR, Kern SE, Preisinger AC, Leppert M, Nakamura Y, White R, Smits AM, Bos JL. Genetic alterations during colorectal-tumor development. *N Engl J Med* 1988; **319**: 525-532
- Bishop JM**. Molecular themes in oncogenesis. *Cell* 1991; **64**: 235-248
- Hunter T**. Cooperation between oncogenes. *Cell* 1991; **64**: 249-270
- Steffensen IL**, Paulsen JE, Alexander J. Genetic and environmental factors in colorectal cancer. Mutations in the familial adenomatous polyposis gene. *Tidsskr Nor Laegeforen* 1997; **117**: 2046-2051
- Shih IM**, Zhou W, Goodman SN, Lengauer C, Kinzler KW, Vogelstein B. Evidence that genetic instability occurs at an early stage of colorectal tumorigenesis. *Cancer Res* 2001; **61**: 818-822
- Marshall CJ**. Tumor suppressor genes. *Cell* 1991; **64**: 313-326
- Loeb LA**. Microsatellite instability: Marker of a mutator phenotype in cancer. *Cancer Res* 1994; **54**: 5059-5063
- Potter JD**. Colorectal Cancer: Molecules and Populations. *J Natl Cancer Inst* 1999; **91**: 916-932
- Sapkota GP**, Boudeau J, Deak M, Kieloch A, Morrice N, Alessi DR. Identification and characterization of four novel phosphorylation sites (Ser31, Ser325, Thr336 and Thr366) on LKB1/STK11, the protein kinase mutated in Peutz-Jeghers cancer syndrome. *Biochem J* 2002; **362**(Pt 2): 481-490
- Al-Jaberi TM**, El-Shanti H. Diversity in polyp pathology and distribution of Familial Juvenile Polyposis Syndrome. *Saudi Med J* 2002; **23**: 328-331
- Cahill DP**, Lengauer C, Yu J, Riggins GJ, Willson JK, Markowitz SD, Kinzler KW, Vogelstein B. Mutations of mitotic checkpoint genes in human cancers. *Nature* 1998; **392**: 300-303
- Zheng S**. Recent study on colorectal cancer in China: early detection and novel related gene. *Chin Med J (Engl)* 1997; **110**: 309-310
- Saha D**, Roman C, Beauchamp RD. New Strategies for Colorectal Cancer Prevention and Treatment. *World J Surg* 2002; **26** [epub ahead of print]
- Parkin DM**, Muir CS. Cancer Incidence in Five Continents. Comparability and quality of data. *IARC Sci Publ* 1992: 145-173
- Whittemore AS**. The Eighth AACR American Cancer Society Award lecture on cancer epidemiology and prevention. Genetically tailored preventive strategies: an effective plan for the twenty-first century? American Association for Cancer Research. *Cancer Epidemiol Biomarkers Prev* 1999; **8**: 649-658
- Lynch HT**, Smyrk TC, Watson P, Lanspa SJ, Lynch JF, Lynch PM, Cavalieri RJ, Boland CR. Genetics, natural history, tumor spectrum, and pathology of hereditary nonpolyposis colorectal cancer: a updated review. *Gastroenterology* 1993; **104**: 1535-1549
- Vasen HF**, Mecklin JP, Khan PM, Lynch HT. The international collaborative group on hereditary nonpolyposis colorectal cancer. *Dis Colon Rectum* 1991; **34**: 424-425
- Han HJ**, Yuan Y, Ku JL, Oh JH, Won YJ, Kang KJ, Kim KY, Kim S, Kim CY, Kim JP, Oh NG, Lee KH, Choe KJ, Nakamura Y, Park JG. Germline mutations of hMLH1 and hMSH2 genes in Korean hereditary nonpolyposis colorectal cancer. *J Natl Cancer Inst* 1996; **88**: 1317-1319
- Yuan Y**, Zheng S. Mutations of hMLH1 and hMSH2 genes in suspected hereditary nonpolyposis colorectal cancer. *Zhonghua Yi xue Zazhi* 1999; **79**: 346-348
- Huang J**, Wu JM, Yang G. Prognostic Significance of Clinico-pathological Variables in Colorectal Carcinoma, Analyzed by CoX Model. *Zhongguo Zhongliu Linchuang* 1997; **23**: 156-162
- Marra G**, Boland CR. Hereditary nonpolyposis colorectal cancer: the syndrome, the genes, and historical perspectives. *J Natl Cancer Inst* 1995; **87**: 1114-1125
- Boland CR**, Troncale FJ. Familial colonic cancer without antecedent polyposis. *Ann Intern Med* 1984; **100**: 700-701
- Jass JR**, Smyrk TC, Stewart SM, Lane MR, Lanspa SJ, Lynch HT. Pathology of hereditary nonpolyposis colorectal cancer. *Anticancer Res* 1994; **14**(4B): 1631-1634
- Fitzgibbons RJ Jr**, Lynch HT, Stanislav GV, Watson PA, Lanspa SJ, Marcus JN, Smyrk T, Kriegler MD, Lynch JF. Recognition and treatment of patients with hereditary nonpolyposis colorectal cancer. *Ann Surg* 1987; **206**: 289-295
- Mecklin JP**, Jarvinen HJ. Clinical features of colorectal carcinoma in cancer family syndrome. *Dis Colon Rectum* 1986; **29**: 160-164
- Tomoda H**, Baba H, Oshiro T. Clinical manifestations in

- patients with hereditary nonpolyposis colorectal cancer. *J Surg Oncol* 1996; **61**: 262-266
- 27 **Losi L**, Fante R, Di Gregorio C, Aisoni ML, Lanza G, Maestri I, Roncucci L, Pedroni M, Ponz de Leon M. Biologic characterization of hereditary nonpolyposis colorectal cancer. Nuclear ploidy, AgNOR count, microvessel distribution, oncogene expression, and grade-related parameters. *Am J Clin Pathol* 1995; **103**: 265-270
- 28 **Mo SJ**, Cai H, Cai SJ. Hereditary Nonpolyposis Colorectal Cancer (affiliated report of 10 kindreds). *Chinese Journal of Digestive Diseases* 1996; **16**: 326-328
- 29 **Zhao B**, Wang ZJ, Xu YF, Wan YL, Li P, Huang YT. Report of 16 kindreds and one kindred with hMLH1 germline mutation. *World J Gastroenterol* 2002; **8**: 263-266
- 30 **Lynch HT**, Ens JA, Lynch JF. The Lynch syndrome II and urological malignancies. *J Urol* 1990; **143**: 24-28
- 31 **Wang Q**, Lasset C, Desseigne F, Saurin JC, Maugard C, Navarro C, Ruano E, Descos L, Trillet-Lenoir V, Bosset JF, Puisieux A. Prevalence of germline mutations of hMLH1, hMSH2, hPMS1, hPMS2, and hMSH6 genes in 75 French kindreds with nonpolyposis colorectal cancer. *Hum Genet* 1999; **105**: 79-85
- 32 **Jonas J**, Kruse R, Bahr R. [Article in German] *Chirurg* 2002; **73**: 366-369
- 33 **Cristofaro G**, Lynch HT, Caruso ML, Attolini A, DiMatteo G, Giorgio P, Senatore S, Argentieri A, Sbrano E, Guanti G. New phenotypic aspects in a family with Lynch syndrome II. *Cancer* 1987; **60**: 51-58
- 34 **Yamamoto H**, Itoh F, Nakamura H, Fukushima H, Sasaki S, Peruchio M, Imai K. Genetic and clinical features of human pancreatic ductal adenocarcinomas with widespread microsatellite instability. *Cancer Res* 2001; **61**: 3139-3144
- 35 **Vilotte J**, Bonstein U, Girodet J, De Mestier du Bourg P, Mignon M, Bonfils S. [Familial colonic cancer (Lynch's syndrome) and bile duct cancer. Study of 2 cases]. *Gastroenterol Clin Biol* 1989; **13**: 1072-1074
- 36 **Mecklin JP**, Jarvinen HJ, Virolainen M. The association between cholangiocarcinoma and hereditary nonpolyposis colorectal carcinoma. *Cancer* 1992; **69**: 1112-1114
- 37 **Benatti P**, Roncucci L, Percesepe A, Viel A, Pedroni M, Tamassia MG, Vaccina F, Fante R, De Pietri S, Ponz de Leon M. Small bowel carcinoma in hereditary nonpolyposis colorectal cancer. *Am J Gastroenterol* 1998; **93**: 2219-2222
- 38 **Love RR**. Small bowel cancers, B-cell lymphatic leukemia, and six primary cancers with metastases and prolonged survival in the cancer family syndrome of Lynch. *Cancer* 1985; **55**: 499-502
- 39 **Borg A, Isola J**, Chen J, Rubio C, Johansson U, Werelius B, Lindblom A. Germline BRCA1 and HMLH1 mutations in a family with male and female breast carcinoma. *Int J Cancer* 2000; **85**: 796-800
- 40 **Reinbach D**, McGregor JR, O'Dwyer PJ, George WD. Synchronous male breast carcinoma and soft tissue sarcoma occurring within a cancer family. *Eur J Surg Oncol* 1992; **18**: 624-626
- 41 **Maher ER**, Morson B, Beach R, Hodgson SV. Phenotypic variation in hereditary nonpolyposis colon cancer syndrome. Association with infiltrative fibromatosis (desmoid tumor). *Cancer* 1992; **69**: 2049-2051
- 42 **Wu YM**. [Progress in the study of family planning in China]. *Zhonghua Yixue Zazhi* 1998; **78**: 927-928
- 43 **Qi Cai**, Meng-Hong Sun, Hong-Fen Lu. Clinicopathological and molecular genetic analysis of 4 typical Chinese HNPCC families. *World J Gastroenterol* 2001; **7**: 805-810
- 44 **Mangold E**, Friedl W, Propping P. [Hereditary colorectal carcinoma: predictive diagnosis and genetic counseling]. *Schweiz Rundsch Med Prax* 2001; **90**: 490-496
- 45 **Schiemann U**, Papatheodorou L, Glasl S, Gross M. Hereditary non-polyposis colorectal cancer (HNPCC): new germline mutation (190-191 del AA) in the human MLH1 gene and review of clinical guidelines for surveillance of affected families. *Eur J Med Res* 2001; **6**: 93-100
- 46 **Syngal S**, Weeks JC, Schrag D, Garber JE, Kuntz KM. Benefits of colonoscopic surveillance and prophylactic colectomy in patients with hereditary nonpolyposis colorectal cancer mutations. *Ann Intern Med* 1998; **129**: 787-796
- 47 **Moslein G**, Albrecht J, Ohmann C, Schackert HK. [Preventive therapy of HNPCC-a study concept]. *Kongressbd Dtsch Ges Chir Kongr* 2001; **118**: 213-217
- 48 **Pistorius SR**, Nagel M, Kruger S, Plaschke J, Kruppa C, Wehrmann U, Schackert HK, Saeger HD. Combined molecular and clinical approach for decision making for surgery in HNPCC patients: a report on three cases in two families. *Int J Colorectal Dis* 2001; **16**: 402-407
- 49 **Park JG**. Genetic diagnosis and management of hereditary nonpolyposis colorectal cancer. *World J Gastroenterol* 1998; **4**(Suppl 2): 55

Edited by Zhang JZ

• LARGE INTESTINAL CANCER •

Less cytotoxicity to combination therapy of 5-fluorouracil and cisplatin than 5-fluorouracil alone in human colon cancer cell lines

Xiu-Xu Chen, Mao-De Lai, Yong-Liang Zhang, Qiong Huang

Xiu-Xu Chen, Mao-De Lai, Qiong Huang, Department of Pathology, School of Medicine, Zhe Jiang University, Hang Zhou, 310031, Zhejiang Province, China

Yong-Liang Zhang, Department of Basic Medicine, School of Medicine, Zhe Jiang University, Hang Zhou, 310031, Zhejiang Province, China

Correspondence to: Mao-De Lai, M.D., Professor of Pathology, Department of Pathology, School of Medicine, Zhe Jiang University, Hang Zhou, 310031, Zhejiang Province, China. lmd@sun.zju.edu.cn
Telephone: +86-0571-87217134

Received 2002-03-13 **Accepted** 2002-04-20

Abstract

AIM: Our previous studies showed increased sensitivity to 5-FU in colon cancer cell lines with microsatellite instability, and considered that mutations of TGF β -R II, IGF IIR, RIZ gene might enhance the potentials of cell growth and proliferation, which increased the sensitivity to 5-FU. Here we compared the distribution of cell cycle and P53 status between two human colon cancer cell lines with different sensitivity to 5-FU. Because mechanistic differences exist between 5-FU and CDDP, we also analyzed the efficacy of CDDP and combination therapy on two human colon cancer cell lines.

METHODS: We compared the sensitivity to CDDP of these two cell lines by MTT assay. Distribution of cell cycle under treatment of 5-FU, CDDP alone or both was analyzed by Flow Cytometry, and expression of P53 was detected by immunocytochemical staining.

RESULTS: SW480 cells were more sensitive to CDDP than LoVo cells at the concentrations above 16 μ mol/l (Ratio of absorption is 0.64 and 0.79 at 16 μ mol/l, respectively; $P < 0.01$). Efficacy of combination therapy was conversely lower than that of single-therapy of 5-FU (Ratio of absorption in LoVo+5-FU, SW480+5-FU, LoVo+5-FU+CDDP and SW480+5-FU+CDDP is 0.53, 0.54, 0.72, 0.78, respectively; $P < 0.01$). LoVo cells were negative whereas SW480 cells positive in P53 expression. 5-FU induced G1-phase arrest in both cell lines, but LoVo cells peaked 24 hours earlier than SW480 cells, and 48 hours earlier for an apparent hypodiploid DNA. However, CDDP showed the contrary, inducing S-phase arrest, and SW480 cells peaking 36 hours earlier. Both cell lines showed hypodiploid nuclei 48 hours after CDDP treatment. Percentage of cells in G1-phase and S-phase dominated alternatively under combination therapy in both cell lines.

CONCLUSION: These results suggest that colon cancer cells with microsatellite instability are more sensitive to 5-FU, whereas more resistant to CDDP. Combination therapy of 5-FU and CDDP shows fewer efficacies than 5-FU single-

therapy, although it can render a cell cycle arrest. P53 may be involved in the shift of G1-phase to S-phase, but inessentially.

Chen XX, Lai MD, Zhang YL, Huang Q. Less cytotoxicity to combination therapy of 5-fluorouracil and cisplatin than 5-fluorouracil alone in human colon cancer cell lines. *World J Gastroenterol* 2002; 8(5): 841-846

INTRODUCTION

5-FU is currently the first-line agent for colorectal cancer after surgical cytoreduction with an overall response rate of less than 15 %^[1,2], this has stimulated intensive effort in the development of novel compounds with improved pharmacological properties and new regimens for colorectal cancer patients. Efforts have been made in combination of 5-FU with several second-line agents, such as paclitaxel, mitomycin, calcium folinate, INF- α , irinotecan, leucovorin, suramin and tegafur, and so on, unfortunately, improvement is far from satisfaction. Our studies previously demonstrated that colorectal cancer cell lines with microsatellite instability showed increased sensitivity to 5-FU, and that mutations were found in 8 loci from different genes, among which 3 loci harbored in the exon of TGF-R II, IGF IIR, and RIZ, respectively. All these three genes are closely associated with cell growth and proliferation. On basis of these results, we proposed that these mutations may enhance the proliferative potentials of cancer cells and increase chemosensitivity to 5-FU.

In this study, We explored the differences of cell cycle arrest and apoptosis between two cell lines under 5-FU treatment, and found that in G1-phase arrest and presence of hypodiploid DNA in LoVo cells happened 48 hours earlier than that in SW480 cells. Because the options available to colorectal cancer patients for second-line therapy were limited, and mechanistic differences existed between 5-FU and CDDP, we analyzed the efficacies of CDDP and combination therapy on these two cell lines. Results indicated that SW480 cells were more sensitive to CDDP than LoVo cells, and that combination therapy of 5-FU and CDDP showed less efficacy than single-therapy of 5-FU in both cell lines, although it can render a cell cycle arrest. P53 may be involved in the entry of G1-phase to S-phase, but inessentially.

MATERIALS AND METHODS

Cell lines

LoVo, a human colon adenocarcinoma cell line, was purchased from the Shanghai Institute of Cell Biology, Chinese Academy of Sciences, Shanghai, China; SW480, a human colon adenocarcinoma cell lines, was donated by the Cancer Institute, Zhe Jiang University. They were maintained in RPMI1640 supplemented with 10 % fetal bovine serum in a humidified 5 % CO₂ atmosphere at 37 °C.

Drugs and agents

5-fluorouracil (5-FU), [cis-diamminedichloroplatinum (II)] (cisplatin/CDDP), 3-[4-dimethylthiazol-2-yl]-2,5-diphenyltetrazolium bromide (MTT), dimethylsulfoxide (DMSO) and propidium iodide (PI), were all purchased from the Sigma Chemical Co. The primary mouse antibody of P53 (DO-7), biotinylated anti-mouse immunoglobulin, horseradish peroxidase-conjugated streptavidin, and the chromogenic substrate solution 3,3-diaminobenzidine were bought from Santa Cruz Biotechnology (Santa Cruz, CA, USA).

MTT assay

MTT assay was performed as described by Lu *et al*^[3]. Briefly, logarithmically growing cells were seeded in the 96-well plate at a concentration of 1×10^4 per well and incubated for 12 hours. Then medium with various concentrations of drugs was added in quadruplicate and exposed for 72 hours. The culture medium was then removed and about 300 μ l fresh medium containing 0.5 mg/ml MTT was added to each well. 4 hours later, the medium was replaced with 100 μ l DMSO and vortexed for 10 minutes. Absorbance (A) was then recorded at 570nm using an Enzyme-linked Immunosorbent Assay device DG3022A. Cell viability was assessed as follows: Viability [%] = $A_{\text{treat}}/A_{\text{control}} \times 100\%$.

Immunocytochemical staining

Immunocytochemical staining was performed using DO-7 anti-P53 on logarithmically growing cell lines, LoVo and SW480, on coverslip. Firstly, cells were plated onto coverslips, adhered overnight. Then, rinsed three times with PBS, cells were fixed in cold acetone for 8-10 min. Endogenous peroxidase was blocked with 1 % hydrogen peroxide in absolute methanol for 30 min. The primary antibodies were applied for 2 hours at 37 °C at 1:300 dilution in a humidified chamber. Then the typical SP strategy followed.

Flow Cytometric analysis

Cells were incubated in medium containing 4 μ mol/L 5-FU, 10 μ mol/L CDDP alone or both (4 μ mol/L 5-FU+10 μ mol/L CDDP) continuously, and then were fixed in ice-cold 70 % ethanol at 0, 12, 24, 48, 72 and 96 h after initial treatment. Then approximately 10 000 cells each specimen stained by 10 μ g/ml PI were analyzed by Flow Cytometry (FACS[®]), as described by Bunz *et al*^[4].

Statistical analysis

Data of MTT assay were mean values of at least three different experiments and expressed as mean \pm SD, analyzed by two-tailed Student's *t*-test and General Linear Model, *P* value of less than 0.05 was considered as statistically significant.

RESULTS

Response to CDDP in LoVo cells and SW480 cells

We compared the sensitivity and responsiveness of LoVo cells and SW480 cells to CDDP and the combination of CDDP+5-FU in cytotoxicity assays. As shown by the dose-effect curve, both cell lines are sensitive to CDDP, but more for SW480 cells (Figure 1A). Neither of the cell lines examined showed significantly synergetic response when the two drugs were combined simultaneously, when compared with single-therapy of 5-FU, indicating that CDDP, to some degree, may block the effects of 5-FU (Figure 1B).

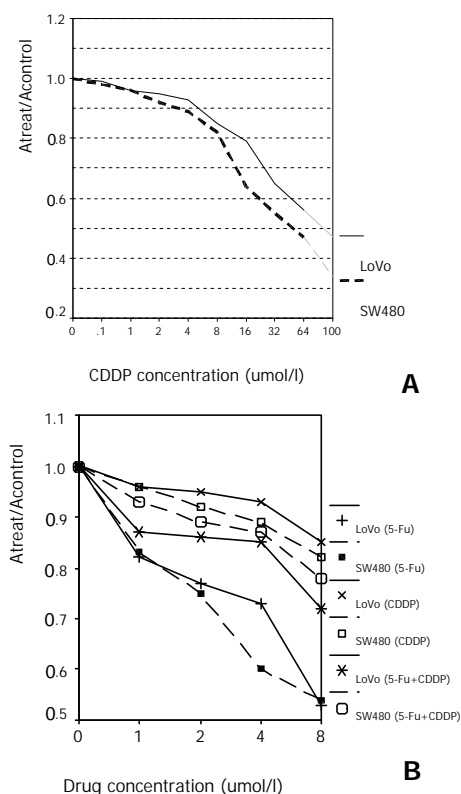


Figure 1 Comparison of sensitivity to 5-FU, CDDP or combination therapy in LoVo cells and SW480 cells. **(A)** SW480 cells show increased sensitivity to CDDP than LoVo cells at the concentrations above 16 μ mol/l (Ratio of absorption is 0.64 and 0.79 at 16 μ mol/l, respectively; $P < 0.01$). **(B)** The dose-effect curve tells that the cytotoxicity diminishes in combination therapy of 5-FU and CDDP in both cell lines when compared with 5-FU single-therapy (Ratio of absorption in LoVo+5-FU, SW480+5-FU, LoVo+5-FU+CDDP and SW480+5-FU+CDDP is 0.53, 0.54, 0.72, 0.78, respectively; $P < 0.01$).

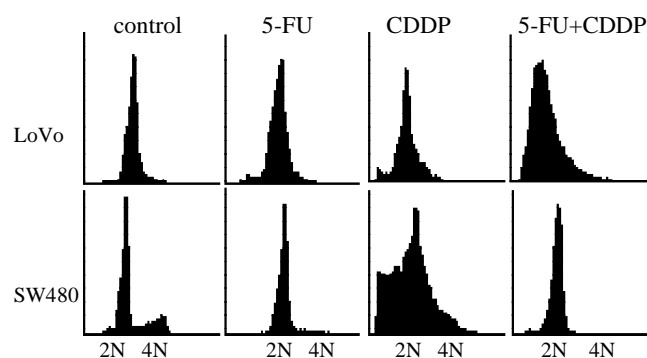


Figure 2 DNA content distribution of LoVo and SW480 cells after 48 hours exposure to 5-FU and/or CDDP. 5-FU causes a more apparent increase of the proportion of hypo diploid DNA cells in LoVo than in SW480. CDDP renders an apparent increase of the hypodiploid DNA cells in both cell lines, but SW480 has more than LoVo cells. Few hypodiploid DNA cells are observed in combination of 5-FU and CDDP treatment.

Distribution of cell cycle by FCM analysis

LoVo cells demonstrated an apparent peak of cells with hypodiploid DNA 48 hours after 5-FU exposure, 48 hours earlier than SW480 cells, which indicated that LoVo cells are more sensitive to 5-FU (Figure 2, 3A). When treated with CDDP for 48 hours, SW480 cells showed more cells with hypodiploid DNA than LoVo cells, about 2-fold increase at 96 hours (55.1 % and 28.5 %, respectively) (Figure 2, 3B).

However, when the two lines were exposed to 5-FU in combination with CDDP, this cytotoxicity significantly diminished. SW480 cells showed an 18 % cells with hypodiploid DNA, but not in LoVo cells in 96 hours (Figure 2, 3C). Both cell lines exposed to 5-FU showed an accumulation

in G1-phase and a significantly decreased proportion of S-phase. On the contrary, CDDP arrests both lines mainly in S-phase instead of G1-phase. Percentage of cells in G1-phase and S-phase dominates alternatively in both lines treated with combination of 5-FU and CDDP (Figure 4).

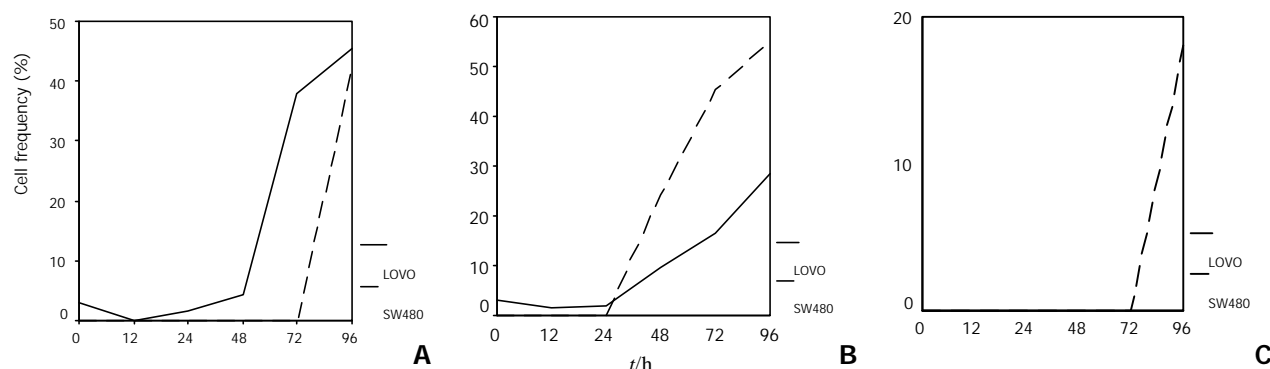


Figure 3 Hypodiploid DNA induced by 5-FU, CDDP or a combination therapy in LoVo cells and SW480 cells. LoVo cells treated with 5-FU show an earlier presence and higher percentage of cells with hypodiploid DNA. **B** When exposed to CDDP, SW480 cells showed a more dramatic increase in presence of hypodiploid DNA than LoVo cells after 48 hours. **C** When the two cell lines were exposed to 5-FU in combination with CDDP, SW480 cells have an 18% hypodiploid DNA, but not in LoVo cells in 96 hours after treatment.

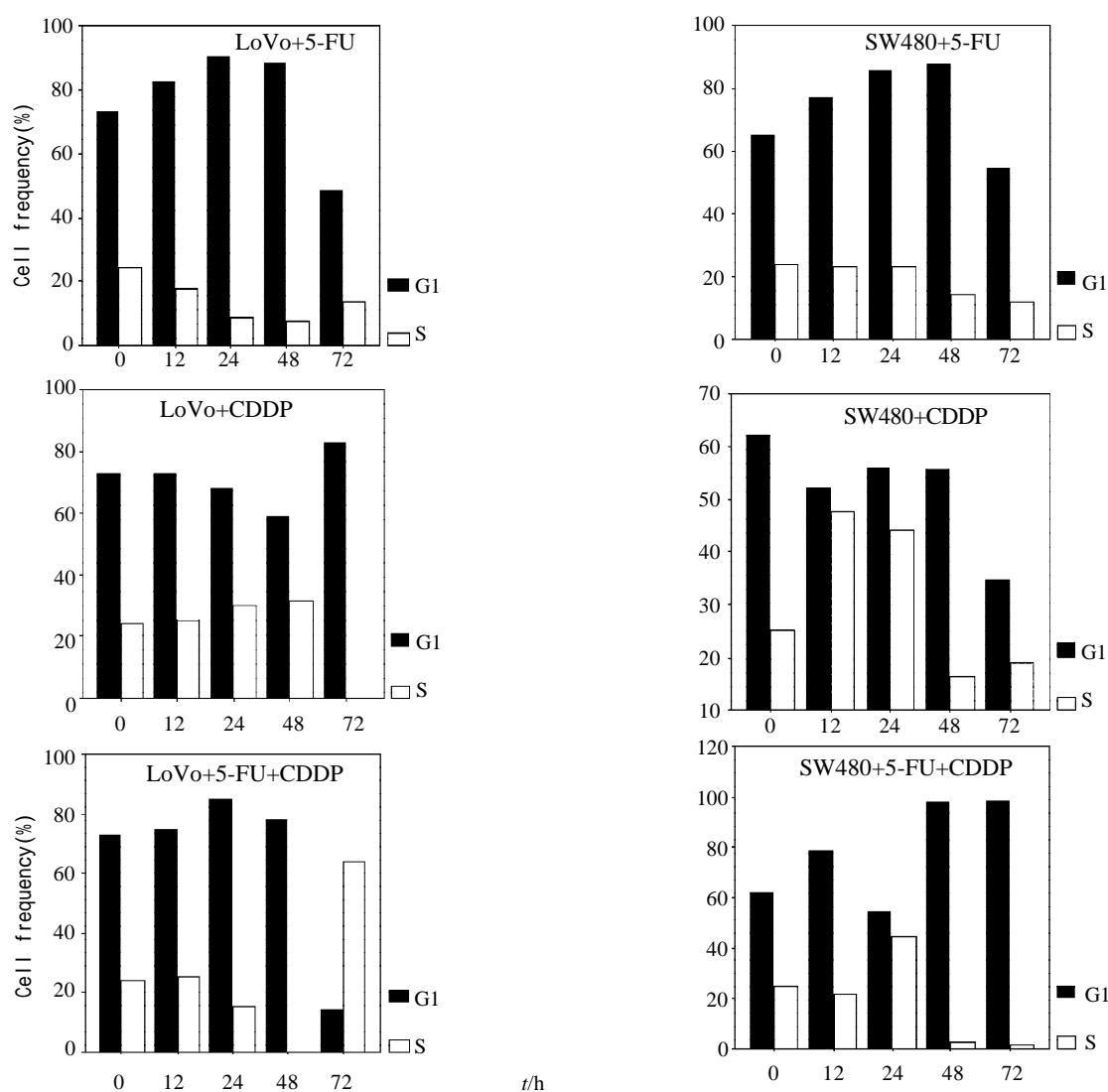


Figure 4 Effects on cell cycle distribution of LoVo cells & SW480 cells treated with 5-FU, CDDP or combination therapy. Both cell lines show an accumulation of G1-phase exposed to 5-FU. On the contrary, CDDP mainly renders an accumulation of S-phase. Percentage of G1- and S-phase dominates alternatively in both lines treated with combination of 5-FU and CDDP.

P53 expression by immunocytochemical staining

P53 staining scattered nestedly in LoVo cells, predominantly in nuclei, and the proportion of positive cells only accounts for less than 1 %, which was thus considered as wtP53. However, SW480 cells showed extensively and strongly P53 expression, and more than 98 % cells were labeled in nuclei, so it suggested a mutated P53 in this cell line (Figure 5).

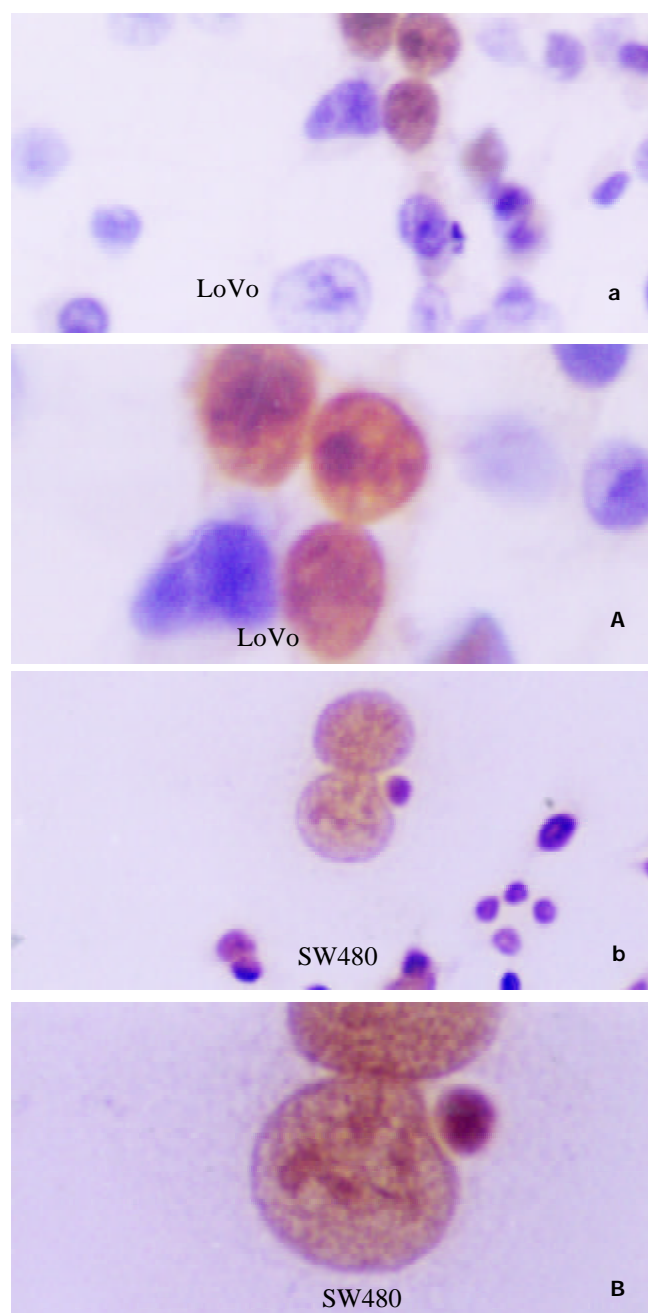


Figure 5 P53 staining with the anti-P53 mAb Do-7 in LoVo and SW480 cells. (a,b $\times 100$; A,B $\times 200$)

DISCUSSION

Our previous studies showed increased sensitivity to 5-FU in colon cancer cell lines with microsatellite instability, and considered that mutations of TGF-R II, IGF II R and RIZ gene maybe enhance the potentials of cell growth and proliferation, which increases the sensitivity to 5-FU. This assumption is supported greatly by findings that the generation time of LoVo

cells is significantly shorter than that of SW480 cells^[4], and by our results here, we found that both cell lines demonstrated an accumulation of G1-phase after 12 hours 5-FU exposure, but apoptosis occurred earlier in LoVo cells.

Many researches have been done to reveal biochemical factors associated with 5-FU response, meanwhile, efforts are made to improve the efficacy of chemotherapy by combining 5-FU with other second-line drugs, such as paclitaxel, oxaliplatin, mitomycin, calcium folinate, INF- α , irinotecan, leucovorin, suramin, tegafur, and so on^[5-10]. Considering mechanistic differences exist between 5-FU and CDDP, we supposed the possibility of their synergism and analyzed the efficacy of combination therapy of these two drugs.

However, our data didn't agree with this supposition. We know that after administration 5-FU is rapidly taken up by cells and metabolized by enzymes by several pathways to produce two active metabolites, i.e. 5-FUTP, which may be incorporated directly into RNA, and 5-FdUMP. 5-FdUMP in the presence of reduced folates inhibits thymidylate synthase (TS) activity and depletes dTTP, a necessary precursor of DNA synthesis. Alternatively, it may be phosphorylated to the triphosphate and 5-FdUTP incorporated directly into DNA, inhibiting chain elongation and altering DNA stability, resulting in the production of single-strand breaks and DNA fragmentation^[11-13]. Thus, 5-FU belongs to the phase-specific anticancer drug that means improved cytotoxicity to cells in S-phase. However, CDDP acts differently, it binds to DNA base pairs, creating adducts, crosslinks, and strand breaks that inhibit DNA replication.

As pointed above, the two cell lines both arrest in G1-phase, and LoVo cells precede SW480 cells in presence of hypodiploid nuclei with treatment of 5-FU. But CDDP rendered an apparent peak of cells with hypodiploid DNA after 48 hour, and LoVo cells showed less percentage of hypodiploid DNA cells, which suggested that, from view of population, SW480 cells are more sensitive to CDDP than LoVo cells. This result is consistent with most reports, i.e. colorectal cancer cells with microsatellite instability are more resistant to CDDP, and several assumptions have been made to explain this phenomenon: firstly, an assumption so-called "Recognition, Excision, Futility of repairing"^[14,15]. The DNA-CDDP adducts are recognized and then excised by the mismatch repair system (MMR), the underlying molecular mechanism responsible for correction of mismatch base pairs or some sorts of DNA damages, but incapable to be repaired because of certain reasons. This failure may then lead to permanent single- or double-strand breaks which are now considered to be the initiation of cell death or apoptosis. Secondly, "Protection mechanism"^[16]. DNA-CDDP adducts are recognized by MMR system or other nuclear factors, then the following binding functions a shelter which protects the damage from repairing by other mechanisms independent of MMR system, which renders cells to death or apoptosis. Thirdly, "Cell cycle pathway". It is supposed that response of cancer cells to CDDP depends on the ability of G2/M arresting. Some workers considered that P53 is responsible for the shift of G1/S phases, whereas MMR system can inactivate CDK1-CyclinB complex by phosphorylation of two amino acid residues, Thr14 and Thr15, of CDK1, and blocks cells in G2/M phase for repair, unrepairable DNA damage often results in activation of the apoptotic pathway (Hawn *et al*, 1995). This assumption is supported by many data^[17-19]. Here, the first explanation disclaims itself because of the homogenous loss of hMSH2, one of most important members responsible for DNA-CDDP adducts recognition in MMR system. We also failed to detect

the G2/M phase arrest which is emphasized in the third assumption. As for the second supposition, further evidences are required to confirm it.

Combination therapy of 5-FU and CDDP showed less efficacy than single-therapy of 5-FU. Here we found that there was less cells with hypodiploid DNA in both cell lines treated with a combination of 5-FU and CDDP, which suggested that the 5-FU-induced cytotoxicity may, at least partially, diminish by the concomitant presence of CDDP. There are at least two mechanisms may explain the observed dominance of CDDP over 5-FU. One may simply involve a CDDP-induced cell cycle blockade, we called it “*cell cycle disturbance*”, analogous to that recently described by Judson *et al* in paclitaxel^[20]. By arresting cells in S-phase of cell cycle, CDDP inhibited both cell lines undergoing apoptosis after exposure to 5-FU. Both cell lines firstly showed a G1-phase increase, a “5-FU-like response”, and then followed by S-phase increase, a “CDDP-like response”. In SW480 cells, particularly in SW480 cells, the percentage of G1-phase and S-phase dominates alternatively. These results demonstrate clearly that disturbance of cell cycle arrest and apoptosis occurred in the combination therapy. An alternative mechanism by which CDDP may exert dominance over 5-FU centers on the ability of each drug to modulate level of many biochemical molecules, we called it “*molecular antagonism*”. CDDP intercalates into DNA, forming adducts, and has been shown to both activate and block a variety of biochemical molecules, including transcription factors, such as *c-myc*, AP-1/AP-2, Oct-1, E2F1, P53 and P73; or molecules involved in cell signal transduction, such as Ras, PKA, EGF4, PKC- α - ϵ - θ ; or factors associated with proliferation, DNA replication and cell cycle regulation, such as PCNA, TS, DNA pol- α / β , Topo I, Cyclin E/D, P16, P21, P27; or Bax and Bcl-2, and so on. We have recently shown that there is a direct correlation between cytotoxicity and 5-FU induced transcriptional activation, i.e. some of these factors are also downstream elements induced by 5-FU and, in turn, affects sensitivity to 5-FU^[21-24], leading us to postulate that at least part of the mechanism involves the antagonism of factors induced by each drug. In fact, these two possibilities are compatible with each other, the latter might just be the underlying biochemical explanation of the former.

Many evidences have shown that sensitivity of cancer cells to 5-FU is associated with a variety of mechanisms, including the key enzyme required for its activation and catabolism, folate substrate and the TS activity, and so on. The concept that P53 is involved in chemotherapy-induced cell cycle arrest and apoptosis is accepted by most scientists^[5,12,25-32]. Yoshikawa *et al*^[1] found there was no relationship between the sensitivity to 5-FU and P53 in colorectal cancer chemotherapy according to evidences from clinical trials, combining with these findings, they proposed that that 5-FU might act via two different pathways, depending on dose: (a) G1/S-phase cell cycle arrest and apoptosis at 1 000 ng/ml, and (b) G2/M-phase cell cycle arrest and mitotic catastrophe at 100 ng/ml in SW480. Our results accord with the higher concentration group they reported, i.e. cells undergo G1-phase or S-phase arrest and apoptosis. Controversies exist in the role of P53 in CDDP chemosensitivity, evidences from malignancies of lung, esophagus, cervix and bladder showed that wtP53 is a favorable prognostic predictor in chemotherapy, and that mutation of P53 will lead cells to chemoresistance^[33-36]. However, in agreement with the findings of Pestell *et al*^[37] in ovarian cancer, colon cancer cell line with mutant P53 exhibited more sensitivity to CDDP. We think this discrepancy may result from the different type of tissue. Up-regulation of P53 in response

to 5-FU/CDDP-induced DNA damage may activates P21 and weel/mik1, which inhibits the CDK activity, and consequentially, E2F1 failed to release itself from E2F1:RB complex due to down-regulation of RB phosphorylation, as a result, cells arrest in G1/S-phase. Alternatively, it is recently reported that P53-induced increase of P21 activity may also be mediated by the PI3K-AKT1/AKT2 signal transduction pathway^[38]. Lin *et al*^[39] found that activation of ATM induced by DNA damage can directly phosphorylate specific residues at the NH₂-terminal of E2F1 and can increase P53 expression. Nagashima *et al* described that P53 can also be acetylated and activated by DNA damage-induced P33^{ING2} in CDDP and paclitaxel exposure^[40]. All these evidences proved that P53 plays an important role in chemotherapy-induced cell cycle arrest and apoptosis. We've known that P21 and P53 are both mutant in SW480 cells, So blockage of cell cycle in G1/S-phase in this cell line may be P53-independent, compared with LoVo cells, apoptosis of SW480 cells treated with 5-FU or CDDP delayed, which may imply that apoptosis induced by P53 pathway is more effective than others. Huang once reported that a few or even one double-strand break of DNA would be enough to increase expression of P53, and led cells to cycle arrest for repairing, if failed, undergoing apoptosis^[21,41,42]. So P53, cell cycle status, damage repair system and apoptotic pathway together determine cells to survive or not.

In conclusion, we have demonstrated that colon cancer cell lines with microsatellite instability are more sensitive to 5-FU, but CDDP goes conversely. Combination therapy of 5-FU and CDDP can lead cells to cycle arrest, but it shows less cytotoxicity than single-therapy of 5-FU. P53 may be involved in cell cycle shift of G1-phase to S-phase, but inessentially.

ACKNOWLEDGEMENTS

We sincerely thank Mrs. Mi-Wei Li, from the Infective Disease Institute of No. 1 Affiliated Hospital of Medical School of Zhe Jiang University, for assistance with Flow Cytometry.

REFERENCES

- 1 **Yoshikawa R**, Kusunoki M, Yanagi H, Noda M, Furuyama JI, Yamamura T, Hashimoto-Tamaoki T. Dual antitumor effects of 5-fluorouracil on the cell cycle in colorectal carcinoma cells: a novel target mechanism concept for pharmacokinetic modulating chemotherapy. *Cancer Res* 2001; **61**:1029-1037
- 2 **Bleiberg H**. Colorectal cancer: the challenge. *Eur J Cancer* 1996; **32A**(Suppl 5): S2-6
- 3 **Lu JG**, Lin C, Huang ZQ, Wu JS, Fu M, Zhang XY, Liang X, Yao X, Wu M. Inhibitory effects of human cholangiocarcinoma cell line by recombinant adenoviruses p16 with CDDP. *Shijie Huaren Xiaohua Zazhi* 2000; **8**: 641-645
- 4 **Bunz F**, Dutriaux A, Lengauer C, Waldman T, Zhou S, Brown JP, Sedivy JM, Kinzler KW, Vogelstein B. Requirement for p53 and p21 to sustain G2 arrest after DNA damage. *Science* 1998; **282**: 1497-1501
- 5 **Trainer DL**, Kline T, McCabe FL, Faucette LF, Field J, Chaikin M, Anazno M, Rieman D, Hoffstein S, Li DJ, Gennoko D, Buscarino C, Lgnch M, Poste G, Greig K. Biological characterization and oncogene expression in human colorectal carcinoma cell lines. *Int J Cancer* 1988; **41**:287-296
- 6 **Kennedy AS**, Harrison GH, Mansfield CM, Zhou XJ, Xu JF, Balcer-Kubiczek EK. Survival of colorectal cancer cell lines treated with paclitaxel, radiation and 5-FU: effect of TP53 or hMLH1 deficiency. *Int J Cancer* 2000; **90**: 175-185
- 7 **Chester JD**, Dent JT, Wilson G, Ride E, Seymour MT. Protracted infusional 5-fluorouracil (5-FU) with bolus with mitomycin in 5-FU-resistant colorectal cancer. *Am Oncol*

- 2000; **11**: 235-237
- 8 **Smith R**, Wickerham DL, Wieand HS, Colangelo L, Mamounas EP. UFT plus calcium folinate vs. 5-FU plus calcium folinate in colon cancer. *Oncol Hungtingt* 1999; **13**: 44-47
- 9 **Sabaawy HE**, Farley T, Ahmed T, Feldman E, Abraham NG. Synergetic effects of retrovirus IFN-alpha gene transfer and 5-FU on apoptosis of colon cancer cells. *Acta Haematol* 1999; **101**: 82-88
- 10 **Van-Cutsem E**, Cunningham D, Ten Bokkel Huinink WW, Punt CJA, Alexopoulos CG, Dirix L, Symann M, Blijham M, Blijham GH, Cholet P, Fillet G, Van Groeningen C, Vannetzel JM, Levi F, Panagos G, Unger C, Wils J, Cote C, Blanc C, Herait P, Bleiberg H. Clinical activity and benefit of irinotecan (CPT-11) in patients with colorectal cancer truly resistant to 5-fluorouracil (5-FU). *Eur J Cancer* 1999; **35**: 54-59
- 11 **Falcone A**, Pfanner E, Brunetti I, Allegrini G, Lencioni M, Galli C, Masi G, Danesi R, Antonuzzo A, Del Tacca M, Conte PF. Suramin in combination with 5-fluorouracil (5-FU) and leucovorin (LV) in metastatic colorectal cancer patients resistant to 5-FU+LV-based chemotherapy. *Tumori* 1998; **84**: 666-668
- 12 **Otake Y**, Tanaka F, Yanagihara K, Hitomi S, Okabe H, Fukushima M, Wada H. Expression of Thymidylate Synthase in Human Non-small Cell Lung Cancer. *Jpn J Cancer Res* 1999; **90**: 1248-1253
- 13 **Kinsella AR**, Smith D, Pickard M. Resistance to chemotherapeutic antimetabolites: a function of salvage pathway involvement and cellular response to DNA damage. *Br J Cancer* 1997; **75**: 935-945
- 14 **Cory JG**, Breland JC, Carter GL. Effect of 5-fluorouracil on RNA metabolism in Novikoff hepatoma cells. *Cancer Res* 1979; **39**:4905-4913
- 15 **Fink D**, Nebel S, Aebi S, Zheng H, Cenni B, Nehme A, Christen RD, Howell SB. The role of DNA mismatch repair in platinum drug resistance. *Cancer Res* 1996; **56**:4881-4886
- 16 **Swann PF**, Waters TR, Moulton DC, Xu YZ, Zheng Q, Edwards M, Mace R. Role of postreplicative DNA mismatch repair in the cytotoxic action of thioguanine. *Science* 1996; **273**:1109-1111
- 17 **Crul M**, Schellens JH, Beijnen JH, Maliepaard M. Cisplatin resistance and DNA repair. *Cancer Treat Rev* 1997; **23**:341-366
- 18 **Brown R**, Hirst GL, Gallagher WM, McIlwrath AJ, Margison GP, van der Zee AG, Anthoney DA. hMLH1 expression and cellular responses of ovarian tumor cells to treatment with cytotoxic cancer agents. *Oncogene* 1997; **15**: 45-52
- 19 **Thiebaut F**, Enns R, Howell SB. Cisplatin sensitivity correlates with its ability to cause cell cycle arrest via a wee1 kinase-dependent pathway in *Schizosaccharmyces Pombe*. *J Cell Physiol* 1994; **159**: 506-514
- 20 **Ikeda M**, Orimo H, Moriyama H, Nakajima E, Matsubara N, Mibu R, Tanaka N, Shimaba T, Kimura A, Shimizu K. Close correlation between mutations of E2F4 and hMSH3 gene in colorectal cancer with microsatellite instability. *Cancer Res* 1998; **58**: 594-598
- 21 **Judson PL**, Watson JM, Gehrig PA, Fowler Jr. WC, Haskill JS. Cisplatin inhibits paclitaxel-induced apoptosis in cisplatin-resistant ovarian cancer cell lines: possible explanation for failure of combination therapy. *Cancer Res* 1999; **59**:2425-2432
- 22 **Dempke W**, Voigt W, Grothey A, Hill BT, Schmoll HT. Cisplatin resistance and oncogenes-a review. *Anticancer Drugs* 2000; **11**: 225-236
- 23 **Jordan P**, Carmo-Fonseca M. Molecular mechanisms involved in cisplatin cytotoxicity. *Cell Mol Life Sci* 2000; **57**: 1229-1235
- 24 **Iqbal S**, Lenz HJ. Determinants of prognosis and response to therapy in colorectal cancer. *Curr Oncol Rep* 2001; **3**: 102-108
- 25 **D'Amico TA**, Harpole DH. Molecular biology of esophageal cancer. *Chest Surg Clin N Am* 2000; **10**: 451-469
- 26 **Iacopetta B**. Tumour site, sex and survival in colorectal cancer. *The Lancet* 2000; **356**: 858
- 27 **Rosty C**, Chazal M, Etienne MC, Letoublon C, Bourgeon A, Delpero JR, Pezet D, Beaune P, Laurent -Puig P, Milano G. Determination of Microsatellite instability, p53 and K-RAS mutation in hepatic metastases from patients with colorectal cancer: relationship with response to 5-fluorouracil and survival. *Int J Cancer* 2001; **95**:162-167
- 28 **Bras-Goncalves RA**, Pocard M, Foormento JL, Poirson-Bichat F, De Pinieux G, Pandrea I, Arvelo F, Ronco G, Villa P, Coquelle A, Milano G, Lesuffleur T, Dutrillaux B, Poupon MF. Synergistic efficacy of 3n-Butyrate and 5-fluorouracil in human colorectal cancer xenografts via modulation of DNA synthesis. *Gastroenterology* 2001; **120**: 874-888
- 29 **Elsaleh H**, Powell B, Soontrapornchai P, Joseph D, Gorla F, Spry N, Iacopetta B. p53 gene mutation, microsatellite instability and adjuvant chemotherapy: impact on survival of 388 patients with Duke's C colon carcinoma. *Oncology* 2000; **58**: 52-59
- 30 **Arango D**, Corner GA, Wadler S, Catalano PJ, Augenlicht LH. *c-myc*/p53 interaction determines sensitivity of human colon carcinoma cells to 5-fluorouracil in vitro and in vivo. *Cancer Res* 2001; **61**:4910-4915
- 31 **Luo F**, Kan B, Lei S, Yan LN, Mao YQ, Zou LQ, Yang YX, Wei YQ. Study on P53 protein and C-erbB2 protein expression in primary hepatic cancer colorectal cancer by flow cytometry. *World J Gastroenterol* 1998; **4**(Suppl 2): 87
- 32 **Xu QW**, Li YS, Zhu HG. Relationship between expression p53 protein, PCNA and CEA in colorectal cancer and lymph node metastasis. *World J Gastroenterol* 1998; **4**:218
- 33 **Choi JH**, Ahn KS, Kim J, Hong YS. Enhanced induction of Bax gene expression in H460 and H1299 cells with the combined treatment of cisplatin and adenovirus mediated wt-p53 gene transfer. *Exp Mol Med* 2000; **32**: 23-28
- 34 **Huang TG**, Ip SM, Yeung WSB, Ngan HYS. Mitomycin C and cisplatin enhanced the antitumor activity of p53-expressing adenovirus in cervical cancer cells. *Cancer Invest* 2001; **19**: 360-368
- 35 **Nakashima S**, Natsugoe S, Matsumoto M, Kijima F, Takebayashi Y, Okumura-H, Shimada M, Nakano S, Kusano C, Baba M, Takao S, Aikou T. Expression of p53 and p21 is useful for the prediction of preoperative chemotherapeutic effects in esophageal carcinoma. *Anticancer Res* 2000; **20**: 1933-1937
- 36 **Miyake H**, Hara I, Hara S, Arakawa S, Kamidono S. Synergistic chemosensitization and inhibition of tumor growth and metastasis by adenovirus-mediated p53 gene transfer in human bladder cancer model. *Urology* 2000; **56**: 332-336
- 37 **Pestell KE**, Hobbs SM, Titley JC, Kelland LR, Walton MI. Effect of p53 status on sensitivity to platinum complexes in a human ovarian cancer cell line. *Mol Pharmacol* 2000; **57**: 503-511
- 38 **Mitsuuchi Y**, Johnson SW, Selvakumaran M, Williams SJ, Hamilton TC, Testa JR. The phosphatidylinositol 3-kinase/AKT signal transduction pathway plays a critical role in the expression of p21^{WAF1/CIP1/SDI1} induced by cisplatin and paclitaxel. *Cancer Res* 2000; **60**: 5390-5394
- 39 **Lin WC**, Lin FT, Nevins JR. Selective induction of E2F1 in response to DNA damage, mediated by ATM-dependent phosphorylation. *Gene Dev* 2001; **15**: 1833-1844
- 40 **Nagashima M**, Shiseki M, Miura K, Hagiwara K, Linke SP, Pedoux R, Wang XW, Yokota J, Riabowol K, Harris CC. DNA damage-inducible gene p33ING2 negatively regulates cell proliferation through acetylation of p53. *Proc Natl Acad Sci USA* 2001; **98**: 9671-9676
- 41 **Bunz F**, Hwang PM, Torrance C, Waldman T, Zhang Y, Dillehay L, Williams J, Lengauer C, Kinzler KW, Vogelstein B. Disruption of p53 in human cancer cells alters the responses to therapeutic agents. *J Clin Invest* 1999; **104**:263-269
- 42 **Hickman JA**, Makin G. Apoptosis and cancer chemotherapy. *Cell Tissue Res* 2000; **301**:143-152

• LARGE INTESTINAL CANCER •

Variability of cell proliferation in the proximal and distal colon of normal rats and rats with dimethylhydrazine induced carcinogenesis

Qing-Yong Ma, Kate E Williamson, Brian J Rowlands

Qing-Yong Ma, Department of Surgery, First Hospital of Xi'an Jiaotong University, Xi'an 710061, Shaanxi Province, China

Kate E Williamson, Brian J Rowlands, Department of Surgery, Institute of Clinical Science, The Queen's University of Belfast, Belfast, UK

Supported in part by DHSS of Northern Ireland.

Correspondence to: Qing-Yong Ma, Department of Surgery, First hospital of Xi'an Jiaotong University, Xi'an 710061, Shaanxi Province, China. qyma0@163.com

Telephone: +86-29-5252911

Received 2002-04-12 **Accepted** 2002-05-20

Abstract

AIM: To investigate the patterns of cell proliferation in proximal and distal colons in normal rats and rats with 1,2-dimethylhydrazine (DMH) induced carcinogenesis using the thymidine analogue bromodeoxyuridine.

METHODS: Colonic crypt cell proliferation was immunohistochemically detected using the anti-bromodeoxyuridine Bu20a monoclonal antibody.

RESULTS: Marked regional differences were found in both groups. Total labelling index (LI) and proliferative zone size in both normal (8.65 ± 0.34 vs 7.2 ± 0.45 , 27.74 ± 1.07 vs 16.75 ± 1.45) and DMH groups (13.13 ± 0.46 vs 11.55 ± 0.45 , 39.60 ± 1.32 vs 35.52 ± 1.58) were significantly higher in distal than in proximal colon ($P < 0.05$), although the number of cells per proximal crypt was greater (31.45 ± 0.20 vs 34.45 ± 0.39 , 42.68 ± 0.53 vs 49.09 ± 0.65 , $P < 0.0001$). Crypt length, total LI and proliferative zone size all increased in both proximal and distal regions of DMH rats compared to normal controls ($P < 0.0001$). In DMH-treated rat colon a shift of labelled cells to higher crypt cell positions was demonstrated distally whilst a bi-directional shift was evident proximally ($P < 0.05$).

CONCLUSION: Our results show that changes in cell proliferation patterns, as assessed by bromodeoxyuridine uptake, can act as a reliable intermediate marker of colonic cancer formation. Observed differences between proliferation patterns in distal and proximal colon may be associated with the higher incidence of tumors in the distal colon.

Ma QY, Williamson KE, Rowlands BJ. Variability of cell proliferation in the proximal and distal colon of normal rats and rats with dimethylhydrazine induced carcinogenesis. *World J Gastroenterol* 2002; 8(5):847-852

INTRODUCTION

Abnormality in epithelial proliferation is considered to be a characteristic of both human diseases associated with higher

risk of colonic cancer and animal colonic cancer models^[1-10]. Hyperproliferation of colonic epithelial cells was observed in tritiated thymidine-labelled colorectal specimens from patients with familial polyposis *Coli*, adenomas and hereditary non-polyposis colon cancer^[11-16]. Assessment of colonic crypt cell proliferation, including detection of increased proliferative state and expansion of the proliferative zone is suggested as a putative intermediate marker of colon cancer risk^[17-19]. Evidence from animal studies showed that experimental colonic tumors induced by procarcinogen 1,2-dimethylhydrazine (DMH) are of epithelial origin with a similar histology, morphology and anatomy to human colonic neoplasms^[20,21]. Furthermore, prior to the development of colonic cancer, DMH injections result in increased colonic crypt cellularity, colonic crypt cell proliferation and colonic crypt proliferative zone^[22,23]. This procarcinogen thus provides an adequate model for kinetic and therapeutic studies of the colorectal cancer^[24-33]. In the normal rat colon, the location of the stem cells and the direction of colonocyte migration differ between the distal colon and the proximal colon^[34]. Interestingly, differences in the incidence, morphology and clinical behaviour of colonic carcinoma have been identified in the proximal and distal colon^[35,36]. However, there are no studies which use bromodeoxyuridine (BrdUrd) to compare cell proliferation patterns in the distal and proximal colonic locations of both normal and colonic cancer animals.

BrdUrd is a thymidine analogue which, after incorporation into normal and malignant cells during the S-phase of the cell cycle, can be detected using a monoclonal antibody. BrdUrd immunohistochemistry offers several advantages over thymidine autoradiography. Firstly, because a radioactive precursor is not required, there is less background interference in the tissue sections. Secondly, a clear distinction between the labelled cells and unlabelled cells is provided. Thirdly, the BrdUrd technique is less time-consuming, thus being more suitable for incorporation into routine diagnostic services. Finally, because BrdUrd is also a therapeutic agent, BrdUrd may be safely injected into the human body to study the cell proliferation in the patients without introducing additional procedures^[37]. Several studies have demonstrated that the LI estimated by BrdUrd immunohistochemistry is equivalent to that obtained by thymidine autoradiography when an *in vitro* labelling technique is used^[38]. This suggests that BrdUrd LI may be used to replace thymidine LI in both *in vitro* and *in vivo* studies.

In the present study, BrdUrd *in vivo* cell labelling was employed to determine the crypt cell proliferation patterns in the proximal and distal rat colons from normal and DMH-induced colon cancer animals.

MATERIALS AND METHODS

Twelve male Wistar rats with initial weight between 180 g and 220 g were housed, 3 in a cage, and maintained on standard laboratory diet (41 B (M)) with free access to water. Six of

these animals received weekly subcutaneous injections of colonic procarcinogen 1,2-dimethylhydrazine (DMH, Aldrich Chemical Company Inc) at a dosage of 20 mg/kg body weight for 20 weeks. The DMH was prepared as a 0.5 % solution in 1 mM ethylenediaminetetra-acetic acid (EDTA, BDH Limited Poole, England) adjusted to pH 7.0 with 10 % sodium bicarbonate immediately before injection. Animals were injected at the same time on the same day each week. Animals were sacrificed 2 weeks after the last DMH injection. Fifteen minutes before removal of the colon, the anaesthetized rats received a peritoneal injection of 5 mg 2 % BrdUrd (Sigma B-5002). This was always done between 9 a.m. and 11 a.m. to avoid diurnal variation. The colon was removed and rinsed with tap water. Following excision of the caecum and rectum, the remaining colon was divided into proximal and distal halves. A 1-2 cm segment of each end of the proximal and distal colon was discarded. After fixation in 70 % ethanol for 4 hours, the segments were rolled prior to processing and embedding in paraffin wax.

BrdUrd immunohistochemistry

Several 3 μ m sections were cut and placed on poly-L-lysine coated slides. The slides were dewaxed before DNA was denatured in 1M HCl at 37 °C for 12 minutes. After rinsing in phosphate buffered saline (PBS, pH 7.1) the sections were incubated with 30 μ l mouse anti-BrdUrd monoclonal antibody (M 744 Dako, Bucks, England) diluted 1:50 in PBS with 0.05 % Tween 20 (PBST) with added normal rat serum diluted 1:25 for 60 minutes at room temperature. After a further rinsing in PBS, the sections were incubated with biotinylated rabbit anti-mouse F(ab')₂ antibody (E 413 Dako, Bucks, England) at a dilution of 1:200 in PBST with added rat serum for 30 minutes at room temperature. Slides were again rinsed in PBS and then incubated with Streptavidin-Biotin Peroxidase complex (K 377 Dako, Bucks, England) for 30 minutes at room temperature. Finally, the reaction product was visualized using diaminobenzidine hydrochloride (DAB) (Sigma, Dorset, England) primed with 100 μ l of 30 % H₂O₂ (diluted 1:20 with distilled water) for approximately 5 minutes. After DAB was washed off with distilled water, the sections were lightly counterstained in Harris haematoxylin before dehydration and mounting in DPX.

Counting and scoring

Only complete well-orientated longitudinally sectioned crypts which displayed lumen at the top and muscularis mucosae at the base was used for analysis. Comparisons between the following 4 groups were undertaken: distal colon from normal rats, proximal colon from normal rats, distal colon from DMH rats and proximal colon from DMH rats. To facilitate scoring, each crypt was divided at the base into 2 crypt columns (hemicypts). Starting at the base of the hemicrypt, cells were numbered up to the luminal surface of the colon to determine the number of cells per hemicrypt (CPC) and then divided into 5 equal compartments each containing the same number of cells. The number and the position of BrdUrd-labelled cells in the hemicrypt were recorded. The proliferative zone, which was expressed as a percentage, was obtained by calculating the difference between the highest and lowest labelled cells in each hemicrypt and dividing this Figureure by the total number of cells in the hemicrypt. Labelling index (LI) was determined for the whole hemicrypt, for each compartment and for the proliferative zone, by dividing the number of labelled cells by the total cells and multiplying by 100. Each hemicrypt was then normalised to a notional 100 cell positions. The frequency of BrdUrd positive cells in each of the 100 positions was recorded.

Statistical analysis

All results are presented as the mean \pm SEM. Two design variables were generated: (1) DMH, where 1 represents a case where DMH has been administered, 0 represents otherwise; and (2) POSITION, where 1 represents a sample from the proximal colonic crypt, while 0 represents one from distal colonic crypt. Multivariate linear regression analyses were performed using the two design variables as covariates against each of the measured parameters (Table 1). Whenever appropriate a two sided Student's *t* test was used to identify the differences between individual variables. Kolmogorov-Smirnov 2 sample test (3) was used to compare the BrdUrd cumulative labelling frequency curves in the four subsets in the sample identified with reference to (1) the presence of DMH treatment, and (2) the site of origin of the sample from the colon. Results were considered to be significant when *P*<0.05 in all cases.

Table 1 Multivariate linear regression analyses with 2 design variables against 7 measured parameters

Response variable	Covariate	Coefficient	<i>P</i> -value
CPC	DMH	12.386	<0.05
	POSITION	5.004	<0.05
TOTLI	DMH	4.433	<0.05
	POSITION	-1.528	<0.05
INDLI 1	DMH	3.915	<0.05
	POSITION	-9.006	<0.05
INDLI 2	DMH	4.504	<0.05
	POSITION	-2.159	0.14
INDLI 3	DMH	10.425	<0.05
	POSITION	3.343	<0.05
PZONE	DMH	18.169	<0.05
	POSITION	-4.454	<0.05
PZONELI	DMH	-18.312	<0.05
	POSITION	1.725	0.43

CPC, cell per hemicrypt; TOTLI, total hemicrypt labelling index; INDLI 1, individual LI in compartment 1; INDLI 2 individual LI in compartment 2; INDLI 3, individual LI in compartment 3; PZONE, proliferative zone; PZONELI, labelling index of proliferative zone.

RESULTS

Proximal compared to distal colon

CPC was significantly greater in the proximal compared to the distal colon in both normal ($t=7.42$, $P<0.0001$) and DMH-treated groups ($t=7.76$, $P<0.0001$, Table 1). The total hemicrypt LI was significantly higher in distal than proximal colon in both normal ($t=2.43$, $P=0.016$) and DMH treated animals ($t=2.47$, $P=0.014$). In the normal controls, BrdUrd labelled cells in the proximal colon were located predominantly in compartment 2 and 3 (88.4 %), whereas the labelled cells in the distal colon were found mostly in compartment 1 and 2 (85.3 %). In compartment 1, LI was significantly higher in distal than in proximal colon ($t=8.05$, $P<0.0001$), while in compartment 3 LI was significantly lower in distal than in proximal colon ($t=-4.46$, $P=0.0001$, Figure 1). Labelled cells

never appeared in compartment 5. The size of the proliferative zone was higher distally ($t=2.57$, $P=0.011$). When the cumulative labelling distribution curves of the proximal and distal colons of normal rats were compared the distal colon showed a significant shift to the left (K-S=2.192, $P<0.0001$, Figure 2).

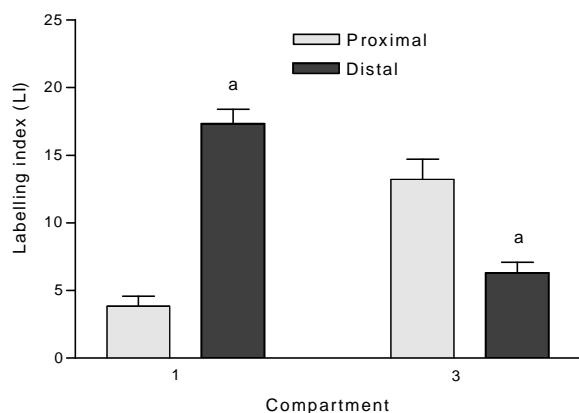


Figure 1 Labelling indices of compartment 1 and compartment 3 in proximal and distal colon of normal rats. ^a $P<0.0001$ when distal is compared to proximal colon in the same compartment. Values are mean \pm SEM.

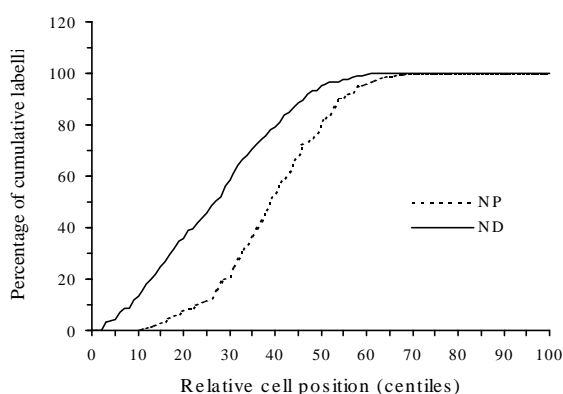


Figure 2 The different patterns of cumulative labelling distributions in proximal (NP) and distal (ND) rat colon of normal controls. The curve is significantly shifted towards the right when the proximal colon is compared to distal colon.

DMH compared with control rats

DMH treatment significantly increased CPC in both proximal ($t=15.9$, $P<0.0001$) and distal colon ($t=20.6$, $P<0.0001$) when compared with normal controls. Total LI was also increased significantly by DMH injections in both proximal ($t=6.23$, $P<0.0001$) and distal colon ($t=7.94$, $P<0.0001$, Table 2). The effects of DMH on the individual LIs for the 5 compartments in the proximal and distal colon are shown in Figures 3 and 4. In proximal colon, the increase in LI was in compartments 1 and 3, whereas in distal colon, the increase in LI in DMH rats was most marked in compartments 2 and 3. The extent of the increase in LI in compartment 3 of the distal colon was significantly greater than the corresponding increase in compartment 3 LI of the proximal colon ($t=3.44$, $P=0.001$). Additionally, DMH increased the size of the proliferative zone in both proximal ($t=7.9$, $P<0.0001$) and distal colonic crypts ($t=10.6$, $P<0.0001$). However the LI of proliferative zone was reduced because of the increased size. Further analysis of the cumulative labelling distributions showed a shift of the DMH distal curve to the 81st centile which was to the right of the

plateau of the normal distal colon located at 61st centile (K-S=1.89, $P=0.001$, Figure 5). In contrast the cumulative labelling distribution curve in proximal colon demonstrated a shift to the left in the lower crypt cell positions and then shifted to the right high up the crypt (K-S=3.625, $P<0.0001$, Figure 6).

Table 2 Comparison of cell proliferation in proximal and distal hemicrypts of normal and DMH rat colon

Parameters	Normal control		DMH	
	Proximal	Distal	Proximal	Distal
Cells/hemi-crypt	34.45 \pm 0.39	31.45 \pm 0.2 ^a	49.09 \pm 0.65 ^b	42.68 \pm 0.53 ^{a,c}
Labelled cells	2.49 \pm 0.16	2.74 \pm 0.11	5.7 \pm 0.24 ^b	5.67 \pm 0.23 ^c
Total LI	7.2 \pm 0.45	8.65 \pm 0.34 ^a	11.55 \pm 0.45 ^b	13.13 \pm 0.46 ^{a,c}
Proliferative zone	16.75 \pm 1.45	21.74 \pm 1.07 ^a	35.52 \pm 1.58 ^b	39.6 \pm 1.32 ^{a,c}
LI of proliferative zone	59.43 \pm 3.39	56.55 \pm 2.13	39.84 \pm 1.77 ^b	38.89 \pm 1.5 ^c

Values expressed as mean \pm SEM. ^a $P<0.05$ when distal is compared to proximal in the same group, ^b $P<0.05$ when DMH proximal is compared to normal proximal, ^c $P<0.05$ when DMH distal compared to normal distal.

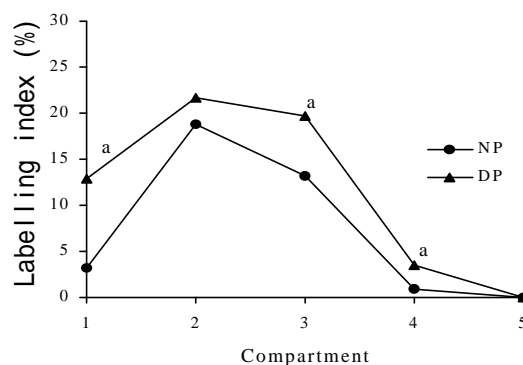


Figure 3 Labelling indices of normal proximal colon (NP) and DMH proximal colon (DP) for the 5 compartments. ^a $P<0.0001$ when labelling indices in the compartments of DMH proximal colons were compared to those found in normal proximal colons in the same compartments.

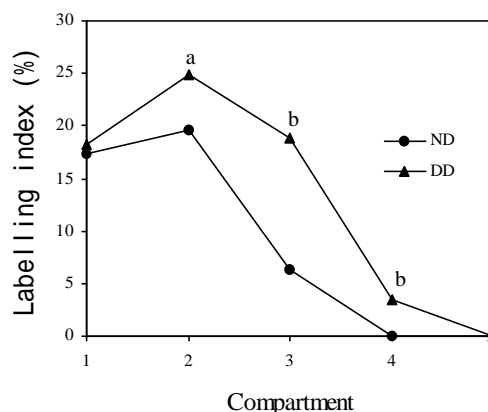


Figure 4 Labelling indices of normal distal colon (ND) and DMH distal colon (DD) for the 5 compartments. ^a $P<0.05$, ^b $P<0.0001$ when labelling indices in the compartments of DMH distal colons were compared to those found in normal distal colons in the same compartments.

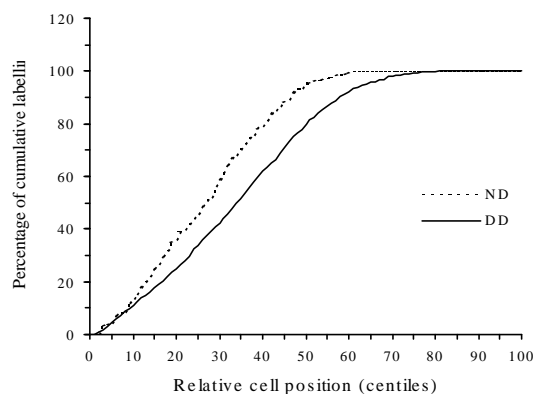


Figure 5 Cumulative labelling distribution in normal (ND) and DMH distal (DD) rat colon. The curve is significantly shifted towards the right in DMH distal colon compared to normal distal colon.

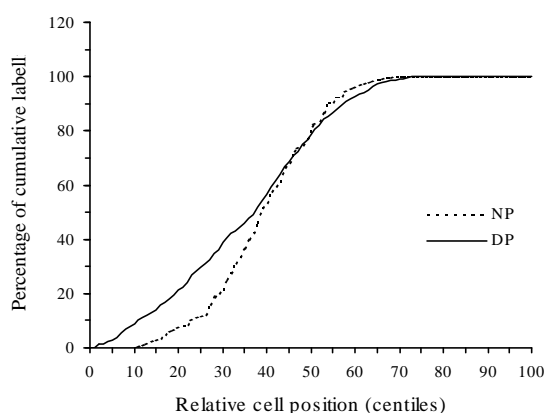


Figure 6 Cumulative labelling distribution in normal (NP) and DMH proximal (DP) rat colon. The curve of DMH treated proximal rat colon is initially significantly shifted towards the left and then in the higher centiles shifted to the right.

DISCUSSION

Significant regional differences in the distribution of BrdUrd-labelled cells located in proximal and distal rat colon have been demonstrated in this study. The total LI and the proliferative zone size are all significantly larger in the distal than in the proximal colonic crypt both in normal and DMH-induced carcinogenesis animals. These regional differences in proliferative cell distribution between proximal and distal colon were previously shown using other markers, e.g. ^3H -thymidine autoradiography and proliferating cell nuclear antigen (PCNA) immunohistochemistry. ^3H -thymidine LI and proliferative zone size have been reported to be significantly larger distally than proximally^[39]. In the distal colon, PCNA expression was strictly confined in the lower third of the crypt, whereas in the proximal colon it was located in the mid-crypt^[23].

Our results show that in the distal colon the proliferative cells are located predominantly in the compartments 1 and 2, whereas in the proximal colon, the proliferative cells are located in the 2nd and 3rd compartments. In earlier studies, using tritiated thymidine, Sunter *et al*^[40] found the differences in the distribution of proliferative activity within the crypt from site to site along the length of the rat colon. In the proximal colon, Sunter noted that the peak LI was located in the middle third of the crypt while in distal colon the peak was located in the lower third near the base of the crypt.

These findings together with ours, tend to support the

explanation of crypt cell origin and colonocyte migration described by Sato and Ahnen^[34]. After double labelling with ^3H -thymidine and BrdUrd, they investigated the location of stem cells and the direction of colonocyte migration in normal rat colonic crypt. They reported that distal stem cells are located in the crypt base while proximal stem cells are located in the mid-crypt. They postulated that colonocytes migrate up toward the luminal surface in distal colon in contrast to the bidirectional migration, i.e. up toward the luminal surface and down toward the crypt base in proximal colon.

Our results show that after DMH injection colonic crypt cell proliferation is significantly increased regardless of the position (proximal or distal) and irrespective of the proliferative parameter assessed except the LI of proliferative zone (Table 1). The LI of the proliferative zone in the DMH animals may not increase because of the concomitant increase of the zone size. DMH treatment not only increases the colonic crypt cellularity, total BrdUrd LI but also increases the size of the proliferative zone in both proximal and distal colon. The LI of each compartment from 1 to 3 is also increased, especially in the distal colon. This can be confirmed by the cumulative labelling distribution curves (Figures 5 and 6). Although DMH treatment increases LI in both proximal and distal colon the cumulative labelling distribution is markedly shifted to the right in distal colon whereas the proximal curve shifts to the left (i.e. downwards in the crypt). These results are interesting because of the differences in colonic cancer distribution between proximal and distal colon. The distribution of DMH-induced colorectal cancer resembles human large bowel carcinoma, in which the majority of tumors are recorded distally^[41,42]. In our previous work when total colon was exposed to the procarcinogen DMH, 73 % tumors occurred distally and only 12 % occurred proximally^[33].

Further investigation is required to resolve the questions concerning the differences of tumor distribution and their relationship to the different crypt cell proliferation patterns observed in proximal and distal colon. It has been shown that in the proximal colon the lower one-third of the crypt contains predominantly mucous cells whereas the upper one-third mainly has columnar cells^[43]. In contrast, crypts of the distal colon contain only a small number of mucous cells in basal positions. The undifferentiated cells or the cells with the lowest level of differentiation (presumptive stem cells) are the vacuolated cells located near or at the crypt base^[44]. When the vacuolated cells migrate upward, they transformed into columnar cells and when they migrate downward, they give rise to mucous cells^[45]. The major role which stem cells play in carcinogenesis is presumably to transform the malignancy^[46]. If this hypothesis is true, there should be more mucinous tumors expected in proximal colon and the tumors in distal colon should originate from columnar cells. In DMH-induced rat colonic carcinogenesis the tumors tended to be more frequently sessile, often mucinous and invasive adenocarcinomas in proximal regions and polyps in distal areas^[42].

In this study we observed a greater baseline value of crypt length in proximal than in distal colon, which is contrary to some other published literature^[39,40]. This disparity may be due to the differences in defining the criteria for handling the overlapping nuclei, selecting crypts or ascertaining the top of the crypt. We have noticed that the nuclei in the proximal colon are not as typical as those in distal colon. In this study longitudinally well-oriented crypts was selected and all visible nuclei were counted.

Our study demonstrated regional differences in crypt cellularity and cell proliferation patterns. Additionally, we can

conclude that the procarcinogen DMH increased crypt cell proliferation and shifted the cumulative BrdUrd labelling distribution in both distal and proximal rat colon. The histochemical similarity of the distal rat colon to the human colon^[43] permits the distal rat colon to be used as a model of colonic cancer^[47-54]. Therefore, BrdUrd is an appropriate intermediate marker for the early detection of colorectal cancer in patients at high risk and the correct assessment of dietary interference.

ACKNOWLEDGEMENT

We thank Dr. LY Hin for his statistical advice and Dr. PW Hamilton for his critical suggestion.

REFERENCES

- 1 **Chapkin RS**, Lupton JR. Colonic cell proliferation and apoptosis in rodent species. Modulation by diet. *Adv Exp Med Biol* 1999; **470**: 105-118
- 2 **Wong WM**, Wright NA. Cell proliferation in gastrointestinal mucosa. *J Clin Pathol* 1999; **52**: 321-333
- 3 **Mills SJ**, Mathers JC, Chapman PD, Burn J, Gunn A. Colonic crypt cell proliferation state assessed by whole crypt microdissection in sporadic neoplasia and familial adenomatous polyposis. *Gut* 2001; **48**: 41-46
- 4 **Zhu JW**, Yu BM, Ji YB, Zheng MH, Li DH. Upregulation of vascular endothelial growth factor by hydrogen peroxide in human colon cancer. *World J Gastroenterol* 2002; **8**: 153-157
- 5 **Peng ZH**, Xing TH, Qiu GQ, Tang HM. Relationship between Fas/FasL expression and apoptosis of colon adenocarcinoma cell lines. *World J Gastroenterol* 2001; **7**: 88-92
- 6 **Xie B**, He SW, Wang XD. Effect of gastrin on protein kinase C and its subtype in human colon cancer cell line SW480. *World J Gastroenterol* 2000; **6**: 304-306
- 7 **Ochsenkuhn T**, Bayerdorffer E, Meining A, Schinkel M, Thiede C, Nussler V, Sackmann M, Hatz R, Neubauer A, Paumgartner G. Colonic mucosal proliferation is related to serum deoxycholic acid levels. *Cancer* 1999; **85**: 1664-1669
- 8 **Akedo I**, Ishikawa H, Ioka T, Kaji I, Narahara H, Ishiguro S, Suzuki T, Otani T. Evaluation of epithelial cell proliferation rate in normal-appearing colonic mucosa as a high-risk marker for colorectal cancer. *Cancer Epidemiol Biomarkers Prev* 2001; **10**: 925-930
- 9 **Barnes CJ**, Hardman WE, Cameron IL. Presence of well-differentiated distal, but not poorly differentiated proximal, rat colon carcinomas is correlated with increased cell proliferation in and lengthening of colon crypts. *Int J Cancer* 1999; **80**: 68-71
- 10 **Kozoni V**, Tsioulas G, Shiff S, Rigas B. The effect of lithocholic acid on proliferation and apoptosis during the early stages of colon carcinogenesis: differential effect on apoptosis in the presence of a colon carcinogen. *Carcinogenesis* 2000; **21**: 999-1005
- 11 **Lipkin M**, Blattner WE, Fraumeni Jr JF, Lynch HT, Deschner E, Winawer S. Tritiated thymidine (phi p, phi h) labeling distribution as a marker for hereditary predisposition to colon cancer. *Cancer Res* 1983; **43**: 1899-1904
- 12 **Sun K**, Jin BQ, Feng Q, Zhu Y, Yang K, Liu XS, Dong BQ. Identification of CD226 ligand on colo205 cell surface. *World J Gastroenterol* 2002; **8**: 108-113
- 13 **Xiao B**, Jing B, Zhang YL, Zhou DY, Zhang WD. Tumor growth inhibition effect of hIL-6 on colon cancer cells transfected with the target gene by retroviral vector. *World J Gastroenterol* 2000; **6**: 89-92
- 14 **Lipkin M**, Blattner WE, Gardner EJ, Burt RW, Lynch H, Deschner E, Winawer S, Fraumeni JF Jr. Classification and risk assessment of individuals with familial polyposis, Gardner's syndrome, and familial non-polyposis colon cancer from [3H]thymidine labeling patterns in colonic epithelial cells. *Cancer Res* 1984; **44**: 4201-4207
- 15 **Wilson RG**, Smith AN, Bird CC. Immunohistochemical detection of abnormal cell proliferation in colonic mucosa of subjects with polyps. *J Clin Pathol* 1990; **43**: 744-747
- 16 **Terpstra OT**, van Blankenstein M, Dees J, Eilers GAM. Abnormal pattern of cell proliferation in the entire colonic mucosa of patients with colon adenoma or cancer. *Gastroenterology* 1987; **92**: 704-708
- 17 **Yamada K**, Yoshitke K, Sato M, Ahnen DJ. Proliferating cell nuclear antigen expression in normal, preneoplastic colonic epithelium of the rat. *Gastroenterology* 1992; **103**: 160-167
- 18 **Colussi C**, Fiumicino S, Giuliani A, Rosini S, Musiani P, Macri C, Potten CS, Crescenzi M, Bignami M. 1,2-Dimethylhydrazine-induced colon carcinoma and lymphoma in msh2(-/-) mice. *J Natl Cancer Inst* 2001; **93**: 1534-1540
- 19 **Anti M**, Armuzzi A, Morini S, Iacone E, Pignataro G, Coco C, Lorenzetti R, Paolucci M, Covino M, Gasbarrini A, Vecchio F, Gasbarrini G. Severe imbalance of cell proliferation and apoptosis in the left colon and in the rectosigmoid tract in subjects with a history of large adenomas. *Gut* 2001; **48**: 238-246
- 20 **Maskens AP**. Histogenesis and growth pattern of 1,2-dimethylhydrazine-induced rat colon adenocarcinoma. *Cancer Res* 1976; **36**: 1585-1592
- 21 **Ma QY**, Hoper M, Anderson N, Rowlands BJ. Effect of supplemental L-arginine in a chemical-induced model of colorectal cancer. *World J Surg* 1996; **20**: 1087-1091
- 22 **Richards TC**. Early changes in the dynamics of crypt cell populations in mouse colon following administration of 12,-dimethylhydrazine. *Cancer Res* 1977; **37**: 1680-1685
- 23 **Heitman DW**, Grubbs BG, Heitman TO, Cameron IL. Effects of 1,2-dimethylhydrazine treatment and feeding regimen on rat colonic epithelial cell proliferation. *Cancer Res* 1983; **43**: 1153-1162
- 24 **Whiteley LO**, Klurfeld DM. Are dietary fiber-induced alterations in colonic epithelial cell proliferation predictive of fiber's effect on colon cancer? *Nutr Cancer* 2000; **36**: 131-149
- 25 **Cascinu S**, Ligi M, Del Ferro E, Foglietti G, Cioccolini P, Staccioli MP, Carnevali A, Luigi Rocchi MB, Alessandrini P, Giordani P, Catalano V, Polizzi V, Agostinelli R, Muretto P, Catalano G. Effects of calcium and vitamin supplementation on colon cell proliferation in colorectal cancer. *Cancer Invest* 2000; **18**: 411-416
- 26 **Pereira MA**. Prevention of colon cancer and modulation of aberrant crypt foci, cell proliferation, and apoptosis by retinoids and NSAIDs. *Adv Exp Med Biol* 1999; **470**: 55-63
- 27 **Schmelz EM**, Sullards MC, Dillehay DL, Merrill AH Jr. Colonic cell proliferation and aberrant crypt foci formation are inhibited by dairy glycosphingolipids in 1, 2-dimethylhydrazine-treated CF1 mice. *J Nutr* 2000; **130**: 522-527
- 28 **Sesink AL**, Termont DS, Kleibeuker JH, Van der Meer R. Red meat and colon cancer: the cytotoxic and hyperproliferative effects of dietary heme. *Cancer Res* 1999; **59**: 5704-5709
- 29 **Stammberger P**, Baczako K. Cytokeratin 19 expression in human gastrointestinal mucosa during human prenatal development and in gastrointestinal tumors: relation to cell proliferation. *Cell Tissue Res* 1999; **298**: 377-381
- 30 **Walker AR**, Segal I. Low-fat dairy foods and colonic epithelial cell proliferation. *JAMA* 1999; **281**: 1274
- 31 **Koh TJ**, Dockray GJ, Varro A, Cahill RJ, Dangler CA, Fox JG, Wang TC. Overexpression of glycine-extended gastrin in transgenic mice results in increased colonic proliferation. *J Clin Invest* 1999; **103**: 1119-1126
- 32 **Caderni G**, Palli D, Lancioni L, Russo A, Luceri C, Saieva C, Trallori G, Manneschi L, Renai F, Zacchi S, Salvadori M, Dolara P. Dietary determinants of colorectal proliferation in the normal mucosa of subjects with previous colon adenomas. *Cancer Epidemiol Biomarkers Prev* 1999; **8**: 219-225
- 33 **Ma Q**, Williamson KE, O' rourke D, Rowlands BJ. The effects of l-arginine on crypt cell hyperproliferation in

- colorectal cancer. *J Surg Res* 1999; **81**: 181-188
- 34 **Sato M**, Ahnen D. Regional variability of colonocyte growth and differentiation in the rat. *Anat Record* 1992; **233**: 409-414
- 35 **Freeman HJ**, Kim YS, Kim YS. Glycoprotein metabolism in normal proximal and distal rat colon and changes associated with 1,2-dimethylhydrazine-induced colonic neoplasia. *Cancer Res* 1978; **38**: 3385-3390
- 36 **Lipkin M**. Update of preclinical and human studies of calcium and colon cancer prevention. *World J Gastroenterol* 1999; **5**: 461-464
- 37 **Ricardi A**, Danova M, Dionigi P, Gaetani P, Cebrelli T, Butti G, Mzzini G, Wilson G. Cell kinetics in leukaemia and solid tumours studied with *in vivo* bromodeoxyuridine and flow cytometry. *Br J Cancer* 1989; **59**: 898-903
- 38 **Qin Y**, Willens G. Comparison of the classical autoradiographic and the immunohistochemical methods with BrdU for measuring proliferation parameters in colon cancer. *Anticancer Res* 1993; **13**: 731-736
- 39 **McGarrity TJ**, Perffer LP, Colony PC. Cellular proliferation in proximal and distal rat colon during 1,2-dimethylhydrazine-induced carcinogenesis. *Gastroenterology* 1988; **95**: 343-348
- 40 **Sunter JP**, Watson AJ, Wright NA, Appleton DR. Cell proliferation at different sites along the length of the rat colon. *Virchows Arch B Cell Path* 1979; **32**: 75-87
- 41 **Rodgers AE**, Nauss KM. Rodent model for carcinoma of the colon. *Dig Dis Sci* 1985; **30**: 87S-102S
- 42 **Shamsuddin AKM**, Trump BF. Colon Epithelium: II. *In vivo* studies of colon carcinogenesis. Light microscopic, histochemical, and ultrastructural studies of histogenesis of azoxymethane-induced colon carcinogenesis in Fischer 344 rats. *JNCI* 1981; **66**: 389-401
- 43 **Shamsuddin AKM**, Trump BF. Colon Epithelium: I. Light microscopic, histochemical, and ultrastructural features of normal colon epithelium of male Fischer 344 rats. *JNCI* 1981; **66**: 375-388
- 44 **Nabeyama A**. Presence of cells combining features of two different cell types in the colonic crypt and pyloric glands of the mouse. *Am J Anat* 1975; **142**: 471-484
- 45 **Chang WWL**, Leblond CP. Renewal of the epithelium in the descending colon of the mouse. I. Presence of three cell populations: vacuolated-columnar, mucous and argentaffin. *Am J Anat* 1971; **131**: 73-100
- 46 **Pierce GB**. Neoplasms, differentiations and mutation. *Am J Pathol* 1974; **77**: 103-118
- 47 **Dashwood RH**, Xu M, Orner GA, Horio DT. Colonic cell proliferation, apoptosis and aberrant crypt foci development in rats given 2-amino-3-methylimidaz. *Eur J Cancer Prev* 2001; **10**: 139-145
- 48 **Holt PR**, Arber N, Halmos B, Forde K, Kissileff H, McGlynn KA, Moss SF, Fan K, Yang K, Lipkin M. Colonic epithelial cell proliferation decreases with increasing levels of serum 25-hydroxy vitamin D. *Cancer Epidemiol Biomarkers Prev* 2002; **11**: 113-119
- 49 **Aly A**, Shulkes A, Baldwin GS. Short term infusion of glycine-extended gastrin(17) stimulates both proliferation and formation of aberrant crypt foci in rat colonic mucosa. *Int J Cancer* 2001; **94**: 307-313
- 50 **Liu Z**, Uesaka T, Watanabe H, Kato N. High fat diet enhances colonic cell proliferation and carcinogenesis in rats by elevating serum leptin. *Int J Oncol* 2001; **19**: 1009-1014
- 51 **Liu Z**, Tomotake H, Wan G, Watanabe H, Kato N. Combined effect of dietary calcium and iron on colonic aberrant crypt foci, cell proliferation and apoptosis, and fecal bile acids in 1,2-dimethylhydrazine-treated rats. *Oncol Rep* 2001; **8**: 893-897
- 52 **Exon JH**, South EH, Magnuson BA, Hendrix K. Effects of indole-3-carbinol on immune responses, aberrant crypt foci, and colonic crypt cell proliferation in rats. *J Toxicol Environ Health A* 2001; **62**: 561-573
- 53 **Jenab M**, Thompson LU. Phytic acid in wheat bran affects colon morphology, cell differentiation and apoptosis. *Carcinogenesis* 2000; **21**: 1547-1552
- 54 **Davidson LA**, Brown RE, Chang WC, Morris JS, Wang N, Carroll RJ, Turner ND, Lupton JR, Chapkin RS. Morphodensitometric analysis of protein kinase C beta(II) expression in rat colon: modulation by diet and relation to *in situ* cell proliferation and apoptosis. *Carcinogenesis* 2000; **21**: 1513-1519

Edited by Ma JY

• LARGE INTESTINAL CANCER •

Angiogenesis inhibitor TNP-470 suppresses growth of peritoneal disseminating foci of human colon cancer line Lovo

Ying-Fang Fan, Zong-Hai Huang

Ying-Fang Fan, Zong-Hai Huang, Department of Surgery, Zhujiang Hospital, First Military Medical University, Guangzhou 510282, China
Supported by the Natural Science Foundation of Guangdong Province, No. 013072

Correspondence to: Dr. Ying-Fang Fan, Department of Surgery, Zhujiang Hospital, The First Military Medical University, Guangzhou 510282, Guangdong Province, China. fynyf@yahoo.com.cn
Telephone: +86-20-61643211

Received 2002-02-28 **Accepted** 2002-05-25

Abstract

AIM: To study the effect of angiogenesis inhibitor TNP-470 on peritoneal dissemination of colon cancer in nude mice.

METHODS: The MTT assay was used to evaluate the inhibitory effect of TNP-470 on human colon cancer cell line Lovo. Lovo cells were injected into the peritoneal cavity of BABL/C nu/nu mice and the models of peritoneal dissemination were developed. Thirty nude mice were randomly divided into control and TNP-470-treated group. In TNP-470-treated group, TNP-470 was injected subcutaneously every other day from day 1 until sacrifice or death (30 mg·kg⁻¹). The control group received a sham injection of the same volume saline solution.

RESULTS: *In vitro*, TNP-470 inhibited the growth of Lovo cells, with its IC₅₀ at 2.14×10² μg·L⁻¹. *In vivo*, TNP-470 demonstrated growth inhibition of tumors. Mice body weight and abdominal circumferences were significantly different between TNP-470-treated group (24.5±3.2 g, 7.0±1.1 cm) and control group (29.5±2.1 g, 10.3±1.5 cm), *P*=0.005 and *P*=0.001. The number of disseminated foci was significantly different between the control group (92.1±20.6) and the TNP-470-treated group (40.3±12.3), *P*<0.001. The maximal size of foci was significantly smaller in TNP-470-treated group (3.3±0.7 mm) than that of control (7.3±2.3 mm), *P*=0.004. Mean survival time was significantly longer in TNP-470-treated group (98.00±12.06 d) than that in control group (41.86±9.51 d), *P*<0.001.

CONCLUSION: Angiogenesis inhibitor TNP-470 might be effective in treating peritoneal dissemination of colon cancer and improve the survival rate of nude mice.

Fan YF, Huang ZH. Angiogenesis inhibitor TNP-470 suppresses growth of peritoneal disseminating foci of human colon cancer line Lovo. *World J Gastroenterol* 2002; 8(5):853-856

INTRODUCTION

Colorectal cancer still remains the most frequent malignancy in Japan, United States of America and China. Although combined therapies, including chemotherapy, radiation therapy and immunotherapy are performed in addition to surgical radical resection, nearly 50 % of patients still die of recurrence

and a major form of recurrence was peritoneal dissemination^[1]. Therefore, new therapeutic programs are needed to raise the survival rate of colorectal cancer patients. The importance of tumor angiogenesis is widely accepted in cases of blood-born metastases^[2,3]. Although the form of blood supply is markedly different between metastases in solid organs and those at the peritoneum, it has been generally accepted that any foci larger than 0.2 mm require new tumor vessels for their growth^[1-4]. Thus, inhibition of angiogenesis would prevent the tumor growth and their peritoneal dissemination.

TNP-470 is a semisynthetic analogue of fumagillin isolated from *Aspergillus fumigatus*. TNP-470 has been reported to inhibit neovascularization by preventing endothelial cells growth and proliferation^[5-9]. Recently, the therapeutic effects of TNP-470 on various human and rodent tumors have been reported and this agent shows a marked inhibitory effect on tumor growth and metastasis *in vivo*^[10-11]. However, the importance of angiogenesis in the establishment and growth of peritoneal dissemination remains unknown and there has been no report that evaluates the effect of TNP-470 on establishment and growth of peritoneal dissemination and ascites production of human colon cancer.

In this study, we investigated the inhibitory effects of TNP-470 on an establishment and growth of intraperitoneally inoculated human colon cancer cell line, Lovo, and survival of nude mice with this tumor *in vivo*. We also examined the inhibitory effect of TNP-470 on cell growth *in vitro*.

MATERIALS AND METHODS

Drug and reagents

TNP-470 was a generous gift from Takeda Chemical Industries (Osaka, Japan). 3-(4,5-Dimethylthiazole-2-yl)-2,5-diphenyl-tetrazolium bromide (MTT), gum arabic and dimethyl sulfoxide (DMSO) were purchased from Sigma (St. Louis, MO); RPMI 1640 and heat-inactivated fetal calf serum (FCS) were purchased from Gibco (Grand Island, NY).

TNP-470 was stored dry at -20 °C. *in vitro* experiments, TNP-470 was dissolved in DMSO and RPMI 1640 medium supplemented with 10 % FCS. The final concentration of DMSO was 0.1 %, while *in vivo* experiments, TNP-470 was suspended in a vehicle of 3 % ethanol and 5 % gum arabic in saline.

Cell line

Human colon adenocarcinoma cell line, Lovo was kindly provided by the Department of Pathology, Cancer Center, First Military Medical University (FIMMU). Cells were cultured in RPMI 1640 supplemented with 10 % FCS, and were maintained at 37 °C in 5 % CO₂. All experiments were performed using cells harvested at the 80-90 % subconfluent stage.

Animals

Female BALB/c nude mice were obtained from the Experimental Animal Center, FIMMU, and reared under specific pathogen-free condition. Four-week-old mice weighing 17-22 g were used in the experiments.

In vitro experiments

The MTT assays were made to evaluate the sensitivity of TNP-470 to Lovo cells^[8]. Lovo cells were plated in 96-well microtiter plates at a concentration of 5×10^4 cells in 50 μ L of RPMI 1640 medium. After 24 h incubation, the medium was changed to RPMI 1640 medium with various concentrations of TNP-470 (5×10^{-4} μ g \cdot L⁻¹– 5×10^5 μ g \cdot L⁻¹), and the medium was incubated for 48 h. 20 μ L MTT (5 g \cdot L⁻¹) solution was then added to each well. After the plates were incubated for 3 h, 150 μ L DMSO was added. The absorbance at 570 nm was determined using a microplate reader (Bio-Rad Model 3550, Hercules, CA). Dose-response curves were plotted, and the 50 % inhibitory concentration (IC₅₀) was extrapolated as the drug dose causing a 50 % reduction in absorbance as compared with control values. The experiments were repeated in three independent experiments.

In vivo experiments

Lovo cells were harvested after being cultured for 48 h and the model of peritoneal dissemination in nude mice was developed as follows. Approximately 5×10^7 cells in 0.2 mL saline solution were injected into the peritoneal cavity of an nude mouse (day 0). Thirty nude mice were randomly divided into a control group ($n=16$) and a TNP-470-treated group ($n=14$). In the TNP-470-treated group, TNP-470 of 30 mg \cdot kg⁻¹ was injected subcutaneously every other day from day 1 until sacrifice. The control group received a sham injection of the same volume of saline. On day 10, two mice in control group were sacrificed and disseminated nodules on the peritoneum were evaluated. Seven mice each were sacrificed on day 30. Body weight and abdominal circumferences (substitute abdominal circumferences for ascites) of each mouse in two groups were measured. The number and maximum size of disseminated nodules on the peritoneum and mesentery were evaluated. The remaining 14 mice, 7 in each group, were followed for the survival experiment.

Statistical analysis

Data were expressed as mean \pm standard deviation. Comparison between two groups was made by the independent samples t test. The survival curve was calculated by the Kaplan-meier method and compared by the Log-rank test. $P < 0.05$ was considered statistically significant. All statistics were carried out using SPSS10.0 statistics software.

RESULTS

Effects of TNP-470 on cell growth in vitro

In the colorimetric MTT assay, significant growth inhibition was observed in a dose-dependent manner. The IC₅₀ value was 2.14×10^2 μ g \cdot L⁻¹ extrapolated from the dose-response curve following 48 h exposure (Figure 1).

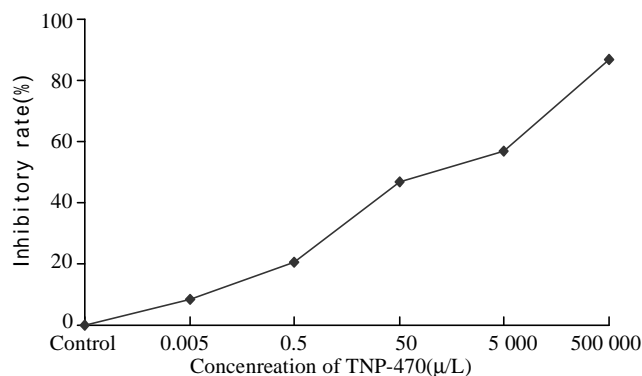


Figure 1 Inhibition curve of Lovo cells after TNP-470 treated 48 h

Effects of TNP-470 on establishment and growth of peritoneal dissemination in vivo

Two mice in control group sacrificed on day 10 developed disseminated nodules, suggesting that small nodules at the peritoneum developed within 10 days after inoculation in this model. Body weight and abdominal circumferences were gained in two groups when mice sacrificed on day 30. Body weight and abdominal circumferences in the control group and the TNP-470-treated group are summarized in Table 1. The difference of body weight and abdominal circumferences were statistically significant ($P=0.005$ and $P=0.001$). The number and maximum size of disseminated foci of the control group and the TNP-470-treated group are shown in Table 2. The difference of foci number and maximal size of disseminated foci were also statistically significant ($P < 0.001$ and $P=0.004$).

Table 1 Body weight and abdominal circumference of two groups ($\bar{x} \pm s$)

Groups	Mice	Body weight (g)	Abdominal circumference (cm)
Control	7	29.5 ± 2.1	10.3 ± 1.5
TNP-470	7	24.5 ± 3.2^a	7.0 ± 1.1^b

^a $t=3.394$, $P=0.005$, ^b $t=4.624$, $P=0.001$, vs control

Table 2 Numbers and Maximum size of disseminated foci of two groups ($\bar{x} \pm s$)

Groups	Mice	Number of foci	Maximum size of foci (mm)
Control	7	92.1 ± 20.6	7.3 ± 2.3
TNP-470	7	40.3 ± 12.3^a	3.3 ± 0.7^b

^a $t=5.715$, $P < 0.001$, ^b $t=4.319$, $P=0.004$, vs control

In the control group, mice died from day 31 to day 57. In a TNP-470-treated group, 5 mice were died from day 74 to day 110. Two mice survived more than 120 days and TNP-470 treatment was continued. These 2 mice did not have any disseminated foci and were sacrificed on day 120 and day 130, respectively. The median survival time in the control group and the TNP-470-treated group were 40 and 92 days, the mean survival time being 41.86 ± 9.51 days and 98.00 ± 12.06 days, respectively ($P < 0.001$). The survival rate was significantly smaller in those in the control group than those of TNP-470-treated group ($P < 0.001$) (Figure 2).

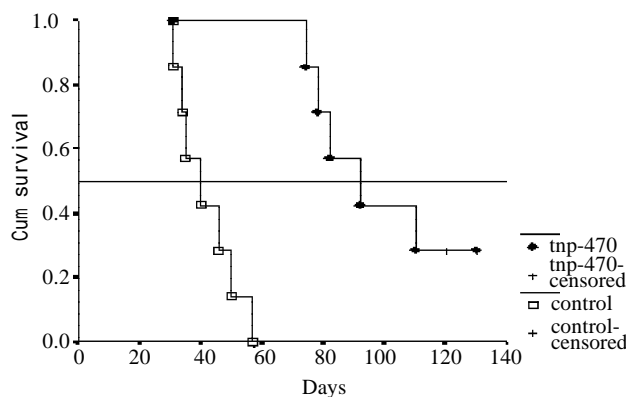


Figure 2 Survival curves in the control and TNP-470-treated groups

DISCUSSION

About 33 % patients with colorectal cancer have recurrence after operation and 50 % patients died of tumor metastasis^[13,14], and the peritoneal dissemination or liver metastasis represents the most common form of recurrence. When the tumor has extended through the serosa or been resected, tumor cells are carried to distant points of the peritoneal cavity and “seeding” on peritoneum. Supported by peritoneal permeability and growth of neovascularization, these tumor cells would develop into micro-metastatic nodules, eventually producing generalized peritoneal dissemination^[15,16]. With tumor recurrence as peritoneal dissemination, patient prognoses are extremely poor. Although combined therapies, including chemotherapy, radiation therapy and immunotherapy are performed in addition to surgical radical resection, no effective treatment can prevent the recurrence. New therapeutic strategies have to be invented to overcome the poor prognosis.

Angiogenesis, has been shown to be essential for tumor growth not only at the primary but also at the site of metastases, and the peritoneum would not be an exception^[17-20]. Inhibition of angiogenesis is emerging as a promising strategy for cancer treatment^[21-24]. Anti-angiogenic agents have demonstrated a remarkable inhibition effect on tumor growth and metastasis, and anti-angiogenic therapy may prevent the tumor recurrence^[25].

Among the most potent inhibitors of angiogenesis is the fumagillin family of natural products. An analog of fumagillin, known as TNP-470 or AGM-1470, has the anti-angiogenic activity by inhibiting endothelial cell growth with high potency both *in vitro* and *in vivo*^[26,27]. Studies have shown that the molecular mechanism of TNP-470 inhibiting endothelial cell proliferation is associated with the two type methionine aminopeptidase (MetAp-2). TNP-470 was found to bind MetAp-2 covalently, leading to specific inhibition of its activity, and strong correlation has been found between inhibition of MetAp-2 enzymatic activity and inhibition of endothelial cell proliferation^[28-33]. Investigators for TNP-470 have demonstrated suppression of neovascularization, tumor growth, and distant metastases *in vivo*^[34-44], and the proliferation of various cancer cell lines *in vitro*^[45-49]. There are very few studies on peritoneal dissemination^[50-52], and no data are available about preventing peritoneal dissemination or survival benefit of colon cancer treated by TNP-470.

Tsujimoto *et al.*^[53] reported that angiogenesis occurred in peritoneal foci 1 week after intraperitoneal inoculation of tumor cells in a mouse model. Our study indicated that TNP-470 inhibited the proliferation of Lovo cells *in vitro*, with its IC₅₀ at 2.14×10² ug/L, and markedly suppressed the growth of peritoneal dissemination *in vivo*. The mice survival time was significantly longer in TNP-470 treated group than that of control. Our results suggest that these effects are exerted not only by inhibiting neovascularization necessary for tumor growth, but also by directly inhibiting the proliferation of Lovo cells.

Body weight loss was known to be the major side effect of TNP-470. There was a slight body weight gain when mice were sacrificed on day 30, and the increase was associated with the production of malignant ascites. In the survival experiments, body weight loss was observed in the control group and 3 tumor-bearing mice became cachectic with the progression of tumor. No body weight loss was observed in the treatment group, suggesting that suppression of the growth of peritoneal dissemination foci by TNP-470 resulted in a preservation of body weight and prevention of cachexia in this model.

In conclusion, angiogenesis inhibitor TNP-470 might be effective in treating peritoneal dissemination of colon cancer by inhibiting the growth of the seeded tumor cells on the peritoneum.

REFERENCES

- 1 **Fan YF**, Huang ZH. Progress in the studies of gene therapy for colorectal cancer. *Shijie Huaren Xiaohua Zazhi* 2001; **9**:427-430
- 2 **Liu H**, Wu JS, Li LH, Yao X. The expression of Platelet-derived growth factor and angiogenesis in human colorectal carcinoma. *Shijie Huaren Xiaohua Zazhi* 2000; **8**:661-664
- 3 **Wu J**, Fan DM. Neoplastic vascularization and vascular inhibitory treatment. *Shijie Huaren Xiaohua Zazhi* 2001; **9**:316-321
- 4 **Blood CH**, Zetter BR. Tumor interactions with the vasculature: angiogenesis and tumor metastasis. *Biochem Biophys Acta* 1990; **1032**: 89-118
- 5 **Kusaka M**, Sudo K, Matsutani E, Kozai Y, Marui S, Fujita T, Ingber D, Folkman J. Cytostatic inhibition of endothelial cell growth by the angiogenesis inhibitor TNP-470 (AGM-1470). *Br J Cancer* 1994; **69**: 212-216
- 6 **Antoine N**, Greimers R, De-Roanne C, Kusaka M, Heinen E, Simar LJ, Castronovo V. AGM-1470, a potent angiogenesis inhibitor, prevents the entry of normal but not transformed endothelial cells into the G₁ phase of the cell cycle. *Cancer Res* 1994; **54**: 2073
- 7 **Abe J**, Zhou W, Takuwa N, Taguchi J, Kurokawa K, Kumada M, Takuwa Y. A fumagillin derivative angiogenesis inhibitor, AGM-1470, inhibits activation of cyclin-dependent kinases and phosphorylation of retinoblastoma gene product but not protein tyrosyl phosphorylation or protooncogene expression in vascular endothelial cells. *Cancer Res* 1994; **54**: 3407-3412
- 8 **Farinelle S**, Malonne H, Chaboteaux C, Decaestecker C, Dedecker R, Gras T, Darro F, Fontaine J, Atassi G, Kiss R. Characterization of TNP-470-induced modifications to cell functions in HUVEC and cancer cells. *J Pharmacol Toxicol Methods* 2000; **43**: 15-24
- 9 **Hotz HG**, Reber HA, Hotz B, Sanghavi PC, Yu T, Foitzik T, Buhr HJ, Hines OJ. Angiogenesis inhibitor TNP-470 reduces human pancreatic cancer growth. *J Gastrointest Surg* 2001; **5**: 131-138
- 10 **Ogawa H**, Sato Y, Kondo M, Takahashi N, Oshima T, Sasaki F, Une Y, Nishihira J, Todo S. Combined treatment with TNP-470 and 5-fluorouracil effectively inhibits growth of murine colon cancer cells *in vitro* and liver metastasis *in vivo*. *Oncol Rep* 2000; **7**: 467-472
- 11 **Yoshizawa J**, Mizuno R, Yoshida T, Hara A, Ashizuka S, Kanai M, Kuwashima N, Kurobe M, Yamazaki Y. Inhibitory effect of TNP-470 on hepatic metastasis of mouse neuroblastoma. *J Surg Res* 2000; **93**: 82-87
- 12 **Verma VN**, Shenoy CN, Nadkarni JJ. Augmentation of cisplatin cytotoxicity using cytokines on cervical carcinoma cell lines. *Cancer Biother Radiopharm* 1996; **11**: 349-354
- 13 **Zaniboni A**. Adjuvant chemotherapy in colorectal cancer with high-dose leucovorin and fluorouracil: impact on disease-free survival and over-survival. *J Clin Oncol* 1997; **15**: 2432-2441
- 14 **Cady B**, Stone MD. The role of surgical resection of liver metastasis in colorectal carcinoma. *Semin Oncol* 1991; **18**:399-406
- 15 **Sayag AC**, Gilly FN, Carry PY, Perdrix JP, Panteix G, Brachet A, Bannissillon V, Braillon G. Intraoperative chemohyperthermia in the management of digestive cancers. *Oncology* 1993; **50**: 333-345
- 16 **Loggie BW**, Perini M, Fleming RA, Russell GB, Geisinger K. Treatment and prevention of malignant ascites associated with disseminated intraperitoneal malignancies by aggressive combined- modality therapy. *Am Surg* 1997; **63**: 137-143
- 17 **Folkman J**. Tumor Angiogenesis Factor. *J Cancer Res* 1974; **34**: 2109-2113
- 18 **Folkman J**. What is the evidence that tumors are angiogenesis dependent? *J Natl Cancer Inst* 1990; **82**:4-6
- 19 **Gengrinovitch S**, Greenberg SM, Cohen T, Gitay-Goren H, Rockwell P, Maione TE, Levi BZ, Neufeld G. Platelet factor-4 inhibits the mitogenic activity of VEGF121 and VEGF165 using concurrent mechanisms. *J Biol Chem* 1995;

- 270: 15059-15065
- 20 **Jia L**, Chen TX, Sun JW, Na ZM, Zhang HH. Relationship between microvessel density and proliferating cell nuclear antigen and prognosis in colorectal cancer. *Shijie Huaren Xiaohua Zazhi* 2000; **8**: 74-76
- 21 **Singh RK**, Gutman M, Bucana CD, Sanchez R, Llansa N, Fidler IJ. Interferons α and β down-regulate the expression of basic fibroblast growth in human carcinoma. *Proc Natl Acad Sci USA* 1995; **92**: 4562-4566
- 22 **Voest EE**, Kenyon BM, Q' Reilly MS, Truitt G, D' Amato RJ, Folkman J. Inhibition of angiogenesis in vivo by interleukin12. *J Natl Cancer Inst* 1995; **87**: 581-586
- 23 **Q' Reilly MS**, Boehm T, Shing Y, Fukai N, Vasios G, Lane WS, Flynn E, Birkhead JR, Olsen BR, Folkman J. Endostatin: an endogenous inhibitor of angiogenesis and tumor growth. *Cell* 1997; **88**: 277-285
- 24 **Wojtowicz-Praga S**, Low J, Marshall J, Ness E, Dickson R, Barter J, Sale M, McCann P, Moore J, Cole A, Hawkins MJ. Phase I trial of a novel matrix metalloproteinase inhibitor batimastat(BB-94) in patients with advanced cancer. *Invest New Drugs* 1996; **14**: 193-202
- 25 **Kanai T**, konno H, Tanaka T, Matsumoto K, Baba M, Nakamura S, Baba S. Effect of angiogenesis inhibitor TNP-470 on the progression of human gastric cancer xenotransplanted into nude mice. *Int J Cancer* 1997; **71**:838-841
- 26 **Ingber D**, Fujita T, Kishimoto S, Sudo K, Kanamaru T, Brem H, Folkman J. Synthetic analogues of fumagillin that inhibit angiogenesis and suppress tumour growth. *Nature* 1990; **48**: 555-557
- 27 **Zhang Y**, Griffith EC, Sage J, Jacks T, Liu JO. Cell cycle inhibition by the anti-angiogenic agent TNP-470 is mediated by p53 and p21WAF1/CIP1. *Proc Natl Acad Sci USA* 2000; **97**: 6427-6432
- 28 **Sin N**, Meng L, Wang MQ, Wen JJ, Bornmann WG, Crews CM. The anti-angiogenic agent fumagillin covalently binds and inhibits the methionine aminopeptidase, MetAP-2. *Proc Natl Acad Sci USA* 1997; **4**: 6099-6103
- 29 **Klinkenberg M**, Ling C, Chang YH. A dominant negative mutation in *Saccharomyces cerevisiae* methionine aminopeptidase-1 affects catalysis and interferes with the function of methionine aminopeptidase-2. *Arch Biochem Biophys* 1997; **347**: 193-200
- 30 **Wang J**, Lou P, Henkin J. Selective inhibition of endothelial cell proliferation by fumagillin is not due to differential expression of methionine aminopeptidases. *J Cell Biochem* 2000; **77**: 465-473
- 31 **Griffith EC**, Su Z, Turk BE, Chen S, Chang YH, Wu Z, Biemann K, Liu JO. Methionine aminopeptidase (type-2) is the common target for angiogenesis inhibitors AGM-1470 and ovalicin. *Chem Biol* 1997; **4**: 461-471
- 32 **Griffith EC**, Su Z, Niwayama S, Ramsay CA, Chang YH, Liu JO. Molecular recognition of angiogenesis inhibitors fumagillin and ovalicin by methionine aminopeptidase 2. *Proc Natl Acad Sci USA* 1998; **95**: 15183-15188
- 33 **Turk BE**, Griffith EC, Wolf S, Biemann K, Chang YH, Liu JO. Selective inhibition of amino-terminal methionine processing by TNP-470 and ovalicin in endothelial cells. *Chem-Biol* 1999; **6**: 823-833
- 34 **Yamaoko M**, Yamamoto T, Masaki T, Ikeyama S, Sudo K, Fujita T. Inhibition of tumor growth and metastasis of rodent tumors by the angiogenesis inhibitor O-(Chloroacetyl-carbamoyl) fumagillol (TNP-470, AGM-1470). *Cancer Res* 1993; **3**: 4262-4267
- 35 **Qian CN**, Min HQ, Lin HL, Hong MH, Ye YL. Primary study in experimental antiangiogenic therapy of nasopharyngeal carcinoma with AGM-1470 (TNP-470). *J Laryngol Otol* 1998; **112**: 849-853
- 36 **Katzenstein HM**, Rademaker AW, Senger C, Salwen HR, Nguyen NN, Thorner PS, Litsas L, Cohn SL. Effectiveness of the angiogenesis inhibitor TNP-470 in reducing the growth of human neuroblastoma in nude mice inversely correlates with tumor burden. *Clin Cancer Res* 1999; **5**: 4273-4278
- 37 **Konno H**. Antitumor effect of the angiogenesis inhibitor TNP-470 on human digestive organ malignancy. *Cancer chemotherapy Pharmacol* 1999; **43**: 885- 889
- 38 **Kanai T**, Konno H, Tanaka T, Matsumoto K, Baba M, Nakamura S, Baba S. Effect of angiogenesis inhibitor TNP-470 on the progression of human gastric cancer xenotransplanted into nude mice. *Int J Cancer* 1997; **71**:838-841
- 39 **Watson JC**, Sutanto-Ward E, Osaku M, Weinstein JK, Babb JS, Sigurdson ER. Importance of timing and length of administration of angiogenesis inhibitor TNP-470 in the treatment of K12/TRb colorectal hepatic metastases in BD-IX rats. *Surgery* 1999; **126**: 358-363
- 40 **Konno H**, Tanaka T, Kanai T, Baba S. Therapeutic effect of angiogenesis inhibitors on liver metastases of human colorectal carcinoma. *Nippon Geka Gakkai asshi* 1998; **99**:441-445
- 41 **Tanaka T**, Konno H, Matsuda I, Nakamura S, Baba S. Prevention of hepatic metastasis of human colon cancer by angiogenesis inhibitor TNP-470. *Cancer Research*, 1995; **55**:836-839
- 42 **Konno H**, Tanaka T, Matsuda I, Kanai T, Maruo Y, Nishino N, Nakamura S, Baba S. Comparison of the inhibitory effect of the angiogenesis inhibitor, TNP-470, and Mitomycin C on the growth and liver metastasis of human colon cancer. *Int J Cancer* 1995; **61**: 268- 271
- 43 **Hori K**, Li HC, Saito S, Sato Y. Increased growth and incidence of lymph node metastases due to the angiogenesis inhibitor AGM-1470. *Br J Cancer* 1997; **75**: 1730-1734
- 44 **Gervaz P**, Scholl B, Padrun V, Gillet M. Growth inhibition of liver metastases by the anti-angiogenic drug TNP-470. *Liver* 2000; **20**: 108-113
- 45 **Emoto M**, Ishiguro M, Iwasaki H, Kikuchi M, Kawarabayashi T. TNP-470 inhibits growth and the production of vascular endothelial growth factor of uterine carcinosarcoma cells in vitro. *Anticancer Res* 2000; **20**:601-604
- 46 **Yamamoto D**, Kiyozuka Y, Adachi Y, Takada H, Hioki K, Tsubura A. Synergistic action of apoptosis induced by eicosapentaenoic acid and TNP-470 on human breast cancer cells. *Breast Cancer Res Treat* 1999; **55**: 149-160
- 47 **Singh Y**, Shikata N, Kiyozuka Y, Nambu H, Morimoto J, Kurebayashi J, Hioki K, Tsubura A. Inhibition of tumor growth and metastasis by angiogenesis inhibitor TNP-470 on breast cancer cell lines in vitro and in vivo. *Breast Cancer Res Treat* 1997; **45**: 15-27
- 48 **Satoh H**, Ishikawa H, Fujimoto M, Fujiwara M, Yamashita YT, Yazawa T, Ohtsuka M, Hasegawa S, Kamma H. Angiocytoxic therapy in human non-small cell lung cancer cell lines-Advantage of combined effects of TNP-470 and SN-38. *Acta Oncol* 1998; **37**:85-90
- 49 **Satoh H**, Ishikawa H, Fujimoto M, Fujiwara M, Yamashita YT, Yazawa T, Ohtsuka M, Hasegawa S, Kamma H. Combined effects of TNP-470 and taxol in human non-small cell lung cell lines. *Anticancer Res* 1998; **18**:1027-1030
- 50 **Yoshikawa T**, Yanoma S, Tsuburaya A, Kobayashi O, Sairenji M, Motohashi H, Noguchi Y. Angiogenesis inhibitor, TNP-470, suppresses growth of peritoneal disseminating foci. *Hepato-gastroenterology* 2000; **47**: 298-302
- 51 **Kato H**, Ishikura H, Kawarada Y, Furuya M, Kondo S, Kato H, Yoshiki T. Anti-angiogenic treatment for peritoneal dissemination of pancreas adenocarcinoma: a study using TNP-470. *Jpn J Cancer Res* 2001; **92**: 67-73
- 52 **Liu B**, Lin Y, Yin H. Experimental study of the effect of angiogenesis inhibitor TNP-470 on the growth and metastasis of gastric cancer in vivo. *Zhonghua Zhongliu Xue* 1998; **20**: 34-36
- 53 **Tsujimoto H**, Hagiwara A, Shimotsuma M, Sakakura C, Osaki K, Sasaki S, Ohyama T, Ohgaki M, Imanishi T, Yamazaki J, Takahashi T. Role of milky spots as selective implantation sites for malignant cells in peritoneal dissemination in mice. *J Cancer Res Clin Oncol* 1996; **122**:590-595

• VIRAL HEPATITIS •

Investigation of HGV and TTV infection in sera and saliva from non-hepatitis patients with oral diseases

Jie Yan, Li-Li Chen, Yong-Liang Lou, Xiao-Zhi Zhong

Jie Yan, Department of Pathogenic Biology, College of Medical Science, Zhejiang University, Hangzhou 310031, Zhejiang Province, China

Li-Li Chen, Department of Stomatology, The Second Affiliated Hospital, College of Medical Science, Zhejiang University, Hangzhou 310009, Zhejiang Province, China

Yong-Liang Lou, Xiao-Zhi Zhong, Wenzhou Medical College, Wenzhou 325000, Zhejiang Province, China

Correspondence to: Jie Yan, Department of Pathogenic Biology, College of Medical Science, Zhejiang University, 353 Yan An Road, Hangzhou 310031, Zhejiang Province, China. yanchen@mail.hz.zj.cn
Telephone: +86-571-87217385 **Fax:** +86-571-87217044

Received 2002-03-11 **Accepted** 2002-04-20

Abstract

AIM: To determine the frequencies of HGV and TTV infections in serum and saliva samples of non-hepatitis patients with oral diseases in Hangzhou area, and to understand the correlation between detected results of HGV RNA and/or TTV DNA in sera and in saliva from the same patients.

METHODS: RT-nested PCR for HGV RNA detection and semi-nested PCR for TTV DNA detection were performed in the serum and saliva samples from 226 non-hepatitis patients with oral diseases, and nucleotide sequence analysis.

RESULTS: Twenty-seven (11.9 %) and 21 (9.3 %) of the 226 serum samples were only positive for HGV RNA and TTV DNA, respectively. 10 (4.4 %) and 9 (3.9 %) of the 226 saliva samples were only positive for HGV RNA and TTV DNA, respectively. And 7 (3.1 %) of the serum samples and 2 (0.9 %) of the saliva samples showed the positive amplification results for both HGV RNA and TTV DNA. 12 saliva samples from the 34 patients (35.3 %) with HGV or HGV/TTV viremia and 11 saliva samples from the 28 patients (39.3 %) with TTV or HGV/TTV viremia were HGV RNA detectable, respectively, including two patients positive for both HGV RNA and TTV DNA in serum and saliva samples. No saliva samples from the 226 patients were found to be HGV RNA or TTV DNA detectable while their serum samples were negative for HGV or TTV. Homologies of the nucleotide sequences of HGV and TTV amplification products from the serum and saliva samples of the two patients compared with the reported sequences were 88.65-91.49 % and 65.32-66.67 %, respectively. In comparison with the nucleotide sequences of amplification products between serum and from saliva sample from any one of the two patients, the homologies were 98.58 % and 99.29 % for HGV, and were 98.65 % and 98.20 % for TTV, respectively.

CONCLUSION: Relatively high carrying rates of HGV and/or TTV in the sera of non-hepatitis patients with oral diseases in Hangzhou area are demonstrated. Parts of the carriers are HGV and/or TTV positive in their saliva. The results of this study indicate that dentists may be one of the populations

with high risk for HGV and/or TTV infection, and by way of saliva HGV and TTV may be transmitted among individuals.

Yan J, Chen LL, Lou YL, Zhong XZ. Investigation of HGV and TTV infection in sera and saliva from non-hepatitis patients with oral diseases. *World J Gastroenterol* 2002; 8(5):857-862

INTRODUCTION

Viral hepatitis is relatively common in China^[1-13]. Except for human A-E hepatitis viruses, hepatitis G virus (HGV) and GB virus C (GBV-C) were recently identified as the causative agents of human non-A-E hepatitis^[14,15]. Transfusion transmitted virus (TTV), another novel virus isolated from a patient suffering from non-A-G hepatitis, was considered to be responsible for human non-A-G hepatitis^[16]. Since the nucleotide sequences and putative amino acid sequences of HGV and GBV-C genomes show high homologies of 85 % and 100 %, respectively, the two viral agents are considered to be the different isolates of the same virus belonging to *Flaviviridae* family^[14,15]. TTV was proposed to be a member of a new virus family temporarily named *Circinoviridae*^[17]. Although HGV is a positive-stranded RNA virus and TTV is a negative-stranded DNA virus, the two viruses are mainly transmitted through a hematogenous pathway^[18-21], especially through blood transfusion^[22-25]. Many investigation data demonstrated that HGV or TTV was able to cause a long-term asymptomatic viremia in non A-E hepatitis patients and only a few patients could suffer from hepatitis with mild liver injury^[26-32]. On the contrary, a few references reported that HGV infection might accelerate the progression of chronic liver diseases and cause fulminant hepatic failure^[33-37]. TTV was frequently found in non-A-G hepatitis patients with a single elevation of alanine aminotransferase (ALT)^[38-40]. Recent published literatures revealed that HGV or TTV infection frequency in peripheral bloods of normal populations including healthy blood donors was found to be relatively high^[41-50] and part of the infected individuals were HGV RNA or TTV DNA detectable not only in the serum samples but also in their saliva samples^[51-55]. Therefore, dentists may be one of the populations at high risk of HGV and TTV infection, and may play an important role in HGV and TTV transmission among individuals. On the other hand, the possibility of HGV and TTV transmission through saliva is also an interesting subject for investigation.

To determine the frequency of HGV or TTV infection in non-hepatitis patients with oral diseases and to understand the correlation of HGV and TTV detection between in sera and in saliva from the same one patients, RT-nested PCR and semi-nested PCR were applied to detect HGV and TTV respectively in the serum and saliva samples from 226 non-hepatitis patients for oral treatment in Hangzhou area. The HGV RNA or TTV DNA positive amplification products from representatives of the serum and saliva samples were cloned and then sequenced. The results of this study may contribute to understand

transmission mechanism of the two viruses and populations with high risk of HGV and TTV infection, and may be helpful for the control of the prevalence of human hepatitis associated with HGV or TTV.

MATERIALS AND METHODS

Materials

Total 226 patients with tooth, pulp or periodontal diseases came from the oral departments of three hospitals in Hangzhou, Zhejiang Province of China, respectively. Each of the patients was told the aim and content of this study and all of them agreed to be the volunteers. A serum sample as well as a saliva sample from each of the patients was collected. These samples were immediately performed for HGV and TTV detection or temporarily stored at -20°C . The patients were confirmed to have no any clinical signals of hepatitis and no elevation of ALT by conventional hepatic examinations, and the serum samples were negative for hepatitis A-C viruses by PCR and EIA. The reagents used in reverse transcription (RT) and PCR were purchased from Boehringer and BMI, and the other reagents used in this study came from Sigma.

Methods

Isolation of total RNA and DNA in sera Total RNA in 200 μl of each serum samples was prepared by Trizol method according to the manufacturer's instruction and then dissolved in 50 μl of DEPC treated super-purified water. 200 μl of each serum samples was mixed with 200 μl DNA extraction solution containing 20 $\text{mmol}\cdot\text{L}^{-1}$ EDTA, 0.5 % (W/W) SDS, 10 $\text{mmol}\cdot\text{L}^{-1}$ Tris-HCl and 40 mg proteinase K (pH8.0) and was treated at 55°C for 30 min. Total DNA in the mixture was extracted by phenol-chloroform method^[56] and then dissolved in 50 μl of TE buffer (pH 8.0).

Isolation of total RNA and DNA in saliva 200 μl of each saliva samples was mixed with 400 μl RNA extraction solution containing 4 $\text{mol}\cdot\text{L}^{-1}$ guanidine thiocyanate, 0.1 $\text{mol}\cdot\text{L}^{-1}$ 2-mercaptoethanol, 0.5 % (W/W) sodium N-lauroylsarcosine and 25 $\text{mmol}\cdot\text{L}^{-1}$ sodium citrate (pH7.0). Vortex the tube gently for 15 min and lay the tube at room temperature for 5 min. 100 mL 2 $\text{mol}\cdot\text{L}^{-1}$ sodium acetate (pH4.0), 600 mL TE buffer (pH8.0) and 200 mL phenol (pH4.5)-chloroform (5:1, V:V) were added into the tube and then mixed. Supernatant of the mixture after centrifugation was added with 400 mL 2-propanol (-20°C) and then mixed. Lay the tube at -20°C for 2 h to precipitate RNA. RNA pellet obtained by using centrifugation at 4°C was washed with 75 % ethanol and then dissolved in 50 μl of DEPC treated super-purified water^[51, 52]. 200 μl of each saliva samples was mixed with 200 mL DNA extraction solution containing 20 $\text{mmol}\cdot\text{L}^{-1}$ EDTA, 100 $\text{mmol}\cdot\text{L}^{-1}$ NaCl, 0.5 % (W/W) SDS, 10 $\text{mmol}\cdot\text{L}^{-1}$ Tris-HCl (pH8.0) and 80 μg proteinase K. Incubate the tube at 55°C for 60 min. Total DNA was obtained by phenol-chloroform method^[56] and then dissolved in 50 μl of TE buffer (pH 8.0)^[53-55].

RT-nested PCR for HGV RNA detection Ten microliters of total RNA preparation was mixed with 10 μl RT master mixture containing 5 $\mu\text{mol}\cdot\text{L}^{-1}$ hexanucleotide as random primers, 12.5 $\text{mol}\cdot\text{L}^{-1}$ each of dNTP, 20U M-MuLV-reverse transcriptase, 20U RNase inhibitor and 4 μl of 5 \times RT buffer (pH8.3). The steps of RT were described as the following: at $70^{\circ}\text{C}\times 5$ min for denaturation, at $42^{\circ}\text{C}\times 60$ min for cDNA synthesis, and at $70^{\circ}\text{C}\times 10$ min to stop the reaction.

Primers derived from HGV 5' -NCR were used in the RT-nested PCR for HGV detection^[13, 50]. The external primers: 5' -ATGACAGGGTTGGTAGGTCGTAAATC -3' (sense), 5' -

CCCCACTGGTCCTTGTCAACTCGCCG-3' (antisense). The internal primers: 5' -TGGTAGCCACTATAGGTGGGTCTTAA -3' (sense), 5' -ACATTGAAGGGCGACGTGGACCGTAC-3' (antisense). For the first round PCR, 10 μl of RT product was mixed with 90 μl PCR master mixture containing 250 $\text{nmol}\cdot\text{L}^{-1}$ each of the external primers, 2.5 $\text{mol}\cdot\text{L}^{-1}$ each of dNTP, 25 $\text{mol}\cdot\text{L}^{-1}$ MgCl_2 , 2.5U of *Taq* DNA polymerase and 10 μl 10 \times PCR buffer (pH8.3). For the second round PCR, 5 μl product from the first round PCR was used as template, and the other reaction reagents were the same as that in the first round PCR except of the primers. DNA Thermal cycler 480 (Perkin Elmer) was used for amplification. The parameters for each of the PCR rounds were described as the following: 94°C 5 min ($\times 1$); 94°C 1 min, 56°C 1 min, 72°C 1.5 min ($\times 35$); 72°C 7 min ($\times 1$). The expected size of target fragments amplified from HGV 5' -NCR RNA was 193bp.

Semi-nested PCR for TTV DNA detection The primers used in the semi-nested PCR for TTV DNA detection were the same described by Okamoto *et al*^[57]. The external primers: 5' -ACAGACAGAGGAGAAGGCAACATG-3' (sense), 5' -CTGGC ATTTTACCATTTCCTCAAAGTT-3' (antisense). The internal primers: 5' -GGCAACAT GTTATGATAGACTGG-3' (sense), 5' -CTGGCATTTCCTCAAAGTT-3' (antisense). Except the primers, MgCl_2 concentration (15 $\text{mol}\cdot\text{L}^{-1}$), total reaction volume (50 μl) and annealing temperature (60°C), the compositions and concentrations of other reaction agents and the parameters for the semi-nested PCR was the same as that of the RT-nested PCR for HGV detection. The expected size of target fragments amplified from TTV DNA was 271bp.

Examination of amplification products The results of amplification reactions were observed on UV light after electrophoresis of 20 $\text{g}\cdot\text{L}^{-1}$ agarose stained with ethidium bromide. 100bp DNA ladder was used as a size marker to estimate the length of products.

Cloning and sequencing of PCR amplification products The target DNA fragments of HGV or TTV amplification products by PCR were cloned into plasmid pGEM-T vector by using T-A cloning kit according to the manufacturer's instruction. The recombinant plasmid was amplified in *E.coli* strain DH 5 α and then recovered by Sambrook's method. A professional company (Sangon) was responsible for the analysis of nucleotide sequences of the inserted fragments. Homology of the nucleotide sequences was compared with those reported respectively^[14, 56].

RESULTS

Positive rates of HGV RNA and TTV DNA detection in the serum and saliva samples

Twenty-seven (11.9 %) and 21 (9.3 %) of the 226 serum samples were only positive for HGV RNA and TTV DNA, respectively. 10 (4.4 %) and 9 (3.9 %) of the 226 saliva samples were only detectable for HGV RNA and TTV DNA, respectively. And 7 (3.1 %) of the serum samples and 2 (0.9 %) of the saliva samples showed the positive results for both HGV RNA and TTV DNA. 171 of the 226 serum samples (75.7 %) and 205 of the 226 saliva samples (90.7 %) were undetectable for both HGV RNA and TTV DNA. Representatives of the target fragments respectively amplified from HGV and TTV genomes in the serum and saliva samples were shown in Figure 1.

Distribution of HGV and TTV detection results in serum and saliva samples

Twelve saliva samples from the 34 patients (35.3 %) positive

for HGV RNA and 11 saliva samples from the 28 patients (39.3 %) positive for TTV DNA in their sera were HGV RNA and TTV DNA detectable respectively, including 2 patients with both HGV RNA and TTV in their serum and saliva samples. No saliva samples from the 226 patients were found to be positive for HGV RNA or TTV DNA but their serum samples were negative for HGV or TTV. Distribution of HGV and TTV detection results in serum and saliva samples of the 226 patients was shown in Table 1.

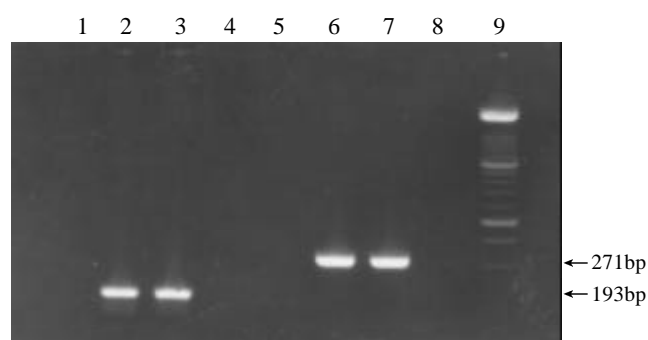


Figure 1 Target fragments respectively amplified from HGV RNA and TTV DNA in serum and saliva samples. (1: HGV negative serum sample; 2 and 3: HGV positive serum sample and saliva sample (No.: 010906); 4: blank control for HGV detection; 5: TTV negative serum sample; 6 and 7: TTV positive serum sample and saliva sample (No.: 011022); 8: blank control for TTV detection; 9: marker)

Table 1 Distribution of HGV and TTV detection results in serum and saliva samples of the 226 patients

serum samples		saliva samples		cases (N)	percentage (%)
HGV	TTV	HGV	TTV		
+	-	-	-	18	8.0
-	+	-	-	13	5.8
+	+	-	-	3	1.3
+	-	+	-	9	4.0
-	+	-	+	8	3.5
+	+	+	+	2	0.9
+	+	+	-	1	0.4
+	+	-	+	1	0.4
-	-	-	-	171	75.7
Total				226	100.0

^a+: positive detection results for HGV or TTV; ^b-: negative detection results for HGV or TTV

Nucleotide sequence analysis and homology comparison

In comparison with the reported HGV^[14] and TTV genotype-1a^[57] nucleotide sequences, the homologies of HGV and TTV amplification products from 2 serum and 2 saliva samples from the two same patients (No.: 010906 and 011022) were 88.65-91.49 % and 65.32-66.67 %, respectively. When to compare the nucleotide sequences of HGV and TTV amplification products between the 2 serum samples and between the 2 saliva samples, the homologies were as high as 98.65 % and 98.20 %, 93.24 % and 94.59 %, respectively. The homology comparison mentioned above did not contain the primer sequences (Figure 2 and 3).

```

1:1 TGGTAGCCACTATAGGTGGGTCTTAAGAGAAGGTTAAGATTCCTCTTGTGCCTGCGGCGA
2:1 ..... G . T T . . C . . . . G . C . . . . . C . . T . . T . . . .
3:1 ..... G . T T . . C . . . . G . C . . . . . C . . T . . T . . . .
4:1 ..... G . . . . C . . . . G . C . . . . . G . C . . . . .
5:1 ..... G . . . . C . . . . G . C . . . . . G . C . . . . .

1:61 GACCGCGCACGGTCCACAGGTGTTGGCCCTACCGGTGGGAATAAGGGCCCGACGTCAGGC
2:61 A . A A ..... T . . . . .
3:61 A . A A ..... T . . . . .
4:61 . . . A A ..... T . . . . . T . . . . .
5:61 . . . A A ..... T . . . . . A . . . . .

1:121 TCGTCGTAAACCGAGCCCGTTACCCACCTGGGCAAACGACGCCACGTACGGTCCACGT
2:121 . G . . . . . A . . . . . A . . . . .
3:121 . . . . . A . . . . . A . . . . .
4:121 . . . . . A . A . . . . .
5:121 . . . . . A . A . . . . .

1:181 CGCCCTTCAATGT
1:181 . . . . .
3:181 . . . . .
4:181 . . . . .
5:181 . . . . .

```

Figure 2 Homology of the nucleotide sequences from HGV RT-nested PCR products of the 2 serum and 2 saliva samples from 2 patients compared with the reported sequence. (1: The reported HGV sequence^[14]; 2 and 3: the sequences of HGV RT-nested PCR products from the serum sample and saliva sample from the patient (No.: 010906); 4 and 5: the sequences of HGV RT-nested PCR products from the serum sample and saliva sample from the patient (No.: 011022). Underlined areas indicate the primer positions.

```

1:1 GGCAACATGTTATGGATAGACTGGCTAAGCAAAAAAACATGAACTATGACAAAGTACAA
2:1 ..... C T . . . G . T G . . T C A G T A . . . . . G C A G . .
3:1 ..... C T . . . G . T G . . T C A G T A . . . . . G C A G . .
4:1 ..... C T . . . . . G G . . T C A G T A . . . . . G C A G . .
5:1 ..... C T . . . . . G G . . T C A G T A . . . . . G C A G . .

1:61 AGTAAATGCTTAATATCAGACCTACCTCTATGGGCAGCAGCATATGGATATGTAGAATTT
2:61 ..... C . . . . . C A . . . . . A . . . C T . . . . . C T . . . T . . . . . C A C . . . A C
3:61 ..... C A . . . . . A . . . C T . . . . . C T . . . . . C A C . . . A C
4:61 ..... T . . T C . . . . . C A . . . . . C T . G . . . . . C T . . . . . C A C . . . A C
5:61 ..... T C . . . . . C A . . . . . C T . G . . . . . C T . . . T . . . . . C A C . . . A C

1:121 TGTGCAAAAAGTACAGGAGACCAAAACATACACATGAATGCCAGGCTACTAATAAGAAGT
2:121 . . C A G C . . . G T A . . . . . A C . . . . . G . A C A C . . T G T . . A T G T G . . . T . . . C
3:121 . . C A G C . . . G T A . . . . . A C . . . . . G . A C A C . . T G T . . A T G T G . . . T . . . C
4:121 . . C A G C . . . G T A . . . C . . . A C . T . . . . . C A . . . . . T G T . . A T G T G . . . T . . .
5:121 . . C A G C . . . G T A . . . C . . . A C . T . . . . . C A . . . . . T G T . . A T G T G . . . T . . .

1:181 CCCTTTACAGACCCACAACACTACTAGTACACACAGACCCACAAAAGGCTTTGTTTCCTTAC
2:181 . . . A . . . . . T A . . T . . G . . . . . A C . . . . . A C A . . A G . . T T . G G . . A . A C . . . G . .
3:181 . . . A . . . . . T A . . T . . G . . . . . A C . . . . . A C A . . A G . . T T . G G . . A . A C . . . C . .
4:181 . G . . . . . T A . . T . . G . . . . . A C . . . . . A C A . . A G . . T T . G G . . A . A C . . . G . .
5:181 . . . . . T A . . T . . G . . . . . A C . . . . . A C A . . A G . . T T . G G . . A . A C . . . C . .

1:241 TCTTTAAACTTTGGAAATGGTAAAATGCCAG
2:241 A G C A . . . . .
3:241 A G C A . . . . .
4:241 A G C A . . . . .
5:241 A G C A . . . . .

```

Figure 3 Homology of the nucleotide sequences from TTV semi-nested PCR products of the 2 serum and 2 saliva samples from 2 patients compared with the reported sequence. (1: The reported TTV sequence^[57]; 2 and 3: the sequences of TTV semi-nested PCR products from the serum sample and saliva sample from the patient (No.: 010906); 4 and 5: the sequences of TTV semi-nested PCR products from the serum sample and saliva sample from the patient (No.: 011022). Underlined areas indicate the primer positions.

DISCUSSION

Viral hepatitis is a common infectious disease of human beings, which is prevalent in all countries of the world and causes a serious healthy problem. Although hepatitis virus A-E have been demonstrated to be the causative agents of human hepatitis A-E respectively, approximately 20 % of acute and 15 % of chronic hepatitis were associated with unknown etiology^[23, 24]. HGV and TTV were recently identified as transfusion-transmitted viruses and were considered to be responsible for human non-A-E hepatitis^[14-17]. Many published literatures reported that among the patients infected with HGV or TTV, a few of them showed mild liver injury, which resulting in a conclusion of a low clinical importance of HGV or TTV infection^[26-32]. However, a wide variety of questions about the potential pathogenicity of HGV and TTV infection still remain unanswered^[13, 23]. So far the assays for HGV and TTV detection are not the routing laboratory examination items in many countries and areas. Not few of investigation data indicated that high frequencies of HGV or TTV infection were frequently found in different normal populations such as in healthy blood donors^[41-50]. Some investigation results revealed that the genomic nuclear of HGV or TTV in saliva of partial infected individuals was also detectable^[51-55], suggesting the possibility by way of saliva for transmission of the two viruses. Although HGV or TTV infection might be not clinically significant, the existence of extensive and potential infectious sources of the two viruses will still generate a great problem for human health.

In the present study, HGV and TTV infection rates in serum samples of the 226 non-hepatitis patients with oral diseases were 15.0 % (34/226) and 12.4 % (28/226) respectively, which indicated that HGV infection rate was obviously higher than that of the reported in other areas of China and abroad (1.3-10.6%)^[7,8], and TTV infection rate was higher than that of the reported abroad (<5 %) ^[41, 43-47] but similar to the reported in China (9.3-16.8 %) ^[42, 48-50]. Such high HGV and TTV infection frequencies in the non-hepatitis population in Hangzhou are probably due to geographic difference. In the previous study, we found 2.5 % of healthy blood donors in Hangzhou coinfectd with both HGV and TTV^[50]. In this study, the serum samples from 7 of the 226 patients (3.1 %) were positive for both HGV RNA and TTV DNA, which offered further evidence for the existence of coinfection of the two viruses. Therefore, it is valuable to make further studies to determine the pathological and clinical significance of the coinfection.

Since the patients with oral diseases in this study did not show any clinical symptoms and laboratory markers for hepatitis, which suggested that most of the patients infected with HGV and/or TTV are usually asymptomatic. However, these asymptomatic patients carrying HGV and/or TTV may be more risky and important for the source of infection. It was worthy to notice that 5.3 % and 4.9 % of the non-hepatitis patients with oral diseases were HGV RNA and/or TTV DNA detectable in the saliva, indicating dentists may be one of the populations at high risk of HGV and/or TTV infection except of blood precipitants and hemodialysed patients^[18, 25, 31, 32, 57, 58].

It was more important that HGV and TTV in saliva might be transmitted among the patients for oral treatment through dentists' hands and therapeutic instruments. So it is necessary to take effective measures to block the possible transmission of HGV and TTV by way of saliva.

In this study, 2 serum samples and 2 saliva samples from the two patients showed positive results for both HGV RNA and TTV DNA. The nucleotide sequences of HGV amplification products from these samples are highly homologous (88.65-91.49 %) to the sequence reported by Linnen *et al.*^[14]. This result of sequence analysis indicates that the RT-nested PCR used in this study is reliable for HGV RNA detection. To analyze the details of the nucleotide sequencing data, it seems to show a HGV genotype different from the reported^[59-62]. Lower homology (65.32-66.67 %) of the nucleotide sequences of TTV Semi-nested PCR products from these samples of the 2 patients compared with the reported TTV genotype 1a sequence^[56] reveals the genomic heterogeneity of TTV isolates from different areas, and this finding accords with the conclusions of previously published literatures^[31, 56]. In this study, no saliva samples from the 226 patients were found to be positive for HGV RNA or TTV DNA while their serum samples were negative for HGV or TTV. Furthermore, the nucleotide sequence homology of HGV amplification products between the serum and saliva samples from any one of the 2 patients is 98.65 % and 98.20 %, respectively, and so is the nucleotide sequence homology of TTV amplification products (93.24 % and 94.59 %), which are much higher than that compared with the reported HGV and TTV sequences^[14, 56]. These data indicate a closely and directly correlation between HGV and TTV genomes detected from serum and saliva from the same one patients.

REFERENCES

- Han FC**, Hou Yu, Yan XJ, Xiao LY, Guo YH. Dot immunogold filtration assay for rapid detection of anti-HAV IgM in Chinese. *World J Gastroenterol* 2000; **6**:400-401
- Zhao YL**, Meng ZD, Xu ZY, Guo JJ, Chai SA, Duo CG, Wang XY, Yao JF, Lin HB, Qi SX, Zhu HB. H2 strain attenuated live hepatitis A vaccines: protective efficacy in a hepatitis A outbreak. *World J Gastroenterol* 2000; **6**:829-832
- Fang JN**, Jin CJ, Cui LH, Quan ZY, Choi BY. A comparative study on serologic profiles of virus hepatitis B. *World J Gastroenterol* 2001; **7**: 107-110
- Tang RX**, Gao FG, Zeng LY, Wang YW, Wang YL. Detection of HBV DNA and its existence status in liver tissues and peripheral blood. *World J Gastroenterol* 1999; **5**:359-361
- Wei J**, Wang YQ, Lu ZM, Li GD, Wang Y, Zhang ZC. Detection of anti-preS1 antibodies for recovery of hepatitis B patients by immunoassay. *World J Gastroenterol* 2002; **8**:276-281
- Xiao LY**, Yan XJ, Mi MR, Han FC, Hou Y. Preliminary study of a dot immunogold filtration assay for rapid detection of anti-HCV IgG. *World J Gastroenterol* 1999; **5**:349-350
- Song YH**, Lin JS, Liu NZ, Kong XJ, Xie N, Wang NX, Jin YX, Liang KH. Anti-HBV hairpin ribozyme-mediated cleavage of target RNA *in vitro*. *World J Gastroenterol* 2002; **8**:91-94
- Li CP**, Wang KX, Wang J, Pan BR. MIL-2R, T cell subsets & hepatitis C. *World J Gastroenterol* 2002; **8**:298-300
- Yan FM**, Chen AS, Hao F, Zhao XP, Gu CH, Zhao LB, Yang DL, Hao LJ. Hepatitis C virus may infect extrahepatic tissues in patients with hepatitis C. *World J Gastroenterol* 2000; **6**: 805-811
- Chen MY**, Huang ZQ, Chen LZ, Gao YB, Peng RY, Wang DW. Detection of hepatitis C virus NS5 protein and genome in Chinese carcinoma of the extrahepatic bile duct and its significance. *World J Gastroenterol* 2000; **6**:800-804
- Wang XZ**, Jiang XR, Chen XC, Chen ZX, Li D, Lin JY, Tao QM. Seek protein which can interact with hepatitis B virus X protein from human liver cDNA library by yeast two-hybrid system. *World J Gastroenterol* 2002; **8**:95-98
- Wang NS**, Liao LT, Zhu YJ, Pan W, Fang F. Follow-up study of hepatitis C virus infection in uremic patients on maintenance hemodialysis for 30 months. *World J Gastroenterol* 2000; **6**: 888-892
- Yan J**, Dennin RH. A high frequency of GBV-C/HGV coinfection in hepatitis C patients in Germany. *World J Gastroenterol* 2000; **6**: 833-841
- Linnen J**, Wages J, Zhang-Kerk ZY, Fry KE, Krawczynski KZ, Alter H, Koonin E, Gallagher M, Alter M, Hadziyannis S, Karayiannis P, Fung K, Nakatsuji Y, Shih JWK, Young L, Piatak M, Hoover C, Fernandez J, Chen S, Zou JC, Morris T, Hyams KC, Ismay S, Lifson JD, Hess G, Fong SKH, Thomas H, Bradley D, Margolis H, Kim JP. Molecular cloning and disease association of hepatitis G virus: a transfusion-transmissible agent. *Science* 1996; **271**: 505-508
- Leary TP**, Muerhoff AS, Simons JN, Pilot-Matias TJ, Erker JC, Chalmer ML, Schlauder GG, Dawson GJ, Desai SM, Mushahwar IK. Sequence and genomic organization of GBV-C: a novel member of the Flaviviridae associated with human non-A-E hepatitis. *J Med Virol* 1996; **48**: 60-67
- Nishizawa T**, Okamoto H, Keinishi K, Yoshizawa H, Miyakawa Y, Mayumi M. A novel DNA virus (TTV) associated with elevated transaminase levels in posttransfusion hepatitis of unknown etiology. *Biochem Biophys Res Commun* 1997; **241**:92-97
- Mushahwar IK**, Erker JC, Muerhoff AS, Leary TP, Simons JN, Birkenmeyer LG, Chalmers ML, Pilot-Matias TJ, Dexai SM. Molecular and biophysical characterization of TT virus: evidence for a new virus family infecting humans. *Proc Natl Acad Sci* 1999; **96**: 3177-3182
- Simmond P**, Smith DB. Structural Constrains on RNA virus evolution. *J Virol* 1999; **73**:5787-5794
- Abe K**, Inami T, Ishikawa K, Nakamura S, Goto S. TT virus infection in nonhuman primates and characterization of the viral genome: identification of simian TT virus isolates. *J Virol* 2000; **74**:1549-1553
- Moaven LD**, Tennakoon PS, Bowden DS, Locarnini SA. Mother-to-baby transmission of hepatitis G virus. *Med J Aust* 1996; **165**: 84-85
- Okamoto H**, Akahane Y, Ukita M, Fukuda M, Tsuda F, Miyakawa Y, Mayumi M. Fecal excretion of a nonenveloped DNA virus (TTV) associated with posttransfusion non-A-G hepatitis. *J Med Virol* 1998; **56**:128-132
- Feucht HH**, Zollner B, Polywka S, Laufs R. Vertical transmission of hepatitis G. *Lancet* 1996; **347**: 615-616
- Mortimer PP**. HGV and the blood supply. *J infect* 1998; **37**: 106-107
- Tanaka H**, Okamoto H, Luengrojanakul P, Chainuvati T, Tusda F, Tanaka T, Miyakawa Y, Mayumi M. Infection with an unenveloped DNA virus (TTV) associated with posttransfusion non-A to G hepatitis in hepatitis patients and healthy blood donors in Thailand. *J Med Virol* 1998; **56**: 234-238
- Yang SS**, Wu CH, Chen TH, Huang YY, Huang CS. TT viral infection through blood transfusion: retrospective investigation on patients in a prospective study of post-transfusion hepatitis. *World J Gastroenterol* 2000; **6**:70-73
- Sarrazin C**, Herrmann G, Roth WK, Lee JH, Marx S, Zeuzem S. Prevalence and clinical and histology manifestation of hepatitis G/GBV-C infections in patients with elevated aminotransferases of unknown etiology. *J Hepatol* 1997; **27**: 276-283
- Alter MJ**. The cloning and clinical implications of HGV and HGBV-C. *N Engl J Med* 1996; **334**: 1536-1537
- Feucht HH**, Zollner B, Polywka S, Knodler B, Schroter M, Nolte H, Laufs R. Prevalence of hepatitis G virus among healthy subjects, individuals with liver disease, and persons at risk for parental transmission. *J Clin Microbiol* 1997; **35**: 767-768
- Naoumov NV**, Petrova EP, Thomas MG, Williams R. Pres-

- ence of a newly described human DNA virus (TTV) in patients with liver disease. *Lancet* 1998; **352**: 195-197
- 30 **Alter MJ**, Gallagher M, Morris TT, Moyer LA, Meeks EL, Krawczynski K, Kim JP, Margolis HS. Acute non-A-E hepatitis in the United States and the role of hepatitis G virus infection. *N Engl J Med* 1997; **336**: 741-746
- 31 **Forns X**, Hegerich P, Darnell A, Emerson SU, Purcell RH, Bukh J. High prevalence of TT virus (TTV) infection in patients on maintenance hemodialysis: frequent mixed infection with different genotypes and lack of evidence of associated liver disease. *J Med Virol* 1999; **59**:313-317
- 32 **Kao JH**, Chen W, Hsiang SC, Chen PJ, Lai MY, Chen DS. Prevalence and implication of TT virus infection: minimal role in patients with non-A-E hepatitis in Taiwan. *J Med Virol* 1999; **59**:307-312
- 33 **Fiordalisi G**, Zanella I, Mantero G, Bettinardi A, Stellini R, Parainfio G, Cadeo G, Primi D. High prevalence of GV virus C infection in a group of Italian patients with hepatitis of unknown etiology. *J Infect Dis* 1996; **174**:181-183
- 34 **Sugai Y**, Nakayama H, Fukuda M, Sawada N, Tanaka T, Tsuda F, Okamoto H, Miyakawa Y, Mayumi M. Infection with GB virus C in patients with chronic liver disease. *J Med Virol* 1997; **51**:175-181
- 35 **Yoshida M**, Okamoto H, Mishiro S. Detection of the GBV-C hepatitis virus genome in serum from patients with fulminant hepatitis of unknown aetiology. *Lancet* 1995; **346**: 1131-1132
- 36 **Heringlake S**, Osterkamp S, Trautwein C, Tillmann HL, Boker K, Muerhoff S, Mushahwar IK, Hunsmann G, Manns MP. Association between fulminant hepatic failure and a stain of GB virus C. *Lancet* 1996; **348**: 1626-1629
- 37 **Tanaka T**, Hess G, Tanaka S, Kohara M. The significance of hepatitis G virus infection in patients with non-A to C hepatic diseases. *Hepatogastroenterology* 1999; **46**: 1870-1873
- 38 **Takayama S**, Miura T, Matsuo S, Taki M, Sugii S. Prevalence and persistence of a novel DNA TT virus (TTV) infection in Japanese haemophiliacs. *Br J Haematol* 1999; **104**: 626-629
- 39 **Sugiyama T**, Shimizu M, Yamauchi O, Kojima M. Seroepidemiologic survey of TT virus (TTV) infection in an endemic area for hepatitis C virus. *Nippon Rinsho* 1999; **57**:1402-1405
- 40 **Cleavinger PJ**, Persing DH, Li H, Moore B, Charlton MR, Sievers C, Therneau TM, Zein NN. Prevalence of TT virus infection in blood donors with elevated ALT in the absence of known hepatitis markers. *Am J Gastroenterol* 2000; **95**:772-776
- 41 **Park YM**, Mizokami M, Nakano T, Choi JY, Cao K, Byun BH, Cho CH, Jung YT, Paik SY, Yoon SK, Mukaide M, Kim BS. GB virus C / hepatitis G virus infection among Korean patients with liver diseases and general population. *Virus Res* 1997; **48**:185-192
- 42 **Ling BH**, Zhuang H, Cui YH, An WF, Li ZJ, Wang SP, Zhu WF. A cross-sectional study on HGV infection in a rural population. *World J Gastroenterol* 1998; **4**:489-492
- 43 **Casteling A**, Song E, Sim J, Blaauw D, Heyns A, Schweizer R, Margolius L, Kuun E, Field S, Schoub B, Vardas E. GB virus C prevalence in blood donors and high risk groups for parenterally transmitted agents from Gauteng, South Africa. *J Med Virol* 1998; **55**:103-108
- 44 **Blair CS**, Davidson F, Lycett C, McDonald DM, Haydon GH, Yap PL, Hayes PC, Simmonds P, Gillon J. Prevalence, incidence, and clinical characteristics of hepatitis G virus / GB virus C infection in Scottish blood donors. *J Infect Dis* 1998; **178**:1779-1782
- 45 **Goubau P**, Andrade FB, Liu HF, Basilio FP, Croonen L, Barreto-Gomes VA. Prevalence of GB virus C/hepatitis G virus among blood donors in north-eastern Brazil. *Trop Med Int Health* 1999; **4**: 365-367
- 46 **Simmonds P**, Davidson F, Lycett C, Prescott LE, MacDonald DM, Ellender J, Yap PL, Ludlam CA, Haydon GH. Detection of a novel DNA virus (TTV) in blood donors and blood products. *Lancet* 1998; **352**:191-195
- 47 **Gad A**, Tanaka E, Orii K, Kafumi T, Serwah AEH, El-Sherif A, Nooman Z, Kiyosawa K. Clinical significance of TT virus infection in patients with chronic liver disease and volunteer blood donors in Egypt. *J Med Virol* 2000; **60**: 177-181A
- 48 **Chen YP**, Liang WF, Zhang L, He HT, Luo KX. Transfusion transmitted virus infection in general populations and patients with various liver diseases in south China. *World J Gastroenterol* 2000; **6**:738-741
- 49 **Huang CH**, Zhou YS, Chen RG, Xie CY, Wang HT. The prevalence of transfusion transmitted virus infection in blood donors. *World J Gastroenterol* 2000; **6**:268-270
- 50 **Yan J**, Chen LL, Luo YH, Mao YF, He M. High frequencies of HGV and TTV infections in blood donors in Hangzhou. *World J Gastroenterol* 2001; **7**:637-641
- 51 **Chen M**, Sonnerborg A, Johansson B, Sallberg M. Detection of hepatitis G virus (GB virus C) RNA in human saliva. *J Clin Microbiol* 1997; **35**: 973-975
- 52 **Seemayer CA**, Viazov S, Philipp T, Roggendorf M. Detection of GBV-C/HGV RNA in saliva and serum, but not in urine of infected patients. *Infection* 1998; **26**:39-41
- 53 **Ross RS**, Viazov S, Runde V, Schaefer UW, Roggendorf M. Detection of TT virus DNA in specimens other than blood. *J Clin Virol* 1999; **13**: 181-184
- 54 **Inami T**, Konomi N, Arakawa Y, Abe K. High prevalence of TT virus DNA in human saliva and semen. *J Clin Microbiol* 2000; **38**:2407-2408
- 55 **Deng X**, Terunuma H, Handema R, Sakamoto M, Kitamura T, Ito M, Akahane. Higher prevalence and viral load of TT virus in saliva than in the corresponding serum: another possible transmission route and replication site of TT virus. *J Med Microbiol* 2000; **62**:531-537
- 56 **Okamoto H**, Takahashi M, Nishizawa T, Ukita M, Fukuda M, Tusa F, Miyakawa Y, Mayumi M. Marked genomic heterogeneity and frequent mixed infection of TT virus demonstrated by PCR with primers from coding and noncoding regions. *Virology* 1999; **259**: 428-436
- 57 **Tian DY**, Yang DF, Xia NS, Zhang ZG, Lei HB, Huang YC. The serological prevalence and risk factor analysis of hepatitis G virus infection in Hubei Province of China. *World J Gastroenterol* 2000; **6**: 585-587
- 58 **Hu ZJ**, Lang ZW, Zhou YS, Yan HP, Huang DZ, Chen WR, Luo ZX. Clinicopathological study on TTV infection in hepatitis of unknown etiology. *World J Gastroenterol* 2002; **8**:288-293
- 59 **Handajani R**, Soetjipito, Lusida MI, Suryohudoyo P, Adi P, Setiawan PB, Nidom CA, Soemarto R, Katayama Y, Fujii M, Hotta H. Prevalence of GB virus C / hepatitis G virus infection among various Population in Surabaya, Indonesia, and Identification of novel groups of sequence variants. *J Clin Microbiol* 2000; **38**: 662-668
- 60 **Wang XT**, Zhuang H, Song HB, Li HM, Zhang HY, Yu Y. Partial sequencing of 5' non-coding region of 7 HGV strains isolated from different areas of China. *World J Gastroenterol* 1999; **5**: 432-434
- 61 **Smith DB**, Cuceanu N, Davidson F, Jarvis LM, Mokili JLK, Hamid S, Ludlam CA, Simmonds P. Discrimination of hepatitis G virus/GBV-C geographical variants by analysis of the 5' non-coding region. *J Gen Virol* 1997; **78**: 1533-1542
- 62 **Lopez-Alcorocho JM**, Castillo I, Tomas JF, Carreno V. Identification of a novel GB type C virus/hepatitis G virus subtype in patients with hemotologic malignancies. *J Med Virol* 1999; **57**:80-84

Edited by Zhao P

• VIRAL HEPATITIS •

Preparation of human single chain Fv antibody against hepatitis C virus E2 protein and its identification in immunohistochemistry

Yan-Wei Zhong, Jun Cheng, Gang Wang, Shuang-Shuang Shi, Li Li, Ling-Xia Zhang, Ju-Mei Chen

Yan-Wei Zhong, Jun Cheng, Gang Wang, Shuang-Shuang Shi, Li Li, Ling-Xia Zhang, Ju-Mei Chen, Gene Therapy Research Center, Institute of Infectious Diseases, 302 Hospital of PLA, 26 Fengtai Road, Beijing 100039, China

Supported by the National Natural Science Foundation of China, No.39900130

Correspondence to: Yan-Wei Zhong, Gene Therapy Research Center, Institute of Infectious Diseases, 302 Hospital of PLA, 26 Fengtai Road, Beijing 100039, China. zyw@genetherapy.com.cn

Telephone: +86-10-66933392 **Fax:** +86-10-63801283

Received 2002-01-28 **Accepted** 2002-03-05

Abstract

AIM: To screen human single chain Fv antibody (scFv) against hepatitis C virus E2 antigen and identify its application in immunohistochemistry.

METHODS: The phage antibody library was panned by HCV E2 antigen, which was coated in microtiter plate. After five rounds of biopanning, 56 phage clones were identified specific to HCV E2 antigen. The selected scFv clones were digested by SfiI/NotI and DNA was sequenced. Then it was subcloned into the vector pCANTAB5E for expression as E-tagged soluble scFv. The liver tissue sections from normal person and patients with chronic hepatitis B and chronic hepatitis C were immunostained with HCV E2 scFv antibody.

RESULTS: The data of scFv-E2 DNA digestion and DNA sequencing showed that the scFv gene is composed of 750 bp. ELISA and immunohistochemistry demonstrated that the human single chain Fv antibody against hepatitis C E2 antigen has a specific binding character with hepatitis virus E2 antigen and paraffin-embedded tissue, but did not react with liver tissues from healthy persons or patients with chronic hepatitis B.

CONCLUSION: We have successfully screened and identified HCV E2 scFv and the scFv could be used in the immunostaining of liver tissue sections from patients with chronic hepatitis C.

Zhong YW, Cheng J, Wang G, Shi SS, Li L, Zhang LX, Chen JM. Preparation of human single chain Fv antibody against hepatitis C virus E2 protein and its identification in immunohistochemistry. *World J Gastroenterol* 2002; 8(5):863-867

INTRODUCTION

Hepatitis C virus (HCV) has been identified as the major etiological agent of post-transfusion non-A non-B hepatitis^[1-10], responsible for most cases of non-A non-B hepatitis. Hepatitis C is a disease of clinical importance because of its high infection rate in blood donors and its persistence as chronic infections

which may lead to cirrhosis and hepatocellular carcinoma in the long term^[11-26]. The variability of the HCV genome has difficulties in serological detection and vaccine design. Recent advance in phage technology offers a means of cloning human anti-HCV antibodies of a defined specificity that may have potential therapeutic use^[27]. We now report the generation of phage display antibody using phage antibody library. From this library we obtained specific single-chain Fv antibody that recognizes the viral envelope protein E2, using HCV E2 protein as the immobilized antigen and proceeding immunohistochemistry.

MATERIALS AND METHODS

Materials

Humanized scFv antibody phage library in which the variable region coding gene of VL and VH were amplified by polymerase chain reaction (PCR) with degenerate primers and connected with a glycine linker [(Gly4Ser)3] was widely used in the screen and identification of humanized scFv to various antigens^[28-34]. The recombinant HCV E2 protein was purchased from Virostat Co, USA. Phage M13K07 was purchased from Pharmacia Co., Sweden. Other reagents used in this experiment are all domestic products of analytical grade.

Biopanning

The phage library was amplified in 37 °C. The host *E. coli* TG1 was infected with phage M13K07 and incubated at 37 °C for 12 hours, the phage in the supernatant was harvested and concentrated by PEG. Culture plate (Nunc) was coated with recombinant HCV E2 protein at the concentration of 80 mg/L. The coating buffer was 0.05 mol/L NaHCO₃, pH 9.6. The plate was blocked with BSA at the concentration of 20 g/L for 2 hours and the concentrated phages were added to the well of the plate, incubated at the room temperature for 90 min. The plates were washed 20 times with PBST and PBS buffer respectively. The bound phage was eluted by the 0.1M of triethylamine, and neutralized with 1M Tris buffer (pH 7.4). Recovered phages were used to infect the host *E. coli* TG1 at the log phase growth and HCV E2 protein-binding phages were amplified. The procedure of absorption-elution-amplification was repeated 5 times.

Identification of phage clones

After 5 rounds of biopanning, 56 phage clones were selected randomly. The clones grew in 400 µl 2×TY-AMP-Glu at 37 °C overnight. The culture was transformed to another Eppendorf tube when its A_{600 nm} reached 0.5. The culture was continued at 30 °C overnight after adding helper phage. ELISA for determining the supernatants was repeated at least two times. The cross-reaction of the supernatants to the BSA antigen was conducted. According to the ELISA results to the HCV E2 and BSA, one clone with high reaction to HCV E2 and low reaction to BSA was selected.

Sequencing analysis

The plasmid DNA was prepared using Wizard plus minipreps DNA Purification System (Promega Co., USA) and sequenced using ABI automated DNA sequencing machine.

Expression of human HCV E2-scFv in *E. coli*

The selected HCV E2 scFv clone was subcloned as *Sfi*I/*Not*I fragments into the vector pCANTAB5E for expression as E-tagged soluble scFv. DNA digestion and electrophoresis confirmed the recombinant vector pCANTAB5E-E2-scFv. Competent *E. coli* XL1-Blue was transformed with pCANTAB5E-E2-scFv and transformed XL1-Blue was induced by IPTG for 20 h. The *E. coli* was harvested by centrifugation at 10 000rpm. The culture supernatant was rendered for ELISA test according to the standard procedure. In ELISA detection, Nunc plate was coated with 1μg/well of recombinant HCV E2 antigen and blocked with 2 % bovine serum albumin (BSA) at 37 °C for 2 h. The supernatants from induced and non-induced transformed *E. coli* were added and incubated at 37 °C for 2 h. The plate was washed with PBS buffer, and 100 μl of HRP/anti-E Tag 1:4000 ratio diluted in PBS buffer containing 1 % BSA was added, and incubated at 37 °C for 1 h. The substrate solution was added and A450nm value was measured.

Immunohistochemical identification of scFv in liver tissue

Paraffin-embedded liver tissue slices were from patients with positive anti-HCV antibodies and HCV-RNA. After deactivating endogenous hyperoxidase, these slices were submersed in the methanol solution with 0.5 % H₂O₂ in the room temperature. Fifty min later, they were washed with PBS buffer for 3 times, 5 % BSA was added and slices were stored overnight at 4 °C. Self-made scFv primary anti- HCV E2 single-chain antibodies were diluted at 1:100 ratio and added on to the slice. They were kept in the 37 °C incubator for 1 h, then 4 °C refrigerator overnight. HRP-sheep anti-M13 antibodies (diluted to 1:200) solutions were dropped on to the tissue sections, incubated at 37 °C for 40 min. After washing 3 times with PBS buffer, DAB solutions (9 mg DAB, 13.5 ml Tris.cl, 1.5 ml CoCl₂, 15 μl 30 % H₂O₂) were dropped on to the tissue sections at room temperature. After ten minutes, the slices were washed with PBS buffer for 3 times again, and 1 % heamatin solution was used to stain the cell nucleus. Gradient ethanol was utilized to dehydrate and dimethylbenzene to clear the sections, then neutral resin to envelope them. The resultant slices were observed under microscope. The controls were set as follows: 1) PBS buffer instead of anti- HCV E2 scFv; 2) HBsAg, HBcAg double-positive liver tissue sections; and 3) Normal liver tissue sections.

RESULTS

Screening and identification phage clones

Using HCV E2 protein as immobilized antigen, the humanized scFv phage library was biopanned. After 5 rounds of biopanning, 56 phage clones were selected randomly. ELISA and cross-reaction of these clones to BSA confirmed their specificity to HCV E2. Among the 56 phage clones, 16 showed good reactivity to the recombinant HCV E2 protein with high A value in the ELISA. In the cross-reaction screen, 6 among the 16 showed low cross-reaction with BSA. The combined results indicated that 1 of the 6 showed the highest reaction to HCV E2 protein and lowest reaction to BSA. One clone has been selected for further DNA digestion and sequence analysis. The DNA sequence digestion was made by *Sfi*I/*Not*I in Figure

1. Its nucleic acid sequence and deduced amino acid sequence about HCV-E2-scFv fragment are shown in Figure 2.

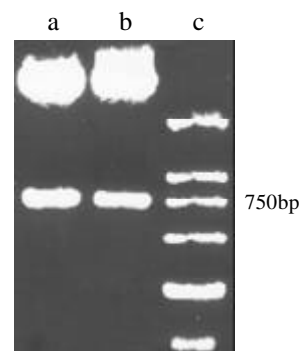


Figure 1 Restriction map of HCV E2-scFv by *Sfi*I/*Not*I digestion. A,B: HCV E2-scFv; C: DNA Marker

```

ATG GCC CAG GTG CAG CTG GTG CAG TCT GGG GCT GAG GTG AAG AAG CCT GGG GCC
M A Q V Q L V Q S G A E V K K P G A
TCA GTG AAG GTT TCC TGC AAG GCT TCT GGA TAC ACC TTC ACT AGC TAT GCT ATG
S V K V S C K A S G Y T F T S Y A M
CAT TGG GTG CGC CAG GCC CCC GGA CAA AGG CTT GAG TGG ATG GGA TGG ATC AAC
H W V R Q A P G Q R L E W M G W I N
GCT GGC AAT GGT AAC ACA AAA TAT TCA CAG AAG TTC CAG GGC AGA GTC ACC ATT
A G N G N T K Y S Q K F Q G R V T I
ACC AGG GAC ACA TCC GCG AGC ACA GCC TAC ATG GAG CTG AGC AGC CTG AGA TCT
T R D T S A S T A Y M E L S S L R S
GAA GAC ACG GCC GTG TAT TAC TGT GCA AGA TCG AGT GGG CCG ATG CAT CGT GAG
E D T A V Y Y C A R S S G P M H R E
TGG GCG CAA GGT ACC CTG GTC ACC GTG TCG AGA GGT GGA GGC GGT TCA GGC GGA
W G Q G T L V T V S R G G G S G G
GGT GGC TCT GGC GGT GGC GGA TCG TCT GAG CTG ACT CAG GAC CCT GCT GTG TCT
G G S G G G S S E L T Q D P A V S
GTG GCC TTG GGA CAG ACA GTC AGG ATC ACA TGC CAA GGA GAC AGC CTC AGA AGC
V A L G Q T V R I T C Q G D S L R S
TAT TAT GCA AGC TGG TAC CAG CAG AAG CCA GGA CAG GCC CCT GTA CTT GTC ATC
Y Y A S W Y Q Q K P G Q A P V L V I
TAT GGT AAA AAC AAC CCG CCC TCA GGG ATC CCA GAC CGA TTC TCT GGC TCC AGC
Y G K N N R P S G I P D R F S G S S
TCA GGA AAC ACA GCT TCC TTG ACC ATC ACT GGG GCT CAG GCG GAA GAT GAG GCT
S G N T A S L T I T G A Q A E D E A
GAC TAT TAC TGT AAC TCC CGG GAC AGC AGT GGT AAC CAT GTG GTA TTC GGC GGA
D Y Y C N S R D S S G N H V V F G G
GGG ACC AAG CTG ACC GTC CTA GGT GCG GCC GCA GAA CAA AAA CTC ATC TCA GAA
G T K L T V L G A A A E Q K L I S E
GAG GAT CTG AAT GGG GCC GCA TAG
E D L N G A A *

```

Figure 2 Nucleic acid and deduced amino acid sequences of scFv for HCV E2 protein GenBank accession number for this sequence is AF317001

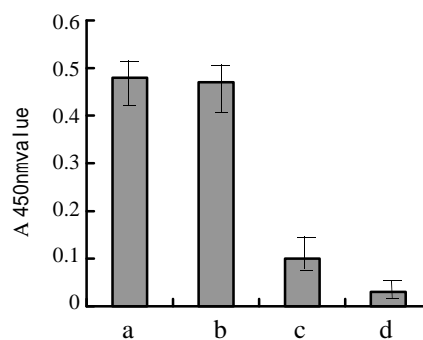


Figure 3 Absorbances of HCV-E2-scFv binding to E2 antigen by ELISA. (a). supernatant from induced XL1-blue transformed with pCANTAB5E-E2-scFv; (b). positive control; (c). supernatant from non-induced XL1-blue transformed with pCANTAB5E-E2-scFv, d. negative control

Expression of human HCV-E2-scFv in *E. coli*.

The expressed HCV-E2-scFv antibody from *E. coli* XL1-blue transformed by pCANTAB5E and induced by IPTG was confirmed by ELISA as shown in Figure 3. The recombinant HCV E2 antigen was taken as the positive control. The protein from induced and non-induced *E. coli* XL1-blue transformed by expression vector was positive. But the protein derived from the *E. coli* non-transformed by pCANTAB5E- HCV E2- scFv was negative. These results indicated that the soluble form of human HCV E2- scFv antibody has been successfully expressed in this procedure.

Immunostaining of HCV E2 antigen of liver tissue sections

The different sections from liver tissues of healthy persons and patients with chronic hepatitis B or C were immunostained. The positive immunostaining was seen only in the liver tissue section of patients with chronic hepatitis C, but not in the liver tissue of normal person and patients with chronic hepatitis B as seen in (Figure 4A). The HCV E2 antigen was mainly located in the cytoplasm of the hepatocytes infected by HCV virus (Figure 4B).

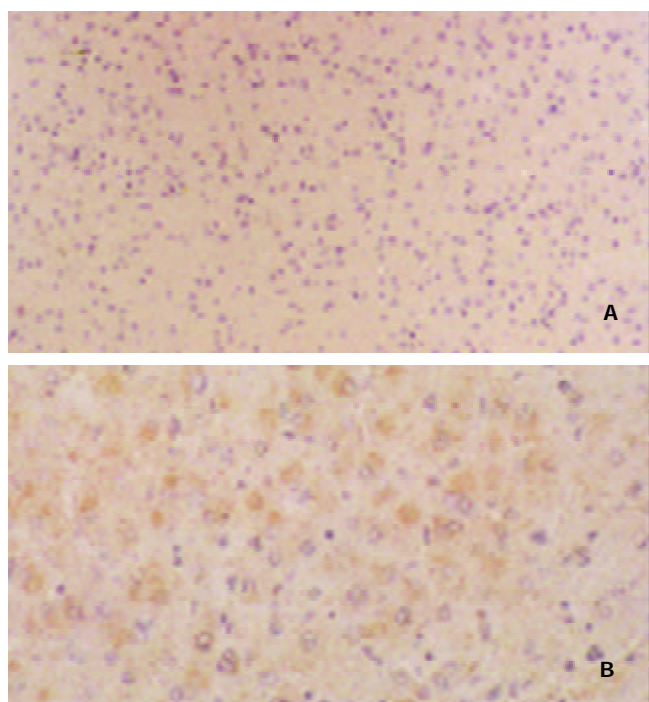


Figure 4 A. Immunohistochemistry of liver tissue from health person. B. Immunohistochemistry of liver tissue from patients with chronic hepatitis C E2 antigen was detected in the cytoplasm of some liver cells

DISCUSSION

HCV is the etiological agent responsible for most cases of non-A non-B hepatitis. It is a blood-related disease of clinical importance since a large number of cases developed chronic infections which may lead to cirrhosis and hepatocellular carcinoma. The variability of the HCV genome has posed serious problems in serological detection of HCV and vaccine design^[27-38]. The possibility of using neutralizing antibodies in passive immunization is also hampered by the existence of genotypes and quasispecies^[39-50]. To circumvent this, it is possible to envisage the use of cross reactive antibodies with a broad reactivity directed against functionally conserved surface domains common to various genotypes. There has been *in vitro*

and *in vivo* evidence that HCV infection elicits a neutralizing antibody response in humans. The virus envelope protein is the primary target for the host immune system. Despite the high variability of the HCV envelope sequence, certain domains of biological importance, e.g. ligands required in viral attachment to host cell receptors, have to be preserved. Antibody specific for the envelope E2 protein has been shown to be cross-reactive HCV E2 and to be able to block viral attachment to cultured human fibroblast cells. However, attempt to obtain human monoclonal anti-HCV antibodies is an urgency.

Phage library is a powerful tool for the selection of important and useful antibody specificities especially for getting humanized scFv^[51-53]. It has many advantages. First, it is the only method to get specific antibody by passing the immunization step. It can mimic the maturation procedure of human antibody *in vivo*, so it is possible to get high affinity antibody from this selection. Second, the scFv with a low molecular weight, can make it potentially applicable in the clinical diagnosis and treatment of both infectious disease and cancer. Finally, it has no Fc fragment, so the background is very low.

The phage technology offers a means of cloning human anti-HCV antibodies of a defined specificity that may be potential for therapeutic and diagnostic use. In this report, we have obtained anti-HCV E2 scFv by affinity selection and purified recombinant hepatitis C virus E2 as coating antigen from synthetic phage display antibody library. After 5 rounds of selection, 56 clones were evaluated by enzyme-linked immunosorbent assay (ELISA). One phage clone was selected from 56 clones according to the highest A450 nm value in the ELISA identification and lowest cross-reaction to the bovine serum albumin (BSA). The coding fragments of scFv were sequenced. The affinity and specificity of scFv were evaluated by ELISA and immunohistochemistry. HCV E2-scFv DNA digestion and sequence data showed that the scFv gene is composed of 750 bp. ELISA and immunohistochemistry demonstrated that the human single chain Fv antibody against HCV E2 antigen has a specific binding activity with hepatitis C virus E2 antigen. This study illustrated the feasibility of using antibody-engineering technology with the phage display library that may be useful for future therapeutic and detection purpose.

REFERENCES

- 1 **Assy N**, Minuk G. A comparison between previous and present histologic assessments of chronic hepatitis C viral infections in humans. *World J Gastroenterol* 1999; **5**:107-110
- 2 **Caselmann WH**, Serwe M, Lehmann T, Ludwig J, Sproat BS, Engels JW. Design, delivery and efficacy testing of therapeutic nucleic acids used to inhibit hepatitis C virus gene expression *in vitro* and *in vivo*. *World J Gastroenterol* 2000; **6**: 626-629
- 3 **Cheng JL**, Liu BL, Zhang Y, Tong WB, Yan Z, Feng BF. Hepatitis C virus in human B lymphocytes transformed by Epstein-Barr virus *in vitro* by *in situ* reverse Transcriptase polymerase chain reaction. *World J Gastroenterol* 2001; **7**: 370-375
- 4 **Dai YM**, Shou ZP, Ni CR, Wang NJ, Zhang SP. Localization of HCV RNA and capsid protein in human hepatocellular carcinoma. *World J Gastroenterol* 2000; **6**:136-137
- 5 **Deng ZL**, Ma Y, Yuan L, Teng PK. The importance of hepatitis C as a risk factor for hepatocellular carcinoma in Guangxi. *World J Gastroenterol* 2000; **6**(Suppl 3):75
- 6 **Feng DY**, Chen RX, Peng Y, Zheng H, Yan YH. Effect of HCV NS3 protein on p53 protein expression in hepatocarcinogenesis. *World J Gastroenterol* 1999; **5**:45-46
- 7 **Gao JE**, Tao QM, Guo JP, Ji HP, Lang ZW, Ji Y, Feng BF.

- Preparation and application of monoclonal antibodies against hepatitis C virus nonstructural proteins. *World J Gastroenterol* 1997; **3**: 114-116
- 8 **Huang F**, Zhao GZ, Li Y. HCV genotypes in hepatitis C patients and their clinical significances. *World J Gastroenterol* 1999; **5**: 547-549
- 9 **Li LF**, Zhou Y, Xia S, Zhao LL, Wang ZX, Wang CQ. The epidemiologic feature of HCV prevalence in Fujian. *World J Gastroenterol* 2000; **6**(Suppl 3):80
- 10 **Maier KP**. Iron, HCV and the liver. *World J Gastroenterol* 1997; **3**: 61-63
- 11 **Song ZQ**, Hao F, Min F, Ma QY, Liu GD. Hepatitis C virus infection of human hepatoma cell line 7721 *in vitro*. *World J Gastroenterol* 2001; **7**: 685-689
- 12 **Sun DG**, Liu CY, Meng ZD, Sun YD, Wang SC, Yang YQ, Liang ZL, Zhuang H. A prospective study of vertical transmission of hepatitis C virus. *World J Gastroenterol* 1997; **3**: 111-113
- 13 **Tang BZ**, Zhuang L, You J, Zhang HB, Zhang L. Seven years follow up on trial of Interferon alpha in patients with HCV RNA positive chronic hepatitis C. *World J Gastroenterol* 2000; **6**(Suppl 3):68
- 14 **Zhao YY**, Yang HY, Liu GX, Li ZQ, Liu L, He LL, Deng WJ. Hepatitis C virus infection in patients with primary liver cancer. *Xin Xiaohuabingxue Zazhi* 1996; **4**(Suppl 5): 43-44
- 15 **Tang ZY**, Qi JY, Shen HX, Yang DL, Hao LJ. Short- and long-term effect of interferon therapy in chronic hepatitis C. *World J Gastroenterol* 1997; **3**: 77
- 16 **Wietzke Braun P**, Meier V, Braun F, Ramadori G. Combination of "low-dose" ribavirin and interferon alfa 2a therapy followed by interferon alfa 2a monotherapy in chronic HCV infected non responders and relapsers after interferon alfa 2a monotherapy. *World J Gastroenterol* 2001; **7**: 222-227
- 17 **Worman HJ**, Lin F. Molecular biology of liver disorders: the hepatitis C virus and molecular targets for drug development. *World J Gastroenterol* 2000; **6**:465-469
- 18 **Worman HJ**, Lin F. Molecular biology of liver disorders: the hepatitis C virus and molecular targets for drug development. *World J Gastroenterol* 2000; **6**:465-469
- 19 **Xiao LY**, Yan XJ, Mi MR, Han FC, Hou Y. Preliminary study of a dot immunogold filtration assay for rapid detection of anti- HCV IgG. *World J Gastroenterol* 1999; **5**: 349-350
- 20 **Yan FM**, Chen AS, Hao F, Zhao XP, Gu CH, Zhao LB, Yang DL, Hao LJ. Hepatitis C virus may infect extrahepatic tissues in patients with hepatitis C. *World J Gastroenterol* 2000; **6**:805-811
- 21 **Yang JM**, Wang RQ, Bu BG, Zhou ZC, Fang DC, Luo YH. Effect of HCV infection on expression of several cancer associated gene products in HCC. *World J Gastroenterol* 1999; **5**: 25-27
- 22 **Yu SJ**. A comparative study on proliferating activity between HBV related and HCV related small HCC. *World J Gastroenterol* 1997; **3**: 236-237
- 23 **Zhang LF**, Peng WW, Yao JL, Tang YH. Immunohistochemical detection of HCV infection in patients with hepatocellular carcinoma and other liver diseases. *World J Gastroenterol* 1998; **4**:64-65
- 24 **Zhang SL**, Liang XS, Lin SM, Qiu PC. Relation between viremia level and liver disease in patients with chronic HCV infection. *World J Gastroenterol* 1996; **2**: 115-117
- 25 **Zhou P**, Cai Q, Chen YC, Zhang MS, Guan J, Li XJ. Hepatitis C virus RNA detection in serum and peripheral blood mononuclear cells of patients with hepatitis C. *World J Gastroenterol* 1997; **3**:108-110
- 26 **Zhu FL**, Lu HY, Li Z, Qi ZT. Cloning and expression of NS3 cDNA fragment of HCV genome of Hebei isolate in *E. coli*. *World J Gastroenterol* 1998; **4**: 165-168
- 27 **Zhong Y**, Cheng J, Shi S, Xia X, Wang G, Yang J, Chen J. Screening and characterization of human phage antibody to hepatitis virus C core antigen. *Zhonghua Gangzhangbing Zazhi* 2001; **9**: 217-219
- 28 **Zhong YW**, Chen J, Shi SS, Wang G, Dong J, Xia XB, Yang JZ, Chen JM. Screening and expression of human phage antibody to hepatitis virus C NS5A antigen. *Chinese J Traditional Western Med* 2001; **2**: 97-99
- 29 **Chen J**, Zhong YW, Shi SS. Screening and characterization of human phage antibody to hepatitis virus C NS5A antigen. *Zhonghua Shiyen He Linchuangbingduxue Zazhi* 2001; **15**: 216-218
- 30 **Zhong Y**, Cheng J, Liu Y, Dong J, Yang J, Zhang L. Expression of human single-chain variable fragment antibody against non-structural protein 3 of hepatitis C virus antigen in *E.coli*. *Zhonghua Gangzhangbing Zazhi* 2000; **8**: 171-173
- 31 **Zhong YW**, Chen J, Xia XB, Wang G, Yang JZ, Chen JM. Screening and characterization of human phage antibody to hepatitis virus C NS4A antigen. *Immunological J* 2000; **16**: 422-428
- 32 **Zhong Y**, Wang S, Zhao J. The preparation of human single-chain Fv antibody specifically against hepatitis C virus NS3 antigen and its application in histochemistry. *Zhonghua Shiyen Yu Bingduxue Zazhi* 2001; **15**:186-188
- 33 **Zhong YW**, Chen J, Liu Y, Dong J, Yang JZ, Zhang LX. Expression of soluble human single chain Fv antibody to hepatitis C NS 3 antigen in *E.coli*. *Ganzhang Zhazhi* 1999; **4**: 71-73
- 34 **Zhong YW**, Chen J, Liu Y, Dong J, Yang JZ, Zhang LX. Screening and characterization of human phage antibody with single-chain variable fragment specific to hepatitis C nonstructural 3 protein. *Zhonghua Chuanranbing Zazhi* 2000; **18**: 84-87
- 35 **He YW**, Liu W, Zen LL, Xiong KJ, Luo DD. Effect of interferon in combination with ribavirin on the plus and minus strands of HCV RNA in patients with chronic hepatitis C. *China Natl J New Gastroenterol* 1996; **2**: 179-181
- 36 **Wei L**, Wang Y, Chen HS, Tao QM. Sequencing of hepatitis C virus cDNA with polymerase chain reaction directed sequencing. *China Natl J New Gastroenterol* 1997; **3**: 12-15
- 37 **Worman HJ**, Feng L, Mamiya N, Mustacchia PJ. Molecular biology and the diagnosis and treatment of liver diseases. *World J Gastroenterol* 1998; **4**: 185-191
- 38 **Chen MY**, Huang ZQ, Chen LZ, Gao YB, Peng RY, Wang DW. Detection of hepatitis C virus NS5 protein and genome in Chinese carcinoma of the extrahepatic bile duct and its significance. *World J Gastroenterol* 2000; **6**: 800-804
- 39 **Han FC**, Hou Y, Yan XJ, Xiao LY, Guo YH. Dot immunogold filtration assay for rapid detection of anti HAV IgM in Chinese. *World J Gastroenterol* 2000; **6**: 400-401
- 40 **Liu LH**, Xiao WH, Liu WW. Effect of 5-Aza-2'-deoxycytidine on the P16 tumor suppressor gene in hepatocellular carcinoma cell line HepG2. *World J Gastroenterol* 2001; **7**: 131-135
- 41 **Meier V**, Mihm S, Ramadori G. HCV-RNA positivity in peripheral blood mononuclear cells of patients with chronic HCV infection: does it really mean viral replication? *World J Gastroenterol* 2001; **7**: 228-234
- 42 **Si XH**, Yang LJ. Extraction and purification of TGF β and its effect on the induction of apoptosis of hepatocytes. *World J Gastroenterol* 2001; **7**: 527-531
- 43 **Wang NS**, Liao LT, Zhu YJ, Pan W, Fang F. Follow-up study of hepatitis C virus infection in uremic patients on maintenance hemodialysis for 30 months. *World J Gastroenterol* 2000; **6**:888-892

- 44 **Yan J**, Dennin RH. A high frequency of GBV-C/HGV coinfection in hepatitis C patients in Germany. *World J Gastroenterol* 2000; **6**: 833-841
- 45 **Chen S**, Wang YM, Li CM, Fang YF. Molecular epidemiology of HCV infection in intravenous drug abusers. *Shijie Huaren Xiaohua Zazhi* 2001; **9**: 526-528
- 46 **Ding HL**, Cheng H, Fu ZZ, Deng QL, Yan L, Yan T. The relationship of α 1mp2 and DR3 genes with susceptibility to type I diabetes mellitus in south China Han population. *World J Gastroenterol* 2000; **6**: 111-114
- 47 **Huang F**, Zhao GZ, Li Y. HCV genotypes in hepatitis C patients and their clinical significances. *World J Gastroenterol* 1999; **5**: 547-549
- 48 **Su YH**, Zhu SN, Lu SL, Gu YH. HCV genotypes expression in hepatocellular carcinoma by reverse transcription in situ polymerase chain reaction. *Shijie Huaren Xiaohua Zazhi* 2000; **8**: 874-878
- 49 **Wang PZ**, Zhou YX. Study on hepatitis C virus genotyping in Xi'an area. *Shijie Huaren Xiaohua Zazhi* 1999; **7**: 757-759
- 50 **Yan XB**, Wu WY, Wei L. Clinical features of infection with different genotypes of hepatitis C virus. *Huaren Xiaohua Zazhi* 1998; **6**: 653-655
- 51 **Marks JD**, Hoogenboom HR, Bonnert TP, McCafferty J, Griffiths AD, Winter G. By-immunization human antibodies from V-gene libraries displayed on phage. *J Mol Biol* 1991; **222**: 581-597
- 52 **Hoogenboom HR**, de Bruine AP, Hufton SE, Hoet RM, Arends JW, Roovers RC. Anti-body phage display technology and its applications. *Immunotechnology* 1998; **4**: 1-20
- 53 **Lamarre A**, Talbot PJ. Characterization of phage-displayed recombinant anti-idiotypic antibody fragments against coronavirus neutralizing monoclonal antibodies. *Viral Immunol* 1997; **10**: 175-182

Edited by Ma JY

• VIRAL HEPATITIS •

Lamivudine does not increase the efficacy of interferon in the treatment of mutant type chronic viral hepatitis B

Sien-Sing Yang, Chao-Tien Hsu, Jui-Ting Hu, Yung-Chih Lai, Chi-Hwa Wu

Sien-Sing Yang, Jui-Ting Hu, Yung-Chih Lai, Chi-Hwa Wu, Liver Unit, Cathay General Hospital, Taipei, Taiwan, China

Sien-Sing Yang, Chao-Tien Hsu, Medical Faculty, China Medical College and Hospital, Taichung, Taiwan, China

Correspondence to: Sien-Sing Yang, MD, Liver Unit, Cathay General Hospital, 280 Sec.4, Jen-Ai Rd., Taipei, Taiwan 10650. yangss@seed.net.tw

Telephone: +886-2-2708-2121 Ext.3121

Fax: +886-2-2707-4949

Received 2002-04-12 **Accepted** 2002-06-11

Abstract

AIM: To study the role of lamivudine in improving the efficiency of interferon for the treatment of mutant type chronic hepatitis B.

METHODS: Fifteen patients with mutant type chronic hepatitis B were prospectively studied. All patients had liver histology and serology to prove the diagnosis of chronic hepatitis B. Each patient received 4.5 million units of interferon alpha-2a thrice weekly and 100 mg of oral lamivudine daily for 24 weeks. Patients were observed and tested for blood chemistry every week for the initial 4 weeks and every 2 weeks thereafter during the treatment until 24 weeks. After the end of treatment, patients were followed up at 4-week intervals for an additional 6 months. Serum HBV DNA levels were tested using the liquid phase molecular hybridization assay. Those with non-detectable HBV DNA were also tested using the real-time polymerase chain reaction. One patient, who did not finish treatment due to depression, was excluded.

RESULTS: At the end of treatment, 7 (50 %) patients had serum ALT levels within normal limits; 12 (86 %) patients had serum HBV DNA levels <5 pg/mL using the liquid phase molecular hybridization assay, but only 8 (67%) were <20 copies/dL using the real-time polymerase chain reaction. Six months after treatment, only two (14 %) patients had a sustained complete response to the combination therapy with serum ALT level <35 IU/L and undetectable serum HBV DNA levels.

CONCLUSION: These pilot data showed that lamivudine did not increase the efficacy of interferon in the treatment of mutant type chronic hepatitis B. The liquid phase molecular hybridization assay was not sensitive enough to detect the low HBV DNA levels during combined interferon and lamivudine therapy.

Yang SS, Hsu CT, Hu JT, Lai YC, Wu CH. Lamivudine does not increase the efficacy of interferon in the treatment of mutant type chronic viral hepatitis B. *World J Gastroenterol* 2002;8(4):868-871

INTRODUCTION

Hepatitis B virus (HBV) is one of the major causes of liver disease worldwide^[1,2], and chronic hepatitis B can progress to cirrhosis and hepatocellular carcinoma^[1,2]. It is thus important to conduct anti-viral therapy against chronic hepatitis B to minimize the amount of liver damage^[4]. Recent studies suggest that around half of all patients with chronic HBV infection responded to a 6 to 12 month course of interferon therapy at the end of treatment with loss of serum hepatitis B viral deoxyribonucleic acid (HBV DNA) and hepatitis B e antigen (HBeAg), as well as normalization of serum alanine aminotransferase (ALT) activity^[5,6]. However, a mutant type of HBV DNA has been identified in serum from patients with chronic hepatitis B, who presented with negative HBeAg and abnormal serum ALT levels^[7]. The mutant type of HBV infection showed mutations at the precore region. Different from those patients with wild type HBV DNA, the response rate of interferon mono-therapy against mutant type chronic hepatitis B was low^[8,9]. Lamivudine has become a recent interest in the treatment of chronic viral hepatitis B^[10,11]. However, the relapse rate after the end of lamivudine therapy is high^[12-14]. Many different regimens, including a longer course of treatment or higher dosages of interferon, have been claimed to improve the interferon therapy, but the sustained response rate is still disappointing^[15,16]. Recent studies from patients with chronic hepatitis C show that the combination of interferon alpha with ribavirin results in a higher sustained response rate than interferon alpha alone^[17,18]. However, the role of combination of interferon and lamivudine against chronic hepatitis B remains uncertain^[19]. We therefore conducted the present pilot study to investigate the possible role of combined interferon and lamivudine to improve the efficiency of interferon in patients with mutant type chronic hepatitis B.

MATERIALS AND METHODS

We prospectively studied 15 documented patients with mutant type chronic hepatitis B at Cathay General Hospital, Taipei, Taiwan between June 1999 and June 2001. All patients were males aged between 20 and 65 years old (mean \pm SD: 44 \pm 8 years), and were naive without prior interferon or other anti-viral therapy. Chronic hepatitis B was defined as positive hepatitis B surface antigen (HBsAg, Auszyme, Abbott Laboratory, Abbott Park, IL 60064) and abnormal serum ALT levels (normal <35 IU/L) for more than 6 months. Mutant type chronic hepatitis B was defined as detectable HBV DNA, positive HBsAg, negative HBeAg [HBeAg; HBe (rDNA) EIA, Abbott Laboratory], and abnormal serum ALT levels in patients having chronic hepatitis B. All patients had at least three documented occasions of abnormal serum ALT levels higher than twice the upper limit of normal with one month apart, within 6 months prior to enrollment. All patients underwent liver biopsy within one month before the start of treatment to confirm the chronic hepatitis without cirrhosis.

None of our patients were alcoholic, intravenous drug users

or homosexual. None had received hepatotoxic drugs, herbal medicine or immuno-suppressive therapy within the past 6 months. Further, none had decompensated liver function (prolonged prothrombin time >3 seconds vs. INR >1.50, serum total bilirubin >3.0 mg/dL, or serum albumin < 3.0 g/dL), cirrhosis, chronic renal failure, clotting abnormalities, hemophiliacs, serious neurological disorders, obesity, chronic viral hepatitis C (Murex anti-HCV, Version III, Murex Diagnostics Ltd., Dartford, England) or delta (Wellcozyme, Wellcome Diagnostics, Dartford, UK), autoimmune disease (anti-nuclear antibody titer >1:40, Fluoro HEPANA, Medical & Biological Lab., Nagoya, Japan), and/or inheritable disorders such as hemochromatosis, alpha-1-antitrypsin deficiency or Wilson's disease. All patients with peripheral white cells <4 000 per mm³ and platelet < 100 000 per mm³ were excluded. Serum HBV DNA was measured using a commercially available liquid phase molecular hybridization assay (Digene Hybrid Capture™ System, Beltsville, MD) according to the manufacturer's instruction. The lowest detectable HBV DNA level was 5 pg/ml. Serum samples with non-detectable HBV DNA were retrospectively tested using the real-time polymerase chain reaction (RT-PCR) methods after the end of clinical follow-up. The lowest detectable HBV DNA level was 20 copies/mL.

All patients received 4.5 millionunits (MU) of interferon alpha-2a (Roferon, F. Hoffmann-La Roche Ltd., Basel, Switzerland) thrice weekly and 100 mg of oral lamivudine daily for 24 weeks. Patients were observed and tested for blood chemistry every week for the initial 4 weeks and every 2 weeks thereafter during the treatment until 24 weeks. After the end of treatment, patients were followed up at 4-week intervals for an additional 6 months.

Normalization of serum ALT levels and absence of serum HBV DNA were assessed for the efficacy of treatment. A complete response was defined as the normalization of serum ALT levels together with the absence of serum HBV DNA by the end of treatment. A sustained complete response was defined as the continuation of the remission for at least 6 months after the end of treatment.

Informed consent was obtained from the patients before treatment. The study protocol was reviewed and approved by the Institutional Review Board of the hospital under the guidelines of the 1975 Declaration of Helsinki.

Statistical analysis

Was performed using two-tailed Student's *t*-test and two-tailed Fisher's exact test where appropriate.

RESULTS

The demographic data, biochemical data and serum HBV DNA levels are shown in Table 1. The total bilirubin were 0.9±0.2 mg/dL (data are presented as mean ±S.D. and so forth; range: 0.4-1.8 mg/dL), and prothrombin time (INR) was 1.01±0.08 seconds (range: 0.81-1.22) before treatment. The mean serum ALT levels were 132±71 IU/L (range: 42-290 IU/L), and mean serum HBV DNA were 224±255 pg/mL (range: 6-1924 pg/ml) before treatment.

The major side effects of treatment were: flu-like symptoms: 8 (53 %), fatigue: 12 (80 %), insomnia: 4 (29 %), hair loss: 5 (33 %), and depression: 1 (7 %). None developed anemia (hemoglobin <11 g/dL), leukopenia (leukocyte <3500/μl), thrombocytopenia (thrombocytes <100×10³/μl), hyperbilirubinemia (>2.0 mg/dL), or pancreatitis during therapy.

Fourteen patients finished a 24-week-course of treatment.

One patient (HSF) discontinued interferon after 2 months of therapy due to interferon-related depression. His serum ALT remained abnormal from 210 IU/L before treatment to 38 IU/L at the end of treatment, and serum HBV DNA levels dropped from 90 pg/mL before treatment to 29 pg/mL at the end of therapy. None of the remaining 14 patients experienced depression, aggression, hostility or hallucination.

The serum ALT levels dropped from 132±71 IU/L before treatment to 46±17 IU/L at the end of treatment (Table 2, *P*=0.0002), and the serum HBV DNA levels decreased from 224±255 pg/ml before treatment to 8±12 pg/mL at the end of treatment (*P*=0.058). At the end of treatment, 7 (50 %) of the 14 patients had serum ALT levels within normal limits. Although 12 (86 %) patients had undetectable serum HBV DNA levels (<5 pg/mL) using the liquid phase molecular hybridization assay, only 8 of them had undetectable HBV DNA (<20 copies/mL) using the RT-PCR. Both of these patients had complete response with normal serum ALT levels and undetectable at the end of treatment. The remaining 12 patients had abnormal serum ALT levels and/or detectable HBV DNA.

Six months after the end of treatment, the mean serum ALT (90±58 IU/L, *P*=0.03) and HBV DNA (63±70 pg/ml, *P*=0.05) levels increased compared to those at the end of treatment. Three patients continued to have undetectable serum HBV DNA using the liquid phase molecular hybridization assay method. However, only two (14 %) of them had both complete response and sustained complete response to the combination therapy with serum ALT level <35 IU/L and undetectable serum HBV DNA levels using the RT-PCR method. One patient with undetectable HBV DNA using the liquid phase molecular hybridization assay had abnormal serum ALT levels after the end of treatment; his serum HBV DNA level was 93 copy/dL using the RT-PCR. All of the remaining 11 patients had abnormal serum ALT levels as well as detectable serum HBV DNA.

Table 1 Demographic data, biochemical data and serum HBV DNA levels of patients

Patient No	Age/Gender (y)	ALT (IU/L)	Total Bilirubin (mg/dL)	Prothrombin time (INR)	HBV DNA (pg/mL)
1*	52/M	210	0.9	1.02	90
2	65/M	42	0.9	0.93	24
3	61/M	162	1.4	1.18	1924
4	43/M	38	0.8	0.91	107
5	45/M	212	0.8	1.00	303
6	34/M	49	0.4	1.02	66
7	38/M	47	0.6	1.05	262
8	36/M	119	0.9	0.81	6
9	35/M	56	0.8	0.90	7
10	48/M	154	0.5	1.12	265
11	46/M	223	1.0	1.14	56
12	38/M	290	1.8	1.16	8
13	41/M	44	1.0	0.93	8
14	39/M	195	0.7	1.03	11
15	60/M	147	0.7	1.07	17

*Patient 1 received only 8 weeks of interferon therapy

Both of the two patients with sustained complete response were less than 40 years old (36 and 38 years old) with higher initial serum ALT levels >100 IU/dL (119 and 290 IU/dL), lower initial serum HBV DNA levels <10 pg/ml (6 and 8 pg/mL), and a histology with moderate intralobular degeneration and focal necrosis (range: 1/3-2/3 of lobules). Using the two-tailed Fisher's exact test, age <40 year-old ($P=0.11$), serum ALT level >100 IU/dL ($P=0.37$), serum HBV DNA < 10 pg/ml ($P=0.07$), and moderate to severe intralobular degeneration and focal necrosis ($P=0.07$) were not significant factors in predicting sustained complete response.

Table 2 Serum ALT and HBV DNA levels of patients before, at the end, and at 6 months after treatment

Patients	ALT (iu/L)			HBV DNA			
	start	end	6M	start	end	6M	
					LPMH PCR	LPMH PCR	
1 ^a	210	38	51	90	29	-	-
2	42	97	166	24	18	-	30
3	162	57	84	1924	ND	24.4	13
4	38	34	37	107	ND	78.8	7
5	212	26	66	303	ND	5.1	27
6	49	46	150	66	63	-	98
7	47	35	43	262	ND	94.7	27
8	119	24	20	6	ND	ND	ND
9	56	80	41	7	ND	43.8	ND
10	154	54	254	265	ND	1.3	128
11	223	48	215	56	ND	1.2	445
12	290	30	24	8	ND	ND	ND
13	44	22	71	8	ND	9.7	10
14	195	56	41	11	ND	2.2	39
15	147	22	47	17	ND	12.6	10
Mean	132	46 ^b	90 ^c	224	8 ^d		63 ^e
S.D.	71	17	58	255	12		70

ND: HBV DNA <5 pg/ml using the liquid phase molecular hybridization assay (LPMH); HBV DNA < 20 copies/dL using the real-time polymerase chain reaction (PCR). ^aPatient 1 received only 8 weeks of interferon therapy; ^b $P=0.0002$, ^d $P=0.05$ compared with those before treatment; ^c $P=0.058$, ^e $P=0.05$ compared with those at the end of treatment

DISCUSSION

At the end of treatment, the mean serum ALT level was decreased, and half of the patients had a serum ALT level within normal limits. Although most patients had undetectable HBV DNA levels using the liquid phase molecular hybridization assay, the change of serum HBV DNA levels was not statistically significant, a finding consistent with studies from patients of chronic viral hepatitis B with wild type HBV DNA^[11,20].

Six months after the end of treatment, the mean serum ALT level was significantly increased compared with those at the end of treatment. Only 14 % of patients had sustained response with normal serum ALT levels as well as undetectable HBV

DNA levels. The low sustained response rate to combined interferon alpha-2a and lamivudine was consistent with those of interferon mono-therapy for patients with mutant type chronic hepatitis B^[8,9]. Our pilot data showed that lamivudine did not increase the efficacy of interferon in the treatment of mutant type chronic hepatitis B, a finding consistent with studies stating those having positive HBeAg that IFN and lamivudine did not offer additional benefit compared with lamivudine monotherapy^[20].

Although 12 of the 14 patients (86 %) had an undetectable HBV DNA level at the end of treatment using the liquid phase molecular hybridization assay, half of them had abnormal serum ALT levels. Only 14 % and 21 % of the 12 patients with undetectable HBV DNA levels using the liquid phase molecular hybridization assay had normal serum ALT levels and undetectable serum HBV DNA using the RT-PCR method. RT-PCR is much more sensitive than liquid phase molecular hybridization assay in the detection of samples with low HBV DNA levels.

For the 15 serum samples with undetectable HBV DNA using the liquid phase molecular hybridization assay, only 10 of them had an undetectable HBV DNA level using the RT-PCR. These four samples were from eight and two patients at the end and 6 months after treatment. Both of these patients had sustained normal serum ALT levels and undetectable serum HBV DNA at 6 months after treatment. For the remaining 5 patients, low titer HBV DNA was identified using the RT-PCR, and all patients developed abnormal serum levels after the end of treatment. Our data showed that the liquid phase molecular hybridization assay was not sensitive enough to detect the low HBV DNA levels during combined interferon alpha-2a and lamivudine therapy. RT-PCR method is better than liquid phase molecular hybridization assay in the detection of low titer HBV DNA. The presentation of low levels of HBV DNA may result in subsequent abnormal serum ALT levels and increasing HBV DNA levels in 6 months.

REFERENCES

- 1 **Chen DS**. Hepatitis B virus infection, its sequelae, and prevention in Taiwan. In: Okuda K, Ishak KG, editors. Neoplasms of the liver. Tokyo: Springer-Verlag 1987: 71-80
- 2 **Margolis HS**, Alter MJ, Hadler SC. Hepatitis B: evolving epidemiology and implications for control. *Seminars Liver Disease* 1991; **11**: 84-89
- 3 **Sherlock S**. Viruses and hepatocellular carcinoma. *Gut* 1994; **35**: 828-832
- 4 **Hoofnagle JH**, di Bisceglie AM. The treatment of chronic viral hepatitis. *N Engl J Med* 1997; **336**: 347-356
- 5 **Carreno V**, Bartolome J, and Castillo I. Long-term effect of interferon therapy in chronic hepatitis B. *J Hepatol* 1994; **20**: 431-435
- 6 **Tine F**, Liberati A, Craxi A, Almasio P, Pagliaro L. Interferon treatment in patients with chronic hepatitis B: a meta-analysis of the published literature. *J Hepatol* 1993; **8**: 154-162
- 7 **Carman WF**, Jacyna MR, Hadziyannis S, Karayiannis P, McGarvey MJ, Makris A, Thomas HC. Mutation preventing formation of hepatitis B e antigen in patients with chronic hepatitis B infection. *Lancet* 1989; **2**: 588-591
- 8 **Lindh M**. HBV precore mutants and response to interferon. *Hepatology* 1997; **25**: 1547-1548
- 9 **Fattovich G**, McIntyre G, Thursz M, Colman K, Giuliano G, Alberti A, Thomas HC, Carman WF. Hepatitis B virus precore/core variation and interferon therapy. *Hepatology* 1995; **22**: 1355-1362
- 10 **Dienstag JL**, Perrillo RP, Schiff ER, Bartholomew M, Vicary C, Rubin M. A preliminary trial of lamivudine for chronic hepatitis B infection. *N Engl J Med* 1995; **333**: 1657-1661

- 11 **Schalm SW**, de Man RA, Heijtkink RA, Niesters HG. New nucleoside analogues for chronic hepatitis B. *J Hepatol* 1995; **22**(1 Suppl):52-56
- 12 **Lau DT**, Khokhar MF, Doo E, Ghany MG, Herion D, Park Y, Kleiner DE, Schmid P, Condreay LD, Gauthier J, Kuhns MC, Liang TJ, Hoofnagle JH. Long-term therapy of chronic hepatitis B with lamivudine. *Hepatology* 2000; **32**: 828-834
- 13 **Song BC**, Suh DJ, Lee HC, Chung YH, Lee YS. Hepatitis B e antigen seroconversion after lamivudine therapy is not durable in patients with chronic hepatitis B in Korea. *Hepatology* 2000; **32**: 803-806
- 14 **Hadziyannis SJ**, Papatheodoridis GV, Dimou E, Laras A, Papaioannou C. Efficacy of long-term lamivudine monotherapy in patients with hepatitis B e antigen-negative chronic hepatitis B. *Hepatology* 2000; **32**: 847-851
- 15 **Di Bisceglie AM**. Long-term outcome of interferon-alpha therapy for chronic hepatitis B. *J Hepatol* 1995; **22**(1 Suppl): 65-67
- 16 **Perrillo RP**. Treatment of chronic hepatitis B with interferon: experience in western countries. *Semin Liv Dis* 1989; **9**: 240-248
- 17 **Kakumu S**, Yoshioka K, Wakita T, Ishikawa T, Takayanagi M, Higashi Y. A pilot study of ribavirin and interferon beta for the treatment of chronic hepatitis C. *Gastroenterology* 1993; **105**: 507-512
- 18 **Lai MY**, Kao JH, Yang PM, Wang JT, Chen PJ, Chan KW, Chu JS, Chen DS. Long-term efficiency of ribavirin plus interferon alpha in the treatment of chronic hepatitis C. *Gastroenterology* 1996; **111**: 1307-1312
- 19 **Terrault NA**. Combined interferon and lamivudine therapy: is this the treatment of choice for patients with chronic hepatitis B virus infection? *Hepatology* 2000; **32**: 675-677
- 19 **Di Bisceglie AM**. Long-term outcome of interferon-alpha therapy for chronic hepatitis B. *J Hepatol* 1995; **22**(1 Suppl): 65-67
- 20 **Farrell G**. Hepatitis B e antigen seroconversion: effects of lamivudine alone or in combination with interferon alpha. *J Med Virol* 2000; **61**: 374-379

Edited by Zhang JZ

Mutational characteristics in consecutive passage of rapidly replicating variants of hepatitis A virus strain H2 during cell culture adaptation

Ning-Zhu Hu, Yun-Zhang Hu, Hai-Jing Shi, Guo-Dong Liu, Su Qu

Ning-Zhu Hu, Yun-Zhang Hu, Hai-Jing Shi, Guo-Dong Liu, Su Qu, Department of Vaccine Research, Institute of Medical Biology, Chinese Academy of Medical Sciences, Peking Union of Medical College, Kunming, 650118, Yunnan Province, China

Correspondence to: Yun-Zhang Hu, Department of Vaccine Research, Institute of Medical Biology, Chinese Academy of Medical Sciences, 379 Jiaoling Road, Kunming, 650118, Yunnan Province, China. huyunz@21cn.com

Telephone: +86-871-8335334 **Fax:** +86-871-8334483

Received 2002-05-16 **Accepted** 2002-06-02

Abstract

AIM: To investigate the molecular mechanism of cell adaptation and rapid replication of hepatitis A virus strain H2 in KBM17 cells.

METHODS: Virus of strain H2 at passage 7 was consecutively passaged in KBM17 cells for 22 passages, every passage was incubated for 14 days. Antigenic and infectious titers of every passage and one-step growth dynamics of passage 22 were determined with ELISA. Genomes of passage 6, passage 12, passage 18 and passage 22 were sequenced and compared with H2K7.

RESULTS: During continuous passage of vaccine strain H2 at passage K7 in KBM17 cells, infectious and antigenic titers increased with the increase of passages, infectious titers at day 14 reached $6.77 \text{ LgCCID}_{50} \text{ ml}^{-1}$ for passage 6 (P6), $7.0 \text{ LgCCID}_{50} \text{ ml}^{-1}$ for passage 12 (P12), $7.33 \text{ LgCCID}_{50} \text{ ml}^{-1}$ for passage 18 (P18) and $7.83 \text{ LgCCID}_{50} \text{ ml}^{-1}$ for passage 22 (P22), respectively. The one-step growth dynamics showed that replicating peak of P22 appeared at day 14 with infectious titers of $7.83 \text{ LgCCID}_{50} \text{ ml}^{-1}$ and antigenic titer of 1:1024. After passage 22 a new cell-adapted variant (P22) of H2K7 with rapid and shortened replication cycle from 28 days to 14 days was obtained. Sequencing and comparisons of genomes of P6, P12, P18 and P22 showed that mutational numbers in genomes of different passages increased with adaptive passages, and mutations scattered over the genome. In comparison with that of K7, P6 had only 6 nucleotides (nt) mutations, P12 had 7 mutational changes, in addition to 6 same mutations with P6, there appeared a new mutation in 5' NTR at nucleotide position 591 resulting in a nucleotide exchange from A to G. P18 had 10 nt mutations, among the 10 mutations, 7 mutational changes were same as with P12, three new mutational changes appeared in the genome, one in 5' NTR, one in 3C coding region, one in 3D coding region, at P22 there appeared 18 nucleotide changes in the genome, on the basis of P18, there occurred additional 8 nucleotide mutations, two in 5' NTR, three in 2C, one in 3A, one in 3C and one in 3D. The results suggested that although H2K7 was already an

attenuated strain, the mutations of genome is not sufficient to completely adapt the KBM17, further mutations caused rapid replication adaptation.

CONCLUSION: 18-nt changes scattering over the genome are cooperatively responsible for further adaptation characterized by rapid and shortened replication cycle from 28 days to 14 days in KBM17 cells. The mutations in 2C coding region play more important role in increase of infectious titer than other mutations, the mutations in 2B coding region show less important role than it usually does in cell adaptation, nucleotide changes in 5' NTR seem to be not relevant to cell adaptation during initial stages (before P6), but do in late stages.

Hu NZ, Hu YZ, Shi HJ, Liu GD, Qu S. Mutational characteristics in consecutive passage of rapidly replicating variants of hepatitis A virus strain H2 during cell culture adaptation. *World J Gastroenterol* 2002; 8(5):872-878

INTRODUCTION

Hepatitis A virus (HAV), one of the two members of genus *Hepatovirus*, is enterically transmitted primarily through the fecal/oral route causing sporadic and epidemic acute hepatitis in humans^[1,2]. Human HAV is a nonenveloped icosahedral particle of 27-32 nm in diameter with a single-stranded, 7.5-kb positive-sense RNA genome with a long 5' -terminal nontranslated RNA segment (5' NTR) and a short 3' NTR with a poly(A) tail^[1]. Similar to other picornaviruses, the HAV genome contains one large open reading frame encoding a polyprotein of about 250 kD, which is co- and posttranslationally cleaved into smaller structural proteins (2A, 2B and 2C) and nonstructural proteins (3A, 3B, 3C and 3D) by virus-encoding proteinases^[3].

HAV has been adapted to grow in a variety of primate cell lines^[4], but in contrast to that of other picornaviruses, the replication cycle of wild-type HAV isolated from infected human in cell culture is extremely low and inefficient. After prolonged incubation and several passages in cell culture, a persistent infection with low virus yields and little apparent impact on cellular growth and metabolism is normally established^[5]. Only a few HAV strains have been reported to cause cytopathesis in vitro^[6,7].

Unlike other picornaviruses, although HAV can be adapted to grow in a variety of primate cell lines, cell-adapted variants still grow poorly in cell culture. The molecular mechanisms of adaptation and slow replication cycle are still not completely understood.

That the genomes of a number of wild types and cell-adapted HAV strains have been completely or almost completely sequenced made it possible to determine the

nucleotide changes responsible for cell adaptation. By sequence comparison of different cell-adapted variants^[8-19], and studies with chimeric HAV composed of sequence from wild-type and cell culture-adapted variants^[20-22], mutations increasing virus replication in cell culture were identified. The adaptation of HAV to grow in cell culture is associated with a number of cooperative mutations over the whole genome, but the mutations within 5' NTR containing regulatory internal ribosome entry segment (IRES) for viral translation^[23], and within 2B and 2C coding regions encoding enzymes for viral RNA replication^[24], play more important role in cell adaptation. Moreover, the mutations in 2B and 2C coding regions were proven to be necessary for adaptation of growth in cell culture of HAV variants^[10,11,21], the mutations in 5' NTR had no independent effect, but cooperatively acted with 2B and 2C coding regions to enhance replication in cell culture^[21,24]. To study further the molecular mechanisms of cell adaptation of HAV in cell culture, a cell-adapted variant of live HAV attenuated vaccine strain H2 was used for consecutive passage for 22 passages in human embryonic lung diploid fibroblast KMB17, during passages the replicating peak cycle was shortened from 28 days to 14 days, the genomes of different passages, 6th passage (HAVH2K7P6), 12th passage (HAVH2K7P12), 18th passage (HAVH2K7P18) and 22nd passage (HAVH2K7P22), were sequenced and compared to identify the adaptive mutations.

MATERIALS AND METHODS

Cell

Human embryo lung diploid fibroblast strain (KMB17)^[25] was used at passage 24-35 in this research.

Virus Strain

Hepatitis A virus strain H2, an attenuated strain at passage K7, was derived from the fecal specimen of a patient with hepatitis A in Hangzhou, China. After isolation and passage in a culture of newborn monkey (*Macaca Mulatta*) kidney cells, adaptation to grow in human embryo lung diploid fibroblast (KMB17), and serial passage at a low temperature (32 °C) in KMB17 cells, the strain became attenuated^[25] and licensed for production of live attenuated HAV vaccine.

H2 strain passage and rapidly replicating adaptation in KMB17 cells

KMB17 cells were grown in 25 cm² flask (Nunc, Weisbaden, germany) using Eagle' Minimal Essential Medium supplemented with penicillin (100 U/ml), streptomycin (100 µg/ml), and 10 % heat-inactivated newborn calf serum, and passaged every four days. HAV H2M20K7 with 28-day replication cycle were seeded onto KMB17 confluent monolayer cells, after 37 °C absorption for 2 hours, maintenance medium with 2 % newborn calf serum were added, and seeded cells were cultured at 35 °C for 14 days. The virus was harvested at the 14th day, and then seeded onto the monolayer cells again, the virus was serially passaged for 22 passages with 14-day cycle. The antigen titers and infectious titers were detected with ELISA^[26, 27]. The virus at 6th, 12th, 18th, 22nd passage were designated as HAVH2K7P6(P6), HAVH2K7P12(P12), HAVH2K7P18(P18) and HAVH2K7P22(P22), respectively. The respective genomes were cloned and sequenced.

One-step growth dynamics

KMB17 cells were infected with a multiplicity of infection (MOI) of 5. The titer was assayed by inoculating the cells grown

in 25 cm² flask (Nunc, Weisbaden, germany), and infection was checked 4 weeks after inoculation by ELISA^[26, 27].

Primers and sequencing strategy

Primers were designed according to the sequence of H2K7^[29] with Goldkey software (Table 1). The sequencing strategy was showed as Figure 1.

Table 1 The primers used for amplification of HAV genomic RNA

Cloned fragments	Primers	Sequences
A (0.8kb)	A1	5'-CGCCGGCGTTCAAGAGGGGTGCCGGAG-3'
	A2	5'-GAATCTCAATGCCAAATCTTGC-3'
B (0.5kb)	B1	5'-TCTGAGGTACTCAGGGGC-3'
	B2	5'-CAGTCAATGATGCTATAGAACC-3'
C (1.1kb)	C1	5'-CCAACAGGGGGGATTGATC-3'
	C2	5'-CGTTAGAAGGAGAGGTCAATC-3'
D (1.0kb)	D1	5'-CCCTGGATTCTGACACTCC-3'
	D2	5'-CAGTGGATAACATGGCATTTG-3'
E (1.1kb)	E1	5'-GTCTGTACAGAACAATCAGAG-3'
	E2	5'-GATCCCAGAACAGATATCTCTTAA-3'
F (1.2kb)	F1	5'-GTTAAGAGATATCTGTCTGGATC-3'
	F2	5'-CCATCTCCAACGAGCACTCC-3'
G (1.2kb)	G1	5'-CAGTTCTTTAGTCATGACAGTTG-3'
	G2	5'-GCCATTGGATCAATTCAGC-3'
H (1.1kb)	H1	5'-GAGTCCCATTATCATCACACA-3'
	H2	5'-GTCCAATCAGATCAAGATTATC-3'
I (0.5kb)	I1	5'-GATTCTCTGTTATGGAGATG-3'
	I2	5'-TTTTTTTTTTTTTTTTTTTTTATT-3'

(1): A-I represent 9 amplified fragments of HAV; (2) 1 and 2 represent positively and negatively oriented primers

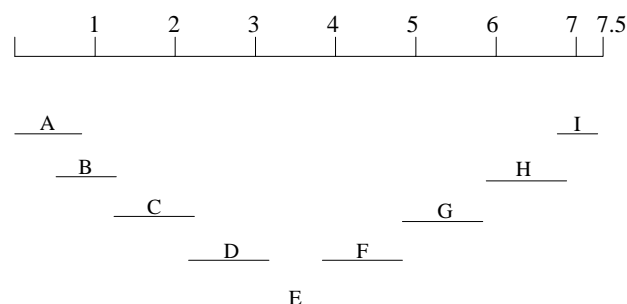


Figure 1 Sequencing strategy of HAV genome. A-I represent 9 amplified fragments of HAV

Antigen-capture PCR amplification of the genomes

cDNA synthesis and cloning Antigen-capture PCR were used to prepare cDNA of genome of different passages^[29] with some modifications. Sterile 0.5-ml conical tube (Eppendorf) was coated 100 µl of human anti-HAV IgG diluted 1:1 000 in 50 mM sodium carbonate buffer (pH 9.6). After 4 h of incubation at 37 °C, the unbound IgG was removed, and 150 µl of 1 % bovine serum albumin (Sigma) diluted in the buffer was added. After 1 h at 37 °C, the tube was washed three times with 300 µl of PBS (pH 7.4) containing 0.05 % Tween 80. purified HAV (100 µl) was then added, and the preparation was incubated overnight at 4 °C. The tube was washed six times with 500 µl of a 40 mM Tris (pH 8.4)-40 mM KCl-7 mM MgCl₂ solution. Then 100 µl of water was added and tube was heated to 95 °C for 5 min to disrupt captured viruses and melt any second structures within the viral RNA. The first strand cDNA was synthesized using SuperScript™ Preamplification System kit (Gibco, Life Technologies), following the instruction by

manufacturer. The clones of different fragments were performed by PCR in a mixture (50 μ l) including 5 μ l 10 \times LA PCR buffer, 8 μ l 2.5mM dNTPs, 2 μ l template of RT-PCR products, 300nM positive-sense primer, 300nM negative-sense primer and 2.5U LA Taq DNA polymerase (TaKaRa), adding water to 50 μ l. The reaction mixture was subjected to 95 $^{\circ}$ C for 5 min, then 30 automated cycles of denaturation at 95 $^{\circ}$ C for 30 sec, annealing at 50 $^{\circ}$ C for 30 sec, and extension at 72 $^{\circ}$ C for 1 min or 1 min 30 sec., The final reaction was incubated at 72 $^{\circ}$ C for 10 min. After the PCR products were recovered and purified, the fragments were ligated into pGEM-T Vector (Promega). The resulting products were transformed into competent *E.coli* DH5 α cells. Three ampicillin-resistant clones were picked out for each fragment. The size of inserts in positive clones was estimated with restriction enzyme site at either side of the inserted fragment. Rapid plasmid preparations were made with the Wizard plasmid purification kit (Promega).

DNA sequencing and analysis

Sequencing strategy was shown in Figure 1. Oligonucleotide primers specific for HAV and primers corresponding to the T7/SP6 promoter region of pGEM \oplus -T Vector were used to sequence the Inserted and identified HAV fragment. a Taq DyeDeoxy Terminator Cycle sequencing kit and a 377 DNA sequencer (Perkin Elmer) were used to determine nucleotide sequences. To eliminate the possibility of errors in the sequence due to Taq polymerase for PCR, at least three clones of each amplified fragment derived from two individual PCR products were sequenced. Also to correctly determine the sequence of extreme 5 terminus of HAV genome, a 5' RACE reaction was used to obtain the a cDNA fragment from 5' NTR of genome with 5' -Full RACE Core Set (TaKaRa). Analysis, alignment and translation in the amino acids of the obtained nucleotide sequences were done using the sequence analysis program OMEGA (Oxford Molecular).

RESULTS

Dynamical characteristics of adaptive enhancement of H2K7 replication in KMB17 cells

Although HAV has been adapted to grow in cell culture, even cell culture adapted variants grow considerably slowly with low virus yields and characterized by an asynchronous onset of replication^[30,31]. HAV usually established persistent infection in cell culture with protracted replication cycle, but replication cycle of maximal accumulation of HAV in cell culture was dually shortened with the increase of passages, even cytopathic effect (CPE) appeared^[32-35]. Attenuated HAV strain H2K7 did not cause CPE in KMB17 cells, its replicating peak of was days, the infectious titer reached. 0LgCCID₅₀ml⁻¹. In this study, attenuated strain H2 at passage K7 were passaged in KMB17 cells every fourteen days. At last the change of incubation cycle, from 28 days to 14 days, resulted in the increase of both antigenic and infectious titers. At first passage of adaptation (P1) the antigenic and infectious titers were only 1:16 ELISA units (ELI.U) and 5.83LgCCID₅₀ml⁻¹, respectively, at P6 the antigenic and infectious titers gradually increased to 1:64 ELI.U and 6.77LgCCID₅₀ml⁻¹, respectively, at P12 obvious enhancement of antigenic and infectious titers (1:256 ELI.U and 7.0 LgCCID₅₀ml⁻¹, respectively) occurred. More enhancement appeared at P18 with 1:512 ELI.U and 7.33 LgCCID₅₀ml⁻¹, respectively, at P22 antigenic and infectious titers reached the highest levels of 1:1024 ELI.U and 7.83 LgCCID₅₀ml⁻¹, respectively (Table 2). During the whole passages no CPE appeared. Furthermore, one-step growth dynamics

showed that at P22 at days 2, 4, 6, 8, 10, 12 14 of culture antigenic and infectious titers gradually increased, at day 14 antigenic and infectious titers reached the highest levels of 1:1024 ELI.U and 7.8 LgCCID₅₀ml⁻¹, respectively, afterwards, the infectious titer gradually decreased, but antigenic titer remained unchanged until day 26 (Table 3). The increases of antigenic and infectious titers with consecutive passage showed that strain H2K7 had been further adapted successfully in KMB17 cells with shortened replication cycle of 28 days to 14days.

Table 2 Titers of different passages of HAVH2K7 on KMB17 for 14d

Passages	Antigen titers	Infectious titers(LgCCID ₅₀ /ml)
1	1:16	5.83
2	1:8	5.5
3	1:16	5.67
4	1:32	6.0
5	1:32	6.5
6	1:64	6.77
7	1:64	6.67
8	1:64	6.5
9	1:64	6.67
10	1:128	6.83
11	1:128	7.0
12	1:256	7.0
13	1:256	7.17
14	1:256	7.0
15	1:256	7.17
16	1:256	7.0
17	1:512	7.17
18	1:512	7.33
19	1:512	7.5
20	1:512	7.67
21	1:1024	7.67
22	1:1024	7.83

Table 3 One-step growth dynamics of HAVH2K7P22 on KMB17 cells

Post inoculation days	Antigen titers	Infectious titers(LgCCID ₅₀ /ml)
2	1:8	ND*
4	1:16	6.0
6	1:32	6.67
8	1:128	7.17
10	1:512	7.5
12	1:1024	7.8
14	1:1024	7.17
16	1:1024	7.0
18	1:1024	7.0
20	1:1024	6.83
22	1:1024	7.0
24	1:1024	6.8
26	1:2048	6.5

*Not determined

Mutational Characteristics in Consecutive Passage of Rapid Replication of Strain H2 during Cell Culture Adaptation

The process of adaptation of HAV in cell culture was also a process of serials of mutations in genome and results in attenuation^[11]. The rapidly adaptive passages of H2K7 in KMB17 cells caused the change of replication cycle, from 28 days to 14 days. The maximal virus yields appeared at 14 days at P22 (Table 3). In order to investigate whether the shortened replication cycle of H2K7P1-22 in cell adaptation was reflected by mutational changes in the genome, which was thought to be responsible for adaptation of HAV, and whether related mutations were responsible for the adjustment of shortened replication cycle, we sequenced and compared the entire genome of four passages (P6, P12, P18, P22), the mutations correlating with adaptation at different passages were identified. The results revealed that mutational numbers in genomes of different passages increased with adaptive passages, and mutations scattered throughout the whole genome. There were only 6 nucleotides mutations appeared in the genome of P6, and nucleotide identity was up to 99.93 % in comparison with that of H2K7, as shown in (Table 4),

Table 4 Differences in the genome sequence and amino acids of the HAV H2 K7 with HAV H2K7 P6, HAV H2K7 P12, HAV H2K7 P18 and HAV H2 K7 P22

Nucleotide position	Location	Nucleotide					Amino acids				
		K7	K7P6	K7P12	K7P18	K7P22	K7	K7P6	K7P12	K7P18	K7P22
33	5' NTR	C	C	C	U	U					
263	5' NTR	U	U	U	U	C					
378	5' NTR	U	U	U	U	C					
591	5' NTR	A	A	G	G	G					
646	5' NTR	A	A	A	U	U					
858	VP2	G	U	U	U	U	A	S	S	S	S
1178	VP2	C	U	U	U	U	I	I	I	I	I
4022	2B	T	C	C	C	C	I	I	I	I	I
4558	2C	A	A	A	A	C	Q	Q	Q	Q	P
4802	2C	U	U	U	U	C	A	A	A	A	A
4949	2C	A	A	A	A	U	T	T	T	T	T
4968	2C	A	C	C	C	C	N	H	H	H	H
5193	3A	C	U	U	U	U	R	C	C	C	C
5217	3A	G	G	G	G	U	A	A	A	A	S
5336	3C	G	G	G	G	A	L	L	L	L	L
5715	3C	A	A	A	G	G	T	T	T	A	A
6427	3D	U	U	U	G	G	V	V	G	G	G
7256	3D	A	U	U	U	U	A	A	A	A	A

two mutations occurred in VP2 coding region (at nucleotide position 858 with exchange from G to U, resulting in amino acid exchange from A to S, at nucleotide position 1178 with silent exchange from C to U, resulting in no amino acid exchange), one mutation in 2B coding region (at nucleotide position 4022 with exchange from U to C, resulting in amino acid exchange from C to I), one mutation in 2C coding region (at nucleotide position 4968 with exchange from A to C, resulting in amino acid exchange from N to H), one in 3A coding region (at nucleotide position 5193 with exchange from C to T, resulting in amino acid exchange from R to C), one in 3D coding region (at nucleotide position 7256 with silent exchange from A to U). When H2K7 was passaged up to P12, 7 mutations appeared, in addition to 6 same mutations with

P6, there was a new mutation appeared in 5' NTR at nucleotide position 591 resulting in a nucleotide exchange from A to G. P18 had 10 nucleotide mutations occurred in the entire genome, among 10 mutations 7 mutational changes were the same with P12, three new mutational changes appeared in genome, one in 5' NTR (one at nucleotide position 33 with nucleotide exchange from C to U), one in 3C coding region (at nucleotide position 5715 with exchange from A to G, resulting in amino acid exchange from U to A), one in 3D coding region (at nucleotide position 6427 with exchange from U to G, resulting in amino acid exchange from V to G). At P22 there were 18 nucleotide changes appeared in the genome, on the basis of P18 additional 8 nucleotide mutations appeared, two in 5' NTR (at nucleotide position 263 with exchange from U to C, and 378 with exchange from U to C), three in 2C coding region (at nucleotide position 4558 with exchange from A to C, resulting in amino acid exchange from Q to R, at nucleotide position 4802 with silent exchange from U to C, resulting in no amino acid exchange, at nucleotide position 4949 with silent exchange from A to U), one in 3A coding region (at nucleotide position 5217 with exchange from G to U, resulting in amino acid exchange from A to S), one in 3C coding region (at nucleotide position 5336 with silent exchange from G to A), one in 3D coding region (at nucleotide position 7256 with silent exchange from A to U).

Identity comparisons of genomes of different passages

Complete nucleotide sequence analysis of four-passages adaptive variants revealed an identity between H2K7 and P6 of 99.93 %, between H2K7 and P12 of 99.9 %, between H2K7 and P18 of 99.87 %, and between H2K7 and P22 of 99.76 %. The identity comparisons showed that mutations increased gradually with the increase of passages, but at high passage obvious mutations were concentrated in 5' NTR region, for example, P22 had 18 nucleotide mutations, 5 of 18 mutations appeared in 5' NTR region, the other mutations scattered throughout the coding region, during adaptive process no mutations appeared in VP4 coding region, VP3 coding region, VP1 coding region, 2A coding region, 3' NTR, the identities were 100 % (Table 5).

Table 5 Identity comparisons of nucleotide sequence of HAVH2K7 with HAVH2K7P6 and HAVH2K7P22

Genomic region	HAVH2K7P6 (%)	HAVH2K7P12 (%)	HAVH2K7P18 (%)	HAVH2K7P22 (%)
GENOME	99.93	99.9	99.87	99.76
5' UTR	100	99.86	99.59	99.32
VP4 ENCODING	100	100	100	100
VP2 ENCODING	99.71	99.71	99.71	99.71
VP3 ENCODING	100	100	100	100
VP1 ENCODING	100	100	100	100
2A ENCODING	100	100	100	100
2B ENCODING	99.74	99.74	99.74	99.74
2C ENCODING	99.9	99.9	99.9	99.6
3A ENCODING	99.42	99.42	98.42	98.84
3B ENCODING	100	100	100	98.53
3C ENCODING	100	100	99.85	99.85
3D ENCODING	99.94	99.86	99.86	99.86
3' UTR	100	100	100	100

DISCUSSION

Although the wild-type HAV grew poorly in cell culture, it usually did not cause CPE, and tended to establish persistent infection, after consecutive passages cell-adaptive variants were characterized with higher replication yield, rapid replication cycle and attenuation^[19], and nucleotide mutations increased with adaptive passages^[17]. On this basis, the development of a live attenuated hepatitis A vaccine (H2 strain) showed good immunogenicity and protective efficacy^[36], a variant of vaccine strain H2 was isolated in the consecutive passages in KMB17 cells without CPE and characterized with rapid replication cycle of 14 days, higher infectious titer of 7.8 LgCCID₅₀ml⁻¹.

From the viewpoint of evolution, cell adaptation of HAV depends on the interaction of HAV and cell, the internal cell environments form a selective pressure on the virus, in order to survive the viral genome gradually mutates to form new phenotype to adapt cell environments, so the accumulations of mutation with increasing passages result in more adaptive phenotype, more rapid replication cycle and higher virus yield. In accordance with this, in a continued passage process of vaccine strain H2 at passage K7 in KMB17 cells, with the increase of infectious titers the mutational numbers of genomes of different passages increased, P6 had 6 mutations with infectious titer of 6.77 LgCCID₅₀ml⁻¹, P12 had 7 mutations with infectious titer of 7.0 LgCCID₅₀ml⁻¹, P18 had 10 mutations with infectious titer of 7.33 LgCCID₅₀ml⁻¹, P22 had 18 mutations with infectious titer of 7.8 LgCCID₅₀ml⁻¹. One-step growth dynamics of P22 also showed that 18 mutations of P22 resulted in shortening the replication cycle from 28 days to 14 days. The results suggested that although H2K7 was already an attenuated strain, the mutations of genome was not sufficient to completely adapt the KMB17, only further mutations increased its adaptive ability in cell KMB17. The sequencing and analysis of genomes of different passages of several cell culture-adapted variants of the HM175 strain of HAV also showed that with the increase of infectious titers the mutational numbers of genomes of different passages increased^[9, 19, 24].

In contrast to the other viruses of picornaviruses, mutations of cell adaptation of HAV scattered throughout the whole genome and cooperatively acted to enhance the growth of virus in cells. sequencing of cell culture-adapted variants of the HM175 strain of HAV showed that P16 had 19 mutations^[24], P35 had 25 mutations^[19] and P59 had 42 mutations^[9], P6 of cell culture-adapted variants of the H2 strain in KMB17 had 6 mutations, P12 had 7 mutations, P18 had 10, P22 had 18, although different strains in different cells had different mutations, these variants shared common mutations in 5' NTR and in 2B, 2C, 3A, 3B, 3C, 3D coding region of the genomes. Experiments with chimeric infectious cDNA clones indicated that the mutations in both 5' NTR and in 2B, 2C, 3A, 3B, 3C, 3D coding region contributed to the ability of the virus to grow in cells of African green monkey kidney lineage^[11, 12]. These results revealed that mutations in 5' NTR and in 2B, 2C, 3A, 3B, 3C, 3D coding region of the genomes played more important role than others in cell adaptation.

The 5' NTR of HAV forms a highly ordered secondary and presumably tertiary structure, and contains elements necessary for both viral translation and RNA replication^[37], HAV translation is initiated in a cap-independent fashion by a mechanism that involves the binding of the 40s ribosomal subunit at a site located hundreds of bases downstream of the 5' end of the RNA which has been termed a ribosomal landing pad or an internal ribosome entry segment (IRES)^[23, 37, 38]. Mutations analysis of 5' NTR showed that the IRES of 450

nucleotides was located downstream of nucleotide (nt)161 and extended to within 40 nt of the first initiator AUG^[38-40]. The efficient translation activity by IRES necessitates the interaction of secondary and presumably tertiary RNA structure with a set of specific eukaryotic translation initiation factors and also noncanonical host factors^[39-41]. Therefore, it is likely that these 5' NTR mutations enhance translation by altering the affinity of the RNA for cellular proteins that either positively or negatively influence the activity of the IRES.

In our study in the continuous cell adaptation of H2K7, the sequencing showed that increased infectious titers with the increased passages of H2K7 in KMB17 cells correlated well with the increased mutations in 5' NTR. P6 had no mutations in 5' NTR with infectious titer of 6.77 LgCCID₅₀ml⁻¹, P12 had 1 mutation in 5' NTR (nt 591) with infectious titer of 7.0 LgCCID₅₀ml⁻¹, P18 had 3 mutations in 5' NTR (nt 33, 591, 646) with infectious titer of 7.33 LgCCID₅₀ml⁻¹, P22 had 5 mutations in 5' NTR (nt 33, 263, 378, 591, 646) with infectious titer of 7.8 LgCCID₅₀ml⁻¹, in addition to 1 mutation (nt 33 of P18 and P22), all mutations appeared in IRES. According to the viewpoint mentioned above, one mutation (nt 591) in IRES of P12 may change the secondary and presumably tertiary structure of 5' NTR of K7, this changed IRES structure enhance the affinity of K7 RNA with cellular proteins, resulting in the enhancement of translation, among 3 mutations in 5' NTR of P18, 2 mutations in IRES further enhance the affinity of K7 RNA with cellular proteins, resulting in further enhancement of translation, among all mutations in 5' NTR of different passages, 4 mutations in IRES of P22 produce the most efficient affinity of RNA with cellular proteins, yielding the maximal progeny virus. A comparison with the model of 5' NTR of RNA secondary structure of the HAV genome, proposed by Ali *et al*^[39], suggest that the G to U mutation (nt 646) of 5' NTR of P22, located in the terminal part of the 5' NTR (loop V), could lead to an RNA duplex folding stabilized by an additional basepairing, resulting in further increase of infectious titer. Consistent with our result, Graff *et al* also showed that increased mutations in IRES of different-passage GBM/Hp8/24 played a role in enhancement of infectious titer and a common G to U mutation (nt 646) of 5' NTR of strain GBM appeared in GBM/Hp8/6, but mutations of different positions of 5' NTR of different HAV strains in different cells may reflect the different interactions of 5' NTR with different cellular proteins. It is worth noting that P6 had no mutation in 5' NTR, but the infectious titer only reached 6.77 LgCCID₅₀ml⁻¹, 0.9 LgCCID₅₀ml⁻¹ more than that at P1, indicating less important role of 5' NTR in early cell adaptation. Consistent with our result, Frings *et al*^[42] found that after 5-passage adaptation of primate cell-adapted hepatitis A virus strain HM175 to its growth in guinea pig cells, the infectious titer reached 6.3 LgCCID₅₀ml⁻¹, but no mutation in 5' NTR. Taken together with our result, it suggest that during early adaptation there were different ways to improve HAV fit with a specific complement of host cell factors and that growth restrictions in defined host cells had not been determined solely by regulatory interactions of cellular factors with 5' NTR sequence, which concerned mainly cap-independent translation initiation.

Previous studies showed that 2B and 2C coding region mutations are essential for cell adaptation of HAV, mutations in other regions have no independent effect, but act cooperatively with mutations in 2B and 2C coding region to enhance replication^[43]. 2B and 2C coding region are found to have 251 and 335 amino acids, respectively. Protein 2B is involved in the rearrangement of cellular membrane^[3]. Protein 2C is considered to have helicase and NTPase activities^[3]. The

functions of 2B and 2C suggest that the mutations in these two regions play important roles in cell adaptation of HAV. During continuous passages from P6-P22 of H2K7, 4 mutations appeared in 2C coding region, two were silent mutations, two resulted in two- amino acid substitutions, one was common in P6, P12, P18 and P22, one mutation at nt 4558 from A to C only appeared in P22, causing amino acid substitution from Q to P, this substitution may enhance the function of 2C, and further increase the infectious titer at P22. In contrast to the previous results^[15], in sequence of entire genome of 4 passages (P6,P12,P18,P22), only one mutation appeared in 2B coding region at nt 4022 from U to C, but not resulting in amino acid mutation, this might suggest that 2B protein play less important role than 2C in KMB17 cell adaptation of H2K7.

Mutations in 3A coding region of the isolate in Italy correlated with CPE^[35], but our result showed that although mutations in 3A coding region appeared, even a unique amino acid mutation from A to S occurred at P22, no CPE appeared at all passages of H2K7 in KMB17 cell culture. The mechanism remains unknown. The other mutations in 3A, 3C, 3D coding region of P22 may cooperatively act to further enhance the virus replication.

Comparisons of entire genome of P22 with those of continuous passages of GBM and HM175 in different cells showed that although the mutations existed in the same 5' NTR, 2B, 2C, 3A, 3B, 3C, 3D coding regions, most of the mutational sites were different, these differences revealed different interaction of HAV with different cellular proteins under different selective pressures.

From our investigations of sequence analysis of consecutive H2K7 passages and a comparison of their growth characteristics, we can conclude that 18-nt changes scattering over the genome are cooperatively responsible for further adaptation characterized by rapid and shortened replication cycle from 28 days to 14 days in KMB17 cells, the mutations in 2C coding region play more important roles in increase of infectious titer than other mutations, the mutations in 2B coding region show less important role than it usually does in cell adaptation, nucleotide changes in 5' NTR seem not to be relevant during initial stages (before P6) of cell adaptation because of the significant enhancement in infectious titer not correlating with the mutations in this region, but in late passage (P22) mutations in 5' NTR which seem to affect obviously the replication cycle of H2K7 in cell adaptation.

REFERENCES

- 1 **Yokosuka O.** Molecular biology of hepatitis A virus: significance of various substitutions in the hepatitis A virus genome. *J Gastroenterol Hepatol* 2000; Suppl: D91-97
- 2 **O'Connor JA.** Acute and chronic viral hepatitis. *Adolesc Med* 2000; **11**:279-292
- 3 **Totsuka A,** Moritsugu Y. Hepatitis A virus proeins. *Interviol* 1999; **42**: 63-68
- 4 **Frings W,** Dotzauer A. Adaptation of primate cell-adapted hepatitis A virus strain HM175 to growth in guinea pig cells is independent of mutations in the 5' nontranslated region. *J Gen Virol* 2001; **82**: 597-602
- 5 **Inoue K,** Yoshiba M, Yotsuyanagi H, Otsuka T, Sekiyama K, Fujita R. Chronic hepatitis A with persistent viral replication. *J Med Virol* 1996; **50**: 322-324
- 6 **Anderson DA.** Cytopathology, plaque assay and heat inactivation of hepatitis A virus strain HM175. *J Med Virol* 1987; **22**: 35-44
- 7 **Cromeans T,** Fields HA, Sobsey MD. Replication kinetics and cytopathic effects of hepatitis A virus. *J Gen Virol* 1989; **70**: 2051-2062
- 8 **Paul AV,** Tada H, von der Helm K, Wissel T, Kiehn R, Wimmer E, Deinhardt F. The entire nucleotide sequence of the genome of hepatitis A virus(isolate MBB). *Virus Res* 1987; **8**: 153-171
- 9 **Ross BC,** Anderson BN, Edwards PC, Gust ID. Nucleotide sequence of high-passaged hepatitis A virus strain HM175: comparison with wild-type and cell culture-adapted strains. *J Gen Virol* 1989; **70**: 2805-2810
- 10 **Emerson SU,** McRill C, Rosenblum B, Feinstone SM, Purcell RH. Mutations responsible for adaptation of hepatitis A virus to efficient growth in cell culture. *J Virol* 1991; **65**: 4882-4886
- 11 **Emerson SU,** Huang YK, McRill C, Lewis M, Purcell RH. Mutations in both the 2B and 2C genes of hepatitis A virus are involved in adaptation to grow in cell culture. *J Virol* 1992; **66**: 650-654
- 12 **Day SP,** Murphy P, Brown EA, Lemon SM. Mutations within the 5, nontranslated region of hepatitis A virus RNA which enhance replication in BS-C-1 cells. *J Virol* 1992; **66**: 6533-6540
- 13 **Chang KH,** Brown EA, Lemon SM. Cell type-specific proteins which interact with the 5, nontranslated region of hepatitis A virus RNA. *J Virol* 1993; **67**: 6716-6725
- 14 **Tedeschi V,** Purcell RH, Emerson SU. Partial characterization of hepatitis A viruses from three intermediate passage levels of a series resulting in adaptation to growth in cell culture and attenuation of virulence. *J Med Virol* 1993; **39**: 16-22
- 15 **Morace G,** Pisani G, Beneduce F, Divizia M, Pana A. Mutations in the 3A genomic region of two cytopathic strains of hepatitis A virus isolated in Italy. *Virus Res* 1993; **28**: 187-194
- 16 **Graff J,** Normann A, Flehmig B. Nucleotide sequence of wild-type hepatitis A virus strain GBM in comparison to two cell culture-adapted variants. *J Virol* 1994; **68**: 548-554
- 17 **Graff J,** Kasang C, Normann A, Pfisterer-Hunt M, Feinstone SM, Flehmig B. Mutational events in consecutive passages of hepatitis A virus strains GBM during cell culture adaptation. *Virol* 1994; **204**: 60-68
- 18 **Cohen JI,** Ticehurst JR, Purcell RH, Buckler-White A, Baroudy BM. Complete nucleotide sequence of hepatitis A virus : comparison of different strains of hepatitis A virus and other picornaviruses. *J Virol* 1987; **61**: 50-59
- 19 **Cohen JI,** Rosenblum B, Ticehurst JR, Daemer RJ, Feinstone SM, Purcell RH. Complete nucleotide sequence of an attenuated hepatitis A virus: comparison with wild-type virus. *Proc Natl Acad Sci USA* 1987; **84**:2497-2501
- 20 **Unkhouser AW,** Purcell RH, Hondt ED, Emerson SU. Attenuated hepatitis A virus : genetic determinants of adaptation to growth in MRC-5 cells. *J Virol* 1994; **68**: 148-157
- 21 **Zhang H,** Chao SF, Ping LH, Grace K, Clarke B, Lemon SM. An infectious cDNA clone of a cytopathic hepatitis A virus: genomic regions associated with rapid replication and cytopathic effect. *Virol* 1995; **212**: 686-697
- 22 **Graff J,** Normann A, Flehmig B. Influence of the 5' nontranslated region of hepatitis A virus strain GBM on its growth in different cell lines. *J Gen Virol* 1997; **78**: 1841-1849
- 23 **Borman AM,** Michel YM, Kean KM. Detailed analysis of the requirements of hepatitis A virus internal ribosome entry segment for the eukaryotic initiation factor complex eIF4F. *J Virol* 2001; **75**: 7864-7871
- 24 **Jansen RW,** Newbold JE, Lemon SM. Complete nucleotide sequence of a cell culture-adapted variant of hepatitis A virus: comparison with wild-type virus restricted capacity for *in vitro* replication. *Virol* 1988; **163**: 299-307
- 25 **Mao JS,** Dong DX, Zhang HY, Chen NL, Zhang XY, Huang HY, Xie RY, Zhou TJ, Wan ZJ, Hu ZH, Cao YY, Li HM, Chu CM. Primary study of attenuated live hepatitis A vaccine (H2 strain) in humans. *J Infect Dis* 1989; **159**: 621-624

- 26 **Chen T**, Zhong G, Yang X, Cao YY. The hepatitis A virus isolated and adapted in human diploid fibroblast cells (KMB17). *Zhongguo Yixue Kexueyuan Yuanbao* 1996; **18**: 29-32
- 27 **Cederna JB**, Klinzman D, Stapleton JT. Hepatitis A virus-specific humoral and cellular immune responses following immunization with a formalin-inactivated hepatitis A vaccine. *Vaccine* 1999; **18**: 892-898
- 28 **Kingsley DH**, Richards GP. Rapid and efficient extraction method for reverse transcription-PCR detection of hepatitis A and Norwalk-like viruses in shellfish. *Appl Environ Microbiol* 2001; **67**: 4152-4157
- 29 **Kusov YY**, Shatirishvili G, Dzagurov G, Gauss-Muller V. A new G-tailing method for the determination of the poly (A) tail length applied to hepatitis A virus RNA. *Nucleic Acids Res* 2001; **29**: E57-57
- 30 **Harmon SA**, Summers DF, Ehrenfeld E. Detection of hepatitis A virus RNA and capsid antigen in individual cells. *Virus Res* 1989; **12**: 361-369
- 31 **Cho MW**, Ehrenfeld E. Rapid completion of the replication cycle of hepatitis A virus subsequent to reversal of guanidine inhibition. *Virology* 1991; **180**: 770-780
- 32 **Cromeans T**, Sobsey MD, Fields HA. Development of a plaque assay for a cytopathic, rapidly replicating isolate of hepatitis A virus. *J Med Virol* 1987; **22**: 45-56
- 33 **Lemon SM**, Murphy PC, Shields PA, Ping LH, Feinstone SM, Cromeans T, Jansen RW. Antigenic and genetic variation in cytopathic hepatitis A virus variants arising during persistent infection: evidence of genetic recombination. *J Virol* 1991; **65**: 2056-2065
- 34 **Nasser AM**, Metcalf TG. Production of cytopathology in Frhk-4 cells by BS-C-1-passaged hepatitis A virus. *Appl Environ Microbiol* 1987; **53**: 2967-2971
- 35 **Venuti A**, Russo CD, Grosso Del M, Patti AM, Ruggeri F, Stasio De PR, Martiniello MG, Pagnotti P, Degener AM, Midulla M, Pana A, Perez-Bercoff R. Isolation and molecular cloning of a fast-growing strain of human hepatitis A virus from its double-stranded replicative form. *J Virol* 1985; **56**: 579-588
- 36 **Zhao YL**, Meng ZD, Xu ZY, Guo JJ, Chai SA, Duo CG, Wang XY, Yao JF, Liu HB, Qi SX, Zhu HB. H2 strain attenuated live hepatitis A vaccines: protective efficacy in a hepatitis A outbreak. *World J Gastroenterol* 2000; **6**: 829-832
- 37 **Funkhouser AW**, Schultz DE, Lemon SM, Purcell RH, Emerson SU. Hepatitis A virus translation is rate-limiting for virus replication in MRC-5 cells. *Virology* 1999; **254**: 268-278
- 38 **Brown EA**, Zajac AJ, Lemon SM. In vitro characterization of an internal ribosome entry site (IRES) present within the 5' nontranslated region of hepatitis A virus RNA: comparison with the IRES of encephalomyocarditis virus. *J Virol* 1994; **68**: 1066-1074
- 39 **Ali IK**, McKendrick L, Morley SJ, Jackson RJ. Activity of the hepatitis A virus IRES requires association between the cap-binding translation initiation factor (eIF4E) and eIF4G. *J Virol* 2001; **75**: 7854-7863
- 40 **Gosert R**, Egger D, Bienz K. A cytopathic and a cell culture adapted hepatitis A virus strain differ in cell killing but not in intracellular membrane rearrangements. *Virology* 2000; **266**: 157-169
- 41 **Yi M**, Lemon SM. Replication of subgenomic hepatitis A virus RNAs expressing firefly luciferase is enhanced by mutations associated with adaptation of virus to growth in cultured cells. *J Virol* 2002; **76**: 1171-1180
- 42 **Frings W**, Dotzauer A. Adaptation of primate cell-adapted hepatitis A virus strain HM175 to growth in guinea pig cells is independent of mutations in the 5' nontranslated region. *J Gen Virol* 2001; **82**: 597-602
- 43 **Emerson SU**, Huang YK, Purcell RH. 2B and 2C mutations are essential but mutations throughout the genome of HAV contribute to adaptation to cell culture. *Virology* 1993; **194**: 475-480

Edited by Wu XN

• *H.pylori* •

Azithromycin in a triple therapy for *H.pylori* eradication in active duodenal ulcer

Vladimir T. Ivashkin, Tatiana L. Lapina, Oksana Yu. Bondarenko, Olga A. Sklanskaya, Petr Ya. Grigoriev, Yuri V. Vasiliev, Emilia P. Yakovenko, Pavel V. Gulyaev, Valeri I. Fedchenko

Vladimir T. Ivashkin, Tatiana L. Lapina, Oksana Yu. Bondarenko, V.Vasilenko Clinic of internal diseases, gastroenterology and hepatology of the Moscow Sechenov Medical Academy, 119881 Pogodinskaya 5, Moscow, Russia

Olga A. Sklanskaya, Pathology Department of the Moscow Sechenov Medical Academy, 119881, Trubetskaya 8, Moscow, Russia

Petr Ya. Grigoriev, Emilia P. Yakovenko, Pavel V. Gulyaev, Valeri I. Fedchenko, Gastroenterological Center of the Health Ministry of Russia, 105203, N. Pervomayskaya ul. 70, Moscow, Russia

Yuri V. Vasiliev, Central Institution of Gastroenterology, 111123, Sh. Entusiastov 86, Moscow, Russia

Supported by PLIVA (Croatia).

Correspondence to: Prof. Vladimir T. Ivashkin, V.Vasilenko Clinic of internal diseases, gastroenterology and hepatology of the Moscow Sechenov Medical Academy, 119881 Pogodinskaya 5 Moscow, Russia. good.day@ru.net

Telephone: +95-248-35- 91 **Fax:** +95-248-36-10

Received 2002-01-11 **Accepted** 2002-01-23

Abstract

AIM: To assess and compare the efficacy and safety of two triple regimes: A) metronidazole, amoxicillin and omeprazole, which is still widely used in Russia, and B) azithromycin, amoxicillin and omeprazole in healing active duodenal ulcer and *H.pylori* eradication.

METHODS: 100 patients with active duodenal ulcer were included in the open, multicentre, randomized study with comparative groups. Patients were randomly assigned to one of the following one-week triple regimes: A) metronidazole 500 mg bid, amoxicillin 1 g bid and omeprazole 20 mg bid (OAM, $n=50$) and B) azithromycin 1 g od for the first 3 days (total dose 3 g), amoxicillin 1 g bid and omeprazole 20 mg bid (OAA, $n=50$). Omeprazole 20 mg od was given after the eradication course as a monotherapy for three weeks. The control endoscopy was performed 8 weeks after the entry. *H.pylori* infection was determined in the entry of the study and four weeks after the cessation of treatment by means of histology and CLO-test.

RESULTS: 97 patients completed the study according to the protocol (1 patient of the OAM group did not come to the control endoscopy, 2 patients of the OAA group stopped the treatment because of mild allergic urticaria). Duodenal ulcers were healed in 48 patients of the OAM group (96 %; CI 90.5-100 %) and in 46 patients of the OAA group (92 %; CI 89.5-94.5 %) ($p=ns$). *H.pylori* infection was eradicated in 15 out of 50 patients with OAM (30 %; CI 17-43 %) and in 36 out of 50 patients treated with OAA (72 %; CI 59-85 %) ($P<0.001$)- ITT analysis.

CONCLUSION: The triple therapy with omeprazole, amoxicillin and metronidazole failed to eradicate *H.pylori* in the majority of patients, which is an essential argument to

withdraw this regimen out of the national recommendations. Macrolide with amoxicillin are preferable to achieve higher eradication rates. Azithromycin (1 g od for the first 3 days) can be considered as a successful component of the triple PPI-based regimen.

Ivashkin VT, Lapina TL, Bondarenko OY, Sklanskaya OA, Grigoriev PY, Vasiliev YV, Yakovenko EP, Gulyaev PV, Fedchenko VI. Azithromycin in a triple therapy for *H.pylori* eradication in active duodenal ulcer. *World J Gastroenterol* 2002; 8(5):879-882

INTRODUCTION

A number of antimicrobial agents have been used in various regimens to eradicate *Helicobacter pylori*. The properties of different medications may have some impact on the therapy result. Clinical trials are undertaken to search for simpler but equally effective (or more effective) regimen. The modern macrolides are in the focus of attention from that point of view. Azithromycin, a new generation macrolide, has some special attributes, that makes it a promising compound in the regimens for *H.pylori* eradication. It is acid-stable, has a long half-life and achieves remarkably high concentration in the gastric tissue. Thus after a single oral dose of 500 mg the concentration of azithromycin persisted in the gastric mucosa above the MIC₉₀ for *H.pylori* over a five-day period^[1]. There were several clinical trials with azithromycin in the therapy of *H.pylori* infection. As pharmacological properties of azithromycin make possible to use shorter courses, the problem was to define an optimal dose and duration of azithromycin in the triple therapy. The triple regimens with the total course dose of azithromycin of 1.5 g gave high eradication rates^[2,3], but the result was not stable^[4], the total course dose of 3 g appeared to be more reliable^[5,6].

There were just a few studies of azithromycin in the treatment of *H.pylori* infection in peptic ulcer and chronic gastritis in Russia^[7,8]. The results were satisfactory, and it was clear that further studies to reach the level of evidence-based medicine are needed.

The clinical trial of azithromycin (Sumamed®, PLIVA) in the triple regimen for the eradication of *H.pylori* in active peptic ulcer, that was planned according to the GCP criteria, was of priority significance for Russia. The aim of the study was to assess and compare the efficacy of two triple regimes: (A) omeprazole, amoxicillin and metronidazole, and (B) omeprazole, amoxicillin and azithromycin in healing active duodenal ulcer and *H.pylori* eradication. The safety and tolerability of the two drug combinations were also evaluated and compared.

MATERIALS AND METHODS

Study design

It was an open, randomized study with comparative groups conducted in three Moscow gastroenterological centers: V.

Vasilenko Clinic of internal diseases, gastroenterology and hepatology of the Moscow Sechenov Medical Academy, Gastroenterological Center of the Health Ministry of Russia and Central Institution of Gastroenterology. The study protocol was worked out by PLIVA pharmaceutical company (Zagreb, Croatia).

The study was conducted according to GCP guidelines and the Helsinki Declaration. All patients gave written informed consent and the protocol was approved by the local Ethic Committees of the above-mentioned centers.

Out-patients and in-patients of both sexes aged between 18 and 70 years with endoscopically proven one or more duodenal ulcers were eligible for entry into the study. *H. pylori* presence before the treatment was detected by a rapid urea test and histology. In the CLO-test (Delta-West Ltd, Australia) two biopsy specimens (one from the antrum and one from the corpus on the greater curvature) were examined. The positive result of the CLO-test was needed to involve the patient into the study. Four biopsy specimens (two from the antrum and two from the mid-corpus on the greater and lesser curvature) underwent histopathological assessment. Sections of paraffin-embedded specimens were routinely stained with haematoxylin-eosin for morphologic examination and with Giemsa for *H. pylori* detection.

The information about the study was accessible to all patients before the entry. The written consent was necessary for participation in the clinical trial. The criteria for exclusion were: intake of proton pump inhibitors, antibiotic or bismuth salts within 4 weeks prior to the study, ulcer complications, concomitant gastric ulcer or reflux oesophagitis of grade II or more according to the classification of Savari et Miller, stomach surgery (except for a simple closure of perforation), known hypersensitivity to one of the study medications, severe concomitant diseases with metabolic changes, suspected poor compliance. Patients were required to be a male or nonpregnant, nonlactating females; females were postmenopausal or using a contraceptive.

At the entry the patients had a full physical examination. Routine haematological and biochemical (serum creatinine, urea, transaminases, alkaline phosphatase, total and direct bilirubine) screening was carried out.

The patients, that satisfied the inclusion criteria, were randomly assigned to one of the following one-week triple regimes: (A) metronidazole 500 mg bid, amoxicillin 1 g bid and omeprazole (Losec®, AstraZeneca) 20 mg bid (OAM) and (B) azithromycin (Sumamed®, PLIVA) 1 g od for the first 3 days (total dose 3 g), amoxicillin 1 g bid and omeprazole (Losec®, AstraZeneca) 20 mg bid (OAA).

Omeprazole (Losec®, AstraZeneca) 20 mg od was given after the eradication course as a monotherapy for three weeks.

Control examination was performed 4 weeks after the cessation of omeprazole monotherapy (8 weeks after entry). Physical status, adverse events, haematological and biochemical analysis, endoscopy (ulcer healing) were assessed. *H. pylori* infection was determined by histology and CLO-test: cure of the infection was established if two tests of all biopsy specimens gave negative results (two from the antrum, two from the corpus on the greater and lesser curvature for histology and one from the antrum, one from the corpus on the greater curvature for CLO-test).

Statistical analysis

The duodenal ulcer healing rates and *H. pylori* eradication rates were compared between the two treatment groups using a χ^2 -test. A two-sided 95 % confidence interval (95 % CI) was calculated using the normal approximation to the binominal distribution.

Patient population

100 patients entered the trial: 50 patients were randomized to group A, and 50 to group B. The two treatment groups had similar demographic characteristics.

The patients at the entry usually had the dyspeptic symptoms typical for active duodenal ulcer. The ulcers localized in the duodenum bulb were between 0.3 cm and 1.5 cm in size (the two thirds of patients had ulcers between 0.5 cm and 1.0 cm in size). Three patients with two duodenal ulcers were randomized to group B.

RESULTS

49 patients (out of 50) of group A (metronidazole, amoxicillin and omeprazole) completed the study without contravention to the protocol: one patient was lost for the follow-up. Two patients of group B (azithromycin, amoxicillin and omeprazole) had mild allergic symptoms (urticaria) in the beginning of the eradication course and stopped treatment. A short use of antihistamine medications led to relief of allergy. Thus, 48 patients of group B (out of 50) completed the study according to the protocol.

The efficacy of treatment regimens was assessed by duodenal ulcer healing. Endoscopy performed 4 weeks after the cessation of omeprazole monotherapy revealed that duodenal ulcers healed in 48 patients of the OAM group and in 46 patients of the OAA group. The causes of ulcer persistence were failed *H. pylori* eradication and drop-out from the protocol. A patient with missing data from group A and two patients of group B (drop-outs due to adverse events) were included in the analysis for ulcer healing as "not healed". Ulcer healing rate in group A was 96 % (CI 90.5-100 %) and in group B 92 % (CI 89.5-94.5 %). Statistical difference was not significant.

The main indicator of the triple regimen effectiveness was the rate of *H. pylori* eradication. Eradication rates were estimated for the population that completed the study according to the protocol (per protocol analysis) and for the population that was involved in the study (intention-to-treat analysis). One patient of group A, that did not come to the control examination, and two patients of group B, withdrawn from the study because of the adverse events, were estimated as a negative eradication result. *H. pylori* infection was eradicated in 15 out of 50 patients with OAM: eradication rate was 30.6 % (95 % CI: 17.6 % - 43.6 %) PP and 30 % (95 % CI: 17-43 %) ITT. *H. pylori* infection was eradicated in 36 out of 50 patients treated with OAA: eradication rate was 75 % (95 % CI: 63-87 %) PP and 72 % (95 % CI: 59-85 %) - ITT analysis (Figure 1).

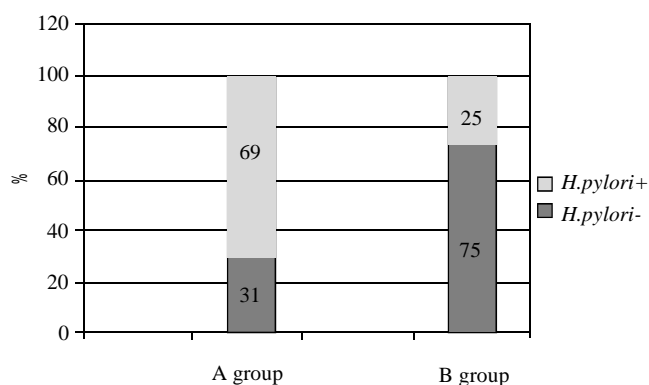


Figure 1 The results (per protocol) of *H. pylori* eradication in the treatment groups.

The difference between the treatment groups was statistically significant: $P < 0.001$.

The treatment safety was assessed by adverse events recording, the laboratory tests deviation of clinical significance were also taken into consideration. The two cases of withdrawal because of an allergic urticaria were registered in group B. Quick relief of the allergic symptoms due to the antihistamine preparations allowed us to consider this adverse events as mild. The laboratory parameters of haematological and biochemical tests (serum creatinine, urea, transaminases, alkaline phosphatase, total and direct bilirubine) were usually normal. There was no clinically significant changes from the baseline in the laboratory results.

DISCUSSION

The new triple regime for *H. pylori* eradication with new macrolide azithromycin was compared with the combination of metronidazole, amoxicillin and omeprazole, which is still widely used in Russia.

Both combinations were highly effective in ulcer healing. The analysis of cases with persistent duodenal ulceration revealed that most of them were connected with protocol nonfulfilment and failed eradication. High healing rates are expected results of triple therapies based on proton pump inhibitors. Both proton pump inhibitors action and the effect of *H. pylori* eradication are of importance in ulcer healing. Persistence of *H. pylori* infection in gastric mucosa is considered now as one of the factors preventing ulcer healing, or to be more precise, as a factor of distortion of the normal regeneration process^[9]. This molecular events are not so evident in everyday clinical practice as potent effect of omeprazole. Proton pump inhibitors-based triple therapies even without "posteradical" antisecretory monotherapy are advantageous in active duodenal ulcer. Rapid symptoms relief and ulcer healing in 96 % patients of group A and in 96 % patients of group B (per protocol) once more proved the effectiveness of eradication therapy based on omeprazole. Rapid ulcer healing did not depend on antibiotic composition.

There are no therapies that eradicate *H. pylori* infection in every case. That is why the search for better anti-*H. pylori* regimes is of present interest. Clinical experience of the Russian trials that are organized according to the principals of evidence-based medicine is of great importance. They give information about the possibility of application of foreign data to the Russian patient population. The therapy used in group A "metronidazole 500 mg bid, amoxicillin 1 g bid and omeprazole 20 mg bid" is widely used in the Russian practice. This regime is well-known to general practitioners and is included in "The guidelines for the management of *Helicobacter pylori* infection" of the Russian *Helicobacter pylori* Study Group and Russian Gastroenterological Association, adopted in 1997^[10]. Since that time there were some reports that informed about very low eradication rates with proton pump inhibitor, metronidazole and amoxicillin^[11, 12]. The present clinical trial demonstrated (by the example of the patients from three Moscow gastroenterological centers) discouraging eradication rate in the OAM triple therapy. This is a real argument in favour of withdrawing regime "proton pump inhibitor, metronidazole and amoxicillin" from the national guidelines as it was done in the Maastricht 2-2000 European Consensus report^[13].

Antimicrobial resistance of *H. pylori* strains is one of the main causes of treatment failure. *H. pylori* resistance to nitroimidazoles (metronidazole and tinidazole) is quite an often event in the Russian populations. Thus, in Moscow *H. pylori* strains with primary metronidazole resistance were found in

more than 50 % of isolates^[14]. Unsuccessful anti-*H. pylori* course of metronidazole-containing regimen usually leads to secondary resistance. One-third of the patients in the present study had a long duration of peptic ulcer disease (>5 years), almost all of them had used metronidazole. *H. pylori* susceptibility testing was not considered in the present trial, but we could suspect, with high probability, nitroimidazole resistance as a cause of eradication failure in two-thirds of the group A patients.

The proton pump inhibitor-based triple therapy with amoxicillin and clarithromycin gives steady high eradication rates. The European clinical trial MACH1 demonstrated the best result using omeprazole 40 mg with amoxicillin 1 g bid and clarithromycin 500 mg bid among five omeprazole-based combinations with different antimicrobials for seven days^[15]. The proton pump inhibitor (or ranitidine bismuth citrate) in combination with clarithromycin 500 mg bid and amoxicillin 1 g bid were named the preferable regimen for first-line eradication therapy in the Maastricht-2 Consensus report^[13]. The real chance to enhance the eradication rates in the countries with high levels of metronidazole resistance is to avoid metronidazole in the anti-*H. pylori* treatment. Provided the levels of clarithromycin resistance are low the macrolide and amoxicillin regimens would be the most beneficial.

The treatment regimen of group B "azithromycin 1 g od for the first 3 days, amoxicillin 1 g bid and omeprazole 20 mg bid for 7 days" eradicated *H. pylori* infection in 72 % of patients, the result is good for the Russian populations. This rate of *H. pylori* eradication seems to be lower that is acceptable. But according to some publications it is quite common with accepted PPI-based triple therapies. Thus J.P. Gisbert *et al*^[16] gave mean eradication rate (weighted mean) as 71 % for ITT analysis for 7-day to 14-day omeprazole-based therapies.

H. pylori has cross resistance to macrolides: the strain resistant e.g. to clarithromycin is resistant to every other macrolide. The level of clarithromycin resistance in Moscow is 8-14 %, unfortunately with the tendency for an increase^[14]. The effect of drug synergism is of great value in combination treatment to heal *H. pylori* infection. P.M. Lepper *et al*^[17] demonstrated in vitro synergistical effect of azithromycin and proton pump inhibitor lansoprazole. They speculate that this effect may enhance eradication rates even with macrolide-resistant *H. pylori* strains because of the unique pharmacological properties of the combination. Azithromycin could provide a potent anti-*H. pylori* effect and could simplify the bulky triple therapy. Of macrolides azithromycin develops the highest concentration in gastric tissue and mucus, its pharmacokinetic properties makes it possible to take azithromycin only once a day and only during three days in a week course. Clarithromycin for standard eradication is administered for 7 days twice a day (usually 4 tablets of 250 mg). Azithromycin is really an advantageous medication to reach simpler therapy, improving both tolerability and compliance. The correctness of the azithromycin dose chosen in our trial - 1 g daily for three days - was confirmed by recent results^[18].

In conclusion, we have shown that azithromycin has clinical (*in vivo*) activity against *H. pylori* infection. Azithromycin (1 g od for the first 3 days in a week course) can be considered as a successful component of the triple proton pump inhibitor-based regimen. It is necessary to eradicate *H. pylori* in peptic ulcer patients, using effective and simple regimens.

REFERENCES

- 1 **Harrison JD**, Jones JA, Morris DL. Azithromycin levels in plasma and gastric tissue, juice and mucus. *Eur J Clin Microbiol Infect Dis* 1991; **10**: 862-864

- 2 **Bertoni G**, Sassatelli R, Nigrisoli E, Tansini P, Bianchi G, Della Casa G, Bagni A, Bedogni G. Triple therapy with azithromycin, omeprazole and amoxicillin is highly effective in the eradication of *Helicobacter pylori*: a controlled trial versus omeprazole plus amoxicillin. *Am J Gastroenterol* 1996; **91**: 258-263
- 3 **Labenz J**, Tillenburg B, Stolte M. Azithromycin as a substitute for clarithromycin in French triple therapy for *Helicobacter pylori*: a randomized study (abstr.). *Gut* 1999; **45** (Suppl. III): A115
- 4 **Di Mario F**, Dal Bo N, Grassi SA, Rugge M, Casarro M, Donisi PM, Vianello, Kusstatcher S, Saladin S, Grasso GA, Ferrana M, Battaglia G. Azithromycin for the cure of *Helicobacter pylori* infection. *Am J Gastroenterol* 1996; **91**: 264-267
- 5 **Vcev A**, Stimac D, Vceva A, Takac B, Pezerovic D, Ivandic A. High dose omeprazole plus amoxicillin and azithromycin in eradication of *Helicobacter pylori* in duodenal ulcer. *Helicobacter* 1999; **4**: 54 - 57
- 6 **Chey WD**, Fisher L, Barnett J, Delvalle J, Elta GH, Hasler WL, Nostrant T, Palaniappan J, Scheiman J. Low- versus high-dose azithromycin triple therapy for *Helicobacter pylori* infection. *Aliment Pharmacol Ther* 1998; **12**: 1263-1267
- 7 **Loginov AS**, Vasiliev YV. The complex use of azithromycin (Sumamed), amoxicillin and metronidazole in *Helicobacter pylori* eradication. *Rus Gastroenterol J* 1998; **3**: 35-41
- 8 **Vasiliev YuV**. Sumamed and new perspectives in rational *Helicobacter pylori* eradication in peptic ulcer and gastritis. *Moscow Med J* 1999; **6**: 19-21
- 9 **Aruin LI**, Kapuller LL, Isakov VA. Morphological diagnostics of gastrointestinal diseases. Moscow: Triada-X, 1998: 174 -182
- 10 The guidelines for the management of *Helicobacter pylori* infection in peptic ulcer disease in adult population. *Rus J Gastroenterol Hepatol Coloproctol* 1998; **1**: 105-107
- 11 **Kurilovich SA**, Shlykova LG, Kopychko TA. Real problems of *H. pylori* eradication (abstr.). *Rus J Gastroenterol Hepatol Coloproctol* 2000; **5** (Suppl. 11): 25
- 12 **Bondarenko OY**, Ivashkin VT, Lapina TL, Sklanskaya OA, Charikova SYu. Efficacy of *Helicobacter pylori* treatment, based on Lansoprazole produced in Russia. *Siberian J Gastroenterol Hepatol* 2000; **10**: 10-11
- 13 **Malfertheiner P**, Megraud F, O' Morain C, Hungin P, Jones R, Axon A. Current concepts in the management of *Helicobacter pylori* infection - the Maastricht 2 - 2000 Consensus Report. *Aliment Pharmacol Ther* 2002; **16**: 167-180
- 14 **Koudryavtseva LV**, Isakov VA, Ivanikov IO, Zaitseva SV. Evolution of *H. pylori* primary resistance to antimicrobial agents in Moscow (Russia) in 1996-1998 (abstr.). *Gut* 2000; **47** (Suppl. I): A8
- 15 **Lind T**, Veldhuizen van Zanten S, Unge P, Spiller R, Bayerdorffer E, O' Morain C, Bardhan KD, Bradette M, Chiba N, Wrangstad M, Cederberg C, Idstrom J-P. Eradication of *Helicobacter pylori* using one-week triple therapies combining omeprazole with two antimicrobials: the MACH1 study. *Helicobacter* 1996; **1**: 138-144
- 16 **Gisbert GP**, Pajares JM, Racz I. Therapy. *Current Opinion Gastroenterol* 2001; **17** (Suppl. 1): S47-S54
- 17 **Lepper PM**, Moricke A, Glasbrenner B, Trautman M. Demonstration of in-vitro synergism between proton-pump inhibitors and macrolides against *Helicobacter pylori* (abstr.). *Gut* 2000; **47** (Suppl. I): A110
- 18 **Bazzoli F**, Zagari R, Albanese R, Pozzato P, Fossi S, Berretti D, Martuzzi C, Lunedei V, Antonini F, Roda E. Three days 1000 vg vs 500 mg daily Azithromycin with tinidazole and omeprazole for *Helicobacter pylori* eradication: a double blind randomized, placebo controlled multicenter study (abstr.). *Gut* 2001; **49** (Suppl. 11): A84

Edited by Xia HHX

• BASIC RESEARCH •

Estrogen reduces CCL₄- induced liver fibrosis in rats

Jun-Wang Xu, Jun Gong, Xin-Ming Chang, Jin-Yan Luo, Lei Dong, Zhi-Ming Hao, Ai Jia, Gui-Ping Xu

Jun-Wang Xu, Jun Gong, Jin-Yan Luo, Lei Dong, Department of Gastroenterology, Second Hospital of Xi'an Jiaotong University, Xi'an 710031, Shaanxi Province, China

Xin-Ming Chang, Zhi-Ming Hao, Ai Jia, Gui-Ping Xu, Department of Gastroenterology, First Hospital of Xi'an Jiaotong University, Xi'an 710061, Shaanxi Province, China

Supported by the Doctorate Foundation of Xi'an Jiaotong University, No.2001-13.

Correspondence to: Dr. Jun-Wang Xu, Department of Gastroenterology, First Hospital of Xi'an Jiaotong University, Xi'an 710061, Shaanxi Province, China. xujw@pub.xaonline.com

Telephone: +86-29-5252911-2401 **Fax:** +86-29-5263190

Received 2002-05-14 **Accepted** 2002-06-03

Abstract

AIM: Chronic liver diseases, such as fibrosis or cirrhosis, are more common in men than in women. This gender difference may be related to the effects of sex hormones on the liver. The aim of the present work was to investigate the effects of estrogen on CCL₄-induced fibrosis of the liver in rats.

METHODS: Liver fibrosis was induced in male, female and ovariectomized rats by CCL₄ administration. All the groups were treated with estradiol (1 mg/kg) twice weekly. And tamoxifen was given to male fibrosis model. At the end of 8 weeks, all the rats were killed to study serum indicators and the livers.

RESULTS: Estradiol treatment reduced aspartate aminotransferase (AST), alanine aminotransferase (ALT), hyaluronic acid (HA) and type IV collagen (CIV) in sera, suppressed hepatic collagen content, decreased the areas of hepatic stellate cells (HSC) positive for α -smooth muscle actin (α -SMA), and lowered the synthesis of hepatic type I collagen significantly in both sexes and ovariectomy fibrotic rats induced by CCL₄ administration. Whereas, tamoxifen had the opposite effect. The fibrotic response of the female liver to CCL₄ treatment was significantly weaker than that of male liver.

CONCLUSION: Estradiol reduces CCL₄-induced hepatic fibrosis in rats. The antifibrogenic role of estrogen in the liver may be one reason for the sex associated differences in the progression from hepatic fibrosis to cirrhosis.

Xu JW, Gong J, Chang XM, Luo JY, Dong L, Hao ZM, Jia A, Xu GP. Estrogen reduces CCL₄- induced liver fibrosis in rats. *World J Gastroenterol* 2002; 8(5): 883-887

INTRODUCTION

Estrogen is frequently used for anticonception and treatments of menopausal disorders. Its clinical use has increased steadily during the last years due to reports of decreased morbidity and mortality during postmenopausal estrogen treatment^[1]. There have been reports of decreased morbidity in cardiovascular

disease, suggesting estrogenic effects on tissues other than on the classic reproductive organs.

Population data have long suggested that chronic liver disease progresses at unequal rates in both sexes for viral hepatitis and other forms of injury with a similar incidence in males and females. In chronic viral hepatitis the major sequelae, such as fibrosis or cirrhosis, are more common in men than in women^[2,3]. Although establishing the actual rate of fibrosis in a patient would require serial liver biopsy, which is seldom done, a reasonable approximation can be inferred from the incidence of fibrosis-related complications^[4-6]. The development of cirrhosis is more common in men than in women (2.3 to 2.6:1). Although the liver is not a classic sex hormone target, livers in both men and women have been shown to contain estrogen receptors and respond to estrogens by regulating liver function. Therefore, sex hormones may play a role in the progression from hepatic fibrosis to cirrhosis. It showed that estradiol treatment resulted in reducing hepatic fibrosis in rats induced by dimethylnitrosamine (DMN). However, much current evidence suggests that women develop alcoholic liver disease at lower levels of alcohol intake and over a shorter period of time as compared to men. In other words, females are more susceptible to alcohol-induced liver injury than males^[7]. The specific mechanisms concerning a gender-related difference in susceptibility are largely unknown.

CCL₄-induced fibrosis shares several characteristics with human fibrosis of different etiologies; thus, it is an adequate model of human fibrosis^[8-10]. The aim of the present work was to study the effects of estrogen on CCL₄-induced fibrosis of the liver in rats, and to investigate the possible mechanisms.

MATERIALS AND METHODS

Animals

Male and female Sprague-Dawley rats (Experimental Animal Holding Unit of Shaanxi Province, China) were housed in a temperature-humidity-controlled environment with 12-h light-dark cycles (lights on from 07:00 to 19:00) and had unrestricted access to food and water. Forty male rats, weighing 220±21 g, corresponding to an age of approximately 10 weeks, were divided into four groups of ten each. For CCL₄ group, 400 mL/L CCL₄ in peanut oil were injected subcutaneously at a dose of 2 mL/kg twice weekly, and the first dosage was doubled. The estrogen group, apart from the use of CCL₄, was treated subcutaneously with estradiol 1 mg/kg twice weekly (The Ninth Pharmaceutical Plant of Shanghai, China). The anti-estrogen group, along with the CCL₄ treatment described above, was given Tamoxifen 6 mg/kg every day orally (The First Pharmaceutical Plant of Suzhou, China). The rats were fed a modified high fat diet containing 5 g/kg cholesterol and 200 g/kg pig oil. The control group was given normal food and water, and received injection of peanut oil vehicle twice weekly.

Fifty female rats 10 weeks old, weighing 208±17 g, were divided into five groups with ten each. The ovariectomy (Ovx) group was initiated with a bilateral ovariectomy and the sham operation group was initiated with just a sham operation. The

two estrogen groups, with bilateral ovariectomy and with sham operation, were treated subcutaneously with estradiol (1 mg/kg twice weekly). All of the above four groups received 400 ml/L of CCL₄ in peanut oil at a dose of 2 ml/kg twice weekly, and were fed with a high fat diet containing 5 g/kg cholesterol and 200 g/kg pig oil. The CCL₄ and estradiol were used after 2 weeks of operation. The control group was given normal food and water, and received injection of peanut oil vehicle twice weekly.

At the end of the 8-week experimental period, all the rats were fasted overnight and put to death by cervical dislocation after anaesthetised by intramuscular injection of sodium pentobarbital (40 mg/kg). Blood was collected from the animals and the serum obtained was analysed. The liver was removed rapidly.

Estimation of serum indicators

In serum, activities of aspartate aminotransferase (AST) and alanine aminotransferase (ALT) were assayed by a 917-Hitachi Automatic Analyzer. Serum hyaluronic acid (HA) and type IV collagen (CIV) concentrations were measured radioimmunologically using commercial kit (Shanghai Navy Medical Institute, China).

Parameters of hepatic antioxidation

Parameters of antioxidation in the liver was determined by measuring the levels of hepatic malondialdehyde (MDA) and superoxide dismutase (SOD) (kit: Jiancheng Medical Institute, Nanjing, China).

Histopathological study

Excised liver tissues from each rat were fixed in 100 ml/L neutral formalin, embedded in paraffin, and stained with hematoxylin-eosin (HE) and masson's trichrome. The evaluation of hepatic fibrosis was determined by a semi-quantitative method to assess the degree of histologic injury in chronic hepatic fibrosis^[11,12].

Immunohistochemical examination

Liver tissue sections were mounted on slides, deparaffinized in xylene, and rehydrated in alcohol. The level of α -smooth muscle actin (α -SMA) (Neomarkers, USA), type I collagens (Boster, Wuhan, China), transforming growth factor β_1 (TGF β_1) and platelet-derived growth factor (PDGF) (Dako, USA) were determined by immunohistochemical methods in female

groups. Based on the extent of histological staging, the α -SMA, type I collagens, TGF β_1 and PDGF positive cells were expressed as a percentage of the total area of the specimen.

Statistical analysis

Data are presented as $\bar{x} \pm s$ unless otherwise indicated. The Mann-Whitney *u* test for nonparametric and unpaired values, student's *t*-test or Fisher's exact test was used as appropriate. Results were considered significant when $P < 0.05$.

RESULTS

Changes of serum indicators and hepatic antioxidation data

At the end of 8-week experimental period, 8 rats were dead because of infection at the region of injection and hepatic crack by unsuitable handling. Table 1 gives the values for the activities of the serum indicator enzymes, the markers of hepatic fibrosis, and the hepatic antioxidation data.

It is evident that CCL₄ produced a marked increase in the activities of serum ALT and AST in both male and female rats. Although the extent of that was lower in female group than in male group, it was not statistically significant ($P > 0.05$). The CCL₄ plus estradiol group showed a significant decrease in the enzyme levels, but the levels were still higher than those of control groups. In ovariectomy rats, when CCL₄ were given, the enzyme levels were higher than those of the sham operation rats in both estradiol used or none-used groups, but the differences were not statistically significant ($P > 0.05$). The levels of serum ALT and AST in Tamoxifen group were significantly higher than those of the CCL₄ group and estrogen used groups.

As for the changing trend of fibrotic markers in serums, HA and CIV were similar with those of the enzyme levels in all groups. The results showed that the levels of HA and CIV in CCL₄ used groups were significantly higher than those of control groups, especially in male group. Tamoxifen could increase the extent of that and estrogen could decrease it significantly. In ovariectomy groups, the HA and CIV were significantly higher than those of sham operation groups.

Tissue antioxidation data indicated that MDA was increased and SOD was decreased in CCL₄ treated rats significantly, whereas estradiol had the opposite effect. The MDA was higher and SOD was lower in males than those of females treated with CCL₄.

Table 1 Liver enzymes, serum fibrosis indicators and hepatic antioxidation ($\bar{x} \pm s$)

Group	<i>n</i>	ALT (nkat/L)	AST (nkat/L)	HA (μ g/L)	CIV (μ g/L)	MDA (nmol/g)	SOD (kNU/g)
Males							
Control	10	31 \pm 6	66 \pm 18	115 \pm 31	18 \pm 5	3.1 \pm 0.9	8.0 \pm 1.6
CCL ₄	10	576 \pm 262 ^a	699 \pm 241 ^a	530 \pm 122 ^a	54 \pm 14 ^a	10.5 \pm 3.4 ^a	2.2 \pm 1.1 ^a
CCL ₄ +E	8	355 \pm 125 ^c	314 \pm 179 ^c	232 \pm 78 ^c	30 \pm 10 ^c	6.6 \pm 2.8 ^c	5.0 \pm 1.6 ^c
CCL ₄ +Tam	8	884 \pm 294 ^c	1073 \pm 453 ^c	703 \pm 187 ^c	69 \pm 15 ^c		
Females							
Control	10	35.8 \pm 7.9	64.5 \pm 20.8	121 \pm 26	17 \pm 4	3.0 \pm 0.8	8.7 \pm 2.8
CCL ₄	9	540 \pm 252 ^a	631 \pm 268 ^a	388 \pm 81 ^a	41 \pm 11 ^a	7.1 \pm 2.1 ^a	4.0 \pm 1.5 ^a
CCL ₄ +Ovx	10	658 \pm 220	697 \pm 240	586 \pm 145 ^c	53 \pm 14 ^c	9.1 \pm 2.9 ^c	2.8 \pm 1.0 ^c
CCL ₄ +E	8	314 \pm 163 ^c	302 \pm 153 ^c	267 \pm 83 ^c	29 \pm 7 ^c	4.7 \pm 2.2 ^c	5.9 \pm 2.0 ^c
CCL ₄ +Ovx+E	9	311 \pm 146 ^c	321 \pm 121 ^c	236 \pm 119 ^c	31 \pm 7 ^c	4.8 \pm 2.3 ^c	6.2 \pm 2.5 ^c

^a $P < 0.05$, vs control; ^c $P < 0.05$, vs CCL₄

Histopathological and immunohistochemical changes

The control livers showed normal lobular architecture with central veins and radiating hepatic cords (Figure 1A). Prolonged administration of CCL₄ causes severe pathological damages: inflammation, necrosis, and collagen deposition (Figure 1B,male). The semiquantitative hepatic collagen staging value was 3.3 ± 0.7 in males, and 2.4 ± 1.1 in females. It was showed that the staging value was significantly decreased in female rats. After administration of estradiol, the extent of hepatic fibrosis was significantly weaker than that of CCL₄ groups (Figure 1C:male): the semiquantitative staging value was 2.0 ± 1.1 in males and 1.6 ± 0.9 in females respectively. Ovariectomy significantly increased the staging value (3.1 ± 0.7). Moreover, the staging value was highest when given Tamoxifen to the experimented rats (3.7 ± 0.5 Figure 1D).

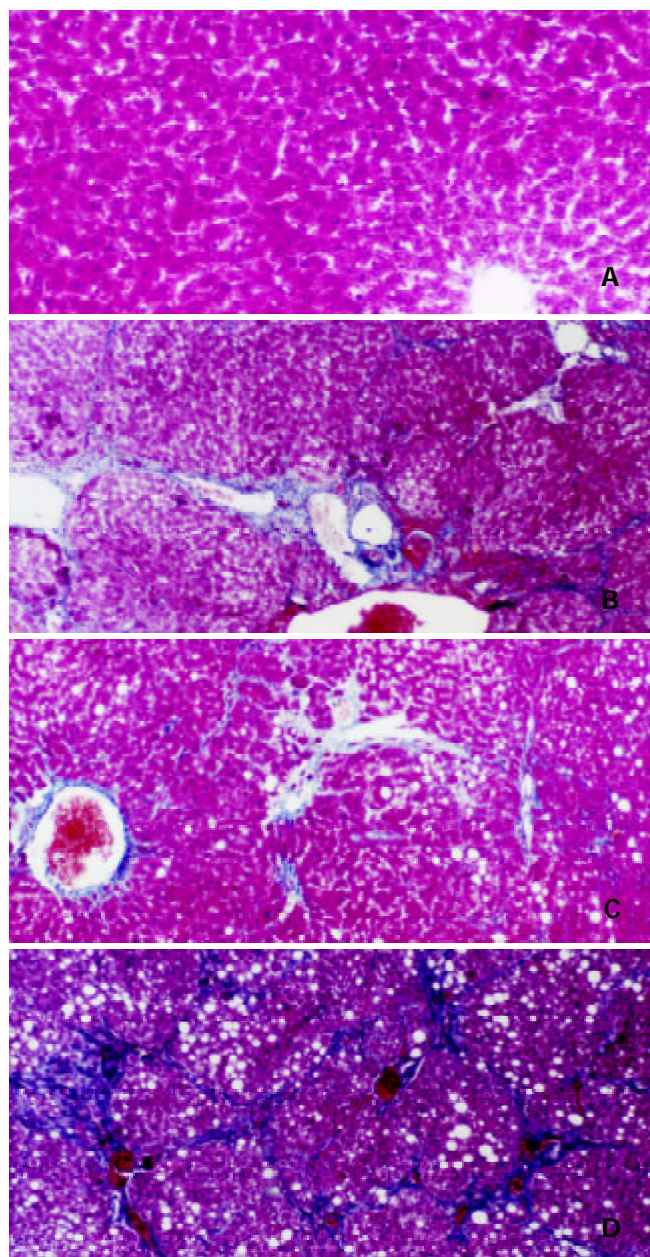


Figure 1 Effects of estradiol and tamoxifen on the histology of CCL₄ induced fibrotic rat liver. Masson trichome stain, scale bar=40 μ m, original magnification, $\times 100$
1A: Normal rat liver; 1B: CCL₄ group shows fibrosis; 1C: Estrogen group with less fibrosis than in group B; 1D: Tamoxifen group shows marked fibrosis than in group B.

Analysis of α -SMA, an activation marker of rat hepatic stellate cells (HSC) by immunohistochemistry showed staining in vascular smooth muscle cell of control rat livers, but not in sinusoids. In the CCL₄ model, the positive cells of α -SMA, type I collagen, TGF β ₁ and PDGF within centrilobular and periportal fibrotic bands. The percentage areas of these staining in the liver of female rats were showed in Figure 2. The results suggest that administration of CCL₄ significantly increased the percentage areas of all of the four marker staining. Ovariectomy group has a marked higher percentage area than that of CCL₄ group and it could be significantly suppressed by estradiol used.

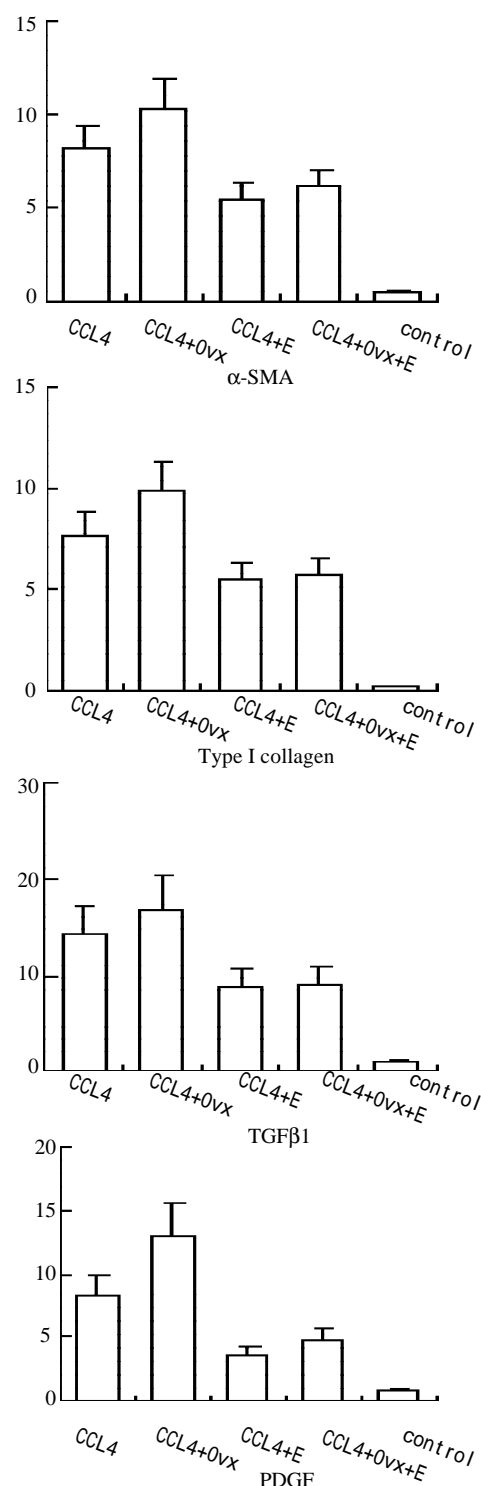


Figure 2 Percentage area (%) of α -SMA, type I collagen, TGF β ₁, and PDGF in female rats

DISCUSSION

Hepatic fibrosis is usually initiated by hepatocyte damage, leading to recruitment of inflammatory cells and platelets, activation of kupffer cells and subsequent release of cytokines and growth factors (e.g. TGF β_1 and PDGF)^[13,14]. These factors probably link the inflammatory and reparative phase of liver cirrhosis, by activating HSC^[15-18]. Upon activation, HSC proliferate and transform into myofibroblast-like cells that deposit large amounts of connective tissue components^[19-27].

The present study showed that estradiol reduces CCL₄-induced hepatic fibrosis in rats. Estradiol administration reduces HA and CIV in serums, suppresses hepatic collagen content, reduces the areas of HSC positive for α -SMA, and lowers the synthesis of hepatic type I collagen in both sexes. The fibrotic response of the female liver to CCL₄ treatment was significantly weaker than that of male liver. It suggested that physiological levels of estrogen have an antifibrogenic effect. These effects of estrogen were also confirmed by ovariectomy in female rats at the time of CCL₄ administration. These findings suggest that the antifibrogenic role of estrogen in the liver may be one reason for the sex associated differences in the progression from hepatic fibrosis to cirrhosis.

Hepatic fibrogenesis is often associated with hepatocellular necrosis and inflammation accompanied by the repair processes^[28-29]. Chronic administration of CCL₄ caused fibrosis as indicated by an increase in serum marker enzymes. Raised serum enzyme levels in CCL₄-injected rats can be attributed to the damaged hepatocellular structural integrity^[30-32]. The administration of estradiol in this study seems to decrease the serum enzymes (ALT, AST), and then preserve the structural integrity of the hepatocellular membrane. Decreased hepatocyte damage suppressing the stimulant effect to the Kupffer cells and subsequent by lower the HSC activation^[33].

Peroxidation of lipids can dramatically change the properties of biological membranes, resulting in severe cell damage and could play a significant role in the pathogenesis of disease. It has showed that lipid peroxidation, free-radical-mediated process, and certain lipid peroxidation products induce genetic overexpression of fibrogenic cytokines and increase the synthesis of collagen. Free radicals and MDA can stimulate the synthesis of collagen and initiate the activation of HSC^[34,35]. Relevant to the latter findings, estradiol and its derivatives are strong endogenous anti-oxidants that reduce lipid peroxide levels in liver and serum. Free radicals, generated mainly by Kupffer cells, are thought to cause tissue injury by initiating lipid peroxidation and irreversibly modifying membrane structure. The present study shows that CCL₄ administration leads to parallel increase in MDA and collagen, and subsequent decrease in SOD, a radical scavenging agent, and that estradiol had the opposite effect. These findings suggest that the antifibrotic effect of estradiol may be caused, at least in part, by its radical scavenging action or antioxidant activity.

Cell proliferation, α -SMA expression, retinoid disappearance, and the formation of collagens and other ECM materials are characteristics of the activated phenotype of HSC^[36]. So HSC are regarded as the primary target cells of hepatic fibrogenesis. Studies in vitro have shown that HSC and their activated counterparts may be induced to proliferate by polypeptide growth factors and cytokines, such as TGF β_1 and PDGF^[37,38]. As these growth factors are produced by infiltrating inflammatory cells, Kupffer cells and sinusoidal endothelial cells, they might act as paracrine mediators which trigger the transformation of HSC *in vivo*. The present data show that estradiol suppresses HSC proliferation and parallel with inhibit TGF β_1 and PDGF expression in CCL₄-induced

fibrosis in male and female rats. These findings suggest that estrogen may exert its suppressive effect on hepatic fibrosis by indirectly modulating the synthesis and releasing of cytokines and other growth factors which in turn altering HSC activation and proliferation.

Chronic fibrotic diseases can differ from each other in etiology. But, in terms of pathogenesis, they share some basic common features^[1]. For instance, three serious chronic disease-atherosclerosis, glomerulosclerosis, and liver fibrosis-may appear very different in their development. In all three, though, a central, and indeed an essential, role is played by macrophages and by ECM-producing cells: smooth muscle cells (SMC) in atherosclerosis, mesangial cell in glomerulosclerosis, and HSC in liver fibrosis. The three types of cells have many properties in common both structurally and functionally, including a changes in cell biology with deposition of matrix proteins. Therefore, factors which affect the development of atherosclerosis or glomerulosclerosis may affect liver fibrosis by similar mechanisms. Studies show that estradiol suppresses atherosclerosis and glomerulosclerosis in rats by directly affecting the estrogen receptor on SMC and mesangial cell. Livers in both male and Female rats have shown to contain high affinity, low capacity estrogen receptors and respond to estrogen by regulating liver function. In the present study, Tamoxifen, an antiestrogen act by occupying the estrogen-binding site of the receptor protein, increases fibrogenesis in CCL₄-induced fibrosis of the liver. It suggests that estradiol may suppress hepatic fibrosis also by a direct receptor mechanism. This remains to be confirmed.

In conclusion, estrogen may play an important role as an endogenous fibrosuppressant, accounting for sex-associated differences in the progression from hepatic fibrosis to cirrhosis. The following mechanisms have been hypothesized to explain the antifibrogenic effect of estrogens: (A) a hepatocellular membrane protection and radical scavenging action, (B) a modulation of HSC proliferation and collagen synthesis, (C) a modulation in the expression of pro-and anti-fibrogenic cytokines and may be (D) a estrogen receptor mechanism. However, the real importance of these mechanisms is still to be elucidated.

REFERENCES

- 1 **Tan E**, Gurjar MV, Sharma RV, Bhalla RC. Estrogen receptor- α gene transfer into bovine aortic endothelial cells induces eNOS gene expression and inhibits cell migration. *Cardiovas Res* 1999; **43**: 788-797
- 2 **Pinzani M**, Romanelli RG, Magli S. Progression of fibrosis in chronic liver diseases: time to tally the score. *J Hepatol* 2001; **34**: 764-767
- 3 **Yan JC**, MA JY, Pan BR, MA LS. Study of hepatitis B in China. *Shijie Huaren Xiaohua Zazhi* 2001; **9**: 611-616
- 4 **Ji XL**. Fine-needle aspiration cytology of liver diseases. *World J Gastroenterol* 1999; **5**: 95-97
- 5 **Nie QH**, Cheng YQ, Xie YM, Zhou YX, Cao YZ. Inhibiting effect of antisense oligonucleotides phosphorothioate on gene expression of TIMP-1 in rat liver fibrosis. *World J Gastroenterol* 2001; **7**: 363-369
- 6 **Dai WJ**, Jiang HC. Advances in gene therapy of liver cirrhosis: a review. *World J Gastroenterol* 2001; **7**: 1-8
- 7 **Jarvelainen HA**, Lukkari TA, Heinaro S, Sippel H, Lindros KO. The antiestrogen toremifene protects against alcoholic liver injury in female rats. *J Hepatol* 2001; **35**: 46-52
- 8 **Du WD**, Zhang YE, Zhai WR, Zhou XM. Dynamic changes of type I, III and IV collagen synthesis and distribution of collagen-producing cells in carbon tetrachloride induced rat liver fibrosis. *World J Gastroenterol* 1999; **5**: 397-403

- 9 **Wu CH.** Fibrodynamics-elucidation of the mechanisms and sites of liver fibrogenesis. *World J Gastroenterol* 1999; **5**: 388-390
- 10 **Liu HL, Li XH, Wang DY, Yang SP.** Matrix metalloproteinase-2 and tissue inhibitor of metalloproteinase-1 expression in fibrotic rat liver. *World J Gastroenterol* 2000; **6**: 881-884
- 11 **George J, Rao KR, Stern R, Chandrakasan G.** Dimethylnitrosamine-induced liver injury in rats: the early deposition of collagen. *Toxicology* 2001; **156**: 129-138
- 12 **Pilette C, Rousselet MC, Bedossa P, Chappard D, Oberti F, Rifflet H, Maiga MY, Gallois Y, Cales P.** Histopathological evaluation of liver fibrosis: quantitative image analysis vs semi-quantitative scores. *J Hepatol* 1998; **28**: 439-446
- 13 **Gao ZL, Li DG, Lu HM, Gu XH.** The effect of retinoic acid on Ito cell proliferation and content of DNA and RNA. *World J Gastroenterol* 1999; **5**: 443-444
- 14 **Bruck R, Shirin H, Aeed H, Matas Z, Hochman A, Pines M, Avni Y.** Prevention of hepatic cirrhosis in rats by hydroxyl radical scavengers. *J Hepatol* 2001; **35**: 457-464
- 15 **Bauer M, Schuppan D.** TGF β_1 in liver fibrosis: time to change paradigms. *FEBS Letters* 2001; **502**: 1-3
- 16 **Wei HS, Li DG, Lu HM, Zhan YT, Wang ZR, Huang X, Zhang J, Cheng JL, Xu QF.** Effects of AT1 receptor antagonist, losartan, on rat hepatic fibrosis induced by CCl₄. *World J Gastroenterol* 2000; **6**: 540-545
- 17 **Huang X, Li DG, Wang ZR, Wei HS, Cheng JL, Zhan YT, Zhou X, Xu QF, Li X, Lu HM.** Expression changes of activin A in the development of hepatic fibrosis. *World J Gastroenterol* 2001; **7**: 37-41
- 18 **Li X, Meng Y, Yang XS, Wu PS, Li SM, Lai WY.** CYP11B2 expression in HSCs and its effect on hepatic fibrogenesis. *World J Gastroenterol* 2000; **6**: 885-887
- 19 **Huang GC, Zhang JS, Zhang YE.** Effects of retinoic acid on proliferation, phenotype and expression of cyclin-dependent kinase inhibitors in TGF- β_1 stimulated rat hepatic stellate cells. *World J Gastroenterol* 2000; **6**: 819-823
- 20 **Wei HS, Lu HM, Li DG, Zhan YT, Wang ZR, Huang X, Cheng JL, Xu QF.** The regulatory role of AT1 receptor on activated HSCs in hepatic fibrogenesis: effects of RAS inhibitors on hepatic fibrosis induced by CCl₄. *World J Gastroenterol* 2000; **6**: 824-828
- 21 **Chen PS, Zhai WR, Zhou XM, Zhang JS, Zhang YE, Ling YQ, Gu YH.** Effects of hypoxia, hyperoxia on the regulation of expression and activity of matrix metalloproteinase-2 in hepatic stellate cells. *World J Gastroenterol* 2001; **7**: 647-651
- 22 **Wang JY, Zhang QS, Guo JS, Hu MY.** Effects of glycyrrhetic acid on collagen metabolism of hepatic stellate cells at different stages of liver fibrosis in rats. *World J Gastroenterol* 2001; **7**: 115-119
- 23 **Xie YM, Nie QH, Chou YX, Cheng YQ, Kang WZ.** Detection of TIMP-1 and TIMP-2 RNA expressions in cirrhotic liver tissue using digoxigenin labelled probe by *in situ* hybridization. *Shijie Huaren Xiaohua Zazhi* 2001; **9**: 251-254
- 24 **Lu X, Liu CH, Xu GF, Chen WH, Liu P.** Successive observation of laminin and collagen IV on hepatic sinusoid during the formation of the liver fibrosis in rats. *Shijie Huaren Xiaohua Zazhi* 2001; **9**: 260-262
- 25 **Yao XX, Tang YW, Yao DM, Xiu HM.** Effect of Yigan Decoction on the expression of type I, III collagen proteins in experimental hepatic fibrosis in rats. *Shijie Huaren Xiaohua Zazhi* 2001; **9**: 263-267
- 26 **Huang GC, Zhang JS.** Intercellular signal transduction of activated hepatic stellate cells. *Shijie Huaren Xiaohua Zazhi* 2001; **9**: 1056-1060
- 27 **Liu T, Hu JH, Cai Q, Ji YP.** Signal conducting molecule in hepatic stellate cells. *Shijie Huaren Xiaohua Zazhi* 2001; **9**: 805-807
- 28 **Lei DX, Peng CH, Peng SY, Jiang XC, Wu YL, Shen HW.** Safe upper limit of intermittent hepatic inflow occlusion for liver resection in cirrhotic rats. *World J Gastroenterol* 2001; **7**: 713-717
- 29 **Li D, Zhang LJ, Chen ZX, Huang YH, Whang XZ.** Effects of TNF α IL-6 and IL-10 on the development of experimental rat liver fibrosis. *Shijie Huaren Xiaohua Zazhi* 2001; **9**: 1242-1245
- 30 **Wang LT, Zhang B, Chen JJ.** Effect of anti-fibrosis compound on collagen expression of hepatic cells in experimental liver fibrosis of rats. *World J Gastroenterol* 2000; **6**: 877-880
- 31 **Zhang YT, Chang XM, Li X, Li HL.** Effects of spironolactone on expression of type I/III collagen proteins in rat hepatic fibrosis. *Shijie Huaren Xiaohua Zazhi* 2001; **9**: 1120-1124
- 32 **Yang Q, Yan YC, Gao YX.** Inhibitory effect of Quxianruangan capsulae on liver fibrosis in rats and chronic hepatitis patients. *Shijie Huaren Xiaohua Zazhi* 2001; **9**: 1246-1249
- 33 **Yao XX, Tang YW, Yao DM, Xiu HM.** Effects of Yigan Decoction on proliferation and apoptosis of hepatic stellate cells. *World J Gastroenterol* 2002; **8**: 511-514
- 34 **Parola M, Robino G.** Oxidative stress-related molecules and liver fibrosis. *J Hepatol* 2001; **35**: 297-306
- 35 **Chen WH, Liu P, Xu GF, Lu X, Xiong WG, Li FH, Liu CH.** Role of lipid peroxidation in liver fibrogenesis induced by dimethylnitrosamine in rats. *Shijie Huaren Xiaohua Zazhi* 2001; **9**: 645-648
- 36 **Akiyoshi H, Terada T.** Centrilobular and perisinusoidal fibrosis in experimental congestive liver in the rat. *J Hepatol* 1999; **30**: 433-439
- 37 **Gandhi CR, Kuddus RH, Uemura T, Rao AS.** Endothelin stimulates transforming growth factor- β_1 and collagen synthesis in stellate cells from control but not cirrhotic rat liver. *Eur J Pharmacol* 2000; **406**: 311-318
- 38 **Gabriel A, Kuddus RH, Rao AS, Gandhi CR.** Down-regulation of endothelin receptor by transforming growth factor β_1 in hepatic stellate cells. *J Hepatol* 1999; **30**: 440-450

Edited by Zhao M

• BASIC RESEARCH •

Establishment of a transgenic cell line stably expressing human cytochrome P450 2C18 and identification of a *CYP2C18* clone with exon 5 missing

Jian Zhu-Ge, Ying-Nian Yu, Yu-Li Qian, Xin Li

Jian Zhu-Ge, Ying-Nian Yu, Department of Pathophysiology and Laboratory of Medical Molecular Biology, Zhejiang University School of Medicine, Hangzhou 310031, Zhejiang Province, China
Yu-Li Qian, Present address: Center of laboratory, Women's hospital, School of Medicine, Zhejiang University, Hangzhou 310031, Zhejiang Province, China

Xin Li, Department of pharmaceutical analysis & drug metabolism, College of Pharmacology Science, Zhejiang University, Hangzhou 310031, Zhejiang Province, China

Supported by National Natural Science Foundation of China, No. 39770868 and Natural Science Foundation of Zhejiang Province, No.397490.

Correspondence to: Prof. Ying-Nian Yu, Department of Pathophysiology and Laboratory of Medical Molecular Biology, Zhejiang University School of Medicine, Hangzhou 310031, Zhejiang Province, China. ynyu@mail.hz.zj.cn

Telephone: +86-571-87217149 **Fax:** +86-571-87217149

Received 2002-03-30 **Accepted** 2002-04-20

Abstract

AIM: The human cytochrome P-450 2C18(CYP2C18) has been characterized. However, the protein has not been purified from liver and very little is known regarding the specific substrate of CYP2C18. In order to study its enzymatic activity for drug metabolism, the *CYP2C18* cDNA was cloned and a stable CHL cell line expressing recombinant CYP 2C18 was established.

METHODS: The human *CYP2C18* cDNA was amplified with reverse transcription-polymerase chain reaction (RT-PCR) from total RNAs extracted from human liver and cloned into pGEM-T vector. The cDNA segment was identified by DNA sequencing and subcloned into a mammalian expression vector pREP9. A transgenic cell line was established by transfecting the recombinant plasmid of pREP9-*CYP2C18* to Chinese hamster lung (CHL) cell. The enzyme activity of *CYP2C18* catalyzing oxidation of tolbutamide to hydroxytolbutamide in postmitochondrial supernant(S9) fraction of the cell was determined by high performance liquid chromatography(HPLC).

RESULTS: The amino acid sequence predicted from the cloned cDNA segment was identical to that of reported by Romkes *et al* (GenBank accession number: M61856, J05326). The S9 fraction of the established cell line metabolizes tolbutamide to hydroxytolbutamide. Tolbutamide hydroxylase activity was found to be $0.509 \pm 0.052 \mu\text{mol} \cdot \text{min}^{-1} \cdot \text{g}^{-1}$ S9 protein or $8.82 \pm 0.90 \text{ mol} \cdot \text{min}^{-1} \cdot \text{mol}^{-1}$ CYP, but was undetectable in parental CHL cell. In addition, we have identified a *CYP2C18* cDNA clone with exon 5 missing.

CONCLUSION: The cDNA of human *CYP2C18* was successfully cloned and a cell line, CHL-CYP2C18, efficiently

expressing the protein of *CYP2C18*, was established. A spliced variant of CYP2C18 with exon 5 missing was identified in the cloning process.

Zhu-Ge J, Yu YN, Qian YL, Li X. Establishment of a transgenic cell line stably expressing human cytochrome P450 2C18 and identification of a *CYP2C18* clone with exon 5 missing. *World J Gastroenterol* 2002; 8(5):888-892

INTRODUCTION

Cytochrome P450 (CYP) is a heme-containing enzyme widely distributed from bacteria to mammals, and catalyzes the oxidative and reductive metabolism of a wide variety of compounds including endogenous as well as exogenous compounds. Mammalian CYP present in liver microsomes is characteristic of its nature in metabolizing exogenous compounds including drugs, pesticides, environmental pollutants, and carcinogens^[1]. Mammals contain at least 17 distinct *CYP* gene families that together code for an estimated 50-60 individual *CYP* genes in any given species^[2]. The human CYP2C subfamily comprises four members, CYP2C8, CYP2C9, CYP2C18 and CYP2C19^[3], accounting for 20 % of the total CYP in human liver. CYP2C18 mRNA was found in liver, albeit at mean levels 7-8-fold lower than those of mRNAs encoding CYP2C8 and CYP2C9^[4,5]. The cDNA encoding human *CYP2C18* has been characterized, but the protein has not been purified from liver, and very little is known regarding the specific substrate of CYP2C18^[4].

The combination of gene technology and cell culture technology has provided new opportunities for studying proteins because any gene from any species encoding a protein may be cloned and expressed in bacterial, yeast, or mammalian cell in a defined way^[6-11]. This approach in drug metabolism is of particular importance because some of the enzymes are difficult to purify and to prepare in sufficient quantities, for its low expression levels, organ-specificity of its expression, or low abundance of native organ material. These restrictions apply especially for human enzymes. The heterologous expression of the cDNA bypasses these restrictions^[12]. The human *CYP2C18* cDNA had been expressed in yeast^[13,14], COS-1 cells^[3], lymphoblast cells^[15], and human liver epithelial cells THLE^[16]. Several cell lines stably expressing human CYP1A1^[17], CYP2B6^[17], CYP2A6^[18], CYP3A4^[19], CYP2C9^[20] and a phase II metabolism enzyme UDP-glucuronosyltransferase, UGT1A9^[21] have been established in our laboratory. In this study human *CYP2C18* cDNA was amplified with reverse transcription-polymerase chain reaction (RT-PCR), and a transgenic cell line stably expressing CYP2C18 was established. In the cloning process, we have identified a spliced variant of CYP2C18 with exon 5 missing.

MATERIALS AND METHODS

Materials

Restriction endonucleases, moloney murine leukemia virus (M-MuLV) reverse transcriptase were supplied by MBI Fermentas AB, Lithuania. PCR primers, DNA sequence primers, random hexamer primer, Taq plus I, and dNTPs were synthesized or supplied by Shanghai Sangon Biotechnology Corp. DNA sequencing kit was purchased from Perkin-Elmer Corp. The TRIzol Reagent, G418, Minimum Essential Media (MEM) and newborn bovine calf sera were from Gibco. NADPH was from Roche molecular biochemicals. Diethyl pyrocarbonate (DEPC), tolbutamide and hydroxytolbutamide were purchased from Sigma Chemical Company. T4 DNA ligase and pGEM-T vector system were from Promega. Other chemical reagents used are all of analytical purity from the commercial sources.

Methods

Cloning of human CYP2C18 cDNA from a Chinese human liver The total RNA was extracted from a surgical specimen of human liver with TRIzol reagent according to the manufacturer's instructions. The RT-PCR amplifications were described before^[20]. Two specific 28 mer oligonucleotide PCR primers were designed according to the mRNA sequence of CYP2C18 reported by Romkes *et al.*^[3] (GenBank accession no. M61856, J05326). The sense primer corresponding to base position 38 to 65 was 5'-TTATCTTCTTCAGCTAGCCAATGTTTCAT-3', with a restriction site of *Nhe* I, and the anti-sense primer, corresponding to the base position from 1681 to 1708, was 5'-TGACAGCACTCGAGCAGCCAACTATCT-3', with a restriction site of *Xho* I. The PCR was performed at 94 °C 2 min, then 35 cycles of 94 °C 60 s, 55 °C 60 s, 72 °C 2 min, and lastly 72 °C 10 min. An aliquot (10 µl) from the PCR was subjected to electrophoresis in a 1 % agarose gel stained with ethidium bromide.

Construction of recombinant pGEM-CYP2C18 and sequencing of CYP2C18 cDNA^[22] The PCR products were ligated with pGEM-T vector, and transformed to the *E. coli* DH5a. Several cDNAs of *CYP2C18* cloned in pGEM-T were sequenced on both strands by dideoxy chain-termination method marked with BigDye with primers of T7 and SP6 promoters and two specific primers of 5'-GGACATGAGCAAATCCTTA-3' (343-361), and 5'-TGGGGATGAGGTAGTTTTTG-3' (1327-1346). The termination products were resolved and detected using an automated DNA sequencer (Perkin-Elmer-ABI Prism 310).

Construction of the pREP9 based expression plasmid for CYP2C18^[22] The *Nhe* I/ *Xho* I fragment having the total span of human *CYP2C18* cDNA and the correctly deduced amino acids sequence in pGEM-*CYP2C18* was subcloned to a mammalian expression vector pREP9 (Invitrogen). The recombinant was transformed to *E. coli* Top 10, and screened by ampicillin resistant. The recombinant was identified by restriction mapping.

Transfection and selection^[20,22] Chinese hamster lung (CHL) cells were transfected with the resultant recombinant plasmid, pREP9-*CYP2C18*, using a modified calcium phosphate method. A transgenic cell line named CHL-*CYP2C18* was established.

Preparation of postmitochondrial supernant (S9) of CHL-CYP2C18 The procedure of preparation of the S9 fraction was described before^[20]. The protein in S9 was determined by the Lowry's method, with bovine serum albumin as standard. CYP was measured spectrally using the method of Johannesen *et al.*^[23].

Tolbutamide hydroxylase assays^[20,24,25] The CYP2C18 tolbutamide hydroxylase activity of S9 was determined by high performance liquid chromatography (HPLC) as described before^[20].

RESULTS

Construction of recombinants and detection of an exon 5 skipping in transcripts of the human CYP2C18 gene

The recombinant of pGEM-*CYP2C18* (Figure 1) was constructed with the human *CYP2C18* cDNA inserted into the cloning site of pGEM-T vector. Selection and identification of the recombinant was carried out by *Nhe* I/ *Xho* I endonuclease digestion and agarose gel electrophoresis (Figure 2). Two cloned cDNA segments were sequenced completely. Comparing with the cDNA sequence reported by Romkes *et al.*^[3] (GenBank accession no. M61856, J05326), one has two base differences, 222T>C, 828C>T, while the encoding amino acid sequence was the same, I74 and H276. However, another cDNA clone was found to have only 8 exons (Figure 3). There is no base difference between this cDNA and the wild type one except the missing exon 5.

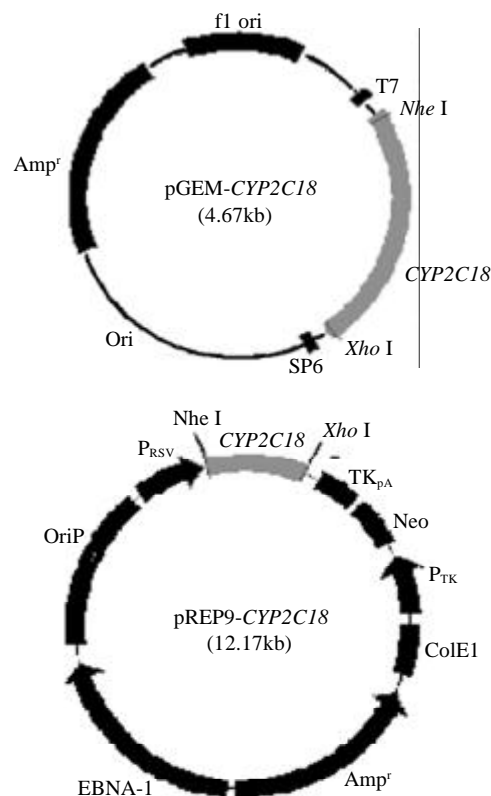


Figure 1 Scheme of recombinants of pGEM-*CYP2C18* and pREP9-*CYP2C18*

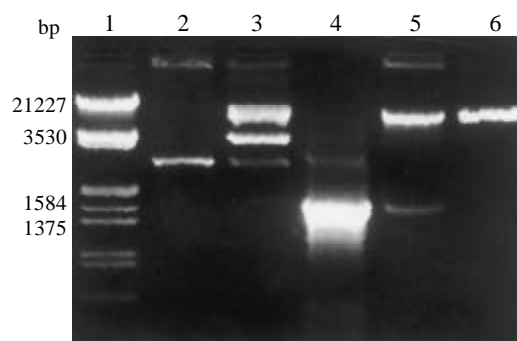


Figure 2 Electrophoresis identification of recombinants of pGEM-*CYP2C18* and pREP9-*CYP2C18*. Lane 1: Marker (λ /EcoR I and Hind III); 2: pGEM-T vector; 3: Recombinant of pGEM-*CYP2C18* digested by *Nhe* I and *Xho* I (incomplete digestion); 4: PCR products of *CYP2C18* (1.67 kb); 5: Recombinant of pREP9-*CYP2C18* digested by *Nhe* I and *Xho* I; 6: pREP9 vector.

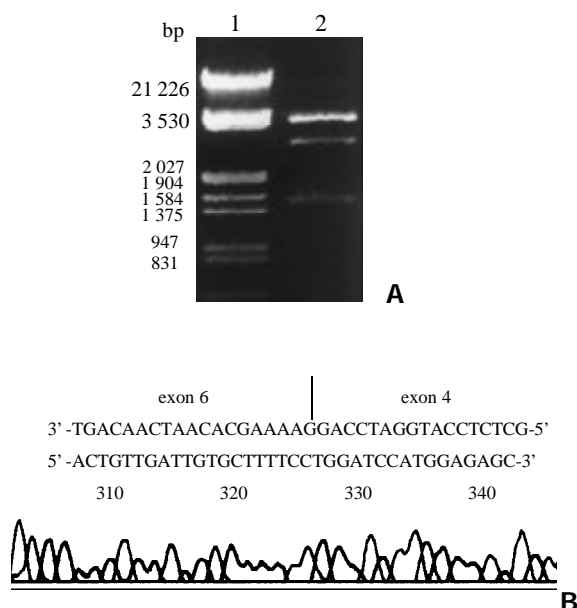


Figure 3 Electrophoresis and sequencing identification of a *CYP2C18* clone with exon 5 missing. A: Electrophoresis identification of a *CYP2C18* clone with an exon 5 being skipped; Lane 1: Marker (λ /EcoR I and Hind III); 2: Recombinant of pGEM-*CYP2C18* digested by *Nhe* I and *Xho* I (incompleted digestion); B: Partial sequencing of an *CYP2C18* cDNA clone with an exon 5 being skipped. The upper sequence represent the sense strand and the underside sequence represent the anti-sense strand being sequenced.

The *Nhe* I/*Xho* I fragment (1.65 kb) containing the complete *CYP2C18* cDNA was subcloned into the *Nhe* I/*Xho* I site of mammalian expression vector pREP9 (Figure 1). Selection and identification of the recombinant was carried out by *Nhe* I/*Xho* I endonuclease digestion and agarose gel electrophoresis (Figure 2). The resulting plasmid was designated as pREP9-*CYP2C18* and contains the entire coding region, along with 162 bp of the 5' and 36 bp of the 3' untranslated region of the *CYP2C18* cDNA, respectively.

Establishment of transgenic cell lines with *CYP2C18* enzyme activity

CHL cells were transfected with pREP9-*CYP2C18*, and selected with G418. The surviving clones were propagated and the cell line termed CHL-*CYP2C18* was established. The tolbutamide hydroxylase activity of *CYP2C18* in S9 of CHL-*CYP2C18* cells was assayed by HPLC. A typical elution profile of hydroxytolbutamide in extracts was shown (Figure 4).

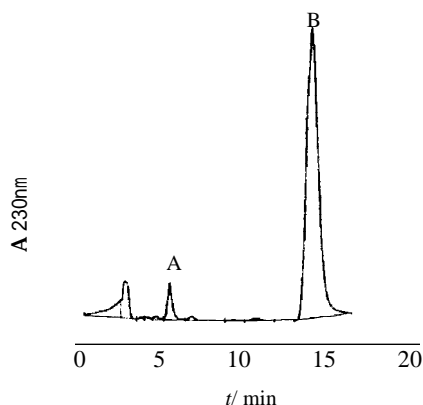


Figure 4 Representative chromatogram of extracts. A Shim-pack CLC-ODS column (15×0.6 cm i.d.) was used. The mobile

phase was constituted with 0.05 % phosphoric acid (pH 2.6), acetonitrile (6:4/V/V) with the flow rate of 1 mL·min⁻¹. Hydroxytolbutamide was monitored at 230 nm. A: hydroxytolbutamide; B: tolbutamide

The *CYP2C18* enzyme activity towards tolbutamide was found to be 0.509 ± 0.052 mmol·min⁻¹·g⁻¹ S9 protein or 8.82 ± 0.90 mol·min⁻¹·mol⁻¹ CYP ($n=3$), but was not detectable in parental CHL cells. The CYP content was 53.9 pmol·mg⁻¹ S9 protein from CHL-*CYP2C18* and no detectable CYP was present in CHL cells.

DISCUSSION

The human *CYP2C18* gene is located on chromosome 10q24. Four *CYP2C18* alleles have been reported. T385 and M385 alleles exhibited the same regio- and stereoselectivities for warfarin^[25]. There was no substantial difference in the ability of the T385 and M385 of *CYP2C18* to metabolize mephenytoin^[26]. *CYP2C18_{m1}*, a substitution of 204T>A in exon 2, which creates a stop codon that yields a truncated protein lacking the heme-binding site^[27]. *CYP2C18_{mFR}*, consisting of -460A>T substitution in the 5' -flanking region, the functional property of this mutant allele remains unclear^[28]. One of the *CYP2C18* cDNA cloned by us belongs to the T385 allele in amino acids sequence. Although there are two base substitutions, 222T>C, 828C>T, the encoding amino acids have not been changed.

To express the functional activity of a CYP, a cell must have adequate heme biosynthetic capabilities and ample intracellular membrane^[29]. CYPs also require other enzymatic components for full activity, including the flavoprotein NADPH-P450 oxidoreductase (OR) and, in some cases, cytochrome b₅. The OR must interact directly with the CYP to transfer the required two electrons from NADPH. Cytochrome b₅ is necessary for increasing electron transfer for certain CYP forms and specific substrates. The CHL is a cell line originally derived from the lung of a newborn female Chinese hamster and has no or very limited activities of CYP enzymes, but has adequate OR and cytochrome b₅ levels to support CYP activities.

To achieve high expression levels of *CYP2C18*, the *CYP2C18* cDNA was cloned into the eukaryotic expression vector pREP9, which had previously been used in this laboratory for the expression of human CYP1A1^[17], CYP2B6^[17], CYP3A4^[18], CYP2A6^[19], CYP2C9^[20] and UGT1A9^[21] in CHL cells. The salient feature of this vector has an EBV origin of replication and nuclear antigen (EBNA-1) to allow high-copy episomal replication in mammal cell lines. The Rous sarcoma virus long terminal repeat (RSV LTR) early promoter controls the expression of the *CYP2C18* cDNA.

CYP2C18 was expressed at a very low level in human liver^[4]. Its protein had not been detected and its mRNA can not be induced by rifampicin or phenobarbital in human livers and cultured primary hepatocytes^[5]. But it seems to be a major CYP2C in the skin and the lung judged by its mRNA levels^[30]. Its mRNA was found in the brain, uterus, mammary gland, kidney, and duodenum^[31]. It has been reported that *CYP2C18* can metabolize (S)-mephenytoin^[26], tolbutamide^[26], warfarin^[25], tienilic acid^[20], diclofenac^[13], aminopyrine^[32], and bisphenol A^[14] by yeast expression and metabolize all-trans-retinoic acid^[15] by lymphoblast expression. Cyclophosphamide (CPA) and ifosfamide can be metabolized by M385 *CYP2C18*. *CYP2C18*-M385 plus CYP OR appear to be excellent gene combinations for use with CPA in P450/prodrug activation-based cancer gene therapy^[33]. A 2-aryloxythiophenes derived from tienilic acid by replacement of its OCH₂COOH substituent with O(CH₂)₃OH function, appears to be a particularly good

substrate of CYP2C18^[34].

Tolbutamide (1-butyl-3-p-tolylsulfonylurea) is an oral hypoglycemic agent which is being used in the treatment of diabetes. In humans it undergoes CYP-catalyzed hydroxylation of the tolyl methyl group which is the initial and rate-limiting reaction followed by further oxidation by cytosolic dehydrogenases yielding carboxytolbutamide. Overall this pathway accounts for up to 85 % of tolbutamide clearance in humans^[35]. We used tolbutamide as a substrate for evaluating the expression of human CYP2C18 activity in CHL-CYP2C18 cells. The tolbutamide hydroxylase activity was 0.509 ± 0.052 mmol·min⁻¹·g⁻¹ S9 protein or 8.82 ± 0.90 mol·min⁻¹·mol⁻¹ CYP, which is slightly higher than that of our cloned human CYP2C9: 0.465 ± 0.109 μmol·min⁻¹·g⁻¹ S9 protein or 8.62 ± 2.02 mol·min⁻¹·mol⁻¹ CYP^[20]. The tolbutamide hydroxylase activity was reported to be 0.273 ± 0.066 ^[36] or 0.189 ± 0.008 ^[37] mmol·min⁻¹·g⁻¹ of human liver microsomes. Considering the low expression of CYP2C18 in liver, the tolbutamide hydroxylase activity in human liver might be contributed by CYP2C9. CHL-CYP2C18 cells efficiently expressing the CYP2C18 may be a useful tool for further studies of its enzymatic function and mechanism.

Interestingly, we find one of our cloned *CYP2C18* cDNAs has only 8 exons by DNA sequencing. This cDNA clone is identical to the wild-type one except the missing exon 5. This is consistent with Zaphiropoulos's report that an exon 5 skipping of human *CYP2C18* gene in epidermis^[30]. The exon is spliced at the predicted sites indicating that it pre-exists in the mRNA samples and is not a PCR artifact. Transcripts that have skipped *CYP2C18* exon 4, exon 4,5 and 6, or exon 4,5,6, and 7 were also identified in epidermis^[30]. The splicing process in higher eukaryotes is characterized by the precise excision of introns that can be longer than 50 000 bases and the joining of exons that are rarely over 300 bases. Yet the mechanisms that regulate the splicing process and the generation of alternatively spliced mRNA products are still poorly understood^[38]. In addition to alternative splicing in intragenic RNA molecule, chimeric RNA production had been detected in *CYP2Cs*^[39-41] and *CYP3As*^[42] genes. This finding suggests that intergenic mRNA formation may represent a generalized splicing pathway that deepens the complexity of splicing patterns in gene families^[42] and the concept of gene transcription may not suffice to include all variations in expressed genomic sequences. Finta and Zaphiropoulos^[43] proposed a more general term, "genome transcription".

The difference in enzyme activity between the full length clone and the spliced variant will be studied in the future.

REFERENCES

- 1 **Anzenbacher P**, Anzenbacherova E. Cytochromes P450 and metabolism of xenobiotics. *Cell Mol Life Sci* 2001; **58**: 737-747
- 2 **Nelson DR**. Cytochrome P450 and the individuality of species. *Arch Biochem Biophys* 1999; **369**: 1-10
- 3 **Romkes M**, Faletto MB, Blaisdell JA, Raucy JL, Goldstein JA. Cloning and expression of complementary DNAs for multiple members of the human cytochrome P450IIC subfamily. *Biochemistry* 1991; **30**: 3247-3255
- 4 **Richardson TH**, Griffin KJ, Jung F, Raucy JL, Johnson EF. Targeted antipeptide antibodies to cytochrome P450 2C18 based on epitope mapping of an inhibitory monoclonal antibody to P450 2C51. *Arch Biochem Biophys* 1997; **338**: 157-164
- 5 **Gerbal-Chaloin S**, Pascussi JM, Pichard-Garcia L, Daujat M, Waechter F, Fabre JM, Carrere N, Maurel P. Induction of CYP2C genes in human hepatocytes in primary culture. *Drug Metab Dispos* 2001; **29**: 242-251
- 6 **Liu XF**, Zou SQ, Qiu FZ. Construction of HCV-core gene vector and its expression in cholangiocarcinoma. *World J Gastroenterol* 2002; **8**: 135-138
- 7 **Wu C**, Zou QM, Guo H, Yuan XP, Zhang WJ, Lu DS, Mao XH. Expression, purification and immuno-characteristics of recombination UreB protein of *H. pylori*. *World J Gastroenterol* 2001; **7**: 389-393
- 8 **Li XJ**, Wu JG, Si JL, Guo DW, Xu JP. High-level expression of human calmodulin in *E. coli* and its effects on cell proliferation. *World J Gastroenterol* 2000; **6**: 588-592
- 9 **Cheng J**, Zhong YW, Liu Y, Dong J, Yang JZ, Chen JM. Cloning and sequence analysis of human genomic DNA of augments of liver regeneration. *World J Gastroenterol* 2000; **6**: 275-277
- 10 **Lu JG**, Lin C, Huang ZQ, Wu JS, Fu M, Zhang XY, Liang X, Yao X, Wu M. Inhibitory effects of human cholangiocarcinoma cell line by recombinant adenoviruses P16 with CDDP. *Shijie Huaren Xiaohua Zazhi* 2000; **8**: 641-645
- 11 **Qin XY**, Shen KT, Zhang X, Cheng ZH, Xu XR, Han ZG. Establishment of an artificial β-cell line expressing insulin under the control of doxycycline. *World J Gastroenterol* 2002; **8**: 367-370
- 12 **Crespi CL**, Miller VP. The use of heterologously expressed drug metabolizing enzymes-state of the art and prospects for the future. *Pharmacol Therapeutics* 1999; **84**: 121-131
- 13 **Mancy A**, Antignac M, Minoletti C, Dijols S, Mouries V, Duong NT, Battioni P, Dansette PM, Mansuy D. Diclofenac and its derivatives as tools for studying human cytochromes P450 active sites: particular efficiency and regioselectivity of P450 2Cs. *Biochemistry* 1999; **38**: 14264-14270
- 14 **Niwa T**, Fujimoto M, Kishimoto K, Yabusaki Y, Ishibashi F, Katagiri M. Metabolism and interaction of bisphenol A in human hepatic cytochrome P450 and steroidogenic CYP17. *Biol Pharm Bull* 2001; **24**: 1064-1067
- 15 **Marill J**, Cresteil T, Lanotte M, Chabot GG. Identification of human cytochrome P450s involved in the formation of all-trans-retinoic acid principal metabolites. *Mol Pharmacol* 2000; **58**: 1341-1348
- 16 **Bort R**, Castell JV, Pfeifer A, Gomezlechón MJ, Mace K. High expression of human CYP2C in immortalized human liver epithelial cells. *Toxicol Vitro* 1999; **13**: 633-638
- 17 **Wu J**, Dong H, Cai Z, Yu Y. Stable expression of human cytochrome CYP2B6 and CYP1A1 in chinese hamster CHL cells: their use in micronucleus assays. *Chin Med Sci J* 1997; **12**: 148-155
- 18 **Yan LQ**, Yu YN, Zhuge J, Xie HY. Cloning of human cytochrome P450 2A6 cDNA and its expression in mammalian cells. *Zhongguo Yaolixue Yu Dulixue Zazhi* 2000; **14**: 31-35
- 19 **Chen Q**, Wu J, Yu Y. Establishment of transgenic cell line CHL-3A4 and its metabolic activation. *Zhonghua Yufang Yixue Zazhi* 1998; **32**: 281-284
- 20 **Zhu GJ**, Yu YN, Li X, Qian YL. Cloning of cytochrome P-450 2C9 cDNA from human liver and its expression in CHL cells. *World J Gastroenterol* 2002; **8**: 318-322
- 21 **Li X**, Yu YN, Zhu GJ, Qian YL. Cloning of UGT1A9 cDNA from liver tissues and its expression in CHL cells. *World J Gastroenterol* 2001; **7**: 841-845
- 22 **Sambrook J**, Fritsch EF, Maniatis T. Molecular Cloning, A Laboratory Manual; 2nd ed. New York: Cold Spring Harbor Laboratory Press 1989; **6**: 28-29
- 23 **Johannessen KA**, DePierre JW. Measurement of cytochrome P-450 in the presence of large amounts of contaminating hemoglobin and methemoglobin. *Anal Biochem* 1978; **86**: 725-732
- 24 **Ho JW**, Moody DE. Determination of tolbutamide hydroxylation in rat liver microsomes by high-performance liquid chromatography: effect of psychoactive drugs on *in vitro* activity. *Life Sci* 1993; **52**: 21-28
- 25 **Kaminsky LS**, de-Morais SM, Faletto MB, Dunbar DA, Goldstein JA. Correlation of human cytochrome P4502C

- substrate specificities with primary structure: warfarin as a probe. *Mol Pharmacol* 1993; **43**: 234-239
- 26 **Goldstein JA**, Faletto MB, Romkes-Sparks M, Sullivan T, Kitareewan S, Raucy JL, Lasker JM, Ghanayem BI. Evidence that CYP2C19 is the major (S)-mephenytoin 4'-hydroxylase in humans. *Biochemistry* 1994; **33**: 1743-1752
- 27 **Komai K**, Sumida K, Kaneko H, Nakatsuka I. Identification of a new non-functional CYP2C18 allele in Japanese: Substitution of T204 to A in exon 2 generates a premature stop codon. *Pharmacogenetics* 1996; **6**: 117-119
- 28 **Tsuneoka Y**, Matsuo Y, Okuyama E, Watanabe Y, Ichikawa Y. Genetic analysis of the cytochrome P-450IIC18 (CYP2C18) gene and a novel member of the CYP2C subfamily. *FEBS Lett* 1996; **384**: 281-284
- 29 **Correia MA**, Farrell GC, Schmid R, Ortiz-de-Montellano PR, Yost GS, Mico BA. Incorporation of exogenous heme into hepatic cytochrome P-450 *in vivo*. *J Biol Chem* 1979; **254**: 15-17
- 30 **Zaphiropoulos PG**. Exon skipping and circular RNA formation in transcripts of the human cytochrome P-450 2C18 gene in epidermis and of the rat androgen binding protein gene in testis. *Mol Cell Biol* 1997; **17**: 2985-2993
- 31 **Klose TS**, Blaisdell JA, Goldstein JA. Gene structure of CYP2C8 and extrahepatic distribution of the human CYP2Cs. *J Biochem Mol Toxicol* 1999; **13**: 289-295
- 32 **Niwa T**, Sato R, Yabusaki Y, Ishibashi F, Katagiri M. Contribution of human hepatic cytochrome P450s and steroidogenic CYP17 to the N-demethylation of aminopyrine. *Xenobiotica* 1999; **29**: 187-193
- 33 **Jounaidi Y**, Hecht JE, Waxman DJ. Retroviral transfer of human cytochrome P450 genes for oxazaphosphorine-based cancer gene therapy. *Cancer Res* 1998; **58**: 4391-4401
- 34 **Minoletti C**, Dijols S, Dansette PM, Mansuy D. Comparison of the substrate specificities of human liver cytochrome P450s 2C9 and 2C18: application to the design of a specific substrate of CYP 2C18. *Biochemistry* 1999; **38**: 7828-7836
- 35 **Miners JO**, Birkett DJ. Cytochrome P450 2C9: an enzyme of major importance in human drug metabolism. *Br J Clin Pharmacol* 1998; **45**: 525-538
- 36 **Miners JO**, Smith KJ, Robson RA, McManus ME, Veronese ME, Birkett DJ. Tolbutamide hydroxylation by human liver microsomes. *Biochem Pharmacol* 1988; **37**: 1137-1144
- 37 **Easterbrook J**, Fackett D, Li AP. A comparison of arclor 1254-induced and uninduced rat liver microsomes to human liver microsomes in phenytoin O-deethylation, coumarin 7-hydroxylation, tolbutamide 4-hydroxylation, S-mephenytoin 4'-hydroxylation, chloroxazone 6-hydroxylation and testosterone 6beta-hydroxylation. *Chem Biol Interact* 2001; **134**: 243-249
- 38 **Zaphiropoulos PG**. Mechanisms of pre-mRNA splicing: classical versus non-classical pathways. *Histol Histopathol* 1998; **13**: 585-589
- 39 **Zaphiropoulos PG**. RNA molecules containing exons originating from different members of the cytochrome P450 2C gene subfamily (CYP2C) in human epidermis and liver. *Nucleic Acids Res* 1999; **27**: 2585-2590
- 40 **Finta C**, Zaphiropoulos PG. The human CYP2C locus: a prototype for intergenic and exon repetition splicing events. *Genomics* 2000; **63**: 433-438
- 41 **Warner SC**, Finta C, Zaphiropoulos PG. Intergenic transcripts containing a novel human cytochrome P450 2C exon 1 spliced to sequences from the CYP2C9 gene. *Mol Biol Evol* 2001; **18**: 1841-1848
- 42 **Finta C**, Zaphiropoulos PG. Intergenic mRNA molecules resulting from trans-splicing. *J Biol Chem* 2002; **277**: 5882-5890
- 43 **Finta C**, Zaphiropoulos PG. A statistical view of genome transcription? *J Mol Evol* 2001; **53**: 160-162

Edited by Bo XN

• BASIC RESEARCH •

Effects of electroporation on primary rat hepatocytes *in vitro*

Yun-Qing Yao, Ding-Feng Zhang, Ai-Long Huang, Yun Luo, Da-Zhi Zhang, Bo Wang, Wei-Ping Zhou, Hong Ren, Shu-Hua Guo

Yun-Qing Yao, Department of Infectious Diseases of the First Affiliated Hospital, Chongqing University of Medical Sciences, Chongqing 400016, China

Ding-Feng Zhang, Ai-Long Huang, Yun Luo, Da-Zhi Zhang, Bo Wang, Wei-Ping Zhou, Hong Ren, Shu-Hua Guo, Institute for Viral Hepatitis, Chongqing University of Medical Sciences, Chongqing 400010, China

Supported by the National Natural Science Foundation of China, No. 39670340

Correspondence to: Dr. Yun-Qing Yao, Department of Infectious Diseases of the First Affiliated Hospital, Chongqing University of Medical Sciences, Chongqing 400016, China. sigyaoyq@public.cta.cq.cn

Telephone: +86-23-69012273

Received 2001-08-09 **Accepted** 2002-05-15

Abstract

AIM: To investigate the effects of electroporation on primary rat hepatocyte and to optimize the electroporation conditions introducing foreign genes into primary hepatocytes.

METHODS: A single-pulse procedure was performed at low voltage (220-400 V) but with high capacitance (500-950 μF). Hepatocytes were divided into 4 groups according to the electroporation conditions: group I, 220 V and 500 μF ; group II, 220 V and 950 μF ; group III, 400 V and 950 μF , and group IV. The control group was freshly isolated hepatocytes and directly cultured under the same conditions as those of electroporation groups. The effects of electroporation on primary rat hepatocytes were detected by trypan blue exclusion (TBE) and MTT analysis. Besides, albumin (Alb), alanine transaminase (ALT) and lactate dehydrogenase (LDH) in the supernatants of cultured hepatocytes were measured by biochemical assay.

RESULTS: Between day 1 and day 15 after incubation, primary rat hepatocytes of each electroporation group appeared normal, being the same with those of control group. TBE staining showed that slight hepatocyte damage and high survival rate were found in the electroporation groups and the control group. Cultured for 3, 7, 11 and 15 days, hepatocyte viability was approximately $92.6 \pm 2.5\%$, $89.5 \pm 3.3\%$, $82.0 \pm 3.5\%$ and $74.3 \pm 1.2\%$, respectively. MTT analysis indicated that the viabilities of hepatocytes had no significant difference between each electroporation group, and those were similar to that of control group. At the 36th hour after electroporation, Alb, ALT and LDH in the supernatants of control group were $5.3 \pm 0.1 \text{ g} \cdot \text{L}^{-1}$, $183.7 \pm 8.4 \text{ nkat} \cdot \text{L}^{-1}$ and $896.8 \pm 58.5 \text{ nkat} \cdot \text{L}^{-1}$; those of group II were $5.7 \pm 0.1 \text{ g} \cdot \text{L}^{-1}$, $215.4 \pm 16.7 \text{ nkat} \cdot \text{L}^{-1}$ and $1063.8 \pm 51.8 \text{ nkat} \cdot \text{L}^{-1}$; and those of group III were $5.8 \pm 0.2 \text{ g} \cdot \text{L}^{-1}$, $217.1 \pm 8.4 \text{ nkat} \cdot \text{L}^{-1}$ and $1063.8 \pm 10.0 \text{ nkat} \cdot \text{L}^{-1}$. Statistically, the proteins of group II and group III were significantly higher than those of control group ($P < 0.05$), whereas the protein production of group I, Alb, ALT and LDH were $5.3 \pm 0.2 \text{ g} \cdot \text{L}^{-1}$, $205.4 \pm 3.3 \text{ nkat} \cdot \text{L}^{-1}$ and $1035.4 \pm 116.9 \text{ nkat} \cdot \text{L}^{-1}$, were similar to those of control group. At the same time,

TBE and MTT analysis indicated that there was no significant cell viability difference between electroporation groups and control group.

CONCLUSION: This single-pulse electroporation procedure performed at low voltage (220-400 V) but with high capacitance (950 μF) is one of the optimal choices to introduce foreign genes into primary rat hepatocyte.

Yao YQ, Zhang DF, Huang AL, Luo Y, Zhang DZ, Wang B, Zhou WP, Ren H, Guo SH. Effects of electroporation on primary rat hepatocytes *in vitro*. *World J Gastroenterol* 2002; 8(5):893-896

INTRODUCTION

Electroporation technique has been widely used in the experiments of foreign gene transfection into cultural cells. Little is known about the effect of electroporation on the primary culture cells, especially on the primary hepatocytes, for most of the target cells are immortal carcinoma cells. At present, in the *in vitro* study of liver diseases, primary cultured hepatocytes have been used as one of the most important target cells, which are increasingly used in the research of basic and clinical medicine^[1-17], and electroporation has also been used as preferred means introducing foreign genes into primary hepatocytes. It is known that primary hepatocyte does not proliferate in common culture, so the biological activities of electroporated hepatocytes must be the key points affecting the efficiency of transfection and expression of foreign genes in the target cells. In order to optimize the electroporation conditions introducing foreign genes into hepatocytes, we studied the effect of electroporation on the biological activities of primary cultured rat hepatocyte.

MATERIALS AND METHODS

Isolation and culture of hepatocytes

Wistar rats, male, about 200 g of body mass, were provided by the Center for Laboratory Animal at Chongqing University of Medical Sciences. Hepatocytes were harvested from adult Wistar rats using the *in situ* collagenase perfusion technique^[18]. Injected into the peritoneal cavity with pentobarbital sodium (100 $\text{mg} \cdot \text{kg}^{-1}$ body weight) and heparin (200 $\text{IU} \cdot \text{kg}^{-1}$ body weight), the abdomen of the animals were opened and the portal vein was exposed and cannulated. Then the liver was perfused at 37°C *in situ* first with a calcium-free Hanks' Balanced Salt Solution (HBSS) for 10 min, next with $0.2 \text{ g} \cdot \text{L}^{-1}$ collagenase (Type IV, 390 $\text{kU} \cdot \text{g}^{-1}$) in calcium-presented HBSS for 15 min. The liver was removed and the cells were combed gently in tissue culture medium. Hepatocytes were pelleted, washed, and separated from nonparenchymal cells by differential centrifugations at $50 \times g$. Viability of hepatocytes exceeded 98 % as determined by trypan blue exclusion (TBE).

Electroporation

Freshly isolated hepatocytes were diluted into $1 \times 10^{10} \text{ cells} \cdot \text{L}^{-1}$ suspension with serum-free RPMI 1640 medium for

electroporation (electroporation apparatus is Bio Rad Gene Pulser II), and were divided into three groups. In group I, voltage was 220 V, and capacitance was 500 μF , in group II, 220 V and 950 μF , and in group III, 400 V and 950 μF . All of three groups were electroporated by single-pulse procedure, and electroporation time was about 19 ms. Before and after electroporation hepatocytes were put onto ice for 10 min. Electroporated hepatocytes diluted into $3 \times 10^8 \text{ cells} \cdot \text{L}^{-1}$ suspension with hepatocyte culture medium was inoculated into 96-well plastic cell-culture plates (3×10^4 cells in each well). Medium contained RPMI 1640 with insulin ($100 \text{ U} \cdot \text{L}^{-1}$), penicillin, streptomycin and $100 \text{ ml} \cdot \text{L}^{-1}$ fetal bovine serum. Control group, group IV, was freshly isolated hepatocytes and was directly cultured under the same conditions as those of electroporation groups. The medium was changed after 36 h incubation and later changed every two days.

Hepatocyte viability and function

To detect the viabilities of hepatocytes of electroporation groups and control group, TBE staining was used from day 1 to day 15 after incubation. Besides, MTT analysis was also used to measure the cell viability. At 36 h after incubation, the medium was changed with phenol red-free RPMI 1640 medium (0.1 mL each well), 10 μL MTT ($5 \text{ g} \cdot \text{L}^{-1}$) was added into each well, and incubated for another 4 h. Then discard the supernatants, add 0.1 mL dimethyl sulfoxide into each well and oscillate the culture plate for 5 min. Next, the 96-well culture plate was put into Elx800 type automatic reader and absorbance values in each well was detected at 405 nm wave length. Each group had more than 6 wells each time. Three more of these tests were repeated. To measure albumin (Alb), alanine aminotransferase (ALT) and lactic dehydrogenase (LDH) in the supernatants of cultured hepatocytes of electroporation groups and control group, biochemical assays were used.

RESULTS

Effect of electroporation on the viability of hepatocytes

From day 1 to day 15 after incubation, primary rat hepatocytes of each electroporation group appeared normal, the same as those of control group. TBE staining showed that the viabilities of hepatocytes had no significant difference between each electroporation group, which were similar to that of control group (Table 1). Culture for 7 d showed that hepatocyte viability was still around 90 %, and about 74 % hepatocytes survived 15 d after electroporation. MTT analysis also showed the same results, after 36 h of culture, primary rat hepatocytes of electroporation groups had the same viabilities as that of control group ($P > 0.05$, Student's *t* test), the absorbance values (405 nm wave length) of group I to IV were 0.317 ± 0.069 , 0.369 ± 0.059 , 0.279 ± 0.085 and 0.332 ± 0.072 , respectively.

Table 1 Viabilities of electroporated hepatocytes measured by TBE

Culture time (day)	Survival rate (%)
1	95.4 ± 1.8
3	92.6 ± 2.5
5	91.3 ± 2.4
7	89.5 ± 3.3
9	87.2 ± 4.6
11	82.0 ± 3.5
13	77.0 ± 0.9
15	74.3 ± 1.2

Effect of electroporation on hepatocyte function

To detect the effect of electroporation on Alb, ALT and LDH production of primary rat hepatocytes, biochemical assays were used to measure these proteins in the supernatants of cultured hepatocytes. Amounts of Alb, ALT and LDH in the supernatants were assayed 36 h after incubation. The results (Table 2) showed that Alb, ALT and LDH production of electroporation groups II and III were significantly higher than those of control group, whereas the protein production of group I was similar to those of control group.

Table 2 Alb, ALT and LDH production in the supernatants of primary cultured rat hepatocytes

Groups	Alb/($\text{g} \cdot \text{L}^{-1}$)	ALT/($\text{nkatal} \cdot \text{L}^{-1}$)	LDH/($\text{nkatal} \cdot \text{L}^{-1}$)
I	5.3 ± 0.2	205.4 ± 3.3	1035.4 ± 116.9
II	5.7 ± 0.1^a	215.4 ± 16.7	1063.8 ± 51.8^a
III	5.8 ± 0.2^a	217.1 ± 8.4^a	1063.8 ± 10.0^a
IV	5.3 ± 0.1	183.7 ± 8.4	896.8 ± 58.5

^a $P < 0.05$, vs control.

DISCUSSION

Primary hepatocytes have been increasingly used in basic and clinical medicine researches, such as the study of hepatocyte function, the mechanism of hepatocyte injuries and the protective approaches of hepatocyte biological activities^[19-25], and the use of hepatocytes in bioartificial liver support system (BALSS)^[26,27] and gene therapy^[28]. Besides, more and more researchers utilize primarily cultured hepatocyte model to study foreign genes' activities and effects on host cells, for example, hepatitis B and C viruses replication and expression in hepatocytes^[29-31]. In order to keep the normal biological activities and functions *in vitro* of hepatocytes, more methods have been used to optimize primary hepatocyte model, especially the introduction techniques of foreign genes into hepatocytes.

The introduction and stable expression of foreign genes in mammalian hepatocytes have been demonstrated by several techniques^[32-37], including the use of physical approaches such as direct injection of a DNA calcium phosphate precipitate, electroporation of plasmid DNA and the exposure to liposome-erythrocyte ghost complexes as well as the biological approach of infection of primary hepatocyte cultured with retrovirus vectors. Among these techniques, electroporation has been considered as one of the most useful methods introducing foreign into target cells^[38-41]. However, it is not defined that which electroporation condition is the best one under which foreign genes can be efficiently transduced into primarily cultured hepatocytes, and this condition could cause little damage to target cells.

It is known that primarily cultured hepatocytes are well-differentiated cells, most of which are resting cells, arrested in G₀, and do not proliferate in common culture conditions. To be an ideal model, in which foreign gene can get highly efficient transfection and expression, primarily cultured hepatocytes after electroporation could not only keep a high survival rate, but also maintain excellent cellular functions. Therefore, optimizing electroporation conditions has become the key point affecting the biological activities of primary hepatocytes.

Our results showed that a single-pulse procedure performed at low voltage (220-400 V) but with a high capacitance (950

μF) caused minimal cell damage and kept hepatocyte with a high survival rate, cultured for 7 d and 15 d, greater than 90 % and 74 % respectively, and hepatocyte viabilities of electroporation groups were similar to that of control group and much higher than those reported by other savants. Our current data further indicated that this electroporation procedure could not only maintain hepatocyte function, but also facilitate Alb, ALT and LDH expression in hepatocytes and production in the culture medium. Its mechanism is not clear, possibly related to two reasons: first, Alb, ALT and LDH might leak into culture medium through electroporated hepatocyte membrane, while minimal cell damage had been found by TBE and MTT assay. Second, this electroporation condition may have a potentiation to stimulate wave of DNA synthesis in electroporated rat hepatocytes. In conclusion, this single-pulse procedure performed at low voltage (220-400 V) but with a high capacitance (950 μF) could not only cause minimal cell damage, but also potentiate DNA synthesis in rat hepatocytes. For instance, up to date, we have used this electroporation procedure in transducing hepatitis B virus gene into primary rat hepatocytes and primary duck hepatocytes and successfully observed that hepatocytes are competent for transfection with HBV gene, which can stably replicate and express in primary hepatocytes^[42,43]. Therefore, this single-pulse procedure can be used as one of the optimized electroporation procedures introducing foreign genes into primarily cultured hepatocytes.

REFERENCES

- 1 **Yao YQ**, Zhang DF, Luo Y, Zhang DZ, Huang AL, Zhou WP, Ren H. Fas Ligand expression and apoptosis in primary rat hepatocytes induced by lipopolysaccharide. *Zhonghua Ganzangbing Zazhi* 2000; **8**: 285-287
- 2 **Yao YQ**, Zhang DF, Luo Y, Huang AL, Zhou WP, Ren H. Research on Optimization of Cryopreservation Techniques of Primary Rat Hepatocytes. *Zhonghua Wuli Yixue Yu Kangfu Zazhi* 2001; **23**: 290
- 3 **Yao YQ**, Zhang DF, Luo Y, Zhang DZ, Huang AL, Zhou WP, Ren H. Influence of electroporation on the biological activities of primary rat hepatocytes. *Zhonghua Ganzangbing Zazhi* 2001; **9**: 178-180
- 4 **Yao YQ**, Zhang DF, Luo Y, Huang AL, Zhou WP, Ren H. Primary Rat Hepatocytes Isolated by in situ Recirculating Perfusion with Low Concentration Collagenase. *Xiandai Yiyao Weisheng Zazhi* 2001; **17**: 84-85
- 5 **Li ZY**, Otto K, Richard RE, Ni S, Kirillova I, Fausto N, Blau CA, Lieber A. Dimerizer-induced proliferation of genetically modified hepatocytes. *Mol Ther* 2002; **5**: 420-426
- 6 **Wang YJ**, Liu GD, Liu J, Li MD. Large-scale isolation of suckling pig hepatocytes. *Shijie Huaren Xiaohua Zazhi* 1999; **7**: 661-662
- 7 **Lee JH**, Kim WH, Park H, Yun C, Kim BH, Kwak SJ, Cho H, Kim MW. Production and characterization of immortalized rat hepatocytes secreting hepatocyte growth factor/scatter factor. *Hepatogastroenterology* 2000; **47**: 978-983
- 8 **Gao Y**, Hu HZ, Chen K, Yang JZ. Primary porcine hepatocytes with portal vein serum cultured on microcarriers or in spheroidal aggregates. *World J Gastroenterol* 2000; **6**: 365-370
- 9 **Beck NB**, Sidhu JS, Omiecinski CJ. Baculovirus vectors repress phenobarbital-mediated gene induction and stimulate cytokine expression in primary cultures of rat hepatocytes. *Gene Ther* 2000; **7**: 1274-1283
- 10 **Einarsson C**, Ellis E, Abrahamsson A, Ericzon BG, Björkhem I, Axelsson M. Bile acid formation in primary human hepatocytes. *World J Gastroenterol* 2000; **6**: 522-525
- 11 **Parker JC**, McPherson RK, Andrews KM, Levy CB, Dubins JS, Chin JE, Perry PV, Hulín B, Perry DA, Inagaki T, Dekker KA, Tachikawa K, Sugie Y, Treadway JL. Effects of skyrin, a receptor-selective glucagon antagonist, in rat and human hepatocytes. *Diabetes* 2000; **49**: 2079-2086
- 12 **Zang GQ**, Zhou XQ, Yu H, Xie Q, Zhao GM, Wang B, Guo Q, Xiang YQ, Liao D. Effect of hepatocyte apoptosis induced by TNF- α on acute severe hepatitis in mouse models. *World J Gastroenterol* 2000; **6**: 688-692
- 13 **Xie Q**, Liao D, Zhou XQ, Qian SB, Cheng SS. Transduction of primary rat hepatocytes with bicistronic retroviral vector. *World J Gastroenterol* 2000; **6**: 725-729
- 14 **Nelsen CJ**, Hansen LK, Rickheim DG, Chen C, Stanley MW, Krek W, Albrecht JH. Induction of hepatocyte proliferation and liver hyperplasia by the targeted expression of cyclin E and skp2. *Oncogene* 2001; **20**: 1825-1831
- 15 **Ouyang EC**, Wu CH, Walton C, Promrat K, Wu GY. Transplantation of human hepatocytes into tolerized genetically immunocompetent rats. *World J Gastroenterol* 2001; **7**: 324-330
- 16 **Si XH**, Yang LJ. Extraction and purification of TGF β and its effect on the induction of apoptosis of hepatocytes. *World J Gastroenterol* 2001; **7**: 527-531
- 17 **Min F**, Hao F, Liu B, Liu GD, Huang JM, Jiang TL. Isolation and culture of Tupaia hepatocytes. *Shijie Huaren Xiaohua Zazhi* 2001; **9**: 627-630
- 18 **Yao YQ**, Zhang DF, Luo Y, Huang AL, Zhou WP, Ren H. Primary Rat Hepatocytes Isolated by in situ Recirculating Perfusion with Low Concentration Collagenase. *Xiandai Yiyao Weisheng Zazhi* 2001; **17**: 84-85
- 19 **Wang XL**, Liu P, Liu CH, Liu C. Effects of coordination of FZHY decoction on functions of hepatocytes and hepatic satellite cells. *Shijie Huaren Xiaohua Zazhi* 1999; **7**: 663-665
- 20 **Liu XL**, Fan DM. Protective effects of prostaglandin E1 on hepatocytes. *World J Gastroenterol* 2000; **6**: 326-329
- 21 **Hu YY**, Liu CH, Wang RP, Liu C, Liu P, Zhu DY. Protective actions of salvianolic acid A on hepatocyte injured by peroxidation in vitro. *World J Gastroenterol* 2000; **6**: 402-404
- 22 **Chen XJ**, Ai ZL, Liu ZS. Apoptosis: a study on mechanism of injuries in human hepatocyte induced by mitomycin. *Shijie Huaren Xiaohua Zazhi* 2000; **8**: 746-750
- 23 **Takayama F**, Egashira T, Yamanaka Y. Protective effect of Ninjin-yoei-to on damage to isolated hepatocytes following transient exposure to tert-butyl hydroperoxide. *Jpn J Pharmacol* 2001; **85**: 227-233
- 24 **Stanca C**, Jung D, Meier PJ, Kullak-Ublick GA. Hepatocellular transport proteins and their role in liver disease. *World J Gastroenterol* 2001; **7**: 157-169
- 25 **Zhang GL**, Wang YH, Teng HL, Lin ZB. Effects of aminoguanidine on nitric oxide production induced by inflammatory cytokines and endotoxin in cultured rat hepatocytes. *World J Gastroenterol* 2001; **7**: 331-334
- 26 **Hu HZ**, Xu XP, Gao Y, Yang JZ. Experimental study of treatment of acute liver failure with bioartificial liver in pigs. *Shijie Huaren Xiaohua Zazhi* 2001; **9**: 139-143
- 27 **Chen XP**, Xue YL, Li XJ, Zhang ZY, Li YL, Huang ZQ. Experimental research on TECA-I bioartificial liver support system to treat canines with acute liver failure. *World J Gastroenterol* 2001; **7**: 706-709
- 28 **Allen KJ**, Reyes R, Demmler K, Mercer JF, Williamson R, Whitehead RH. Conditionally immortalized mouse hepatocytes for use in liver gene therapy. *J Gastroenterol Hepatol* 2000; **15**: 1325-1332
- 29 **Jiang YG**, Li QF, Mao Q, Wang YM. Primary human fetal hepatocytes with HBV infection in vitro. *Shijie Huaren Xiaohua Zazhi* 2000; **8**: 403-405
- 30 **Sprinzl MF**, Oberwinkler H, Schaller H, Protzer U. Transfer of hepatitis B virus genome by adenovirus vectors into cultured cells and mice: crossing the species barrier. *J Virol* 2001; **75**: 5108-5118
- 31 **Min F**, Hao F, Liu B, Liu GD, Huang JM, Wang YM, Song MN. A promotion of PEG and DMSO in HCV infection of adult normal Tupaia hepatocytes in primary culture in vitro. *Shijie Huaren Xiaohua Zazhi* 2001; **9**: 631-634
- 32 **Bilello JP**, Delaney WE 4th, Boyce FM, Isom HC. Transient disruption of intercellular junctions enables

- baculovirus entry into nondividing hepatocytes. *J Virol* 2001; **75**: 9857-9871
- 33 **Wade-Martins R**, Smith ER, Tyminski E, Chiocca EA, Saeki Y. An infectious transfer and expression system for genomic DNA loci in human and mouse cells. *Nat Biotechnol* 2001; **19**: 1067-1070
- 34 **Glebe D**, Berting A, Broehl S, Naumann H, Schuster R, Fiedler N, Tolle TK, Nitsche S, Seifer M, Gerlich WH, Schaefer S. Optimised conditions for the production of hepatitis B virus from cell culture. *Intervirology* 2001; **44**: 370-378
- 35 **Deng X**, Cagen LM, Wilcox HG, Park EA, Raghow R, Elam MB. Regulation of the rat SREBP-1c promoter in primary rat hepatocytes. *Biochem Biophys Res Commun* 2002; **290**: 256-262
- 36 **Riley NE**, Li J, Worrall S, Rothnagel JA, Swagell C, van Leeuwen FW, French SW. The Mallory body as an aggresome: *in vitro* studies. *Exp Mol Pathol* 2002; **72**: 17-23
- 37 **He Y**, Zhou J, Dou KF. Construction of hepatocyte growth factor expression vector and detection of expression in human hepatocytes. *Shijie Huaren Xiaohua Zazhi* 2001; **9**: 1143-1146
- 38 **Raptis L**, Brownell HL, Vultur AM, Ross GM, Tremblay E, Elliott BE. Specific inhibition of growth factor-stimulated extracellular signal-regulated kinase 1 and 2 activation in intact cells by electroporation of a growth factor receptor-binding protein 2-Src homology 2 binding peptide. *Cell Growth Differ* 2000; **11**: 293-303
- 39 **Yamamoto M**, Sakuma T, Ichimaru H, Nemoto N. Localization of estradiol-responsive region in the phenobarbital-responsive enhancer module of mouse Cyp2b-10 gene. *J Biochem Mol Toxicol* 2001; **15**: 76-82
- 40 **Jiang WG**, Grimshaw D, Lane J, Martin TA, Abounader R, Laterra J, Mansel RE, Abounder R. A hammerhead ribozyme suppresses expression of hepatocyte growth factor/scatter factor receptor c-MET and reduces migration and invasiveness of breast cancer cells. *Clin Cancer Res* 2001; **7**: 2555-2562
- 41 **Xue F**, Takahara T, Yata Y, Minemura M, Morioka CY, Takahara S, Yamato E, Dono K, Watanabe A. Attenuated acute liver injury in mice by naked hepatocyte growth factor gene transfer into skeletal muscle with electroporation. *Gut* 2002; **50**: 558-562
- 42 **Yao YQ**, Tang N, Huang AL, Wang B, Zhang DF. Study on the replication of hepatitis B virus compared with that of duck hepatitis B virus in primary duck hepatocytes. *Zhonghua Yixue Zazhi* 2001; **81**: 1157-1161
- 43 **Yao YQ**, Huang AL, Tang N, Wang B, Zhang DF. Replication and transfection of hepatitis B virus DNA into primary duck hepatocytes. *Zhonghua Ganzangbing Zazhi* 2002; **10**: 34-36

Edited by Ma JY

• BASIC RESEARCH •

Effect of N-desulfated heparin on hepatic/renal ischemia reperfusion injury in rats

Tong Zhou, Jin-Lian Chen, Wei Song, Feng Wang, Ming-Jun Zhang, Pei-Hua Ni, Jian-Guo Geng

Tong Zhou, Wei Song, Feng Wang, Department of Nephrology, Ruijin Hospital, Shanghai Second Medical University, Shanghai 200025, China

Jin-Lian Chen, Department of Gastroenterology, Shanghai Sixth People's Hospital, Shanghai 200233, China

Ming-Jun Zhang, Animal Laboratory, Ruijin Hospital, Shanghai Second Medical University, Shanghai 200025, China

Pei-Hua Ni, Department of Biochemistry, Shanghai Second Medical University, Shanghai 200025

Jian-Guo Geng, Institute of Biochemistry and Cell Biology, Shanghai 200030, China

Supported by grants from the National Nature Scientific Funds of China (39970340) and the Scientific Funds of the Chinese Ministry of Health.

Correspondence to: Tong Zhou, Department of Nephrology, Ruijin Hospital, Shanghai Second Medical University, Shanghai 200025, China. zhoutong_cn@hotmail.com

Telephone: +86-21-64370045 **Fax:** +86-21-64333548

Received 2002-03-25 **Accepted** 2002-04-20

Abstract

AIM: To investigate the effect of N-desulfated heparin on hepatic/renal ischemia and reperfusion injury in rats.

METHODS: Using rat models of 60 minutes hepatic or renal ischemia followed by 1 h, 3 h, 6 h and 24 h reperfusion, animals were randomly divided into following groups, the sham operated controls, ischemic group receiving only normal saline, and treated group receiving N-desulfated heparin at a dose of 12 mg/kg at 5 minutes before reperfusion. P-selectin expression was detected in hepatic/renal tissues with immunohistochemistry method.

RESULTS: P-selectin expression, serum ALT, AST, BUN and Cr levels were significantly increased during 60 minute ischemia and 1 h, 3 h, 6 h and 24 h reperfusion, while the increment was significantly inhibited, and hepatic/renal pathology observed by light microscopy was remarkably improved by treatment with the N-desulfated heparin. Furthermore, the heparin was found no effects on PT and KPTT.

CONCLUSION: P-selectin might mediate neutrophil infiltration and contribute to hepatic/renal ischemia and reperfusion. The N-desulfated heparin might prevent hepatic/renal damage induced by ischemia and reperfusion injury without significant anticoagulant activity.

Zhou T, Chen JL, Song W, Wang F, Zhang MJ, Ni PH, Geng JG. Effect of N-desulfated heparin on hepatic/renal ischemia reperfusion injury in rats. *World J Gastroenterol* 2002; 8(5):897-900

INTRODUCTION

Hepatic/renal ischemia-reperfusion injury is very common

clinically. So far, no effective treatment for this pathological injury is available. It has been found that cell adhesion molecule P-selectin plays an important role in hepatic/renal ischemia-reperfusion injury by mediating the interactions of polymorphonuclear neutrophils with endothelium. P-selectin monoclonal antibody has been demonstrated to prevent effectively reperfusion-induced hepatic/renal tissue damage^[1-22]. Heparin, a highly sulfated proteoglycan, has anti-inflammatory activity besides its anticoagulant function. Recently reports suggested that heparin could prevent leukocyte adhesion through inhibiting the role of P-selectin and might be used to treat inflammatory diseases^[23]. However, the clinical use of heparin for treatment of inflammation is impeded by its strong anticoagulant activity^[24]. Chemically modified heparins which have been developed have relatively low anticoagulant activity remain their anti-inflammatory activities^[25,26]. In this study, we investigated the effect of N-desulfated heparin (NNH) on hepatic/renal ischemia-reperfusion injury in rats.

MATERIALS AND METHODS

Animal model

Ninety male Wistar rats (Shanghai Experimental Animal Centers of Chinese Academy of Sciences), weighing 200±10 g, were given free access to food and water for three days before the experiments. The rats were anesthetized with 2.5 % sodium pentobarbital intraperitoneally, and randomly divided into 2 groups. In one group of rats, the ligament linking liver, diaphragm and abdominal wall were separated, portal vein and liver artery that drain blood to left hepatic lobe were freed by blunt dissection and then blocked with a microvascular clamp for 60 minutes, after that clamp was removed, and reperfusion was started; while in another group, the left renal artery was freed, blocked with a microvascular clamp for 60 minutes, then the clamp was removed and reperfusion was started, simultaneously, the right kidney was cut off. The two groups of rats were randomly divided into NNH-treated group (n=20) and non-treated group (n=20). They were divided into subgroups according to the indicated time: 1, 3, 6, 24 hours after reperfusion. NNH (12 mg/kg, Institute of Biochemistry and Cell Biology, Chinese Academy of Sciences), or saline were injected by veins five minutes before reperfusion. A sham-operated group (n=5, anesthesia and opening celiac cavity, no blocking of hepatic or renal blood flow) served as control.

Collection and measurement methods of specimens

Blood, hepatic and renal tissues were harvested at the indicated time. Serum levels of aspartate aminotransferase (AST) and alanine aminotransferase (ALT), and blood urea nitrogen (BUN) and creatinine (Cr) were measured with a 747 automatic analyzer (Hitachi boehringer Mannheim, Mannheim, Germany). Hepatic and renal tissue samples were fixed in 10 % formalin and embedded in paraffin. Sections were cut 5 µm thick and stained with hematoxylin and eosin for light microscope examination. Expression of P-selectin in hepatic/renal tissue

was detected by an immunohistochemistry method with a labelled streptavidin biotin (LSAB) kit (Fujian Maixin Biotechnology Co., products of Biotechnology co. CA, USA). Activated partial thromboplastin time (APTT) and prothrombin time (PT) were also measured.

Statistical analysis

Data was presented with $\bar{x} \pm s$, and Student's *t* test was used to determine changed between different groups. $P < 0.05$ was considered significant.

RESULTS

Histopathologic evaluation

One hour after reperfusion, visual observation revealed that the left hepatic lobe was more swollen than the right lobe, and was dark in color. Under the light microscope, interstitial congestion and infiltration of inflammatory cells were observed. 1 hour after reperfusion, with the observation of naked eyes, the renal cortex was pale, the renal medulla displayed blood stagnation and was dark in color. Under the light microscope, edema, denaturation with different extent and necrosis of renal tubular epithelial cells were observed. Simultaneously, interstitial congestion, edema and infiltration of inflammatory cells were also observed. However, in the N-desulfated heparin-treated group. The outward appearance of the liver and kidney was similar to that of normal control. Hepatic cells and tubular cells showed less swelling and no denaturation or necrosis, and interstitial changes were not obvious.

Hepatic and renal function evaluation

Twenty four hours after hepatic reperfusion, the serum levels of ALT (628 ± 91 μ L) and AST (1608 ± 199 μ L) in the saline-treated group were much higher than the sham-operated group (52 ± 11 μ L and 80 ± 17 μ L respectively, $P < 0.01$). The NNH-treated group revealed significantly lower levels of ALT (161 ± 24 μ L) and AST (360 ± 49 μ L) compared with saline-treated group ($P < 0.01$).

Twenty four hours after renal reperfusion, the serum levels of BUN (14.54 ± 0.67 mmol/L) and Cr (102.2 ± 4.67 μ mol/L) were much higher than the sham-operated group (7.88 ± 0.57 mmol/L and 39.00 ± 4.47 μ mol/L, respectively, $P < 0.01$). The NNH-treated group presented with significantly lower levels of BUN (10.60 ± 0.80 mmol/L) and Cr (67.78 ± 5.01 μ mol/L) compared with saline-treated group ($P < 0.01$).

P-selectin expression in hepatic and renal tissues

P-selectin was expressed widely within hepatic and renal tissues 1 hour after reperfusion, which was mainly distributed on small vessels of left hepatic lobe and tubular epithelium. In addition, it was also expressed on part of hepatic cellular membrane, glomerulomesangium, capillary loops, and interstitium. After treatment with the NNH, there were no obvious yellow-brown positive granules in the hepatic and renal tissue, suggesting that the P-selectin expression was not displayed.

PT and KPTT assays

Twenty four hours after hepatic reperfusion, PT (15.0 ± 1.6 s) and KPTT (21.9 ± 4.1 s) in the saline-treated group were similar to that of sham-operated group (13.4 ± 1.7 s and 17.9 ± 2.9 s respectively, $P > 0.05$). PT (14.6 ± 1.9 s) and KPTT (18.7 ± 3.7 s) in NNH-treated group did not differ from those in saline-treated group ($P > 0.05$). 24 hours after renal reperfusion, PT and KPTT were 13.7 ± 1.4 s and 17.6 ± 3.1 s respectively, while in NNH-treated group they were 13.3 ± 1.6 s and 17.1 ± 3.5 s respectively ($P > 0.05$).

DISCUSSION

Recently, the role of cell adhesion molecules and neutrophil in organ ischemia and reperfusion injury has attracted attention^[27-48]. As a potential member of the selectin family, P-selectin is found in both weibel-plade body of epithelial cell of middle and small blood vessels and a-granule of platelet. It is expressed rapidly on the surface of these cells after their activation. P-selectin plays an important role in inflammation by initiating neutrophil rolling, adhesion and recruitment to injured tissue^[27]. Blockade of P-selectin expression or interaction with its ligands can attenuate leukocyte adherence and infiltration during ischemia and reperfusion injury. And P-selectin monoclonal antibody was found to have protective effects on the injury^[21,22].

Heparin and its analogue have been shown to bind to cell adhesion molecule P-selectin. The binding can inhibit adhesion of leukocytes mediated specifically by the adhesion molecules and are of anti-inflammatory activity^[25,26]. Although heparin can be used to treat inflammatory diseases, their clinical potentials are limited due to their potent anticoagulant activity. Several chemical modifications of heparin that have reduced anticoagulant activities while preserving their anti-inflammatory activities have been reported. For example, the O-desulfated heparin derivatives have been shown to be of treatment for inflammation, while they still retained 5-30 % anticoagulant activities as compared with heparin^[49]. Further, N-acetylheparin is known to have lower anticoagulant activity while preserving the anti-inflammatory activity^[50]. N-desulfated heparin has been reported to have significantly reduced anticoagulant activity^[51,52]. However, the anti-inflammatory roles of the heparin have not been extensively studied before.

The effect of N-desulfated heparin on ischemia and reperfusion injury was observed in this study based on the established rat model of hepatic/renal ischemia-reperfusion.

Hepatic and renal tissue displayed significant histopathologic damage after hepatic/renal ischemia-reperfusion while the serum levels of ALT and AST as well as BUN and Cr were increased. We showed that ischemia-reperfusion induced hepatic/renal injury was remarkably attenuated when NNH was given 5 min before reperfusion as shown by improved hepatic/renal function and less pathologic damage. The results suggest that the NNH has a protective effect on hepatic/renal reperfusion injury by inhibiting the interaction of neutrophils and endothelium.

After ischemia and reperfusion, P-selectin expression was up-regulated in hepatic and renal tissue, suggesting that P-selectin is related to hepatic/renal reperfusion injury. It has been found that leukocyte rolling and recruitment was delayed when deficient mice were infected, suggesting that P-selectin is involved in the early events of inflammation mediated by leukocytes^[53]. Results from this study showed that P-selectin expression in hepatic and renal tissue was inhibited in NNH-treated group. This is consistent with down-regulated expression of sialyl lewis X, a ligand for P-selectin located mainly in neutrophils, as with anti-P-selectin therapy (unpublished data). These suggest that P-selectin might mediate neutrophil infiltration within the liver and kidney in the early stage of hepatic/renal reperfusion injury. Furthermore, blockade of P-selectin can attenuate inflammatory cell infiltration and pathological damage. N-desulfated heparin can be of protective role in the hepatic and renal injury caused by ischemia-reperfusion by inhibiting the adhesion and activation of neutrophils mediated by P-selectin. In addition, we found the heparin had no significant effects on PT and KPTT. It is

consistent with Bjornsson's study^[51]. Therefore, the N-desulfated heparin might be an efficient approach for the treatment of reperfusion injury with no obvious anticoagulant activity.

REFERENCES

- Jaeschke H.** Is anti-P-selectin therapy effective in hepatic ischemia-reperfusion injury because it inhibits neutrophil recruitment? *Shock* 1999; **12**: 233-234
- Sawaya DE Jr,** Zibari GB, Minardi A, Bilton B, Burney D, Granger DN, McDonald JC, Brown M. P-selectin contributes to the initial recruitment of rolling and adherent leukocytes in hepatic venules after ischemia/reperfusion. *Shock* 1999; **12**: 227-232
- Yadav SS,** Howell DN, Steeber DA, Harland RC, Tedder TF, Clavien PA. P-Selectin mediates reperfusion injury through neutrophil and platelet sequestration in the warm ischemic mouse liver. *Hepatology* 1999; **29**: 1494-1502
- Singh I,** Zibari GB, Brown MF, Granger DN, Eppihimer M, Zizzi H, Cruz L, Meyer K, Gonzales E, McDonald JC. Role of P-selectin expression in hepatic ischemia and reperfusion injury. *Clin Transplant* 1999; **13**: 76-82
- Young CS,** Palma JM, Mosher BD, Harkema J, Naylor DF, Dean RE, Crockett E. Hepatic ischemia/reperfusion injury in P-selectin and intercellular adhesion molecule-1 double-mutant mice. *Am Surg* 2001; **67**: 737-744
- Amersi F,** Dulkanchainun T, Nelson SK, Farmer DG, Kato H, Zaky J, Melinek J, Shaw GD, Kupiec-Weglinski JW, Horwitz LD, Horwitz MA, Busuttil RW. A novel iron chelator in combination with a P-selectin antagonist prevents ischemia/reperfusion injury in a rat liver model. *Transplantation* 2001; **71**: 112-118
- Liu P,** Xu B, Hock CE, Nagele R, Sun FF, Wong PY. NO modulates P-selectin and ICAM-1 mRNA expression and hemodynamic alterations in hepatic I/R. *Am J Physiol* 1998; **275**: H2191-H2198
- Yoshidome H,** Kato A, Edwards MJ, Lentsch AB. Interleukin-10 suppresses hepatic ischemia/reperfusion injury in mice: implications of a central role for nuclear factor kappaB. *Hepatology* 1999; **30**: 203-208
- Kojima N,** Sato M, Suzuki A, Sato T, Satoh S, Kato T, Senoo H. Enhanced expression of B7-1, B7-2, and intercellular adhesion molecule 1 in sinusoidal endothelial cells by warm ischemia/reperfusion injury in rat liver. *Hepatology* 2001; **34**: 751-777
- Young CS,** Palma JM, Mosher BD, Harkema J, Naylor DF, Dean RE, Crockett E. Hepatic ischemia/reperfusion injury in P-selectin and intercellular adhesion molecule-1 double-mutant mice. *Am Surg* 2001; **67**: 737-744
- Serracino-Inglott F,** Habib NA, Mathie RT. Hepatic ischemia-reperfusion injury. *Am J Surg* 2001; **181**: 160-166
- Ghobrial R,** Amersi F, Stecker K, Kato H, Melinek J, Singer J, Mhoyan A, Busuttil RW, Kupiec-Weglinski JW, Stepkowski SM. Amelioration of hepatic ischemia/reperfusion injury with intercellular adhesion molecule-1 antisense oligodeoxynucleotides. *Transplant Proc* 2001; **33**: 538
- Kuzume M,** Nakano H, Yamaguchi M, Matsumiya A, Shimokohbe G, Kitamura N, Nagasaki H, Kumada K. A monoclonal antibody against ICAM-1 suppresses hepatic ischemia-reperfusion injury in rats. *Eur Surg Res* 1997; **29**: 93-100
- Yadav SS,** Howell DN, Gao W, Steeber DA, Harland RC, Clavien PA. L-selectin and ICAM-1 mediate reperfusion injury and neutrophil adhesion in the warm ischemic mouse liver. *Am J Physiol* 1998; **275**: G1341-G1352
- Colletti LM,** Cortis A, Lukacs N, Kunkel SL, Green M, Strieter RM. Tumor necrosis factor up-regulates intercellular adhesion molecule 1, which is important in the neutrophil-dependent lung and liver injury associated with hepatic ischemia and reperfusion in the rat. *Shock* 1998; **10**: 182-191
- Meyer K,** Brown MF, Zibari G, Panes J, McMillan RW, McDonald JC, Granger DN. ICAM-1 upregulation in distant tissues after hepatic ischemia/reperfusion: a clue to the mechanism of multiple organ failure. *J Pediatr Surg* 1998; **33**: 350-353
- Nemoto T,** Burne MJ, Daniels F, O'Donnell MP, Crosson J, Berens K, Issekutz A, Kasiske BL, Keane WF, Rabb H. Small molecule selectin ligand inhibition improves outcome in ischemic acute renal failure. *Kidney Int* 2001; **60**: 2205-2214
- Fuller TF,** Sattler B, Binder L, Vetterlein F, Ringe B, Lorf T. Reduction of severe ischemia/reperfusion injury in rat kidney grafts by a soluble P-selectin glycoprotein ligand. *Transplantation* 2001; **72**: 216-222
- Singbartl K,** Green SA, Ley K. Blocking P-selectin protects from ischemia/reperfusion-induced acute renal failure. *FASEB J* 2000; **14**: 48-54
- Zizzi HC,** Zibari GB, Granger DN, Singh I, Cruz LD, Abreo F, McDonald JC, Brown MF. Quantification of P-selectin expression after renal ischemia and reperfusion. *J Pediatr Surg* 1997; **32**: 1010-1013
- Zhou T,** Li X, Wu P, Zhang D, Zhang M, Chen N, Dong D. Effect of anti-P-selectin monoclonal antibody on renal ischemia/reperfusion injury in rats. *Chin Med J (Engl)* 2000; **113**: 790-793
- Wu P,** Li X, Zhou T, Zhang MJ, Chen JL, Wang WM, Chen N, Dong DC. Role of P-selectin and anti-P-selectin monoclonal antibody in apoptosis during hepatic/renal ischemia reperfusion injury. *World J Gastroenterol* 2000; **6**: 244-247
- Nelson RM,** Cecconi O, Roberts WG, Aruffo A, Linhardt RJ, Bevilacqua MP. Heparin oligosaccharides bind L- and P-selectin and inhibit acute inflammation. *Blood* 1993; **82**: 3253-3258
- Bourin MC,** Lindahl U. Glycosaminoglycans and the regulation of blood coagulation. *Biochem J* 1993; **289**: 313-330
- Wang L,** Brown JR, Varki A, Esko JD. Heparin's anti-inflammatory effects require glucosamine 6-O-sulfation and are mediated by blockade of L- and P-selectins. *J Clin Invest* 2002; **110**: 127-136
- Xie X,** Rivier AS, Zakrzewicz A, Bernimoulin M, Zeng XL, Wessel HP, Schapira M, Spertini O. Inhibition of selectin-mediated cell adhesion and prevention of acute inflammation by nonanticoagulant sulfated saccharides. Studies with carboxyl-reduced and sulfated heparin and with trestatin a sulfate. *J Biol Chem* 2000; **275**: 34818-34825
- Rabb H,** O'Meara YM, Maderna P, Coleman P, Brady HR. Leukocytes, cell adhesion molecules and ischemic acute renal failure. *Kidney Int* 1997; **51**: 1463-1468
- Burne MJ,** Elghandour A, Haq M, Saba SR, Norman J, Condon T, Bennett F, Rabb H. IL-1 and TNF independent pathways mediate ICAM-1/VCAM-1 up-regulation in ischemia reperfusion injury. *J Leukoc Biol* 2001; **70**: 192-198
- Daemen MA,** de Vries B, van't Veer C, Wolfs TG, Buurman WA. Apoptosis and chemokine induction after renal ischemia-reperfusion. *Transplantation* 2001; **71**: 1007-1011
- Downey P,** Tolley DA, Johnston SR, Young M. Ischemia-reperfusion injury after relief of ureteral obstruction: an animal study. *J Endourol* 2001; **15**: 209-211
- Ghielli M,** Verstrepen WA, De Greef KE, Helbert MH, Ysebaert DK, Nouwen EJ, De Broe ME. Antibodies to both ICAM-1 and LFA-1 do not protect the kidney against toxic (HgCl₂) injury. *Kidney Int* 2000; **58**: 1121-1134
- Rabb H,** Wang Z, Postler G, Soleimani M. Possible molecular basis for changes in potassium handling in acute renal failure. *Am J Kidney Dis* 2000; **35**: 871-877
- Donnahoo KK,** Meldrum DR, Shenkar R, Chung CS, Abraham E, Harken AH. Early renal ischemia, with or without reperfusion, activates NFkappaB and increases TNF-alpha bioactivity in the kidney. *J Urol* 2000; **163**: 1328-1332

- 34 **Gong JP**, Wu CX, Liu CA, Li SW, Shi YJ, Li XH, Peng Y. Liver sinusoidal endothelial cell injury by neutrophils in rats with acute obstructive cholangitis. *World J Gastroenterol* 2002; **8**: 342-345
- 35 **Lopez S**, Prats N, Marco AJ. Expression of E-selectin, P-selectin, and intercellular adhesion molecule-1 during experimental murine listeriosis. *Am J Pathol* 1999; **155**: 1391-1397
- 36 **Tsujino K**, Kodama A, Kanaoka N, Maruta T, Kono M. Expression of pulmonary mRNA encoding ICAM-1, VCAM-1, and P-selectin following thoracic irradiation in mice. *Radiat Med* 1999; **17**: 283-287
- 37 **Chu A**, Hong K, Berg EL, Ehrhardt RO. Tissue specificity of E- and P-selectin ligands in Th1-mediated chronic inflammation. *J Immunol* 1999; **163**: 5086-5093
- 38 **Morise Z**, Granger DN, Fuseler JW, Anderson DC, Grisham MB. Indomethacin induced gastropathy in CD18, intercellular adhesion molecule 1, or P-selectin deficient mice. *Gut* 1999; **45**: 523-528
- 39 **Levesque JP**, Zannettino AC, Pudney M, Niutta S, Haylock DN, Snapp KR, Kansas GS, Berndt MC, Simmons PJ. PSGL-1-mediated adhesion of human hematopoietic progenitors to P-selectin results in suppression of hematopoiesis. *Immunity* 1999; **11**: 369-378
- 40 **Thorlacius H**, Zhang XW. P-selectin-mediated rolling is a prerequisite for ICAM-1-independent firm adhesion in arterioles provoked by tumor necrosis factor-alpha *in vivo*. *Microvasc Res* 1999; **58**: 193-196
- 41 **Kamochi M**, Kamochi F, Kim YB, Sawh S, Sanders JM, Sarembock I, Green S, Young JS, Ley K, Fu SM, Rose CE Jr. P-selectin and ICAM-1 mediate endotoxin-induced neutrophil recruitment and injury to the lung and liver. *Am J Physiol* 1999; **277**: L310-L319
- 42 **Kalff JC**, Carlos TM, Schraut WH, Billiar TR, Simmons RL, Bauer AJ. Surgically induced leukocytic infiltrates within the rat intestinal muscularis mediate postoperative ileus. *Gastroenterology* 1999; **117**: 378-387
- 43 **McCafferty DM**, Smith CW, Granger DN, Kubes P. Intestinal inflammation in adhesion molecule-deficient mice: an assessment of P-selectin alone and in combination with ICAM-1 or E-selectin. *J Leukoc Biol* 1999; **66**: 67-74
- 44 **Scalia R**, Armstead VE, Minchenko AG, Lefer AM. Essential role of P-selectin in the initiation of the inflammatory response induced by hemorrhage and reinfusion. *J Exp Med* 1999; **189**: 931-938
- 45 **Farooque M**, Isaksson J, Olsson Y. Improved recovery after spinal cord trauma in ICAM-1 and P-selectin knockout mice. *Neuroreport* 1999; **10**: 131-134
- 46 **Mizgerd JP**, Bullard DC, Hicks MJ, Beaudet AL, Doerschuk CM. Chronic inflammatory disease alters adhesion molecule requirements for acute neutrophil emigration in mouse skin. *J Immunol* 1999; **162**: 5444-5448
- 47 **Mori N**, Horie Y, Gerritsen ME, Anderson DC, Granger DN. Anti-inflammatory drugs and endothelial cell adhesion molecule expression in murine vascular beds. *Gut* 1999; **44**: 186-195
- 48 **Hu S**, Sheng ZY. The effects of anisodamine and dobutamine on gut mucosal blood flow during gut ischemia/ reperfusion. *World J Gastroenterol* 2002; **8**: 555-557
- 49 **Thourani VH**, Brar SS, Kennedy TP, Thornton LR, Watts JA, Ronson RS, Zhao ZQ, Sturrock AL, Hoidal JR, Vinten-Johansen J. Nonanticoagulant heparin inhibits NF-kappaB activation and attenuates myocardial reperfusion injury. *Am J Physiol Heart Circ Physiol* 2000; **278**: H2084-H2093
- 50 **Kouretas PC**, Kim YD, Cahill PA, Myers AK, To LN, Wang YN, Sitzmann JV, Hannan RL. Nonanticoagulant heparin prevents coronary endothelial dysfunction after brief ischemia-reperfusion injury in the dog. *Circulation* 1999; **99**: 1062-1068
- 51 **Bjornsson TD**, Schneider DE, Hecht AR. Effects of N-deacetylation and N-desulfation of heparin on its anticoagulant activity and in vivo disposition. *J Pharmacol Exp Ther* 1988; **245**: 804-808
- 52 **Sache E**, Maillard M, Malazzi P, Bertrand H. Partially N-desulfated heparin as a non-anticoagulant heparin: some physico-chemical and biological properties. *Thromb Res Suppl* 1989; **55**: 247-258
- 53 **Frenette PS**, Mayadas TN, Rayburn H, Hynes RO, Wagner DD. Susceptibility to infection and altered hematopoiesis in mice deficient in both P- and E-selectins. *Cell* 1996; **84**: 563-574

Edited by Zhao M

Expression of exogenous rat collagenase *in vitro* and in a rat model of liver fibrosis

Ji-Yao Wang, Jin-Sheng Guo, Chang-Qing Yang

Ji-Yao Wang, Jin-Sheng Guo, Chang-Qing Yang, Division of Gastroenterology, Zhongshan Hospital, Fu Dan University, Shanghai 200032, China

Supported by National Fund of Natural Science of China, NO. 39570336

Correspondence to: Ji-Yao Wang, M.D. MSc, Chief of Division of Gastroenterology, Zhongshan Hospital, Fu Dan University, 180 Feng Lin Road, Shanghai 200032, China. jiyao_wang@hotmail.com

Telephone: +86-21-34140200 **Fax:** +86-21-34160980

Received 2002-04-13 **Accepted** 2002-05-10

Abstract

AIM: The present study was conducted to test the hypothesis that the introduction of the collagenase gene into tissue culture cells and into a rat model of liver fibrosis would result in the expression of enzymatically active product.

METHODS: FLAG-tagged full-length rat collagenase cDNA was PCR amplified and cloned into a mammalian expression vector. NIH3T3 cells were then transiently transfected with this construct. Expression of exogenous collagenase mRNA was assessed by RT-PCR, and the exogenous collagenase detected by Western blotting using anti-FLAG monoclonal antibody. Enzymatic activity was detected by gelatin zymography. To determine the effects of exogenous collagenase production *in vivo*, the construct was bound to glycosyl-poly-L-lysine and then transduced into rats that had developed liver fibrosis as a result of CCl₄ plus ethanol treatment. The hepatic expression of the construct and its effect on the formation of liver fibrosis were demonstrated using RT-PCR and immunohistochemistry.

RESULTS: It was found that exogenously expressed rat collagenase mRNA could be detected in NIH3T3 cells following transfection. Enzymatically active collagenase could also be detected in the culture medium. The recombinant plasmid was also expressed in rat liver after *in vivo* gene transfer. Expression of exogenous rat collagenase correlated with decreased deposition of collagen types I and III in the livers of rats with experimentally induced liver fibrosis.

CONCLUSION: The expression of active exogenous rat collagenase could be achieved *in vitro* and *in vivo*. It was suggested that *in vivo* expression of active exogenous collagenase may have therapeutic effects on the formation of liver fibrosis.

Wang JY, Guo JS, Yang CQ. Expression of exogenous rat collagenase *in vitro* and in a rat model of liver fibrosis. *World J Gastroenterol* 2002; 8(5):901-907

INTRODUCTION

Matrix metalloproteinases (MMPs) are a group of proteolytic enzymes that require zinc ions for their activities, they take part in a variety of normal and disease-associated matrix lysis

and remodeling events^[1-3]. For example, interstitial collagenase, one member of MMPs, also called collagenase, mainly initiates the degradation of collagen types I, II, III, V, VII, and X, which are fibrillar collagens^[4-6]. Interstitial collagenase probably contributes importantly to tissue repair, embryogenesis, bone renewal, and to some pathogenic processes such as rheumatoid arthritis, tumor metastasis, and also organ fibrosis^[7-10]. Changing the expression or the activities of interstitial collagenase by regulatory factors or by gene transfer may have therapeutic effects on those disease processes.

Liver cirrhosis often shortens life expectancy and decreases the quality of life. In liver cirrhosis, a major pathological feature is the accumulation of extracellular matrix (ECM). Within the major components of ECM, collagen types I and III constitute more than 95 % of the total content of increased collagen in fibrotic liver. The abnormal accumulation of ECM may reflect alterations in the synthesis of matrix proteins, their degradation, or both^[11,12]. The reversibility of liver fibrosis/ cirrhosis has been found in patients with various chronic hepatopathy^[13, 14] and in experimental cirrhotic animals^[15], indicating a therapeutic approach of this disease condition through improving ECM degradation. It has been reported that the mRNA transcription of interstitial collagenase is not up-regulated in experimental hepatic fibrosis^[16,17] and the interstitial collagenase proteins in cirrhotic human livers and in serum of chronic hepatitis patients decrease^[18,19]. Previous study also shows that the activity of collagenase decreases in advanced liver fibrosis^[20-22] and in serum from patients with chronic liver disease^[23,24]. Therefore, we proposed that exogenous gene expression of active collagenase might have therapeutic effects on the chronic liver diseases processes. The present experiments were performed to test the hypothesis that the introduction of a collagenase expression vector into tissue culture cells resulted in the enzyme expression, and that similar introduction of exogenous collagenase into a rat model of chemically induced liver fibrosis, altered the development of fibrosis. The *in vitro* results suggest that rat collagenase could be transiently expressed in NIH3T3 cells, and that rat liver fibrosis could be delayed by transducing the collagenase gene *in vivo*.

MATERIALS AND METHODS

Vector construction

A 6 amino acids deleted rat collagenase cDNA containing plasmid (UMR5.4) was kindly provided by Dr John J. Jeffrey^[25] and used as starting material. Full-length rat collagenase cDNA was PCR amplified using the primers RIC-UP1 and RIC-DP1 with UMR5.4 as the DNA template (Table 1). The sense primer RIC-UP1 contained the sequences of the deleted 6 amino acids. The PCR fragments were then inserted into the PCR2.1 vector (Invitrogen, Carlsbad, CA, USA) to form PCR2.1-RIC. Using PCR2.1-RIC as template, the cDNA was further PCR amplified with RIC-UP2 and RIC-DP2 as primers (Table 1). The FLAG epitope was added to the C-terminus of the rat collagenase

gene in this construct by using RIC-DP2 that contained the FLAG sequence at the 3' end adjacent to the translation stop codon TAA (Table 1). The PCR reaction was performed as follows: the total reaction volume was 100 μ l which contained 1ng DNA template (PCR2.1-RIC), 10 pmol \cdot L⁻¹ of each primer of RIC-UP2 and RIC-DP2, 2.5 μ mol \cdot L⁻¹ dNTP, 10 \times PCR buffer and 5U Taq polymerase; 35 PCR cycles at 95 $^{\circ}$ C for 1.5 min, 55 $^{\circ}$ C for 1.5 min, and 72 $^{\circ}$ C for 2 min. The 1400 kb PCR product was purified and inserted into mammalian expression vector pTargeTM by the method of TA cloning following the protocol suggested by manufacture (Promega, Madison, Wis, USA) and named as pCMV-RC-F (Figure 1, Map of the plasmid pCMV-RC-F). The pCMV-RC-F was DNA sequenced using T7 primer. The large-scale of plasmid DNA was prepared using Qiagen tip100 (Qiagen, Hilden, Germany). The vector pTargeTM that was self-ligated without any inserted DNA was also isolated and used as control in the transfection study.

Table 1 Primer pairs for PCR and RT-PCR reactions

RIC-UP1: 5' -CATGCATTCAGCTATCCTGGCCACCTTCTTCTGTG-3'
RIC-DP1: 5' -CTCCATAGATGAACTCCCC-3'
RIC-UP2: 5' -CCACCATGCATTCAGCTATCCTGG-3'
RIC-DP2: 5' -GTTACTTATCATCGTCGTCCTTGTAGTCACACCAC AATAAGGAATTC-3'
RIC-UP3: 5' -GAATCCAGTCTCTCTATGGTCCAG-3' (785-808)
RIC-DP3: 5' -TCATCGTCGTCCTTGTAGTCACAC-3' (1413-1436)
IC-UP4: 5' -TGGAGCCCTGATGTTTCCCATCTA--3' (693-717)
IC-DP4: 5' -ACCCAAATACTCTTTGGGAGATAA--3' (1423-1446)
β -UP5: 5' -AACCGCGAGAAGATGAACCAGATCATGTTT-3' (2135-2164)
β -DP5: 5' -AGCAGCCGTGGCCATCTCTTGCTCGAAGTC-3' (2456-2485)

(): binding location of primer in relative cDNA sequence

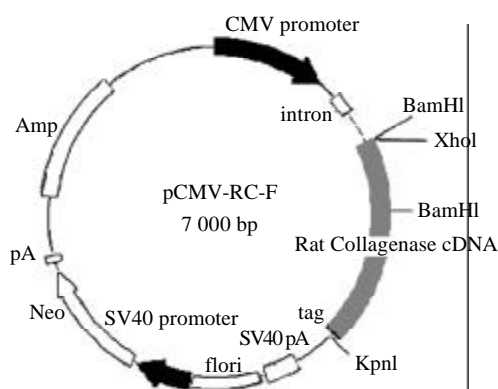


Figure 1 Map of plasmid pCMV-RC-F. The FLAG tagged full length rat collagenase cDNA was inserted into a mammalian expression plasmid vector PtargeTM which carries the human cytomegalovirus (CMV) immediate-early enhancer/promoter region.

In vitro transfection

Exponentially growing NIH 3T3 cells were seeded into 6-well tissue culture dishes at 5×10^5 cells/well and grown overnight to 60 % confluency in culture medium supplemented with 10 % FCS. Each well was then transfected with 5 μ g DNA constructs using lipofectamine according to the instruction provided by the manufacturer (Gibco BRL, Eggenstein, Germany). Encapsulated DNA was incubated for 5 h on cells in serum free medium, then in medium containing 10 % bovine serum. After further incubation of the cells for 24 h, the culture medium

was discarded and replaced by normal culture medium. Fifty-six h after transfection, the NIH 3T3 cells and their media were harvested for further analysis.

RT-PCR analysis for mRNA expression

The collected cells were washed twice with ice-cold phosphate-buffered saline (PBS), and the mRNA extracted with mRNA Capture Kit (Boehringer Mannheim). The samples were further incubated with biotin-labeled oligo (dT)₂₀ working solution for 5 min to hybridize the mRNA with oligo (dA)_n. The mixture was added to a streptavidin-coated PCR tube, and incubated for 3 min at 37 $^{\circ}$ C to immobilize the poly (A)_n RNA. Tubes were then washed three times and amplified by RT-PCR. The RT-PCR reaction system contained 0.3 μ mol \cdot L⁻¹ each of the primer pairs RIC-UP3 and RIC-DP3 (corresponded to nucleotides 785-808 of the collagenase encoding region and the FLAG domain coding region, amplified a PCR product of 652 bp), 5 mmol \cdot L⁻¹ DTT, 6 U RNasin, 1.5 mmol \cdot L⁻¹ MgCl₂, 5 \times RT-PCR buffer and 1 μ l TitanTM Enzyme mix provided with the TitanTM RT-PCR System (Boehringer Mannheim). Samples were placed in a thermocycler equilibrated at 50 $^{\circ}$ C for 30 min, at 94 $^{\circ}$ C for 5 min, then for 34 cycles at 94 $^{\circ}$ C for 1 min, 55 $^{\circ}$ C for 2 min, and 72 $^{\circ}$ C for 3 min, with a final extension at 72 $^{\circ}$ C for 10 min. The amplification products were then analyzed on 10 g \cdot L⁻¹ agarose gels containing 0.5 mg \cdot L⁻¹ ethidium bromide.

Western blot analysis of FLAG-tagged rat collagenase expression

The amount of protein in the collected culture medium of transfected cells was determined with Dye-binding method (Bio-Rad, Hercules, CA, USA). For each samples 30 μ g total protein was electrophoresed on sodium dodecyl sulfate-polyacrylamide gel and then transferred to polyvinylidene difluoride (PVDF) membrane (Gelman Inc, Ann Arbor, MI, USA) by electroblotting. Pre-stained rainbow recombinant protein molecular weight markers (Amersham International plc, Little Chalfont, Buckinghamshire, England) were used for molecular weight determinations. Membranes were blocked with a blocking buffer containing 50 g \cdot L⁻¹ non-fat milk powder, 10 mmol \cdot L⁻¹ Tris/HCl (pH 7.5), 100 mmol \cdot L⁻¹ NaCl and 1 g \cdot L⁻¹ Tween 20 and incubated with 1 : 100 diluted solution of anti-FLAG M₂ McAb^[26] (Kodak, New Haven, CT, USA) at 37 $^{\circ}$ C for 1 h. After washing for 30 min the membranes were treated with HRP-conjugated secondary antibody (1:5000) (Bio-Rad) for 1 h at room temperature followed by another 30 min of washings. The ECL Western blotting system (Amersham Life Sciences) was used in accordance to the manufacturer's instructions for chemiluminescence of proteins, and the blots were then exposed to photographic films (Fuji Photo Film Co., Tokyo, Japan).

Gelatin zymography assay for the enzyme activity

The activity of collagenase was detected by gelatin zymography as previously described^[27, 28] with minor modifications. Culture supernatants that contained 60 μ g /lane total protein were prepared and mixed with 5 \times zymogram sample buffer consisting of 0.4 mol \cdot L⁻¹ Tris (pH 6.8), 50 g \cdot L⁻¹ SDS, 200 g \cdot L⁻¹ glycerol, and 0.3 g \cdot L⁻¹ bromphenol blue, then electrophoresed with protein molecular weight markers as described before on 100 g \cdot L⁻¹ sodium dodecyl sulfate-polyacrylamide gels containing 10 g \cdot L⁻¹ gelatin under an ice water cycle. After electrophoresis, the position of molecular weight markers were marked and the gels were rinsed in washing buffer consisting of 50 mmol \cdot L⁻¹ Tris, pH 7.6, 1 μ mol \cdot L⁻¹ ZnCl₂, 5 mmol \cdot L⁻¹ CaCl₂, 250 g \cdot L⁻¹ TritonX-100 at 4 $^{\circ}$ C on a rotary shaker. The Triton X-100 solution was decanted and replaced with rinsing

buffer consisting of 50 mmol·L⁻¹ Tris (pH 7.6), 1 μmol·L⁻¹ ZnCl₂, 5 mmol·L⁻¹ CaCl₂ for further washing. The gel was then incubated with enzyme buffer containing 50 mmol·L⁻¹ Tris (pH 7.6), 1 μmol·L⁻¹ ZnCl₂, 5 mmol·L⁻¹ CaCl₂, 0.2 g·L⁻¹ Brij-35 at 37 °C for 42 h. Each gel was stained with 0.5 g·L⁻¹ Coomassie blue G-250 in an aqueous solution of 300 g·L⁻¹ methanol and 100 g·L⁻¹ acetic acid and destained with three changes of 300 g·L⁻¹ methanol, 100 g·L⁻¹ acetic acid. Areas of digestion were visualized as non-staining regions of the gel and photographed.

Animal model of liver fibrosis

Thirty-six male Wistar rats (Shanghai Experimental Animal Center, Chinese Academy of Sciences) weighing 130±10 g were randomly distributed into four groups, 6 in a normal control group (A), 10 in an experimental liver fibrosis model without plasmid treatment as disease control group (B), and 10 in each of two pCMV-RC-F plasmid transfection as treatment groups (C1 and C2). Animals in the normal control group were treated with olive oil and received food and water *ad libitum*. Rats in the other three groups received a subcutaneous injection of CCl₄ solution (500 g·L⁻¹ in olive oil) twice a week for eight weeks at a dose of 0.3 ml per 100 g of body weight after an initial dose of 0.6 ml per 100 g. The only source of fluid for the rats was 100 g·L⁻¹ ethanol in water during the entire period of experiment. In addition, animals in the C1 group were intravenous injected with 100 μg of galactosyl poly-L-lysine (G-PLL, obtained from Dr. Wen Shouming, The Air Force General Hospital of Chinese Peoples Liberation Army, Beijing, China) encapsulated recombinant plasmid through tails vein every two weeks, beginning two weeks after the start of treatment with CCl₄. G-PLL was included to accelerate the targeting effect of the transduced plasmid to the livers^[29-31]. Animals in the C2 group received the same treatment as those in group C1 but the plasmid was administrated four weeks after starting the treatment with CCl₄. Animals in the B group received G-PLL encapsulated pTargetTM empty plasmid vector at the same dosage and the same time as those in the C1 group. The molecular ratio of galactose and poly-L-lysine is 15:28 and the average molecular weight of the G-PLL is *M_r* 8 500.

After weeks 8 treatment, the surviving 6 or 7 rats in each of the C1, C2, B groups and all the 6 rats in the A group were narcotized with 20 g·L⁻¹ pentobarbital sodium. The middle lobes of the livers were removed and specimens were fixed in Carnoy's fixative (glacial acetic acid, chloroform, and ethanol in volume ratio of 1:3:6) and then embedded in paraffin for histological analysis. The remaining tissue was quickly partitioned and immediately frozen and stored under liquid nitrogen for RNA extraction and RT-PCR analysis. Then the animals were humanly killed.

Collagenase mRNA expression in rat liver

Total RNA was isolated from the liver tissues using Trizol (Gibco BRL) according to the manufacturer's directions. Integrity of RNA was confirmed by visual examination on an ethidium bromide-stained 10 g·L⁻¹ Tris-acetate and EDTA agarose gel. Total RNA of 1 mg from each sample was used for reverse transcription and amplification using a RT-PCR kit (Sino-American Biotechnology Co. Shanghai, China). The RT-PCR reaction contained 10 pmol each of the primer pairs RIC-UP3 and RIC-DP3 for detecting the recombinant collagenase mRNA (a product of 652 bp), or each primer pairs of IC-UP4 and IC-DP4 (designed within nucleotides 711-734 of the coding region and nucleotides 1440-1463 of 3' untranslated region of collagenase, Table 1) for amplifying the endogenous collagenase mRNA (a product of 753 bp)^[25].

The later primer pairs could not amplify the expression of recombinant collagenase that was lack of the nature 3' untranslated region of collagenase gene. Additionally primer pairs β-UP5 and β-DP5 were included for amplifying the expression of b-actin 335 bp DNA fragment) as internal control^[32]. Samples were placed in a thermocycler with the incubation programme of 37 °C for 40 min, 94 °C for 7 min, then 36 cycles of 94 °C for 1 min, 56 °C for 1 min, and 72 °C for 1 min, with a final extension of 72 °C for 10 min. Products of RT-PCR were electrophoresed on a 20 g·L⁻¹ agarose gel to show the amplified bands.

Histology and Immunohistochemistry

For immunohistochemical staining, 5 mm sections of each group were treated with anti-FLAG M₂ McAb to assay the expression of recombinant collagenase. After dewaxed with xylene and rehydrated through a graded alcohol series, sections were digested with 4 g·L⁻¹ trypsin. Nonspecific binding was blocked with calf serum 1:5 in PBS. The sections were incubated with mouse anti-FLAG M₂ McAb (1:100) overnight at 4 °C and then with biotinylated horse anti-mouse IgG (Vector) for 30 min, avidin-peroxidase complex for 30 min, and the substrate solution (3,3'-diaminobenzidine tetrahydrochloride in H₂O₂ in Tris buffer, pH 7.4) for 10 min, followed by counterstaining with hematoxylin. The sections were washed with 0.01 mol·L⁻¹ PBS (pH 7.4) three times after each step. Finally, ten high power fields of each section were observed under microscope and the positive signals were counted.

Some sections of each group were treated with the monoclonal antibodies against collagen types I and III (1:100), then with secondary antibody and the procedure of the immunostaining were same to the above-mentioned except without counterstaining with hematoxylin. The slides were then analyzed with an Image Analyzing system (TJTY 300 System) to obtain the integral light density (ILD) of stained collagen types I and III.

Morphological examination was performed with Hematoxylin and Eosin staining (H&E) for histological changes of liver fibrosis.

Statistical analysis

The ILD values of collagen types I and III were analyzed by one-way ANOVA. The statistics were calculated by software SPSS 7.0 for Windows. The data are expressed as mean ± S.E. M. Values of *P*<0.05 were considered statistically significant.

RESULTS

In vitro expression and secretion of active FLAG-tagged rat collagenase

After *in vitro* transfection of plasmid in NIH 3T3 cells, the transcription of recombinant collagenase gene was confirmed by RT-PCR amplification of 652 bp cDNA fragment from cells transfected with pCMV-RC-F, but not from cells transfected with control plasmid pTargetTM (Figure 2). This product was of the size expected from mRNA of the tagged collagenase. Further demonstration of transfected gene expression was performed by Western blot analysis using anti-FLAG McAb. The immunoreactive band at about *M_r* 55 000 was observed in the culture supernatant of cells transfected with pCMV-RC-F but not in that with pTargetTM transfection or in culture medium alone (Figure 3). Collagenase activities were also found around the *M_r* 55 000 in gelatin zymogram analysis of the culture supernatant of pCMV-RC-F transfected cells and still could be observed after 1:64 dilution. A weak activity of collagenase was also observed in the culture supernatant of pTargetTM

transfected cells but was almost undetectable after 1:2 dilution. No enzyme activity of M_r 55 000 collagenase could be detected in culture medium alone (Figure 4).

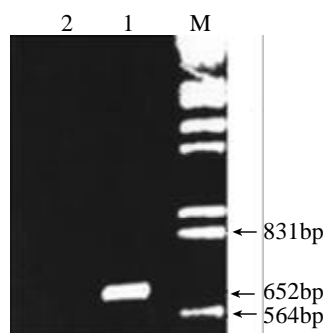


Figure 2 RT-PCR assay of the mRNA expression of recombinant collagenase in NIH 3T3 cells. The PCR-amplified 652 bp fragment of recombinant collagenase cDNA derived from their respective mRNA was found in NIH 3T3 cells which were transfected with pCMV-RC-F (lane 1), while no signal was detected in cells which transfected with control plasmid pTargetTM (lane 2). Lane M is the molecular weight marker (DNA/*Hind* III, *Bam*H I).

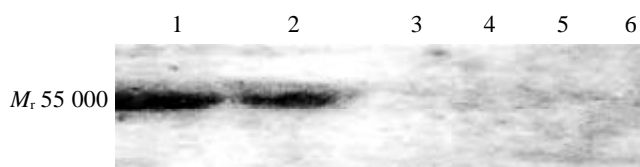


Figure 3 Westernblot analysis of the FLAG-tagged rat collagenase expression using mouse anti-FLAG M_2 McAb. The immunoreactive band with anti-FLAG M_2 McAb at about M_r 55 000 was observed in the culture supernatant of cells transfected with pCMV-RC-F (lane 1) and the supernatant of 1:2 dilution (lane 2). No immunoreactive was found in the supernatant of cells transfected with pTargetTM (lane 3, 4) or in culture medium alone (lane 5, 6).

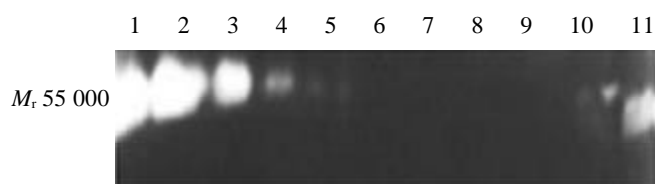


Figure 4 Gelatin zymography analysis for the activity of collagenase. The enhanced gelatin degradation activity was found in the culture supernatant of pCMV-RC-F transfected cells (lane 1-7 represent the zymograph of 1:1, 1:2, 1:4, 1:8, 1:16, 1:32, 1:64 diluted solutions of the supernatant) when compared with pTargetTM transfected cells (lane 10,11 represent the zymograph of 1:2 and 1:1 diluted solutions of the supernatant). No activity was found at about M_r 55 000 in the culture medium (lane 8, 9).

In vivo expression of FLAG-tagged rat collagenase in rat livers and its effects on liver fibrosis

The 650bp amplified product was detected in the RT-PCR samples from pCMV-RIC-F plasmid transduced rat groups (C1 and C2 group) but not in the control animal groups (A and B

groups) (Figure 5). The 753 bp amplified product by primer IC-UP4 and IC-DP4 which represent the endogenous collagenase gene expression was detected in all samples (Figure 6). In addition to RT-PCR, the expression of exogenous collagenase was observed in C1 and C2 groups by immunostaining with anti-FLAG antibody (Figure 7). Nearly about 30 percent of total cells presented positive signals in C1 and C2 groups, and the distributions of positive signals were found in both the hepatocytes and the perisinusoidal cells.

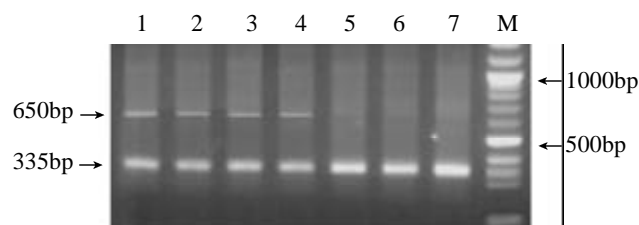


Figure 5 RT-PCR assay for the expression of recombinant interstitial collagenase in rat livers. The 652bp PCR amplified fragment of recombinant collagenase cDNA which was derived from their respective mRNA could be detected in liver samples from pCMV-RIC-F plasmid transduced rat groups C1 (lane 1, 2) and C2 (lane 3, 4) but not in the normal control group A (lane 5, 6) and disease control group B (lane 7). 335 bp fragment was PCR amplified b-actin cDNA. Lane M was 100 bp-1200 bp DNA marker ladders.

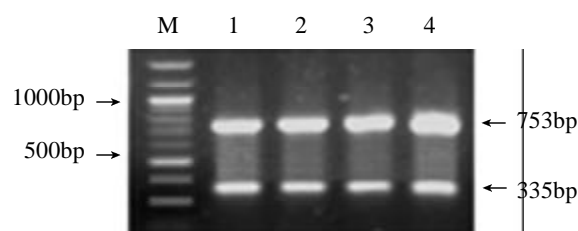


Figure 6 RT-PCR assay for the endogenous expression of collagenase in rat livers. The 753bp PCR-amplified fragment of endogenous collagenase cDNA which was derived from their respective mRNA could be detected in all liver samples from the normal control groups A (lane 1) and disease control group B (lane 4), as well as pCMV-RIC-F plasmid transduced rat groups C1 (lane 3) and C2 (lane 4). 335 bp fragment was PCR amplified b-actin cDNA. Lane M was 100bp-1200bp DNA marker ladders.

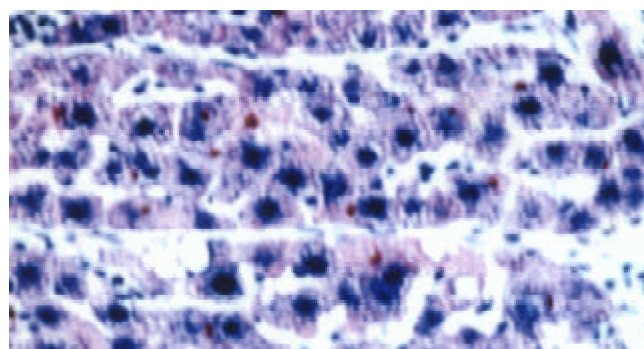


Figure 7 Immunohistochemical analysis of the expression of recombinant plasmid with anti-FLAG antibody in pCMV-RIC-F plasmid transduced group C1 ($\times 400$). Nearly about 30 percent of total cells presented positive signals. The distributions of positive signals were found in both the hepatocytes and the perisinusoidal cells.

The accumulation of collagen types I and III in the livers of animals in group B was more severe than that in group C1 and C2 according to the quantitative analysis of the immunohistochemical findings ($P<0.05$) (Table 2, Figure 8A-D).

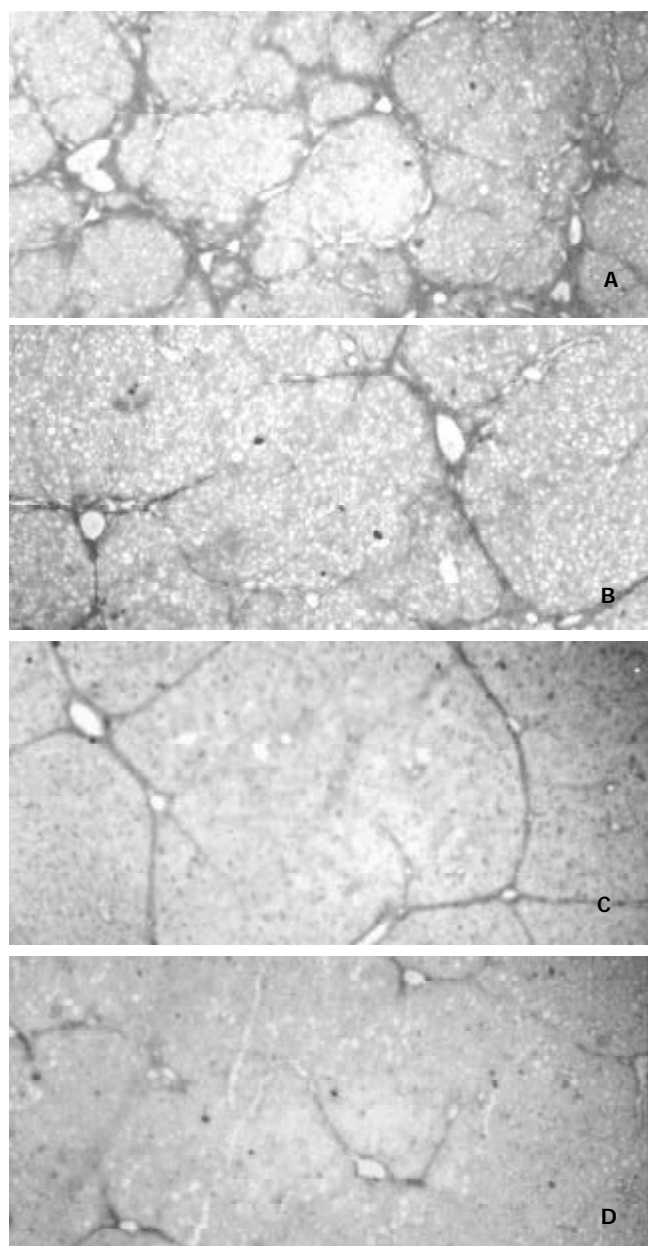


Figure 8 Immunohistochemical analysis of collagen types I (A, B) and III (C, D) in livers ($\times 100$). The accumulations of collagen in the disease control group (A, C) were more severe than that in the pCMV-RIC-F plasmid transduced C1 group (B, D).

Table 2 Effects of *in vivo* transfection of FLAG-tagged rat collagenase on the accumulation of collagen type I and III in experimental liver fibrosis

Group	<i>n</i>	ILD of collagen I	ILD of collagen III
A	6	17.35 \pm 2.62	18.94 \pm 3.78
B	6	86.83 \pm 11.93 ^a	75.21 \pm 10.07 ^a
C1	7	69.25 \pm 12.31 ^{ab}	62.10 \pm 9.72 ^{ab}
C2	7	72.18 \pm 14.18 ^{ab}	64.80 \pm 11.69 ^{ab}

^a $P<0.05$ when compared with normal control group (group A);

^b $P<0.05$ when compared with disease control group (group B).
ILD: Integral Light Density; N: number of rats in each group

DISCUSSION

In the present study the expression of FLAG-fusion rat collagenase was detected in pCMV-RIC-F transfected NIH 3T3 cells and the secreted FLAG-fusion collagenase was found in the culture supernatant. This recombinant collagenase also exhibited enhanced gelatin degradation activity. These results suggest that the construction of recombinant collagenase plasmid is successfully function *in vitro* and could be used in further study *in vivo*. NIH 3T3 cell is a cell line of mouse embryonic fibroblasts. The mouse and the rat interstitial collagenase share highly homology when comparison was made between the amino acid sequences of their active forms^[33]. Constitutive expression of collagenase gene had been found in NIH 3T3 cells before^[34]. In our study, the weak activity of collagenase found in the culture supernatant of pTargetTM transfected cells in our gelatin zymography study might reflect this constitutive expression of mouse collagenase. Similar situation may also exist in liver tissues *in vivo*. Using anti-FLAG McAb we can easily distinct the recombinant rat collagenase that is tagged with FLAG domain from the natural mouse collagenase or the natural rat collagenase.

Collagen types I and III constituted the main components found in the increase of ECM^[35, 36]. It has been proposed that the degradation of collagen types I and III is very important in the reversion of liver fibrosis. Theoretically the degradation of collagen could be enhanced if the expression of active collagenase increases. In this study, it was found that the recombinant plasmid could be delivered to liver by G-PLL and could be expressed in the tissue of liver. It was observed immunohistochemically that there were significant decrease of collagen types I and III deposition after transducing the recombinant collagenase plasmid into fibrotic livers. This suggests that the exogenous collagenase gene was able to degrade collagen.

Experimental gene therapies of liver cirrhosis have been tried by other research groups with different gene transfer methods and targeted genes^[37-42]. In our study glycosyl-poly-L-lysine was used in the recombinant collagenase gene transfer into the livers since hepatocytes possess receptors that recognize galactose-terminal (asialo-) glycoproteins and thus they are particularly well suited for receptor-mediated methods of gene transfer. In our previous study it was proved that the recombinant plasmid could be delivered to liver and hepatocytes more specifically by G-PLL than lipofectamine^[33]. In the present study it was also found that the positive signals of anti-FLAG McAb binding protein were in the hepatocytes of the rats of C1 and C2 groups. The less amounts of perisinusoidal cells which had positive signals as well might be the activated kupffer cells that had the function of phagocytosis. In addition, the previous study also observed the obvious expression of recombinant FLAG-tagged rat collagenase in liver at 24 h after plasmid transfection and persisting for longer than three weeks^[31]. No detrimental effects of the transfection and expression of plasmid on important organs of normal rats such as liver, lung, heart and kidney were found by monitoring the serum levels of alanine transaminase, aspartic transaminase and creatinine and by observing the histological manifestation of these organs before and after transfection. These results indicated that the *in vivo* transfection of recombinant collagenase in liver that was mediated by glycosyl-poly-L-lysine was functionally expressed in liver and safe for other tissues.

The regulation of collagenase activity was affected by multiple factors^[43, 44]. These include regulation of gene-transcription and protein-biosynthesis by cytokines or other factors, transformation of proenzymes into active forms, the

influence of specific or non-specific inhibitors on the activity of activated enzyme. Some studies have shown that the level of tissue inhibitor of metalloproteinase-1 (TIMP-1), which is a specific inhibitor of metalloproteinase, became very high during progressive liver fibrosis^[45-49]. However the changes of regulation mechanisms such as the expression of TIMP-1 after collagenase gene transduction are still unknown. Whether the treatment effect on liver fibrosis by transferring an antisense gene of TIMP-1 is better than directly transferring collagenase gene as it was performed in this study worth further investigation.

In summary, the exogenous FLAG-tagged rat collagenase can be transferred by a recombinant plasmid and is expressed functionally in NIH3T3 cells and in a rat liver fibrosis model. As the result demonstrated that *in vivo* transduction of exogenous FLAG-tagged rat collagenase reduced liver fibrosis, this may stimulate the effort for which, the new therapeutic strategies in the management of liver fibrosis through regulation of collagenase activity and/or its inhibitors.

ACKNOWLEDGEMENTS

We gratefully acknowledge professor John J. Jeffrey (Departments of Biochemistry and Medicine, Albany Medical Center, USA) for his kind provision of rat collagenase UMR5.4 plasmid. Dr Shouming Wen (Air Force General Hospital of PLA, Beijing, China) for his supply of galactosyl-poly-L-lysine. Dr. Wei-tian Liu and Dr. Lin-Xun Duan (GenWay Biotech Inc Suite E2, Welsh Commons, PA 19454, USA) for the helping construction of plasmid. We also gratefully thank Dr. Arkady Mak, Dr. M. W. L. Koo and Professor M. A. Zern for their critical review of the manuscript.

REFERENCES

- Friedman SL.** The cellular basis of hepatic fibrosis: mechanisms and treatment strategies. *N Engl J Med* 1993; **323**: 1828-1835
- Matrisian LM.** The matrix-degrading metalloproteinases. *Bioessays* 1992; **14**: 455-463
- Ries C,** Petrides PE. Cytokine regulation of matrix metalloproteinase activity and its regulatory dysfunction in disease. *Biol Chem Hoppe Seyler* 1995; **376**: 345-355
- Varghese S,** Rydzziel S, Jeffrey JJ, Canalis E. Regulation of interstitial collagenase expression and collagen degradation by retinoic acid in bone cells. *Endocrinology* 1994; **134**: 2438-2444
- Sires UI,** Schmid TM, Fliszar CJ, Wang ZQ, Gluck SL, Welgus HG. Complete degradation of type X collagen requires the combined action of interstitial collagenase and osteoclast-derived cathepsin-B. *J Clin Invest* 1995; **95**: 2089-2095
- Nikkari ST,** O'Brien KD, Ferguson M, Hatsukami T, Welgus HG, Alpers CE, Clowes AW. Interstitial collagenase (MMP-1) expression in human carotid atherosclerosis. *Circulation* 1995; **92**: 1393-1398
- Arthur MJP.** Collagenases and liver fibrosis. *J Hepatol* 1995; **22** (Suppl. 2): 43-48
- Woessner JF.** Matrix metalloproteinases and their inhibitors in connective tissue remodeling. *FASEB J* 1991; **5**: 2145-2154
- Sodek J,** Overall CM. Matrix metalloproteinases in periodontal tissue remodelling. *Matrix Suppl* 1992; **1**: 352-362
- Okazaki I,** Watanabe T, Hozawa S, Arai M, Maruyama K. Molecular mechanism of the reversibility of hepatic fibrosis: with special reference to the role of matrix metalloproteinases. *J Gastroenterol Hepatol* 2000; **15**(Suppl.): D26-D32
- Scott JE,** Bosworth TR, Cribb AM, Gressner AM. The chemical morphology of extracellular matrix in experimental rat liver fibrosis resembles that of normal developing connective tissue. *Virchows Arch* 1994; **424**: 89-98
- Kovalszky I.** Fibrogenesis in the liver fibrosis, cirrhosis. *Orv Hetil* 1993; **134**: 59-64
- Defour JF,** Delellis R, Kaplan MM. Regression of hepatic fibrosis in hepatic fibrosis in hepatitis C with long-term interferon treatment. *Dig Dis Sci* 1998; **43**: 2573-2576
- Dufour JF,** Delellis R, Kaplan MM. Reversibility of hepatic fibrosis in autoimmune hepatitis. *Ann intern Med* 1997; **127**: 981-985
- Fort J,** Pilette C, Veal N, Oberti F, Gallois Y, Douay O, Rosenbaum J, Cales P. Effects of long-term administration of interferon alpha in two models of liver fibrosis in rats. *J Hepatol* 1998; **29**: 263-270
- Kossakowska AE,** Edwards DR, Lee SS, Urbanski LS, Stabler AL, Zhang CL, Phillips BW, Zhang YK, Urbanski SL. Altered balance between matrix metalloproteinases and their inhibitors in experimental biliary fibrosis. *Am J Pathol* 1998; **153**: 1895-1902
- Watanabe T,** Niioka M, Hozawa S, Kameyama K, Hayashi T, Aria M, Ishikawa A, Maruyama K, Okazaki I. Gene expression of interstitial collagenase in both progressive and recovery phase of rat liver fibrosis induced by carbon tetrachloride. *J Hepatol* 2000; **33**: 224-235
- Lichtinghagen R,** Breitenstein K, Arndt B, Kühbacher T, Böker KHW. Comparison of matrix metalloproteinase expression in normal and cirrhotic human liver. *Virchows Arch* 1998; **432**: 153-158
- Murawaki Y,** Ikuta Y, Idobe Y, Kawasaki H. Serum matrix metalloproteinase-1 in patients with chronic viral hepatitis. *J Gastrol Hepatol* 1999; **14**: 138-145
- Maruyama K,** Feinman L, Fainsilber Z, Nakano M, Okazaki I, Lieber CS. Mammalian collagenase increases in early alcoholic liver disease and decreases with cirrhosis. *Life Sci* 1982; **30**: 1379-1384
- Perez-Tamayo R,** Montfort I, Gonzalez E. Collagenolytic activity in experimental cirrhosis of the liver. *Exp Mol Pathol* 1987; **47**: 300-308
- Giménez A,** Parés A, Alié S, Camps J, Deulofeu R, Caballería J, Rodés J. Fibrogenic and collagenolytic activity in carbon-tetrachloride-injured rats: beneficial effects of zinc administration. *J Hepatol* 1994; **21**: 292-298
- Murawaki Y,** Koda M, Yamada S, Kawasaki H, Shima H, Burkhardt H. Serum collagenase activity in patients with chronic liver disease. *J Hepatol* 1993; **18**: 328-334
- Murawaki Y,** Kawasaki H, Burkhardt H. Serum collagenase activity in chronic liver diseases. *Pathol Res Pract* 1994; **190**: 929-933
- Quinn CO,** Scott DK, Brinckerhoff CE, Matrisian LM, Jeffrey JJ, Partridge NC. Rat collagenase cloning, amino acid sequence comparison, and parathyroid hormone regulation in osteoblastic cells. *J Biol Chem* 1990; **265**: 22342-22348
- Brizzard BL,** Chubet RG, Vizard DL. Immunoaffinity purification of FLAG epitope-tagged bacterial alkaline phosphatase using a novel monoclonal antibody and peptide elution. *Biotechniques* 1994; **16**: 730-735
- Kleiner DE,** Stetler-Stevenson WG. Quantitative zymography: Detection of picogram quantities of gelatinases. *Anal Biochem* 1994; **218**: 325-329
- Tyagi SC,** Matsubara L, Weber KT. Direct extraction and estimation of collagenase (s) activity by zymography in microquantities of rat myocardium and uterus. *Clin Biochem* 1993; **26**: 191-198
- Perales JC,** Ferkol T, Beegen H, Ratnoff OD, Hanson RW. Gene transfer in vivo: sustained expression and regulation of genes introduced into the liver by receptor-targeted uptake. *Proc Natl Acad Sci USA* 1994; **91**: 4086-4090
- Nishikawa M,** Takemura S, Takakura Y, Hashida M. Targeted delivery of plasmid DNA to hepatocytes *in vivo*: optimization of the pharmacokinetics of plasmid DNA/galactosylated poly (L-lysine) complexes by controlling

- their physicochemical properties. *J Pharmacol Exp Ther* 1998; **287**: 408-415
- 31 **Yang C**, Wang J, He B, Liu J, Guo J. Glyco-poly-L-lysine is better than liposomal delivery of exogenous genes to rat liver. *World J Gastroenterol* 2000; **6**: 526-531
 - 32 **Nudel U**, Zakut R, Shani M, Neuman S, Levy Z, Yaffe D. The nucleotide sequence of the rat cytoplasmic beta-actin gene. *Nucleic Acids Res* 1983; **11**: 1759-1771
 - 33 **Henriet P**, Rousseau GG, Eeckhout Y. Cloning and sequencing of mouse collagenase cDNA divergence of mouse and rat collagenases from the other mammalian collagenases. *FEBS L* 1992; **310**: 175-178
 - 34 **Aho S**, Rouda S, Kennedy SH, Qin H, Tan EM. Regulation of human interstitial collagenase (matrix metalloproteinase-1) promoter activity by fibroblast growth factor. *Eur J Biochem* 1997; **247**: 503-510
 - 35 **Rojkind M**. Role of metalloproteinases in liver fibrosis. *Alcohol Clin Exp Res* 1999; **23**: 934-939
 - 36 **Arthur MJ**. Degradation of matrix proteins in liver fibrosis. *Pathol Res Pract* 1994; **190**: 825-833
 - 37 **Garcia-Banuelos J**, Siller-Lopez F, Miranda A, Aguilar LK, Aguilar-Cordova E, Armendariz-Borunda J. Cirrhotic rat livers with extensive fibrosis can be safely transduced with clinical-grade adenoviral vectors. Evidence of cirrhosis reversion. *Gene Ther* 2002; **9**: 127-134
 - 38 **Salgado S**, Garcia J, Vera J, Siller F, Bueno M, Miranda A, Segura A, Grijalva G, Segura J, Orozco H, Hernandez-Pando R, Fafutis M, Aguilar LK, Aguilar-Cordova E, Armendariz-Borunda J. Liver cirrhosis is reverted by urokinase-type plasminogen activator gene therapy. *Mol Ther* 2000; **2**: 545-551
 - 39 **Rudolph KL**, Chang S, Millard M, Schreiber-Agus N, DePinho RA. Inhibition of experimental liver cirrhosis in mice by telomerase gene delivery. *Science* 2000; **287**: 1253-1258
 - 40 **Ukei T**, Kaneda Y, Tsutui H, Nakanishi K, Sawa Y, Morishita R, Matsumoto K, Nakamura T, Takahashi H, Okamoto E, Fujimoto J. Hepatocyte growth factor gene therapy of liver cirrhosis in rats. *Nat Med* 1999; **5**: 226-230
 - 41 **Qi Z**, Atsuchi N, Ooshima A, Takeshita A, Ueno H. Blockage of type beta transforming growth factor signaling prevents liver fibrosis and dysfunction in the rat. *Proc Natl Acad Sci USA* 1999; **96**: 2345-2349
 - 42 **Ueno H**, Sakamoto T, Nakamura T, Qi Z, Astuchi N, Takeshita A, Shimizu K, Ohashi H. A soluble transforming growth factor beta receptor expressed in muscle prevents liver fibrogenesis and dysfunction in rats. *Hum Gene Ther* 2000; **11**: 33-42
 - 43 **DeCarlo AA Jr**, Windsor LJ, Bodden MK, Harber GJ, Birkedal Hansen B, Birkedal Hansen H. Activation and novel processing of matrix metalloproteinases by a thiol-proteinase from the oral anaerobe *Porphyromonas gingivalis*. *J Dent Res* 1997; **76**: 1260-1270
 - 44 **Schwartz JD**, Monea S, Marcus SG, Patel S, Eng K, Galloway AC, Mignatti P, Shamamian P. Soluble factor(s) released from neutrophils activates endothelial cell matrix metalloproteinase-2. *J Surg Res* 1998; **76**: 79-85
 - 45 **Benyon RC**, Iredale JP, Goddard S, Winwood PJ, Arthur MJ. Expression of tissue inhibitor of metalloproteinase 1 and 2 is increased in fibrotic human liver. *Gastroenterology* 1996; **110**: 821-831
 - 46 **Murawaki Y**, Ikuta Y, Idobe Y, Kitamura Y, Kawasaki H. Tissue inhibitor of metalloproteinase-1 in the liver of patients with chronic liver disease. *J Hepatol* 1997; **26**: 1213-1219
 - 47 **Dudas J**, Kovalszky I, Gallai M, Nagy JO, Schaff Z, Knittel T, Mehde M, Neubauer K, Szalay F, Ramadori G. Expression of decorin, transforming factor -beta 1, tissue inhibitor metalloproteinase 1 and 2, and type IV collagenases in chronic hepatitis. *Am J Clin Pathol* 2001; **115**: 725-735
 - 48 **Lichtinghagen R**, Michels D, Haberkorn CI, Arndt B, Bahr M, Flemming P, Manns MP, Boeker KH. Matrix metalloproteinase (MMP)-2, MMP-7, and tissue inhibitor of metalloproteinase-1 are closely related to the fibroproliferative process in the liver during chronic hepatitis C. *J Hepatol* 2001; **34**: 239-247
 - 49 **Boeker KH**, Haberkorn CI, Michels D, Flemming P, Manns MP, Lichtinghagen R. Diagnostic potential of circulating TIMP-1 and MMP-2 as markers of liver fibrosis in patients with chronic hepatitis C. *Clin Chim Acta* 2002; **316**: 71-81

Edited by Zhao M

• BASIC RESEARCH •

The immunotherapeutic effect of dendritic cells vaccine modified with interleukin-18 gene and tumor cell lysate on mice with pancreatic carcinoma

Zhao-Hui Tang, Wen-Hong Qiu, Gao-Song Wu, Xiang-Ping Yang, Sheng-Quan Zou, Fa-Zu Qiu

Zhao-Hui Tang, Gao-Song Wu, Sheng-Quan Zou, Fa-Zu Qiu, Department of Surgery of Tong Ji Hospital; **Wen-Hong Qiu**, Department of immunology, Tongji Medical College, Huazhong University of Science and Technology, Wuhan 430030, Hubei Province, China

Xiang-Ping Yang, Department of Biochemistry, Rheinisch-Westfälische Technische Hochschule(RWTH), D-52074 Aachen, Germany

Correspondence to: Zhao-Hui Tang, Department of General surgery, Tongji Hospital, 1095 Jiefang Road, Wuhan 430030, Hubei Province, China. tangzh45@sina.com

Telephone: +86- 27-83660374

Received 2002-04-26 **Accepted** 2002-06-10

Abstract

AIM: To estimate the effect of a therapeutic vaccine against pancreatic carcinoma based on dendritic cell (DC) vaccine modified with tumor lysate and Interleukin-18 gene.

METHODS: The BALB/C mice model of pancreatic carcinoma was induced with DMBA. DC vaccine was constructed through pulsed with tumor lysate and transfected by the recombinant adenoviral vector encoding IL-18 gene. The immunotherapeutic effects of DC vaccine on mice with pancreatic carcinoma were assessed (divided into DC-IL18-Lysate group, DC-Lysate group, DC-IL18 group, DC group, PBS group).

RESULTS: After vaccination of the DC vaccine, the concentration of IL-18 and IFN- γ were 2161 ± 439 ng \cdot L⁻¹ and 435 ± 72 ng \cdot L⁻¹ in DC-IL18-Lysate group and there was significant difference compared with other groups ($P < 0.01$). After vaccination of the DC vaccine, the transplanted tumors were observed on 30 days in DC-Lysate groups, on 16 days in DC-IL18 groups, on 3 days in control group, but mice remained tumor-free for at least 50 days in DC-IL18-Lysate group and there was significant difference between DC-IL18-Lysate group and other groups ($P < 0.01$). The median survival exceeds 62 days in DC-IL18-Lysate group. But the median survival was 48.6 days in DC-Lysate group, 33 days in DC-IL18 group, 17 days in PBS group. The survival period was obviously prolonged in DC-IL18-Lysate group than in other groups ($P < 0.05$, $P < 0.01$). The weight of pancreatic tumor was 0.22 ± 0.083 g in DC-IL18-Lysate group, 1.45 ± 0.74 g in DC-Lysate group, 1.89 ± 1.34 g in DC-IL18 group, 3.0 ± 1.6 g in DC group, 2.9 ± 2.0 g in PBS group and the weight of tumor obviously reduced in DC-IL18-Lysate group than in other groups ($P < 0.05$, $P < 0.01$).

CONCLUSION: DC vaccine modified with tumor lysate and Interleukin-18 gene can induce a specific and effective immune response against pancreatic carcinoma cell.

Tang ZH, Qiu WH, Wu GS, Yang XP, Zou SQ, Qiu FZ. The immunotherapeutic effect of dendritic cells vaccine modified with interleukin-18 gene and tumor cell lysate on mice with pancreatic carcinoma. *World J Gastroenterol* 2002; 8(5):908-912

INTRODUCTION

Because of the lack of methods for early diagnosis and the limited effects of surgical treatment, chemotherapy and radiation therapy, about 98 % of the patients with pancreatic carcinoma don't live more than 5 years^[1-4]. So we clearly need the new therapies to improve the prognosis of the patients with pancreatic carcinoma. Immunotherapy is moving close to become a promising approach of anticancer therapy as it has fewer side effects and, more importantly, the opportunity to generate long-term immunity^[5-7]. Dendritic cell (DC) is highly effective antigen presenting cell (APC) with the unique capability of inducing primary immune response against tumor-associated antigens. Animal studies have shown that the DC vaccine pulsed with tumor antigen could elicit specific T-cell response against tumor^[8-12]. Recently, *Geiger et al*^[13] reported that they have completed the first phase trial of tumor lysate-pulsed DC vaccine in the therapy of pediatric solid tumor, including osteosarcoma and fibrosarcoma, which were partial or complete regression.

Interleukin-18 (IL-18), originally termed IFN-inducing factor, induces IFN- γ production in both T cells and NK cells^[14-15]. In addition, IL-18 induces T cells to produce GM-CSF, and enhances the cytolytic activity of T cells and NK cells^[16]. In some animal model systems, IL-18 gene transfected into tumor cells should enhance both specific and nonspecific antitumor immune responses, which indicate if IL-18 gene were transferred into DC, it should induce highly effective antitumor immune responses^[17-20].

In this study, an *in vivo* model to estimate the effect of a therapeutic vaccine against pancreatic carcinoma based on DC vaccine modified with tumor lysate and Interleukin-18 gene was designed. We hope those results should provided a scientific basis for our next step, clinical trials, in the future.

MATERIALS AND METHODS

Materials

BALB/c mice (6-8 week old, male) were purchased from the experimental animal center of the Tongji Medical College. ³H-TdR, ⁵¹Cr was from Beijing Institute of Atomic Energy, 7,12-Dimethylbenzanthracene(DMBA) from Aldrich Co. Germany. IL-18, IFN- γ ELISA Kits from Zhongke Biotech Co. Wuhan. A recombinant adenoviral vector encoding IL-18 gene termed pCR3.1-IL-18 was kind gift from Dr. Chenwen Ye (Department of Immunology, Institut Pasteur de Lille, Paris, France). The mouse dendritic cell line MTSC4 derived from

the thymic of BALB/c mice (4 week old) were obtained from the department of immunology of Beijing medical university, which were maintained in CM.

Methods

The mice model of pancreatic carcinoma The membrane and partial parenchyma of BALB/c mice's pancreas were opened about 1 mm depth and the DMBA (7 mg) was put into there, as previously described^[21]. After 3-4 months, the mice developed pancreatic ductal adenocarcinomas with glandular duct-like distribution of cancer cells. The tumors from mice's pancreas were removed, carefully detached with a cell scraper, washed twice in PBS, and resuspended at a density of 2×10^7 /ml in serum-free medium. 0.5 ml (2×10^7 /ml) viable tumor cells were injected into the left flank of BALB/c to develop the mice model of pancreatic carcinoma.

DC pulsed with tumor lysate Pancreatic carcinoma cells from the fresh solid tumor of mice were incubated with 0.01 % EDTA-solution for 10 min, washed twice in PBS, and resuspended at a density of 5×10^6 /ml in serum-free medium. The cell suspensions were frozen at -80°C (2 min) and thawed in 37°C water (4 min), which were disrupted by four freeze-thaw cycles. For the removal of crude debris, the lysate was centrifuged for 10 min at $300 \times g$. The supernatant was collected and passed through a 0.2- μm filter for later use. Dendritic cells (DCs) were incubated with tumor lysates at a ratio of three tumor cells equivalents to one DC (i.e., 3:1) in CM. After 18 hr of incubation, DCs were harvested, washed twice in HBSS, and resuspended in HBSS for further study.

Cell transfection A recombinant adenoviral vector encoding IL-18 gene termed pCR3.1-IL-18 was kind gift from Dr. Chemen Ye (Immunology, Paris, France). For the transfection, DC and DC pulsed with tumor lysates were washed twice in HBSS, and incubated at 37°C with the adenoviral vectors, respectively. Virus was used at a dose of 100 multiplicity of infection (MOI). Under these conditions, more than 80 % of DCs were infected.

Induction of tumor-specific CTL *in vivo* 30 BALB/c mice were at random divided into five groups. Every group included 6 mice, which were immunized s.c. in the right flank, (1) 0.2 ml DC-IL18-Lysate (2×10^4 DCs modified with tumor lysate and IL-18, DC-IL18-Lysate group); (2) 0.2 ml DC-Lysate (2×10^4 DCs modified with tumor lysate, DC-lysate group); (3) 0.2 ml DC-IL18 (2×10^4 DCs modified with IL-18, DC-IL18 group); (4) 0.2 ml DC (2×10^4 DCs, DC group); (5) 0.2 ml PBS (control group), respectively, twice at 7 days. After 7 days, spleen-derived T cells were isolated from mice by Nylon wool-separated and were cocultured *in vitro* with tumor cells for 5 days. After 5 days, T cells were tested for cytolytic activity in a standard 4-hr ^{51}Cr -release assay. Effector-to target (E/T) ratio were from 20:1 to 100:1. Each assay was performed in triplicate and triplicate wells were averaged and percentage of special CTL was calculated by the formula [(sample-spontaneous release)/(maximum release-spontaneous release) $\times 100$ %]^[22].

Immunological protection of DCs vaccine 30 BALB/c mice were at random divided into five groups and were immunized s.c. in the right flank with DC-IL18-Lysate, DC-Lysate, DC-IL18, DC, PBS, respectively, twice at 7 days (described above). These mice were challenged 7 days after the last immunization with 0.5 ml (1×10^7 /ml) viable tumor cells from mice pancreas by s.c. in the left flank. The development of pancreatic carcinoma was observed in every mice.

Immunotherapeutic effect of DCs vaccine 30 mice from the mice model of pancreatic carcinoma with average tumor size $0.3 \times 0.5 \text{ cm}^2$ were at random divided into five groups

(described above), which were respectively injected in the right flank with 2×10^4 DC-IL18-Lysate, DC-Lysate, DC-IL18, DC, PBS, respectively, twice at 7 days. The size of the tumors was recorded twice weekly by measuring the largest perpendicular diameters (PD) and transverse diameter (TD) with calipers. The weight of the tumor was calculated by the formula $[(PD \times TD^2)/2]$.

Cytokine analysis After 7 days of the mice with pancreatic carcinoma immunized (described above), serum was obtained from the carotid artery of mice. The concentration of IL-18 and IFN- γ in the serum were measured by ELISA.

Statistical analysis

Data were expressed as the mean \pm SEM and were analyzed by *t* test or ANOVA. Differation were considered significant when P was <0.05 . Tests were performed using SAS (Statistical Analysis Software).

RESULTS

Tumor-specific CTL *in vivo*

Spleen cells obtained from mice at 7 days after the final immunization were cocultured with pancreatic carcinoma cells for 5 days. T cells of DC-IL18-Lysate group, DC-Lysate group and DC-IL18 groups were able to efficiently lyse the pancreatic carcinoma cells. The lytic efficiency increases following the rise of E/T ratio. The lytic efficiency of DC-IL18-Lysate group was the best, DC-Lysate group was the subsequence, and DC-IL18 group was the final. But T cells from additional groups obviously lack this ability ($P < 0.01$, Figure 1).

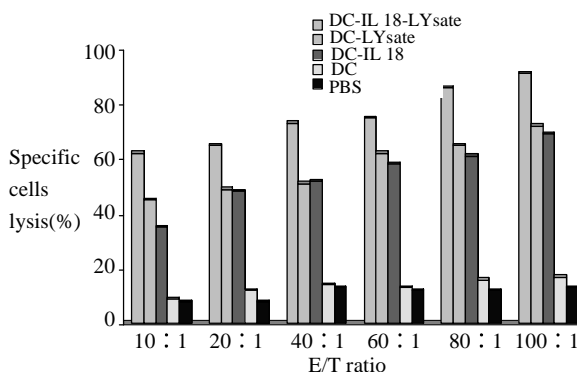


Figure 1 T cells were tested for cytolytic activity in a standard 4-hr ^{51}Cr -release assay. Effector-to target (E/T) ratio were from 20:1 to 100:1.

Cytokine analysis

After 7 days of the mice immunized, the concentration of IL-18 and IFN- γ in the serum were measured by ELISA. The concentration of IL-18 and IFN- γ were $2161 \pm 439 \text{ ng} \cdot \text{L}^{-1}$ and $435 \pm 72 \text{ ng} \cdot \text{L}^{-1}$ in DC-IL18-Lysate group. There were significant differences in DC-IL18-Lysate group versus other groups ($P < 0.05$, $P < 0.01$, Figure 2a-2b).

Immunological protection of DCs vaccine

The transplanted tumors were not observed in DC-IL18-Lysate group after the viable tumor cells from mice pancreas injected into the left flank 50 days. After 30 days, the transplanted tumors were observed in DC-Lysate groups. The first time was 16 days the transplanted tumor observed in DC-IL18 groups after the tumor cells injected into mice. Additional

groups all were observed the development of transplanted tumors from 3 to 9 days ($P<0.01$, Figure 3).

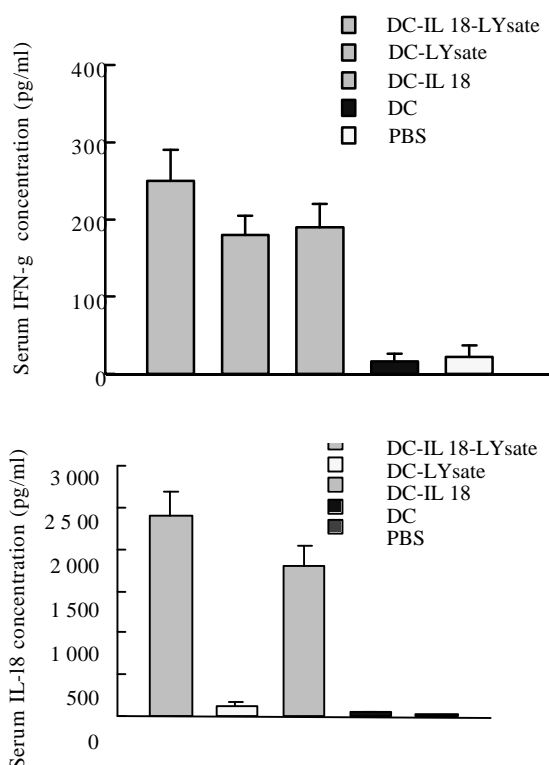


Figure 2a,2b The concentration of IL-18 and IFN- γ in the serum were measured by ELISA

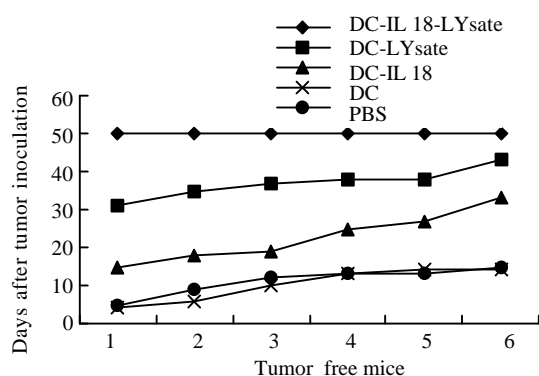


Figure 3 The development of the transplanted tumors was observed in every day

Immunotherapeutic effect of DCs vaccine

The growth velocity of tumor was observed obviously slowing in the mice immunized with DC-IL18-Lysate, DC-Lysate and DC-IL18. There were 3 cases in DC-IL18-Lysate group and 1 case in DC-Lysate group observed almost complete regression of the tumors. In contrast, the tumor cells displayed infiltrating style and adherent with nearby tissue in the mice immunized with PBS and DC. There was significant difference in the weight of tumor between the DC-IL18-Lysate group and the other groups ($P<0.01$, versus PBS group, DC group and DC-IL18 group; $P<0.05$, versus DC-Lysate group). The median survival exceeds 62 days in DC-IL18-Lysate group. But the median survival was only 48.6 days in DC-Lysate group, 33 days in DC-IL18 group, 17 days in PBS group (Table 1).

Table 1 Immunotherapeutic Effect of DCs Vaccine in Mice with Pancreatic Carcinoma

	DC-IL18-Lysate I group	DC-Lysate II group	DC-IL18 III group	DC IV group	PBS V group
Tumor Weight (g)	0.22±0.083 ^a	1.45±0.74 ^{bc}	1.89±1.34 ^d	3.0±1.6	2.9±2.0
Median Survival (d)	>62 ^a	48.6±9.4 ^{bc}	33±12.3 ^d	17±3.2	19.6±5.4

^a $P<0.01$, vs the other groups; ^b $P<0.05$, vs III group; ^c $P<0.01$, vs IV and V groups; ^d $P<0.05$, vs IV and V group

DISCUSSION

Dendritic cells (DCs) play an important role as primary antigen-presenting cell to initiate and maintain T-cell responses^[23-25]. In our study, we designed an *in vivo* model to estimate the effect of a therapeutic vaccine against pancreatic carcinoma based on DCs modified with tumor lysate and Interleukin-18 gene. It was observed that DCs were pulsed with tumor lysate could obviously increase the efficiency against the pancreatic carcinoma cells.

At present, potential targets for the immunotherapy of pancreatic carcinoma are antigens such as carcinoembryonic antigen^[26], HER-2/neu^[27], mutant ras^[28], p53^[29]. However, vaccinating a single antigen has disadvantages, because it is unknown which of the identified antigens was the potential to induce an effective antitumor immune response. Furthermore, immunity against a single antigen maybe ineffective in tumors with pancreatic carcinoma and carries the risk of inducing tumor antigen escape variant^[30,31]. In addition, this strategy is restricted to those patients with a specific HLA type.

In our research, we selected the tumor lysate as the target antigen because these unfractionated tumor-derived antigens could circumvent these disadvantages. Tumor lysates contain multiple known as well as unknown antigens that could be presented to T cells by MHC class I- and class II-pathways^[32-35]. Therefore, lysate-load DCs are more likely to induce a polyclonal expansion of T cells, including MHC class II restricted T-helper cells. These have been recognized to play an important role in the activation of CTLs, which were probably the most important cells in antitumor immune response. The generation of CTL clones with multiple specificities may be an advantage in heterogeneous tumors and could also reduce the risk of tumor escape variants. Furthermore, lysate from the autologous tumor can be used independently of the HLA type the patient. A major drawback of unfractionated tumor antigens is the possibility of inducing an autoimmune reactivity to epitopes that are shared by normal tissues^[36]. However, in clinical trials using lysate as the source of antigen, no clinically relevant autoimmune responses were detected^[37-44].

IL-18 is a recently discovered cytokine cloned from mice with fluminant hepatitis induced by challenge with propionibacterium acnes and subsequent administration of LPS^[14]. IL-18 lacks a signal sequence and is processed into the mature form by an IL-1 β -converting enzyme (ICE)^[15]. IL-18 is produced by cells of monocyte lineage, augments NK cytolytic activity, and enhances proliferation of T cells. IL-18 also promotes NK and T cells to secrete IFN- γ and GM-CSF. Based on those findings, IL-18 was demonstrated to confer a superior antitumor activity in some murine tumor systems. However, the systemic administration of recombinant IL-18 proteins, though effectively inhibited the tumor growth, resulted in death of all animals because of toxicity^[45-47].

Systemic administration of IL-18 also was associated with severe dose-dependent toxicity in patient during the first human trial. The transfer of cytokine genes may circumvent the toxicity of systemic IL-18, at same time, may delivery and provide adequate local cytokine levels for immune cell activation.

In our study, the IL-18 gene was transfected into DCs by recombinant adenoviral vector and we observed cytokine releases in serum of the mice were immunized with DCs modified with IL-18 and tumor lysate by ELISA. After 7 days of the mice immunized, the concentration of IL-18 and IFN- γ was obviously increased in DC-IL18-Lysate group. This indicated DCs transfected with the cytokines gene exhibited significant levels of IL-18 production. At same time, augmented the production of IFN- γ .

In our research, the effect of immunological protection and immunotherapy of DCs vaccines was obviously increased when DCs were modified with IL-18 gene and tumor lysate than IL-18 gene alone, tumor lysate alone. Especially, from the results of our study we found DCs modified with IL-18 gene alone induced a limited antitumor immunologic reaction. These findings strongly suggest that IL-18, tumor lysate and DC interacted and there were congenous effect against pancreatic carcinoma. At first, IL-18 enhanced NK cytolytic activity to induce more frequent and effective tumor cell death and promoted NK and T cells to secrete IFN- γ . Zitvoet *et al*^[48] reported the antitumor effect of DC-based vaccination was dependent on production of Th1-associated cytokines such as IFN- γ . Therefore, IL-18 may play an important role in antitumor activity of DCs through enhancing the production of IFN- γ ^[49]. In turn, DCs sever as effective antigen-presenting cells to induce potent and specific immunologic reaction. At same time, DCs expressed more ICE that was required when the preprotein of IL-18 was processed into the biological activity form. As shown in a recent study, the functions of DCs were affected by contact with tumor cells. Dynamic changes in chemokine receptor expression (up-regulation of CCR7) were identified on DCs following contact apoptotic tumor cells^[50]. Fumiaki *et al*^[51] also demonstrated that direct contact with DCs and tumor cell could be important for generating CTLs. Thus, the implications are that IL-18/Tumor cell/DC plays a critical inductive and interactive role in promoting the efficiency of immunotherapy against pancreatic carinoma.

In summary, DC vaccines modified with tumor lysate and Interleukin-18 gene can induce a specific and effective immune response against pancreatic carcinoma cells. However, the feasibility and security of this DCs vaccine still need to be observed in additional experiments.

REFERENCES

- Fuyahiko M**, Makoto S, Lianghao D, Peron JM, Cai Q, Robbins PD, Lotze MT. Effective gene therapy for pancreatic cancer by cytokines mediated by restricted replication competent adenovirus. *Hum Gene Ther* 2000; **11**: 223-235
- Zhou ZH**, Song MZ. Current therapies of pancreatic cancer. *Shijie Huaren Xiaohua Zazhi* 2000; **8**: 214-215
- Liu JW**, Li KZ. Pancreatic cancer, oncogene and anti oncogene. *Shijie Huaren Xiaohua Zazhi* 2001; **9**: 72-73
- Zhang SN**, Yuan SZ. Gene therapy for pancreatic carcinoma. *Shijie Huaren Xiaohua Zazhi* 1999; **7**: 269-270
- Liu MP**, Zhou JC, Guo XZ, Chen W, Dai B, An TY, Ma SY. Purification and characterization of antigen SC6 for pancreatic cancer. *Shijie Huaren Xiaohua Zazhi* 1999; **7**: 593-595
- Leng JJ**, Chen YQ, Leng XS. Genetic therapy for pancreatic neoplasms. *Shijie Huaren Xiaohua Zazhi* 2000; **8**: 916-918
- Jia L**, Yuan SZ. Progress of treatment of advanced pancreatic carcinoma with gemcitabine. *Shijie Huaren Xiaohua Zazhi* 1999; **7**: 985-986
- Lambert LA**, Gibson GR, Maloney M, Durell B, Noelle RJ, Barth RJ Jr. Intranodal Immunization with Tumor Lysate-pulsed Dendritic Cells Enhances Protective Antitumor Immunity. *Cancer Res* 2001; **61**: 641-646
- Shimizu K**, Thomas EK, Giedlin M, Mule JJ. Enhancement of Tumor Lysate- and Peptide-pulsed Dendritic Cell-based Vaccines by the Addition of Foreign Helper Protein. *Cancer Res* 2001; **61**: 2618-2624
- Li MS**, Yuan AL, Zhang WD. Low immune function of peripheral blood dendritic cells in hepatocarcinoma patients. *Shijie Huaren Xiaohua Zazhi* 1998; **6**: 240-241
- Li MS**, Yuan AL, Zhang WD, Liu SD, Lu AM, Zhou DY. Dendritic cells in vitro induce efficient and special antitumor immune response. *Shijie Huaren Xiaohua Zazhi* 1999; **7**: 161-163
- Chen HB**, Zhang JK, Huang ZL, Sun JL, Zhou YQ. Effects of cytokines on dendritic cells against human hepatoma cell line. *Shijie Huaren Xiaohua Zazhi* 1999; **7**: 191-193
- Geiger JD**, Hutchinson RJ, Hohenkirk LF, McKenna EA, Yanik GA, Levine JE. Treatment of solid tumors in children with tumor-lysate-pulsed dendritic cells. *Lancet* 2000; **326**: 1163-1165
- Okamura H**, Tsutsui H, Komatsu T, Yutsudo M, Hakura A, Tanimoto T, Torigoe K, Okura T, Nukada Y, Namba M, Kurimoto M. Cloning of a new cytokine that induces IFN- γ production by T cells. *Nature* 1995; **378**: 88-91
- Okamura H**, Tsutsui H, Kashiwamura SI, Hakura A, Tanimoto T, Torigoe K, Okura T. IL-18: a novel cytokine that augments both innate and acquired immunity. *Adv Immunol* 1998; **70**: 281-288
- Wu HG**, Zhou LB, Pan YY, Huang C, Chen HP, Shi Z, Hua XG. Study of the mechanisms of acupuncture and moxibustion treatment for ulcerative colitis rats in view of the gene expression of cytokines. *World J Gastroenterol* 1999; **5**: 515-517
- Akita K**, Ushio S, Ohtsuki T, Tsutsui H, Adarki O, Yoshida N, Tanabe F. Comparison between the biological and biochemical aspects of IL-18 (IFN- γ -inducing factor) and IL-1 β . *Proc Am Assoc Cancer Res* 1997; **38**: 357-362
- Hanlon L**, Argyle D, Bain D, Nicolson L, Dunham S, Golder MC, McDonald M, McGillivray C, Jarrett O, Neil JC, Onions DE. Feline leukemia virus DNA vaccine efficacy is enhanced by coadministration with interleukin-12 (IL-12) and IL-18 expression vectors. *J Virol* 2001; **75**: 8424-8433
- Grimm CF**, Ortmann D, Mohr L, Michalak S, Krohne TU, Meckel S, Eisele S, Encke J, Blum HE, Geissler M. Mouse alpha-fetoprotein-specific DNA-based immunotherapy of hepatocellular carcinoma leads to tumor regression in mice. *Gastroenterology* 2000; **119**: 1104-1112
- Golab J**. Interleukin 18-interferon gamma inducing factor-a novel player in tumour immunotherapy? *Cytokine* 2000; **12**: 332-338
- Qin RY**, Ai DI, Zou SQ, Qiu FZ. Development of a new rat model of pancreatic cancer. *Zhonghua Shiyian Waik Zazhi* 2000; **17**: 462-463
- Kirk CJ**, Hartigan D, Nickoloff BJ, Bonini C, Lee SP, Riddell SR, Greenberg PD. T Cell-dependent Antitumor Immunity Mediated by Secondary Lymphoid Tissue Chemokine: Augmentation of Dendritic Cell-based Immunotherapy. *Cancer Res* 2001; **61**: 2062-2070
- Zhang JK**, Chen HB, Sun JL, Zhou YQ. Effect of dendritic cells on LPAK cells induced at different times in killing hepatoma cells. *Shijie Huaren Xiaohua Zazhi* 1999; **7**: 673-675
- Li MS**, Yuan AL, Zhang WD, Chen XQ, Tian XH, Piao YJ. Immune response induced by dendritic cells induce apoptosis and inhibit proliferation of tumor cells. *Shijie Huaren Xiaohua Zazhi* 2000; **8**: 56-58
- Luo ZB**, Luo YH, Lu R, Jin HY, Zhang BP, Xu CP. Immunohistochemical study on dendritic cells in gastric mucosa of patients with gastric cancer and precancerous

- lesions. *Shijie Huaren Xiaohua Zazhi* 2000; **8**: 400-402
- 26 **Nestle FO**, Alijagic S, Gilliet M, Sun Y, Grabbe S, Dummer R, Burg G, Schadendorf D. Vaccination of melanoma patients with peptide- or tumor lysate-pulsed dendritic cells. *Nat Med* 1998; **4**: 328-332
- 27 **Nukaya I**, Yasumoto M, Iwasaki T, Ideno M, Sette A, Celis E, Takesako K, Kato I. Identification of HLA-A24 epitope peptides of carcinoembryonic antigen which induce tumor-reactive cytotoxic T lymphocyte. *Int J Cancer* 1999; **80**: 92-97
- 28 **Peiper M**, Goedegebuure PS, Izbicki JR, Eberlein TJ. Pancreatic cancer associated ascites-derived CTL recognize a nine-amino-acid peptide GP2 derived from HER2/neu. *Anticancer Res* 1999; **19**: 2471-2475
- 29 **Gjertsen MK**, Bjorheim J, Saeterdal I, Myklebust J, Gaudernack G. Cytotoxic CD4+ and CD8+ T lymphocytes, generated by mutant p21-ras (12Val) peptide vaccination of a patient, recognize 12Val-dependent nested epitopes present within the vaccine peptide and kill autologous tumour cells carrying this mutation. *Int J Cancer* 1997; **72**: 784-790
- 30 **Thumer B**, Haendle I, Roder C, Hubert P, Jacobs N, Giannini SL, Havard L, Renard I, Saboulard D. Vaccination with mage-3A1 peptide-pulsed mature, monocyte-derived dendritic cells expands specific cytotoxic T cells and induces regression of some metastases in advanced stage IV melanoma. *J Exp Med* 1999; **190**: 1669-1678
- 31 **Schnurr M**, Galambos P, Scholz C, Fiander A, Man S, Jasani B, Navabi H, Lipetz C, Evans AS, Mason M. Tumor Cell Lysate-pulsed Human Dendritic Cells Induce a T-Cell Response against Pancreatic Carcinoma Cells: an *in vitro* Model for the Assessment of Tumor Vaccines. *Cancer Res* 2001; **61**: 6445-6450
- 32 **Schnurr M**, Galambos P, Scholz C, Fiander A, Man S, Jasani B, Navabi H, Lipetz C, Evans AS, Mason M. Tumor Cell Lysate-pulsed Human Dendritic Cells Induce a T-Cell Response against Pancreatic Carcinoma Cells: an *in vitro* Model for the Assessment of Tumor Vaccines. *Cancer Res* 2001; **61**: 6445-6450
- 33 **Fields RC**, Shimizu K, Mulé JJ. Murine dendritic cells pulsed with whole tumor lysates mediate potent antitumor immune responses *in vitro* and *in vivo*. *Proc Natl Acad Sci USA* 1998; **95**: 9482-9487
- 34 **Timmerman JM**, Czerwinski DK, Davis TA, Hsu FJ, Benike C, Hao ZM, Taidi B, Rajapaksa R, Caspar CB, Okada CY, van Beckhoven A, Liles TM, Engleman EG, Levy R. Idiotypic-pulsed dendritic cell vaccination for B-cell lymphoma: clinical and immune responses in 35 patients. *Blood* 2002; **99**: 1517-1526
- 35 **Jiao X**, Lo-Man R, Guermonprez P, Fiette L, Deriaud E, Burgaud S, Gicquel B, Winter N, Leclerc C. Dendritic cells are host cells for mycobacteria *in vivo* that trigger innate and acquired immunity. *J Immunol* 2002; **168**: 1294-301
- 36 **Udewig B**, Ochsenbein A F, Odermatt B, Paulin D, Hengartner H, Zinkernagel RM. Immunotherapy with dendritic cells directed against tumor antigens shared with normal host cells results in severe autoimmune disease. *J Exp Med* 2000; **191**: 795-804
- 37 **Holdt L**, Rieser C, Papesch C, Gilligan MG, Knox PG, Searle PF. Cellular and humoral immune responses in patients with metastatic renal cell carcinoma after vaccination with antigen pulsed dendritic cells. *J Urol* 1999; **161**: 777-782
- 38 **Li J**, Holmes LM, Franek KJ, Burgin KE, Wagner TE, Wei Y. Purified hybrid cells from dendritic cell and tumor cell fusions are superior activators of antitumor immunity. *Cancer Immunol Immunother* 2001; **50**: 456-462
- 39 **Tanigawa K**, Takeshita N, Eickhoff GA, Shimizu K, Chang AE. Antitumor reactivity of lymph node cells primed *in vivo* with dendritic cell-based vaccines. *J Immunother* 2001; **24**: 493-501
- 40 **Kammerer R**, Stober D, Riedl P, Oehninger C, Schirmbeck R, Reimann J. Noncovalent association with stress protein facilitates cross-priming of CD8+ T cells to tumor cell antigens by dendritic cells. *J Immunol* 2002; **168**: 108-117
- 41 **Orentas RJ**, Schauer D, Bin Q, Johnson BD. Electrofusion of a weakly immunogenic neuroblastoma with dendritic cells produces a tumor vaccine. *Cell Immunol* 2001; **213**: 4-13
- 42 **Steinman RM**, Dhodapkar M. Active immunization against cancer with dendritic cells: the near future. *Int J Cancer* 2001; **94**: 459-473
- 43 **Foley HD**, Otero M, Orenstein JM, Pomerantz RJ, Schnell MJ. Rhabdovirus-based vectors with human immunodeficiency virus type 1 (HIV-1) envelopes display HIV-1-like tropism and target human dendritic cells. *J Virol* 2002; **76**: 19-31
- 44 **Biragyn A**, Surenhu M, Yang D, Ruffini PA, Haines BA, Klyushnenkova E, Oppenheim JJ, Kwak LW. Mediators of innate immunity that target immature, but not mature, dendritic cells induce antitumor immunity when genetically fused with nonimmunogenic tumor antigens [J]. *J Immunol* 2001; **167**: 6644-6653
- 45 **Hara I**, Nagai H, Miyake H, Yamanaka K, Hara S, Micallef MJ, Kurimoto M, Gohji K, Arakawa S, Ichihashi M, Kamidono S. Effectiveness of cancer vaccine therapy using cells transduced with the interleukin-12 gene combined with systemic interleukin-18 administration. *Cancer Gene Ther* 2000; **7**: 83-90
- 46 **Heuer JG**, Tucker-McClung C, Hock RA. Neuroblastoma cells expressing mature IL-18, but not proIL-18, induce a strong and immediate antitumor immune response. *J Immunother* 1999; **22**: 324-335
- 47 **Osaki T**, Peron JM, Cai Q, Okamura H, Robbins PD, Kurimoto M, Lotze MT, Tahara H. IFN-gamma-inducing factor/IL-18 administration mediates IFN-gamma- and IL-12-independent antitumor effects. *J Immunol* 1998; **160**: 1742-1749
- 48 **Zitvogel L**, Mayordomo J I, Tjandrawan T, Gilmore RD Jr, Dolan M, Piesman J, Titus RG. Therapy of murine tumors with tumor peptide-pulsed dendritic cells: dependence on T cells, B7 costimulation, and T helper cell 1-associated cytokines. *J Exp Med* 1996; **183**: 87-97
- 49 **Kohyama M**, Saijyo K, Hayasida M, Yasugi T, Kurimoto M, Ohno T. Direct activation of human CD8+ cytotoxic T lymphocytes by interleukin-18. *Jpn J Cancer Res* 1998; **89**: 1041-1046
- 50 **Hirao M**, Onai N, Hiroishi K, Lee C, Schechner J, Glusac E, Christensen I, Snyder E, Holloway V, Tigelaar R, Edelson RL. Chemokine receptor-7 on dendritic cells is induced after interaction with apoptotic tumor cells: critical role in migration from the tumor site to draining lymph nodes. *Cancer Res* 2000; **60**: 2209-2217
- 51 **Fumiaki T**, Wataru H, Haruki O, Ohta M, Fujie T, Tanaka F, Inoue H, Takesako K. Rapid generation of potent and tumor specific CTL by interleukin 18 using dendritic cells and natural killer cells. *Cancer Res* 2000; **60**: 4838-4844

Edited by Qi QH

• BASIC RESEARCH •

Synthesis of an enzyme-dependent prodrug and evaluation of its potential for colon targeting

Yi-Nuo Pang, Yan Zhang, Zhi-Rong Zhang

Yi-Nuo Pang, Yan Zhang, West China School of Pharmacy, Sichuan University, Chengdu, 610041, Sichuan Province, China

Supported by the National Distinguished Youth Scientific Fund, No. 39925039

Correspondence to: Prof. Zhi-Rong Zhang, West China School of Pharmacy, Sichuan University, Chengdu, 610041, Sichuan Province, China. zrzsl@mail.sc.cninfo.net

Telephone: +86-28-85501566 **Fax:** +86-28-85456898

Received 2002-03-22 **Accepted** 2002-04-20

Abstract

AIM: To synthesize dexamethasone-succinate-dextran (DSD) conjugate and to evaluate the potentiality of DSD for the treatment of inflammatory bowel diseases.

METHODS: Dexamethasone was attached to dextran (average molecular weight=70 400 Dalton) using succinate anhydride in an anhydrous environment catalyzed by 4-dimethylaminopyridine and 1, 1'-carbonyldiimidazole. The chemical structure of DSD was identified by UV, IR and NMR, and the *in vivo* drug release behavior of this prodrug was investigated after oral administration of DSD suspension.

RESULTS: The DSD conjugate was obtained in two steps and the content of dexamethasone in DSD was 11.28 %. The dextran prodrug was stable in rat stomach and small intestine and negligibly absorbed from these tracts. Four to nine hours after the oral administration, most of the prodrug (>95 %) had moved to the cecum and colon, and was easily hydrolyzed by an endodextranase. Recover of dexamethasone from colon and cecum after administration of DSD conjugate was 6-12 folds higher than the recovery after administration of unmodified dexamethasone ($t=2.74$, $P<0.05$). The preferential release of free dexamethasone in cecum and colon over that in the small intestine was statistically significant ($t=2.27$, $P<0.05$).

CONCLUSION: The results of this study indicate that dextran conjugates may be useful in selectively delivering glucocorticoids to the colon.

Pang YN, Zhang Y, Zhang ZR. Synthesis of an enzyme-dependent prodrug and evaluation of its potential for colon targeting. *World J Gastroenterol* 2002; 8(5):913-917

INTRODUCTION

Inflammatory bowel diseases, which include ulcerative colitis and Crohn's disease are currently treated with glucocorticoids and other anti-inflammatory agents^[1,2]. For a steroidal anti-inflammatory drug, e.g. dexamethasone or prednisolone, a long-term administration would produce systemic side effects, including adrenosuppression, Cushingoid symptoms, immunosuppression, and diabetes. In this case, it is desirable

to localize the release of dexamethasone insofar as possible to the afflicted sites in the colon. Release of drug in the proximal GI tract should be avoided to circumvent absorption from the small intestine, and consequent drug wastage and systemic side effects^[2]. Because of the unique physiological characteristics of the large intestine, drug delivery to the colon can be achieved in different ways, including pH dependent approaches utilizing the changes in pH along the GI tract^[3-12], coated dosage forms^[13-17], time-controlled or pulsatile release systems^[18-24], pressure-controlled colon delivery systems^[25-30], coating drugs with bacterially degradable polymers^[31-40], and delivery of drugs as prodrugs^[41-47].

The bacterial count in the colon is higher than that in the preceding sections of the GI tract by many orders of magnitude in humans and other animals. Enzymes of the colonic bacteria can specifically degrade some kind of polysaccharides and azopolymers or break the chemical bonds between the parent drug and the carrier, and then the pharmacological active component can be released from natural and synthetic prodrugs. The most important issue for this approach is a selection of the functional groups that can survive the passage through stomach and small intestine, but are degraded by enzymes of the colonic microflora thus specifically releasing the drug into the colon^[2].

This project used dexamethasone as the model drug to synthesize a prodrug via a succinate tetracarbon-bridge that links the parent drug to the dextran carrier. Compared with unmodified dexamethasone, dexamethasone-succinate-dextran conjugate is more hydrophilic and has a larger molecular weight, which may decrease its possibility of being absorbed into the systemic circulation through the small intestinal epithelial cells. When it arrives to the colon, the dextran structure is hydrolyzed quickly by endogenous dextranase and then the esterase breaks the ester bond to release the dexamethasone. Distributions of dexamethasone in plasma and luminal contents were investigated after gastric intubation of DSD suspension or equivalent dose of dexamethasone to male SD rats.

MATERIALS AND METHODS

Material and apparatus

Dexamethasone was purchased from Tianjin Pharmacy Ltd., China. 4-dimethylaminopyridine (DMPA), 1,1'-carbonyldiimidazole and dextran (weight-average molecular weight=70 400 Dalton) were obtained from Sigma Chemical Company, St. Louis, MO. Succinate anhydride was purchased from Beijing Medicine Corporation, China. Molecular sieve (5Å) was obtained from Shitian Chemical Ind. China.

Methods

Synthesis of dexamethasone-dextran conjugate

Dexamethasone 3.98 g, succinate anhydride 1.27 g and 4-dimethylaminopyridine 1.55 g were dissolved in 400 ml anhydrous acetone over 5Å molecular sieves. The reaction solution was stirred at 25 °C for 30 minutes, and the resulting solution was evaporated in a rotary evaporator to produce light

yellow solid. After the solid was dissolved in anhydrous ethanol, distilled water was added to achieve a solution of ethanol and water (29:71 v/v). The solution was kept at -4°C for 48 h to crystallize and filtered under reduced pressure. The resulting crystals were dried in a P_2O_5 drying pistol with refluxing of 95 % ethanol under vacuum (10 mmHg) for 24 h to produce dexamethasone succinate hemiester (DS). The yield is $85.28 \pm 4.57\%$.

3.08 g of DS and 1.78 g of 1,1'-carbonyldiimidazole were dissolved in 15 ml of anhydrous dimethyl sulfoxide (DMSO). The reaction was run at 25°C with stirring for 30 min. Then a solution of dextran in anhydrous DMSO (200 ml) and triethylamine (17.5 ml) was added, and the mixture was stirred at 25°C for 21 h. The dextran conjugate was precipitated by adding 300 ml of ethanol/ether (50:50 v/v) to the DMSO solution with stirring. The resulting polymer was dispersed in ethanol again and filtered under a stream of dry nitrogen. The precipitate was collected by filtration under reduced pressure, then washed with anhydrous ether three times to produce DSD white powder (yield: $81.27 \pm 5.09\%$): UV λ_{max} : 242 nm (ϵ 14 500); IR (KBr): 3420(OH), 2930(CH_2), 1740($\text{C}=\text{O}$), 1660($\text{C}=\text{C}$), 1020($\text{C}-\text{O}-\text{C}$) 898 cm^{-1} ; ^1H NMR (DEXO- d_6): δ 7.310, 7.285(d, 1H, C-1), 6.233, 6.207(d, 1H, C-2), 6.002(s, 1H, C-4), 3.488, 3.508, 3.623, 3.742, 4.668(s, 1H, C-5', C-4', C-3', C-2', C-1'), 3.202(s, 2H, C-6'), 2.054(s, 2H, C-21), 1.464(s, 3H, C-19), 0.860(s, 3H, C-18), 0.758, 0.774(d, 3H, C-16).

The content of dexamethasone in DSD was measured by HPLC after alkaline hydrolysis.

Preparation of DSD granules and DSC test To evaluate the potential colon specificity of DSD *in vivo* test, granules of DSD or dexamethasone were prepared with the following ingredients: DSD or dexamethasone, cornstarch and lactose (5:50:45). A wet granulation method was applied. The granules were partially dissolved and suspended in water before dosing. Before granulation, all the ingredients were subjected to Differential Scanning Calorimetry (DSC). Measurements were performed on a calorimeter DSC7 connected to a Thermal Analysis Data Station 3 700 (Perkin-Elmer, Germany). Five mg of bulk materials were accurately weighed into standard aluminum pans. Thermograms were recorded from 303 to 573 K at a heating rate of $10\text{ K} \cdot \text{min}^{-1}$.

In vivo test Male SD rats (weighing about 150 g) were fed a standard diet (R-2, Chengdu) and were fasted for 18 h prior to drug administration with free access to drinking water. The rats were divided into the test group and control group randomly. Each group was subdivided further into seven subgroups. The test groups were administered with suspension of DSD (equivalent to 3 mg of dexamethasone per Kg of rat body weight) by gastric intubation, and the control groups were administered with suspension of dexamethasone. After the drug administration, blood samples of the test subgroups and the control subgroups were collected at each predetermined time (1, 3, 4, 5, 6, 7, 9 h). Then the rats were sacrificed by decapitation and the stomach, proximal small intestine (PSI), distal small intestine (DSI), cecum and colon were removed. The contents of the GI tract were removed by gently squeezing the GI segments. The separated contents and tissues were quickly frozen to -20°C and stored until analysis. Rat blood samples were collected and centrifuged at 700 g for 10 min. The plasma was frozen to -20°C and stored until analysis was performed.

Analysis The frozen intestinal contents were thawed, weighed, and diluted to 50 % (w/v) with phosphate buffer (pH 6.8). The suspended samples were homogenized by vortexing, and then 0.5 g of the diluted contents was placed in a 5-ml centrifuge tube. 200 μl of isotonic phosphate buffer (pH 2), 100 μl of internal

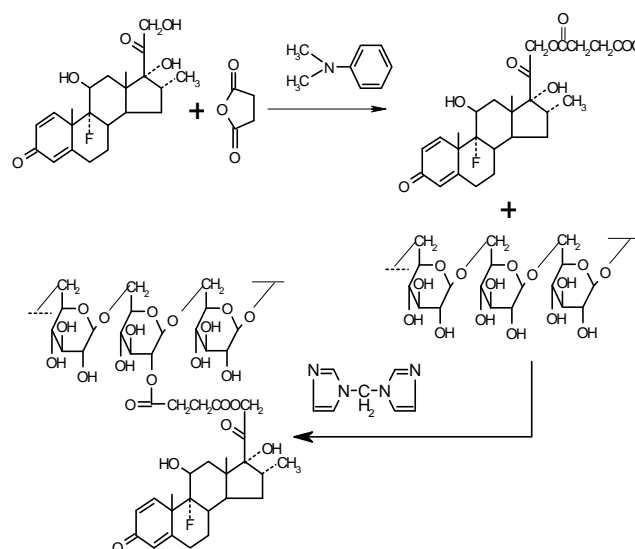
standard solution ($0.1336\text{ mg} \cdot \text{ml}^{-1}$) and dexamethasone solution in different concentrations were added to the 5-ml centrifuge tube. The samples were extracted with acetic ester (3 ml) by vortexing for 2 min. After centrifuging for 10 min at 1000 g, 2 ml of the organic phase was removed and evaporate at 45°C under vacuum. The residue was redissolved in mobile phase solution and centrifuged for 10 min at 1000 g. 20 μl of the supernatant fluid was subjected to HPLC analysis under the following conditions: Shimadzu CTO-10A system controller, LC-10AT pumps, SPD-10A variable wavelength detector, a Shimpack CLC C18 column ($5\text{ }\mu\text{m}$, $4.6 \times 150\text{ mm}$). The mobile phase consisted of 35 % acetonitrile and 65 % buffer (50 mM trisodium citrate adjusted to pH 4.6 with phosphoric acid). A flow rate of $1\text{ ml} \cdot \text{min}^{-1}$ and a detection wavelength of 241 nm were used. Prednisolone acetate was used as the internal standard. The plasma samples were treated by the same method described above.

RESULTS

Chemistry

DSD was prepared in two steps with a modified Mcleod reaction^[2]. It is essential to keep the reaction continuing under the anhydrous condition to ensure high yield. Succinate anhydride was coupled to the dexamethasone hydroxyl group in anhydrous acetone in the presence of 4-dimethylaminopyridine to produce hemiester. Then the hemiester was coupled to dextran in DMSO using 1,1'-carbonyldiimidazole as catalyzer (Scheme 1).

The chemical structure was identified by ^1H NMR and IR, confirming the procedure of scheme 1. The content of dexamethasone in DSD was 11.28 equals to about 20 dexamethasone (molecular weight=392 Dalton) molecules were coupled to one dextran molecule (average molecular weight=70 400 Dalton).



Scheme 1 Preparation of DSD

Differential scanning calorimetry (DSC)

Study on interaction between the supplementary ingredients of suspension and DSD was performed by DSC. The thermogram displayed two transition peaks at 343K and 561K corresponding to DSD, and another two peaks at 420K and 486K corresponding to mixed ingredients. No new transition peak was observed when the physical mixture of DSD and ingredients were subjected to DSC, indicating that there was no interaction between DSD and the supplementary ingredients.

In vivo testing

The recovery of free dexamethasone from rat blood and GI tract at various times following oral administration of DSD suspensions is shown in Table 1. During the whole observation period (0-9 h), no dexamethasone was detected in blood. This observation indicated that DSD conjugate was so stable that it could not be degraded in upper GI tract and could not be absorbed into blood. Three hours after dosing, only very small amount (<3 % of total recovery) of dexamethasone was detected in small intestine in spite of the high level of esterase in small intestine. After 6h, the recovery of dexamethasone in small intestine further decreased. At the same time, a large portion (>95 % of total recovery) of the prodrug reached the cecum and colon intact.

Control experiments in which unmodified dexamethasone was administered showed that dexamethasone was absorbed primarily from the small intestine and the blood concentration of dexamethasone was much higher than test groups. Meanwhile, very small amount of dexamethasone was observed either in the cecum or in the colon (Table 2).

Table 1 Recovery of free dexamethasone from the rat blood and GI tract at various times after administration of DSD suspensions^{a, b} (equivalent to 15mg of dexamethasone per Kg body weight)

t h	T μg	Recovery of dexamethasone(%)					
		B	S	PSI	DSI	Ce	Co
1	5.2	nd	74	26	nd	nd	nd
3	7.3	nd	54	nd	46	nd	nd
4	14	nd	8.8	6.6	10.2	54	20.5
5	27.6	nd	9.2	5.0	13.4	54.4	18.0
6	133	nd	4.0	0.27	2.2	83	10.2
7	128	nd	4.5	nd	0.557	80	15.2
9	105	nd	12.4	3.49	3.72	62	18.2

Table 2 Recovery of free dexamethasone from the rat blood and GI tract at various times after administration of dexamethasone suspensions^{a, b} (equivalent to 15 mg of dexamethasone per Kg body weight)

t h	T μg	Recovery of dexamethasone (%)					
		B	S	PSI	DSI	Ce	Co
1	1076	8.9	54	15.8	20.8	0.05	nd
3	857	4.58	94.6	0.05	1.08	nd	nd
4	390	26	58	10.2	5.0	0.40	nd
5	230	36	22	1.19	4.2	16	2.56
6	203	33	30	6.7	3.63	24.7	2.25
7	139	39	49	2.02	5.6	3.74	0.79
9	134	40	42	1.52	7.8	6.0	3.1

^aValues represent the average of three animals. ^bt, Time; T, Total recovery; B, Blood; S, Stomach; PSI, Proximal small intestine; DSI, Distal small intestine; Ce, Cecum; Co, Colon. nd: Not detected

The dexamethasone recoveries from cecum and colon after the oral administration of DSD suspensions or dexamethasone suspensions were also shown graphically (Figure 1 and Figure 2). It was obvious that the recovery of test groups from cecum and colon after administration were higher than that of control groups by 6-12 folds ($t=2.74$, $P<0.05$).

The specificity of dexamethasone release was further evaluated by comparing the amount of free dexamethasone recovered in the small intestine with that in the colon in the test group. A paired *t*-test indicated that the preferential release of free dexamethasone in cecum and colon over that in the small intestine was statistically significant ($t=2.27$, $P<0.05$). Meanwhile, a similar analysis in the control group showed that the difference between the dexamethasone concentration in the colon and that in the small intestine was not statistically significant.

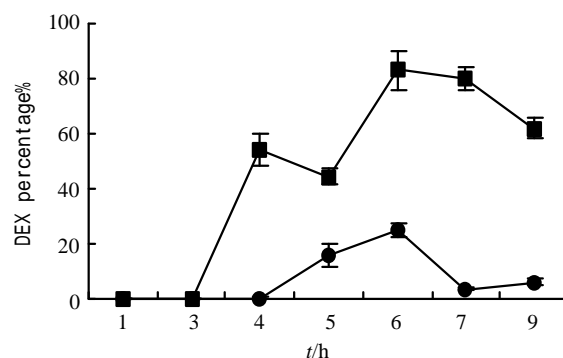


Figure 1 The dexamethasone contents-time curves in cecum after the oral administration dexamethasone suspensions (●) and DSD suspensions (■)

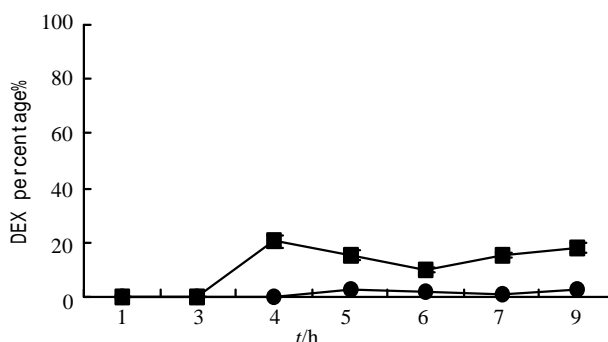


Figure 2 The dexamethasone contents-time curves in colon after the oral administration dexamethasone suspensions (●) and DSD suspensions (■)

DISCUSSION

The bacterial count in the colon is much higher than that in upper GI tract^[2]. The colonic micro flora produce a variety of enzymes, including azoreductase, various glycosidases and amidases, which are not present in the stomach or the small intestine. Therefore, enzyme dependent drug release, which relies on the existence of enzyme-producing microorganisms in the colon, could be used to deliver drug to the colon after enzymatic cleavage of degradable carrier bonds and premature drug release does not occur in this case.

Besides treating inflammatory bowel diseases, colon-specific drug delivery system might be useful in other situations. The delivery of certain antineoplastic agents to the

colon might be beneficial in controlling colon cancer^[48]. Enzyme prodrug gene therapy for colon cancer is also investigated by several researchers^[49,50]. Antibiotics might be delivered specifically to the colon via cyclodextrin carriers^[51-53]. In each of these cases, colon-specific delivery would allow the use of higher doses of potent agents with fewer systemic side effects.

The present results showed that the ester type prodrugs of dexamethasone/dextran release dexamethasone preferentially on cecal and colonic contents after the hydrolysis of dextran to small oligosaccharides, suggesting that dextran could serve as a new class of colon-specific drug carrier. The dextran conjugate survives the passage through upper GI tract although the high level of esterase in small intestine, indicating that dextran protects ester bond from hydrolysis by esterase. This result, together with the observation mentioned above, suggests that bacterial enzymes in the colon are responsible for hydrolysis of dextran conjugates. When DSD reached the colon, dextran was completely hydrolyzed into smaller oligosaccharides and exposed the ester bonds to esterase, which led to the rapid release of dexamethasone.

In summary, a colon-specific drug-delivery system has been developed based on drug-dextran conjugation and the unique glycosidase activity of the colonic microflora. Colonic drug delivery can be achieved with carriers by making prodrugs that survive the passage through stomach and small intestine, but the active moiety is released by enzymes specifically produced in colon.

REFERENCES

- 1 **Jiang XL**, Cui HF. An analysis of 10218 ulcerative colitis cases in China. *World J Gastroenterol* 2002; **8**: 158-161
- 2 **Mcleod AD**, Friend DR, Tozer TN. Glucocorticoid-dextran conjugates as potential prodrugs for colon-specific delivery: hydrolysis in rat gastrointestinal tract contents. *J Pharm Sci* 1994; **83**: 1284-1288
- 3 **Rudolph MW**, Klein S, Beckert TE, Petereit HU, Dressman JB. A new 5-aminosalicylic acid multi-unit dosage form for the therapy of ulcerative colitis. *Eur J Pharm Biopharm* 2001; **51**: 183-190
- 4 **Khan MZI**, Prebeg Z, Kurjakovic N. A pH-dependent colon targeted oral drug delivery system using methacrylic acid copolymers. *J Control Release* 1999; **58**: 215-222
- 5 **Gupta VK**, Beckert TE, Price JC. A novel pH- and time-based multi-unit potential colonic drug delivery system. I. development. *Int J Pharm* 2001; **213**: 83-91
- 6 **Gupta VK**, Assmus MW, Beckert TE, Price JC. A novel pH- and time-based multi-unit potential colonic drug delivery system. II. Optimization of multiple response variables. *Int J Pharm* 2001; **213**: 93-102
- 7 **Ishibashi T**, Pitcairn GR, Yoshino H, Mizobe M, Wilding IR. Scintigraphic evaluation of a new capsule-type colon specific drug delivery system in healthy volunteers. *J Pharm Sci* 1998; **87**: 531-537
- 8 **Nykanen P**, Krogars AK, Sakkinen M, Heinamaki J, Jurjensson H, Veski P, Marvola M. Organic acids as excipients in matrix granules for colon-specific drug delivery. *Int J Pharm* 1999; **184**: 251-261
- 9 **Cole ET**, Robert AS, Alyson LC, Ian RW, Hans UP, Carsten S, Thomas B, Dominique C. Enteric coated HPMC capsules designed to achieve intestinal targeting. *Int J Pharm* 2002; **231**: 83-95
- 10 **Marta R**, Vila-Jato JV, Dolores T. Design of a new multiparticulate system for potential site-specific and controlled drug delivery to the colonic region. *J Control Rel* 1998; **55**: 67-77
- 11 **Lorenao-lamosa ML**, Remunan LC, Vila-Jato JLL, Alonso MJ. Design of microencapsulated chitosan microsphere for colonic drug delivery. *J Control Rel* 1998; **52**: 109-118
- 12 **Rodriguez M**, Antunez JA, Taboada C, Seijo B, Torres D. Colon-specific delivery of budesonide from microencapsulated cellulosic cores: evaluation of the efficacy against colonic inflammation in rats. *J Pharm Pharmacol* 2001; **53**: 1207-1215
- 13 **Leopold CS**, Eikeler D. Basic coating polymers for the colon-specific drug delivery in inflammatory bowel disease. *Drug Dev Ind Pharm* 2000; **26**: 1239-1246
- 14 **Cavalcanti OA**, Van D, Caramico-Soares I, Kinget R. Polysaccharides as excipients for colon-specific coatings. Permeability and swelling properties of films. *Drug Dev Ind Pharm* 2002; **28**: 157-164
- 15 **Nykanen P**, Lempaa S, Aaltonen ML, Jurjensson H, Veski P, Marvola M. Citric acid as excipient in multiple-unit enteric-coated tablets for targeting drugs on the colon. *Int J Pharm* 2001; **229**: 155-162
- 16 **Villar-Lopez ME**, Nieto-Reyes L, Anguiano-Igea S, Otero-Espinar FJ, Blanco-Mendez J. Formulation of triamcinolone acetonide pellets suitable for coating and colon targeting. *Int J Pharm* 1999; **179**: 229-235
- 17 **Tozaki H**, Fujita T, Komoike J, Kim SI, Terrashima H, Muranishi S, Okabe S, Yamamoto A. Colon-specific delivery of budesonide with a novel dosage form against 2,4,6-trinitrobenzenesulphonic acid-induced colitis in rats. *J Pharm Pharmacol* 1999; **51**: 257-261
- 18 **Fukui E**, Miyamura N, Kobayashi M. An *in vitro* investigation of the suitability of press-coated tablets with hydroxypropylmethylcellulose acetate succinate (HPMCAS) and hydrophobic additives in the outer shell for colon targeting. *J Control Release* 2001; **70**: 97-107
- 19 **Fukui E**, Miyamura N, Uemura K, Kobayashi M. Preparation of enteric coated timed-release press-coated tablets and evaluation of their function by *in vitro* and *in vivo* tests for colon targeting. *Int J Pharm* 2000; **204**: 7-15
- 20 **Sangalli ME**, Maroni A, Zema L, Busetti C, Giordano F, Gazzaniga A. In vitro and in vivo evaluation of an oral system for time and/or site-specific drug delivery. *J Control Release* 2001; **73**: 103-110
- 21 **Ishibashi T**, Ikegami K, Kubo H, Kobayashi M, Mizobe M, Yoshino H. Evaluation of colonic absorbability of drugs in dogs using a novel colon-targeted delivery capsule (CTDC). *J Control Release* 1999; **59**: 361-376
- 22 **Sangalli ME**, Maroni A, Busetti C, Zema L, Giordano F, Gazzaniga A. In vitro and in vivo evaluation of oral systems for time and site specific delivery of drugs. *Boll Chim Farm* 1999; **138**: 68-73
- 23 **Yang L**, Chu JS, Fix JA. Colon-specific drug delivery: new approaches and *in vitro/in vivo* evaluation. *Int J Pharm* 2002; **235**: 1-15
- 24 **Hebden JM**, Wilson CG, Spiller RC, Gilchrist PJ, Blackshaw E, Fried ME, Perkin AC. Regional differences in quinine absorption from the undisturbed human colon assessed using a timed release delivery system. *Pharm Res* 1999; **16**: 1087-1092
- 25 **Takaya T**, Niwa K, Muraoka M, Ogita I, Nagai N, Yano Ri, Kimura G, Yoshikawa Y, Yoshikawa H, Takada K. Importance of dissolution process on systemic availability of drugs delivered by colon delivery system. *J Control Release* 1998; **50**: 111-122
- 26 **Muraoka M**, Hu ZP, Shimokawa T, Sekino SI, Kurogoshi RE, Kuboi Y, Yoshikawa Y, Takada K. Evaluation of intestinal pressure controlled colon delivery capsule containing caffeine as a model drug in human volunteers. *J Control Rel* 1998; **52**: 119-129
- 27 **Takaya T**, Sawada K, Suzuki H, Funaoka A, Matsuda KI, Takada K. Application of a colon delivery capsule to 5-aminosalicylic acid and evaluation of the pharmacokinetic profile after oral administration to beagle dogs. *J Drug Target* 1997; **4**: 271-276
- 28 **Hu ZP**, Kimura G, Mawatari SS, Shimokawa T, Yoshikawa Y, Takada K. New preparation method of intestinal pres-

- sure controlled colon delivery capsules by coating machine and evaluation in beagle dogs. *J Control Rel* 1998; **56**: 293-302
- 29 **Shibata N**, Ohno T, Shimokawa T, Hu ZP, Yoshikawa Y, Koga K, Murakami M, Takada K. Application of pressure-controlled colon delivery capsule to oral administration of glycyrrhizin in dogs. *J Pharm Pharmacol* 2001; **53**: 441-447
 - 30 **Jeong YI**, Ohno T, Hu ZP, Yoshikawa Y, Shibata N, Nagata S, Takada K. Evaluation of an intestinal pressure controlled colon delivery capsules prepared by a dipping method. *J Control Rel* 2001; **71**: 175-182
 - 31 **Chavan MS**, Sant VP, Nagarsenker MS. Azo-containing urethane analogues for colonic drug delivery: synthesis, characterization and *in vitro* evaluation. *J Pharm Pharmacol* 2001; **53**: 895-900
 - 32 **Tozaki H**, Nishioka J, Komoike J, Okada N, Fujita T, Muranishi S, Kim SI, Terashima H, Yamamoto A. Enhanced absorption of insulin and (Asu(1,7))el-calcitonin using novel azopolymer-coated pellets for colon-specific drug delivery. *J Pharm Sci* 2001; **90**: 89-97
 - 33 **Tozaki H**, Fujita T, Odoriba T, Terabe A, Okabe S, Muranishi S, Yamamoto A. Validation of a pharmacokinetic model of colon-specific drug delivery and the therapeutic effects of chitosan capsules containing 5-aminosalicylic acid on 2,4,6-trinitrobenzenesulphonic acid-induced colitis in rats. *J Pharm Pharmacol* 1999; **51**: 1107-1112
 - 34 **Macleod GS**, Fell JT, Collett JH, Sharma HL, Smith AM. Selective drug delivery to the colon using pectin:chitosan: hydroxypropyl methylcellulose film coated tablets. *Int J Pharm* 1999; **187**: 251-257
 - 35 **Brondsted H**, Andersen C, Hovgaard L. Crosslinked dextran-a new capsule material for colon targeting of drugs. *J Control Rel* 1998; **53**: 7-13
 - 36 **Kakoulides EP**, Smart JD, Tsibouklis J. Azocrosslinked poly(acrylic acid) for conic delivery and adhesion specificity: *in vitro* degradation and preliminary *ex vivo* bioadhesion studies. *J Control Rel* 1998; **54**: 95-109
 - 37 **Stubbe B**, Maris B, Mooter GV, Smedt SCD, Demeester J. The *in vitro* evaluation of 'azo containing polysaccharide gels' for colon delivery. *J Control Rel* 2001; **75**: 103-114
 - 38 **Adkin DA**, Kenyon CJ, Lerner EI, Landau I, Strauss E, Caron D, Penhas A, Rubinstein A, Wilding IR. The use of scintigraphy to provide "proof of concept" for novel polysaccharide preparations designed for colonic drug delivery. *Pharm Res* 1997; **14**: 103-107
 - 39 **Krishnaiah YSR**, Raju PV, Dinesh Kumar B, Bhaskar P. Development of colon targeted drug delivery systems for mevendazole. *J Control Rel* 2001; **77**: 87-95
 - 40 **Krishnaiah YSR**, Satyanarayana S, Rama Prasad YV, Narasimha Rao S. Gamma scintigraphic studies on guar gum matrix tablets for colonic drug delivery in healthy human volunteers. *J Control Rel* 1998; **55**: 245-252
 - 41 **Davaran S**, Hanaee J, Khosravi A. Release of 5-amino salicylic acid from acrylic type polymeric prodrugs designed for colon-specific drug delivery. *J Control Release* 1999; **58**: 279-287
 - 42 **Maris B**, Verheyden L, Van Reeth K, Samyn C, Augustijns P, Kinget R, Van den, Mooter G. Synthesis and characterisation of inulin-azo hydrogels designed for colon targeting. *Int J Pharm* 2001; **213**: 143-152
 - 43 **Lee JS**, Jung YJ, Kim YM. Synthesis and evaluation of N-acyl-2-(5-fluorouracil-1-yl)-D, L-glycine as a colon-specific prodrug of 5-fluorouracil. *J pharm Sci* 2001; **90**: 1787-1794
 - 44 **Jung YJ**, Lee JS, Kim YM. Colon-specific prodrugs of 5-aminosalicylic acid: synthesis and *in vitro/in vivo* properties of acidic amino acid derivatives of 5-aminosalicylic acid. *J Pharm Sci* 2001; **90**: 1767-1775
 - 45 **Sinha VR**, Kumria R. Polysaccharides in colon-specific drug delivery. *Int J Pharm* 2001; **224**: 19-38
 - 46 **Sinha VR**, Kumria R. Colonic drug delivery: prodrug approach. *Pharm Res* 2001; **18**: 557-564
 - 47 **Goto M**, Okamoto Y, Yamamoto M, Aki H. Anti-inflammatory effects of 5-aminosalicylic acid conjugates with chenodeoxycholic acid and ursodeoxycholic acid on carageenan-induced colitis in guinea-pigs. *J Pharm Pharmacol* 2001; **53**: 1711-1720
 - 48 **Ichinose K**, Tomiyama N, Nakashima M, Ohya Y. Anti-tumor activity of dextran derivatives immobilizing platinum complex. *Anticancer Drugs* 2000; **11**: 33-38
 - 49 **Wang S**, Low PS. Folate-mediated targeting of antineoplastic drugs, imaging agent, and nucleic acids to cancer cells. *J Control Rel* 1998; **53**: 39-48
 - 50 **Kievit E**, Bershad E, Ng E, Sethna P. Superiority of yeast over bacterial cytosine deaminase for enzyme/prodrug gene therapy in colon cancer xenografts. *Cancer Res* 1999; **59**: 1417-1421
 - 51 **Minami K**, Hirayama F, Uekama K. Colon-specific drug delivery based on a cyclodextrin prodrug: release behavior of biphenylacetic acid from its cyclodextrin conjugates in rat intestinal tracts after oral administration. *J Pharm Sci* 1998; **87**: 715-720
 - 52 **Yano H**, Hirayama F, Arima H, Uekama K. Prednisolone-appended alpha-cyclodextrin: alleviation of systemic adverse effect prednisolone after intracolonic administration in 2,4,6-trinitrobenzenesulfonic acid-induced colitis rats. *J Pharm Sci* 2001; **90**: 2103-2112
 - 53 **Yano H**, Hirayama F, Arima H, Uekama K. Preparation of prednisolone-appended alpha-beta-and gamma-cyclodextrins: substitution at secondary hydroxyl groups and *in vitro* hydrolysis behavior. *J Pharm Sci* 2001; **90**: 493-503

Edited by Bo XN

• BASIC RESEARCH •

The pre-synaptic blocker toosendanin does not inhibit secretion in exocrine cells

Zong-Jie Cui, Xue-Hui He

Zong-Jie Cui, Xue-Hui He, Institute of Cell Biology, Beijing Normal University, Beijing 100875, China

Supported by Natural Science Foundation of China Grant No. 39870367, 39825112, 30070286, and The Ph.D. Program of the Ministry of Education, China.

Correspondence to: Zong-Jie Cui, Ph.D. (Cantab.), Professor, Institute of Cell Biology, Beijing Normal University, Beijing 100875, China. zjcui@bnu.edu.cn

Telephone: +86-10-6220 9162 **Fax:** +86-10-6220 9162

Received 2002-04-18 **Accepted** 2002-06-08

Abstract

AIM: Toosendanin is a pre-synaptic blocker at the neuromuscular junction and its inhibitory effect is divided into an initial facilitative/stimulatory phase followed by a prolonged inhibitory phase. The present study investigated whether the subsequent inhibitory phase was due to exhaustion of the secretory machinery as a result of extensive stimulation during the initial facilitative phase. More specifically, this paper examined whether toosendanin could directly inhibit the secretory machinery in exocrine cells.

METHODS: Rat pancreatic acinar cells were isolated by collagenase digestion. Secretion was assessed by measuring the amount of amylase released into the extracellular medium as a percentage of the total present in the cells before stimulation. Cholecystokinin (CCK)-induced increases in intracellular calcium in single cells were measured with fura-2 microfluorometry.

RESULTS: Effects of toosendanin on CCK-induced amylase secretion and calcium oscillations were investigated. Toosendanin of 87-870 μ M had no effect on 10 pM-100 nM CCK-stimulated amylase secretion, nor did 8.7-870 μ M toosendanin inhibit 5 pM CCK-induced calcium oscillations. In contrast, 10 nM CCK₁ receptor antagonist FK 480 completely blocked 5 pM CCK-induced calcium oscillations.

CONCLUSION: The pre-synaptic "blocker" toosendanin is a selective activator of the voltage-dependent calcium channels, but does not interfere with the secretory machinery itself.

Cui ZJ, He XH. The pre-synaptic blocker toosendanin does not inhibit secretion in exocrine cells. *World J Gastroenterol* 2002; 8(5):918-922

INTRODUCTION

Toosendanin is a tetracyclic triterpenoid isolated from the seeds and barks of *Melia toosendan* Seib. et Zucc and *Melia azedarach* L. It has been used as an anthelmintic for many centuries, and has also been found to have pesticidal effects^[1-5], and have anti-botulismic and other effects in whole animals^[6,7]. Work on nerve-muscle and other preparations (neuromuscular junction)^[8-14] has established that toosendanin is a potent, long-lasting pre-synaptic

inhibitor. The neuromuscular blocking effect of toosendanin is divided into two phases: an early stimulatory phase that is due to direct activation of voltage-dependent calcium channels^[8, 12-18], and a delayed inhibition^[9, 14]. However, it is not known whether or not the delayed blockade of the neuromuscular transmission is due to direct interference with the secretory machinery involved in neurotransmitter release.

Whether toosendanin has any direct effect on the secretory machinery can only be examined in secretory cells with no voltage-dependent calcium channels. If indeed the delayed blocking effect of toosendanin is due to direct inhibition of the secretory machinery, only will an inhibitory phase be observed in secretory cells which lack voltage-dependent calcium channels. The pancreatic acinar cell is an ideal model in which to address this question. The molecular mechanisms of secretion in pancreatic acinar cells are well elucidated^[19-24], and these non-excitabile cells have no voltage-dependent calcium channels^[25, 26]. Therefore, this study examined if toosendanin has any inhibitory effect on secretion induced by a physiological secretagogue, cholecystokinin (CCK), in freshly isolated rat pancreatic acinar cells.

MATERIALS AND METHODS

Materials

CCK octapeptide, α -amylase and amylose azure were purchased from Sigma (St. Louis, MO, USA), Cell-Tak was purchased from Collaborative Biomedicals (Bedford, MA, USA). Toosendanin was a gift from Professor He LI (Department of Chemistry, Beijing Normal University). Collagenase P was bought from Boehringer Mannheim (Mannheim, Germany). Fura-2 AM was purchased from Molecular Probes (Eugene, OR, USA). (s)-N-[1-(2-fluorophenyl)-3,4,6,7-tetrahydro-4-oxo-pyrrolo[3,2,1-jk][1,4]benzodiazepin-3-yl]-1H-indole-2-carboximide (FK480) was donated by Fujisawa Pharmaceutical Co. Ltd. (Osaka, Japan). Toosendanin and FK480 were both dissolved in DMSO as stock solutions before dilution to final concentration.

Isolation of rat pancreatic acini

Pancreatic acini were isolated from male Sprague-Dawley rats with body weight ranged from 170 g to 250 g according to the method reported previously^[23, 27, 28].

Measurement of amylase secretion

Isolated acini were aliquoted into 2 ml portions and stimulated at 37 °C in a shaking water bath (50 cycle \cdot min⁻¹) for 30 min. The amylase secreted into the buffer was assayed according to the procedures reported previously^[29-32] and expressed as percentage of the total present in the acini before stimulation.

Measurement of intracellular calcium [Ca²⁺]_i

Ten microlitre of 1mM Fura-2 AM was added to 1 ml of isolated acini (final concentration 10 μ M) and the mixture was incubated in a shaking water bath at 37 °C and 50 cycle \cdot min⁻¹ for 40 min.

Fura-2-loaded acini were attached to the cover-slip of a Sykus-Moore chamber and perfused on the stage of an Olympus fluorescence microscope (IX70) attached to a microfluorometric calcium measurement system (M40, Photon Technology International, NJ, USA). Calcium increases were expressed as fluorescence ratios measured at 510 nm (F340/F380)^[23, 27, 33-35].

Standard buffer used in this work was composed of (all in mM) NaCl 118, KCl 4.7, MgCl₂ 1.16, CaCl₂ 2.5, NaH₂PO₄ 1.16, glucose 5.6, bovine serum albumin 2 mg · ml⁻¹, soybean trypsin inhibitor 0.1 mg · ml⁻¹, N-(2-hydroxyethyl) piperazine-N'-(2-ethanesulfonic acid) (HEPES) 10, MEM amino acid mixture (GIBCOBRL, Grand Island, NY, USA) 2 % and glutamine 2. The buffer was adjusted for pH to 7.4 with 4 mM NaOH and oxygenated with O₂ for 30 min before use.

RESULTS

Effects of toosendanin on CCK-induced amylase secretion

CCK stimulated amylase secretion from the freshly isolated rat pancreatic acini in a concentration-dependent manner (Figure 1). The maximum stimulation was achieved at CCK concentration of 100 pM, with a percentage secretion of 33 ± 1.6 ($n=6$). This bell-shaped dose response curve is consistent with previous report^[36].

In separate experiments, acini were first incubated with toosendanin at 870 μ M or 87 μ M for 10 min before stimulation with CCK for a further 30 min in the continued presence of toosendanin (Figure 2). When toosendanin was added at 87 μ M, the maximum stimulating CCK concentration shifted from 100 pM (18.2 ± 1.6 , $n=6$) to 1 nM (19.7 ± 1.2 , $n=6$). With the addition of toosendanin at 870 μ M, the maximum CCK concentration also shifted from 100 pM (18.2 ± 1.6 , $n=6$) to 1 nM (19.2 ± 1.9 , $n=4$). The slight rightward shift indicates a mild but statistically insignificant inhibition (Student's *t* test, $P>0.05$). In control experiments, neither 0.01 % solvent DMSO nor toosendanin at each concentration used had any effect on amylase secretion (data not shown).

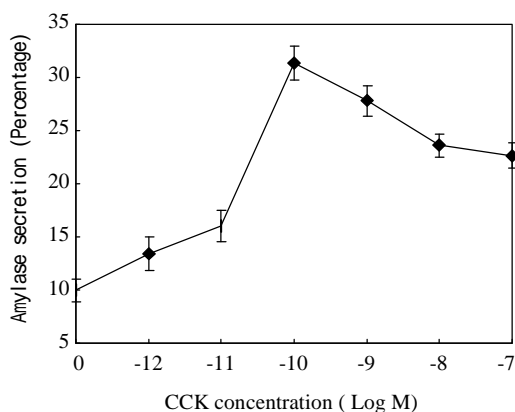


Figure 1 Concentration dependence of cholecystokinin (CCK)-stimulated amylase secretion. Note that maximum secretion was achieved at 100 pM of CCK. $n=6$

Effects of toosendanin on CCK-induced $[Ca^{2+}]_i$ oscillations

CCK of 5 pM induced regular calcium oscillations in perfused rat pancreatic acinar cells (Figure 3), which is consistent with previous reports^[27, 28]. Addition of toosendanin at 8.7 μ M to the CCK-stimulated acinar cells for 10-20 min had no apparent effect on CCK-induced calcium oscillations (Figure 3A, $n=4$). Even when toosendanin was increased to 87 μ M, there was still no obvious inhibition observed (Figure 3B, $n=7$). At 870 μ M, toosendanin induced a very mild inhibition: a single spike

appeared missing in the trace shown (Figure 3C, $n=8$).

For comparison, FK480, an antagonist for CCK₁ receptors^[37-39], produced immediate and complete inhibition of 5 pM CCK-induced calcium oscillations (Figure 4, $n=5$). FK480 at 10 nM abolished 5 pM CCK-induced calcium oscillations immediately upon addition, reducing the calcium to pre-stimulation level (Figure 4). After washout of FK480, calcium oscillations did not re-appear immediately, indicating that FK480 might bind to the acinar cells very tightly. It was possible, however, to re-introduce calcium oscillations when CCK was increased to 100 pM. At a lower FK480 concentration of 1 nM, a much longer time was needed before complete abolition of 5 pM CCK-induced Ca^{2+} oscillations was observed (data not shown).

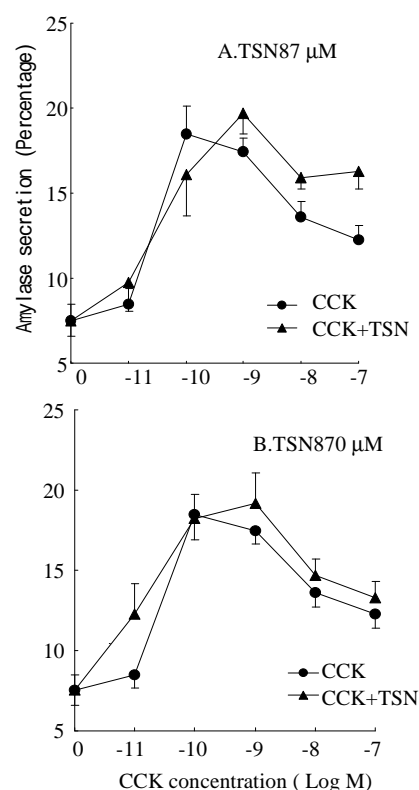
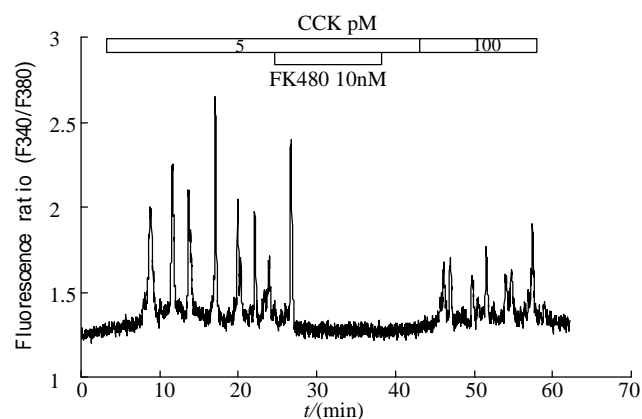


figure 2 Effect of toosendanin (TSN) on CCK-stimulated amylase secretion. TSN was added to the pancreatic acini 10 min before stimulation with CCK which was maintained for another 30 min. A. TSN 87 μ M, $n=6$. B. TSN 870 μ M, $n=4$. Note that, for clarity, the same CCK dose-response curve ($n=6$) was



the horizontal bars. $n=5$.

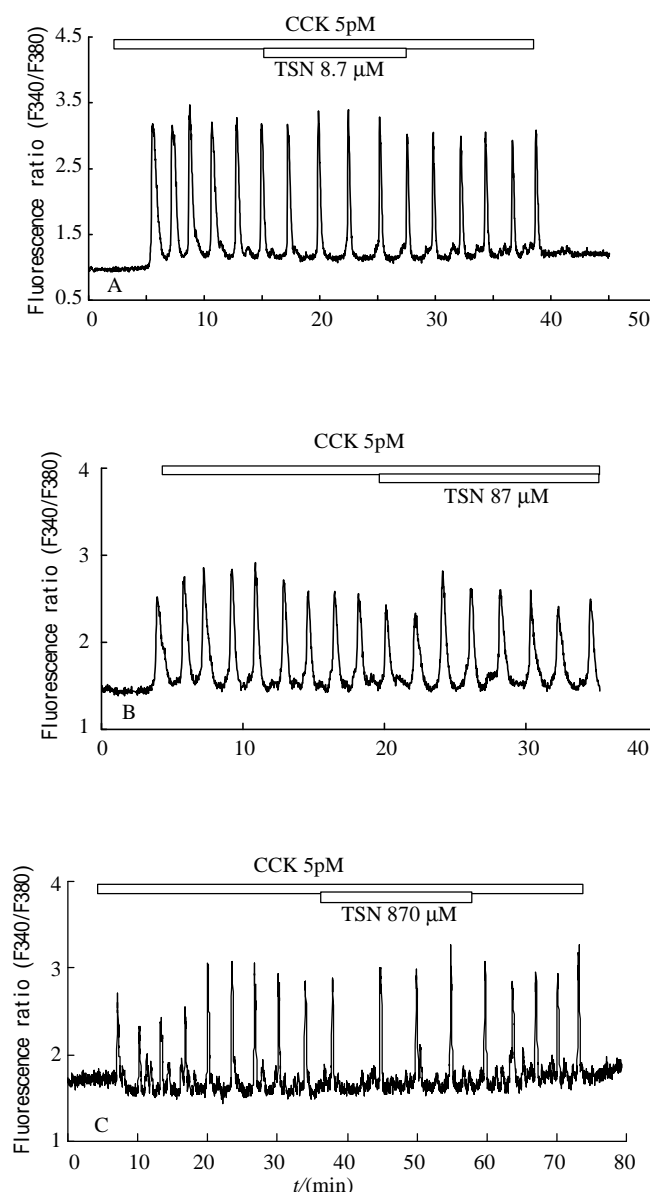


Figure 3 Effect of toosendanin on 5 pM CCK-induced calcium oscillations. CCK and TSN were added as indicated by the horizontal bars. A. TSN 8.7 μ M, $n=4$. B. TSN 87 μ M, $n=7$. C. TSN 870 μ M, $n=8$.

DISCUSSION

The present work demonstrated that toosendanin, a pre-synaptic inhibitor of the neuromuscular transmission^[7, 9, 13, 14], had little effect on CCK-stimulated amylase secretion. Although treatment with toosendanin at both concentrations tested (87 μ M, 870 μ M) resulted in a rightward shift in concentration of CCK that was needed to induce a maximum stimulation, i.e. from 100 pM in untreated cells to 1 nM in treated cells (Figure 2)^[36], the toosendanin inhibition was not statistically significant for each CCK concentration ($P>0.05$).

Toosendanin of 8.7- 87 μ M had no effect on 5 pM CCK-induced calcium oscillations. At a much higher concentration of 870 μ M, a mild inhibition was observed because one spike seemed missing (Figure 4). This lack of marked inhibition of toosendanin on CCK-induced calcium oscillations is in sharp contrast with the complete blockade of CCK-induced calcium oscillations by FK480, a CCK₁ receptor antagonist^[38, 40, 41]. Toosendanin at the neuromuscular junction had dual effects, a fast-onset stimulation which lasts about 40 min followed by a

long-lasting inhibition^[7-9, 12-14]. The fast phase has been postulated to be due to activation of voltage-dependent calcium channels^[8, 12-18]. However, toosendanin had no effect on CCK-induced calcium oscillations in rat pancreatic acinar cells. This indicates that toosendanin had no effect on stores-operated calcium channels as they are the only calcium channels existing in the freshly isolated pancreatic acinar cells^[20, 26] and are important for the continued presence of calcium oscillations^[23, 27].

In view of the above findings, the pre-synaptic blocking effect of toosendanin should be looked at under a new light. The delayed inhibition of neuromuscular transmission could just be due to massive stimulation of synaptic vesicle fusion after activation of the voltage-dependent calcium channels at the nerve terminal, resulting in the depletion of synaptic vesicles and delayed depression. The fact that toosendanin administration in rat leads to a decrease in synaptic vesicles^[42, 43] strongly supports this hypothesis. The initial strong stimulation of voltage-dependent calcium channels would afford the early stimulatory effects of toosendanin, providing an antidote to botulism^[6, 18].

An activator for voltage-dependent calcium channels as toosendanin may be, a long-lasting inhibition of the neuromuscular junction^[7-9, 12-14] or an extended period of synaptic vesicle depletion would require the stimulatory effect of toosendanin to be long-lasting. This stimulatory effect has indeed been found to last 40 min in nerve-muscle preparations^[7-9, 12-14]. It is well known that voltage-dependent calcium channels inactivate rather quickly after opening, although with different kinetics^[44-49]. Therefore, the long-lasting effect must be due to something other than constant opening of the calcium channels. It is known that intracellular calcium signals are subsequently encoded into activation of calcium/calmodulin-dependent protein kinases^[50-52], and short-duration calcium signals could be transformed into long-lasting activation of calcium/calmodulin-dependent protein kinase II^[53], therefore it would be interesting in the future to further investigate the possible effect of toosendanin on calcium oscillations in excitable cells, and on oscillation-associated activation of calcium/calmodulin-dependent protein kinase II. It would also be interesting to identify which types of voltage-dependent calcium channels are activated by toosendanin since a number of them are involved in neurotransmitter release^[54-56]. In this conjunction, it is important to note that decreased calcium influx into motor nerve terminals has been found to recruit additional neuromuscular junctions during the synapse elimination period^[57].

REFERENCES

- 1 **Wang WL**, Wang Y, Chiu S. The toxic chemical factors in the fruits of *Melia Azadarach* and their bioactivities toward *Pieris rapae*. *Kunchong Xuebao* 1994; **37**: 20-24
- 2 **Cespedes CL**, Alarcon J, Aranda E, Becerra J, Silva M. Insect growth regulator and insecticidal activity of beta-dihydroagarofurans from *Maytenus* spp. (Celastraceae). *Z Naturforsch* 2001; **56**: 603-613
- 3 **Cespedes CL**, Martinez-Vazquez M, Calderon JS, Salazar JR, Aranda E. Insect growth regulatory activity of some extracts and compounds from *Parthenium argentatum* on fall armyworm *Spodoptera frugiperda*. *Z Naturforsch* 2001; **56**: 95-105
- 4 **Cespedes CL**, Calderon JS, Lina L, Aranda E. Growth inhibitory effects on fall armyworm *Spodoptera frugiperda* of some limonoids isolated from *Cedrela* spp. (Meliaceae). *J Agric Food Chem* 2000; **48**: 1903-1908
- 5 **Tada K**, Takido M, Kitanaka S. Limonoids from fruit of *Melia toosendan* and their cytotoxic activity. *Phytochemistry* 1999; **51**: 787-791

- 6 **Zou J**, Miao WY, Ding FH, Meng JY, Ye HJ, Jia GR, He XY, Sun GZ, Li PZ. The effect of toosendanin on monkey botulism. *J Tradit Chin Med* 1985; **5**: 29-30
- 7 **Zhao WQ**, Feng H, Bennett P, Ng KT. Inhibition of intermediate-term memory following passive avoidance training in neonate chicks by a presynaptic cholinergic blocker. *Neurobiol Learn Mem* 1997; **67**: 207-213
- 8 **Ding J**, Xu TH, Shi YL. Different effects of toosendanin on perineurially recorded Ca^{2+} currents in mouse and frog motor nerve terminals. *Neurosci Res* 2001; **41**: 243-249
- 9 **Wang ZF**, Shi YL. Modulation of inward rectifier potassium channel by toosendanin, a presynaptic blocker. *Neurosci Res* 2001; **40**: 211-215
- 10 **Wang ZF**, Shi YL. Inhibition of large-conductance Ca^{2+} -activated K^{+} channels in hippocampal neurons by toosendanin. *Neuroscience* 2001; **104**: 41-47
- 11 **Wang ZF**, Shi YL. Toosendanin-induced inhibition of small-conductance calcium-activated potassium channels in CA1 pyramidal neurons of rat hippocampus. *Neurosci Lett* 2001; **303**: 13-16
- 12 **Huang HY**, Zhou CW, Shi YL. Toosendanin facilitates [^3H] noradrenaline release from rat hippocampal slices. *Natural Toxins* 1996; **4**: 92-95
- 13 **Xu Y**, Shi Y. Action of toosendanin on the membrane current of mouse motor nerve terminals. *Brain Res* 1993; **631**: 46-50
- 14 **Shih YL**. Abolishment of non-quantal release of acetylcholine from the mouse phrenic nerve endings by toosendanin. *Jpn J Physiol* 1986; **36**: 601-605
- 15 **Shi YL**, Furuya K, Wang WP, Terekawa S, Xu K, Yamagishi S. Calcium conductance increase by toosendanin in NG108-15 cells. *Kexue Tongbao* 1993; **38**: 836-839
- 16 **Ye Q**, Qu AL, Zhang CG, Xu T, Zhou Z. Effects of toosendanin on the $[\text{Ca}^{2+}]_i$ on rat chromaffin cells. *Zhongguo Shenjing Kexue Zazhi* 2001; **17**: 105-108
- 17 **Shi YL**, Chen WY. Effect of Toosendanin on acetylcholine level of rat brain, a microdialysis study. *Brain Res* 1999; **850**: 173-178
- 18 **Shih YL**, Hsu K. Anti-botulismic effect of toosendanin and its facilitatory action on miniature end-plate potentials. *Jpn J Physiol* 1983; **33**: 677-680
- 19 **Schulz I**, Krause E, Gonzalez A, Gobel A, Sternfeld L, Schmid A. Agonist-stimulated pathways of calcium signaling in pancreatic acinar cells. *Biol Chem* 1999; **380**: 903-908
- 20 **Camello C**, Pariente JA, Salido GM, Camello PJ. Sequential activation of different Ca^{2+} entry pathways upon cholinergic stimulation in mouse pancreatic acinar cells. *J Physiol* 1999; **516**: 399-408
- 21 **Cancela JM**, Van Coppenolle F, Galione A, Tepikin AV, Petersen OH. Transformation of local Ca^{2+} spikes to global Ca^{2+} transients: the combinatorial roles of multiple Ca^{2+} releasing messengers. *EMBO J* 2002; **21**: 909-919
- 22 **Leite MF**, Burgstahler AD, Nathanson MH. Ca^{2+} waves require sequential activation of inositol trisphosphate receptors and ryanodine receptors in pancreatic acini. *Gastroenterology* 2002; **122**: 415-427
- 23 **Cui ZJ**, Kanno T. Cholecystokinin analog JMV-180-induced intracellular calcium oscillations are mediated by inositol 1,4,5-trisphosphate in rat pancreatic acini. *Acta Pharmacol Sin* 2000; **21**: 377-380
- 24 **Burdakov D**, Galione A. Two neuropeptides recruit different messenger pathways to evoke Ca^{2+} signals in the same cell. *Curr Biol* 2000; **10**: 993-996
- 25 **Petersen OH**, Findlay I. Electrophysiology of the pancreas. *Physiol Rev* 1987; **67**: 1054-1116
- 26 **Tsunoda Y**, Tashiro Y. Distinct characteristics of receptor-operated Ca^{2+} influx and refilling in pancreatic acinar cells. *Biochem Biophys Res Commun* 1999; **256**: 579-583
- 27 **Cui ZJ**, Kanno T. Photodynamic triggering of calcium oscillation in the isolated rat pancreatic acini. *J Physiol* 1997; **504**: 47-55
- 28 **Cui ZJ**, Habara Y, Wang DY, Kanno T. A novel aspect of photodynamic action: induction of recurrent spikes in cytosolic calcium concentration. *Photochem Photobiol* 1997; **65**: 382-386
- 29 **Cui ZJ**. Types of voltage-dependent calcium channels involved in high potassium depolarization-induced amylase secretion in the exocrine pancreatic tumour cell line AR4-2J. *Cell Res* 1998; **8**: 23-31
- 30 **Matthews EK**, Cui ZJ. Photodynamic action of rose bengal on isolated rat pancreatic acini: stimulation of amylase release. *FEBS Lett* 1989; **256**: 29-32
- 31 **Matthews EK**, Cui ZJ. Photodynamic action of sulphonated aluminium phthalocyanine (SALPC) on isolated rat pancreatic acini. *Biochem Pharmacol* 1990; **39**: 1445-1457
- 32 **Matthews EK**, Cui ZJ. Photodynamic action of sulphonated aluminium phthalocyanine (SALPC) on AR4-2J cells, a carcinoma cell line of rat exocrine pancreas. *Br J Cancer* 1990; **61**: 695-701
- 33 **Cui ZJ**, Guo LL. Assessing physiological concentrations of endogenous substances *in situ* by inducing calcium oscillations in vitro. Case of liver. *Acta Pharmacol Sin* 2002; **23**: 27-32
- 34 **Hashikura S**, Satoh Y, Cui ZJ, Habara Y. Photodynamic action inhibits compound 48/80-induced exocytosis in rat peritoneal mast cells. *Jpn J Vet Res* 2001; **49**: 239-247
- 35 **Cui ZJ**, Habara Y, Satoh Y. Photodynamic modulation of adrenergic receptors in the isolated rat hepatocytes. *Biochem Biophys Res Commun* 2000; **277**: 705-710
- 36 **Murai A**, Satoh S, Okumura J, Furuse M. Factors regulating amylase secretion from chicken pancreatic acini *in vitro*. *Life Sci* 2000; **66**: 585-591
- 37 **Satoh Y**, Matsuo T, Sogabe H, Itoh H, Tada T, Kinoshita T, Yoshida K, and Takao Takaya T. Studies on a novel, potent and orally effective cholecystokinin A antagonist, FK-480. Synthesis and structure-activity relationships of FK480 and related compounds. *Chem Pharm Bull* 1994; **42**: 2071-2083
- 38 **Kuno M**, Sogabe H, Ito H, Matsuo T, Satoh Y, Motoyama Y, Tanaka H. Augmentation of the inhibitory effect of FK480, a CCK-A receptor antagonist, on pancreatic exocrine secretion by achlorhydria. *Pancreas* 1998; **17**: 57-64
- 39 **Kihara Y**, Otsuki M. Different inhibitory effects of the newly developed CCK receptor antagonists FK480 and KSG-504 on pancreatic exocrine and endocrine secretion in the isolated perfused rat pancreas. *Pancreas* 1995; **10**: 109-117
- 40 **Akiyama T**, Otsuki M. Characterization of a new cholecystokinin receptor antagonist FK480 in *in vitro* isolated rat pancreatic acini. *Pancreas* 1994; **9**: 324-331
- 41 **Ito H**, Sogabe H, Nakarai T, Sato Y, Tomoi M, Kadowaki M, Matsuo M, Tokoro K, Yoshida K. Pharmacological profile of FK480, a novel cholecystokinin type-A receptor antagonist: comparison to lorglumide. *J Pharmacol Exp Ther* 1994; **268**: 571-575
- 42 **Xiong CS**. Effect of toosendanin on the ultrastructure of the rat neuromuscular junction. *Yaoxue Xuebao* 1982; **17**: 407-412
- 43 **Xiong CS**. The interaction between toosendanin and botulinum toxin at the neuromuscular junction; an ultrastructural observation. *Yaoxue Xuebao* 1985; **20**: 495-499
- 44 **Bernatchez G**, Berrou L, Benakezouh Z, Ducay J, Parent L. Role of Repeat I in the fast inactivation kinetics of the $\text{Ca}_v2.3$ channel. *Biochim Biophys Acta* 2001; **1514**: 217-229
- 45 **Berjukow S**, Marksteiner R, Sokolov S, Weiss RG, Margreiter E, Hering S. Amino acids in segment IVS6 and beta-subunit interaction support distinct conformational changes during $\text{Ca}_v2.1$ inactivation. *J Biol Chem* 2001; **276**: 17076-17082
- 46 **Lee A**, Scheuer T, Catterall WA. Ca^{2+} /calmodulin-dependent facilitation and inactivation of P/Q-type Ca^{2+} channels. *J Neurosci* 2000; **20**: 6830-6838
- 47 **Lee A**, Wong ST, Gallagher D, Li B, Storm DR, Scheuer T, Catterall WA. Ca^{2+} /calmodulin binds to and modulates

- P/Q-type calcium channels. *Nature* 1999; **399**: 155-159
- 48 **Peterson BZ**, DeMaria CD, Adelman JP, Yue DT. Calmodulin is the Ca^{2+} sensor for Ca^{2+} -dependent inactivation of L-type calcium channels. *Neuron* 1999; **22**: 549-558
- 49 **Villarroya M**, Olivares R, Ruiz A, Cano-Abad MF, de Pascual R, Lomax RB, Lopez MG, Mayorgas I, Gandia L, Garcia AG. Voltage inactivation of Ca^{2+} entry and secretion associated with N- and P/Q-type but not L-type Ca^{2+} channels of bovine chromaffin cells. *J Physiol* 1999; **516**: 421-432
- 50 **Cui ZJ**. Ca^{2+} /calmodulin-dependent protein kinase II and its functions. *Shengli Kexue Jinzhan* 1997; **28**: 61-63
- 51 **Cui ZJ**. Muscarinic stimulation of calcium/calmodulin-dependent protein kinase II in isolated rat pancreatic acini. *Acta Pharmacol Sin* 1997; **18**: 255-258
- 52 **Cui ZJ**, Gorelick FS, Dannies PS. Calcium/calmodulin-dependent protein kinase-II activation in rat pituitary cells in the presence of thyrotropin-releasing hormone and dopamine. *Endocrinology* 1994; **134**: 2245-2250
- 53 **Lisman J**, Schulman H, Cline H. The molecular basis of CaMKII function in synaptic and behavioral memory. *Nat Rev Neurosci* 2002; **3**: 175-190
- 54 **Yan Z**, Chi P, Bibb JA, Ryan TA, Greengard P. Roscovitine: a novel regulator of P/Q-type calcium channels and transmitter release in central neurons. *J Physiol* 2002; **540**: 761-770
- 55 **Kato A**, Ohkubo T, Kitamura K. Algogen-specific pain processing in mouse spinal cord: differential involvement of voltage-dependent Ca^{2+} channels in synaptic transmission. *Br J Pharmacol* 2002; **135**: 1336-1342
- 56 **Rathmayer W**, Djokaj S, Gaydukov A, Kreissl S. The neuromuscular junctions of the slow and the fast excitatory axon in the closer of the crab *Eriphia spinifrons* are endowed with different Ca^{2+} channel types and allow neuron-specific modulation of transmitter release by two neuropeptides. *J Neurosci* 2002; **22**: 708-717
- 57 **Santafe MM**, Garcia N, Lanuza MA, Uchitel OD, Salon I, Tomas J. Decreased calcium influx into the neonatal rat motor nerve terminals can recruit additional neuromuscular junctions during the synapse elimination period. *Neuroscience* 2002; **110**: 147-154

Edited by Liu HX

• BASIC RESEARCH •

Intestinal damage mediated by Kupffer cells in rats with endotoxemia

Jian-Ping Gong, Chuan-Xin Wu, Chang-An Liu, Sheng-Wei Li, Yu-Jun Shi, Kang Yang, Yue Li, Xu-Hong Li

Jian-Ping Gong, Chuan-Xin Wu, Chang-An Liu, Sheng-Wei Li, Yu-Jun Shi, Kang Yang, Yue Li, Xu-Hong Li, Department of General Surgery, The Second College of Clinical Medicine & the Second Affiliated Hospital of Chongqing University of Medical Science, 74 Linjiang Road, Chongqing 400010, China

Supported by the National Natural Science Foundation of China, No.39970719,30170919

Correspondence to: Dr Jian-Ping Gong, Department of General Surgery, The Second College of Clinical Medicine & the Second Affiliated Hospital of Chongqing University of Medical Science, 74 Linjiang Road, Chongqing 400010, China. gongjianping11@hotmail.com

Telephone: +86-28-85541610 **Fax:** +86-23-63822815

Received 2001-09-26 **Accepted** 2001-11-08

Abstract

AIM: To determine the *in vivo* effects of phagocytic blockade of Kupffer cell (KC) on the release of proinflammatory cytokines in small intestinal lesion and on the integrity of intestinal tract by using gadolinium chloride (GdCl₃) during early endotoxemia.

METHODS: Wistar rats were divided into three groups: Group A, rats were injected with endotoxin (*E. coli* O111:B₄, a dose of 12 mg.kg⁻¹) only; Group B, rats were pretreated intravenously with 25 mg of GdCl₃ per kg 24 h are given endotoxin; and Group C, sham operation only. All animals were sacrificed 4 h after endotoxin injection. In portion of the rats of three groups, bile duct was cannulated, which the bile was collected externally. Morphological changes of ileum were observed under light microscopy and electronic microscopy. The KC were isolated from rats by collagenase perfusion and in KC, expression of TNF- α and IL-6 mRNA were determined by RT-PCR analysis. Plasma and bile TNF- α and IL-6 Levels were determined by enzyme-linked immunosorbent assay (ELISA).

RESULTS: In group A, there were neutrophil infiltration and superficial epithelial necrosis of the ileal villi, sloughing of mucosal epithelium, and disappearance of some villi. In group B, the ileal mucosal damage was much reduced. which in group C, no significant morphological changes were seen. GdCl₃ pretreatment decreased significantly the expression of TNF- α and IL-6 mRNA in group B (4.32 \pm 0.47 and 4.05 \pm 0.43) when compared to group A (9.46 \pm 1.21 and 9.04 \pm 1.09) ($P<0.05$). There was no significant expression of TNF- α and IL-6 mRNA in group C (1.03 \pm 0.14 and 10.4 \pm 0.13). In rats of group A, the levels of TNF- α and IL-6 in bile and plasma were 207 \pm 29 ng \cdot L⁻¹, 1032 \pm 107 ng \cdot L⁻¹, 213 \pm 33 ng \cdot L⁻¹, and 1185 \pm 127 ng \cdot L⁻¹, respectively. In group B, they were 113 \pm 18 ng \cdot L⁻¹, 521 \pm 76 ng \cdot L⁻¹, 147 \pm 22 ng \cdot L⁻¹, and 572 \pm 54 ng \cdot L⁻¹, respectively. In group C, they were 67 \pm 10 ng \cdot L⁻¹, 72 \pm 13 ng \cdot L⁻¹, 109 \pm 18 ng \cdot L⁻¹, and 118 \pm 22 ng \cdot L⁻¹ respectively. There were significant difference between the three group ($P<0.05$).

CONCLUSION: KC release cytokines TNF- α and IL-6 causing damage to the integrity of intestinal epithelium and play a crucial role in the initiation and progression of intestinal mucosal damage during early endotoxemia.

Gong JP, Wu CX, Liu CA, Li SW, Shi YJ, Yang K, Li Y, Li XH. Intestinal damage mediated by Kupffer cells in rats with endotoxemia. *World J Gastroenterol* 2002; 8(5):923-927

INTRODUCTION

LPS (lipopolysaccharide) is now considered to be a potent inducer of a series of inflammatory mediators^[1-6]. In the early as infection, the main symptoms can be ascribed in part to the inflammatory cytokines as tumor necrosis factor alpha (TNF- α), interleukin-1 (IL-1), IL-6 and platelet-activating factor^[7-9]. Recently, Jackson *et al*^[10] reported that intestinal damage is mediated by factors derived from the bile. KC (Kupffer cell) constitute 80-90 % of the fixed tissue macrophages of the reticuloendothelial system (RES) and their activation and subsequent release of cytokines have great influence on the systemic response during sepsis^[11-14]. KC has been shown to be a major source of released IL-6 following traumatic or hemorrhagic shock and after resuscitation^[15]. Since LPS has been removed from the blood by the liver, we speculated the cytokines from KC in the bile may likely cause the damage to the intestinal during endotoxemia. Therefore, the aim of this study was to determine whether the *in vivo* phagocytic blockade of KC by using gadolinium chloride (GdCl₃) had any effects on intestinal integrity during early endotoxemia and whether the proinflammatory cytokines played crucial role in small intestinal lesions.

MATERIALS AND METHODS

Animals model

Wistar rats 10 wk old, weighing 220 g to 250 g were used in this experiment. The rats were obtained from Laboratory Animal Center of Chongqing University of Medical Science. These animals were divided into three groups: Group A, rats injected endotoxin only; Group B, rats pretreated with GdCl₃ and given endotoxin; and group C, sham operation only.

In vivo blockade of Kupffer cells by gadolinium chloride

In group B, animals were treated intravenously with 25 mg of GdCl₃ per kg 24 h prior to the operation as described by Koo *et al*^[15]. In the preliminary experiment, the optimum dose and time of administration of GdCl₃ were determined by assessment of loss of KC labeled with India ink. In some of animals, in order to collect the bile, the animals were fasted overnight with free access to water. Bile duct was cannulated in rats of the three groups under ether anesthesia as described by Jackson *et al*^[10]. Briefly, the abdomen was opened through a midline incision of 1.5-2.0 cm immediately below the sternum. The

bile duct was located, and approximately 1 to 1.5 cm of a 25 cm polyethylene cannulation tube (external diameter, 0.8 mm; internal diameter, 0.4 mm) was inserted into bile duct and tied in place, the other end of the tube was exteriorized through an opening in the right flank by an 18-gauge needle, allowing bile to be collected externally. The abdominal incision was then sutured, and the rats were held in restraining cages. Rats from group A and B were then injected iv with LPS from *E. coli* serotype O111: B4 (Sigma, St. Louis, Mo. USA), using a dose of 12 mg · kg⁻¹. Animals from group C were infused with some dose of pyrogen-free sterile saline. Plasma were separated from tail vein blood, and bile was collected 4 h after LPS administration when these rats were killed and the macroscopic appearance of the whole small intestine was assessed.

Morphological observation of ileum

One-to two-centimeter segments of the ileum from each rats were fixed in 100 ml · L⁻¹ buffered formalin or 25 g · L⁻¹ glutaraldehyde immediately. For light microscopy, the tissue blocks were embedded in paraffin, and the 5-um sections were stained with HE. For electronic microscopy, the tissue blocks were embedded in Epon 618 resin and ultrathin sections stained with uranyl acetate and lead citrate. A H-2000 transmission electronmicroscope was used.

Kupffer cell isolation

KC were isolated as described previously^[16,17]. In brief, the livers were removed after a portal vein perfusion with Hanks' balanced salt solution (HBSS) and the homogenate was digested in a solution of 5 g · L⁻¹ collagenase (Type IV, Sigma). The digest was washed thoroughly and plated on plastic dishes in RPMI medium containing 50 ml · L⁻¹ fetal calf serum (FCS). After 3 h incubation at 37 °C in O₂ and CO₂ (0.95/0.05), nonadherent cells were removed with pipet. The adherent cells were collected with a rubber policeman. 70 % to 90 % viable KC was obtained in this manner. GdCl₃-treated and control cells exhibited similar viability, morphology, and *in vitro* phagocytosis, although the livers from GdCl₃-treated rats yielded 10-20 % fewer KC than saline-injected rats.

Expression of TNF-α and IL-1 mRNA in kupffer cell

RNA isolation and C-complementary DNA synthesis Total RNA was isolated from KC by using the Trizol Reagent (Life Technologies, USA). The quality of RNA was controlled by the intactness of ribosomal RNA bands. A total of 0.5 mg of each intact total RNA samples was reverse-transcribed to complementary DNA (cDNA) by using the reverse transcription polymerase chain reaction (RT-PCR) kit (Roche, USA). cDNA was stored at -70 °C till polymerase chain reaction (PCR) analysis.

Determination of TNF-α and IL-6 mRNA by RT-PCR The PCR primers used were TNF-α: sense (5'-CACCATGAGCACGGA AAGCA-3'), antisense (5'-GCAATGACTCCAAAGTAGAC-3'); IL-6: sense (5'-CTTCCAGCCAGTTGCCTTCT-3'), anti-sense (5'-AGCCAGAGTCATTCAAGAGCA-3'); β-actin: sense (5'-ACCACAGCTGAGAGGGAAATCG-3'), antisense (5'-AGAGGTCTTTACGGATGTCAACG-3'). The sizes of the amplified PCR products were 692 bp for TNF-α, 309 bp for IL-6, and 281 bp for β-actin. The conditions for amplification were as follows: denaturation at 94 °C for 1 min, annealing at 57 °C for 2 min, and extension at 72 °C for 2 min for 31 cycles. The PCR products were electrophoresed in 15 g · L⁻¹ % agarose gels, and the gels were ethidium bromide stained and video photographed on an ultraviolet transilluminator.

Bioassay for cytokines in plasma and bile

Plasma and bile levels of TNF-α and IL-6 were determined by enzyme-linked immunosorbent assay (ELISA) kits according to the manufacture's instructions and guidelines (Biosource International, Camarillo, CA).

Statistical analysis

All data were expressed as $\bar{x} \pm s$ and compared by one-way analysis of variance (ANOVA). Differences in values were considered significant if $P \leq 0.05$.

RESULTS

Effect of phagocytotic blockade of Kupffer cells on the intestinal integrity

We investigated the effect of phagocytotic blockade of Kupffer cells by GdCl₃ on the histological appearance of the ileum. 4 h after inoculation with LPS, macroscopic examination showed marked hyperemia, edema, and fluid accumulation within the lumen of small bowel in rats of group A. In contrast, in animals of group B, there was substantial reduction in hyperemia and no fluid accumulation. There was neither hyperemia nor fluid accumulation in group C.

In group A, there was marked tissue damage. Under light microscope, there were neutrophil infiltration in the villi, severely damaged epithelial layer with superficial necrosis and sloughing, some villi completely disappeared (Figure 1A). In contrast, the rats of group B, intestinal mucosal damage were much reduced, there was no evidence of hyperemia, vasodilatation or edema in the lamina propria, and the epithelial layer was intact, only modest hyperemia in the submucosa, only occasional edematous apex at the villi (Figure 1B). In group C, The histological appearance was normal (Figure 1C).



Figure 1A Superficial epithelial necrosis of villi and complete absence of some villi (HE×198).



Figure 1B In intestinal mucosal damage much reduced (HE×198)

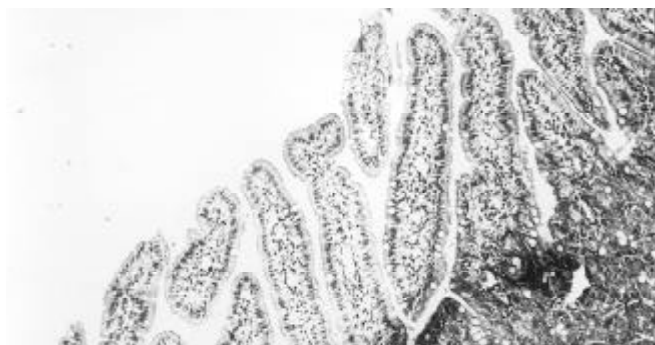


Figure 1C Normal appearance of intestinal mucosa (HE × 198).

Effect of $GdCl_3$ on expression of $TNF-\alpha$ and $IL-6$ mRNA in Kupffer cells

$GdCl_3$ clearly resulted in sustained loss of phagocytic activity of KCs diminishing concentrations of $TNF-\alpha$ and $IL-6$ in bile and plasma. We found that $GdCl_3$ pretreatment decreased KCs cytokines transcripts after injection of LPS so that expression of $TNF-\alpha$ and $IL-6$ mRNA in group B were significantly less than those in group A ($P < 0.05$). There were no expression of $TNF-\alpha$ and $IL-6$ genes in rats of group C (Figure 2).

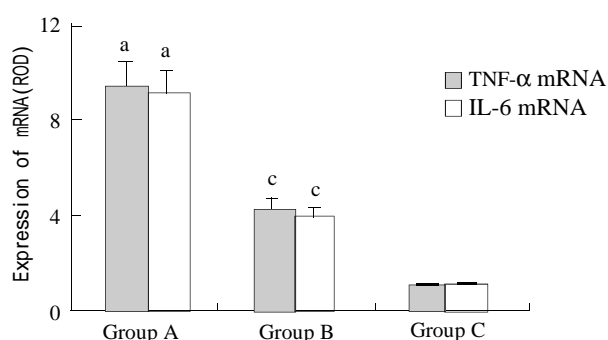


Figure 2 Expression of $TNF-\alpha$ and $IL-6$ mRNA. ^a $P < 0.05$, vs other two groups, ^c $P < 0.05$, vs group C.

Cytokines production in bile and plasma

$TNF-\alpha$ and $IL-6$ in the bile and plasma of above three groups were measured by bioassay (Table 1). In rats of group A, there were significant increase of $TNF-\alpha$ and $IL-6$ in bile and plasma, the concentration of the two cytokines in the bile were over 5-fold and 4-fold higher than those at in the plasma, respectively. In animals of group B, $GdCl_3$ given 24 h prior to LPS markedly reduced the levels of $TNF-\alpha$ and $IL-6$ in bile and plasma when compared to those in group A ($P < 0.05$). Low levels of $TNF-\alpha$ and $IL-6$ were detectable in bile and plasma in rats of group C.

Table 1 Plasma and bile $TNF-\alpha$ and $IL-6$ levels of in rats ($\bar{x} \pm s$, $n = 7$)

Group	$TNF-\alpha$ (ng.L ⁻¹)		$IL-6$ (ng.L ⁻¹)	
	Plasma	Bile	Plasma	Bile
A	207 ± 29 ^a	1032 ± 107 ^a	213 ± 33 ^a	1185 ± 127 ^a
B	113 ± 18 ^c	521 ± 76 ^c	147 ± 22 ^c	572 ± 54 ^c
C	67 ± 10	72 ± 13	109 ± 18	118 ± 22

^a $P < 0.05$, vs other two groups; ^c $P < 0.05$, vs Group C

DISCUSSION

The role of cytokines in the bile causing gastrointestinal damage during sepsis has received little attention to date, and the bile continues to be viewed upon as having a purely digestive function. Other investigators reported after the relief of obstructive jaundice by internal drainage, endotoxemia could be reversed. But, the ratio of villous height to crypt depth in the mucosa of the terminal ileum was decreased in the rats with external drainage. The absence of bile from the gut may promote bacterial translocation to visceral organs^[10,18]. These findings implicate the use of bile to prevent intestinal mucosal damage and reduce postoperative complications of jaundiced patient with endotoxemia. In fact, a growing body of evidence points to the presence of inflammatory mediators and other factors in bile. These factors include cytokines $IL-1$, $IL-6$, $TNF-\alpha$, and epidermal growth factor, complement components, and acute-phase proteins, which are released by KC and other macrophages^[13,19-27]. Recently, Jackson *et al*^[10] reported the involvement of bile in gastrointestinal tract damage in endotoxemia. External drainage of bile or bile duct occlusion markedly reduced the effects of LPS to the intestine and prolonged survival of the animals^[13,19-27]. These studies indicate that after treatment with LPS, the bile contains substances that are capable of mediating intestinal damage. Our results showed there were higher concentrations of $TNF-\alpha$ and $IL-6$ in rats with endotoxemia than those in the control rats, and there were 5-fold and 6-fold higher levels of $TNF-\alpha$ and $IL-6$ in bile than in plasma. The intestinal mucosal epithelia of these animals were severely damaged. These findings suggest the luminal cytokines derived from the bile, contribute to the intestinal damage during early endotoxemia.

Where do these cytokines in bile come from? The precise molecular mechanism of the cytokines in bile is uncertain. There are several reasons to believe that cytokines in the bile originate from synthesis by KC in the bile rather than extracted from the circulating blood. First, The KC are the main site for the clearance of endotoxin, they constitute about 80-90 % of sessile macrophages of the RES. LPS is taken up by KC and leads to production of cytokines by these cells^[12,15-16,19,21,28,29]. Second, the concentration of $TNF-\alpha$ and $IL-6$ in the bile was more markedly increased than those in the plasma. Finally, the levels of these cytokines were significantly reduced by treatment with $GdCl_3$ which preferentially inhibited the KC function, again supporting the concept of production of cytokines by the hepatic KC. A number of studies had been conducted to examine the role of KC function during endotoxemia and other circulatory conditions. Studies dealing with the blockade of KCs phagocytosis in lethal endotoxic shock models had shown increased animal survival that underwent $GdCl_3$ pretreatment^[30-32]. Moreover, utilizing KC blockade by $GdCl_3$ revealed the mediators released by KC during sepsis played a significant role^[33]. Although studies had shown that intestinal damage occurred during sepsis, it remained unknown whether blockade of KC prior to the onset of endotoxemia could prevent the occurrence of intestinal damage. The present study was designed to determine whether the *in vivo* phagocytic blockade of KC by $GdCl_3$ prior to the onset of sepsis had any salutary effects on intestinal integrity and expression of proinflammatory cytokines such as $TNF-\alpha$ and $IL-6$, their genes and proteins. Our results indicated that expression of $TNF-\alpha$ and $IL-6$ mRNA significantly increased 4 h after the induction of LPS. However, rats that underwent $GdCl_3$ treatment prior to LPS demonstrated significantly reduced expression of the genes and proteins of these cytokines in bile and plasma. Thus, KC can play a crucial role in the

initiation and progression of intestinal damage following endotoxemia^[34-38].

The role of cytokines in intestinal pathology has not been well elucidated. But, cytokines in intestinal tract could promote bacterial association with the epithelium, or might act upon luminal microorganism to enhance their invasive characteristics^[39-43]. There are evidences that TNF- α is able to affect directly the virulent properties of some organisms. For example, TNF- α enhances the invasion of cultured cells, promoted by cytokines. IL-1 has been shown to act as a growth factor for pathogenic *E. coli*. Fluid accumulation in the intestine of LPS-treated rats indicates presence of altered permeability. Furthermore, TNF- α can affect directly the permeability of epithelial barriers, and loosening of the tight junction so as to facilitate the early entry of bacteria into the mesenteric lymph nodes and other target organs. TNF- α can induce expression of adhesion molecules ICAM-1 and LFA-3 in human intestinal epithelial cell lines. It can also influence cytokines production and proliferation in intestinal cell lines^[44-48]. These findings reveals the presence of specific receptors on such cells, the TNF- α receptors are predominantly located on the basolateral aspect of intestinal epithelial cells, as are receptors for IL-1. After LPS stimulation, macrophages release cytokines damaging the intestinal epithelial integrity, allowing luminal TNF- α and IL-6 to gain access to their receptors on the basolateral aspect of the epithelial cells and increase epithelial permeability, finally cause the intestinal damage.

REFERENCES

- 1 **Parker SJ**, Watkins PE. Experimental models of Gram-negative sepsis. *Br J Surg* 2001; **88**: 22-30
- 2 **Angus DC**, Linde-Zwirble WT, Lidicker J, Clermont G, Carcillo J, Pinsky MR. Epidemiology of severe sepsis in the United States: Analysis of incidence, outcome, and associated costs of care. *Crit Care Med* 2001; **29**: 1303-1310
- 3 **Fan K**. Regulatory effects of lipopolysaccharide in murine macrophage proliferation. *World J Gastroenterol* 1998; **4**: 137-139
- 4 **Liu BH**, Chen HS, Zhou JH, Xiao N. Effects of endotoxin on endothelin receptor in hepatic and intestinal tissues after endotoxemia in rats. *World J Gastroenterol* 2000; **6**: 298-300
- 5 **Zhang SC**, Dai Q, Wang JY, He BM, Zhou K. Gut derived endotoxemia: one of the factors leading to production of cytokines in liver diseases. *World J Gastroenterol* 2000; **6** (Suppl 3): 16
- 6 **Lin E**, Calvano SE, Lowry SF. Inflammatory cytokines and cell response in surgery. *Surgery* 2000; **127**: 117-126
- 7 **Bone-Larson CL**, Simpson KJ, Colletti LM, Lukacs NW, Chen SC, Lira S, Kunkel SL, Hogaboam CM. The role of chemokines in the immunopathology of the liver. *Immunol Rev* 2000; **177**: 8-20
- 8 **Kono H**, Wheeler MD, Rusyn I, Lin M, Seabra V, Rivera CA, Bradford BU, Forman DT, Thurman RG. Gender differences in early alcohol-induced liver injury: role of CD14, NF- κ B, and TNF- α . *Am J Physiol Gastrointest Liver Physiol* 2000; **278**: G652-G661
- 9 **Roy DL**, Padova FD, Adachi Y, Glauser MP, Calandra T, Heumann D. Critical role of lipopolysaccharide-binding protein and CD14 in immune responses against gram-negative bacteria. *J Immunol* 2001; **167**: 2759-2765
- 10 **Jackson GDF**, Dai Y, Sewell WA. Bile mediates intestinal pathology in endotoxemia in rats. *Infect Immun* 2000; **68**: 4714-4719
- 11 **Knolle PA**, Gerken G. Local control of the immune response in the liver. *Immunol Rev* 2000; **174**: 21-34
- 12 **Seki S**, Habu Y, Kawamura T, Takeda K, Dobashi H, Ohkawa T, Hiraide H. The liver as a crucial organ in the first line of host defence: the role of Kupffer cells, natural killer (NK) cells and NK1.1 Ag+ T cells in T helper 1 immune responses. *Immunol Rev* 2000; **174**: 35-46
- 13 **Enomoto N**, Ikejima K, Yamashina S, Enomoto A, Nishiura T, Nishimura T, Brenner DA, Schemmer P, Bradford BU, Rivera CA, Zhong Z, Thurman RG. Kupffer cell-derived prostaglandin E₂ is involved in alcohol-induced fat accumulation in rat liver. *Am J Physiol Gastrointest Liver Physiol* 2000; **279**: G100-G106
- 14 **Xu MQ**, Gong JP, Xue L, Han BL, Hu F. Effects of Kupffer cell NF- κ B activation on liver regeneration after partial hepatectomy in biliary obstructive rats. *Di-San Junyi Daxue Xuebao* 2001; **23**: 1143-1145
- 15 **Koo DJ**, Chaudry IH, Wang P. Kupffer cells are responsible for producing inflammatory cytokines and hepatocellular dysfunction during early sepsis. *J Surg Res* 1999; **83**: 151-157
- 16 **Gong JP**, Xu MQ, Li K, Zhu J, Han BL. Expression of CD14 in Kupffer's cells induced by lipopolysaccharide. *Di-San Junyi Daxue Xuebao* 2001; **23**: 425-428
- 17 **Gong JP**, Han BL. Technique of isolation, culture, and identification of liver cells. *Shijie Huaren Xiaohua Zazhi* 1999; **7**: 417-419
- 18 **Islam AFMW**, Moss ND, Dai Y, Smith MSR, Collins AM, Jackson GDF. Lipopolysaccharide-induced biliary factors enhance invasion of *Salmonella enteritidis* in a rat model. *Infect Immun* 2000; **68**: 1-5
- 19 **Guo XW**, Dudman NP. Homocysteine induces expressions of adhesive molecules on leukocytes in whole blood. *Chin Med J* 2001; **114**: 1235-1239
- 20 **Enomoto N**, Yamashina S, Kono H, Schemmer P, Rivera CA, Enomoto A, Nishiura T, Nishimura T, Brenner DA, Thurman RG. Development of a new, simple rat model of early alcohol-induced liver injury based on sensitization of kupffer cells. *Hepatology* 1999; **29**: 1680-1689
- 21 **Mack C**, Jungermann K, Gotze O, Schieferdecker HL. Anaphylatoxin C5a actions in rat liver: synergistic enhancement by C5a of lipopolysaccharide-dependent α_2 -macroglobulin gene expression in hepatocytes via IL-6 release from Kupffer cells. *J Immunol* 2001; **167**: 3972-3979
- 22 **Gong JP**, Liu CA, Wu CX, Li SW, Shi YJ, Yang K, Li Y, Li XH. Liver sinusoidal endothelial cell injury by neutrophils in rats with acute obstructive cholangitis. *World J Gastroenterol* 2002; **8**: 342-345
- 23 **Han DW**. The clinical sine of subsequent liver injury induced by gut derived endotoxemia. *Shijie Huaren Xiaohua Zazhi* 1999; **7**: 1055-1058
- 24 **Wu RQ**, Xu YX, Song XH, Chen LJ, Meng XJ. Adhesion molecule and proinflammatory cytokine gene expression in hepatic sinusoidal endothelial cells following cecal ligation and puncture. *World J Gastroenterol* 2001; **7**: 128-130
- 25 **Emmanuilidis K**, Weighardt H, Maier W, Gerauer K, Fleischmann T, Zheng XX, Hancoc WW, Holzmann B, Heidecke CD. Critical role of Kupffer cell-derived IL-10 for host defense in septic peritonitis. *J Immunol* 2001; **167**: 3919-3927
- 26 **Ling YL**, Meng AH, Zhao XY, Shan BE, Zhang JL, Zhang XP. Effect of cholecystokinin on cytokines during endotoxemic shock in rats. *World J Gastroenterol* 2001; **7**: 667-671
- 27 **Wang LS**, Zhu HM, Zhou DY, Wang YL, Zhang WD. Influence of whole peptidoglycan of bifidobacterium on cytotoxic effectors produced by mouse peritoneal macrophages. *World J Gastroenterol* 2001; **7**: 440-443
- 28 **Bai XY**, Jia XH, Cheng LZ, Gu YD. Influence of IFN- α -2b and BCG on the release of TNF and IL-1 by Kupffer cells in rats with hepatoma. *World J Gastroenterol* 2001; **7**: 419-421
- 29 **Gong JP**, Han BL. Effects of CD14 in LPS mediating activation of Kupffer cells. *Shijie Huaren Xiaohua Zazhi* 1999; **7**: 875-877
- 30 **Watanabe M**, Chijiwa K, Kameoka N, Yamaguchi K, Kuroki S, Tanaka M. Gadolinium pretreatment decreases

- survival and impairs liver regeneration after partial hepatectomy under ischemia/reperfusion in rats. *Surgery* 2000; **127**: 456-463
- 31 **Takeyama O**, Ikai I, Yamamoto M, Kanazawa A, Yagi T, Uesugi T, Nishitai R, Satoh S, Terajima H, Yamaoka Y. The protective role of Kupffer cells in humoral injury of xenoperfused rat livers. *Transplantation* 2000; **69**: 1283-1289
- 32 **Arai M**, Peng XX, Currin RT, Thurman RG, Lemasters JJ. Protection of sinusoidal endothelial cells against storage/reperfusion injury by prostaglandin E₂ derived from Kupffer cells. *Transplantation* 1999; **68**: 440-445
- 33 **Roland CR**, Naziruddin B, Mohanakumar T, Flye MW. Gadolinium blocks rat Kupffer cell calcium channels: relevance to calcium-dependent prostaglandin E₂ synthesis and septic mortality. *Hepatology* 1999; **29**: 756-765
- 34 **Zuo GQ**, Gong JP, Liu CA, Li SW, Wu XC, Yang K, Li Y. Expression of lipopolysaccharide binding protein and its receptor CD14 in experimental alcoholic disease. *World J Gastroenterol* 2001; **7**: 836-840
- 35 **Okada K**, Marubayashi S, Fukuma K, Yamada K, Dohi K. Effect of the 21-aminosteroid on nuclear factor-kB activation of Kupffer cells in endotoxin shock. *Surgery* 2000; **127**: 79-86
- 36 **Tomioka M**, Linuma H, Okinaga K. Impaired Kupffer cell function and effect of immunotherapy in obstructive jaundice. *J Surg Res* 2000; **92**: 276-282
- 37 **Calne RY**. Immunological tolerance-the liver effect. *Immunol Rev* 2000; **174**: 280-282
- 38 **Ikejima K**, Enomoto N, Seabra V, Ikejima A, Brenner DA, Thurman RG. Pronase destroys the lipopolysaccharide receptor CD14 on Kupffer cells. *Am J Physiol Gastrointest Liver Physiol* 1999; **276**: G591-G598
- 39 **Rocha F**, Laughlin R, Musch MW, Hendrickson BA, Chang EB, Alverdy J. Surgical stress shifts the intestinal Escherichia coli population to that of a more adherent phenotype: role in barrier regulation. *Surgery* 2001; **130**: 65-73
- 40 **Echtenacher B**, Weigl K, Lehn N, Mannel DN. Tumor necrosis factor-dependent adhesions as a major protective mechanism early in septic peritonitis in mice. *Infect Immun* 2001; **69**: 3550-3555
- 41 **Gil LT**, Rosello AM, Torres AC, Moreno RL, Orihuela JAF. Modulation of soluble phases of endothelial/leukocyte adhesion molecule 1, intercellular adhesion molecule 1, and vascular cell adhesion molecule 1 with interleukin-1 β after experimental endotoxemic challenge. *Crit Care Med* 2001; **29**: 776-781
- 42 **Sims CA**, Wattanasirichaigoon S, Menconi MJ, Ajami AM, Fink MR. Ringer's ethyl pyruvate solution ameliorates ischemia/reperfusion-induced intestinal mucosal injury in rats. *Crit Care Med* 2001; **29**: 1513-1518
- 43 **Lehmann C**, Konig JP, Dettmann J, Birnbaum J, Kox WJ. Effects of iloprost, a stable prostacyclin analog, on intestinal leukocyte adherence and microvascular blood flow in rat experimental endotoxemia. *Crit Care Med* 2001; **29**: 1412-1416
- 44 **Funda DP**, Tuckova L, Farre MA, Iwase T, Moro I, Tlaskalova-Hogenova H. CD14 is expressed and released as soluble CD14 by human intestinal epithelial cells in vitro: lipopolysaccharide activation of epithelial cells revisited. *Infect Immun* 2001; **69**: 3772-3781
- 45 **Gong JP**, Liu CA, Wu CX, Li SW, Shi YJ, Li XH. Nuclear factor kB activity in patients with acute severe cholangitis. *World J Gastroenterol* 2002; **8**: 346-349
- 46 **Baykal A**, Iskit AB, Hamaloglu E, Guc MO, Hascelik G, Sayek I. Melatonin modulates mesenteric blood flow and TNF- α concentrations after lipopolysaccharide challenge. *Eur J Surg* 2000; **166**: 722-727
- 47 **Assy N**, Jacob G, Spira G, Edoute Y. Diagnostic approach to patients with cholestatic jaundice. *World J Gastroenterol* 1999; **5**: 252-262
- 48 **Li SW**, Gong JP, Wu CX, Shi YJ, Liu CA. Lipopolysaccharide induced synthesis of CD14 proteins and its gene expression in hepatocytes during endotoxemia. *World J Gastroenterol* 2002; **8**: 124-127

Edited by Wu XN

• BASIC RESEARCH •

Epidemiological survey of *Blastocystis hominis* in Huainan City, Anhui Province, China

Ke-Xia Wang, Chao-Pin Li, Jian Wang, Yu-Bao Cui

Ke-Xia Wang, Chao-Pin Li, Jian Wang, Yu-Bao Cui, School of Medicine, Anhui University of Science & Technology, Huainan 232001, Anhui Province, China

Correspondence to: Dr. Chao-Pin Li, Department of Etiology and Immunology, School of Medicine, Anhui University of Science & Technology, Huainan 232001, Anhui Province, China. cpli@aust.edu.cn

Telephone: +86-554-6658770 **Fax:** +86-554-6662469

Received 2002-03-09 **Accepted** 2002-08-15

Abstract

AIM: To provide scientific evidence for prevention and controlling of blastocystosis, the infection of *Blastocystis hominis* and to study its clinical significance in Huainan City, Anhui Province, China.

METHODS: *Blastocystis hominis* in fresh stools taken from 100 infants, 100 pupils, 100 middle school students and 403 patients with diarrhea was smeared and detected with method of iodine staining and hematoxylin staining. After preliminary direct microscopy, the shape and size of *Blastocystis hominis* were observed with high power lens. The cellular immune function of the patients with blastocystosis was detected with biotin-streptavidin (BSA).

RESULTS: The positive rates of *Blastocystis hominis* in fresh stools taken from the infants, pupils, middle school students and the patients with diarrhea, were 1.0 % (1/100), 1.0 % (1/100), 0 % (0/100) and 5.96 % (24/403) respectively. Furthermore, the positive rates of *Blastocystis hominis* in the stool samples taken from the patients with mild diarrhea, intermediate diarrhea, severe diarrhea and obstinate diarrhea were 6.03 % (14/232), 2.25 % (2/89), 0 % (0/17) and 12.31 % (8/65) respectively. The positive rates of *Blastocystis hominis* in fresh stools of male and female patients with diarrhea were 7.52 % (17/226) and 3.95 % (7/177) respectively, and those of patients in urban and rural areas were 4.56 % (11/241) and 8.02 % (13/162) respectively. There was no significant difference between them ($P>0.05$). The positive rates of CD_3^+ , CD_4^+ , CD_8^+ in serum of *Blastocystis hominis*-positive and -negative individuals were 0.64 ± 0.06 , 0.44 ± 0.06 , 0.28 ± 0.04 and 0.60 ± 0.05 , 0.40 ± 0.05 and 0.30 ± 0.05 respectively, and the ratio of CD_4^+/CD_8^+ of the two groups were 1.53 ± 0.34 and 1.27 ± 0.22 . There was significant difference between the two groups ($P<0.05$, $P<0.01$).

CONCLUSION: The prevalence of *Blastocystis hominis* as an enteric pathogen in human seems not to be associated with gender and living environment, and that *Blastocystis hominis* is more common in stool samples of the patients with diarrhea, especially with chronic diarrhea or obstinate diarrhea. When patients with diarrhea infected by *Blastocystis hominis*, their cellular immune function decreases, which make it more difficult to be cured.

Wang KX, Li CP, Wang J, Cui YB. Epidemiological survey of *Blastocystis hominis* in Huainan City, Anhui Province, China. *World J Gastroenterol* 2002;8(5):928-932

INTRODUCTION

Blastocystis hominis (B.h) is increasingly recognized to be a cause of human enteric disease. Its presence has been reported in a wide variety of intestinal disorders resembling irritable bowel syndrome (IBS) such as bloating, flatulence, mild to moderate diarrhea, abdominal pain, and nausea^[1-35]. The geographic distribution of *Blastocystis hominis* appears to be global, with infections common in tropical, subtropical and developing countries^[36-40]. In general, studies from developed countries report approximately a 1.5 % to 10 % overall prevalence of *Blastocystis hominis*^[41-45]. However, few reports of the prevalence and the importance of the protozoan *Blastocystis hominis* as an intestinal pathogen in China have been found. In order to explore the epidemiological characteristics and clinical significance of blastocystosis in population of the city of Huainan, a prospective study was carried out from July to August in 2001.

MATERIALS AND METHODS

Population

The study was performed in the following groups of the population in Huainan: in a healthy population ($n=300$, normal group), including infants in day-care centers ($n=100$), pupils ($n=100$) and middle school students ($n=100$), and in outpatients with diarrhea ($n=403$, male 226 and female 177, aged from 6 to 52 years). In addition, we paid more attention to the patients with intractable diarrhea.

Methods

A questionnaire, administered by a nurse, was used to collect detailed information of each subject investigated. Information was collected by means of in-person, telephone and interview, including age, gender, history of present illness, anamnesis, symptomatology (i.e. fever, upper respiratory tract infection, nausea, diarrhea, abdominal cramps, bloating, steatorrhea), date of symptom onset, duration of symptoms, personal health habits, and living environmental condition and the date of stool sample collected.

Stool examination All individuals were asked to provide one stool sample in disposable stool boxes for analysis. Samples were sent to the Department of Etiology and Immunology, School of Medicine, Anhui University of Science & Technology in Huainan for *Blastocystis hominis*. Then the sample was smeared to semitransparent feces membrane on the surface of sheet slides. After these smears were left to dry naturally and fixed with methanol, iodine solution and hematoxylin staining were made, and examination under microscope was carried out. The shape and size of *Blastocystis hominis* were observed.

Detection of T lymphocyte subsets To investigate possible changes of cellular immune function in *Blastocystis hominis*-infected individuals, the level of CD_3^+ , CD_4^+ , CD_8^+ and CD_4^+/CD_8^+ in peripheral blood of *Blastocystis hominis*-positive individuals were tested with biotin-streptavidin (BSA) method. Firstly, peripheral venous blood of subjects was withdrawn, anticoagulated with heparin, and diluted with fluid free of Ca^{2+} , Mg^{2+} . Secondly, peripheral blood mononuclear cells were separated with lymphocytes separating medium, cleaned, and the number of cells was adjusted to $(1-3) \times 10^9/L$ of which $10 \mu l$ was taken and smeared in an acid-proof varnish circle on the surface of the slides. When it dried naturally, McAb of anti- CD_3^+ , anti- CD_4^+ and anti- CD_8^+ and sheep anti-guineapig IgG, SA-HRP were added into the circle. After development with DAB, the slides were observed under microscope. Only brown cytomembrane staining was regarded as positive, otherwise, as negative specimen. A total of 200 cells were counted, and the positive percentage of cells were analyzed respectively.

Statistical analysis

The positive rates were expressed as percentage, and the statistical analysis was carried out by using χ^2 and *t*-test. A probability value of less than 0.05 was considered statistically significant.

RESULTS

Stool examination

Of the 703 stool samples examined, 3.70 % (26/703) were found to be positive for *Blastocystis hominis*. Furthermore, the positive rate of *Blastocystis hominis* in 300 stools of healthy people was 0.67 % (2/300); and those of infants, pupils and middle school students were 1.00 % (1/100), 0 (0/100) and 1.00 % (1/100) respectively. In addition, The positive rates of *Blastocystis hominis* in the stools taken from the outpatients with mild diarrhea, intermediate diarrhea, severe diarrhea and obstinate diarrhea were 6.03 % (14/232), 2.25 % (2/89), 0 % (0/17) and 12.31 % (8/65) respectively. There was significant difference in the positive rates between each type of patients ($P < 0.05$). The detailed results are showed in Table 1.

Table 1 The detective results of *B.h* in fresh feces (n, %)

Group	n	B.h positive	
		n	rate
^b Normal	300	2	0.67
Infants	100	1	1.00
Pupils	100	1	1.00
Middle school students	100	0	0.00
^b Diarrheic outpatients	403	24	5.96
^a Mild	232	14	6.03
^a Intermediate	89	2	2.25
^a Severe	17	0	0.00
^a Obstinate	65	8	12.31

^a $P < 0.05$, $\chi^2 = 7.9475$; ^b $P < 0.01$, $\chi^2 = 13.5181$ vs: comparison with normal and abnormal and different diarrhea

Relationship between gender and infection of *Blastocystis hominis*

Of the 403 outpatients, the positive rates of *Blastocystis hominis* in male and female patients were 7.52 % (17/226) and 3.95 % (7/177) respectively. Statistics found no significant difference in positive rate between male and female.

Relationship between living place and infection of *Blastocystis hominis*

The positive rates of *Blastocystis hominis* in stools taken from patients with diarrhea living in urban and in rural areas were 7.52 % (17/226) and 3.95 % (7/177) respectively. There was no significant difference between the two groups ($P > 0.05$).

Relationship between types of diarrhea and infection of *Blastocystis hominis*

The positive rate of *Blastocystis hominis* in stools of healthy people was 0.67 % (2/300), while that of diarrheic patients was 5.96 % (24/403). Among the patients with diarrhea, the positive rates of *Blastocystis hominis* in loose stools, watery stools and mucopurulent bloody stools were 3.70 % (21/305), 4.23 % (3/81) and 0 % (0/17) respectively. There was no significant difference between each type of patients ($P > 0.05$). Results are showed in Table 2.

Table 2 Relationship between types of diarrhea and infection of *B.h* (n, %)

Group	n	B.h positive	
		n	rate
Normal	300	2	0.67
Diarrhea	403	24	5.96
Loose stool	305	21	3.70
Watery stool	81	3	4.23
Mucopurulent bloody stool	17	0	0.00

$P > 0.05$, $\chi^2 = 2.2767$ vs: comparison with different diarrhea

Changes of cellular immune function in *Blastocystis hominis*-infected individuals

Compared with the negative group, the level of CD_3^+ , CD_4^+ and CD_4^+/CD_8^+ of *Blastocystis hominis*-infected individuals decreased, but that of CD_8^+ did not change.

Table 3 Tlymphocyte subsets of patients with *B.h* in faeces ($\bar{x} \pm s$, number fraction)

B.h	n	CD_3^+	CD_4^+	CD_8^+	CD_4^+/CD_8^+
Positive	26	0.64 ± 0.06	0.44 ± 0.06^a	0.28 ± 4.44	1.53 ± 0.34^b
Negative	30	0.60 ± 0.05	0.40 ± 0.05^a	0.30 ± 5.12	1.27 ± 0.22^b

^a $P < 0.05$, ^b $P < 0.01$, vs negative

DISCUSSION

Results from this study showed that *Blastocystis hominis* as an intestinal pathogen in humans was found in Huainan area by stool examination, and the prevalence was not related to gender

and living circumstances, and that statistically significant association was observed between the presence of diarrhea and infection with *Blastocystis hominis*.

In this study, *Blastocystis hominis* was found in 26 (3.70 %) of the 703 stool specimens examined. The positive rates of male was similar to that of female, and there is no significant difference in the positive rates between the diarrhea patients living in urban areas and those in rural areas ($P>0.05$), which showed the prevalence of the organism was not related to gender and living environment of the individuals examined.

The results of this study supported the idea that *Blastocystis hominis* was associated with diarrhea. The positive rates of *Blastocystis hominis* in stools of the healthy people was 0.67 % (2/300), while that of the diarrheic patients was 5.96 % (24/403), and the difference between them was significant ($P<0.05$). To be exact, the positive rates of *Blastocystis hominis* was high in stools of the patients with mild diarrhea, intermediate diarrhea and obstinate diarrhea, but there was no *Blastocystis hominis* found in stools of patients with severe diarrhea. In accordance with other reports^[46-49], vacuolar *Blastocystis hominis* were found in stools of patients with diarrhea with iodine solution and hematoxylin staining. This finding suggested that vacuolar *Blastocystis hominis* might be the main type of *Blastocystis hominis* causing diarrhea. Although the reasons why the organism had been found in both symptomatic and asymptomatic individuals have been largely unknown^[50-56], one possibility was that it was due to infection time, infection dose, poly-infection with bacteria and the ability of host immunity that might decide whether the symptom turned up or not, because only over 24 h could the cysts of *Blastocystis hominis* develop into a large number of vacuolar forms^[57-58].

In addition, this experiment demonstrated that the hematoxylin staining offered a very convenient and easy method to differentiate the various stages of *Blastocystis hominis*. As a matter of fact, there is high affinity between hematoxylin and *Blastocystis hominis*. By hematoxylin staining, the walls, nucleus, chromatoid bodies and other structures of *Blastocystis hominis* can be observed clearly, and vacuolar, granular, metamorphic *Blastocystis hominis* can be easily differentiated from small amebae which do not cause any disease^[59-61].

Our study provided evidence for the changes of cellular immune function in *Blastocystis hominis*-infected individuals. In this paper, the level of CD_3^+ , CD_4^+ , and CD_4^+/CD_8^+ decreased in *Blastocystis hominis*-infected individuals, but that of CD_8^+ was normal. Compared with the *Blastocystis hominis* negative group, the difference was significant ($P<0.05$). Recent advances in *Blastocystis hominis* found that in subjects suffering from immunodepression *Blastocystis hominis* showed a significant association with gastrointestinal symptoms^[62-71]. All of these showed that the infection of *Blastocystis hominis* was related to the hosts' cellular immune function.

The level of CD_4^+/CD_8^+ is key to immunoregulation. When decreased, it suggested that T helper lymphocytes took part in the course of diarrhea caused by *Blastocystis hominis*. Indeed, both the ability of humoral immunity and that of cellular immunity decreased in the patients with low level of CD_4^+/CD_8^+ , which made it difficult to cure diarrhea^[72-75]. Because of low ability of immunological kill mediated by CD_8^+ cell, the cellular immunity of human bodies played an important role in the course of diarrhea.

In conclusion, *Blastocystis hominis* should be kept in mind of parasitologists and physicians when dealing with patients with diarrhea. *Blastocystis hominis* has long been described

as a non-pathogenic protozoan parasite until recently, when claims have been made that it can result in pathogenic conditions^[76-78]. Many labs do not know that it is now considered harmful to human bodies, or do not know how to test for it. Moreover, because of absence of specific symptoms, the disease was easily confused with other intestinal diseases and was easily misdiagnosed. The authors suggested that stool examination should be carried out on patients with diarrhea in order to decide whether or not the patients were infected by *Blastocystis hominis*, and the stool samples should be collected more than once from patients showing clinical signs and symptoms.

ACKNOWLEDGEMENTS

We thank Associate Professors Zhu Yu-Xia, Xu Li-Fa, Tang Xiao-Long, Cai Ru, Qian Zhong-Qing, Yang Qing-Gui, He Ji, Zhang Xiu-Yun, Zhou Hui-Sheng, Lu Jun (Department of Etiology and Immunology, School of Medicine, Anhui University of Science & Technology) and some students of our college for their help in sample collection and experimental studies.

REFERENCES

- 1 **Rajah Salim H**, Suresh Kumar G, Vellayan S, Mak JW, Khairul Anuar A, Init I, Vennila GD, Saminathan R, Ramakrishnan K. Blastocystis in animal handlers. *Parasitol Res* 1999; **85**: 1032-1034
- 2 **Zaman V**, Howe J, Ng M, Goh TK. Scanning electron microscopy of the surface coat of Blastocystis hominis. *Parasitol Res* 1999; **85**: 974-976
- 3 **Yoshikawa H**, Abe N, Iwasawa M, Kitano S, Nagano I, Wu Z, Takahashi Y. Genomic analysis of Blastocystis hominis strains isolated from two long-term health care facilities. *J Clin Microbiol* 2000; **38**: 1324-1330
- 4 **Cheng YQ**, Nie QH. Treatment of infectious diarrhea with microecosystem. *Shijie Huaren Xiaohua Zazhi* 2001; **9**: 932-934
- 5 **Dagci H**, Ustun S, Taner MS, Ersoz G, Karacasu F, Budak S. Protozoan infections and intestinal permeability. *Acta Trop* 2002; **81**: 1-5
- 6 **Bhattacharya SK**. Therapeutic methods for diarrhoea in children. *World J Gastroenterol* 2000; **6**: 497-500
- 7 **He ST**, He FZ, Wu CR, Li SX, Liu WX, Yang YF, Jiang SS, He G. Treatment of rotaviral gastroenteritis with Qiwei Baizhu powder. *World J Gastroenterol* 2001; **7**: 735-740
- 8 **Ho LC**, Armiugam A, Jeyaseelan K, Yap EH, Singh M. Blastocystis elongation factor-1alpha: genomic organization, taxonomy and phylogenetic relationships. *Parasitology* 2000; **121**: 135-144
- 9 **Nasirudeen AM**, Singh M, Yap EH, Tan KS. Blastocystis hominis: evidence for caspase-3-like activity in cells undergoing programmed cell death. *Parasitol Res* 2001; **87**: 559-565
- 10 **Iqbal J**, Hira PR, Al-Ali F, Philip R. Cryptosporidiosis in Kuwaiti children: seasonality and endemicity. *Clin Microbiol Infect* 2001; **7**: 261-266
- 11 **Cao YL**. Laboratory diagnosis of infectious diarrhea. *Shijie Huaren Xiaohua Zazhi* 2001; **9**: 927-928
- 12 **Windsor JJ**, Macfarlane L, Whiteside TM, Chalmers RM, Thomas AL, Joynson DH. Blastocystis hominis: a common yet neglected human parasite. *Br J Biomed Sci* 2001; **58**: 12-18
- 13 **Force M**, Sparks WS, Ronzio RA. Inhibition of enteric parasites by emulsified oil of oregano in vivo. *Phytother Res* 2000; **14**: 213-214
- 14 **Katz DE**, Taylor DN. Parasitic infections of the gastrointestinal tract. *Gastroenterol Clin North Am* 2001; **30**: 797-815
- 15 **Taamasri P**, Mungthin M, Rangsin R, Tongupprakarn B, Areekul W, Leelayoova S. Transmission of intestinal

- blastocystosis related to the quality of drinking water. *Southeast Asian J Trop Med Public Health* 2000; **31**: 112-117
- 16 **Xia B**, Shivananda S, Zhang GS, Yi JY, Crusius JBA, Peka AS. Inflammatory bowel disease in Hubei Province of China. *China Natl J New Gastroenterol* 1998; **3**: 119-120
 - 17 **Giacometti A**, Cirioni O, Fiorentini A, Fortuna M, Scalise G. Irritable bowel syndrome in patients with Blastocystis hominis infection. *Eur J Clin Microbiol Infect Dis* 1999; **18**: 436-439
 - 18 **Zhou JL**, Xu CH. The method of treatment on protozoon diarrhea. *Huaren Xiaohua Zazhi* 2000; **8**: 93-95
 - 19 **Zhou X**, Li N, Li JS. Growth hormone stimulates remnant small bowel epithelial cell proliferation. *World J Gastroenterol* 2000; **6**: 909-913
 - 20 **Barrett KE**. New insights into the pathogenesis of intestinal dysfunction: secretory diarrhea and cystic fibrosis. *World J Gastroenterol* 2000; **6**: 470-474
 - 21 **Tan KS**, Singh M, Yap EH. Recent advances in Blastocystis hominis research: hot spots in terra incognita. *Int J Parasitol* 2002; **32**: 789-804
 - 22 **Fan WG**, Long YH. Diarrhea in travelers. *Shijie Huaren Xiaohua Zazhi* 2000; **8**: 937-938
 - 23 **Arisue N**, Hashimoto T, Yoshikawa H, Nakamura Y, Nakamura G, Nakamura F, Yano TA, Hasegawa M. Phylogenetic position of Blastocystis hominis and of stramenopiles inferred from multiple molecular sequence data. *J Eukaryot Microbiol* 2002; **49**: 42-53
 - 24 **Tan KS**, Ng GC, Quek E, Howe J, Ramachandran NP, Yap EH, Singh M. Blastocystis hominis: A simplified, high-efficiency method for clonal growth on solid agar. *Exp Parasitol* 2000; **96**: 9-15
 - 25 **Feng ZH**. Application of gene vaccine and vegetable gene in infective diarrhea. *Shijie Huaren Xiaohua Zazhi* 2000; **8**: 934-936
 - 26 **Chen XQ**, Singh M, Ho LC, Tan SW, Yap EH. Characterization of protein profiles and cross-reactivity of Blastocystis antigens by sodium dodecyl sulfate-polyacrylamide gel electrophoresis and immunoblot analysis. *Parasitol Res* 1999; **85**: 343-346
 - 27 **Scringeour**. Chronic intermittent diarrhoea and fatigue. *Aust Fam Physician* 2001; **30**: 897-903
 - 28 **Zaman V**, Howe J, Ng M. Scanning electron microscopy of Blastocystis hominis cysts. *Parasitol Res* 1998; **84**: 476-477
 - 29 **Xiao YH**. Treatment of infective Diarrhea with antibiotic. *Shijie Huaren Xiaohua Zazhi* 2000; **8**: 930-932
 - 30 **Moe KT**, Singh M, Gopalakrishnakone P, Ho LC, Tan SW, Chen XQ, Yap EH. Cytopathic effect of Blastocystis hominis after intramuscular inoculation into laboratory mice. *Parasitol Res* 1998; **84**: 450-454
 - 31 **Ok UZ**, Girginkardesler N, Balcioglu C, Ertan P, Pirildar T, Kilimcioglu AA. Effect of trimethoprim-sulfamethaxazole in Blastocystis hominis infection. *Am J Gastroenterol* 1999; **94**: 3245-3247
 - 32 **Fryauff DJ**, Prodjodipuro P, Basri H, Jones TR, Mouzin E, Widjaja H, Subianto B. Intestinal parasite infections after extended use of chloroquine or primaquine for malaria prevention. *J Parasitol* 1998; **84**: 626-629
 - 33 **Horiki N**, Kaneda Y, Maruyama M, Fujita Y, Tachibana H. Intestinal blockage by carcinoma and Blastocystis hominis infection. *Am J Trop Med Hyg* 1999; **60**: 400-402
 - 34 **Lanuza MD**, Carbajal JA, Villar J, Mir A, Borrás R. Soluble-protein and antigenic heterogeneity in axenic Blastocystis hominis isolates: pathogenic implications. *Parasitol Res* 1999; **85**: 93-97
 - 35 **Haresh K**, Suresh K, Khairul Anus A, Saminathan S. Isolate resistance of Blastocystis hominis to metronidazole. *Trop Med Int Health* 1999; **4**: 274-277
 - 36 **Hoevers J**, Holman P, Logan K, Hommel M, Ashford R, Snowden K. Restriction-fragment-length polymorphism analysis of small-subunit rRNA genes of Blastocystis hominis isolates from geographically diverse human hosts. *Parasitol Res* 2000; **86**: 57-61
 - 37 **Lee JD**, Wang JJ, Chung LY, Chang EE, Lai LC, Chen ER, Yen CM. A survey on the intestinal parasites of the school children in Kaohsiung county. *Kaohsiung J Med Sci* 2000; **16**: 452-458
 - 38 **Romero Cabello R**, Guerrero LR, Munoz Garcia MR, Geyne Cruz A. Nitazoxanide for the treatment of intestinal protozoan and helminthic infections in Mexico. *Trans R Soc Trop Med Hyg* 1997; **91**: 701-703
 - 39 **Yoshikawa H**, Nagano I, Wu Z, Yap EH, Singh M, Takahashi Y. Genomic polymorphism among Blastocystis hominis strains and development of subtype-specific diagnostic primers. *Mol Cell Probes* 1998; **12**: 153-159
 - 40 **Barret JP**, Dardano AN, Hegggers JP, McCauley RL. Infestations and chronic infections in foreign pediatric patients with burns: is there a role for specific protocols? *J Burn Care Rehabil* 1999; **20**: 482-486
 - 41 **Kaneda Y**, Horiki N, Cheng XJ, Fujita Y, Maruyama M, Tachibana H. Ribodemes of Blastocystis hominis isolated in Japan. *Am J Trop Med Hyg* 2001; **65**: 393-396
 - 42 **Tasova Y**, Sahin B, Koltas S, Paydas S. Clinical significance and frequency of Blastocystis hominis in Turkish patients with hematological malignancy. *Acta Med Okayama* 2000; **54**: 133-136
 - 43 **Jensen B**, Kepley W, Guarner J, Anderson K, Anderson D, Clairmont J, De L' aune W, Austin EH, Austin GE. Comparison of polyvinyl alcohol fixative with three less hazardous fixatives for detection and identification of intestinal parasites. *J Clin Microbiol* 2000; **38**: 1592-1598
 - 44 **Herwaldt BL**, de Arroyave KR, Wahlquist SP, de Merida AM, Lopez AS, Juranek DD. Multiyear prospective study of intestinal parasitism in a cohort of Peace Corps volunteers in Guatemala. *J Clin Microbiol* 2001; **39**: 34-42
 - 45 **Guignard S**, Arienti H, Freyre L, Lujan H, Rubinstein H. Prevalence of enteroparasites in a residence for children in the Cordoba Province, Argentina. *Eur J Epidemiol* 2000; **16**: 287-293
 - 46 **Garcia LS**, Shimizu RY. Evaluation of intestinal protozoan morphology in human fecal specimens preserved in EcoFix: comparison of Wheatley's trichrome stain and EcoStain. *J Clin Microbiol* 1998; **36**: 1974-1976
 - 47 **Tan KS**, Howe J, Yap EH, Singh M. Do Blastocystis hominis colony forms undergo programmed cell death? *Parasitol Res* 2001; **87**: 362-367
 - 48 **Abou El Naga IF**, Negm AY. Morphology, histochemistry and infectivity of Blastocystis hominis cyst. *J Egypt Soc Parasitol* 2001; **31**: 627-635
 - 49 **Vdovenko AA**. Blastocystis hominis: origin and significance of vacuolar and granular forms. *Parasitol Res* 2000; **86**: 8-10
 - 50 **Brandonisio O**, Maggi P, Panaro MA, Lisi S, Andriola A, Acquafredda A, Angarano G. Intestinal protozoa in HIV-infected patients in Apulia, South Italy. *Epidemiol Infect* 1999; **123**: 457-462
 - 51 **Amin AM**. Blastocystis hominis among apparently healthy food handlers in Jeddah, Saudi Arabia. *J Egypt Soc Parasitol* 1997; **27**: 817-823
 - 52 **Vennila GD**, Suresh Kumar G, Khairul Anuar A, Rajah S, Saminathan R, Sivanandan S, Ramakrishnan K. Irregular shedding of Blastocystis hominis. *Parasitol Res* 1999; **85**: 162-164
 - 53 **Hellard ME**, Sinclair MI, Hogg GG, Fairley CK. Prevalence of enteric pathogens among community based asymptomatic individuals. *J Gastroenterol Hepatol* 2000; **15**: 290-293
 - 54 **Walderich B**, Bernauer S, Renner M, Knobloch J, Burchard GD. Cytopathic effects of Blastocystis hominis on Chinese hamster ovary (CHO) and adeno carcinoma HT29 cell cultures. *Trop Med Int Health* 1998; **3**: 385-390
 - 55 **Svenungsson B**, Lagergren A, Ekwall E, Evengard B, Hedlund KO, Karnell A, Lofdahl S, Svensson L, Weintraub A. Enteropathogens in adult patients with diarrhea and healthy control subjects: a 1-year prospective study in a

- Swedish clinic for infectious diseases. *Clin Infect Dis* 2000; **30**: 770-778
- 56 **Gericke AS**, Burchard GD, Knobloch J, Walderich B. Isoenzyme patterns of *Blastocystis hominis* patient isolates derived from symptomatic and healthy carriers. *Trop Med Int Health* 1997; **2**: 245-253
- 57 **Zaman V**, Zaki M, Manzoor M, Howe J, Ng M. Postcystic development of *Blastocystis hominis*. *Parasitol Res* 1999; **85**: 437-440
- 58 **Moe KT**, Singh M, Howe J, Ho LC, Tan SW, Chen XQ, Yap EH. Development of *Blastocystis hominis* cysts into vacuolar forms *in vitro*. *Parasitol Res* 1999; **85**: 103-108
- 59 **Vdovenko AA**, Williams JE. *Blastocystis hominis*: neutral red supravital staining and its application to *in vitro* drug sensitivity testing. *Parasitol Res* 2000; **86**: 573-581
- 60 **Zaman V**. The differential identification of *Blastocystis hominis* cysts. *Ann Trop Med Parasitol* 1998; **92**: 233-235
- 61 **Leber AL**. Intestinal amebae. *Clin Lab Med* 1999; **19**: 601-619
- 62 **Amenta M**, Dalle Nogare ER, Colomba C, Prestileo TS, Di Lorenzo F, Fundaro S, Colomba A, Ferrieri A. Intestinal protozoa in HIV-infected patients: effect of rifaximin in *Cryptosporidium parvum* and *Blastocystis hominis* infections. *J Chemother* 1999; **11**: 391-395
- 63 **Wilcox CM**. Etiology and evaluation of diarrhea in AIDS: a global perspective at the millennium. *World J Gastroenterol* 2000; **6**: 177-186
- 64 **Lebbad M**, Norrgren H, Naucler A, Dias F, Andersson S, Linder E. Intestinal parasites in HIV-2 associated AIDS cases with chronic diarrhoea in Guinea-Bissau. *Acta Trop* 2001; **80**: 45-49
- 65 **Menon BS**, Abdullah MS, Mahamud F, Singh B. Intestinal parasites in Malaysian children with cancer. *J Trop Pediatr* 1999; **45**: 241-242
- 66 **Germani Y**, Minssart P, Vohito M, Yassibanda S, Glaziou P, Hocquet D, Berthelemy P, Morvan J. Etiologies of acute, persistent, and dysenteric diarrheas in adults in Bangui, Central African Republic, in relation to human immunodeficiency virus serostatus. *Am J Trop Med Hyg* 1998; **59**: 1008-1014
- 67 **Ghosh K**, Ayyaril M, Nirmala V. Acute GVHD involving the gastrointestinal tract and infestation with *Blastocystis hominis* in a patient with chronic myeloid leukaemia following allogeneic bone marrow transplantation. *Bone Marrow Transplant* 1998; **22**: 1115-1117
- 68 **Cimerman S**, Cimerman B, Lewi DS. Prevalence of intestinal parasitic infections in patients with acquired immunodeficiency syndrome in Brazil. *Int J Infect Dis* 1999; **3**: 203-206
- 69 **Li MD**. Diarrhea in AIDS. *Shijie Huaren Xiaohua Zazhi* 2000; **8**: 937-938
- 70 **Prasad KN**, Nag VL, Dhole TN, Ayyagari A. Identification of enteric pathogens in HIV-positive patients with diarrhoea in northern India. *J Health Popul Nutr* 2000; **18**: 23-26
- 71 **Mathewson JJ**, Salameh BM, DuPont HL, Jiang ZD, Nelson AC, Arduino R, Smith MA, Masozera N. HEP-2 cell-adherent *Escherichia coli* and intestinal secretory immune response to human immunodeficiency virus (HIV) in outpatients with HIV-associated diarrhea. *Clin Diagn Lab Immunol* 1998; **5**: 87-90
- 72 **Kaneda Y**, Horiki N, Cheng X, Tachibana H, Tsutsumi Y. Serologic response to *Blastocystis hominis* infection in asymptomatic individuals. *Tokai J Exp Clin Med* 2000; **25**: 51-56
- 73 **Nasirudeen AM**, Tan KS, Singh M, Yap EH. Programmed cell death in a human intestinal parasite, *Blastocystis hominis*. *Parasitology* 2001; **123**: 235-246
- 74 **Long HY**, Handschack A, Konig W, Ambrosch A. *Blastocystis hominis* modulates immune responses and cytokine release in colonic epithelial cells. *Parasitol Res* 2001; **87**: 1029-1030
- 75 **Tan KS**, Ibrahim M, Ng GC, Nasirudeen AM, Ho LC, Yap EH, Singh M. Exposure of *Blastocystis* species to a cytotoxic monoclonal antibody. *Parasitol Res* 2001; **87**: 534-538
- 76 **Cirioni O**, Giacometti A, Drenaggi D, Ancarani F, Scalise G. Prevalence and clinical relevance of *Blastocystis hominis* in diverse patient cohorts. *Eur J Epidemiol* 1999; **15**: 389-393
- 77 **Waring L**, Reed C. *Blastocystis hominis*: causative organism or harmless commensal? *Aust Fam Physician* 2001; **30**: 374-378
- 78 **Koutsavlis AT**, Valiquette L, Allard R, Soto J. *Blastocystis hominis*: a new pathogen in day-care centers? *Can Commun Dis Rep* 2001; **27**: 76-84

Edited by Zhang JZ

• CLINICAL RESEARCH •

Pancreatic microcirculatory impairment in experimental acute pancreatitis in rats

Zong-Guang Zhou, You-Dai Chen, Wei Sun, Zhong Chen

Zong-Guang Zhou, You-Dai Chen, Wei Sun, Zhong Chen, III
Department of General Surgery (Gastroenteric Surgery), West China Hospital, Sichuan University, Chengdu 610041, Sichuan, China

Supported by the National Natural Science Foundation of China, No.39770722, and by the key project of National Outstanding Young Foundation of China, No. 39925032

Correspondence to: Professor. Zong-Guang Zhou, III Department of General Surgery, West China Hospital, Sichuan University, Chengdu 610041, China. zhou767@21cn.com

Received 2001-11-02 **Accepted** 2001-12-05

Abstract

AIM: To study the feature of pancreatic microcirculatory impairment, especially the initial changes, in caerulein-induced experimental acute pancreatitis (AP).

METHODS: The pancreatic microcirculation of caerulein-induced AP model was studied by intravital fluorescence microscopy with FITC-labeled erythrocytes (FITC-RBC), scanning electron microscopy of vascular corrosion casts, and light microscopy of Chinese ink-injected/cleared tissues.

RESULTS: Animals in caerulein-treated group showed hyperamylemia ($\times 2$), pancreatic oedema, infiltration of inflammatory cells in pancreas. Constrictions of intralobular arteriolar sphincters, presence of vacuoles in all layers of sphincter, and gross irregularity in capillary network of acini were found in the AP specimens. The decrease of pancreatic capillary blood flow ($0.34 \pm 0.10 \text{ nl} \cdot \text{min}^{-1}$ vs $0.91 \pm 0.06 \text{ nl} \cdot \text{min}^{-1}$ of control, $P < 0.001$), reduction of functional capillary density ($277 \pm 13 \text{ cm}^{-1}$ vs $349 \pm 8 \text{ cm}^{-1}$ of control, $P < 0.001$), and irregular intermittent perfusion were observed in caerulein-induced groups.

CONCLUSION: Impairment and constriction of pancreatic intralobular arteriolar sphincter are the initial microcirculatory lesions in the early phase of acute pancreatitis, and play a key role in the pancreatic ischaemia and pancreatic microvascular failure in acute pancreatitis.

Zhou ZG, Chen YD, Sun W, Chen Z. Pancreatic microcirculatory impairment in experimental acute pancreatitis in rats. *World J Gastroenterol* 2002; 8(5):933-936

INTRODUCTION

Etiopathology of acute pancreatitis (AP) is not fully understood^[1-19]. Microcirculatory impairment has long been recognized as one of the etiological factors of acute pancreatitis^[20]. Pancreatic microcirculatory disturbance may act as initiating factor or aggravating/continuing factor. However, the mechanism of microcirculatory impairment in

acute pancreatitis is complex; there are questions concerning local pancreatic microcirculatory change in acute pancreatitis and the features of pancreatic microcirculatory disturbance in various stages of AP remain subject to further study^[21-28]. To investigate the feature of the pancreatic microcirculatory impairment in the early-stage of caerulein-induced experimental acute pancreatitis, dynamic method of microcirculatory research combined with static method had been carried out in this study.

MATERIALS AND METHODS

Animals

48 adult male Wistar rats, weighing 250-350 g, were randomly assigned to 4 groups: (1) control group (group 1, $n=12$). (2) intravital study group, pancreatic microcirculation observed with FITC-labeled RBC and intravital fluorescence microscope (group 2, $n=12$). (3) light microscopy and scanning electron microscopy study group, pancreatic microvasculature perfused with ink and methylmethacrylate (group 3, $n=12$). (4) histocellular study group (group 4, $n=12$).

Experimental pancreatitis

Caerulein used to induce acute pancreatitis was obtained from Sigma Co.. All experimental groups were injected caerulein subcutaneously 5.5 and $7.5 \mu\text{g} \cdot \text{kg}^{-1}$ 1 and 2 h after the beginning of experiment respectively, while control group was injected physiological saline solution subcutaneously. All groups were observed 4 after the beginning of the experiment.

Erythrocytes labeling

Erythrocytes were labeled by fluorescein isothiocyanate (FITC, purchased from Sigma Co.) using a combined approach of the procedures of Klar (1995). The labeled cells were stored a maximum of 24h before use.

In vivo microscopy

The pancreas of the studied animal was exteriorized on a stage, then FITC-labeled RBC was intravenously injected and intravital fluorescence microscope (Olympus X-70) were used to dynamically observe the pancreatic microcirculatory indices, and the images were simultaneously picked up by high-resolution video cassette recorder.

Morphology of microvasculature

Thoracic aortas of the studied animal were cannulated for perfusion. After flushing the vessels with warmed heparinized physiological saline solution, a diluted resin mixture or China ink was injected through the cannula with an injection pressure of $12-16 \text{ kPa}$, until the portal vein and inferior vena cava was filled with the injected resin or ink.

The pancreas of resin-injected animal was corroded overnight or longer in a hot $300-400 \text{ g} \cdot \text{L}^{-1}$ KOH solution, washed in running water and rinsed again several times in distilled

water, air-dried, coated with gold in a vacuum evaporator, and observed in a scanning electron microscope.

The pancreas of ink-injected animal was fixed overnight or longer in Bouins solution, cleared in trichloromethane, embedded in paraffin, serially sectioned (thin sections of 5-7 μm for observation of the relationship between capillaries and cells, thick sections of 50-100 μm for observation of the vessel continuation), and observed with an Olympus X-60/50 light microscope. Serial reconstruction was carried out, camera lucida tracings of photographs were made at x330 final magnification on transparent sheets and superimposed for analysis.

Assays

Serum amylase level was determined and adopted as an indicator of AP. The increase in water content of pancreatic tissue served to indicate the formation and severity of pancreatic edema. The wet weight/dry weight ratio was expressed in per cent. Pancreatic tissue blocks of all groups were routinely paraffin wax-embedded, sliced, stained with hematoxylin/eosin and toluidine blue/basic fuchsin, then the sections were microscopically studied.

Statistical analysis

The results were expressed in mean \pm standard deviation, and *t*-test was used to evaluate differences between control and AP groups. Difference was considered significant at the $P < 0.05$ level.

RESULTS

Pancreatic edema

Gross appearance of pancreatic tissue of control group remained normal, and presented 72 % of water content. In comparison, pancreatic edema gradually appeared in Group2, 3 and 4 four hours after subcutaneous injection of caerulein, in parallel with an increase in pancreatic tissue volume. Edema of pancreatic head and body was much prominent, and the water content increased to 75 %. Inflammatory exudate accumulated in the anterior pararenal space and lesser omental sac in 50 % cases.

Morphology

Injury of intralobular arteriolar sphincter became visible 4 h after animal model established, and numerous cytoplasmic vacuoles formed; massive interstitial edema and inflammatory cell infiltration gradually emerged at 6 h. While in control group, pancreatic acini, tubules and blood vessels were normal microscopically.

Serum amylase

Serum amylase measurement in control group presented normal level (20.8 $\mu\text{kat} \cdot \text{L}^{-1}$). Serum amylase in all AP groups showed hyperamylasemia (45.0 $\mu\text{kat} \cdot \text{L}^{-1}$), significant higher than that of control group ($P < 0.01$).

Light microscopy and scanning electron microscopy

Animals in the caerulein-treated group showed constriction of intralobular arteriolar sphincter 4 h after beginning of the experiment, presence of vacuoles in all the layers of sphincter, gross irregularity in capillary network of acini, reduction of capillary density, and blebs protruded from the surface of casts reflecting a substantial increase in capillary permeability.

In vivo fluorescence microscopy

Comparing with the control group, 4 hours after the start of

experiment in AP groups the pancreatic microcirculatory in the caerulein-treated group showed the reduction of the velocity of FITC-labeled RBC, decrease of pancreatic capillary blood flow ($P < 0.01$, Table 1), reduction of functional capillary density and arterioles diameter ($P < 0.05$), and irregular intermittent perfusion of capillary network ($P < 0.05$). Arterioles of pancreatic lobules and capillary density experienced significant changes at 6 h. The calibers of venules and capillaries showed no marked change in 6 h, while there was significant change by 8 h ($P < 0.05$, Table 2).

Table 1 Intravital fluorescence microscopy of pancreatic microcirculation with FITC-labeled erythrocytes

t/h	Group	d(FITC-RBC)/ ($\times 10^6 \text{ cell/L}$)	Velocity of FITC-RBC/ ($\text{cell} \cdot \text{min}^{-1}$)	RBC flow/ ($\text{nl} \cdot \text{min}^{-1}$)	Microcirculatory blood flow/ ($\text{nl} \cdot \text{min}^{-1}$)
4	Control	113 \pm 5	86 \pm 3	0.28 \pm 0.01	0.88 \pm 0.06
	AP ^b	85 \pm 9	43 \pm 2	0.12 \pm 0.03	0.56 \pm 0.09
6	Control	104 \pm 4	81 \pm 4	0.31 \pm 0.02	0.99 \pm 0.07
	AP ^b	68 \pm 7	36 \pm 5	0.09 \pm 0.03	0.45 \pm 0.12
8	Control	96 \pm 6	84 \pm 5	0.29 \pm 0.04	0.91 \pm 0.06
	AP ^b	59 \pm 9	30 \pm 5	0.07 \pm 0.03	0.34 \pm 0.10

^b $P < 0.001$ vs control.

Table 2 Intravital observation of pancreatic microcirculation

t/h	Group	D(arteriole) / μm	D(venule) / μm	D(capillary) / μm	d(Capillary) / cm^{-1}	Capillary perfusion
4	Control	23.5 \pm 8	28 \pm 3	6.7 \pm 1.5	394 \pm 7	Stable
	AP	20.2 \pm 5.1	29.1 \pm 2	7 \pm 1.4	381 \pm 9	Unstable
6	Control	24.1 \pm 8	28 \pm 2.7	6.9 \pm 1.48	400 \pm 5.8	Stable
	AP	16.4 \pm 3.1 ^a	27.5 \pm 3	6 \pm 0.3	291 \pm 16 ^a	Intermittent & irregular
8	Control	23.2 \pm 5.5	27.4 \pm 1.6	7.3 \pm 1	349 \pm 8	Relatively stable
	AP	18.2 \pm 3.5 ^a	29 \pm 1.5 ^a	5.2 \pm 0.3 ^b	277 \pm 13 ^b	Intermittent & irregular

^a $P < 0.05$, ^b $P < 0.001$ vs control.

DISCUSSION

In 1862 Panum demonstrated that acute hemorrhagic pancreatitis could be induced with wax droplets injected into pancreatic arteries. From then on, the etiological role which pancreatic ischaemia and tissue hypoperfusion plays in AP has been extensively discussed^[29]. Many researches suggested that local microcirculatory disturbance, not insufficient blood flow in peripheral circulation, was responsible for perfusion failure of pancreatic tissue. In recent years, various animal models such as hemorrhagic shock, embolization of pancreatic microvasculature by minute particles and ligation of pancreatic arteries, have been used to verify that microcirculatory impairment of pancreas is the initial stage of AP. But the following questions haven't been answered conclusively: whether all types of AP are initiated by pancreatic microcirculatory impairment? What are the characteristics of early-stage pancreatic microcirculatory change? And what are the features of pancreatic microcirculatory disturbance in the natural process of AP? Insights into all these areas are crucial to the development of prevention and treatment measures.

Animal model

Sodium taurocholate-induced experimental pancreatitis was used by many authors to investigate microcirculatory change of AP; this model can reflect soundly the pathological features of acute necrotizing pancreatitis. Since direct injury to pancreatic ductules, acini and blood vessels may happen in several minutes, the gradual evolution of early-stage pathological change of pancreas in AP cannot be explored. In addition, modulation of intraductal pressure in the process of retrograde pancreatobiliary injection of sodium taurocholate also poses a real challenge. In this study, caerulein-induced experimental pancreatitis was chosen to investigate the features of early-stage pancreatic microcirculatory change. Subcutaneous administration of caerulein is easy to operate, and can result in acute edematous pancreatitis similar to that induced by intravenous injection of caerulein. In this model, the pathological changes develop slowly and gradually, the microcirculatory and histological changes of pancreas become prominent 4 h after the beginning of experiment, and pancreatic edema reaches its zenith by 8 h. This gradual development course allows us to study the triggering factor and the features of early-stage pancreatic microcirculatory impairment without haste.

Study techniques

For decades, pancreatic microcirculatory study heavily depended on the following techniques: injection of minute particles, Indian ink and methylthionine chloride into pancreatic arteries; measurement of pancreatic blood flow through pancreatoduodenal arteries and veins; measurements of relative blood flow and tissue perfusion of pancreas with intravenous injection of nuclide Rb-86, etc. Since acute necrotizing pancreatitis is characterized with progressive regional or focal necrosis of pancreatic tissue, observation with a single method has the following disadvantages: (1) dynamic and direct observation of local microcirculatory change of pancreas is impossible, since the animal must be sacrificed at a specific time; (2) observation of local blood flow of pancreas and tissue perfusion cannot be made simultaneously on the same specimen; (3) as to traditional intravital observation of pancreatic microcirculation, quantitative study cannot be effective due to dim image. This experiment has solved the above problems by developing a new approach; this approach combined intravital microcirculation observation technique, using selective blood element fluorescent marker, with another technique-maintaining dynamic and tissue message on static specimen.

Pancreatic microcirculatory impairment in AP

In recent years, applied basic researches on the morphology of pancreatic microcirculation revealed that the blood supply of pancreatic lobule, in most cases, is provided by a single intralobular arteriole. This arteriole sends forth tree-like branches when entering pancreatic lobule; it has no anastomosis with adjacent intralobular arterioles and their branches, and can be considered end-artery^[30]. This characteristic suggested that pancreatic lobules are susceptible to ischaemic injury due to spasm of intralobular arterioles, embolization of arterioles by emboli, formation of microthrombi or compression by interstitial edema. However, causative factors of early-stage ischaemia and the precise triggering factor of local microcirculatory disturbance are not evident.

This study showed that, manifested as lasting spasm of arteriolar sphincter and multiple cytoplasmic vacuoles within smooth muscle cells of sphincter, the main feature of early-stage pancreatic microcirculatory impairment of AP is injury of sphincter of pancreatic intralobular arteriole. This

experiment also demonstrated that among many factors causing early-stage ischaemia, the key one is injury and spasm of sphincter of pancreatic intralobular arteriole. In this study, injury of arteriolar sphincter occurred earlier than microcirculatory impairment, which reflected that injury of intralobular arteriolar sphincter was the initial stage of pancreatic perfusion failure and local microcirculatory disturbance. Microcirculatory hypoperfusion happened almost simultaneously with injury and spasm of arteriolar sphincter, indicating that pancreatic tissue is highly sensitive to ischaemic stress and has no compensatory reserve. Since sphincter of pancreatic intralobular arteriole serves as main lockgate to control blood flow to pancreatic lobule, and intralobular arteriole has characteristics of end-artery, even sphincter spasm of very short time will quickly evoke obvious pancreatic microcirculatory impairment. Other factors causing ischaemia^[31-37], such as compression from interstitial edema, microemboli or obstruction due to thrombosis, tend to be secondary ones, which may happen gradually in the course of pathological change of AP. These traumatic factors help to sustain and aggravate pancreatic microcirculatory impairment. To clarify relationship between traumatic factors of pancreatic microcirculatory impairment and pathological evolution of AP has guiding value in making treatment plans for clinical AP cases of various development stages. Features of early-stage microcirculatory change of experimental pancreatitis suggested that early adoption of spasm relieving and counter-injury measures are of vital importance in prevention and treatment of local microcirculatory disturbance of AP.

REFERENCES

- 1 **Chen QP**. Enteral nutrition and acute pancreatitis. *World J Gastroenterol* 2001; **7**: 185-192
- 2 **Fleischer F**, Dabew R, Göke B, Wagner ACC. Stress kinase inhibition modulates acute experimental pancreatitis. *World J Gastroenterol* 2001; **7**: 259-265
- 3 **Zhang WZ**, Han TQ, Tang YQ, Zhang SD. Rapid detection of sepsis complicating acute necrotizing pancreatitis using polymerase chain reaction. *World J Gastroenterol* 2001; **7**: 289-292
- 4 **Luo Y**, Yuan CX, Peng YL, Wei PL, Zhang ZD, Jiang JM, Dai L, Hu YK. Can ultrasound predict the severity of acute pancreatitis early by observing acute fluid collection? *World J Gastroenterol* 2001; **7**: 293-295
- 5 **Slavin J**, Ghaneh P, Sutton R, Hartley M, Rowlands P, Garvey C, Hughes M, Neoptolemos J. Management of necrotizing pancreatitis. *World J Gastroenterol* 2001; **7**: 476-481
- 6 **Wu XN**. Current concept of pathogenesis of severe acute pancreatitis. *World J Gastroenterol* 2000; **6**: 32-36
- 7 **Xia Q**, Jiang JM, Gong X, Chen GY, Li L, Huang ZW. Experimental study of "Tong Xia" purgative method in ameliorating lung injury in acute necrotizing pancreatitis. *World J Gastroenterol* 2000; **6**: 115-118
- 8 **Tiscornia OM**, Hamamura S, Lehmann ES, Otero G, Waisman H, Tiscornia Wasserman P, Bank S. Biliary acute pancreatitis: a review. *World J Gastroenterol* 2000; **6**: 157-168
- 9 **Wu JX**, Xu JY, Yuan YZ. Effect of emodin and sandostatin on metabolism of eicosanoids in acute necrotizing pancreatitis. *World J Gastroenterol* 2000; **6**: 293-294
- 10 **Qin RY**, Zou SQ, Wu ZD, Qiu FZ. Influence of splanchnic vascular infusion on the content of endotoxins in plasma and the translocation of intestinal bacteria in rats with acute hemorrhage necrosis pancreatitis. *World J Gastroenterol* 2000; **6**: 577-580
- 11 **Wu XN**. Treatment revisited and factors affecting prognosis of severe acute pancreatitis. *World J Gastroenterol* 2000; **6**: 633-635
- 12 **Chen DL**, Wang WZ, Wang JY. Epidermal growth factor

- prevents gut atrophy and maintains intestinal integrity in rats with acute pancreatitis. *World J Gastroenterol* 2000; **6**:762-765
- 13 **Wu XN**. The mechanism of actions of Octreotide, Bupleurum. Peony Cheng Qi decoction and Dan Shan in severe acute pancreatitis. *World J Gastroenterol* 1999; **5**: 249-251
- 14 **Pezzilli R**, Mancini F. Assessment of severity of acute pancreatitis: a comparison between old and most recent modalities used to evaluate this perennial problem. *World J Gastroenterol* 1999; **5**: 283-285
- 15 **Yuan YZ**, Lou KX, Gong ZH, Tu SP, Zhai ZK, Xu JY. Effects and mechanisms of emodin on pancreatic tissue EGF expression in acute pancreatitis in rats. *Shijie Huaren Xiaohua Zazhi* 2001; **9**: 127-130
- 16 **Xia SH**, Zhao XY, Guo P, Da SP. Hemocirculatory disorder in dogs with severe acute pancreatitis and intervention of platelet activating factor antagonist. *Shijie Huaren Xiaohua Zazhi* 2001; **9**: 550-554
- 17 **Wu CT**, Li ZL. Effect of DAO on intestinal damage in acute necrotizing pancreatitis in dogs. *Shijie Huaren Xiaohua Zazhi* 1999; **7**: 64-65
- 18 **Gong ZH**, Yuan YZ, Lou KX, Tu SP, Zhai ZK, Xu JY. Effects and mechanisms of somatostatin analogues on apoptosis of pancreatic acinar cells in acute pancreatitis in mice. *Shijie Huaren Xiaohua Zazhi* 1999; **7**: 964-966
- 19 **Qin RY**, Zou SQ, Wu ZD, Qiu FZ. Effect of splanchnic vascular perfusion on production of TNF α and OFR in rats with acute hemorrhagic necrotic pancreatitis. *Huaren Xiaohua Zazhi* 1998; **6**: 831-833
- 20 **Kaska M**, Pospisilova B, Slizova D. Pathomorphological changes in microcirculation of pancreas during experimental acute pancreatitis. *Hepatogastroenterology* 2000; **47**:1570-1574
- 21 **Hirano T**, Hirano K. Thromboxane A2 receptor antagonist prevents pancreatic microvascular leakage in rats with caerulein-induced acute pancreatitis. *Int J Surg Investig* 1999; **1**: 203-210
- 22 **Bhatia M**, Saluja AK, Singh VP, Frossard JL, Lee HS, Bhagat L, Gerard C, Steer ML. Complement factor C5a exerts an anti-inflammatory effect in acute pancreatitis and associated lung injury. *Am J Physiol Gastrointest Liver Physiol* 2001; **280**: G974-978
- 23 **Bhatia M**, Brady M, Zagorski J, Christmas SE, Campbell F, Neoptolemos JP, Slavin J. Treatment with neutralising antibody against cytokine induced neutrophil chemoattractant (CINC) protects rats against acute pancreatitis associated lung injury. *Gut* 2000; **47**: 838-844
- 24 **Leung PS**, Chan WP, Nobiling R. Regulated expression of pancreatic renin-angiotensin system in experimental pancreatitis. *Mol Cell Endocrinol* 2000; **166**: 121-128
- 25 **Gomez-Cambronero L**, Camps B, de La Asuncion JG, Cerda M, Pellin A, Pallardo FV, Calvete J, Sweiry JH, Mann GE, Vina J, Sastre J. Pentoxifylline ameliorates cerulein-induced pancreatitis in rats: role of glutathione and nitric oxide. *J Pharmacol Exp Ther* 2000; **293**: 670-676
- 26 **al-Eryani S**, Payer J, Huorka M, Duris I. Etiology and pathogenesis of acute pancreatitis. *Bratisl Lek Listy* 1998; **99**: 303-311
- 27 **Sunamura M**, Yamauchi J, Shibuya K, Chen HM, Ding L, Takeda K, Kobari M, Matsuno S. Pancreatic microcirculation in acute pancreatitis. *J Hepatobiliary Pancreat Surg* 1998; **5**: 62-68
- 28 **Plusczyk T**, Rathgeb D, Westermann S, Feifel G. Somatostatin attenuates microcirculatory impairment in acute sodium taurocholate-induced pancreatitis. *Dig Dis Sci* 1998; **43**: 575-585
- 29 **Plusczyk T**, Westermann S, Bersal B, Menger M, Feifel G. Temporary pancreatic duct occlusion by ethibloc: cause of microcirculatory shutdown, acute inflammation, and pancreas necrosis. *World J Surg* 2001; **25**: 432-437
- 30 **Zhou Z**, Zeng Y, Yang P, Cheng Z, Zhao J, Shu Y, Gao X, Yan L, Zhang Z. Structure and function of pancreatic microcirculation. *Shengwu Yixue Gongchengxue Zazhi* 2001; **18**: 195-200
- 31 **Klar E**, Werner J. New pathophysiologic knowledge about acute pancreatitis. *Chirurg* 2000; **71**: 253-264
- 32 **Skoromnyi AN**, Starosek VN. Hemodynamic changes in the liver, kidney, small intestine and pancreas in experimental acute pancreatitis. *Klin Khir* 1998; **12**: 46-48
- 33 **Obermaier R**, Benz S, Kortmann B, Benthues A, Ansorge N, Hopt UT. Ischemia/reperfusion-induced pancreatitis in rats: a new model of complete normothermic *in situ* ischemia of a pancreatic tail-segment. *Clin Exp Med* 2001; **1**: 51-59
- 34 **Mayer H**, Schmidt J, Thies J, Ryschich E, Gebhard MM, Herfarth C, Klar E. Characterization and reduction of ischemia/reperfusion injury after experimental pancreas transplantation. *J Gastrointest Surg* 1999; **3**: 162-166
- 35 **von Dobschuetz E**, Hoffmann T, Messmer K. Inhibition of neutrophil proteinases by recombinant serpin Lex032 reduces capillary no-reflow in ischemia/reperfusion-induced acute pancreatitis. *J Pharmacol Exp Ther* 1999; **290**: 782-788
- 36 **Vollmar B**, Janata J, Yamauchi J, Wolf B, Heuser M, Menger MD. Exocrine, but not endocrine, tissue is susceptible to microvascular ischemia/reperfusion injury following pancreas transplantation in the rat. *Transpl Int* 1999; **12**: 50-55
- 37 **Benz S**, Schnabel R, Morgenroth K, Weber H, Pfeffer F, Hopt UT. Ischemia/reperfusion injury of the pancreas: a new animal model. *J Surg Res* 1998; **75**: 109-115

Edited by Pagliarini R

• CLINICAL RESEARCH •

A ten-year study on non-surgical treatment of postoperative bile leakage

Xiao-Peng Chen, Shu-You Peng, Cheng-Hong Peng, Yin-Bi Liu, Liu-Bin Shi, Xian-Chuan Jiang, Hong-Wei Shen, Yuan-Liang Xu, Shu-Bin Fang, Jing Rui, Xiang-Hou Xia, Guo-Hai Zhao

Xiao-Peng Chen, Shu-You Peng, Cheng-Hong Peng, Yin-Bi Liu, Liu-Bin Shi, Xian-Chuan Jiang, Hong-Wei Shen, Yuan-Liang Xu, Department of Surgery, Second Affiliated Hospital, Medical School of Zhejiang University, Hangzhou 310009, Zhejiang Province, China
Xiao-Peng Chen, Shu-Bin Fang, Jing Rui, Xiang-Hou Xia, Guo-Hai Zhao, Department of Surgery, Affiliated Yijishan Hospital, Wannan Medical College, Wuhu 241001, Anhui Province, China
Correspondence to: Dr. Xiao-Peng Chen, Department of Surgery, Second Affiliated Hospital, Medical School of Zhejiang University, Hangzhou 310009, Zhejiang Province, China. drcxp@sohu.com
Telephone: +86-553-5866103
Received 2001-12-20 **Accepted** 2002-04-08

Abstract

AIM: To summarize systematically our ten-year experience in non-surgical treatment of postoperative bile leakage, and explore its methods and indications.

METHODS: The clinical data of 57 patients with postoperative bile leakage treated non-surgically from January 1991 to December 2000 were reviewed retrospectively.

RESULTS: The site of the leakage was mainly the disrupted or damaged fistulous tracts of T tube in 25 patients (43.9 %), the fossae of gallbladder in 14 cases (24.6 %), the cut surface of liver in 7 cases (12.3 %), and it was undetectable in the other 2 cases. Besides bile leakage, the wrong ligation of bile ducts was found in 3 patients, residual stones of the distal bile duct in 5 patients, benign papillary strictures in 3, and biloma resulting from bile collections in 2. The diagnoses were made according to the history of surgery, clinical situation, abdominal paracentesis, ultrasonography, ERCP, PTC, MRI/MRCP, gastroscopy and percutaneous fistulography. All 57 patients were treated non-surgically at the beginning of bile leakage. The non-surgical methods included keeping original drainage unobstructed, percutaneous abdominal paracentesis or drainage, percutaneous transhepatic cholangial/biliary drainage (PTCD/PTBD), endoscopic management, traditional Chinese medicine and so on. Of the 57 patients, 2 patients died, 5 were converted to reoperation later, the other 50 were directly cured by non-surgical methods without any complication. The cure rate of the non-surgery was 82.5 % (50/57).

CONCLUSION: Many nonoperative methods are available to treat postoperative bile leakage. Non-surgical treatment may serve as the first choice for the treatment of bile leakage for its advantages in higher cure rate, convenience and safety in practice. It is important to choose the specific non-surgical method according to the volume, site of bile leakage and patient's condition.

Chen XP, Peng SY, Peng CH, Liu YB, Shi LB, Jiang XC, Shen HW, Xu YL, Fang SB, Rui J, Xia XH, Zhao GH. A ten-year study on non-surgical treatment of postoperative bile leakage. *World J Gastroenterol* 2002; 8(5):937-942

INTRODUCTION

Bile leakage is one of the most common and serious complications after hepatobiliary surgery. In recent years, the treatment strategy of bile leakage has generated fundamental changes due to the excellent effect of non-surgical therapy and its minimally invasive intervention^[1-6]. Non-surgical treatment has been regarded as the first choice in the management of postoperative bile leakage in many cases. Only when there is no essential condition or no effect by non-surgery, will operation be considered^[1,2]. Although there are many nonoperative approaches that could be used to cure bile leakage, most literatures only reported one of these methods^[7-53], being deficient in systematization and comprehensiveness. Thus, surgeons could not often apply them synthetically and reasonably. Over the past decade from 1991 to 2000, we treated 57 patients with postoperative bile leakage non-surgically in our two hospitals. In this article, we summarized the methods and indications of the non-surgical treatment for postoperative bile leakage.

MATERIALS AND METHODS

Patients

From January 1991 to December 2000, a total of 57 patients with postoperative bile leakage, including 23 males and 34 females, were treated non-surgically in the Department of Surgery of the Second Affiliated Hospital, Medical School of Zhejiang University and the Affiliated Yijishan Hospital of Wannan Medical College. The mean age of the patients was 46 years, with a range from 25 to 73 years. All of them belonged to postoperative bile leakage. The original operations were performed with simple open cholecystectomy (OC) in 21 cases, OC plus choledochotomy with T tube drainage in 25, simple hepatectomy in 7, hepatectomy plus Roux-en-Y cholangiojejunostomy in 3, and repair of bile duct injury plus choledochoduodenostomy in 1, respectively. The clinical presentations were diverse. Most patients were presented with sudden or gradual abdominal pain after operation, and T tube removal/slippage or U tube exchange. Almost half of the cases had much bile-like liquid outflowing from the original drainage tubes or the fistulous tracts of T tube. Twelve patients had light to moderate fever, four hyperpyrexia, six jaundice, and two had nausea and vomiting.

Diagnosis

The diagnoses were made according to the operational history, clinical situation, abdominal paracentesis (21 person times), ultrasonography (17), ERCP (8), PTC (5), MRI/MRCP (3), gastroscopy (3), and percutaneous fistulography (2). The site of the leakage was the cystic duct in 3 cases, the fossae of gallbladder in 14 (Figure 1), the disrupted or damaged fistulous tracts of T tube in 25 (Figures 2 and 3), the damaged bile duct in 3 (Figures 4 and 5), the cut surface of liver in 7 (Figure 6), the stomas of bilioenteric anastomosis in 3 and it was

undetectable in the other 2 cases. Besides bile leakage, the wrong ligation of bile ducts beyond the leakages was also found in 3 patients with common bile duct injury. Of the 25 patients with bile leakage following T tube removal, residual stones of the distal bile duct were also found in 5 cases (Figures 3 and 7) and benign papillary strictures were detected in 3 (Figure 5). Bile collections in 2 patients developed biloma, which oppressed pylorus, resulting in pyloric obstruction. Bile collections at two different sites, including hepatorenal recess and hepatogastric interspace with only a slender and bent tract (diameter <0.5 cm) between them, were confirmed in one patient undergoing hepatectomy, whose original subphrenic drainage was removed owing to occlusion before the bile leakage was found. Although the drainage on the anterior abdominal wall was still retained, it only drained bile from hepatogastric interspace.

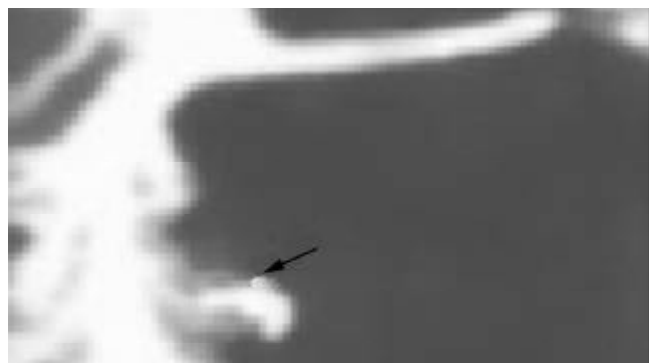


Figure 1 ERCP showed a bile leak from the fossae of gallbladder (↑).



Figure 2 Cholangiography through T tube showed a leak from common bile duct (↑).

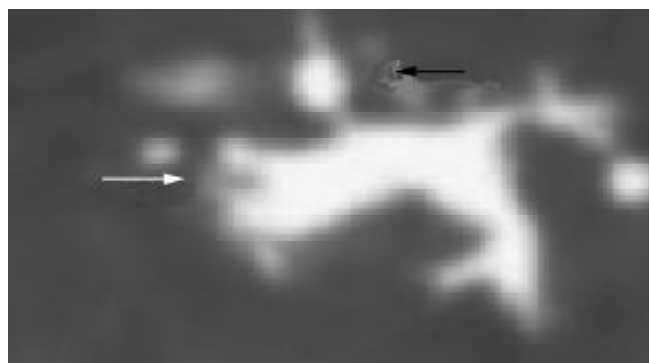


Figure 3 ERCP showed a leak from the fistulous tract of T tube (↑) and stones at distal duct (⊕).

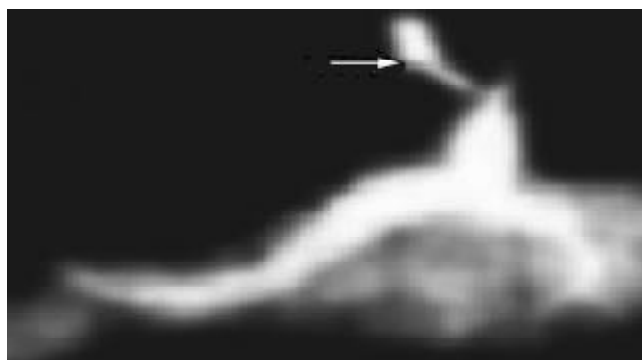


Figure 4 ERCP showed a leak from right hepatic duct (⊕).



Figure 5 MRCP showed stricture at distal duct (↑) and liquid collection in the right subhepatic region (⊕).



Figure 6 CT showed bile accumulating in the cut surface of right liver (↑).



Figure 7 The distal duct stones was removed with choledochoscope (⊕).

Management

When patients revealed the symptoms of bile leakage or biliary peritonitis, some essential disposal measures were immediately used such as right lateral decubitus position, semi-reclining position, gastrointestinal decompression, complementing water-electrolyte, antibiotic and appropriate nutritional support^[1,2]. After that, specific non-surgical methods were chosen according to the volume, site of bile leakage and patient's condition. The original drainage in 19 patients undergoing OC or hepatectomy were kept unobstructed because they still produced some effect of drainage. The cannulae were changed in 5 cases of OC or hepatectomy due to their occlusion. In addition, washing with antibiotic was performed through the cannulae. In all the 25 patients with bile leakage following T tube removal or slippage, a new drainage was once again placed into the fistulous tract of T tube. Repeated abdominal cavity suction and drainage with a percutaneous catheter were performed by percutaneous abdominal paracentesis in 3 of 25 patients while percutaneous transhepatic cholangial drainage (PTCD) or percutaneous transhepatic biliary drainage (PTBD) were performed in 2 patients whose intrahepatic bile ducts were dilated. The residual ductal stones in 5 patients were eliminated by choledochoscope (Figure 7), endoscopic sphincterotomy (EST) and the traditional Chinese medicine, respectively. The traditional Chinese medicines included bitter orange, costusroot, mongolian milkvetch, rhubarb, christina loosestrife herb, etc. In order to maintain the pressure of bile duct and facilitate stones passage, it was necessary to obstruct the T tube at intervals when the Chinese medicines were administered. The bile duct stricture in 3 cases was relieved by choledochoscope and EST, respectively. Percutaneous catheter drainages guided by ultrasound were used in one patient with biloma and 3 patients with common bile leakage. As to the patient with subhepatic fluid accumulations at two different sites detected by ultrasonography, MRI and percutaneous fistulography, it was inappropriate to reoperate on him or her due to the postoperative weak health, and it was very dangerous to apply abdominal paracentesis because the hepatorenal recess was just near the right thoracic cavity. A new drain tube was first placed into hepatogastric interspace and afterwards into the bent tract and hepatorenal recess through the fistulous tract on the anterior abdominal wall. The whole process was guided by gastroscope and X-ray. Flushing with antibiotic was performed everyday.

RESULTS

In the early stage of our study, one patient with stoma leakage died of infectious shock, and one with post-hepatectomy bile leakage died of multiple organ failure (MOF). After 1996, no patient died of bile leakage. Five patients were converted to operation due to ineffective non-surgical management, presentation of jaundice or concomitant wrong ligation of bile duct. All the 5 patients were cured by late reoperation. Of the 5 cases, one with biloma belonged to the early stage of our study. Owing to the absence of experience in the non-surgical treatment at that time (1993), he only received some essential disposals except percutaneous catheter drainage at the beginning of bile leakage. He underwent exploratory laparotomy plus drainage a week later because nausea and vomiting were not relieved. Two patients with bile leakage from cystic duct stump underwent exploratory laparotomy plus re-ligation of cystic duct after 2-3 days drainage. The other two patients all underwent hepatojejunostomy 2-3 months later due to concomitant wrong ligation of bile duct. The other 50

patients were directly cured by non-surgical treatment without correlated complications. The mean closure time of bile leakage was 9 days, with a range from 5 days to 3 months. The cure rate of non-surgical treatment was 82.5 % (50/57).

DISCUSSION

When bile leakage occurs, it is necessary to adopt some essential disposals such as gastrointestinal decompression, fluid replacement, antibiotic therapy, etc. However, it is important to choose operation or nonoperation according to the volume of bile leakage and patient's condition. In recent years, the treatment strategy of bile leakage has generated fundamental changes due to the invention or finding of some new non-surgical methods, which have further improved the therapeutic effect of bile leakage with minimal invasive intervention or no trauma. Non-surgical treatment has been regarded as the first choice in the management of postoperative bile leakage in many cases, and it is acceptable by such patients. Only when there is no essential condition for non-surgery, or no effect, will operation be considered^[1-6].

Non-surgical methods

In our study, the 57 patients with postoperative bile leakage were all managed by non-surgical treatment at the beginning of bile leakage. Fifty patients were cured except that two died and five were converted to reoperation later. The cure rate of non-surgical treatment was 82.5 % (50/57). The total therapeutic efficacy is satisfactory. Based on our data, the following non-surgical methods could be used in the treatment of bile leakage. (1) Keep the original drain tube unobstructed or change it^[1,2,5]. The original drainage should be maintained when it still drains some bile, and should be changed for a new drain tube when obstructed. In addition, we think it is equally of importance to wash with antibiotic through the cannulae^[9], because it could increase the local concentration of antibiotic and improve anti-infection effect. It was difficult for the bile leakage to heal in patients of older age, malnutrition, complicated diabetes and using hormone. Besides drainage, some related therapy should be continued in these cases, the hormone should be cancelled, and the time of drainage be properly prolonged. (2) Insert a new catheter through the fistulous tract of T tube^[1,5,16,17]. It is necessary to place a new catheter immediately through the fistulous tract of T tube if the bile leakage occurs after a T tube removal or slippage. The procedure should be performed as early as possible to prevent the occlusion of fistulous tract. Suction with negative pressure could be additionally used when necessary^[1,16,18]. (3) Percutaneous abdominal paracentesis^[1,5,6,8,10-13]. As an important nonoperative method, abdominal paracentesis can be applied because it does not need special device except an injection syringe. If the site of leakage was deep or near important organs, abdominal paracentesis should be guided by ultrasound. It is helpful to not only the diagnosis of bile leakage but also the abdominal cavity suction or percutaneous catheter drainage. In this group, abdominal paracentesis was performed in five patients (4 with bile leakage after T tube removal and 1 with post-cholecystectomy biloma). Among them, the biloma was punctured under the guidance of ultrasound^[1]. All 5 were cured. (4) PTCD/PTBD or placement of a percutaneous transhepatic stent^[1,14,15]. Owing to some dangers (including hemorrhage, new bile leakage and so on), it should be generally performed under the guidance of ultrasound in patients with intrahepatic cholangiectasis^[5,4]. PTCD is helpful to the healing of bile leakage because it may reduce the volume of leakage. In our

study, PTCs were used in 2 cases because both abdominal drainages were insufficient. Two weeks later, both patients were cured. (5) Endoscopic management^[1,6,8,24-53]. As a new progression in the nonoperative treatment of bile leakage, endoscopic management generally means EST, endoscopic nasobiliary tube drainage (ENBD) and endoscopic biliary stent (EBS)^[32,33,55], which are all finished by duodenoscope. It is mainly applied to the patients with bile duct stone, stricture or biloma^[32,33,55]. These endoscopic methods could effectively remove the residual ductal stones, relieve the stricture of bile duct and facilitate the healing of leakage. However, endoscopes include choledochoscope and gastroscope besides duodenoscope. Because choledochoscope may not only get rid of the residual stones but also dilate the narrow bile duct, it should also play an important role in the nonoperative treatment of bile leakage, and should not be neglected. In our study, choledochoscopic treatments were given to 4 patients (2 with residual stones, 2 with bile duct stenosis). All were cured. Gastroscope may occasionally be used in the nonoperative treatment of bile leakage. In this group, the new drain tube in the patient with bile accumulations at two different sites was placed under the guidance of gastroscope and X-ray. The leakage closed 3 months later. Thus, we should not confine our sights to the duodenoscope when using endoscopic treatment. Besides duodenoscope, gastroscope and choledochoscope may also be applied. (6) Traditional Chinese medicines^[1]. It is mainly applied to the patients with bile duct stone. Some Chinese medicines may facilitate the passage of residual stones, resulting in accelerated healing of leakage. In this group, after Chinese medicines were administered to 2 patients for 5-7 days, the residual stones were all precluded that was confirmed by ultrasound and contrast examination. Both leakages closed within 2 weeks. In addition, there are some other non-surgical methods including laparoscopy^[19-22], ethanol ablation^[23] and so on.

Indications

Non-surgical treatment therapy plays an important role in the management of bile leakage due to its many advantages. First, the cure rate is high^[33,39]. Binmoeller *et al*^[33] reported that the total cure rate of endoscopic management was 86 %. In Fuji's study, all 8 postoperative bile leakages were cured by endoscopic treatment^[39]. In our study, 57 patients were treated with various non-surgical methods, 50 were directly cured, the rate being 82.5 %. Next, non-surgical treatment is convenient, safe^[1,10,40,41], atraumatic or micro-traumatic^[43]. If only it is properly used, reoperation could be avoided in most patients with postoperative bile leakage, and the pain and costs of patients could be reduced. Thus, it is acceptable by patients, and fits the general trend and direction of modern surgery. The non-surgical therapy is especially suitable for the elderly patients who are physically weak, poor in common state, complicated by other serious diseases, unbearable or unwilling to accept reoperation in a short time. In this group, more than half of the patients belonged to such cases. Owing to correct choice of treatment, they not only avoided reoperation, but also safely passed the dangerous period. As for the patients who need surgery but could not be operated on at the early stage of bile leakage due to their conditions, non-surgical treatment can not only serve as interim measure before operation but also wins precious time for preoperative preparation. It was quite obvious that such condition was present in the 5 patients who were converted to late reoperation. When the patients with bile leakage were treated non-surgically, its indications should be strictly controlled. Based

on our data, we think that nonoperative therapy could be first attempted in the following cases^[1]. (1) Patients with early bile leakage^[2] (within 4-6 hours), relatively minor leakage, rather light or local peritonitis and no infectious shock or following shock by estimation; (2) Postoperative early patients who are poor in general state, complicated with other serious diseases, unbearable or unwilling to accept reoperation in a short time; (3) Patients whose original subhepatic drainages were still reserved and unobstructed; (4) Patients who suffer from bile leakages after T tubes removal or slippage and can be implanted with new drain tubes through the fistulous tracts of T tubes; (5) Patients who can be treated with percutaneous abdominal paracentesis or drainage; (6) Patients with intrahepatic bile duct dilatation who can be managed by PTC/PTBD; (7) Patients whose residual bile duct stones or strictures can be cured by endoscopic management or traditional Chinese Medicine. Of course, it is essential to pay close attention to the change of patient's condition and complications during nonoperative treatment, and it also necessary to be simultaneously ready to reoperate at any time. Surgery should be considered as soon as possible if the patient's condition has not improved even aggravated such as abdominal pain degree worsening, scope expanding, temperature apparently rising and so on^[1,10]. Reoperation should also be considered if only the patient's condition goes beyond the limit of nonoperative therapy such as relatively major bile leakage, serious peritonitis^[1,2], persistent leakage or concomitant wrong ligation of bile duct. In our study, 5 patients were converted to reoperation later due to inefficiency of non-surgical management, occurrence of jaundice or wrong ligation of bile duct.

REFERENCES

- 1 **Chen XP**, Peng SY. Causes and treatment of bile leakage (a report of 22 cases). *Zhongguo Shiyong Waikē Zazhi* 2001; **21**: 102-104
- 2 **Hu CG**, Xing CG, Liu GS, Jiang GQ. Postoperative biliary leak in early stage of cholecystectomy: clinical analysis of 16 cases. *Quanke Yisheng* 1999; **8**: 125-126
- 3 **Johnston TD**, Gates R, Reddy KS, Nickl NJ, Ranjan D. Nonoperative management of bile leaks following liver transplantation. *Clin Transplant* 2000; **14**: 365-369
- 4 **Gahukamble DB**, Khamage AS, Gahukamble LD. Outcome of minimal surgery for hydatid cysts of the liver in children with reference to post-operative biliary leakage. *Ann Trop Paediatr* 2000; **20**: 147-151
- 5 **Ge BJ**, Xing HL, Cai TN. The surgical treatment of bile peritonitis after removal of T-tubes from the common bile duct. *Shanxi Yike Daxue Xuebao* 2001; **32**: 233-234
- 6 **De Backer A**, Fierens H, De Schepper A, Pelckmans P, Jorens PG, Vaneerdeweg W. Diagnosis and nonsurgical management of bile leak complicated by biloma after blunt liver injury: report of two cases. *Eur Radiol* 1998; **8**: 1619-1622
- 7 **Dou KF**, Li KZ, Fu YC, Wang JY, Wang WZ, Yan B. Diagnosis and management of bile duct injury and bile leakage in laparoscopic cholecystectomy. *Shanxi Yixue Zazhi* 1996; **25**: 142-144
- 8 **Chen CY**, Lin XZ. Percutaneous and endoscopic management of bile leak following endoscopic stone retrieval—a case report. *Hepatogastroenterology* 1999; **46**: 2199-2201
- 9 **Sun B**, Jiang HC, Pu DX, Xu J. The clinical application of surgical drainage for hepatectomy. *Linchuang Waikē Zazhi* 2000; **8**: 338-339
- 10 **Tepetes K**, Karavias D, Felekouras E, Jabour N, Tzakis A, Starzl E. Bile leakage following T-tube removal in orthotopic liver transplantation. *Hepatogastroenterology* 1999; **46**: 425-427

- 11 **Blasco J**, Real MI, Montana X, Macho J, Arguis P, Burrel M, Bianchi L, Grande L. Percutaneous repair of an iatrogenic laceration of the left bile duct with a covered stent. *J Vasc Interv Radiol* 2001; **12**: 1112-1115
- 12 **VanSonnenberg E**, D'Agostino HB, Casola G, Hoyt DB, Lurie A, Varney RR. Gallbladder perforation and bile leakage: percutaneous treatment. *Radiology* 1991; **178**: 687-689
- 13 **Mansour AY**, Stabile BE. Extrahepatic biliary obstruction due to post-laparoscopic cholecystectomy biloma. *JSLs* 2000; **4**: 167-171
- 14 **Lillemoe KD**, Petrofski JA, Choti MA, Venbrux AC, Cameron JL. Isolated right segmental hepatic duct injury: a diagnostic and therapeutic challenge. *J Gastrointest Surg* 2000; **4**: 168-177
- 15 **Ernst O**, Sergeant G, Mizrahi D, Delemazure O, L'Hermine C. Biliary leaks: treatment by means of percutaneous transhepatic biliary drainage. *Radiology* 1999; **211**: 345-348
- 16 **Jiang XC**. Bile peritonitis following T-tube olisthy or removal. *Zhejiang Yike Daxue Xuebao* 1996; **25**: 16-18
- 17 **Qian J**, Lin SQ. Analysis of 15 cases with T-tubes that are incorrectly treated. *Hangzhou Yixue Gaodeng Zhuanke Xuexiao Xuebao* 2001; **22**: 164-165
- 18 **Yu WP**, Ding JM, Cai ZF, Ling JX. Treatment of postoperative bile leakage by low negative pressure vacuum. *Gandan Waikie Zazhi* 2000; **8**: 106-107
- 19 **Dexter SP**, Miller GV, Davides D, Martin IG, Sue Ling HM, Sagar PM, Larvin M, McMahon MJ. Relaparoscopy for the detection and treatment of complications of laparoscopic cholecystectomy. *Am J Surg* 2000; **179**: 316-319
- 20 **Wills VL**, Jorgensen JO, Hunt DR. Role of relaparoscopy in the management of minor bile leakage after laparoscopic cholecystectomy. *Br J Surg* 2000; **87**: 176-180
- 21 **Ruan JD**, Wan XP, Zhang XB, Shen H, Xia Z, Liu S. Use laparoscopic exploration to treat complications after laparoscopic cholecystectomy. *Zhongguo Neijing Zazhi* 1998; **4**: 8-10
- 22 **Fan YL**, Xu YR, Wang JM, Gong RH. Clinical analysis of 27 cases with bile leaks after laparoscopic cholecystectomy (LC). *Zhongguo Zonghe Linchuang* 2001; **17**: 213
- 23 **Kyokane T**, Nagino M, Sano T, Nimura Y. Ethanol ablation for segmental bile duct leakage after hepatobiliary resection. *Surgery* 2002; **131**: 111-113
- 24 **Rerknimitr R**, Sherman S, Fogel EL, Kalayci C, Lumeng L, Chalasani N, Kwo P, Lehman GA. Biliary tract complications after orthotopic liver transplantation with choledochocholedochostomy anastomosis: endoscopic findings and results of therapy. *Gastrointest Endosc* 2002; **55**: 224-231
- 25 **El-Youssef M**, Parsons WG, Whittington PF. Endoscopic retrograde cholangiopancreatography and endobiliary stenting for the treatment of a bile leak in a child. *J Pediatr Gastroenterol Nutr* 1999; **29**: 350-353
- 26 **Poddar U**, Thapa BR, Bhasin DK, Prasad A, Nagi B, Singh K. Endoscopic retrograde cholangiopancreatography in the management of pancreaticobiliary disorders in children. *J Gastroenterol Hepatol* 2001; **16**: 927-931
- 27 **Morelli J**, Mulcahy HE, Willner IR, Baliga P, Chavin KD, Patel R, Payne M, Cotton PB, Hawes R, Reuben A, Cunningham JT. Endoscopic treatment of post-liver transplantation biliary leaks with stent placement across the leak site. *Gastrointest Endosc* 2001; **54**: 471-475
- 28 **Ponchon T**, Baillie J. An elderly man with a postcholecystectomy bile leak. *Endoscopy* 2000; **32**: 585-588
- 29 **Prat F**, Pelletier G, Ponchon T, Fritsch J, Meduri B, Boyer J, Person B, Bretagne JF. What role can endoscopy play in the management of biliary complications after laparoscopic cholecystectomy? *Endoscopy* 1997; **29**: 341-348
- 30 **Pfau PR**, Kochman ML, Lewis JD, Long WB, Lucey MR, Olthoff K, Shaked A, Ginsberg GG. Endoscopic management of postoperative biliary complications in orthotopic liver transplantation. *Gastrointest Endosc* 2000; **52**: 55-63
- 31 **Sugiyama M**, Mori T, Atomi Y. Endoscopic nasobiliary drainage for treating bile leak after laparoscopic cholecystectomy. *Hepatogastroenterology* 1999; **46**: 762-765
- 32 **Mortensen J**, Kruse A. Endoscopic management of postoperative bile leaks. *Br J Surg* 1992; **79**: 1339-1341
- 33 **Binmoeller MD**, Ronald M, Katon MD. Endoscopic management of postoperative biliary leaks: review of 77 cases and report of two cases with biloma formation. *Am J Gastroenterol* 1991; **86**: 227-231
- 34 **Mergener K**, Strobel JC, Suhocki P, Jowell PS, Enns RA, Branch M S, Baillie J. The role of ERCP in diagnosis and management of accessory bile duct leaks after cholecystectomy. *Gastrointest Endosc* 1999; **50**: 527-531
- 35 **Chow S**, Bosco JJ, Heiss FW, Shea JA, Qaseem T, Howe II D. Successful treatment of post-cholecystectomy bile leaks using nasobiliary tube drainage and sphincterotomy. *Am J Gastroenterol* 1997; **92**: 1839-1843
- 36 **Sugiyama M**, Atomi Y, Matsuoka T, Yamaguchi Y. Endoscopic biliary stenting for treatment of persistent biliary fistula after blunt hepatic injury. *Gastrointest Endosc* 2000; **51**: 42-44
- 37 **Saraswat VA**, Choudhuri G, Sharma BC, Agarwal DK, Gupta R, Baijal SS, Sikora SS, Saxena R, Kapoor V K. Endoscopic management of postoperative bile leak. *J Gastroenterol Hepatol* 1996; **11**: 148-151
- 38 **Dauids PH**, Rauws EA, Tytgat GN, Huibregtse K. Postoperative bile leakage: endoscopic management. *Gut* 1992; **33**: 1118-1122
- 39 **Fujii T**, Maguchi H, Obara T, Tanno S, Itoh A, Shudo R, Takahashi K, Saito H, Ura H, Kohgo Y. Efficacy of endoscopic diagnosis and treatment for postoperative biliary leak. *Hepatogastroenterology* 1998; **45**: 656-661
- 40 **Sreenivas DV**, Kumar YR, Kumar A. Endoscopic treatment of postoperative biliary leak. *Trop Gastroenterol* 1996; **17**: 225-226
- 41 **Zhang W**, Hu ZQ. Endoscopic nasobiliary drainage in the treatment of postoperative biliary fistula. *Zhonghua Putong Waikie Zazhi* 1999; **14**: 336-337
- 42 **Wang TZ**, Zhang X, Wang N, Tao SB, Zou LC. The evaluation of nasobiliary drainage in the treatment of biliary fistula. *Zhongguo Xiandai Putong Waikie Jinzhan* 2001; **4**: 60
- 43 **Foco A**, Garbarini A, Franchello A, Orlando E, Festa T, Gandini G, Righi D, Comotti F, Massaglia F, Drago D. Management of postoperative bile leakage with endoscopic sphincterotomy (EST) and a naso-biliary drain (NBD). *Hepatogastroenterology* 1992; **39**: 301-303
- 44 **De Luca N**, Bourke M, Williams SJ. Endoscopic treatment of bile leak caused by gunshot injury. *Gastrointest Endosc* 2001; **53**: 778
- 45 **Ikematsu Y**, Ito Y, Yuzawa H, Nishiwaki Y, Kida H, Waki S, Nakamura T, Uchimura M. Late-onset biliary leakage after laparoscopic cholecystectomy using laparoscopic coagulating shears. Report of a case. *Surg Endosc* 2001; **15**: 1228
- 46 **Saab S**, Martin P, Soliman GY, Machicado GA, Roth BE, Kunder G, Han SH, Farmer DG, Ghobrial RM, Busuttil RW, Bedford RA. Endoscopic management of biliary leaks after T-tube removal in liver transplant recipients: nasobiliary drainage versus biliary stenting. *Liver Transpl* 2000; **6**: 627-632
- 47 **Shuhart MC**, Kowdley KV, McVicar JP, Rohrmann CA, McDonald MF, Wadland DW, Emerson SS, Carithers RL Jr, Kimmey MB. Predictors of bile leaks after T-tube removal in orthotopic liver transplant recipients. *Liver Transpl Surg* 1998; **4**: 62-70

- 48 **Braghetto I**, Bastias J, Csendes A, Debandi A. Intraperitoneal bile collections after laparoscopic cholecystectomy: causes, clinical presentation, diagnosis, and treatment. *Surg Endosc* 2000; **14**: 1037-1041
- 49 **Prasad H**, Poddar U, Thapa BR, Bhasin DK, Rao KL, Singh K. Endoscopic management of post laparoscopic cholecystectomy bile leak in a child. *Gastrointest Endosc* 2000; **51**: 506-507
- 50 **Banzo I**, Blanco I, Gutierrez-Mendiguchia C, Gomez-Barquin R, Quirce R, Carril JM. Hepatobiliary scintigraphy for the diagnosis of bile leaks produced after T-tube removal in orthotopic liver transplantation. *Nucl Med Commun* 1998; **19**: 229-236
- 51 **Ryan ME**, Geenen JE, Lehman GA, Aliperti G, Freeman ML, Silverman WB, Mayeux GP, Frakes JT, Parker HW, Yakshe PN, Goff JS. Endoscopic intervention for biliary leaks after laparoscopic cholecystectomy: a multicenter review. *Gastrointest Endosc* 1998; **47**: 261-266
- 52 **Griffen M**, Ochoa J, Boulanger BR. A minimally invasive approach to bile peritonitis after blunt liver injury. *Am Surg* 2000; **66**: 309-312
- 53 **Aru GM**, Davis CR Jr, Elliott NL, Morris SJ. Endoscopic retrograde cholangiopancreatography in the treatment of bile leaks and bile duct strictures after laparoscopic cholecystectomy. *South Med J* 1997; **90**: 705-708
- 54 **Fan YZ**, Cai TN, Wang BC. Studies on surgical operations and prognosis of extrahepatic bile duct cancer. *World J Gastroenterol* 1996; **2**: 27-29
- 55 **Hong DF**, Gao M, Bryner U, Cai XJ, Mou YP. Intraoperative endoscopic sphincterotomy for common bile duct stones during laparoscopic cholecystectomy. *World J Gastroenterol* 2000; **6**: 448-450

Edited by Ma JY

• CLINICAL RESEARCH •

Multivariate statistical analysis of clinicopathologic factors influencing survival of patients with bile duct carcinoma

Ping He, Jin-Sen Shi, Wu-Ke Chen, Zuo-Ren Wang, Hong Ren, Hua Li

Ping He, Jin-Sen Shi, Wu-Ke Chen, Zuo-Ren Wang, Hong Ren, Hua Li, Hepato-Biliary Research Lab, the First Hospital of Xi'an Jiaotong University, Xi'an 710061, Shanxi Province, China

Correspondence to: Dr. Ping He, Hepato-Biliary Research Lab, the First Hospital of Xi'an Jiaotong University, Xi'an 710061, Shanxi Province, China. heping99@263.net

Telephone: +86-29-5252981 Ext 2327(O) +86-29-7724595(H)

Received 2001-08-09 **Accepted** 2001-09-12

Abstract

AIM: To evaluate the influence of various clinicopathologic factors on survival of patients with bile duct carcinoma after curative resection.

METHODS: A retrospective analysis was made for 86 cases of bile duct carcinoma treated from January 1981 to September 1995. Fifteen clinicopathologic factors possibly influencing survival were selected. Independent variables were first analyzed by univariate methods. Survival for variable was estimated by the method of Kaplan and Meier. The variables that were statistically significant by univariate analysis were included in a multivariate analysis, which were confirmed using the Cox stepwise proportion hazard model with the help of SPSS 10.0 for Windows software.

RESULTS: The overall cumulative survival rate was 72.6 % at 1 year, 32.4 % at 3 years, and 18.7 % at 5 years. The results of univariate analysis showed that the major significant prognostic factors influencing survival of these patients were histological type of lesion, lymph node metastasis, pancreatic invasion, duodenal invasion, perineural invasion, macroscopic vessel involvement, resected surgical margin and depth of cancer invasion ($P=0.02, 0.02, 0.004, 0.005, 0.01, 0.43, 0.03$ and 0.04). Age, sex, location of tumor, size of tumor, macroscopic type of lesions, hepatic metastasis, and hepatic invasion were not significantly associated with prognosis ($P>0.05$). Pancreatic invasion, perineural invasion and lymph node metastases were the three most important prognostic factors by multivariate analysis using the Cox proportional hazards model.

CONCLUSION: Pancreatic invasion, perineural invasion and lymph node metastases are the most important prognostic factors for bile duct carcinoma after curative resection.

He P, Shi JS, Chen WK, Wang ZR, Ren H, Li H. Multivariate statistical analysis of clinicopathologic factors influencing survival of patients with bile duct carcinoma. *World J Gastroenterol* 2002; 8(5):943-946

INTRODUCTION

With the recent improvement of surgical techniques in hepatobiliary surgery, a curative surgical resection of bile duct

carcinoma can be accomplished with acceptable morbidity and mortality^[1-8]. However, the prognosis for such patients is frustrating, although this tumor is small, grows slowly and metastasizes late^[7-13]. In the present article, an effort is made to evaluate the influence of various clinicopathologic factors on survival of patients with bile duct carcinoma using the Cox proportional hazards model. The results of these analyses were used when surgical treatment was performed for patients with bile duct carcinoma.

MATERIALS AND METHODS

General data

Eighty-six cases of bile duct carcinomas were resected in the Department of Hepatobiliary Surgery, First Hospital of Xi'an Jiaotong University from January 1981 through September 1995. The resected specimens were examined pathologically, and the relation between clinicopathologic findings and patient survival was studied.

Variables

The following clinicopathologic variables were considered for prognosis: age, sex, location of primary tumor, size of the tumor, macroscopic type of lesion (papillary, nodular, infiltrating), histological type of lesion (papillary adenocarcinoma, well-differentiated, moderately differentiated, and poorly differentiated adenocarcinoma, and adenosquamous cell carcinoma), hepatic metastasis, lymph node metastasis, hepatic invasion, pancreatic invasion, duodenal invasion, perineural invasion, vascular invasion, resected margin of the bile duct, depth of cancer invasion (invasion limited to fibromuscular layer, to adventitia and subserosal layer, to and beyond the serosal exposure).

Analysis

Independent variables were first analyzed by univariate methods. Statistical significance of the variables was determined by *t*-test and Chi-square test. Survival for variable was estimated by the method of Kaplan and Meier. The variables with statistical significance in univariate analysis were included in a multivariate analysis, which were further confirmed using the Cox stepwise proportion hazard model with the help of SPSS 10.0 for Windows software.

RESULTS

Clinical findings

Of the 86 surgically treated patients, 51 were male and 35 female aged from 33 to 78 years, averaging 58.6 years. The patients aged from 50 to 78 years made up 66.5 %. Of the lesions, 40 (47 %) were upper bile duct cancer, 13 (15.2 %) were middle bile duct cancer, and 33 (38.8 %) lower bile duct cancer. All the lesions were resected at operation. The type of operation depends on the site and extent of tumor. Bile duct resection was done with cholangiojejunostomy in 17 patients,

bile duct resection in 26 with irregular hepatectomy and choledochoduodenostomy, pancreatoduodenectomy in 42 patients, and hepatopancreatoduodenectomy in one.

Overall survival

The overall cumulative survival rates were 72.6 % at 1 year, 32.4 % at 3 years, and 18.7 % at 5 years. Fifteen clinicopathologic factors were analyzed, and the prognoses were significantly related to 8 of the 15 variables analyzed by univariate method (Table 1).

Table 1 Univariate analysis of the clinicopathologic factors for the survival of 86 patients with bile duct carcinoma

Factors	No. of patients	P value
Sex		0.90
Male	51	
Female	35	
Age (yrs)		0.33
<50	29	
≥50	57	
Location of tumor		0.15
Upper	40	
Middle	13	
Lower	33	
Size of tumor		0.21
<2cm	11	
2 - 4cm	62	
>4cm	13	
Macroscopic type of lesions		0.43
Papillary	17	
Nodular	32	
Infiltrating	37	
Histological type of lesion		0.02
Papillary adenocarcinoma	7	
Well differentiated adenocarcinoma	27	
Moderately differentiated adenocarcinoma	36	
Poorly differentiated adenocarcinoma	14	
Adenosquamous cell carcinoma	2	
Hepatic metastasis		0.88
Present	2	
Absent	84	
Lymph node metastasis		0.02
Present	37	
Absent	49	
Hepatic invasion		0.36
Present	29	
Absent	57	
Pancreatic invasion		0.004
Present	21	
Absent	65	
Duodenal invasion		0.005
Present	14	
Absent	72	
Resected margin of the bile duct		0.03
Present	19	
Absent	67	
Perineural invasion		0.01
Present	65	
Absent	21	
Vascular invasion		0.04
Present	17	
Absent	69	
Depth of cancer invasion		0.04
Invasion limited to fibromuscular layer	9	
Invasion limited to adventitia and subserosal layer	59	
Invasion to and beyond the serosal exposure	18	

The significant variables were lymph node metastasis, duodenal invasion, pancreatic invasion, perineural invasion, vascular invasion, resected margin of the bile duct, histological type of lesion, and depth of cancer invasion. The following factors were not significantly associated with prognosis: age, sex, location of tumor, size of tumor, macroscopic type of lesions, hepatic metastasis, and hepatic invasion.

Multivariate analysis using the Cox proportional hazards model involving the 8 significant factors determined by univariate analysis identified the three prognostic variables (Table 2). They were the pancreatic invasion, the perineural invasion and the lymph node metastasis. Pancreatic invasion was observed in 21(24.4 %) of the 86 patients with bile duct carcinoma. The 5-year survival rates for patients with negative and positive pancreatic invasion were 36 % and 2 %, respectively. A statistically significant difference in survival could be observed between the patient with positive and negative pancreatic invasion ($P=0.005$). Perineural invasion was seen in 75.6 % of the patients with bile duct cancer. Univariate analysis showed a statistically significant difference of survival between the perineural invasion and perineural noninvasion groups ($P=0.01$) (Table 1). The 5-year survival rate was 47 % for patients without perineural invasion, whereas 13 % for the perineural invasion-positive patients. Lymph node metastasis was observed in 37(43 %) of the 86 patients with bile duct carcinoma. The 5-year survival rate was 44 % for patients without lymph node metastasis, and 11 % for patients with lymph node metastasis.

Table 2 Relative values of three prognostic variables derived from Cox stepwise proportional hazards model

Variables	β	SE	Sig(P)	Exp(B)	95%CI for Exp(B)
Pancreatic invasion	0.226	0.084	0.007 ^b	1.254	(1.064-1.479)
Perineural invasion	0.691	0.236	0.012 ^a	2.408	(1.221-4.753)
Lymph node metastasis	0.894	0.489	0.023 ^a	2.762	(1.164-6.557)

^a $P<0.05$, ^b $P<0.01$, vs control

DISCUSSION

With the continuing progress of diagnostic and surgical techniques in biliary surgery, a great deal of biliary cancers can be resected with acceptable morbidity and mortality. However, the 5-year survival was only 10-20 %, and only one-third of the patients could be treated surgically at the time of diagnosis^[14-18]. The local recurrence of bile duct cancer is relatively high even after curative resection of this lesion. Therefore, a proper surgical procedure should be considered for preventing this undesirable outcome. It is important to know what prognostic factors relate to the survival of the patients with bile duct cancer.

In our study, the overall cumulative survival rates for 86 patients with bile duct carcinoma were 72.6 % at 1 year, 32.4 % at 3 years, and 18.7 % at 5 years. This study showed that the prognoses for patients with bile duct cancer were significantly associated with pancreatic invasion, perineural invasion, duodenal invasion, histological type of lesion, lymph node metastasis, vascular invasion, resected margin of the bile duct, and depth of cancer invasion ($P<0.05$). Age, sex, location and size of tumor, macroscopic type of lesions, hepatic metastasis, and hepatic invasion were not significantly associated with survival ($P>0.05$).

Our study also showed that pancreatic invasion, perineural invasion and lymph node metastases were the three most important prognostic factors by multivariate analysis using the Cox proportional hazards model (Table 2). Todoroki *et al* revealed that the primary tumor and tumor node metastasis (TNM) stage were independent predictors of survival using multivariate analysis of 67 patients with bile duct cancer^[19]. Havlik *et al* found that lymph nodes, vascular invasion, advanced tumor stage, positive tumor margins, and p53 mutation were associated with poor survival by multivariate analyses^[20]. Inoue *et al* identified that surgical margin, lymph node metastasis, lymph node dissection, vascular invasion, and left-side location of the main tumor were significant risk factors for overall survival using univariate analysis and confirmed that surgical margin, lymph node metastasis, and vascular invasion were independently significant variables for overall survival using multivariate analysis^[21]. All of them did not mention pancreatic and perineural invasion were prognostic factors for the survival of patients with bile duct carcinoma. Other scholars^[22,23] and we, however, have all observed a significant correlation between perineural invasion and postoperative survival.

Pancreatic invasion is the first prognostic variable (Table 2). Patients with negative pancreatic invasion survived significantly longer than those with positive pancreatic invasion after resection of the lesion. Our findings show that the 5-year survival rate for patients with negative pancreatic invasion was 36 %, whereas it was 2 % for patients with positive pancreatic invasion. This poor prognosis might be due to the fact that when the bile duct cancer invades pancreatic tissue it behaves like a primary pancreatic cancer, and the 5-year survival rate was only around 6 %^[24-28], leading to a worse prognosis. Since bile duct cancer possess biological characteristic of the invasive growth and anatomical location, lower bile duct carcinoma mostly invade pancreas, making that the 5-year survival rate for postoperative patients with lower bile duct carcinoma less than 10 %^[29].

Perineural invasion and lymph node metastasis were also determined to be the independent prognostic factors for survival by the multivariate analysis (Table 2). Some scholars had studied extensively the clinicopathologic significance of perineural invasion, and the results of this study substantiated these findings^[22,23]. In our study, the 5-year survival rate for patients with negative perineural invasion was 47 %, whereas it was 13 % for patients with positive perineural invasion. It is well accepted that lymph node metastasis is an independent prognostic factor for bile duct cancer patients^[19-21,30]. According to our study, the 5-year survival rate was 44 % for patients without lymph node metastasis, and 11 % for patients with lymph node metastasis. As a result of abundant lymphatic, blood vessel, nerve fibers and loose connective tissue around the bile duct, the cancer cells provided with the way of 'jump model' growth. The excessive metastasis fashion results in the inevitable local recrudescence postoperatively. Consequently, we emphasize the need for dissection of autonomic nerve fibers and plexuses around the hepatic and celiac arteries and the portal vein during operation. In addition the lymph nodes, lymphatic vessels, and connective tissues must be dissected for radical operation on bile duct carcinoma.

REFERENCES

- 1 **Huang ZQ**, Zhuo LX, Wang DD, Lu JG, Chen YM. Clinical and laboratory research of hilar cholangiocarcinoma surgical treatment. *Shijie Huaren Xiaohua Zazhi* 2000; **8**: 961-964
- 2 **Gerhards MF**, van Gulik TM, de Wit LT, Obertop H, Gouma DJ. Evaluation of morbidity and mortality after resection for hilar cholangiocarcinoma-a single center experience. *Surgery* 2000; **127**: 395-404
- 3 **Nimura Y**, Kamiya J, Kondo S, Nagino M, Uesaka K, Oda K, Sano T, Yamamoto H, Hayakawa N. Aggressive preoperative management and extended surgery for hilar cholangiocarcinoma: Nagoya experience. *J Hepatobiliary Pancreat Surg* 2000; **7**: 155-162
- 4 **Nagino M**, Kamiya J, Uesaka K, Sano T, Yamamoto H, Hayakawa N, Kanai M, Nimura Y. Complications of hepatectomy for hilar cholangiocarcinoma. *World J Surg* 2001; **25**: 1277-1283
- 5 **Tang D**, Liang LJ, Huang JF. The preoperative assessment and surgical treatment of hilar cholangiocarcinoma: a study of 86 cases. *Zhonghua Putong Waikexue* 2001; **16**: 517-519
- 6 **Doglietto GB**, Alfieri S, Pacelli F, Mutignani M, Costamagna G, Carriero C, Di Giorgio A, Papa V. Extrahepatic bile duct carcinoma: A western experience with 118 consecutive patients. *Hepatogastroenterology* 2000; **47**: 349-354
- 7 **Yoshimi F**, Asato Y, Amemiya R, Shioyama Y, Itabashi M. Comparison between pancreatoduodenectomy and hepatopancreatoduodenectomy for bile duct cancer. *Hepatogastroenterology* 2001; **48**: 994-998
- 8 **Launois B**, Reding R, Lebeau G, Buard JL. Surgery for hilar cholangiocarcinoma: French experience in a collective survey of 552 extrahepatic bile duct cancers. *J Hepatobiliary Pancreat Surg* 2000; **7**: 128-134
- 9 **Blom D**, Schwartz SI. Surgical treatment and outcomes in carcinoma of the extrahepatic bile ducts: the University of Rochester experience. *Arch Surg* 2001; **136**: 209-215
- 10 **Mena FJ**, Velicia R, Valbuena MC, Gonzalez JM, Caropaton A, Perez-Miranda M, Bellido J. Carcinoma of the extrahepatic biliary tree: analysis of 15 cases. *Rev Esp Enferm Dig* 1999; **91**: 297-304
- 11 **Ahrendt SA**, Nakeeb A, Pitt HA. Cholangiocarcinoma. *Clin Liver Dis* 2001; **5**: 191-218
- 12 **Blanchet MC**, Ducerf C, Benoit L, Gerard JP, Baulieux J. Proximal bile duct cholangiocarcinomas. *Ann Chir* 2000; **125**: 825-831
- 13 **Gerhards MF**, van Gulik TM, de Wit LT, Obertop H, Gouma DJ. Evaluation of morbidity and mortality after resection for hilar cholangiocarcinoma-a single center experience. *Surgery* 2000; **127**: 395-404
- 14 **Launois B**, Terblanche J, Lakehal M, Catheline JM, Bardaxoglou E, Landen S, Campion JP, Sutherland F, Meunier B. Proximal bile duct cancer: high resectability rate and 5-year survival. *Ann Surg* 1999; **230**: 266-275
- 15 **Blom D**, Schwartz SI. Surgical treatment and outcomes in carcinoma of the extrahepatic bile ducts: the University of Rochester experience. *Arch Surg* 2001; **136**: 209-215
- 16 **Reed DN Jr**, Vitale GC, Martin R, Bas H, Wieman TJ, Larson GM, Edwards M, McMasters K. Bile duct carcinoma: trends in treatment in the nineties. *Am Surg* 2000; **66**: 711-715
- 17 **Lillemoe KD**, Cameron JL. Surgery for hilar cholangiocarcinoma: the Johns Hopkins approach. *J Hepatobiliary Pancreat Surg* 2000; **7**: 115-121
- 18 **Burke EC**, Jarnagin WR, Hochwald SN, Pisters PW, Fong Y, Blumgart LH. Hilar Cholangiocarcinoma: patterns of spread, the importance of hepatic resection for curative operation, and a presurgical clinical staging system. *Ann Surg* 1998; **228**: 385-394
- 19 **Todoroki T**, Kawamoto T, Koike N, Fukao K, Shoda J, Takahashi H. Treatment strategy for patients with middle and lower third bile duct cancer. *Br J Surg* 2001; **88**: 364-370
- 20 **Havlik R**, Sbisá E, Tullo A, Kelly MD, Mitry RR, Jiao LR, Mansour MR, Honda K, Habib NA. Results of resection for hilar cholangiocarcinoma with analysis of prognostic factors. *Hepatogastroenterology* 2000; **47**: 927-931

- 21 **Inoue K**, Makuuchi M, Takayama T, Torzilli G, Yamamoto J, Shimada K, Kosuge T, Yamasaki S, Konishi M, Kinoshita T, Miyagawa S, Kawasaki S. Long-term survival and prognostic factors in the surgical treatment of mass-forming type cholangiocarcinoma. *Surgery* 2000; **127**: 498-505
- 22 **Bortolasi L**, Burgart LJ, Tsiotos GG, Luque-De Leon E, Sarr MG. Adenocarcinoma of the distal bile duct. A clinico-pathologic outcome analysis after curative resection. *Dig Surg* 2000; **17**: 36-41
- 23 **Wang DD**, Huang ZQ, Wang JX, Wang YS, Chen LZ. Relationship between perineural invasion and the coupling expression of DPC4 with NCAM in cholangiocarcinoma. *Zhonghua Shiyan Wake Zazhi* 2000; **17**: 12-13
- 24 **Lu XH**. Development of diagnosis and treatment in pancreatic and bile duct carcinoma. *Zhonghua Xiaohua Zazhi* 1999 ; **19**: 8-10
- 25 **Cooperman AM**, Kini S, Snady H, Bruckner H, Chamberlain RS. Current surgical therapy for carcinoma of the pancreas. *J Clin Gastroenterol* 2000; **31**: 107-113
- 26 **Ginsberg GG**. New developments in pancreatic cancer. *Semin Gastrointest Dis* 2000; **11**: 162-167
- 27 **Meyer W**, Jurowich C, Reichel M, Steinhäuser B, Wunsch PH, Gebhardt C. Pathomorphological and histological prognostic factors in curatively resected ductal adenocarcinoma of the pancreas. *Surg Today* 2000; **30**: 582-587
- 28 **Shankar A**, Russell RCG. Recent advances in the surgical treatment of pancreatic cancer. *World J Gastroenterol* 2001; **7**: 622-626
- 29 **Ouyang YZ**, Sun WB. The diagnosis and treatment of lower bile duct carcinoma: result of 85 cases. *Zhonghua Putong Waiké Zazhi* 2000; **15**: 555-557
- 30 **Kitagawa Y**, Nagino M, Kamiya J, Uesaka K, Sano T, Yamamoto H, Hayakawa N, Nimura Y. Lymph node metastasis from hilar cholangiocarcinoma: audit of 110 patients who underwent regional and paraaortic node dissection. *Ann Surg* 2001; **233**: 385-392

Edited by Ma JY

• CLINICAL RESEARCH •

Abdominal pain among children re-evaluation of a diagnostic algorithm

Hong Zhou, Yi-Chen Chen, Jin-Zhe Zhang

Hong Zhou, Yi-Chen Chen, Jin-Zhe Zhang, Department of Pediatric Surgery, Beijing Children's Hospital, Affiliated to Capital University of Medical Sciences, Beijing 100045, China

Correspondence to: Dr. Hong Zhou, Department of Pediatric Surgery, Beijing Children's Hospital, 56 Nan Lishi Road, Beijing 100045, China. hzhou@163bj.com

Telephone: +86-10-68028401 **Fax:** +86-10-68011503

Received 2001-08-08 **Accepted** 2001-08-28

Abstract

AIM: To re-evaluate the algorithm that has been used for over 40 years for diagnosis of acute abdominal pain among children.

METHODS: Among the 937 cases admitted to the surgical emergency ward in 2000, 656 cases of acute appendicitis were studied to evaluate the usefulness of the present algorithm for its calculated accuracy, false positive and false negative rates, the sensitivity and specificity in the instant diagnosis of various types of acute appendicitis in different age groups. The algorithm used was established in 1958 and revised for this study in 1999. It includes a 3-step analysis of clinical presentations, i.e.: firstly, a diagnosis of surgical pain by definite organic abdominal signs; then a diagnosis of the subgroup of surgical condition by special signs; and finally the diagnosis of the present disease by specific signs. A footnote describes a "comparative technique" of abdominal examination in non-cooperative children.

RESULTS: The general accuracy of diagnosis was 92.8 %, overall mortality 0.1 % among 973 cases of abdominal pain in 2000. 373 attending surgeons and 241 residents including trainees joined the diagnosis and treatment with no remarkable difference in the results. The incidence of acute appendicitis, 656 in 973 cases, was 67.4 % representing the majority of abdominal pain. In the series of 656 cases, the accuracy of diagnosis of acute appendicitis was 93.6 %, false positive 6.4 %, false negative 0.9 %, sensitivity at first visit 82.7 %, specificity for appendicitis 98.0 %, no death or documentary complication.

CONCLUSION: The present algorithm used for diagnosis of acute abdominal pain is effective and preferable in reducing misdiagnosis and maltreatment at emergency. The use of some modern technology should be further explored.

Zhou H, Chen YC, Zhang JZ. Abdominal pain among children re-evaluation of a diagnostic algorithm. *World J Gastroenterol* 2002; 8(5): 947-951

INTRODUCTION

In recent literature, the incidence of perforated appendicitis seems to be rising, and most of the late cases are due to

misdiagnosis^[1-3]. In China, we have not yet had the similar poor impression^[4]. For many years, we've achieved good results in the management of acute abdomen in pediatric surgery^[5]. The best results as reported by Beijing Children's Hospital (BCH) are: no death in 20 years in 10 000 consecutive cases of acute appendicitis^[6], no death in 3 years in 100 consecutive cases of strangulated intestinal obstruction including all those cases that came in shock state^[7], and over 90 % of cases of early intussusception that were reduced without emergency surgery even in county hospitals^[8,9]. In 1958, a systematical analysis method, the algorithm, for diagnosis of acute abdominal pain among children was published^[10], and popularized in many places of China. It has been generally followed, with timely revisions, for over 40 years. However, with the rapid progress of the modern diagnostic tools in recent years, it is necessary to have a re-evaluation of the above mentioned diagnostic algorithm for abdominal pain among children and try to find out some reasonable modern technology to make it further improved and popularized.

MATERIALS AND METHODS

This is a prospective study of the diagnostic algorithm, which was established in 1958. With the improvement of medical sciences, and changes in the incidence of common diseases in pediatric surgical emergency clinic, the algorithm has been revised many times. Generally, for over 40 years, it has been proved helpful in the diagnosis of acute abdomen of children. For this study, the algorithm was revised again in 1999 as shown in Table 1.

Table 1 Algorithm for diagnosis of abdominal pain

Abdominal Pain		
Acute abdomen (long time pain definite signs)	Non-acute abdomen (short pain no definite sign)	
1 Focal inflammation	2 Intestinal obstruction	1 Primary enterospasm (allergic, idiopathic)
(1) local tenderness (appendicitis, etc.)	(1) intestinal pattern (adhesive obstruction)	(1) weaning colic
(2) tender mass (torsion ovarian cyst)	(2) movable mass (intussusception)	(2) school-boy colic
3 generalized peritonitis (full and silent abdomen)	2 secondary enterospasm (organic, non-acute)	
(1) spreading peritonitis (inflamed organ)	(2) gangrenous peritonitis (strangulation)	(1) chronic G-I ulcers (2) pancreaticobiliary colic
(3) perforating peritonitis (peptic ulcer, typhoid)	(4) primary peritonitis (bacteremia, vaginitis)	(3) chronic gastritis (4) cerebrospinal colic (5) hemo-vascular disease (6) metabolic disease (7) auto-immune disorder (8) intoxication

*Footnote: (1) "comparative technique" of abdominal palpation, watching different reaction of the child on different part of abdomen. (2) "dynamic comparison" of clinical presentation, is today better or worse than yesterday?

It consists of a 3-step analysis of clinical presentations. The first step is to make the diagnosis of a surgical abdomen by finding definite abdominal signs indicating organic lesion, i.e. tenderness, spasm, intestinal pattern and mass. The second step is to make the diagnosis of the subgroup of surgical abdomen, namely organ inflammation, intestinal obstruction and generalized peritonitis by their special signs respectively. The third step is to make the diagnosis of the present disease, like acute appendicitis or intussusception by their specific cardinal signs. In the footnote, the “comparative technique” of abdominal examination for non-cooperative children and its “comparative dynamic evaluation” are described.

Strictly following the above algorithm, 973 cases of acute abdominal pain admitted to the surgical emergency ward of BCH in 2000 (Table 2) were reviewed. The overall rate of misdiagnosis and a general status of the diagnosis and result of treatment were studied (Table 3). In order to make a differential evaluation, 614 cases of acute appendicitis which is the representative disease occupying 68.0 % in 2000 (Table 4) were investigated in detail. The accuracy of diagnosis, the false positives, false negatives, the sensitivity and the specificity of the use of the diagnostic algorithm were calculated accordingly. Different-level doctors concerned in making diagnosis were also recorded.

Table 2 Came with abdominal pain to emergency ward, BCH, 2000

Category	n	%
Organ inflammation ^a	637	65.5
Intestinal obstruction ^b	160	16.5
Traumatic abdomen	28	2.9
GI hemorrhage	38	3.9
Primary peritonitis	5	0.5
Perforation peritonitis	8	0.8
Tumor twisting or rupturing	14	1.4
Torsion testes or appendage	8	0.8
Other organic lesion	5	0.5
Non organic pain	70	7.2
Total	973	100.0

^aIncluded 614 appendicitis ^bIncluded 57 intussusception

Table 3 Outcome of 973 cases of acute abdominal pain admitted to surgical emergency ward in 2000

Outcome	n	%
Cure	894	91.9
Improved ^a	67	6.9
Unimproved ^a	11	1.1
Died	1	0.1
Total	973	100.0

^aMost are chronic traumatic, inflammatory, and malignancy cases with acute pain

Table 4 Number of operated patients of common surgical abdomen, 2000

Disease	n	%
Acute appendicitis	614	68.0
Intussusception ^a	57	6.3
Incarcerated hernia	45	5.0
Traumatic abdomen	28	3.1
Adhesive obstruction	25	2.8
Fecalith obstruction	19	2.1
Miscellaneous	115	12.7
Total	903	100.0

^aThe other 90 % of early cases cured in OPD by rectal insufflation

RESULTS

Among 973 cases in 2000, the overall mortality was 0.1 %. It was a boy aged 6 yr, who died of strangulation perforation of stomach in uncontrolled Crohn's disease. There was still no death of acute appendicitis. The general accuracy of diagnosis of acute abdomen was 94.5 %. Concerning the 656 cases of acute appendicitis in 2000, the following figures were calculated: Diagnosis at discharge (614)/Diagnosis on admission (656)=93.6 % overall accuracy; Non-surgical abdomen (42)/Appendicitis admitted (656)=6.4 % false positive at admission; Admission after 2nd visit (196)/Appendicitis admitted (656)=29.9 % false negative at the 1st visit, mostly delayed in other hospital due to transfer; Second visits in BCH surgery (6)/Appendicitis admitted (656)=0.9 % false negative BCH; Admitted by 1st visit (258)/Appendicitis in 24 h (312)=82.7 % sensitivity (It means, 82.7 % of early appendicitis within 24 h can be diagnosed at first visit); Proved appendicitis (542)/Cases operated (553)=98.0 % specificity (It means, 98.0 % of appendicitis can be differentiated from other surgical conditions); Ratio between cases diagnosed at first visit by surgeons of high level and low level=373:241 cases (in BCH, surgeons under 3 years of training are not allowed to manage on-call emergency); Acute appendicitis (656)/Abdominal pain (973)=67.4 % incidence at admission. There was no mortality, no documentary complication, but 5 perforated cases in moderate postoperative morbidity. Pathology of 614 case of acute appendicitis in 2000 is shown in Table 5.

Table 5 Pathology of 614 cases of operated appendicitis (2000)

Pathology	Simple	Suppurative	Gangrenous	Perforative	Recurrent	Abscess	Infiltrative	Total
Cases	166	254	7	103	38	42 ^a	4	614
%	27.0	41.4	1.1	16.8	6.2	6.8	0.7	100.0

^aSimple drainage only

DISCUSSION

Theoretic basis of the diagnostic algorithm

Because the basic pathology of surgical conditions must be an organic lesion inside the abdomen, the chief symptoms and signs must be persistent and definite^[11]. Acute pain shorter than

6 hours is hard to rule out from the more common abdominal pain due to functional intestinal spasm unless some specific abdominal signs are found^[12,13]. By the term “definite”, it means definite pain, definite location and definite area involved. Therefore, the child has to be examined many times in an appropriate period of time. In BCH, people usually do the 1st time examination at the first visit, the 2nd examination after laboratory tests, and the 3rd repeat of examination before sending the patient to the ward or back home. Full agreement of the positive findings in the 3 examinations will make the final diagnosis. If negative sign appears in any one examination, further observation and re-examination should be made. The common positive abdominal signs indicating surgical condition are local tenderness, muscular spasm, palpable intestinal pattern and mass. By a soft flat abdomen without the above mentioned signs, people can rule out acute surgical abdomen.

According to common presentations of surgical abdomen, it can be classified into 3 sub-groups: (1) Definite local tenderness and spasm usually indicate a focal inflammation. (2) A palpable distended intestinal loop or a movable solid sausage mass indicates intestinal obstruction. (3) A resistant and silent abdomen indicates generalized peritonitis. These practically cover up all common diseases seen in children. (1) In the sub-group of focal inflammation, the diagnosis depends on the location of tenderness, e.g. in RLQ of abdomen which is usually acute appendicitis; pelvic rectal tenderness with mass is usually torsion of ovarian tumor; flank tenderness is usually renal colic or perinephretic abscess; (2) In the sub-group of intestinal obstruction, a distended intestinal pattern indicates extraluminal obstruction of intestine, e.g. adhesional strangulation, or a solid mass usually indicates intraluminal obstruction, e.g. intussusception or ascaris bezoar; (3) In the sub-group of generalized peritonitis: a marked tender point indicates the focus of spreading peritonitis, e.g. perforated appendicitis; a palpable loop or mass indicates gangrenous peritonitis, e.g. strangulated intestinal obstruction. Pneumoperitoneum by percussion or X-ray indicates perforating peritonitis, e.g. peptic ulcer perforation; thin pus by abdominal puncture aspiration indicates most probably primary peritonitis.

After 3-step analysis, the final diagnosis of a surgical disease is usually made. And then, a comparison between the cardinal signs of the disease and the signs found in this particular patient should be made as a feed-back checking. Any disagreement must be carefully investigated or the diagnosis be reconsidered otherwise.

Method of abdominal assessment in non-cooperative children

Examination of abdomen needs cooperation of the patient. Answering tenderness must be accurate. A crying kid always makes the palpation confused. Even the school-boy may not be able to give an accurate answer to abdominal examination. So the surgeon has to try all means to search for cooperation of a bigger child and to evaluate the findings carefully by repeated examinations. At the same time, he has to observe every action of the kid carefully. Quick squatting or jumping up and down from the examination table without hesitation may rule out abdominal tenderness^[14]. For examination of crying kids, a 3-step “comparative technique” of abdominal palpation has been practiced satisfactory in BCH. (1) The 1st step: the mother stands by the head to beguile the baby and hold both its hands. The surgeon stands by the right side of the examination table and palpates the abdomen from LLQ, LUQ, RUQ to RLQ subsequently. Carefully watching the reaction of baby, a high pitch crying might be the answer of tenderness. (2) The 2nd step: let baby’s left hand free, surgeon presses the abdomen with two hands on RLQ and LLQ. Baby naturally

uses his free hand to push away the hand in the tender point, e.g. RLQ. (3) The 3rd step: surgeon makes a finger press at the tender area, e.g. McBurney’s point. Baby will try all means to get rid of the finger. By this time, the surgeon may press all other parts of abdomen, to make sure no tenderness beside McBurney’s point or elsewhere.

By the same way, surgeon’s two hands press on both sides of the baby’s abdomen. After several cryings, people may find the hand on left side having pressed much deeper than that on the right side if there is spasm in RLQ of abdomen.

In difficult cases, a dose of short action sedative can be used, e.g. 10 % choral hydrate by dose 1 ml/mos of age. This is limited only to the last examination. Under sedation, deep palpation in six parts (4 quadrants, periumbilical and pelvis) can be made. In order to feel the deep structures in abdomen, the abdominal aorta or other landmarks of posterior abdominal wall should be reached. In rectal pelvic bimanual examination, infiltration or abscess of peri-appendiceal structure can be felt in right iliac fossa and incarcerated inguinal hernia can be felt at the middle along the inguinal ligament from interior by the endo-rectal examination finger^[15,16]. It must be kept in mind that the pathology of an acute abdomen is continuously changing. Therefore dynamic comparative observation and evaluation are essential. For making an instant diagnosis in emergency clinic, the information from mother’s impression about baby’s appetite and general activity, whether today is better or worse than yesterday, will be very helpful in making decision of emergency surgery^[17].

Supplementary diagnostic techniques (Table 5)

By quick plane X-ray film of erect position, especially in suspected intestinal obstruction, preferably with low pressure barium enema, perforating peritonitis, intestinal obstruction and intussusception can be well demonstrated (Figure 1, 2)^[18]. By ultrasound, acute appendicitis and abscess, intussusception, peritoneal fluid, and ovarian cyst or tumor, and perinephretic lesions may be demonstrated (Figure 3, 4)^[19-32]. By paracentesis, the abdominal puncture fluid may tell the peritonitis, strangulation of intestine, perforation of intestine or gall bladder^[33,34]. Bloody aspirate always calls for an immediate surgical exploration. In case of fine needle puncture getting into intestine under pressure, don’t hurry, keeping on aspiration until negative pressure will prevent intestinal leakage after withdrawal of needle. CT, MRI, Scintiscanning and other fantastic modern tools are used only occasionally^[35-38]. But dramatic improvement of the diagnosis of acute abdomen in children must depend on further exploration for the use of high technology. e.g. laparoscopy and portable ultrasound computerized^[39-44].

Table 6 Confirmatory diagnostic method used in 973 admissions, 2000

Diagnostic method	n	%
Physical exam	630	64.7
Paracentesis ^a	58	6.0
Imaging	285	29.3
Plane film	93	
Rectal insufflation ^b	48	
Barium enema	8	
Barium meal ^a	33	
Sonography	90	
Tc ^{99m} scintiscan ^a	13	
Total	973	100.0

^aAfter admission ^bReduction failed cases in O.P.D.



Figure 1 Small empty colon

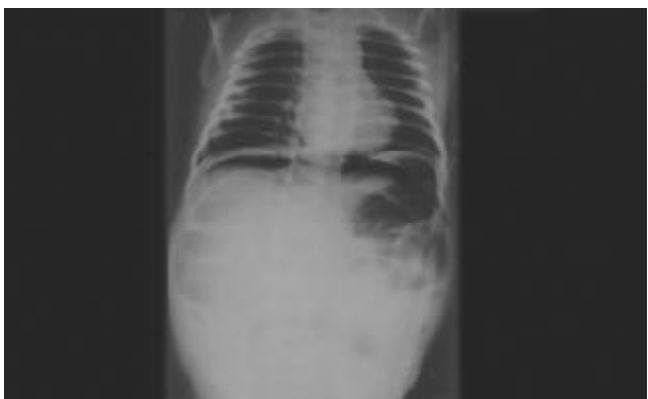


Figure 2 Pneumoperitoneum



Figure 3 Appendiceal abscess

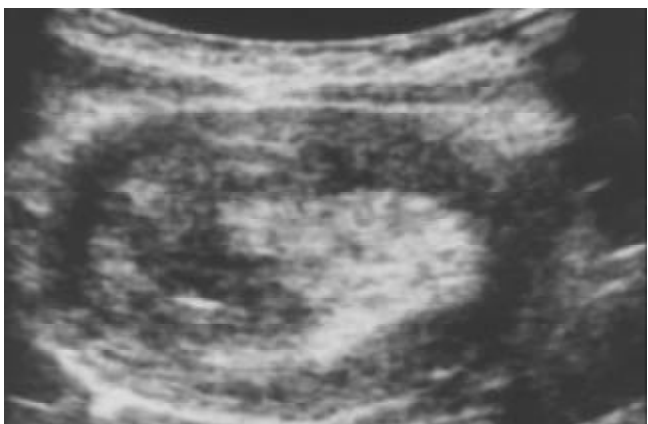


Figure 4 Intussusception-target sign

We conclude that the algorithm has been used and accepted for more than 40 years in thousands of patients by hundreds of surgeons of different levels. It proves helpful in handling acute abdominal pain among children. The prospective study of appendicitis in 2000, has proved its accuracy, false positive, false negative, specificity and sensitivity, all being of acceptable value. However, there are still doubtful cases needing observation, especially in cases with 6 hrs duration without definite signs, partial intestinal obstruction without toxic reactions, and late appendicitis may not need operation. Besides, in the other half of the algorithm (Table1), non-surgical abdominal pain, it includes a large number of diseases needing systemic examination and investigation. However none of them need immediate surgical operation. The most common "school-boy colic" (or primary intestinal spasm) characterized by short pain in attacks, normal appetite and activities in intervals, repeated attacks for months without impairment of nutrition or growth occupies about 60 % of school-boy abdominal pain. Keep this in mind, and it may reduce the false positive diagnosis of acute abdomen.

PROSPECTIVE TECHNOLOGY

(1) Since this algorithm is simple and regular, it can be put into a software of computer to up-grade it into high technology; (2) Portable ultrasonography machine to be used on emergencies examination table could take place of manual palpation of abdomen for uncooperative kids, making the examination more objective; (3) Further improvement of laparoscopy, exploratory laparotomy in acute abdominal pain may be unnecessary.

REFERENCES

- 1 **Krasna IH.** Abdominal pain and appendicitis: Is there a difference in referrals between HMO pediatricians and private pediatricians. *J Pediatr Surg* 2000; **35**: 1084-1086
- 2 **Rothrock SG,** Pagane J. Acute appendicitis in children: emergency department diagnosis and management. *Ann Emerg Med* 2000; **36**: 39-51
- 3 **Gofrit ON,** Abu-Dalu K. Perforated appendicitis in the child: contemporary experience. *Isr Med Assoc J* 2001; **3**: 262-265
- 4 **Zhang JZ.** Digestive surgery in Chinese children. *Shijie Huaren Xiaohua Zazhi* 2000; **8**: 489-490
- 5 **Zhang JZ.** Treatment of acute appendicitis in children with combined traditional Chinese and western medicine. *Zhonghua Yixue Zazhi* 1977; **3**: 373-378
- 6 **Zhang JZ,** Xie XY. A 20-year review of acute appendicitis in children. *Zhonghua Xiaoer Waike Zazhi* 1987; **8**: 149-151
- 7 **Zhou H,** Zhang JZ. Enterectomy, exteriorization of intestine and delayed entero-anastomosis for intestinal necrosis in children. *Zhonghua Xiaoer Waike Zazhi* 1992; **13**: 323-324
- 8 **Guo JZ,** Ma XY, Zhou QH. Results of air pressure enema reduction of intussusception: 6,396 cases in 13 years. *J Pediatr Surg* 1986; **21**: 1201-1203
- 9 **Zhou H,** Zhang JZ. Rectal insufflation reduction of intussusception: further improvement on the basis of spasm theory. *Asian J Surg* 1999; **22**: 136-141
- 10 **Zhang JZ.** Diagnosis and treatment of acute abdomen in pediatric surgery. *Zhonghua Waike Zazhi* 1958; **6**: 890-894
- 11 **Wade S,** Kilgour T. Extracts from "clinical evidence": infantile colic. *BMJ* 2001; **25**: 437-440
- 12 **Rasquin-Weber A,** Hyman PE, Cucchiara S, Fleisher DR, Hyams JS, Milla PJ, Staiano A. Childhood functional gastrointestinal disorders. *Gut* 1999; **45**: 1160-1168
- 13 **Riddell A,** Carr SB. Recurrent abdominal pain in

- childhood. *Practitioner* 2000; **244**: 346-350
- 14 **Irish MS**, Pearl PH, Caty MG, Glick PL. The approach to common abdominal diagnoses in infants and children. *Pediatr Clin Nor Amer* 1998; **45**: 729-771
 - 15 **Scholer SJ**, Pituch K, Orr DP, Dittus RS. Use of the rectal examination on children with acute abdominal pain. *Clin Pediatr* 1998; **37**: 311-316
 - 16 **Jesudason EC**, Walker J. Rectal examination in paediatric surgical practice. *Brit J Surg* 1999; **86**: 376-378
 - 17 **Bachoo P**, Mahomed AA, Ninan GK, Youngson GG. Acute appendicitis: the continuing role for observation. *Pediatr Surg Int* 2001; **17**: 125-128
 - 18 **Suri S**, Gupta S, Sudhakar PJ, Venkataramu NK, Sood B, Wig JD. Comparative evaluation of plain films, ultrasound and CT in the diagnosis of intestinal obstruction. *Acta Radiol* 1999; **40**: 422-428
 - 19 **Axelrod DA**, Sonnad SS, Hirschl RB. An economic evaluation of sonographic examination of children with suspected appendicitis. *J Pediatr Surg* 2000; **35**: 1236-1241
 - 20 **Emil S**, Mikhail P, Laberge JM, Flageole H, Nguyen LT, Shaw KS, Baican L, Oudjhane K. Clinical versus sonographic evaluation of acute appendicitis in children: a comparison of patient characteristics and outcomes. *J Pediatr Surg* 2001; **36**: 780-783
 - 21 **Dilley A**, Wesson D, Munden M, Hicks J, Brandt M, Minifee P, Nuchtern J. The impact of ultrasound examinations on the management of children with suspected appendicitis: a 3-year analysis. *J Pediatr Surg* 2001; **36**: 303-308
 - 22 **Smoljanic Z**, Zivic G, Krstic Z, Milanovic D, Vukanic D, Lukac R. Intestinal intussusception in children. Ultrasonic diagnosis. *Srp Arh Celok Lek* 2000; **128**: 259-261
 - 23 **Dugougeat F**, Navarro O, Daneman A. The role of sonography in children with abdominal pain after recent successful reduction of intussusception. *Pediatr Radiol* 2001; **30**: 654
 - 24 **Tiao MM**, Wan YL, Ng SH, Ko SF, Lee TY, Chen MC, Shieh CS, Chuang JH. Sonographic features of small-bowel intussusception in pediatric patients. *Acad Emerg Med* 2001; **8**: 368-373
 - 25 **Sirlin CB**, Casola G, Brown MA, Patel N, Bendavid EJ, Hoyt DB. Quantification of fluid on screening ultrasonography for blunt abdominal trauma: a simple scoring system to predict severity of injury. *J Ultrasound Med* 2001; **20**: 359-364
 - 26 **Ma OJ**, Kefer MP, Stevison KF, Mateer JR. Operative versus nonoperative management of blunt abdominal trauma: Role of ultrasound-measured intraperitoneal fluid levels. *Am J Emerg Med* 2001; **19**: 284-286
 - 27 **Rathaus V**, Zissin R, Werner M, Erez I, Shapiro M, Grunebaum M, Konen O. Minimal pelvic fluid in blunt abdominal trauma in children: the significance of this sonographic finding. *J Pediatr Surg* 2001; **36**: 1387-1389
 - 28 **Kokoska ER**, Keller MS, Weber TR. Acute ovarian torsion in children. *Am J Surg* 2000; **180**: 462-465
 - 29 **Chiaramonte C**, Piscopo A, Cataliotti F. Ovarian cysts in newborns. *Pediatr Surg Int* 2001; **17**: 171-174
 - 30 **Yip WC**, Ho TF, Yip YY, Chan KY. Value of abdominal sonography in the assessment of children with abdominal pain. *J Clin Ultrasound* 1998; **26**: 397-400
 - 31 **Puylaert JB**. Ultrasound of acute GI tract conditions. *Eur Radiol* 2001; **11**: 1867-1877
 - 32 **Li YM**, Zhao HB, Cui L, Jin P, Xia HW. An analysis of sonographic examination in gastrointestinal perforation diseases. *Shijie Huaren Xiaohua Zazhi* 1998; **6**: 446
 - 33 **Haecker FM**, Berger D, Schumacher U, Friess D, Schweizer P. Peritonitis in childhood: aspects of pathogenesis and therapy. *Pediatr Surg Int* 2000; **16**: 182-188
 - 34 **Zhou H**, Cheng W. Primary peritonitis in children. *Ann Coll Surg HK* 2000; **4**: 53-56
 - 35 **John SD**. Trends in pediatric emergency imaging. *Radiol Clin North Am* 1999; **37**: 995-1034
 - 36 **Klein MD**, Rabbani AB, Rood KD, Durham T, Rosenberg NM, Bahr MJ, Thomas RL, Langenburg SE, Kuhns LR. Three quantitative approaches to the diagnosis of abdominal pain in children: practical applications of decision theory. *J pediatr Surg* 2001; **36**: 1375-1380
 - 37 **Sivit CJ**, Siegel MJ, Applegate KE, Newman KD. When appendicitis is suspected in children. *Radiographics* 2001; **21**: 247-262
 - 38 **Turan C**, Tutus A, Ozokutan BH, Yolcu T, Kose O, Kayseri MK. The evaluation of technetium 99m-citrate scintigraphy in children with suspected appendicitis. *J Pediatr Surg* 1999; **34**: 1272-1275
 - 39 **Sun XL**, Xu HB. Comparative study among open, laparoscopic and video-assisted appendectomies. *Shijie Huaren Xiaohua Zazhi* 1998; **6**: 710-711
 - 40 **Xu HB**. Problems and strategies of laparoscopic surgery. *Shijie Huaren Xiaohua Zazhi* 1999; **7**: 1059-1060
 - 41 **Liu GL**. Advancement of laparoscopic surgery in China. *Shijie Huaren Xiaohua Zazhi* 1999; **7**: 260-261
 - 42 **Zou YT**. Application of laparoscopy in diagnosis and treatment of abdominal injuries. *Shijie Huaren Xiaohua Zazhi* 2000; **8**: 1261-1262
 - 43 **Huang ZH**, Qian WF, Jiang ZS. Application of laparoscopy in gastrointestinal surgery. *Shijie Huaren Xiaohua Zazhi* 2000; **8**: 1263-1265
 - 44 **Zhou H**, Zhang JZ, Jia LQ. The use of portable B-mode ultrasound in a acute abdomen among children. *Zhonghua Xiaer Waike Zazhi* 1995; **16**: 216-217

Edited by Hu DK

• CLINICAL RESEARCH •

Study on the function of pharynx & upper esophageal sphincter in globus hystericus

Jing Sun, Bin Xu, Yao-Zong Yuan, Jia-Yu Xu

Jing Sun, Bin Xu, Yao-Zong Yuan, Jia-Yu Xu, Department of Gastroenterology, Ruijin hospital, Shanghai Second Medical University, Shanghai 200025, China

Correspondence to: Yao-Zong Yuan, Department of Gastroenterology, Ruijin hospital, Shanghai Second Medical University, Shanghai 200025, China. yyz28@hotmail.com

Telephone: +86-21-64370045-665242 **Fax:** +86-21-64150773

Received 2001-12-20 **Accepted** 2002-02-19

Abstract

AIM: Globus pharyngeus is not an uncommon symptom. Presently, its unclear dated pathophysiology remains unclear and the disease can not be evaluated correctly with routine diagnostic methods. The objective of this study is to establish the normal values of pharyngeal and UES pressure, pharyngeal transit time in healthy volunteers and to compare the differences between healthy volunteers and patients with globus pharyngeus.

METHODS: Twenty-four healthy volunteers and thirty-two patients clinically diagnosed as globus pharyngeus entered the study. Pressures of pharynx and UES were measured. Pharyngeal transit time was measured by videofluoroscopic procedure.

RESULTS: Normal pressure of pharynx, and normal resting pressure of UES were 157.81 ± 63.86 mmHg and 68.33 ± 37.56 mmHg, respectively. The corresponding values in the patients were 175.50 ± 93.47 mmHg and 71.38 ± 41.42 mmHg. The pharyngeal transit time was 1.44 ± 0.30 s in normal control group, among them there were 4 cases with stasis of barium in the valleculae and one in the piriform sinus. No laryngeal penetration or aspiration was found. In the patient group, the pharyngeal transit time was 1.37 ± 0.41 s, among them there were 6 cases with stasis of barium in the valleculae and 5 in the piriform sinus. 9 cases had laryngeal penetration and 2 had aspiration. There were no statistical differences of pressures of pharynx, UES and the pharyngeal transit time between the two groups. But there was an association between laryngeal penetration and globus pharyngeus.

CONCLUSION: Radiographic examination of the pharynx show specific findings of pharyngeal dysfunction in patients with globus pharyngeus. UES pressure is normal in most patients. Hence, we find no role for UES hypertonicity as an etiologic factor in globus pharyngeus.

Sun J, Xu B, Yuan YZ, XU JY. Study on the function of pharynx & upper esophageal sphincter in globus hystericus. *World J Gastroenterol* 2002; 8(5):952-955

INTRODUCTION

Globus sensation (globus pharyngitis, globus pharyngeus) is best described as a constant sensation of something stuck or a lump or tightness in the throat. Typically, a lump, or crumb-like (foreign body) sensation, a constriction or choking^[1-3] is complained. Nearly half of the general population has had intermittent symptoms resembling globus^[4-6]. More severe and distressing symptoms comprise up to 4 % of referrals to otolaryngological specialists^[4]. In addition to emotional stress, mood, and personality disorders, it has been attributed to a high upper esophageal sphincter (UES) resting pressure, gastroesophageal reflux (GER)^[7,8], esophageal dysmotility, hiatal hernia, kinematic pharyngeal transit time and local anatomic abnormalities^[9-16]. Although the associations are diverse and broadly investigated, the etiology of globus still remains unclear^[4].

The aim of our study was to investigate the association of globus pharyngeus with UES resting pressure and kinematic pharyngeal transit time.

MATERIALS AND METHODS

Study subject

Two groups of persons were studied: globus pharyngeus patients and the control group. The globus pharyngeus group comprised thirty-two consecutive patients presenting themselves to the otolaryngology and gastroenterology departments with predominant symptom of globus pharyngeus with no abnormality on examination of neck, larynx, or pharynx between December 2000 and March 2001. The diagnostic criteria of the globus sensation is in accordance with Rome II criteria: At least 12 weeks, which need not be consecutive, in the preceding 12 months of: (1) The persistent or intermittent sensation of a lump or foreign body in the throat; (2) Occurrence of the sensation between meals; (3) Absence of pathologic gastroesophageal reflux, achalasia, or other motility disorder with a recognized pathologic basis as scleroderma of the esophagus. The control group consisted of twenty-four healthy volunteers. The male: female ratio in the globus pharyngeus group was 1:1.29, as compared with 1:1.4 in the control group. The mean age in the globus pharyngeus group was 47 ± 11 years (range: 28-73 years), as compared with 49 ± 17 years (range: 21-77 years). These differences were not significant. A single investigator examined all patients by videofluoroscopy and esophageal manometry.

Esophageal manometry

After an overnight fast, manometry was performed using a solid-state intraluminal transducer assembly (Konigsberg Instruments, Inc., Pasadena, USA). The catheter consists of a flexible tube containing four pressure microtransducers. The distal two are circumferential transducers that record the average pressure over 360°. The circumferential transducer consists of a 4.6-mm-diameter silastic annulus enclosing a small transducer within a castor oil-filled chamber. The two

proximal transducers with a single sensor oriented in one direction. The transducers, starting at the distal end, are separated by 3, 2 and 5 cm. Pressure data are collected on-line by means of a computerized motility system and analyzed using Polygram equipment and software [Synectics (Medtronics), Shoreview, Minnesota].

Before the examination, the transducers were calibrated at 0 mmHg and 50 mmHg after balneum in 37 °C water 10 minutes. Manometry of the UES and pharynx was performed in the upright position. The catheter was passed through a nostril into the stomach. Then it was withdrawn in 1-cm increments every 20 seconds back into the esophagus. UES resting pressure was assessed using a station pull-through of the distal transducer with at least 15-sec intervals for stabilization between each 1-cm movement of the catheter, since the UES is somewhat reactive to the catheter movement. After identifying the high-pressure zone during this slow pull-through, at least 15-sec is allowed to elapse before measuring the resting UES pressure. Maximal stable pressure is recorded in millimeters of mercury using esophageal pressure just distal to the UES as zone baseline. Five 5-ml water (room temperature) swallows were used to assess UES relaxation, pharyngeal contraction, and UES/pharyngeal coordination. Swallows were 30 seconds apart. The swallows were performed with the circumferential transducer placed just proximal to the high-pressure zone of the UES to allow accurate recording of the pressure throughout the cycle of elevation of the sphincter during deglutition. Placement of the circumferential transducer proximal to the high-pressure zone of the sphincter compensates for oral movement during swallowing.

Mamometry helped clarify the specific timing of pressure events during pharyngeal contraction and UES relaxation^[17].

Videofluoroscopy

Detailed sequential analysis of videofluoroscopic images recorded at 25 frames/s clarifies timing of the events that occur during pharyngeal contraction and UES opening. It clearly defines the key role of muscle contraction occurring early in the swallowing sequences that produce the elevation of the hyoid and larynx, which is an essential element in the opening of the UES^[18-20].

Kinematic pharyngeal transit time is defined as the time from the first movement of the bolus, which results in a complete swallow, to the time the epiglottis returns to its initial position. The definition excludes oral preparation time and tongue movements that do not result in a complete swallow^[21].

Videofluoroscopy was completed in both anteroposterior and lateral projections with 5-ml thin barium at room temperature^[22-23]. To standardize the evaluations in our study, timing measurements were completed in the lateral projection.

The following data were collected by one physician evaluator: (1) quantitative kinematic pharyngeal transit times including the time of arrival of the head of the bolus reaching the level of the posterior inferior border of C₂ vertebral body (C₂L), the inferior level of the valleculae (BV), the posterior inferior border of C₄ vertebral body (C₄L), and the time at which the epiglottis returned to its original position (Em); These data points were selected to provide more easily identifiable radiologic landmarks for measurement^[21,24-26]. (2) The presence or absence of vallecular or piriform pooling, and (3) the presence or absence of penetration of part of the bolus to or through the true vocal cord^[27-29].

Statistical analysis

Fisher *P* test was used to compare patients and controls, with statistical significance set at the level of 0.05.

RESULTS

Kinematic pharyngeal transit time

The data of kinematic pharyngeal transit time from the control group and globus pharyngeus group were presented in Table 1.

Table 1 Kinematic pharyngeal transit time

	Control group(n=24)	Globus sensation group(n=32)	<i>P</i>
C ₂ L	0.50±0.27	0.45±0.33	>0.05
BV	0.57±0.26	0.51±0.34	>0.05
C ₄ L	0.67±0.27	0.63±0.36	>0.05
EM	1.44±0.30	1.37±0.41	>0.05

Note: Times are given in seconds.

There was no statistically significant difference between the control group and globus pharyngeus group, which showed ^a*P*>0.05. There were four cases of volunteers presenting stasis of barium in the valleculae and one in the piriform sinus. No laryngeal penetration and aspiration were found. Meanwhile, there were six and five of patients representing stasis of barium in the valleculae and piriform sinus respectively. Nine and two of patients had laryngeal penetration and aspiration. The results of valleculae and piriform sinus stasis and airway aspiration had no statistically significant differences between the two groups. But there was an association between laryngeal penetration and globus pharyngeus.

Esophageal manometry

The data of esophageal manometry from the control group and globus pharyngeus group were presented in Table 2.

Table 2 Data of esophageal mamometry

	Control group (n=24)	Globus pharyngeus group(n=32)
UES		
Resting pressure	68.33±37.56mmHg	71.38±41.42mmHg
Residual pressure	-7.30±6.48mmHg	-11.04±6.90mmHg
Relaxation time (from the beginning of relaxation to the nadir)	0.27±0.06s	0.28±0.15s
Duration (time from beginning of relaxation to the end)	0.54±0.08s	0.59±0.15s
Recovery (time from nadir of relaxation to the end)	0.27±0.08s	0.33±0.15s
Pharynx		
Peak pressure	157.81±63.86mmHg	175.50±93.47mmHg
contraction time (from the beginning of contraction to the nadir)	0.20±0.06s	0.22±0.08s
duration (time from beginning of contraction to the end)	0.42±0.08s	0.44±0.12s
Recovery (time from peak of contraction to the end)	0.22±0.05s	0.22±0.06s

There was no significant difference between the two groups ($P>0.05$). And also no difference in gender in the two groups (Table 3)

Table 3 Data of male and female in two groups

	Control group		Globus pharyngeus group	
	Male	Female	Male	Female
UES resting pressure(mmHg)	65.55±34.02	70.32±38.49	67.61±34.39	73.65±44.00
UES residual pressure (mmHg)	-9.33±6.80	-5.84±5.82	-8.80±6.98	-12.39±6.49
Pharyngeal peak pressure(mmHg)	165.72±69.19	151.45±57.36	163.19±105.47	182.89±81.99

DISCUSSION

Globus pharyngeus is a common disorder, accounting for 3-10 % of otolaryngologic outpatient referrals^[1,4]. The cause is unknown, and is likely to be of multifactorial origin. Abnormal function of the upper esophageal sphincter (UES) may produce the globus sensation symptom^[14,30]. Disorders of the UES include the hypertonic and hypotonic sphincter and various abnormalities of relaxation. Globus sensation has been associated with hypertonic upper esophageal sphincter and a persistent cricopharyngeal impression (i.e., bar), and Zenker diverticulum may be seen in patients with abnormal sphincter relaxation^[9-13,30-31].

Hypertonicity of the UES was suggested as an etiologic factor in the genesis of globus sensation by Watson and Sullivan^[32] in a study involving only nine patients suggested hypertonicity of the UES as an etiologic factor in the genesis of globus pharyngeus. This observation was in contradiction with a previous controlled study by Calderelli *et al*^[33], who found normal UES pressures in their patients with globus sensation. The techniques used for UES manometry in both studies might have questionable accuracy, as they did not count for the radial asymmetry of the UES pressure profile. In a more recent study, Cook *et al*^[34] failed to demonstrate any difference in resting UES pressure between normal controls and those with a history of globus sensation. Our study, using computerized solid-state manometry with a circumferentially recording transducer has not shown increased prevalence of UES hypertonicity in patients with globus sensation.

Through studies using multi-lumen catheters, radial asymmetry of the UES has been demonstrated over a number of years^[35,36]. Pressures recorded in the anterior and posterior directions were usually two or three times greater than pressures recorded laterally. This was believed to result from the anatomical disposition of the cricopharyngeus, but might be due in some extent to the compressive effect of the posterior lamina of the cricoid cartilage against the vertebral bodies of the cervical spine. So we believe that values for UES pressure are best obtained using a circumferential sensing solid-state transducer^[37]. In addition to radial asymmetry, oral movement of the sphincter during deglutition complicates the manometric assessment of the UES. With the transducer located in the sphincter high-pressure zone, a recording artifact will usually occur. As the swallow is initiated, the sphincter moves oral, leaving the transducer recording esophageal pressure. This fall in pressure may be erroneously interpreted as sphincter relaxation. If, however, the transducer is located proximal to the high pressure zone, when the subject swallows and the

larynx elevates, the UES (which has not yet relaxed) moves onto the transducer, which then records a rise in pressure followed by a fall in pressure as the sphincter relaxes. The pressure rises again as the sphincter regains tone and falls as the larynx returns to its original position, moving the sphincter distal to the transducer. The manometric recording in the UES that results from this sequence of events resembles the letter 'M' and this configuration can be used to ascertain correct transducer placement^[38-41].

The manometric findings in our study did not demonstrate any possible origin for the globus sensation. Detailed sequential analyses of videofluoroscopic images recorded at 25 frames/s have clarified timing of the events that occur during pharyngeal contraction and UES opening^[42,43]. These studies have clearly defined the key role of muscle contractions occurring early in the swallowing sequence that produce the elevation of the hyoid and larynx which is an essential element in the opening of the UES^[44,45]. Videofluoroscopy was completed in both anteroposterior and lateral projections with 5 ml 250 % barium sulfate liquid^[27].

The initiating event in our kinematic times is approximately at the beginning of the oropharynx. Consequently, BV in our study represents transit time through the oropharynx and mesopharynx. Pharyngeal dysfunction was defined as the presence of one or more of the following findings: (1) poor laryngeal elevation and epiglottic motion, (2) laryngeal penetration or aspiration, and (3) stasis of barium in the vallecula and piriform sinuses^[46,47].

Radiographic evidence of pharyngeal dysfunction such as stasis and aspiration was seen in patients, but these findings were not specific for upper esophageal sphincter dysfunction. Batch and Wilson *et al* also found that pharyngeal abnormalities were rarely seen at radiography in patients with globus pharyngeus^[48-50]. Thus, radiographic findings suggestive of upper esophageal sphincter dysfunction were rarely present in patients with globus sensation^[30].

In conclusion, findings by radiographic examination of the pharynx may show specific findings of pharyngeal dysfunction in patients with globus pharyngeus. Results of the pressures of the UES are normal in most patients with this symptom. So we find no role for UES hypertonicity as an etiologic factor for globus, but a strong association between laryngeal penetration and globus pharyngeus.

REFERENCES

- 1 **Clouse RE**. Functional esophageal disorders. *Gut* 1999; **45**: II 31- II 36
- 2 **Batch AJR**. Globus pharyngeus I . II. *J Laryngol Otol* 1988; **102**: 152-158, 227-230
- 3 **Wilson JA**, Heading RC, Maran AGD. Globus sensation is not due to gastro-esophageal reflux. *Clin Otolaryngol* 1987; **12**: 271-275
- 4 **Corso MJ**, Pursnani KG, Mohiuddin MA, Gideon RM, Castell JA, Katzka DA, Katz PO, Castell DO. Globus Sensation is associated with hypertensive upper esophageal sphincter but not with gastroesophageal reflux. *Dig Dis Sci* 1998; **43**: 1513-1517
- 5 **Thompson WG**, Heaton KW. Heartburn and globus is apparently in healthy people? *Can Med Assoc J* 1982; **126**: 46-48
- 6 **Moloy PJ**, Charter R. The globus symptom. *Arch Otolaryngol* 1982; **108**: 740-744
- 7 **Shaker R**, Milbrath M, Ren J, Toohill R, Hogan WJ, Li Q. Esophagopharyngeal distribution of refluxed gastric acid in patients with reflux laryngitis. *Gastroenterology* 1995; **109**: 1575-1582

- 8 **Smit CF**, Tan J, Devriese PP, Mathus LM, Brandsen M, Schouwenburg PF. Ambulatory pH monitoring at the upper esophageal sphincter. *Laryngoscope* 1998; **108**: 299-302
- 9 **Logemann JA**, Veis S, Colangelo L. A screening procedure for oropharyngeal dysphagia. *Dysphagia* 1999; **14**: 44-51
- 10 **Wilson JA**, White A, von Heacke NP, Marnn AGD, Heading RC, Pryde A, Dphil JR. Gastroesophageal reflux and posterior laryngitis. *Ann Otol Rhinol Laryngol* 1989; **98**: 405-410
- 11 **Jacob P**, Kahrilas PJ, Herzog G. Proximal esophageal pH-metry in patients with reflux laryngitis. *Gastroenterology* 1991; **100**: 305-310
- 12 **Koufman JA**. The otolaryngologic manifestations of gastroesophageal reflux disease (GERD): a clinical investigation of 225 patients using ambulatory 24-h pH monitoring and an experimental investigation of the role of acid and pepsin in the development of laryngeal injury. *Laryngoscope* 1991; **101**(Suppl 53): 1-78
- 13 **Dodds WJ**, Stewart E, Logeman J. Pathophysiology and radiology of the normal oral and pharyngeal phases of swallowing. *AJR* 1990; **154**: 953
- 14 **Hill J**, Stuart RC, Fung HK, Ng EK, Cheung FM, Chung SC, Hassett A. Gastroesophageal reflux, motility disorders and psychological profiles in the etiology of globus pharyngis. *Laryngoscope* 1997; **107**: 1373-1377
- 15 **Weisskopf A**. Reflux esophagitis: a cause of globus. *Otolaryngol Head Neck Surg* 1981; **89**: 780-782
- 16 **Wilson JA**, Pryde A, Pirus J, Allan PL, Macintyre CCA, Maram AGD, Heading RC. Pharyngoesophageal dysmotility in globus sensation. *Arch Otolaryngol Head Neck Surg* 1987; **115**: 1086-1090
- 17 **Linsell JC**, Anggiansah A, Owen WJ. Manometric findings in patients with globus sensation [abstract]. *Gut* 1987; **28**: 1378
- 18 **Jones B**, Donner MW. Examination of the patient with dysphagia. *Radiology* 1988; **167**: 319-326
- 19 **Robbins J**, Hamilton JW, Lof GL, Kempster GB. Oropharyngeal swallowing in normal adults of different ages. *Gastroenterology* 1992; **103**: 823-829
- 20 **Jones B**, Kramer SS, Donner MW. Dynamic imaging of the pharynx. *Gastrointest Radiol* 1985; **10**: 213-224
- 21 **Johnson ER**, McKenzie SW, Rosenquist CJ, Lieberman JS, Sievers AE. Dysphagia following stroke: quantitative evaluation of pharyngeal transit times. *Arch Phys Med Rehabil* 1992; **73**: 419-422
- 22 **Mujica VR**, Conklin J. When it's hard to swallow, what to look for patients with dysphagia. *Postgrad Med* 1999; **105**: 131-134, 141-142, 145
- 23 **Dantas RO**, Dodds WJ, Massey BT, Kern MK. The effect of high-vs-low-density barium preparations on the quantitative features of swallowing. *AJR* 1989; **153**: 1191-1195
- 24 **Cook IJ**, Dodds WJ, Dantas RO, Kern MK, Massey BT, Shaker R. Timing of videofluoroscopic manometric events and bolus transit during the oral and pharyngeal phases of swallowing. *Dysphagia* 1989; **4**: 8-15
- 25 **Woo P**, Noordzij P, Ross J. Association of esophageal reflux and globus symptom: comparison of laryngoscopy and 24-hour manometry. *Otolaryngol, Head Neck Surg* 1996; **115**: 502-507
- 26 **McConnel FMS**, Cerenko D, Jackson RT, Guffin TN. Timing of major events of pharyngeal swallowing. *Arch Otolaryngol Head Neck Surg* 1988; **114**: 1413-1418
- 27 **Ekberg BO**, Nylander G. Cineradiography of the pharyngeal stage of deglutition in 150 individuals without dysphagia. *British J Radiol* 1982; **55**: 253-257
- 28 **Logemann JA**. Screening, diagnosis, and management of neurogenic dysphagia. *Seminars in Neurology* 1996; **16**: 319-327
- 29 **Levine MS**, Rubesin SE. Radiologic investigation of dysphagia. *AJR* 1990; **154**: 1157-1163
- 30 **Ott DJ**, Ledbetter MS, Koufman JA, Chen MY. Globus pharyngeus: Radiographic evaluation and 24-hour pH monitoring of the pharynx and esophagus in 22 patients. *Radiology* 1994; **191**: 95-97
- 31 **Mason RJ**, Bremner CG, Demeester TR, Crookes PF, Peters JH, Hagen JA, Demeester SR. Pharyngeal swallowing disorders. *Ann Surg* 1998; **228**: 598-608
- 32 **Aviv JE**. Clinical assessment of pharyngolaryngeal sensitivity. *Am J Med* 2000; **108**: 68s-72s
- 33 **Smit CF**, Leeuwen JA, Mathus LM, Devriese PP, Semin A, Tan J, Schouwenburg PF. Gastropharyngeal and gastroesophageal reflux in globus and hoarseness. *Arch Otolaryngol, Head Neck Surg* 2000; **126**: 827-830
- 34 **Cook IL**, Dent J, Collins SM. Upper esophageal sphincter tone and reactivity to stress in patients with a history of globus sensation. *Dig Dis Sci* 1989; **34**: 672-676
- 35 **Triadafilopoulos G**, Hallstone A, Nelson-abbott H, Bedinger K. Oropharyngeal and esophageal interrelationships in patients with nonobstructive dysphagia. *Dig Dis Sci* 1992; **37**: 551-557
- 36 **Sears VW**, Castell JA, Castell DO. Radial and longitudinal asymmetry of human pharyngeal pressures during swallowing. *Gastroenterology* 1991; **101**: 1559-1563
- 37 **Castell LA**, Castell DO. Recent developments in the manometric assessment of upper esophageal sphincter function and dysfunction. *Dig Dis* 1997; **15**(Suppl): 28-39
- 38 **Welch RW**, Luchmann K, Ricks PM, Drake ST, Gates GA. Manometry of the normal upper esophageal sphincter and its alteration in laryngectomy. *J Clin Invest* 1979; **63**: 1036-1041
- 39 **McConnel FMS**. Analysis of pressure generation and bolus transport during pharyngeal swallowing. *Laryngoscope* 1988; **98**: 71-78
- 40 **Knauer CM**, Castell JA, Dalton CB, Nowak L, Shaker R. Pharyngeal/upper esophageal sphincter pressure dynamics in humans-effects of pharmacologic agents and thermal stimulation. *Dig Dis Sci* 1990; **35**: 774-779
- 41 **Kahrilas PJ**, Dodds WJ, Dent J, Logemann JA, Shaker R. Upper esophageal sphincter function during deglutition. *Gastroenterology* 1988; **95**: 52-62
- 42 **Kahrilas PJ**. A method for continuous monitoring of upper esophageal sphincter pressure. *Dig Dis Sci* 1987; **32**: 121-128
- 43 **Curtis DJ**, Cruess DF, Berg T. The cricopharyngeal muscle: a video recording review. *AJR* 1984; **142**: 497-500
- 44 **Johnson ER**, McKenzie SW, Sievers A. Aspiration pneumonia in stroke. *Arch Phys Med Rehabil* 1993; **74**: 973-975
- 45 **Dodds WJ**, Logemann JA, Stewart ET. Radiologic assessment of abnormal oral and pharyngeal phases of swallowing. *AJR* 1990; **154**: 965-974
- 46 **Jones B**. The pharynx disorders of function. *Radiol Clin Nor Am* 1994; **32**: 1103-1115
- 47 **Ott DJ**, Pikna LA. Clinical and videofluoroscopic evaluation of swallowing disorders. *AJR* 1993; **161**: 507-513
- 48 **Ekberg O**, Olsson R. Dynamic radiology of swallowing disorders. *Endoscopy* 1997; **29**: 439-446
- 49 **Isberg A**, Nilsson ME, Schiratzki H. Movement of the upper esophageal sphincter and a manometric device during deglutition. *Acta Radiol Diag* 1985; **26**: 381-388
- 50 **Färkkilä MA**, Ertama L, Katila H. Globus pharyngis, commonly associated with esophageal motility disorders. *AJR* 1994; **89**: 503-507

Edited by Wu XN

• CLINICAL RESEARCH •

Combined small bowel and reduced auxiliary liver transplantation: case report

Wei-Jie Zhang, Dun-Gui Liu, Qi-Fa Ye, Bo Sha, Fan-Jun Zhen, Hui Guo, Sui-Sheng Xia

Wei-Jie Zhang, Dun-Gui Liu, Qi-Fa Ye, Bo Sha, Fan-Jun Zhen, Hui Guo, Sui-Sheng Xia, Institute of Organ Transplantation, Tongji Hospital, Huazhong University of Science and Technology, Wuhan 430030, Hubei Province, China

Correspondence to: Dr. Wei-Jie Zhang, Institute of Organ Transplantation, Tongji Hospital, 1095 Jie Fang Da Dao, Wuhan 430030, China. wjzhang@public.wh.hb.cn

Telephone: +86-27-83662655 **Fax:** +86-27-83662892

Received 2001-05-31 **Accepted** 2001-09-22

Abstract

AIM: To present a case of combined small bowel and reduced auxiliary liver transplantation.

METHODS: A 55-year-old patient with short bowel syndrome and TPN-related liver dysfunction received small bowel transplantation combined with a reduced auxiliary liver graft. A liver was added to restore the patient's liver function and to protect the intestinal allograft from rejection. His own liver was not removed.

RESULTS: Without donor pretreatment and by conventional immunosuppressive therapy following transplantation, the patient experienced had only one episode of mild intestinal rejection, which was easily reversed by treatment with Methylprednisolone. No liver rejection occurred. Unfortunately, the patient died of heart and lung failure 30d after transplantation, despite successful graft replacement. Histopathologic examination of specimens after death demonstrated normal structure in both intestinal and liver grafts.

CONCLUSION: The auxiliary liver graft might play a role in preventing intestinal allograft rejection. However, the observation period in this case is short. Further study is needed to determine the risks, effect on the protecting the small-bowel from rejection, and feasibility of general application of this procedure.

Zhang WJ, Liu DG, Ye QF, Sha B, Zhen FJ, Guo H, Xia SS. Combined small bowel and reduced auxiliary liver transplantation: case report. *World J Gastroenterol* 2002; 8(5):956-960

INTRODUCTION

Small bowel transplantation is a possible choice of treatment for patients with irreversible failure of the intestine^[1-8]. Compared with the success in other solid organ allografts, attempts at small bowel transplantation in human have got poor results in terms of patient and graft survival^[9-17]. Rejection, immunosuppression-related infections and graft-versus-host reaction (GVHR) are the main obstacles to clinical application^[18-30].

In 1990, Grant *et al*^[31] first reported a case of successful small-bowel transplantation combined with a liver graft. This patient had only one episode of mild intestinal rejection, which was easily reversed by treatment with OKT₃. She had maintained normal nutrition for more than 2 years after surgery. The authors considered that the lack of serious intestinal rejection in this case may be due to immunological protection provided by the liver graft. Subsequently, some investigators demonstrated the same observations^[32-38], others reported that combined liver-bowel transplantation has no immunologic advantage over bowel transplantation alone^[39-41]. Furthermore, it has been shown that auxiliary liver transplantation had a slight protective effect on simultaneously transplanted small bowel, and it was not as strong as has been observed with orthotopic liver transplantation^[42].

We report a case of short-bowel syndrome and secondary TPN-related hepatic dysfunction who received small-bowel transplantation combined with a reduced auxiliary liver graft in our institute. After operation, only one episode of mild intestinal rejection occurred without liver rejection.

CASE REPORT

Case history

A 55 year old patient has had the short-bowel syndrome since February 1999 after the resection of whole small bowel and right colon because of thrombosis of the superior mesenteric artery. He was then alive on total parenteral nutrition (TPN), but was not discharged from hospital due to uncontrollable diarrhea. Besides, the TPN-related liver impairment developed. After extensive discussion with the patient and his family, small-bowel transplantation was performed on April 15, 1999. An auxiliary liver was simultaneously transplanted for the purpose of both restoring his liver function and protecting the intestinal graft from rejection. We did not remove his own liver.

Transplantation procedures

The donor is a brain death adult. Both donor and recipient were blood group O. The donor's HLA phenotype was A11,-; B75,-; DR12, 15 and DQ6 (1),-. The recipient's HLA phenotype was A2,23;B44,62;DR7,- and DQ2,5. The lymphocytotoxic crossmatch was negative. No pretreatment was given to alter the graft immunogenicity with antilymphocyte or other modalities.

To reduce the volume of donor liver, left lateral lobectomy and right frontal lobectomy were performed. The reduced liver and small bowel including the duodenum, jejunum and partial ileum were grafted into the abdominal cavity of the recipient. The donor's abdominal aorta duct containing the origins of the superior mesenteric artery and coeliac artery was anastomosed end-to-side to the recipient's infrarenal aorta. The donor's infrahepatic vena cava was anastomosed end-to-side to the recipient's infrarenal vena cava. The end of the donor

jejunum was anastomosed to recipient's duodenum; intestinal continuity was restored with an end-to-side ileocolic anastomosis. The end of the donor's ileum was exteriorized as an ileostomy (Figure 1).

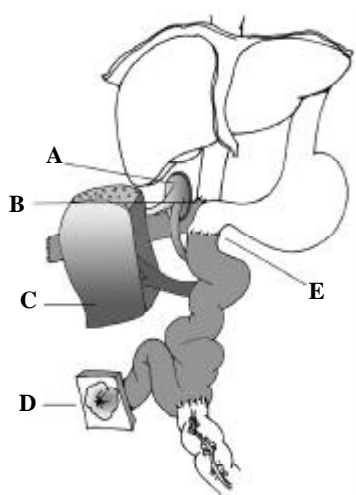


Figure 1 Small-bowel and auxiliary liver allograft. A. Carrel patch containing the origin of the superior mesenteric artery and the coeliac artery is anastomosed to the recipient's aorta; B. Anastomosis of end of the donor infrahepatic vena cava to the side of recipient's vena cava; C. The reduced liver; D. Ileostomy; E. Anastomosis of donor jejunum to the recipient's duodenum

Immunosuppression management

Methylprednisolone was given intravenously 30 min before graft revascularization (first dose of 500mg bolus) and rapidly tapered to 20 mg·d⁻¹ over the next 10 days. Cyclosporin A by continuous intravenous infusion was begun intraoperatively (3mg·kg·d⁻¹) to maintain the whole blood concentration of 350–450 µg·L⁻¹ by monoclonal radioimmunoassay. Cyclophosphamide 100 mg was also given intravenously daily for the first 3 days. Prostaglandin E₁ (600 µg·d⁻¹) was begun intraoperatively and continued for 20 days.

Postoperative course

Detection of graft rejection was based primarily on clinical observations and mucosal biopsies. During his postoperative course, the bowel graft developed only one histologic evidence of rejection. Mucosal biopsy on the seventh postoperative day showed lymphocyte infiltration in epithelium, slight fattening of the villi, decreased numbers of goblet cells, but the mucosal destruction and necrosis were not observed (Figure 2). The rejection was successfully reversed by a 3 day course of methylprednisolone bolus (15mg·kg·d⁻¹ per day in tapering doses).

There was no clinical or histological evidence of liver rejection. The liver function including ALT, AST, Tbil, cholesterol, triglyceride returned to the normal range 5 days after surgery. On the 9th and 23rd postoperative day, laparotomy was performed because of surgical complications. During the operation, the liver was biopsied, and a normal histological appearance was found (Figure 3).

The patient did not receive any specific treatment for preventing graft-versus-host disease (GVHD) other than the immunosuppression therapy previously described. No sign of GVHD developed. Unfortunately, some severe complications occurred including intestinal fistula, stress ulcer and bleeding,

ARDS, pulmonary and abdominal infection. The patient died of heart and lungs failure 30 days after transplantation despite successful graft replacement. The histopathologic examination of specimens after death demonstrated normal structure in both intestinal and liver grafts.

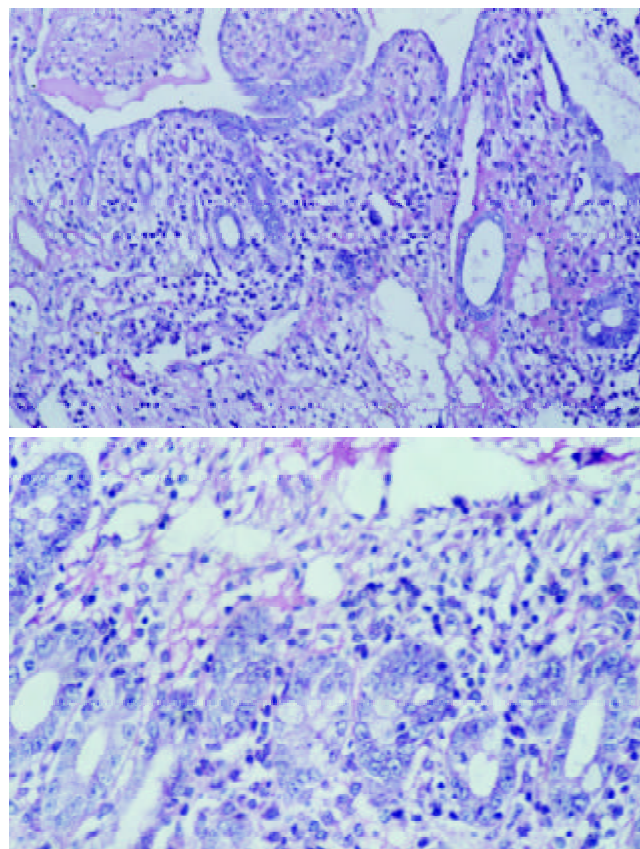


Figure 2 Photomicrographs showing acute rejection with lymphocytic cryptitis on the 7th postoperative day, the mucosal destruction and necrosis were not observed (H&E, A, ×200; B, ×400).

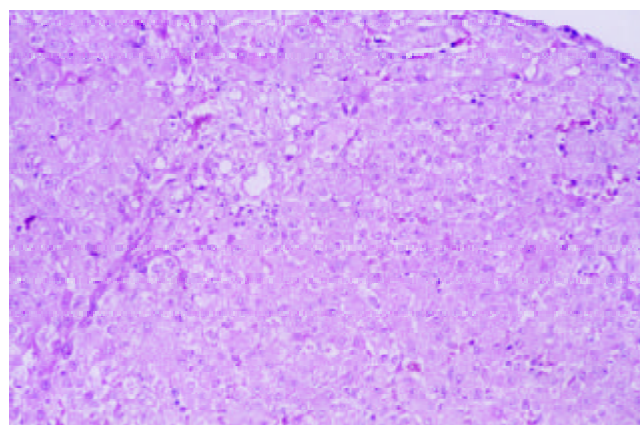


Figure 3 Liver biopsy specimens on the 9th postoperative day showed normal appearance of the allograft (×200), no inflammatory infiltrate in the portal tract.

DISCUSSION

Liver dysfunction is a well-recognized complication of intestinal failure. Advances in TPN have allowed the patient

suffering from short bowel syndrome to survive. However, in many instances total parenteral nutrition causes severe liver damage leading to cirrhosis. Thus, combined liver and small bowel transplantation becomes an established life-saving therapy for the treatment of liver disease and intestinal failure^[43-46]. In the general, an orthotopic liver and small bowel are transplanted. To our knowledge, this case is the first report of transplantation of combined auxiliary reduced liver and small bowel in human. We tried to restore the patient's liver function and to protect the intestinal allograft from rejection. For these reasons, an auxiliary liver was simultaneously transplanted. The auxiliary reduced liver-small bowel transplantation model represents a new, less aggressive possibility for multiorgan transplantation^[31,47,48]. It offers some advantages over multivisceral transplants, including simplicity and less mortality than the combined orthotopic liver-intestinal transplantation. This procedure is useful for the patients with reversible hepatopathy associated with intestinal insufficiency because it can offer temporal or definitive hepatic support.

Without donor pretreatment and under conventional immunosuppressive therapy, this patient had only one episode of mild intestinal rejection, which was easily reversed by treatment with Methylprednisolone. These data indicate a possible role of the auxiliary liver graft in preventing intestinal allograft rejection. In fact, the immunoprotecting effect of the liver was first described by Calne in 1969 in a porcine model^[49]. The animal can reject skin, kidney and hearts rapidly. However, orthotopic and accessory heterotopic liver allografts can protect preferentially from rejection grafts of donor specific skin, kidney and heart. Injected soluble liver antigen may also protect donor specific tissue from rejection. It suggested that allogeneic liver can induce immunological tolerance in immunologically mature pigs^[49]. Subsequent studies demonstrate that specific tolerance can be achieved in combined liver/small bowel transplantation after a transient rejection crisis^[32-38].

The mechanism of immunological protection of the liver is not very clearly until now^[50-52]. Apoptosis of T lymphocytes may be involved in graft rejection and tolerance induction^[50]. Apoptosis is a mechanism for eliminating autoreactive cells during T cell maturation in the thymus. T cells themselves use apoptosis to eliminate alloantigen-expressing donor cells during rejection responses. Apoptosis of parenchymal cells in the grafted livers correlated directly with interleukin-2 receptor expression of the infiltrating T cells. In the late phase of rejection, a peak of apoptosis in the lymphocyte infiltrate was demonstrated, characterized as predominantly apoptotic CD8⁺ T lymphocytes. T cell inactivation seems to result in apoptosis of cytotoxic T cell and tolerance^[50]. In addition, microchimerism is associated with long-term graft acceptance in combined liver/small bowel transplantation^[51,52]. Donor specific leucocytes could be detected immunohistochemically in the combined liver/small bowel group and isolated liver group in spleen, host Peyer patches, and mesenteric lymph nodes. Particularly in the liver sinusoids investigators^[52] found a great number of persisting donor leukocytes in all long-term survivors in combined liver/small bowel rats. The persisting leucocytes obviously originate from the initially transplanted white cell population of the liver. The liver as constant source of antigen plus a persisting and obviously active leukocyte population may provide the basis for a long-term survival of the liver graft and any cotransplanted organ.

However, the observation period in this case was short and

it is difficult to extrapolate that the complex immune responses between the donor and recipient are affirmatively associated with adding a liver graft. Moreover, other studies found that liver grafting failed to prevent intestinal rejection in human and large animal model^[39-41]. Further studies are needed to determine the risks, effect on the protecting the small bowel from rejection, and feasibility of general application of this procedure.

REFERENCES

- 1 **Johnson CP**, Sarna SK, Zhu YR, Buchmann E, Bonham L, Telford GL, Roza AM, Adams MB. Effects of intestinal transplantation on postprandial motility and regulation of intestinal transit. *Surgery* 2001; **129**: 6-14
- 2 **Tzakis AG**, Kato T, Nishida S, Mittal N, Neff G, Nery J, O'Brien C, Ruiz P, Levi D, Pinna A. Evolution of gastrointestinal transplantation at the University of Miami. *Transplant Proc* 2001; **33**: 1545-1549
- 3 **Kaufman SS**. Small bowel transplantation: selection criteria, operative techniques, advances in specific immunosuppression, prognosis. *Curr Opin Pediatr* 2001; **13**: 425-428
- 4 **Quigley EM**. Small intestinal transplantation. *Curr Gastroenterol Rep* 2001; **3**: 408-411
- 5 **Sudan DL**, Kaufman SS, Shaw BW Jr, Fox IJ, McCashland TM, Schafer DF, Radio SJ, Hinrichs SH, Vanderhoof JA, Langnas AN. Isolated intestinal transplantation for intestinal failure. *Am J Gastroenterol* 2000; **95**: 1506-1515
- 6 **Sudan DL**, Iverson A, Weseman RA, Kaufman S, Horslen S, Fox IJ, Shaw BW Jr, Langnas AN. Assessment of function, growth and development, and long-term quality of life after small bowel transplantation. *Transplant Proc* 2000; **32**: 1211-1212
- 7 **Pakarinen MP**, Halttunen J. The physiology of the transplanted small bowel: an overview with insight into graft function. *Scand J Gastroenterol* 2000; **35**: 561-577
- 8 **Garrido V**, Bond GJ, Mazariegos G, Wu T, Martin D, Colangelo J, Ezzelarab M, Fung J, Reyes J, Abu-Elmagd K. Late severe rejection of intestinal allografts: risks and survival outcome. *Transplant Proc* 2001; **33**: 1556-1557
- 9 **Bramhall SR**, Minford E, Gunson B, Buckels J. Liver transplantation in UK. *World J Gastroenterol* 2001; **7**: 602-611
- 10 **Cavallari A**, Nardo B, Caraceni P. Arterialization of the portal vein in a patient with a dearterialized liver graft and massive necrosis. *N Engl J Med* 2001; **345**: 1352-1353
- 11 **Zhu XF**, Chen GH, He XS, Lu MQ, Wang GD, Cai CJ, Yang Y, Huang JF. Liver transplantation and artificial liver support in fulminant hepatic failure. *World J Gastroenterol* 2001; **7**: 566-568
- 12 **Tang ZY**. Hepatocellular carcinoma-Cause, treatment and metastasis. *World J Gastroenterol* 2001; **7**: 445-454
- 13 **Grant D**. Intestinal transplantation: 1997 report of the international registry. Intestinal Transplant Registry. *Transplantation* 1999; **67**: 1061-1064
- 14 **Bueno BJ**, Ohwada S, Kocoshis S, Mazariegos GV, Dvorchik I, Sigurdsson L, Di Lorenzo C, Abu-Elmagd K, Reyes J. Factors impacting the survival of children with intestinal failure referred for intestinal transplantation. *J Pediatr Surg* 1999; **34**: 27-33
- 15 **Thompson JS**. Intestinal transplantation. Experience in the United States. *Eur J Pediatr Surg* 1999; **9**: 271-273
- 16 **Dionigi P**, Alessiani M, Ferrazi A. Irreversible intestinal failure, nutrition support, and small bowel transplantation. *Nutrition* 2001; **17**: 747-750

- 17 **Silver HJ**, Castellanos VH. Nutritional complications and management of intestinal transplant. *J Am Diet Assoc* 2000; **100**: 680-684
- 18 **Cicalese L**, Sileri P, Asolati M, Rastellini C, Abcarian H, Benedetti E. Infectious complications following living-related small bowel transplantation in adults. *Transplant Proc* 2001; **33**: 1554-1555
- 19 **Delis S**, Kato T, Ruiz P, Mittal N, Babinski L, Tzakis A. Herpes simplex colitis in a child with combined liver and small bowel transplant. *Pediatr Transplant* 2001; **5**: 374-377
- 20 **Song WL**, Wang WZ, Wu GS, Dong GL, Ling R, Ji G, Zhao JX. Evaluation of perioperative serum cytokine level in acute rejection in human living related small bowel transplantation. *Shijie Huaren Xiaohua Zazhi* 2001; **9**: 401-404
- 21 **Li YX**, Li JS, Li N. Improved technique of vascular anastomosis for small intestinal transplantation in rats. *World J Gastroenterol* 2000; **6**: 259-262
- 22 **Farmer DG**, McDiarmid SV, Smith C, Stribling R, Seu P, Ament MA, Vargas J, Yersiz H, Markmann JF, Ghobriel RM, Goss JA, Martin P, Busuttil RW. Experience with combined liver-small intestine transplantation at the University of California, Los Angeles. *Transplant Proc* 1998; **30**: 2533-2534
- 23 **Khan FA**, Kato T, Pinna AD, Berho M, Nery JR, Colombani P, Tzakis AG. Graft failure in multivisceral transplantation recipients secondary to necrotizing enterocolitis. *Transplant Proc* 2000; **32**: 1204-1205
- 24 **Muiesan P**, Dhawan A, Novelli M, Mieli-Vergani G, Rela M, Heaton ND. Isolated liver transplant and sequential small bowel transplantation for intestinal failure and related liver disease in children. *Transplantation* 2000; **69**: 2323-2326
- 25 **Cicalese L**, Sileri P, Green M, Abu-Elmagd K, Kocoshis S, Reyes J. Bacterial translocation in clinical intestinal transplantation. *Transplantation* 2001; **71**: 1414-1417
- 26 **Li YS**, Li JS, Li N, Jiang ZW, Zhao YZ, Li NY, Liu FN. Evaluation of various solutions for small bowel graft preservation. *World J Gastroenterol* 1998; **4**: 140-143
- 27 **Dong GL**, Wang WZ, Wu GS, Song WL, Ji G, Luo L, Xu JL, Zhao CH. Strategy of nutritional support for a patient with partial live small bowel transplantation during perioperation. *Shijie Huaren Xiaohua Zazhi* 2000; **8**: 539-541
- 28 **Raofi V**, Holman DM, Dunn TB, Fontaine MJ, Mihalov MM, Vitello JM, Asolati M, Benedetti E. Comparison of rejection rate and functional outcome of small bowel transplantation alone or in conjunction with the ileocecal valve versus combined small and large bowel transplantation. *Clin Transplant* 1999; **13**: 389-394
- 29 **Todo S**, Tzakis AG, Abu-Elmagd K, Reyes J, Nakamura K, Casavilla A, Selby R, Nour BM, Wright H, Fung JJ, Demetris AJ, Van-Thiel DH, and Trarzl TE. Intestinal transplantation in composite visceral grafts or alone. *Ann Surg* 1992; **216**: 223-233
- 30 **Goulet O**. Intestinal failure in children. *Transplant Proc* 1998; **30**: 2523-2525
- 31 **Grant D**, Wall W, Mimeault R, Zhong R, Ghent C, Garcia B, Stiller C, Duff J. Successful small-bowel/liver transplantation. *Lancet* 1990; **335**: 181-184
- 32 **Zhong R**, He G, Sakai Y, Li XC, Garcia B, Wall W, Duff J, Stiller C, Grant D. Combined small bowel and liver transplantation in the rat: possible role of the liver in preventing intestinal allograft rejection. *Transplantation* 1991; **52**: 550-576
- 33 **Li X**, Zhong R, He G, Sakai Y, Quan D, Garcia B, Duff J, Grant D. Host immunosuppression after combined liver/intestine transplantation in the rat. *Transplant Proc* 1992; **24**: 1206-1207
- 34 **Meyer D**, Gassel HJ, Timmermann W, Otto C, Ulrichs K, Thiede A. Rejection rate of a small bowel allografts is reduced by liver transplantation. *Transplant Proc* 2000; **32**: 1287
- 35 **Gassel HJ**, Timmermann W, Meyer D, Gassel AM, Thiede A. Investigations of the immunoprotective role of the liver after allogeneic orthotopic combined liver-small-bowel transplantation in the rat. *Transplant Proc* 1997; **29**: 693-694
- 36 **de Vera ME**, Reyes J, Demetris J, Mazariegos G, Schaefer N, Vargas H, Bond G, Wu T, Fung J, Starzl TE, Abu-Elmagd K. Isolated intestinal versus composite visceral allografts: causes of graft failure. *Transplant Proc* 2000; **32**: 1221-1222
- 37 **Loffeler S**, Meyer D, Otto C, Gassel HJ, Timmermann W, Ulrichs K, Thiede A. Different kinetics of donor cell populations after isolated liver and combined liver/small bowel transplantation. *Transpl Int* 2000; **13**(Suppl 1): 537-540
- 38 **Meyer D**, Otto C, Rummel C, Gassel HJ, Timmermann W, Ulrichs K, Thiede A. "Tolerogenic effect" of the liver for a small bowel allograft. *Transpl Int* 2000; **13** (Suppl 1): 123-126
- 39 **Gruessner RWG**, Nakhleh RE, Benedetti E, Pirenne J, Belani KG, Beebe D, Carr R, Troppmann C, Gruessner AC. Combined liver-total bowel transplantation has no immunologic advantage over total bowel transplantation alone: A prospective study in a porcine model. *Arch Surg* 1997; **132**: 1077-1085
- 40 **Abu-Elmagd K**, Todo S, Tzakis A, Furukawa H, Nour B, Reyes J, Nakamura K, Scotti-Foglieni C, El-Hammadi H, Kadry Z, Fung J, Demetris J, Starzl TE. Rejection of human intestinal allografts: alone or in combination with the liver. *Transplant Proc* 1994; **26**: 1430-1431
- 41 **Velio P**, Bertoglio C, Bardella MT, Bianchi PA, Andreoni B, Biffi R, Marzona L, Gatti SO, Pozzi S, Tiberio G, Galmarini D, Rossi G, Piazzini A, and Orsenigo R. Histologic findings after orthotopic small bowel transplantation alone or with the liver. *Transplant Proc* 1994; **26**: 1632-1633
- 42 **Theal M**, McAlister VC, He G, Wright J, MacDonald AS, Bitter-Suermann H, Lee TDG. Effect of auxiliary liver transplantation on the simultaneously transplanted small bowel allograft. *Transplant Proc* 1994; **26**: 1620
- 43 **Bueno J**, Abu-Elmagd K, Mazariegos G, Madariaga J, Fung J, Reyes J. Composite liver-small bowel allografts with preservation of donor duodenum and hepatic biliary system in children. *J Pediatr Surg* 2000; **35**: 291-296
- 44 **de Ville de Goyet J**, Mitchell A, Mayer AD, Beath SV, McKiernan PJ, Kelly DA, Mirza D, Buckles JA. En block combined reduced-liver and small bowel transplants: from large donors to small children. *Transplantation* 2000; **69**: 555-559
- 45 **Gilroy R**, Sudan D. Liver and small bowel transplantation: therapeutic alternatives for the treatment of liver disease and intestinal failure. *Semin Liver Dis* 2000; **20**: 437-450
- 46 **Sudan DL**, Iyer KR, Deroover A, Chinnakotla S, Fox II Jr, Shaw BW Jr, Langnas AN. A new technique for combined liver/small intestinal transplantation. *Transplantation* 2001; **72**: 1846-1848
- 47 **Calleja-Kempin J**, Martin-Cavanna J, Vazquez-Estevez J, Alvarez E. Small bowel transplant combined with a reduced auxiliary liver graft. *Transplant Proc* 1997; **29**: 1823-1825

- 48 **Benedetti E**, Pirenne J, Chul SM, Fryer J, Fasola C, Hakim NS, Troppmann C, Beebe DS, Carr RJ, Belani KGW. Simultaneous en bloc transplantation of liver, small bowel and large bowel in pigs-technical aspects. *Transplant Proc* 1995; **27**: 341-343
- 49 **Calne RY**, Sells RA, Pena JR, Davis DR, Millard PR, Herbertson BM, Binns RM, Davies DA. Induction of immunological tolerance by porcine liver allografts. *Nature* 1969; **223**: 472-476
- 50 **Meyer D**, Baumgardt S, Loeffeler S, Czub S, Otto C, Gassel HJ, Timmermann W, Thiede A, Ulrichs K. Apoptosis of T lymphocytes in liver and/or small bowel allografts during tolerance induction. *Transplantation* 1998; **66**: 1530-1536
- 51 **Meyer D**, Loeffeler S, Otto C, Czub S, Gassel HJ, Timmermann W, Thiede A, Ulrichs K. Donor-derived alloantigen-presenting cells persist in the liver allograft during tolerance induction. *Transpl Int* 2000; **13**:12-20
- 52 **Loeffeler S**, Meyer D, Rolleke G, Gassel HJ, Ulrichs K, Thiede A. Microchimerism is associated with long-term graft acceptance in combined liver/small bowel transplantation. *Transplant Proc* 1998; **30**: 2555-2556

Edited by Ma JY

Intestinal endotoxemia as a pathogenetic mechanism in liver failure

De-Wu Han

De-Wu Han, Institute of Hepatology, Shanxi Medical University, Taiyuan 030001, Shanxi Province, China

Correspondence to: De-Wu Han, M.D., Professor of Pathophysiology, Director of Institute of Hepatology, Shanxi Medical University, 86 Xin Jian Nan Road, Taiyuan 030001, Shanxi Province, China. smuhan@public.ty.sx.cn

Telephone: +86-351-4690082 **Fax:** +86-351-4690865

Received 2002-07-17 **Accepted** 2002-08-20

Abstract

Liver injury induced by various pathogenic factors (such as hepatitis virus, ethanol, drugs and hepatotoxicants, etc.) through their respective special pathogenesis is referred to as “primary liver injury” (PLI). Liver injury resulted from endotoxin (lipopolysaccharide, LPS) and the activation of Kupffer cells by LPS while intestinal endotoxemia (IETM) occurred during the occurrence and development of hepatitis is named the “secondary liver injury” (SLI). The latter which has lost their own specificities of primary pathogenic factors is ascribed to IETM. The “secondary liver injury” is of important action and impact on development and prognosis of hepatitis. More severe IETM commonly results in excessive inflammatory responses, with serious hepatic necrosis, further severe hepatitis and even induces acute liver failure. The milder IETM successively precipitates a cascade, including repeated and persistent hepatocytic impairment accompanied by infiltration of inflammatory cells, hepatic fibrosis, cirrhosis and hepatocarcinoma. Generally, the milder IETM ends with chronic hepatic failure. If PLI caused by various pathogenic factors through their independent specific mechanisms is regarded as “the first hit” on liver, then SLI mediated by different chemical mediators from KCs activated by IETM in the course of hepatitis is “the second hit” on liver. Thus, fusing and overlapping of the primary and secondary liver injuries determine and influence the complexity of the illness and outcome of the patient with hepatitis. For this reason, the viewpoint of “SLI” induced by the “second hit” on liver inflicted by IETM suggests that medical professionals should attach great importance to both “PLI” and “SLI” caused by IETM. That is, try to adjust the function of KCs and eliminate endotoxemia of the patient.

Han DW. Intestinal endotoxemia as a pathogenetic mechanism in liver failure. *World J Gastroenterol* 2002; 8(6): 961-965

INTRODUCTION

Gut is a vast pool of bacteria and endotoxins (lipopolysaccharide, LPS) in the body. There are endotoxemia in severe trauma, burn or scald, intestinal ischemia and liver diseases. They are mainly resulted from large quantities of endotoxin produced by overgrowth of gram-negative bacteria in gut that are

increasingly taken into portal vein because of the increased permeability of intestinal wall. Endotoxemia will be generated if the level of endotoxin surpasses the hepatic capacity for endotoxin scavenging due to decreased phagocytic ability of liver kupffer cells (KCs) and then endotoxin spills over into systemic circulation. For these reasons, it is named IETM because endotoxin comes from gut.

In recent years, the relationship between IETM and liver diseases has been increasingly paid much attention to. Animal studies have demonstrated that various experimental liver diseases were commonly accompanied by IETM. Clinical observations have also showed evidences that the highest incidence (80-100 %) and severe degree of IETM in patients with severe hepatitis was generally recognized, though the incidences of IETM in patients with acute or chronic hepatitis, severe hepatitis, cirrhosis and hepatocarcinoma were not reported equally. Incidences of IETM investigated in our institute in acute or chronic hepatitis, severe hepatitis and cirrhosis were 75 %, 79 %, 93.3 % and 84.3 % respectively^[1].

LPS activates KCs via two pathways: one is membrane attachment from mCD₁₄ which is the classical CD₁₄ dependent pathway, that requires LPS binding protein (LBP) as a cofactor carrying LPS to the membrane of KCs bound to the receptor CD₁₄; the soluble compound formed by combining LBP with LPS increases affinity of LPS with CD₁₄. Whereas the other pathway-sCD₁₄ may not require LBP, combines with corresponding receptor on KCs by aid of other proteins (such as HDL, LDL etc). These two pathways finally activate signal transduction system and trigger the synthesis and release of cytokines and inflammatory mediators^[2].

KCs stimulated by LPS release chemostatic substances such as TNF- α , interleukins, leukotriene B₄ and complement C₅, which attract circulating neutrophilic leucocytes. Activated neutrophilic leucocytes up-regulate adhesion molecules receptor (CD_{11b}/CD₁₈) on its membrane surface, then adhere to endothelial cells of hepatic sinusoids. In the meanwhile, adhesion molecules ICAM-1 and ELAM-1 on surface of endothelial cells are also up-regulated and precipitate neutrophilic leucocytes moving to hepatic sinusoids. Oxygen-derived free radicals produced by these activated neutrophilic leucocytes cause lipid peroxidation of cells. Moreover, toxic mediators (PAF, NO, ET-1 etc) released from KCs enhance further liver injury and make platelets aggregated into microthrombi. Hepatic sinusoids being blocked by adhering neutrophilic leucocytes, platelets and swelling KCs induce slowing of blood flow with following hypoxia. The onset of liver necrosis in this situation is ascribed mainly to abnormal microcirculation. Therefore, liver damage is an overall outcome that is induced by the interactions between inherent KCs, immigrating neutrophilic leucocytes and hepatocytes^[3].

Additionally, it should be mentioned that LPS not only induces liver necrosis directly or indirectly by chemical mediators released from activated KCs, but also is a promoting factor for other hepatotoxicants (such as D-galactosamine, tetrachloride [CCl₄], ethanol, etc) to induce liver necrosis. The

use of anti-LPS antibody can significantly attenuate liver necrosis induced by hepatotoxicants and prevent from the occurrence of acute liver failure^[4].

There are still some arguments on whether or not LPS directly injures hepatocytes at present. It is reported that there is high content of lipid (phospholipid mainly) in the membrane of hepatocellular mitochondria. The affinity of diphosphatidyl glycerol, which is the special component of the lipid, with is the special component of the lipid, with LPS is very strong. Its acyl group that binds to LPS induces the structural damage of mitochondria, interferes with biological oxidation, inhibits production of ATP and causes hepatocellular injury. LPS can directly insert into double layers of lipid molecule of membrane or conjugate to membrane receptors and initiate the metabolism of membrane phosphatidyl inositol. Large quantities of phosphatidic acid (PA) and inositol triphosphate (IP₃) are produced. Degeneration and necrosis of hepatocytes are induced by elevated Ca²⁺ in cytoplasm, which is resulted from PA with Ca²⁺ carrier-like action and IP₃ which causes the opening of Ca²⁺ channel in membrane, with great deal of Ca²⁺ flowing the cell. Structural and functional injuries of hepatocytes and mitochondria can also be caused by degradation of membrane phospholipid and lipid peroxidation mediated by PLA₂ activation induced by LPS. LPS phagocytosed by KCs can damage the membrane of lysosome and lead to release of various lysosomal enzymes resulting in cell autolysis.

To explore LPS directly acting on hepatocytes *in vitro*, we found that hepatocytes showed typical ladder pattern of apoptotic cells morphologically and this process could be inhibited by apoptotic inhibitor ATA. The number of apoptotic hepatocytes was proportional with the dosage of LPS; the number of apoptotic hepatocytes treated with LPS within 24 hours was also in positive ratio with time. It implicated that LPS could directly induce apoptosis of hepatocytes and this action was more prominent at the early phase of treatment^[5].

The interaction of LPS with KCs plays a determinant role during the occurrence of liver injury and acute liver failure. It was confirmed in a large number of animal experiments that liver injury induced by CCl₄, D-galactosamine, thioacetamide (TAA), ethanol, etc. could be reduced or prevented by performing colectomy or administering antibiotics (such as polymyxin B, mycifradin) to decrease the level of intestinal LPS, or by administering gadolinium chloride (GdCl₃), silica (SiO₂) to block KCs.

The research performed by Ahmad et al. indicated that there was high expression of ICAM-1 on hepatocytes, KCs, endothelial cells during acute endotoxemia; there was no expression of ICAM-1 on hepatocytes and KCs when KCs were blocked by GdCl₃; there is no occurrence of TNF- α and LTB₄, which is released from KCs activated by LPS, attracting neutrophilic leucocytes to infiltrate into liver. These results implicated that KCs played a vital role in hepatitis and liver injury induced by LPS^[6].

Many researches suggested that ethanol can increase permeability of intestinal mucosa, macromolecules such as LPS were intaken into blood and the plasma level of LPS thus rose up. While phagocytosing LPS, KCs released chemical mediators such as TNF- α , PGE₂ to promot oxidation of alcohol in the liver. Owing to increased oxygen consupsion, hepatocytes was injured by free radicals formed in the state of hypoxia. Experiments verified that the level of plasma LPS in alcoholism animals was significantly correlated with hepatic pathological change (cellular steatosis and necrosis, inflammatory infiltration); the steatosis and necrosis of liver

induced by alcohol could be prevented by administering GdCl₃ to block KCs^[7].

D-galactosamine can induce focal necrosis of whole hepatic lobule with severe infiltration of neutrophilic leucocytes, but liver injury can be thoroughly prevented by GdCl₃ injection in caudal vein before D-galactosamine injection intraperitoneally in rats. Liver injury and apoptosis induced by D-galactosamine and small dose of LPS can be markedly alleviated via treatment with TNF- α antiserum, so did alcoholic liver injury. Because TNF- α was mainly stemmed from activated KCs, the key role of KCs played in the liver injury was thus certified^[8,9].

In summary, previous researches on mechanism of liver injury were mostly confined to parenchymal liver cells, whereas large amount of current experiments have demonstrated that activation of KC by LPS plays a more important role in the occurrence and development of liver injury.

Based upon the above-mentioned understanding we have conceived the following hypothesis on liver injury induced by various pathogenic factors and the development and prognosis of hepatitis (Figure 1)

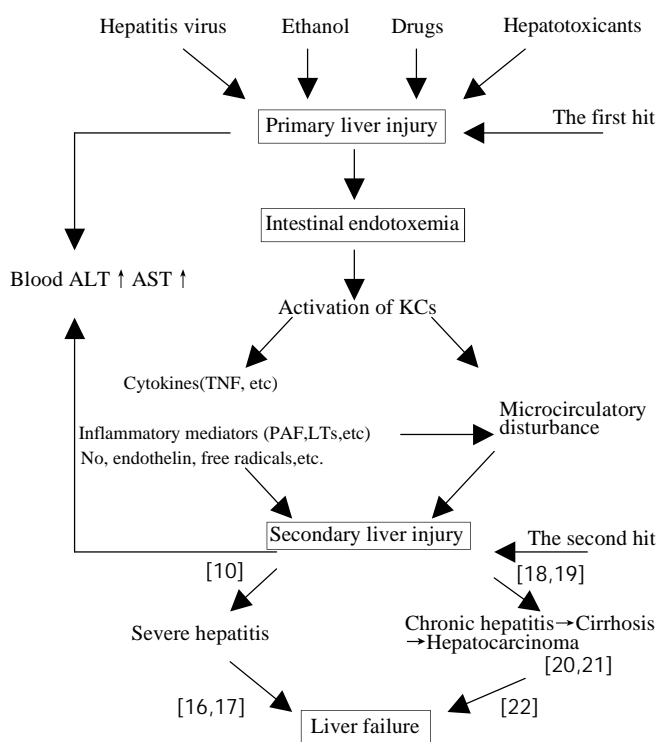


Figure 1 Diagram of the hypothesis of IETM in liver failure

The “primary liver injury (PLI)” is the hepatic damage that various pathogenic factors (such as hepatitis virus, alcohol, drugs, hepatotoxicants, etc.) induced by specific mechanism separately. In contrast, IETM is formed in the course of the development of hepatitis. Liver injury, which is resulted from LPS, activation of KCs by LPS and others, is referred to as “secondary liver injury (SLI)” The SLI which has lost their own specificities of primary pathogenic factors is ascribed to IETM.

The SLI has an important effect on the development and prognosis of various hepatitis. The severe IETM, which commonly causes over-inflammatory reaction and serious hepatic necrosis, will lead to severe hepatitis and even acute hepatic failure^[10]. The mild IETM will successively precipitate a cascade, including the repeated and persistent hepatocellular injury accompanied by infiltration of inflammatory cells,

hepatic fibrosis, cirrhosis and even hepatocarcinoma. Generally, it ends with chronic hepatic failure^[11].

Certainly, the mechanism of occurrence and development of various viral hepatitis is not so simple but a considerably complicated issue related to virus itself, host immune state, etc. It is difficult to cover it by only one hypothesis.

PRIMARY LIVER INJURY

Hepatic damage induced by various pathogenic factors (such as hepatitis virus, alcohol, drugs, hepatotoxicants, etc) via specific mechanism separately is named the "primary liver injury (PLI)".

Hepatic damage resulted from various hepatitis virus is mainly ascribed to host immune reaction. Cytotoxic T lymphocytes (CTLs) attack hepatocytes with HbcAg, HLA-1 and ICAM-1. It results in lysis and apoptosis of a large amount of hepatocytes. Drugs cause hepatic damage either by direct action, metabolic product or immune mechanism. Ethanol may give rise to be oxidative stress and direct necrosis of hepatocytes in alcoholic liver injury. The new antigen formed by the combination of lipid peroxide products, acetaldehyde (ethanol-derived metabolite) and protein triggers immunity reaction and makes CTLs to attack hepatocytes. TAA, a hepatotoxicant, is taken by liver then is metabolized into TAA-sulfoxide by cytochrome P₄₅₀ mixed-function oxidase and further transformed into the intermediates and other polar molecules, which irreversibly combine with intrahepatic biomacromolecules to cause hepatic necrosis. Moreover, TAA also activates PLA₂ which can increase lysolecithin and destroy hepatocellular membrane. CCl₄ is biotransformed into active trichloromethyl free radical by intrahepato cellular cytochrome P₄₅₀, which may lead to lipid peroxide and injury of cell membrane. In brief, various pathogenic factors may all induce the liver damage by their own mechanism respectively.

IETM INDUCED BY KCs WITH PHAGOCYTIC DYSFUNCTION

When PLI is present, the structural and functional injuries of KCs occur at the same time with injuries of hepatic parenchymal cells. Our research indicated that mitochondria swelled, decreased and phagocytosis of KCs was markedly weakened during acute hepatic failure resulted from galactosamine or TAA. Other researchers observed KCs injury under electronmicroscopy at the first hour and almost all cells were necrotic at about the second hour after exposure to a lethal dose of ranine virus. The damage of hepatic parenchymal cells emerged at the fourteenth hour under the same circumstance. The function of mononuclear phagocyte system was inhibited in mice vaccinated with sub-lethal dose of ranine virus within 24 hours in other reports^[10].

Because of the serious destruction of tissues in severe hepatitis, KCs are overburdened in that they not only must phagocytize virus and immune complexes, but also remove cellular debris and other foreign bodies. Thus, the function of phagocytosis and elimination of endotoxin by KCs were impaired badly.

In physiological condition, the powerful phagocytosis of KCs require the help of nonspecific opsonin (such as fibronectin, Fn). In acute hepatic failure, the level of plasma Fn showed a significantly reduction due to the decline or loss of function that Fn is synthesized and secreted by hepatocytes. Experimental results revealed that there was a positive correlation between the decrease of Fn and phagocytosis of KCs^[1]. In conclusion, IETM is further aggravated by the impaired phagocytosis of KCs after "Primary liver injury".

SECONDARY LIVER INJURY

The SLI refers to the liver damage mediated by a battery of chemical mediators that were synthesized and released from KCs activated through IETM induced by PLI.

The SLI has been confirmed in a large number of animal experiments and clinical studies. First, In rats colectomized before administration of TAA, the level of plasmic endotoxin had no statistical difference from that in control group, the content of TNF- α was markedly lower and plasmic ALT activity was only one fifth of that in TAA group. Our findings indicated that severity of PLI induced by TAA was only one fifth of that by SLI^[12]. Second, it has been demonstrated in our extensive experiments that either inhibiting the function of KCs (GdCl₃ and SiO₂) or lightening IETM can attenuate the release of chemical mediators from KC and subsequent hepatic injury^[10]. Third, it has been reported from plenty of domestic and foreign clinical data that there are a battery of chemical mediators, which were released by activated KC in plasma of patients with various hepatitis (derived from virus, alcohol etc.) and hepatic diseases (such as posthepatic cirrhosis) in variable degrees, correspondingly brought about sorts of clinical signs and symptoms^[13]. The "second liver injury" makes a great impact on the development and prognosis of hepatitis.

Severe hepatitis

The plasma endotoxin level in patients with severe hepatitis was approximately five to eight times that of the normal person. The higher the level of endotoxin was, the severer the hepatitis would be. These data suggested that IETM had a great impact on the progress of hepatitis. KCs activated by LPS released a great deal of proinflammatory cytokines (TNF- α , IL-1, IL-6, etc.), lipid inflammatory mediators (LTs, PAF, TXA₂, etc.), NO, endothelin and oxygen-derived free radicals, which further amplified the inflammatory reaction. TNF- α , the most crucial proinflammatory cytokine of all, could mobilize neutrophilic leukocytes chemotactically into liver and initiated a series of reactions, i.e. respiratory burst, release of oxygen-derived free radical, lipid peroxide and hepatocellular necrosis. It also could induce considerable intercellular adhesion molecule-1 (ICAM-1) expression on sinusoidal endothelia and hepatocytes and promote CTLs to attack hepatocytes and led to massive hepatocellular necrosis. It was reported that there was a significantly positive correlation between TNF- α level and ICAM-1 mRNA content. Whereas ICAM-1 level also showed a significantly accordant positive correlation with serum ALT activity, the degree of hepatic necrosis, the degree of neutrophilic leucocytes infiltration in liver tissues. 67 percent of the necrotic area will be decreased if pretreated with anti-ICAM-1 antibody. These findings demonstrated that ICAM-1 played a vital role during the transformation of severe hepatitis into acute liver failure^[6].

Liu *et al*^[14] have observed that endotoxin-induced liver injury predominantly accounted for severe microcirculatory disturbance of liver. The response of hepatic microvasculature to LPS was directly related to the quantity and activated degree of KCs. The stronger the activated degree of KC was, the severer the hepatic microcirculatory disorder was. The histological observation showed that there was a large number of filiform ball microthrombi within hepatic sinusoids and micrangiums. The hemagglutination and the adhesion of activated leukocytes to vascular endothelium in sinusoids were observed too. The area of hepatic necrosis reached beyond 50 percent. The activity of plasmic ALT was significantly elevated. Obviously, the microcirculatory disturbance induced by LPS is predominantly responsible for hepatic persistent

necrosis and the further development of acute liver failure.

Ren *et al*^[15] used intoxication by TAA to duplicate rat model of severe hepatitis. The results indicated that in the TAA group, the level of plasmic endotoxin and the serum ALT activity were all significantly higher than those in the control group, the arterial ketone body ratio of acetoacetate to β -hydroxybutyrate(AKBR) decreased below 0.4, the ATP content of hepatocellular mitochondria was notably lower. While in the TAA plus colectomy group, there was no endotoxemia, the ATP content of hepatocellular mitochondria was sharply higher than that in the TAA group, but the serum ALT activity significantly lower than that in the TAA group. Thus, we might conclude that IETM played a key role in the occurrence of acute liver failure, the metabolic imbalance and dysfunction of liver might be caused by IETM through damaging hepatic energy metabolism.

We further investigated the role that functional state of KCs played in the occurrence of acute liver failure. The findings suggested that though a large single dose of CCL₄ could induce severe injury of hepatic parenchymal cells, no liver failure occurred in rats, because the structure and function of KCs were not affected. At the twenty fourth hour after intragastric infusion of rats, the granular turbid fluid of silica (18 μ g/100 g B.W.) was injected into caudal vein the level of plasma endotoxin was remarkably increased due to inhibition of KCs. At the twenty seventh hour urine volume, excretion of urea nitrogen and creatinine decreased markedly, with marked increase of blood urea nitrogen and creatinine indicating renal failure. Obvious lethargic phenomenon in rats with electroencephalograph (EEG) showing specific triphasic wave of the early stage of hepatic coma was observed at the 36th hour. EEG presented large and slow alternative wave after 40th hour. These findings suggested hepatic coma had occurred in rats. All these results demonstrated that although there was not significant change in parenchymal liver cells, rats experienced hepatic failure quickly, presenting as renal failure and coma in comparison with rats intragastrically infused with CCL₄ but without treatment with SiO₂^[16]. Similar results could be observed in the model of fulminant hepatic failure induced by TAA. In rats intragastrically infused with TAA but preceded by injection of SiO₂ in caudal vein, hepatic failure occurred rapidly. There was no significant difference in the injury extent of hepatic parenchymal cells as compared with rats without pretreatment with SiO₂. These findings demonstrated that IETM induced by KCs dysfunction played a determinative role in promoting hepatic insufficiency to develop into hepatic failure^[17].

Chronicity of hepatitis (acute hepatitis \rightarrow chronic hepatitis \rightarrow hepatic fibrosis \rightarrow cirrhosis of liver \rightarrow hepatocarcinoma or hepatic failure)

In the presence of persistent and mild IETM, repeated and sustained hepatocellular injury and concomitant inflammatory cell infiltration frequently develops and transforming growth factor β (TGF- β) controls the repairment of liver tissues via restricting the regeneration of hepatocytes and increasing extracellular matrix (ECM). Long-term injection of CCL₄ in small dose or oral intake of TAA in low concentration can cause chronic mild IETM with continuous expression of TGF- β in the experiment rats which successively result in hepatic fibrosis, micronodular cirrhosis then hepatocarcinogenesis in part and hepatic failure often resulted from some inducing factors within 2-6 months.

Jia *et al.* had established rat model of hepatic fibrosis induced by compound factor(CCL₄ mainly). Liver tissues were

characterized by steatosis and necrosis attended by inflammatory infiltration within 1-2 weeks. Then hepatic fibrotic proliferation developed within 3-4 weeks. Hepatic fibrosis continuously became aggravated, pseudulobuli were formed and hepatocirrhosis eventually developed within 5-8 weeks. In the meanwhile, IETM became increasingly serious and the level of plasma endotoxin rose gradually, which was positively correlated with the amount of hepatic collagen. It was indicated through immunohistochemical location that TNF- α was involved in the liver fibrosis mediated by endotoxin. By ultrastructural observation, the phenotype transformation of fat-storing cells suggested that functional state of fat-storing cells was closely related to endotoxin in the development of hepatic fibrosis^[18]. Cirrhosis which developed in rats drinking 0.03 % TAA for four months was accompanied by IETM with higher plasma levels of TNF- α , endothelin, NO, MDA, and hepatic collagen contents simultaneously in experiment performed by Zhao *et al*^[19]. Under electronmicroscopy, fat-storing cell nucleus showed the shape of star, cytoplasm projected outwardly, fat drop in cytoplasm diminished, its morphology was gradually transformed into that of myofibroblast. Collagen fibres apparently were increased around cell body. It was demonstrated by animal experiments that endotoxin could aggravate proliferation of hepatic fibers that developed into cirrhosis.

In the experiment by Yang *et al*^[20,21], 41.7 percent of rats drinking 0.03 % TAA for 6 months developed hepatocarcinoma on the basis of cirrhosis with elevation of endotoxin. Endotoxin could increase both overexpressions of bcl-2, P53 protein and point mutation of N-ras, P53 genes; increase the generation of free radicals and reduce antioxidase activity with aggravation of injury of DNA. These results provided evidences that endotoxin could precipitate cancerous change induced by TAA.

In above experiments, drugs against intestinal endotoxemia (such as herbal mixture "shuang Li Gan") could alleviate cirrhosis, and bring about decreased incidence of hepatocarcinoma. It was demonstrated again that prevention and treatment of IETM could stop the progress of hepatitis into chronicity.

Li *et al* have found that rats with cirrhosis became wilted somnolent and comatous and showed typical EEG changes at the fourth hour after a small dose of endotoxin injected once intraperitoneally. These manifestations suggested that hepatic encephalopathy (HE) had occurred in rats with cirrhosis. At this time blood ammonia level was elevated more than twice and plasma glucagons elevated more than ten times of that in normal rats. Glutamine contents of plasma and cerebrum were obviously higher than that in the cirrhotic control group. There were significant positive correlations between the levels of plasma endotoxin and plasma glucagon or ammonia, between the level of plasma ammonia and that of glutamine in cerebral homogenate. Apart from these, the contents of 5-hydroxytryptamin(5-HT), free tryptophan and 5-hydroxyindole acetic acid were all increased, whereas the contents of noradrenaline and dopamine were reduced in cerebral cortex.

It was exhibited from ultrastructural analysis that cellular swell and the diminished number of organelles in astrocytes of cerebral cortex markedly appeared in rats with HE induced by endotoxin. Immunohistochemical staining of TNF- α indicated that there was positive staining on endothelial cells of intracerephalic micrangium and some astrocytes of cerebral cortex.

Based on the above results, HE in rats with cirrhosis induced by endotoxin might be associated with sharp rise of plasma glucagons and subsequent rise of blood ammonia. Owing to the high level of blood ammonia, a great deal of

ammonia accumulated in cerebra and were transformed into glutamine under the action of glutamine synthetase of astrocytes. A great amount of glutamine was excreted from cerebra via blood-brain barriers (BBB) and resulted in a great amount of neutral amino acids transported into cerebra through the mechanism of carriers exchange. Great quantities of aromatic amino acids might inhibit tyrosine hydroxylase, and keep aromatic amino acids (phenylalanine, tyrosine) from synthesizing true neurotransmitter-noradrenaline and dopamine, but transformed into false neurotransmitter. Besides, tryptophan entering into the cerebra might form 5-HT under the action of corresponding enzyme. Thus, decreased true neurotransmitter with a coexisting increased inhibitory and(or) false neurotransmitter led to the functional inhibition of central nervous system followed by HE^[22].

In summary, if PLI caused by various pathogenic factors through their independent specific mechanism is regarded as “the first hit” on liver, then SLI mediated by different chemical mediators from KCs activated by IETM in the course of hepatitis is “the second hit” on liver. Thus fusing and overlapping of the primary and secondary liver injuries determine and influence the complexity of the illness and outcome of the patient with hepatitis.

For this reason, the viewpoint of “secondary liver injury” induced by “the second hit” on liver inflicted by IETM suggests that medical professionals should attach great importance to both “primary liver injury”, and “secondary liver injury” caused by IETM. That is, try to adjust the function of KCs and eliminate endotoxemia of the patient. Thus, it is beneficial in the short term to the cure of hepatitis and prevention from developing to severe hepatitis. it facilitates blocking the risk of development from hepatitis to cirrhosis and hepatocarcinoma in the long term. So the defence line against liver failure should be constructed through clearing IETM.

REFERENCES

- 1 **Zhao LF**, Han DW. Clinical significance of endotoxemia in liver diseases. *Shijie Huaren Xiaohua Zazhi* 1999; **7**: 391-393
- 2 **Grace LS**, Richard DK, Alireza A, Zang HY, Steintroeffer L, Alarcon WH, Remick DG, Wang SC. Kupffer cell activation by lipopolysaccharide in rats: role for lipopolysaccharide binding protein and Toll-like receptor 4. *Hepatology* 2000; **31**: 932-936
- 3 **Hoek JB**. Endotoxin and alcoholic liver disease: tolerance and susceptibility. *Hepatology* 1999; **29**: 1602-1604
- 4 **Charles BC**, Eva XB, Patricia EG, Kunkel SL, Roth RA. Bacterial lipopolysaccharide enhances aflatoxin B1 hepatotoxicity in rats by a mechanism that depends on tumor necrosis factor α . *Hepatology* 2001; **33**: 66-73
- 5 **Liang XB**, Qiao ZD, Yin L, Zhao JH, Han DW. Lipopolysaccharide induced apoptosis of rat hepatocyte *in vitro*. *Zhughua Ganzangbing Zazhi* 1999; **7**: 72-73
- 6 **Ahmad N**, Gazdner CR, Yurkow EJ, Laskin DL. Inhibition of macrophages with gadolinium chloride alters intercellular adhesion molecule-1 expression in the liver during acute endotoxemia in rats. *Hepatology* 1999; **29**: 728-736
- 7 **Thurman RG**, Bardford BU, Limuro Y. The role of gut-derived bacterial toxin and free radicals in alcohol-induced liver injury. *J Gastroenterol Hepatol* 1998; **13**(Suppl): S39-50
- 8 **Stachlewitz RF**, Sealra V, Bradford B, Bardham CA, Rusyn I, Germolec D, Thurman RG. Glycine and uridine prevent D-galactosamine hepatotoxicity in the rat: role of kupffer cells. *Hepatology* 1999; **29**: 737-745
- 9 **Winwood PJ**, Arthur HJP. Kupffer cells: their activation and role in animal models of liver injury and human liver disease. *Semin Liver Dis* 1993; **13**: 50-59
- 10 **Han DW**. Studies on pathogenesis of hepatic failure: hypothesis of intestinal endotoxemia. *Zhughua Ganzangbing Zazhi* 1995; **3**: 134-137
- 11 **Han DW**, Zhao LF. Effects of intestinal endotoxemia on chronicity of hepatitis. *Jichu Yixue Yu Linchuang* 1999; **19**: 482-487
- 12 **Liu LX**, Han DW, Ren DB. Effects of intestinal endotoxemia on pathogenesis of liver injury induced by thioacetamide. *Zhughua Ganzangbing Zazhi* 2000; **8**: 174-175
- 13 **Han DW**. Clinical basis for “secondary injury” induced by intestinal endotoxemia. *Shijie Huaren Xiaohua Zazhi* 1999; **7**: 1055-1058
- 14 **Liu LX**, Han DW, Ma XH. Role of hepatic microcirculatory disturbance induced by intestinal endotoxemia in liver injury. *Zhoughua Zhuanranbing Zazhi* 2001; **19**: 94-96
- 15 **Ren DB**, Han DW, Zhao YC. Effect of intestinal endotoxemia on hepatic energy metabolism in acute liver failure. *Zhongguo Binglishengli Zazhi* 2001; **17**: 890-892
- 16 **Han DW**, Fu ST, Ma XH, Zhao YC, Yin L. The Role of Kuffer cells in acute liver failure. *Zhonghua Ganzangbing Zazhi* 1994; **2**: 71-74
- 17 **Jian SY**, Han DW, Ma XH, Zhao YC, Yin L. Studies on actions of functional status of kupffer cells on experimental acute hepatic failure in rat. *Zhughua Ganzangbing Zazhi* 1995; **3**: 80-82
- 18 **Jia JB**, Han DW, Xu RL, Chen XM, Zhao YC, Ma XH, Yan JP. Role of gut-derived endotoxemia in the pathogenesis of experimental hepatic fibrosis. *Zhongguo Bialishengli Zazhi* 1998; **14**: 396-399
- 19 **Zhao LF**, Li H, Han DW. Effects of intestinal endotoxemia on the development of cirrhosis in rats. *Zhughua Ganzangbing Zazhi* 2001; **9**(Suppl): 21-23
- 20 **Yang JM**, Han DW, Liang QC, Zhao JL, Hao SY, Ma XH, Zhao YC. Effects of endotoxin on expression of ras, P53 and bcl-2 oncoprotein in hepatocarcinogenesis induced by thioacetamide in rats. *Chin Natl new Gastroenterol* 1997; **3**: 213-217
- 21 **Yang JM**, Han DW, Xie CM, Liang QC, Zhao YC, Ma XH. Endotoxin enhances hepatocarcinogenesis induced by oral intake of thioacetamide in rats. *World J Gastroenterol* 1998; **4**: 128-132
- 22 **Li XQ**, Han DW, Xu RL, Zhao YC, Ma XH. Hepatic encephalopathy in cirrhotic rats induced by endotoxin injection. *Zhongguo Binglishengli Zazhi* 1999; **15**: 151-153

Edited by Xu JY

• ESOPHAGEAL CANCER •

Down-regulation of gut-enriched Krüppel-like factor expression in esophageal cancer

Nan Wang, Zhi-Hua Liu, Fang Ding, Xiu-Qin Wang, Chuan-Nong Zhou, Min Wu

Nan Wang, Zhi-Hua Liu, Fang Ding, Xiu-Qin Wang, Chuan-Nong Zhou, Min Wu, National Laboratory of Molecular Oncology, Cancer Institute, Chinese Academy of Medical Sciences, Beijing 100021, China

Supported by China Key Program on Basic Research, No. G1998051021 and National Natural Science Foundation of China, No. 39993420

Correspondence to: Dr. Zhi-Hua Liu, National Laboratory of Molecular Oncology, Cancer Institute, Chinese Academy of Medical Sciences, 17 Panjiayuan, Chaoyang District, Beijing 100021, China. liuzh@pubem.cicams.ac.cn

Telephone: +86-10-67723789 **Fax:** +86-10-67715058

Received 2002-06-28 **Accepted** 2002-08-09

Abstract

AIM: Esophageal carcinoma is one of the most common malignant tumors in China. But the molecular mechanisms of esophageal carcinoma remains unclear. Gut-enriched Krüppel-like factor (GKLF) is a newly identified transcription factor which is expressed abundantly in the epithelial cells of the gastrointestinal tract and deregulation of GKLF was linked to several types of cancer. It is of interest to study the expression and role of GKLF in esophageal carcinoma.

METHODS: Semi-quantitative RT-PCR was used to compare GKLF expression in esophageal squamous cell carcinoma to normal mucosa of the same patients. The serum deprivation inducibility of GKLF was observed in an esophageal squamous cancer cell line by comparison to the primary culture of human fibroblast. The effect of antisense GKLF transfection on the proliferation and adhesion of esophageal squamous cancer cell line was also observed.

RESULTS: The level of GKLF transcript is lower in esophageal squamous cell carcinoma compared to paired normal-appearing mucosa in 14 of 17 of the tumors analyzed. The serum deprivation inducibility of GKLF was greatly decreased in an esophageal squamous cancer cell line compared to the primary culture of human fibroblast. Decreased expression of GKLF in the esophageal cancer cell by antisense GKLF transfection increased its proliferation rate compared with that of vector transfected cell control ($P < 0.05$). Transfection of antisense GKLF decreased its adhesion ability ($P < 0.05$).

CONCLUSION: The findings of this study demonstrate the down-regulation of GKLF in esophageal squamous cancer, and suggest that deregulation of GKLF may play a role in initiation and/or progression as well as the metastasis of esophageal squamous cancer.

Wang N, Liu ZH, Ding F, Wang XQ, Zhou CN, Wu M. Down-regulation of gut-enriched Krüppel-like factor expression in esophageal cancer. *World J Gastroenterol* 2002; 8(6):966-970

INTRODUCTION

The gut-enriched Krüppel-like factor (GKLF), also named as epithelial zinc finger (EZF) or KLF4, is a recently identified transcription factor with three C₂H₂ zinc fingers in the carboxyl terminus^[1-3]. The expression of GKLF is enriched in the epithelial cells of the gastrointestinal tract and skin^[1,2]. Although the physiological role of GKLF is not clear, experimental evidences^[1] suggest that GKLF is potentially a negative regulator of cell proliferation and involves in the differentiation process of epithelial cells. In the gene targeting experiment^[4], GKLF knockout mice showed the impairment of skin barrier function, indicating that GKLF is both vital to and selective for the barrier acquisition.

GKLF expression is decreased in the intestinal adenomas of mice and colon adenomas of patients^[5,6]. Experimental data^[7] also suggest that down-regulation of GKLF may play a role in the initiation stage of tumorigenesis of colon. In oral dysplastic epithelium and squamous cell carcinoma, GKLF expression was increased and diffusely distributed^[8,9]. In breast cancer, GKLF expression was increased and associated with the stages of tumor progression in the breast^[9]. These observations indicated that GKLF expression is regulated during neoplastic progression in a tissue and tumor type-specific fashion.

GKLF expression was enriched in esophageal epithelia^[2]. In esophageal cancer cell lines, abundant GKLF expression was also observed^[10,11]. The regulating effect of GKLF on the squamous epithelium-specific keratin 4 and Epstein-Barr virus ED-L2 promoters^[10] suggests GKLF plays an important role in the differentiation of esophageal squamous epithelium. The human GKLF gene was mapped onto chromosome 9q31^[3], which is a hot site of chromosome abnormality in esophageal cancer^[12,13]. GKLF gene aberration was observed in colon cancer in which the function of GKLF was demolished^[14]. These evidences led us to the research on the expression of GKLF in esophageal cancer, and consequent effect on the cancer cells. To our knowledge, this is the first report on the down-regulation of GKLF in esophageal cancer, and the first evidence of association of GKLF function with cell adhesion ability.

MATERIALS AND METHODS

Tissue samples and cell culture

Fresh surgical specimens of 17 pairs of esophageal squamous cell carcinoma and corresponding normal tissues were immediately frozen and stored in liquid nitrogen after resection. Squamous esophageal cancer cell line EC9706 was kindly provided by Dr. Mingrong Wang in the lab. The cell was grown in M199 (Gibco BRL, Gaithersburg, MD) supplemented with 15 % FCS. Primary culture of fibroblast was derived from resected normal esophageal tissue of an esophageal cancer patient, and maintained in McCoy 5A (Gibco BRL, Gaithersburg, MD) supplemented with 10 % FBS. Cells were incubated at 37 °C with 5 % CO₂. For the serum deprivation experiments, cells were seeded into 25 ml flasks with 4 ml full medium and cultured until 50 % confluency. The content of

FCS in the cell media was reduced to 0.5 %. Cells were then incubated continuously at 37 °C, in 5 % CO₂ for various periods.

RNA preparation and RT-PCR

Total RNA was extracted by TRIzol method (Gibco BRL, Gaithersburg, MD). Up to 5 µg of total RNA was reverse transcribed in 20 µl volume of reaction with both oligo (dT) and random primers, using SuperScript Preamplification System (Gibco BRL, Gaithersburg, MD) according to the instruction.

PCR was carried out in 30 µl total reaction mixture which contains 10 mmol/L Tris-HCL, pH 8.3, 50 mmol/L KCL, 1.75 mmol/L MgCl₂, 0.1 % Triton X-100, 200 µmol/L each of dGTP, dATP, dTTP, and dCTP, and 200 nmol/L each of the forward and reverse primers; 0.5-2 µl of cDNA template after RNase-free DNase I digestion was added. The primers used in the PCR reaction were synthesized according to the published cDNA sequences encoding human GKLF and GAPDH (GeneBank Accession numbers AF105036 and NM_002046, respectively). For the measurement of GKLF mRNA expression in tissue and cell samples, forward primer 5'-GTC GGA CCA CCT CGC CTT ACA CAT-3' and reverse primer 5'-GGT CTT CCC TCC CCC AAC TCA CG-3' of GKLF were used which amplify the region containing 3' noncoding sequence of GKLF cDNA (+1 374 to +1 749) and the expected PCR product was 376 bp; For the measurement of GKLF mRNA expression in cells after transfection of GKLF cDNA, forward primer 5'-CCA CCG GCC GGC TGC ACA CGA CT-3' and reverse primer 5'-TCA TCT GAG CGG GCG AAT TTC CAT CCA CA-3' of GKLF were used which amplify the coding sequence of GKLF cDNA (+864 to +1 298) and the expected PCR product was 435 bp. GAPDH primers (forward primer 5'-GGC AAA TTC CAT GGC ACC GTC AAG-3' and reverse primer 5'-GCA ATG CCA GCC CCA GCG TCA AA-3') were added in the same PCR reaction, and the expected PCR product of 746 bp was used as internal control. PCR was set up for 27 cycles: 30 s at 94 °C, 30 s at 56 °C 45 s at 72 °C.

GKLF cDNA cloning and sequencing

The full length GKLF cDNA coding sequence was amplified from reverse transcribed cDNA of EC9706. The forward primer 5'-CTG CTT CGG GCT GCC GAG GAC CTT CTG GG-3' and reverse primer 5'-GGC AGT GTG GGT CAT ATC CAC TGT CTG GGA-3' of GKLF were used and the expected PCR product was 1511 bp (-67 to +1444 nucleotides). The cycling condition was 30 s at 94 °C, 30 s at 63 °C 1 min at 72 °C for 30 cycles. The PCR product was electrophoresed onto 0.9 % agarose and 1.5 kb fragment was purified with the purification system (Qiagen, Hilden, Germany). The fragment was then cloned into PCR cloning vector pMD18T (TaKaRa, Dalian, China) and sequenced commercially (TaKaRa, Dalian, China).

Transfection

DNA fragment containing GKLF cDNA (-67 to +1444 nucleotides) was cut out from pMD18T vector by *Bam*HI and *Hind*III digestion and subcloned into pCDNA3.1 expression vector (Invitrogen, San Diego, CA) in antisense orientation. EC9706 cells were transfected with antisense GKLF cDNA as well as pCDNA3.1 vector using the Lipofectamine method according to the manufacture's protocol (Gibco BRL, Gaithersburg, MD). Briefly, cells were incubated with 1 ml of the transfection mixture containing 4.0 µg plasmid DNA and 25 µl Lipofectamine reagents in serum-free medium for 6 h, followed by adding 1 ml fresh media supplemented with 30 % FCS. The medium was exchanged with fresh complete media after overnight incubation.

RNA content determination

For semi-quantification of GKLF mRNA expression, the PCR products were electrophoresed onto 1.2 % agarose gel containing ethidium bromide. The images were analyzed with Multi-Analyst software (Bio-Rad, Hercules, CA) after scanned and the densities of GKLF and GAPDH bands were determined. The ratios of GKLF to GAPDH were compared in each paired sample.

Cell proliferation assay

Cells were inoculated into 96 well plates (2000/well) 36 h after transfection and incubated for further 24 h at 37 °C in CO₂ incubator. CellTiter 96 AQuous One Reagent (Promega, Madison, WI) was added into each well and OD490 was measured according to manufacture's method. The cells were washed three times with PBS and incubated in complete media for another 24 h. The assay was repeated and the ratio of OD490 to that of the first assay was calculated as the relative cell proliferate rate.

Cell adhesion assay

Cells were detached from culture flasks by trypsinisation 48 h after transfection and inoculated into 96 well plates (5000/well). After 2 h incubation, unattached cells were then removed by washing 3 times with PBS. CellTiter 96 AQuous One Reagent was added into each well and OD490 was measured. The percentage adhesion was determined by comparing the OD490 of attached cells to that of corresponding cells without washing.

Statistics

Results are expressed as mean \pm S.E.M. The statistical significance was determined with paired or grouped *t*-test.

RESULTS

GKLF expression in esophageal cancer

The GKLF mRNA expression was determined semi-quantitatively using RT-PCR method. In 17 pairs of tissue specimens, GKLF expression was detected in all samples as an expected PCR product of 376 bp in length, and 14 of them showed decreased expression in cancer sample compared to corresponding normal tissue. Paired *t*-test has a significant difference ($P < 0.05$) between cancer sample and normal tissue. Representative cases of GKLF expression detected by RT-PCR are shown in Figure 1.

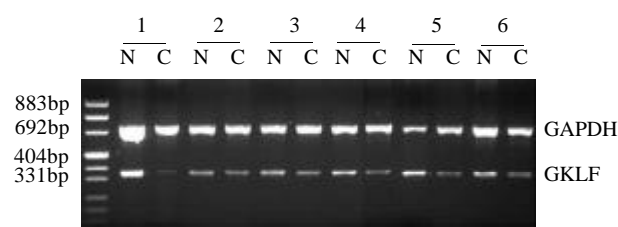


Figure 1 Semi-quantitative RT-PCR of GKLF in esophageal squamous cancer patients. RNA from specimens of normal appearing mucosa (N) and cancer (C) were extracted and GKLF as well as GAPDH were amplified. This figure showed the representative results from several individual patients.

GKLF cDNA coding sequence

GKLF gene resides at 9q31 of human genome^[3], which is a frequent site of LOH in esophageal cancer^[15,16]. Gene mutation

of GKLf coding sequence was also reported in a colon cancer cell line^[14]. In this Laboratory, the genomic alterations were observed in squamous esophageal cancer cell line EC9706 which includes 9q region by comparative genomic hybridization (unpublished data). To find out if GKLf cDNA was mutated in esophageal cancer cell line EC9706, the full length cDNA of coding region of GKLf was amplified by RT-PCR from cDNA of EC9706. An 1.5 kb length of PCR product was detected as expected. The single band was cloned into pMD18T vector and sequenced. The sequence conformed to cDNA of GKLf (GeneBank Accession number AF105036) completely without any mutation.

Serum deprivation induction of GKLf

GKLf expression was induced in murine fibroblast by serum deprivation^[1]. As GKLf expression was down-regulated in esophageal squamous cell carcinoma, we were interested in observing the inducibility of GKLf expression in esophageal cancer by serum deprivation. The cell line EC9706 was serum deprived and GKLf mRNA expression was detected by RT-PCR at 0 h, 6 h, 1 d, 2 d and 3 d. A primary culture of human fibroblast was also serum deprived as a positive control. Figure 2 showed the inducibility of GKLf by serum deprivation in both EC9706 and fibroblast. Although GKLf was induced in EC9706, the level was greatly decreased compared to that in human fibroblast.

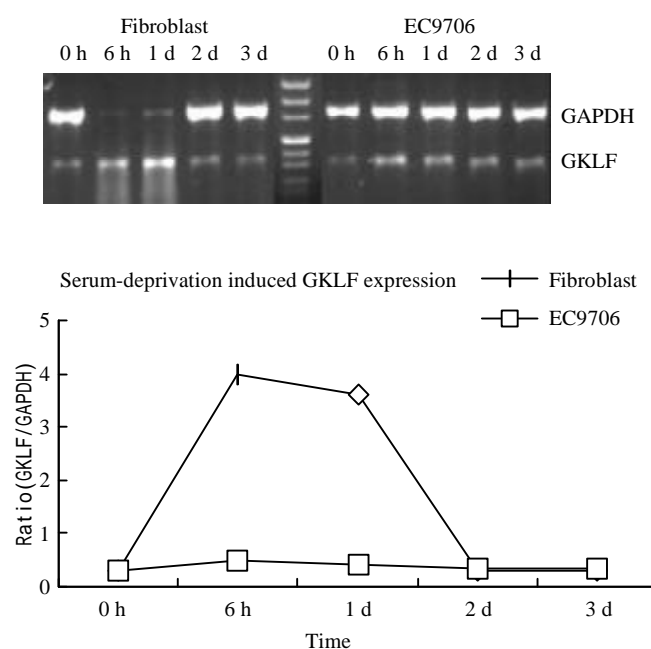


Figure 2 Serum deprivation induced GKLf expression. Both human primary cultured fibroblast and an esophageal squamous cancer cell line EC9706 was underwent serum deprivation. GKLf expression was measured semi-quantitatively by RT-PCR. The magnitude of GKLf expression was calculated as ratio of GKLf to GAPDH.

Cell growth and adhesion properties in esophageal cancer cells with low GKLf expression

It was reported that forced overexpression of GKLf inhibited DNA synthesis^[1] and decreased cell proliferation^[17]. We transiently transfected the esophageal cancer cell line EC9706 with antisense GKLf expression vector, which caused low expression of GKLf in the transfected cells (shown in Figure 3). The cell proliferative rate was assayed as described above.

Compared to the controlled cells, the low GKLf expression cells grew at a greater rate with a significant difference ($P < 0.05$). As we noticed that cell adhesion ability changed in individual stable transfectants of EC9706 with GKLf expression vectors (data not shown), cell adhesion assay was also carried out in these transiently transfected cells with low GKLf expression. In these cells, the adhesion ability was decreased significantly compared to the controlled cells ($P < 0.05$) (Figure 3).

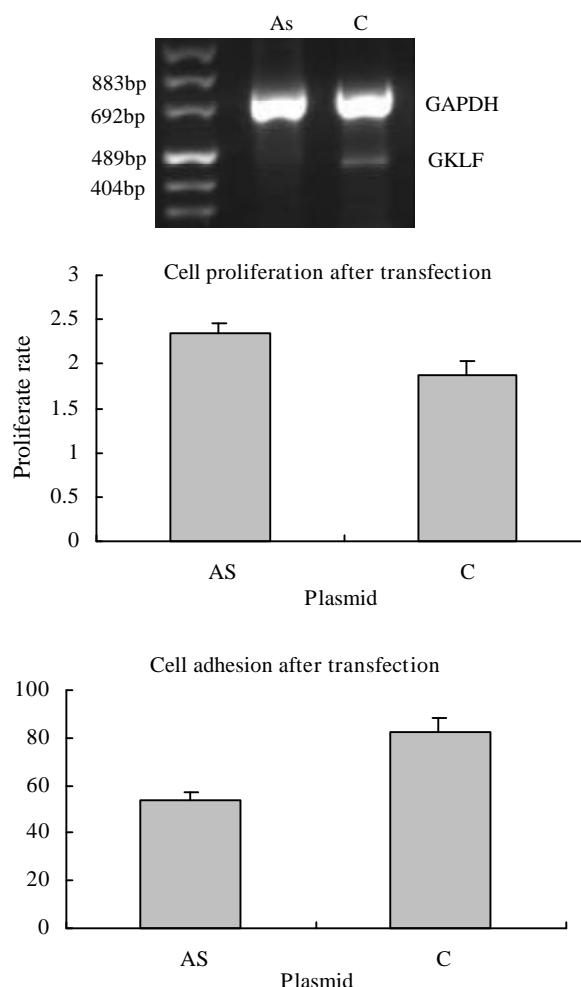


Figure 3 Cell growth and adhesion in GKLf transfected EC9706 cells. The cells were transiently transfected with antisense GKLf expression plasmid (AS) and pCDNA3.1 as control (C). The GKLf expression levels detected by RT-PCR were shown in the upper panel. The cell growth rates were shown in the middle panel; each data point represents mean \pm S.E.M. of 7 repeats; there was a significant difference between AS and C ($P < 0.05$). The cell adhesions were shown in the lower panel; each data point represents mean \pm S.E.M. of 4 repeats; AS had significant difference compared to C ($P < 0.05$).

DISCUSSION

Alterations of GKLf expression in cancer cells are tissue and tumor type-specific. Our current findings showed that GKLf was down-regulated in esophageal squamous cell carcinoma. It is known that down-regulation of GKLf occurred in intestinal adenoma and colonic adenoma^[6] while up-regulation of GKLf occurred in breast carcinomas and oral squamous cell carcinoma^[9]. The mechanism of altered GKLf expression and its difference among different tumor type is not clear yet. The results from colon cancer cells^[6] showed that no involvement of DNA methylation in the down-regulation of GKLf, while

mutated CDX2 expression in some colon cancer cell lines may help to explain the low levels of GKLF expression^[18].

Serum deprivation induces growth arrest and apoptosis in normal cells while the inducibility of serum deprivation is usually decreased in cancer cells. Experimental evidence showed that p21^[19] and cyclin D1^[20] involved in the serum deprivation induces growth arrest and apoptosis. In some kind of cancer cells, serum deprivation did not induce the expression of p21^[21]. As a transcription factor, GKLF involves in the p53-p21 regulating pathway^[22]. It also regulates the cell cycle factors such as cyclin D1^[23]. Decreased inducibility of GKLF by serum deprivation in EC9706 cells may suggest a role of GKLF in decreased response of cancer cells to serum deprivation.

GKLF overexpression inhibits proliferation of NIH3T3 and of HT-29 colon cancer cells^[1,7]. Similar to the report^[7], we found that antisense expression of GKLF promotes cellular proliferation of EC9706 cells. Combined with the finding that GKLF was down-regulated in esophageal cancer tissues, the result suggested that GKLF might play a role in the initiation and/or progression of esophageal cancer. It was shown that GKLF exerted its effect on cell proliferation at G₁ phase of cell cycle^[7,24]. That GKLF mediates the p53-p21 regulating pathway^[22] could be a mechanism of its cell cycle effect as this pathway is important for the regulation of G1/S transition^[25]. Cyclin D1-RB pathway is another possible effecting pathway of GKLF for its cell cycle regulation, since GKLF directly down-regulates cyclin D1 expression^[23] while cyclin D1 facilitates progression through the G1 phase which plays a role in the initiation of esophageal cancer^[26]. Overexpression of cyclin D1 was observed in the early phase of esophageal tumors in zinc-deficient rat model^[27], suggesting an important role of zinc proteins in regulating cyclin D1 expression, and conforming to our proposition that down-regulation of GKLF plays a role in the initiation and/or progression of esophageal cancer.

The basic mechanism of tumour cell metastasis is reduced expression of adhesion molecules which results in an increased migratory ability of the cancer cells^[28]. We showed here that alteration of GKLF expression in EC9706 cell decreased its adhesion, implicating that GKLF involves in the metastasis of esophageal cancer. Abnormal expression of such cell adhesion molecules as cadherin, integrin and mucin has definite relationship with cancer metastasis^[29-31]. It is known that GKLF could regulate MUC5B gene transcription directly^[32]. GKLF also regulates laminin expression^[33,34] while laminin is a component of extracellular matrix which plays a key role in cell adhesion and migration. More frequent allelic loss at 9q region where the GKLF gene located was reported in esophageal squamous cell carcinoma patients with metastasis^[15], suggesting a clinically significant role of GKLF gene in esophageal cancer.

GKLF belongs to a family of Krüppel-like factors that is the most abundant transcription factors in human cells^[35]. It targets to the specific DNA sequence^[36] which represents one of the most abundant classes of conserved motifs of intergenic regions over the human genome^[37], besides to the common DNA sequences through which this family of factors binds and acts^[36,38]. More and more target genes are being discovered^[39,40], that will expedite our understandings of GKLF mediated action in both normal and malignant cells.

In summary, the results of this study showed that GKLF is down-regulated in esophageal squamous cell carcinoma, and GKLF deregulation in esophageal cancer cell line EC9706 shows a manner of decrease inducibility to serum deprivation. Furthermore, down-regulation of GKLF in EC9706 cells results in the proliferation and decreased adhesion of cancer cells, suggesting that down-regulation of GKLF may contribute to malignant phenotype of esophageal cancer.

REFERENCES

- 1 **Shields JM**, Christy RJ, Yang VW. Identification and characterization of a gene encoding a gut-enriched Krüppel-like factor expressed during growth arrest. *J Biol Chem* 1996; **271**: 20009-20017
- 2 **Garrett-Sinha LA**, Eberspaecher H, Seldin MF, de Crombrughe B. A gene for a novel zinc-finger protein expressed in differentiated epithelial cells and transiently in certain mesenchymal cells. *J Biol Chem* 1996; **271**: 31384-31390
- 3 **Yet SF**, McA' Nulty MM, Folta SC, Yen HW, Yoshizumi M, Hsieh CM, Layne MD, Chin MT, Wang H, Perrella MA, Jain MK, Lee ME. Human EZF, a Krüppel-like zinc finger protein, is expressed in vascular endothelial cells and contains transcriptional activation and repression domains. *J Biol Chem* 1998; **273**: 1026-1031
- 4 **Segre JA**, Bauer C, Fuchs E. Klf4 is a transcription factor required for establishing the barrier function of the skin. *Nat Genet* 1999; **22**: 356-360
- 5 **Ton-That H**, Kaestner KH, Shields JM, Mahatanankoon CS, Yang VW. Expression of the gut-enriched Krüppel-like factor gene during development and intestinal tumorigenesis. *FEBS Lett* 1997; **419**: 239-243
- 6 **Dang DT**, Bachman KE, Mahatan CS, Dang LH, Giardiello FM, Yang VW. Decreased expression of the gut-enriched Krüppel-like factor gene in intestinal adenomas of multiple intestinal neoplasia mice and in colonic adenomas of familial adenomatous polyposis patients. *FEBS Lett* 2000; **476**: 203-207
- 7 **Shie JL**, Chen ZY, O'Brien MJ, Pestell RG, Lee ME, Tseng CC. Role of gut-enriched Krüppel-like factor in colonic cell growth and differentiation. *Am J Physiol Gastrointest Liver Physiol* 2000; **279**: G806-G814
- 8 **Foster KW**, Ren S, Louro ID, Lobo-Ruppert SM, McKie-Bell P, Grizzle W, Hayes MR, Broker TR, Chow LT, Ruppert JM. Oncogene expression cloning by retroviral transduction of adenovirus E1A-immortalized rat kidney RK3E cells: transformation of a host with epithelial features by c-MYC and the zinc finger protein GKLF. *Cell Growth Differ* 1999; **10**: 423-434
- 9 **Foster KW**, Frost AR, McKie-Bell P, Lin CY, Engler JA, Grizzle WE, Ruppert JM. Increase of GKLF messenger RNA and protein expression during progression of breast cancer. *Cancer Res* 2000; **60**: 6488-6495
- 10 **Jenkins TD**, Opitz OG, Okano J, Rustgi AK. Transactivation of the human keratin 4 and Epstein-Barr virus ED-L2 promoters by gut-enriched Krüppel-like factor. *J Biol Chem* 1998; **273**: 10747-10754
- 11 **Brembeck FH**, Rustgi AK. The tissue-dependent keratin 19 gene transcription is regulated by GKLF/KLF4 and Sp1. *J Biol Chem* 2000; **275**: 28230-28239
- 12 **Miura K**, Suzuki K, Tokino T, Isomura M, Inazawa J, Matsuno S, Nakamura Y. Detailed deletion mapping in squamous cell carcinomas of the esophagus narrows a region containing a putative tumor suppressor gene to about 200 kilobases on distal chromosome 9q. *Cancer Res* 1996; **56**: 1629-1634
- 13 **Hu N**, Roth MJ, Polymeropolous M, Tang ZZ, Emmert-Buck MR, Wang QH, Goldstein AM, Feng SS, Dawsey SM, Ding T, Zhuang ZP, Han XY, Ried T, Giffen C, Taylor PR. Identification of novel regions of allelic loss from a genomewide scan of esophageal squamous-cell carcinoma in a high-risk Chinese population. *Genes Chromosomes Cancer* 2000; **27**: 217-228
- 14 **Shie JL**, Tseng CC. A nucleus-localization-deficient mutant serves as a dominant-negative inhibitor of gut-enriched Krüppel-like factor function. *Biochem Biophys Res Commun* 2001; **283**: 205-208
- 15 **Hu N**, Roth MJ, Emmert-Buck MR, Tang ZZ, Polymeropolous M, Wang QH, Goldstein AM, Han XY, Dawsey SM, Ding T, Giffen C, Taylor PR. Allelic loss in esophageal squamous cell carcinoma patients with and without family history of upper gastrointestinal tract cancer. *Clin Cancer Res* 1999; **5**: 3476-3482
- 16 **Roth MJ**, Hu N, Emmert-Buck MR, Wang QH, Dawsey SM, Li G, Guo WJ, Zhang YZ, Taylor PR. Genetic progression and heterogeneity associated with the development of esophageal squamous cell carcinoma. *Cancer Res* 2001; **61**: 4098-4104
- 17 **Chen ZY**, Shie J, Tseng C. Up-regulation of gut-enriched Krüppel-like factor by interferon-gamma in human colon carcinoma cells. *FEBS Lett* 2000; **477**: 67-72

- 18 **Dang DT**, Mahatan CS, Dang LH, Agboola IA, Yang VW. Expression of the gut-enriched Krüppel-like factor (Krüppel-like factor 4) gene in the human colon cancer cell line RKO is dependent on CDX2. *Oncogene* 2001; **20**: 4884-4890
- 19 **Duttaroy A**, Qian JF, Smith JS, Wang E. Up-regulated P21CIP1 expression is part of the regulation quantitatively controlling serum deprivation-induced apoptosis. *J Cell Biochem* 1997; **64**:434-446
- 20 **Driscoll B**, Buckley S, Barsky L, Weinberg K, Anderson KD, Warburton D. Abrogation of cyclin D1 expression predisposes lung cancer cells to serum deprivation-induced apoptosis. *Am J Physiol* 1999; **276**: L679-L687
- 21 **Modiano JF**, Ritt MG, Wojcieszyn J, Smith R 3rd. Growth arrest of melanoma cells is differentially regulated by contact inhibition and serum deprivation. *DNA Cell Biol* 1999; **18**: 357-367
- 22 **Zhang W**, Geiman DE, Shields JM, Dang DT, Mahatan CS, Kaestner KH, Biggs JR, Kraft AS, Yang VW. The gut-enriched Krüppel-like factor (Krüppel-like factor 4) mediates the transactivating effect of p53 on the p21WAF1/Cip1 promoter. *J Biol Chem* 2000; **275**: 18391-18398
- 23 **Shie JL**, Chen ZY, Fu M, Pestell RG, Tseng CC. Gut-enriched Krüppel-like factor represses cyclin D1 promoter activity through Sp1 motif. *Nucleic Acids Res* 2000; **28**: 2969-2976
- 24 **Chen X**, Johns DC, Geiman DE, Marban E, Dang DT, Hamlin G, Sun R, Yang VW. Krüppel-like factor 4 (gut-enriched Krüppel-like factor) inhibits cell proliferation by blocking G1/S progression of the cell cycle. *J Biol Chem* 2001; **276**: 30423-30428
- 25 **Bartek J**, Lukas J. Pathways governing G1/S transition and their response to DNA damage. *FEBS Lett* 2001; **490**: 117-122
- 26 **Nakagawa H**, Wang TC, Zukerberg L, Odze R, Togawa K, May GH, Wilson J, Rustgi AK. The targeting of the cyclin D1 oncogene by an Epstein-Barr virus promoter in transgenic mice causes dysplasia in the tongue, esophagus and forestomach. *Oncogene* 1997; **14**: 1185-1190
- 27 **Fong LY**, Nguyen VT, Farber JL, Huebner K, Magee PN. Early deregulation of the p16ink4a-cyclin D1/cyclin-dependent kinase 4-retinoblastoma pathway in cell proliferation-driven esophageal tumorigenesis in zinc-deficient rats. *Cancer Res* 2000; **60**: 4589-4595
- 28 **Cavallaro U**, Christofori G. Cell adhesion in tumor invasion and metastasis: loss of the glue is not enough. *Biochim Biophys Acta* 2001; **1552**: 39-45
- 29 **Madhavan M**, Srinivas P, Abraham E, Ahmed I, Mathew A, Vijayalekshmi NR, Balaram P. Cadherins as predictive markers of nodal metastasis in breast cancer. *Mod Pathol* 2001; **14**: 423-427
- 30 **Li G**, Satyamoorthy K, Herlyn M. N-cadherin-mediated intercellular interactions promote survival and migration of melanoma cells. *Cancer Res* 2001; **61**: 3819-3825
- 31 **Kim YS**, Gum JR Jr, Crawley SC, Deng G, Ho JJ. Mucin gene and antigen expression in biliopancreatic carcinogenesis. *Ann Oncol* 1999; **10** (Suppl 4): 51-55
- 32 **Seuningen IV**, Perrais M, Pigny P, Porchet N, Aubert JP. Sequence of the 5'-flanking region and promoter activity of the human mucin gene MUC5B in different phenotypes of colon cancer cells. *Biochem J* 2000; **348**: 675-686
- 33 **Miller KA**, Eklund EA, Peddinghaus ML, Cao Z, Fernandes N, Turk PW, Thimmapaya B, Weitzman SA. Krüppel-like factor 4 regulates laminin α 3A expression in mammary epithelial cells. *J Biol Chem* 2001; **276**: 42863-42868
- 34 **Higaki Y**, Schullery D, Kawata Y, Shnyreva M, Abrass C, Bomsztyk K. Synergistic activation of the rat laminin γ 1 chain promoter by the gut-enriched Krüppel-like factor (GKLF/KLF4) and Sp1. *Nucleic Acids Res* 2002; **30**: 2270-2279
- 35 **Bieker JJ**. Krüppel-like factors: three fingers in many pies. *J Biol Chem* 2001; **276**: 34355-34358
- 36 **Shields JM**, Yang VW. Identification of the DNA sequence that interacts with the gut-enriched Krüppel-like factor. *Nucleic Acids Res* 1998; **26**: 796-802
- 37 **Kondrashov AS**, Shabalina SA. Classification of common conserved sequences in mammalian intergenic regions. *Hum Mol Genet* 2002; **11**: 669-674
- 38 **Philipsen S**, Suske G. A tale of three fingers: the family of mammalian Sp/XKLF transcription factors. *Nucleic Acids Res* 1999; **27**: 2991-3000
- 39 **Chen ZY**, Shie JL, Tseng CC. Gut-enriched Krüppel-like factor represses ornithine decarboxylase gene expression and functions as check point regulator in colonic cancer cells. *J Biol Chem* 2002; In press
- 40 **Zelko IN**, Folz RJ. MZF-like, Krüppel-like and Ets-family of transcription factors determine the cell-specific expression of mouse extracellular superoxide dismutase. *Biochem J* 2002; In press

Edited by Zhang JZ

• ESOPHAGEAL CANCER •

Relationship between Egr-1 gene expression and apoptosis in esophageal carcinoma and precancerous lesions

Ming-Yao Wu, Ying-Rui Liang, Xian-Ying Wu, Chu-Xiang Zhuang

Ming-Yao Wu, Ying-Rui Liang, Xian-Ying Wu, Department of Pathology, Shantou university Medical College, Shantou 515031, Guangdong Province, China

Chu-Xiang Zhuang, Department of physiology, Shantou university Medical College, Shantou 515031, Guangdong Province, China

Supported by the National Natural Science Foundation of China, No. 39670298

Correspondence to: Ming-Yao Wu, Department of Pathology, Shantou University Medical College, 22 Xinling Road, Shantou 515031, Guangdong Province, China. mywu@stu.edu.cn

Telephone: +86-754-8900486 **Fax:** +86-754-8557562

Received 2002-06-14 **Accepted** 2002-07-26

Abstract

AIM: To study the expression of early growth response gene-1 (Egr-1 gene) and Bcl-X_L protein and its relationship with the cell apoptosis in human esophageal carcinoma(EC) and precancerous lesions.

METHODS: *In situ* hybridization(ISH), immunohistochemistry (IHC) and TUNEL method were used respectively to detect Egr-1mRNA, Egr-1 protein, apoptosis related-protein Bcl-X_L and cell apoptosis *in situ* from 66 cases of esophageal squamous cell carcinoma and their upper cut edge and paracancerous mucosa.

RESULTS: Egr-1 gene *in situ* hybridization, Bcl-X_L immunohistochemistry positive products were located in the cytoplasm, while Egr-1 immunohistochemistry and TUNEL positive signal were located in the nuclei. The apoptosis index(AI) and the frequency of apoptosis occurrence were increased gradually from precancerous lesion to cancer ($P<0.01$) and the expression of Egr-1mRNA and Egr-1 protein in dysplasia was the highest among all specimens ($P<0.01$). The AI of Egr-1 positive cancer tissues was much higher than that of Egr-1 negative cancer tissues ($P<0.01$), while the AI of Bcl-X_L positive cancer tissues was much lower than that of Bcl-X_L negative cancer tissues ($P<0.01$). The AI and Egr-1 expression were not correlated with invasiveness and lymphatic metastasis in EC.

CONCLUSION: Cell apoptosis was present through esophageal carcinogenesis. The expression of Egr-1 mRNA and Egr-1 protein were high in precancerous lesion of esophagus. The AI was increased significantly in Egr-1 positive squamous cell carcinoma. Egr-1 might promote apoptotic effect. Egr-1 expression and cell apoptosis may have an important biological significance in esophageal carcinogenesis.

Wu MY, Liang YR, Wu XY, Zhuang CX. Relationship between Egr-1 gene expression and apoptosis in esophageal carcinoma and precancerous lesions. *World J Gastroenterol* 2002; 8(6): 971-975

INTRODUCTION

Esophageal carcinoma is one of the most common malignant tumors in China^[1-5]. Its pathogenesis and development are closely related to the expression of some proto-oncogenes and their products and apoptosis of the cancer cells^[6-19]. The expression of oncogenes and tumor suppressor genes in esophageal carcinoma has been studied; the relationship between Egr-1 and carcinoma has been reported as well^[20]. Our previous studies have indicated that Egr-1 gene inhibited the growth of Eca109 after the exogenous introduction of Egr-1 gene^[21]. But the relationship between expression of Egr-1 and cell apoptosis in esophageal carcinoma is not well understood so far. In this paper, we have performed the examination of Egr-1mRNA and Egr-1protein expression, apoptosis related-protein Bcl-X_L expression and cell apoptosis of the carcinoma tissue, upper cut edge mucosa and paracancerous lesions from 66 cases esophageal carcinoma using *In situ* hybridization, immunohistochemistry and terminal deoxynucleotidyl transferase (TdT)-mediated dUTP-digoxigenin nick end labeling method (TUNEL) respectively. The purpose is to understand the correlation of Egr-1 expression and cell apoptosis in esophageal carcinogenesis.

MATERIALS AND METHODS

Sample collecting and processing

Fresh esophagus specimens after operation including esophageal mucosa at the upper cut edge, cancer tissue and mucosa just adjacent to the tumor mass were taken from 66 patients of esophageal carcinomas who had not received accepted chemotherapy or radiotherapy before operation. All specimens were from Department of Pathology Shantou University Medical College, from January to December, 2000. The specimens were fixed in 40 mL/L neutral formalin; the slides were applied by 1/1 000 diethyl pyrocarbonate (DEPC, Sigma Chemical Co, USA), paraffin embedded, cut in 4 μ m, HE stained.

Histopathology analysis

Histopathological diagnosis of esophageal para-cancer epithelia was made according to Liu *et al*'s criteria including 39 cases of normal epithelium, 52 cases of simple hyperplasia and 41 cases of dysplasia. 66 cases of esophageal carcinoma were diagnosed using WHO histological tumor classification including 2 cases of carcinoma *in situ*, 18 cases of grade I squamous cell carcinoma, 33 cases of grade II and 13 cases of grade III. 22 cases had invaded the superficial muscular layer, and others had invaded the serosa. 36 of 66 cases had lymphatic metastasis.

In situ hybridization

Eukaryotic expression vector of PCMV-Egr-1 plasmid was donated by Dr RP Huang (Molecular Medicine, Northwest Hospital, WA, USA). The plasmid was confirmed by amplification, purification and endonuclease cutting, then

retrieved the DNA. The expression of Egr-1 was detected by digoxigenin-labeled gene probe from a commercial kit (Boster company, China) according to the manufacturer's instructions. Sections were dewaxed in xylene, then into graduated ethanol, and then into 30 mL/L hydrogen peroxide methanol for 30 min. Proteinase K at 37 °C for 20 min in 20 µg/ml and then fixed in 40 g/L PFA for 10 min in sequence. 90 % ethanol 5 min at -20 °C precool, digoxigenin-labeled cDNA probe (1:40) were denatured in hybridization buffer at 95-100 °C for 10 min, then -20 °C for 3 min, added on tissues and cover slipped at 42 °C overnight. Sections were washed with SSC and then mouse anti-digoxigenin antibody, biotinylated goat anti-mouse and then streptavidin-biotin complex(SABC) for 30 min, finally, with 3.3'-diaminobenzidine (DAB) visualization. Human breast tissue and the mouse brain tissue were used as the positive control. Incubation solution instead of the probe and sections digested by RNase (10 µg/ml) before Egr-1 detection were designed for the negative control.

Immunohistochemistry

Egr-1 and Bcl-X_L were analyzed by using Egr-1(588): cat#SC-110 rabbit polyclonal antiserum (1:200, Santa Cruz Biot Co, USA) and Bcl-X_L(H-62): sc-7195 polyclonal antibody (ready to use) with the SABC method according to the manufacturer's instructions (Boster company, China), and finally DAB visualization. The human breast tissue and the esophageal carcinoma tissue were used as the positive control. Negative control was designed by using PBS instead of Egr-1 antiserum or instead of Bcl-X_L polyclonal antibody.

Detection of cell apoptosis

Apoptosis was detected by the TdT-mediated dUTP nick end labeling (TUNEL) method using a detection kit from Boster company (China) according to the manufacturer's instructions. Section were dewaxed in xylene, then into graduated ethanol, and then into Fresh 30 mL/L hydrogen peroxide in room temperature for 10 min, washed with PBS, digested by proteinase K(20 µg/ml) at 37 °C for 10 min, and incubated with TdT and DIG-dUTP reaction mixture at 37 °C for 2 h. Samples were washed with PBS, and then biotinylated mouse anti-digoxigenin antibody, and then streptavidin-biotin complex(SABC) at 37 °C for 30 min, and finally, with DAB visualization. The small intestine mucosa of mouse was used as the positive control. Negative control was designed by PBS instead of TdTase.

Judgement of the results

The Egr-1mRNA positive expression showed brown stained signal in the cytoplasm; the Egr-1 protein positive signal showed brown stained signal in the nucleus. Either Egr-1mRNA positive or Egr-1 protein positive was considered to be positive result. Bcl-X_L positive expression showed brown stained signal in the cytoplasm; the result was considered positive if the positive cells accounted for more than 20 % in each slide. The nuclei of apoptotic cells were stained brown as detected under light microscopy(Olympus CHK). Apoptotic cells were counted according to the Schepop's method. Ten optical fields which were the strongest positive areas were counted (×400, field diameter 0.545 mm, area 2.33 mm²) and the vicinity of the necrotic areas were not evaluated in each slide. The apoptosis index (AI) was the average of positive cells per mm² in the slide.

Statistical analysis

Statistical significance was determined by χ^2 test or Student's *t* test.

RESULTS

Changes of cell apoptosis in esophageal precancerous lesions and cancer tissues

Apoptotic cells were observed in tissues with different lesions of esophageal epithelia and cancer tissues(Figure 1, 2). The AI and the frequency of apoptosis occurrence were low in the normal epithelia, but they were increased gradually from normal epithelia to dysplasia and to cancer tissues. The AI and the frequency of apoptosis occurrence of dysplasia lesions group was significantly higher than that of normal epithelia group ($P<0.01$, $P<0.01$, Table 1).

Table 1 Changes of cell apoptosis in esophageal precancerous lesions and cancer tissues

Groups	<i>n</i>	Apoptosis cases (%)	AI (cells/mm ²)
Normal epithelia	39	8 (20.5)	8.2±3.1
Simple hyperplasia	52	17 (32.7)	13.4±4.3
Dysplasia	41	31 (75.6) ^a	17.8±8.3 ^b
Carcinoma <i>in situ</i>	2	2 (100)	20.3±5.1
Invasive carcinoma	64	64 (100)	25.2±9.8

^a $P<0.01$, $\chi^2=24.29$ vs normal epithelia, χ^2 test; ^b $P<0.01$, $t=5.19$ vs normal epithelia, Student's *t* test.

The relationship between the expressions of Egr-1mRNA and Egr-1 protein and cell apoptosis in esophageal precancerous lesion and cancer tissues

The expressions of Egr-1mRNA and Egr-1 protein were observed in the cytoplasm and nuclei in different lesions of esophageal epithelia and cancer lesions respectively (Figure 3). The positivity results of Egr-1 ISH and Egr-1 IHC were nearly identical, but ISH showed slightly higher. The AI and the rate of Egr-1 positivity were increased gradually from normal epithelia to simple hyperplasia and to dysplasia; the AI and the rate of Egr-1 positive expression of dysplasia lesions group was significant higher than that of normal epithelia group ($P<0.01$, $P<0.01$); the Egr-1 positivity rate of invasive carcinoma group was significant lower than that of dysplasia lesions group ($P<0.01$, Table 2).

Table 2 The relationship between the expressions of Egr-1 and cell apoptosis in esophageal precancerous lesions and cancer tissues

Groups	<i>n</i>	Egr-1 positive		Egr-1 negative	
		<i>n</i> (%)	AI(cells/mm ²)	<i>n</i> (%)	AI(cells/mm ²)
Normal epithelia	39	9(23.1)	10.2±4.1	30(76.9)	3.8±2.5
Simple hyperplasia	52	20(38.5)	16.4±5.6	30(60.0)	7.2±4.3
Dysplasia	41	27(65.9) ^a	25.4±9.2 ^b	14(34.1)	10.9±7.4
Carcinoma <i>in situ</i>	2	1(50.0)	29.3±5.6	1(50.0)	11.5±3.7
Invasive carcinoma	64	17(26.6) ^c	30.8±6.8	47(73.4)	21.4±9.1

^a $P<0.01$, $\chi^2=14.78$ vs normal epithelia, χ^2 test; ^b $P<0.01$, $t=6.80$ vs normal epithelia, Student's *t* test; ^c $P<0.01$, $\chi^2=15.84$ vs Dysplasia, χ^2 test.

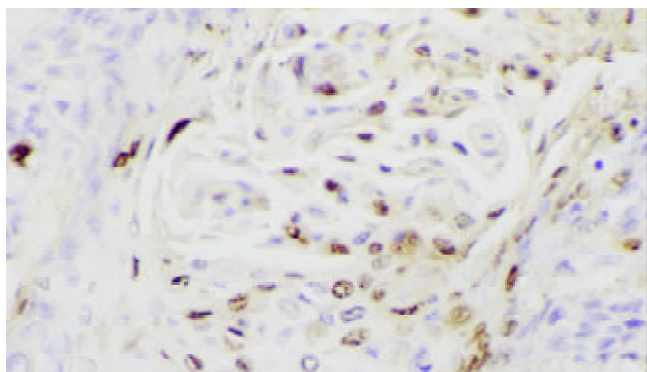


Figure 1 Positive apoptotic cell in nuclei of esophageal epithelial dysplasia. TUNEL×200.

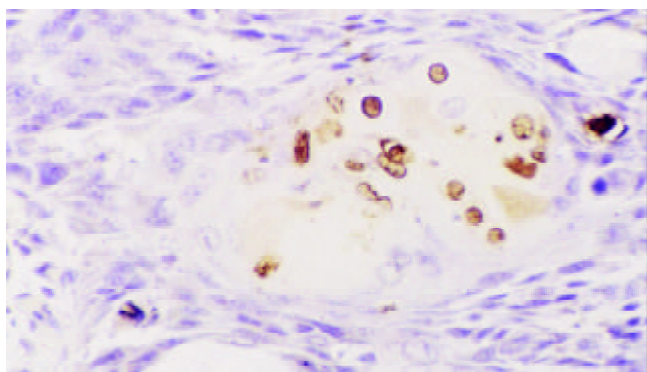


Figure 2 Positive apoptotic cell in nuclei of esophageal squamous cell carcinoma. TUNEL×200.

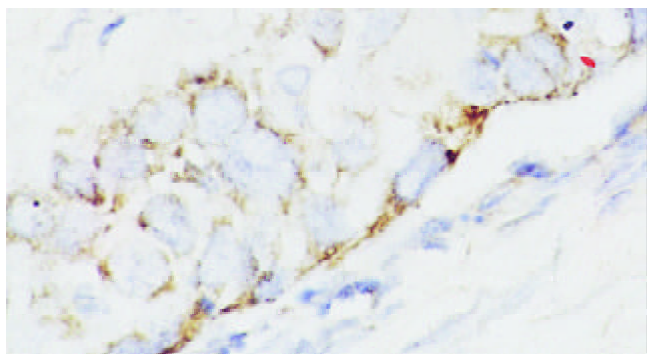


Figure 3 Positive Egr-1 mRNA in cytoplasm of esophageal squamous cell carcinoma. ISH ×400.

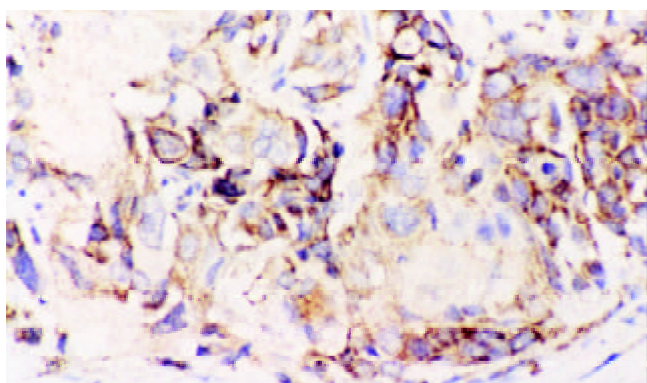


Figure 4 Positive Bcl-X_L protein in cytoplasm of esophageal squamous cell carcinoma. IHC×200.

The relationship between the protein expression of Bcl-X_L and cell apoptosis in esophageal precancerous lesions and cancer tissues

The expression of Bcl-X_L protein was observed in tissues with different lesion of esophageal epithelia and cancer tissues. The AI and Bcl-X_L immunostaining positivity rate were increased gradually as the lesion progressed. The AI and the rate of Bcl-X_L positive expression of dysplasia lesions group was significantly higher than that of normal epithelia group ($P<0.01$, $P<0.01$). In the Bcl-X_L(+) cases (Figure 4) the AI was low, while in the Bcl-X_L(-) cases had higher AI in the cancer tissues ($P<0.01$, Table 3).

Table 3 The relationship between the protein expression of Bcl-X_L and cell apoptosis in esophageal precancerous lesions and cancer tissues

Groups	n	Bcl-X _L positive		Bcl-X _L negative	
		n (%)	AI(cells/mm ²)	n (%)	AI(cells/mm ²)
Normal epithelia	39	4(10.3)	1.4±1.2	35(89.7)	8.3±4.3
Simple hyperplasia	52	11(21.2)	3.7±3.6	41(82.0)	14.5±3.7
Dysplasia	41	28(68.3) ^a	18.9±8.2 ^b	13(31.7)	20.6±6.3
Carcinoma <i>in situ</i>	2	1(50.0)	11.8±3.3	1(50.0)	29.0±5.7
Invasive carcinoma	64	46(71.9)	14.5±7.5 ^c	18(28.1)	28.6±8.6

^a $P<0.01$, $\chi^2=28.06$ vs normal epithelia, χ^2 test; ^b $P<0.01$, $t=10.53$ vs normal epithelia, Student's *t* test; ^c $P<0.01$, $t=6.10$ vs compared with Bcl-X_L protein negative group, Student's *t* test.

Table 4 The relationship between the expression of Egr-1 and cell apoptosis and biological behavior in esophageal squamous cell carcinoma

Clinicopathologic data	n	Egr-1 positive n(%)	AI(cells/mm ²)
Age(years)			
≤50	20	6(30.0)	21.5±7.9
>50	46	12(26.1)	24.3±8.8
Tumor site			
Upper segment	4	0 (0)	20.4±6.2
Middle segment	50	14(28.0)	23.7±9.3
Lower segment	12	4(33.3)	21.5±8.4
Lesion's diameter(cm)			
≤5	45	10(22.2)	22.6±8.5
>5	21	8(38.1)	22.3±9.2
Differentiation degrees			
Grade I	18	7(38.9)	31.6±9.3
Grade II	33	10(30.3)	28.5±8.9
Grade III	13	0(0)	7.2±3.5
Keratinization			
Negative	15	1(6.7)	8.6±3.2
Positive	51	17(33.3) ^a	34.7±9.4 ^b
Invasive depth			
Upper muscular layer	22	5(22.7)	18.7±7.5
Serosa	44	13(29.5)	26.1±9.2
Lymphatic metastasis			
Negative	30	11(36.7)	23.4±8.6
Positive	36	7(19.4)	20.8±7.5
Bcl-X _L protein			
Negative	19	10(52.6)	29.4±8.8
Positive	47	8(17.0) ^c	13.5±4.2 ^d

^a $P<0.05$, $\chi^2=4.15$ vs compared with non-keratinized squamous carcinoma group, χ^2 test; ^b $P<0.01$, $t=16.79$ vs compared with non-keratinized squamous carcinoma group, Student's *t* test; ^c $P<0.01$, $\chi^2=8.65$ vs compared with Bcl-X_L protein negative group, χ^2 test; ^d $P<0.01$, $t=7.54$ vs compared with Bcl-X_L protein negative group, Student's *t* test.

The relationship between the expression of Egr-1 and cell apoptosis and biological behavior in esophageal squamous cell carcinoma

All Egr-1 positive cases were of keratinized squamous cell carcinoma (grade I,II). The AI and Egr-1 positivity rate of keratinized squamous cell carcinoma group were significantly higher than that of the non-keratinized squamous cell carcinoma group ($P<0.05$, $P<0.01$). In Bcl-X_L protein positive group, the AI and the Egr-1 positivity rate were lower significantly than those in Bcl-X_L(-)group ($P<0.01$, $P<0.01$, Table 4).

DISCUSSION

Modern molecular biology investigations have indicated that proliferative inhibition of some neoplasm cells is related to apoptosis induction by the oncogene expression of these cells^[22-28]. Apoptosis, or programmed cell death, is a process in which a genetic program is activated, may be positively or negatively modulated by several oncogenes and tumor suppressor genes. The cancerigenic course of esophageal carcinoma has been identified as a successive course from simple hyperplasia of basal cell, dysplasia, carcinoma *in situ* to invasive carcinoma. Our studies suggest that The AI and the frequency of apoptosis occurrence increased gradually in esophageal carcinogenesis.

Egr-1 is one of the immediate early gene family, the Egr-1 gene was localized in human chromosome 5q31.1. Egr-1 is a nuclear protein that contains three zinc-finger domains, which regulate the cellular growth and differentiation by activating Cyclin D1 to promote the cell from the G0/G1 phase into the G2/M phase^[29]. It was reported^[30,31] that Egr-1 was originally in dormancy, and would be activated by the induction of stress, ischemia, hypoxia, bacterial toxin, cell factors, ionizing radiation and some oncogenic factors through membrane depolarization. We have detected tissue series of esophageal carcinogenesis using *In situ* hybridization and immunohistochemistry, and found that the rate of Egr-1 positive expression in dysplasia was the highest among all specimens (65.9 %). This might be explained that the paracancerous mucosa is much more stimulated, and this is in accordance with that Egr-1 expression is activated by many factors. High expression of Egr-1 might preserve the stabilization of chromosome and suppress proliferation, and also improve differentiation and apoptosis of the cell. Egr-1 expression is decreased significantly from dysplasia to cancer tissues^[32,33].

Recent studies have shown^[34] that there are several genes which participate in apoptosis regulation. Apoptosis regulation genes are divided into two groups: existence gene and death gene. Living gene includes cell promoting gene, while death gene includes proliferation suppressing gene. Studies using diverse tumor cells suggest that endogenous levels of Egr-1 act to impede proliferation^[21,29]. Consistent with its anti-tumor role, Egr-1 has been identified an important gene for impeding proliferation, and apoptosis of certain tumor cells needs Egr-1. Some studies indicated that the mechanism of Egr-1 inducing apoptosis might be involved by the activation of some oncogenes, e.g. wild type P53 gene, TNF- α and the concentration of calcium ions^[35,36]. Another gene that implicates apoptotic pathway is bcl-2. Bcl-2 has been identified to be an apoptosis inhibitor. Recently, a new bcl-2 relayed gene Bcl-X was identified. Alternative splicing results in two bcl-X-derived mRNA species, called bcl-X_L and bcl-X_S. Bcl-X_L appears to have functions similar to Bcl-2 in that it is capable of suppressing cell apoptosis in cancer cells^[37].

Abnormal hyperplasia and cell apoptosis of cancer cell are the dynamic process in the pathogenesis and development of esophageal carcinoma. Many studies indicated that cell hyperplastic cycle and cell apoptosis were two importance essential portions to maintain homostasis by many genes constituted complex modulation system. Our studies detected that cell apoptosis existed in normal epithelia and different lesion of esophagus, but AI and the frequency of apoptosis occurrence were increased gradually as the lesions progressed. In the similar lesions, the AI in Egr-1 positive group was higher than that in Egr-1 negative group. In contrast, the AI of Bcl-X_L positive group was lower than that of Bcl-X_L negative group. The AI and the expression of Egr-1 were not correlated with invasiveness and lymphatic metastasis of the cancer tissues. Our study suggests that cell apoptosis might be an important process in esophageal carcinogenesis. Egr-1 might promote apoptosis effect while Bcl-X_L inhibit it. But further study is necessary to explore the mechanism and significance of Egr-1 and Bcl-X_L improving or suppressing apoptosis in esophageal carcinogenesis.

REFERENCES

- 1 **Su M**, Lu SM, Tian DP, Zhao H, Li XY, Li DR, Zheng ZC. Relationship between ABO blood groups and carcinoma of esophagus and cardia in Chaoshan inhabitants of China. *World J Gastroenterol* 2001; **7**: 657-661
- 2 **Gao SS**, Zhou Q, Li YX, Bai YM, Zheng ZY, Zou JX, Liu G, Fan ZM, Qi YJ, Zhao X, Wang LD. Comparative studies on epithelial lesions at gastric cardia and pyloric antrum in subjects from a high incidence area for esophageal cancer in Henan, China. *World J Gastroenterol* 1998; **4**: 332-333
- 3 **Qiao GB**, Han CL, Jiang RC, Sun CS, Wang Y, Wang YJ. Overexpression of P53 and its risk factors in esophageal cancer in urban areas of Xi'an. *World J Gastroenterol* 1998; **4**: 57-60
- 4 **Chen KN**, Xu GW. Diagnosis and treatment of esophageal cancer. *Shijie Huaren Xiaohua Zazhi* 2000; **8**: 196-202
- 5 **Zheng ZY**, Wang LD, Shi ST, Yang GY, Xue ZH, Gao SS, Li YX, Yang CS. p53 gene mutations in multifocal esophageal precancerous and cancerous lesions in patients with esophageal cancer in high-risk northern China. *Shijie Huaren Xiaohua Zazhi* 1999; **7**: 280-284
- 6 **Wang LD**, Zhou Q, Wei JP, Yang WC, Zhao X, Wang LX, Zou JX, Gao SS, Li YX, Yang CS. Apoptosis and its relationship with cell proliferation, p53, Waf1p21, bcl-2 and c-myc in esophageal carcinogenesis studied with a high-risk population in northern China. *World J Gastroenterol* 1998; **4**: 287-293
- 7 **Li J**, Feng CW, Zhao ZG, Zhou Q, Wang LD. A preliminary study on ras protein expression in human esophageal cancer and precancerous lesions. *World J Gastroenterol* 2000; **6**: 278-280
- 8 **Zhang LJ**, Chen KN, Xu GW, Xing HP, Shi XT. Congenital expression of mdm-1 gene in tissues of carcinoma and its relation with pathomorphology and prognosis. *World J Gastroenterol* 1999; **5**: 53-56
- 9 **Casson AG**. Molecular biology of Barrett's esophagus and esophageal cancer: role of p53. *World J Gastroenterol* 1998; **4**: 277-279
- 10 **Xu CT**, Yan XJ. P53 anti-cancer gene and digestive system neoplasms. *Shijie Huaren Xiaohua Zazhi* 1999; **7**: 77-79
- 11 **Lin J**, Deng CS, Sun J, Zhou Y, Xiong P, Wang YP. Study on the genetic susceptibility of HLA-DQB1 alleles in esophageal cancer of Hubei Chinese Hans. *Shijie Huaren Xiaohua Zazhi* 2000; **8**: 965-968
- 12 **Qin HY**, Shu Q, Wang D, Ma QF. Study on genetic polymorphisms of DCC gene VNTR in esophageal cancer. *Shijie Huaren Xiaohua Zazhi* 2000; **8**: 782-785
- 13 **Wang LD**, Chen H, Guo LM. Alteration of tumor suppressor gene system p53-Rb and human esophageal carcinogenesis. *Shijie Huaren Xiaohua Zazhi* 2001; **9**: 367-371
- 14 **Yu GQ**, Zhou Q, Ivan D, Gao SS, Zheng ZY, Zou JX, Li YX, Wang LD. Changes of p53 protein blood level in esophageal cancer

- patients and normal subjects from a high incidence area in Henan, China. *World J Gastroenterol* 1998; **4**: 365-366
- 15 **Zhou YA**, Gu ZP, Wang XN, Ma QF. WAF1 gene suppresses growth of human esophageal carcinoma cell line EC109. *Shijie Huaren Xiaohua Zazhi* 2002; **10**: 628-632
 - 16 **Zhou YA**, Gu ZP, Wang XN, Ma QF, Huang LJ. Re-expression of p16^{INK4a} gene suppresses growth of human esophageal carcinoma cells. *Shijie Huaren Xiaohua Zazhi* 2001; **9**: 877-881
 - 17 **Liu J**, Chen SL, Zhang W, Su Q. P21^{WAF1} gene expression with P53 mutation in esophageal carcinoma. *Shijie Huaren Xiaohua Zazhi* 2000; **8**: 1350-1353
 - 18 **Tan LJ**, Jiang W, Zhang N, Zhang XR, Qiu DH. Fas/FasL expression of esophageal squamous cell carcinoma, dysplasia tissues and normal mucosa. *Shijie Huaren Xiaohua Zazhi* 2001; **9**: 15-19
 - 19 **Sarbia M**, Bittinger F, Grabellus F, Verreet P, Dutkowski P, Willers R, Gabbert HE. Expression of Bax, a pro-apoptotic member of the Bcl-2 family, in esophageal squamous cell carcinoma. *Int J Cancer* 1997; **73**: 508-513
 - 20 **Levin WJ**, Press MF, Gaynor RB, Sukhatme VP, Boone TC, Reissmann PT, Figlin RA, Holmes EC, Souza LM, Slamon DJ. Expression patterns of immediate early transcription factors in human non-small cell lung cancer. *Oncogene* 1995; **11**: 1261-1269
 - 21 **Wu MY**, Chen MH, Liang YR, Meng GZ, Yang HX, Zhuang CX. Experimental and clinicopathologic study on the relationship between transcription factor Egr-1 and esophageal carcinoma. *World J Gastroenterol* 2001; **7**: 490-495
 - 22 **Li HL**, Chen DD, Li XH, Zhang HW, Lu YQ, Ye CL, Ren XD. Changes of NF-KB, p53, Bcl-2 and caspase in apoptosis induced by JTE-522 in human gastric adenocarcinoma cell line AGS cells: role of reactive oxygen species. *World J Gastroenterol* 2002; **8**: 431-435
 - 23 **Xu AG**, Li SG, Liu JH, Gan AH. Function of apoptosis and expression of the proteins Bcl-2, p53 and C-myc in the development of gastric cancer. *World J Gastroenterol* 2001; **7**: 403-406
 - 24 **Sun BH**, Zhao XP, Wang BJ, Yang DL, Hao LJ. FADD and TRADD expression and apoptosis in primary human hepatocellular carcinoma. *World J Gastroenterol* 2000; **6**: 223-227
 - 25 **Peng ZH**, Xing TH, Qiu GQ, Tang HM. Relationship between Fas/FasL expression and apoptosis of colon adenocarcinoma cell lines. *World J Gastroenterol* 2001; **7**: 88-92
 - 26 **Si XH**, Yang LJ. Extraction and purification of TGF β and its effect on the induction of apoptosis of hepatocytes. *World J Gastroenterol* 2001; **7**: 527-531
 - 27 **Xu HY**, Yang YL, Guan XL, Song G, Jiang AM, Shi LJ. Expression of regulation apoptosis gene and apoptosis index in primary liver cancer. *World J Gastroenterol* 2000; **6**: 721-724
 - 28 **Li J**, Yang XK, Yu XX, Ge ML, Wang WL, Zhang J, Hou YD. Overexpression of p27KIP1 induced cell cycle arrest in G1 phase and subsequent apoptosis in HCC-9204 cell line. *World J Gastroenterol* 2000; **6**: 513-521
 - 29 **Nair P**, Muthukkumar S, Sells SF, Han SS, Sukhatme VP, Rangnekar VM. Early growth response-1-dependent apoptosis is mediated by p53. *J Biol Chem* 1997; **272**: 20131-20138
 - 30 **Yan SF**, Lu J, Zou YS, Soh WJ, Cohen DM, Buttrick PM, Cooper DR, Steinberg SF, Mackman N, Pinsky DJ, Stern DM. Hypoxia-associated induction of early growth response-1 gene expression. *J Biol Chem* 1999; **274**: 15030-15040
 - 31 **Bae SK**, Bae MH, Ahn MY, Son MJ, Lee YM, Bae MK, Lee OH, Park BC, Kim KW. Egr-1 mediates transcriptional activation of IGF-II gene in response to hypoxia. *Cancer Res* 1999; **59**: 5989-5994
 - 32 **Huang RP**, Fan Y, Belle I, Niemeyer C, Gottardis MM, Mercola D, Adamson ED. Decreased Egr-1 expression in human, mouse and rat mammary cells and tissues correlates with tumor formation. *Int J Cancer* 1997; **72**: 102-109
 - 33 **Huang RP**, Liu C, Fan Y, Mercola D, Adamson ED. Egr-1 negatively regulates human tumor cell growth via the DNA-binding domain. *Cancer Res* 1995; **55**: 5054-5062
 - 34 **Peter ME**, Heufelder AE, Hengartner MO. Advances in apoptosis research. *Proc Natl Acad Sci U S A* 1997; **94**: 12736-12737
 - 35 **Ahmed MM**, Sells SF, Venkatasubbarao K, Fruitwala SM, Muthukkumar S, Harp C, Mohiuddin M, Rangnekar VM. Ionizing radiation-inducible apoptosis in the absence of p53 linked to transcription factor Egr-1. *J Biol Chem* 1997; **272**: 33056-33061
 - 36 **Woronicz JD**, Calnan B, Ngo V, Winoto A. Requirement for the orphan steroid receptor Nur77 in apoptosis of T-cell hybridomas. *Nature* 1994; **367**: 277-281
 - 37 **Schott AF**, Apel II, Nunez G, Clarke MF. Bcl-X_L protects cancer cells from p53-mediated apoptosis. *Oncogene* 1995; **11**: 1389-1394

Edited by Xu JY

• ESOPHAGEAL CANCER •

Progressive transformation of immortalized esophageal epithelial cells

Zhong-Ying Shen, Li-Yan Xu, Min-Hua Chen, Jian Shen, Wei-Jia Cai, Yi Zeng

Zhong-Ying Shen, Li-Yan Xu, Min-Hua Chen, Jian Shen, Wei-Jia Cai, Department of Tumor Pathology; Medical College of Shantou University, Shantou 515031, Guangdong Province, China

Yi Zeng, Institute of Virology, Chinese Academy of Preventive Medicine, Beijing 100052, China

Supported by the National Natural Science Foundation of Chinese No. 39830380

Correspondence to: Dr. Zhong-Ying Shen, Department of Tumor Pathology, Medical College of Shantou University, 22 Xinling Road, Shantou 515031, Guangdong Province, China. zhongyingshen@yahoo.com

Telephone: +86-754-8538621 **Fax:** +86-754-8537516

Received 2002-07-12 **Accepted** 2002-08-09

epithelial cells with transduction of HPV18E₆E₇, cells from the 10th to the 85th passage were changed gradually from preimmortal, immortal, precancerous to malignantly transformed stages. All of these changes were in a dynamic progressive process. The establishment of a continuous line of esophageal epithelium may provide a *in vitro* model of carcinogenesis induced by HPV.

Shen ZY, Xu LY, Chen MH, Shen J, Cai WJ, Zeng Y. Progressive transformation of immortalized esophageal epithelial cells. *World J Gastroenterol* 2002; 8(6): 976-981

Abstract

AIM: To investigate the progressive transformation of immortal cells of human fetal esophageal epithelium induced by human papillomavirus, and to examine biological criteria of sequential passage of cells, including cellular phenotype, proliferative rate, telomerase, chromosome and tumorigenicity.

METHODS: The SHEE cell series consisted of immortalized embryonic esophageal epithelium which was in malignant transformation when cultivated over sixty passages without co-carcinogens. Cells of the 10th, 31st, 60th and 85th passages were present in progressive development after being transfected with HPV. Cells were cultivated in a culture flask and 24-hole cultural plates. Progressive changes of morphology, cell growth, contact-inhibition, and anchorage-dependent growth characteristics were examined by phase contrast microscopy. The cell proliferation rate was assayed by flow cytometry. The modal number of chromosomes was analyzed. HPV18E₆E₇ was detected by Western blot methods and activities of telomerase were analyzed by TRAP. Tumorigenicity of cells was detected with soft agar plates cultivated and with tumor formation in SCID mice.

RESULTS: In morphological examination the 10th passage cells were in good differentiation, the 60th and 85th passages cells were in relatively poor differentiation, and the 31st passage cells had two distinct differentiations. The characteristics of the 85th and 60th passage cells were weakened at contact-inhibition and anchorage-dependent growth. Karyotypes of four stages of cells belonged to hyperdiploid or hypotriploid, and bimodal distribution of chromosomes appeared in the 31st and 60th passage cells. All of these characteristics combined with a increasing trend. The activities of telomerase were expressed in the latter three passages. Four fourths of SCID mice in the 85th passage cells and one fourth of SCID mice in the 60th passage cells developed tumors, but the cells in the 10th and 31st passage displayed no tumor formation.

CONCLUSION: In continual cultivation of fetal esophageal

INTRODUCTION

The cell line SHEE was derived from immortalized embryonic esophageal epithelium induced by gene E6E7 of HPV 18 in our laboratory^[1,2] being cultivated and propagated over 100 passages. The 31st generation (SHEE31) had begun to express partial cell differentiation into two directions with some nests of cells with good differentiation and some with poor differentiation^[3]. The 61st generation cells (SHEE61) were premalignant cells^[4], and displayed a fully malignant transformation with a strong invasive potency at the 85th passage (SHEE85)^[5]. We believe that this established cell line (SHEE), continually affected by expression of HPV, would change its biological characters such as cell proliferation, differentiation, chromosome and telomerase, and that this might be controlled by cytogenesis (chromosomes) and molecular genetics (genes).

In general, the immortalized or transformed cells caused by carcinogens are always accompanied by chromosome abnormality and mutation of gene^[6]. The chromosome's changes are manifested in structure and the number of chromosomes^[7,8]. All of these changes appear in the procedure from quantitative to qualitative changes. The length of telomere in living cells was continually shortened after cellular mitosis^[9]. Because the somatic cells have no or lower levels of telomerase activity, telomere would be shortened, so it limits the division and lifespan of cells^[10,11]. Immortal or malignant cells manifest telomerase activities, which can maintain the telomere length^[12,13], so they will be immortal. With exposure of the early passage of immortal cell line to viral oncogenes, HPV or SV40T, conversion of these telomerase from negative expression to high levels of telomerase activity resulted^[14]. Telomerase would be present in benign lesions and activated during the late stage of carcinogenesis^[15].

Changes occurred in SHEE cells from the 10th to the 85th passage, with emphasis on their phenotypes, cytogenetic changes, telomerase activity and tumorigenicity, were studied in this paper. Phenotype of cells included the morphological changes of proliferation and contact-inhibition growth, and the modal number of chromosomes and the tumorigenicity, especially soft-agar culture and tumor formation in severely combined immuno-deficient (SCID) mice.

MATERIALS AND METHODS

Cell culture

The SHEE cells were routinely cultivated in culture medium 199 (GIBCO) with 10 % bovine serum, 100 units of penicillin and streptomycin in a humidified atmosphere of 5 % CO₂. Selected generations at the 10th passage (SHEE10), 31st passage (SHEE31), 60th passage (SHEE60) and 85th passage (SHEE85) were inoculated in culture flask and 24-hole culture plate with glass slide inside.

Living cell examination

The cell shape, anchorage dependent and contact-inhibited growth were examined by phase-contrast microscopy.

Cell cycle analysis

Cultured cells of each passage were collected from suspended and digested cells, fixed by 70 % alcohol, then filtered through nylon mesh, to generate single-cell suspension (1×10^6 /ml). The cells were stained with propidium iodide (Sigma) and were analyzed using flow cytometry (FCM) (FACSort Becton-Dickinson). Data of DNA of cells were collected and analyzed with Lysis II software, then a histogram was drawn and the cell percentages of each proliferation stage in the cell cycle and the number of cells more than 4n of DNA were calculated. The proliferation index formula: $S+G_2M/G_0G_1+S+G_2M$ and the cell amount at preG₀G₁ stage, the apoptotic cells, were calculated.

Cytogenetic analysis

Metaphase spreads were obtained using standard cytogenetic methods. Briefly, the culturing cells of each passage were preserved at 3–4 °C for 3–4 h to make cells on synchronous stage, then cultivated at 37 °C for 3–4 h, and added in 0.05 µg/ml colchicine for 1 h. Harvesting was by standard method and stained with Giemsa, 50–100 metaphases were scored for each line.

Telomerase activity assay^[16]

Telomerase activity was measured using the telomeric repeat amplification protocol (TRAP). Frozen samples were homogenized in 10–50 µL of ice-cold lyses buffer (10 mmol·L⁻¹ Tris-HCl, pH7.5, 1 mmol·L⁻¹ EGTA, 0.1 mmol·L⁻¹ Benzimidazole, 5 mmol·L⁻¹ βmercaptoethanol, 5 g·L⁻¹ CHAPS, 100 mL·L⁻¹ glycerol). After 30 min of incubation on ice, the lysate was centrifuged at 12 000 g for 20 min at 4 °C. TRAP-eze Telomerase Detection Kit (Oncor Inc.) reaction was performed using 1 µL lysate or 1/10 diluted lysate, 2.5 µL 10×TRAP buffer (200 mmol·L⁻¹ Tris-HCl, pH8.3, 15 mmol·L⁻¹ MgCl₂, 630 mmol·L⁻¹ KCl, 0.5 % Tween 20, 10 mmol·L⁻¹ EGTA, 1 g·L⁻¹ BSA), 0.5 µL 2.5 mmol·L⁻¹ dNTP, 0.5 µL Ts primer, 0.5 µL TRAP primer mix, 19.5 µL water, 0.5 µL taq (2 µ·L⁻¹). After incubation at 30 °C for 30 min, the reaction mixture was immediately transferred to 94 °C and performed PCR (GenAmp PCR System 2400, PE, USA) at 94 °C for 30s, 55 °C for 30s, for 35 cycles. PCR products were separated in a non-denaturing 125 g·L⁻¹ PAGE in 1×TBE at 5V·cm⁻¹. The gel was stained using AgNO₃ and was photographed.

Soft agar assays

Four passages of cells (1×10^4) were cultivated in each hole of the 6-hole plastic plate (Corning Co.) which was covered with two layers agarose (Agarose, V312A, Promega), the bottom, 1 % and the upper, 0.5 %. The cells were incubated in 5 % CO₂ at 37 °C incubator for 40 d and the cell colony

formations were scored every ten days. Each soft-agar cloning experiment was carried out at least in duplicate.

Tumorigenicity assays

In vivo tumor graft experiments were performed on the severely combined immunodeficient (SCID) mice (C.B-17/IcrJ-scid, Animal Lab of Chinese Academy of Medical Sciences). Cells of each passage were injected into the subaxillary skin of four mice with 1×10^6 cells for every one. Mice were observed weekly for two months and the tumor tissues were examined histopathologically.

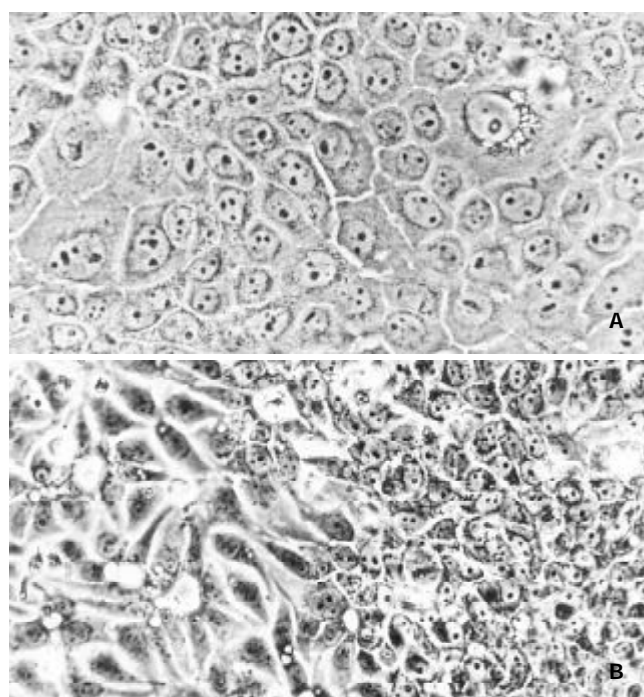
HPV18E₆E₇ assays

The protein expression of HPV18E₆E₇ was detected by Western blot method. The cells were washed three times with ice-cold PBS, then were lysed in buffer [50mM Tris-HCl, pH8.0, 150mM NaCl, 100 µg/ml phenyl-methyl-sulfonyl fluoride (PMSF), 1 % TritonX-100] for 30 min at ice. After removal of cell debris by centrifugation (12 000 g, 5 min), the protein concentration of lysates was measured by Bradford method. 50 µg proteins of different passage boiled for 5 min in sample buffer were separated by 10 % SDS-PAGE, transferred onto nitrocellulose membrane (Bio-Rad). Nonspecific reactivity was blocked by incubation overnight at 4 °C in buffer (10mM Tris-HCl, pH7.5, 150mM NaCl, 2 % Tween-20, 4 % bovine serum albumin). The membrane was then incubated with antibody of mouse anti HPV18E₆, (SC-264, Zhong Shan Biotech Co.), followed by reaction with anti-mouse IgG antibody. Reactive protein was detected by ECL chemiluminescence system (Amersham).

RESULTS

Proliferation and differentiation of SHEES

The cells of SHEE10 grew evenly on the flask. Cells appeared to have the characteristics of squamous epithelium (Figure 1, A) with multiangular outline and oval nucleus. SHEE31 were attached to the dish with partial differentiating into squamous epithelium and partial undifferentiated basal cells (Figure 1, B). The cells of SHEE60 and SHEE85 were differently shaped and sized and cells were crowded and overlapped (Figure 1C, D).



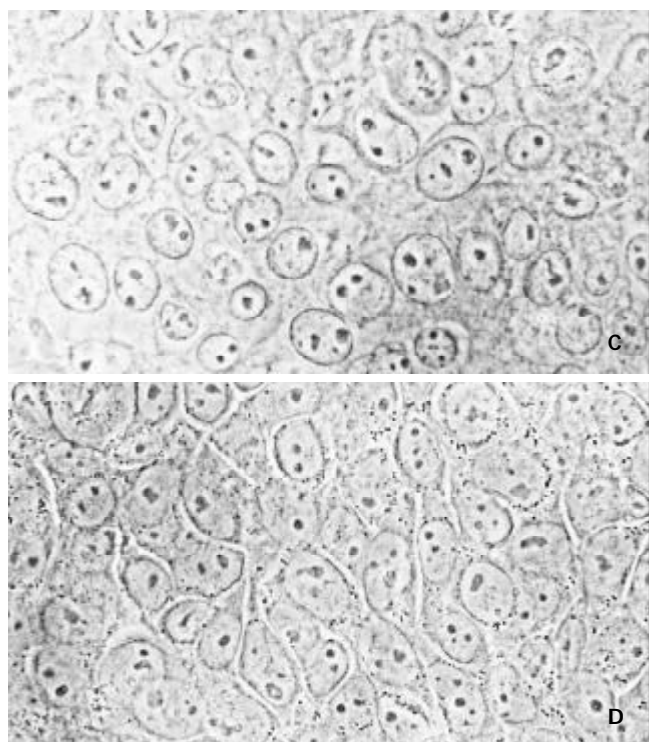


Figure 1 Morphology of SHEE cell (photographs of phase contrast microscope) A, SHEE10, good differentiation ($\times 400$); B, SHEE31, differentiated to two directions, well differentiated (left), and poorly differentiated (right) ($\times 200$); C, SHEE60, poor differentiation ($\times 400$); D, SHEE85 shows different shape and size with larger nucleolus ($\times 400$)

FCM analyzed cell cycle

In the DNA histogram (Figure 2), the distribution of DNA content of SHEE31 was similar to that of SHEE10, the proliferative indexes of SHEE10 and SHEE 31 were at the same level (32.0 %, 35.2 %), but different from SHEE60 (47.5 %) and SHEE85 (54.3 %). Of all DNA $>4n$ cells there were SHEE10, 2.5 %; SHEE31, 4.7 %; SHEE60, 6.1 % and SHEE85, 7.2 %. This showed that heteroploid and hyperploid tumor cells increased with progressive culture of SHEE.

The modal number of chromosome

The number of chromosomes in SHEE10, SHEE31, SHEE60 and SHEE85 (Table 1) ranged between 32 and 196, and these chromosomes were mainly hyperdiploids and hypotriploids. Most cells of hypertriploids were found at SHEE60. Modal number of chromosomes at SHEE10 was 58-62, at SHEE31 and SHEE60 were bimodal distribution, 55-57, 61-63, and 58-60, 63-65 respectively, at SHEE85 was 59-65. The modal number from the 10th passage to the 85th passage increased slowly.

Table 1 Number of Chromosome in SHEE Series

Number of passage	Number of cell	≤ 46	47-57	58-68	≥ 69	modal number
SHEE10	91	17(18.7%)	45(49.5%)	22(27.7%)	4 (4.3%)	58-62
SHEE31	100	12(12.0%)	38(38.0%)	46(46.0)	4 (4.0%)	55-57,61-63
SHEE60	52	5 (9.6%)	13(25.0%)	22(42.3%)	12(23.1%)	58-60,63-65
SHEE85	85	4 (4.7%)	16(18.8%)	54(63.5%)	11 (12.9)	59-65

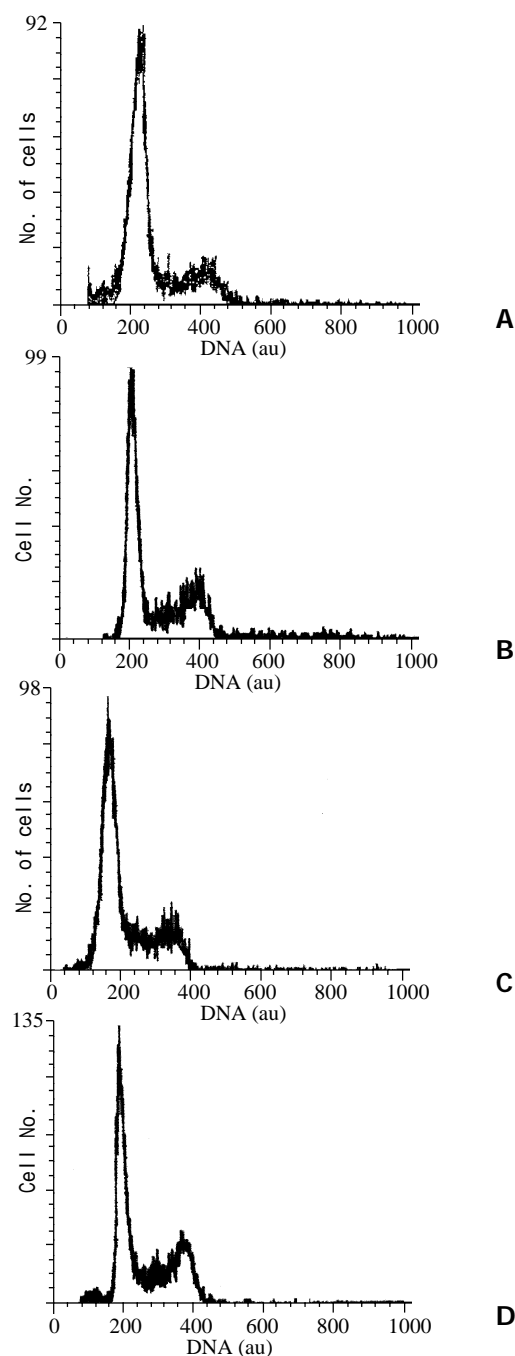


Figure 2 DNA histograms of SHEE. A, SHEE10; B, SHEE31; C, SHEE60; D, SHEE85; au, arbitrary unit.

Telomerase activity

Telomerase activation was absent in normal esophageal epithelium and SHEE10. The activity of telomerase appeared in the 31st passage, and it was strongly positive in SHEE60 and SHEE85.

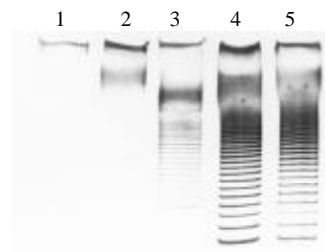


Figure 3 Activity of telomerase SHEE series 1, normal esophageal epithelium; 2, SHEE10; 3, SHEE31; 4, SHEE60; 5, SHEE85.

Expression of HPV18E₆E₇

The expression of HPV18E₆E₇ was examined by Western blot method. The figure (Figure 4) showed the expression of protein of HPV18E₆E₇ at cells of four stages of SHEE cell lines.

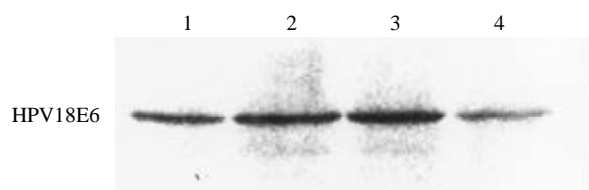


Figure 4 Western blot analysis of protein of HPV18E6 in SHEE 1, SHEE10; 2, SHEE31; 3, SHEE60; 4, SHEE85.

Tumorigenicity

SHEE10 could not grow on soft agar, but SHEE31, SHEE60 and SHEE85 could. SHEE31 formed small colonies, (less than 20 cells in a colony) compared to SHEE60 and SHEE85 in which large colonies (more than 50 cells in a colony) were formed. SCID mice inoculated with cells of SHEE10 and SHEE31 did not form tumors, but one quarter of SCID mice with inoculation of SHEE60 cells formed tumors with a latency period of over 2 months (data not shown). It was determined that a percentage of cells of SHEE60 manifested malignancy. All SCID mice inoculated with SHEE85 cells manifested tumor formation, which infiltrated into muscular layer histopathologically (Figure 5).

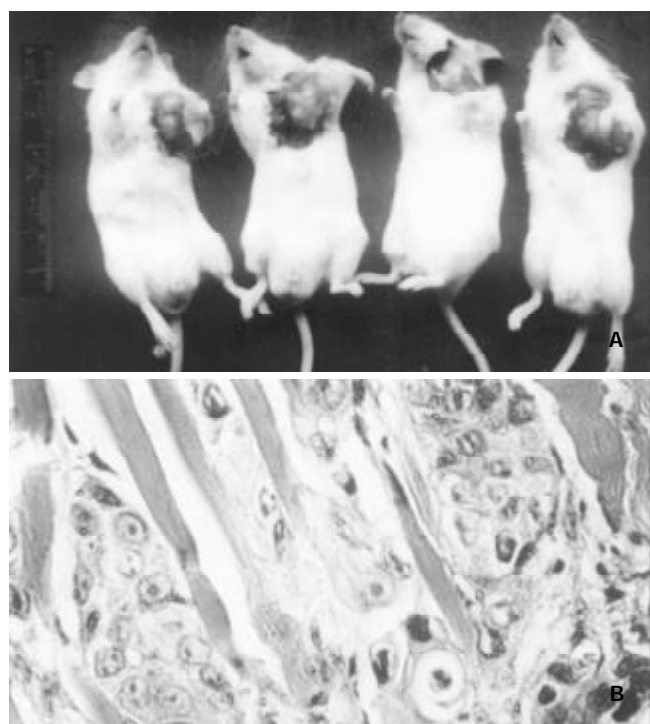


Figure 5 Heterotransplanting SHEE85 cells into SCID mice Tumors in right axia (arrow) of SCID mice are found (A). Invasion of tumor cells is found in muscular layer (B). HE, ×400

DISCUSSION

Cellular proliferation, differentiation and apoptosis are fundamental life activities, and are also the growth markers of immortal cells. According to the DNA content and proliferation index, the cells of SHEE10, SHEE31, SHEE60 and SHEE85 all show proliferative characteristics. The proliferation index

and cell numbers of polyploid (DNA>4n) of each passage were compared as a result of SHEE10<SHEE31<SHEE60<SHEE85. SHEE31 cells showed differentiation in two directions: one displayed relatively large and multiangular cells with abundant cytoplasm and oval nucleus; the others displayed small cells with less cytoplasm and small round nucleus. SHEE60 cells overlapped to grow, which were differently shaped and poorly differentiated. SHEE85 cells were crowded in cultivation with cells of poor differentiation and received less contact-inhibition. Detecting anchorage growth and contact inhibition specificity by cultivation on the soft agar is of help to judge its malignant character^[17,18]. The small colony formation of SHEE10 and SHEE31 cultivated in soft agar, and large colonies in SHEE85 and SHEE60 showed that the characteristics of anchorage-dependent growth decreased but tumorigenicity increased. A few tumors are formed in SCID mice incubated with SHEE60. So we judged that they were not at a fully malignant stage but at a premalignant stage. SHEE85 cells, which were transplanted into 4 SCID mice and developed tumors in all mice, expressed malignant transformation.

There were more hyperdiploid and hypotriploid in the chromosomes of four stages of SHEE cell lines. The separate modal number of chromosomes first appeared in SHEE31 and continued to SHEE60. The number of chromosomal sets and the percentage of hyperploid in SHEE31 varied between SHEE10 and SHEE60, and SHEE85 has more hypotriploid cells than the others. All above showed that chromosomes of SHEE series cell lines were unstable and more susceptible to malignant transformation by promoters^[19, 20]. The changes of cytogenetics will control the proliferation and differentiation of cells^[21].

In 1965, Hayflick reported that the culture life of human diploid fibroblast was limited to 50-100 generations, the same to epithelial cells. In 1985, Greider discovered the activity of telomerase. In 1994, Kim also identified a specific association between the telomerase activity and immortal cells or cancer cells. Telomerase activity was demonstrated in cancers of the digestive tract^[22-24], such as gastric^[25-29], hepatic^[30-32] colorectal^[33-35] and esophageal cancer^[36-38]. The telomerase activity is possibly both a prerequisite and a diagnostic criterion for immortal cells^[39]. Weitzman and Hahn believed T-antigen of SV40 and *ras* gene induce transformation of normal epithelium cells which require expression of telomerase activity^[40,41], so over-expression of telomerase related to proliferation is the early event of cancer^[42]. In our data the telomere was 30kb in length in the normal fetal esophageal cell, shortened to 17kb in SHEE 10, then further shortened to 3.5kb in SHEE 31, and then maintained at this level continually^[43]. The telomerase, first appeared in the 20th passage, could not prevent shortening of telomere, because it was in a low-or noncatalytic function, therefore cells had difficulty to survive in cultivation before the 20th passage. The cells grew stably after the 31st passage. Our results indicated that immortalization of SHEE might require activation of telomerase.

Infection of HPV can cause karyotype confusion, such as breaking of chromosome, abnormal structure and number of chromosomes^[44]. It also suggests that immortal esophageal cells induced by HPV18 E6E7 may affect the changes of chromosomes, and cause instability of genetic characters^[45]. Viruses can cause loss of contact inhibition, decrease of adhesion between cells, confusion of cellular skeletal structure, and loss requiring to growth factor^[46]. The virus genome inserts and integrates with the chromosome of host, causing the activation and expression of oncogenes^[47]. HPV E6E7 protein is conjugated with anti-oncoprotein p53 and pRb^[48], thus

causing loss of control of cellular growth, and encouraging the phenotyping production of cellular transformation. Previous reports have shown that activation of telomerase can be achieved by the E₆ and E₇ proteins of HPV^[49]. It has been reported that E₆ could promote malignant change, while E₇ may cause benign neoplasm^[50]. It has been indicated elsewhere that virogene HPV16 E6 alone can cause cellular malignant change^[51]. In this experiment, we found that immortal cells contained HPV18 E6E7 and that, therefore, the SHEE series can gradually lead to the malignant transformation. It is also postulated that HPV is likely be a major risk factor for esophageal cancer^[52].

In summary, of all these cells, some underwent aging, apoptosis and died, whereas others proceeded to malignant transformation. To search the direction of development of cells, we evaluated these changes by referring to the cytogenetic index. In these four series of immortal cells, the chromosomes presented characteristics of hyperdiploid and hypotriploid along with separation of modal number. The positive activity of telomerase can help determine the cells that are progressing from preimmortal toward immortal stages. The SHEE60 passage showed initial partial malignant change which could be regarded as premalignancy. The cells of SHEE85 were in fully malignant transformation with tumor formation and invasive potential. In conclusion, it is possible to demonstrate multiple stages in the transformation process that are associated with different genetic and phenotypic characteristics.

REFERENCES

- Shen ZY, Cen S, Cai WJ, Ten ZP, Shen J, Hu Z, Zeng Y. Immortalization of human fetal esophageal epithelial cells induced by E6 and E7 genes of human papilloma virus. *Zhonghua Shiyen He Linchuang Bingduxue Zazhi* 1999; **13**: 121-123
- Shen ZY, Shen J, Cai WJ, Cen S, Zeng Y. Biological characteristics of human fetal esophageal epithelial cell line immortalized by the E6 and E7 gene of HPV type 18. *Zhonghua Shiyen He Linchuang Bingduxue Zazhi* 1999; **13**: 209-212
- Shen ZY, Xu LY, Chen MH, Cai WJ, Chen JY, Hon CQ, Shen J, Zeng Y. Biphasic differentiation of immortalized esophageal epitheliums induced by HPV 18E6E7. *Bingdu Xuebao* 2001; **17**: 210-214
- Shen ZY, Chen XH, Shen J, Cai WH, Chen JY, Huang TH, Zeng Y. Malignant transformation of immortalized human embryonic esophageal epithelial cells induced by human papillomavirus. *Bingdu Xuebao* 2000; **16**: 97-101
- Shen ZY, Shen J, Cai WJ, Chen JY, Zeng Y. Malignant transformation of the immortalized esophageal epithelial cells. *Zhonghua Zhongliuxue Zazhi* 2002; **24**: 107-109
- Evan G, Littlewood T. A matter of life and cell death. *Science* 1998; **281**: 1317-1322
- Shen ZY, Xu LY, Chen XH, Cai WJ, Shen J, Chen JY, Huang TH, Zeng Y. The genetic events of HPV-immortalized esophageal epithelium cells. *Int J Mol Med* 2001; **8**: 537-542
- Fusenig NE, Boukamp P. Multiple stages and genetic alterations in immortalization, malignant transformation and tumor progression of human skin keratinocytes. *Mol Carcinog* 1998; **23**: 144-158
- Shen ZY, Xu LY, Li EM, Cai WJ, Chen MH, Shen J, Zeng Y. Telomere and telomerase in the initial stage of immortalization of esophageal epithelial cell. *World J Gastroenterol* 2002; **8**: 357-362
- Tsao SW, Zhang DK, Cheng RY, Wan TYS. Telomerase activation in human cancer. *Chin Med J* 1998; **111**: 745-750
- Jones CJ, Kipling D, Morris M, Hepburn P, Skinner J, Bounacer A, Wyllie FS, Ivan M, Bartek J, Wynford-Thomas D, Bond JA. Evidence for a telomere-independent "clock" limiting RAS oncogene-driven proliferation of human thyroid epithelial cells. *Mol Cell Biol* 2000; **20**: 5690-5699
- Zhang DK, Ngan HY, Cheng RY, Cheang AN, Liu SS, Tsao SW. Clinical significance of telomerase activation and telomeric restriction fragment (TRF) in cervical cancer. *Eur J Cancer* 1999; **35**: 154-160
- Hsieh HF, Harn HJ, Chiu SC, Liu YC, Lui WY, Ho LI. Telomerase activity correlates with cell cycle regulators in human hepatocellular carcinoma. *Liver* 2000; **20**: 143-151
- Mutirangura A, Sriuranpong V, Termrung graunglert W, Tresukosol D, Lertsaguansinchai P, Voravul N, Niruthisard S. Telomerase activity and human papillomavirus in malignant, premalignant and benign cervical lesions. *Br J Cancer* 1998; **78**: 933-939
- Nowak JA. Telomerase, cervical cancer, and human papillomavirus. *Clin Lab Med* 2000; **20**: 369-382
- Hou M, Xu D, Bjorkholm M, Gruber A. Real-time quantitative telomeric repeat amplification protocol assay for the detection of telomerase activity. *Clin Chem* 2001; **47**: 519-524
- Sakaguchi M, Miyazaki M, Inoue Y, Tsuji T, Kouchi H, Tanaka T, Yamada H, Namba M. Relationship between contact inhibition and intranuclear S100C of normal human fibroblasts. *J Cell Biol* 2000; **149**: 1193-1206
- Calaf G, Russo J, Tait L, Estrad S, Alvarado ME. Morphological phenotypes in neoplastic progression of human breast epithelial cells. *J Submicrosc Cytol Pathol* 2000; **32**: 83-96
- Shen ZY, Cai WJ, Shen J, Xu JJ, Cen S, Ten ZP, Hu Z, Zeng Y. Human papilloma virus 18E6E7 in synergy with TPA induced malignant transformation of human embryonic esophageal epithelial cells. *Bingdu Xuebao* 1999; **15**: 1-6
- Shen ZY, Shen J, Cai WJ, Wu XY, Zheng RM, Zeng Y. The promoter effects of malignant transformation of sodium butyrate on the immortalized esophageal epithelium induced by human papillomavirus. *Zhonghua Binglixue Zazhi* 2002; **31**: 39-41
- Weitzman JB, Yaniv M. Rebuilding the road to cancer. *Nature* 1999; **400**: 401-402
- Yakoob J, Hu GL, Fan XG, Zhang Z. Telomere, telomerase and digestive cancer. *World J Gastroenterol* 1999; **5**: 334-337
- He XX, Wang JL. Activity of telomerase and oncogenesis. *Huaren Xiaohua Zazhi* 1998; **6**: 1100-1101
- Yang SM, Fang DC, Luo YH, Lu R, Liu WW. Telomerase activity in gastrointesind submucosal tumors and its clinical significance. *Huaren Xiaohua Zazhi* 1998; **6**: 765-767
- Zhan WH, Ma JP, Peng JS, Gao JS, Cai SR, Wang JP, Zheng ZQ, Wang L. Telomerase activity in gastric cancer and its clinical implications. *World J Gastroenterol* 1999; **5**: 316-319
- He XX, Wang JL, Wu JL, Yuan SY, Ai L. Telomerase expression, Hp infection and gastric mucosal carcinogenesis. *Shijie Huaren Xiaohua Zazhi* 2000; **8**: 505-508
- He XX, Wang JL, Wu JL, Yuan SY, Ai L. Telomere, cellular DNA content and gastric mucosal carcinogenesis. *Shijie Huaren Xiaohua Zazhi* 2000; **8**: 509-512
- Yao XX, Yin L, Zhang SY, Bai WY, Li YM, Sun ZC. hTERT expression and cellular immunity in gastric cancer and precancerosis. *Shijie Huaren Xiaohua Zazhi* 2001; **9**: 508-512
- Xia ZS, Zhu ZH, He SG. Effects of ATRA and 5 Fu on growth and telomerase activity of xenografts of gastric cancer in nude mice. *Shijie Huaren Xiaohua Zazhi* 2000; **8**: 674-677
- Meng ZQ, Yu EX, Song MZ. Inhibition of telomerase activity of human liver cancer cell SMMC 7721 by chemotherapeutic drugs. *Shijie Huaren Xiaohua Zazhi* 1999; **7**: 252-254
- Fu JM, Yu XF, Shao YF. Telomerase and primary liver cancer. *Shijie Huaren Xiaohua Zazhi* 2000; **8**: 461-463
- Qu B, Li BJ, Lu ZW, Pan HL. Clinical significance of telomerase activity detected in fine-needle aspiration specimens to liver cancer diagnosis. *Shijie Huaren Xiaohua Zazhi* 2001; **9**: 538-541
- Qiu SL, Huang JQ, Wang YF, Peng ZH. Analysis of telomerase activity in colorectal cancer, precancerous lesions and cancer washings. *Shijie Huaren Xiaohua Zazhi* 1998; **6**: 992-993
- Sobti RC, Kochar J, Singh K, Bhasin D, Capalash N. Telomerase activation and incidence of HPV in human gastrointestinal tumors in North Indian population. *Mol Cell Biochem* 2001; **217**: 51-56
- Jia L, Li YY. Telomerase activity of exfoliated cancer cells in colonic luminal washings. *Huaren Xiaohua Zazhi* 1998; **6**: 955-957
- Koyanagi K, Ozawa S, Ando N, Takeuchi H, Ueda M, Kitajima M. Clinical significance of telomerase activity in the non-cancerous epi-

- thelial region of oesophageal squamous cell carcinoma. *Br J Surg* 1999; **86**: 674-679
- 37 **Hiyama T**, Yokozaki H, Kitadai Y, Haruma K, Yasui W, Kajiyama G, Takara E. Overexpression of human telomerase RNA is an early oesophageal carcinogenesis. *Virchows Arch* 1999; **434**: 483-487
 - 38 **Kiyoizuka Y**, Asai A, Yamamoto D, Senzaki H, Yoshioka S, Takahashi H, Hioki K, Tsubura A. Establishment of novel human esophageal cancer cell relation to telomere dynamics and telomerase activity. *Dig Dis Sci* 2000; **45**: 870-879
 - 39 **Koyanagi K**, Ozawa S, Ando N, Mukai M, Kitagawa Y, Ueda M, Kilajima M. Telomerase activity as an indicator of malignant in iodine-nonreactive lesions of the esophagus. *Cancer* 2000; **88**: 1524-1529
 - 40 **Hahn WC**, Counter CM, Lundberg AS, Beijersbergen RL, Brooks MW, Weinberg RA. Creation of human tumour cells with defined genetic elements. *Nature* 1999; **400**: 464-468
 - 41 **Xu LY**, Shen ZY, Li EM, Cai WJ, Shen J, Li C, Hong CQ, Chen JY, Zeng Y. Telomere length and telomerase activity in immortalized and malignant transformed human embryonic esophageal epithelial cell lines by E6 and E7 genes of HPV 18 type. *Aibian Qibian Tubian* 2001; **13**: 137-140
 - 42 **Morales CP**, Lee EL, Shay JW. *In situ* hybridization for the detection of telomerase RNA in the progression from Barrett's esophagus to esophageal adenocarcinoma. *Cancer* 1998; **83**: 652-659
 - 43 **Shen ZY**, Xu LY, Li C, Cai WJ, Shen J, Chen JY, Zeng Y. A comparative study of telomerase activity and malignant phenotype in multistage carcinogenesis of esophageal epithelial cells induced by human papillomavirus. *Int J Mol Med* 2001; **8**: 633-639
 - 44 **Steenbergen RD**, Hermsen MA, Walboomers JM, Meijer GA, Baak JP, Meijer CJ. Non-random allelic losses at 3p 11p and 13p during HPV-mediated immortalization and concomitant loss of terminal differentiation of human keratinocytes. *Int J cancer* 1998; **76**: 412-417
 - 45 **Duensing S**, Lee LY, Duensing A, Basile J, Piboonniyom S, Gonzalez S, Crum CP, Munger K. The human papillomavirus type 16E₆ and E₇ oncoproteins cooperate to induce mitotic defects and genomic instability by uncoupling centrosome duplication from the cell division cycle. *Proc Natl Acad Sci USA* 2000; **29**: 10002-10007
 - 46 **Garbe J**, Wong M, Wigington D, Yaswen P, Stampfer MR. Viral oncogenes accelerate conversion to immortality of cultured conditionally immortal human mammary epithelium cells. *Oncogen* 1999; **18**: 2169-2180
 - 47 **Wang P**, Peng ZL, Wang H, Liu SL. Study on the carcinogenic mechanism of human papillomavirus type 16 E7 protein in cervical carcinoma. *Zhonghua Shiyan He Linchuang Bingduxue Zazhi* 2000; **14**: 117-120
 - 48 **Zur Hausen H**. Papillomaviruses in human cancers. *Proc Assoc Am Physicians* 1999; **111**: 581-587
 - 49 **Song S**, Liem A, Miller JA, Lambert PF. Human papillomavirus types 16 E6 and E7 contribute differently to carcinogenesis. *Virology* 2000; **26**: 141-150
 - 50 **Song S**, Pitot He, Lambert PF. The human papillomavirus type 16 E6 gene alone is sufficient to induce carcinomas in transgenic animals. *J Virol* 1999; **73**: 5887-5893
 - 51 **Shen ZY**, Cen S, Shen J, Cai WJ, Xu JJ, Teng ZP, Hu Z, Zeng Y. Study immortalization and malignant transformation of human embryonic esophageal epithelial cells induced by HPV18E6E7. *J Cancer Res Clin Oncol* 2000; **126**: 589-594
 - 52 **Shen ZY**, Hu SP, Shen J, Lu LC, Tang CZ, Kuang ZS, Zhong SP, Zeng Y. Detection of human papillomavirus in esophageal carcinoma. *J Med Virol* 2002; **68**: 412-416

Edited by Zhang JZ

• GASTRIC CANCER •

Roles of Fas signaling pathway in vitamin E succinate-induced apoptosis in human gastric cancer SGC-7901 cells

Kun Wu, Yao Li, Yan Zhao, Yu-Juan Shan, Wei Xia, Wei-Ping Yu, Lan Zhao

Kun Wu, Yao Li, Yan Zhao, Yu-Juan Shan, Wei Xia, Lan Zhao, Department of Nutrition and Food Hygiene, Public Health School, Harbin Medical University, Harbin 150001, Heilongjiang Province, China

Wei-Ping Yu, Genetics Institute, Texas University of USA, Austin, USA
Supported by National Natural Science Foundation of China, No. 39970647

Correspondence to: Prof. Kun Wu, Department of Nutrition and Food Hygiene, Public Health School, Harbin Medical University, Harbin 150001, Heilongjiang Province, China. wukun@public.hr.hl.cn
Telephone: +86-451-3648665

Received 2002-03-29 **Accepted** 2002-05-26

Abstract

AIM: To investigate the roles of Fas signaling pathway in vitamin E succinate-induced apoptosis in human gastric cancer SGC-7901 cells.

METHODS: Human gastric cancer SGC-7901 cells were treated with VES at 5, 10, 20 mg·L⁻¹, succinic acid and vitamin E as vehicle control and condition media only as untreated (UT) control. Apoptotic morphology was observed by DAPI staining. Western blot analysis was applied to measure the expression of Fas, FADD and caspase-8 proteins. After the cells were transiently transfected with Fas and FADD antisense oligonucleotides, respectively, caspase-8 activity was determined by flurometric method.

RESULTS: The morphologically apoptotic changes were observed after VES treatment by DAPI staining. 23.7 % and 89.6 % apoptosis occurred after 24 h and 48 h of 20 mg·L⁻¹ VES treatment, respectively. The protein levels of Fas, FADD and caspase-8 were evidently increased in a dose-dependent manner after 24 h of VES treatment. The blockage of Fas by transfection with Fas antisense oligonucleotides obviously inhibited the expression of FADD protein. After SGC-7901 cells were transfected with Fas and FADD antisense oligonucleotides, caspase-8 activity was obviously decreased ($P < 0.01$), whereas Fas blocked more than FADD.

CONCLUSION: VES-induced apoptosis in human gastric cancer SGC-7901 cells involves Fas signaling pathway including the interaction of Fas, FADD and caspase-8.

Wu K, Li Y, Zhao Y, Shan YJ, Xia W, Yu WP, Zhao L. Roles of Fas signaling pathway in vitamin E succinate-induced apoptosis in human gastric cancer SGC-7901 cells. *World J Gastroenterol* 2002; 8(6): 982-986

INTRODUCTION

RRR- α -tocopheryl succinate (vitamin E succinate, VES), a derivative of natural vitamin E, has been shown to be a potent growth inhibitor of many kinds of cancer cell types^[1-5].

Antiproliferative effects of VES on tumor cells are diverse, including G1 cell cycle blockage^[6-8], DNA synthesis arrest^[9-11], induction of differentiation^[12-14] and apoptosis^[15-17]. Meanwhile, tumor cell growth inhibition by VES has also been demonstrated *in vivo*^[18,19]. VES is noteworthy for its non-toxic and non-inhibitory effects on normal cell types, indicating that VES can be used as a chemopreventive/chemotherapeutic agent against tumors.

Up to date, the precise mechanisms of VES-induced inhibition of tumor cell growth are not well understood, but some studies show that VES can increase the secretion and activation of transforming growth factor- β s (TGF- β s) and enhance the expression of TGF- β receptor II^[10,20]. Yu *et al*^[21] reported that VES-triggered apoptosis in human breast cancer cell lines is inhibited by 50 % with antibody neutralization of TGF- β ligand and transient transfection of TGF- β antisense oligonucleotides, implicating that TGF- β plays a crucial role in VES-induced apoptosis and VES may induce cancer cells to undergo apoptosis through other pathways as well. Turley *et al*^[22] observed that the expression of Fas, a cell surface receptor, is increased after treatment of breast cancer cells with VES and VES-induced apoptosis in breast cancer cells is inhibited when Fas neutralized antibody or transfection of Fas antisense oligonucleotides are applied to cancer cells, showing that Fas-mediated apoptosis may be another important pathway by which VES inhibits tumor cell growth.

Gastric cancer is one of the most common malignant tumors in China^[23-32]. Our previous studies found that VES can block cell cycle, arrest DNA synthesis and induce apoptosis in human gastric cancer SGC-7901 cells, therefore inhibiting cell growth^[33-36]. In addition, our *in vivo* research demonstrated that VES inhibits benzo(a)pyrene (B(a)P)-induced forestomach carcinogenesis in female mice^[37]. The exact mechanisms of apoptosis are not clearly known, but we found that VES can secrete and activate biologically active TGF- β and then TGF- β increases the kinase activity of c-Jun N-terminal kinase (JNK) followed by phosphorylation of c-Jun, and finally activated c-Jun triggers apoptosis in human gastric cancer SGC-7901 cells^[38]. In this study, signaling pathway of Fas-induced apoptosis in VES-treated SGC-7901 cells is determined to further investigate the mechanisms of VES-induced growth inhibition.

MATERIALS AND METHODS

Materials

VES was purchased from Sigama Co. Ltd. RPMI 1640 media and LIPOFECTAMINE PLUS™ Reagent were obtained from Gibco BRL, ApoAlert™ Caspase-8 Fluorescent Assay kit from Clontech, Inc. DAPI (4',6-diamidine-2'-phenylindole dihydrochloride), FADD and caspase-8 rabbit polyclonal antibodies, Fas antisense (GAG GGT CCA GAT GCC CAG CAT) and FADD antisense (CAG CAC CAG GAA CGG GTC CAT) oligonucleotides were gifts from Dr. Sanders BG (University of Texas, Austin, USA). Fas rabbit polyclonal antibody was from Santa Cruz Biotechnology, Inc.

Methods

Cell culture Human gastric cancer cell lines SGC-7901 were maintained in RPMI 1640 medium supplemented with 100 mL · L⁻¹ fetal calf serum (FCS), 100 kU · L⁻¹ penicillin, 100 mg · L⁻¹ streptomycin and 2 mmol · L⁻¹ L-glutamine under 50 mL · L⁻¹ CO₂ in a humidified incubator at 37 °C. SGC-7901 cells were incubated for different time periods in the presence of VES at 5, 10 and 20 mg · L⁻¹ (VES was dissolved in absolute ethanol and diluted in RPMI 1640 complete condition media correspondingly to a final concentration of VES and 1 mL · L⁻¹ ethanol), succinic acid, vitamin E and ethanol equivalents as vehicle (VEH) control and condition media only as untreated (UT) control.

Determination of apoptosis Cells were treated with VES at 20 mg/L for 48 h, then harvested, washed with PBS and stained with 2 mg · L⁻¹ DAPI in 100 % methanol for 30 min at 37 °C. Cells were viewed using a fluorescence microscope with ultraviolet (UV) excitation at 300-500 nm. Cells with nuclei that contained clearly condensed chromatin or cells with fragmented nuclei were scored as apoptotic.

Western blot analysis SGC-7901 cells treated with VES were harvested, washed in PBS and lysed in lysis buffer containing 150 mmol · L⁻¹ NaCl, 1 mL · L⁻¹ NP-40, 5 mg · L⁻¹ sodium deoxycholate, 1 g · L⁻¹ SDS, 50 mmol · L⁻¹ Tris (pH 7.4), 1 mmol · L⁻¹ DTT, 0.5 mmol · L⁻¹ Na₃VO₄, 10 mmol · L⁻¹ phenylmethylsulfonyl fluoride (PMSF), 10 mg · L⁻¹ trypsin, 10 mg · L⁻¹ aprotinin and 5 mg · L⁻¹ leupeptin. Following the centrifugation of 12 000×g for 30 min at 4 °C, the amount of protein in the supernatant was determined using Biorad DC protein assay. Equal amount of protein was separated on 10 % SDS-PAGE and transferred to nitrocellulose filter (Gibco BRL, USA) overnight. Blocked with 50 g · L⁻¹ defatty milk, the filter was incubated with Fas, FADD and caspase-8 rabbit polyclonal antibodies, respectively, and horseradish peroxidase-conjugated IgG, finally developed with DAB.

Transient transfection The cells were washed twice with serum-free medium without antibiotics and incubated for 3 h in 2 ml of serum-free medium containing 30 ul of LIPOFECTAMINE Reagent and 2 ug of Fas or FADD antisense oligonucleotides. After 3 h, the cells were treated with VES.

Caspase-8 activity assay Caspase-8 activity was determined according to the manufacturer's instructions. Briefly, 50 ul of supernatant from VES-treated cell extracts were mixed with 50 ul of a mixture of 2× reaction buffer and DTT, then 1 ul of 1 mmol · L⁻¹ IETD-fmk and incubated for 30 min at 37 °C in water bath. Next, 5 ul of 1 mmol · L⁻¹ IETD-AFC was added, followed by incubation for 1 h at 37 °C in water bath. The fluorescent absorbance (A) was measured at 400nm for emission and at 505nm for excitation.

Statistical analysis

The data were expressed as $\bar{x} \pm s$. Statistical analysis was performed using student's *t*-test. *P* < 0.05 was considered significant.

RESULTS

VES induced apoptosis in SGC-7901 cells

SGC-7901 cells in untreated control group and 20 mg · L⁻¹ VES group were cultured for 48 h, collected and stained with DAPI. The morphological changes were observed with fluorescent microscope at 300-500nm (Figure 1). The nuclei in UT control group exhibited circular-like shape, clear edge, and homogeneous staining; while those treated with

VES showed uneven edge, chromatin condensation, pyknosis and formation of apoptotic body. 23.7 % and 89.6 %.

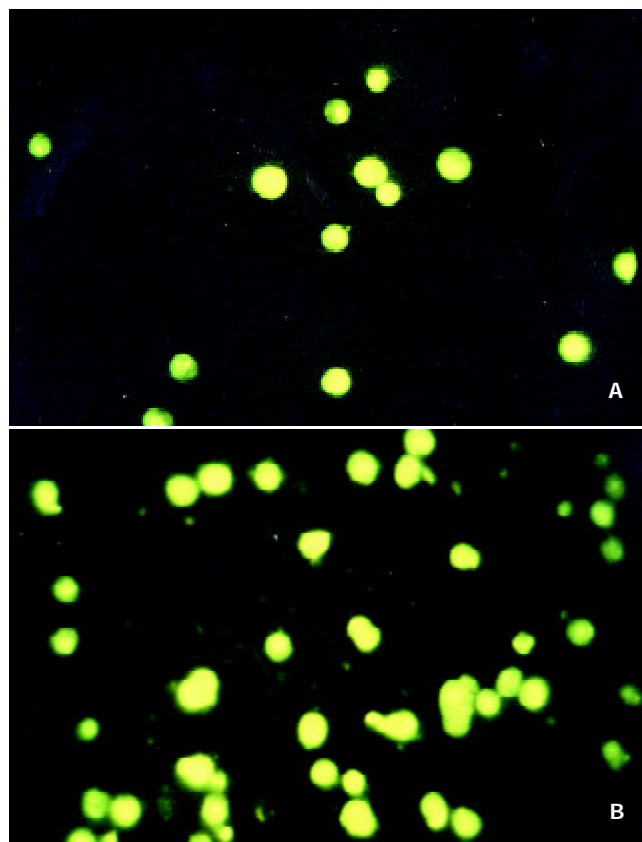


Figure 1 SGC-7901 cells stained with DAPI. A: UT control; B: VES at 20 mg · L⁻¹

Effects of VES on protein expression

The protein levels of Fas, FADD and caspase-8, as determined by western blot analysis of cells extracts obtained from VES-treated SGC-7901 cells, were evidently increased in a dose-dependent manner after 24 h of VES treatment (Figure 2,3,4).

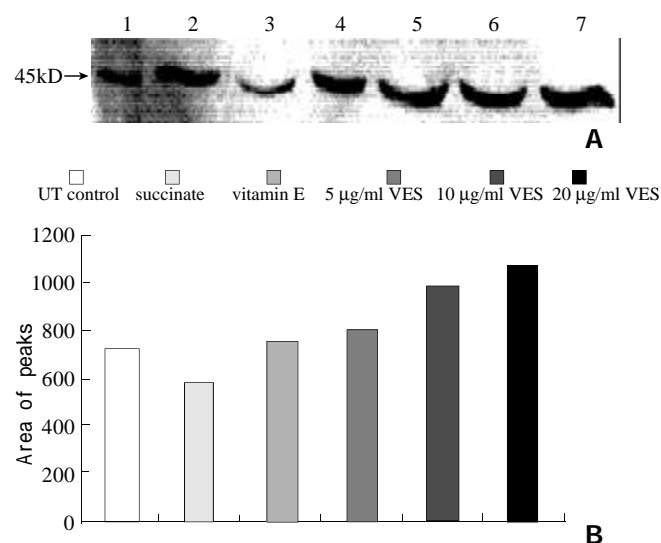


Figure 2 The expression of Fas protein in SGC-7901 cells following treatment of VES for 24 h. Lane1: Molecular weight marker; Lane2: UT control; Lane3: succinate; Lane4: vitamin E; Lane5: VES at 5 mg · L⁻¹; Lane6: VES at 10 mg · L⁻¹; Lane7: VES at 20 mg · L⁻¹.

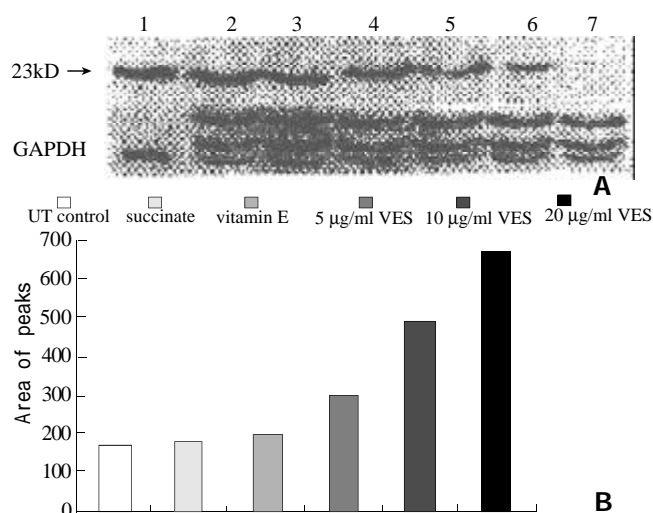


Figure 3 The expression of FADD protein in SGC-7901 cells following treatment of VES for 24 h. Lane1: Molecular weight marker; Lane2: VES at 20 mg·L⁻¹; Lane3: VES at 10 mg·L⁻¹; Lane4: VES at 5 mg·L⁻¹; Lane5: vitamin E; Lane6: succinate; Lane7: UT control.

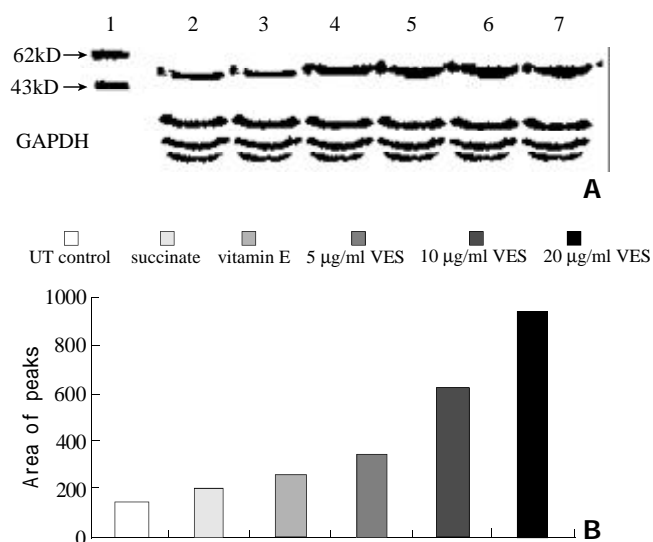


Figure 4 The expression of caspase-8 protein in SGC-7901 cells following treatment of VES for 24 h. Lane1: Molecular weight marker; Lane2: UT control; Lane3: succinate; Lane4: vitamin E; Lane5: VES at 5 mg·L⁻¹; Lane6: VES at 10 mg·L⁻¹; Lane7: VES at 20 mg·L⁻¹.

The expression of FADD protein when Fas was blocked in VES-treated SGC-7901 cells

SGC-7901 cells were transiently transfected with antisense oligonucleotides to Fas, followed by 20 mg·L⁻¹ VES treatment for 24 h. The expression of FADD protein was decreased by 77 % compared with that in control group (Figure 5), indicating that the blockage of Fas signal obviously inhibited the expression of FADD protein.

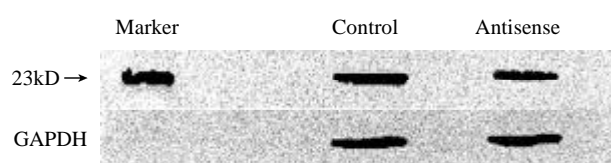


Figure 5 The expression of FADD protein when Fas antisense was transfected into SGC-7901 cells following treatment of VES for 24h.

Effects of blockage of Fas and FADD on caspase-8 activity in VES-treated SGC-7901 cells

SGC-7901 cells were transfected with Fas and FADD antisense oligonucleotides, respectively, followed by VES treatment for 24 h at different doses. Caspase-8 activity in both cases was decreased with significant differences compared with the activity in the same dose of VES-treated cells untransfected in an obviously dose-dependent manner (Table 1). Meanwhile, caspase-8 activity in Fas antisense-transfected cells was reduced more than that in FADD antisense-transfected cells and the differences were significant.

Table 1 Effects of blockage of Fas and FADD on caspase-8 activity in VES-treated SGC-7901 cells

Groups	Doses (mg·L ⁻¹)	Caspase-8 activity
VES	5	12.1±0.70
	10	21.6±0.88
	20	32.4±1.71
Fas antisense +VES	5	5.1±0.35 ^b
	10	10.9±0.39 ^b
	20	16.9±0.87 ^b
FADD antisense +VES	5	9.6±0.34 ^{bd}
	10	15.7±0.29 ^{bd}
	20	21.9±0.83 ^{bd}

^b*P*<0.01, vs VES at the same dose; ^d*P*<0.01, vs Fas antisense at the same dose.

DISCUSSION

Fas (also called CD95/APO-1), a 45kDa type I transmembrane protein, belongs to the nerve growth factor(NGF)/tumor necrosis factor (TNF) receptor superfamily. As a member of five death domain-containing receptors, Fas initiates a signal-transduction cascade leading to programmed cell death^[39-42]. In this study, we determined the expression of Fas protein in VES-treated SGC-7901 cells. The data showed that after 24 h of VES treatment, the expression of Fas protein was evidently increased with a marked dose-dependent relationship in comparison with control, indicating that Fas signal pathway is initiated in the course of VES-triggered apoptosis. After VES treatment following transfection of Fas antisense oligonucleotides into SGC-7901 cells, the expression of Fas protein and caspase-8 activity were obviously reduced and VES-induced apoptosis was inhibited by 50 %, implicating that Fas may play an essential role in VES-mediated apoptosis in human gastric cancer SGC-7901 cells.

All the death receptors' cytoplasmic regions contain a death domain (DD) required for cytotoxic signal transduction. Engagement of death receptors by their ligands can lead death receptors to oligomerization; then an adaptor protein is required to recruit death receptors to their effectors. Engagement of Fas by Fas ligand or agonistic anti-Fas antibodies can induce apoptosis in Fas-bearing cells^[43-46]. The main death pathway initiated from Fas activation involves a series of death associated molecules including FAP-1 (Fas-associated protein 1), RIP (receptor interaction protein) and FADD (Fas-associated death domain-containing protein)^[47]. Therefore, the roles of FADD in VES-treated SGC-7901 cells were also investigated in the present study.

FADD (also known as MORT1), a cytoplasmic protein,

contains 208 amino acids and N-terminal amino acids of FADD constitute a death effector domain (DED) essential to death signal transduction^[47-50]. We treated SGC-7901 cells with VES and found that the level of FADD protein was obviously elevated compared with control in an evident dose-dependent manner, showing that FADD was also involved in the signaling pathway of VES-mediated apoptosis in SGC-7901 cells. In addition, we transfected SGC-7901 cells with FADD antisense oligonucleotides followed by treating them with VES. The results showed that the expression of FADD protein and caspase-8 activity was obviously inhibited, further suggesting that FADD was associated with VES-triggered apoptosis in human gastric cancer SGC-7901 cells.

Caspase-8 (MACH1/FLICE), a member of interleukin 1 β -converting enzyme family of proapoptotic proteases, contains two N-terminal stretches that are apparently homologous to death effector domain (DED) of FADD through which FADD recruits to caspase-8 leading to the activation of the proteolytic cascade of caspases^[51-54]. Kim *et al.*^[55] found that Fas-mediated apoptosis was completely blocked in caspase-8-deficient Jurkat T lymphocytes and restored in the case of recruitment of wild-type caspase-8, indicating that caspase-8 is an important mediator of Fas-induced apoptosis. We show here that the expression and activity of caspase-8 in SGC-7901 cells were apparently elevated, demonstrating that caspase-8 is associated with VES-induced apoptosis. In order to explore the relationship among Fas, FADD and caspase-8 in VES-induced apoptosis in SGC-7901 cells, we determined the activity of caspase-8 following transfection of SGC-7901 cells with Fas and FADD antisense oligonucleotides. The data showed that the blockage of Fas and FADD obviously reduced the activity of caspase-8 in VES-treated SGC-7901 cells, while the blockage of Fas did more than that of FADD.

In summary, the adaptor protein FADD is recruited to Fas receptor via mutual interaction of their DDs. FADD in turn recruits procaspase-8 through interaction between DEDs of FADD and procaspase-8. Upon formation of this death-inducing signaling complex, procaspase-8 is activated leading to the activation of the proteolytic cascade of caspases, so Fas may play a crucial role in VES-mediated apoptosis in human gastric cancer SGC-7901 cells. VES-mediated apoptosis is very complex. It is reported that mitochondria permeability transition (MPT) participates in apoptosis^[56-61]. Therefore, additional studies should provide insight into the role of the biological significance of mitochondria in the mechanisms of tumor cell growth inhibition by VES in future.

REFERENCES

- 1 **Fariss MW**, Merson MH, Hara TM. The selective antiproliferation effects of α -tocopheryl hemisuccinate and cholesteryl hemisuccinate on murine leukemia cells result from the action of the intact compounds. *Cancer Res* 1994; **54**: 3346-3357
- 2 **Ottino P**, Duncan JR. Effect of α -tocopheryl succinate on free radical and lipid peroxidation levels in BL6 melanoma cells. *Free Radical Biol & Med* 1997; **22**: 1145-1151
- 3 **Kogure K**, Morita M, Nakashima S, Hama S, Tokumura A, Fukuzawa K. Superoxide is responsible for apoptosis in rat vascular smooth muscle cells induced by α -tocopheryl hemisuccinate. *Biochim Biophys Acta* 2001; **1528**: 25-30
- 4 **Turley JM**, Ruscetti FW, Kim SJ, Fu T, Gao FV, Rirchenall-Roberts MC. Vitamin E succinate inhibits proliferation of BT-20 human breast cancer cells: increased binding of cyclin A negatively regulates E2F transactivation activity. *Cancer Res* 1997; **57**: 2668-2675
- 5 **Neuzil J**, Weber T, Gellert N, Weber C. Selective cancer cell killing by α -tocopheryl succinate. *Br J Cancer* 2000; **84**: 87-89
- 6 **Pussinen PJ**, Lindner H, Glatter O, Reicher H, Kostner GM, Wintersperger A, Malle E, Sattler W. Lipoprotein-associated α -tocopheryl-succinate inhibits cell growth and induces apoptosis in human MCF-7 and HBL-100 breast cancer cells. *Biochim Biophys Acta* 2000; **1485**: 129-144
- 7 **Kline K**, Yu W, Zhao B, Turley JM, Sanders BG. Vitamin E Succinate: Mechanisms of action as tumor cell growth inhibitor. In: *Nutrients in Cancer Prevention and Treatment*. Prasad KN, Santamaria L and Williams RM (eds). Totowa, NY: Humana 1995: 39-56
- 8 **Israel K**, Sanders BG, Kline K. RRR- α -Tocopheryl Succinate inhibits the proliferation of human prostatic tumor cells with defective cell cycle/differentiation pathway. *Nutr Cancer* 1995; **24**: 161-169
- 9 **Yu W**, Sanders BG, Kline K. RRR- α -tocopheryl succinate inhibits EL4 thymic lymphoma cell growth by inducing apoptosis and DNA synthesis arrest. *Nutr Cancer* 1997; **27**: 92-101
- 10 **Simmons-Menchaca M**, Qian M, Yu W, Sanders BG, Kline K. RRR- α -Tocopheryl succinate inhibits DNA synthesis and enhances the production and secretion of biologically active transforming growth factor- β by avian retrovirus-transformed lymphoid cells. *Nutr Cancer* 1995; **24**: 171-185
- 11 **Wu K**, Zhao Y, Liu BH, Li Y, Liu F, Guo J, Yu W. RRR- α -tocopheryl succinate inhibits human gastric cancer SGC-7901 cell growth by inducing apoptosis and DNA synthesis arrest. *World J Gastroenterol* 2002; **8**: 26-30
- 12 **Kim SJ**, Bang OS, Lee YS, Kang SS. Production of inducible nitric oxide is required for monocytic differentiation of U937 cells induced by vitamin E-succinate. *J Cell Sci* 1998; **111**: 435-441
- 13 **You H**, Yu W, Sanders BG, Kline K. RRR- α -tocopheryl succinate induces MDA-MB-435 and MCF-7 human breast cancer cells to undergo differentiation. *Cell Growth Differ* 2001; **12**: 471-480
- 14 **Yu W**, Sanders BG, Kline K. Modulation of murine EL-4 thymic lymphoma cell proliferation and cytokine production by Vitamin E succinate. *Nutr Cancer* 1996; **25**: 137-149
- 15 **Yu W**, Israel K, Liao QY, Aldaz CM, Sanders BG, Kline K. Vitamin E succinate (VES) induces Fas sensitivity in human breast cancer cells: role for Mr 43 000 Fas in VES-triggered apoptosis. *Cancer Res* 1999; **59**: 953-961
- 16 **Yu W**, Liao QY, Hantash FM, Sanders BG, Kline K. Activation of extracellular signal-regulated kinase and c-Jun-NH(2)-terminal kinase but not p38 mitogen-activated protein kinases is required for RRR- α -tocopheryl succinate-induced apoptosis of human breast cancer cells. *Cancer Res* 2001; **61**: 6569-6576
- 17 **Neuzil J**, Weber T, Schroder A, Lu M, Ostermann G, Gellert N, Mayne GC, Olejnicka B, Negre-Salvayre A, Sticha M, Coffey RJ, Weber C. Induction of cancer cell apoptosis by α -tocopheryl succinate: molecular pathways and structural requirements. *FASEB J* 2001; **15**: 403-415
- 18 **Schwartz J**, Shklar G. The selective cytotoxic effect of carotenoids and α -tocopherol on human cancer cell lines *in vitro*. *J Oral Maxillofac Surg* 1992; **50**: 367-373
- 19 **Malafa MP**, Neitzel LT. Vitamin E succinate promotes breast cancer tumor dormancy. *J Surg Res* 2000; **93**: 163-170
- 20 **Ariazi EA**, Satomi Y, Ellis MJ. Activation of the transforming growth factor beta signaling pathway and induction of cytostasis and apoptosis in mammary carcinomas treated with the anti-cancer agent perillyl alcohol. *Cancer Res* 1999; **59**: 1917-1928
- 21 **Kline K**, Yu W, Sanders BG. Vitamin E: Mechanisms of Action as Tumor Cell Growth Inhibitors. *Cancer and Nutrition*. K.N. Prasad and W.C. Cole(Eds). IOS Press 1998: 37-53
- 22 **Turley JM**, Fu T, Ruscetti FW, Mikovits JA, Bertolette DC, Birchenall-Roberts MC. Vitamin E succinate induces Fas-mediated apoptosis in estrogen receptor-negative human breast cancer cells. *Cancer Res* 1997; **57**: 881-890
- 23 **Liu HF**, Liu WW, Fang DC. Study of the relationship between apoptosis and proliferation in gastric carcinoma and its precancerous lesion. *Shijie Huaren Xiaohua Zazhi* 1999; **7**: 649-651
- 24 **Zhuang XQ**, Lin SR. Progress in research on the relationship between Hp and stomach cancer. *Shijie Huaren Xiaohua Zazhi* 2000; **8**: 206-207
- 25 **Zhu ZH**, Xia ZS, He SG. The effects of ATRA and 5Fu on telomerase activity and cell growth of gastric cancer cells *in vitro*.

- Shijie Huaren Xiaohua Zazhi* 2000; **8**: 669-673
- 26 **Xia JZ**, Zhu ZG, Liu BY, Yan M, Yin HR. Significance of immunohistochemically demonstrated micrometastases to lymph nodes in gastric carcinomas. *Shijie Huaren Xiaohua Zazhi* 2000; **8**: 1113-1116
- 27 **Tu SP**, Zhong J, Tan JH, Jiang XH, Qiao MM, Wu YX, Jiang SH. Induction of apoptosis by arsenic trioxide and hydroxy camptothecin in gastric cancer cells *in vitro*. *World J Gastroenterol* 2000; **6**: 532-539
- 28 **Cai L**, Yu SZ, Zhang ZF. *Helicobacter pylori* infection and risk of gastric cancer in Changde County, Fujian Province, China. *World J Gastroenterol* 2000; **6**: 374-376
- 29 **Yao XX**, Yin L, Zhang JY, Bai WY, Li YM, Sun ZC. hTERT expression and cellular immunity in gastric cancer and precancerosis. *Shijie Huaren Xiaohua Zazhi* 2001; **9**: 508-512
- 30 **Xu AG**, Li SG, Liu JH, Gan AH. Function of apoptosis and expression of the proteins Bcl-2, p53 and C-myc in the development of gastric cancer. *World J Gastroenterol* 2001; **7**: 403-406
- 31 **Wang X**, Lan M, Shi YQ, Lu J, Zhong YX, Wu HP, Zai HH, Ding J, Wu KC, Pan BR, Jin JP, Fan DM. Differential display of vincristine-resistance-related genes in gastric cancer SGC7901 cell. *World J Gastroenterol* 2002; **8**: 54-59
- 32 **Liu JR**, Li BX, Chen BQ, Han XH, Xue YB, Yang YM, Zheng YM, Liu RH. Effect of cis-9,trans-11-conjugated linoleic acid on cell cycle of gastric adenocarcinoma cell line (SGC-7901). *World J Gastroenterol* 2002; **8**: 224-229
- 33 **Wu K**, Ren Y, Guo J. The effects of vitamin E succinate on the cyclic regulation protein of human gastric cancer cells. *Weisheng Dulixue Zazhi* 1998; **12**: 203-207
- 34 **Liu BH**, Wu K, Zhao DY. Inhibition of human gastric cancer SGC-7901 cell growth by vitamin E succinate. *Weisheng Yanjiu* 2000; **29**: 172-174
- 35 **Wu K**, Guo J, Shan YJ, Liu BH. The effects of vitamin E succinate on apoptosis in human gastric cancer. *Weisheng Dulixue Zazhi* 1999; **13**: 84-90
- 36 **Liu BH**, Wu K. Study on the growth inhibition of Vitamin E Succinate in human gastric cancer cell. *Aibian Jibian Tubian* 2000; **12**: 79-81
- 37 **Wu K**, Shan YJ, Zhao Y, Yu JW, Liu BH. Inhibitory effects of RRR- α -tocopheryl succinate on benzo(a)pyrene (B(a)P)-induced forestomach carcinogenesis in female mice. *World J Gastroenterol* 2001; **7**: 60-65
- 38 **Wu K**, Liu BH, Zhao DY, Zhao Y. The effect of vitamin E succinate on the expression of TGF- β 1, c-Jun and JNK1 in human gastric cancer SGC-7901 cells. *World J Gastroenterol* 2001; **7**: 83-87
- 39 **Zhao Y**, Wu K. Cell death molecule Fas/CD95 and apoptosis. *Aibian Jibian Tubian* 2001; **13**: 55-58
- 40 **Droin N**, Bichat F, Rebe C, Wotawa A, Sordet O, Hammann A, Bertrand R, Solary E. Involvement of caspase-2 long isoform in Fas-mediated cell death of human leukemic cells. *Blood* 2001; **97**: 1835-1844
- 41 **Wei HS**, Li DG, Lu HM. Hepatic cell apoptosis and fas gene. *Shijie Huaren Xiaohua Zazhi* 1999; **7**: 531-532
- 42 **Chatterjee D**, Schmitz I, Krueger A, Yeung K, Kirchhoff S, Krammer PH, Peter ME, Wyche JH, Pantazis P. Induction of apoptosis in 9-nitrocamptothecin-treated Du145 human prostate carcinoma cells correlates with de novo synthesis of CD95 and CD95 ligand and down-regulation of cFLIP(short). *Cancer Res* 2001; **61**: 7148-7154
- 43 **Liu HF**, Liu WW, Fang DC. Effect of combined anti Fas mAb and IFN- γ on the induction of apoptosis in human gastric carcinoma cell line SGC-7901. *Shijie Huaren Xiaohua Zazhi* 2000; **8**: 1361-1364
- 44 **Tan LJ**, Jiang W, Zhang N, Zhang XR, Qiu DH. Fas/FasL expression of esophageal squamous cell carcinoma, dysplasia tissues and normal mucosa. *Shijie Huaren Xiaohua Zazhi* 2001; **9**: 15-19
- 45 **Peng ZH**, Xing TH, Qiu GQ, Tang HM. Relationship between Fas/FasL expression and apoptosis of colon adenocarcinoma cell lines. *World J Gastroenterol* 2001; **7**: 88-92
- 46 **Boldrini L**, Faviana P, Pistolesi F, Gisfredi S, Di Quirico D, Lucchi M, Mussi A, Angeletti CA, Baldinotti F, Fogli A, Simi P, Basolo F, Fontanini G. Alterations of Fas (APO-1/CD95) gene and its relationship with p53 in non small cell lung cancer. *Oncogene* 2001; **20**: 6632-6637
- 47 **Hu WH**, Johnson H, Shu HB. Activation of NF-kappaB by FADD, Casper and caspase-8. *J Biol Chem* 2000; **275**: 10838-10844
- 48 **Sun BH**, Zhao XP, Wang BJ, Yang DL, Hao LJ. FADD and TRADD expression and apoptosis in primary human hepatocellular carcinoma. *World J Gastroenterol* 2000; **6**: 223-227
- 49 **AaStrasser A**, Newton K. FADD/MORT1, a signal transducer that can promote cell death or cell growth. *Int J Biochem Cell Biol* 1999; **31**: 533-537
- 50 **Kabra NH**, Kang C, Hsing LC, Zhang J, Winoto A. T cell-specific FADD-deficient mice: FADD is required for early T cell development. *Proc Natl Acad Sci USA* 2001; **98**: 6307-6312
- 51 **Engels IH**, Stepczynska A, Stroch K, Lauber K, Berg C, Schwenzer R, Wajant H, Janicke RU, Porter AG, Belka C, Gregor M, Schulze-Osthoff K, Wesselborg S. Caspase-8/FLICE functions as an executioner caspase in anticancer drug-induced apoptosis. *Oncogene* 2000; **19**: 4563-4573
- 52 **Gomez-Angelats M**, Cidlowski JA. Protein kinase C regulates FADD recruitment and death-inducing signaling complex formation in Fas/CD95-induced apoptosis. *J Biol Chem* 2001; **276**: 44944-44952
- 53 **Krueger A**, Schmitz I, Baumann S, Krammer PH, Kirchhoff S. Cellular FLICE-inhibitory protein splice variants inhibit different steps of caspase-8 activation at the CD95 death-inducing signaling complex. *J Biol Chem* 2001; **276**: 20633-20640
- 54 **Packard BZ**, Komoriya A, Brotz TM, Henkart PA. Caspase-8 activity in membrane blebs after anti-Fas ligation. *J Immunol* 2001; **167**: 5061-5066
- 55 **Kim IK**, Chung CW, Woo HN, Hong GS, Nagata S, Jung YK. Reconstitution of caspase-8 sensitizes JB6 cells to TRAIL. *Biochem Biophys Res Commun* 2000; **277**: 311-316
- 56 **Halestrap AP**, Doran E, Gillespie JP, O'Toole A. Mitochondria and cell death. *Biochem Soc Trans* 2000; **28**: 170-177
- 57 **Tafani M**, Schneider TG, Pastorino JG, Farber JL. Cytochrome c-dependent activation of caspase-3 by tumor necrosis factor requires induction of the mitochondrial permeability transition. *Am J Pathol* 2000; **156**: 2111-2121
- 58 **Costantini P**, Jacotot E, Decaudin D, Kroemer G. Mitochondrion as a novel target of anticancer chemotherapy. *J Natl Cancer Inst* 2000; **92**: 1042-1049
- 59 **Zamzami N**, Hamel CE, Maisse C, Brenner C, Munoz-pinedo C, Belzacq AS, Costantini P, Vieira H, Loeffler M, Molle G, Kroemer G. Bid acts on the permeability transition pore complex to induce apoptosis. *Oncogene* 2000; **19**: 6342-6350
- 60 **Petronilli V**, Penzo D, Scorrano L, Bernardi P, Lisa FD. The mitochondrial permeability transition, release of cytochrome c and cell death. *J Biol Chem* 2001; **276**: 12030-12034
- 61 **Li HL**, Chen DD, Li XH, Zhang HW, Lü JH, Ren XD, Wang CC. JTE-522-induced apoptosis in human gastric adenocarcinoma cell line AGS cells by caspase activation accompanying cytochrome C release, membrane translocation of Bax and loss of mitochondrial membrane potential. *World J Gastroenterol* 2002; **8**: 217-223

Edited by Pang LH

• GASTRIC CANCER •

Expression of E-cadherin and β -catenin in gastric carcinoma and its correlation with the clinicopathological features and patient survival

Yong-Ning Zhou, Cai-Pu Xu, Biao Han, Min Li, Liang Qiao, Dian-Chun Fang, Jian-Min Yang

Yong-Ning Zhou, Cai-Pu Xu, Dian-Chun Fang, Jian-Min Yang,
Department of Gastroenterology, Southwest Hospital, the Third
Military Medical University, Chongqing, 400038, China

Yong-Ning Zhou, Biao Han, First Teaching Hospital, Lanzhou
Medical College, Lanzhou, Gansu Province, 730000, China

Min Li, Department of Pathology, Lanzhou Medical College,
Lanzhou, Gansu Province, 730000, China

Liang Qiao, Massey Cancer Center, Medical College of Virginia,
Virginia Commonwealth University, Richmond, VA 23298, USA

Correspondence to: Prof. Cai-Pu Xu, Department of Gastroenterology,
Southwest Hospital, the Third Military Medical University, Chongqing,
400038, China. yongningzhou@sina.com.cn

Telephone: +86-23-68754143

Received 2002-07-04 **Accepted** 2002-07-30

Abstract

AIM: The E-cadherin-catenin complex is important for cell-cell adhesion of epithelial cells. Impairment of one or more components of this complex is associated with poor differentiation and increased invasiveness of carcinomas. We evaluated the expression pattern of E-cadherin and β -catenin in gastric carcinoma and dysplasia and analyzed their relationship with tumor clinicopathological features and patient survival.

METHODS: Immunohistochemical staining of E-cadherin and β -catenin was performed from paraffin specimens of 163 gastric carcinomas, 44 gastric mucosal dysplasia, and 25 intestinal metaplasia, 28 atrophic gastritis and 12 healthy controls.

RESULTS: Normal membrane staining was observed in intestinal metaplasia, atrophic gastritis and control biopsy specimens for E-cadherin and β -catenin. 36 % and 16 % of gastric dysplasia were stained abnormally for E-cadherin and β -catenin respectively. Abnormal expression of E-cadherin and β -catenin was demonstrated in 46 % and 44 % of gastric carcinoma respectively. Abnormal expression of E-cadherin and β -catenin occurred more significantly in Borrmann III/IV than in Borrmann I / II type ($P < 0.005$, respectively). A significantly higher proportion of signet-ring, mucinous and tubular adenocarcinomas were abnormally expressed for E-cadherin and β -catenin as compared with papillary adenocarcinomas ($\chi^2 = 8.47, P < 0.005$, and $\chi^2 = 7.05, P < 0.01$, respectively). Moreover, abnormal E-cadherin and β -catenin staining occurred more frequently in diffuse than in intestinal type of tumor ($\chi^2 = 18.18$ and $17.79, P < 0.005$, respectively). There was a significant correlation between abnormal β -catenin expression and positive lymph node metastasis. A survival advantage was noted in tumors retaining normal membranous expression of β -catenin, independent of type, grade, or stage of the disease ($P < 0.0005$).

CONCLUSION: Abnormal expression of the E-cadherin-catenin complex occurs frequently in gastric carcinoma, closely related to its histogenesis. Abnormal expression of the E-cadherin-catenin complex in gastric dysplasia may be an early event in the tumorigenesis. The close correlation with poor survival suggests that abnormal β -catenin may be a useful prognostic marker.

Zhou YN, Xu CP, Han B, Li M, Qiao L, Fang DC, Yang JM. Expression of E-cadherin and β -catenin in gastric carcinoma and its correlation with the clinicopathological features and patient survival. *World J Gastroenterol* 2002; 8(6):987-993

INTRODUCTION

It is well-known that anchorage of cells to substrate is critical for the integrity of many cell types including epithelial cells. The cadherins are a major class of adhesion molecules which play an important role in the homotypic cell-cell adhesion and hence cancer cell metastasis and invasion. E-cadherin is a member of the cadherin family which is expressed in all epithelial cells^[1,2]. It is a calcium-dependent cell adhesion molecule that binds to other E-cadherin molecules on adjacent cells and is located at the adhesion junction of epithelial cells^[1]. Functional cadherin-dependent cell adhesion requires the formation of complexes between E-cadherin and the cytoplasmic proteins known as the catenins. The catenin, which interacts with the cytoplasmic domain of E-cadherin, consists of at least three proteins: α -, β -, and γ -catenin. β -catenin forms a complex with E-cadherin, while α -catenin links this complex to the actin cytoskeleton^[3,4]. It is postulated that changes in cell-cell and cell-matrix interactions account for the ability of cancer cells to cross normal tissue boundaries and metastasize^[5]. In addition, loss of cell adhesion may contribute to loss of contact inhibition and thus play a role at the earlier stage of the neoplastic process.

Previous studies have provided evidence that perturbation of E-cadherin-mediated cell adhesion is involved in tumor progression and metastasis^[6,7]. Loss of E-cadherin expression or function *in vitro* has been associated with loss of differentiation and increased invasive capacity of cancer cell lines^[8,9]. A variety of human cancers exhibit altered expression of E-cadherin that correlates with high grade and advanced tumor stage^[10-12]. These changes may result from deletions, point mutations of the E-cadherin genes or CpG methylation of the promoter region.

β -catenin appears to bind directly and most tightly to E-cadherin and so affects the strength of cell-cell adhesion^[13]. It is also involved in the Wntless/Wnt signaling pathway and interacts with epidermal growth factor receptor^[14,15], with the APC tumor suppressor gene, and with two novel nuclear transcription factors, T-cell factor (TCF)-4 and lymphoid enhancing factor (LEF)-1^[16,17].

Gastric cancer is the second most common malignancy worldwide, and is among the leading causes of mortality in countries such as Japan, China, and Chile. Even in the developed Western countries, the 5-year survival rate for gastric cancer is only 10-19 %^[18]. In China, gastric cancer is the most common malignancy diagnosed annually, with a high cancer-related mortality (25 %)^[19]. Among the highly prevalent geographic areas of gastric cancer is Lanzhou, a city of northwest China. It is currently unknown what factors contribute to the development, progression, and metastasis of gastric cancers in this geographic area^[20,21].

Reduced or completely lost E-cadherin-catenin complex expression has been found in gastric, although results regarding the degree of aberrant E-cadherin-catenin complex expression and its relationship with clinicopathological features and patient survival are contradictory. In this study, by using the immunohistochemical staining, we investigated the expression pattern of E-cadherin or β -catenin in gastric cancers, dysplasia, intestinal metaplasia, atrophic gastritis and normal gastric mucosa and the possible role of E-cadherin-catenin complex in the pathogenesis of gastric cancers in Lanzhou area. The possible relationship between the expression of the E-cadherin and β -catenin and the tumor clinicopathology, as well as its potential value in the evaluation of patient survival were also discussed.

MATERIALS AND METHODS

Patients and tissue samples

The specimens of gastric cancers were obtained from 185 consecutive patients who underwent gastrectomy at the Department of Surgery (First Teaching Hospital, Lanzhou Medical College, Lanzhou, P. R. China) between January 1995 and December 1996. None of the patients received chemotherapy or radiotherapy before surgery. Clinicopathological information and survival data were obtained from hospital records and patients' doctor in charge. Six patients who died within 4 weeks following surgery were excluded from the survival analysis for the purpose of eliminating bias caused by surgical operation-related death. In sixteen cases, suitable well-preserved blocks could not be obtained, thus a total of 163 patients were included in the final study. There were 123 males and 40 females (3.08:1), with median age of 54.5 years (range, 28-77 years). Samples were taken from the representative cancerous lesions as well as adjacent non-cancerous mucosa. In addition, mucosal biopsy specimens from 32 patients with dysplasia (plus 12 cases from gastrectomy, total 44 cases), 25 with intestinal metaplasia, 28 with atrophic gastritis and 12 healthy controls were examined.

For microscopic examination, tissues were routinely fixed with formalin before being embedded in paraffin. A 4- μ m section from each specimen block was stained with H & E for histological evaluation, and representative blocks were chosen for immunohistochemical study. In addition, normal colonic epithelium was used as positive control and adjacent normal gastric mucosa as internal control. Negative controls included adjacent section of the same block in which the primary antibody was replaced by phosphate-buffered saline (PBS).

Tumor staging and classification

Tumors were staged at the time of surgery by the standard criteria for TNM staging using the unified international gastric cancer staging classification^[22] and the following morphological details were recorded: depth of invasion (pT category), lymph node involvement (pN category). By Lauren system^[23], tumors were classified into intestinal and diffuse

types. According to the criteria of WHO classification, tumors were classified into adenocarcinoma, which was defined as papillary adenocarcinoma, tubular adenocarcinoma, mucinous adenocarcinoma and signet-ring cell carcinoma, and undifferentiated carcinoma. The gross appearance of tumors was diagnosed using the Borrmann's classification. Dysplasia was diagnosed according to the Padova International Classification^[24] for gastric dysplasia.

Antibodies and other chemicals

The following items were purchased from Maxim Biotech (Maxim Biotech Inc., South San Francisco, CA, USA): mouse monoclonal antibodies against human E-cadherin and β -catenin; UltraSensitive S-P Kit; and peroxidase-conjugated streptavidin. Diaminobenzidine tetrahydrochloride (DAB) and other routine chemicals were obtained from Sigma-Aldrich Corp. (St. Louis, MO, USA).

Immunohistochemical staining

To detect the presence and patterns of E-cadherin and β -catenin, we utilized the peroxidase-conjugated streptavidin immunostaining technique, as previously described by others^[25]. Briefly, 4 μ m tissue sections were dewaxed and rehydrated through changes of xylene and graded alcohol, then to water. Endogenous peroxidase activity was blocked by incubating the sections with 0.6 % hydrogen peroxide for 10 min. Heat-mediated antigen retrieval was performed by heating the sections (immersed in 0.01M citrate buffer, pH 6.0) in a microwave oven (750 W) for 20 min. The slides were then washed with PBS before being exposed to 10 % normal goat serum for 10 min to block the non-specific background reaction. The slides were then incubated with respective primary antibody overnight at 4 °C. Following washes with PBS, the slides were incubated for 15 min with the secondary antibody, biotinylated goat anti-mouse IgG. The slides were further washed for 3 \times 10 min in PBS, followed by incubation with peroxidase-conjugated streptavidin for 10 min. The peroxidase reaction was developed in PBS using hydrogen peroxide as substrate and DAB as a chromogen. Sections were counterstained with haematoxylin, dehydrated, and evaluated under a light microscope.

Evaluation of immunostaining

Slides were independently examined by two experienced pathologists who were blinded to the stage of the tumor and to the initial score of the other observer, and a high level of concordance (90 %) was achieved. In case of disagreement, the slides were reviewed and a consensus view achieved. Staining intensity was graded semiquantitatively from 0 to 3, as previously described^[25,26]. 0: negative staining; 1: cytoplasmic staining; 2: heterogeneous staining (tumors composing of both normal and abnormal staining areas); and 3: a normal membranous staining. Because the staining pattern sometimes varied within the same tumor particularly when the differentiation status varied, the final score was based on the dominant pattern. For the ease of data analysis, all tumors with loss of membranous expression were classified as abnormal which included those with absent, heterogeneous or cytoplasmic staining patterns.

Statistical analysis

The correlation between the expression of the E-cadherin or β -catenin and clinicopathological features was analysed for statistical significance by the χ^2 (chi-square) test. Survival curves were constructed according to the method of Kaplan

and Meier. For differences between curves, the *P* value was calculated using the log rank test. A multivariate Cox regression analysis was performed to assess the prognostic significance of different staining patterns and their relationship with other pathological variables. A *P* value of less than 0.05 was considered as statistically significant. All statistical analyses were performed using the SPSS 8.0 statistical package (USA).

RESULTS

Immunohistochemical staining of E-cadherin and β -catenin

Normal gastric mucosa Gastric mucosa specimen from 12 normal health controls were examined. E-cadherin and β -catenin stained intensely in a membranous distribution throughout the epithelium in all the normal control cases (Figure 1).

Atrophic gastritis, intestinal metaplasia, dysplasia and gastric cancer Areas of atrophic gastritis, intestinal metaplasia showed normal membranous distribution of staining for E-cadherin and β -catenin in all cases. Abnormal expression was shown in 36.4 % (16/44) of dysplasia for E-cadherin, and in 15.9 % (7/44) for β -catenin. Of the total of 163 primary tumors examined, the abnormal expression rate of E-cadherin and β -catenin were 46.0 % and 44.8 %, respectively (Table 1). Representative examples were shown in Figure 1.

Table 1 Abnormal expression of E-cadherin and β -catenin in gastric carcinoma and precancerous condition

	Total <i>n</i>	E-cadherin <i>n</i> (%)	β -catenin <i>n</i> (%)
Gastric carcinoma	163	75 (46.0)	73 (44.8)
Dysplasia	44	16 (36.4)	7 (15.9)
Intestinal metaplasia	25	0	0
Atrophic gastritis	28	0	0
Health controls	12	0	0

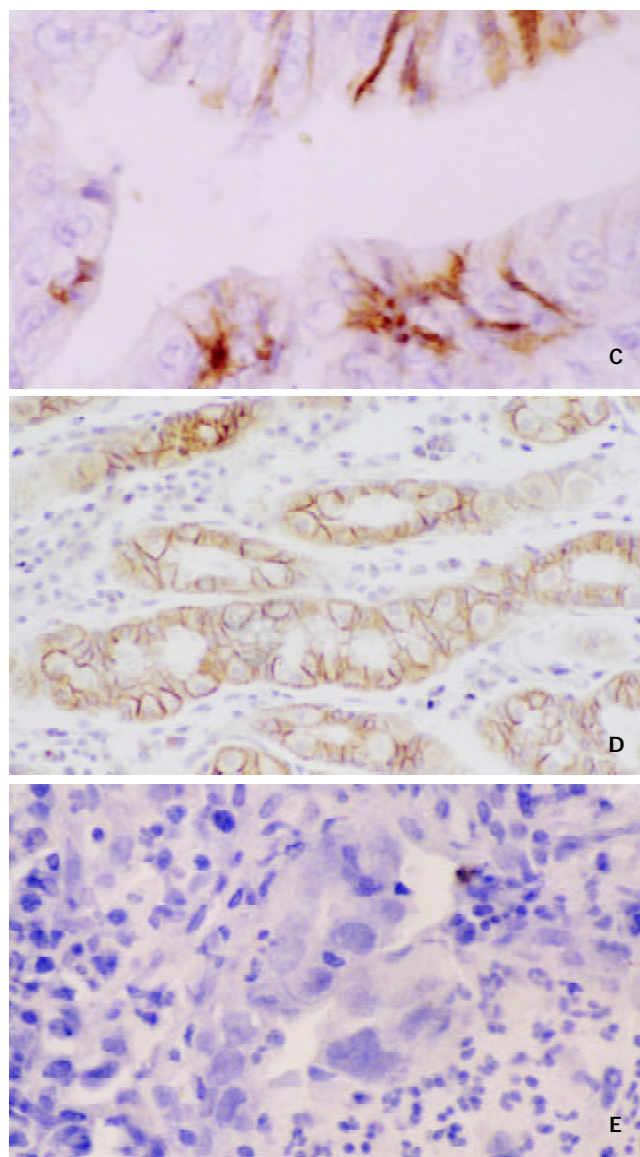
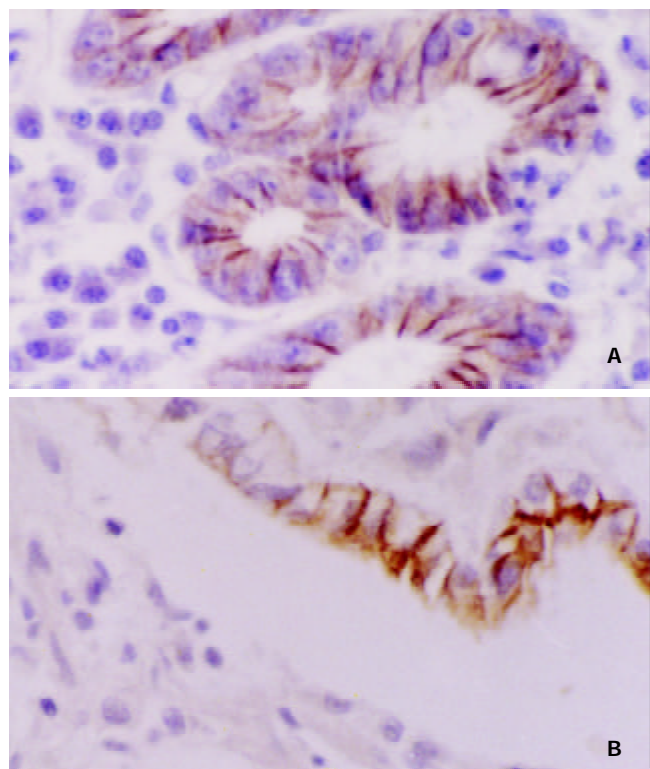


Figure 1 Immunoreactivity of E-cadherin and β -catenin in Gastric Carcinoma. A. Normal membranous staining pattern of E-cadherin (SP×200); B. Poorly differentiated tumor with complete loss of membranous staining with E-cadherin in the majority of cells. Membranous staining can be seen in a few cells retaining gastric gland (SP×400); C. Moderately differentiated tumor showing cytoplasmic staining with β -catenin, partly nuclear β -catenin expression (SP×400); D. Staining of E-cadherin showing preserved strong membranous expression in gastric mucosa with intestinal metaplasia (SP×200); E. Mucosal biopsy specimen with dysplasia (high grade) showing loss of membranous expression of E-cadherin (SP×400)

Expression of E-cadherin or β -catenin and gross appearance in gastric cancer

The frequencies of abnormal expression in tumors less than 5 cm, 5.1-10 cm and more than 10 cm in length were 33.3 %, 35.5 %, and 74.4 % for E-cadherin, respectively, and 28.2 %, 36.2 %, and 78.9 % for β -catenin, respectively (Table 2). The rate of abnormal expression in tumors more than 10 cm was significantly higher than that in tumors less than 10 cm in length (*P*<0.005, respectively). As shown in Table 2, analysis of 139 cases of gastric cancer (24 cases were excluded from 163 cases because of incomplete surgical record) revealed that the expression of E-cadherin and β -catenin were significantly

correlated with the Borrmann classification: Abnormal expression occurred more significantly often in Borrmann III and Borrmann IV than in Borrmann I and Borrmann II type ($P<0.005$, respectively).

Table 2 Expression of E-cadherin or β -catenin and Gross Appearance

	No	E-cadherin expression (%)		β -catenin expression (%)	
		Abnormal	P value	Abnormal	P value
Tumor size (cm)	163				
0-4.9	48	16 (33.3)		14 (28.2)	
5.0-9.9	76	30 (35.5)	16.58	29 (36.2)	21.41
≥ 10.0	39	29 (74.4)	$<0.005^a$	30 (78.9)	$<0.005^a$
Gross appearance	139				
Borrmann I	12	1 (8.3)		2 (16.7)	
Borrmann II	16	3 (18.8)		3 (18.8)	
Borrmann III	80	35 (43.8)	11.92	32 (40.0)	9.65
Borrmann IV	31	21 (67.7)	$<0.005^b$	24 (77.4)	$<0.005^b$

^a ≥ 10.0 group vs 0-4.9 or 5-9.9 group; ^bBorrmann III and Borrmann IV groups vs Borrmann I and Borrmann II groups

Expression of E-cadherin or β -catenin and histopathological findings

Table 3 shows no correlation could be verified between expression of E-cadherin or β -catenin and the invasion depth of the tumor (T_1/T_2 vs T_3/T_4). Among the 163 cases of gastric cancers in our series, lymphatic metastasis was observed in 92 cases (56.4 %). We found that there was no correlation between the abnormal expression of E-cadherin and the positivity of lymphatic metastasis. However, the expression of β -catenin was closely correlated with lymphatic metastasis ($P<0.005$).

According to the WHO classification, papillary adenocarcinoma showed abnormal expression of E-cadherin and β -catenin more frequently compared with signet-ring carcinoma and mucinous and tubular adenocarcinoma ($P<0.005$ and $P<0.01$, respectively). Furthermore, according to the histological classification of Lauren, abnormal expression of E-cadherin and β -catenin was significantly higher in diffuse than in intestinal types ($P<0.005$, respectively).

Survival analysis

Survival data were obtained for 113 of the patients. Kaplan-Meier curves were computed to compare survival of patients with normal versus abnormal expression of E-cadherin and β -catenin. The overall median survival of patients in this study was 1067 days (range 78-2365). Average survival time for patients showing abnormal expression of E-cadherin was 1065 ± 118 days, normal expression of E-cadherin was 1508 ± 121 days. Patients with normal expression of E-cadherin appeared to have a longer survival time compared with those who have abnormal E-cadherin expression, although the difference was not statistically significant ($P=0.058$). The average survival time for patients with abnormal expression of β -catenin was 764 ± 110 days, as opposed to the survival time of 1798 ± 105 days for patients with normal expression ($P<0.0005$) (Figure 2). A multivariate Cox regression analysis confirmed statistically significant association of abnormal β -catenin expression with poor survival ($P<0.0005$), independent of tumor type, grade, or stage.

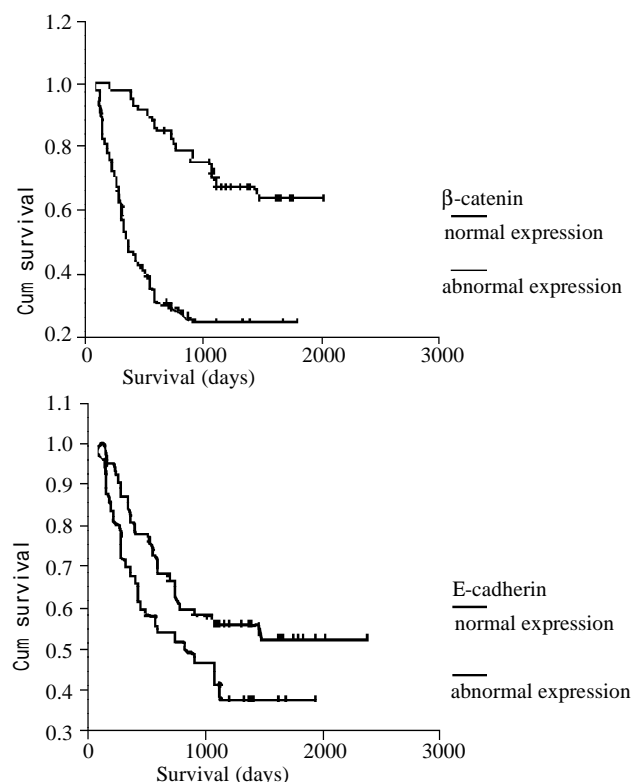


Figure 2 Kaplan-Meier survival curves showing a statistically significant survival advantage found in all tumors with normal membranous expression of β -catenin (B) compared with those with loss of membranous expression ($P<0.0005$). Abnormal E-cadherin (A) staining pattern showed a trend toward worse survival, but not statistically significant ($P=0.058$).

Table 3 Relationship Between Expression of E-cadherin or β -catenin and Histopathological Features in Gastric Carcinoma

	No	E-cadherin expression (%)		β -catenin expression (%)	
		Abnormal	P value	Abnormal	P value
pT category					
T ₁ /T ₂	65	28 (43.1)		29 (44.6)	
T ₃ /T ₄	98	47 (48.0)	NS	44 (44.9)	NS
pN category					
N-negative	71	29 (40.8)		20 (28.2)	14.56
N-positive	92	46 (50.0)	NS	53 (57.6)	<0.005
WHO classification					
Adenocarcinoma	160				
Papillary	16	3 (18.8) ^a		2 (7.1) ^a	
Tubular	109	48 (44.0)		46 (42.2)	
Mucinous	24	13 (54.2)	8.47	15 (62.5)	7.05
Signet ring	11	8 (72.7)	<0.005	7 (63.3)	<0.01
Undiff. carcinoma	3	3 (100)		3 (100)	
Lauren classification					
Intestinal type	108	36 (33.3) ^b	18.18	34 (31.5) ^b	17.79
Diffuse type	40	29 (72.5)	<0.005	28 (70.0)	<0.005
Mixed type	15	10 (66.7)		11 (73.3)	

^aPapillary vs Tubular, Mucinous and Signet ring; ^bIntestinal type vs Diffuse type. NS: No Significance

DISCUSSION

Aberrant expression of E-cadherin and β -catenin with loss of membranous localization has been detected in a number of human cancers. Previous studies^[27-30] have shown variable abnormal expression of E-cadherin-catenin complex ranging from 20 % up to 90 % of tumors. In gastric carcinoma or other human carcinomas, the overall expression of E-cadherin-catenin complex as reported in different studies is difficult to compare due to different score systems and different antibodies used. In this study, 46 % of gastric carcinomas showed abnormal E-cadherin expression and 44 % showed abnormal β -catenin expression, so our data are in line with previous reports which revealed alteration of E-cadherin and β -catenin expression in gastric carcinomas. In addition, by using the Kaplan-Meier curve and A multivariate Cox regression analysis, we found that β -catenin but not E-cadherin expression abnormalities were associated with poor survival, confirming the findings of Jawhari *et al*^[25] and Ramesh *et al*^[48]. However, the use of E-cadherin as a patient survival indicator needs to be further verified, as previous findings by Gabbert *et al*^[30], Shun *et al*^[29], and Grabsch *et al*^[31] indicated that there was correlation between abnormal E-cadherin expression and patient survival in gastric carcinoma.

We demonstrated a significant correlation between expression of E-cadherin-catenin complex and tumor differentiation. Aberrant E-cadherin or β -catenin expression was associated with diffuse-type (poorly differentiated) carcinomas. Similarly, abnormal expression rate of E-cadherin and β -catenin was significantly higher in low- and undifferentiated adenocarcinomas than in well-differentiated adenocarcinomas. Previous *in vitro* studies^[8] have shown that loss of E-cadherin in human carcinoma cell lines is associated with poor differentiation and fibroblastoid morphology. Furthermore, down-regulation of E-cadherin protein product after E-cadherin-specific antisense RNA transfection results in an invasive and de-differentiated phenotype^[9]. Transfection of E-cadherin cDNA into undifferentiated carcinoma cells produces an epithelioid morphology and increases intercellular adhesion. These effects are reversible using anti-E-cadherin antibodies and provide direct *in vitro* evidence of the crucial role of E-cadherin in the regulation of cell polarity, cellular differentiation, and epithelial morphology^[9,32]. Our results support the above findings, suggesting that E-cadherin-catenin complex may play an important role in the genesis of histological differentiation and may be used as a differentiation marker in gastric carcinoma^[33,34].

The E-cadherin-mediated cell adhesion system is known to act as an "invasive suppressor system"^[24,35,36] and tumors with reduced E-cadherin expression were also reported to have a higher frequency of lymph node involvement, distant metastasis and morphologic degree of invasiveness than those with preserved E-cadherin expression^[37,38]. In this study, decreased E-cadherin expression occurred more frequently in tumors of more infiltrative growth on gross appearance or in those of larger size than in their counterparts, but showed no association with the invasion depth of the tumor, and lymph node metastasis. This findings strongly suggests that the presence of E-cadherin as revealed by immunohistochemistry might not indicate that E-cadherin is necessarily functional. For instance, certain mutations in the E-cadherin gene or changes in E-cadherin associated cytoplasmic proteins, the catenin, may alter their adhesive functions. Mutations affecting intercellular adhesion mechanisms have emerged as important steps in the development and progression of many human epithelial tumors. In gastric carcinomas, mutations of the E-

cadherin gene have been reported^[39-42]. A germline mutation in E-cadherin associated with familial gastric carcinoma was recently reported in a New Zealand kindred^[43]. Moreover, *in vitro* studies with E-cadherin-negative carcinoma cell lines suggested that methylation around the promoter region CpG island may be one mechanism of E-cadherin inactivation in human carcinomas^[44,45]. Catenins have been classified into α , β , and γ . The cytoplasmic tail of E-cadherin interacts with either β - or γ -catenins which bridge E-cadherin to the cytoskeleton through α -catenin^[46,47]. Many studies indicate that the association of E-cadherin with catenins is essential for their cell-cell adhesion^[25,48]. Mutations in α - and β -catenins have not been convincingly demonstrated^[49], but protein expression abnormalities are relatively frequent, and occur in both diffuse and intestinal carcinomas^[50,51]. As the function of E-cadherin is modulated by α -catenin, loss of α -catenin expression or deletion of α -catenin could suppress E-cadherin-mediated cell-cell adhesion activity, despite normal E-cadherin and β -catenin expression^[52]. β -catenin is a multifunctional protein, and plays an important role in Wntless/Wnt signal transduction in addition to its function as a cell-adhesion components^[53]. Posttranslation modification of β -catenin molecule by phosphorylation has been shown to disrupt the interaction between E-cadherin and α -catenin, causing loss of E-cadherin-dependent intercellular adhesiveness and in turn potentiating the neoplastic process^[53,54]. Furthermore, the association of abnormal β -catenin expression with a worse survival, independent of tumor type, grade, or stage, seems to suggest that it acts as an independent prognostic variable.

The pathogenesis of gastric carcinoma remains largely unknown. Although a number of genetic and molecular alterations have been described in gastric carcinoma^[55-57], the exact sequence and number of genetic or molecular alterations are not yet known. There were several patterns postulated on how histomorphological changes of the gastric mucosa will progress to the development of gastric carcinoma. The best known was proposed by Correa *et al*^[58] who described the development of gastric tumors from gastritis through intestinal metaplasia, dysplasia, and eventually to gastric carcinoma. Recent *in vitro* and *in vivo* studies have shown that alteration or loss of E-cadherin expression seems to be critical for the development of gastric carcinomas. Furthermore, Ohene *et al*^[59], Xiangming *et al*^[60], Blok *et al*^[61] and Shun *et al*^[62] reported that abnormal E-cadherin-catenin complex expression occurred in early gastric carcinomas and changes in E-cadherin expression might be early events in gastric carcinoma. Our analysis aimed at investigating E-cadherin-catenin complex expression in the possible precancerous conditions, such as atrophic gastritis, intestinal metaplasia and dysplasia and evaluating the role of E-cadherin-catenin complex expression in the development of gastric carcinoma. In this study, we found that abnormal expression was shown in 36.4 % of dysplasia for E-cadherin and 16 % for β -catenin, respectively, while atrophic gastritis, intestinal metaplasia showed normal expression. Our observations of decreased E-cadherin and β -catenin expression in dysplasia raises the possibility that changes in the E-cadherin-catenin complex occur at an early stage in the neoplastic process.

In conclusion, abnormal expression of E-cadherin and β -catenin occurs in a considerable proportion of gastric carcinomas and correlates with loss of differentiation. Loss of normal β -catenin expression showed a close correlation with poor survival, independent of tumor type, grade, and stage, suggesting that it may be an independent prognostic marker. Our results also indicate that changes in abnormal expression of E-cadherin-catenin complex may be early events in gastric carcinomas.

ACKNOWLEDGEMENT

We are grateful to Drs. M. Jiang, MT. Gao and JS. Wang, Department of Pathology, Lanzhou Medical College, Lanzhou, China, for providing the tissue specimens.

REFERENCES

- 1 **Uemura T.** The cadherin superfamily at the synapse: more members, more missions. *Cell* 1998; **93**: 1095-1098
- 2 **Takeichi M.** Cadherin cell adhesion receptors as a morphogenetic regulator. *Science* 1991; **251**: 1451-1455
- 3 **Zhou YN, Wu ZD, Xu CP, Fang DC.** E-cadherin-catenin complex in gastric carcinoma. *Shijie Huaren Xiaohua Zazhi* 2002; **10**: 436-440
- 4 **Jawhari A, Farthing M, Pignatelli M.** The importance of the E-cadherin-catenin complex in the maintenance of intestinal epithelial homeostasis: more than intercellular glue. *Gut* 1997; **41**: 581-584
- 5 **Pignatelli M, Vessey CJ.** Adhesion molecules: novel molecular tools in tumor pathology. *Hum Pathol* 1994; **25**: 849-856
- 6 **Oka H, Shiozaki H, Kobayashi K, Inoue M, Tahara H, Kobayashi T, Takatsuka Y, Matsuyoshi N, Hirano S, Takeichi M.** Expression of E-cadherin cell adhesion molecules in human breast cancer tissues and its relationship to metastasis. *Cancer Res* 1993; **53**: 1696-1701
- 7 **Pignatelli M, Ansari TW, Gunter P, Liu D, Hirano S, Takeichi M, Kloppel G, Lemoine NR.** Loss of membranous E-cadherin expression in pancreatic cancer: correlation with lymph node metastasis, high grade, and advanced stage. *J Pathol* 1994; **174**: 243-248
- 8 **Frixen UH, Behrens J, Sachs M, Eberle G, Voss B, Warda A, Lochner D, Birchmeier W.** E-cadherin-mediated cell-cell adhesion prevents invasiveness of human carcinoma cells. *J Cell Biol* 1991; **113**: 173-185
- 9 **Vlemminckx K, Vakaet L Jr, Mareel M, Fiers W, van-Roy F.** Genetic manipulation of E-cadherin expression by epithelial tumor cells reveals an invasion suppressor role. *Cell* 1991; **66**: 107-119
- 10 **Richmond PJ, Karayiannakis AJ, Nagafuchi A, Kaisary AV, Pignatelli M.** Aberrant E-cadherin and alpha-catenin expression in prostate cancer: correlation with patient survival. *Cancer Res* 1997; **57**: 3189-3193
- 11 **Syrigos KN, Krausz T, Waxman J, Pandha H, Rowlinson-Busza G, Verne J, Epenetos AA, Pignatelli M.** E-cadherin expression in bladder cancer using formalin-fixed, paraffin-embedded tissues: correlation with histopathological grade, tumour stage and survival. *Int J Cancer* 1995; **64**: 367-370
- 12 **Siitonen SM, Kononen JT, Helin HJ, Rantala IS, Holli KA, Isola JJ.** Reduced E-cadherin expression is associated with invasiveness and unfavorable prognosis in breast cancer. *Am J Clin Pathol* 1996; **105**: 394-402
- 13 **Tanaka M, Kitajima Y, Edakuni G, Sato S, Miyazaki K.** Abnormal expression of E-cadherin and beta-catenin may be a molecular marker of submucosal invasion and lymph node metastasis in early gastric cancer. *Br J Surg* 2002; **89**: 236-244
- 14 **Katoh M.** Frequent up-regulation of WNT2 in primary gastric cancer and colorectal cancer. *Int J Oncol* 2001; **19**: 1003-1007
- 15 **Korinek V, Barker N, Molin PJ, Van wichen D, de Weger R, Kinzler KW, Vogelstein B, Clevers H.** Constitutive transcriptional activation by a β -catenin-Tcf complex in APC-/- colon carcinoma. *Science* 1997; **275**: 1784-1787
- 16 **Morin PJ, Sparks AB, Korinek V, Barker N, Clevers H, Vogelstein B, Kinzler KW.** Activation of β -catenin-Tcf signaling in colon cancer by mutations in β -catenin or APC. *Science* 1997; **275**: 1787-1790
- 17 **Porfiri E, Rubinfeld B, Albert I, Hovanes K, Waterman M, Polakis P.** Induction of a beta-catenin-LEF-1 complex by wnt-1 and transforming mutants of beta-catenin. *Oncogene* 1997; **15**: 2833-2839
- 18 **Hansson LE, Sparen P, Nyren O.** Survival in stomach cancer is improving: results of a nationwide population-based Swedish study. *Ann Surg* 1999; **230**: 162-169
- 19 **Sun XD, Mu R, Zhou YS, Dai XT, Qiao YL, Zhang SW, Huangpu XM, Sun J, Li LD, Lu FZ.** 1990-1992 mortality of stomach cancer in China. *Zhonghua Zhongliu Zazhi* 2002; **24**: 4-8
- 20 **Werner M, Becker KF, Keller G, Hofler H.** Gastric adenocarcinoma: pathomorphology and molecular pathology. *J Cancer Res Clin Oncol* 2001; **127**: 207-216
- 21 **Becker KF, Keller G, Hofler H.** The use of molecular biology in diagnosis and prognosis of gastric cancer. *Surg Oncol* 2000; **9**: 5-11
- 22 **Kennedy BJ.** The unified international gastric cancer staging classification. *Scand J Gastroenterol* 1987; **22**: 11-13
- 23 **Lauren P.** The two histological main types of gastric carcinoma. *Acta Pathol Microbiol Scand* 1965; **64**: 31-49
- 24 **Rugge M, Correa P, Dixon MF.** Gastric Dysplasia. The international classification. *Am J Surg Pathol* 2000; **124**: 167-176
- 25 **Jawhari A, Jordan S, Poole S, Browne P, Pignatelli M, Farthing MJ.** Abnormal immunoreactivity of the E-cadherin-catenin complex in gastric carcinoma: relationship with patient survival. *Gastroenterology* 1997; **112**: 46-54
- 26 **Shiozaki H, Tahara H, Oka H, Miyata M, Kobayashi K, Tamura S, Iihara K, Doki Y, Hirano S, Takeichi M.** Expression of immunoreactive E-cadherin adhesion molecule in human cancer. *Am J Pathol* 1991; **139**: 17-23
- 27 **Mayer B, Johnson JP, Leitl F, Jauch KW, Heiss MM, Schildberg FW, Birchmeier W, Funke I.** E-cadherin expression in primary and metastatic gastric cancer: down-regulation correlates with cellular dedifferentiation and glandular disintegration. *Cancer Res* 1993; **53**: 1690-1695
- 28 **Karayannakis AJ, Syrigos KN, Chatzigianni E, Papanikolaou S, Karatzas G.** E-cadherin expression as a differentiation marker in gastric cancer. *Hepatogastroenterology* 1998; **45**: 2437-2442
- 29 **Shun CT, Wu MS, Lin JT, Wang HP, Hounng RL, Lee WJ, Wang TH, Chuang SM.** An immunohistochemical study of E-cadherin expression with correlations to clinicopathological features in gastric cancer. *Hepatogastroenterology* 1998; **45**: 944-949
- 30 **Gabbert HE, Mueller W, Schneiders A, Meier S, Moll R, Birchmeier W, Hommel G.** Prognostic value of E-cadherin expression in 413 gastric carcinomas. *Int J Cancer* 1996; **69**: 184-189
- 31 **Grabsch H, Takeno S, Noguchi T, Hommel G, Gabbert HE, Mueller W.** Different patterns of beta-catenin expression in gastric carcinomas: relationship with clinicopathological parameters and prognostic outcome. *Histopathology* 2001; **39**: 141-149
- 32 **Fleming S.** Cell adhesion and epithelial differentiation. *J Pathol* 1991; **164**: 95-100
- 33 **Chan AO, Lam SK, Chu KM, Lam CM, Kwok E, Leung SY, Yuen ST, Law SY, Hui WM, Lai KC, Wong CY, Hu HC, Lai CL, Wong J.** Soluble E-cadherin is a valid prognostic marker in gastric carcinoma. *Gut* 2001; **48**: 808-811
- 34 **Ougolkov A, Mai M, Takahashi Y, Omote K, Bilim V, Shimizu A, Minamoto T.** Altered expression of beta-catenin and c-erbB-2 in early gastric cancer. *J Exp Clin Cancer Res* 2000; **19**: 349-355
- 35 **Shiozaki H, Oka H, Inoue M, Tamura S, Monden M.** E-cadherin mediated adhesion system in cancer cells. *Cancer* 1996; **77**: 1605-1613
- 36 **Lee JH, Koh JT, Shin BA, Ahn KY, Roh JH, Kim YJ, Kim KK.** Comparative study of angiostatic and anti-invasive gene expressions as prognostic factors in gastric cancer. *Int J Oncol* 2001; **18**: 355-361
- 37 **Takeichi M.** Cadherins in cancer: implications for invasion and metastasis. *Curr Opin Cell Biol* 1993; **5**: 806-811
- 38 **Birchmeier W, Behrens J.** Cadherin expression in carcinomas: role in the formation of cell junctions and the prevention of invasiveness. *Biochim Biophys Acta* 1994; **1198**: 11-26
- 39 **Machado JC, Soares P, Carneiro F, Rocha A, Beck S, Blin N, Bex G, Sobrinho-Simoes M.** E-cadherin gene mutations provide a genetic basis for the phenotypic divergence of mixed gastric carcinomas. *Lab Invest* 1999; **79**: 459-465
- 40 **Fukudome Y, Yanagihara K, Takeichi M, Ito F, Shibamoto S.** Characterization of a mutant E-cadherin protein encoded by a mutant gene frequently seen in diffuse-type human gastric carcinoma. *Int J Cancer* 2000; **88**: 579-583
- 41 **Chun YS, Lindor NM, Smyrk TC, Petersen BT, Burgart LJ, Guilford PJ, Donohue JH.** Germline E-cadherin gene mutations: is prophylactic total gastrectomy indicated? *Cancer* 2001; **92**: 181-187

- 42 **Zheng ZH**, Sun XJ, Qiu GR, Liu YH, Wang MX, Sun KL. E-cadherin gene mutation in precancerous condition, early and advanced stages of gastric cancer. *Shijie Huaren Xiaohua Zazhi* 2002; **10**: 153-156
- 43 **Guilford P**, Hopkins J, Harraway J, McLeod M, McLeod N, Harawira P, Taite H, Scoular R, Miller A, Reeve AE. E-cadherin germline mutations in familial gastric cancer. *Nature* 1998; **392**: 402-405
- 44 **Tamura G**, Yin J, Wang S, Fleisher AS, Zou T, Abraham JM, Kong D, Smolinski KN, Wilson KT, James SP, Silverberg SG, Nishizuka S, Terashima M, Motoyama T, Meltzer SJ. E-Cadherin gene promoter hypermethylation in primary human gastric carcinomas. *J Natl Cancer Inst* 2000; **92**: 569-573
- 45 **Leung WK**, Yu J, Ng EK, To KF, Ma PK, Lee TL, Go MY, Chung SC, Sung JJ. Concurrent hypermethylation of multiple tumor-related genes in gastric carcinoma and adjacent normal tissues. *Cancer* 2001; **91**: 2294-2301
- 46 **Ozawa M**, Baribault H, Kemler R. The cytoplasmic domain of the cell adhesion molecule uvomorulin associates with three independent proteins structurally related in different species. *EMBO J* 1989; **8**: 1711-1717
- 47 **Hinck L**, Nathke IS, Papkoff J, Nelson WJ. Dynamics of cadherin/catenin complex formation: novel protein interactions and pathways of complex assembly. *J Cell Biol* 1994; **125**: 1327-1340
- 48 **Ramesh S**, Nash J, McCulloch PG. Reduction in membranous expression of beta-catenin and increased cytoplasmic E-cadherin expression predict poor survival in gastric cancer. *Br J Cancer* 1999; **81**: 1392-1397
- 49 **Tong JH**, To KF, Ng EK, Lau JY, Lee TL, Lo KW, Leung WK, Tang NL, Chan FK, Sung JJ, Chung SC. Somatic beta-catenin mutation in gastric carcinoma--an infrequent event that is not specific for microsatellite instability. *Cancer Lett* 2001; **163**: 125-130
- 50 **Karatzas G**, Karayiannakis AJ, Syrigos KN, Chatzigianni E, Papanikolaou S, Simatos G, Papanikolaou D, Bogris S. Expression patterns of the E-cadherin-catenin cell-cell adhesion complex in gastric cancer. *Hepatogastroenterology* 2000; **47**: 1465-1469
- 51 **Joo YE**, Rew JS, Kim HS, Choi SH, Park CS, Kim SJ. Changes in the E-cadherin-catenin complex expression in early and advanced gastric cancers. *Digestion* 2001; **64**: 111-119
- 52 **Yu J**, Ebert MP, Miehlik S, Rost H, Lendeckel U, Leodolter A, Stolte M, Bayerdorffer E, Malfertheiner P. alpha-catenin expression is decreased in human gastric cancers and in the gastric mucosa of first degree relatives. *Gut* 2000; **46**: 639-644
- 53 **Behrens J**, von Kries JP, Brunh L. Functional interaction of beta-catenin with the transcription factor LEF-1. *Nature* 1996; **382**: 638-642
- 54 **Takayama T**, Shiozaki H, Doki Y, Oka H, Inoue M, Yamamoto M, Tamura S, Shibamoto S, Ito F, Monden M. Aberrant expression and phosphorylation of β -catenin in human colorectal cancer. *Br J Cancer* 1998; **77**: 605-613
- 55 **Yokozaki H**, Yasui W, Tahara E. Genetic and epigenetic changes in stomach cancer. *Int Rev Cytol* 2001; **204**: 49-95
- 56 **Tamura G**, Sato K, Akiyama S, Tsuchiya T, Endoh Y, Usuba O, Kimura W, Nishizuka S, Motoyama T. Molecular characterization of undifferentiated-type gastric carcinoma. *Lab Invest* 2001; **81**: 593-598
- 57 **Gao HJ**, Yu LZ, Bai JF, Peng YS, Sun G, Zhao HL, Miu K, L XZ, Zhang XY, Zhao ZQ. Multiple genetic alterations and behavior of cellular biology in gastric cancer and other gastric mucosal lesions: *H. pylori* infection, histological types and staging. *World J Gastroenterol* 2000; **6**: 848-854
- 58 **Correa P**. Human gastric carcinogenesis: a multistep and multifactorial process--first American Cancer Society Award Lecture on cancer epidemiology and prevention. *Cancer Res* 1992; **52**: 6735-6740
- 59 **Ohene-Abuakwa Y**, Noda M, Perenyi M, Kobayashi N, Kashima K, Hattori T, Pignatelli M. Expression of the E-cadherin/catenin (alpha-, beta-, and gamma-) complex correlates with the macroscopic appearance of early gastric cancer. *J Pathol* 2000; **192**: 433-439
- 60 **Xiangming C**, Hokita S, Natsugoe S, Tanabe G, Baba M, Takao S, Kuroshima K, Aikou T. Cooccurrence of reduced expression of alpha-catenin and overexpression of p53 is a predictor of lymph node metastasis in early gastric cancer. *Oncology* 1999; **57**: 131-137
- 61 **Blok P**, Craanen ME, Dekker W, Tytgat GN. Loss of E-cadherin expression in early gastric cancer. *Histopathology* 1999; **34**: 410-415
- 62 **Shun CT**, Wu MS, Lin MT, Chang MC, Lin JT, Chuang SM. Immunohistochemical evaluation of cadherin and catenin expression in early gastric carcinomas: correlation with clinicopathologic characteristics and *Helicobacter pylori* infection. *Oncology* 2001; **60**: 339-345

Edited by Xu JY

• GASTRIC CANCER •

Expression of vascular endothelial growth factor and its receptors KDR and Flt-1 in gastric cancer cells

Hua Zhang, Jian Wu, Lin Meng, Cheng-Chao Shou

Hua Zhang, Jian Wu, Lin Meng, Cheng-Chao Shou, Peking University School of Oncology, Beijing Institute for Cancer Research, Beijing 100034, China

Supported by National Nature Science Foundation for Outstanding Young Scientist of China (to S. CC., No. 39525021), National 863 program of China (2002 AA 216111) and Beijing Laboratory of Cancer Molecular Biology.

Correspondence to: Dr. Cheng-Chao Shou, Department of Biochemistry and Molecular Biology, Peking University School of Oncology, Beijing Institute for Cancer Research, No.1 Da-Hong-Luo-Chang Street, Western District, Beijing 100034, China. cshou_9@hotmail.com

Telephone: +86-10-66160960 **Fax:** +86-10-66175832

Received 2002-04-25 **Accepted** 2002-06-12

Abstract

AIM: The expression of vascular endothelial growth factor (VEGF) and its receptors KDR and Flt-1 by gastric carcinoma tissues and different gastric carcinoma cell lines was detected to elucidate the molecular mechanism of this growth factor in promoting tumor growth.

METHODS: The expression of VEGF, Flt-1 and KDR was determined by reverse transcription-polymerase chain reaction (RT-PCR) in gastric cancer cell lines RF-1, RF-48, AGS-1, NCI-N87, NCI-SNU-1, NCI-SNU-5, NCI-SNU-16 and KATO-III. The expression of Flt-1 and KDR in paraffin-embedded specimens of gastric cancer was determined by immunohistochemistry. The 3-(4,5-dimethylthiazol-2-yl)-2,5-diphenyltetrazolium bromide (MTT) assay was used to assess the role of VEGF in tumor cell proliferation.

RESULTS: All 8 gastric cancer cell lines analyzed expressed VEGF₁₂₁ and VEGF₁₆₅ and six of them expressed both Flt-1 and KDR, while cell line NCI-SNU-5 expressed Flt-1 only and cell line KATO-III expressed neither Flt-1 nor KDR. The gastric carcinoma tissues expressed Flt-1 and KDR widely, with the positive rate of expression of Flt-1 and KDR being 84.6 % and 70 % respectively. The exogenous VEGF stimulated the growth of KDR-positive cell lines NCI-N87 and AGS-1 in a dose-dependent manner but exhibited no effect on the growth of KDR-negative cell line NCI-N87.

CONCLUSION: VEGF and its receptors KDR and Flt-1 were expressed widely in gastric carcinoma cells and the VEGF stimulated KDR-positive tumor cell growth directly. These results suggest that VEGF may play a role in promoting tumor growth and metastasis by participating in both paracrine and autocrine pathways.

Zhang H, Wu J, Meng L, Shou CC. Expression of vascular endothelial growth factor and its receptors KDR and Flt-1 in gastric cancer cells. *World J Gastroenterol* 2002; 8(6):994-998

INTRODUCTION

Angiogenesis is essential for the continued growth of solid

tumors. Among the factors contributing to angiogenesis, vascular endothelial growth factor (VEGF, also called vascular permeability factor) is recognized as one of the most important molecules in the formation of new blood vessels^[1-8]. A variety of malignant human tumors, including breast, lung and prostate carcinomas, are known to secrete VEGF. The level of VEGF expression correlates with tumor progression and metastasis. Moreover, over-expression of VEGF was suggested to participate in carcinogenic processes. Different investigators reported that VEGF might play an important role during the pre-malignant stages of tumorigenesis in colon, pancreas, and cervix.

VEGF binds with high affinity to its cognate VEGF receptors (VEGFRs) Flt-1/VEGFR-1, flk-1/KDR/VEGFR-2, and neuropilin-1^[9,10]. KDR is responsible for mitogenic signaling, and plays an important role in vasculogenesis and blood island formations. However, Flt-1 does not mediate cell growth when introduced into NIH3T3 cells or into porcine aortic endothelial cells that do not express VEGFRs, but regulates the assembly of endothelial cells and tissue factor production in endothelial cells. Recently the third receptor of VEGF, neuropilin-1, was purified from tumor cells. It binds VEGF₁₆₅ but not VEGF₁₂₁, and modulates VEGF binding to VEGFR-2/Flk-1 and the subsequent bioactivity^[9].

Recently a few studies have proved that Flt-1 and/or KDR were also expressed in tumor cells, such as hematopoietic malignancies^[11-14], pancreatic cancer^[15], breast cancer^[16], neuroblastoma^[17], Kaposi sarcoma^[18], and lung carcinomas induced by N-nitrosobis (2-hydroxypropyl) amine in rats^[19]. We previously demonstrated that the VEGF and KDR were co-expressed in gastric adenocarcinoma MGC803 cells, and exogenous recombinant human VEGF₁₆₅ stimulated growth of MGC803 cells directly^[20]. The present study extended our previous work and detected the expression of VEGF, Flt-1 and KDR in eight gastric cancer cell lines by RT-PCR, and the expression of Flt-1 and KDR in gastric tumor specimens by immunohistochemistry. The results showed that VEGF and VEGFR were co-expressed in gastric tumor cells widely, and exogenous VEGF₁₆₅ stimulated the growth of KDR-positive gastric carcinoma cells, indicating that there is a possible autocrine pathway for VEGF in gastric cancer.

MATERIALS AND METHODS

Cell culture and reagents

Human gastric cancer cell lines from American Type Culture Collection (ATCC) were generously supplied by Dr. Ji JF. The cell lines RF-1 and RF-48 were cultured in Leibovitz' s L-15 medium containing 10 % fetal calf serum (FCS), AGS-1, NCI-N87, NCI-SNU-1 and NCI-SNU-16 were cultured in RPMI1640 medium containing 10 %FCS and NCI-SNU-5 and KATO-III were cultured in RPMI1640 medium containing 20 % FCS. Anti-Flt-1 rabbit polyclonal antibody was purchased from Santa Cruz Biotechnology, Inc. Anti-KDR mouse monoclonal antibody 6E2 was prepared in our laboratory. Recombinant human VEGF₁₆₅ was purchased from Sigma Inc.

RT-PCR

Total RNA was extracted from eight carcinoma cell lines of 2×10^6 cells each using TRIZOL following the manufacturer's instructions. First-strand cDNA was synthesized from 10 μ g of total RNA in a 50 μ l reaction volume by reverse transcription (RT) using random hexamer and MMLV reverse transcriptase (GIBCO BRL) as described by the manufacturer. The cDNA of 2 μ l was amplified by PCR in a 25 μ l reaction volume with primers designed to span intron-exon boundaries to distinguish amplified cDNA from genomic DNA (Table 1). VEGF was amplified for 40 cycles at 94 °C for 45 sec, 55 °C for 40 sec and 72 °C for 1 min and its primers were chosen to recognize all the known VEGF splice variants according to the published sequences (GenBank: AF022375). GAPDH was amplified for 30 cycles using the same cycling conditions as for VEGF. Flt-1 and KDR were amplified by semi-nest PCR. The Flt-1 was first amplified with forward-1 (corresponding to nucleotides 1-15, GenBank: AF063657) and reverse primers (corresponding to nucleotides 1287-1270) for 30 cycles at 94 °C for 45 sec, 64 °C for 1 min and 72 °C for 2 min, then amplified with forward-2 (corresponding to nucleotides 94-109) and reverse primers for 30 cycles. The KDR was first amplified with forward (corresponding to nucleotides 1316-1330, GenBank: AF063658) and reverse-2 (corresponding to nucleotides 2275-2260) primers for 30 cycles at 94 °C for 45 sec, 52 °C for 1 min and 72 °C for 2 min, and then amplified with the forward and reverse-1 (corresponding to nucleotides 2225-2207) primers for 30 cycles at 94 °C for 45 sec, 64 °C for 1 min and 72 °C for 2 min.

The PCR products of Flt-1 were analyzed by restriction endonuclease digestion with *SacI* and *PstI* (New England Biolabs Inc.) and KDR were analyzed with *HindIII* (New England Biolabs Inc.). The amplified cDNA of Flt-1 and KDR from AGS-1 cells were cloned into pGEM-T Easy vector (Promega) and sequenced.

Table 1 Gene specific primers for PCR

gene	GenBank	Orientation	Sequence
VEGF	AF022375	Forward	5'-GGGGGATCCGCCTCCGAAACCATGAACCTT-3'
		Reverse	5'-CCCGAATTCCTCGGTGAGAGATCTGGTT-3'
Flt-1	AF063657	Forward-1	5'-TCTAGGATCCATGGTCAGTACTGGGACACC-3'
		Forward-2	5'-AAGGGATCCCTGAACCTGAGTTTAAAA-3'
		Reverse	5'-GGCGAATTCCTGGGTTTCACATTGAC-3'
KDR	AF063658	Forward	5'-TAAGGATCCCACTCAACGCTGAC-3'
			5'-GGAGAATTCCTCAACTGCATGCCTGGCAG-3'
			5'-TCCTGGGCACCTTCTA-3'
GAPDH	AF261085	Forward	5'-ACCACAGTCCATGCCATCAC-3'
			5'-TCCACCACCTGTTGCTGTA-3'

(Underlined sequences are restriction endonuclease recognition sites, which were added for further cloning).

Immunohistochemical analysis

Paraffin-embedded gastric carcinoma specimens were collected from the Department of Pathology, Beijing Institute for Cancer Research. The tissue sections were deparaffinized, treated with 3 % H₂O₂ to inhibit endogenous peroxidase and incubated in 0.1M sodium citrate buffer, pH6.0, at 92-98 °C for 10 min for antigen retrieval. The tissues were blocked with 10 % normal goat serum at 37 °C for 30 min and stained for Flt-1 with rabbit polyclonal antibody at 1:200 dilution, or for KDR with mouse monoclonal antibody 6E2 at 4 μ g/ml, at 4 °C overnight. This was followed by sequential incubations in biotin-conjugated secondary antibody, streptavidin-peroxidase and 3, 3'-diaminobenzidine

(DAB) for visualization. Normal rabbit serum (1:10 000 dilution) or normal mouse IgG (4 μ g/ml) was used as negative controls.

Cell proliferation assay

Cells AGS-1 and NCI-N87 were seeded into 96-well plates with 2×10^4 and 5×10^4 cells per well respectively and incubated in 10 % RPMI1640 medium for 24 hours. The culture medium was then replaced with serum-free medium and cells cultured for another 24 hours. KATO III cells were seeded at 2×10^4 /well and incubated in serum-free medium for 24 hours. All these cells were then treated with varying concentrations of VEGF₁₆₅ (0-10 ng/ml) for 72 hours followed by treatment with 3-(4,5-dimethylthiazol-2-yl)-2, 5-diphenyl tetrazolium bromide (MTT) for 4 hours. The medium was gently aspirated, cells were lysed in 150 μ l of dimethylsulfoxide and the cell lysates were measured for absorbance at 492 nm with a Model 550 microplate reader. (Bio-Rad Co.). The viability was expressed as mean percentage of untreated controls \pm SE ($n=4$). Statistical analysis was performed by means of Student's *t*-test.

RESULTS

Expression of VEGF and its receptors in human gastric carcinoma cell lines

RT-PCR with primers designed to amplify all 5 known splicing variants of VEGF generated two products of 531bp and 663bp in size corresponding to VEGF isoforms VEGF₁₂₁ and VEGF₁₆₅ in all eight gastric carcinoma cell lines (Figure 1A). Flt-1 of the expected size (1212 bp) was amplified in all cell lines except KATOIII cells (Figure 1B) and the amplified products were successfully digested with *SacI* and *PstI* respectively (data not shown). KDR of the expected sized (927bp) was amplified in all cell lines except SNU-5 and KATOIII cells (Figure 1C) and the amplified products were successfully digested with *HindIII* (data not shown).

The fragments of Flt-1 and KDR amplified from AGS-1 were cloned into pGEM-T Easy vector and sequenced.



Figure 1 Detection of expression of VEGF and VEGFR in eight gastric carcinoma cell lines by RT-PCR. A. VEGF was amplified using primers designed to detect all known splicing variants and two isoforms 531bp and 663bp corresponding to VEGF₁₂₁ and VEGF₁₆₅ were obtained in all cell lines. B. Flt-1 of the expected size (1212bp) was amplified in all cell lines except KATOIII. C. KDR of the expected size (927bp) was amplified in all cell lines except SNU-5 and KATOIII. D. GAPDH was amplified in each cell line as a positive control for RT-PCR.

Flt-1 and KDR were widely expressed in gastric carcinoma

Specimens from 52 cases of gastric carcinoma were examined by immunohisto-chemistry to detect the expression of Flt-1. The results showed that Flt-1 was not only expressed in endothelial cells, but also in the tumor cells with a positivity of 84.6 % (44cases/52cases) (Figure 2A). The intensity of immunostaining was stronger in well-differentiated adenocarcinomas than in poorly differentiated adenocarcinomas. The vascular smooth muscles were also positive for Flt-1, consistent with published report^[21], so were some normal cells in the bottom of gastric gland. Immunostaining was not observed on tumor tissues when normal rabbit serum was used as primary antibody.

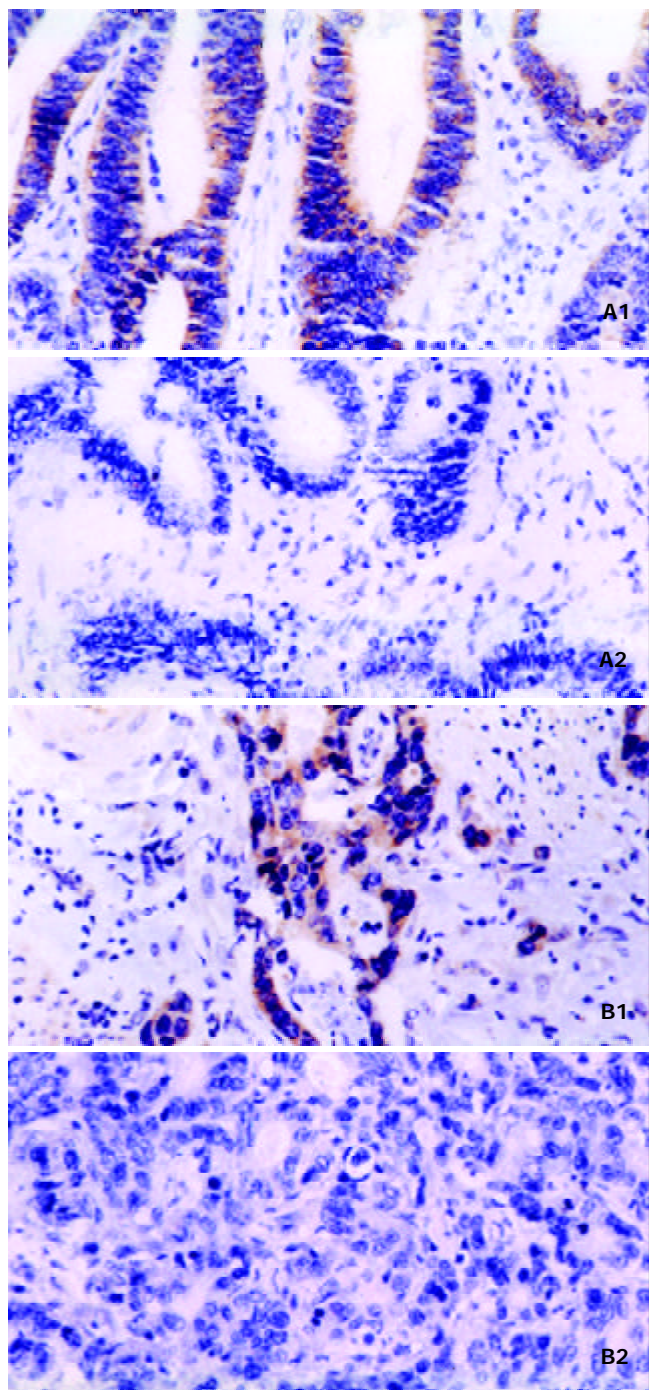


Figure 2 Immunohistochemical analysis of Flt-1 and KDR on gastric carcinoma specimens (x400). A. Expression of Flt-1. B. Expression of KDR. below sections are respectively negative controls of the left-hand side sections of the same specimens.

Specimens from 30 cases of gastric carcinoma were detected for expression of KDR and the results were similar to those of Flt-1 except that the positive rate was slightly lower (70 %) (Figure 2B). Among 24 cases detected for both receptors, Flt-1 was always positive when KDR was positive (Table 2).

Table 2 Expression of Flt-1 and KDR on gastric carcinoma specimens

Expression of Flt-1 and KDR	n	Percentage of 24 cases
Flt-1(+) KDR(+)	15	62.5
Flt-1(-) KDR(-)	5	20.8
Flt-1(+) KDR(-)	4	16.7
Flt-1(-) KDR(+)	0	0

VEGF stimulated growth of KDR-positive gastric carcinoma cell lines

To determine whether the exogenous recombinant human VEGF₁₆₅ was able to stimulate proliferation of gastric carcinoma cells through KDR receptor, AGS-1, NCI-N87 and KATOIII cells were incubated with varying concentrations of VEGF₁₆₅ and its effects were measured using MTT assay (Figure 3). The results showed dose-dependent effect of VEGF₁₆₅ on the growth of KDR-positive cells NCI-N87 and AGS-1 and the maximum dose of 10 ng/ml VEGF stimulated the growth of KDR-positive cells NCI-N87 and AGS-1 to 131.5 % (± 5.4 %) and 130.8 % (± 11.3 %), of controls respectively ($P < 0.01$). However, VEGF₁₆₅ had no effect on KDR-negative KATOIII cells ($P > 0.05$).

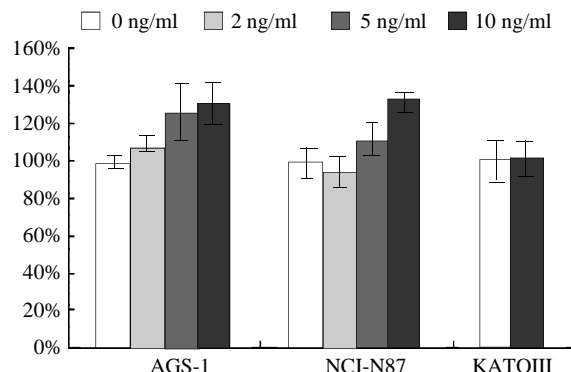


Figure 3 Effects of recombinant human VEGF₁₆₅ on proliferation of AGS-1, NCI-N87 and KATOIII cells. The cells were treated with concentrations of VEGF₁₆₅ indicated, and their viability was assessed using MTT and expressed as mean percentage of the untreated controls \pm SE ($n=4$).

DISCUSSION

It is well known that tumor cells can secrete VEGF, and its receptors KDR and Flt-1 are primarily expressed in endothelial cells. Therefore, it seems that the receptors of VEGF are endothelial cell-specific. However, recent emerging evidences have shown that VEGFRs are expressed in cell types other than endothelial cells, especially in tumor cells, indicating there is an autocrine pathway of VEGF on tumor cells. The presence of VEGF autocrine growth factor activity has been demonstrated in 5 different human tumor types, including melanoma, ovarian and pancreatic carcinoma, Kaposi sarcoma, and leukemia^[11-19]. Gastric cancer is common in China and abroad^[22-36]. Our previous study by Tian *et al*^[20] demonstrated that VEGF acted as an

autocrine growth factor for human gastric adenocarcinoma cell MGC803. To investigate whether this is a common mechanism in gastric carcinoma, we determined the expression of VEGF and VEGFRs in eight gastric carcinoma cell lines at mRNA level. It was found that all the cell lines examined expressed VEGF₁₂₁ and VEGF₁₆₅. Meanwhile, both Flt-1 and KDR were expressed in these tumor cells, except that NCI-SNU-5 cells expressed Flt-1 only, and KATOIII expressed neither of the receptors. It seems that the co-expression of VEGF and VEGFR is common in gastric carcinoma cell lines. To investigate this phenomenon further, we detected the expression of VEGFRs in gastric carcinoma specimens. The immunohistochemical analysis showed similar results to that from cell lines, e.g. VEGFRs were expressed in endothelial cells of tumor tissue as well as in tumor cells. The positive rate of Flt-1 expression was slightly higher than that of KDR expression and the KDR-positive specimens were always Flt-1 positive. These results suggest that VEGF acted not only as a paracrine factor on endothelial cells, but also as an autocrine factor on tumor cells.

It has been reported that the expression of KDR in non-endothelial cells is associated with increase in DNA synthesis in response to VEGF stimulation. We therefore investigated whether the exogenous VEGF could stimulate the growth of KDR-positive tumor cells. VEGF₁₆₅ of 10 ng/ml increased the growth of AGS-1 and NCI-N87 cells, which were KDR positive, to 130.8 % and 131.5 % of the control unstimulated cells respectively, but showed no effect on KDR-negative KATOIII cells, indicating that the KDR receptor on gastric carcinoma is functional. Although the concentrations of VEGF in different cell cultures reported were lower (from 0.1 ng/ml to 2.8 ng/ml^[11,12,14,17]) than what we used in this experiments, it is believed that the VEGF is actively secreted by tumor cells and its local concentration might be much higher, so that an autocrine pathway through KDR receptor for the growth factor is possible in gastric carcinoma. The expression of VEGF is regulated by several factors, including hypoxia, cytokines such as interleukin (IL)-1, activation of certain oncogenes (Ras, Raf, Src), and loss-of-function mutations of p53 and the von Hippel-Lindau genes. Mutation of ras and p53 is usually seen in early stage of gastric carcinogenesis^[37], which can result in significant up-regulation of VEGF. Therefore, autocrine pathway of VEGF may play an important role in the progression of early stage gastric carcinoma and the antagonist of VEGF/VEGFR may inhibit tumor progression by directly inhibiting angiogenesis. In fact, this has been confirmed in animal model of human leukemia^[13]. Dias *et al* used neutralizing antibodies specific for murine endothelial cell or human endothelial cell VEGFR-2 to inhibit the paracrine or autocrine VEGF/VEGFR pathway. They showed that blocking either the paracrine pathway or the autocrine VEGF/VEGFR-2 pathway delayed leukemic growth and engraftment *in vivo* but failed to cure inoculated mice, and long-term remission with no evidence of disease was achieved only if mice were treated with antibodies against both murine and human VEGFR-2.

In conclusion, we first demonstrated that VEGF and VEGFR were co-expressed in gastric cancer, and the exogenous VEGF could stimulate the growth of KDR-positive tumor cells. These results suggest that there might exist an autocrine mechanism of VEGF in gastric carcinoma, and VEGF could promote tumor growth and metastasis by both direct and indirect pathways.

REFERENCES

- Song ZJ**, Gong P, Wu YE. Relationship between the expression of iNOS, VEGF, tumor angiogenesis and gastric cancer. *World J Gastroenterol* 2002; **8**: 591-595
- Mao H**, Yuan AL, Zhao MF, Lai ZS, Zhang YL, Zhou DY. Effect of p38MAPK signal pathway on ultrastructural change of liver cancer cells induced by VEGF. *Shijie Huaren Xiaohua Zazhi* 2000; **8**: 536-538
- Qin LX**, Tang ZY. The prognostic molecular markers in hepatocellular carcinoma. *World J Gastroenterol* 2002; **8**: 385-392
- Tian XJ**, Wu J, Meng L, Dong ZW, Shou CC. Expression of VEGF₁₂₁ in gastric carcinoma MGC803 cell line. *World J Gastroenterol* 2000; **6**: 281-283
- Yan JC**, Chen WB, Ma Y, Shun XH. Expression of vascular endothelial growth factor in liver tissues of hepatitis B. *Shijie Huaren Xiaohua Zazhi* 1999; **7**: 837-840
- Zhao MF**, Mao H, Zheng JX, Yuan YW. Effect of vascular endothelial growth factor on adhesion of large intestine cancer cell HT-29. *Shijie Huaren Xiaohua Zazhi* 2000; **8**: 646-649
- Tang YC**, Li Y, Qian GX. Reduction of tumorigenicity of SMMC-7721 hepatoma cells by vascular endothelial growth factor antisense gene therapy. *World J Gastroenterol* 2001; **7**: 22-27
- Gu ZP**, Wang YJ, Li JG, Zhou YA. VEGF₁₆₅ antisense RNA suppresses oncogenic properties of human esophageal squamous cell carcinoma. *World J Gastroenterol* 2002; **8**: 44-48
- Soker S**, Takashima S, Miao HQ, Neufeld G, Klagsbrun M. Neuropilin-1 is expressed by endothelial and tumor cells as an isoform-specific receptor for vascular endothelial growth factor. *Cell* 1998; **92**: 735-745
- Griffioen AW**, Molema G. Angiogenesis: potentials for pharmacologic intervention in the treatment of cancer, cardiovascular diseases, and chronic inflammation. *Pharmacol Rev* 2000; **52**: 237-268
- Bellamy WT**, Richter L, Frutiger Y, Grogan TM. Expression of vascular endothelial growth factor and its receptors in hematopoietic malignancies. *Cancer Res* 1999; **59**: 728-733
- Dias S**, Hattori K, Zhu ZP, Heissig B, Choy M, Lane W, Wu Y, Chadburn A, Hyjek E, Gill M, Hicklin DJ, Witte L, Moore M. A.S., Rafii S. Autocrine stimulation of VEGFR-2 activates human leukemic cell growth and migration. *J Clin Invest* 2000; **106**: 511-521
- Dias S**, Hattori K, Heissig B, Zhu ZP, Wu Y, Witte L, Hicklin DJ, Tateno M, Bohlen P, Moore M.A.S., Rafii S. Inhibition of both paracrine and autocrine VEGF/VEGFR-2 signaling pathways is essential to induce long-term remission of xenotransplanted human leukemias. *Proc Natl Acad Sci USA* 2001; **98**: 10857-10862
- Hayashibara T**, Yamada Y, Miyaniishi T, Mori H, Joh T, Maeda T, Mori N, Maita T, Kamihira S, Tomonaga M. Vascular endothelial growth factor and cellular chemotaxis: a possible autocrine pathway in adult T-cell leukemia cell invasion. *Clin Cancer Res* 2001; **7**: 2719-2726
- Marschall ZV**, Cramer T, Hocker M, Burde R, Plath T, Schirner M, Heidenreich R, Breier G, Riecken EO, Wiedenmann B, Rosewicz S. De novo expression of vascular endothelial growth factor in human pancreatic cancer: evidence for an autocrine mitogenic loop. *Gastroenterology* 2000; **119**: 1358-1372
- De Jong JS**, Van Diest PJ, Van der Valk P, Baak JPA. Expression of growth factors, growth inhibiting factors, and their receptors in invasion breast cancer. I: an inventory in search of autocrine and paracrine loops. *J Pathol* 1998; **184**: 44-52
- Meister B**, Grunebach F, Bautz F, Brugger W, Fink F-M, Kanz L, Mohle R. Expression of vascular endothelial growth factor (VEGF) and its receptor in human neuroblastoma. *Eur J Cancer* 1999; **35**: 445-449
- Masood R**, Cai J, Zheng T, Smith DL, Hinton DR, Gill PS. Vascular endothelial growth factor (VEGF) is an autocrine growth factor for VEGF receptor-positive human tumors. *Blood* 2001; **98**: 1904-1913
- Takahama M**, Tsutsumi M, Tsujiuchi T, Kido A, Sakitani H, Iki K, Taniguchi S, Kitamura S, Konishi Y. Expression of vascular endothelial growth factor and its receptors during lung carcinogenesis by *N*-nitrosobis(2-hydroxypropyl)amine in rats. *Mol Carcinog* 1999; **24**: 287-293
- Tian X**, Song S, Wu J, Meng L, Dong Z, Shou C. Vascular endothelial growth factor: acting as an autocrine growth factor for human gastric adenocarcinoma cell MGC803. *Biochem Biophys Res Commun* 2001; **286**: 505-512

- 21 **Wang H**, Keiser JA. Vascular endothelial growth factor upregulates the expression of matrix metalloproteinases in vascular smooth muscle cells: role of flt-1. *Circ Res* 1998; **83**: 832-840
- 22 **Cai L**, Yu SZ. A molecular epidemiologic study on gastric cancer in Changle, Fujian Province. *Shijie Huaren Xiaohua Zazhi* 1999; **7**: 652-655
- 23 **Wong BC**, Lam SK, Ching CK, Hu WH, Kwok E, Ho J, Yuen ST, Gao Z, Chen JS, Lai KC, Ong LY, Chen BW, Wang WH, Jiang XW, Hou XH, Lu JY. Differential *Helicobacter pylori* infection rates in two contrasting gastric cancer risk regions of South China. China Gastric Cancer Study Group. *J Gastroenterol Hepatol* 1999; **14**: 120-125
- 24 **Gao GL**, Yang Y, Yang SF, Ren CW. Relationship between proliferation of vascular endothelial cells and gastric cancer. *Shijie Huaren Xiaohua Zazhi* 2000; **8**: 282-284
- 25 **Zou SC**, Qiu HS, Zhang CW, Tao HQ. A clinical and long term follow up study of peri operative sequential triple therapy for gastric cancer. *World J Gastroenterol* 2000; **6**: 284-286
- 26 **Zhang XQ**, Lin SR. The study advance of *Helicobacter pylori* and gastric cancer. *Shijie Huaren Xiaohua Zazhi* 2000; **8**: 206-207
- 27 **Xue XC**, Fang GE, Hua JD. Gastric cancer and apoptosis. *Shijie Huaren Xiaohua Zazhi* 1999; **7**: 359-361
- 28 **Cai L**, Yu SZ, Zhang ZF. *Helicobacter pylori* infection and risk of gastric cancer in Changle Country, Fujian Province, China. *World J Gastroenterol* 2000; **6**: 374-376
- 29 **Harrig XH**. Association between *Helicobacter pylori* and gastric cancer: current knowledge and future research. *World J Gastroenterol* 1998; **4**: 93-96
- 30 **Folli S**, Morgagni P, Roviello F, De Manzoni G, Marrelli D, Saragoni L, Di Leo A, Gaudio M, Nanni O, Carli A, Cordiano C, Dell'Amore D, Vio A. Risk factors for lymph node metastases and their prognostic significance in early gastric cancer (EGC) for the Italian Research Group for Gastric Cancer (IRGGC). *Jpn J Clin Oncol* 2001; **31**: 495-499
- 31 **Yokota T**, Kunii Y, Teshima S, Yamada Y, Saito T, Takahashi M, Kikuchi S, Yamauchi H. Significant prognostic factors in patients with early gastric cancer. *Int Surg* 2000; **85**: 286-290
- 32 **Kocher HM**, Linklater K, Patel S, Ellul JP. Epidemiological study of oesophageal and gastric cancer in south-east England. *Br J Surg* 2001; **88**: 1249-1257
- 33 **Barchielli A**, Amorosi A, Balzi D, Crocetti E, Nesi G. Long-term prognosis of gastric cancer in a European Country: a population-based study in Florence (Italy). 10-year survival of cases diagnosed in 1985-1987. *Eur J Cancer* 2001; **37**: 1674-1680
- 34 **Xu CT**, Huang LT, Pan BR. Current gene therapy for stomach carcinoma. *World J Gastroenterol* 2001; **7**: 752-759
- 35 **Niu WX**, Qin XY, Liu H, Wang CP. Clinicopathological analysis of patients with gastric cancer in 1200 cases. *World J Gastroenterol* 2001; **7**: 281-284
- 36 **Li XY**, Wei PK. Diagnosis of stomach cancer by serum tumor markers. *Shijie Huaren Xiaohua Zazhi* 2001; **9**: 568-570
- 37 **Er Z**. Aibian Jili Yanjiou. *Beijing: Beijing press*, 1999: 447-449

Edited by Liu HX

• GASTRIC CANCER •

Effect of apoptosis on gastric adenocarcinoma cell line SGC-7901 induced by *cis*-9, *trans*-11-conjugated linoleic acid

Jia-Ren Liu, Bing-Qing Chen, Yan-Mei Yang, Xuan-Ling Wang, Ying-Ben Xue, Yu-Mei Zheng, Rui-Hai Liu

Jia-Ren Liu, Bing-Qing Chen, Yan-Mei Yang, Xuan-ling Wang, Ying-ben Xue, Yu-Mei Zheng, Public Health College, Harbin Medical University, Harbin 150001, Heilongjiang Province, China
Rui-Hai Liu, Food Science and Toxicology, Department of Food Science, Cornell University, Ithaca, NY 14853-7201, USA

Supported by the National Natural Science Foundation of China, No. 39870661

Correspondence to: Dr. Jia-Ren Liu. Public Health College, Harbin Medical University, 199 Dongdazhi Street, Nangang District, Harbin 150001, Heilongjiang Province, China. jiaarenliu@yahoo.com

Telephone: +86-451-3641309 **Fax:** +86-451-3648617

Received 2002-05-18 **Accepted** 2002-08-03

Abstract

AIM: To determine the effect of apoptosis on gastric cancer cells (SGC-7901) induced by *cis*-9, *trans*-11-conjugated linoleic acid (c9, t11-CLA) and its possible mechanism in the inhibition of cancer cells growth.

METHODS: Using cell culture, flow cytometry and immunocytochemical techniques, we examined the cell growth, frequency of apoptosis and distribution of cell cycle, expression of ki67, bcl-2, Fas, and *c-myc* of SGC-7901 cells which were treated with various c9, t11-CLA concentrations (25, 50, 100 and 200 $\mu\text{mol} \cdot \text{L}^{-1}$) of c9, t11-CLA for 24 h and 48 h, with a negative control (0.1 % ethanol).

RESULTS: The growth of SGC-7901 cells was inhibited by c9, t11-CLA. Eight days after treatment with various concentrations of c9, t11-CLA, as mentioned above, the inhibition rates were 5.9 %, 20.2 %, 75.6 % and 82.4 %, respectively. The frequency of apoptosis on SGC-7901 cells induced by different concentrations of c9, t11-CLA (except for 25 $\mu\text{mol} \cdot \text{L}^{-1}$, 24 h) was significantly greater than that in the negative control ($P < 0.01$). To further investigate the influence of the cell cycle progression, we found that apoptosis induced by c9, t11-CLA may be involved in blocking the cell cycle of SGC-7901 cells. Immunocytochemical staining demonstrated that SGC-7901 cells preincubated in media supplemented with different c9, t11-CLA concentrations for various time periods significantly decreased the expressions of ki67 (the expression rates were 18.70-3.20 %, at 24 h and 8.10-0.20 % at 48 h, respectively), bcl-2 (4.30-0.15 % at 24 h and 8.05 %-0 at 48 h), and *c-myc* (4.85-2.20 % at 24 h and 4.75-0.30 % at 48 h) as compared with those in the controls (the expressions of ki67, bcl-2, and *c-myc* were 15.1 % at 24 h and 13.5 % at 48 h, 6.80 % at 24 h and 8.00 % at 48 h, 5.50 % at 24 h and 5.30 % at 48 h, respectively) ($P < 0.01$), whereas the expressions of Fas were increased (0.60-2.75 %, 24 h and 0.45-5.95 %, 48 h).

CONCLUSION: The growth and proliferation of SGC-7901 cells are inhibited by c9, t11-CLA via blocking the cell cycle, pathways of bcl-2-associated mitochondria with reduced

expression of bcl-2 and Fas-associated death domain protein (FADD) with enhanced expression of Fas. But expression of *c-myc* on SGC-7901 cells is lower than that in negative control, which needs to be studied further.

Liu JR, Chen BQ, Yang YM, Wang XL, Xue YB, Zheng YM, Liu RH. Effect of apoptosis on gastric adenocarcinoma cell line SGC-7901 induced by *cis*-9, *trans*-11-conjugated linoleic acid. *World J Gastroenterol* 2002; 8(6):999-1004

INTRODUCTION

Conjugated linoleic acid (CLA), a derivative of a fatty acid linoleic acid (LA), is a minor fatty acid found especially in red meat and in dairy products. The biosynthesis of CLA in ruminants is the result of a rumen bacterium, which is known to convert linoleic acid to stearic acid via CLA. In recent years, CLA has received considerable attention as a chemopreventive agent. This is because CLA was shown to inhibit in vitro the proliferation of human gastric cancer cells (SGC-7901)^[1,2], mammary cancer cells (MCF-7)^[3-7], of human malignant melanoma cells, colorectal cancer cells^[8], and rat hepatoma cells^[9] and in animal studies to prevent the development of mouse epidermal carcinogenesis, mouse forestomach cancer^[10,11] and of rat mammary tumorigenesis^[12-15].

Although the exact mechanisms are not clear, the inhibitory effect of CLA on the proliferation of rapidly dividing cells has been attributed to the induction of cell cycle arrest^[1] and the induction of apoptosis^[2,16]. In many instances, growth inhibition following terminal differentiation or anticancer drug treatment results in apoptosis. Apoptosis, namely, programmed cell death, is an active and physiological process characterized by a series of morphological and biological alterations in which the cells become smaller, shrinking, the nuclei round up, the chromatin becomes agglutinated and marginated, the nuclear membrane breaks down, and followed by the degenerative changes of the cells. The exact mechanisms of apoptosis are still unclear, but our earlier studies indicated that CLA can induce apoptosis in human gastric cancer SGC-7901 cells^[2].

Gastric cancer is both common in China and the other parts of the world^[17-30], and chemoprevention is always used as the main treatment for advanced cancer so far, which has become a focus topic in this area^[31-54]. In this study, we investigate the pathways of apoptosis induced by *cis*-9, *trans*-11-CLA (c9, t11-CLA) which are thought to be high in proportion and activation as potential antioxidant and anticarcinogenic agents in CLA's isomers and probe into the possible mechanism of apoptosis on human gastric adenocarcinoma cells SGC-7901.

MATERIALS AND METHODS

Materials

c9, t11-CLA, a monoisomer of c-9, t11-octadecadienoic acid with 98 % purity, was obtained from Dr. Ruihai Liu (Food Science and Toxicology, Department of Food Science, Cornell

University, Ithaca, NY, USA). The c9, t11-CLA was dissolved in 96 mL \cdot L⁻¹ ethanol, and diluted to the following concentrations: 25, 50, 100 and 200 μ mol \cdot L⁻¹.

Methods

Cell culture Human gastric adenocarcinoma cells (SGC-7901), purchased from Cancer Research Institute of Beijing (China), were cultured in RPMI 1640 (Gibco) medium, supplemented with calf serum 100 mL \cdot L⁻¹, penicillin (100 \times 10³ U \cdot L⁻¹) and streptomycin (100 mg \cdot L⁻¹). The pH was maintained at 7.2-7.4, by equilibration with 5 % CO₂. The temperature was kept at 37 °C. The cells were sub-cultured with a mixture of Ethylenedinitrile tetraacetic acid (EDTA) and trypsin.

Cell growth curve The SGC-7901 cells were seeded in six 24-well plates (Nuc, Co.), each well containing 2 \times 10⁴ cells. After 24 h, the medium of different plates was replaced with media supplemented with c9, t11-CLA at different concentrations. On the next day, the numbers of cells of 3 wells from each plate was determined by using the trypan blue staining. The means were obtained on each of eight days and were used to draw a cellular growth curve. The inhibitory rates (IR) on the 8th day was calculated as follows:

$$IR(\%) = \frac{\frac{\text{Total number of cells in negative control (8d)} - \text{Number of cells in test groups (8d)}}{\text{Total number of cells in negative control (8d)}} \times 100\%$$

Apoptosis detection and cell cycle analysis

SGC-7901 cells (5 \times 10⁵ cells in 25 ml bottles) were seeded in appropriate medium for 24 h prior to the beginning of the experiment. The medium was then replaced with different concentrations of c9, t11-CLA. After 24 h and 48 h, the cells were harvested using a mixture of trypsin/EDTA, washed twice with cold PBS, fixed in 70 % ethanol on ice for 30 minutes, and washed once again. Cells were then stained by adding 1 ml of PI mixture (containing 50 μ g propidium iodide, 0.2 mg RNase, 5 μ L Triton X-100, and 1 mg citromalic acid) in the dark (4 °C, 30 minutes). Cell apoptosis and cell cycle analysis were subsequently performed by flow cytometry using a FACSCalibur Analyzer (BD Biosciences) with a 15-milliwatt air-cooled argon laser (excitation=488 nm). Sub G₁ peak was observed and DNA content in phases of cell cycle was analyzed using software of Modifix LT.

Cell samples

SGC-7901 cells were treated for 24 h and 48 h with various concentrations of c9, t11-CLA and collected by centrifugation. Specimens were fixed immediately in 40 g \cdot L⁻¹ formaldehydum polymerisatum and embedded in paraffin. Gastric cancer tissue from a patient served as a reference.

Primary antibody

To examine the expression of Ki67 cell proliferation and the expression of bcl-2, c-myc and Fas in SGC-7901 cells, we used four primary antibodies: corresponding rabbit polyclonal antibodies for bcl-2 and Fas and corresponding mouse monoclonal antibodies for ki67 and c-myc. Antibodies of bcl-2 and Fas were purchased from the Calbiochem Co. USA; and others from Zhongshan Co. China.

Immunocytochemistry

Immunocytochemical staining was performed on serial sections at room temperature using the horseradish peroxidase method. The sections were deparaffinized in xylene and rehydrated through graded alcohol. The sections were incubated for 10 min at 95 °C in 10 mmol \cdot L⁻¹ sodium citrate (pH 6.0) buffer for ki67

staining. Endogenous peroxidases were inactivated by immersing the sections in hydrogen peroxide for 10 min, and then were incubated for 10 min with 100 mL \cdot L⁻¹ normal goat serum in PBS to block the non-specific binding. The sections were subsequently incubated overnight at 4 °C with relevant antibodies (1:50 dilution) respectively. The next day, the sections were incubated with biotinylated anti-mouse or anti-rabbit IgG (Zhongshan Co., China) for 30 min, followed by peroxidase-conjugated streptavidin (Zhongshan Co., China) for 30 min. The chromogenic reaction was developed with DAB (diaminobenzidine) for 10 min, and all sections were counterstained with hematoxylin. Controls consisted of omission of the primary antibody. The positive rate (PR) was calculated as follows:

$$PR(\%) = \frac{\text{Number of positive cells}}{\text{Total number (2} \times 10^4)} \times 100$$

Statistical analysis

Analysis of data was performed using the Student's *t* test or χ^2 test. A value of *P* < 0.05 is considered to be statistically significant.

RESULTS

Effect of c9, t11-CLA on SGC-7901 cell growth

As shown in Figure 1, growth of the cells in various concentrations (except for 25 μ mol \cdot L⁻¹ and 50 μ mol \cdot L⁻¹) of c9, t11-CLA did differ from the negative control within 8d. SGC-7901 cells incubated in 25 μ mol \cdot L⁻¹ of c9, t11-CLA grew at a higher rate than that of the negative control, while in 100 and 200 μ mol \cdot L⁻¹ concentrations of c9, t11-CLA, proliferation of SGC-7901 cell was significantly inhibited. The inhibitory rate of various c9, t11-CLA concentrations were 5.9 %, 20.2 %, 75.6 % and 82.4 %, respectively.

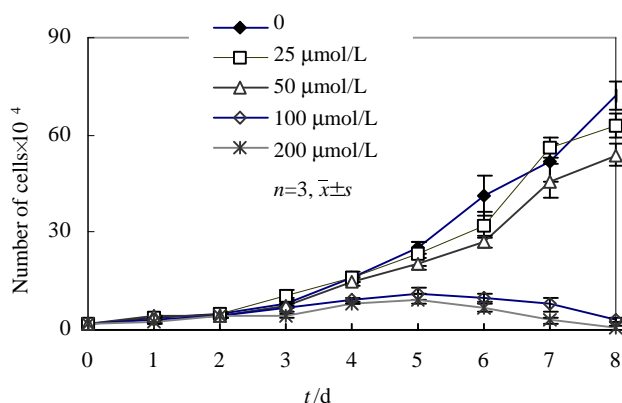


Figure 1 Growth curve of SGC-7901 cells cultured in various concentrations of c9, t11-CLA

Analysis of flow cytometry

To investigate the influence of c9, t11-CLA on apoptosis and cell cycle progression of SGC-7901 cells, we determined apoptosis and cell cycle distribution by flow cytometry. The results are shown in Table 1. We observed that apoptotic peaks and intention of the cells accumulating in the G₀/G₁ phases and of cells decreased in the S phase of the cell cycle in SGC-7901 cells with different c9, t11-CLA concentrations at various time periods, whereas G₂/M did not. The results suggested that c9, t11-CLA may induce apoptosis and arrest the progression of cell cycle of SGC-7901 cells.

Cell proliferation

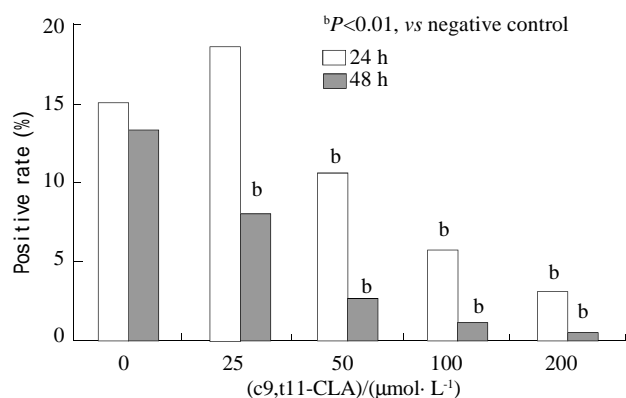
Ki67 is a marker for the proliferation of cells. To determine the

Table 1 Cell cycle analysis of SGC-7901 cells induced by c9, t11-CLA at 24 h and 48 h ($\bar{x} \pm s$, $n=4$)

c9,t11-CLA(μmol)	Apoptosis		G_0/G_1		G_2/M		S	
	24 h	48 h	24 h	48 h	24 h	48 h	24 h	48 h
0	0.55 \pm 0.09	0.69 \pm 0.21	53.13 \pm 3.44	58.57 \pm 0.90	11.13 \pm 2.75	12.64 \pm 1.18	35.74 \pm 2.04	28.80 \pm 0.89
25	1.27 \pm 0.73	3.89 \pm 2.12	53.00 \pm 8.35	56.81 \pm 1.09	15.55 \pm 1.11	15.95 \pm 0.36	31.40 \pm 9.23	26.52 \pm 1.46
50	4.12 \pm 0.55 ^a	8.18 \pm 1.55 ^b	56.58 \pm 0.87	56.32 \pm 0.78	14.55 \pm 3.45	15.17 \pm 0.61	28.87 \pm 3.32	28.51 \pm 1.32
100	7.95 \pm 0.31 ^b	12.33 \pm 1.53 ^b	58.35 \pm 2.44	61.18 \pm 4.94	13.12 \pm 1.50	14.49 \pm 3.10	28.52 \pm 0.96	25.08 \pm 2.85
200	12.79 \pm 3.12 ^b	14.75 \pm 5.97 ^b	60.67 \pm 4.28 ^a	63.82 \pm 7.84 ^a	12.95 \pm 4.48	13.35 \pm 3.91	26.38 \pm 0.92 ^b	22.82 \pm 4.63 ^b

^a $P<0.05$, ^b $P<0.01$ vs negative control

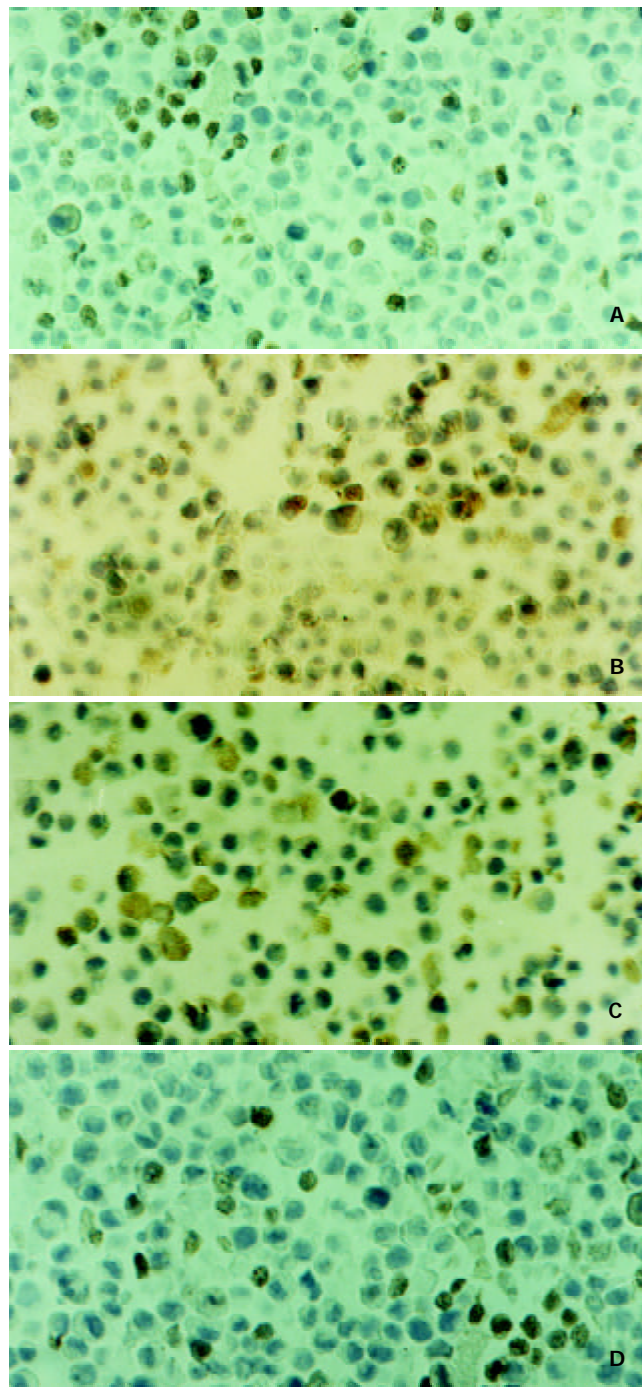
effect of c9, t11-CLA on the proliferation of SGC-7901 cells, we investigated the expression of ki67 using immunocytochemistry. The results are shown in Figure 2. Expression rates of ki67(Figure 3A) on SGC-7901 cells gradually decreased after SGC-7901 cells were incubated with different concentrations of c9,t11-CLA at various time periods. Moreover, SGC-7901 cells expressed significantly less ki67 than did the negative control ($P<0.01$). The expression rate of ki67 on SGC-7901 cells displayed a dose-response relationship as the concentrations of CLA increased.

**Figure 2** Expression of ki67 on SGC-7901 cells treated with c9, t11-CLA**Expressions of bcl-2, Fas and c-myc**

We detected the expression of bcl-2, Fas, and c-myc on SGC-7901 cells treated by various concentrations of c9, t11-CLA with immunocytochemical technique. The expression rates of bcl-2 and c-myc (Figure 3B, 3D) on SGC-7901 cells was decreased (Table 2) after SGC-7901 cells were incubated with different concentrations of c9, t11-CLA for 24 h and 48 h while expression of Fas increased (Table 2; Figure 3C). In the meantime, there was no expression of Fas at doses of c9,t11-CLA (25 and 50 $\mu\text{mol} \cdot \text{L}^{-1}$ at 24 h).

Table 2 Positive rates of bcl-2, Fas and c-myc on SGC-7901 cells treated with c9, t11-CLA (%)

C9,t11-CLA ($\mu\text{mol/L}$)	24 h			48 h		
	bcl-2	Fas	c-myc	bcl-2	Fas	c-myc
0	6.80	0.60	5.50	8.00	0.45	5.30
25	4.30	0	4.85	8.05	0.85	4.75
50	2.50 ^b	0	4.20 ^a	3.80 ^b	2.75 ^b	3.70 ^a
100	1.45 ^b	1.95 ^b	3.80 ^a	0.30 ^b	4.10 ^b	1.35 ^b
200	0.15 ^b	2.75 ^b	2.20 ^b	0	5.95 ^b	0.30 ^b

^a $P<0.05$, ^b $P<0.01$ vs negative control.**Figure 3** A: The expression of Ki67 on SGC-7901 cells of the negative control. Immunocytochemistry staining SP method, original magnification, $\times 400$; B: The expression of bcl-2 on

SGC-7901 cells of the negative control. Immunocytochemistry staining SP method, original magnification, $\times 400$; C: The expression of Fas on SGC-7901 cells of c9, t11-CLA group ($200 \mu\text{mol} \cdot \text{L}^{-1}$ 48 h). Immunocytochemistry staining SP method, original magnification, $\times 400$; D: The expression of *c-myc* on SGC-7901 cells of the negative control. Immunocytochemistry staining SP method, original magnification, $\times 400$

DISCUSSION

CLA is a natural fatty acid in animal's food. CLA has a mixture of positional (9/11 or 10/12 double bonds) and geometric (various *cis/trans* combinations) isomers of linoleic acid (LA) formed by rumen and colonic bacteria. There are eight potential isomers of CLA, but the *cis* 9, *trans* 11 and *trans* 9, *cis* 11 isomers are thought to be active as potential antioxidant and anticarcinogenic agents. Therefore, it is of interest to investigate extensively the mechanism of anticancer activities of CLA.

Over the past ten years, a number of animal experiments have supported the observation that CLA is an effective chemopreventive agent for cancer, and that it can inhibit carcinogenesis of different tissues at various stages of induction by chemical agents^[14,15]. Several investigators in our group have reported that c9, t11-CLA is an effective agent to prevent carcinogenesis^[10,11] and cancer^[1-3,7]. Zhu's study^[10] demonstrated that c9, t11-CLA could significantly inhibit the mice forestomach neoplasia induced by B(a)P ($50 \text{ mg} \cdot \text{kg}^{-1}$) in post-initiation in short term (23 weeks). The incidences of tumors in mice of B(a)P group, B(a)P with high dose CLA ($5 \mu\text{L} \cdot \text{g}^{-1}$) group and B(a)P with low dose CLA ($2.5 \mu\text{L} \cdot \text{g}^{-1}$) group were 100 %, 60 % and 69 %, respectively ($P < 0.05$). Xue's study^[10] also indicated that the incidence of neoplasm in mouse forestomach in the B(a)P group, 75 % pure c9, t11-CLA group, 98 % pure c9, t11-CLA group and 98 % pure t10, c12-CLA group were 100.0 %, 75.0 %, 69.2 % and 53.8 %, respectively. This may be due to an inhibiting mitogen of activated protein kinase (MAPK)- an approach to reduce carcinogenesis.

The data in this series suggested that c9, t11-CLA could inhibit the proliferation of cancer cells, i.e. SGC-7901 cells^[1,2] and MCF-7 cells^[3,7], and induced cancer cell (SGC-7901) apoptosis^[2]. Liu's study^[1] indicated that cell growth and proliferation and DNA synthesis of SGC-7901 cells were inhibited and SGC-7901 cells preincubated in media supplemented with different c9, t11-CLA concentrations at various time periods significantly decreased the expressions of PCNA (the expression rates were 7.2-3.0 %, at 24 h and 9.1-0.9 % at 48 h, respectively), Cyclin A (11.0-2.3 %, at 24 h and 8.5-0.5 %, at 48 h), B₁ (4.8-1.8 % at 24 h and 5.5-0.6 % at 48 h) and D₁ (3.6-1.4 % at 24 h and 3.7 %-0 at 48 h) as compared with those in the negative controls (the expressions of PCNA, cyclin A, B₁ and D₁ were 6.5 % at 24 h and 9.0 % at 48 h, 4.2 % at 24 h and 5.1 % at 48 h, 9.5 % at 24 h and 6.0 % at 48 h, respectively) ($P < 0.01$), whereas the expressions of p16^{ink4a} and p21^{cip1/waf1}, cyclin-dependent kinases inhibitors (CDKI) were increased. Our results showed that the proliferation marker Ki67 was inhibited and the cells were accumulating in the G₀/G₁ phase and cells decreasing in the S phases of the cell cycle on SGC-7901 cells with different c9, t11-CLA concentrations at various time periods, whereas G₂/M did not have. All these results suggested that c9, t11-CLA may arrest the progression of cell cycle of SGC-7901 cells. Our previous works^[2] indicated that at the early stage morphological changes of cell apoptosis were observed using fluorescent dye (Hoechst 33342) under electronic microscope and SGC-7901 cells preincubated in media supplemented with different c9, t11-CLA concentrations

at various times significantly decreased the expressions of mutant p53 as compared with those in the negative control. The inhibitory rates of mutant p53 on SGC-7901 cells induced by various c9, t11-CLA concentrations ($25-200 \mu\text{mol} \cdot \text{L}^{-1}$) were -19.2 %, 13.7 %, 53.4 %, and 89.0 % at 24 h and 1.8 %, 29.1 %, 87.3 %, and 86.8 % at 48 h, respectively. p53 is one of the major factors controlling cell proliferation, suppressing both growth and transformation of cells. A common idea^[55] is that p53 acts as "guardian of the genome" by preventing damaging of DNA in cell proliferation or DNA damage leads to an increase in the level of p53, resulting in p21^{CIP1/WAF1}-mediated cell cycle arrest in the G₁ phase, which persists until DNA repair is completed or by arresting the cell division cycle induces damaged-cell apoptosis. In the absence of functional wild-type p53, the "guardian" function is lost; cells accumulate genetic damage and show marked genetic instability, often to the extent of gross aneuploidy. However, wild-type p53 protein has a very short half-time, many point mutants have a greatly enhanced stability, allowing for the immunohistochemical detection of mutant p53 in clinical material. Mutant p53 protein loses its biochemical functions which may facilitate DNA repair as well as apoptosis, and displayed over-proliferation of cancer cells. In addition, Natalie *et al*^[56] found that a fraction of p53 protein localizes to mitochondria at the onset of p53-dependent apoptosis. The accumulation of p53 to mitochondria is rapid (within 1 h after p53 activation) and precedes changes in mitochondrial membrane potential, cytochrome c release, and procaspase-3 activation. Overexpression of anti-apoptotic bcl-2 inhibits signal-mediated mitochondrial p53 accumulation and apoptosis but not cell cycle arrest. Our results showed that c9, t11-CLA may reduce the expression of mutant p53 protein and may recover the bio-function of wild p53 protein that blocks the cell cycle of SGC-7901 cells by p21^{CIP1/WAF1} and processes to another apoptotic pathway of mitochondria by bcl-2.

At the same time, we investigated further the expressions of bcl-2 and Fas from pathways of cell apoptosis such as mitochondria and Fas-associated death domain (FADD) as well as expression of *c-myc* on SGC-7901 cells treated with various concentrations of c9, t11-CLA. Bcl-2 is an inhibitor of apoptosis and shown to exert anti-apoptotic activity by one of the following mechanisms^[57]: 1) sequestration of the proforms of two major initiator caspases, pro-caspase-9 (through binding to Apaf-1) and pro-caspase-8 (through unidentified molecules); 2) inhibition of apoptogenic mitochondrial changes, including cytochrome c release and the mitochondrial membrane potential ($\Delta \Psi$) loss resulting in AIF (apoptosis-inducing factor) release, as demonstrated using isolated mitochondria bearing endogenous bcl-2 and recombinant forms of these proteins, and 3) Inhibition of accumulation of p53 in mitochondrial membrane^[56]. Fas is a potent inducer of apoptosis in tumor cells but not in normal cells. Fas/CD95 requires ligand receptor (FasL/CD95L) which binds to FasL and via downstream signaling molecules FADD activates caspase-8. Fas binding to FasL can activate two routes downstream of caspase-8 activation^[58]: type I apoptosis signaling: direct activation of effector's caspases by caspase-8; type II apoptosis (inhibition of bcl-2 overexpression): cleavage of proapoptotic members of bcl-2 family, $\Delta \Psi$, release of cytochrome c and activation of caspase-9. The present study indicated that expression of bcl-2 protein decreased and expression of Fas increased on SGC-7901 cells induced by c9, t11-CLA as compared with that in negative control. c9, t11-CLA may induce apoptosis via pathways of bcl-2-associated mitochondria, p53-associated cell cycle and FADD on SGC-7901 cells. The relationship among p53, bcl-2 and Fas is still

unclear in the effect of apoptosis on SGC-7901 cells induced by c9,t11-CLA. The *c-myc* oncogene product (*c-myc*) is a transcription factor that dimerizes with Max and recognized E-box sequence, and it plays key functions in cell proliferation, differentiation and apoptosis^[59]. *C-myc* expression can not only promotes proliferation but also induce or sensitize cells to apoptosis. Overexpression of *c-myc* under the circumstances that this gene is usually down regulated such as serum deprivation, results in apoptotic cells in nonhepatic cells and in a hepatoma cell line^[60]. But our result showed that expression of *c-myc* with 10 % calf serum was lowered with c9, t11-CLA in SGC-7901 cells. We have not known the reason why expression of *c-myc* on SGC-7901 cells is lower than that in negative control, and this needs further studies.

In conclusion, c9, t11-CLA may inhibit proliferation and induce apoptosis by decreasing in the expression of ki67, bcl-2 and increasing that of Fas in SGC-7901 cells. This result suggested that the inhibition effect of c9, t11-CLA on SGC-7901 cell proliferation is related to the pathways of bcl-2-associated mitochondria, p53-associated cell cycle and FADD on SGC-7901 cells. In the meantime, we found that expression of *c-myc* was lowered, but we do not know its action how to regulate apoptotic progression in SGC-7901 cells. The apoptotic mechanism of c9, t11-CLA in SGC-7901 cells awaits further studies.

REFERENCES

- Liu JR, Li BX, Chen BQ, Han XH, Xue YB, Yang YM, Zheng YM, Liu RH. Effect of cis-9, trans-11-conjugated linoleic acid on cell cycle of gastric adenocarcinoma cell line (SGC-7901). *World J Gastroenterol* 2002; **8**: 224-229
- Liu JR, Chen BQ, Deng H, Han XH, Liu RH. Cell Apoptosis Induced by Conjugated Linoleic Acid in Human Gastric Cancer (SGC-7901) Cells. *Gongye Weisheng Yu Zhiyebing* 2001; **27**:129-133
- Liu JR, Chen BQ, Xue YB, Han XH, Yang YM, Liu RH. Inhibitory effect of conjugated linoleic acid on the in vitro growth of human mammary cancer cells (MCF-7). *Zhonghua Yufang Yixue* 2001; **35**: 244-247
- O'Shea M, Devery R, Lawless F, Murphy J, Stanton C. Milk fat conjugated linoleic acid (CLA) inhibits growth of human mammary MCF-7 cancer cells. *Anticancer Res* 2000; **20**: 3591-3601
- Park Y, Allen KG, Shultz TD. Modulation of MCF-7 breast cancer cell signal transduction by linoleic acid and conjugated linoleic acid in culture. *Anticancer Res* 2000; **20**: 669-676
- Miller A, Stanton C, Devery R. Modulation of arachidonic acid distribution by conjugated linoleic acid isomers and linoleic acid in MCF-7 and SW480 cancer cells. *Lipids* 2001; **36**: 1161-1168
- Liu JR, Chen BQ, Han XH, Yang YM, Zheng YM, Liu RH. Effect of cis9, trans 11- conjugated linoleic acid on cell cycle of human mammary cancer cells (MCF-7). *Chinese J Cancer Res* 2002; **14**: 93-99
- Palombo JD, Ganguly A, Bistrrian BR, Menard MP. The antiproliferative effects of biologically active isomers of conjugated linoleic acid on human colorectal and prostatic cancer cells. *Cancer Lett* 2002; **177**: 163-172
- Yamasaki M, Ikeda A, Hirao A, Tanaka Y, Miyazaki Y, Rikimaru T, Shimada M, Sugimachi K, Tachibana H, Yamada K. Effect of dietary conjugated linoleic acid on the in vivo growth of rat hepatoma dRLh-84. *Nutr Cancer* 2001; **40**: 140-148
- Zhu Y, Qiu J, Chen BQ, Liu RH. The inhibitory effect of CLA on mice forestomach neoplasia induced by benzo(a)pyrene. *Zhong Hua Yu Fang Yi Xue* 2001; **35**: 19-22
- Xue YB, Chen BQ, Liu JR, Zheng YM, Liu RH. The inhibition of mouse forestomach neoplasm induced by B(a)p through MAPKs pathway by conjugated linoleic acid. *Zhonghua Yufang Yixue* 2001; **35**: 1-4
- Park HS, Ryu JH, Ha YL, Park JH. Dietary conjugated linoleic acid (CLA) induces apoptosis of colonic mucosa in 1,2-dimethylhydrazine-treated rats: a possible mechanism of the anticarcinogenic effect by CLA. *Br J Nutr* 2001; **86**: 549-555
- Ip C, Ip MM, Loftus T, Shoemaker S, Shea-Eaton W. Induction of apoptosis by conjugated linoleic acid in cultured mammary tumor cells and premalignant lesions of the rat mammary gland. *Cancer Epidemiol. Biomarkers Prev* 2000; **9**: 689-696
- Kimoto N, Hirose M, Futakuchi M, Iwata T, Kasai M, Shirai T. Site-dependent modulating effects of conjugated fatty acids from safflower oil in a rat two-stage carcinogenesis model in female Sprague-Dawley rats. *Cancer Lett* 2001; **168**: 15-21
- Futakuchi M, Cheng JL, Hirose M, Kimoto N, Cho YM, Iwata T, Kasai M, Tokudome S, Shirai T. Inhibition of conjugated fatty acids derived from safflower or perilla oil of induction and development of mammary tumors in rats induced by 2-amino-1-methyl-6-phenylimidazo[4,5-b] pyridine (PhIP). *Cancer Lett* 2002; **178**: 131-139
- Miner JL, Cederberg CA, Nielsen MK, Chen X, Baile CA. Conjugated linoleic acid (CLA), body fat, and apoptosis. *Obes Res* 2001; **9**: 129-134
- Tovey FI, Hobsley M. Post-gastrectomy patients need to be followed up for 20-30 years. *World J Gastroenterol* 2000; **6**: 45-48
- Pan QS, Fang ZP, Zhao YX. Immunocytochemical identification and localization of APUD cells in the gut of seven stomachless teleost fishes. *World J Gastroenterol* 2000; **6**: 96-101
- Chen GY, Wang DR. The expression and clinical significance of CD44v in human gastric cancers. *World J Gastroenterol* 2000; **6**: 125-127
- Xu CT, Huan LT, Pan BR. Current gene therapy for stomach carcinoma. *World J Gastroenterol* 2001; **7**: 752-759
- Fang DC, Yang SM, Zhou XD, Wang DX, Luo YH. Telomere erosion is independent of microsatellite instability but related to loss of heterozygosity in gastric cancer. *World J Gastroenterol* 2001; **7**: 522-526
- Xu AG, Li SG, Liu JH, Gan AH. Function of apoptosis and expression of the proteins Bcl-2, p53 and *C-myc* in the development of gastric cancer. *World J Gastroenterol* 2001; **7**: 403-406
- Morgner A, Miehle S, Stolte M, Neubauer A, Alpen B, Thiede C, Klann H, Hierlmeier FX, Ell C, Ehninger G, Bayerdrffer E. Development of early gastric cancer 4 and 5 years after complete remission of *Helicobacter pylori* associated gastric low grade marginal zone B cell lymphoma of MALT type. *World J Gastroenterol* 2001; **7**: 248-253
- Niu WX, Qin XY, Liu H, Wang CP. Clinicopathological analysis of patients with gastric cancer in 1200 cases. *World J Gastroenterol* 2001; **7**: 281-284
- Xin Y, Li XL, Wang YP, Zhang SM, Zheng HC, Wu DY, Zhang YC. Relationship between phenotypes of cella2function differentiation and pathobiological behavior of gastric carcinomas. *World J Gastroenterol* 2001; **7**: 53-59
- Yao YL, Xu B, Song YG, Zhang WD. Overexpression of cyclin E in Mongolian gerbil with *Helicobacter pylori*- induced gastric precancerosis. *World J Gastroenterol* 2002; **8**: 60-63
- Gao HJ, Yu LZ, Bai JF, Peng YS, Sun G, Zhao HL, Miu K, Lü XZ, Zhang XY, Zhao ZQ. Multiple genetic alterations and behavior of cellular biology in gastric cancer and other gastric mucosal lesions: *H. pylori* infection, histological types and staging. *World J Gastroenterol* 2000; **6**: 848-854
- Deng DJ. Progress of gastric cancer etiology: N-nitrosamides 1999s. *World J Gastroenterol* 2000; **6**: 613-618
- Liu ZM, Shou NH, Jiang XH. Expression of lung resistance protein in patients with gastric carcinoma and its clinical significance. *World J Gastroenterol* 2000; **6**: 433-434
- Zou SC, Qiu HS, Zhang CW, Tao HQ. A clinical and long-term follow-up study of peri-operative sequential triple therapy for gastric cancer. *World J Gastroenterol* 2000; **6**: 284-286
- Wang X, Liu FK, Li X, Li JS, Xu GX. Inhibitory effect of endostatin expressed by human liver carcinoma SMMC7721 on endothelial cell proliferation in vitro. *World J Gastroenterol* 2002; **8**: 253-257
- Cao WX, Ou JM, Fei XF, Zhu ZG, Yin HR, Yan M, Lin YZ. Methionine-dependence and combination chemotherapy on human gastric cancer cells in vitro. *World J Gastroenterol* 2002; **8**: 230-232
- Li Y, Lu YY. Applying a highly specific and reproducible cDNA

- RDA method to clone garlic up-regulated genes in human gastric cancer cells. *World J Gastroenterol* 2002; **8**: 213-216
- 34 **Sun ZJ**, Pan CE, Liu HS, Wang GJ. Anti-hepatoma activity of resveratrol *in vitro*. *World J Gastroenterol* 2002; **8**: 79-81
- 35 **Wang X**, Lan M, Shi YQ, Lu J, Zhong YX, Wu HP, Zai HH, Ding J, Wu C, Pan BR, Jin JP. Differential display of vincristine-resistance-related genes in gastric cancer SGC-7901 cell. *World J Gastroenterol* 2002; **8**: 54-59
- 36 **Gao F**, Yi J, Shi GY, Li H, Shi XG, Tang XM. The sensitivity of digestive tract tumor cells to As₂O₃ is associated with the inherent cellular level of reactive oxygen species. *World J Gastroenterol* 2002; **8**: 36-39
- 37 **Liu DH**, Zhang XY, Fan DM, Huang YX, Zhang JS, Huang WQ, Zhang YQ, Huang QS, Ma WY, Chai YB, Jin M. Expression of vascular endothelial growth factor and its role in oncogenesis of human gastric carcinoma. *World J Gastroenterol* 2001; **7**: 500-505
- 38 **Liu S**, Wu Q, Chen ZM, Su WJ. The effect pathway of retinoic acid through regulation of retinoic acid receptor α in gastric cancer cells. *World J Gastroenterol* 2001; **7**: 662-666
- 39 **Wu K**, Shan YJ, Zhao Y, Yu JW, Liu BH. Inhibitory effects of RRR- α -tocopheryl succinate on benzo(a)pyrene (B(a)P) induced forestomach carcinogenesis in female mice. *World J Gastroenterol* 2001; **7**: 60-65
- 40 **Wu YL**, Sun B, Zhang XJ, Wang SN, He HY, Qiao MM, Zhong J, Xu JY. Growth inhibition and apoptosis induction of Sulindac on Human gastric cancer cells. *World J Gastroenterol* 2001; **7**: 796-800
- 41 **Cui M**, Zhang HJ, An LG. Tumor growth Inhibition by polysaccharide from *Coprinus comatus*. *Shijie Huaren Xiaohua Zazhi* 2002; **9**: 287-290
- 42 **Wang XB**, Wang X, Zhang NZ. Inhibition of somatostatin analog Octreotide on human gastric cancer cell MKN45 growth *in vitro*. *Xin Xiaohua Bingxue Zazhi* 2002; **10**: 40-42
- 43 **Zhan J**, Xie DR, Yao HR, Lin XG, Liang XW, Xiang YQ. Apoptosis of large intestine cancer cells (SW620) induced by As₂O₃. *Shijie Huaren Xiaohua Zazhi* 2001; **9**: 228-229
- 44 **Yu LF**, Wu YL, Zhang YP. Reversal of drug resistance in the vincristine-resistant human gastric cancer cell lines MKN28/VCR by emulsion of seminal oil of *Brucea Javanica*. *Shijie Huaren Xiaohua Zazhi* 2001; **9**: 376-378
- 45 **Liu WC**, Mu HX, Ren J, Zhang XY, Pan BR. Anti-tumor activity of defensin on gastric cancer cell line *in vitro*. *Shijie Huaren Xiaohua Zazhi* 2001; **9**: 622-626
- 46 **Chen JP**, Shen DM, Yang ZB. CagA⁺ *Hp* broth culture filtrates induced malignant transformation on human gastric epithelial cells. *Shijie Huaren Xiaohua Zazhi* 2001; **9**: 617-621
- 47 **Qin YC**, Yuan YQ, Si JL, Lin J, Zhu J, Liu JY. The effects of Apoptosis and activation of telomerase on human gastric cancer cells induced by paclitaxel. *Shijie Huaren Xiaohua Zazhi* 2001; **9**: 1086-1087
- 48 **Zhang L**, Fu HM, Jin SZ, Hang R, Zhou CG. Overexpression of P53 and relationship between extracellular matrix and differentiation, invasion and metastasis of gastric carcinoma. *Shijie Huaren Xiaohua Zazhi* 2001; **9**: 992-996
- 49 **Sun B**, Wu YL, Zhang XJ, Wang SN, He HY, Qiao MM, Zhang YP, Zhong J. Effects of Sulindac on growth inhibition and apoptosis induction in human gastric cancer cells. *Shijie Huaren Xiaohua Zazhi* 2001; **9**: 997-1002
- 50 **Liu HF**, Liu WW, Fang DC, Gao JH, Wang ZH. Apoptosis and proliferation induced by *Helicobacter pylori* and its association with p53 protein expression in gastric epithelial cells. *Shijie Huaren Xiaohua Zazhi* 2001; **9**: 1265-1268
- 51 **Tu SP**, Jiang SH, Qiao MM, Cheng SD, Wang LF, Wu YL, Yuan YZ, Wu YX. Effect of trichosanthin on cytotoxicity and induction of apoptosis of multiple drugs resistance cells in gastric cancer. *Shijie Huaren Xiaohua Zazhi* 2000; **8**: 150-152
- 52 **Xia ZS**, Zhu ZH, He SG. Effects of ATRA and 5-Fu on growth and telomerase activity of xenografts of gastric cancer in nude mice. *Shijie Huaren Xiaohua Zazhi* 2000; **8**: 674-677
- 53 **Zhao AG**, Yang JK, Zhao HL. Chinese Jianpi herbs induce apoptosis of human gastric cancer grafted onto nude mice. *Shijie Huaren Xiaohua Zazhi* 2000; **8**: 737-740
- 54 **Liu HF**, Liu WW, Fang DC, Yang SM, Zhao L. Gastric epithelial apoptosis induced by *Helicobacter pylori* and its relationship with Bax protein expression. *Shijie Huaren Xiaohua Zazhi* 2000; **8**: 860-862
- 55 **Koutsodontis G**, Tentes I, Papakosta P, Moustakas A, Kardassis D. Sp1 plays a critical role in the transcriptional activation of the human cyclin-dependent kinase inhibitor p21(WAF1/Cip1) gene by the p53 tumor suppressor protein. *J Biol Chem* 2001; **276**: 29116-29125
- 56 **Marchenko ND**, Zaika A, Moll UM. Death signal-induced localization of p53 protein to mitochondria. A potential role in apoptotic signaling. *J Biol Chem* 2000; **275**: 16202-16212
- 57 **Wang NS**, Unkila MT, Reineks EZ, Distelhorst CW. Transient expression of wild-type or mitochondrially targeted Bcl-2 induces apoptosis, whereas transient expression of endoplasmic reticulum-targeted Bcl-2 is protective against Bax-induced cell death. *J Biol Chem* 2001; **276**: 44117-44128
- 58 **Luschen S**, Ussat S, Scherer G, Kabelitz D, Adam-Klages S. Sensitization to death receptor cytotoxicity by inhibition of fas-associated death domain protein (FADD)/caspase signaling. Requirement of cell cycle progression. *J Biol Chem* 2000; **275**: 24670-24678
- 59 **Fujioka Y**, Taira T, Macda Y, Tanaka S, Nishihara H, Iguchi-Ariga SM, Nagashima K, Ariga H. MM-1, a c-Myc-binding protein, is a candidate for a tumor suppressor in leukemia/lymphoma and tongue cancer. *J Biol Chem* 2001; **276**: 45137-45144
- 60 **Liu HL**, Lo CR, Jones BE, Pradhan Z, Srinivasan A, Valentino KL, Stockert RJ, Czaja MJ. Inhibition of c-Myc Expression Sensitizes Hepatocytes to Tumor Necrosis Factor-induced Apoptosis and Necrosis. *J Biol Chem* 2000; **275**: 40155-40162

Edited by Ma JY

• GASTRIC CANCER •

Mast cell density and the context of clinicopathological parameters and expression of p185, estrogen receptor, and proliferating cell nuclear antigen in gastric carcinoma

Ying-An Jiang, You-Yuan Zhang, He-Sheng Luo, Shou-Fu Xing

Ying-An Jiang, He-Sheng Luo, Department of Gastroenterology, Renming Hospital of Wuhan University, Wuhan 430060, Hubei Province, China

You-Yuan Zhang, Department of Pathology, Central Hospital of Huangshi City, Huangshi 435000, Hubei Province, China

Shou-Fu Xing, Department of Pathology, Medical College of Wuhan University, Wuhan 430071, Hubei Province, China

Correspondence to: Ying-An Jiang, Central Hospital of Huangshi City, 43 Wuhan Road, Huangshi 435000, Hubei Province, China. hszxyy@public.hs.hb.cn

Telephone: +86-714-6283783 **Fax:** +86-714-6233931

Received 2002-04-26 **Accepted** 2002-06-10

Abstract

AIM: To investigate the relationship between the mast cell density (MCD) and the context of clinicopathological parameters and expression of p185, estrogen receptor (ER), and proliferating cell nuclear antigen (PCNA) in gastric carcinoma.

METHODS: Mast cell, p185, ER, and PCNA were detected using immunohistochemical S-P labeling method. Mast cell was counted in tissue of gastric carcinoma and regional lymph nodes respectively, and involved lymph nodes (ILN) were examined as usual.

RESULTS: MCD was significantly related to both age and depth of penetration ($\chi^2=4.688, P<0.05$ for age and $\chi^2=9.350, P<0.01$ for depth of penetration) between MCD $>21/0.03$ mm² and MCD $\leq 21/0.03$ mm² in 100 patients; MCD in 1-6 ILN group patients was significantly higher than that in 7-15 ILN or >15 ILN group patients ($u=6.881, 8.055, P<0.01$); There were significant differences intergroup in positive expression rate of p185, ER and PCNA between MCD $>21/0.03$ mm² and MCD $\leq 21/0.03$ mm² in 100 patients.

CONCLUSION: Mast cell may have effect on inhibiting invasive growth of tumor, especially in the aged patients; The number of mast cells, in certain degree, may predicate the number of involved lymph nodes, which is valuable for assessment of prognosis; MCD was related to the expression of p185, ER, and PCNA in gastric carcinoma. It suggests that mast cell accumulation may inhibit the proliferation and the dissemination of the gastric carcinoma.

Jiang YA, Zhang YY, Luo HS, Xing SF. Mast cell density and the context of clinicopathological parameters and expression of p185, estrogen receptor, and proliferating cell nuclear antigen in gastric carcinoma. *World J Gastroenterol* 2002; 8(6):1005-1008

INTRODUCTION

Recently, many studies have reported on the association of

mast cell with various tumors^[1-9]. In several malignancies, mast cell has been found to correlate with growth, penetration and prognosis of tumor^[10-13]. Therefore, our study was undertaken to investigate the relationship between the mast cell density (MCD) and the context of clinicopathological parameters and expression of p185, estrogen receptor (ER), and proliferating cell nuclear antigen (PCNA) in gastric carcinoma.

MATERIALS AND METHODS

Materials

The specimens of gastric carcinoma, histologically confirmed, were surgically obtained from 421 patients. The patients had undergone curative tumor resection at our hospital between 1984 and 1998. And only 100 patients were chosen at random in our study. Among 100 patients, 41 patients had lymph node metastases. All resected tissue specimens were fixed in formalin, embedded in paraffin, and cut into 3-4 μ m serial sections. 459 lymph nodes were collected from 41 patients (range, 8-26 per patient).

Methods

Mast cell, p185, ER, and PCNA were detected using immunohistochemical method (agents from Maixin-Bio Corp. Fuzhou, China). The count of mast cells in the tissue of gastric carcinoma was as described by Takanami *et al*^[10]. A grid (0.15 mm by 0.2 mm) which was defined an area of 0.03 mm² per field was used for to count mast cells. Similarly, that of mast cells in regional lymph nodes was described by Bowers *et al*^[14]. A grid which defined an area of mm² per field was used. ILN was examined using routine pathological method. The results were expressed as the means \pm SD. Statistical analyses were performed using the Chi-square and *u* test. A *P* value less than or equal to 0.05 was considered significant.

RESULTS

Table 1 showed the clinicopathologic parameters for two groups (high MCD group, MCD was more than 21/0.03 mm², and low MCD group, MCD was equal to 21/0.03 mm² or less). There were no significant differences between two groups regarding both degree of differentiation and largest dimension of tumor. However, MCD was significantly related to both age and depth of penetration ($P<0.05$ for age and $P<0.01$ for depth of penetration) (Figure 1).

Table 2 showed correlation between MCD and cancerous metastases in regional lymph nodes. MCD in 1-6 ILN group patients ($n=21$) was 12 ± 3.11 , 7-15 ILN ($n=14$), 6 ± 2.06 , >15 ILN ($n=6$), 5 ± 1.33 , respectively. MCD in 1-6 ILN group patients was significantly higher than that in 7-15 ILN or >15 ILN group patients ($P<0.01$), but, MCD in 7-15 ILN group patients was not significantly higher than that in >15 ILN group patients ($P>0.05$) (Figure 2).

Table 1 Correlation between MCD and Clinicopathologic finding of gastric carcinoma (n=100)

Variable	MCD>21/0.03 mm ²	MCD≤21/0.03 mm ²	P Value
Age (yrs)			
<60	16	25	<0.05
≥60	36	23	
Degree of differentiation			
Well	18	14	>0.05
Moderately	23	21	
Poorly	11	13	
Largest dimension of tumor (in mm)			
≤30	30	36	>0.05
>30	22	12	
Depth of penetration			
Involved serosa	21	34	<0.01
Not involved serosa	31	14	

Table 2 Correlation between MCD and cancerous metastases in regional lymph nodes (n=41)

Variable	n	MCD ($\bar{x}\pm s$, /mm ²)
1-6 ILN	21	12±3.11
7-15 ILN	14	6±2.06
> 15 ILN	6	5±1.33

ILN: involved lymph nodes

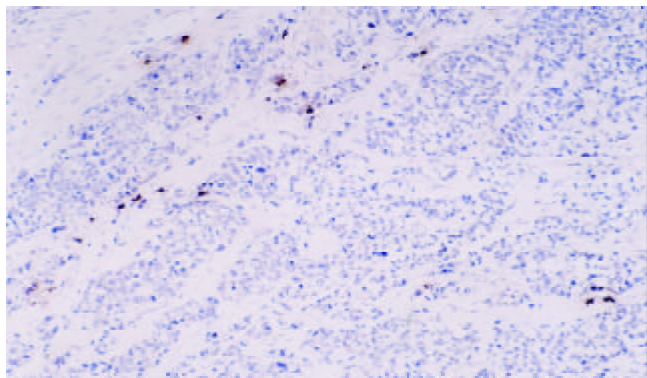


Figure 1 Mast cells of gastric carcinoma (Tryptase labeling, DAB staining, original magnification, ×100)

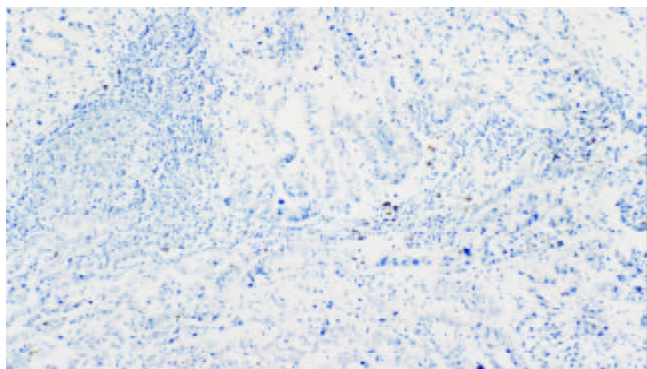


Figure 2 Mast cells of regional lymph nodes of gastric carcinoma (Tryptase labeling, original magnification, ×100)

There were significant differences intergroup in positive expression rate of p185, ER and PCNA between high MCD group (the MCD was more than 21/0.03 mm²) and low MCD group (the MCD was equal to 21/0.03 mm² or less) ($P<0.01$). As was shown in Table 3 (Figure 3,4,5).

Table 3 Correlation between MCD and the positive expression rate of p185, ER, and PCNA in the gastric carcinoma tissues

MCD	n	Positive expression rate (%)		
		p185	ER	PCNA
>21/0.03 mm ²	52	22(42.31)	11(21.15)	12(23.08)
≤21/0.03 mm ²	48	31(59.62)	28(53.84)	27(51.92)
P Value		<0.01	<0.001	<0.01

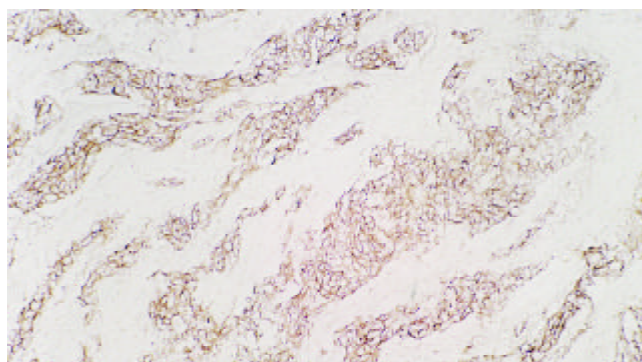


Figure 3 p185 of gastric carcinoma (Original magnification,×100)

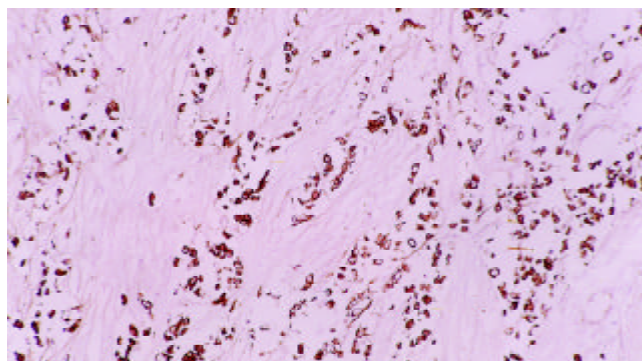


Figure 4 Estrogen receptor of gastric carcinoma (Original magnification, ×100)

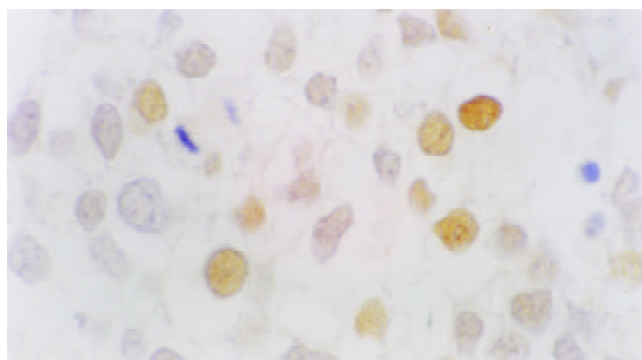


Figure 5 PCNA of gastric carcinoma (Original magnification,×400)

DISCUSSION

Numerous studies have shown that mast cell plays an important role in tumor growth. Dabbou *et al*^[15,16] found that mast cells were accumulated around the periphery of the invasive and metastatic rat mammary adenocarcinoma, and they believed that interactions between mast cell and tumor cell were important for the growth and invasive properties of the tumor. Nakamura *et al*^[17] found the mechanism of mast cell accumulation at sites of tumors was that tumor cells could produce a factor which might not be the already known mast cell growth factors. Wang *et al*^[18] found that the anti-tumor effect of mast cell might be related to releasing of tumor necrosis factor (TNF) and non-TNF cytotoxicity. Our results revealed there were no significant differences intergroup regarding both degree of differentiation and largest dimension of tumor between $MCD > 21/0.03 \text{ mm}^2$ and $MCD \leq 21/0.03 \text{ mm}^2$. MCD was significantly related to both age and depth of penetration ($P < 0.05$ for age and $P < 0.01$ for depth of penetration).

The data indicate the lymph node status is associated with the patients' prognoses in many malignancies, and may be useful in assessing the outcome of this disease^[19-28]. The treatment regimen was depended on not only whether involved lymph node was present or not, but also the number of involved lymph node^[20,29]. Maurel *et al*^[30] had examined 7.7 ± 0.2 lymph nodes per specimen in 851 patients with resected colorectal carcinoma, the results strongly pointed out that at least eight lymph nodes must be examined and they called the number of eight as a "golden number". At least eight lymph nodes per specimen were examined in our study as done by Maurel *et al*^[30]. Roder *et al*^[20] followed up 477 patients with gastric carcinoma of lymph node metastasis, and they found that 5-year survival rates were as follows (1) 1-6 involved lymph nodes: 45.5 %; (2) 7-15 involved lymph nodes: 29.7 %; (3) > 15 involved lymph nodes: 10.4 %. There was a highly significant difference in survival ($P < 0.0001$). Our results indicated that MCD in 1-6 ILN group patients was 12 ± 3.11 , 7-15 ILN, 6 ± 2.06 , > 15 ILN, 5 ± 1.33 , respectively. MCD in 1-6 ILN group patients was significantly higher than that in 7-15 ILN or > 15 ILN group patients ($P < 0.01$), but, MCD in 7-15 ILN group patients was not significantly higher than that in > 15 ILN group patients ($P > 0.05$). In other words, the higher MCD was in regional lymph nodes, the lower number of ILN of gastric cancerous metastases was. It demonstrates that the number of mast cells, in certain degree, may predicate the number of involved lymph nodes of gastric cancerous metastases. Therefore, MCD is a valuable parameter for assessing the prognosis of patients with gastric carcinoma.

The C-erbB-2 was first identified in ethylnitrosourea-induced rat neuroblastoma. It encodes a 185 kilodalton (kDa) glycoprotein. It was reported recently that overexpression and gene amplification of C-erb B-2 were frequently observed in the intestinal type gastric adenocarcinoma, and it was a prognostic indicator in tumor^[31-33]. ER is commonly known to be present in the cell of the breast and endometrium, but have also been identified in diverse normal and neoplastic nonreproductive tissues. The expression of ER has been considered to be a favorable prognostic factor in breast carcinoma and endometrial carcinoma but a poor prognostic factor in gastric carcinoma^[34]. PCNA is an auxiliary protein of DNA polymerase delta which plays a major role in synthesizing DNA and is expressed in the nuclei, particularly in the late phase of G₁ and S. Therefore PCNA is a useful marker for proliferative activity^[35-37]. Our results showed there were significant differences intergroup in the positive expression rate of p185, ER and PCNA between $MCD > 21/0.03 \text{ mm}^2$ and $MCD \leq 21/0.03 \text{ mm}^2$. It suggests that mast cell

accumulation may inhibit the proliferation and the dissemination of gastric carcinoma. This finding may provide a molecular foundation of the further study on relation between mast cell and gastric carcinoma.

REFERENCES

- 1 Tomita M, Matsuzaki Y, Edagawa M, Shimizu T, Hara M, Sekiya R, Onitsuka T. Association of mast cells with tumor angiogenesis in esophageal squamous cell carcinoma. *Dis Esophagus* 2001; **14**: 135-138
- 2 Tomita M, Matsuzaki Y, Onitsuka T. Effect of mast cells on tumor angiogenesis in lung cancer. *Ann Thorac Surg* 2000; **69**: 1686-1690
- 3 Erkilic S, Erbagci Z. The significance of mast cells associated with basal cell carcinoma. *J Dermatol* 2001; **28**: 312-315
- 4 Terada T, Matsunaga Y. Increased mast cells in hepatocellular carcinoma and intrahepatic cholangiocarcinoma. *J Hepatol* 2000; **33**: 961-966
- 5 Wilkins BS, Buchan SL, Webster J, Jones DB. Tryptase-positive mast cells accompany lymphocytic as well as lymphoplasmacytic lymphoma infiltrates in bone marrow trephine biopsies. *Histopathology* 2001; **39**: 150-155
- 6 Hart PH, Grimbaldeston MA, Finlay-Jones JJ. Sunlight, immunosuppression and skin cancer: role of histamine and mast cells. *Clin Exp Pharmacol Physiol* 2001; **28**: 1-8
- 7 Terada T, Matsunaga Y. Increased mast cells in hepatocellular carcinoma and intrahepatic cholangiocarcinoma. *J Hepatol* 2000; **33**: 961-966
- 8 Sawatsubashi M, Yamada T, Fukushima N, Mizokami H, Tokunaga O, Shin T. Association of vascular endothelial growth factor and mast cells with angiogenesis in laryngeal squamous cell carcinoma. *Virchows Arch* 2000; **436**: 243-248
- 9 Johansson S, Landstrom M, Bjerner L, Henriksson R. Effects of tobacco smoke on tumor growth and radiation response of dunning R3327 prostate adenocarcinoma in rats. *Prostate* 2000; **42**: 253-259
- 10 Takanami I, Takeuchi K, Naruke M. Mast cell density is associated with angiogenesis and poor prognosis in pulmonary adenocarcinoma. *Cancer* 2000; **88**: 2686-2692
- 11 Imada A, Shijubo N, Kojima H, Abe S. Mast cells correlate with angiogenesis and poor outcome in stage I lung adenocarcinoma. *Eur Respir J* 2000; **15**: 1087-1093
- 12 Tomita M, Matsuzaki Y, Onitsuka T. Correlation between mast cells and survival rates in patients with pulmonary adenocarcinoma. *Lung Cancer* 1999; **26**: 103-108
- 13 Elpek GO, Gelen T, Aksoy NH, Erdogan A, Dertsiz L, Demircan A, Keles N. The prognostic relevance of angiogenesis and mast cells in squamous cell carcinoma of the oesophagus. *J Clin Pathol* 2001; **54**: 940-944
- 14 Bowers HM Jr, Mahapatro RC, Kennedy JW. Numbers of mast cells in the axillary lymph nodes of breast cancer patients. *Cancer* 1979; **43**: 568-573
- 15 Dabbous MK, Haney L, Nicolson GL, Eckley D, Woolley DE. Mast cell modulation of tumour cell proliferation in rat mammary adenocarcinoma 13762NF. *Br J Cancer* 1991; **63**: 873-878
- 16 Hultsch T, Brand P, Lohmann S, Saloga J, Kincaid RL, Knop J. Direct evidence that FK506 inhibition of FcεpsilonRI-mediated exocytosis from RBL mast cells involves calcineurin. *Arch Dermatol Res* 1998; **290**: 258-263
- 17 Nakamura K, Tanaka T, Morita E, Kameyoshi Y, Yamamoto S. Enhancement of fibroblast-dependent mast cell growth in mice by a conditioned medium of keratinocyte-derived squamous cell carcinoma cells. *Arch Dermatol Res* 1994; **287**: 91-96
- 18 Wang X, Ruan Y, Wu Z. Studies of mast cell-mediated cytotoxicity to hepatoma cells *in vitro*. *Zhonghua Zhongliu Zazhi* 1996; **18**: 276-278
- 19 Xu Y, Guo Z. The number of lymph node with metastases influences survival in patients with cancer of the thoracic esophagus. *Zhonghua Zhongliu Zazhi* 2000; **22**: 244-246
- 20 Roder JD, Bottcher K, Busch R, Wittekind C, Hermanek P, Siewert JR. Classification of regional lymph node metastasis from gas-

- tric carcinoma. German Gastric Cancer Study Group. *Cancer* 1998; **82**: 621-631
- 21 **Lanza G**, Gafa R, Decarli N. Pathological factors involved in lymph node status determination in colorectal carcinoma: analysis of 166 cases with long-term follow-up. *Pathologica* 2001; **93**: 631-639
- 22 **Nakajima Y**, Nagai K, Miyake S, Ohashi K, Kawano T, Iwai T. Evaluation of an indicator for lymph node metastasis of esophageal squamous cell carcinoma invading the submucosal layer. *Jpn J Cancer Res* 2002; **93**: 305-312
- 23 **Wong JH**, Steinemann S, Tom P, Morita S, Tauchi -Nishi P. Volume of lymphatic metastases does not independently influence prognosis in colorectal cancer. *J Clin Oncol* 2002; **20**: 1506-1511
- 24 **Rouzier R**, Extra JM, Klijanienko J, Falcou MC, Asselain B, Vincent-salomon A, Vielh P, Boursstyn E. Incidence and prognostic significance of complete axillary downstaging after primary chemotherapy in breast cancer patients with T1 to T3 tumors and cytologically proven axillary metastatic lymph nodes. *J Clin Oncol* 2002; **20**: 1304-1310
- 25 **Katai H**, Maruyama K, Sasako M, Sano T. Incidence of nodal metastasis around the superior border of the pancreas based on number of metastatic perigastric nodes. *Gastric Cancer* 1998; **1**: 115-117
- 26 **Ichikura T**, Morita D, Uchida T, Okura E, Majima T, Ogawa T, Mochizuki H. Sentinel node concept in gastric carcinoma. *World J Surg* 2002; **26**: 318-322
- 27 **Lau WK**, Blute ML, Bostwick DG, Weaver AL, Sebo TJ, Zincke H. Prognostic factors for survival of patients with pathological Gleason score 7 prostate cancer: differences in outcome between primary Gleason grades 3 and 4. *J Urol* 2001; **166**: 1692-1697
- 28 **Sasatomi E**, Finkelstein SD, Woods JD, Bakker A, Swalsky PA, Luketich JD, Fernando HC, Yousem SA. Comparison of accumulated allele loss between primary tumor and lymph node metastasis in stage II non-small cell lung carcinoma: implications for the timing of lymph node metastasis and prognostic value. *Cancer Res* 2002; **62**: 2681-2689
- 29 **Niemann TH**, Yilmaz AG, Marsh WL Jr, Lucas JG. A half a node or a whole node: a comparison of methods for submitting lymph nodes. *Am J Clin Pathol* 1998; **109**: 571-576
- 30 **Maurel J**, Launoy G, Grosclaude P, Gignoux M, Arveux P, Mathieu-Daude H, Raverdy N, Faivre J. Lymph node harvest reporting in patients with carcinoma of the large bowel: a French population-based study. *Cancer* 1998; **82**: 1482-1486
- 31 **Dursun A**, Poyraz A, Celik B, Akyol G. Expression of c-erbB-2 oncoprotein in gastric carcinoma: correlation with histopathologic characteristics and analysis of Ki-67. *Pathol Oncol Res* 1999; **5**: 104-106
- 32 **Aoyagi K**, Kohfuji K, Yano S, Murakami N, Miyagi M, Takeda J, Shirouzu K. Evaluation of the epidermal growth factor receptor (EGFR) and c-erbB-2 in superspreading-type and penetrating-type gastric carcinoma. *Kurume Med J* 2001; **48**: 197-200
- 33 **Oshima CT**, Lanzoni VP, Iriya K, Forones NM. C-erbB-2 oncoprotein in gastric carcinoma: correlation with clinical stage and prognosis. *Int J Biol Markers* 2001; **16**: 250-254
- 34 **Xin Y**, Li XL, Wang YP, Zhang SM, Zheng HC, Wu DY, Zhang YC. Relationship between phenotypes of cell-function differentiation and pathobiological behavior of gastric carcinomas. *World J Gastroenterol* 2001; **7**: 53-59
- 35 **Noda H**, Maehara Y, Irie K, Kakeji Y, Yonemura T, Sugimachi K. Increased proliferative activity caused by loss of p21(WAF1/CIP1) expression and its clinical significance in patients with early-stage gastric carcinoma. *Cancer* 2002; **94**: 2107-2112
- 36 **Tao K**, Chen D, Tian Y, Lu X, Yang X. The relationship between apoptosis and the expression of proliferating cell nuclear antigen and the clinical stages in gastric carcinoma. *J Tongji Med Univ* 2000; **20**: 222-224
- 37 **Konno S**, Takebayashi Y, Aiba M, Akiyama S, Ogawa K. Clinicopathological and prognostic significance of thymidine phosphorylase and proliferating cell nuclear antigen in gastric carcinoma. *Cancer Lett* 2001; **166**: 103-111

Edited by Liu HX

• GASTRIC CANCER •

Expression of gastric cancer-associated MG7 antigen in gastric cancer, precancerous lesions and *H. pylori*-associated gastric diseases

Dong-Li Guo, Ming Dong, Lan Wang, Li-Ping Sun, Yuan Yuan

Dong-Li Guo, Ming Dong, Lan Wang, Li-Ping Sun, Yuan Yuan, Cancer Institute, First Affiliated Hospital, China Medical University, Shenyang, 110001, Liaoning Province, China

Supported by The National Basic Research Program (973) of China, No.G1998051203

Correspondence to: Dr. Yuan Yuan, No.3 gastric cancer laboratory, Cancer Institute, First Affiliated Hospital, China Medical University, 155 Northern Nanjing Street, Heping District, Shenyang 110001, Liaoning Province, China. yyuan@mail.cmu.edu.cn

Received 2002-05-13 **Accepted** 2002-06-03

Abstract

AIM: To investigate the relationship between the antigen MG7 antigen expression and gastric cancer as well as precancerous condition; to study the relationship between the MG7 antigen expression and *H. pylori* infection in benign gastric lesions in order to find out the effect of *H. pylori* infection on the process of gastric cancer development.

METHODS: The level of MG7 antigen expression was determined by immunohistochemical method in 383 gastric biopsied materials. The intestinal metaplasia was determined by histochemistry method. The *H. pylori* infection was determined by HE stain, PCR and ELISA in 291 specimens, among which only 34 cases of *H. pylori*-associated gastric lesions were followed up.

RESULTS: The positive rate of MG7 expression in normal gastric mucosa, intestinal metaplasia, dysplasia and gastric cancer increased gradually in ascending order ($P < 0.01$). The positive rate of MG7 antigen expression in type III intestinal metaplasia of gastric mucosa was higher than that of type I and II intestinal metaplasia, being highly significant ($P < 0.05$). The positive rate of MG7 antigen expression in superficial gastritis, atrophic gastritis and gastric cancer increased gradually (11.9 %, 64.8 %, 91.2 %, $P < 0.01$). There was no significant difference between *H. pylori*-negative and *H. pylori*-positive intestinal metaplasia, atrophic gastritis and dysplasia of gastric epithelium in the positive rate of MG7 antigen expression. There was no expression of MG7 antigen in *H. pylori*-negative superficial gastritis. The positive rate of MG7 expression in *H. pylori*-positive superficial gastritis was 20.5 %, and the difference between them was significant ($P < 0.05$). During following up, one of the three *H. pylori* negative cases turned positive again, and its MG7 antigen expression turned to be stronger correspondingly. 3 of 31 *H. pylori* positive cases were detected as early gastric cancer, among which one with “+++” MG7 antigen expression was diminished after *H. pylori* eradication.

CONCLUSION: MG7 antigen expression is highly specific in gastric cancer and can be used as a good marker for

screening of gastric cancer; type III intestinal metaplasia, atrophic gastritis and dysplasia should be followed up and MG7 antigen expression has high clinical value in the dynamic follow-up study; although the positive -MG7 in positive -*H. pylori* superficial gastritis show benign morphology in features, there is still the potential risk of developing into gastric cancer, hence special attention should be paid to those showing increasing MG7 antigen expression.

Guo DL, Dong M, Wang L, Sun LP, Yuan Y. Expression of gastric cancer-associated MG7 antigen in gastric cancer, precancerous lesions and *H. pylori*-associated gastric diseases. *World J Gastroenterol* 2002; 8(6):1009-1013

INTRODUCTION

Gastric monoclonal antibody MG7 was first gotten by immunizing the BALB/C mice directly with poor-differentiated adenocarcinoma gastric cancer cell line MKN-46-9^[1]. By immunohistochemistry method the MG7 antigen is distinguished limited in the gastric cancer tissue^[2-5], which is specific and serves as a marker of gastric cancer. *Helicobacter pylori* (*H. pylori*) infection is established as a major cause of gastritis, peptic ulcer disease and gastric cancer^[6-8]. The current study is to investigate the dynamic expression of MG7 antigen in different gastric mucosa, including the normal gastric tissue, *H. pylori*-associated gastric lesions as well as other precancerous conditions and gastric cancer, also to investigate the influence of *H. pylori* on MG7 antigen expression.

MATERIALS AND METHODS

Clinical data

The gastric cancer-associated antigen MG7 expression was studied in 383 gastric mucosal biopsied materials, including 26 normal gastric mucosa, 67 superficial gastritis, 21 gastric ulcer, 71 atrophic gastritis, 82 intestinal metaplasia, 59 dysplasia, and 57 gastric cancerous tissue, among which 29 were differentiated and 28 undifferentiated.

Reagents

The MoAb MG7 was gifted by Professor Fan Daiming in No. 4 China Military Medical University; The ABC kit was the product of American Vector Company.

HID-ABpH2.5-PAS mucin histochemistry stain

82 IM were categorized into three types according to the morphology, degree of differentiation and mucin-protein secreted. These were stained with Alicant blue pH 2.5/ periodic acid Schiff (AB/PAS) to visualize neutral mucin and some acidic mucins, and with high iron diamine/Alcant blue pH 2.5 (HID/AB) to identify sulphomucin and sialomucin^[9]. Type I

(complete) was characterized by mature absorptive and goblet cells, the latter secreted sialomucin. Paneth's cells were often present. Type II (incomplete) showed few or no absorptive cells, but with 'intermediate' columnar cells in various differentiated stages, secreting neutral and sialomucins, while Paneth's cells might not be present. In type III (incomplete), cell dedifferentiation was more obvious than that in type II, with 'intermediate' cells secreting predominantly sulphomucin and goblet cells containing sialo- and/or sulphomucin. Paneth's cells were usually absent. A variable degree of disorganized architecture was often present in type III IM.

H. pylori examination

The *H. pylori* infection was detected by HE stain, PCR and ELISA. *H. pylori* was considered positive if two of the above three methods were positive. *H. pylori* could be found in the gastric epithelium or in the mucus by histological examination. Detection of *H. pylori* with *H. pylori*-DNA-PCR method followed the protocol of kit. The band in the same position as the positive control was defined as positive. When ELISA method was performed, the sample with OD value/OD average value of negative controls ≥ 2.1 was defined as positive.

Immunohistochemistry stain (ABC method) of gastric cancer-associated antigen MG7

4 μ m thick sections were cut from paraffin wax blocks, mounted on acid cleaned glass slides, and heated at 55 °C for 60 minutes. The slides were dewaxed and dehydrated, then the endogenous peroxidase activity was inhibited by incubation with 3 % H₂O₂ (20 minutes at room temperature). To reduce the non-specific background staining, the slides were incubated with 2 % horse serum (20 minutes at room temperature), then were incubated with MG7 antibody in a moist chamber at 4 °C overnight. The avidin-biotin-peroxidase complex procedure was then performed as described by ABC immunohistochemistry kit. Peroxidase activity was detected with diaminobenzidine as substrate. Finally, the sections were weakly counterstained with Harris' s haematoxylin. Negative controls with PBS replacing specific primary antibodies were included in each run. Positive controls were cases of undifferentiated gastric cancer with MG7 expression. The sections were considered positively stained only when unequivocal cellular membrane and cytoplasm staining for MG7 were present. Diagnosis was made by brown coloration with varied intensities and the number of cells with brown coloration^[10]. score 1: light brown; score 2: brown; score 3: deep brown. score 1: stained cells <30 %; score 2: stained cells 30-70 %; score 3: stained cells >70 %. According to the sum of the two index, as that comprehensive scores were made. Comprehensive score 0 was defined as negatively expressed, comprehensive scores 2-4 were defined positively expressed, the cases and that above 4 was defined as over-expressed.

Statistical analysis

The results were analyzed by χ^2 test.

RESULTS

The expression of gastric cancer-associated MG7 antigen in different gastric mucosal tissues

The coloration in gastric cancerous tissue was often brown or deep brown, which was mainly located in the cellular membrane, cytoplasm and the glandular lumen, but not in the nucleus. The brown coloration was usually diffusely and non-polar distributed in the cytoplasm of cancer cells and might

also be present in the luminal surface of the glands, sometimes it was located in some cancer cell nests or glands. The coloration in benign gastric lesions was often light brown, which was mainly located at the apex of the cytoplasm, the luminal surface membrane, none was seen in the cell nucleus. There were less positive cells in benign gastric lesions.

There was no expression of MG7 antigen in normal gastric mucosa. The positive rate of MG7 antigen expression in gastric cancer was 91.2 %. The level of MG7 antigen expression in undifferentiated gastric cancer was higher than that of differentiated gastric cancer (89.7 %, 92.3 %, $P>0.05$). From the viewpoint of histology, the positive rates of MG7 expression in normal gastric mucosa, metaplasia/dysplasia and gastric cancer increased gradually ($P<0.01$), see Table 1. From clinical viewpoint the positive rates of MG7 expression in superficial gastritis, atrophic gastritis and gastric cancer also increased gradually ($P<0.01$), see Table 2. The expression rates of MG7 antigen in the increasing order were normal gastric mucosa, superficial gastritis, intestinal metaplasia, atrophic gastritis, dysplasia and gastric cancer, there was significant difference between gastric cancer and other benign gastric lesion groups ($P<0.05$), see Table 1 and 2.

Table 1 The expression of MG7 antigen in various gastric lesions

Gastric lesions	n	No. of cases with MG7expression				Positive rate(%)	Over-expression rate(%)
		-	+	++	+++		
Normal gastric mucosa	26	26	0	0	0	0.0 ^b	0.0 ^b
Intestinal metaplasia	82	34	43	4	1	58.5 ^{bd}	6.1 ^b
Dysplasia	59	30	23	4	2	49.2 ^{bd}	10.2 ^b
Gastric cancer	57	5	23	18	11	91.2 ^d	50.9 ^d

^b $P<0.01$ vs: compared with gastric cancer; ^d $P<0.01$ vs: compared with normal gastric mucosa

Table 2 The expression of MG7 antigen in different gastric diseases

Gastric lesions	n	No. of cases with MG7expression				Positive rate(%)	Over-expression rate(%)
		-	+	++	+++		
Superficial gastritis	67	59	7	0	1	11.9 ^b	1.5 ^b
Atrophic gastritis	71	25	39	7	0	64.8 ^{bd}	9.9 ^b
Gastric cancer	57	5	23	18	11	91.2 ^d	50.9 ^d

^b $P<0.01$ vs: compared with gastric cancer; ^d $P<0.01$ vs: compared with superficial gastritis

The expression of gastric cancer-associated MG7 antigen in different types of intestinal metaplasia

According to different mucin secreted, the intestinal metaplasia of gastric mucosa could be categorized into three types. The positive rate of MG7 antigen expression in type III intestinal metaplasia of gastric mucosa was significantly different as compared with type I and type II intestinal metaplasia ($P<0.05$), but was close to gastric cancer ($P>0.05$). The over-expression rate of MG7 antigen in type I, type II, type III intestinal metaplasia and gastric cancer increased gradually, and there was significant difference between gastric cancer group and other groups respectively ($P<0.05$), see Table 3.

Table 3 The expression of MG7 in different types of intestinal metaplasia and gastric cancer

Types of intestinal metaplasia	n	No. of cases with MG7 expression				Positive rate(%)	Over-expression rate(%)
		-	+	++	+++		
type I and II intestinal metaplasia	53	28	24	1	0	47.2 ^{bb}	1.9 ^b
type III intestinal metaplasia	29	6	19	3	1	79.3 ^{dd}	13.8 ^b
gastric cancer	57	5	23	18	11	91.2 ^{dd}	50.9 ^d

^b $P<0.01$ vs compared with gastric cancer; ^{bb} $P<0.05$ vs compared with gastric cancer; ^a $P<0.01$ vs compared with superficial gastritis; ^{dd} $P<0.05$ vs compared with superficial gastritis

The expression of MG7 antigen in *H. pylori*-associated gastric diseases

On examination, *H. pylori* infection was detected in 291 specimens of different gastric mucosa tissues including 66 superficial gastritis, 20 gastric ulcer, 70 atrophic gastritis, 80 intestinal metaplasia and 55 dysplasia. The MG7 antigen expression was also examined in *H. pylori*-positive and *H. pylori*-negative groups of different gastric diseases. It was found that the positive rates of MG7 antigen expression in *H. pylori*-positive and *H. pylori*-negative cases of superficial gastritis, gastric ulcer, atrophic gastritis, intestinal metaplasia and dysplasia were 20.5 %/0, 25 %/12.5 %, 62.5 %/65.8 %, 52 %/66.7 %, 30.3 %/54.5 %, respectively. The positive rate of MG7 expression in *H. pylori*-positive superficial gastritis (20.5 %) was significantly higher than that in *H. pylori*-negative superficial gastritis ones (0), ($P<0.05$). There was no significant differences between *H. pylori*-negative and *H. pylori*-positive atrophic gastritis, intestinal metaplasia and dysplasia of gastric epithelium in positive rates of MG7 antigen expression, see table 4. In the MG7 antigen expression positive ones, positive-*H. pylori* in superficial gastritis, intestinal metaplasia, atrophic gastritis and dysplasia of gastric epithelium was counted as 8/8, 26/46, 20/45, 10/22 respectively. Among the 8 superficial gastritis with MG7 expression, the rate of *H. pylori* infection was 100 %.

Table 4 The expression of MG7 antigen in *H. pylori*-associated gastric lesions

Gastric lesions	n	<i>H. pylori</i> -positive		<i>H. pylori</i> -negative	
		MG7 expression		MG7 expression	
		No. of cases	rate (%)	No. of cases	rate (%)
superficial gastritis	39	8	20.5	27	0
gastric ulcer	12	3	25	8	12.5
atrophic gastritis	32	20	62.5	38	25
intestinal metaplasia	50	26	52.0	30	20
dysplasia	33	10	30.3	22	12

^a $P<0.05$ vs compared with *H. pylori*-positive cases of the same gastric lesion

The follow-up of cases with *H. pylori*-associated gastric diseases

34 cases were followed up for 2 years, among which 3 cases without *H. pylori* infection and 31 cases with *H. pylori* infection. There were 19 with negative MG7 antigen expression (-); 13 with weakly positive MG7 antigen expression (+); (++) and

(+++ each. One year later, among the 3 without *H. pylori* infection, 1 case was found newly *H. pylori* infected accompanied by increased MG7 expression. Among 31 cases of *H. pylori*-positive diseases, early gastric cancer was detected in 3 with MG7 antigen expression, of which one with weakly positive MG7 antigen expression (+) was atrophic gastritis, one with MG7 antigen expression (++) was also atrophic gastritis but one case with MG7 antigen expression (+++) was superficial gastritis, see Table 5. After surgical operation and drug treatment, the reduced MG7 expression with *H. pylori* eradication was found in a case of superficial gastritis.

Table 5 The follow-up results of 34 cases with *H. pylori*-associated gastric diseases

Change of <i>H. pylori</i> status	No. of cases	MG7 antigen expression			
		mitigated	unchanged	aggravated	malignant change
<i>H. pylori</i> infection unchanged	19	4	13	1	1
<i>H. pylori</i> eradicated	14	4	7	1	2
<i>H. pylori</i> newly infected	1	0	0	1	0

DISCUSSION

Gastric cancer is still a major health problem and the leading cause of cancer mortality despite a worldwide decline in incidence. Early detection and early diagnosis are important in prevention and treatment of gastric cancer. The antigen recognized by gastric monoclonal antibody MG7^[1] is different from other gastrointestinal tumor markers as reported^[11,12]. It has been taken as a promising index in gastric cancer screening because of its specificity^[1-4,13,14]. In this study, we found that the expression of MG7 antigen in different gastric tissue was different. The positive rate of MG7 antigen expression in gastric cancer is 91.2 %. The positive rate of MG7 expression in normal gastric mucosa, metaplasia/dysplasia and gastric cancer increased in ascending order ($P<0.01$). The positive rate of MG7 expression in superficial gastritis, atrophic gastritis and gastric cancer increased in succession ($P<0.01$). The expression rate of MG7 antigen in undifferentiated gastric cancer was higher than that of differentiated gastric cancer ($P>0.05$), cases with positive expression cells are more above 70 % in undifferentiated gastric cancer than that in differentiated gastric cancer ($P<0.05$), showing the presence of somewhat tendency of certain histopathologic type. The dynamic changes in expression of MG7 antigen in normal gastric mucosa, precancerous lesions and gastric cancer implicated that in the gastric precancerous conditions, MG7 antigen increased gradually with the development and progression of gastric cancer and its sensitivity was higher in gastric cancer, and could be used as a marker for screening.

This study showed that among the benign gastric lesions the positive rate of MG7 expression in atrophic gastritis and dysplasia were significantly higher than that in superficial gastritis but significantly lower than that in gastric cancer, implicating there were more gastric cancer-associated antigens in the cell membrane and cytoplasm of atrophic gastritis and dysplasia which was in access to gastric cancer. Intestinal metaplasia is taken as gastric precancerous lesion^[16,17]. It was found that type III (incomplete) intestinal metaplasia had cancerous potential, our study demonstrated the positive rate of MG7 antigen expression in type III intestinal metaplasia of gastric mucosa was significantly different compared with type I and type II intestinal metaplasia ($P<0.05$), and was

analogous, even more closed to gastric cancer ($P<0.05$). Since the dynamic changes in of MG7 antigen expression was closely related with the development and progression of gastric cancer, cases with atrophic gastritis, dysplasia and type III intestinal metaplasia should be closely followed up for the early detection of gastric cancer.

The development of gastric cancer is a multistep process that is multifactorial. Several factors may act in stages of development of cancer^[9]. Epidemiology data show the close relationship between *H. pylori* and gastric cancer^[18,19]. *H. pylori* has been assigned as a class I carcinogen by WHO, and acts as the initiating agent. It virulence factors can damage gastric epithelial cells^[20-22], break the balance between proliferation and apoptosis^[23-33], but it is still unclear whether *H. pylori* plays a role after development of atrophic gastritis and intestinal metaplasia^[34,35].

Our study found that the positive rate of MG7 expression in *H. pylori*-positive superficial gastritis was higher than that in *H. pylori*-negative cases ($P<0.05$). There were 8 cases of positive *H. pylori* superficial gastritis with MG7 antigen expression, which suggested that *H. pylori* infection was directly stated to MG7 antigen expression. But there was no significant difference between *H. pylori*-negative and *H. pylori*-positive atrophic gastritis, intestinal metaplasia and dysplasia in the positive rate of MG7 antigen expression. This might be due to the change of the environment in atrophic gastritis, intestinal metaplasia and dysplasia, which was unsuitable for the growth of *H. pylori*.

By following up of the 34 cases of *H. pylori*-associated disease, we detected early gastric cancer in 3 *H. pylori*-positive cases with MG7 antigen expression, (2 cases of atrophic gastritis, one case of superficial gastritis). After surgical operation and drug treatment with *H. pylori* eradication reduced MG7 expression was found in the case of superficial gastritis. Among the 3 cases without *H. pylori* infections, 1 case had newly emerged *H. pylori* infection accompanied by increased MG7 expression. These implicated the close relationship between the *H. pylori* infection and the expression of MG7 antigen in gastric mucosa, although some *H. pylori*-positive gastric lesions with MG7 antigen expression showed benign morphology, there is still the potential risk of developing into gastric cancer, hence follow up study is essential; more attention should be paid to those with increased MG7 antigen expression.

REFERENCES

- 1 **Fan DM**, Zheng XY, Chen XT, Mu ZX, Hu JL, Qiao TD, Chen BJ, Wang JY, Zhang ZQ, Gao ZQ. Preparation of anti-undifferentiated gastric cancer cell line MKN-46-9 monoclonal antibody and immunohistochemical identification. *Jiefangjun Yixue Zaizhi* 1988; **13**: 12-13
- 2 **Jin N**, Shen MC. Distribution of monoclonal antibodies MG7 and MGd-1 against gastric carcinoma in stomach cancer. *Zhonghua Zhongliu Zazhi* 1990; **12**: 193-195
- 3 **Hu JL**, Mu ZX, Zhou SJ, Fan DM, Chen XT, Zhang XY, Wang YX, Wang WL, Zhu XS. Expression of MG7 antigen in the atypical dysplasia of the gastric mucosa. *Zhonghua Yixue Zazhi* 1988; **68**: 363-365
- 4 **Ren Q**, Zhang XY, Chen XT, Liu J. The immunoelectromicroscopic studies on the distribution of MG7, MG9, MGd1 antigens with monoclonal antibodies against gastric cancers. *Aizheng* 1990; **9**: 100-102
- 5 **Qiao TD**, Zhang XY, Hu JL, Fan DM, Chen BJ, Chen XT, Zhou SJ, Mu ZX. Expression of the tumor-associated antigen (MG7-Ag) in 1000 cases of atypical dysplasia of the gastric mucosa. *Jiefangjun Yixue Zazhi* 1993; **18**: 121-123
- 6 **Kang SP**, Chang QL, He HM, Li SP, Zhang KQ, Kang P, Liu YS. Epidemiologic investigation of upper gastrointestinal diseases in Liulin county Shanxi Province. *Shijie Huaren Xiaohua Zazhi* 1998; **6**(Suppl 7): 210-211
- 7 **Guo CQ**, Wang YP, Liu GY, Ma SW, Ding GY, Li JC. Study on *Helicobacter pylori* infection and -p53, c-erbB-2 gene expression in carcinogenesis of gastric mucosa. *Shijie Huaren Xiaohua Zazhi* 1999; **7**: 313-315
- 8 **Lu SY**, Pan XZ, Peng XW, Shi ZL. Effect of *Hp* infection on gastric epithelial cell kinetics in stomach diseases. *Shijie Huaren Xiaohua Zazhi* 1999; **7**: 760-762
- 9 **Correa P**. Human gastric carcinogenesis: a multistep and multifactorial process-first American cancer society award lecture on cancer epidemiology and prevention. *Cancer Res* 1992; **52**: 6735-6740
- 10 **Filipe MI**, Potet F, Bogomoletz WV, Dawson PA, Fabiani B, Chauveinc P, Fenzy A, Gazzard B, Goldfain D, Zeegen R. Incomplete sulphmucin-secreting intestinal metaplasia for gastric cancer. Preliminary data from a prospective study from three centrals. *Gut* 1985; **26**: 1319-1326
- 11 **Fang DC**, Liu WW. The expression of 8 kinds of tumor-associated antigen in gastric lesions. *Neijing* 1994; **11**: 259-262
- 12 **Zhang JR**, Zhang XY, Chen XT, Fan DM. The purification and analysis of new gastric cancer-associated antigen MG5-Ag, MG7-Ag and MG9-Ag. *Disi Junyi Daxue Xuebao* 1988; **9**: 282
- 13 **Ren J**, Chen Z, Zhou SJ, Zhong XY, Pan BR, Fan DM. Detection of circulating gastric carcinoma-associated MG7 -Ag in human sera using an established single determinant immuno-polymerase chain reaction technique. *Cancer* 2000; **88**: 280-285
- 14 **Chen SZ**, Liu ZZ, Qiao TD, Chen BJ, Hu JL, Zhang XY. The expression of MG7 corresponding antigen in gastrointestinal polyps and its relation with cancer. *Zhonghua Waike Zazhi* 1992; **30**: 716-718
- 15 **Fang DC**, Liu WW. Subtypes of intestinal metaplasia and gastric carcinoma. *Chin Med J* 1991; **104**: 467-471
- 16 **Wu MS**, Shun CT, Lee WC, Chen CJ, Wang HP, Lee WJ, Sheu JC, Lin JT. Gastric cancer risk in relation to *Helicobacter pylori* infection and subtypes of intestinal metaplasia. *Br J Cancer* 1998; **78**: 125-128
- 17 **Filipe MI**, Munoz N, Matko I, Kato I, Pompe-Kirn V, Jutersek A, Teuchmann S, Benz M, Prijon T. Intestinal metaplasia types and the risk of gastric cancer: a cohort study in Slovenia. *Int J Cancer* 1994; **57**: 324-329
- 18 **Chang WK**, Kim HY, Kim DJ, Lee J, Park CK, Yoo JY, Kim HJ, Kim MK, Choi BY, Choi HS, Park KN. Association between *Helicobacter pylori* infection and the risk of gastric cancer in the Korean population: prospective case-controlled study. *J Gastroenterol* 2001; **36**: 816-822
- 19 **Uemura N**, Okamoto S, Yamamoto S, Matsumura N, Yamaguchi S, Yamakido M, Taniyama K, Sasaki N, Schlemper RJ. *Helicobacter pylori* infection and the development of gastric cancer. *N Engl J Med* 2001; **345**: 829-832
- 20 **Kohda K**, Tanaka K, Aiba Y, Yasuda M, Miwa T, Koga Y. Role of apoptosis induced by *Helicobacter pylori* infection in the development of duodenal ulcer. *Gut* 1999; **44**: 456-462
- 21 **Peng H**, Pan GZ, Lu CM. Relationship between gastric *H. pylori* infection and cell apoptosis. *Zhonghua Xiaohua Zazhi* 1999; **19**: 154-155
- 22 **Suganuma M**, Kurusu M, Okabe S, Sueoka N, Yoshida M, Wakatsuki Y, Fujiki H. *Helicobacter pylori* Membrane Protein 1: A New Carcinogenic Factor of *Helicobacter pylori*. *Cancer Research* 2001; **61**: 6356-6359
- 23 **Moss SF**, Sordillo EM, Abdalla AM, Makarov V, Hanzely Z, Perez-Perez GI, Blaser MJ, Holt PR. Increased gastric epithelial cell apoptosis associated with colonization with cagA + *Helicobacter pylori* strains. *Cancer Res* 2001; **61**: 1406-1411
- 24 **Szaleczky E**, Pronai L, Molnar B, Berczi L, Feher J, Tulassay Z. Increased cell proliferation in chronic *Helicobacter pylori* positive gastritis and gastric carcinoma-correlation between immuno-histochemistry and Tv image cytometry. *Anal Cell Pathol* 2000; **20**: 131-139
- 25 **Moss SF**, Calam J, Agarwal B, Wang S, Holt PR. Induction of gastric epithelial apoptosis by *Helicobacter pylori*. *Gut* 1996; **38**: 498-501

- 26 **Nardone G**, Staibano S, Rocco A, Mezza E, D' Armiento FP, Insabato L, Coppola A, Salvatore G, Lucariello A, Figura N, Rosa GD, Budillon G. Effect of *Helicobacter pylori* infection and its eradication on cell proliferation, DNA status, and oncogene expression in patients with chronic gastritis. *Gut* 1999; **44**: 789-799
- 27 **Dong QJ**, Liu WZ, Zheng X, Xiao SD, Shi R, Peng YS. Effect of *Helicobacter pylori* on gastric epithelial apoptosis. *Zhonghua Neike Zazhi* 1997; **36**: 751-753
- 28 **Li ZJ**, Lin QX, Nie YQ, Chen YF, Wang QY. Apoptosis and proliferation in gastric epithelial cells is induced by *Helicobacter pylori* and accompanied by increased expression of p53. *Linchuang Xiahuabing Zazhi* 1999; **11**: 102-104
- 29 **Zhang Z**, Yuan Y, Gao H, Dong M, Wang L, Gong YH. Apoptosis, proliferation and p53 gene expression of *H. pylori* associated gastric epithelial lesions. *World J Gastroenterol* 2001; **7**: 779-782
- 30 **Gao H**, Yuan Y, Wu YQ, Wang L, Dong M, Zhang Z. Effect of the eradication of *Helicobacter pylori* on PCNA, p53 protein and p16 protein expression. *Zhonghua Yufang Yixue Zazhi* 1999; **33**: 14-17
- 31 **Konturek PC**, Konturek SJ, Pierzchalski P, Bielanski W, Duda A, Marlicz K, Starzynska T, Hahn EG. Cancerogenesis in *Helicobacter pylori* infected stomach-role of growth factors, apoptosis and cyclooxygenases. *Med Sci Monit* 2001; **7**: 1092-1107
- 32 **Lu XL**, Qian KD, Tang XQ, Zhu YL, Du Q. Detection of *H. pylori* DNA in gastric epithelial cells by in situ hybridization. *World J Gastroenterol* 2002; **8**: 305-307
- 33 **Yao YL**, Xu B, Song YG, Zhang WD. Overexpression of cyclin E in Mongolian gerbil with *Helicobacter pylori*-induced gastric precancerosis. *World J Gastroenterol* 2002; **8**: 60-63
- 34 **Asaka M**, Kimura T, Kato M, Kudo M, Miki K, Ogoshi K, Kato T, Tatsuta M, Graham DY. Possible role of *Helicobacter pylori* infection in early gastric cancer development. *Cancer* 1994; **73**: 2691-2694
- 35 **Forman D**, Newell DG, Fullerton F, Yarnell JWG, Stacey AR, Wald N, Sitas F. Association between infection with *Helicobacter pylori* and risk of gastric cancer:evidence from a prospective investigation. *BMJ* 1991; **302**: 1302-1305

Edited by Wu XN

• GASTRIC CANCER •

Activation of JNK by TPA promotes apoptosis via PKC pathway in gastric cancer cells

Yan Chen, Qiao Wu, Si-Yang Song, Wen-Jin Su

Yan Chen, Qiao Wu, Si-Yang Song, Wen-Jin Su, Key Laboratory of the Ministry of Education for Cell Biology and Tumor Cell Engineering, The School of Life Sciences, Xiamen University, Xiamen, Fujian Province, 361005, China

Supported by the National Outstanding Youth Science foundation of China, No. 39825502; the National Natural Science Foundation of China, No.39880015, 30170477; the Natural Science Foundation of Fujian Province, No.C0110004

Correspondence to: Dr. Qiao Wu, Key Laboratory of the Ministry of Education for Cell Biology and Tumor Cell Engineering, The School of Life Sciences, Xiamen University, Xiamen, Fujian Province, 361005, China. xgwu@xmu.edu.cn

Telephone: +86-592-2187959 **Fax:** +86-592-2086630

Received 2002-01-28 **Accepted** 2002-04-20

Abstract

AIM: JNK cascade plays an important role in cell proliferation, differentiation and apoptosis. However, the exact function of JNK cascade for apoptosis induction remains largely unknown. In this study, the role of JNK activation stimulated by TPA in the process of apoptosis induction and its signaling transduction pathway in gastric cancer cells were investigated and determined.

METHODS: Expressions of mRNA and protein were detected by Northern blot and Western blot. Transcription activity was measured by transient transfection and CAT assay. Apoptotic cells were displayed through staining the nucleus with DAPI and were observed under fluorescence microscope. The apoptotic index was determined by counting 1000 cells randomly.

RESULTS: JNK protein was stimulated rapidly by TPA, and reached its highest peak within 3 hr, then decreased in a time-dependent manner, but the expression level of JNK protein induced by TPA was always keeping higher than that in untreated cells. Similar pattern was seen in *c-jun* mRNA level induced by TPA. TPA significantly activated the transcriptional activity of activator protein-1 with a TPA-dose-dependent manner. Furthermore, activation of JNK was mediated through PKC pathway. Treatment of cells with PKC specific inhibitor, Wortmannin, led to repression of JNK even in the presence of TPA. More importantly, all these effects were associated with induction of apoptosis in gastric cancer cells. TPA induced apoptosis obviously in gastric cancer cells. The apoptotic cells became smaller and rounded, and their nuclei became condensation and fragmentation with brightly stained chromatin. However, suppression of JNK by PKC specific inhibitor, Wortmannin, resulted in the decrease of apoptosis induced by TPA in a time-dependent manner, apoptotic index dramatically decreased from 32.56 % to 8.71 %.

CONCLUSION: TPA stimulates JNK cascade, including up-regulation of JNK protein expression level and *c-jun* mRNA expression level, and activation of activator protein-1

transcriptional activity. Activation of JNK is mediated through PKC pathway, which has an association with induction of apoptosis by TPA. Thus, activation of JNK via PKC pathway may represent one of important mechanisms for TPA to induce apoptosis in gastric cancer cells.

Chen Y, Wu Q, Song SY, Su WJ. Activation of JNK by TPA promotes apoptosis via PKC pathway in gastric cancer cells. *World J Gastroenterol* 2002; 8(6):1014-1018

INTRODUCTION

Mitogen-activated protein kinase (MAPK) pathway is an important signal transduction pathway that transduces extracellular signals in intracellular responses and has been implicated in a wide array of physiological processes including cell growth, differentiation, and apoptosis^[1-6]. The extracellular signal-regulated kinase (ERK), the *c-jun* N-terminal kinase (JNK) and the p38 MAPK are the members of MAPK family^[7-9]. Among them, JNK is one of the key mediators of stress signal and inflammatory response evoked by a variety of agents such as UV-irradiation, γ -irradiation, heat shock, and inflammatory cytokine^[10,11]. Once activated by specific kinases, JNK mediates the phosphorylation and activation of the transcription factors, such as *c-Jun*, ATF2, and Elk1^[12,13].

JNK can be strongly activated through stress signal that ultimately leads to apoptosis. Accumulating reports have recently been focused on the potential role of JNK in apoptotic signaling. In PC12 cells, JNK plays a critical role in mediating apoptosis caused by nerve growth factor withdrawal^[14]. The JNK pathway is also required for the induction of apoptosis by ceramide, γ - and UV-irradiation, some chemotherapeutic drugs^[15-17]. Inversely, other reports have shown evidences that activation of JNK is not mechanistically implicated in the apoptotic process. activation of JNK does not correlate with apoptosis induced by the detachment of epithelial cells^[18]. Inhibition of JNK activity by the expression of *c-jun* mutant does not prevent TNF-mediated cell death^[19,20].

The present study investigates the effects of 12-O-tetradecanoyl-Phorbol-13-acetate (TPA) on activation of JNK and its role in apoptosis induction in gastric cancer cells. Our results indicated that TPA activated the expressions of JNK protein, which led to induction of *c-jun* mRNA expression, and was associated with activation of activator protein-1 transcriptional activity. Furthermore, activation of JNK cascade was mediated through protein kinase C (PKC) pathway. All these effects had an association with induction of apoptosis by TPA. Thus, activation of JNK via PKC pathway might represent one of mechanisms for TPA to induce apoptosis in gastric cancer cells.

MATERIALS AND METHODS

Cell line and culture condition

Human gastric cancer cell line, MGC80-3 was established by

Cancer Research Center, Xiamen University^[21]. Cells were maintained in RPMI-1640 medium, supplemented with 10 % FCS, 1 m mol/L glutamine, and 100 u/ml penicillin. The concentration of TPA was 100 ng/ml.

Western blot analysis^[22]

Cells treated by TPA were harvested, and suspended in RIPA buffer (10 m mol/L Tris (pH7.4), 150 m mol/L NaCl, 1 % Triton X-100, 1 % Deoxycholic Acid, 0.1 % SDS, 5 m mol/L EDTA (pH8.0), 1 m mol/L PMSF). Protein concentration was determined by using the Bio-Rad protein assay system according to the manufacturer's direction (Bio-Rad Hereules, CA). Total protein (50 µg) was subjected to SDS-PAGE and transferred to nitrocellulose membrane for western blot analysis. The membrane was subsequently blocked with 5 % dry milk in TBS-T and then immunoblotted with the corresponding antibody. Protein was detected by using the ECL kit (Amersham Inc.) according to the manufacturer's direction. Before incubation with antibody, the same membrane was stained by ponceau S. (Sigma) to show the amount of protein used in each well. The intensities of bands indicated by Western blot were quantified by densitometer.

RNA preparation and northern blotting

Extraction of total RNA was performed by the guanidine hydrochloride/ultracentrifugation method. Total RNA (20 µg) was separated on 1 % agarose gel containing formaldehyde, and then transferred to nylon membrane, hybridized with α -³²p-dATP and α -³²p-dCTP labeled *c-jun* probe (Zhong Shang Biotec. CO., China), washed, and autoradiographed as described previously^[23]. The same membrane was probed again with β -actin cDNA to show the amount of RNA used in each well. The intensities of bands indicated by Northern blot were quantified by densitometer.

Transient transfection and CAT assay^[24]

Cells were seeded in a six-well plate and were approximately 70 % confluent at the time of transfection. Cells were transfected by CeLLFECTINtm (Gibco/BRI Life Technologies) by the following procedure: 6 µl CeLLFECTINtm in 1.0 ml standard medium was added to each well containing 1.0 ml of standard medium supplemented with the -73Col-CAT reporter plasmid (100 ng), β -galactosidase expression vector (400 ng, pCH110, pharmacia). CAT activity was determined using ³H-acetyl-CoA as substrate. β -galactosidase activity was measured to normalize transfection efficiency.

Apoptosis analysis^[25]

Cells were treated with TPA, trypsinized, washed with PBS. The harvested cells were fixed in 3.7 % paraformaldehyde on ice, washed with PBS, then stained with 50 µg/mL of 4,6-diamidino-2-phenylindole (DAPI, Sigma) containing 100 µg/mL of DNase-free RNase A to facilitate the examination of nuclei under fluorescence microscope. Apoptotic cells were investigated and counted among 1000 cells randomly. The apoptotic index was a mean of three independent experiments.

RESULTS

Stimulation of JNK expression by TPA

To determine whether TPA activates the JNK expression in gastric cancer cells, MGC80-3 cells were treated with TPA in a time course, and the expression level of JNK protein was detected by western blot analysis. As shown in Figure 1, JNK expressed in MGC80-3 cells, after cells were treated with TPA,

the JNK expression was stimulated markedly. It was noted simultaneously that JNK expression was stimulated rapidly by TPA and reached a highest peak within 3 hr. After 3 hr treatment of TPA, although TPA-stimulated JNK expression decreased in a time course manner, the level of JNK protein was always keeping higher than that in MGC80-3 cells (Figure 1). Thus, the result clearly indicates the activation of JNK by TPA.

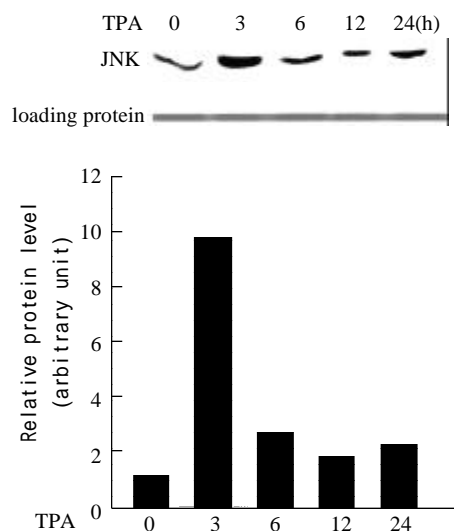


Figure 1 Expression of JNK protein in response to TPA induction. Cells treated with TPA for different time indicated. Expression of JNK protein was detected by Western blot. Amount of protein used in each lane was indicated by staining with ponceau S. The intensity of each band was quantified by densitometer.

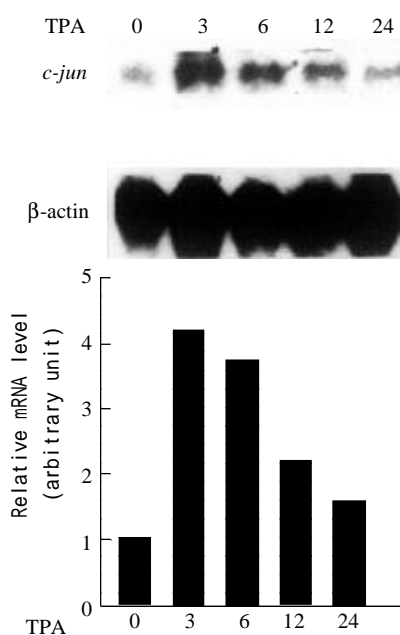


Figure 2 Expression of *c-jun* mRNA in response to TPA induction. Cells treated with TPA for different time indicated. Expression of *c-jun* mRNA was revealed by Northern blot. The same membrane was probed again with β -actin cDNA to show the amount of RNA used in each well. The intensity of each band was quantified by densitometer.

Effect of TPA on *c-jun* mRNA expression

Since activation of the JNK cascade is known to induce *c-jun* expression in several cell systems^[26,27], we examine whether *c-jun* expression in mRNA level is also induced by TPA in gastric cancer cells. Northern blot analysis, using *c-jun* as a probe, revealed that MGC80-3 cells expressed *c-jun* mRNA at lower level, after treatment of TPA, expression level of *c-jun* mRNA was upregulated in a time-dependent manner (Figure 2). More interestingly, the induction patterns between JNK and *c-jun* by TPA were very similar. *c-jun* mRNA also reached its maximal peak induced by TPA within 3 hr, followed by a decrease with extension of TPA treatment in a time-course. Taken together, the data with Figure 1 demonstrate that JNK cascade indeed plays a role in TPA signaling in gastric cancer cells.

Transcriptional activity of activator protein-1 in response to TPA

Activator protein-1 is composed of products of the proto-oncogenes *c-jun* and *c-fos*^[28]. The result mentioned above implies that TPA may affect transcriptional activity of activator protein-1 due to the activation of *c-jun*. To further determine whether TPA activates the transcriptional activity of activator protein-1, we measured transcriptional activity of activator protein-1 in MGC80-3 cells treated with various concentrations of TPA by the methods of transient transfection and CAT assay. When the reporter -73Col-CAT expression vector that contains an AP-1 binding site^[29] was transfected into MGC80-3 cells, a strong induction of reporter transcriptional activity was observed when cells were treated by TPA. This induction of reporter transcriptional activity was TPA-dose-dependent obviously (Figure 3). Thereby, TPA had a capability of activating the transcriptional activity of activator protein-1.

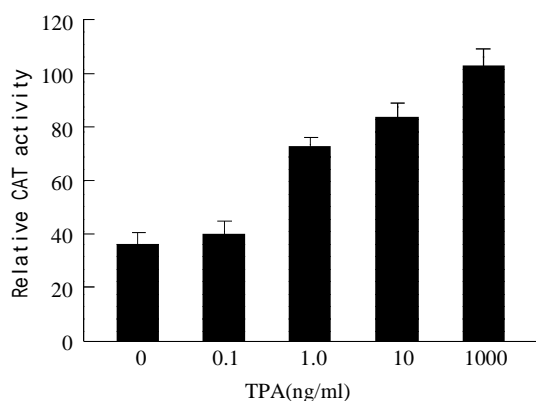


Figure 3 Effect of TPA on transcriptional activity of activator protein-1. Cells were treated with various concentrations of TPA indicated. Various expression vectors were transfected into cells as described in materials and methods. Transcriptional activity was measured by the method of transient transfection and CAT assay. Data shown represent mean of duplicate experiments (\pm SE).

TPA activates JNK cascade through PKC pathway

Since the target of TPA is protein kinase C (PKC)^[30,31], we examine whether stimulation of JNK cascade by TPA is through PKC pathway in gastric cancer cells. When MGC80-3 cells were pretreated with PKC specific inhibitor, Wortmannin^[32,33] for 2 hr, and then treated with TPA for another 3 hr, there was a significant inhibition observed in TPA-stimulated JNK protein expression (Figure 4, lane 4). As controls, JNK expression was clearly detected in MGC80-3 cells (Figure 4, lane 1) and TPA-

stimulated JNK expression was seen obviously in the TPA-treated cells (Figure 4, lane 3), and Wortmannin alone slightly repressed JNK expression (Figure 4, lane 2), respectively. The similar result was observed in MGC80-3 cells treated with another PKC inhibitor, PKC inhibitor peptide^[34] (data not shown). These results suggest that activation of JNK by TPA is mediated through PKC pathway.

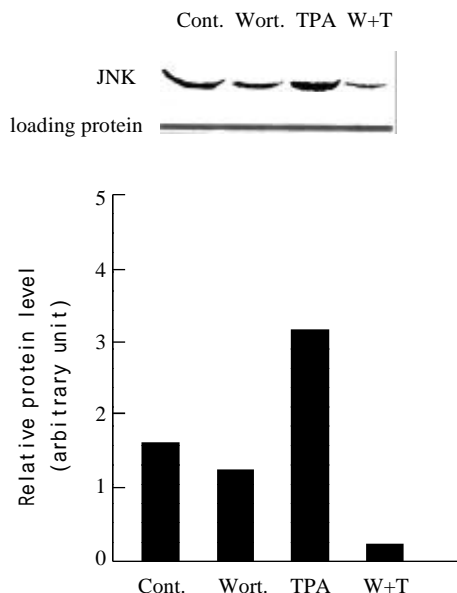


Figure 4 Effect of various agents, including Wortmannin (shown by Wort. or W), a PKC specific inhibitor, on expression of JNK protein. Cells were treated with Wortmannin for 2 hr, following by TPA induction for another 3 hr. Protein was detected by Western blot. Amount of protein used in each lane was indicated by staining with ponceau S. The intensity of each band was quantified by densitometer.

TPA-induced apoptosis is correlated with JNK expression through PKC pathway

To determine the effects of TPA on JNK and PKC functions, and their relationship with induction of apoptosis in gastric cancer cells, we analyzed apoptotic rate in MGC80-3 cells treated with relevant agents. Compared to the untreated MGC80-3 cells, treatment of cells with TPA caused the classical morphological characteristics of apoptosis, cells became smaller and rounded, and their nuclei became condensation and fragmentation with brightly stained chromatin (Figure 5A). However, when treatment of cells with PKC specific inhibitor, Wortmannin, subsequently with TPA, the apoptotic cells were decreased obviously, cells displayed a normal nuclear morphology similar to that of untreated cells (Figure 5A). In addition, the number of apoptotic cells was increased by the induction of TPA in a time-dependent manner. The highest apoptotic rate reached 32.56 % after treating cells with TPA for 48 hr, but only 5.46 % in untreated MGC80-3 cells (Figure 5B).

Since TPA-activated JNK cascade was mediated through PKC pathway in MGC80-3 cells (Figure 4), we analyzed whether this pathway was an association with apoptosis induced by TPA. Compared to TPA that induced apoptosis obviously, pretreated cells with PKC specific inhibitor, Wortmannin, significantly inhibited apoptosis induced by TPA, apoptotic rate was rather low, the highest apoptotic rate was only 8.71 %, although those cells were treated subsequently by TPA for another 48 h (Figure 5B). Accordingly, all these data further suggest that induction

of apoptosis by TPA is through PKC pathway, which may associate with the activation of JNK cascade.

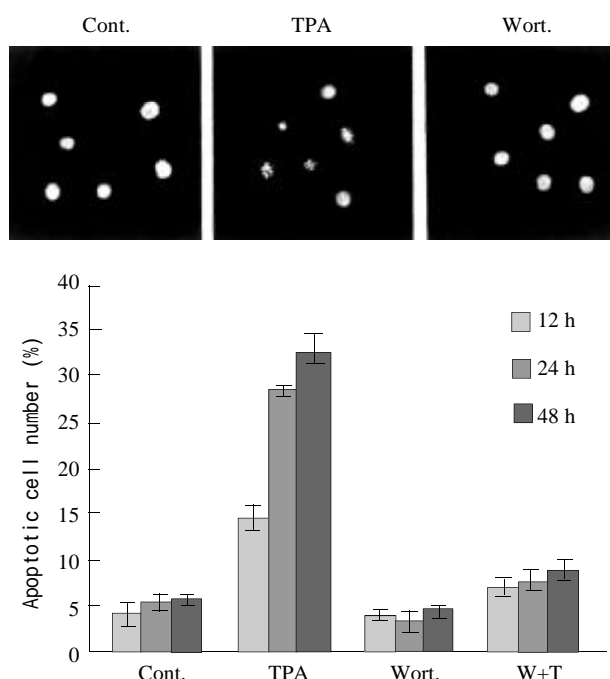


Figure 5 Effect of various agents, including TPA and Wortmannin, on apoptosis induction. Cells were treated with TPA and/or Wortmannin for different time indicated, and then the apoptotic rate was analyzed as described in material and methods. (A) The morphological changes in nucleus in response to different agents. (B) Apoptosis index.

DISCUSSION

The dynamic balance among the extracellular signal-regulated kinase (ERK), the *c-jun* N-terminal kinase (JNK) and the p38 Mitogen-activated protein kinase (p38 MAPK) activities critically determines the cellular fate in response to stimuli of proliferation, differentiation and apoptosis^[35,36]. The role of ERK signaling in the processes of cell differentiation and proliferation has been clearly recognized^[37,38], while requirement of JNK and p38 MAPK activations for apoptosis remains controversy. In some cases, JNK and p38 MAPK activity is strictly required for apoptosis^[39-41]. However, in other circumstances, they are not associated with the induction of apoptosis^[42]. In this study, we demonstrate that TPA stimulates JNK cascade through PKC pathway, which is associated with induction of apoptosis in gastric cancer cells.

JNK cascade plays an important role in cell proliferation, differentiation and apoptosis^[43,44]. In HeLa cells, the activation of JNK was very rapid and sustained for at least 24 hr post-irradiation^[45]. We also found that JNK activity was activated by TPA in gastric cancer cells, MGC80-3. This activation occurred very rapidly within 3 hr of the TPA addition (Figure 1), suggesting that JNK protein may be one of the TPA primary response targets. More importantly, JNK expression level activated by TPA was always keeping higher than that in untreated MGC80-3 cells. This evidence also suggests that the JNK pathway is a major one for mediating TPA effect, which should be functional in gastric cancer cells.

JNK cascade involves many factors. Activated transcription factor 2 (ATF-2) and *c-jun* are activated mainly by JNK^[43]. Transcriptional regulation of *c-jun* expression is mainly mediated by a TPA-response element in its promoter, which binds to *c-jun*/ATF-2 heterodimers^[46]. Increase of *c-jun* mRNA

by various stimuli is highly regulated by phosphorylation of *c-jun* or ATF-2 that bind to the activator protein-1 binding sites present in the *c-jun* promoter^[47]. Our observation showed a possible interrelation between JNK and *c-jun*, which were activated rapidly by TPA and reach its maximal peak within 3 hr, and then decreased with time-dependent manner (Figure 1, 2). Activator protein-1 is a transcriptional factor mainly composed of the *c-jun/c-jun* homodimer or *c-jun/c-fos* heterodimer. The fact that TPA also activated the transcriptional activity of activator protein-1 significantly in MGC80-3 cells (Figure 3) suggests that signaling that causes the transcriptional activity of activator protein-1 is functional in gastric cancer cells. Thus, induction of *c-jun* by TPA in MGC80-3 cells is likely due to the activation of JNK, which led to the activation of activator protein-1 transcriptional activity. This is a JNK cascade stimulated by TPA indeed.

How to function for JNK activation by TPA in gastric cancer cells is still largely unknown. MGC80-3 cells underwent apoptosis in response to TPA, as evidenced by typical morphological changes (Figure 5A, B), which is consistent with our previous observation^[48,49]. Our results demonstrated that apoptosis induction by TPA was associated with JNK activation via PKC pathway. When PKC specific inhibitor, Wortmannin was used to treat MGC80-3 cells prior to TPA treatment, it would prevent TPA further to activate JNK expression (Figure 4). In this case, apoptotic cells were much fewer than that in TPA-treated cells, apoptotic index dramatically decreased from 32.56 % to 8.71 % (Figure 5A, B). Thus, these data not only confirm that TPA-induced apoptosis is associated with JNK activation through PKC pathway, but also indicate that JNK cascade is required for apoptosis induction by TPA, which may be one mechanism for TPA to inhibit the growth of gastric cancer cells.

In summary, the present study demonstrates that the activation of JNK cascade is mediated through a signaling transduction pathway that involves PKC-dependent pathway, which leads to activation of JNK, induction of the *c-jun* expression and activation of activator protein-1 transcriptional activity in response to TPA. The activation of JNK cascade is closely associated with induction of apoptosis by TPA in gastric cancer cells.

ACKNOWLEDGEMENT

We acknowledge the kind gift of reporter plasmid from Dr. Xiao-Kun Zhang (The Burnham Institute, CA, USA).

REFERENCES

- 1 Brunet A, Roux D, Lenormand P, Dowd S, Keyse S, Pouyssegur J. Nuclear translocation of p42/p44 mitogen-activated protein kinase is required for growth factor-induced gene expression and cell cycle entry. *The EMBO J* 1999; **18**: 664-674
- 2 Feng DY, Zheng H, Tan Y, Cheng RX. Effect of phosphorylation of MAPK and Stat3 and expression of *c-fos* and *c-jun* proteins on hepatocarcinogenesis and their clinical significance. *World J Gastroenterol* 2001; **7**: 33-36
- 3 Robinson MJ, Cobb MH. Mitogen-activated protein kinases pathways. *Cur Opin Cell Biol* 1997; **9**: 180-186
- 4 Nishida E, Gotoh Y. The MAP kinase cascade is essential for diverse signal transduction pathways. *Trends Biochem Science* 1993; **18**: 128-131
- 5 Mao H, Yuan AL, Zhao MF, Lai ZS, Zhang YL, Zhou DY. Effect of p38MAPK signal pathway on ultrastructural change of liver cancer cells induced by VEGF. *Shijie Huaren Xiaohua Zazhi* 2000; **8**: 536-538
- 6 Fleischer F, Dabew R, Ke BG, Wagner ACC. Stress kinases inhibition modulates acute experimental pancreatitis. *World J Gastroenterol* 2001; **7**: 259-265

- 7 **Frost JA**, Xu SC, Michele RH, Marcus S, Cobb MH. Actions of Rho family small G proteins and p21-Activated protein kinases on mitogen-activated protein kinase family members. *Mol Cell Biol* 1996; **16**: 3707-3713
- 8 **Vrana JA**, Grant S. Synergistic induction of apoptosis in human Leukemia cells (U937) exposed to bryostatin1 and the proteasome inhibitor lactacystin involves dysregulation of the PKC/MAPK cascade. *Blood* 2001; **97**: 2105-2115
- 9 **Cano E**, Mahadevan LC. Parallel signal processing among mammalian MAPKs. *Trends Biochem Science* 1995; **20**: 117-122
- 10 **Hibi M**, Lin A, Smeal T, Minden A, Karin M. Identification of an oncoprotein and UV-responsive protein kinase that binds and potentiates the *c-jun* activation domain. *Genes Dev* 1993; **7**: 2135-2148
- 11 **Ham J**, Eiler A, Whitefield J, Neame SJ, Shah B. *c-jun* and the transcriptional control of neuronal apoptosis. *Biochem Pharmacol* 2000; **60**: 1015-1021
- 12 **Marais R**, Wynne J, Treisman R. The SRF accessory protein Elk-1 contains a growth factor regulated transcriptional activation domain. *Cell* 1993; **73**: 381-393
- 13 **Gupta S**, Campbell D, Derijard B, Daris RJ. Transcription factor ATF-2 regulation by the JNK signal transduction pathway. *Science* 1995; **267**: 389-393
- 14 **Xia Z**, Dickens M, Ringeaud JJ, Daris RJ, Grenberg ME. Opposing effects of ERK and JNK, p38 MAPKs on apoptosis. *Science* 1995; **270**: 1326-1331
- 15 **Verheij M**, Bose A, Lin XH, Yao B, Jarvis WD, Grant S, Birrer MJ, Szabo E, Zon LI, Kyriakis JM, Haimovitz FA, Fuks Z, Kolesnick RN. Requirement for ceramide-initiated SAPK/JNK signaling in stress-induced apoptosis. *Nature* 1996; **380**: 75-79
- 16 **Chen YR**, Wang X, Templeton D, Davis RJ, Tan TH. The role of *c-jun* N-terminal kinase (JNK) in apoptosis induced by ultraviolet C and gamma radiation. Duration of JNK activation may determine cell death and proliferation. *J Biol Chem* 1996; **271**: 31929-31936
- 17 **Osborn MT**, Chambers TC. Role of the stress-activated/*c-jun* N-terminal protein kinase pathway in the cellular response to adriamycin and other chemotherapeutic drugs. *J Biol Chem* 1996; **271**: 30950-30955
- 18 **Khawaja A**, Downward J. Lack of correlation between activation of Jun N-terminal kinase and induction of apoptosis after detachment of epithelial cells. *J Cell Biol* 1997; **139**: 1017-1023
- 19 **Liu ZG**, Hsu H, Goeddel DV, Karin M. Dissection of TNF receptor 1 effector functions: JNK activation is not linked to apoptosis while NF- κ B activation prevents cells death. *Cell* 1996; **87**: 565-576
- 20 **Lenczowski JM**, Dominguez Z, Eder AM, King LB, Zarchchuk CM, Ashwell JD. Lack of a role for Jun kinase and AP-1 in Fas-induced apoptosis. *Mol Cell Biol* 1997; **17**: 170-181
- 21 **Wang KH**. An *in vitro* cell line (MGc80-3) of a poorly differentiated mucoid adenocarcinoma of human stomach. *Shiyan Shengwu Xiebao* 1983; **16**: 257-267
- 22 **Wu Q**, Chen ZM, Su WJ. Growth inhibition of gastric cells by all-trans retinoic acid through arresting cell cycle progression. *Chin Med J* 2001; **114**: 958-961
- 23 **Wu Q**, Chen ZM, Su WJ. Mechanism of inhibition on activator protein-1 activity by all-trans retinoic acid in gastric cancer cells. *Chin Med J* 2000; **113**: 972-976
- 24 **Wu Q**, Li Y, Liu R, Agadir A, Lee MO, Liu Y, Zhang XK. Modulation of retinoic acid sensitivity in lung cancer cells through dynamic balance of orphan receptors nur77 and COUP-TF and their heterodimerization. *EMBO J* 1997; **16**: 1656-1667
- 25 **Liu Y**, Lee M, Wang HG, Li Y, Hashimoto Y, Klaus M, Reed JC, Zhang XK. Retinoic acid receptor β mediates the growth-inhibitory effect of retinoic acid by promoting apoptosis in human breast cancer cells. *Mol Cell Biol* 1996; **16**: 1138-1149
- 26 **Li Y**, Lin BZ, Agadir A, Liu R, Dawson MI, Reed JC, Fontana JA, Bost F, Hobbs PD, Zheng Y, Chen GQ, Shroot B, Mercola D, Zhang XK. Molecular Determinants of AHPN (CD437)-induced growth arrest and apoptosis in human lung cancer cell lines. *Mol Cell Biol* 1998; **18**: 4719-4731
- 27 **Karin M**. The regulation of AP-1 activity by mitogen-activated protein kinases. *J Biol Chem* 1995; **270**: 16843-16846
- 28 **Tsuneo KQ**, Xu AF, Kenji N, Masanori K. Selective roles of retinoic acid receptor and retinoid X receptor in the suppression of apoptosis by all-trans-retinoic acid. *J Biol Chem* 2001; **276**: 12697-12701
- 29 **Yang-Yen HF**, Zhang XK, Graupner G, Tzukerman M, Sakamoto B, Karin M, Pfahl M. Antagonism between retinoic acid receptors and AP-1: implications for tumor promotion and inflammation. *New Biol* 1991; **3**: 1206-1219
- 30 **Goodnight JA**, Mischak H, Kolch W, Mushinski JF. Immunocytochemical localization of eight protein kinase C isoforms overexpressed in NIH 3T3 fibroblasts. *J Biol Chem* 1995; **270**: 9991-10001
- 31 **Mischak H**, Pierce JH, Goodnight J, Martiny BG, Schaechtle C, Kazanieta MG, Blumberg PM, Pierce JH, Mushinski JF. Overexpression of protein kinase C-delta and epsilon in NIH-3T3 cells induces opposite effects on growth, morphology, anchorage dependence, and tumorigenicity. *J Biol Chem* 1993; **268**: 6090-6096
- 32 **Cross MJ**, Stewart A, Hodgkin MN, Kerr DJ, Wakelam MJ. Wortmannin and its structural analogue demethoxyviridin inhibit stimulated phospholipase A2 activating in Swiss 3T3 cells. *J Biol Chem* 1995; **270**: 25352-25355
- 33 **Bandyopadhyay G**, Standaer ML, Galloway L, Moscat J, Farese RV. Evidence for involvement of protein kinase C (PKC) -zeta and noninvolvement of diacylglycerol-sensitive PKCs in insulin-stimulated glucocorticoid transport in L6 myotubes. *Endocrinology* 1997; **138**: 4721-4731
- 34 **House C**, Kemp BE. Protein kinase C contains a pseudosubstrate prototypic in its regulatory domain. *Science* 1987; **238**: 1726-1728
- 35 **Beatrice C**, Manuel P, Heid SA, Marie M, Violette B, Brnard R, Annie SA. Signal transduction pathways involved in soluble fractalkine-induced monocytic cell adhesion. *Blood* 2001; **97**: 2031-2038
- 36 **Zhou H**, Lin AN, Gu ZN, Chen S, Park H, Chiu R. 12-O-tetradecanoylphorbol-13-acetate (TPA)-induced *c-jun* N-terminal kinase (JNK) phosphatase renders immortalized or transformed epithelial cells refractory to TPA-inducible JNK activity. *J Biol Chem* 2000; **275**: 22868-22874
- 37 **Elisabetta R**, Fabio M, Manuela B, Deriso DS. Constitutive activation of the MAPK pathway mediates v-fes-induced mitogenesis in murine macrophages. *Blood* 2000; **95**: 3959-3963
- 38 **Olson NE**, Kozlowski I, Reidy MA. Proliferation of intimal smooth muscle cells. *J Biol Chem* 2000; **275**: 11270-11277
- 39 **Sluss HK**, Barrett T, Derijard B, Davis RJ. Signal transduction by tumor necrosis factor mediated by JNK protein kinases. *Mol Cell Biol* 1994; **14**: 8376-8384
- 40 **Butterfield L**, Storey B, Maas L, Heasley LE. *c-jun* N-terminal kinase regulation of the apoptotic response of small cell lung cancer cells to ultraviolet radiation. *J Biol Chem* 1997; **272**: 10110-10116
- 41 **Victoria MM**, Yoshihisa I, Javier LCa, Masanori K. Suppression of apoptosis by all-trans retinoic acid. *J Biol Chem* 1999; **274**: 20251-20258
- 42 **Sakata N**, Patel HR, Terada N, Araffo A, Johnson GL, Gelfand W. Selective activation of *c-jun* kinase mitogen-activated protein kinase by CD40 on human B cells. *J Biol Chem* 1995; **270**: 30823-30828
- 43 **Agadir A**, Chen GQ, Frederic B, Li Y, Mercola D, Zhang XK. Differential effect of retinoic acid on growth regulation by phorbol ester in human cancer cell lines. *J Biol Chem* 1999; **274**: 29779-29785
- 44 **Huang CS**, Li JX, Ma WY, Dong ZG. JNK activation is required for JB6 cell transformation induced by tumor necrosis factor- α but not by TPA. *J Biol Chem* 1999; **274**: 29672-29676
- 45 **Assefa Z**, Vantighem A, Declercq W, Vandenabeele P, Vandenheede JR, Merlevede W, Witte Peter, Agostinis P. The activation of the JNK and p38 MAPK signaling pathways protects Hela cells from apoptosis following photodynamic therapy with hypericin. *J Biol Chem* 1999; **274**: 8788-8796
- 46 **Karin M**. Signal transduction from the cell surface to the nucleus through the phosphorylation of transcription factors. *Curr Opin Cell Biol* 1994; **6**: 415-424
- 47 **Van DH**, Wilhelm D, Herr I, Steffwn A, Herrlich P, Angel P. ATF-2 is preferentially activated by stress-activated protein kinases to mediate *c-jun* induction in response to genotoxic agents. *EMBO J* 1995; **14**: 1798-1811
- 48 **Wu Q**, Liu S, Ding L, Ye XF, Su WJ. PKC α translocation from mitochondria to nucleus is closely related to induction of apoptosis in gastric cancer cells. *Zhongguo Kexue* 2002; **32**: 40-45
- 49 **Liu S**, Wu Q, Ye XF, Cai JH, Huang ZW, Su WJ. Induction of apoptosis by TPA and VP-16 is through the translocation of TR3. *World J Gastroenterol* 2002; **8**: 446-450

• GASTRIC CANCER •

Efficacy of intraperitoneal thermochemotherapy and immunotherapy in intraperitoneal recurrence after gastrointestinal cancer resection

Qing-Guo Fu, Fan-Dong Meng, Xiao-Dong Shen, Ren-Xuan Guo

Qing-Guo Fu, Fan-Dong Meng, Xiao-Dong Shen, Ren-Xuan Guo,
The Second General Surgery Department of The First Clinical College,
China Medical University, Shenyang 110001, Liaoning Province, China
Correspondence to: Dr. Qing-Guo Fu, The Second General Surgery
Department of The First Clinical College, China Medical University,
Shenyang 110001, Liaoning Province, China. qingguofu@hotmail.com
Telephone: +86-24-23256666-6237
Received 2002-04-24 **Accepted** 2002-06-03

Abstract

AIM: To investigate the prophylactic and therapeutic efficacy of intraperitoneal IL-2 immunotherapy following intraperitoneal thermochemotherapy in the metastasis and recurrence of gastric and colorectal cancer after operation.

METHODS: Forty-two gastric cancer patients at T₃II-T₄III_B stages and 96 patients with colorectal cancer at B to D stages admitted from January 1996 to October 1998 were randomly divided into control group (group I, 65 cases) receiving intraperitoneal thermochemotherapy, and group II (73 cases) receiving both intraperitoneal thermochemotherapy and intraperitoneal IL-2 immunotherapy. Distilled water at 43-45 °C containing 5-Fu 0.5 g/L and MMC 8 mg/L was perfused into peritoneal cavity before closure at the end of operation for 1 h, and from the third day, IL-2 10 million IU in 500 ml 0.9 % sodium chloride was intraperitoneally administered daily for 10 times. One month after operation, all the patients underwent regular intravenous chemotherapy. Before and after the IL-2 immunotherapy, some Th1 type cytokines in the peripheral blood of the patients in the two groups were detected by ELISA, and the intraperitoneal recurrence and liver metastasis rates and the 3-year survival rate were statistically evaluated after intensive follow-up.

RESULTS: IL-2 intraperitoneal immunotherapy significantly elevated the level of some Th1 type cytokines ($P < 0.01$ compared with that of control group), and the 3-year survival rate of group II was 18.1 % higher and the rates of intraperitoneal recurrence and liver metastasis were 16.9 % and 6.0 % lower than those of group I significantly ($P < 0.05-0.01$).

CONCLUSION: The combination of intraperitoneal IL-2 immunotherapy and thermochemotherapy could promote Th1 immune paradigm and enforce anti-tumor activity of bodies, which plays a positive role in preventing gastric and colorectal cancer from intraperitoneal recurrence and development.

Fu QG, Meng FD, Shen XD, Guo RX. Efficacy of intraperitoneal thermochemotherapy and immunotherapy in intraperitoneal recurrence after gastrointestinal cancer resection. *World J Gastroenterol* 2002; 8(6):1019-1022

INTRODUCTION

Occurring frequently, that the gastrointestinal cancers spread in abdominal cavity and metastasize to the liver after resection, and in a number of cases, the lesion penetrated to serosa and implanted to peritoneum before operation. More and more clinical studies have revealed that postoperative intraperitoneal thermochemotherapy was obviously efficient in reducing the intraperitoneal recurrence and liver metastasis incidence^[1-7]. Intraperitoneal thermochemotherapy can increase the sensitivity of tumor cells to chemotherapy drugs^[8], and simultaneously enhance the antigenicity of tumor cells^[9] which would be conducive to immunotherapy, therefore, based on this hypothesis, we conducted a clinical study on the efficacy of intraperitoneal thermochemotherapy and intraperitoneal immunotherapy involved in 42 cases of gastric cancer and 96 cases of colorectal cancer, and reported below.

MATERIALS AND METHODS

From January 1996 to October 1998, 42 cases of gastric cancer at T₃II-T₄III_B stages and 96 cases of colorectal cancer at B-D stages were randomly divided into 2 groups (control group, group I and treatment group, group II, Table 1), among whom 87 cases were males, and 51 cases females, with an age from 21 to 73 years, averaging 64.4±7.1 years.

Method

Therapeutic method Radical operation was performed on 35 gastric cancer patients and the B-C₂ stage colorectal cancer patients, and palliative operation on 4 gastric cancer and colorectal patients of D-stage. The localized mesenteric and peritoneal infiltration lesions were removed as clear as possible or electrically burned if the lesions were at feasible locus. Before closure under general anesthesia, 4000 ml distilled water at 43-45 °C containing 5-Fu 0.5 g/l and MMC 8 mg/l was perfused in 4 equal volumes into peritoneal cavity, 1000 ml per quarter for an hour. Ice bags were put at groins, axilla and lateral chest and with ice cap on the head. Patients with heart, kidney, lung diseases or diabetes were not accepted in the study. Blood pressure, pulse, ECG and saturation of oxygen in blood were closely monitored during the treatment. On the 3rd day after operation, Group II was treated with IL-2, 1 million u dissolved in 0.9 % sodium chloride 500 ml, through trocars fastened in the abdominal wall. Patients were directed to change body positions to help defuse the drug. The puncture spots were adjusted to the tumor sites, and the therapy was carried out once a day and 10 times in all.

Both groups were administered intravenous chemical therapy from the 1st month after operation, which lasted one year. Routine of blood and urine, function of liver and kidney, CT, and B-ultrasound were performed regularly.

Evaluation of patients' immune function Both before and after intraperitoneal thermochemotherapy and immunotherapy,

Table 1 The clinicopathological stages and surgical procedures in each group

Groups	n	Male	Female	Age(yrs)	Stages(n)	Radical	Non-radical
Group I	65	39	26	62.5±6.6	-	57	8
Gastric cancer	19	12	7	61.7±5.5	T ₃ II (9)T ₄ III _A (7)T ₄ III _B (3)	16	3
Colorectal cancer	46	27	19	64.4±3.9	B(20)C1(12)C2(9)D(5)	41	5
Group II	73	48	25	65.4±8.7	-	62	11
Gastric cancer	23	16	7	67.1±7.6	T ₃ II (11)T ₄ III _A (8)T ₄ III _B (4)	19	4
Colorectal cancer	50	32	18	63.3±5.2	B(22)C1(13)C2(8)D(7)	43	7

Control group: (1) Gastric cancer: papilloadenocarcinoma, 7 cases; tuboadenocarcinoma, 6 cases; lowly-differentiated adenocarcinoma, 2 cases; mucoadenocarcinoma, 1 case; signet ring cell carcinoma, 2 cases; and undifferentiated carcinoma 1 case; (2) Colorectal cancer: highly and intermediately differentiated adenocarcinoma, 29 cases; mucoadenocarcinoma, 12 cases; and undifferentiated carcinoma 5 cases. Therapy group: (1) Gastric cancer: papilloadenocarcinoma, 9 cases; tuboadenocarcinoma, 6 cases; lowly-differentiated adenocarcinoma, 2 cases; mucoadenocarcinoma, 2 cases; signet ring cell carcinoma, 2 cases; and undifferentiated carcinoma 2 cases; Colorectal cancer: highly and intermediately differentiated adenocarcinoma, 33 cases; mucoadenocarcinoma, 12 cases; and undifferentiated carcinoma 5 cases.

Table 2 The levels of some Th1 cytokines in peripheral blood of patients before and after immunotherapy (pg/ml)

Groups	<i>n</i>	The level of the cytokines						<i>P</i>
		IL-2		TNF-β		IFN-γ		
		Pre-therapy	Post-therapy	Pre-therapy	Post-therapy	Pre-therapy	Post- therapy	
group I	(65)	10.2±3.7	9.5±3.8	25.3±7.4	24.9±4.5	29.5±6.9	27.7±7.3	>0.25
group II	(73)	13.5±6.7	38.4±6.2	18.0±4.6	55.4±10.1	27.4±7.1	77.1±18.2	<0.01

serum levels of several Th1 type cytokines (IL-2, TNF-β, IFN-γ) were detected with ELISA techniques in both groups to contrast results and evaluate the anti-tumor immune activity of the patients in two groups. The ELISA Kit was bought from Bangding Biotechnic Company in Beijing, and the results were recognized with a mean value of A450nm.

Method of follow-up The follow-up was made by a group of experienced doctors. Patients were checked regularly at a 3-6 month interval after operation in the outpatient department. Checking items included general physical examination such as supraclavicular lymph nodes and anus digital palpation, blood and urine routine, liver and kidney function, serum CEA, B-ultrasound of liver and spleen, also CT when necessary. We managed to keep in corresponding and phonic touch with these patients. Patient's situation and tumor status were determined according to the clinical manifestation and associated examinations. The death time and cause were defined and recorded carefully. Those who lost to follow-up were also recognized as dead.

Statistical methods

The result of cytokine detection was analyzed with Student *t* test, the recurrent rate in abdominal cavity and metastasis rate in liver with χ^2 test, and 3-year-survival rate with survival curve.

RESULTS

The changes of some Th1 cytokine levels in the peripheral blood of the patients after intraperitoneal immunotherapy with IL-2

The levels of IL-2, TNF-β, INF-γ in the peripheral blood of the patients who received IL-2 intraperitoneal therapy were

obviously increased as compared with the control group. The difference was significant ($P < 0.01$). And there were no significant changes in the levels of the same cytokines in control group ($P > 0.25$, Table 2).

The effect of IL-2 intra-peritoneal immunotherapy

The 3-year follow-up ratio of the cases was 91.3 %, the result is shown in Table 3.

Table 3 The therapeutic efficiency of intraperitoneal thermochemotherapy combined with IL-2 immunotherapy

Groups	n	Intraperitoneal recurrent rate (%)	Hepatic metastasis rate(%)	3-year survival rate(%)
Group I	65	29.2(19/65)	16.9(11/65)	47.7(31/65)
Group II	73	12.3(9/73) ^b	10.9(8/73) ^a	65.8(48/73) ^a

^a $P < 0.05$ vs control group, ^b $P < 0.01$ vs control group

Based on the comparison of intra-peritoneal recurrence rate, hepatic metastasis rate and 3-year survival rate, we could draw a conclusion that intraperitoneal thermochemotherapy combined with immunotherapy was effective in decreasing intraperitoneal recurrence and hepatic metastasis rate and raising 3-year survival rate ($P < 0.01-0.05$ contrasted with control group). In our study, 4 cases were lost in group I and 8 in group II, and they were calculated as dead cases. Intraperitoneal spread, metastasis in liver and lung, uncontrollable hydrothorax and hydroperitoneum and dyscrasia at the end of advanced-stage cancer were accounted

for the death. In group I, only one patient with gastric carcinoma who received palliative operation survived for 2 years, while there were 2 cases in group II. And 4 (4/5) colorectal cancer cases of D-stage and 3 (3/7) in group II died from intraperitoneal spread. Although the number of cases was not big enough for statistical study, the therapeutic effect was indicated in some degree.

DISCUSSION

Nowadays in most of formal hospitals, there are no technological difficulties with the radical operation of gastrointestinal cancer. Thus, how to raise the survival rate and the life quality of these patients depends much on the compound therapy following operation. Although routine chemotherapy (intravenously or orally) could help inhibit the liver metastasis, intraperitoneal spread and recurrence, its effect is still not satisfactory. In recent ten years, a large number of clinical studies have proved that postoperative intra-abdominal thermochemotherapy has exerted obvious therapeutic effect in inhibiting the recurrence of gastrointestinal cancer in abdominal cavity and liver metastasis^[10-15], which is routinely applied in many hospitals. Intra-abdominal chemotherapy can be given at any time, but it can cause peritonitis, abdominal pain, and sometimes overlapped at short interval with intravenous or oral chemotherapy. Meanwhile, being a single therapy, it would bring about severe adverse effect following a long-term administration. On the other hand, intraperitoneal thermochemotherapy should be administered under general anesthesia and could not be applied repeatedly. Although its therapeutic effect is among the best, the low frequency of administration is its unavoidable defect. Based on this idea, more research should be made to seek a compound strategy with complementary therapeutic effect^[16-24].

The intraperitoneal thermochemotherapy can increase the sensitivity of tumor cells to chemotherapy drugs and kill even more tumor cells than routine administration, and can efficiently lower the incidence of intraperitoneal recurrence and liver metastasis^[24-27]. More importantly, thermal effect can increase the antigenicity of tumor cells and facilitate the expression of tumor antigens (such as heat shock proteins), which is conducive to immune effector cells to recognize and kill the tumor cells^[28-30].

IL-2 is an effective anti-tumor cytokine, and it can induce and promote the activation and proliferation of T lymphocytes, increase the tumor-killing effect of effector cells, such as TIL, CTL, LAK and NK, and improve the general anti-tumor immune function of the body^[31-37]. There are many lymph nodes and abundant lymphatic network in the abdominal cavity, and lots of lymph organs in the intestinal wall. When a high concentration of IL-2 is administered into the abdominal cavity and act on those lymphatic tissues and organs, the proliferation and killing capacity of lymphocytes is efficaciously promoted, under the background that the antigenicity of residual cancer cells has already increased due to the thermal effect, the anti-tumor effect of IL-2 would be maximized. The lymphocytes activated by IL-2 spreading with blood circulation will kill the metastatic foci in liver or other sites. In this study, the level of major Th1 cytokines in peripheral blood was significantly increased after immunotherapy, demonstrating that IL-2 could activate anti-tumor immune effect cells, induce the production of Th1 cytokines, enhance the anti-tumor immune function of the body, and kill tumor cells. In the immunotherapy group, the intra-abdominal recurrence and the incidence of liver metastasis were decreased by 16.9 % and 6.0 %, respectively as compared with the control group, which support the point that IL-2 immunotherapy combined with intraperitoneal

thermochemotherapy is effective and applicable, and that it is appropriate to perform immunotherapy after thermochemotherapy, which may be a more scientific and reasonable strategy than other combinations and may contribute to the immunotherapeutic function and the complementation of the two therapies. Because IL-2 could promote the proliferation of lymphocytes and the latter might be inhibited by chemotherapy drugs, we did not combine IL-2 with chemotherapy drugs. This is worth of further research. During immunotherapy, most patients could tolerate and no obvious side-effect was observed. The common side-effect was the increase of body temperature (4 cases reached 38.8 °C and others in the range of 38.2-38.6 °C) and physical cooling could take effect. Fever is another common side-effect of IL-2, which may disappear after the withdrawal of IL-2.

In this study, we found that, in the patients with peritoneal infiltration, the removal of the tumor as complete as possible during operation combining with thermochemotherapy and immunotherapy could produce satisfactory therapeutic effect. Four patients of this type survived for more than 3 years. So the intra-abdominal therapy for the gastrointestinal cancers should be paid enough attention, even to the intraperitoneal metastasis and infiltration in certain degree, resection or partial resection should be performed as completely as possible other than giving up. Immediate postoperative thermochemotherapy and immunotherapy could also improve the prognosis of some patients.

In conclusion, intra-abdominal metastasis of gastrointestinal cancer is an important factor in affecting the prognosis of the patients. In our study, the intraperitoneal thermochemotherapy and intraperitoneal immunotherapy have displayed a promising therapeutic and prophylactic effect, and research is need on this compound therapy upon our observation.

REFERENCES

- 1 **Beaujard AC**, Glehen O, Caillot JL, Francois Y, Bienvenu J, Panteix G, Garbit F, Grandclement E, Vignal J, Gilly FN. Intraperitoneal chemohyperthermia with mitomycin C for digestive tract cancer patients with peritoneal carcinomatosis. *Cancer* 2000; **88**:2512-2519
- 2 **Kim JY**, Bae HS. A controlled clinical study of serosa-invasive gastric carcinoma patients who underwent surgery plus intraperitoneal hyperthermo-chemo-perfusion (IHCP). *Gastric Cancer* 2001; **4**: 27-33
- 3 **Witkamp AJ**, de Bree E, Kaag MM, Boot H, Beijnen JH, van Slooten GW, van Coevorden F, Zoetmulder FA. Extensive cytoreductive surgery followed by intra-operative hyperthermic intraperitoneal chemotherapy with mitomycin-C in patients with peritoneal carcinomatosis of colorectal origin. *Eur J Cancer* 2001; **37**: 979-984
- 4 **Sugarbaker PH**, Yonemura Y. Palliation with a glimmer of hope: management of resectable gastric cancer with peritoneal carcinomatosis. *Hepatogastroenterology* 2001; **48**: 1238-1247
- 5 **Elias DM**, Ouellet JF. Intraperitoneal chemohyperthermia: rationale, technique, indications, and results. *Surg Oncol Clin N Am* 2001; **10**: 915-933
- 6 **Chen J**, Wang S, Xu H. Curative effect of radical gastrectomy combined with peritoneal lavage with thermal hypoosmotic solution in treatment of gastric cancer. *Zhonghua Yixue Zazhi* 2001; **81**: 730-732
- 7 **Takahashi I**, Emi Y, Hasuda S, Kakeji Y, Maehara Y, Sugimachi K. Clinical application of hyperthermia combined with anticancer drugs for the treatment of solid tumors. *Surgery* 2002; **131**: S78-84
- 8 **Chen ZX**, Chen JP, Chen Z, Peng DS, Zhen JX, Tan JS. Treatment of cancerous ascites and radical gastrectomy with intraperitoneal hyperthermic double distilled water and cis-diaminodichloro-platinum perfusion. *China Natl J New Gastroenterol* 1997; **3**: 246-248

- 9 **Rau B**, Gaestel M, Wust P, Stahl J, Mansmann U, Schlag PM, Benndorf R. Preoperative treatment of rectal cancer with radiation, chemotherapy and hyperthermia: analysis of treatment efficacy and heat-shock response. *Radiat Res* 1999; **151**: 479-488
- 10 **Feng GG**, Zhou XG, Yu BM. Prevention of metastasis to liver by using 5-FU intraperitoneal chemotherapy in nude mice inoculated with human colonic cancer cells. *China Natl J New Gastroenterol* 1996; **2**: 134-135
- 11 **Cavaliere F**, Perri P, Di Filippo F, Giannarelli D, Botti C, Cosimelli M, Tedesco M, Principi F, Laurenzi L, Cavaliere R. Treatment of peritoneal carcinomatosis with intent to cure. *J Surg Oncol* 2000; **74**: 41-44
- 12 **Ceelen WP**, Hesse U, de Hemptinne B, Pattyn P. Hyperthermic intraperitoneal chemoperfusion in the treatment of locally advanced intra-abdominal cancer. *Br J Surg* 2000; **87**: 1006-1015
- 13 **Fujimura T**, Yonemura Y, Nakagawara H, Kitagawa H, Fushida S, Nishimura G, Miyazaki I, Shibata K. Subtotal peritonectomy with chemohyperthermic peritoneal perfusion for peritonitis carcinomatosa in gastrointestinal cancer. *Oncol Rep* 2000; **7**: 809-814
- 14 **Sugarbaker PH**, Yonemura Y. Clinical pathway for the management of resectable gastric cancer with peritoneal seeding: best palliation with a ray of hope for cure. *Oncology* 2000; **58**: 96-107
- 15 **Piso P**, Bektas H, Werner U, Schlitt HJ, Kubicka S, Bornscheuer A, Manns M, Klempnauer J. Improved prognosis following peritonectomy procedures and hyperthermic intraperitoneal chemotherapy for peritoneal carcinomatosis from appendiceal carcinoma. *Eur J Surg Oncol* 2001; **27**: 286-290
- 16 **Sobat H**, Juretic A, Samija M. Combined modality therapy of rectal cancers. *Ann Oncol* 1999; **10**: 99-103
- 17 **Cavaliere F**, Di Filippo F, Cosimelli M, Aloe L, Arcuri E, Anza M, Callopoli A, Di Lauro L, Morace E, Botti C, Natoli S, Tedesco M, Giunta S, Cavaliere R. The integrated treatment of peritoneal carcinomatosis. A preliminary experience. *J Exp Clin Cancer Res* 1999; **18**: 151-158
- 18 **Yonemura Y**, Fujimura T, Fushida S, Fujita H, Bando E, Nishimura G, Miwa K, Endou Y, Tanaka M, Sasaki T. A new surgical approach (peritonectomy) for the treatment of peritoneal dissemination. *Hepatogastroenterology* 1999; **46**: 601-609
- 19 **Samel S**, Singal A, Becker H, Post S. Problems with intraoperative hyperthermic peritoneal chemotherapy for advanced gastric cancer. *Eur J Surg Oncol* 2000; **26**: 222-226
- 20 **Rau B**, Wust P, Tilly W, Gellermann J, Harder C, Riess H, Budach V, Felix R, Schlag PM. Preoperative radiochemotherapy in locally advanced or recurrent rectal cancer: regional radiofrequency hyperthermia correlates with clinical parameters. *Int J Radiat Oncol Biol Phys* 2000; **48**: 381-391
- 21 **Shido A**, Ohmura S, Yamamoto K, Kobayashi T, Fujimura T, Yonemura Y. Does hyperthermia induce peritoneal damage in continuous hyperthermic peritoneal perfusion? *World J Surg* 2000; **24**: 507-511
- 22 **Abe T**, Sakaguchi Y, Ohno S, Ikeda Y, Kitamura K, Maehara Y, Sugimachi K. Apoptosis and p53 overexpression in human rectal cancer; relationship with response to hyperthermo-chemo-radiotherapy. *Anticancer Res* 2001; **21**: 2115-2120
- 23 **Kunisaki C**, Shimada H, Nomura M, Akiyama H, Takahashi M, Matsuda G. Lack of efficacy of prophylactic continuous hyperthermic peritoneal perfusion on subsequent peritoneal recurrence and survival in patients with advanced gastric cancer. *Surgery* 2002; **131**: 521-528
- 24 **Zhang GQ**, Qing SH, Zhou ZD, Qi DL, Hou BH. Animal experiment study of toxin of regional and system of MMC intraperitoneal hyperthermotherapy perfusion. *Shijie Huaren Xiaohua Zazhi* 2000; **8**: 592-593
- 25 **Sayag-Beaujard AC**, Francois Y, Glehen O, Sadeghi-Looyeh B, Bienvenu J, Panteix G, Garbit F, Grandclement E, Vignal J, Gilly FN. Intraperitoneal chemo-hyperthermia with mitomycin C for gastric cancer patients with peritoneal carcinomatosis. *Anticancer Res* 1999; **19**: 1375-1382
- 26 **Hou BH**, Qing SH, Dong FY, Qi DL, Zhang GQ, Zhao F, Yao XQ, Peng M. Effects of continuous hyperemia peritoneal perfusion chemotherapy on peritoneal implantation of human colonic cancer cells in nude mice. *Shijie Huaren Xiaohua Zazhi* 2000; **8**: 650-653
- 27 **Luo F**, Sun JL, Ren DM, Cai D, Shen M. Effect of hyperthermia on telomerase activity and genes expression in human gastric cancer cell line. *Shijie Huaren Xiaohua Zazhi* 2001; **9**: 1261-1264
- 28 **Okamoto M**, Tazawa K, Kawagoshi T, Maeda M, Honda T, Sakamoto T, Tsukada K. The combined effect against colon-26 cells of heat treatment and immunization with heat treated colon-26 tumour cell extract. *Int J Hyperthermia* 2000; **16**: 263-273
- 29 **Sinha P**, Poland J, Schnolzer M, Celis JE, Lage H. Characterization of the differential protein expression associated with thermoresistance in human gastric carcinoma cell lines. *Electrophoresis* 2001; **22**: 2990-3000
- 30 **Wang XY**, Kazim L, Repasky EA, Subjeck JR. Characterization of heat shock protein 110 and glucose-regulated protein 170 as cancer vaccines and the effect of fever-range hyperthermia on vaccine activity. *J Immunol* 2001; **166**: 490-497
- 31 **Han DM**, Zhu XN, Huang ZG, Wang JJ, Cheng J, Fan EZ, Pian YS, Li Y, Zhang W. The observation on treatment effects of local adoptive immunotherapy in 33 cases with head and neck cancer. *Zhonghua Zhongliu Zazhi* 1997; **19**: 454-456
- 32 **Gravis G**, Viens P, Vey N, Blaise D, Stoppa AM, Olive D, Maraninchi D. Pilot study of immunotherapy with interleukin-2 after autologous stem cell transplantation in advanced breast cancers. *Anticancer Res* 2000; **20**: 3987-3991
- 33 **Rosenberg SA**. Progress in human tumour immunology and immunotherapy. *Nature* 2001; **411**: 380-384
- 34 **Buzio C**, Andrulli S, Santi R, Pavone L, Passalacqua R, Potenzoni D, Ferrozzi F, Giacosa R, Vaglio A. Long-term immunotherapy with low-dose interleukin-2 and interferon-alpha in the treatment of patients with advanced renal cell carcinoma. *Cancer* 2001; **92**: 2286-2296
- 35 **Mantovani G**, Maccio A, Madeddu C, Massa E, Mudu MC, Mulas C, Gramignano G, Massidda S, Murgia V, Lusso MR, Mura L. Immunotherapy (recombinant interleukin 2), hormone therapy (medroxyprogesterone acetate) and antioxidant agents as combined maintenance treatment of responders to previous chemotherapy. *Int J Oncol* 2001; **18**: 383-391
- 36 **Rosenberg SA**. Progress in the development of immunotherapy for the treatment of patients with cancer. *J Intern Med* 2001; **250**: 462-475
- 37 **Atkins MB**. Interleukin-2: clinical applications. *Semin Oncol* 2002; **29**: 12-17

Edited by Ma JY

• GASTRIC CANCER •

Intravenous chemotherapy for resected gastric cancer: meta-analysis of randomized controlled trials

Jian-Kun Hu, Zhi-Xin Chen, Zong-Guang Zhou, Bo Zhang, Jing Tian, Jia-Ping Chen, Li Wang, Chao-Hua Wang, Hong-Yan Chen, You-Ping Li

Jian-Kun Hu, Zhi-Xin Chen, Zong-Guang Zhou, Bo Zhang, Jing Tian, Jia-Ping Chen, Chao-Hua Wang, Hong-Yan Chen, General Surgery Department, West China Hospital of Sichuan University, Chengdu 610041, Sichuan Province, China

Li Wang, You-Ping Li, Chinese Evidence-Based Medicine/Cochrane Center, Chengdu 610041, Sichuan Province, China

Supported by the Scientific Foundation of Chinese Cochrane Center (EBM200114) and the key project of national outstanding young foundation of China (No39925032).

Correspondence to: Drs. Jian-Kun Hu and Zong-Guang Zhou, General Surgery Department, West China Hospital of Sichuan University, Chengdu 610041, Sichuan Province, China. fjkclm1111@hotmail.com

Telephone: +86-28-85422479

Received 2002-03-13 **Accepted** 2002-04-20

Abstract

AIM: To assess the safety and efficacy of different intravenous chemotherapeutic regimens in patients with gastric carcinomas who had undergone gastrectomy.

METHODS: A meta-analysis of all the relevant randomized controlled trials (RCTs) was performed. Language was restricted to Chinese and English. RCTs were identified from Medline and Embase (1980-2001/4), and Chinese Bio-medicine Database (1990-2001/1). Literature references were checked at the same time. We included randomized and quasi-randomized trials comparing the efficacy of intravenous chemotherapy after gastrectomy with that of surgery alone in patients with confirmed gastric carcinomas who had undergone gastrectomy. Selection criteria were: randomized or quasi-randomized trials with following-up results; Trials could be double-blind, single-blind or not blind; Chemotherapy groups were given intravenous chemotherapy after gastrectomy without neo-adjuvant chemotherapy, intraperitoneal hyperthermic perfusion, radiotherapy or chemoimmunotherapy; Controlled group included those receiving gastrectomy alone. The following data were extracted: the number of survival and death by the end of the follow-up; the different agents and doses of the intravenous chemotherapy; the baseline of the chemotherapy group and the controlled arm; the serious adverse events; the statistical consideration; cost-effectiveness analysis. The statistical analysis was performed by RevMan4.1 software which was provided by the Cochrane Collaboration. A *P* value of <0.05 was considered statistically significant. Meta-analysis was done with random effects model. Heterogeneity was checked by chi-square test. Sensitivity analysis was performed by excluding the trials in which Jadad-scale was only 1 score. The result was expressed with odds ratio (OR) for the categorical variable.

RESULTS: Fourteen trials involving 4543 patients were included. Meta-analysis was done with random effects model.

Heterogeneity and sensitivity analysis were performed also. The effect of intravenous chemotherapy after gastrectomy was better than surgery alone (odds ratio 0.56, 95 % CI 0.40-0.79). There was a significant difference between the two groups by u-test (*P*=0.0008). Sensitivity analysis revealed the same difference (odds ratio 0.81, 95 % CI 0.70-0.94). Of fourteen trials, only three studies were of high quality according to the Jadad-scale (with three score). There was one meta-analysis trial and the others, about ten trials, were of low quality. There was no trial which mentioned sample-size calculation, allocation concealment, intention-to-treat analysis. Most of the trials didn't describe the blind-procedure. There were five trials which detailed the side-effects according to the toxicity grade by WHO standard. The side-effects halting treatment were haematologic and biochemical toxicity, debilitating nausea and vomiting. There were two patients died of chemotherapy toxicity.

CONCLUSION: Based on the review, intravenous chemotherapy after gastrectomy may have positive treatment effect on gastric cancer. However, the evidence is not strong because of the general low methodologic quality of the RCTs. Therefore, we can't make the conclusion that intravenous chemotherapy after gastrectomy may have better treatment effect on gastric cancer than that of surgery alone. Rigorously designed, randomised, double-blind, placebo-controlled trials are required.

Hu JK, Chen ZX, Zhou ZG, Zhang B, Tian J, Chen JP, Wang L, Wang CH, Chen HY, Li YP. Intravenous chemotherapy for resected gastric cancer: meta-analysis of randomized controlled trials. *World J Gastroenterol* 2002; 8(6):1023-1028

INTRODUCTION

Gastric cancer is one of the most common cancers worldwide. The outcome of patients with gastric carcinoma has recently been significantly improved with advances in experimental researches, early diagnosis and surgical techniques^[1-44]. Although chemotherapy and radiation therapy have been tried as either an adjuvant or palliative treatment, their values are limited by toxicity or the lack of efficacy^[45]. While surgery remains the mainstay of potentially curative treatment, survival rates for patients able to undergo complete resection are poor^[46]. The five year survival rate for resected gastric cancer is about 30-60 % which has been disappointing. A number of studies have investigated whether intravenous chemotherapy after a resection improves the survival rate or not, but the results are different and disputed. Hermans *et al*^[47] reviewed the randomized controlled trials by meta-analysis, the results indicated that postoperative chemotherapy in general offered no additional survival benefit for patients with curatively resected gastric cancer. Janunger *et al*^[48] performed a systematic overview of chemotherapy effects in gastric cancer by the Swedish Council

of Technology Assessment in Health Care(SBU). A meta-analysis of 21 randomised adjuvant studies revealed a statistically significant survival benefit (OR=0.84, 95 % CI 0.74-0.96).

The aim of meta-analysis is to summarize the results of randomized trials performed to evaluate the effect of intravenous chemotherapy for gastric cancer^[47]. The analysis is restricted to trials published since 1980. Surgical resection without any adjuvant therapy is considered standard treatment. Only intravenous chemotherapy trials with gastrectomy control arm were taken into consideration in this meta-analysis.

MATERIALS AND METHODS

Materials

Randomized or quasi-randomized trials comparing the efficacy of intravenous chemotherapy after gastrectomy with that of surgery alone in patients with confirmed gastric carcinomas who had received gastrectomy were included in this meta-analysis. Language was restricted to Chinese and English.

Selection criteria were: randomized or quasi-randomized trials with following-up results; Trials could be double-blind, single-blind or not blind; Chemotherapy groups were given intravenous chemotherapy after gastrectomy without neo-adjuvant chemotherapy, intraperitoneal hyperthermic perfusion, radiotherapy or chemoimmunotherapy; Controlled group included those receiving gastrectomy alone.

Exclusion criteria were prior malignancy; neo-adjuvant chemotherapy, intraperitoneal hyperthermic perfusion, radiotherapy or chemoimmunotherapy; patients who didn't receive gastrectomy; the controlled studies also included those without gastrectomy.

Methods

Search strategy Search was applied to the following electronic databases: the Cochrane Library, MEDLINE (1980-2001.4), EMBASE (1980-2001.4) and Chinese Bio-medicine Database (1990-2001/1). Literature reference proceedings were handsearched at the same time. The searching words were chemotherapy, stomach neoplasms and surgery.

Data collection and analysis Data were extracted independently by two reviewers. The methodological quality of trials was evaluated using the Jadad-scale plus allocation concealment. Intention-to-treat analyses were performed.

The following data were extracted: the number of survival and death by the end of the follow-up; the different agents and doses of the intravenous chemotherapy; the baseline of the chemotherapy group and the controlled arm; the serious adverse events; the statistical consideration; cost-effectiveness analysis.

The statistical analysis was performed by RevMan4.1 software which was provided by the Cochrane Collaboration. A *P* value of <0.05 was considered statistically significant. Meta-analysis was done with random effects model. Heterogeneity was checked by chi-square test. If the results of the trials had heterogeneity, random effects model was used for meta-analysis. Sensitivity analyses was performed by excluding the trials which Jadad-scale was only 1 score. The result was expressed with odds ratio(OR) for the categorical variable.

RESULTS

There were 1076 papers relevant to the searching words. Through the steps of screening the title, reading the abstract and the entire article, twenty-seven randomized trials were identified. Only fourteen randomized trials comparing the efficacy of intravenous chemotherapy after gastrectomy with that of surgery alone in patients with confirmed gastric carcinomas, including 4543

patients, met the inclusion criteria^[47,49-56,1A-5A]. There were six trials which were excluded for repetitive studies^[57-60,6A,7A], five for having been included in the result of the Hermans' meta-analysis^[61-65], two for no available data^[66,67]. Of fourteen included trials, four trials were conducted in China (see appendix)^[2A-5A], three in England^[50,55,1A], two in Italy^[49,54], two in Spain^[51,56], one in Korea^[52], Germany^[53] and Netherlands^[47] respectively. The average sample size was 324 patients (from 25 to 1967 patients). The follow-up time was from forty-eight months to one hundred and twenty months. The chemotherapy regimens used were FAM,MMC,MFV,MFC,FEM and 5-FU+BCNU(Table 1). All the baselines of the trials were parallel. None of them performed the cost- effectiveness analysis.

Table 1 Data from 14 trials on intravenous chemotherapy versus surgery alone after resection for gastric cancer

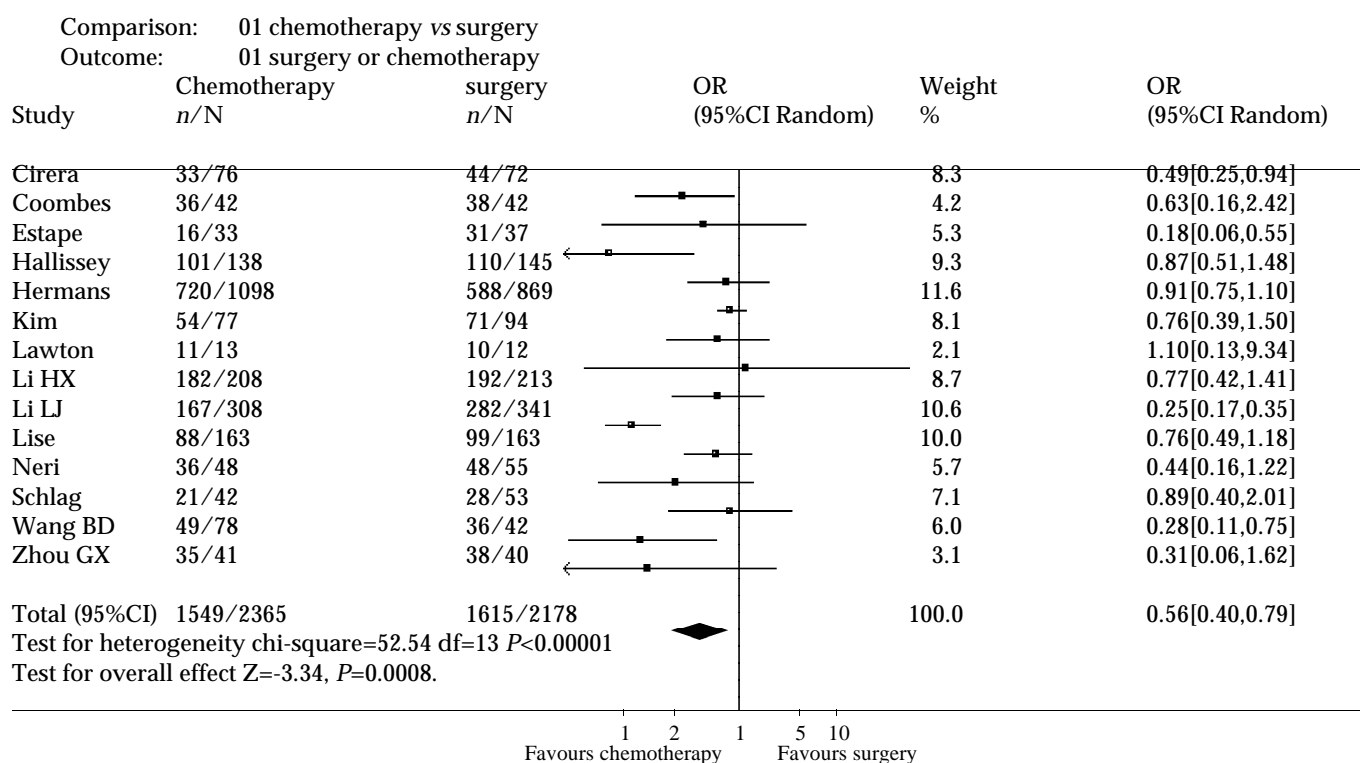
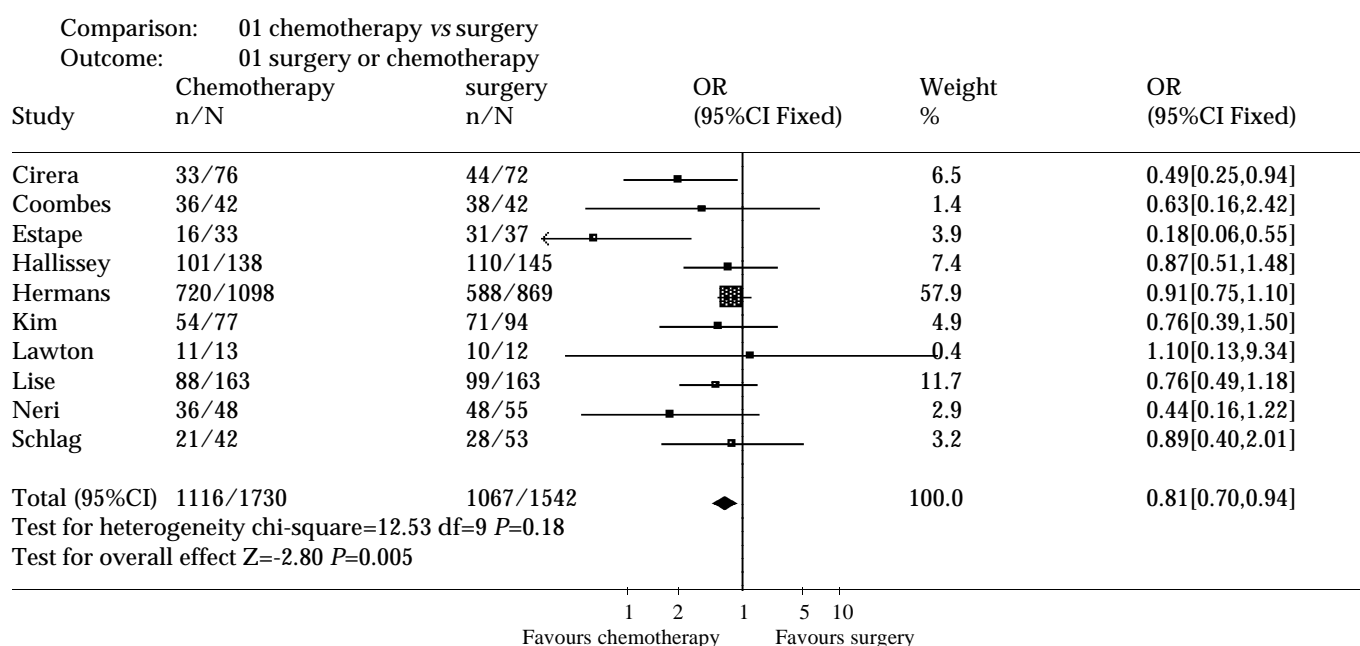
Author	Published time	Chemotherapy regimens	Chemotherapy group (number of death/total)	Surgery group (number of death/total)	Follow-up time (months)
Lise	1995	FAM	88/163	99/163	78
Hallisey	1994	FAM	101/138	110/145	60
Estate	1991	MMC	16/33	31/37	120
Kim	1992	FM	54/77	71/94	60
Li LJ	1994	MFV/MFC/FAM	167/308	282/341	60
Wang BD	1994	FM+Ara-C	49/78	36/42	36
Li HX	1994	FM	182/208	192/213	60
Coombes	1998	FEM	36/42	38/42	60
Schlag	1987	5Fu+BCNU	21/42	28/53	72
Neri	1996	Epidoxorubicin	36/48	48/55	36
Zhou GX	1998	FM	35/41	38/40	60
Lawton	1981	5Fu+BCNU	11/13	10/12	60
Cirera	1999	MMC+Tegafur	33/76	44/72	37
Hermans	1993	Meta-analysis	720/1098	588/869	NA

Abbreviations: F/5-Fu, fluorouracil; A,doxorubicin; M/ MMC, mitomycin; C/Ara-C,cytarabine; E,etoposide; V,vinblastine; BCNU,1,3-bis-(2-chloroethyl)-1-(nitrosourea); NA,no available.

The effectiveness of intravenous chemotherapy after gastrectomy was better than surgery alone (odds ratio 0.56, 95 % CI 0.40-0.79). The results of the trials showed inconsistency, as checked by the chi-square test ($\chi^2=52.54$, $P<0.00001$). There was a significant difference between the two groups by u-test ($P=0.0008$) (Figure 1). By excluding the low quality trials^[2A-5A], the sensitivity analysis was performed and revealed the same difference between chemotherapy and surgery alone (odds ratio 0.81, 95 % CI 0.70-0.94, $P=0.005$) (Figure 2).

Of fourteen trials, only three studies^[49,50,56] were of high quality according to the Jadad-scale (with three score). There was one meta-analysis trial^[47] and the others, about ten trials were of low quality. There was no trial which mentioned sample-size calculation, allocation concealment, intention-to-treat analysis. Most of the trials didn't describe the blind-procedure. Therefore, the methodologic quality of the RCTs is not strong enough to testify the conclusion.

There were five trials^[49,53-56] which detailed the side-effects of medicine according to World Health Organization grade. The side-effects halting treatment were haematologic and biochemical toxicity, debilitating nausea and vomiting. There were two patients died of chemotherapeutic toxicity (one died of cardiac toxicity and the other of massive alimentary tract

**Figure 1** The effectiveness of intravenous chemotherapy versus surgery alone**Figure 2** Sensitivity analysis

hemorrhage because of thrombopenia). Severe toxicity (grade 3 or 4 according to the WHO scale) occurred in 5.33 %, with alopecia in 39 patients, leucopenia (WBC values less than 2 000/ μ L) in 18, nausea in 21, thrombopenia (platelet count less than 50 000/ μ L) in 13, anemia in 9, vomiting in 5, diarrhea in 5, gastritis in 5, stomatitis in 4, cardiac toxicity in 4, septicemia in 2 and neural toxicity in 1.

DISCUSSION

It is well recognized that most patients who undergo curative resection of gastric carcinoma remain at high risk of local and systematic relapse. Thus, a worldwide effort has been done to develop effective adjuvant therapy to reduce this risk^[68].

The aim of meta-analysis is to summarize the results of randomized trials performed to evaluate the effect of intravenous chemotherapy for gastric cancer. Surgical resection without any adjuvant therapy is considered standard treatment. Only intravenous chemotherapy trials with gastrectomy control arm were taken into consideration in this meta-analysis. There are two meta-analyses to assess the effect of intravenous chemotherapy for gastric cancer with gastrectomy. Hermans *et al*^[47] researched the randomized controlled trials by meta-analysis; the results indicated that postoperative chemotherapy in general offered no additional survival benefit for patients with curatively resected gastric cancer. Janunger *et al*^[48] performed a systematic overview of chemotherapy effects in gastric cancer by the Swedish Council of Technology

Assessment in Health Care (SBU). A meta-analysis of 21 randomised adjuvant studies revealed a statistically significant survival benefit (OR=0.84, 95%CI 0.74-0.96). But we couldn't get the original article of Janunger, therefore we didn't include the trials in this meta-analysis.

Measuring an effect on survival by calculating the odds ratios was proved to be effective in an analysis^[47]. Only four trials which were performed by Cirera^[56], Estape^[51], Li *et al*^[2A] and Wang *et al*^[4A] respectively, demonstrated a positive effect of intravenous chemotherapy versus the controlled group by calculating the odds ratios.

Of included fourteen trials, only three studies were of high quality according to the Jadad-scale. There was one meta-analysis trial and the others, about ten trials were of low quality. There was no trial which mentioned sample-size calculation, allocation concealment, intention-to-treat analysis. Therefore, the methodologic quality of the RCTs is not strong enough to testify the conclusion. Based on the review, intravenous chemotherapy after gastrectomy may have positive treatment effect on gastric cancer. However, the evidence is not strong because of the general low methodologic quality of the RCTs. Rigorously designed, randomised, double-blind, placebo-controlled trials are required.

The toxicity of medicine is an important factor to influence the outcome of the chemotherapy. But unfortunately, there were only five trials which detailed the side effects of medicine according to World Health Organization grade in this meta-analysis. Hence, in the future research, we should put in mind to observe the side effects carefully and describe them by the WHO grade standard.

Recently, such therapies as intraperitoneal hyperthermic perfusion^[69-74], neo-adjuvant chemotherapy^[75-84], radiotherapy^[85-89] and chemoimmunotherapy^[52] are demonstrated with a positive effect to reduce the relapse risk. Tao *et al*^[90] revealed that preoperative regional artery chemotherapy had the effect to induce growth inhibition and apoptosis of gastric carcinoma cells. Cao *et al*^[91] found that human primary gastric cancer cell *in vitro* were methionine-dependent; methionine-free environment might strengthen the killing effect of chemotherapy on human primary gastric cancer cells. But, the scientific conclusion should be supported by the high quality randomized, double-blind, controlled trials.

Appendix A. RCT reports retrieved in Chinese of chemotherapy for resected gastric cancer

- 1A **Zhai Y**, Ding DS. A controlled, randomised trial of adjuvant chemotherapy using FEM combination protocol in resectable gastric cancer. *Guowai Yiyao Kangshengsu Zazhi* 1998; **19**: 150-151
- 2A **Li LJ**, Wang LY, Cai L, Chao GF, Shi YQ, Wang ZY, Lin YJ. Combined treatment of surgery with chemotherapy of stomach cancer: an analysis 5-year following up of 649 patients. *Shiyong Zhongliuxue Zazhi* 1994; **8**: 57-58,79
- 3A **Li HX**, Wang YB, Zhuang YZ. Clinical trial of perioperative chemotherapy using FM combination protocol in patient with gastric cancer. *Zhongguo Zhongliu Linchuang* 1994; **21**: 604-606
- 4A **Wang BD**, Zhang GY, Leng GZ. The effect of chemotherapy in respectable gastric cancer. *Dangdai Zhongliuxue Zazhi* 1994; **1**: 137-138
- 5A **Zhou GX**, Peng YM. Clinical study on the effect of chemical therapy to stomach cancer after operation. *Zhongliu Fangzhi Zazhi* 1998; **25**: 294-295
- 6A **Wang ZY**, Jia SW, Li LJ, Cai YH, Bai YX, Li L, Yan ZJ, Dai HX. Combined treatment of surgery with chemotherapy of stomach cancer: an analysis 5-year following up of 170 patients. *Haerbing Yike Daxue Xuebao* 1990; **24**: 30-33
- 7A **Chen W**, Li RL, Sui GJ. Adjuvant chemotherapy can improve the late result of radical operation in patients with gastric cancer. *Zhongliu Fangzhi Yanjiu* 1994; **21**: 163-165

REFERENCES

- 1 **Wang X**, Lan M, Shi YQ, Lu J, Zhong YX, Wu HP, Zai HH, Ding J, Wu KC, Pan BR, Jin JP, Fan DM. Differential display of vincristine-resistance-related genes in gastric cancer SGC7901 cell. *World J Gastroenterol* 2002; **8**: 54-59
- 2 **Zhang XY**. Some recent works on diagnosis and treatment of gastric cancer. *World J Gastroenterol* 1999; **5**: 1-3
- 3 **Zou SC**, Qiu HS, Zhang CW, Tao HQ. A clinical and long-term follow-up study of peri-operative sequential triple therapy for gastric cancer. *World J Gastroenterol* 2000; **6**: 284-286
- 4 **Li Y**, Yang L, Cui JT, Li WM, Guo RF, Lu YY. Construction of cDNA representational difference analysis based on two cDNA libraries and identification of garlic inducible expression genes in human gastric cancer cells. *World J Gastroenterol* 2002; **8**: 208-212
- 5 **Li Y**, Lu YY. Applying a highly specific and reproducible cDNA RNA method to clone garlic up-regulated genes in human gastric cancer cells. *World J Gastroenterol* 2002; **8**: 213-216
- 6 **Liu JR**, Li BX, Chen BQ, Han XH, Xue YB, Yang YM, Zheng YM, Liu RH. Effect of cis-9, trans-11-conjugated linoleic acid on cell cycle of gastric adenocarcinoma cell line (SGC-7901). *World J Gastroenterol* 2002; **8**: 224-229
- 7 **Tovey FI**, Hobsley M. Post-gastrectomy patients need to be followed up for 20-30 years. *World J Gastroenterol* 2000; **6**: 45-48
- 8 **Hou P**, Tu ZX, Xu GM, Gong YF, Ji XH, Li ZS. *Helicobacter pylori* vacA genotypes and cagA status and their relationship to associated diseases. *World J Gastroenterol* 2000; **6**: 605-607
- 9 **Deng DJ**. Progress of gastric cancer etiology: N-nitrosamides in the 1990s. *World J Gastroenterol* 2000; **6**: 613-618
- 10 **Yin F**, Shi YQ, Zhao WP, Xiao B, Miao JY, Fan DM. Suppression of P-gp induced multiple drug resistance in a drug resistant gastric cancer cell line by overexpression of Fas. *World J Gastroenterol* 2000; **6**: 664-670
- 11 **Cai L**, Yu SZ, Ye WM, Yi YN. Fish sauce and gastric cancer: an ecological study in Fujian Province, China. *World J Gastroenterol* 2000; **6**: 671-675
- 12 **Li QF**, Ou-Yang GL, Li CY, Hong SG. Effects of tachyplesin on the morphology and ultrastructure of human gastric carcinoma cell line BGC-823. *World J Gastroenterol* 2000; **6**: 676-680
- 13 **Zhu JS**, Su Q, Zhou JG, Hu PL, Xu JH. Study of primary leiomyosarcoma induced by MNNG in BALB/C nude mice. *World J Gastroenterol* 2000; **6**: 128-130
- 14 **Cao WX**, Cheng QM, Fei XF, Li SF, Yin HR, Lin YZ. A study of preoperative methionine-depleting parenteral nutrition plus chemotherapy in gastric cancer patients. *World J Gastroenterol* 2000; **6**: 255-258
- 15 **Tian XJ**, Wu J, Meng L, Dong ZW, Shou CC. Expression of VEGF121 in gastric carcinoma MGC803 cell line. *World J Gastroenterol* 2000; **6**: 281-283
- 16 **Cai L**, Yu SZ, Zhang ZF. *Helicobacter pylori* infection and risk of gastric cancer in Changle County, Fujian Province, China. *World J Gastroenterol* 2000; **6**: 374-376
- 17 **Zhang FX**, Zhang XY, Fan DM, Deng ZY, Yan Y, Wu HP, Fan JJ. Antisense telomerase RNA induced human gastric cancer cell apoptosis. *World J Gastroenterol* 2000; **6**: 430-432
- 18 **Gu QL**, Li NL, Zhu ZG, Yin HR, Lin YZ. A study on arsenic trioxide inducing in vitro apoptosis of gastric cancer cell lines. *World J Gastroenterol* 2000; **6**: 435-437
- 19 **Wang ZN**, Xu HM. Relationship between collagen IV expression and biological behavior of gastric cancer. *World J Gastroenterol* 2000; **6**: 438-439
- 20 **Han FC**, Yan XJ, Su CZ. Expression of the CagA gene of *H. pylori* and application of its product. *World J Gastroenterol* 2000; **6**: 122-124
- 21 **Chen GY**, Wang DR. The expression and clinical significance of CD44v in human gastric cancers. *World J Gastroenterol* 2000; **6**: 125-127
- 22 **Tuo BG**, Yan YH, Ge ZL, Ou GW, Zhao K. Ascorbic acid secretion in the human stomach and the effect of gastrin. *World J Gastroenterol* 2000; **6**: 704-708
- 23 **Huang XQ**. *Helicobacter pylori* infection and gastrointestinal hormones: a review. *World J Gastroenterol* 2000; **6**: 783-788
- 24 **Gao HJ**, Yu LZ, Bai JF, Peng YS, Sun G, Zhao HL, Miu K, Lü XZ, Zhang XY, Zhao ZQ. Multiple genetic alterations and behavior

- of cellular biology in gastric cancer and other gastric mucosal lesions: *H. pylori* infection, histological types and staging. *World J Gastroenterol* 2000; **6**: 848-854
- 25 **Chen JP**, Lin C, Xu CP, Zhang XY, Wu M. The therapeutic effects of recombinant adenovirus RA538 on human gastric carcinoma cells *in vitro* and *in vivo*. *World J Gastroenterol* 2000; **6**: 855-860
 - 26 **Zhou HP**, Wang X, Zhang NZ. Early apoptosis in intestinal and diffuse gastric carcinomas. *World J Gastroenterol* 2000; **6**: 898-901
 - 27 **Chen XQ**, Zhang WD, Song YG, Zhou DY. Induction of apoptosis of lymphocytes in rat mucosal immune system. *World J Gastroenterol* 1998; **4**: 19-23
 - 28 **Xiao B**, Shi YQ, Zhao YQ, You H, Wang ZY, Liu XL, Yin F, Qiao TD, Fan D M. Transduction of Fas gene or Bcl-2 antisense RNA sensitizes cultured drug resistant gastric cancer cells to chemotherapeutic drugs. *World J Gastroenterol* 1998; **4**: 421-425
 - 29 **Wang XW**, Xie H. Presence of Fas and Bcl-2 proteins in BEL-7404 human hepatoma cells. *World J Gastroenterol* 1998; **4**: 540-543
 - 30 **Lu YF**, Zhao G, Guo CY, Jia SR, Hou YD. Vagus effect on pylorus-preserving gastrectomy. *World J Gastroenterol* 1999; **5**: 177-178
 - 31 **Liu HF**, Liu WW, Fang DC, Men RP. Expression and significance of proapoptotic gene Bax in gastric carcinoma. *World J Gastroenterol* 1999; **5**: 15-17
 - 32 **Li HL**, Chen DD, Li XH, Zhang HW, Lu YQ, Ye CL, Ren XD. Changes of NF- κ B, p53, Bcl-2 and caspase in apoptosis induced by JTE-522 in human gastric adenocarcinoma cell line AGS cells: role of reactive oxygen species. *World J Gastroenterol* 2002; **8**: 431-435
 - 33 **He XS**, Su Q, Chen ZC, He XT, Long ZF, Ling H, Zhang LR. Expression, deletion and mutation of p16 gene in human gastric cancer. *World J Gastroenterol* 2001; **7**: 515-521
 - 34 **Han Y**, Han ZY, Zhou XM, Shi R, Zheng Y, Shi YQ, Miao JY, Pan BR, Fan DM. Expression and function of classical protein kinase C isoenzymes in gastric cancer cell line and its drug-resistant sublines. *World J Gastroenterol* 2002; **8**: 441-445
 - 35 **Ji F**, Peng QB, Zhan JB, Li YM. Study of differential polymerase chain reaction of C-erbB-2 oncogene amplification in gastric cancer. *World J Gastroenterol* 1999; **5**: 152-155
 - 36 **Xia L**, Yuan YZ, Xu CD, Zhang YP, Qiao MM, Xu JX. Effects of epidermal growth factor on the growth of human gastric cancer cell and the implanted tumor nude mice. *World J Gastroenterol* 2002; **8**: 455-458
 - 37 **Zhang Z**, Yuan Y, Gao H, Dong M, Wang L, Gong YH. Apoptosis, proliferation and p53 gene expression of *H. pylori* associated gastric epithelial lesions. *World J Gastroenterol* 2001; **7**: 779-782
 - 38 **Liu LX**, Liu ZH, Jiang HC, Qu X, Zhang WH, Wu LF, Zhu AL, Wang XQ, Wu M. Profiling of differentially expressed genes in human gastric carcinoma by cDNA expression array. *World J Gastroenterol* 2002; **8**: 580-585
 - 39 **Xue FB**, Xu YY, Wan Y, Pan BR, Ren J, Fan DM. Association of *H. pylori* infection with gastric carcinoma: a Meta analysis. *World J Gastroenterol* 2001; **7**: 801-804
 - 40 **Miehlke S**, Kirsch C, Dragosics B, Gschwandler M, Oberhuber G, Antos D, Dite P, Luter J, Labenz J, Leodolter A, Malfertheiner P, Neubauer A, Ehninger G, Stolte M, Bayerdorfer E. *Helicobacter pylori* and gastric cancer: current status of the Austrian Czech German gastric cancer prevention trial (PRISMA Study). *World J Gastroenterol* 2001; **7**: 243-247
 - 41 **Yao XX**, Yin L, Sun ZC. The expression of hTERT mRNA and cellular immunity in gastric cancer and precancerosis. *World J Gastroenterol* 2002; **8**: 586-590
 - 42 **Song ZJ**, Gong P, Wu YE. Relationship between the expression of iNOS, VEGF, tumor angiogenesis and gastric cancer. *World J Gastroenterol* 2002; **8**: 591-595
 - 43 **Ren J**, Dong L, Xu CB, Pan BR. The role of KDR in the interactions between human gastric carcinoma cell and vascular endothelial cell. *World J Gastroenterol* 2002; **8**: 596-601
 - 44 **Ren J**, Dong L, Xu CB, Pan BR. Expression of sphingosine kinase gene in the interactions between human gastric carcinoma cell and vascular endothelial cell. *World J Gastroenterol* 2002; **8**: 602-607
 - 45 **Cunningham D**, Hole D, Taggart DJ, Soukop M, Carter DC, Mcardle CS. Evaluation of the prognostic factors in gastric cancer: the effect of chemotherapy on survival. *Br J Surg* 1987; **74**: 715-720
 - 46 **Averbach AM**, Jacquet P. Strategies to decrease the incidence of intra-abdominal recurrence in resectable gastric cancer. *Br J Surg* 1996; **83**: 726-733
 - 47 **Hermans J**, Bonenkamp JJ, Boon MC, Bunt AMG, Ohyama S, Sasako M, Van de Velde CJH. Adjuvant therapy after curative resection for gastric cancer: meta-analysis of randomized trials. *J Clin Oncol* 1993; **11**: 1441-1447
 - 48 **Janunger KG**, Hafstrom L, Nygren P, Glimelius B. A systematic overview of chemotherapy effects in gastric cancer. *Acta Oncol* 2001; **40**: 309-326
 - 49 **Lise M**, Nitti D, Marchet A, Sahmoud T, Buyse M, Duez N, Fiorentino M, Santos JGD, Labianca R, Rougier P, Gignoux M. Final results of a phase III clinical trial of adjuvant chemotherapy with the modified fluorouracil, doxorubicin, and mitomycin regimen in resectable gastric cancer. *J Clin Oncol* 1995; **13**: 2757-2763
 - 50 **Hallisey MT**, Dunn JA, Ward LC, Allum WH. The second British stomach cancer group trial of adjuvant radiotherapy or chemotherapy in resectable gastric cancer: five-year follow-up. *Lancet* 1994; **343**: 1309-1312
 - 51 **Estape J**, Grau JJ, Lcobendas F, Curto J, Daniels M, Vinolas N, Pera C. Mitomycin C as an adjuvant treatment to resected gastric cancer: a 10-year follow-up. *Ann Surg* 1991; **213**: 219-221
 - 52 **Kim JP**, Kwon OH, Oh ST, Yang HK. Results of surgery on 6589 gastric cancer patients and immunochemosurgery as the best treatment of advanced gastric cancer. *Ann Surg* 1992; **216**: 269-279
 - 53 **Schlag P**. Adjuvant chemotherapy in gastric cancer. *World J Surg* 1987; **11**: 473-477
 - 54 **Neri B**, Leonardi VD, Romano S, Andreoli F, Pernice LM, Bruno L, Borrelli D, Valeri A, Fabbri S, Intini C, Cini G. Adjuvant chemotherapy after gastric resection in node-positive cancer patients: a multicentre randomised study. *Br J Cancer* 1996; **73**: 549-552
 - 55 **Lawton JO**, Giles GR, Hall R, Bird GG, Matheson T. Chemotherapy following palliative resection of gastric cancer. *Br J Surg* 1981; **68**: 397-399
 - 56 **Cirera L**, Balil A, Alentorn EB, Tusquets I, Cardona T, Arcusa A, Jolis L, Saigi E, Guasch I, Badia A, Boleda M. Randomized clinical trial of adjuvant mitomycin plus Tegafur in patients with resected stage III gastric cancer. *J Clin Oncol* 1999; **17**: 3810-3815
 - 57 **Allum WH**, Hallisey MT, Ward LC, Hockey MS. A controlled, prospective, randomised trial of adjuvant chemotherapy or radiotherapy in resectable gastric cancer: interim report. *Br J Cancer* 1989; **60**: 739-744
 - 58 **Allum WH**, Hallisey MT, Kelly KA. Adjuvant chemotherapy in operable gastric cancer: 5 year follow-up of first British stomach cancer group trial. *Lancet* 1989; **1**: 571-574
 - 59 **Yu CCW**, Levison DA, Dunn JA, Ward LC, Demonakou M, Allum WH, Hallisey MT. Pathological prognostic factors in the second British stomach cancer group trial of adjuvant therapy in resectable gastric cancer. *Br J Cancer* 1995; **71**: 1106-1110
 - 60 **Pignon JP**, Ducreux M, Rougier P. Meta-analysis of adjuvant chemotherapy in gastric cancer: a critical reappraisal. *J Clin Oncol* 1994; **12**: 877-878
 - 61 **Engstrom PF**, Lavin PT, Douglass HO, Brunner KW. Postoperative adjuvant 5-fluorouracil plus methyl-CCNU therapy for gastric cancer patients. *Cancer* 1985; **55**: 1868-1873
 - 62 **Higgins GA**, Amadeo JH, Smith DE, Humphrey EW, Keehn RJ. Efficacy of prolonged intermittent therapy with combined 5-FU and methyl-CCNU following resection for gastric carcinoma. *Cancer* 1983; **52**: 1105-1112
 - 63 **Bonfanti G**, Tumori N. Adjuvant treatments following curative resection for gastric cancer. *Br J Surg* 1988; **75**: 1100-1104
 - 64 **Douglass HO**, Stablein DM. Controlled trial of adjuvant chemotherapy following curative resection for gastric cancer. *Cancer* 1982; **49**: 1116-1122
 - 65 **Coombes RC**, Schein PS, Chilvers CED, Wils J, Beretta G, Bliss JM, Rutten A, Amadori D, Cortes-Funes H, Villar-Grimalt A, Meftakle C, Rauschecker HF, Boven E, Vassilopoulos P, Welvaart K, Ferreira EP, Wiig J, Gisselbrecht C, Rougier P, Woods EMA. A randomized trial comparing adjuvant fluorouracil, doxorubicin, and mitomycin with no treatment in operable gastric cancer. *J Clin Oncol* 1990; **8**: 1362-1369
 - 66 **Fielding JW**, Fagg SL, Jones BG, Ellis D, Hockey MS, Minawa

- A, Brookes VS, Craven JL, Mason MC, Timothy A, Waterhouse JAH, Wrigley PFM. An interim report of a prospective, randomized, controlled study of adjuvant chemotherapy in operable gastric cancer: British stomach cancer group. *World J Surg* 1983; **7**: 390-399
- 67 **Krook JE**, O'Connell MJ, Wieand HS, Beart RW, Leigh JE, Kugler JW, Foley JF, Pfeifle DM, Twito DI. A prospective, randomized evaluation of intensive-course 5-Fluorouracil plus Doxorubicin as surgical adjuvant chemotherapy for resected gastric cancer. *Cancer* 1991; **67**: 2454-2458
- 68 **Shimada K**, Ajani JA. Adjuvant therapy for gastric carcinoma patients in the past 15 years. *Cancer* 1999; **86**: 1657-1668
- 69 **Fujimoto S**, Takahashi M, Mutou T, Kobayashi K, Toyosawa T. Successful intraperitoneal hyperthermic chemoperfusion for the prevention of postoperative peritoneal recurrence in patients with advanced gastric carcinoma. *Cancer* 1999; **85**: 529-534
- 70 **Yu W**, Whang I, Suh I, Averbach A, Chang D, Sugarbaker PH. Prospective randomized trial of early postoperative intraperitoneal chemotherapy as an adjuvant to resectable gastric cancer. *Ann Surg* 1998; **228**: 347-354
- 71 **Rosen HR**, Jatzko G, Repse S, Potrc S, Neudorfer H, Sandbichler P, Zacherl J, Rabl H, Holzberger P, Lisborg P, Czejka M. Adjuvant intraperitoneal chemotherapy with carbon-adsorbed mitomycin in patients with gastric cancer: results of a randomized multicenter trial of the Austrian working group for surgical oncology. *J Clin Oncol* 1998; **16**: 2733-2738
- 72 **Sautner T**, Hofbauer F, Depisch D, Schiessel R, Jakesz R. Adjuvant intraperitoneal cisplatin chemotherapy does not improve long-term survival after surgery for advanced gastric cancer. *J Clin Oncol* 1994; **12**: 970-974
- 73 **Yonemura Y**, Fujimura T, Fushida S, Takegawa S, Kamata T, Katayama K, Kosaka T, Yamaguchi A, Miwa K, Miyazaki I. Hyperthermo-chemotherapy combined with cytoreductive surgery for the treatment of gastric cancer with peritoneal dissemination. *World J Surg* 1991; **15**: 530-536
- 74 **Hagiwara A**, Takahashi T, Ueda T, Lee R, Takeda M, Itoh T. Intraoperative chemotherapy with carbon particles adsorbing mitomycin C for gastric cancer with peritoneal dissemination in rabbits. *Surg* 1988; **104**: 874-881
- 75 **Leichman L**, Silberman H, Leichman CG, Spears CP, Ray M, Muggia FM, Kiyabu M, Radin R, Laine L, Stain S, Fuerst M, Groshen S, Donovan A. Preoperative systemic chemotherapy followed by adjuvant postoperative intraperitoneal therapy for gastric cancer: a university of Southern California pilot program. *J Clin Oncol* 1992; **10**: 1933-1942
- 76 **Kiyabu M**, Leichman L, Chandrasoma P. Effects of preoperative chemotherapy on gastric adenocarcinomas: a morphologic study of 25 cases. *Cancer* 1992; **70**: 2239-2245
- 77 **Ajani JA**, Ota DM, Jessup JM, Ames FC, McBride C, Boddie A, Levin B, Jackson DE, Roh M, Hohn D. Resectable gastric Carcinoma: an evaluation of preoperative and postoperative chemotherapy. *Cancer* 1991; **68**: 1501-1506
- 78 **Yonemura Y**, Sawa T, Kinoshita K, Matsuki N, Fushida S, Tanaka S, Ohoyama S, Takashima T, Kimura H, Kamata T, Fujimura T, Sugiyama K, Shima K, Miyazaki I. Neoadjuvant chemotherapy for high-grade advanced gastric cancer. *World J Surg* 1993; **17**: 256-262
- 79 **Ajani JA**, Mansfield PF, Lynch PM, Pisters PW, Feig B, Dumas P, Evans DB, Rajman I, Hargraves K, Curley S, Ota DM. Enhanced staging and all chemotherapy preoperatively in patients with potentially resectable gastric carcinoma. *J Clin Oncol* 1999; **17**: 2403-2411
- 80 **Fink U**, Schuhmacher C, Stein HJ, Busch R, Feussner H, Dittler HJ, Helmberger A, Bottcher K, Siewert JR. Preoperative chemotherapy for stage III-IV gastric carcinoma: feasibility, response and outcome after complete resection. *Br J Surg* 1995; **82**: 1248-1252
- 81 **Wilke H**, Preusser P, Fink U, Gunzer U, Meyer HJ, Meyer J, Siewert JR, Achterrath W, Lenaz L, Knipp H, Schmoll HJ. Preoperative chemotherapy in locally advanced and nonresectable gastric cancer: a phase II study with etoposide, doxorubicin, and cisplatin. *J Clin Oncol* 1989; **7**: 1318-1326
- 82 **Melcher AA**, Mort D, Maughan TS. Epirubicin, cisplatin and continuous infusion 5-fluorouracil (ECF) as neoadjuvant chemotherapy in gastro-oesophageal cancer. *Br J Cancer* 1996; **74**: 1651-1654
- 83 **Sugamura K**, Makino M, Shirai H, Kimura O, Maeta M, Itoh H, Kaibara N. Enhanced induction of apoptosis of human gastric carcinoma cells after preoperative treatment with 5-fluorouracil. *Cancer* 1997; **79**: 12-17
- 84 **Becker K**, Fumagalli U, Mueller JD, Fink U, Siewert JR, Hofler H. Neoadjuvant chemotherapy for patients with locally advanced gastric carcinoma. *Cancer* 1999; **85**: 1484-1489
- 85 **Lokich JJ**, Shea M, Chaffey J. Sequential infusional 5-fluorouracil followed by concomitant radiation for tumors of the esophagus and gastroesophageal junction. *Cancer* 1987; **60**: 275-279
- 86 **Gill PG**, Jamieson GG, Denham J, Devitt PG, Ahmad A, Yeoh E, Jones AM. Treatment of adenocarcinoma of the cardia with synchronous chemotherapy and radiotherapy. *Br J Surg* 1990; **77**: 1020-1023
- 87 **Coia LR**, Paul AR, Engstrom PF. Combined radiation and chemotherapy as primary management of adenocarcinoma of the esophagus and gastroesophageal junction. *Cancer* 1988; **61**: 643-649
- 88 **Haas CD**, Mansfield CM, Leichman LP, Considine B, Bukowski RM. Combined nonsimultaneous radiation therapy and chemotherapy with 5-FU, Doxorubicin, and Mitomycin for residual localized gastric adenocarcinoma: a southwest oncology group pilot study. *Cancer Treat Rep* 1983; **67**: 421-424
- 89 **Weissberg JB**. Role of radiation therapy in gastrointestinal cancer. *Arch Surg* 1983; **118**: 96-104
- 90 **Tao HQ**, Zou SC. Effect of preoperative regional artery chemotherapy on proliferation and apoptosis of gastric carcinoma cells. *World J Gastroenterol* 2002; **8**: 451-454
- 91 **Cao WX**, Ou JM, Fei XF, Zhu ZG, Yin HR, Yan M, Lin YZ. Methionine-dependence and combination chemotherapy on human gastric cancer cells *in vitro*. *World J Gastroenterol* 2002; **8**: 230-232

Edited by Lu HM

• LIVER CANCER •

Mechanism of 5-fluorouracil required resistance in human hepatocellular carcinoma cell line Bel₇₄₀₂

Jing Jin, Min Huang, Huai-Ling Wei, Geng-Tao Liu

Jing Jin, Huai-Ling Wei, Geng-Tao Liu, Department of Pharmacology, Institute of Materia Medica, Peking Union Medical College & Chinese Academy of Medical Sciences, Beijing 100050, People's Republic of China

Min Huang, Department of Pharmacology, University of North Carolina at Chapel Hill, 7365, North Carolina, USA

Correspondence to: Prof. Geng-Tao Liu, Institute of Materia Medica, 1 Xian Nong Tan Street, Beijing 100050, China. liugt@imm.ac.cn

Telephone: +86-10-63165178 **Fax:** +86-10-63017757

Received 2002-03-11 **Accepted** 2002-06-15

Abstract

AIM: To investigate the resistance mechanism of 5-fluorouracil (5-FU) in Bel₇₄₀₂/5-FU cells which was established in our lab by *in vitro* continuous stepwise exposure of human hepatocellular carcinoma (HCC) cell line Bel₇₄₀₂ to 5-FU.

METHODS: The expression of multidrug resistance-associated protein (MRP) and thymidylate synthase (TS) in Bel₇₄₀₂ cells was detected by immunocytochemistry. The fluorescein (FLU) accumulation, an index of MRP functional activity, was determined by flow cytometry. The distribution of FLU was observed by confocal laser scanning microscope. The spectrofluorometry was used to show the intracellular content of glutathione (GSH). Cell growth inhibition was determined by MTT assay. The activity of glutathione S-transferases (GSTs) was determined by spectrophotometry.

RESULTS: A higher expression of MRP in the Bel₇₄₀₂/5-FU cells was observed by using monoclonal mouse anti-MRP antibody, MRPr-1, in comparison with Bel₇₄₀₂ cells. Bel₇₄₀₂/5-FU cells also showed a significant decrease of FLU accumulation. FLU mainly accumulated in the nucleus with a high nuclear/cytoplasmic ratio in Bel₇₄₀₂ cells, whereas there was no difference of FLU accumulation between the nucleus and cytoplasm in Bel₇₄₀₂/5-FU cells. The intracellular GSH content in Bel₇₄₀₂/5-FU cells was almost 3 folds higher than that in Bel₇₄₀₂ cells. Addition of D, L-buthione-S, R-sulfoximine (BSO) dose-dependently reduced the GSH content in Bel₇₄₀₂/5-FU cells, however, only a weak enhancement on the cytotoxicity of 5-FU and doxorubicin (Dox) to Bel₇₄₀₂/5-FU cells was observed. Bel₇₄₀₂/5-FU cells also exhibited 29.1 % higher total GSTs activity than Bel₇₄₀₂ cells. Immunocytochemical staining by using anti-TS monoclonal antibody TS 106 showed that the level of TS in Bel₇₄₀₂/5-FU cells elevated markedly as compared with Bel₇₄₀₂ cells.

CONCLUSION: The continuous exposure of Bel₇₄₀₂ cells to 5-FU led to overexpression of TS and MRP, as well as increased intracellular GSH content and total GST activity.

Jin J, Huang M, Wei HL, Liu GT. Mechanism of 5-fluorouracil required resistance in human hepatocellular carcinoma cell line Bel₇₄₀₂. *World J Gastroenterol* 2002; 8(6):1029-1034

INTRODUCTION

It is well known that HCC is one of the malignant tumors with poor chemosensitivity to anticancer agents. To date, the fluoropyrimidine fluorouracil, such as 5-FU, is still the first choice drug in the treatment of HCC^[1-3]. However, its usage is limited because of the rapid development of acquired resistance. So far, there is no paper dealing with the establishment of acquired resistance of 5-FU in HCC and its active mechanism of resistance in the literature. Then we established a 160-fold 5-FU resistant cell line named Bel₇₄₀₂/5-FU from the parental HCC Bel₇₄₀₂ cell line through about 6 months of continuous 5-FU selection. In addition to resistance to 5-FU, the Bel₇₄₀₂/5-FU cells also showed 3-4-fold cross-resistance to Dox and cytarabine, but no cross-resistance to vincristine, taxol, cisplatin and hydroxycamptothecine. Our prior study revealed that Bel₇₄₀₂ and Bel₇₄₀₂/5-FU cells showed no difference in P-glycoprotein (P-gp) levels.

Nishiyama^[4] showed that the increased expression of MRP was closely related to 5-FU resistance in gastrointestinal cancer cell lines. MRP is also a member of the ABC superfamily of membrane transport proteins, which has certain sequence homology with P-gp. The drug-resistance pattern conferred by MRP is similar but not identical to that of P-gp^[5,6]. It is believed that MRP prefers to transport anionic drugs and neutral drugs conjugated to acidic ligands, such as GSH, glucuronate, or sulfate^[7,8]. GSH has been suggested as an important component of MRP-mediated MDR and drug transport^[9]. GSH can combine with anticancer drugs to form less toxic and more water soluble GSH conjugates, which can be exported from cells by MRP^[10,11]. The conjugation reaction is catalyzed by GSTs. The elevation of cellular GSH and the elevated expression and activity of GSTs are associated with the development of drug-resistance phenotype of tumor cells to alkylating compounds, including melphalan, cyclophosphamide, chlorambucil, nitrogen mustard, doxorubicin^[12-14].

TS catalyses the reductive methylation of deoxyuridine monophosphate to deoxythymidine monophosphate using 5, 10-methylene-tetrahydrofolate as a methyl donor co-substrate. This reaction provides the only *de novo* source of dTMP and is an essential step in DNA biosynthesis. TS is a critical target for fluoropyrimidine, including 5-FU. *In vitro* and *in vivo* studies have reported that increased TS protein levels and gene amplification and/or decreased inhibition of TS activity may be associated with the resistance to 5-FU^[15,16].

The purpose of the present study was to determine whether the change of MRP, GSH/GST and TS contributed to the 5-FU resistance observed in Bel₇₄₀₂/5-FU cells.

MATERIALS AND METHODS

Materials

Drugs and reagents 5-FU was purchased from Xudong Haipu Pharmaceutical Inc. (Shanghai, China). 1-chloro-2,4-dinitrobenzene (CDNB) and O-phthalaldehyde (OPT), GSH and 3-4,5-dimethyl-thiazol-2,5-diphenyl tetrazolium bromide

(MTT) was obtained from Sigma Chemical Co. (St. Louis, MO). Monoclonal mouse anti-MRP, MRP-r1 and FITC-labeled goat anti-mouse IgG were obtained from Zhong Shan Biotechnology Co., LTD (Beijing, China). Thymidylate synthase Ab-1 TS 106 was obtained from Neomarker (Fremont, CA). Fluorescein (FLU) was obtained from Amresco (Solon, Ohio).

Cell lines The parental human hepatocellular carcinoma Bel₇₄₀₂ cells and the 5-FU selected drug-resistant Bel₇₄₀₂/5-FU cells were grown in RPIM1640 (GIBCO) media containing 10 % newborn calf serum, 100 unit/mL penicillin and 100 µg/mL streptomycin. Cells were kept at 37 °C in a 5 % CO₂-95 % air atmosphere, and passaged by 0.25 % trypsin plus 0.02 % EDTA treatment. Bel₇₄₀₂/5-FU cells were routinely maintained in the presence of 10 µg/mL 5-FU. Cells were however cultured in the absence of 5-FU for at least 3 days before their use for experiments.

Methods

Immunofluorescence assay of MRP expression Bel₇₄₀₂ and Bel₇₄₀₂/5-FU cells were seeded on to sterilized slides. After 24hr of incubation, cells were washed twice with cold PBS and fixed with 70 % methanol at -20 °C for 10 min. All subsequent procedures were done at room temperature. All slides were washed once with blocking solution (1 % bovine serum albumin/5 % normal goat serum/PBS), incubated in blocking solution with 0.1 % Tween 20 for 30 min, followed by incubation with MRPr1 which was diluted 1:30 in blocking solution with 0.1 % Tween 20 for 1 hour. Then slides were washed once with blocking solution and incubated with FITC-conjugated goat anti-mouse IgG which was diluted 1:50 in blocking solution at room temperature for 1 hour. Finally, Slides were examined under confocal laser scanning microscope (BIO-RAD MRC1024) for fluorescence intensities^[17].

FLU accumulation Assessment of MRP functional activity was carried out by measuring the intracellular accumulation of FLU^[18]. The confluent Bel₇₄₀₂ and Bel₇₄₀₂/5-FU monolayers were preincubated for 30 min at 37 °C in the culture medium, then exposed to 100 µmol·L⁻¹ FLU for 3hr at 37 °C. After washing for three times with ice-cold PBS, cells were rapidly collected and intracellular fluorescence of FLU was immediately measured with flow cytometer (Coulter, EPICS XL).

Cellular FLU distribution Bel₇₄₀₂ or Bel₇₄₀₂/5-FU cells were plated onto 6-multiwell plate (Coster) for examining FLU distribution by using confocal laser scanning microscopy. The cells were exposed to 100 µmol·L⁻¹ FLU for 3hr at 37 °C. After this incubation period, the loading solutions were removed and cells were washed for three times with ice-cold PBS containing 1 % bovine serum albumin and examined under confocal laser scanning microscope (MERIDIAN™ Ultima 212)^[19].

Measurement of cellular GSH content Bel₇₄₀₂/5-FU cells incubated with or without different concentrations of BSO for 24 hrs and Bel₇₄₀₂ cells were lysed by addition of 0.2 % Triton X-100 in PBS. Afterwards, 20 % HPO₃ was added to precipitate proteins. The cells were centrifuged at 4 °C at 10 000 r.p.m. for 10 min and the supernatant fraction was used for the measurement of GSH^[20]. Briefly, to 0.4 mL of the supernatant, 0.1 mL OPT (containing 0.1 mg OPT) and 2.5 mL PBS (0.1 mol·L⁻¹)-EDTA (5 mmol·L⁻¹) buffer (pH 8.0) were added. After thorough mixing and incubation at room temperature for 15 min, the solution was transferred to a quartz cuvette. Its fluorescence intensity at 420nm was determined with the excitation at 350nm by a fluorescence spectrophotometer (HITACHI, MPF-4).

Chemoresensitivity testing The effect of BSO on the cytotoxicity of Dox and 5-FU to Bel₇₄₀₂/5-FU cells was assayed by a MTT method^[21]. Briefly, Bel₇₄₀₂/5-FU cells were plated in 96-well plates at 3000 cells per well. After 24hr, various

concentrations of the test drugs were added in quadruplicate samples for each concentration. The cells were exposed to drugs for continuous 3 days. Then MTT (0.5 mg·mL⁻¹) was added and the plates were incubated at 37 °C in 5 % CO₂ for 4hr before 150 µL 100 % dimethyl sulfoxide was added to each well. The optical density of each well was determined by a microplate reader (Bio-Rad Model 450) at a wavelength of 570nm.

Total GST activity Bel₇₄₀₂ and Bel₇₄₀₂/5-FU cells were washed with PBS and resuspended in 200 µL TMS solution (50 mmol·L⁻¹ Tris, pH 7.5, 3 mmol·L⁻¹ MgCl₂, 200 mmol·L⁻¹ sucrose). After sonication at 4 °C (60sec), they were centrifuged at 10 000rpm for 25 min. To 10 µL cell supernatant, 2.9mL sodium phosphate buffer (0.1 mol·L⁻¹, pH 6.5) and 0.1mL reduced GSH were added. The reaction was carried out at room temperature by the addition of 30mM CDNB (in DMSO). Formation of S-2,4 dinitrophenyl glutathione was monitored spectrophotometrically by the increase in absorbance at 340nm ($\epsilon_{340}=9.6 \text{ mM}^{-1} \cdot \text{CM}^{-1}$). GST activity was expressed as nmol·min⁻¹·mg⁻¹ protein in the cells^[22].

TS expression Bel₇₄₀₂ and Bel₇₄₀₂/5FU cells in the exponential phase of growth were seeded onto sterile slides and incubated at 37 °C in 5 % CO₂ for 24hr. After washing with cold PBS, cells were fixed in cold acetone for 10 min. The cells were subsequently rinsed in PBS and incubate with normal goat serum (10 % in PBS) at room temperature for 30 min to reduce nonspecific binding. Cells were then incubated with TS 106 (1:50 dilution) at 37 °C for 2hr. After being washed with PBS, all slides were incubated with FITC-labeled goat anti-mouse IgG at 37 °C for 1hr. All slides were washed with PBS again and examined under confocal laser scanning microscope (BIO-RAD MRC1024)^[23].

RESULTS

Expression of MRP

Fluorescence immunostaining signal was weakly detectable in Bel₇₄₀₂ cells and a denser staining was found in plasma membrane of Bel₇₄₀₂/5-FU cells. The resistant Bel₇₄₀₂/5-FU cells (Figure 1B) showed an enhanced immunoreactivity to MRP compared to that of sensitive Bel₇₄₀₂ cells (Figure 1A), which indicated that the resistant cells contained elevated level of MRP.

FLU accumulation as an index of MRP functional activity

The previous result showed that Bel₇₄₀₂ and Bel₇₄₀₂/5-FU cells differed in MRP expression, then we performed the functional MRP assay to demonstrate if the established difference in the levels of MRP in the two cells were indicative for differences in the MRP activity. FLU is a well-recognized substrate of MRP but not of P-gp. The use of FLU and FLU analogs as probes for MRP functional activity has been reported by Huai-Yun *et al*^[24]. The results of flow cytometry showed that the accumulation of FLU in Bel₇₄₀₂ cells was almost two times higher than that in Bel₇₄₀₂/5-FU cells (Figure 2). In other word, MRP functional activity in the resistant Bel₇₄₀₂/5-FU cells was higher than that in the parental cells.

FLU redistribution

In drug-selected MRP-overexpressing cells, alterations in drug localization have been observed in addition to decreased accumulation^[25]. The intracellular distribution of FLU was directly examined by confocal laser scanning microscopy (Figure 3). When exposed to FLU for 3 hours, besides the difference in FLU accumulation between the two cell lines, different localization of FLU in both cell lines was also

observed. FLU mainly accumulated in the nucleus with a high nuclear/cytoplasmic ratio in Bel₇₄₀₂ cells (Figure 3A), whereas there was no difference of location between nucleus and cytoplasm in Bel₇₄₀₂/5-FU cells (Figure 3B).

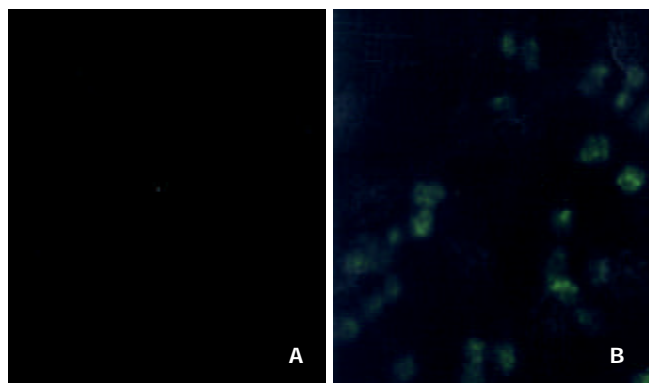


Figure 1 Immunocytochemical detection of MRP in Bel₇₄₀₂ and its 5-FU resistant cells in cytoprep slides. (A) Bel₇₄₀₂ cells; (B) Bel₇₄₀₂/5-FU cells. The cells were fixed in 70 % methanol, and incubated with anti-MRP monoclonal antibody MRPr-1 for 1 hr at room temperature. FITC-conjugated goat anti-mouse IgG was added to examine the fluorescence staining of MRP under confocal laser scanning microscope

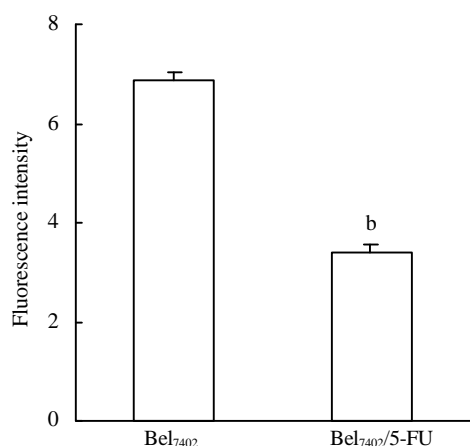


Figure 2 FLU accumulation in Bel₇₄₀₂ and Bel₇₄₀₂/5-FU cells. The cells were incubated with 100 $\mu\text{mol} \cdot \text{L}^{-1}$ FLU for 3 hr. After washing, the cells were trypsinized and intracellular fluorescence of FLU was determined with a flow cytometer. Data were pooled from three independent experiments. ^b $P < 0.001$ vs Bel₇₄₀₂ cells

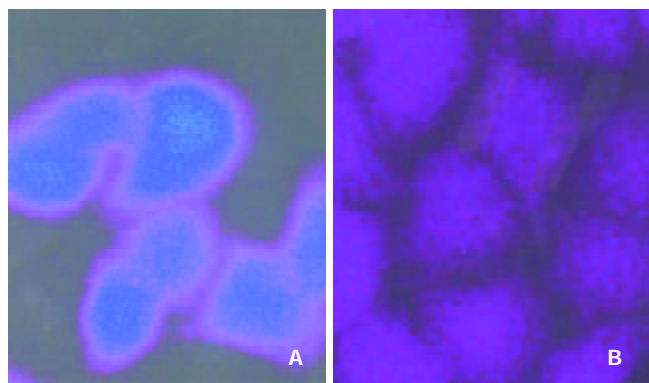


Figure 3 FLU distribution in Bel₇₄₀₂ and Bel₇₄₀₂/5-FU cells. The cells were incubated with 100 $\mu\text{mol} \cdot \text{L}^{-1}$ FLU for 3 hr. Then the intracellular distribution of FLU was revealed by confocal laser scanning microscopy. (A) Bel₇₄₀₂ cells; (B) Bel₇₄₀₂/5-FU cells.

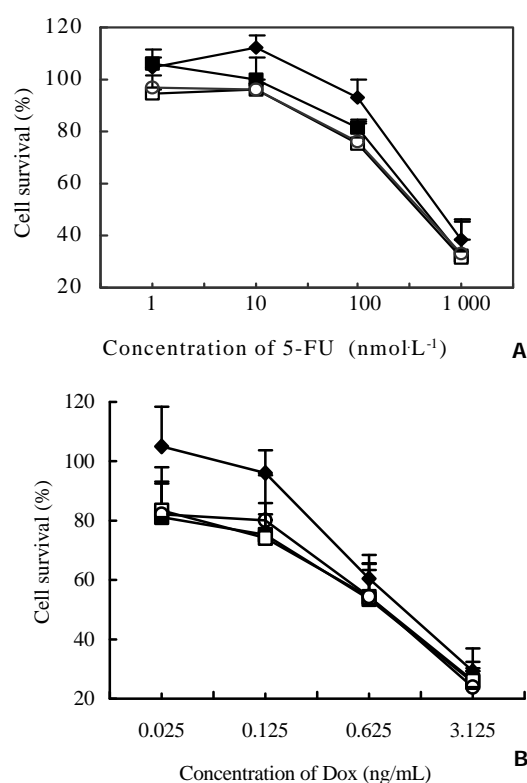


Figure 4 Effect of BSO on the cytotoxicity of 5-FU and Dox to Bel₇₄₀₂/5-FU cells. The cells were incubated with different concentrations of 5-FU (Figure 4A) or Dox (Figure 4B) in the absence (◆) or presence of BSO at the concentration of 5 $\mu\text{mol} \cdot \text{L}^{-1}$ (□), 50 $\mu\text{mol} \cdot \text{L}^{-1}$ (○) and 100 $\mu\text{mol} \cdot \text{L}^{-1}$ (■) respectively for 72 hr. Cell survival was determined by MTT assay. The values represent the means \pm SD of three experiments.

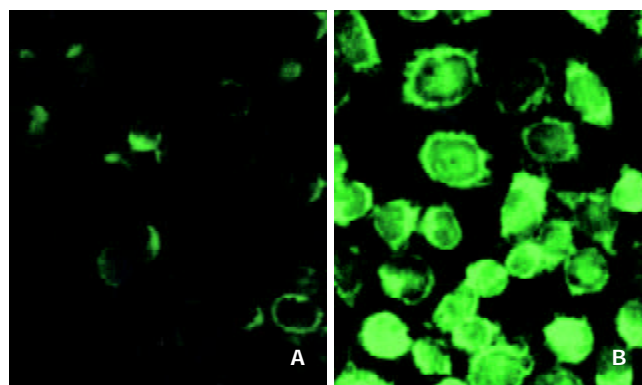


Figure 5 Immunocytochemical analysis of TS from parental and 5-FU resistant Bel₇₄₀₂ cells. The cytoprep slides were made as described in "Methods". The slides were fixed in acetone, incubated with TS 106 and stained by using FITC-conjugated goat anti-mouse IgG. TS expression was determined by confocal laser scanning microscopy. (A) Bel₇₄₀₂ cells; (B) Bel₇₄₀₂/5-FU cells.

GSH levels and depletion of GSH by BSO

Since GSH implicates in the mechanism of MRP-mediated drug resistance, the intracellular GSH content was determined in Bel₇₄₀₂ and Bel₇₄₀₂/5-FU cells. As shown in Table 1, the GSH content in Bel₇₄₀₂/5-FU cells increased almost two folds in comparison with that in Bel₇₄₀₂ cells. When Bel₇₄₀₂/5-FU cells were incubated with BSO, an inhibitor of GSH biosynthesis, at 5, 50 and 100 $\mu\text{mol} \cdot \text{L}^{-1}$ for 24 hours, the GSH content in the cells decreased in a dose-dependent manner.

Table 1 GSH content and GSTs activity in Bel₇₄₀₂ and Bel₇₄₀₂/5-FU cells and the effect of BSO on the intracellular GSH content in Bel₇₄₀₂/5-FU cells

	BSO (μmol·L ⁻¹)	Subline	
		Bel ₇₄₀₂ /5-FU	Bel ₇₄₀₂
GSH content (mg/mg protein)	-	0.952±0.257	0.322±0.196 ^b
	5	0.520±0.107	
	50	0.427±0.200 ^a	
	100	0.403±0.135 ^a	
GSTs activity (nmol/min/mg protein)	-	19.1±1.9	14.8±1.2 ^c

GSH content was determined in Bel₇₄₀₂/5-FU cells treated with or without BSO for 24 hr and Bel₇₄₀₂ cells. GSTs activity was assayed by the method of Ghalia *et al*^[22] using 30 mmol·L⁻¹ GSH and 30 mmol·L⁻¹ CDNB as substrates. Results are presented as mean ±SD from three independent experiments, each performed in triplicates. Differences for significance were tested by using a Student's *t*-test: ^a*P*<0.05, ^b*P*<0.01 vs Bel₇₄₀₂/5-FU cells without the addition of BSO; ^c*P*<0.05 vs the GSTs activity in Bel₇₄₀₂/5-FU cells

Effect of BSO on the resistance of Bel₇₄₀₂/5-FU cells

Sublethal concentrations of BSO (5, 50, 100 μmol·L⁻¹) were added to test the role of GSH in the sensitivity of Bel₇₄₀₂/5-FU cells to 5-FU and Dox. As a result, the addition of BSO caused a slight left shift in the dose-effect pattern of 5-FU (Figure 4A) and Dox (Figure 4B) in Bel₇₄₀₂/5-FU cells, indicating that the inhibition of GSH biosynthesis by BSO only had a weak reversal activity on the resistance of Bel₇₄₀₂/5-FU cells.

GST enzymatic activity

GSTs catalyze the coupling reaction of intracellular electrophiles with GSH. Elevation of GSTs particularly GSTp is associated with an acquired resistance of cells to certain anticancer drugs. Table 1 showed the total GST activity in Bel₇₄₀₂/5-FU cells were 29.1 % higher than that in Bel₇₄₀₂ cells. The difference between both cell lines was significant (*P*<0.05).

TS levels

In order to determine whether there is difference of TS expression in Bel₇₄₀₂ and Bel₇₄₀₂/5-FU cell lines, an immunocytochemical analysis was performed by using MAb TS 106. As shown in Figure 5, the pattern of TS 106 reactivity was a dark granular appearance and diffusely spread throughout the cytoplasm in Bel₇₄₀₂/5-FU cells. The cytochemical staining intensity of TS 106 in Bel₇₄₀₂/5-FU cells (Figure 5B) markedly increased as compared with the parental Bel₇₄₀₂ cells (Figure 5A).

DISCUSSION

In vitro continuous stepwise exposure of HCC cell line Bel₇₄₀₂ to 5-FU for 6 months resulted in a 160 fold resistant subline Bel₇₄₀₂/5-FU in our laboratory. The established resistance to 5-FU only slightly decreased or remained unchanged without continuous exposure to 5-FU for one month. Verapamil, a classical MDR reversal agent, significantly reversed the resistance to VCR, taxol and Dox with similar fold reversal in Bel₇₄₀₂ and Bel₇₄₀₂/5-FU cell lines, but it only had little effect on the chemosensitivity to 5-FU and hydroxycamptothecine in both cells. In our previous study on the required resistant mechanism of Bel₇₄₀₂/5-FU cells to 5-FU, we found that there was no difference in the expression level of the *mdr-1* product P-gp between the two cells by immunocytochemical staining

and Western-blotting analysis.

Up-regulation of MRP protein was observed by using the monoclonal antibody against MRP, MRPr-1 in this study. It was reported that^[26] the gene expression of MRP correlated well with 5-FU resistance in 7 human gastrointestinal cancer cell lines. In some multidrug resistance cancer cells without alterations in levels of MRP, no resistance to 5-FU was found^[27,28]. MRP has been postulated to cause multidrug resistance by exporting the anticancer drugs out of the cells, then the accumulation of drugs in cells decreased. Unlike P-gp, MRP can be localized in both the plasma membrane and membranes of intracellular organelles, including the endoplasmic reticulum and Golgi apparatus, thus cause intracellular or cytoplasmic sequestration of drug and prevent pharmaceuticals from reaching their cellular targets^[25,29]. Anticancer drugs such as anthracyclines localize to the nucleus and cytoplasm with a high nuclear/cytoplasmic ratio in sensitive cancer cells. In contrast, anthracyclines accumulate mainly in the perinuclear region or in cytoplasmic vesicles in drug-selected MRP-overexpressing cells, and much less in the nucleus. In our experiments, the functional activity of MRP was investigated by flow cytometry using FLU accumulation as a probe. The accumulation of FLU in Bel₇₄₀₂/5-FU cells was only about half of the amount of FLU in the parental Bel₇₄₀₂ cells, suggesting an increased activity of MRP in the resistant Bel₇₄₀₂/5-FU cells. Furthermore, decreased nuclear/cytoplasmic ratio of FLU fluorescence was observed in Bel₇₄₀₂/5-FU cells as compared to that in the parental Bel₇₄₀₂ cells. All of these observations indicated that the decreased accumulation of FLU and the alteration in FLU distribution in Bel₇₄₀₂/5-FU cells may stem from up-regulated MRP.

MRP has been suggested to be the GS-X pump for multivalent organic anions such as cysteinyl leukotrienes, GSH disulfide and various GSH S-conjugates^[8,30]. Intracellular GSH content is closely related to MRP-mediated multidrug resistance, since GSH interacts directly with MRP and this interaction causes a change in MRP structure that facilitates the binding and/or transport of anticancer drugs. Alternatively, GSH and anticancer drugs may spontaneously form a complex that behaves as a MRP substrate^[31,32]. Using selective GSH modulators to decrease cellular GSH levels can sensitize tumor cells to the killing effects of chemotherapeutics^[33]. BSO is a specific inhibitor of the rate-limiting enzyme of the GSH biosynthetic pathway, γ-glutamylcysteine synthetase. Treatment of either drug-selected or transfected resistant cells with BSO markedly depletes GSH and restores sensitivity to anticancer drugs that are transported by MRP^[34-36]. In the present report, the resistant Bel₇₄₀₂/5-FU cells exhibited a significantly higher intracellular GSH content and higher overall GST activity than 5-FU sensitive Bel₇₄₀₂ cells. Addition of BSO dose-dependently reduced the GSH content in Bel₇₄₀₂/5-FU cells. However, only a weak enhancement in the cytotoxicity of 5-FU and Dox to Bel₇₄₀₂/5-FU cells by BSO was observed in growth inhibition assay. Moreover, BSO restores sensitivity to Dox more effectively than to 5-FU. Till now there is no direct evidence that 5-FU is a substrate of GSTs or MRP. It appeared that the elevated levels of the GSH/GST system and higher expression of MRP did not to play an important role in the 5-FU resistance development. These alterations maybe associated with the cross-resistance of Dox and cytarabine in the Bel₇₄₀₂/5-FU cells.

5-FU is widely used in the treatment of breast, gastrointestinal, and head and neck cancers. The induction of TS following short-term 5-FU exposure is a generally observed phenomenon in malignant breast and colon cells^[37]. A number of clinical

evaluations referred to the relationship of TS expression in tumors to clinical response and survival of cancer patients receiving 5-FU-based chemotherapy^[38,39]. Fukushima *et al*^[40] established a human tumor sub-line resistant to 5-FU by using colorectal xenografts in nude mice and an increase in TS activity was observed in this resistant cell. According to our study, the 5-FU resistant HCC cells exhibited the elevated levels of TS protein by immunocytochemical detection, which is a sensitive and quantitative method of detecting human TS by monoantibody TS 106 by a direct comparison of Western blotting and biochemical TS assay^[22]. Although it has been demonstrated a close correlation between TS protein levels and sensitivity to 5-FU in clinic, several other mechanisms of acquired resistance to 5-FU have been attributed to TS, such as gene amplification, increased dUMP levels, decreased FdUMP accumulation, decreased stability of ternary complex, depletion of intracellular folates and so on^[41]. Only TS protein expression was investigated in this research. Further investigations should be performed to determine whether other altered effects on TS occur in this Bel₇₄₀₂/5-FU cells.

In summary, our results clearly showed that TS expression increased remarkably in 5-FU resistant Bel₇₄₀₂/5-FU cells. In addition, the expression of MRP as well as GSTs activity and GSH content also increased. The overexpression of TS may be the main cause for the resistance development of 5-FU. The changes in MRP and GSH/GST system seemed to result in the cross-resistance of Dox in Bel₇₄₀₂/5-FU cells.

REFERENCES

- 1 Tono T, Hasuiki Y, Ohzato H, Takatsuka Y, Kikkawa N. Limited but definite efficacy of prophylactic hepatic arterial infusion chemotherapy after curative resection of colorectal liver metastases: A randomized study. *Cancer* 2000; **88**: 1549-1556
- 2 Guo WJ, Yu EX. Evaluation of combined therapy with chemoembolization and irradiation for large hepatocellular carcinoma. *Br J Radiol* 2000; **73**: 1091-1097
- 3 Aguayo A, Patt YZ. Nonsurgical treatment of hepatocellular carcinoma. *Semin Oncol* 2001; **28**: 503-513
- 4 Nishiyama M, Yamamoto W, Park JS, Okamoto R, Hanaoka H, Takano H, Saito N, Matsukawa M, Shirasaka T, Kurihara M. Low-dose cisplatin and 5-fluorouracil in combination can repress increased gene expression of cellular resistance determinants to themselves. *Clin Cancer Res* 1999; **5**: 2620-2628
- 5 Kuwano M, Toh S, Uchiyumi T, Takano H, Kohno K, Wada M. Multidrug resistance-associated protein subfamily transporters and drug resistance. *Anticancer Drug Des* 1999; **14**: 123-131
- 6 van Zuylen L, Nooter K, Sparreboom A, Verweij J. Development of multidrug-resistance converters: sense or nonsense? *Invest New Drugs* 2000; **18**: 205-220
- 7 Borst P, Evers R, Kool M, Wijnholds J. A family of drug transporters: the multidrug resistance-associated proteins. *J Natl Cancer Inst* 2000; **92**: 1295-1302
- 8 Gottesman MM. Mechanisms of cancer drug resistance. *Ann Rev Med* 2002; **53**: 615-627
- 9 Krishna R, Mayer LD. Multidrug resistance (MDR) in cancer. Mechanisms, reversal using modulators of MDR and the role of MDR modulators in influencing the pharmacokinetics of anti-cancer drugs. *Eur J Pharm Sci* 2000; **11**: 265-283
- 10 Rappa G, Finch RA, Sartorelli AC, Lorico A. New insights into the biology and pharmacology of the multidrug resistance protein (MRP) from gene knockout models. *Biochem Pharmacol* 1999; **58**: 557-562
- 11 Keppler D. Export pumps for glutathione S-conjugates. *Free Radic Biol Med* 1999; **27**: 985-991
- 12 Akiyama SI, Chen ZS, Sumizawa T, Furukawa T. Resistance to cisplatin. *Anticancer Drug Des* 1999; **14**: 143-151
- 13 Panasci L, Paiement JP, Christodoulou G, Belenkov A, Malapetsa A, Aloyz R. Chlorambucil drug resistance in chronic lymphocytic leukemia: the emerging role of DNA repair. *Clin Cancer Res* 2001; **7**: 454-461
- 14 Breidel M. Anticancer drug resistance in primary human brain tumors. *Brain Res Rev* 2001; **35**: 161-204
- 15 Mirjoleit JF, Barberi-Heyob M, Merlin JL, Marchal S, Etienne MC, Milano G, Bey P. Thymidylate synthase expression and activity: relation to S-phase parameters and 5-fluorouracil sensitivity. *Br J Cancer* 1998; **78**: 62-68
- 16 van Triest B, Pinedo HM, van Hensbergen Y, Smid K, Telleman F, Schoenmakers PS, van der Wilt CL, van Laar JA, Noordhuis P, Jansen G, Peters GJ. Thymidylate synthase level as the main predictive parameter for sensitivity to 5-fluorouracil, but not for folate-based thymidylate synthase inhibitors, in 13 nonselected colon cancer cell lines. *Clin Cancer Res* 1999; **5**: 643-654
- 17 Wada H, Saikawa Y, Niida Y, Nishimura R, Noguchi T, Matsukawa H, Ichihara T, Koizumi S. Selectively induced high MRP gene expression in multidrug-resistant human HL60 leukemia cells. *Exp Hematol* 1999; **27**: 99-109
- 18 Decleves X, Regina A, Laplanche JL, Roux F, Boval B, Launay JM, Scherrmann JM. Functional expression of P-glycoprotein and multidrug resistance-associated protein (Mrp1) in primary cultures of rat astrocytes. *J Neurosci Res* 2000; **60**: 594-601
- 19 Miller DW, Batrakova EV, Kabanov AV. Inhibition of multidrug resistance-associated protein (MRP) functional activity with pluronic block copolymers. *Pharm Res* 1999; **16**: 396-401
- 20 Rappa G, Lorico A, Flavell RA, Sartorelli AC. Evidence that the multidrug resistance protein (MRP) functions as a co-transport of glutathione and natural product toxins. *Cancer Res* 1997; **57**: 5232-5237
- 21 Benderra Z, Trussardi A, Morjani H, Villa AM, Doglia SM, Manfait M. Regulation of cellular glutathione modulates nuclear accumulation of daunorubicin in human MCF7 cells overexpressing multidrug resistance associated protein. *Eur J Cancer* 2000; **36**: 428-434
- 22 Ghalia AA, Rabboh NA, el Shalakani A, Seada L, Khalifa A. Estimation of glutathione S-transferase and its Pi isoenzyme in tumor tissues and sera of patients with ovarian cancer. *Anticancer Res* 2000; **20**: 1229-1235
- 23 Johnston PG, Liang CM, Henry S, Chabner BA, Allegra CJ. Production and characterization of monoclonal antibodies that localize human thymidylate synthase in the cytoplasm of human cells and tissue. *Cancer Res* 1991; **51**: 6668-6676
- 24 Huai-Yun H, Secrest DT, Mark KS, Carney D, Brandquist C, Elmquist WF, Miller DW. Expression of multidrug resistance-associated protein (MRP) in brain microvessel endothelial cells. *Biochem Biophys Res Commun* 1998; **243**: 816-820
- 25 Ross DD. Novel mechanisms of drug resistance in leukemia. *Leukemia* 2000; **14**: 467-473
- 26 Kirihaara Y, Yamamoto W, Toge T, Nishiyama M. Dihydropyrimidine dehydrogenase, multidrug resistance-associated protein, and thymidylate synthase gene expression levels can predict 5-fluorouracil resistance in human gastrointestinal cancer cells. *Int J Oncol* 1999; **14**: 551-556
- 27 Iida N, Takara K, Ohmoto N, Nakamura T, Kimura T, Wada A, Hirai M, Sakaeda T, Okumura K. Reversal effects of antifungal drugs on multidrug resistance in MDR1-overexpressing HeLa cells. *Biol Pharm Bull* 2001; **24**: 1032-1036
- 28 Liu B, Staren ED, Iwamura T, Appert HE, Howard JM. Mechanisms of taxotere-related drug resistance in pancreatic carcinoma. *J Surg Res* 2001; **99**: 179-186
- 29 Aszalos A, Ross DD. Biochemical and clinical aspects of efflux pump related resistance to anti-cancer drugs. *Anticancer Res* 1998; **18**: 2937-2944
- 30 Bradshaw DM, Arceci RJ. Clinical relevance of transmembrane drug efflux as a mechanism of multidrug resistance. *J Clin Oncol* 1998; **16**: 3674-3690
- 31 Loe DW, Deeley RG, Cole SP. Characterization of vincristine transport by the Mr 190,000 multidrug resistance protein (MRP): evidence for cotransport with reduced glutathione. *Cancer Res* 1998; **58**: 5130-5136
- 32 Salerno M, Garnier-Suillerot A. Kinetics of glutathione and daunorubicin efflux from multidrug resistance protein

- overexpressing small-cell lung cancer cells. *Eur J Pharmacol* 2001; **421**: 1-9
- 33 **Chen X**, Carystinos GD, Batist G. Potential for selective modulation of glutathione in cancer chemotherapy. *Chem Biol Interact* 1998; **111-112**: 263-275
- 34 **Cole SP**, Deeley RG. Multidrug resistance mediated by the ATP-binding cassette transporter protein MRP. *Bioessays* 1998; **20**: 931-940
- 35 **Benderra Z**, Trussardi A, Morjani H, Villa AM, Doglia SM, Manfait M. Regulation of cellular glutathione modulates nuclear accumulation of daunorubicin in human MCF7 cells overexpressing multidrug resistance associated protein. *Eur J Cancer* 2000; **36**: 428-434
- 36 **Lewandowicz GM**, Britt P, Elgie AW, Williamson CJ, Coley HM, Hall AG, Sargent JM. Cellular glutathione content, *in vitro* chemoresponse, and the effect of BSO modulation in samples derived from patients with advanced ovarian cancer. *Gynecol Oncol* 2002; **85**: 298-304
- 37 **Parr AL**, Drake JC, Gress RE, Schwartz G, Steinberg SM, Allegra CJ. 5-Fluorouracil-mediated thymidylate synthase induction in malignant and nonmalignant human cells. *Biochem Pharmacol* 1998; **56**: 231-235
- 38 **Kuniyasu T**, Nakamura T, Tabuchi Y, Kuroda Y. Immunohistochemical evaluation of thymidylate synthase in gastric carcinoma using a new polyclonal antibody: the clinical role of thymidylate synthase as a prognostic indicator and its therapeutic usefulness. *Cancer* 1998; **83**: 1300-1306
- 39 **Yeh KH**, Shun CT, Chen CL, Lin JT, Lee WJ, Lee PH, Chen YC, Cheng AL. High expression of thymidylate synthase is associated with the drug resistance of gastric carcinoma to high dose 5-fluorouracil-based systemic chemotherapy. *Cancer* 1998; **82**: 1626-1631
- 40 **Fukushima M**, Fujioka A, Uchida J, Nakagawa F, Takechi T. Thymidylate synthase (TS) and ribonucleotide reductase (RNR) may be involved in acquired resistance to 5-fluorouracil (5-FU) in human cancer xenografts *in vivo*. *Eur J Cancer* 2001; **37**: 1681-1687
- 41 **Peters GJ**, Backus HH, Freemantle S, van Triest B, Codacci-Pisanelli G, van der Wilt CL, Smid K, Lunec J, Calvert AH, Marsh S, McLeod HL, Bloemena E, Meijer S, Jansen G, van Groeningen CJ, Pinedo HM. Induction of thymidylate synthase as a 5-fluorouracil resistance mechanism. *Biochim Biophys Acta* 2002; **1587**: 194-205

Edited by Bo XN

• LIVER CANCER •

An implantable rat liver tumor model for experimental transarterial chemoembolization therapy and its imaging features

Xin Li, Chuan-Sheng Zheng, Gan-Sheng Feng, Chen-Kai Zhuo, Jun-Gong Zhao, Xi Liu

Xin Li, Chuan-Sheng Zheng, Gan-Sheng Feng, Chen-Kai Zhuo, Jun-Gong Zhao, Xi Liu, Department of Interventional Radiology, Union Hospital, Tongji Medical College, Huazhong University of Science and Technology, Wuhan 430022, Hubei Province, China
Supported by the National Natural Science Foundation of China, No.39770839

Correspondence to: Dr. Xin Li, Department of Interventional Radiology, Union Hospital, Tongji Medical College, Huazhong University of Science and Technology, Wuhan 430022, Hubei Province, China. wxyao2001@yahoo.com.cn

Telephone: +86-27-85726432

Received 2002-07-04 **Accepted** 2002-07-25

Abstract

AIM: To establish an ideal implantable rat liver tumor model for interventional therapy study and examine its angiographic signs and MRI, CT features before and after embolization.

METHODS: Forty male Wistar rats were implanted with Walker-256 tumor in the left lateral lobe of liver. Digital subtraction angiography (DSA) and transarterial chemoembolization were performed on day 14 after implantation. Native computer tomography (CT, $n=8$) and native magnetic resonance (MR, $n=40$) were performed between the day 8 and day 21 after implantation. The radiological morphological characteristics were correlated with histological findings.

RESULTS: Successful implantation was achieved in all forty rats, which was confirmed by CT and MRI. MR allowed tumor visualization from day 8 while CT from day 11 after implantation. The tumors were hypodensity on CT, hypointense on MR T1-weighted and hyperintense on T2-weighted. The model closely resembled human hepatocarcinoma in growth pattern and the lesions were rich in vasculature on angiography and got its filling mainly from the hepatic artery. Before therapy, tumor size was $211.9 \pm 48.7 \text{ mm}^3$. No ascites, satellite liver nodules or lung metastasis were found. One week after therapy, tumor size was $963.6 \pm 214.8 \text{ mm}^3$ in the control group and $356.5 \pm 78.4 \text{ mm}^3$ in TACE group. Ascites (4/40), satellite liver nodules (7/40) or lung metastasis (3/40) could be seen on day 21.

CONCLUSION: Walker-256 tumor rat model is suitable for the interventional experiment. CT and MRI are helpful in animal optioning and evaluating experimental results.

Li X, Zheng CS, Feng GS, Zhuo CK, Zhao JG, Liu X. An implantable rat liver tumor model for experimental transarterial chemoembolization therapy and its imaging features. *World J Gastroenterol* 2002; 8(6):1035-1039

INTRODUCTION

Hepatocellular carcinoma (HCC) is a relatively common malignant tumor and its prognosis is poor^[1,2]. The first choice

of treatment is hepatectomy, but most cases are considered inoperable due to extreme tumor extension at the time of diagnosis and/or accompanying advanced cirrhosis^[2,3]. Moreover, it will respond neither to radiotherapy nor to systemic chemotherapy, the most frequently applied palliative treatment option for locally advanced tumors is transarterial chemoembolization (TACE)^[3-7]. Various protocols have been proposed with different chemotherapeutic agent, different embolization materials and different approaches. Lack of carefully designed, prospective and randomized trials has caused the most suitable scheme of TACE not yet established^[8]. In order to accelerate the study of TACE strategies for HCC, it is necessary to have a suitable and reproducible animal model.

The aim of the present study was to establish an implantable rat liver tumor model for experimental TACE therapy, and deliberate its angiographic signs and MRI, CT features before and after TACE.

MATERIALS AND METHODS

Tumor and animals

The Walker-256 carcinosarcoma cell line was obtained from the Cell Preservation Center of Wuhan University (Wuhan, Hubei, P. R. China). Forty male Wistar rats weighing $200 \pm 20 \text{ g}$ (experiment animal center, Tongji Medical College, Huazhong University of Science and Technology) were used.

Tumor implantation

Tumor implantation was performed using a modification of the technique described by Yang *et al*^[9]. A 2-week-old subcutaneously growing solid tumor was explanted from a donor animal and minced into small cubes of about 2 mm^3 . The recipient animals were laparotomized through a midline abdominal incision under intraperitoneal anesthesia with 1 % pentobarbital sodium (30 mg/kg body weight). The left lateral lobe of the liver was protruded out of the abdominal cavity and a subcapsular tunnel about 3-5 mm depth was made by a fine-point tweezer. Then a solid tumor fragment was inserted into the subcapsular tunnel and fixed with a small piece of gelfoam on the liver surface. No hemostasis was necessary.

Catheterization of the hepatic artery

14 days after the implantation, a second laparotomy was performed for angiographic studies and TACE therapy^[10]. Another midline abdominal incision was performed under the general anesthesia. The common hepatic artery, the gastroduodenal artery and the right hepatic artery were isolated using a binocular operative microscope (Suzhou Medical Instruments Factory, Jiansu, China). Through an arteriotomy of the gastroduodenal artery, a polyethylene catheter (0.3 mm in inside diameter and 0.5 mm in outside diameter) was inserted retrogradely into the gastroduodenal artery and temporarily fixed by a suture.

Animal group and drugs doses

Forty rats were randomly divided into two groups (Control

group and TACE group) of twenty rats each. Control group received 0.3 ml normal saline and TACE group received 0.5 ml/kg of iodized oil (Lipiodol UltraFluid, Andre Guerbet, Aulnay-sous-Bois, France) which were given by slow retrograded manual injected into the gastroduodenal artery while the common hepatic artery and right hepatic artery were temporarily ligated.

Imaging

Hepatic artery angiography was performed by using a digital angiographic unit (Bicor Top, Siemens, Germany). A 0.3 ml bolus of contrast medium (300 mg iodine/ml, Ultravist 300, Schering, Germany) was manually injected retrogradely via the surgically implanted catheter into the gastroduodenal artery. CT ($n=8$) and MR imaging ($n=40$) were performed at 8, 11, 14 days after the implantation and 7 or 8 days after the angiography and TACE therapy. Animals were anesthetized as described earlier prior to imaging. CT scans were performed on Somatom Plus 4 spiral Scanner (Siemens, Germany) with 3.0 mm scan thickness and 3.0 increments (pitch=1.0), a field of view of 150 mm, 140 mA and 80kVp. Documentation was performed with a window width of 250 and a center of 50 Hounsfield units. MR images were performed on 1.5-Tesla system (Siemens Vision, Siemens, Germany) supplemented by a cervical coil. T1-weighted (TR/TE, 450/12 msec) and T2-weighted (TR/TE, 2800/96 msec) transverse SE images (slice thickness 2mm) were acquired using acquisition times of 7:25 and 6:16 min, respectively.

Tumor volume was determined from MR measurements of the largest and smallest diameter and calculated according to the following formula: Tumor volume (mm^3)=largest diameter (mm) \times [smallest diameter (mm)]²/2.

Histologic evaluation

Forty rats were sacrificed at 2 (ten rats) and 7 (thirty rats) days after TACE, respectively. Samples of liver tumors were fixed in 10 % formalin, dehydrated and embedded in paraffin; 5- μm sections were stained with hematoxylin-eosin for light microscopy and measurement of the degree of tumor necrosis.

RESULTS

Tumor uptake, Tumor growth, and Histopathological findings

Tumor implantation led to the outgrowth of liver tumor nodules in all forty rats. The lesions were located in the left lobe of the liver as a solitary mass. Mean volume of the tumor measured by MR examination was $211.9 \pm 48.7 \text{ mm}^3$ 14 days after implantation, there was no statistic difference between the control and the TACE groups. No ascites, satellite liver nodules or lung metastasis was found. One week after therapy, mean volume of the tumor were $963.6 \pm 214.8 \text{ mm}^3$ in the control group and $356.5 \pm 78.4 \text{ mm}^3$ in TACE group and there were significant statistic differences between them ($t=8.396$, $P<0.001$). Ascites (4/40), satellite liver nodules (7/40) or lung metastasis (3/40) could be seen in some models at day 21.

Hematoxylin-eosin (H & E) stained sections of the liver specimens showed a poorly differentiated carcinoma, which were usually roughly spherical or ovoid in shape. Tumor cells arranged in irregular groups and the signs of malignancy, including hyperchromatosis, polymorphism and numerous mitoses were detected. The mass had a sharp demarcation from the surrounding normal hepatic parenchyma; its capsules were thin and composed of collagen fibers, which were caused by the compression of the tumor. The tumor showed inhomogeneous signs of hypervascularization consisting mainly

of small arteries and capillaries. Satellite nodules or portal vein tumor embolization could be seen in some models (Figure 1).

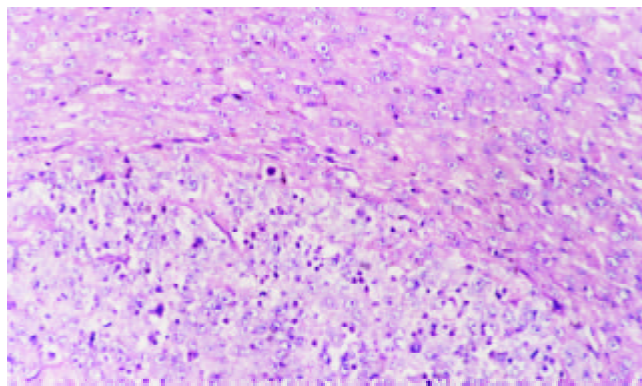


Figure 1 Control group, 7 days after hepatic artery infusion, show tumor and thin capsule. Hematoxylin-eosin $\times 200$

Spontaneous spotty, scattered necrosis were seen in all cases of the control group 7 days after the therapy. 2 days after iodized oil embolization, the range of tumor central necrosis obviously enlarged to moderate (16/20) or even severe degree (4/20). Intra-tumor hemorrhage and bile stasis were seen in some cases. Tumor cells tended to remain viable in the periphery of nodules in the samples 7 days after embolization. We also found thick fibrous capsules around the tumor with chronic inflammation and granulomatosis. Different degree of degeneration or necrosis were seen in normal hepatic parenchyma adjacent the tumor (Figure 2).

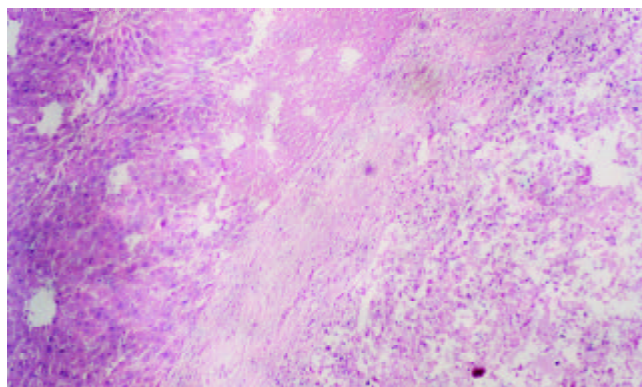


Figure 2 TACE group, 7 days after hepatic artery embolization, show tumor center necrosis, thick fibrous capsules, and degeneration or necrosis in normal hepatic parenchyma adjacent the tumor. Hematoxylin-eosin $\times 100$.

Tumor imaging

8 days after the implantation, MR could show node with clear shape in some cases, which showed hypointensity on T1-weighted and hyperintensity on T2-weighted (Figure 3). 14 days after the implantation, MR could detect lesions in all cases. Some degree of necrosis was seen in the center of the mass in 17 cases, presented as a lower intensity on T1 and T2-weighted as compared with the pathologic tissue without necrosis (Figure 4).

One week after hepatic artery infusions, necrosis was found in all cases of control group and little change was found before and after therapy. While in TACE group, MR features were as follows: the signal in the center of lesion was asymmetrical

and mixed (high, intermediate, and low) on T2-weighted. Rim sign with varying thickness of slight high signal intensity was seen on T1 and T2-weighted (Figure 5). In addition, the presence of ascites, satellite liver nodules or lung metastasis could be shown well on MR imaging.

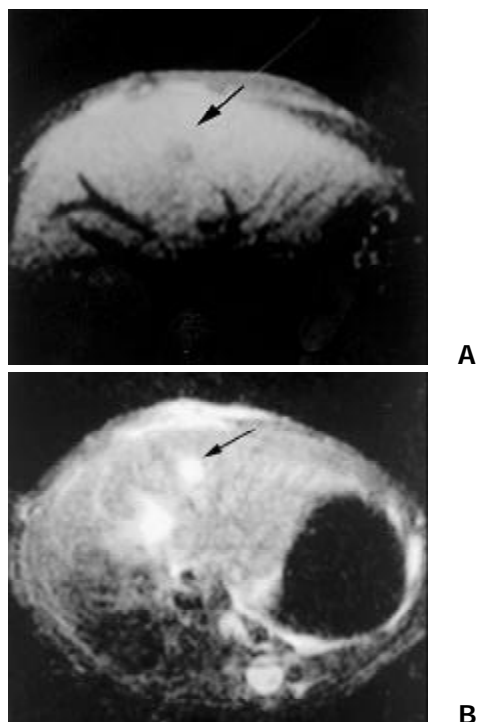


Figure 3 8 days after the implantation, MR demonstrate a node with clear shape, hypointensity on T1- weighted (A) and hyperintensity on T2 - weighted (B)

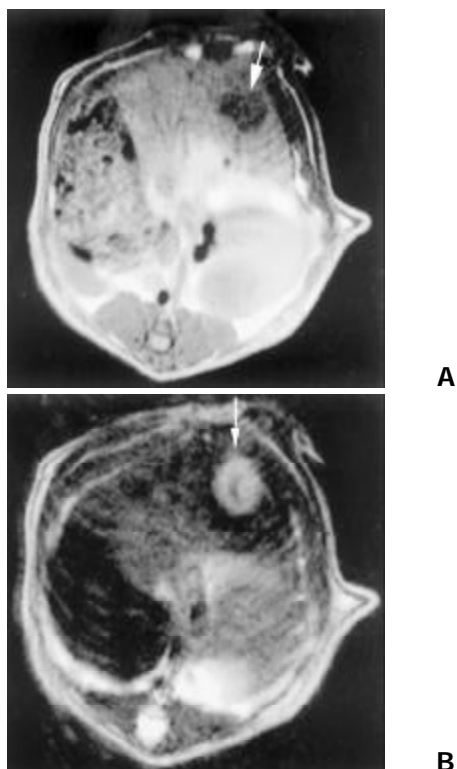


Figure 4 14 days after the implantation, tumor center showed lower intensity on T1 (A) and T2-weighted (B) than that of periphery, which indicate coagulation necrosis

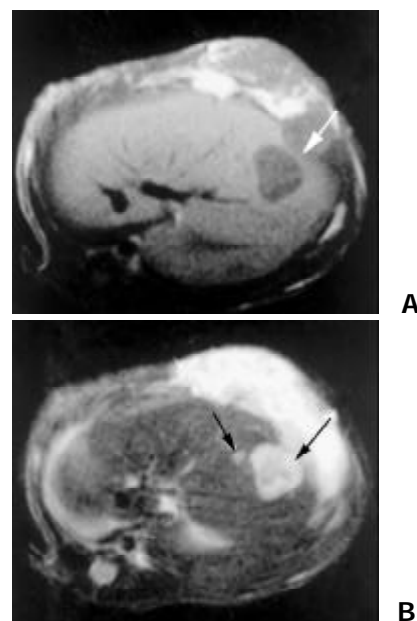


Figure 5 One week after TACE, MR showed center necrosis, periphery rim sign of slight higher T1 (A) and T2 (B) intensity, and the satellite nodular (B)

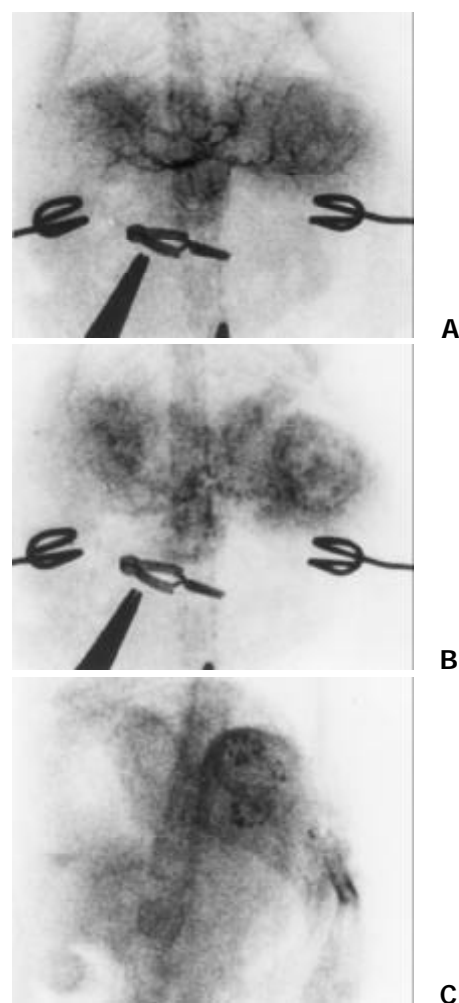


Figure 6 The tumor were mainly fed by the hepatic artery. Angiography features including hypervascularity, irregular tortuous and convoluted vessels (A), tumor stain (B) and the deposition of iodized oil in tumor after embolization (C)

Tumor could first be identified at day 11 after implantation on native CT. CT depicted the tumor as hypodensity masses and well discernible from the surrounding liver tissues. Some lesions were less dense in the central areas. After TACE, CT scans showed the dense deposition of iodized oil in tumor.

The hepatic artery mainly fed the tumors. Angiographic features included neovascularity, hypervascularity, irregular tortuous and convoluted vessels, tumor stain and sometime with contrast puddling. But no arteriovenous shunts or early venous drainage were seen. Those with central necrosis showed a contrast-enhancing periphery and a nonenhancing center. After embolization, main branches of the left hepatic artery were occluded and the deposition of iodized oil in tumor could be seen (Figure 6).

Comparative study of image and pathologic findings

The clear border shown by MR represented the fiber septum caused by the compression of the tumor on neighboring normal liver tissue. Central areas of lower density in CT, lower signal intensity on T1-weighted images and T2-weighted images were compatible with central necrosis. After therapy, central areas of high signal intensity on T2-weighted images correlated with areas of liquefaction necrosis, which were more common in larger lesion. Areas of low or intermediate signal intensity of the lesion on T2-weighted images corresponded to coagulation necrosis. The peripheral rim with varying thickness of slight high signal intensity on T1 and T2-weighted images correlated with the thick fibrous capsules and the granulation tissues.

DISCUSSION

TACE has been widely carried out and is considered an effective treatment for HCC patients who are not candidates for surgery^[3-8]. But as to selection of patient, TACE approaches and therapeutic efficacy, there were great variation by the different studies reported to date^[5,11-13]. Standardization of proper patient selection and choice of optimal TACE methods selection remain to be determined, which severely embarrass the further progress of TACE in HCC therapy. Many scholars advocate prospective randomized controlled trials to assess the efficacy of different TACE strategies^[8,14,15]. But the reaction to TACE is influenced by many factors, such as tumor differentiation, size, blood supply, liver function and adverse effect to the treatment make it difficult to judge the real efficacy of a certain TACE regime^[16-21]. Replication a suitable animal model for TACE therapy can overcome these shortages. We can study the efficacy of TACE on tumor of same differentiation and similar size, location and number. Experiments on tumor model will help in exploring new technique of TACE, studying the effectiveness of different therapeutic strategies and evaluating TACE related adverse effect.

Various methods have been introduced to develop intrahepatic tumor models. Nude rats transplantation models are relatively hard to feed, need more complicate manipulation in tumor implantation and hepatic artery therapy and were more expensive^[22-24]. Induction with hepatocarcinogens (such as diethylnitrosamine or aflatoxin) will produce multifocal liver tumors^[25,26]. Many implantation tumors (such as Novikoff hepatoma or DHD K12 colon carcinoma cells) show early central necrosis, early systemic metastasis, or appear hypovascular^[27-29]. All of these models were not suitable for TACE study. In the present study we establish Walker-256 transplanted liver tumor model and examine its tumor growth characteristic, blood supply and imaging features to judge the potential of this model in the experimental study of TACE^[30].

The models show reproducibility on tumor growth rate and growth characteristic. The lesions get its blood supply mainly from hepatic artery, rich in vasculature and had similar angiographic features similar to that of HCC^[31,32]. We concluded the tumor around 14 days after implantation was suitable for TACE experimental study-by the time the tumor had proper size, hypervascularization and no evident central necrosis.

Imaging procedures allowed monitoring of tumor size at the time of intervention and during the follow-up period without sacrificing animal and thus reduced the number of animals needed. In this series, we investigated the visualization and sizing of tumors using native CT and MR, which had been proven very useful for the clinical assessment of the effects of TACE in HCC^[33-35]. The CT and MR appearance of Walker-256 carcinoma before and after TACE is similar to that of HCC in humans. It can reflect the histopathologic changes in some degree and determine the treatment efficacy preliminarily. We found MR is superior to CT in tumor detection. In further studies, MR and CT features before and after contrast media administration will be carried out to obtain further information^[36-38].

The left lateral lobe is the largest one in many rat liver lobes and the left hepatic artery has a larger caliber than the right one. So we chose the left lateral lobe as the target during the tumor implantation. After the liver was returned to the abdominal cavity, the implantation site was spontaneous covered by parts of the median lobe. Simultaneously, we fixed the tumor fragment with a small piece of gelfoam on the liver surface. Our implantation techniques guaranteed the intra-parenchyma tumor growth and avoided the artificial technique-induced tumor dissemination.

According to our trial experiment and literature, the iodized oil dosage chosen for embolization was 0.5 ml / kg, which can obstruct the secondary branches of the left hepatic artery^[39]. When the embolic agent was injected retrograded slowly into the gastroduodenal artery, the common hepatic artery was temporarily ligated to avoid reflux of embolic agent into the celiac trunk. Simultaneously, for the purpose of segmental embolization, we temporarily ligated right hepatic artery and this could help the rat to survive after embolization.

By the study of the imaging and pathological features, we considered the advantages of the model are: (1) We can choose the position of implantation as designed. (2) It has a high tumor uptake rate and high reproducibility of tumor growth characteristics, the procedure of implantation is simple and can be performed quickly. (3) Blood supply of the tumors mainly comes from hepatic artery and the lesions were rich in vasculature, indicating that the model is suitable for TACE experimental study. (4) The experimental methods (including tumor implantation and hepatic artery catheterization) guarantee a high post-therapy survival rate and allow the dynamic evaluation of image characteristics and treatment efficacy possible. (5) MR and CT scan can display the lesion clearly and show ascites, satellite liver nodules or lung metastasis in some models. These are helpful in animal optioning and allows noninvasive evaluation of treatment efficacy.

We conclude that the model can resemble the natural course of human HCC and have similar angiographic, CT and MR features. This tumor model has the potential to be effectively used in the experimental study of TACE.

REFERENCES

- 1 **Pisani P**, Parkin DM, Bray FI, Ferlay J. Estimates of the world-wide mortality from twenty-five major cancers in 1990. *Int J Cancer* 1999; **83**: 18-29

- 2 **Akriviadis EA**, Llovet JM, Efremidis SC, Shouval D, Canelo R, Ringes B, Meyers WC. Hepatocellular carcinoma. *Br J Surg* 1998; **85**: 1319-1331
- 3 **Liu CL**, Fan ST. Nonresectional therapies for hepatocellular carcinoma. *Am J Surg* 1997; **173**: 358-365
- 4 **Sangro B**, Herraiz M, Martinez-Gonzalez MA, Bilbao I, Herrero I, Belouqui O, Betes M, de-la-Pena A, Cienfuegos JA, Quiroga J, Prieto J. Prognosis of hepatocellular carcinoma in relation to treatment: A multivariate analysis of 178 patients from a single European institution. *Surgery* 1998; **124**: 575-583
- 5 **Ueno K**, Miyazono N, Inoue H, Nishida H, Kanetsuki I, Nakajo M. Transcatheter arterial chemoembolization therapy using iodized oil for patients with unresectable hepatocellular carcinoma: evaluation of three kinds of regimens and analysis of prognostic factors. *Cancer* 2000; **88**: 1574-1581
- 6 **Chia-Hsien Cheng J**, Chuang VP, Cheng SH, Lin YM, Cheng TI, Yang PS, Jian JJ, You DL, Horng CF, Huang AT. Unresectable hepatocellular carcinoma treated with radiotherapy and/or chemoembolization. *Int J Cancer* 2001; **96**: 243-252
- 7 **Fan J**, Ten GJ, He SC, Guo JH, Yang DP, Wang GY. Arterial chemoembolization for hepatocellular carcinoma. *World J Gastroenterol* 1998; **4**: 33-37
- 8 **Okada S**. Transcatheter arterial embolization for advanced hepatocellular carcinoma: the controversy continues. *Hepatology* 1998; **27**: 1743-1744
- 9 **Yang R**, Rescorla FJ, Reilly CR, Faught PR, Sanghvi NT, Lumeng L, Franklin TD, Grosfeld JL. A reproducible rat liver cancer model for experimental therapy: introducing a technique of intrahepatic tumor implantation. *J Surg Res* 1992; **52**: 193-198
- 10 **Kamphorst EJ**, Bodeker H, Koroma S, Linnemann U, Berger MR. New technique for superselective arterial (chemo-) embolization of the rat liver. *Lab Anim Sci* 1999; **49**: 216-219
- 11 **Kamada K**, Nakanishi T, Kitamoto M, Aikata H, Kawakami Y, Ito K, Asahara T, Kajiyama G. Long-term prognosis of patients undergoing transcatheter arterial chemoembolization for unresectable hepatocellular carcinoma: comparison of cisplatin lipiodol suspension and doxorubicin hydrochloride emulsion. *J Vasc Interv Radiol* 2001; **12**: 847-854
- 12 **Zhang Z**, Liu Q, He J, Yang J, Yang G, Wu M. The effect of preoperative transcatheter hepatic arterial chemoembolization on disease-free survival after hepatectomy for hepatocellular carcinoma. *Cancer* 2000; **89**: 2606-2612
- 13 **Chen MS**, Li JQ, Zhang YQ, Lu LX, Zhang WZ, Yuan YF, Guo YP, Lin XJ, Li GH. High-dose iodized oil transcatheter arterial chemoembolization for patients with large hepatocellular carcinoma. *World J Gastroenterol* 2002; **8**: 74-78
- 14 **Llado L**, Virgili J, Figueras J, Valls C, Dominguez J, Rafecas A, Torras J, Fabregat J, Guardiola J, Jaurieta E. A prognostic index of the survival of patients with unresectable hepatocellular carcinoma after transcatheter arterial chemoembolization. *Cancer* 2000; **88**: 50-57
- 15 **Trevisani F**, De Notariis S, Rossi C, Bernardi M. Randomized control trials on chemoembolization for hepatocellular carcinoma: is there room for new studies? *J Clin Gastroenterol* 2001; **32**: 383-389
- 16 **Chan AO**, Yuen MF, Hui CK, Tso WK, Lai CL. A prospective study regarding the complications of transcatheter intraarterial lipiodol chemoembolization in patients with hepatocellular carcinoma. *Cancer* 2002; **94**: 1747-1752
- 17 **Lee SH**, Hahn ST, Park SH. Intraarterial lidocaine administration for relief of pain resulting from transarterial chemoembolization of hepatocellular carcinoma: its effectiveness and optimal timing of administration. *Cardiovasc Intervent Radiol* 2001; **24**: 368-371
- 18 **Lee JK**, Chung YH, Song BC, Shin JW, Choi WB, Yang SH, Yoon HK, Sung KB, Lee YS, Suh DJ. Recurrences of hepatocellular carcinoma following initial remission by transcatheter arterial chemoembolization. *J Gastroenterol Hepatol* 2002; **17**: 52-58
- 19 **Caturelli E**, Siena DA, Fusilli S, Villani MR, Schiavone G, Nardella M, Balzano S, Florio F. Transcatheter arterial chemoembolization for hepatocellular carcinoma in patients with cirrhosis: evaluation of damage to nontumorous liver tissue-long-term prospective study. *Radiology* 2000; **215**: 123-128
- 20 **Lee HS**, Kim JS, Choi IJ, Chung JW, Park JH, Kim CY. The safety and efficacy of transcatheter arterial chemoembolization in the treatment of patients with hepatocellular carcinoma and main portal vein obstruction. A prospective controlled study. *Cancer* 1997; **79**: 2087-2094
- 21 **Poon RT**, Ngan H, Lo CM, Liu CL, Fan ST, Wong J. Transarterial chemoembolization for inoperable hepatocellular carcinoma and postresection intrahepatic recurrence. *J Surg Oncol* 2000; **73**: 109-114
- 22 **Selzner M**, Bielawska A, Morse MA, Rudiger HA, Sindram D, Hannun YA, Clavien PA. Induction of apoptotic cell death and prevention of tumor growth by ceramide analogues in metastatic human colon cancer. *Cancer Res* 2001; **61**: 1233-1240
- 23 **Gervaz P**, Scholl B, Padrun V, Gillet M. Growth inhibition of liver metastases by the anti-angiogenic drug TNP-470. *Liver* 2000; **20**: 108-113
- 24 **Shiba H**, Okamoto T, Futagawa Y, Ohashi T, Eto Y. Efficient and cancer-selective gene transfer to hepatocellular carcinoma in a rat using adenovirus vector with iodized oil esters. *Cancer Gene Ther* 2001; **8**: 713-718
- 25 **Tang ZY**, Sun FX, Tian J, Ye SL, Liu YK, Liu KD, Xue Q, Chen J, Xia JL, Qin LX, Sun SL, Wang L, Zhou J, Li Y, Ma ZC, Zhou XD, Wu ZQ, Lin ZY, Yang BH. Metastatic human hepatocellular carcinoma models in nude mice and cell line with metastatic potential. *World J Gastroenterol* 2001; **7**: 597-601
- 26 **Yang CF**, Liu J, Wasser S, Shen HM, Tan CE, Ong CN. Inhibition of ebselen on aflatoxin B (1)-induced hepatocarcinogenesis in Fischer 344 rats. *Carcinogenesis* 2000; **21**: 2237-2243
- 27 **Kurth S**, Bulian D, Kreft B, Riemenschneider T. Intraarterial hepatic chemotherapy with fluorouracil, fluorodeoxyuridine, mitomycin C, cisplatin or methotrexate as single-agent anticancer drugs for a transplanted experimental liver tumor in rats. *J Cancer Res Clin Oncol* 1996; **122**: 421-426
- 28 **Bastian P**, Bartkowski R, Kohler H, Kissel T. Chemo-embolization of experimental liver metastases. Part I: distribution of biodegradable microspheres of different sizes in an animal model for the locoregional therapy. *Eur J Pharm Biopharm* 1998; **46**: 243-254
- 29 **Gervaz P**, Scholl B, Padrun V, Gillet M. Growth inhibition of liver metastases by the anti-angiogenic drug TNP-470. *Liver* 2000; **20**: 108-113
- 30 **Guo WJ**, Li J, Ling WL, Bai YR, Zhang WZ, Cheng YF, Gu WH, Zhuang JY. Influence of hepatic arterial blockage on blood perfusion and VEGF, MMP-1 expression of implanted liver cancer in rats. *World J Gastroenterol* 2002; **8**: 476-479
- 31 **Krinsky GA**, Nguyen MT, Lee VS, Rosen RJ, Goldenberg A, Theise ND, Morgan G, Rofsky NM. Dysplastic nodules and hepatocellular carcinoma: sensitivity of digital subtraction hepatic arteriography with whole liver explant correlation. *J Comput Assist Tomogr* 2000; **24**: 628-634
- 32 **Chuang VP**. Hepatic tumor angiography: a subject review. *Radiology* 1983; **148**: 633-639
- 33 **Takayasu K**, Arii S, Matsuo N, Yoshikawa M, Ryu M, Takasaki K, Sato M, Yamanaka N, Shimamura Y, Ohto M. Comparison of CT findings with resected specimens after chemoembolization with iodized oil for hepatocellular carcinoma. *Am J Roentgenol* 2000; **175**: 699-704
- 34 **Vogl TJ**, Trapp M, Schroeder H, Mack M, Schuster A, Schmitt J, Neuhaus P, Felix R. Transarterial chemoembolization for hepatocellular carcinoma: volumetric and morphologic CT criteria for assessment of prognosis and therapeutic success-results from a liver transplantation center. *Radiology* 2000; **214**: 349-357
- 35 **De Santis M**, Alborino S, Tartoni PL, Torricelli P, Casolo A, Romagnoli R. Effects of lipiodol retention on MRI signal intensity from hepatocellular carcinoma and surrounding liver treated by chemoembolization. *Eur Radiol* 1997; **7**: 10-16
- 36 **Colagrande S**, Fargnoli R, Dal Pozzo F, Bindi A, Rega L, Villari N. Value of hepatic arterial phase CT versus lipiodol ultrafluid CT in the detection of hepatocellular carcinoma. *J Comput Assist Tomogr* 2000; **24**: 878-883
- 37 **Kubota K**, Hisa N, Nishikawa T, Fujiwara Y, Murata Y, Itoh S, Yoshida D, Yoshida S. Evaluation of hepatocellular carcinoma after treatment with transcatheter arterial chemoembolization: comparison of Lipiodol-CT, power Doppler sonography, and dynamic MRI. *Abdom Imaging* 2001; **26**: 184-190
- 38 **Katyal S**, Oliver JH, Peterson MS, Chang PJ, Baron RL, Carr BI. Prognostic significance of arterial phase CT for Prediction of response to transcatheter arterial chemoembolization in unresectable hepatocellular carcinoma: a retrospective analysis. *Am J Roentgenol* 2000; **175**: 1665-1672
- 39 **Kan Z**, Sato M, Ivancev K, Uchida B, Hedgpeth P, Lunderquist A, Rosch J, Yamada R. Distribution and effect of iodized poppyseed oil in the liver after hepatic artery embolization: experimental study in several animal species. *Radiology* 1993; **186**: 861-866

• LIVER CANCER •

Pathological characteristics, PCNA labeling index and DNA index in prognostic evaluation of patients with moderately differentiated hepatocellular carcinoma

Wen-Jiao Zeng, Guo-Yuan Liu, Jie Xu, Xin-Da Zhou, Yue-E Zhang, Nong Zhang

Wen-Jiao Zeng, Guo-Yuan Liu, Jie Xu, Yue-E Zhang, Nong Zhang, Department of Pathology, Medical School of Fudan University, Shanghai, China

Xin-Da Zhou, Liver Cancer Research Institute of Fudan University, Shanghai, China

Supported by the Foundation of the Minister of Science and Technology, No 96-906-01-15

Correspondence to: Dr. Nong Zhang, Department of Pathology, Medical School of Fudan University, 138 Yi Xue Yuan Road, Shanghai 200032, China. zhangnong@shmu.edu.cn

Telephone: +86-21-54237537 **Fax:** +86-21-65649416

Received 2002-05-11 **Accepted** 2002-06-09

Abstract

AIM: To study the relationship between prognosis and pathological characteristics, proliferating cell nuclear antigen labeling index (PCNA-LI) and DNA index (DI) in patients with moderately differentiated hepatocellular carcinoma (HCC).

METHODS: 51 cases of moderately differentiated HCC were analyzed with respect to the relation between their clinical follow-up data and pathological characteristics. Meanwhile, PCNA-LI of HCC cells was detected by immunohistochemistry assay and DI was measured by Feulgen staining and automatic image analysis technique.

RESULTS: Patients with a single tumor nodule, less than 5 cm in diameter, no tumor emboli, no daughter nodules and necrosis had relatively better prognosis; patients with euploidy HCC had better prognosis than those with aneuploidy; among the aneuploidy patients those with DI <1.5 had better prognosis than the cases with DI >1.5; The higher the PCNA-LI, the worse would be the prognosis. The increase in DI was correlated with the increase in PCNA-LI, and both of them were correlated with the pathological changes of the tumor.

CONCLUSION: A composite analysis of the pathological characteristics of tumor tissue, DI and PCNA-LI might be useful in predicting the prognosis of HCC patients.

Zeng WJ, Liu GY, Xu J, Zhou XD, Zhang YE, Zhang N. Pathological characteristics, PCNA labeling index and DNA index in prognostic evaluation of patients with moderately differentiated hepatocellular carcinoma. *World J Gastroenterol* 2002; 8(6):1040-1044

INTRODUCTION

Hepatocellular carcinoma (HCC) is one of the most common malignant tumors in the world. Since 1990s HCC has become

the second killer in various cancers in China^[1]. Metastasis and recurrence of the neoplasm after surgical removal is still high. The frequency of 5-year recurrence after radical resection is 61.5 % overall^[2]. So the knowledge of the indexes related to recurrence and survival is very helpful in predicting the prognosis of patients with HCC and to make decision on adjuvant therapies for those patients. It has been generally accepted that the degree of differentiation of tumor cells is one of the most important aspects affecting the prognosis, but even among patients of a similar differentiation of HCC, the survival period is quite different. To explore this difference, we analyzed 51 cases of moderately differentiated HCC with respect to their clinical follow-up data, the histopathological characteristics, proliferating cell nuclear antigen labeling index (PCNA-LI) and DNA index (DI). We expected to find some simple and applicable indexes for estimating the prognosis of HCC by examining the surgical specimens of HCC.

MATERIALS AND METHODS

Materials

Formalin-fixed and paraffin-embedded HCC tissues blocks from 51 cases of patients with moderately differentiated HCC, the clinical data, data of the specimens (tumor size, portal vein tumor emboli, daughter nodules and so on) and follow-up data (including ultrasound examinations of liver every half a year after surgery) were collected in Zhongshan Hospital affiliated to Fudan University during 1989-1990. We used tumor-free survival (TFS) to estimate prognosis in order to eliminate the affection of various therapies after tumor recurrence. TFS was recorded dating from the time of operation, up to the time of death or detection of HCC recurrence by ultrasound examination. The follow-up ended in December, 1999 (2 cases were lost to follow up at 67, 88 months respectively). The TFS time ranged from 8 days to more than 129 months. The probability of 1-year TFS was 62.7 %, that of 3-year TFS was 35.3 % and that of 5-year TFS was 27.5 %. 8 cases had no recurrence and were still alive at the end of the follow-up.

Histopathological inspection

4 µm tissue thick sections were cut from each block and stained with hematoxylin-eosin. We examined morphological characteristic and arrangements of tumor cells, infiltration of mononuclear cells in the stroma, tumor capsules formation and its thickness, state of tumor cells invasion, and tumor emboli and microscopic daughter nodule in vein around the cancer. The infiltration of mononuclear cells was graded as follow: 0, none or occasionally found; 1, diffuse; 2, crowded together or even lymphoid follicles formed. Tumor without capsule was defined as tumor tissue directly bordering on normal liver tissue. If ten or more layers of stratified fibrous collagen together with fibroblasts separate them, it was defined as thick

capsule; less than this was defined as thin capsule. The diameter of cancer was indicated with geometric mean of three-dimensional parameters of single cancer nodule and cube root of total volume of multiple ones.

Immunohistochemical staining

Formalin-fixed and paraffin-embedded liver tissue sections of 4 μ m thickness were dewaxed in xylene and graded alcohols, hydrated, and washed in phosphate-buffered saline. The endogenous peroxidase was inhibited by 0.6 % H_2O_2 for 30 minutes, and the sections were incubated with normal goat serum (1:20 for 20 minutes). A 1:40 diluted rabbit polyclonal antibody to PCNA was applied 1 hour at 37 °C and then at 4 °C overnight in a moist chamber. Phosphate-buffered saline replaced the first antibody as blank control. A standard avidin-biotin peroxidase technique (ABC assay) was applied. Briefly, biotinylated goat anti-rabbit Ig and avidin-biotin peroxidase complex were applied for 1 hour each, with 15 minute washing in phosphate-buffered saline. The reaction was finally developed with 3-3' diaminobenzidine solution in 0.003 % H_2O_2 buffer phosphate (PH 7.8) for 10 minutes. Sections were counterstained with hematoxylin, dehydrated in alcohol, cleared in xylene, and mounted in DPX. The antibody and ABC kit were purchased from Dako Co. Copenhagen, Denmark.

To get average positive level of each case, six microscopic fields of 400 \times magnification were selected which included two representative fields each of considerable, medium and a few positive cells. PCNA-LI is the percentage of immunohistochemical staining positive cells in 1 000 HCC cells counted. The criterion to evaluate the expression of PCNA-LI was as following: 1, >15 % (high); 2, 5-15% (medium); 3, <5 % (low).

Determine of DNA-index

Feulgen staining was applied on 4 μ m thick sections, and IMS Cell Analysis System (Shenteng Co. Shanghai, P.R. China) was used to detect DNA index. In each case six representative microscopic fields were chosen and the integral optical density (IOD) of 100 discrete HCC cells was measured with lymphocyte nuclei in stroma as diploidy control. Then the DNA index was automatically calculated.

Statistical analysis

SPSS for windows 10.0 software was used in statistical analysis. Data were expressed as means \pm SD in the presence of continuous variables and as counts (percentages) for the categorical variables. Continuous variables were compared with the student *t* test, and categorical variables were compared with χ^2 test. The probability of TFS time was calculated using the Kaplan-Meier approach and differences between survival curves were tested by the Log-rank test.

RESULTS

General conditions

51 patients were from 27 to 71 years old, median 53 years old. 48 cases were male (94.1 %). The probability of 3-year TFS in single nodule group was 44.4 %, significantly higher than multiply nodules group 13.3 % ($P < 0.05$). The probability of 5-year TFS in tumor size ≤ 5 cm was 43.3 %, higher than group with tumor size > 5 cm 4.8 % ($P < 0.01$) (Table 1).

Inspection of tissue section

Tumor emboli were found in 19 cases and tumor necrosis in 16 cases during surgical operation and/or in pathological

sections. The probability of 5-year TFS in those without tumor emboli was obviously higher than those with them ($P < 0.01$). The probability of 1-year TFS in those without tumor necrosis was significantly higher than those with it ($P < 0.01$). 45 of 51 cases had well-preserved wax blocks and had one or two sections available to show capsules and tissues around tumor. We found that the probability of 1-year TFS in those with daughter nodules was lower than those without them ($P < 0.01$) and the probability of TFS in those with thick capsule was slightly higher than those with thin capsule or no capsule. The mononuclear cells infiltrating in the tumor and surroundings were mainly lymphocytes, mixing with fibrous collagen and fibroblasts, which were mostly distributed at the interface between HCC and the surroundings (Figure 1). They formed thin or thick capsule, some of which extended to tumor tissue and connected with stroma in HCC. Various degrees of lymphocytic infiltration occurred in tumor stroma (Figure 2), coordinated with that of the interface area. Only very few of the lymphocytes infiltrating tumor parenchyma showed direct contact with tumor cells. The probability of TFS in those with more heavy lymphocytic infiltration was slightly higher. (Table 1).

Table 1 The relationship between pathological characteristics and TFS

Variables	<i>n</i>	The probability of TFS (%)		
		1-year	3-year	5-year
Tumor nodule				
Single	36	72.2	44.4	33.3
Multiple	15	40.0 ^a	13.3 ^a	6.7
Tumor diameter				
≤5 cm	30	86.7	53.3	43.3
>5 cm	21	33.3 ^b	9.5 ^b	4.8 ^b
Tumor necrosis				
No	35	77.1	42.9	34.3
Yes	16	31.3 ^b	18.8	12.5
Tumor emboli				
No	26	76.9	50.0	42.3
Yes	19	36.8 ^b	10.5 ^b	0 ^b
Daughter nodules				
No	30	80.0	40.0	30.0
Yes	15	20.0 ^b	20.0	13.3
Infiltrated lymphocytes				
Many	9	88.9	66.7	44.4
A few or none	42	59.5	31.0	23.8
Capsule				
Thick	13	69.2	46.2	30.8
None or thin	32	56.3	28.1	21.9

^a $P < 0.05$ vs the above group, ^b $P < 0.01$ vs the above group.

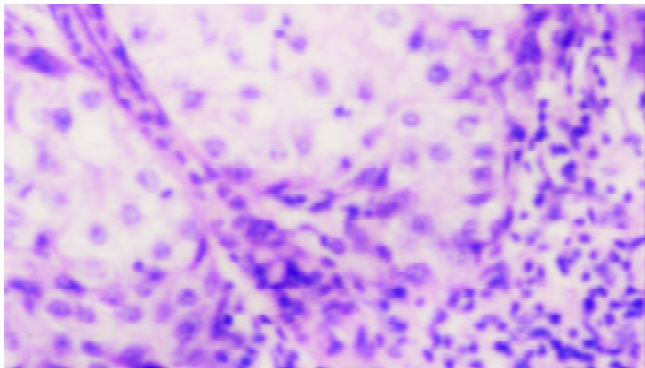


Figure 1 Massive lymphocytes infiltrating the interface between HCC and surroundings (HE, ×100)

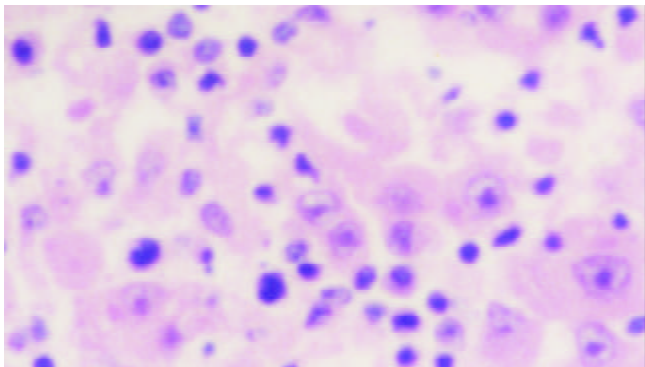


Figure 2 Many lymphocytes infiltrating tumor stroma (HE, ×100)

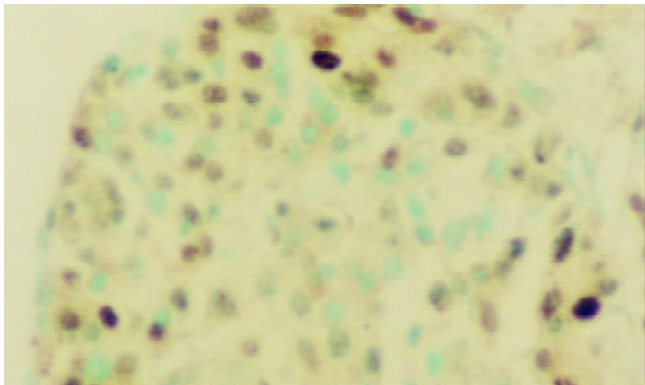


Figure 3 PCNA positive cells mainly distributed in the peripheral area of tumor nest (PCNA immunohistochemical staining, ×200)

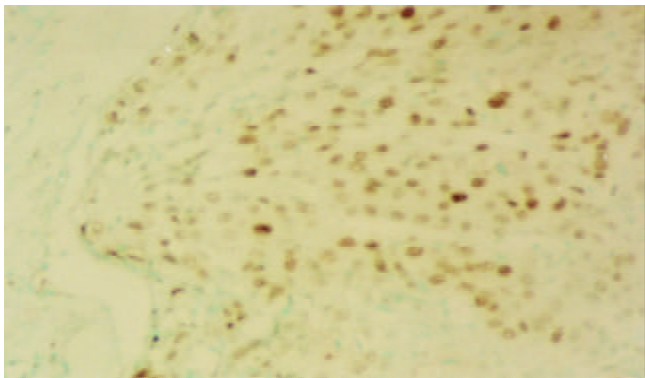


Figure 4 HCC invasion in capsule (HE, ×100)

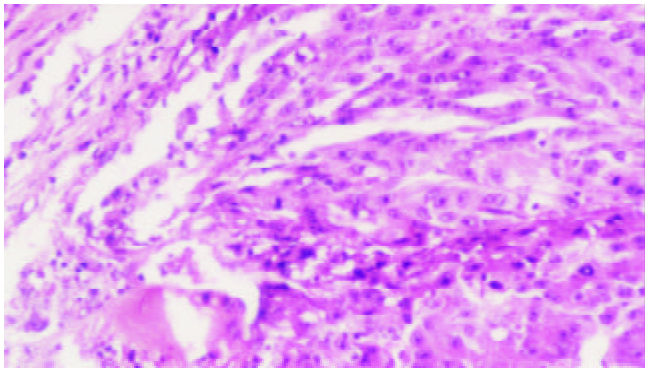


Figure 5 PCNA positive cells (the continuous section of Figure 4, PCNA immunohistochemical staining, ×100)

PCNA-Labeling Index

PCNA positive granules were found in the nuclei, and all cells with recognizable nuclear stain were considered as positive. PCNA positive cells were mainly distributed in the peripheral area of tumor nest and also in tumor emboli and at the site of HCC invasion (Figure 3,4,5). The prognosis in the case with higher PCNA-LI was worse, $P<0.01$ (Figure 6). With a higher PCNA-LI, the tumor size was usually larger and the probability of tumor emboli, daughter nodules and tumor necrosis was also higher ($P<0.05$, Table 2).

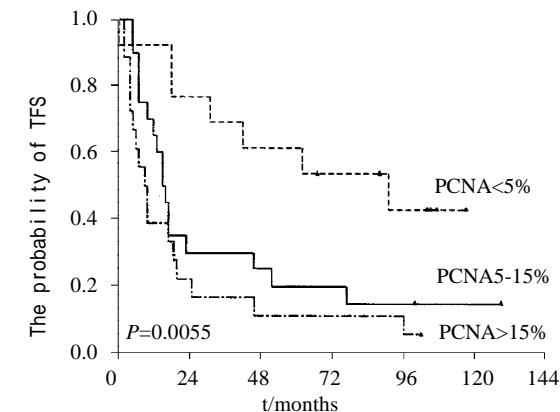


Figure 6 The Kaplan-Meier curves of different PCNA-LI groups

Table 2 The relationship of pathological characteristics to DI and PCNA-LI

Variables	<i>n</i>	Diameter (cm)	Multiple nodules	Tumor necrosis	Tumor emboli ^a	Daughter nodules ^a
DI						
Euploid	8	4.30±1.97	2	1	0/6	0/6
Aneuploid DI<1.5	22	3.64±1.29	5	4	8/19	4/19
Aneuploid DI>1.5	21	6.34±2.65 ^{bc}	8	11	11/20	11/20 ^d
PCNA-LI						
<5 %	13	4.09±1.44	0	1	0/10	2/10
5-15 %	20	4.53±2.50	10 ^c	4	8/18	3/18
>15 %	18	5.78±2.60 ^b	5	11 ^{ce}	11/17 ^c	10/17 ^e

^aThe denominator was the number of observed cases, the numerator was the number of those presenting tumor emboli or satellite nodules. ^b $P<0.05$, ^c $P<0.01$ compared with the first group; ^d $P<0.05$, ^e $P<0.01$ compared with the second group.

DNA-index

In diploidy $DI=1 \pm 0.1$, and in tetraploidy $DI=2 \pm 0.1$. DI out of the above range was aneuploidy. The prognosis of HCC cases with euploidy was better than those with aneuploidy, and in the latter $DI<1.5$ was better than $DI>1.5$, $P<0.001$ (Figure 7). In the group of $DI>1.5$ aneuploidy, tumor size was larger and the probability of tumor emboli, daughter nodules and tumor necrosis was higher (Table 2).

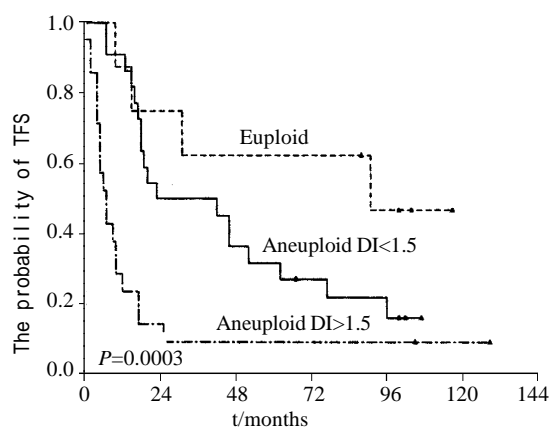


Figure 7 The Kaplan-Meier curves of different DI groups

The relationship between PCNA-LI and DI

The PCNA-LI in $DI<1.5$ aneuploidy group was obviously higher than in euploidy group ($P<0.05$), and that in $DI>1.5$ aneuploidy group was also higher than $DI<1.5$ aneuploidy group ($P<0.05$, Table 3). Aneuploidy $DI>1.5$ was seen more in higher PCNA-LI cases ($P<0.01$), and no euploidy was found in 18 cases with high PCNA-LI (Table 4). The TFS time in 13 aneuploidy cases with high PCNA-LI and $DI>1.5$ was from 2 to 25 months; their average TFS time was 8.1 months and the probability of 1-year TFS was only 15 %, much lower than that of the total cases (62.7 %, $P<0.01$).

Table 3 PCNA-LI in different DI groups

DI	n	PCNA-LI (%)
Euploid	8	5.076±3.904
Aneuploid $DI<1.5$	22	9.300±6.896 ^a
Aneuploid $DI>1.5$	21	15.113±9.527 ^{bc}

^a $P<0.05$, ^b $P<0.01$ compared with the first group, respectively;

^c $P<0.05$ compared with the second group.

Table 4 The DNA-index distribution in different PCNA groups

PCNA-LI	n	Euploidy	Aneuploidy $DI<1.5$	Aneuploidy $DI>1.5$
<5%	13	5	6	2
5-15%	20	3	11	6
>15%	18	0	5	13

χ^2 test $P<0.01$, compared aneuploidy $DI>1.5$ and the others among the groups.

DISCUSSION

According to pathomorphological inspection of HCC, the TFS of patients with single tumor nodule (diameter ≤ 5 cm, no tumor

emboli, no daughter nodules and tumor necrosis) was obviously high and these factors are indicators of better prognosis, which are consistent with results of other retrospective researches^[3-6]. The mononuclear cells reaction may represent the response to local irritation by the tumor, but it also may be a host immunological defense mechanism against the neoplastic process. Tumor-infiltrating lymphocytes are important in immunotherapy for tumors^[7-9]. The presence of collagen I and III in tumor tissues may inhibit tumor cell infiltration and metastasis and such patients may have a better prognosis^[10]. The expression of MMPs (a matrix-degrading enzyme family) in tumor and its relation to prognosis is one of hot points in tumor research^[11-16]. Our studies also implied that patients with more mononuclear cells infiltrating in the tumor and surrounding tissue had better prognosis, and those with a thick capsule also had a longer TFS, though the differences were not statistically significant because of small number of cases.

Detection of DNA content and ploidy of tumor cells is still a common method to evaluate tumor malignancy and patient's prognosis^[17-22]. Our studies demonstrated that the prognosis of patients with euploidy HCC was better than that of patients with aneuploidy HCC, and in the latter the prognosis of $DI<1.5$ cases was better than that of $DI>1.5$ ones. In aneuploidy, $DI=1.5$ seemed to be a borderline, and the probability of 3-year TFS in $DI>1.5$ cases (13.6 %) was obviously lower than in $DI<1.5$ cases (52.4 %, $P<0.01$).

PCNA, auxiliary protein of DNA polymerase delta, accumulates in the nuclei during the S-phase of the cell-cycle, i.e., proliferating cells^[23]. PCNA-LI can explicitly reflect proliferating degree of tumor. It was reported that PCNA-LI >2.0 % was the strongest independent predictor of HCC in patients with compensated cirrhosis^[24]. Previous research found that PCNA-LI was closely related with HCC differentiation, but others reached a conclusion that PCNA was not related with patients survival^[25]. We found that PCNA-LIs were very different even in the similar moderately differentiated HCC cases, and the prognosis was worse in patients with higher PCNA-LI, and the probability of 5-year TFS in PCNA-LI >15 % group was only 11.1 % which was far lower than that in PCNA-LI <5 % group (61.5 %, $P<0.01$). Closset et al reported that PCNA-LI <30 % appeared to be a good prognostic factor in patients without cirrhosis^[26]. Besides differentiation of HCC, the difference of PCNA-LI borderline is most closely due to fields selection. We noticed that PCNA positive cells often mainly distributed in the peripheral area of tumor nest and also in tumor emboli and at the site of HCC invasion, while seldom in the middle of tumor nest. Such uneven distribution caused difficulty in selecting fields for immunohistochemistry. We applied an objective way to solve the problem: firstly, we went over the whole section, then selected six microscopic fields of $400\times$ magnification, including two representative fields for each one of a considerable number, medium and a few positive cell areas, and finally calculated positive ones in 1 000 tumor cells.

Both PCNA-LI and DI can reflect the degree of tumor proliferation^[19]. Studies in 51 cases HCC showed a certain relationship between them: the PCNA-LI in aneuploidy group was higher than in euploidy group, and a higher PCNA-LI had a higher proportion of aneuploidy. In 18 cases with a high PCNA-LI not a single case of euploidy was detected and the proportion of $DI>1.5$ aneuploidy was also high ($P<0.05$). However, it should be pointed out that merely judged by PCNA-LI or DI a few exceptions were found, for example, the TFS of 2 cases in the high PCNA-LI group was more than 5 years and one of them was still alive at the end of follow-up, and similarly 2 cases in $DI>1.5$ aneuploidy group were alive

at the end of follow-up. But all 13 cases with high PCNA-LI and $DI > 1.5$ aneuploidy had bad prognosis. So we consider that PCNA-LI and DI should be applied together in evaluating HCC patient's prognosis.

Surely other indexes, for instance, microvessel density, etc, are also helpful for evaluating prognosis through pathological examinations of HCC surgical specimens^[2, 27-30]. We believe that a composite prospective analysis of the pathological characteristics of tumor tissue, DI and PCNA-LI is a simple and objective means to evaluate the risk of recurrence and prognosis for those patients with HCC after surgery.

REFERENCES

- Tang ZY.** Hepatocellular carcinoma-cause, treatment and metastasis. *World J Gastroenterol* 2001; **7**: 445-454
- Niu Q, Tang ZY, Ma ZC, Qin LX, Zhang LH.** Serum vascular endothelial growth factor is a potential biomarker of metastatic recurrence after curative resection of hepatocellular carcinoma. *World J Gastroenterol* 2000; **6**: 565-568
- Giannelli G, Pierri F, Trerotoli P, Marinosci F, Serio G, Schiraldi O, Antonaci S.** Occurrence of portal vein tumor thrombus in hepatocellular carcinoma affects prognosis and survival. A retrospective clinical study of 150 cases. *Hepatol Res* 2002; **24**: 50-59
- Dohmen K, Shirahama M, Onohara S, Miyamoto Y, Torii Y, Irie K, Ishibashi H.** Differences in survival based on the type of follow-up for the detection of hepatocellular carcinoma: an analysis of 547 patients. *Hepatol Res* 2000; **18**: 110-121
- Fan J, Wu ZQ, Tang ZY, Zhou J, Qiu SJ, Ma ZC, Zhou XD, Ye SL.** Multimodality treatment in hepatocellular carcinoma patients with tumor thrombi in portal vein. *World J Gastroenterol* 2001; **7**: 28-32
- Zhao WH, Ma ZM, Zhou XR, Feng YZ, Fang BS.** Prediction of recurrence and prognosis in patients with hepatocellular carcinoma after resection by use of CLIP score. *World J Gastroenterol* 2002; **8**: 237-242
- Yoong KF, McNab G, Hübscher SG, Adams DH.** Vascular adhesion protein-1 and ICAM-1 support the adhesion of tumor-infiltration lymphocytes to tumor endothelium in human hepatocellular carcinoma. *J Immunol* 1998; **160**: 3978-3988
- Yoong KF, Afford SC, Jones R, Aujla P, Qin S, Price K, Hübscher SG, Adams DH.** Expression and function of CXCL and CC chemokines in human malignant liver tumors: a role for human monokine induced by γ -interferon in lymphocyte recruitment to hepatocellular carcinoma. *Hepatology* 1999; **30**: 100-111
- Takayama T, Sekine T, Makuuchi M, Yamasaki S, Kosuge T, Yamamoto J, Shimada K, Sakamoto M, Hirohashi S, Ohashi Y, Kakizoe T.** Adoptive immunotherapy to lower postsurgical recurrence rates of hepatocellular carcinoma: a randomised trial. *Lancet* 2000; **356**: 802-807
- Lara-Pezzi E, Majano PL, Yáñez-Mó M, Gómez-Gonzalo M, Carretero M, Moreno-Otero R, Sánchez-Madrid F, López-Cabrera M.** Effect of the hepatitis B virus HBx protein on integrin-mediated adhesion to and migration on extracellular matrix. *J Hepatol* 2001; **34**: 409-415
- Westermarck J, Kähäri V-M.** Regulation of matrix metalloproteinase expression in tumor invasion. *The FASEB J* 1999; **13**: 781-792
- McKenna GJ, Chen Y, Smith RM, Meneghetti A, Ong C, McMaster R, Scudamore CH, Chung SW.** A role for matrix metalloproteinases and tumor host interaction in hepatocellular carcinomas. *Am J Surg* 2002; **183**: 588-594
- Brew K, Dinakarandian D, Nagase H.** Tissue inhibitors of metalloproteinases: evolution, structure and function. *Biochim Biophys Acta* 2000; **1477**: 267-283
- Lichtinghagen R, Musholt PB, Lein M, Römer A, Rudolph B, Kristiansen G, Hauptmann S, Schnorr D, Loening SA, Jung K.** Different mRNA and Protein Expression of Matrix Metalloproteinases 2 and 9 and Tissue Inhibitor of Metalloproteinases 1 in Benign and Malignant Prostate Tissue. *Eur Urol* 2002; **42**: 398-406
- Davidson B, Goldberg I, Gotlieb WH, Kopolovic J, Ben-Baruch G, Nesland JM, Reich R.** The prognostic value of metalloproteinases and angiogenic factors in ovarian carcinoma. *Mol Cell Endocrinol* 2002; **187**: 39-45
- Ohmiya N, Matsumoto S, Yamamoto H, Baranovskaya S, Malkhosyan SR, Perucho M.** Germline and somatic mutations in hMSH6 and hMSH3 in gastrointestinal cancers of the microsatellite mutator phenotype. *Gene* 2001; **272**: 301-313
- Martin G, Halwani F, Shibata H, Meterissian S.** Value of DNA ploidy and S-phase fraction as prognostic factors in stage III cutaneous melanoma. *Can J Surg* 2000; **43**: 29-33
- Gschwendtner A, Fend F, Hoffmann Y, Krugmann J, Klingler PJ, Mairinger T.** DNA-ploidy analysis correlates with the histogenetic classification of thymic epithelial tumours. *J Pathol* 1999; **189**: 576-580
- Matturri L, Biondo B, Cazzullo A, Colombo B, Giordano F, Guarino M, Pallotti F, Turconi P, Lavezzi AM.** Prognostic significance of different biological markers (DNA index, PCNA index, apoptosis, p53, Karyotype) in 126 adenocarcinoma gastric biopsies. *Anticancer Res* 1998; **18**: 2819-2826
- Mastronardi L, Guiducci A, Buttaro FM, Cristallini EG, Puzzilli F, Maira G.** Relationships among DNA Index, S-Phase, and invasive behavior in anterior pituitary adenomas. A cytometric study of 61 cases with Feulgen-positive DNA analysis. *Surg Neurol* 2001; **56**: 27-32
- Imai Y, Sasaki T, Fujibayashi T.** Volume-corrected mitotic index as a prognostic factor in oral squamous cell carcinomas. *Oral Oncol* 2001; **37**: 72-76
- Krušlin B, Višnjie A, Cizmie A, Tomicic I, Kos M, Jukie S, Seiwerth S.** DNA ploidy analysis and cell proliferation in congenital sacrococcygeal teratomas. *Cancer* 2000; **89**: 932-937
- Celis JE, Madsen P, Celis A, Nielsen HV, Gesser B.** Cyclin (PCNA, auxiliary protein of DNA polymerase δ) is a central component of the pathway(s) leading to DNA replication and cell division. *FEBS Lett* 1987; **220**: 1-7
- Donato MF, Arosio E, Ninno ED, Ronchi G, Lampertico P, Morabito A, Balestrieri MR, Colombo M.** High rates of hepatocellular carcinoma in cirrhotic patients with high liver cell proliferative activity. *Hepatology* 2001; **34**: 523-528
- Wu P-C, Lau VK-T, Fang JW-S, Lai VC-H, Lai C-L, Lau JY-N.** Imbalance between cell proliferation and cellular DNA fragmentation in hepatocellular carcinoma. *Liver* 1999; **19**: 444-451
- Closset J, Van de Stadt J, Delhay M, El Nakadi I, Lambilliotte JP, Gelin M.** Hepatocellular carcinoma: surgical treatment and prognostic variables in 56 patients. *Hepatogastroenterology* 1999; **46**: 2914-2918
- Tamano M, Sugaya H, Oguma M, Iijima M, Yoneda M, Murohisa T, Kojima K, Kuniyoshi T, Majima Y, Hashimoto T, Terano A.** Serum and tissue PIVKA-II expression reflect the biological malignant potential of small hepatocellular carcinoma. *Hepatol Res* 2002; **22**: 261-269
- Aoyagi Y, Mita Y, Suda T, Kawai K, Kuroiwa T, Igarashi M, Kobayashi M, Waguri N, Asakura H.** The fucosylation index of serum α -fetoprotein as useful prognostic factor in patients with hepatocellular carcinoma in special reference to chronological changes. *Hepatol Res* 2002; **23**: 287-295
- Zheng Q, Tang ZY, Xue Q, Shi DR, Song HY, Tang HB.** Invasion and metastasis of hepatocellular carcinoma in relation to urokinase-type plasminogen activator, its receptor and inhibitor. *J Cancer Res Clin Oncol* 2000; **126**: 641-646
- Shimada M, Rikimaru T, Hamatsu T, Yamashita Y, Terashi T, Taguchi K, Tanaka S, Shirabe K, Sugimachi K.** The role of macroscopic classification in nodular-type hepatocellular carcinoma. *Am J Surg* 2001; **182**: 177-182

Edited by Lu HM

• LIVER CANCER •

Retrovirus-mediated gene transfer of human endostatin inhibits growth of human liver carcinoma cells SMMC7721 in nude mice

Xuan Wang, Fu-Kun Liu, Xi Li, Jie-Shou Li, Gen-Xin Xu

Xuan Wang, Fu-Kun Liu, Xi Li, Jai-Sou Li, Research Institute of General Surgery, Clinical School of Medicine, Nanjing University, Nanjing 210002, Jiangsu Province, China

Gen-Xin Xu, Department of Molecular Biology, Nanjing Military Medical School, Nanjing 210002, Jiangsu Province, China

Correspondence to: Dr. Xuan Wang, Research Institute of General Surgery, Clinical School of Medicine, Nanjing University, No.305, Eastern Road of Zhongshan, Nanjing 210002, Jiangsu Province, China. wx58cn@yahoo.com.cn

Telephone: +86-25-4513749 **Fax:** +86-25-4364753

Received 2002-01-26 **Accepted** 2002-03-06

Abstract

AIM: To study the effect of human endostatin mediated by retroviral gene transfer on the growth of human hepatocarcinoma cell line SMMC7721 in nude mice.

METHODS: Human endostatin gene together with rat serum albumin signal peptide was transferred into human liver carcinoma SMMC7721 cells by retroviral vector pLncx to build a stable transfectant (SMMC-endo). PCR and Western blot analysis were used to verify the transfection and secretion of human endostatin gene in SMMC7721 cells. The endothelial cell proliferation assay *in vitro* was conducted to test the biological activity of the expressed human endostatin. The inhibitory effect of endostatin expressed by transfected SMMC7721 on the growth rates of tumor cells *in vivo* was observed. The mean microvessel density in the specimen was also counted.

RESULTS: PCR amplification proved that the genome of SMMC-endo cells contained a 550bp specific fragment of endostatin gene. Western blot analysis confirmed the secretion of human endostatin gene in the conditioned medium of transfected SMMC-endo cells. The endothelial proliferation assay showed that the conditioned medium of SMMC-endo cells significantly inhibited the proliferation of human umbilical vein endothelial cells by 48 %, significantly higher than that of SMMC-pLncx (10.2 %, $P < 0.01$). *In vivo* experiments revealed that only in 3 out of 5 mice tumors were formed and the mean size of flank tumors from SMMC-endo cells was 94.5 % smaller than that from the control SMMC-pLncx cells 22 days after tumor inoculation ($P < 0.001$). The mean microvessel density in tumor samples from SMMC-endo cells was only 8.6 ± 1.1 , much fewer than that of 22.6 ± 4.5 from SMMC-pLncx cells ($P < 0.01$).

CONCLUSION: Human endostatin mediated by retroviral gene transfer can inhibit human liver carcinoma cell SMMC7721 growth in nude mice.

Wang X, Liu FK, Li X, Li JS, Xu GX. Retrovirus-mediated gene transfer of human endostatin inhibits growth of human liver carcinoma cells SMMC7721 in nude mice. *World J Gastroenterol* 2002; 8(6):1045-1049

INTRODUCTION

It has become clear that angiogenesis not only is essential for a number of physiological processes such as embryonic development, organ and tissue regeneration, but also plays a pivotal role in tumor growth and metastases^[1-4]. Folkman^[2] demonstrated that suppression of tumor angiogenesis leads to tumor starvation and tumor regression. Thus, the tumor vascular system has become an important target for cancer therapy, and methods to inhibit angiogenic process provide an unique opportunity to inhibit tumor growth^[4]. An increasing number of antiangiogenic agents have been discovered recently. These included angiostatin, endostatin and interleukin-12^[5-7]. Among them, endostatin is one of the most hopeful antiangiogenic proteins. Its antiangiogenic effect, most potent discovered so far, can specifically inhibit the proliferation and migration of endothelial cell, and subsequently promote the development of apoptosis and regression of tumor^[8-14]. However, antiangiogenic therapy with endostatin requires multiple and prolonged administrations, and the problems of such as bioactive protein production in large quantities, high costs and the cumbersome daily administration can often be met during cancer therapy^[15]. Gene transfer therapy could provide an alternative approach to continuous local delivery of this antiangiogenic factor *in vivo*^[16]. So, in order to explore the effect of human endostatin expressed by human liver carcinoma cell on tumor growth, stable transfectant from human liver carcinoma cell line SMMC7721 transferred with human endostatin gene was built and the inhibitory effect of endostatin on tumor growth *in vitro* and *in vivo* were observed.

MATERIALS AND METHODS

Cell culture

Human liver carcinoma cell line SMMC7721 was kept by our laboratory. Human umbilical vein endothelial cell line (HUVEC) was purchased from Institute of Cell Biology, Chinese Academy of Sciences. HUVEC and human liver carcinoma cell line SMMC7721 were maintained in RPMI 1640 medium (Gibco) supplemented with $100 \text{ mL} \cdot \text{L}^{-1}$ FBS, 100 units/mL penicillin and 100 $\mu\text{g/mL}$ streptomycin. Retrovirus packaging cell line PA317 was kindly provided by Dr. Qian Qijun (Second Military Medical University, Shanghai, China), and maintained in DMEM (Gibco) supplemented with $100 \text{ mL} \cdot \text{L}^{-1}$ FBS, 100 units/mL penicillin and 100 $\mu\text{g/mL}$ streptomycin.

Plasmid

The recombinant retroviral plasmid pLncx-endo containing the cDNA for human endostatin gene with a HA tag attached to the C-terminus as a fusion protein was engineered by our laboratory^[17]. In this plasmid, human endostatin cDNA was put downstream of rat serum albumin signal peptide.

Generation of stable transfectants

Recombinant plasmid pLncx-endo was transferred into PA317

cells by Lipofectamine (Gibco) following the manufacturer's instructions. G418 selection at 500 $\mu\text{g}/\text{mL}$ was added at the same time. Two weeks after transfection, G418-resistant colonies emerged and were expanded respectively. The supernatants of G418-resistant PA317 colony were collected and stored at $-80\text{ }^{\circ}\text{C}$ for usage. 5×10^5 SMMC7721 cells were plated on 6-well plate and incubated for 24 h. The cells were rinsed with serum-free RPMI 1640 medium twice, and 100 μL supernatant of endostatin-transfected PA317 colony was added and incubated for 3 h. Another 3 mL 1640 medium was added with the final concentration of polybrene at $2\text{ mg} \cdot \text{L}^{-1}$ and G418 at $500\text{ mg} \cdot \text{L}^{-1}$. Four weeks after transfection, G418-resistant cells were expanded for preservation and tested for endostatin-HA fusion protein by immunohistochemistry and Western blot analysis. The endostatin-transfected colony was designated as SMMC-endo. Control transfectant (SMMC-pLncx) was generated in a similar way except the parent plasmid pLncx-endo was replaced by empty plasmid pLncx.

PCR amplification of endostatin from transfected SMMC7721 cells

According to human endostatin sequence, two primers were devised. The primers used were E1: 5' CCG GAA TTC ATG CAC AGC CAC CGC GAC TTC CAG CCG and E2: 5' GCC GGA TCC CTA CTT GGA GGC AGT CAT GAA GCT. SMMC-endo and SMMC-pLncx cells were harvested and DNA extracted. PCR was performed in 50 μL reactive volume containing 2 μL cDNA, 2 μL $10 \times$ PCR buffer, 2 μL $4 \times$ dNTP ($2\text{ mmol} \cdot \text{L}^{-1}$), 50 $\text{pmol} \cdot \text{L}^{-1}$ primer, and 1 μL *Tag* DNA polymerase. The samples were subjected to 30 thermal cycles of 5 min at $94\text{ }^{\circ}\text{C}$ for predenaturation, 1 min at $94\text{ }^{\circ}\text{C}$ for denaturing, 1 min at $60\text{ }^{\circ}\text{C}$ for annealing, 1 min at $72\text{ }^{\circ}\text{C}$ for extension, and 10 min at $72\text{ }^{\circ}\text{C}$ for final extension after the last cycle. PCR products were checked on $10\text{ g} \cdot \text{L}^{-1}$ agarose gels (containing $0.5\text{ mg} \cdot \text{L}^{-1}$ ethidium bromide).

Western blot analysis

SMMC-endo and SMMC-pLncx cells were plated in six-well plates at 2.5×10^5 cells/well respectively and incubated for 24 h. The medium was replaced with 1 mL serum-free RPMI 1640 and collected after 48 h. One mL of conditioned medium was concentrated in a microcon 10 microconcentrator (Amicon, Beverly, MA) to 20 μL and subjected to a $120\text{ g} \cdot \text{L}^{-1}$ reducing SDS/PAGE gel. Protein was transferred to a nitrocellulose membrane and incubated overnight in 50 $\text{mL} \cdot \text{L}^{-1}$ nonfat milk in PBS at $4\text{ }^{\circ}\text{C}$. After briefly washing in $10\text{ mL} \cdot \text{L}^{-1}$ fat-free milk, the membrane was incubated with anti-HA mouse monoantibody diluted 1:500. After three 10-min washes in $1\text{ mL} \cdot \text{L}^{-1}$ fat-free milk, membrane was incubated in horseradish peroxidase-conjugated antimouse immunoglobulin diluted 1:1000. After three 10-min washes in TBS, proteins were detected using 3,3'-diaminobenzidine as the chromagen.

Endothelial cell proliferation assay

SMMC-endo, SMMC-pLncx and SMMC7721 cells were plated onto six-well culture plates at a density of 2.5×10^5 cells/well and incubated for 24 h. The cells were washed with PBS, and 1.5 mL of serum-free RPMI 1640 were added and incubated for another 48 h. The total of 9 mL serum-free RPMI 1640 were collected and concentrated to 1.8 mL using Centrplus 10 concentrator (Amicon), and stored at $-80\text{ }^{\circ}\text{C}$ for usage. HUVEC cells were seeded at a density of 4000 cells/well into gelatinized 40-well culture plates and incubated ($37\text{ }^{\circ}\text{C}$, $50\text{ mL} \cdot \text{L}^{-1}\text{CO}_2$) for 24 h in 100 μL RPMI 1640 medium. The medium was replaced with 20 μL of above concentrated conditioned medium and incubated for 30 min. 80 μL of RPMI 1640 supplemented with $100\text{ mL} \cdot \text{L}^{-1}$ fetal bovine serum and

$1\text{ }\mu\text{g} \cdot \text{L}^{-1}$ bFGF (Sigma) was then added for 72 h. The numbers of cells were determined using a colorimetric MTT assay. Tests were conducted in quadruplicate.

In vivo evaluation of tumor growth

To test whether endostatin expressed by host cells could inhibit tumor growth *in vivo*, we used the human liver carcinoma cell line SMMC7721. This model has been widely used in experiment. 4-week-old female BALB/c (nu/nu) mice (purchased from Shanghai Institute of Cancer Research) were chosen. SMMC7721 cells were inoculated s.c. into the right flank of nude mice and changes in tumor growth were monitored. In this experiment, flank tumors were generated by s.c. injection of 5×10^5 cells in 100 μL of HBSS into the right flank of athymic BALB/c (nu/nu) mice for SMMC-endo and control SMMC-pLncx cells ($n=5$). Tumors were measured by calipers in two dimensions every 2 days, and the volume was calculated as $\text{length} \times \text{width}^2 \times 0.52$.

Histological analysis

To determine the effect of endostatin on vascular growth *in vivo*, microvessel density counting was conducted on frozen sections of tumors from SMMC-endo and SMMC-pLncx cells as described previously^[18] by immunostaining with anti CD₃₄ (Gibco). Anti-CD₃₄ antibody was used at a dilution of 1:500. Immunohistochemistry was accomplished utilizing an avidin-biotin technique. SMMC-endo and control SMMC-pLncx were grown on six-well glass slides and fixed in acetone at room temperature. After washing in PBS, the cells were incubated with a $10\text{ mL} \cdot \text{L}^{-1}$ H_2O_2 solution at room temperature for ten minutes to quench endogenous peroxidases. Nonspecific binding was blocked with $50\text{ mL} \cdot \text{L}^{-1}$ normal horse serum at room temperature for five minutes. The cells were then incubated with anti-HA at a 1:300 dilution at $4\text{ }^{\circ}\text{C}$ overnight. Following washing in PBS, the secondary antibody, biotinylated antimouse, was added and the cells were incubated at room temperature for one hour. After washes in PBS, Vectastain reagent (a solution containing streptavidin-horseradish peroxidase) was added and then incubated at room temperature for ten minutes. 3,3'-diaminobenzidine was used as the chromagen. After ten minutes, the brown color signifying the presence of antigen bound to antibodies was detected by light microscopy and photographed at $\times 200$. The blood vessels were counted from five areas in each tumor section.

RESULTS

Generation of stable transfectants

A 550-bp fragment was seen in the PCR product from DNA of SMMC-endo cells, but not from the control (Figure 1). On a reducing $120\text{ g} \cdot \text{L}^{-1}$ SDS/PAGE gel, a distinct band at around $M_{22\text{ }000}$, corresponding to the size of endostatin, was only visualized in the supernatant of SMMC-endo cells. Monoclonal mouse anti-HA antibody reacted positively in a Western blot with the $M_{22\text{ }000}$ protein only. It confirmed that endostatin protein expressed by transfected SMMC-endo cells could be secreted into the supernatant of cells (Figure 2).

Antiangiogenic effect of human endostatin expressed by endostatin-transfected cells

The effect of expressed endostatin on HUVEC proliferation was tested. The result showed that there were no significant differences among the concentrated conditioned media from SMMC7721, SMMC-pLncx cells and RPMI 1640 medium in inhibiting the growth of HUVEC. Compared to RPMI 1640 medium, the inhibitory rate on HUVEC proliferation for conditioned medium from SMMC-endo cells was 48 %,

significantly higher than that of 10.2 % for control SMMC-pLncx. There was a significant difference on the antiangiogenic effect between conditioned medium from SMMC-endo and SMMC-pLncx ($P<0.01$, Figure3).

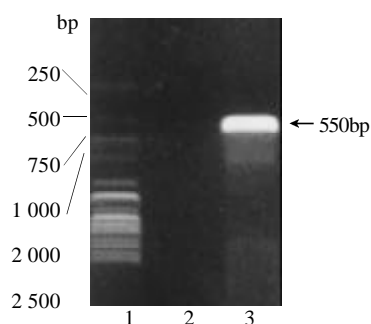


Figure 1 Analysis of PCR product of endostatin-transfected SMMC7721 cells by 1 % agarose gel electrophoresis. 1: DNAMarker. 2: PCR product of SMMC-pLncx. 3: PCR product of SMMC-endo.

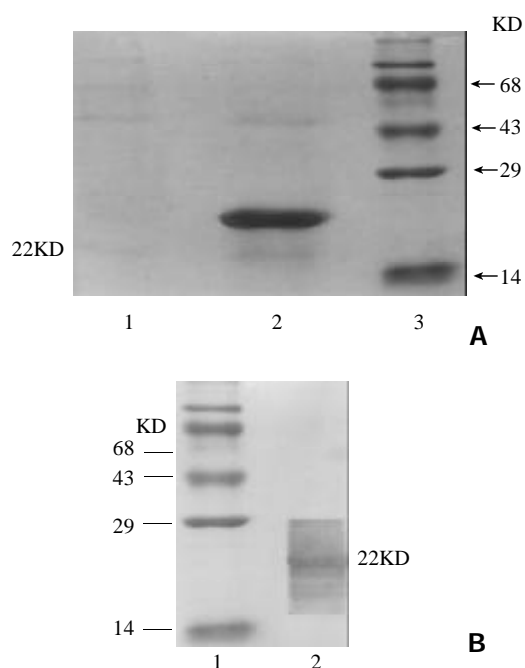


Figure 2 SDS-PAGE analysis and Western blot of endostatin expressed in supernatant of virally transduced SMMC7721 cells (A) SDS-PAGE analysis; 1, supernatant of control SMMC-pLncx cells; 2, supernatant of endostatin-transfected SMMC-endo cells; 3, protein marker; (B) Western blot analysis; 1 protein marker; 2, supernatant of endostatin-transfected SMMC-endo cells.

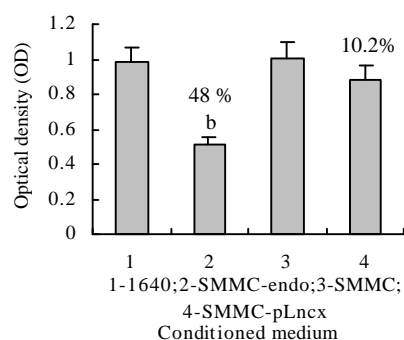


Figure 3 Inhibition of endothelial cell proliferation by conditioned medium from SMMC-endo cells. Conditioned medium

from SMMC-endo (2), SMMC7721 (3) and SMMC-pLncx (4) were concentrated and applied to HUVEC cells grown in 40-well plate. Three days later, cell number, as measured by absorbance(OD), was then quantified by using a colorimetric MTT assay. Bars, SD. ^b $P<0.01$, compared with conditioned medium from control SMMC-pLncx.

Human endostatin inhibits tumor growth in nude mice

To determine the anti-tumor effect of endostatin expressed by transfected SMMC7721 cell, 5×10^5 cells were injected s.c. into right flanks of nude BALB/c mice. SMMC7721 cells and SMMC-pLncx cells formed tumor rapidly within 14 days. While flank tumors from SMMC-endo cells grew very slowly in nude mice. The first palpable tumor from SMMC-endo cells appeared 16 days after injection and only in 3 out of 5 nude mice formed tumors. The mean size of flank tumors from SMMC-endo cells was 94.5 % smaller than that from SMMC-pLncx cells 22 days after tumor inoculation, a significant difference between SMMC-endo and SMMC-pLncx groups ($P<0.001$, Figure 4). The mean microvessel density(MVD) in tumors was determined by utilizing anti- CD₃₄. The number of vessels was counted and the results showed that the MVD in tumor samples from SMMC-endo cells was only 8.6 ± 1.1 , much fewer than that of 22.6 ± 4.5 from SMMC-pLncx cells ($P<0.01$, Figure 5). It meant that endostatin expressed by SMMC-endo cells could decrease tumor vascularization.

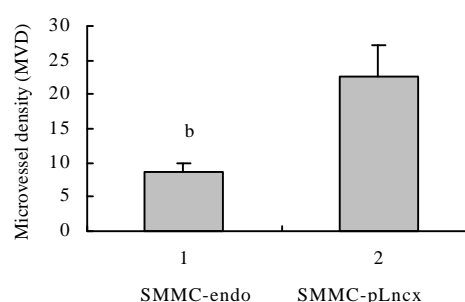
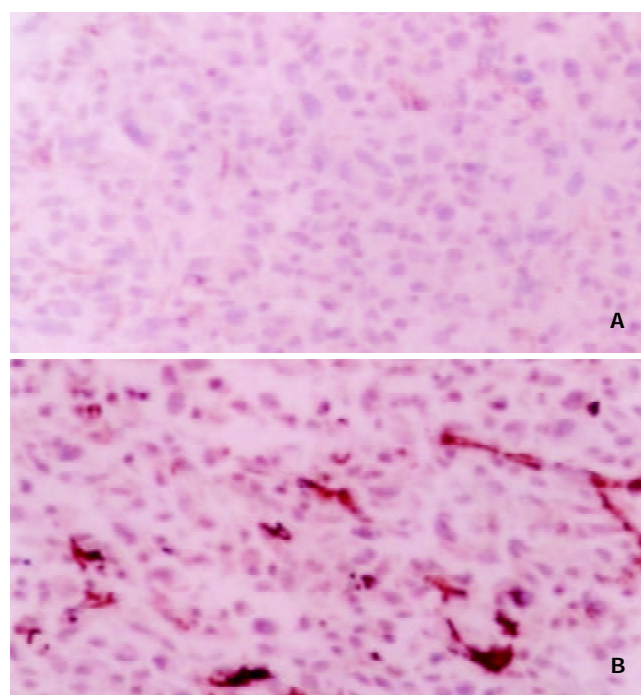


Figure 5 Tumor sections were stained with an antibody reactive to CD₃₄. A: Tumor section from endostatin-transfected

group showed only a few positively stained vascular endothelial cells. B: Similar section of the control group showed highly vascularized tumor tissue. C: Microvessel density (MVD) was quantified by counting of positively stained endothelial cells from 5 fields in each tumor section. Bars, SD. ^b $P < 0.01$, compared with control SMMC-pLncx. $\times 200$.

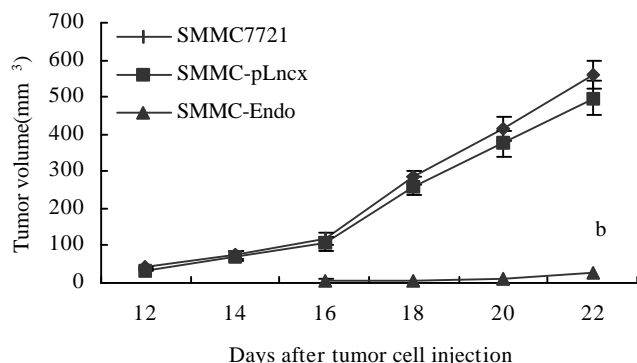


Figure 4 Inhibition on the growth of human liver carcinoma implanted in nude mice by human endostatin. ^b $P < 0.001$, SMMC-endo compared with control SMMC-pLncx.

DISCUSSION

It is known to all that blood supply is necessary for tumor progression and metastasis^[1-4]. Folkman^[2] noted that tumor will stop growing or die when it exceeds 2 mm to 3 mm in diameter if new blood vessel for tumor is not formed. Numerous studies have also shown that inhibition of tumor growth and metastases could be reached by administration of recombinant antiangiogenic proteins^[15,19-21]. Moreover, the genome of endothelial cells, targeted by antiangiogenic proteins has a stable inheritance property and rare mutation rate. So, unlike tumor cells in chemotherapy, acquired resistance to recombinant antiangiogenic protein is rarely developed during antiangiogenic therapy. Therefore, antiangiogenic therapy is probably one of the most effective and promising approaches to cancer treatment^[14].

Antiangiogenic therapy will require sustained maintenance of therapeutic levels *in vivo*^[22,23]. Continuous delivery and high doses of recombinant antiangiogenic protein in circulation by repeated administrations seem expensive and impossible. Gene therapy transfer of foreign antiangiogenic gene into host cells represents an alternative method to tumor therapy. The aim of generating high efficient protein in areas around tumor with no toxin and keeping long time relatively high expression of antiangiogenic protein can be achieved by a single administration of gene transfer. There have been successful reports of antiangiogenic gene therapy with viral vectors being used to treat tumor^[24-27]. Endostatin is a new kind of potent antiangiogenic factor consisting of 184 amino acids in C-terminal fragment of endogenous collagen18 a. It was first isolated as a M_r 20 000 protein from conditioned medium of the EOMA murine hemangioendothelioma cell line by Professor O' Reilly in 1997^[28-33]. *In vivo* and *in vitro* experiments had demonstrated that endostatin has specific inhibitory effect on the formation of new blood vessel. It could inhibit tumor growth with reduction of virtually all tumor neovascularization and without detectable systemic sign of toxicity^[34-37]. In the same way, antiangiogenic therapy with endostatin in cancer requires prolonged administration and high doses of recombinant protein. Furthermore, the production of soluble functional polypeptide endostatin has proven difficult and nearly 95 % of the recombinant protein used will be excreted

out of the body because of its insoluble and instable property^[38]. However, all of the above problems can be overcome by gene transfer of endostatin gene. As gene transfer mediated by retroviral is most commonly used among the various ways of transducing methods and retroviral can be integrated into chromosome of host cells. So, gene transfer mediated by retrovirus can be inherited to next generation and stably expressed in host cells for a long duration^[27]. In this experiment, recombinant retroviral plasmid pLncx-endo was transferred into human liver carcinoma cell SMMC7721 by using lipofectamine. The following PCR examination and Western blot analysis confirmed the transfection and stable expression of human endostatin by SMMC-endo cells. The expressed protein was secreted outside of cells under the influence of rat albumin signal peptide^[10,39]. It revealed that a stable transfectant that could secrete human endostatin was built. *In vitro* endothelial cell proliferation assay verified the biological activity of endostatin, which showed that conditioned medium from SMMC-endo could significantly inhibit the proliferation of endothelial cells by 48 %, while the inhibitory rate for conditioned medium from control SMMC-pLncx was only 10.2 %. It suggested that the secreted protein expressed by the stable transfectant had a potent antiangiogenic effect^[40,41]. *In vivo* experiments showed that tumor formations from SMMC-endo cells were dramatically inhibited. Compared to control group, only in 3 out of 5 mice inoculated with SMMC-endo cells tumors were formed and a remarkable reduction in tumor size was also exhibited 22 days after tumor injection. The mean size of tumors from SMMC-endo cells was about 94.5 % smaller than that from control SMMC-pLncx. Meanwhile, histological analysis showed that the MVD in tumors from SMMC-endo cells was also remarkably decreased compared to control SMMC-pLncx. It meant that human endostatin expressed by SMMC7721 could indeed inhibit the formation of tumor *in vivo*. In another word, endostatin arrests tumor growth by inhibiting the formation of microvessels *in vivo*, and gene transfer therapy mediated by retrovirus could meet the requirements for tumor treatment. But we also noted that the expressed endostatin did not completely inhibit the formation of tumor in nude mice. Some proangiogenic factors such as VEGF and bFGF, produced by SMMC7721 cell itself may be responsible for this phenomenon^[42,43]. Another probable reason is the low amount of endostatin expressed by retroviral plasmid pLncx. So, in a word, gene transfer of endostatin mediated by retroviral pLncx could significantly inhibit the growth of SMMC7721 cells in nude mice by affecting angiogenesis and is probable one of the effective ways to deal with tumor. But the application of new efficient expression plasmid and combined therapy with multiple genes may further improve the therapeutic effect of endostatin in the future.

REFERENCES

- Hahnfeldt P, Panigrahy D, Folkman J, Hlatky L. Tumor development under angiogenic signaling: a dynamical theory of tumor growth, treatment response and postvascular dormancy. *Cancer Res* 1999; **59**: 4770-4775
- Folkman J, Watson K, Ingber D, Hanahan D. Induction of angiogenesis during the transition from hyperplasia to neoplasia. *Nature* 1989; **339**: 58-62
- Liekens S, De Clercq G, Neyts J. Angiogenesis: regulators and clinical applications. *Biochem Pharmacol* 2001; **61**: 253-270
- Wu J, Fang DM. Angiogenesis and antiangiogenesis therapy. *Shijie Huaren Xiaohua Zazhi* 2001; **9**: 316-321
- Yanagi K, Onda M, Uchida E. Effect of angiostatin on liver metastasis of pancreatic cancer in hamsters. *Jpn J Cancer Res* 2000; **91**: 723-730

- 6 **Sacco MG**, Caniutti M, Cato EM, Frattini A, Chiesa G, Ceruti R, Adorui F, Zecca L, Scanziani E, Vezzoni P. Liposome-delivered angiostatin strongly inhibits tumor growth and metastatization in a transgenic model of spontaneous breast carcinoma. *Cancer Res* 2000; **60**: 266-265
- 7 **Wang Z**, Qiu SJ, Ye SL, Tang ZY, Xiao X. Combined IL-12 and GM-CSF gene therapy for murine hepatocarcinoma. *Cancer Gene Ther* 2001; **8**: 751-758
- 8 **O'reilly MS**, Bohem T, Shing Y, Fukai N, Vasios G, Lane WS, Flynn E, Folkman J. Endostatin: an endogenous inhibitor of angiogenesis and tumor growth. *Cell* 1997; **88**: 277-285
- 9 **Berger AC**, Feldman AL, Gnant MF. The angiogenesis inhibitor, endostatin, does not affect murine cutaneous wound healing. *J Surg Res* 2000; **91**: 26-31
- 10 **Dhanabal M**, Volk R, Ramchandran R, Simons M, Sukhatme V. Cloning, expression, and *in vitro* activity of human endostatin. *Biochem and Biophys Res Commun* 1999; **258**: 345-352
- 11 **Chen QR**, Kumar D, Stass SA, Mixson AJ. Liposomes complexed to plasmids encoding angiostatin and endostatin inhibit breast cancer in nude mice. *Cancer Res* 1999; **59**: 3308-3312
- 12 **Taddei L**, Chiarugi P, Brogelli L. Inhibitory effect of full-length human endostatin on *in vitro* angiogenesis. *Biochem and Biophys Res Commun* 1999; **263**: 340-345
- 13 **Blezinger P**, Wang J, Gondo M, Quezada A, Mehrens D, French M, Singhai A, Sullivan S, Rolland A, Ralston R, Min W. Systemic inhibition of tumor growth and tumor metastases by intramuscular administration of the endostatin gene. *Nat Biotechnol* 1999; **17**: 343-348
- 14 **Yoon SS**, Eto H, Lin CM, Nakamura H, Pawlik TM, Song SU, Tanabe KK. Mouse endostatin inhibits the formation of lung and liver metastases. *Cancer Res* 1999; **59**: 6251-6256
- 15 **Oehler MK**, Blicknell R. The promise of anti-angiogenic cancer therapy. *Br J Cancer* 2000; **82**: 749-752
- 16 **Folkman J**. Antiangiogenic gene therapy. *Proc Natl Acad Sci USA* 1998; **95**: 9064-9066
- 17 **Wang X**, Liu FK, Li X, Li JS, Xu GX. Inhibitory effect of endostatin expressed by human liver carcinoma SMMC7721 on endothelial cell proliferation *in vitro*. *World J Gastroenterol* 2002; **8**: 253-257
- 18 **Tanigawa N**, Lu C, Mitsui T, Miura S. Quantitation of sinusoid-like vessels in hepatocellular carcinoma: its clinical and prognostic significance. *Hepatology* 1997; **26**: 1216-1223
- 19 **Feldman AL**, Restifo NP, Alexander HR, Bartlett DL, Hwu P, Seth P, Libutti K. Antiangiogenic gene therapy of cancer utilizing a recombinant adenovirus to elevate systemic endostatin levels in mice. *Cancer Res* 2000; **60**: 1503-1506
- 20 **Indraco S**, Morini M, Gola E, Carrozzino F, Habeler W, Minghelli S, Santi L, Bianchi LC, Cao Y, Albini A, Noonan DM. Effects of angiostatin gene transfer on functional properties and *in vivo* growth of Kaposi' sarcoma cells. *Cancer Res* 2001; **61**: 5441-5446
- 21 **Shi W**, Teschendorf C, Muzyczka N, Siemann DW. Adeno-associated virus-mediated gene transfer of endostatin inhibits angiogenesis and tumor growth *in vivo*. *Cancer Gene Ther* 2002; **9**: 513-521
- 22 **Huang X**, Wong MKK, Zhao Q, Zhu Z, Wang KZQ, Huang N, Ye C, Gorelik E, Li M. Soluble recombinant endostatin purified from *Escherichia coli*: antiangiogenic activity and antitumor effect. *Cancer Res* 2001; **61**: 478-481
- 23 **Feldman AL**, Pak H, Yang JC, Alexander HR, Libutti SK. Serum endostatin levels are elevated in patients with soft tissue sarcoma. *Cancer* 2001; **91**: 1525-1529
- 24 **Naguen JT**. Adeno-associated virus and other potential vectors for angiostatin and endostatin gene therapy. *Adv Exp Med Bio* 2000; **465**: 457-466
- 25 **Sauter BV**, Martinet O, Zhang WJ, Mandeli J, Woo SLC. Adenovirus-mediated gene transfer of endostatin *in vivo* results in high level of transgene expression and inhibition of tumor growth and metastases. *Proc Natl Acad Sci USA* 2000; **97**: 4802-4807
- 26 **Ma GZ**, Liu SZ, Chiang YH, Li J, Chen SL, Tsao YP, Xiao X. Intratumoral gene therapy of malignant brain tumor in a rat model with angiostatin delivered by adeno-associated viral (AAV) vector. *Gene Ther* 2002; **9**: 2-11
- 27 **Qian WF**, Huang ZH, Chi DB. Herpes simplex virus thymidine kinase/ganciclovir system combined with 5-Fu for the treatment of experimental colorectal cancer. *Shijie Huaren Xiaohua Zazhi* 2001; **9**: 190-193
- 28 **Sasaki T**, Fukai N, Mann K, Gohring W, Olsen BR, Timpl R. Structure, function and tissue forms of the C-terminal globular domain of collagen XVIII containing the angiogenesis inhibitor endostatin. *Embo J* 1998; **17**: 4249-4256
- 29 **Wen W**, Moses MA, Wiederschain D, Arbiser JL, Folkman J. The generation of endostatin is mediated by elastase. *Cancer Res* 1999; **59**: 6052-6056
- 30 **Strik H**, Schluesener HJ, Seid K, Meyermann R, Deininger M. Localization of endostatin in rat and human gliomas. *Cancer* 2001; **91**: 1013-1019
- 31 **Musso O**, Theret N, Heljasvaara R, Rehn M, Turlin B, Campion JP, Pihlajaniemi T, Clement B. Tumor hepatocytes and basement membrane-producing cells specifically express two different forms of the endostatin precursor, collagen XVIII, in human liver cancers. *Hepatology* 2001; **33**: 868-876
- 32 **Musso O**, Rehn M, Theret N, Turlin B, Paulette BS, Lotrian D, Campion JP, Pihlajaniemi T, Clement B. Tumor progression is associated with a significant decrease in the expression of the endostatin precursor collagen XVIII in human hepatocellular carcinomas. *Cancer Res* 2001; **61**: 45-49
- 33 **Lietard J**, Theret N, Rehn M, Musso O, Dargere D, Pihlajaniemi T, Clement B. The promoter of the long variant of collagen XVIII, the precursor of endostatin, contains liver-specific regulatory elements. *Hepatology* 2000; **33**: 1377-1385
- 34 **Ding I**, Sun JZ, Fenton B, Liu WM, Kinsely P, Okunieff P, Min W. Intratumoral administration of endostatin plasmid inhibits vascular growth and perfusion in Mca-4 murine mammary carcinomas. *Cancer Res* 2001; **61**: 526-531
- 35 **Kim YM**, Jang JW, Lee OH, Yeon J, Choi EY, Kim EW, Lee ST, Kwon YG. Endostatin inhibits endothelial and tumor cellular invasion by blocking the activation and catalytic activity of matrix metalloproteinase. *Cancer Res* 2000; **60**: 5410-5413
- 36 **Yokoyama Y**, Green JE, Sukhatme VP, Ramakrishnan S. Effect of endostatin on spontaneous tumorigenesis of mammary adenocarcinomas in a transgenic mouse model. *Cancer Res* 2000; **60**: 4362-4365
- 37 **Yokoyama Y**, Dhanabal M, Griffioen AW. Synergy between angiostatin and endostatin: inhibition of ovarian cancer growth. *Cancer Res* 2000; **60**: 2190-2196
- 38 **Felbor U**, Dreier L, Bryant RA, Ploegh HL, Olsen BR, Moths W. Secreted cathepsin L, generates endostatin from collagen XVIII. *Embo J* 2000; **19**: 1187-1194
- 39 **Cao MM**, Pan W, Chen QL, Ma ZC, Ni ZI, Wu WB, Pan X, Cao GW, Qi ZT. Construction of the eukaryotic expression vector expressing the fusion protein of human endostatin protein and IL-3 signal peptide. *Shijie Huaren Xiaohua Zazhi* 2001; **9**: 43-46
- 40 **Perletti G**, Concar P, Giardini R, Marras E, Piccinini F, Folkman J, Chen L. Antitumor activity of endostatin against carcinogen-induced rat primary mammary tumors. *Cancer Res* 2000; **60**: 1793-1796
- 41 **Dhanabal M**, Ramchandra R, Waterman MJF, Lu H, Knebelmann B, Segal M, Sukhatme VP. Endostatin induce endothelial cell apoptosis. *J Biol Chem* 1999; **274**: 1721-1726
- 42 **Tang YC**, Li Y, Qian GX. Reduction of tumorigenicity of SMMC7721 hepatoma cells by vascular endothelial growth factor antisense gene therapy. *World J Gastroenterol* 2001; **7**: 22-27
- 43 **Tang ZY**, Sun FX, Tian J, Ye SL, Liu YK, Liu KD, Chen J, Xia JL, Qin LX, Sun HC, Wang L, Zhou J, Li Y, Ma ZC, Zhou XD, Wu ZQ, Lin ZY, Yang BH. Metastatic human hepatocellular carcinoma models in nude mice and cell line with metastatic potential. *World J Gastroenterol* 2001; **7**: 597-601

Edited by Wu XN

Over-expression of LPTS-L in hepatocellular carcinoma cell line SMMC-7721 induces crisis

Cheng Liao, Mu-Jun Zhao, Jing Zhao, Di Jia, Hai Song, Zai-Ping Li

Cheng Liao, Mu-Jun Zhao, Jing Zhao, Di Jia, Hai Song, Zai-Ping Li, State Key Laboratory of Molecular Biology, Institute of Biochemistry and Cell Biology, Shanghai Institutes for Biological Sciences, Chinese Academy of Sciences, Shanghai 200031, China
Supported by a grant from National High Technology "863" Program of China No. 2001AA221021, a grant from Special Funds for Major State Basic Research "973" of China No. 001CB510205 and a grant from the National Natural Sciences Foundation of China No. 30170524.
Correspondence to: Professor Mu-Jun Zhao, State Key Laboratory of Molecular Biology, Institute of Biochemistry and Cell Biology, Shanghai Institutes for Biological Sciences, Chinese Academy of Sciences, Shanghai 200031, China. mjzhao@sunm.shnc.ac.cn
Telephone: +86-21-64315030 Ext 5295 **Fax:** +86-21-64338357
Received 2002-05-16 **Accepted** 2002-06-03

Abstract

AIM: To evaluate the function of the longer transcripts LPTS-L in hepatocellular carcinoma cell line SMMC-7721.

METHODS: SMMC-7721 cells were transfected with LPTS-L expression construct and stably transfected cells were selected by G418. Multiple single clones formed and were checked for their phenotype. In the study of the effect on telomerase activity of LPTS-L *in vitro*, GST-LPTS-L fusion protein was expressed in *E.coli* and purified by glutathione-agarose column. Telomeric repeat amplification protocol (TRAP) assays were performed to study the influence of telomerase activity in SMMC-7721 cells.

RESULTS: Over-expression of LPTS-L induced SMMC-7721 cells into crisis. LPTS-L could inhibit the telomerase activity in SMMC-7721 cells *in vitro*.

CONCLUSION: LPTS-L is a potent telomerase inhibitor. Over-expression of LPTS-L can induce hepatoma cells into crisis due to the reduction of telomerase activity.

Liao C, Zhao MJ, Zhao J, Jia D, Song H, Li ZP. Over-expression of LPTS-L in hepatocellular carcinoma cell line SMMC-7721 induces crisis. *World J Gastroenterol* 2002; 8(6):1050-1052

INTRODUCTION

Telomeres are a specialized structure composed of deoxyribonucleic acid (DNA) with associated proteins in the ends of chromosomes in the nuclei of all eukaryotic organisms^[1]. Telomeric DNA consists of long head-to-tail arrays of repeated DNA sequences and the repetitive hexanucleotide in human is TTAGGG^[2]. Telomeres provide a mechanism to compensate for under-replication of the linear DNA ends, distinguish true chromosome ends from breaks in DNA, and protect chromosome ends from fusing with others or broken chromosomes. In some cells, telomeres also control the positions of chromosomes within the nucleus^[3, 4].

Telomerase, a special reverse transcriptase enzyme, extends the telomeric DNA using intrinsic RNA template and helps stabilization of telomere length in human stem cells, reproductive cells and cancer cells^[5-7]. Telomerase activity has been found in almost all human tumors, while in most somatic tissues, including the liver, it cannot be detected, and telomere length is shortened by 50-200 nucleotides with each cell division^[8-10].

The telomere and telomerase serve as a kind of clock controlling life span, which forms the telomere and telomerase hypothesis of cell aging and tumorigenesis. The prominent hypothesis states that a signal is initiated to cease cell dividing and induce cell senescence when the telomere is shortened with cell doubling and reach to a certain threshold level. The maintenance of telomere stability is required for the long-term proliferation of tumor cells. Thus, escaping from cell senescence and becoming immortal by activating telomerase, or an alternative mechanism to maintain telomeres, constitutes an additional step in tumorigenesis^[8, 9].

LPTS gene is a human novel liver-related putative tumor suppressor gene (LPTS), identified by our laboratory^[10]. It is located in chromosome 8p23, a hot spot of tumor suppressor in hepatocellular carcinoma (HCC) with a high frequency of loss of heterozygosity (LOH). LPTS gene is transcribed to two isoforms of mRNA. The longer transcript, referred to as LPTS-L, encodes a 328-a.a. protein and is down-regulated in HCC cell lines and tissues at both RNA and protein levels (unpublished data). LPTS-L is highly homologous with PinX1, identified as a telomerase inhibitor recently^[12], with quite different sequences in 3' untranslated region.

In this study, we determined the function of LPTS-L through transfecting the LPTS-L into hepatoma cell line SMMC-7721, and analyzing its effect of cell proliferation and morphology. We also detected the effect of LPTS-L to the telomerase activity. The results clearly showed that LPTS-L is a potent telomerase inhibitor and could induce hepatoma cells into crisis.

MATERIALS AND METHODS

Cell line

The previously characterized hepatoma cell line SMMC-7721 was obtained from the Cell Bank of the Chinese Academy of Sciences (Shanghai, China) and cultured in RPMI medium 1640 (Life Technologies Inc.) plus 10 % new-born calf serum at 37 °C at a 5 % carbon dioxide atmosphere in a humidified incubator.

Transfection of LPTS-L into SMMC-7721

The coding region of LPTS-L was subcloned into eukaryotic expression vector pcDNA₃ (Invitrogen, Inc., Carlsbad CA) and constructed pcDNA₃-LPTS-L. The plasmids were purified with QIAGEN Plasmid Kit (QIAGEN Inc.) and transfected with 2 mg of plasmid with LipofectAMIN (Life Technologies, Inc.) according to the manufacturer's protocols. Twenty-four hours after transfection, G418 (Life Technologies, Inc.) was added to the medium at a final concentration of 700 mg/L to kill untransfected cells.

Expression and purification of GST fusion protein

The coding sequence of LPTS-L was cloned in frame into the *E.coli* GST fusion expression vector pGEX-4T2 (Amersham Pharmacia Biotech Inc.), then the construct was transfected into *E.coli* BL21(DE3). The protein was expressed with IPTG induction for 3 hours and purified by glutathione-agarose (Sigma) column.

TRAP telomerase activity assay^[13]

HCC cells SMMC-7721 were lysed in lysis buffer (10 mM TrisHCl pH7.5, 1 mM MgCl₂, 1 mM EGTA, 0.1 mM PMSF, 5 mM 2-mercaptoethanol, 0.5 % CHAPS, 10 % glycerol) on ice for 30 min and centrifuged at 13 000 rpm for 30 min, the telomerase was contained in the suspension of cell extract. The protein of LPTS-L was incubated with cell extract for 10 min at 4 °C before subjecting to telomerase extension according the reference^[11]. Telomerase products were separated on 10 % polyacrylamide gels, which were stained with silver.

RESULTS

Over-expression of LPTS-L in SMMC-7721 induces crisis

To investigate the function of LPTS-L in hepatoma cells, 987-bp coding region of LPTS-L was subcloned into pcDNA₃ eukaryotic expression vector to construct pcDNA₃-LPTS-L, then the construct was transfected into SMMC-7721 cell lines, with pcDNA₃ vector as control. The growth of hepatoma cells transfected with LPTS-L became slow, possibly due to an increase rate of cell death, as compared with control. In most cases, the cells transfected with LPTS-L exhibited increased size and flattened-morphology, with the characteristics associated with crisis (Figure 1).

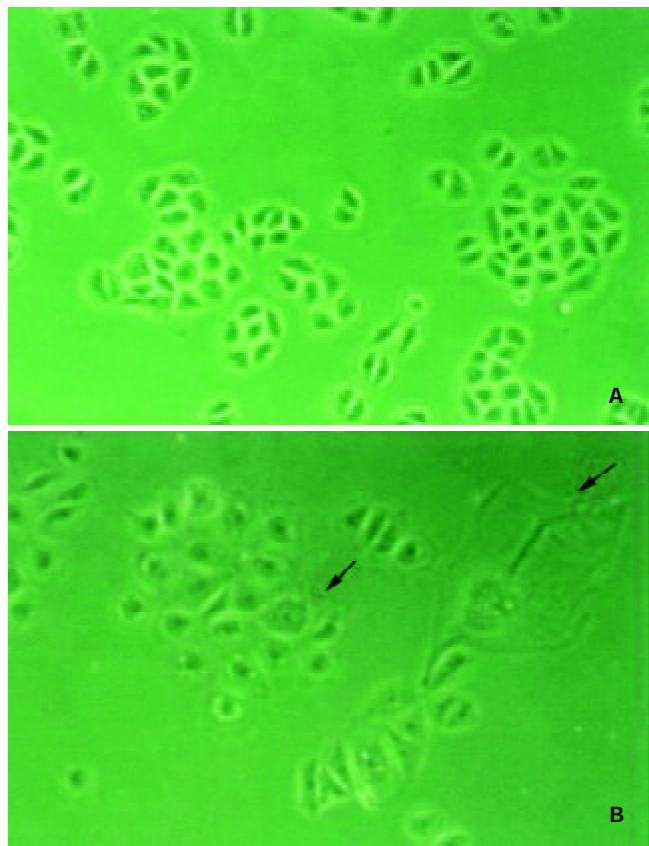


Figure 1 Morphologic changes induced by LPTS-L in hepatoma cell line SMMC-7721. A. cells expressing control vector; B. large flat cells in crisis expressing LPTL.

LPTS-L could inhibit telomerase activity of SMMC-7721 cell extract *in vitro*

To study the mechanism of the induction of the hepatoma cells into crisis by LPTS-L, we used telomerase activity assay *in vitro* to determine the correlation between LPTS-L protein and telomerase. Firstly, we subcloned the coding sequence of LPTS-L into GST fusion protein expression vector in frame and purified the GST-LPTS-L fusion protein by affinity chromatography (Figure 2). The purity of the fusion protein was enough for the next telomerase activity assay. We next added the GST-LPTS-L protein into the cell extract of SMMC-7721 and then performed the TRAP assay. The results showed clearly that LPTS-L inhibited telomerase activity greatly, 1 mg fusion protein could almost inhibit the telomerase activity, while 10 µg GST protein had no effect at all (Figure 3).

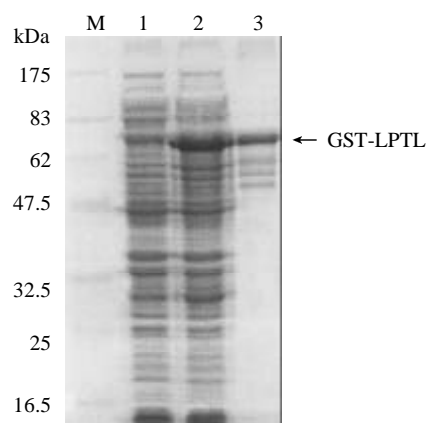


Figure 2 The expression of GST fusion protein with LPTS-L. M: protein marker; 1. total protein before IPTG induction; 2. total protein after IPTG induction for 3 hours; 3. purified GST fusion protein by affinity chromatography on glutathione-agarose column.

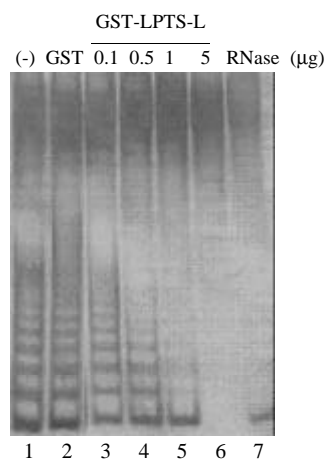


Figure 3 LPTS-L fusion protein inhibits telomerase activity in hepatocellular carcinoma cell line SMMC-7721 by TRAP assay *in vitro*. 1. SMMC-7721 cell extract alone; 2. plus 10 µg GST protein; 3-6. plus 0.1, 0.5, 1, 5 µg GST-LPTS-L fusion protein and the lane 7 is cell extract plus RNase.

DISCUSSION

Normal hepatocytes seldom divide, which is reflected by a fact that their telomeres length does not decrease with age. Telomerase activity is absent in the resting liver but transiently reappears during hepatic regeneration. The telomere length of

HCC cells is relatively shorter than that of the normal hepatocytes, but is stable due to the activation of telomerase activity^[14,15]. The telomerase activity could be detected in all HCC tissue samples smaller than 3 cm, regardless of the patient's age, sex, viral marker and degree of tumor differentiation^[16]. Telomerase activity was also detectable in hepatoma cell line SMMC-7721 as assayed by TRAP assay. Over-expression of LPTS-L in SMMC-7721 cells could inhibit telomerase activity, and induce cells into crisis. From the results above, we can conclude that LPTS-L encoded by LPTS gene is expressed in normal liver cells and serves as a telomerase inhibitor. In the HCC cells, LPTS-L was down-regulated or absent, while transformed LPTS-L into HCC cells could stop the cell proliferation and the cells became large, flat and dead. LPTS gene must be inactivated to depress the telomerase inhibitory activity during hepatocarcinogenesis.

Recently, the correlation between telomerase and immortalization of tumor cells, makes the telomere and telomerase a hotspot in tumor molecule pathological study. Reactivation of telomerase appears to be a universal and obligatory step towards cell immortalization. Telomerase activity has been found in about 85-90 % of all human tumors, including liver cancer, but not in adjacent normal cells. As a result, telomerase has become a novel target not only for cancer diagnosis but also for the development of novel therapeutic agents^[17,18]. LPTS-L encoded by LPTS gene, which could inhibit the activity of the telomerase directly, is an important protein inhibiting telomerase activity. LPTS gene might be a new target in the "battle" against hepatocellular carcinoma, and could be used in tumor gene therapy through reactivation of its expression in tumor cells.

REFERENCES

- 1 **Blackburn EH.** Structure and function of telomeres. *Nature* 1991; **350**: 569-573
- 2 **Moyzis RK,** Buckingham JM, Cram LS, Dani M, Deaven LL, Jones MD, Meyne J, Ratliff RL, Wu JR. A highly conserved repetitive DNA sequence, (TTAGGG)_n, present at the telomeres of human chromosomes. *Proc Natl Acad Sci USA* 1988; **85**: 6622-6626
- 3 **Blackburn EH.** Telomeres: structure and synthesis. *J Biol Chem* 1990; **265**: 5919-5921
- 4 **Blackburn EH.** Switching and signaling at the telomere. *Cell* 2001; **106**: 661-673
- 5 **Greider W,** Blackburn EH. Identification of a specific telomere terminal transferase activity in Tetrahymena extracts. *Cell* 1985; **43**: 405-413
- 6 **Nugent CI,** Lundblad V. The telomerase reverse transcriptase: components and regulation. *Genes Dev* 1998; **12**: 1073-1085
- 7 **Feng J,** Funk WD, Wang SS, Weinrich SL, Avilion AA, Chiu CP, Adams RR, Chang E, Allsopp RC, Yu J. The RNA component of human telomerase. *Science* 1995; **269**: 1236-1241
- 8 **Shay JW,** Zou Y, Hiyama E, Wright WE. Telomerase and cancer. *Hum Mol Genet* 2001; **10**: 677-685
- 9 **Stewart SA,** Weinberg RA. Telomerase and human tumorigenesis. *Semin Cancer Biol* 2000; **10**: 399-406
- 10 **Meyerson M.** Role of telomerase in normal and cancer cells. *J Clin Oncol* 2000; **18**: 2626-2634
- 11 **Liao C,** Zhao M, Song H, Uchida K, Yokoyama KK, Li T. Identification of the gene for a novel liver-related putative tumor suppressor at a high-frequency loss of heterozygosity region of chromosome 8p23 in human hepatocellular carcinoma. *Hepatology* 2000; **32**: 721-727
- 12 **Zhou XZ,** Lu KP. The Pin2/TRF1-interacting protein PinX1 is a potent telomerase inhibitor. *Cell* 2001; **107**: 347-359
- 13 **Kim NW,** Piatyszek MA, Prowse KR, Harley CB, West MD, Ho PL, Coviello GM, Wright WE, Weinrich SL, Shay JW. Specific association of human telomerase activity with immortal cells and cancer. *Science* 1994; **266**: 2011-2015
- 14 **Miura N,** Horikawa I, Nishimoto A, Ohmura H, Ito H, Hirohashi S, Shay JW, Oshimura M. Progressive telomere shortening and telomerase reactivation during hepatocellular carcinogenesis. *Cancer Genet Cytogenet* 1997; **93**: 56-62
- 15 **Huang GT,** Lee HS, Chen CH, Chiou LL, Lin YW, Lee CZ, Chen DS, Sheu JC. Telomerase activity and telomere length in human hepatocellular carcinoma. *Eur J Cancer* 1998; **34**: 1946-1949
- 16 **Erlitzki R,** Minuk GY. Telomeres, telomerase and HCC: the long and the short of it. *J Hepatol* 1999; **31**: 939-945
- 17 **Zhang FX,** Zhang XY, Fan DM, Deng ZY, Yan Y, Wu HP, Fan JJ. Antisense telomerase RNA induced human gastric cancer cell apoptosis. *World J Gastroenterol* 2000; **6**: 430-432
- 18 **Yakoob J,** Hu GL, Fan XG, Zhang Z. Telomere, telomerase and digestive cancer. *World J Gastroenterol* 1999; **5**: 334-337

Edited by Ma JY

• LIVER CANCER •

Effects of tachyplesin on proliferation and differentiation of human hepatocellular carcinoma SMMC-7721 cells

Gao-Liang Ouyang, Qi-Fu Li, Xuan-Xian Peng, Qing-Rong Liu, Shui-Gen Hong

Gao-Liang Ouyang, Shui-Gen Hong, Laboratory of Cell Biology, School of Life Sciences, Xiamen University, Xiamen 361005, Fujian Province, China

Qi-Fu Li, Xuan-Xian Peng, Qing-Rong Liu, The Key Laboratory of China Education Ministry for Cell Biology and Tumor Cell Engineering, School of Life Sciences, Xiamen University, Xiamen 361005, Fujian Province, China

Supported by the National Natural Science Foundation of China, No. 30170724 and Natural Science Foundation of Fujian Province, No. C97015.

Correspondence to: Dr. Qi-Fu Li, The Key Laboratory of China Education Ministry for Cell Biology and Tumor Cell Engineering, School of Life Sciences, Xiamen University, Xiamen 361005, Fujian Province, China. chifulee@163.net

Telephone: +86-592-2183619 **Fax:** +86-592-2186392

Received 2002-05-02 **Accepted** 2002-06-11

Abstract

AIM: To investigate the antitumor activities of tachyplesin on human hepatocellular carcinoma (HCC) cells.

METHODS: Tachyplesin, isolated from acid extracts of Chinese horseshoe crab (*Tachyplesus tridentatus*) hemocytes, was used to treat the human HCC cell line SMMC-7721. Effects of tachyplesin on the proliferation of SMMC-7721 cells were measured with trypan blue dye exclusion test and HE staining. The morphology and ultrastructure of the cells were examined by light microscopy and transmission electron microscopy, respectively. The activities of γ -glutamyltransferase (γ -GT) and tyrosine aminotransferase (TAT) were assayed with biochemical methods. The levels of alpha fetoprotein (α -FP), proliferating cell nuclear antigen (PCNA), p21^{WAF1/CIP1} and *c-myc* were examined by immunocytochemistry.

RESULTS: After treatment with tachyplesin 3.0 mg/L, the proliferation of SMMC-7721 cells was inhibited significantly, with the cell growth inhibitory rate amounted to 55.57 % and the maximum cell mitotic index declined by 43.68 %. The morphology and ultrastructure underwent restorational alteration. The activity of γ -GT declined while TAT activity increased obviously, and the levels of α -FP and PCNA decreased. Moreover, the expression of p21^{WAF1/CIP1} protein was up-regulated and that of *c-myc* protein was down-regulated.

CONCLUSION: Tachyplesin could effectively inhibit the proliferation of hepatocarcinoma cells, reverse the malignant morphological and ultrastructural characteristics, alter the levels of enzymes and antigens, regulate the expression of differentiation-associated oncogene and tumor suppressor gene, and induce hepatocarcinoma cell differentiation.

Ouyang GL, Li QF, Peng XX, Liu QR, Hong SG. Effects of tachyplesin on proliferation and differentiation of human hepatocellular carcinoma SMMC-7721 cells. *World J Gastroenterol* 2002; 8(6): 1053-1058

INTRODUCTION

The induction of tumor cell differentiation is a new strategy of drug therapy of tumors. In recent years, many studies showed that malignant tumor cells could be induced to terminal differentiation by some inducers. Differentiation-inducing therapy has already been applied to leukemias, lymphomas, and other solid tumors^[1]. On the other hand, the study on antitumor activities of marine bioactive substances has become an important field in exploiting marine bioactive substances and antitumor drugs^[2-4]. In order to explore the method and means of regulating the proliferation of tumor cell and reversing its malignant phenotypes artificially, we focus on screening and identifying marine bioactive substances, especially those with low molecular weight which can adjust cell signal transduction and regulate cell proliferation and differentiation.

Horseshoe crab, a kind of marine animal, which has survived relatively unchanged for the past 350 million years, now is at the center of a resource tug of war. During the past two decades, many bioactive substances with special functions, including clotting factors, lectins, proteinase inhibitors, defensins, tachyplesin and tachystatins, have been found in the hemocytes and hemolymph plasma of horseshoe crab^[5-9]. In our previous works, we reported that tachyplesin could alter the malignant morphological and ultrastructural characteristics and regulate the proliferation and differentiation of human gastric carcinoma cells^[10,11]. In this paper, the antitumor activities of tachyplesin on hepatocellular carcinoma cell line SMMC-7721 were investigated to further clarify the antitumor mechanism of tachyplesin.

MATERIALS AND METHODS

Drugs and reagents

Tachyplesin was isolated from acid extracts of Chinese horseshoe crab (*Tachyplesus tridentatus*) hemocytes as described by Nakamura *et al*^[12]. RPMI-1640 medium were obtained from Gibco. Fetal calf serum was supplied by Si-Ji-Qing Biotechnology Co. (Hangzhou, China). Trypan blue were purchased from Sigma Co. γ -GT kit was purchased from Shanghai Lianyang Biotechnical Co. Mouse anti-human α -FP, PCNA, p21^{WAF1/CIP1}, *c-myc* monoclonal antibodies were purchased from Santa Cruz. SP detection kit and DAB kit were purchased from Beijing Zhongshan Biotechnology Co.

Cell culture and treatment

SMMC-7721 cells, provided by the Institute of Biochemistry and Cell Biology, Shanghai Institute of Biological Sciences, Chinese Academy of Sciences, were maintained in RPMI-1640 medium supplemented with 20 % heat-inactivated fetal calf serum, 100 units/mL penicillin, 100 mg/L streptomycin and 50 mg/L kanamycin at 37 °C, 5 % CO₂ in air atmosphere. SMMC-7721 cells were treated with culture medium containing tachyplesin after being seeded for 24 hours.

Determination of cell growth curve and cell mitotic index

SMMC-7721 cells ($5 \times 10^4/\text{mL}$) were seeded in small culture flasks or in little penicillin bottles with cover slips respectively. Tachyplesin treatment was performed after cells being subcultured for 24 hours. From the first to seventh day, three flasks of untreated or tachyplesin-treated cells were harvested every day, and the viable cells were counted by the trypan blue dye exclusion test. Meanwhile, the cover slips with untreated or tachyplesin-treated cells were also taken out every day, fixed in Bouin-Hollande fixative, and stained with Hematoxylin-Eosin (HE) staining. The mitotic cells in 1000 cells on each cover slip were counted.

Sample preparation for the light microscopy

SMMC-7721 cells and the cells treated with 3.0 mg/L tachyplesin for 5 days were seeded in little penicillin bottles with cover slips, and grown in the normal culture medium or in the medium containing 3.0 mg/L tachyplesin for 48 hours, respectively. The cells on cover slips were rinsed with D-Hank's solution twice at 37°C , fixed overnight in Bouin-Hollande fixative, stained with Hematoxylin-Eosin staining, and observed under light microscope.

Sample preparation for transmission electron microscopy

SMMC-7721 cells and the cells treated with 3.0 mg/L tachyplesin for 7 days were rinsed with D-Hank's solution twice at 37°C , shaved into centrifuge tubes with plastic scraper. Cells were centrifuged at 2000 rpm for 15 min, and the supernatants were removed. The precipitates were prefixed in 2.5 % glutaraldehyde for 2 hours and postfixed in 1 % osmium tetroxide for 2 hours, dehydrated in ethanol series, embedded in epoxy resin 618, stained with lead citrate and uranyl acetate, and observed under the JEM-100CX II transmission electron microscope.

Assays for the activities of γ -glutamyltransferase (γ -GT) and tyrosine aminotransferase (TAT)

SMMC-7721 cells and the cells treated with 3.0 mg/L tachyplesin for 7 days were harvested, counted, and sonicated in ice-cooled 0.1 mol/L PBS. The homogenates were centrifuged and the supernatants were subjected to assay of enzymatic activities. The γ -GT activity was determined with γ -GT reagent kit and the TAT activity was detected according to the method described by Marston *et al*^[13]. The activities of γ -GT and TAT were valued as OD unit per 1×10^6 cells.

Immunocytochemistry analysis

SMMC-7721 cells and the cells treated with 3.0 mg/L tachyplesin for 5 days were seeded in little penicillin bottles with cover slips for 48 hours respectively. The cells grown on cover slips were fixed with cold acetone for 10 min, rinsed twice in PBS for 15 min. They were then immersed in 3 % hydrogen peroxide for 10 min, washed with distilled water and PBS for 15 min, blocked with 10 % normal goat serum for 10 min at room temperature, and incubated with the monoclonal mouse anti-human α -FP, PCNA, p21^{WAF1/CIP1}, *c-myc* antibodies at 4°C overnight. After incubation with primary antibodies, cover slips were rinsed twice in PBS for 15 min, incubated with biotin-labeled secondary antibody at 37°C for 10 min, rinsed twice in PBS for 15 min, and then incubated in streptavidin-peroxidase at 37°C for 10 min. The antigen-antibody complex was visualized with diaminobenzidine (DAB) substrate. Negative controls were incubated in the absence of primary antibodies.

Statistical analysis

Student's *t* test was used to compare the difference between control group and tachyplesin treatment group. The data of cell growth, mitotic index and enzymatic activities were presented as the mean with the corresponding standard deviation. *P* value of less than 0.05 is considered statistically significant.

RESULTS

Effects of tachyplesin on the proliferation of SMMC-7721 cells

Under concentration of 2.5, 3.0, 3.5 mg/L, tachyplesin significantly inhibited the proliferation of SMMC-7721 cells. The growth inhibitory rates on SMMC-7721 cells on the seventh day were 47.09 %, 55.57 % and 62.77 %, respectively ($P < 0.05$) (Figure 1). According to the principle of induced differentiation treatment, we chose 3.0 mg/L tachyplesin for induced treatment. Cell mitotic index determination showed that SMMC-7721 cells had vigorous proliferation capability, reached to the divided peak on the fourth day, and the maximum mitotic index amounted to $35.19 \pm 2.17\%$. However the mitotic index of the cells treated with 3.0 mg/L tachyplesin was only $19.82 \pm 1.89\%$ at the divided peak, declined by 43.68 % ($P < 0.05$), and the divided peak was on the third day after tachyplesin treatment (Figure 2).

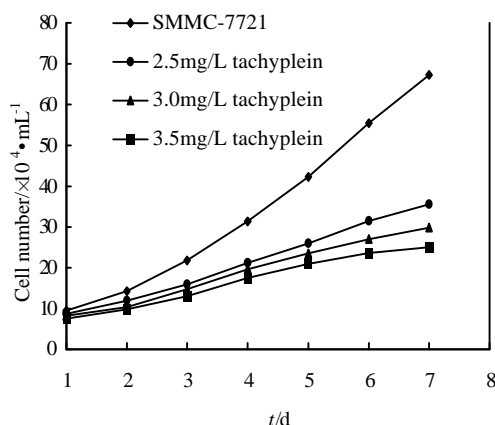


Figure 1 Effect of tachyplesin on the growth of SMMC-7721 cells

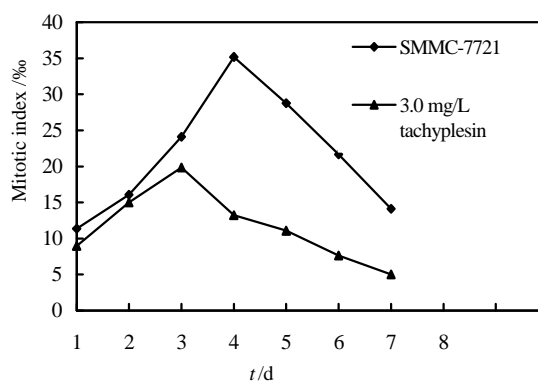


Figure 2 Effect of tachyplesin on the mitotic index of SMMC-7721 cells

Effects of tachyplesin on the morphology and ultrastructure of SMMC-7721 cells

SMMC-7721 cells showed typical malignant morphological and ultrastructural characteristics in SMMC-7721 cells like other epithelial cancer cells. Under light microscope, the volume of SMMC-7721 cells was relatively small, nuclei were

large and irregular with several nucleoli in it, and cytoplasm volume was small (Figure 3A). And it was revealed by transmission electron microscope that the nucleocytoplasmic ratio of SMMC-7721 cells was relatively large, nuclei were irregular with many heterochromatins and few euchromatins and large nucleolus in it, while cell organelles were not well-developed in the cytoplasm (Figure 3C). However, after being treated with 3.0 mg/L tachyplesin, SMMC-7721 cells had undergone a significant morphological and ultrastructural changes and appeared as normal differentiated epithelial cells. The cells turned to be more spread and flat, the nucleocytoplasmic ratio was reduced, the shape of nuclei became regular, heterochromatin in nucleus decreased while euchromatin increased, the volume of nucleolus was reduced, and cytoplasm was abundant with well-developed cell organelles (Figure 3B,D).

Effects of tachyplesin on the activities of γ -GT and TAT in SMMC-7721 cells

The human hepatocarcinoma SMMC-7721 cells had high γ -GT activity and low TAT activity. After treatment with 3.0 mg/L tachyplesin, the activity of γ -GT in SMMC-7721 cells were declined from 0.48 ± 0.04 Unit to 0.30 ± 0.02 Unit ($P < 0.05$) while TAT activity increased from 0.44 ± 0.04 Unit to 0.90 ± 0.04 Unit ($P < 0.05$) as shown in Figure 4.

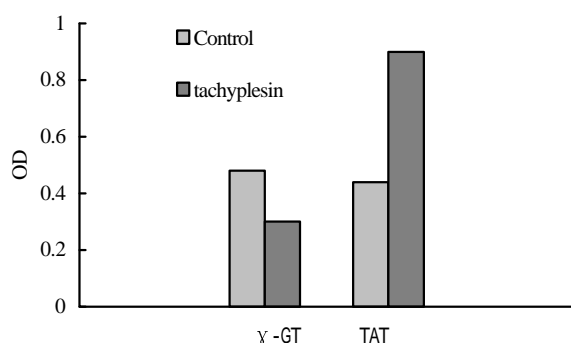


Figure 4 Effects of tachyplesin on the activities of γ -GT and TAT in SMMC-7721 cells

Effects of tachyplesin on α -FP, PCNA levels in SMMC-7721 cells

High level of α -FP was detected in the cytoplasm and nucleus of SMMC-7721 cells (Figure 5A). However, after being treated with 3.0 mg/L tachyplesin, the cells had a very low level of α -FP (Figure 5B). The PCNA level was also high and mainly distributed in the nucleus of SMMC-7721 cells, especially in the spherical cells, while the immunocytochemical signal was weak in the tachyplesin-treated cells (Figure 5C,D).

Effects of tachyplesin on protein p21^{WAF1/CIP1}, c-myc levels in SMMC-7721 cells

To investigate the effects of tachyplesin on the expression of differentiation-associated tumor suppressor gene and oncogene, the levels of p21^{WAF1/CIP1} and c-myc proteins were also examined. Immunocytochemistry showed that the level of p21^{WAF1/CIP1} protein was low in the nucleus and cytoplasm of the untreated cells while it was very high in the cells treated with tachyplesin (Figure 5E,F). High level of c-myc was observed in SMMC-7721 cells and exposure of the cells to tachyplesin resulted in an obvious decrease of c-myc protein (Figure 5G,H).

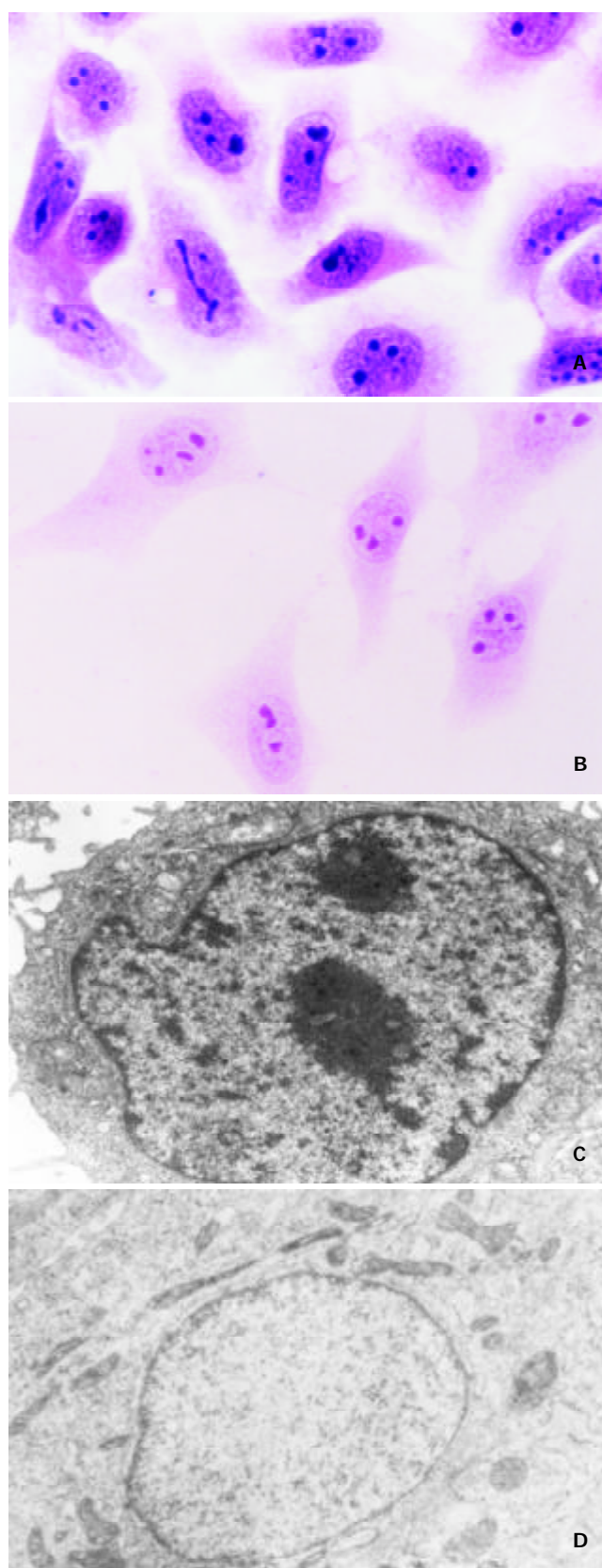


Figure 3 Effects of tachyplesin on the morphology and ultrastructure of SMMC-7721 cells. A: SMMC-7721 cells ($\times 536$); B: SMMC-7721 cells treated with tachyplesin ($\times 536$); C: The nucleocytoplasm ratio is large, the shape of nucleus is irregular and cell organelles are not well-developed in the cytoplasm of SMMC-7721 cell ($\times 8800$); D: The nucleocytoplasm ratio decreased, the shape of nucleus is regular and cell organelles are well-developed in the cytoplasm of tachyplesin-treated SMMC-7721 cell ($\times 11000$)

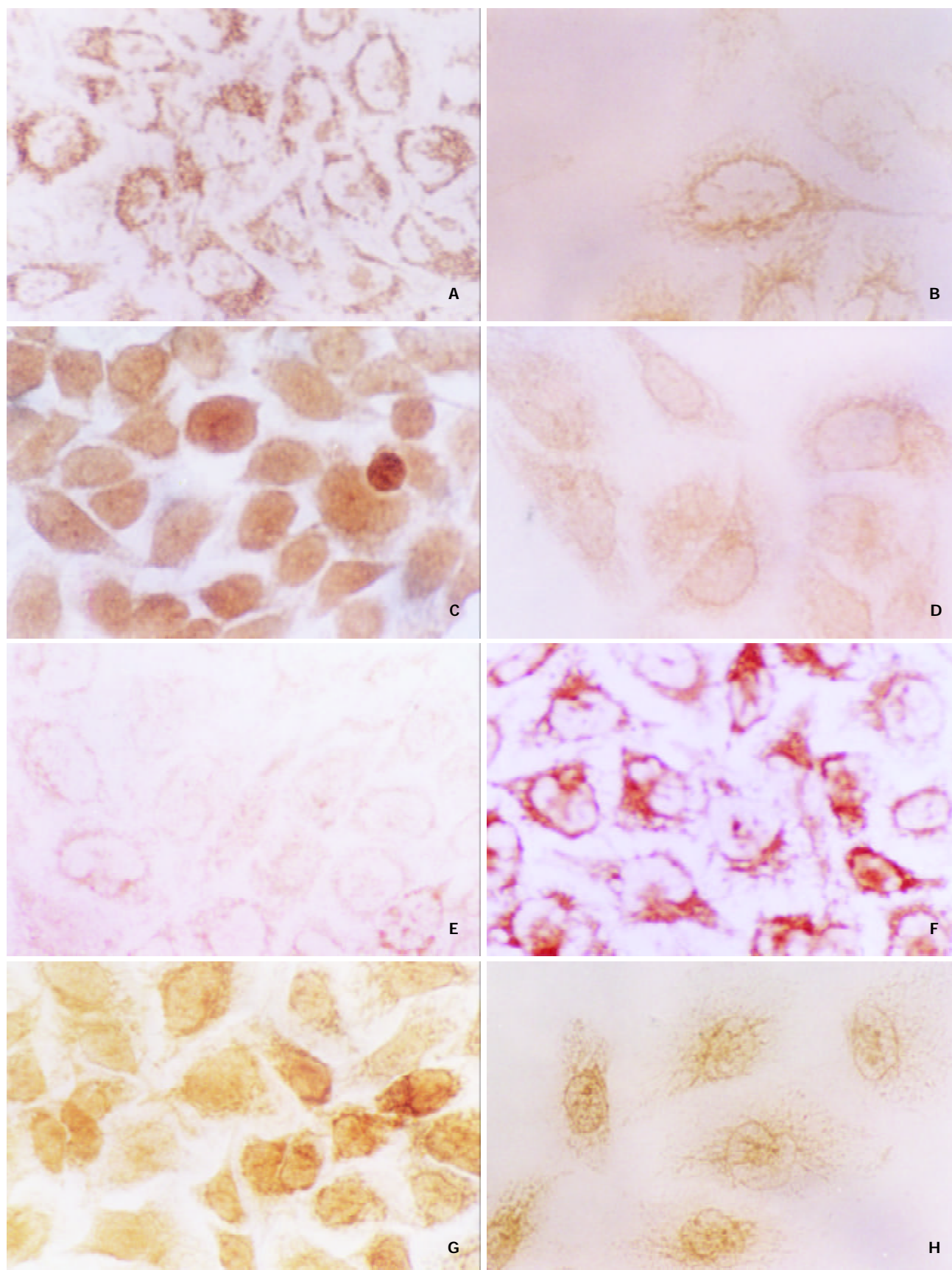


Figure 5 Effects of tachyplesin on the levels of α -FP, PCNA, p21^{WAF1/CIP1}, c-myc proteins in SMMC-7721 cells ($\times 536$). A: The high level of α -FP in SMMC-7721 cells detected by immunocytochemistry; B: The level of α -FP in the tachyplesin-treated SMMC-7721 cells is decreased; C: The high level of PCNA in SMMC-7721 cells; D: The level of PCNA in the tachyplesin-treated SMMC-7721 cells is decreased; E: The low level of p21^{WAF1/CIP1} in SMMC-7721 cells; F: The level of p21^{WAF1/CIP1} in the tachyplesin-treated SMMC-7721 cells is increased; G: The high level of c-myc in SMMC-7721 cells; H: The level of c-myc in the tachyplesin-treated SMMC-7721 cells is decreased.

DISCUSSION

It is important to examine the changes of the main malignant characteristics of cancer cells in order to evaluate the malignant phenotype reversion. Continual division and constant proliferation are important characteristics of tumor cells. The proliferating activity of cells is inversely correlated with the degree of differentiation. Therefore, inhibiting the proliferation of tumor cells is a significant index in induction of differentiation^[1,14]. In the present study, the results of the cell growth curve and mitotic index assay indicated that tachyplesin could inhibit the multiplicative activity of hepatocarcinoma cells effectively, with similar effects of growth inhibition as retinoic acid, HMBA and dimethyl sulphoxide on human hepatocarcinoma cells HepG2 and SMMC-7721^[15-20]. It suggests that tachyplesin could suppress tumor cell growth as other differentiation inducers.

Malignant morphology and ultrastructure are other important characteristics of tumor cells. Previous studies had revealed that lots of differentiation inducers could reverse the morphology and ultrastructure of tumor cells. Therefore, evaluating the changes of these two characteristics in tumor cells is important in determining the effects of exotic substances, especially differentiation inducers on tumor cells. Our results showed that tachyplesin could reverse the malignant morphological and ultrastructural characteristics of SMMC-7721 cells as it did on gastric carcinoma cells or other inducers on hepatocarcinoma cells and other tumor cells^[10,18,19].

α -FP, an oncofetal antigen, is as an important tumor-specific marker for the diagnosis of hepatocellular carcinoma and has been widely used in clinical setting^[21-25]. PCNA, the auxiliary protein of DNA polymerase δ , ϵ , plays an important role in DNA replication, repair and cell cycle control, and can be used as differentiation marker of hepatocarcinoma^[26-30]. The increased levels of α -FP and PCNA are correlated with hepatocyte malignancy, and many differentiation inducers such as HMBA, retinoic acid and sodium butyrate could decrease their levels in hepatocarcinoma cells^[18-20]. γ -GT and TAT also can be used as tumor markers of hepatocellular carcinoma^[31-33]. The decreased activity of TAT and the increased levels of α -FP, PCNA and γ -GT activities are correlated with hepatocyte malignancy. Many differentiation inducers, such as retinoic acid and HMBA, could reduce the levels of α -FP and PCNA and γ -GT while increase the level of TAT in hepatocarcinoma cells^[18,19,34]. Our results revealed that the levels of α -FP and PCNA and γ -GT were down-regulated and the activity of TAT was increased in the tachyplesin-treated cells, indicating that tachyplesin could alter the activities of differentiation-associated enzymes and decrease the levels of tumor-associated antigens as many differentiation inducers.

In addition, many tumor suppressor genes and oncogenes, which were correlative with the tumorigenesis and progression and prognosis of hepatocarcinoma, also could serve as index of induced differentiation. p21^{WAF1/CIP1}, the pioneer member of p21 family of cyclin-cdk inhibitor class of proteins, has been implicated as a growth arrest mediator in cell terminal differentiation and apoptosis^[1,30,35]. Many inducers such as sodium butyrate could increase the expression of p21^{WAF1/CIP1} of hepatocarcinoma cells^[20]. In the meantime, *c-myc* gene also plays an essential role in cell proliferation, differentiation, and apoptosis^[36,37]. Down-regulation of *c-myc* expression induced by differentiation signals is regarded as a hallmark of cell differentiation^[38-40]. The expression of *c-myc* level was reduced in sodium butyrate-induced differentiation of human hepatoma cells^[41], and in *all-trans* retinoic acid-induced differentiation of human leukemic U937 cells with an increase in p21^{WAF1/CIP1}

expression^[42]. Our results showed that tachyplesin could increase the expression of p21^{WAF1/CIP1} and down-regulate the levels of *c-myc* protein in SMMC-7721 cells, and induce the cells to terminal differentiation as other differentiation inducers^[42,43].

Taken together, the results of the current study indicated that tachyplesin could effectively inhibit the proliferation of human hepatoma SMMC-7721 cells, reverse the malignant morphological and ultrastructural characteristics, alter the activities of differentiation-associated enzymes and the levels of tumor-associated antigens, adjust the expression of oncogenes and tumor suppressor gene correlative with hepatocellular carcinoma, and so induce hepatocarcinoma cell differentiation.

REFERENCES

- 1 Yoneda K, Yamamoto T, Ueta E, Osaki T. Induction of cyclin-dependent kinase inhibitor p21 in vesnarinone-induced differentiation of squamous cell carcinoma cells. *Cancer Lett* 1998; **133**: 35-45
- 2 Schwartzmann G, da-Rocha AB, Berlinck RGS, Jimeno J. Marine organisms as a source of new anticancer agents. *Lancet Oncol* 2001; **2**: 221-225
- 3 Schwartzmann G. Marine organisms and other novel natural sources of new cancer drugs. *Ann Oncol* 2000; **11**: 235-243
- 4 Munro MHG, Blunt JW, Dumdei EJ, Hickford SJH, Lill RE, Li SX, Battershill CN, Duckworth AR. The discovery and development of marine compounds with pharmaceutical potential. *J Biotechnol* 1999; **70**: 15-25
- 5 Iwanaga S, Kawabata S, Muta T. New types of clotting factors and defense molecules found in horseshoe crab hemolymph: their structures and functions. *J Biochem* 1998; **123**: 1-15
- 6 Kawabata S, Iwanaga S. Role of lectins in the innate immunity of horseshoe crab. *Dev Comp Immunol* 1999; **23**: 391-400
- 7 Osaki T, Omotezako M, Nagayama R, Hirata M, Iwanaga S, Kasahara J, Hattori J, Ito I, Sugiyama H, Kawabata S. Horseshoe crab hemocyte-derived antimicrobial polypeptides, tachystatins, with sequence similarity to spider neurotoxins. *J Biol Chem* 1999; **274**: 26172-26178
- 8 Iwanaga S. The molecular basis of innate immunity in the horseshoe crab. *Cur Opin Immunol* 2002; **14**: 87-95
- 9 Berkson J, Shuster CN. The horseshoe crab: the battle for a true multiple-use resource. *Fisheries* 1999; **24**: 6-10
- 10 Li QF, Ouyang GL, Li CY, Hong SG. Effects of tachyplesin on the morphology and ultrastructure of human gastric carcinoma cell line BGC-823. *World J Gastroenterol* 2000; **6**: 676-680
- 11 Li QF, Ouyang GL, Li CY, Chen RC, Hong SG. Effects of tachyplesin on the proliferation and expression of C-erbB-2 and p53 genes in human gastric carcinoma cell line BGC-823. *Int J Modern Cancer Therapy* 2000; **3**: 30-33
- 12 Nakamura T, Furunaka H, Miyata T, Tokunaga F, Muta T, Iwanaga S, Niwa M, Takao T, Shimonishi Y. Tachyplesin, a class of antimicrobial peptide from the hemocytes of the horseshoe crab (*Tachyplus tridentatus*), isolation and chemical structure. *J Biol Chem* 1988; **263**: 16709-16713
- 13 Marston FA, Pogson CI. A simple and rapid assay for tyrosine aminotransferase. *FEBS Lett* 1977; **83**: 277-280
- 14 Li QF, Wang DY. The differentiation of human gastric adenocarcinoma cell line MGC80-3 induced by dBcAMP *in vitro*. *Chin J Cancer Res* 1991; **3**: 4-10
- 15 Li C, Wan YJY. Differentiation and antiproliferation effects of retinoic acid receptor beta in hepatoma cells. *Cancer Lett* 1998; **124**: 205-211
- 16 Falasca L, Marcellini P, Ara C, Rufo A, Devirgiliis LC. Growth inhibition and induction of specific hepatic phenotype expression by retinoic acid in HEPG2 cells. *Anticancer Res* 1999; **19**: 3283-3292
- 17 Vesey DA, Cunningham JM, Selden AC, Woodman AC, Hodgson HJ. Dimethyl sulphoxide induces a reduced growth rate, altered cell morphology and increased epidermal-growth-factor binding in Hep G2 cells. *Biochem J* 1991; **277**: 773-777

- 18 **Ouyang GL**, Li QF, Peng XX, Hong SG. Differentiation of human hepatocarcinoma SMMC-7721 cells induced by HMBA. *Shiyan Shengwu Xuebao* 2001; **34**: 269-273
- 19 **Zhang XW**. Recent advances in study of drugs that affects differentiation induction on hepatoma. *Zhongguo Zhongliu Linchuang* 1999; **26**: 389-392
- 20 **Yamamoto H**, Fujimoto J, Okamoto E, Furuyama J, Tamaoki T, Hashimoto-Tamaoki T. Suppression of growth of hepatocellular carcinoma by sodium butyrate in vitro and in vivo. *Int J Cancer* 1998; **76**: 897-902
- 21 **Wang XW**, Xu B. Several new targets of antitumor agents. *Zhongguo Yaoli Xuebao* 1997; **18**: 289-292
- 22 **Lee KC**, Crowe AJ, Barton MC. p53-mediated repression of alpha-fetoprotein gene expression by specific DNA binding. *Mol Cell Biol* 1999; **19**: 1279-1288
- 23 **Yoshida S**, Kurokohchi K, Arima K, Masaki T, Hosomi N, Funaki T, Murota M, Kita Y, Watanabe S, Kuriyama S. Clinical significance of lens culinaris agglutinin-reactive fraction of serum alpha-fetoprotein in patients with hepatocellular carcinoma. *Int J Oncol* 2002; **20**: 305-309
- 24 **Jiang YF**, Yang ZH, Hu JQ. Recurrence or metastasis of HCC: predictors, early detection and experimental antiangiogenic therapy. *World J Gastroenterol* 2000; **6**: 61-65
- 25 **He P**, Tang ZY, Ye SL, Liu BB. Relationship between expression of alpha-fetoprotein messenger RNA and some clinical parameters of human hepatocellular carcinoma. *World J Gastroenterol* 1999; **5**: 111-115
- 26 **Cao JQ**, Hu XY, Xie M, Sun JY, Cheng H. Expression of proliferating cell nuclear antigen and alpha-fetoprotein in hepatocellular carcinoma and its clinical significance. *Shiyong Aizheng Zazhi* 1998; **13**: 105-107
- 27 **Na IO**, Lai EC, Fan ST, Ng M, Chan AS, So MK. Prognostic significance of proliferating cell nuclear antigen expression in hepatocellular carcinoma. *Cancer* 1994; **73**: 2268-2274
- 28 **Jonsson ZO**, Hindges R, Hubscher U. Regulation of DNA replication and repair proteins through interaction with the front side of proliferating cell nuclear antigen. *EMBO J* 1998; **17**: 2412-2425
- 29 **Wang LQ**, Yu YZ, Sell S. p53 and PCNA as differentiation markers of hepatocellular carcinomas. *J Tumor Marker Oncol* 1998; **13**: 5-13
- 30 **Qin LF**, Ng IOL, Fan ST, Ng M. p21/WAF1, p53 and PCNA expression and p53 mutation status in hepatocellular carcinoma. *Int J Cancer* 1998; **79**: 424-428
- 31 **Kang JH**, Shi YM, Zheng RL. Effects of ascorbic acid and DL- α -tocopherol on human hepatoma cell proliferation and redifferentiation. *Zhongguo Yaoli Xuebao* 2000; **21**: 348-352
- 32 **Chen RC**, Xie XC, Ouyang GL, Cai KX, Su JH, Fu YG. Induction of differentiation in human hepatocarcinoma SMMC-7721 cell by natural antioxidant Isoverbascoside. *Int J Modern Cancer Therapy* 2000; **3**: 29-33
- 33 **Chen RC**, Su JH, Ouyang GL, Cai KX, Li JQ, Xie XG. Induction of differentiation in human hepatocarcinoma cells by isoverbascoside. *Planta Med* 2002; **68**: 370-372
- 34 **Wasserman L**, Nordenberg J, Beery E, Deutsh AA, Novogrodsky A. Differentiation effects of sodium butyrate and dimethyl sulfoxide on gamma-glutamyl transpeptidase and alkaline phosphatase activities in MCF breast cancer cells. *Exp Cell Biol* 1987; **55**: 188-193
- 35 **Hui AM**, Kanai Y, Sakamoto M, Tsuda H, Hirohashi S. Reduced p21(WAF1/CIP1) expression and p53 mutation in hepatocellular carcinomas. *Hepatology* 1997; **25**: 575-579
- 36 **Bartova E**, Kozubek S, Kozubek M, Jirsova P, Lukasova E, Skalninkova M, Cafourkova A, Koutna I. Nuclear topography of the c-myc gene in human leukemic cells. *Gene* 2000; **244**: 1-11
- 37 **Heath VJ**, Gillespie DAF, Crouch DH. Inhibition of the terminal stages of adipocyte differentiation by cMyc. *Exp Cell Res* 2000; **254**: 91-98
- 38 **He Y**, Zhang JR, Zhang J, Yuan YW. The role of c-myc in regulating mdm-1 gene expression in tumor cell line KB. *Chin Med J* 2000; **113**: 848-851
- 39 **Jiang N**, Zhan FH, Cao L, Yao KT, Li GY. c-myc gene inactivation during inducing of nasopharyngeal carcinoma cells with retinoic acid. *Chin Med J* 2000; **113**: 823-826
- 40 **Xu HY**, Yang YL, Guan XL, Song G, Jiang AM, Shi LJ. Expression of regulating apoptosis gene and apoptosis index in primary liver cancer. *World J Gastroenterol* 2000; **6**: 721-724
- 41 **Ebinuma H**, Saito H, Saito Y, Wakabayashi K, Nakamura M, Kurose I, Ishii H. Antisense oligodeoxynucleotide against c-myc mRNA induces differentiation of human hepatocellular carcinoma cells. *Int J Oncol* 1999; **15**: 991-999
- 42 **Dimberg A**, Bahram F, Karlberg I, Larsson LG, Nilsson K, Oberg F. Retinoic acid-induced cell cycle arrest of human myeloid cell lines is associated with sequential down-regulation of c-Myc and cycle E and posttranscriptional up-regulation of p27(Kip1). *Blood* 2002; **99**: 2199-2206
- 43 **Yuan SL**, Huang RM, Wang XJ, Song Y, Huang GQ. Reversing effect of Tanshinone on malignant phenotypes of human hepatocarcinoma cell line. *World J Gastroenterol* 1998; **4**: 317-319

Edited by Bo XN

• LIVER CANCER •

Effect of bax, bcl-2 and bcl-xL on regulating apoptosis in tissues of normal liver and hepatocellular carcinoma

Xiao-Zhong Guo, Xiao-Dong Shao, Min-Pei Liu, Jian-Hua Xu, Li-Nan Ren, Jia-Jun Zhao, Hong-Yu Li, Di Wang

Xiao-Zhong Guo, Xiao-Dong Shao, Min-Pei Liu, Jian-Hua Xu, Li-Nan Ren, Jia-Jun Zhao, Hong-Yu Li, Di Wang, Department of Gastroenterology, General Hospital of Shenyang Military Region, Shenyang 110016, Liaoning Province, China

Correspondence to: Dr. Xiao-Zhong Guo, Department of Gastroenterology, General Hospital of Shenyang Military Region, Shenyang 110016, Liaoning Province, China

Telephone: +86-24-23056230

Received 2002-03-11 **Accepted** 2002-05-11

Abstract

AIM: To investigate the expression of bax, bcl-2 and bcl-xL mRNA in the tissues of normal liver and hepatocellular carcinoma (HCC), and analyze the relationship between the expression of bax, bcl-2 and bcl-xL mRNA and clinical parameters of HCC patients.

METHODS: The expression of bax, bcl-2 and bcl-xL mRNA of normal liver and HCC was measured by Northern blot. Statistical analyses were made by *t* test and correlation analysis.

RESULTS: A very low mRNA level was indicated at bax, bcl-2 and bcl-xL in the HCC tissues in contrast to the tissues of normal liver by Northern blot analysis. The analyses of mRNA level revealed that HCC tissues exhibited a mean 7.6-fold decrease in bax, 4.2-fold in bcl-2 and 3.5-fold in bcl-xL in comparison with normal control tissues, respectively. Positive correlation was found between bax and bcl-xL ($r=0.7061, P<0.01$). There was no significance between the mRNA expression of these three genes and age, gender, tumor differentiation and tumor stage of HCC patients.

CONCLUSION: The results are consistent with the fact that apoptosis rarely occurs in normal livers but increases in HCC, indicating that bcl-2 and bcl-xL may play a very important role in regulating the apoptosis of normal liver and HCC.

Guo XZ, Shao XD, Liu MP, Xu JH, Ren LN, Zhao JJ, Li HY, Wang D. Effect of bax, bcl-2 and bcl-xL on regulating apoptosis in tissues of normal liver and hepatocellular carcinoma. *World J Gastroenterol* 2002; 8(6):1059-1062

INTRODUCTION

Apoptosis is a highly regulated form of programmed cell death defined by distinct morphological and biochemical features. Programmed cell death is involved in a type of cell death, in which the cell actively uses a genetically controlled program to cause its own demise during the tissue remodeling of embryogenesis^[1]. Apoptosis is a key mechanism causing cell death and organ diseases, failure of apoptosis is now understood to contribute to the development of human malignancies^[2-5].

The bcl-2 family is the best characterized group of apoptosis-mediating factors, which include bcl-2, mcl-1, bcl-x, bax, bak, and several others. Although its members share close structural homologies, their biologic functions differentiate into apoptosis-promoting (bax, bak, bcl-xS) or apoptosis-inhibiting (bcl-2, mcl-1, bcl-xL) properties^[1, 6]. The bcl-2 related genes regulate cell death and are considered to correlate with the pathogenesis and progression of cancers^[7-14]. Since the relationship between bcl-2 family and HCC is still unclear, we investigated the expression of the three genes in HCC and normal controls and evaluated the mediating action in HCC and the relationship between the genes and clinical parameters as well.

MATERIALS AND METHODS

Patients

Ten cases of (4 women, 6 men) normal liver tissues were obtained. The median age in the control group was 57 years, with a range of 39-75 years. HCC tissues were obtained from 21 patients (9 women, 12 men) undergoing surgery for HCC. The median age of the HCC patients was 64 years (a range of 33-76 years). According to the TNM classification of the International Union against Cancer, there were 6 patients with stage II, 13 with stage III, and 2 with stage IV disease. Tissues destined for RNA extraction were frozen in the operating room in liquid nitrogen immediately on surgical removal and maintained at -80 °C until use.

Northern blot analysis

Total RNA was extracted by the guanidinium isothiocyanate method, fractionated on 1.2 % agarose. 1.8 mol·L formaldehyde gels, and stained with ethidium bromide for verification of RNA integrity and loading equivalence^[15]. The RNA was electrotransferred to Nylon membranes (GeneScreen; DuPont, Boston, Massachusetts, USA) and cross linked by UV irradiation. The filters were then prehybridized, hybridized, and washed under conditions appropriate for digoxigenin labelled antisense riboprobes (bcl-2 and bax) or the ³²P labelled antisense riboprobe (bcl-xL) and cDNA probe (7S) as previously described^[15, 16].

In the case of the digoxigenin-labelled bcl-2 and bax cRNA probes, the filters were prehybridized and hybridized overnight at 68 °C (bcl-2) or 65 °C (bax) in a buffer containing 50 % formamide, 2×SSC (1×SSC is 0.15M NaCl/0.015 M sodium citrate buffer) (bcl-2) or 5×SSC (bax), 2 % blocking reagent (Boehringer Mannheim, Mannheim, Germany), 0.1 % N-lauroylsarcosine, and 0.02 % sodium dodecyl sulphate (SDS). The filters were then washed in 2×SSC/0.1 % SDS at room temperature, followed by three 15 minute washing at 68 °C (bcl-2) or 65 °C (bax) in 0.065×SSC/0.065% SDS/35% formamide (bcl-2) or 0.1×SSC/0.1 % SDS (bax). The filters were then incubated in a blocking buffer (1 % blocking reagent in 100 mmol·L maleic acid/150 mmol·L NaCl, pH 7.5) for 30 minutes, and in blocking buffer containing anti-digoxigenin alkaline phosphatase antibody (1:20 000; Boehringer

Mannheim) for 30 minutes, washed three times with maleic acid buffer for 15 minutes, and incubated with 25 mmol/L CDP-Star (Boehringer Mannheim). The membranes were then exposed to X ray films.

For the ^{32}P labelled antisense riboprobe (bcl-xL), the blots were prehybridized for 6 hours in 50 % formamide, 0.5 % sodium dodecyl sulfate (SDS), $5\times$ SSC (sodium chloride/sodium citrate buffer), $5\times$ Denhardt's solution ($1\times$ Denhardt's solution=0.02 % ficoll, 0.02 % polyvinylpyrrolidone, and 0.02 % bovine serum albumin), 250 mg/L salmon sperm DNA, and 50 mmol/L sodium phosphate buffer (pH 6.5). The blots were then hybridized for 18 hours at 65 °C in the presence of 1×10^6 cpm/ml labeled antisense riboprobe, washed twice at 65 °C in a solution containing $1\times$ SSPE (150 mmol/L NaCl, 10 mmol/L NaH_2PO_4 , and 1 mmol/L EDTA) and 0.5 % SDS, and twice at 65 °C in a solution containing $0.1\times$ SSPE and 0.5 % SDS.

In the case of the 7S cDNA probe, blots were prehybridized for eight hours at 42 °C in a buffer which contained 50 % formamide, 1 % SDS, 0.75 mol/L NaCl, 5 mmol/L EDTA, $5\times$ Denhardt's solution, 100 mg/L salmon sperm DNA, 10 % dextran sulfate, and 50 mmol/L phosphate buffer (pH 7.4). The hybridization was carried out at 42 °C for 18 hours by adding the ^{32}P labelled cDNA probe (1×10^5 cpm/mL). The blots were rinsed twice in $2\times$ SSC at room temperature and washed three times at 55 °C in $0.2\times$ SSC/2 % SDS under conditions appropriate for cDNA probes. Blots were then exposed at -80 °C to Fuji X ray films with intensifying screens (DuPont).

For statistical analysis of the Northern blot results, the intensity of the radiographic bands was quantified by laser densitometry (Bio-Rad 620; Richmond, California, USA). The ratio between the bax, bcl-2 or bcl-xL and the corresponding 7s signal was calculated in each sample.

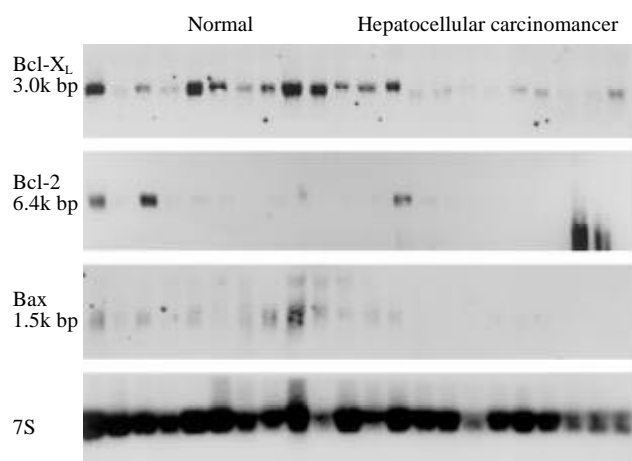
Statistical analysis

The data were expressed as median and range. Statistical analyses were carried out using the SPLM software (Statistical Department of Fourth Military Medical University). For statistical analysis, the *t* test and correlation analysis were used. Significance was defined as $P<0.05$.

RESULTS

Northern blot analysis

Northern blot analysis was carried out to determine bax, bcl-2 and bcl-xL mRNA expression in the normal and the cancerous liver. In contrast, hybridization signals of mRNA of three genes were higher in normal liver tissues as compared with the signals in cancerous samples (Figure 1). A low mRNA level of bax, bcl-2 and bcl-xL mRNA was almost present in all HCC tissue samples. In some HCC tissues the expression levels for all three genes were very faint and were only visible on the original autoradiographs. None of the normal or cancer samples showed any aberrant bax, bcl-2 or bcl-xL mRNA transcripts, and bax and bcl-2 mRNA were reduced in 100 % of cancer samples, and bcl-xL mRNA was reduced in 95 % of cancer samples in contrast with the normal controls. Densitometric analysis of the Northern blots indicated that the bax and bcl-2 mRNA levels in all cancer samples were 7.6- and 5.4-fold ($P=0.0002$; $P=0.00887$) higher than those in the matched control samples; bcl-xL mRNA levels in all cancer samples were 3.5-fold lower ($P=0.0002$) than those in the normal samples (Table 1). The expression of bax and bcl-xL mRNA was positively correlated in HCC ($r=0.7061$, $P<0.01$), but there was no correlation between bax and bcl-2 or bcl-2 and bcl-xL ($r=0.1637$, $r=0.4830$).



Normal Hepatocellular carcinoma
Figure 1 result of Northern blot analysis

Table 1 The expression of bax, bcl-2 and bcl-xL mRNA in hepatocellular carcinoma and normal liver

	Hepatocellular carcinoma (21 cases)	normal liver (10 cases)	<i>t</i> value	<i>P</i> value
Bax	0.929 ± 1.233	7.060 ± 6.574	4.197	0.0002
Bcl-2	1.414 ± 1.331	5.930 ± 7.227	2.815	0.0087
Bcl-xL	2.433 ± 2.218	8.500 ± 5.743	4.277	0.0002

Correlation of Northern blot analysis with clinical pathological parameters

To determine whether the presence of bax, bcl-2 or bcl-xL mRNA in the HCC tissues is of clinical significance, the Northern blot data were statistically analysed in patient data (sex, age) and clinical data (tumor stage, tumor differentiation). No significance was found between the expression of bax, bcl-2 or bcl-xL and these parameters (Table 2).

Table 2 The relationship between the expression of bax, bcl-2 and bcl-xL and clinical parameters of patients with hepatocellular carcinoma

	<i>n</i>	bax	bcl-2	bcl-xL
Age				
≤65	10	0.980 ± 1.530	1.960 ± 1.678	3.020 ± 2.549
>65	11	0.882 ± 0.962	0.918 ± 0.663	1.900 ± 1.825
gender				
male	13	1.100 ± 1.471	1.654 ± 1.532	2.600 ± 2.645
female	8	0.650 ± 0.699	1.025 ± 0.871	2.163 ± 1.386
grading				
well and moderate	12	0.975 ± 1.384	1.592 ± 1.540	2.775 ± 2.453
poor and undifferentiated	9	0.867 ± 1.076	1.178 ± 1.028	1.978 ± 1.901
tumor stage				
I II	6	0.583 ± 0.454	0.700 ± 0.616	2.000 ± 1.616
III IV	15	1.067 ± 1.423	1.700 ± 1.445	2.607 ± 2.445

Statistical analysis revealed no relationship between bax, bcl-2 or bcl-xL expression and these parameters.

DISCUSSION

Apoptosis is a central regulator of tissue homeostasis. It contributes to the elimination of damaged cells in normal tissues and balances the appropriate cell number under the circumstances of physiologic cell proliferation and tissue repair.

In the past few years, scientific interest has focused on the process of apoptosis. Like cell replication, apoptosis is controlled by the network of positive and negative growth signals. Based on the currently prevailing views, it is assumed that malignant cells should be incapable of apoptosis and /or not responsive to death signals, thereby allowing unrestrained growth of cancer. Recently, more and more studies indicated that apoptosis is of importance in the growth and development of many tumors, but the pattern of apoptosis varies in different tumors^[11-19]. In contrast with normal tissues, there is often reduction of apoptosis in most cancerous tissues^[20-23], but hepatic cancer is different. HCC is one of the most common and aggressive tumors in the world today, and little is known about the cellular pathogenesis^[24-34]. The apoptosis is rare in normal liver tissues (there is only 2-4 apoptotic cells per 10 000 hepatic or biliary cells^[35]), while the HCC tissues have higher rates of apoptosis^[37]. These findings indicate that the apoptosis-related genes are expressed in various frequencies in different cancers, and a general pattern of activation or inactivation of these genes in malignant tumors cannot be defined. Therefore, the function of apoptotic genes in different human cancers must be evaluated individually.

In this study, we analysed the concomitant expression of bax, bcl-2 and bcl-xL in the HCC tissues and normal liver. These genes belong to the same family of apoptotic genes. Although the structures are similar, they exert opposite effects on apoptosis. bcl-2 and bcl-xL inhibit apoptosis and contribute to cell survival and the resistance of cells against damaging influences. In contrast, bax, which is considered to be a central regulator of apoptosis, is a promoter of programmed cell death^[37]. The relationship between bcl-2 related genes and HCC is still unclear.

By the analysis of 21 HCC patients, reduced bax and bcl-2 signals were present in all samples and reduced bcl-xL signals were present in 95 % of the cancer samples. The low expression of bcl-2 and bcl-xL is consistent with enhanced apoptosis in the HCC, but the low expression of bax does not account for this phenomenon. The findings revealed that anti-apoptotic genes, but not apoptosis-promoting genes, might play a more important role in regulating the apoptosis of normal liver and HCC. There was no correlation between bax, bcl-2 and bcl-xL and age, gender, differentiation or stage of tumor in HCC patients. We can not give a reasonable explanation for the finding that the expression of bax and bcl-xL was positively correlated in HCC. We concluded that anti-apoptotic genes do not influence the differentiation and development of HCC, but these genes can increase the rate of apoptosis in HCC by reducing their expression or changing the ratio with other genes. The influencing factors of apoptosis increased in HCC are not known, which may include 1) inherent metabolic process of tumor tissues; 2) hypoxia of tumor tissues; 3) some cytokines such as tumor necrosis factor; 4) attack of CTL, etc.

The low expression of anti-apoptotic genes, which increase apoptosis in HCC, may have negative impact on growth of tumors as a homeostasis mechanism that inhibits cell group with extensive growth, and this effect can delay the development of tumors. But it may also be a selective pressure, which removes the aging tumor cells or some tumor cells with phenotype similar to normal cells and selects more aggressive and prosperous clone of tumor cells, accelerating the development of tumors. Further studies on the regulating action of apoptotic genes will deepen the understanding about the growth and development of HCC and offer valuable information to genetic therapy of HCC, thus enhancing the sensibility to radiotherapy and chemotherapy.

REFERENCES

- 1 **Que FG**, Gores GJ. Cell death by apoptosis: basic concepts and disease relevance for the gastroenterologist. *Gastroenterology* 1996; **110**: 1238-1243
- 2 **Friess H**, Lu Z, Graber HU, Zimmermann A, Adler G, Kore M, Schmid RM, Buchler MW. Bax, but not bcl-2, influences the prognosis of human pancreatic cancer. *Gut* 1998; **43**: 414-421
- 3 **Deng LY**, Zhang YH, Xu P, Yang SM, Yuan XB. Expression of interleukin 1 β converting enzyme in 5-FU induced apoptosis in esophageal carcinoma cells. *World J Gastroenterol* 1999; **5**: 50-52
- 4 **Zhao AG**, Yang JK, Zhao HL. Chinese Jianpi herbs induce apoptosis of human gastric cancer grafted onto nude mice. *Shijie Huaren Xiaohua Zazhi* 2000; **8**: 737-740
- 5 **Xin ZP**, Xu CF, Huang YX, Wen QS, Xu CZ, Zhao YF. Experimental study on induction of apoptosis by cisplatin in human gastric carcinoma cell line SGC-7901. *Huaren Xiaohua Zazhi* 1998; **6**: 844-846
- 6 **Friess H**, Lu Z, Andren-Sandberg A, Berberat P, Zimmermann A, Adler G, Schmid R, Buchler MW. Moderate activation of the apoptosis inhibitor bcl-xL worsens the prognosis in pancreatic cancer. *Ann Surg* 1998; **228**: 780-787
- 7 **Xiao B**, Shi YQ, Zhao YQ, You H, Wang ZY, Liu XL, Yin F, Qiao TD, Fan DM. Transduction of Fas gene or bcl-2 antisense RNA sensitizes cultured drug resistant gastric cancer cells to chemotherapeutic drugs. *World J Gastroenterol* 1998; **4**: 421-425
- 8 **Wu JY**, Zhou XF, Jiang WX, Wang JL, Yang F, Cai XS, Zhang ZG. The impact of chemotherapeutic drugs on the expression of bcl-2, p53 and Ki-67 in gastric cancer cells. *Shijie Huaren Xiaohua Zazhi* 1999; **7**: 589
- 9 **Yuan RW**, Ding Q, Jiang HY, Tan XF, Zou SQ, Xia HS. Apoptosis and the expression of bcl-2 and p53 in pancreatic cancer. *Shijie Huaren Xiaohua Zazhi* 1999; **7**: 851-854
- 10 **Qiao Q**, Wu JS, Zhang J, Ma QJ, Lai DN. The expression of bcl-2 and bax in human colon cancer. *Shijie Huaren Xiaohua Zazhi* 1999; **7**: 936-938
- 11 **Chen XJ**, Ai ZL, Liu ZS. Apoptosis-study on the mechanism of hepatic cell injury by mitomycin. *Shijie Huaren Xiaohua Zazhi* 2000; **8**: 746-750
- 12 **Yang JQ**, Yang LE, Zhu HC. Mitomycin induces apoptosis of human hepatic cancer cell. *Shijie Huaren Xiaohua Zazhi* 2001; **9**: 268-272
- 13 **Guo WJ**, Yu EX, Zheng SG, Shen ZZ, Luo JM, Wu GH, Xia SA. Study on Jianpi Liqi medicine inducing apoptosis in human hepatic cancer cell SMMC7721. *Shijie Huaren Xiaohua Zazhi* 2000; **8**: 52-55
- 14 **Chen HY**, Liu WH, Qin SD. Induction of arsenic trioxide on apoptosis of hepatic cancer cell strain. *Shijie Huaren Xiaohua Zazhi* 2000; **8**: 532-535
- 15 **Liang WJ**, Huang ZY, Ding YQ, Zhang WD. Lovo cell line apoptosis induced by cycloheximide combined with TNF α . *Shijie Huaren Xiaohua Zazhi* 1999; **7**: 326-328
- 16 **Lin JK**, Chou CK. *In vitro* apoptosis in the human hepatoma cell line induced by transforming growth factor β 1. *Cancer Res* 1992; **52**: 385-388
- 17 **Tu SP**, Jiang SH, Tan JH, Jiang XH, Qiao MM, Zhang YP, Wu YL, Wu YX. Proliferation inhibition and apoptosis induction by arsenic trioxide on gastric cancer cell SGC-7901. *Shijie Huaren Xiaohua Zazhi* 1999; **7**: 18-21
- 18 **Thompson CB**. Apoptosis in the pathogenesis and treatment of disease. *Science* 1995; **267**: 1456-1462
- 19 **Fukuda K**, Kojiro M, Chiu JF. Demonstration of extensive chromatin cleavage in transplanted morris hepatoma 7777 tissue: apoptosis or necrosis? *Am J Pathol* 1993; **142**: 935-946
- 20 **Xiao B**, Xiao LC, Lai ZS, Zhang YL, Zhang ZS, Zhang WD. *In vitro* experimental study on Zhen'ailing inhibiting growth of gastric cancer cells. *Shijie Huaren Xiaohua Zazhi* 1999; **7**: 951-954
- 21 **Li LP**, Zhang Z, Han SX. Retinoic acid inhibits proliferation of tumor cells and induces apoptosis. *Shijie Huaren Xiaohua Zazhi* 2001; **9**: 437-440
- 22 **Liu HF**, Liu WW, Fang DC. Anti-Fas monoclonal antibody induces apoptosis of human gastric cancer cell line SGC-7901. *Shijie*

- Huaren Xiaohua Zazhi* 1999; **7**: 476-478
- 23 **Zhan J**, Xie DR, Yao HR, Lin XG, Liang XW, Xiang YQ. Arsenic trioxide induces apoptosis of colon cancer line SW620. *Shijie Huaren Xiaohua Zazhi* 2001; **9**: 228-229
- 24 **Liu HF**, Liu WW, Fang DC, Yang SM, Wang RQ. The expression of bax in gastric precancerous and cancerous tissues and its relation with apoptosis. *Shijie Huaren Xiaohua Zazhi* 2000; **8**: 665-668
- 25 **Xu AG**, Li SG, Liu JH, Gan AH. The function of apoptosis and protein expression of bcl-2, p53 and C-myc in the development of gastric cancer. *World J Gastroenterol* 2000; **6**(Suppl 3):27
- 26 **Lai DN**, Wu JS, Wu YZ. The relationship between the expression of bcl-2 and differentiation of colon and rectum cancer. *Shijie Huaren Xiaohua Zazhi* 1999; **7**: 91-92
- 27 **Soini Y**, Virkajarvi N, Lehto VP, Paakko P. Hepatocellular carcinomas with a high proliferation index and a low degree apoptosis and necrosis are associated with a shortened survival. *Br J Cancer* 1996; **73**: 1025-1030
- 28 **Friess H**, Yamanaka Y, Buchler M. Enhanced expression of the type II transforming growth factor beta receptor in human pancreatic cancer cells without alteration of type III receptor expression. *Cancer Res* 1993; **53**: 2704-2707
- 29 **Guo XZ**, Friess H, Graber HU. Kai1 expression is up-regulated in early pancreatic cancer and decreased in the presence of metastases. *Cancer Res* 1996; **56**: 4876-4880
- 30 **Zang GQ**, Yu H, Zhou XQ, Liao D, Xie Q, Wang B. TNF- α in vitro induces apoptosis and necrosis of rat hepatic cell. *Shijie Huaren Xiaohua Zazhi* 2000; **8**: 303-306
- 31 **James SJ**, Muskhelishvili L. Rates of apoptosis and proliferation vary with caloric intake and may influence incidence of spontaneous hepatoma in C57BL/6 \times C3H F₁ mice. *Cancer Res* 1994; **54**:5508-5510
- 32 **Mills JJ**, Chari RS, Boyer LJ, Gould MN, Jirtle RL. Induction of apoptosis in liver tumors by the monoterpene perillyl alcohol. *Cancer Res* 1995; **55**: 979-983
- 33 **Tanaka S**, Wands JR. Insulin receptor substrate 1 overexpression in human hepatocellular carcinoma cells prevents transforming growth factor β 1. *Cancer Res* 1996; **56**: 3391-3394
- 34 **Patel T**, Gores GJ. Apoptosis and hepatobiliary disease. *Hepatology* 1995; **21**: 1725-1741
- 35 **Peng LM**, Wang ZL. Foundation and clinic of apoptosis. 1st eds. *Beijing:Renmin Weisheng Chubanshe*, 2000: 394
- 36 **Grasl-Kraupp B**, Ruttkay-Nedecky B, Mullaer L, Taper H, Huber W, Bursch W, Schulte-hermann R. Inherent increase of apoptosis in liver tumors: implication for carcinogenesis and tumor regression. *Hepatology* 1997; **25**: 906-912
- 37 **Walton MI**, Whyson D, O' Connor PM, Hockenbery D, Korsmeyer SJ, Kohn KW. Constitutive expression of human bcl-2 modulates nitrogen mustard and camptothecin induced apoptosis. *Cancer Res* 1993; **53**: 1853-1861

Edited by Ma JY

• LIVER CANCER •

Etiology and management of hemorrhage in spontaneous liver rupture: a report of 70 cases

Zhe-Yu Chen, Qing-Hui Qi, Zuo-Liang Dong

Zhe-Yu Chen, Qing-Hui Qi, Zuo-Liang Dong, Department of surgery, General Hospital of Tianjin Medical University, Tianjin 300052, China

Correspondence to: Qing-Hui Qi, Department of surgery, General Hospital, Tianjin Medical University, Tianjin 300052, China

Telephone: +86-22-27812608 Ext 2580 **Fax:** +86-22-27813550

Received 2002-04-29 **Accepted** 2002-06-25

Abstract

AIM: To analyze the causes and management of hemorrhage in spontaneous liver rupture.

METHODS: Seventy cases of spontaneous liver rupture were retrospectively analyzed for causes of hemorrhage and therapeutic effects of surgical approaches.

RESULTS: It was demonstrated that the causes of spontaneous liver rupture were primary liver cancer in 60 cases (85.7 %), cirrhosis in 3 cases (4.3 %), liver angioma in 2 cases (2.9 %), liver adenoma in 4 cases (5.7 %), and secondary liver cancer in 1 case (1.4 %). Hemostasis was achieved with surgical approaches in 68 cases (97.1 %) and non-surgical approaches in 2 cases (2.9 %). Surgical interventions included suture, ligation of hepatic artery, hepatic artery chemoembolization and partial hepatic resection.

CONCLUSION: The results suggest that surgical intervention is still the main therapeutic method and the best procedure that should be selected according to causes of disease and patient's condition and history.

Chen ZY, Qi QH, Dong ZL. Etiology and management of hemorrhage in spontaneous liver rupture: a report of 70 cases. *World J Gastroenterol* 2002; 8(6):1063-1066

INTRODUCTION

Bleeding of spontaneous liver rupture is a severe complication in liver diseases, owing to its clinical signs being usually not specific. Therefore, correct diagnosis and management are very important. At present, it is a difficult problem in surgery for the diagnosis and therapy of spontaneous liver rupture. In this paper, the etiology and management in seventy cases of spontaneous liver rupture treated in Tian Jin medical university general hospital in ten years were analysed.

MATERIALS AND METHODS

Seventy patients with spontaneous liver rupture (41 male and 29 female) with a median age of 49±4.3year (range,17-75years) were admitted from January 1992 to December 2001. There were 68 cases with surgical intervention and 2 cases with non-surgical therapy.

Majority of patients initially experienced some abdominal complaints, such as abdominal pain, anorexia, vomiting and abdominal distention. The serious cases had signs of anemia, shock and acute peritonitis (Table1).

Table 1 Clinical symptoms of spontaneous liver rupture in 70 cases

	Abdominal pain	anemia	shock	acute peritonitis
number	63	48	37	19
percentage	90.0%	68.6%	52.9%	27.1%

Twenty one patients had hepatitis history and 1 patient had undergone Mile's operation two years ago because of rectum carcinoma before the liver rupture. Abdominal paracentesis showed that blood was incoagulable in 61 patients. B type ultrasonography and/or computed tomography (CT) displayed hydroperitonitis and liver tumor or liver cirrhosis in 68 patients. Thirty seven patients had hemoglobin(Hb) below 100 g/L. Liver functions of all patients were classified according to Child's criteria: Child A in 17 patients, Child B 39 patients, Child C 14 patients. Alpha-fetoprotein(AFP) was positive in 41 cases. Sixty eight cases had diagnosed pathological diagnosis: primary liver carcinoma 60 cases, liver cirrhosis 3 cases, liver angioma 2 cases, liver adenoma 4 cases, secondary liver cancer 1 case (Table2). Twenty six patients had history of slight injury.

Table 2 Cause of spontaneous liver rupture in 70 cases

	Primary liver cancer	cirrhosis	liver angioma	liver adenoma	secondary liver cancer
number	60	3	2	4	1
percentage	85.7%	4.3%	2.9%	5.7%	1.4%

Two patients were treated by non-surgical method, selective hepatic artery chemoembolization via femoral artery. Sixty-eight patients had undergone operation and surgical methods included partial resection of liver and ligation of hepatic artery (Table3).

Table 3 Therapeutic methods of spontaneous liver rupture in 68 patients

	suture	packing	ligation of hepatic artery	hepatic artery chemoembolization	hepatic partial resection
number	17	7	23	2	40
percentage	24.3%	10.0%	32.9%	2.9%	57.1%

Operative methods were as follow: (1) suture: Long and thin needles with thick silk were selected to enter the normal liver tissue near the lesion in one side of the split and came out

of the other side through the health tissue after hepatic artery and portal vessels were blocked. Silk was finally ligated after suture of the split had been finished. (2) packing: If bleeding of the gap had not been controlled completely after ligation of hepatic artery, suture should be applied to the lesion and if the patient was too weak to undergo the complicated operation, packing with gauze cushion should be used to procure hemostasis. The edge of gauze cushion was let out from the incision and left there for three days after surgery. Finally, if hemostasis was successful, the gauze cushion should be pulled out. (3) ligation of hepatic artery: When the hepato-duodenal ligament was pulled up near the Winslow pole, the pulse of hepatic artery could be palpated, the artery was then isolated and ligated. It should be prudent to ligate the stem of the hepatic artery in cirrhosis, lest hepatic coma would occur after the procedure. (4) hepatic artery chemoembolization: The catheter was inserted to proper hepatic artery or right and left hepatic artery, gelfoam and iodized oil were used as suppository, and injected via gastroduodenal artery or right gastro-epiploic artery. Methylene blue was injected to locate the site of embolization before procedure. (5) liver partial resection: Eleven, seven, two and twenty one patients had received hepatic left lateral lobectomy, left hemihepatectomy, right hemihepatectomy and non-regular hepatic partial resection respectively.

RESULTS

Two patients (AFP positive) who were given non-surgical intervention with bleeding entirely controlled could not survive over one year. All the rest adopted surgical therapeutic methods. Suture with addition of ligation of hepatic artery were performed in seventeen patients, with their primary diseases proved by pathology. There were 16 cases of primary liver cancer, and one liver cirrhosis. Hemostasis was achieved in 13 patients, bleeding of three patients could not be controlled and one patient developed liver failure and died during seven days after operation. Only one patient survived about one year. Ligation of hepatic artery supplemented with packing was used in seven patients with four died of hemorrhagic recurrence. The mean survival time in the seven patients was about nine months. Single ligation of hepatic artery was applied in two patients with primary carcinoma and their survival time was less than one year. Two patients of primary liver carcinoma were given hepatic artery chemoembolization and died within one year. Bleeding in forty patients was controlled by partial hepatectomy, but liver failure took place in two patients who died ten days after the surgery. Fourteen patients with four patients of hepatic adenoma among them lived more than one year.

DISCUSSION

Spontaneous liver rupture can happen not only in the primary liver cancer but also in liver benign tumor and liver cirrhosis. Careful history, physical and examination with necessary laboratory tests and imaging examination can provide enough clue for the diagnosis of liver rupture without difficulty. A typical patient usually presented with severe upper abdominal pain, abdominal distension, anorexia and vomiting. Rupture usually occurred during working or after slight injury. Facial pallor, cold sweat, pulse >100 times/minute, systolic pressure <90 mmHg, tenderness, rebound tenderness and muscular tension over upper abdomen, positive abdominal paracentesis, Hb<100 g/L and hematocrit 25-30 % suggest that the disease would be quite serious. B-ultrasonography(B-us) can detect 72.5 % tumor of liver and is a helpful and simple method to

diagnose liver cancer, detect cancerous embolus of portal vein and evaluate the degree of intraperitoneal hemorrhage^[1]. However, computed tomography (CT) especially helical CT is more sensitive to diagnosis liver tumor than B-us owing to its higher resolving power^[2,3]. CT can detect tumors as small as 1 cm in diameter, and it may also differentiate the quality, the position and the invasion range of the tumor accurately^[4]. Patient's therapy should be individualized because each case is not exactly similar.

Spontaneous rupture of primary liver carcinoma

As we know that hepatocellular carcinoma (HCC) is the most common primary liver tumor. Worldwide annual incidence of HCC was estimated to be at least one million new patients^[5]. Its incidence of spontaneous rupture was about 10 %^[6,7]. Liver rupture is short of special symptoms, especially it can usually be misdiagnosed if liver cancer is not diagnosed before rupture. But it is not very difficult if the diagnosis of intraperitoneal hemorrhage is made and examinations of B-us and CT are done. Primary liver cancer accompanied with cirrhosis accounted 53.9-85.0 % of liver malignancies. Because liver function in these cases is generally poor, the principle of treatment is to resuscitate rapidly, control bleeding, resect cancerous tissue and to retain as much healthy liver tissue as possible^[8-10]. Firstly the vital physical signs and blood loss should be evaluated; Secondly the number of tumors, its size, location, invasive range, and the possible presence of cancerous in portal vein should all be considered. Thirdly, liver function must be assessed, and presence or not jaundice and ascitic fluid as well as the degree of cirrhosis should be evaluated. The liver functional status should be classified according to Child's criterion. Hepatic partial resection should be performed immediately if patients's vital physical signs are stable, Child's classification was A or B, tumor's range is localized in one hepatic segment or lobe, and the first or the second hepatic hilus and the inferior vena cava are not invaded. Operation program include hepatic lobe or segment resection and non-regular hepatic partial resection^[11-14]. If a great deal of blood is lost, despite the rest conditions are better or Child's classification of liver is C, tumor is too massive to be resected and tumor invades the hepatic portal vessels and the inferior vena cava, hemostasis should be considered first. In this situation the most simple surgical methods such as ligation of hepatic artery and hepatic artery chemoembolization should be selected^[15-19]. Because blood supply of primary liver carcinoma is mainly by hepatic artery, ligation of hepatic artery can thus block the blood supply and nutrition of the carcinoma. If bleeding can not be controlled by blocking or embolization of hepatic artery, suture should be used in addition, and packing would be the final choice^[20-23].

Spontaneous rupture of cirrhosis without malignant change

Liver cirrhosis usually supervenes hemorrhage of upper digestive tract^[24], but rarely supervenes spontaneous rupture. Macronodular cirrhosis or varicose veins and lymphatic vessels can occasionally produce spontaneous rupture and leads to bloody abdomen. Once rupture in macronodular cirrhosis happens, the patient would die of liver failure in a short time. Rupture of varicose veins and lymphatic vessels is manifestation of terminal hepatic disease owing to high pressure of portal vein, therefore its prognosis is very poor^[25]. Hepatic partial resection is not indicated in this kind of rupture, and control of hemorrhage by ligation of hepatic artery with packing and suture is the best choice. Liver tissue of cirrhosis is very crisp, inappropriate manipulation can lead to

uncontrollable bleeding. Thin bending needle and thick silk should be selected in suture, and silk should be ligated after suture.

Rupture of liver angioma

Hemangiomas which arise from mesenchymal cells are the most common benign tumor of the liver^[26,27]. It can occur in all age groups, with incidence of 7 % in general population. The circumscribed lesions are composed mostly of closely packed hyperplastic vascular channels lined by a single layer of normal appearing endothelial cells. The majority of hemangiomas are small without symptom. However, it may be enlarged and associated with diffuse hemangiomatosis and even nearly replace the liver. Spontaneous rupture in hemangiomas is not usual but can be dramatic and very dangerous. Patients can die of massive hemorrhage in a short time. In this condition patients are too weak to endure massive operation owing to hematemesis. Therefore, hemostasis is the first choice of treatment^[28,29]. Ligation of hepatic artery or packing should be performed to control bleeding instantly as soon as shock is being treated. If the hemorrhage is stopped and the patient's condition is good, secondary operation to cure angioma should be selected. Suturing the split should be between healthy liver tissue, otherwise the massive bleeding may recur.

Rupture of liver adenoma

Liver adenomas which arise from epithelial tissue are relatively common benign tumors of liver^[30]. Majority of adenoma have capsules and minority of adenoma without capsule are prone to malignant change. Liver adenoma usually is solitary and varies in size. Occasionally they may be multiple and cluster within families. Tumor rupture or dramatic bleeding occurs in approximately one third of patients. Microscopically, the adenoma are closely approximated cords of hepatocytes that have vacuolated sinusoidal borders. Centers of adenomas may undergo degenerative changes. Some adenoma have abundant blood supply which are separate from adjacent normal hepatic tissue^[31]. At present, adenomas are associated with the use of oral contraceptives and usually occur in young women^[32]. The incidence goes up gradually. For rupture of adenoma the treatment principle is similar to that of primary liver cancer. If patients's conditions are stable and tumors are localized in one lobe or segment of liver, partial hepatectomy should be performed instantly. If blood loss is big, and the tumors are unresectable, then therapy should be ligation or embolization of hepatic artery to control bleeding^[33,34]. Delayed resection can be prepared after successful hemostasis^[35]. Liver transplantation can be considered for diffuse adenomatosis or the tumor exceeds half of the liver in diameter^[36].

Rupture of secondary liver carcinoma

Liver is a frequent site for metastases arising from gastrointestinal cancers, which is a significant oncologic problem. Secondary liver carcinomas are generally diffuse but may present as a single cirrhotic nodule which is distinguished from healthy liver tissue with degenerative changes in its center. The histological structures of metastatic carcinoma resemble the primary cancer outside the liver. Secondary liver cancers grow slower than primary liver carcinoma and are usually unresectable. Ligation or chemoembolization of the hepatic artery should be selected to control bleeding first, then the next step in treatment will be decided. Cancer should be resected, if the patients's condition gets better and the metastatic cancer may be limited to one

lobe or a segment of the liver, the partial hepatectomy can be selected as emergency operation.

REFERENCES

- 1 **Bennett WF**, Bova JG. Review of hepatic imaging and a problem-oriented approach to liver masses <special article>. *Hepatology* 1990; **12**: 761
- 2 **Choi BG**, Park SH, Byun JY, Jung SE, Choi KH, Han JY. The finds of ruptured hepatocellular carcinoma on helical CT. *Br J Radiol* 2001; **74**: 142-146
- 3 **Coakley FV**, Schwartz LH. Imaging hepatocellular carcinoma: a practical approach. *Semin Oncol* 2001; **28**: 460-473
- 4 **Ishihara M**, Kobayashi H, Ichikawa, Cho K, Gemma K, Kumazaki T. The value of emergency CT studies in spontaneous rupture of hepatocellular carcinoma. Analysis for tumor protrusion and hemorrhagic acties. *Nippon Ika Daigaku Zasshi* 1997; **64**: 532-537
- 5 **Bridbord K**. Pathogenesis and prevention of hepatocellular carcinoma. *Cancer Detect Prev* 1989; **14**: 191
- 6 **Lai EC**, Wu KM, Choi TK. Spontaneous ruptured hepatocellular carcinoma. An appraisal of surgical treatment. *Ann Surg* 1989; **210**: 24
- 7 **Migamoto M**, Sudo T, Kuyama T. Spontaneous rupture of hepatocellular carcinoma: a review of 172 Japanese cases. *Am J Gastroenterol* 1991; **86**: 68
- 8 **Vergara V**, Muratore A, Bouzari, Polastri R, Ferrero A, Galatola G, Capussotti L. Spontaneous rupture of hepatocellular carcinoma: surgical resection and long-term survival. *Eur J Oncol* 2000; **26**: 770-772
- 9 **Zhu LX**, Wang GS, Fan ST. Spontaneous rupture of hepatocellular carcinoma. *Br J Surg* 1996; **83**: 602
- 10 **Zhu LX**, Geng XP, Fan ST. Spontaneous rupture of hepatocellular carcinoma and vascular injury. *Arch surg* 2001; **136**: 682-687
- 11 **Furuse J**, Iwasaki M, Yoshino M, Konishi M, Kawano N, Kinoshita T, Ryu M, Satake M, Morigama M. Hepatocellular carcinoma with portal vein tumor thrombus: embolization of arterioportal Shunts. *Radiology* 1997; **204**: 787-790
- 12 **Liu CL**, Fan ST, Lo CM, Tso WK, Poon RT, Lan CM, Wong J. Management of spontaneous rupture of hepatocellular carcinoma single-center experience. *J Clin Oncol* 2000; **19**: 3725-3732
- 13 **Zhu LX**, Wang GS, Fan ST. Spontaneous rupture of hepatocellular carcinoma. *Br J Surg* 1996; **83**: 602-607
- 14 **Chen TZ**, Wu JC, Chan CY, Sheng WY, Yen FS, Chiang JH, Chau GY, Lui UY, Lee SD. Ruptured hepatocellular carcinoma: treatment strategy and prognostic factor analysis. *Zhonghua Yixue Zazhi* 1996; **57**: 322-328
- 15 **Castells L**, Moreiras M, Quiroga S, Alvarez-Castells A, Segarra A, Esteban R, Guardia J. Hemoperitoneum as a first manifestation of hepatocellular carcinoma in western patients with liver cirrhosis: effectiveness of emergency treatment with transcatheter arterial embolization. *Dig Dis Sci* 2001; **46**: 555-562
- 16 **Leung KL**, Lau WY, Lai PB, Yiu RY, Meng WC, Leow CK. Spontaneous rupture of hepatocellular carcinoma: conservative management and selective intervention. *Arch Surg* 1999; **134**: 1103-1107
- 17 **Gates J**, Hartnell GG, Stuart KE, Clouse ME. Chemoembolization of hepatic neoplasms: safety, complication, and when to worry. *Aadiographics* 1999; **19**: 399-414
- 18 **Recordare A**, Bonariol L, Caratozzlo E, Callegari F, Bruno G, Dipaola F, Bassi N. Management of spontaneous bleeding due to hepatocellular carcinoma. *Minerva Chir* 2002; **57**: 347-356
- 19 **Kodama Y**, Shimizu T, Endo H, Hige S, Kamishima T, Holland GA, Miyamoto N, Miyasaka K. Spontaneous rupture of hepatocellular carcinoma supplied by the right renal capsular artery treated by transcatheter arterial embolization. *Cardiovasc Intervent Radiol* 2002; **25**: 137-140
- 20 **Chiappa A**, Zbar A, Audisio RA, Dipalo S, Bertani E, Staudacher C. Emergency liver resection for ruptured hepatocellular carcinoma: complicating cirrhosis. *Hepatogastroenterology* 1999; **46**: 1145-1150
- 21 **Shuto T**, Hirohashi K, Kubo S, Tanaka H, Hamba H, Kubota D, Kionshita H. Delayed hepatic resection for ruptured hepatocel-

- lular carcinoma. *Surgery* 1998; **124**: 33-37
- 22 **Fan ST**, Ng IO, Poon RT, Lo CM, Liu CL, Wong J. Hepatectomy for hepatocellular carcinoma: the surgeon's role in long-term survival. *Arch Surg* 1999; **134**: 1124-1130
- 23 **Yoshida H**, Onda M, Tajiri T, Umehara M, Mamada Y, Matsumoto S, Yamamoto K, Kaneko M, Kumazaki T. Treatment of spontaneous ruptured hepatocellular carcinoma. *Hepatogastroenterology* 1999; **46**: 2451-2453
- 24 **Ruiz D**, Farran L, Ramo SE, Bi0ndo S, Moreno P, Bettonica C, Jorba R, Borobia FG, Jaurrieta E. Results of management of upper gastrointestinal bleeding from gastroesophaged varices. *Rev Esp Enferm Dig* 2001; **93**: 433-444
- 25 **Kosowsky JM**, Gibler WB. Massive hemoperitoneum due to rupture of a retroperitoneal varix. *J Emery Med* 2000; **19**: 347-349
- 26 **Capplani A**, Zanghi A, Dilita M, Zanghi G, Tomarchio G, Petrillo G. Spontaneous rupture of a giant hemangioma of the liver. *Ann Ital Chir* 2000; **71**: 379-383
- 27 **Weimann A**, Ringe B, Klempnauer J, Lamesch P, Gratz KF, Prokop M, Maschek H, Tush G, Pichlmayr R. Benign liver tumors: differential diagnosis and indications for surgery. *World J Surg* 1997; **21**: 983
- 28 **Iqbal N**, Saleem A. Hepatic hemangioma: a review. *Tex Med* 1997; **93**: 48-50
- 29 **Krasuski P**, Poniecka A, Wali A. Intrapartum spontaneous rupture of liver hemangioma. *J Matern Fetal Med* 2001; **10**: 290-292
- 30 **Cheng PN**, Shin JS, Lin XZ. Hepatic adenoma: an observation from asymptomatic stage to rupture. *Hepatogastroenterology* 1996; **43**: 245-248
- 31 **Chiappa A**, Zbar A, Audisio RA, Paties C, Bertani E, Staudocher C. Ruptured hepatic adenoma in liver adenomatosis: a case report of emergency surgical management. *Hepatogastroenterology* 1999; **46**: 1942-1943
- 32 **Meissner K**. Hemorrhage caused by ruptured liver cell adenoma following long-term oral contraceptive: a case report. *Hepatogastroenterology* 1998; **45**: 224-225
- 33 **Pawarode A**, Voravud N. Ruptured primary hepatocellular carcinoma at chulalongkorn University Hospital: a retrospective study of 32 cases. *J Med Thai* 1997; **80**: 706-714
- 34 **Terkivatan T**, de Wilt JH, de Man RA, van Rijn RR, Zonder van PE, Tilanus HW, Ijzermans JN. Treatment of ruptured hepatocellular adenoma. *Br J Surg* 2001; **88**: 207-209
- 35 **Marini P**, Vilgrain V, Belghiti J. Management of spontaneous rupture of liver tumors. *Dig Surg* 2002; **19**: 109-113
- 36 **Muller J**, Keeffe EB, Esquivel CO. Liver transplantation for treatment of giant hepatocellular adenomas. *Liver Transpl Surg* 1995; **1**: 99

Edited by Xu JY

• COLORECTAL CANCER •

Transfection of colorectal cancer cells with chemokine MCP-3 (monocyte chemotactic protein-3) gene retards tumor growth and inhibits tumor metastasis

Jin-Yue Hu, Guan-Cheng Li, Wen-Meng Wang, Jian-Gao Zhu, Yue-Fei Li, Guo-Hua Zhou, Qu-Bing Sun

Jin-Yue Hu, Guan-Cheng Li, Jian-Gao Zhu, Yue-Fei Li, Guo-Hua Zhou, Qu-Bing Sun, Laboratory of Tumor Immunobiology, Cancer Research Institute, Xiangya Medical School, Central South University, Changsha 410078, Hunan Province, China

Wen-Meng Wang, Department of Internal Medicine, Hunan Armed Police Force Hospital, Changsha 410006, Hunan Province, China

Correspondence to: Professor Qu-Bing Sun, Lab of Tumor Immunobiology, Cancer Research Institute, Xiangya Medical School, Central South University, 88 Xiangya Road, Changsha 410078, Hunan Province, China. libsun@public.cs.hn.cn

Telephone: +86-731-4805445 **Fax:** +86-731-4372793

Received 2002-05-16 **Accepted** 2002-06-12

Abstract

AIM: To evaluate the possibility of the induction of anti-tumor immune response by transfecting the colorectal cancer cells with chemokine MCP-3 gene.

METHODS: Mouse MCP-3 gene was transduced into mouse colorectal cancer cells CMT93 by using of Liposome. G418-resistant clones were selected and the MCP-3 mRNA expression was detected by RT-PCR. The chemotactic activity of MCP-3 in the cell culture supernatant was detected by Chemotaxis assay. The tumorigenicity of wild type CMT93 and CMT93 gene transfectants were detected by *in vivo* experiments. The immune cell infiltrations in tumor tissue and tumor metastasis were detected histopathologically.

RESULTS: MCP-3 mRNA expression was detected by RT-PCR in gene-transfected cells (CMT93/MCP-3), but not in control groups. And MCP-3 secreted in the cell culture supernatant possessed chemotactic activity. The results from *in vivo* experiments showed that the tumorigenicity of CMT93/MCP-3 had not decreased, but the tumors derived from CMT93/MCP-3 cells grew more slowly than those from CMT93 cells (1.021 ± 0.253 cm² vs 1.769 ± 0.371 cm², $P < 0.05$) or CMT93/mock cells (1.021 ± 0.253 cm² vs 1.680 ± 0.643 cm², $P < 0.05$). Histopathological results showed few immune cells infiltrating in the tumor tissue derived from the controls. In the tumor tissue derived from CMT93/MCP-3, infiltrating immune cells increased. In addition, no tumor metastasis was found in all mice inoculated with CMT93/MCP-3 tumor cells. But all mice had tumor metastasis in CMT93 controls and 4 in 5 mice had tumor metastasis in CMT93/mock controls.

CONCLUSION: The results suggested that the transfection of chemokine MCP-3 gene could promote the induction of anti-colorectal cancer immunity, but the tumor growth could not be inhibited completely by merely MCP-3 gene transfection.

Hu JY, Li GC, Wang WM, Zhu JG, Li YF, Zhou GH, Sun QB. Transfection of colorectal cancer cells with chemokine MCP-3 (monocyte chemotactic protein-3) gene retards tumor growth and inhibits tumor metastasis. *World J Gastroenterol* 2002; 8 (6):1067-1072

INTRODUCTION

Chemokines, a kind of polypeptide with low molecular weight, can activate and chemoattract immune cells and play a pivotal role in host defense and in immunological conditions such as autoimmune reaction and malignant tumors^[1]. Chemokines such as monocyte chemotactic protein-1 (MCP-1) is produced by a variety of tumors such as ovarian carcinoma^[2] Kaposi's sarcoma^[3], cervical carcinoma^[4], and melanoma^[5]. There are evidences suggesting that chemokines play an important role in immune cells infiltrating in tumor tissue. Chemokine gene transferred into tumor cells elicits anti-tumor effect such as reducing tumorigenicity and inhibiting tumor growth^[1].

MCP-3 is a CC chemokine identified from osteosarcoma supernatant^[6]. By binding to CCR1, CCR2, and CCR3^[7-11], MCP-3 acts on a lot of immune cells. Tumor gene therapy with MCP-3 had been reported in p815 mastocytoma mouse model^[12] and human cervical carcinoma xenografts^[13]. But the anti-tumor effect by MCP-3 gene transfer in colorectal cancer model has not been determined. In our study, we found that after the transfecting of CMT93 colorectal cancer cell with MCP-3 gene, tumor growth was retarded and tumor metastasis was inhibited completely by promoting immune cells infiltration in tumor tissue.

MATERIALS AND METHODS

Materials

Male or female C57BL/6 mice, 6-8 weeks old, were purchased from Shanghai Experimental Animal Center of Chinese Academy of Sciences. CMT93 is a mouse colon cancer cell line from an induced carcinoma of mouse rectum^[14], which was purchased from ATCC in America. Plasmid pCMV/MCP3 containing mouse MCP3 gene and plasmid pCDNA/YT4 containing mouse CCR1 (C-C chemokine receptor 1) gene were presented kindly by Dr. Ji Ming Wang in NCI in America. MCP-3 RT-PCR primers were presented kindly by Dr. Ji Ming Wang as well.

Transfection of tumor cells with MCP-3 gene

According to the LipofectAMINE (Gibco) kit protocol. Briefly, (1) 2 μ g plasmid DNA and 15 μ l LipofectAMINE are added to 200 μ l DMEM without FCS, mix gently, and incubate at 37 °C for 30min. (2) Wash the CMT93 cells in 6 well plate with FCS-free DMEM. (3) Add 0.8ml of serum-free DMEM to the tube containing the DNA and lipofectAMINE complexes, mix gently and overlay the rinsed cells. (4) Incubate the cells with complexes for 5 h at 37 °C in CO₂ incubator. (5) Add 1ml of DMEM containing 200 mL⁻¹ serum, incubate overnight. (6)

Replace the medium with fresh DMEM. (7) Digest the cells and plate them to the 100 ml bottles, incubate 24 h. (8) Replace the medium with fresh DMEM containing 800 µg/ml G418 and select the positive clones.

RNA preparation and reverse transcription polymerase chain reaction (RT-PCR)

The Total RNA from cells was extracted with RNeasy Mini kit (QIAGEN) according to the manufacture's instructions. Total of 0.5 µg RNA was used for RT-PCR. For mouse MCP-3, sense primer 5'-TCTGTGCCTGCTGCTCATAG-3' (nucleotide 73-92) and antisense primer 5'-CTTTGGAGTTGGGGTTTTCA-3' (nucleotide 321-340) were used to yield a 268-base pair product. For mouse β-actin, sense primer 5'-TGTGATGGTGGGAATGGGTCGG-3' and antisense primer 5'-TTTGATGTCACGCACGATTTC-3' were purchased from STRATAGENE to amplify a 514-base pair fragment. RT-PCR was performed with high fidelity ProSTRAR™ HF single-tube RT-PCR system (STRATAGENE), consisting of a 15-min reverse transcription at 37 °C, 1 min of inactivation of Moloney murine leukemia virus reverse transcriptase at 95 °C, 40 cycles of denaturing at 95 °C (30 s), annealing at 60 °C (30 s), and extension at 68 °C (2 min), as well as a final extension for 10 min at 68 °C.

Chemotaxis assay

Chemotaxis assays were performed using 48-well chemotaxis chambers (Neuro probe, Cabin John, MD, USA). As described previously^[15]. First 27-29 µl cell culture supernatants from CMT93 and its gene transfectants were placed in the wells of the lower compartment of the chamber. 50 µl cells (1×10^6 /ml in binding medium, BM: RPMI1640 containing 10 mL · L⁻¹ BSA, 25 mmol · L⁻¹ HEPES) were plated in the wells of the upper compartment. The upper and lower compartments were separated by a polycarbonate filter (Osmonics, Livermore, CA, USA; 10 µm pore-size) which was pre-coated with 50 µg · mL⁻¹ collagen type I (Collaborative Biomedical Products, Bedford, MA, USA). After incubation at 37 °C for 5 h, the filter was removed, stained, and the cells migrated across the filter were counted under light microscope after coding the samples. The results were expressed as chemotaxis index (CI), which represents the fold increase in the number of migrated cells in response to chemoattractants over the spontaneous cell migration in response to control medium.

Tumorigenicity

As previously reported^[16], Balb/c mice were inoculated subcutaneously on the back with 5×10^6 CMT93/MCP-3 cells (8 mice), or CMT93/mock cells (7 mice) or CMT93 cells (5 mice). Tumor sizes were assessed for every 5 days by measuring perpendicular diameters with caliper (0.002 cm). The tumor sizes from each groups were expressed as mean square (long diameter × short diameter). On day 14, one mice in each groups was selected randomly and sacrificed for histologic evaluation. The other mice were observed and the tumor metastasis was measured.

Histologic evaluation

Tissues were removed from the site of tumor cell inoculation 14 days after injection, or from the drainage lymph node of the site of tumor cell inoculation. Then fixed in 100 mL · L⁻¹ formalin, blocked in paraffin, sectioned at 4-6 µm, and stained with hematoxylin and eosin. The infiltrating leukocytes in tumor tissue were observed and evaluated, and the tumor metastasis in the drainage lymph node was determined.

RESULTS

RT-PCR

After gene transfection and the following G418-resistant clone selection, we detected MCP-3 mRNA expression in MCP-3 gene transfected CMT93 cells by RT-PCR using one-step kit. In contrast, the wild type CMT93 cells and the mock transfected CMT93 cells did not express MCP-3 (Figure 1).

Chemotaxis

After the detection of MCP-3 mRNA expression, we tested the biological function of MCP-3 secreted in the culture supernatant. Chemotaxis analyses revealed that the RBL/2H3 cells transfected with CCR1, which is one of the receptors of MCP-3, migrated when supernatants from MCP-3 transfected CMT93 (CMT93/MCP-3) cells were present in the lower wells of the chemotaxis chamber (Figure 2, 3D). No increased cell migration occurred when supernatants from mock transfected CMT93 (CMT93/mock) or wild type CMT93 cells were present in the lower wells of the chemotaxis chamber (Figure 2, 3C,3B). These results showed that not only the transfected MCP-3 gene expressed but also the expressed protein possessed biological function.

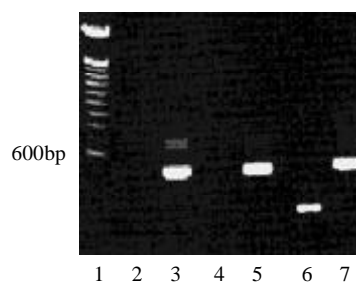
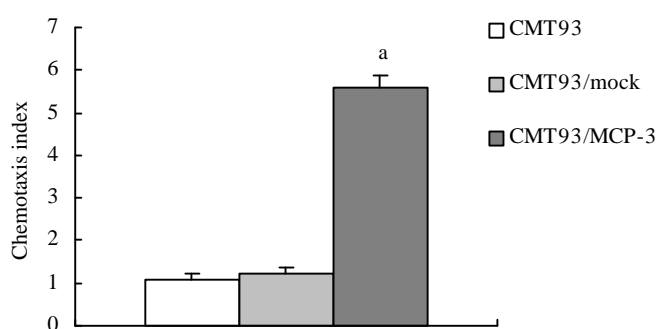


Figure 1 MCP-3 mRNA expression of CMT93 or its gene transfectants (RT-PCR). Lane 1: 100bp DNA ladder marker; Lane 2: CMT93+Primer MCP-3; Lane 3: CMT93+Primer β-actin; Lane 4: CMT93/Mock + Primer MCP-3; Lane 5: CMT93/Mock + Primer β-actin; Lane 6: CMT93/MCP-3+Primer MCP-3; Lane 7: CMT93/MCP-3+Primer β-actin.



from CMT93 cells or its gene transfectants. ^a*P* < 0.05 vs CMT93 or CMT93/mock group.

MCP-3 retards tumor growth

To examine whether MCP-3 secretion retard tumor growth, we injected MCP-3 transfectants subcutaneously into Balb/c mice to test their tumorigenicity. As showed in Figure 4, all mice had tumor growth on day 5 after tumor cell inoculation. But tumors from CMT93/MCP-3 grew more slowly than that from mock transfectants or wild type CMT93 (*P* < 0.05, Table 1). These results suggested though MCP-3 secretion could not inhibit tumor formation completely; it retarded tumor growth.

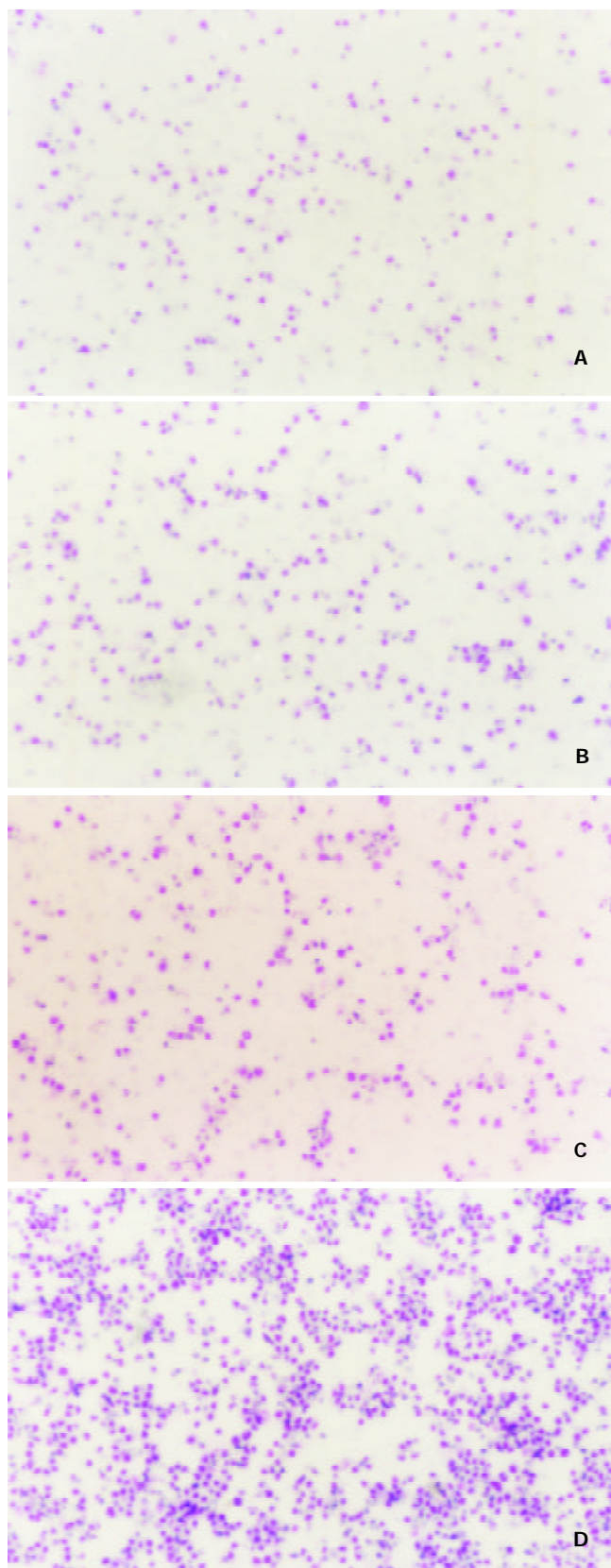


Figure 3 Chemotactic activity of MCP-3 in supernatant from CMT93 or its transfectants (Wright staining showed the chemoattracted target cells $\times 25$). A: medium; B: CMT93 supernatant. The chemoattracted cells were not increased significantly; C: CMT93/Mock supernatant. The chemoattracted cells were not increased significantly; D: CMT93/MCP-3 supernatant. The chemoattracted cells were increased significantly.

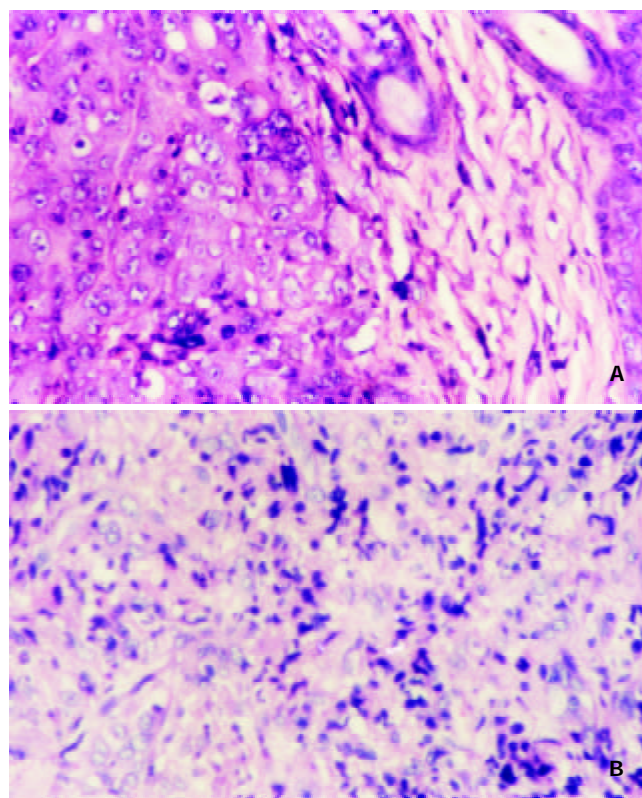


Figure 5 Histopathology of the tumors derived from CMT93 or CMT93/MCP3 (HE staining $\times 200$). A: tumor derived from CMT93 cells; few infiltrated immune cells were found; B: tumor derived from CMT93/MCP-3 cells, the infiltrated immune cells were increased.

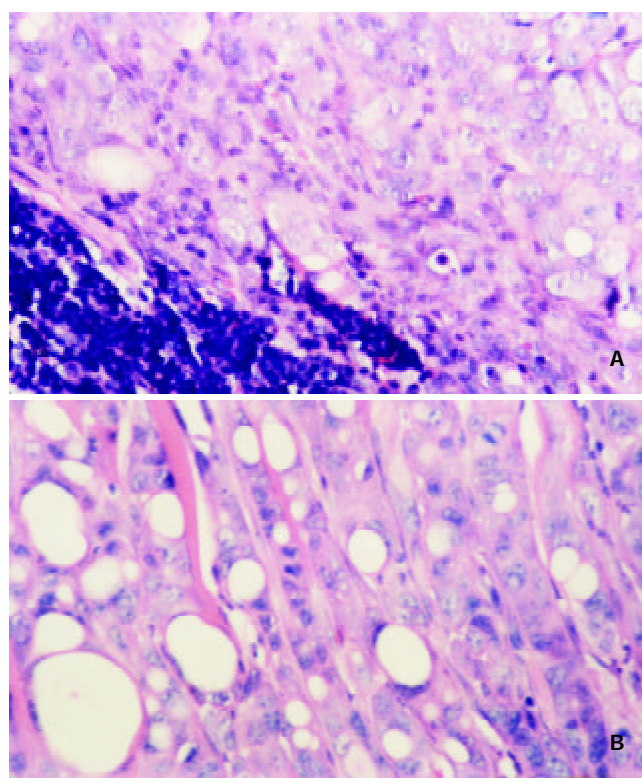


Figure 6 Histopathology of tumor derived from CMT93 metastasized to the local drainage lymph node (HE staining $\times 200$). A: up-left is the lymph tissue, down-right is the tumor tissue; B: tumor infiltrated to the muscle tissue.

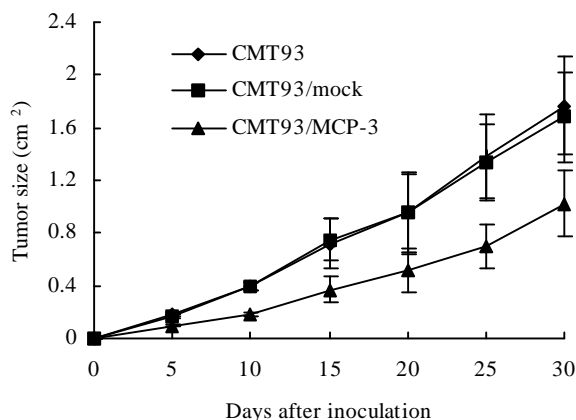
Table 1 Tumor size in the mice inoculated with CMT93 or its gene transfectants (cm², $\bar{x} \pm s$)

Days after tumor injection	Tumor size in the mice inoculated with		
	CMT93	CMT93/mock	CMT93/MCP-3
5	0.181±0.020	0.170±0.012	0.097±0.012 ^a
10	0.398±0.030	0.397±0.025	0.186±0.019 ^a
15	0.720±0.185	0.751±0.157	0.372±0.104 ^a
20	0.950±0.303	0.954±0.309	0.416±0.167 ^a
25	1.385±0.222	1.335±0.292	0.699±0.170 ^a
30	1.769±0.371	1.680±0.643	1.021±0.253 ^a

^a*P*<0.05 vs CMT93 or CMT93/mock group

Immune cells infiltration

MCP-3 gene transfer profoundly altered leukocyte recruitment in tumors grown in syngeneic Balb/c mice. On day 14 after tumor inoculation, all the mice showed tumor growths of about (0.6-0.8)×(0.6-0.8) cm² in size, which allowed a histologic study. Histologic results showed that tumor derived from MCP-3 gene transfected CMT93 cells contained much more infiltrating leukocytes, but tumor derived from the wild type CMT93 cells contained less leukocytes (Figure 5). Infiltrating leukocytes were located in the cancer nests mainly. The tumors derived from mock transfectants contained less leukocytes as well (data not shown). These results suggested that the effect of MCP-3 gene transfer in retarding tumor growth maybe related to the infiltration of leukocytes which were chemoattracted by MCP-3.

**Figure 4** The tumor growth curves of CMT93 or its gene transfectants

Tumor metastasis

On day 30, tumors in all 4 mice inoculated with CMT93 cells into the backs metastasized, two to inguinal drainage lymph node, other two to cervical drainage lymph node. Of tumors in 5 mice inoculated with CMT93/mock cells in the backs, 4 metastasized to inguinal drainage lymph node, and the other one did not metastasize. Tumors in all 7 mice inoculated with CMT93/MCP-3 did not metastasize. Histological study showed a metastatic lymph node (Figure 6a). In another metastasis lesion, tumor cells went out of the lymph node to invade the muscle tissue (Figure 6b). The percentage of tumor metastasis of MCP-3 gene transfectants was significantly lower than that of wild type or mock transfected CMT93 tumor cells (Table 2, *P*<0.05).

Table 2 Tumor metastasis in mice inoculated with CMT93 or its gene transfectants

Mice inoculated with	No. metastasized	No. not metastasized	Percentage (%)
CMT93	4	0	100
CMT93/Mock	4	1	80
CMT93/MCP-3	0	7	0 ^{a,b}

^a*P*<0.001 vs CMT93 group; ^b*P*<0.05 vs CMT93/Mock group

DISCUSSION

Chemokines characterized by their ability to induce directional migration and activation of leukocytes comprise the superfamily of polypeptides which is the largest family of cytokines. Produced by a variety of cell types including hematopoietic and non-hematopoietic origin, chemokines regulate leukocyte adhesion, trafficking, homing and angiogenesis, and contribute to lymphopoiesis and hematopoiesis. *In vivo* studies using neutralizing antibodies, antagonists, or by deletion of chemokines and their receptors have revealed that chemokines and their receptors play a pivotal role in host defense and in immunological conditions^[1].

The fact that chemokines attract different leukocyte populations and promote their functions has prompted a number of studies on the effect of chemokine gene transduction into tumor cells. Not only CC chemokines such as MCP-1 (monocyte chemoattractant protein-1)^[17,18], MCP-3 (monocyte chemoattractant protein-3)^[12,13], MIP-1α (macrophage inflammatory protein-1α)^[19], MIP-1β (macrophage inflammatory protein-1β)^[20], SLC (secondary lymphoid tissue chemokine)^[21], MIP-3α (macrophage inflammatory protein 3α)^[22], TCA3 (T-cell activation gene 3)^[23], RANTES (regulated on activation normally T cell expressed and secreted)^[24], but also CXC chemokines including ELR- (angiostatic) chemokines such as IP10 (interferon-inducible protein 10)^[25-28], MIG (monokine induced by interferon gamma)^[29,30], PF4 (platelet factor 4)^[31], and ELR+ (angiogenic) chemokines such as IL-8 (interleukin-8)^[32-33] had been selected for tumor gene immunotherapy. In addition, C chemokine lymphotactin^[34-36] had been reported in tumor gene therapy as well. Divergent results were obtained depending on the tumor models and whether human or murine chemokine genes were used.

MCP-3 had a wide spectrum of action on different immune cells, including monocytes^[10], T cells^[37,38], NK cells^[39], basophils^[40], eosinophils^[40], and neutrophils^[10]. In addition, MCP-3 was active on DC as well^[41-43]. In P815 mastocytoma mouse model, MCP-3 gene transfer reduced tumorigenicity by augmenting immune cell infiltration in tumor tissue and dendritic cells accumulation in peritumorous tissue^[12]. MCP-3 gene transfer also induced leukocyte infiltration and reduces growth of human cervical carcinoma cell xenografts^[13].

In our study, MCP-3 gene was transduced into mouse colorectal cancer CMT93 tumor cells to determine the anti-tumor activity of MCP-3 in colorectal cancer model. Though tumorigenicity of CMT93 was not reduced, and the tumors can't be rejected completely after MCP-3 gene transfer, but the tumors grew more slowly than those of controls. And MCP-3 gene transfer inhibited tumor metastasis thoroughly. In the tumor tissue from MCP-3 gene transfectants, infiltrated immune cells increased. We speculate that the anti-tumor immunity elicited by MCP-3 gene transfer is type I T cell-dependent just as reported^[12]. We found the humoral response against CMT93 tumor cells in the serum from CMT93/MCP-

3 primed mouse did not increase (data not shown), and few neutrophils was found in tumor tissue. These results reversely suggested a type I T cell-dependent response was contributed to the anti-tumor immunity in MCP-3 gene transfer. Further study is needed to prove whether dendritic cells contribute to the anti-tumor immunity elicited by MCP-3 gene transfer or not.

REFERENCES

- 1 **Wang JM**, Deng X, Gong W, Su S. Chemokines and their role in tumor growth and metastasis. *J Immunol Methods* 1998; **220**: 1-17
- 2 **Negus RP**, Stamp GW, Relf MG, Burke F, Malik ST, Bernasconi S, Allavena P, Sozzani S, Mantovani A, Balkwill FR. The detection and localization of monocyte chemoattractant protein-1 (MCP-1) in human ovarian cancer. *J Clin Invest* 1995; **95**: 2391-2396
- 3 **Sciaccia FL**, Sturzl M, Bussolino F, Sironi M, Brandstetter H, Zietz C, Zhou D, Matteucci C, Peri G, Sozzani S. Expression of adhesion molecules, platelet-activating factor, and chemokines by Kaposi's sarcoma cells. *J Immunol* 1994; **153**: 4816-4825
- 4 **Riethdorf L**, Riethdorf S, Gutzlaff K, Prall F, Loning T. Differential expression of the monocyte chemoattractant protein-1 gene in human papillomavirus-16-infected squamous intraepithelial lesions and squamous cell carcinomas of the cervix uteri. *Am J Pathol* 1996; **149**: 1469-1476
- 5 **Graves DT**, Barnhill R, Galanopoulos T, Antoniadis HN. Expression of monocyte chemotactic protein-1 in human melanoma *in vivo*. *Am J Pathol* 1992; **140**: 9-14
- 6 **Van Damme J**, Proost P, Lenaerts JP, Opdenakker G. Structural and functional identification of two human, tumor-derived monocyte chemotactic proteins (MCP-2 and MCP-3) belonging to the chemokine family. *J Exp Med* 1992; **176**: 59-65
- 7 **Sozzani S**, Zhou D, Locati M, Rieppi M, Proost P, Magazin M, Vita N, van Damme J, Mantovani A. Receptors and transduction pathways for monocyte chemotactic protein-2 and monocyte chemotactic protein-3. Similarities and differences with MCP-1. *J Immunol* 1994; **152**: 3615-3622
- 8 **Neote K**, DiGregorio D, Mak JY, Horuk R, Schall TJ. Molecular cloning, functional expression, and signaling characteristics of a C-C chemokine receptor. *Cell* 1993; **72**: 415-425
- 9 **Gao JL**, Kuhns DB, Tiffany HL, McDermott D, Li X, Francke U, Murphy PM. Structure and functional expression of the human macrophage inflammatory protein 1 alpha/RANTES receptor. *J Exp Med* 1993; **177**: 1421-1427
- 10 **Xu LL**, McVicar DW, Ben-Baruch A, Kuhns DB, Johnston J, Oppenheim JJ, Wang JM. Monocyte chemotactic protein-3 (MCP3) interacts with multiple leukocyte receptors: binding and signaling of MCP3 through shared as well as unique receptors on monocytes and neutrophils. *Eur J Immunol* 1995; **25**: 2612-2617
- 11 **Ponath PD**, Qin S, Post TW, Wang J, Wu L, Gerard NP, Newman W, Gerard C, Mackay CR. Molecular cloning and characterization of a human eotaxin receptor expressed selectively on eosinophils. *J Exp Med* 1996; **183**: 2437-2448
- 12 **Fioretti F**, Fradelizi D, Stoppacciaro A, Ramponi S, Ruco L, Minty A, Sozzani S, Garlanda C, Vecchi A, Mantovani A. Reduced tumorigenicity and augmented leukocyte infiltration after monocyte chemotactic protein-3 (MCP-3) gene transfer: perivascular accumulation of dendritic cells in peritumoral tissue and neutrophil recruitment within the tumor. *J Immunol* 1998; **161**: 342-346
- 13 **Wetzel K**, Menten P, Opdenakker G, Van Damme J, Grone HJ, Giese N, Vecchi A, Sozzani S, Cornelis JJ, Rommelaere J, Dinsart C. Transduction of human MCP-3 by a parvoviral vector induces leukocyte infiltration and reduces growth of human cervical carcinoma cell xenografts. *J Gene Med* 2001; **3**: 326-337
- 14 **Franks LM**, Hemmings VJ. A cell line from an induced carcinoma of mouse rectum. *J Pathol* 1978; **124**: 35-37
- 15 **Deng X**, Ueda H, Su SB, Gong W, Dunlop NM, Gao JL, Murphy PM, Wang JM. A synthetic peptide derived from human immunodeficiency virus type 1 gp120 downregulates the expression and function of chemokine receptors CCR5 and CXCR4 in monocytes by activating the 7-transmembrane G-protein-coupled receptor FPRL1/LXA4R. *Blood* 1999; **94**: 1165-1173
- 16 **Hu JY**, Wang S, Zhu JG, Zhou GH, Sun QB. Expression of B7 costimulation molecules by colorectal cancer cells reduces tumorigenicity and induces anti-tumor immunity. *World J Gastroenterol* 1999; **5**: 147-151
- 17 **Sakai Y**, Kaneko S, Nakamoto Y, Kagaya T, Mukaida N, Kobayashi K. Enhanced anti-tumor effects of herpes simplex virus thymidine kinase/ganciclovir system by codelivering monocyte chemoattractant protein-1 in hepatocellular carcinoma. *Cancer Gene Ther* 2001; **8**: 695-704
- 18 **Nakashima E**, Kubota Y, Matsushita R, Ozaki E, Ichimura F, Kawahara S, Nakanishi I, Kuno K, Matsushima K. Synergistic antitumor interaction of human monocyte chemoattractant protein-1 gene transfer and modulator for tumor-infiltrating macrophages. *Pharm Res* 1998; **15**: 685-689
- 19 **Nakashima E**, Oya A, Kubota Y, Kanada N, Matsushita R, Takeda K, Ichimura F, Kuno K, Mukaida N, Hirose K, Nakanishi I, Ujiiie T, Matsushima K. A candidate for cancer gene therapy: MIP-1 alpha gene transfer to an adenocarcinoma cell line reduced tumorigenicity and induced protective immunity in immunocompetent mice. *Pharm Res* 1996; **13**: 1896-1901
- 20 **Miyata T**, Yamamoto S, Sakamoto K, Morishita R, Kaneda Y. Novel immunotherapy for peritoneal dissemination of murine colon cancer with macrophage inflammatory protein-1beta mediated by a tumor-specific vector, HVJ cationic liposomes. *Cancer Gene Ther* 2001; **8**: 852-860
- 21 **Kirk CJ**, Hartigan-O'Connor D, Nickoloff BJ, Chamberlain JS, Giedlin M, Aukerman L, Mule JJ. T cell-dependent antitumor immunity mediated by secondary lymphoid tissue chemokine: augmentation of dendritic cell-based immunotherapy. *Cancer Res* 2001; **61**: 2062-2070
- 22 **Fushimi T**, Kojima A, Moore MA, Crystal RG. Macrophage inflammatory protein 3alpha transgene attracts dendritic cells to established murine tumors and suppresses tumor growth. *J Clin Invest* 2000; **105**: 1383-1393
- 23 **Laning J**, Kawasaki H, Tanaka E, Luo Y, Dorf ME. Inhibition of *in vivo* tumor growth by the beta chemokine, TCA3. *J Immunol* 1994; **153**: 4625-4635
- 24 **Mule JJ**, Custer M, Averbook B, Yang JC, Weber JS, Goeddel DV, Rosenberg SA, Schall TJ. RANTES secretion by gene-modified tumor cells results in loss of tumorigenicity *in vivo*: role of immune cell subpopulations. *Hum Gene Ther* 1996; **7**: 1545-1553
- 25 **Feldman AL**, Friedl J, Lans TE, Libutti SK, Lorang D, Miller MS, Turner EM, Hewitt SM, Alexander HR. Retroviral gene transfer of interferon-inducible protein 10 inhibits growth of human melanoma xenografts. *Int J Cancer* 2002; **99**: 149-153
- 26 **Palmer K**, Hitt M, Emtage PC, Gyorffy S, Gaudie J. Combined CXC chemokine and interleukin-12 gene transfer enhances anti-tumor immunity. *Gene Ther* 2001; **8**: 282-290
- 27 **Narvaiza I**, Mazzolini G, Barajas M, Duarte M, Zaratiegui M, Qian C, Melero I, Prieto J. Intratumoral coinjection of two adenoviruses, one encoding the chemokine IFN-gamma-inducible protein-10 and another encoding IL-12, results in marked antitumoral synergy. *J Immunol* 2000; **164**: 3112-3122
- 28 **Luster AD**, Leder P. IP-10, a C-X-C-chemokine, elicits a potent thymus-dependent antitumor response *in vivo*. *J Exp Med* 1993; **178**: 1057-1065
- 29 **Ruehlmann JM**, Xiang R, Niethammer AG, Ba Y, Pertl U, Dolman CS, Gillies SD, Reisfeld RA. MIG (CXCL9) chemokine gene therapy combines with antibody-cytokine fusion protein to suppress growth and dissemination of murine colon carcinoma. *Cancer Res* 2001; **61**: 8498-8503
- 30 **Addison CL**, Arenberg DA, Morris SB, Xue YY, Burdick MD, Mulligan MS, Iannettoni MD, Strieter RM. The CXC chemokine, monokine induced by interferon-gamma, inhibits non-small cell lung carcinoma tumor growth and metastasis. *Hum Gene Ther* 2000; **11**: 247-261
- 31 **Tanaka T**, Manome Y, Wen P, Kufe DW, Fine HA. Viral vector-mediated transduction of a modified platelet factor 4 cDNA inhibits angiogenesis and tumor growth. *Nat Med* 1997; **3**: 437-442
- 32 **Yamanaka R**, Tanaka R, Yoshida S, Saitoh T, Fujita K. Growth inhibition of human glioma cells modulated by retrovirus gene transfection with antisense IL-8. *J Neurooncol* 1995; **25**: 59-65

- 33 **Hirose K**, Hakozaki M, Nyunoya Y, Kobayashi Y, Matsushita K, Takenouchi T, Mikata A, Mukaida N, Matsushima K. Chemokine gene transfection into tumour cells reduced tumorigenicity in nude mice in association with neutrophilic infiltration. *Br J Cancer* 1995; **72**: 708-714
- 34 **Xia DJ**, Zhang WP, Zheng S, Wang J, Pan JP, Wang Q, Zhang LH, Hamada H, Cao X. Lymphotactin cotransfection enhances the therapeutic efficacy of dendritic cells genetically modified with melanoma antigen gp100. *Gene Ther* 2002; **9**: 592-601
- 35 **Emtage PC**, Wan Y, Hitt M, Graham FL, Muller WJ, Zlotnik A, Gauldie J. Adenoviral vectors expressing lymphotactin and interleukin 2 or lymphotactin and interleukin 12 synergize to facilitate tumor regression in murine breast cancer models. *Hum Gene Ther* 1999; **10**: 697-709
- 36 **Huang H**, Li F, Gordon JR, Xiang J. Synergistic enhancement of antitumor immunity with adoptively transferred tumor-specific CD4+ and CD8+ T cells and intratumoral lymphotactin transgene expression. *Cancer Res* 2002; **62**: 2043-2051
- 37 **Loetscher P**, Seitz M, Clark-Lewis I, Baggiolini M, Moser B. Monocyte chemotactic proteins MCP-1, MCP-2, and MCP-3 are major attractants for human CD4+ and CD8+ T lymphocytes. *FASEB J* 1994; **8**: 1055-1060
- 38 **Taub DD**, Proost P, Murphy WJ, Anver M, Longo DL, van Damme J, Oppenheim JJ. Monocyte chemotactic protein-1 (MCP-1), -2, and -3 are chemotactic for human T lymphocytes. *J Clin Invest* 1995; **95**: 1370-1376
- 39 **Allavena P**, Bianchi G, Zhou D, van Damme J, Jilek P, Sozzani S, Mantovani A. Induction of natural killer cell migration by monocyte chemotactic protein-1, -2 and -3. *Eur J Immunol* 1994; **24**: 3233-3236
- 40 **Dahinden CA**, Geiser T, Brunner T, von Tscharner V, Caput D, Ferrara P, Minty A, Baggiolini M. Monocyte chemotactic protein 3 is a most effective basophil- and eosinophil-activating chemokine. *J Exp Med* 1994; **179**: 751-756
- 41 **Sozzani S**, Sallusto F, Luini W, Zhou D, Piemonti L, Allavena P, Van Damme J, Valitutti S, Lanzavecchia A, Mantovani A. Migration of dendritic cells in response to formyl peptides, C5a, and a distinct set of chemokines. *J Immunol* 1995; **155**: 3292-3295
- 42 **Vecchi A**, Massimiliano L, Ramponi S, Luini W, Bernasconi S, Bonecchi R, Allavena P, Parmentier M, Mantovani A, Sozzani S. Differential responsiveness to constitutive vs. inducible chemokines of immature and mature mouse dendritic cells. *J Leukoc Biol* 1999; **66**: 489-494
- 43 **Xu LL**, Warren MK, Rose WL, Gong W, Wang JM. Human recombinant monocyte chemotactic protein and other C-C chemokines bind and induce directional migration of dendritic cells *in vitro*. *J Leukoc Biol* 1996; **60**: 365-371

Edited by Lu HM

• VIRAL HEPATITIS •

ROC curves in evaluation of serum fibrosis indices for hepatic fibrosis

Min Zheng, Wei-Min Cai, Hong-Lei Weng, Rong-Hua Liu

Min Zheng, Wei-Min Cai, Hong-Lei Weng, Rong-Hua Liu, Institute of Infectious Diseases, First Affiliated Hospital, School of Medicine, Zhejiang University, Hangzhou 310003 Zhejiang Province, China
Correspondence to: Dr. Min Zheng, Institute of Infectious Diseases, First Affiliated Hospital, School of Medicine, Zhejiang University, Hangzhou 310003, Zhejiang Province, China. charming-hz@163.net
Telephone: +86-571-87236580 **Fax:** +86-571-87068731
Received 2002-03-14 **Accepted** 2002-04-20

Abstract

AIM: Use Receiver operating characteristic (ROC) curves to find out the relationship between serum level of hyaluronic acid (HA), type III procollagen (PCIII), N-terminal procollagen III peptide (PIIINP), laminin (LN), type IV collagen (C-IV) and hepatic fibrosis, as well as to determine their value in clinical practice.

METHODS: 114 serum samples from chronic hepatitis patients were assayed for fibrosis indices including HA, PCIII, PIIINP, LN and IV-C with radioimmunoassay (RIA). Liver biopsy was also performed in all these patients and the biopsy material was examined histopathologically.

RESULTS: ROC curves analysis showed that area under the curve (AUC) of PIIINP, HA, PCIII, C-IV and LN was 0.800, 0.728, 0.727, 0.583 and 0.463, respectively. The analysis also showed that PIIINP ($r=0.452$), HA ($r=0.497$) and PCIII ($r=0.404$) have greater diagnosis performances than C-IV ($r=0.238$) and LN ($r=0.128$) according to fibrosis staging. The sensitivity of HA plus PIIINP was 55.1 %, it was the most sensitive combination. Combined three or more than three indices that based on HA, the specificity was 100 %. Using combination assays can improve the specificity, but its sensitivity was not high. Serum fibrosis indices increased as the grade of inflammation aggravated. But only PIIINP and PCIII had significant difference between G1 and G2 (PIIINP: 13.16 ± 8.07 vs 8.32 ± 5.09 ; PCIII: 164.22 ± 65.69 vs 138.23 ± 77.63). The coefficient correlation of the results of inflammation grade and fibrosis staging to HA was 0.525 and 0.553 respectively, that to PCIII, 0.446 and 0.412, that to LN, 0.234 and 0.194, and that to IV-C, 0.363 and 0.351, respectively.

CONCLUSION: Serum fibrosis indices can indicate tendency of hepatic fibrosis, but it cannot replace liver biopsy. However, as diagnostic markers, more efficient serum fibrosis indices for the diagnosis of hepatic fibrosis need to be explored.

Zheng M, Cai WM, Weng HL, Liu RH. ROC curves in evaluation of serum fibrosis indices for hepatic fibrosis. *World J Gastroenterol* 2002; 8(6):1073-1076

INTRODUCTION

Chronic injury leading to fibrosis in the liver^[1-11]. Liver biopsy has traditionally been the standard method for assessing hepatic fibrosis, but the procedure is associated with complications in patient under biopsy and so it is difficult to put into practice. Reports showed that serum fibrosis indices, including PCIII, PIIINP, LN, HA and C-IV and others, can reflect the activity of hepatic fibrosis to some extent^[12-19]. Mean \pm SD has always been used to express the standard for hepatic fibrosis^[20]. In recent years, some scientists have recommended to use Receiver operating characteristic (ROC) curves in determination of indices of hepatic fibrosis in clinical practice^[21]. Reports using ROC curves to evaluate fibrosis indices were seen, but histopathological results of the liver have not been used as control. In this study, levels of all the five fibrosis indices were measured in patients with chronic hepatitis B and comparison with biopsy results of the liver was carried out to determine if the measurements of these indices have any clinical value as markers of chronic hepatic fibrosis. ROC analysis was used to determine the sensitivity and specificity of the assays in detecting the liver disease.

MATERIALS AND METHODS

Subjects

During the Sixth National Conference for Infectious and Parasitic Diseases, the protocol of prevention and treatment for virus hepatitis was modified in 2000 (abbreviated as “2000 criteria”)^[22]. According to the “2000 criteria”, 114 patients had typical presentations of chronic hepatitis. 99 were males and 15, females. Among them, 75, 30 and 9 showed mild, moderate and severe degree of the disease, respectively. The patients’ histories were mainly collected from the First Affiliated Hospital of School of Medicine, Zhejiang University and several hospitals in Zhejiang Province between July, 1998 and September, 1999. Their age ranged between 16 and 57 years and the disease course was from one to 30 years. All patients showed positive in HBV markers (HBVM) and the diagnosis was made by liver biopsy according to the “2000 criteria”^[22].

Histology

Biopsy fragments of the livers were fixed in 10 % neutralized formaldehyde, embedded in paraffin, and then stained with hematoxylin and eosin. Reticulation fibrosis stain and the Sirius red method were used specially for staining fibrous tissue components. Histological assessment of the liver was done according to Wang’s report^[23], and the stage of fibrosis was divided into four, expressed as S1 to S4 according to the “2000 criteria”^[22]. S1 shows expansion in portal tract areas with fibrosis; S2, fibrosis around portal tract areas with fibrosis segregation formation, while maintaining lobule structure; S3, formation of fibrosis segregation and disorder of lobule structure without hepatic cirrhosis, and S4, early stage or confirmed cirrhosis. S0 shows no fibrosis.

Determination of serum fibrosis indices

The serum specimens were divided into five proportions and stored at -20 °C. The assay of the levels of serum HA, PCIII, PIIINP, IV-C and LN was done by RIA. The kits of HA, IV-C and LN were provided by the Shanghai Navy Medical Institute. The kit of PCIII was provided by the Chongqing Tumor Institute. The kit of PIIINP was provided by the Shanghai Orion Diagnostic Reagent Corporation (produced by Finland Orion Corporation). The operations were performed according to the user's manual.

Statistical analysis

Results were expressed as mean \pm standard deviation ($\bar{x} \pm s$) and compared when necessary. The relationship between noninvasive markers and stage of histological liver fibrosis was analyzed by the Spearman rank-correlation test and nonparametric one-way ANOVA for nonparametric data. Tests were considered statistically significant at $P < 0.05$. Sensitivity of the assays was plotted against the false positivity (1-specificity) using ROC curves using SPSS 10.5 statistical program. Comparison of AUC was performed, which compares the AUC to the diagonal line of no information (AUC 0.5). The pathologist was blind to the results of serum indices in the study subjects. In order to determine the specificity and sensitivity of the assays, $S \geq 1$ for one with hepatic fibrosis was arbitrarily defined. Take (1-specificity) as x-axis, and take sensitivity as y-axis. If AUC=1.0, the index is an ideal test, and if AUC<0.5, the index has no diagnostic value.

RESULTS

ROC curves of five serum fibrosis indices

From Figure 1 the AUC of serum fibrosis indices in ROC curves is in the order of PIIINP>HA>PCIII>C-IV>LN. It means that PIIINP, HA and PCIII are more useful than C-IV and LN in terms of the fibrosis index for diagnosis. PIIINP is the most sensitive index among the five indices, but its specificity is not as high as HA and PCIII. Take both sensitivity and specificity into account, the cut-off point was selected according to max number of sensitivity add specificity. Table 1 shows the cut-off point, sensitivity, specificity and correct diagnosis index of the five indices.

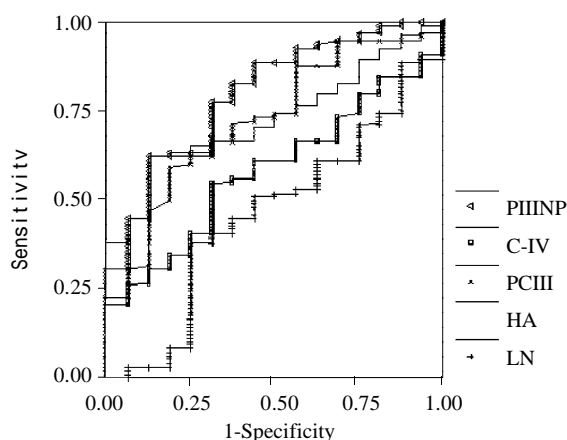


Figure 1 ROC curves of five serum fibrosis indices

The value of combination of the five indices for diagnosis

HA is the generally used index for diagnosis. From Figure 1, HA is the best one among the five indices. So HA was taken as a basic index and was used in combination with other indices

for the diagnosis of hepatic fibrosis. Each index result of ROC analysis is shown in Table 1. Table 2 shows the sensitivity and specificity of combination diagnosis. Among two index combination groups HA+PIIINP is better than HA+PCIII and HA+C-IV and HA+LN. In combinations of the above three indices, specificity is all 100 %. The best sensitivity was seen in HA+C-IV+PIIINP and HA+C-IV+ PCIII combinations.

Table 1 ROC curves of five serum fibrosis indexes

Indices	AUC	P Vaule	cut-off point	Sensitivity	Specificity	r Vaule
PIIINP	0.800	0.000	5.61 μ g/L	82.7%	62.5%	0.452
HA	0.728	0.003	145.2 ng/ml	62.2%	87.5%	0.497
PCIII	0.727	0.004	137.4 μ g/L	59.2%	81.2%	0.404
C-IV	0.583	0.287	74.2 μ g/L	55.1%	68.7%	0.238
LN	0.463	0.636	156.65 ng/ml	37.8%	75.0%	0.128

Right diagnosis index (r)=sensitivity+specificity - 1

Table 2 Parameter of combination diagnosis with several fibrosis indexes

Combination	Sensitivity (%)	Specificity (%)
HA + PIIINP	55.1	87.5
HA + PCIII	50.0	87.5
HA + LN	27.6	100
HA + C-DIV	42.9	100
HA + LN+C-IV	21.4	100
HA + LN+ PIIINP	24.5	100
HA + LN+ PCIII	24.5	100
HA + C-IV+PIIINP	38.8	100
HA + C-IV+PCIII	38.8	100
HA + LN+C-IV+ PIIINP	19.4	100
HA + LN+C-IV+PCIII	19.4	100

The relationship between hepatic fibrosis indices and inflammation grades

Table 3 shows that numerical value of serum fibrosis indices, excluding LN, increased along with the development of inflammation grades. Only PIIINP and PCIII, but not others, have significant difference between G2 and G1. Values of PIIINP, PCIII, HA and C-IV in the stage G3 and G4 have significant differences as compared to those in the stage G1.

Table 3 The relationship between hepatic fibrosis indexes and inflammation grades

G	n	PIIINP(μ g/L)	HA(ng/ml)	PCIII(μ g/L)	C-IV(μ g/L)	LN(ng/ml)
1	45	8.32 \pm 5.09	144.78 \pm 123.31	138.23 \pm 77.63	73.89 \pm 23.61	155.43 \pm 55.48
2	36	13.16 \pm 8.07 ^b	211.26 \pm 187.17	164.22 \pm 65.69 ^b	6.26 \pm 52.56	138.76 \pm 43.42
3	27	15.61 \pm 7.05 ^b	476.26 \pm 296.44 ^b	190.06 \pm 75.10 ^b	109.75 \pm 42.12 ^b	161.52 \pm 34.25
4	6	15.60 \pm 5.41 ^b	562.08 \pm 274.47 ^b	261.68 \pm 127.77 ^b	123.10 \pm 41.60 ^b	154.60 \pm 20.03

^b $P < 0.01$; Compare to G1

Correlation between serum fibrosis indices and histological classification (*r*)

Table 4 shows the details of relationship between serum fibrosis indices and liver inflammation grades and fibrosis staging.

Table 4 Correlation between serum fibrosis indexes and histology classification

	PIIINP	HA	PCIII	C-IV	LN
Inflammation grads	0.463 ^b	0.523 ^b	0.446 ^b	0.363 ^b	0.234
Fibrosis stages	0.403 ^b	0.553 ^b	0.412 ^b	0.351 ^b	0.194

^b $P < 0.01$

DISCUSSION

Hepatic fibrosis is a result in loss of normal liver cell function due to the disorganized over-accumulation of extracellular matrix (ECM) components in the liver^[24-29]. It is clear that the increase production and decrease degradation of ECM components are responsible for the altered ECM metabolism in fibrotic liver. So the metabolism production of ECM in serum can be regarded as the indices of hepatic fibrosis. Different serum fibrosis indices represent different ECM metabolism. Such as PIIINP and PCIII reflect collagen metabolism^[30], and HA reflects hepatic fibrosis activity and liver injury^[31,32]. LN reflects basement membrane transformation and has some relation to portal hypertension^[32,33]. We have reported an integral project for the diagnosis of hepatic fibrosis and serum fibrosis index spectrum for the serodiagnosis of hepatic fibrosis^[34]. But along with the development of the technology of testing and statistic, new evaluation for serum hepatic fibrosis indices is necessary. ROC curves and AUC of ROC curves can assess the value of one test^[35,36]. ROC curves can do comparison of several diagnostic techniques for one disease. In this way, clinicians can get help for screening out the most suitable scheme. So ROC analysis has become an important method for the assessment of diagnostic markers for hepatic fibrosis.

From Figure 1 and Table 1 it is clear that PIIINP is the most sensitive index among the five indices. However, its specificity is comparatively low. Also a conclusion can be got from Figure 1 and Table 1 that HA is the most specific index. This is consistent with the results of our previous study on the relationship between serum fibrosis indices and liver histological changes^[37], and is also consistent with other reports^[38,39]. The cut-off point is used in our study to confirm the critical value of serum fibrosis indices when they are used in the diagnosis of hepatic fibrosis. Not only the cut-off point meets the requirement of study on clinical epidemiology, but also it can get more reliable result. One may get conclusion from the figure that using only one index to diagnose fibrosis may be prejudicial. From the ROC curves we can see, no single serum index has both ideal sensitivity and specificity. Our results also showed that excluding LN, other serum indices have close relation with inflammation. This is also the reason why the specificity is low if only one serum fibrosis index is used in the diagnosis. Ye *et al.* reported that serum PCIII index can exclude the influence of hepatocyte inflammation and necrosis. But their results just took serum alanine aminotransferase (ALT), bilirubin, albumin, HBVDNA and HBVM as standards for estimation. As we know that serum liver function tests and HBVDNA are not very objective indices. Our results based on histological examination of the liver hinted that PCIII also has

close relation with inflammation grades of chronic hepatitis. The correlation coefficient of PCIII is just lower than HA and PIIINP. So PCIII examination cannot get rid of interference of inflammation. And PIIINP is more sensitive than PCIII in early hepatic fibrosis^[40].

As influenced by the metabolism of connective tissue in the body, one index can only reflect one aspect of synthesis or degradation of ECM. So combined test of several indices for the diagnosis of hepatic fibrosis is the way of choice. Use several noninvasive markers combination to diagnose hepatic fibrosis have been reported^[37,41]. However, no identical standard has been made in terms of index selecting. Positive rate of HA in the diagnosis was 91-94 % in liver cirrhosis, so it is the most sensitive index to screen hepatic fibrosis and cirrhosis. According to the cut-off point and take HA as the basis index to combined with other indices to diagnose hepatic fibrosis, our study was carried out. From Table 2 tests of HA plus PIIINP or PCIII are the most sensitive combination with rather high specificity. Although other combinations seem to be more specific, their sensitivity is quite low. The sensitivity of our combinations is lower than other report, but the specificity is higher^[42]. Reports already published usually took $\bar{x} \pm s$ of serum indices for the diagnosis of chronic active hepatitis. However, using serum markers to diagnose fibrosis caused by chronic hepatitis without liver histological results for control may be over-estimated the sensitivity of the diagnosis. This study divided different groups by stage according to histological results and utilized ROC curves concatenation variable to ascertain cut-off point and in doing so attention was paid to both sensitivity and specificity. One of the reasons of low sensitivity may be due to patient selection for the study among them most were cases of chronic hepatitis. As we only use fibrosis stage $S \geq 1$ as grouping standard, the inflammation in the groups between $S=0$ and $S \geq 1$ may influence the result of sensitivity.

In conclusion, serum HA, PIIINP, PCIII, C-IV and LN levels reflect some aspects of ECM synthesis and degradation. Although serum fibrosis indices can reflect degree of fibrosis impersonally, the stage classification of fibrosis is too simple. And, as a result, fibrosis in the same stage may have considerable difference. So if quantified measurement of liver fiber with computer analysis is done first^[43-45], and then followed by using ROC curves to assess the serum fibrosis indices, as a noninvasive diagnosis technique, serum fibrosis indices will have more significant meaning in clinical evaluation of the liver disease.

REFERENCES

- 1 **Yao SK**, Yin F. Diagnosis and treatment of hepatic fibrosis. *Shijie Huaren Xiaohua Zazhi* 2000; **8**: 681-683
- 2 **Liu F**, Liu JX, Cao ZC, Li BS, Zhao CY, Kong L, Zhen Z. Relationship between TGF- β 1, serum indexes of liver fibrosis and hepatic tissue pathology in patients with chronic liver diseases. *Shijie Huaren Xiaohua Zazhi* 1999; **7**: 519-521
- 3 **Bai WY**, Yao XX, Feng LY. The situation of hepatic fibrosis research. *Shijie Huaren Xiaohua Zazhi* 2000; **8**: 1267-1268
- 4 **Friedman SL**. Molecular mechanisms of hepatic fibrosis and principles of therapy. *J Gastroenterol* 1997; **32**: 424-430
- 5 **Assy N**, Paizi M, Gaitini D, Baruch Y, Spira G. Clinical implication of VEGF serum levels in cirrhotic patients with or without portal hypertension. *World J Gastroenterol* 1999; **5**: 296-300
- 6 **Yan JC**, Ma Y, Chen WB, Shun XH. Dynamic observation on liver fibrosis and cirrhosis of hepatitis B. *Huaren Xiaohua Zazhi* 1998; **6**: 699-702
- 7 **Chen WX**, Li YM, Yu CH, Cai WM, Zheng M, Chen F. Quantitative analysis of transforming growth factor beta 1 mRNA in patients with alcoholic liver disease. *World J Gastroenterol* 2002; **8**: 379-381

- 8 **Piscaglia F**, Gaiani S, Gramantieri L, Zironi G, Siringo S, Bolondi L. Superior mesenteric artery impedance in chronic liver diseases: relationship with disease severity and portal circulation. *Am J Gastroenterol* 1998; **93**: 1925-1930
- 9 **Du LJ**, Tang WX, Dan ZL, Zhang WY, Li SB. Protective effect of ganyanping on CCl₄ induced liver fibrosis in rats. *Shijie Huaren Xiaohua Zazhi* 1998; **6**: 21-22
- 10 **Lin H**, Lu M, Zhang YX, Wang BY, Fu BY. Induction of a rat model of alcoholic liver diseases. *Shijie Huaren Xiaohua Zazhi* 2001; **9**: 24-28
- 11 **Peng YZ**, Huang QT, Yan SN, Deng B, Hu JJ. Effect of RNA against hepatic fibrosis in rabbits infected with *Schistosoma japonicum*. *Zhongguo Jishengchongxue Yu Jishengchongbing Zazhi* 1998; **16**: 214-218
- 12 **Shen M**, Qiu DK, Chen Y, Xiong WJ. Effects of recombinant augment of liver regeneration protein, danshen and oxymatrine on rat fibroblasts. *Shijie Huaren Xiaohua Zazhi* 2001; **9**: 1129-1233
- 13 **Guechot J**, Serfaty L, Bonnard AM, Chazouilleres O, Poupon RE, Poupon R. Prognostic value of serum hyaluronan in patients with compensated HCV cirrhosis. *J Hepatol* 2000; **32**: 447-452
- 14 **He Y**, Wang JB, Wang YM. The diagnosis development of hepatic fibrosis with chronic hepatitis. *Shijie Huaren Xiaohua Zazhi* 2001; **9**: 1305-1309
- 15 **Leroy V**, De Traversay C, Barnoud R, Hartmann J D, Baud M, Ouzan D, Zarski J P. Changes in histological lesions and serum fibrogenesis markers in chronic hepatitis C patients non-responders to interferon alpha. *J Hepatol* 2001; **35**: 120-126
- 16 **Luo RH**, Yang SJ, Xie JQ, Zhao ZX, He YC, Yao JL. Diagnostic value of five serum markers for liver fibrosis. *Zhonghua Ganzangbing Zazhi* 2001; **9**: 148-150
- 17 **Deng LX**, Zhou YP, Peng XM, Deng H, Deng Y, Yao JL. Serum markers and pathological evaluation in hepatitis fibrosis of chronic hepatitis B treated with interferon alpha. *Zhonghua Ganzangbing Zazhi* 2001 (Suppl): 66-67
- 18 **Lu X**, Liu CH, Xu GF, Chen WH, Liu P. Successive observation of laminin and collagen IV on hepatic sinusoid during the formation of the liver fibrosis in rats. *Shijie Huaren Xiaohua Zazhi* 2001; **9**: 260-262
- 19 **Wang X**, Chen YX, Xu CF, Zhao GN, Huang YX, Wang QL. Relationship between tumor necrosis factor- α and liver fibrosis. *World J Gastroenterol* 1998; **4**: 18
- 20 **Cai WM**. Assay of serum hepatic fibrosis markers. In: Ye WF, Zhong ZY, eds. Diagnosis of liver and biliary diseases. Tianjin: Tianjin Publ Hou Sci Technol 1998: 190-200
- 21 **Walsh KM**, Timms P, Campbell S, Macsween RNM, Morris AJ. Plasma levels of matrix metalloproteinases-2 (MMP-2) and tissue inhibitors of metalloproteinases-1 and -2 (TIMP-1,2) as noninvasive markers of liver disease in chronic hepatitis C disease in chronic hepatitis C comparison using ROC analysis. *Dig Dis Sci* 1999; **44**: 624-630
- 22 **Society of Infectious Diseases and Parasitic Diseases, CMA**. Criteria on the prevention and treatment for virus hepatitis. *Zhonghua Neike Zazhi* 2001; **40**: 62-68
- 23 **Wang TL**, Wang BE, Liu X, Jia JD, Zhao JB, Li XM, Zhang J, Li NZ. Correlation of serum mark with fibrosis in chronic viral hepatitis. *Zhonghua Binglixue Zazhi* 1998; **27**: 185-190
- 24 **Sun DL**, Sun SQ, Li TZ, Lu XL. Serologic study on extracellular matrix metabolism in patients with viral liver cirrhosis. *Shijie Huaren Xiaohua Zazhi* 1999; **7**: 55-56
- 25 **Ueki N**, Taguchi T, Takahashi M, Adachi M, Ohkawa T, Amuro Y, Hada T, Higashino K. Inhibition of hyaluronan synthesis by vesnarinone in cultured human myofibroblasts. *Biochim Biophys Acta* 2000; **1495**: 160-167
- 26 **Apte MV**, Haber PS, Darby SJ, Rodgers SC, McCaughan GW, Korsten MA, Pirola RC, Wilson JS. Pancreatic stellate cells are activated by proinflammatory cytokines: implications for pancreatic fibrogenesis. *Gut* 1999; **44**: 534-541
- 27 **Bissell DM**. Hepatic fibrosis as wound repair: a progress report. *J Gastroenterol* 1998; **33**: 295-302
- 28 **Li C**, Wan M, Zeng M, Su B, He Q, Lu L, Mao Y. A preliminary study of the combination of noninvasive parameters in the diagnosis of liver fibrosis. *Zhonghua Ganzangbing Zazhi* 2001; **9**: 261-263
- 29 **Cai WM**, Chen Z, Chen F, Zhou C, Liu RH, Wang JX. Changes of ultrasonography and two serum biochemical indices for hepatic fibrosis in schistosomiasis japonica patients one year after praziquantel treatment. *Clin Med J(Engl)* 1997; **110**: 797-800
- 30 **Iredale JP**, Benyon RC, Pickering J, McCullen M, Northrop M, Pawley S, Hovell C, Arthur MJP. Mechanisms of spontaneous resolution of rat liver fibrosis. *J Clin Invest* 1998; **102**: 538-549
- 31 **Pares A**, Deulofeu R, Gimenez A, Caballeria L, Bruguera M, Caballeria J, Ballesta AM, Rodes J. Serum hyaluronate reflects hepatic fibrogenesis in alcoholic liver disease and is useful as a marker of fibrosis. *Hepatology* 1996; **24**: 1399-1403
- 32 **Li Y**, Yao ZM, Yu T. Influence of BOL on hyaluronic acid, laminin and hyperplasia in hepatofibrotic rats. *World J Gastroenterol* 2001; **7**: 872-875
- 33 **Cui DL**, Yao XX. Serum diagnosis of hepatic fibrosis. *Shijie Huaren Xiaohua Zazhi* 2000; **8**: 683-684
- 34 **Cai WM**, Sun YL, Zhang LH, Liu RH, Wang GY, Yu YX, Yang HQ, Zhu LZ. Primary discussion on serum fibrosis index diagnosis spectrum: analysis on the results of 11 serum indices from 612 cases with chronic hepatitis. *Zhongxiyi Jiehe Ganbing Zazhi* 1995; **5**: 3-6
- 35 **Xu YQ**, Wang BE, Cao HG. An ultrasound scoring system for the diagnosis of liver fibrosis and cirrhosis. *Chin Med J (Engl)* 1999; **112**: 1125-1128
- 36 **Walsh KM**, Fletcher A, MacSween RN, Morris AJ. Basement membrane peptides as markers of liver disease in chronic hepatitis C. *J Hepatol* 2000; **32**: 325-330
- 37 **Cai WM**, Zheng M, Weng HL, Liu RH. Determination and significance of serum markers for fibrosis in patients with chronic hepatitis. *Zhonghua Neike Zazhi* 2001; **40**: 448-451
- 38 **Gu SW**, Zhang H, Zhang L, Luo KX, Yang SC, Wu EH, Peng TT. Relationship between serum fibrosis markers and fibrosis quantitative analysis of liver tissue *Zhonghua Ganzangbing Zazhi* 1999; **7**: 199-200
- 39 **Tang ZM**, Ru QJ, Zhang ZE, Zhu QG, Wang PX. Clinical study on relationship between liver-blood stasis and liver fibrosis. *Zhongguo Zhongxiyi Jiehe Zazhi* 1997; **17**: 81-83
- 40 **Zheng M**, Cai WM, Weng HL, Liu RH. Determination and significance of serum PCIII and PIIINP in patients with chronic hepatitis. *Linchuang Gandanbing Zazhi* 2002; **18**: 89-91
- 41 **Weng HL**, Cai WM, Liu RH. Animal experiment and clinical study of effect of gamma-interferon on hepatic fibrosis. *World J Gastroenterol* 2001; **7**: 42-48
- 42 **Oberti F**, Valsesia E, Pilette C, Rousselet MC, Bedossa P, Aube C, Gallois Y, Rifflet H, Maiga MY, Penneau Fontbonne D, Cales P. Noninvasive diagnosis of hepatic fibrosis or cirrhosis. *Gastroenterol* 1997; **113**: 1609-1616
- 43 **Zhang FK**, Wang BE, Wang TL, Jia JD, Dong Z, Zhang J. Three-dimensional reconstruction of experimental fibrotic liver tissue and effect of herbal compound on it. *Zhonghua Ganzangbing Zazhi* 2000; **8**: 355-357
- 44 **Xie SB**, Yao JL, Zheng SS, Yao CL, Zheng RQ. The relationship between the levels of serum fibrosis marks and morphometric quantitative measurement of hepatic histological fibrosis. *Zhonghua Ganzangbing Zazhi* 2000; **8**: 203-205
- 45 **Pilette C**, Rousselet MC, Bedossa P, Chappard D, Oberti F, Rifflet H, Maiga MY, Gallois Y, Cales P. Histopathological evaluation of liver fibrosis: quantitative image analysis vs semi-quantitative scores. Comparison with serum markers. *J Hepatol* 1998; **28**: 439-446

Edited by Pang LH

• VIRAL HEPATITIS •

Detection of soluble TRAIL in HBV infected patients and its clinical implications

Li-Hui Han, Wen-Sheng Sun, Chun-Hong Ma, Li-Ning Zhang, Su-Xia Liu, Qiu Zhang, Li-Fen Gao, You-Hai Chen

Li-Hui Han, Wen-Sheng Sun, Chun-Hong Ma, Li-Ning Zhang, Su-Xia Liu, Qiu Zhang, Li-Fen Gao, Institute of Immunology, Medical College of Shandong University, Jinan 250012, Shandong Province, China

You-Hai Chen, Institute for Human Gene Therapy, University of Pennsylvania, Philadelphia PA19104, USA

Supported by the National Natural Science Foundation Community, No.30128023

Correspondence to: Prof Wen-Sheng Sun, Institute of Immunology, Medical College of Shandong University, Jinan 250012, Shandong Province, China. wsu@sdu.edu.cn

Telephone: +86-531-8382038 **Fax:** +86-0531-8382588

Received 2002-04-18 **Accepted** 2002-06-12

Abstract

AIM: To detect the expression of soluble TRAIL (TNF-related apoptosis inducing ligand, TRAIL) in the peripheral blood of HBV infected patients and try to elucidate whether the expression level of sTRAIL have any correlativity with the clinical staging, the expression level of HBV markers and the degree of liver damage.

METHODS: 52 cases of HBV infected patients were investigated, including 8 HBV carriers, 30 chronic hepatitis B, 11 cirrhotics and 3 HBV infection related hepatocellular carcinoma. Expression of soluble TRAIL and markers of the hepatitis B were measured by enzyme-linked immunosorbent assay.

RESULTS: The expression level of sTRAIL in the peripheral blood of the HBV infected patients was significantly higher than that of healthy controls (1378.35 ± 540.23 pg/ml vs 613.75 ± 175.80 pg/ml, $P < 0.001$). In the group of chronic hepatitis, the expression level of sTRAIL was coincident with the status of the disease and was significantly correlated with the level of ALT. In the group of cirrhosis and liver cancer, its expression level was significantly higher than that of the healthy persons and HBV carriers, but lower than that of the hepatitis B patients; meanwhile, the expression of sTRAIL did not have any correlativity with the functional indexes of the liver.

CONCLUSION: The soluble TRAIL in the HBV infected people may participate in the liver damage. Our results indicated that the expression level of soluble TRAIL may reflect the ravage of liver caused by host immune reaction to a certain degree.

Han LH, Sun WS, Ma CH, Zhang LN, Liu SX, Zhang Q, Gao LF, Chen YH. Detection of soluble TRAIL in HBV infected patients and its clinical implications. *World J Gastroenterol* 2002; 8(6): 1077-1080

INTRODUCTION

TRAIL (TNF-Related Apoptosis Inducing Ligand), a new member of the TNF superfamily that could induce apoptosis,

was first cloned and identified by Wiley in 1995^[1]. TRAIL can potentially interact with five different receptors. These receptors include death receptor 4, death receptor 5, decoy receptor 1, decoy receptor 2^[2-8], and a soluble receptor called osteoprotegerin^[9]. TRAIL can induce rapid and effective apoptosis of tumor cells while spare normal tissue cells successfully, which makes it a novel molecule that has the potential for treatment of malignant tumors. *In vivo* investigation of rTRAIL revealed that TRAIL could selectively kill tumor cells, but not normal cells, leaving the host organ systems unharmed^[10,11]. However, since TRAIL is also an effective molecule participating in the immune surveillance, it is not known whether it takes part in the pathogenesis caused by hepatitis B virus and what role it may play in the HBV infection related inflammation. The expression level of soluble TRAIL in the peripheral blood of the HBV infected patients was detected and analyzed in our experiments. We tried to find out whether there is any relationship between the expression of soluble TRAIL and liver damage caused by hepatitis B virus.

MATERIALS AND METHODS

Cases and specimens

52 HBV infected patients with an average age of 41.9 years from Jinan Infectious Hospital and Shandong University Qilu Hospital were investigated, including 8 HBV carrier, 30 chronic hepatitis B patients, 11 cirrhotics and 3 HBV-related liver cancer. The diagnosis of hepatitis and cirrhosis were in accordance with the criteria emended in the Third National Conference of Infectious and parasitic held in Beijing 1995. 24 healthy blood donors with an average age of 31.4 years were taken as controls.

Major reagents

Soluble TRAIL ELISA detection kit was the product of Diaclone company in France with the detection range from 64 pg/ml to 3000 pg/ml. The HBsAg and HBeAg detection kits were the products of Lizhu Group.

Detection of soluble TRAIL in the peripheral blood

The standard specimen was diluted to 3000, 1500, 750, 375, 187.5, 93.5 pg/ml in turn. Specimens, diluted standards and the negative control were put into the 96 wells plate coated with the antibody of TRAIL. The specimens were detected according to the procedures described in the protocol. A_{450} value was utilized to draw the standard curve and the expression level of sTRAIL was obtained from the curve.

Detection of Hepatitis B viral particles

Specimens, negative control and positive control were put into the ELISA kit coated with antibodies to HBsAg and HBeAg, respectively. The type B hepatitis markers were obtained from the ratio of A_{450} value of specimens to A_{450} value of negative control (S/N value).

Evaluation of liver function

The indexes that could reflect the function of the liver including alanine transaminase (ALT), albumin (ALB) and total bilirubin (Tbil) were assayed by the automatic biochemical analyzer equipment according to its protocol.

Statistical analysis

The results were expressed as means \pm SD, and statistical analysis was performed with the analysis of variance (ANOVA). A value of $P < 0.05$ was considered statistically significant.

RESULTS

Comparison of the expression level of sTRAIL in the chronic hepatitis patients and that of the healthy control

The expression level of sTRAIL was much higher in the HBV infected group than that of the healthy controls (1378.35 ± 540.23 pg/ml vs 613.75 ± 175.80 pg/ml, $P < 0.001$).

Study on the correlation between the expression of sTRAIL and the clinical staging of hepatitis B patients

There was significant difference in sTRAIL expression among the groups of hepatitis patients divided by the stage and severity of the illness. The expression level of sTRAIL became higher gradually with the change of severity of the ailment in the group of chronic hepatitis patients. In the group of liver cirrhosis and liver cancer, the expression level of sTRAIL was significantly higher than that of the healthy controls and the HBV carriers, but lower than that of chronic hepatitis patients group. The statistical analysis of the expression level of sTRAIL and the status of the HBV infected patients was referred to Table 1.

Table 1 Statistical analysis of the relevance of expression of sTRAIL and clinical staging of hepatitis B

	<i>n</i>	sTRAIL ($\times 10^{-9}$ μ g/ml)
HBV carriers	8	876.88 \pm 369.59
Chronic hepatitis	30	1494.97 \pm 533.24
Mild chronic hepatitis	9	1138.90 \pm 424.90
Moderate chronic hepatitis	12	1558.65 \pm 489.87 ^a
Severe chronic hepatitis	9	1812.78 \pm 499.99 ^b
HBV infectious related cirrhosis	11	1375.00 \pm 526.08 ^c
HBV related infectious liver cancer	3	1561.00 \pm 449.56 ^d

^a $P < 0.01$ vs mild chronic hepatitis group; ^b $P < 0.001$ vs mild chronic hepatitis group; ^c $P < 0.05$ vs severe chronic hepatitis group; ^d $P < 0.05$ vs severe chronic hepatitis group

Study on the relationship between the expression of sTRAIL and clinical indices of the hepatitis B patients

In all the HBV infected patients, the expression level of sTRAIL was positively correlated with the ALT ($r = 0.425$, $P < 0.01$). But not with the level of Albumin and Tbil. Further study indicated that in hepatitis patients, the expression level of sTRAIL was positively correlated with the value of ALT and AIB, but not between sTRAIL and any of the clinical indices in the group of HBV carrier and cirrhosis. In the HBV infection related liver cancer group, it could not be analyzed because the number was too small. The related results referred to Table 2.

Table 2 Analysis of correlation between the expression of sTRAIL and clinical indices of hepatitis B

	sTRAIL	clinical indices	Correlativity coefficient
HBV carrier	876.88 \pm 369.59	ALT 28.38 \pm 5.09 Tbil 17.73 \pm 3.34 ALB 39.5 \pm 1.20	
Chronic hepatitis	1494.97 \pm 533.24	ALT 173.61 \pm 135.32 Tbil 66.79 \pm 61.73 ALB 32.95 \pm 5.86	$r = 0.496$ ($P < 0.01$) $r = -0.392$ ($P < 0.05$)
HBV infectious related cirrhosis	1375.00 \pm 526.08	ALT 150.36 \pm 132.72 Tbil 82.83 \pm 118.00 ALB 34.01 \pm 5.79	
HBV infectious related liver cancer	1561 \pm 449.56	ALT 85.67 \pm 48.76 Tbil 58.81 \pm 24.43 ALB 36.63 \pm 10.07	

Relationship between sTRAIL and the expression level of HBV markers

Our results indicated that the expression level of sTRAIL was positively correlated with the level of HBeAg ($r = 0.3$, $P < 0.05$), but it not with the level of HBsAg. The statistical analysis please referred to Table 3 and Table 4.

Table 3 Analysis of correlation between the expression of HBsAg and that of sTRAIL

Group divided by S/N	<i>n</i>	Expression of HBsAg(S/N)	Expression of sTRAIL in peripheral blood ($\times 10^{-9}$ μ g/ml)
<2.1(-)	2	0.5 \pm 0.7	1852.50 \pm 123.74
>2.1 and <10(+)	0		
>10 and <30(++)	0		
>30 and <50(+++)	4	43.25 \pm 3.78	1693.75 \pm 547.76
>50(++++)	46	61.48 \pm 5.19	1330.30 \pm 537.80

Table 4 Analysis of the correlation between Expression of HBeAg and that of sTRAIL

Group divided by S/N	cases	The expression of HBeAg(S/N)	Expression of sTRAIL in peripheral blood ($\times 10^{-9}$ μ g/ml)
<2.1(-)	14	0.86 \pm 0.51	1166.81 \pm 448.84
>2.1 and <10(+)	9	5.47 \pm 2.88	1088.33 \pm 528.27 ^a
>10 and <30(++)	19	20.79 \pm 5.39	1590.26 \pm 474.81 ^{ab}
>30 and <50(+++)	4	36.06 \pm 4.82	1655.00 \pm 534.48 ^a
>50(++++)	6	54.69 \pm 4.49	1730.83 \pm 652.64 ^{bc}

^a $P < 0.05$ vs the negative group; ^b $P < 0.01$ vs the negative group; ^c $P < 0.05$ vs the mildly positive group(+)

DISCUSSION

It was believed in the past that the HBV related liver damage was caused by hepatocytic necrosis. With the development of investigation methods, more and more researchers realized that

the hepatic dysfunction was caused by apoptosis rather than necrosis^[1,12,13]. Many apoptosis inducing molecules have been found to participate in the progress. FasL was the first apoptosis inducing ligand found to play a role in apoptosis elicited by HBV. With the cloning and definition of TRAIL, it was found that many apoptosis reactions caused by combination of FasL were indeed induced by FasL and TRAIL, furthermore, TRAIL played a key role in many reactions^[12-14].

FasL was proven to participate in the pathogenesis of HBV infection related disease^[15-17], but it had not been elucidated whether TRAIL also played a role in the HBV infection related illness. Our results indicated that the expression level of soluble TRAIL in the circulating blood of the HBV infected patients was significantly higher than that of the healthy controls. In the patients whose livers were severely damaged, the expression level of sTRAIL was even higher, which suggested that sTRAIL might be activated by the HBV infection and played a role in the immune reaction elicited by HBV leading to liver damage.

It was reported that soluble TRAIL could induce massive and rapid apoptosis of the tumor cells at pmol concentration but spared the normal tissue cells. Soluble TRAIL may exert its function by binding with the death receptors in the liver cells after secreting into the circulating blood. TRAIL may act as an effective immune molecule after HBV infection, its mechanism may be explained in two ways. On the one hand, the HBV infected cells may be eliminated by the apoptosis inducing effect of sTRAIL; on the other hand, when the apoptosis reaction induced by sTRAIL is excessive, it may cause massive destruction of the liver tissue and lead to persistence of HBV infection related inflammation.

Our results indicated that sTRAIL was greatly upregulated in chronic hepatitis and was positively correlated with the liver damage. However, in cirrhotic and carcinoma patients, the level of sTRAIL fell somewhat. This indicated that the body immune surveillance would be activated after HBV infection, thereafter TRAIL and many other immune molecules could eliminate the virus from the body. On the other hand, HBV itself still replicates and become persistent in the body. The liver damage is caused mainly by the associated immunologic reaction rather than by the virus itself. It indicated that the immune reactions elicited by HBV would determine the outcome of the infection to a certain degree. Since TRAIL was an immune surveillant molecule widely expressed throughout the body, which probably participated in the HBV infection related immune reaction. Our results indicated that in case of chronic infection, liver damage was positively correlated with the expression of sTRAIL which suggested that sTRAIL may participate in the immune destruction elicited by HBV. This is the first report in the world concerning the role of the sTRAIL plays in HBV infection and only FasL was reported to have some effect on the HBV infection in the past^[15-19].

To further analyze the mechanism of the upregulation of sTRAIL, secretion of HBsAg and HBeAg were detected. It showed that the expression of sTRAIL had no correlation with the secretion of HBsAg, but was positively correlated with the secretion of HBeAg. This suggested that HBeAg may play an even more important role in the activation of TRAIL than HBsAg. HBeAg is a secreted nonparticulate version of hepatitis B core Ag (HBcAg), and its function is not completely known. It was reported that HBeAg may have an immunoregulatory function in promoting viral persistence^[20-22]. Since HBeAg was reported to induce T-cell tolerance to HBV infected cells^[21], we propose that the upregulation of sTRAIL correlated to the secretion of HBeAg maybe some immune regulation elicited to rectify the virus evasion caused by HBeAg.

HBV carrier also had an upregulated expression of sTRAIL compared with the healthy control, which indicated that the immune system of these HBV carrier was also activated though they had not yet shown any symptoms of the disease. If this activation did not break the balance between HBV replication and the immune destruction, the hepatitis virus would persist in the body for a long time. However, it also indicated that the HBV carrier already had slight or undetectable immune destruction before the appearance of clinical symptoms, they were at risk of developing into the chronic hepatitis. Once the balance between the viral replication and immune destruction being broken, hepatitis symptoms would appear.

It is the first report that HBV infection may activate the expression of sTRAIL and the HBV infected hepatocytes can be killed by the upregulated expression of sTRAIL. The inappropriate upregulation of sTRAIL can lead to the liver damage and the spreading of the virus. Our results indicated that the expression of sTRAIL could reflect the liver damage to a certain degree which may help estimate the status and prognosis of the disease.

REFERENCES

- 1 **Wiley SR**, Schooley K, Smolak PJ, Din WS, Huang CP, Nicholl JK, Sutherland GR, Smith TD, Rauch C, Smith CA. Identification and characterization of new member of the TNF family that induces apoptosis. *Immunity* 1995; **3**: 673-682
- 2 **Pan G**, Ni J, Wei YF, Gentz R, Dixit VM. An antagonist decoy receptor and a death domain-containing receptor for TRAIL. *Science* 1997; **277**: 815-818
- 3 **Pan GJ**, Ni G, Yu YF, Yu G, Gentz R, Dixit VM. TRUND, a new member of the TRAIL receptor family that antagonizes TRAIL signalling. *FEBS Lett* 1998; **424**: 41-45
- 4 **Schneider P**, Bodmer JL, Thome M, Hoffmann K, Holler N, Tschopp J. Characterization of two receptors for TRAIL. *FEBS Lett* 1997; **416**: 329-334
- 5 **Sheikh MS**, Burns TF, Huang Y, Wu GS, Amundson S, Brooks KS, Fornace AJ Jr, el-Deriy WS. p53-dependent and -independent regulation of the death receptor KILLER/DR5 gene expression in response to genotoxic stress and tumor necrosis factor α . *Cancer Res* 1998; **58**: 1593-1598
- 6 **Sheridan JP**, Marsters SA, Pitti RM, Gurney A, Schubatch M, Baldwin D, Ramakrishnan L, Gray CL, Baker K, Wood WI, Goddard AD, Godowski P, Ashkenazi K. Control of TRAIL-induced apoptosis by a family of signaling and decoy receptors. *Science* 1997; **277**: 818-821
- 7 **Walczak H**, Degli-Esposti MA, Johnson RS, Smolak PJ, Waugh JY, Boiani N, Timour MS, Gerhart MJ, Schooler KA, Smith CA, Goodwin RJ, Rauch CT. TRAIL-R2: a novel apoptosis-mediating receptor for TRAIL. *EMBO J* 1997; **16**: 5386-5397
- 8 **Screaton GR**, Mongkolsapaya J, Xu XN, Cowper AE, McMichael AJ, Bell JI. TRICK2, a new alternatively spliced receptor that transduces the cytotoxic signal from TRAIL. *Curr Biol* 1997; **7**: 693-696
- 9 **Dul E**, Averbaut ER, Eichman C, DiPrinzio R, Dodds RA, James RE, Rosenberg M, Lee JC, Young PR. Osteoprotegerin is a receptor for the cytotoxic ligand TRAIL. *J Biol Chem* 1998; **273**: 14363-14367
- 10 **Walczak H**, Miller RE, Ariail K, Gliniak B, Griffith TS, Kubin M, Chin W, Jones J, Woodward A, Le T, Smith C, Smolak P, Goodwin RG, Rauch CT, Schuh JC, Lynch DH. Tumoricidal activity of tumor necrosis factor-related apoptosis-inducing ligand *in vivo*. *Nat Med* 1999; **5**: 157-163
- 11 **Ashkenazi A**, Pai RC, Fong S, Leung S, Lawrence DA, Marsters SA, Blackie C, Chang L, McMurtrey AE, Hebert A, DeForge L, Koumenis IL, Lewis D, Harris L, Bussiere J, Koeppen H, Shahrokhi Z, Schwall RH. Safety and antitumor activity of recombinant soluble Apo2 ligand. *J Clin Invest* 1999; **104**: 155-162
- 12 **Velthuis JH**, Rouschop KM, De Bont HJ, Mulder GJ, Nagelkerke JF. Distinct Intracellular Signaling in Tumor Necrosis Factor-re-

- lated Apoptosis-inducing Ligand- and CD95 Ligand-mediated Apoptosis. *J Biol Chem* 2002; **277**: 24631-24637
- 13 **Knight MJ**, Riffkin CD, Muscat AM, Ashley DM, Hawkins CJ. Analysis of FasL and TRAIL induced apoptosis pathways in glioma cells. *Oncogene* 2001; **20**: 5789-5798
- 14 **Raftery MJ**, Schwab M, Eibert SM, Samstag Y, Walczak H, Schonrich G. Targeting the function of mature dendritic cells by human cytomegalovirus: a multilayered viral defense strategy. *Immunity* 2001; **15**: 997-1009
- 15 **Siegmund D**, Mauri D, Peters N, Juo P, Thome M, Reichwein M, Blenis J, Scheurich P, Tschopp J, Wajant H. Fas-associated death domain protein (FADD) and caspase-8 mediate up-regulation of *c-Fos* by Fas ligand and tumor necrosis factor-related apoptosis-inducing ligand (TRAIL) via a FLICE inhibitory protein (FLIP)-regulated pathway. *J Biol Chem* 2001; **276**: 32585-32590
- 16 **Ehrmann Jr**, Galuszkova D, Ehrmann J, Krc I, Jezdinska V, Vojtesek B, Murray PG, Kolao Z. Apoptosis-related proteins, BCL-2, BAX, FAS, FAS-L and PCNA in liver biopsies of patients with chronic hepatitis B virus infection. *Pathol Oncol Res* 2000; **6**: 130-135
- 17 **Hayashi N**, Mita E. Involvement of Fas system-mediated apoptosis in pathogenesis of viral hepatitis. *J Viral Hepat* 1999; **6**: 357-365
- 18 **Hayashi N**, Mita E. Fas system and apoptosis in viral hepatitis. *J Gastroenterol Hepatol* 1997; **12**: S223-226
- 19 **Mochizuki K**, Hayashi N, Hiramatsu N, Katayama K, Kawanishi Y, Kasahara A, Fusamoto H, Kamada T. Fas antigen expression in liver tissues of patients with chronic hepatitis B. *J Hepatol* 1996; **24**: 1-7
- 20 **Milich DR**, Jones J, Hughes J, Maruyama T. Role of T cell tolerance in the persistence of hepatitis B virus infection. *J Immunother* 1993; **14**: 226-233
- 21 **Milich DR**, Jones JE, Hughes JL, Price J, Raney AK, McLachlan A. Is a function of the secreted hepatitis B e antigen to induce immunologic tolerance in utero? *Proc Natl Acad Sci U S A* 1990; **87**: 6599-6603
- 22 **Thomas HC**, Jacyna M, Waters J, Main J. Virus-host interaction in chronic hepatitis B virus infection. *Semin Liver Dis* 1988; **8**: 342-349

Edited by Wu XN

• VIRAL HEPATITIS •

Prevalence of hepatitis G virus infection and homology of different viral strains in Southern China

Gang Li, Hui-Hui Ma, Geroge KK Lau, Yin-Kit Leung, Chun-Lan Yao, Yu-Tian Chong, Wen-Hui Tang, Ji-Lu Yao

Gang Li, Hui-Hui Ma, Chun-Lan Yao, Yu-Tian Chong, Ji-Lu Yao, Department of Infectious Diseases, the Third Affiliated Hospital, Zhongshan University, Guangzhou 510630, Guangdong Province, China

Geroge KK Lau, Division of Gastroenterology and Hepatology, University Department of Medicine, Queen Mary Hospital, Hong Kong Special Administrative Region, China

Yin-Kit Leung, Viral Hepatitis Research Center of Guangdong-Hong Kong, Hong Kong Division, Hong Kong Special Administrative Region, China

Wen-Hui Tang, Department of Infectious Diseases, the First Affiliated Hospital, Kunming Medical College, Yunnan Province, China

Supported by the National Natural Science Foundation of China, NO. 39600130 and the grant from the Department of Health of Guangdong Province.

Correspondence to: Dr. Gang Li, Department of Infectious Diseases, the Third Affiliated Hospital, Zhongshan University, Gangding, Shipai, Guangzhou 510630, Guangdong Province, China. ligangzh@pub.guangzhou.gd.cn

Telephone: +86-20-85516867-2019 **Fax:** +86-20-87544614

Received 2002-04-10 **Accepted** 2002-05-18

Abstract

AIM: To investigate the prevalence of hepatitis G virus (HGV) infection and to analyse the homology of different HGV strains in Southern China.

METHODS: A total of 1993 sera from different groups in Guangdong, Hong Kong, and Yunnan were detected by reverse transcription polymerase chain reaction (RT-PCR). The nucleotide sequences of 5' untranslated region (5' UTR) derived from 20 strains and NS5 region from 3 strains were determined.

RESULTS: The positive rate of HGV RNA was 0.89 % in community population, 2.57 % in blood donors, 17.86 % in intravenous drug abusers, 14.13 % in patients with hemodialysis, 13.66 % in those with hepatocellular carcinoma, 25.30 % in non A-E hepatitis, 7.22 % in hepatitis B, 12.73 % in hepatitis C, 41.67 % in patients received bone marrow transplantation, respectively. The homology was 90.40-100 % in 5' UTR among different strains, while that of NS5 region was 93.3-94 % in nucleotide sequence, and 97-99.2 % in amino acid sequence.

CONCLUSION: These results showed that there was a high incidence of HGV infection in patients from Southern China, being treated for bone marrow transplantation, hepatocellular carcinoma and those on haemodialysis. Furthermore, there was also a high frequency of co-infection of HGV with HBV, HCV, non A-E viral hepatitis and that among intravenous drug abusers. The study also showed that sequence variation in different strains was associated with geographical factors but there was no significant difference in 5' UTR in circulating viruses between different patient groups. Finally, by

sequential analysis of viral species present in individual patients over a three months period there was no evidence of sequence variation in the 5' UTR.

Li G, Ma HH, Lau GKK, Leung YK, Yao CL, Chong YT, Tang WH, Yao JL. Prevalence of hepatitis G virus infection and homology of different viral strains in Southern China. *World J Gastroenterol* 2002; 8(6):1081-1087

INTRODUCTION

Recently, a novel RNA virus of the Flaviviridae family has been identified by two groups of researchers working independently and designated as GBV-C or HGV^[1,2]. These viruses are now considered to be different isolates of the same virus. The predominant route of transmission of HGV appears to be parenteral by contaminated blood and blood products although other routes, such as vertical transmission or through saliva may also exist^[3-14]. HGV contains a positive-sense, single stranded RNA genome approximately 9.4kb in length that encodes a single long open reading frame (ORF) coding for two putative envelope proteins (E1 and E2), and several nonstructural proteins (NS1-NS5) (Figure 1). The coding region is flanked by a long 5' -untranslated region (5' UTR) and 3' -untranslated region (3' UTR). The putative core protein which has been described in related viruses such as HCV appears to be truncated or even absent in different isolates of HGV^[15]. 1-3 % of healthy blood donors are infected with HGV in the USA and in Europe and HGV infection was found to be common in subjects with various forms of chronic liver disease^[16,17]. It has been reported that HGV can be associated with either acute or persistent infection^[18,19]. Some studies suggested the possibility of a link between fulminant hepatitis and HGV infection^[20-22]. However, the clinical implications of HGV infection have not been clearly determined since the vast majority of infected individuals do not show liver injury^[23-28]. In this report, HGV prevalence in Southern China was investigated using an RT-PCR-based survey of different patient populations. Furthermore, sequence analysis of some PCR products from the 5' UTR and NS5A regions allowed homology comparisons to be carried out for epidemiological analysis.

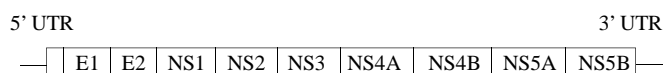


Figure 1 Structure of HGV genome

MATERIALS AND METHODS

Subjects

From 1994 to 1997, 1993 serum samples from 1991 subjects were obtained from Guangdong province, Yunnan province, and Hong Kong Special Administrative Region in Southern

China. These serum samples were stored at -70 °C. Hepatitis C virus infection was confirmed by RT-PCR and enzyme-linked immunosorbent assay (ELISA, second-generation). Commercially available ELISAs were used for immunoglobulin M (IgM) antibodies to hepatitis A virus, for hepatitis B surface antigen (HBsAg) and antibodies to hepatitis B core antigen (HBcAb), hepatitis D virus and hepatitis E virus. Patients with hepatocellular carcinoma were histologically confirmed.

In 2 patients serial serum samples were collected 3 months after the first sample. In addition, 22 different samples derived from 20 subjects were analysed by nucleotide sequencing of either PCR fragments from the 5' UTR (19 patients), the NS5A region (2 patients) or both (1 patient) (Table 1).

Table 1 Samples for sequencing

Sample	Sex	Age (yrs)	Origin	Diagnosis	Regions for sequencing
GD1	F	58	Guangdong	non A-E hepatitis	5' UTR
GD3027	M	47	Guangdong	hepatitis B	5' UTR, NS5A
GD3040	M	76	Guangdong	hepatitis B	5' UTR
GD3064	F	20	Guangdong	non A-E hepatitis	5' UTR
GDCA	M	26	Guangdong	hepatocellular carcinoma	5' UTR
YN1	M	26	Yunnan	intravenous drug user	5' UTR
YN2	M	38	Yunnan	intravenous drug user	5' UTR
YN3	M	45	Yunnan	intravenous drug user	5' UTR
HKC9	F	42	Hong Kong	hepatitis C	5' UTR
HKC16	M	38	Hong Kong	hepatitis C	5' UTR
HK8	M	56	Hong Kong	recipient of bone marrow	5' UTR
HK9	M	42	Hong Kong	recipient of bone marrow	5' UTR
HK10	M	38	Hong Kong	recipient of bone marrow	5' UTR
HK11	M	42	Hong Kong	recipient of bone marrow	5' UTR
HK12	M	42	Hong Kong	recipient of bone marrow	5' UTR
HK24	F	42	Hong Kong	recipient of bone marrow	5' UTR
HK80	M	40	Hong Kong	recipient of bone marrow	5' UTR
HK108	M	18	Hong Kong	recipient of bone marrow	5' UTR
HK116	M	42	Hong Kong	recipient of bone marrow	5' UTR
HK120	M	40	Hong Kong	recipient of bone marrow	5' UTR
A132	M	20	Hong Kong	blood donor	NS5A
A711	M	25	Hong Kong	blood donor	NS5A

HK9 and HK12 were derived from the same patient after a 3-month interval; HK11 and HK116 were also from a patient after a 3-month interval

Detection of HGV RNA by reverse transcriptase-polymerase chain reaction

RNA was extracted from 100 µl of serum using a modification of the enzyme digestion and heat-denaturation method. The serum was added to 10 µl enzyme digestive mixture (Tris 10mM pH 7.8, EDTA 5mM, proteinase K 300 µg/ml) at 55 °C for 30 min and then 98 °C for 15 min. After centrifugation, 5 µl of supernatant were used for the synthesis of cDNA. The synthesis was performed at 42 °C for 45 min with 2.5U AMV reverse transcriptase (Promega) in a 10 µl reaction mixture

containing 1 × buffer, 0.25mM dNTPs, 8U RNasin (Promega) and 100 ng specific antisense external primer (G2 or 36) (Table 2).

PCR amplification was performed using primers specific for 5' UTR and NS5A region (Table 2). The first-round PCR amplification of the cDNA was carried out in 20 µl of reaction mixture containing 5 µl of cDNA product, 1 × PCR buffer (Promega), 1.5mM MgCl₂, 100pmoles of each sense and antisense external primers (G1 and G2, or 35 and 36), 20 µM each dNTP and 2U Taq DNA polymerase (Promega). PCR was performed for 30 cycles with the following reaction cycle: 94 °C for 40 secs, 55 °C for 40secs, 72 °C for 60secs (2 min for NS5A amplification). 5 µl of the first PCR product were subjected to a second amplification for 35 cycles under the same condition as for the first PCR, using sense and antisense inner primers (G3 and G4, or 33 and 34). The amplified products were visualized by 2 % agarose gel electrophoresis and ethidium bromide staining.

Table 2 Primers used in RT-PCR

Primer	Polarity	Position	Nucleotide sequence
G1	+	117-136	5' ATGCGTGATGACAGGGTTGG 3'
G2	-	451-471	5' TAGGTGGCCCCATGCATTTC 3'
G3	+	161-180	5' GGTAGCCACTATAGGTGGGT 3'
G4	-	379-398	5' CACTGGTCCTGTCAACTCG 3'
33	+	6672-6697	5' GTTGAATTCGCGATGGAGCGCTACAC 3'
34	-	7267-7292	5' CTGGGATCCGTATCATGTATGGTTCT 3'
35	+	6573-6592	5' TCGATTGCTGTAGCTGAGCC 3'
36	-	7327-7346	5' GGTAAGTTCATTGCCACCA 3'

The numbering is identical to that of the PNF2161 strain of HGV^[1].

Cloning of HGV NS5A PCR fragments

The PCR products of HGV NS5A were purified by phenol-chloroform extraction, precipitated by ethanol, dissolved in water and digested with EcoRI and BamHI (Boehringer Mannheim). The fragments were recovered from low melting point agarose gels and cloned into vector pUC19. Resulting recombinants were identified by enzyme-digestion and the same NS5A-specific second PCR procedure as that described above.

Sequence determination and homology analysis

The 238-base pair amplification products of HGV 5' UTR were directly sequenced by HGV 5' UTR-specific inner primers (G3 and G4), while the NS5A clones were sequenced using pUC19-specific primers hybridizing to sequences flanking the cloned fragment. The sequencing was performed using a double-strand DNA cycle sequencing system by the dye termination method in a ABI 310 automated DNA sequencer (Applied Biosystems Inc.). Nucleotides obtained and putative amino acid sequences were then compared with each other and with the published HGV prototype sequences by program DNASIS, program PROSIS and program Lasergene.

RESULTS

Prevalence of HGV in Southern China

Statistical analyses were performed using Fisher's exact tests and a significance level was set at $P=0.05$. The prevalence of

HGV infection from different groups in Southern China was shown in Table 3.

The infectious rate of HGV in general population from Southern China is 0.89 %. The following groups were highly significantly different from both the blood donors and general population group: recipient of bone marrow transplantation, haemodialysis patients, intravenous drug abusers, patients with hepatocellular carcinoma, non A-E hepatitis, hepatitis B ($P<0.0001$), and hepatitis C ($P<0.002$). Patients with bone marrow transplantation had the highest carrier rate of 41 %, which was significantly higher than the other groups ($P<0.05$). The following groups were not significantly different from the blood donors or general population group: hepatitis B+A, hepatitis B+C, hepatitis B+E, hepatitis E ($P>0.05$). There was no significant difference between the blood donor and general population groups ($P=0.054$).

Table 3 Prevalence of HGV infection from different groups in Southern China

Group	cases	HGV RNA Positive cases(%)
Bone marrow transplantation	108	45(41.67)
Haemodialysis	92	13(14.13)
Intravenous drug users	84	15(17.86)
Hepatocellular carcinoma	161	22(13.66)
Hepatitis B	263	19(7.22)
Hepatitis C	55	7(12.73)
Hepatitis B + Hepatitis A	16	1(6.25)
Hepatitis B + Hepatitis C	6	1(16.67)
Hepatitis B + Hepatitis E	26	3(11.54)
Hepatitis E	29	2(6.90)
Non A-E hepatitis	83	21(25.30)
Blood donors	506	13(2.57)
General population	562	5(0.89)
Total	1991	

Nucleotide sequence of the 5' UTR from 20 HGV isolates

An alignment of the nucleotide sequence of the 5' UTR from the 20 HGV isolates we studied being presented in Figure 2. Sequence analysis demonstrated that the 5' UTR was highly conserved and the homology varied between 90.4 % and 100 % among different isolates from Southern China. We found that the 5' UTR of HGV consisted of highly conserved domains interspersed between variable domains. The most variable domain spans 38 nucleotides (positions 187 to 222). Molecular evolutionary phylogenetic tree was constructed to clarify the relationship among different HGV strains, using Clustal method with Weighted residue weight table.

Some highly conserved regions were observed, including No.223 to No.298, No.327 to No.345, No.349 to No.372, but relative diversity regions were also observed, such as the regions from No.187 to No.222, No.299 to No.306. Some isolates had 100 % identical sequence in 5' UTR, such as GD3040, GD3064 from Guangdong and HKC16, HK9, HK12, HK108 from Hong Kong.

Geographical variability was also demonstrated: greater homology was seen in strains obtained from Southern China, the homology was from 95 % to 100 % among Guangdong

strains, 93 % to 100 % within Hong Kong strains, 94 % to 100 % between Guangdong and Hong Kong strains. While a lower level of homology compared to the strain from Northern China, which was 90 % to 94 % between Southern China and Northern China strains, with even lower homology when compared with those from other countries, which was 85 % to 92 % between Southern China and the reported prototype strains from USA and West Africa.

We also studied the HGV 5' UTR sequence in the same patients over a period of 3 months and observed no mutation, as shown in Figure 2. HK9 and HK12 were from one patient, HK11 and HK116 from another one.

Nucleotide sequence of partial NS5A region from 3 HGV isolates

Similar to 5' UTR, 621 base pair of NS5A region from 3 HGV isolates in Southern China are well conserved with the homology of 93.3-94.0 % (Figure 3). While a lower homology was seen when compared to those in USA and West Africa, which was from 87.3 % to 93.5 %. Different nucleotides were randomly distributed throughout the sequences and most mutations were silent, with the result of deduced amino acid homology of 97.9-98.9 % (Figure 4). The study also suggests that the variation may be associated with geographical factor.

DISCUSSION

We studied 1993 sera from 1991 patients with various forms of viral hepatitis, hepatocellular carcinoma, intravenous drug abusers, recipients of bone-marrow transplantation, blood donors and general population from 3 different regions in Southern China, including Guangdong, Hong Kong and Yunnan. HGV RNA was detected in as high as 41.67 % (45/108), 14.13 % (13/92), 17.86 % (15/84), 13.66 % (22/161), 12.73 % (7/55), 25.30 % (21/83) of patients with bone-marrow transplantation, hemodialysis, intravenous drug abusers, hepatocellular carcinoma, hepatitis C and non A-E hepatitis, respectively. It is noteworthy that nearly 42 % of recipients of bone-marrow transplantation were HGV RNA positive. This is understandable, because these patients have usually received many transfusions or blood products from a large number of donors. This also demonstrated the fact, that HGV was transmissible via blood transfusion^[29].

13 (2.57 %) out of 506 blood donors were positive for HGV RNA, the difference of the positive rate from the general population (0.89 %) was statistically not significant. In addition, HGV RNA was found to be 7.22 % (19/263) among patients with hepatitis B, 6.90 % (2/29) among patients with hepatitis E, 6.25 % (1/16) among patients with coinfection of hepatitis B and hepatitis A, 16.67 % (1/6) among coinfection of hepatitis B and hepatitis C, and 11.54 % (3/26) among coinfection of hepatitis B and hepatitis E. Using Fisher's exact tests to work out the exact P-values in situations where the number of positive cases was less than 5, the P-values obtained were dependent on the magnitude of the difference in prevalence of HGV infection between those groups, but also on the total number of cases in each group. Hence, although the prevalence of HGV infection was 16.7 % in hepatitis B+C group, we were not able to show it was different from either blood donors or the general population because the number was small (only 6 cases) in hepatitis B+C group. Same situations occurred in groups of hepatitis B+A, hepatitis B+E, and hepatitis E. However, the difference between hepatitis B and the general population was significant even though the prevalence of HGV infection was only 7.22 % because of large number of cases (263 cases) in hepatitis B group.

GD1	CTTAAGGGTT	GGTCAAGGTC	CCTCTAGCGC	TTGTGGCGAG	AAAGCGCACG	GTCCACAGGT	GTTGGCCCTA	250
GD3027T.G...	
GD3040G.....	
GD3064G.....	
GDCAG	...T.....	...G.....T	C.....	
YN1T	...G.....	
YN2GT	...TA...	C.....G	.C.....	
YN3G.....	
HKC9G.....	
HKC16G.....	
HK8T.....	...G.....T	
HK9G.....	
HK10G.....TT	
HK11G.....	
HK12G.....	
HK24T.....	...G.....	
HK80T.....	...G.....	
HK108G.....	
HK116	
HK120T.....	...G.....A	T.TT.....CG.....	
C964C.....A.....	...T.T...	...C.....	
PNF2161A.AA	...T...A.T	...T.T...	C...C.....	.CC.....	
R10291A.AA	...T...A.T	...T.T...	C...C.....	.CC.....	
GBV-CGA	.CT.C.....	...T.....	A.A...A.GAT.....	
GD1	CCGGTGTGAA	TAAGGGCCCCG	ACGTCAGGCT	CGTCGTTAAA	CCGAGCCCAT	TACCCACCTG	GGCAAACAGC	320
GD3027CA	
GD3040A	
GD3064A	
GDCAC	.A.....A	
YN1GA	
YN2A.....G.....GA	
YN3GA	
HKC9GA	
HKC16A	
HK8A	
HK9A	
HK10A	
HK11C	.TA.....GA	
HK12A	
HK24A	
HK80A	
HK108A	
HK116C	.TA.....GA	
HK120	A.....A	
C964G.....G	A...G.....GA	
PNF2161G.....GGA	
R10291G.....G	A...G.....GA	
GBV-CA.....	G...CT...A	.C.....G	...T.C.....GA	
GD1	GCCCACGTAC	GGTCCACGTC	GCCCTACAAT	GTCTCTCTTG	ACCAATAGGC	TTTGCCGG	378	
GD3027		
GD3040		
GD3064		
GDCAT.....		
YN1	...T.....T.....		
YN2T.....		
YN3	...T.....		
HKC9		
HKC16		
HK8T.....A.....		
HK9		
HK10		
HK11T.....		
HK12		
HK24T.....A.....		
HK80T.....AA.....		
HK108		
HK116T.....		
HK120T.....A.....		
C964T.....	...G.....A.....		
PNF2161T.....	G.A.....		
R10291T.....	...G.....A.....		
GBV-CT.....	G.A.....		

Figure 2 Alignment of 5' UTR cDNA sequences of 20 HGV isolates from Southern China. GD stands for Guangdong, YN for Yunnan, HK for Hong Kong. C964 was derived from Northern China, PNF2161 and R10291 from United States^[1], GBV-C from West Africa^[2]. Identical nucleotides are shown as dots. The numbering is according to Linnen *et al*^[1].

A132	gttgaattcgcgatggagcgctacacTCTTCGCGCCAACTGCGGATGAGGAACGTGGCG	60
A711C..C...A...GT.....T....C	
GD3027C.....A.....T.....	
C964C.....A.....T.....	
PNF2161CT.G..T..AT.....A..C.C...T....A	
R10291C..G...AT.....C.C...T...A...	
GBV-CC.....A...GT.....C...T.....	
A132	CCCTCTGAGGTTTCATCTGAGGTCAGCATCGAGATCGGGACGGAGACTGAGGATTCAGAA	120
A711	..T.....G..A.....T.....A..C.....	
GD3027A.....C.....	
C964G.....T.....A..C.....	
PNF2161C.....GTC...T..C..T.....A..C.....	
R10291C.....GTC...A..C..T.....A..C.....	
GBV-CA.....C.....	
A132	CTGACTGAGGCAGATCTGCCACCCGAGCTGCGGCCCTTCAGGCGATCGAGAATGCTGCG	180
A711T.....T.....T..C..A...A.....	
GD3027A.....C..A.....	
C964A.....	
PNF2161C.....G..G..G...T..T..C..A.....	
R10291C..C...G..G...A...C...T.....	
GBV-CC...T...A..G...T...C..A...A.....	
A132	AGAATTCTTGAGCCGCACATTGATGTCATCATGGAGGACTGCAGTACACCCTCTCTCTGT	240
A711C..A.....	
GD3027C..A...T.....A.....	
C964A.....T.....	
PNF2161	..G.....A.....T.....	
R10291	..G.....T..T.....T.....T.....	
GBV-CC..A...C.....Y.....T.....	
A132	GGGAGTAGCCGAGAGATGCCTGTGTGGGGAGAAGACGTACCCCGCACTCCATCGCCTGCA	300
A711	..T.....A.....A.....	
GD3027	..A.....A.....C.....A.....	
C964	..T.....A.....A..C.....A...	
PNF2161	..T.....A.....A..C...T.....A...	
R10291	..T.....A.....A..C.....A...	
GBV-C	..T.....A.....A.....	
A132	CTTATCTCGGTTACGGAGAGCAGCTCAGATGAGAAGACCCCGTCGGTGTCTCTTCGCAG	360
A711C.....	
GD3027C.....	
C964C.....T.....C.....	
PNF2161T.....C.....	
R10291C.....C.....	
GBV-CT.....A...C.....	
A132	GAGGATACCCCGTCTCGGACTCATTGAAGTCATCCAAGAGTCTGATACTGCTGAGAGT	420
A711A..G.....G.....	
GD3027C.....T.....G.....C..G..A..C..A..CG	
C964C.....T.....C..G.....C..G..A..C..AG..G	
PNF2161T.....C.....G.....A..A.....	
R10291T.....C.....G.....A..A.....	
GBV-CC.....A.....ATCA	
A132	GAGGAAAGCGTCTTCAACGTGGCTCTTTCCGTAATAAAGCCTTATTTCCACAAAGCGAT	480
A711T.....C.....G.....	
GD3027C.....G.....G.....	
C964G.....C.....G.....C	
PNF2161T.....T.....G.....C	
R10291T.....G.....G.....G..T...	
GBV-CG.....	
A132	GCTACGCGTAAGCTCACAGTCAAGATGTCATGCTGTGTGGAGAAGAGCGTCACGCGCTTC	540
A711	..C.....T..T.....A.....	
GD3027	..C..A.....A..G..T..G.....A.....	
C964	..G..TA..G.....T..C.....G.....C..T..A.....T	
PNF2161	..G..CA..G.....T..C.....G.....C..T..A.....T	
R10291	..C..TA..A.....T..C.....G.....AAT.....C..T.....	
GBV-C	..C..A..A.....A..G..T.....T.....T.....A..A.....	
A132	TTTTCCTTAGGGTTGACTGTAGCTGATGTGGCTAGCTTGTGTGAGATGGAAATCCagaaccatacatgatacggatccag	621
A711A..G.....TC..A.....	
GD3027C.....C..G..C..C.....A.....	
C964	..C..A..G.....G..G.....T.....C.....G.....	
PNF2161	..C..A..G.....G..G.....T.....C.....	
R10291T..G...C.....G..G.....C..TC.....G.....	
GBV-CT.....C..G.....C.....C.....G.....	

Figure 3 Comparison of NS5 cDNA sequence of HGV A132 (HongKong strain) with the corresponding sequences from GD3027 (Guangdong strain), A711 (Hong Kong strain) and the reported isolates (C964, PNF2161, R10291, GBV-C). Dots indicate identity with sequence of HGV A132.

A132	LPRQLRMRNV	APSEVSSEVS	IEIGTETEDS	ELTEADLPPA	AAALQAIENA	ARILEPHIDV	60
A711	..H.....	
GD3027	..H.....	
C964	..H.....	
PNF2161	..H...L...D.....	
R10291	..H...L...D.....	
GBV-C	..H.....	
A132	IMEDCSTPSL	CGSSREMPVW	GEDVPRTPSP	ALISVTESSS	DEKTPSVSSS	QEDTPSSDSF	120
A711I.....G..	
GD3027	
C964I.....L....L	
PNF2161I.....	
R10291I.....	
GBV-CI.....L..T..	
A132	EVIQESDTAE	SEESVFNVAL	SVLKALFPQS	DATRKLTVKM	SCCVEKSVTR	FFSLGLTVAD	180
A711	...G.....	
GD3027R.....	
C964E...TE..F...	
PNF2161E...G	
R10291E...GE.....R..N.....	
GBV-C	
A132	VASLCEME	I	189				
A711						
GD3027						
C964						
PNF2161						
R10291						
GBV-C						

Figure 4 Comparison of deduced amino acid sequence of HGV A132 NS5 with the corresponding sequences from A711, GD3027 strains and C964, PNF2161, R10291, GBV-C isolates.

In this study we determined the nucleotide sequence of the 5' UTR spanned 238 nucleotides with positions 161 to 398 from 20 HGV isolates in Southern China. The data confirmed that the 5' UTR of the HGV genome was well conserved among HGV isolates from Southern China, with homology more than 90.4 %, even 100 % identical sequence in some strains, such as GD3040, GD3064, HKC16, HK9 and HK108. Phylogenetic analysis here supported the conclusion that sequence variation in different HGV strains was associated with geographical factors because greater homology was seen between the Southern China strains, while a lower homology when compared to the strains from Northern China, even lower homology was observed in comparison with those from other countries^[30,31].

Partial sequences of NS5A gene region flanking positions 6672 to 7292 from 3 HGV strains were also determined. Nucleotide variations from each other were seen at 6.3 % to 7.1% scattered along the genome and most of them had not caused change in amino acid, which implied that this region might have a biological role.

Sequencing samples for 5' UTR were derived from different patient groups, including non A-E hepatitis, hepatitis B, hepatitis C, hepatocellular carcinoma, intravenous drug abusers, recipient of bone marrow transplantation and blood donor. However, no apparent variation in 5' UTR was found between different groups in Southern China, which suggested that the heterogeneity among different HGV isolates was not related to patient groups in the same geographical area.

HK9 and HK12 were from one patient over a period of three months, HK11 and HK116 from another patient in the same interval. The follow-up study of HGV 5' UTR sequence changes in the two patients with bone-marrow transplantation from Hong Kong suggested that the 5' UTR was not susceptible to mutations as frequently observed in other RNA viruses during a 3-month interval. However, this is only within a

relatively short period and whether it has the potential to mutate over a longer period remains to be seen.

REFERENCES

- 1 **Linnen J**, Wages Jr, Zhang-Keck ZY, Fry KE, Krawczynski KZ, Alter H, Koonin E, Gallagher M, Alter M, Hadziyannis S, Karayiannis P, Fung K, Nakatsuji Y, Shih JW, Young L, Piatak M Jr, Hoover C, Fernandez J, Chen S, Zou JC, Morris T, Hyams KC, Ismay S, Lifson JD, Kim JP. Molecular cloning and disease association of hepatitis G virus: a transfusion-transmissible agent. *Science* 1996; **271**: 505-508
- 2 **Leary TP**, Muerhoff AS, Simons JN, Pilot Matias TJ, Erker JC, Chalmers ML, Schlauder GG, Dawson GJ, Desai SM, Mushahwar IK. Sequence and genomic organization of GBV-C: a novel member of the Flaviviridae associated with human non A-E hepatitis. *J Med Virol* 1995; **48**: 60-67
- 3 **Lefrere JJ**, Roudot-Thoraval F, Morand-Joubert L, Brossard Y, Parnet-Mathieu F, Mariotti M, Agis F, Rouet G, Lerable J, Lefevre G, Girot R, Loiseau P. Prevalence of GB virus type C/hepatitis G virus RNA and of anti-E2 in individuals at high or low risk for blood-borne or sexually-transmitted viruses: evidence of sexual and parenteral transmission. *Transfusion* 1999; **39**: 83-94
- 4 **Lefrere JJ**, Sender A, Mercier B, Mariotti M, Pernot F, Soulie JC, Malvoisin A, Berry M, Gabai A, Lattes F, Galiay JC, Pawlak C, de Lachaux V, Chauveau V, Hreiche G, Larsen M, Ferec C, Parnet-Mathieu F, Roudot-Thoraval F, Brossard Y. High rate of GB virus type C/HGV transmission from mother to infant: possible implications for the prevalence of infection in blood donors. *Transfusion* 2000; **40**: 602-607
- 5 **Chen M**, Sonnerborg A, Johansson B, Sallberg M. Detection of hepatitis G virus (GB virus C) RNA in human saliva. *J Clin Microbiol* 1997; **35**: 973-975
- 6 **Seemayer CA**, Viazov S, Philipp T, Roggendorf M. Detection of GBV-C/HGV RNA in saliva and serum, but not in urine of infected patients. *Infection* 1998; **26**: 39-41
- 7 **Ohto H**, Ujiie N, Sato A, Okamoto H, Mayumi M. Mother-to-infant transmission of GB virus type C/HGV. *Transfusion* 2000; **6**: 725-730

- 8 **Fischler B**, Lara C, Chen M, Sonnerborg A, Nemeth A, Sallberg M. Genetic evidence for mother-to-infant transmission of hepatitis G virus. *J Infect Dis* 1997; **176**: 281-285
- 9 **Tian DY**, Yang DF, Xia NS, Zhang ZG, Lei HB, Huang YC. The serological prevalence and risk factor analysis of hepatitis G virus infection in Hubei Province of China. *World J Gastroenterol* 2000; **6**: 585-587
- 10 **Zhong RX**, Luo HT, Zhang RX, Li GR, Lu L. Investigation on infection of hepatitis G virus in 105 cases of drug abusers. *World J Gastroenterol* 2000; **6**(Suppl 3): 63
- 11 **Bourlet T**, Berthelot P, Grattard F, Genin C, Lucht FR, Pozzetto B. Detection of GB virus C/hepatitis G virus in semen and saliva of HIV type-1 infected men. *Clin Microbiol Infect* 2002; **8**: 352-357
- 12 **Frey SE**, Homan SM, Sokol-Anderson M, Cayco MT, Cortorreal P, Musial CE, Di Bisceglie A. Evidence for probable sexual transmission of the hepatitis G virus. *Clin Infect Dis* 2002; **34**: 1033-1038
- 13 **Clevenberg P**, Durant J, Halfon P, Tran A, Manos T, Rahelinirina V, Yang G, Benzaken S, Ouzan D, Rampal P, Dellamonica P. High prevalence of GB virus C/hepatitis G virus infection in different risk groups of HIV-infected patients. *Clin Microbiol Infect* 1998; **4**: 644-647
- 14 **Eugenia QR**, Ana QR, Carmen M. Investigation of saliva, faeces, urine or semen samples for the presence of GBV-C RNA. *Eur J Epidemiol* 2001; **17**: 271-274
- 15 **Katayama K**, Kageyama T, Fukushi S, Hoshino FB, Kurihara C, Ishiyama N, Okamura H, Oya A. Full-length GBV-C/HGV genomes from nine Japanese isolates: characterization by comparative analyses. *Arch Virol* 1998; **143**: 1063-1075
- 16 **Marrone A**, Shih JW, Nakatsuji Y, Alter HJ, Lau D, Vergalla J, Hoofnagle JH. Serum hepatitis G virus RNA in patients with chronic viral hepatitis. *Am J Gastroenterol* 1997; **92**: 1992-1996
- 17 **Zhong RX**, Luo HT, Zhang RX, Li GR, Lu L. Investigation on infection of hepatitis G virus in 105 cases of drug abusers. *World J Gastroenterol* 2000; **6**(Suppl 3): 63
- 18 **Yashina TL**, Favorov MO, Khudyakov YE, Fields HA, Znoiko OO, Shkurko TV, Bonafonte T, Sevall JS, Agopian MS, Peter JB. Detection of hepatitis G virus (HGV) RNA: clinical characteristics of acute HGV infection. *J Infect Dis* 1997; **175**: 1302-1306
- 19 **Ling BH**, Zhuang H, Cui YH, An WF, Li ZJ, Wang SP, Zhu WF. A cross-sectional study on HGV infection in a rural population. *World J Gastroenterol* 1998; **4**: 489-492
- 20 **Moaven LD**, Locarnini SA, Bowden DS, Kim JP, Breschkin A, McCaw R, Yun A, Wages Jr, Jones B, Angus P. Hepatitis G virus and fulminant hepatic failure: evidence for transfusion-related infection. *J Hepatol* 1997; **27**: 613-619
- 21 **Sheng L**, Soumillion A, Beckers N, Wu CG, Verslype C, Nevens F, Pirenne J, Aerts R, Kosala H, Fevery J, Yap SH. Hepatitis G virus infection in acute fulminant hepatitis: prevalence of HGV infection and sequence analysis of a specific viral strain. *J Viral Hepatitis* 1998; **5**: 301-306
- 22 **Anastassopoulou CG**, Delladetsima JK, Anagnostopoulos G, Katsoulidou A, Papachristopoulos A, Tassopoulos NC, Theodoridou M, Hatzakis A. Fulminant hepatic failure in a pediatric patient with active GB virus C (GBV-C)/hepatitis G virus (HGV) infection. *Hepatol Res* 2002; **23**: 85-89
- 23 **Kao J**, Chen D. GB virus-C/hepatitis G virus infection in Taiwan: a virus that fails to cause a disease? *J Biomed Sci* 1999; **6**: 220-225
- 24 **Yu JG**, Hou XR, Pan W, Zhang GS, Zhou XM. PCR detection of hepatitis G virus RNA in sera and liver tissues from patients with chronic hepatitis C. *Shijie Huaren Xiaohua Zazhi* 1998; **6**: 580
- 25 **Zhao XP**, Yang DL, Wang BJ, Yang Y, Shen HX, Peng ZH, Hao LJ. Immunohistochemical study of HGV expression in liver of patients with hepatitis G. *Shijie Huaren Xiaohua Zazhi* 1998; **6**: 586
- 26 **Xu JZ**, Yang ZG, Le MZ, Wang MR, He CL, Sui YH. A study on pathogenicity of hepatitis G virus. *World J Gastroenterol* 2001; **7**: 547-550
- 27 **Reshetnyak VI**, Sharafanova TI, Ilchenko LU, Golovanova EV, Poroshenko GG. Peripheral blood lymphocytes DNA in patients with chronic liver diseases. *World J Gastroenterol* 2001; **7**: 235-237
- 28 **Ren H**, Zhu FL, Zhu SY, Song Y, Qi ZT. Immunogenicity of HGV NS5 protein expressed from Sf9 insect cells. *World J Gastroenterol* 2001; **7**: 98-101
- 29 **Yan J**, Chen LL, Luo YH, Mao YF, He M. High frequencies of HGV and TTV infections in blood donors in Hangzhou. *World J Gastroenterol* 2001; **7**: 637-641
- 30 **Wang XT**, Zhuang H, Song HB, Li HM, Zhang HY, Yu Y. Partial sequencing of 5' non-coding region of 7 HGV strains isolated from different areas of China. *World J Gastroenterol* 1999; **5**: 432-434
- 31 **Ling B**, Zhuang H, Wang L. Analysis of hepatitis G virus genotypes in some areas of China. *Zhonghua Yufang Yixue Zazhi* 2000; **34**: 354-357

Edited by Wu XN

• VIRAL HEPATITIS •

Establishment of a simple assay *in vitro* for hepatitis C virus NS3 serine protease based on recombinant substrate and single-chain protease

Gui-Xin Du, Li-Hua Hou, Rong-Bin Guan, Yi-Gang Tong, Hai-Tao Wang

Gui-Xin Du, Li-Hua Hou, Rong-Bin Guan, Yi-Gang Tong, Hai-Tao Wang, Department of Applied Molecular Biology, Institute of Microbiology and Epidemiology, Fengtai, Beijing 100071, China
Supported by the National Natural Science Foundation of China, No.39630020.

Correspondence to: Dr. Gui-Xin Du, Department of Applied Molecular Biology, Institute of Microbiology and Epidemiology, Fengtai, Beijing 100071, China. dugx@hotmail.com

Telephone: +86-10-66948580 **Fax:** +86-10-66948563

Received 2002-07-18 **Accepted** 2002-08-09

Abstract

AIM: To establish a simple and convenient assay *in vitro* for the Hepatitis C virus NS3 serine protease based on the recombinant protease and substrate, and to evaluate its feasibility in screening the enzyme inhibitors.

METHODS: Based on the crystallographic structure of hepatitis C virus (HCV) serine protease, a novel single-chain serine protease was designed, in which the central sequence of cofactor NS4A was linked to the N-terminus of NS3 serine protease domain via a flexible linker GSGS. The fusion gene was obtained by two-step PCR that was carried out with three primers and then cloned into the prokaryotic expression vector pQE30, and the recombinant clone was verified by DNA sequencing. The single-chain recombinant protease was expressed when the *E.coli* was induced with IPTG and the expression conditions were optimized to produce large amount of soluble protease. The recombinant substrate NS5ab that covers the cleavage point NS5A/B was also expressed in *E.coli*. Both of the protease and substrate were purified by using Ni-NTA agarose metal affinity resin, then they were mixed together in a specific buffer, and the mixture was analyzed by SDS-PAGE. The cleavage system was used to evaluate some compounds for their inhibitory activity on serine protease.

RESULTS: The single-chain recombinant protease was over-expressed as soluble protein when the *E.coli* was induced at a low dosage of IPTG (0.2 mM) and cultured at a low temperature (15 °C). The protease was purified by using Ni-NTA agarose metal affinity resin (the purity is over 95 %). The recombinant substrate NS5ab was expressed in an insoluble form and could refold successfully after purification and dialysis. A simple and convenient assay *in vitro* was established, in which the purified single-chain serine protease could cleave the recombinant substrate NS5ab into two fragments that were visualized by SDS-PAGE. PMSF had an effect on inhibiting activity of serine protease, while EDTA had not.

CONCLUSION: A simple and convenient assay *in vitro* for hepatitis C virus NS3 serine protease is based on recombinant

substrate NS5ab and single-chain serine protease. This assay can be used in screening of enzyme inhibitors.

Du GX, Hou LH, Guan RB, Tong YG, Wang HT. Establishment of a simple assay *in vitro* for hepatitis C virus NS3 serine protease based on recombinant substrate and single-chain protease. *World J Gastroenterol* 2002; 8(6):1088-1093

INTRODUCTION

Hepatitis C virus (HCV) is a member of the *Flaviviridae* and now recognized as the major aetiological agent of post-transfusion non-A non-B hepatitis^[1-3]. The viral genome is a 9.6-kb, positive-sense single-stranded RNA molecule that contains a single open reading frame encoding a polyprotein of 3010 to 3030 amino acids^[4-6]. The polyprotein undergoes proteolytic processing by both host signal peptidases and viral proteases, giving rise to at least 10 mature proteins, and the cleavage of the 5 nonstructural proteins (NS3, NS4A, NS4B, NS5A and NS5B) were carried out by viral protease NS3/4A^[7,8]. Since NS3/4A serine protease is very important for releasing functional proteins from the polyprotein, which are essential for replication and maturation of virus, it is currently being targeted in the development of drugs and diagnostics^[9-11].

Previous studies indicate that the NS3/4A serine protease is a heterodimer formed by NS3 protein and its cofactor NS4A^[12]. Analysis of the X-ray structures of the truncated NS3 protein complexed with the NS4A-derived peptide revealed that the serine protease domain adopts a chymotrypsin-like fold that means the NS3/4A is a member of chymotrypsin-like serine protease^[13,14]. Although the protease domain of NS3 expressed without its cofactor is enzymatic active, its activity is partial and it can only recognize and cleave the NS5A/B site while the other two sites (NS4A/B and NS4B/5A) can not be cleaved^[15,16]. That is, the NS4A enhances the cleavage at NS5A/B site and is absolutely required for cleavage at the NS4B/5A site^[17,18]. In order to carry out detailed characterization of this enzyme and develop the antiviral agent, a reproducible and convenient large-scale production of the purified enzyme and its substrate is essential^[19]. In this report, we constructed and over-expressed a novel single-chain serine protease in a soluble form in *E.coli*, and established a simple assay *in vitro* for HCV serine protease based on the recombinant substrate NS5ab and single-chain protease. In addition, we examined the effect of several well-known protease inhibitors by the established assay system.

MATERIALS AND METHODS

Materials

Prokaryotic expression vector pQE30, *E.coli* M15 cells and metal affinity chromatography resins (Ni-NTA agarose) were obtained from Qiagen Inc. (Chatsworth, California). Restriction

enzymes (BamHI and HindIII), T4 DNA ligase and Ex. Taq DNA polymerase were purchased from Takara Inc. (Dalian, Liaoning). PCR Pure[®] PCR purification kit were obtained from Clontech Inc. The prokaryotic expression plasmid pGEX-3X-NS3N that carries the gene of amino terminal 181 amino acids of HCV NS3 protein is a gift from Dr. Chen *et al.*^[20].

Methods

Construction of expression plasmids pQENS3N4A To generate fusion gene of NS4A₂₁₋₃₂-GSGS-NS3₃₋₁₈₁, three primers were designed. Primers P2 (5'-ATT ATT TTA TCT GGT AGT GGT AGT ATC ACG GCC TAC TCC CAA-3') and P3 (5'-CCC AAGCTT TTA GGA CCG CAT GGT AGT TTC-3') were used to amplify the NS4A₂₉₋₃₂-GSGS-NS3₃₋₁₈₁ using the plasmid pGEX-3X-NS3N as template. After that the PCR products were used as template to generate NS4A₂₁₋₃₂-GSGS-NS3₃₋₁₈₁ with primers P1 (5'-C GGATCC GGT TCT GTT GTT ATT GTT GGT AGA ATT ATT TTA TCT GGT-3') and P3. Underlined sequences represents HindIII and BamHI restriction sites, respectively. The highlighted sequences represents overlapping region of primers P1 and P2. The fusion gene NS4A₂₁₋₃₂-GSGS-NS3₃₋₁₈₁ contained the sequence encoding the NS4A peptide, GSVVIVGRILS (NS4A a.a 21-32), the linker, glycine-serine-glycine-serine (GSGS)^[21], and the NS3 a.a 3-181. The expression vector pQE30 and fusion gene were both digested with BamHI and HindIII, then they were ligated after purification. The resulting plasmid was used to transform competent *E.coli* M15 and the recombinant clones were selected on LB agar plates with ampicillin (100 mg/mL) and kanamycin (25 mg/mL), and identified by restriction enzyme mapping and sequencing. The resulting recombinant plasmid is termed as pQENS3N4A.

Construction of expression plasmids pQENS5ab To construct the expression plasmid pQENS5ab, a cDNA fragment encoding amino acid residues 2263-2498 in the HCV polyprotein was isolated from the serum of a healthy HCV carrier in China by nested PCR using appropriate oligonucleotides, (1: 5'-AGT (G/A)AT (C/T)CT GGA CTC TTT CG-3', 2: 5'-TGC TGG ATA GGT TCC TGA CGT-3', 3: 5'-TAT GGTACC GAG GA(C/T) GAG AGG GAA GTA TC-3', 4: 5'-TGC AAGCTT AAC TGT GGA CGC CT 3'), which was inserted a *KpnI* site at the 5'-end and *HindIII* site at the 3'-end of the sequence. The PCR product amplified using Ex. Taq (Takara) was cloned into expression plasmid pQE30 that was digested with *KpnI* and *HindIII*. The resulting plasmid pQENS5ab encodes the cleavage site of NS5A/B with a N-terminal 20 non-virus encoded amino acids possessing a consecutive stretch of 6 His residues, which allows fusion protein to be purified in a single step by metal chelating affinity chromatography. The cloned DNA fragment was sequenced in order to exclude the introduction of mutations by PCR and also to confirm the in-frameness of the insert.

Expression and purification of recombinant single-chain serine protease in *E.coli* A single clone from *E.coli* M15 transformed with the recombinant plasmid pQENS3N4A was used to initiate growth in Luria broth supplemented with 100 µg/mL ampicillin and 25 µg/mL kanamycin. When the absorbance reached a value of 0.8 OD₆₀₀, IPTG was added to give a final concentration of 0.2 mM and the incubation continued for additional 6 h at 20 °C. Under this condition a high level expression of NS3N4A in a soluble form was observed. The cells were harvested by centrifugation and washed extensively with PBS (20 mM sodium phosphate; pH7.4, 140 mM NaCl). The cell pellet was resuspended in lysis buffer (50 mM Tris·HCl; pH7.4, 10 % glycerol, 0.3M NaCl,

2 mM β-mercaptoethanol, 0.5 % NP-40) and disrupted by sonication on ice using sonifier (60s×10 strokes at 150W output with 30s intervals). The homogenate was centrifuged at 15000×g for 30 min to remove cell debris and was chromatographed on a nickel-agarose column (Qiagen). The column was washed extensively with 10 column volumes of lysis buffer and subsequently washed using 20 column volumes of buffer W (50 mM Tris·HCl; pH7.4, 10 % glycerol, 1M NaCl, 20 mM imidazole, 2mM β-mercaptoethanol, 0.5 % NP-40) and finally eluted with buffer E (50 mM Tris·HCl; pH7.4, 10 % glycerol, 1M NaCl, 250 mM imidazole, 2mM β-mercaptoethanol, 0.5 % NP-40). Eluted fractions were subjected to SDS-PAGE and the pooled enzyme was dialyzed against buffer D (50 mM Tris·HCl; pH7.4, 10 % glycerol, 1M NaCl, 2mM β-mercaptoethanol, 0.5 % NP-40) to remove imidazole before stored in aliquots at -20 °C.

Protein concentrations were estimated from UV absorbance at 280 nm and 260 nm and calculated according to the formula: concentration of protein (g/L)= 1.45×A₂₈₀-0.74×A₂₆₀.

Expression, purification and refolding of recombinant substrate NS5ab The transformed cells were grown at 37 °C in Luria broth supplemented with 100 µg/mL ampicillin and 25 µg/mL kanamycin. When cell density reached an OD₆₀₀ of 0.8-1.0, induction was initiated by the addition of 1mM IPTG. Cells of 500 mL culture were harvested 5 hours after induction and resuspended in 10 mL lysis buffer (50 mM sodium phosphate; pH7.8, 300 mM NaCl). After disruption by sonication on ice, the inclusion bodies were collected by centrifugation at 12 000×g for 15 min and washed three times in the lysis buffer. The inclusion body was solubilized in 8M urea (50 mM sodium phosphate; pH8.0, 300 mM NaCl, 8M urea) and was chromatographed on a nickel-agarose column (Qiagen). The purification was performed according to the manual of Qiaexpressionist[®]. To refold the purified NS5ab protein, the protein was dialyzed against refolding buffer with a stepwise gradient of urea from 6M to 4M, 2M, 1M, 0.5M, 0.25M and finally to TBS (50 mM Tris·HCl; pH7.4, 140 mM NaCl). The concentration of substrate NS5ab was calculated according to the foregoing formula on the basis of UV absorbance at 280 nm and 260 nm. The purified recombinant substrate NS5ab was stored in aliquots at -20 °C.

***In vitro* proteolytic assay for HCV NS3 serine protease** 20 µg of purified single-chain serine protease was incubated with 20 µg of recombinant substrate NS5ab in 100 µl of 25 mM Tris·HCl (pH7.4), 10 % glycerol, 0.5M NaCl, 10mM DTT and 0.5 % NP-40 at room temperature. After the reaction was terminated at various time points, there were mixed with same volume of 2×loading buffer and heated at 90 °C for 10 min, then analyzed by SDS-PAGE and stained with Coomassie brilliant blue R-250 (CBB R-250).

Effects of some known serine protease inhibitors In this assay, the single-chain serine protease was mixed with appropriate amount of PMSF or EDTA at room temperature for 30 min before they were incubated with recombinant substrate NS5ab to pursue the reaction. 45 min later, the reaction was terminated and analyzed with SDS-PAGE and CBB R-250.

RESULTS

Cloning and expression of recombinant single-chain serine protease

To produce a recombinant HCV NS3N4A protein complex with structural confirmation similar to its biological counterpart, an expression plasmid encoding HCV NS4A central peptide GSGVVIVGRILS (NS4A a.a. 21-32)

covalently jointed to a NS3 N-terminal protease domain via an flexible amino acid linker GSGS was engineered^[22]. The cDNA fragment encoding this single-chain protease was inserted into a pQE30 expression vector that provided additional six amino acids and six histidine residues at the amino terminus of the NS4A peptide (Figure 1). Induction of the bacteria harboring this expression plasmid with a low concentration of IPTG (0.2 mM) at low temperature (20 °C) resulted in the production of a 23 kDa recombinant protein (Figure 2, lane 2). Much of the expressed recombinant protein existed in the soluble fraction of the bacterial lysate (Figure 2, lane 3). Further purification of the expressed protein using nickel-affinity chromatography yielded a product with greater than 95 % homogeneity as measured by SDS-PAGE and thin layer scanning assay (Figure 2, lane 5). Approximately 7.5 mg of protein was obtained from 500 ml culture following purification.

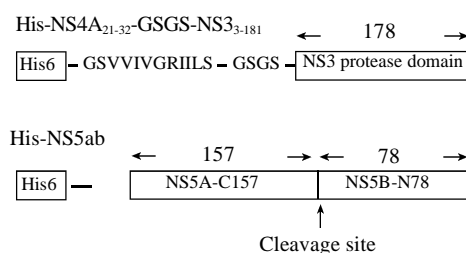


Figure 1 Schematic diagram of constructs expressing single-chain serine protease NS3N4A and substrate NS5ab. His6, the hexahistidine metal chelation tag; GSVVIVGRILS, NS4A central peptide (a.a. 21-32) and GSGS, an amino acid linker connecting the NS4A peptide to the NS3 serine protease domain. Cleavage site, representing the cleavage site between NS5A and NS5B.

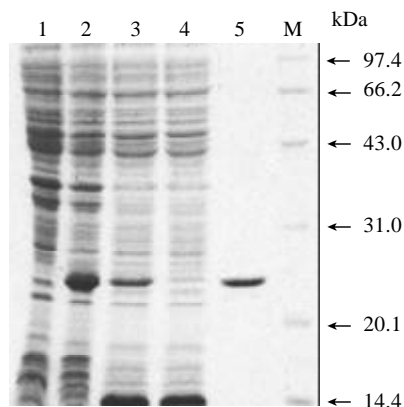


Figure 2 SDS-PAGE analysis for the expression and purity of single-chain serine protease. Lane 1, Noninduced cells; lane 2, Cells induced with IPTG; lane 3, Cleared lysate; lane 4, Flow-through; lane 5, Purified single-chain serine protease; M, low molecular weight markers.

Cloning and expression of recombinant substrate NS5ab

To produce a recombinant substrate of HCV NS3 serine protease, the gene that encoding HCV NS5A C-terminal 157 amino acids residues, cleavage site of NS5A/B, and NS5B N-terminal 78 amino acids residues was isolated by nested RT-PCR from the serum of a healthy HCV carrier in China. The cDNA fragment was inserted into pQE30 expression vector that provided additional 20 amino acids residues (including six histidine residues) at the amino terminal of the viral peptide (Figure 1). Induction of the bacteria harboring expression plasmid pQENS5ab resulted in the production of recombinant protein of 35kDa (Figure 3, lane 2). The majority of the

expressed recombinant protein existed in the insoluble fraction of the bacteria lysate. After purification of the recombinant protein NS5ab using nickel-affinity resin, the purified protein was refolded by dialysis method to produce soluble substrate with greater than 90 % homogeneity (Figure 3, lane 3). Approximately 7.6 mg of protein per liter of culture was obtained by following purification and refolding.

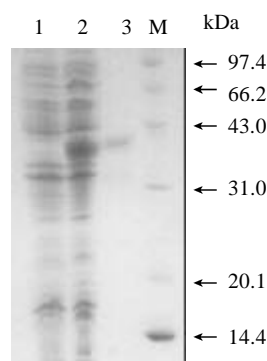


Figure 3 SDS-PAGE analysis for the expression and purity of HCV NS5ab protein. Lane 1, noninduced *E.coli* M15 cell lysate; lane 2, lysate of *E.coli* M15 cells transformed with pQENS5ab plasmids after induction; lane 3, purified HCV NS5ab protein; M, Low molecular weight markers.

In vitro proteolytic assay for HCV NS3 serine protease

The soluble single-chain serine protease and soluble substrate NS5ab was incubated in a reaction buffer and then investigate whether the enzyme can process the substrate correctly and efficiently^[23]. Figure 4 showed that the single-chain serine protease could cleave the substrate NS5ab into two fragments with molecular weight about 24kDa and 11kDa respectively. In addition, the amount of products increased and the substrate decreased along with reaction time (Figure 4, lane 1-5). That means the single-chain serine protease has highly active proteolytic activity and the substrate is active, too.

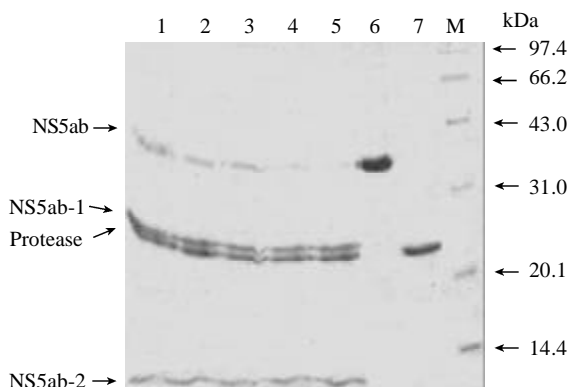


Figure 4 In vitro trans-cleavage at the NS5A/5B site of single-chain serine protease. Lane 1-5, cleavage reaction after 10, 20, 30, 45 and 60 mins; lane 6, protein substrate NS5ab; lane 7, single-chain serine protease; M, low molecular weight markers.

Effects of some known serine protease inhibitors

The *in vitro* trans-cleavage assay system described made it possible to examine the effect of known serine protease inhibitors^[24]. Two kinds of known proteinase inhibitors (PMSF and EDTA) were added to the reaction system and the effect visualized by SDS-PAGE and CBB R-250 staining. It was shown that the well-characterized inhibitor PMSF could inhibit

proteolytic activity at 5 mM *in vitro* (Figure 5, lane 4), while the metal chelator EDTA had no observable effect on the protease activity even at a concentration of 5 mM (Figure 5, lane 6).

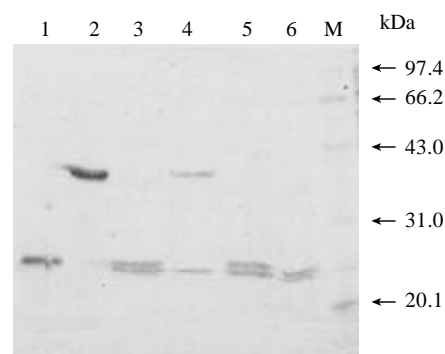


Figure 5 The inhibitory effects of PMSF and EDTA on single-chain protease activity. M, low molecular weight markers; lane 1, single-chain serine protease; lane 2, protein substrate NS5ab; lane 3, without PMSF; lane 4, with 5 mmol/L PMSF; lane 5, without EDTA; lane 6, with 5 mmol/L EDTA.

DISCUSSION

This study aimed at establishing a simple *in vitro* assay for hepatitis C virus NS3 serine protease, since such an assay is the most important for screening specific antiviral inhibitors from combinatorial chemical library and random biological library^[25-27]. To accomplish this object we have to obtain substantial amounts of purified NS3 serine protease with complete functional activity. Previous studies had shown that there are two methods to produce fully active HCV serine protease. The first method is to express full length NS3₁₋₆₃₁ which was fused to the N-terminal of NS4A₁₋₅₄ in eukaryotic cells^[28], and the second one is to express protease domain in *E.coli* and mix them with excessive synthetic NS4A core peptide to form heterodimer^[29]. Although the two methods work, there still are many shortages. The former can only provide little amount of protein and the enzymatic activity of protein produced by later method is very low^[28,29]. According to Yan's report^[30], the reason that poor activity of the heterodimer formed *in vitro* by synthetic peptide and protease domain lies in that the affinity of synthetic peptide is much lower than that of the full-length NS4A, which makes the complex is unstable. So it is reasonable to express the fusion protein of NS3 protease domain and NS4A in *E.coli*.

Inoue and his colleague^[31] expressed NS3 protease fused at the amino terminal of NS4A in *E.coli*, which showed ideal stability and activity, but the products existed in inclusion bodies that lead to the poor productivity. In addition, the crystallographic structure of NS3 serine protease domain complexed with synthetic peptide indicated that it might be better for NS4A fused to amino terminal of NS3 protease domain^[21,22]. Since the central part of NS4A is embedded in the cleft formed by NS3 protease domain and its C-terminus lies close to the amino terminus of NS3 (Figure 6A), it is reasonable to fuse the NS4A central peptide to amino terminal of NS3 via a flexible linker. This fusion format will change the natural intermolecular interaction to intramolecular interaction (Figure 6B), which will increase the stability of NS4A-NS3N complex. In this study, we constructed a single-chain serine protease that contained central peptide of NS4A fused to amino terminal of NS3 protease domain via GSGS linker, and it could process the recombinant substrate NS5ab efficiently.

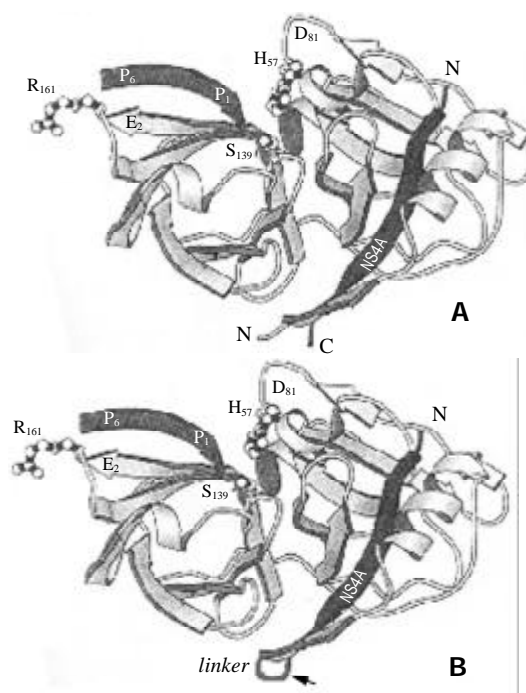


Figure 6 The crystal structure of serine protease domain and NS4A central sequence. A, cocrystal structure of the NS3₁₋₁₈₁/NS4A₂₁₋₃₂ complex (adapted from reference 11). B, cocrystal structure of the NS3₁₋₁₈₁/NS4A₂₁₋₃₂ complex with a flexible linker

The reason that single-chain serine protease can express in a soluble form at high level in *E.coli* lies in two points: 1) the low concentration of inducer and low temperature culture reduced the synthesis speed of peptide, which enhance the folding of protein^[32-34]; 2) the central sequences of NS4A may increase the solubility of the single-chain serine protease. The NS3 domain was in various prokaryotic expression vectors with failures to produce soluble recombinant protein in this study, though various measures had been taken, such as lowering temperature and lowering concentration of IPTG (unpublished materials). In the same condition, the protease domain that fused to the C-terminal of NS4A central segment could express in a soluble form, which means that the central sequences of NS4A may increase the solubility of NS3 protease domain. Previous studies had confirmed that NS3 protease's N-terminus would be changed from disordered structure to regular structure when it formed a complex with the NS4A peptide, that is why the NS4A central peptide is capable of promoting the folding of protein^[35,36]. In addition, the NS4A central peptide is highly hydrophobic, which will reduce the synthesis of peptide in host and be beneficial to protein's refolding^[37].

Based on the recombinant single-chain protease and substrate protein NS5ab, we established a simple and cheap *in vitro* assay for HCV NS3 protease. In this assay system, the results were analyzed by SDS-PAGE and visualized by Coomassie brilliant blue R-250 staining (CBB R-250), which make it an attractive system because of its convenience, low cost and intuitiveness. To assess the applicability of this assay system in identification of serine protease inhibitors, we examined the effects of two known serine protease inhibitors on the activity of HCV protease. The results confirmed that the PMSF could inhibit the proteolytic activity of HCV serine protease completely at 5 mM, while the metal chelator EDTA had no observable effect on it, which had been observed by other researchers^[38,39]. In conclusion, the *in vitro* assay

established here is applicable in evaluating the effect of chemical compounds and biological molecules on the activity of HCV serine protease. Furthermore, this assay can be used in high throughput screening of the potential inhibitors of HCV protease^[40,41].

REFERENCES

- 1 **Choo QL**, Kuo G, Weiner AJ, Overby LR, Bradley DW, Houghton M. Isolation of a cDNA clone derived from a blood-borne non-A, non-B viral hepatitis genome. *Science* 1989; **244**: 359-362
- 2 **Alter MJ**, Margolis HS, Krawczynski K, Judson FN, Mares A, Alexander WJ, Hu PY, Miller JK, Gerber MA, Sampliner RE. The natural history of community-acquired hepatitis C in the United States. The Sentinel Counties Chronic non-A, non-B Hepatitis Study Team. *N Engl J Med* 1992; **327**: 1899-1905
- 3 **Kuo G**, Choo QL, Alter HJ, Gitnick GL, Redeker AG, Purcell RH, Miyamura T, Dienstag JL, Alter MJ, Stevens CE. An assay for circulating antibodies to a major etiologic virus of human non-A, non-B hepatitis. *Science* 1989; **244**: 362-364
- 4 **Kato N**, Hijikata M, Nakagawa M, Ootsuyama Y, Muraiso K, Ohkoshi S, Shimotohno K. Molecular structure of the Japanese hepatitis C viral genome. *FEBS Lett* 1991; **280**: 325-328
- 5 **Okamoto H**, Okada S, Sugiyama Y, Kurai K, Iizuka H, Machida A, Miyakawa Y, Mayumi M. Nucleotide sequence of the genomic RNA of hepatitis C virus isolated from a human carrier: comparison with reported isolates for conserved and divergent regions. *J Gen Virol* 1991; **72**: 2697-2704
- 6 **Takamizawa A**, Mori C, Fuke I, Manabe S, Murakami S, Fujita J, Onishi E, Andoh T, Yoshida I, Okayama H. Structure and organization of the hepatitis C virus genome isolated from human carriers. *J Virol* 1991; **65**: 1105-1113
- 7 **Grakoui A**, Wychowski C, Lin C, Feinstone SM, Rice CM. Expression and identification of hepatitis C virus polyprotein cleavage products. *J Virol* 1993; **67**: 1385-1395
- 8 **Shimotohno K**, Tanji Y, Hirowatari Y, Komoda Y, Kato N, Hijikata M. Processing of the hepatitis C virus precursor protein. *J Hepatol* 1995; **22**: 87-92
- 9 **Llinas-Brunet M**, Bailey M, Fazal G, Ghire E, Gorys V, Goulet S, Halmos T, Maurice R, Poirier M, Poupert MA, Rancourt J, Thibeault D, Wernic D, Lamarre D. Highly potent and selective peptide-based inhibitors of the hepatitis C virus serine protease: towards smaller inhibitors. *Bioorg Med Chem Lett* 2000; **10**: 2267-2270
- 10 **Dymock BW**, Jones PS, Wilson FX. Novel approaches to the treatment of hepatitis C virus infection. *Antivir Chem Chemother* 2000; **11**: 79-96
- 11 **De Francesco R**, Steinkuhler C. Structure and function of the hepatitis C virus NS3-NS4A serine proteinase. *Curr Top Microbiol Immunol* 2000; **242**: 149-169
- 12 **Bartenschlager R**. The NS3/4A proteinase of the hepatitis C virus: unravelling structure and function of an unusual enzyme and a prime target for antiviral therapy. *J Viral Hepat* 1999; **6**: 165-181
- 13 **Kim JL**, Morgenstern KA, Lin C, Fox T, Dwyer MD, Landro JA, Chambers SP. Crystal structure of the hepatitis C virus NS3 protease domain complexed with a synthetic NS4A cofactor peptide. *Cell* 1996; **87**: 343-355
- 14 **Yan Y**, Li Y, Munshi S, Sardana V, Cole JL, Sardana M, Steinkuehler C, Tomei L, De Francesco R. Complex of NS3 protease and NS4A peptide of BK strain hepatitis C virus: a 2.2 Å resolution structure in a hexagonal crystal form. *Protein Sci* 1998; **7**: 837-847
- 15 **Grakoui A**, McCourt DW, Wychowski C, Feinstone SM, Rice CM. Characterization of the hepatitis C virus-encoded serine proteinase: determination of proteinase-dependent polyprotein cleavage sites. *J Virol* 1993; **67**: 2832-2843
- 16 **Bartenschlager R**, Ahlborn-Laake L, Mous J, Jacobsen H. Kinetic and structural analyses of hepatitis C virus polyprotein processing. *J Virol* 1994; **68**: 5045-5055
- 17 **Landro JA**, Raybuck SA, Luong YP, O' Malley ET, Harbeson SL, Morgenstern KA, Rao G, Livingston DJ. Mechanistic role of an NS4A peptide cofactor with the truncated NS3 protease of hepatitis C virus: elucidation of the NS4A stimulatory effect via kinetic analysis and inhibitor mapping. *Biochemistry* 1997; **36**: 9340-9348
- 18 **Barbato G**, Cicero DO, Nardi MC, Steinkuhler C, Cortese R, De Francesco R, Bazzo R. The solution structure of the N-terminal proteinase domain of the hepatitis C virus (HCV) NS3 protein provides new insights into its activation and catalytic mechanism. *J Mol Biol* 1999; **289**: 371-384
- 19 **Steinkuhler C**, Koch U, Narjes F, Matassa VG. Hepatitis C virus protease inhibitors: current progress and future challenges. *Curr Med Chem* 2001; **8**: 919-932
- 20 **Chen Z**, Xu J, Song HB, Zhou YS, Wang HT. Cloning and sequence analysis of hepatitis C virus NS3 serine protease. *Zhonghua Ganzangbing Zazhi* 1998; **6**: 114-115
- 21 **Taremi SS**, Beyer B, Maher M, Yao N, Prosis W, Weber PC, Malcolm BA. Construction, expression, and characterization of a novel fully activated recombinant single-chain hepatitis C virus protease. *Protein Sci* 1998; **7**: 2143-2149
- 22 **Howe AY**, Chase R, Taremi SS, Risano C, Beyer B, Malcolm B, Lau JY. A novel recombinant single-chain hepatitis C virus NS3-NS4A protein with improved helicase activity. *Protein Sci* 1999; **8**: 1332-1341
- 23 **Koch JO**, Bartenschlager R. Determinants of substrate specificity in the NS3 serine proteinase of the hepatitis C virus. *Virology* 1997; **237**: 78-88
- 24 **Mori A**, Yamada K, Kimura J, Koide T, Yuasa S, Yamada E, Miyamura T. Enzymatic characterization of purified NS3 serine proteinase of hepatitis C virus expressed in *Escherichia coli*. *FEBS Lett* 1996; **378**: 37-42
- 25 **Ingallinella P**, Fattori D, Altamura S, Steinkuhler C, Koch U, Cicero D, Bazzo R, Cortese R, Bianchi E, Pessi A. Prime site binding inhibitors of a serine protease: NS3/4A of hepatitis C virus. *Biochemistry* 2002; **41**: 5483-5492
- 26 **Fowler A**, Price-Jones M, Hughes K, Anson J, Lingham R, Schulman M. Development of a high throughput scintillation proximity assay for hepatitis C virus NS3 protease that reduces the proportion of competitive inhibitors identified. *J Biomol Screen* 2000; **5**: 153-158
- 27 **Fukuda K**, Vishnuvardhan D, Sekiya S, Hwang J, Kakiuchi N, Taira K, Shimotohno K, Kumar PK, Nishikawa S. Isolation and characterization of RNA aptamers specific for the hepatitis C virus nonstructural protein 3 protease. *Eur J Biochem* 2000; **267**: 3685-3694
- 28 **Sali DL**, Ingram R, Wendel M, Gupta D, McNemar C, Tsarbopoulos A, Chen JW, Hong Z, Chase R, Risano C, Zhang R, Yao N, Kwong A D, Ramanathan L, Le H V, Weber P C. Serine protease of hepatitis C virus expressed in insect cells as the NS3/4A complex. *Biochemistry* 1998; **37**: 3392-3401
- 29 **Vishnuvardhan D**, Kakiuchi N, Urvil PT, Shimotohno K, Kumar P K, Nishikawa S. Expression of highly active recombinant NS3 protease domain of hepatitis C virus in *E. coli*. *FEBS Lett* 1997; **402**: 209-212
- 30 **Yan Y**, Li Y, Munshi S, Sardana V, Cole J L, Sardana M, Steinkuehler C, Tomei L, De Francesco R. Complex of NS3 protease and NS4A peptide of BK strain hepatitis C virus: a 2.2 Å resolution structure in a hexagonal crystal form. *Protein Sci* 1998; **7**: 837-847
- 31 **Inoue H**, Sakashita H, Shimizu Y, Yamaji K, Yokota T, Sudo K, Shigeta S, Shimotohno K. Expression of a hepatitis C virus NS3 protease-NS4A fusion protein in *Escherichia coli*. *Biochem Biophys Res Commun* 1998; **245**: 478-482
- 32 **Swartz JR**. Advances in *Escherichia coli* production of therapeutic proteins. *Curr Opin Biotechnol* 2001; **12**: 195-201
- 33 **Weickert MJ**, Doherty DH, Best EA, Olins PO. Optimization of

- heterologous protein production in *Escherichia coli*. *Curr Opin Biotechnol* 1996; **7**: 494-499
- 34 **Hockney RC**. Recent developments in heterologous protein production in *Escherichia coli*. *Trends Biotechnol* 1994; **12**: 456-463
- 35 **Kwong AD**, Kim JL, Rao G, Lipovsek D, Raybuck SA. Hepatitis C virus NS3/4A protease. *Antiviral Res* 1999; **41**: 67-84
- 36 **Mossakowska DE**. Expression of nuclear hormone receptors in *Escherichia coli*. *Curr Opin Biotechnol* 1998; **9**: 502-505
- 37 **Tomei L**, Failla C, Vitale RL, Bianchi E, De Francesco R. A central hydrophobic domain of the hepatitis C virus NS4A protein is necessary and sufficient for the activation of the NS3 protease. *J Gen Virol* 1996; **77**: 1065-1070
- 38 **Steinkuhler C**, Tomei L, De Francesco R. In vitro activity of hepatitis C virus protease NS3 purified from recombinant Baculovirus-infected Sf9 cells. *J Biol Chem* 1996; **271**: 6367-6373
- 39 **Shoji I**, Suzuki T, Chieda S, Sato M, Harada T, Chiba T, Matsuura Y, Miyamura T. Proteolytic activity of NS3 serine proteinase of hepatitis C virus efficiently expressed in *Escherichia coli*. *Hepatology* 1995; **22**: 1648-1655
- 40 **Kakiuchi N**, Nishikawa S, Hattori M, Shimotohno K. A high throughput assay of the hepatitis C virus nonstructural protein 3 serine proteinase. *J Virol Methods* 1999; **80**: 77-84
- 41 **Cerretani M**, Di Renzo L, Serafini S, Vitelli A, Gennari N, Bianchi E, Pessi A, Urbani A, Colloca S, De Francesco R, Steinkuhler C, Altamura S. A high-throughput radiometric assay for hepatitis C virus NS3 protease. *Anal Biochem* 1999; **266**: 192-197

Edited by Zhang JZ

• VIRAL HEPATITIS •

p73b inhibits transcriptional activities of enhancer I and X promoter in hepatitis B virus more efficiently than p73a

Zhen-Hua Xu, Mu-Jun Zhao, Tsai-Ping Li

Zhen-Hua Xu, Mu-Jun Zhao, Tsai-Ping Li, State Key Laboratory of Molecular Biology, Institute of Biochemistry and Cell Biology, Shanghai Institutes for Biological Sciences, Chinese Academy of Sciences, Shanghai 200031, China

Supported by special funds for Major State Basic Research “973” of China, No. 2001CB510205.

Correspondence to: Professor Mu-Jun Zhao, P.O. Box 35, State Key Laboratory of Molecular Biology, Institute of Biochemistry and Cell Biology, Shanghai Institutes for Biological Sciences, Chinese Academy of Sciences, 320 Yue-Yang Road, Shanghai 200031, China. mjzhao@sunm.shnc.ac.cn

Telephone: +86-21-64374430 Ext 5295 **Fax:** +86-21-64338357

Received 2002-07-23 **Accepted** 2002-08-09

Abstract

AIM: p73, as a novel member of a family of p53-related transcription factors, shares redundant functions with p53, such as the abilities of inducing apoptosis and suppressing growth. It is well known that p53 can repress HBV expression and transcription efficiently. The aim of this paper is to investigate the transcriptional effect of p73 α and p73 β on hepatitis B virus (HBV) and to understand the correlation between HBV and p73.

METHODS: To construct an x-gene inactivated HBV plasmid which was cotransfected with p73 α or p73 β expression vectors into HepG2 cells. After transiently transfection, HBV surface antigen (HBsAg) and HBV e antigen (HBeAg) were detected by ELISA. Viral transcripts synthesized by HBV were evaluated by Northern blotting analysis. The activities of HBV regulatory elements, including enhancer I/X promoter (ENI/Xp) and enhancer II/core promoter (ENII/Cp) were monitored by luciferase assays.

RESULTS: Both p73 α and p73 β could repress HBsAg and HBeAg expression by downregulating the ENI/Xp and ENII/Cp activities. But p73 β exerted stronger inhibition on the activity of ENI/Xp than p73 α , resulting in much lower level of viral transcripts and the antigens expression.

CONCLUSION: p73 β as a novel member of p53 family can efficiently inhibit HBV transcription mainly through downregulating the activities of the HBV ENI/Xp regulatory elements.

Xu ZH, Zhao MJ, Li TP. p73 β inhibits transcriptional activities of enhancer I and X promoter in hepatitis B virus more efficiently than p73 α . *World J Gastroenterol* 2002; 8(6):1094-1097

INTRODUCTION

p73 gene maps to chromosome 1p36.1, a region which was frequently deleted in several tumors, including neuroblastoma, colorectal cancer and breast cancer^[1]. Moreover, it has been found to share significant homology with the tumor suppressor

gene p53 within the transactivation domain, DNA binding domain and oligomerization domain. Both p53 and p73 have redundant functions in the regulation of gene expression, because they have amino acid sequence identity reaching to 63 % in the DNA binding domain^[2]. p73 can activate p53-regulated genes and suppress growth or induce apoptosis, and expression of p73 can be induced by DNA damage as p53 does^[3,4]. Although deletion of p73 gene is observed in neuroblastoma and a subtype of T-cell lymphoma, it is rarely mutated in human cancer^[5-9], unlike p53 which is mutated in about 50 % of human cancers^[5,7,10-12]. Other evidence suggests that p73 is important for regulation of normal development^[13]. p73 gene is expressed as p73 α , a 636 amino acid polypeptide, and p73 β , a 499 amino acid polypeptide that is encoded by an alternatively spliced transcript lacking 96 nucleotides corresponding to exon 13^[11]. Until now, at least six different p73 proteins (α - ζ) have been found^[14].

Hepatitis B virus^[15-17] is a causative agent of chronic hepatitis and hepatocellular carcinoma. Upon infection or DNA transfection, four major viral transcripts are detected. The largest 3.5 kb mRNA is composed of precore and pregenomic mRNA, that direct the synthesis of HBV e antigen (HBeAg) and HBV core antigen (HBcAg) respectively. Pregenomic RNA also serves as a template for reverse-transcription to synthesize the viral DNA genome. The largest surface antigen is synthesized from 2.4 kb mRNA, and the middle and major surface antigen are synthesized from 2.1 kb mRNA. The smallest transcript is a 0.7 kb mRNA, which is responsible for HBx protein production^[18]. The transcription of these RNAs are governed by the core, S1, S2 and X promoters, respectively. The activities of these promoters are under the control of enhancer I and II^[19].

In addition to a function as a tumor suppressor, p53 can defend host cell from the invading virus. p53 actively inhibits viral replication as in the case of SV40 and HBV^[20,21]. p53 binds to a sequence adjacent to the replication origin of SV40 and abrogates the helicase activity of T antigen by directly binding to it. It has been reported that p53 can bind specifically to the HBV enhancer I and repress the activity of enhancer I and X promoter, resulting in HBV gene expression downregulated^[22]. In addition, p53 can interfere with the life cycle of HBV through down-regulation of the enhancer II and pregenomic/core promoter. Although p53 can not directly bind the enhancer II, it represses the transcriptional activity of HBV through protein-protein interaction^[23].

p73, as a novel member of a family of p53-related transcription factors, has attracted more attention during these years. However the relationship between p73 and the hepatitis B virus is not elucidated. Based on the similarity between p53 and p73, we examined whether p73, mainly p73 α and p73 β , can affect HBV antigens expression and the viral transcription.

MATERIALS AND METHODS

Construction of plasmid

p3.8II, kindly provided by Prof. Wang Yuan, is an HBV plasmid which contains terminally redundant HBV genome

and can replicate in liver cell. The x-gene inactivated p3.8IIXm was constructed by changing the start codon of the X open reading frame on p3.8II. The pENI/XpLuc and pENII/CpLuc reporter plasmids were constructed by inserting nt1067-1403 and nt1430-1879 which contain enhancer I/X promoter and enhancer II/core promoter respectively in front of the pGL3 basic vector (Promega). The mammalian expression vectors pcDNA3-HA-73 α and pcDNA3-HA-73 β encode epitope tagged p73 proteins which were kind gifts from Dr. Lu Hua. p53 expression plasmid pRC/CMV hp53 was provided by Dr. Judith Roth. All the constructs were confirmed by restriction enzyme analysis and DNA sequencing.

Cell culture and transfection

HepG2 cells were cultured in DMEM supplemented with kanamycin (250 IU/ml), gentamycin (40 IU/ml) and 10 % fetal calf serum in 5 % CO₂ at 37 °C. Transfection was carried out by the calcium phosphate method^[24]. Each transfection reaction contained a constant amount of 10 μ g DNA per 6 cm dish.

Preparation of cell lysate and measurement of HBV antigens

Five days after transfection, cells were washed twice with PBS and were detached from dishes with 10 mM EDTA in PBS. After centrifugation (5 000 rpm, 1 min), cells were resuspended in 100 μ l 250 mM Tris-HCl (pH7.5) and lysed by three thawing and freezing cycles. After centrifugation, the supernatant was transferred and stored at 4 °C. The protein concentration was estimated by Bradford method (Biocolor). Culture medium was collected every day after transfection. HBsAg and HBeAg were measured with ELISA kits (Sino-America). All procedures were performed according to the descriptions of the manufacturers.

RNA analysis

Total RNA was extracted from transfected cells using TRIzol reagent (Gibco BRL). The RNA samples were treated with RNase-free DNaseI (Pharmacia). For Northern blotting analysis, 20 μ g of total cellular RNA per sample was separated on 1 % formaldehyde-agarose gel and blotted to a Hybond-N nylon membrane (Amersham). The membrane was prehybridized in Quick-Hyb buffer (Amersham) for at least 1 hour, followed by 2 hr hybridization at 65 °C with the probes of α -³²p-dCTP labeled 3.2 kb HBV DNA and G3PDH fragments. After hybridization, the membrane was washed in 2 % SSC, 0.1 % SDS buffer (RT, 20 min), 0.2 % SSC, 0.1 % SDS (65 °C, 30 min), then exposed to an X-ray film at -70 °C.

Luciferase assay

Cells were lysed and analyzed with a luciferase assay system (Promega). Corrections of the luciferase activity were made based on the protein concentrations of the lysates. The luciferase activity was measured with a Lumat LB9507 luminometer (Berthold) in 10 μ l of the lysate after addition of 100 μ l assay reagent.

RESULTS

p73 β represses HBsAg and HBeAg expression more efficiently than p73 α

Before investigating whether p73 could affect HBV transcription like p53, we established the X protein-minus HBV mutant p3.8IIXm to avoid the interaction between p73 and the HBV X protein. This HBV mutant had no ATG start codon of the X-ORF (Figure1). ELISA results revealed that the HBV antigens expression in mutant type of p3.8IIXm was just a half of that in wild type p3.8II.

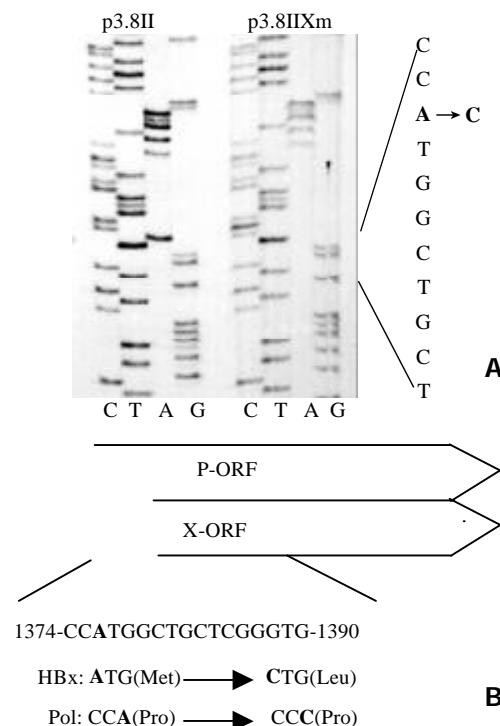


Figure 1 Partial DNA sequences of p3.8II and p3.8IIXm is indicated in the left panel (A). The point mutation A→C results in the amino acid changes in the ORF of HBV polymerase (P) and X protein(X) (B).

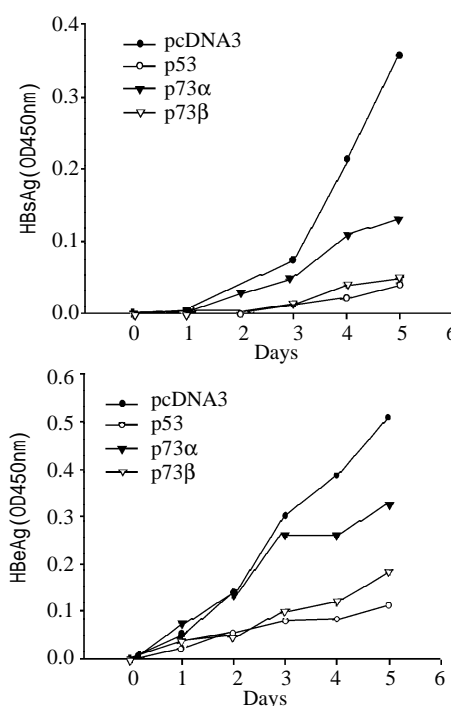


Figure 2 Time course of HBV antigen expression. HepG2 cells were transiently transfected with X-minus p3.8IIXm, and cotransfected with pcDNA3, p53, p73 α , or p73 β individually. Culture medium were harvested at certain days, and detected by ELISA kit.

As shown in Figure2A, P3.8IIXm could secrete HBsAg into the medium continuously starting from day 2. Cotransfection of p3.8IIXm with p73 β expression plasmid resulted in a reduced level of HBsAg (87 % reduction on day 5 post transfection), which was similar to p53 (89 % reduction on

day 5 post transfection). Cotransfection of p3.8IIXm with p73 α expression plasmid exhibited weak repression on HBsAg synthesis (only 63 % reduction on day 5 post transfection). The time-dependent alteration in the level of HBeAg (Figure 2B) displayed a similar pattern to that of HBsAg. On day 5 post transfection, the expression of HBeAg was changed at the level of 36 % reduction for p73 α and 64 % reduction for p73 β . Also as shown in Figure 2B, p53 could inhibit HBeAg more efficiently (78 % reduction on day 5 post transfection) than p73 α and p73 β . It is concluded that both p73 α and p73 β can downregulate HBV expression including HBsAg and HBeAg, but p73 β can repress the HBV antigens expression more efficiently than p73 α .

p73b can repress the synthesis of viral transcripts including pregenomic/precore RNA and preS/S RNA

The roles of p73 α and p73 β in viral transcription were assessed at the HBV RNA levels after cotransfection of p3.8IIXm and p73 expression plasmids. Using Northern blot hybridization with ³²P-labeled 3.2 kb HBV fragment as a probe, we detected the pregenomic RNA and precore RNA as well as preS/S mRNA. As Figure 3 shown, cotransfection of p73 β resulted in the reduction of the viral transcript level like p53, but p73 α seems to exhibit very weak repression on HBV transcription. These results are in accordance with the above ELISA data.

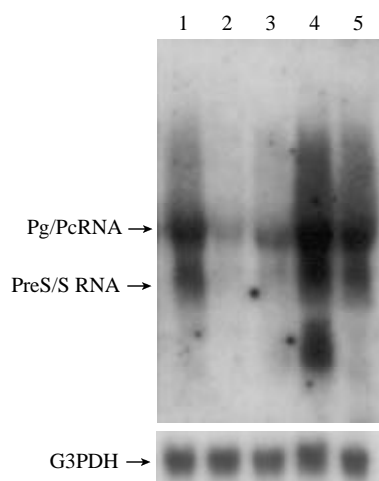


Figure 3 Northern blotting analysis of HBV viral transcripts, including pregenomic/precore RNA and preS/S RNA. HepG2 cells were transiently transfected with p3.8IIXm, and also with the expression plasmids. Lane 1 represents pcDNA3, lane 2, p53, lane 3, p73 β , lane 4, p73 α and lane 5, p73 α respectively. Total cellular RNA were extracted and α -³²p-dCTP labeled 3.2 kb HBV DNA or G3PDH used as probe.

p73b inhibits HBV transcription mainly through downregulating the activity of HBV ENI/Xp regulatory elements

To explain the molecular mechanism of the p73 β mediated repression of HBV transcription, we investigated the possibility of p73 regulating the enhancer and promoter activity. pENI/Xp reporter plasmid containing HBV enhancer I and X promoter was cotransfected into HepG2 cells with p73 α and p73 β expression plasmids, and the levels of luciferase activity were determined. As shown in Figure 4A, the luciferase activity of the pENI/Xp was decreased with transfection of p73 β and p73 α , down to 65 % and 35 % of the control value respectively. Therefore, p73 β can repress the activity of enhancer I and X promoter more efficiently than p73 α . The activity of HBV enhancer II and core promoter were repressed by p73 α and p73 β at a similar level, but the effects of inhibition were weaker

than that by p53 (Figure 4B). Therefore, it is concluded that p73 β represses HBV gene expression mainly through the enhancer I and X promoter.

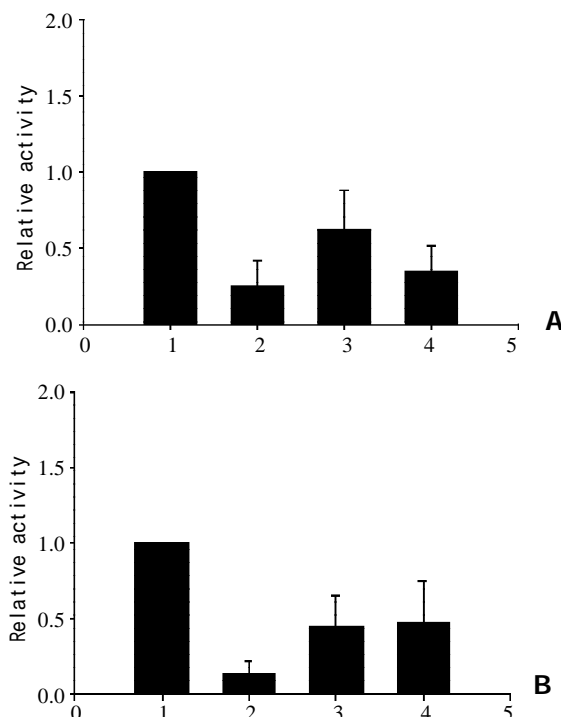


Figure 4 Effects of p73 α and p73 β on the regulatory sequences of hepatitis B virus. HepG2 cells were transfected with expression plasmids, pcDNA3(1), p53(2), p73 α (3), and p73 β (4). In each case, 1 μ g of reporter plasmids, pENI/XpLuc, containing the enhancer I/X promoter (A) and pENII/CpLuc, containing the enhancer II/core promoter (B), were individually cotransfected. 42 hours after transfection, the cells were harvested and luciferase activity was determined. The value obtained with reporters alone was arbitrarily set to 100 %, and the other values were normalized accordingly. The column heights reflect the average of at least three independent experiments.

DISCUSSION

HBV, an important risk factor of hepatitis and hepatocellular carcinoma, employs a reverse transcription step which is controlled by cellular transcription factors and some cellular signal transduction pathways, including the tumor suppressor gene p53^[25,26]. Physiologically activated p53 can repress HBV transcription, and this repression can be abrogated by physiological levels of HBx protein. It is generally believed that p53 can interact with HBx, and the latter destroys p53 function, including the repression of virus transcription. To exclude the interaction between p73 and the X protein, we constructed the X-minus HBV strain p3.8IIXm which could replicate in hepatoma cells without producing X protein.

HBsAg and HBeAg are translated from preS/S mRNA and precore mRNA individually. HBV core promoter is in charge of the transcription of pregenomic RNA as well as precore mRNA. ENI and ENII are the two enhancers in the viral genome. ENI is usually able to upregulate all the HBV promoters, and ENII has a particularly significant stimulatory effect upon the core promoter. In this report, we found that p73 β repressed HBsAg and HBeAg expression more efficiently, and it inhibited the viral transcripts level mainly through downregulating the enhancer I and X promoter. In the ENI/Xp construct, there were two sites with homology to

the 10 bp half-consense (RRRCWWGYYY) for p53 binding, which had been reported to bind specifically to the HBV enhancer I and repress its activity^[22]. Liver-specific enhancer II had also been found to be the target for the p53-mediated inhibition of hepatitis B viral gene expression. p53 could not directly bind to the enhancer II, and it repressed the ENII activity through protein-protein interaction^[23]. p73 protein has significant homology with p53, and p73 can interact with the consensus p53-responsive sequences. But that whether the mechanism of repression on enhancer of HBV by p73 and p53 is the same awaits further investigation. In our results, p73 α exerted a very weak repression on HBV transcription and antigen expression, while Doitsh *et al* reported that p73 β did not repress but activated HBV transcription^[27], probably due to the high dose of the protein we used in this study.

It was noted that p73 was less active than p53, whereas p73 β displayed stronger transcriptional activity than p73 α . The difference between p73 α and p73 β in the potential to regulate transcription may be due to the ability of these proteins to form oligomers. p73 β is the truncated form of full-length p73 α . While p73 β is known to oligomerize with itself efficiently, p73 α forms oligomers with a poor efficiency, at least when assayed in the yeast two-hybrid system^[2]. Therefore it can be used to explain why p73 β exerts more efficient inhibition on HBV transcription than p73 α .

Although p73 β has been found to interfere with the HBV transcription in this report, whether HBV can inactivate the function of p73 to affect the viral-infected cell fate, and the relationship between the X protein and p73 β remain to be investigated.

ACKNOWLEDGEMENTS

The authors would like to thank Prof. Wang Yuan for providing p3.8II plasmid, Dr. Lu Hua for pcDNA3-HA-p73 α , pcDNA3-HA-p73 β , and Dr. Vogelstein for the pRC/CMV-p53.

REFERENCES

- Ikawa S, Nakagawara A, Ikawa Y. p53 family genes: structural comparison, expression and mutation. *Cell Death Differ* 1999; **6**: 1154-1161
- Kaghad M, Bonnet H, Yang A, Creancier L, Biscan JC, Valent A, Minty A, Chalon P, Ferrara P, McKeon F, Caput D. Monoallelically expressed gene related to p53 at 1p36, a region frequently deleted in neuroblastoma and other human cancers. *Cell* 1997; **90**: 809-819
- Steegenga WT, Shvarts A, Riteo N, Bos JL, Jochemsen AG. Distinct regulation of p53 and p73 activity by adenovirus E1A, E1B, and E4orf6 proteins. *Mol Cell Biol* 1999; **19**: 3885-3894
- Jost CA, Marin MC, Kaelin WJ. p73 is a human p53-related protein that can induce apoptosis. *Nature* 1997; **389**: 191-194
- Ichimiya S, Nimura Y, Kageyama H, Takada N, Sunahara M, Shishikura T, Nakamura Y, Sakiyama S, Seki N, Ohira M, Kaneko Y, McKeon F, Caput D, Nakagawara A. p73 at chromosome 1p36.3 is lost in advanced stage neuroblastoma but its mutation is infrequent. *Oncogene* 1999; **18**: 1061-1066
- Nimura Y, Mihara M, Ichimiya S, Sakiyama S, Seki N, Ohira M, Nomura N, Fujimori M, Adachi W, Amano J, He M, Ping YM, Nakagawara A. p73, a gene related to p53, is not mutated in esophageal carcinomas. *Int J Cancer* 1998; **78**: 437-440
- Nomoto S, Haruki N, Kondo M, Konishi H, Takahashi T, Takahashi T, Takahashi T. Search for mutations and examination of allelic expression imbalance of the p73 gene at 1p36.33 in human lung cancers. *Cancer Res* 1998; **58**: 1380-1383
- Mihara M, Nimura Y, Ichimiya S, Sakiyama S, Kajikawa S, Adachi W, Amano J, Nakagawara A. Absence of mutation of the p73 gene localized at chromosome 1p36.3 in hepatocellular carcinoma. *Br J Cancer* 1999; **79**: 164-167
- Alonso ME, Bello MJ, Lomas J, Gonzalez-Gomez P, Arjona D, De Campos JM, Gutierrez M, Isla A, Vaquero J, Rey JA. Absence of mutation of the p73 gene in astrocytic neoplasms. *Int J Oncol* 2001; **19**: 609-612
- Yang SM, Zhou H, Chen RC, Wang YF, Chen F, Zhang CG, Zhen Y, Yan JH, Su JH. Sequencing of p53 mutation in established human hepatocellular carcinoma cell line of HHC4 and HHC15 in nude mice. *World J Gastroenterol* 1998; **4**: 506-510
- Peng XM, Peng WW, Yao JL. Codon 249 mutations of p53 gene in development of hepatocellular carcinoma. *World J Gastroenterol* 1998; **4**: 125-127
- Wang D, Shi JQ. Overexpression and mutations of tumor suppressor gene p53 in hepatocellular carcinoma. *China Natl J New Gastroenterol* 1996; **2**: 161-164
- Yang A, Walker N, Bronson R, Kaghad M, Oosterwegel M, Bonin J, Vagner C, Bonnet H, Dikkes P, Sharpe A, McKeon F, Caput D. p73-deficient mice have neurological phenomonal and inflammatory defects but lack spontaneous tumors. *Nature* 2000; **404**: 99-103
- Ueda Y, Hijikata M, Takagi S, Chiba T, Shimotohno K. New p73 variants with altered C-terminal structures have varied transcriptional activities. *Oncogene* 1999; **18**: 4993-4998
- Wands JR, Blum HE. Primary hepatocellular carcinoma. *N Engl J Med* 1991; **325**: 729-731
- Tang ZY. Hepatocellular carcinoma-cause, treatment and metastasis. *World J Gastroenterol* 2001; **7**: 445-454
- Feitelson MA, Sun B, Satioglu Tufan NL, Liu J, Pan J, Lian Z. Genetic mechanisms of hepatocarcinogenesis. *Oncogene* 2002; **21**: 2593-2604
- Nassal M, Schaller H. Hepatitis B virus replication. *Trends Microbiol* 1993; **1**: 221-226
- Seeger C, Mason WS. Hepatitis B virus biology. *Micro MolBioRev* 2000; **64**: 51-68
- Bargonetti J, Friedman PN, Kern SE, Volgestin B, Prives C. Wild-type But Not Mutant p53 Immunopurified Proteins Bind to Sequences Adjacent to the SV40 Origin of Replication. *Cell* 1991; **1083**: 1091
- Wang EH, Friedman PN, Prives C. The Murine p53 Protein Blocks Replication of SV40 DNA *In Vitro* by Inhibiting the Initiation Functions of SV40 Large Antigen. *Cell* 1989; **57**: 379-392
- Ori A, Zauberman A, Doitsh G, Paran N, Oren M, Shaul Y. p53 binds and represses the HBV enhancer: an adjacent enhancer element can reverse the transcription effect of p53. *EMBO J* 1998; **17**: 544-553
- Lee H, Kim HT, Yun YD. Liver-specific enhancer II is the target for the p53-mediated inhibition of hepatitis B viral gene expression. *J Biol Chem* 1998; **273**: 19786-19791
- Sambrook J, Fritsch EF, Maniatis T. Molecular Cloning, a Laboratory Manual, 2nd edn. New York: Cold Spring Harbor Laboratory Press 1989: 788-791
- Arbuthnot P, Kew M. Hepatitis B virus and hepatocellular carcinoma. *Int J Exp Pathol* 2001; **82**: 77-100
- Brechot C, Gozuacik D, Murakami Y, Paterlini-Brechot P. Molecular bases for the development of hepatitis B virus (HBV)-related hepatocellular carcinoma (HCC). *Semin Cancer Biol* 2000; **10**: 211-231
- Doitsh G, Shaul Y. HBV transcription repression in response to genotoxic stress is p53-dependent and abrogated by pX. *Oncogene* 1999; **18**: 7506-7513

Edited by Zhang JZ

• *H. pylori* •

PELA microspheres loaded *H. pylori* lysates and their mucosal immune response

Jian-Min Ren, Quan-Ming Zou, Fu-Kun Wang, Qiang He, Wei Chen, Wen-Kun Zen

Jian-Min Ren, Quan-Ming Zou, Fu-Kun Wang, Wen-Kun Zen,
Faculty of Medical Laboratory Science, Third Military Medical
University, Chongqing 400038, China

Qiang He, Wei Chen, Department of Radiology, southwest Hospital,
Third Military Medical University, Chongqing 400038, China

Correspondence to: Jian-Min Ren, Faculty of Medical Laboratory
Science, Third Military Medical University, Chongqing, 400038,
China. renjianmin123@sina.com

Telephone: +86-23-68753046 **Fax:** +86-23-68753046

Received 2001-08-24 **Accepted** 2001-09-05

Abstract

AIM: To prepare poly (D,L-lactide)-polyethylene glycol copolymer (PELA) microspheres loaded *H. pylori* lysates or *Cystografin* and observe their targeting in gastrointestinal mucous membrane or analyze the mucosal immune responses by oral administration.

METHODS: PELA microspheres loaded *H. pylori* lysates or *Cystografin* were prepared by double emulsion evaporation method. Their distribution in gastrointestinal mucous membrane was observed by CT. Balb/c mice orally immunized in mucosal immune responses, whose antibody production in salivary and gut washing and antibody secreting cells in Peyer's patches (PP) were estimated by ELISA and ELISPOT, respectively. The microspheres' physical properties, such as particle size, protein level and morphology were investigated.

RESULTS: All prepared microspheres were found to have a smooth surface morphology from 3.20-4.05 μm in diameter and high encapsulation efficiency from 74.9-82.2 %. No significant correlation in their physical properties was shown, depending on their molecular weight at the similar composition ratio. Immunization with all types of PELA-*Hp* microspheres elevated the saliva sIgA level at week 3 by approximately 3-4 times that with soluble antigen, which was greatly enhanced after boosting. At one week after last immunization with all types of PELA-*Hp* microspheres (week 8), the specific sIgA-ASCs, IgG-ASCs and sIgA in salivary rose obviously. In intestinal Peyer's patches, the specific sIgA-ASCs were $5.92-6.98 \times 10^4/\text{ml}$ cell and IgG-ASCs were $3.47-4.02 \times 10^4/\text{ml}$ cell, about 5-9 times higher than those with soluble antigen ($P < 0.01$). ASCs in intestine were more than those in stomach and the majority of the ASCs were sIgA-ASCs. The sIgA in gut washing fluid was 1.62-1.85 OD, about 3-6 times that of those with soluble antigen. There were significant differences of the ASCs and sIgA in gut washing fluid as compared with those of PBS and MS-0 ($P < 0.05$). There appeared to be good correlation between sIgA level in gut washing fluid and sIgA-ASCs in intestinal Peyer's patches.

CONCLUSION: PELA microspheres may be used as vehicle to delivery antigen and adjuvant in designing oral vaccination.

Ren JM, Zou QM, Wang FK, He Q, Chen W, Zen WK. PELA microspheres loaded *H. pylori* lysates and their mucosal immune response. *World J Gastroenterol* 2002; 8(6):1098-1102

INTRODUCTION

Helicobacter pylori (*Hp*) is a major pathogen causing type B gastritis, peptic ulcer and mucosa-associated lymphoid tissue gastric lymphoma^[1-12]. A triple antimicrobial therapy is often adopted for patients with infection^[13-16], for *Hp* reinfection easily occurs and the drug resistance strains are increasing, therefore, antimicrobial treatment may be ineffective in prevention of reinfection^[17-21]. Oral immunization is considered a convenient and safe method to induce mucosal immunity against infection. This has become a focus topic among the researchers^[22-26].

The biodegradable and biocompatible microsphere as a vaccine delivery vehicle has many advantages^[26]. The biodegradable polyesters (including polylactic acid (PLA), polyglycolic acid (PGA) and their copolymers (PLGA)) had been widely studied and used in biomedical engineering^[27-30]. For hydrophobicity of the PLA and the PLGA, this type of material is usually not desirable for protein and peptide. Their degraded products, lactic acids or glycolic acids will create a local acidic environment that may be harmful to the surrounding tissues^[31]. These microspheres loaded vaccines can be rapidly captured by phagocyte in the reticulo-endothelial system, while the microspheres (nanospheres) prepared with PLA-PEG-PLA (type A-B-A) triblock copolymers, which was produced by copolymerization of hydrophilic polyethylene glycol with lactide, showed longer circulating half life of the proteins *in vivo*^[32]. They can overcome the disadvantages of the PLA or PLGA microspheres as drug vehicle.

MATERIALS AND METHODS

Bacterial culture

*Hp*971023, *Hp*980706, *HpM* bacterial strains were isolated by our laboratory. The strains were inoculated onto blood plat in the microaerobic cultivation at 37 °C for 48 h. The organisms were washed 3 times with 0.15 mol/L phosphate buffered saline (PBS, pH7.4) and were harvested by centrifugation at 5 000rpm for 10 minutes at 4 °C. The resulting suspensions was added to 0.15 mol/L PBS(pH7.4), EDTA 0.65 g/L and phenylmethylsulfonyl fluoride (PMSF) 1 mmol/L and sonicated (200W \times 30s \times 10 times). The *Hp* lysate was collected by centrifugation at 12 000 rpm for 20 minutes. The protein concentration was determined by UV spectrophotometer (Beckman DU-640, USA).

Preparation of the PELA microspheres loaded *Hp*

PELA (weight ratio of D, L-lactide to PEG-2000, 95:5; the inherent viscosity of the PELA ranged from 0.1271 to 0.3329 dL/g measured in tetrahydrofuran at 25 °C) was synthesized

according to procedures described in literature^[32]. The PELA microspheres loaded *Hp* were manufactured using double emulsion evaporation method as described^[32,33]. One ml aqueous solution mixed 4 % *Hp* lysate (inter-water phase) was emulsified with 10 ml of 6 % (w/v) PELA in methylene chloride using T25B homogenizer (USA) at 8 000 rpm for 5 min (w/o). After homogenization, 30 ml aqueous solution of 2 % PVA (degree of polymerization $n = 1\ 500\text{--}1\ 800$) was added to the primary water-in oil (w/o) emulsion and the stirring was continued further for 5 min. The resulting w/o/w suspensions were stirred magnetically at 1 200 rpm for 10–12 h at room temperature (over 25 °C) to evaporate the solvent. The microspheres were obtained by centrifugation and washed three to eight times with distilled water. The cleaned microspheres were lyophilized and stored at 4 °C under desiccation. If the aqueous solution mixed *Hp* lysate (inter-water phase) was replaced by pure water or some concentration of *cystografin*, the blank PELA microspheres and PELA-*cystografin* microspheres can be obtained respectively. The amount of protein loaded in the PELA microspheres was determined by dissolving a fixed amount of microspheres in methylene chloride, the protein content was measured with UV spectrophotometer (Beckman DU-640, USA). The protein loading efficiency was calculated directly by recovering the protein from the microspheres^[34].

Measurement of microsphere size and morphology

The mean size of microspheres and distribution were calculated using a LeitzDiaplan light microscope (Wild MPS52, Japan) to measure the diameter of microspheres, whose amount was no less than 200. The surface structure of microspheres was examined by scanning electron microscopy (AMRAY, USA-China).

PELA-*cystografin* microspheres targeting

Minature pigs (*sus scorfa domestica*) weighing 15–20 kg were used in the study. PELA-*cystografin* microspheres (mean diameter of 3.72 µm, the amount of *cystografin* loaded was about 16 %) were suspended in 7.5 % sodium bicarbonate solution and 100 ml suspension (10 g PELA-*cystografin* microspheres) was orally administered by intubation feeding to minature pigs. After 0, 3, 8 and 15 days, the distribution of PELA-*cystografin* microspheres in the all gastrointestinal tract was observed by CT. The pigs were killed and the images of all gastrointestinal tract were taken after being washed up.

Immunization procedures

BALB/c mice (female, 6–8 weeks old, and 18–25 g in weight) were offered by our experimental animal center. Mice were randomly assigned to one of the seven immunization groups (twenty mice per group). Before administration, mice stopped feeding for 2 h and then took orally 0.5 ml mixture of the Hanks' equilibration salt and 7.5 % sodium bicarbonate solution (4:1 ratio) in order to neutralize gastric acid fluids. Each experimental group was orally immunized on week 0, 1 and 2. The immunized mice were given a booster immunization on week 7 with the same agents as the primary immunization. The first four groups were immunized by oral administration with different PELA-*Hp* microspheres (that is MS-1, MS-2, MS-3 and MS-4 group, 1mg *Hp* per mouse). The fifth group, sixth and seventh group of mice received free 1 mg of soluble *Hp* lysate antigen, PBS solution or blank PELA microspheres under similar conditions, respectively. One week after the last immunizations (week 8), mice were killed and assayed by indirect ELISA and ELISPOT.

Detection of ASCs in lymphocytes from intestine and gastric mucosa

Peyer's patches (PP) in intestine and gastric mucosa were selected^[35] and placed into 0.5 ml 5 % FCS RPMI-1640 medium. The tissues were ground and recovered on 70 µm cell strainer. The recovered tissues were harvested by centrifugation at 1 500rpm for 15 minutes and washed two times to collect suspensions, which were added 15 ml 70 % Percoll medium and centrifuged at 1500rpm for 15 minutes. Cell pellets are resuspended in 0.5 ml RPMI-1640 medium to form $5 \times 10^5/\text{ml}$. The cell suspensions were stained with 2 % trypan blue. The cell viability and purity were assessed. The ELISPOT assay^[36] was used to detect ASCs in the intestine and gastric tissues of the mice. Briefly, 96-well (Millipore) were coated with 0.2 ml *H. pylori* sonicate preparations dissolved in 0.05 mol/L sodium bicarbonate solution (50 µg protein per well) and left overnight at 4 °C. After washed three times in PBS, well plates were saturated with 2 % BSA (100 µl per well) and incubated at 37 °C for 1 hour. The plates were washed once in RPMI-1640 and each well was added 0.2 ml $5 \times 10^5/\text{ml}$ of the cell suspensions.

The cells were incubated at 37 °C in 10 % CO₂ for 4 hours. The plates were washed three times in PBS-Tween and then added 100 µl biotinylated monoclonal IgA or IgG antibodies to specific mouse, which had been diluted 1:1500 and 1:2000 in 10 % FCS-PBS, respectively. The plates were incubated at 37 °C for 2 hours. After three washes, the avidinperoxidase solution, diluted 1:2 000 in PBS, was incubated at 37 °C for 30 minutes. After three washes in PBS-Tween, 100 µl substrate solution (containing 7.5 % gelatin, 1 g/L 3,3', 5,5'-tetramethylbenzidine (TMB), 0.03 % H₂O₂) was added to each well. The reaction was coagulated quickly in ice-water bath. After 10–30 minutes, the immunospots were counted under inverted microscope (Olymps, Tokyo, Japan). The number of ASC was the mean number of immunospots deducting the mean number of each contrast.

Assay of saliva sIgA and gut sIgA by ELISA

Saliva was collected from immunized mice^[37]. Gut washing fluids was collected after the last immunization one week (week 8). Each well was coated with 100 µl of *H. pylori* lasate solution at concentration of 50 µg/ml in 0.05 mol/L sodium carbonate-bicarbonate buffer (pH 9.6) overnight at 4 °C. After suction and three washes in PBS-Tween, 100 µl of 2 % BSA solution in PBS was added to each well and further incubated for 1 hour at 37 °C. The initial dilution of sample (saliva and gut washing fluids) was 1:20. 100 µl diluted samples was added to wells and incubated for 1 hour at 37 °C. After three washes in PBS-Tween, 100 µl of biotinylated goat anti-mouse IgA incubated for 1 hour at 37 °C. After washing three times with PBS-Tween, 100 µl of the avidinperoxidase solution was added and incubated for 1 hour at 37 °C. Then washed and added 100 µl substrate solution. The plates were incubated for 20 minutes at 37 °C. The reaction was stopped by addition of 100 µl of 0.5 mol/L hydrochloric acid, and the color development was measured by plate reader set at 405 nm.

Statistical analysis

Data were analyzed using Student's *t* test. Results were expressed as mean ± standard error. Differences were considered significant for values $P < 0.05$.

RESULTS

Properties and morphology of PELA-*Hp* microspheres

The properties of PELA-*Hp* microspheres prepared with

different inherent viscosity of PELA (ranged from 0.1271-0.3329 dL/g) are shown in Table 1. The properties of microspheres were examined under light microscope in particle size and by UV spectrophotometer in protein loading and encapsulation efficiency. The morphology of microspheres was examined under scanning electron microscopy. The morphology of MS-2 is shown Figure 1.

Table 1 The properties of the PELA-*Hp* microspheres

Lot	PELA[η] (dL/g)	Mean dimeter(μ m)	Protein loading (%,w/w)	Encapsulation efficiency (%,w/w)
MS-1	0.1271	3.87	5.06	77.6
MS-2	0.2083	3.20	5.53	82.2
MS-3	0.3054	3.53	5.40	74.9
MS-4	0.3329	4.05	5.27	79.5

*The inherent viscosity of PELA is measured in tetrahydrofuran at 25 °C.

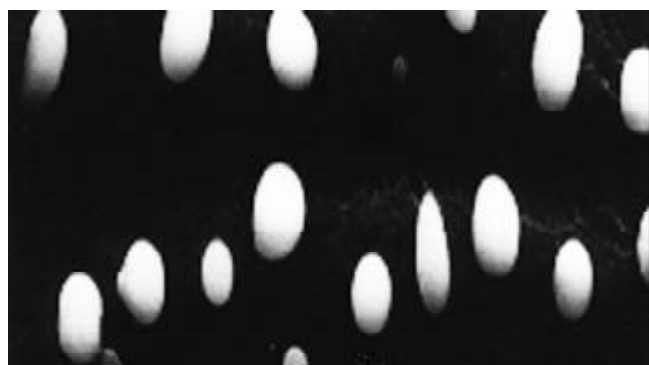


Figure 1 Scanning electron micrographs of MS-2 loaded *Hp*.

PELA-cystografin microsphere targeting

The images of the miniature pig by oral administration with PELA-cystografin microsphere were observed by CT. The experiment could indirectly obtain the distribution of PELA microsphere in all gastrointestinal tract as time (day). The results suggested that PELA-cystografin microsphere mainly was distributed in the gastric cavity and at the surface of gastric mucosa after oral administration for three days. Then part of the microspheres gradually moved to enter the intestine by the stomach peristalsis and adhered to their surface (images not shown). After 15 days, the microspheres were found mainly distributed at the surface of intestine. The images are shown Figure 2.

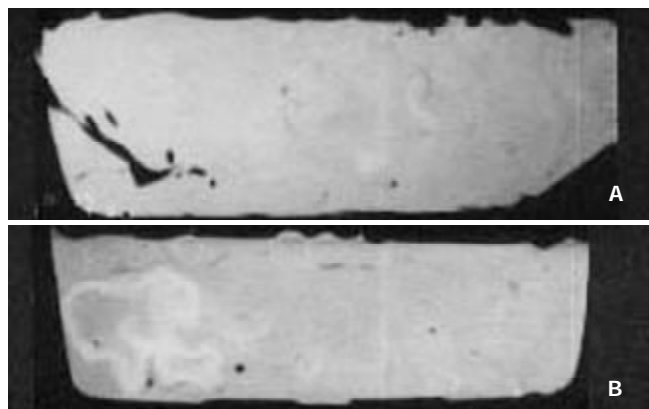


Figure 2 Images of pig stomach and gut after oral administration. (a) blank PELA microsphere; (b) PELA-cystografin microsphere.

Mucosal immune responses of orally immunized PELA-*Hp* microspheres

Saliva sIgA responses after oral immunization with soluble antigen, PELA-*Hp* microspheres with different inherent viscosities of PELA (ranged from 0.1271 to 0.3329 dL/g) were measured at week 3, week 5 and week 8 (Table 2). Immunization with soluble antigen induced weak saliva IgA antibodies. Immunization with all types of PELA-*Hp* microspheres elevated saliva sIgA level at week 3 (approximately 3-4 times higher than those with soluble antigen) and greatly enhanced after boosting (week 8). The changes of saliva sIgA at different stages after oral immunization related to the properties of PELA.

Table 2 Comparison of sIgA titres in saliva at different stages after oral immunization ($\bar{x} \pm s$)

Groups	Week 3	Week 5	Week 8
PBS	0.081 \pm 0.026	0.074 \pm 0.023	0.080 \pm 0.011
Ag	0.197 \pm 0.177	0.199 \pm 0.093	0.225 \pm 0.029
MS-0	0.090 \pm 0.041	0.071 \pm 0.013	0.110 \pm 0.046
MS-1	0.416 \pm 0.183	0.567 \pm 0.136	0.891 \pm 0.215
MS-2	0.399 \pm 0.179	0.608 \pm 0.209	0.882 \pm 0.264
MS-3	0.346 \pm 0.126	0.674 \pm 0.128	0.957 \pm 0.238
MS-4	0.304 \pm 0.105	0.523 \pm 0.211	0.944 \pm 0.143

At one week after last immunization with all types of PELA-*Hp* microspheres (week 8), the specific sIgA-ASCs, IgG-ASCs and sIgA were estimated by ELISPOT and ELISA. The results are shown in Table 3.

Table 3 Immune response induced with PELA-*Hp* microspheres at week 8 ($n=20$, $\bar{x} \pm s$)

Groups	PP sIgA-ASCs	(1×10^4) IgG-ASCs	Stomach sIgA-ASCs	(1×10^3) IgG-ASCs	Gut sIgA
PBS	0.13 \pm 0.04	0.16 \pm 0.07	0.19 \pm 0.08	0.23 \pm 0.06	0.234 \pm 0.08
Ag	0.27 \pm 0.11	0.29 \pm 0.09	0.35 \pm 0.11	0.36 \pm 0.15	0.34 \pm 0.17
MS-0	0.16 \pm 0.07	0.17 \pm 0.05	0.15 \pm 0.06	0.21 \pm 0.07	0.25 \pm 0.08
MS-1	6.58 \pm 1.38	3.78 \pm 0.82	4.17 \pm 1.09	0.74 \pm 0.29	1.75 \pm 0.46
MS-2	6.92 \pm 1.77	4.02 \pm 0.93	3.80 \pm 1.34	1.02 \pm 0.44	1.85 \pm 0.38
MS-3	6.77 \pm 1.46	3.56 \pm 1.10	4.12 \pm 0.83	1.81 \pm 0.73	1.62 \pm 0.81
MS-4	5.92 \pm 1.92	3.47 \pm 0.82	3.65 \pm 1.04	1.88 \pm 0.23	1.71 \pm 0.70

DISCUSSION

The relationship between the properties of PELA-*Hp* microspheres and molecular weight of PELA copolymer are shown Table 1. All types of PELA-*Hp* microspheres prepared with the same component PELA, whose protein loading, encapsulation efficiency and size were 5.06-5.40 %, 74.9-82.2 % and 3.20-4.05 μ m, respectively, were not significantly different. This confirmed the previous investigations^[38]. Morphology of PELA microspheres using double emulsion evaporation method were investigated under scanning electron microscopy. The obtained microspheres were all spherical, homogeneous particles and had smooth surface (as shown in Figure 1). The results coincided with the report of SY Kim *et al*^[39], while Kofler *et al*^[40] reported that the microspheres were

porous particles with a rough surface. This is likely that different processing and manufacturing conditions of microspheres (such as $o/w_{\text{out-water phase}}/w_{\text{inter-water phase}}$, stirring velocity, temperature etc), which result in morphologies of microspheres.

The images of the miniature pigs by oral administration of PELA-*cystografin* microspheres are shown in Figure 2. This indirectly clarified the conclusion arrived by Eldridge *et al*^[41], which was that microspheres (mean diameter <10 μm) after oral administration firstly adhered to the surface of the gastrointestinal mucous membrane, then arrived at their Peyer's patches (PP) to induce mucosal and systemic immune responses. Therefore, our obtained microspheres (mean diameter <5 μm) could induce mucosal and systemic immune responses by particle uptake into the PP. After oral administration, all types of PELA-*Hp* microspheres (week 8), the specific sIgA-ASCs, IgG-ASCs and sIgA in gut washing fluids obviously rose by ELISA and ELISPOT. The specific sIgA-ASCs and IgG-ASCs were approximately 5-9 times that with soluble antigen. ASCs in the intestine were more than those in stomach, and the majority of the ASCs were sIgA-ASCs. This result indicated that there appeared to be a good correlation between sIgA level in gut washing fluid and sIgA-ASCs in intestinal PP. The sIgA in gut washing fluid was about 3-6 times higher than those with soluble antigen (as shown in Table 3), that is very important for oral immunization to effectively induce mucosal immune response and protect against *Hp* infection^[21,35]. The protein release of PELA-*Hp* microspheres was influenced by several parameters including PELA copolymer molecular weight, diameter, the ratio of lactide/PEG and the manufacturing technology. Immunization with all types of PELA-*Hp* microspheres elevated the saliva sIgA level at week 3 (approximately 3-4 times higher than those with soluble antigen) and greatly enhanced after boosting (week 8) (Table 2). At the same components of PELA (feed ratio of lactide/PEG=95:5 in this study), after oral immunization for 3 weeks, mice with PELA-*Hp* microspheres prepared with lower molecular weight of PELA, the saliva sIgA level became higher than the mice with PELA-*Hp* microspheres prepared with higher molecular weight of PELA. However, after oral immunization for 8 weeks, there was no differences in antibody production level between those formulations. This result can be explained as follows: the initial burst release of *Hp* was bigger from PELA-*Hp* microspheres prepared with lower molecular weight PELA, meanwhile because low molecular weight of PELA was degraded easily and can not effectively protect *Hp* release from microspheres ($t_{1/2}$ was short)^[36], this means that mice orally immunized with PELA-*Hp* microspheres prepared with lower molecular weight PELA induced stronger mucosal and systemic immune responses after oral immunization in earlier stages. All types of PELA-*Hp* microspheres ($\eta=0.1271-0.3329$ dL/g PELA, 1-2 month degradation *in vitro*) were degraded fully and released encapsulated antigens at week 8 irrespective of differences of copolymer molecular weights. We also found in this study that antigen release from microspheres can be controlled and accommodated by dictating the component and molecular weight of polymer. This will play an important role in designing oral vaccines for the protection against diseases in the future.

REFERENCES

- 1 Sepulveda AR, Graham DY. Role of *Helicobacter pylori* in gastric carcinogenesis. *Gastroenterol Clin North Am* 2002; **31**: 517-535
- 2 Vandeplass Y. *Helicobacter pylori* infection. *World J Gastroenterol* 2000; **6**: 20-31
- 3 Nakamura S, Aoyagi K, Furuse M, Suekane H, Matsumoto T, Yao T, Sakai Y, Fuchigami T, Yamamoto I, Tsuneyoshi M, Fujishima M. B-cell monoclonality precedes the development of gastric MALT lymphoma in *Helicobacter pylori*-associated chronic gastritis. *Am J Pathol* 1998; **152**: 1271-1279
- 4 Hiyama T, Haruma K, Kitadai Y, Miyamoto M, Tanaka S, Yoshihara M, Sumii K, Shimamoto F, Kajiyama G. B-cell monoclonality in *Helicobacter pylori*-associated chronic atrophic gastritis. *Virchows Arch* 2001; **438**: 232-237
- 5 Wu C, Zou QM, Guo H, Yuan XP, Zhang WJ, Lu DS, Mao XH. Expression, purification and immuno-characteristics of recombinant UreB protein of *H. pylori*. *World J Gastroenterol* 2001; **7**: 389-393
- 6 Miyamoto M, Haruma K, Hiyama T, Kamada T, Masuda H, Shimamoto F, Inoue K, Chayama K. High incidence of B-cell monoclonality in follicular gastritis: a possible association between follicular gastritis and MALT lymphoma. *Virchows Arch* 2002; **440**: 376-380
- 7 Wildner-Christensen M, Touborg Lassen A, Lindebjerg J, Schaffalitzky De Muckadell OB. Diagnosis of *Helicobacter pylori* in Bleeding Peptic Ulcer Patients, Evaluation of Urea-Based Tests. *Digestion* 2002; **66**: 9-13
- 8 Bobrzynski A, Beben P, Budzynski A, Bielanski W, Plonka M, Konturek S. Incidence of complications of peptic ulcers in patients with *Helicobacter pylori* (*Hp*) infection and/or NSAID use in the era of *Hp* eradication. *Med Sci Monit* 2002; **8**: CR554-557
- 9 Sato Y, Iwafuchi M, Ueki J, Yoshimura A, Mochizuki T, Motoyama H, Sugimura K, Honma T, Narisawa R, Ichida T, Asakura H, Van T. Gastric carcinoid tumors without autoimmune gastritis in Japan: a relationship with *Helicobacter pylori* infection. *Dig Dis Sci* 2002; **47**: 579-585
- 10 Gomollon F, Sicilia B. *Helicobacter pylori*: strategies for treatment. *Expert Opin Investig Drugs* 2001; **10**: 1231-1241
- 11 Zhuang XQ, Lin SR. Research of *Helicobacter pylori* infection in precancerous gastric lesions. *World J Gastroenterol* 2000; **6**: 428-429
- 12 Peng ZS, Liang ZC, Liu MC, Ouyang NT. Studies on gastric epithelial cell proliferation and apoptosis in *Hp* associated gastric ulcer. *Shijie Huaren Xiaohua Zazhi* 1999; **7**: 218-219
- 13 Kawakami E, Ogata SK, Portorreal AC, Magni AM, Pardo ML, Patricio FR. Triple therapy with clarithromycin, amoxicillin and omeprazole for *Helicobacter pylori* eradication in children and adolescents. *Arq Gastroenterol* 2001; **38**: 203-206
- 14 Fanti L, Ieri R, Mezzi G, Testoni PA, Passaretti S, Guslandi M. Long-term follow-up and serologic assessment after triple therapy with omeprazole or lansoprazole of *Helicobacter*-associated duodenal ulcer. *J Clin Gastroenterol* 2001; **32**: 45-48
- 15 Buzas Gyorgy M, Szekeley E, Illyes G, Szeles I. Lansoprazole versus ranitidine bismuth citrate containing triple regimens for *Helicobacter pylori* eradication in patients with duodenal ulcer. *Orv Hetil* 2000; **141**: 1711-1714
- 16 Catalano F, Catanzaro R, Bentivegna C, Brogna A, Condorelli G, Cipolla R. Ranitidine bismuth citrate versus omeprazole triple therapy for the eradication of *Helicobacter pylori* and healing of duodenal ulcer. *Aliment Pharmacol Ther* 1998; **12**: 59-62
- 17 Ruggiero P, Peppoloni S, Berti D, Rappuoli R, Giudice GD. New strategies for the prevention and treatment of *Helicobacter pylori* infection. *Expert Opin Investig Drugs* 2002; **11**: 1127-1138
- 18 Velasco Benitez CA, Amorcho Perez RD. Treatment of gastritis-associated *Helicobacter pylori* infection in children. *Rev Gastroenterol Peru* 2002; **22**: 159-163
- 19 Catalano F, Branciforte G, Catanzaro R, Bentivegna C, Cipolla R, Nuciforo G, Brogna A. Comparative treatment of *Helicobacter pylori*-positive duodenal ulcer using pantoprazole at low and high doses versus omeprazole in triple therapy. *Helicobacter* 1999; **4**: 178-184
- 20 Osato MS, Reddy SG, Piergies AA, Bochenek WJ, Testa RT, Graham DY. Comparative efficacy of new investigational agents against *Helicobacter pylori*. *Aliment Pharmacol Ther* 2001; **15**: 487-492
- 21 Kim BO, Shin SS, Yoo YH, Pyo S. Peroral immunization with *Helicobacter pylori* adhesin protein genetically linked to cholera toxin A2B subunits. *Clin Sci (Lond)* 2001; **100**: 291-298

- 22 **Challacombe SJ**, Sweet SP. Oral mucosal immunity and HIV infection: current status. *Oral Dis* 2002; **8** Suppl 2: 55-62
- 23 **van Ginkel FW**, Nguyen HH, McGhee JR. Vaccines for mucosal immunity to combat emerging infectious diseases. *Emerg Infect Dis* 2000; **6**: 123-132
- 24 **Mutwiri G**, Bowersock T, Kidane A, Sanchez M, Gerdtz V, Babiuk LA, Griebel P. Induction of mucosal immune responses following enteric immunization with antigen delivered in alginate microspheres. *Vet Immunol Immunopathol* 2002; **87**: 269-276
- 25 **Ishizaka ST**, Israel ZR, Gettie A, Mishkin EM, Staas JK, Gilley RM, Dailey PJ, Montefiori DC, Marx PA, Eldridge JH. Induction of mucosal antibody responses by microsphere-encapsulated formalin-inactivated simian immunodeficiency virus in a male urethral challenge model. *Vaccine* 1999; **17**: 2817-2825
- 26 **Allaoui-Attarki K**, Pecquet S, Fattal E, Trolle S, Chachaty E, Couvreur P, Andreumont A. Protective immunity against *Salmonella typhimurium* elicited in mice by oral vaccination with phosphorylcholine encapsulated in poly(DL-lactic-co-glycolide) microparticles. *Infect. Immun* 1997; **65**: 853-857
- 27 **Wang MY**, Levi AD, Shah S, Green BA. Polylactic acid mesh reconstruction of the anterior iliac crest after bone harvesting reduces early postoperative pain after anterior cervical fusion surgery. *Neurosurgery* 2002; **51**: 413-416
- 28 **Camargo PM**, Lekovic V, Weinlaender M, Vasilic N, Madzarevic M, Kenney EB. Platelet-rich plasma and bovine porous bone mineral combined with guided tissue regeneration in the treatment of intrabony defects in humans. *J Periodontol Res* 2002; **37**: 300-306
- 29 **Giardino R**, Fini M, Nicoli Aldini N, Giavaresi G, Rocca M. Polylactide bioabsorbable polymers for guided tissue regeneration. *J Trauma* 1999; **47**: 303-308
- 30 **Hoffman GT**, Soller EC, McNally-Heintzelman KM. Biodegradable synthetic polymer scaffolds for reinforcement of albumin protein solders used for laser-assisted tissue repair. *Biomed Sci Instrum* 2002; **38**: 53-58
- 31 **Huang YY**, Chung TW, Tzeng TW. A method using biodegradable polylactides/polyethylene glycol for drug release with reduced initial burst. *Int J Pharm* 1999; **182**: 93-100
- 32 **Deng X**, Zhou S, Li X, Zhao J, Yuan M. *In vitro* degradation and release profiles for poly-DL-lactide-poly(ethylene glycol) microspheres containing human serum albumin. *J Control Release* 2001; **71**: 165-173
- 33 **Yang YY**, Chung TS, Ng NP. Morphology, drug distribution, and in vitro release profiles of biodegradable polymeric microspheres containing protein fabricated by double-emulsion solvent extraction/evaporation method. *Biomaterials* 2001; **22**: 231-241
- 34 **Yang YY**, Chia HH, Chung TS. Effect of preparation temperature on the characteristics and release profiles of PLGA microspheres containing protein fabricated by double-emulsion solvent extraction/evaporation method. *J Control Release* 2000; **69**: 81-96
- 35 **Ferrero RL**, Thiberge JM, Labigne A. Local immunoglobulin G antibodies in the stomach may contribute to immunity against *Helicobacter* infection in mice. *Gastroenterology* 1997; **113**: 185-194
- 36 **Mattsson A**, Lonroth H, Quiding Jarbrink M, Svennerholm AM. Induction of B cell responses in the stomach of *Helicobacter pylori*-infected subjects after oral cholera vaccination. *J Clin Invest* 1998; **102**: 51-56
- 37 **Ishii H**, Nakagawa Y. Stress response to surgical procedures in the submandibular region and its influence on salivary secretion in mice. *Arch Oral Biol* 2001; **46**: 387-390
- 38 **Matsumoto J**, Nakada Y, Sakurai K, Nakamura T, Takahshi Y. Preparation of nanoparticles consisted of poly(L-lactide)-poly(ethylene glycol)-poly(L-lactide) and their evaluation in vitro. *Int J Pharm* 1999; **185**: 93-101
- 39 **Kim SY**, Doh HJ, Ahn JS, Ha YJ, Jang MH, Chung SI, Park HJ. Induction of mucosal and systemic immune response by oral immunization with *H. pylori* lysates encapsulated in poly(DL-lactide-co-glycolide) microparticles. *Vaccines* 1999; **17**: 607-616
- 40 **Kofler N**, Ruedl C, Klima J, Recheis H, Bock G, Wick G, Wolf H. Preparation and characterization of poly(DL-lactic-co-glycolide) and poly(L-lactic acid) microspheres with entrapped pneumotropic bacterial antigens. *J Immunol Meth* 1996; **192**: 25-35
- 41 **Eldridge JH**, Staas JK, Meulbroek JA, Tice TR, Gilley RM. Biodegradable and biocompatible poly(DL-lactide-co-glycolide) microspheres as an adjuvant for staphylococcal enterotoxin B toxoid which enhances the level of toxin-neutralizing antibodies. *Infect Immun* 1991; **59**: 2978-2986

Edited by Ma JY

• *H. pylori* •

***Helicobacter pylori* infection and gastric cancer: evidence from a retrospective cohort study and nested case-control study in China**

Run-Tian Wang, Tao Wang, Kun Chen, Ji-Yao Wang, Jie-Ping Zhang, San-Ren Lin, Yi-Min Zhu, Wen-Ming Zhang, Yu-Xin Cao, Chou-Wen Zhu, Hai Yu, Yu-Jun Cong, Shu Zheng, Bing-Quan Wu

Run-Tian Wang, Tao Wang, Jie-Ping Zhang, San-Ren Lin, Bing-Quan Wu, Health Science Center, Peking University, Beijing, 100083, China

Kun Chen, Yi-Min Zhu, Shu Zheng, School of Medicine, Zhejiang University, Hangzhou, 310031, China

Ji-Yao Wang, Chou-Wen Zhu, Zhongshan Hospital, Fudan University, Shanghai, 200032, China

Wen-Ming Wang, The First People's Hospital of Changzhou, Jiangsu, 213003, China

Yu-Xin Cao, The First People's Hospital of Muping, Shandong, 264100, China

Yu-Jun Cong, The Third People's Hospital of Muping, Shandong, 264107, China

Supported by Chinese Medical Board of New York, Inc., No.96-628

Correspondence to: Run-Tian Wang, Prof., Department of Epidemiology and Health Statistics, School of Public Health, Peking University, Beijing, 100083, China. twang@bjmu.edu.cn

Telephone: +86-10-62091525 **Fax:** +86-10-62015583

Received 2002-04-29 **Accepted** 2002-06-12

followed up for 1-19 years, averaged 10.88 years. The outcome of death from stomach cancer in the exposure cohort was 33, and in the non-exposure cohort 11. After adjustment for age and sex, RR=1.9850 ($P=0.0491$), 95 % CI was 1.0026, and 3.9301. The results of conditional logistic regression showed an OR of 4.467 and 95 % CI of 1.161, and 17.190 for the nested case control study.

CONCLUSION: The results from the retrospective cohort study and the nested-case control study on the association of *H. pylori* infection and gastric cancer in China suggested that *Helicobacter pylori* infection might increase the risk of stomach cancer.

Wang RT, Wang T, Chen K, Wang JY, Zhang JP, Lin SR, Zhu YM, Zhang WM, Cao YX, Zhu CW, Yu H, Cong YJ, Zheng S, Wu BQ. *Helicobacter pylori* infection and gastric cancer: evidence from a retrospective cohort study and nested case-control study in China. *World J Gastroenterol* 2002; 8(6):1103-1107

Abstract

AIM: To explore the association between *Helicobacter pylori* (*Hp*) infection and risk of gastric cancer in China.

METHODS: Utilizing gastroendoscopic biopsy tissue banks accumulated from 1980 to 1988 in Shandong, Zhejiang, and Jiangsu, where stomach cancer incidence was high, during stomach cancer screening conducted by Health Science Center of Peking University, School of Medicine of Zhejiang University, and Zhongshan Hospital of Fudan University. Warthin Starry silver staining method was applied to determine *H. pylori* infection status of biopsies collected during gastroendoscopic examination. In the retrospective study, the subjects were divided into two cohorts, the exposure cohort was positive *H. pylori* infection, and the non-exposure cohort was negative. Death from stomach cancer was determined as the outcome of the study. Logistic regression and Cox regression were applied to analyze the association between *Helicobacter pylori* infection and gastric cancer risk. In the nested case-control study, there were 28 deaths from gastric cancer in the fields of Muping, Shandong province, and Zhoushan, Zhejiang provinces. 4 controls were matched to each case on the basis of age (± 5 years old), sex, residential place at the same time entered into the study. Conditional logistic regression analysis was used to analyze the data.

RESULTS: There were a total of 2 719 subjects (male 1 399, female 1 320) with gastroendoscopic biopsies stored available treated as a cohort. *H. pylori* positive cohort included 1 671 subjects (61.5 %) and *H. pylori* negative cohort 1 048 subjects (38.5 %). These subjects were

INTRODUCTION

Large volume of literature on the association of *H. pylori* infection and gastric cancer has been published since Warren and Marshall first isolated *Helicobacter pylori* from human gastric mucosa in 1983^[1]. The first compelling evidence linking *H. pylori* infection to gastric cancer was obtained from seroepidemiologic studies using nested case-control study design in the United States and Britain^[2-4]. Although there were discrepancy among epidemiological studies^[5-22], some meta-analyses indicated the magnitude of the association *H. pylori* infection and risk of gastric cancer was ORs=2-6^[23-27]. Most of the studies based on serological data; the status of whether the *H. pylori* harbored in gastric mucosa at the time of sample collection was uncertain and it only indicated past infection of *H. pylori*. Using the *H. pylori* detected by microscopy from biopsy had some limitations because only several specimens were taken during endoscopy underwent, which might lead to underestimation. However, the bacilli found under microscope might reveal actual status of *H. pylori* harbored in the gastric mucosa. Under the support of foundation of Chinese Medical Board of New York Inc., Health Science Center of Peking University, Medical School of Zhejiang University and Zhongshan Hospital of Fudan University cooperated in the study of the association of *H. pylori* infection and gastric cancer. The subjects of *H. pylori* infection was positive when there were bacilli found under the microscope, the outcome of the study was gastric cancer death. A nested case-control design was carried out using gastric cancer death from Muping, Shandong province and Zhoushan, Zhejiang province where most of the subjects resided in the rural areas.

MATERIALS AND METHODS

Field of investigation

The field of Health Science Center of Peking University is Gaoling town in Muping County of Yantai City of Shandong province (short for Muping below), the mortality rate of gastric cancer was averaging 40/100 000 population during the last two decades. Screening and early diagnosis program were undertaken for those over 35 years old in 1987 and 1988. 2200 subjects' biopsies were taken and underwent histopathological diagnosis. The field of School of Medicine of Zhejiang University is Daishan county in Zhoushan archipelago of Zhejiang Province (short for Zhoushan below), the mortality rate of gastric cancer was about 50/100 000 population, gastric cancer screening had been conducted and gastroendoscopy and histological diagnosis had been done on about 1800 subjects from 1980 to 1983. The field of Zhongshan Hospital of Fudan University is Changzhou city in Jiangsu province (short for Changzhou below), the mortality rate of gastric cancer was about 40/100 000 population, gastroendoscopy had been carried out in 1500 subjects.

Pathological and laboratory examination criteria

The histologic sections stained by H&E was according to the National Gastric Cancer Prevention Study Pathological Diagnostic Criteria, and gastric cancer was confirmed by pathological diagnosis. The *H. pylori* infection was determined by histologic assessment. Warthin Starry silver staining was applied to the histologic section of endoscopic biopsies and to determine the status of *H. pylori* infection of the subjects. The diagnostic criteria followed the Criteria for diagnosis on histologic sections on the first meeting of experts when an agreement was reached in April 1999^[28].

Subjects of retrospective cohort study

Biopsies were available for histologic sections and Warthin Starry silver staining from Muping, Zhoushan and Changzhou comprised the cohort. There were 1055, 875 and 793 subjects' biopsies available, respectively. The pathologic diagnosis was retrieved according to the record of diagnosis, and gastric cancer patients were excluded either for those diagnosed at the time of screening or diagnosed within one year after screening program. The histologic assessment of *H. pylori* infection was conducted by pathologists well trained on diagnosing *H. pylori* infection with Warthin Starry silver staining slides. The exposure cohort was *H. pylori* infection positive after the histologic section assessment, and the non-exposure cohort was negative.

Subjects of nested case-control study

The cases were those who died from gastric cancer during the following period after the screening program and met the criteria set forth above in Muping and Zhoushan. For each case of gastric cancer death, we matched 4 controls on the basis of age (not ± 5 years), sex, date of biopsy specimen sampling and residential place, who were gastric cancer-free at the end of 1999.

Questionnaire survey

All subjects whose biopsies for histologic assessment were given a questionnaire interview, which included demographic data, family history of gastric cancer, life style such as smoking habit etc., and diagnosis and treatment of *H. pylori* infection in the past. The interviewers were village doctors trained on the interviewing skills. The interviews started from 1998 to the end of 1999. The subjects died and those who could not answer the questions while interviewing, was helped by their relatives familiar with them.

Statistical analysis

A database was established by the EPI info package, was put in according to standard procedure after the questionnaires evaluation and met the requirements. The SPSS package was used to conduct logistic regression analysis of the cohort and the Egret package (A Commercial System for Advanced Epidemiologic Statistics 1999) was applied to conduct Cox regression analysis of the survival data of the cohort, conditional logistic regression was used to compute the asymptotic ORs for the nested case control data.

RESULTS

General information of the cohort

The total subjects of the cohort were 2 719. There were 1 055 subjects from Muping, 875 subjects from Zhoushan and 793 subjects from Changzhou.

1 399 (51.5 %) subjects were male, and 1 320 (48.5 %) female. 1 671 (61.5 %) subjects were *H. pylori* positive; 1 048 (38.5 %) were *H. pylori* negative. Table 1 listed the general information of the three cohorts.

Table 1 The general information of the *H. pylori* positive and *H. pylori* negative cohorts

	<i>H. pylori</i> positive cohort	<i>H. pylori</i> negative cohort	Total	<i>P</i>
Gender (male/female)	1671(881/790)*	1048(520/528)	2719 (1399/1320)	>0.05
Muping	675(424/251)	380(239/141)		=1.000
Zhoushan	501(285/216)	370(183/187)		=0.033*
Changzhou	495(172/323)	298(98/200)		=0.643
Age (<50, 50-60, ≥ 60)	1671 (604,505,562)	1048 (366,310,372)	2719 (970,815,934)	>0.05
Muping	675(216,189,270)	380(102,110,168)		0.082,0.096
Zhoushan	501(221,138,142)	370(142,109,119)		0.097,0.224
Changzhou	495(167,178,150)	298(112,91,85)		0.108,0.131
Economic Status (well,poor)	1612 (1513,99)	1007 (949,58)	2619 (2462,157)	>0.05 (0.719-0.734)
Smoking (yes, no)	1610 (877,733)	1006 (566,450)	2616 (1433,1183)	>0.05 (0.123-1.0)
Alcohol drinking (yes, no)	1610 (624,986)	1006 (384,622)	2616 (1008,1608)	>0.05 (0.07-0.814)
Family history of gastric cancer (yes, no)	1670 (167,1503)	1046 (98,948)	2716 (265,2451)	>0.05 (0.277-0.948)

*The number in the parenthesis indicated the relevant number of each category defined in the first column.

Average follow-up duration of the subjects (Table 2)

Table 2 Follow-up duration of the cohort

Fields	<i>n</i>	Average follow-up duration(yrs)	Standard devision
Muping	1055	11.1496	2.8798
Zhoushan	871	14.1883	2.5603
Changzhou	793	6.5596	2.1343
Total	2719	10.8805	4.0358

There were 2 719 subjects' biopsies available for histologic assessment of *H. pylori* infection in the three fields where the prevalence rate of gastric cancer was high in China and were followed up to observe the outcome. The average follow-up duration was 10.88 years.

Number of gastric cancer deaths observed in cohort

The number of gastric cancer deaths observed in each field in *H. pylori* positive and *H. pylori* negative cohorts was listed in Table 3.

Table 3 The distribution of gastric cancer deaths observed in the follow-up period of the cohorts

Field	<i>H. pylori</i> positive cohort		<i>H. pylori</i> negative cohort		Total	
	<i>n</i>	No. of gastric cancer death	<i>n</i>	No. of gastric cancer death	<i>n</i>	No. of gastric cancer death
Muping	675	9	380	3	1055	12
Zhoushan	501	10	370	6	871	16
Changzhou	495	14	298	2	793	16
Total	1671	33	1048	11	2719	44

There were 1 671 subjects in the exposure cohort and 1 048 subjects in the non-exposure cohort, 33 and 11 cases respectively died from gastric cancer during the follow-up period.

The results of cohort study

The average age of gastric cancer death cases of the *H. pylori* positive and *H. pylori* negative cohorts was 60.41 and 69.18, respectively. The *t* test showed that there was significant difference between the two cohorts ($t=2.494$, $P=0.017$). The results of logistic regression analysis of association of *H. pylori* infection and gastric cancer death of different age groups were shown in Table 4. The results of Cox regression analysis was shown in Table 5.

Table 4 Result of logistic regression analysis of different age groups

Variables	OR	95 %
<50 years old	4.601	1.885,11.229
50-60 years old	1.916	0.961,3.822
≥60 years old	Do not convergence	

Table 5 The results of Cox regression analysis with adjustment of age and sex

Variable	β	S.E	Wald	df	<i>P</i>	RR	95%CI	
							lower	upper
<i>H. pylori</i>	0.6856	0.3485	3.8705	1	0.0491	1.9850	1.0026	3.9301
Age	0.9062	0.5005	3.2773	1	0.0702	2.4748	0.9278	6.6010
Sex	-0.3237	0.3203	1.0215	1	0.3122	0.7234	0.3861	1.3554

The RR=1.9850, $P=0.0491$, 95 % CI is 1.0026 to 3.9301 for exposure of *H. pylori* infection cohort to non-exposure cohort with adjustment of age and sex.

The cumulative hazard function for positive and negative *H. pylori* infection and gastric cancer death adjusted age and sex was shown in Figure 1: a higher hazard for subjects with positive *H. pylori* infection, the difference was statistically different.

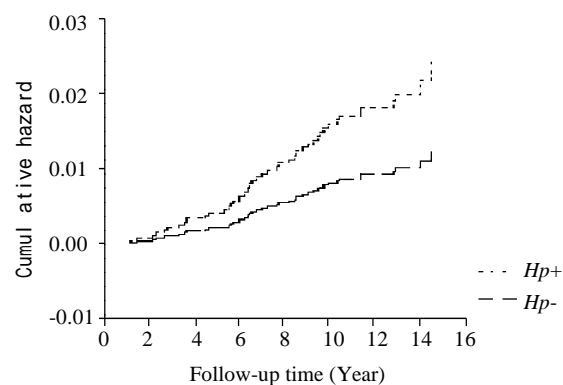


Figure 1 Cumulative hazard function for subjects with positive and negative *H. pylori* infection

The results of nested case-control study

The total number of gastric cancer death within the cohort of Muping and Zhoushan was 28, and 21 were male, 7 female. The average age of the subjects of cases and controls was 65.89 and 65.21, and the statistical analysis showed no difference between the two cohorts.

After univariate analysis, the result of multivariate analysis with adjustment of potential confounding factors was shown in Table 6.

Table 6 The result of conditional logistic analysis of *H. pylori* and gastric cancer risk

	β	<i>P</i>	OR	95% CI (lower)	95% CI (upper)
<i>H. pylori</i> infection	1.497	0.0295	4.467	1.1610	17.1900
Non-farmer	-1.415	0.0669	0.243	0.0535	1.1040
Poor economic condition	1.287	0.2022	3.620	0.5011	26.1600
Usually drank unboiled water	1.099	0.1565	3.000	0.6564	13.710
Wash hands before meals	-1.896	0.0241	0.150	0.0289	0.7798
Like to eat smoked food	0.913	0.2102	2.492	0.5974	10.3900
Lower vegetables intake	0.5153	0.4542	1.674	0.4342	6.4550
Smoking	5.808	0.0037	332.800	6.5840	1.683e+004
Older age started to smoke	-0.145	0.0137	0.865	0.7707	0.9707
Lower fruits intake	-0.524	0.4836	0.592	0.1367	2.5660
History of upper abdominal pain	0.678	0.3027	1.970	0.5425	7.1530

After adjusted some potential confounding factors, it showed that *H. pylori* infection was significantly associated with gastric cancer death, the OR was 4.467, 95 % CI was 1.161-17.19, $P<0.05$.

DISCUSSION

The aim of this study was to explore the association between *H. pylori* infection and gastric cancer risk. The average follow up duration was 10.8 years. The results of retrospective analysis showed that the risk of death from gastric cancer in the *H. pylori*

positive cohort was 1.985 times to *H. pylori* negative cohort (95 % CI (1.0026, 3.9301)); the results of the nested case-control showed the association between *H. pylori* infection and gastric cancer risk increased after adjustment of some potential confounding factor, the OR was 4.467, 95 % CI was 1.161 to 17.190. The result suggested that the *H. pylori* infection was associated with gastric cancer death. The results were in accordance with those retrospective and nested case control studies^[2-4,10,12,14,18,19, 21,22] and meta-analyses of *H. pylori* infection and gastric cancer risk published recently^[23-27]. It was also similar to the magnitude of association between *H. pylori* infection and non-cardia gastric cancer 2.29^[29] in Linxian of China reported by Limburg *et al* in a nested case control study and the results of Hansen *et al*^[14]. The average age of gastric death in the *H. pylori* infection cohort was younger than that of negative cohort, the difference was statistically significant, the ORs of different age groups were in favor of that *H. pylori* infection was risk factor for the young^[10,30,31]. Because the carcinogenesis of gastric cancer was of multiple stages and multiple factors involvement, *H. pylori* infection is not an independent risk factors on the carcinogenesis of gastric cancer. The prevalence of *H. pylori* infection is high in developing counties, only a small proportion of people infected with the bacteria develop gastric cancer. The biological mechanism of gastric carcinogenesis remains unclear. Our results suggested that *H. pylori* infection played different role at different ages of life.

The gastric cancer death in this study was those histologically confirmed cases and excluding those followed after gastroendoscopic screening within one year in each field and cardia gastric cancer, all these limitations might strengthen the virtual epidemiological evidence generated by this study.

There are several methods to determine the *H. pylori* infection of the stomach; the sensitivity and specificity are approximate^[32-34]. The application of these methods would render different results' false negative results in different population^[7,13,33,34], and the use of multiple tests may help to provide a more accurate diagnosis of *H. pylori* infection^[35]. Although the seroconversion rate was a bit lower^[36,37]. The loss of *H. pylori* infection may occur earlier in those using serological assessment of *H. pylori* infection than using histological assessment of *H. pylori* infection, because sera *H. pylori* IgG can be detected after the eradication of *H. pylori*. Histologic assessment of biopsies was more reliable and with less information bias. The data of this study was a combined analysis in high gastric cancer prevalence areas in China. The recent mortality rate of gastric cancer was about 40-50/100 000 persons by screening and early diagnostic program carried out in the three regions and the biopsies reserved made such a study feasible. Although the subjects screened could not represent the natural population and some biopsies used by other studies, there might be selection bias, which could result some bias in the estimation the association between *H. pylori* infection and gastric cancer risk. Since strict quality control and the confounding factors controlled during the analysis were conducted, the chance of misclassification of diagnosis and exposure was minimized, and the overall result was reliable.

Although we had provided evidence for positive association between *H. pylori* infection and gastric cancer risk based on histologic assessment of *H. pylori* infection by limited cohort subjects, it needs to expand the study in a natural population to minimize the selection bias. The association between *H. pylori* *Cag A* positive strain, which is considered more virulent than others, and gastric cancer should be further investigated. More convincing evidence of *H. pylori* infection and gastric cancer risk would be gained by *H. pylori* eradication interventional study.

REFERENCES

- 1 Warren JR, Marshall BJ. Unidentified curved bacilli on gastric epithelium in active chronic gastritis. *Lancet* 1983; **1**: 1273-1275
- 2 Forman D, Newell DG, Fullerton F, Yarnell JWG, Stacey AR, Wald N, Sitas F. Association between infection with *Helicobacter pylori* and risk of gastric cancer: evidence from a prospective investigation. *British Med J* 1991; **302**: 1302-1305
- 3 Parsonnet J, Friedman GD, Vandersteen DP, Chang Y, Vogelmann JH, Orentreich N, Sibley RK. *Helicobacter pylori* infection and the risk of gastric carcinoma. *N Engl J Med* 1991; **325**: 1127-1131
- 4 Nomura A, Stemmermann GN, Chyou PH, Kato I, Perez-Perez GI, Blaser MJ. *Helicobacter pylori* infection and gastric carcinoma among Japanese Americans in Hawaii. *N Engl J Med* 1991; **325**: 1132-1136
- 5 Muszynski J, Dzierzanowska D, Sieminska J, Bogdanska M, Vogt E, Ehrmann A. Is *Helicobacter pylori* infection a real risk factor for gastric carcinoma? *Scand J Gastroenterol* 1995; **30**: 647-651
- 6 Rudi J, Muller M, von Herbay A, Zuna I, Raedsch R, Stremmel W, Rath U. Lack of association of *Helicobacter pylori* seroprevalence and gastric cancer in a population with low gastric cancer incidence. *Scand J Gastroenterol* 1995; **30**: 958-963
- 7 Webb PM, Yu MC, Forman D, Henderson BE, Newell DG, Yuan JM, Gao YT, Ross RK. An apparent lack of association between *Helicobacter pylori* infection and risk of gastric cancer in China. *Int J Cancer* 1996; **67**: 603-607
- 8 Kim HY, Cho BD, Chang WK, Kim DJ, Kim YB, Park CK, Shin HS, Yoo JA. *Helicobacter pylori* infection and the risk of gastric cancer among the Korean population. *J Gastroenterol Hepatol* 1997; **12**: 100-103
- 9 Watanabe Y, Kurata JH, Mizuno S, Mukai M, Inokuchi H, Miki K, Ozasa K, Kawai K. *Helicobacter pylori* infection and gastric cancer. A nested case-control study in a rural area of Japan. *Dig Dis Sci* 1997; **42**: 1383-1387
- 10 Whiting JL, Hallissey MT, Fielding JWL, Dunn J. Screening for gastric cancer by *Helicobacter pylori* serology: a retrospective study. *British J Surg* 1998; **85**: 408-411
- 11 Wu MS, Shun CT, Lee WC, Chen CJ, Wang HP, Lee WJ, Sheu JC, Lin JT. Gastric cancer risk in relation to *Helicobacter pylori* infection and subtypes of intestinal metaplasia. *Brit J Cancer* 1998; **78**: 125-128
- 12 Azuma T, Ito S, Sato F, Yamazaki Y, Miyaji H, Ito Y, Suto H, Kuriyama M, Kato T, Kohli Y. The role of HLA-DQA1 gene in resistance to atrophic gastritis and gastric adenocarcinoma induced by *Helicobacter pylori* infection. *Cancer* 1998; **82**: 1013-1018
- 13 Yuan JM, Yu MC, Xu WW, Cockburn M, Gao YT, Ross RK. *Helicobacter pylori* infection and risk of gastric cancer in Shanghai, China: updated results based upon a locally developed and validated assay and further follow-up of the cohort. *Cancer Epidemiology, Biomarkers & Prevention* 1999; **8**: 621-624
- 14 Hansen S, Melby KK, Aase S, Jellum E, Vollset SE. *Helicobacter pylori* infection and risk of cardia cancer and non-cardia gastric cancer. A nested case-control study. *Scand J Gastroenterol* 1999; **34**: 353-360
- 15 Inoue M, Tajima K, Matsuura A, Suzuki T, Nakamura T, Ohashi K, Nakamura S, Tominaga S. Severity of chronic atrophic gastritis and subsequent gastric cancer occurrence: a 10-year prospective cohort study in Japan. *Cancer Lett* 2000; **161**: 105-112
- 16 Enroth H, Kraaz W, Engstrand L, Nyren O, Rohan T. *Helicobacter pylori* strain types and risk of gastric cancer: a case-control study. *Cancer Epidemiol Biomarkers Prev* 2000; **9**: 981-985
- 17 Plummer M, Vivas J, Fauchere JL, Del Giudice G, Pena AS, Ponzetto A, Lopez G, Miki K, Oliver W, Munoz N. *Helicobacter pylori* and stomach cancer: a case-control study in Venezuela. *Cancer Epidemiol Biomarkers Prev* 2000; **9**: 961-965
- 18 Yamagata H, Kiyohara Y, Aoyagi K, Kato I, Iwamoto H, Nakayama K, Shimizu H, Tanizaki Y, Arima H, Shinohara N, Kondo H, Matsumoto T, Fujishima M. Impact of *Helicobacter pylori* infection on gastric cancer incidence in a general Japanese population: the Hisayama study. *Arch Intern Med* 2000; **160**: 1962-1968
- 19 Wang T, Chen K, Wang RT, Zhu YM, Cong YJ, Zhou YN, Zhang JP, Yu H, Cao YX, Zheng S. Nested case-control study on the

- relationship of *Hp* infection and gastric cancer risk. *Zhongguo Yufang Yixue Zazhi* 2001; **2**: 27-29
- 20 **Jiang YW**, Wang RT, Wang T, Zhang JP, Lei DN. Multi-groups controlled study on the association of *Helicobacter pylori* infection with gastric cancer and stomach diseases. *Beijing Daxue Xuebao(Yixue Ban)* 2001; **33**: 160-163
 - 21 **Wang RT**, Chen K, Wang JY, Wang T, Zhu YM, Zhang WM, Cao YX, Zhang JP, Zhu CW, Yu H, Zheng S, Wu BQ. Retrospective study on *Helicobacter pylori* infection and gastric cancer risk. *Zhonghua Yixue Zazhi* 2001; **81**: 1458-1459
 - 22 **Uemura N**, Okamoto S, Yamamoto S, Matsumura N, Yamaguchi S, Yamakido M, Taniyama K, Sasaki N, Schlemper RJ. *Helicobacter pylori* Infection and the development of gastric cancer. *N Engl J Med* 2001; **345**: 784-789
 - 23 **Huang JQ**, Sridhar S, Chen Y, Hunt RH. Meta-analysis of the relationship between *Helicobacter pylori* seropositivity and gastric cancer. *Gastroenterology* 1998; **114**: 1169-1179
 - 24 **Danesh J**. *Helicobacter pylori* infection and gastric cancer: systematic review of the epidemiological studies. *Aliment Pharmacol Ther* 1999; **13**: 851-856
 - 25 **Eslick GD**, Lim LL, Byles JE, Xia HH, Talley NJ. Association of *Helicobacter pylori* infection with gastric carcinoma: a meta-analysis. *Am J Gastroenterol* 1999; **94**: 2373-2379
 - 26 **Helicobacter and Cancer Collaborative Group**. Gastric cancer and *Helicobacter pylori*: a combined analysis of 12 case control studies nested within prospective cohorts. *Gut* 2001; **49**: 347-353
 - 27 **Xue FB**, Xu YY, Wan Y, Pan BR, Ren J, Fan DM. Association of *H. pylori* infection with gastric carcinoma: a meta analysis. *World J Gastroenterol* 2001; **7**: 801-804
 - 28 **National H. pylori Research Group**. Agreement and comments on some *H. pylori* issues. *Chinese Medical Journal* 2000; **80**: 394-395
 - 29 **Limburg PJ**, Qiao YL, Mark SD, Wang GQ, Perez-Perez GI, Blaser MJ, Wu YP, Zou XN, Dong ZW, Taylor PR, Dawsey SM. *Helicobacter pylori* Seropositivity and subsite-specific gastric cancer risks in Linxian, China. *J Natl Cancer Instit* 2001; **93**: 226-233
 - 30 **Haruma K**, Komoto K, Kamada T, Ito M, Kitadai Y, Yoshihara M, Sumii K, Kajiyama G. *Helicobacter pylori* infection is a major risk factor for gastric carcinoma in young patients. *Scand J Gastroenterol* 2000; **35**: 255-259
 - 31 **Imrie C**, Rowland M, Bourke B, Drumm B. Is *Helicobacter pylori* infection in childhood a risk factor for gastric cancer? *Pediatriscs* 2001; **107**: 373-380
 - 32 **Logan RPH**, Walker MM. ABC of the upper gastrointestinal tract: Epidemiology and diagnosis of *Helicobacter pylori* infection. *BMJ* 2001; **323**: 920-922
 - 33 **Miwa H**, Kikuchi S, Ohtaka K, Kobayashi O, Ogihara A, Hojo M, Nagahara A, Sato N. Insufficient diagnostic accuracy of imported serological kits for *Helicobacter pylori* infection in Japanese population. *Diagn Microbiol Infect Dis* 2000; **36**: 95-99
 - 34 **Ohara S**, Kato M, Asaka M, Toyota T. Studies of ¹³C-urea breath test for diagnosis of *Helicobacter pylori* infection in Japan. *J Gastroenterol* 1998; **33**: 6-13
 - 35 **Tabata H**, Fuchigami T, Kobayashi H, Sakai Y, Nakanishi M, Tomioka K, Nakamura S, Fujishima M. *Helicobacter pylori* and mucosal atrophy in patients with gastric cancer: a special study regarding the methods for detecting *Helicobacter pylori*. *Dig Dis Sci* 1999; **44**: 2027-2034
 - 36 **Rosenstock S**, Jorgensen T, Andersen L, Bonnevie O. Seroconversion and seroreversion in IgG antibodies to *Helicobacter pylori*: a serology based prospective cohort study. *J Epidemiol Community Health* 2000; **54**: 444-450
 - 37 **Kumagai T**, Malaty HM, Graham DY, Hosogaya S, Misawa K, Furihata K, Ota H, Sei C, Tanaka E, Akamatsu T, Shimizu T, Kiyosawa K, Katsuyama T. Acquisition versus loss of *Helicobacter pylori* infection in Japan: results from an 8-year birth cohort study. *J Infect Dis* 1998; **178**: 717-721
 - 38 **Sung JY**, Lin SR, Ching JYL, Zhou LY, To KF, Wang RT, Leung WK, Ng EKW, Lau JYW, Lee YT, Yeung CK, Chao W, Chung SCS. Atrophy and intestinal metaplasia one year after cure of *H. pylori* infection: a prospective, randomized study. *Gastroenterology* 2000; **119**: 7-14

Edited by Wu XN

• BASIC RESEARCH •

Mutation of RET gene in Chinese patients with Hirschsprung's disease

Ji-Cheng Li, Shi-Ping Ding, Ying Song, Min-Ju Li

Ji-Cheng Li, Shi-Ping Ding, Ying Song, Department of Lymphology, Department of Histology and Embryology, Zhejiang University Medical College, Hangzhou 310031, Zhejiang Province, China

Min-Ju Li, Children's Hospital, Zhejiang University Medical College, Hangzhou 310006, Zhejiang Province, China

Supported by Excellent Young Talented Person by Chinese Health Ministry and Analysis and Testing Foundation of Zhejiang Province
Correspondence to: Dr. Ji-Cheng Li, Department of Lymphology, Department of Histology and Embryology, Zhejiang University Medical College, Hangzhou 310031, Zhejiang Province, China. lijc@mail.hz.zj.cn

Telephone: +86-571-87217139 **Fax:** +86-571-87217139

Received 2002-03-30 **Accepted** 2002-04-20

Abstract

AIM: To investigate the pathogenic mechanism of Hirschsprung's disease (HD) at the molecular level and to elucidate the relationship between RET oncogene and Chinese patients with HD.

METHODS: Exon 13 of RET oncogene from 20 unrelated HD patients was analyzed with polymerase chain reaction-single strand conformation polymorphism (PCR-SSCP). The positive amplifying products were then sequenced. According to the results of SSCP and DNA sequence, SSCP was done as well for the samples from the family other members of some cases with mutated RET gene.

RESULTS: SSCP analysis indicated that mobility abnormality existed in 4 unrelated HD patients. Direct DNA sequence analysis identified a missense mutation, T to G at the nucleotide 18 888 and a frameshift mutation at the nucleotide 18 926 insG. In a HD family, the sicked child and his father were the same heterozygous missense mutation (T to G at nucleotide 18 888).

CONCLUSION: Among Chinese HD patients, RET gene mutations may exist in considerable proportion with different patterns. These new discoveries indicate that RET mutations may play an important role in the pathogenesis of unrelated HD in the Chinese population. PCR-SSCP combined with DNA sequence can be used as a tool in the genetic diagnosis of HD.

Li JC, Ding SP, Song Y, Li MJ. Mutation of RET gene in Chinese patients with Hirschsprung's disease. *World J Gastroenterol* 2002; 8(6):1108-1111

INTRODUCTION

Hirschsprung's disease (HD), with the incidence of 1/5 000, occupies the second in the congenital malformation, manifests as complete or incomplete ileus clinically^[1-5]. As a complex disease, HD has been ascribed to the absence in the terminal

hindgut of ganglion cells from the neural crest, which causes the abnormal contraction of involved intestines, and then the proximal end of the sick colon appears compensatory dilated thickness and forms megacolon. However, the reason for the deficit of ganglion cells remains in dispute^[5]. With the development of the molecular biology, the molecular pathogenesis of HD have attracted the attention of many scholars. In 1993, Genetic mapping in multiplex families and the mutational analysis of candidate genes have led to the definitive identification of the defects that contribute to the HD risk. It has been found that the gene defects present in a major proportion of Hirschsprung's disease families are mutations in chromosome 10q11.2, which have now been found to be associated with RET gene^[6-9]. Subsequently, various kinds of mutation of RET gene have been reported abroad^[10-19]. However, there existed less reports about HD in Chinese population. In order to further investigate the pathogenic mechanism of HD, we examined exon 13 mutations of RET gene in 20 unrelated patients with the single strand conformation polymorphism analysis of polymerase chain reaction products (PCR-SSCP).

MATERIALS AND METHODS

Case selection and extraction of DNA

Twenty unrelated cases with HD by pathological verification were collected after operation at Zhejiang Children's Hospital during 1998 to 2000. Four milliliters of peripheral blood samples used for the experiment were obtained from each patient and the control blood samples were taken from anonymous donors provided by Zhejiang Children's Hospital. The blood samples were anti-coagulated by sodium citrate and DNA was extracted according to the standard protocols.

PCR amplification

The designed primers were synthesized by Shanghai Shengong Biology Company. The primer sequence of exon 13: (Forward) 5'-GACCTGGTATGGTCATGGA-3', (Reverse) 5'-AAGAGGGAGAACAGGGCTGTA-3'. The PCR mixture contained 200 ng of template-DNA and PCR reaction buffer containing 50 mmol/L KCl, 10 mmol/L Tris-HCl (pH 8.4), 1.5 mmol/L MgCl₂, 0.5 μmol/L each of two fragment-specific primers, 100 μmol/L each of dATP, dGTP, dTTP and dCTP, and 2 units of Taq DNA polymerase (provided by Shanghai Shengong Biology Company) for a reaction volume of 50 μL. The conditions for temperature cycling for all PCR amplifications were 94 °C for 5 min for pre-denaturation, 94 °C for 45 second, 58 °C for 45 second and 72 °C for 45 second. Amplifications were carried out for 30 cycles with a final extension for 10 min at 72 °C. The amplified fragments were run in 1 % agarose gel, and were confirmed to be 253bp in size using 100-bp ladder markers.

SSCP analysis

SSCP analysis of fragments was performed on a Mini

Electrophoresis Unit (Bio-Rad Company, U.S.A). 10 μ l of the PCR product was diluted with 10 μ l of sample buffer containing 90 % formamide, 0.05 % Bromphenol Blue dye and 0.05 % xylene cyanol. The samples were heated at 100 °C for 8 min, transferred into an ice-cold water bath for 3 min, and analysed by 8 % PAGE in 45 mM-Tris-borate (pH8.0)/1mM-EDTA (TBE) buffer under 13 v·cm⁻¹ at 10 °C.

DNA silver staining

Gels were stained with silver as follows: fixed in 100 ml·L⁻¹ alcohol for 10 min→oxidized in 100 ml·L⁻¹ nitric acid for 3 min→drip washed for 1 min with double distilled water→stained in 2 g·L⁻¹ silver nitric acid for 5 min→drip washed for 1 min with double distilled water →showed appropriated color in 15 g·L⁻¹ anhydrous sodium carbonate and 4 ml·L⁻¹ formalin →ended reducing response by 7.5 ml·L⁻¹ glacial acetic acid→drip washed with double distilled water →analysis results and photographed.

Purification of PCR product , T clone and DNA sequence

Abnormal PCR products screened by SSCP was cut from gel and purified by VIOGENE kit. Agarose gel-purified PCR products was subcloned to pUCm-T vector through TA clone. Sequence analysis was carried out with a PE377 automated sequencer.

RESULTS

The analysis of PCR products

The increment of all DNA samples from HD patients was a single strand with the length of 253 bp, and so was that from normal control, which indicated that a large fragment insertion and deletion did not exist in the region of exon 13 of RET gene among 20 HD patients.

Results of SSCP-Ag dying and DNA sequencing

Of all the patients and normal control analyzed, four showed abnormal SSCP patterns in exon 13. In Figure 1,2, the mobility of one single-strand was abnormal in case 2,3,4. In case 6, the mobility of two single-strand was abnormal. DNA sequence analysis showed nucleotide changes in all variable SSCP bands. Of the two patterns of nucleotide change, one was missense mutation, and the other was frameshift mutation (Figure 3, Table 1).

Table 1 The mutation analysis of exon 13 of RET gene from four cases

case	he heterozygous of allele gene	Nucleotide change	Amino acid change	Mutation types
case2	Heterozygote	18 888 T→G	Cys→Phe	missense mutation
case3	Heterozygote	18 888 T→G	Cys→Phe	missense mutation
case4	Heterozygote	18 888 T→G	Cys→Phe	missense mutation
case6	Homozygote	18 926 ins G	--	frameshift mutation

The parents genotypes of the case 2,3 and 4 were also examined by SSCP. We found that the mobility pattern of the father was in coincidence with his son in case 4, while the mobility pattern of the mother was normal (Figure 4). DNA sequence analysis showed the same mutation between the father and the son, implied that the exon 13 of RET gene in case 4 was originated from his paternal heredity. No abnormal patterns of DNA migration was observed in the parents of the case2,3.

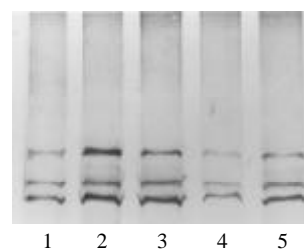


Figure 1 The abnormal shifted SSCP bands in exon 13. Lanes 1,2:normal control; Lanes3-5:case 1,2,3.

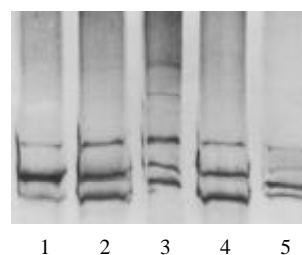


Figure 2 The abnormal shifted SSCP bands in exon 13. Lanes 1,2:normal control; Lanes 3-5:case 4-6.

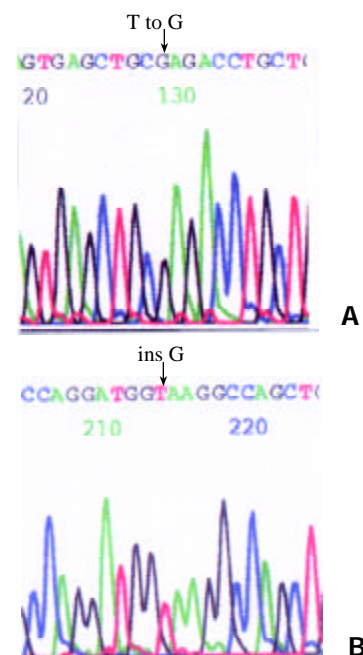


Figure 3 A fragment of sequence in exon 13 of case2(a),3(a),4(a),6(b). The arrows indicate the position of mutation.

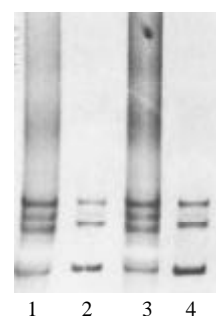


Figure 4 The abnormal shifted SSCP bands in exon 13 of case 4 and his parents. Lanes1: normal control; Lane2: case 4; Lane3: mother of case 4; Lane4: father of case 4.

DISCUSSION

The human RET gene lies on chromosome band 10q11.2 and comprises 20 exons, with the length about 80 kb^[20-26]. The RET gene encodes a receptor tyrosine kinase consisting of an intracellular tyrosine kinase domain, a transmembrane domain and an extracellular domain which includes a "cadherin-like" region. Receptor tyrosine kinases generally function as ligand dependent dimers, which phosphorylate "second messenger" proteins in the cytoplasm and they are commonly associated with regulation of cell growth and differentiation, the development of normal nerves, and expressed in gangliogenic source cells (such as neurogenic ganglia and ganglia of peripheral nerve system, neuroendocrine cells, epidermic pigment cells, etc.). Mutations of the RET gene may lead to the premature termination of the transcription and translation procedures or the alteration of amino acid sequence, and thus, during the embryogenesis, the signal conduction was obstructed, causing the nerve cells migration stagnated and the colonic nerves defected.

Exon 13 of RET gene played a key role in encoding the tyrosine kinase domain and therefore the exon 13 on 20 unrelated Chinese HD patients was examined with PCR-SSCP in the present study. The PCR result revealed that the increment of all DNA samples from HD patients was a single strand with the same length of 253 bp as that of the samples from the control, which indicated that a large fragment insertion and deletion did not exist in the exon 13 region among 20 HD cases. The SSCP analysis indicated that the mobility abnormality existed in 4 cases and further DNA sequencing analysis exhibited two novel mutations: a transition, T to G at the nucleotide 18888, which lead to a Cysteine transformed phenylalanine and the disulfide bond was disrupted of the receptor tyrosine kinase. And thus the RET protein was destroyed and the signal conduction was obstructed which finally caused HD. Another frameshift insert G at the nucleotide 18 926, which could altered the amino acid sequence and thus Hirschsprung's disease arose from the abnormal RET protein as mentioned above. In 4 HD cases, among which 3 cases were heterozygous mutation and 1 case who was two-day-old child was homozygous mutation, accompanied by serious icterus. It has been reported that only a half quantity of RET gene mutation are likely to cause HD and homozygous mutation of RET gene may be fetal in human^[24-26], which has been confirmed by our finding.

So far, a variety of frameshift, nonsense, or missense mutations scattered along the entire RET proto-oncogene have been identified in HD patients. However, the 'hot spot' region has not been found, which causes the difficulties in the design of specific primer and the detection of the RET gene mutation by routine diagnostic method. Single-strand conformation polymorphism (SSCP) analysis enables the discrimination of DNA fragments of the same size containing sequence variations and has been employed in the investigation of the monogenic and polygenic diseases as well as the oncogene and anti-oncogene studies^[27-38]. The technique is based on the facts that partially denatured double stranded DNA (dsDNA) migrates as two single stranded DNA (ssDNA) in non-denaturing polyacrylamide gel electrophoresis (PAGE), and that small changes in the nucleotide sequence may alter the ssDNA conformation and therefore its electrophoretic profiles. Thus, the single-strand conformational polymorphism analysis is useful to screen out the mutations in a small region with 150-500bp in size on a gene of interest with the rapid, economic and sensitive characteristics. Because of the fragment of RET gene exon 13 being 253bp, it is therefore suitable to take the

PCR-SSCP analysis in our experiment. Furthermore, we found that increasing the concentrations of acrylamide and methylene bisacrylamide, using the thin gel (0.75 mm-thick) and applying the 100 ml·L⁻¹ glycerin made the straps obtained more be clear and distinguishable.

Hirschsprung's disease is considered a heterogeneous genetic disorder with dominant, recessive, sex-linked and polygenic forms, and associated with a number of other genetic disorders including Down's syndrome^[39], familial leukoplakia, congenital central dysfunction of ventilation, etc. Up to now, it has not been reported yet on the inheritance patterns in the Chinese patients with HD. In the present study, SSCP analysis was performed as well for the samples from the family members of some cases with mutated RET gene. The results showed that in a HD family, the sicked child and his father were the same heterozygous missense mutation (Cys→Phe). However, the inheritance patterns for the family remain to be investigated. Besides, the sequencing analysis proved that even the same exon 13 on the RET gene manifested the allele heterogeneity in the sites and ways of mutation (missense mutation and frameshift mutation). Therefore, congenital megacolon is a highly heterogenous disease.

At present, the clinical therapy for Hirschsprung's disease includes early diagnosis and excision of involved intestine segments^[40-42]. But as for the patients with the long segment or the whole colon involved, the effect of the surgical intervention is extremely poor. In the present case, there were 4 cases of mutation screened out by the exon 13 on RET gene from 20 HD cases. The mutation rate of RET gene was 20 %. Considering the false-negative result by SSCP analysis, the rate of the RET mutation should be higher. The higher mutation rate of RET gene implied that the check-out of gene mutation can be taken as a routine technique of molecular genetics for diagnosing congenital megacolon; together with the chromosome aberration analysis, the method can be applied in the clinical prenatal diagnosis.

REFERENCES

- 1 Amiel J, Lyonnet S. Hirschsprung disease, associated syndromes, and genetics: a review. *J Med Genet* 2001; **38**: 729-739
- 2 Li JC, Mi KH, Zhou JL, Busch L, Kuhnelt W. The development of colon innervation in trisomy 16 mice and Hirschsprung disease. *World J Gastroenterol* 2001; **7**: 16-21
- 3 Li JC, Busch LC, Kuhnelt W. The development of the enteric nervous system in trisomy 16 mice with the occurrence of congenital megacolon. *Zhonghua Yixue Zazhi* 1999; **79**: 466-469
- 4 Won KJ, Torihashi S, Mitsui-Saito M, Hori M, Sato K, Suzuki T, Ozaki H, Karaki H. Increased smooth muscle contractility of intestine in the genetic null of the endothelin ETB receptor: a rat model for long segment Hirschsprung's disease. *Gut* 2002; **50**: 355-360
- 5 Martucciello G, Ceccherini I, Lerone M, Jasonni V. Pathogenesis of Hirschsprung's disease. *J Pediatr Surg* 2000; **35**: 1017-1025
- 6 Munnes M, Fanaei S, Schmitz B, Muiznieks I, Holschneider AM, Doerfler W. Familial form of hirschsprung disease: nucleotide sequence studies reveal point mutations in the RET proto-oncogene in two of six families but not in other candidate genes. *Am J Med Genet* 2000; **94**: 19-27
- 7 Davenport MP, Ward RL, Hawkins NJ. The null oncogene hypothesis and protection from cancer. *J Med Genet* 2002; **39**: 12-15
- 8 Kerstjens-Frederikse WS, Hofstra RMW, Essen AJ, Meijers JHC, Buys CHCM. A hirschsprung disease locus at 22qll? *J Med Genet* 1999; **36**: 221-224
- 9 Borrego S, Ruiz A, Saez ME, Gimm O, Gao X, Lopez-Alonso M, Hernandez A, Wright FA, Antinolo G, Eng C. RET genotypes comprising specific haplotypes of polymorphic variants predispose to isolated Hirschsprung disease. *J Med Genet* 2000; **37**: 572-578
- 10 Gath R, Goessling A, Keller KM, Koletzko S, Coerdet W,

- Muntefering H, Wirth S, Hofstra RMW, Mulligan L, Eng C, von Deimling A. Analysis of the RET, GDNF, EDN3, and EDNRB genes in patients with intestinal neuronal dysplasia and Hirschsprung disease. *Gut* 2001; **48**: 671-675
- 11 **Sakai T**, Nirasawa Y, Itoh Y, Wakizaka A. Japanese patients with sporadic Hirschsprung: mutation analysis of the receptor tyrosine kinase proto-oncogene, endothelin-B receptor, endothelin-3, glial cell line-derived neurotrophic factor and neurturin genes: a comparison with similar studies. *Eur J Pediatr* 2000; **159**: 160-167
 - 12 **Julies MG**, Moore SW, Kotze MJ, du Plessis L. Novel RET mutations in Hirschsprung's disease patients from the diverse South African population. *Eur J Hum Genet* 2001; **9**: 419-423
 - 13 **Inoue K**, Shimotake T, Tomiyama H, Iwai N. Mutational analysis of the RET and GDNF gene in children with hypoganglionosis. *Eur J Pediatr Surg* 2001; **11**: 120-123
 - 14 **Shimotake T**, Go S, Inoue K, Tomiyama H, Iwai N. A homozygous missense mutation in the tyrosine kinase domain of the RET proto-oncogene in an infant with total intestinal aganglionosis. *Am J Gastroenterol* 2001; **96**: 1286-1291
 - 15 **Sancandi M**, Ceccherini I, Costa M, Fava M, Chen B, Wu Y, Hofstra R, Laurie T, Griffiths M, Burge D, Tam PKH. Incidence of RET mutations in patients with Hirschsprung's disease. *J Pediatr Surg* 2000; **35**: 139-142
 - 16 **Myers SM**, Salomon R, Goessling A, Pelet A, Eng C, Deimling AV, Lyonnet S, Mulligan LM. Investigation of germline GFR α -1 mutations in Hirschsprung disease. *J Med Genet* 1999; **36**: 217-220
 - 17 **Inoue K**, Shimotake T, Inoue K, Tokiwa K, Iwai N. Mutational analysis of the RET proto-oncogene in a kindred with multiple endocrine neoplasia type 2A and Hirschsprung's disease. *J Pediatr Surg* 1999; **34**: 1552-1554
 - 18 **Borrego S**, Saez ME, Ruiz A, Gimm O, Lopez-Alonso M, Antinolo G, Eng C. Specific polymorphisms in the RET proto-oncogene are over-represented in patients with Hirschsprung disease and may represent loci modifying phenotypic expression. *J Med Genet* 1999; **36**: 771-774
 - 19 **Pigny P**, Bauters C, Wemeau JL, Houcke ML, Crepin M, Caron P, Giraud S, Calender A, Buisine MP, Kerckaert JP, Porchet N. A novel 9-base pair duplication in RET exon 8 in familial medullary thyroid carcinoma. *J Clin Endocrinol Metab* 1999; **84**: 1700-1704
 - 20 **Lui VC**, Samy ET, Sham MH, Mulligan LM, Tam PK. Glial cell line-derived neurotrophic factor family receptors are abnormally expressed in aganglionic bowel of a subpopulation of patients with Hirschsprung's disease. *Lab Invest* 2002; **82**: 703-712
 - 21 **Zhan J**, Xiu Y, Gu J, Fang Z, Hu XL. Expression of RET proto-oncogene and GDNF deficit in Hirschsprung's disease. *J Pediatr Surg* 1999; **34**: 1606-1609
 - 22 **Iwashita T**, Kurokawa K, Qiao S, Murakami H, Asai N, Kawai K, Hashimoto M, Watanabe T, Ichihara M, Takahashi M. Functional analysis of RET with Hirschsprung mutations affecting its kinase domain. *Gastroenterology* 2001; **121**: 24-33
 - 23 **Lesueur F**, Corbex M, McKay JD, Lima J, Soares P, Griseri P, Burgess J, Ceccherini I, Landolfi S, Papotti M, Amorim A, Goldgar DE, Romeo G. Specific haplotypes of the RET proto-oncogene are over-represented in patients with sporadic papillary thyroid carcinoma. *J Med Genet* 2002; **39**: 260-265
 - 24 **Melillo RM**, Santoro M, Ong SH, Billaud M, Fusco A, Hadari YR, Schlessinger J, Lax I. Docking protein FRS2 links the protein tyrosine kinase RET and its oncogenic forms with the mitogen-activated protein kinase signaling cascade. *Mol and Cell Biol* 2001; **21**: 4177-4187
 - 25 **Hansford JR**, Mulligan LM. Multiple endocrine neoplasia type 2 and RET: from neoplasia to neurogenesis. *J Med Genet* 2000; **37**: 817-827
 - 26 **Mograbi B**, Boccardi R, Bourget I, Juhel T, Farahi-far D, Romeo G, Ceccherini I, Rossi B. The sensitivity of activated cys RET mutants to glial cell line derived neurotrophic factor is mandatory to rescue neuroectodermic cells from apoptosis. *Mol and Cell Biol* 2001; **21**: 6719-6730
 - 27 **Zhu Y**, Wang DY, Sugimura H, Fan GY, Wang XD, Ren CS. Mutation analysis of tumor suppressor gene PTEN in bone and soft tissue tumors. *Zhonghua Yixue Zazhi* 2001; **81**: 715-718
 - 28 **Xiao JF**, Tang BS, Xia JH, Xiao P, Xie GJ. PCR in the gene diagnosis of charcot-marc-tooth disease. *Zhonghua Yixue Zazhi* 2001; **81**: 138-141
 - 29 **Qin Y**, Li B, Tan YS, Sun ZL, Zuo FQ, Sun ZF. Polymorphism of p16INK4a gene and rare mutation of p15INK4b gene exon2 in primary hepatocarcinoma. *World J Gastroenterol* 2000; **6**: 411-414
 - 30 **Gong K**, Zhang ZW, Xin DQ, Na X, Wu G, Na YQ. Frequent somatic mutations of the von Hippel-Lindau tumor suppressor gene in primary sporadic human renal clear cell carcinomas. *Zhonghua Yixue Zazhi* 2001; **81**: 142-144
 - 31 **He XS**, Su Q, Chen ZC, He XT, Long ZF, Ling H, Zhang LR. Expression, deletion and mutation of p16 gene in human gastric cancer. *World J Gastroenterol* 2001; **7**: 515-521
 - 32 **She FF**, Su DH, Lin JY, Zhou LY. Virulence and potential pathogenicity of coccoid *Helicobacter pylori* induced by antibiotics. *World J Gastroenterol* 2001; **7**: 254-258
 - 33 **Yip SP**. Single-tube multiplex PCR-SSCP analysis distinguishes 7 common ABO alleles and readily identifies new alleles. *Blood* 2000; **95**: 1487-1492
 - 34 **Eng C**, Brody LC, Wagner TMU, Devilee P, Vijg J, Szabo C, Tavtigian SV, Nathanson KL, Ostrander E, Frank TS. Interpreting epidemiological research: blinded comparison of methods used to estimate the prevalence of inherited mutations in *BRCA1*. *J Med Genet* 2001; **38**: 824-833
 - 35 **Pitcher D**, Sillis M, Robertson JA. Simple method for determining biovar and serovar types of ureaplasma urealyticum clinical isolates using PCR-single-strand conformation polymorphism analysis. *J Clin Microbiol* 2001; **39**: 1840-1844
 - 36 **Emeny RT**, Herron JR, Xi LF, Koutsky LA, Kiviat NB, Wheeler CM. Comparison of variant-specific hybridization and single-strand conformational polymorphism methods for detection of mixed human papillomavirus type 16 variant infections. *J Clin Microbiol* 1999; **37**: 3627-3633
 - 37 **Gillman LM**, Gunton J, Turenne CY, Wolfe J, Kabani AM. Identification of *mycobacterium* species by multiple-fluorescence PCR-single-strand conformation polymorphism analysis of the 16S rRNA gene. *J Clin Microbiol* 2001; **39**: 3085-3091
 - 38 **Hall JS**, French R, Morris TJ, Stenger DC. Structure and temporal dynamics of populations within wheat streak mosaic virus isolates. *Journal of Virology* 2001; **75**: 10231-10243
 - 39 **Parisi MA**, Kapur RP. Genetics of Hirschsprung disease. *Curr Opin Pediatr* 2000; **12**: 610-617
 - 40 **Baranyay F**, Bogar G, Sebestyen M. Adult Hirschsprung's disease with mental retardation and microcephaly. *Orv Hetil* 2000; **141**: 1673-1676
 - 41 **Koletzko S**, Jesch I, Faus-Keßler T, Briner J, Meier-ruge W, Muntefering H, Coerd W, Wessel L, Keller KM, Nutzenadel W, Schmittenebecher P, Holschneider A, Sacher P. Rectal biopsy for diagnosis of intestinal neuronal dysplasia in children: a prospective multicentre study on interobserver variation and clinical outcome. *Gut* 1999; **44**: 853-861
 - 42 **Ludman L**, Spitz L, Tsuji H, Pierro A. Hirschsprung's disease: functional and psychological follow up comparing total colonic and rectosigmoid aganglionosis. *Arch Dis Child* 2002; **86**: 348-351

Edited by Zhu L

• BASIC RESEARCH •

Effect of matrine on Kupffer cell activation in cold ischemia reperfusion injury of rat liver

Xin-Hua Zhu, Yu-Dong Qiu, Hao Shen, Ming-Ke Shi, Yi-Tao Ding

Xin-Hua Zhu, Yu-Dong Qiu, Ming-Ke Shi, Yi-Tao Ding, Department of Hepatobiliary Surgery, Affiliated Drum Tower Hospital, Medical Department of Nanjing University, Nanjing 210008, Jiangsu Province, China

Hao Shen, Biochemistry Department of Nanjing University, Nanjing 210008, China

Supported by the Chinese Medicine Administration Bureau of Jiangsu Province, No SZ 9902

Correspondence to: Dr. Xin-Hua Zhu, Department of Hepatobiliary Surgery, Affiliated Drum Tower Hospital, Medical College of Nanjing University, Zhongshang Road 321, Nanjing 210008, Jiangsu Province, China. drzhu@elong.com

Telephone: +86-25-3304616 Ext. 11601 **Fax:** +86-25-3317016

Received 2002-06-01 **Accepted** 2002-06-26

Abstract

AIM: To study the effect of matrine on activation of Kupffer cell during cold ischemia and reperfusion injury in rat orthotopic liver transplantation (OLT).

METHODS: 168 syngeneic SD rats were randomly divided into four groups: untreated group, small-dose treated group, large-dose treated group and sham operation group. After 5 hours of preservation in Ringer's (LR) solution, orthotopic implantation of the donor liver was performed. At 1 h, 2 h, 4 h and 24 h after reperfusion of the portal vein, 6 rats were killed in each group to collect the serum and the liver for assay and pathology.

RESULTS: Matrine markedly inhibited the activation of Kupffer cells and their release of tumor necrosis factor (TNF). TNF cytotoxicity level at 2 h decreased significantly by matrine treatment (7.94 ± 0.42 , 2.39 ± 0.19 and 2.01 ± 0.13 U/ml, respectively; $P < 0.01$), so did the other three time points. The level of hyaluronic acid (HA) and alanine transaminase (ALT) decreased significantly in both treated groups, and matrine treatment markedly ameliorated focal necrosis of hepatocytes, inflammatory cells aggregating, rounding and detachment of sinusoidal endothelial cells (SEC). And no significant difference was observed between the treated groups.

CONCLUSION: Matrine can inhibit the activation of Kupffer cell and prevent the donor liver from cold preservation and reperfusion injury in rat orthotopic liver transplantation.

Zhu XH, Qiu YD, Shen H, Shi MK, Ding YT. Effect of matrine on Kupffer cell activation in cold ischemia reperfusion injury of rat liver. *World J Gastroenterol* 2002; 8(6):1112-1116

INTRODUCTION

Preservation injury continues to be a major clinical problem in orthotopic liver transplantation (OLT) with a 10 % incidence of primary nonfunction^[1,2]. Additionally, there is clinical

evidence that severe preservation injury is associated with an increase in liver graft rejection^[3]. Therefore, it is clinically and pathophysiologically important to elucidate the mechanism and prevention of cellular injury during hepatic ischemia and the subsequent reperfusion. Kupffer cells become activated during cold preservation and subsequent reperfusion, as has been demonstrated by enhanced endocytosis of carbon particles^[4], an increased release of TNF- α ^[5-8] and ultrastructural changes^[9]. When activated, they generate a plethora of inflammatory cytokines and oxygen-derived free radicals, which play a particularly important part in the pathogenesis of hepatic ischemia and reperfusion injury^[10].

Matrine (matridin-15-one) is a typical lupine alkaloid along with lupinine, sparteine and cytisine, and has an absolute structure of 5S, 6S, 7R, 11R^[11] (Figure 1). This alkaloid, isolated from kinds of *Sophora* plants in *Leguminosae*, shows pharmacological effects as anti-inflammation^[12], immunity-inhibition^[13], B and C hepatitis virus inhibition^[14], anti-tumor^[15] and anti-arrhythmia activity^[16], and has been used in treatment of chronic viral hepatitis. Pharmacological studies revealed no obvious side-effect of matrine^[17]. The present study was designed to evaluate the effects of matrine on Kupffer cell activation caused by preservation and reperfusion with an orthotopic liver transplantation model.

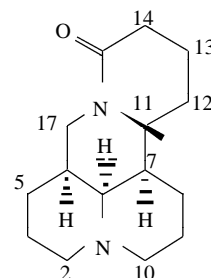


Figure 1 Chemical structure of (+)-Matrine

MATERIALS AND METHODS

Reagents

Matrine, a parenteral solution (50 mg/5 ml), was purchased from Ming Xing Pharmaceutical Factory, Guangzhou, China. HA RIA kit was from Shanghai Ocean Research Biomedical Technology Center, China. Recombinant human TNF (1000 units/ml) was from Genzyme Co. in Boston, America. Rat TNF- α ELISA kit was purchased from Bender MedSystems Co. in Vienna, Austria. Endotoxin quantitation kit was from Shanghai Medical Test Center, China.

Animals

168 male inbred SD rats weighing 200 to 220 g were purchased from the Animal Center of Jin Ling Hospital (Nanjing, China). All rats were provided with standard laboratory chow and water and housed in accordance with institutional animal care

policies. Prior to being used in the study, the rats were fasted for 12 hours and were allowed free access to water.

Experimental design

Rat orthotopic liver transplantation was performed using the technique of Kamada and Calne^[18] under ether anesthesia, and the hepatic artery was not reconstructed. Ringer's (LR) solution was used for perfusion. The liver graft was preserved for 5 h in Ringer's solution at 4 °C, then transplanted orthotopically. The explantation of the recipient liver required <10 minutes and the rewarming time of the graft (i.e., clamping of the portal vein and the subhepatic vena cava during implantation) did not exceed 18 minutes.

The animals were randomly assigned into four experimental groups as follows: (1) a control group in which the recipients were injected ip Normal Saline (N.S, 1ml) before laparotomy. (2) a small-dose treated group (ST) in which the recipients were injected ip matrine (40 mg·Kg⁻¹) before surgery. (3) a large-dose treated group (LT), in which the transplantation was performed following the injection of matrine (80 mg·Kg⁻¹) as above. (4) a sham operation group (Normal), in which the liver was mobilized as the others without hepatectomy to exclude the influence of surgery.

At 1 h, 2 h, 4 h and 24 h after reperfusion of the portal vein, 6 rats were killed in each group to collect the blood sample via the infrahepatic vena cava and the median lobe of liver for assay. The serum was separated and stored at -70 °C until analysis. Washed with cold Saline solution, the liver samples were stored immediately in liquid nitrogen until analysis.

Hepatic enzyme assays

Alanine aminotransferase (ALT) activity of the serum samples collected at 4 h and 24 h after reperfusion was determined by automatic biochemistry analyzer (HITACHI 7 600).

Assessment of HA plasma level

HA plasma levels of those samples collected at 1 h, 2 h, and 4 h after reperfusion were determined in duplicate using a HA RIA kit according to the manufacturer's protocols.

Plasma endotoxin level

Endotoxin plasma levels of the samples collected at 1h and 2h were determined in duplicate using a limulus amebocyte lysate assay kit according to the manufacturer's instruction.

Plasma TNF cytotoxicity determination

Plasma TNF cytotoxicity of all samples were determined with TNF cytotoxicity L929 assays as described^[19,20]. Each sample was assayed in duplicate wells.

Hepatic TNF- α assay

Coomassie Light Blue assay was used for protein quantitation of all hepatic samples. Hepatic levels of TNF- α were assayed with a rat TNF- α ELISA kit from the Bender MedSystems corporation. This was an enzyme-linked immunoabsorbent assay for the quantitation of natural or recombinant rat TNF- α levels. The assay was carried out according to the manufacturer's instructions.

Light microscopy

Six hepatic specimens were collected at 4 hr after reperfusion of portal vein in each group. The liver specimens for light microscopy were fixed with 10 % formalin and then embedded in paraffin. The sections were stained with hematoxylin and eosin for histologic examination.

Transmission electron microscopy

For transmission electron microscopy, liver fragments of approximately 1 mm³ were fixed in 2 % glutaraldehyde containing 0.1 M phosphate buffer for 3 hours. After washing in phosphate buffer, specimens were postfixed with osmium tetroxide, dehydrated in graded alcohols, and embedded in Epon 812. Ultrathin sections were stained with uranyl acetate and lead citrate and examined under an electron microscope (JEM-1200EX).

Statistical analysis

The results are expressed as mean \pm SD. Data were analyzed using Statistical Analysis System (SAS). One-way analysis of variance (ANOVA) was used for multiple comparisons with Student-Newman-Keuls (snk) test. A *P* value of < 0.05 was considered statistically significant.

RESULTS

Effect of matrine on ALT serum levels

ALT serum levels in both treated groups decreased significantly compared with control values at different time points after reperfusion, and two folds-dose matrine provided the large-dose treated group with a significant decrease in ALT. (Figure 2).

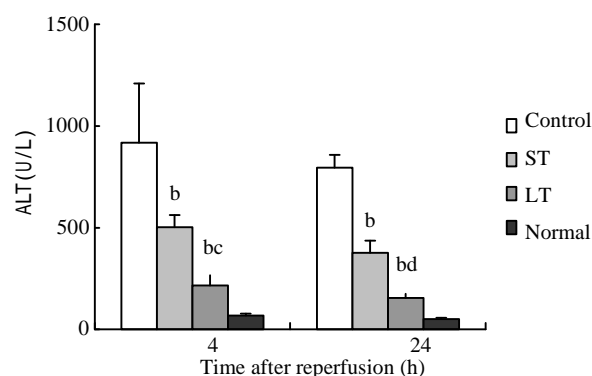


Figure 2 Effect of matrine on ALT plasma level after 5-hour cold preservation and reperfusion in rat orthotopic liver transplantation. (*n*=6 at each time); b: very significantly different from control (*P*<0.01); c: significantly different from the small-dose treated group (*P*<0.05); d: very significantly different from the small-dose treated group (*P*<0.01).

Effect of matrine on HA plasma levels

Compared with the sham operation group, a significant elevation of serum HA was observed in the other three groups at different time points, with the peak level at 2 h after surgery. HA levels at different time points were ameliorated markedly by matrine treatment, and two folds-dose matrine provided the large-dose treated group with a significant elevation in HA. (Figure 3).

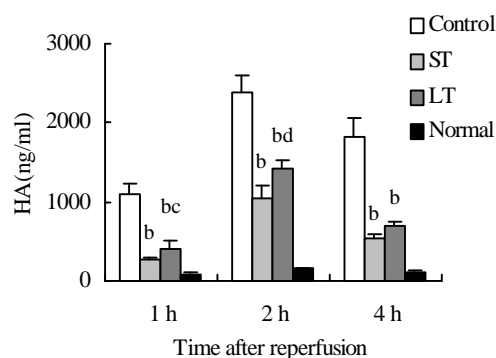


Figure 3 Effect of matrine on plasma HA level after 5-hour cold preservation and reperfusion in rat orthotopic liver

transplantation. ($n=6$ at each time); b: very significantly different from control ($P<0.01$); d: very significantly different from the small-dose treated group ($P<0.01$).

Effect of matrine on plasma endotoxin levels

In both treated groups, plasma endotoxin levels increased significantly compared with control values at 1 h and 2 h after reperfusion. No significant difference was noted between the two treated groups (Figure 4).

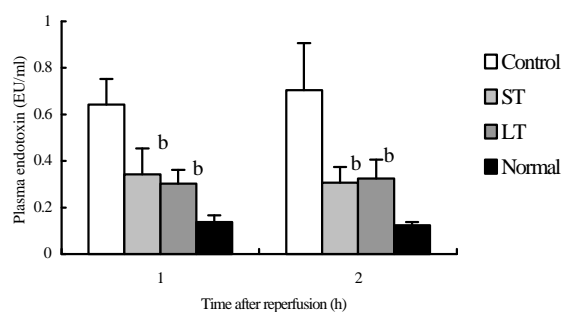


Figure 4 Effect of matrine on endotoxin plasma level after 5-hour cold preservation and reperfusion in rat orthotopic liver transplantation. ($n=6$ at each time) b: very significantly different from control ($P<0.01$)

Effect of matrine on plasma TNF cytotoxicity

Almost no plasma TNF cytotoxicity was detected in the sham operation group. In the other three groups, the maximum TNF values were obtained 2 h after surgery as shown in Figure 5. TNF cytotoxicity level at 2 h decreased significantly by matrine treatment (7.94 ± 0.42 , 2.39 ± 0.19 and 2.01 ± 0.13 U/ml, respectively; $P<0.01$), so did the other three time points. No significant difference was noted between the two treated groups.

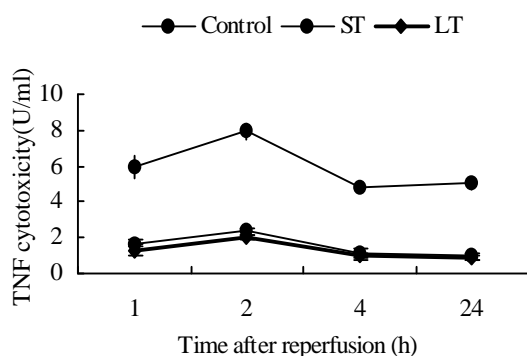


Figure 5 Effect of matrine on TNF cytotoxicity after 5-hour cold preservation and reperfusion in rat orthotopic liver transplantation. ($n=6$ at each time).

Effect of matrine on hepatic TNF- α levels

The hepatic TNF- α level of sham operation group was low (56.8 ± 13.2 pg/mgprot). In the other three groups, the maximum TNF- α levels were obtained at 2 h after surgery as shown in Figure 6, and TNF- α levels at different time points post reperfusion were significantly decreased by matrine treatment, but no significant difference was noted between the two treated groups.

Light microscopy

In sham operation group, the histological findings indicated that the degree of liver cell injury, Kupffer cell hyperplasia,

and inflammatory cell infiltration in portal areas and sinusoids were mild. As shown in Figure 7, histological examination revealed some focal necrosis of hepatocytes, extensive congestion, and inflammatory cells aggregating in hepatic sinusoid lumen in the control group, and the obvious Kupffer cell hyperplasia and rounding and detachment of SEC were observed, too. These were ameliorated markedly in both treated groups, and no significant difference was observed between the two treated groups.

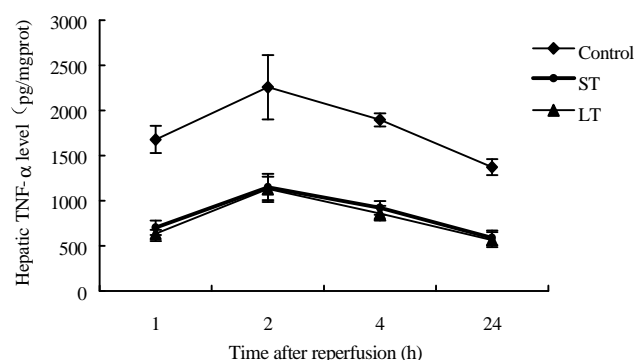


Figure 6 Effect of matrine on hepatic TNF- α level after 5-hour cold preservation and reperfusion in rat orthotopic liver transplantation. ($n=6$ at each time)

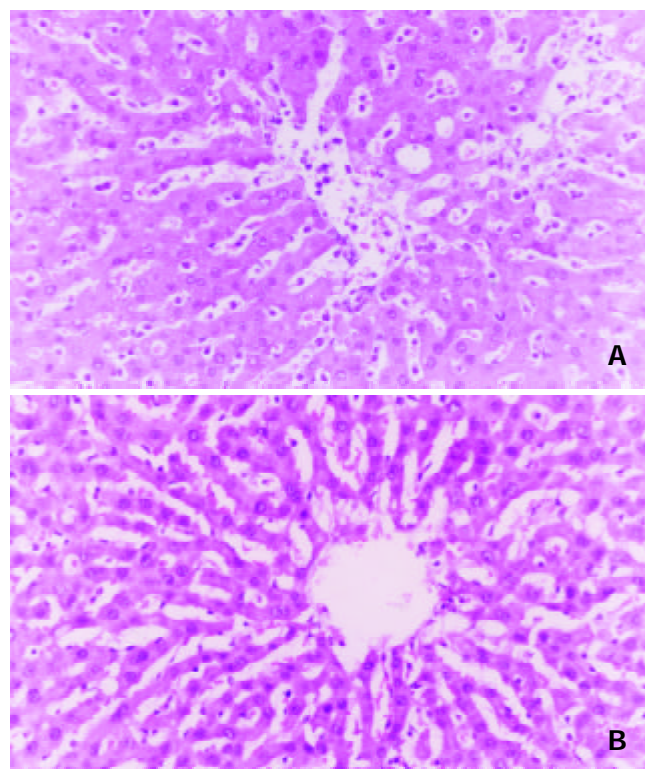


Figure 7 Histological appearance of the rat liver at 4 hours after reperfusion A: control group; B: a small-dose treated group. (HE staining paraffin-embedded 5 μ m thick-sections. $\times 200$)

Transmission electron microscopy

Samples taken from the control group showed obvious activation of Kupffer cells, including increase of cytoplasmic processes, irregular nucleus and many phagolysosomes, hyaline vacuoles, and granules in cytoplasm. (Figure 8) The treated groups showed a nearly normal ultrastructure of Kupffer cells in the samples examined compared with the control. This was reflected in

rounding of Kupffer cell, regular nucleus, and a reduction in the amount of cytoplasmic processes. No significant differences were noted between the two treated groups.

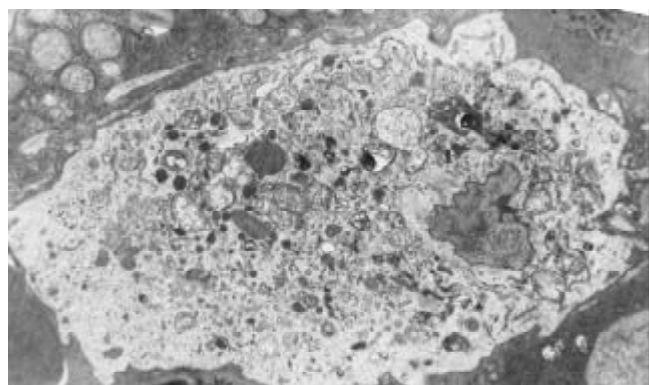


Figure 8 Electron microscopic pictures of rat liver in control group 4 hours after reperfusion. (Original magnifications: $\times 6\,000$)

DISCUSSION

With donor shortage becoming worse, preservation injury continues to be a major clinical problem with a 10 % incidence of primary nonfunction^[1,2]. Kupffer cells play an important part in mediating ischemia and reperfusion injury after hepatic transplantation. It is likely that they are primed during cold preservation and then activated at the time of reperfusion. The addition of an inhibitor of Kupffer cell activation to liver preservation solutions may further increase the duration of cold storage times and also improve the outcome of grafts^[21-23].

In the present investigation, rat livers were kept for 5 hours in cold Ringer's solution (4 °C), exceeding the safe limit of 4 hours^[24]. Under these preservation and transplantation conditions (i.e., a portal vein clamping time of less than 20 minutes), a postoperative survival rate of about 40 % was obtained. Thus, 5 hours in cold Ringer's solution, although a severely compromising condition, should allow an adequate assessment of the mechanisms of cold ischemia and reperfusion injury that lead to primary nonfunction. Usually, the rats without matrine treatment recovered well from anesthesia; however, their clinical status began to deteriorate within 4 to 6 hours, and nonsurvivors died within 24 hours, mostly between 10 to 20 hours.

After reperfusion, serum endotoxins immediately bind to lipopolysaccharides binding protein (LPSBP) and are usually trapped by Kupffer cells^[25]. Kupffer cells exhibited progressive rounding, ruffling of the cell surface, polarization, appearance of wormlike densities, vacuolization, and degranulation. After activation, Kupffer cells produce TNF- α and induce neutrophil chemotaxis and activation^[5,26]. TNF- α has potent proinflammatory actions, which can induce IL-8 synthesis and up-regulate the expression of adhesion molecules giving rise to increased leukocyte-sinusoidal endothelial cell interactions^[23,27], which result in further cytokine production. In our study, serum endotoxin levels at different time points post transplantation were ameliorated markedly by matrine treatment, and the results have confirmed matrine markedly inhibited the activation of Kupffer cells and their release of TNF, inflammatory cell infiltration and injury of sinusoidal endothelial cell.

The serum ALT and HA levels were determined as functional indices of hepatocyte and sinusoidal endothelial cell damage, respectively. ALT and HA levels at different time

points post-transplantation improved markedly by matrine treatment, and their pathological changes of liver graft ameliorated, too. Two folds-dose matrine treatment can't give rats the better therapeutic effect, and no obvious side effect was noted in our study.

In conclusion, the results of this study demonstrated the inhibition effect of matrine on Kupffer cell activation and its protective effect against the cold ischemia reperfusion injury of the graft in liver transplantation.

REFERENCES

- 1 **Greig PD**, Woolf GM, Sinclair SB, Abecassis M, Strasberg SM, Taylor BR, Blendis LM, Superina RA, Glynn MFX, Langer B, Levy GA. Treatment of primary liver graft nonfunction with prostaglandin E1. *Transplantation* 1989; **48**: 447-453
- 2 **Ploeg RJ**, D' Alessandro AM, Knechtle SJ, Stegall MD, Pirsch JD, Hoffmann RM, Sasaki T, Sollinger HW, Belzer FO, Kalayoglu M. Risk factors for primary dysfunction after liver transplantation-a multivariate analysis. *Transplantation* 1993; **55**: 807-813
- 3 **Howard TK**, Klintmalm GBG, Cofer JB, Husberg BS, Goldstein RM, Gonwa TA. The influence of preservation injury on rejection in the hepatic transplant recipients. *Transplantation* 1990; **49**: 103-107
- 4 **Lindert KA**, Caldwell-Kenkel JC, Nukina S, Lemasters JJ, Thurman RG. Activation of Kupffer cells on reperfusion following hypoxia: partial phagocytosis in a low-flow, reflow model. *Am J Physiol* 1992; **262**: 345-350
- 5 **Shibuya H**, Ohkohchi N, Tsukamoto S, Satomi S. Tumor necrosis factor- α induced, superoxide-mediated neutrophil accumulation in cold ischemic/reperfusion rat liver. *Hepatology* 1997; **26**: 113-120
- 6 **Zhang SC**, Dai Q, Wang JY, He BM, Zhou K. Gut-derived endotoxemia: One of the factors leading to production of cytokines in liver diseases. *World J Gastroenterol* 2000; **6**(Suppl 3):16
- 7 **Arii S**, Monden K, Adachi Y, Zhang W, Higashits H, Furutani M, Mise M, Fujita S, Nakamura T. Pathogenic role of kupffer cell activation in the reperfusion injury of cold-preserved liver. *Transplantation* 1994; **58**: 1072-1077
- 8 **Xu MQ**, Xue L, Gong JP. Significance of Kupffer cell NF- κ B activation during hepatic ischemia/reperfusion in rats. *Shijie Huaren Xiaohua Zazhi* 2001; **9**: 1250-1253
- 9 **Caldwell-Kenkel JC**, Currin RT, Tanaka T, Thurman RG, Lemasters JJ. Kupffer cell activation and endothelial cell damage after storage of rat livers: effects of reperfusion. *Hepatology* 1991; **13**: 83-95
- 10 **Shiratori Y**, Kiriya H, Fukushima Y, Nagura T, Takada H, Hai K, Kamii K. Modulation of ischemia-reperfusion-induced hepatic injury by Kupffer cells. *Dig Dis Sci* 1994; **39**: 1265-1272
- 11 **Okuda S**, Yoshimoto M, Tsuda K, Utzugi N. Über die absolute Konfiguration des Matrine. *Chem. Pharm Bull* 1966; **14**: 314-318
- 12 **Hu ZL**, Zhang JP, YU XB, Lin W, Qian DH. Effect of matrine on lipopolysaccharides/D-galactosamine-induced hepatitis and tumor necrosis factor release from macrophages *in vitro*. *Acta Pharm Sin* 1996; **17**: 351-353
- 13 **Liang P**, Bo AH, Xue GP, Han R, Li HF, Xu YL. Study on the mechanism of matrine on immune liver injury in rats. *Shijie Huaren Xiaohua Zazhi* 1999; **7**: 104-108
- 14 **Chen XS**, Wang GJ, Cai X, Yu HY, Hu YP. Inhibition of hepatitis B virus by oxymatrine *in vivo*. *World J Gastroenterol* 2001; **7**: 49-52
- 15 **Si WK**, Pan J, Lu H, Li ZQ. Study on matrine inhibiting proliferation of HepG2 cell and the relation between its dosage and inhibiting style. *Shijie Huaren Xiaohua Zazhi* 2001; **9**: 185-189
- 16 **Ai J**, Gao HH, He SZ, Wang L, Luo DL, Yang BF. Effects of matrine, artemisinin, and tetrandrine on cytosolic $[Ca^{2+}]_i$ in guinea pig ventricular myocytes. *Acta Pharmacol Sin* 2001; **22**: 512-515
- 17 **Ye M**. Pharmacological study of matrine injection. *Guangdong Yi Xue* 1997; **18**: 793
- 18 **Kamada N**, Calne RY. Orthotopic liver transplantation in the rat: Technique using cuff for portal vein anastomosis and biliary drainage. *Transplantation* 1979; **28**: 47-51

- 19 **Chang NS**. TGF- β 1 induction of novel extracellular proteins that trigger resistance to TNF cytotoxicity in murine L929 fibroblasts. *J Biol Chem* 1995; **270**: 7765-7772
- 20 **Chang NS**. Hyaluronidase induces murine L929 fibrosarcoma cells resistant to tumor necrosis factor and Fas cytotoxicity in the presence of actinomycin D. *Cell Biochem. Biophys* 1996; **27**: 109-132
- 21 **Shiratori Y**, Kiriya H, Fukushi Y. Modulation of ischemia-reperfusion-induced hepatic injury by Kupffer cells. *Dig Dis Sci* 1994; **39**: 1265-1272
- 22 **Marzi I**, Cowper K, Takei Y, Lindert K, Lemasters JJ, Thurman RG. Methylpalmitate prevents Kupffer cell activation and improves survival after aorthotopic liver transplantation in the rat. *Transplant Int* 1991; **4**: 215-220
- 23 **Li XK**, Matin AFM, Suzuki H, Uno T. Effect of protease inhibitor on ischemia-reperfusion injury of the rat liver. *Transplantation* 1993; **56**: 1331-1336
- 24 **Sumimoto R**, Jamieson NV, Wake K. 24 -hour rat liver preservation using UW solution and some simplified variants. *Transplantation* 1989; **48**: 144-146
- 25 **Vajdová K**, Smreková R, Kukan M, Jakubovsky J, van Rooijen N, Horecky J, Lutterova M, Wsolová L. Endotoxin-induced aggravation of preservation-reperfusion injury of rat liver and its modulation. *Hepatology* 2000; **32**:112-120
- 26 **Takei Y**, Marzi I, Kauffman FC. Increase in survival time of liver transplants by protease inhibitors and a calcium channel blocker nisoldipine. *Transplantation* 1990; **50**: 14-20
- 27 **Arii S**, Monden K, Adachi Y. Pathogenic role of Kupffer cell activation in the reperfusion injury of cold-preserved liver. *Transplantation* 1994; **58**: 1072-1077

Edited by Wu XN

• BASIC RESEARCH •

Effects of hydrogen peroxide on mitochondrial gene expression of intestinal epithelial cells

Jian-Ming Li, Qian Cai, Hong Zhou, Guang-Xia Xiao

Jian-Ming Li, Qian Cai, Hong Zhou, Guang-Xia Xiao, Institute of Burn Research, Southwest Hospital, Third Military Medical University, Chongqing 400038, China

Supported by the Special Funds for Major State Basic Research of China, No.G1999054202

Correspondence to: Professor Hong Zhou, Institute of Burn Research, Southwest Hospital, Third Military Medical University, Chongqing 400038, China. zhouh64@mail.tmmu.com.cn

Received 2001-12-05 **Accepted** 2002-03-05

Abstract

AIM: To study the effects of hydrogen peroxide on mitochondrial gene expression of intestinal epithelial cells in *in vitro* model of hydrogen peroxide-stimulated SW-480 cells.

METHODS: RNA of hydrogen peroxide-induced SW-480 cells was isolated, and reverse-transcriptional polymerase chain reaction was performed to study gene expression of ATPase subunit 6, ATPase subunit 8, cytochrome c oxidase subunit I (COI), cytochrome c oxidase subunit II (COII) and cytochrome c oxidase subunit III (COIII). Mitochondria were isolated and activities of mitochondrial cytochrome c oxidase and ATPase were also measured simultaneously.

RESULTS: Hydrogen peroxide led to differential expression of mitochondrial genes with some genes up-regulated or down-regulated in a dose dependent manner. Differences were very obvious in expressions of mitochondrial genes of cells treated with hydrogen peroxide in a concentration of 400 μ mol/L or 4 mmol/L. In general, differential expression of mitochondrial genes was characterized by up-regulation of mitochondrial genes in the concentration of 400 μ mol/L and down-regulation in the concentration of 4 mmol/L. In consistence with changes in mitochondrial gene expressions, hydrogen peroxide resulted in decreased activities of cytochrome c oxidase and ATPase.

CONCLUSIONS: The differential expression of mitochondrial genes encoding cytochrome c oxidase and ATPase is involved in apoptosis of intestinal epithelial cells by affecting activities of cytochrome c oxidase and ATPase.

Li JM, Cai Q, Zhou H, Xiao GX. Effects of hydrogen peroxide on mitochondrial gene expression of intestinal epithelial cells. *World J Gastroenterol* 2002; 8(6):1117-1122

INTRODUCTION

Hidden injuries of gut during early stage of severe burn may occur, and lead to endogenous translocation of intestinal endotoxin or bacteria. But factors contributing to gut barrier dysfunction are multiple and its mechanism is unclear^[1-10]. Apoptosis of intestinal epithelial cells induced by excessive

reactive oxygen species released by activated polymorphonuclear cells and vascular endothelial cells plays a role in the pathogenesis of intestinal mucosal dysfunction. The role of mitochondria in the development of apoptosis has been well clarified recently^[11-15]. As we know, there are some proteins related to mitochondrial electron transport chain such as cytochrome c oxidase subunits and ATP synthase subunits encoded by mitochondrial genome, which may be involved in mitochondrial injuries of intestinal epithelial cells. Our study focused on the effects of hydrogen peroxide on mitochondrial gene expression of intestinal epithelial cells.

MATERIALS AND METHODS

Cell line and culture

Human intestinal epithelial cell line SW-480 stored routinely in our laboratory was cultured in RPMI1640 supplemented with 10 % (v/v) heat inactivated newborn calf serum (Hyclone), 100 units/ml of penicillin, 0.1 mg/ml streptomycin and 2 mM L-glutamine at 37 °C in a humidified 5 % CO₂, 95 % air incubator. Confluent cells were prepared for further studies.

Treatment and groups

Cells were treated with 4 mmol/L or 400 μ mol/L hydrogen peroxide. Cells without any hydrogen peroxide were prepared as control.

Primers design

WWW primer picking software (primer3) from Whitehead Institute for Biomedical Research was used to design the primers of ATPase6, ATPase8, COI, COII and COIII genes encoded by mitochondrial genome in accordance with the latest Human Mitochondrial DNA "Cambridge" Sequence (Table 1). Housekeeping gene β -actin was regarded as internal control.

Table 1 Primers of ATPase6, ATPase8, COI, COII and COIII genes encoded by mitochondrial genome

Target genes	Sequence of base pairs	Size of PCR products(bp)
COI	5'-GTTGTAGCCCACTTCCAC-3' 5'-CATCGGGGTAGTCCGAGTAA-3'	222
COII	5'-TTCATGATCACGCCCTCATA-3' 5'-TAAAGGATGCGTAGGGATGG-3'	187
CO III	5'-AAAGCACATACCAAGGCCAC-3' 5'-CTTCTAGGGGATTTAGCGGG-3'	195
ATPase 6	5'-GCCCTAGCCCACTTCTTACC-3' 5'-TTAAGGCGACAGCGATTCT-3'	256
ATPase 8	5'-CCCACCATAATTACCCCAT-3' 5'-TTTATGGGCTTTGGTGAGG-3'	102
β -actin	5'-TGACGGGGTCACCCACACTGTGCCCATCTA-3' 5'-CTAGAAGCATTGCGGTGGACGATGGAGGG-3'	661

Isolation of total RNA

Total RNA was isolated by Tripure isolation reagent (Roche) according to manual provided by the kit. Any subject used in RNA isolation was treated with DEPC (Sigma) followed by vapor sterilization. A260/A280 of RNA samples were between 1.6 and 2.0.

Expression of ATPase6, ATPase8, COI, COII and COIII genes

Titan One Tube RT-PCR Kit (Roche) was applied according to manual for studying expression of mRNA of ATPase6, ATPase8, COI, COII and COIII genes. The PCR profile was as follows: a reverse-transcription reaction at 50 °C for 30 min and initial denaturation at 94 °C for 2 min, followed by 35 cycles of denaturation at 94 °C for 30 s, annealing at 56 °C for 30 s, primer extension at 68 °C for 45 s and a final extension at 68 °C for 10 min. PCR products were separated by electrophoresis on a 1 % vertical agarose electrophoresis and observed under ultraviolet and stored in computer by gel imaging system. Relative density of genes was calculated by dividing density of respective gene with density of β -actin.

Isolation of mitochondria

Mitochondria were isolated as described previously^[16]. Cells about 1×10^7 were trypsinized followed by washing for one time, and then cells suspended in ice-cold isolation buffer (0.25 M sucrose, 10 mM Tris-HCl, pH 7.4) were homogenized with a glass homogenizer for 10 strokes in ice. The supernatants was further centrifuged at $1\,500 \times g$ for 10 min at 4 °C, the pellet was suspended again in ice-cold isolation buffer and homogenized in ice. Two supernatants were mixed and centrifuged at $17\,000 \times g$ for 10 min at 4 °C. Fresh isolated mitochondria was suspended in isolation buffer, protein concentration were determined by Folin-Phen assay and adjusted to 4 mg/ml. Activities of cytochrome c oxidase and ATPase were measured within 6 h after isolation of mitochondria.

Cytochrome c oxidase activity

In 1 ml reaction volume, 70 μ l reduced ferrocyanochrome c, 10 μ l isolation mitochondria (4 mg/ml) and 920 μ l 10 mM K_2HPO_4 (pH 7.4) were mixed at room temperature, and the absorbance was measured every 30 seconds. The decreased absorbance represents activity of cytochrome c oxidase^[17].

ATPase activity

Ten micro-liter of isolated mitochondria (4 mg/ml) and 1 ml of 10 % TCA were mixed in Eppendorf tubes at 37 °C for 60 min, and the reaction was terminated by incubation in ice. Then 250 μ l of 0.02 mol/L ATP- Na_2 and 100 μ l of 0.05 mol/L $MgCl_2$ were added respectively, and the reaction was ended by adding 1 ml of 10 % TCA after 5 min at 37 °C, followed by centrifugation at 3 000 rpm for 15 min at 4 °C. The contents of inorganic phosphorus in supernatants representing ATPase activity were determined^[18].

Statistical analysis

Data were expressed as $mean \pm SD$. To analyze the data statistically, student's *t* test was used to determine statistical differences, and $P < 0.05$ was considered significant.

RESULTS

Expression of house-keeping gene β -actin mRNA

After treating with hydrogen peroxide, no significant changes of house-keeping gene β -actin mRNA could be observed, indicating its value as an internal control (Figure 1).

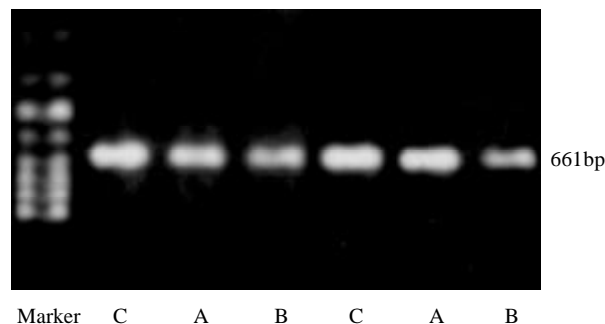


Figure 1 Effects of hydrogen peroxide on expression of house-keeping gene β -actin mRNA.

C: control cells; A: 4 mM H_2O_2 -treated cells (3 h); B: 400 mM H_2O_2 -treated cells (3 h).

Expression of COI mRNA

Cells from normal control expressed certain amount of COI mRNA. Increasing expression of COI mRNA was found after treating with hydrogen peroxide in the concentration of 400 μ mol/L, but no significant changes could be observed in the concentration of 4 mmol/L (Figure 2).

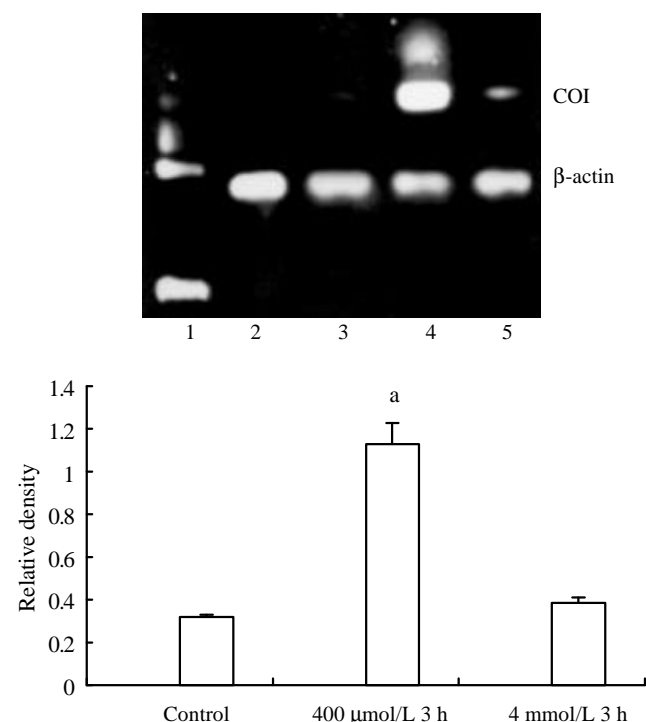


Figure 2 Effects of hydrogen peroxide on expression of COI mRNA (^a $P < 0.05$, vs. normal control).

1 DNA marker: 1 DNA/Hind III, 2 positive control, 3 normal control, 4 400 μ mol/L 3 h, 5 4 mmol/L 3 h.

Expression of COII mRNA

Weak expression of COII mRNA was found in control cells. Significant increase could be found in both 400 μ mol/L and 4 mmol/L hydrogen peroxide-stimulated cells (Figure 3).

Expression of COIII mRNA

Stable expression of COIII mRNA was found in control cells. Significant decrease could be found in 400 μ mol/L hydrogen peroxide-stimulated cells (Figure 4).

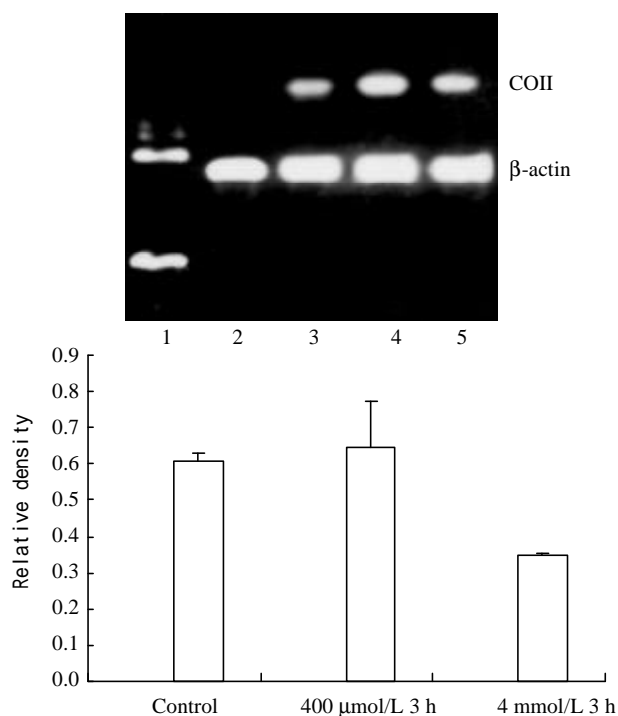


Figure 3 Effects of hydrogen peroxide on expression of COII mRNA ($^*P<0.05$, vs normal control). 1 DNA marker; 1DNA/Hind III, 2 positive control, 3 normal control, 4 400 $\mu\text{mol/L}$ 3 h, 5 4 mmol/L 3 h.

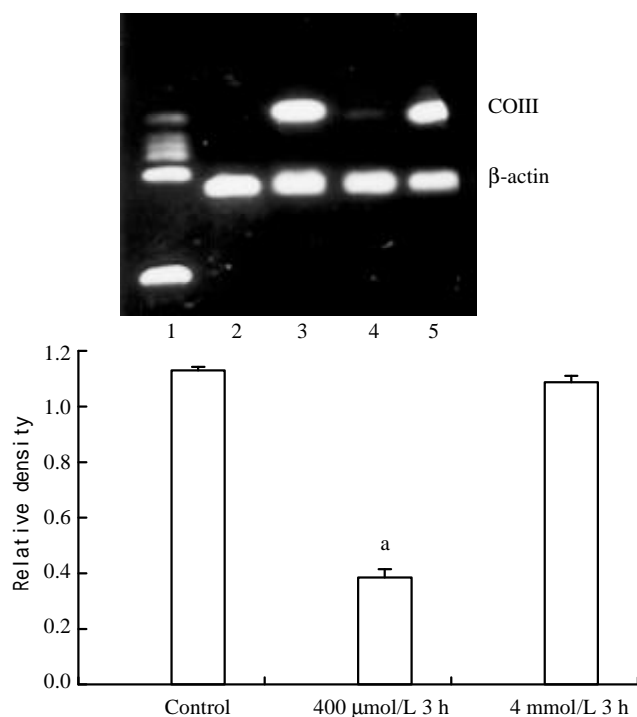


Figure 4 Effects of hydrogen peroxide on expression of COIII mRNA ($^*P<0.05$, vs normal control). 1 DNA marker: 1DNA/Hind III, 2 positive control, 3 normal control, 4 400 $\mu\text{mol/L}$ 3 h, 5 4 mmol/L 3 h.

Expression of ATPase6 mRNA

Expression of ATPase6 mRNA increased significantly in 400 $\mu\text{mol/L}$ hydrogen peroxide stimulated-cells, meanwhile decreased expression could also be found in 4 mmol/L hydrogen peroxide-stimulated cells (Figure 5).

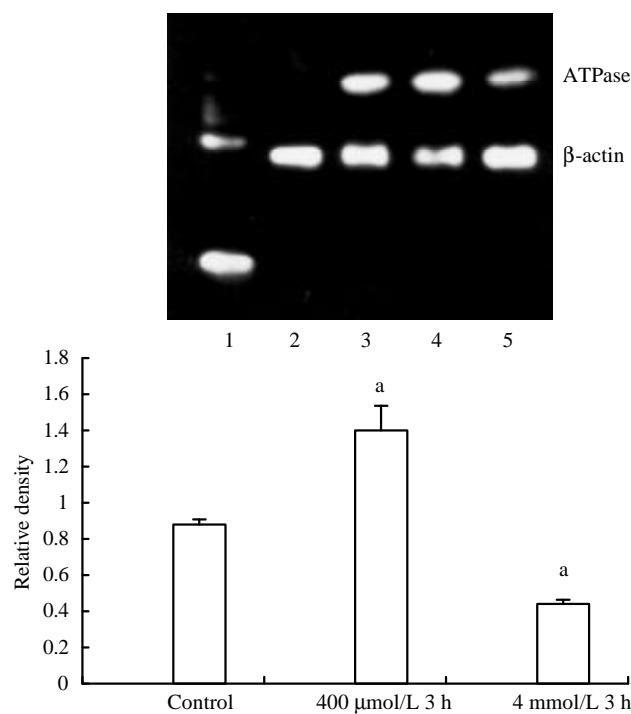


Figure 5 Effects of hydrogen peroxide on expression of ATPase6 mRNA ($^*P<0.05$, vs normal control). 1 DNA marker: 1DNA/Hind III, 2 positive control, 3 normal control, 4 400 $\mu\text{mol/L}$ 3 h, 5 4 mmol/L 3 h.

Expression of ATPase8 mRNA

Stable expression of ATPase8 mRNA was found in control cells. No significant increase could be found in 400 $\mu\text{mol/L}$ hydrogen peroxide-stimulated cells. Decreased expression of ATPase8 mRNA in 4 mmol/L hydrogen peroxide-stimulated cells was found (Figure 6).

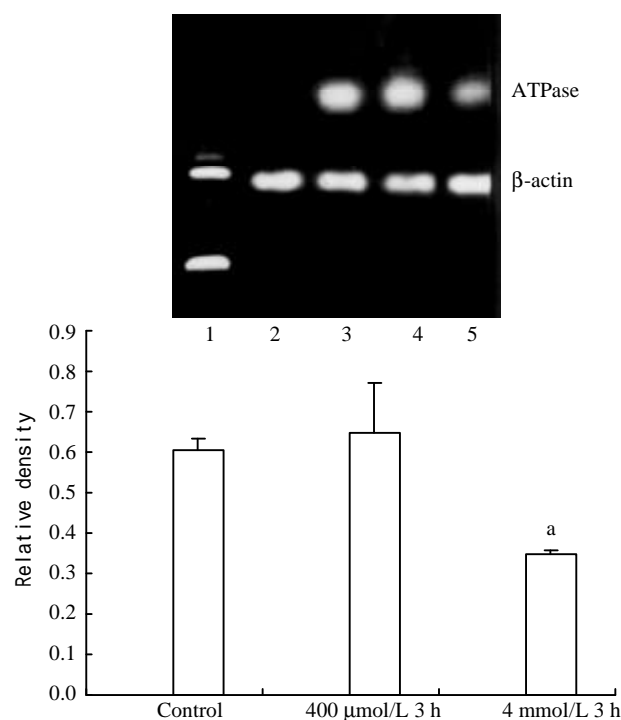


Figure 6 Effects of hydrogen peroxide on expression of ATPase8 mRNA ($^*P<0.05$, vs. normal control). 1 DNA marker: 1DNA/Hind III, 2 positive control, 3 normal control, 4 400 $\mu\text{mol/L}$ 3 h, 5 4 mmol/L 3 h.

Activity of cytochrome c oxidase

Activities of cytochrome c oxidase decreased significantly in both 400 $\mu\text{mol/L}$ and 4 mmol/L hydrogen peroxide-stimulated cells (Figure 7).

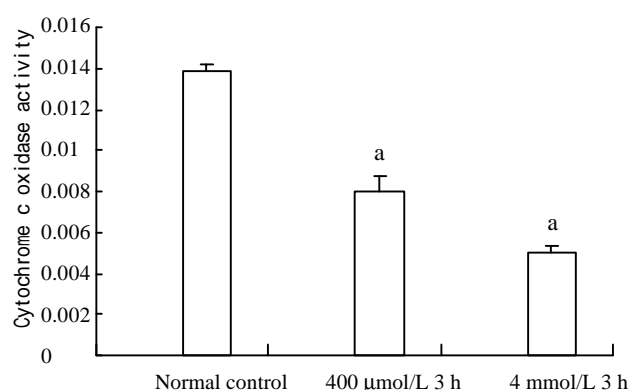


Figure 7 Activity of cytochrome c oxidase in hydrogen peroxide-stimulated SW-480 cells (^a $P < 0.05$, vs. normal control).

ATPase activity

Although only ATPase activity in 4 mM hydrogen peroxide-stimulated cells decreased significantly on the view of statistics, the trend is very obvious (Figure 8).

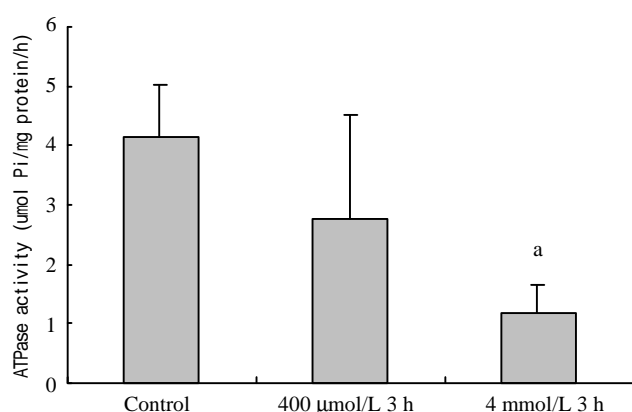


Figure 8 Activity of ATPase in hydrogen peroxide-stimulated SW-480 cells (^a $P < 0.05$, vs. normal control).

DISCUSSION

The role of mitochondrion in the pathogenesis of apoptosis has been well defined. Mitochondrion, a kind of organelle controlling growing, breeding and dying of eukaryocyte, embodies its functions through: (1) production of ATP; (2) production of ROS, which regulates nuclear gene expression; (3) link between cytoplasm and nucleus; (4) sensitive response to stimulator or signals outside cytoplasm; (5) triggering of cell death^[19, 20]. Evidences show the central role of mitochondria in the development of apoptosis. Many stimulators like ROS, Ca^{2+} and cytokines lead to activation of caspases by inducing release of cytochrome C and thereby trigger a cascade in apoptosis^[11].

Release of mitochondrial apoptosis-inducing substance caused by collapse of mitochondrial membrane potential and open of mitochondrial permeability transition pore controlled by Bcl 2 family is the key step to initiate apoptosis. Mitochondrial respiration depends on maintenance of mitochondrial membrane potential.

Now the relationship between DNA injuries and apoptosis

has been recognized^[21]. Although mitochondrial genome was sequenced in 1981^[22], there is little study on function of mitochondrial genes. Thirteen proteins encoded by mitochondrial genome make up parts of enzymes involving mitochondrial oxidative phosphorylation. Without protection of histone, mitochondrial genome is much easier to be injured compared with nuclear genome. Our research also confirmed this (results to be published). Many researches indicated that oxidative stress led to mutation of mitochondrial genes^[23-32]. The relationship between mutation of DNA and expression of genes needs to be well investigated.

Hydrogen peroxide led to differential expression of mitochondrial genes with some genes up-regulated or down-regulated in a dose-dependent manner. Differences were very obvious in expression of mitochondrial genes of cells treated with hydrogen peroxide in the concentration of 400 $\mu\text{mol/L}$ or 4 mmol/L . In general, differential expression of mitochondrial genes was characterized by up-regulation of mitochondrial genes in the concentration of 400 $\mu\text{mol/L}$ and down-regulation in the concentration of 4 mmol/L . In consistence with changes of mitochondrial gene expression, hydrogen peroxide led to similar decreased activities of cytochrome C oxidase and ATPase. Differential expression reflected the difference in the sensitivity of gene responding to oxidative stress, which may relate greatly to cellular physiological process next. In rat lung epithelial cells treated with hydrogen peroxide for 8 or 24 h, the differential display of genes showed that mutation of genes from mitochondrial genome encoding NADH dehydrogenase subunit 5, subunit 6 and 16 S ribosome could be detected; the results also suggested that mitochondrial genes played a role in the control of apoptosis^[33]. Researches showed that there were some links between mitochondrial dysfunction and injuries of mitochondrial DNA or expression of mitochondrial genes in hydrogen peroxide-stimulated vascular endothelial cells and smooth muscle cells^[34].

Meanwhile we also found a large scale of point mutation of mitochondrial gene such as ATPase8 subunit in 4 mmol/L hydrogen peroxide treated SW-480 cells, suggesting its correlation with down-regulation of ATPase expression.

It is considered now that the mitochondrial permeability transition (MPT) plays a key role in the pathogenesis of apoptosis and necrosis^[35-38]. If MPT initiates rapidly with depletion of ATP, cells undergo necrosis, and if MPT occurs without depletion of ATP, cells evolved into apoptosis. So we may conclude that complete inhibition of ATPase would lead to necrosis and partially inhibition of ATPase would lead to apoptosis. Consistent with this conclusion, our study proved a partially inhibition of ATPase in both 4 mmol/L and 400 $\mu\text{mol/L}$ hydrogen peroxide-treated SW-480 cells, suggesting its potential role in apoptosis. But there are still many problems to be clarified, including the relationship between different expressions of mitochondrial genes, activities of cytochrome C oxidase and ATPase, oxidative phosphorylation and regulation of apoptosis.

Studies including ours showed that mitochondrial genes played the role in apoptosis. To establish mtDNA deletion cells (ρ^0 cells) provided in our studies more direct evidences^[39-42].

It is unclear about the pathway leading to increasing expression of mitochondrial genes. Defects of mitochondrial energy supply may be one of the compensatory mechanisms leading to increasing expression of mitochondrial genes^[43].

Our results showed that differential expression seemed to be incompatible with decreasing activities of cytochrome C oxidase or ATP synthase. To answer this question, we should

pay attention to mitochondrial proteins encoded by the nuclear genome, which form main parts of mitochondrial proteins. For example, only subunits 6 and 8 of ATP synthase were encoded by mitochondrial genome, which may also be controlled by some nuclear transcriptional factors^[44-46]. Meanwhile most parts of ATPase were encoded by the nuclear genome. Cross-talk between mitochondrial genes and nuclear genes will be the next key or difficult question to be answered^[47-50]. It will become available to study cross-talk between mitochondrial genes and nuclear genes from the view of genome and proteome by the developing techniques of genome and proteome.

REFERENCES

- Zuo GQ**, Gong JP, Liu CA, Li SW, Wu XC, Yang K, Li Y. Expression of lipopolysaccharide binding protein and its receptor CD14 in experimental alcoholic liver disease. *World J Gastroenterol* 2001; **7**: 836-840
- Meng AH**, Ling YL, Zhang XP, Zhao XY, Zhang JL. CCK-8 inhibits expression of TNF- α in the spleen of endotoxic shock rats and signal transduction mechanism of p38 MAPK. *World J Gastroenterol* 2002; **8**: 139-143
- Wu RQ**, Xu YX, Song XH, Chen LJ, Meng XJ. Relationship between cytokine mRNA expression and organ damage following cecal ligation and puncture. *World J Gastroenterol* 2002; **8**: 131-134
- Li SW**, Gong JP, Wu CX, Shi YJ, Liu CA. Lipopolysaccharide induced synthesis of CD14 proteins and its gene expression in hepatocytes during endotoxemia. *World J Gastroenterol* 2002; **8**: 124-127
- Yu PW**, Xiao GX, Qin Xj X, Zhou LX, Wang ZQ. The effects of PAF antagonist on intestinal mucosal microcirculation after burn in rats. *World J Gastroenterol* 2000; **6**: 906-908
- Qin RY**, Zou SQ, Wu ZD, Qiu FZ. Influence of splanchnic vascular infusion on the content of endotoxins in plasma and the translocation of intestinal bacteria in rats with acute hemorrhage necrosis pancreatitis. *World J Gastroenterol* 2000; **6**: 577-580
- Wang QG**, He LY, Chen YW, Hu SL. Enzymohistochemical study on burn effect on rat intestinal NOS. *World J Gastroenterol* 2000; **6**: 421-423
- Fu XB**, Yang YH, Sun TZ, Gu XM, Jiang LX, Sun XQ, Sheng ZY. Effect of intestinal ischemia-reperfusion on expressions of endogenous basic fibroblast growth factor and transforming growth factor betain lung and its relation with lung repair. *World J Gastroenterol* 2000; **6**: 353-355
- Fu WL**, Xiao GX, Yue XL, Hua C, Lei MP. Tracing method study of bacterial translocation *in vivo*. *World J Gastroenterol* 2000; **6**: 153-155
- Yang YH**, Fu XB, Sun TZ, Jiang LX, Gu XM. bFGF and TGF β expression in rat kidneys after ischemic/reperfusional gut injury and its relationship with tissue repair. *World J Gastroenterol* 2000; **6**: 147-149
- Green DR**, Reed JC. Mitochondria and apoptosis. *Science* 1998; **281**: 1309-1312
- Hengartner MO**. The biochemistry of apoptosis. *Nature* 2000; **407**: 770-776
- Desagher S**, Martinou JC. Mitochondria as the central control point of apoptosis. *Trends Cell Biol* 2000; **10**: 369-377
- Petit PX**, Susin SA, Zamzami N, Mignotte B, Kroemer G. Mitochondria and programmed cell death: back to the future. *FEBS Letters* 1996; **396**: 7-13
- Finkel E**. The mitochondrion: is it central to apoptosis? *Science* 2001; **292**: 624-626
- Koya RC**, Fujita H, Shimizu S, Ohtsu M, Takimoto M, Tsujimoto Y, Kuzumaki N. Gelsolin inhibits apoptosis by blocking mitochondrial membrane potential loss and cytochrome c release. *J Biol Chem* 2000; **275**: 15343-15349
- Barazzoni R**, Short KR, Nair KS. Effects of aging on mitochondrial DNA copy number and cytochrome c oxidase gene expression in rat skeletal muscle liver and heart. *J Biol Chem* 2000; **275**: 3343-3347
- Buchet K**, Godinot C. Functional F1-ATPase essential in maintaining growth and membrane potential of human mitochondrial DNA-depleted p0 cells. *J Biol Chem* 1998; **273**: 22983-22989
- Kluck RM**, Bossy Wetzel E, Green DR, Newmeyer DD. The release of cytochrome C from mitochondria: a primary site for Bcl-2 regulation of apoptosis. *Science* 1997; **275**: 1132-1136
- Susin SA**, Zamzami N, Castedo M, Hirsch T, Marchetti P, Macho A, Daugas E, Geuskens M, Kroemer G. Bcl-2 inhibits the mitochondrial release of an apoptogenic protease. *J Exp Med* 1996; **184**: 1331-1341
- Rich T**, Allen RL, Wyllie AH. Defying death after DNA damage. *Nature* 2000; **407**: 777-783
- Anderson S**, Bankier AT, Barrell BG, de Bruijn MH, Coulson AR, Drouin J, Eperon IC, Nierlich DP, Roe BA, Sanger F, Schreier PH, Smith AJ, Staden R, Young IG. Sequence and organization of the human mitochondrial genome. *Nature* 1981; **290**: 457-465
- Simon DK**, Lin MT, Ahn CH, Liu GJ, Gibson GE, Beal MF, Johns DR. Low mutational burden of individual acquired mitochondrial DNA mutations in brain. *Genomics* 2001; **73**: 113-116
- Wallace DC**. A mitochondrial paradigm for degenerative diseases and ageing. *Novartis Found Symp* 2001; **235**: 247-263
- Chang SW**, Zhang D, Chung HD, Zassenhaus HP. The frequency of point mutations in mitochondrial DNA is elevated in the Alzheimer's brain. *Biochem Biophys Res Commun* 2000; **273**: 203-208
- Esposito LA**, Melov S, Panov A, Cottrell BA, Wallace DC. Mitochondrial disease in mouse results in increased oxidative stress. *Proc Natl Acad Sci USA* 1999; **96**: 4820-4825
- Lu CY**, Lee HC, Fahn HJ, Wei YH. Oxidative damage elicited by imbalance of free radical scavenging enzymes is associated with large-scale mtDNA deletions in aging human skin. *Mutat Res* 1999; **423**: 11-21
- Bhat HK**, Hiatt WR, Hoppel CL, Brass EP. Skeletal muscle mitochondrial DNA injury in patients with unilateral peripheral arterial disease. *Circulation* 1999; **99**: 807-812
- Swerdlow RH**, Parks JK, Cassarino DS, Shilling AT, Bennett JP, Harrison MB, Parker WD. Characterization of cybrid cell lines containing mtDNA from Huntington's disease patients. *Biochem Biophys Res Commun* 1999; **261**: 701-704
- Wei YH**. Oxidative stress and mitochondrial DNA mutations in human aging. *Proc Soc Exp Biol Med* 1998; **217**: 53-63
- Ide T**, Tsutsui H, Hayashidani S, Kang D, Suematsu N, Nakamura K, Utsumi H, Hamasaki N, Takeshita A. Mitochondrial DNA damage and dysfunction associated with oxidative stress in failing hearts after myocardial infarction. *Circ Res* 2001; **88**: 529-535
- Swerdlow RH**, Parks JK, Davis JN, Cassarino DS, Trimmer PA, Currie LJ, Dougherty J, Bridges WS, Bennett JP, Wooten GF, Parker WD. Matrilineal inheritance of complex I dysfunction in a multigenerational Parkinson's disease family. *Ann Neurol* 1998; **44**: 873-881
- Janssen YM**, Driscoll KE, Timblin CR, Hassenbein D, Mossman BT. Modulation of mitochondrial gene expression in pulmonary epithelial cells exposed to oxidants. *Environ Health Perspect* 1998; **106**(Suppl 5): 1191-1195
- Ballinger SW**, Patterson C, Yan CN, Doan R, Burow DL, Young CG, Yakes FM, Van Houten B, Ballinger CA, Freeman BA, Runge MS. Hydrogen peroxide and peroxynitrite induced mitochondrial DNA damage and dysfunction in vascular endothelial and smooth muscle cells. *Circ Res* 2000; **86**: 960-966
- Hatano E**, Bradham CA, Stark A, Iimuro Y, Lemasters JJ, Brenner DA. The mitochondrial permeability transition augments Fas-induced apoptosis in mouse hepatocytes. *J Biol Chem* 2000; **275**: 11814-11823
- Lemasters JJ**. V.Necrapoptosis and the mitochondrial permeability transition: shared pathways to necrosis and apoptosis. *Am J Physiol* 1999; **276**: G1-G6
- Lemasters JJ**, Qian T, Bradham CA, Brenner DA, Cascio WE, Trost LC, Nishimura Y, Nieminen AL, Herman B. Mitochondrial dysfunction in the pathogenesis of necrotic and apoptotic cell death. *J Bioenerg Biomembr* 1999; **31**: 305-319
- Pastorino JG**, Tafani M, Rothman RJ, Marcinkeviciute A, Hoek JB, Farber JL, Marcinkeviciute A. Functional consequences of the sustained or transient activation by Bax of the mitochondrial per-

- meability transition pore. *J Biol Chem* 1999; **274**: 31734-31739
- 39 **Wang J**, Silva JP, Gustafsson CM, Rustin P, Larsson NG. Increased *in vivo* apoptosis in cells lacking mitochondrial DNA gene expression. *Proc Natl Acad Sci U S A* 2001; **98**: 4038-4043
- 40 **Appleby RD**, Porteous WK, Hughes G, James AM, Shannon D, Wei YH, Murphy MP. Quantitation and origin of the mitochondrial membrane potential in human cells lacking mitochondrial DNA. *Eur J Biochem* 1999; **262**: 108-116
- 41 **Tang JT**, Yamazaki H, Inoue T, Koizumi M, Yoshida K, Ozeki S, Inoue T. Mitochondrial DNA influences radiation sensitivity and induction of apoptosis in human fibroblasts. *Anticancer Res* 1999; **19**: 4959-4964
- 42 **Suzuki A**, Tsutomi Y, Yamamoto N, Shibutani T, Akahane K. Mitochondrial regulation of cell death: mitochondria are essential for procaspase 3-p21 complex formation to resist Fas-mediated cell death. *Mol Cell Biol* 1999; **19**: 3842-3847
- 43 **Wiesner RJ**, Hornung TV, Garman JD, Clayton DA, O'Gorman E, Wallimann T. Stimulation of mitochondrial gene expression and proliferation of mitochondria following impairment of cellular energy transfer by inhibition of the phosphocreatine circuit in rat hearts. *J Bioenerg Biomembr* 1999; **31**: 559-567
- 44 **Herzig RP**, Scacco S, Scarpulla RC. Sequential serum-dependent activation of CREB and NRF-1 leads to enhanced mitochondrial respiration through the induction of cytochrome c. *J Biol Chem* 2000; **275**: 13134-13141
- 45 **Miranda S**, Foncea R, Guerrero J, Leighton F. Oxidative stress and upregulation of mitochondrial biogenesis genes in mitochondrial DNA-depleted HeLa cells. *Biochem Biophys Res Commun* 1999; **258**: 44-49
- 46 **Wu Z**, Puigserver P, Andersson U, Zhang C, Adelmant G, Mootha V, Troy A, Cinti S, Lowell B, Scarpulla RC, Spiegelman BM. Mechanisms controlling mitochondrial biogenesis and respiration through the thermogenic coactivator PGC-1. *Cell* 1999; **98**: 115-124
- 47 **Traven A**, Wong JM, Xu D, Sopta M, Ingles CJ. Interorganellar communication: Altered nuclear gene expression profiles in a yeast mitochondrial DNA mutant. *J Biol Chem* 2001; **276**: 4020-4027
- 48 **Kaasik A**, Veksler V, Boehm E, Novotova M, Minajeva A, Ventura-Clapier R. Energetic crosstalk between organelles: architectural integration of energy production and utilization. *Circ Res* 2001; **89**: 153-159
- 49 **Poyton RO**, Dagsgaard CJ. Mitochondrial-nuclear crosstalk is involved in oxygen-regulated gene expression in yeast. *Adv Exp Med Biol* 2000; **475**: 177-184
- 50 **Poyton RO**, McEwen JE. Crosstalk between nuclear and mitochondrial genomes. *Annu Rev Biochem* 1996: 65563-65607

Edited by Lu HM

Analysis of Heme oxygenase isomers in rat

Zhen-Wei Xia, Wen-Jun Cui, Xue-Hong Zhang, Qing-Xiang Shen, Jian Wang, Yun-Zhu Li, Shen-Nian Chen, Shan-Chang Yu

Zhen-Wei Xia, Yun-Zhu Li, Shun-Nian Chen, Shan-Chang Yu, Department of Pediatrics, Rui Jin Hospital, Shanghai Second Medical University, Shanghai 200025, China

Wen-Jun Cui, Xue-Hong Zhang, College of Life Science and Biotechnology, Shanghai Jiaotong University & The Chinese Academy of Science, Shanghai Branch, Shanghai 200030, China

Qing-Xiang Shen, Jian Wang, Shanghai Institute of Planned Parenthood Research, Shanghai 200032, China

Supported by National Natural Scientific Foundation of China, No. 39600159

Correspondence to: Dr. Zhen-Wei Xia, Department of Pediatrics, Rui Jin Hospital, Shanghai Second Medical University, 197 Rui Jin Er Road, Shanghai 200025, China. xzw63@hotmail.com

Telephone: +86-21-64333414 **Fax:** +86-21-64333414

Received 2002-06-11 **Accepted** 2002-07-26

Abstract

AIM: To purify and identify heme oxygenase (HO) isomers which exist in rat liver, spleen and brain treated with hematin and phenylhydrazine and in untreated rat liver and to investigate the characteristics of HO isomers, to isolate and confirm the rat HO-1 cDNA that actually encodes HO-1 by expressing cDNA in monkey kidney cells (COS-1 cells), to prepare the rat heme oxygenase-1 (HO-1) mutant and to detect inhibition of HO-1 mutated enzyme.

METHODS: First, rat liver, spleen and brain microsomal fractions were purified by DEAE-Sephacel and hydroxylapatite. The characteristics including activity, immunity and inducibility of two isomers (HO-1 and HO-2), and their apparent molecular weight were measured by detecting enzymatic activities, SDS-polyacrylamide gel electrophoresis (SDS-PAGE) and Western blotting analysis, respectively. Second, plasmid pcDNA3HO1 containing native rat HO-1 cDNA and pcDNA3HO1D25 carrying mutated rat HO-1 cDNA (His25Ala) were constructed by site-directed mutagenesis. COS-1 cells transfected with pcDNA3HO1 and pcDNA3HO1D25 were collected and disrupted by sonication, the microsomes were prepared by ultracentrifugation. Third, the inhibition of rat HO-1 mutant was analyzed.

RESULTS: Two isomers were purified and identified in treated rat liver, spleen, brain and untreated rat liver. HO-1 was the predominant form with a ratio of 2.0:1 and 3.2:1 of HO-1 and HO-2 in liver and spleen, respectively, but only the activity of HO-2 in the brain and untreated liver could be detected. The apparent molecular weights of HO-1 and HO-2 were about M_r 30 000 and M_r 36 000 under reducing conditions, respectively. The antiserum against liver HO-2 was employed in Western blotting analysis, the reactivity of HO-1 in the liver was not observed. The plasmid pcDNA3HO1 was highly expressed in endoplasmic reticulum of transfected COS-1 cells. The specific activity was \approx 5-fold higher than that of the control. However, the enzyme activity of mutated HO-1 declined. While an equal amount of mutant was added to the enzyme reaction system, the levels of bilirubin decreased 42 %.

CONCLUSION: The studies suggest that HO-1 and HO-2 exist in the hematin and phenylhydrazine treated rat liver and spleen, but only HO-2 in the brain and untreated liver. Two constitutive forms are different in molecular weight, inducibility and immunochemical properties. The activity of expressed HO-1 in COS-1 cells is higher than that of purified enzyme from rat spleen tissue. It suggests that this clone has an insert of 1030 base-pairs encodes HO-1. His25Ala mutant reduced the formation of bilirubin and it suggests that the mutant could completely bind the heme with native enzyme.

Xia ZW, Cui WJ, Zhang XH, Shen QX, Wang J, Li YZ, Chen SN, Yu SC. Analysis of Heme oxygenase isomers in rat. *World J Gastroenterol* 2002; 8(6):1123-1128

INTRODUCTION

Cellular levels of heme are regulated by the rates of its synthesis and degradation. Heme catabolism occurs by oxidative cleavage of the -methene bridge of the tetrapyrrole, eventually leading to the formation of equimolar amounts of biliverdin and the release of contained iron atom. Biliverdin is then rapidly reduced to form bilirubin. The heme oxygenase (HO) system controls the rate-limiting step in heme catabolism. Three isomers (HO-1, HO-2 and HO-3) have been identified that catalyze this reaction. HO-1 is a M_r 30 000 that is inducible by heme and other numerous stimuli being the predominant form in liver and spleen. HO-2 is a constitutively synthesized M_r 36 000 protein that is abundant in brain and testis. HO-3 is a M_r 33 000 protein that, so far, has only been expressed constitutively in rat neurones. They are the products of different genes^[1-32].

Overexpression of HO-1 gene can lead to hyperbilirubinemia in human with certain hepatic disorder, especially patients in whom bilirubin disposition is impaired for developmental or genetic reasons, i.e., in newborns and in patients with Crigler-Najjar type I syndrome. So, the characterization of the two constitutive forms and the expression of HO-1 gene would have considerable experimental value in elucidating the role of the enzyme in physiological and pathological processes and finally in effective prevention and treatment of hyperbilirubinemia.

The objective of this study was to purify and identify HO isomers (HO-1 and HO-2) in treated rat liver, spleen, brain and untreated rat liver, to construct the expression plasmid pcDNA3HO1 carrying HO-1 cDNA and to confirm that the cDNA actually encodes HO-1 by expressing cDNA in COS-1 cells. On the basis of these findings, we have expected the substitution of histidine residues essential for heme binding would eliminate HO activity, so site-directed mutagenesis was applied to construct mutated rat HO-1 cDNA (Histidine25→Alanine, His25Ala), then the activity of mutant was detected and compared with that of native enzyme. The inhibition of this mutant was also examined by determining the levels of bilirubin in the enzymatic reaction mixture.

MATERIALS AND METHODS

Preparation of tissue

The rats (purchased from Shanghai Institute of Cell Biology,

Academia Sinica) were allowed to food and water *ad libitum* and were injected with 40 $\mu\text{mol/kg}$ hematin (pH 7.4), intraperitoneally; 100 mg/kg phenylhydrazine, intravenously. The animals were killed 20 hours after treatment.

Purification and identification of HO-1 and HO-2

All operations were carried out below 4 °C. The rat liver, spleen and brain tissues were added 2 volumes of 0.25 mol/L sucrose solution containing 0.1 mmol/L EDTA. The mixture was homogenized and centrifuged at 9 000 g for 5 minutes. The supernatant fractions were collected and subsequently centrifuged at 150 000 g for 1 hour. The microsomal pellet was treated according to the method described by Maines *et al.* The solubilized microsomes were diluted with 1 volume of 0.05 mmol/L DTT solution, with pH adjusted to 8 and loaded onto DEAE-Sephacel column (2.5 \times 13.6 cm) that was previously equilibrated with 20 mmol/L Tris-HCl buffer (pH 7.5) containing 0.05 mmol/L EDTA, 0.5 % TritonX-100, 0.1 % sodium cholate and 0.05 mmol/L DTT. The column was eluted with concurrent linear gradients of KCl (0-0.4 mol/L) and TritonX-100 (0.5-0.9 %) prepared with the equilibration buffer. 3-4 ml fractions were collected and analyzed for HO activity.

The pooled DEAE-Sephacel fractions containing the first peak of HO activity and the second peak of HO activity were dialyzed against distilled water for 24 hours below 4 °C, and then concentrated and loaded onto a hydroxylapatite column equilibrated with 10 mmol/L potassium phosphated buffer, pH 7.5, respectively. The column was washed with 10 mmol/L potassium phosphate buffer, pH 7.2, containing 0.05 mmol/L EDTA, 0.4 % TritonX-100 and 0.1 % sodium cholate, followed by the same solution containing 20 % glycerol. The column was eluted with a linear gradient of 10-260 mmol/L potassium phosphate in the above buffer. The fractions containing HO activity were collected.

Construction of expression plasmid carrying native rat HO-1 cDNA

The expression vector pcDNA3 was linearized by digestion with BamHI and the single-stranded ends were filled in by treatment with DNA polymerase I (Klenow fragment). The resulting blunt ends were used for ligation with XhoI (-59) / HindIII (971) cDNA fragment isolated from pRHO1, which was provided by Shibahara. Both ends of the fragment were converted to blunt ends before ligation. The plasmid pcDNA3HO1 that encodes native HO-1 was constructed.

Mutagenesis of cDNA for rat HO-1 and construction of pcDNA3HO1D25

The expression vector pcDNA3HO1 was cleaved with XbaI. The region of the template was amplified in polymerase chain reaction. 5' -terminal primers was T7 and 3' -terminal primer was a synthetic oligonucleotide (5' -CTCAGAAATCTCTGCA CGGGTGGCCACCTCC-3'). The amplified products were digested by HindIII/EcoRI and the resulting DNA fragments (HindIII \rightarrow EcoRI, 171bp) were ligated to pBS KS which had been pretreated with HindIII/EcoRI. The recombinant plasmid (pBS KSHO1-171) was digested with EcoRI and the single stranded ends were filled in by treatment with Klenow fragment followed by dephosphorylation with calf intestinal alkaline phosphatase.

To construct the plasmid pBS KSHO1D25 (4034bp), the pcDNA3HO1 was digested with EcoRI. The DNA fragments (EcoRI \rightarrow EcoRI, 932bp) from pcDNA3HO1 was purified and inserted into EcoRI site of pBS KSHO1-171.

Finally, the vector pBS KSHO1D25 was cut with HindIII

and BamHI, and ligated to pcDNA3, which had been also pretreated with HindIII and BamHI, to construct pcDNA3HO1D25 (6525bp).

Transfection of COS-1 cells

COS-1 cells, which were provided by Shanghai Institute of Cell Biology, Academia Sinica, were maintained in Dulbecco's modified Eagle's medium containing 2.5 % newborn calf serum. Confluent cells, seeded in 75 ml culture flask, were fed with medium 4 hours before addition of plasmid DNA. Plasmid DNA (10 μg per flask) was used to transfect COS-1 cells by the calcium phosphate method. DNA (at 10 $\mu\text{g/ml}$) was adjusted to 250 mmol/L CaCl_2 and added slowly to an equal volume of sterile 2 \times HBS with constant agitation. The calcium phosphate-DNA precipitate was allowed to form for 30 minutes, and 1 ml of precipitate was added to an adequate volume of medium that covered recipient cells. After 4 hours of exposure to DNA, the medium was replaced with fresh medium, and the cells were allowed to incubate for an additional 48 hours, then cells were collected and stored at -70 °C until assay for HO-1. The cells were disrupted by sonication and pellets (microsomes) were prepared by centrifugation at 105 000 g, 0-4 °C, 1 hour. The microsomes were suspended in 50 mmol/L potassium phosphate buffer, pH 7.4/0.1 % Triton X-100, subjected to SDS-PAGE to confirm whether the specific band was located in the position of M_r 30 000.

Measurement of heme oxygenase isomers and expressed products activity

The activity of HO isomers and expressed products was determined by measuring the bilirubin formation monitored as an absorbance increase at 464 nm. One unit of the enzyme was defined as the amount catalyzing the formation of 1 nmol of bilirubin per 1 hour.

SDS-polyacrylamide gel electrophoresis of HO isomers and expressed products

Electrophoretic procedures were performed according to Laemmli's method in order to identify HO isomers and their molecular weight.

Production of antiserum

The purified rat liver HO-2 fraction mixed with 100 μl of 0.9 % NaCl solution and injected intraperitoneally into Kunming mice (10-15 g) purchased from Shanghai Institute of Cell Biology, Academia Sinica. Then these mice were boosted with antigen every second week, for three times. The mice were bled 10 days after the final boost and sera were collected and stored under -20 °C.

Western blotting

Western blotting was performed as follows. Protein samples, rat liver HO-1 and rat brain HO-2 fractions, were subjected to SDS-polyacrylamide gel electrophoresis (SDS-PAGE) in 1.5 mm slab gels according to the procedure of Laemmli and the separated polypeptides were then transferred electrophoretically from the gel to a nitrocellulose sheet using a transfer buffer consisting of 48 mmol/L Tris base, 39 mmol/L glycine, 20 % (v/v) methanol and 0.07 % (w/v) SDS, pH 8.3. Following electroblotting, the nitrocellulose paper was stained with Ponceau S for protein detection. Destaining was performed with distilled water. For immunostaining the nitrocellulose blot was incubated at 37 °C for 1 hour with bovine serum albumin in 20.0 mmol/L Tris-HCl buffer, pH 7.5, containing 0.5 mol/L sodium chloride in order to saturate all protein binding sites.

The nitrocellulose blot was then incubated with antiserum against rat liver HO-2 at 37 °C for 1 hour, and washed several times with peroxidase-anti-mouse IgG diluted with PBS solution. The blot was stained with diaminobenzidine (DAB) solution, washed with distilled water.

RESULTS

Purification and identification of the two forms of HO from different tissues

Two peaks exhibiting HO activity from rat liver and spleen treated with hematin and phenylhydrazine were eluted using DEAE-Sephacel chromatography. The peaks were designated as HO-1 and HO-2 according to the sequence of their elution from column. The pooled DEAE-Sephacel fractions containing HO-1 and HO-2 activities were loaded onto hydroxylapatite column, and the final purified HO-1 and HO-2 products exhibited only a single band when visualized by staining of SDS-PAGE with Coomassie Blue. The values obtained for HO-1 and HO-2 activities were shown in the Figure 1, with the ratio of HO-1 to HO-2 being approximately 2.0:1 and 3.2:1, respectively.

The treated rat brain and untreated rat liver microsomal fractions were also solubilized and subjected to ion-exchange chromatography of DEAE-sephacel, respectively. The chromatography elution patterns of HO activity were compared with those of treated rat liver and spleen. Only one peak of HO activity was detected from the treated rat brain and untreated rat liver (Figure 1). An activity peak was not present in the elution at the inducible isomer of HO (HO-1) region.

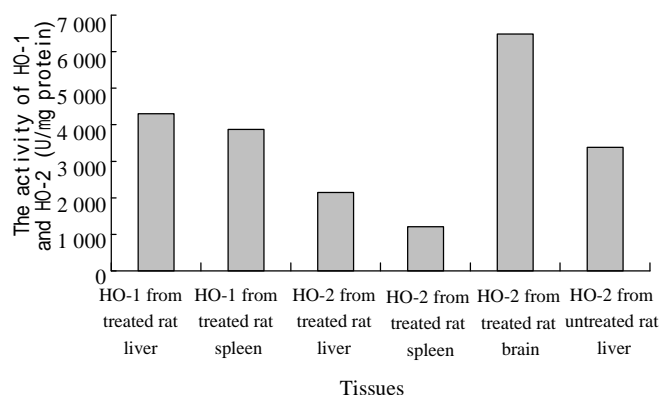


Figure 1 The measurement of HO isomers from different tissues

Characterization of HO-1 and HO-2

Two forms of HO were subjected to electrophoresis, in which two distinct bands exhibiting HO activity were detected, the migration patterns of HO-1 and HO-2 being different. The purified HO-2 on SDS-PAGE displayed a higher monomeric molecular weight. The apparent molecular weight of HO-1 and HO-2 were M_r 30 000 and M_r 36 000, respectively. The apparent molecular weight in treated brain microsomal preparation was identical to the purified liver and spleen HO-2. The HO-1 activity was increased in response to hematin and phenylhydrazine, while that of HO-2 was fully refractory to these agents. The blot was treated with anti-rat liver HO-2 serum followed by anti-mouse IgG-peroxidase conjugate and then stained for peroxidase activity. As expected, rat brain HO-2 preparation gave a reddish brown band in the region of molecular weight M_r 36 000. However, the rat HO-1 preparation failed to show a stained band.

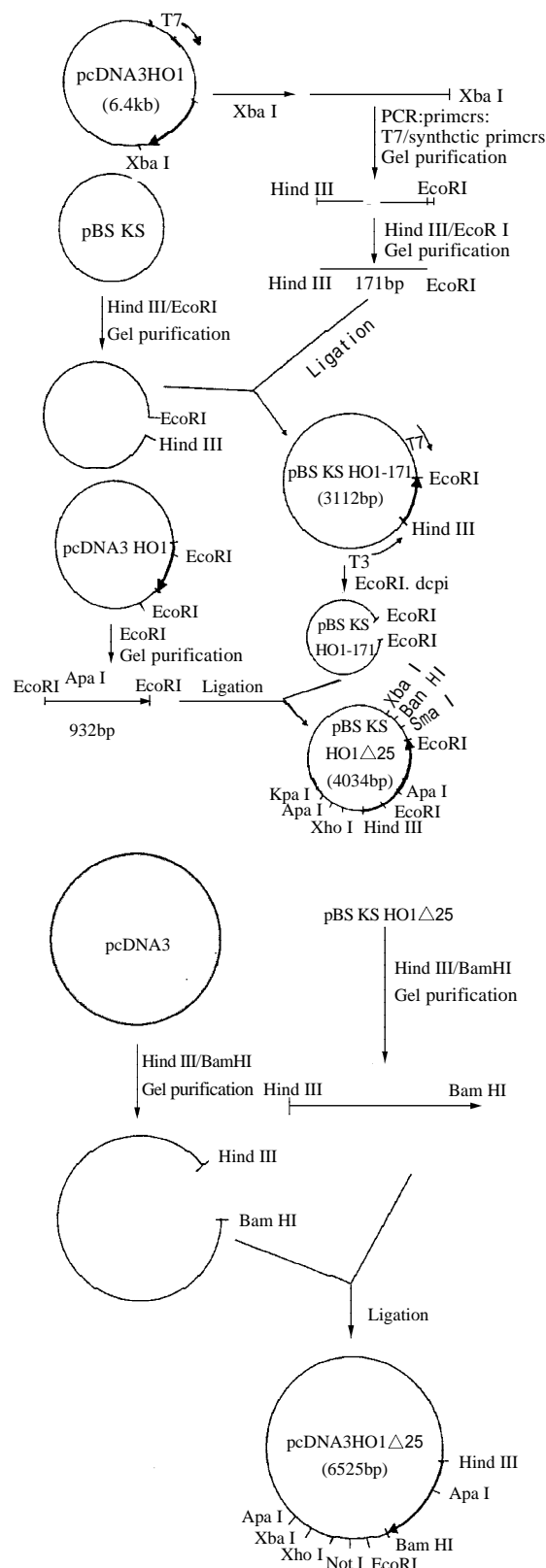


Figure 2 The strategy for construction of the expression vector of pcDNA3HO1 Δ25

Construction of plasmid pcDNA3HO1 containing rat HO-1 cDNA

The pcDNA3HO1 containing HO-1 cDNA was screened out. The fragments of 916 bp and 5 567 bp were observed after digestion of the resulting plasmid with EcoRI indicating that the plasmid had HO-1 cDNA in a correct direction.

Expression of native rat HO-1 cDNA in COS-1 cells

The activity of HO-1 product transiently expressed in COS-1 cells was detected. The results suggested that the specific band was located in the position of M_r 30 000, the specific activities of HO-1 in COS-1 cells transfected with plasmid pcDNA3HO1 and plasmid pcDNA3 were 13 688 and 2 920 units/mg of protein/hour, respectively. The activity of expressed enzyme was 4.5-fold, 3.1-fold and 3.5-fold higher in comparison with that of the control transfected with plasmid pcDNA3, purified HO-1 from rat liver and spleen tissue, respectively.

Construction of mutated rat HO-1 cDNA (His25Ala) and assay of its activity

Figure 2. showed the strategy for construction of the expression vector of pcDNA3HO1D25. The histidine-25 residue was replaced with an alanine residue by site-directed mutagenesis. The whole nucleotide sequence of insert of mutant rat HO-1 was confirmed by the dideoxynucleotide chain-termination method. COS-1 cells transfected with pcDNA3HO1D25 were harvested by centrifugation. The activity of mutant rat HO-1 was detected and the value was 1 948-2 160 units/mg protein per hour.

The molecular weight and mobility of native and mutant rat HO-1

The protein concentrations from native and mutant rat HO-1 were 7.38 mg/ml and 7.22 mg/ml, respectively. 10 μ l samples were subjected to SDS-PAGE for detecting their molecular weight and mobility. The results revealed that native and mutant rat HO-1 had the same mobility and molecular weight as that of rat liver HO-1 with a molecular mass of about M_r 30 000.

The inhibition of mutant to native HO-1

The inhibition of His25Ala mutant was confirmed by detecting the levels of bilirubin. Formation in the reaction system decreased to 42 % after addition of the mutant.

DISCUSSION

The oxidation of heme is carried out by three isozymes of microsomal HO. HO-1 is inducible by inflammatory cytokines and oxidants, including nitric oxide (NO), whereas HO-2 and HO-3 are expressed constitutively^[31,32]. They are the key enzymes in the catabolic pathway of heme, and the conversion of biliverdin to bilirubin is catalysed by biliverdin reductase^[33,34]. So it is highly important to inhibit the activities of HO isomers for reducing the products of bilirubin^[35,36], finally to prevent and treat hyperbilirubinemia.

The microsomal HO isomers had been purified in other laboratory. The results showed HO-1, which is inducible and highly expressed in liver and spleen tissues, and HO-2, which is constitutive and distributed throughout the body. HO-3 has only been expressed constitutively in rat neurones^[31,32]. The isomers have different molecular masses and are products of distinctly different genes^[37]. HO-1 gene from a rat genomic DNA library was isolated using cloned cDNA as hybridization probes and determined its complete nucleotide sequence. The gene is composed of 6 830 nucleotides and consists of four introns and five exons^[37]. Preliminary mutagenesis studies on rat HO-1 by Ito-Maki *et al*^[38] have shown that the His25→Ala25 mutation completely abolished the enzyme activity, and histidine has been considered to be an essential residue for the enzyme activity.

In our studies, we have purified and identified two constitutive forms of HO in rat liver, spleen and brain tissues and provided evidences for a decidedly different

characterization for the two forms, HO-1 and HO-2. The results indicate that in the treated rat liver and spleen, there exist two different molecular species of HO. It appears that HO-1 and HO-2 substantially differ in their molecular composition and structure as judged by their chromatographic behavior and electrophoretic migration patterns. Difference in amino acid composition or sequence usually results in such observation. In the induced liver and spleen, the microsomes contain mostly the HO-1, with the ratio of HO-1 being approximately 2.0:1 and 3.2:1, it suggests that the liver and spleen are among the main sites of haemoglobin heme degradation. Hematin and phenylhydrazine are the inducers known for their ability to increase the activity of the microsomal HO-1 in the liver, the activity of which can be induced by up to 100-fold, but the spleen HO-1 activity could not be increased after treatment of hematin and phenylhydrazine, in comparison with the results reported by Maines and Braggins. It suggests that HO activity is constantly maintained in the induced state as a result of sustained exposure to haemoglobin released in the course of disruption of senescent erythrocytes.

With the same procedure, only the form of HO, HO-2, could be clearly detected and the HO-1 was absent in the brain after inducement with hematin and phenylhydrazine. The result, however, does not suggest that this isomer is absent in the tissue, rather, it may reflect the inability of the presently used procedures to detect the exceedingly low level of HO-1, and the expression of the HO-1 isomer in the brain may be suppressed under most conditions. Surprisingly, the brain displayed a higher HO-2 activity than the liver, possibly reflecting a major biological adaptation. HO-1 and HO-2 preparation were analysed by the Western immunoblotting technique. The rat brain HO-2 preparation exhibited immunological reactivity with antibody to rat liver HO-2, but not to the rat liver HO-1, indicating that these two HO preparations are antigenically different.

pRHO1 contains 1 557 nucleotides excluding the dG tail and the poly (dA) tract (\approx 150 residues). The vector pcDNA3 is designed for eukaryotic expression and has an expanded multiple cloning sites to facilitate cloning of inserts besides having the same characterization of other vectors. pcDNA3HO1 harbouring the rat HO-1 cDNA. was constructed and transfected into COS-1 cells for confirming that the isolated cDNA, XhoI(-59)/HindIII(971) fragment, actually encodes HO-1. COS-1 cells have endogenous HO-1 activity and this basal activity did not change after transfection with plasmid pcDNA3HO1. Accordingly, the activity of HO-1 in cells transfected with pcDNA3 was used as control. The results indicated clearly that isolated cDNA encoded HO-1. Furthermore, these results also show that the expressed HO-1 was actually incorporated into the endoplasmic reticulum of COS -1 cells, as we isolated microsomes for assay of HO-1. Shibahara *et al.* constructed the pKCRHO21 carrying the entire protein-coding region in correct orientation as pcDNA3HO1, XhoI(-59)/HindIII(971) fragment. The cells transfected with pKCRHO21 have 2-fold higher activity than that of rat spleen. Ishikawa *et al.* reported that during cultivation, a few degraded forms of HO-1 that had lost their membrane-associating, C-terminal region appeared. Among these soluble enzymes, a degraded form of HO-1 with molecular mass of M_r 30 000 was found to retain ability to decomposed heme to biliverdin^[37,38]. These results are in accordance with ours^[39]. So it clearly indicates that isolated cDNA encodes HO-1.

There are 10 histidine residues in HO-1 and 5 of them are located between amino acid residues 100-132. Up-to-date, the report showed that the axial heme ligand in the ferrous

heme-HO-1 complex is a neutral form of the imidazole of a histidine using optical absorption, EPR, and resonance Raman scattering^[38,40,41]. Histidine residues at positions 25, 84, 119 and 132 in the HO-1 sequence are conserved in rat, human, mouse and chicken HO-1. These histidines may be important for heme-binding. Preliminary mutagenesis studies on rat HO-1 by Ito-Maki *et al* have shown that the His25Ala mutation completely abolished the enzyme activity but that the replacement of either His84 or His119 by Ala did not alter the enzyme activity. On the basis of this work, His25 has been considered to be an essential residue for the enzyme activity. In this study, pcDNA3HO1D25, containing the mutated rat HO-1 cDNA (His25Ala), was constructed using site-directed mutagenesis and transfected to COS-1 cells. The activity of mutant declined but did not completely abolish. At present, no reasoning can be offered for this discrepancy. Maybe it is because the enzyme reaction system is different.

After successfully expressing mutant protein, an equal amount of mutant HO-1 was added in reaction system. The result showed that His25Ala mutant reduced the formation of bilirubin. This suggests that the mutant may completely bind the substrate-heme with native enzyme. Some researches found that the precursor of bilirubin, heme, could be discharged from bile while the metabolic procedure of heme to bilirubin was inhibited by Sn-protoporphyrin.

Further studies are required to identify His25Ala mutant characteristics before using this mutant to prevent and treat hyperbilirubinemia.

REFERENCES

- Hill-Kapturczak N, Chang SH, Agarwal A. Heme oxygenase and the kidney. *DNA Cell Biol* 2002; 307-321
- Botros FT, Laniado-Schwartzman M, Abraham NG. Regulation of cyclooxygenase-and cytochrome p450-derived eicosanoids by heme oxygenase in the rat kidney. *Hypertension* 2002; 39: 639-644
- Motterlini R, Clark JE, Foresti R, Sarathchandra P, Mann BE, Green CJ. Carbon monoxide-releasing molecules: characterization of biochemical and vascular activities. *Circ Res* 2002; 90: E17-24
- Gildemeister OS, Pepe JA, Lambrecht RW, Bonkovsky HL. Induction of heme oxygenase-1 by phenylarsine oxide. Studies in cultured primary liver cells. *Mol Cell Biochem* 2001; 226: 17-26
- Guo X, Shin VY, Cho CH. Modulation of heme oxygenase in tissue injury and its implication in protection against gastrointestinal diseases. *Life Sci* 2001; 69: 3113-3119
- Haider A, Olszanecki R, Gryglewski R, Schwartzman ML, Lianos E, Kappas A, Nasjletti A, Abraham NG. Regulation of cyclooxygenase by the heme-heme oxygenase system in microvessel endothelial cells. *J Pharmacol Exp Ther* 2002; 300: 188-194
- Lo S, Bell HS, Yamaguchi S, Wharton SB, Whittle IR. Heme oxygenase (HO) isoforms in experimental C6 glioma: an immunocytochemical study. *Br J Neurosurg* 2001; 15: 416-418
- Parfenova H, Neff RA 3rd, Alonso JS, Shlopov BV, Jamal CN, Sarkisova SA, Leffler CW. Cerebral vascular endothelial heme oxygenase: expression, localization, and activation by glutamate. *Am J Physiol Cell Physiol* 2001; 281: C1954-1963
- Vaccari A, Rui S, Saba P, Fa M, Cagiano R, Coluccia A, Mereu G, Steardo L, Tattoli M, Trabace L, Cuomo V. Prenatal low-level exposure to CO alters postnatal development of hippocampal nitric oxide synthase and haem-oxygenase activities in rats. *Int J Neuropsychopharmacol* 2001; 4: 219-222
- Yoshiki N, Kubota T, Aso T. Identification of heme oxygenase in human endometrium. *J Clin Endocrinol Metab* 2001; 86: 5033-5038
- Leplingard A, Brung-Lefebvre M, Guedon C, Savoye G, Dechelotte P, Lemoine F, Lebreton JP, Lerebours E. Increase in cyclooxygenase-2 and nitric oxide-synthase-2 mRNAs in pouchitis without modification of inducible isoenzyme heme-oxygenase-1. *Am J Gastroenterol* 2001; 96: 2129-2136
- Vicente AM, Guillen MI, Alcaraz MJ. Modulation of haem oxygenase-1 expression by nitric oxide and leukotrienes in zymosan-activated macrophages. *Br J Pharmacol* 2001; 133: 920-926
- Sharma HS, Westman J, Gordh T, Alm P. Topical application of brain derived neurotrophic factor influences upregulation of constitutive isoform of heme oxygenase in the spinal cord following trauma an experimental study using immunohistochemistry in the rat. *Acta Neurochir Suppl* 2000; 76: 365-369
- Ding S, Yao D, Deeni YY, Burchell B, Wolf CR, Friedberg T. Human NADPH-P450 oxidoreductase modulates the level of cytochrome P450 CYP2D6 holoprotein via haem oxygenase-dependent and -independent pathways. *Biochem J* 2001; 356: 613-619
- Barber A, Robson SC, Myatt L, Bulmer JN, Lyall F. Heme oxygenase expression in human placenta and placental bed: reduced expression of placenta endothelial HO-2 in preeclampsia and fetal growth restriction. *FASEB J* 2001; 15: 1158-1168
- Stevenson DK, Vreman HJ, Wong RJ, Contag CH. Carbon monoxide and bilirubin production in neonates. *Semin Perinatol* 2001; 25: 85-93
- Miller SM, Reed D, Sarr MG, Farrugia G, Szurszewski JH. Haem oxygenase in enteric nervous system of human stomach and jejunum and co-localization with nitric oxide synthase. *Neurogastroenterol Motil* 2001; 13: 121-131
- Alcaraz MJ, Habib A, Creminon C, Vicente AM, Lebreton M, Levy-Toledano S, Maclouf J. Heme oxygenase-1 induction by nitric oxide in RAW 264.7 macrophages is upregulated by a cyclo-oxygenase-2 inhibitor. *Biochim Biophys Acta* 2001; 1526: 13-16
- da Silva JL, Zand BA, Yang LM, Sabaawy HE, Lianos E, Abraham NG. Heme oxygenase isoform-specific expression and distribution in the rat kidney. *Kidney Int* 2001; 59: 1448-1457
- Navarra P, Miceli F, Tringali G, Minici F, Pardo MG, Lanzzone A, Mancuso S, Apa R. Evidence for a functional link between the heme oxygenase-carbon monoxide pathway and corticotropin-releasing hormone release from primary cultures of human trophoblast cells. *J Clin Endocrinol Metab* 2001; 86: 317-323
- Giordano A, Nisoli E, Tonello C, Canello R, Carruba MO, Cinti S. Expression and distribution of heme oxygenase-1 and -2 in rat brown adipose tissue: the modulatory role of the noradrenergic system. *FEBS Lett* 2000; 487: 171-175
- Takahashi M, Dore S, Ferris CD, Tomita T, Sawa A, Wolosker H, Borchelt DR, Iwatsubo T, Kim SH, Thinakaran G, Sisodia SS, Snyder SH. Amyloid precursor proteins inhibit heme oxygenase activity and augment neurotoxicity in Alzheimer's disease. *Neuron* 2000; 28: 461-473
- Liu H, Song D, Lee SS. Role of heme oxygenase-carbon monoxide pathway in pathogenesis of cirrhotic cardiomyopathy in the rat. *Am J Physiol Gastrointest Liver Physiol* 2001; 280: G68-74
- Lim S, Groneberg D, Fischer A, Oates T, Caramori G, Mattos W, Adcock I, Barnes PJ, Chung KF. Expression of heme oxygenase isoenzymes 1 and 2 in normal and asthmatic airways: effect of inhaled corticosteroids. *Am J Respir Crit Care Med* 2000; 162: 1912-1918
- Yoshiki N, Kubota T, Aso T. Expression and localization of heme oxygenase in human placental villi. *Biochem Biophys Res Commun* 2000; 276: 1136-1142
- Alm P, Sharma HS, Sjoquist PO, Westman J. A new antioxidant compound H-290/51 attenuates nitric oxide synthase and heme oxygenase expression following hyperthermic brain injury. An experimental study using immunohistochemistry in the rat. *Amino Acids* 2000; 19: 383-394
- Gordh T, Sharma HS, Azizi M, Alm P, Westman J. Spinal nerve lesion induces upregulation of constitutive isoform of heme oxygenase in the spinal cord. An immunohistochemical investigation in the rat. *Amino Acids* 2000; 19: 373-381
- Beschorner R, Adjodah D, Schwab JM, Mittelbronn M, Pedal I, Mattern R, Schluesener HJ, Meyermann R. Long-term expression of heme oxygenase-1 (HO-1, HSP-32) following focal cerebral infarctions and traumatic brain injury in humans. *Acta Neuropathol (Berl)* 2000; 100: 377-384
- Kobayashi Y, Ohshiro N, Okui E, Sasaki T, Tokuyama S, Yoshida T, Yamamoto T. Concurrent induction of rat hepatic microsomal cytochrome P450 and haem oxygenase by 2,2'-dipyridyl ketone: comparison with the effect of 2,2'-dipyridyl amine. *Xenobiotica*

- 2000; **30**: 683-692
- 30 **Maines MD**. The heme oxygenase system and its functions in the brain. *Cell Mol Biol (Noisy-le-grand)* 2000; **46**: 573-585
- 31 **Donnelly LE**, Barnes PJ. Expression of heme oxygenase in human airway Epithelial cells. *Am J Respir Cell Mol Biol* 2001; **24**: 295-303
- 32 **McCoubrey WK**, Huang TJ, Maines MD. Isolation and characterization of a cDNA from the rat brain that encodes hemoprotein heme oxygenase-3. *Eur J Biochem* 1997; **247**: 725-732
- 33 **Sugishima M**, Omata Y, Kakuta Y, Sakamoto H, Noguchi M, Fukuyama K. Crystal structure of rat heme oxygenase-1 in complex with heme. *FEBS Let* 2000; **471**: 61-66
- 34 **Ahmad Z**, Salim M, Maines MD. Human biliverdin reductase is a leucine zipper-like DNA-binding protein and functions in transcriptional activation of heme oxygenase-1 by oxidative stress. *J Biol Chem* 2002; **277**: 9226-9232
- 35 **Montellano PR**. The mechanism of heme oxygenase. *Curr Opin Chem Biol* 2000; **4**: 221-227
- 36 **Sugishima M**, Sakamoto H, Kakuta Y, Omata Y, Hayashi S, Noguchi M, Fukuyama K. Crystal structure of rat apo-heme oxygenase-1 (HO-1): mechanism of heme binding in HO-1 inferred from structural comparison of the apo and heme complex forms. *Biochemistry* 2002; **41**: 7293-7300
- 37 **Ishikawa K**, Sato M, Yoshida T. Expression of rat heme oxygenase in *Escherichia coli* as a catalytically active, full-length form that binds to bacterial membranes. *Eur J Biochem* 1991; **202**: 161-165
- 38 **Ito-Maki M**, Ishikawa K, Matera KM, Sato M, Ikeda-Saito M, Yoshida T. Demonstration that histidine 25, but not 132, is the axial heme ligand in rat heme oxygenase-1. *Arch Biochem Biophys* 1995; **317**: 253-258
- 39 **Xia ZW**, Li YZ, Chen SN, Shen QX, Li CL, Shen H, Yu SC. The purification and identification of heme oxygenase isoforms from spleen tissue of rat and the expression of heme oxygenase-1 cDNA in COS-1 cells. *Chin Med J* 1998; **111**: 842-846
- 40 **Wilks A**, Moenne-Loccoz P. Identification of the proximal ligand His-20 in heme oxygenase (Hmu O) from *Corynebacterium diphtheriae*. Oxidative cleavage of the heme macrocycle does not require the proximal histidine. *J Biol Chem* 2000; **275**: 11686-11692
- 41 **Liu Y**, Moenne-Loccoz P, Hildebrand DP, Wilks A, Loefer TM, Mauk AG, Ortiz de Montellano PR. Replacement of the proximal histidine iron ligand by a cysteine or tyrosine converts heme oxygenase to an oxidase. *Biochemistry* 1999; **38**: 3733-3743

Edited by Xu JY

• BASIC RESEARCH •

Shedding of TNFR1 in regenerative liver can be induced with TNF α and PMA

Min Xia, Shao-Bai Xue, Cun-Shuan Xu

Min Xia. College of Life Science, Henan Normal University, Xinxiang 453002, Henan province, China; The Institute of Cell Research, Beijing, Normal University, Beijing100875, China

Shao-Bai Xue, The Institute of Cell Research, Beijing Normal University, Beijing 100875, China

Cun-Shuan Xu, College of Life Science, Henan Normal University, Xinxiang 453002, Henan Province, China

Supported by Chinese National Natural Science Foundation, No. 39970362 and the Foundation of Bioengineering Key Laboratory in Henan Province, No. PKL99003

Correspondence to: Professor Cun-Shuan Xu, College of Life Science, Henan normal University, Xinxiang 453002, Henan Province, China. aihua@henannu.edu.cn

Telephone: +86-373-3326524 **Fax:** +86-373-3326524

Received 2002-05-18 **Accepted** 2002-06-26

Abstract

AIM: Liver regeneration is associated with apoptosis of hepatocytes, which is mediated via tumor necrosis factor receptor 1 (TNFR1). The shedding of TNFR1 in liver regeneration and its mechanism to regulate this shedding were investigated.

METHODS: The shedding of TNFR1 in liver regeneration and changes of TNF- α , PMA and plasma membrane purified from hepatocytes on this shedding process were measured with Western blot. Then, the relationship between TNFR1 shedding and apoptosis of hepatocytes induced by TNF α was studied by detecting apoptotic index.

RESULTS: The shedding of TNFR1 began at 4 hours and terminated before 2 months after partial hepatectomy. In culture system, serum from rats at 36 h after partial hepatectomy could also promote this shedding process. With the stimulation of TNF α , PMA or purified plasma membrane from hepatocytes at 36 h after partial hepatectomy or from hepatocytes treated with TNF α for 2 h, membranous TNFR1 was also shed. With the stimulation of both TNF α and plasma membrane from hepatocytes affected with TNF α for 2 h or from hepatocytes at 36 h after partial hepatectomy, apoptotic index of hepatocytes decreased from 21 % to 7.52 % and 8.45 %, respectively. PMA could also reduce apoptotic index to 13.67 %. This descent occurred in hepatocytes cultured in serum from rats at 36 h after partial hepatectomy too, but not in serum from rats at 2 months after partial hepatectomy and sham-operated rats.

CONCLUSION: Shedding of TNFR1 may help reduce apoptosis of hepatocytes induced by TNF α . Membrane-anchored metalloproteases could play a role in shedding membranous TNFR1. At the same time, PKC may take part in regulation of this shedding process.

Xia M, Xue SB, Xu CS. Shedding of TNFR1 in regenerative liver can be induced with TNF α and PMA. *World J Gastroenterol* 2002; 8(6):1129-1133

INTRODUCTION

Tumor necrosis factor alpha (TNF- α), secreted predominantly by monocytes and macrophages, is an important mediator of various inflammatory and immune responses^[1]. During liver regeneration after a partial hepatectomy, TNF α levels are elevated leading to the activation of a number of transcription factors such as STAT-3, *c-jun*, *c-fos*, activating protein-1 (AP-1) and nuclear factor- κ B (NF κ B)^[2-4]. And soluble TNF- α exerts its biological functions by binding to special target cell surface receptors^[5] which have been identified as TNFR1 (p55) and TNFR2 (p75)^[6,7]. After ligand binding, TNFR1 or TNFR2 can be bound by TNFR-associated protein-2 and the serine/threonine kinase receptor-interacting protein, and then mediate survival and proliferating signals via the transcription factor NF κ B and via activation of jun N-terminus kinase (JNK), which in turn mediates new gene transcription via AP-1^[8]. On the other hand, TNFR1, not TNFR2, could be bound by the death domain of the Fas-associated death domain protein (FADD) via the adapter protein TNF-R1-associated death domain protein (TRADD), which mediates its interaction with caspase 8 and activates the caspase cascade during apoptosis.

Membranous proteins undergo shedding of ectodomain extensively, among these are cytokines such as TNF α ^[9,10] and kit ligand^[11], cytokine receptors like the TNF α receptors^[12] and the p75 nerve growth factor receptor^[13], adhesion proteins such as L-selectin^[14,15], and other proteins, including the β -amyloid precursor protein^[16,17], the angiotensin-converting enzyme^[18,19], and the protein tyrosine phosphatases LAR and PTP σ ^[20]. It has been postulated that shedding of membranous protein ectodomain might play a role in controlling a cell's survival^[21]. And this shedding of membranous protein happens extensively in miscellaneous cells, such as monocytes and hepatocytes. For TNFR, both the p55 and p75 form could be shed on the surface of a cell^[22-25]. Recently, there had been several reports demonstrating that TNF α could induce the shedding of its own receptor in lymphocyte^[26,27]. However, whether membranous TNFR1 of hepatocyte is shed during liver regeneration remains unclear. In present study, we examined this issue in rat regenerative liver.

To clarify which elements affected the shedding of membranous TNFR1, we also determined the shedding of membranous TNFR1 of hepatocyte under stimulations of TNF α , phorbol 12-myristate 13-acetate (PMA) or metalloprotease inhibitors. And then the effect of TNFR1 shedding on the apoptosis of hepatocytes was investigated.

MATERIALS AND METHODS

Partial hepatectomy

Partial hepatectomy (PH) was performed on *Sprague-Dawley Rattus norvegicus* according to Higgins' method^[28].

Separation and purification of parenchymal hepatocytes

After isolated with collagenase according to the method as

described previously^[29], 4 ml suspension of hepatocytes was laid on 15 ml 60 % (v/v) Percoll (Sigma) in 30 ml centrifuge tube, and then centrifugated at 400 g for 5 min at 4 °C. Finally, obtained precipitate was washed three times with PBS at 50 g for 2 min at 4 °C.

Primary culture of hepatocytes and treatment

After isolation, hepatocytes were cultured in 50 mL · L⁻¹ CO₂ at 37 °C in RPMI1640 containing 10 % fetal bovine serum (BSA) and penicillin/streptomycin for 2 h according to standard protocols. Then the medium was replaced by fresh RPMI 1640 deprived of BSA to remove the non-attached cells.

To determine the effect of serum on shedding of TNFR1, serum from rats after partial hepatectomy for 36 h was added into culture medium. Thirty minutes later, cultured hepatocytes were harvested with policeman from culture dish.

For other incubations, plasma membrane purified from hepatocytes after partial hepatectomy for 48 h or from cultured hepatocytes induced by TNF-α at a concentration of 5 nmol · L⁻¹ for 2 h were added at a concentration of 2 μg membranous protein per milliliter culture medium. Addition of plasma membrane boiled for 5 min and plasma membrane from hepatocytes of rats without partial hepatectomy were used as control. Then 2 mmol · L⁻¹ BB-1101 (Sigma), and staurosporine at 5 ng · L⁻¹ were respectively added into culture medium. Two hours later after various stimulations as above, hepatocytes were collected.

Phorbol 12-myristate 13-acetate (PMA, Sigma) alone concentrated at 10 μmol · L⁻¹ (in DMSO) or PMA accompanied with staurosporine (3 nmol · L⁻¹, Sigma) were added into culture medium of attached hepatocytes for 30 min.

Purification of plasma membrane and membranous protein

Isolated or cultured hepatocytes (1 × 10⁷) were homogenized in buffer A (1 mmol · L⁻¹ NaHCO₃, pH7.5; 0.5 mmol · L⁻¹ CaCl₂; 2 μmol · L⁻¹ aprotinin, 10 μmol · L⁻¹ E-64, 100 μmol · L⁻¹ PMSF, 100 μmol · L⁻¹ TPCK) on ice. After centrifuged at 1 500 g for 3 × 10 min at 4 °C, the precipitate was suspended with 5 ml buffer A, and then mixed with 5 ml 69 % (w/v) sucrose solution. And 5 ml 42.3 % (w/v) sucrose solution was added on top of the mixture. They were then centrifuged at 100 000 g for 2 h at 4 °C. The snip on the top of centrifugal solution was washed with buffer A at 100 000 g for 3 × 10 min at 4 °C. Finally, the membranes were purified about 25-fold from homogenate, judging by their 5' -nucleatidase activity. Obtained membranes were resolved in 1 ml TrittonX114 buffer (2 % TrittonX114, 50 mmol · L⁻¹ Tris- HCL, pH7.5) on ice for 15 min, then centrifuged at 10 000 g for 5 min at 4 °C, and then incubated at 37 °C for 10 min and centrifuged at 2 000 g at 37 °C for 5 min. Detergent fraction was collected to perform procedures as described above once again. Finally, pure membranous proteins were in TrittonX114 detergent phase.

TNFR1 and membrane-anchored metalloprotease assays

Total membranous proteins were prepared as described above. Concentration of protein was determined according to described method^[30]. Ninety micrograms membranous protein was separated by SDS-PAGE and electroblotted to nitrocellulose. After incubation with fresh blocking solution, blots were exposed to TNFR1 primary antibody (1:1 000, Santa cruz, USA). Blots were then incubated with a 1:1 000 dilution of rat alkaline phosphatase-colligated secondary antibody (Zhong Shan Biotech Co. China) for 1 h at 37 °C. Blots were again washed for 3 × 5 min in PBS and then developed by NBT/BcIp III (Dingguo Biotech Co. China).

Assessment of apoptosis

The percentage of apoptotic cells was determined by evaluating propidium iodide and Hoechst 33 342 stained preparations by fluorescent microscopy and scoring 8-10 randomly selected fields containing more than 1 000 cells. In the meantime, the results were confirmed by DNA fragmentation by agarose electrophoresis^[31].

Statistical analysis

All data values are expressed as means ± SE for statistical analysis, the significance of differences between experimental conditions was determined using the Student's test for unpaired observations. A *P* value (two tailed) of less than 0.05, compared with hepatocytes cultured in RPMI1640 with 10 % BSA, was considered significant.

RESULTS

Shedding of TNFR1

Shedding of membranous TNFR1 ectodomain after partial hepatectomy was examined by Western blotting. Shedding of TNFR1 began at 4 h after hepatectomy, but not at 2 h, in which process a 55 kD form of TNFR1 was shed into a 39 kD form. And this process lasted at least for 144 h and ended before 2 months after hepatectomy (Figure 1). In culture system *in vitro*, serum from rats at 36 h after partial hepatectomy could also promote this shedding process. However, serum from sham-operated rats and from rats at 2 months after partial hepatectomy could not (Figure 2). And with the stimulation of TNFα, PMA and purified plasma membrane from hepatocytes at 36 h after partial hepatectomy and from hepatocytes treated with TNFα for 2 h, TNFR1 also could be shed. But this shedding of membranous TNFR1 was inhibited by staurosporine and BB1101 (Figure 2-5).

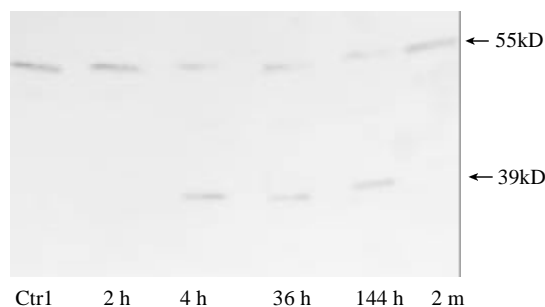


Figure 1 TNFR1 shedding on the surface of parenchymal hepatocytes occurs in regenerative liver. Data shown represent time course of TNFR1 shedding after partial hepatectomy. Plasma membrane from normal liver was used as control.

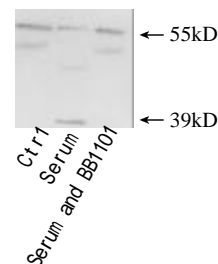


Figure 2 TNFR1 shedding under the stimulation of serum from rats after partial hepatectomy. Cultured hepatocytes were treated with serum from regenerative liver at 36 h for 30min, or the serum accompanied with metalloprotease inhibitor BB1101 at 2mmol · L⁻¹. Cultured hepatocytes under no any treatments were used as control.

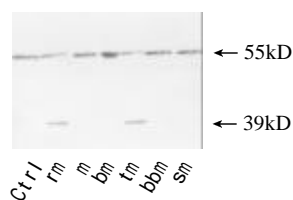


Figure 3 TNFR1 shedding induced with plasma membrane of hepatocytes from regenerative liver. Cultured hepatocytes were treated for 30 min with plasma membrane from hepatocytes at 36 h after hepatectomy (rm) or sham-operated (m) or from hepatocytes treated with TNF α at 10 $\mu\text{g}\cdot\text{mL}^{-1}$ for 2 h (tm). Plasma membrane boiled for 5 min (bbm) as control. Then metalloprotease inhibitor BB1101 at 2 $\text{mmol}\cdot\text{L}^{-1}$ (bbm), or staurosporine at 5 $\text{ng}\cdot\text{mL}^{-1}$ (sm) was added into culture medium. Cultured hepatocytes under no any treatments were as control.

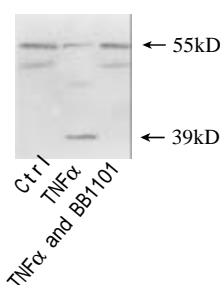


Figure 4 TNFR1 shedding under the stimulation of TNF α . Cultured hepatocytes were treated respectively with TNF α at 10 $\mu\text{g}\cdot\text{mL}^{-1}$ for 2 h, or TNF α accompanied with metalloprotease inhibitor BB1101 at 2 $\text{mmol}\cdot\text{L}^{-1}$. Cultured hepatocytes under no any treatments were as control.

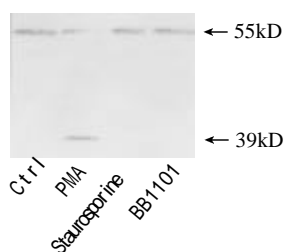


Figure 5 Effect of PMA on TNFR1 shedding. Cultured hepatocytes were treated with PMA at 10 $\mu\text{g}\cdot\text{mL}^{-1}$ for 30 min, staurosporine accompanied with PMA at 5 $\text{ng}\cdot\text{mL}^{-1}$, or PMA accompanied with BB1101 at 2 $\text{mmol}\cdot\text{L}^{-1}$. Cultured hepatocytes without any treatment were used as control.

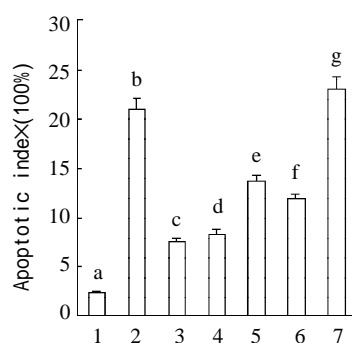


Figure 6 Induction of apoptosis after treatment with TNF α . Means of data shown in figure were: 1. Control; 2. Treated

with TNF α at 10 $\mu\text{g}\cdot\text{mL}^{-1}$; 3. Treatment with TNF α at 10 $\mu\text{g}\cdot\text{mL}^{-1}$ after treated with plasma membrane purified from liver at 36 h after partial hepatectomy at 2 $\mu\text{g}\cdot\text{mL}^{-1}$; 4. Treated with plasma membrane at 2 $\mu\text{g}\cdot\text{mL}^{-1}$ purified from hepatocytes induced with TNF α accompanied with TNF α at 10 $\mu\text{g}\cdot\text{mL}^{-1}$; 5. Treated with PMA at a concentration of 10 $\mu\text{mol}\cdot\text{L}^{-1}$ (in DMSO) accompanied with TNF at 10 $\mu\text{g}\cdot\text{mL}^{-1}$; 6. Treated with serum from rat after partial hepatectomy for 36 h at 5 % accompanied with TNF α at 10 $\mu\text{g}\cdot\text{mL}^{-1}$; 7. Treated with TNF α at 10 $\mu\text{g}\cdot\text{mL}^{-1}$ after treated with plasma membrane purified from rat liver regenerated for 2 months at 2 $\mu\text{g}\cdot\text{mL}^{-1}$. Apoptotic index=(numbers of apoptotic cells/total cells numbers per well) $\times 100$. Data were means from 6 separate experiments \times SE ($n=6$ wells). Different letters over bars indicate significant differences, $P<0.05$. The results are confirmed by DNA fragmentation by agarose electrophoresis (data not provided).

Effects of TNFR1 shedding on apoptosis of hepatocyte

Purified plasma membrane from hepatocytes at 36 h after partial hepatectomy or from hepatocytes induced with TNF α or PMA reduced the apoptotic index induced by TNF α from 21 % to 7.52 %, 8.45 % and 13.67 %, respectively. This descent also occurred in hepatocytes cultured in serum from rats after partial hepatectomy for 36 h. But cultured in serum from rats at 2 months after partial hepatectomy, apoptotic index of hepatocytes was even higher than that in serum from sham-operated rats (Figure 6).

DISCUSSION

In adult liver, hepatocytes are highly differentiated and predominantly in G_0 state of cell cycle. Partial hepatectomy can induce these hepatocytes to undergo rapid proliferation, leading to organ regeneration^[3,32,33]. However, the exact mechanisms that initiate and terminate this highly regulated proliferative event remain unclear. In present studies, we assessed the shedding of TNFR1 during liver regeneration and the association between this shedding and apoptosis of hepatocytes.

Several recent works had provided obvious evidences that tumor necrosis factor- α (TNF- α) functioned as a two-edged sword in the liver. It is an important cytokine of the early signaling pathways leading to regeneration and an antiapoptotic effector. On the other hand, it is also an intensive mediator of apoptosis^[2,3]. TNFR should be involved in all these process above because TNF α must bind to TNFR before it can exert its roles. And down-regulation of membranous TNFR1 expression levels of hepatocyte had been previously confirmed as an important pathway to regulate the role of TNF- α ^[34]. Our results demonstrated that the shedding of TNFR1 occurred during liver regeneration. This shedding of TNFR1 could reduce apoptotic rate of hepatocytes induced by TNF- α . These results suggested that TNFR1 shedding might also be a pathway to down-regulate membranous TNFR1 levels of hepatocyte. Our finding that shedding of TNFR1 induced by serum from rats after partial hepatectomy progressively suggested that some factors were secreted into serum during liver regeneration. These factors might regulate liver regeneration by inducing the shedding of TNFR1.

Several peptide hormones had been shown to down-modulate their own receptors^[35-38]. This down-modulation was believed to require the binding of the ligand with its receptor, followed by internalization of the ligand-receptor complex into the cell. After the dissociation of the receptor from its ligand inside the lysosome, the receptor was either degraded or recycled back to the cell surface^[39]. Our results showed that the TNFR1 shedding was induced by TNF- α , though only parts

of membranous receptor were shed. Higuchi reckoned that TNFR2, not TNFR1, was shed in lysosome^[40]. However, our results showed that membranous TNFR1 could be shed on the cell surface.

Our results also showed that metalloprotease inhibitor inhibited the shedding of TNFR1. This suggested that some metalloproteases played a role in this shedding process. Two possible sources of these metalloprotease could be proposed for the shedding of TNFR1. One possibility was that these metalloproteases presented in serum because the shedding of TNFR1 could be induced by serum from rats after partial hepatectomy and inhibited by BB1101. It was also possible that these metalloproteases were membrane-anchored proteins. TNFR1 was shed when cells were treated with plasma membrane purified from hepatocytes of regenerative liver. At the same time, this shedding of TNFR1 could be inhibited by metalloprotease inhibitor either.

We also found that PMA could induce the shedding of TNFR1. This shedding of TNFR1 was inhibited by staurosporine. These results suggested that PKC was involved in regulating the shedding of TNFR1. Perhaps phosphorylating of TNFR1 by PKC made it sensitive to metalloprotease. However, further investigations are needed to identify which protease should be responsible for the shedding of TNFR1.

REFERENCES

- 1 **Old LJ**. Tumor necrosis factor. *Science* 1985; **230**: 630-632
- 2 **Brucoleri A**, Gallucci R, Germolec DR, Blackspair P, Simeonova P. Induction of early-immediate genes by tumor necrosis factor- α contributes to liver repair following chemical-induced hepatotoxicity. *Hepatology* 1997; **25**: 133-141
- 3 **Diehl AM**, Rai RM. Liver regeneration 3: regulation of signal transduction during liver regeneration. *FASEB J* 1996; **10**: 215-227
- 4 **Diehl AM**, Yin M, Fleckenstein J, Yang SQ, Lin HZ, Brenner DA, Westwick J. Tumor necrosis factor- α induces c-jun during the regenerative response to liver injury. *Am J Physiol* 1994; **267**: 552-561
- 5 **Decker K**. Biologically active products of stimulated liver macrophages (Kuffer cells). *Eur J Biochem* 1990; **192**: 245-261
- 6 **Himmler A**, Maurer-Fogy I, Könke M, Scheurich P, Plizenmaier K, Lantz M, Olsson I, Hauptmann R, Stratowa C, Adolf GR. Molecular cloning and expression of human and rat tumor necrosis factor receptor chain (p60) and its soluble derivative, tumor necrosis factor-binding protein. *DNA Cell Biol* 1990; **9**: 705-715
- 7 **Brockhaus M**, Schoenfeld HJ, Schlaeger EJ, Hunziker W, Lesslauer W, Loetscher H. Identification of two types of tumor necrosis factor receptors on human cell lines by monoclonal antibodies. *Proc Natl Acad Sci USA* 1990; **87**: 3127-3131
- 8 **Douglas AW**, Neil HJ, Sabina CC, Peter RH, Richard B, Mark R, Ruth AR. Role for tumor necrosis factor α receptor 1 and interleukin-1 receptor in the suppression of mouse hepatocyte apoptosis by the peroxisome proliferator nafenopin. *Hepatology* 1999; **30**: 1417-1424
- 9 **Hooper NM**, Karran EH, Turner AJ. Membrane protein secretases. *Biochem J* 1997; **321**: 265-279
- 10 **Black R**, Rauch CT, Kozlosky CJ, Peschon J, Slack JL, Wolfson MF. A metalloproteinase disintegrin that releases tumour-necrosis factor- α from cells. *Nature* 1997; **385**: 733-736
- 11 **Huang EJ**, Nocka KH, Buck J, Besmer P. Differential expression and processing of two cell associated forms of the kit-ligand: KL-1 and KL-2. *Mol Biol Cell* 1992; **3**: 349-362
- 12 **Porteu F**, Nathan C. Shedding of tumor necrosis factor receptors by activated human neutrophils. *J Exp Med* 1990; **172**: 599-607
- 13 **DiStefano PS**, Johnson EM Jr. Identification of a truncated form of the nerve growth factor receptor. *Proc Natl Acad Sci USA* 1988; **85**: 270-274
- 14 **Kishimoto TK**, Jutila MA, Berg EL, Butcher EG. Neutrophil Mac-1 and MEL-14 adhesion proteins inversely regulated by chemotactic factors. *Science* 1989; **245**: 1238-1241
- 15 **Kahn J**, Walcheck B, Migaki GI, Jutila MA, Kishimoto TK. Calmodulin regulates L-selectin adhesion molecule expression and function through a protease-dependent mechanism. *Cell* 1998; **92**: 809-818
- 16 **Selkoe DJ**. Amyloid beta-protein and the genetics of Alzheimer's disease. *J Biol Chem* 1996; **271**: 18295-18298
- 17 **Sisodia SS**. Beta-amyloid precursor in cleavage by a membrane-bound protease. *Proc Natl Acad Sci USA* 1992; **89**: 6075-6079
- 18 **Oppong SY**, Hooper NM. Characterization of a secretase activity which releases angiotensin-converting enzyme from the membrane. *Biochemistry J* 1993; **292**: 597-603
- 19 **Ramchandran R**, Sen I. Cleavage processing of angiotensin-converting enzyme by a membrane-associated metalloprotease. *Biochemistry* 1995; **34**: 12645-12652
- 20 **Aicher B**, Lerch MM, Muller T, Schilling J, Ullrich A. Cellular redistribution of protein tyrosine phosphatases LAR and PTP sigma by inducible proteolytic processing. *J Cell Biol* 1997; **138**: 681-696
- 21 **Stone AL**, Kroeger M, Sang QXA. Structure-function analysis of the ADAM family of disintegrin-like and metalloproteinase-containing proteins. *Pro Chem J* 1999; **4**: 447-465
- 22 **Kohno T**, Brewer MT, Baker SL, Schwartz PE, Schwartz PE, King MW, Hal KK, Squires CH, Thompson RC, Vannice J. A second tumor necrosis factor receptor gene product can be shed a naturally occurring tumor necrosis factor inhibitor. *Proc Natl Acad Sci USA* 1990; **87**: 8325-8331
- 23 **Porteu F**, Nathan C. Shedding of tumor necrosis factor receptors by activated human neutrophils. *J Exp Med* 1990; **172**: 593-598
- 24 **Porteu F**, Brockhaus M, Wallach D, Englemann H, Nathan CF. Human neutrophil releases a ligand-binding fragment from the 75-kDa tumor necrosis factor (TNF) receptor. *J Biol Chem* 1991; **266**: 18839-18846
- 25 **Aderka D**, Englemann H, Maor Y, Brakebysch C, Wallach D. Stabilization of the bioactivity of tumor necrosis factor by its soluble receptors. *J Exp Med* 1992; **175**: 318-324
- 26 **Higuchi M**, Aggarwal BB. Inhibition of ligand binding and antiproliferative effects of tumor necrosis factor and lymphotoxin by soluble forms of recombinant p60 and p80 receptors. *Biochem Biophys Res Commun* 1992; **182**: 632-636
- 27 **Zhang LS**, Aggarwal BB. Role of sulfhydryl groups in induction of cell surface down-modulation and shedding of extracellular domain of human TNF receptors in human histiocyte lymphoma U937 cells. *J Immunol* 1994; **153**: 3746-3751
- 28 **Higgins GM**, Anderson RM. Experimental pathology of the liver I: Restoration of the liver of white rat following partial surgical removal. *Arch Pathol* 1931; **12**: 186-189
- 29 **Zhou JX**, Xia M. Rapid isolation and primary culture of the rat hepatocytes. *Henan Shifan Daxue Xuebao* 1989; **2**: 46-49
- 30 **Marshak DR**, Kadonaga JT, Burgess RR, Knuth MW. Strategies for protein purification and characterization: a laboratory course manual. Cold Spring Harbor: Cold Spring Harbor Laboratory Press 1996: 82-83
- 31 **Martin SJ**. Protein or RNA synthesis inhibition induces apoptosis of mature human CD4+ T cell blasts. *Immunol Lett* 1993; **35**: 125-129
- 32 **Akerman P**, Cote P, Yang SQ, McClain C, Nelson S, Bagby GJ, Diehl AM. Antibodies to tumor necrosis factor- α inhibit liver regeneration after partial hepatectomy. *Am J Physiol* 1992; **263**: G579-G583
- 33 **Bradham CA**, Plumpe J, Manns MP, Brenner DA, Trautwein C. Mechanisms of hepatic toxicity I. TNF-induced liver injury. *Am J*

- Physiol* 1998; **275**: G387-G391
- 34 **Aggarwal BB**, Eessalu TE. Effect of phorbol esters on down-regulation and redistribution of cell surface receptors for tumor necrosis factor- α . *J Biol Chem* 1987; **262**: 16450-16457
- 35 **Kosmakos FC**, Roth J. Insulin-induced loss of the insulin receptor in IM-9 lymphocytes: a biological process mediated through the 4 insulin receptor. *J Biol Chem* 1980; **255**: 9860-9866
- 36 **Guibert LJ**, Stanley ER. Modulation of receptor for colony-stimulating factor, CSF-1, by bacterial lipopolysaccharide and CSF-1. *J Immunol Method* 1984; **73**: 17-22
- 37 **Lloyd CE**, Ascoli M. On the mechanisms involved in the regulation of the cell surface receptors for human choriogonadotropin and mouse epidermal growth factor in cultured Leydig tumor cells. *J Cell Biol* 1983; **96**: 521-527
- 38 **Heldin CH**, Wasteson A, Westermark B. Interaction of platelet-derived growth factor with its fibroblast receptor: demonstration of ligand degradation and receptor modulation. *J Biol Chem* 1983; **257**: 4216-4221
- 39 **Wiley HS**. Receptors as models for the mechanisms of membrane protein turnover and dynamics. *Curr Top Membr Transp* 1985; **24**: 36-41
- 40 **Higuchi M**, Aggarwal BB. TNF induces internalization of the p60 receptor and shedding of the receptor. *J Immunol* 1994; **152**: 3550-3558

Edited by Zhang JZ

• BASIC RESEARCH •

Effects of recombinant human growth hormone on rat septic shock with intraabdominal infection by *E. coli*

Ying Huang, Shu-Ren Wang, Cheng Yi, Ming-Ying Ying, Ying Lin, Mao-Hui Zhi

Ying Huang, Shu-Ren Wang, Department of Pathophysiology, Huaxi School of Basic Medical Sciences and Forensic Medicine, Sichuan University, Chengdu 610041, Sichuan Province, China

Cheng Yi, Cancer Center, Huaxi Hospital, Sichuan University, Chengdu 610041, Sichuan Province, China

Ming-Ying Ying, Ying Lin, ICU, Huaxi Hospital, Sichuan University, Chengdu 610041, Sichuan Province, China

Mao-Hui Zhi, Lab of Functional Sciences, Huaxi School of Basic Medical Sciences and Forensic Medicine, Sichuan University, Chengdu 610041, Sichuan Province, China

Correspondence to: Shu-Ren Wang, Department of Pathophysiology, Huaxi School of Basic Medical Sciences and Forensic Medicine, Sichuan University, Chengdu 610041, Sichuan Province, China. wansuren@mail.sc.cninfo.net

Telephone: +86-28-85501268

Received 2002-07-23 **Accepted** 2002-08-16

Abstract

AIM: To investigate the therapeutic effects of recombinant human growth hormone (rhGH) on rat septic shock with intraabdominal infection by *E. coli* and its possible mechanism.

METHODS: 76 SD rats were divided into 3 groups randomly: control group (group C, $n=16$) without any special treatment, septic shock group (group S, $n=30$) received bolus injection of *E. coli* (1×10^{10} cfu \cdot L $^{-1}$, 15 ml \cdot kg $^{-1}$, ip), treated group (group T, $n=30$) received bolus injection of *E. coli*, and then followed by rhGH injection (2.25 U \cdot kg $^{-1}$ \cdot d $^{-1}$, im). Group S and group T were further divided into 1d and 3d subgroups, respectively ($n=15$ each). Mean arterial pressure (MAP), levels of plasma TNF α and endotoxin and leukocyte count were determined on 1st day and 3rd day after *E. coli* injection. Another 39 SD rats were divided into groups C, S and T ($n=13$ each) just for observing survival rate within 1 week.

RESULTS: (1) On 1st and 3rd day, MAP in group S decreased markedly, and MAP on 1st day lowered more than that of 3rd day ($P<0.01$), while MAP in group T just decreased slightly. The survival rate within 1 week was much higher in group T (84.6 %) than in group S (46.2 %) ($P<0.01$). (2) On 1st day, plasma TNF α and endotoxin elevated significantly in group S and group T ($P<0.05$), and endotoxin in group S had more increase ($P<0.01$). On 3rd day, TNF α in group S returned to the level of group C ($P>0.05$), while TNF α in group T went down below the level of group C ($P<0.01$). On 3rd day, endotoxin in group S declined, but was still higher than that of group C ($P<0.01$), endotoxin in group T returned to the level of group C ($P>0.05$). (3) On 1st day, neutrophil ratio in total leukocyte count in both group S and group T increased significantly ($P<0.05$ vs group C).

CONCLUSION: rhGH showed beneficial effects on rat septic shock. The possible mechanisms may involve the attenuation of bacteria/endotoxin translocation and decreased systemic

endotoxin level; inhibition of the production and release of TNF α ; improved circulatory function; improved systemic host defenses and maintenance of intestinal mucosa barrier.

Huang Y, Wang SR, Yi C, Ying MY, Lin Y, Zhi MH. Effects of recombinant human growth hormone on rat septic shock with intraabdominal infection by *E. coli*. *World J Gastroenterol* 2002; 8(6):1134-1137

INTRODUCTION

Septic shock is a common and severe disease, the incidence and mortality of septic shock are still very high now-a-days. Growth hormone is an important anabolic hormone. Experimental study showed that recombinant human growth hormone (rhGH) enhanced protein synthesis^[1], promoted tissue recovery, improved host defenses^[2-4], decreased stress and maintained intestinal mucosa barrier^[5,6]. The present study was to investigate the therapeutic effects of rhGH on rat septic shock with intraabdominal infection by *E. coli* and its possible mechanism.

MATERIALS AND METHODS

Animal models and groups

76 female Sprague-Dawley rats weighing between 200 and 240 g were obtained from the Animal Center of Sichuan University. The rats were divided randomly into 3 groups: control group (group C, $n=16$) without any special treatment; septic shock group (group S, $n=30$), injected intraperitoneally with a bolus of *E. coli* (1×10^{10} cfu \cdot L $^{-1}$, 15 ml \cdot kg $^{-1}$); treated group (group T, $n=30$) received a bolus injection of *E. coli*, and then followed by rhGH intramuscular injection (2.25 U \cdot kg $^{-1}$ \cdot d $^{-1}$). Group S and group T were further divided into 1d and 3d subgroups, respectively ($n=15$ each).

Another 39 female Sprague-Dawley rats weighing between 200 and 240 g were divided into groups C, S and T ($n=13$ each) just for observing the survival rate within 1 week.

Reagents

rhGH (Saizen) was obtained from Serono Co. in Switzerland. Bacterial suspension of *E. coli* was supplied by Dept. of Microbiology in Huaxi School of Basic Medical Sciences and Forensic Medicine. Limulus ameocyte lysate (LAL) kit and radioimmunoassay (RIA) kit of rat TNF α were purchased from Shanghai Laboratory of Medical Science and Institute of Radioimmunology, Chinese PLA General Hospital, respectively.

Methods

Measurement of blood pressure Rats were anesthetized with sodium pentobarital (15 ml \cdot kg $^{-1}$, ip) on 1st day or 3rd day after receiving *E. coli*. An arterial cannula connected with Four-Channel Physiological Measuring Instrument (RM-6200, Japan) was inserted into a carotic artery for recording mean arterial pressure (MAP).

Leukocyte count 0.5 ml blood anticoagulated by heparin was collected through a venous cannula which was inserted into an external jugular vein. Leukocyte count was measured by using CELL-DYN 1600.

Plasma endotoxin determination Levels of plasma endotoxin was determined by LAL test, according to the manual of the kit.

Measurement of plasma TNF α Concentrations of plasma TNF α was measured using RIA, according to the manual of the kit.

Statistical analysis

All data except survival rate were expressed as mean \pm standard deviation ($\bar{x} \pm s$). Data were analyzed by *t*-test or variance analysis using SPSS 10.0 software, and $P < 0.05$ was considered as the significant level of difference.

RESULTS

Mean arterial pressure (MAP) and survival rate

On 1st day and 3rd day, MAP in group S decreased obviously, and MAP on 1st day showed a 46 % decrease ($P < 0.01$, vs group C). MAP in group T was just about 10 % reduction ($P < 0.05$, vs group C). These results suggested that rhGH could attenuate the hypotension induced by septic infection. 7 Rats in group S were dead within 1 week, the survival rate was 46.2 % (6/13). 2 Rats in group T were dead within 1 week, the survival rate was 84.6 % (11/13). All rats in group C survived. The survival rate was much higher in group T than in group S ($P < 0.01$, See Table 1). These findings indicated that rhGH could improve the outcome of septic shock significantly.

Table 1 Effects of rhGH on mean arterial pressure (MAP) ($\bar{x} \pm s$) and survival rate within 1 week in rat septic shock

Group	MAP (mmHg)		Survival rate within 1 week (%)
	1 d	3 d	
C	124.6 \pm 13.9		100.0
S	67.4 \pm 22.6 ^b	98.9 \pm 23.2 ^{a,d}	46.2
T	114.4 \pm 15.9 ^{a,d}	109.9 \pm 10.2 ^a	84.6 ^f

^a $P < 0.05$, ^b $P < 0.01$, vs group C; ^d $P < 0.01$, vs group S in 1 d; ^f $P < 0.01$, vs group S.

Leukocyte count

On 1st day, the numbers of leukocyte in both group S and group T showed no significant difference from that of group C ($P > 0.05$), while neutrophil ratio in total leukocytes was higher in both group S and group T than in group C, and more in group T ($P < 0.05$). On 3rd day, both the numbers of leukocyte and neutrophil ratio in total leukocytes had no significant changes among the three groups ($P > 0.05$, See Table 2).

Table 2 Effect of rhGH on leukocyte count in rat septic shock ($\bar{x} \pm s$)

Time	Leukocyte ($\times 10^9/L$)			Neutrophil (%)		
	Group C	Group S	Group T	Group C	Group S	Group T
1 d	8.42 \pm 2.44	9.61 \pm 3.58		28.75 \pm 8.83 ^a	36.77 \pm 11.84 ^c	
	7.73 \pm 4.57			16.14 \pm 6.0		
3 d	6.75 \pm 2.18	6.07 \pm 2.45		13.74 \pm 7.06	14.96 \pm 5.35	

^a $P < 0.05$, ^b $P < 0.01$, vs group C; ^c $P < 0.05$, vs 1 d in group S.

Plasma endotoxin and TNF α

On 1st day, plasma TNF α and endotoxin increased significantly in group S and group T ($P < 0.05$), and endotoxin in group S had more increase ($P < 0.01$). On 3rd day, TNF α in group S returned to the level of group C ($P > 0.05$), while TNF α in group T went down below the level of group C ($P < 0.01$). Endotoxin in group S decreased, but was still higher than that of group C ($P < 0.01$). Endotoxin in group T returned to the value of group C ($P > 0.05$, See Table 3). These results suggested that rhGH could extinguish plasma endotoxin and inhibit the production and release of TNF α .

Table 3 Effects of rhGH on the concentrations of plasma endotoxin and TNF α in rat septic shock

Time	Endotoxin (U \cdot L ⁻¹)			TNF α (μ g \cdot L ⁻¹)		
	Group C	Group S	Group T	Group C	Group S	Group T
1 d		256 \pm 52 ^a	150 \pm 39 ^{b,c}		3.59 \pm 0.69 ^b	3.66 \pm 1.33 ^b
	111 \pm 53			2.88 \pm 0.74		
3 d		189 \pm 52 ^a	108 \pm 42 ^d		2.23 \pm 1.09	1.54 \pm 0.36 ^{a,d}

^a $P < 0.01$, ^b $P < 0.05$, vs group C; ^c $P < 0.01$, vs group S in 1 d; ^d $P < 0.01$, vs group S in 3 d.

DISCUSSION

When acute peritoneal bacterial infection happens, there are two lines of host defense against peritoneal bacterial invasion. The first line of host defense is peritoneal resident cells, which consist mainly of macrophages. Peritoneal macrophages begin the process of phagocytosis and killing of bacteria immediately after bacterial inoculation^[7]. Inoue T *et al* demonstrated that administration of rhGH augmented the numbers of peritoneal macrophages significantly in gram-negative sepsis model. The second line of host defense is an acute inflammatory response involving the influx of neutrophils. Neutrophils are attracted to the site of infection by chemotactic factors, then phagocytize, kill and eliminate bacteria^[7]. In our study, neutrophil ratio in total leukocyte count in both group S and group T increased significantly than that in group C on 1st day, and more in group T. Our results indicated that rhGH could significantly increase neutrophil ratio in total leukocytes. Taken together, it could be inferred that rhGH could enhance the two lines of host defense, accelerate the clearance of bacteria from the peritoneal cavity, minimize the spread of bacteria to blood, and then diminish plasma endotoxin and proinflammatory cytokines levels.

Endotoxin, the main toxic component of gram-negative bacteria, is the leading cause of sepsis or septic shock^[8-10]. Our experiment showed that plasma endotoxin levels both in group S and group T elevated obviously after *E.coli* challenge. The main reason of higher endotoxin level in plasma was related to the proliferation of *E.coli* in blood and peritoneal cavity. In addition, it was also associated with the impairment of intestinal mucosa barrier, which may cause and accelerate bacteria/endotoxin translocation^[11].

An important function of intestinal mucosa barrier is to prevent translocation of bacteria/toxins from gut lumen into circulation^[12-23]. Glutamine (Gln), the preferred fuel for gut^[24], is a required nutrient for maintaining the normal structure and function of intestinal mucosa barrier^[25,26]. The ability of intestinal mucosa uptaking and utilizing Gln directly influences the function of intestinal mucosa barrier. In septic shock, ischemia, hypoxia and proinflammatory cytokines may result in impairment of intestinal mucosa barrier, meanwhile, Gln

intake by intestinal mucosa and the activity of glutaminase, which catalyzes the hydrolysis of Gln to glutamate and ammonia, could also be injured, so result in marked reduction of the utilization of Gln by gut. An injured Gln metabolism may be another contributor in the breakdown of the intestinal mucosa barrier. The impairment of intestinal mucosa barrier facilitating the entering of bacteria/endotoxin into portal venous and lymphatic systems was defined as bacteria/endotoxin translocation^[27-29]. Moreover, higher systemic endotoxin level could significantly compromise the integrity of intestinal mucosa barrier, and further enhanced the translocation of bacteria/endotoxin^[30].

On 1st day, plasma endotoxin increased significantly in group S than in group T. On 3rd day, endotoxin in group S remained at higher level, while endotoxin in group T returned to control level. These results suggested that rhGH could decrease plasma endotoxin level, which might be due to: (1) rhGH binding growth hormone receptors localized extensively in intestinal mucosa could increase the activity of glutaminase, promote intestinal mucosa to uptake and utilize Gln, ameliorate the impairment of intestinal mucosa barrier. (2) rhGH could also protect intestinal mucosa barrier by enhancing the paracrine and autocrine mechanism of IGF-1 and upregulate the expression of IGF-1 mRNA in intestine^[31]. Thereby, rhGH administration showed beneficial effects in maintaining the integrity of intestinal mucosal barrier^[32,33], attenuating bacteria/endotoxin translocation^[27,34,35] and decreasing plasma endotoxin level^[31]. In addition, Prieto *et al*^[7] also demonstrated that rhGH could promote the release and chemotaxis of neutrophils, minimize the spread of bacteria and attenuate bacteria/endotoxin translocation, and then reduce plasma endotoxin level.

Endotoxin could trigger a series of inflammatory processes, leading to release of many other proinflammatory cytokines^[34]. TNF, a central mediator of the complex network of proinflammatory cytokines^[35], plays a critical role in the pathogenesis of gram-negative-induced sepsis. Our results showed plasma TNF α increased significantly on 1st day after *E. coli* injection. The mechanism of higher plasma TNF may be due to^[35]: (1) TNF released from macrophages in gut wall and peritoneal cavity in response to endotoxin stimulation, which may be one of the reasons of early higher TNF level in portal vein and systemic circulation. (2) Endotoxin entering liver via portal venous, stimulated Kupffer cells to produce more TNF α and then further elevated plasma TNF α level^[36-38]. On 3rd day, TNF α in group S returned to the level of group C, while TNF α in group T reduced even lower than that in group C, suggesting that rhGH could inhibit the production and release of TNF α . The mechanism may involve: rhGH maintained intestinal mucosa barrier, diminished bacteria/endotoxin translocation and downregulated the production of TNF.

After *E. coli* injection, MAP in rats of group S decreased obviously, MAP declined even more obviously on 1st day than on 3rd day; while MAP in group T just decreased slightly on 1st day and 3rd day. The data revealed that rhGH could attenuate the decline of blood pressure in septic shock. The mechanism of rhGH improving circulatory function may be related to inhibition of production and release of proinflammatory cytokines and decrease of systemic endotoxin level.

The survival rate within 1 week was much higher in group T (84.6 %) than in group S (46.2 %), which indicated that rhGH could increase survival rate and improve outcome in septic shock.

In summary, the above results showed that rhGH treatment had desirable beneficial effects on rat septic shock, which may involve the following mechanism that rhGH administration

could improve host defenses^[2-4]; maintain intestinal mucosa barrier^[5,6]; diminish bacteria/endotoxin translocation^[17-19]; decrease systemic endotoxin level^[18]; inhibit the production and release of TNF α and improve circulatory function.

REFERENCES

- 1 **Kolstad O**, Jenssen TG, Ingebretsen OC, Vinnars E, Revhaug A. Combination of recombinant human growth hormone and glutamine-enriched total parenteral nutrition to surgical patients: effects on circulating amino acids. *Clin Nutr* 2001; **20**: 503-510
- 2 **Van den Berghe G**. Novel insights into the neuroendocrinology of critical illness. *Eur J Endocrinol* 2000; **143**: 1-13
- 3 **Heemskerk VH**, Daemen MA, Buurman WA. Insulin-like growth factor-1 (IGF-1) and growth hormone (GH) in immunity and inflammation. *Cytokine Growth Factor Rev* 1999; **10**: 5-14
- 4 **Hattori N**, Saito T, Yagyu T, Jiang BH, Kitagawa K, Inagaki C. GH, GH receptor, GH secretagogue receptor, and ghrelin expression in human T cells, B cells, and neutrophils. *J Clin Endocrinol Metab* 2001; **86**: 4284-4291
- 5 **Mylonas PG**, Matsouka PT, Papandoniou EV, Vagianos C, Kalfarentzos F, Alexandrides TK. Growth hormone and insulin-like growth factor I protect intestinal cells from radiation induced apoptosis. *Mol Cell Endocrinol* 2000; **160**: 115-122
- 6 **Zhou X**, Li N, Li JS. Growth hormone stimulates remnant small bowel epithelial cell proliferation. *World J Gastroenterol* 2000; **6**: 909-913
- 7 **Prieto I**, Gomez de Segura IA, Garcia Grande A, Guerra A, Pozo F, Garcia P, de Miguel E. Growth hormone reduces bacterial translocation in radiation enteritis in the rat. *Rev Esp Enferm Dig* 1998; **90**: 353-360
- 8 **Meng AH**, Ling YL, Zhang XP, Zhao XY, Zhang JL. CCK-8 inhibits expression of TNF-alpha in the spleen of endotoxic shock rats and signal transduction mechanism of p38 MAPK. *World J Gastroenterol* 2002; **8**: 139-143
- 9 **Ling YL**, Meng AH, Zhao XY, Shan BE, Zhang JL, Zhang XP. Effect of cholecystokinin on cytokines during endotoxic shock in rats. *World J Gastroenterol* 2001; **7**: 667-671
- 10 **Fan K**. Regulatory effects of lipopolysaccharide in murine macrophage proliferation. *World J Gastroenterol* 1998; **4**: 137-139
- 11 **Forsythe RM**, Xu DZ, Lu Q, Deitch EA. Lipopolysaccharide-induced enterocyte-derived nitric oxide induces intestinal monolayer permeability in an autocrine fashion. *Shock* 2002; **17**: 180-184
- 12 **Ersin S**, Tuncyurek P, Esassolak M, Alkanat M, Buke C, Yilmaz M, Telefoncu A, Kose T. The prophylactic and therapeutic effects of glutamine- and arginine-enriched diets on radiation-induced enteritis in rats. *J Surg Res* 2000; **89**: 121-125
- 13 **Sun XQ**, Fu XB, Zhang R, Lu Y, Deng Q, Jiang XG, Sheng ZY. Relationship between plasma D(-)-lactate and intestinal damage after severe injuries in rats. *World J Gastroenterol* 2001; **7**: 555-558
- 14 **Dong HL**. Intestinal permeability test and its clinical significance. *Shijie Huaren Xiaohua Zazhi* 2000; **8**: 562-563
- 15 **Luo H**, Wang LF, Imoto T, Hiji Y. Inhibitory effect and mechanism of acarbose combined with gymnemic acid on maltose absorption in rat intestine. *World J Gastroenterol* 2001; **7**: 9-15
- 16 **Qin RY**, Zou SQ, Wu ZD, Qiu FZ. Influence of splanchnic vascular infusion on the content of endotoxins in plasma and the translocation of intestinal bacteria in rats with acute hemorrhage necrosis pancreatitis. *World J Gastroenterol* 2000; **6**: 577-580
- 17 **Hess DJ**, Henry-Stanley MJ, Erickson EA, Wells CL. Effect of tumor necrosis factor alpha, interferon gamma, and interleukin-4 on bacteria-enterocyte interactions. *J Surg Res* 2002; **104**: 88-94
- 18 **Sileri P**, Morini S, Sica GS, Schena S, Rastellini C, Gaspari AL, Benedetti E, Cicalese L. Bacterial translocation and intestinal morphological findings in jaundiced rats. *Dig Dis Sci* 2002; **47**: 929-934
- 19 **Mosenthal AC**, Xu D, Deitch EA. Elemental and intravenous total parenteral nutrition diet-induced gut barrier failure is intestinal site specific and can be prevented by feeding nonfermentable fiber. *Crit Care Med* 2002; **30**: 396-402
- 20 **Kouris GJ**, Liu Q, Rossi H, Djuricin G, Gattuso P, Nathan C, Weinstein RA, Prinz RA. The effect of glucagon-like peptide 2

- on intestinal permeability and bacterial translocation in acute necrotizing pancreatitis. *Am J Surg* 2001; **181**: 571-575
- 21 **Parks RW**, Stuart Cameron CH, Gannon CD, Pope C, Diamond T, Rowlands BJ. Changes in gastrointestinal morphology associated with obstructive jaundice. *J Pathol* 2000; **192**: 526-532
 - 22 **Erbil Y**, Berber E, Ozarmagan S, Seven R, Eminoglu L, Calis A, Olgac V, Gurler N. The effects of sodium deoxycholate, lactulose and glutamine on bacterial translocation in common bile duct ligated rats. *Hepatogastroenterology* 1999; **46**: 2791-2795
 - 23 **Gork AS**, Usui N, Ceriati E, Drongowski RA, Epstein MD, Coran AG, Harmon CM. The effect of mucin on bacterial translocation in I-407 fetal and Caco-2 adult enterocyte cultured cell lines. *Pediatr Surg Int* 1999; **15**: 155-159
 - 24 **Gu Y**, Wu ZH. The anabolic effects of recombinant human growth hormone and glutamine on parenterally fed, short bowel rats. *World J Gastroenterol* 2002; **8**: 752-757
 - 25 **Neu J**, DeMarco V, Li N. Glutamine: clinical applications and mechanisms of action. *Curr Opin Clin Nutr Metab Care* 2002; **5**: 69-75
 - 26 **Li YS**, Li JS, Jiang JW, Liu FN, Li N, Qin WS, Zhu H. Glycyl-glutamine-enriched long-term total parenteral nutrition attenuates bacterial translocation following small bowel transplantation in the pig. *J Surg Res* 1999; **82**: 106-111
 - 27 **Li JY**, Lu Y, Hu S, Sun D, Yao YM. Preventive effect of glutamine on intestinal barrier dysfunction induced by severe trauma. *World J Gastroenterol* 2002; **8**: 168-171
 - 28 **Antequera R**, Bretana A, Cirac A, Brito A, Romera MA, Zapata R. Disruption of the intestinal barrier and bacterial translocation in an experimental model of intestinal obstruction. *Acta Cient Venez* 2000; **51**: 18-26
 - 29 **Yu P**, Martin CM. Increased gut permeability and bacterial translocation in *Pseudomonas pneumonia*-induced sepsis. *Crit Care Med* 2000; **28**: 2573-2577
 - 30 **Dickinson E**, Tuncer R, Nadler E, Boyle P, Alber S, Watkins S, Ford H. NOX, a novel nitric oxide scavenger, reduces bacterial translocation in rats after endotoxin challenge. *Am J Physiol* 1999; **277**: G1281-G1287
 - 31 **Wang X**, Wang B, Wu J, Wang G. Beneficial effects of growth hormone on bacterial translocation during the course of acute necrotizing pancreatitis in rats. *Pancreas* 2001; **23**: 148-156
 - 32 **Scopa CD**, Koureleas S, Tsamandas AC, Spiliopoulou I, Alexandrides T, Filos KS, Vagianos CE. Beneficial effects of growth hormone and insulin-like growth factor I on intestinal bacterial translocation, endotoxemia, and apoptosis in experimentally jaundiced rats. *J Am Coll Surg* 2000; **190**: 423-431
 - 33 **Zhou X**, Li YX, Li N, Li JS. Effect of bowel rehabilitative therapy on structural adaptation of remnant small intestine: animal experiment. *World J Gastroenterol* 2001; **7**: 66-73
 - 34 **Wang P**, Li N, Li JS, Li WQ. The role of endotoxin, TNF-alpha, and IL-6 in inducing the state of growth hormone insensitivity. *World J Gastroenterol* 2002; **8**: 531-536
 - 35 **Luo ZY**. Shock. 1st ed. Tianjin. *Tianjin Science and Technology Press* 2001: 432-440
 - 36 **Gong JP**, Wu CX, Liu CA, Li SW, Shi YJ, Yang K, Li Y, Li XH. Intestinal damage mediated by Kupffer cells in rats with endotoxemia. *World J Gastroenterol* 2002; **8**: 923-927
 - 37 **Su GL**. Lipopolysaccharides in liver injury: molecular mechanisms of Kupffer cell activation. *Am J Physiol Gastrointest Liver Physiol* 2002; **283**: G256-G265
 - 38 **Su GL**, Goyert SM, Fan MH, Aminlari A, Gong KQ, Klein RD, Myc A, Alarcon WH, Steinstraesser L, Remick DG, Wang SC. Activation of human and mouse Kupffer cells by lipopolysaccharide is mediated by CD14. *Am J Physiol Gastrointest Liver Physiol* 2002; **283**: G640-G645

Edited by Xu JY

• CLINICAL RESEARCH •

Expression of MMP-2, TIMP-2 protein and the ratio of MMP-2/TIMP-2 in gallbladder carcinoma and their significance

Yue-Zu Fan, Jing-Tao Zhang, Hu-Chuan Yang, Yao-Qin Yang

Yue-Zu Fan, Jing-Tao Zhang, Department of surgery, Tongji Hospital of Tongji University, Shanghai 200065, China

Hu-Chuan Yang, Yao-Qin Yang, Institutes of Tumor, Medical College of Tongji University, Shanghai 200065, China

Supported by Scientific Research Foundation of the Railway Ministry, China, No. TDB99-69

Correspondence to: Professor Yue-Zu Fan, Department of surgery, Tongji Hospital of Tongji University, 389 Xincun Road, Shanghai 200065, China

Telephone: +86-21-56051080-1107 **Fax:** +86-21-56050502

Received 2002-01-11 **Accepted** 2002-02-19

Abstract

AIM: To study the correlation between expression of MMP-2, TIMP-2 protein and the ratio of MMP-2/TIMP-2 and clinical-pathological parameters of patients with gallbladder carcinoma.

METHODS: Carcinomas ($n=45$) and polypoid lesions ($n=15$) of the gallbladder were studied for the expression of MMP-2 and TIMP-2 protein by immunohistochemical avidin-biotin-complex method and image analysis. Clinical-pathological data of patients with gallbladder carcinoma such as histological type, grade of differentiation, level of infiltration, liver invasion and lymph node involvement, etc, were recorded.

RESULTS: There was significant difference between the average level (1.123 ± 0.108 vs 1.030 ± 0.054 , $P=0.002$) of MMP-2, the ratio (1.050 ± 0.013 vs 0.937 ± 0.078 , $P=0.003$) of MMP-2/TIMP-2 in gallbladder carcinomas and in polypoid lesions of the gallbladder. Significant difference was found between the expression of MMP-2 in early stage and advanced tumors, but there was no correlation between MMP-2 protein expression and histological type, differentiation degree, infiltration level, lymph node involvement or liver invasion. Although no difference was observed between TIMP-2 expression and histological type or differentiation degree, significant difference was found between TIMP-2 expression and different Nevin stage, infiltration level, local lymph node involvement or liver invasion (1.168 ± 0.067 vs 1.048 ± 0.075 , 1.170 ± 0.062 vs 1.039 ± 0.069 , 1.039 ± 0.076 vs 1.147 ± 0.083 , 1.048 ± 0.074 vs 1.103 ± 0.095 , $P<0.05$). MMP-2/TIMP-2 ratio did not correlate with histological type, grade of differentiation and liver invasion, but significant differences were found between MMP-2/TIMP-2 ratio and different Nevin stage, infiltration level and lymph node involvement in patients with carcinoma of gallbladder.

CONCLUSION: TIMP-2 and MMP-2/TIMP-2 ratio could reflect more accurately biological characteristic of gallbladder carcinoma and MMP-2/TIMP-2 ratio might be a new

significant marker in early diagnosis, in the judgment of invasion or metastasis and the estimate of prognosis in patients with gallbladder carcinomas.

Fan YZ, Zhang JT, Yang HC, Yang YQ. Expression of MMP-2, TIMP-2 protein and the ratio of MMP-2/TIMP-2 in gallbladder carcinoma and their significance. *World J Gastroenterol* 2002; 8(6):1138-1143

INTRODUCTION

Primary carcinoma of gallbladder represents a very lethal malignant tumor because of its early metastasis, strong invasion and poor prognosis^[1-3]. It is very important to estimate the malignant degree and invasion tendency in order to guide clinical diagnosis and treatment of gallbladder carcinoma. Breakage or degradation of ECM (extracellular matrix) and BM (basement membrane) is necessary in the process of tumor invasion^[4,5]. Matrix metalloproteinases (MMPs) and their tissue inhibitors of metalloproteinases (TIMPs), specially, MMP-2 and its tissue inhibitor (TIMP-2), take important roles in degradation of ECM and BM^[6,7] and relating to tumor invasion^[8-11]. So far, there are no reports on the expression of MMP-2, TIMP-2 and the ratio of MMP-2/TIMP-2 in gallbladder carcinoma. An effort is presently made to examine expression of MMP-2 and TIMP-2 protein and ratio of MMP-2/TIMP-2 in carcinomas and polypoid lesions of the gallbladder, to study correlation between expression of MMP-2, TIMP-2 and ratio of MMP-2/TIMP-2 and clinical-pathological parameters of patients with gallbladder carcinoma and to evaluate their clinical significance.

MATERIALS AND METHODS

Materials

45 carcinomas and 15 polypoid lesion of the gallbladder underwent operational resection and confirmed histopathologically at Tongji hospital of Tongji University from 1995 to 2000 were studied. All samples were fixed in 10 % formalin and embedded in paraffin. In 45 patients with carcinoma of gallbladder, there were 6 males and 39 females with a mean age of 61.9 years (range 36-80 years). Of these, there were histologically 30 adenocarcinomas, 6 papillary carcinomas and 9 others (squamous, mucinous, undifferentiated and clear cell carcinoma); there were 24 G1 (well differentiation), 11 G2 (moderate differentiation) and 10 G3 (poor differentiation), according to the criteria established by World Health Organization for histological type of tumors of the gallbladder and extrahepatic bile ducts. Clinical-pathological dates of each patient with carcinoma of gallbladder, such as histological type, grade of differentiation, level of infiltration, liver invasion and lymph node involvement, etc, were recorded. 15 polypoid lesions of the gallbladder were used as controls. Of them, there were 7 males, 8 females with a mean age of 45.5 years (range 27-74 years).

Methods

Immunohistochemistry Immunohistochemical staining was performed on sections from formalin-fixed paraffin-embedded blocks by the avidin-biotin-complex method (*SABC kit*, BOSTER). Monoclonal MMP-2 antibody (*Neomarker's*) was used at a concentration of 1:100 and TIMP-2 antibody (*Antibody Diagnostic*) at 1:20. Goat serum, biotinylated secondary antibody (goat anti-mouse IgG) and DAB are all purchased from BOSTER. For negative control, the slides were treated with PBS in place of primary antibody.

Quantified analysis of stained intensity^[12] Stained intensity was quantified with the software Analysis System of Clinicopathological Image (*version 2, for windows 95/OSR*). The methods were as follows: (1) estimating the percentage of positive tumor cells, no positive cells, regarded as 0 %. (2) examining average gray value of positive cells of individual slide with image analysis system to be used as antigen concentration. (3) calculating antigen content: Content=gray value×percentage of positive cells. Control samples were examined with the same methods.

Data alternating and statistical analysis Because some samples were negative the examined data needed to be alternated. Regarding examined data as X, alternated data as Y. Alternating method was as following:

$$Y=e^x \quad e=2.71828$$

In this way MMP-2/TIMP-2 ratio was calculated.

All the statistical analyses were performed using *SPSS 10.0* for windows. $P<0.05$ or $F<0.05$ was considered to be of statistical significance.

RESULTS

Expression of MMP-2 and TIMP-2 protein and the ratio of MMP-2/TIMP-2 in carcinomas and polypoid lesions of the gallbladder

Expression of MMP-2 and TIMP-2 protein was observed in tumor cells and epithelial cells of benign lesions, tumor stromal tissues, muscularis of gallbladder and vas wall. Some endangium of vas wall were stained. The protein of MMP-2 and TIMP-2 was mainly expressed in cytoplasm of positive cells (Figure 1-4). Although the expressing pattern of MMP-2 and TIMP-2 protein in carcinomas of gallbladder was identical to that in polypoid lesions of gallbladder, expressed value of MMP-2 in carcinoma was significantly higher than that in polypoid lesions while there was no difference in TIMP-2 protein expression between the two groups (Table 1). In addition, the ratio of MMP-2/TIMP-2 in carcinoma of gallbladder was significantly higher than that in polypoid lesions of gallbladder ($P=0.003$, Table 1).

Table 1 Expression of MMP-2, TIMP-2 and ratio of MMP-2/TIMP-2 in carcinoma and polypoid lesions of gallbladder ($\bar{x}\pm s$)

	<i>n</i>	MMP-2	TIMP-2	MMP-2/TIMP-2
PLG	15	1.030±0.054	1.104±0.072	0.937±0.078
GBC	45	1.123±0.108 ^a	1.077±0.090	1.050±0.013 ^b

PLG: polypoid lesions of the gallbladder; GBC: gallbladder carcinoma.

^a $P=0.002$, ^b $P=0.003$.

Correlation between expression of MMP-2, TIMP-2 protein and ratio of MMP-2/TIMP-2 and clinical-pathological parameters in patients with carcinoma of gallbladder

Correlation between expression of MMP-2, TIMP-2 protein

and ratio of MMP-2/TIMP-2 and clinical-pathological parameters in patients with carcinoma of gallbladder were shown in Table 2 and Figure 3-8. There were no correlation between expression of MMP-2 or TIMP-2 protein and ratio of MMP-2/TIMP-2 and the patients' histological type or degree of differentiation (F test, $P>0.05$). Based on Nevin stage criteria, our files included early stage (S1, S2, $n=11$) and advanced stage tumors (S3-S5, $n=34$). Expression of MMP-2 protein was only correlated with Nevin stage ($P<0.05$); while expression level of TIMP-2 protein was positively correlated with Nevin stage and infiltration level ($P<0.05$), but was reversely correlated with lymph node metastasis and liver invasion ($P<0.05$). There were significant differences between ratio of MMP-2/TIMP-2 and different Nevin stages, infiltration levels, lymph node metastasis and liver invasion in patients with gallbladder carcinoma.

Table 2 Expression and correlation of MMP-2 and TIMP-2 proteins and ratio of MMP-2/TIMP-2 and clinical-pathological parameters of patients with carcinoma of the gallbladder ($\bar{x}\pm s$)

	<i>n</i>	MMP-2	TIMP-2	MMP-2/TIMP-2
histological type				
adenocarcinoma	30	1.140±0.113	1.077±0.089	1.064±0.143
papillary carcinoma	6	1.101±0.106	1.117±0.094	0.990±0.106
others	9	1.082±0.086	1.042±0.084	1.043±0.101
differentiated degree				
well	24	1.117±0.099	1.089±0.095	1.031±0.114
moderate	11	1.041±0.131	1.062±0.083	1.081±0.159
poor	10	1.120±0.110	1.064±0.086	1.059±0.144
Nevin stage				
S1, S2	11	1.063±0.077	1.168±0.067	0.914±0.086
S3-S5	34	1.143±0.110 ^a	1.048±0.075 ^b	1.094±0.112 ^c
Infiltration level				
muscular	13	1.088±0.099	1.170±0.062	0.932±0.093
serosal	32	1.137±0.109	1.039±0.069 ^b	1.097±0.114 ^c
Lymph node				
LN (+)	29	1.131±0.109	1.039±0.076	1.092±0.12
LN (-)	16	1.120±0.107	1.147±0.083 ^b	0.973±0.114 ^c
Liver invasion				
(+)	21	1.136±0.107	1.048±0.074	1.087±0.107
(-)	24	1.112±0.110	1.103±0.095 ^b	1.017±0.143

^a $P<0.05$, ^b $P<0.05$, ^c $P<0.05$.

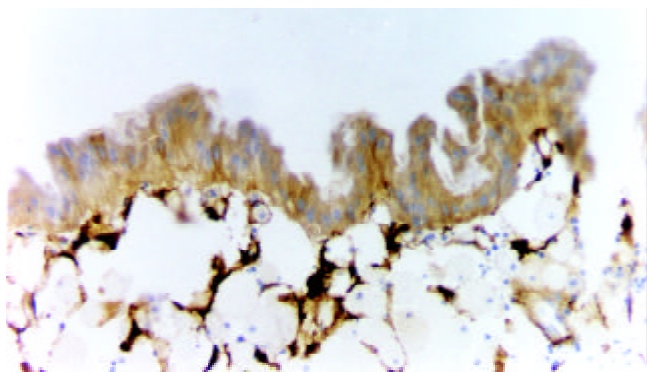


Figure 1 Expression of MMP-2 proteins in polypoid lesion cells of the gallbladder ($\times 200$).

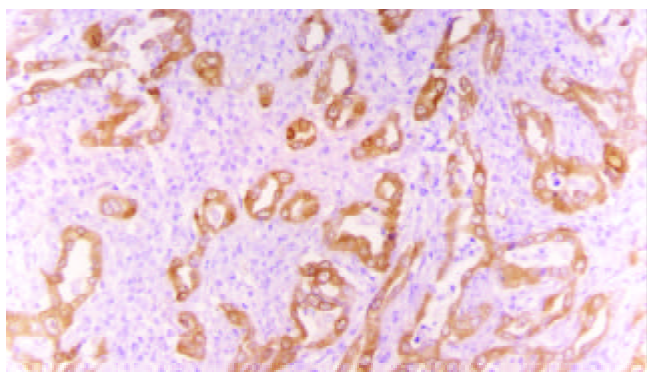


Figure 2 Expression of MMP-2 proteins in adenocarcinoma cells of the gallbladder ($\times 200$).

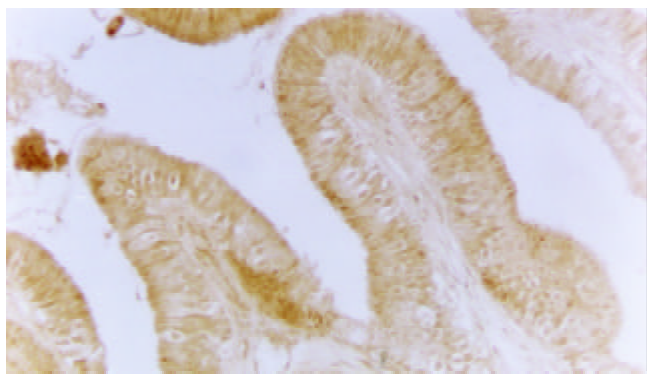


Figure 3 Expression of TIMP-2 protein in polypoid lesion cells of the gallbladder ($\times 200$).

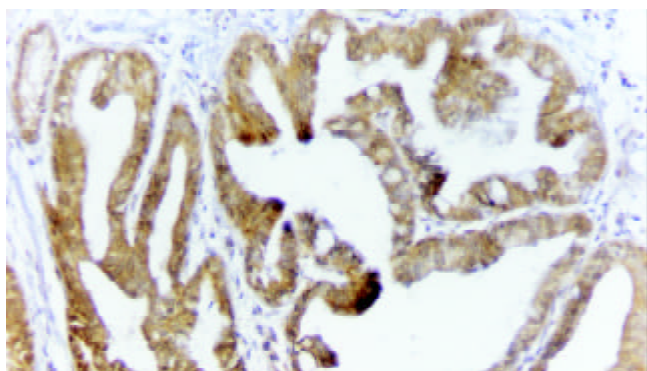


Figure 4 Expression of TIMP-2 protein in adenocarcinoma cells of the gallbladder ($\times 200$).

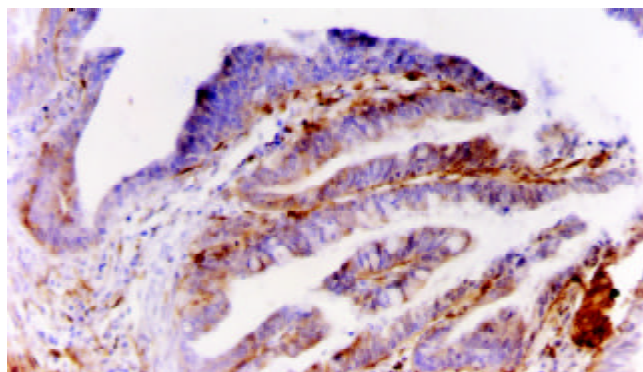


Figure 5 Expression of MMP-2 protein in adenocarcinomas of the gallbladder with LN (-) (Expression level 1.101, $\times 200$).

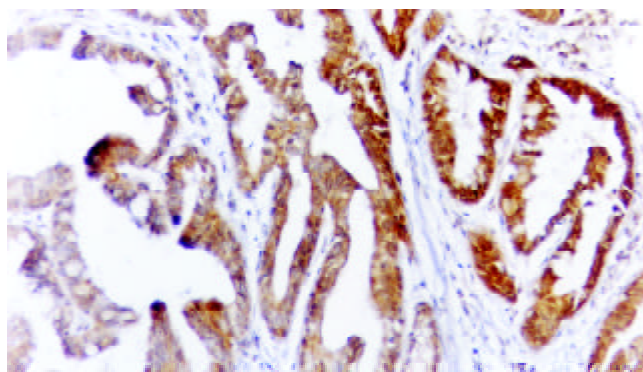


Figure 6 Expression of TIMP-2 protein in adenocarcinomas of the gallbladder with LN (-) (Expression level 1.268, $\times 200$).

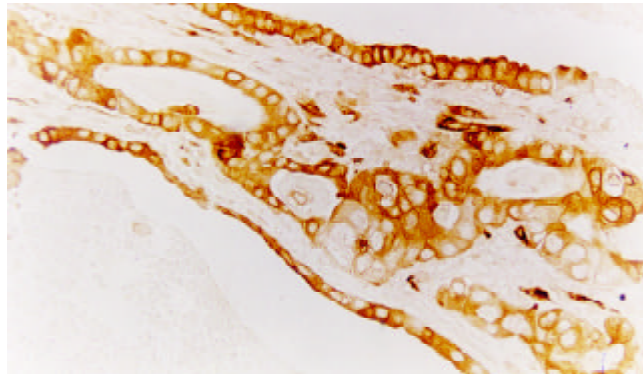


Figure 7 Expression of MMP-2 protein in adenocarcinomas of the gallbladder with LN (+) (Expression level 1.270, $\times 200$).

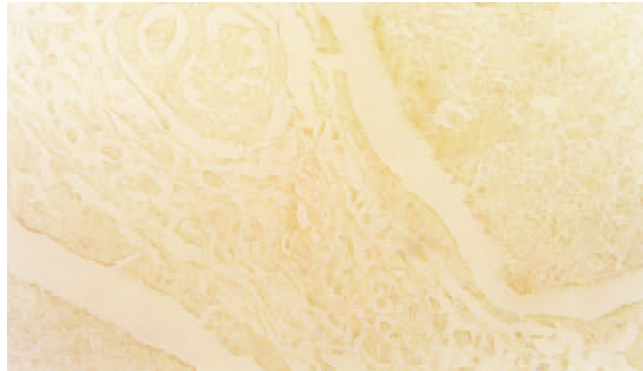


Figure 8 Expression of TIMP-2 protein in adenocarcinomas of the gallbladder with LN (+) (Expression level 1.000, $\times 200$).

DISCUSSION

One of the typical characteristics of malignant tumor is invasion and metastasis. Its ability of invasion and metastasis is mainly responsible for their lethality. So it is necessary to understand the molecular and cellular mechanism of tumor dissemination so as to develop novel therapies basing on this knowledge. Tumor invasion is considered to be a dynamic, complex and multi-step process^[13], but the essential step is the degradation of extracellular matrix (ECM) and basement membrane (BM)^[13,14]. It was reported that MMPs (matrix metalloproteinases) are important for the degradation of ECM. MMPs hydrolyze specifically type IV, V, VII, X collagens and fibronectin, elastin *et al*, which are all important components of ECM and BM, and are closely associated with the invasiveness and metastasis of tumor^[15-20]. TIMPs (tissue inhibitors of metalloproteinases), as the specific inhibitors of MMPs, have such ability to form tight binding, non-covalent inhibitory complexes with multiple members of the MMP family that they inhibit MMP activity of ECM degradation and have anti-metastasis function^[21,22].

There have been many reports about correlation between expression of MMP-2 and TIMP-2 and tumor development^[22-28]. However, no reports concerning correlation between expression of MMP-2 and TIMP-2 and clinicopathological parameters in gallbladder carcinoma have been found. In an immunohistochemical study of 27-pancreatic cancers conducted by Branhall^[29], a strong correlation was found between over-immunoreactivity of MMP-2 and the aggressive phenotype of pancreatic carcinoma. Another study of 177 breast cancer consisting mainly of invasive ductal carcinoma showed that the activation rate of pro-MMP-2 is significantly higher in node-positive carcinomas than in nod-negative cancers or benign neoplasms. Patients with positive staining for MMP-2 were significantly associated with shortened survival and a 3.6 fold increase in the risk of death. MMP-2 was an independent prognostic indicator in multivariate analysis^[30]. Transfection of TIMP-2 gene into HT-1080 cell line and C-H-ras transformed rat embryo fibroblast inhibited their invasion potential in a murine tumor model. Ara *et al*^[4] have observed the expression of high level of TIMP-2 in early stage and the inverse correlation with the corresponding MMP-2 in cases of neuroblastoma, which may represent a mechanism by which tumor cells and stromal tissues control the proteolysis and remodeling of ECM that occurs during invasion and advancement of stages. Also, the correlation of TIMP-2 over-expression with better chance of survival seemed to be associated with the ability of TIMP-2 to inhibit MMP-2 activities and tumor invasion. But recently some studies have suggested that the expression level of TIMP-2 relates to poor prognosis. Ree *et al*^[31] showed that TIMP-2 mRNA level correlated with the development of distant metastases. It was reported in another study that TIMP-1 and TIMP-2 mRNA levels were positively correlated with lymph node metastasis, reduced 5-year survival and Duke's classification in primary colorectal carcinomas. A study on stomach cancer showed that TIMP-1 and TIMP-2 were identified in 41 % and 57 % of tumors, respectively, whereas normal gastric mucosa was negative. No correlation was observed between the presence of TIMP-2 and tumor stage, histological type, lymph node status or survival^[32].

Primary carcinoma of the gallbladder represents a lethal malignant tumor because of its early metastasis, poor prognosis and great difficulties in management^[1-3]. Focusing on the key step of ECM degradation in metastasis, studying on the expression of MMP-2 and TIMP-2 and evaluating the

correlation between these expression levels and clinicopathological parameters would be important for early diagnosis, judgment of invasion or metastasis and prognosis in patients with carcinoma of gallbladder. The present study examined the expression of MMP-2 and TIMP-2 in primary carcinoma of gallbladder by immunohistochemical and image analysis methods in order to evaluate accurately the invasive potential of tumor cells. Results showed that several types of tissues expressed MMP-2 and TIMP-2 protein, such as tumor cells, muscularis of gallbladder and vas wall, stromal cells and epithelial cells of benign lesions, indicating that MMP-2 and TIMP-2 are from epithelial cells (normal or transformed) and other stromal cells. The staining pattern of tumor cells and epithelial cells of benign lesions was cytoplasmic type, identical to previous immunohistochemical studies^[33]. Although the expression of MMP-2 and TIMP-2 could be observed in carcinomas and polypoid lesions of the gallbladder, the expression level of MMP-2 and the ratio of MMP-2/TIMP-2 in tumor was significantly lower than those in benign lesions. But there was no difference in TIMP-2 levels between the two groups, indicating that the relatively high expression of MMP-2 was the basis of tumor invasion and metastasis.

With regard to correlations between the expression of MMP-2 or TIMP-2 and clinicopathological parameters of patients with carcinoma of gallbladder, the present study showed that the expression of MMP-2 related to Nevin stage. Expression value in advanced stage was obviously higher than in early stage (1.143 ± 0.110 vs 1.063 ± 0.077 , $P < 0.05$), but had no correlation with lymph node status and infiltration level. These seemed in contradiction with above reports. The reasons were, on one hand, difference of study method and antibody^[14], on the other hand, double effects of TIMP-2. TIMP-2 not only inhibits MMP-2 activities but also takes part in activation of MMP-2 on the cell surface. If the relationship between MMP-2 and TIMP-2 was not considered, invasive characteristic of cancer cells would not be reflected completely by only examining the expression of MMP-2. In addition, there was no significant difference in the expression value of TIMP-2 between groups of different histological type and grade of differentiation. Expression of TIMP-2 in early stage was obviously higher than in advanced stage, and correlated with infiltration level, local lymph node metastasis and liver invasion. All these suggested that there was a correlation between TIMP-2 expression and the clinicopathological parameters standing for the patients' prognosis. TIMP-2 may be one of indicators in the judgment of Nevin stage, invasion and lymph node metastasis in patients with carcinoma of gallbladder.

MMPs play a major role in ECM degradation while TIMPs are the specific regulators of MMPs. The balance of MMPs/TIMPs is the decisive factor for the maintenance of ECM steadiness and integrity, and the roles of MMPs in tumor metastasis do not depend on the absolute concentration of MMPs in local area, but the MMPs/TIMPs ratio. The expression levels of MMPs and TIMPs would alter in varying degrees in many biological or pathological processes, such as blastocyst implantation, embryonic development, never growth, tissue remodeling, wound healing and the breakdown of blood brain barrier, ulceration, liver fibrosis *et al*^[34-41], but the MMPs/TIMPs balance is controlled accurately. During tumor metastasis the balance of MMPs/TIMPs is broken, favoring ECM degradation without regulation. A study demonstrated recently that the increased adhesion of A2058 cells was associated with increased secretion of MMP-2, which was then inhibited by the increase of TIMP-2. The author

believed the imbalance of MMP-2 and TIMP-2 was critical for tumor cells to have strong invasive potential. Thus examining the absolute concentration of MMPs in local area had no significance and could not reflect the invasive potential of tumor cells. MMPs/TIMPs might act as a prognostic factor indicating malignant invasion and metastasis.

Based on this point, the author evaluated for the first time the correlation between the ratio of MMP-2/TIMP-2 and the clinicopathological parameters of gallbladder carcinoma when examining the expression of MMP-2 and TIMP-2 protein. The results showed that the ratio of MMP-2/TIMP-2 was obviously lower in ploid lesions of the gallbladder than that in carcinoma of gallbladder ($P=0.003$). The ratio of MMP-2/TIMP-2 related to Nevin stage and was significantly higher in advanced cases than in early cases. Significant difference of the ratio between lymph involvement (+) and (-) was also observed (1.092 ± 0.122 vs 0.973 ± 0.114 , $P<0.05$). Moreover, the ratio of MMP-2/TIMP-2 also correlated with infiltration level. Gohji and coworkers^[42] have examined MMP-2/TIMP-2 of 53 advanced urothelial cancers, and reported that MMP-2/TIMP-2 ratio was obviously higher in 31 patients with recurrence than that in patients without recurrence. COX multiple regression analysis showed MMP-2/TIMP-2 as a new marker predicting recurrence in urothelial tumors. They^[43] also found the higher the serum MMP-2/TIMP-2 ratio of advanced bladder cancer, the earlier recurrence and the poorer prognosis. Serum MMP-2/TIMP-2 ratio could exert a predictive role, identical to our conclusion. We propose that, compared with the expression of MMP-2 or TIMP-2, the ratio of MMP-2/TIMP-2 could reflect more accurately the biological characteristics of invasion and metastasis in patients with carcinoma of the gallbladder. As a new prognostic marker, the ratio of MMP-2/TIMP-2 might be useful in early diagnosis and in estimating the invasion and metastasis or survival crisis in patients with carcinoma of the gallbladder.

REFERENCES

- 1 He XD, Zhao YP, Gao P, Zheng CJ, Zhang ZH, Zhang JX. Experience in diagnosis and treatment of primary carcinoma of gallbladder: a report of 52 cases. *Zhonghua Putong Waiké Zazhi* 2001; **7**: 0-72
- 2 Zheng CJ, He XD, Xiao Y, Zhang ZH, Zhang JX. Surgical treatment of gallbladder cancer in 69 cases. *Zhonghua Putong Waiké Zazhi* 2001; **16**: 76-78
- 3 Xu YH, Guo RX, Tian YL, He SG, Shen K, Duan YW. Surgical treatment of gallbladder carcinoma: result of 89 cases. *Zhonghua Gandan Waiké Zazhi* 2001; **16**: 73-75
- 4 Ara BT, Fukuzawa M, Kusafuka T, Komoto Y, Oue T, Inoue M, Okada A. Immunohistochemical expression of MMP-2, MMP-9, and TIMP-2 in neuroblastoma: Association with tumor progression and clinical outcome. *J Pediatr Surg* 1998; **33**: 1272-1278
- 5 Ellenrieder V, Alber B, Lacher U, Hendler SF, Menke A, Boeck W, Wagner M, Wilda M, Friess H, Buchler M, Adler G, Gress TM. Role of MT-MMPs and MMP-2 in pancreatic cancer progression. *In J Cancer* 2000; **85**: 14-20
- 6 Zhang SG, Wu MC, Tan JW, Chen H, Yang JM, Qian QJ. Expression of perforin and granzyme B mRNA in judgment of immunosuppressive effect in rat liver transplantation. *World J Gastroenterol* 1999; **5**: 217-220
- 7 Fingleton BM, Heppner Goss KJ, Crawford HC, Matrisian LM. Matrilysin in early stage intestinal tumorigenesis. *APMIS* 1999; **107**: 102-110
- 8 Maatta M, Soini Y, Liakka A, Autio-Harmainen H. Differential expression of matrix metalloproteinase (MMP)-2, MMP-9, and membrane type 1-MMP in hepatocellular and pancreatic adenocarcinoma: Implications for tumor progression and clinical prognosis. *Clin Cancer Res* 2000; **6**: 2726-2734
- 9 Hofmann UB, Westphal JR, Muijen GNP van, Ruiter DJ. Matrix Metalloproteinases in human melanoma. *J Invest Dermatol* 2000; **115**: 337-344
- 10 Hong ZY, Yu JL, Zhang YS, Gao Y. Relationship between the expression of matrix metalloproteinase-9 and CD-34 and invasion and metastasis of hepatocellular cancer (HCC). *Shijie Huaren Xiaohua Zazhi* 2001; **9**: 170-174
- 11 Stamenkovic I. Matrix metalloproteinases in tumor invasion and metastasis. *Semin Cancer Biol* 2000; **10**: 415-433
- 12 Herbst RS, Yano S, Kuniyasu H, Khuri FR, Bucana CD, Guo F, Liu D, Kemp B, Lee JJ, Hong WK, Fidler IJ. Differential expression of E-cadherin and type IV collagenase genes predicts outcome in patients with stage I non-small cell lung carcinoma. *Clin Cancer Res* 2000; **6**: 790-797
- 13 Meyer T, Hart IR. Mechanisms of tumor metastasis. *Eur J Cancer* 1998; **34**: 214-221
- 14 Kleiner DE, Stetler-Stevenson WG. Matrix metalloproteinases and metastasis. *Cancer Chemother Pharmacol* 1999; **43** (Suppl): s42-s51
- 15 Stock UA, Wiederschain D, Kilroy SM, Shum-Tim D, Khalil PN, Vacanti JP, Mayer Jr JE, Moses MA. Dynamics of extracellular matrix production and turnover in tissue engineered cardiovascular structures. *J Cell Biochem* 2001; **81**: 220-228
- 16 Uria JA, Lopez-Otin C. Matrilysin -2, a new matrix metalloproteinase expressed in human tumors and showing the minimal organization required for secretion, latency, and activity. *Cancer Res* 2000; **60**: 4745-4751
- 17 Deng SJ, Bickett DM, Mitchell JL, Lambert MH, Blackburn RK, Carter III HL, Neugebauer J, Pahel G, Weiner MP, Moss ML. Substrate specificity of human collagenase 3 assessed using a phage-displayed peptide library. *J Biol Chem* 2000; **275**: 31422-31427
- 18 Stracke JO, Hutton M, Stewart M, Pendas AM, Smith B, Lopez-Otin C, Murphy G, Knauper V. Biochemical characterization of the catalytic domain of human matrix metalloproteinase 19. Evidence for a role as a potent basement membrane degrading enzyme. *J Biol Chem* 2000; **275**: 14809-14816
- 19 Marchenko GN, Ratnikov BI, Rozanov DV, Godzik A, Deryugina EI, Strongin AY. Characterization of matrix metalloproteinase-26, a novel metalloproteinase widely expressed in cancer cell of epithelial origin. *Biochem J* 2000; **356**: 705-718
- 20 Nar H, Werle K, Bauer MMT, Dollinger H, Jung B. Crystal structure of human macrophage elastase (MMP-12) in complex with a hydroxamic acid inhibitor. *J Mol Biol* 2001; **312**: 743-751
- 21 Butler GS, Butler MJ, Atkinson SJ, Will H, Tamura T, Westrum SS van, Crabbe T, Clements J, Ortho MP, Murphy G. The TIMP-2 membrane type 1 metalloproteinase "receptor" regulates the concentration and efficient activation of progelatinase A. A kinetic study. *J Biol Chem* 1998; **273**: 871-880
- 22 Zucker S, Cao J, Chen WT. Critical appraisal of the use of matrix metalloproteinase inhibitors in cancer treatment. *Oncogene* 2000; **19**: 6642-6650
- 23 Caenazzo C, Onisto M, Sartor L, Scalera R, Giraldo A, Nitti D, Garbisa S. Augmented membrane type 1 matrix metalloproteinase (MT1-MMP): UMM-2 messenger RNA ratio in gastric carcinomas with poor prognosis. *Clin Cancer Res* 1998; **4**: 2179-2186
- 24 Wang ZN, Xu HM. Relationship between collagen IV expression and biological behavior of gastric cancer. *World J Gastroenterol* 2000; **6**: 438-439
- 25 Ji F, Wang WL, Yang ZL, Li YM, Huang HD, Chen WD. Study on the expression of matrix metalloproteinase-2 mRNA in human gastric cancer. *World J Gastroenterol* 1999; **5**: 455-457
- 26 He YD, Zhao YW, Kong LF, Yin PZ. Activity alternating of matrix metalloproteinase-2 in hepatocellular carcinoma. *Shijie Huaren Xiaohua Zazhi* 2000; **8**: 952-953
- 27 Jiang ZS, Gao Y. Biological characteristics of matrix metalloproteinases and their roles in invasion and metastasis in hepatocellular carcinoma. *Shijie Huaren Xiaohua Zazhi* 2000; **8**: 1403-1404
- 28 Zhu ZY, Du Z, Wang YJ, Zhang W, Sun BC. Examination of E-cadherin and matrix metalloproteinases and its significance in primary HCC. *Shijie Huaren Xiaohua Zazhi* 2001; **9**: 839-840

- 29 **Bramhall SR**, Stamp GWH, Dunn J, Lemoine NR, Neoptolemos JP. Expression of collagenase (MMP-2), stromelysin (MMP-3) and tissue inhibitor of the metalloproteinases (TIMP1) in pancreatic and ampullary disease. *Br J Cancer* 1996; **73**: 972-978
- 30 **Talvensaari-Mattila A**, Paakko P, Hoyhtya M, Blanco-Sequeiros G, Turpeenniemi-Hujanen T. Matrix metalloproteinase-2 immunoreactive protein: A marker of aggressiveness in breast carcinoma. *Cancer* 1998; **83**: 1153-1162
- 31 **Ree AH**, Florenes VA, Berg JP, Malandsmo GM, Nesland JM, Fodstad O. High levels of messenger RNA for tissue inhibitors metalloproteinases (MMP-1 and TIMP-2) in primary breast carcinomas are associated with development of distant metastases. *Clin Cancer Res* 1997; **3**: 1623-1628
- 32 **Murray GI**, Duncan ME, Arbuckle E, Melvin WT, Fothergill JE. Matrix metalloproteinases and their inhibitors in gastric cancer. *Gut* 1998; **43**: 791-797
- 33 **Vaisanen A**, Kallioinen M, Taskinen PJ, Turpeenniemi-Hujanen T. Prognostic value of MMP-2 immunoreactive protein (72kD type IV collagenase) in primary skin melanoma. *J Pathol* 1998; **186**: 51-58
- 34 **Benyon RC**, Arthur MJP. Extracellular matrix degradation and the role of hepatic stellate cell. *Semin Liver Dis* 2001; **21**: 373-384
- 35 **Fini ME**, Cook JR, Mohan R. Proteolytic mechanism in corneal ulceration and repair. *Arch Dermatol Res* 1998; **290** (Suppl): s12-s23
- 36 **Harkness KA**, Adamson P, Sussman JD, Davies-Jones GAB, Greenwood J, Woodroffe MN. Dexamethasone regulation of matrix metalloproteinase expression in CNS vascular endothelium. *Brain* 2000; **123**: 698-709
- 37 **Ozenci V**, Rinaldi L, Teleshova N, Matusevicius D, Kivisakk P, Kouwenhoven M, Link H. Metalloproteinases and their inhibitors in multiple sclerosis. *J Autoimmun* 1999; **12**: 297-303
- 38 **Ninomiya T**, Yoon S, Nagano H, Kumon Y, Seo Y, Kasuga M, Yano Y, Nakaji M, Hayashi Y. Significance of serum matrix metalloproteinases and their inhibitors on the antifibrogenetic effect of interferon-alfa in chronic hepatitis C patients. *Intervirology* 2001; **44**: 227-231
- 39 **Rosenberg GA**, Estrada EY, Dencoff JE. Matrix metalloproteinases and TIMPs are associated with blood-brain barrier opening after reperfusion in rat brain. *Stroke* 1998; **29**: 2189-2195
- 40 **Liu HL**, Li XH, Wang DY, Yang SP. Matrix metalloproteinase-2 and tissue inhibitor of metalloproteinase-1 expression in fibrotic rat liver. *World J Gastroenterol* 2000; **6**: 881-884
- 41 **Lü XH**, Xie YH, Fu BY, Liu CR, Wang BY. Dynamic expression of tissue inhibitor of metalloproteinase-1 in alcoholic liver disease in rats. *Shijie Huaren Xiaohua Zazhi* 2001; **9**: 29-33
- 42 **Gohji K**, Fujimoto N, Fujii A, Komiyama T, Ohkawa J, Nakajima M. Prognostic significance of circulating matrix metalloproteinase-2 to tissue inhibitor of metalloproteinases-2 ratio in recurrence of urothelial cancer after complete resection. *Cancer Res* 1996; **56**: 3196-3198
- 43 **Gohji K**, Fujimoto N, Ohkawa J, Fujii A, Nakajima M. Imbalance between serum matrix metalloproteinase-2 and its inhibitor as a predictor of recurrence of urothelial cancer. *Br J Cancer* 1998; **77**: 650-655

Edited by Pang LH

• CLINICAL RESEARCH •

Cyclospore cayetanensis in Anhui, China

Ke-Xia Wang, Chao-Pin Li, Jian Wang, Ye Tian

Ke-Xia Wang, Chao-Pin Li, Jian Wang, Ye Tian, School of Medicine, Anhui University of Science & Technology Huainan 232001, Anhui Province, China

Correspondence to: Dr. Chao-Pin Li, Department of Etiology and Immunology, School of Medicine, Anhui University of Science and Technology Huainan 232001, Anhui Province, China. cpli@aust.edu.cn

Telephone: +86-554-6658770 **Fax:** +86-554-6662469

Received 2002-05-11 **Accepted** 2002-06-09

Abstract

AIM: To investigate the infection of *Cyclospore cayetanensis* in Anhui Province.

METHODS: Identification of *Cyclospore cayetanensis* was made microscopically by finding the oocysts of *Cyclospore cayetanensis* in fecal smears taken from the infants, pupils and adults with obstinate diarrhea, and immunocompromised individuals by using a auramine-phenol stain and modified acid-fast stain. Cellular immune function was detected with biotin-streptavidin (BSA), and the specific antibody against *Cyclospore cayetanensis* was detected with method of ELISA.

RESULTS: (1) The positive rates of *Cyclospore cayetanensis* infection in infants, pupils, infants and adults with obstinate diarrhea and with immunocompromised individuals were significantly different ($P < 0.01$), with the rates of 0 %, 0.50 % (1/200), 5.62 % (10/178), and 9.38 % (3/32) respectively. (2) The infection rates of males and females were 2.61 % (10/383) and 1.44 % (4/227) respectively, with no significant difference ($P < 0.05$). (3) The positive rates of population with oocysts in urban and rural areas were 0.92 % (3/325) and 3.86 % (11/285) respectively. (4) The positive rates of CD₃⁺, CD₄⁺, CD₈⁺ and the ratio of CD₄⁺/CD₈⁺ of individuals with and without oocysts were significantly different ($P < 0.05$, $P < 0.01$), and their values were (64.28±6.55) %, (43.55±5.80) %, (28.23±4.32) %, 1.52±0.32 and (58.97±5.23) %, (39.26±4.93) %, (30.54±5.17) %, 1.26±0.21, respectively. (5) Specific IgG, IgM and IgG+IgM in serum of the patients with oocyst were significantly different ($P < 0.01$) with the positive rates of 63.41 % (9/14), 17.07 % (1/14) and 19.51 % (4/14) respectively.

CONCLUSION: *Cyclospore cayetanensis* infection is present in Anhui, China and it was confirmed to be a new pathogen associated with children diarrhea, adults obstinate diarrhea and diarrhea in immunocompromised individuals. Among all the infected individuals, adult obstinate diarrhea patients and immunocompromised individuals are common. Feces examination of oocysts and serological examination of the specific antibody will be of much help in the diagnosis of *Cyclospore cayetanensis* infection.

Wang KX, Li CP, Wang J, Tian Y. *Cyclospore cayetanensis* in Anhui, China. *World J Gastroenterol* 2002; 8(6):1144-1148

INTRODUCTION

Cyclospore cayetanensis is an emerging protozoan pathogen associated with diarrhea and human immune function^[1-16]. It is a kind of enteric parasite that infests in the gastrointestinal tract of human causing severe diarrhea. Jejunal biopsies showed an altered mucosal architecture with shortening and widening of the intestinal villi due to diffuse edema and infiltration by a mixed inflammatory cell infiltrate^[17,18]. There was reactive hyperemia with vascular dilatation and congestion of villous capillaries. Cyclosporiasis occurs in persons of all ages and in either immunocompetent or immunocompromised hosts^[19-30]. Human being is the only natural host for this parasite^[31]. Clinical symptoms of Cyclosporiasis are characterized by watery diarrhea (approximately 6 stools/day), nausea, anorexia, abdominal cramping, fatigue, and weight loss, and they are not so specific and can often be misdiagnosed^[32-37]. So cyclospora oocysts detection is needed by phase contrast microscopy, modified acid-fast staining, autofluorescence, and amplification by the polymerase chain reaction^[38-48].

In order to investigate the infection of *Cyclospore cayetanensis* in Anhui Province, we took an investigation of *Cyclospore cayetanensis* in rural and urban areas of Anhui Province. The results of our investigation showed that *Cyclospore cayetanensis* infection was present in Anhui Province and it was confirmed to be a new pathogen associated with children diarrhea and adult obstinate diarrhea.

MATERIALS AND METHODS

Materials

A total of 610 individuals from 11 cities, including Huainan, Hefei, Bengbu, were involved in this investigation. All of them aged from 1 to 55 years, 383 male and 227 female. And they were divided into 2 groups (control group and experimental group).

Screening population (Control group) 400 individuals (infants and pupils) were included in the control group, 217 male and 183 female.

Diarrhea patients (Experimental group) 178 individuals with undefined diarrhea from outpatients (infants and adult with obstinate diarrhea) as well as 32 immunocompromised individuals with obstinate diarrhea were involved in the experimental group, 166 male and 44 female. And 210 feces specimens from the experimental group were collected. Those who had any 2 of the following 5 criteria were considered as immunocompromised individuals: (1) weakened proliferation reaction in lymphocyte transformation test, reduction or lopsided development in T-cell subsets; (2) lower expression of one or more immune globulin (IgG, IgM, IgA, IgD and IgE); (3) deficiency in cytokine, such as IL-2, IFN- γ as well as loss of expression in IL-1R and in IL-2R; (4) weakened function of phagocyte and (5) frequent occurrence of infection such as opportunistic pathogen, virus, fungi and parasites.

Methods

Inquiry of diarrhea history Histories of present illness, anamnesis, symptoms, personal hygiene habits, living

environmental hygiene of the objects and so on were inquired. **Feces examination** 2-3 g fresh feces per person was collected with disposable boxes and smeared into translucent layers. Then the smears were microscopically examined after auramine-phenol stain and modified acid-fast stain. It was described as positive when oocysts were found with apparent internal structure in red, but other non-specific granules revealed black-blue, which was significantly different from the oocysts.

Serological examination Oocysts of *Cyclospore cayetanensis* were taken as antigen from artificially infected guinea pigs and embraced on polystyrene board. Serological examination was performed with ELISA to detect the specific antibody of IgG and IgM in individuals with oocysts. Each time, values of OD of 3 holes (empty, positive, and negative respectively) were read from enzyme labeling meter, and it was judged to be positive when it was 2.1 times as much as the negative.

Detection of T lymphocyte cell subsets Cellular immune function of the individuals with oocysts was detected. The percentage of CD₃⁺, CD₄⁺ and CD₈⁺, and the ratio of CD₄⁺/CD₈⁺ were detected with biotin-streptavidin (BSA) method. Mixed with heparin, peripheral blood was taken and diluted with an equivalence of liquid free of Ca²⁺ and Mg²⁺, then mononuclear cells were separated with lymphocytes separating medium and were made into cell suspension with concentration of (1-3)×10⁶ cells per ml after washing and adjustment. 10 µl of the cell suspension was smeared in acid-proof varnish rings on the surface of slides each time, and when it dried naturally, McAb of anti-CD₃⁺, anti-CD₄⁺ and anti-CD₈⁺, IgG of sheep against guinea pig, and SA-HRP were added. After development with DAB, the smears were observed under microscope. Cytoplasm in brown was regarded as positive, and non-pigmenting as negative. Each time a total of 200 cells were counted for statistics of the positive percentage of cells.

Statistical analysis

Data were expressed as mean ± standard deviation. And multiple comparison tests were performed with χ^2 test and *t* test.

RESULTS

Feces examination

The positive rates of *Cyclospore cayetanensis* from feces taken from the control group and the experimental group were 0.25 % (1/400) and 6.19 % (13/210) respectively. To be exact, the positive rates of the diarrheal and immunocompromised individuals were 5.62 % (10/178) and 9.38 % (3/32) respectively. And the positive rates of the two groups were significantly different ($P < 0.01$). The results are shown in Table 1.

Table 1 Feces examination of *Cyclospore cayetanensis* in different groups (n, %)

Group	n	Auramine-phenol stain+Modified acid-fast stain	
		Positive number	Positive rate
Control group ^b	400	1	0.25
Infants	200	0	0.00
Pupils	200	1	0.50
Experimental group ^b	210	13	6.19
Diarrheal patients	178	10	5.62
Immunocompromised individuals	32	3	9.38
Total	610	14	2.30

^b $P < 0.01$, $\chi^2 = 21.6684$ vs: control group

Common clinical symptoms

Among individuals with *C. cayetanensis*, some had no or slight symptoms in early stage. In our survey, healthy pupils and immunocompromised individuals had no self-conscious symptoms. However, others had clinical symptoms mainly in lower digestive tract (60 %), such as abdominal distention, abdominal pain, loose stool and watery stool. After retrospective studies on 14 cases of *Cyclospore cayetanensis* infection, it was found that 10 of them (71.43 %) were misdiagnosed as bacterial enteritis ($n=5$), viral enteritis ($n=3$), non-specific enteritis ($n=2$), parasitic infection ($n=2$) and abdominal discomfort ($n=2$). The results are shown in Table 2.

Table 2 Clinical symptoms caused by *Cyclospore cayetanensis* (n, %)

Group	Case number	Case Percentage
Non-self-conscious symptom	4	28.57
Self-conscious symptom	10	71.43
General symptom	2	14.29
Upper digestive tract symptom	1	7.14
Lower digestive tract symptom	4	28.57
Upper and lower digestive tract symptom	1	7.14
General and upper digestive tract symptom	1	7.14
General and upper, lower digestive tract symptom	1	7.14
Total	14	100

General symptom: acratia and fever;

Upper digestive tract symptom: anorexia, nausea and vomiting;

Lower digestive tract symptom: abdominal distention, abdominal pain, loose stool and watery stool.

Relationship between infection of *Cyclospore cayetanensis* and gender

Total 610 individuals from different population groups were involved in this investigation on oocysts of *C. cayetanensis* in stools. It was shown that the total positive rate of oocysts was 2.30 % (14/610). In detail, the positive rates were 2.61 % (10/383) in male and 1.44 % (4/227) in female, and there was no significant difference between them ($P > 0.05$). The results are shown in Table 3.

Table 3 Feces examination of *Cyclospore cayetanensis* of different gender

Group	n	Auramine-phenol stain+Modified anti-acid stain	
		Positive number	Positive rate (%)
Male	383	10	2.61
Female	227	4	1.44
Total	610	14	2.30

$P > 0.05$, $\chi^2 = 0.4581$

Relationship between infection of *Cyclospore cayetanensis* and living environmental condition as well as personal hygiene habits

It was shown that the positive rate of oocysts in rural areas was significantly higher than that in urban areas ($P < 0.05$). The

survey showed that there were much difference in living environmental condition and personal hygiene habits between the individuals in rural areas and in urban. In rural areas, plenty of simple toilets, deficiency of sanitary facilities and diffusing feces contamination were commonly seen, and most people were unaware of health knowledge and good hygiene habits. Thus, higher infection rate occurred in rural areas. The results are shown in Table 4.

Table 4 Feces examination of *Cyclospore cayetanensi* in different areas

Group	n	Auramine-phenol stain+Modified acid-fast stain	
		Positive number	Positive rate (%)
Urban area	325	3	0.92
Rural area	285	11	3.86
Total	610	14	2.30

$P < 0.05$, $\chi^2 = 5.8419$

Detection of specific antibody

It was shown that specific antibody of IgG was frequently positive in oocysts-positive individuals, and those of both IgG and IgM were positive in some cases. The results are shown in Table 5.

Table 5 Detection of specific antibody of individuals with *Cyclospore cayetanensis* (n, %)

Group	n	IgG ^b		IgM ^b		IgG+IgM ^b	
		Number	Rate	Number	Rate	Number	Rate
Oocysts positive	14	9	63.41	1	17.07	4	19.51
Oocysts negative	20	0	0.00	0	0.00	0	0.00

^b $P < 0.01$, $\chi^2 = 10.4962$ vs: oocyst negative

Detection of cellular immune function

It was found that the levels of CD₃⁺, CD₄⁺ and CD₄⁺/CD₈⁺ decreased compared with those of the oocysts-negative individuals ($P < 0.05$, $P < 0.01$). And the expression of CD₈⁺ seemed to be stable. The results are shown in Table 6.

Table 6 Detection of T lymphocyte cell subsets of individuals with *Cyclospore cayetanensis* (n, $\bar{x} \pm s$, %)

Group	n	CD ₃ ⁺	CD ₄ ⁺	CD ₈ ⁺	CD ₄ ⁺ /CD ₈ ⁺
Oocysts positive	14	64.28±6.55 ^a	43.55±5.80 ^c	28.23±4.32	1.52±0.32 ^b
Oocysts negative	20	58.97±5.23	39.26±4.93	30.54±5.17	1.26±0.21

^a $P < 0.05$, $t = 2.6213$; ^c $P < 0.05$, $t = 2.3226$ and ^b $P < 0.01$, $t = 2.8666$ vs: negative group

DISCUSSION

Cyclospore cayetanensis is a new human coccidian parasite associated with human prolonged diarrhea. Twenty years ago, the first known human cases of cyclosporiasis were reported in medical literature^[11,18,32]. And prevalence or case reports about it were presented only in about 20 countries^[49-58]. Its

characteristics of pathogenic immune had not been clarified until now. In 1986, Soave separated a kind of “coccidian-like body” for the first time, later more and more people found similar organisms in stools of diarrheic patients. Accordingly, a kind of round granular coccidian-like body was found in stools of patients with diarrhea in Peru in 1992, then it was termed *Cyclospore cayetanensis* and confirmed to be a new kind of pathogen that caused human coccidiosis enteritis^[59,60]. Later, Chinese scholars Chen and Han *et al* verified the presence of infection caused by *C. cayetanensis* in China after comparing the feces specimens between those collected from different areas of China and those from America by Cterling. In survey of cryptosporidium in 2001, we isolated red and round granular coccidian-like bodies from feces of patients with diarrhea, and considered 14 cases of them to be *Cyclospore cayetanensis* infection.

Cyclospore cayetanensis has a worldwide distribution. Patients with this prolonged diarrheal illness are described in North, Central and South America, the Caribbean, Africa, Bangladesh, Southeast Asia, Australia, England, and Eastern Europe^[49,58]. Routes of transmission are still unknown, although the fecal-oral route, either directly or via water, is probably the major one. And it was considered that there were two sources of infection: contaminated drinking water and fruits^[61-68].

This investigation showed that the infection rate of *Cyclospore cayetanensis* was 0.25 % in normal population including infants and pupils, but 5.62 % in patients with diarrhea and 9.32 % in immunocompromised individuals, which was significantly different from normal population. The results showed that the positive rates of oocysts had no significantly different between males and females, but was significantly different between individuals in rural and urban areas, which was 0.92 % and 3.86 % respectively. So infection of *Cyclospore cayetanensis* is present in both urban and rural areas in Anhui Province, and it seemed to be related to personal hygiene habits and immune functions. When ingesting *Cyclospore cayetanensis* oocysts contaminated food and becoming immunocompromised, one could be infected. Individuals only infected by *Cyclospore cayetanensis* were fewer, and they were chiefly non-apparently infected with slight or no symptoms. On the other hand, multi-infection was very common. *Cyclospore cayetanensis* usually co-infected with bacteria and caused non-specific symptoms, including inertia, anorexia, abdominal distention, abdominal pain, loose and watery stool, which could easily be confused with other common intestinal diseases^[69]. So it should be considered as *Cyclospore cayetanensis* infection if individuals experienced prolonged diarrhea.

Detection of cellular immune function in this study showed that the level of CD₃⁺, CD₄⁺ and CD₄⁺/CD₈⁺ in the individuals with oocysts decreased, and the expression of CD₈⁺ seemed to be stable. It indicated that *Cyclospore cayetanensis* infection was related to cellular immune function of individuals, and it appeared with the decrease of CD₃⁺ and CD₄⁺ cells, which was associated with the decrease of immune defense, immune clearance and immune reaction to invading *Cyclospore cayetanensis*. CD₄⁺/CD₈⁺ is the hub of immunoregulation network. The decrease of CD₄⁺ cells indicated that auxiliary T lymphocyte cell took part in the pathogenesis process of diarrhea, and that both humoral immunity of *Cyclospore cayetanensis* antibody and cellular immunity response to *Cyclospore cayetanensis* infection were limited. So it made prolonged diarrhea and led to weak immunological killer effect. Thus we concluded that cellular immune took part in pathogenic process of diarrhea caused by *Cyclospore cayetanensis*.

The specific antibody detection showed that after *Cyclospore cayetanensis* infection, the specific antibody was mainly of IgG, sometimes both IgG and IgM, in rare cases of IgM only. It indicated that *Cyclospore cayetanensis* infection was a kind of chronic infection, and present infection should be considered even if there was IgG (+) only. ELISA usually served in the specific antibody detection, and it was more simple, practical, specific and sensitive. Furthermore, it was convenient to perform and capable of being widely used. Serological examination of specific antibody performed among patients with prolonged diarrhea would be more effective at early diagnosis and treatment.

Cyclospore cayetanensis discussed in the present study was encountered in our survey of *Cryptosporidium* in 2001. We found that auramine-phenol stain could be used in the detection of *Cyclospore cayetanensis* as well. More attention should be paid to the distinction between *Cyclospore cayetanensis* and *Cryptosporidium*: (1) The average diameter of the former (7.953×8.253 mm) was larger than that of the latter (about 5mm); (2) The internal structure of the former was not too clear to be seen any feature of the oocysts of the latter; (3) The density and quantity of the former was less than the latter and (4) The brightness of fluorescence under cryptoscope of the oocysts after auramine-phenol stain of the former was weaker than that of the latter. It remained to be further confirmed that the wall of the oocysts and its structure of *Cyclospore cayetanensis* might vary in different stages of the development of the protozoa. *Cyclospore cayetanensis* is differentiated from other coccidians by its sporulation characteristics and autofluorescence. Because of the autofluorescent properties of the oocysts, particular attention should be drawn to the role of fluorescent microscopy in providing a rapid, inexpensive, and sensitive technique for diagnosis of Cyclospora infections in stool samples^[50].

We've tried to deal with the disease caused by *Cyclospore cayetanensis* with spiramycin, and it seemed to be effective. It was reported that oral trimethoprim-sulfamethoxazole was a better choice in the treatment for Cyclospora infection^[70-76]. Sometimes, it can also be healed with non-antibacterial therapy. In immunocompetent individuals, diarrhea is usually self-limited but might last for several weeks. In immunocompromised hosts it is prolonged, severe and can be associated with biliary tract involvement.

In conclusion, *Cyclospore cayetanensis* infection may not be so rare in China, and further studies should be carried out on its prevalence areas, prevalence principle, life history, mode of transmission and prevention.

ACKNOWLEDGEMENTS

We thank Associate Professors Zhu Yu-Xia, Xu Li-Fa, Tang Xiao-Long, Cai Ru, Qian Zhong-Qing, Yang Qing-Gui, He Ji, Zhang Xiu-Yun, Zhou Hui-Sheng, Lu Jun (Department of Etiology and Immunology, School of Medicine, Anhui University of Science & Technology) and some students of our college for their help in sample collection and experimental studies.

REFERENCES

- 1 **Curry A**, Smith HV. Emerging pathogens: Isospora, Cyclospora and microsporidia. *Parasitology* 1998; **117**: 143-159
- 2 **Serpentini A**, Dutoit E, Camus D. *Cyclospora cayetanensis*: review of an emerging intestinal pathogen. *Ann Biol Clin (Paris)* 1999; **57**: 677-683
- 3 **Eberhard ML**, Nace EK, Freeman AR, Streit TG, da Silva AJ, Lammie PJ. *Cyclospora cayetanensis* infections in Haiti: a common occurrence in the absence of watery diarrhea. *Am J Trop Med Hyg*

- 1999; **60**: 584-586
- 4 **Lindhorst E**, Long EG. *Cyclospora cayetanensis*-an intestinal protozoan pathogenic for humans which is of increasing clinical significance. *Dtsch Med Wochenschr* 1998; **123**: 504-509
- 5 **Mezzari A**, Antunes HB, Wiebbelling AM. *Cyclospora cayetanensis*, a new protozoan to be researched. *Rev Assoc Med Bras* 1999; **45**: 347-348
- 6 **Xia B**, Shivananda S, Zhang GS, Yi JY, Crusius JBA, Peka AS. Inflammatory bowel disease in Hubei Province of China. *China Natl J New Gastroenterol* 1998; **3**: 119-120
- 7 **Cao YL**. Laboratory diagnosis of infectious diarrhea in microorganism. *Shijie Huaren Xiaohua Zazhi* 2001; **9**: 929-930
- 8 **Albert MJ**, Faruque AS, Faruque SM, Sack RB, Mahalanabis D. Case-control study of enteropathogens associated with childhood diarrhea in Dhaka, Bangladesh. *J Clin Microbiol* 1999; **37**: 3458-3464
- 9 **Ranjitham M**, Madan M, Chandrasekharan S. *Cyclospora cayetanensis*, a new emerging coccidian parasite. *J Commun Dis* 1999; **31**: 137-139
- 10 **Barrett KE**. New insights into the pathogenesis of intestinal dysfunction: secretory diarrhea and cystic fibrosis. *World J Gastroenterol* 2000; **6**: 470-474
- 11 **Fan WG**, Long YH. Diarrhea in travelers. *Shijie Huaren Xiaohua Zazhi* 2000; **8**: 937-938
- 12 **Feng ZH**. Application of gene vaccine and vegetable gene in infective diarrhea. *Shijie Huaren Xiaohua Zazhi* 2000; **8**: 934-936
- 13 **Katz DE**, Taylor DN. Parasitic infections of the gastrointestinal tract. *Gastroenterol Clin North Am* 2001; **30**: 797-815
- 14 **Nunez FA**, Finlay CM. Training for diagnosis of intestinal parasitic diseases in the national laboratory system of Cuba. *Cad Saude Publica* 2001; **17**: 719-724
- 15 **Sterling CR**, Ortega YR. Cyclospora: an enigma worth unraveling. *Emerg Infect Dis* 1999; **5**: 48-53
- 16 **Brown GH**, Rotschafer JC. Cyclospora: review of an emerging parasite. *Pharmacotherapy* 1999; **19**: 70-75
- 17 **Ortega YR**, Sterling CR, Gilman RH. *Cyclospora cayetanensis*. *Adv Parasitol* 1998; **40**: 399-418
- 18 **Ortega YR**, Nagle R, Gilman RH, Watanabe J, Miyagui J, Quispe H, Kanagusuku P, Roxas C, Sterling CR. Pathologic and clinical findings in patients with cyclosporiasis and a description of intracellular parasite life-cycle stages. *J Infect Dis* 1997; **176**: 1584-1589
- 19 **Mosimann M**, Nguyen XM, Furrer H. Excessive watery diarrhea and pronounced fatigue due to *Cyclospora cayetanensis* infection in an HIV infected traveler returning from the tropics. *Schweiz Med Wochenschr* 1999; **129**: 1158-1161
- 20 **O'Mahony C**, Mannion PT. *Cyclospora cayetanensis* and HIV-related diarrhoea. *Int J STD AIDS* 1998; **9**: 59
- 21 **Wilcox CM**. Etiology and evaluation of diarrhea in AIDS: a global perspective at the millennium. *World J Gastroenterol* 2000; **6**: 177-186
- 22 **Parija SC**, Bhattacharya S. Pictorial CME. Isospora belli and cyclospora cayetanensis in a case of chronic diarrhoea in an immunocompromised host. *J Assoc Physicians India* 2000; **48**: 1192
- 23 **Ali MS**, Mahmoud LA, Abaza BE, Ramadan MA. Intestinal spore-forming protozoa among patients suffering from chronic renal failure. *J Egypt Soc Parasitol* 2000; **30**: 93-100
- 24 **Madrid V**, Torrejon E, Rivera N, Madrid M. Cyclosporiasis. Report of a clinical case in Concepcion, Chile. *Rev Med Chil* 1998; **126**: 559-562
- 25 **Ferreira MS**. Infections by protozoa in immunocompromised hosts. *Mem Inst Oswaldo Cruz* 2000; **95**: 159-162
- 26 **Santana Ane M**, Nunez Fernandez FA, Perez Avila J, Barrero Bringuez M, Velazquez Viamontes B. Emergence of a new pathogen: *Cyclospora cayetanensis* in patients infected with human immunodeficiency virus. *Rev Cubana Med Trop* 2000; **52**: 66-69
- 27 **Escobedo AA**, Nunez FA. Prevalence of intestinal parasites in Cuban acquired immunodeficiency syndrome (AIDS) patients. *Acta Trop* 1999; **72**: 125-130
- 28 **Moreno-Camacho A**, Lopez-Velez R, Munoz Sanz A, Labarga-Echevarria P. Intestinal parasitic infections and leishmaniasis in patients with HIV infection. *Enferm. Infecc Microbiol Clin* 1998; **16**: 52-60
- 29 **Verdier RI**, Fitzgerald DW, Johnson WD Jr, Pape JW. Trimethoprim-sulfamethoxazole compared with ciprofloxacin for treatment and prophylaxis of Isospora belli and *Cyclospora cayetanensis* infection in HIV-infected patients. A randomized, controlled trial. *Ann Intern Med* 2000; **132**: 885-888

- 30 **Fernandes AO**, Carollo MC, Braz LM, Amato Neto V, Villela MS. Human cyclosporiasis diagnosis: report of a case in Sao Paulo, SP, Brazil. *Rev Inst Med Trop Sao Paulo* 1998; **40**: 391-394
- 31 **Eberhard ML**, Nace EK, Freeman AR. Survey for *Cyclospora cayetanensis* in domestic animals in an endemic area in Haiti. *J Parasitol* 1999; **85**: 562-563
- 32 **Ranjitham M**, Madan M, Chandrasekharan S. *Cyclospora cayetanensis*-an emerging coccidian parasite. *J Assoc Physicians India* 1999; **47**: 1198-1199
- 33 **Connor BA**, Johnson EJ, Soave R. Reiter syndrome following protracted symptoms of *Cyclospora* infection. *Emerg Infect Dis* 2001; **7**: 453-454
- 34 **Connor BA**, Reidy J, Soave R. Cyclosporiasis: clinical and histopathologic correlates. *Clin Infect Dis* 1999; **28**: 1216-1222
- 35 **Fleming CA**, Caron D, Gunn JE, Barry MA. A foodborne outbreak of *Cyclospora cayetanensis* at a wedding: clinical features and risk factors for illness. *Arch Intern Med* 1998; **158**: 1121-1125
- 36 **Abou EL**, Naga IF. Studies on a newly emerging protozoal pathogen: *Cyclospora cayetanensis*. *J Egypt Soc Parasitol* 1999; **29**: 575-586
- 37 **Looney WJ**. *Cyclospora* species as a cause of diarrhoea in humans. *Br J Biomed Sci* 1998; **55**: 157-161
- 38 **el Naga IF**, Negm AY, Awadalla HN. Preliminary identification of an intestinal coccidian parasite in man. *J Egypt Soc Parasitol* 1998; **28**: 807-814
- 39 **Di Gliullo AB**, Cribari MS, Bava AJ, Cicconetti JS, Collazos R. *Cyclospora cayetanensis* in sputum and stool samples. *Rev Inst Med Trop Sao Paulo* 2000; **42**: 115-117
- 40 **Nace EK**, Steurer FJ, Eberhard ML. Evaluation of Streck tissue fixative, a nonformalin fixative for preservation of stool samples and subsequent parasitologic examination. *J Clin Microbiol* 1999; **37**: 4113-4119
- 41 **Eberhard ML**, da Silva AJ, Lilley BG, Pieniazek NJ. Morphologic and molecular characterization of new *Cyclospora* species from Ethiopian monkeys: *C. cercopithecus* sp.n., *C. colobi* sp.n., and *C. papionis* sp.n. *Emerg Infect Dis* 1999; **5**: 651-658
- 42 **Orlandi PA**, Lampel KA. Extraction-free, filter-based template preparation for rapid and sensitive PCR detection of pathogenic parasitic protozoa. *J Clin Microbiol* 2000; **38**: 2271-2277
- 43 **Rigo CR**, Franco RM. Comparison between the modified Ziehl-Neelsen and Acid-Fast-Trichrome methods for fecal screening of *Cryptosporidium parvum* and *Isospora belli*. *Rev Soc Bras Med Trop* 2002; **35**: 209-214
- 44 **Dalton C**, Goater AD, Pethig R, Smith HV. Viability of *Giardia intestinalis* cysts and viability and sporulation state of *Cyclospora cayetanensis* oocysts determined by electrorotation. *Appl Environ Microbiol* 2001; **67**: 586-590
- 45 **Adam RD**, Ortega YR, Gilman RH, Sterling CR. Intervening transcribed spacer region 1 variability in *Cyclospora cayetanensis*. *J Clin Microbiol* 2000; **38**: 2339-2343
- 46 **Jinneman KC**, Wetherington JH, Hill WE, Adams AM, Johnson JM, Tenge BJ, Dang NL, Manger RL, Wekell MM. Template preparation for PCR and RFLP of amplification products for the detection and identification of *Cyclospora* sp. and *Eimeria* spp. Oocysts directly from raspberries. *J Food Prot* 1998; **61**: 1497-1503
- 47 **Negm AY**. Identification of *Cyclospora cayetanensis* in stool using different stains. *J Egypt Soc Parasitol* 1998; **28**: 429-436
- 48 **Ponce de Leon P**, Flaherty P, Zdero M. A new trichromatic safranin stain for the detection of *Cryptosporidium parvum*, *Cyclospora cayetanensis*, species of *Microsporidia* and *Isospora belli* in fecal material. *Rev Latinoam Microbiol* 1999; **41**: 211-214
- 49 **Bern C**, Hernandez B, Lopez MB, Arrowood MJ, de Mejia MA, de Merida AM, Hightower AW, Venczel L, Herwaldt BL, Klein RE. Epidemiologic studies of *Cyclospora cayetanensis* in Guatemala. *Emerg Infect Dis* 1999; **5**: 766-774
- 50 **Gascon J**, Alvarez M, Eugenia Valls M, Maria Bords J, Teresa Jimenez De Anta M, Corachan M. Cyclosporiasis: a clinical and epidemiological study in travellers with imported *Cyclospora cayetanensis* infection. *Med Clin (Barc)* 2001; **116**: 461-464
- 51 **Fryauff DJ**, Krippner R, Prodjodipuro P, Ewald C, Kawengian S, Pegelow K, Yun T, von Heydowolf-Wehnert C, Oyofu B, Gross R. *Cyclospora cayetanensis* among expatriate and indigenous populations of West Java, Indonesia. *Emerg Infect Dis* 1999; **5**: 585-588
- 52 **Rizk H**, Soliman M. Coccidiosis among malnourished children in Mansoura, Dakahlia Governorate, Egypt. *J Egypt Soc Parasitol* 2001; **31**: 877-886
- 53 **Cann KJ**, Chalmers RM, Nichols G, O'Brien SJ. *Cyclospora* infections in England and Wales: 1993 to 1998. *Commun Dis Public Health* 2000; **3**: 46-49
- 54 **Sherchand JB**, Cross JH. Emerging pathogen *Cyclospora cayetanensis* infection in Nepal. *Southeast Asian J Trop Med Public Health* 2001; **32**: 143-150
- 55 **Chacin-Bonilla L**, Estevez J, Monsalve F, Quijada L. *Cyclospora cayetanensis* infections among diarrheal patients from Venezuela. *Am J Trop Med Hyg* 2001; **65**: 351-354
- 56 **Chalmers RM**, Nichols G, Rooney R. Foodborne outbreaks of cyclosporiasis have arisen in North America. Is the United Kingdom at risk? *Commun Dis Public Health* 2000; **3**: 50-55
- 57 **Pradesaba RA**, Gonzalez M, Piedrasanta E, Merida C, Contreras K, Vela C, Culajay F, Flores L, Torres O. *Cyclospora cayetanensis* in three populations at risk in Guatemala. *J Clin Microbiol* 2001; **39**: 2951-2953
- 58 **Zar FA**, El-Bayoumi E, Yungbluth MM. Histologic proof of acalculous cholecystitis due to *Cyclospora cayetanensis*. *Clin Infect Dis* 2001; **33**: 140-141
- 59 **Herwaldt BL**. *Cyclospora cayetanensis*: a review, focusing on the outbreaks of cyclosporiasis in the 1990s. *Clin Infect Dis* 2000; **31**: 1040-1057
- 60 **Vazquez Tsuji O**, Jimenez Dominguez R, Campos Rivera T, Valencia Rojas S, Romero Cabello R, Gamez Aranda V, Martinez-Barbosa I. *Cyclospora cayetanensis* infection. Laboratory diagnosis. *Rev Latinoam Microbiol* 2000; **42**: 45-52
- 61 **Sturbaum GD**, Ortega YR, Gilman RH, Sterling CR, Cabrera L, Klein DA. Detection of *Cyclospora cayetanensis* in wastewater. *Appl Environ Microbiol* 1998; **64**: 2284-2286
- 62 **Sherchand JB**, Cross JH, Jimba M, Sherchand S, Shrestha MP. Study of *Cyclospora cayetanensis* in health care facilities, sewage water and green leafy vegetables in Nepal. *Southeast Asian J Trop Med Public Health* 1999; **30**: 58-63
- 63 **Nichols GL**. Food-borne protozoa. *Br Med Bull* 2000; **56**: 209-235
- 64 **Graczyk TK**, Ortega YR, Conn DB. Recovery of waterborne oocysts of *Cyclospora cayetanensis* by Asian freshwater clams (*Corbicula fluminea*). *Am J Trop Med Hyg* 1998; **59**: 928-932
- 65 **Lepes T**. Newly established causes of diarrhea: the protozoan *Cyclospora cayetanensis* (Coccidia, Apicomplexa). *Med Pregl* 1998; **51**: 242-244
- 66 **Caceres VM**, Ball RT, Somerfeldt SA, Mackey RL, Nichols SE, MacKenzie WR, Herwaldt BL. A foodborne outbreak of cyclosporiasis caused by imported raspberries. *J Fam Pract* 1998; **47**: 231-234
- 67 **Mota P**, Rauch CA, Edberg SC. Microsporidia and *Cyclospora*: epidemiology and assessment of risk from the environment. *Crit Rev Microbiol* 2000; **26**: 69-90
- 68 **Quintero-Betancourt W**, Peele ER, Rose JB. *Cryptosporidium parvum* and *Cyclospora cayetanensis*: a review of laboratory methods for detection of these waterborne parasites. *J Microbiol Methods* 2002; **49**: 209-224
- 69 **Egloff N**, Oehler T, Rossi M, Nguyen XM, Furrer H. Chronic watery diarrhea due to co-infection with *Cryptosporidium* spp and *Cyclospora cayetanensis* in a Swiss AIDS patient traveling in Thailand. *J Travel Med* 2001; **8**: 143-145
- 70 **Varea M**, Clavel A, Doiz O, Castillo FJ, Rubio MC, Gomez-Lus R. Fuchsin fluorescence and autofluorescence in *Cryptosporidium*, *Isospora* and *Cyclospora* oocysts. *Int J Parasitol* 1998; **28**: 1881-1883
- 71 **Bhattacharya SK**. Therapeutic methods for diarrhoea in children. *World J Gastroenterol* 2000; **6**: 497-500
- 72 **Zhou X**, Li N, Li JS. Growth hormone stimulates remnant small bowel epithelial cell proliferation. *World J Gastroenterol* 2000; **6**: 909-913
- 73 **Chen YQ**, Nie QH. Treatment of infectious diarrhea with micro-ecosystem. *Shijie Huaren Xiaohua Zazhi* 2001; **9**: 932-934
- 74 **Xiao YH**. Treatment of infective Diarrhea with antibiotic. *Shijie Huaren Xiaohua Zazhi* 2000; **8**: 930-932
- 75 **Eberhard ML**, Ortega YR, Hanes DE, Nace EK, Do RQ, Robl MG, Won KY, Gavidia C, Sass NL, Mansfield K, Gzalo A, Griffiths J, Gilman R, Sterling CR, Arrowood MJ. Attempts to establish experimental *Cyclospora cayetanensis* infection in laboratory animals. *J Parasitol* 2000; **86**: 577-582
- 76 **Zhou JL**, Xu CH. The method of treatment on protozoon diarrhea. *Shijie Huaren Xiaohua Zazhi* 2000; **8**: 93-95

• CLINICAL RESEARCH •

Sequential changes of body composition in patients with enterocutaneous fistula during the 10 days after admission

Xin-Bo Wang, Jian-An Ren, Jie-Shou Li

Xin-Bo Wang, Jian-An Ren, Jie-Shou Li, Clinical School of Medical College, Nanjing University, Research Institute of General Surgery, Nanjing General Hospital, People's Liberation Army, Nanjing 210002, Jiangsu Province, China

Correspondence to: Dr. Xin-Bo Wang, Research Institute of General Surgery, Nanjing General Hospital, People's Liberation Army, 305 East Zhongshan Road, Nanjing 210002, Jiangsu Province, China. wang_xb@sohu.com

Fax: +86-25-4803956

Received 2002-06-01 **Accepted** 2002-07-22

Abstract

AIM: To investigate the sequential changes of body composition in the metabolic response that occurred in a group of patients with enterocutaneous fistula after admission to the hospital.

METHODS: Sixty-one patients with enterocutaneous fistula admitted to our hospital had measurements of body composition by multiple-frequency bioelectrical impedance analysis after admission and 5, 10 days later. Sequential measurements of plasma constitutive proteins were also made.

RESULTS: The body weight, fat-free mass, body mass index, and body cell mass were initially well below the normal range, especially the body mass index and body cell mass. And all the data gradually moved up over the 10-day study period, only a highly significant difference was found in body cell mass. Once the patients received nutrition supplement, ECW began to return to normal range slowly as well as ICW and TBW began to rise up, and ECW/TBW significantly declined to near normal level by day 10 in either male or female patients. There was a reprioritization of plasma constitutive protein synthesis that was obligatory and independent of changes in FFM.

CONCLUSION: Serial measurements can quantify the disturbance of body composition in enterocutaneous fistula patients. The early nutritional intervention rapidly ameliorates the abnormal distribution of body water while the state-of-the-art surgical management prevents the further deterioration in cellular composition.

Wang XB, Ren JA, Li JS. Sequential changes of body composition in patients with enterocutaneous fistula during the 10 days after admission. *World J Gastroenterol* 2002; 8(6):1149-1152

INTRODUCTION

Malnutrition is common in patients with enterocutaneous fistula, over a period of time, giving rise to alterations in body composition, as well as systemic and multiorgan manifestations. Malnutrition is also associated with adverse outcomes, whereas clinical stability is associated with

nutritional stability^[1]. Unfortunately, accurate nutritional assessment is difficult in patients with enterocutaneous fistula because standard laboratory methods are inaccurate and the techniques used to precisely assess metabolic compartments are complex, expensive, and of limited availability, especially in China. Assessment of body composition may provide important information about the nutritional status^[2]. The applicability of one safe and convenient methods for body composition analysis, multiple-frequency bioelectrical impedance analysis (MF-BIA) in malnourished patients with enterocutaneous fistula has been sparsely elucidated^[3].

Thus, the aim of the present study is to investigate the sequential changes of body composition in the metabolic response that occurred in a group of patients with enterocutaneous fistula after admission to the hospital.

MATERIALS AND METHODS

Patients

Between December 1, 2000, and November 30, 2001, 86 patients suffering from enterocutaneous fistula (EF) were admitted to the EF Treatment Group of Institute of General Surgery at Jinling Hospital, Nanjing, China. All of these patients wholly recruited from other inpatient clinic were included in the study. EF care at our hospital took place more than thirty years ago in a well coordinated system of pre-hospital and in-hospital care that includes good co-operation with other hospitals, radio-telephone communication, and a high-level, in-hospital EF team response and experience, which includes rapid assessment, resuscitation, stabilization, and sequential therapeutics according to well-established principles^[4].

At the time of admission, all patients studied were able to accomplish the analysis of body composition in standing position for 3 minutes. None of the patients were treated with diuretics and prednisolone and they had exclusion of any metabolic disease. For each patient, diagnosis was made on clinical presentation: definite history of operation, temperature spikes, elevated white cell counts, increasing abdominal tenderness, wound infection, and drainage of succus entericus from intraperitoneal drains. Initial management of the patients invariably involved fluid resuscitation, repletion of depleted electrolytes, maintenance of systemic and multi-organic function, active suction drainage of succus entericus, appropriate broad-spectrum antibiotic therapy to control sepsis, pharmacological approaches including H₂ antagonists, somatostatin and growth hormone if needed^[5], and nutritional supplementation. Some patients who needed prompt exploration of the abdominal cavity to control generalized peritonitis or definitive pus were excluded from the study.

Nutrition was given enterally (Peptide, Nutricia, Dutch) when possible^[4]. The caloric distribution of the formula was 16.5 % protein, 22.7 % fat, and 60.8 % carbohydrate administered by the nasogastric, nasojejunal, gastrostomic, jejunostomic, or any available intestinal route^[4,6]. Nutritional intake was increased up to 2000Kcal/d according a standard

protocol. Patients with contraindications to enteral feeding were given parenteral nutrition by dedicated single-lumen central venous catheters. The initial daily prescription of 17 g nitrogen, 1000Kcal from glucose, and 500Kcal from fat was modified on the basis of size, renal function, and indirect calorimetry.

Study protocol

Patients underwent serial measurements of plasma protein concentrations and body composition during a period of 10 days. The first studies were performed as soon as hemodynamic stability was achieved without either colloid infusion or increasing inotropic support (day 0). The body composition measurements were repeated 5, 10 after admission in the Department of General Surgery by one medician. Measurements of the plasma protein were also made 10 days later.

Techniques of body composition analysis

Body composition measurements were made in all subjects using an multiple-frequency bioelectrical impedance (MFBIA) model InBody 3.0 (Biospace, Seoul, Korea). As one of the latest impedance analyzers, InBody 3.0 uses state-of-the-art technology, an 8-point tactile electrode system that measures the total and segmental impedance and phase angle of alternating electric current at four different frequencies (5 kHz, 50 kHz, 250 kHz, and 500 kHz).

Impedance measurements were made with the subject standing in an upright position, on foot electrodes in the platform of the instrument, with the legs not touching the thighs and the arms not touching the torso. The subject stood on the four foot electrodes: two oval shape electrodes and two heel shape electrodes, and gripped the two Palm-and-Thumb electrodes in order to yield two thumb electrodes and two palm electrodes, without shoes or excess clothing (coats, sweaters, vests). The skin and the electrodes were precleaned using the specific electrolyte tissue according to the manufacturer's instructions. Prior to this, height (stadiometry) was recorded to the nearest 0.1 cm. All the subjects were instructed to fast and to avoid exercise 8 h before measurement and had been resting for at least 30 min before measurement.

All the body composition data were performed in the instrument by inner software and typed in the result sheet immediately after measuring. The software performs provides a plot of reactive and resistive components of the measured impedance at each frequency, as well as body weight, fat-free mass (FFM), total body water (TBW), intra-/extra-cellular water (ICW/ECW), segmental fluid distribution, fat mass (FM), body cell mass (BCM) and body mass index (BMI).

Plasma proteins

Fibronectin, transferrin, and prealbumin were measured as markers of the constitutive plasma proteins. These were determined by ELISA assay using kits of Pointe, UK.

Statistical methods

Analyses were performed using SPSS10.0. Paired student's *t* test was used to detect significant changes over time. Values are expressed as means \pm SD. *P* values less than 0.05 were considered significant.

RESULTS

Patients

Sixty-one of the 86 patients who were recruited into the study completed the protocol, and their clinical diagnostic details are listed in Table 1. During the 10 days after admission, Of the 25

patients who did not complete the protocol, 11 underwent prompt laparotomy exploration to control sepsis, the remaining 14 were too weakness to stand up to complete the body composition measurement. The 61 enterocutaneous fistula patients were all secondary to alimentary tract operation, 18 secondary to cancer, 10 secondary to inflammatory bowel diseases, 2 secondary to pancreatitis, 5 secondary to digestive ulcer, 26 secondary to trauma, intestinal obstruction, and cholelithiasis.

Of the 51 male patients, 24 received total parenteral nutrition, the remaining 27 received enteral nutrition with or without parenteral feeding. Of the 10 female patients, 3 received TPN, and the remaining 7 received total or partial enteral feeding. Nutrition was administered continuously. There was no apparent clinical manifestation of peripheral extremity edema, ascites, or other intra-abdominal fluid collections just before body composition measurement. The median time from admission to receiving the nutritional support was 2 days (range 1 to 3 days).

Table 1 Clinical data of patients recruited for the study

	Male	Female
Esophageal and gastric fistula	4	0
Duodenal fistula	11	3
High-output intestinal fistula	9	2
Low-output intestinal fistula	18	4
Colonic fistula	10	2
Pancreatic and biliaric fistula	5	0
Total	51 ^a	10 ^a

^aSome patients had multiple-origin enterocutaneous fistulas.

Body composition measurements

The body weight, BMI, FFM, and BCM in the male patients were initially well below the normal range (in our own data), especially BMI and BCM, which can be accounted for the severely malnutritional state of these enterocutaneous fistula patients. All the data gradually moved up over the 10-day study period (in Table 2), only a highly significant difference was found in BCM. As is also shown in Table 3, except for the female patients received a significant increase in FFM as well as in BCM. As to the differences of FFM in gender-specific, the causes may be attributed to the small case number, the gentle state of illness, and the high proportion of enteral feeding of the female patients. The latter intensifies the benefits of enteral nutrition in the treatment of enterocutaneous fistula in early course and needs further refinement in future research.

Once the patients received nutrition supplement, ECW began to return to normal slowly as well as ICW and TBW began to raise to normal, and ECW/TBW (which should be the index of edema) significantly declined to near normal by day 10 in either male or female patients. Finally, TW and TW/TBW in male patients significantly increased on Day 5 and then slowly decreased on Day 10, which may be attributable to excess fluid locating in the trunk for abdominal infection or intolerance to early enteral feeding.

Plasma proteins

Twenty of 61 patients at random underwent serial measurement of plasma protein concentration (Shown in Table 4). We found that fibronectin, transferrin, and prealbumin concentrations, which were initially well below the normal range increasingly raised up without significance by Day 10 (*P*>0.05).

Table 2 Demographic and body composition data for male (*n*=51)

Age (years)	41.9±13.5			
Height (cm)	170.2±8.5			
	Day0	Day5	Day10	<i>P</i>
Weight (kg)	51.19±11.00	51.09±10.88	51.39±10.89	0.58
BMI (kg/m ²)	17.62±3.08	17.56±3.06	17.71±3.00	0.44
TBW (kg)	29.41±5.09	29.61±5.03	29.61±5.07	0.18
ECW (kg)	10.51±1.97	10.43±1.91	10.35±1.87	0.12
ICW (kg)	18.89±3.26	19.16±3.23 ^b	19.24±3.31 ^b	0.005
ECW/TBW	0.357±0.0171	0.351±0.0194 ^b	0.350±0.0161 ^b	<0.0001
FFM (kg)	42.55±7.27	42.84±7.16	42.80±7.25	0.21
FM (kg)	8.64±5.00	8.27±4.67 ^b	8.59±4.68	0.009
% FM (wt/wt)	15.97±6.47	15.26±6.15 ^b	15.82±5.97	0.006
BCM (kg)	29.61±5.10	29.98±5.04 ^b	30.02±5.14 ^a	0.010
TW (kg)	13.71±2.41	13.92±2.34 ^b	13.84±2.42	0.007
TW/TBW (%)	46.58±2.25	47.00±1.76 ^a	46.69±1.90	0.015

BMI=body mass index, TBW=total body water, ECW=extracellular water, ICW=intracellular water, FM=fat mass, FFM=fat-free mass, BCM=body cell mass, TW=trunk water ^a*P*<0.05, ^b*P*<0.01 vs Day0.

Table 3 Demographic and body composition data for female (*n*=10)

Age (years)	50.1±11.4			
Height (cm)	157.9±5.4			
	Day0	Day5	Day10	<i>P</i>
Weight (kg)	46.78±8.52	46.92±8.83	47.63±8.57 ^a	0.04
BMI (kg)	18.81±3.74	19.11±3.60	19.18±3.69 ^a	0.04
TBW (kg)	23.44±4.38	24.29±3.54	24.86±3.29	0.057
ECW (kg)	8.59±1.09	8.53±1.25	8.56±1.20	0.38
ICW (kg)	15.54±2.18	15.75±2.32	16.19±2.12 ^b	0.001
ECW/TBW	0.358±0.0157	0.351±0.015 ^a	0.348±0.0127 ^a	0.017
FFM (kg)	35.11±4.49	35.26±5.04	36.09±4.68 ^b	0.005
FM (kg)	10.59±7.11	11.64±6.02	11.56±4.68	0.31
% FM (wt/wt)	23/.26±9.89	23.90±8.82	23.24±8.83	0.49
BCM (kg)	24.48±3.21	24.71±3.52	25.36±3.22 ^b	0.004
TW (kg)	11.26±1.46	11.48±1.81	11.21±1.56	0.07
TW/TBW (%)	48.98±7.80	46.06±1.21	46.18±1.24	0.30

BMI=body mass index, TBW=total body water, ECW=extracellular water, ICW=intracellular water, FM=fat mass, FFM=fat-free mass, BCM=body cell mass, TW=trunk water, ^a*P*<0.05, ^b*P*<0.01 vs Day0.

Table 4 Results of plasma proteins over 10 days

	Day0	Day5	Day10	^a <i>P</i>
FN (mg/L)	109.4±36.4	117.9±37.4	128.6±46.6	0.06
TF (mg/dl)	232.2±40.7	230.4±48.0	243.4±44.2	0.07
PA (mg/dl)	17.4±7.5	19.4±7.1	21.0±6.9	0.054

FN=fibronectin, TF=transferrin, PA=prealbumin ^a*P* vs Day0.

DISCUSSION

Estimation of body composition is important in the assessment

and monitoring of enterocutaneous fistula patients. Enterocutaneous fistula is a condition in which overnutrition, edema, and undernutrition can coexist simultaneously, or successively, over a period of time, giving rise to alterations in body composition, as well as systemic and multiple-organic manifestations. The development of a noninvasive, inexpensive, and accurate technique to assess body water and nutritional compartment would be of great clinical value to identify those patients with impaired morbidity and mortality in enterocutaneous fistula, and enhanced nutritional support is indicated in those patients with persisting nutritional deficits^[4,7].

Bioelectrical impedance analysis is a technique of assessing body composition such as total body water and thus fat-free mass in the healthy population^[8]. And in a number of conditions such as hemodialysis^[9], pregnancy^[10], hepatic cirrhosis^[11], after surgery^[12], and in critical illness^[13], changes in TBW have been shown to be accompanied by changes in impedance. However, in situations where there are clinically important changes in intracellular and extracellular water distribution, such as ascites^[11] and critical illness^[14], the value of single-frequency BIA is limited. It is proposed that multiple-frequency BIA (MFBI) may be of particular use in patients with altered distribution of body water^[2]. At low frequency, the current passes through the extracellular fluids because of the capacitance effect of cell membranes and tissue interfaces, whereas at high frequencies, the current is conducted through both intra- and extracellular fluids. The Biospace InBody 3.0 body-composition analyzer is a novel device to estimate body water compartments and body fat. It differs from other impedance systems, which uses an 8-point tactile electrode system that measures the total and segmental impedance and phase angle of alternating electric current at four different frequencies between 5 and 500 kHz.

BMI was found to be an important predictor of mortality in clinic study, with the association between body mass index and mortality suggesting the U-shaped relation corroborated by many studies^[15]. Although BMI in our study was initially well below the normal range, there were no significant differences in BMI over the study period for male and female patients as well as in body weight and FFM. However, there were highly significant differences in BCM changes over the study period (Table 2 and Table 3). Weight and BMI do not definitely evaluate changes in body compartments and therefore do not reveal if loss of FFM or gain in FM occurs^[16]. The keenness and speediness in the response of BCM to medical intervention made a strong impression on us. BCM provides an ideal reference for metabolic studies in enterocutaneous fistula, while less specific parameters such as body weight, BMI or FFM (which include non-metabolic compartments such as ECW) should be interpreted with caution^[17]. Therefore, we emphasize the importance of measurement of the growth of the metabolically active body compartment, the BCM, in accurately assessing nutritional status in enterocutaneous fistula. And it would be useful in future research to investigate whether the relation between BCM and mortality is also U-shaped in critical illness especially in enterocutaneous fistula. This question may be more amenable to investigate in relatively small, short studies, provided that an appropriate tool for assessment of body composition in enterocutaneous fistula patients is used.

Our results show once again that there is a reprioritization of hepatic protein synthesis in enterocutaneous fistula^[18] that is obligatory and independent of changes in FFM. Concentrations of the constitutive plasma proteins fallen initially raised up over the study period without significance (*P*>0.05) because of their well known turnover rates. There were no significant correlations between the changes of FFM and those of the constitutive plasma proteins. These obligatory

changes may occur in face of continuing proteolysis and high energy expenditure in critical illness. And our results confirm that the measurements of the constitutive plasma proteins have no significant values in demonstrating changes in cellular composition early in the course of enterocutaneous fistula.

Once the patients received nutrition supplement, ECW began to return to normal slowly as well as ICW and TBW began to rise to normal, while ECW/TBW (which should be the index of edema) significantly declined to near normal range by day 10 in either male or female patients ($P<0.0001$ in male, and $P=0.017$ in female). These results are partially similar to those obtained in the critical illness study^[19,20]. In our experience, these findings may be relevant to the clinical manifestations of enterocutaneous fistula patients, especially when persistent severe malnutrition was detected. There may be a reduction in ICW by a compensation for increased ECW in the patients especially those received inappropriate nutritional supplement. And in the early course of nutritional intervention, the rapid amelioration was found not in body protein but in body water compartments. These findings in our study have two implications. First, the present understanding of the degree of abnormal body water distribution that occurs in such patients is largely correct. In the second, it is clear from this study that most effects of the early administered nutritional intervention lie in the rapid improvement of body water distribution. It seems unlikely that much more can be done to preserve cellular composition in early stage of treatment, but state-of-the-art surgical management appears to have prevent further deterioration.

Finally, BIA is a technique that can be readily applied in clinical situations, easy, portable, noninvasive, and inexpensive. Because of these advantages, it can be repeated frequently as necessary and therefore gives a picture of the patient's body composition status and responses to therapy. However, there are still many debates on the validity of MFBIA in clinical assessment of nutritional status especially body water compartment^[21, 22]. MFBIA may not accurately predict water compartments in critically illness especially in those with greatly altered distribution of water, which may alter the capacitance effect of all membranes on conductance through the fluid compartment, although this is highly speculative. It is also recognized that the whole-body BIA is insensitive to fluid changes in the trunk. In our data, we found that the BCM correlated with resting energy expenditure ($r^2=0.61$, $P<0.001$ on Day0, and $r^2=0.59$, $P<0.001$ on Day10) in 12 enterocutaneous fistula patients who were admitted to our hospital consecutively. The slope of the line relating BCM to REE was the same on Day0 and on Day10 ($P=0.34$) in these 12 patients. These findings encouraged us to elucidate the applicability of MFBIA in the enterocutaneous fistula patients. We also suggest that patients with enterocutaneous fistula during treatment phases be followed periodically with BIA measurements. Longitudinal follow-up would permit evaluation of treatment side effects (eg, overfeeding, undernutrition) or sepsis, which are known to have catabolic effects on FFM and FM. And in the future, we will introduce more sophisticated and more invasive techniques such as dual-energy x-ray absorptiometry (DXA).

In conclusion, we have for the first time quantified the changes of body composition during 10 days after admission in enterocutaneous fistula patients by use of MFBIA and have shown that the early nutritional intervention rapidly ameliorates the disturbance of body water while the state-of-the-art surgical management prevents the further deterioration in cellular composition.

REFERENCES

- Huang YC. Malnutrition in the critically ill. *Nutrition* 2001; **17**: 263-264
- Ellis K. Human body composition: In vivo methods. *Physiol Rev* 2000; **80**: 649-680
- Gross E, Holbrook IB, Thornton M. Assessment of the nutritional state of patients with an intestinal fistula. *Br J Surg* 1978; **65**: 740-743
- Li JS, Ren JA, Yin L, Han JM. Management of enteric fistula- Thirty year's experience. *Zhonghua Waike Zazhi* 2002; **40**: 100-103
- Li JS, Ren JA, Wang XB, Gu J, Jiang J. Somatostatin and growth hormone promote spontaneous closure of enterocutaneous fistula. *Zhonghua Waike Zazhi* 2000; **38**: 447-449
- Levy E, Frileux P, Cugnenc PH, Honigor J, Olivier JM, Parc R. High-output external fistulae of the small bowel: Management with continuous enteral nutrition. *Br J Surg* 1989; **76**: 676-679
- Dudrick SJ, Maharaj AR, McKelvey AA. Artificial nutritional support in patients with gastrointestinal fistulas. *World J Surg* 1999; **23**: 570-576
- Kyle UG, Genton L, Karsegard L, Slosman DO, Pichard C. Single prediction equation for bioelectrical impedance analysis in adults aged 20-94 years. *Nutrition* 2001; **17**: 248-253
- Cooper BA, Aslani A, Ryan M, Zhu FYP, Ibels LS, Allen BJ, Pollock AP. Comparing different methods of assessing body composition in end-stage renal failure. *Kidney Int* 2000; **58**: 408-414
- Lukaski HC, Siders WA, Nielsen EJ, Hall CB. Total body water in pregnancy: Assessment by using bioelectrical impedance. *Am J Clin Nutr* 1994; **59**: 578-585
- Lehnert ME, Clarke DD, Gibbons JG, Ward LC, Golding SM, Shepherd RW, Cornish BH, Crawford DHG. Estimation of body water compartments in cirrhosis by multiple-frequency bioelectrical impedance analysis. *Nutrition* 2001; **17**: 31-34
- Meguid MM, Lukaski HC, Tripp MD, Rosenberg JM, Parker FB. Rapid bedside method to assess changes in postoperative fluid status with bioelectrical impedance analysis. *Surgery* 1992; **112**: 502-508
- Sluys TEMS, Ende MEVD, Swart GR, van den Berg JWO, Wilson JHP. Body composition in patients with acquired immunodeficiency syndrome: A validation study of bioelectrical impedance analysis. *JPEN* 1993; **17**: 404-408
- Foley K, Keegan M, Campbell I, Murby B, Hancox D, Bpharm BP. Use of single-frequency bioimpedance at 50 kHz to estimate total body water in patients with multiple organ failure and fluid overload. *Crit Care Med* 1999; **27**: 1472-1477
- Apovian CM. Nutritional assessment in the elderly: Facing up to the challenges of developing new tools for clinical assessment. *Nutrition* 2001; **17**: 62-63
- Frankenfield D, Rowe WA, Cooney RN, Smith JS, Becker D. Limits of body mass index to detect obesity and predict body composition. *Nutrition* 2001; **17**: 26-30
- Shepherd RW, Greer RM, McNaughton SA, Wotten M, Cleghorn GJ. Energy Expenditure and the Body Cell Mass in Cystic Fibrosis. *Nutrition* 2001; **17**: 22-25
- Kuvshinov BW, Brodish RJ, McFadden DW, Fischer JE. Serum transferrin as a prognostic indicator of spontaneous closure and mortality in gastrointestinal cutaneous fistulas. *Ann Surg* 1993; **217**: 615-623
- Plank LD, Hill GL. Sequential metabolic changes following induction of systemic inflammatory response in patients with severe sepsis or major blunt trauma. *World J Surg* 2000; **24**: 630-638
- Cheng ATH, Plank LD, Hill GL. Prolonged overexpansion of extracellular water in elderly patients with sepsis. *Arch Surg* 1998; **133**: 745-751
- Haderslev KV, Staun M. Comparison of dual-energy X-ray absorptiometry to four other methods to determine body composition in underweight patients with chronic gastrointestinal disease. *Metabolism* 2000; **49**: 360-366
- Ellis KJ, Shypailo RJ, Wong WW. Measurement of body water by multifrequency bioelectrical impedance spectroscopy in a multiethnic pediatric population. *Am J Clin Nutr* 1999; **70**: 847-853

Edited by Ren SY